Can. J. Chem. Downloaded from www.nrcresearchpress.com by 210.87.254.5 on 09/05/12
For personal use only.

Canadian Journal of Chemistry

Published by THE NATIONAL RESEARCH COUNCIL OF CANADA

VOLUME 46 JANUARY 1, 1968 NUMBER 1

Reaction mechanism studies. 4. The diaxial → diequatorial rearrangement of β-chlorothioethers

J. F. KING,[1] K. ABIKAR, DONNA M. DEAKEN, AND R. G. PEWS[2]

Department of Chemistry, University of Western Ontario, London, Ontario

Received August 23, 1967

Benzenesulfenyl chloride adds diaxially to 5α-cholest-2-ene (**1**) yielding 2β-chloro-3α-(phenylthio)-5α-cholestane (**3**). Assuming that the reaction proceeds via the episulfonium ion (**2**), this allows the inclusion of these species within the scope of the diaxial opening rule. On heating, **3** undergoes rearrangement to 3β-chloro-2α-(phenylthio)-5α-cholestane (**4**). This reaction is the first instance of a diaxial → diequatorial rearrangement of β-halothioethers.

Mild oxidation of **3** gives a mixture of the two sulfoxides epimeric at the sulfur atom (**16***a* and **16***b*). On heating, both sulfoxides suffer pyrolytic elimination, without any sign of diaxial → diequatorial rearrangement. A major product of the elimination, evidently 2-chloro-5α-cholest-2-ene (**18**), was found to be formed a little more readily from the *S*-sulfoxide (**16***b*) than from the *R*-isomer (**16***a*). This observation is in accord with the conclusion of previous investigators that the elimination of the sulfenic acid from an alkyl sulfoxide involves bond formation between the hydrogen and sulfinyl oxygen during the rate determining stage (cf. **19**).

Canadian Journal of Chemistry, 46, 1 (1968)

The diaxial → diequatorial rearrangement (1) has been shown to take place with dihalides (2–4), and carboxylic (1, 5) and sulfonic esters (6) of halohydrins. Our interest in this reaction has led us to consider the possibility of such rearrangement with other types of compounds, not only to discover the full scope of the reaction but also with an eye to elucidating details of its mechanism (cf. (7)). From the examples already known it appeared that a sufficient—though not necessarily exclusive—requirement for the rearrangement was the presence in a 1,2-diaxial relationship of a good leaving group and a function capable of neighboring group participation. We therefore expected that β-halothioethers should be capable of undergoing the diaxial → diequatorial rearrangement. In addition, these species possess structural features which we hoped would be helpful to us in our general study (and which are discussed, in part, in the following paper), and we set out to make 2β-chloro-3α-(phenylthio)-5α-cholestane (**3**) as an appropriate substrate with which to test these notions. This account describes the preparation of this compound, its thermal rearrangement, and the proof of structure of these materials, together with some observations on the corresponding sulfoxides. The following paper outlines experiments designed to shed light on the mechanism of this reaction, and upon the diaxial → diequatorial rearrangement in general.

Electrophilic attack on 5α-cholest-2-ene is well known to take place preferentially from the α face, which is presumably less hindered than the β face because of the absence of angular methyl groups. As it is believed that sulfenyl chlorides react with simple olefins with initial formation of an episulfonium ion (8–10), it was therefore anticipated that the reaction of 5α-cholest-2-ene with benzenesulfenyl chloride would lead first to the episulfonium ion (**2**). It would further be expected that **2** would open according to the "diaxial opening rule" giving the corresponding diaxial compound, 2β-chloro-3α-(phenylthio)-5α-cholestane (**3**). This expectation is based on

[1]Fellow of the Alfred P. Sloan Foundation, 1966–1968.

[2]Holder of a Dow Chemical of Canada Limited Postgraduate Fellowship, 1961–1962, and a National Research Council of Canada Studentship, 1962–1963. Present address: Dow Chemical Co., Midland, Michigan, U.S.A.

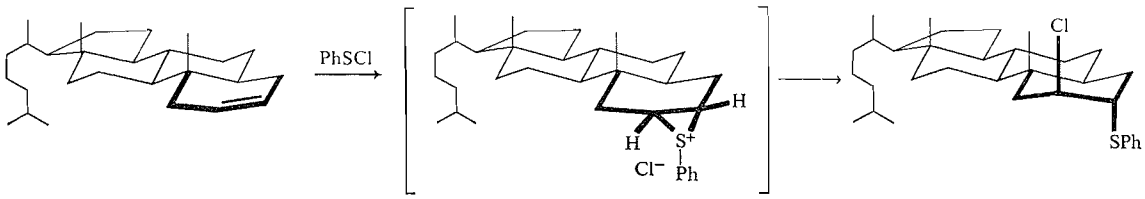

1 2 3

analogy with the observed behavior of other three-membered ring species, such as epoxides (11), halonium ions (12), and ethylenimines (13), and not on any direct evidence from episulfonium ions themselves. Therefore, when the reaction was in fact found to yield a 1:1 adduct, the compound was subjected to careful scrutiny in order to be entirely certain the structure was indeed **3**.

As the usefulness of the compound to us depended on whether or not it would undergo diaxial → diequatorial rearrangement, it was immediately subjected to the appropriate conditions and found to isomerize. Among the dozen examples of diaxial → diequatorial rearrangement reported with 2,3-disubstituted 5α-cholestane derivatives (4–7), the molecular rotation difference ($[\phi]_{Eq} - [\phi]_{Ax}$) varies from −290° to −730°, with most in the range of roughly −400° to −550°. The difference in the present instance is −410°, in excellent agreement with the expectation that the 5α-cholest-2-ene – benzenesulfenyl chloride adduct is in fact diaxial, and rearranging to a diequatorial isomer.

Comparison of the nuclear magnetic resonance (n.m.r.) spectra of the two compounds confirmed this. The diaxial isomer showed bands centered near 4.4 and 3.75 p.p.m. and assigned to the methine protons on C-2 and C-3 respectively.[3] Both bands showed as unresolved humps with widths measured at one-half their heights ("half-widths") of less than 9 c.p.s. Hassner and Heathcock (15) have examined the spectra of a number of analogous steroids and have found that such methine hydrogen atoms when equatorial have half-widths of from 5 to 12 c.p.s., whereas axial protons, presumably because of the greater coupling with vicinal axial protons, show much broader bands, viz. from 15 to 30 c.p.s. The rearranged compound (**4**) showed only a single broad band (half-width > 40 c.p.s.) around 4.4 p.p.m. but the picture was somewhat clearer with the sulfone (**12**), obtained by oxidation of **4**. The spectrum of **12** has broad bands centered around 3.9 and 3.25 p.p.m. with half-widths of about 15 and 20 c.p.s. respectively, clearly indicating that the protons at C-2 and C-3 in the sulfone (**12**) and hence in the rearranged thioether (**4**) are axial.

The above argument establishes that the 5α-cholest-2-ene – benzenesulfenyl chloride adduct is diaxial and rearranges thermally to a diequatorial isomer. No data, however, have been presented to show that the compound is in fact **3**, and not the diaxial compound in which the positions of the substituents are reversed, i.e. 3α-chloro-2β-(phenylthio)-5α-cholestane. The required evidence was obtained from a sequence of reactions beginning with the oxidation of **3** to the corresponding sulfone (**5**). Hydrogenation of **5** in the presence of Raney nickel gave the dechloro-sulfone (**6**), together with a somewhat larger amount of 5α-cholestane. The structure of the dechloro-sulfone was established by independent synthesis from 5α-cholestan-3β-yl phenylmethanesulfonate (**8**) as in the reaction scheme. The assignment of the stereochemistry of 7 (and hence of **6**) follows from the well-known predilection of thiophenoxide ions to attack with inversion of configuration at carbon atoms bearing easily displaced groups, as in the closely related example of the 4-*t*-butylcyclohexyl tosylates studied by Eliel and Ro (16). As a check on this point 5α-cholestan-3α-yl mesylate (**11**) was treated with sodium thiophenoxide and the product (**10**) oxidized to the sulfone (**9**). This material was clearly different from **6** but could be obtained from **6** by treatment with strong base, which allows the phenylsulfonyl group to epimerize to the less compressed equatorial position.

As a final check that the diaxial compound (**3**)

[3]This assignment, rather than the reverse, is made on the basis of (*i*) the greater deshielding effect of chlorine as compared with sulfur (14), and (*ii*) the observation that the band at 3.75 p.p.m. is shifted to 3.95 p.p.m. in the *p*-nitro analogue of **3** (see J. F. King and K. Abikar, Can. J. Chem. This issue.) while the 4.4 p.p.m. band is unchanged.

Can. J. Chem. Downloaded from www.nrcresearchpress.com by 210.87.254.5 on 09/05/12
For personal use only.

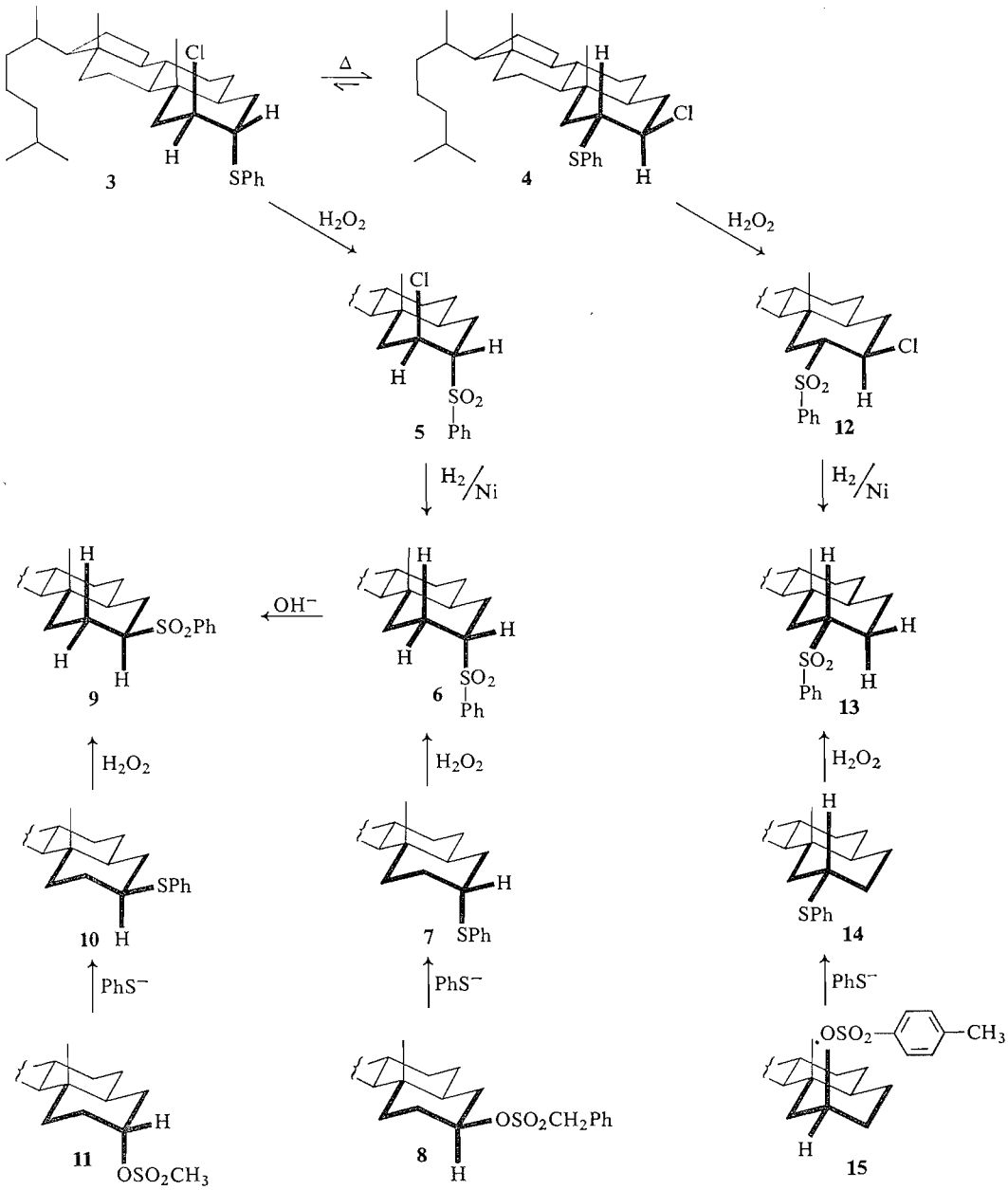

Can. J. Chem. Downloaded from www.nrcresearchpress.com by 210.87.254.5 on 09/05/12
For personal use only.

Can. J. Chem. Downloaded from www.nrcresearchpress.com by 210.87.254.5 on 09/05/12
For personal use only.

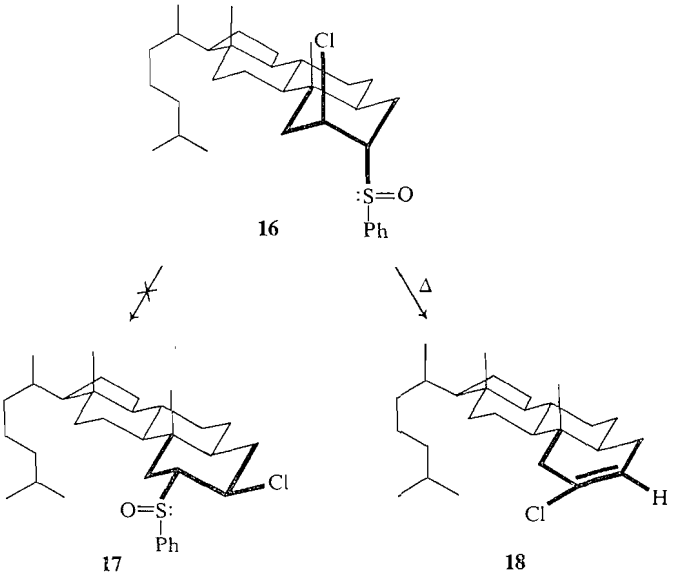

was in fact, undergoing a diaxial → diequatorial rearrangement, the product (**4**) was oxidized to **12** which was then hydrogenolyzed giving 2α-(phenylsulfonyl)-5α-cholestane (**13**). Sulfone **13** was synthesized from 5α-cholestan-2β-yl tosylate (**15**) via the sulfide (**14**) in a manner similar to the preparation of **6** and **9**. In agreement with the assigned stereochemistry, **13** was stable to the conditions under which **6** isomerized to **9**.

The above results, coupled with the recent discovery of neighboring group participation by sulfinyl groups (17), prompted us to determine whether or not the corresponding β-chlorophenylsulfoxides would undergo diaxial → diequatorial rearrangement. Accordingly sulfides **3** and **4** were subjected to mild oxidation to yield the corresponding sulfoxides. The material from **3** was found to be a roughly 2:1 mixture of the two sulfoxides epimeric at the sulfur atom, and which proved to be separable on thin-layer chromatography. The major component melted at 125° and showed a strong positive Cotton effect ($a = +300$). Following the work of Mislow and co-workers on optically active aryl alkyl sulfoxides (18, 19), it was assigned the *R* configuration at the sulfur atom, as in **16***a*. The other diaxial sulfoxide (m.p. 160°) showed a very strong negative Cotton effect ($a = -1432$) and was accordingly formulated as the *S*-isomer (**16***b*). Further oxidation of the original mixture of the two epimeric sulfoxides gave a virtually quantitative yield of sulfone **5**. The diequatorial chloro-sulfide (**4**) was also oxidized under mild conditions giving what appeared from its sharp melting point and chromatographic behavior to be a single product (**17**), though no very serious attempts were made to determine whether or not the product was in fact composed of epimeric materials.

On heating, neither **16***a* nor **16***b* gave any detectable quantity of **17**. The major isolated

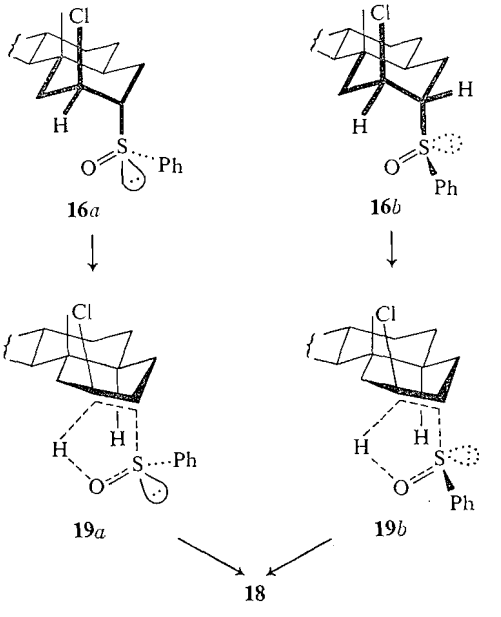

Can. J. Chem. Downloaded from www.nrcresearchpress.com by 210.87.254.5 on 09/05/12
For personal use only.

product (in 40–50% yield) from the sulfoxide mixture was evidently derived from pyrolytic elimination of the elements of benzenesulfenic acid (PhSOH). The presence of one olefinic hydrogen (at 5.7 p.p.m.) and the known propensity of sulfoxides to undergo cis elimination (20) indicate the vinyl chloride structure (**18**) for the pyrolysis product.

Kingsbury and Cram (20) have suggested that such eliminations proceed via a transition state in which the hydrogen becomes bonded to the *oxygen* atom of the sulfinyl group rather than the sulfur atom, and two recent papers supply stereochemical support for this idea (21, 22). For the pyrolysis of **16***a* and **16***b*, these transition states may be formulated as in **19***a* and **19***b*, respectively. On such a basis it would be expected that the *S*-sulfoxide (**16***b*) would form **18** more readily than the *R*-sulfoxide (**16***a*), because **19***b* lacks the non-bonding repulsion between the phenyl group and the 5α-hydrogen present in **19***a* (and which is probably not present in the starting material (**16***a*)). This expectation was, in fact, realized. Upon heating a toluene solution of each sulfoxide at 95° for a number of hours, taking samples at intervals for assay by thin-layer chromatography, we found in each sample that the *S*-sulfoxide (**16***b*) produced more **18** than did the *R*-isomer (**16***a*). Accompanying **18** in the pyrolysis and running at only slightly slower rate on the chromatogram, was a second material which appeared to be formed in larger amount from the *R*-sulfoxide than from the *S*-compound. No attempt was made to characterize this material owing to the small quantities at hand. The observation, however, raises the interesting possibility that the material is 2-chloro-5α-cholest-3-ene, an allylic isomer of **18**, which for a reason similar to that given for the relative ease of forming **18**, might be expected to be produced more readily from **16***a* than from **16***b*.

Experimental

Melting points were determined on a Kofler hot stage and are uncorrected. Infrared spectra were obtained with a Beckman IR-7 instrument equipped with sodium chloride optics. Nuclear magnetic resonance spectra were measured on a Varian A-60 instrument with tetramethylsilane as internal standard. Optical rotations at the D line were determined with a Rudolph model 80 polarimeter using approximately 1% solutions in chloroform; all other rotations were obtained using a Jasco ORD/UV-5-CD spectropolarimeter.

Petroleum ether refers to the fraction of boiling range 35–60°. Thin-layer chromatography was carried out on Camag Kieselgel DF 5. A multiple development technique was employed to separate compounds with very similar R_f values. In these cases the plate was developed using solvent which gave a low R_f value, then air-dried and redeveloped, the procedure being repeated until the desired separation had been achieved.

2β-Chloro-3α-(phenylthio)-5α-cholestane (3)

5α-Cholest-2-ene was prepared by the method of Alt and Barton (4), and benzenesulfenyl chloride by chlorination of diphenyl disulfide (23). A solution of 5α-cholest-2-ene (**1**) (2.7 mmole) in methylene chloride (60 ml) was cooled in an ice bath. Benzenesulfenyl chloride (3.0 mmole) in methylene chloride (30 ml) was added with stirring over a period of 15 min. The brownish-red color of the sulfenyl chloride disappeared rapidly as long as there was any unreacted cholest-2-ene; the conversion of all of the olefin was marked by persistence of the color. The reaction mixture was quickly washed with two 50 ml portions of water, the methylene chloride layer dried with sodium sulfate, and the solvent evaporated under reduced pressure. The product (1.35 g, 90%) crystallized in the flask immediately. Recrystallization from acetone gave needles melting at 109–110°, $[\alpha]_D$ +20.5°.

Anal. Calcd. for $C_{33}H_{51}SCl$: C, 76.92; H, 9.98; S, 6.22; Cl, 6.88. Found: C, 76.98; H, 9.96; S, 6.29; Cl, 6.87.

3β-Chloro-2α-(phenylthio)-5α-cholestane (4)

2β-Chloro-3α-(phenylthio)-5α-cholestane (**3**) (0.90 g) was dissolved in 1-butanol and heated at 80° for 1½ h. The solvent was removed under reduced pressure and the residue chromatographed on silica gel. The fraction (651 mg) eluted with petroleum ether was recrystallized from ether–methanol; m.p. 74°, $[\alpha]_D$ −57°.

Anal. Calcd. for $C_{33}H_{51}SCl$: C, 76.92; H, 9.98; S, 6.22; Cl, 6.88. Found: C, 76.94; H, 10.01; S, 6.38; Cl, 6.63.

2β-Chloro-3α-(phenylsulfonyl)-5α-cholestane (5)

2β-Chloro-3α-(phenylthio)-5α-cholestane (**3**) (100 mg) in acetic acid (10 ml) was heated at 91° with excess 30% hydrogen peroxide (~1 ml) for 2 h. The reaction mixture was poured into water and extracted with chloroform. The chloroform extract was washed successively with dilute NaOH, dilute HCl, and water. The solvent was removed under reduced pressure leaving a product (96 mg) which was then recrystallized from acetone. The compound melted at 154°, solidified and melted again at 165°; $[\alpha]_D$ +53°.

Anal. Calcd. for $C_{33}H_{51}SO_2Cl$: C, 72.43; H, 9.40; S, 5.86; Cl, 6.48. Found: C, 72.62; H, 9.38; S, 6.08; Cl, 6.62.

3α-(Phenylthio)-5α-cholestane (7)

5α-Cholestan-3β-yl phenylmethanesulfonate (**8**) was prepared by the reaction of cholestan-3β-ol, phenylmethanesulfonyl chloride, and triethylamine, as described by Durst (24). A portion (250 mg) of the sulfonate was added to a solution prepared by mixing benzenethiol (0.50 g), metallic sodium (40 mg), 95% ethanol (2 ml) with tetrahydrofuran (10 ml), and the mixture refluxed in a nitrogen atmosphere for 9 h. The reaction mixture was then poured into dilute aqueous NaOH and extracted with chloroform. The extract was washed with dilute

Can. J. Chem. Downloaded from www.nrcresearchpress.com by 210.87.254.5 on 09/05/12
For personal use only.

HCl and water and dried over Na_2SO_4. The crude product (256 mg) obtained on evaporation of the solvent was purified by thin-layer chromatography giving a material (174 mg, 81%) which on recrystallization from ether–ethanol melted at 105–106°, $[\alpha]_D$ +19.5°.

Anal. Calcd. for $C_{33}H_{52}S$: C, 82.44; H, 10.90; S, 6.66. Found: C, 82.18; H, 10.65; S, 6.94.

3α-(Phenylsulfonyl)-5α-cholestane (6)

3α-(Phenylsulfonyl)-5α-cholestane was prepared by oxidation of 3α-(phenylthio)-5α-cholestane (**7**) with hydrogen peroxide as already described in the preparation of 2β-chloro-3α-(phenylsulfonyl)-5α-cholestane (see above). The yield was virtually quantitative. The analytical specimen was obtained by recrystallization from ether–ethanol, m.p. 159–160°, $[\alpha]_D$ +17.5°.

Anal. Calcd. for $C_{33}H_{52}SO_2$: C, 77.29; H, 10.22; S, 6.24. Found: C, 77.17; H, 9.79; S, 6.24.

Hydrogenation of 2β-Chloro-3α-(phenylsulfonyl)-5α-cholestane

2β-Chloro-3α-(phenylsulfonyl)-5α-cholestane (**5**) (157 mg) was dissolved in 2-methoxyethanol and shaken with hydrogen at atmospheric pressure in the presence of Raney nickel catalyst (ca. 3.3 g) and calcium carbonate (200 mg). The crude product obtained after filtration and evaporation of the solvent from the filtrate, was separated by thin-layer chromatography into two components. The major component (85 mg) was shown to be cholestane and the minor component (23 mg) to be 3α-(phenylsulfonyl)-5α-cholestane (**6**), in each case by comparison of specific rotation, infrared spectrum, melting point, and mixture melting point with that of an authentic specimen.

3β-(Phenylthio)-5α-cholestane (10)

3β-(Phenylthio)-5α-cholestane was prepared in 76% yield from 5α-cholestan-3α-yl methanesulfonate (**11**) by the method given for 3α-(phenylthio)-5α-cholestane (see above), m.p. 79–80°, $[\alpha]_D$ +18°. The reaction mixture also contained a small amount (12%) of 5α-cholest-2-ene.

Anal. Calcd. for $C_{33}H_{52}S$: C, 82.44; H, 10.90; S, 6.66. Found: C, 82.23; H, 11.21; S, 7.05.

3β-(Phenylsulfonyl)-5α-cholestane (9)

Oxidation of 3β-(phenylthio)-5α-cholestane (**10**) with hydrogen peroxide as described above in the preparation of 2β-chloro-3α-(phenylsulfonyl)-5α-cholestane gave a 70% yield of crude 3β-(phenylsulfonyl)-5α-cholestane. Recrystallization from methylene chloride – ethanol gave the pure material, m.p. 182°, $[\alpha]_D$ +20.5°.

Anal. Calcd. for $C_{33}H_{52}SO_2$: C, 77.29; H, 10.22; S, 6.24. Found: C, 77.54; H, 9.88; S, 6.59.

Epimerization of 3α-(Phenylsulfonyl)-5α-cholestane

3α-(Phenylsulfonyl)-5α-cholestane (**6**) (25 mg) was heated with potassium hydroxide (135 mg) in distilled dimethyl sulfoxide at ~75° for 16 h. The reaction mixture was poured into water and extracted with chloroform. The extract was washed with dilute hydrochloric acid and water, dried, and the solvent evaporated. The material (21 mg, 84%), melting at 182–183°, obtained on recrystallization from ether–ethanol, was shown by infrared spectrum and mixture melting point to be identical to 3β-(phenylsulfonyl)-5α-cholestane obtained by hydrogen peroxide oxidation of 3β-(phenylthio)-5α-cholestane (see above).

2α-(Phenylthio)-5α-cholestane (14)

Benzenethiol (2.0 ml) and tetrahydrofuran (80 ml) were added to a solution (5 ml) of sodium ethoxide (from 300 mg of sodium) in ethanol. 5α-Cholestan-2β-yl tosylate (865 mg) was added and the mixture refluxed under nitrogen for 6 h. It was then poured into dilute NaOH, extracted with methylene chloride, and the extract washed with dilute HCl and water, and dried over sodium sulfate. The crude product, which was contaminated with phenyl disulfide, was subjected to thin-layer chromatography using cyclohexane–ether (9:1) and developing two or three times. The purified material (136 mg) so obtained, was recrystallized from ether–methanol and acetone–methanol; m.p. 85–86°.

Anal. Calcd. for $C_{33}H_{52}S$: C, 82.44; H, 10.90; S, 6.66. Found: C, 82.15; H, 10.66; S, 6.90.

2α-(Phenylsulfonyl)-5α-cholestane (13)

2α-(Phenylthio)-5α-cholestane was oxidized in good yield with hydrogen peroxide as in the preparation of 2β-chloro-3α-(phenylsulfonyl)-5α-cholestane (see above). The product was chromatographed and then recrystallized from ether–methanol giving an analytical sample melting at 167–168°; $[\alpha]_D$ +9°.

Anal. Calcd. for $C_{33}H_{52}O_2S$: C, 77.29; H, 10.22; S, 6.24. Found: C, 77.47; H, 10.15; S, 6.39.

Hydrogenation of 3β-Chloro-2α-(phenylsulfonyl)-5α-cholestane

3β-Chloro-2α-(phenylsulfonyl)-5α-cholestane (**12**) (317 mg) was dissolved in 2-methoxyethane (50 ml) and shaken with hydrogen in the presence of Raney nickel catalyst (~1.0 g) and lithium carbonate (0.2 g) for 46 h. On thin-layer chromatography the crude product (270 mg) was separated into unreacted **12** (116 mg), cholestane (72 mg, 53% yield, on the basis of unrecovered starting material), and 2α-(phenylsulfonyl)-5α-cholestane (**13**) (45 mg, 24% yield, on the basis of unrecovered starting material) identified by melting point, mixture melting point, and specific rotation.

2β-Chloro-3α-(phenylsulfinyl)-5α-cholestane (R- and S-isomers, 16a and 16b)

2β-Chloro-3α-(phenylthio)-5α-cholestane (**3**) (682 mg, 1.32 mmoles) was suspended in glacial acetic acid (200 ml) and 30% hydrogen peroxide solution (2.0 ml) added. The solid particles were scratched with a glass rod to aid dissolution, and the reaction mixture was then let stand for 2 h at room temperature. The material was then poured into water (ca. 300 ml) and the mixture extracted with methylene chloride. The extracts were washed successively with dilute NaOH, water, dilute HCl, and water again. The methylene chloride layer was then dried with anhydrous $MgSO_4$ and the solvent evaporated giving the crude product (701 mg). On recrystallization from ether–methanol a crystalline product (591 mg) melting from 115 to 130° was obtained. This material was used directly in both the preparative pyrolysis forming **18**, and the oxidation to sulfone **5**. It showed only one spot on thin-layer chromatography with a number of solvents, but was found to be resolved into two components with cyclohexane–ether (3:1). A portion (200 mg) of the recrystallized sulfoxide mixture was placed on thin-layer plates and developed two or three times with the cyclo-

Can. J. Chem. Downloaded from www.nrcresearchpress.com by 210.87.254.5 on 09/05/12
For personal use only.

hexane–ether mixture. The front-running material (63 mg) melted at 160° after recrystallization from ether–methanol. The n.m.r. spectrum showed unresolved peaks at 3.1 and 4.9 p.p.m. with widths at half-heights of 8 c.p.s. each. The optical rotatory dispersion (o.r.d.) curve of an ethanol solution showed a trough at 270 mμ, [φ] −9202°, and a peak at 221 mμ, [φ] +20770°, ([α]$_D$ −4° in chloroform); on the basis of the work of Mislow *et al.* (18), it was assigned the *S* configuration at the sulfur atom.

Anal. Calcd. for $C_{33}H_{51}ClOS$: C, 74.61; H, 9.68; Cl, 6.68; S, 6.04. Found: C, 74.33; H, 9.64; Cl, 6.72; S, 5.91.

The slower-running component (139 mg) was recrystallized from ether–methanol, m.p. 125°. The n.m.r. spectrum showed humps at 3.0 and 4.1 p.p.m., half-widths roughly 10 c.p.s. each. The o.r.d. curve (ethanol) showed a peak at 270 mμ, [φ] +24 980°, and a trough at 221 mμ, [φ] −118 200° ([α]$_D$ +118° in chloroform); it was assigned the *R*-configuration at the sulfur atom.

Anal. Calcd. for $C_{33}H_{51}ClOS$: C, 74.61; H, 9.68; Cl, 6.68; S, 6.04. Found: C, 74.60; H, 9.86; Cl, 6.45; S, 6.01.

*Pyrolysis of 2β-Chloro-3α-(phenylsulfinyl)-5α-cholestane (**16**)*

The diaxial sulfoxide (**16**, mixture of epimers at the sulfur atom) (250 mg) was heated in a mixture of nitromethane (8 ml) and chloroform (2 ml) for 21 h at 98 ± 2°. The solution was evaporated to dryness. Thin-layer chromatography of the residue showed no material corresponding to either the starting material (**16**) or the diequatorial sulfoxide (**17**); most of the product appeared to run near the front and only slightly more slowly than 5α-cholest-2-ene. A benzene solution of the residue was filtered through silica gel and the solvent evaporated. This material was chromatographed on alumina (grade I); elution with petroleum ether yielded 80 mg of a product which after four recrystallizations from ether–methanol melted at 122°; [α]$_D$ +71°. The n.m.r. spectrum showed unresolved humps at ~5.7 p.p.m. and 2.1 p.p.m. in addition to the complex absorption from 0.5 to 2.0 p.p.m.

Anal. Calcd. for $C_{27}H_{45}Cl$: C, 80.04; H, 11.19; Cl, 8.75. Found: C, 80.47; H, 11.21; Cl, 8.44.

To determine the relative ease with which each of the two sulfoxides (**16***a* and **16***b*) formed the compound melting at 122° (**18**), 6 mg samples of each sulfoxide were dissolved in dry toluene (5 ml) and each solution divided into five ampoules. Each ampoule was flushed with dry nitrogen, sealed, and heated in a water bath at 95°. An ampoule of each sulfoxide was opened after 1 h, 2 h, and 4 h and the remaining two after 10½ h. In each case the solvent was removed with a stream of nitrogen, and a portion of the residue analyzed by thin-layer chromatography. Development with cyclohexane–ether (3:1) showed the reaction to be nearly complete after 10½ h, and that there was no detectable amount of material running at the same rate on the chromatogram as 3β-chloro-2α-(phenylsulfinyl)-5α-cholestane (**17**) in any of the samples. Development with petroleum ether showed a material from each sulfoxide with the same R_f value as **18**; for each pair of samples the intensity of that spot from the *S*-sulfoxide (**16***b*, m.p. 160°) was distinctly greater than that from the *R*-sulfoxide (**16***a*, m.p. 125°). In the chromatogram of each reaction product there appeared another spot immediately following that corresponding to **18**. The intensity of this spot in the material from the *R*-sulfoxide was greater than that of the corresponding spot from the *S*-sulfoxide. From the *R*-sulfoxide the spots due to **18** and the slower moving material appeared to be of very similar intensities, whereas from the *S*-sulfoxide the spot due to **18** was a good deal more intense than that of the slower moving material.

*Oxidation of the 2β-Chloro-3α-(phenylsulfinyl)-5α-cholestane Mixture (**16**)*

The crystalline mixture of the two sulfoxides epimeric at the sulfur atom (100 mg) was dissolved in glacial acetic acid (10 ml). Hydrogen peroxide solution (30%, 1.0 ml) was added and the mixture heated for 2 h at 91°. It was then poured into water and extracted with chloroform. The extract was washed with dilute NaOH, water, dilute HCl, and water, respectively, and dried over $MgSO_4$. The solvent was evaporated giving the crude product (96 mg). Recrystallization from acetone gave the pure product, melting at 165° with a transition at 154°. Its infrared spectrum was identical to that of the material obtained directly by oxidation of the diaxial chlorosulfide (**3**).

*3β-Chloro-2α-(phenylsulfinyl)-5α-cholestane (**17**)*

3β-Chloro-2α-(phenylthio)-5α-cholestane (**4**) was oxidized in good yield with hydrogen peroxide in glacial acetic acid in a manner similar to that used in the preparation of 2β-chloro-3α-(phenylsulfinyl)-5α-cholestane (**16**). On recrystallization from methylene chloride – methanol the product melted at 201–202°; [α]$_D$ −184°.

Anal. Calcd. for $C_{33}H_{51}ClOS$: C, 74.61; H, 9.68; Cl, 6.68; S, 6.04. Found: C, 74.56; H, 9.65; Cl, 6.78; S, 6.18.

Acknowledgments

This work was supported by grants-in-aid from the Ontario Research Foundation and the Department of University Affairs of the Province of Ontario, and by the National Research Council of Canada.

1. D. H. R. Barton. *In* Theoretical organic chemistry papers presented to the Kekule Symposium. Butterworths, London. 1959. p. 127.
2. D. H. R. Barton and E. Miller. J. Am. Chem. Soc. **72**, 1066 (1950).
3. K. Hattori and T. Kawasaki. Yakugaku Zasshi, **57**, 115 (1937).
4. G. H. Alt and D. H. R. Barton. J. Chem. Soc. 4284 (1954).
5. D. H. R. Barton and J. F. King. J. Chem. Soc. 4398 (1958).
6. J. F. King, R. G. Pews, and R. A. Simmons. Can. J. Chem. **41**, 2187 (1963).
7. J. F. King and R. G. Pews. Can. J. Chem. **43**, 847 (1965).
8. N. Kharasch. *In* Organic sulfur compounds. Vol. 1. *Edited by* N. Kharasch. The Pergamon Press, Ltd., London. 1961. p. 375.
9. D. J. Pettit and G. K. Helmkamp. J. Org. Chem. **29**, 2702 (1964).

10. W. H. MUELLER and P. E. BUTLER. J. Am. Chem. Soc. **88**, 2866 (1966).
11. A. FURST and P. A. PLATTNER. Intern. Congr. Pure and Appl. Chem., 12th Congr., New York. 1951. Abstracts of papers. p. 409.
12. D. H. R. BARTON and R. C. COOKSON. Quart. Rev. London, **10**, 44 (1956).
13. A. HASSNER and C. HEATHCOCK. Tetrahedron Letters, 393 (1963); *also* J. Org. Chem. **30**, 1748 (1965).
14. L. M. JACKMAN. Applications of nuclear magnetic resonance spectroscopy in organic chemistry. The Pergamon Press, Ltd., London. 1959. p. 53.
15. A. HASSNER and C. HEATHCOCK. J. Org. Chem. **29**, 1350 (1964).
16. E. L. ELIEL and R. S. RO. J. Am. Chem. Soc. **79**, 5995 (1957).
17. H. HOGEVEEN, G. MACCAGNANI, and F. MONTANARI. Bull. Sci. Fac. Chim. Ind. Bologna, **21**, 257 (1963).
18. K. MISLOW, M. M. GREEN, P. LAUR, J. T. MELILLO, T. SIMMONS, and A. L. TERNAY, JR. J. Am. Chem. Soc. **87**, 1958 (1965).
19. P. BICKART, M. AXELROD, J. JACOBUS, and K. MISLOW. J. Am. Chem. Soc. **89**, 697 (1967).
20. C. A. KINGSBURY and D. J. CRAM. J. Am. Chem. Soc. **82**, 1810 (1960).
21. D. N. JONES and M. A. SAEED. Proc. Chem. Soc. 81 (1964).
22. S. I. GOLDBERG and M. S. SAHLI. Tetrahedron Letters, 4441 (1965).
23. H. LECHER. Ber. **58**, 409 (1925).
24. T. DURST. Ph.D. Thesis, University of Western Ontario, London, Ontario. 1964.

Can. J. Chem. Downloaded from www.nrcresearchpress.com by 210.87.254.5 on 09/05/12
For personal use only.

Reaction mechanism studies. 5. The mechanism of the diaxial → diequatorial rearrangement of β-chlorothioethers

J. F. KING[1] AND K. ABIKAR
Department of Chemistry, University of Western Ontario, London, Ontario
Received August 23, 1967

p-Methoxy- and *p*-nitro substituted analogues (**1***b* and **1***c*) of the diaxial β-chlorothioether 2β-chloro-3α-(phenylthio)-5α-cholestane (**1***a*), have been prepared and found to undergo the diaxial → diequatorial rearrangement. The rates of rearrangement of these compounds show the sequence *p*-methoxy > H > *p*-nitro. It is concluded that the transition state for the rearrangement is polarized in the sense of a sulfonium chloride (**3**). The rearrangement of **1***a* is 1600 times faster in butanol than in decalin (at 110°). There is thus no inherent insensitivity to solvent change in a rearrangement in which there may be a "four-atom arrangement" in the transition state, a conclusion relevant to previous work on the diaxial → diequatorial rearrangement of 1,2-dibromides (1). It was further found that the nitro group slowed the rearrangement (at 110°) more in butanol than in decalin, an observation regarded as consistent with, but not requiring, the incursion of a merged ion-pair, cyclic concerted mechanism.

Canadian Journal of Chemistry, **46**, 9 (1968)

Can. J. Chem. Downloaded from www.nrcresearchpress.com by 210.87.254.40 on 09/05/12
For personal use only.

The previous paper (2) describes the synthesis of a diaxial β-halothioether (**1***a*) by the action of benzenesulfenyl chloride on 5α-cholest-2-ene, and the thermal rearrangement of this product to its diequatorial isomer (**2***a*). In the present account we outline experiments which provide some definition of the mechanism of this transformation.

From what is known of the relative capacities of chlorine and arylthio groups to function as leaving groups and as participating functions at neighboring centers, it seemed highly likely that ionization of **1***a* would proceed in the sense of a sulfonium chloride (**3**), rather than a chloronium sulfide (**4**). To obtain experimental evidence on the point we prepared the corresponding *p*-methoxy and *p*-nitro derivatives, **1***b* and **1***c*, respectively, and found that both of these materials rearrange on heating.

The structures of these compounds follow from the close similarities between them and the unsubstituted compounds (**1***a* and **2***a*), both in method of synthesis and in properties. The nuclear magnetic resonance (n.m.r.) spectra of all of the sulfenyl chloride adducts (**1***a–c*) are very similar except, of course, for those differences expected as a result of the substitution in the aromatic ring; the spectra of the rearrangement products are also correspondingly similar. In addition, the change in molecular rotation accompanying the transformation **1** → **2** was found to be ca. −600° for **1***b* → **2***b*[2] and −830° for **1***c* → **2***c*, as compared with −410° for the reaction of the unsubstituted compound.

Measurement of the rates of rearrangement indicated the reactions to be first order. As may be seen in Table I, in all of the solvents and at all of the temperatures at which the rates were studied, the rate constants followed the sequence *p*-methoxy > the unsubstituted compound > *p*-nitro. This is readily interpreted in terms of charge separation in the transition state in the sense of a sulfonium chloride (**3**), and not that of a chloronium sulfide (**4**).

As mentioned at the beginning of the previous paper (2), the reason for investigating this reaction was to gain information relevant to our general study of the diaxial → diequatorial rearrangement. We had found (1) that the rates of rearrangement of **5***a*, **5***b*, **6***a*, and **6***b* were much more sensitive to a change in solvent than was the rate of rearrangement of the analogous dibromide (**5***c*). Though the exact positions of the rearranging atoms in the transition states of these reactions are not known, it could have been argued that the difference between the dibromide reaction on the one hand and that of the bromohydrin esters on the other, derived from a different geometrical arrangement in the transition

[1]Fellow of the Alfred P. Sloan Foundation, 1966–1968.

[2]Compound **2***b* was not obtained in a pure, crystalline state, but was characterized as the sulfone. The molecular rotation change quoted is that for the conversion of **1***b* into the equilibrium mixture of **1***b* and **2***b*, which is probably at least 90% **2***b*.

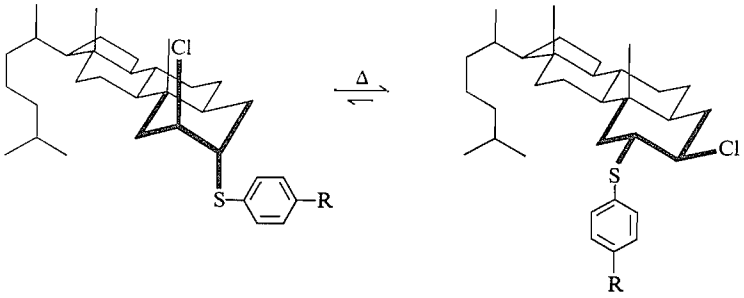

1 **2**

a) R = H
b) R = CH_3O
c) R = NO_2

state. Thus perhaps C-2, C-3, and the two bromine atoms of the dibromide form a four-center arrangement in the transition state, whereas C-2, C-3, the bromine, the two oxygens, and the sulfur (or carbon) of the esters become ordered in a six-membered ring pattern. It is further at least conceivable that such six-atom transition states would (by some unspecified process) be more susceptible to interaction with solvent, and hence lead to a greater sensitivity of the rate of reaction to change in solvent. In the system under discussion in the present study, C-2, C-3, and the chlorine and sulfur atoms are the only atoms directly involved in bond breaking and forming processes. Therefore, if the geometrical effect of the type just indicated were significant, it would be expected that the rate of rearrangement of the β-chlorothioethers would be as insensitive to change in solvent as that of the dibromide (**5***c*). We have previously shown that on changing the solvent from nitromethane to decalin (at 99°), the rate of rearrangement of the dibromide **5***c* decreased 22-fold, whereas those of the bromohydrin esters (**5***a*, **5***b*, **6***a*, and **6***b*) decreased 100- to nearly 300-fold. The β-chlorothioethers (**1**) in this study were not sufficiently soluble in nitromethane for the rate to be measured in that solvent. However, the rate was measured in a mixture of nitromethane and chloroform (60:40) and also in butanol (both at 60°) and the rates were found to be very similar in these solvents (see Table I). As may be further seen in Table I, the rate of rearrangement of **1***a* is reduced about 1600-fold on changing from butanol to decalin (at 110°). It is therefore concluded that the "four-atom arrangement" in the transition state has no intrinsic features rendering it significantly less responsive to a change in the reaction medium, and that the smaller change in sensitivity to solvent change shown by the dibromide rearrangement compared with that of the bromohydrin esters, does not have its origin in differences in geometrical arrangement of the atoms in the transition state.

The question of whether or not the diaxial → diequatorial rearrangement proceeds under any circumstances via a merged ion-pair, cyclic concerted mechanism was taken up in Part 3 of this series (1). After a discussion of some length it was concluded that the data available at that time were consistent with the incursion of a "merged" mechanism, but that it was also at least conceivable that the reaction was proceeding in all cases via an ion-pair mechanism in which the ratio of ion-pairs returning to starting material to ion-pairs giving product was varying with changes in medium and substrate. In the course of the present study we wondered if the β-chlorothioether system might not be used to obtain evidence on the question.

In particular we were interested to see if the presence of a *p*-nitro group, especially in a solvent of very low ionizing power such as decalin, might lead to a manifestly "merged-mechanism" process. We found that the introduction of a nitro group had a smaller effect on the rate of rearrangement in decalin solution than in butanol. Thus the ratio k_{NO_2}/k_H is 0.11 in decalin and 0.053 in butanol (at 110°). This change in the k_{NO_2}/k_H ratio, though small, is qualitatively what would be expected from a "merged" reaction. In such a process complete ionization to an ion-pair would not occur in less polar media. Thus when the reaction is carried out in decalin, the magnitude of the charge on the sulfur atom in the transition state would be

Can. J. Chem. Downloaded from www.nrcresearchpress.com by 210.87.254.40 on 09/05/12
For personal use only.

TABLE I

Rate constants for the diaxial → diequatorial rearrangement of the 2β-chloro-3α-(phenylthio)-cholestanes (**1**)

	Solvent	Temperature (°C)	k_{equil}* (s^{-1})	k/k_{1a}†
2β-Chloro-3α-(phenylthio)-5α-cholestane (**1***a*)	Nitromethane–chloroform (3:2)	60	1.51×10^{-4}	(1.00)
2β-Chloro-3α-(phenylthio)-5α-cholestane (**1***a*)	1-Butanol	50	4.7×10^{-5}	(1.00)
2β-Chloro-3α-(phenylthio)-5α-cholestane (**1***a*)	1-Butanol	60	1.55×10^{-4}	(1.00)
2β-Chloro-3α-(phenylthio)-5α-cholestane (**1***a*)	1-Butanol	80	9.2×10^{-4}	(1.00)
2β-Chloro-3α-(phenylthio)-5α-cholestane (**1***a*)	1-Butanol	110	1.36×10^{-2} (estimated)‡	(1.00)
2β-Chloro-3α-(phenylthio)-5α-cholestane (**1***a*)	Decalin	110	8.5×10^{-6}	(1.00)
2β-Chloro-3α-(*p*-methoxyphenylthio)-5α-cholestane (**1***b*)	Nitromethane–chloroform (3:2)	60	4.5×10^{-4}	3.0
2β-Chloro-3α-(*p*-nitrophenylthio)-5α-cholestane (**1***c*)	Nitromethane–chloroform (3:2)	60	5.1×10^{-6}	0.034
2β-Chloro-3α-(*p*-nitrophenylthio)-5α-cholestane (**1***c*)	1-Butanol	110	7.3×10^{-4}	0.053
2β-Chloro-3α-(*p*-nitrophenylthio)-5α-cholestane(**1***c*)	Decalin	110	9.3×10^{-7}	0.11

*k_{equil} is the first order rate constant for the rate of formation of the equilibrium mixture of **1** and **2**.
†The ratio of k_{equil} for the compound to k_{equil} for **1***a* under the same conditions.
‡Estimated by extrapolation of the plot of log k_{equil} for the other three temperatures vs. $1/T$.

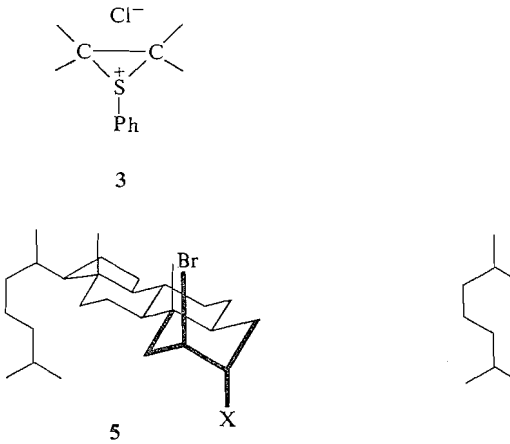

less than in butanol. Accordingly in decalin the presence of the nitro group would have a smaller effect on the reaction rate than in butanol. It must be pointed out, however, that the above experimental result is in effect a small change in the Hammett ρ value accompanying a change in solvent. In view of the difficulties generally associated with determining the origin of small variations in ρ, there seems little point in elaborating the discussion any further than merely pointing out that the results qualitatively agree with what would be expected of a "merged-mechanism", but can probably be accounted for in other ways as well.

Experimental

The general techniques, apparatus, and terminology are the same as in the previous paper (2).

The solvents used in the kinetic measurements were purified as follows. 1-Butanol (British Drug Houses "Analar" grade was shaken with 10% sulfuric acid, 5% sodium bisulfite, and 5% sodium hydroxide solutions, respectively. It was then washed with two portions of water and dried over anhydrous sodium carbonate; final drying was effected by refluxing over calcium hydride

Can. J. Chem. Downloaded from www.nrcresearchpress.com by 210.87.254.40 on 09/05/12
For personal use only.

Can. J. Chem. Downloaded from www.nrcresearchpress.com by 210.87.254.40 on 09/05/12
For personal use only.

followed by distillation under reduced pressure. Fisher "spectranalyzed" grade chloroform was washed five times with water, dried over anhydrous magnesium sulfate, and refluxed over calcium hydride and distilled. Fisher reagent grade nitromethane was distilled from calcium hydride. Decalin was purified as described previously (1).

2β-Chloro-3α-(p-nitrophenylthio)-5α-cholestane (1c)

Freshly crystallized *p*-nitrothiophenol (462 mg, 2.98 mmole) was chlorinated in methylene chloride at 0°. The solvent and excess chlorine were evaporated quickly. The resulting sulfenyl chloride was dissolved in methylene chloride and added to 5α-cholest-2-ene (1.0 g, 2.7 mmole) in methylene chloride little by little with shaking. The mixture was washed quickly three times with water. The solvent was removed after drying over anhydrous magnesium sulfate. The crude product was crystallized from ether–methanol; yield 1.01 g (67%), m.p. 55–60°. Recrystallization from methylene chloride – petroleum ether yielded pure product, m.p. 129°, $[\alpha]_D$ +28.5°. The nuclear magnetic resonance (n.m.r.) spectrum showed bands at 3.95 and 4.35 p.p.m., each with "half-width" of 8 c.p.s. and each corresponding in area to one hydrogen.

Anal. Calcd. for $C_{33}H_{50}NO_2SCl$: C, 70.73; H, 9.00; N, 2.50; S, 5.73; Cl, 6.33. Found: C, 70.88; H, 8.82; N, 2.67; S, 5.95; Cl, 6.45.

2β-Chloro-3α-(p-methoxyphenylthio)-5α-cholestane (1b)

A saturated solution of chlorine in carbon tetrachloride at 0° was added slowly and with shaking to a well-cooled solution of *p*-methoxythiophenol in carbon tetrachloride until a permanent deep red color was obtained. The excess chlorine and solvent were removed quickly by evaporation under reduced pressure. The residue was distilled under reduced pressure; b.p. 118° at 5 mm.

A solution of 5α-cholest-2-ene (500 mg, 1.35 mmole) in methylene chloride was cooled to −5° and the similarly cooled solution of the sulfenyl chloride in the same solvent, was added gradually with shaking until the mixture acquired permanent yellow color. The mixture was washed twice with water. The solvent was removed after drying over anhydrous magnesium sulfate. The residue was crystallized from methylene chloride – petroleum ether; yield 448 mg (60%), m.p. 109–113°. After further crystallization from ether–methanol, the compound melted at 113–115°; $[\alpha]_D$ +16.0°. The n.m.r. spectrum showed bands at 3.53 and 4.33 p.p.m., each with "half-widths" of 10 c.p.s., and each corresponding in area to one hydrogen.

Anal. Calcd. for $C_{34}H_{53}SOCl$: C, 74.89; H, 9.98; S, 5.88; Cl, 6.50. Found: C, 75.34; H, 9.54; S, 6.16; Cl, 6.53.

3β-Chloro-2α-(p-nitrophenylthio)-5α-cholestane (2c)

2β-Chloro-3α-(*p*-nitrophenylthio)-5α-cholestane was heated for about 2 h (*ca.* 8 half-lives) in 1-butanol at 110°. The solvent was removed under reduced pressure. The residue was dissolved in benzene and filtered through silica gel; yield 170 mg (85%). Recrystallization from acetone yielded a product melting at 131°; $[\alpha]_D$ −120°. The only absorption in the n.m.r. spectrum between 2.5 and 7.3 p.p.m. was a broad band from 3.2–4.2 p.p.m. having an area consistent with the presence of two hydrogen atoms.

Anal. Calcd. for $C_{33}H_{50}NO_2SCl$: C, 70.73; H, 9.00; N, 2.50; S, 5.73; Cl, 6.33. Found: C, 71.07; H, 8.89; N, 2.64; S, 5.91; Cl, 6.68.

3β-Chloro-2α-(p-methoxyphenylthio)-5α-cholestane (2b)

2β-Chloro-3α-(*p*-methoxyphenylthio)-5α-cholestane (300 mg, 0.55 mmoles) was heated in nitromethane–chloroform (3:2) for 4 h at 60°. The solvent was evaporated to dryness. Thin-layer chromatography showed only one major spot. The n.m.r. spectrum indicated diaxial methine protons showing a broad band from 2.8 to 3.9 p.p.m. partly obscured by the methoxyl peak at 3.75 p.p.m. The compound was not obtained in the crystalline state and for the purposes of characterization was oxidized by heating with hydrogen peroxide in acetic acid as described in the previous paper, whereupon the sulfone was obtained in 77% yield. Crystallization from ether–methanol yielded a compound melting at 181°; $[\alpha]_D$ −30.5°. The n.m.r. spectrum showed the broad absorption band from 3.1–4.1 p.p.m., again partly obscured by the methoxyl peak at 3.83 p.p.m.

Anal. Calcd. for $C_{34}H_{53}SO_3Cl$: C, 70.73; H, 9.25; S, 5.55; Cl, 6.14. Found: C, 70.78; H, 9.16; S, 5.45; Cl, 6.05.

Rate Measurements and Determination of the Composition of the Pyrolytic Equilibrium Mixtures

The rate measurements were carried out in sealed Pyrex ampoules in the manner previously described (1, 3) except that the samples were heated in an ethylene glycol bath maintained at the specified temperature ±0.1°. The extent of reaction was determined polarimetrically, the rotation being measured in the solvent of the reaction together with an equal volume of chloroform.

The equilibrium values for the *p*-nitro and unsubstituted materials in nitromethane–chloroform (3:2) were determined by pyrolyzing two or three samples each of the diaxial and diequatorial compounds for a period corresponding to 8 half-lives and averaging their optical rotations. For the equilibrium **1***a* ⇌ **2***a*, the $[\alpha]_D$ values starting from **1***a* were −57, −51, and −60°, and those from **2***a*, −57, −58, and −58°; the average (−57°) corresponds to an equilibrium mixture containing 98 ± 2% **2***a*. For the equilibrium **1***c* ⇌ **2***c*, the $[\alpha]_D$ values from **1***c* were −99 and −106, and from **2***c*, −112, −108, and −114°; the average (−110°) corresponds to an equilibrium mixture with 93 ± 5% **2***c*. In the *p*-methoxy series the diequatorial isomer (**2***b*) was not obtained pure. To obtain a reasonable approximation of the equilibrium rotation, six samples of the diaxial isomer (**1***b*) were pyrolyzed as above. The $[\alpha]_D$ values so obtained were −36, −30, −32, −38, −35, and −33°; the average, −34°. In butanol the pyrolyses were accompanied by a larger measure of decomposition. The samples were accordingly heated for relatively short times and the equilibrium rotation found by plotting the $[\alpha]_D$ values vs. time and visually estimating the convergence point of the curves. In this way the following values were obtained: **1***a* ⇌ **2***a*, −44 ± 3° (corresponding to 87 ± 4% **2***a*), and **1***c* ⇌ **2***c*, −97 ± 15° (corresponding to 87 ± 10% **2***c*). As in our previous study of the halohydrin esters (1), the direct determination of the equilibrium rotation in decalin was found to be impracticable, owing to decomposition accompanying the long reaction times. As before (1), it was assumed that no important error would

be introduced by taking the same equilibrium composition as in another solvent; in this case the data from nitromethane–chloroform were used.

Acknowledgments

This work was supported by grants-in-aid from the Ontario Research Foundation and the Department of University Affairs of the Province of Ontario, and by the National Research Council of Canada.

1. J. F. KING and R. G. PEWS. Can. J. Chem. **43**, 847 (1965).
2. J. F. KING, K. ABIKAR, D. M. DEAKEN, and R. G. PEWS. Can. J. Chem. This issue.
3. J. F. KING, R. G. PEWS, and R. A. SIMMONS. Can. J. Chem. **41**, 2187 (1963).

Can. J. Chem. Downloaded from www.nrcresearchpress.com by 210.87.254.40 on 09/05/12
For personal use only.

The alkaloids of *Lycopodium alopecuroides* L.

W. A. AYER, B. ALTENKIRK, AND S. VALVERDE-LOPEZ
Department of Chemistry, University of Alberta, Edmonton, Alberta

AND

B. DOUGLAS, R. F. RAFFAUF, AND J. A. WEISBACH
Smith, Kline, and French Laboratories, Philadelphia, Pennsylvania

Received August 15, 1967

The alkaloids of *Lycopodium alopecuroides* L. have been examined and seven alkaloids isolated. These include the known alkaloids lycopodine, lycodoline, and clavolonine, and three previously unreported alkaloids, alopecurine, debenzoylalopecurine, and alopecuridine. Anhydrolycodoline, previously obtained as a degradation product of lycodoline, was also isolated. The properties of the new alkaloids are described.

Canadian Journal of Chemistry, **46**, 15 (1968)

Can. J. Chem. Downloaded from www.nrcresearchpress.com by 210.87.254.6 on 09/05/12
For personal use only.

The members of the genus *Lycopodium* (family Lycopodiaceae) thus far examined have proved to be a rich source of alkaloids (1). To date, however, only 16 species and varieties have been examined in any detail, although there are possibly well over 400 species (2). The presence of alkaloids in *L. alopecuroides* L. has been noted previously (3) but no detailed study appears to have been carried out. We have now examined the alkaloids of this species in some detail and have isolated a total of seven alkaloids, four of which have not been obtained previously from natural sources.

The separation of the alkaloids was achieved by adsorption chromatography on alumina. A preliminary separation was carried out by eluting with solvents of increasing polarity, and the fractions thus obtained were further separated by "dry-column" chromatography (4) and by crystallization. The progress of the separation was monitored by thin-layer chromatography (t.l.c.). In order to facilitate the presentation, the alkaloids will be discussed in order of decreasing R_f value.

The first substance eluted was an oil, somewhat unstable in air, which was best isolated as its crystalline hydrochloride. The mass spectrum of the free base was almost identical with that of anhydrolycodoline (**1**) (5) and comparison of the melting point and infrared spectrum of the hydrochloride with those of authentic anhydrolycodoline hydrochloride confirmed the identity. The natural occurrence of anhydrolycodoline has not been noted previously.

One of the most abundant alkaloids present was lycopodine (**2**), the most widely distributed of the *Lycopodium* alkaloids (1). Lycopodine was closely followed by a compound, m.p. 244–245°, which could be separated from lycopodine by virtue of its slight solubility in cold acetone. The properties of this compound (*vide infra*) do not correspond to any previously reported *Lycopodium* alkaloid, and we suggest the name alopecurine for this substance.

Alopecurine was assigned the molecular formula $C_{23}H_{29}O_3N$ on the basis of the analytical and mass spectral data. The presence of a benzoyloxy group was indicated by the infrared, ultraviolet, and mass spectra. The infrared spectrum (Fig. 1) showed bands at 1705, 1595, 1580, 1270, and 1110 cm^{-1} characteristic (6) of benzoates, the ultraviolet spectrum showed typical (7) benzoate absorption at 230, 272, and 280 mμ, and the mass spectrum showed strong peaks at *m/e* 245 (loss of benzoic acid), 122, 105, and 77 (8). The third oxygen of alopecurine is present as part of a hydroxyl group as shown by the presence of OH absorption in the infrared spectrum and by the formation of a mono *O*-acetyl derivative on acetylation. Lack of NH absorption in the infrared spectrum of *O*-acetyl alopecurine indicates that the nitrogen is tertiary.

Alkaline hydrolysis of alopecurine yielded benzoic acid and debenzoylalopecurine, $C_{16}H_{25}O_2N$, m.p. 230–232°, which does not seem to be identical with any known *Lycopodium* alkaloid or derivative of the same molecular formula. Debenzoylalopecurine was also isolated in small amounts directly from the plant extract, but

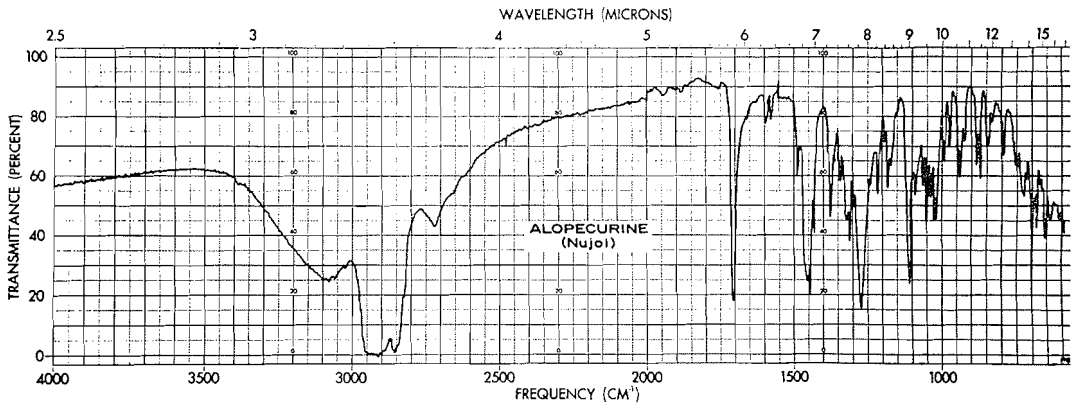

FIG. 1

whether it occurs as such or is formed by hydrolysis of alopecurine during the isolation procedure is not known. Since debenzoylalopecurine does not seem to contain a carbon–carbon double bond (attempted catalytic hydrogenation, nuclear magnetic resonance (n.m.r.) and infrared evidence) it appears that the molecule is pentacyclic. Although acetates are quite common among the *Lycopodium* alkaloids (1), alopecurine is the first benzoylated *Lycopodium* alkaloid to be reported.

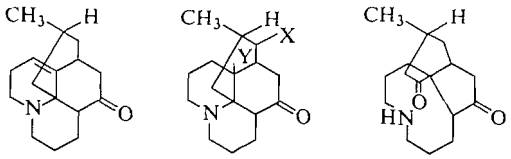

1 **2** X = Y = H; **3** X = H, Y = OH; **4** X = OH, Y = H; **5**

Alopecurine was followed off the column by lycodoline (**3**) (5) and then clavolonine (**4**) (9), both of which were identified by comparison with authentic samples. Further elution provided another new alkaloid, m.p. 171–172°, which we have called alopecuridine. Analytical and mass spectral data indicated the molecular formula $C_{16}H_{25}O_3N$ for alopecuridine. The infrared spectra of this substance were unusual. The spectrum determined in chloroform (Fig. 2) showed strong OH absorption at 3575 cm^{-1} and weak absorption at 3330 cm^{-1} (NH?). In the carbonyl region there was strong absorption at 1740 cm^{-1}, medium intensity absorption at 1690 cm^{-1}, and weak absorption at 1595 cm^{-1}. The spectrum (Nujol mull, Fig. 3) of alopecuridine which had been crystallized from acetone exhibited a series of bands in the OH, NH region, as well as carbonyl absorption at 1730 (strong) and 1640 cm^{-1} (medium intensity). The Nujol spectrum of a sublimed sample of alopecuridine (Fig. 4) showed a sharp band at 3480 cm^{-1} and a single carbonyl band at 1710 cm^{-1}. Both of these crystalline forms exhibited the solution spectrum mentioned above. The infrared spectra of the hydroperchlorate and the hydrobromide (Nujol) showed a single carbonyl band at 1750 cm^{-1}. Acetylation of alopecuridine yielded a neutral *N*-acetyl derivative $C_{18}H_{27}O_4N$ (Fig. 5) which showed hydroxyl absorption, as well as carbonyl absorption at 1740, 1685, and 1620 cm^{-1} (both in solution and in Nujol mull). We feel that these spectra are best interpreted on the basis of a transannular interaction (10) between a secondary amino group and a carbonyl group of alopecuridine.

The results may be summarized in terms of the part structures A and B. The chloroform spectrum of the base and the nujol spectrum of the crystallized material represent form A or an

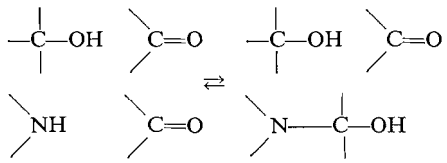

A B

equilibrium mixture of A and B, whereas the sublimed sample must be entirely in form B. The salts are of form B, but the acetyl derivative is of form A. The fact that the non-interacting carbonyl group absorbs at different positions (e.g. 1730 cm^{-1} in the crystallized base, 1710 cm^{-1} in the sublimed base) may be due to

Can. J. Chem. Downloaded from www.nrcresearchpress.com by 210.87.254.6 on 09/05/12
For personal use only.

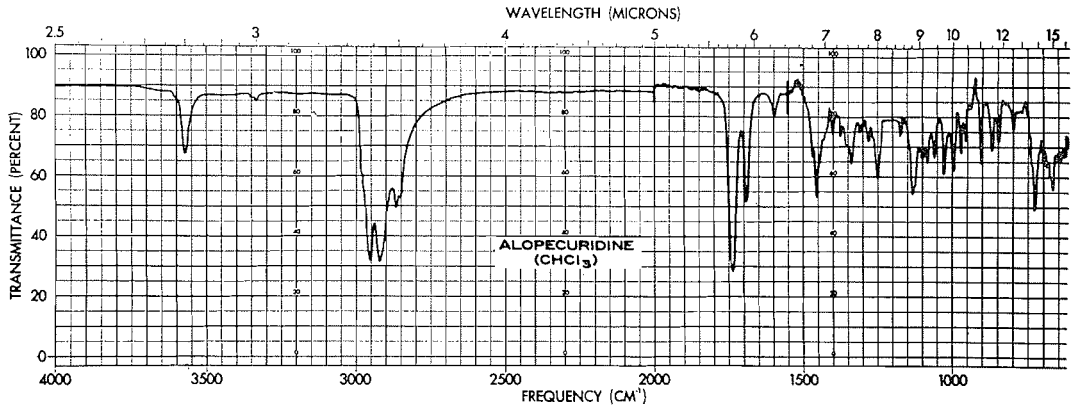

FIG. 2

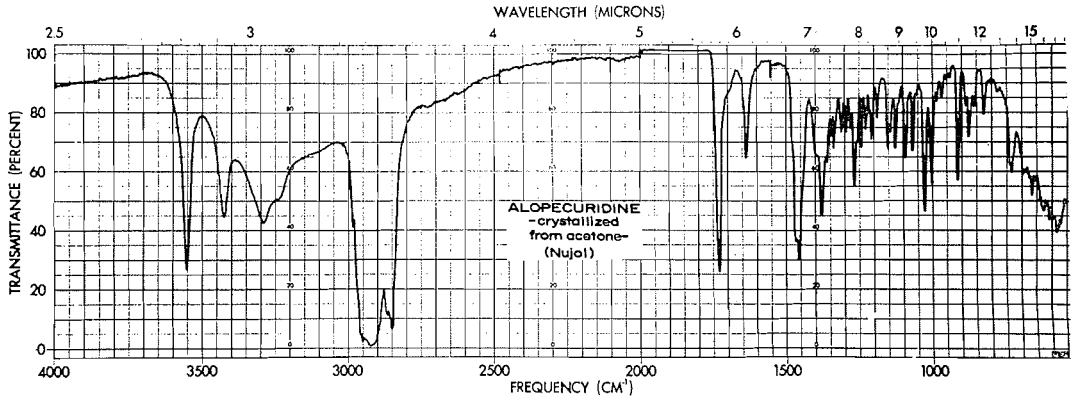

FIG. 3

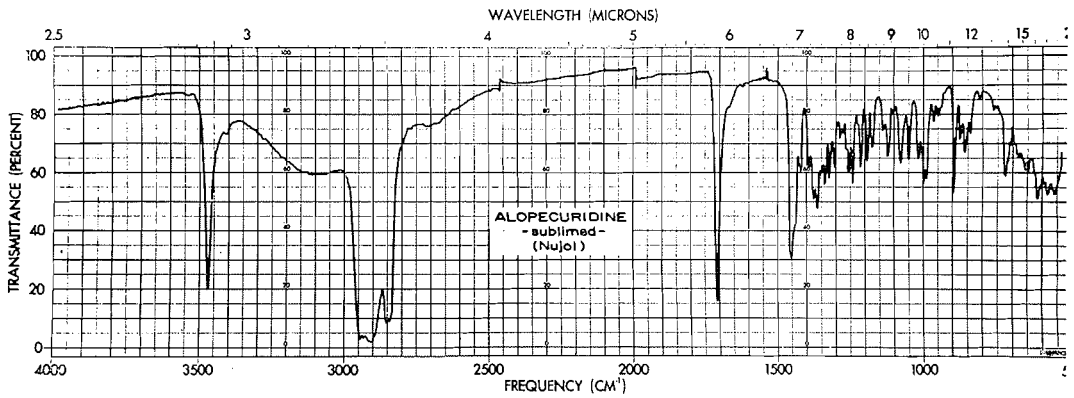

FIG. 4

varying degrees of intermolecular hydrogen-bonding in the crystal. The possibility that one of the carbonyl groups in part structure A is an aldehyde carbonyl is excluded by the fact that the nuclear magnetic resonance (n.m.r.) spectrum of *N*-acetylalopecuridine shows no absorption below τ 6.0. The n.m.r. spectrum does show the presence of a secondary *C*-methyl group (3-proton doublet at τ 8.92) as well as the acetyl methyl (singlet at τ 7.91). It thus appears that alopecuridine has two ketonic carbonyl groups, one of which is present in an 8–10-membered ring which contains a transannular secondary amino group (10). The other keto group gives rise to absorption at 1740 cm^{-1} in the infrared and hence may be located in a five-membered ring.

Can. J. Chem. Downloaded from www.nrcresearchpress.com by 210.87.254.6 on 09/05/12
For personal use only.

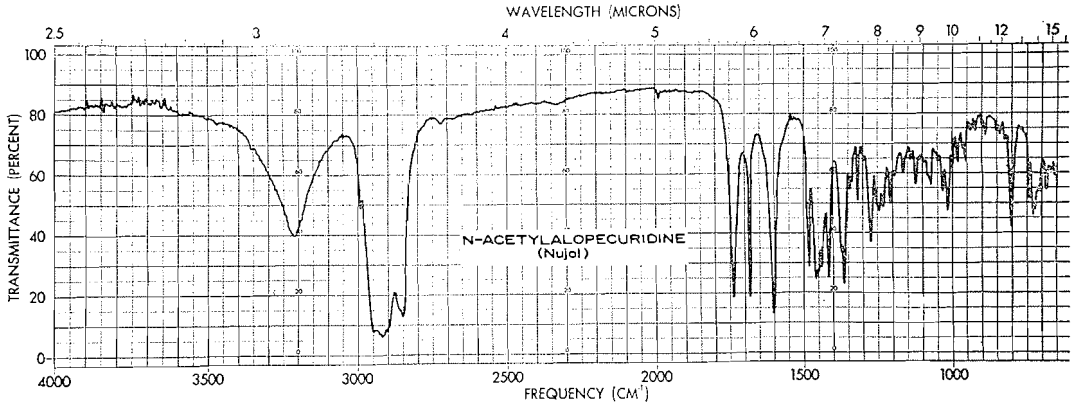

FIG. 5

The hydroxyl group in alopecuridine is not readily acetylated and thus is either tertiary or highly hindered, or both. Since there does not appear to be a carbon–carbon double bond in alopecuridine, the molecule is tricyclic.

Many of the properties of alopecuridine are similar to those described for fawcettimine (11, 12) which has been shown to possess structure **5**. Alopecuridine contains one oxygen more than fawcettimine and it seems possible that alopecuridine is a hydroxylated fawcettimine.

Chemical and *x*-ray crystallographic studies aimed at the elucidation of the structures of alopecurine and alopecuridine are in progress.

Experimental[1]

Plant Collection

The material used was collected by Drs. R. K. Godfrey and S. McDaniel in pine flatwoods near Tallahassee, Florida, during September, 1964, and a voucher specimen (No. 5255) is on file in the Florida State University Herbarium.

Isolation of the Crude Alkaloids

The ground whole plant of *Lycopodium alopecuroides* L. (6.8 kg) was extracted for three days with 10:1 ethanol–methanol in a large Soxhlet apparatus. The extract was concentrated at atmospheric pressure and any remaining solvent was removed by agitation with a stream of air. The residue was treated with ethyl acetate (4 l) and concentrated aqueous ammonia (20 ml) and the mixture stirred and refluxed for 2 h. The solution was filtered and the separated solid washed with additional ethyl acetate (2 × 500 ml). The combined organic layers were extracted with dilute sulfuric acid (5%, total of 2.8 l), which was then washed with benzene (3 × 500 ml, discarded). The acidic solution was cooled and taken to pH 9 with concentrated aqueous ammonia; the alkaline mixture was extracted with chloroform until further extracts gave a negative test with Mayer's reagent. The combined chloroform layers were washed with saturated salt solution, dried over Na_2SO_4, and concentrated *in vacuo* to yield the total, non-quaternary bases (12.9 g).

Separation of the Alkaloids

The crude alkaloid (4.5 g) was placed on a column of basic alumina (150 g, Activity III) and eluted in 13 fractions as shown in Table I.

TABLE I

Fraction	Eluant	Volume (ml)	Weight of fraction (g)
1	benzene	150	0.02
2	benzene	150	0.06
3	benzene	150	0.16
4	benzene	150	0.15
5	benzene–ether (4:1)	150	0.16
6	benzene–ether	150	0.23
7	ether	150	0.10
8	ether	150	0.43
9	chloroform	450	0.31
10	chloroform–methanol (99:1)	200	0.25
11	chloroform–methanol (49:1)	200	1.06
12	chloroform–methanol (24:1)	200	0.91
13	chloroform–methanol (9:1)	300	0.29

Fractions 1 and 2 contained non-basic material and were not further investigated. Fraction 3 showed two spots, R_f 0.9 and 0.5 (solvent system *a*), on t.l.c. Fraction 3

[1]Melting points were determined on a hot stage and are uncorrected. Infrared spectra were measured on a Perkin–Elmer model 441 spectrophotometer; ultraviolet spectra with a Cary model 14 spectrophotometer; nuclear magnetic resonance spectra with a Varian Associates model A-60 spectrometer; mass spectra with an AEI MS2-H mass spectrometer. Thin-layer chromatograms were carried out on 0.25 mm layers of Alumina G (Research Specialties Co., Richmond, California) which were dried for several hours at 100° and were developed with Dragendorff's reagent or with iodine vapor. The solvent systems used were benzene:ether (1:1) (solvent system *a*) and chloroform:methanol (49:1) (solvent system *b*). Microanalyses are by C. Daessle, Montreal.

Can. J. Chem. Downloaded from www.nrcresearchpress.com by 210.87.254.6 on 09/05/12
For personal use only.

Can. J. Chem. Downloaded from www.nrcresearchpress.com by 210.87.254.6 on 09/05/12
For personal use only.

was combined with similar material from another chromatogram (total, 0.5 g), dissolved in benzene (5 ml), and applied to the top of a dry-packed alumina (250 g) column (4). The chromatogram was developed with ether (200 ml), the column extruded and the components located by t.l.c. of appropriate aliquots washed off the alumina with methanol. The component of R_f 0.9 was obtained as a yellow oil (0.1 g) which slowly turned dark on exposure to air. This material was converted to the hydrochloride and crystallized from methanol–acetone to yield off-white crystals of anhydrolycodoline hydrochloride, m.p. 274–276° (decomp.). Identity was established by comparison of the infrared spectrum of the salt with that of an authentic sample, and by mixture melting point determination. The mass spectrum of the free base was identical to that of anhydrolycodoline (5). The component of R_f 0.5 was lycopodine (determined by infrared).

Fractions 4, 5, and 6 contained mainly lycopodine. Fraction 7 contained five components (t.l.c.) none of which could be isolated in pure form.

Fraction 8 showed three spots (R_f's 0.98, 0.90, 0.82, solvent system *b*) on t.l.c., the first of which is probably lycopodine. The material was dissolved in hot acetone and allowed to cool. Colorless crystals of *alopecurine* (0.10 g) separated which, after recrystallization from acetone, melted at 244–245°. Spectral details are described in the text, R_f 0.90.

Anal. Calcd. for $C_{23}H_{29}O_3N$ (mol. wt., 367): C, 76.17; H, 7.95; N, 3.81. Found (mol. wt., mass spectrometry, 367): C, 75.52; H, 7.94; N, 3.67.

Concentration of the acetone mother liquors obtained above yielded crystalline lycodoline, m.p. 179–180°, identical (t.l.c. behavior, infrared spectrum, mixture melting point) with an authentic sample.

Fraction 9 showed two spots corresponding to lycodoline (R_f 0.82) and clavolonine (R_f 0.58) on t.l.c. (solvent *b*). These two components were separated by dry column chromatography as described above except that chloroform:methanol (49:1) was used as developing solvent.

Fractions 10, 11, and 12 all showed the presence of a component of R_f 0.29 (solvent *b*) which crystallized from acetone and acetone–ether solutions of these fractions. A total of 0.75 g of alopecuridine, which melted at 171–172° after recrystallization from acetone, was obtained in this way. Further small amounts of alopecuridine were obtained by rechromatography of the mother liquors, but the bulk of the remaining material, which was a dark brown resin and which did not move from the origin on t.l.c. (solvent *b*), could not be separated into pure components. The nuclear magnetic resonance spectrum of alopecuridine (pyridine solution) showed a doublet at τ 9.12 (CH—CH_3) as the only cleanly resolved peak. The mass spectrum showed intense peaks (percentage of base peak in brackets) at *m/e* 279 (3, parent peak), 223 (26), 220 (21), 165 (70), 150 (100), 127 (97), 98 (69), and 97 (47). The remaining spectral properties are discussed in the text,

Anal. Calcd. for $C_{16}H_{25}O_3N$: C, 68.79; H, 9.02; N. 5.01. Found: C, 68.63; H, 8.88; N, 5.31.

Crystallization of fraction 13 from acetone yielded a small amount (20 mg) of material R_f 0.08 (solvent *b*), m.p. 230–232° which proved to be identical with the debenzoylalopecurine described below. The remainder of the fraction could not be separated into pure components.

Acetylation of Alopecurine

Alopecurine (50 mg) was dissolved in acetic anhydride – pyridine (6 ml. of 1:1) and the solution kept at room temperature for 24 h. The solvents were then removed at the pump, the residue dissolved in chloroform, and the resulting solution washed first with sodium bicarbonate solution, then with water. Evaporation of the chloroform left a glassy material which could not be crystallized but which yielded a crystalline hydroperchlorate, m.p. > 300°, from aqueous acetone. Infrared spectrum (Nujol mull): 3175 (+NH), 1725 (*O*-acetyl), 1700 (*O*-benzoyl), 1595, 1580, 1500 (phenyl), 1275 (*O*-benzoyl), 1250 (*O*-acetyl), 1100 cm^{-1} (ClO_4). The infrared spectrum of the free base showed no OH or NH absorption.

Anal. Calcd. for $C_{25}H_{31}O_4N \cdot HClO_4$: C, 58.87; H, 6.32. Found: C, 59.59; H, 6.11.

Hydrolysis of Alopecurine

Alopecurine (100 mg) was dissolved in alcohol (9 ml) and 4% aqueous KOH (6 ml) added. The resulting solution was refluxed for 1½ h, then concentrated at the pump, diluted with water, and extracted with chloroform. Evaporation of the chloroform left a solid (50 mg) which was purified by sublimation and then crystallization from acetone. The debenzoylalopecurine thus obtained melted at 230–232°. Infrared spectrum (Nujol): 3350 (broad OH absorption). No bands in the 1500 to 1800 cm^{-1} region. The mass spectrum showed a parent peak at *m/e* 263 corresponding to $C_{16}H_{25}O_2N$ and a base peak at *m/e* 216.

Acidification of the aqueous hydrolysis solution and extraction with chloroform afforded benzoic acid (13 mg), identical in melting point and infrared spectrum with an authentic sample.

Acetylation of Alopecuridine

Alopecuridine (55 mg) was dissolved in acetic anhydride – pyridine (6 ml of 1:1) and heated on the steam bath for 24 h (the same result was obtained at room temperature). The solvent was removed at the pump and the residue dissolved in chloroform and washed with bicarbonate solution, dilute hydrochloric acid, and water. Evaporation of the chloroform left a solid which was crystallized from acetone to give colorless, fine needles (50 mg), m.p. 223–224°. Details of the infrared and nuclear magnetic resonance spectra are described in the text.

Anal. Calcd. for $C_{18}H_{27}O_4N$ (mol. wt., 321): C,67.26; H, 8.47; N, 4.36. Found (mol. wt., mass spectrometry, 321): C, 67.01; H, 8.75; N, 4.18.

Acknowledgments

We wish to thank Drs. R. K. Godfrey and S. McDaniel, Department of Biological Sciences, Florida State University, for their cooperation in the collection of the plant material, and Dr. R. H. Burnell, Laval University, for an exchange of information regarding fawcettimine. We also wish to thank Messrs. R. N. Swindlehurst and G. Bigam and their associates for most of the infrared and nuclear magnetic resonance spectra, and W. Duholke and A. T. Budd for the mass spectra.

1. H. G. BOIT. Ergebnisse der alkaloid chemie bis 1960. Akademie-Verlag, Berlin. 1961. pp. 916, 1011.
2. W. HERTER. Index Lycopodiorum. Montevideo, Uruguay. 1949.
3. M. E. WALL, C. E. FENSKE, J. W. GARVIN, J. J. WILLAMEN, Q. JONES, B. G. SCHUBERT, and H. S. GENTRY. J. Am. Pharm. Assoc. Sci. Ed. **48**, 695 (1959).
4. B. LOEV and K. M. SNADER. Chem. Ind. London, 15 (1965).
5. W. A. AYER and G. G. IVERACH. Can. J. Chem. **42**, 2514 (1964).
6. L. J. BELLAMY. The infrared spectra of complex molecules. John Wiley and Sons, Inc., New York. 1958. pp. 71, 179.
7. A. I. SCOTT. Interpretation of the ultraviolet spectra of natural products. The Pergamon Press, Ltd., New York. 1964. p. 115.
8. H. BUDZIKIEWICZ, C. DJERASSI, and D. H. WILLIAMS. Interpretation of mass spectra of organic compounds. Holden-Day, Inc., San Francisco. 1964. p. 194.
9. R. H. BURNELL and D. R. TAYLOR. Tetrahedron, **15**, 173 (1961).
10. N. J. LEONARD. Record Chem. Progr. Kresge-Hooker Sci. Lib. **17**, 243 (1956).
11. R. H. BURNELL, C. G. CHIN, B. S. MOOTOO, and D. R. TAYLOR. Can. J. Chem. **41**, 3091 (1963).
12. Y. INUBUSHI, H. ISHII, T. HARAYAMA, R. H. BURNELL, W. A. AYER, and B. ALTENKIRK. Tetrahedron Letters, 1069 (1967).

Can. J. Chem. Downloaded from www.nrcresearchpress.com by 210.87.254.6 on 09/05/12
For personal use only.

Can. J. Chem. Downloaded from www.nrcresearchpress.com by 210.87.254.5 on 09/05/12
For personal use only.

Hydrogen bonding and conformation in *cis*- and *trans*-2-alkoxy-3-hydroxytetrahydrofurans

W. W. ZAJAC, JR.,[1] F. SWEET,[2] AND R. K. BROWN
Department of Chemistry, University of Alberta, Edmonton, Alberta

Received July 14, 1967

Infrared spectra show both free and hydrogen bonded hydroxyl absorption in several *trans*-2-alkoxy-3-hydroxytetrahydrofurans. The extent of non-bonded hydroxyl is greater than that of bonded hydroxyl. Suggestions are made of possible conformations which might account for the infrared data.

Canadian Journal of Chemistry, **46**, 21 (1968)

Introduction

Relatively little consideration has been given to the correlation of conformation with physical and chemical properties in cyclopentane and even less to the saturated five-membered ring heterocycles (1, 2). Having previously synthesized a series of 2-alkoxy-3-hydroxytetrahydrofurans (3), we undertook an investigation of the conformations of these compounds. Of the physical methods available, infrared spectroscopy (4) and proton nuclear magnetic resonance are particularly well-suited for the conformational studies of 2-alkoxy-3-hydroxytetrahydrofurans. The present paper reports the results of an examination of the hydrogen bonding in these molecules to obtain information concerning their conformation. Proton magnetic resonance studies will be presented in a later paper.

Experimental

Infrared spectra were obtained with a Perkin–Elmer model 421 grating spectrophotometer. Carbon tetrachloride, used as solvent, was dried and distilled from phosphorus pentoxide. Concentrations of the alcohols were 0.005 *M* or less and 1 cm or 2 cm cells were used, depending upon concentration of the solutions. Generally, successive dilutions were made to ensure that intramolecular and not intermolecular hydrogen bonding was being observed. The instrument was calibrated in the 3600 cm^{-1} region with carbon dioxide. Spectra for ethylene glycol were also obtained. The values for free and bonded hydroxyl agreed with literature values to ± 2 cm^{-1} (5).

The 2-alkoxy-3-hydroxytetrahydrofurans were prepared according to published directions. The remaining compounds listed in Table I were prepared as described in the accompanying references.

3-Hydroxytetrahydrofuran (item 3, Table I) was prepared by a more productive route than previously reported (8, 9). *2-Chloro-3-hydroxytetrahydrofuran* was obtained in 62% yield according to published directions (18) by addition of hypochlorous acid (19) to 2,5-dihydrofuran (Aldrich Chemical Co.); b.p., 80° at 4 mm, 101° at 14 mm; n_D^{25}, 1.4789 (lit. b.p., 102–103° at 14 mm (18); 99–103° at 12 mm, n_D^{20}, 1.4883 (20)).

The above chlorohydrin (9.5 g, 0.078 mole) was dissolved in 50 ml of dry 1,2-dimethoxyethane (distilled from lithium aluminium hydride) contained in a 200 ml round bottom flask equipped with a magnetic stirrer, reflux condenser, and drying tube. To this was added slowly 3.97 g (0.093 mole) of sodium hydride (a 56% dispersion in mineral oil) while the flask was kept at 0–5° with an ice bath. After hydrogen evolution had ceased the mixture was refluxed for 12 h, during which time sodium chloride precipitated. The mixture was cooled and diluted with ether to complete precipitation of the chloride and excess sodium hydride and then filtered by gravity. The filtrate was freed from solvents on a spinning band column and the residue was distilled giving 6.3 g (94%) of *3,4-epoxytetrahydrofuran*; b.p., 45° at 14 mm; n_D^{25}, 1.4439; (lit. b.p., 143–145°; n_D^{20}, 1.4442 (20)). This was shown to contain only one component when subjected to gas–liquid chromatography using a Burrell model K-2 Kromo-Tog equipped with a 2.5 m column packed with 20% butanediol succinate on Gas-Chrom P (60-80 mesh); column temperature, 125°; helium carrier gas at a flow rate of 60 ml/min.

The above epoxide (2.0 g, 0.023 mole) in 25 ml of dry ether was added slowly to a mixture of 0.40 g (0.01 mole) of lithium aluminium hydride in 50 ml of ether at room temperature. After addition was complete (~30 min), the solution was diluted with 25 ml of ether and the mixture stirred overnight at room temperature. The mixture was then cooled to about −10° with a dry ice – acetone bath and the complex decomposed by the successive addition of 1 ml of water, then 3 ml of 15% aqueous sodium hydroxide, followed by 1 ml of water. The mixture was filtered free of solids, and the solid washed with ether, then with chloroform. The combined filtrate and washings were dried over $MgSO_4$ and freed from solvent by fractional distillation and the residue was distilled to give 1.9 g (96%) of *3-hydroxytetrahydrofuran* boiling at 87° at 24 mm; n_D^{24}, 1.4482; (lit. b.p., 84–88° at 24 mm, n_D^{20}, 1.4507 (8); 82–88° at 24 mm, n_D^{25}, 1.4497 (21)). Gas–liquid chromatography showed that this alcohol contained a trace of impurity which was not unreacted

[1]On leave during 1965–1966 from Villanova University, Villanova, Pennsylvania.

[2]Doctoral candidate in the Department of Chemistry, University of Alberta, Edmonton, Alberta.

TABLE I
Infrared spectral data

Item	Compound		ν_{OH} in cm^{-1} Free (ϵ)	Bonded (ϵ)	$\Delta\nu$*	$r_{OH}\cdots O$ in Å Ref. 5†	Ref. 12‡	Reference
1	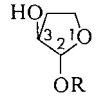	R = CH_3	3628 (30)	3604 (24)	24	2.5	2.9	This work
		R = C_2H_5	3628 (43)	3604 (32)	24	2.5	2.9	This work
		R = $CH(CH_3)_2$	3629 (43)	3604 (35)	25	2.5	2.9	This work
		R = $C(CH_3)_3$	3628 (40)	3604 (35)	24	2.5	2.9	This work
2	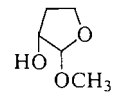		3620 (<5)	3565 (80)	55	2.0	2.2	This work
3	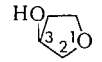		3628					8
			3625	3612	13	2.9	3.9	9
			3624 (60)	3599 (32)	25	2.5	2.9	This work
4	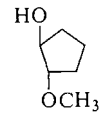		3627	—				10
5	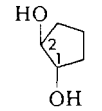		3620	—				5
6	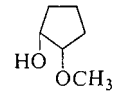		—	3570	59	1.9	2.1	10
7	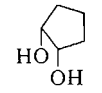		3633	3572	57	1.9	2.1	5

*$\Delta\nu = \nu_{free} - \nu_{bonded}$: ν_{free} taken as 3 629 cm^{-1} (13).
†Calculated from $\Delta\nu = (250/r) - 74$.
‡Calculated from $\Delta\nu = [42.5/(r - 1.4)] - 3.5$.

epoxide. Pure 3-hydroxytetrahydrofuran was obtained by gas–liquid chromatography using an Aerograph Autoprep model A-700 with a 20 ft × 1/4 in. (O.D.) column filled with 25% Carbowax 20 M on Gas-Chrom P (60–80 mesh) with helium as the carrier gas at a flow rate of 110 ml/min.

Results and Discussion

The infrared spectra were obtained in carbon tetrachloride at concentrations below 0.005 *M*, conditions which suppress intermolecular hydrogen bonding (4–7).

In Table I are recorded the infrared absorption frequencies in the hydroxyl stretching region. Also included are the literature data for 3-hydroxytetrahydrofuran (8, 9), *cis*- and *trans*-cyclopentane-1,2-diol (5) and *cis*- and *trans*-2-methoxycyclopentanol (10). The data (items 1 and 2, Table I), clearly show that both the *cis*- and *trans*-2-alkoxy-3-hydroxytetrahydrofurans have an hydroxyl group which is intramolecularly bonded to oxygen. Although the extinction coefficients are good only to ±10%, the figures show a somewhat higher proportion of the conformer with a free hydroxyl group in the *trans* compound, while the *cis* isomer is essentially devoid of unbonded hydroxyl.

It has been established that no intramolecular hydrogen bonding occurs in either *trans*-2-methoxycyclopentanol (10) or in *trans*-cyclopentane-1,2-diol (5), the minimum distance between hydroxyl hydrogen of one substituent and oxygen of the second substituent being too large for such bonding (⩾3.3 Å). Yet in our *trans*-2-alkoxy-3-hydroxytetrahydrofurans con-

Can. J. Chem. Downloaded from www.nrcresearchpress.com by 210.87.254.5 on 09/05/12
For personal use only.

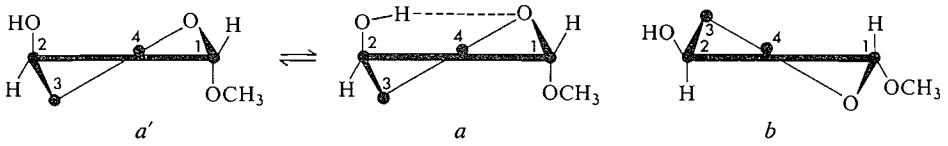

SCHEME I

siderable bonding does occur. Since the 3-hydroxyl and 2-alkoxy groups are *trans*, no bonding is possible between them. Accordingly, hydrogen bonding must occur between the hydroxyl group at position-3 and the ring oxygen.

Barker *et al.* (8) have reported only free hydroxyl absorption for 3-hydroxytetrahydrofuran (item 3, Table I) whereas Eugster and Allner (9) detected both free and bonded hydroxyl absorption for this compound. We have obtained the infrared spectrum of 3-hydroxytetrahydrofuran and found both free and bonded hydroxyl absorption in roughly the same proportion as found by Eugster and Allner.[3] There is a discrepancy between the value reported by the latter authors (9) for bonded hydroxyl (3612 cm^{-1}) and that found in our work (3599 cm^{-1}). This we have been unable to resolve. It is noteworthy that our value gives a $\Delta\nu$ of 25 cm^{-1} which is consistent with the $\Delta\nu$ values found for the *trans*-2-alkoxy-3-hydroxytetrahydrofurans.

Comparison of the extinction coefficients for 3-hydroxytetrahydrofuran and the *trans*-2-alkoxy-3-hydroxytetrahydrofurans shows that introduction of the alkoxy group at position-2 causes an *increase* in the proportion of the conformer having a bonded hydroxyl (free/bonded = 60/32 in the former vs. 30–43/24 in the latter).

Kuhn (5) has shown that the hydrogen bond is stronger the larger the difference ($\Delta\nu$) between the non-bonded and bonded absorption frequencies. Comparison of $\Delta\nu$ for each pair of *cis-trans* isomers listed in Table I shows that $\Delta\nu$ is greater for the *cis*- than for the *trans*-2-alkoxy-3-hydroxytetrahydrofuran. This further corroborates the original assignment of configuration made for these compounds based on nuclear magnetic resonance data (3). Using either the equation derived by Kuhn (5) or the modified equation by Brutcher and Bauer (12) relating the $\Delta\nu$ to the hydrogen bonded distance between H and O, it is seen that these distances are greater in the *trans* compounds than they are in the *cis* isomers. These are in reasonable agreement with the distances found in accurate scale models. For these simple calculations we chose 3629 cm^{-1} as the absorption frequency of the non-bonded secondary hydroxyl group as suggested by Cole and Jeffries (13).

To account for the free and bonded hydroxyl absorption found for the *trans*-2-alkoxy-3-hydroxytetrahydrofurans, two possible situations arise. In the first of these we envisage two molecular conformations[4]—one in which the hydroxyl group is in a position which permits hydrogen bonding (*a* in Scheme I) and one in which such bonding is not possible (*b* in Scheme I). Each of these two conformations can be obtained by rotation about the C_1—C_2 bond. Clockwise rotation[5] of C_2 (sighting from C_1 to C_2), which is accompanied by *anticlockwise* rotation of C_1, removes the hydrogen–oxygen eclipsing interaction and both the hydroxyl and alkoxy groups assume a quasiaxial (or axial)[6] orientation (*a* in Scheme I). Hydrogen bonding with the ring oxygen is possible in this conformation. The reverse rotation about C_1—C_2, which also decreases eclipsed hydrogen–oxygen interaction, places the two substituents in a quasiequatorial (or equatorial) arrangement (*b* in Scheme I). In this conformation no intramolecular hydrogen bonding can occur. One

[3]Both free and bonded hydroxyl absorption has been found for the analogous heterocycle, 3-hydroxytetrahydrothiophene and some of its derivatives (11).

[4]Nuclear magnetic resonance data suggests that the molecule is probably not in the simple envelope conformation.

[5]For convenience in this part of the discussion we have numbered the tetrahydrofuran as shown in Scheme I with the carbon atom adjacent to the oxygen, and bearing the alkoxy group, labelled C_1 and the vicinal carbon (bearing the OH group) as C_2, etc. Names and numbering of the ring atoms of compounds in Table I follow the normal rules.

[6]We assume the half chair conformation. The infrared data do not permit one to discern between the axial and quasiaxial arrangement. The same is true for the equatorial and quasiequatorial conformation.

Can. J. Chem. Downloaded from www.nrcresearchpress.com by 210.87.254.5 on 09/05/12
For personal use only.

might expect the latter conformation to be less stable because of gauche oxygen–oxygen interaction at C_1 and C_2 which is about 0.35 kcal/mole in the cyclitols (14). Furthermore, the anomeric effect (15) should tend to stabilize the former conformation (*a* in Scheme I) in which the substituents are quasiaxial (or axial). Hence conformer *a* should be more stable than conformer *b*. Use of the extinction coefficients for the bonded and non-bonded hydroxyl groups (item 1, Table I) to calculate the proportion of the two conformers suggested above is not justified since it is known that bonded hydroxyl has a higher extinction coefficient than does free hydroxyl (16, 17). However, it is clear from the extinction coefficients that if one assumes that free and bonded hydroxyls are due only to the two conformers above, conformer *b* (free hydroxyl) is in greater proportion.

The alternate possibility, which might account for the hydrogen bonding data, assumes that essentially one conformer exists (i.e. *a*, Scheme I) because of the reasons cited above (gauche O,O interaction; anomeric effect). Rotation about the C_2—O bond would then permit both free and bonded hydroxyl (*a* and *a'*) with the conformer *a'* in greater abundance. It should be pointed out that the OH - - - O distance (Table I) of 2.5 Å to 2.9 Å indicates no particularly strong hydrogen bond. If this second alternative (*a* and *a'*) is the one which is responsible for the observed bonded and free hydroxyl, then it follows that the hydrogen bonding in the *trans*-2-alkoxy-3-hydroxytetrahydrofurans is a consequence of the conformational preference for *a*, which in turn is due to the anomeric effect and minimization of O,O gauche interaction.

Acknowledgment

The authors thank the National Research Council of Canada for financial support during the course of this work.

1. E. L. Eliel, N. L. Allinger, S. J. Angyal, and G. A. Morrison. Conformational analysis. John Wiley and Sons, Inc., New York. 1965.
2. M. Hanack. Conformation theory. Academic Press, Inc., New York. 1965.
3. F. Sweet and R. K. Brown. Can. J. Chem. **44**, 1571 (1966).
4. M. Tichy. Advances in organic chemistry. Vol. 5. Interscience Publishers, Inc., New York. 1965. pp. 115–298.
5. L. P. Kuhn. J. Am. Chem. Soc. **74**, 2492 (1952).
6. L. P. Kuhn. J. Am. Chem. Soc. **76**, 4323 (1954).
7. L. P. Kuhn. J. Am. Chem. Soc. **80**, 5950 (1958).
8. S. A. Barker, J. S. Brimacombe, A. B. Foster, D. H. Whiffen, and G. Zweifel. Tetrahedron, **7**, 10 (1959).
9. C. H. Eugster and K. Allner. Helv. Chim. Acta, **45**, 1750 (1962).
10. K. W. Buck, A. B. Foster, A. Labib, and M. Webber. J. Chem. Soc. 2846 (1964).
11. A. Lutringhaus, S. Kabuss, H. Prinzback, and F. Langenbucher. Ann. **653**, 195 (1962).
12. F. V. Brutcher, Jr. and W. Bauer, Jr. J. Am. Chem. Soc. **84**, 2236 (1962).
13. A. R. H. Cole and P. R. Jeffries. J. Chem. Soc. 4391 (1956).
14. S. J. Angyal and D. J. Hough. Chem. Ind. London, 1147 (1956).
15. J. T. Edward and J. Puskas. Can. J. Chem. **40**, 711 (1962).
16. A. D. Cross. Introduction to practical infrared spectroscopy. 2nd ed. Butterworths, London. 1964. p. 40.
17. G. C. Pimentel and A. L. McClellan. The hydrogen bond. W. H. Freeman and Co., San Francisco. 1960. p. 170.
18. W. Reppe. Ann. **596**, 138 (1955).
19. G. H. Coleman and H. F. Johnston. *In* Organic synthesis. Coll. Vol. I. John Wiley and Sons, Inc., New York. 1941. p. 158.
20. E. G. E. Hawkins. J. Chem. Soc. 248 (1959).
21. H. Wynberg. J. Am. Chem. Soc. **80**, 364 (1958).

Can. J. Chem. Downloaded from www.nrcresearchpress.com by 210.87.254.5 on 09/05/12
For personal use only.

Can. J. Chem. Downloaded from www.nrcresearchpress.com by 210.87.254.5 on 09/05/12
For personal use only.

Preparation and base-catalyzed reactions of some β-halohydroperoxides

KARL R. KOPECKY, JOHAN H. VAN DE SANDE,[1] AND CEDRIC MUMFORD
Department of Chemistry, University of Alberta, Edmonton, Alberta

Received July 26, 1967

The reaction between olefins, *N*-chloroacetamide or 1,3-dibromo-5,5-dimethylhydantoin, and hydrogen peroxide affords β-halohydroperoxides in good yields. These compounds react extremely rapidly in basic solution to give products which depend upon their structure. The 3-halo-2,3-dimethyl-2-butyl hydroperoxides form 2,3-dimethyl-3-hydroperoxy-1-butene and from the 2-halo-1,2-dimethylcyclohexyl hydroperoxides 1-methyl-2-methylene-cyclohexyl hydroperoxide is obtained. No allylic hydroperoxide can be detected from the reaction between base and 3-bromo-2-methyl-2-butyl hydroperoxide. Mainly cleavage products, acetone and acetaldehyde, are formed together with some 2,3-epoxy-2-methylbutane. The reaction between base and 2-bromo-1-phenylethyl hydroperoxide gives styrene oxide, benzoic acid, and some benzaldehyde. From *trans*-2-bromocyclohexyl hydroperoxide, *trans*-2-bromocyclohexanol, cyclohexene oxide, and some *trans*-1,2-cyclohexanediol are obtained upon reaction with base. No evidence for the formation of the allylic hydroperoxide was obtained.

Canadian Journal of Chemistry. **46**, 25 (1968)

Introduction

The dye-photosensitized oxidation of olefins affords a unique route to allylic hydroperoxides of definite structure (1, 2). The hydroperoxy group is always introduced at one of the originally olefinic carbon atoms and a shift of the double bond always occurs, eq. [1], so that the reaction is very useful from a synthetic point of view.

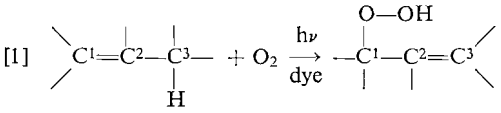

While the reaction proceeds well with tetrasubstituted olefins and somewhat less so with trisubstituted olefins, disubstituted and monosubstituted olefins are oxidized very slowly (3). The latter require very long irradiation times for significant yields of products so that other reactions of the olefins and further reactions of the product become important. This led to a consideration of other routes which would be as specific and more generally useful for the conversion of olefins to allylic hydroperoxides. It appeared that a reaction between base and β-halohydroperoxides could yield allylic hydroperoxides. Thus, conversion of an olefin to the β-halohydroperoxide and then the elimination of the elements of halogen acid would constitute a simple, two step, chemical transformation of the olefin to an allylic hydroperoxide. This transformation could introduce the hydroperoxy group and relocate the double bond of an olefin into the same positions as is observed in the photosensitized oxidation, eq. [2].

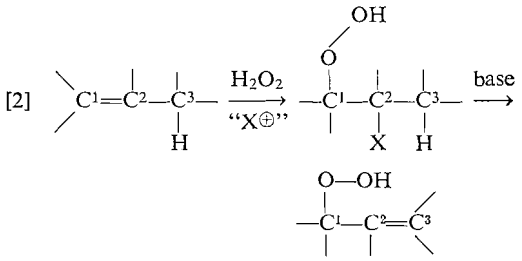

This paper reports some of the results obtained in the study of this approach. After work had begun there appeared several reports on the reactions of β-halo- and β-cyanohydroperoxides with base (4–6). It is reported that 1-chloro-2-methyl-2-propyl hydroperoxide is rapidly decomposed by base to acetone and formaldehyde (4), while other workers report that upon treatment with base the bromo analogue, 1-bromo-2-methyl-2-propyl hydroperoxide is converted partly to isobutylene oxide as well as to acetone and formaldehyde (5). A similar cleavage reaction was observed when 2-methyl-2-hydroperoxypropionitrile was treated with base (6). Acetone and cyanate ion are produced. The above β-halohydroperoxides have halogen on the terminal carbon atom and a simple elimination route is not available to these materials.

Results and Discussion

Preparation of β-Halohydroperoxides

β-Halohydroperoxides have been prepared by

[1]Holder of a National Research Council of Canada Studentship, 1964–1967 and a University of Alberta Dissertation Fellowship, 1967.

Can. J. Chem. Downloaded from www.nrcresearchpress.com by 210.87.254.5 on 09/05/12
For personal use only.

autoxidation of halogenated hydrocarbons (7, 8), by the acid-catalyzed addition of hydrogen peroxide to allylic halides (4), by the reaction between olefins, hydrogen peroxide, and *t*-butyl hypochlorite (9), and by the addition of bromine or chlorine to olefins in the presence of hydrogen peroxide (5, 10). In the present study it has been found that β-halohydroperoxides can be prepared conveniently and in good yield by the reaction between olefins, *N*-haloamides, and excess 98% hydrogen peroxide in ether solution. The reaction appears to be general and gives essentially no dihalogenated adducts, which are major by-products in Rieche's method (5, 10).

β-Chlorohydroperoxides were prepared by the reaction between equivalent amounts of *N*-chloroacetamide and olefin and a 10-fold excess of 98% hydrogen peroxide in ether solution. The reaction was very slow at room temperature; however, a very vigorous, exothermic reaction occurred when a trace of *p*-toluenesulfonic acid was added to the reaction mixture at 0°. The β-bromohydroperoxides were prepared by the reaction between equivalent amounts of 1,3-dibromo-5,5-dimethylhydantoin and olefin and a 5-fold excess of hydrogen peroxide in ether. This reaction proceeded very rapidly at 0°, but some coloring occurred and some dibromide was produced. Dibromide formation could be entirely eliminated by adding the brominating agent to a solution of olefin and hydrogen peroxide in ether at −40°. Excess hydrogen peroxide and amide were removed by washing the reaction mixtures with water.

The β-halohydroperoxides prepared are listed in Table I. The 3-halo-2,3-dimethyl-2-butyl hydroperoxides, **1***a* and **1***b* (10), could be isolated as crystalline solids. This was done by concentration of the ether solution and crystallization from pentane. Several attempts at isolation of 2-chloro-1,2-dimethylcyclohexyl hydroperoxide, **2***a*, resulted in explosions, so that neither **2***a* nor 2-bromo-1,2-dimethylcyclohexyl hydroperoxide, **2***b*, were isolated or characterized. The remaining compounds, 3-bromo-2-methyl-2-butyl hydroperoxide (**3**), *trans*-2-bromocyclohexyl hydroperoxide (**4**), and 2-bromo-1-phenylethyl hydroperoxide (**5**), were isolated as liquids which gave clean nuclear magnetic resonance (n.m.r.) spectra and had 80–90% of the theoretical active oxygen content. These materials were isolated by removing the ether under 0.5 mm pressure at

TABLE I

Yield of β-halohydroperoxides from olefins

Olefin	Halogen source*	β-Halohydroperoxide	% yield†
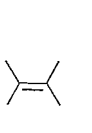	A	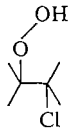 **1***a*	60‡
	B	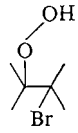 **1***b*	76§
	A	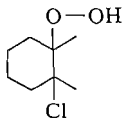 **2***a*	57‖
	B	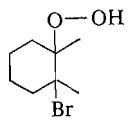 **2***b*	86
	B	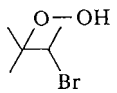 **3**	80
	B	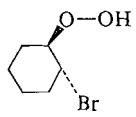 **4**	73
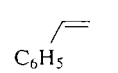	B	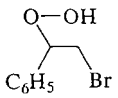 **5**	55

*A, *N*-chloroacetamide; B, 1,3-dibromo-5,5-dimethylhydantoin.
†Yields based on starting olefin and determined by iodometric titration unless otherwise indicated.
‡Also isolated as a solid in 30% yield.
§Isolated yield of crystalline product.
‖By difference from unreacted starting material as determined by gas chromatography.

TABLE II

Products from reaction between β-halohydroperoxides and base

β-Halohydroperoxide	Total % yield	Product composition	% yield*
1*a*	70	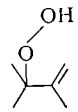 **6**	70†
1*b*	77	**6**	77†
2*a*	33	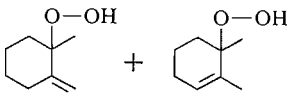 **7**‡ **8**	33†, 1
2*b*	66	**7**‡ **8**	66(42†), 2
3	87	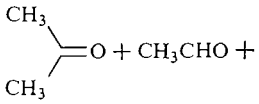	76, 77
			10
4	58	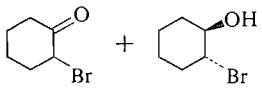	trace, 27
		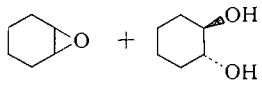	29, 2
5	94	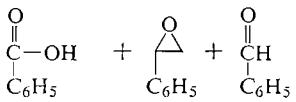	45†, 45, 4

*As determined by gas chromatographic analysis unless otherwise indicated.
†Yield of isolated product.
‡Characterized as the alcohol 9 after reduction.

30°. β-Bromohydroperoxides are formed in higher yields than β-chlorohydroperoxides.

All of the β-halohydroperoxides isolated were characterized by iodometric titration and by their nuclear magnetic resonance spectra. All showed broad singlet absorption of relative peak area ca. 1 in the range τ 1 to 2 in the n.m.r. spectrum. This is the characteristic region for the absorption of the hydroperoxy proton (11). Other features of the n.m.r. spectra of these compounds are straightforward and will not be discussed. In addition **1***a*, **4**, and **5** were further characterized by reduction to the corresponding halohydrins which proved in each case to be identical with authentic material.

Reaction of β-Halohydroperoxides with Base

It was found that all the β-halohydroperoxides reacted extremely rapidly with base. The products formed are listed in Table II. The reactions were carried out by mixing the β-halohydroperoxide in methanol or ether solution with a methanolic

Can. J. Chem. Downloaded from www.nrcresearchpress.com by 210.87.254.5 on 09/05/12
For personal use only.

Can. J. Chem. Downloaded from www.nrcresearchpress.com by 210.87.254.5 on 09/05/12
For personal use only.

solution of base at temperatures ranging from 0° to 30°. After about 1 to 2 h the reaction mixtures were poured into water and extracted with ether, except in the reaction of **2***a*. In this reaction sodium borohydride was added to the reaction mixture prior to workup to reduce the allylic hydroperoxide. The yields of products obtained from **1***a*, **1***b*, **2***a*, and **2***b* are yields of products actually isolated by distillation. The yields of products from the other reactions were determined by gas–liquid chromatography (g.l.c.) using internal standards.

The product from **1***a* and **1***b* was identical in every respect with authentic 2,3-dimethyl-2-hydroperoxy-1-butene (**6**), prepared by photosensitized oxidation of 2,3-dimethyl-2-butene (12).

The allylic hydroperoxides, 2-methylene-1-methylcyclohexyl hydroperoxide (**7**) and 1,2-dimethyl-2-cylohexenyl hydroperoxide (**8**) were reduced to the corresponding alcohols, 2-methylene-1-methylcyclohexanol (**9**) and 1,2-dimethyl-2-cyclohexen-1-ol (**10**), and characterized as such. Essentially the same ca. 97–3 mixture of alcohols was produced in 80% yield by the photosensitized oxidation of 1,2-dimethylcyclohexene followed by reduction of the hydroperoxides formed. The product (**9**), always the major one, was identified by its n.m.r. spectrum and by comparison with authentic material (13) which was prepared by the Grignard reaction between methyl magnesium iodide and 2-methylenecyclohexanone. The n.m.r. spectrum showed two one proton absorptions at τ 5.15 and 5.39 characteristic of a terminal olefin.

Compound **10** was present in such a small amount in every case that it appeared not to affect the spectral properties of **9** and was only detectable by gas chromatography. It was identified in the reaction mixtures only by comparison of its gas chromatographic retention time with that of an authentic sample of **10** (14) prepared by reaction of methyllithium with 2-methyl-2-cyclohexenone. It is estimated that only ca. 3% to 5% of **10** was present in any of the product mixtures from **2***a* or **2***b* or from the photooxidation–reduction sequence.

Thus, the addition–elimination sequence outlined in eq. [2] can, in fact, be used to transform 2,3-dimethyl-2-butene and 1,2-dimethylcyclohexene to the corresponding allylic hydroperoxides in good yield. The products are the same as those obtained from the photosensitized reaction, and in the case of 1,2-dimethylcyclohexene even the selectivities of the two processes are similar. The photosensitized reaction of 1,2-dimethylcyclohexene is rather selective when compared with other examples in which more than one product is possible (1, 2).

9 **10**

However, the situation in the case of 2-methyl-2-butene and cyclohexene is quite different. Although a rapid reaction took place, no evidence was found for the formation of any allylic hydroperoxide from the base-catalyzed reactions of **3** and **4**. Portions of the reaction mixture were reduced with sodium borohydride and analyzed by gas chromatography for the products of reduction of the allylic hydroperoxides, 3-methyl-1-butene-3-ol (**11**) and 2-methyl-1-butene-3-ol (**12**) in the case of the reaction mixture from **3**, and cyclohexene-3-ol (**13**) in the case of the reaction mixture from **4**. In neither case was any of the allylic alcohol detectable. Less than 0.5% of any of these compounds could have been detected.

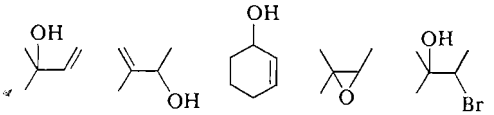

11 **12** **13** **14** **15**

Instead, the products from **3**, found in the unreduced reaction mixture, consisted mainly of acetone and acetaldehyde, together with 2,3-epoxy-2-methylbutane (**14**). Thus, cleavage of the 2,3-carbon – carbon bond was the predominant reaction. This is the same type of reaction previously reported for the 1-bromo- and 1-chloro-2-methyl-2-propyl hydroperoxides (4, 5). It has been suggested (4, 5) that the cleavage proceeds via a four-atom cyclic peroxide. The oxide (**14**), must have resulted from ring closure of the intermediate bromohydrin, **15**. The bromohydrin could have resulted from a base-catalyzed reduction of the bromohydroperoxide, a reaction which is known to occur with tertiary hydroperoxides (15). Another, more likely, mode of formation of **15** is discussed below.

The predominant reaction of *trans*-2-bromocyclohexyl hydroperoxide (**4**) in the presence

Can. J. Chem. Downloaded from www.nrcresearchpress.com by 210.87.254.5 on 09/05/12
For personal use only.

of base appears to be reduction to the bromohydrin which, in turn, is partly converted to cyclohexene oxide. A small amount of the latter is further converted to *trans*-1,2-cyclohexanediol. A search was made for adipaldehyde which might result from ring cleavage, and possible products derived from it, but no such material could be identified. Also, a search was made for 2-bromocyclohexanone, which would be expected to be formed by base-catalyzed elimination of hydroxide ion from the secondary hydroperoxide, **4**, (16). Again, although traces of a strongly lachrymatory substance were produced, no further evidence of it or products derived from it was obtained. The material balance in this reaction is not satisfactory, however, and some of the latter reactions may have occurred (see below).

Both reduction and carbon–carbon bond cleavage reactions were observed in the reaction between 2-bromo-1-phenylethyl hydroperoxide, (**5**), and base. An elimination pathway is not available to **5**. Products identified were styrene oxide, 2-bromo-1-phenylethanol, and benzoic acid. The latter may have resulted from a Cannizzaro reaction between formaldehyde and benzaldehyde which would be the primary products of carbon–carbon bond cleavage.

However, the benzoic acid may also be formed from oxidation of benzaldehyde by unreacted bromohydroperoxide, **5**. The other product of this reaction would be the bromohydrin, 2-bromo-1-phenylethanol, which, in turn, could be converted to styrene oxide under the reaction conditions. Such a sequence also seems to be a more plausible route to the oxides formed in the base-catalyzed reactions of **3** and **4** rather than the base-catalyzed reduction (15) of the hydroperoxy group mentioned in discussing the products formed from **3**. Such reactions, in the case of tertiary hydroperoxides without other functional groups (15), seem to require much higher temperatures than those used here, and it is not obvious that halogen substitution should speed the reaction.

The reactions between β-halohydroperoxides and base may take a variety of paths and the products of these reactions depend upon structure. Although it is probably too early to generalize, it appears that β-halohydroperoxides formed from tetrasubstituted olefins give almost exclusively elimination products, allylic hydroperoxides, when treated with base. Only trace amounts of cleavage product, acetone, were detected from reaction of the tetrasubstituted β-halohydroperoxides, **1***a* and **1***b*. Nor could the yield of any cleavage products from **2***b* have been significant, since a 66% yield (by analysis) of elimination product was formed. Also, β-halohydroperoxides of tetrasubstituted olefins suffer little, if any, reduction with base. No evidence for the formation of any halohydrin or epoxide from **1***a*, **1***b*, **2***a*, or **2***b* was found.

In contrast, neither **3** or **4**, which have, in principle, elimination pathways available to them, gave any trace of elimination product with base. The difference in behavior toward base between **1***a* or **1***b* and **3** is striking since the only difference between these materials is a methyl group.

The addition–elimination sequence outlined in eq. [2] is thus seen to lead to the desired allylic hydroperoxide only with tetrasubstituted olefins where it works very well.

The conversion of a trisubstituted or a *gem*-disubstituted olefin to the β-halohydroperoxide followed by the reaction of the latter with base may be a useful process for the cleavage of olefinic bonds.

Experimental

Melting points and boiling points are uncorrected. Infrared spectra were recorded on Perkin–Elmer model 421 and model 337 spectrophotometers. Nuclear magnetic resonance (n.m.r.) spectra were determined with a Varian A-60 analytical spectrometer with tetramethylsilane as internal standard. Gas–liquid chromatography (g.l.c.) was carried out on Aerograph 202 and A-90-P3 gas chromatographs. Quantitative g.l.c. analyses were made with calibrated internal standards. Microanalyses were determined by Mrs. D. Mahlow of these laboratories. Solutions were dried using anhydrous magnesium sulfate.

All preparations of β-haloperoxides were carried out behind shields. Apparatus containing these compounds was manipulated with the aid of tongs and hands were protected with heavy canvas gloves.

N-Chloroacetamide was prepared according to the method of Orton (17), m.p. 111°. Reported (18) m.p. 110°. Iodometric analysis showed 38.18% Cl; required 37.97% Cl.

The 1,3-dibromo-5,5-dimethylhydantoin used was obtained from Matheson, Coleman, and Bell and contained 98% of the theoretical amount of active bromine by iodometric analysis.

3-Chloro-2,3-dimethyl-2-butyl Hydroperoxide, 1a

The 2,3-dimethyl-2-butene was prepared from 2,3-dimethyl-2-butanol by dehydration over 85% phosphoric acid. The crude product was fractionally distilled through a Nestor–Faust annular teflon spinning band distillation column. The product had b.p. 70–71° (700 mm), n_D^{25}

Can. J. Chem. Downloaded from www.nrcresearchpress.com by 210.87.254.5 on 09/05/12
For personal use only.

1.4075. Reported (19) b.p. 73°, n_D^{25} 1.4094. Analysis by g.c. using a 5 ft × 1/4 in. FFAP column indicated that the material was > 99% pure.

To a solution of 9.0 g (107 mmole) of 2,3-dimethyl-2-butene, 9.45 g (101 mmole) *N*-chloroacetamide and 50 ml ether in a three-necked flask, fitted with a thermometer and reflux condenser and cooled in an ice bath, was added 15 g (400 mmole) of 98% hydrogen peroxide (FMC Corp.) at a rate to keep the temperature from rising above 10°. After the resulting solution had cooled to 0° ca. 1 g of *p*-toluenesulfonic acid was added. The temperature rose rapidly and the solution began to boil. It was stirred in the ice bath for 1 h. (Usually, the solution ceased boiling after a few minutes. However, in some reactions the reaction was so exothermic that all the ether was driven out and temperatures of up to 150° were observed in the reaction flask.) The reaction mixture was then washed with several portions of water and with 10% sodium bicarbonate solution. In separate exeriments it was determined that four washings with water were sufficient to remove all the hydrogen peroxide and 5,5-dimethylhydantoin or acetamide from ether.

Twenty per cent of the dried ethereal solution was concentrated on a bath at 40° and the residue taken up in 15 ml pentane. The pentane solution was cooled to −65°. The precipitate, which formed over several hours, was filtered in a low-temperature filtration apparatus. This material, (1.0 g, 30%), m.p. 72–73° (decomposition), appeared to be hygroscopic. The n.m.r. spectrum (CCl_4) showed absorption at τ 1.9–2.1 (broad singlet) for the hydroperoxy proton and at τ 8.38 (singlet) and 8.60 (singlet) for the protons of the two *gem*-dimethyl groups with relative peak areas 0.9:6.4:6.0, required 1:6:6. A satisfactory elemental analysis could not be obtained on this material, but it had 99% of the theoretical active oxygen content as determined by iodometric titration. The *p*-nitrobenzoate ester was prepared, m.p. 104.5–105°. The n.m.r. spectrum (benzene) showed absorption at τ 2.40 (singlet) for the aromatic protons and at τ 8.43 (singlet) and 8.68 (singlet) for the protons of the two *gem*-dimethyl groups with relative peak areas 4.28:6.0:5.65, required, 4:6:6.

Anal. Calcd. for $C_{13}H_{16}NO_5Cl$: C, 51.75; H, 5.35. Found: C, 51.25; H, 5.56.

Ten per cent of the ether solution of **1***a* was added to a stirred slurry of 0.3 g of lithium aluminium hydride in 20 ml ether at 0°. The mixture was hydrolyzed after 10 min with 15% potassium hydroxide. Gas–liquid chromatographic analysis using a 5 ft × 1/4 in. column of 10% DEGS on Chromosorb W at 70° showed the presence of only one product in addition to some 2,3-dimethyl-2-butene. The product, 3-chloro-2,3-dimethyl-2-butanol, was collected from the effluent stream of the g.l.c. and had n.m.r. and infrared spectra identical with those of an authentic (20) sample.

*2,3-Dimethyl-3-hydroperoxy-1-butene (**6**) from **1***a*

Sixty per cent of the solution of **1***a* prepared above was added to a solution of 4.0 g sodium hydroxide in 100 ml methanol at 0° and the resulting mixture was stirred for 1 h. The reaction mixture was then poured into ice-water. This mixture was extracted twice with ether. The combined ether layers were washed several times with water and dried. After careful distillation of the ether through a 4 ft Podbielniak column the residual oil was distilled to yield 3.6 g (48%) of **6**, b.p. 56–57° (16 mm), n_D^{25} 1.4390. Reported (12) b.p. 55° (12 mm), n_D^{20} 1.4428. The n.m.r. spectrum (CCl_4) showed absorption at τ 1.6–1.8 (broad singlet) for the hydroperoxy proton, τ 5.1–5.2 (multiplet) for the vinyl protons, τ 8.22 (multiplet) for the protons of the allylic methyl group, and τ 8.70 (singlet) for the protons of the *gem*-dimethyl groups with relative peak areas 1.05:1.88:3.0:5.8, required, 1:2:3:6. This material was identical (n.m.r. and infrared spectra) with a sample of **6** prepared by the photosensitized oxidation (12) of 2,3-dimethyl-2-butene.

Another solution of **1***a* prepared as described above from 5.0 g of 2,3-dimethyl-2-butene was shown by iodometric titration to contain a 60% yield of chlorohydroperoxide, **1***a*. Four-fifths of this solution was reacted with methanolic base and the product isolated as described above. There was obtained 2.3 g (42% overall, 70% based on **1***a* formed) of **6**, n_D^{25} 1.4385, identical (n.m.r. and infrared spectra) with authentic **6**.

Gas–liquid chromatographic analysis of the reaction mixtures containing **6** before distillation indicated only traces of material with the retention-time of acetone. No evidence for the formation of any chlorohydrin or oxide was obtained.

*3-Bromo-2,3-dimethyl-2-butyl Hydroperoxide, **1***b*

To a solution of 4.8 g (57 mmole) of 2,3-dimethyl-2-butene and 9.0 g (260 mmole) of 98% hydrogen peroxide in 50 ml ether stirred at −40° was added 8.1 g (57 mmole) of 1,3-dibromo-5,5-dimethylhydantoin in small portions over a 10 min period. The reaction mixture, protected with a calcium chloride tube, was allowed to warm to room temperature, washed with 25 ml cold, saturated sodium bicarbonate solution and several times with water. Ether was distilled from the dried organic layer through a 2 ft Podbielniak column using a 40° water bath. The residual oil crystallized when the remainder of the ether was removed under vacuum. Two recrystallizations from pentane gave 8.5 g (76%) of constant melting product, m.p. 93–94°. Reported (5) m.p. 93°. Two iodometric titrations indicated 96.77% and 96.75% of the theoretical amount of active oxygen. The n.m.r. (CCl_4) spectrum showed absorption at τ 1.8–2.3 (broad singlet) for the hydroperoxy proton and at τ 8.19 (singlet) and 8.55 (singlet) for the protons of the two *gem*-dimethyl groups with relative peak areas of 0.7:6.0:6.1, required 1:6:6.

The reaction as carried out above gave colorless solutions. No dibromide and no gas evolution could be detected. Addition of the brominating agent at 0° resulted in a vigorous reaction with the evolution of gas and the generation of a bromine color. Considerable amounts of dibromide were also produced.

*2,3-Dimethyl-3-hydroperoxy-1-butene from **1***b*

Four grams of **1***b* gave 1.8 g (77%) of the allylic hydroperoxide **6**, n_D^{25} 1.4385, when treated with base in the manner described for **1***a*. The product was identical (n.m.r. and infrared spectra) with authentic **6**.

*1-Methyl-2-methylenecyclohexanol, **9***

*(a) From 2-Bromo-1,2-dimethylcyclohexyl Hydroperoxide, **2***b*

The method due to Hammond (21) was used to prepare 1,2-dimethylcyclohexene. The product was fractionally distilled through the annular teflon spinning band distillation column and had b.p. 133° (700 mm), n_D^{24} 1.4573.

Can. J. Chem. Downloaded from www.nrcresearchpress.com by 210.87.254.5 on 09/05/12
For personal use only.

Reported (21) b.p. 136.2° (745 mm), n_D^{25} 1.4587. Gas chromatographic analysis using a 5 ft × 1/4 in. column of dinonylphthalate on Chromosorb P at 110° showed that less than 1% of the isomeric olefins were present in the fraction collected.

A solution of **2***b* in ether was prepared from 2.0 g (18.2 mmole) 1,2-dimethylcyclohexene, 2 ml (82 mmole) of 98% hydrogen peroxide and 2.6 g (9.1 mmole) of 1,3-dibromo-5,5-dimethylhydantoin in 20 ml ether using the procedure described above for the preparation of **1***b*. Iodometric titration of an aliquot of the solution showed that 86% of hydroperoxide had formed. The solution was added to a solution of 2 g sodium hydroxide in 100 ml methanol at 0°. After stirring for 90 min at 0° the reaction mixture was poured into 200 ml ice-water. The resulting mixture was extracted twice with 100 ml ether and the combined organic layers were washed three times with 100 ml water. The dried solution was added slowly to a stirred slurry of 1.5 g lithium aluminium hydride in 35 ml ether. This mixture was heated under reflux for 1 h and then a solution of 15% potassium hydroxide was added dropwise until the organic layer became clear. The organic layer was decanted and the precipitate slurried several times with ether and the combined organic solutions were dried. An aliquot of the solution was analyzed by g.l.c. on a 5 ft × 1/4 in. column of 10% FFAP on Chromosorb W at 120°. There were present 12% 1,2-dimethylcyclohexene and 66% of product, **9**, based on the hydroperoxide yield. Also present was ca. 2% of a material with the same g.c. retention time as the isomeric alcohol, 1,2-dimethyl-2-cyclohexenol (**10**).

Ether was distilled from the solution and the residual oil was distilled to give 0.85 g (42% based on the hydroperoxide content of the starting solution) of **9**, b.p. 58–61° (15 mm), n_D^{25} 1.4799. Reported (13) b.p. 58° (10 mm). The n.m.r. spectrum (CCl_4) showed absorption at τ 5.15 (multiplet) and 5.39 (multiplet) for the olefinic protons, τ 7.6 to 8.6 (broad) for the ring and hydroxyl protons and τ 8.72 (singlet) for the protons of the methyl group with relative peak areas of 1.0:0.92:9.2:2.84, required: 1:1:9:3. The infrared spectrum (neat) showed hydroxyl absorption at 3660 (sharp) and 3550 to 3200 (broad) cm^{-1} and absorption characteristic of a terminal olefin at 1640 (strong) and 990 (strong) cm^{-1}. There was no absorption at τ 4.68 in the n.m.r. spectrum where the olefinic proton of the isomeric alcohol **10** absorbs.

This product was identical (g.l.c. retention time, n.m.r. and infrared spectra) with authentic **9** (13) prepared by the addition of methylmagnesium iodide to 2-methylenecyclohexanone as described below.

(b) From 2-Chloro-1,2-dimethylcyclohexyl Hydroperoxide, 2a

The procedure described for the preparation of **1***a* was used to prepare a solution of **2***a* from 9.6 g (86 mmole) of 1,2-dimethylcyclohexene, 11 g (500 mmole) of 98% hydrogen peroxide, and 8.4 g (86 mmole) of *N*-chloroacetamide. An aliquot of the dried solution, after removal of hydrogen peroxide and acetamide, was analyzed by g.c. on the FFAP column using chlorobenzene as an internal standard. It was found that 43% of the original 1,2-dimethylcyclohexene had not reacted. The solution containing **2***a* was then added to 4 g sodium hydroxide in 100 ml methanol at 0° and the resulting mixture was stirred at 0° for 1 h. To this mixture was added 0.25 g sodium borohydride dissolved in a little methanol. After 1 h at room temperature the reaction mixture was poured into ice-water. The resulting mixture was extracted twice with ether. The combined ether extracts were washed several times with water and dried. The ether was distilled and the residual oil adsorbed on a 2.5 × 30 cm column of basic alumina. The column was washed with 200 ml pentane to remove the unreacted 1,2-dimethylcyclohexene and then the product was eluted with 200 ml ether. The ether was removed and the residual oil distilled to give 1.1 g (19% based on reacted olefin) of **9**, n_D^{25} 1.4813. This material was identical (n.m.r. and infrared spectra) with authentic **9**. The n.m.r. spectrum showed no absorption at τ 4.68 where the olefinic proton of the isomeric alcohol **10** absorbs. Gas-chromatographic analysis indicated the presence of *ca.* 1% of a material with the same retention time as the isomeric alcohol **10**. Several attempts to isolate **2***a* resulted in explosions.

(c) From Sensitized Oxidation of 1,2-Dimethylcyclohexene

The photolysis cell consisted of a 2.5 cm × 25 cm water-jacketed test tube fitted with a ground glass stopper containing an outlet tube and an inlet tube with a fritted disk which reached to the bottom of the test tube. The inlet tube was connected to the exhaust port of a Dynaport air pump. The outlet tube was connected to a T-tube which was, in turn, connected to an oxygen buret and to the inlet port of the air pump.

A solution of 3.0 g 1,2-dimethylcyclohexene and 30 mg of methylene blue in 30 ml methanol was placed in the photolysis cell. The pump was turned on and after pressure equilibrium was reached the cell was illuminated with two 100 W frosted light bulbs placed against the cell on either side. Aluminium foil was placed around the apparatus. Oxygen uptake became very slow after 70 min when 610 ml (STP) had been consumed (theoretical 570 ml). This solution was poured into 100 ml ice-water and the resulting mixture extracted twice with 30 ml pentane. The combined pentane extracts were washed with water and with saturated sodium chloride. The dried solution was added slowly to a slurry of 1 g lithium aluminium hydride in 50 ml ether. The mixture was heated under reflux for 2 h and then worked up as described under A. The product was separated from olefin on alumina as described under B. The product was distilled to give 2.4 g (71%) of an oil, b.p. 88–90° (85 mm), n_D^{25} 1.4786. The product was identical (n.m.r. and infrared spectra) with authentic **9**. The n.m.r. spectrum showed no absorption at τ 4.68 where the vinylic proton of the isomeric alcohol **10** absorbs. Gas–liquid chromatographic analysis indicated the presence of ca. 5% of a material with the same retention time as **10**.

(d) From 2-Methylenecyclohexanone

The 2-methylenecyclohexanone was prepared according to the procedure of Mannich (22). A mixture of 9 g 37% formaldehyde solution, 9 g dimethylamine hydrochloride, and 48 g cyclohexanone was heated on the steam bath. Water (50 ml) was added to the cooled mixture and the aqueous layer extracted several times with ether. The aqueous layer was concentrated using a rotatory evaporator. The crystals which formed were recrystallized from acetone–alcohol to give 10 g (54%) of salt, m.p. 150–151° (reported (22) m.p. 152°).

This salt (5 g) was pyrolyzed under vacuum (0.15 mm). The pyrolysate was caught in a trap at −70°, redistilled and stored at −70° until a solution of methylmagnesium

Can. J. Chem. Downloaded from www.nrcresearchpress.com by 210.87.254.5 on 09/05/12
For personal use only.

iodide made from 0.5 g magnesium and 3 g methyl iodide in 50 ml ether was added. The reaction mixture was allowed to warm to room temperature and then hydrolyzed with water. The ether layer was dried and the solvent removed. The small amount of residual oil had two high-boiling components in a 60:40 ratio which were isolated by trapping the effluent from g.l.c. (FFAP column). A sufficient quantity of each was isolated for spectral analysis. The major component had a g.l.c. retention time and n.m.r. and infrared spectra which were identical with **9** prepared by methods (*a*)–(*c*) above. The second component was not identified. It had hydroxyl but no olefinic absorption in the infrared spectrum and no absorbtion in the n.m.r. spectrum below τ 6.

1,2-Dimethyl-2-cyclohexene-1-ol, 10

The procedure of Warnhoff and Johnson (23) was used for the preparation of 2-methylcyclohexenone, b.p. 95–100° (75 mm), n_D^{25} 1.4820. Reported (23) b.p. 98–101 (77 mm), n_D^{25} 1.4836.

2-Methylcyclohexenone (1 g) in 5 ml ether was added to 4 ml of 0.24 *M* methyllithium at −40° under a nitrogen atmosphere. The reaction mixture was allowed to warm to room temperature and was then hydrolyzed with 10% potassium hydroxide solution. The organic layer was dried, the ether was removed, and the residual oil was distilled to give 0.4 g material b.p. 82–85° (25 mm). Reported (14) for **10**, b.p. 132° (180 mm). Gas chromatographic analysis on the FFAP column at 120° showed two components in a *ca.* 60:40 ratio in addition to a small amount of starting material. The two products were collected from the effluent of the g.l.c. The major product, n_D^{26} 1.4764 (reported (14) for **10**, n_D^{20} 1.4844), had the same g.c. retention time as the minor product formed with **9** in the various oxidations of 1,2-dimethylcyclohexene described above. Its n.m.r. spectrum (CCl_4) showed absorption at τ 4.68 (multiplet) for the olefinic proton, τ 7.9–8.6 (b) for the ring, hydroxyl, and allylic methyl protons and τ 8.80 (singlet) for the protons of the other methyl group with relative peak areas of 1:11.3:3.5, required: 1:10:3, consistent with the structure of **10**. The infrared spectrum (CCl_4) showed hydroxyl absorptions at 3600 (sharp) and 3500–3300 (broad) cm^{-1} as well as olefinic CH stretching absorption at 3160–3120 cm^{-1}.

The minor product, n_D^{25} 1.4616, showed hydroxyl absorptions but no absorption characteristic of an olefin in the infrared spectrum and had no absorption in the n.m.r. spectrum below τ 6. It was not investigated further.

trans-2-Bromocyclohexyl Hydroperoxide, 4

The procedure described for the preparation of **1***b* was used to prepare an ether solution of *trans*-2-bromocyclohexyl hydroperoxide from 8.2 g (100 mmole) of redistilled cyclohexene, 14.3 g (50 mmole) of 1,3-dibromo-5,5-dimethylhydantoin, and 17 g (500 mmole) of 98% hydrogen peroxide. The dried solution was concentrated under aspirator pressure using a rotary evaporator on a water bath at 30°. The crude product, 19.8 g, contained 72% of the theoretical amount of hydroperoxide by iodometric titration. It was taken up in 100 ml pentane and the resulting solution was cooled to −78°. The pentane was decanted from the crystals which formed. These melted at ca. −20°. The hydroperoxide content of this oil was 88% of the theoretical. The n.m.r. spectrum (CCl_4) showed absorption at τ 1.04 (broad singlet) for the hydroperoxy proton, τ 5.80 (multiplet) for the methine protons, and τ 7.4–9.0 (broad) for the methylene protons of the ring with relative peak areas 0.89:2.0:8.1, required 1:2:8.

Hydrogenation of 1.95 g (0.01 mole) of this oil in 25 ml ether over platinum oxide at 0° and one atmosphere resulted in the rapid uptake of 178 ml (STP), 80% (based on weight of starting material) of hydrogen. The reaction mixture was filtered, the filtrate dried, and the ether removed. Gas–liquid chromatographic analysis of the residual oil on a 5 ft × 1/4 in. column of 10% QF-1 on Chromosorb W at 150° showed the presence of a trace of dibromocyclohexane in addition to the major product which had a retention time identical with authentic *trans*-2-bromo-cyclohexanol (24). The *p*-bromobenzenesulfonyl ester was prepared, m.p. and mixture melting point with authentic material 90.0–90.5°; reported (24) m.p. 90–90.5°.

Reaction of trans-2-Bromocyclohexyl Hydroperoxide with Base

A solution of 5.6 g potassium hydroxide in 25 ml ethanol was added to a solution of 19.5 g *trans*-2-bromocyclohexyl hydroperoxide (80% hydroperoxide) in 100 ml ether at 25°. The resulting mixture began to boil and deposit a precipitate. Boiling continued for ca. 30 min, and the solution was allowed to stir overnight at 25°. Titration of an aliquot showed that 95% of the hydroperoxide had been consumed. The mixture was filtered and the filtrate stirred vigorously with 50 ml of 2 *M* sodium sulfite for 1 h. The organic layer was then washed twice with water, dried, and the ether was removed through a vigreaux column.

The residual oil had a pungent odor. The infrared spectrum (neat) showed broad, strong absorption in the region 3600–3200 cm^{-1} and a medium intensity absorption with several maxima at 1735–1715 cm^{-1}. The major volatile components were found by g.l.c. analysis to be cyclohexene oxide and *trans*-2-bromocyclohexanol. These compounds were identified by comparison of their retention times with authentic cyclohexene oxide (25) and *trans*-2-bromocyclohexanol (24) on the QF-1 column and on a 5 ft × 1/4 in. column of 20% DEGS on Chromosorb W. Quantitative g.l.c. analysis using the QF-1 column showed that 29% cyclohexene oxide and 27% *trans*-2-bromocyclohexanol had been formed (based on the hydroperoxide content of the starting material). No trace of any material with the retention time of authentic cyclohexen-3-ol could be found.

Attempted distillation of a portion of the oil resulted in decomposition soon after boiling began (pot temperature 100°, 10 mm). A small amount of material which had collected in the condenser was taken up in carbon tetrachloride. The infrared spectrum of this material was identical with that of authentic cyclohexene oxide.

The combined aqueous extracts were extracted several times with ether and the combined ether extracts were concentrated. The viscous oil, 0.3 g which remained crystallized on standing, and was recrystallized from benzene, m.p. 96.0–97.5°. The mass spectrum of this material showed a parent peak at *m/e* 116.0835 corresponding to a molecular formula of $C_6H_{12}O_2$ which requires 116.0837. It was identified as *trans*-1,2-cyclo-

Can. J. Chem. Downloaded from www.nrcresearchpress.com by 210.87.254.5 on 09/05/12
For personal use only.

hexanediol by its melting point behavior, mixture melting point with authentic *trans*-1,2-cyclohexanediol (26) 96–101° and mixture melting point with authentic *cis*-1,2-cyclohexanediol[2] (27) 65–74°. The authentic diols had m.p. 98–101°, reported (26) m.p. 104°, and 96–98°, reported (28) m.p. 98°, respectively.

The precipitate obtained on filtering the initial reaction mixture was taken up in a small amount of water. The resulting solution was made acid with 6 *N* hydrochloric acid and extracted with chloroform. The organic layer was dried and the solvent was removed to leave 0.8 g of a viscous oil. A thin-layer chromatogram of this material using silica gel G.F. 254 as adsorbent and ether as eluent indicated that at least six components were present. The material was not investigated further.

Several other reactions between *trans*-2-bromocyclohexyl hydroperoxide and base were carried out. The reaction temperature and time, concentrations of reactants, and method of reduction (sodium borohydride, lithium aluminium hydride) of the crude reaction mixture were varied. In no case was any trace of cyclohexen-3-ol found.

Cyclohexen-3-ol

A solution of 8 g (0.05 mole) 3-bromocyclohexene (29) and 4.1 g (0.05 mole) of sodium acetate in 50 ml acetic acid was heated on the steam bath for 5 min. The resulting mixture was filtered and the filtrate was slowly poured into an aqueous slurry of sodium carbonate. The resulting mixture was extracted with 100 ml ether. The dried ether solution was added to a slurry of 1 g lithium aluminium hydride in 50 ml ether. The reaction mixture was hydrolyzed by dropwise addition of saturated potassium carbonate until the organic layer became clear. The solution was decanted, the precipitate washed with a little ether, and the combined ether solutions were concentrated. Distillation of the residue gave 2.0 g, 45%, of colorless oil, b.p. 53° (6 mm). Reported (30) b.p. 63–65° (12 mm). The n.m.r. spectrum (neat) showed absorption at τ 4.32 (multiplet) for the olefinic protons, τ 4.97 (singlet) for the hydroxyl proton, τ 5.89 (b) for the methine proton and τ 7.8–8.8 (b) for the ring methylene protons with relative peak areas 2.0:0.96:0.96:6.3, required 2:1:1:6.

2-Bromo-1-phenylethyl Hydroperoxide, 5

The procedure described for the preparation of **1***b* was used to prepare an ethereal solution of **5** from 10.4 g (0.1 mole) of purified styrene, 14.3 g (0.05 mole) of 1,3-dibromo-5,5-dimethylhydantoin, and 17 g (0.5 mole) of 98% hydrogen peroxide. The dried solution was concentrated to constant weight under 0.5 mm pressure on a water bath at 30° using a rotary evaporator. The residual oil, 14.1 g, and 86% of the theoretical hydroperoxide content. The n.m.r. spectrum (CCl_4) showed absorption at τ 1.00 (b) for the hydroperoxy proton, τ 2.80 (singlet) for the phenyl protons, τ 5.07 (triplet, $J = 6.5$ c.p.s.) for the methine proton, and τ 6.48 (doublet, $J = 6.5$ c.p.s.) and τ 6.53 (doublet, $J = 6.5$ c.p.s.) for the non-equivalent methylene protons. The relative peak areas were 0.57:5.0:0.85:1.8, required 1:5:1:2. A mixture of 13.0 g of this material in 100 ml ether and 31 g sodium bisulfite was stirred vigorously overnight. The organic layer was separated, dried, and concentrated. Distillation of the residual oil yielded 9.2 g, 87% (based on hydroperoxide content) of 2-bromo-1-phenylethanol, b.p. 78–79° (0.3 mm), n_D^{26} 1.5763. Reported (31) b.p. 120–123° (5 mm), $n_D^{19} = 1.5785$. The n.m.r. and infrared spectra were identical with those of an authentic sample (31).

Reaction of 2-Bromo-1-phenylethyl Hydroperoxide with Base

A solution of 4 g sodium hydroxide in 15 ml methanol was added to 20.6 g of **5**, 78% hydroperoxide content, in 100 ml methanol at 0°. A white precipitate soon began to form. The mixture was stirred at 0° for 2 h. Water (200 ml) was added and the mixture extracted four times with 100 ml pentane. The aqueous layer was concentrated to a small volume and made acidic with 6 *N* hydrochloric acid. An oil separated which began to crystallize. The mixture was extracted with 100 ml ether and the ether was dried. Evaporation of the ether left an oil which crystallized on standing, 4.3 g. The solid, recrystallized from methanol, had m.p. and mixture melting point with benzoic acid 119–120°. The yield was 45% based on the hydroperoxide content of the starting material.

The dried organic layer was concentrated to a small volume through a 4 ft Podbielniak column. The odor of benzaldehyde was detected in the concentrate. 1,2-Dianilinoethane (2 g) (32) in 20 ml methanol was added to 21% of the concentrate. The solution was left at 0° overnight. The crystals which separated were filtered to give 0.133 g, 2.9% (based on the hydroperoxide content of the starting material **5**), of 1,2,3-triphenyltetrahydroimidazole, melting point and mixture melting point with authentic (32) material 131–131.5°. Reported (32) m.p. 137°.

The remainder of the concentrate was adsorbed on a 1.5 × 30 cm column of neutral alumina. The column was washed with 100 ml pentane and with 200 ml ether. The eluents were analyzed by g.l.c. on a 9.5 ft × 1/4 in. column of 10% Ucon-50-HB-5100 on Chromosorb W at 158°. The pentane eluent contained only styrene and the ether eluent only benzaldehyde and styrene oxide. Further elution of the column with 200 ml ether gave no more product. Quantitative g.l.c. analysis showed that 4% benzaldehyde and 45% styrene oxide (based on the hydroperoxide content of the starting material) had been formed in the reaction.

Concentration of 63% of the ether eluent and distillation of the residual oil yielded 1.34 g, 33%, of styrene oxide, b.p. 53° (2.8 mm), n_D^{26} 1.5312. Reported (31) b.p. 65° (5 mm), n_D^{20} 1.5340. The n.m.r. spectrum of this product was identical with authentic (31) material as was the infrared spectrum except for a weak absorption at 1 700 cm^{-1}.

3-Bromo-2-methyl-2-butyl Hydroperoxide, 3

The procedure described for the preparation of **1***b* was used to prepare an ether solution of **2** from 7.0 g (0.1 mole) of 2-methyl-2-butene, 14.3 g (0.05 mole) of 1,3-dibromo-5,5-di-methylhydantoin, and 17 g (0.5 mole) of 98% hydrogen peroxide. The dried solution was concentrated to constant weight under 0.5 mm pressure on a water bath at 30° using a rotary evaporator. The residual oil, 16 g, had 92% of the theoretical hydroperoxide content. The n.m.r. spectrum (CCl_4) showed absorption at τ 1.40 (b) for the hydroperoxy proton, τ 5.56 (quartet, $J = 7$ c.p.s.) for the methine proton τ 8.32 (doublet, $J = 7$ c.p.s.) for the terminal methyl protons, and τ 8.63

[2]Kindly donated by Mr. S. Evani.

and 8.72 for the protons of the non-equivalent *gem*-dimethyl groups. The relative peak areas were 0.77: 1.0:3.3:5.9, required 1:1:3:6.

Reaction of 3-Bromo-2-methyl-2-butyl Hydroperoxide with Base

A solution of 4.4 g sodium hydroxide in 16 ml methanol was added slowly to a well-stirred solution of 18 g of **3** in 100 ml ether kept at 0°. The solution was stirred at 0° for 1½ h after addition was complete. Gas–liquid chromatographic analysis of an aliquot on a 5 ft × 1/4 in. column of 10% Carbowax 1500 on Chromosorb W at 50° indicated that 76% acetone and 77% acetaldehyde had been formed. Acetaldehyde and acetone were identified by comparison of their retention times on the Carbowax column and on a 5 ft × 1/4 in. column of 10% glycerol on Chromosorb W. Thin-layer chromatography on silica gel GF-254 using benzene as eluent of a mixture of 2,4-dinitrophenylhydrazones obtained from an aliquot of the reaction mixture gave two partially resolved spots. The R_f values were equal to those of the 2,4-dinitrophenylhydrazones of acetone and acetaldehyde.

The reaction mixture was poured into 200 ml water and the mixture was extracted with ether. An aliquot of the dried organic layer analyzed by g.l.c. on the Carbowax column at 50° showed that 10% of 2,3-epoxy-2-methylbutane had been formed.

The organic layer was carefully concentrated through a 4 ft Podbielniak column. From the residual oil 2,3-epoxy-2-methylbutene was isolated by trapping it from the effluent of the g.l.c. column. Its n.m.r. and infrared spectra were identical with those of authentic (33) material.

Acknowledgment

This work was supported in part by a grant from the National Research Council of Canada.

1. G. O. SCHENCK. Angew. Chem. **69**, 579 (1957).
2. K. GOLLNICK and G. O. SCHENCK. Rev. Pure Appl. Chem. **9**, 507 (1964).
3. K. R. KOPECKY and H. J. REICH. Can. J. Chem. **43**, 2265 (1965).
4. W. H. RICHARDSON, J. W. PETERS, and W. P. KONOPKA. Tetrahedron Letters, No. **45**, 5531 (1966).
5. M. SCHULZ, A. RIECHE, and K. KIRSCHKE. Chem. Ber. **100**, 370 (1967).
6. L. DULOG and W. VOGHT. Tetrahedron Letters, No. **42**, 5169 (1966).
7. E. R. BELL, F. H. DICKEY, J. H. RALEY, F. F. RUST, and W. B. VAUGHN. Ind. Eng. Chem. **41**, 2597 (1949).
8. A. RIECHE, E. SCHMITZ, and M. SCHULZ. Z. Chem. **3**, 443 (1963).
9. K. WEISSERMEL and M. LEDERER. Chem. Ber. **96**, 77 (1963).
10. A. RIECHE, M. SCHULZ, and K. KIRSCHKE. Chem. Ber. **99**, 3244 (1966).
11. S. FUJIWARA, M. KATAYAMA, and S. KAMIO. Bull. Chem. Soc. Japan, **32**, 655 (1959).
12. G. O. SCHENCK and K. SCHULTE-ELTE. Ann. **618**, 185 (1958).
13. C. MANNICH. Chem. Ber. **74**, 554 (1941).
14. W. N. HAWORTH. J. Chem. Soc. **103**, 1242 (1913).
15. M. S. KHARASCH, A. FONO, W. NUDENBERG, and B. BISCHOF. J. Org. Chem. **17**, 20 (1952).
16. (*a*) N. KORNBLUM and H. E. DE LA MARE. J. Am. Chem. Soc. **73**, 880 (1951). (*b*) S. S. MEDWEDEW and E. ALEXEJEWA. Chem. Ber. **65**, 133 (1932).
17. K. J. ORTON and A. E. BRADFIELD. J. Chem. Soc. 993 (1927).
18. A. HANTSCH and T. E. DOLLFUS. Chem. Ber. **35**, 252 (1902).
19. F. D. ROSSINI *et al.* Selected values of chemical thermodynamic properties. U.S. Government Printing Office, Washington, D.C. 1955. p. 55.
20. A. DETOEUF. Bull. Soc. Chim. France [4], **31**, 169 (1922).
21. G. S. HAMMOND and T. D. NEVITT. J. Am. Chem. Soc. **76**, 4121 (1954).
22. C. MANNICH and R. BRAUN. Chem. Ber. **53**, 1874 (1920).
23. E. W. WARNHOFF and W. S. JOHNSON. J. Am. Chem. Soc. **75**, 494 (1953).
24. S. WINSTEIN and R. B. HENDERSON. J. Am. Chem. Soc. **65**, 2196 (1943).
25. Org. Syn. Coll. Vol. I, 185 (1944).
26. S. WINSTEIN. J. Am. Chem. Soc. **64**, 2792 (1942).
27. K. B. WIBERG and K. A. SAEGEBARTH. J. Am. Chem. Soc. **74**, 6256 (1957).
28. M. F. CLARKE and L. N. OWEN. J. Chem. Soc. 315 (1949).
29. H. J. DAUBEN, JR. and L. L. MCCOY. J. Am. Chem. Soc. **81**, 4863 (1959).
30. R. CRIEGEE. Ann. **481**, 263 (1931).
31. C. O. GUSS and R. ROSENTHAL. J. Am. Chem. Soc. **77**, 2549 (1955).
32. H.-W. WANZLICK and W. SOCHEL. Chem. Ber. **86**, 1463 (1963).
33. J. READ and W. G. REID. J. Chem. Soc. 1487 (1928).

Can. J. Chem. Downloaded from www.nrcresearchpress.com by 210.87.254.5 on 09/05/12
For personal use only.

Can. J. Chem. Downloaded from www.nrcresearchpress.com by 210.87.254.6 on 09/05/12
For personal use only.

Cyclohexane compounds. VII. Nucleophilic scission of the stereoisomeric 3-methoxycyclohexene oxides[1]

R. A. B. BANNARD AND A. A. CASSELMAN
Defence Chemical, Biological, and Radiation Laboratories, Ottawa, Canada

AND

E. J. LANGSTAFF AND R. Y. MOIR
Department of Chemistry, Queen's University, Kingston, Ontario

Received June 12, 1967

The mode of scission of *cis*- and *trans*-3-methoxycyclohexene oxides by hydrogen chloride, hydrogen bromide, ammonia, acetic acid, and methanol (under both acidic and alkaline conditions) has been examined using vapor-phase chromatography to detect and isolate minor isomers. Approximately 10% of the product from opening of the *trans* oxide is formed by attack at position-2 with each of these nucleophiles, whereas opening of the *cis* oxide proceeds exclusively by attack at position-1. The results are interpreted as reflecting very similar transition states for all of these reactions, with differences in product distributions for the two oxides being governed by the inductive effect of the methoxyl group and by steric factors in the corresponding transition states.

Canadian Journal of Chemistry, 46, 35 (1968)

For the past several years we have been interested in finding a reasonable, quantitative explanation for the product distribution and differences in reaction rates for the scission and formation of the oxirane ring in the stereoisomeric oxides of 3-methoxycyclohexene (**1** and **2**). We have attempted to utilize measurable steric and electronic data from the formation step to explain the product distribution found experimentally for the oxide scission. In the early stages of the investigation progress was hampered by the difficulty of separating the oxides in a pure condition and in establishing their structures (1–3). Similar separation and structural identification problems arose each time the behavior of a new nucleophile was examined. Nevertheless, investigations by McRae, Moir, and co-workers (1), Lemieux, Kullnig, and Moir (2), and by Bannard and Hawkins (3) made it evident that under alkaline conditions these oxides are attacked by nucleophiles such as methanol, water, and ammonia predominantly, if not exclusively, at position-1. More recently (4, 5), examination of the scission of these compounds by hydrobromic and hydrochloric acids again demonstrated an overwhelming preference for attack at position-1 and showed that there is apparently no marked tendency toward a change in the direction of opening of the oxirane ring in these alicyclic epoxides under acidic conditions as has frequently been observed for unsymmetrical aliphatic oxides (6–8).

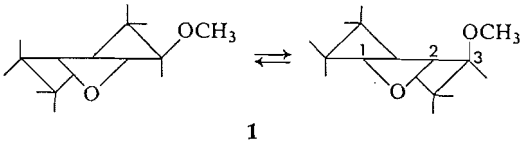

1

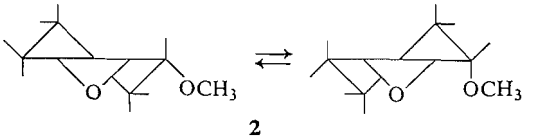

2

A major step forward in the analysis of product mixtures from the halogen hydracid scission of the oxides was made possible by the application of preparative vapor-phase chromatography to the purification and elucidation of structure of the chlorohydrins and bromohydrins, which are formed by the action of aqueous *N*-chloro- and *N*-bromosuccinimide on the two conformers **3** and **4** of 3-methoxycyclohexene as shown in Fig. 1. In connection with the latter work, Bannard, Casselman, and Hawkins (9) interpreted the distribution of bromohydrin isomers (**5***b*–**8***b*) obtained by assuming the formation of bromonium ion intermediates from the two conformers of 3-methoxycyclohexene which then underwent scission with hydroxide ion in a manner analogous to the opening of the corresponding oxides. It was assumed (*a*) that the electron-withdrawing effect of the methoxyl

[1]Issued as DCBRL Report No. 541.

TABLE I

Nucleophilic scission of *trans*-oxide

Nucleophile X	Percentage yield of products: 6	5	Total percentage yield
a Cl	84.9	8.1	93.0
b Br	86.6	10.2	96.8
c OAc*	76.5	10.9	87.4
d OMe	69.4	8.1	77.5
e NH_2	80.2	9.0	94.1†
d OMe	82.1	8.4	90.5

*Isolated as diacetyl derivative.
†4.9% secondary amine also formed.

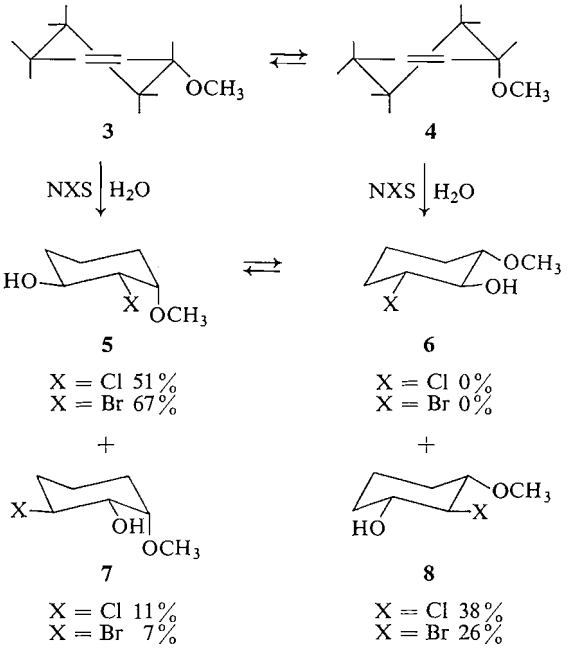

FIG. 1. The action of aqueous *N*-chloro- and *N*-bromosuccinimide on conformers **3** and **4**.

group establishes a very strong preference for nucleophilic attack at position-1 by exerting a greater inhibitory influence on the development of carbonium ion character at position-2 in the transition state of a "borderline S_N2" mechanism (2, 7); (*b*) that the ring opens with a great preference for the initial formation of diaxially-oriented products in chair forms (10, 11), and (*c*) that the reaction rates of conformers of the bromonium ions may be adversely affected by steric interference in the transition state. Langstaff, Hamanaka, Neville, and Moir (5) examined an almost identical interpretation for the distribution of the chlorohydrin isomers (**5***a*–**8***a*) involving chloronium ion intermediates. Both groups of workers (5, 9) agreed that the observed differences in the distribution of the isomers in the two series might be ascribed to the well known low participation energy of chlorine (12) relative to bromine, but also that the apparently exclusive formation of 1-substituted derivatives during scission of the oxides (1–5, 9) constitutes rather strong evidence against the analogy suggested (5, 9) between the oxide scissions and the *N*-haloimide – olefin reactions. With the object of clarifying the situation, it was decided to reexamine the oxide cleavage reactions with a variety of nucleophiles under both acidic and basic conditions, this time using vapor-phase chromatography to detect, isolate, and identify any minor products formed by attack at position-2.

The hydrochloric acid cleavages were conducted in anhydrous ether at −50° and the hydrobromic acid experiments in the same solvent at −15°. Acetolyses were conducted at 70° in the presence of a catalytic amount of sulfuric acid and the methanolyses were performed at room temperature and under reflux conditions respectively in the presence of catalytic quantities of sulfuric acid or sodium methoxide. Ammonolyses were performed in aqueous ethanolic ammonia at 110°. In connection with these experiments, it should be pointed out that the minor products from the acetolysis, methanol-

Can. J. Chem. Downloaded from www.nrcresearchpress.com by 210.87.254.6 on 09/05/12
For personal use only.

TABLE II

Nucleophilic scission of *cis*-oxide

Nucleophile X	Percentage yield of products: 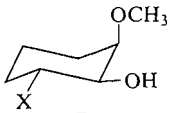 7	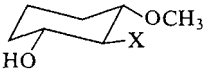 8	Total percentage yield
a Cl	100	*	100
b Br	97.3	*	97.3
c OAc†	86.2	*	86.2
d OMe	‡	*	
e NH_2	92.0	*	96.7§
d OMe	82.0	*	82.0

*Not detected.
†Isolated as diacetyl derivative.
‡High (see Experimental Section).
§4.7% secondary amine also isolated.

ysis, and ammonolysis of the *trans* oxide had not been obtained nor characterized previously. The structures of these compounds were readily established from their nuclear magnetic resonance (n.m.r.) spectra after the preparation of suitable derivatives to remove extraneous hydroxylic proton resonances.

Considering the *trans* oxide scissions first, it is clear from Table I that although there is a very great preference for attack at position-1, approximately 10% of the product results from reaction at position-2. Yields are, in general, quite high and the product distribution remains relatively constant regardless of the size and strength of the nucleophile and the acidity or basicity of the reaction medium. In relation to the ammonlyses it is noteworthy that in addition to the primary amines, 4.9% of secondary amine is also formed. This result agrees with the observation made by Hawkins and Bannard (13) that 3–5% of secondary amine is formed during the ammonlysis of cyclohexene oxide under identical conditions.

In the *cis* oxide ring openings summarized in Table II, *exclusive* attack occurs at position-1 to within the limits of detection of the minor products **8***a*–**8***e* by vapor-phase chromatography.[2]

[2]Experiments on the bromohydrins and aminoalcohols indicated that the lower limit of detectability was approximately 0.5–1.0%. In the scission of the *cis* oxide **2** by acetic acid (followed by acetylation) in addition to **7***c*, 2.2% of an unidentified product was obtained. This substance cannot be the compound arising from abnormal opening at position-2 since this would furnish **8***c* identical with the major isomer **6***c* isolated from the similar scission of the *trans* oxide **1**.

The results from all these oxide scissions indicate that the transition states in all these kinetically controlled reactions are equivalent about the reactive centers, although they differ in gross structure due to the position and orientation of the methoxyl group. Assuming as before (2, 7) that the electron-withdrawing effect of the methoxyl group exerts a constant inductive influence in favor of attack at position-1 in a "borderline S_N2" mechanism in both isomers, and that preference is shown for initial diaxial opening to yield chair forms (10, 11), it follows that the transition states for the opening of the *trans* oxide approximate to structures **9** and **10** and those for the *cis* oxide approximate to structures **11** and **12**. In these transition states, the presence or absence of a proton on the leaving group seems immaterial for transition-state

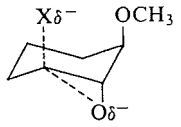

9

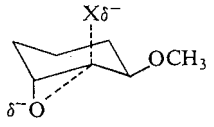

10

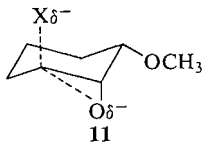

11

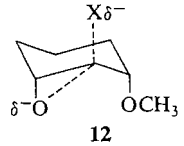

12

geometry in view of the results just reported. If it is assumed that the inductive effect of the methoxyl group is constant, the difference observed in the product distribution from the

Can. J. Chem. Downloaded from www.nrcresearchpress.com by 210.87.254.6 on 09/05/12
For personal use only.

Can. J. Chem. Downloaded from www.nrcresearchpress.com by 210.87.254.6 on 09/05/12
For personal use only.

trans and *cis* oxides must be the result of steric factors such as the presence of axially-oriented substituents, gauche substituent interactions, and 1,3-diaxial interactions in the transition state.[3] Kinetic studies of the reverse reaction suggest that the transition states must be much more product-like than oxide-like. For both oxides scission at position-1 is favored by a very large inductive effect.[4] Qualitatively it would be anticipated that **9** would have a higher energy content than **10** because of the extra axial group and the 1,3-diaxial interaction in the former. Consequently, scission at position-1 in the *trans* oxide would be less favored to this extent, i.e. unfavorable steric interactions in the transition state **9** impede the normally favored opening at position-1. In the *cis* oxide openings, **12** would be expected to have a higher energy content than **11** because of the same unfavorable steric factors mentioned above. Steric interactions in transition state **11** therefore reinforce the inductive effect which already favors opening at position-1. It is therefore not surprising that the *trans* oxide leads to two products by a competition process involving **9** and **10**, and that the scission of the *cis* oxide leads to only one product because no such competition is involved since the formation of **11** is overwhelmingly favored over **12**. It is noteworthy that a complete qualitative correspondence exists between the products from the epoxide scissions just described and those from the reactions between aqueous *N*-haloimides and 3-methoxycyclohexene (5, 9). This can be construed as strong evidence in favor of the bromonium and chloronium ion intermediates suggested earlier for the *N*-haloimide – olefin reactions.

In connection with these studies on the distribution of products from the oxide ring openings, the reverse reactions were studied kinetically for the chlorohydrins and bromohydrins to place the qualitative interpretation just presented on a firmer foundation, and the results of these investigations will be reported in detail elsewhere. With these kinetic data in mind, we are now convinced that the product distribution from these reactions is governed by an intricate but predictable interplay of substituent inversion effects (A-factors), gauche substituent interactions (G-factors), and 1,3-diaxial interactions (Z-factors), together with an inductive parameter involving the methoxyl substituent and the nucleophile in the transition states **9** to **12.** Clearly it is now important to examine the influence of other substituent groups at position-3 on the nature of the products formed during the scission of alicyclic epoxides.

[3]Ground state effects have no influence on the product ratio since the ground state may be taken as common to both modes of scission of a given oxide. It is true that different conformations are involved, but they are in rapid equilibrium, so that either one, or the equilibrium mixture of both, may be used in expressing the rate law for both scissions.

[4]We use this term in its most general sense to include electrostatic effects transmitted though single bonds as well as directly through space.

Experimental[5,6,7]

DL-*trans-3-Methoxycyclohexene Oxide (1)*

The *trans* oxide was prepared by the addition at 20–32° over a 30 min period of 12.0 g (0.30 mole) of sodium hydroxide dissolved in 30 ml of water, to a mechanically-stirred suspension of DL-(1,3/2)-1-bromo-2-hydroxy-3-methoxycyclohexane (*6b*) (4) (41.8 g, 0.200 mole) in 30 ml of water, followed by heating at 50° with stirring for 30 min. Extraction with ether (5 × 50 ml), followed by drying over anhydrous magnesium sulfate and distillation *in vacuo*, gave 24.9 g (97.3%) of colorless fragrant oil, b.p. 56.5–57.0° at 10 mm; n_D^{25} 1.4516 (3).

DL-*cis-3-Methoxycyclohexene Oxide (2)*

The *cis* oxide was prepared in exactly the same manner as the *trans* oxide except that DL-(1/2,3)-1-bromo-2-hydroxy-3-methoxycyclohexane (*7b*) (4) was used as the starting material, and the addition of the alkali was completed over a period of 12 min. Stirring was continued at 28° for a further 15 min, following which the oxide was immediately extracted and isolated as described for its isomer. The yield of colorless fragrant oil was 24.8 g (97.0%), b.p. 74–75° at 10 mm, n_D^{25} 1.4582 (3). The purity of both isomers was verified by comparison of their infrared spectra with those of authentic samples (3) and by vapor-phase chromatography (v.p.c.) in the Wilkens Autoprep model A-700 gas chromatograph at 150° (10 ft 3/8 in. diameter aluminium column, Anakrom 60/70 mesh, impregnated with 30% diethyleneglycol succinate). The retention times for the *trans* and *cis* oxides respectively were 2 and 4 min.

Hydrochloric Acid Scission of DL-*trans-3-Methoxycyclohexene Oxide (1)*

DL-*trans*-3-Methoxycyclohexene oxide (16.7 g, 0.130 mole) was weighed into a long-necked flask and 30 ml of anhydrous diethyl ether was added. The resultant solution was cooled to −50° and saturated with anhydrous hydrogen chloride, then allowed to warm to room temperature (1½ h). Most of the ether and hydrogen chloride was removed by bubbling air through the solution and the remainder was removed by evaporation *in vacuo* on the rotary evaporator. The residual thick yellow oil (19.8 g, 93.0%) was subjected to v.p.c. analysis on a 10% Versamid-900 column (5 ft 3/8 in. diameter, 150°) and

[5]All melting points are uncorrected.

[6]Analyses by J. Helie of these laboratories.

[7]Helium flow rates in v.p.c. experiments were 300 ml/min unless otherwise specified.

Can. J. Chem. Downloaded from www.nrcresearchpress.com by 210.87.254.6 on 09/05/12
For personal use only.

found to consist of 84.9% DL-(1,3/2)-1-chloro-2-hydroxy-3-methoxycyclohexane (**6***a*) (5) and 8.1% DL-(1/2,3)-1-hydroxy-2-chloro-3-methoxycyclohexane (**5***a*), the unexpected isomer. Both compounds were identified by comparison of the retention times and peak enhancement found for the mixture with those of previously synthesized and identified samples of the same compounds.

Hydrochloric Acid Scission of DL-*cis-3-Methoxycyclohexene Oxide (2)*

DL-*cis*-3-Methoxycyclohexene oxide (30.2 g, 0.236 mole) was treated in the same manner as described for the *trans* oxide. After the removal of excess reagent and solvent there remained 38.9 g, (100%) of yellow oil, which when analyzed by v.p.c. on a neopentyl glycol sebacate (4 ft) column at 70 °C. and 40 pounds per square inch (p.s.i.) proved to be pure DL-(1/2,3)-1-chloro-2-hydroxy-3-methoxycyclohexane (**7***a*) (5). The compound was identified by comparison of its retention time and peak enhancement with an authentic sample, and proven to be free of the minor product **8***a* by the same means, i.e. the column used was shown to be capable of separating mixtures of the two isomers prepared from authentic samples.

Hydrobromic Acid Scission of DL-*trans*-3-*Methoxycyclohexene Oxide (1)*

DL-*trans*-3-Methoxycyclohexene oxide (6.40 g, 0.500 mole) was transferred in 30 ml of anhydrous ether to a 500 ml three-neck flask equipped with a magnetic stirrer, thermometer, reflux condenser, and pressure-equalizing dropping funnel. A solution of anhydrous hydrogen bromide in anhydrous ether (350 ml, 0.21 *N*) was added to the stirred solution at −10° to −15° over a period of 35 min. Stirring was continued while the temperature of the clear solution was allowed to rise spontaneously to room temperature (4 h). The solution was heated at 35° with stirring for another hour, following which the ether was removed *in vacuo*, furnishing 11.4 g of crystalline solid. Recrystallization from ether and ether–pentane gave 8.17 g of colorless stout needles, m.p. 67.5–69°, which was identified as DL-(1,3/2)-1-bromo-2-hydroxy-3-methoxycyclohexane (**6***b*) by a mixture melting point determination and by comparison of infrared spectra. The residual oil, 2.18 g, was analyzed by v.p.c. in the Wilkens Autoprep model A-700 gas chromatograph at 150° (5 ft column, Chromosorb P, 45/60 mesh, impregnated with 10% Versamid-900). The chromatogram showed two peaks with retention times of 17 and 22 min respectively[8] which were identified as **6***b* (4) (m.p. 67.5–69°) and DL-(1/2,3)-1-hydroxy-2-bromo-3-methoxycyclohexane (**5***b*) (9) (n_D^{25} 1.5148) respectively by actual recovery and comparison of their properties with authentic samples. The relative proportions were found to be 1:1 by peak area measurements after calibration experiments had been performed with the authentic compounds. Thus, the yields of **6***b* and **5***b* are 9.26 g (86.6%) and 1.09 g (10.2%) respectively.

Isomerization of DL-*(1,3/2)-1-Bromo-2-hydroxy-3-methoxycyclohexane (6b). Vapor-phase Chromatography on Versamid-900 at 170°*

Vapor-phase chromatography of a 60% methanolic solution of DL-(1,3/2)-1-bromo-2-hydroxy-3-methoxycyclohexane (**6***b*) at 170° in the Wilkens model A-700 gas chromatograph using a 5-ft, 3/8 in. diameter, aluminium column packed with Chromosorb P which had been impregnated with 15% Versamid-900 gave a broad peak with retention time 18–48 min together with a broad shoulder at 9–18 min. Serial injections of 150 μl of the methanol solution were made and collected as one fraction with a retention time of 9–48 min; recovery was 41%. Serial injections of a 45% methanol solution of the recovered oil were made employing the same apparatus at 150°, but substituting an Anakrom column impregnated with 30% diethyleneglycol succinate. The two fractions, which had retention times of 15 (55%) and 25 min (45%), were collected separately; recovery was 65%. The slower-moving fraction crystallized and was identified as **6***b* by comparison of the melting points and infrared spectra. The faster-moving fraction was a colorless oil isomeric with the starting material but different from the other three methoxybromocyclohexanols described previously (4, 9).

Anal. Calcd. for $C_7H_{13}O_2Br$: C, 40.22; H, 6.27; Br, 38.22. Found: C, 40.05; H, 6.08; Br, 38.05.

Acetylation of 250 mg of this substance in the usual manner furnished 265 mg (88.3%) of colorless oil which was purified by preparative v.p.c. at 150° (retention time 15 min) using a 5 ft Fluoropak 80 column which had been impregnated with 10% SE30.[9]

Anal. Calcd. for $C_9H_{15}O_3Br$: C, 43.04; H, 6.02; Br, 31.82. Found: C, 43.23; H, 5.92; Br, 31.81.

Hydrobromic Acid Scission of DL-*cis-3-Methoxycyclohexene Oxide (2)*

The reaction conditions and method of isolation were identical with those used for the *trans* oxide. The product was a liquid and was distilled *in vacuo* using a micro "Bantamware" distillation assembly, yielding 10.4 g (97.3%) of DL-(1/2,3)-1-bromo-2-hydroxy-3-methoxycyclohexane (**7***b*) (4), b.p. 59° at 0.005 mm pressure; n_D^{25} 1.5082. The compound was identified by comparison of its infrared spectrum with that of an authentic sample and showed only 1 peak on v.p.c. at 150° in the Autoprep model A-700 gas chromatograph (10 ft column Anakrom 60/70 mesh, impregnated with 30% diethyleneglycol succinate) with a retention time of 13.5 min. An authentic sample of DL-(1,3/2)-1-hydroxy-2-bromo-3-methoxycyclohexene (**8***b*) (9) had retention time 18.0 min under identical conditions and synthetic mixtures were resolvable.

[8]A shoulder on this peak at 13 min was subsequently shown to owe its origin to a reproducible isomerization of **6***b* to DL-(1,2/3)-1-bromo-2-hydroxy-3-methoxycyclohexane on the chromatographic column as described below. It was, therefore, necessary to confirm the relative proportions of **6***b* and **5***b* by chromatography at 150° on Anakrom impregnated with 30% diethyleneglycol succinate, under which conditions no isomerization of **6***b* occurs.

[9]The nuclear magnetic resonance spectrum of this substance in deuteriochloroform (15% solution) showed an acetoxyl methyl at τ 7.90, methoxyl methyl at τ 6.65, and methine protons at τ 6.55, 5.50, and 5.15. The methine proton resonance at lowest field clearly must be due to the proton attached to the carbon atom which bears the acetoxyl group (14). The multiplet pattern for this proton is a quartet with $J_{1,2} = 3.0$ c.p.s. and $J_{2,3} = 6.7$ c.p.s. From these data the structure of the isomeric bromohydrin is concluded to be DL-(1,2/3)-1-bromo-2-hydroxy-3-methoxycyclohexane.

Can. J. Chem. Downloaded from www.nrcresearchpress.com by 210.87.254.6 on 09/05/12
For personal use only.

Acetolysis of DL-*cis*-3-*Methoxycyclohexene Oxide (2)*

DL-*cis*-3-Methoxycyclohexene oxide (10.5 g, 0.082 mole) was treated with glacial acetic acid (100 ml) and concentrated sulfuric acid (0.10 g) at 70° for 6 h. Acetic anhydride (25 ml) was added and the solution was kept for 36 h at room temperature. The acid and excess anhydride were largely removed *in vacuo* on the rotary evaporator and the residue was neutralized with sodium bicarbonate and potassium carbonate to pH 8. The resultant solution was extracted with ether (6 × 30 ml) and dried over anhydrous magnesium sulfate. Removal of the ether furnished 16.3 g (86.2%) of an oil, analysis of which by v.p.c. at 85° on a 6 ft column of Chromosorb P impregnated with 10% neopentyl glycol sebacate showed it to consist of a single diacetate isomer. The structure of the diacetate was established as DL-(1/2,3)-1,2-diacetoxy-3-methoxycyclohexane (**7***c*) by its n.m.r. spectrum.

Anal. Calcd. for $C_{11}H_{18}O_5$: C, 57.35; H, 7.88. Found: C, 57.31; H, 7.81.

A small quantity of a second product (2.2%) was separated from **7***c* by preparative v.p.c. This substance was not identified but it cannot be the minor isomer **8***c* formed by opening at position-2 since its v.p.c. characteristics differ markedly from those of the latter substance which is identical with the major isomer **6***c* obtained by scission of the *trans* oxide at position-1 (see below).

Acetolysis of DL-*trans*-3-*Methoxycyclohexene Oxide (1)*

DL-*trans*-3-Methoxycyclohexene oxide (60.8 g, 0.475 mole) was treated with acetic acid as described for its isomer except that the addition of acetic anhydride was omitted. After isolation in the manner indicated above, 78.0 g (87.4%) of a mixture of oil and crystals was obtained. Vapor-phase chromatographic analysis of this mixture under the same conditions as mentioned in the scission of the *cis* isomer indicated the presence of two isomers in the ratio 87.5:12.5. Fractional distillation of the mixture at 75–90° at 0.02 mm pressure gave 7.60 g of an oil which was further acetylated and redistilled in a Späth tube (air-bath temperature 90–100°) at 0.02 mm yielding 8.85 g of oily product. Analysis of the latter material by v.p.c. at 85° as described above gave two peaks with retention times of 15.75 and 20 min respectively. When pure DL-(1/2,3)-1,2-diacetoxy-3-methoxycyclohexane (**5***c*) was added to a sample of the oil, the first peak was reinforced, strongly suggesting that the first peak is **5***c*[10] formed by attack at position-2. Analysis of the oil showed it to consist solely of diacetate so that the second peak must be DL-(1,3/2)-1,2-diacetoxy-3-methoxycyclohexane (**6***c*) formed by normal opening at position-1.

Anal. Calcd. for $C_{11}H_{18}O_5$: C, 57.36; H, 7.88. Found: C, 57.47, 57.43; H, 8.13, 8.04.

The crystalline compound recovered from the pot residue from the first distillation was recrystallized twice from ligroin, had m.p. 73.5–75.0°, and was identified as DL-(1,3/2)-1-acetoxy-2-hydroxy-3-methoxycyclohexane by its n.m.r. spectrum.

Anal. Calcd. for $C_9H_{16}O_4$: C, 57.41; H, 8.57. Found C, 57.29, 57.43; H, 8.43, 8.27.

Methanolysis of DL-*cis*-3-*Methoxycyclohexene Oxide (2)*

Basic Conditions

DL-*cis*-3-Methoxycyclohexene oxide (9.63 g, 0.075 mole) was heated under reflux for 48 h in methanol (35 ml) containing sodium (0.651 g). The solution was then kept at room temperature for 5 days, acidified with acetic acid, and distilled through an 8 in. Vigreux column until a colorless mushy solid remained in the pot. The latter was collected by filtration, washed with ether, and the filtrate and washings were fractionated yielding 1.55 g of colorless oil, b.p. 45° at 0.03 mm pressure, n_D^{25} 1.4558, identified by v.p.c. as unreacted *cis* oxide (5); and 8.28 g (82.0%) of colorless oil, b.p. 45–53° at 0.03 mm, n_D^{25} 1.4592, identified as DL-(1/2,3)-1,3-dimethoxy-2-hydroxycyclohexane (**7***d*) by the n.m.r. spectrum of its *p*-nitrobenzoate. Vapor-phase chromatographic analysis at 85° on a 6-ft column of Chromosorb P impregnated with 10% neopentyl glycol sebacate indicated the fraction to consist of only one isomer.

Acidic Conditions

DL-*cis*-3-Methoxycyclohexene oxide (3.00 g, 0.0234 mole) was added to anhydrous methanol (15 ml) containing one drop of concentrated sulfuric acid. The solution warmed spontaneously to 60°, and was allowed to cool to room temperature and kept overnight. The methanol was removed *in vacuo* on the rotary evaporator and the residue was distilled yielding 3.98 g[11] of DL-(1/2,3)-1,3-dimethoxy-2-hydroxycyclohexane (**7***d*) as a colorless oil, b.p. 42–48° at 0.02 mm. Identification was made as described above and v.p.c. analysis again indicated that **7***d* was the only isomer formed.

Methanolysis of DL-*trans*-3-*Methoxycyclohexene Oxide (1)*

Basic Conditions

DL-*trans*-3-Methoxycyclohexene oxide (25.2 g, 0.197 mole) was treated with a solution of sodium methoxide as described for its stereoisomer. After neutralization with acetic acid, the solution was distilled yielding 2.51 g of unreacted oxide identified by v.p.c. analysis, and 25.7 g (90.5%) of colorless oil, b.p. 80–85° at 0.01 mm, n_D^{25} 1.4585, which by v.p.c. analysis proved to be a mixture of DL-(1,3/2)-1,3-dimethoxy-2-hydroxycyclohexane (**6***d*) and DL-(1/2,3)-2,3-dimethoxy-1-hydroxycyclohexane (**5***d*) in the ratio 90.7:9.3. Several attempts were made to separate this mixture on the Fisher Preparative Partitioner but only **6***d* was obtained pure by this means, n_D^{25} 1.4584. This compound was identified by its n.m.r. spectrum (2).

The second isomer was isolated only in an enriched form and was further purified by conversion to the *p*-nitrobenzoyl derivative, followed by fractional crystallization. The pure derivative had m.p. 71.2–71.8° and was identified by its n.m.r. spectrum.[12]

Anal. Calcd. for $C_{15}H_{19}O_6N$: C, 58.22; H, 6.20; N, 4.53. Found: C, 58.25; H, 5.99; N, 4.54.

Acidic Conditions

DL-*trans*-3-Methoxycyclohexene oxide (16.0 g, 0.125 mole) was subjected to acidic methanolysis in the same manner as described for its stereoisomer. Isolation by distillation *in vacuo* afforded 15.5 g (77.5%) of colorless

[10]This material was identical with the diacetylated compound **7***c* obtained from scission of the *cis* oxide with acetic acid followed by subsequent acetylation.

[11]The % yield was high but indeterminate due to error in weights.

[12]The n.m.r. spectrum of this substance did not show the expected quartet for the C-2 methine proton of **5***d* because of overlap with another peak. However, it did show two non-equivalent methoxyl methyl proton resonances at τ 6.60 and 6.52 respectively in contrast to that of **6***d* which showed only one methoxyl methyl proton resonance equivalent to 6 protons at τ 6.64.

Can. J. Chem. Downloaded from www.nrcresearchpress.com by 210.87.254.6 on 09/05/12
For personal use only.

oil, b.p. 80–85° at 0.01 mm pressure, n_D^{25} 1.4593. Vapor-phase chromatographic analysis revealed it to contain the same two compounds as the product from the basic cleavage of the same oxide but in the ratio 89.5:10.5.

Ammonolysis of DL-*trans-3-Methoxycyclohexene Oxide (1)*

The procedure was identical with that reported by Bannard and Hawkins (3) except that 20.5 g (0.160 mole) of oxide was used and heating was conducted at 110°. Removal of the excess ammonia and ethanol *in vacuo* followed by recrystallization from absolute methanol, with addition of decolorizing charcoal, furnished 21.3 g of pale-yellow crude crystalline material together with 1.74 g of dark residue. Recrystallization of the former from absolute methanol furnished 18.3 g of DL-(1,3/2)-1-amino-2-hydroxy-3-methoxycyclohexane (**6***e*) (3), as colorless platelets, m.p. 111.5–112.5°[13] alone, and in admixture with an authentic sample. The dark residue, on heating at 10^{-3} mm pressure furnished two sublimates, one a colorless crystalline solid at 40–60° (m.p. 60–95°), and the other a more waxy solid at 80–100° (m.p. 95–125°). Similar treatment of the residue obtained on evaporation to dryness *in vacuo* of the mother liquor from the recrystallization of the major product yielded identical sublimates. Recombination of corresponding fractions followed by resublimation and fractional recrystallization of the lower-melting sublimate from anhydrous ether gave a further 700 mg of **6***e* as colorless leaflets, m.p. 111.5–112.5° and 1.75 g of the previously unreported DL-(1/2,3)-1-hydroxy-2-amino-3-methoxycyclohexane (**5***e*), as long thick leaflets, m.p. 89.5–90.5°.[14]

Anal. Calcd. for $C_7H_{15}O_2N$: C, 57.90; H, 10.41; N, 9.65. Found: C, 57.78; H, 10.42; N, 9.73.

The residue (680 mg) recovered by evaporation to dryness of the mother liquors was analyzed by v.p.c. at 165° in the Autoprep A-700 gas chromatograph (10 ft column, Chromosorb P 45/60 mesh, impregnated with 5% potassium hydroxide and 25% polyethylene glycol 20 000) after suitable calibration experiments with the pure 1-amino (55.5 min) and 2-amino (66 min) isomers in question. The relative amounts were found to be 33.6% and 66.4% respectively. Thus, the yields of 1-amino- and 2-amino derivatives were 19.2 g (80.2%) and 2.20 g (9.0%) respectively.

The higher-melting sublimate was recrystallized from anhydrous ether, yielding 1.10 g (4.9%) of colorless crystalline substance, m.p. 95–125°, which was concluded to be a mixture of stereoisomeric secondary amines, judging from its analysis and chromatographic properties. This mixture was not eluted from the above-mentioned chromatographic column at temperatures up to 195° and similar behavior was exhibited by an analogous secondary amine obtained previously by Hawkins and Bannard (13) from the ammonolysis of cyclohexene oxide. The primary and secondary amines could be separated, however, by paper chromatography on Whatman No. 1 paper using *n*-butanol:acetic acid:water (4:1:5). Under these conditions, the 1-amino derivative, the 2-amino derivative and the secondary amine mixture had R_f values 0.50, 0.60, and 0.70 respectively (chromogen, bromcresol green). Consequently, paper chromatography was used to check for the presence of secondary amine in the primary amines.

Anal. Calcd. for $C_{14}H_{27}O_4N \cdot 1/2\ H_2O$: C, 59.56; H, 10.00; N, 4.96. Found: C, 59.40; H, 10.12; N, 4.75.

DL-*(1/2,3)-1-Acetoxy-2-acetamido-3-methoxycyclohexane*

This substance was obtained in quantitative yield by heating DL-(1/2,3)-1-hydroxy-2-amino-3-methoxycyclohexane (**5***e*) under reflux for 1 h with a large excess of acetic anhydride as described previously (16). Recrystallization from anhydrous ether gave colorless rosettes, m.p. 108–108.5°.

Anal. Calcd. for $C_{11}H_{19}O_4N$: C, 57.62; H, 8.35; N, 6.11. Found: C, 57.52; H, 8.46; N, 6.10.

DL-*(1/2,3)-2-Amino-1,3-cyclohexanediol*

DL-(1/2,3)-1-Hydroxy-2-amino-3-methoxycyclohexane hydrobromide, m.p. 234–235.5°, (248 mg, 1.1×10^{-3} mole) and 68% aqueous hydrobromic acid (1.0 ml) were heated together in a Carius tube at 68° for 1.5 h. The pale-yellow solution was evaporated to dryness *in vacuo* and the crystalline residue was pumped at a pressure of 1.0×10^{-3} mm to remove traces of excess hydrogen bromide. The residual tan-colored rosettes (221 mg) were dissolved in water (10 ml) and the solution was passed through Amberlite IRA-400 (OH) resin (5 ml), after which the resin was washed with water (50 ml). Evaporation of the combined eluates to dryness *in vacuo* furnished a colorless crystalline residue, sublimation of which at 60–65° at 1.0×10^{-3} mm pressure gave 151 mg (95.0%) of DL-(1/2,3)-2-amino-1,3-cyclohexanediol, as colorless crystals, m.p. 112–113°. Suami and Ogawa (15) report 112–113° for this compound. Acetylation of the aminediol (136 mg) gave 260 mg (97.4%) of a crystalline triacetyl derivative (sublimes at 110–120° at 1.0×10^{-3} mm pressure), which had m.p. 144–146° alone and in admixture with an authentic sample of DL-(1/2,3)-2-acetamido-1,3-diacetoxycyclohexane (15). The infrared spectra of the two specimens were also identical.

Ammonolysis of DL-*cis-3-Methoxycyclohexene Oxide (2)*

The procedure was the same as described for the *trans* oxide except that 2.05 g (0.0160 mole) of *cis* oxide was used. Removal of the ethanol and excess ammonia *in vacuo* from the pale-yellow solution left an almost colorless residue, heating of which at 65° at 10^{-3} mm pressure furnished 2.21 g (92.0%) of colorless crystalline sublimate, m.p. 95–97°, which was identified as DL-(1/2,3)-1-amino-2-hydroxy-3-methoxycyclohexane (**7***e*) (3) by mixture melting point determination with an authentic specimen, and by comparison of infrared spectra. Vapor-phase chromatographic analysis on the Autoprep A-700 gas chromatograph at 165° (10 ft column, 45/60 mesh Chromosorb P impregnated with 5% potassium hydroxide and 25% polyethylene glycol 20 000) gave a single peak with retention time 49 min. Its R_f value in paper chromatograms on Whatman No. 1 paper using *n*-butanol:

[13]The m.p. of this compound was erroneously reported earlier (3) as 107–108°.

[14]The structure of **5***e* was established by deetherification to DL-(1/2,3)-2-amino-1,3-cyclohexanediol, m.p. 112–113°, in 95% yield (15) and conversion of the latter to a triacetyl derivative, m.p. 144–146°, in 98% yield, which was identical with an authentic specimen of DL-(1/2,3)-2-acetamido-1,3-diacetoxycyclohexane kindly provided by Prof. S. Ogawa. Confirmation of the structure was obtained from the 60 Mcycle/s n.m.r. spectrum of DL-(1/2,3)-1-acetoxy-2-acetamido-3-methoxycyclohexane. The spectrum exhibited a double quartet at τ 4.07 due to the methine proton at C-2 which was collapsed to a quartet ($J_{2,3} = 2.8$ c.p.s. and $J_{1,2} = 9.3$ c.p.s.) by spin decoupling the proton attached to nitrogen.

acetic acid: water (4:1:5) was 0.52 (chromogen, bromcresol green). No indication of the presence of a minor product was observed in any of these experiments.

The residue from the sublimation on heating at 80–100° at 10^{-3} mm pressure, furnished an oily base, 106 mg (4.7%), which was concluded to be the corresponding secondary amine mixture, judging from its analysis and chromatographic behavior.

Anal. Calcd. for $C_{14}H_{27}O_4N \cdot 1/2\ H_2O$: C, 59.56; H, 10.00; N, 4.96. Found: C, 59.73; H, 10.31; N, 4.70.

This substance, like its counterpart from the *trans* oxide was not eluted from the column during v.p.c. analysis as described above using temperatures up to 195°. It was, however, separable from the primary amine by paper chromatography using the above-mentioned solvent system. (R_f 0.70, chromogen, bromcresol green).

Acknowledgments

We are indebted to Prof. S. Ogawa for providing us with an authentic sample of DL-(1/2,3)-2-acetamido-1,3-diacetoxycyclohexane, and to Dr. M. Weinberger and Miss P. Lutley for recording the n.m.r. spectra of DL-(1/2,3)-1-acetoxy-2-acetamido-3-methoxycyclohexane and DL-(1,2/3)-1-bromo-2-acetoxy-3-methoxycyclohexane.

Thanks are extended to the National Research Council of Canada for the award of a scholarship to one of us (E. J. L.) and for partial financial support of the work.

1. J. A. McRae, R. Y. Moir, J. W. Haynes, and L. G. Ripley. J. Org. Chem. **17**, 1621 (1952).
2. R. U. Lemieux, R. K. Kullnig, and R. Y. Moir. J. Am. Chem. Soc. **80**, 2237 (1958).
3. R. A. B. Bannard and L. R. Hawkins. Can. J. Chem. **36**, 1241 (1958).
4. R. A. B. Bannard and L. R. Hawkins. Can. J. Chem. **39**, 1530 (1961).
5. E. J. Langstaff, E. Hamanaka, G. Neville, and R. Y. Moir. Can. J. Chem. **45**, 1907 (1967).
6. R. G. Kadesch. J. Am. Chem. Soc. **68**, 41 (1946).
7. R. E. Parker and N. S. Isaacs. Chem. Rev. **59**, 737 (1959).
8. A. A. Frost and R. G. Pearson. Kinetics and mechanism. John Wiley and Sons, Inc., New York. 1961. Chap. 12.
9. R. A. B. Bannard, A. A. Casselman, and L. R. Hawkins. Can. J. Chem. **43**, 2398 (1965).
10. A. Fürst and Pl. A. Plattner. 12th Intern. Congr. Pure and Appl. Chem. New York. 1951. Abstr. Papers, p. 405.
11. S. J. Angyal. Chem. Ind. London, 1230 (1954).
12. S. Winstein, E. Grunwald, and L. L. Ingraham. J. Am. Chem. Soc. **70**, 821 (1948).
13. L. R. Hawkins and R. A. B. Bannard. Can. J. Chem. **36**, 220 (1958).
14. R. A. B. Bannard. Can. J. Chem. **44**, 775 (1966).
15. T. Suami and S. Ogawa. Bull. Chem. Soc. Japan, **37**, 194 (1964).
16. R. A. B. Bannard. Can. J. Chem. **42**, 744 (1964).

Can. J. Chem. Downloaded from www.nrcresearchpress.com by 210.87.254.6 on 09/05/12
For personal use only.

Photochemical rearrangement and dimerization of 1,1-disubstituted indenes

JOHN J. MCCULLOUGH
Department of Chemistry, McMaster University, Hamilton, Ontario

Received July 26, 1967

The photochemical behavior of 1,1-diphenylindene and 1,1-dimethylindene has been studied. The former undergoes efficient rearrangement on direct irradiation or on acetophenone sensitization, forming 2,3-diphenylindene and 1,2-diphenylindene. In contrast, 1,1-dimethylindene gave no detectable products of methyl migration but formed dimeric cyclobutanes on sensitized and direct photolysis. The structures of the two dimers formed in the sensitized reaction were assigned from their nuclear magnetic resonance spectra. It was also demonstrated that hydrogen, like methyl, migrated inefficiently if at all in this system. This difference in migratory aptitudes is discussed in terms of orbital symmetry of the indene system.

Canadian Journal of Chemistry. 46, 43 (1968)

Can. J. Chem. Downloaded from www.nrcresearchpress.com by 210.87.254.105 on 09/05/12
For personal use only.

Introduction

Indene is capable of reacting by several photochemical pathways. For example, on sensitized photolysis, with light absorbed by acetophenone or Michler's ketone, the *cis-anti-cis* cyclobutane dimer (1–4), with head-to-head orientation (4) is formed in high yield. However, on direct irradiation in which the light is absorbed by indene, extensive polymerization occurs. Cyclobutanes can also be obtained by sensitized cross-addition reactions of indene with coumarin (1, 4) or acrylonitrile (5). Photolysis of indene and acrylonitrile with no sensitizer results in the formation of 2-(1-indenyl)-propionitrile as the major product (5).

In order to obtain further information on the photochemical behavior of the indene system, a study of 1,1-diphenylindene and 1,1-dimethylindene was undertaken. In these two cases there were the following *a priori* possibilities. First, the compounds could dimerize, rearrange,[1] polymerize, or give products of all three reactions. If rearrangement or dimerization occurred, there was the question as to what the products would be. Second, it was of considerable interest to make a comparison of the reactions with and without a sensitizer, since the parent compound behaves differently in the two reactions.

Results

Synthetic and Structural Aspects

The two model compounds for photolysis, 1,1-diphenylindene and 1,1-dimethylindene were prepared by similar routes from the appropriate indanones. For example, 3,3-diphenyl-1-indanone obtained by cyclization of 3,3,3-triphenyl propionic acid with stannic chloride, was reduced by sodium borohydride in ethanol, and the 3,3-diphenyl-1-indanol was dehydrated on treatment with *p*-toluenesulfonic acid in acetic acid at reflux to give 1,1-diphenylindene m.p. 89–90° (lit. 91–92°, (6)); the route is essentially that of Brown and Jackman (6). The method of Bosch and Brown (7) was followed in obtaining 1,1-dimethylindene, and the nuclear magnetic resonance (n.m.r.) spectrum of the product was identical with the published spectrum (7).

On photolysis in hexane or ethanol, 1,1-diphenylindene gave products of phenyl and hydrogen migration which were identified as 2,3-diphenylindene (**1**) and 1,2-diphenylindene (**2**). These were formed in the ratio 75:25 as determined by gas chromatography (Column A, 220°) and were isolated by chromatography on alumina. Reduction of 2,3-diphenylindenone with zinc and hydrochloric acid as described by Shriner and Knox afforded 1,2-diphenylindene, m.p. 175° (8). The reactions are shown in Scheme I.

This had λ_{max}(hexane) 237, 305 mμ log ϵ 4.11 and 4.28 respectively. The n.m.r.[2] was in accord with this structure and had a rather broad singlet at 4.90 (1 proton, benzylic) as well as a multiplet centered at 7.10 (15 protons, aromatics and vinyl proton).[3] This synthetic material was identical in all respects, with the minor photolysis product of 1,1-diphenylindene. On treatment of 1,2-diphenylindene with dimethylamine (9) in pyridine

[1]Photolysis of 1,1,3-triphenylindene leads to phenyl migration; see ref. (13).

[2]Chemical shifts are given in p.p.m., see experimental.

[3]There is at least one precedent for this n.m.r. pattern in the 2-substituted indene system (24).

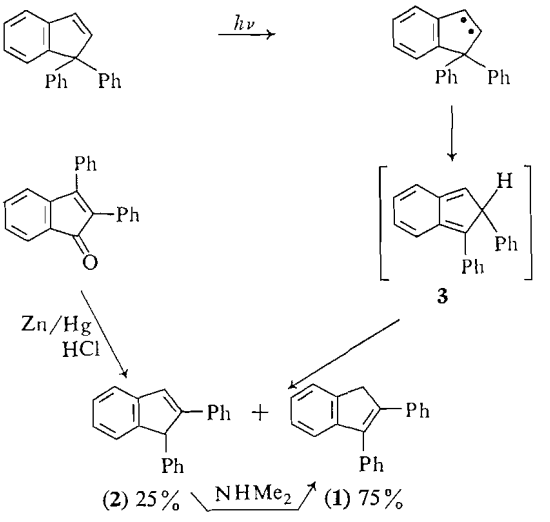

SCHEME I

the 2,3-isomer m.p. 108° was formed in quantitative yield.[4] The latter, which was the major product of the photolytic migration, had λ_{max}(hexane) 237 and 305 mμ, log ε 4.30 and 4.26 respectively, and showed n.m.r. peaks at 3.75, (two-proton singlet, methylene group) and at 7.15 and 7.25 (14 protons, aromatics).

These same rearrangement products were obtained on photosensitization with acetophenone. A dimer was also obtained, m.p. 160–162°, the n.m.r. of which showed that it was not derived directly from 1,1-diphenylindene, but from one of the rearrangement products.

The photochemical behavior of 1,1-dimethylindene was quite different. No products of methyl migration could be detected. These were sought for by gas chromatography (Column A, 110°) and by n.m.r. spectroscopy. No peaks of retention time similar to 1,1-dimethylindene were observed, and no trace of allylic methyl resonance was seen in the n.m.r. spectra of aliquots taken at all stages of the reaction. Gas chromatography (Column B, 200°) did show that several compounds, presumably dimers were formed.

As in the case of indene (1–4) the mixture of products of photosensitization was simpler. Two dimers (Scheme II) formulated as the head-to-head isomer (**4**) and the head-to-tail compound (**5**) were isolated by alumina chromatography. The former was non-crystalline and was the major product; the latter had m.p. 92–95° and was the only other significant product. The above structures for these dimers are derived from infrared and n.m.r. spectra. Both compounds had two bands of equal intensity at 1362 and 1383 cm^{-1} in the infrared, showing that the *gem*-dimethyl system (10) was intact. The n.m.r. of the major, low-melting dimer showed singlets at 1.31 and 0.95 (6 protons per peak, methyl group) and a multiplet at 7.15 (8, protons, aromatic). The methine protons of the cyclobutane system appeared as two doublets at 3.47 (2 benzylic protons) and 2.52 (2 protons), the splitting for each doublet being 4.5 Hz. Although these protons belong to an AA^1XX^1 system, there is only one large coupling constant between protons of different chemical shifts. Inspection of a related case, the head-to-head dimers of coumarin (11), leads to the conclusion that the A and X portions could appear as doublets.

The crystalline dimer of dimethylindene shows singlets at 1.14 and 1.57 (6 protons per peak, methyl protons) and at 7.18 (8 aromatic protons). The methine protons gave rise to two quartets centered at 3.76 (2 benzylic protons) and at 2.42 (2 protons), which had an object–image relationship. This pattern is consistent with the head-to-tail orientation, since the corresponding coumarin dimer (11) has an AA^1XX^1 spectrum with a similar appearance.

Support for the above assignment of structures to the dimethylindene dimers derives from the n.m.r. of the photo-dimer of indene itself. The latter was shown to be the head-to-head compound (4), and in the n.m.r. the signal from the benzylic methines appears as a doublet, centered at 3.64, with a splitting of 5.4 Hz. The corresponding protons of the major, low-melting dimer of dimethylindene give rise to a similar doublet at 3.47 (*vide supra*). The signal at 3.76 from the crystalline dimer is a quartet. These facts point to the head-to-head structure for the low-melting dimer of dimethylindene.

In order to determine whether photolytic hydrogen migration occurs in the indene system, 1,1,3-trideuterioindene was prepared by the method of Bergson (12). This was photolyzed to 80% polymerization, and the residual indene recovered by distillation. Nuclear magnetic resonance spectroscopy showed that no change

[4]In our hands, use of potassium hydroxide in ethanol to effect isomerization gave intractable material.

Can. J. Chem. Downloaded from www.nrcresearchpress.com by 210.87.254.105 on 09/05/12
For personal use only.

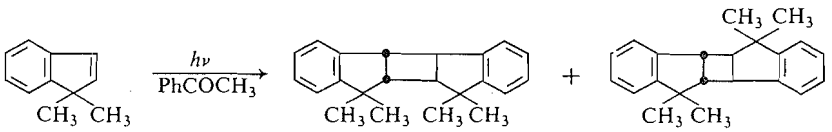

(4) 83% (5) 17%

SCHEME II

in deuterium distribution had occurred. It was also found that the 1,2- and 2,3-diphenylindene isomers did not interconvert on irradiation.

Discussion

Mechanistic Aspects

There are a number of reports in the recent literature of photolytic migration of hydrogen, methyl, and phenyl groups in unsaturated hydrocarbon systems. Specifically, Griffin and coworkers have found that all three of the above groups migrate in suitably substituted alkenes (13–15) and Jones and Jones reported similar migrations of methyl and hydrogen in the trimethylcycloheptatriene system (16).

In this work it has been demonstrated that while rearrangement is the exclusive photochemical process of 1,1-diphenylindene, no rearrangement products of the 1,1-dimethyl derivative could be found, nor could evidence for hydrogen migration in indene be produced. The low migratory aptitudes of hydrogen and methyl relative to phenyl cannot be an inherent quality in the former two, since all three groups migrate readily in other systems (13–16).

The difference in migratory aptitudes can be understood if the selection rules for sigmatropic reactions (17) are applied to the indene system. A model for the transition state for migration (see Fig. 1), following the suggestion of Woodward and Hoffmann (17), would consist of an indenyl radical and a methyl radical, hydrogen atom, or phenyl radical. The symmetry of the lowest unoccupied molecular orbital of the indenyl radical then determines whether migrations in the excited state are permitted. This radical has 9 π electrons, hence the orbital in question is ψ_6 which has the symmetry shown in (**6**) and (**7**). It can be seen that the coefficients at the migration start and terminus are of opposite sign (18), and suprafacial migrations from C_1 to C_2 of groups which interact with the indene π system only through σ orbitals, such as methyl or hydrogen, are forbidden. In considering the same

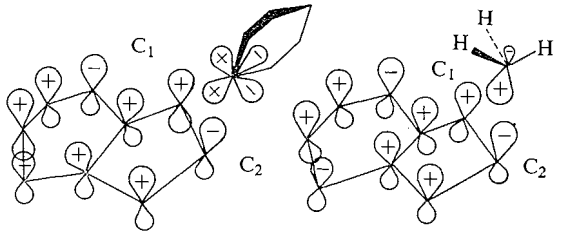

(6) (7)

FIG. 1. Models for transition states for phenyl and methyl migration.

migration of aryl groups, the π system of the migrating group must be taken into account. In this case the *p*-orbitals of the π system are of the correct symmetry for positive overlap with ψ_6 at C_1 and C_2, as shown in (**6**). Also, the lowest antibonding orbitals of benzene have nearly the same energy (-1.00β) as ψ_6 of the indenyl radical (-0.90β) (18) hence the overlap will cause a significant energy lowering in the transition state, resulting in the facile migration of a phenyl group.[5]

Migration of a phenyl group would result in the formation of an *o*-quinodimethane, or isoindene structure. Such species intervene in several reactions including photochemical (19–21), thermal (22–24), and elimination (24, 25) processes. The isoindene[6] (**3**) could undergo a hydrogen shift to form the products, (**1**) and (**2**). This shift probably occurs in the ground state of (**3**), since the photochemical process, which is just the reverse of photo-migration of hydrogen in indene, is symmetry forbidden. On the other hand, the ground state process is well known;

[5]Woodward and Hoffmann (17) have pointed out that for migrating groups with π systems, reversal of the selection rules from those for σ-bonded groups can be envisaged.

[6]Griffin *et al.* (13) suggested these same steps in a mechanism for the rearrangement of 1,1,3-triphenylindene, but did not discuss the mechanism in any detail. We have been unable to trap the isoindene intermediate using dienophiles as trapping agents.

Can. J. Chem. Downloaded from www.nrcresearchpress.com by 210.87.254.105 on 09/05/12
For personal use only.

Can. J. Chem. Downloaded from www.nrcresearchpress.com by 210.87.254.105 on 09/05/12
For personal use only.

Roth (22) found that deuterium scrambling occurred on heating deuterioindene and Alder and Fremery (25) generated isoindene by a debromination reaction to obtain indene as the product. The mixture of diphenylindenes is not a photostationary state, for the products do not interconvert on irradiation. The ratio is therefore that of kinetically controlled hydrogen shift, which of course can occur in either of two senses giving (**1**) and (**2**).

The sensitized dimerization of 1,1-dimethylindene gives two products, while the same reaction of indene yields a single dimer (1–4). The major dimer in both cases is the head-to-head compound, formed via the more stable diradical intermediate (27). Steric interaction between methyl groups may be responsible for the formation of some head-to-tail product in the dimethylindene dimerization.

Experimental

The nuclear magnetic resonance (n.m.r.) spectra were obtained with a Varian A-60 spectrometer. The chemical shifts are δ values measured against tetramethylsilane ($\delta = 0$) as internal standard. Infrared spectra were run on a Beckman IR 5 or on a Perkin–Elmer 521 instrument.

Gas chromatography was performed with a Varian-Aerograph 202B instrument, with 60–70 ml/min of helium, using Column A (5 ft × 1/4 in. 20% SE 30 on Chromosorb W) or Column B (5 ft × 1/4 in. 15% carbowax on Chromosorb W). Melting points were taken on a Kofler hot stage and are uncorrected.

Nitrogen was Canadian Liquid Air certified grade and was further purified by passage through vanadous sulfate (26) solution, concentrated sulfuric acid, and then over potassium hydroxide pellets.

Alumina used was Adsorption Fisher Alumina and the Ethanol (95%) was distilled before use.

Microanalyses were by the Spang Micro-analytical Laboratory, Ann Arbor, Michigan.

Photolysis of 1,1-Diphenylindene

A solution of 1,1-diphenylindene (1.054g; 0.00393 mole) in ethanol (400 ml) was photolyzed through quartz with a type L450W Hanovia lamp in the usual water-cooled immersion apparatus. The vessel was fitted with a magnetic stirrer, an inlet and capillary outlet for nitrogen, and a means of withdrawing aliquots by a syringe. The solution was purged with purified nitrogen for 1 h prior to and during the photolysis. Aliquots were removed and monitored by ultraviolet absorption and by gas chromatography. The ultraviolet spectrum showed considerable absorption at 305–325 mμ after 10 min photolysis. By gas chromatography (Column A, 220°) the 1,2-diphenylindene peak (retention time, 20 min) was seen to decrease, while the two product peaks (28 min and 34 min) increased. When the 1,1-diphenylindene had all reacted (2 h), the solvent was removed and the mixture chromatographed on a 4.0 × 90 cm column of alumina slurry packed in hexane. The column was eluted with 10% benzene–hexane, and 250 ml fractions were collected. Fractions 7–10 contained 2,3-diphenylindene (700 mg, m.p. 95–105°). The m.p. was raised to 108–110°, lit. 108° (8), by one crystallization from light petroleum, b.p. 80–100°. Fractions 11–15 were mainly 1,2-diphenylindene (200 mg, m.p. 100–125°). Crystallization from light petroleum gave material of m.p. 175–176°, lit. 175–177° (8).

Sensitized Photolysis of 1,1-Diphenylindene

Acetophenone (26.75 g, 0.222 mole) and 1,1-diphenylindene (0.9454 g, 0.00353 mole) in ethanol (400 ml) were photolyzed as above except that a Vycor sleeve was used. The reaction was essentially complete after 3 h as shown by the absence of the 1,1-diphenylindene peak on gas chromatography, in which the same products in the same ratio as in the direct photolysis were observed. After distillation of solvent and acetophenone, chromatography as described above gave 2,3-diphenylindene (fractions 10–17) 180 mg, m.p. 105–110°. Fractions 25–30 contained dimer, 400 mg, m.p. 156–160° (160–162° from ethanol–benzene).

Anal. Calcd. for $C_{42}H_{32}$: C, 93.99; H, 6.01. Found: C, 94.09; H, 5.86.

The n.m.r. spectrum ($CDCl_3$) was simple, having a sharp singlet at 4.0 (4 protons) and a series of multiplets between 7.2 and 8.2 (28 protons, aromatic). This spectrum shows that the dimer is not formed directly from 1,1-diphenylindene since such a dimer would not give a singlet from the methine protons (cf. dimethylindene dimers).

Irradiation of 2,3-Diphenylindene

2,3-Diphenylindene (138.9 mg, 4.86×10^{-4} mole as above) in ethanol (350 ml) was irradiated for 2 h, aliquots being taken at 30 min intervals. No peak corresponding to 1,2-diphenylindene was observed on gas chromatography. On terminating the photolysis the solvent was removed and the residue, in benzene solution, was filtered through alumina. The benzene was evaporated to give 110.9 mg of oil which crystallized m.p. 100–115° on adding light petroleum b.p. 80–100°. The n.m.r. of the crystalline material showed no peak at 4.90, which would have been present if isomerization to 1,2-diphenylindene had occurred.

Irradiation of 1,2-Diphenylindene

1,2-Diphenylindene (140 mg, 5.24×10^{-4} mole) in ethanol (300 ml) was irradiated (quartz) with the usual apparatus. Aliquots were taken and checked by gas chromatography for 2,3-diphenylindene; none of the latter was detected, after short (30 min) or longer (6 h) photolysis times.

Base-catalyzed Isomerization of 1,2-Diphenylindene to 2,3-Diphenylindene

1,2-Diphenylindene (66.0 mg) was treated with dimethylamine (0.5 ml) in pyridine (3.0 ml) for 12 h at 25°. Benzene and water were added, the organic layer was separated, washed with 2 *N* H_2SO_4 and water, and dried ($MgSO_4$). The residue on evaporation of the solvent was crystalline m.p. 102–108°, 60 mg (91%). Recrystallization from light petroleum b.p. 80–100° raised the m.p. to 108–109°.

Sensitized Photolysis of 1,1-Dimethylindene

1,1-Dimethylindene (2.083 g, 0.0144 mole) and acetophenone (19.425 g, 0.0162 mole) in *t*-butyl alcohol (380 ml) and methanol (20 ml) were photolyzed in the usual apparatus for 5 h using a Vycor filter. Aliquots were withdrawn at 30 min intervals and analyzed for products of rearrangement (Column A, 110°) and dimerization (Column B, 220°). The latter showed a major peak, retention time 7 min, accounting for about 90% of the total peak areas. The solvent and acetophenone were removed and the residue chromatographed on a 4.0 × 90 cm column of alumina, slurry-packed in hexane. The column was eluted with 250 ml fractions of this solvent. Fractions 6–11 contained 900 mg of material which declined to crystallize and gave a single peak on gas chromatography (Column B, 220°). This was shown by n.m.r. to be the head-to-head dimer of 1,1-dimethylindene.

Anal. Calcd. for $C_{22}H_{24}$: C, 91.61; H, 8.29. Found: C, 91.45; H, 8.57.

Fractions 13–17 contained 150 mg of the head-to-tail dimer, m.p. 50–70° (92–95° from aqueous ethanol).

Anal. Calcd. for $C_{22}H_{24}$: C, 91.61; H, 8.39. Found: C, 91.68; H, 8.43.

Direct Irradiation of 1,1-Dimethylindene

Photolysis of 2.0 g of 1,1-dimethylindene in ethanol (400 ml) as described for 1,1-diphenylindene resulted in disappearance of starting material. No allylic proton signals were observed in the n.m.r. of aliquots taken at 20 min intervals; these aliquots showed one peak on gas chromatography (Column B, 110°) corresponding to 1,1-dimethylindene. Several peaks were observed on this column at 220°, one of which had the same retention time as the head-to-head dimer from the sensitized reaction.

Irradiation of 1,1,3-Trideuterioindene

1,1,3-Trideuterioindene (5.363 g, 90% deuterium substituted) in ethanol (400 ml) was irradiated until about 80% of the indene had reacted, as estimated by gas chromatography. The solvent was removed, and the indene distilled at 1 mm, b.p. 35°. About 0.5 g of deuterated indene was recovered, and the n.m.r. was identical with that of starting material, demonstrating that hydrogen migration had not occurred.

Acknowledgments

The author thanks Mr. C. W. Huang for help in obtaining the n.m.r. spectra. Financial support from the National Research Council of Canada is gratefully acknowledged.

1. G. O. Schenck, W. Hartmann, S. P. Mannsfeld, W. Metzner, and C. H. Krauch. Ber. **95**, 1642 (1962).
2. C. H. Krauch, W. Metzner, and G. O. Schenck. Naturwiss. **50**, 710 (1963).
3. Belg. Pat. 630,110 (1963); Chem. Abstr. **60**, 15801 (1964).
4. J. Bowyer and Q. N. Porter. Australian J. Chem. **19**, 1455 (1966).
5. J. J. McCullough and C. W. Huang. Chem. Commun. 815 (1967).
6. R. F. Brown and L. M. Jackman. J. Chem. Soc. 3147 (1960).
7. A. Bosch and R. K. Brown. Can. J. Chem. **42**, 1718 (1964).
8. R. L. Shriner and W. R. Knox. J. Org. Chem. **16**, 1064 (1951).
9. G. Bergson. Acta Chem. Scand. **17**, 2691 (1963).
10. L. J. Bellamy. The infrared spectra of complex molecules. Methuen and Co., Ltd., London. 1959. p. 13.
11. C. H. Krauch, S. Farid, and G. O. Schenck. Ber. **99**, 625 (1966).
12. G. Bergson. Acta Chem. Scand. **18**, 2003 (1964).
13. G. W. Griffin, A. F. Marcantonio, H. H. Kristinsson, R. C. Petterson, and C. S. Irving. Tetrahedron Letters, 2951 (1965).
14. G. W. Griffin, J. Cavell, R. C. Petterson, R. M. Dodson, and G. Klose. J. Am. Chem. Soc. **87**, 1410 (1965).
15. H. Kristinsson and G. W. Griffin. J. Am. Chem. Soc. **88**, 378 (1966).
16. L. B. Jones and V. K. Jones. J. Am. Chem. Soc. **89**, 1880 (1967).
17. R. B. Woodward and R. Hoffmann. J. Am. Chem. Soc. **87**, 2511 (1965).
18. C. A. Coulson and A. Streitwieser. Dictionary of π-electron calculations. W. H. Freeman and Co., San Francisco. 1965. p. 210.
19. N. C. Yang and C. Rivas. J. Am. Chem. Soc. **83**, 2213 (1961).
20. G. Quinkert. Pure Appl. Chem. **9**, 607 (1964); G. Quinkert, W. W. Wiersdorf, M. Finke, and K. Opitz. Tetrahedron Letters, 2193 (1966).
21. H. A. Staab and J. Ipaktschi. Angew. Chem. Intern. Ed. Engl. **5**, 321 (1966).
22. W. R. Roth. Tetrahedron Letters, 1009 (1964).
23. J. A. Berson and M. Pomerantz. J. Am. Chem. Soc. **86**, 3896 (1964).
24. C. F. Huebner, P. L. Strachan, E. M. Donoghue, N. Cahoon, L. Dorfman, R. Margerison, and E. Wenkert. J. Org. Chem. **32**, 1126 (1967).
25. K. Alder and M. Fremery. Tetrahedron **14**, 190 (1961).
26. L. Meites and T. Meites. Anal. Chem. **20**, 984 (1948).
27. N. J. Turro and P. D. Bartlett. J. Org. Chem. **30**, 1849 (1965).

Can. J. Chem. Downloaded from www.nrcresearchpress.com by 210.87.254.105 on 09/05/12
For personal use only.

Low molecular weight carbohydrates from potato (*Solanum tuberosum*)[1]

BRANKO URBAS
Food Research Institute, Canada Department of Agriculture, Ottawa, Canada
Received August 30, 1967

An investigation was made of the low molecular weight carbohydrates of potato, Netted Gem variety. The material soluble in 80% alcohol was fractionated and separated by a combination of charcoal–Celite column and paper chromatography. Fifteen major components were isolated and characterized, and five minor components were detected. The major components were galactose, glucose, fructose, myoinositol, and eleven oligosaccharides, namely, sucrose, melibiose (Gal_p 1 → 6 G_p), maltotriose (G_p 1 → 4 G_p 1 → 4 G_p), digalactosyl glycerol (Gal_p 1 → 6 Gal_p 1 → 1 Glyc), glucosyl → myoinositol, raffinose (Gal_p 1 → 6 G_p 1 → 2 Fru_f), planteose (Gal_p 1 → 6 Fru_f 2 → 1 G_p), galactinol (D-1-*O*-α-D-galactopyranosyl-myoinositol), manninotriose (Gal_p 1 → 6 Gal_p 1 → 6 G_p), stachyose (Gal_p 1 → 6 Gal_p 1 → 6 G_p 1 → 2 Fru_f), and trigalactosyl glycerol (Gal_p 1 → 6 Gal_p 1 → 6 Gal_p 1 → 1 Glyc). The five components detected in small amounts were: three disaccharides, ribosyl-glucose, xylosyl-glucose, and arabinosyl-glucose, and two trisaccharides both made up of fructose and glucose units in the ratio of 2:1.

Canadian Journal of Chemistry, 46, 49 (1968)

The carbohydrates of low molecular weight present in potato, as exemplified by the Netted Gem variety, were studied in this investigation. The potatoes were harvested at Fredericton, New Brunswick, in October, 1966. The purpose of the investigation was to determine the nature of the mono- and oligosaccharides found in potato.

In the literature (1–3), potato carbohydrates of low molecular weight were considered to be a mixture of xylose, fructose, glucose, mannose, sucrose, maltose, raffinose, heptulose, melezitose, inositol, and fructan. The evidence for the presence of these sugars was based solely on the paper chromatography technique and the reaction of the sugars to various spray reagents.

In this study, a mixture of neutral carbohydrates was obtained by extracting the raw potato with 80% aqueous alcohol. The mixture was fractionated on a carbon/Celite column and subfractionated by paper chromatography and thin-layer chromatography. The isolated oligosaccharide material was divided into four groups of compounds based on their composition.

The first group of oligosaccharides contained sucrose and members of the raffinose family. The latter occurs, probably as reserve carbohydrate, in a wide variety of plant sources, notably seeds and roots (4). The members of the family isolated in this study were melibiose, raffinose, planteose, manninotriose, stachyose, and two trisaccharides made up of fructose and glucose units in a ratio of 2:1 but whose structure was not completely defined due to lack of material.

The second group of oligosaccharides contained myoinositol, D-1-*O*-α-D-galactopyranosyl-myoinositol (galactinol), and glucopyranosyl-myoinositol.

Myoinositol occurs widely in nature in both free and bound forms. The bound form has a varied composition but the phosphate esters are a major component. This form can be easily hydrolyzed by strong acid and partially hydrolyzed by phosphatases and glycosidases. Structural studies on inositol containing phosphatides indicate that the myoinositol is chemically joined in these compounds through glucosidic bonds and phosphate ester links. It is quite possible, therefore, that galactinol and newly isolated glucosyl-myoinositol represents one of the building units present in the phosphoinositides.

Methylation of the galactinol showed that this compound has the same structure as the compound found earlier in sugar beet juice (5, 6). The glucopyranosyl-myoinositol gave glucose and myoinositol on hydrolysis. Its structure was further investigated, particularly with respect to the point of attachment of the glucosidic linkage to the myoinositol. Exhaustive methylation failed to give nonamethylated ether. Hydrolysis of the methylated glucosyl-myoinositol gave three products. The glucose unit was identified as crystalline 2,3,4,6-tetra-*O*-methyl-*N*-phenyl-D-glucosylamine. There was insufficient material to separate the fraction containing pentamethyl and tetramethyl myoinositol. Only myoinositol was present on demethylation of the mixture. Until enough material becomes available to elucidate

[1]Issued as Contribution No. 61 of the Food Research Institute.

Can. J. Chem. Downloaded from www.nrcresearchpress.com by 210.87.254.6 on 09/05/12
For personal use only.

Can. J. Chem. Downloaded from www.nrcresearchpress.com by 210.87.254.6 on 09/05/12
For personal use only.

its structure completely, this naturally occurring glycoside of myoinositol is tentatively assigned the structure β-D-glucopyranosyl-myoinositol.

The third group of compounds contained digalactosyl glycerol and trigalactosyl glycerol. Monogalactosyl and digalactosyl glycerol occur widely in plants and glycolipids. They constitute a major class of lipids in photosynthetic tissues and algae. Monogalactosyl and digalactosyl glycerol, as glycolipids, have recently been reported in potato by Lepage (7, 8). A higher member of this homologous series, trigalactosyl monoglyceride, was reported by Benson *et al.* (9) in the lipids of Chlorella. As far as the author is aware, the free carbohydrate moiety of these glycolipids has not as yet been reported, although Sastry and Kates (10) isolated specific enzymes from runner-bean leaves which catalyze the hydrolysis of monogalactosyldilinolenin and digalactosyldilinolenin to corresponding galactosylglycerols and free linolenic acid. This suggests that the compounds isolated from potato could be the products of enzymic hydrolysis of the glycolipids. A methylation study of the digalactosyl glycerol showed it to have the structure galactopyranosyl 1 → 6 galactopyranosyl 1 → 1 glycerol. Thus, this compound in the potato extract has the same structure as that previously found for a carbohydrate moiety of known glycolipids from wheat flour (11, 12) and from runner-bean leaves (13). On methylation the trigalactosyl glycerol gave a dodecamethylated product which on hydrolysis yielded 2,3,4,6-tetra-*O*-methyl-D-galactose, 2,3,4-tri-*O*-methyl-D-galactose, and 2,3-di-*O*-methyl glycerol, in the proportion of 1:2:1. This indicated that the trigalactosyl glycerol had a straight chain structure containing two 1 → 6 and one 1 → 1 glycosidic linkages, and was a higher member of the homologous series of galactosyl glycerols.

The fourth group of oligosaccharides consisted of three disaccharides: ribosyl-glucose, xylosyl-glucose, and arabinosyl-glucose, and one trisaccharide, maltotriose. The disaccharides were studied by hydrolysis both with and without prior borohydride reduction. The products were then investigated by means of paper electrophoresis.

Experimental

Solutions were concentrated on a rotatory-type evaporator under reduced pressure and below 40 ° unless otherwise stated. Melting points were determined on a Thomas–Kofler micro hot-stage apparatus, and are corrected. Optical rotations were recorded on a Carl Zeiss polarimeter with circular scale reading. Glass plates coated with silica gel G were used for thin-layer chromatography (t.l.c.). The solvent systems used were (*i*) 6% methanol in benzene and (*ii*) 10% methanol in benzene (14). Paper chromatograms were run by the descending method using the following solvent systems (v/v): (*a*) butan-1-ol – pyridine – water (10:3:3); (*b*) ethyl acetate – pyridine – water (2.5:1:2.5); and (*c*) butanone – water azeotrope containing ammonia. Paper electrophoresis was done on Whatman 3MM paper in 0.2 *M* sodium tetraborate buffer (15) at 800 V for 2–3 h. Reducing sugars were detected with aniline hydrogen phthalate (16); keto sugars with naphthoresorcinol (17); and non-reducing sugars by alkaline silver nitrate (18).

Isolation of Carbohydrate Fraction

The potatoes, of the Netted Gem variety, were harvested at Fredericton, New Brunswick, in October, 1966, and stored for two months at 4 °. The potato sample (50 kg) was hand-peeled, diced, and ground up by means of an Urschel dicer and a Fitz-Mill grinder. The slurry was extracted with 95% ethanol (220 l), filtered, and the residue washed with 80% ethanol (2 × 20 l). The alcohol extract was concentrated to a volume of 2 l and filtered through a mat of Celite 545. Methanol (5 l) and chloroform (2.5 l) were added to the filtrate. The solution was shaken for 5 min and left to stand for 2 h. Addition of water (2.5 l) and chloroform (2.5 l) followed by shaking and standing gave a two-phase system. The chloroform phase was discarded and the methanol–water phase was concentrated to a volume of 800 ml and deionized by passage through columns of Rexyn 101 (H^+) and Rexyn AG5 (OH^-) ion exchange resins. The neutral solution was freeze-dried to yield a crude mixture of carbohydrate components as a yellow powder (250 g). This was dissolved in water (2 l) and fractionated on a charcoal/Celite column (8 × 50 cm) by elution with, respectively, water, 2.5% and 40% aqueous ethanol (19).

Paper chromatography of the fraction (200 g) eluted with water (25 l) showed that it contained fructose (40.5%), glucose (45.5%), myoinositol (0.6%), galactose (0.35%), and small amounts of organic and inorganic material. A portion of this fraction was further separated by paper chromatography in solvent *a*.

The fraction (22 g) eluted with 2.5% aqueous ethanol (12 l) showed by paper chromatography mainly sucrose with traces of fructose and glucose. This fraction was purified by crystallization from aqueous ethanol.

The fraction (14 g) eluted with 40% aqueous ethanol gave definite oligosaccharide material with traces of the material eluted earlier. This fraction was separated by a combination of paper chromatography (solvents *a* and *b*) for the sugars and t.l.c. (solvent (*i*)) for their acetylated products.

The products described below are in the order of their elution from the carbon/Celite column.

Identified Components

D-*Fructose*

The syrup showed $[\alpha]_D^{25}$ −90 ° (*c*, 2.2 in water) and yielded crystalline 1,3,4,6-tetra-*O*-benzoyl-D-fructofuranose, with m.p. and mixture melting point 122–123 ° (20).

Can. J. Chem. Downloaded from www.nrcresearchpress.com by 210.87.254.6 on 09/05/12
For personal use only.

D-*Glucose*

The syrup, with $[\alpha]_D^{26}$ +50 ° (*c*, 1.4 in water), was identified as crystalline *N*(*p*-nitrophenyl)-D-glucopyranosylamine, m.p. 184–186 °, undepressed on admixture with an authentic sample (21).

D-*Galactose*

The syrup failed to crystallize and was converted to crystalline β-D-galactopyranose pentaacetate, m.p. 142 ° and $[\alpha]_D^{25}$ +25 ° (*c*, 3.2 in chloroform) (22, 23).

Myoinositol

This compound was chromatographically and electrophoretically indistinguishable from an authentic sample and had m.p. and mixture melting point 225–226 °. On acetylation it gave myoinositol hexaacetate with m.p. 218–219 °(24, 25).

Sucrose

This fraction crystallized when kept in a desiccator; it was recrystallized from aqueous ethanol to yield 19.7 g of pure material; m.p. and mixture melting point 184–185 ° and $[\alpha]_D^{22}$ +66 ° (*c*, 2.6 in water) (26, 27).

Ribosyl-glucose

This was a reducing sugar (6 mg) having $R_{sucrose}$ 0.79 and 0.81 in solvents *a* and *b* respectively. Mild acid hydrolysis with 0.1 *N* sulfuric acid gave approximately equimolar amounts of ribose and glucose. Reduction with borohydride and hydrolysis of the product yielded ribose as the only reducing sugar.

Xylosyl-glucose

This reducing disaccharide (5 mg) had $R_{sucrose}$ 0.82 and 0.84 in solvents *a* and *b* respectively. On hydrolysis it gave xylose and glucose (1:1). Reduction followed by hydrolysis yielded xylose as the reducing sugar.

Arabinosyl-glucose

The syrupy disaccharide (15 mg) had a mobility on paper chromatograms $R_{sucrose}$ 0.56 and 0.60 in solvents *a* and *b* respectively. Location of glucose as the reducing end group was established by hydrolysis both before and after borohydride reduction.

Trisaccharides ***1*** *and* ***2***

These were non-reducing sugars. Compounds **1** (16 mg) and **2** (20 mg) reacted slowly with alkaline silver nitrate spray reagent, while with naphthoresorcinol spray reagent they gave a purple color characteristic for fructose-containing sugars. Mild acid hydrolysis (0.1 *N* sulfuric acid at 100 ° for 5 min) gave glucose and fructose (1:2). Emulsin had no effect on the sugars whereas amyloglucosidase produced complete hydrolysis to glucose and fructose.

The mobilities of the sugars on paper chromatograms were, for compound **1**, $R_{sucrose}$ 0.54 (*a*) and 0.58 (*b*), for compound **2**, $R_{sucrose}$ 0.47 (*a*) and 0.53 (*b*). M_g values by paper electrophoresis were 0.07 for compound **1** and 0.11 for compound **2**. Insufficient material for determination of the linkages precluded further study of these sugars.

Melibiose

This was a reducing sugar (25 mg) which on complete hydrolysis gave glucose and galactose (1:1). The sequence of monosaccharides in the sugar was determined by borohydride reduction, followed by hydrolysis. Paper chromatography of the products showed galactose and sorbitol, thus establishing glucose as the reducing sugar portion of the disaccharide. The mobility of this disaccharide was the same as melibiose in solvents *a* and *b*. It was characterized as β-melibiose octaacetate having $[\alpha]_D^{28}$ +103.6 ° (*c*, 0.9 in chloroform) and m.p. 177–178 ° (28).

Maltotriose

This was a reducing sugar (12 mg) which on partial acid hydrolysis gave glucose, maltose, and the original sugar. Complete hydrolysis was achieved both by acid and amyloglucosidase, giving glucose as the parent sugar. Its mobilities on paper chromatograms and on a paper electrophorogram were the same as maltotriose. On acetylation it gave β-maltotriose hendecaacetate, m.p. and mixture melting point 134–136 ° (29).

Digalactosyl glycerol

This component (420 mg) was obtained as an amorphous powder. On paper chromatograms it had $R_{raffinose}$ values of 1.0 in solvent *a*, and 0.84 in solvent *b*; on paper electrophorogram, M_g value was 0.52. This component gave a positive reaction only with alkaline silver nitrate spray reagent. Partial hydrolysis yielded glycerol, galactose, reducing disaccharide, and unchanged products, whereas complete hydrolysis produced galactose and glycerol.

The amorphous product was crystallized and recrystallized by dissolving in a minimum quantity of water, adding absolute ethanol to turbidity, and allowing to stand at room temperature overnight. The digalactosyl glycerol (α-D-galactopyranosyl-1,6-β-D-galactopyranosyl-1-glycerol) crystallized in fine needles, m.p. 194–195 ° and $[\alpha]_D^{27}$ +87.7 ° (*c*, 1.7 in water). Reported values for m.p. 182–184 ° (12), 195–197 ° (30), and 188–189 ° (13).

Anal. Calcd. for $C_{15}H_{28}O_{13}$: C, 43.27; H, 6.68; Found: C, 43.27; H, 6.78.

A portion (250 mg) of digalactosyl glycerol was methylated in dimethyl formamide (8 ml) with methyl iodide (5 ml) and silver oxide (2 g), according to Kuhn's procedure (31). The syrupy product was then methylated twice by Purdie's reagent (32) giving 165 mg of a yellow oil with $[\alpha]_D^{27}$ +65 ° (*c*, 2.0 in chloroform).

Anal. Calcd. for $C_{24}H_{46}O_{13}$ (mol. wt., 542): OCH_3, 51.4. Found (mol. wt., 560): OCH_3, 51.4.

The methylated product (150 mg) was hydrolyzed with *N* hydrochloric acid (10 ml) for 10 h at 100 °, cooled, neutralized (Ag_2CO_3), filtered, and concentrated to a syrup (145 mg). Chromatographic analysis in solvent *c* showed two methylated sugars which by their mobility were identified as: 2,3,4,6-tetra-*O*-methyl-D-galactose and 2,3,4-tri-*O*-methyl-D-galactose.

The mixture was fractionated on a silica gel column, using solvent (*i*), and yielded three fractions. The first fraction (25 mg) was identified as 1-*p*-nitrobenzoyloxy-2,3-di-*O*-methyl glycerol, m.p. 42–44 °, a value in agreement with that of the *p*-nitrobenzoic acid ester of 2,3-di-*O*-methyl glycerol (33).

The second fraction (60 mg) had the same R_g value as an authentic sample of 2,3,4,6-tetra-*O*-methyl-D-galactose. The sugar was further identified as crystalline 2,3,4,6-tetra-*O*-methyl-*N*-phenyl-D-galactosylamine, m.p. and mixture melting point 193–195 ° (34).

The third fraction (63 mg) had the same mobility by paper chromatography, solvent *c*, as an authentic 2,3,4-tri-*O*-methyl-D-galactose. The sugar was further identified as a crystalline 2,3,4-tri-*O*-methyl-*N*-phenyl-D-galactosylamine and had m.p. 170–172 °, undepressed on admixture with an authentic specimen (m.p. 166–168 °) (35).

Can. J. Chem. Downloaded from www.nrcresearchpress.com by 210.87.254.6 on 09/05/12
For personal use only.

β-D-Glucopyranosyl-myoinositol

The material (50 mg) had $R_{raffinose}$ 1.0 (*a*), and 0.86 (*b*) on paper chromatograms and on paper electrophoresis M_g of 0.52. It did not react with aniline hydrogen phthalate and naphthoresorcinol spray reagents but gave a positive reaction with alkaline silver nitrate. On complete hydrolysis it gave glucose and myoinositol in a ratio of 1:1. It was recrystallized from methanol and had m.p. 264–266 ° and $[\alpha]_D^{27}$ −17.8 ° (*c*, 1.4 in water).

Anal. Calcd. for $C_{12}H_{22}O_{11}$: C, 42.11; H, 6.48. Found: C, 42.14; H, 7.06.

The above compound (45 mg) was acetylated with sodium acetate and acetic anhydride at 110–120 ° for 2 h. The reaction mixture was poured into ice water. The solid acetate was recovered by filtration and recrystallized from ethanol to yield 102 mg of pure material; m.p. 165–167 ° and $[\alpha]_D^{25}$ −39 ° (*c*, 1.2 in chloroform).

Anal. Calcd. for $C_{30}H_{40}O_{20}$ (mol. wt., 720): C, 50.00; H, 5.60; CH_3CO, 53.7. Found (mol. wt., vapor pressure, 710): C, 50.20; H, 5.89; CH_3CO, 53.3.

The deacetylated product (40 mg) was methylated first by Kuhn's procedure then exhaustively by Purdie's reagent to give a syrup (30 mg).

Anal. Calcd. for OCH_3: 59.5. Found: 54.02.

Further methylation with sodium and methyl iodide in ether solution failed to increase the methoxy content (36). The partially methylated product (30 mg) was hydrolyzed under reflux with *N* hydrochloric acid for 4 h, neutralized (Ag_2CO_3), and concentrated under reduced pressure. The syrupy product showed, by paper chromatography in solvent *c*, a mobility corresponding to 2,3,4,6-tetra-*O*-methyl-D-glucose. Examination of the product by t.l.c. in solvent (*ii*) showed that, besides 2,3,4,6-tetra-*O*-methyl-D-glucose, two additional products were present. They were not detectable with aniline hydrogen phthalate spray reagent and could only be detected by spraying the plate with 5% sulfuric acid in ethanol and charring. The hydrolyzed product (30 mg) was refluxed with aniline (20 mg) in ethanol (1 ml) for 2 h. The anilide formed was separated from the tetra- and pentamethyl myoinositols by t.l.c. in solvent (*ii*). 2,3,4,6-Tetra-*O*-methyl-*N*-phenyl-D-glucosylamine after recrystallization from ether – light petroleum (1:1) had m.p. 136–137 °, in agreement with the reported value (37). Efforts to crystallize or separate the methylated myoinositol fraction were unsuccessful due to lack of material and therefore the fraction was demethylated with boron trichloride (38) to give myoinositol having m.p. and mixture melting point 225–227 °.

Raffinose

This non-reducing sugar (800 mg) on partial hydrolysis with 0.1 *N* hydrochloric acid (100 °, 5 min) gave only melibiose and fructose. Complete hydrolysis afforded galactose, glucose, and fructose (1:1:1). The mobility of this trisaccharide in solvents *a* and *b* was the same as for raffinose. The product after recrystallization from aqueous ethanol had m.p. and mixture melting point 134–138 °, and $[\alpha]_D^{25}$ +105 ° (*c*, 2.62 in water) (39).

Planteose

This was a non-reducing sugar (12 mg) ($R_{raffinose}$ 1.0 (*a*) and 0.85 (*b*)) which gave a positive test with naphthoresorcinol spray reagent indicating that it contained sucrose. On partial hydrolysis it gave glucose, disaccharide, and unchanged material, and, on complete hydrolysis it yielded fructose, glucose, and galactose (1:1:1). Hydrolysis by emulsin for two weeks yielded unchanged planteose, sucrose, galactose, and traces of glucose and fructose. On the basis of these observations the sugar was identified as planteose.

Galactinol

This non-reducing component (40 mg) had $R_{raffinose}$ 0.60 and 0.56 in solvents *a* and *b*, respectively. M_g value by paper electrophoresis was 0.34. On acid hydrolysis it gave galactose and myoinositol (1:1). The compound was recrystallized from water–ethanol and had m.p. 218–222 °, and $[\alpha]_D^{27}$ +130.5 ° (*c*, 1.2 in water).

Methylation of this compound (38 mg) by the Kuhn and the Purdie procedure, respectively, gave a nonamethyl ether (30 mg) which was recrystallized from pentane and had m.p. 88–93 °, $[\alpha]_D^{27}$ +115.2 ° (*c*, 0.72 in water). Reported values for m.p. 96.5–98 ° and $[\alpha]_D$ +119 ° (5).

The nonamethyl ether of galactinol (30 mg) was hydrolyzed with *N* hydrochloric acid (4 ml) for 10 h. The reaction mixture was neutralized (Ag_2CO_3), filtered, and concentrated under reduced pressure to a syrup (30 mg). The mixture was separated by t.l.c. using solvent (*ii*) giving equimolar amounts of 2,3,4,6-tetra-*O*-methyl-D-galactose and pentamethyl myoinositol.

The 2,3,4,6-tetra-*O*-methyl-D-galactose was converted into its anilide derivative which after recrystallization from ethanol had m.p. 193–195 °, undepressed on admixture with an authentic specimen. 2,3,4,5,6-Penta-*O*-methyl myoinositol was recrystallized from hot pentane to give fine needles with m.p. 117 °. Reported m.p. 117–117.5 ° (6).

Manninotriose

This reducing component (21 mg) with $R_{raffinose}$ 0.37 (*a*) and 0.39 (*b*) gave on complete hydrolysis galactose and glucose (2:1). On partial hydrolysis it gave galactose, glucose, melibiose, and an additional disaccharide having R_g value less than melibiose. On reduction with borohydride, followed by complete acid hydrolysis, galactose was found as the only reducing sugar, showing that glucose was the reducing end of the trisaccharide. The trisaccharide had the same mobility on paper chromatograms and paper electrophorogram as manninotriose (manninotriose was prepared from stachyose by hydrolysis with 20% acetic acid).

Stachyose

This non-reducing component (480 mg) had $R_{raffinose}$ 0.22 in solvent *a* and 0.41 in solvent *b*. M_g value for paper electrophorogram was 0.33. Hydrolysis by emulsin for 10 days yielded fructose, galactose, sucrose, and raffinose. Complete hydrolysis gave galactose, glucose, and fructose (2:1:1). Amorphous material obtained after separation from paper chromatograms was crystallized from 91% ethanol on seeding and had $[\alpha]_D^{27}$ +132 ° (*c*, 2.3 in water), m.p. and mixture melting point 150 ° (40).

Trigalactosyl Glycerol

This compound (98 mg) was isolated as a glass-like material. It was non-reducing and on paper chromatograms had $R_{raffinose}$ 0.23 and 0.34 in solvents *a* and *b* respectively. On paper electrophorogram its M_g value was 0.48. Acid hydrolysis gave galactose and glycerol. The product, α-D-galactopyranosyl-1,6-α-D-galactopyra-

nosyl-1,6-β-D-galactopyranosyl-1-glycerol, could not be induced to crystallize and had specific rotation of $[\alpha]_D^{25}$ +114 ° (*c*, 2.0 in water).

A portion (80 mg) of trigalactosyl glycerol was methylated initially by Kuhn's procedure and then by Purdie's, as described before for digalactosyl glycerol. The fully methylated product (65 mg) was a syrup and had $[\alpha]_D^{25}$ +79.8 ° (*c*, 1.4 in chloroform).

Anal. Calcd. for $C_{33}H_{62}O_{18}$ (mol. wt., 746): OCH_3, 49.8. Found (mol. wt., vapor pressure, 740): OCH_3, 49.5.

The methylated product (65 mg) was hydrolyzed with *N* hydrochloric acid (5 ml) for 10 h at 100 °, cooled, neutralized (Ag_2CO_3), and concentrated to a syrup (60 mg). Chromatographic analysis in solvent *c* showed two methylated sugars whose mobilities were the same as 2,3,4,6-tetra-*O*-methyl-D-galactose and 2,3,4-tri-*O*-methyl-D-galactose (1:2). The mixture was separated by t.l.c. using solvent (*ii*) into three fractions, (*a*) 2,3-di-*O*-methyl-D-glycerol (8 mg), identified as a 1-*p*-nitrobenzoyl derivative with m.p. 42–44 °; (*b*) 2,3,4,6-tetra-*O*-methyl-D-galactose (17.8 mg), which was converted to 2,3,4,6-tetra-*O*-methyl-*N*-phenyl-D-galactosylamine and had m.p. and mixture melting point 193–195 °; and 2,3,4-tri-*O*-methyl-D-galactose (32 mg), identified as an anilide with m.p. and mixture melting point 170–172 °.

Acknowledgments

The author is indebted to Dr. M. Kates for a sample of digalactosyl glycerol. Analyses were performed by Mr. George Morris, Analytical Chemistry Research Service, Canada Department of Agriculture, and Mr. A. E. Castagne, Division of Biosciences, National Research Council of Canada, Ottawa.

1. K. T. Williams, E. F. Potter, and A. Bevenue. J. Assoc. Offic. Agr. Chemists, **35**, 483 (1952).
2. S. Schwimmer, A. Bevenue, W. J. Weston, and A. L. Potter. J. Agr. Food Chem. **2**, 1284 (1954).
3. A. T. Habib and H. D. Brown. Food Technol. **11**, 85 (1957).
4. D. French. Advan. Carbohydrate Chem. **9**, 149 (1954).
5. R. J. Brown and R. F. Serro. J. Am. Chem. Soc. **75**, 1040 (1953).
6. E. A. Kabat, D. L. MacDonald, C. E. Ballou, and H. O. L. Fischer. J. Am. Chem. Soc. **75**, 4507 (1953).
7. M. Lepage. J. Chromatog. **13**, 99 (1964).
8. M. Lepage. Private communication.
9. A. A. Benson, R. Wiser, R. A. Ferrari, and J. A. Miller. J. Am. Chem. Soc. **80**, 4740 (1958).
10. P. S. Sastry and M. Kates. Biochemistry, **3**, 1280 (1964).
11. H. E. Carter, R. H. McCluer, and E. D. Slifer. J. Am. Chem. Soc. **78**, 3735 (1956).
12. H. E. Carter, R. A. Hendry, and N. Z. Stanacev. J. Lipid Res. **2**, 223 (1961).
13. P. S. Sastry and M. Kates. Biochemistry, **3**, 1271 (1964).
14. M. E. Tate and C. T. Bishop. Can. J. Chem. **40**, 1043 (1962).
15. A. B. Foster. J. Chem. Soc. 982 (1953).
16. S. M. Partridge. Nature, **164**, 443 (1949).
17. J. L. Bryson and T. J. Mitchell. Nature, **167**, 864 (1951).
18. W. E. Trevelyan, D. P. Procter, and J. S. Harrison. Nature, **166**, 444 (1950).
19. R. L. Whistler and D. F. Durso. J. Am. Chem. Soc. **72**, 677 (1950).
20. P. Brigl and R. Schinle. Chem. Ber. **67**, 127 (1934).
21. F. Weygand, W. Perkow, and P. Kuhner. Chem. Ber. **84**, 594 (1951).
22. E. Erwig and W. Koenigs. Chem. Ber. **22**, 2207 (1889).
23. C. S. Hudson and H. O. Parker. J. Am. Chem. Soc. **37**, 1589 (1915).
24. F. A. Hoglan and E. Bartow. Ind. Eng. Chem. **31**, 749 (1939).
25. G. E. McCasland and S. Boutsicaris. J. Am. Chem. Soc. **75**, 3845 (1953).
26. F. J. Bates and R. F. Jackson. Bull. Natl. Bur. Std. **13**, 125 (1916).
27. R. U. Lemieux and G. Huber. J. Am. Chem. Soc. **75**, 4118 (1953).
28. H. G. Fletcher, Jr. and H. W. Diehl. J. Am. Chem. Soc. **74**, 5774 (1952).
29. M. L. Wolfrom, L. W. Georges, A. Thompson, and I. L. Miller. J. Am. Chem. Soc. **71**, 2873 (1949).
30. B. Wickberg. Acta Chem. Scand. **12**, 1183 (1958).
31. R. Kuhn, H. Trischmann, and I. Low. Angew. Chem. **67**, 32 (1955).
32. T. Purdie and J. C. Irvine. J. Chem. Soc. 1021 (1903).
33. A. Fairbourne, G. P. Gibson, and D. W. Stephens. J. Chem. Soc. 445 (1931).
34. D. McCreath and F. Smith. J. Chem. Soc. 387 (1939).
35. F. Smith. J. Chem. Soc. 1724 (1939).
36. K. Freudenberg and R. M. Hixon. Chem. Ber. **56**, 2119 (1923).
37. J. C. Irvine and A. M. Moodie. J. Chem. Soc. 95 (1908).
38. S. Allen, T. G. Bonner, E. J. Bourne, and N. M. Saville. Chem. Ind. London, 630 (1958).
39. H. Assarsson and O. Theander. Acta Chem. Scand. **12**, 1319 (1958).
40. A. K. Mitra and A. S. Perlin. Can. J. Chem. **35**, 1079 (1957).

Can. J. Chem. Downloaded from www.nrcresearchpress.com by 210.87.254.6 on 09/05/12
For personal use only.

Can. J. Chem. Downloaded from www.nrcresearchpress.com by 210.87.254.40 on 09/05/12
For personal use only.

Photochemical synthesis.[1] 19. The flash photolysis of unsaturated sultones

J. L. CHARLTON AND P. DE MAYO
Department of Chemistry, University of Western Ontario, London, Ontario

Received August 22, 1967

The hypothesis that the irradiation of unsaturated sultones gives the final products, the ketosulfonic esters, via a sulfene intermediate has been reexamined. In the case of sultone (**4**), it has been shown that, if such a species be an intermediate, it must have a lifetime, in cyclohexane solution, of less than 20 μs. The consequenes of this observation are discussed.

The flashing of sultone (**4**) in methanol generates the enol of the keto ester end product (**13**) which decays with a half life of about 20 s

Canadian Journal of Chemistry, **46**, 55 (1968)

In a previous paper (1), the possible photochemical generation of sulfenes was discussed. It was considered possible that since unsaturated sultones of type (**1**) contained the homoannular diene system in a six-membered ring, irradiation might induce the ring opening, known to occur in such systems, to give the sulfenes (**2**). In the presence of methanol these intermediates would be expected to react further to give the corresponding esters (**3**) (and/or isomers).

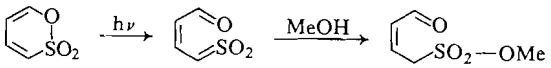

1 **2** **3**

Upon irradiation, the sultones (**4**) (5), (**5**), and (**6**) did indeed give the predicted esters in methanol, whilst in the case of (**4**) irradiation in ether containing two equivalents of benzylamine gave the corresponding sulfonamide, characterized as the 2,4-dinitrophenylhydrazone.

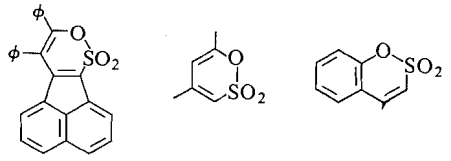

4 **5** **6**

In view of this evidence, the generation of a sulfene intermediate seemed probable. Further evidence in support if this hypothesis was that irradiation of (**4**) in diglyme was found to give up to 23% mole of sulfur dioxide.

The evidence for the existence of the sulfene intermediate was, nonetheless, circumstantial and in the intervening years it became clear that other processes were, in principle, possible. With the availability of apparatus for flash photolysis a reexamination of the system was considered desirable.

Sultone (**4**) was chosen for examination because its absorption fell at a convenient wavelength. Prior to the investigation however, it was necessary to clarify the isomerism (positional and geometrical) possible in the photochemical end products; a matter not clearly resolved previously (1).

Solutions of sultone (**4**) in methanolic base gave a deep blue solution containing, presumably, the anion (**7**). Simple acidification and isolation of the product gave a mixture of three esters (**8**) which could be separated by thin-layer chromatography. These were the two isomers with the double bond exocyclic to the five-membered ring (**8***a* and **8***b*), and the endo isomer (**8***c*). Dissolution of the three esters, separately, in base followed by re-isolation, gave the same mixture of all three components,

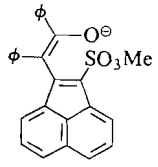

7

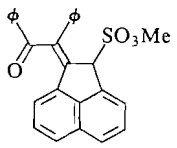

8*a*

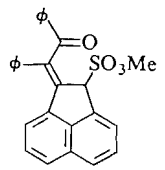

8*b*

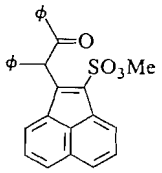

8*c*

[1]For the preceding paper in this series, see P. de Mayo and J. S. Wasson, Chem. Commun. 970, (1967).

Can. J. Chem. Downloaded from www.nrcresearchpress.com by 210.87.254.40 on 09/05/12
For personal use only.

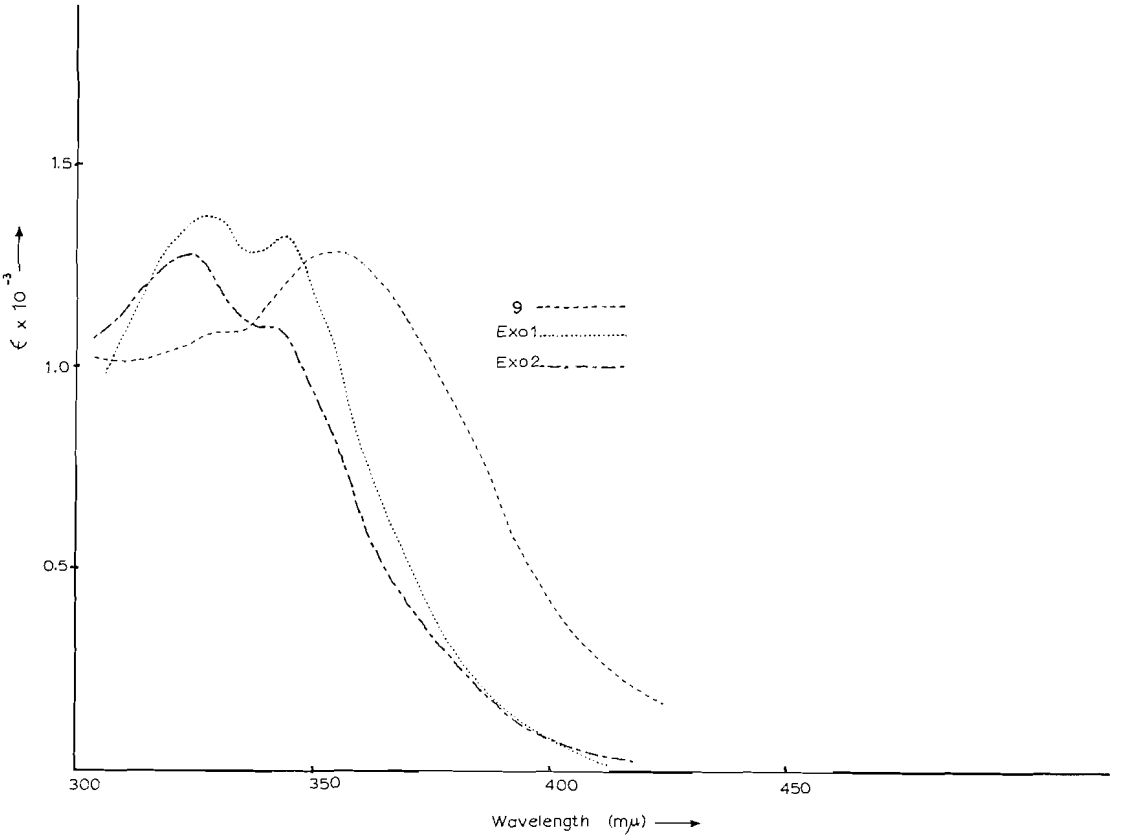

FIG. 1. The ultraviolet spectra of **9** and exo-ester 1 and exo-ester 2.

lending support to the conclusion, based on analytical data, that they are indeed isomers.

The formation of the esters, directly from the sultone by the action of methoxide ion must result from direct substitution on the sulfur. This is in direct contrast with saturated sulfonic esters where substitution on the carbon bearing oxygen would be expected to occur.

The two isomers (**8***a* and **8***b*) were recognized by the general resemblance of their ultraviolet spectra to that of (**9**), the latter being obtained by the dehydration of (**10**) (5) with phosphorus oxychloride and pyridine. Both had carbonyl absorption at 1660 cm^{-1}, to be compared with 1657 for (**9**). The stereochemistry about the double bond is not known in (**9**) but it is believed to be a single isomer as the nuclear magnetic resonance (n.m.r.) exhibits a singlet for the non-aromatic hydrogens. The stereochemistry of (**8***a* and **8***b*) could not be assigned unambiguously from spectral data.

The endo isomer (**8***c*) was recognized by its higher carbonyl absorption (1685 cm^{-1}) and the

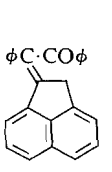

9

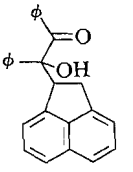

10

difference in ultraviolet spectrum. The latter resembled the spectrum of (**11**), a substance previously obtained from the ester mixture (**8**) by alkaline hydrolysis (1). The position of the double bond in (**11**) had been shown by ozonolysis to the diketone followed by cyclization to the perinaphthenone (**12**).

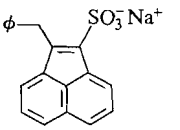

11

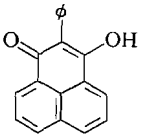

12

Chemical evidence as to the structure of (**8***c*) was also obtained. Ozonolysis in ethanolic

Can. J. Chem. Downloaded from www.nrcresearchpress.com by 210.87.254.40 on 09/05/12
For personal use only.

solution followed by treatment with base, gave, after isolation and sublimation, naphthalic anhydride. The generation of this substance may be formulated as follows.

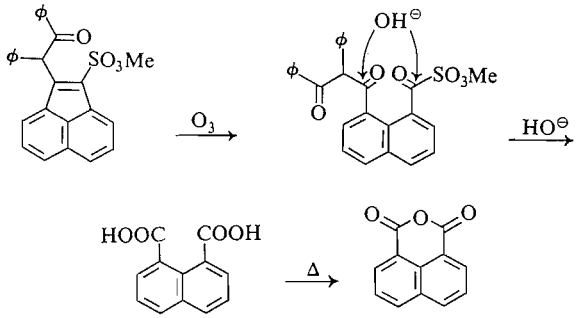

With the nature of the methanolysis products of the sultone clarified, those obtained by irradiation were now examined. This process was now facilitated by the use of thin-layer chromatography, a process not employed in the original study.

By running successive chromatograms of irradiated methanolic solutions it was found that addition proceeded rapidly to give, first, exo-ester 1 followed by the appearance of exo-ester 2 (see Experimental regarding nomenclature). The endo ester (**8***c*) could not be detected. Irradiation of either (**8***a*) or (**8***b*) generated the other exo ester, but, again, no endo ester was observed. Prolonged irradiation led to the formation of a further, non-isomeric substance (which will be the subject of another communication), and the further accumulation of other unidentified compounds.

The background chemistry now having been resolved it was possible to attempt the flash study. It was found that exposure of solutions of the sultone (**4**) to flashes of up to 10^3 J produced no transient with absorption at longer wavelength than that of the sultone itself. However, it was by no means clear that a sulfene or other intermediate would necessarily absorb at such a wavelength.

The only method of detection available then was by complete annihilation of the starting sultone. Flashing a 5×10^{-7} *M* solution of the sultone in methanol with increasing power showed that the (rapid) disappearance of the absorption at 4500 Å reached a maximum at 1100 J, increased power thereafter having on further effect.

On flashing at 1100 J the decrease in absorption at 4500 Å reached, as stated, a maximum and was not further reduced with increased power. Nevertheless, some absorption still remained at this wavelength. Since the exo esters have no absorption in this region, the absorption was evidently that of an intermediate. Indeed, the residual absorption at 4500 Å decayed to near zero within a minute of flashing. Similarly a band produced at 3370 Å on flashing, also slowly decreased in intensity at the same rate. An approximate rate constant for the disappearance of this transient was obtained by monitoring the change at 4500 Å, and was found to be 3 min^{-1}. The spectrum of the transient was obtained both by spectrographic and photoelectric recording (see Experimental).

The lifetime and nature of the transient appeared, hopefully, to be compatible with naive expectation for a sulfene intermediate. It was soon apparent, however, that such optimism was unjustified since the formation of the sulfene, if not its decay, should be essentially independent of the solvent. In an inert solvent, therefore, the formation of the same transient was to be expected, followed by reversion to the original absorption. In cyclohexane, however, no transient could be detected down to 20 μs after the initiating flash. From this is was concluded (*a*) that the transient in methanol was not the sulfene, and (*b*) that if a sulfene were an intermediate, its lifetime was exceedingly short.

The question then arose as to the nature of the observed intermediate. The fact that it decayed under mild conditions to the exo ester limited the number of possibilities. Further, the absorption at long wavelength was significant, requiring a more extended chromophore than found in the exo or endo esters. The starting sultone (**4**) was the only other compound in this series having significant absorption at this wavelength. A plausible intermediate fitting all the available data was the enol (**13**). The slowness of the tautomerism in a neutral medium is not surprising, and has recent analogy in the formation of (**15**) from (**14**) (4).

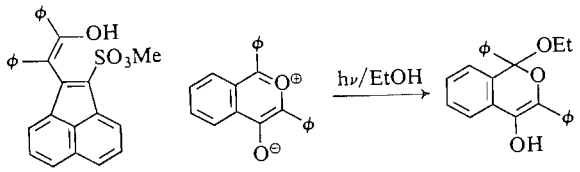

13 **14** **15**

Can. J. Chem. Downloaded from www.nrcresearchpress.com by 210.87.254.40 on 09/05/12
For personal use only.

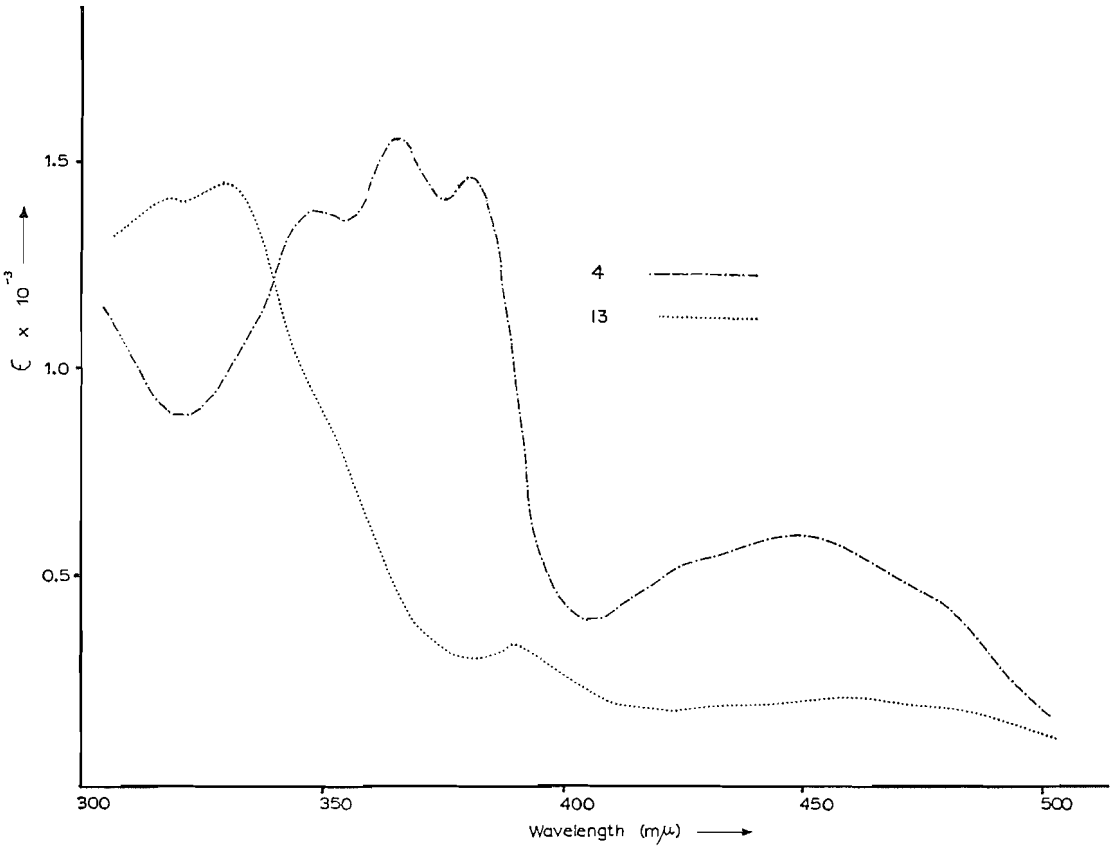

FIG. 2. The ultraviolet spectra of sultone **4** and enol **13.**

If this structure be accepted, then a possible pathway could involve addition of methanol to the activated sultone in two steps; the addition of methoxyl being separated, though briefly, from protonation. (The addition to a sulfene is merely a particular instance of the general pathway.) If the addition of the two moieties were separated in time, an intermediate carbanion became a possibility, and this species could be the same as that observed on dissolution of the esters in alkali. Since this has high intensity absorption at 625 mμ ($\epsilon \approx 10^4$ in 3.3 *N* methanolic potassium hydroxide) it should be readily detectable. Experimentally, however, no such transient could be observed.

It must be concluded, therefore, that the methanolysis of (**4**) occurs by either direct addition of methanol to the excited sultone, or that any ground state intermediate formed from the sultone, if there be one, is separated energetically from that sultone by an activation barrier of less than about 10 kcal/mole.

Exposure of sultones (**5**) and (**6**) in concentrations of 6×10^{-5} and 6×10^{-4} *M* to comparable flashes revealed no transient of wavelength longer than 320 mμ and lifetime longer than about 20 μs.

The sultam (**16**) has been found to give the pyrol on irradiation and the solvent does not participate. Again a mechanism passing through a sulfene is conceivable but not obligatory. In this case, however, the sultene should have a greatly extended chromophore, and if formed should be readily detected. Again, no transient with a longer wavelength than 3200 Å could be observed. It must be concluded that the participation of a sulfene in these reactions is improbable.

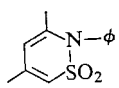

16

Can. J. Chem. Downloaded from www.nrcresearchpress.com by 210.87.254.40 on 09/05/12
For personal use only.

Experimental

Flash Apparatus

The technique and general arrangement has been described by Porter (2) and was modified slightly in the present study.

Stainless steel O-ring fittings with tungsten inserts were used for electrodes in the flash lamps. A vacuum connection at the fitting allowed evacuation and filling of the lamps with Argon (10–100 mm). Both of the capacitor banks, spectroflash (10μF/10kV, General Electric) and photoflash (two, 5μF/20kV, General Electric) were charged by Sorenson high voltage power supplies (230-6P, 30kV/8 mA). Quartz cells of 20 cm path length were used with a reservoir to permit degassing. A tungsten quartz lamp (Phillips 7023F5) was used as the source in the photoelectric arrangement.

The transmitted beam was passed into a Spex 1700-II monochromator. With a swing-away mirror it could be used as a spectrograph or a recording spectrometer. In the spectrographic mode, the spectrum was recorded on Polaroid film (P/N55) and plate densities were recorded with a Kipps and Zonen densitometer (BDII). A Hilger and Watts 7-step neutral density filter was used for calibration. In the photoelectric mode the signal was monitored with an EMI 6256 B photomultiplier connected directly to a RM 503 Tetronix oscilloscope. Permanent records of the oscilloscope traces were made with a Polaroid Tetronix C-27 camera. The delay circuit used was similar to that of Goodfriend and Woods (3) and had a range of 2 to 250 μs.

The sultone (8.6×10^{-7} *M*) was flashed with complete annihilation of the starting material. Flashing a fresh solution and monitoring the transmittance before and 0.5 s after the flash at intervals of 50A yielded a spectrum of the intermediate. It was plotted with reference to a standard spectrum of the sultone by the equation

$$A_1 - \log \frac{I_2}{I_1} = A_2$$

where A_1 is the absorbance of the sultone, A_2 is that of the intermediate, I_2 the transmittance of the sultone before the flash, and I_1 is the transmittance of the intermediate 0.5 s after the flash. Using the spectrograph and densitometer similar results were obtained.

*Dehydration of Ketol (**10**)*

The ketol (350 mg) was dissolved in pyridine (50 ml) containing phosphorus oxychloride (10 ml) at 0 °C and the mixture then heated under reflux for 6 h. After pouring onto ice the product was isolated with ether, the solvent washed, and after evaporation the residue was crystallized from chloroform. About 50% of the starting material was recovered. Crystallization of the mother liquors from methanol–chloroform, and then benzene – light petroleum gave the conjugated ketone (**9**) (100 mg) m.p. 153–156°; λ_{max} (MeOH) 342 (ϵ 13 200), 327 (ϵ 13 700), 249 (ϵ 30 400), 236 (ϵ 29 400) mμ; ν_{max} 1 657 cm^{-1}.

Anal. Calcd. for $C_{26}H_{18}O$: C, 89.82; H, 5.25. Found: C, 90.14; H, 5.24.

*Acetylation of Ketol (**10**)*

The Ketol (350 mg) was stirred in suspension in acetyl chloride (15 ml) and zinc chloride (50 mg) for 4 h, until all the starting material was dissolved. The mixture was then poured onto ice and the product isolated with ether. The extract was washed with sodium hydrogen carbonate solution, water, and dried over $MgSO_4$. The residue was chromatographed on silicic acid (100 g).

Elution with benzene gave the chloride (**17**; R = Cl) (100 mg) which, (crystallized from benzene – light petroleum) had m.p. 142 – 145°; ν_{max} 1678 cm^{-1}; λ_{max} (MeOH) 288 (ϵ 9200), 276 (ϵ 9700), 255 (ϵ 13 400), 226 (ϵ 71 500) mμ; nuclear magnetic resonance (n.m.r.) δ 7.4 (m), 5.2 (t, 1H), 3.2 (s, 1H), 3.1 (qu, 1H).

Anal. Calcd. for $C_{26}H_{19}OCl$: C, 81.56; H, 5.00; Cl, 9.27. Found: C, 81.64; H, 5.10; Cl, 9.39.

Further elution with benzene then gave the acetate (**17**; R = OAc) (50 mg) which, (crystallized from benzene – light petroleum) had m.p. 186–189°; ν_{max} 1740, 1680 cm^{-1}; λ_{max} (MeOH) 280 (ϵ 8900), 290 (ϵ 9300) mμ; n.m.r.: δ 7.7 (m), 5.2 (qu, 1H), 3.7 (m, 2H), 1.7 (s, 1H).

Anal. Calcd. for $C_{28}H_{22}O_3$: C, 82.73; H, 5.45. Found: C, 82.65; H, 5.40.

Hydrolysis of the acetate (0.0125 *N* NaOH in 1:1 aqueous ethanol) at room temperature regenerated the starting ketol. Pyrolysis of the acetate in the gas phase (.005 mm) by sublimation through a quartz tube at 400° gave a mixture. Separation by thin-layer chromatography (eluant: benzene) gave, as the main component, benzil, identified by comparison with an authentic specimen.

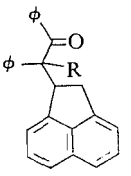

17

*Methanolysis of Sultone (**4**)*

The sultone (220 mg) was dissolved in ca. 3 ml dioxane and this solution added to a methanolic solution of potassium hydroxide (100 ml; 2.5 *N*). The solution immediately became dark blue. After 1 min the solution was acidified with slightly more than one equivalent of hydrochloric acid in water (250 ml). The yellow solution was extracted with chloroform, the solvent removed and the residue separated by preparative thin-layer chromatography. [Eluant: ethyl acetate – light petroleum (1:4)]. In order of increasing R_f, the following were obtained.

(a) Exo-ester 2

Exo-ester 2 was crystallized from chloroform in white needles, with m.p. 202–204° (decomp.); ν_{max} 1660, 1360, 1170, 995 cm^{-1}; λ_{max} (MeOH) 338 (ϵ 10 900), 328 (ϵ 11 800), 320 (ϵ 12 700), 254 (ϵ 24 000), 233 (ϵ 43 400) mμ; n.m.r.: δ 3.3 (s), 6.2 (s), 7.4 (m), 8.2 (m).

Anal. Calcd. for $C_{27}H_{20}O_4S$: C, 73.62; H, 4.58; S, 7.28. Found: C, 73.21; H, 4.50; S, 7.41.

(b) Exo-ester 1

Exo-ester 1 was crystallized from chloroform – ethyl acetate in yellow needles that had m.p. 179–180.5° (decomp.); ν_{max} 1660, 1360, 1170, 995 cm^{-1}, λ_{max} (MeOH), 353 (ϵ 12 800), 328 (ϵ 10 900), 256 (ϵ 24 300), 231 (ϵ 49 300) mμ; n.m.r.: δ 3.5 (s), 6.5 (s), 7.5 (m).

Anal. Calcd. for $C_{27}H_{20}O_4S$: C, 73.62; H, 4.58; S, 7.28. Found: C, 73.60; H, 4.65; S, 7.06.

Treatment of the separated esters (1 mg, in 1 ml dioxane) with base (5 ml 1*N* KOH in MeOH) and isolation gave in each case a mixture of the three esters as indicated by thin-layer chromatography (eluant: ethyl acetate – light petroleum, 1:4). All three esters gave the same absorption spectrum in base (0.67 *N* in KOH/MeOH), λ_{max} 346 (ϵ 10 200, broad), 625 (ϵ 2200) mμ.

Ozonolysis of Endo-ester (8c)

The ester (27.1 mg) was treated with a stream of ozone at −20° in ethanolic solution (10 ml) for 70 min. Base (2% sodium hydroxide; 12 ml) was added and the mixture heated to 65° for 30 min. The acidic material was isolated in the usual way and crystallized from methanol (10 mg) m.p. 264–268°. Sublimation gave needles, m.p. 272–274°. A mixture melting point with naphthalic anhydride in an evacuated capillary showed no depression.

Irradiation of Sultone (4) and Exo-esters 1 and 2

Irradiation of a solution of the Sultone (**4**) (1 mg in 25 cm^3 MeOH) proceeded rapidly and gave first exo-ester 1, followed, more slowly, by exo-ester 2. No endo ester was detectable on thin-layer chromatograms. Irradiation of either exo-ester generated, under the same conditions, a mixture of exo-esters. Again, no endo isomer was produced.

Prolonged irradiation led to the formation of a new substance. This material, m.p. 180–183° (from benzene) was not isomeric with the other substances. Its structure will be the subject of a later communication.

1. J. F. KING, P. DE MAYO, E. MORKVED, A. B. M. A. SATTAR, and A. STOESSEL, Can. J. Chem. **41**, 100 (1963).
2. G. PORTER. *In* Technique of organic chemistry. Vol. VIII. Part II. *Edited by* S. L. Friess, E. S. Lewis, and A. Weissberger. Interscience Publishers, Inc., New York. 1963. p. 1056.
3. P. L. GOODFRIEND and H. P. WOODS. Rev. Sci. Instr. **36**, (1) 10 (1965).
4. E. F. ULLMAN and W. A. HENDERSON. J. Am. Chem. Soc. **88**, 4942 (1960).
5. P. DE MAYO and A. STOESSEL. Can. J. Chem. **40**, 57 (1962).

Can. J. Chem. Downloaded from www.nrcresearchpress.com by 210.87.254.40 on 09/05/12
For personal use only.

Can. J. Chem. Downloaded from www.nrcresearchpress.com by 210.87.254.40 on 09/05/12
For personal use only.

Preparation of unsaturated carbohydrates. A facile synthesis of methyl 4,6-*O*-Benzylidene-D-hex-2-enopyranosides

R. U. LEMIEUX, E. FRAGA, AND K. A. WATANABE[1]
Department of Chemistry, University of Alberta, Edmonton, Alberta

Received August 21, 1967

A simple method was explored for the preparation of methyl 4,6-*O*-benzylidene-hex-2-enopyranosides. Methyl 2,3-anhydro-4,6-*O*-benzylidene-D-hexopyranosides were converted to diaxial iodohydrins using sodium iodide in acetone which contained sodium acetate and acetic acid. Treatment of the iodohydrins with either methane- or *p*-toluenesulfonyl chloride in refluxing pyridine yielded the 2,3-unsaturated derivative in excellent yield. The four isomers for methyl 4,6-*O*-benzylidene-D-hex-2-enopyranoside were thus prepared. The rotations of the anomeric pairs followed Hudson's rules of isorotation. Evidence is provided that, in the absence of strong destabilizing interactions in the product, the epoxide ring of one of the above-mentioned 2,3-anhydroglycosides is opened by lithium iodide in ether to form the iodohydrin as the lithium alkoxide in high yield. This observation provides an explanation for the reduction of methyl 2,3-anhydro-4,6-*O*-benzylidene-α-D-allopyranoside to 4,6-*O*-benzylidene-D-allal. Reaction of methyl 4,6-*O*-benzylidene-2-deoxy-2-iodo-α-D-idopyranoside with methyl lithium provided 4,6-*O*-benzylidene-D-gulal. The conformational properties of a number of the compounds prepared and of acetylated methyl pentopyranosides, as derived from their nuclear magnetic resonance parameters, are discussed with particular reference to the role that geminal coupling constants may play in the determination of configuration and conformational equilibria.

Canadian Journal of Chemistry, 46, 61 (1968)

It has been suggested that 2,3-unsaturated sugars play significant biological roles in metabolic pathways. For example, ribonucleosides may be converted into deoxyribonucleosides through the 2′,3′-unsaturated intermediate (1, 2). The antibiotic cordycepin (3, 4) is formed from adenosine (5) probably via 2′,3′-dehydrodeoxyadenosine (6). Unsaturated compounds of this type occur naturally, for example, ascorbic acid (7–9) and a nucleoside antibiotic blasticidin S (6, 10).

Two methods have been used to prepare derivatives of 2,3-unsaturated sugars. One is the acid-catalyzed double bond shift in derivatives of glycals. Thus, already in 1914, Fischer (11) prepared 4,6-di-*O*-acetyl-D-*erythro*-hex-2-enopyranose and the compound has since served as a precursor to the α-ethyl (12, 13), α-phenyl (14), α- and β-*p*-nitrophenyl (15, 16) glycosides and to the 4,6-di-*O*-acetyl and 4,6-di-*O*-benzoyl derivatives of D-*erythro*-hex-2-enopyranosyl fluoride (17). The 2-acetoxy derivative of both the anomers of 1,4,6-tri-*O*-acetyl-D-*erythro*-hex-2-enopyranose was obtained by acid isomerization of 2-acetoxy-3,4,6-tri-*O*-acetyl-D-glucal (18, 20). The α-*threo* isomer was also prepared from the corresponding galactal derivative (19). Also, a derivative of an unsaturated nucleoside was prepared by the acid-catalyzed reaction between tri-*O*-acetyl-D-glucal and theophylline (21).

The second method involves direct introduction of a 2,3-olefinic double bond. Thus, methyl 4,6-*O*-benzylidene-α-D-*erythro*-hex-2-enopyranoside was first prepared by Bolliger and Prins (22) from methyl 4,6-*O*-benzylidene-3-deoxy-2-*O*-*p*-toluenesulfonyl-α-D-mannopyranoside. This compound has since been prepared in a variety of other ways including epoxide (23), iodohydrin (24), episulfide (25, 26), thionocarbonate (26), sulfonate (26, 27), xanthate (16), thiouronium (28), and aziridine (29) intermediates. Unsaturated nucleosides have also been synthesized (30–36).

On repeating the preparation of 4,6-*O*-benzylidene-D-allal (4,6-*O*-benzylidene-1,2-dideoxy-D-*ribo*-hex-1-enopyranose) (**3***b*) reported by Feast, Overend, and Williams (37), which involves reaction of methyl 2,3-anhydro-4,6-*O*-benzylidene-α-D-allopyranoside (**1**) with methyl lithium in ether (prepared from methyl iodide and lithium), methyl 4,6-*O*-benzylidene-2-deoxy-2-iodo-α-D-altropyranoside (**2***b*) (38) was isolated as the product of the reaction and utilization of this compound as starting material gave the product (**3***b*) in higher yield. Evidently, lithium iodide, in contrast to sodium iodide (39), is capable of reacting with an epoxide under basic conditions to yield the lithium alkoxide (e.g., **2***a*)

[1]University of Alberta Postdoctorate Fellow, 1966–1968.

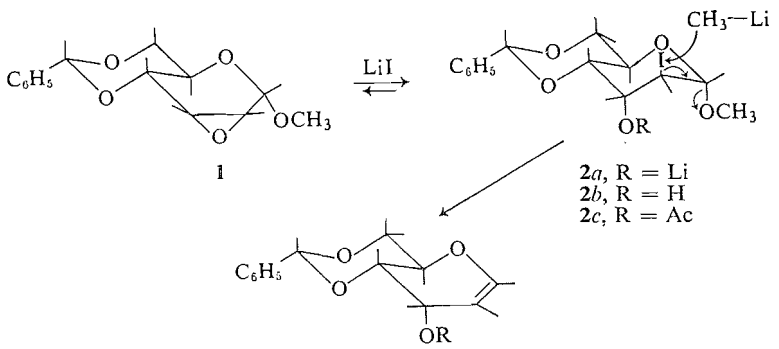

of the iodohydrin. With sodium iodide, acid is required to neutralize the product. The formation of the allal derivative (**3***a*) could now be appreciated as involving nucleophilic attack on the iodine atom of **2***a* leading to elimination of the methoxy group.[2] On applying the reaction to methyl 4,6-*O*-benzylidene-2-deoxy-2-iodo-α-D-idopyranoside (**7**), as expected from the above considerations, 4,6-*O*-benzylidene-D-gulal (4,6-*O*-benzylidene-1,2-dideoxy-D-*xylo*-hex-1-enopyranose) was formed. Nuclear magnetic resonance (n.m.r.) parameters for this compound and its 3-*O*-acetyl derivative and the corresponding derivatives of D-allal are given in Table I. The general characteristics of the n.m.r. parameters for the gulal derivative as compared to those of the allal compound leave no doubt that the former compound is also a 4,6-*O*-benzylideneglycal. The magnitude of $J_{2,3}$ requires the equatorial orientation for H-3. The values for $J_{5,6e}$ and $J_{5,6a}$ require that H-5 be in axial orientation to be in gauche relationship with both the neighboring H-6's. Since H-5 is axial and weakly coupled ($J_{4,5}$ = 1.5 c.p.s. for the monoacetate) with H-4, H-4 must be equatorially oriented as required for the assigned D-*xylo* configuration. The assignments and n.m.r. parameters in Table I are based on unequivocal evidence derived from appropriate spin decoupling experiments. In the case of the 4,6-*O*-benzylidene-D-gulal, the signals for H-3 and H-4 were almost exactly superimposed. For this reason, the signal for H-2 appeared as a rough septet of lines and the coupling constant reported in Table I for $J_{2,3}$ was derived from the spacing of the outer strong lines in the quartet obtained when H-1 was spin decoupled.

The iodohydrin **2***b* was obtained in quantitative yield from **1** using five molar equivalents of lithium iodide in ether at room temperature for 30 min. That the reaction leads to the alkoxide (**2***a*) was apparent from the fact that the addition of acetic anhydride to the reaction mixture gave an immediate formation of the 3-*O*-acetate (**2***c*)—a transformation which did not occur at a comparable rate when acetic anhydride was added to the iodohydrin dissolved in the solution of lithium iodide in ether. A compound identical to the iodohydrin **2***b* was obtained by iodomethoxylation (41) of the allal derivative **3***b*.

On the other hand, the isomeric methyl 2,3-anhydro-4,6-*O*-benzylidene-α-D-mannopyranoside (**4**) reacted very slowly with lithium iodide leading after 9 days to an equilibrium mixture which appeared (n.m.r.) to contain an about 3:2 ratio of **4** and the adduct (**5***a*), respectively. The non-bonded interaction in the product between the axial iodine atom and the axial methoxy group allows the rationalization of the results and appears to be present in the transition state. Since the formation of the iodohydrin (**5***b*) became quantitative when acetic acid was added to the reaction mixture, there can be little doubt that in fact the lithium alkoxide (**5***a*) of the iodohydrin was the product of the reaction in absence of acid—a matter of considerable theoretical interest and of possible synthetic value.

In order to prepare iodohydrins from epoxides, the conditions prescribed by Cornforth (39), which employ sodium iodide, sodium acetate, and acetic acid in acetone, are most convenient.

[2]Sharma and Brown (40) have commented on the reaction of lithium iodide with **1** and the conversion of **2***a* to **3***a*, reactions which were discovered as reported in this publication.

Can. J. Chem. Downloaded from www.nrcresearchpress.com by 210.87.254.40 on 09/05/12
For personal use only.

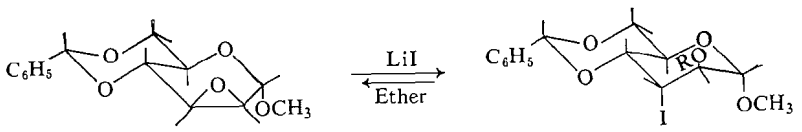

4

5*a*, R = Li
5*b*, R = H

TABLE I

Nuclear magnetic resonance parameters for 4,6-*O*-benzylidene-1,2-dideoxy-hex-1-enopyranoses and their 3-*O*-acetyl derivatives

	Chemical shifts (τ)							
Compound	H-1	H-2	H-3	H-4	H-5	H-6*e*	H-6*a*	Ref.
D-*ribo*	3.62	5.05	5.81	6.23	5.83	5.57	6.20	40
D-*ribo*-3-*O*-acetate	3.54	5.01	4.57	6.05	5.80	5.53	6.18	40
D-*xylo*	3.45	5.12	6.08	6.08	6.29	5.66	6.03	
D-*xylo*-3-*O*-acetate	3.37	4.99	5.07	5.95	6.24	5.65	6.01	

	Coupling constants (c.p.s.)							
Compound	$J_{1,2}$	$J_{2,3}$	$J_{3,4}$	$J_{4,5}$	$J_{5,6e}$	$J_{5,6a}$	$J_{6a,6e}$	Ref.
D-*ribo*	6.0	6.0	3.5	9.5	4.5	9.5	−10.0	40
D-*ribo*-3-*O*-acetate	6.0	5.7	3.5	9.5	4.4	9.5	−9.6	40
D-*xylo*	6.4	6.8	—	—	1.8	1.5	−12.5	
D-*xylo*-3-*O*-acetate	5.8	5.6	2.0	1.5	1.8	1.5	−12.5	

The known iodohydrins **2***b* and **5***b* (23, 38) were obtained from the epoxides **1** and **4**, respectively, in quantitative yield. Nuclear magnetic resonance parameters for these compounds are reported in Table II.

In order to test more extensively the synthetic methods developed in this research and also to achieve the synthesis of all the methyl 4,6-*O*-benzylidene-D-hex-2-enopyranosides, the methyl 2,3-anhydro-4,6-*O*-benzylidene-glycopyranosides with the β-D-*allo* (42), α-D-*gulo* (43, 44), and β-D-*talo* (45, 46) configurations were prepared following the published procedures. These epoxides all underwent ready conversion to iodohydrins using Cornforth's reagent. Except for the compound with the β-D-*allo* configuration, as for compounds **2***b* and **5***b*, the diaxial products (**6**, **7**, and **8**) were formed in near quantitative yield as expected on the basis of the Fürst–Plattner rule (47). In the case of the β-D-*allo* compound about 20% of 2,3-di-equatorial product was formed. The structures of the iodohydrins were established as follows.

Reaction of the 2,3-anhydro-β-D-*allo* compound with sodium iodide gave a mixture of iodohydrins. The β-D-*gluco* configuration was required for the higher melting (m.p. 230°) isomer (**9**) in view of the coupling interactions observed in the n.m.r. spectrum of its *O*-acetyl derivative. The quartet signal at τ 4.62 with spacings of 10.8 and 7.5 c.p.s. was assigned to the 2-proton since it is coupled with the doublet signal for the anomeric proton at τ 6.28 with the spacing of 7.5 c.p.s. (deuterated benzene as solvent). Thus, both H-2 and H-3 must be in axial orientation. The isomer (**6**) (m.p. 175–176°) was assigned the β-D-*altro* configuration on a similar basis. The *O*-acetyl derivative (benzene-d_6 as solvent) gave signals at τ 4.25 (triplet), 5.52 (quartet), 5.87 (quartet), and 6.41 (doublet) assigned to the protons at positions 3, 4, 2, and 1, respectively, on the basis of unequivocal spin decoupling experiments. First order analysis indicated coupling constants, $J_{1,2} = 2.0$, $J_{2,3} = 3.1$, $J_{3,4} = 3.0$, and $J_{4,5} = 9.2$ c.p.s., which are compatible with the structure and conformation indicated in **6** (48, 49). The occurrence of appreciable (about 20%) oxide ring-opening to di-equatorial product (**9**) in this reaction is readily understood since the methoxy group must be expected to destabilize the transition state leading to the diaxial product by non-bonded interaction with the entering iodide ion. The reactions of the other epoxides all proceeded to diaxial product

Can. J. Chem. Downloaded from www.nrcresearchpress.com by 210.87.254.40 on 09/05/12
For personal use only.

Can. J. Chem. Downloaded from www.nrcresearchpress.com by 210.87.254.40 on 09/05/12
For personal use only.

TABLE II

Nuclear magnetic resonance parameters for methyl 4,6-*O*-benzylidene-2(or 3)-deoxy-2(or 3)-iodo-D-glycopyranosides in benzene-d_6 and Methyl 4,6-*O*-Benzylidene-D-hex-2-enopyranosides* in Pyridine-d_5

	Chemical shifts (τ)					Coupling constants (c.p.s.)			
Iodohydrins	H-1	H-2	H-3	H-4	H-5	$J_{1,2}$	$J_{2,3}$	$J_{3,4}$	$J_{4,5}$
2-*O*-acetyl-*β-gluco*	6.05	4.61	6.22	6.04		7.5	10.8	10.2	
2-*O*-acetyl-*α-altro*	5.48	4.58	5.68	5.85	6.39	1.1	2.2	3.5	
3-*O*-acetyl-*α-altro*	5.18	5.57	4.49	5.57	5.70	0.5	2.0	2.5	
3-*O*-acetyl-*β-altro*	6.41	5.87	4.24	5.52	6.17	2.0	3.1	3.0	9.0
2-*O*-acetyl-*β-ido*	4.92	4.76	5.52	6.28	5.93	1.1	2.1	2.5	
3-*O*-acetyl-*α-ido*	4.93	5.93	4.60	6.36	6.56	2.9	4.6	2.7	3.0

	Chemical shifts (τ)					Coupling constants (c.p.s.)				
Alkenes	H-1	H-2	H-3	H-4	H-5	$J_{1,2}$	$J_{1,3}$	$J_{1,4}$	$J_{2,4}$	$J_{6a,6e}$
α-erythro (**12**)	5.05	4.23	3.80	5.70	5.70	2.2	<0.3	1.5	−2.2	−9.9
β-erythro (**13**)	4.66	4.30	3.81	5.66	5.90	1.3	−1.2	2.6	−2.5	−9.7
α-threo† (**14**)	4.91	3.88	3.86	5.85	6.16	2.0	<0.3	<0.3	<0.3	−12.5
β-threo‡ (**15**)	4.82	3.88	3.86	5.80	6.57	0.75	−0.8	1.7	~0	−12.5

*$J_{2,3}$ = 10 c.p.s.
†$J_{3,4}$ = 5.0, $J_{4,5}$ = 2.0, $J_{1,6a}$ = ±0.6 c.p.s.
‡$J_{3,4}$ = 4.2, $J_{4,5}$ = 1.7 c.p.s.

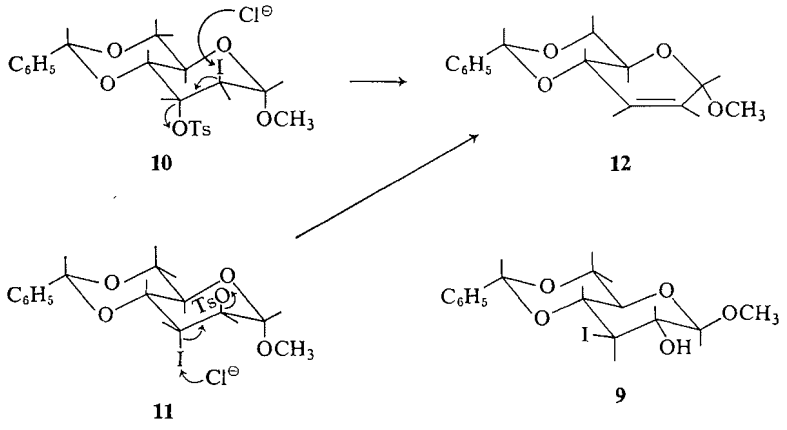

in high yield since the n.m.r. spectra of the crude products were virtually identical with those of the purified compounds. These results are in general agreement with considerations based on conformational analysis.

The α-D-*altro* iodohydrins **2***b* and **5***b* provided the mono-*O*-*p*-toluenesulfonyl derivatives **10** and **11** when the reaction was carried out near 0° for 44 h. At room temperature, the iodo-*p*-toluenesulfonates were reduced to methyl 4,6-*O*-benzylidene-α-D-*erythro*-hex-2-enopyranoside (**12**) at an appreciable rate. After 3 days, the yield of **12** was near quantitative. Neither the *p*-toluenesulfonyl nor methanesulfonyl derivatives of the iodohydrins **6**, **7**, and **8** could be obtained. Instead the olefinic compounds **13**, **14**, and **15**, respectively, were produced. The methanesulfonations gave the better yields which were nearly quantitative. Although the reactions proceeded to completion at room temperature, several days were

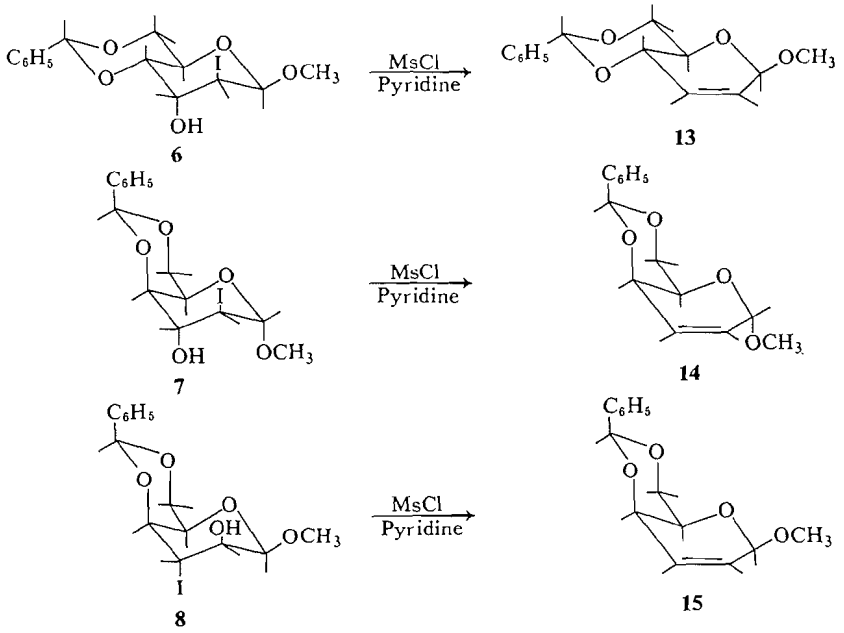

required. Only several minutes were required at the boiling point of the mixture to achieve similar yields.

The *p*-toluenesulfonate (**10**) was only very slowly converted to the olefin **12** when refluxed in pure pyridine. However, when an equimolar amount of tetraethylammonium chloride was added to **10** dissolved in pyridine, the olefin was rapidly formed. It is evident, therefore, that the reaction proceeds by nucleophilic attack by chloride ion on the iodine as indicated in the equation **10** → **12**. Under the preferred conditions, pyridinium hydrochloride formed in the course of the sulfonylation is the source of chloride ion. An attempt to prepare the olefin **12** from either the epoxide **1** or the iodohydrin **2***b* using Cornforth's procedures (39) failed. Furthermore, the procedure used by Albano, Horton, and Tsuchiya (26) to convert methyl 4,6-*O*-benzylidene-2,3-di-*O*-*p*-toluenesulfonyl-α-D-glucopyranoside to **12** and which involves treatment of the ditosylate with sodium iodide and zinc dust in dimethylformamide did not, in our hands, prove useful for the conversion of the 4,6-*O*-benzylidene-2,3-di-*O*-*p*-toluenesulfonyl derivatives of methyl β-D-glucopyranoside and methyl α-D-galactopyranoside to the olefins **13** and **14**, respectively.

The structures assigned to the olefins **12** to **15** are completely in accord with the compositions and n.m.r. parameters (see Table II) obtained for the compounds. The 2-*O*-methanesulfonyl derivative of the β-D-*gluco* iodohydrin (**9**) was highly resistant to attack by chloride ion to form the olefin **13**. This observation is in keeping with the requirement of an antiparallel arrangement of the iodine atom and the methanesulfonyldeoxy group for facile reaction.

The rotations of a number of anomeric pairs of 2,3-unsaturated pyranoid structures are listed in Table III. It is of interest to note that Hudson's rules of isorotation do not apply when there is present an acyloxy group at the 2-position.

The signs for the $^5J_{H-H}$ couplings are reported as positive in view of the recent publication by Coxon, Jennings, and McLauchlan (50) on a related compound. Hall and Manville (51) have recently reported on the relative signs of proton–proton coupling constants in saturated and unsaturated carbohydrate derivatives. It is of interest to note that the $J_{6a,6e}$ geminal coupling constants for the C-4 epimers reported in Table I are larger for the *xylo* than for the *ribo* configuration. This finding is in accord with the suggestion (52) that the $^2J_{H-H}$ coupling constant will depend in part upon the relative orientation of an electronegative vicinal substituent with the coupling being numerically larger when the electronegative substituent is *gauche* to only one of the geminal hydrogens than when it is in

Can. J. Chem. Downloaded from www.nrcresearchpress.com by 210.87.254.40 on 09/05/12
For personal use only.

TABLE III

Specific rotations of anomeric pairs of 2,3-unsaturated pyranoid structures

Compound	[α]	Solvent	Ref.
Methyl 4,6-*O*-benzylidene-α-D-*erythro*-hex-2-enopyranoside	+129°	$CHCl_3$	
Methyl 4,6-*O*-benzylidene-β-D-*erythro*-hex-2-enopyranoside	+45°	$CHCl_3$	
Methyl 4,6-*O*-benzylidene-α-D-*threo*-hex-2-enopyranoside	−130°	$CHCl_3$	
Methyl 4,6-*O*-benzylidene-β-D-*threo*-hex-2-enopyranoside	−172°	$CHCl_3$	
p-Nitrophenyl 4,6-di-*O*-acetyl-α-D-*erythro*-hex-2-enopyranoside	+174°	Benzene	14
p-Nitrophenyl 4,6-di-*O*-acetyl-β-D-*erythro*-hex-2-enopyranoside	+51°	Benzene	14
1,2,4-Tri-*O*-acetyl-2-hydroxy-α-D-*glycero*-pent-2-enopyranose	+15°	$CHCl_3$	19
1,2,4-Tri-*O*-acetyl-2-hydroxy-β-D-*glycero*-pent-2-enopyranose	+169°	$CHCl_3$	19
1,2,4,6-Tetra-*O*-acetyl-2-hydroxy-α-D-*erythro*-hex-2-enopyranose	+50°	$CHCl_3$	18
1,2,4,6-Tetra-*O*-acetyl-2-hydroxy-β-D-*erythro*-hex-2-enopyranose	+146°	$CHCl_3$	18, 20
1-*O*-Acetyl-2,4,6-tri-*O*-benzoyl-2-hydroxy-α-D-*erythro*-hex-2-enopyranose	+52°	$CHCl_3$	15
1-*O*-Acetyl-2,4,6-tri-*O*-benzoyl-2-hydroxy-β-D-*erythro*-hex-2-enopyranose	+91°	$CHCl_3$	15

gauche relationship to both the geminal protons. Coxon (53) has observed examples with ribopyranose derivatives and Hall and Manville (54) with 2-deoxyhexopyranose derivatives. It is seen from Table II that this situation is also present for the $J_{6a,6e}$ couplings observed for the *erythro* and *threo*-hex-2-enopyranose derivatives. Dr. Harold Spedding, in an unpublished work performed in this laboratory in 1962, observed $J_{5a,5e}$ coupling constants for the α and β forms of methyl tri-*O*-acetyl-D-xylopyranoside in chloroform of −10.7 and −11.8 c.p.s., respectively. In contrast, for the corresponding α and β derivatives of L-arabinopyranose wherein the 4-acetoxy group is *gauche* to only H-5*e*, the values for $J_{5a,5e}$ were −13.1 and −13.2 c.p.s., respectively. As expected, the value of $J_{5a,5e}$ for methyl tri-*O*-acetyl-α-D-lyxopyranoside was numerically small, −10.7 c.p.s. However, the value for this coupling constant was −12.3 c.p.s. for the β anomer. This result may indicate (53) an appreciable abundance of the compound in the 1C as well as the C1 conformation. This may also be the situation for methyl tri-*O*-acetyl-β-D-ribopyranoside since $J_{5a,5e}$ was −12.6 c.p.s. for this compound. Recently, Holland, Horton, and Jewell (55) reported $J_{5a,5e}$ to be 12.9 c.p.s. for tri-*O*-acetyl-β-D-xylopyranosyl chloride both in chloroform and in benzene. This result obviously is in support of their contention, based on vicinal coupling constants, that the compound exists to a large extent in the 1C-conformation. It may be noted in this regard that the value of 11.8 c.p.s. observed for methyl tri-*O*-acetyl-β-D-xylopyranoside is suggestive of a considerable abundance of the 1C conformation for this compound as well. In fact, the value $J_{4,5a} = 7.8$ c.p.s. is small as compared to that expected (about 9 c.p.s.) for the C1 conformation. Also, the value $J_{4,5e} = 6.0$ c.p.s. is large as compared to the value expected (about 3 c.p.s.) for protons in *gauche* relationship. The role of the anomeric effect (56) in controlling these conformational equilibria is apparent.

Experimental

Methyl 4,6-O-Benzylidene-2-deoxy-2-iodo-α-D-altropyranoside (2b)

(a) From Methyl 2,3-Anhydro-4,6-O-benzylidene-α-D-allopyranoside (1)

Compound **1** (57) (2.64 g, 0.01 mole) was dissolved in acetone (50 ml) and gently refluxed for 1 h with sodium iodide (7.5 g, 0.05 mole), sodium acetate (0.41 g, 0.005 mole), and acetic acid (12 ml, 0.2 mole). The mixture was evaporated to dryness *in vacuo* and the residue was dissolved in a mixture of chloroform (70 ml) and water (100 ml). The aqueous layer was separated and extracted with chloroform (70 ml). The combined chloroform solutions were washed with water (100 ml), dried over sodium sulfate, and evaporated to dryness *in vacuo*. The residue was crystallized from ethanol to yield **2b** (3.72 g, 95%); m.p. 105–106°, $[\alpha]_D^{25}$ +35.0° (*c*, 2.0 in chloroform). [Lit. (38), m.p. 105–106°, $[\alpha]_D^{20}$ +39.0° (*c*, 1.3 in chloroform).]

Anal. Calcd. for $C_{14}H_{17}O_5I$: C, 42.86; H, 4.34. Found: C, 42.73; H, 4.31.

Compound **1** (0.264 g, 0.001 mole) was added to 50 ml of 0.1 *M* lithium iodide in ether (58). After 30 min, a clear yellow solution was obtained and thin-layer chromatography showed the reaction to be virtually complete. Acetic acid was added to neutralize the solution and work-up in the usual manner gave 0.390 g (99%) of **2b**.

In a second experiment, 1.2 ml of acetic anhydride was added to the reaction mixture instead of the acetic acid. After 2 min water was added and the product was isolated. The n.m.r. spectrum of the syrup was identical to that of the acetate **2c**. In a control experiment, the iodohydrin **2b** (0.392 g, 0.001 mole) was treated with 50 ml of 0.1 *M* lithium iodide in ether. After 30 min 1.2 ml

Can. J. Chem. Downloaded from www.nrcresearchpress.com by 210.87.254.40 on 09/05/12
For personal use only.

Can. J. Chem. Downloaded from www.nrcresearchpress.com by 210.87.254.40 on 09/05/12
For personal use only.

of acetic anhydride was added and after 2 min the product was isolated. The iodohydrin **2***b* was recovered in near quantitative yield.

*(b) From 4,6-O-Benzylidene-*D*-allal (**3***b*)*

A mixture of **3***b* (37), (0.86 g, 0.0036 mole) and silver acetate (0.71 g, 0.0042 mole) in methanol (50 ml) was cooled to 0°. Iodine (0.5 g, 0.0042 mole) was added over a period of 5 min. The product, isolated in the usual manner as a syrup, was found by n.m.r. analysis to be a 1:1 mixture of two isomers. Crystallization from ethanol gave a 0.33 g (23%) yield of compound **2***b*.

Reaction of Methyl Lithium with 2b

The ether solution containing 5.25% of methyl lithium (32 ml, 0.079 mole) was added to a solution of compound **2***b* (1.00 g, 0.0025 mole) in ether (100 ml) under stirring. The reaction mixture, after being gently refluxed for 18 h, was neutralized with acetic acid (0.9 ml) and was worked up in usual manner. The product (0.502 g, 85%) was isolated as colorless, fluffy needles, m.p. 83.5°, $[\alpha]_D^{25}$ +209.5° (*c*, 2.0 in ethanol).

Anal. Calcd. for $C_{13}H_{14}O_4$: C, 66.68; H, 6.03. Found: C, 66.51; H, 5.90.

This product was identical with 4,6-*O*-benzylidene-D-allal (**3**) prepared, in a 72% yield, following the published procedure (37) by mixture melting point, n.m.r., and infrared spectra. [Lit. (37), m.p. 84–84.5°, $[\alpha]_D^{25}$ +210° (*c*, 0.44 in ethanol).]

*4,6-O-Benzylidene-*D*-gulal*

Compound **7** (0.90 g, 2.3 mmoles) was treated with methyl lithium (12 ml, 5.25% ether solution) as described above. The reaction mixture, after being refluxed for 2 h, was worked up as usual. The crystalline product (349 mg) was recrystallized from ether–Skellysolve B; colorless needles, m.p. 128.5–129.5°, $[\alpha]_D^{25}$ +192° (*c*, 1.4 in chloroform). The n.m.r. parameters are reported in Table I.

Anal. Calcd. for $C_{13}H_{14}O_4$: C, 66.68; H, 6.03. Found: C, 66.70; H, 5.81.

*Methyl 4,6-O-Benzylidene-2-deoxy-2-iodo-3-O-(p-toluenesulfonyl)-α-*D*-altropyranoside (**10**)*

Compound **2***b* (1.96 g, 0.05 mole) and *p*-toluenesulfonyl chloride (1.05 g, 0.055 mole) were dissolved in pyridine (20 ml) and the reaction was stored at near 0° for 44 h. The mixture was poured onto an ice-water mixture (100 ml) and extracted with two 100-ml portions of chloroform. The extracts were combined and washed with water (100 ml), dried over sodium sulfate, then evaporated *in vacuo* at room temperature. Ethanol (10 ml) was added to the residue and evaporated. This procedure was repeated several times until the odor of pyridine had disappeared. During this treatment, crystallization occurred. The crystals were well triturated with cold ethanol (20 ml), filtered, and washed with ethanol. The yield was 2.07 g, (76%); m.p. 122–123° (decomp.), $[\alpha]_D^{25}$ +28.4° (*c*, 1.0 in chloroform). Richards and Wiggins (38) reported m.p. 114.5–115° (decomp.), $[\alpha]_D^{18}$ −15.6° in chloroform for the iodotosylate **10**.

Anal. Calcd. for $C_{21}H_{22}O_7I$: C, 46.24, H, 4.04. Found: C, 46.39; H, 4.17.

Prolonged reaction at 0° or at room temperature caused the formation of the olefin **12**. Thus, from the reaction after four days at room temperature a 73% yield of **12** was obtained. Although **10** could be stored in the dark below −5°, it changed to a dark tar within a few days at room temperature.

*Methyl 4,6-O-Benzylidene-3-deoxy-3-iodo-α-*D*-altropyranoside (**5***b*)*

Methyl 2,3-anhydro-4,6-*O*-benzylidene-α-D-mannopyranoside (**4**) (59) reacted considerably more slowly with sodium iodide, under the conditions described above for the preparation of **2***b*, than did the *allo* epoxide **1**. A 20 h period of reflux was used to prepare a 91% yield of rods, m.p. 163.5–164.5°, $[\alpha]_D^{25}$ +116° (*c*, 1.2 in chloroform) recrystallized from ethyl acetate. Literature (60) m.p. 163–163.5°, $[\alpha]_D^{22}$ +111° (*c*, 4 in chloroform).

Anal. Calcd. for $C_{14}H_{17}O_5I$: C, 42.86; H, 4.34. Found: C, 42.41; H, 4.24.

Reaction of 4 with Lithium Iodide

Compound **4** (26.4 mg 0.1 mmole) was dissolved in ether (4.5 ml) in a 5-ml polarimeter tube. To this was added a 1 *M* solution of lithium iodide in ether (0.5 ml, 0.5 mmole). Change of optical rotation was checked at intervals. The value of rotation reached constant after 9 days. The reaction mixture was neutralized with a drop of acetic acid and extracted with water. After being dried over sodium sulfate, the ether solution was evaporated to dryness. The n.m.r. spectrum indicated that the residue was a 3:2 mixture of **4** and **5***b*.

*Methyl 4,6-O-Benzylidene-3-deoxy-3-iodo-2-(O-p-toluenesulfonyl)-α-*D*-altropyranoside (**11**)*

Compound **5***b* (1.96 g, 0.05 mole) and *p*-toluenesulfonyl chloride (1.05 g, 0.055 mole) were dissolved in pyridine (20 ml). After being kept for 44 h at near 0°, the reaction mixture was worked up as described above for the preparation of **10**. Trituration of the product with cold ethanol (20 ml), provided 1.56 g (53%) of fine needles, m.p. 128–129°; $[\alpha]_D^{25}$ +37.5° (*c*, 1.0 in chloroform). [Lit. (23) m.p. 127.5–129°, $[\alpha]_D^{23}$ +46.4 in chloroform.]

Anal. Calcd. for $C_{21}H_{22}O_7SI$: C, 46.24; H, 4.04. Found: C, 45.92; H, 4.20.

This compound was unstable to storage at room temperature and decomposed to a dark tar within a few days.

*Methyl 4,6-O-Benzylidene-α-*D*-erythro-hex-2-enopyranoside (**12**)*

(a) From the Iodohydrin 2b

2 (1.96 g, 0.005 mole) was refluxed in pyridine (15 ml) with *p*-toluenesulfonyl chloride (1.05 g, 0.0055 mole) for 20 min. After cooling to room temperature, the dark-brown reaction mixture was partitioned between water (100 ml) and ether (100 ml). The aqueous layer was separated and washed with ether (100 ml). The combined ether solutions were washed with 0.1 *M* sodium thiosulfate (100 ml) and water (100 ml) and dried over sodium sulfate. The solvent was evaporated *in vacuo*. Pyridine was removed by azeotropic distillation with ethanol. The solid residue was recrystallized from ethanol (15 ml). Long needles 1.17 g (95%) were obtained; m.p. 119.5–120°, $[\alpha]_D^{25}$ +129.0°, (*c*, 1.4 chloroform).

Anal. Calcd. for $C_{14}H_{16}O_4$: C, 67.72; H, 6.47. Found: C, 67.67; H, 6.23.

(b) From the Iodohydrin 5b

In the manner described above, *p*-toluenesulfonylation of 1.96 g of **5***b* gave a 1.18 g (95%) yield of the olefin **12**.

Can. J. Chem. Downloaded from www.nrcresearchpress.com by 210.87.254.40 on 09/05/12
For personal use only.

Methyl 2,3-Anhydro-4,6-O-benzylidene-β-D-allopyranoside

This compound was prepared by Peat and Wiggins (42) by treatment of methyl 4,6-*O*-benzylidene-3-*O*-*p*-toluenesulfonyl-β-D-glucopyranoside with base. This latter compound was obtained by *O*-benzylidenation of the methyl 3-*O*-toluenesulfonyl-β-D-glucopyranoside prepared by Oldham and Oldham (61). We have observed that the compound can be prepared in 20% yield by mono-*p*-toluenesulfonylation of methyl 4,6-*O*-benzylidene-β-D-glucopyranoside (62). Treatment with base gave a product with the same melting point and rotation as those reported by Peat and Wiggins for the title compound. However, the compound was more readily prepared as follows.

Methyl 4,6-*O*-benzylidene-2,3-di-*O*-*p*-(toluenesulfonyl)-β-D-glucopyranoside (63) (15 g, 0.025 mole) was suspended in 1,2 dichloroethane (200 ml). To the ice-cold mixture, 100 ml of a cold 1.9 *M* solution of sodium methoxide in methanol was added. After shaking at room temperature for 48 h, water (400 ml) and 1,2-dichloroethane (100 ml) was added and the organic layer processed in the usual manner. Solvent removal left a colorless solid which was extracted with boiling Skellysolve B. Evaporation of the extract gave 6.5 g (93%) of crude methyl 2,3-anhydro-4,6-*O*-benzylidene-β-D-allopyranoside, m.p. 130–132°. Recrystallization from ethanol raised the melting point to 133–135°, $[\alpha]_D^{25}$ −15° (*c*, 1.5 in chloroform). Peat and Wiggins (42) reported m.p. 138°, $[\alpha]_D^{19}$ −15.6°.

Methyl 4,6-O-Benzylidene-2-deoxy-2-iodo-β-D-altropyranoside (6) and Methyl 4,6-O-Benzylidene-3-deoxy-3-iodo-β-D-glucopyranoside

Treatment of the above epoxide (2.64 g) under the conditions used to convert **4** to **5***b* gave a product which was fractionally crystallized from ethanol (50 ml). The first crop, 187 mg, m.p. 225–227° gave, on further purification by recrystallization from ethanol, needles m.p. 230°, $[\alpha]_D^{25}$ −135° (*c*, 1.0 in pyridine) to which the β-D-*gluco* configuration was assigned on the basis of the n.m.r. parameters reported in the discussion.

Anal. Calcd. for $C_{14}H_{17}O_5I$: C, 42.86; H, 4.34. Found: C, 42.99; H, 4.29.

The monoacetate derivative melted at 165–166°, $[\alpha]_D^{25} = -148°$ (*c*, 4.3 in chloroform).

Anal. Calcd. for $C_{16}H_{19}O_6I$: C, 44.24; H, 4.38. Found: C, 43.98; H, 4.17.

The mother liquor from the above crystallization yielded cubic crystals (743 mg, m.p. 168–171°) which were purified by recrystallization from ethanol. The constants for the analytical sample were m.p. 175–176°, $[\alpha]_D^{25}$ −91° (*c*, 2.8 in chloroform) and the n.m.r. parameters used to assign the β-D-*altro* configuration (**6**) are reported in the discussion.

Anal. Calcd. for $C_{14}H_{17}O_5I$: C, 42.86; H, 4.34. Found: C, 42.99; H, 4.29.

The monoacetate derivative was obtained as needles, m.p. 123–123.5°, $[\alpha]_D^{25} = -109°$ (*c*, 3.0 in chloroform).

Anal. Calcd. for $C_{16}H_{19}O_6I$: C, 44.24; H, 4.38. Found: C, 44.42; H, 4.34.

Methyl 4,6-O-Benzylidene-β-D-erythro-hex-2-enopyranoside (13)

To the solution of the iodohydrin **6** (196 mg, 0.0005 mole) in pyridine (4 ml) was added methanesulfonyl chloride (0.05 ml) and the mixture was refluxed for 10 min. The reaction was diluted with ice-water (20 ml), then extracted with ether (10 ml × 2). The combined extracts were washed successively with 10 ml portions of water, 0.1 *N* hydrochloric acid, water, 0.1 *M* sodium thiosulfate, and finally with water. After being dried over sodium sulfate, the ether was evaporated to dryness. Upon recrystallization of the residue from a small amount of ethanol, **13** was obtained as fine needles; 98 mg, (79%), m.p. 94–95°, $[\alpha]^{25}$ +45° (*c*, 1.3 in chloroform).

Anal. Calcd. for $C_{14}H_{16}O_4$: C, 67.74; H, 6.45. Found: C, 67.67; H, 6 29.

Methyl 4,6-O-Benzylidene-2-deoxy-2-iodo-α-D-idopyranoside (7)

Methyl 2,3-anhydro-4,6-*O*-benzylidene-α-D-gulopyranoside (43, 44) (1.76 g) was converted to the iodohydrin (**7**) with sodium iodide under the conditions used to prepare **5***b* from **4**. The colorless solid product was recrystallized from ethanol to give colorless needles, (1.60 g, 61.3%), m.p. 162–163°, $[\alpha]_D^{25}$ +28° (*c*, 1.2 in chloroform).

Anal. Calcd. for $C_{14}H_{17}O_5I$: C, 42.86; H, 4.34. Found: C, 43.08; H, 4.15.

The monoacetate derivative was obtained as leaflets, m.p. 142–143°, $[\alpha]_D^{25}$ +31° (*c*, 2.3 in chloroform).

Anal. Calcd. for $C_{16}H_{19}O_6I$: C, 44.24; H, 4.38. Found: C, 44.52; H, 4.31.

Methyl 4,6-O-Benzylidene-α-D-threo-hex-2-enopyranoside (14)

Compound **7** (0.196 g, 0.005 mole) was treated with methanesulfonyl chloride (0.045 ml, 0.006 mole) in pyridine for 20 min as described for the preparation of **13**. The product isolated as fine needles, 0.112 g, (90%), m.p. 163–164°, $[\alpha]_D^{25}$ −130° (*c*, 3.0 in chloroform).

Anal. Calcd. for $C_{14}H_{16}O_4$: C, 67.74; H, 6.45. Found: C, 67.55; H, 6.45.

Methyl 4,6-O-Benzylidene-3-deoxy-3-iodo-β-D-idopyranoside (8)

Methyl 2,3-anhydro-4,6-*O*-benzylidene-β-D-talopyranoside (45, 46) (1.76 g, 0.0067 mole) was treated with sodium iodide (5.0 g, 0.033 mole) as described for the preparation of **6**. The product obtained as long needles, 1.82 g (70%), m.p. 132–133°, $[\alpha]_D^{25}$ −30° (*c*, 2.8 in chloroform).

Anal. Calcd. for $C_{14}H_{17}O_5I$: C, 42.86; H, 4.34. Found: C, 43.15; H, 4.45.

The mono-*O*-acetyl derivative was prepared as cubes, m.p. 174–175°, $[\alpha]_D^{25}$ −28° (*c*, 2.4 in chloroform).

Anal. Calcd. for $C_{16}H_{19}O_6I$: C, 44.24; H, 4.38. Found: C, 44.30; H, 4.24.

Methyl 4,6-O-Benzylidene-β-D-threo-hex-2-enopyranoside (15)

Compound **8** (0.196 g, 0.005 mole) was treated with methanesulfonyl chloride (0.045 ml, 0.006 mole) in pyridine for 5 min as described for the preparation of **13**. Fine needles for the product (96 mg, 76%) had m.p. 122–123°, $[\alpha]_D^{25}$ −172° (*c*, 1.1 in chloroform).

Anal. Calcd. for $C_{14}H_{16}O_4$: C, 67.74; H, 6.45. Found: C, 67.42; H, 6.35.

Acknowledgments

The authors are grateful for grants to R. U. L. from the National Research Council of Canada (T-172) in support of this research. The micro-

Can. J. Chem. Downloaded from www.nrcresearchpress.com by 210.87.254.40 on 09/05/12
For personal use only.

analyses and n.m.r. spectra were determined in this department.

1. P. Reichardt. J. Biol. Chem. **237**, 3513 (1962).
2. J. P. H. Verheyden and J. G. Moffatt. J. Am. Chem. Soc. **86**, 1236 (1964).
3. K. G. Cunningham, S. A. Hutchinson, W. Mason, and F. S. Spring. J. Chem. Soc. 2299 (1951).
4. E. A. Kaczka, E. L. Dulaney, C. O. Gitterman, H. B. Woodruff, and K. Folkers. Biochem. Biophys. Res. Commun. **14**, 452 (1964).
5. R. J. Suhadolnik, G. Weinbaum, and H. P. Moloche. J. Am. Chem. Soc. **86**, 948 (1964).
6. J. J. Fox, K. A. Watanabe, and A. Bloch. Progr. Nucleic Acid Res. Mol. Biol. **5**, 251 (1966).
7. T. Reichstein, A. Grussner, and R. Oppenauer. Helv. Chim. Acta, **17**, 510 (1934).
8. R. G. Ault, D. K. Baird, H. C. Carrington, W. N Haworth, R. Herbert, E. L. Hirst, E. G. V. Percival, F. Smith, and M. Stacey. J. Chem. Soc. 1419 (1933).
9. D. K. Baird, W. N. Haworth, R. W. Herbert, E. L. Hirst, F. Smith, and M. Stacey. J. Chem. Soc. 62 (1934).
10. H. Yonehara and N. Otake. Tetrahedron Letters, 3785 (1966).
11. E. Fischer. Ber. **47**, 196 (1914).
12. M. Bergmann. Ann. **443**, 223 (1925).
13. S. Laland, W. G. Overend, and M. Stacey. J. Chem. Soc. 738 (1950).
14. R. J. Ferrier, W. G. Overend, and A. E. Ryan. J. Chem. Soc. 3667 (1962).
15. R. J. Ferrier, W. G. Overend, and G. H. Sankey. J. Chem. Soc. 2830 (1965).
16. R. J. Ferrier. J. Chem. Soc. 5443 (1964).
17. I. Lundt and C. Pedersen. Acta Chem. Scand. **20**, 1369 (1966).
18. R. U. Lemieux, D. R. Lineback, M. L. Wolfrom, F. B. Moody, E. G. Wallace, and F. Komitzky. J. Org. Chem. **30**, 1092 (1965).
19. R. J. Ferrier, W. G. Overend, and G. H. Sankey. J. Chem. Soc. 2339 (1966).
20. R. U. Lemieux and R. J. Bose. Can. J. Chem. **44**, 1855 (1966).
21. W. A. Bowels and R. K. Robins. J. Am. Chem. Soc. **86**, 1252 (1964).
22. H. R. Bolliger and D. A. Prins. Helv. Chim. Acta, **29**, 1061 (1946).
23. G. N. Richards. J. Chem. Soc. 4511 (1954).
24. F. H. Newth. J. Chem. Soc. 471 (1956).
25. J. E. Christensen and L. Goodman. J. Am. Chem. Soc. **83**, 3827 (1961).
26. E. Albano, D. Horton, and T. Tsuchiya. Carbohydrate Res. **2**, 349 (1966).
27. D. Horton and W. N. Turner. Tetrahedron Letters, 2531 (1964).
28. R. D. Guthrie and D. Murphy. J. Chem. Soc. 6666 (1965).
29. R. D. Guthrie and D. King. Carbohydrate Res. **3**, 128 (1966).
30. C. L. Stevens, N. A. Nielsen, and P. Blumbergs. J. Am. Chem. Soc. **86**, 3592 (1964).
31. J. P. Horwitz, J. Chua, M. A. DaRooge, M. Noel, and I. L. Klundt. J. Org. Chem. **31**, 205 (1966).
32. J. P. Horwitz, J. Chua, and M. Noel. Tetrahedron Letters, 1343 (1966).
33. J. R. McCarthy, Jr., M. J. Robins, L. B. Townsend, and R. K. Robins. J. Am. Chem. Soc. **88**, 1549 (1966).
34. J. J. Fox and I. Wempen. Tetrahedron Letters, 643 (1965).
35. G. L. Tong, W. W. Lee, and L. Goodman. J. Org. Chem. **30**, 2854 (1965).
36. W. V. Rugle, T. Y. Shen, and A. A. Patchett. J. Org. Chem. **30**, 4353 (1965).
37. A. A. Feast, W. G. Overend, and N. A. Williams. J. Chem. Soc. 7378 (1965).
38. G. N. Richards and L. F. Wiggins. J. Chem. Soc. 2442 (1953).
39. J. W. Cornforth, R. H. Cornforth, and K. K. Mathew. J. Chem. Soc. 112 (1959).
40. M. Sharma and R. K. Brown. Can. J. Chem. **44**, 2825 (1966).
41. R. U. Lemieux and B. Fraser-Reid. Can. J. Chem. **42**, 532 (1964).
42. S. Peat and L. F. Wiggins. J. Chem. Soc. 1088 (1938).
43. M. Gyr and T. Reichstein. Helv. Chim. Acta, **28**, 226 (1945).
44. A. C. Maehly and T. Reichstein. Helv. Chim. Acta, **30**, 496 (1947).
45. E. Sorkin and T. Reichstein. Helv. Chim. Acta, **28**, 1 (1945).
46. F. Reber and T. Reichstein. Helv. Chim. Acta, **28**, 1114 (1945).
47. A. Fürst and P. A. Plattner. 12th Intern. Congr. Pure and Appl. Chem., New York. 1951. Abstr. Papers, p. 409.
48. R. U. Lemieux, R. K. Kullnig, H. J. Berstein, and W. G. Schneider. J. Am. Chem. Soc. **80**, 6098 (1958).
49. R. U. Lemieux and J. D. Stevens. Can. J. Chem. **43**, 2059 (1965).
50. B. Coxon, H. J. Jennings, and K. A. McLauchlan. Tetrahedron, **23**, 2395 (1967).
51. L. D. Hall and J. F. Manville. Carbohydrate Res. **4**, 271 (1967).
52. J. A. Pople and A. A. Bothner-By. J. Chem. Phys. **42**, 1339 (1965).
53. B. Coxon. Tetrahedron, **22**, 2281 (1966).
54. L. D. Hall and J. F. Manville. Can. J. Chem. **45**, 1299 (1967).
55. C. V. Holland, D. Horton, and J. S. Jewell. J. Org. Chem. **32**, 1818 (1967).
56. R. U. Lemieux and J. Hayami. Can. J. Chem. **43**, 2162 (1965).
57. N. K. Richtmyer. Methods Carbohydrate Chem. **1**, 107 (1962).
58. M. D. Taylor and L. R. Grant. J. Am. Chem. Soc. **77**, 1507 (1955).
59. L. F. Wiggins. Methods Carbohydrate Chem. **2**, 189 (1963).
60. G. N. Richards, L. F. Wiggins, and W. S. Wise. J. Chem. Soc. 496 (1956).
61. J. W. H. Oldham and M. A. Oldham. J. Am. Chem. Soc. **61**, 1112 (1939).
62. K. Freudenberg. Ber. **61**, 1743 (1928).
63. H. Ohle and K. Spenker. Ber. **61**, 2387 (1928).

Can. J. Chem. Downloaded from www.nrcresearchpress.com by 210.87.254.6 on 09/05/12
For personal use only.

NOTES

Thiohydantoins. VI. Hydrolysis of 1-acyl-2-thiohydantoins: reported anomalies

J. T. EDWARD AND J. K. LIU
Department of Chemistry, McGill University, Montreal, Quebec

Received August 4, 1967

Two reports in which it was claimed that the 1-acyl group of a 1-acyl-2-thiohydantoin was not rapidly removed by dilute acid or alkali were investigated and found erroneous.

Canadian Journal of Chemistry, 46, 71 (1968)

1-Acyl-2-thiohydantoins are rapidly hydrolyzed in dilute acid (1) or alkali (2, 3) to carboxylic acids and 2-thiohydantoins. The latter are slowly hydrolyzed further to α-thioureido acids by alkali (1, 4), but are stable in mineral acids at ordinary temperatures[1] (4). Use is made of these properties in Schlack and Kumpf's procedure (2) for identifying the *C*-terminal amino acid of a polypeptide or protein: this amino acid residue is converted into a 1-acyl-2-thiohydantoin, and the 2-thiohydantoin can then be detached from the remainder of the peptide chain by mild acid or alkaline hydrolysis. However, there are two anomalous cases of 1-acyl-2-thiohydantoin behavior reported in the literature (5, 6). The work described below shows that in both cases the results reported are probably erroneous.

The first case is the report of Dains *et al.* (5) that acid hydrolysis of 1-benzoyl-3-phenyl-2-thiohydantoin (**3**) yields, not benzoic acid and 3-phenyl-2-thiohydantoin (**4**), but benzoic acid, aniline, and hippuric acid. Dains claimed to prepare 1-benzoyl-3-phenyl-2-thiohydantoin, m.p. 177–179°, by heating hippuric acid (**1**) with phenyl isothiocyanate to 150°. Under these conditions carboxylic acids are known to react with phenyl isothiocyanate to give carbon oxysulfide and anilides (7), and indeed we found that hippuric acid gave hippuranilide (**2**) (8), m.p. 212–213°. The possibility that in the hands of Dains the reaction had taken a different course to give 1-benzoyl-3-phenyl-2-thiohydantoin was excluded by preparing an authentic specimen of this compound (**3**) by treating 3-phenyl-2-thiohydantoin (**4**) with benzoyl chloride in pyridine. The compound melted at 132–133°, and was hydrolyzed almost instantaneously by 0.05 *N* sodium hydroxide to benzoic acid and 3-phenyl-2-thiohydantoin.

It accordingly seems likely that the product, m.p. 177–179°, obtained by Dains *et al.* was impure hippuranilide, which would be expected to give benzoic acid, hippuric acid, and aniline on acid hydrolysis.

A second apparent anomaly is the report of Johnson and O'Brien (6) that 5-benzal-1-benzoyl-2-thiohydantoin (**6**) is hydrolyzed by dilute sodium hydroxide to the thioureido acid (isolated as the yellow sodium salt **7**), and not to benzoic acid and 5-benzal-2-thiohydantoin (**8**). The salt (**7**) was reported to give the latter compound when treated with hydrochloric acid, the benzoyl group being apparently split off at this stage.

In an attempt to check this work, 1-benzoyl-2-thiohydantoin (**5**) was allowed to react with benzaldehyde in acetic acid containing sodium acetate, under the conditions claimed by Johnson and O'Brien to give **6**. A yellow solid was obtained which decomposed at about 260–262° (Johnson and O'Brien reported no melting point) and which showed some of the properties reported by Johnson and O'Brien for **6**. However, it was shown by its analysis (Johnson and O'Brien reported no analysis) and nuclear magnetic resonance spectrum to be not **6** but 5-benzal-2-thiohydantoin (**8**). It is likely that the 1-benzoyl derivative **6** is formed first, but that it loses the benzoyl group by acetolysis under the catalytic influence of the acetate ion. Analogously, 1-acetyl-2-thiohydantoin has been found to condense with benzaldehyde in acetic

[1]J. T. Edward and I. Lantos, unpublished results.

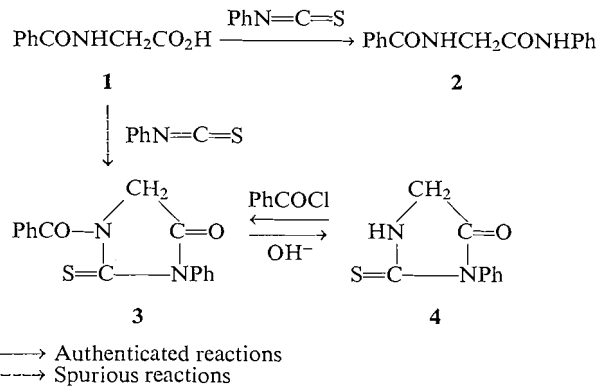

acid containing sodium acetate to give **8**, the 1-acetyl group being lost in this case (9). Regardless of the precise mechanism, the results show the extreme ease with which the 1-acyl group is removed from 1-acyl-2-thiohydantoins.

Treatment of 5-benzal-2-thiohydantoin (**8**) with sodium hydroxide according to the directions of Johnson and O'Brien gave a yellow sodium salt having some of the properties of the compound which they formulated as **7**. However, the analytical data excluded this formula, and indicated formula **9** (plus 0.5 molecule of water of crystallization); the spectroscopic data were in agreement with this structure. The ionization of 2-thiohydantoins at the 3-position as in **8** → **9**, is now well established (10), but this appears to be the first report of the isolation of the sodium salt **9**. It is possible that Johnson and O'Brien were misled by a faulty analysis of their compound (they reported only one nitrogen analysis) into thinking it the carboxylate salt **7**.

Experimental

Hippuranilide (2)

A mixture of hippuric acid (17.9 g) and phenyl isothiocyanate (13.5 g) was heated to 150–154° for 1.5 h. The dark red product was dissolved in hot ethanol (50 ml), and treated with charcoal. Colorless needles of hippuranilide (7.5 g), m.p. 212–213° (lit. 208.5° (8)) separated from the solution when cool; λ_{max} (EtOH) 241 mμ; ϵ_{max} 24 000.

Anal. Calcd. for $C_{15}H_{14}N_2O_2$: C, 70.85; H, 5.55; N, 11.02; O, 12.58. Found: C, 71.07; H, 5.73; N, 10.95; O, 12.42.

1-Benzoyl-3-phenyl-2-thiohydantoin (3)

A mixture of 3-phenyl-2-thiohydantoin (11) (0.4 g) and benzoyl chloride (0.5 ml) in pyridine (10 ml) was warmed to 80–90° for 30 min. The resultant solution was poured into 5% aqueous sodium bicarbonate (20 ml) and the mixture extracted with diethyl ether (25 ml). The ether layer was washed with water and diluted with methanol. The solution was concentrated, treated with charcoal, and filtered. Overnight the filtrate deposited pale-yellow crystals of 1-benzoyl-3-phenyl-2-thiohydantoin (0.34 g), m.p. 132–133°; λ_{max} (EtOH) at 375, 285, and 245 mμ (ϵ_{max} 123, 9200, and 18 300) (cf. 1-benzoyl-2-thiohydantoin: λ_{max} (EtOH) at 373, 280, and 240 mμ; ϵ_{max} 132, 10 200, and 25 000).

Anal. Calcd. for $C_{16}H_{12}N_2O_2S$: C, 64.86; H, 4.32; N, 9.46. Found: C, 64.78; H, 4.48; N, 9.51.

Reaction of 1-Benzoyl-2-thiohydantoin with Benzaldehyde

A solution of 1-benzoyl-2-thiohydantoin (12) (2.0 g), benzaldehyde (2.8 g) and anhydrous sodium acetate (4.0 g) in glacial acetic acid (10 ml) was heated under reflux for 3 h. The solution was cooled and diluted with water (20 ml). A yellow solid separated which decomposed at 260–261° (lit. m.p. of 5-benzal-2-thiohydantoin, 258° (12)); λ_{max} (EtOH) 294, 265, and 245 mμ; ϵ_{max} 5160, 29 400, and 9400; ν_{max} (KBr) 1715 (C=O), 1630 (C=C) cm^{-1}. Nuclear magnetic resonance spectrum:[2] δ 6.60 (1H), 7.53 (5H), and 12.53 (2H).

Anal. Calcd. for $C_{10}H_8N_2OS$: C, 58.82; H, 3.95; N, 13.72. Found: C, 59.01; H, 4.08; N, 13.66.

Sodium Salt of 5-Benzal-2-thiohydantoin

5-Benzal-2-thiohydantoin (1 g) dissolved in warm 0.2 *N* sodium hydroxide solution (20 ml). The solution when cool deposited yellow prisms (1.1 g). These were recrystallized from water and dried for 72 h over phosphorus pentoxide under a pressure of 1.0 mm. The crystals sintered at 85–88°, melted at 90°, partially resolidified at 132–136°, and finally melted at 306°, ν_{max} (KBr) 1626 cm^{-1}. (Johnson and O'Brien (6) reported their yellow salt to sinter at 85°, decomp. at 88–89 to an oil which partially resolidified at 115–120° and did not melt up to 260°.) The ultraviolet spectrum of the salt in dilute ethanol solution was identical with that of 5-benzal-2-thiohydantoin.

Anal. Calcd. for $C_{10}H_7N_2OSNa \cdot \frac{1}{2}H_2O$: C, 51.00; H, 3.41. Found: C, 50.75, 50.88; H, 3.51, 3.54.

Acknowledgment

The financial support of the National Research Council of Canada is gratefully acknowledged.

[2]Downfield from tetramethylsilane, in p.p.m.

Can. J. Chem. Downloaded from www.nrcresearchpress.com by 210.87.254.6 on 09/05/12
For personal use only.

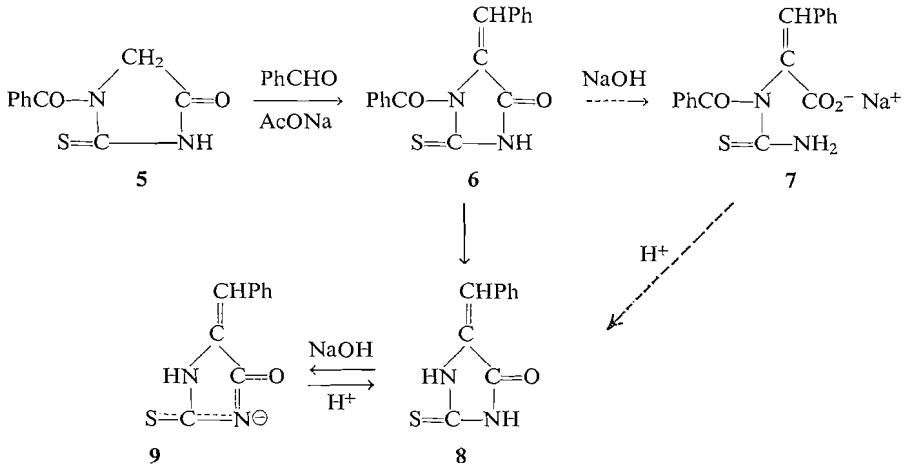

1. E. WARE. Chem. Rev. **46**, 403 (1950). V. H. BAPTIST and H. B. BULL. J. Am. Chem. Soc. **75**, 1727 (1953).
2. P. SCHLACK and W. KUMPF. Z. Physiol. Chem. **154**, 125 (1926).
3. S. G. WALEY and J. WATSON. J. Chem. Soc. 2394 (1951). A. KJAER and P. ERIKSEN. Acta Chem. Scand. **6**, 448 (1952). G. W. KENNER, H. G. KHORANA, and R. J. STEDMAN. J. Chem. Soc. 673 (1953). E. SCOFFONE and A. TURCO. Ric. Sci. **26**, 865, 1506 (1965).
4. J. T. EDWARD and S. NIELSEN. J. Chem. Soc. 5080 (1957).
5. F. B. DAINS, R. THOMPSON, and W. ASENDORF. J. Am. Chem. Soc. **44**, 2310 (1922).
6. T. B. JOHNSON and W. B. O'BRIEN. J. Biol. Chem. **12**, 205 (1912).
7. E. A. WERNER. J. Chem. Soc. **59**, 544 (1891). F. KRAFFT and H. KARSTEUS. Chem. Ber. **25**, 452 (1892).
8. T. CURTIUS. J. Prakt. Chem. [2] **52**, 243 (1895).
9. H. SHIRAI and T. YASHIRO. Nagoya Shiritsu Daigaku Yakugabuka Kiyo **8**, 30 (1960); Chem. Abstr. **55**, 11 396 (1961).
10. J. T. EDWARD and S. NIELSEN. J. Chem. Soc. 5075 (1957).
11. P. EDMAN. Acta. Chem. Scand. **4**, 283 (1950).
12. T. B. JOHNSON and B. H. NICOLET. J. Am. Chem. Soc. **33**, 1973 (1911).

The effect of tetra-*n*-butylammonium salts on the nuclear magnetic resonance of nitrobenzene

J. B. HYNE AND A. R. FABRIS
Department of Chemistry, University of Calgary, Calgary, Alberta

Received July 6, 1967

Tetra-*n*-butylammonium salts effect the nuclear magnetic resonance response of the para and meta protons of nitrobenzene to a greater extent than that of the ortho protons in solutions in carbon tetrachloride. It is suggested that this effect may be due to a specific interaction between the salt, in ion-pair form, and the aromatic ring of nitrobenzene.

Canadian Journal of Chemistry, 46, 73 (1968)

In connection with our studies of tetraalkylammonium salts in various solvents, we have observed the nuclear magnetic resonance (n.m.r.) spectra of tetra-*n*-butylammonium bromide and iodide in 10% nitrobenzene/CCl_4 solvent mixtures. We wish to report briefly an apparent unusual effect of the quaternary ammonium salts on the aromatic proton resonances of the nitrobenzene component of the binary solvent.

Figure 1 illustrates the effect of addition of tetra-*n*-butylammonium bromide on the n.m.r. proton shifts of nitrobenzene (10% solution in CCl_4). Peak assignments for the various ring protons are those of Corio and Dailey (1). Virtually identical behavior was observed for the iodide salt. The shift change for the ortho aromatic protons ($\sim$1 c.p.s.) over the salt concentration range used is barely outside the experimental uncertainty (A-60 nuclear magnetic resonance spectrometer, sweep width 50 c.p.s.,

Can. J. Chem. Downloaded from www.nrcresearchpress.com by 210.87.254.6 on 09/05/12
For personal use only.

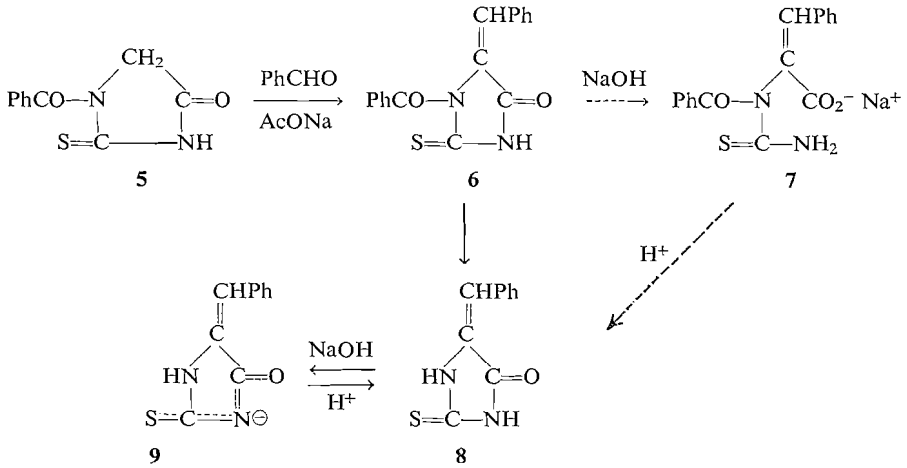

1. E. WARE. Chem. Rev. **46**, 403 (1950). V. H. BAPTIST and H. B. BULL. J. Am. Chem. Soc. **75**, 1727 (1953).
2. P. SCHLACK and W. KUMPF. Z. Physiol. Chem. **154**, 125 (1926).
3. S. G. WALEY and J. WATSON. J. Chem. Soc. 2394 (1951). A. KJAER and P. ERIKSEN. Acta Chem. Scand. **6**, 448 (1952). G. W. KENNER, H. G. KHORANA, and R. J. STEDMAN. J. Chem. Soc. 673 (1953). E. SCOFFONE and A. TURCO. Ric. Sci. **26**, 865, 1506 (1965).
4. J. T. EDWARD and S. NIELSEN. J. Chem. Soc. 5080 (1957).
5. F. B. DAINS, R. THOMPSON, and W. ASENDORF. J. Am. Chem. Soc. **44**, 2310 (1922).
6. T. B. JOHNSON and W. B. O'BRIEN. J. Biol. Chem. **12**, 205 (1912).
7. E. A. WERNER. J. Chem. Soc. **59**, 544 (1891). F. KRAFFT and H. KARSTEUS. Chem. Ber. **25**, 452 (1892).
8. T. CURTIUS. J. Prakt. Chem. [2] **52**, 243 (1895).
9. H. SHIRAI and T. YASHIRO. Nagoya Shiritsu Daigaku Yakugabuka Kiyo **8**, 30 (1960); Chem. Abstr. **55**, 11 396 (1961).
10. J. T. EDWARD and S. NIELSEN. J. Chem. Soc. 5075 (1957).
11. P. EDMAN. Acta. Chem. Scand. **4**, 283 (1950).
12. T. B. JOHNSON and B. H. NICOLET. J. Am. Chem. Soc. **33**, 1973 (1911).

The effect of tetra-*n*-butylammonium salts on the nuclear magnetic resonance of nitrobenzene

J. B. HYNE AND A. R. FABRIS
Department of Chemistry, University of Calgary, Calgary, Alberta

Received July 6, 1967

Tetra-*n*-butylammonium salts effect the nuclear magnetic resonance response of the para and meta protons of nitrobenzene to a greater extent than that of the ortho protons in solutions in carbon tetrachloride. It is suggested that this effect may be due to a specific interaction between the salt, in ion-pair form, and the aromatic ring of nitrobenzene.

Canadian Journal of Chemistry, 46, 73 (1968)

In connection with our studies of tetraalkylammonium salts in various solvents, we have observed the nuclear magnetic resonance (n.m.r.) spectra of tetra-*n*-butylammonium bromide and iodide in 10% nitrobenzene/CCl_4 solvent mixtures. We wish to report briefly an apparent unusual effect of the quaternary ammonium salts on the aromatic proton resonances of the nitrobenzene component of the binary solvent.

Figure 1 illustrates the effect of addition of tetra-*n*-butylammonium bromide on the n.m.r. proton shifts of nitrobenzene (10% solution in CCl_4). Peak assignments for the various ring protons are those of Corio and Dailey (1). Virtually identical behavior was observed for the iodide salt. The shift change for the ortho aromatic protons ($\backsim$1 c.p.s.) over the salt concentration range used is barely outside the experimental uncertainty (A-60 nuclear magnetic resonance spectrometer, sweep width 50 c.p.s.,

Can. J. Chem. Downloaded from www.nrcresearchpress.com by 210.87.254.5 on 09/05/12
For personal use only.

sweep time 0.2 c.p.s./s, radio frequency field 0.13 MG., response 0.4 c.p.s.) whereas the shift for the meta and para protons (~6 c.p.s.) is clearly significantly greater. The downfield shift of the meta and para protons is essentially a linear function of the salt concentration. Solubility limitations precluded studies at a higher salt concentration.

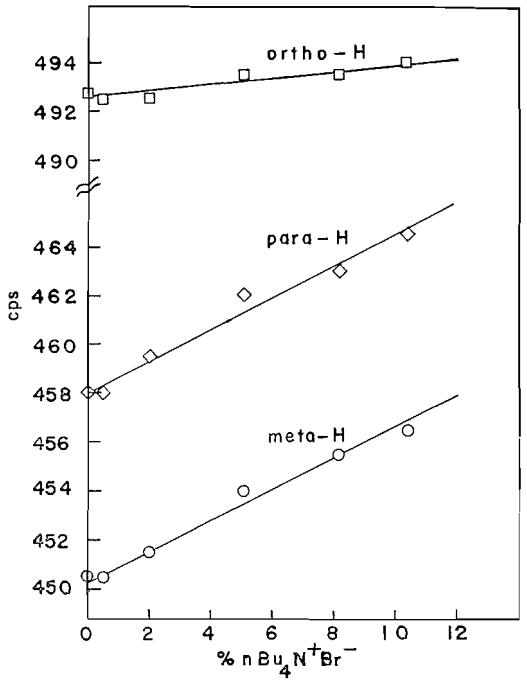

FIG. 1. The effect of added salt on the proton resonances of nitrobenzene. The shifts are in c.p.s. at 60 Mcycles relative to internal TMS. The ortho proton values are given as the center of the multiplet.

We consider this observation interesting because of the possible importance of a specific interaction between the quaternary ammonium salts, largely in the ion-pair form in this low dielectric medium, and the strongly dipolar nitrobenzene. Nicholls and Szwarc (2) have recently reported the observation of similar effects on the proton shifts of cyclic ethers on the addition of salts to these solvents. Lithium perchlorate and silver tetrafluoroboride both caused downfield shifts of the ether solvent protons, the effects being greatest on the protons α to the ethereal oxygen which is presumably the site of specific interaction with the salt. Lithium and sodium tetraphenylborides, however, produced upfield shifts which were greater for the more remote β protons than for the protons α to the ethereal oxygen. These authors suggest that this reversal of behavior is caused by the anisotropy of the aromatic rings of the salt anion which avoid the vicinity of the ether oxygen atoms and adopt a preferred orientation with respect to the β protons.

We have previously suggested that the unusually high ion-pair association constant for the tetra-*n*-butylammonium salts in nitrobenzene may be due to the nitrobenzene acting as a 'template' for the ion pair thus favoring its formation (3). The observed downfield shift of the meta and para protons, but not the ortho protons, cannot be the result of interaction solely between the nitro substituent and the salt ion pair. This would be expected to have the most pronounced effect on the n.m.r. shift of the ortho protons in a similar manner to the α proton effect in the ethers observed by Nicholls and Szwarc. If, however, the halide ion of the ion pair occupied a preferred location at the meta/para end of the aromatic ring, polarization of the molecule in the direction of the electron flow toward the nitro substituent or simple Van der Waals interaction would deshield the para and meta protons leading to a small downfield shift. The effect at the ortho protons would be small due to the dominant influence of the proximate nitro group and steric inhibition of close approach of either component of the ion pair. We have examined the effect of added salt on the ultraviolet spectrum of nitrobenzene in the hope of obtaining some evidence for a weak interaction of the type suggested. No convincing evidence was obtained. The n.m.r. results, however, appear to be beyond question and it may well be that whereas the interaction between the salt and the aromatic ring is strong enough to elicit a small shift in the proton resonance it is too weak effectively to influence the electronic transitions responsible for the ultraviolet absorption.

1. P. L. CORIO and B. P. DAILEY. J. Am. Chem. Soc. **78**, 3043 (1956).
2. D. NICHOLLS and M. SZWARC. J. Phys. Chem. **71**, 2727 (1967).
3. J. B. HYNE. J. Am. Chem. Soc. **85**, 304 (1963).

Can. J. Chem. Downloaded from www.nrcresearchpress.com by 210.87.254.5 on 09/05/12
For personal use only.

Convenient synthesis of myristicinaldehyde

ALEXANDER T. SHULGIN
1483 Shulgin Road, Lafayette, California

Received August 8, 1967

The conversion of isomyristicin to a Schiff base of myristicinaldehyde is described. The subsequent hydrolysis of this base to the free aldehyde establishes a convenient preparation of this material. Apiolealdehyde is similarly generated from isoapiole, suggesting that this procedure may have general application in the conversion of the natural aromatic ethers of essential oils to the correspondingly substituted benzaldehydes.

Canadian Journal of Chemistry, 46, 75 (1968)

Can. J. Chem. Downloaded from www.nrcresearchpress.com by 210.87.254.6 on 09/05/12
For personal use only.

In connection with a study of the syntheses of alkaloids related to *Anhalonium lewinii*, the need arose for appreciable quantities of myristicinaldehyde (**4**, R = H). Three preparatory routes were considered: the cyclic ether could be prepared from 5-hydroxyvanillin; 2,3-methylenedioxyanisole could be appropriately formylated; or modifications could be made on the chain of naturally available myristicin.

Examples of the first process which employ methylene bromide (1) and methylene sulfate (2) in the formation of the methylenedioxy ring have been reported. In both instances the yields of myristicinaldehyde were prohibitively poor. Present attempts in this manner employing methylene iodide proved to be equally impractical.

The Vilsmeier reaction, which adds a formyl group to the aromatic ring, has been applied to 2,3-methylenedioxyanisole. The earliest report (3) described a 46% yield of product substituted adjacent to the methoxyl group, but subsequently it was observed that an appreciable percentage of substitution also occured adjacent to the methylenedioxy group (4). A careful gas–liquid chromatographic analysis has been performed of the crude reaction mixture. The two isomers described are indeed the principal components, but a third peak of the desired orientation was consistently present. It amounted to only 5% of the total aldehyde content, however, and no experimental variation could be found to increase this yield.

The third route, that which starts with myristicin, appeared to be the only practical synthesis of the title compound. Base-catalyzed isomerization to isomyristicin (**1**) places the double bond in a position appropriate to an aldehydic end product. $KMnO_4$ has been employed in a number of procedures (5) to provide the final aldehyde, but there is concurrent formation of the corresponding benzoic acid. Hydrogen peroxide with a vanadium catalyst (6) precludes acid formation but still provides only modest yields. It has only been through ozonolysis that sizable quantities of **4** have been prepared (7) but here minor variations in the reaction conditions seriously affect the yields realized (7*c*).

It has been observed in the course of the preparation of a number of β-nitrophenylpropenes from the corresponding olefinic precursors (8), that there was invariably produced a small amount of the aromatic aldehyde that would result from cleavage of the propenylbenzene at the double bond. This hydrolysis of the product nitropropene into its theoretical synthetic precursors (benzaldehyde and nitroalkane) was explored as a preparative route to these aldehydes which are otherwise difficult to obtain.

It has been found that this hydrolytic reaction is the principal reaction to occur when an amine that can form a Schiff base (**3**) is introduced. The completion of the synthetic cycle by the base-catalyzed condensation of the product aldehyde with nitroethane to regenerate the nitropropene (**2**) both verifies the structure of the aldehyde generated and confirms that the action of tetranitromethane is indeed on the β-carbon of the phenylpropene. Of a number of bases explored as agents in this displacement, primary amines related to benzylamine gave the most consistent results, and of these DL-α-methylbenzylamine appeared to be the best.

The reaction is allowed to occur between stoichiometric amounts of the benzylamine and the nitropropene. If the amine is employed in excess as a solvent a material that corresponds to

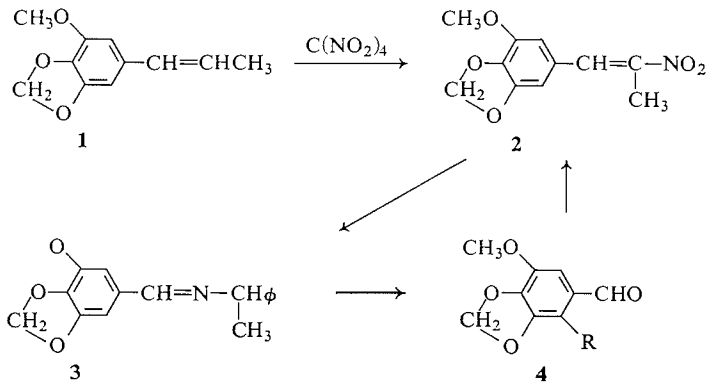

a 1:1 adduct of these two components is obtained as the principal product.

This procedure has been successfully employed in the preparation of apiolealdehyde (**4**, R = OCH_3) from isoapiole (85%) and appears to be generally applicable to nitropropenes derivable from natural essential oils.

Experimental

1-(3-Methoxy4-,5-methylenedioxyphenyl)-2-nitropropene (2)

A solution of 50 g isomyristicin (**1**) in 300 ml dry acetone and 24 g pyridine was cooled to 0 °C with vigorous stirring. There was then added 54 g of cold tetranitromethane which caused a slight temperature rise (to 5°) despite the external cooling. The stirring was continued for 2 min at which time the reaction mixture was quenched with a chilled solution of 16.8 g KOH in 300 ml H_2O. Stirring was continued while the heat of neutralization dissipated, and the product was then removed by filtration. An additional quantity of the nitropropene (for a total of 50.7 g, 82%) was obtained from the filtrates by extraction with methylene chloride. The low melting point (103°) was due to a small contamination with myristicinaldehyde which is generated concurrently. Although it cannot interfere with the subsequent reaction below, it can be removed by recrystallization from methanol to yield yellow needles of **2**, m.p. 110°.

Myristicinaldehyde (4; R = H)

An intimate mixture of 50 g **2** and 26 g DL-α-methylbenzylamine was heated on the steam bath until solution was effected and the evolution of nitroethane was complete. The intermediate Schiff base **3** was hydrolyzed without isolation by the addition of dilute hydrochloric acid and continued heating. At 60 to 80° there was an abrupt solidification of the myristicinaldehyde that had formed and further heating was unnecessary. The aldehyde is removed by filtration of the cooled reaction mixture and could be purified either by crystallization from water, or better by exhaustive extraction of this crude solid product with boiling hexane. The yield thus obtained is 36.9 g (97% of theory and 79% overall from isomyristicin) of a cream-colored solid with m.p. 128–129°.

Complete integrity of the ether orientation was established by the reconversion of **4** to **2** with nitroethane as has been described for the trimethoxy counterpart (8).

Preparation of the Nitropropene: α-Methylbenzylamine Adduct, $C_{19}H_{22}N_2O_5 \cdot xH_2O$

When an excess of the benzylamine is employed as a solvent, the addition of water at the end of the above-mentioned dissolution resulted in an intensely insoluble product, m.p. 161° (decomposition) which is soluble in neither the aqueous nor the organic phase. This white solid, on washing with acetonitrile, showed an analysis that indicated it to be an adduct of one molecule of each of the reactants, with about two molecules of water of hydration.

Anal. Calcd. for $C_{19}H_{22}N_2O_5 \cdot 2H_2O$: C, 57.85; H, 6.39; N, 7.10. Found: C, 58.14; H, 5.99; N, 6.72.

A more convincing argument for this molecular formula comes from mass spectrometric analysis, which showed a molecular ion at *m/e* 358 which corresponds to the water-free 1:1 adduct. A daughter ion at *m/e* 283, corresponding to the loss of the $CH_3CH_2NO_2$ moiety, is confirmed by an appropriate metastable peak. An independent daughter peak at *m/e* 237 indicated the loss of α-methylbenzylamine moiety but with the retention of the nitroethane; this corresponds to the production of an ion corresponding to **2**. The use of benzylamine led to a similar product (m.p. 152° decomposition) and lends weight to the suggested stoichiometry.[1] Although the microanalytical results indicated some two or three molecules of water of hydration, again the mass spectrum showed only the molecular ion peak corresponding to the anhydrous 1:1 adduct ($C_{18}H_{20}N_2O_5$; *m/e* 344), and both daughter ions corresponding to the loss either of nitroethane (*m/e* 269) or of benzylamine (*m/e* 237).

Apiolealdehyde (4, R = OCH_3)

Employing the procedure described above for isomyristicin, isoapiole (m.p. 55–56° obtained from apiole of Oil of Parsley) was nitrated to 1-(2,5-dimethoxy-3,4-methylenedioxyphenyl)-2-nitropropene, and this intermediate was similarly converted to the aldehyde. This

[1]Both of these hydrated adducts showed in their infrared spectra, a salt-like structure involving the N—H bond which indicated an intramolecular interaction with the nitro group.

Can. J. Chem. Downloaded from www.nrcresearchpress.com by 210.87.254.6 on 09/05/12
For personal use only.

product aldehyde (m.p. 102–103°) was obtained in a 75% overall yield from isoapiole.

Formylation of 2,3-Methylenedioxyanisole

The crude reaction product, obtained from the interaction of 2,3-methylenedioxyanisole with the Vilsmeier Complex generated from *N*-methylformanilide and $POCl_3$, was analyzed by gas–liquid chromatography. Complete separation of the three possible benzaldehydes was achieved through the use of an ethylene glycol succinate column (15%, 150 × 1 cm) at 190 °C. The two major peaks emerged at 7.8 min and at 12.0 min, and were readily identified as 2-methoxy-3,4-methylenedioxybenzaldehyde and 4-methoxy-2,3-methylenedioxybenzaldehyde, respectively. The third aldehyde, myristicinaldehyde, occurred as a minor peak at 9.5 min. A characteristic ratio for these materials was 45:9:1, and variation in reaction condition caused marked variation in total yield but little change in this ratio.

1. K. N. CAMPBELL, P. F. HOPPER, and B. K. CAMPBELL. J. Org. Chem. **16**, 1736 (1951).
2. W. BAKER, L. V. MONTGOMERY, and H. A. SMITH. J. Chem. Soc. 1281 (1932).
3. W. B. BROWNELL and A. W. WESTON. J. Am. Chem. Soc. **73**, 4971 (1951).
4. A. F. WAGNER, E. WALTON, A. N. WILSON, J. L. RODIN, F. W. HOLLY, N. G. BRINK, and K. FOLKERS. J. Am. Chem. Soc. **81**, 4987 (1959).
5. (*a*) F. W. SEMMLER. Chem. Ber. **24**, 3818 (1891). (*b*) H. THOMS. Chem. Ber. **36**, 3446 (1903). (*c*) A. H. SALWAY. J. Chem. Soc. **95**, 1204 (1909). (*d*) A. R. SURREY. J. Am. Chem. Soc. **70**, 2887 (1948). (*e*) C. E. REDEMANN, B. B. WISEGARRER, and R. N. ICKE. J. Org. Chem. **13**, 886 (1948).
6. K. E. HAMLIN and A. W. WESTON. J. Am. Chem. Soc. **71**, 2210 (1949).
7. (*a*) E. SPÄTH and J. GANGL. Monatsh. Chem. **44**, 103 (1923). (*b*) F. DALLACKER, F. GOHLKE, and M. LIPP. Monatsh. Chem. **91**, 1089 (1960). (*c*) B. F. ANDERSON, L. H. BRIGGS, T. CEBALO, and M. A. TROTMAN. J. Chem. Soc. 1026 (1964).
8. A. T. SHULGIN. J. Med. Chem. **9**, 445 (1966).

Steroid 16,17-furoxan derivatives

HANS REIMANN AND HELEN SCHNEIDER

Natural Products Research Department, Schering Corporation, Bloomfield, New Jersey

Received August 11, 1967

The syntheses of 3-methoxy-1,3,5(10)-estratrieno[16,17-*c*]furoxan (**3**) and 3-keto-4-androsteno[16,17-*c*]furoxan (**8**) from 16-oximinoestrone methyl ether and 16-oximino-5-androsten-3β-ol-17-one, respectively, are described.

Canadian Journal of Chemistry, **46**, 77 (1968)

In recent years there has been considerable interest in steroid analogues containing a fused heterocyclic ring, particularly at the 2,3- or 16,17-positions of the steroid nucleus (1). We now report the synthesis of [16,17-*c*]furoxans ([16,17-*c*][1′,2′,5′]oxadiazole *N*-oxides) in the androstane and estrane series.

The reaction of 16-oximinoestrone 3-methyl ether (**1**) (2, 3) with hydroxylamine hydrochloride in pyridine afforded the 16,17-bisoximino compound **2** (2, 4) which was oxidized with sodium hypochlorite (5) to give 3-methoxy-1,3,5(10)-estratrieno[16,17-*c*]furoxan (**3**). While compound **3** had a sharp melting point and appeared homogeneous in two chromatographic systems, its nuclear magnetic resonance (n.m.r.) spectrum[1] showed bands for the C-18 protons at 1.21 and 1.18 p.p.m., representing the two possible *N*-oxides **3***a* and **3***b*, the upfield band presumably being due to shielding by the 5′-*N*-oxide in the latter (6). The formation of two isomeric furoxans is in agreement with the observations of Havranek and co-workers (7), who recently described the syntheses of some steroid [2,3-*c*]-furazans ([2,3-*c*][1′,2′,5′]oxadiazoles) and [2,3-*c*]-furoxans ([2,3-*c*][1′,2′,5′]oxadiazole *N*-oxides). The preparation of a series of androstano [2,3-*c*]-furazans and [2,3-*c*]furoxans has also recently been reported by a Japanese group (8).

In a similar manner 16-oximino-5-androsten-3β-ol-17-one (**4**) (9) was converted to the 16,17-bisoxime **5**, which on oxidation afforded 3β-hydroxy-5-androsteno[16,17-*c*]furoxan (**6**). The nuclear magnetic resonance (n.m.r.) spectrum of **6** again showed the presence of both the 2′- and 5′-*N*-oxides, **6***a* and **6***b* (C-18 bands at 1.22 and 1.18 p.p.m., C-19 singlet at 1.08 p.p.m.), with the former predominating. Compound **6** was

[1]We thank Mr. M. Yudis for the nuclear magnetic resonance evaluations. Nuclear magnetic resonance spectra were recorded in deuteriochloroform solution, unless otherwise noted, on a Varian A-60 A instrument.

Can. J. Chem. Downloaded from www.nrcresearchpress.com by 210.87.254.6 on 09/05/12
For personal use only.

Can. J. Chem. Downloaded from www.nrcresearchpress.com by 210.87.254.6 on 09/05/12
For personal use only.

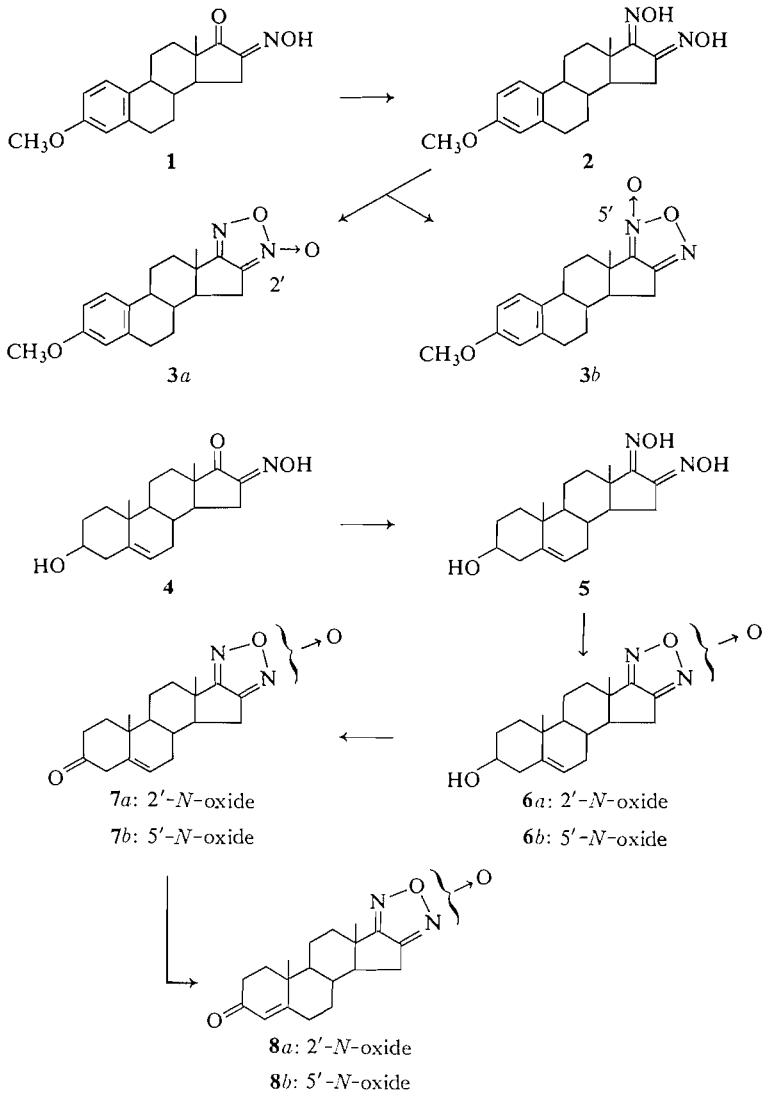

oxidized with Jones' reagent (10) to the 3-keto analogue **7**. The latter was not fully characterized but was isomerized directly to afford the desired 3-keto-4-androsteno[16,17-*c*]furoxan (**8**). The n.m.r. spectrum of **8** in deuteriochloroform showed a summation band for the C-18 and C-19 protons at 1.27 p.p.m. In pyridine, however, this was resolved into a doublet, the more intense, upfield band (1.02 p.p.m.) presumably representing a summation of the C-19 protons and of the C-18 protons of the 5′-*N*-oxide isomer **8***b*, while the lesser, downfield band (1.05 p.p.m.) is due to the C-18 protons of the 2-*N*-oxide isomer **8***a*.

Experimental[2]

3-Methoxy-16,17-bisoximino-1,3,5(10)-estratriene (2)

To a solution of 925 mg of 16-oximinoestrone methyl ether (m.p. 202–205°; $\lambda\lambda_{max}$ (MeOH) 230, 276, 285 mμ

[2]Melting points were determined on a Fisher–Johns apparatus and are uncorrected. Rotations were measured in dioxane unless otherwise noted. Physical and analytical data were obtained by the Physical Chemistry Department, Schering Corporation.

Can. J. Chem. Downloaded from www.nrcresearchpress.com by 210.87.254.6 on 09/05/12
For personal use only.

(ε 13 300, 2500, 2000); λ_{max} (MeOH–NaOH) 287 mμ; $\lambda\lambda_{max}$ (Nujol) 3.05, 5.73, 6.09, 6.17, and 6.64 μ; $[\alpha]_D$ +90° (reported (3, 4): m.p. 180–183°; ·H_2O m.p. 198°)) in 20 ml of pyridine was added 1.0 g of hydroxylamine hydrochloride and the mixture allowed to stand at room temperature for 18 h. The solution was poured into ice water and the resulting precipitate was filtered, washed with water, and dried to give 954 mg of **2**. The product was crystallized from much methanol to afford a total of 673 mg of pure **2**, m.p. 251–255° (decomp.); $[\alpha]_D$ −23° (pyridine); $\lambda\lambda_{max}$ (MeOH) 223, 228, 245, 286 mμ (ε 13 800; 13 400; 9000; 2600); $\lambda\lambda_{max}$ (Nujol) 2.94, 6.16, 6.31, 6.64 μ. (Reported (4): m.p. 230° (decomp.))

Anal. Calcd. for $C_{19}H_{24}N_2O_3$: C, 69.49; H, 7.37; N, 8.53. Found: C, 69.56; H, 7.72; N, 8.42.

3-Methoxy-1,3,5(10)-estratrieno[16,17-c]furoxan (3)

To a suspension of 638 mg of compound **2** in a mixture of 28.8 ml of 10% aqueous sodium hydroxide and 56.4 ml of water, chilled in an ice bath, was added dropwise with stirring 150 ml of a freshly prepared 1.0 *N* solution of sodium hypochlorite. Stirring was continued in the cold for 90 min, then the precipitate was filtered, washed with water and dried, giving 614 mg of **3**, m.p. 182–184°. Crystallization from acetone–hexane, after treatment with decolorizing carbon, afforded analytically pure material,[3] m.p. 185–187°; $[\alpha]_D$ +55°; $\lambda\lambda_{max}$ (MeOH) 223, 261, 286 mμ (ε 10 600, 6500, 2400); $\lambda\lambda_{max}$ (Nujol) 6.00, 6.16, 6.33, 6.50, 6.65 μ.

Anal. Calcd. for $C_{19}H_{22}N_2O_3$: C, 69.92; H, 6.79; N, 8.58. Found: C, 69.77; H, 6.68; N, 8.41.

16,17-Bisoximino-5-androsten-3β-ol (5)

A solution of 3.533 g of 16-oximino-5-androsten-3β-ol-17-one and 3.5 g of hydroxylamine hydrochloride in 75 ml of pyridine was kept at room temperature overnight. The solution was then poured into ice water and the resulting precipitate was filtered, washed with cold water, and dried to give 3.594 g of crude **5**. The material was crystallized from methanol to yield a total of 2.332 g of pure **5**, m.p. 262–263° (decomp.); $[\alpha]_D$ −148° (pyridine); λ_{max} (MeOH) 247 mμ (ε 8200); λ_{max} (MeOH–NaOH) 275 mμ; $\lambda\lambda_{max}$ (Nujol) 2.94, 3.14, 6.0 (w)μ.

Anal. Calcd. for $C_{19}H_{28}N_2O_3 \cdot H_2O$: C, 65.11; H, 8.63; N, 7.99. Found: C, 65.32; H, 8.55; N, 8.21.

3β-Hydroxy-5-androsteno[16,17-c]furoxan (6)

To a suspension of 2.000 g of compound **5** in a mixture of 88 ml of 10% aqueous sodium hydroxide, 160 ml of water and 40 ml of ethanol, chilled in an ice bath, was added dropwise with stirring 312 ml of a freshly prepared 1.0 *N* solution of sodium hypochlorite. The reaction mixture was stirred at 0° for 2 h, then kept in the refrigerator overnight. The precipitated product was filtered, washed with water, and dried, giving 1.839 g, m.p. 172–175°. The material was crystallized from acetone–hexane to yield 1.505 g, m.p. 178–179°. The analytical sample was recrystallized from aqueous methanol, m.p. 178–179°; $[\alpha]_D$ −101°; λ_{max} (MeOH) 259 mμ (ε 5810); $\lambda\lambda_{max}$ (Nujol) 3.03, 6.00, 6.50 μ.

Anal. Calcd. for $C_{19}H_{26}N_2O_3$: C, 69.06; H, 7.93; N, 8.48. Found: C, 68.82; H, 8.03; N, 8.67.

3-Keto-5-androsteno[16,17-c]furoxan (7)

A solution of 300 mg of compound **6** in 15 ml of acetone was chilled in an ice bath and chromic – sulfuric acid reagent (266 mg chromium trioxide/ml solution) was added dropwise with stirring until a permanent orange coloration of the solution was obtained. After standing in the cold for 5 min, some methanol was added, then the mixture was poured into ice water. The resulting precipitate was filtered, washed with water, and dried to afford 225 mg of crude **7**, m.p. about 140–210° (decomp.); [4]λ_{max} (MeOH) 258 mμ (ε 6250); $\lambda\lambda_{max}$ (Nujol) 5.83, 6.00, 6.50 μ. This material was used without further purification in the next experiment.

3-Keto-4-androsteno[16,17-c]furoxan (8)

To a filtered solution of 220 mg of crude 7 in hot methanol was added 5% sodium hydroxide to pH 8–9. The solution was heated on the steam bath for 5 min, then neutralized with acetic acid, concentrated to a low volume and poured into ice water. The resulting precipitate was filtered, washed with water, and dried to afford 180 mg of crude **8**, m.p. 198–200°. The product was dissolved in acetone, treated with decolorizing carbon, and crystallized from acetone–hexane, giving 85 mg, m.p. 208–210° (decomp.) and a second crop of 64 mg. The analytical sample was recrystallized from acetone–hexane, m.p. 212–214° (decomp.); $[\alpha]_D$ +31°; λ_{max} (MeOH) 240 mμ (ε 20 000); $\lambda\lambda_{max}$ (Nujol) 5.98, 6.04, 6.19, 6.50 μ.

Anal. Calcd. for $C_{19}H_{24}N_2O_3$: C, 69.49; H, 7.37; N, 8.53. Found: C, 69.52; H, 7.57; N, 8.69.

1. P. DE RUGGIERI, C. GANDOLFI, V. GUZZI, D. CHIARAMONTI, and C. FERRARI. Farmaco, Pavia, Ed. Sci. **20**, 280 (1965). For a review and leading references.
2. M. N. HUFFMAN. J. Biol. Chem. **167**, 273 (1947).
3. A. BUTENANDT and E. L. SCHÄFFLER. Z. Naturforsch. **1**, 82 (1946).
4. M. N. HUFFMAN. J. Am. Chem. Soc. **64**, 2235 (1942).
5. J. H. BOYER and U. TOGGWEILER. J. Am. Chem. Soc. **79**, 895 (1957).
6. F. B. MALLORY and A. CAMMARATA. J. Am. Chem. Soc. **88**, 61 (1966).
7. R. E. HAVRANEK, G. B. HOEY, and D. H. BAEDER. J. Med. Chem. **9**, 326 (1966).
8. G. OHTA, T. TAKEGOSHI, K. UENO, and M. SHIMIZU. Chem. Pharm. Bull. Tokyo, **13**, 1445 (1965).
9. F. H. STODOLA, E. C. KENDALL, and B. F. MCKENZIE. J. Org. Chem. **6**, 841 (1941).
10. R. G. CURTIS, I. HEILBRON, E. R. H. JONES, and G. F. WOODS. J. Chem. Soc. 461 (1953).
11. K. E. PFITZNER and J. G. MOFFATT. J. Am. Chem. Soc. **87**, 5670 (1965).

[3]Thin-layer chromatography of **3** on silica gel, using triple development with benzene or single development with 0.5% methanol in benzene, showed a single spot by ultraviolet absorption and by staining with 50:50 methanol – sulfuric acid spray.

[4]Compare with ref. 11, in which it is shown that steroid 5-en-3-ones are rearranged to the corresponding 4-en-3-ones in the course of melting point determinations.

Reactions of nitro sugars. VII. A study on acetylation and some chemical properties of acetates[1]

HANS H. BAER, FRANK KIENZLE, AND FAROUK RAJABALEE
Department of Chemistry, University of Ottawa, Ottawa, Canada

Received August 10, 1967

The 2,4,6-tri-*O*-acetates of methyl 3-deoxy-3-nitro-β-D-glucopyranoside, -galactopyranoside, and -mannopyranoside, the 2-*O*-acetates of the 4,6-*O*-benzylidene derivatives of the two first-mentioned glycosides, and the tetra-*O*-acetate of 1,4-dideoxy-1,4-dinitro-*neo*-inositol are prepared by boron trifluoride–catalyzed acetylation. The advantages of the procedure over acetylation in pyridine are pointed out. The *gluco* triacetate, when produced in the presence of pyridine, is accompanied by crystalline by-products of a novel nature. It suffers undetermined changes by the action of activated alumina, and in dilute aqueous alkali it is instantly converted into an unsaturated nitronate.

Canadian Journal of Chemistry, **46**, 80 (1968)

Can. J. Chem. Downloaded from www.nrcresearchpress.com by 210.87.254.42 on 09/05/12
For personal use only.

In recent investigations concerning the acetylation of the hydroxyl group at C-2 of methyl 4,6-*O*-benzylidene-3-deoxy-3-nitro-hexopyranosides, a number of complications to the seemingly simple problem were uncovered. Thus, hot acetic anhydride and sodium acetate effected straightforward acetylation of the β-D-*gluco* isomer, but caused C-2 epimerization in the β-D-*manno* isomer and dehydration in the β-D-*galacto* and α-D-*talo* isomers. Acetylation with acetic anhydride and pyridine gave satisfactory results in the D-*gluco* and D-*manno* series but failed with the β-D-*galacto* and α-D-*talo* isomers (1, 2). Catalysis by acids such as sulfuric or perchloric was deemed inadvisable because of the inherent danger of acetolysis in the glycoside and benzylidene acetal structures. When it became evident that the preparation of 2,4,6-tri-*O*-acetates of methyl 3-deoxy-3-nitrohexopyranosides, which were required for certain synthetic purposes, was attended with similar or even greater difficulties, an alternative method of acetylation was sought.

Using acetic anhydride in the presence of boron trifluoride, a catalyst that has been employed for many purposes (3) but apparently not to any great extent for the esterification of nitro alcohols, we have now been able to prepare, conveniently and with yields of up to 90%, crystalline methyl 2,4,6-tri-*O*-acetyl-3-deoxy-3-nitro-β-D-glucopyranoside, -β-D-mannopyranoside, and -β-D-galactopyranoside. The method is applicable also to cyclic acetal derivatives as was demonstrated with the examples of methyl 4,6-*O*-benzylidene-3-deoxy-3-nitro-β-D-gluco- and β-D-galactopyranosides that were acetylated smoothly with retention of the benzylidene group. Further examples include the *O*-acetylation of an acetamidonitro glycoside[2] and of a dinitroinositol. The latter, 1,4-dideoxy-1,4-dinitro-*neo*-inositol, gave its tetra-*O*-acetate in excellent yield.[3]

It has been reported (6) that some primary and secondary nitroalkanes when treated with acetic anhydride and boron trifluoride undergo a displacement of the nitro group by the acetoxy group. Nitrocyclohexane, for instance, has been stated to give cyclohexyl acetate in yields of up to 58%. Although the same reaction conditions were actually adopted for glycoside acetylations in the present work, no displacement was observed. In fact, attempts to induce it by modifying the conditions were unsuccessful. It would therefore appear that nitro sugars, perhaps because of the abundance of oxygen functions, do not lend themselves to this interesting reaction.

The action of base upon a β-acetoxynitroalkane is known to cause elimination of acetic acid; the α-nitroalkene so generated is prone to immediate nucleophilic addition of the base present, provided the latter is a sufficiently strong nucleophile. The over-all result then is an exchange of the acetoxy group for the nucleophile employed (7). Alcoholic alkoxide or ammonia solutions produce β-nitro ethers and β-nitroamines respectively. Consequently, it is not feasible with these standard reagents to regenerate structurally unchanged nitro glycosides from their *O*-acetates (4, 8). The use of

[1]For part VI in this series, see H. H. Baer, T. Neilson, and W. Rank. Can. J. Chem. **45**, 991 (1967).

[2]This has already been communicated in another connection (4).

[3]This compound can be prepared in equally good yield by catalysis with sulfuric acid, whereas in pyridine, aromatization to 2,5-dinitrophenyl acetate takes place (5).

Can. J. Chem. Downloaded from www.nrcresearchpress.com by 210.87.254.42 on 09/05/12
For personal use only.

aqueous alkali for such regenerations was therefore worth considering, although it was realized that, because of the intermediacy of α-nitroalkene structures, the glycosides would still be subject to epimerizations. A spectroscopic experiment revealed, however, that the action of 0.01 *N* sodium hydroxide at 25° upon methyl 2,4,6-tri-*O*-acetyl-3-deoxy-3-nitro-β-D-glucopyranoside (**1***b*) does not lead to the deacetylated parent glucoside (**1***a*) nor to any epimer thereof. Shortly after being alkalized an aqueous solution of **1***b* exhibits a strong peak in its ultraviolet absorption spectrum at λ_{max}302 mμ (ε, 19 000 after 4 min). No high intensity absorption is seen in the 250 mμ region where the nitronate **2***b* as well as the deacetylated nitronate **2***a* would be expected to absorb. Upon acidification of the alkaline solution, the peak incurs a shift from 302 to 288 mμ and then decreases rapidly in intensity, disappearing within 30 min. Thereafter, if the solution is again made alkaline, the original absorption pattern is not restored. These observations are explicable on the basis of our recent study (9) concerning the formation of allylic glycoside nitronates. It has been shown that the non-acetylated glucoside (**1***a*) is converted *via* **2***a* into the unsaturated nitronate **4***a*, with an α-nitroalkene (**3***a*) postulated as an intermediate. Even at 98° this process was slow enough to permit spectral observation of a gradual disappearance of **2***a* and concurrent production of **4***a*. From the present study it is evident that the reaction of the triacetate **1***b* is too rapid for intermediary, saturated **2***b* to be observed, and the formation of the unsaturated nitronate (**4***b*) is nearly complete within the time required for recording the spectrum. The most likely reason for this acceleration is the superior character of acetoxyl vs. hydroxyl as a leaving group at C-4 in the saturated nitronate and the inductive assistance to proton abstraction from C-5 by the acetoxyl group at C-6 in the intermediate α-nitroalkene.[4] The spectral changes that follow acidification are fully analogous to those occurring with the non-acetylated compound and are seen as a result of the liberation of nitronic acid **5***b* (hypsochromic shift of 14 mμ) with subsequent *aci*-nitro – nitro tautomerization to **6***b* (loss of absorbance at 288 mμ). Since after this transformation, the spectrum characteristic of **4***b* is not restored by the addition of alkali, **6***b* appears to undergo further chemical changes, which are as yet unelucidated.

The considerable sensitivity of **1***b* is also attested to by the finding that it reacts with activated silica gel during thin-layer chromatography in *n*-heptane – 2-butanone. Pure **1***b* gave, in addition to its main spot at R_f 0.6, a weak spot at R_f 0.8. The intensity of the latter increased at the expense of the former by prolonging the time of contact of the material with the silica gel prior to irrigation. When **1***b* was boiled for 15 min in chloroform in the presence of a large excess of the gel, it was converted completely into the fast-moving material. A preparative experiment yielded a colorless, strongly levorotatory syrup ($[\alpha]_D$ −132°) which contained methoxyl and acetyl groups in a ratio of 1:2 as judged from the integration of nuclear magnetic resonance (n.m.r.) signals near τ 6.5 and 7.9. Low-field resonance near τ 2.5 (intensity, 1 H) and an infrared band at 1 530 cm^{-1} may be assigned to a structural element $-C(NO_2):CH-$. These preliminary indications suggest that silica gel effects an elimination of a molecule of acetic acid from **1***b*.

Prior to adopting the superior boron trifluoride method of acetylation, we have acetylated with modest success the glucoside **1***a* in the presence of pyridine. When the crude triacetate **1***b* produced in this manner was recrystallized from hot aqueous ethanol, the mother liquor turned yellow and exhibited a strong absorption peak at λ_{max} 346 mμ. This was not observed when pure **1***b*, or **1***b* prepared with boron trifluoride, were recrystallized. The crude triacetate was therefore suspected of containing a (colorless) by-product which, engendered by an action of pyridine as yet unrecognized, was subsequently transformed into the yellow species under the conditions of recrystallization.[5] Two yellow, crystalline compounds, m.p. 147°–148° and m.p. 119°, were isolated in small amounts and will be shown in a forthcoming paper (10) to possess the

[4]Obviously, the product **4***b* (λ_{max} 302 mμ) is not identical with **4***a* (λ_{max} 297 mμ (9)), although the latter might have been expected to arise by the loss of the remaining two acetyl groups. Hydrolysis of the C-6 acetyl presumably is slow under the conditions of the experiment; it should be faster at higher temperture, and heating (30 min at 100°) did in fact cause a hypsochromic shift of about 4 mμ, which may be interpreted in terms of such hydrolysis. A replacement of the C-2 acetoxyl by hydroxyl through the β-elimination – addition mechanism may of course have occurred in **2***b* at the outset of the reaction, but this aspect, which requires future clarification, is ignored here in a tentative formulation as 2,6-di-*O*-acetates, of all the products originating from **2***b*.

[5]Indeed, heating of pure **1***b* in aqueous ethanol with a small quantity of added pyridine produced the same color.

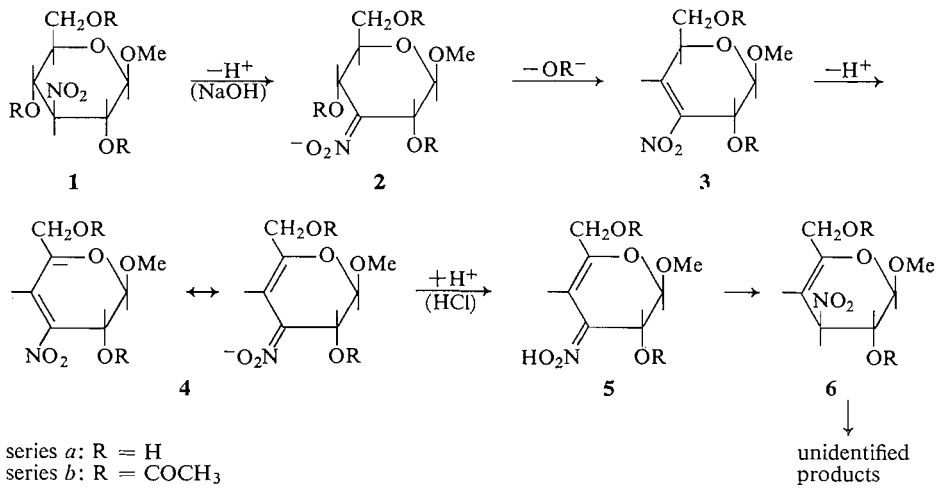

compositions $C_{15}H_{15}NO_8$ and $C_{17}H_{19}NO_8$, with structures derived from 7-nitro-isochromene. One experiment yielded, in addition to **1***b*, a small amount of a colorless product $C_{18}H_{22}N_2O_{12}$, which will be shown (10) to be indeed a precursor of the yellow compounds.

Experimental

*Methyl 2,4,6-Tri-O-acetyl-3-deoxy-3-nitro-β-*D*-gluco-pyranoside (**1***b*)*

(a) Acetylation in the Presence of Pyridine

Acetic anhydride (2 ml) was added to a solution of methyl 3-deoxy-3-nitro-β-D-glucopyranoside (11) (200 mg) in tetrahydrofuran (25 ml) and pyridine (2 ml). The mixture was left at ambient temperature for 1 h and was then stirred vigorously for 5 min with water (50 ml) and chloroform (50 ml). After separation of the phases the aqueous phase was extracted once with chloroform. The combined chloroform extracts were washed twice with 4% sulfuric acid, once with *M* sodium bicarbonate solution, and twice with water. After drying with sodium sulfate, filtering the mixture, and evaporating the solvent, a solid was obtained, which, after recrystallization from 50% aqueous ethanol, gave 125 mg (39%) of **1***b* as colorless prisms of m.p. 149–150°. A subsequent recrystallization gave m.p. 152–153° and $[\alpha]_D^{23}$ −23.5° (*c*, 1 in chloroform) for **1***b*.

Anal. Calcd. for $C_{13}H_{19}NO_{10}$ (349.3): C, 44.75; H, 5.48; N, 4.02. Found: C, 44.83; H, 5.65; N, 4.22.

By-products—The preceding experiment was repeated using fourfold amounts of materials. The crude acetylation product (550 mg) was recrystallized as described. Addition of water to the yellow mother liquor of recrystallization, to incipient turbidity, caused the separation of yellow needles (24 mg) that melted at 147–148° and showed λ_{max} 240 mμ (ε, 9800) and λ_{max} 346 mμ (ε, 11 000) in methanol. No volatile alkyl iodide was formed in a Zeisel alkoxyl determination. The infrared spectrum revealed identity of the substance with compound $C_{15}H_{15}NO_8$ (10).

An acetylation experiment was performed using 2.5 g of nitro glucoside, 5 ml of acetic anhydride, and 7 ml of pyridine in 50 ml of tetrahydrofuran. The reaction time was, however, 18 h at 4°. The crude product (2.2 g) melted below 100°; it was recrystallized several times from boiling 50% ethanol, whereby each time the solvent became yellow during the operation. From the mother liquors was obtained, upon addition of some water, a yellow crystalline material (145 mg) with m.p. 113–115° which rose to 118–119° by one recrystallization. Ultraviolet peaks were at λ_{max} 240 mμ (ε, 10 000) and λ_{max} 345 mμ (ε, 12 000, in methanol). The infrared spectrum revealed identity of the substance with compound $C_{17}H_{19}NO_8$ (10).

In a similar experiment, also performed at 4°, 2 g of nitro glucoside gave only 0.92 g of crude acetylation product in the first crystallization. Addition of water to the mother liquor caused the separation of colorless crystals (70 mg, m.p. 120–121° decomposition). The infrared spectrum differed from that of pure triacetate **1***b* in the fingerprint region, and also, most strikingly, by the presence of *two* asymmetric nitro vibrations (ν_{max} 1553, 1530, in Nujol) of about equal intensities. The spectrum suggested structural identity of the substance with compound $C_{18}H_{22}N_2O_{12}$ (10).

(b) Acetylation Catalyzed by Boron Trifluoride

To a suspension of methyl 3-deoxy-3-nitro-β-D-glucopyranoside (2.4 g) in acetic anhydride (15 ml) were added ten drops of boron trifluoride etherate. The glycoside dissolved rapidly, and the solution, after standing at room temperature for 1 h, was poured into 200 ml of magnetically stirred ice water. The acetate separated in crystalline form while the excess anhydride decomposed. After thorough washing with water and drying *in vacuo* over potassium hydroxide, the isolated material (3.4 g, 90.5%) melted at 153–154°; $[\alpha]_D^{23}$ −24° (*c*,1 in chloroform). The infrared spectrum was identical with that of **1***b* prepared according to (*a*).

In an attempt at displacing the nitro group during the acetylation, nitro glucoside (200 mg) was treated with an excess of acetic anhydride (3.5 ml) and a molar quantity (130 mg) of boron trifluoride etherate for six days at room

Can. J. Chem. Downloaded from www.nrcresearchpress.com by 210.87.254.42 on 09/05/12
For personal use only.

Can. J. Chem. Downloaded from www.nrcresearchpress.com by 210.87.254.42 on 09/05/12
For personal use only.

temperature. The reaction mixture was worked up as just described but the product failed to crystallize. The infrared spectrum of the water-insoluble syrup indicated that the nitro group was still present. A similar result was obtained when the nitro glucoside (180 mg) and the catalyst (130 mg) were refluxed for 3 h in 6 ml of acetic anhydride.

(c) Reactions of ***1b***

The behavior of **1***b* in alkaline solution was investigated by use of a Perkin–Elmer 202 spectrophotometer. The substance (3.49 mg) was dissolved in a few drops of dimethyl sulfoxide and introduced into 200 ml of 0.01 *N* sodium hydroxide to give a solution that was $0.5 \times 10^{-4}M$ in **1***b*. Acidification was effected in the cell with 2 *N* hydrochloric acid in slight excess. Basic conditions were subsequently re-established by adding a drop of 20% sodium hydroxide solution.

For the experiments relating to thin-layer chromatography, silica gel G (E. Merck, Darmstadt) was activated at 140°.[6] The plates were irrigated with *n*-heptane – 2-butanone (1:1). For a preparative conversion into the fast-moving product, a suspension of silica gel (4 g) in chloroform (50 ml, reagent grade) containing 130 mg of **1***b* was briskly stirred and heated under reflux for 15–20 min, after which time **1***b* was no longer detectable. The gel was filtered off and washed with chloroform, and the filtrate was evaporated to give a colorless syrup. Crystallization was attempted from ethyl acetate – petroleum ether, but in the course of several days at 4° only a very small amount of needles was isolated. It represented residual starting material **1***b* of quantity below the level detectable chromatographically. The syrupy product was recovered by evaporation of the solvents and showed $[\alpha]_D^{23}$ −132° (*c*, 1.1 in chloroform). An n.m.r. spectrum was taken in deuteriochloroform.

*Methyl 2,4,6-Tri-O-acetyl-3-deoxy-3-nitro-*D*-β-galactopyranoside*

Methyl 3-deoxy-3-nitro-β-D-galactopyranoside (11) (280 mg) was treated with acetic anhydride (3 ml) and boron trifluoride etherate (4 drops). After 1 h the excess anhydride was destroyed with methanol (3 ml) and the mixture was then diluted with water (15 ml) and extracted four times with chloroform. The combined extracts were washed twice with water and dried with sodium sulfate. The mixture was filtered and solvent evaporated to give a crystalline residue which was triturated with a few milliliters of 50% aqueous ethanol, filtered, and dried. The product (420 mg, 91%) had m.p. 115°, raised to 122° by recrystallization from aqueous ethanol.

Anal. Calcd. for $C_{13}H_{19}NO_{10}$ (349.3): C, 44.75; H, 5.48; N, 4.02. Found: C, 45.01; H, 5.74; N, 4.24.

*Methyl 2,4,6-Tri-O-acetyl-3-deoxy-3-nitro-β-*D*-mannopyranoside*

Methyl 3-deoxy-3-nitro-β-D-mannopyranoside (11) (200 mg) was allowed to react for 1 h with acetic anhydride (2 ml) and boron trifluoride etherate (3 drops). The mixture was then stirred with ice water (50 ml), which caused crystallization of the triacetate, 148 mg (47.5%), m.p. 133–134°. Recrystallization from 50% aqueous ethanol gave plates of unchanged melting point; $[\alpha]_D^{23}$ −66° (*c*, 0.7 in ethanol).

Anal. Calcd. for $C_{13}H_{19}NO_{10}$ (349.3): C, 44.75; H, 5.48; N, 4.02. Found: C, 44.71; H, 5.45; N, 3.86.

*Methyl 2-O-Acetyl-4,6-O-benzylidene-3-deoxy-3-nitro-β-*D*-galactopyranoside*

Methyl 4,6-*O*-benzylidene-3-deoxy-3-nitro-β-D-galactopyranoside (1) (100 mg), acetic anhydride (1.5 ml) and boron trifluoride etherate (1 drop) were allowed to react at ambient temperature for 10 min. The mixture was worked up by stirring with ice water whereby the product separated in crystalline form in a yield of 95 mg (83%). The compound ($[\alpha]_D^{23}$ −4.5° in chloroform, *c*, 0.8) was analytically pure, although it showed a melting range of 142–156° which remained essentially unchanged upon recrystallization from 50% aqueous ethanol. Infrared spectroscopy revealed that heating to the vicinity of the melting point causes a partial decomposition of the pure compound (ν_{max} 1555 cm^{-1} for alkane nitro, no hydroxyl band) into nitroolefin (ν_{max} 1525 cm^{-1}) and acetic acid (broad hydroxyl absorption).

Anal. Calcd. for $C_{16}H_{19}NO_8$ (353.3): C, 54.40; H, 5.42; N, 3.97. Found: C, 54.28; H, 5.26; N, 3.82.

*Methyl 2-O-Acetyl-4,6-O-benzylidene-3-deoxy-3-nitro-β-*D*-glucopyranoside*

Methyl 4,6-*O*-benzylidene-3-deoxy-3-nitro-β-D-glucopyranoside (12) (200 mg) was suspended in a mixture of acetic anhydride (3 ml) and anhydrous ether (4 ml). One droplet of boron trifluoride etherate was added, and the mixture was gently warmed until a clear solution was obtained (5 min). Petroleum ether (b.p. 30–60°) was then added in excess, which caused immediate crystallization of the acetate in a yield of 200 mg (88%), m.p. 189–190°, $[\alpha]_D^{23}$ −79.1° (*c*, 0.8 in chloroform). Reported (12), m.p. 193–194°, $[\alpha]_D^{23}$ −77.7°. The infrared spectrum confirmed the identity of the product with that obtained earlier (12).

2,3,5,6-Tetra-O-acetyl-1,4-dideoxy-1,4-dinitro-neo-inositol

To a suspension of carefully powdered 1,4-dideoxy-1,4-dinitro-*neo*-inositol (5) (238 mg) in acetic anhydride (2.4 ml) was added boron trifluoride etherate (0.13 ml), and the mixture was heated for 5 min on a steam bath. During the heating the inositol dissolved and its acetate began to crystallize. After cooling of the mixture with ice for 5 min, the crystals were isolated, washed well with ether, and dried. The yield was 331 mg, and another 21 mg was obtained from the mother liquor following removal of the excess anhydride by several evaporations with methanol. Yields of 80–90% were also found in several similar experiments using minor variations in the amount of catalyst, reaction time, and isolation procedure.

The infrared spectrum of the product was identical with that of a sample prepared by sulfuric acid catalysis (5). The compound decomposed gradually on heating near 285° (reported (5), above 250°).

[6]It was noticed that a gel which had become deactivated by 3 weeks' exposure to atmospheric moisture did not react with **1***b*, although it was still capable of separating **1***b* and the fast-moving reaction product.

Acknowledgments

This work was supported by research grant A 1350 from the National Research Council of

Canada. The Ogilvie Flourmills Co. is thanked for a postgraduate fellowship to F.K., and the National Research Council of Canada is thanked for a studentship to F.R.

1. H. H. BAER, F. KIENZLE, and T. NEILSON. Can. J. Chem. **43**, 1829 (1965).
2. H. H. BAER and F. KIENZLE. Can. J. Chem. **45**, 983 (1967).
3. A. V. TOPCHIEV, S. V. ZAVGORODNII, and YA. M. PAUSHKIN. Boron fluoride and its compounds as catalysts in organic chemistry. The Pergamon Press, Ltd., London. 1959.
4. H. H. BAER and T. NEILSON. J. Org. Chem. **32**, 1068 (1967).
5. F. W. LICHTENTHALER and H. O. L. FISCHER. J. Am. Chem. Soc. **83**, 2005 (1961).
6. P. K. BHATTACHARYYA, A. C. GHOSH, V. M. SATHE, N. L. DUTTA, and M. RAM. Tetrahedron, **20**, Suppl. No. **1**, 275 (1964).
7. V. V. PEREKALIN. Unsaturated nitro compounds. *Translated by* L. Mandel. Israel Service for Scientific Translations, Jerusalem. 1964.
8. H. H. BAER, T. NEILSON, and W. RANK. Can. J. Chem. **45**, 991 (1967).
9. H. H. BAER and F. KIENZLE. Ann. **695**, 192 (1966).
10. H. H. BAER and F. KIENZLE. Part VIII in this series. To be published.
11. H. H. BAER. Ber. **93**, 2865 (1960); H. H. BAER and F. KIENZLE. Can. J. Chem. **41**, 1606 (1963).
12. H. H. BAER and T. NEILSON. Can. J. Chem. **43**, 840 (1965).

Two-step synthesis of *cis,cis*-1,6-cyclodecadiene

S. N. SHARMA, R. K. SRIVASTAVA, AND D. DEVAPRABHAKARA
Department of Chemistry, Indian Institute of Technology, Kanpur, India

Received September 12, 1967

A convenient synthesis of *cis,cis*-1,6-cyclodecadiene (**3**) has been described starting from *cis,cis*-1,5-cyclononadiene (**1**). This two-step sequence involves the synthesis of 1,2,6-cyclodecatriene (**2**) in one-step followed by chemical reduction with sodium and liquid ammonia.

Canadian Journal of Chemistry, 46, 84 (1968)

Recently we have been investigating the chemistry of the medium-sized ring dienes, *cis*, *cis*-1,5-cyclononadiene (**1**) and *cis,cis*-,1,6-cyclodecadiene (**3**). The molecular model construction of the diene, **3**, suggests that it is capable of existing in one of the Pitzer strain-free conformations (**3***a*) in which the opposite sides of the ring come into close proximity, the condition which is responsible for various transannular reactions observed in the medium-sized ring compounds. The subject of this note deals with a more efficient method of synthesizing *cis,cis*-1,6-cyclodecadiene (**3**) than the two routes described in the literature (1,2) since it requires few good-yield steps.

The one-step allene synthesis described recently by Untch and co-workers (3) was found to be nicely adaptable to the synthesis of 1,2,6-cyclodecatriene (**2**). The treatment of a fourfold excess of *cis,cis*-1,5-cyclononadiene[1] (**1**) (4) with one equivalent of carbon tetrabromide and two equivalents of methyl lithium in diethyl ether at about −65° gave 1,2,6-cyclodecatriene (**2**) in 60% yield based on carbon tetrabromide. The structure of the allene (**2**) was established by elemental analysis, characteristic infrared absorptions at 1 961 and 862 cm^{-1}, and nuclear magnetic resonance signals for two olefinic protons at τ 4.65 and allenic protons at τ 4.89.

We (5) have shown earlier that sodium in liquid ammonia reduces allenes to olefins in good yields. The allene (**2**) on reduction with sodium in liquid ammonia gave the diene (**3**) in 76% yield. The diene (**3**) was characterized thoroughly by physical and chemical data.

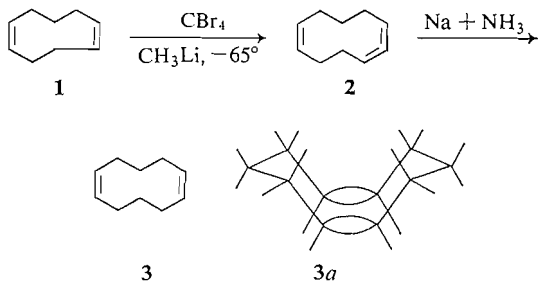

Gas chromatographic analysis of the diene (**3**) on two different columns showed it to be a single substance. The infrared spectrum showed a weak band at 1656 cm^{-1} (C=C stretching) and a strong band at 710 cm^{-1} (out of the plane hydrogen bending) characteristic of the *cis* double bond

[1]This starting material was prepared by similar steps starting from the readily available *cis,cis*-1,5-cyclooctadiene.

Can. J. Chem. Downloaded from www.nrcresearchpress.com by 210.87.254.42 on 09/05/12
For personal use only.

Can. J. Chem. Downloaded from www.nrcresearchpress.com by 210.87.254.42 on 09/05/12
For personal use only.

and the absence of a strong band at 965 cm^{-1} (out of the plane hydrogen bending) characteristic of the *trans* double bond (6). Thus the configurations of the two double bonds in the diene (**3**) were established to be *cis,cis*. The ultraviolet spectrum showed only end absorptions. Nuclear magnetic resonance showed a multiplet at τ 4.64 corresponding to four olefinic protons.

The presence of two double bonds was established by hydrogenation. The hydrogenation value was found to be 1.94. The reduction product was shown to be cyclodecane. The positions of the double bonds were established by ozonolysis followed by oxidation and esterification which gave only dimethyl glutarate. The identity of the product in each case was established by comparison of retention times by gas chromatography and superimposable infrared spectra with those of authentic samples.

Experimental

Boiling points are uncorrected. All infrared spectra were recorded on a Perkin–Elmer Infracord model 137B as films between salt plates. The ultraviolet spectrum was determined in *n*-hexane using a Beckman model DB spectrophotometer. Nuclear magnetic resonance (n.m.r.) spectra were taken on a Varian HR-100 instrument with tetramethylsilane as the internal standard. Gas chromatographic analyses were made with an Aerograph model 90P instrument using 6 ft by 1/4 in. columns. The following liquid phases were employed (percentages by weight on 60/80 mesh chromosorb W): 15% carbowax 20M-silver nitrate, 15% ucon, and 15% polyethylene glycol succinate. Microanalyses were carried out by Mr. A. H. Siddiqui of the Department of Chemistry, Indian Institute of Technology, Kanpur, India.

1,2,6-Cyclodecatriene (2)

Form *cis,cis*-1,5-cyclononadiene (62 g, 0.50 mole), carbon tetrabromide (41.5 g, 0.125 mole), and methyl lithium in diethyl ether (154.5 ml, 0.250 mole), 1,2,6-cyclodecatriene (10.1 g, ~ 60%), b.p. 81–82° at 16 mm, n_D^{29} 1.5230 was prepared by the procedure described by Untch and co-workers (3).

Anal. Calcd. for $C_{10}H_{14}$: C, 89.55; H, 10.44. Found: C, 89.66; H, 10.40.

Examination of the material by means of gas chromatography on a 6 ft by 1/4 in. carbowax 20M-silver nitrate column showed it to be a single substance. The infared spectrum showed strong bands at 1961 and 862 cm^{-1} characteristic of the allene group. The n.m.r. spectrum of the neat sample showed a multiplet at τ 4.65 (two protons) for olefinic protons and another multiplet at τ 4.89 (two protons) for the allenic protons.

cis,cis-1,6-Cyclodecadiene (3)

To a solution of sodium (6.9 g, 0.25 mole) dissolved in liquid ammonia (200 ml) was added 1,2,6-cyclodecatriene (6.7 g, 0.05 mole) in anhydrous ether (30 ml). The solution was stirred at its boiling temperature for 1 h and then treated with excess of ammonium chloride. Evaporation of ammonia and processing of the residue in the usual manner gave *cis,cis*-1,6-cyclodecadiene (5.2 g, 76%), b.p. 66–67° at 12 mm, n_D^{29} 1.4965. The reported (1) values are: b.p. 67° at 11 mm, n_D^{30} 1.4964.

Anal. Calcd. for $C_{10}H_{16}$: C, 88.23; H, 11.76. Found: C, 88.14; H, 11.72.

Gas chromatography on 6 ft by 1/4 in. carbowax 20M-silver nitrate and also on 6 ft by 1/4 in. ucon columns indicated it to be a homogenous substance. The infrared spectrum showed bands at 1656 cm^{-1} (C=C stretching) and 710 cm^{-1} (*cis* double bond). The ultraviolet spectrum showed the following absorptions: λ_{max} (hexane) 220 mμ (log ϵ 2.43), 215 mμ (log ϵ 2.53), 210 mμ (log ϵ 2.67), and 206 mμ (log ϵ 2.92). Nuclear magnetic resonance showed a multiplet at τ 4.64 corresponding to 4 olefinic protons.

Hydrogenation

A solution of *cis,cis*-1,6-cyclodecadiene (200 mg) in methanol (15 ml) was reduced with 5% Pd–C catalyst (100 mg) in a microhydrogenator. The uptake of hydrogen ceased after 1.94 mole-equivalent had been absorbed. The catalyst was filtered off and the filtrate was concentrated to obtain cyclodecane (100 mg). Authenticity was established by comparison of gas chromatographic retention times and superimposable infrared spectra using an authentic sample of cyclodecane.

Ozonation

cis,cis-1,6-Cyclodecadiene (2.7 g) in carbon tetrachloride (30 ml) was ozonized at −30° with approximately 4% ozone–oxygen mixture. The ozone was completely absorbed until 2 moles of ozone had reacted. At this stage ozone passed through was observed to release iodine in the adjoining potassium iodide trap. The reaction mixture was allowed to come to room temperature and was transferred into a 150 ml round bottom flask. To this were added 30 ml of 10% sodium hydroxide and 30 ml of 30% hydrogen peroxide. The flask was fitted with a reflux condenser and gently warmed until a vigorous reaction set in. After the spontaneous reaction had ceased (20–30 min), the reaction mixture was heated under reflux for about 6 h, at which time it gave no peroxide test with sodium iodide. The mixture was cooled and the carbon tetrachloride layer was separated. The aqueous layer was acidified with concentrated hydrochloric acid. The acidified aqueous solution was subjected to continuous hot ether extraction for about 48 h. The ether solution was dried and esterified using diazomethane to give only dimethyl glutarate (1.8 g). Identity was established by gas chromatography and infrared spectra using an authentic sample of dimethyl glutarate.

1. D. J. Cram and N. L. Allinger. J. Am. Chem. Soc. **78**, 2518 (1956).
2. P. Heimbach. Angew. Chem. Intern. Ed. Engl. **5**, 595 (1966).
3. K. G. Untch, D. J. Martin, and N. T. Castellucci J. Org. Chem. **30**, 3572 (1965).
4. D. Devaprabhakara and R. Vaidyanathaswamy. J. Org. Chem. To be published.
5. D. Devaprabhakara and P. D. Gardner. J. Am. Chem. Soc. **85**, 648 (1963).
6. L. J. Bellamy. The infrared spectra of complex molecules. John Wiley and Sons, Inc., New York. 1954.

Can. J. Chem. Downloaded from www.nrcresearchpress.com by 210.87.254.40 on 09/05/12
For personal use only.

A rapid, mild procedure for the preparation of alkyl chlorides and bromides

J. HOOZ AND S. S. H. GILANI
Department of Chemistry, University of Alberta, Edmonton, Alberta

Received May 17, 1967

Primary and secondary alkyl chlorides have been conveniently prepared by the reaction of tri-*n*-octylphosphine with carbon tetrachloride solutions of the corresponding alcohols. This rapid, high yield reaction proceeds with inversion of configuration. By using carbon tetrabromide the method has been extended to the synthesis of alkyl bromides.

Canadian Journal of Chemistry, 46, 86 (1968)

The formation of ylid **1** ($R = C_6H_5$) and triphenylphosphine dihalide (**2**) from the interaction of triphenylphosphine with carbon tetrahalides (eq. [1]) was simultaneously and independently discovered by Rabinowitz and Marcus (1) and Ramirez and co-workers (2). An ionic

$$[1] \quad 2\,R_3P + CX_4 \rightarrow R_3P{=}CX_2 + R_3PX_2$$
$$X = Cl, Br \qquad \mathbf{1} \qquad \mathbf{2}$$

mechanism involving nucleophilic displacement on halogen has been invoked (3) to account for the formation of these products (eqs. [2] and [3]).

$$[2] \quad R_3P{:}\overset{\curvearrowright}{+}X{-}\overset{\curvearrowright}{C}X_3 \rightarrow R_3\overset{+}{P}X\,\overset{-}{C}X_3 \rightarrow R_3\overset{+}{P}CX_3\,\overset{-}{X}$$
$$\mathbf{3} \qquad \mathbf{4}$$

$$[3] \quad R_3P{:}\overset{\curvearrowright}{+}X{-}\overset{\overset{X}{|}}{\underset{\underset{X}{|}}{C}}{-}\overset{+}{P}R_3\overset{-}{X} \rightarrow R_3P{=}CX_2 + R_3PX_2$$

Ylids of structure **1** ($R = C_6H_5$) possess considerable synthetic potential since they provide a route to otherwise difficultly accessible 1,1-dihaloalkenes on reaction with carbonyl compounds (1, 2, 4). Reagents of the type R_3PX_2 ($R = C_6H_5$ or n-C_4H_9) have been demonstrated to permit the conversion of alcohols to alkyl halides to proceed generally without complication of elimination or rearrangement (5, 6); in addition, they convert phenols to aryl halides (6, 7) without formation of position isomers.

The present study arose out of a consideration that intermediates of structure **3** (or **4**) could be trapped by reaction with alcohols to provide **5** (or **6**), e.g.

$$R_3\overset{+}{P}X\,\overset{-}{C}X_3 + R'OH \rightarrow R_3\overset{+}{P}X\,\overset{-}{O}R' \rightarrow R_3\overset{+}{P}OR'\,\overset{-}{X} + HCX_3$$
$$\mathbf{5} \qquad \mathbf{6}$$

The anticipated collapse of **6** to alkyl halide and tertiary phosphine oxide finds ample analogy in a related study (8).

$$[4] \quad R_3\overset{+}{P}OR'\,\overset{-}{X} \rightarrow R'X + R_3PO$$

Accordingly, we have found that phosphines smoothly convert alcohols to chlorides (eq. [5]).

$$[5] \quad R_3P + R'OH + CCl_4 \rightarrow R'Cl + R_3PO + HCCl_3$$
$$\text{where } R = n\text{-}C_8H_{17} \text{ or } C_6H_5$$

Using tri-*n*-octylphosphine (TOP) and primary alcohols, conversions are of the order 90–100% in favorable cases. Triphenylphosphine may also be used at longer reaction times.[1] Although no attempts at optimization have been made, we find that this facile transformation is conveniently accomplished (for chlorides) by adding a slight excess over one mole equivalent of TOP to a solution of alcohol in carbon tetrachloride as solvent. A vigorous reaction ensues which is complete, in the case of primary alcohols, in ca. 5 min. The product is readily isolated by standard methods of distillation and chromatography (cf. Experimental).

Typical results are the formation of n-$C_5H_{11}Cl$ (94%), $C_6H_5CH_2Cl$ (100%), n-$C_8H_{17}Cl$ (93%), and $C_6H_5CH_2CH_2Cl$ (66%).[2]

Secondary alcohols also react. Thus, after ca. 5 min reaction time, *sec*-butyl chloride and 2-chlorooctane were formed in 60% and 80% yields, respectively, from the corresponding alcohols. When (+)-2-octanol was subjected to this reaction, (−)-2-chlorooctane was obtained in 90% optical purity, a result consistent with a bimolecular displacement process accompanied by a Walden inversion in the product determining step (eq. [4]).

The incursion of a competing olefin-forming elimination process renders this method of

[1]Recently, and concurrent with the present work, a similar study has been reported (10) using triphenylphosphine.

[2]Analysis by gas–liquid partition chromatography.

Can. J. Chem. Downloaded from www.nrcresearchpress.com by 210.87.254.40 on 09/05/12
For personal use only.

limited value for the preparation of tertiary chlorides. For example, *t*-butanol gave only 13–15% *t*-butyl chloride, and isobutylene was detected by gas–liquid partition chromatography (g.l.p.c.).

Bromides may also be prepared by this method but in this case the ratio of reagents is ROH: TOP:CBr_4 = 1:2:2. Diethyl ether is a suitable solvent. In this manner *n*-$C_5H_{11}Br$ (97%) and $C_6H_5CH_2Br$ (96%)[2] were formed after ca. 5 min reaction time.

In view of the mild conditions employed and good yields obtained, this method offers considerable promise as a synthetic tool.

Experimental

All melting and boiling points are uncorrected. The alcohols, chlorides, and bromides were commercially available materials whose homogeneity was established by g.l.p.c., using an Aerograph A90-P3 instrument equipped with a thermal conductivity detector. Infrared spectra were recorded on a Perkin–Elmer model 421 spectrophotometer. Nuclear magnetic resonance spectra were recorded on a Varian A-60 analytical spectrometer using tetramethylsilane as internal standard.

All conversions of alcohol to alkyl chloride were accomplished by a procedure similar to that employed for the preparation of 1-chlorooctane which is described in detail. Bromides were prepared by the method described for the synthesis of 1-bromopentane.

Preparation of 1-Chlorooctane

To a magnetically-stirred solution of 1-octanol (10.0 mmoles) in 20 ml carbon tetrachloride was added tri-*n*-octylphosphine (10.5 mmoles). An exothermic reaction ensued. (In larger scale runs it is recommended that the reaction be moderated by a cooling bath.) Approximately 5 min after complete addition of the phosphine an aliquot was analyzed by g.l.p.c. (5 ft × 1/4 in. FFAP on Chromosorb W column operated at 140°, helium flow 55 ml/min). No octanol was present, but a new peak appeared, and was shown to be 1-chlorooctane by comparison of retention time with that of an authentic sample. The yield[3] (as determined by g.l.p.c.) was 94%. By operating at a column temperature of 50° and helium flow of 25 ml/min, the peaks due to carbon tetrachloride and chloroform could be resolved but the yield of the latter was not determined.

Chloroform and carbon tetrachloride were distilled through a 25 cm Vigreaux column and the residue was chromatographed on BDH alumina. The pentane eluate was concentrated and distilled to give an 88% yield of pure 1-chlorooctane.[4]

Isolation of Tri-n-octylphosphine Oxide

The above-described experiment was duplicated, and after ca. 5 min reaction time the crude mixture was distilled to remove all material boiling up to ca. 184°. The residue was triturated with pentane and cooled to −78°. The resulting solid was filtered, washed with cold pentane, and dried. In this manner there was obtained 3.55 g (92%) of solid, m.p. 48–52° (lit. (9) m.p. 48–54°), ν_{max} (Nujol) 1138 cm^{-1} (PO). The nuclear magnetic resonance spectrum ($CDCl_3$) showed absorption for 9 protons as a multiplet centered at τ 9.1 (CH_3) and 42 protons with absorption from ca. τ 8.0–8.92 (CH_2).

Preparation of 1-Bromopentane

Tri-*n*-octylphosphine (20 mmoles) was added to a magnetically-stirred solution of 1-pentanol (10 mmoles) and carbon tetrabromide (20 mmoles) in 20 ml anhydrous ether. An immediate exothermic reaction took place and the initially colorless mixture turned yellow. Five minutes after complete addition of the phosphine an aliquot was analyzed by g.l.p.c.; the yield of 1-bromopentane was 97%. The mixture was worked up in a manner identical to that described for 1-chlorooctane, and upon distillation there was obtained an 80% yield of 1-bromopentane.[4] Since no special precautions were taken to minimize handling losses this yield can doubtless be improved.

Acknowledgment

The financial assistance of the National Research Council of Canada is gratefully acknowledged.

1. R. Rabinowitz and R. Marcus. J. Am. Chem. Soc. **84**, 1312 (1962).
2. F. Ramirez, N. B. Desai, and N. McKelvie. J. Am. Chem. Soc. **84**, 1745 (1962).
3. B. Miller. Topics Phosphorus Chem. **2**, 133 (1965).
4. A. J. Speziale, G. J. Marco, and K. W. Ratts. J. Am. Chem. Soc. **82**, 1260 (1960); A. J. Speziale and K. W. Ratts. J. Am. Chem. Soc. **84**, 854 (1962).
5. L. Horner, H. Oediger, and H. Hoffmann. Ann. **626**, 26 (1959).
6. G. A. Wiley, R. L. Hershkowitz, B. M. Rein, and B. C. Chung. J. Am. Chem. Soc. **86**, 964 (1964).
7. H. Hoffmann, L. Horner, H. G. Wippel, and D. Michael. Chem. Ber. **95**, 523 (1962).
8. J. P. Schaefer and D. S. Weinberg. J. Org. Chem. **30**, 2635 (1965).
9. C. A. Blake, K. B. Brown, and C. F. Coleman. U.S. At. Energy Comm. ORNL-1964 (1955); Chem. Abstr. **50**, 15321b (1956).
10. I. M. Downie, J. B. Holmes, and J. B. Lee. Chem. Ind. London, 900 (1966).

[3]Under otherwise identical conditions, the yield of 1-chlorooctane was 47% after 5 min reaction time employing triphenylphosphine.

[4]The structures of all synthetic materials were secured by comparison of physical properties with those of authentic samples.

Can. J. Chem. Downloaded from www.nrcresearchpress.com by 210.87.254.5 on 09/05/12
For personal use only.

Canadian Journal of Chemistry

Published by THE NATIONAL RESEARCH COUNCIL OF CANADA

VOLUME 46 JANUARY 15, 1968 NUMBER 2

γ-Radiolysis of cyclohexane with electron scavengers. II. Solid cyclohexane at 77 °K[1,2]

N. H. SAGERT

Research Chemistry Branch, Chalk River Nuclear Laboratories, Chalk River, Ontario

Received July 25, 1967

The γ-radiolysis of homogeneous solid solutions of SF_6 and N_2O in cyclohexane has been examined at 77 °K. With SF_6, yields of the major products, hydrogen, bicyclohexyl, and cyclohexene, were all reduced, and no large yields of other products were observed. Thus, since SF_6 reduces hydrogen yields by capturing electrons, combination of the SF_6 anion and cyclohexane cation does not lead to bond breaking. Experimental evidence suggests that the ratio of disproportionation to combination of cyclohexyl radicals in solid cyclohexane at ~ 186 °K is 0.3 ± 0.2.

With N_2O, hydrogen yields are decreased to 3.5 *G* units, but large yields of cyclohexene, bicyclohexyl, and cyclohexanol (4.7, 2.0, and 1.0 *G* units respectively) are produced. Thus combination of O^- and the cyclohexane cation leads to a great deal of bond breaking. The yields are explained by a mechanism similar to Dyne's mechanism for the radiolysis of hydrocarbons. It was, however, necessary to assume that excited states of cyclohexane formed directly behave differently from those formed by electron–cation combination.

Canadian Journal of Chemistry, 46, 89 (1968)

Introduction

Charge separation is important in the radiolysis of liquid hydrocarbons. This charge separation has been studied in our laboratory by using N_2O, SF_6 (1), and CCl_4 (2) to capture the major negatively charged species, the electron. Hydrogen yields were reduced, but with N_2O and CCl_4, secondary reactions occurred which resulted in even more total decomposition than when the scavengers were absent. Consideration of these extra yields has led to the suggestion (1) that the true electron yield is somewhat greater than indicated by the reduction in hydrogen yield when an electron scavenger is added. In the study reported here, the work with electron scavengers is extended to the solid phase using SF_6, a scavenger which gives no detectable yields of secondary products, and N_2O, one which gives large yields of secondary products.

Hydrogen yields from the radiolysis of pure solid cyclohexane are somewhat smaller than those from the radiolysis of the liquid (3). It has been suggested e.g. (4) that such decreases arise because hydrogen atoms combine with each other rather than abstract hydrogen from the hydrocarbon at low temperatures. On the other hand, Dyne and Denhartog (5) found evidence that the hydrogen precursors were probably "hot" hydrogen atoms which had a high probability of reaction before being moderated to thermal energies. It was hoped that by using N_2O and SF_6 to get an estimate of the total electron yield we could gain some insight as to why the yields are lower from the solid.

Homogeneous solid solutions of SF_6 and N_2O in cyclohexane were prepared by slow deposition from the gas phase and were irradiated with ^{60}Co γ-rays. All yields were decreased with SF_6, but the fractional decreases in the yields of the products were not identical, whereas they were in the liquid (1). Thus the mechanism is probably somewhat different in the solid than in the liquid. With N_2O, large yields of liquid products and nitrogen were obtained which could only be explained by assuming $G(e^-)$ to be $\simeq 4$. It is suggested that the smaller yields of hydrogen from the radiolysis of pure solid cyclohexane compared with the liquid result from a smaller efficiency for the production of hydrogen precursors when a positive ion is neutralized by an electron.

[1]Issued as A.E.C.L. No. 2981.
[2]For Part I of this series, see ref. 1.

Can. J. Chem. Downloaded from www.nrcresearchpress.com by 210.87.254.5 on 09/05/12
For personal use only.

Results and Discussion

(a) SF_6 in C_6H_{12}

The hydrogen, bicyclohexyl, and cyclohexene yields are presented in Fig. 1 as a function of the mole fraction of SF_6. These yields are independent of dose up to doses of at least 10^{23} eV/l. As

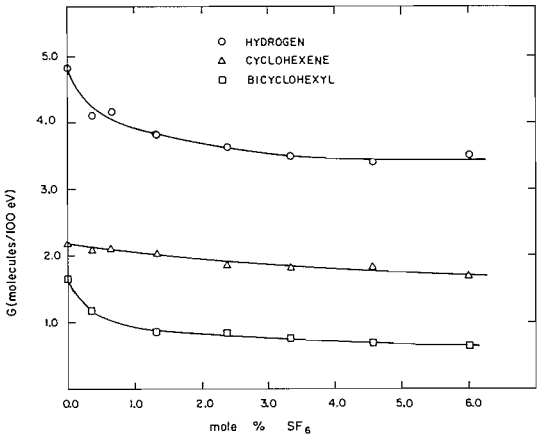

FIG. 1. Yields of hydrogen, cyclohexene, and bicyclohexyl for the cyclohexane–SF_6 system.

with the liquid (1), all yields are reduced by SF_6, but in the solid, bicyclohexyl is reduced much more efficiently than cyclohexene or hydrogen. The yields in the absence of SF_6 compare favorably with those obtained by Stone using large samples (3). Other products include hexene-1 which was reduced from 0.2_5 to 0.1_5 *G* units, *n*-hexane with a yield of 0.1 *G* units which was little affected by SF_6, and, in the presence of SF_6 only, a small ($\sim$ 0.1 *G* units) yield of a product whose retention time on a carbowax column was almost identical with that of benzene. Although the low yield of this product made it difficult to obtain good mass spectra, those that were obtained were more consistent with identification of this product as cyclohexyl fluoride than as benzene. As was found by Stone (3), material balances are poorer than those obtained from radiolysis of the liquid, and almost 1 *G* unit of hydrogen is unaccounted for.

These results will be discussed using Dyne's (6) mechanism for hydrocarbon radiolysis.

[1*a*] [1*b*] $C_6H_{12} \rightsquigarrow \begin{cases} C_6H_{12}^+ + e^- \\ C_6H_{12}^* \end{cases}$

[2] $C_6H_{12}^+ + e^- \rightarrow C_6H_{12}^*$

[3*a*] [3*b*] $C_6H_{12}^* \rightarrow \begin{cases} X_H + C_6H_{11} \\ H_2 + C_6H_{10} \end{cases}$

[4] $X_H + C_6H_{12} \rightarrow H_2 + C_6H_{11}$

[5] $e^- + \text{solute} \rightarrow \text{solute}^-$

[6] $\text{solute}^- + C_6H_{12}^+ \rightarrow \text{not-}C_6H_{12}^*$,

where the initial acts are thought of as being ionization (reaction [1*a*]) and direct excitation (reaction [1*b*]). Recombination of an electron and a positive ion leads to an excited molecule (reaction [2]) which is indistinguishable from one formed initially. The excited molecule decomposes to give cyclohexene and hydrogen or to give cyclohexyl radicals and a species X_H, presumably a hot hydrogen atom, that can further react (reaction [4]) to produce hydrogen and another radical. An electron-capturing solute may form an anion which, when it reacts with the solvent cation (reaction [6]), does not lead to an excited state which decomposes to give X_H or H_2. When SF_6 is used as a solute there is no evidence that reaction [6] leads to more than 0.1 *G* units of bond breaking.

If the solute scavenges all the electrons, the limiting yield of hydrogen, which is 3.4 *G* units, may be equated with the hydrogen from $C_6H_{12}^*$ formed from direct excitation (reaction [1]). Since the yield of hydrogen in the absence of solute is 4.7_5 *G* units, then the difference between this and the limiting yield with solute present, 1.4 *G* units, may be taken as the yield of hydrogen from $C_6H_{12}^*$ produced by ion–electron combination in the absence of solute. Dyne and Denhartog (5) have argued convincingly that the hydrogen is produced at liquid nitrogen temperature so that electron reactions and reactions involving X_H (5) take place at this temperature. The species $C_6H_{12}^+$, SF_6^-, and C_6H_{11} are left trapped in the matrix along with the "molecular" C_6H_{10} formed by reaction [3*b*]. On warming, the positive and negative ions combine giving few products and the C_6H_{11} radicals combine and disproportionate.

To get an estimate of the ratio of disproportionation to combination, an estimate of the "molecular" yield is necessary. The term "molecular" refers to the unimolecular decomposition of $C_6H_{12}^*$ to give hydrogen and cyclohexene (reaction [3*b*]), regardless of

Can. J. Chem. Downloaded from www.nrcresearchpress.com by 210.87.254.5 on 09/05/12
For personal use only.

whether the C_6H_{12}* is produced directly or by ion–electron combination. The results of Dyne and his co-workers on the first-order yield of D_2 (G_1(D)) from 5% C_6D_{12} in C_6H_{12} are of some help. They found that G_1(D) from the liquid is about 0.27 (7), and from the solid is 0.45 to 0.50 (5). Since the total "molecular" yield in liquid cyclohexane is about 1.0 (1, 8), the total "molecular" yield in the solid may be considerably greater and may be estimated to be 1.8 to 2.0. If the yield of C_6H_{12}* is proportional to the yield of hydrogen as required by Dyne's mechanism, the "molecular" yield in the presence of 3% SF_6 is about 1.5. In the solid phase it would appear that C_6H_{12}* produced directly is about twice as likely to decompose "molecularly" as C_6H_{12}* produced by ion–electron combination. This is the simplest explanation for the observation that the radical yield, as manifested in the bicyclohexyl yield, is reduced much more than the total yield of hydrogen or of cyclohexene.

If the above values for the molecular yields are adopted and it is assumed that bicyclohexyl is only produced by radical combination, the ratio of disproportionation to combination is 0.3 ± 0.2. This is much lower than the value of 1.1 found in the liquid phase (9). However, it is known from electron spin resonance (e.s.r.) experiments that the disappearance of radicals formed at low temperatures takes place close to a phase change at 186 °K as the matrix is warmed, and not at the melting point (10). Hence it is not surprising that the liquid phase ratio does not apply, since the radicals may be held in a position favoring combination as they approach each other.

(b) N_2O in C_6H_{12}

Yields of hydrogen and nitrogen for the radiolysis of homogeneous solid solutions of N_2O in C_6H_{12} are shown in Fig. 2, and yields of liquid products are shown in Fig. 3. These yields are also linear with dose up to 10^{23} eV/l. In the presence of N_2O there are also small yields of benzene (< 0.1 G unit), cyclohexylcyclohexene (0.2 G units), hexene-1 (0.1_2 G units), *n*-hexane (0.1 G units), and at high N_2O concentration, cyclohexanone (0.3 G units). No oxygen gas was produced. The solid points are for samples deposited at a flow rate of 1.8 cc/min rather than the more usual rate of 3.5 cc/min. No significant changes in yields resulted, indicating that 3.5 cc/min is a flow rate small enough to ensure a uniform deposit.

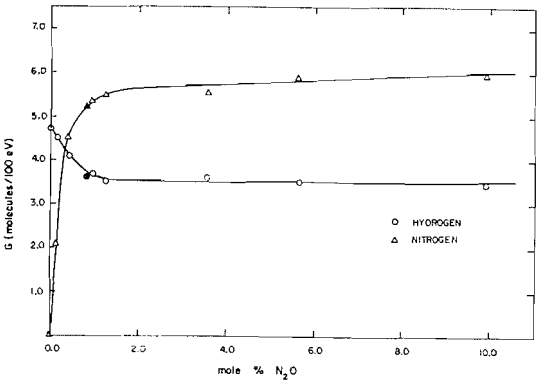

FIG. 2. Yields of gaseous products from the cyclohexane–N_2O system. Open points are samples deposited at 3.5 cc/min. Closed points are the sample deposited at 1.8 cc/min.

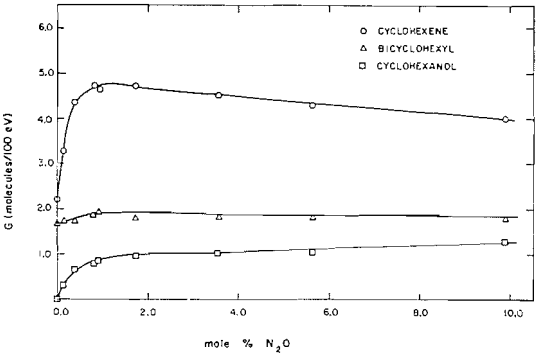

FIG. 3. Yields of liquid products from the cyclohexane–N_2O system. Open points are samples deposited at 3.5 cc/min. Closed points are the sample deposited at 1.8 cc/min.

(i) Low Concentration of N_2O (1%)

With N_2O the hydrogen yield is reduced to 3.5 G units, indicating that the "direct" yield (reaction [1*b*]) of C_6H_{12}* is of this order. The electron and hot hydrogen atom reactions will take place at 77 °K. Scavenging of electrons by N_2O can be considered to take place at 77 °K also.

[7] $$e^- + N_2O \rightarrow [N_2O^-] \rightarrow N_2 + O^-$$

The $C_6H_{12}^+$, C_6H_{11}, and O^- (or N_2O^-) will then be trapped in the matrix and will be released on warming. With N_2O, large yields of liquid products are formed, so that reactions analogous

Can. J. Chem. Downloaded from www.nrcresearchpress.com by 210.87.254.5 on 09/05/12
For personal use only.

to reaction [6] lead to a great deal of bond breaking.

Of the fates considered for O^- in the liquid (1)

[8] $$O^- + C_6H_{12}^+ \rightarrow OH + C_6H_{11}$$

[9] $$O^- + C_6H_{12} \rightarrow OH^- + C_6H_{11},$$

the latter should be suppressed in the solid at low temperature since it is an abstraction and probably requires some activation energy. If the yield of electrons and positive ions is 4 *G* units (1, 11) the yield of OH will be about 4 *G* units. The yield of C_6H_{11} may be as high as 8 *G* units. Of this 4 *G* units are produced by reaction [8] along with OH radicals. The yield of C_6H_{12}* by direct excitation has been shown to be 3.4 *G* units, and of this 1.5 *G* units decompose molecularly. Thus 1.9 *G* units of X_H and C_6H_{11} are formed (reaction [3*a*]) and the X_H will give another 1.9 *G* units of C_6H_{11} when it abstracts hydrogen from cyclohexane (reaction [4]).

These yields are sufficient to explain the enhanced yield of cyclohexanol, bicyclohexyl, and cyclohexene if the ratio of disproportionation to combination of OH and C_6H_{11} (reaction [10]),

[10*a*] $$C_6H_{11} + OH \rightarrow C_6H_{10} + H_2O$$

[10*b*] $$\rightarrow C_6H_{11}OH,$$

is about 3, and if the ratio of disproportionation to combination for two C_6H_{11} radicals is 0.3. It is also necessary that the "molecular" yield of cyclohexene be 1.5 as used above, and that OH + OH be small. Calculations using the gas phase rate constant for OH plus propane measured by Greiner (12), corrected to 186 °K using his estimate of the activation energy (5.6 kcal/mole), show that the abstraction of a hydrogen atom from cyclohexane by a hydroxyl radical cannot compete with reaction [10].

(ii) Higher Concentrations of N_2O (> 5%)

With higher concentrations of N_2O reactions [11],

[11*a*] $$O^- + N_2O \rightarrow N_2 + O_2^-$$

[11*b*] $$\rightarrow NO + NO^-,$$

may become important (13, 14). Reaction [11] produces an increase in N_2 yield and a decrease in OH if it is followed by

[12*a*] $$O_2^- + C_6H_{12}^+ \rightarrow HO_2 + C_6H_{11}$$

and

[12*b*] $$NO^- + C_6H_{12}^+ \rightarrow HNO + C_6H_{11}.$$

The decrease in OH of a *G* unit would explain the decreased yield of C_6H_{10} at high N_2O concentration. The small increase in *G*(cyclohexanol) may result from the combination of HO_2 with C_6H_{11} or from the reaction of C_6H_{11} with O_2 produced from reaction [13] (15).

[13] $$2HO_2 \rightarrow H_2O_2 + O_2$$

Yields of N_2 were about a *G* unit higher than can be readily explained. In the solid phase, as in the liquid, there may be a small amount of chain decomposition of N_2O.

To account for the large increase in the yields of liquid products, as well as the large N_2 yield, it has been necessary to postulate that electrons and ions are produced with *G* values at least as large as those in the liquid, i.e. ~ 4. However, in the absence of scavenger, only about 1.4 *G* units of hydrogen come from ion–electron combination. Thus this process occurs with about 35% efficiency; much less than its efficiency in the liquid ($\sim 75\%$). This efficiency could be less because hydrogen precursors combine with themselves, rather than abstract hydrogen from hydrocarbon. The efficiency could also be less because hydrogen precursors are produced less efficiently from the combination of an electron and a cyclohexane cation. It was not possible to make a clean-cut distinction from this work. However, we had to assume that all the X_H from C_6H_{12}* formed directly was capable of abstracting hydrogen from the hydrocarbon. Thus, most of the X_H can be considered capable of abstracting hydrogen, which supports its identification as a "hot" hydrogen atom, and leads to the suggestion that yields of hydrogen are lower from the solid because hydrogen precursors are produced less efficiently from the combination of an electron and a cation.

Experimental

Cyclohexane (Fisher Spectrograde), N_2O (Canadian Liquid Air), and SF_6 (Matheson) were used as received. The cyclohexane was free of cyclohexene and was not purified further. Cyclohexane samples of 1 ml volume were degassed by the freeze–thaw technique and transferred to a 2 l flask on a mercury-free, grease-free vacuum line. The additives were degassed and transferred to the same flask. The gases were then thoroughly mixed and deposited slowly (about 3.5 cc/min) at 77 °K in the irradiation cell. The design of the cell and the techniques used to ensure a homogeneous deposit have been described in detail by Stone (3). Samples were irradiated at 77 °K in a ^{60}Co γ-source at a dose rate (in cyclohexane) of 6.9×10^{20}

eV/l min to a total dose of about 4.3×10^{22} eV/l unless otherwise specified. All G values reported are partial yields based on energy absorbed in the cyclohexane. The dose rate was determined using ferrous sulfate dosimetry, taking $G(Fe^{3+})$ to be 15.5. After irradiation the samples were melted and refrozen to allow trapped gas to escape. Gases not condensable at 77 °K were measured volumetrically and analyzed mass spectrometrically. Liquid products were analyzed by gas chromatography using columns and conditions similar to those used by Stone (16). The cyclohexanol and cyclohexanone were measurable on the XE-60 column at 160 °C. The gas chromatographic peaks were identified by mass spectrometry where necessary, using a Consolidated 21-130 mass spectrometer. Water was not determined quantitatively.

Acknowledgments

Dr. J. A. Stone originally suggested these experiments. Drs. A. W. Boyd and J. W. Fletcher provided very helpful aid and discussions. The aid of Mr. A. S. Blair, who carried out some preliminary experiments, is also acknowledged. Drs. F. Brown and P. J. Dyne are thanked for their frank comments on an earlier draft of this manuscript.

1. N. H. SAGERT and A. S. BLAIR. Can. J. Chem. **45**, 1351 (1967).
2. J. A. STONE and P. J. DYNE. Can. J. Chem. **42**, 669 (1964).
3. J. A. STONE. Can. J. Chem. **43**, 809 (1965).
4. W. VAN DUSEN, JR. and F. K. TRUBY. J. Am. Chem. Soc. **87**, 188 (1965).
5. P. J. DYNE and J. DENHARTOG. Can. J. Chem. **44**, 461 (1966).
6. P. J. DYNE. Can. J. Chem. **43**, 1080 (1965).
7. P. J. DYNE and W. M. JENKINSON. Can. J. Chem. **38**, 539 (1960).
8. S. Z. TOMA and W. H. HAMILL. J. Am. Chem. Soc. **86**, 1478 (1964).
9. W. A. CRAMER. J. Phys. Chem. **71**, 1112 (1967).
10. H. SZWARC. J. Chim. Phys. **59**, 1067 (1962).
11. G. G. MEISELS. J. Chem. Phys. **41**, 51 (1964).
12. N. R. GREINER. J. Chem. Phys. **46**, 3389 (1967).
13. G. R. A. JOHNSON and J. M. WARMAN. Trans. Faraday Soc. **61**, 1709 (1965).
14. J. M. WARMAN. Nature, **213**, 381 (1967).
15. R. BLACKBURN and A. CHARLESBY. Trans. Faraday Soc. **62**, 1159 (1966).
16. J. A. STONE. Can. J. Chem. **42**, 2873 (1964).

Can. J. Chem. Downloaded from www.nrcresearchpress.com by 210.87.254.5 on 09/05/12
For personal use only.

γ-Radiolysis of cyclohexane with electron scavengers. III. Perfluorocarbons as electron scavengers[1,2]

N. H. SAGERT

Research Chemistry Branch, Chalk River Nuclear Laboratories, Chalk River, Ontario

Received July 28, 1967

The room temperature, liquid phase radiolysis of cyclohexane in the presence of three solutes, perfluorocyclohexane (PCH), perfluoromethylcyclohexane (PMCH), and perfluorocyclobutane (PCB) has been examined. All decrease the hydrogen yield from 5.6 to 2.6 *G* units by capturing electrons. However, with PMCH and PCB the yields of cyclohexene and bicyclohexyl are not decreased as much as the hydrogen yield and with PCH, dimer and olefin yields are increased. Furthermore, large yields of monohydrofluorocarbon (e.g. undecafluorocyclohexane) are produced, indicating that a carbon–fluorine bond has been broken. It is concluded that electron capture by these fluorocarbon compounds causes dissociation; possible mechanisms are discussed, but it was not possible to reach a clear conclusion on the basis of our results.

The radiolysis of homogeneous solid solutions of these solutes at 77 °K has also been studied, but only PMCH was studied in detail. Under these conditions there is no evidence for dissociative electron capture and apparently the combination of solute anion and hydrocarbon cation on warming does not lead to bond breaking.

Canadian Journal of Chemistry, **46**, 95 (1968)

Can. J. Chem. Downloaded from www.nrcresearchpress.com by 210.87.254.6 on 09/05/12
For personal use only.

Introduction

Charge separation is known to play an important part in the radiolysis of hydrocarbons. N_2O, SF_6, and CCl_4 have been used to study this charge separation by capturing the negatively charged species, the electron, thereby reducing hydrogen yields.

In this laboratory more thorough studies of the action of CCl_4 (1), N_2O, and SF_6 (2, 3) have been carried out, and a general mechanism has been proposed (4). With SF_6, all major products, hydrogen, cyclohexene, and bicyclohexyl, are reduced and no large yields of other products can be found. This indicates that SF_6 probably captures electrons non-dissociatively and that neutralization of the SF_6 anion by the cyclohexane cation does not result in bond breaking to give either hydrogen or cyclohexyl radical precursors. With CCl_4 and N_2O, yields of products other than hydrogen increased, indicating that these substances capture electrons dissociatively or that the neutralization of the anion by the cyclohexane cation leads to bond breaking.

Perfluorocycloalkanes have been used as electron scavengers and are known to lower hydrogen yields (5, 6). Rajbenbach (6) has measured hydrogen yields and has concluded that these solutes capture electrons non-dissociatively. It was therefore of interest to measure the yields of all the major liquid products using these perfluorocarbons as solutes to see if evidence for carbon–fluorine bond breaking could be found.

In liquid solutions, irradiated at 25 °C, conclusive evidence was found that carbon–fluorine bonds were broken, and that almost one bond was broken for every electron scavenged. Two possible mechanisms by which this bond breaking might occur are considered. In solid solutions, irradiated at 77 °K, only a small amount of bond breaking took place; less than one bond was broken for every 10 electrons scavenged.

Experimental

Cyclohexane (Fisher Spectrograde), N_2O (Canadian Liquid Air), perfluoromethylcyclohexane (Imperial Smelting), perfluorocyclohexane (Aldrich), and perfluorocyclobutane (Matheson) were used as received. Materials were degassed on a mercury-free, grease-free vacuum line.

Perfluoromethylcyclohexane (PMCH) and perfluorocyclohexane (PCH) solutions were made up by weighing. These solutions were of 2 ml volume and were contained in pyrex cells fitted with a breaking device (7). The samples were irradiated at 25 °C in a ^{60}Co γ-source at dose rates (in cyclohexane) of 6.9×10^{20} eV/l min to total doses of 4×10^{22} eV/l as determined by ferrous sulfate and cyclohexane dosimetry.

Perfluorocyclobutane (PCB) solutions and N_2O–PCH solutions were of 3 ml volume and were contained in the stainless steel cells described previously (2). Concentrations were determined from gas solubilities. The solubility of PCB at 23 °C was determined to be 0.21_3 mole/l atm

---

[1]Issued as A.E.C.L. No. 2982.

[2]Presented in part at 50th Chemical Institute of Canada Conference, Toronto, Ontario, June 1967.

Can. J. Chem. Downloaded from www.nrcresearchpress.com by 210.87.254.6 on 09/05/12
For personal use only.

in cyclohexane. These samples were also irradiated at 25 °C with ^{60}Co γ-rays at dose rates (in cyclohexane) of 5.7×10^{20} eV/l min, as determined by ferrous sulfate and cyclohexane dosimetry using $G(Fe^{3+}) = 15.6$ and $G(H_2) = 5.5_5$ respectively.

Solid samples of 1 ml liquid volume were deposited slowly from the gas phase as described by Stone (8) and were irradiated at 77 °K.

After irradiation, gases not condensable at 77 °K were measured volumetrically and analyzed mass spectrometrically. Liquid products were determined by gas chromatography (9). $C_6F_{11}H$ and C_4F_7H were determined on a squalane column at 70 °C. The $C_6F_{11}H$ was identified by retention time and by mass spectrometry. The mass spectrum on a Consolidated 21-130 mass spectrometer was similar to that of an authentic sample of $C_6F_{11}H$ (Aldrich) and to published spectra (10). C_4F_7H was identified by mass spectrometry. Its spectrum was similar to published spectra (10).

Results

(i) Perfluorocyclohexane in Liquid Cyclohexane

The major products formed in the radiolysis of pure cyclohexane are hydrogen, cyclohexene, and bicyclohexyl (11). Yields of these products in the presence of PCH are shown in Figs. 1 and 2. PCH reduces the hydrogen yield, probably by electron capture as discussed by Rajbenbach (6). However, the yields of the other major products, cyclohexene and bicyclohexyl, are not reduced and the latter yield is actually increased. The hydrogen and bicyclohexyl yields are linear with dose up to 2×10^{23} eV/l. Cyclohexene yields show a small dose dependence: the yield extrapolated to zero dose being 3.2_5 molecules for each 100 eV absorbed by the cyclohexane, or 3.2_5 G units.

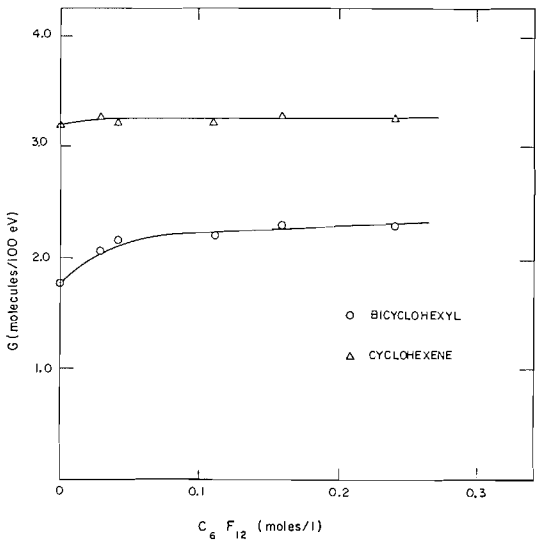

FIG. 2. Bicyclohexyl and cyclohexene yields from the radiolysis of solutions of PCH in cyclohexane at 25 °C. Dose = 2.81×10^{22} eV/l.

$C_6F_{11}H$ is produced in large yields. These yields are shown in Fig. 1 and approach the total electron yield (4.1 G units (2)). The $C_6F_{11}H$ accounts for about half the hydrogen precursors scavenged by PCH. No attempt was made to determine HF, but there are no large yields of *n*-hexane, propane, or other hydrogen-rich products.

In order to show that electrons were precursors of $C_6F_{11}H$, N_2O was added to a 0.1 M solution of PCH. In Fig. 3, it may be seen that N_2O decreases the $C_6F_{11}H$ yield, while at the

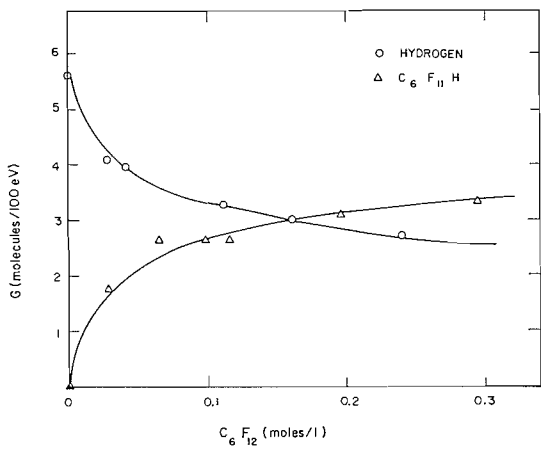

FIG. 1. Hydrogen and $C_6F_{11}H$ yields from the radiolysis of solutions of PCH in cyclohexane at 25 °C. Dose = 2.81×10^{22} eV/l.

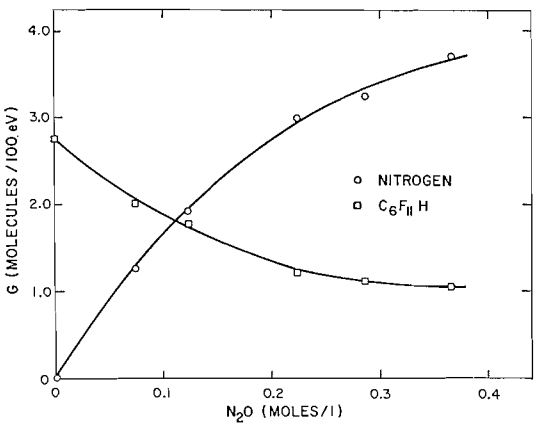

FIG. 3. Hydrogen, nitrogen, and $C_6F_{11}H$ yields from the radiolysis of 0.1 M solutions of PCH in cyclohexane with N_2O at 25 °C. Dose = $3.3_5 \times 10^{22}$ eV/l.

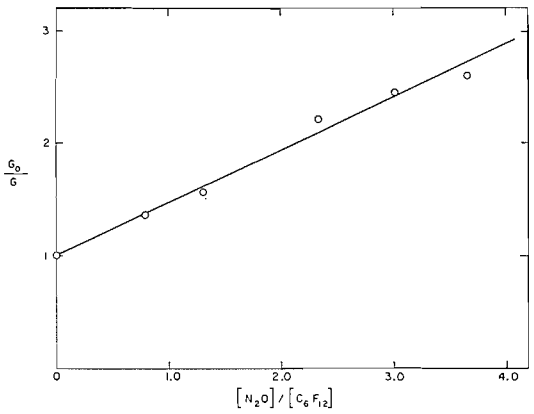

FIG. 4. Stern–Volmer type plot of the $C_6F_{11}H$ yields given in Fig. 3. G_0, the yield of $C_6F_{11}H$ in the absence of N_2O, is 2.7 G units. Slope = 0.47.

same time nitrogen is produced. The $C_6F_{11}H$ yields, plotted in the Stern–Volmer fashion in Fig. 4, imply that electron capture by PCH is twice as efficient as by N_2O in this system.

(ii) Perfluorocyclobutane in Liquid Cyclohexane

Perfluorocyclobutane (PCB) also reduces hydrogen yields from liquid cyclohexane (Fig. 5) as has been noted by Rajbenbach (6). The liquid products, although reduced somewhat, still total 4.4 G units at 0.3 M PCB whereas the hydrogen yield is 2.6 G units. Thus some of the precursors of hydrogen are captured by the PCB and give liquid product precursors, but not hydrogen. The zero-dose yield of liquid products is higher than 4.4 since, although there is no dose effect with hydrogen yields up to 2×10^{23} eV/l, liquid product yields are somewhat dose dependent. G(cyclohexene) extrapolated to zero dose was 2.7_5, and G(bicyclohexyl) similarly extrapolated was 2.1_5.

C_4F_7H was produced. Unfortunately no authentic standards were available. $G(C_4F_7H)$ is 4.5 at 0.2 M PCB if the sensitivity of the hydrogen flame detector is the same for it as for C_4F_8. Since the detector is 2.8 times as sensitive to $C_6F_{11}H$ as to PCH, it is likely that the C_4F_7H yield is from 1.5 to 2.0 G units. This still means that a large number of C—F bonds are broken. This yield is approximately equal to the liquid product yield (4.4) minus the hydrogen yield (2.6) for 0.2 M PCB.

(iii) Perfluoromethylcyclohexane in Liquid Cyclohexane

Yields of hydrogen and the two major liquid products for the radiolysis of liquid cyclohexane with PMCH are shown in Fig. 6. This solute

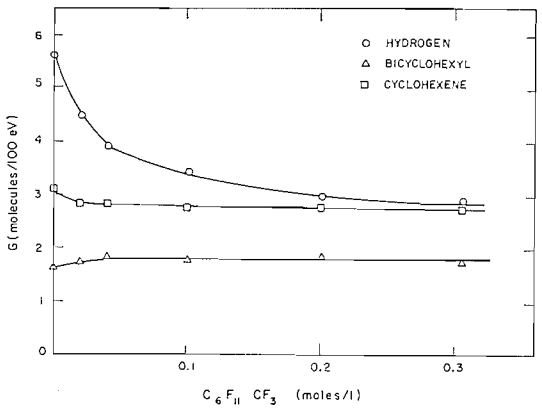

FIG. 6. Hydrogen and liquid product yields from the radiolysis of solutions of PMCH in cyclohexane at 25 °C. Dose = 2.83×10^{22} eV/l.

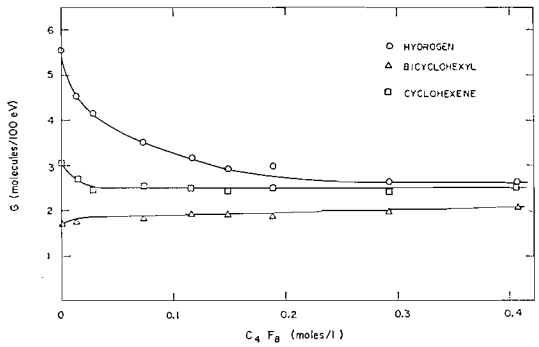

FIG. 5. Hydrogen and liquid product yields from the radiolysis of solutions of PCB in cyclohexane at 25 °C. Dose = 3.42×10^{22} eV/l.

reduces hydrogen yields less efficiently than PCH. Liquid products yields total 4.6 in 0.3 M solution, while the hydrogen yield is 2.9 G units. Thus the captured precursors of hydrogen give liquid product precursors. Hydrogen yields are linear with dose but the zero-dose yields for bicyclohexyl and cyclohexene are 1.8_3 and 3.1_5 G units respectively. This is a somewhat larger dose dependence than noted with other solutes.

(iv) Perfluorocarbons in Solid Cyclohexane

Irradiations of homogeneous solid solutions of all these solutes were carried out. In all cases the hydrogen, cyclohexene, and bicyclohexyl were reduced. PMCH solutions were studied in more

Can. J. Chem. Downloaded from www.nrcresearchpress.com by 210.87.254.6 on 09/05/12
For personal use only.

detail and the results are shown in Fig. 7. As with SF_6, bicyclohexyl was reduced more efficiently than cyclohexene and hydrogen. These results are qualitatively similar to those obtained for solid solutions of SF_6 (3). For a solid solution of PCH in cyclohexane, $G(C_6F_{11}H)$ was about 0.3. These results indicate that much less dissociation takes place in the solid. All yields from the solid were independent of dose up to doses of 10^{23} eV/l.

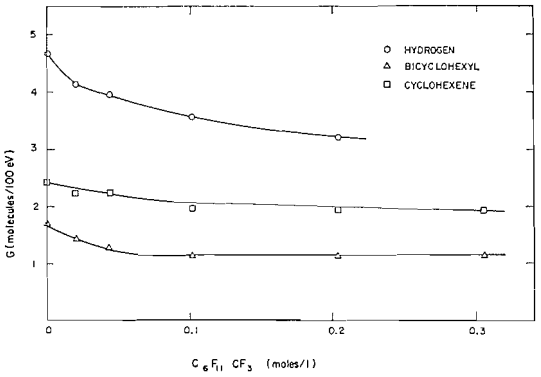

FIG. 7. Hydrogen and liquid product yields from the radiolysis of solid solutions of PMCH in cyclohexane at 77 °K. Dose = 3.18×10^{22} eV/l.

Perfluoroethane was not able to change the yield of any of the products in the solid phase.

Discussion

Arguments in favor of electron capture by perfluorocycloalkanes have been given by Rajbenbach (6). Thermal atom reactions may be ruled out by the high strength of the C—F bond (12). Hot atom reactions are possible, but large effects are noted for small concentrations of additives and there is no apparent reason why hot atoms should selectively attack fluorocarbons. The ionization potentials of fluorocarbons are usually greater than those of the corresponding hydrocarbons (13) so that charge transfer from solvent to solute cannot occur, and charge transfer is considered to be the most common form of "energy transfer" in saturated hydrocarbons (4). There is considerable recent experimental evidence that PMCH attaches thermal electrons very efficiently (14, 15). Thus it is reasonable to conclude that the effects of perfluorocycloalkanes on the radiolysis of hydrocarbons can be attributed to electron capture.

The mechanism of Dyne (4) as used by Sagert and Blair (2) for the radiolysis of liquid cyclohexane will be taken as a basis for discussion.

[1a] $C_6H_{12} \rightsquigarrow \ulcorner C_6H_{12}^+ + e^-$

[1b] $\llcorner C_6H_{12}^*$

[2] $C_6H_{12}^+ + e^- \rightarrow C_6H_{12}^*$

[3a] $C_6H_{12}^* \rightarrow H + C_6H_{11}$

[3b] $C_6H_{12}^* \rightarrow H_2 + C_6H_{10}$

[4] $H + C_6H_{12} \rightarrow H_2 + C_6H_{11}$

[5] $\text{solute} + e^- \rightarrow \text{solute}^-$

[6] $\text{solute}^- + C_6H_{12}^+ \rightarrow \text{not-}C_6H_{12}^*$

The main features of this mechanism are that initially ions and electrons as well as excited molecules are produced (reaction [1]). Ions and electrons which recombine, either in the spur or outside, lead to excited states of the hydrocarbons which, in the liquid, are indistinguishable from those formed initially (reaction [2]). The excited molecules then decompose (reaction [3]) to give either hydrogen and olefin (molecular decomposition), or radicals and bimolecular hydrogen precursors. It is thought that the latter are "hot" hydrogen atoms (16). An electron-capturing solute forms an anion which when it reacts with the positive ion does not form the same excited state of the hydrocarbon (reaction [6]), and thus does not lead to hydrogen production.

In the case of SF_6 as solute (2), reaction [6] not only does not produce hydrogen precursors but also fails to produce cyclohexyl radicals since the yields of cyclohexene and bicyclohexyl are also reduced. Thus the solute anion is neutralized without further detectable reaction. By contrast, the present results show that with perfluorocycloalkanes in solution, electron capture

[7] $C_6F_{12} + e^- \rightarrow C_6F_{12}^-$

leads to an anion that, while not producing hydrogen, does produce at least two cyclohexyl radicals, a $C_6F_{11}H$ molecule and possibly other products. Thus in some way a C—F bond is broken. This might be by

[8] $C_6F_{12}^- \rightarrow C_6F_{11} + F^-$

followed by

[9] $F^- + C_6H_{12}^+ \rightarrow HF + C_6H_{11}$

and

[10] $C_6F_{11} + C_6H_{12} \rightarrow C_6F_{11}H + C_6H_{11}.$

Can. J. Chem. Downloaded from www.nrcresearchpress.com by 210.87.254.6 on 09/05/12
For personal use only.

Can. J. Chem. Downloaded from www.nrcresearchpress.com by 210.87.254.6 on 09/05/12
For personal use only.

However, in the gas phase, the appearance potential for F^- from PCH is 1.8 eV (17). Thus reaction [8] is extremely endothermic. Electrons are initially formed with several eV excess energy and are moderated by collision to thermal energies. It might be thought that electrons could react with solute before being moderated to thermal velocities. However, it would appear that moderation is much too fast a process to allow this at the low solute concentration used (18, and references cited therein, 19). Armstrong *et al.* (20) have discussed the difficulties involved for HCl gas. Thus reaction [8] can only occur if the energetics in the liquid are very much different from those in the gas phase, so that reaction [8] becomes thermoneutral or exothermic in the liquid. This is quite possible since Claridge and Willard (21) have shown that phase changes have a considerable effect on dissociative electron capture processes.

A second proposal is that

[11] $C_6F_{12}^- + C_6H_{12}^+ \rightarrow C_6F_{11} + C_6H_{11} + HF$

occurs, followed by reaction [10]. Reaction [11] would be exothermic if a reasonable electron affinity (<5 eV) is assumed for PCH. Because of the long lifetime measured for $PMCH^-$ (14) this proposal is attractive. The data presented here do not allow a clear choice between these two proposals.

The amount of dissociation may be measured as the liquid product yield minus the hydrogen yield. At 0.3 *M* of solute, the yields of dissociation are 3.1, 1.6_5, and 1.9 *G* units for PCH, PMCH, and PCB respectively, indicating that the efficiency for dissociation is much higher with PCH. For PCH and PCB, these numbers agree very well with the yields of $C_6F_{11}H$ and C_4F_7H, which are 3.3 and 1.5–2.0 *G* units respectively. The total electron yield in cyclohexane is probably around 4 (2), so that the efficiency of dissociation is quite high.

The yields of cyclohexene and bicyclohexyl in the presence of solute are consistent with the ratio of disproportionation to combination for cyclohexyl radicals of 1.3 (22), and a small "molecular" yield (reaction [3*b*]) of 0.1 to 0.3 *G* units of cyclohexene, if it is assumed that the bicyclohexyl yield arises largely from radical combination. They are also consistent with the more recently determined ratio of 1.1 and a slightly larger "molecular" yield (23).

Yields for the homogeneous solid irradiated at 77 °K resemble those from homogeneous solid solutions of SF_6 (3). Furthermore, with PCH, only ~ 0.3 *G* units of $C_6F_{11}H$ were produced. Thus at the low temperature where the ions begin to diffuse in the solid, it would appear that reaction [8] does not occur and that the anion and cation neutralize each other with little bond breaking. As with solid solutions of SF_6, bicyclohexyl was reduced more quickly than cyclohexene. This behavior has been interpreted (3) as implying that there is a larger "molecular" yield in the solid at low temperature and that there may be two or more distinguishable types of C_6H_{12}*. C_2F_6 did not affect any yield, and so appears not to attach electrons at low temperature.

Acknowledgments

The author would like to thank Drs. A. W. Boyd, J. W. Fletcher, and P. J. Dyne for helpful discussions and encouragement.

1. J. A. Stone and P. J. Dyne. Can. J. Chem. **42**, 669 (1964).
2. N. H. Sagert and A. S. Blair. Can. J. Chem. **45**, 1351 (1967).
3. N. H. Sagert. Can. J. Chem. **46**, 89 (1968).
4. P. J. Dyne. Can. J. Chem. **43**, 1080 (1965).
5. P. J. Dyne and J. Denhartog. Unpublished work.
6. L. A. Rajbenbach. J. Am. Chem. Soc. **88**, 4275 (1966); J. Chem. Phys. **47**, 242 (1967).
7. Farhataziz and P. J. Dyne. An anthology of experimental techniques in radiation chemistry. A.E.C.L. Rept. CRC-1205. 1964. p. 7.
8. J. A. Stone. Can. J. Chem. **43**, 809 (1965).
9. J. A. Stone. Can. J. Chem. **42**, 2872 (1964).
10. J. R. Majer. Advan. Fluorine Chem. **2**, 55 (1961).
11. P. J. Dyne and J. A. Stone. Can. J. Chem. **39**, 2381 (1961).
12. M. M. Bibby and G. Carter. Trans. Faraday Soc. **59**, 2455 (1963).
13. V. I. Vedeneyev, L. V. Gurvich, V. N. Kondrat'yev, V. A. Medvedev, and Ye. L. Frankevich. Bond energies, ionization potentials, and electron affinities. Edward Arnold (Publishers) Ltd. London. 1966. pp. 153–165.
14. B. H. Mahan and C. E. Young. J. Chem. Phys. **44**, 2192 (1966).
15. R. K. Asundi and J. D. Craggs. Proc. Phys. Soc. London, **83**, 611 (1964).
16. P. J. Dyne and J. Denhartog. Can. J. Chem. **44**, 461 (1966).
17. M. M. Bibby and G. Carter. Trans. Faraday Soc. **62**, 2637 (1966).
18. T. L. Cottrell and I. C. Walker. Quart. Rev. **20**, 153 (1966).
19. R. H. Healey and J. W. Reed. The behaviour of slow electrons in gases. Amalgamated Wireless, (Australasia) Ltd. 1941.
20. R. S. Davidow, R. A. Lee, and D. A. Armstrong. J. Chem. Phys. **45**, 3364 (1966).
21. R. F. C. Claridge and J. E. Willard. J. Am. Chem. Soc. **87**, 4992 (1965).
22. C. E. Klots and R. H. Johnsen. Can. J. Chem. **41**, 2702 (1963).
23. W. A. Cramer. J. Phys. Chem. **71**, 1112 (1967).

Some observations on the ion–molecule reactions in ethylene

J. J. MYHER[1] AND A. G. HARRISON
Department of Chemistry, University of Toronto, Toronto, Ontario
Received August 15, 1967

The ion–molecule reactions in ethylene have been studied under conditions where $C_2H_4^+$ was the only primary ion. In addition to the expected secondary ions $C_3H_5^+$ and $C_4H_7^+$, the $C_3H_4^+$, $C_2H_2^+$, and $C_2H_3^+$ ions have been detected, presumably formed by the reactions

[*a*] $C_2H_4^+ + C_2H_4 \rightarrow C_3H_4^+ + CH_4$

[*b*] $\rightarrow C_2H_2^+ + C_2H_6$

[*c*] $\rightarrow C_2H_3^+ + C_2H_5$.

Reactions [*b*] and [*c*] are endothermic for ground state reactants and it has been shown that the kinetic energy of the reactant ion plays a major role in determining the relative importance of these endothermic reactions.

The $C_5H_9^+$ ion has been shown to originate by further reaction of the $C_3H_5^+$ secondary ion rather than by reaction of the $(C_4H_8^+)^*$ collision complex. The reversion of the $(C_4H_8^+)^*$ complex to reactants has been confirmed by the observation of isotopically mixed ethylene ions in C_2H_4–C_2D_4 mixtures.

Canadian Journal of Chemistry, **46**, 101 (1968)

Introduction

Although the ion–molecule reactions in gaseous ethylene have been studied extensively (1–9), a number of features of the reactions remain uncertain. The present study of the ionic reactions in ethylene was carried out under conditions where $C_2H_4^+$ was the only significant primary ion and the results obtained permit clarification of a number of these uncertainties.

It has been well established that the major secondary ions in the high pressure mass spectrum of ethylene originating from reaction of the $C_2H_4^+$ ions are the $C_3H_5^+$ and $C_4H_7^+$ ions resulting from the reaction sequence,

[1] $C_2H_4^+ + C_2H_4 \rightarrow (C_4H_8^+)^*$

[2] $(C_4H_8^+)^* \rightarrow C_3H_5^+ + CH_3$

[3] $\rightarrow C_4H_7^+ + H$.

Recently, Szabo (10) has reported that the reaction of $C_2H_4^+$ with ethylene leads to formation of $C_2H_3^+$ and $C_2H_2^+$ as product ions, presumably by the reactions

[4] $C_2H_4^+ + C_2H_4 \rightarrow C_2H_3^+ + C_2H_5$

[5] $C_2H_4^+ + C_2H_4 \rightarrow C_2H_2^+ + C_2H_6$.

The occurrence of these apparently endothermic reactions has been confirmed in the present work and it is shown that the kinetic energy of the reactant ion plays a major role in determining the relative importance of these reactions.

At elevated ethylene pressures product ions of higher order have been observed by numerous workers (2, 4, 6–10). The two major higher-order ions at medium pressures, originating from a $C_2H_4^+$ precursor, are $C_4H_8^+$ and $C_5H_9^+$. It has been conclusively established that the $C_4H_8^+$ ion is third order in pressure and originates by collisional stabilization of the complex formed in reaction [1], viz.[2]

[6] $(C_4H_8^+)^* + C_2H_4 \rightarrow C_4H_8^+ + C_2H_4^*$.

Although the origin of $C_4H_8^+$ appears to be established, the mechanism of formation of $C_5H_9^+$ has been in dispute. Field (4) has proposed that it originates by the reaction sequence

[7*a*] $(C_4H_8^+)^* + C_2H_4 \rightarrow (C_6H_{12}^+)^*$

[7*b*] $(C_6H_{12}^+)^* \rightarrow C_5H_9^+ + CH_3$,

while Wexler and Marshall (6) have proposed that it originates by the reaction sequence

[8*a*] $C_3H_5^+ + C_2H_4 \rightarrow (C_5H_9^+)^*$

[8*b*] $(C_5H_9^+)^* + C_2H_4 \rightarrow C_5H_9^+ + C_2H_4^*$.

Basically the two mechanisms differ in the lifetime and/or reactivity assigned to the collision complex $(C_4H_8^+)^*$. The Field mechanism requires that the complex reacts by collision with C_2H_4 before dissociation to $C_3H_5^+$ or other products occurs, while the Wexler mechanism

[1]Present address: Department of Physical Chemistry, Cambridge University, Cambridge, England.

[2]Szabo (10) has concluded that $C_4H_8^+$ is a secondary ion while $C_3H_5^+$ and $C_4H_7^+$ are tertiary ions. This conclusion is in disagreement with all previous studies and also with the results obtained in the present work.

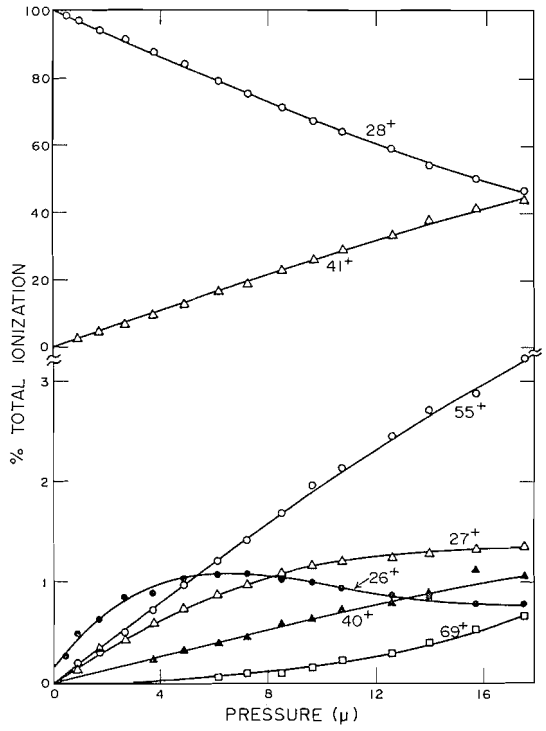

FIG. 1. Normalized ion intensities as a function of pressure 3.4 eV ion exit energy.

assumes that $(C_4H_8^+)^*$ has such a short lifetime (or is sufficiently unreactive) that dissociation to $C_3H_5^+$ (and other products) occurs before further significant reaction is possible. Convincing evidence for either mechanism has been lacking. Results will be presented in the following which provide strong support for reaction [8] as the major path for formation of $C_5H_9^+$.

The present work also provides evidence that a significant fraction of the $(C_4H_8^+)^*$ collision complexes revert to reactants, in some cases with isotopic mixing of the hydrogens in the complex.

Experimental

The present experiments were carried out on the medium pressure instrument previously described (11). The pertinent operating conditions were a source temperature of approximately 100 °C and a primary ion travel distance of 0.54 cm. Pressure studies were carried out at various repeller fields and hence various ion exit energies as detailed in the following section. The electron beam was pulsed and the primary ion residence times were measured by the deflection technique previously described (11). The source pressures were measured directly using an MKS Baratron capacitance micromanometer.

Phillips research grade ethylene was used without further purification. Ethylene-d_4 was obtained from Merck, Sharp and Dohme of Canada. Low energy analysis showed it to be 98.6% C_2D_4 and 1.4% C_2D_3H.

Results and Discussion

A typical pressure plot obtained at 3.4 eV ion exit energy and an electron energy where $C_2H_4^+$ was the only significant primary ion is shown in Fig. 1. In addition to the $C_3H_5^+$ (*m/e* 41) and $C_4H_7^+$ (*m/e* 55) ions, which are the expected secondary ions (reactions [2] and [3]), the $C_2H_3^+$ (*m/e* 27) and $C_3H_4^+$ (*m/e* 40) ion intensities increase with pressure in a manner characteristic of secondary ions, while $C_2H_2^+$ (*m/e* 26) increases initially and then decreases as expected for a reactive secondary ion. In addition to these ions significant ion currents were noted at *m/e* ratios of 69 ($C_5H_9^+$), 56 ($C_4H_8^+$), 39 ($C_3H_3^+$), and 29 ($C_2H_5^+$); only the results for *m/e* 69 are shown in Fig. 1. The zero initial slope and upward curvature are characteristic of ions formed by processes which are greater than second order in ethylene pressure. The remaining ions not shown in Fig. 1 exhibited a similar behavior with increasing pressure.

For the case of one reactant ion leading to a number of product ions by competing reactions, i.e.

$$\begin{aligned} P^+ + M &\xrightarrow{k_1} S_1^+ + N_1 \\ &\xrightarrow{k_2} S_2^+ + N_2 \\ &\xrightarrow{k_j} S_j^+ + N_j, \end{aligned}$$

we may write for any given pressure

$$[9] \qquad I_{P^+} + I_{S_1^+} + \cdots + I_{S_j^+} = I_{P^+}{}^0,$$

where I_{X^+} is the normalized intensity of the ion X^+, i.e. fraction of total measured ion current, and $I_{P^+}{}^0$ is the normalized intensity of the reactant ion extrapolated to zero pressure (i.e. no reaction). Rearrangement yields

$$[10] \qquad I_{P^+}{}^0 - I_{P^+} = \Delta I_{P^+} = \sum_1^j I_{S_j^+}.$$

Since the concentration of M is much larger than that of P^+ we may consider the competing reactions as being quasi-first order and can write

$$[11] \qquad I_{S_1^+} = \frac{k_1}{\sum_1^j k_j} \sum_1^j I_{S_j^+} = \frac{k_1}{\sum_1^j k_j} \Delta I_{P^+}.$$

Equation [11] predicts that a plot of $I_{S_1^+}$ versus ΔI_{P^+} should be a straight line the slope of which

gives the fraction of the total reaction producing that secondary ion.

TABLE I

Fractional yields for reactions of $C_2H_4^+$ with C_2H_4

m/e	Secondary ion	Fractional yield, Exit energy 3.5 eV	Fractional yield, Exit energy 0.85 eV
26	$C_2H_2^+$	0.09	—
27	$C_2H_3^+$	0.04	—
40	$C_3H_4^+$	0.01_9	0.02_0
41	$C_3H_5^+$	0.81	0.88_5
55	$C_4H_7^+$	0.05_9	0.07_5

Figure 2 shows a plot of I_{41+} ($C_3H_5^+$), I_{40+} ($C_3H_4^+$), and I_{55+} ($C_4H_7^+$) as a function of ΔI_{28+} for the results at 3.4 eV ion exit energy. As predicted straight lines are observed, the slopes of which give the fractional yields recorded in Table I, Column 2. The similar plot for the remaining ions is shown in Fig. 3. The *m/e* 27 ($C_2H_3^+$) ion shows an initial quasi-linear rise followed by a dropoff from the linear relation. This is to be expected if the secondary ion reacts further and a similar behavior has been noted for a number of secondary ions in propyne and allene (12). From the initial slope the fractional yield given in Table I has been determined. The *m/e* 26 ($C_2H_2^+$) ion shows an initial increase followed by a rapid falloff. From the initial slope

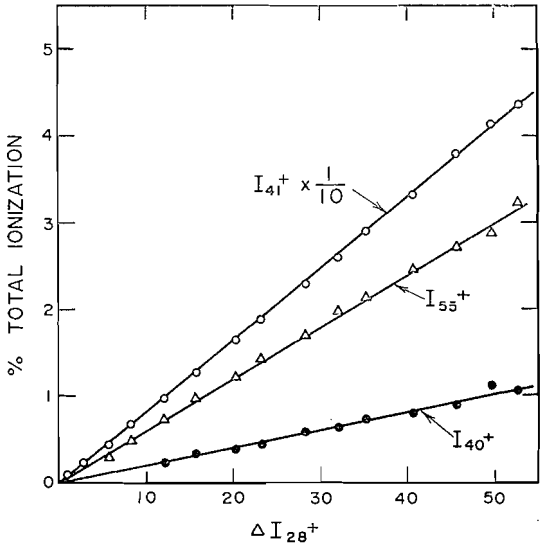

FIG. 2. Product ion intensities versus ΔI_{28+}, 3.4 eV ion exit energy.

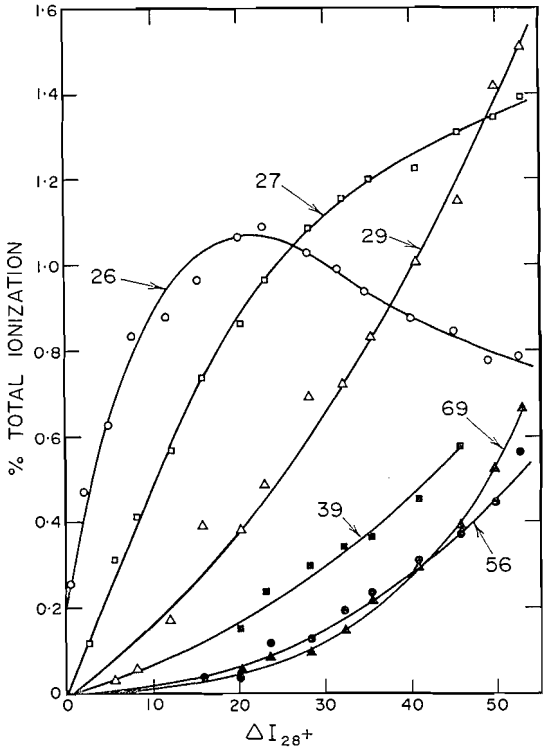

FIG. 3. Product ion intensities versus ΔI_{28+}, 3.4 eV ion exit energy.

we estimate that approximately 9% of the $C_2H_4^+$ ion reacts to form $C_2H_2^+$, although this estimate is obviously subject to large error. The *m/e* 56 ($C_4H_8^+$) and 69 ($C_5H_9^+$) ions show an initial slope of zero followed by a rapid increase in slope at higher conversions, a behavior which is to be expected for tertiary or higher order ions. The situation for the *m/e* 39 ($C_3H_3^+$) and *m/e* 29 ($C_2H_5^+$) ions is not completely clear since the initial slopes (particularly for $C_2H_5^+$) are not zero. It is possible that $C_2H_5^+$ may be formed to a slight extent ($\backsim$ 1% of total reaction) by reaction of $C_2H_4^+$ with C_2H_4, although from the upward curvature it is clear that the major part of the $C_2H_5^+$ originates by a tertiary reaction, presumably

[12] $$C_2H_3^+ + C_2H_4 \rightarrow C_2H_5^+ + C_2H_2 .$$

It should be noted that $C_2H_2^+$ is not entirely absent from the primary spectrum and the reaction

[13] $$C_2H_2^+ + C_2H_4 \rightarrow C_3H_3^+ + CH_3$$

probably accounts for both the apparent secondary and tertiary $C_3H_3^+$ formation.

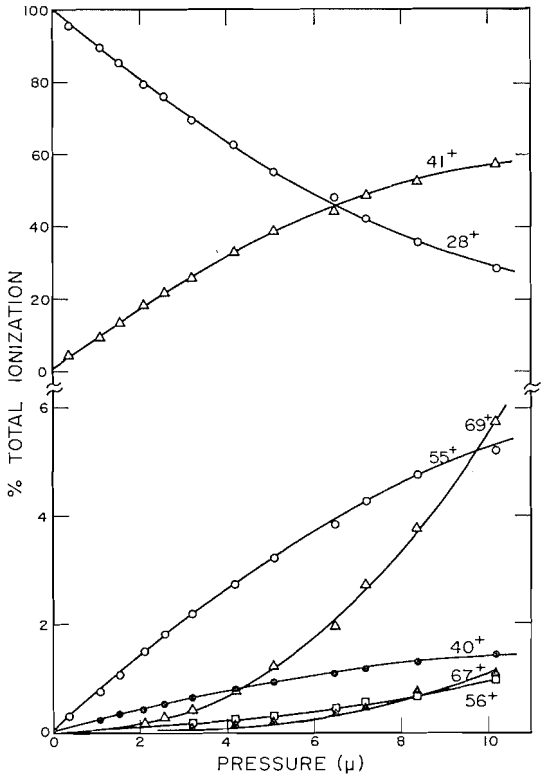

FIG. 4. Ion intensities as a function of pressure, 0.85 eV ion exit energy.

In contrast to the above results, the results obtained at 0.85 eV ion exit energy are considerably simpler with only the $C_3H_4^+$ (*m/e* 40), $C_3H_5^+$ (*m/e* 41), and $C_4H_7^+$ (*m/e* 55) ions being observed as secondary ions while $C_4H_8^+$ (*m/e* 56) and $C_5H_9^+$ (*m/e* 69) are formed as higher order ions. The pressure plot is shown in Fig. 4 while the plot of the normalized product ion intensities as a function of the $C_2H_4^+$ reacted, ΔI_{28+}, is shown in Fig. 5. From the slopes of the straight lines of Fig. 5 the fractional yields given in Column 3 of Table I were obtained.

The results obtained at 3.4 eV support the observations of Szabo (10) that reactions [4] and [5] do occur. However, comparison of the results at 0.85 eV and 3.4 eV ion exit energy shows that the importance of the reactions is strongly dependent on the kinetic energy of the reactant $C_2H_4^+$ ion. Using heats of formation tabulated by Field and Franklin (13) reaction [4] is calculated to be 40 kcal/mole endothermic while reaction [5] is calculated to be 29 kcal/mole endothermic for ground state reactants. Although there must be some internal excitation of the $C_2H_4^+$ ion, even at these low electron energies, the run at 0.85 eV ion exit energy ($\backsim$ 10 kcal/mole maximum available kinetic energy) shows that the internal energy is insufficient to drive reactions [4] and [5]. The run at 3.4 eV ion exit energy ($\backsim$ 40 kcal/mole maximum available kinetic energy) shows that the utilization of both the kinetic and internal energies of the reactant ion is very important to bring about an otherwise endothermic reaction.

One further point of interest concerning the results summarized in Table I is the observation of $C_3H_4^+$ (*m/e* 40) as a product ion, presumably formed by the reaction

$$[14] \qquad C_2H_4^+ + C_2H_4 \rightarrow C_3H_4^+ + CH_4,$$

$$\Delta H = -1 \text{ to } -5 \text{ kcal/mole}.$$

This reaction, accounting for approximately 2% of the total reaction, of $C_2H_4^+$, has not been reported previously, although examination of the high pressure mass spectra reported by Field (4) and Wexler and Marshall (6) indicates in both cases a significant ion current at *m/e* 40. The spectrum given by Field yields a ratio $C_4H_7^+/C_3H_4^+ \approx 3.6$ compared with a ratio of 3.0 to 3.7 obtained in the present work. The $C_3H_4^+$ intensity reported by Wexler and Marshall is considerably lower.

Mechanism of Formation of $C_5H_9^+$

As shown in Fig. 5 I_{55+} and I_{40+} are linear functions of ΔI_{28+} over the entire range covered (up to $\backsim$ 70% conversion of $C_2H_4^+$). This indicates, first, that these ions are not formed by tertiary reactions and, second, that they do not react appreciably with C_2H_4. On the other hand the plot of I_{41+} ($C_3H_5^+$) versus ΔI_{28+} begins to show a negative deviation from linearity at approximately 40% conversion of the $C_2H_4^+$ reactant. This is to be expected only if the $C_3H_5^+$ product ion is reacting further with C_2H_4. The only significant higher-order ion present in the spectrum is $C_5H_9^+$ and, indeed, the sum $I_{41+} + I_{69+}$ (dotted line of Fig. 5) is a linear function of ΔI_{28+} up to 70% conversion. This material balance suggests that $C_5H_9^+$ is produced by reaction of $C_3H_5^+$ with C_2H_4 and therefore favors reaction [8] over reaction [7] as the mechanism of formation of $C_5H_9^+$.

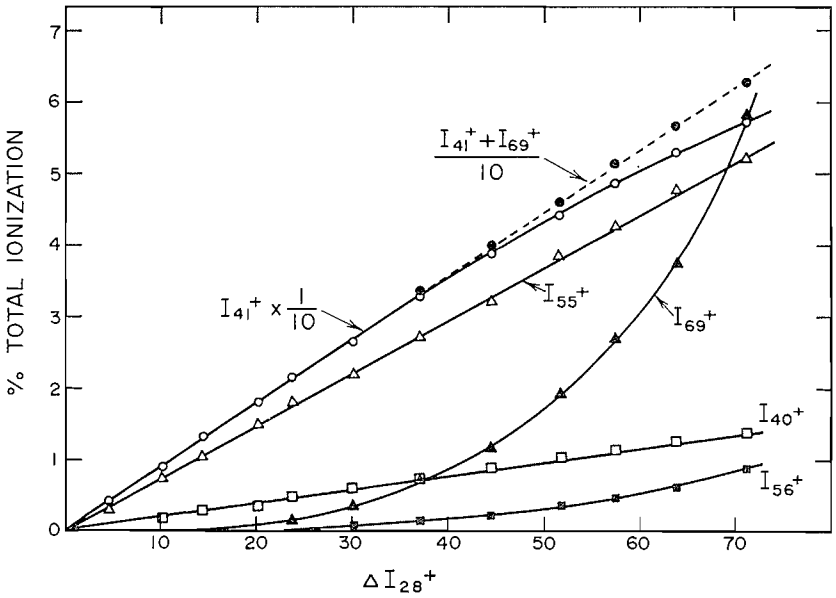

FIG. 5. Product ion intensities versus $\Delta I_{28}+$, 0.85 eV ion exit energy.

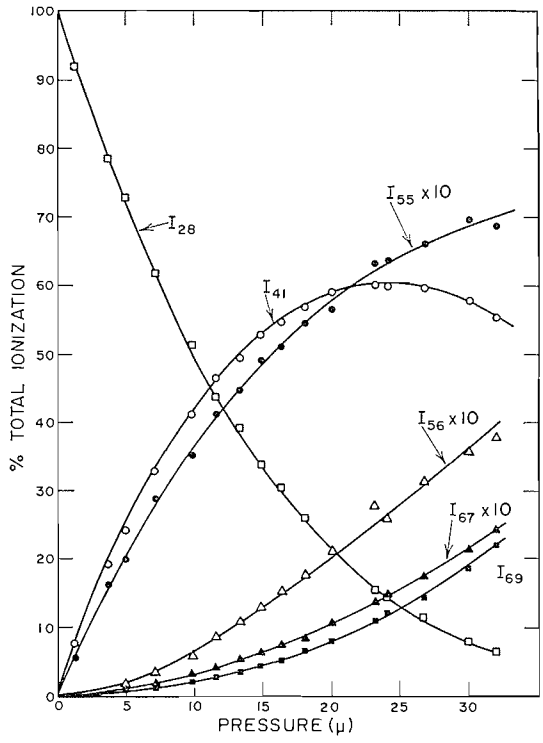

FIG. 6. Ion intensities as a function of pressure, 0.80 eV ion exit energy.

To obtain further evidence a run was carried out at 0.80 eV ion exit energy (and low electron energy) which extended to considerably higher conversion of the $C_2H_4^+$ ion. As shown by the pressure plot (Fig. 6) approximately 94% of the $C_2H_4^+$ ion has reacted at the highest pressures studied and the $C_5H_9^+$ (*m/e* 69) ion has reached approximately 22% of the total ionization, indeed it is the second largest peak in the mass spectrum. In addition the $C_3H_5^+$ ion intensity passes through a maximum and then decreases with increasing ethylene pressure.

The plot of these results as a function of $\Delta I_{28}+$ is shown in Fig. 7. The *m/e* 55 ($C_4H_7^+$) ion intensity is a linear function of the $C_2H_4^+$ reacted over the entire range examined indicating that the $C_4H_7^+$ ion is quite unreactive. Similarly the $C_3H_4^+$ (*m/e* 40) ion intensity is linear over most of the range although it shows a slight dropoff at higher conversion. On the other hand, as in Fig. 5, the *m/e* 41 ($C_3H_5^+$) ion intensity deviates from a linear relation with $\Delta I_{28}+$ at approximately 40% conversion. The sum $I_{41}+ + I_{69}+$ ($C_3H_5^+ + C_5H_9^+$) is linear with $\Delta I_{28}+$ up to ca. 80% conversion following which a slight negative deviation is observed. This deviation may be due to formation of higher order ions (e.g. $C_7H_{13}^+$) by further reaction of $C_5H_9^+$ (the higher mass region was not examined). However,

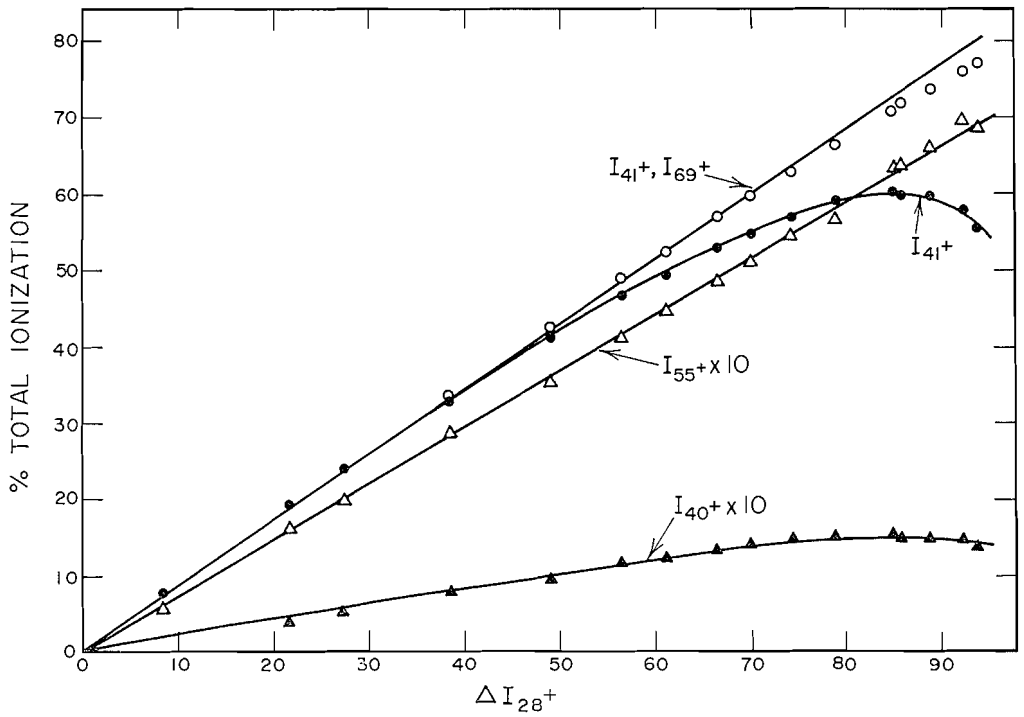

FIG. 7. Product ion intensities versus ΔI_{28+}, 0.80 eV ion exit energy.

the $C_5H_7^+$ (*m/e* 67) ion accounts for $\backsim 2\%$ of the total ionization at higher pressures (Fig. 6) and the sum $C_3H_5^+ + C_5H_7^+ + C_5H_9^+$ is a linear function of ΔI_{28+} over the entire range.[3]

The essential observations relevant to the mechanism of formation of $C_5H_9^+$ are that the $C_3H_4^+$ and $C_4H_7^+$ ion intensities are linear functions of the $C_2H_4^+$ reacted while the $C_3H_5^+$ intensity shows the characteristic dropoff expected for a reactive secondary ion with the sum of the $C_3H_5^+$ and $C_5H_9^+$ intensities being essentially linear with the $C_2H_4^+$ reacted. These observations cannot be explained by assuming a single collision complex $(C_4H_8^+)^*$ which may either dissociate to form the secondary ions (reactions [2], [3], and [14]) or react further with C_2H_4 to form $C_5H_9^+$ (reaction [7]). If these two channels for reaction of $(C_4H_8^+)^*$, i.e. decomposition versus further reaction, were competitive one would expect the intensity of all secondary ions to deviate from a linear relation with ΔI_{28+} as an increasing fraction of the collision complex reacted to form $C_5H_9^+$. However, one observes that only the $C_3H_5^+$ ion intensity deviates from a linear relation with ΔI_{28+}.

One can explain this observation in two possible ways. It can be explained by assuming that more than one collision complex is formed by collision of $C_2H_4^+$ with C_2H_4. In this case it is necessary to assume further that one of these complexes forms only $C_4H_7^+$ and $C_3H_4^+$ by dissociation and does not react further with ethylene to form $C_5H_9^+$, while a second complex either dissociates to form $C_3H_5^+$ or reacts further (reaction [7]) to form $C_5H_9^+$. In this case the formation of $C_3H_5^+$ and $C_5H_9^+$ are competitive and the linearity of $I_{41+} + I_{69+}$ with ΔI_{28+} would be expected.

Alternatively the results can be simply explained by assuming that the $C_5H_9^+$ ion is formed by reaction [8] rather than reaction [7], i.e. that $C_5H_9^+$ originates by reactions of the secondary $C_3H_5^+$ ion with C_2H_4 rather than by reaction of the $(C_4H_8^+)^*$ collision complex. Although the

[3]Previous workers (4, 6) have attributed formation of $C_5H_7^+$ to reactions involving a $C_2H_3^+$ precursor ion. The observation of $C_5H_7^+$ in the present case where $C_2H_4^+$ is the only reactant ion indicates that at least part of the $C_5H_7^+$ ion is formed in a reaction chain involving the $C_2H_4^+$ ion.

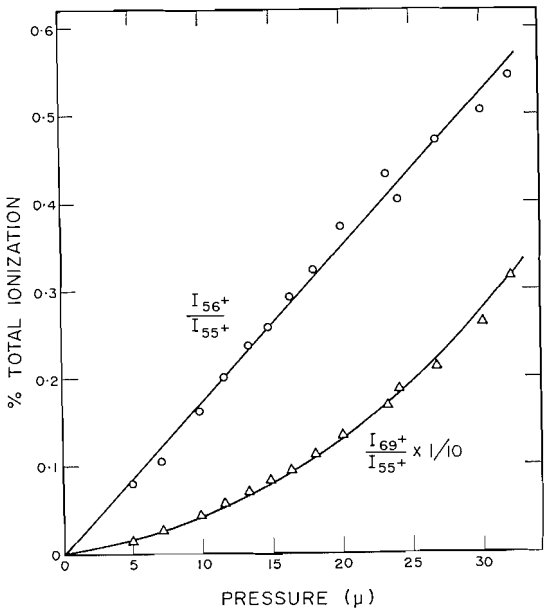

FIG. 8. I_{56+}/I_{55+} and I_{69+}/I_{55+} as a function of pressure.

explanation in terms of two complexes, outlined above, cannot be completely eliminated, the explanation in terms of the occurrence of reaction [8] is preferred. Some independent evidence in favor of this explanation is found in the kinetic order of the $C_5H_9^+$ ion. The reaction scheme [7] predicts that $C_5H_9^+$ should be third order overall in pressure while reaction scheme [8] predicts that $C_5H_9^+$ should be fourth order in pressure. Field (4) observed some years ago that the $C_5H_9^+$ intensity increased more rapidly with pressure than expected for a third order reaction and this has been confirmed in the present work. Figure 8 shows plots of I_{56+}/I_{55+} ($C_4H_8^+/C_4H_7^+$) and I_{69+}/I_{55+} ($C_5H_9^+/C_4H_7^+$) as a function of pressure. Since $C_4H_8^+$ is well known to be third order in pressure and $C_4H_7^+$ is second order in pressure the ratio should increase linearly with pressure and, within experimental error, this behavior is observed experimentally. On the other hand the ratio I_{69+}/I_{55+} shows a curved relationship as a function of pressure indicating that $C_5H_9^+$ is formed by a reaction which is greater than third order in pressure. A plot of I_{69+}/I_{55+} against P^2 does not lead to a straight line and the apparent order of $C_5H_9^+$ would appear to be between 3 and 4. Whether this apparent non-integral order is real or an experimental artifact is not known. If some of the $C_5H_9^+$ collision complexes formed in [8*a*] have sufficient lifetimes to be detected then a kinetic order of less than 4 would be observed.

The conclusion that $C_5H_9^+$ is formed by reaction [8] rather than by reaction [7] can be stated in other terms that the rate of reaction [8] is much greater than the rate of reaction [7]. This appears to be so even though reaction [8] is presumably of higher order in ethylene pressure than [7]. No conclusive independent evidence on the relative rates of these reactions is available. Kebarle *et al.* (8) have shown that $C_4H_8^+$ ions produced by electron impact react very slowly with ethylene (the cross section being 1/400 that for reaction of $C_2H_4^+$ with ethylene); however, it does not necessarily follow that $(C_4H_8^+)^*$ also reacts slowly. For reaction [8] to be responsible for the relatively high yield of $C_5H_9^+$ the reaction must obviously be very efficient. Our opinion is that this apparent high efficiency may be due in part to a relatively long lifetime for the $(C_5H_9^+)^*$ collision complex. Indeed as pointed out above the experimental kinetic order suggests that we may be observing directly some of the collision complexes. Further experiments to study more directly the reaction of $C_3H_5^+$ with ethylene are planned which it is hoped will provide more conclusive evidence on this point.

Decomposition of Collision Complex into Reactants

The present results lead to rate constants for the disappearance of $C_2H_4^+$ of 5.7×10^{-10} cm^3 molecule^{-1} s^{-1} at 3.5 eV ion exit energy and 8.3×10^{-10} cm^3 molecule^{-1} s^{-1} at 0.85 eV ion exit energy. These results are to be compared with a rate constant of 2.8×10^{-10} cm^3 molecule^{-1} s^{-1} obtained by Field *et al.* (1) and 8.3×10^{-10} cm^3 molecule^{-1} s^{-1} calculated from the date of Wexler *et al.* (9). All of these rate constants are considerably lower than the collision rate constant of 13.1×10^{-10} cm^3 molecule^{-1} s^{-1} calculated from the ion-induced dipole model (14). Although the applicability of the theory to such a complex system is perhaps questionable the results suggest the possibility that an appreciable fraction of the collision complexes may revert to reactants and led us to examine this possibility by searching for isotopically mixed ethylene ions in the spectra of C_2H_4–C_2D_4 mixtures.

Table II records the spectrum obtained

TABLE II

Partial mass spectrum of C_2H_4–C_2D_4 mixtures (intensities in arbitrary units)

m/e	1.0 μ C_2D_4 + 1.1 μ C_2H_4	1.0 μ C_2D_4	1.1 μ C_2H_4	Difference spectrum	Ionic assignment
26	3.26	0.0	2.6	0.66	$C_2H_2^+$
27	1.28	0.46	0.39	0.43	$C_2H_3^+$, C_2DH^+
28	666.7	1.48	665.2	0.0	$C_2H_4^+$, $C_2D_2^+$, $C_2H_2D^+$
29	1.20	0.0	0.23	0.97	$C_2DH_3^+$, $C_2D_2H^+$
30	3.29	0.34		2.95	$C_2D_2H_2^+$, $C_2D_3^+$
31	8.36	7.61		0.75	$C_2D_3H^+$
32	580.8	580.8		0.0	

between *m/e* 26 and 32 for a mixture of 1.0 μ C_2D_4 and 1.1 μ C_2H_4 at 3.4 eV ion exit energy and a continuous 1.2 μA ionizing electron current at 11 V nominal electron energy. Also given in Table II are the spectra obtained under identical conditions for 1.0 μ C_2D_4 and 1.1 μ C_2H_4 run separately. All spectra have been corrected for natural abundance ^{13}C and those for the pure components have been normalized so that the intensities of *m/e* 28 ($C_2H_4^+$) and *m/e* 32 ($C_2D_4^+$) are equal to the respective intensities in the mixture. Subtraction of the spectra found for the pure C_2H_4 and pure C_2D_4 from the spectrum obtained for the mixture leaves the residual spectrum recorded in Table II, Column 5.

The excess ion currents observed at *m/e* 26 and *m/e* 27 in the mixture presumably originate by the reactions

$$[5a] \quad (C_2H_4 + C_2D_4)^+ \rightarrow C_2H_2^+ + C_2H_2D_4$$

$$[4a] \quad \rightarrow C_2H_3^+ + C_2HD_4 .$$

The same reactions can be expected to contribute to formation of *m/e* 28 ($C_2D_2^+$) and *m/e* 30 ($C_2D_3^+$). It cannot be determined from the present experiments whether reactions [4*a*] and [5*a*] proceed with or without isotopic mixing. If they proceed with complete isotopic mixing one would expect the intensity distributions $C_2H_2^+$:C_2DH^+:$C_2D_2^+$ = 3:8:3 and $C_2H_3^+$:$C_2H_2D^+$:$C_2HD_2^+$:$C_2D_3^+$ = 1:6:6:1. In the absence of any isotopic mixing one would anticipate, since all concentrations are similar, that $C_2H_2^+$:$C_2D_2^+$ $\approx$ 1:1 and $C_2H_3^+$:$C_2D_3^+$ $\approx$ 1:1. Thus in either case the maximum contribution of $C_2D_3^+$ at *m/e* 30 should be approximately the same at that of $C_2H_3^+$ at *m/e* 27 or approximately 0.4_3 intensity units leaving approximately 2.5 intensity units to be ascribed to $C_2H_2D_2^+$.

The observation of significant intensity which must be ascribed to the $C_2H_2D_2^+$ ion indicates that some back reaction must occur to give isotopically mixed products. If we assume complete isotopic scrambling in the $(C_4H_4D_4^+)^*$ collision complex we calculate C_2H_4:C_2H_3D:$C_2H_2D_2^+$:$C_2HD_3^+$:$C_2D_4^+$ = 1:16:36:16:1, hence $C_2H_2D_2^+$ would be the most abundant species formed in the back reaction. Excess intensities are found in the spectra of the mixture at *m/e* 29 and *m/e* 31. That at *m/e* 29 may correspond, in fact, to $C_2D_2H^+$, however, the importance of this fragment cannot be determined without knowing the extent of isotopic scrambling in reaction [4*a*]. If we assume that the total intensities at *m/e* 29 and 31 correspond respectively to $C_2DH_3^+$ and $C_2D_3H^+$ we calculate the intensity distribution $C_2H_3D^+$:$C_2H_2D_2^+$:$C_2HD_3^+$ = 20:53:16 which is not greatly different from the predicted distribution of 16:36:16 although there appears to be a slight preference for formation of the $C_2H_2D_2^+$ ion.

TABLE III

Intensity distribution for $C_3H_5^+$ type ions in C_2H_4–C_2D_4 mixture

Ion	Calculated	Experimental, this work	Ref. 15
$C_3D_4H^+$	1.0	1.0	1.0
$C_3D_3H_2^+$	6.0	4.53	3.76
$C_3D_2H_3^+$	6.0	4.56	3.77
$C_3DH_4^+$	1.0	0.99	0.91

The results with C_2H_4–C_2D_4 mixtures show that the formation of condensation products proceeds with extensive isotopic mixing. Table III compares the measured distribution of isotopically mixed $C_3H_5^+$ type ions formed in C_2H_4–C_2D_4 mixtures with that calculated on the basis of complete scrambling in the $(C_4H_4D_4^+)^*$ complex. The experimental distribution is reasonably close to that calculated on the basis of

complete scrambling and indicates extensive scrambling of the hydrogen atoms in the complex. The distribution found in the present work indicates relatively greater scrambling than found by Meisels (15) whose results are given in the final column. The reasons for this difference are not clear.

Acknowledgments

The authors are indebted to the National Research Council of Canada for financial support of this work and for the award of Studentships (1963–1966) to J. J. M.

1. F. H. FIELD, J. L. FRANKLIN, and F. W. LAMPE. J. Am. Chem. Soc. **79**, 2419 (1957).
2. C. E. MELTON and P. S. RUDOLPH. J. Chem. Phys. **32**, 1128 (1960).
3. R. FUCHS. Z. Naturforsch. **16a**, 1026 (1961).
4. F. H. FIELD. J. Am. Chem. Soc. **83**, 1523 (1961).
5. A. G. HARRISON. Can. J. Chem. **41**, 236 (1963).
6. S. WEXLER and R. MARSHALL. J. Am. Chem. Soc. **86**, 781 (1964).
7. P. KEBARLE and A. M. HOGG. J. Chem. Phys. **42**, 668 (1965).
8. P. KEBARLE, R. M. HAYNES, and S. SEARLES. Advan. Chem. Ser. **58**, 210 (1966).
9. S. WEXLER, A. LIFSHITZ, and A. QUATTROCHI. Advan. Chem. Ser. **58**, 193 (1966).
10. I. SZABO. Arkiv Fysik, **33**, 57 (1966).
11. S. K. GUPTA, E. G. JONES, A. G. HARRISON, and J. J. MYHER. Can. J. Chem. **45**, 3107 (1967).
12. J. J. MYHER and A. G. HARRISON. To be published.
13. F. H. FIELD and J. L. FRANKLIN. Electron impact phenomena and the properties of gaseous ions. Academic Press, New York. 1957.
14. G. GIOUMOUSIS and D. P. STEVENSON. J. Chem. Phys. **29**, 294 (1958).
15. G. G. MEISELS. Advan. Chem. Ser. **58**, 243 (1966).

Can. J. Chem. Downloaded from www.nrcresearchpress.com by 210.87.254.40 on 09/05/12
For personal use only.

Theory of nucleation in solid state reactions

A. R. ALLNATT[1] AND P. W. M. JACOBS
Department of Chemistry, University of Western Ontario, London, Ontario

Received July 14, 1967

The theory of nucleation in solid state reactions is formulated in a general way and a solution to the problem of multi-step nucleation obtained. Two special cases of the general formulation are considered: the second of these corresponds to Bagdassarian's approximate model and some corrections to his treatment are pointed out. A new equation describing the kinetics of a solid state reaction, which involves multi-step nucleation followed by a constant and isotropic rate of growth, is derived. This equation is termed the generalized Avrami equation since it removes the restriction, in Avrami's treatment, of a single-step nucleation process. Erofeev's analysis of the problem is shown to be valid only in the limit of short times: the generalized Avrami equation reduces to Erofeev's equation in this limit.

Canadian Journal of Chemistry, 46, 111 (1968)

It is generally accepted that in the decomposition of a solid to yield a second product phase, the chemical reaction initiates at certain discrete points in the reactant called nucleus-forming sites. This results in the formation of sub-microscopic particles of the solid product phase called nuclei which are distributed over the surface of, or embedded in the bulk of, the reactant. Further chemical reaction is localized at the interface between the nuclei and the reactant matrix so that the nuclei grow in size as the reaction proceeds. As the nuclei grow, the area of this interface increases, thus accounting for the rapid acceleratory stage which is usually a feature of the isothermal kinetics. Further growth leads to overlap of the nuclei, resulting in a reduction in the area of the interface and a consequent deceleration of the reaction, which continues until the reactant is consumed. If nucleation occurs over the whole surface, or if the growth of surface nuclei is unusually rapid, then the surface soon becomes covered by a product layer and the kinetics are governed by the rate of inward propagation of this contracting envelope. Thus the reaction is entirely decelerator in character. A constant rate of propagation leads to the familiar 'contracting volume' expression (1, 2).

The conventional theory of the decomposition of solids distinguishes between formation and growth of nuclei in a very real way by ascribing different rate constants k_t and k_g to these two processes. This is a realistic procedure if a nucleus can be formed as a result of a single reaction step because the first molecular decomposition at a nucleus-forming site is clearly occurring in a different environment from that for subsequent ones. If the presence of a single product molecule provides the autocatalytic conditions necessary for nucleus growth, then one might expect that $k_g > k_t$. On the other hand if the nucleus-forming site contains some special structural feature which is eliminated or altered by the act of decomposition, then k_t might well be $> k_g$. The latter situation is essential for the kinetics to be entirely deceleratory.

An important advance was made by Bagdassarian (3) who introduced the concept of multi-step nucleation. He proposed that, in general, p successive molecular decompositions at a single site are required to form a stable growth nucleus and that nuclei containing less than p product atoms are not growth nuclei, but germ nuclei, which may become growth nuclei by acquiring the requisite number of product atoms. Bagdassarian considered only the special case

$$k_0 = k_1 = k_2 \text{ --- } = k_{p-1}$$
$$k_p = k_{p+1} = k_{p+2} \text{ --- } = k, \qquad [1]$$

where k_i is the rate constant for the addition of a product atom to a nucleus containing i atoms. Bagdassarian recognized that [1] was an approximation but evidently believed that a knowledge of the dependence of k_i on i was necessary to make the problem soluble. In this paper we present the general solution to the problem of multi-step nucleation. This falls into two parts: first we consider the situation in which the rate constants are all different and then we consider the modifications to the theory which are necessary when the k's are all different up to $i = r$ and

[1]Permanent address: Department of Chemistry, The University, Manchester 13, England.

Can. J. Chem. Downloaded from www.nrcresearchpress.com by 210.87.254.40 on 09/05/12
For personal use only.

equal for $i > r$. We also reconsider the Bagdassarian special case in greater detail, since his solution, though correct, is incomplete.

Multi-Step Nucleation

General Solution

The differential equation controlling the number of nuclei n_i which contain i product atoms is

$$[2] \qquad \frac{dn_i(t)}{dt} = k_{i-1}n_{i-1}(t) - k_i n_i(t).$$

This equation is to be solved subject to the boundary conditions $n_i = 0$ for $i < 0$; $n_i = 0$ for $i > 0$ at $t = 0$, $n_i = n_0(0)$ for $i = 0$ at $t = 0$; $n_i = 0$ for $i = 0$ at $t = \infty$. Let

$$[3] \qquad \tilde{n}_i(s) = \int_0^\infty e^{-st} n_i(t)\, dt$$

denote the Laplace transform of $n_i(t)$. Then [2] transforms to

$$[4] \qquad s\tilde{n}_i - n_i(0) = k_{i-1}\tilde{n}_{i-1} - k_i\tilde{n}_i,$$

which has the solution

$$[5] \quad (s + k_i)\tilde{n}_i = n_i(0) + k_{i-1}\tilde{n}_{i-1} = n_i(0) + k_{i-1}\left[\frac{n_{i-1}(0) + k_{i-2}\tilde{n}_{i-2}}{s + k_{i-1}}\right], \text{ etc.}$$

The solution may be continued down to $n_0(0)$ by repeated use of [5]. But according to the boundary conditions $n_i(0) = 0$ for all i except $i = 0$ and therefore

$$[6] \quad (s + k_i)\tilde{n}_i = \left(\frac{k_{i-1}}{s + k_{i-1}}\right)\left(\frac{k_{i-2}}{s + k_{i-2}}\right) \cdots \left(\frac{k_0}{s + k_0}\right) n_0(0).$$

Therefore

$$n_i(t) = k_{i-1}k_{i-2} \cdots k_0 n_0(0)\ \mathrm{Tr}\ \frac{1}{(s + k_i)(s + k_{i-1}) \cdots (s + k_0)},$$

where Tr denotes the inverse transform. Thus

$$[7] \quad n_i(t) = n_0(0)k_0k_1k_2 \cdots k_{i-1}\left\{\sum_{l=0}^{l=i} \frac{e^{-k_l t}}{\left(\prod_{\substack{j=0 \\ (j\neq l)}}^{i} (k_j - k_l)\right)}\right\}.$$

The solutions for $i = 0$, 1, 2 are

$$[8] \qquad n_0(t) = n_0(0)\, e^{-k_0 t}$$

$$[9] \qquad n_1(t) = n_0(0)k_0\left[\frac{e^{-k_0 t} - e^{-k_1 t}}{k_1 - k_0}\right]$$

$$[10] \quad n_2(t) = n_0(0)k_0k_1\left[\frac{e^{-k_0 t}}{(k_1 - k_0)(k_2 - k_0)} + \frac{e^{-k_1 t}}{(k_2 - k_1)(k_0 - k_1)} + \frac{e^{-k_2 t}}{(k_0 - k_2)(k_1 - k_2)}\right].$$

These results for $i = 0$, 1, 2 are identical with those obtained by direct solution (4) of the differential eq. [2], but the direct method becomes impractical for large i and so does not lead to a general solution to the problem.

The form of these solutions is particularly interesting for $k_i t \ll 1$. Equations [9] and [10] then simplify to

$$[11] \qquad n_1(t) = n_0(0)k_0 t = K_1 t$$

and

$$[12] \qquad n_2(t) = \frac{n_0(0)k_0k_1}{2!} t^2 = K_2 t^2,$$

suggesting the basis for a general power law for nucleation: if the formation of a stable growth nucleus requires the successive decomposition of p molecules of reactant, and if the nucleation rate constants are such that $k_i t \ll 1$, then the number of growth nuclei formed in time t is proportional to t^p.

The general proof follows by induction; application of the Faltung theorem to the result [6] gives

$$[13] \quad n_i(t) = k_{i-1} \int_0^t d\tau\, e^{-k_i(t-\tau)} n_{i-1}(\tau).$$

We desire to show that if, in the limit $t \to 0$, n_{i-1} behaves like t^{i-1} then n_i behaves like t^i. Suppose

$$[14] \quad n_{i-1}(\tau) = a_{i-1}\tau^{i-1} + b_{i-1}\tau^i + \cdots.$$

Then [13], [14] give

$$[15] \quad \frac{n_i(t)}{k_{i-1}} = e^{-k_i t} \int_0^t d\tau\, e^{k_i \tau} [a_{i-1}\tau^{i-1} + b_{i-1}\tau^i + \cdots].$$

Expand both exponentials as far as the second term and integrate, giving

$$\frac{n_i(t)}{k_{i-1}} = \frac{a_{i-1}t^i}{i} + O(t^{i+1}),$$

so that

$$[16] \quad \lim_{t\to 0} n_i(t) = \left\{\lim_{t\to 0} n_{i-1}(t)\right\} \frac{k_{i-1}t}{i}.$$

Can. J. Chem. Downloaded from www.nrcresearchpress.com by 210.87.254.40 on 09/05/12
For personal use only.

In view of [11] and [16] it follows that

$$[17]\quad n_i(t) = \frac{k_{i-1}k_{i-2}\cdots k_0 n_0(0)}{i!}t^i = K_i t^i$$

$$(k_j t \ll 1 \text{ for all } j),$$

which is the general power law for nucleation.

$(k_i = k,\ i \geqslant r+1)$

The solution [7] for $n_i(t)$ is inconvenient in the limiting case when any two of the nucleation rate constants are equal. We therefore consider the situation in which the k_i are all different for $i = 0, 1, 2 \cdots r$, but $k_i = k$ for $i \geqslant r+1$. It follows then from the general formula [6] that, for $i > r$,

$$[18]\quad \tilde{n}_i = \left(\frac{1}{s+k}\right)\left(\frac{k}{s+k}\right)^{i-r-1}\left(\frac{k_r}{s+k_r}\right)\cdots\left(\frac{k_0}{s+k_0}\right)n_0(0).$$

Transforming [18] gives

$$[19]\quad n_i(t) = n_0(0)k_0k_1k_2\cdots k_r k^{i-r-1} \times I_i(t),$$

where

$$[20]\quad I_i(t) = \int_0^t d\tau\, \mathrm{Tr}\left[\frac{1}{s+k}\right]^{i-r}_{\mathrm{at}\,(t-\tau)} \times \mathrm{Tr}\left[\left(\frac{1}{s+k_r}\right)\cdots\left(\frac{1}{s+k_0}\right)\right]_{\mathrm{at}\,\tau}$$

or

$$[21]\quad I_i(t) = \int_0^t d\tau\left[\frac{(t-\tau)^{i-r-1}}{(i-r-1)!}e^{-k(t-\tau)}\right]\times\left[\sum_{l=0}^{r}\frac{e^{-k_l\tau}}{\prod_{\substack{j=0\\(j\neq l)}}^{r}(k_j-k_l)}\right]$$

on substituting the inverse transforms. Integrating gives

$$[22]\quad I_i(t) = \sum_{l=0}^{r}\frac{e^{-k_l t}}{(k-k_l)^{i-r}\prod_{\substack{j=0\\(j\neq l)}}^{r}(k_j-k_l)}\times\left[1-e^{-(k-k_l)t}\left\{\frac{[(k-k_l)t]^{i-r-1}}{(i-r-1)!}+\frac{[(k-k_l)t]^{i-r-2}}{(i-r-2)!}+\cdots 1\right\}\right].$$

Equations [19] and [22] give the general solution to the problem of multi-step nucleation when the rate constants are all different at the start, but after the nucleus contains more than r atoms, the nucleation rate constants have a constant value k for the addition of successive atoms of product.

The limit for short times may be obtained by a technique similar to that already used. We have that

$$[14']\quad n_i(t) = a_i t^i + b_i t^{i+1} + \cdots$$

for $i \leqslant r$. For $i > r$, one requires (see [7] and [21])

$$[23]\quad I_i(t) = \int_0^t\left[d\tau\frac{(t-\tau)^{i-r-1}}{(i-r-1)!}e^{-k(t-\tau)}\right]\times\frac{n_r(\tau)}{n_0(0)\prod_{j=0}^{r-1}k_j} = \frac{1}{(i-r-1)!\,n_0(0)\prod_{j=0}^{r-1}k_j}\times e^{-kt}t^{i-r-1}\left[\frac{a_r t^{r+1}}{r+1}+0(t^{r+2})\right],$$

so that

$$[24]\quad \lim_{t\to 0} I_i(t) = \frac{1}{(i-r-1)!\,n_0(0)\prod_{j=0}^{r-1}k_j}\times\left[\frac{a_r}{r+1}\right]t^i.$$

Substituting from [24] in [19] gives

$$[25]\quad n_i(t) = \frac{k^{i-r-1}k_r}{(i-r-1)!}\left(\frac{a_r}{r+1}\right)t^i \qquad (kt,\ k_i t \ll 1).$$

But

$$\lim_{t\to 0} n_r(t) = a_r t^r$$

and so [25] and [17] give

$$[26]\quad n_i(t) = \frac{k^{i-r-1}k_r k_{r-1}\cdots k_0 n_0(0)}{(i-r-1)!\,(r+1)!}t^i = K_i t^i, \text{ provided } kt,\ k_i t \ll 1.$$

Thus the power law for nucleation is still valid, but note that the meaning of the constant K_i

Can. J. Chem. Downloaded from www.nrcresearchpress.com by 210.87.254.40 on 09/05/12
For personal use only.

depends on whether the k_i are all unequal or whether $k_i = k$ for $i > r$ (see eqs. [17] and [26] respectively).

Bagdassarian Model

Bagdassarian assumed (3) that

$$[1] \qquad k_0 = k_1 \text{ --- } = k_{p-1}$$
$$k_p = k_{p+1} \text{ --- } = k.$$

The general expression [6] for the transform of n_i reduces in this case to

$$[27] \quad \tilde{n}_i = \frac{{k_0}^i}{(s + k_0)^{i+1}} n_0(0) \quad \text{for } i < p,$$

and so

$$[28] \quad n_i(t) = n_0(0) \frac{(k_0 t)^i}{i!} e^{-k_0 t} \quad (i < p).$$

For $i \geqslant p$,

$$[29] \quad \tilde{n}_i = \frac{k^{i-p}}{(s + k)^{i-p+1}} \frac{{k_0}^p}{(s + k_0)^p} n_0(0)$$

and

$$[30] \qquad n_i(t) = k^{i-p} k_0^p n_0(0) I_i(t),$$

where

$$[31] \quad I_i(t) = \int_0^t d\tau \frac{(t - \tau)^{i-p}}{(i - p)!} \frac{\tau^{p-1}}{(p - 1)!} \times e^{-k(t-\tau)} e^{-k_0 \tau}.$$

Evaluating the integral and substituting the result in [30] gives

$$[32] \quad n_i(t) = \left(\frac{k_0}{k}\right)^p \left(\frac{k}{k_0 - k}\right)^i n_0(0) \times e^{-kt} \sum_{m=0}^{i-p} \frac{[(k_0 - k)t]^{i-p-m}}{(i - p - m)!} \times \frac{(m + p - 1)!}{m!\,(p - 1)!} \left\{1 - e^{(k-k_0)t} \left[1 + \text{---} + \frac{[(k_0 - k)t]^{m+p-2}}{(m + p - 2)!} + \frac{[(k_0 - k)t]^{m+p-1}}{(m + p - 1)!}\right]\right\},$$

which holds for $i \geqslant p$.

The total number of growth nuclei formed in time t is

$$n(t) = \sum_{i=p}^{\infty} n_i(t).$$

Now

$$\tilde{n}(t) = \sum_{i=p}^{\infty} \tilde{n}_i;$$

on substituting from [29] and evaluating the inverse transform, we have

$$[33] \quad n(t) = n_0(0)\left[1 - e^{-k_0 t} \sum_{j=0}^{p-1} \frac{(k_0 t)^j}{j!}\right],$$

which is identical with Bagdassarian's formula [4']. However, his formula on page 447 of ref. 3 for $n_i(t)$ is valid only for $i < p$. The result [33] is clearly correct, since

$$[34] \quad \sum_{i=0}^{\infty} n_i(t) = n_0(0) = \sum_{i=0}^{p-1} n_i(t) + n(t),$$

whence [33] follows immediately on substituting for $n_i(t)$ from [28]. Bagdassarian used this method to evaluate $n(t)$ and thus obtained the correct result [33], since his formula for $n_i(t)$ is correct if $i < p$. It is important to recall that Bagdassarian's theory was one of photographic development but that we are utilizing his basic idea of multi-step nucleation in solid state thermal reactions. Thus in Bagdassarian's theory nuclei go on growing after they contain p atoms of product but with a different rate constant k ($\neq k_0$). All nuclei with $i \geqslant p$ will then undergo development when the grains are exposed to the developer. In our theory, as soon as a nucleus reaches the size characterized by p atoms, it becomes a stable growth nucleus and no further assumptions about k_i, $i \geqslant p$, are necessary since k_i is automatically determined by whatever assumptions are made concerning the nuclear growth rates. For example, a constant growth rate means that $k_i \propto i^{2/3}$.

Growth of Nuclei

The two main theories of nucleus growth are those due to Avrami (5) and to Erofeev (6). Avrami assumed that germ nuclei are converted into growth nuclei in a single activated step. However, some unactivated germ nuclei are lost through incorporation into growing nuclei. Also growth nuclei formed from germ nuclei, which happen to be near one another in the reactant, will impinge together and overlap during growth. This ingestion and overlap result in the fractional decomposition α being smaller than α_{ex}, the extended fractional decomposition, which Avrami defines as the fractional decomposition which would have occurred without ingestion and overlap. If we assume that de-

Can. J. Chem. Downloaded from www.nrcresearchpress.com by 210.87.254.40 on 09/05/12
For personal use only.

composition is a purely random phenomenon[2] then

$$[35] \qquad d\alpha = d\alpha_{ex}(1 - \alpha).$$

Formula [35] is the simplest expression that satisfies the required boundary conditions $d\alpha/dt = d\alpha_{ex}/dt$ at $\alpha = 0$, $d\alpha/dt = 0$, but $d\alpha_{ex}/dt$ finite at $\alpha = 1$. It follows from [35] that the fractional decomposition α is given by the Avrami equation

$$[36] \quad -\log(1 - \alpha) = k' n_0(0) \times \left[e^{-k_0 t} - 1 + k_0 t - \frac{(k_0 t)^2}{2!} + \frac{(k_0 t)^3}{3!} \right].$$

[See refs. 1, 2, 4, and 5 for the detailed arguments and for explicit expressions for the constant k'.] k_0 is the nucleation rate constant.

The approach used by Erofeev (6) is to take the rate of formation of growth nuclei as

$$[37] \quad \left[\frac{dn}{dt} \right]_{t=\tau} = \frac{n_0(0) k_0 k_1 \cdots k_{p-1}}{(p-1)!} t^{p-1},$$

which we have shown to be the correct form for small t, eq. [17]. The extended fractional decomposition is then

$$[38] \quad \alpha_{ex} = [V(\infty)]^{-1} \int_0^t d\tau \times \left[\frac{dn}{dt} \right]_{t=\tau} \frac{4}{3} \pi [G(t - \tau)]^3$$

if the nuclei are assumed to be spherical with a constant growth rate in a radial direction of G. $V(\infty)$ is the total volume of product when reaction is complete. Integrating [38] and substituting in the integral of [35], $-\log(1 - \alpha) = \alpha_{ex}$, gives the Erofeev equation

$$[39] \qquad -\log(1 - \alpha) = (\bar{k}_n t)^n,$$

where $n = p + 3$, and $\bar{k}_n$ is the overall rate constant for the reaction determined by analyzing the kinetic data by plotting $[-\log(1 - \alpha)]^{1/n}$ against t. Equation [39] is one of the most commonly used formulae in solid state reaction kinetics; it is frequently referred to as the Avrami–Erofeev equation on the grounds that the Avrami eq. [36] would reduce to this form for either short times, $kt \ll 1$, or for long times, $kt \gg 1$. As this approximation is clearly not valid when kt is of order unity, it seems better to drop this nomenclature and to preserve the name Avrami equation for [36].

The nucleation law used by Erofeev is, however, only approximate, since it is of the correct form for a multi-step nucleation process, with the k's all different, only if $k_i t \ll 1$ (see eq. [17]). It will now be shown that the use of the exact form of the nucleation law for multi-step nucleation leads to a generalized Avrami equation which, for small t, reduces to the Erofeev equation. This new development also replaces the weak point in Avrami's formulation which lies in restricting the nucleation law to a single-step process.

Suppose that nucleation is a multi-step process characterized by rate constants $k_0, k_1 \cdots k_p$, and that once a nucleus containing p atoms of product is formed it becomes an active growth nucleus. The rate of formation of active growth nuclei is therefore

$$[40] \qquad \frac{dn_p(t)}{dt} = k_{p-1} n_{p-1}(t) = n_0(0) \sum_{l=0}^{p-1} B_{pl} e^{-k_l t},$$

where the general result [7] has been used for $n_{p-1}(t)$ and

$$[41] \qquad B_{pl} = k_l \prod_{\substack{j=0 \\ (j \neq l)}}^{p-1} \frac{k_j}{k_j - k_l}.$$

The extended fractional decomposition α_{ex} is then

$$[42] \quad \alpha_{ex} = \frac{\sigma}{V(\infty)} \int_0^t d\tau \left[\frac{dn_p}{dt} \right]_{t=\tau} \times [G(t - \tau)]^3,$$

where G is the constant radial growth rate and σ is a shape factor ($= 4\pi/3$ for spherical nuclei).

[2]Following Avrami, both nucleation and subsequent decomposition are assumed to be random in both space and time. The latter assumption is well grounded in statistical mechanics: spatial randomness will be valid for exactly equivalent segments of reactant. In real crystals, however, topochemical equivalence may not be a realistic assumption in view of the occurrence of point defects, dislocations, and grain boundaries together with grosser imperfections such as cracks or scratches. In fine powders the particle size distribution may also be important. Alignment of nuclei along dislocations or grosser imperfections can lead to non-random overlap and hence to substantial modifications in the observed time dependence of the reaction rate. Some special cases of this are discussed in ref. 4.

Substituting from [40] in [42], integrating, and evaluating α from α_{ex} in the usual way gives

$$[43] \quad -\log(1-\alpha) = 6\sigma[V(\infty)]^{-1}n_0(0)G^3 \times \sum_{l=0}^{p-1} k_l^{-4}B_{pl}\left\{e^{-k_l t} - 1 + k_l t - \frac{(k_l t)^2}{2!} + \frac{(k_l t)^3}{3!}\right\}.$$

Equations [43] and [41] give the general solution to the problem of multi-step nucleation followed by a constant rate of growth in three dimensions. Equation [43] is of the same form as eq. [36] and we therefore term it the generalized Avrami equation. The limit for short times is of interest: as $t \to 0$, [43] becomes

$$[44] \quad -\log(1-\alpha) = 6\sigma[V(\infty)]^{-1}n_0(0)G^3 \sum_{l=0}^{p-1} B_{pl}\frac{t^4}{4!} + 0(t^5).$$

But from [7],

$$[45] \quad k_{p-1}n_{p-1} = n_0(0)\sum_{l=0}^{p-1} B_{pl}e^{-k_l t} = n_0(0)\left[\sum_{l=0}^{p-1} B_{pl} + \left\{\sum_{l=0}^{p-1} B_{pl}(-k_l)\right\}t + \left\{\sum_{l=0}^{p-1} B_{pl}\left(\frac{k_l^2}{2!}\right)\right\}t^2 + \cdots\right].$$

But we have already proved (see [17]) that n_i behaves like t_i as $t \to 0$, so that the first $p-1$ coefficients in [45] must be zero. Therefore [44] becomes

$$[46] \quad -\log(1-\alpha) = 6\sigma[V(\infty)]^{-1}n_0(0)G^3 \times \sum_{l=0}^{p-1} B_{pl}\frac{(-k_l t)^{p+3}}{(p+3)!}\frac{1}{k_l} \quad (k_l t \ll 1).$$

Thus $-\log(1-\alpha)$ behaves like t^{p+3} when $k_l t \ll 1$, if there are p steps in forming a growth nucleus. But this is just Erofeev's conclusion, which is therefore exact in the limit of short times.

1. P. W. M. Jacobs and F. C. Tompkins. *In* Chemistry of the solid state. *Edited by* W. E. Garner. Butterworths, London. 1955. Chap. 7.
2. D. A. Young. Decomposition of solids. Pergamon, Oxford. 1966.
3. Ch. Bagdassarian. Acta Physicochim. U.R.S.S. **20,** 441 (1945).
4. P. W. M. Jacobs. Kinetics of the thermal decomposition of solids. Kinetics of reactions in ionic systems. Plenum Press, New York. To be published.
5. M. Avrami. J. Chem. Phys. **7,** 1103 (1939); **8,** 212 (1940); **9,** 177 (1941).
6. B. V. Erofeev. Compt. Rend. Acad. Sci. U.R.S.S. **52,** 511 (1946).

Can. J. Chem. Downloaded from www.nrcresearchpress.com by 210.87.254.40 on 09/05/12
For personal use only.

Can. J. Chem. Downloaded from www.nrcresearchpress.com by 210.87.254.6 on 09/05/12
For personal use only.

Coordination compounds of norbornadiene with silver tetrafluoroborate[1]

HAROLD W. QUINN
Exploratory Research Laboratory, Dow Chemical of Canada, Limited, Sarnia, Ontario

Received August 8, 1967

Crystalline complexes of norbornadiene with silver tetrafluoroborate have been obtained both from anhydrous and aqueous solution. While both solutions yield complexes of stoichiometry $AgBF_4 \cdot C_7H_8$ and $2AgBF_4 \cdot 3C_7H_8$, those from the aqueous solutions also contain water of crystallization. The infrared spectra show that norbornadiene is similarly complexed in both the anhydrous and hydrated complexes but that the coordination in the 1:1 complex is different from that in the 2:3 complex. The anhydrous and hydrated 1:1 complexes have the same X-ray diffraction powder patterns while those of 2:3 complexes are different.

Canadian Journal of Chemistry, 46, 117 (1968)

Introduction

The addition of norbornadiene (bicyclo[2.2.1]-hepta-2,5-diene) to an aqueous silver nitrate solution has been observed to produce a mixture of $AgNO_3 \cdot C_7H_8$ and $2AgNO_3 \cdot C_7H_8$ (1). Recrystallization of the product from ethanol yielded $2AgNO_3 \cdot C_7H_8$ (the complex observed by a number of investigators (2–4)), the structure of which has been reported (5) to involve a cross-linking of $AgNO_3$ chains with norbornadiene molecules.

In view of the differing stoichiometry of the butadiene-1,3 complex of $AgNO_3$ and $AgBF_4$ (6), it was considered to be desirable to investigate the norbornadiene complexes of $AgBF_4$. Consequently a study has been made of those complexes obtained from both aqueous and non-aqueous solutions of silver tetrafluoroborate.

Experimental

Anhydrous silver tetrafluoroborate was prepared as previously described (6). Saturated aqueous solutions containing about 47% by weight of $AgBF_4$ were obtained from Fairmount Chemical Company. The solution was filtered and the filtrate analyzed at 28.0 weight % Ag.

Norbornadiene (N_D^{20} 1.4703) was obtained from Aldrich Chemical Company. Prior to use it was vacuum distilled to free it of polymeric products and stored in a refrigerator.

The solvents employed, nitromethane and toluene, were Eastman Spectro grade and Fisher certified reagent grade respectively. They were used without further purification.

Complex Formation from Anhydrous Solution

The calculated compositions (weight %) of the complexes which, on the basis of the literature, one might anticipate are as follows:

$2AgBF_4 \cdot C_7H_8$: Ag, 44.80; C, 17.46; H, 1.67.

$AgBF_4 \cdot C_7H_8$: Ag, 37.61; C, 29.31; H, 2.81.

$2AgBF_4 \cdot 3C_7H_8$: Ag, 32.40; C, 37.88; H, 3.63.

Attempted Preparation of $2AgBF_4 \cdot C_7H_8$

$AgBF_4$ (2.151 g, 0.0110 mole) was dissolved in 3 ml toluene and 0.455 g (0.0049 mole) norbornadiene dissolved in 1 ml toluene added with shaking. A greyish-white precipitate was obtained, filtered under vacuum, washed twice with 1 ml quantities of toluene and thrice with petroleum ether, and vacuum dried at room temperature.

Anal. Found: Ag, 37.9; C, 28.4; H, 2.80 (corresponds to $AgBF_4 \cdot 0.962C_7H_8$).

It was noted that the toluene washings did not mix readily with the original filtrate. Addition of more norborandiene to this filtrate resulted in further precipitation of white solid, indicating an incomplete initial complexing of the $AgBF_4$.

Preparation of $AgBF_4 \cdot C_7H_8$ (I)

$AgBF_4$ (1.038 g, 0.0053 mole) was dissolved in 2.5 ml toluene and 0.455 g (0.0049 mole) norbornadiene added with shaking. The white precipitate obtained was separated by vacuum filtration, washed four times with petroleum ether, and vacuum dried at room temperature. The product, which was somewhat hygroscopic, showed no melting point but discolored at about 110 °C and decomposed rapidly at about 150 °C.

Anal. Found: Ag, 37.5; C, 29.7; H, 2.85 (corresponds to $AgBF_4 \cdot 1.016C_7H_8$).

Preparation of $2AgBF_4 \cdot 3C_7H_8$ (II)

$AgBF_4$ (0.723 g, 0.0037 mole) was dissolved in 2 ml toluene. Upon addition of 0.910 g (0.0099 mole) norbornadiene with shaking a fine white precipitate was obtained. The toluene was removed by vacuum filtration and the precipitate was washed four times with petroleum ether and vacuum dried at room temperature. The product, which showed no tendency to be hygroscopic, did not melt but began to discolor at about 140 °C and rapidly decomposed at about 165 °C.

Anal. Found: Ag, 32.6; C, 37.6; H, 3.70 (corresponds to $AgBF_4 \cdot 1.469C_7H_8$).

Preparation of $2AgBF_4 \cdot 3C_7H_8$ from Nitromethane Solution

Norbornadiene (1.090 g, 0.012 mole) was added to 0.767 g (0.0039 mole) $AgBF_4$ dissolved in 2 ml CH_3NO_2.

[1]Contribution No. 152.

Can. J. Chem. Downloaded from www.nrcresearchpress.com by 210.87.254.6 on 09/05/12
For personal use only.

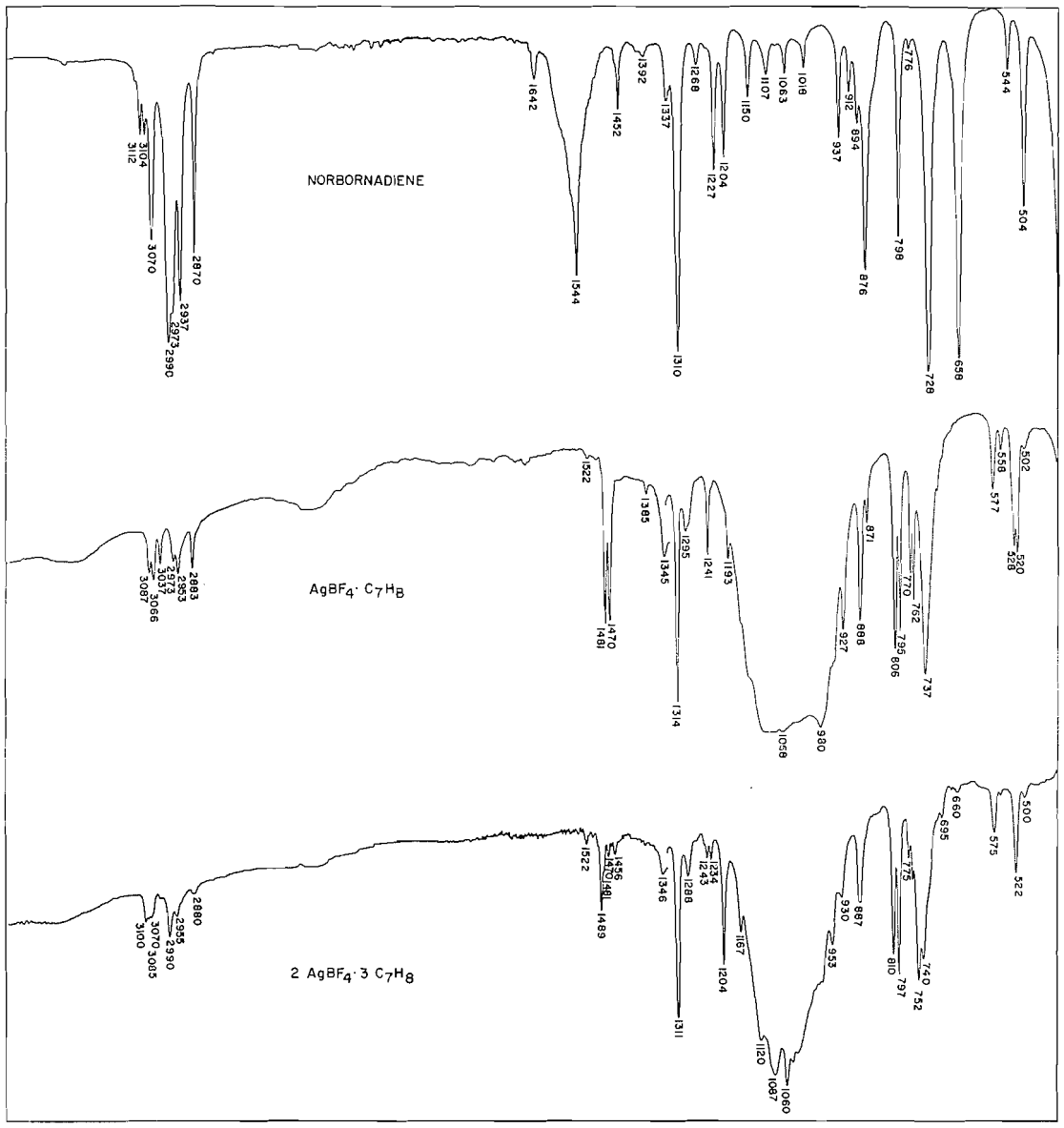

FIG. 1. Infrared spectra of norbornadiene and the complexes $AgBF_4 \cdot C_7H_8$ and $2AgBF_4 \cdot 3C_7H_8$ obtained from anhydrous solution.

The white crystalline product obtained was dissolved by heating to about 80 °C. Upon cooling, fine needles were obtained. One milliliter of CH_3NO_2 was added and the system warmed to effect solution; upon slow cooling, large needle-like crystals were obtained. The crystals were filtered, washed twice with petroleum ether, and vacuum dried (weight 0.248 g).

Anal. Found: Ag, 32.35; C, 36.05; H, 3.60.

Complex Formation from Aqueous Solution

Preliminary experimentation established that the norbornadiene complexes obtained from aqueous solution were hydrated and that a mixture of complexes of differing stoichiometry was usually obtained. Over a period of time, techniques were developed which permitted isolation of single complexes.

Preparation of $AgBF_4 \cdot C_7H_8$ Hydrate (III)

Norbornadiene (5.144 g, 0.056 mole) dissolved in 6.58 g petroleum ether was added to 23.169 g aqueous $AgBF_4$ containing 0.060 mole $AgBF_4$ and shaken for 10 min. (Preliminary experiments had established the

Can. J. Chem. Downloaded from www.nrcresearchpress.com by 210.87.254.6 on 09/05/12
For personal use only.

desirability of dissolving norbornadiene in petroleum ether in order to prevent a marked precipitation of complex at the organic–aqueous interface.) A significant evolution of heat was observed. The aqueous layer was removed with a hypodermic syringe, filtered, and refrigerated at about 10 °C for 48 h. Transparent crystals ranging from about 0.5 to 3 mm in diameter were obtained, vacuum filtered, and surface dried on filter paper. Some crystals were blocky, while others were long. Employing a microscope, some of the longer crystals (III) were removed from the mass (III*a*) and analyzed.

Anal. Found for III: Ag, 33.55; C, 26.25; H, 2.97; H_2O, 9.68. Anal. Found for III*a*: Ag, 29.35; C, 31.0; H, 3.99; H_2O, 11.65.

III corresponds to $AgBF_4 \cdot 1.004C_7H_8 \cdot 1.729H_2O$ and III*a* to $AgBF_4 \cdot 1.355C_7H_8 \cdot 2.379H_2O$.

Preparation of $2AgBF_4 \cdot 3C_7H_8$ Hydrate (IV)

Aqueous $AgBF_4$ (30.369 g) containing 0.080 mole $AgBF_4$ was diluted with 16.741 g distilled water. To this was added 3.786 g (0.041 mole) norbornadiene dissolved in 5.331 g petroleum ether and the system shaken for 5 min. The aqueous layer was separated, filtered, and refrigerated at 10 °C for 18 h with no crystal growth observed. An additional 2.864 g (0.031 mole) norbornadiene dissolved in 4.061 g petroleum ether was added and the same treatment applied. Over a period of 3 days at 10 °C, transparent blocky crystals of 3 to 4 mm diameter were obtained, removed from the supernatant, and surface dried with filter paper, whereupon the surface became opaque.

Anal. Found: Ag, 31.0; C, 34.9; H, 4.06; H_2O, 7.7 (corresponds to $AgBF_4 \cdot 1.444C_7H_8 \cdot 1.489H_2O$).

Both III and IV show partial melting between 95 and 105 °C, followed by discoloration above 120 °C and rapid decomposition above 150 °C.

Ethanol Recrystallization of Complex from Aqueous Solution

Norbornadiene (4.568 g, 0.050 mole) was added to 10.422 g aqueous $AgBF_4$ containing 0.015 mole $AgBF_4$. The massive white precipitate obtained was filtered on a sintered disc and dissolved in 5 ml of hot ethanol. Upon cooling a mass of white needle-like crystals was obtained, filtered, and dried on filter paper (weight 1.304 g). The product did not melt but decomposed rapidly at about 170 °C.

Anal. Found: Ag, 26.35; C, 36.6; H, 3.27.

Infrared Spectra

All infrared spectra were obtained on a Beckman IR9 spectrophotometer employing AgCl windows for the hydrated complexes and KBr windows for all others. The complexes were run as Nujol and fluorolube mulls prepared in a nitrogen-blanketed dry box. The spectrum of norbornadiene was obtained from CCl_4 and CS_2 solutions.

Nuclear Magnetic Resonance Spectra

The proton resonance spectra of I, II, and norbornadiene dissolved in nitromethane were determined at room temperature on a Varian A60 spectrometer.

X-Ray Diffraction

Debye–Scherrer patterns were obtained on all samples using a General Electric camera of 143.2 mm diameter.

Results

Complexes from Anhydrous Solution

The complex obtained from a preparation employing toluene as solvent and a 3:1 mole ratio of norbornadiene:$AgBF_4$ shows an analysis corresponding essentially to $2AgBF_4 \cdot 3C_7H_8$ (II), while that obtained employing a ratio of 1:1 or lower appears to be $AgBF_4 \cdot C_7H_8$ (I). The complex obtained with a mole ratio of $\backsim$ 0.5:1 had an infrared spectrum and a Debye–Scherrer pattern identical with those of I, while the product of reactions employing mole ratios of 1:1 to 1.5:1 was observed to be a mixture of I and II.

With nitromethane as solvent, the product analysis indicated some possible incorporation of solvent. While the infrared spectrum showed bands attributable to nitromethane, it was otherwise identical with that of II, as was the Debye–Scherrer pattern.

Infrared Spectra

Each of the complex species I and II has its characteristic infrared spectrum shown in Fig. 1.

In the C—H stretching region for norbornadiene, the bands at 3070 and 2990 cm^{-1}, at 2980 cm^{-1}, and at 2937 and 2870 cm^{-1} are probably assignable (7) to the bonds involving olefinic, bridgehead, and bridging hydrogens respectively. In this region the primary differences between the spectra of I and II are the presence of the band at 3037 cm^{-1} and the absence of the band at about 2990 cm^{-1} in I. The spectrum of II is more akin to that of the uncomplexed diene than is that of I.

The bands at 1642 and 1544 cm^{-1} in norbornadiene have been assigned to the C=C stretching vibration split by vibrational coupling (3). Complex I has bands of equal intensity at 1470 and 1481 cm^{-1}. While it is not certain that both of these bands are due to C=C stretching vibrations, it has definitely been established that they decrease identically in intensity with decreasing amount of I in the complex; II shows a single band at 1489 cm^{-1}. (The spectrum of II in Fig. 1 shows the presence of a small amount of I.) The complex spectra show no bands near 1550 cm^{-1}, indicating the presence of uncoordinated double bonds, as has been observed with $CuCl \cdot C_7H_8$ (8). Increasing intensity of the band at 1489 cm^{-1} is accompanied by some intensity increase of the weak bands at 1522 cm^{-1} and 1456 cm^{-1}.

Can. J. Chem. Downloaded from www.nrcresearchpress.com by 210.87.254.6 on 09/05/12
For personal use only.

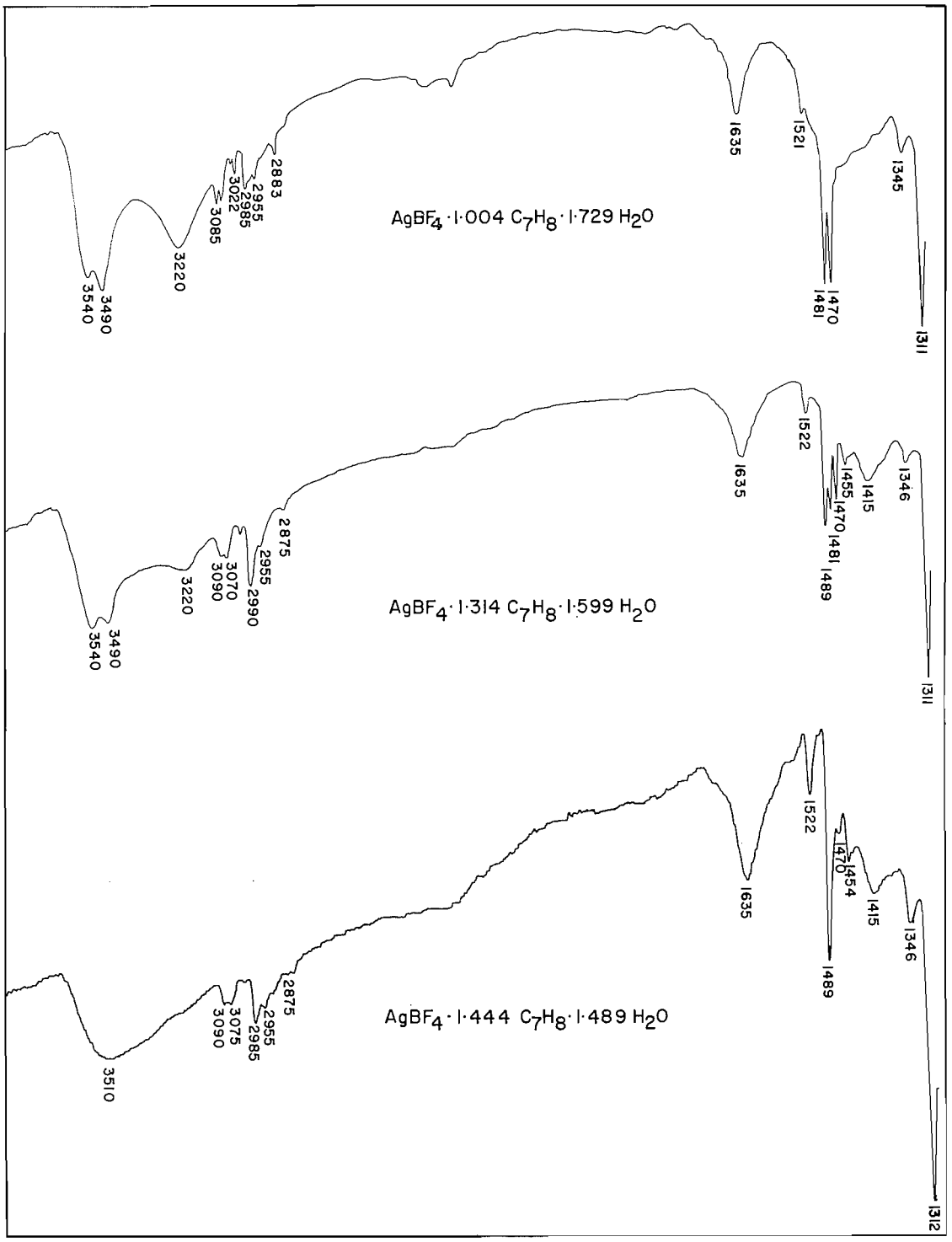

FIG. 2. Infrared spectra of the fluorolube mulls of complexes obtained from aqueous solution.

TABLE I

Stoichiometric and X-ray diffraction data for hydrated complexes

Sample	C_7H_8:$AgBF_4$	Mole fraction		H_2O:$AgBF_4$		X-ray phase
		III	IV	Calcd.*	Obs.	
66–18A	1.004	0.99	0.01	1.99	1.73	B
66–20B	1.206	0.59	0.41	1.79	1.51	B
66–22A	1.291	0.44	0.56	1.72	1.57	B
66–12	1.314	0.37	0.63	1.68	1.60	B + C
66–20C	1.325	0.35	0.65	1.67	1.48	B + C
67–20	1.360	0.28	0.72	1.64	1.81	B + C
66–22	1.378	0.24	0.76	1.62	1.73	C
67–21	1.444	0.11	0.89	1.56	1.49	C

*Calculated on basis $x = 2$ and $y = 3$.

A number of other bands, which have not been assigned, appear at somewhat different frequencies in I than in II. The band at 1227 cm^{-1} in the diene appears at 1241 cm^{-1} in I and 1236 cm^{-1} in II, while the band at 1204 cm^{-1} in C_7H_8 appears at 1193 and 1204 cm^{-1} in I and II respectively. Also the band at 798 cm^{-1} in the diene appears to be split in the complexes into bands with a frequency difference of about 11 cm^{-1}.

The intense band at 658 cm^{-1} in norbornadiene, which may represent the out-of-plane deformation vibration of the olefinic hydrogens, is shifted to about 735 to 750 cm^{-1} in the complexes. It is not possible to establish which band in this region corresponds to that particular deformation.

The bands at about 520, 770, 1060, and 1345 can be assigned to $AgBF_4$.

X-Ray Diffraction

The diffraction pattern of II shows a single phase A, while that of I shows another single phase B. Samples of complex which show significant amounts of both I and II (as indicated by the infrared spectrum) contain both phase A and phase B. Such samples can be obtained by exposing a sample of II to the nitrogen atmosphere of a dry box.

Nuclear Magnetic Resonance Spectra

A comparison of the proton chemical shifts of the complexes dissolved in nitromethane with the diene in the same solvent shows a deshielding of the olefinic, the bridgehead, and bridging protons (9) amounting to 40, 28, and 6 c.p.s. for I and to 34, 22, and 6 c.p.s. for II. Because the complexes are essentially insoluble in an n.m.r. solvent such as chloroform, it was necessary to employ nitromethane, which is known to compete to some extent with olefins for complexing at the silver ion. The addition of surplus norbornadiene to the nitromethane solutions produces a spectrum with smaller chemical shifts, indicating a rapidly established equilibrium between complexed and uncomplexed diene molecules (10). Thus one cannot conclude that the lesser deshielding of II indicates less strongly complexed norbornadiene, since in nitromethane solution a complex dissociation equilibrium is probably established.

Complexes from Aqueous Solution

Crystallization from aqueous solution always produced hydrated complexes. While the product usually appeared to be a mixture of hydrated I and II, it was possible in certain instances to obtain crystals that could be represented essentially by one of the formulae $AgBF_4 \cdot C_7H_8 \cdot xH_2O$ (III) or $2AgBF_4 \cdot 3C_7H_8 \cdot yH_2O$ (IV). While integral values of x and y have not been observed, there is an indication that x may have an upper limiting value of 2 while y appears to have a value between 2 and 4.

In Table I are reported the mole fractions of III and IV, calculated from the observed C_7H_8:$AgBF_4$ mole ratio, encountered in the mixtures obtained from several preparations. A comparison is made of the observed H_2O:$AgBF_4$ ratio with that calculated on the basis that $x = 2$ and $y = 3$.

It was found that, even from systems with a C_7H_8:$AgBF_4$ mole ratio of less than 1, the first hydrated complex to crystallize was IV, indicating a lower aqueous solubility, probably as a result of its higher organic character.

Recrystallization of the product from ethanol resulted in a complex which appeared to contain

Can. J. Chem. Downloaded from www.nrcresearchpress.com by 210.87.254.6 on 09/05/12
For personal use only.

Can. J. Chem. Downloaded from www.nrcresearchpress.com by 210.87.254.6 on 09/05/12
For personal use only.

both ethanol and water molecules in addition to norbornadiene.

Infrared Spectra

The spectra of the region between 4000 and 1300 cm^{-1} of III, IV, and a mixture of III and IV (of composition $AgBF_4 \cdot 1.314C_7H_8 \cdot 1.599H_2O$) are depicted in Fig. 2. Except for the bands assignable to the vibrational modes of the water molecules, the spectra of III and IV are essentially identical with those of I and II respectively. The bands assigned to the C=C stretching vibrations are at exactly the same frequency in both the anhydrous and hydrated complexes, i.e. at 1470 and 1481 cm^{-1} for III and at 1489 cm^{-1} for IV. The pattern of the C—H stretching region in III is somewhat different from that in I.

The bands appearing at 3540, 3490, 3220, 1635, 1415, 655, and 430 cm^{-1} are considered to be due to vibrational modes involving the water molecules. In general the bands in the 3000 cm^{-1} region, i.e. the O—H stretching bands, appear to become less well-resolved with increasing diene content of the complex, with the spectrum of IV showing a broad band extending from about 3680 to 3120 cm^{-1} with a maximum at about 3510 cm^{-1}. Also the band at 3220 cm^{-1} appears to decrease in intensity with increasing diene content (decreasing H_2O content) of the complex, while simultaneously there appears to be some decrease in the intensity of the 3490 cm^{-1} band relative to the 3540 cm^{-1} band. In III, the bands in this region and that at 1635 cm^{-1} (due to the in-plane bending mode (γ_2)) are quite analogous to the water bands shown by compounds such as $[Zn(H_2O)_6]SiF_6$ or $[Fe(H_2O)_6]SiF_6$ (11).

While the low frequency bands at 655 and 420 cm^{-1} may be due to librational modes (12) of hydrogen-bonded water molecules, the assignment of the band at 1415 cm^{-1} remains uncertain. In general, its intensity appears to increase with increasing ratio of IV to III in the complex.

X-Ray Diffraction

As indicated in Table I, the complex III shows the same solid phase B as does the anhydrous complex I. In fact, this phase only is observed to the point where the overall complex stoichiometry is equivalent to a mixture of about 40% of III and 60% of IV. Another solid phase C then appears and increases in proportion to phase B until the overall stoichiometry corresponds to about 25% of III and 75% of IV and represents the only solid phase at higher diene levels.

Discussion

The anhydrous silver tetrafluoroborate complexes of norbornadiene correspond exactly in stoichiometry to those of the conjugated diolefin, 1,3-butadiene (6). The differing stoichiometry of the complexes of norbornadiene with $AgBF_4$ and $AgNO_3$ (1–4) is probably due to the differing coordination of the silver ion with the respective anion, as has been suggested earlier for 1,3-butadiene (6). The structural investigation of Baenziger *et al.* (5) has established a bonding between the silver ion and the nitrate ion in $2AgNO_3 \cdot C_7H_8$.

With the exception of the presence of the water molecules in III, it would appear that exactly the same 1:1 complex species is produced both from anhydrous and aqueous solutions of $AgBF_4$. The similarity of the infrared spectra and of the X-ray diffraction pattern for I and III indicates that norbornadiene is similarly coordinated in both and that the water molecules of III must occupy sites that were available in the lattice of I.

Also, the infrared spectra indicate that the diene molecules are similarly complexed in II and IV species. However, the difference in the diffraction patterns, showing phase A for II and phase C for IV, indicates that the lattice of II cannot accommodate the water of crystallization found in IV without undergoing some change.

The differences between the infrared spectra of I and II are such as to suggest that there is some basic difference between the coordination of norbornadiene in the two complexes. This observation is in contrast to that made with 1,3-butadiene (6), wherein it was suggested that the formation of the 2:3 complex resulted from weaker complexation of additional diene molecules without significant change in the steric configuration of the 1:1 complex. The result was a 2:3 complex with two differently coordinated types of diene molecules.

The infrared spectrum of $2AgBF_4 \cdot 3C_7H_8$, with only a single band at 1489 cm^{-1}, representing the C=C stretching vibration, suggests a complex with all double bonds equivalently

Can. J. Chem. Downloaded from www.nrcresearchpress.com by 210.87.254.6 on 09/05/12
For personal use only.

coordinated. The two bands at 1470 and 1481 cm^{-1}, representing the C=C stretching bands in $AgBF_4 \cdot C_7H_8$, suggests on the other hand two differently coordinated double bonds in that complex. While the question of complex structure can be adequately answered only by complete structural analysis, it is quite reasonable to believe that the 1:1 complex exists in the solid state as a polymeric chain with alternating $AgBF_4$ and C_7H_8 units, as suggested by Traynham (1). The 2:3 complex might then be formed by cross-linking of the chains by additional diene molecules. The configuration of the norbornadiene molecule is such that the spatial arrangement of the diene molecules about the silver ion may be quite different in II than in I. The ease of interconversion of I and II by simple addition or removal of norbornadiene suggests that the basic structure of I is perhaps not too markedly changed upon formation of II.

The observation, particularly with the hydrated complex, that a significant quantity of norbornadiene can be added to III before the crystal structure, phase B, converts to that of IV, phase C, indicates that the lattice of I or III is sufficiently open to accommodate some additional norbornadiene without a major reorganization being necessary. Similarly phase C can lose some norbornadiene without reverting to phase B.

The frequencies of the well-defined O—H stretching bands shown by III are very similar to those observed for several hydrated salts (11, 13). On the basis of the assignments made by Balicheva and Andreev (13), it would be suggested that the band at 3490 cm^{-1} represents the stretching frequency when the proton is hydrogen bonded to another water molecule, while the band at 3540 cm^{-1} indicates that the proton is hydrogen bonded to the anion. It is, however, more probable that the bands at 3540 and 3490 cm^{-1} can be assigned to the asymmetric (γ_3) and symmetric (γ_1) stretching modes respectively of water molecules interstitially held in the crystal lattice, perhaps through weak interaction with the anions. While it has been shown (14) that BF_4^- demonstrates some electron donor property, it is not so marked that one would expect strong hydrogen bonding between water molecules and the anions.

While one might expect to observe a weak bond at about 3200 cm^{-1} attributable to the overtone ($2\gamma_2$) of the bending mode at 1635 cm^{-1}, it is surprising to observe that, in III, the 3220 cm^{-1} band is of similar intensity to the 1635 cm^{-1} band.

Furthermore, it has been observed in this laboratory that the infrared spectrum of a sample of anhydrous $AgBF_4$ exposed for a few minutes to the atmosphere shows rather strong water absorption bands only at 3560, 3480, and 1635 cm^{-1}. Since the band at about 3220 cm^{-1} is only very weak and since, relative to the band at 3540 cm^{-1}, that band in III decreases in intensity with increasing diene content (decreasing water content), it is suggested that in III it represents more strongly interacting water molecules, perhaps hydrogen bonded to the interstitial water molecules. The spectral broadening observed with increasing amount of IV (phase C) in the system is perhaps indicative of less discretely different types of water molecules in that structure.

The somewhat higher C=C stretching frequencies demonstrated by II and IV than by I and III indicate slightly weaker complexing of the diene in the 2:3 than in the 1:1 complexes. This is to be expected. It is, however, somewhat surprising, that hydration of the complexes results in no change in the C=C stretching frequency. This observation leads one to suggest that there is, at most, only a weak interaction between the silver ions and water molecules and that the interstitial water molecules may be held in the lattice largely by weak interaction with the anions and by hydrogen bonding with one another.

Acknowledgments

The author is greatly indebted to D. J. Peterson of the Analytical Laboratory, Dow Chemical of Canada, Ltd., for the infrared spectra and to L. E. Swim and H. W. Rinn of the Dow Chemical Company, Midland, Michigan, for analytical and X-ray diffraction data respectively. The helpful discussion of D. N. Glew and J. H. Tsai of this laboratory is also much appreciated.

1. J. G. TRAYNHAM. J. Org. Chem. **26**, 4694 (1961).
2. E. W. ABEL, M. A. BENNETT, and G. WILKINSON. J. Chem. Soc. 3178 (1959).
3. C. F. WILCOX, S. WINSTEIN, and W. G. MCMILLEN. J. Am. Chem. Soc. **82**, 5450 (1960).

4. M. AVRAM, E. SLIAM, and C. D. NENITZESCU. Ann. **636**, 184 (1960).
5. N. C. BAENZIGER, H. L. HAIGHT, R. ALEXANDER, and J. R. DOYLE. Inorg. Chem. **5**, 1399 (1966).
6. H. W. QUINN. Can. J. Chem. **45**, 1329 (1967).
7. R. ZBINDEN and H. K. HALL. J. Am. Chem. Soc. **82**, 1215 (1960).
8. G. N. SHRAUZER and S. EICHLER. Chem. Ber. **95**, 260 (1962).
9. K. TORI, Y. HATA, R. MUNEYUKI, Y. TAKANO, T. TSUJI, and H. TANIDA. Can. J. Chem. **42**, 926 (1964).
10. H. W. QUINN, J. S. MCINTYRE, and D. J. PETERSON. Can. J. Chem. **43**, 2896 (1965).
11. Y. KERMARREC. Compt. Rend. **258**, 5836 (1964).
12. K. NAKAMOTO. Infrared spectra of inorganic and coordination compounds. Wiley, New York. 1963. p. 156.
13. T. G. BALICHEVA and S. N. ANDREEV. Zh. Strukt. Khim. **5**, 29 (1964).
14. S. BROWNSTEIN and J. PAASIVIRTA. Can. J. Chem. **43**, 1645 (1965).

Can. J. Chem. Downloaded from www.nrcresearchpress.com by 210.87.254.6 on 09/05/12
For personal use only.

Can. J. Chem. Downloaded from www.nrcresearchpress.com by 210.87.254.42 on 09/05/12
For personal use only.

Enthalpy and entropy of activation for benzyl chloride solvolysis in various alcohol–water solvent mixtures

H. S. GOLINKIN[1] AND J. B. HYNE
Department of Chemistry, University of Calgary, Calgary, Alberta

Received July 24, 1967

The first order rate constants for the solvolysis of benzyl chloride in a series of mixtures of methyl, ethyl, *i*-propyl, and *t*-butyl alcohols with water are reported at 40.05 and 60.50 °C. The ΔH^* and ΔS^* values are calculated using these rate constants and those previously reported at 50.25 °C (1, 2). The dependence of these parameters on solvent composition is discussed.

Canadian Journal of Chemistry, **46**, 125 (1968)

Introduction

We previously reported the solvent dependence of activation volumes for benzyl chloride solvolysis in aqueous binary solvents (1, 2). The negative value of the activation volume was found to pass through a minimum as solvent composition was varied. It was also found that the position and depth of the extremum varies in a characteristic manner as the nonaqueous component of the solvent is varied. We were interested in determining whether a parallel effect would be observed in the extremum behavior of the activation enthalpy and entropy, as has been demonstrated for other solvolytic reactions (3–10).

Arnett *et al.* (11–13) have demonstrated that the extrema observed in ΔH^* in aqueous ethyl alcohol can arise as the result of variation of solvation of the initial state, the transition state, or both. We have demonstrated that the behavior of ΔV^*_0 for benzyl chloride solvolysis in the solvent systems studied is due mainly to variation of solvation of the initial state (2). Recently, Martin and Robertson (14) demonstrated that ΔC^*_p for *t*-butyl chloride solvolysis in aqueous ethyl alcohol also shows extremum behavior. The question as to which state causes this extremum must await further calorimetric measurements, but by analogy with the ΔH^* behavior of this reaction (11) it is to be expected that the initial state solvation variation will be found responsible.

If the extrema in the various activation parameters are related to the same physical phenomena, it is to be expected that the variation of these extrema with changes in the organic component of the solvent should parallel one another. It is the purpose of this work to investigate the reality of this expectation.

Experimental

The conductimetric technique for determining the solvolysis rates at 40.05 and 60.50 °C was similar to that reported previously (8).

Results

The conductimetric data were analyzed by the method of Guggenheim (15) using a least squares calculation (1). The observed first order rate constants at 40.05 and 60.50 °C are presented in Table I. Those at 50.25 °C have been reported previously (1, 2).

Activation enthalpies were calculated from the rate constants in Table I using eq. [1]. Activation entropies

$$[1] \quad \Delta H^* = -R\{[\ln (k_2/k_1) - \ln (T_2/T_1)]/[1/T_2 - 1/T_1]\}$$

were then calculated by eq. [2] using the rate constants

$$[2] \quad \Delta S^* = R[\ln k - \ln (\kappa T/h) + \Delta H^*/RT]$$

at 50.25 °C. The results for both ΔH^* and ΔS^* are presented in Table II. The reported error limits were estimated by the method previously reported for activation volumes (16).

The use of only two rates at temperatures 20° apart for the evaluation of ΔH^* requires some justification. Robertson and Scott (17) have reported a value of ΔC^*_p of −40.4 cal/deg mole for benzyl chloride solvolysis in water. The Arrhenius plot of $\ln k$ versus $1/T$ is therefore

[1]Present address: Division of Pure Chemistry, National Research Council of Canada, Ottawa, Canada.

Can. J. Chem. Downloaded from www.nrcresearchpress.com by 210.87.254.42 on 09/05/12
For personal use only.

TABLE I

Rate constants for the solvolysis of benzyl chloride

Mole fraction	$10^5 \times \kappa$ (s^{-1}) 40.05 °C	60.50 °C
	Methyl alcohol	
0.000	7.527 ±0.002	59.4 ±0.5
0.100	4.74 ±0.08	34.6 ±0.2
0.200	2.51 ±0.02	17.8 ±0.4
0.300	1.41 ±0.02	9.8 ±0.2
0.400	0.7803±0.0001	5.71±0.03
	Ethyl alcohol	
0.100	2.54 ±0.03	17.2 ±0.1
0.200	0.677±0.002	4.71 ±0.04
0.300	0.283±0.001	2.18 ±0.01
0.400	0.159±0.001	1.273±0.006
	i-Propyl alcohol	
0.050	3.51 ±0.06	22.58 ±0.002
0.100	0.904 ±0.007	6.17 ±0.03
0.200	0.158 ±0.002	1.30 ±0.02
0.300	0.073 ±0.002	0.566±0.008
0.400	0.0428±0.0004	0.362±0.002
	t-Butyl alcohol	
0.050	1.630 ±0.001	9.78 ±0.04
0.100	0.236 ±0.002	1.803±0.008
0.200	0.0611±0.0007	0.577±0.007
0.300	0.0299±0.0002	0.258±0.003

TABLE II

Activation parameters for the solvolysis of benzyl chloride

Mole fraction	$\Delta H^*_{50.28}$ (kcal/mole)	$\Delta S^*_{50.25}$ (cal/deg mole)
	Methyl alcohol	
0.000	20.3 ±0.3	−12.5±0.9
0.100	19.54±0.08	−16.1±0.3
0.200	19.3 ±0.3	−18. ±1.
0.300	19.0 ±0.3	−20.1±0.8
0.400	20.1 ±0.3	−18.2±0.8
	Ethyl alcohol	
0.100	18.8±0.1	−19.7±0.4
0.200	19.1±0.2	−21.3±0.8
0.300	20.1±0.2	−19.9±0.7
0.400	20.5±0.2	−19.8±0.6
	i-Propyl alcohol	
0.050	18.26±0.02	−20.72±0.06
0.100	18.45±0.07	−23.1 ±0.2
0.200	20.8 ±0.03	−19.1 ±1.
0.300	20.16±0.07	−22.3 ±0.2
0.400	21.0 ±0.2	−20.6 ±0.5
	t-Butyl alcohol	
0.050	17.6±0.2	−24.5±0.7
0.100	20.0±0.2	−20.5±0.5
0.200	22.2±0.2	−16.4±0.7
0.300	21.2±0.3	−20.7±0.8

nonlinear. By taking the slope of the straight line drawn between the two ln k values at 40.05 and 60.50 °C as the *tangent* to the ln k versus $1/T$ plot at 50.28 °C a very good value for ΔH^* at the median temperature is obtained.

Although the activation enthalpies are associated with a mean temperature of 50.28 °C, the difference of 0.03° is negligible for calculating the ΔS^* values at 50.25 °C. Indeed, the ΔC^*_p value of −40.4 cal/deg mole reported by Robertson and Scott (17) for benzyl chloride solvolysis in water predicts an error of only 0.005 e.u. in ΔS^* due to this temperature difference.

Comparison of the ΔH^* and ΔS^* values in Table II with those reported by other workers shows good agreement. Robertson and Scott (17) report values of 20 370 cal/mole for $\Delta H^*_{50.28}$ and −12.4 e.u. for $\Delta S^*_{50.25}$ in water. Hyne, Wills, and Wonkka (8) report $\Delta H^*_{51.65}$ values of 20 367 cal/mole in water and 19 555 cal/mole in 0.203 mole fraction ethyl alcohol.

Discussion

Enthalpy of Activation

The dependence of ΔH^* on the composition and nature of the solvent is illustrated in Fig. 1. It can be seen that in each of the four systems a minimum occurs. The observed minimum in aqueous methyl alcohol is contrary to the findings of Tommila *et al.* (18–20), who observed no minimum in this medium and concluded that both the substrate and the organic component of the solvent had to possess large hydrophobic groups in order that a minimum be observed (21). The appearance of the minimum in aqueous methyl alcohol in our work signifies that this explanation is an oversimplification. Nonetheless the depth of the minimum in ΔH^*, relative to pure water, does increase as the hydrophobic character of the alcohol molecule increases. The activation volume for this reaction (2) and the enthalpy of activation for *p*-methylbenzyl chloride (22) behave in a similar manner. As the depth of the minimum increases its position is shifted toward the pure water end of the solvent composition scale. Such behavior was predicted by Arnett and McKelvey (23) on the basis of the behavior of heats of solution in aqueous alcohols. These workers found that the heat of solution of sodium tetraphenylboride has an endothermic maximum relative to pure water of 16.9 kcal/mole in aqueous *t*-butyl alcohol as compared with the value of 10.7 kcal/mole in aqueous ethyl alcohol (23). In *t*-butyl alcohol

the extremum occurs at 0.045 mole fraction alcohol, whereas it was observed at 0.12 mole fraction alcohol in the ethyl alcohol media.

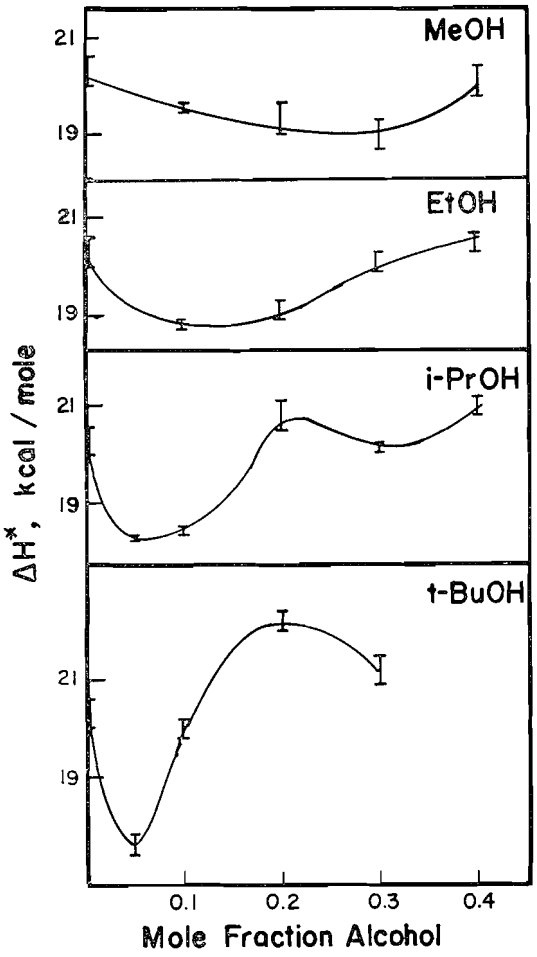

FIG. 1. Dependence of ΔH^* on solvent composition.

In order to dissect the contributions of the initial and transition states to the behavior of ΔH^* in the manner now well established by Arnett and co-workers (13), values for the heat of solution of benzyl chloride in each of the solvent systems are required. Arnett and McKelvey (13) presented a preliminary dissection of this type for benzyl chloride in ethanol–water, but the limited solubility of the halide in the highly aqueous end of the solvent range renders the heat measurements at least suspect if not unobtainable.

Entropy of Activation

The variation of ΔS^* with solvent composition is shown in Fig. 2. It is apparent that the behavior of this parameter parallels that of both ΔH^* and ΔV^*_0 in that a minimum is observed, the depth and position of which are dependent upon the nature of the alcohol in the solvent. However, the positions of the ΔH^* and ΔS^* minima do not appear to coincide in all cases. In the ethyl and *i*-propyl alcohol systems the entropy minimum occurs at higher alcohol concentrations than the enthalpy minimum. Hyne and Wills (7) also found that coincidence of these minima is not a general phenomenon; only two of the systems studied by these authors coincided.

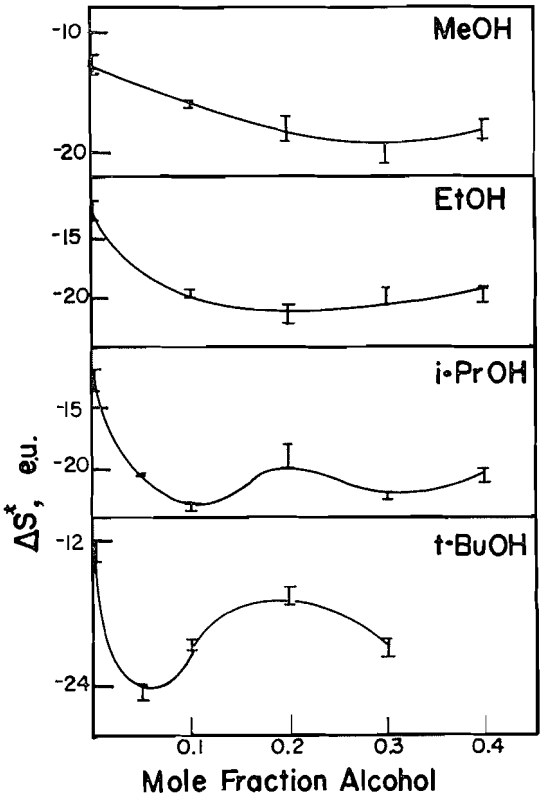

FIG. 2. Dependence of ΔS^* on solvent composition.

Due to the lack of available data, no dissection of ΔS^* into initial state and transition state contributions is possible.

Burris and Laidler (24) have suggested that since ΔS^* and ΔV^* both reflect solvent behavior for ionic reactions, they should parallel one another in sign and magnitude. In fact these authors obtained a linear relation between these parameters for six different reactions in water. The question then arises as to the possibility of a similar linear relationship between ΔS^* and ΔV^* for a single reaction in several solvents. The

Can. J. Chem. Downloaded from www.nrcresearchpress.com by 210.87.254.42 on 09/05/12
For personal use only.

present data, available for 17 solvents, represent a fair test of this postulate. The results are shown in Fig. 3. The ΔV^* values for 0.05 mole fraction isopropyl and *t*-butyl alcohols are interpolated (see ref. 2).

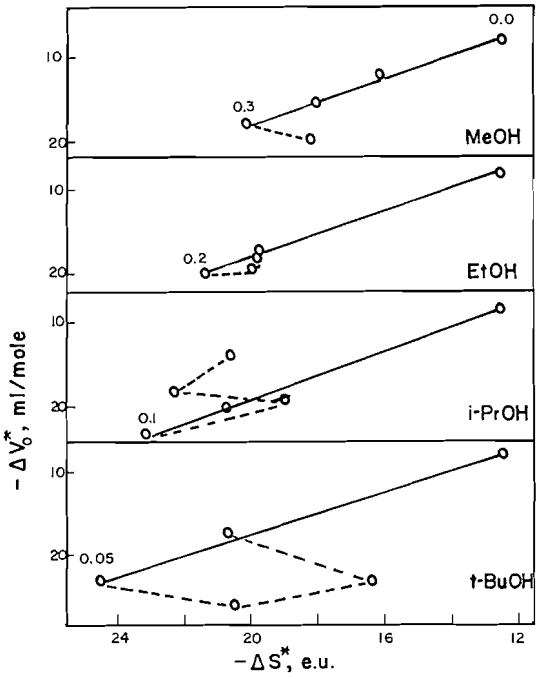

FIG. 3. Partial linear relationships (full line) between ΔV^*_0 and ΔS^*. Value shown above points is mole fraction of solvent mixture for point.

It is at once apparent that overall linearity is not observed. Instead we find quite complex curves similar to the so-called isokinetic relationships (25, 26). Despite the apparent complexity, however, the linearity of the ΔS^* versus ΔV^*_0 plot from pure water to approximately that solvent composition at which the extremum is found in the behavior of the parameters with respect to solvent composition should be noted. These portions of the plots are shown in full line in Fig. 3. Furthermore the *slopes* of these sections of the plots are identical within the limits of uncertainty of the data. In these solvent composition ranges, therefore, ΔS^* and ΔV^* do indeed parallel one another in both sign and magnitude, suggesting similar solvent behavior in all four cases. It is in this region of initial cosolvent addition to water that the structure-making effect of the cosolvent is considered to be effective (27). On a mole fraction composition basis *t*-butyl alcohol maximizes water structure at lowest mole fraction (circa 0.05) and methyl alcohol at highest mole fraction (circa 0.3). It is, therefore, not surprising that in each binary solvent mixture, while the cosolvent is enhancing the water structure, the entropy and volumes of activation should manifest such parallelism in behavior. Over the different solvent composition ranges the solvent structure is passing through the same change from pure water structure to enhanced water structure brought about by the added cosolvent. The similarity of the ΔS^* versus ΔV^* slope in all cases reflects this common solvent behavior. Beyond the solvent composition corresponding to maximum cosolvent-induced structuredness the bulk effect of the cosolvent becomes predominant and the solvent structures begin to diverge toward those characteristic of the pure cosolvent. Parallelism in the behavior of ΔS^* and ΔV^* would therefore not be expected.

Comparison of Activation Parameters and Mixing Parameters

Available data on the position of the extremum of the activation and thermodynamic parameters of mixing for the various binary solvent systems discussed in this work are collected in Table III. It is immediately obvious that the position of the extremum in the heat and entropy of mixing does not always occur at the same solvent composition. The tendency is for the entropy extremum to occur at somewhat higher cosolvent mole fraction. Insofar as both the activation parameters and thermodynamic parameters of mixing reflect the structural properties of the binary solvent system it is not surprising that this same tendency is shown in the relative positions of the enthalpy and entropy of activation.

TABLE III

Mole fraction of organic cosolvent at which high aqueous region extremum in parameter appears

	Activation parameters		Binary solvent mixing parameters	
Organic cosolvent	ΔH^*	ΔS^*	ΔH^M	ΔS^E
Methyl alcohol	0.28	0.3	0.3	0.3
Ethyl alcohol	0.12	0.2	0.22	0.31
i-Propyl alcohol	0.06	0.1	0.10	—
t-Butyl alcohol	0.05	0.05	0.10	0.23

Can. J. Chem. Downloaded from www.nrcresearchpress.com by 210.87.254.42 on 09/05/12
For personal use only.

Acknowledgment

The authors gratefully acknowledge the financial assistance of the National Research Council of Canada.

1. J. B. HYNE, H. S. GOLINKIN, and W. G. LAIDLAW. J. Am. Chem. Soc. **88**, 2101 (1966).
2. H. S. GOLINKIN, IKCHOON LEE, and J. B. HYNE. J. Am. Chem. Soc. **89**, 1307 (1967).
3. A. H. FAINBERG and S. WINSTEIN. J. Am. Chem. Soc. **78**, 2770 (1956).
4. A. H. FAINBERG and S. WINSTEIN. J. Am. Chem. Soc. **79**, 1597, 1602, 5937 (1957).
5. E. TOMMILA. Suomen Kemistilehti, **B25**, 37 (1952).
6. E. TOMMILA and M. MURTO. Acta Chem. Scand. **17**, 1947, 1957, 1985 (1963).
7. J. B. HYNE and R. WILLS. J. Am. Chem. Soc. **85**, 3650 (1963).
8. J. B. HYNE, R. WILLS, and R. E. WONKKA. J. Am. Chem. Soc. **84**, 2914 (1962).
9. J. B. HYNE. J. Am. Chem. Soc. **82**, 5129 (1960).
10. J. B. HYNE and R. E. ROBERTSON. Can. J. Chem. **34**, 931 (1956).
11. E. M. ARNETT, P. M. DUGGLEBY, and J. J. BURKE. J. Am. Chem. Soc. **85**, 1350 (1963).
12. E. M. ARNETT, W. G. BENTRUDE, J. J. BURKE, and P. M. DUGGLEBY. J. Am. Chem. Soc. **87**, 1541 (1965).
13. E. M. ARNETT and D. R. MCKELVEY. Record Chem. Progr. Kresge-Hooker Sci. Lib. **26**, 185 (1965).
14. J. G. MARTIN and R. E. ROBERTSON. J. Am. Chem. Soc. **88**, 5353 (1966).
15. E. A. GUGGENHEIM. Phil. Mag. [7], **2**, 538 (1926).
16. H. S. GOLINKIN, W. G. LAIDLAW, and J. B. HYNE. Can. J. Chem. **44**, 2193 (1966).
17. R. E. ROBERTSON and J. M. W. SCOTT. J. Chem. Soc. 1596 (1961).
18. E. TOMMILA, A. KOIVISTO, J. P. LYRRA, L. ANTELL, and S. HEIMO. Ann. Acad. Sci. Fennicae, Ser. AII, 47 (1952).
19. L. PEKKARINEN and E. TOMMILA. Acta Chem. Scand. **13**, 1019 (1955).
20. E. TOMMILA and S. MALTAMO. Suomen Kemistilehti, **B28**, 118 (1955).
21. E. TOMMILA and S. MALTAMO. Suomen Kemistilehti, **B28**, 73 (1955).
22. J. B. HYNE and R. WILLS. Unpublished results.
23. E. M. ARNETT and D. R. MCKELVEY. J. Am. Chem. Soc. **87**, 1393 (1965).
24. C. T. BURRIS and K. J. LAIDLER. Trans. Faraday Soc. **51**, 1497 (1955).
25. J. E. LEFFLER. J. Org. Chem. **20**, 1202 (1955).
26. J. E. LEFFLER and E. GRUNWALD. Rates and equilibria of organic reactions. John Wiley and Sons, Inc., New York, N.Y. 1963. Chap. 9.
27. F. FRANKS and D. J. G. IVES. Quart. Rev. London, **20**, 1 (1966).

Can. J. Chem. Downloaded from www.nrcresearchpress.com by 210.87.254.42 on 09/05/12
For personal use only.

Nature of the coordination bond in metal complexes of substituted pyridine derivatives. I. The substituent effect on the coordination bond

PATRICK T. T. WONG[1] AND D. G. BREWER
Department of Chemistry, University of New Brunswick, Fredericton, New Brunswick
Received May 29, 1967

The nature of the coordination bond in some metal complexes of 4-substituted pyridines has been investigated by thermodynamic and infrared spectroscopic methods. The effects of the substituents upon the coordination bond strength in the copper(II) complexes of these ligands have been found by direct measurement of the heats of coordination. These effects have been further described by the substituent effect upon the change in free energy of the coordination center in the ligands. A new parameter, R_π, measuring the relative π bonding in the complexes of 4-substituted pyridines has been introduced. For this purpose a series of complexes of the types $[M(4\text{—}R\text{—}C_5H_4N)_2Cl_2]$ and $[(4\text{—}R\text{—}C_5H_4N)\cdot HCl]$ ($R = CH_3$, CH_2OH, H, $COCH_3$, $CONH_2$, $COOCH_3$, CN; M = Cu(II), Zn(II)) has been isolated, and the infrared spectra of these complexes and the free ligands have been examined.

Canadian Journal of Chemistry, 46, 131 (1968)

Can. J. Chem. Downloaded from www.nrcresearchpress.com by 210.87.254.6 on 09/05/12
For personal use only.

Introduction

Although metal complexes of pyridine derivatives have been studied for years, only one systematic study (1) has attempted to estimate the coordination bond strength as affected by the substituents on the pyridine ring. In that investigation, the relative bond strength of silver complexes of substituted pyridines was studied by comparing their stability constants in aqueous solution. The absence of a linear relationship between these stability constants and the basicity of the free ligands was attributed to the formation of a π bond.

Recently Da Silva (2, 3) analyzed the data from this same study and suggested a π factor, S_t, which was related to the additional stabilization caused by the formation of a π bond. For silver-substituted pyridine systems, S_t was defined as

$$S_t = \log \beta_2 - 2pK_a - (\log \beta_2^0 - 2pK_a^0),$$

where β_2 and β_2^0 are overall stability constants for the substituted pyridine and for pyridine itself respectively and the K_a's are the acid dissociation constants of the corresponding pyridinium ions. When this "π factor" was plotted versus the Hammett's substituent constants, the slope of the line obtained was in the opposite direction to that for the logarithmic plot of the K_a versus the substituent constants. This reversal was explained as being the consequence of substituent-aided back donation. However, a conclusion was reached upon reinvestigation (4) of these arguments that this "π factor" was unacceptable, since the same inverse relationship was obtained for aliphatic amine – silver complexes, where there is no opportunity for π bonding.

In the present work, the substituent effect on the bond strength between the pyridine ring and the metal ion was studied directly by the measurement of the heats of coordination. The ligands $4\text{—}R\text{—}C_5H_4N$ ($R = CH_3$, CH_2OH, H, $COCH_3$, $CONH_2$, $COOCH_3$, CN) were selected for this study.

Since Hammett's substituent constants did not satisfactorily describe the effects of substituents upon the reactivity of ligands in the previous studies (3), an attempt was made to correlate the bond strength in these substituted pyridine complexes to a new substituent constant. This constant, designated σ_H, measures the substituent effect on the free energy change of the coordination center in the ligands, viz. the ring nitrogen atom.

Furthermore, the effects of substituents upon the relative π contribution to the coordination bond were determined by an infrared spectroscopic method. In order to deduce a general equation for the correlation of the infrared data of the complexes with a new parameter, R_π, measuring the relative magnitude of π bonding, the infrared frequencies of the ring vibrational mode, ν_{12}, of the free ligands, their hydrochlorides, and the corresponding zinc and copper complexes were determined.

---

[1]Present address: Division of Applied Chemistry, National Research Council of Canada, Ottawa, Canada.

TABLE I

Preparation of complexes of zinc chloride with heterocyclic bases, $[ZnL_2Cl_2]$

L	Calculated (%)			Found (%)		
	C	H	N	C	H	N
Pyridine	40.78	3.42	9.51	40.78	3.42	9.39
4-Methylpyridine	44.68	4.38	8.69	44.50	4.29	8.49
4-Cyanopyridine	41.84	2.34	16.27	41.77	2.36	16.18
4-Acetylpyridine	44.41	3.73	7.40	44.42	3.67	7.31
4-Carbinylpyridine	40.65	3.98	7.90	40.50	3.89	7.79
4-Pyridinecarboxamide	37.87	3.18	14.72	38.14	3.05	14.82
4-Carbomethoxypyridine	40.95	3.44	6.82	43.39	3.71	6.82

TABLE II

Preparation of complexes of cupric chloride with heterocyclic bases, $[CuL_2Cl_2]$

L	Calculated (%)					Found (%)				
	C	H	Cl	N	Cu	C	H	Cl	N	Cu
Pyridine	41.04	3.44	24.23	9.57	21.71	40.93	3.46	24.19	9.41	21.56
4-Methylpyridine	44.94	4.40	22.11	8.74	19.81	44.88	4.32	22.08	8.76	19.76
4-Cyanopyridine	42.06	2.35	20.70	16.35	18.54	42.07	2.42	20.58	16.32	18.56
4-Acetylpyridine	44.63	3.75	18.82	7.44	16.87	44.46	3.78	18.82	7.34	16.67
4-Carbinylpyridine	40.86	4.00	20.11	7.94	18.02	40.69	3.98	20.23	7.90	17.82
4-Pyridinecarboxamide	38.06	3.19	18.73	14.80	16.78	37.84	3.29	18.71	14.72	16.43
4-Carbomethoxypyridine	41.14	3.45	17.35	6.85	15.55	41.15	3.23	17.45	6.84	15.51

Experimental

I. Reagents

The 4-substituted pyridines were supplied by Aldrich Chemical Company Incorporated. 4-Methylpyridine, 4-acetylpyridine, 4-carbomethoxypyridine, and pyridine were dried over potash overnight and then distilled twice. 4-Cyanopyridine and 4-carbinylpyridine were recrystallized twice from benzene, and 4-pyridinecarboxamide twice from absolute alcohol.

The cupric nitrate solution for the determination of the heat of coordination was prepared by dissolving the recrystallized cupric nitrate in water and then determining the metal content gravimetrically by the pyridine method (5).

II. Preparation of Zinc Complexes

The pyridine, 4-methylpyridine, 4-acetylpyridine, and 4-carbomethoxypyridine complexes of the form ZnL_2Cl_2 were prepared by adding the ligand (2 moles) into an aqueous solution of zinc chloride (1 mole). The resulting precipitates were recrystallized from absolute alcohol.

The 4-cyanopyridine and 4-pyridinecarboxamide complexes were obtained by mixing a 50% alcoholic solution of the ligand (2 moles) and an aqueous solution of zinc chloride (1 mole). The complexes were recrystallized from 95% alcohol.

The 4-carbinylpyridine complex was prepared by adding aqueous solution of 4-carbinylpyridine (2 moles) to an aqueous solution of zinc chloride (1 mole) with constant stirring in an ice bath. The resulting precipitate was dissolved in 95% alcohol and reprecipitated out by adding ethyl ether into the solution of the complex. Microanalysis data are listed in Table I.

III. Preparation of Copper Complexes

Complexes of the form CuL_2Cl_2 were prepared by a method similar to that for the preparation of dichlorobis(pyridine)copper(II) (6), where L was pyridine or 4-substituted pyridines. The ligand (2 moles) was added dropwise into the cupric chloride (1 mole) solution in absolute alcohol with constant stirring (4-cyanopyridine, 4-carbinylpyridine, and 4-pyridinecarboxamide were dissolved in absolute alcohol before addition to the cupric chloride solution). The complex was separated by filtration, washed with absolute alcohol and anhydrous ether several times, and dried in a vacuum desiccator over sulfuric acid.

Microanalysis for carbon, hydrogen, nitrogen, chlorine, and copper gave values close to theoretical ones (Table II).

IV. Preparation of Pyridine and 4-Substituted Pyridine Hydrochlorides

The white precipitates of the hydrochlorides were obtained by passing anhydrous hydrogen chloride gas into anhydrous ether solutions of the ligands (absolute alcohol solutions in the cases of 4-carbinylpyridine and 4-pyridinecarboxamide). The precipitates were recrystallized from a methanol–acetone mixture.

Microanalysis results for carbon, hydrogen, nitrogen, and chlorine are listed in Table III.

V. Determination of the Heat of Coordination

The calorimeter consisted of a Dewar flask (approximately 500 ml capacity) containing a Beckman calibrated thermometer, a motor-driven stirrer, an inner sample holder with an outlet hole on the bottom plugged by silicone stopcock grease (which can be blown out by applying air pressure at the top), and a glass coil connected

Can. J. Chem. Downloaded from www.nrcresearchpress.com by 210.87.254.6 on 09/05/12
For personal use only.

TABLE III

Preparation of hydrochlorides of heterocyclic bases, [LHCl]

L	Calculated (%)				Found (%)			
	C	H	N	Cl	C	H	N	Cl
Pyridine	51.96	5.23	12.12	30.68	51.51	5.63	11.47	30.00
4-Methylpyridine	55.61	6.22	10.80	27.36	51.46	6.53	9.64	26.50
4-Cyanopyridine	51.26	3.56	19.93	25.22	51.07	3.45	20.28	25.24
4-Acetylpyridine	53.34	5.12	8.89	22.50	53.33	5.03	9.14	22.69
4-Carbinylpyridine	49.49	5.54	9.62	24.36	49.43	5.45	9.69	24.45
4-Pyridinecarboxamide	45.44	4.45	17.67	22.36	46.25	4.47	17.75	22.08
4-Carbomethoxypyridine	48.43	4.65	8.07	20.44	48.44	4.59	8.10	19.64

to a thermostated bath, maintaining the contents of the calorimeter at an original temperature of 25.0± 0.1 °C.

The heat capacity of the calorimeter was determined by neutralizing 10 ml of standard 2 *N* sodium hydroxide with a slight excess of standard hydrochloric acid at 25 °C. The heat capacity of the calorimeter thus obtained was 86.85 cal/°K.

In a typical run, the covered calorimeter was placed in a thermostated bath at 25.0 ± 0.1 °C. A 10 ml aliquot of copper nitrate solution, with a precisely known concentration around 1.5 *M*, was introduced into the inner sample holder. Then 500 ml of a solution, 0.2 *M* in ligand and 0.01 *M* in nitric acid, were measured into the calorimeter. After a suitable interval of time for temperature equilibration, the glass coil was disconnected from the thermostated bath and the copper nitrate solution was allowed to mix with the ligand by blowing out the silicone plug. The increase in temperature was recorded every 30 s and the temperature change for the reaction was then calculated using the standard method (7).

The heat of dilution for cupric nitrate in 0.01 *M* nitric acid was determined in a separate experiment (using 10 ml of copper nitrate solution with the same concentration as that in each run) and was found to be 113.3 cal/mole. The heat of dilution of the ligand solution by the water contained in the copper nitrate solution was found to be negligible.

VI. Dissociation Constants of Pyridinium and 4-Substituted Pyridinium Ions

The dissociation constants were determined by the usual pH titration method (8). The nature of the systems was kept similar to those in the ΔH determination, viz. a 0.2 *M* solution of the ligands was titrated with standard nitric acid. Using those points from the buffer region of the titration curves, the dissociation constants were calculated according to the following equation (8).

$$K_D = \frac{[H^+]\{C_{Py} - (C_{HNO_3} - [H^+])\}}{(C_{HNO_3} - [H^+])},$$

where C_{Py} and C_{HNO_3} are the original concentration of the ligands and of the nitric acid added respectively.

VII. Infrared Absorption Spectra

To obtain the infrared spectra in the region between 4000 and 300 cm^{-1}, a Beckman IR-12 filter/grating spectrophotometer was used. The solid samples were measured using the potassium bromide disc method, and the liquid free ligands as capillary films. The spectrophotometer was continually purged with dry air and the calibration of the spectrophotometer was checked against the rotational spectra of water vapor and ammonia gas.

Results and Discussion

I. Relative Coordination Bond Strength

The calorimetric data for the formation of the copper complexes of pyridine and 4-substituted pyridines are listed in Table IV. The values of the heat evolved in each experiment have been corrected for the heat of dilution of the metal salts and are given in column five. The third column gives the amount of nitric acid added to the ligand solutions to keep the pH value of the solutions below 6, so that the hydrolysis of cupric ion in these systems can be neglected.

Since successive enthalpies, ΔH_1, for a given metal ion with neutral ligands are approximately constant (9, 10), the relative magnitude of the coordination bond strength of copper–pyridine complexes can be determined by the corresponding values of the average heat of coordination per mole of ligand bonded to the metal, viz. $\Delta H_a \equiv \Delta H_c/\bar{n}$, which are shown in column seven.

Bjerrum's degree of formation, $\bar{n}$, can be obtained by means of the following equation (derived in the normal way from appropriate totality expressions, electrical neutrality expressions, etc.)

$$\bar{n} = \frac{[L]_B}{C_M} = \frac{C_{Py} - \left(\frac{[H^+]}{K_D} + 1\right)\left\{\frac{C_{HNO_3} - [H^+] + \frac{K_w}{[H^+]}}{\frac{[H^+]}{K_D}}\right\}}{C_M},$$

Can. J. Chem. Downloaded from www.nrcresearchpress.com by 210.87.254.6 on 09/05/12
For personal use only.

TABLE IV
Heat of coordination

L	$C_{Cu^{2+}}$ (M)	C_{HNO_3} (M)	C_L (M)	ΔH_c (kcal/mole)	$\bar{n}$	ΔH_a (kcal/mole)
4-Methylpyridine	3.0835×10^{-2}	9.980×10^{-3}	0.19598	16.120	3.44	4.70
			0.19595	16.197	3.44	4.71
			0.19590	16.111	3.43	4.70
4-Carbinylpyridine	3.0835×10^{-2}	9.980×10^{-3}	0.19609	13.544	3.06	4.43
			0.19607	13.537	3.06	4.42
			0.19607	13.535	3.06	4.42
Pyridine	3.0835×10^{-2}	9.980×10^{-3}	0.19600	13.132	2.98	4.39
			0.19598	13.133	2.98	4.38
			0.19596	13.128	3.00	4.37
4-Acetylpyridine	3.0835×10^{-2}	9.980×10^{-3}	0.19599	7.031		
			0.19595	7.058	—	—
			0.19500	7.091		
4-Pyridinecarboxamide	3.0835×10^{-2}	9.980×10^{-3}	0.19590	6.800	2.20	3.10
			0.19590	6.773	2.20	3.08
			0.19597	6.785	2.21	3.07
4-Carbomethoxypyridine	3.0835×10^{-2}	9.980×10^{-3}	0.19594	6.656	2.20	3.03
			0.19596	6.647	2.20	3.02
			0.19595	6.647	2.20	3.02
4-Cyanopyridine	3.0835×10^{-2}	9.980×10^{-3}	0.19592	3.350	1.34	2.50
			0.19590	3.336	1.34	2.49
			0.19587	3.309	1.34	2.47

where C_{Py}, C_M, and C_{HNO_3} are the original concentration of ligand, cupric nitrate, and nitric acid respectively.

Obviously any inaccuracy in the K_D value results in a considerable error in the calculation of the $\bar{n}$ value. Therefore, the K_D values of the pyridines were redetermined under the same conditions as those in heat of coordination determination and are shown in Table V.

TABLE V
Dissociation constants of heterocyclic bases

Heterocyclic bases	K_D
4-Methylpyridine	9.40×10^{-7}
4-Carbinylpyridine	3.92×10^{-6}
Pyridine	5.42×10^{-6}
4-Acetylpyridine	3.19×10^{-4}
4-Pyridinecarboxamide	3.75×10^{-4}
4-Carbomethoxypyridine	5.69×10^{-4}
4-Cyanopyridine	1.26×10^{-2}

The uncertainty of the $\bar{n}$ value for the 4-acetylpyridine system may be due to the fact that some side equilibria are involved in this system (11).

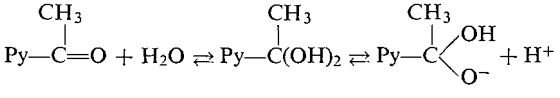

An examination of the ΔH_a values as well as the ΔH_c values in Table IV shows that 4-substitution of $-CH_3$ and $-CH_2OH$ groups on the pyridine ring increases the coordination bond strength, whereas 4-substitution of $-COCH_3$, $-CONH_2$, $-COOCH_3$, and $-CN$ groups gives a lower coordination bond strength. The relative magnitude of the coordination bond strength in these complexes is

$$4\text{-}CH_3Py > 4\text{-}CH_2OHPy > Py > 4\text{-}COCH_3Py > 4\text{-}CONH_2Py \approx 4\text{-}COOCH_3Py > 4\text{-}CNPy.$$

The difference in the coordination bond strength of these complexes is entirely dependent upon the substituents on the pyridine ring. This effect can be understood without any difficulty by using a molecular orbital model (12) and the relative energy levels of the orbitals on the pyridine ring and the substituents (13, 14). The direction of the migration of electron density between the pyridine ring and the substituents influences the availability of the "non-bonding" pair of electrons at the pyridine nitrogen.

The substitution of electron-attracting groups (such as $-COCH_3$, $-CONH_2$, $-COOCH_3$, and $-CN$) causes the electron density on the pyridine ring to be lowered. Therefore, the σ-coordination bond in cupric complexes of these

Can. J. Chem. Downloaded from www.nrcresearchpress.com by 210.87.254.6 on 09/05/12
For personal use only.

Can. J. Chem. Downloaded from www.nrcresearchpress.com by 210.87.254.6 on 09/05/12
For personal use only.

ligands is weaker than that in the cupric–pyridine complex. The electron-releasing substituents (—CH_3 and —CH_2OH) result in a migration in the opposite direction, and enhance the σ-coordination bond strength.

Furthermore, by consideration of the relative ability of these substituents to either release or attract electron density, as measured by the acid dissociation constants of the corresponding free ligand, one may predict that the relative magnitude of σ bonding in cupric complexes of these ligands is as follows.

$$4\text{-}CH_3Py > 4\text{-}CH_2OHPy > Py > 4\text{-}COCH_3Py > 4\text{-}CONH_2Py > 4\text{-}COOCH_3Py > 4\text{-}CNPy$$

With respect to the π-bonding contribution, the increase in electron density on the pyridine ring caused by the —CH_3 and —CH_2OH substituents inhibits the back donation of π-electron density from the metal. Therefore, the π bonding between the metal and the ligands with these substituents is probably not important. However, the electron density on the pyridine ring is lowered by the substitution of —$COCH_3$, —$CONH_2$, —$COOCH_3$, and —CN groups, and the π contribution to the coordination bond of the complexes involving these ligands becomes appreciable.

In this kind of coordination bond, σ bonding plays the predominant part in determining the total bond strength (12). Therefore, in a series such as the one under study, the relative total bond strength should follow the same order as that for σ bonding. This prediction is identical to the bond strength order as determined by the ΔH values, except in the case of the 4-pyridinecarboxamide and 4-carbomethoxypyridine complexes. In these complexes, π bonding becomes important and is higher in the 4-pyridinecarboxamide complex. It turns out that the net bond strength in these two complexes is very similar, even though the σ bonding in the former complex is a little lower than in the latter (by comparison of their K_D value).

It was reported (3, 15) that there is no direct correlation of the stability of metal complexes of substituted pyridines with Hammett's substituent constants. The only known case of such a direct relationship was given by May and Jones (16) for cupric complexes of substituted benzoic acid.

The absence of this correlation in pyridine complexes system is expected, since the original Hammett's σ factor is related only to the change in free energy of a side chain in a benzene series. In substituted pyridines, the reaction center for complex formation is the nitrogen atom which is within the ring, rather than in a side chain. Therefore, a different balance between the inductive and resonance effects is involved. Furthermore, the polarization of the aromatic ring by the nitrogen atom will likely result in different substituent effects than are encountered in benzene systems.

In the present study, it was also not possible to find a direct correlation between the bond strength and Hammett's substituent constants. However, the effect of the substituents on the complex formation in the pyridine series can be described by a new substituent constant, defined as $\sigma_H \equiv \log K - \log K^0$ (where K and K^0 are acid dissociation constants of the substituted and unsubstituted pyridinium ions respectively).

A plot of the values of $\delta \equiv \Delta H - \Delta H^0$ (where ΔH and ΔH^0 are heats of coordination of cupric complexes of substituted and unsubstituted pyridines respectively) against the corresponding σ_H values gives a fairly good linear relationship, as shown in Fig. 1. The "goodness of the fit" in the cases of 4-methylpyridine and

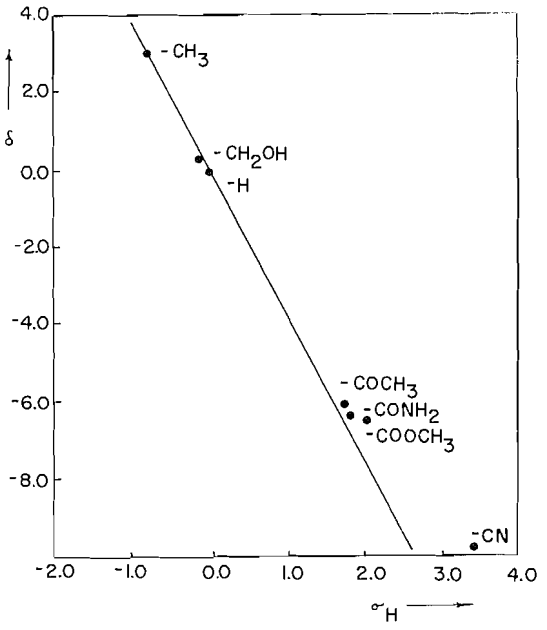

FIG. 1. The correlation between the change of ΔH_0 and substituent constant σ_H.

Can. J. Chem. Downloaded from www.nrcresearchpress.com by 210.87.254.6 on 09/05/12
For personal use only.

4-carbinylpyridine systems indicates that the π bonding in these complexes is not important. The higher δ values of those electron-attracting substituent systems are due to the π contribution in their coordination bonds.

II. Correlation of the Ring Vibration with the Relative π-Contribution in the Metal–Nitrogen Coordination Bond

The infrared vibrational frequencies of the ν_{12} mode of some 4-substituted pyridines and their copper complexes, zinc complexes, and hydrochlorides are listed in Table VI. It was reported (17) that this vibrational mode was an aromatic ring vibration, without any mass effect of the substituents, and did not involve any substituent-ring and hydrogen-ring bending. The normal coordinate calculation of these systems in a sequential paper of this series, to be submitted shortly, shows that the vibrational frequency of this mode is mainly affected by the aromatic CN stretching force constant. The intensity of this mode, however, was found to be affected very much by the substituents on the 4-position of the pyridine ring. Electron-attracting substituents decreased the intensity a great deal, due to the lower mesomeric moment of these substituted pyridines (18). For instance, the electronic dipole moment of the pyridine molecule is decreased from 2.22 to 1.61 D by the substitution of a —CN group on the 4-position of the ring (19). It was also found that the ν_{12} intensity of these substituted pyridines appeared to be increased when they coordinated with copper(II) or zinc(II) ion. This is expected, since the coordination causes a strong perturbation of one of the centers of polarity, the lone-pair electrons of the nitrogen atom, which contributes about 80% of the total dipole moment of the pyridine molecule (20).

It is seen in Table VI that the frequency of the ν_{12} mode is greatly shifted by complex formation with both copper and zinc ions. The results show that the frequencies of the complexes with electron-attracting substituents are higher than, and those with electron-releasing substituents are a little lower than, that of the pyridine complex, except for the 4-carbinylpyridine complex of copper(II). The relative magnitude of the frequency is in the order

$$4\text{-}CH_3Py < 4\text{-}CH_2OHPy < Py < 4\text{-}COCH_3Py \approx 4\text{-}CONH_2Py \approx 4\text{-}COOCH_3Py < 4\text{-}CNPy.$$

This order can again be interpreted by rationalizing the migration of electron density. For electron-releasing substituents, the electron density migrates to the delocalized system in the pyridine ring, which cannot further transfer to the metal because of filled d orbitals. It can only enhance the donation of the non-bonding electron pair of the nitrogen atom to the metal. Furthermore, the migration of electron density from the substituent to the ring inhibits the back donation of electron density from the metal to the ring. Therefore, the electron density on the ring and thus the ring vibrational frequency in these complexes is similar to, or a little lower than, that of the pyridine complex.

The high ν_{12} frequency of 4-carbinylpyridine–copper complex compared with that of pyridine–copper complex, as shown in Table VI, is due to the fact that the CH_2OH group is an electron-releasing group, which gives a higher electron density on the pyridine ring of the 4-carbinylpyridine complex than that of the pyridine complex, even though the back donation is less in the former complex.

In the case of the complexes with electron-attracting substituents, the strong back donation of electron density by the metal to the delocalized system on the ring causes the electron density near the nitrogen atom to increase, and thus increases the ν_{12} frequency in these complexes over that in the pyridine complex.

In order to obtain information about the relative π contribution to the coordination bond in these complexes, the ν_{12} vibrational frequencies of the free ligands and their hydrochlorides were compared. Only the wavenumber for 4-methylpyridine hydrochloride is uncertain, since it was overlapped by other peaks and appeared as a shoulder.

The data in Table VI indicate that the frequencies of both the free ligands and their hydrochlorides follow a similar trend. This is strong evidence that the higher ν_{12} frequencies for the complexes with these electron-attracting substituents are caused mainly by the back donation of electron density from the metal. In hydrochlorides of these ligands, the back donation of electron density from the proton to the ring can be neglected, and with the migration of electron density from the ring to the substituents resulting in a lower ring vibrational frequency.

Can. J. Chem. Downloaded from www.nrcresearchpress.com by 210.87.254.6 on 09/05/12
For personal use only.

TABLE VI

Vibrational frequencies of ν_{12} mode

R	[Cu(4—R—Py)$_2$Cl$_2$] (cm^{-1})	[Zn(4—R—Py)$_2$Cl$_2$] (cm^{-1})	[4—R—Py·HCl] (cm^{-1})	[4—R—Py] (cm^{-1})
CH_3	1042	1033	1033	1040
CH_2OH	1049	1035	1037	1038
H	1043	1043	1028	1029
$COCH_3$	1055	1058	1018	1020
$CONH_2$	1055	1057	1023	1025
$COOCH_3$	1056	1055	1023	1024
CN	1063	1063	1003	1006

A plot of the frequency (in wavenumbers) of the ν_{12} mode of the hydrochlorides against that of the free ligands gives a straight line (Fig. 2), indicating that the back donation in the hydrochlorides of these ligands is, in fact, negligible, and the electron density on the ring of the hydrochlorides is therefore similar to that of the corresponding free ligands. The same plots for the copper and zinc complexes are also shown in Fig. 2.

From such a plot, it is seen that the relative electron density on the ring of the complexes of pyridine derivatives can be determined directly from the ν_{12} vibration frequencies of the complexes and the free ligands. This correlation can be expressed by the general equation

$$R = \nu_{ML} - (A\nu_L + B),$$

where R is a parameter related to the relative electron density on the pyridine ring. ν_{ML} and ν_L are the ν_{12} frequencies in cm^{-1} of metal complex and the corresponding free ligand respectively, and A and B are constants.

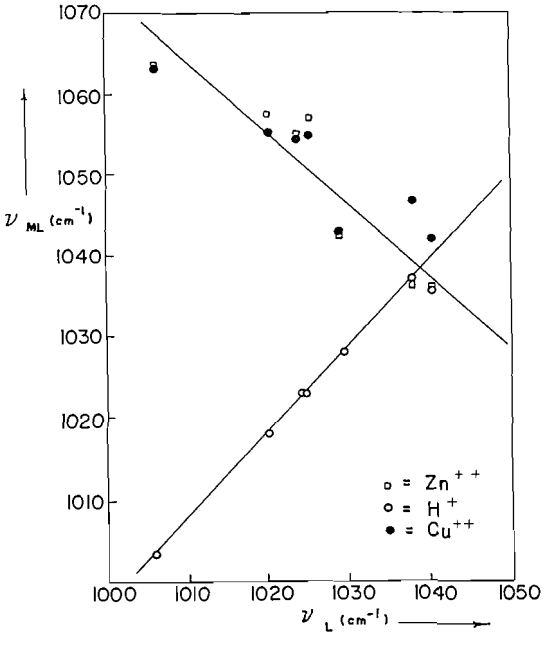

FIG. 2. A plot of the ring vibrational frequencies of the hydrochlorides, copper complexes, and zinc complexes of 4-substituted pyridines vs. those of the free ligands.

TABLE VII

The R_π values of Zn(II) and Cu(II) complexes of 4-substituted pyridines

Ligands	R_π values Zn(II)	Cu(II)
4-Methylpyridine	−5.5	3.5
4-Carbinylpyridine	−1.5	12.5
Pyridine	15.5	15.5
4-Acetylpyridine	39.6	36.6
4-Pyridinecarboxamide	33.5	31.6
4-Carbomethoxypyridine	32.5	33.5
4-Cyanopyridine	58.6	58.6

If the interaction between the delocalized system of the ring and the lone-pair electrons of the nitrogen atom is negligible, R becomes a parameter measuring the relative magnitude of the π contribution to the coordination bond of the complexes, since the higher electron density on the ring in these complexes over that of the corresponding free ligands is mainly caused by back donation from the metal. For the 4-substituted pyridine series, A and B are equal to 1.002 and −3.60 respectively. Therefore the relative magnitude of π bonding in the coordination bond of the complexes of 4-substituted pyridines is directly related to the ν_{12} frequencies of the corresponding complex and the related free ligand by the following equation.

$$R_\pi = \nu_{ML} - (1.002\nu_L - 3.60)$$

With the R_π values in Table VII, it is seen that the relative magnitude of π bonding in the coordination bond for both copper and zinc complexes is in the order

$$4\text{-CNPy} > 4\text{-COCH}_3\text{Py} > 4\text{-COOCH}_3\text{Py} \approx 4\text{-CONH}_2\text{Py} > \text{Py} > 4\text{-CH}_2\text{OHPy} > 4\text{-CH}_3\text{Py}.$$

The R_π values of the zinc complexes of 4-carbinylpyridine and 4-methylpyridine are smaller than those of the corresponding copper complexes, and the ν_{12} frequencies of the zinc complexes are almost the same as those of the corresponding hydrochlorides. This indicates that the back-donating ability of the zinc ion in the complexes is much lower than that of copper ion, which is identical with the prediction on the basis of their first ionization potentials (12).

The extension of these R_π calculations to other metal complexes of these ligands is currently under way in this laboratory.

Acknowledgments

We are indebted to the National Research Council of Canada and the University of New Brunswick for the necessary funds for this investigation.

1. R. K. MURMANN and F. BASOLO. J. Am. Chem. Soc. **77**, 3484 (1955).
2. H. IRVING and J. J. R. F. DA SILVA. Proc. Chem. Soc. 250 (1962).
3. J. J. R. F. DA SILVA and J. G. CALADO. J. Inorg. Nucl. Chem. **28**, 125 (1966).
4. A. YINGST and D. H. MCDANIEL. J. Inorg. Nucl. Chem. **28**, 2919 (1966).
5. A. I. VOGEL. A textbook of quantitative inorganic analysis. Longmans Co., London. 1962. p. 499.
6. W. LANG. Ber. **21**, 1578 (1888).
7. J. M. STURTEVANT. *In* Physical methods of organic chemistry. *Edited by* A. Weisshergen. Vol. I. Part I. Interscience Publishers, New York, N.Y. 1959. p. 54.
8. S. CHABEREK, JR., R. C. COURTNEY, and A. E. MARTELL. J. Am. Chem. Soc. **74**, 5057 (1952).
9. A. A. GRIMBERG and K. B. YATSIMIRSKII. Bull. Acad. Sci. USSR, Div. Chem. Sci. 239 (1952).
10. F. J. C. ROSSOTTI. *In* Modern coordination chemistry. *Edited by* J. Lewis and R. G. Wilkins. Interscience Publishers, New York, N.Y. 1960. p. 27.
11. E. LAVIRON. Bull. Soc. Chim. France, 2325 (1961).
12. D. G. BREWER and P. T. T. WONG. Can. J. Chem. **44**, 1407 (1966).
13. S. NAGAKURA and J. TANAKA. J. Chem. Phys. **22**, 236 (1954).
14. R. J. THOMPSON and A. B. F. DUNCAN. J. Chem. Phys. **14**, 573 (1946).
15. W. MAY and M. JONES. J. Inorg. Nucl. Chem. **25**, 507 (1963).
16. W. MAY and M. JONES. J. Inorg. Nucl. Chem. **24**, 511 (1962).
17. E. SPINNER. J. Chem. Soc. 3860 (1963).
18. C. M. BAX, A. R. KATRITZKY, and L. E. SUTTON. J. Chem. Soc. 1257 (1958).
19. D. G. LIRS and B. C. CURRAN. J. Am. Chem. Soc. **67**, 79 (1945).
20. R. D. BROWN and M. L. HEFFERNAN. Australian J. Chem. **10**, 493 (1957).

Can. J. Chem. Downloaded from www.nrcresearchpress.com by 210.87.254.6 on 09/05/12
For personal use only.

Can. J. Chem. Downloaded from www.nrcresearchpress.com by 210.87.254.105 on 09/05/12
For personal use only.

Nature of the coordination bond in metal complexes of substituted pyridine derivatives. II. The far infrared spectra and metal–ligand force constants of copper complexes of 4-substituted pyridines

PATRICK T. T. WONG[1] AND D. G. BREWER
Department of Chemistry, University of New Brunswick, Fredericton, New Brunswick

Received June 1, 1967

Infrared spectra, including the lower frequency region, of copper (II) complexes of the type $[CuL_2Cl_2]$, where L = 4-methylpyridine, 4-carbinylpyridine, pyridine, 4-acetylpyridine, 4-pyridinecarboxamide, 4-carbomethoxypyridine, and 4-cyanopyridine have been measured. The substituent effect upon the copper–nitrogen (ligand) and copper–chlorine stretching frequencies has also been examined. It was found that the substituents on the pyridine ring not only affected the nature of copper–nitrogen bond, but also the copper–chlorine bond. It appears that an entirely delocalized system exists, involving the chlorine atoms and the substituents in the complexes. Force constants associated with the coordination bond between copper and the nitrogen of the ligands have been calculated by means of an IBM 1620 computer. By comparison of the copper–nitrogen stretching frequencies with the corresponding force constants, and the heats of coordination, it may be concluded that the magnitude of the metal–ligand stretching frequency is directly related to the metal–ligand coordination bond strength for the systems under study.

Canadian Journal of Chemistry, 46, 139 (1968)

Introduction

The effects of substituents upon the coordination bond strength and upon the relative π contribution to that bond in a series of metal complexes of 4-substituted pyridines have been studied in a previous paper (1). The present work has been undertaken to study the substituent effects upon the metal–nitrogen (ligand) and metal–chlorine stretching frequencies in the far infrared region, as well as the metal–nitrogen (ligand) stretching force constants of a series of complexes of the form $[CuL_2Cl_2]$, where L is 4-methylpyridine, 4-hydroxymethylpyridine, pyridine, 4-acetylpyridine, 4-pyridinecarboxamide, 4-carbomethoxypyridine, and 4-cyanopyridine.

Recently, during this experimental work, a study (2) reported spectra in the 667–150 cm^{-1} region on metal complexes of some pyridines, including two of the 4-substituted pyridines in the present study (4-methylpyridine and 4-cyanopyridine). Tentative assignments were made for M—N (ligand), M—NCS, M—ONO_2, and M—Cl stretching vibrations. An attempt to correlate the metal stretching band positions with the base strengths of the substituted pyridines was also made. However, no direct relationship between these two factors was found, when copper complexes of pyridine, 4-aminopyridine, 2-methylpyridine, 3-methylpyridine, 4-methylpyridine, 2,4-lutidine, 2,5-lutidine, 2,6-lutidine, 3,4-lutidine, and 3,5-lutidine were examined. The failure in this correlation is probably due to the fact that the bascity of a ligand, in terms of protonation, does not involve π bonding, which plays a very important role in complex formation of pyridine derivatives. Furthermore, solvent effects might complicate the relationship between the basicity of the ligands and the metal–ligand stretching frequencies, experimentally determined from solid state spectra.

In the present investigation, the metal–nitrogen (ligand) stretching frequencies are correlated with both the heat of coordination data (1) and the metal–nitrogen (ligand) stretching force constants. In order to obtain the force constants a normal coordinate analysis has been carried out using an IBM 1620 computer. The final *G* matrix elements are tabulated in the Appendix[2], which can be used for other similar systems.

Experimental

All the reagents and the preparation of cupric complexes of the type $[CuL_2Cl_2]$, where L is 4-methylpyridine, 4-hydroxymethylpyridine, pyridine, 4-acetylpyridine, 4-pyridinecarboxamide, 4-carbomethoxypyridine, and 4-cyanopyridine, have been described in a previous paper (1).

[1]Present address: Division of Applied Chemistry, National Research Council of Canada, Ottawa, Canada.

[2]This Appendix has been placed in the Depository of Unpublished Data. Photocopies may be obtained, upon request, from: Depository of Unpublished Data, National Science Library, National Research Council of Canada, Ottawa, Canada.

Can. J. Chem. Downloaded from www.nrcresearchpress.com by 210.87.254.105 on 09/05/12
For personal use only.

TABLE I

Infrared absorption bands of heterocyclic bases and their cupric complexes in the 343–162 cm^{-1} region*

	Absorption bands (cm^{-1})						
	[Cu—Cl]		[Cu—N]	[CuCl bridge]			
4-CH_3Py						206 m	167 w
[Cu(4-CH_3Py)$_2Cl_2$]	296 s[299]		285 m[266]		259 s	207 m[209]	168 m[170]
4-CH_2OHPy				258 w		209 w	174 w
[Cu(4-CH_2OHPy)$_2Cl_2$]	295 s		276 s	252 w	240 s		183 s
Py							
[$CuPy_2Cl_2$]	293 s		268 s		235 s	203 w	178 m
4-$COCH_3$Py						219 m	
[Cu(4-$COCH_3$Py)$_2Cl_2$]	296 s		265 m		241 s		173 s
4-$CONH_2$Py		274 w				225 sh	178 w
[Cu(4-$CONH_2$Py)$_2Cl_2$]	301 s	275 m	264 m		249 w	190 s	168 w
4-$COOCH_3$Py						215 s	174 w
[Cu(4-$COOCH_3$Py)$_2Cl_2$]	301 s		264 w		235 s		164 m
4-CNPy							172 s
[Cu(4-CNPy)$_2Cl_2$]	304 s[307]		243 s[242]		236 s	217 s[217]	169 m[171]

*Data in brackets from ref. 2. Py = pyridine, s = strong, m = medium, w = weak, sh = shoulder.

Can. J. Chem. Downloaded from www.nrcresearchpress.com by 210.87.254.105 on 09/05/12
For personal use only.

A Perkin–Elmer 521 spectrophotometer was used to record the infrared spectra in the region between 4 000 and 300 cm^{-1}. The instrument was purged with dry air and was calibrated against water vapor, methane, ammonia gas, and methanol vapor. The infrared spectra of the complexes were measured using the potassium bromide disk method.

To obtain the far infrared spectra of the complexes and the free ligands in the region between 343 and 162 cm^{-1}, a Perkin–Elmer model 301 spectrophotometer was used. The solid samples were measured as mulls in Nujol, which were placed between two polyethylene windows and then inserted into the cell holder. For the liquid samples, polyethylene liquid cells were used. No absorption was found in the region examined for both the polyethylene and Nujol. The spectrophotometer was continually purged with dry nitrogen and was calibrated with water vapor.

Results and Discussion

I. Far Infrared Spectra

The observed frequencies in the 343–162 cm^{-1} region of some 4-substituted pyridines and their cupric chloride complexes are given in Table I. Bands for the complexes of 4-cyanopyridine and 4-methylpyridine, reported by Frank and Rogers (2) recently, are also included. However, two new bands, one in the 4-cyanopyridine complex (236 cm^{-1}) and one in the 4-methylpyridine complex (285 cm^{-1}) are found in the present work.

By comparing the spectra of the metal complexes versus the free ligands, the chloride complex of copper(II) (3), and the recent studies (2, 4–6) of the metal stretching vibration of dichlorobis(pyridine)copper(II), the bands in the 296–304 cm^{-1} region and the 219–236 cm^{-1} region for the complexes under study can be assigned to the Cu—Cl stretching modes. The new bands at 285–243 cm^{-1}, which are not available in the spectra of the $[CuCl_4]^{2-}$ complex and the free ligands, arise from a mode involving copper–nitrogen stretching.

A recent study (5) of halogen–metal stretching vibration spectra for pyridine complexes of the form $[MX_2Py_{2-4}]$ showed that only one X-sensitive band was observed for monomeric octahedral complexes and planar complexes in the 400–200 cm^{-1} region, whereas two X-sensitive bands were available for tetrahedral and distorted polymeric octahedral complexes. In the spectra of tetrahedral complexes, both X—M stretching bands are located between 400–290 cm^{-1}, but in the case of distorted polymeric octahedral complexes, these two bands are separated into two regions, 400–290 cm^{-1} and near 240 cm^{-1}.

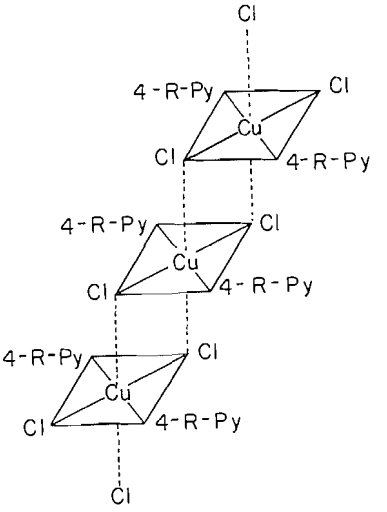

FIG. 1. Stereo-configuration of the copper complexes.

The presence of two chlorine–copper stretching bands for all the 4-substituted pyridine copper chloride complexes and the separation of these two bands into 343–290 cm^{-1} and 259–236 cm^{-1} regions indicate that the stereo-configuration of all the complexes under study is a distorted polymeric octahedral (Fig. 1). The band at 296–304 cm^{-1} is assigned to the stretching of the shorter chlorine–copper bonds and that at 259–236 cm^{-1} is assigned to the bridging chlorine–copper bonds.

The data in Table I show that the metal–nitrogen stretching frequency is appreciably changed by the effect of different substituents in the 4-position of the pyridine ring and decreases in the order

$$CH_3 > CH_2OH > H > COCH_3 > CONH_2 \approx COOCH_3 > CN.$$

This is identical to the bond strength trend determined by the values of the heat of coordination. Therefore, apparently, these metal–nitrogen stretching frequencies play an important role in indicating the relative magnitude of coordination bond strength in metal complexes of pyridine derivatives.

The data in Table I also show that not only ν_{Cu-N}, but also ν_{Cu-Cl}, of the complexes is very sensitive to the nature of the groups substituted on the pyridine ring. The effect of the substituents is to produce a shift of the chlorine–copper stretching frequency in dichlorobis(4-substituted

Can. J. Chem. Downloaded from www.nrcresearchpress.com by 210.87.254.105 on 09/05/12
For personal use only.

pyridine)Cu(II) complexes according to the order

$$CH_3 > CH_2OH > H < COCH_3 < CONH_2 \approx COOCH_3 < CN.$$

Since the metal–ligand stretching frequency is related to the metal–ligand bond strength, the relative magnitude of the chlorine–copper bond strength in the complexes should also follow this order.

It is interesting that the effects of both the electron-releasing and electron-attracting groups appear to increase the chlorine–copper stretching frequencies and the strengthening of the copper–chlorine bonds. The substitution of electron-releasing groups on the pyridine ring gives a stronger copper–nitrogen σ bond; thus a higher electron density on the copper atom results, which in turn enhances the drift of electron density from copper to chlorine and strengthens the $d\pi$–$d\pi$ copper to chlorine bonding. Stronger electron-releasing groups give a higher π contribution in the copper–chlorine coordination bond, so that the copper–chlorine bond strength of these complexes is in the order

4-methylpyridine > 4-hydroxymethylpyridine > pyridine.

On the other hand, electron-attracting groups lower the electron density on the copper atom and result in a strengthening of the π contribution and a weakening of the σ contribution in the copper–nitrogen bond. Therefore the back donation of electron density from copper to chlorine in these systems becomes unimportant. Moreover the donation of electron density from the chlorine to the copper is much enhanced and results in a strengthening of the σ bonding between copper and chlorine. Stronger electron-attracting groups on the pyridine ring give a stronger copper–chlorine bond and the above ν_{Cu-Cl} trend for these complexes is expected.

II. Normal Coordinate Analysis

In order to study the substituent effects upon the copper–nitrogen stretching force constants for a series of 4-substituted pyridine – Cu(II) complexes, as well as other force constants of the pyridine ring, a normal coordinate calculation was carried out. For such a complicated molecule as the dichlorobis(4-substituted pyridine)Cu(II) complex, a reasonable assumption is desirable to simplify the calculation. Since most of the vibrational absorptions in the infrared spectra of the copper complexes are similar to those of the corresponding free ligands, and thus coupling between ligands in a molecule is expected to be small, a simple 1:1 complex model may be sufficient as a first approximation (7).

The 1:1 complex model shown in Fig. 2 has 30 normal vibrations, in which R is a substituent and is treated as a single "atom" having a mass of the particular substituent. These 30 normal vibrations are grouped into four species ($11A_1 + 3A_2 + 6B_1 + 10B_2$) of the point group C_{2v}. Since the in-plane vibrations ($11A_1 + 10B_2$) are separable from the out-of-plane vibrations ($3A_2 + 6B_1$), only the 21 in-plane vibrations are calculated in this paper.

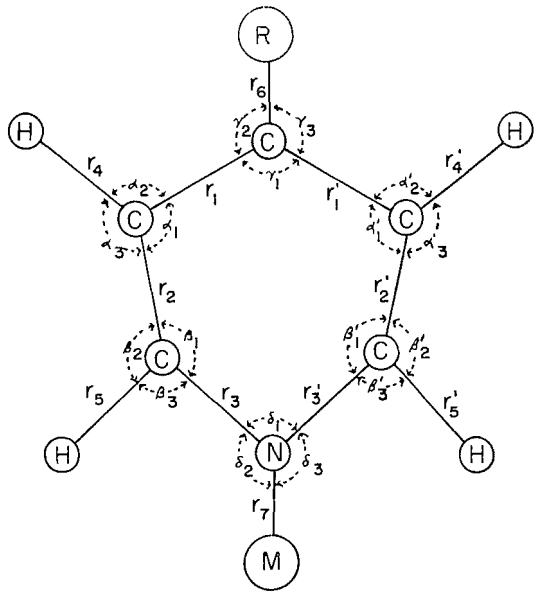

FIG. 2. The 1:1 complex model of 4-substituted pyridine – Cu(II) complexes and the 30 internal coordinates.

The original G and F matrices were constructed (11) according to the 30 internal coordinates for the 21 in-plane vibrations, as shown in Fig. 2. These matrices are further reduced and separated into 12th order A_1 and 11th order B_2 matrices by coordinate transformations. The elements of the final G matrices are tabulated in the Appendix.

Apparently 9 redundant conditions are involved in the 30 internal coordinates; viz. there are 30 internal coordinates, but only 21 vibra-

Can. J. Chem. Downloaded from www.nrcresearchpress.com by 210.87.254.105 on 09/05/12
For personal use only.

tions. Seven of them can be easily found from Fig. 2.

$$[1]\quad \Delta\alpha_1 + \Delta\alpha_2 + \Delta\alpha_3 = 0$$

$$[2]\quad \Delta\alpha'_1 + \Delta\alpha'_2 + \Delta\alpha'_3 = 0$$

$$[3]\quad \Delta\beta_1 + \Delta\beta_2 + \Delta\beta_3 = 0$$

$$[4]\quad \Delta\beta'_1 + \Delta\beta'_2 + \Delta\beta'_3 = 0$$

$$[5]\quad \Delta\gamma_1 + \Delta\gamma_2 + \Delta\gamma_3 = 0$$

$$[6]\quad \Delta\delta_1 + \Delta\delta_2 + \Delta\delta_3 = 0$$

$$[7]\quad \Delta\alpha_1 + \Delta\alpha'_1 + \Delta\beta_1 + \Delta\beta'_1 + \Delta\gamma_1 + \Delta\delta_1 = 0$$

However, it is difficult to deduce the remaining 2 redundant conditions directly from Fig. 2. These redundant conditions can be left in the secular equations to be used as a check on the calculations, since these redundancies must yield frequencies equal to zero in the final results.

Removal of the [1]–[6] redundancies can be accomplished by a linear combination of the internal coordinates (8). The transformation matrix, T, for this coordinate transformation is shown in Table II. The redundancy concerning the sum of all the six angles in the ring (eq. [7]) can be removed by a symmetry coordinate transformation. The corresponding symmetry coordinates are given in Table III.

To construct the F matrix, the modified Urey–Bradley force field (9) of the following type was used.

$$\begin{aligned}
2U = &\sum_i [K_i + \sum_{j\neq i} (t^2_{ij} F'_{ij} + s^2_{ij} F_{ij})] (\Delta r_i)^2 \\
&+ \sum_{i<j} [H_{ij} - s_{ij}s_{ji}F'_{ij} + t_{ij}t_{ji}F_{ij}] (r_{ij}\Delta\alpha_{ij})^2 \\
&+ 2 \sum_{i<j} [-t_{ij}t_{ji}F'_{ij} + s_{ij}s_{ji}F_{ij}] (\Delta r_i)(\Delta r_j) \\
&+ 2 \sum_{i\neq j} [t_{ij}s_{ji}F'_{ij} + t_{ji}s_{ij}F_{ij}] (r_j/r_i)^{1/2}(\Delta r_i)(r_{ij}\Delta\alpha_{ij}) \\
&+ 2\rho(\Delta r'_3\Delta r_3 + \Delta r'_3\Delta r'_2 + \Delta r_2\Delta r_3 + \Delta r'_2\Delta r'_1 + \Delta r_1\Delta r_2 + \Delta r'_1\Delta r_1) \\
&- 2\rho(\Delta r'_3\Delta r'_1 + \Delta r_1\Delta r_3 + \Delta r'_2\Delta r_1 + \Delta r'_1\Delta r_2 + \Delta r'_3\Delta r_2 + \Delta r'_2\Delta r_3) \\
&+ 2\rho(\Delta r'_3\Delta r_1 + \Delta r'_1\Delta r_3 + \Delta r'_2\Delta r_2),
\end{aligned}$$

where $s_{ij} = (r_i - r_j\cos\alpha_{ij})/q_{ij}$ $\qquad$ $t_{ji} = (r_i\sin\alpha_{ij})/q_{ij}$

$s_{ji} = (r_j - r_i\cos\alpha_{ij})/q_{ij}$ $\qquad$ $q_{ij}^2 = r_i^2 + r^2_j - 2r_ir_j\cos\alpha_{ij}.$

$t_{ij} = (r_j\sin\alpha_{ij})/q_{ij}$

Furthermore, K, H, and F are the force constants for the bond stretching, angle deformation and repulsion between the nearest non-bonded atoms. F' is introduced as a force constant associated with the linear term of the repulsive energy and remains in the above equation as an internal tension term. Its value is assumed to be $-0.1F$, as usual (9). ρ is an average "Kekule" force constant.

The secular equation $|GF - E\lambda| = 0$ was set up according to Wilson's method (10). By using a "high-frequency separation" method (11) for the C—H stretching modes, the order of both A_1 and B_2 matrices was reduced. To find the eigenvalues of the final secular equations of 10th order and 9th order, the QR transformation method (12) was used.

Numerical values of all the matrix elements were calculated using the parameters in Tables IV and V. Since no structural data are available for these substituted pyridine complexes and small changes in bond lengths do not affect the calculated frequencies at all, it is assumed that the bond distances in the complexes do not change appreciably by substitution.

The eigenvalues, λ's, thus obtained, are converted into wavenumbers, and can then be compared with the observed frequencies. These are shown in Table VI. The agreement between calculated and observed values is seen to be satisfactory. A refinement of the force constants has been made only for the metal–nitrogen stretching

Can. J. Chem. Downloaded from www.nrcresearchpress.com by 210.87.254.105 on 09/05/12
For personal use only.

TABLE II

Transformation matrix T

T	r_1	r'_1	r_2	r'_2	r_3	r'_3	r_4	r'_4	r_5	r'_5	r_6	r_7	α_1	α_2	α_3	α'_1	α'_2	α'_3	β_1	β_2	β_3	β'_1	β'_2	β'_3	γ_1	γ_2	γ_3	δ_1	δ_2	δ_3
t_1	+1																													
t_2		+1																												
t_3			+1																											
t_4				+1																										
t_5					+1																									
t_6						+1																								
t_7							+1																							
t_8								+1																						
t_9									+1																					
t_{10}										+1																				
t_{11}											+1																			
t_{12}												+1																		
t_{13}													+1	+1	+1															
t_{14}													+1	0	0															
t_{15}													0	+1	−1															
t_{16}																+1	+1	+1												
t_{17}																+1	0	0												
t_{18}																0	+1	−1												
t_{19}																			+1	+1	+1									
t_{20}																			+1	0	0									
t_{21}																			0	+1	−1									
t_{22}																						+1	+1	+1						
t_{23}																						+1	0	0						
t_{24}																						0	+1	−1						
t_{25}																									+1	+1	+1			
t_{26}																									+1	0	0			
t_{27}																									0	+1	−1			
t_{28}																												+1	+1	+1
t_{29}																												+1	0	0
t_{30}																												0	+1	−1

(Zero)

(Zero)

TABLE III

Symmetry coordinates for in-plane vibrations of the 1:1 complex model

A_1 species	Symmetry coordinates	Vibration modes	B_2 species	Symmetry coordinates	Vibration modes
s_1	$\frac{1}{\sqrt{2}}(\Delta r_1+\Delta r'_1)$	V_s C—C	s_1	$\frac{1}{\sqrt{2}}(\Delta r_1-\Delta r'_1)$	V_{as} C—C
s_2	$\frac{1}{\sqrt{2}}(\Delta r_2+\Delta r'_2)$	V_s C—C	s_2	$\frac{1}{\sqrt{2}}(\Delta r_2-\Delta r'_2)$	V_{as} C—C
s_3	$\frac{1}{\sqrt{2}}(\Delta r_3+\Delta r'_3)$	V_s C—N	s_3	$\frac{1}{\sqrt{2}}(\Delta r_3-\Delta r'_3)$	V_{as} C—N
s_4	$\frac{1}{\sqrt{2}}(\Delta r_4+\Delta r'_4)$	V_s C—H	s_4	$\frac{1}{\sqrt{2}}(\Delta r_4-\Delta r'_4)$	V_{as} C—H
s_5	$\frac{1}{\sqrt{2}}(\Delta r_5+\Delta r'_5)$	V_s C—H	s_5	$\frac{1}{\sqrt{2}}(\Delta r_5-\Delta r'_5)$	V_{as} C—H
s_6	Δr_6	V_s C—R	s_6	$\frac{1}{\sqrt{2}}(\Delta\alpha_2-\Delta\alpha_3-\Delta\alpha'_2+\Delta\alpha'_3)$	δ_{as} C—H
s_7	Δr_7	V_s N—Cu	s_7	$\frac{1}{\sqrt{2}}(\Delta\beta_2-\Delta\beta_3-\Delta\beta'_2+\Delta\beta'_3)$	δ_{as} C—H
s_8	$\frac{1}{\sqrt{2}}(\Delta\alpha_2-\Delta\alpha_3+\Delta\alpha'_2-\Delta\alpha'_3)$	δ_s C—H	s_8	$\frac{1}{\sqrt{2}}(\Delta\gamma_2-\Delta\gamma_3-\Delta\delta_2+\Delta\delta_3)$	δ_{as} C—R, C—N
s_9	$\frac{1}{\sqrt{2}}(\Delta\beta_2-\Delta\beta_3+\Delta\beta'_2-\Delta\beta'_3)$	δ_s C—H	s_9	$\frac{1}{2}(\Delta\alpha_1-\Delta\alpha'_1+\Delta\beta_1-\Delta\beta'_1)$	Ring def.
s_{10}	$\frac{1}{2}(\Delta\alpha_1+\Delta\alpha'_1-\Delta\beta_1-\Delta\beta'_1)$	Ring def.	s_{10}	$\frac{1}{2}(\Delta\alpha_1-\Delta\alpha'_1-\Delta\beta_1+\Delta\beta'_1)$	Ring def.
s_{11}	$\frac{1}{\sqrt{2}}(\Delta\delta_1-\Delta\gamma_1)$	Ring def.			
s_{12}	$\frac{1}{\sqrt{12}}(2\Delta\gamma_1+2\Delta\delta_1-\Delta\alpha_1-\Delta\alpha'_1-\Delta\beta_1-\Delta\beta'_1)$	Ring def.			
s_{13}	$\frac{1}{\sqrt{6}}(\Delta\alpha_1+\Delta\alpha'_1+\Delta\beta_1+\Delta\beta'_1+\Delta\gamma_1+\Delta\delta_1)$	Redundant			

TABLE IV

Molecular parameters used in the calculation (13–17)

$\alpha_1=\alpha'_1=118°32'$	$r'_1=r_1=1.3944$ Å
$\alpha_2=\alpha'_2=121°18'$	$r_2=r'_2=1.3945$ Å
$\alpha_3=\alpha'_3=120°10'$	$r_3=r'_3=1.3402$ Å
$\beta_1=\beta'_1=123°53'$	$r_4=r'_4=1.0805$ Å
$\beta_2=\beta'_2=120°14'$	$r_5=r'_5=1.0803$ Å
$\beta_3=\beta'_3=115°53'$	$r_6=2.02$ Å
$\gamma_1=118°20'$	$r_7(CH_3)=r_7(CH_2OH)=1.53$ Å
$\gamma_2=\gamma_3=120°50'$	$r_7(COCH_3)=r_7(CONH_2)=1.50$ Å
$\delta_1=116°50'$	$r_7(COOCH_3)=1.50$ Å
$\delta_2=\delta_3=121°35'$	$r_7(CN)=1.46$ Å

mode. The descriptions of the fundamental vibrations in Table VI are according to the previous assignments (18, 19). It was found that the lowest band of the B_2 species is sensitive to the mass of the metal ion in the complex, and therefore it might be assigned to the metal–ligand asymmetric vibration. However, this band for some complexes is not observed.

The results shown in Table V indicate that the copper–nitrogen stretching force constants of the complexes of 4-methylpyridine and 4-hydroxymethylpyridine are larger than, and those of the remaining 4-substituted pyridines are smaller than, that of the pyridine complex. Comparing these force constants, it gives the same order as those obtained by both the heat of coordination data and the copper–nitrogen stretching frequencies, viz.

$$CH_3Py > CH_2OHPy > Py > COCH_3Py > CONH_2Py \approx COCH_3Py > CNPy.$$

Moreover, the computation shows that the copper–nitrogen stretching frequency is mainly affected by the metal–ligand stretching force constant and, furthermore, is directly dependent upon it. Therefore, the normal coordinate treatment provides strong evidence that the magnitude of the metal–ligand stretching frequency in the far infrared region may be used as a measure of the coordination bond strength for complexes of pyridine derivatives.

The force constants for the repulsive interaction between the nearest non-bonded carbon and nitrogen atoms in the pyridine ring, F_{CC} and F_{CN}, are larger in the substituted pyridine complexes than in the pyridine complex itself. This is

Can. J. Chem. Downloaded from www.nrcresearchpress.com by 210.87.254.105 on 09/05/12
For personal use only.

Can. J. Chem. Downloaded from www.nrcresearchpress.com by 210.87.254.105 on 09/05/12
For personal use only.

TABLE V

Force constants (10^5 dyn/cm)

	K_1	K_2	K_3	K_6	K_7	$H\alpha_1$	$H\alpha_2$	$H\alpha_3$	$H\beta_1$	$H\beta_2$	$H\beta_3$	$H\gamma_1$	$H\gamma_2$	$H\gamma_3$
$[Cu(4\text{-}CH_3Py)_2Cl_2]$	3.65	3.65	4.50	5.32	1.86	0.30	0.23	0.23	1.10	0.23	0.19	0.30	0.19	0.19
$[Cu(4\text{-}CH_2OHPy)_2Cl_2]$	3.41	3.41	4.50	6.80	1.74	0.30	0.23	0.23	1.10	0.23	0.19	0.30	0.19	0.19
$[Cu(Py)_2Cl_2]$	4.35	4.35	4.50	4.54	1.58	0.48	0.23	0.23	1.16	0.23	0.21	0.48	0.38	0.38
$[Cu(4\text{-}COCH_3Py)_2Cl_2]$	3.32	3.32	4.50	6.82	1.50	0.30	0.23	0.23	1.10	0.23	0.19	0.30	0.19	0.19
$[Cu(4\text{-}CONH_2Py)_2Cl_2]$	3.32	3.32	4.50	6.82	1.49	0.30	0.23	0.23	1.10	0.23	0.19	0.30	0.19	0.19
$[Cu(4\text{-}COOCH_3Py)_2Cl_2]$	3.32	3.32	4.50	6.82	1.49	0.30	0.23	0.23	1.10	0.23	0.19	0.30	0.19	0.19
$[Cu(4\text{-}CNPy)_2Cl_2]$	4.30	4.30	4.90	5.45	1.05	0.30	0.23	0.23	1.16	0.23	0.24	0.30	0.25	0.25

	$H\delta_1$	$H\delta_2$	$H\delta_3$	F_1	F_2	F_3	F_4	F_5	F_6	F_7	F_8	F_9	F_{10}	ρ
$[Cu(4\text{-}CH_3Py)_2Cl_2]$	0.40	0.45	0.45	1.00	0.43	0.55	1.00	1.00	0.43	0.43	1.00	0.52	0.22	0.29
$[Cu(4\text{-}CH_2OHPy)_2Cl_2]$	0.40	0.45	0.45	1.00	0.43	0.55	1.00	1.00	0.43	0.43	1.00	0.52	0.35	0.29
$[Cu(Py)_2Cl_2]$	0.50	0.45	0.45	0.80	0.43	0.43	0.80	0.71	0.43	0.43	0.80	0.52	0.22	0.31
$[Cu(4\text{-}COCH_3Py)_2Cl_2]$	0.40	0.45	0.45	1.00	0.43	0.55	1.00	1.00	0.43	0.43	1.00	0.52	0.27	0.29
$[Cu(4\text{-}CONH_2Py)_2Cl_2]$	0.40	0.45	0.45	1.00	0.43	0.55	1.00	1.00	0.43	0.43	1.00	0.52	0.27	0.29
$[Cu(4\text{-}COOCH_3Py)_2Cl_2]$	0.40	0.45	0.45	1.00	0.43	0.55	1.00	1.00	0.43	0.43	1.00	0.52	0.35	0.29
$[Cu(4\text{-}CNPy)_2Cl_2]$	0.40	0.45	0.45	1.00	0.43	0.65	1.00	1.00	0.43	0.43	1.00	0.52	0.25	0.29

TABLE VI

Fundamental vibrational frequencies of copper complexes of 4-substituted pyridines

Description	$[Cu(4\text{-}CH_3Py)_2Cl_2]$		$[Cu(4\text{-}CH_2OHPy)_2Cl_2]$		$[Cu(Py)_2Cl_2]$		$[Cu(4\text{-}COCH_3Py)_2Cl_2]$	
	Obs. (cm^{-1})	Calcd. (cm^{-1})	Obs. (cm^{-1})	Calcd. (cm^{-1})	Obs. (cm^{-1})	Calcd. (cm^{-1})	Obs. (cm^{-1})	Calcd. (cm^{-1})
A_1 species								
ν(M—N)	285	285	276	276	268	268	265	265
ν_{6a}, ring, R-sens.	550	650	611	566	643	713	—	536
ν_1, ring, β(C—M)	1033	992	1032	1006	1016	1010	1027	996
ν_{12}, ring	1042	1059	1049	1046	1042	1046	1055	1043
ν_{18}, ν(C—R), β(C—H)	1190	1163	1184	1158	3036	3040	1148	1151
ν_{9a}, β(C—H)	1231	1231	1224	1228	1216	1216	1228	1230
R-sens.	1432	1427	1419	1415	1400	1367	1420	1416
ν_{19a}, ν(C—C, C—N)	1506	1524	1508	1519	1490	1499	1497	1519
ν_{8a}, ν(C—C)	1621	1617	1621	1622	1605	1597	1614	1626
B_2 species								
M-sens.	207	251	—	221	203	318	—	219
ν_{15}, R-sens.	418	424	417	404	1152	1154	391	406
ν_{6b}, ring	669	775	663	770	655	780	667	772
ν_{18b}, β(C—H)	1101	1075	1099	1086	1123	1119	1061	1039
ν_3, β(C—H)	1119	1145	1111	1151	1239	1301	1101	1127
ν_{14}, ν(C—C, C—N)	1335	1342	1338	1341	1365	1393	1333	1341
ν_{19b}, ν(C—C, C—N) β(C—R, C—H)	1439	1398	1430	1403	1450	1510	1416	1390
ν_{8b}, ν(C—C)	1563	1551	1562	1553	1574	1642	1562	1547

Description	$[Cu(4\text{-}COOCH_3Py)_2Cl_2]$		$[Cu(4\text{-}COOCH_3Py)_2Cl_2]$		$[Cu(4\text{-}CNPy)_2Cl_2]$	
	Obs. (cm^{-1})	Calcd. (cm^{-1})	Obs. (cm^{-1})	Calcd. (cm^{-1})	Obs. (cm^{-1})	Calcd. (cm^{-1})
A_1 species						
ν(M—N)	264	264	264	264	243	243
ν_{6a}, ring, R-sens.	—	533	—	516	559	534
ν_1, ring, β(C—M)	1027	1001	1027	1001	1025	997
ν_{12}, ring	1055	1043	1055	1035	1063	1055
ν_{18}, ν(C—R), β(C—H)	1149	1150	1149	1166	1189	1194
ν_{9a}, β(C—H)	1226	1229	1228	1228	1219	1228
R-sens.	1419	1415	1420	1415	1425	1404
ν_{19a}, ν(C—C, C—N)	1499	1519	1497	1507	1534	1536
ν_{8a}, ν(C—C)	1611	1626	1614	1626	1611	1601
B_2 species						
M-sens.	190	219	—	214	217	248
ν_{15}, R-sens.	414	406	393	413	401	437
ν_{6b}, ring	666	772	666	773	665	791
ν_{18b}, β(C—H)	1041	1043	1062	1043	1115	1149
ν_3, β(C—H)	1094	1128	1101	1129	1233	1220
ν_{14}, ν(C—C, C—N)	1331	1340	1333	1340	1325	1364
ν_{19b}, ν(C—C, C—N) β(C—R, C—H)	1419	1392	1416	1393	1415	1415
ν_{8b}, ν(C—C)	1555	1548	1562	1553	1601	1596

probably due to the charge density at the carbon and nitrogen atoms in the ring being affected by the substituents.

The aromatic CN stretching force constant is larger in the complex of 4-cyanopyridine, which indicates that the back donation in this complex is much greater. This is identical with the results obtained from the comparison of the frequencies of the ν_{12} mode in the previous paper (1).

Acknowledgments

It is a pleasant duty to express our sincere gratitude to Dr. M. Falk, Dr. J. E. Bertie, and

Can. J. Chem. Downloaded from www.nrcresearchpress.com by 210.87.254.105 on 09/05/12
For personal use only.

Dr. E. Whalley of the National Research Council of Canada for the use of their instruments.

We wish to thank the University of New Brunswick and the National Research Council of Canada for their financial assistance for this work.

1. P. T. T. Wong and D. G. Brewer. Can. J. Chem. **46**, 131 (1968).
2. C. W. Frank and L. B. Rogers. Inorg. Chem. **5**, 615 (1966).
3. R. J. H. Clark and T. M. Dunn. J. Chem. Soc. 1198 (1963).
4. G. E. Coates and D. Ridley. J. Chem. Soc. 166 (1964).
5. R. J. H. Clark and C. S. Williams. Inorg. Chem. **4**, 350 (1965).
6. M. Goldstein, E. F. Mooney, A. Anderson, and H. A. Gebbie. Spectrochim. Acta, **21**, 105 (1965).
7. K. Nakamoto, P. J. McCarthy, R. Ruby, and A. E. Martell. J. Am. Chem. Soc. **83**, 1066 (1961).
8. K. Nakamoto and A. E. Martel. J. Chem. Phys. **32**, 588 (1960).
9. G. Zerbi, Bryce Crawford, Jr., and J. Overend. J. Chem. Phys. **38**, 127 (1963).
10. E. B. Wilson, Jr. J. Chem. Phys. 7, 1047 (1939); **9**, 76 (1941).
11. E. B. Wilson, Jr., J. C. Decius, and P. C. Cross. Molecular vibration. McGraw-Hill Book Co., Inc., New York. 1955. p. 74.
12. J. G. F. Francis. Computer J. **4**, 265 (1961).
13. B. Bak, L. Hansen-Hygard, and J. Rastup-Anderson. J. Mol. Spectry. **2**, 361 (1958).
14. J. D. Dunitz. Acta Cryst. **10**, 307 (1957).
15. L. O. Brockway and J. Monteath Robertson. J. Chem. Soc. 1324 (1939).
16. D. R. Lide, Jr. Tetrahedron, **17**, 125 (1962).
17. B. Bak, D. Christensen, W. B. Dixon, L. H. Nygard, and J. R. Anderson. J. Chem. Phys. **37**, 2027 (1962).
18. E. Spinner. J. Chem. Soc. 3860 (1963).
19. J. H. S. Green, W. Kynaston, and H. M. Paisley. Spectrochim. Acta, **19**, 549 (1963).

Can. J. Chem. Downloaded from www.nrcresearchpress.com by 210.87.254.105 on 09/05/12
For personal use only.

Can. J. Chem. Downloaded from www.nrcresearchpress.com by 210.87.254.42 on 09/05/12
For personal use only.

New polyatomic cations of the group VI B elements: I. Solutions of selenium in highly acidic solvents

J. Barr, R. J. Gillespie, R. Kapoor, and K. C. Malhotra
Department of Chemistry, McMaster University, Hamilton, Ontario

Received September 7, 1967

Colored solutions of selenium in fluorosulfuric, sulfuric, and disulfuric acids have been investigated by conductometric, cryoscopic, spectrophotometric, and magnetic methods. Evidence is presented for the new species Se_4^{2+} and Se_8^{2+} in the yellow and green solutions respectively.

Canadian Journal of Chemistry, 46, 149 (1968)

Introduction

Sulfur, selenium, and tellurium dissolve in certain strongly acidic solvents to form intensely colored solutions. The reaction of tellurium with concentrated sulfuric acid to produce a red solution was one of the first recorded properties of the element (1); in sulfuric acid or oleum, selenium produces green or yellow solutions (2–4) and sulfur gives blue solutions in oleum (4, 5). Similar reactions have been reported with SO_3 (4–7), although the presence of a small quantity of water is necessary for this reaction (8). From the reactions of the elements with SO_3, compounds analyzing as S_2O_3 (8, 9), $TeSO_3$ (6, 10, 11), and $SeSO_3$ (7) have been reported. A green and a yellow form of $SeSO_3$ have been described (7) and the colors of the solutions in sulfuric acid and oleum have frequently been attributed to S_2O_3, $SeSO_3$, and $TeSO_3$ or polymeric forms of them. The colors have also been attributed to unoxidized forms of the elements, e.g. in the form of polyatomic radicals (12).

Some quantitative measurements on the blue sulfur solutions have been published (12–17); these will be discussed in a later paper, but quantitative information on the selenium and tellurium solutions is very limited and inconclusive (12, 18).

We have recently examined the colored solutions of all three elements in the three solvents sulfuric acid, disulfuric acid, and fluorosulfuric acid: this paper reports our results and conclusions for the selenium solutions.

Experimental

Electrical Conductivity Measurements

The apparatus used has been described previously (19–21). Additions of selenium and of selenium dioxide to all three solvents were made from a weight burette: peroxydisulfuryl difluoride was added as a solution in fluorosulfuric acid from a glass syringe with a stainless steel needle.

Measurements at −86.35 °C were made by immersing the cell in a trichlorethylene slush-bath: the temperature was measured with a platinum resistance thermometer, and was reproducible to ±0.05°.

The green solutions of selenium in both H_2SO_4 and $H_2S_2O_7$ were unstable with time, undergoing a slow further oxidation to the yellow solution. Conductivity measurements were recorded over several hours and extrapolated to zero time: only one addition could therefore be made to each sample of solvent. The yellow solutions were stable.

Magnetic Susceptibility Measurements

Magnetic susceptibilities were determined by the standard Gouy method using a permanent magnet and a sample tube calibrated with standardized nickel dichloride solutions. The usual corrections for the susceptibility of the sample tube and the air displaced by the sample were applied.

Cryoscopic Measurements

The techniques for all three solvents have been described previously (21–23).

Spectrophotometric Measurements

Measurements were made in 1 cm rectangular cells with silica inserts to give path lengths from 0.1 to 1 mm, enabling comparatively concentrated solutions to be used. Optical densities were measured against a reference cell containing solvent on a Bausch and Lomb Spectronic 505 recording spectrophotometer, or on a Cary model 14 recording instrument from 240 to 700 mμ.

Materials

Selenium

Commercially available pure selenium was dried in a vacuum desiccator over P_2O_5.

Peroxydisulfuryl Difluoride

This was made by an electrolytic method similar to that described by Dudley (24): the product was condensed in the anodic compartment cold-trap, purified by trap-to-trap distillation in a vacuum line, and distilled into a weighed quantity of fluorosulfuric acid.

Selenium Dioxide

Commercially available pure selenium dioxide was purified by evaporation with fuming nitric acid, and then

Can. J. Chem. Downloaded from www.nrcresearchpress.com by 210.87.254.42 on 09/05/12
For personal use only.

sublimed in a dry atmosphere at 200 °C. The white, needle-like crystals were stored over P_2O_5 in a desiccator.

Results and Discussion

Qualitative Observations

Our qualitative observations of the reactions of selenium with the various solvents are set out below and are in general agreement with previously reported observations.

Selenium reacts with disulfuric acid at room temperature and with 100% sulfuric acid at 50–60° to form green solutions with evolution of SO_2; the disulfuric acid solutions are unstable and slowly change to yellow. These solutions produce an immediate quantitative precipitation of red Se when added to water. It is known that at much higher temperatures oxidation to SeO_2 occurs with these solvents (25, 26) and the solutions are colorless. The previously reported yellow color of solutions of SeO_2 in sulfuric acid (27) is now attributed to the presence of trace amounts of selenium impurity.

With highly purified fluorosulfuric acid selenium dissolves slowly to form a green solution. With acid containing a small quantity of SO_3 the same reaction is much more rapid, and in both cases SO_2 is evolved.

The green selenium solutions change to yellow on addition of oxidizing agents such as selenium dioxide, potassium persulfate, or peroxydisulfuryl difluoride. With SeO_2 as oxidizing agent, no further change can be effected, but an excess of the other two oxidizing agents converts the yellow solution to a colorless solution of SeO_2. Addition of a reducing agent, e.g. hydrazine sulfate, reverses these changes.

Selenium will not dissolve in 95% sulfuric acid at room temperature, but on addition of ceric sulfate the green solution is produced. Green, yellow, or colorless solutions can similarly be produced by potassium persulfate in 95% sulfuric acid. This shows that SO_3 is not essential for the production of the colored species, but that an oxidizing agent is necessary. In all cases there is clear indication of an oxidation process in the formation of the colored species from Se, and this has often been overlooked in previous interpretations.

The general conclusions to be drawn from these observations are: 1. The colored species correspond to positive oxidation states of selenium. 2. The oxidation states are less than IV, since selenium dioxide can be used as an oxidizing agent to produce them. 3. The yellow species is a higher oxidation state than the green.

Magnetic Susceptibility Measurements

The magnetic susceptibilities of both the green and yellow species were measured for 10% wt./wt. solutions of selenium in disulfuric acid. In calculating χ for the solute the relationship

$$\chi_{Se} = \frac{\chi_{solution} - \chi_{solvent} \cdot w_{solvent}}{w_{Se}}$$

was used, where w's represent weight fractions and χ's represent mass susceptibilities.

The susceptibilities per g-atom selenium were found to be -17×10^{-6} c.g.s. units for the yellow species and -12×10^{-6} c.g.s. units for the green species at 28.5 °C, i.e. both are diamagnetic.

Absorption Spectra

By studying the absorption spectra under various conditions in all three solvents it is possible to attribute to the yellow species an intense absorption with a maximum at 410 mμ and a very weak absorption at 330 mμ. The green species has peaks at 295 mμ (intense) and at 470 mμ (weak) and a broad band with a maximum at 685 mμ. Removal of any SO_2 from the solutions by pumping had no effect on the intensity of the 295 mμ peak, which cannot therefore be attributed to the 280 mμ absorption of SO_2 (17). The spectra were essentially the same in all three solvents, and Table I shows the maximum-observed extinction coefficients.[1]

TABLE I

Extinction coefficients for green and yellow species in HSO_3F, H_2SO_4, and $H_2S_2O_7$, expressed in terms of concentration in g-atom Se/liter

	ϵ		
λ (mμ)	HSO_3F	H_2SO_4	$H_2S_2O_7$
A. Yellow solutions			
410	2 120	1 920	1 850
330	170	170	170
B. Green solutions			
295	930	890	760
470	260	200	270
685	380	250	220

[1]Extinction coefficients are quoted in terms of selenium concentration in g-atom/l, although it is obvious later that monatomic selenium is not the species present in solution.

Can. J. Chem. Downloaded from www.nrcresearchpress.com by 210.87.254.42 on 09/05/12
For personal use only.

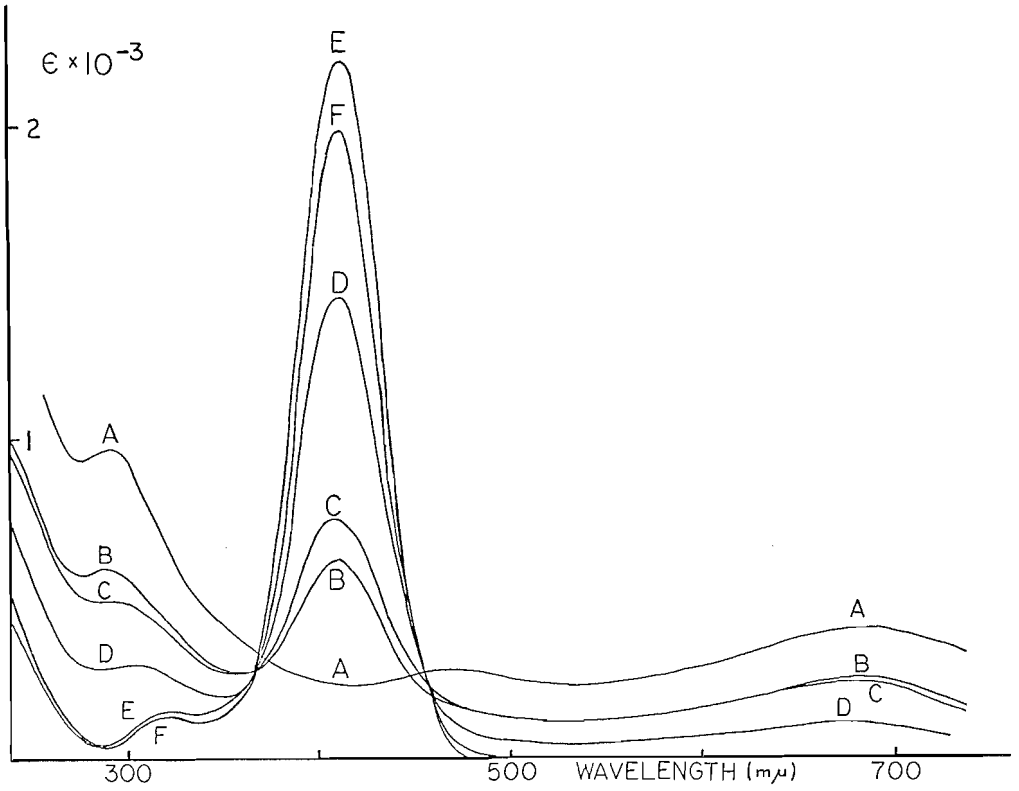

FIG. 1. Absorption spectra of $Se/S_2O_6F_2$ mixtures in HSO_3F. $Se/S_2O_6F_2$ = (A) 10.25, (B) 8.00, (C) 7.34, (D) 5.39, (E) 4.00, (F) 3.50.

Figure 1 shows the spectra of selenium in fluorosulfuric acid containing various amounts of peroxydisulfuryl difluoride; Fig. 2 shows the extinction coefficients of the various peaks as a function of the ratio of selenium to peroxydisulfuryl difluoride. The intensity of the 410 mμ peak of the yellow species reaches a clear maximum at the 4:1 $Se:S_2O_6F_2$ ratio. On adding more selenium the 410 mμ intensity decreases and that of the 295 peak increases, suggesting that the green species is formed by the reaction between the yellow species and selenium: the final solution is almost blue. However, no clear indication could be obtained of the ratio of selenium to oxidizing agent required for formation of the green species, although a solution with $Se:S_2O_6F_2$ ratio 10.25:1 showed no trace of the 410 mμ peak. It is probable that some oxidation of selenium by the solvent occurs in solutions of high selenium content, and this would complicate the interpretation.

On adding excess oxidizing agent to the yellow solution the intensity of the 410 mμ peak decreases and becomes zero at $Se:S_2O_6F_2 = 0.5:1$.

As $S_2O_6F_2$ behaves as an oxidizing agent according to

$$[1] \qquad S_2O_6F_2 + 2e \rightarrow 2SO_3F^-,$$

it is clear from the spectrophotometric data that the yellow species corresponds to an oxidation state of $+1/2$ for selenium, while the green species has an oxidation state less than this. With an excess of oxidizing agent the final product is Se^{IV}, presumably SeO_2 formed by reaction [2].

$$[2] \qquad Se + 2S_2O_6F_2 \rightarrow SeO_2 + 2S_2O_5F_2$$

An oxidation state of $+1/2$ cannot be explained in terms of the known compounds of selenium; no compounds analogous to thiosulfate, polythionates, etc. give the required oxidation state: an ion such as $Se_8O_3^{2-}$ similar to the ion $S_8O_3^{2-}$ suggested as an intermediate

Can. J. Chem. Downloaded from www.nrcresearchpress.com by 210.87.254.42 on 09/05/12
For personal use only.

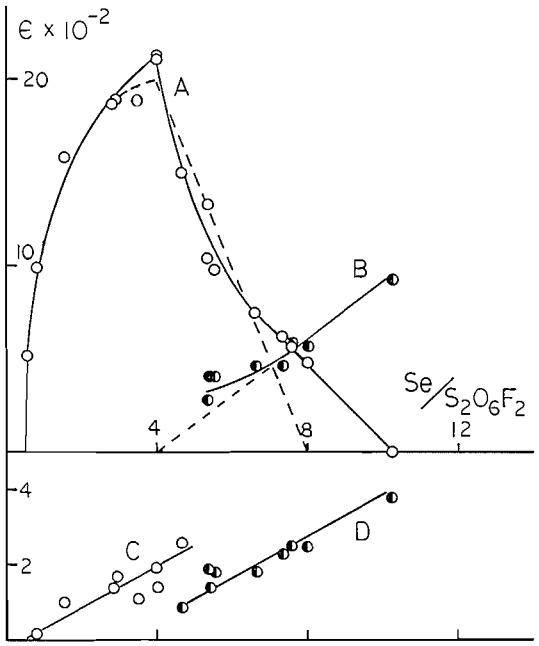

FIG. 2. Variation of intensities of peaks in the absorption spectrum with $Se/S_2O_6F_2$ ratio: A, 410 mμ; B, 295 mμ; C, 330 mμ; D, 685 mμ. (--) Calculated curves for formation of SeO_2, Se_4^{2+}, and Se_8^{2+} with ϵ_{max} (Se_4^{2+}) = 2 000.

in the reaction of sulfur with sulfite to form thiosulfate (28) would not be expected to be stable under strongly acidic conditions. More feasible are polyatomic cations of the type $Se_n^{\frac{1}{2}n+}$, e.g. Se_2^{+}, Se_4^{2+}, Se_6^{3+}, etc., similar to the ions formed by iodine under the same conditions (29) and to those formed by bismuth in melts (30–32).

Conductometric and Cryoscopic Measurements

Fluorosulfuric Acid

Conductometric measurements were carried out on 4:1 $Se:S_2O_6F_2$ solutions at 25 °C and at −86.35 °C; the results are given in Table II and Fig. 3. The solutions are conducting and a plot of "equivalent" conductance (Λ) against $\sqrt{c}$, where c is the concentration of selenium in g-atom/kg solvent, is linear, and extrapolates to a value $\Lambda_0 = 125$ at 25 °C.

The value for KSO_3F at this temperature and on the same concentration scale is 262 (20). A similar plot gave $\Lambda_0(KSO_3F) = 19.2$, $\Lambda_0(Se) = 8.8$ at −86.3 °C.

Values of γ, the number of fluorosulfate ions produced per selenium atom, were calculated by

TABLE II

Specific conductances of 4:1 $Se:S_2O_6F_2$ solutions in $HFSO_3$ at 25 °C and −86.35 °C, and of KSO_3F at −86.35°

$Se/S_2O_6F_2$		
Concentration (g-atom Se/kg)	$10^4\kappa$ (ohm^{-1} cm^{-1}) (25°)	$10^4\kappa$ (ohm^{-1} cm^{-1}) (−86.35°)
0.00	1.09	0.004
0.0189	22.43	1.55
0.0362	37.62	2.91
0.0587	65.69	4.67
0.0886	95.89	6.80
0.1201	126.40	8.90
0.1362	142.52	10.00
0.0027	3.55	0.20
0.0078	9.62	0.63
0.0177	21.12	1.47
0.0344	39.79	2.81
0.0018	2.63	0.11
0.0048	6.09	0.37
0.0092	11.43	0.77
0.0116	14.26	0.95
0.0196	23.14	1.59
0.0425	48.41	3.38
0.0718	79.13	5.53
0.0829	90.43	6.30
0.1046	111.89	7.76
0.1214	127.99	8.83
0.1445	149.58	10.27

KSO_3F (−86.35°)	
Molality	$10^4\kappa$ (ohm^{-1} cm^{-1})
0.00	0.004
0.0056	1.00
0.0155	2.74
0.0364	6.14
0.0536	8.66
0.0729	11.32
0.1056	15.21
0.1365	18.30
0.1672	20.81

the conventional method of comparing the concentrations of a strong base with that of the unknown required to produce the same conductance; values of γ of 0.47–0.45 at 25 °C and 0.45–0.48 at −86.3 °C, were obtained using KSO_3F as a reference. Values of γ were also obtained by comparing values of Λ_0 for Se and for KSO_3F; $\gamma = 0.48$ at 25 °C and $\gamma = 0.46$ at −86.3 °C. For the formation of an ion $Se_n^{\frac{1}{2}n+}$ the reaction would be

$$[3] \qquad n\mathrm{Se} + \tfrac{n}{4}S_2O_6F_2 = Se_n^{\frac{1}{2}n+} + \tfrac{n}{2}SO_3F^-.$$

For all values of n, γ would be 0.5, and the experimental values are in reasonable agreement with this.

Can. J. Chem. Downloaded from www.nrcresearchpress.com by 210.87.254.42 on 09/05/12
For personal use only.

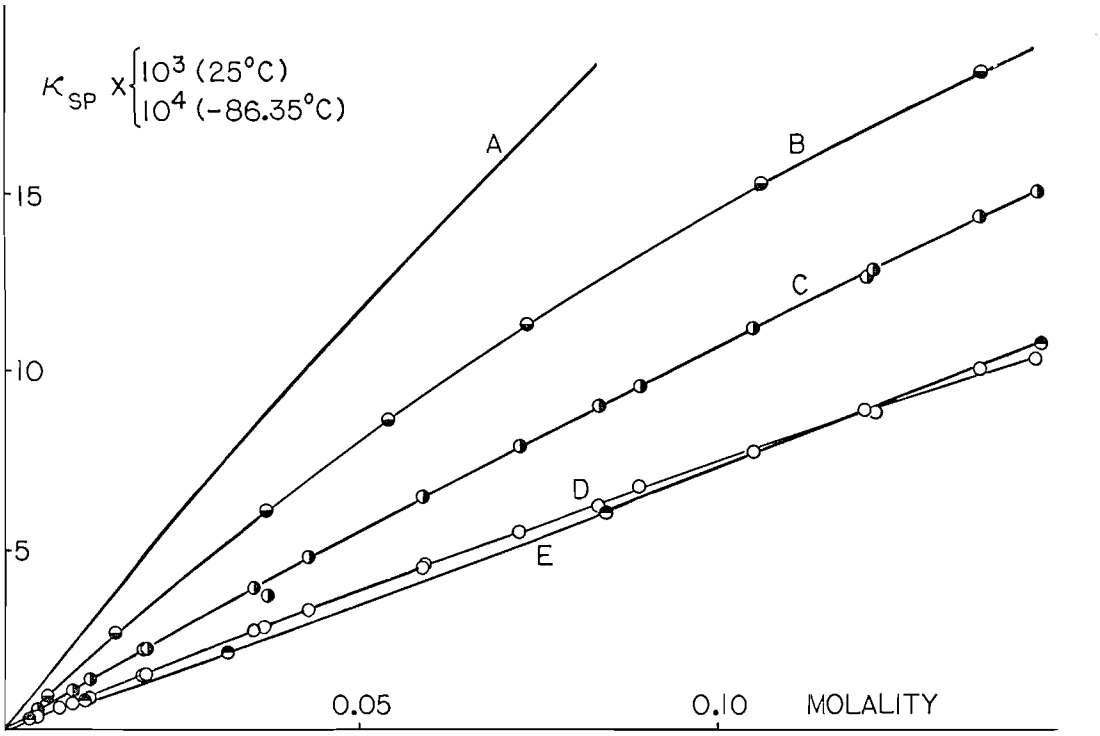

FIG. 3. Conductivities in HSO_3F at 25 °C and −86.35 °C. A, KSO_3F (25 °C). B, KSO_3F (−86.35 °C). C, 4/1 $Se/S_2O_6F_2$ solutions (25 °C). D, 4/1 $Se/S_2O_6F_2$ solutions (−86.35 °C). E, green solutions of Se in HSO_3F (25 °C).

TABLE III

Freezing points of 4:1 $Se:S_2O_6F_2$ solutions in $HFSO_3$

Concentration (g-atom Se/kg solvent)	Freezing point (°C)
0.0000	−89.019
0.02546	−89.103
0.04962	−89.140
0.06616	−89.188
0.09900	−89.294
0.12561	−89.353
0.15082	−89.439

The results of cryoscopic measurements on the 4:1 solutions are given in Table III. A value of 0.75 for ν, the number of particles produced by one atom of selenium, was obtained from the slope of the linear freezing-point concentration plot using the value of 3.93 °K $mole^{-1}$ kg^{-1} for the cryoscopic constant (23). For reaction according to eq. [3] ν would have the value $(n + 2)/2n$, and would be 0.75 for Se_4^{2+} or 0.67 for Se_6^{3+}. The observed value of ν thus strongly suggests that the Se_4^{2+} ion is formed and the less probable Se_6^{3+} ion can also be eliminated on the grounds that it would be paramagnetic, in contrast to the observed diamagnetism. Thus the reaction can be written

$$[4] \qquad 4Se + S_2O_6F_2 = Se_4^{2+} + 2SO_3F^-.$$

For a doubly charged cation the conventional method of calculating γ would not be expected to give wholly accurate results if a 1:1 electrolyte is used for comparison. Using barium fluorosulfate, $Ba(SO_3F)_2$, as a reference electrolyte γ values ranged from 0.48–0.54 at 25 °C: however, since the Ba^{2+} cation is so much smaller than a polyatomic selenium cation and since there is cryoscopic evidence that barium fluorosulfate may be incompletely dissociated in fluorosulfuric acid (33), even this comparison is somewhat imperfect. Using *o*-phenylenediamine, a strong diprotonated base (34), as reference gave γ values 0.49 ± 0.005 at 25 °C and 0.47 ± 0.01 at −86.35 °C.

Less certain information on the nature of the green species could be obtained in fluorosulfuric acid. More selenium will dissolve in the yellow

Can. J. Chem. Downloaded from www.nrcresearchpress.com by 210.87.254.42 on 09/05/12
For personal use only.

TABLE IV

Conductivities of solutions obtained by adding selenium to 4:1 $Se:S_2O_6F_2$ solution*

Ratio $Se:S_2O_6F_2$	Time after addition (h)	$10^4\kappa$ (ohm^{-1} cm^{-1})
4.000	—	142.54
4.059	1	143.00
4.315	1	144.60
	2	144.64
4.932	1	147.29
5.848	1	150.56
	16	151.13
6.888	1	154.98
7.710	1	157.46
8.276	1	159.21†
	2	161.20†
9.046	1	165.15†
	3½	168.31†
	18	170.55†
	66	171.97

*Concentration Se in original solution = 0.1362 *m*.
†Contained undissolved selenium.

solution with only a small increase in conductance. Up to a ratio $Se:S_2O_6F_2$ about 8:1 the selenium dissolves readily to produce stable green solutions; beyond this value, further selenium dissolves only very slowly and produces a marked increase in conductance (Table IV) suggesting reaction with the solvent. Both the conductivity and spectrophotometric results are consistent with a reaction of the type

$$Se_4^{2+} + mSe = Se^{2+}{}_{(4+m)}$$

and the value of m would thus appear to be about 4, i.e. the green species is probably Se_8^{2+}. This species would be expected to be diamagnetic in agreement with our experimental observations.

TABLE V

Conductivities of green solutions of selenium in HSO_3F at 25 °C

Concentration (g-atom Se/kg solvent)	$10^4\kappa$ (ohm^{-1} cm^{-1})
0.0000	1.194
0.00348	3.230
0.0114	8.894
0.0313	22.03
0.0843	61.75
0.1448	108.7

Selenium dissolves in fluorosulfuric acid to produce the green solution, but this reaction is almost eliminated by the addition of potassium fluoride and thus appears to involve oxidation by sulfur trioxide which is normally present in small amounts even in the carefully purified solvent (23). Only with acid of the highest purity is this reaction negligible. For reaction with sulfur trioxide to produce a polyatomic, doubly charged cation,

$$[5]\quad nSe + 3HSO_3F + SO_3 = Se_n^{2+} + 3SO_3F^- + H_3O^+ + SO_2,$$

the value of γ is given by $2.58/n$ (35), allowing for the hydrolysis reaction

$$H_3O^+ + SO_3F^- \rightleftarrows HF + H_2SO_4.$$

Table V and Fig. 3 show the conductivity results at 25 °C for this green solution. The conductance drifted considerably with time over a period up to 24 h as reaction [5] is relatively slow, and the results are the final, stable figures. The value of γ is 0.32 ± 0.01, which corresponds to $n = 8.1 \pm 0.3$.

Sulfuric Acid

Reaction of selenium with sulfuric acid at 50–60 °C produces the green species. Freezing points and conductivities interpolated from a larger number of measurements obtained in several experiments are given in Table VI.

For the formation of $SeSO_3$, the reaction would be

$$Se + 2H_2SO_4 = SeSO_3 + H_3O^+ + HSO_4^-$$

with values $\gamma = 1.0$ and $\nu = 3.0$. This is not in agreement with the experimental values of γ and ν and the fact that SO_2 is a known product rules out the possibility of this reaction.

For the formation of polymeric cations, Se_n^{x+}, a series of reactions can be visualized:

$$2nSe + 5xH_2SO_4 = 2Se_n^{x+} + 2xH_3O^+ + 4xHSO_4^- + xSO_2.$$

As it has a very low solubility in sulfuric acid, essentially all the sulfur dioxide formed in the above reactions is evolved from the solution, so that the expected values of γ and ν would be $2x/n$ and $(3x + 1)/n$ respectively. The observed value of $\gamma = 0.5$ shows that $x/n = 0.25$, i.e. the cation contains selenium in the $+\frac{1}{4}$ oxidation state and is of the form Se_4^+, Se_8^{2+}, Se_{12}^{3+}, etc. The ν values for these ions would be 1.0, 0.875, and 0.833 respectively, and hence the observed

TABLE VI
Conductivities and freezing point of green solutions of selenium in 100% sulfuric acid

Molality	Freezing point (°C)	θ	ν	$10^2\kappa$ (ohm^{-1} cm^{-1})	γ
0.1	9.974	0.651	0.90	1.475	0.51
0.2	9.483	1.142	0.89	2.150	0.50
0.3	8.988	1.637	0.88	2.765	0.50
0.4	8.463	2.162	0.88	3.305	0.49
0.5	7.950	2.675	0.87	—	—

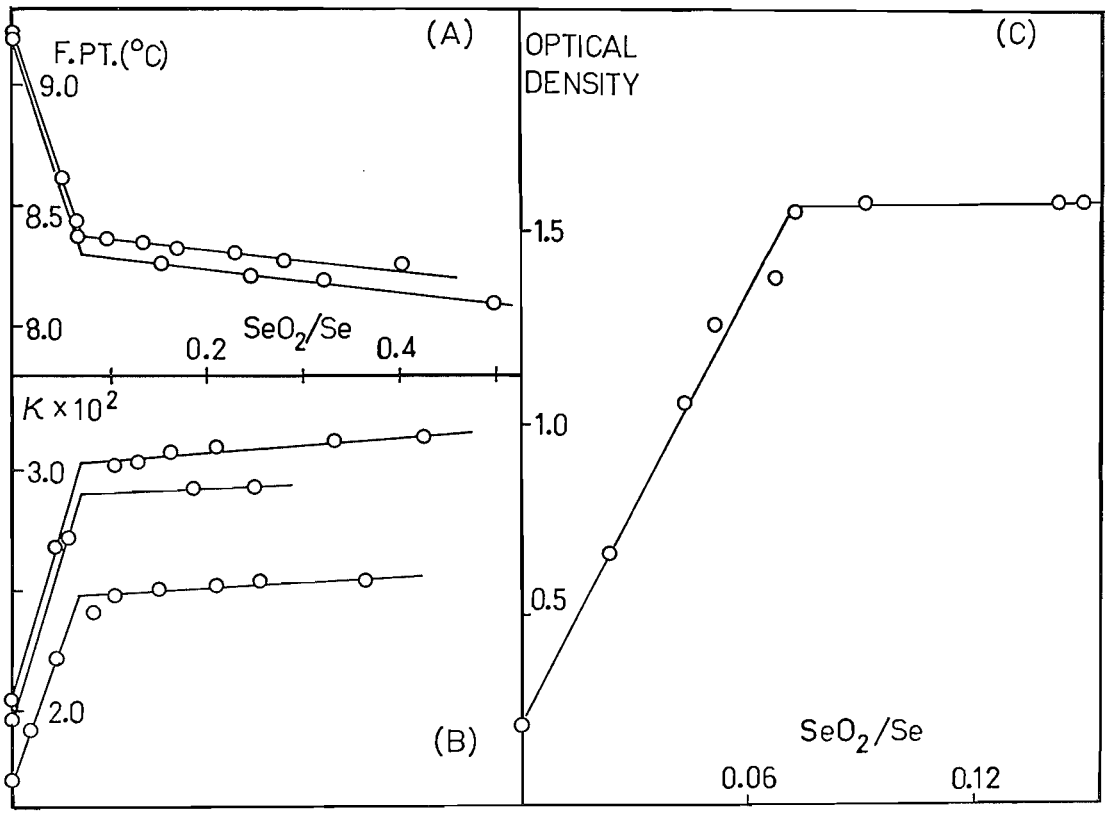

FIG. 4. Titrations of green selenium solutions with SeO_2 in H_2SO_4. A, cryoscopic titration. B, conductometric titration. C, photometric titration at 410 mμ.

value of 0.87–0.90 strongly suggests that the cation is Se_8^{2+}.

[6] $8Se + 5H_2SO_4 = Se_8^{2+} + 2H_3O^+ + 4HSO_4^- + SO_2$

The less probable Se_{12}^{3+} can also be ruled out by the magnetic measurements.

The green solution can be oxidized to the yellow solution with selenium dioxide, and Fig. 4 gives the results of conductometric, spectrophotometric, and cryoscopic titrations of the green solution. There is a clear change of slope in all cases at a ratio of $Se:SeO_2 = 1:0.07$. Beyond this end-point the changes in both conductivity and freezing point are those expected for addition of SeO_2, and the 410 mμ peak is of unchanged intensity.

On the basis of the formula Se_4^{2+} for the yellow species and Se_8^{2+} for the green, SeO_2 would be expected to oxidize $14Se(+\frac{1}{4})$ to $14Se(+\frac{1}{2})$, being itself reduced to $Se(+\frac{1}{2})$. Thus

[7] $7Se_8^{2+} + 4SeO_2 + 24H_2SO_4 = 15Se_4^{2+} + 8H_3O^+ + 24HSO_4^-$.

Can. J. Chem. Downloaded from www.nrcresearchpress.com by 210.87.254.42 on 09/05/12
For personal use only.

TABLE VII

Freezing points and conductivities at the mole ratio $SeO_2/Se = 0.071$

Moles Se	Moles SeO_2	Total moles selenium	m	Freezing point (°C)	ν	$10^2\kappa$ (ohm^{-1} cm^{-1})	γ
0.03386	0.00242	0.03628	0.2401	8.384	1.49		
0.02752	0.00196	0.02949	0.2431	8.350	1.49		
0.02400	0.00171	0.02569	0.1869			3.055	0.90
0.02618	0.00187	0.02805	0.1695			2.881	0.90
0.02482	0.00177	0.0260	0.1496			2.503	0.85
0.01443	0.00103	0.01546	0.0913			1.890	0.89
0.00894	0.00638	0.00958	0.0547			1.443	0.88

TABLE VIII

Conductivities of solutions of selenium in $H_2S_2O_7$ at 25 °C

Green solutions		Yellow solutions	
Molality × 10^2	$10^3\kappa$ (ohm^{-1} cm^{-1})	Molality × 10^2	$10^3\kappa$ (ohm^{-1} cm^{-1})
3.74	3.9521	1.90	4.0077
5.10	4.0430	3.88	4.2797
8.33	4.3010	8.05	4.9132
9.97	4.4196	10.70	5.4592
14.15	4.8163	12.10	5.7138
15.25	4.9152	19.77	6.9795
21.31	5.4054	22.33	7.4251
27.94	6.0298	27.06	8.2053
31.44	6.3501	34.52	9.4033
38.52	6.9377	41.26	10.4095
50.57	7.9517	45.21	11.0310
57.99	8.5674	47.71	11.4273
		54.82	12.3750
		57.40	12.7692
		63.52	13.4172

TABLE IX

Freezing points of solutions of selenium in $H_2S_2O_7$

Green solutions		Yellow solutions	
$10^2\ m$	Freezing point (°C)	$10^2\ m$	Freezing point (°C)
4.52	35.05	3.03	35.01
9.36	34.97	8.72	34.79
20.16	34.77	11.39	34.68
28.86	34.57	14.84	34.51
36.55	34.38	19.68	34.25
48.24	34.03	25.12	33.92
58.05	33.66	31.67	33.43
		37.22	33.07
		44.51	32.49
		53.42	31.72

Can. J. Chem. Downloaded from www.nrcresearchpress.com by 210.87.254.42 on 09/05/12
For personal use only.

Can. J. Chem. Downloaded from www.nrcresearchpress.com by 210.87.254.42 on 09/05/12
For personal use only.

The calculated ratio SeO_2:Se at the equivalence point is 1:14 or 0.071:1, in excellent agreement with the observed value.

From the freezing points and conductivities of the end-point solutions in these titrations the values of γ and ν given in Table VII were obtained. The equation for the overall reaction is obtained by combining eqs. [6] and [7],

[8] $$56Se + 59H_2SO_4 + 4SeO_2 = 15Se_4^{2+} + 22H_3O^+ + 52HSO_4^- + 7SO_2,$$

hence the expected values for γ and ν are 0.87 and 1.48 respectively. The experimental results are in good agreement with these values and thus provide support for both the proposed species Se_8^{2+} and Se_4^{2+}.

Disulfuric Acid

Both green and yellow solutions of selenium can be obtained in disulfuric acid at room temperature. The green solutions are not very stable and on long standing (2–3 weeks) become oxidized to yellow solutions. The conductivity and the freezing points of the green solutions at first drift rapidly, but change only slowly after 12–14 h. The method for obtaining the conductivity and freezing point data for the green species by extrapolating to zero time has already been discussed. The yellow solutions are stable and their freezing points and conductivities do not change with time. The yellow solutions were prepared by keeping the green solutions at 60° for several hours. The conductivity results are given in Table VIII and the cryoscopic results are in Table IX. It is not possible to calculate values of ν and γ from the results of cryoscopic and conductimetric measurements in disulfuric acid in the same straightforward manner as for sulfuric and fluorosulfuric acid, mainly because of the extensive solvent self-dissociation. The mode of ionization of a solute is best established by comparison of the observed freezing point and conductivity curves with "theoretical curves" constructed from the results obtained with certain reference solutes (21). In Figs. 5 and 6 the results for the green solutions are compared with the predicted curves for a solute ionizing according to eq. [9].

[9] $$nS \rightarrow A^{2+} + 2HS_3O_{10}^- + 5H_2SO_4 + B,$$

where $n = 4$ and 8 and B is a nonelectrolyte.

The good agreement between the observed and "theoretical" curves clearly establishes that the

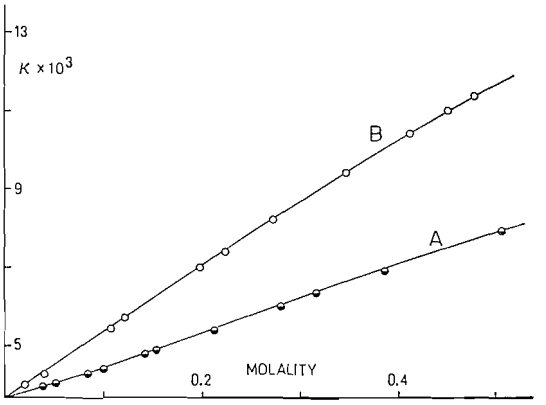

FIG. 5. Conductivities of selenium solutions in disulfuric acid at 25 °C. The curves are calculated for a solute ionizing according to eq. [9] with $n = 8$ (Curve A) and $n = 4$ (Curve B). ◒ Experimental points for green solutions of selenium. ○ Experimental points for yellow solutions of selenium.

overall reaction to produce the green solution is

[10] $$8Se + 6H_2S_2O_7 \rightarrow Se_8^{2+} + 2HS_3O_{10}^- + 5H_2SO_4 + SO_2.$$

Sulfur dioxide is very soluble in disulfuric acid and behaves as a nonelectrolyte (21).

The amount of sulfuric acid formed was determined by cryoscopic titration with SO_3. The freezing point rises, passes through a maximum, and then decreases on addition of SO_3. The titration exhibits a maximum in freezing point at molar ratio $SO_3/Se = 0.7$, which suggests that selenium is reacting according to eq. [10], for which the expected value is $5/8 = 0.63$. The somewhat high experimental value is probably explained by partial reaction to Se_4^{2+}, which involves formation of more H_2SO_4 per gram atom of Se. The rise in the freezing point also agrees with the formation of 5 moles of H_2SO_4 from 8 moles of selenium according to the above equation.

Comparison of the freezing points and conductivities of the yellow solutions with the "theoretical" curves in Figs. 5 and 6 establishes that the overall reaction can be represented by the equation

[11] $$4Se + 6H_2S_2O_7 \rightarrow Se_4^{2+} + 2HS_3O_{10}^- + 5H_2SO_4 + SO_2.$$

The amount of sulfuric acid formed was determined by cryoscopic titration with SO_3; the end-point occurs at $SO_3/Se = 1.3$, which agrees

Can. J. Chem. Downloaded from www.nrcresearchpress.com by 210.87.254.42 on 09/05/12
For personal use only.

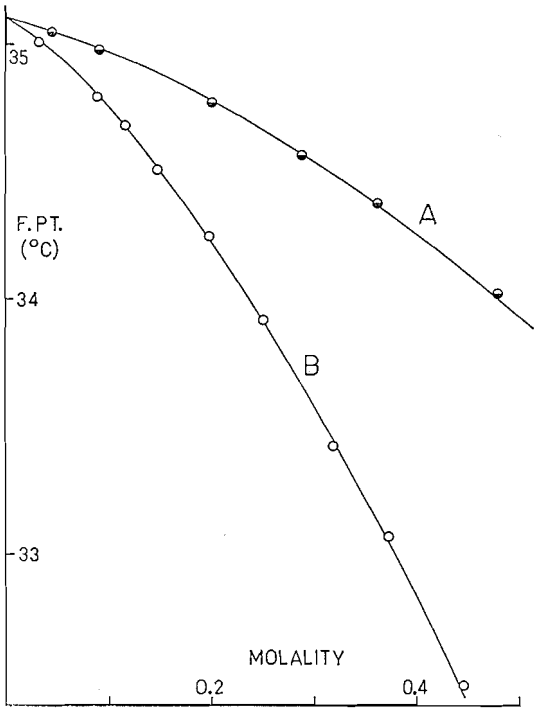

FIG. 6. Freezing points of selenium solutions in disulfuric acid. The curves are calculated for a solute ionizing according to eq. [9] with $n = 8$ (Curve A) and $n = 4$ (Curve B). ◒ Experimental points for green solutions of selenium. ○ Experimental points for yellow solutions of selenium.

well with the value of $5/4 = 1.25$ expected for reaction according to eq. [11].

Conclusions

Our results show conclusively that the yellow species in solutions of selenium in strongly acidic solvents is Se_4^{2+} and the corresponding green species is Se_8^{2+}. We could find no evidence of other similar species in the solutions, the product of further oxidation of Se_4^{2+} being Se^{IV}. Our results cannot be explained in terms of formation of $SeSO_3$ or in terms of uncharged radicals. The compound analyzing as $SeSO_3$ seems well-established, but we feel that this is most unlikely to represent the true structure. In view of the fact that this compound is produced by reaction of Se with SO_3 in the presence of traces of water, a formulation such as $Se_4^{2+}.S_4O_{13}^{2-}$, with a very similar analysis, would seem more acceptable. We hope to be able to report more conclusively on this point at a later date. Solid compounds which appear to contain the Se_4^{2+} cation have been isolated from the fluorosulfuric acid and oleum solutions. The composition and structure of these compounds is under investigation. We are not able to assign structures to either Se_4^{2+} or Se_8^{2+} but structural investigations are being undertaken.

Acknowledgment

We thank the National Research Council of Canada for financial support of this work.

1. M. H. KLAPROTH. Phil. Mag. **1**, 78 (1798).
2. G. MAGNUS. Ann. Physik, [2] **10**, 491 (1827); [2] **14**, 328 (1828).
3. N. W. FISCHER. Ann. Physik, [2] **12**, 153 (1828); [2] **15**, 77 (1829); [2] **16**, 118 (1829).
4. J. W. MELLOR. Comprehensive treatise on inorganic and theoretical chemistry. Longmans, Green and Co., London. 1930. Vol. 10. pp. 184–186, 922; Vol. 11. pp. 116–117.
5. F. C. VOGEL. J. für Chemie u. Physik, **4**, 121 (1812).
6. R. WEBER. J. Prakt. Chem. **133**, 218 (1882).
7. E. DIVERS and M. SHIMOSE. J. Chem. Soc. **43**, 329 (1883); **45**, 194, 201 (1884).
8. I. VOGEL and J. R. PARTINGTON. J. Chem. Soc. **127**, 1514 (1925).
9. R. WEBER. Ann. Physik, [2] **156**, 531 (1875).
10. E. DIVERS and M. SHIMOSE. J. Chem. Soc. **43**, 319, 323 (1883).
11. J. J. DOOLAN and J. R. PARTINGTON. J. Chem. Soc. **125**, 1402 (1924).
12. R. AUERBACH. Z. Physik. Chem. Leipzig, **121**, 337 (1926).
13. J. AROTSKY and M. C. R. SYMONS. Trans. Faraday Soc. **56**, 1426 (1960).
14. J. R. BRAYFORD and P. A. H. WYATT. Trans. Faraday Soc. **52**, 642 (1956).
15. B. DACRE and P. A. H. WYATT. Trans. Faraday Soc. **57**, 1958 (1961).
16. H. LUX and E. BOHM. Chem. Ber. **98**, 3210 (1965).
17. M. C. R. SYMONS. J. Chem. Soc. 2440 (1957).
18. E. MOLES. Anales Real Soc. Espan. Fis. Quim. Madrid, **13**, 134 (1915).
19. R. J. GILLESPIE, J. V. OUBRIDGE, and C. SOLOMONS. J. Chem. Soc. 1804 (1957).
20. J. BARR, R. J. GILLESPIE, and R. C. THOMPSON. Inorg. Chem. **3**, 1149 (1964).
21. R. J. GILLESPIE and K. C. MALHOTRA. J. Chem. Soc. In press.
22. R. J. GILLESPIE, E. D. HUGHES, and C. K. INGOLD. J. Chem. Soc. 2473 (1950).
23. R. J. GILLESPIE, J. B. MILNE, and R. C. THOMPSON. Inorg. Chem. **5**, 468 (1966).
24. F. B. DUDLEY. J. Chem. Soc. 3407 (1963).
25. L. S. GETSKIN and V. V. YATSUK. Zh. Prikl. Khim. **35**, 2546 (1962).
26. E. SHULEK and L. BARCZA. Acta Chim. Acad. Sci. Hung. **37**, 351 (1963).
27. R. H. FLOWERS, R. J. GILLESPIE, and E. A. ROBINSON. J. Inorg. Nucl. Chem. **9**, 155 (1959).
28. M. SCHMIDT and H. HEINRICH. Angew. Chem. **70**, 572 (1958).
29. R. A. GARRETT, R. J. GILLESPIE, and J. B. SENIOR. Inorg. Chem. **4**, 563 (1965). R. J. GILLESPIE and J. B. MILNE. Inorg. Chem. **5**, 1577 (1966).

30. L. E. TOPOL, S. J. YOSIM, and R. A. OSTERYOUNG. J. Phys. Chem. **65**, 1511 (1961).
31. C. R. BOSTON, G. P. SMITH, and L. C. HOWICK. J. Phys. Chem. **67**, 1849 (1963). N. J. BJERRUM, C. R. BOSTON, G. P. SMITH, and H. L. DAVIS. Inorg. Nucl. Chem. Letters, **1**, 141 (1965). N. J. BJERRUM and G. P. SMITH. Inorg. Nucl. Chem. Letters, **3**, 165 (1967).
32. A. HERSHAFT and J. D. CORBETT. Inorg. Chem. **2**, 979 (1963). J. D. CORBETT. Inorg. Nucl. Chem. Letters, **3**, 173 (1967).
33. R. J. GILLESPIE and R. C. THOMPSON. Unpublished.
34. J. BARR and R. J. GILLESPIE. Unpublished.
35. R. J. GILLESPIE, J. B. MILNE, and J. B. SENIOR. Inorg. Chem. **5**, 1233 (1966).

Can. J. Chem. Downloaded from www.nrcresearchpress.com by 210.87.254.42 on 09/05/12
For personal use only.

Can. J. Chem. Downloaded from www.nrcresearchpress.com by 210.87.254.42 on 09/05/12
For personal use only.

Catalytic hydrogenation of allene

R. S. MANN AND D. E. TO
Department of Chemical Engineering, University of Ottawa, Ottawa, Canada

Received June 1, 1967

The reaction between allene and hydrogen over pumice-supported metals of the eighth group has been investigated in a constant volume reactor for a wide range of temperature and reactant ratios. The shape of the pressure–time curves were found to be dependent upon the reactant ratios and their order of admission. The reaction over nickel–pumice is principally a selective formation of propylene with small yields of propane and reduced polymers of allene. The orders of hydrogenation reaction are first, or slightly higher, and zero with respect to hydrogen and allene respectively. The apparent activation energies for Pd, Pt, Co, Fe, Ni, Rh, Ir, Ru, and Os are 13, 17.4, 10.8, 9.4, 7.8, 9.6, 5.3, 3.0, and 4.6 kcal/mole respectively. The catalytic activities of the metals are in the sequence

$$Pt > Pd > Rh > Ir > Ni > Co > Fe > Ru > Os.$$

While selectivity was found to decrease with increasing initial hydrogen pressures, it increased with increasing temperatures.

Canadian Journal of Chemistry, **46**, 161 (1968)

Introduction

Though several papers have appeared in the last 30 years describing the kinetics of catalytic hydrogenation of olefins and alkynes, very little work has been reported about the kinetics of the hydrogenation of allene over metal catalysts. Bond and Sheridan (1) studied the hydrogenation of allene over pumice-supported nickel, palladium, and platinum catalysts. The order of reactions were found to be one and about zero with respect to hydrogen and allene respectively. Kistiakowsky and co-workers (2) hydrogenated allene with a large excess of hydrogen. They did not specify the catalyst used. Recently Bond and co-workers (3) have reported about the selectivities observed in the first stage of the reaction, for alumina-supported ruthenium, rhodium, osmium, iridium, and platinum catalysts. No mention has been made about the effect of reactant ratios and temperature on the selectivity.

This paper describes a detailed study of the kinetics of allene hydrogenation over pumice-supported metals of the eighth group and the effect of the various experimental variables upon the selectivity of the reaction in presence of nickel–pumice catalyst.

Experimental

The apparatus, materials, and experimental techniques used were the same as reported by Mann and Naik (4) for methylacetylene hydrogenation. All catalysts, except osmium, were prepared by impregnating and evaporating solutions containing the calculated weight of Analar grade chemicals, in presence of pumice. While iron, cobalt, and nickel catalysts were prepared from their nitrates, ruthenium, rhodium, palladium, and platinum were prepared from their chlorides. Iridium catalyst was prepared from iridic ammonium chloride. Osmium catalyst was prepared by adding the required amount of aqueous solution of ammonium chlorosmate to the pumice granules, and the mixture kept in a warm water bath, while being dried by a stream of nitrogen.

The reactions were followed by measuring the pressure fall using a mercury manometer. The product compositions were obtained by gas chromatography using a Fisher gas partitioner, mounted on the top of a model 27 Fisher thermal stabilizer maintained at 30 °C. A 14 ft long 30% hexamethyl phosphoramide on 60–80 mesh Fisher Columpak and 8 ft long 30–60 mesh activated 13 X molecular sieve columns were used to separate allene, propylene, propane, and hydrogen. Helium at the rate of 70 mm/min at a pressure of 20 p.s.i.g. was used as the carrier gas.

Results and Discussions

(a) Pressure–Time Curves

The pressure drop – time curves observed in the hydrogenation of allene over metal catalysts were found to be dependent upon (i) initial hydrogen/allene ratios and (ii) the order of admission of reactants. Type I pressure time curves (4, 5) almost invariably resulted when allene was admitted first into the reaction vessel, provided that the initial hydrogen/allene ratio was greater than about two. Type III curves were always obtained, regardless of the order of admission of the reactants into the reaction vessel, provided that hydrogen/allene ratio was smaller than about two. The inflection point, $-\Delta p_\alpha$, was found to increase with increased hydrogen pressures. The pressure–time curves

obtained for allene hydrogenation over nickel at 75 °C for several hydrogen/allene ratios ($\bar{R}$) are shown in Fig. 1.

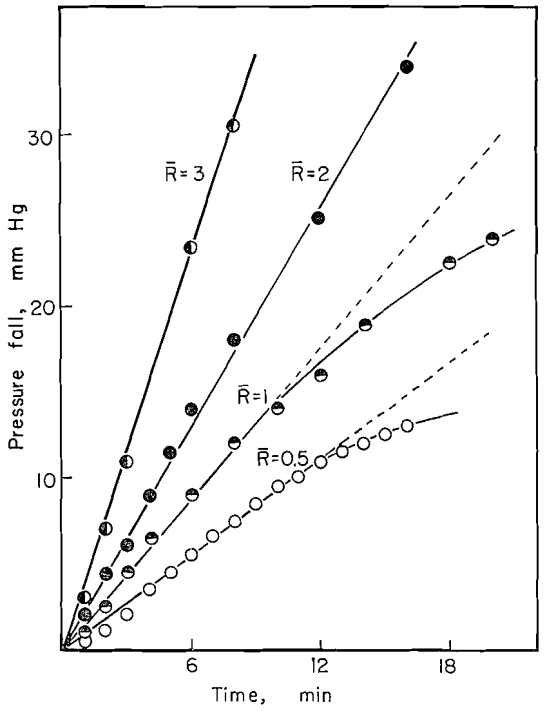

FIG. 1. Pressure–time curves of different initial H_2/C_3H_4 ratios, $\bar{R}$, for nickel–pumice catalyst at 75 °C using $P_{C_3H_4} = 60 \pm 1$ mm Hg.

(b) Orders of Reaction with Respect to Hydrogen and Allene

Using a fixed allene pressure of 60 mm, and a wide range of hydrogen pressures (30–300 mm), orders in hydrogen were determined at several temperatures. Similarly the order of reaction with respect to allene was obtained by using 60 mm hydrogen and varying the allene pressures between 30 and 300 mm. The dependence of initial rates upon the initial pressures of hydrogen and allene over nickel–pumice catalysts at 75 and 90 °C is shown in Fig. 2.

The orders of reaction with respect to hydrogen (n) and allene (m) are given in Table I for the metal catalysts. While the orders with respect to allene were zero and almost independent of temperature, the order of reaction with respect to hydrogen varied between 0.8 and 1.6, and

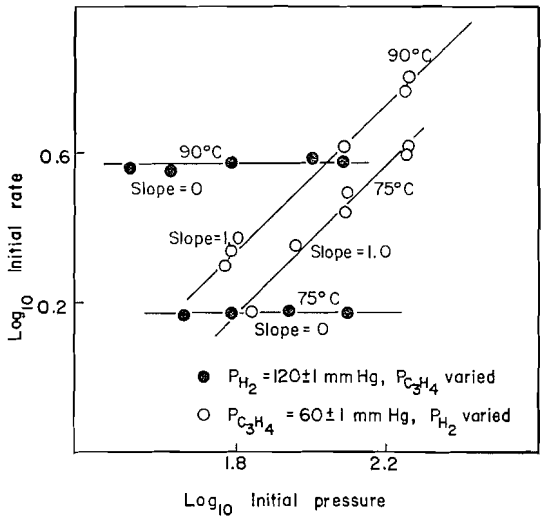

FIG. 2. Dependence of initial rates upon initial pressures of hydrogen and allene over nickel–pumice at 75 and 90 °C.

increased very slightly with increasing temperatures.

(c) Activation Energy

Plots of $\log_{10}$ specific reaction rates against the absolute temperature were very good straight lines over a wide range of temperatures. The derived apparent activation energies for group VIII metals are given in Table I.

(d) Compensation Effect

A "compensation effect" (6) was observed to exist among various catalysts tested. A plot of $\log_{10} A_l$ against apparent activation energy for these catalysts gave a straight line, giving the relation

$$\log_{10} A_l = 0.81\, E_l - 2.0.$$

(e) The Effect of Experimental Variables upon Selectivity for Nickel–Pumice Catalyst

Selectivity (S) is defined as the ratio of propylene to propylene plus propane, $P_{\text{propylene}}/(P_{\text{propylene}} + P_{\text{propane}})$. Propylene, propane, and some polymers were observed as initial products of the reaction under all conditions studied, propylene being the major product.

(i) Dependence of Selectivity upon Pressure Fall

The dependence of selectivity upon pressure fall and the course of reaction were investigated for various hydrogen/allene ratios between 40

Can. J. Chem. Downloaded from www.nrcresearchpress.com by 210.87.254.42 on 09/05/12
For personal use only.

TABLE I

Orders of reaction and activation energies for catalysts

Catalyst	Temperature range (°C)	Average order		Activation energy (kcal/mole)
		m	*n*	
Pd	21–40	0	1.03±0.06	13. ±0.2
Pt	112–147	0	1.04±0.04	17.4±0.2
Co	104–126	0	1.05±0.05	10.8±0.2
Fe	74–114	0	1.53±0.12	9.4±0.2
Ni	40–130	0	1.0 ±0.08	7.8±0.2
Rh	42–63	0	0.82±0.02	9.6±0.2
Ir	25–45	0	1.05±0.03	5.3±0.2
Ru	81–145	0	1.38±0.03	3.0±0.2
Os	125–200	0	0.90±0.03	4.6±0.2

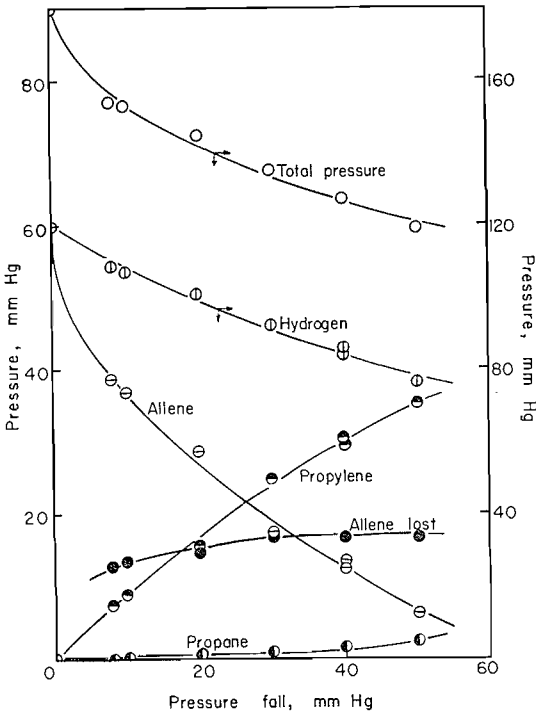

FIG. 3. Course of reaction over nickel–pumice at 75 °C.

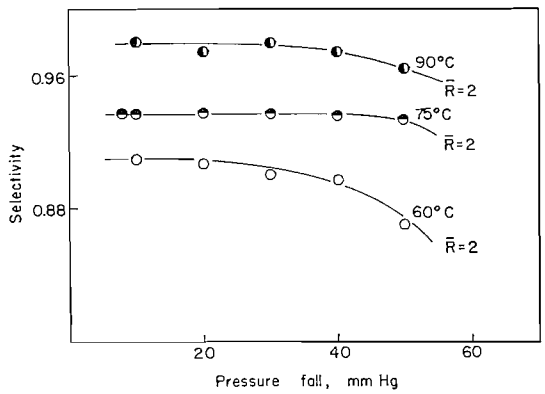

FIG. 4. Dependence of selectivity upon pressure falls using initial H_2/C_3H_4, $\bar{R}$, equal to 2.

and 100 °C. The course of the reaction was followed by means of an analysis of the reaction products for various reactant ratios for different pressure falls. With an initial hydrogen/allene ratio of 2 at 75 °C, the main initial reaction is the selective formation of propylene with relatively little propane (Fig. 3). The selectivity was fairly constant (Fig. 4) till the pressure had fallen by about 45 mm, when it started dropping rapidly with further pressure falls. The dependence of selectivity on pressure fall at several temperatures is shown in Fig. 4.

(ii) Dependence of Selectivity upon Initial Pressures of Hydrogen and Allene

The dependence of selectivity on the initial hydrogen pressures was studied between 40 and 100 °C. While initial allene pressure was kept constant at 60 mm, the pressure of hydrogen was varied between 60 and 300 mm. The products were analyzed when the total pressure fall was equal to 40 mm. Selectivity decreased with increasing hydrogen pressures, and all the curves were concave towards the origin over the entire range of temperature and pressures studied (Fig. 5). It was found that for a particular hydrogen/allene ratio, higher selectivities could be achieved by increasing the reaction temperature. No significant variation in the selectivity

Can. J. Chem. Downloaded from www.nrcresearchpress.com by 210.87.254.42 on 09/05/12
For personal use only.

TABLE II

Dependence of selectivity upon temperature ($P_{H_2} = 180 \pm 1$ mm; pressure fall = 30 mm; $P_{C_3H_4} = 60 \pm 1$ mm)

Temp. (°C)	Pressure of product stream (mm) H_2	C_3H_8	C_3H_6	C_3H_4	Allene lost (polymer) (mm)	Selectivity (S)
40	123	3	16	20	21.5	0.842
60	110	2.5	16	15.1	26.4	0.865
75	140	0.9	18	13.5	26.4	0.952
90	150	0.8	20	14.0	25.2	0.961
100	132	0.8	19.9	14.5	25.8	0.962
115	138	0.7	18.0	14.5	26.8	0.962
130	135	0.7	18.0	13.5	27.8	0.962

TABLE III

Comparison of results of present investigations with those of Bond and Sheridan

	Present results			Bond and Sheridan		
Type of catalyst studied	Pu–Ni	Pu–Pd	Pu–Pt	Pu–Ni	Pu–Pd	Pu–Pt
Type of P–t curves	1+III	III	1+III	—	—	—
Temperature range (°C)	40–130	21.5–40	112–147	0–114	89–197	48–173
Order with respect to H_2	1±0.08	1.03±.06	1.04±.04	1	1	1
Order with respect to C_3H_4	0	0	0	0	0	0
Activation energy (kcal/mole)	7.8±.2	13.00±.2	17.4±.2	12.9±.5	12.3±.5	17.1±.5

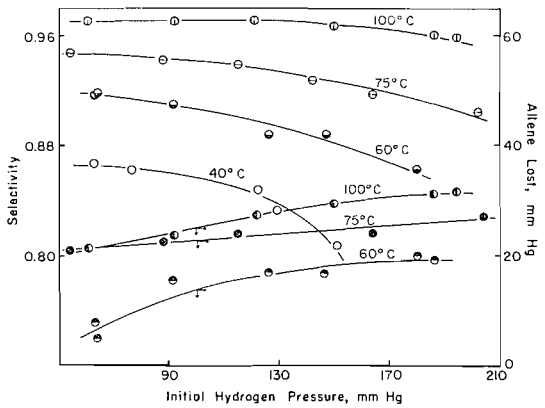

FIG. 5. Dependence of selectivity and hydrocarbon lost (polymers) on initial H_2/C_3H_4 ratios.

with increasing allene pressure was observed at 90 °C. Figure 6 shows the effect of allene pressures on the polymer formation. The amount of polymers formed (allene lost) increased with allene pressures, giving almost a linear relationship in the lower allene pressure ranges.

(iii) Dependence of Selectivity upon Temperature

The temperature dependence of the selectivity for a hydrogen/allene ratio of 3 was studied between 40 and 130 °C. The products were analyzed for a total pressure fall of 30 mm. The results are given in Table II. Selectivity increased very rapidly in the lower temperature (40–75 °C) and subsequently levelled off at higher temperatures (100–130 °C).

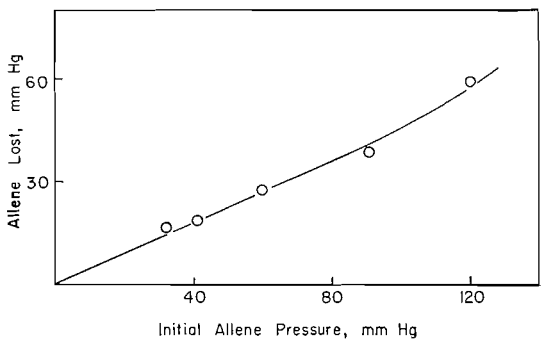

FIG. 6. Dependence of polymers on initial allene pressure at $P_{H_2} = 120 \pm 1$ mm Hg and total pressure fall of 25 mm Hg.

(f) Comparison with the Results of Previous Investigators and General Discussions

Bond and Sheridan (1) studied the kinetics of hydrogenation of allene over pumice-supported nickel, palladium, and platinum catalysts only.

Can. J. Chem. Downloaded from www.nrcresearchpress.com by 210.87.254.42 on 09/05/12
For personal use only.

Can. J. Chem. Downloaded from www.nrcresearchpress.com by 210.87.254.42 on 09/05/12
For personal use only.

A comparison of our results with those of Bond and Sheridan is given in Table III.

No comparison could be made for other catalysts besides platinum, palladium, and nickel, since no published data are available. Bond and Sheridan (1) do not give any information about the shape of the pressure–time curves they obtained for allene hydrogenation and hence no direct comparison of the pressure–time curves obtained in this investigation can be made with their work.

The activation energies for platinum and palladium were nearly the same as obtained by Bond and Sheridan. However, the activation energy for nickel is much lower. There was no sign of a fall in the energy of activation of allene hydrogenation even at higher temperature.

The use of higher partial pressures of hydrogen tended to slightly enhance the activity of the catalysts reversibly, while higher partial pressures of allene often poisoned the catalyst reversibly thus suppressing its catalytic acitivity. It was also noticed that under similar conditions slightly higher rates were obtained by admitting hydrogen first into the reaction vessel rather than allene.

Though Bond and Sheridan (1) studied the general course of reaction for hydrogen/allene ratio of 1:1 at 66 and 73 °C, and the effect of reactant ratios on the yield of propylene and propane at 74 °C, they did not study the dependence of selectivity on temperature for various reactant ratios and the effect of reactant ratios on the selectivity and polymer formation. In the present investigations, the general characteristics and product analysis of allene hydrogenation on nickel between 40 and 100 °C were found to be similar to those obtained by Bond and Sheridan. While following the course of reaction for allene hydrogenation in a 1:1 ratio at 100 °C, we found that the formation of propylene ranged from 35 to 40 times that of propane, as compared with Bond and Sheridan, who reported the formation of propylene to be 14 times that of propane.

Selectivity increased with increasing temperature in the lower temperature range (40–75 °C) and then at higher temperatures (100–140 °C) subsequently levelled off. This is very similar to the observation of Bond and Turkevitch (7), who noted that the rate of propylene exchange on platinum increased relative to the rate of deuteration as the temperature was raised. This is probably due to a decrease in the surface coverage of hydrogen as the temperature is raised.

The reaction in almost all respects closely resembles the acetylene–hydrogen reaction. This similarly suggests that the mechanism of reaction is essentially the same as that proposed for acetylene hydrogenation by Bond and Wells (8).

The zero or slightly negative order in allene and the positive order in hydrogen show that allene is more strongly adsorbed on the catalyst surface. Bond and Sheridan (9), while studying the hydrogenation of a mixture of hydrocarbons, found that allene was more strongly adsorbed than propylene. Added propylene did not show appreciable effect on the hydrogenation of allene. These results support the theory of associative adsorption. The very high selectivity observed in the present investigation also supports the associative adsorption of allene, and a Twigg-type (10) associative mechanism for the hydrogenation, involving the addition of hydrogen in two steps.

The similarities between acetylene hydrogenation and allene hydrogenation suggests that the mechanism of allene hydrogenation is one in which gaseous allene and hydrogen are adsorbed on the surface of the catalyst to form the half-hydrogenated state $H_2C{=}\overset{*}{\underset{*}{C}}{-}CH_3$, which in turn is further hydrogenated to form gaseous propylene or isomerizes to form a free radical $H_2\overset{*}{C}{-}\overset{*}{C}{-}CH_3$. The radical either reacts further with adsorbed hydrogen ($\overset{*}{H}$) to form adsorbed propylene, which is hydrogenated further to propane or combines with adsorbed allene to form polymers.

The small amount of propane that is formed is attributed to the further hydrogenation of adsorbed propylene. The longer the propylene remains adsorbed on the surface, the greater will be its chance of undergoing further hydrogenation and isomerization, thus causing a reduction in the selectivity.

Acknowledgments

The authors are grateful to the Chemical Society, London, and Esso (Imperial Oil Company of Canada) for the award of a grant (to R. S. M.) and the National Research Council of Canada for a bursary (to D. E. T.).

1. G. C. BOND and J. SHERIDAN. Trans. Faraday Soc. **48**, 658 (1952).
2. G. B. KISTIAKOWSKY, J. R. RUHROFF, H. A. SMITH, and W. E. VAUGHAM. J. Am. Chem. Soc. **58**, 146 (1936).
3. G. C. BOND, G. WEBB, P. B. WELLS, and J. M. WINTERBOTTOM. J. Catalysis, **1**, 74 (1964).
4. R. S. MANN and S. C. NAIK. Can. J. Chem. **45**, 1023 (1967).
5. G. C. BOND. J. Chem. Soc. 2075 (1958).
6. E. CREMER. Advan. Catalysis, **7**, 77 (1955).
7. G. C. BOND and J. TURKEVICH. Trans. Faraday Soc. **49**, 281 (1953).
8. G. C. BOND and P. B. WELLS. Advan. Catalysis, **15**, 91 (1965).
9. G. C. BOND and J. SHERIDAN. Trans. Faraday Soc. **48**, 664 (1952).
10. G. H. TWIGG. Discussions Faraday Soc. **8**, 152 (1950).

Can. J. Chem. Downloaded from www.nrcresearchpress.com by 210.87.254.42 on 09/05/12
For personal use only.

Can. J. Chem. Downloaded from www.nrcresearchpress.com by 210.87.254.105 on 09/05/12
For personal use only.

Reflectance spectroscopic determination of cobalt, nickel, and copper with pyridine-2-aldehyde-2-quinolylhydrazone[1]

R. W. Frei, R. Liiva, and D. E. Ryan
Department of Chemistry, Dalhousie University, Halifax, Nova Scotia

Received July 25, 1967

Nickel, cobalt, and copper are separated from interfering metals by thin-layer chromatography on silica gel and cellulose layers. The metals are sprayed with pyridine-2-aldehyde-2-quinolylhydrazone solution and determined by diffuse reflectance spectroscopy. Under optimum conditions, 0.01 μg per spot can be determined easily and with good reproducibility.

Canadian Journal of Chemistry, 46, 167 (1968)

Compounds capable of behaving as tridentate chelating agents can be selective in their reactions with metal ions; a number of such compounds (substituted hydrazones) were described in an earlier paper (1). One of these, pyridine-2-aldehyde-2-quinolylhydrazone (PAQH), has been used to develop sensitive and highly selective spectrophotometric methods for palladium, nickel, and cobalt (2, 3). PAQH gives visible colors with nine metal ions but, by combining PAQH with chromatographic techniques, it was hoped to take advantage of the high sensitivity of the reagent and to simultaneously determine nickel, cobalt, and copper without interference. Diffuse reflectance spectroscopy was used previously (4) in a quantitative investigation of the rubeanic acid complexes of cobalt, copper, and nickel adsorbed on thin-layer chromatographic (t.l.c.) adsorbents. In this study the suitability of PAQH as a spray reagent for cobalt, copper, and nickel (after thin-layer chromatographic separation of these ions) has been investigated by the same technique.

Experimental

Reagents

Stock solutions containing 1 g metal per liter of solution were prepared from reagent grade chlorides. PAQH was prepared as previously described (1) and the reagent solution was 0.03% w/v in ethanol. Thin-layer chromatographic grade silica gel G from "Merck" Darmstadt with particle size of 10–40 μ maximum and containing 15% plaster of paris as a binder was used. The cellulose layers were made from MN cellulose 300 manufactured by Macherey, Nagel and Co., Dueren, Germany, without binder and with a particle size of 10 μ maximum. The solvent systems for the chromatographic separation were described in a previous paper (4) and consisted of 0.5% concentrated hydrochloric acid (specific gravity, 1.19) in acetone for silica gel plates and a freshly prepared mixture of methylethylketone : concentrated hydrochloric acid : water in the ratio 15:3:2 by volume for cellulose plates.

Apparatus

Diffuse reflectance spectra and transmission spectra were measured with a Bausch and Lomb Spectronic 505 recording spectrophotometer equipped with the standard reflectance attachment for the ultraviolet and visible regions; barium sulfate plates made with a powder press were used as reference standards. Quantitative photometric studies were done with a Beckman DU spectrophotometer, equipped with a reflectance attachment, at wavelength settings determined previously from the reflectance spectra. The cells used to hold the sample and reference material have been described elsewhere (5); although the prepared barium sulfate plates were occasionally used, the plate adsorbent usually served as reference standard. The chromatoplates were coated using a "Desaga" thin-layer chromatography applicator with the layer thickness adjusted to 0.25 mm.

General Procedure

The 20 × 5 cm plates, after coating, were heated at 110 °C (1 h for silica gel and 15 min for cellulose) and were stored in a dry cabinet over silica gel adsorbent. The metals were applied to the plate by spotting with a 10 μl Hamilton micro-syringe; the samples were dried for 5 min at 110 °C, were cooled to room temperature, and then chromatographed in a preconditioned (12 h) chromatography chamber. After separation (20 to 30 min), the plates were air dried for 15 min or heated to 110 °C for 5 min and treated as described in the various sections to follow. The optimum conditions have been determined for each adsorbent and are discussed in the corresponding sections.

The technique used in quantitative analysis of the separated material has been described previously (5). The 20–30 mg samples removed from the plates for analysis of the spots were weighed to ±0.1 mg and were ground in a small agate mortar for two periods of 1 min each to insure homogeneity and a more uniform particle size. Samples that were not analyzed immediately were stored in a desiccator over silica gel.

[1]Paper presented at the 18th Mid-America Symposium on Spectroscopy in Chicago, May 1967.

Can. J. Chem. Downloaded from www.nrcresearchpress.com by 210.87.254.105 on 09/05/12
For personal use only.

Results and Discussion

Reagent

Figure 1 shows the spectra of solutions of PAQH in ethanol; acidic and basic solutions contained 1 ml of 0.1 *N* hydrochloric acid or sodium hydroxide per 100 ml of solution. The reagent is strongly yellow in fresh basic solution but fading occurs within a few hours (Fig. 2). An acidic solution is less intensely colored (Fig. 1) and is stable for several months. The stock solution of the reagent was therefore kept in ethanol containing 1 ml of 0.1 *N* hydrochloric acid per 100 ml of solution.

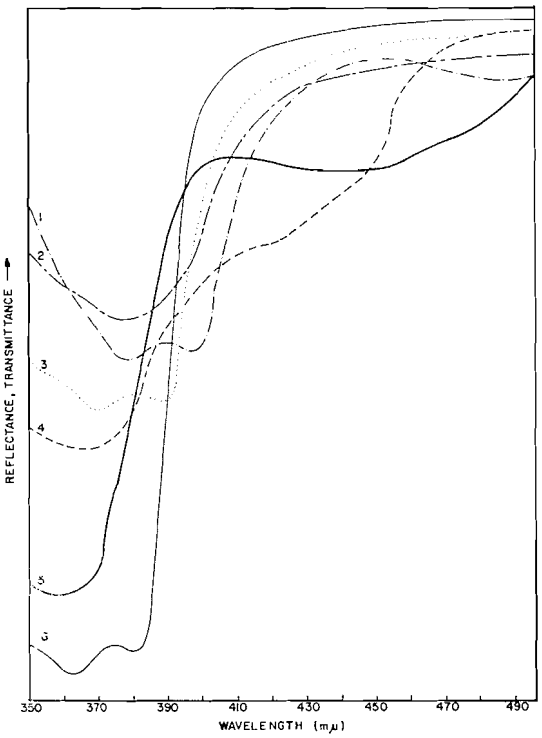

FIG. 1. Spectra of reagent. Legend: on cellulose (1, acidic; 2, basic); on silica gel (3, acidic; 4, basic); in ethanol solution (5, basic; 6, acidic).

Figure 1 shows also the reflectance spectra of the reagent on basic silica gel and cellulose (adsorbent first sprayed with 0.03% reagent solution and then with 0.1 *N* sodium hydroxide); the spectra are similar to the transmission spectrum in basic solution but the maxima are shifted slightly to higher wavelengths and bands are broadened due to light scattering. The reagent is stable for several weeks on basic silica gel but on cellulose, as in solution, the color fades rapidly.

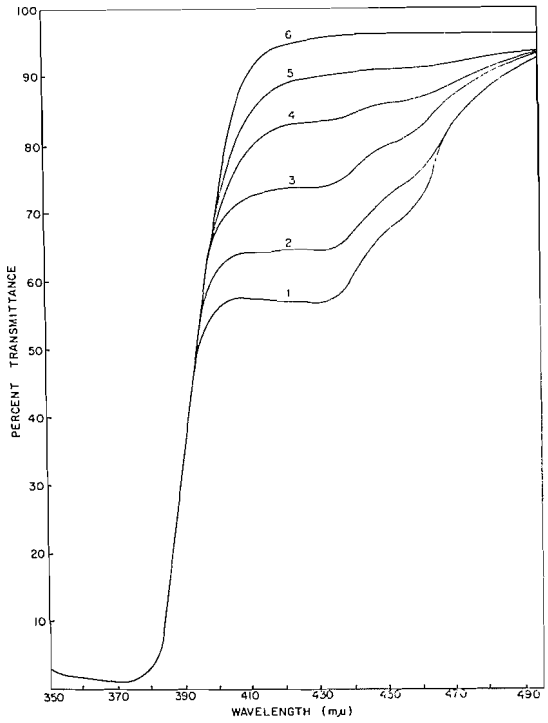

FIG. 2. Time study of 0.03% PAQH in basic ethanol. Legend: 1, start; 2, 1 h; 3, 2 h; 4, 3.5 h; 5, 5 h; 6, 12 h.

The same characteristic double peak in the near ultraviolet is observed on neutral and acidic adsorbent as in acidic solution (Fig. 1). An additional minimum at 490 mμ appears on cellulose which accounts for the orange color of the plate. The cellulose is not likely to contain significant transition metal impurities and it is probable that a chemical reaction occurs between the reagent and cellulose; further support for such an assumption is given later by the unusual behavior of the metal chelates on cellulose.

The optimum reagent concentration in the spray solution for maximum color formation with the metal ions is 0.03%. No significant increase in spot intensity occurs at reagent concentrations greater than 0.03% w/v for the three cations and a spray solution of this concentration was used in further studies.

Cobalt Complex

pH Study

The chromatograms, after separation and neutralization of the plates in ammonia vapor,

TABLE I

Absorption maxima (mμ) of PAQH complexes

	Aqueous solution	Silica gel	Cellulose
Co	500 (pH, 7–8)	508 (0.01 *N* NaOH)	536 (0.01 *N* NaOH)
Ni	480 (pH, 9)	490 (1.0 *N* NaOH)	520 (1.0 *N* NaOH)
Cu	475 (pH, 9)	485 (1.0 *N* NaOH)	505 (1.0 *N* NaOH)

were sprayed with reagent solutions which were made 0.01 to 1.0 *M* in sodium hydroxide shortly before use. The highest spot intensity was observed for a 0.01 *M* solution. Under these conditions the reagent was colorless on silica gel but an orange background, as previously mentioned, was observed on cellulose (Fig. 3).

Temperature Study

Heating of the plates at 110 °C for 5 min immediately after application of the reagent solution resulted in a 2–3% *R* increase in spot intensity on silica gel and about 1–2% *R* increase on cellulose. The intensity increased by another 1% on heating for 30 min at 110 °C but no changes were observed on heating for longer periods. Heating of the plates for 5 min at 110 °C is recommended, therefore, as a standard procedure.

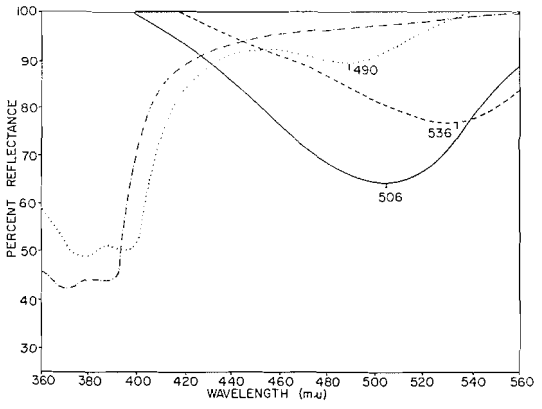

FIG. 3. Reflectance spectra for reagent and for cobalt complexes on silica gel and cellulose. Legend: on cellulose (. . . . reagent, --- complex); on silica gel (-.- reagent, — complex).

Spectra

The reflectance spectra of the reagent and the cobalt complex (1 μg/spot), under optimum pH and temperature conditions, are shown in Fig. 3. Little interference from the reagent is observed for silica gel plates. Similarly, although there is a reagent maximum at 490 mμ, there is no interference on cellulose because the absorption maximum of the cobalt complex is shifted considerably to 536 mμ. This bathochromic shift was observed for all three metals (Table I) but its magnitude, on cellulose, is rather unusual. Thus, for rubeanic acid complexes (4), a 10–20 mμ bathochromic shift of the reflectance spectra in the order cellulose < silica gel < alumina was reported as due to adsorbent–adsorbate interaction; cellulose, being the weakest adsorbent, showed the smallest shift. For PAQH complexes a chemical reaction between the cellulose–water complex and the metal chelate is probably responsible for the unusually large shift.

Reflectance–Concentration Relationship

Reflectance spectra of a dilution series ranging from 0.01 to 2 μg per spot are shown in Fig. 4. No significant peak shifts with concentration are observed and a working wavelength of 508 mμ for silica gel and 536 mμ for cellulose seems appropriate for the entire concentration range. The sensitivity is 0.01 μg per spot at a 50% accuracy level.

Figure 5 shows calibration curves for *R* versus concentration and for the Kubelka–Munk function $(1 - R)^2/2R$ versus concentration. A linear relationship is obtained for the latter at concentrations up to 1.3 μg per spot.

The reproducibility of reflectance measurements for samples of equal concentrations is given in Table II; a significant improvement is

TABLE II

Reproducibility of reflectance measurements for complexes

	Average standard deviations for six 1 μg samples	
	Spraying technique	Dipping technique
Co	±0.85% *R*	±0.55% *R*
Ni	±0.78% *R*	±0.50% *R*
Cu	±1.02% *R*	±0.58% *R*

Can. J. Chem. Downloaded from www.nrcresearchpress.com by 210.87.254.105 on 09/05/12
For personal use only.

Can. J. Chem. Downloaded from www.nrcresearchpress.com by 210.87.254.105 on 09/05/12
For personal use only.

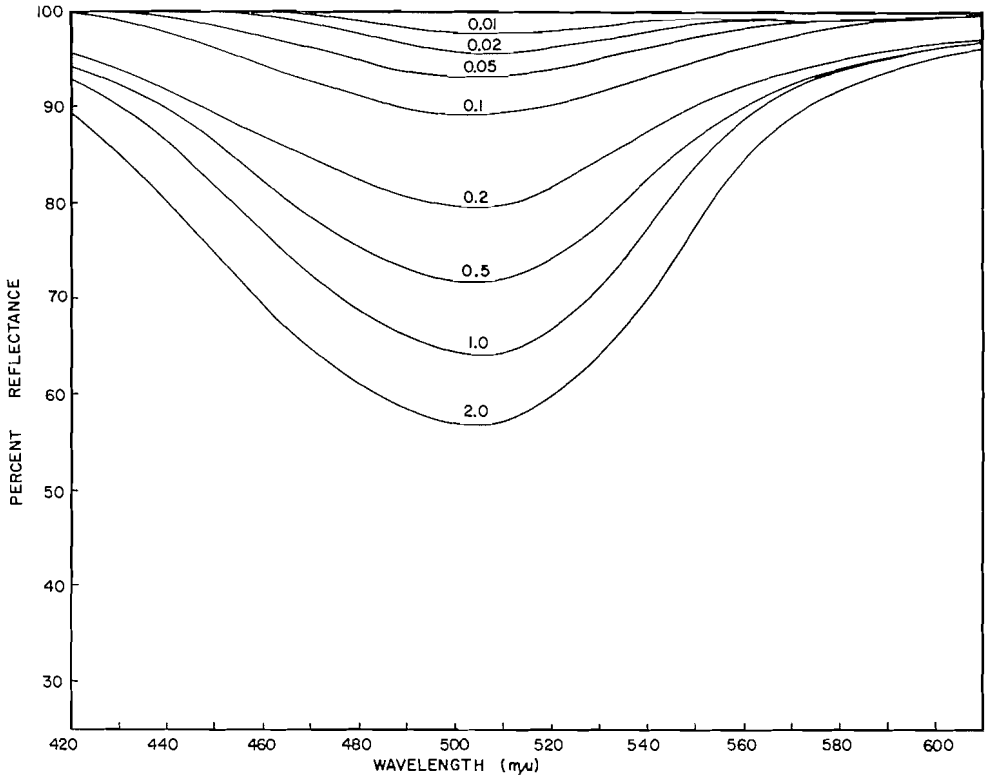

FIG. 4. Reflectance spectra of a dilution series of cobalt complexes adsorbed on silica gel.

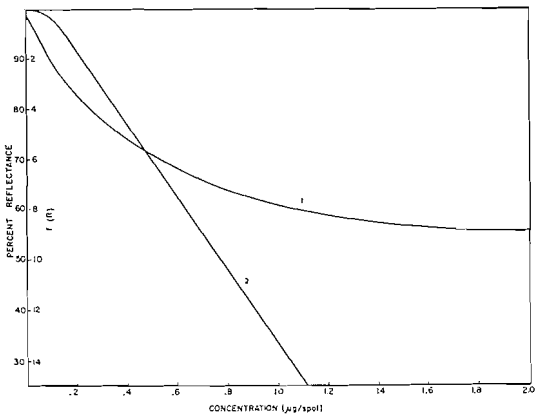

FIG. 5. Calibration curves for cobalt on silica gel. Legend: 1, % R vs. concentration; 2, Kubelka–Munk function vs. concentration.

observed with the dipping technique. Best results are obtained when standards are processed with the samples although a calibration curve can be used over an extended period with some loss in accuracy. The samples, when stored in a desiccator in the dark, remain stable for weeks.

Nickel Complex

PAQH reacts as a tridentate reagent to form either square planar (coordination number four) or octahedral (coordination number six) complexes with metals; both 1:1 and 2:1 (reagent to metal) complexes would be expected for nickel. Figure 6 shows the reflectance spectra for nickel on silica gel after spraying with solutions varying from 0.025 to 1.0 N in sodium hydroxide. A red complex with a maximum at 520 mμ is predominant at low basicity but conversion to a brown species (maximum 480–490 mμ) occurs with increasing sodium hydroxide concentration; maximum sensitivity is obtained with 1.0 N sodium hydroxide spray solution when nearly quantitative formation of the brown species has occurred. The brown complex is the 2:1 species normally encountered in solution (1). The red species observed at low basicity on silica gel is presumably the 1:1 planar complex; unlike in solution, the 1:1 species is readily observed on silica gel and the pronounced influence of adsorbent on equilibrium conditions is evident.

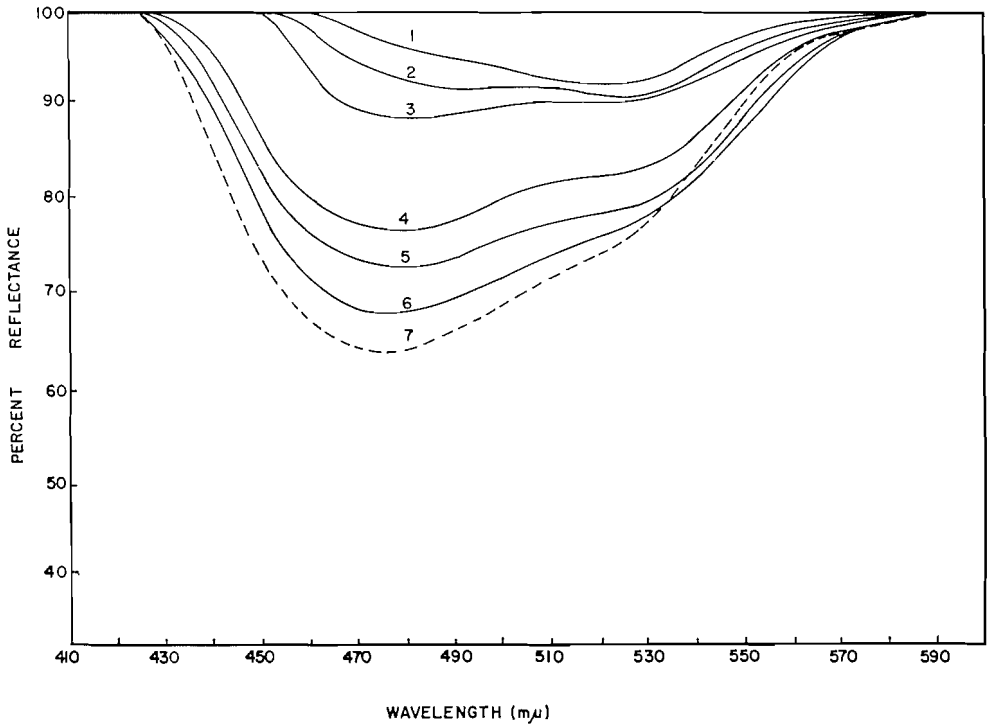

FIG. 6. Reflectance spectra of nickel complex adsorbed on silica gel and sprayed with NaOH solutions. Legend: 1, 0.025 *N* NaOH; 2, 0.05 *N* NaOH; 3, 0.10 *N* NaOH; 4, 0.25 *N* NaOH; 5, 0.50 *N* NaOH; 6, 0.75 *N* NaOH; 7, 1.0 *N* NaOH.

On cellulose, however, only the red species is observed and the absorption maximum (520 mμ) is independent of basicity; a higher sensitivity is obtained by spraying with a 1.0 *N* sodium hydroxide solution. It was reported earlier that reagent and complex behavior on cellulose is unusual and that a chemical, rather than adsorption, interaction was suspected. Stabilization of the 1:1 species on cellulose can be attributed to occupation of coordination sites by the cellulose–water complex.

Temperature Study

Figure 7 shows spectra obtained for various treatment after spraying. Immediate heating of the plate results in a considerable loss in sensitivity (curve 1). If the plate is allowed to stand for 1 h there is a sensitivity increase of at least 5% (curve 2) since the reaction is not quantitative immediately after spraying; curve 2 also shows that a significant portion of the nickel seems to be present in the red complex form after 1 h standing. However, if the sample is now heated at 110 °C for 5 min the intensity increases and the red complex disappears to a large extent (curve 3); the increase in peak height at 480 mμ occurs at the expense of the red modification which is converted to the brown species. Further heating results only in a minor increase of the peak and the red complex disappears completely (curve 4); a small bathochromic shift is also observed upon prolonged heating.

On cellulose, the samples are air dried for 1 h. Heating of the cellulose plates results in a dark yellow background coloration that is probably due to attack of the cellulose by sodium hydroxide. As mentioned previously, only the red species is obtained.

Reflectance–Concentration Relationship

Figure 8 shows the spectra of a dilution series of nickel under optimum conditions (sprayed with a 1.0 *N* sodium hydroxide solution, air dried for 1 h after spraying, and heated for 5 min at 110 °C before measuring spectra). The sensitivity is 0.01 μg per spot. Calibration curves similar to those for cobalt are obtained when *R* or the Kubelka–Munk function of *R* is plotted against concentration. Reproducibility data for nickel are shown in Table II.

Can. J. Chem. Downloaded from www.nrcresearchpress.com by 210.87.254.105 on 09/05/12
For personal use only.

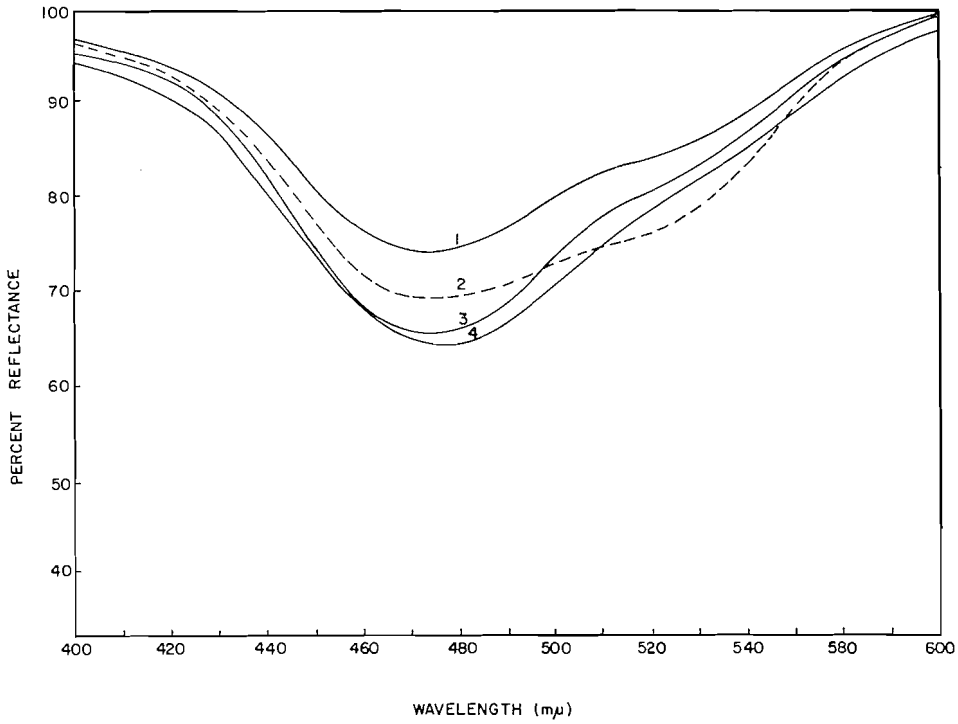

FIG. 7. Reflectance spectra of nickel complex on silica gel. Legend: 1, heated at 110 °C for 5 min immediately after spraying; 2, air dried for 1 h; 3, as 2 and then heated for 5 min at 110 °C; 4, as 2 and then heated for 30 min at 110 °C.

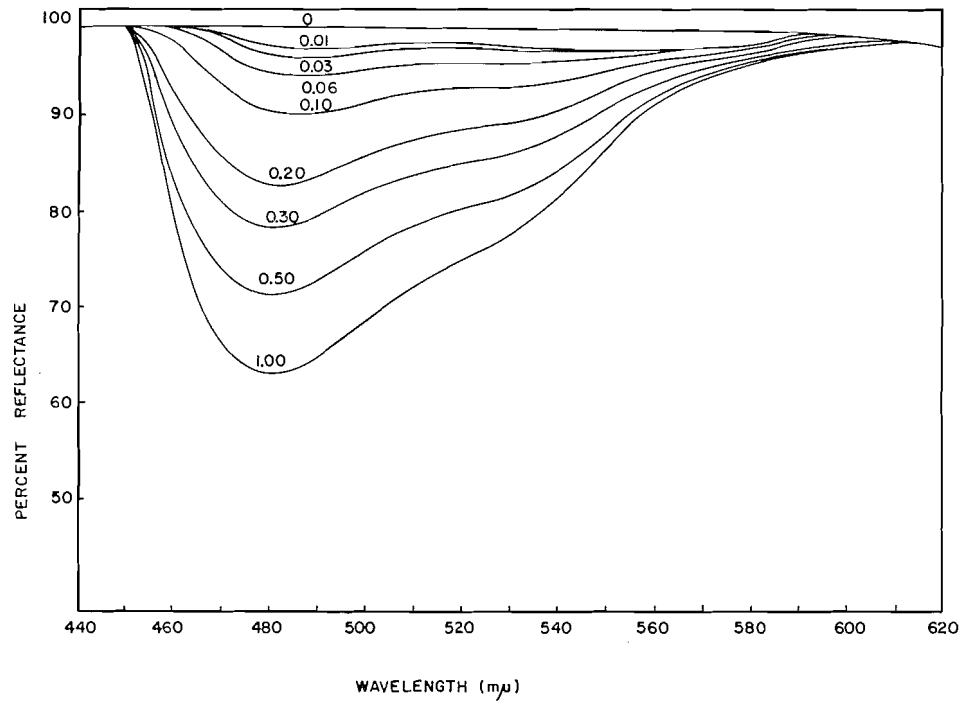

FIG. 8. Reflectance spectra of a dilution series of nickel complex on silica gel. Legend: numbers on spectra refer to concentration of nickel in μg per spot.

Can. J. Chem. Downloaded from www.nrcresearchpress.com by 210.87.254.105 on 09/05/12
For personal use only.

Copper Complex

Copper, like nickel, forms square planar and octahedral complexes and the behavior of copper is very similar to nickel. On silica gel two species are observed but only one is found on cellulose. The optimum conditions for nickel also seem to be best for copper. Under these conditions a brown complex, with an absorption maximum at 485 mμ, is predominant on silica gel; an orange-to-reddish colored species (absorption maximum at 505 mμ) is observed on cellulose. The sensitivity is 0.02 μg per spot; reproducibility data are given in Table II. The Kubelka–Munk law is also valid for copper and a linear calibration curve is obtained up to 1.5 μg per spot.

Other Metal Ions

Iron, zinc, manganese, cadmium, and lead ions react with PAQH to form colored products but do not interfere in the determination of cobalt, nickel, and copper. Iron in commercial silica gel can be removed by chromatographing the plates with the solvent mixture; iron impurities moving with the solvent front are then cut off and the plate used for analysis. Cadmium, lead, and iron in the sample move with the solvent front. Zinc and cadmium are chromatographically separated from nickel, cobalt, and copper and, in addition, even 10-fold excesses of these metal complexes fade almost completely on silica gel upon heating at 110 °C.

Acknowledgments

The authors are grateful to the National Research Council of Canada and the Defence Research Board of Canada for financial support.

1. M. L. Heit and D. E. Ryan. Anal. Chim. Acta, **32**, 448 (1965).
2. M. L. Heit and D. E. Ryan. Anal. Chim. Acta, **34**, 407 (1966).
3. S. P. Singhal and D. E. Ryan. Anal. Chim. Acta, **37**, 91 (1967).
4. R. W. Frei and D. E. Ryan. Anal. Chim. Acta, **37**, 187 (1967).
5. R. W. Frei and M. M. Frodyma. Anal. Chim. Acta, **32**, 5016 (1965).

Can. J. Chem. Downloaded from www.nrcresearchpress.com by 210.87.254.105 on 09/05/12
For personal use only.

Can. J. Chem. Downloaded from www.nrcresearchpress.com by 210.87.254.6 on 09/05/12
For personal use only.

Primary process in the photolysis of hexafluoroacetone in the presence of mercury vapor[1]

R. K. BOYD,[2] G. B. CARTER,[3] AND K. O. KUTSCHKE
Division of Pure Chemistry, National Research Council of Canada, Ottawa, Canada

Received May 23, 1967

Studies have been made of the variation with ketone pressure of the quantum yield for the decomposition of hexafluoroacetone, excited by 3130 Å, at 25 and 78 °C, and of the relative yield of the total emission at several temperatures. These are described in considerable detail with a view to discerning possible sources of systematic error. No large systematic error could be identified except that of decreased yields caused by deactivation by mercury vapor. The decomposition data support the weak collision mechanism for vibrational relaxation in the excited singlet state unless an as yet unknown source of large systematic error can be identified.

A description is offered of the path of the decomposition in terms of simplified diatomic representations of the $n\pi^*$ singlet and triplet states and of a repulsive state arising from the radicals CF_3 and CF_3CO in their ground electronic states. On the basis of that description an activation energy $\geqslant 11$ kcal mole^{-1}, derived from the combined decomposition and emission data, is to be ascribed to the first-order decomposition of triplet state molecules in vibrational equilibrium with their surroundings.

Canadian Journal of Chemistry, 46, 175 (1968)

Introduction

An earlier publication (1) offered a reinterpretation of literature data as they pertain to the mechanism of the primary process in the photolysis of hexafluoroacetone following excitation by the 3130 Å group of the mercury arc. The present paper describes in detail the new data cited there, reports additional new data bearing on the primary photodecomposition, and describes a study of some aspects of the emission from the excited states of this ketone. Two brief studies of other aspects of the overall investigation of the primary process have been reported recently (2, 3).

Near the completion of the present work the investigations of Bowers and Porter, which are now published (4, 5), came to our attention. There are two important quantitative discrepancies between those results and those reported here. One of these discrepancies can be attributed to the quenching of the triplet state of this ketone by mercury vapor, which was reported recently (3) and since has been confirmed (6, 7). It seems probable that the method used by Bowers and Porter (8) to fill photolysis cells coincidentally also eliminated a substantial fraction of the mercury from their reactant. Thus their result that $\phi_\infty \sim 0.2$ at room temperature is closer to the unquenched value than that found here (~ 0.025). The discrepancy (9) regarding the shape of plots of $1/\phi$ vs. pressure at low pressures cannot be explained as readily.

Because of the unexplained discrepancies the experimental work is described in greater detail here than is usually the case and a discussion is given of possible sources of systematic errors. This description is divided into two sections of which the first describes the experiments on the photodecomposition and the second those on the emission.

Experimental

(I) Photodecomposition

The cylindrical quartz photolysis cell (10 cm long, 5 cm diameter) was housed in a cylindrical aluminium block furnace whose temperature was regulated with a Fenwall Series 560 controller and monitored by two thermocouples. The block and cell were placed in an air thermostat maintained several degrees below the temperature of the block. Also in the thermostat were a magnetically driven impeller to circulate gases through the cell and three metal valves (Hoke 413) which separated the cell from the storage manifold, from the analytical section, and from a cold finger which extended beyond the walls of the thermostat. When not in use as a condensation point, the finger was maintained near the temperature of the thermostat.

A manometer and a multi-range McLeod gauge were used to measure pressures of reactants. These were attached to the storage manifold and, in pressure ranges where comparisons of reasonable precision could be made,

---

[1]Issued as NRCC No. 9755.

[2]NRCC Postdoctorate Fellow, 1962–1964. Present address: Dept. of Chemistry, University of Toronto, Toronto 2, Ontario.

[3]NRCC Postdoctorate Fellow, 1962–1964. Present address: Imperial Chemical Industries, Ltd., Petrochemical and Polymer Laboratory, The Heath, Runcorn, Cheshire.

Can. J. Chem. Downloaded from www.nrcresearchpress.com by 210.87.254.6 on 09/05/12
For personal use only.

agreement well within 1% was obtained between adjacent ranges of the McLeod gauge and between the McLeod and the manometer. The usual series of traps, a LeRoy–Ward still, and a solid nitrogen trap in the analytical section could be evacuated by a small mercury diffusion pump backed by a Toepler pump – gas burette combination. Samples could be taken from the burette for combustion over hot copper oxide or withdrawn for gas chromatographic or mass spectrometric analysis. A more detailed description of the apparatus for handling the product gases is given in ref. 10.

The entire apparatus could be evacuated below 10^{-5} mm as read on a McLeod gauge but was, of course, saturated with mercury vapor at its equilibrium vapor pressure at room temperature.

The light source was a 550W Hanovia Type A medium pressure mercury arc fed from a regulated a.c. supply. Filters described by Kasha (11) isolated the 3130 Å group in the slightly divergent beam which just filled the reaction vessel at the entrance window. A quartz lens collected the emerging beam and focussed it onto an RCA 935 photocell whose output was measured with a critically damped galvanometer. The linearity of the photometric apparatus was checked with calibrated neutral density filters and wire gauzes. A Beer's law plot for hexafluoroacetone vapor gave values for the decadic extinction coefficient of 6.8_3, 7.5_8, and 8.0_4 $(\text{mole/l})^{-1}$ cm^{-1} at room temperature, 78 °C, and 107 °C respectively for the "3130" radiation isolated in this way. Such plots were linear to optical densities near unity and were assumed to remain linear at very small densities.

Hexafluoroacetone (HFA) from two sources was used. In early experiments it was generated from the hydrate (Merck, Sharpe and Dohme) and subjected to careful fractionation at low temperatures to remove the ethylene which presumably was produced in the dehydration procedures from the small amounts of ethanol usually present in the hydrate. Traces of carbon dioxide were found in the purified material. Later experiments were done with anhydrous HFA from Allied Chemical Co. A substantial impurity of fluoroform usually was present and was removed by distillation at −155 °C. Mass spectra of the purified material from the two sources were in complete agreement as were the kinetic results. Acetone-d_6 had been carefully dried and outgassed by earlier workers and was merely outgassed further before use. Reagent grade acetone was dried and distilled from a trap at −78 °C. Decafluorobutane and carbon dioxide were taken from commercial cylinders; large head and tail fractions were rejected during outgassing procedures.

Galvanometer readings Δ_t^0 and Δ_t, proportional to the light intensity transmitted by the empty cell and the cell containing ketone, were used to calculate a corrected fractional absorption $f = \Delta_a/\Delta_t^0$, where Δ_a is proportional to the absorbed light intensity. "Typical" values of reflectance and transmittance of quartz windows as cited by Hunt and Hill (12) were used; measurements made on similar optical components yielded results in complete agreement with the typical values. Because of the furnace windows it was necessary to correct the measurements for that light which was reflected back into the cell from those windows as well as for internal reflections within the cell. The rigorous type of treatment used by Hunt and Hill (12, 13) becomes unwieldy when four windows are involved. Consequently a simplified expression was obtained in which only first reflections at each window were considered (compare ref. 10, p. 303). If second and third reflections were included the expression became too cumbersome to use, yet differed in its numerical value for a wide range of trial values of $r = \Delta_t/\Delta_t^0$ by less than 1.5%. These higher-order reflections were, therefore, omitted and the expression used was $\Delta_a = \Delta_t^0(1-r)(T_1T_2)^{-1}(1 + (R_1 + R_2T_1)^2r)$. T_1 and T_2 are the fractions of a monochromatic, parallel beam which are transmitted by a cell window and by a furnace window, respectively, and R_1 and R_2 are the similar fractions which are reflected. It is implicit in the derivation that the two cell windows are identical to one another as are the two furnace windows. In fact, the measured values of R and T for all windows tried were identical (±2%) and, when these values are inserted, the expression for Δ_a becomes $\Delta_a = 1.21\Delta_t^0(1-r)(1 + 0.130r)$. At very high and very low pressures r was calculated from the measured pressure and the extinction coefficient obtained for data in the regions where r could be measured precisely.

A sample of ketone from storage was allowed to expand into the reaction cell and storage manifold to the desired pressure; this was measured after temperature equilibration. If no additive was to be used the valve from the storage manifold was closed and the exposure begun. If an additive was to be used, the ketone was condensed into the cold finger and isolated by a valve. The additive was introduced as above, the cold finger opened, and mixing of the gases was carried out for a suitable time. A small correction to the initial pressures involving the volumes and temperatures of the cold finger and the cell was evaluated separately.

The value of Δ_t was monitored throughout the exposure and maintained constant by minor adjustments of the lamp current. Values of Δ_t^0 were taken immediately after the photolysis before the lamp was extinguished.

Products were transferred to the gas burette through several traps at −196 °C and a final trap at −210 °C. Several trap-to-trap distillations were done to ensure the complete removal of physically occluded volatile material. That this procedure was successful was demonstrated in a few experiments with HFA in which several less volatile fractions were taken as well. These fractions always contained in total less than 3%, and usually less than 1%, of the carbon monoxide found in the first fraction. In experiments with acetone or acetone-d_6 the composition of the first fraction was determined by combustion over hot copper oxide; in a few experiments a mass spectrometric analysis yielded a composition within ±1/2% of that obtained by combustion.

It is assumed that ϕ, the quantum yield for the primary decomposition, is equal to the measured Φ_{CO}, as discussed earlier (1). The method of actinometry employed evaluates ϕ in terms of ϕ_D or ϕ_A, the primary quantum yields for the decomposition of acetone-d_6 or acetone respectively, through the following expression.

$$\phi = \left(\frac{\mu_{HFA}}{\mu_D}\right)\left(\frac{t_D}{t_{HFA}}\right)\left(\frac{V_D}{V_{HFA}}\right)\left(\frac{\Delta^0_{t,D}}{\Delta^0_{t,HFA}}\right)\left(\frac{f_D}{f_{HFA}}\right)\phi_D$$

Can. J. Chem. Downloaded from www.nrcresearchpress.com by 210.87.254.6 on 09/05/12
For personal use only.

The subscript HFA refers to quantities measured in the photolysis of hexafluoroacetone and D to those in the actinometric experiments with acetone-d_6; for actinometric experiments with acetone, the subscript D is replaced by A. μ represents the number of moles of carbon monoxide produced in a time t when the illuminated volume was V. The product $\Delta_t{}^0 f$ is proportional to the absorbed intensity and was used in arbitrary units of galvanometer deflection. Most actinometric experiments were done with acetone-d_6 because it was conveniently available on the apparatus from previous work, but some later experiments were done with natural acetone as well. ϕ_D, or ϕ_A, was taken to be unity and to be equal to Φ_{CO} for the conditions used (3130 Å; several pressures in the range 50 to 100 mm; temperatures near 150 and 180 °C).

A brief discussion of possible systematic errors in the calculation of ϕ is considered to be worthwhile. No significant systematic errors should arise in the first two factors in the expression for ϕ; in particular μ_{HFA} and μ_D always were measured on the same volume of the gas burette so that, even if the calibration of this volume were to be in error, no error would be introduced into the final value calculated. The illuminated volumes V_D and V_{HFA} were geometrically identical so that the ratio was taken as unity. This assumption neglects at least three phenomena which might give rise to error. (i) Because the lifetimes of the excited state intermediates for HFA and acetone-d_6, or acetone, are not identical, the mean diffusion distances of these differ. If the light beam does not fill the cell then V_D might differ from V_{HFA}; if it does fill the cell, different fates of the excited species on the walls might give rise to an effective value of $V_{HFA}/V_D \neq 1$. The light beam filled the cell in the present experiments but no assessment has been made of the possible effect of the walls. (ii) Strong absorption in the rotational fine structure of the absorption spectrum of the ketone or of the actinometric gas could cause V_{HFA} to differ from V_D. In fact, it is probable that both spectra are highly pressure broadened, and perhaps diffuse, so that this effect should be negligible. (iii) The bulk of the products are formed in a smaller volume at pressures for which the optical density is higher. Because no attempt was made to ensure that the fractional absorptions in the actinometric experiments was the same as in those with HFA, this effect of Beer's law and of the slight polychromaticity of the light could cause changes in the effective value of V_{HFA}/V_D if either or both systems involve bimolecular reactions between excited species, or between an excited species and a free radical. The absence of an effect of I_a on ϕ eliminates these latter possibilities and thus also any effective volume effect for the conditions used here.

Because galvanometer deflections were shown to be linear in incident intensity, because attempts were made to hold $\Delta_t{}^0$ constant from one experiment to the next, and because the small changes which in fact occurred could be allowed for in a linear manner, no significant systematic errors can be ascribed to the factor $\Delta^0{}_{t,D}/\Delta^0{}_{t,HFA}$. Systematic errors are present, but almost certainly are not significant, in the ratio f_D/f_{HFA}. Because it was impractical to arrange $f_D = f_{HFA}$ for all pressures of HFA studied, the type of correction discussed above was employed. The actual corrections to be applied to $(1-r_D)/(1-r_{HFA})$ to obtain f_D/f_{HFA} are near unity because only the ratio of the corrections to the individual $(1-r)$ enters the calculation. Thus much of any systematic error which might enter because of the approximate formulation used is expected to cancel. The actual corrections to $(1-r_D)/(1-r_{HFA})$ range from 0.91 at low pressures through unity at a pressure of HFA such that its optical density was 0.2 (the optical density of acetone at the pressures used in the actinometry) to 1.03 at high pressures.

The possibility exists that neither ϕ_D nor ϕ_A, taken to be equal to unity and to be proportional to the rate of formation of carbon monoxide in the photolysis of acetone-d_6 or acetone, is not unity for the conditions used in the actinometric experiments. Indeed, Hoare has suggested that the extinction coefficient of acetone changes when carbon dioxide is present and that Φ_{CO} varies with the amount of carbon dioxide added (14, 15). These observations cast considerable doubt on the assumption that $\phi_D = \phi_A =$ unity so that several tests were made to check them.

The value of f_{HFA} for mixtures of HFA and carbon dioxide at 78 °C was as much as 25% lower than that of HFA alone; the magnitude of the decrease was smaller at lower values of $[CO_2]/[HFA]$. Eventually it was observed that mixing, as judged by light absorption, was a very slow process (> 16 h in the reaction system used) and that the operation or not of the impeller had little effect on the time required for complete mixing. A second impeller proved to be similarly inefficient. The sign of the effect observed here is opposite to that reported by Hoare (14) but this probably merely reflects differences in the geometry of the two reaction systems or in the methods of filling the cells. Slow mixing was also observed when acetone, or acetone-d_6, was mixed with carbon dioxide at 151 °C, but for all three ketones, the observed fractional absorption was independent (±1%) of the amount of carbon dioxide added, provided that sufficient time was allowed for complete diffusive mixing. A similar observation was made with 20 mm of acetone and 161 mm of carbon dioxide at 107 °C in the apparatus, described below, used for emission studies. In this respect our observations agree with those of Martin and Sutton (16).

Moreover, the rate of formation of carbon monoxide (R_{CO}) from the photolysis of acetone (36 mm, 151 °C) was independent (±0.5%) of the addition of ~ 58 mm of carbon dioxide, provided that mixing was complete. Martin and Sutton (16) made a similar observation at 120 °C.

A series of experiments was done under the conditions, and with the results, tabulated in Table I.

TABLE I

No.	Ketone	Pressure (mm)	T (°C)	$(R_{CO}/\Delta_t{}^0 f)$*
A1	Acetone-d_6	76.9	149	1.99
A2	Acetone-d_6	50.4	175	2.00
A36	Acetone	60.5	144.5	1.94
A39	Acetone-d_6	60.6	"	1.91
A38	Acetone	134.0	"	1.93
A37	Acetone	134.0	"	1.99

*Proportional to Φ_{CO}; units are 10^{-10} mole s^{-1} (react. vol.)$^{-1}$ (cm deflection)$^{-1}$.

Can. J. Chem. Downloaded from www.nrcresearchpress.com by 210.87.254.6 on 09/05/12
For personal use only.

The optical train was different for A1 and A2 than for the last four experiments; hence the entries in the last column are expected to be different in the two sets. For A37, Δ_t^0 was adjusted so that $\Delta_t^0 f$ was the same as for A36; the decreased Δ_t^0 could not be read as precisely so that $R_{CO}/\Delta_t^0 f$ for this experiment carries a greater uncertainty than do the others. It is apparent that $R_{CO}/\Delta_t^0 f$ does not depend on whether acetone or acetone-d_6 is used (A36 and A39), is independent of temperature (A1 and A2), of ketone pressure at constant incident intensity (A36 and A38), and, probably, but with rather less precision, is independent of ketone pressure at constant absorbed intensity (A36 and A37). The simplest interpretation of these observations is that ϕ_D and ϕ_A are each very close to unity for the conditions cited. Herr and Noyes (17) found $\Phi_{CO} = 1 \pm 10\%$ at 120 °C. This observation is irreconcilable with the 40% increase in Φ_{CO} in the acetone photolysis at 100 °C reported by Hoare and Caldwell (15) to be caused by the addition of ~ 150 mm of carbon dioxide. It is concluded that the latter results are suspect because of the possibility of incomplete mixing and that our assumption of $\phi_D = \phi_A = 1$ is not invalidated by those results.

It is concluded that systematic errors in the present results, aside from the quenching caused by mercury vapor, are not important and probably are no greater than the scatter in the data. The latter can be assessed from the various plots of the data and, except at the lowest pressures, is probably less than 2%.

It was noted in early experiments that analysis of the condensable fraction by gas chromatography indicated the presence of trace amounts of C_3F_8 and C_4F_{10} among the products. These were not formed if the cell had been evacuated overnight with the first analytical trap held at −196 °C. Each experiment reported here was done after this pretreatment of the reaction cell. On several occasions a cell which had been evacuated for only a short time after a photolysis at high pressure was exposed without addition of ketone; some carbon monoxide invariably was formed. It is thought that a cyclic trimer of HFA of low volatility was responsible for these effects, but no definite conclusion was reached. In any event, the pretreatment of the reaction vessel prevented the formation of spurious products and the matter was not pursued further.

(II) Emission

The emission from HFA following excitation at 3130 Å consists of a broad, essentially structureless, band extending from below 3500 Å to above 8000 Å (4, 7, 18, 19): some disagreement exists regarding the exact shape and extent of the emission spectrum (7), but the general description above suffices for present purposes. Contrary to a conclusion reached in the early work (18) the emission consists of at least two components, a fluorescence of short lifetime whose intensity is unaffected by the presence of moderate quantities of oxygen and a phosphorescence of much longer lifetime (3, 5, 7) which is quenched by a few mm of oxygen (4, 19, 20). The quantum yield of the total emission, $\phi_e = \phi_f + \phi_p$, is about 0.01 with some variation with conditions of excitation (4).

In the present work measurements were made of $Q = \beta\phi_e$ as a function of [HFA] at several temperatures. The numerical factor of proportionality, β, depends on the geometry of the apparatus, on the unknown absolute quantal sensitivity of the light detecting devices, and on the variations of that sensitivity over the wavelength region of interest. It is not frequently noted explicitly that if the emission spectrum changes with excitation conditions the value of β also changes, so that Q need not be the same function of ϕ_e for all excitation conditions.

The apparatus used for the measurement of Q was of conventional basic design but contained sufficient useful modifications to warrant some discussion; most of these modifications were based on experience gained in earlier work (19).

Exciting light at 3130 Å, isolated by filters (11), was taken from a modified Hanovia lamp of the type used in the photodecomposition work. The modification consisted in replacing the middle ~ 4.5 cm length of ~ 24 mm outside diameter quartz tubing comprising the envelope of the lamp by a similar length of ~ 12 mm outside diameter quartz tubing. At the two seals the envelope was further restricted to ~ 7 mm inside diameter. While this modification decreased the useful life of the lamp, geometrical stability of the arc was greatly increased in that wandering of the central core of the arc within the envelope was minimized (19)[4]. Thus the lamp could be used with a very small (3 mm) aperture in a mask which almost touched the lamp envelope near the middle of the narrow tubing. In this way a homogeneous, stable, and quite parallel beam could be obtained with a single lens and several stops.

In most experiments a fused quartz cell 15 cm long and 5 cm in diameter was used. A quartz viewing window (4 cm diameter) was attached to a short sidearm at the middle of the cell; diametrically opposite the viewing window was a second sidearm which terminated in a Wood's horn. The cell was housed in the center half of an aluminium block furnace with end windows. Exciting light entered the furnace as a beam 1 cm in diameter and left the furnace with a diameter of 1.5 cm.

A small fraction of the incident light was reflected by a quartz plate to a collecting lens and an RCA 935 photocell which thus could be used to monitor the incident intensity, Δ_0. The transmitted light, Δ_t, was focussed onto a second 935 photocell without casting a shadow of the anode onto the cathode. Measurements of Δ_t^0, the transmitted light with the cell empty, and the transmission of the cell calculated from the typical values for window transmission given by Hunt and Hill (12), permitted calculation of the fraction of light absorbed by the gas from the measured Δ_t values. Because internal actinometry was not used, it was important to correct the absorbed light intensity, Δ_a, for reflections from the cell and furnace windows. The value of Δ_a was obtained from the same expression as that used in the photodecomposition experiments.

The photometric arrangements used in the emission studies were superior to those employed in the photodecomposition work largely because of the smaller diameter of the light beam; consequently the extinction coefficients obtained are considered to be more reliable. Plots were made of $\log_{10} \Delta_t^0/\Delta_t$ vs. p_{HFA} over a wide

[4]We are greatly indebted to Mr. G. Ensell for modifying the commercial lamps used in this study.

Can. J. Chem. Downloaded from www.nrcresearchpress.com by 210.87.254.6 on 09/05/12
For personal use only.

range of pressures. At optical densities greater than ~ 2.5 the plot deviated significantly from linearity in a direction which suggested the presence in the beam of small amounts of wavelengths not absorbed by the ketone; this since has been shown to be the case (6, 7). Therefore this curvature was ignored in the calculations of Q and fractional absorptions have been calculated for high and low pressures by extrapolation from the linear portion of the curve. The decadic extinction coefficients, in (mole $l^{-1})^{-1}$ cm^{-1}, were 6.92 at 25 °C, 7.42 at 78 °C, 7.76 at 107 °C, 7.91 at 119 °C, 8.22 at 140 °C, and 8.47 at 170 °C.

A portion of the column of emitting vapor was focussed through the viewing window to an image of unit magnification at the aperture of a 1P21 photomultiplier tube. A mask with an opening of dimensions equal to those of the free aperture of the photomultiplier was placed on the viewing window. This had been shown (19) to decrease the photomultiplier signal from the empty cell, Δ_e^0, 20 times, but to decrease the signal due to emission, Δ_e, by only a few percent. This confirms that the portion of the emitting column of vapor viewed was limited by the aperture of the photomultiplier and thus had an area ~ 1 cm $\times$ 1 cm at the center of the cell. A Corning 7380 filter, which is "opaque" below $\sim 3\,400$ Å, further reduced Δ_e^0, so that for the lowest emitted intensity studied, i.e. lowest pressure of HFA, $\Delta_e^0/\Delta_e < 5\%$. All photocell and photomultiplier currents were detected with a Victoreen VTE-1 electrometer and recorded on a Leeds and Northrup recorder using a Leeds and Northrup microvolt amplifier as a preamplifier. These instruments were greatly superior in stability and ease of reading to the galvanometer and potentiometer systems used earlier (19).

Because the emitted light was viewed a considerable distance from the entrance and exit windows of the cell whereas only the total absorption could be measured, it was necessary to calculate that fraction, g, of the total absorption which occurred in the viewed region (19). The fraction of a parallel, monochromatic beam which is absorbed in a short length, δ cm, situated at the middle of a cell of total length l cm, is given by $g = (\sinh(\epsilon c\delta/2)/(\sinh(\epsilon cl/2)$, in which $\epsilon = 2.303\alpha$; α is the decadic molar extinction coefficient in $(\text{mole/l})^{-1}$ cm^{-1} and c is the ketone concentration in mole/l. At high pressures g is very small and subject to large errors because the experimental quantities occur in the argument of exponential functions. The data reported here have been corrected for both reflection and local absorption phenomena and are recorded as $Q = (\Delta_e - \Delta_e^0)/g\Delta_a$.

The cell was attached to a grease-free vacuum system which was saturated with mercury vapor. Pressures could be read on a mercury manometer, or a multi-range McLeod gauge reading to ~ 10 mm, which were attached to a storage manifold. Small quantities of various gases could be added to the cell contents from calibrated volumes, attached to the storage manifold, by means of a Toepler pump which connected the manifold to the cell system. The latter consisted of the cell, a cold finger, and an all-glass piston pump which served to mix the cell contents very efficiently, provided the total pressure was greater than ~ 10 mm. Constancy of fractional absorption and emission was attained a few minutes after mixing was begun.

The hexafluoroacetone used was from the same sources as those employed in the photodecomposition work and purification procedures were identical.

The data are given here in graphical form only (see Discussion). Copies of the tabulated results are available from the last-named author.

Discussion

There is disagreement between the results obtained here and those reported by Porter and his co-workers in respect to two observations. A discussion of one of these is given now while that of the other fits more naturally in a later section.

The data of Bowers and Porter (5) led to an extrapolated value of the quantum yield at infinite concentration of HFA of $\phi_\infty \simeq 0.2$ at room temperature. Figure 1 shows the higher pressure data obtained in the present study in the form of plots of ϕ vs. $[A]^{-1}([A] \equiv [(CF_3)_2CO])$; the intercept at $[A]^{-1} = 0$ for the data at room temperature is $\phi_\infty = 0.025$. The greater part, and perhaps all, of this discrepancy can be attributed to the presence in the present apparatus of mercury vapor, which now is known to cause a decrease in the phosphorescence lifetime (3, 7), to decrease the ratio of the intensities phosphorescence/fluorescence (7), and to cause the quantum yields for decomposition to be too low under several experimental conditions (6). As noted in the Introduction it appears that the procedures used by Bowers and Porter essentially prevented the entry of nearly all the mercury vapor into the reaction vessel. Hence their higher value for ϕ_∞ is more nearly correct for the uninhibited system.

Bowers and Porter (5) also report that ϕ_∞ ("b" in their Table 1) is ~ 0.2 when excitation was at 3130 Å and 3340 Å, but that it decreased to ~ 0.1 and zero for excitation at 2804 Å and 2652 Å respectively; all measurements were made at 25 °C. On the other hand the data of Ayscough and Steacie (21), taken at 3130 Å, and of Giacometti, Okabe, and Steacie (22), taken at $\sim$ 2650 Å, can be plotted in the form ϕ vs. $[A]^{-1}$ and extrapolated with no injustice to the data to a common intercept at 25 °C; this also is true at 53 °C. Some scatter exists in those data and data were not taken at sufficiently high pressures to establish with certainty the conclusion that ϕ_∞ depends only on temperature; nevertheless it is difficult to reconcile the earlier data with those of Bowers and Porter. Although those earlier data (21, 22) are incorrect because of

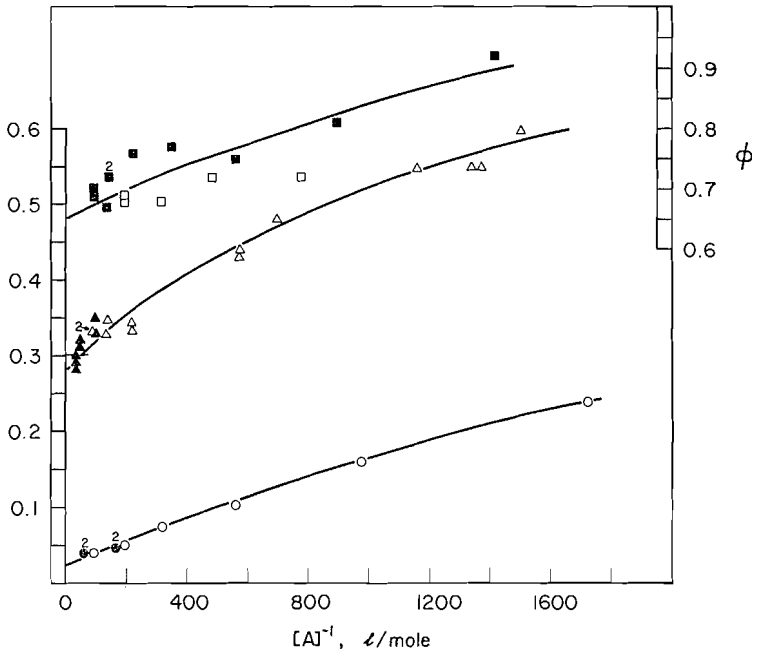

FIG. 1. Plots of ϕ vs. $[A]^{-1}$. (○), (●) Left ordinate; two separate series at 25 °C. (△), (▲) Left ordinate; two separate series at 78 °C; the filled triangle with the horizontal line was in the second series but represents an experiment in which the incident intensity was ~ 7.7% the usual value. (□), (■) Right ordinate; two separate series at 107 °C. At 107 °C the two series were done consecutively but changes were made in the optical arrangements between series. At 25 °C and 78 °C the two series were separated by several months and several changes in the optical arrangements intervened.

quenching by mercury vapor, it seems unreasonable to expect that an effect of exciting wavelength (λ_e) on ϕ_∞ should be obscured by that phenomenon.

Moreover, it is difficult to reconcile a change of ϕ_∞ with λ_e with the usual postulate that absorption over the whole of the first absorption band of the ketone corresponds to a single electronic transition. Indeed, the mechanism discussed below, which, aside from the quenching by mercury vapor, is essentially identical with that discussed by Bowers and Porter, predicts that ϕ_∞ depends only on temperature. The effect of a decrease of λ_e is predicted to be an increase in the initial slope of ϕ vs. $[A]^{-1}$ but to leave ϕ_∞ unaffected. As λ_e is made longer and longer this initial slope is expected to decrease and to reach zero for excitation in the zero–zero band, in which case $\phi = \phi_\infty$ for all pressures. In practice, of course, the energy spread in λ_e and in the absorbing molecules prevents the attainment of such an ideal condition of excitation even if the absorption were large enough to observe.

Because it might be important to compare data taken in the presence of mercury vapor with those taken in the future with mercury absent, Fig. 1 also includes the higher pressure data at two higher temperatures. At 78 °C, $\phi_\infty = 0.28$ and at 107 °C, $\phi_\infty = 0.65$, but the latter is subject to considerable error because inadequate temperature control introduced an unacceptable amount of scatter into the data. For this reason other deductions based on the data at 107 °C will not be given.

The Overall Mechanism

It is thought that reactions [1] through [10] are those which are important in the primary process under the conditions used here. In the mechanism, A represents a molecule of HFA in its ground electronic state, S_1^n a molecule in the lowest excited singlet state containing n quanta of vibrational energy, S_1^0 a molecule in low lying vibrational levels of that excited state from which decomposition cannot occur for energetic, or other, reasons, and T_1^0 a molecule in the lowest excited triplet state which essentially has reached vibrational equilibrium with its surroundings.

Can. J. Chem. Downloaded from www.nrcresearchpress.com by 210.87.254.6 on 09/05/12
For personal use only.

Can. J. Chem. Downloaded from www.nrcresearchpress.com by 210.87.254.6 on 09/05/12
For personal use only.

[1] $A + h\nu \rightarrow S_1^n$

[2,n] $S_1^n \rightarrow CF_3 + CF_3CO \rightarrow 2CF_3 + CO$

[3,n] $S_1^n + A \rightarrow S_1^{n-1} + A$

⋮ ⋮

[2,1] $S_1^1 \rightarrow CF_3 + CF_3CO \rightarrow 2CF_3 + CO$

[3,1] $S_1^1 + A \rightarrow S_1^0 + A$

[4] $S_1^0 \rightarrow A + h\nu_f$

[5] $S_1^0 \rightarrow A$

[6] $S_1^0 \rightarrow T_1^0$

[7] $T_1^0 \rightarrow A + h\nu_p$

[8] $T_1^0 \rightarrow CF_3 + CF_3CO \rightarrow 2CF_3 + CO$

[9] $T_1^0 \rightarrow A$

[10] $T_1^0 + Hg \rightarrow A + Hg$

The series of reactions [3,i] ($i = 1$ to n) represent the multistage deactivation proposed earlier (1). An internal conversion from S_1 to the ground state, [5], has been shown (5) to be important and is included here. The intersystem crossings [6] and [9] and the internal conversion [5] presumably occur as more complicated sets of reactions, but in the absence of evidence to the contrary, it is assumed that they may be represented over the whole range of pressure studied by the simple first-order processes shown. The decomposition reactions [2,i] ($i = 1$ to n) and [8] are written to imply that the free radicals are formed in their ground, or very low-lying, electronic states, perhaps with excess vibrational energy although the amount cannot be specified, and that the lifetime of the CF_3CO radical with respect to decomposition is so small that none of its other possible reactions need be considered. A more detailed discussion of this latter point has been given earlier (1, 2). Recently Amphlett and Whittle (23) have reached a similar conclusion regarding the fate of the trifluoroacetyl radical in this system. Reaction [10] is included to give a phenomenological representation of the effect of mercury vapor; the path of the reaction cannot be specified in detail.

It can be shown (1) that the mechanism predicts that

$$\phi = 1 - (1 - \phi_\infty)\prod_{i=1}^{n}([A]/([A] + p_i))$$

in which $\phi_\infty = k_6k_8/(k_4 + k_5 + k_6)(k_7 + k_8 + k_9 + k_{10}[Hg])$ and $p_i = k_{2,i}/k_{3,i}$. Obviously ϕ_∞ will decrease when Hg is present so that [10] correctly represents the effect of mercury in a general way.

An overall qualitative description of the pressure dependence of the decomposition is as follows. At very low pressures molecules decompose from the higher vibrational levels of S_1 before collisions can remove sufficient vibrational energy to prevent that decomposition. At sufficiently high pressures collisions efficiently remove vibrational energy from molecules in S_1 before decomposition can occur. A pressure-independent fraction of molecules in S_1^0 are transferred to T_1^0 and decompose from there. This latter decomposition, corresponding to ϕ_∞, is envisaged to be a unimolecular decomposition in its high pressure region, and thus of the first order, proceeding with an activation energy of about 10–15 kcal mole^{-1} (5, 21). At intermediate pressures a transition occurs from the situation in which singlet decomposition dominates to that in which decomposition from the triplet is of major importance. Figures 2 and 3 show plots of ϕ vs. [A] at 25 °C and 78 °C respectively; the data of Ayscough and Steacie (21) are included to demonstrate the excellent quantitative agreement between the two studies. It is seen that the deductions from the mechanism do indeed predict correctly the trend of the data.

A further point merits consideration at this juncture. It is, in fact, rather surprising that [8], which has a relatively low activation energy and thus a relatively small value of E/RT, should remain first order over the range of pressures used here. The present data including those on the relative emission yield as a function of pressure which are discussed in a later section, require that reactions [7], [8], and [9] all exhibit the same pressure dependence. On the basis only of the data presented here it is not possible to decide whether all reactions of the triplet state, including phosphorescence, require a collision or whether none do. However, it has been shown that τ_p (the lifetime of the phosphorescence) is independent of pressure in the region 4–760 mm (3); this independence has been verified with data which extend to $\sim$ 0.5 mm (7). The present mechanism, from which one obtains $\tau_p = (k_7 + k_8 + k_9 + k_{10}[Hg])^{-1}$ and thus is independent of ketone pressure, is in agreement with this observation.

Vibrational Relaxation in S_1

Conflicting conclusions have been reached concerning the question whether the vibrational

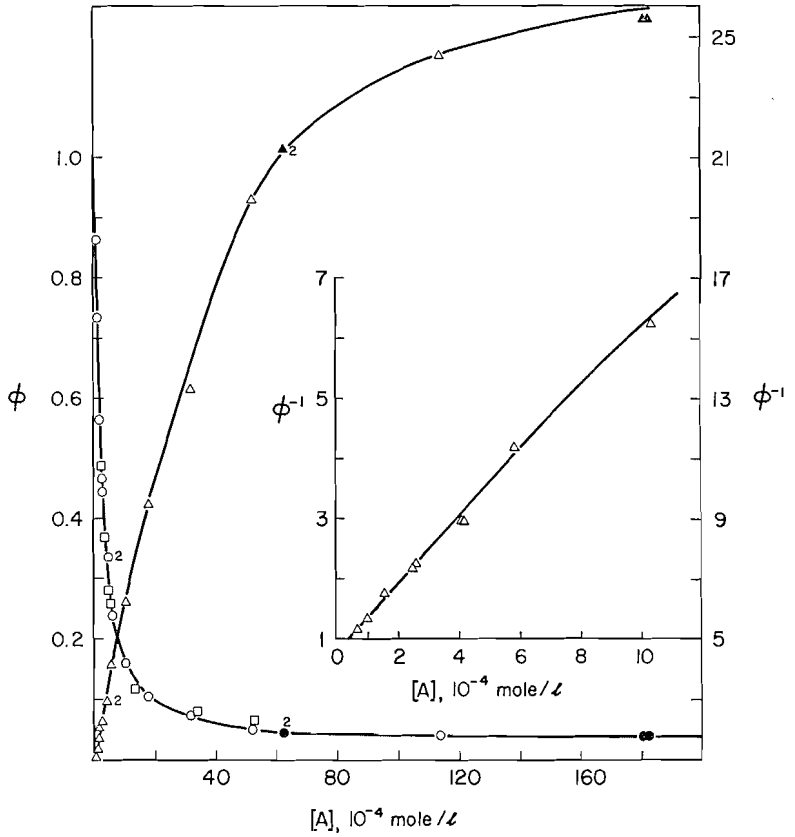

FIG. 2. Data at 25 °C ϕ vs. [A]. Left ordinate: (○), (●) present work; (□) Ayscough and Steacie. ϕ^{-1} vs. [A]. Right ordinate: (△), (▲) present work; Ayscough and Steacie data not included. Filled symbols show second series done several months after first (open symbols). Inset: ϕ^{-1} vs. [A] in low pressure region. Approximate pressures in mm Hg can be obtained by multiplication of [A], in 10^{-4} mole/l, by 2.

relaxation in S_1 is best represented by a cascade of weak collisions (1), as is shown in the mechanism offered here, or by strong collisions (5, 9), in which case the series of reactions [2,*i*] and [3,*i*] ($i = 1$ to n) should be replaced by the pair of reactions [2] and [3].

[2] $\quad S_1^n \rightarrow CF_3 + CF_3CO \rightarrow 2CF_3 + CO$

[3] $\quad S_1^n + A \rightarrow S_1^0 + A$

Two experimental tests have been discussed. One involves the shape of plots of ϕ^{-1} vs. [A] at low pressures, and the second that of plots of $(1 - \phi)/[A]$ vs. [A].

Considerations (1) of the mechanism show that if a cascade of weak collisions is involved, plots of ϕ^{-1} vs. [A] rise from unity at [A] = 0 with a slope which increases from zero at [A] = 0 until ϕ^{-1} reaches a point of inflection whence the plot continues to rise with decreasing slope to approach the asymptote, ϕ_∞^{-1}, as [A] is increased without limit. If a single strong collision is involved in the relaxation, the curve rises with a finite, positive slope, which always decreases as [A] increases, to approach the same asymptote. The pressure at which any point of inflection might occur is rather low and its presence might not be demonstrable in an experimentally accessible region. Indeed Porter and co-workers (5, 9) have not detected such a point of inflection down to pressures of 0.1 mm at room temperature. Figures 2 and 3 also include plots of ϕ^{-1} vs. [A] for the present data. It is to be noted that the plots remain approximately linear in the low pressure region (see insets in Figs. 2 and 3) but extrapolate to values of $\phi^{-1} < 1$ at [A] = 0. These linearly extrapolated intercepts are 0.74 at 25 °C and 0.86 at 78 °C.

An intercept less than unity suggests either

Can. J. Chem. Downloaded from www.nrcresearchpress.com by 210.87.254.6 on 09/05/12
For personal use only.

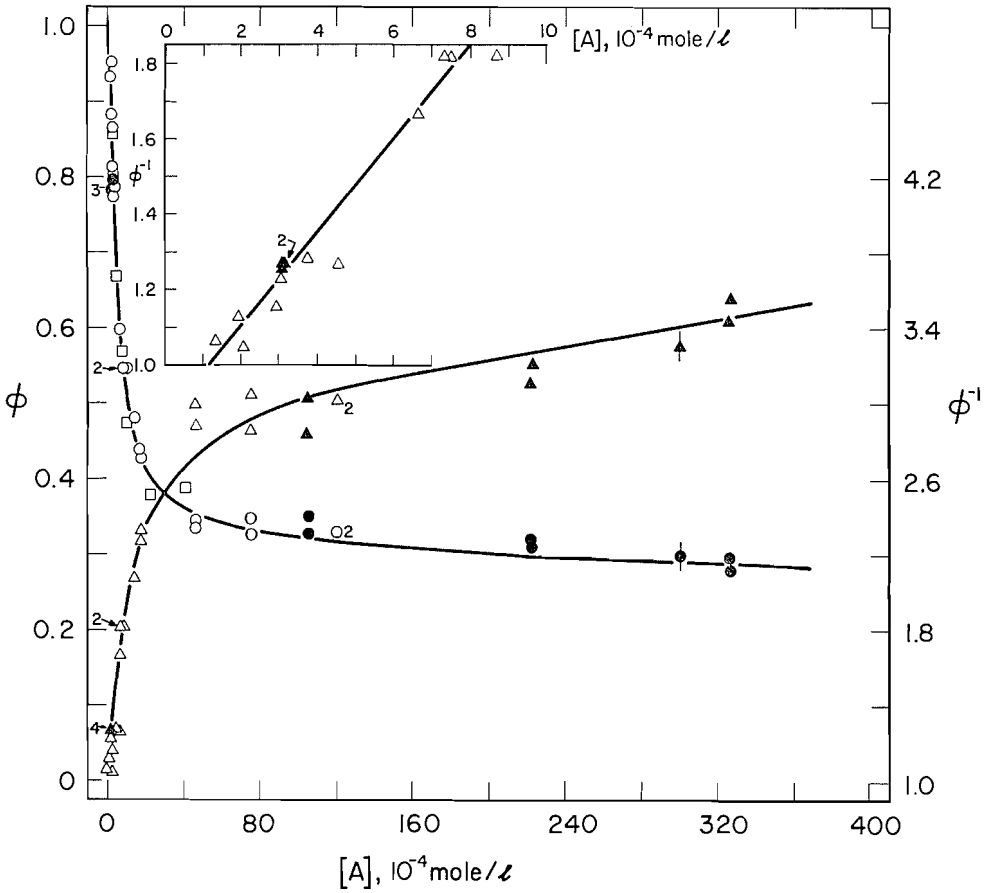

FIG. 3. Data at 78 °C. Symbols and scales as in Fig. 2 except that filled symbols with a vertical line represent an experiment at ~ 7.7% of the usual incident intensity in second series.

that the curve will pass through a point of inflection at a still lower pressure and then through $\phi^{-1} = 1$ at [A] = 0, or that a systematic error exists in the measurements so that the values of ϕ reported are systematically too large. The former interpretation is consistent with the occurrence of a weak collision mechanism; the latter merits further consideration.

If, because of systematic errors, the quantity actually measured was $w = (1 + x)\phi$, where $x > 0$, rather than ϕ itself, the intercept obtained by linear extrapolation would indeed fall below unity on the w^{-1} scale. The observed intercepts require that $x = 0.35$ at 25 °C and $x = 0.16$ at 78 °C. In view of the discussion of possible systematic errors given in the Experimental section, it is not reasonable to ascribe systematic errors of this magnitude to the present data. Moreover, the change of the systematic error with temperature is even more difficult to explain because the technique and procedures used in the experiments at the two temperatures were identical.

One possible explanation for the change of x with temperature might involve the effect of mercury vapor. If the deactivation reaction has a negative activation energy then its rate will be lower at the higher temperature. It should be recognized that the apparent collisional efficiency of deactivation is expected to be less at higher temperatures because of the positive activation energy of the competing reaction [8], and possibly of [9], as well as because of any negative temperature coefficient for [10]. Thus, although the effect of mercury vapor is to decrease ϕ, the magnitude of the effect could be less at higher

Can. J. Chem. Downloaded from www.nrcresearchpress.com by 210.87.254.6 on 09/05/12
For personal use only.

Can. J. Chem. Downloaded from www.nrcresearchpress.com by 210.87.254.6 on 09/05/12
For personal use only.

temperature and, coupled with some unknown, larger, temperature-independent effect giving rise to a positive x, the mercury effect conceivably could account for a smaller x at higher temperature. However, in the lower pressure region only a small fraction of the molecules which decompose do so from $T_1{}^0$, which, it is assumed, is the only state affected by mercury vapor, so that this possible explanation of the temperature dependence of x is not realistic. Moreover, the larger, temperature-independent effect, which must also be present to give x a large overall positive value, has not been identified.

It is worth emphasizing that Porter and Uchida's data (9) were obtained at pressures lower than were used here and the absence of a point of inflection in their data is strong evidence against the weak collision mechanism. However, it is also worth reemphasizing, as they do, that their data were adjusted to pass through $\phi^{-1} = 1$ at [A] = 0, so that only the shape of their plot, and not the absolute values of ϕ quoted, is significant. Indeed, a valid criticism of their data standing alone is simply that the point of inflection exists at a still lower pressure and that their method of adjusting the data to pass through $\phi^{-1} = 1$ disguises this possibility. However, the present data are such that the point of inflection is indeed expected in the region they studied.

Another point should be made in connection with systematic errors. If w, rather than ϕ, was the quantity measured, and if the strong collision mechanism operates so that only [2] and [3] remain as reactions for the vibrationally excited singlet state, then it is easy to show that $(w - w_\infty)[A] = (1 + x)p - pw$, in which $p = k_2/k_3$. Obviously this expression will be most sensitive to random errors at high pressures. Hence four plots were made of the data taken at 78 °C using $w_\infty = 0.26$, 0.27, 0.28, and 0.29; the visually estimated scatter in the high pressure region was least for that in which $w_\infty = 0.28$ and this particular plot is shown in Fig. 4. The slope and intercept yielded $p = 280 \times 10^{-6}$ mole/l and $x = 0.37$. A similar treatment of the data taken at 25 °C led to $w_\infty = 0.025$, $p = 140 \times 10^{-6}$ mole/l, and $x = 0.25$. The agreement between these two independent determinations of x, while probably fortuitous at 78 °C, and with the less precisely determined estimates cited earlier (1), supports the conclusion that a very large, positive, systematic error in the present measurements must be accepted if these data are to be interpreted in terms of the strong collision mechanism.

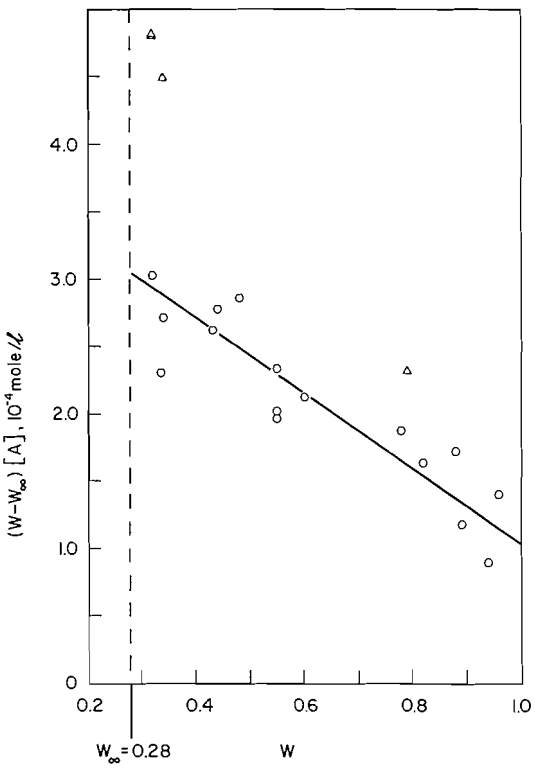

FIG. 4. Evaluation of x at 78 °C if systematic error present. Experiments shown as triangles assumed to have large random error and were disregarded in drawing the line. Line corresponds to $(w - w_\infty)[A] = 3.85 \times 10^{-4} - 2.81 \times 10^{-4} w$ mole/l, whence $x = 0.37$; w_∞ taken as 0.28.

Plots of the function $(1 - \phi)/[A]$ vs. [A] for the data taken at the two temperatures are shown in Figs. 5 and 6; the plot reported earlier (1) used raw data which had not been corrected for reflections. The existence of a maximum in these plots, again supporting a weak collision mechanism or an unreasonably large systematic error if the strong collision mechanism is valid, seems reasonably well established at 78 °C and, with rather less certainty, at 25 °C. It should be noted that the pressure at which the maximum occurs, $\sim 1.5 \times 10^{-4}$ mole/l at 25 °C and $\sim 4 \times 10^{-4}$ mole/l at 78 °C, changes with temperature in the sense predicted by qualitative considerations of the mechanism (1).

Can. J. Chem. Downloaded from www.nrcresearchpress.com by 210.87.254.6 on 09/05/12
For personal use only.

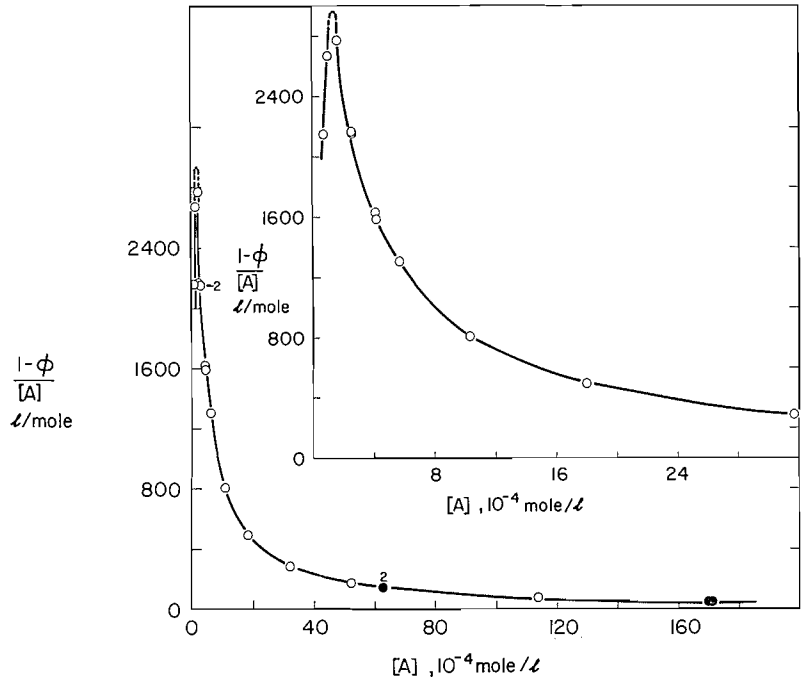

FIG. 5. Plot of $(1 - \phi)/[A]$ vs. [A] at 25 °C. Inset shows low pressure region. Symbols as for Fig. 2.

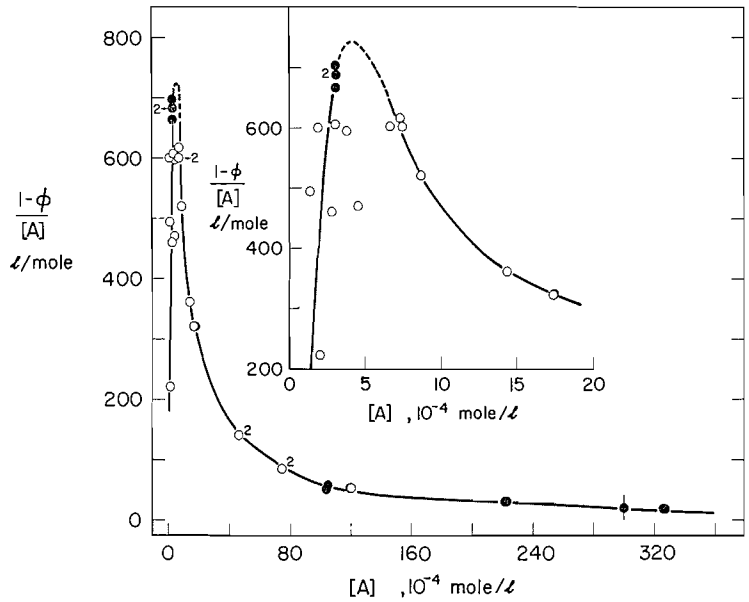

FIG. 6. Plot of $(1 - \phi)/[A]$ vs. [A] at 78 °C. Inset shows low pressure region. Symbols as for Fig. 3.

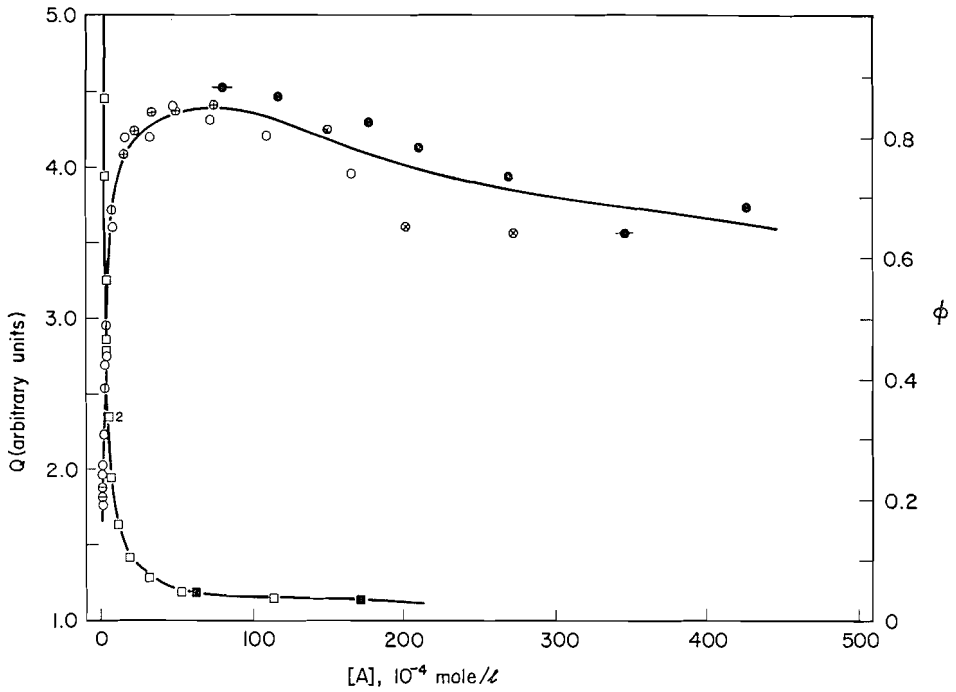

FIG. 7. Variation of Q and ϕ with [A] at 25 °C. Q vs. [A] (left ordinate). (○) Series 1; [A] changed by expansion but each new value measured; the same procedure was used in all series. (⊕) Series 2 at ~ 50% incident intensity of series 1. (⊖) Series 3. (⊗) Fresh ketone from storage for each experiment. The following experiments were done several weeks after those already mentioned and after the outside of the viewing window had become partially fogged by an oily condensate which presumably distilled from the cell insulation during the high temperature work done in the interim. The fogging remained undiscovered until the apparatus was disassembled. Therefore, all the following Q values have been multiplied by a factor of 1.23 which was obtained by normalizing series 4 to series 1. (⊕) Series 4. (●) Done with fresh ketone for each experiment; symbols with a short horizontal line represent experiments done at ~ 7.7% usual incident intensity. Not all data taken at low pressure are shown (see Fig. 9). ϕ vs. [A] (right ordinate): (□) first series; (■) second series. See caption to Fig. 2; data of Ayscough and Steacie are omitted.

It is concluded that the present data favor the weak collision mechanism. The source of the discrepancy between this conclusion and that reached by Porter and co-workers (5, 9) remains disturbingly unresolved.

The Emission

The dependence of Q on [A] as predicted by the mechanism can be described as follows, if it is assumed that the numerical factor β is independent of [A]. Q is expected to rise from zero at [A] = 0 with a slope which increases from zero at [A] = 0 to a maximum and then to decrease as [A] is increased further; at very high pressures Q approaches an asymptotic limit of

$$Q_\infty = \beta(k_4/(k_4 + k_5 + k_6)) \times [1 + (k_6/k_4)(k_7/(k_7 + k_8 + k_9 + k_{10}[\mathrm{Hg}]))].$$

Figures 7 and 8, in which Q is plotted in arbitrary units against [A], show approximately the predicted behavior; a plot of ϕ vs. [A] is included on the same pressure scale. It is seen that Q and ϕ essentially have reached their respective limits at approximately the same pressure. However, there are two respects in which the shape of the Q plots is not exactly as predicted.

At the highest pressures Q falls slightly (~ 20%) as [A] increases rather than continuing to rise slowly to a definite limit. It is just in this region where the correction for local absorption becomes most inaccurate because small errors in the measured extinction coefficients are magnified greatly; at the highest pressure the relative error in Q is some three times that of the extinction coefficient. It is believed that this, rather than a real decrease in Q or a change of β with pressure in this region, is the cause for the apparent decrease. An alternative possibility is that the length, δ, of the emitting vapor which actually was viewed was not situated exactly at

Can. J. Chem. Downloaded from www.nrcresearchpress.com by 210.87.254.6 on 09/05/12
For personal use only.

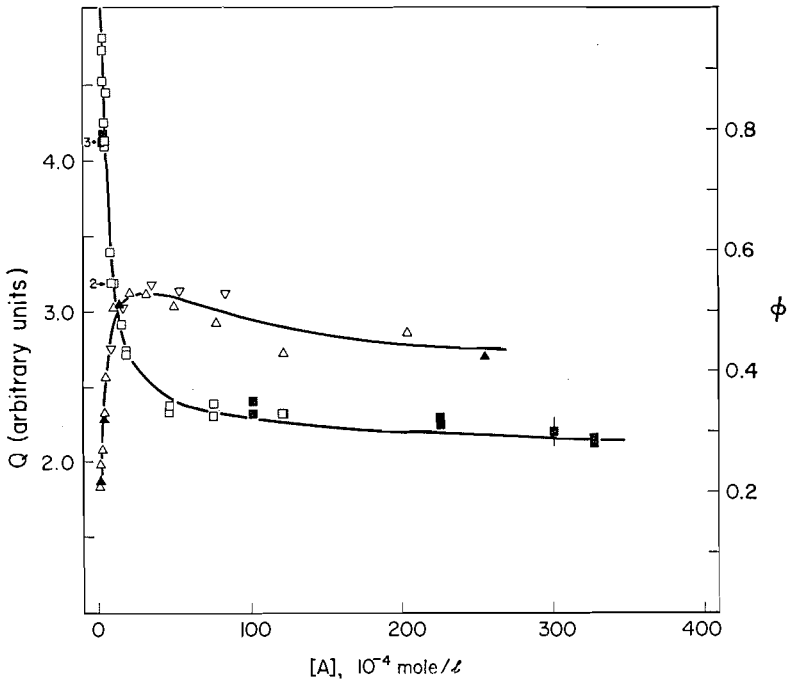

FIG. 8. Variation of Q and ϕ with [A] at 78 °C. Q vs. [A] (left ordinate). (△) Series 1; pressure changed by expansion but each value measured. (▲) Fresh ketone from storage used for each of these experiments. (▽) Series 2 done several weeks after first. Second series normalized to first with a factor of 1.19 to allow for partial fogging of viewing window (see caption to Fig. 7). Not all data taken at low pressures are shown (see Fig. 9). ϕ vs. [A] (right ordinate): (□) first series; (■) second series. See caption to Fig. 3; data of Ayscough and Steacie are omitted.

the midpoint of the cell. In that case the functional form of the local absorption correction factor, g, is no longer that cited and a systematic error in Q, if calculated with g as given, would result. Henriques and Noyes (24) offer a solution for the form of g for apparatus of a more general geometry. The geometry of the present apparatus was not sufficiently well defined to permit an application of this more sophisticated treatment. A final conclusion on this matter must await the data, soon to be obtained (7), with short cells for which the local absorption correction remains relatively small and more accurately calculable.

Figure 9 shows plots of Q vs. log [A] at several temperatures; logarithmic units are used to encompass the large range of [A] studied. It is seen that, even at the lowest pressures studied, Q does not tend toward zero, contrary to a prediction of the mechanism. The observation persists in plots using a linear pressure scale over a small range of low pressures. If this is a real phenomenon it suggests that emission occurs from all vibrational levels of S_1. On the other hand the data are less reliable in this region of pressure and a more careful study than has been done previously of the p/f ratio as a function of pressure will be required to decide whether or not the observation is an experimental artifact.

Energetics

It might be useful to consider a simplified picture of the energetics of the excited states involved and a hypothesis concerning the path by which the decomposition might occur. The picture turns out to be a simplified analogy of the molecular orbital description since advanced by Abrahamson, Littler, and Vo (25) for the photochemistry of the simplest carbonyl compound, formaldehyde.

A "diatomic" approximation of the states involved is depicted schematically in Fig. 10. The diagram is constructed largely by analogy with the known energy and geometry of the analogous states of formaldehyde (see ref. 26 for reviews). Thus S_1 is shown with a larger equilibrium CF_3—$COCF_3$ distance than that of the gound state and is correlated at high energies with some unknown electronically excited states

Can. J. Chem. Downloaded from www.nrcresearchpress.com by 210.87.254.6 on 09/05/12
For personal use only.

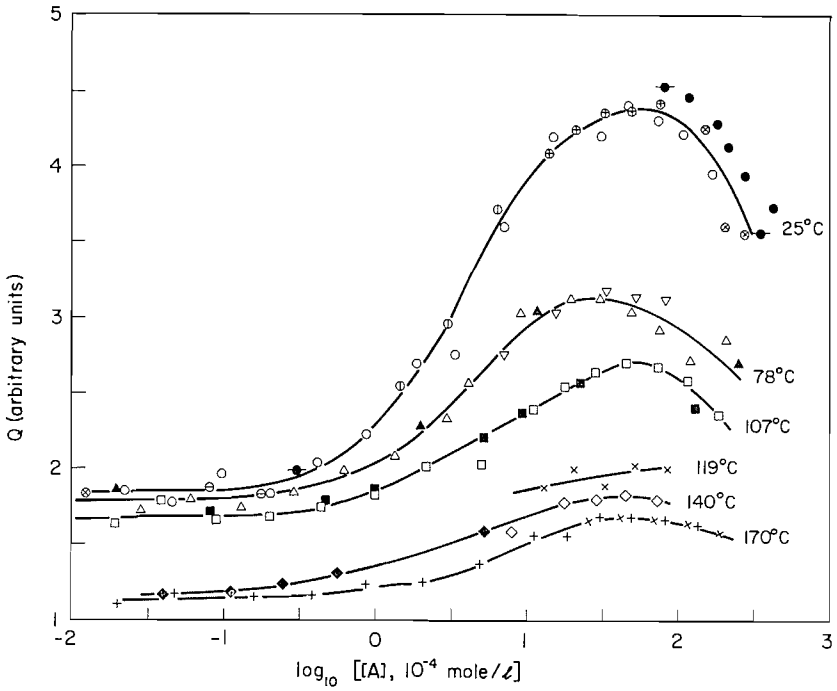

FIG. 9. Q vs. $\log_{10}$ [A] at various temperatures. Note that the logarithmic scale accentuates the decrease in Q at high pressure. Symbols for data at 25 °C and 78 °C are same as used in Figs. 7 and 8 respectively. 107 °C: (□) first series; (■) done with fresh ketone for each experiment. 140 °C: (◇) series 1. Each point represents two experiments one at normal, and one at ~ 50% normal incident intensity; greatest spread observed was 1.5%. (◆) Series 2. 170 °C: (+) series 1; (×) series 2.

of one or both of the fragments. Okabe and Steacie (18) locate the S_1 state about 82 kcal mole^{-1} above the ground state so that the minimum of S_1 lies approximately at the level of the dissociation limit of the ground state ($D(CF_3—COCF_3) \simeq 80$ kcal mole^{-1} assumed). The $n\pi^*$ triplet state, T_1, is shown with similar geometry, i.e. equilibrium $CF_3—COCF_3$ distance, to that of the S_1 state. It is not necessary to specify whether T_1 correlates with the same, or different, electronically excited state of the fragments as does S_1; it seems unlikely that T_1 should correlate directly with the ground electronic state of the fragments. As is the case for formaldehyde the S_1–T_1 separation is set at ~ 9 kcal mole^{-1}. The analogue of the $\sigma^*_{CH_2*}$ orbital discussed by Abrahamson *et al.* (25) is represented by the repulsive curve rising from the fragments in their ground electronic states and crossing T_1 and S_1 at distances only slightly larger than the bonding distances. As discussed there (25) placing the repulsive curve as shown implies a large stabilization of the repulsive orbital at near-bonding distances. The low energy, and thus this large stabilization, of the repulsive curve is of fundamental importance for the validity of the overall scheme to be discussed here.

Excitation at 3130 Å (92 kcal mole^{-1}) introduces a maximum of 10 kcal mole^{-1} vibrational energy into the symmetrical C—C stretching vibration represented in Fig. 10. It is probable that many other vibrations and rotations are excited in the transition (cf. the progression in the carbonyl stretching frequency which is prominent in the absorption spectrum of formaldehyde (26) and propynal (27)), so that the vibrational energy initially present in the C—C mode must be considerably less than the maximum. This maximum C—C vibrational energy is represented by the upper limit of the shaded area in S_1 in Fig. 10. The lower limit of the shaded area is set by the point at which the repulsive curve crosses S_1; the energy level at which this occurs is not known and has been drawn arbitrarily in the diagram. Decomposition from the singlet state is envisaged to occur as

Can. J. Chem. Downloaded from www.nrcresearchpress.com by 210.87.254.6 on 09/05/12
For personal use only.

Can. J. Chem. Downloaded from www.nrcresearchpress.com by 210.87.254.6 on 09/05/12
For personal use only.

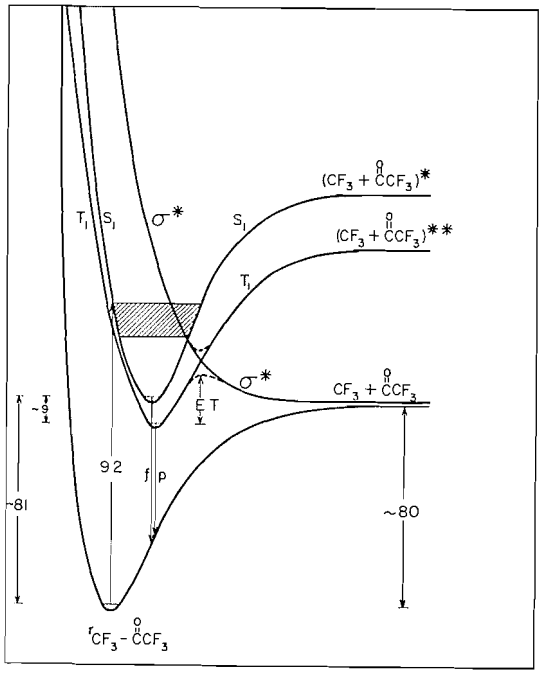

FIG. 10. Diatomic approximation to potential energy surfaces for hexafluoroacetone. The diagram is schematic and not to scale. Energy values indicated are in kcal mole^{-1}. f and p represent fluorescence and phosphorescence, respectively. S_1 represents the lowest excited singlet state of HFA, T_1 the lowest excited triplet, and σ^* the repulsive state formed from the fragments in their ground, or low-lying, electronic states.

follows. During the presumably rapid exchange of vibrational energy among the various modes, sufficient energy will from time to time accumulate in the C—C stretching mode to energize it above the lower limit of the shaded area from which a transition to the repulsive curve can occur. This crossing need not occur whenever the energetic requirements are met but a specification of other requirements which might be necessary cannot be given at this time. Collisions reduce the total vibrational energy of the molecule and, thus, the probability that sufficient energy can accumulate in the C—C mode to permit the transition to the repulsive curve. It is this loss of vibrational energy to which the strong or weak collision mechanism applies. After the molecule has lost some large amount of vibrational energy, so that the accumulation of sufficient energy in the C—C mode to exceed the lower limit of the shaded area becomes an extremely improbable event, the molecule is referred to as being in the $S_1{}^0$ state. It is from this region that the internal conversion and the fluorescence are thought to originate, although evidence that the fluorescence spectrum remains independent of pressure to very low pressures has not been obtained (18, 22), so that the possibility of fluorescence from levels above $S_1{}^0$ cannot be ruled out on the basis of published data (see above discussion of the emission).

A detailed description of the intersystem crossing reaction [6] cannot be given. Presumably the crossing first produces molecules in high vibrational levels of T_1 from which vibrational energy is lost rapidly by collision; *a priori* it is expected that if collisions do not intervene, the reverse transition would occur eventually. The fact that it is unnecessary to postulate a collision in [6] merely indicates that collisions are sufficiently frequent not to be rate determining.

A molecule in the state $T_1{}^0$ is in a potential well from which it can escape by emission of phosphorescence, by undergoing a second intersystem crossing, [9], whose details cannot be specified, by deactivation through a collision with an atom of mercury, by reaction with, or energy transfer to, an active addend (2, 3), or by unimolecular decomposition over the barrier E_T indicated in Fig. 10. The height of this barrier is not known *a priori* but the general picture, if correct, requires that E_T be rather greater than the S_1–T_1 separation; the energy of activation, which may approximately be associated with ϕ_∞, of 10–15 kcal mole^{-1} (5, 22) is in agreement with this requirement.

An approximate evaluation of E_T can be made from the data given here. It is clear that $k_8/k_7 = \phi_\infty/\phi_{p,\infty}$, in which $\phi_{p,\infty}$ is the unknown absolute quantum yield of phosphorescence at infinite pressure. However, $\phi_{p,\infty} = Q_\infty\beta^{-1}(1 + (\phi_{f,\infty}/\phi_{p,\infty}))^{-1}$, in which $\phi_{f,\infty}$ is the, also unknown, absolute quantum yield of fluorescence at infinite pressure. If it is assumed that β and the ratio $\phi_{f,\infty}/\phi_{p,\infty}$ are independent of temperature, $E_8 - E_7$, but not A_8/A_7, can be obtained from the data. *A priori* it is not unreasonable to expect β to be relatively independent of temperature, since the maxima in the intensities of the fluorescence and the phosphorescence have only a small wavelength separation (4, 7, 19). On the other hand, $\phi_{f,\infty}/\phi_{p,\infty}$ is expected to increase as temperature increases and has a value near 1/4 at room temperature (4). Thus the energy difference derived will be a minimum. Q_∞ is estimated as $\sim$4.0 at

25 °C and ~ 2.8 at 78 °C so that, using ϕ_∞ data cited earlier, $E_8 - E_7 \geqslant 11$ kcal mole^{-1}. This is also a minimum value for $E_T = E_8$.

Finally it should be noted that it is impossible to decide from the data available whether decomposition from S_1 proceeds directly to the repulsive state, as suggested above, or whether intersystem crossing occurs from many high vibrational levels of S_1 to high vibrational levels of T_1. Molecules in these states would have a very high probability to accumulate sufficient energy in the C—C bond to overcome the barrier E_T. Indeed, assuming, as is likely, that the repulsive curve is triplet, the non-crossing rule might be invoked, in which case the shape of T_1 in the region of the original crossing point is changed to that shown as broken lines in Fig. 10. These two suggestions bring the representation of the potential energy diagram offered here into general agreement with that advanced recently by Larson and O'Neal (28) for the mechanism of the primary process in acetone. It is thought, however, that the stability of T_1 in both acetone and hexafluoroacetone is too great to be represented by their Fig. 7, in which T_1 is shown to correlate directly with the fragments in their ground electronic states without an intervening barrier.

Many, if not most, of the suggestions and interpretations made in this section are highly speculative. It is hoped that some of the areas of uncertainty have been defined more precisely and that the general picture offered, while obviously oversimplified, will stimulate further consideration of these processes.

1. A. N. STRACHAN, R. K. BOYD, and K. O. KUTSCHKE. Can. J. Chem. **42**, 1345 (1964).
2. S. N. KHANNA and K. O. KUTSCHKE. Can. J. Chem. **44**, 1465 (1966).
3. A. GANDINI and K. O. KUTSCHKE. Can. J. Chem. **44**, 1720 (1966).
4. P. G. BOWERS and G. B. PORTER. J. Phys. Chem. **68**, 2982 (1964).
5. P. G. BOWERS and G. B. PORTER. J. Phys. Chem. **70**, 1692 (1966).
6. D. A. WHYTOCK. Unpublished work in these laboratories.
7. A. GANDINI. Unpublished work in these laboratories.
8. P. G. BOWERS and G. B. PORTER. Private communication.
9. G. B. PORTER and K. UCHIDA. J. Phys. Chem. **70**, 4079 (1966).
10. H. W. MELVILLE and B. G. GOWENLOCK. Experimental methods in gas reactions. McMillan and Co., Ltd., New York. 1964. p. 242.
11. M. KASHA. J. Opt. Soc. Am. **38**, 929 (1948).
12. R. E. HUNT and T. L. HILL. J. Chem. Phys. **15**, 111 (1947).
13. J. G. CALVERT and J. N. PITTS, JR. Photochemistry. Wiley and Sons, Inc., New York. 1966. p. 793.
14. D. E. HOARE. Trans. Faraday Soc. **53**, 791 (1957).
15. D. E. HOARE and J. CALDWELL. J. Am. Chem. Soc. **84**, 3987 (1962).
16. G. R. MARTIN and H. C. SUTTON. Trans. Faraday Soc. **48**, 812 (1952).
17. D. S. HERR and W. A. NOYES, JR. J. Am. Chem. Soc. **62**, 2052 (1940).
18. H. OKABE and E. W. R. STEACIE. Can. J. Chem. **36**, 137 (1958).
19. H. W. HOLDEN. Unpublished work in these laboratories.
20. R. E. REBBERT. Private communication.
21. P. B. AYSCOUGH and E. W. R. STEACIE. Proc. Roy. Soc. London, Ser. A, **234**, 476 (1956).
22. G. GIACOMETTI, H. OKABE, and E. W. R. STEACIE. Proc. Roy. Soc. London, Ser. A, **250**, 287 (1959).
23. J. C. AMPHLETT and E. WHITTLE. Trans. Faraday Soc. **63**, 80 (1967).
24. F. C. HENRIQUES and W. A. NOYES, JR. J. Am. Chem. Soc. **62**, 1038 (1940).
25. E. W. ABRAHAMSON, J. G. F. LITTLER, and KIM-PHAN VO. J. Chem. Phys. **44**, 4082 (1966).
26. D. A. RAMSAY. *In* Determination of organic structure by physical methods. Vol. 2. *Edited by* F. C. Nachod and W. D. Phillips. Academic Press, New York. 1962. Chap. 4. J. C. D. BRAND and D. G. WILLIAMSON. *In* Advances in physical organic chemistry. Vol. I. *Edited by* V. Gold. Academic Press, New York. 1963. Chap. 5.
27. J. C. D. BRAND, J. H. CALLOMON, and J. K. G. WATSON. Can. J. Phys. **39**, 1508 (1961).
28. C. W. LARSON and H. E. O'NEAL. J. Phys. Chem. **70**, 2475 (1966).

Can. J. Chem. Downloaded from www.nrcresearchpress.com by 210.87.254.6 on 09/05/12
For personal use only.

Pyrolysis of phenylmercaptoacetic acid[1,2]

A. T. C. H. TAN AND A. H. SEHON
Department of Chemistry, McGill University, Montreal, Quebec

Received March 23, 1967

The pyrolysis of phenylmercaptoacetic acid was investigated by the toluene-carrier technique over the temperature range 760–835 °K. The main products of the decomposition were phenyl mercaptan, carbon dioxide, acetic acid, phenyl methyl sulfide, carbon monoxide, and dibenzyl.

The overall decomposition was a first-order reaction with respect to phenylmercaptoacetic acid and could be represented by the two parallel steps:

[1] $$C_6H_5SCH_2COOH \xrightarrow{k_1} C_6H_5S\cdot + \cdot CH_2COOH$$

[2] $$C_6H_5SCH_2COOH \xrightarrow{k_2} C_6H_5SCH_3 + CO_2$$

Reaction [1] was shown to be a homogeneous first-order dissociation process, and its rate constant was represented by the expression

$$k_1 = 1.0 \times 10^{15} \exp(-58000/RT)\ s^{-1}.$$

The activation energy of this reaction, i.e. 58 kcal/mole, was identified with $D(C_6H_5S—CH_2COOH)$.

Canadian Journal of Chemistry, 46, 191 (1968)

Introduction

In a previous investigation (1) the experimentally determined stabilization energy of the phenylsulfide radical, $C_6H_5S\cdot$, was estimated to be about 13 kcal/mole. Hence, the weakest bond in a compound of the type $C_6H_5S—R$ would be expected to be the bond between the phenylsulfide and R radicals.

The thermal decomposition of phenylmercaptoacetic acid was investigated in the present study, with the toluene-carrier technique, with a view to determining the C—S bond dissociation energy in this compound, i.e. $C_6H_5S—CH_2COOH$, and in the hope of elucidating the reactivity of the $\cdot CH_2COOH$ radical.

Experimental

Materials

Phenylmercaptoacetic acid, m.p. 63 °C, was obtained from Evans Chemetics, Inc., and was recrystallized three times from a solution of benzene and petroleum ether. The purity of the compound, as determined by titration against standard sodium hydroxide, was better than 99%. The toluene was generously supplied by the Gulf Petroleum Company, Pittsburgh, Pa. It was stirred for 20 h with calcium chloride and distilled through an efficient column. The fraction boiling at 110.5 °C was collected and used in all experiments.

Apparatus

The pyrolysis was studied over the temperature range 760–835 °K in an apparatus similar to those used in previous investigations employing the toluene-carrier technique (2). The toluene pressure was varied from 7 to 18 mm. Known weights of the acid were introduced into a U-tube in the form of pellets. One arm of the U-tube was connected to the toluene reservoir and the other led to the furnace. During an experiment, the U-tube was heated by a removable oil bath maintained at constant temperature. The partial pressure of acid was varied from 0.08 to 0.44 mm by varying the temperature of the oil bath between 138 and 165 °C. The time of residence of the reactants in the reaction vessel was varied from about 0.2 to 1.4 s by changing the size of the capillary in the outlet of the tube connected to the reaction vessel.

Gas Chromatography

The apparatus for vapor–liquid chromatography was essentially similar to that described by Callear and Cvetanović (3). Helium was used as the carrier gas. For the analysis of the products condensed at liquid air temperature, a column made of pyrex glass tubing ($\frac{1}{4}$ in. i.d.) filled with 10 g of dinonylphthalate on 24 g of celite 505 was used.

Analysis

The products of the pyrolysis were separated from the remaining undecomposed portion of phenylmercaptoacetic acid and unreacted toluene by fractional distillation through a series of three traps maintained at −5, −78, and −188 °C, respectively. The noncondensable gases were transferred with the help of two diffusion pumps connected in series and collected into calibrated bulbs. The materials collected at −5 °C consisted of dibenzyl and undecomposed phenylmercaptoacetic acid. This trap

[1]Presented at the 47th Canadian Chemical Conference, Kingston, Ontario, June 1964.

[2]These results were incorporated in the thesis submitted by A. T. C. H. Tan in partial fulfillment of the requirements for the M.Sc. degree, McGill University, 1962. Present address: Department of Biochemistry, University of Vermont, Burlington, Vermont 05401, U.S.A.

Can. J. Chem. Downloaded from www.nrcresearchpress.com by 210.87.254.6 on 09/05/12
For personal use only.

Can. J. Chem. Downloaded from www.nrcresearchpress.com by 210.87.254.6 on 09/05/12
For personal use only.

TABLE I

Products of the decomposition of phenylmercaptoacetic acid*

Expt. No.	Temp. (°K)	Acid (mmole)		C_6H_5SH (mmole)	CH_3COOH (mmole)	$(C_6H_5CH_2)_2$ (mmole)	CO_2 (mmole)	Noncondensable gases			
		Initial	Decomposed					Total (mmole)	% H_2	% CH_4	% CO
75	760	1.065	0.171	0.018	0.015	—	0.07	0.005	—	—	—
74	767	0.888	0.116	0.015	0.007	—	0.13	0.006	—	—	—
66p	779	0.926	0.103	0.027	0.005	0.011	0.07	0.025	—	—	—
60	783	0.540	0.057	0.012	0.010	—	—	0.002	—	—	—
63	783	0.859	0.108	0.032	0.020	—	0.08	0.009	—	—	—
64	783	1.040	0.141	0.038	0.016	0.014	0.07	0.014	—	—	—
65	783	0.852	0.108	0.034	0.013	0.012	0.07	0.015	—	27.8	72.2
67	793	0.944	0.160	0.052	0.030	0.035	0.10	0.018	—	28.6	71.4
68	793	0.982	0.143	0.045	0.030	0.029	0.09	0.017	—	28.6	71.4
87	795	0.605	0.236	0.082	0.035	0.075	0.15	0.045	3.7	22.5	73.8
73	804	0.296	0.067	0.029	0.010	0.032	0.04	0.013	4.7	13.3	82.0
69	813	0.666	0.191	0.081	0.050	0.069	0.12	0.027	4.2	20.5	75.3
70	813	0.601	0.161	0.058	0.042	0.058	0.09	0.018	3.9	24.1	72.0
86	813	1.065	0.149	0.067	0.040	0.026	0.10	0.024	5.7	11.2	83.1
89p	813	0.573	0.379	0.154	0.012	0.137	0.22	0.140	3.7	6.8	89.5
88p	815	0.692	0.474	0.184	0.022	0.133	0.30	0.153	1.1	10.7	88.2
72	823	0.285	0.110	0.051	0.025	0.039	0.07	0.021	10.1	23.5	66.4
80	828	0.577	0.273	0.104	0.052	0.095	0.18	0.033	9.8	19.5	70.7
79	829	0.255	0.114	0.055	0.030	0.047	0.07	0.017	9.4	23.4	67.2
84	833	0.591	0.496	0.287	0.200	0.205	0.28	0.076	11.7	21.2	67.1
85	833	0.849	0.234	0.086	0.040	0.057	0.15	0.034	10.0	18.4	71.6
81	833	0.353	0.192	0.097	0.060	0.077	0.13	0.024	10.2	20.0	69.8
91p	833	0.309	0.258	0.110	0.005	0.076	0.16	0.095	1.0	10.8	88.2
82	835	0.867	0.415	0.216	0.220	0.160	0.21	0.049	12.3	19.2	71.5

*The — indicates that products were not large enough to be measured; p refers to experiments done in the packed reaction vessel.

Can. J. Chem. Downloaded from www.nrcresearchpress.com by 210.87.254.6 on 09/05/12
For personal use only.

was weighed before and after an experiment and its contents were dissolved in ethanol, then diluted with water, and titrated with standard sodium hydroxide. The number of milliequivalents of sodium hydroxide used was considered to be equal to the amount of unreacted acid and the amount of dibenzyl was taken as the difference between the total weight of the contents trapped at −5 °C and the weight corresponding to the unreacted acid. The validity of this procedure was established in "control" experiments, performed with the furnace temperature at 200 °C, where no decomposition occurred; it was thus shown that the acid could be trapped quantitatively at −5 °C and thus removed from the stream of toluene.

The trap at −78 °C contained toluene, acetic acid, phenyl mercaptan, and phenyl methyl sulfide. Acetic acid was demonstrated by gas chromatography and was determined by titration with standard sodium hydroxide. Phenyl mercaptan was determined as previously described (4) by amperometric titration with a 0.1 *N* silver nitrate solution using a rotating platinum electrode and a microammeter. The contents of the trap at −78 °C gave a deep-red color with chloranil and an orange-yellow color with quinone, which indicated the presence of phenyl methyl sulfide (5). However, the presence of the large excess of toluene did not permit the use of the latter procedure for the quantitative determination of phenyl methyl sulfide.

The contents of the trap at −188 °C were separated by gas chromatography. One large and three tiny peaks were obtained. On the basis of the elution time, as determined from the gas chromatogram, and of infrared (i.r.) analysis, the major component in this trap was identified as carbon dioxide. The i.r. spectrum of a cumulative sample of the contents of the trap at −188 °C, collected for several experiments, also revealed a strong absorption at 2150 cm^{-1}, which could be assigned to the —C=C=O asymmetric stretching vibration of ketene (6); the other three smaller absorption peaks of this i.r. spectrum (at 3070, 1388, and 1120 cm^{-1}) confirmed further the presence of ketene in this sample (7, 8).

The amount of carbon monoxide and the ratio of hydrogen to methane in the noncondensable gases was established by combustion over copper oxide at 350 °C.

Results

The main products of the decomposition were carbon dioxide, phenyl mercaptan, acetic acid, dibenzyl, phenyl methyl sulfide, and carbon monoxide. Small quantities of ketene, methane, and traces of hydrogen were also found. Table I shows the main products and the amounts of acid decomposed under different experimental conditions.

The contents of the trap at −5 °C, when warmed to room temperature, in the presence of air, turned slightly yellow. However, the infrared analysis of the contents of this trap revealed the presence of undecomposed acid and dibenzyl only. It is, therefore, concluded that the yellow color was due to substances produced in negligible amounts.

The amount of the total noncondensable gases varied between 23 and 54% of the phenylmercaptan and it increased up to 90% in the experiments performed in the packed reaction vessel. Carbon monoxide constituted about 60 to 70% of the total noncondensable gases and the remainder consisted of methane. The percentage of carbon monoxide rose to about 90% in the experiments performed in the packed reaction vessel. At the highest temperatures used, a small amount of hydrogen was also formed.

Discussion

Mechanism of Decomposition

The analytical results suggested that the pyrolysis of phenylmercaptoacetic acid occurred primarily by two simultaneous processes [1] and [2], involving a free radical and a molecular dissociation reaction, respectively.

[1] $C_6H_5SCH_2COOH \xrightarrow{k_1} C_6H_5S + CH_2COOH$

[2] $C_6H_5SCH_2COOH \xrightarrow{k_2} C_6H_5SCH_3 + CO_2$

From the relative amounts of the products formed, reaction [2] appears to predominate in the temperature range studied. If each phenylsulfide radical abstracted a hydrogen atom from toluene, i.e. by reaction [3],

[3] $C_6H_5S + C_6H_5CH_3 \rightarrow C_6H_5SH + C_6H_5CH_2,$

the sum of the phenyl mercaptan and of the carbon dioxide formed in reactions [3] and [2] would be expected to be equal to the total amount of phenylmercaptoacetic acid decomposed. In actual fact, as can be seen from the data listed in the last two columns of Table II, this expectation was supported by experimental results.

Furthermore, if each of the CH_2COOH radicals abstracted a hydrogen atom from toluene in reaction [4], the ratio of phenyl mercaptan to acetic acid would be unity.

[4] $CH_2COOH + C_6H_5CH_3 \rightarrow CH_3COOH + C_6H_5CH_2$

However, as shown in Table I, the amount of acetic acid was always less than that of phenyl mercaptan and, therefore, it must be concluded that reaction [4] was not sufficiently rapid to remove all the CH_2COOH radicals and that some of these disappeared also by other reactions.

TABLE II

$[C_6H_5SH + (CO_2 - CH_4^*)]$/acid decomposed†

Expt.‡ No.	Temp. (°K)	C_6H_5SH (mmole)	Total CO_2 (mmole)	Acid decomposed (mmole)	$\frac{C_6H_5SH + CO_2}{\text{acid decomposed}}$	$\frac{C_6H_5SH + (CO_2 - CH_4^*)}{\text{acid decomposed}}$
74	767	0.015	0.13	0.116	1.25	1.25
66p	779	0.027	0.07	0.103	0.94	0.87
63	783	0.032	0.08	0.108	1.03	1.01
64	783	0.038	0.07	0.141	0.77	0.77
65	783	0.034	0.07	0.108	0.96	0.91
67	793	0.052	0.10	0.160	0.95	0.93
68	793	0.045	0.09	0.143	0.95	0.93
87	795	0.082	0.15	0.236	0.98	0.96
73	804	0.029	0.04	0.067	1.03	0.97
69	813	0.081	0.12	0.191	1.05	1.01
70	813	0.058	0.09	0.161	0.92	0.90
86	813	0.067	0.10	0.149	1.12	1.08
89p	813	0.154	0.22	0.379	0.99	0.95
88p	815	0.184	0.30	0.474	1.02	0.98
72	823	0.051	0.07	0.110	1.10	1.03
80	828	0.104	0.18	0.273	1.04	1.03
79	829	0.055	0.07	0.114	1.10	1.08
84	833	0.287	0.28	0.496	1.14	1.10
85	833	0.086	0.15	0.234	1.01	0.99
81	833	0.097	0.13	0.192	1.18	1.01
91p	833	0.110	0.16	0.258	1.04	0.96
82	835	0.216	0.21	0.415	1.02	1.00

†CH_4^* = [total CH_4] − [CH_4 from the decomposition of toluene]. This calculation was based on the assumption that all the hydrogen formed resulted from the decomposition of toluene and that for each 1.5 moles of hydrogen formed, 1 mole of methane was formed (11).
‡The experiments marked p refer to those done in the packed reaction vessel.

Fate of the CH_2COOH Radicals

The CH_2COOH radicals may have abstracted one hydrogen atom according to reaction [4],

[4] $CH_2COOH + C_6H_5CH_3 \rightarrow CH_3COOH + C_6H_5CH_2$,

or may have decomposed according to reactions [5] and [6].

[5] $CH_2COOH \rightarrow CH_3 + CO_2$

[6] $CH_2COOH \rightarrow CH_2CO + OH$

The methyl and hydroxyl radicals produced in reactions [5] and [6] would be expected to abstract a hydrogen atom from toluene to yield methane (9) and water (2), respectively.

[7] $CH_3 + C_6H_5CH_3 \rightarrow CH_4 + C_6H_5CH_2$

[8] $OH + C_6H_5CH_3 \rightarrow C_6H_5CH_2 + H_2O$

Owing to technical difficulties to establish a water-free system, all attempts to detect among the products the presence of small quantities of water, which might have been formed, were unsuccessful. Nevertheless, reaction [8] is believed to be a probable reaction responsible for the removal of hydroxyl radical.

The benzyl radicals were assumed to dimerize to give dibenzyl.

[9] $2C_6H_5CH_2 \rightarrow (C_6H_5CH_2)_2$

If reactions [1] to [9] represent the mechanism of the decomposition of phenylmercaptoacetic acid in a stream of toluene, the following stoichiometry should have been observed.

$$[C_6H_5SH] = [(C_6H_5CH_2)_2] = [CH_3COOH] + [CH_2CO] + [CH_4]$$

However, the data listed in Table I indicate that

$$[C_6H_5SH] > [(C_6H_5CH_2)_2] > [CH_3COOH] + [CH_4].$$

In actual fact, the ratio of dibenzyl to phenyl mercaptan was, in most experiments conducted at the higher temperatures, somewhat smaller than unity, varying between 0.7 and 0.9. In previous studies it was shown that dibenzyl could not be trapped quantitatively at −5 °C from a stream of toluene and that its recovery was usually not better than 90% of the theoretical amount (10). It is clear that the relative losses in

Can. J. Chem. Downloaded from www.nrcresearchpress.com by 210.87.254.6 on 09/05/12
For personal use only.

Can. J. Chem. Downloaded from www.nrcresearchpress.com by 210.87.254.6 on 09/05/12
For personal use only.

the recovery of dibenzyl would be larger at the lower temperatures and higher flow rates, since the absolute amount of dibenzyl formed would be smaller under these conditions. In consequence it seems reasonable to conclude that the amount of dibenzyl actually formed in this investigation approached the amount of phenyl mercaptan formed.

Since the amount of ketene produced was small and since it did not account for the difference between the phenyl mercaptan and [acetic acid plus methane], it is considered reasonable to postulate that some ketene was either dimerized or decomposed. On concentration grounds alone, dimerization of ketene would not be too likely to occur. Moreover, the large amounts of carbon monoxide in the reaction would support the alternate explanation that a large fraction of the ketene formed in reaction [6] had decomposed.

It is difficult to propose a mechanism for the formation of carbon monoxide. However, considering that the ratio of carbon monoxide to phenyl mercaptan increased considerably in the experiments performed in the packed reaction vessel[3], it would appear that the carbon monoxide was due to some heterogeneous decomposition reaction of the ketene on the wall of the reaction vessel.

Calculation of $D(C_6H_5S—CH_2COOH)$

The overall rate constant, k, for the pyrolysis of phenylmercaptoacetic acid was expressed as

$$[10] \qquad k = 1/t \ln [(A)/(A - X)],$$

where t is the time of contact in seconds, (A) and (A − X) represent the amounts of phenylmercaptoacetic acid passed through the reaction vessel and recovered in the trap at −5 °C, respectively. If the two parallel reactions [1] and [2] were also first-order processes, and if reaction [3] were very rapid by comparison with reaction [1], one could write the additional rate expressions

$$[11] \quad k_1 = \frac{(C_6H_5SH)}{(A)} k[1 - \exp(-kt)]^{-1}$$

$$[12] \quad k_2 = \frac{(CO_2)}{(A)} k[1 - \exp(-kt)]^{-1},$$

where (C_6H_5SH) and (CO_2) represent the amounts of phenyl mercaptan and of carbon dioxide formed during time t, respectively.

The first-order rate constants, k and k_1, calculated for experiments under different conditions are listed in Table III. Both rate constants were almost unaffected by the variation of the partial pressure of the acid by a factor of 5.5, of the toluene pressure by a factor of 2, of the time of contact by a factor of 6.5, and of the surface/volume ratio of the reaction vessel by a factor of 27 in the higher temperature range. However, at the lower temperature used, the scatter of the data suggest some heterogeneity. It is, therefore, concluded that the use of eqs. [10] and [11] was justifiable in the higher temperature range, and that reaction [1], as well as the overall decomposition of phenylmercaptoacetic acid, were homogeneous first-order processes in this range. Moreover, because of the scatter of the data at the lower temperature, these were neglected for the calculation of the Arrhenius equation for the rate constant k of the overall decomposition.

Since phenyl methyl sulfide could not be determined quantitatively, and since carbon dioxide was not produced exclusively in reaction [2], no attempt was made to calculate k_2 with the help of eq. [12]. The rate constant k_2 represents the small difference between k and k_1; however, because of the inherently large error involved in such a calculation, such computations were not attempted.

The Arrhenius plots of log k and log k_1 vs. $1/T$ are shown in Figs. 1 and 2 respectively, and the corresponding rate constants computed from these graphs are given by the expressions

$$k = 2 \times 10^{12} \exp(-46000/RT) \text{ s}^{-1} \text{ and}$$

$$k_1 = 1.0 \times 10^{15} \exp(-58000/RT) \text{ s}^{-1}.$$

With the usual assumption that the recombination of radicals requires no activation energy, the value of 58 kcal/mole, with an estimated uncertainty of ±2 kcal/mole, may be identified with the dissociation energy of the $C_6H_5S—CH_2COOH$ bond. By comparison, the C—S bond dissociation energy in phenyl methyl sulfide had been found to be 60 kcal/mole (1). This difference of 2 kcal/mole is obviously within experimental error of the technique. Nevertheless, it is in the right direction, since it is reasonable to expect that the CH_2COOH radical is slightly resonance stabilized with reference to the methyl radical.

[3]For example, at 833 °K, in experiment No. 85, the carbon monoxide formed was only about 0.25 of the amount of phenyl mercaptan formed; while in experiment No. 91p the ratio was increased to 0.77.

Can. J. Chem. Downloaded from www.nrcresearchpress.com by 210.87.254.6 on 09/05/12
For personal use only.

TABLE III

Rate constants for the pyrolysis of phenylmercaptoacetic acid

Expt.* No.	Temp. (°K)	Toluene press. (mm Hg)	Acid press. (mm Hg)	Toluene press. / Acid press.	Time of contact (s)	Overall % decomposition	k (s^{-1})	k_1 (s^{-1})
75	760	11.72	0.29	40	0.44	16.1	0.40	0.04
74	767	13.09	0.27	48	0.46	13.1	0.30	0.04
66p	779	10.74	0.18	60	0.44	11.1	0.27	0.07
60	783	17.97	0.11	163	0.55	10.6	0.21	0.04
63	783	15.33	0.17	90	0.61	12.6	0.22	0.07
64	783	14.90	0.17	88	0.65	13.5	0.23	0.06
65	783	11.18	0.24	47	0.61	12.7	0.23	0.07
67	793	9.85	0.19	52	0.46	16.9	0.40	0.13
68	793	15.33	0.24	64	0.37	14.6	0.43	0.14
87	795	11.72	0.22	53	1.11	39.0	0.45	0.15
73	804	10.85	0.12	90	0.45	22.6	0.57	0.25
69	813	9.63	0.17	57	0.47	28.7	0.73	0.31
70	813	17.34	0.16	108	0.33	26.8	0.95	0.34
86	813	5.04	0.24	21	0.21	14.0	0.95	0.33
89p	813	10.85	0.22	49	1.17	66.3	0.92	0.38
88p	815	11.81	0.23	51	1.04	68.5	1.04	0.42
72	823	7.83	0.17	46	0.46	38.6	1.06	0.49
80	828	7.42	0.44	17	0.48	47.3	1.33	0.51
79	829	9.12	0.08	114	0.41	44.7	1.44	0.70
84	833	15.51	0.18	86	1.34	84.0	1.36	0.79
85	833	5.80	0.10	58	0.21	27.6	1.52	0.57
81	833	7.87	0.13	60	0.49	54.4	1.60	0.81
91p	833	11.85	0.17	70	1.08	83.7	1.66	0.71
82	835	15.00	0.06	250	0.38	47.9	1.73	0.90

*p refers to experiments done in the packed reaction vessel.

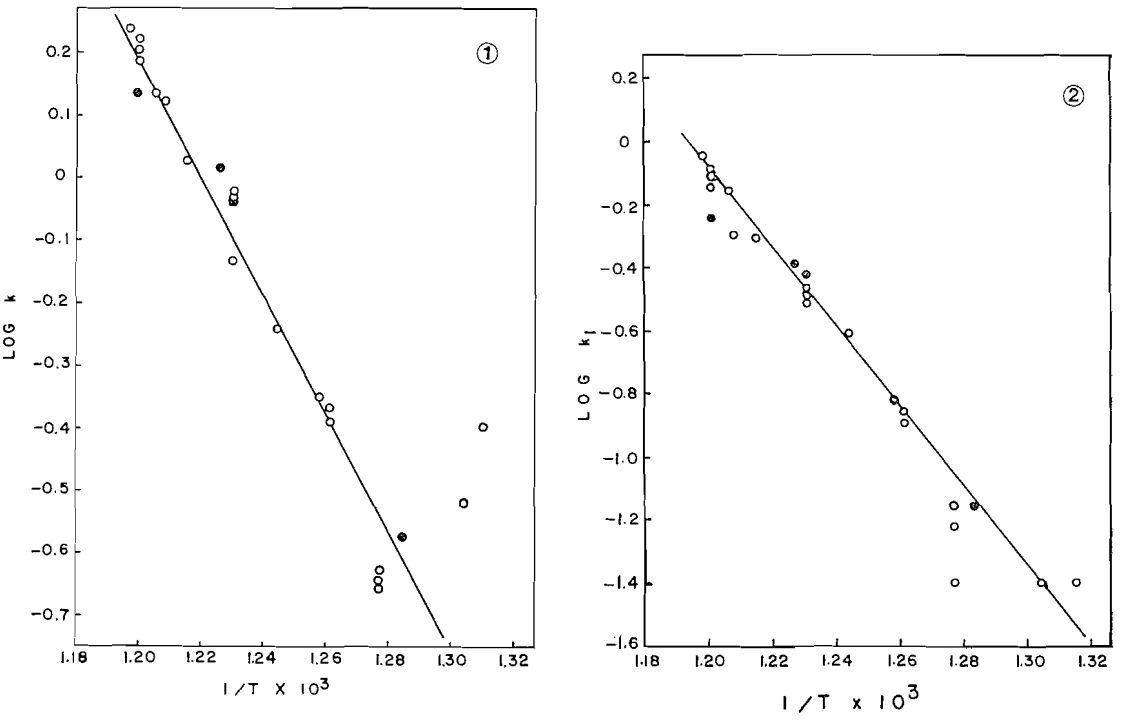

FIG. 1. Plot of log k vs. $1/T$. Experiments done in the packed reaction vessel are indicated by the filled circles.
FIG. 2. Plot of log k_1 vs. $1/T$. Experiments done in the packed reaction vessel are indicated by the filled circles.

Acknowledgments

The authors wish to thank the National Research Council of Canada for continued financial assistance. This work was also supported in part by the Petroleum Research Fund administered by the American Chemical Society; grateful acknowledgment is hereby made to the donors of said fund.

1. M. H. BACK and A. H. SEHON. Can. J. Chem. **38**, 1076 (1960).
2. M. H. BACK and A. H. SEHON. Can. J. Chem. **38**, 1261 (1960).
3. A. B. CALLEAR and R. J. CVETANOVIĆ. Can. J. Chem. **33**, 1256 (1955).
4. I. M. KOLTHOFF and W. E. HARRIS. Ind. Eng. Chem. Anal. Ed. **18**, 161 (1946).
5. R. PUMMER. Ber. **43**, 1402 (1910).
6. R. N. JONES and C. SANDORFY. Chemical applications of spectroscopy. Interscience, New York. 1956.
7. A. P. COX and A. S. ESBITT. J. Chem. Phys. **38**, 1636 (1963).
8. INFRARED SPECTRAL DATA. American Petroleum Institute Research Project 44, Texas A & M University, College Station, Texas. Curve 699, Ketene.
9. M. SZWARC. J. Chem. Phys. **17**, 431 (1949).
10. E. H. BRAYE, A. H. SEHON, and B. deB. DARWENT. J. Am. Chem. Soc. **77**, 5283 (1955).
11. M. SZWARC. J. Chem. Phys. **16**, 128 (1948).

Can. J. Chem. Downloaded from www.nrcresearchpress.com by 210.87.254.6 on 09/05/12
For personal use only.

The role of Hg 6^3P_0 atoms in mercury photosensitization. IV. Origin of the 4850 Å and 3350 Å bands

J. E. McAlduff,[1] D. D. Drysdale,[2] and D. J. Le Roy
Lash Miller Chemical Laboratories, University of Toronto, Toronto, Ontario

Received May 16, 1967

The continuous emission bands at 4850 Å and 3350 Å, attributed to the decay of electronically excited mercury molecules, have been studied in a flow system in which Hg 6^3P_1 atoms were generated in the presence of nitrogen. The mechanism presented to account for the formation and decay of these eximers incorporates the assumption that these bands are derived by spontaneous emission from the $A^30_u^-$ and A^31_u states of the mercury molecule respectively. It is proposed that the A^31_u state is the precursor of the $A^30_u^-$ state.

Canadian Journal of Chemistry, **46**, 199 (1968)

Can. J. Chem. Downloaded from www.nrcresearchpress.com by 210.87.254.42 on 09/05/12
For personal use only.

In Part III of this series (1) we postulated the formation of an electronically excited Hg_2 molecule to account for the steady-state concentration of Hg 6^3P_0 atoms in a system comprising mercury vapor and nitrogen illuminated by the mercury resonance line at 2537 Å. At that time, we suggested that this molecule might be the species responsible for the visible continuum emitted by mercury vapor in the region of 4850 Å. The present communication is a report on the results and interpretation of an investigation of the bands at 4850 Å and 3350 Å and of the dependence of their intensities on the concentrations of mercury and nitrogen.

The fluorescence continua associated with electronically excited states of Hg_2 have been studied extensively in systems containing mercury vapor alone at relatively high temperatures (2). The species responsible for the continuum at 4850 Å appears to have a long lifetime; thus Rayleigh (3) and Phillips (4) were able to observe it in a flowing stream of gas some distance downstream from the region of excitation. Rayleigh (5) also showed that the gas giving rise to this continuum downstream contained metastable Hg 6^3P_0 atoms. In the presence of nitrogen, which is known to produce Hg 6^3P_0 atoms by quenching of the 6^3P_1 state, the continuum can also be observed at the low mercury pressures obtaining at room temperature. For these reasons it has usually been assumed that the species responsible for the 4850 Å band is the $A^30_u^-$ state of Hg_2, which has as its dissociation products a metastable 6^3P_0 atom and a ground state 6^1S_0 atom.

McCoubrey (6), with a system containing pure mercury vapor at 200 °C, found a common persistence time for the 4850 Å band and the ultraviolet band at 3350 Å. To account for this close relationship, he postulated that the 3350 Å band arises by spontaneous emission from the $A^30_u^-$ state while the 4850 Å band results from a triple collision involving an Hg_2 $A^30_u^-$ molecule and two mercury atoms in the ground state. This explanation was a departure from the earlier postulate of Mrozowski (7) that the 3350 Å band originates by spontaneous emission from the A^31_u state, for which the dissociation products are a 6^3P_1 atom and a 6^1S_0 atom.

Berberet and Clark (8) studied the 4850 Å band in the presence of nitrogen and postulated the formation of an electronically excited Hg_2 molecule in a triple collision of a 6^3P_0 atom, a 6^1S_0 atom, and a nitrogen molecule. The excited Hg_2 molecule was then assumed to decay by either spontaneous emission of the 4850 Å band or diffusion to the walls.

The purpose of the present investigation was, then, to resolve the problem of the origins of the 4850 Å and 3350 Å bands and, if possible, to correlate the dependence of their intensities with the reactions of Hg^3P_0 atoms studied previously (1).

Experimental

The apparatus was almost identical with that used previously by Kimbell and Le Roy (9) in studying the emission of the forbidden line (Hg $6^3P_0 \rightarrow 6^1S_0$). Initially quantitative measurements on the 4850 Å band were made by isolating a single relatively narrow portion of the band in the region of 4850 Å by using a GL-935 photocell

[1]Present address: Department of Chemistry, St. Francis Xavier University, Antigonish, Nova Scotia.
[2]Present address: Department of Physical Chemistry, The University, Leeds, 2, England.

Can. J. Chem. Downloaded from www.nrcresearchpress.com by 210.87.254.42 on 09/05/12
For personal use only.

and a filter combination of an 8K2 and a 47C-5 Wratten filter. Subsequently an EMI-5683 photomultiplier was used in conjunction with a series of five filter combinations to isolate narrow portions of the emission band. These combinations, together with their regions of maximum transmission, are recorded in Table I.

TABLE I

Filter combinations used in isolating regions of the 4850 Å band

Filter combination	Wavelength range (Å)	λ_{max} (Å)
Corning 3385 Corning 5113	4550 – 4800	4660
Wratten 8K2 Wratten 50	4645 – 4975	4750
Wratten 47 Corning 3384	4885 – 5315	5030
Wratten 47 Wratten 62	5085 – 5340	5200
Dal # 062901 (Interference filter)	5720 – 6140	5930

All measurements on the 3350 Å band were made using a Hilger Model E-517 quartz spectrograph and Kodak 103-F spectrographic plates. The plates were developed in Kodak D-19 developer for 4 min at 20 °C and photometered on a Joyce-Loebel Mk III C double beam microdensitometer. Since the plate sensitivity is dependent on wavelength, all measurements of optical density were made at the arbitrary wavelength 3400 Å. For this wavelength, the value of γ_λ was determined as the slope of the plot of log (exposure time) (as abscissa) vs. resultant optical density, D_λ (as ordinate), for a constant intensity I_λ:

$$D_\lambda = b_\lambda + \gamma_\lambda \log I_\lambda + \gamma_\lambda \log t.$$

Thus for a constant exposure time, the intensities of the emission at various nitrogen pressures relative to the intensity at $N_2 = 97$ mm could be calculated from optical densities by the expression

$$\frac{I_\lambda^{N_2}}{I_\lambda^{N_2=97\text{ mm}}} = \text{antilog}\,\frac{D_\lambda^{N_2} - D_\lambda^{N_2=97}}{\gamma_\lambda}.$$

A constant mercury pressure of 9.30×10^{-4} mm was used.

Scattered light from the walls of the reaction vessel was eliminated by the use of suitable apertures and in the case of the photometric measurements corrections were made for dark current and for fluorescence from the quartz windows.

A quantity directly proportional to the concentration of metastable atoms, [Hg^0], was calculated for part of the present work making use of data evaluated in III and elsewhere (1). Briefly, the product $K^0[Hg^0]L$ was obtained from the expression

$$\psi = \frac{[Hg]}{K^0[Hg^0]L} \cdot 10^{-K^*[Hg]x},$$

where K^0 is the extinction coefficient for the absorption of 4047 Å by Hg^0 atoms, L is the path length of the analysis radiation (4047 Å), K^* is the effective extinction coefficient of 2537 Å radiation, and x is the path length of the exciting radiation in the present apparatus. ψ is a function of nitrogen and mercury concentrations, otherwise containing only known rate constants and quantities that have been evaluated experimentally (1). Thus $K^0[Hg^0]L$ can be calculated for various nitrogen and mercury pressures under conditions where its experimental determination would be adversely affected by pressure broadening of the absorption lines.

Results

The 4850 Å Band

In order to ascertain whether or not the *shape* of this emission band was dependent on the concentrations of nitrogen and mercury, relative intensity measurements were made in five different regions of the band. These were made in two series: in the first the mercury pressure was kept constant at $10.7_8 \times 10^{-4}$ mm and the nitrogen pressure was varied from 19.5 mm to 124.5 mm; in the second the nitrogen pressure was kept constant at 60.0 mm and the mercury pressure varied from $3.3_1 \times 10^{-4}$ mm to $10.7_8 \times 10^{-4}$ mm. The results are shown in Table II and Table III.

The intensities were measured in arbitrary units. In columns 7 to 11 of Table II intensities are given relative to those for a nitrogen pressure of 124.5 mm. It is evident that the relative intensities, while strongly dependent on nitrogen pressure, are essentially independent of wavelength. We therefore conclude that the shape of the emission band is independent of nitrogen pressure. The average values of the relative intensities, together with their standard deviations, are given for each nitrogen pressure in the last column of Table II and are plotted in Fig. 1. It can be seen that the scatter of the points from a smooth curve is, in every case, less than the standard deviations given in Table II.

From Table III it is evident the intensities, relative to those for a mercury pressure of $10.7_8 \times 10^{-4}$ mm, are strongly dependent on mercury pressure but essentially independent of wavelength. In these measurements the standard deviations are somewhat larger but here also the scatter of the average relative intensities from a smooth curve was considerably less than the standard deviations of Table III, as shown in Fig. 2.

The fact that the shape of the band was independent of both nitrogen and mercury pressure greatly simplified the analysis of the

Can. J. Chem. Downloaded from www.nrcresearchpress.com by 210.87.254.42 on 09/05/12
For personal use only.

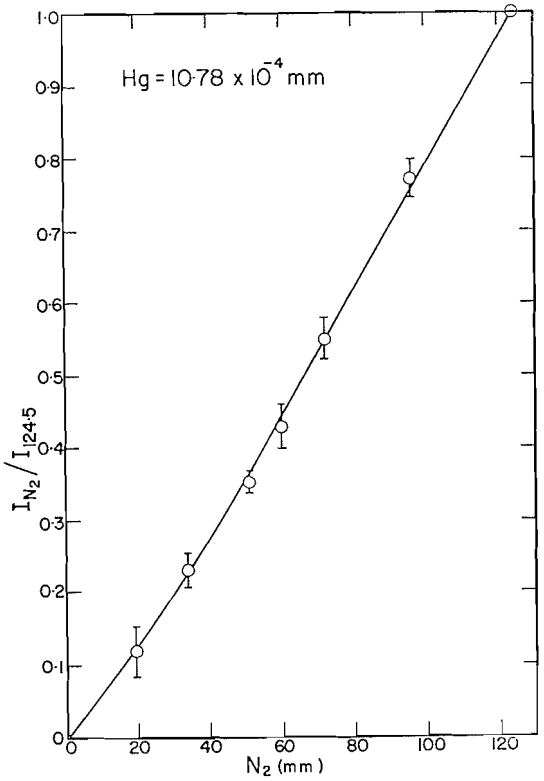

FIG. 1. Dependence of 4850 Å band intensity on $[N_2]$ for $[Hg] = 10.78 \times 10^{-4}$ mm. The ordinate is the ratio of the intensity at $[N_2]$ to the intensity at $[N_2] = 124.5$ mm.

results, because it was then unnecessary to take into account the variation of the sensitivity of the photomultiplier with wavelength in order to obtain the (integrated) band intensity as a function of nitrogen and mercury pressure.

Because of the rather low intensity of the 4850 Å band it was not possible to investigate it, in the present research, at nitrogen pressures less than about 20 mm. At this and higher pressures we felt that K^0 was likely to be influenced by pressure broadening and that the optical density for the absorption of 4047 Å would no longer be a very accurate measure of the concentration of Hg^0. We have, therefore, *calculated* the values of $K^0[Hg^0]L$ using the rate constants given previously (1), together with the pressures of nitrogen and mercury used in the present experiments.

In Fig. 3 the relative band intensities taken from Table II are plotted against the product of the relative concentration of Hg^0 times the nitrogen pressure. The latter is simply the value of $K^0[Hg^0]L[N_2]$ for the nitrogen pressure concerned divided by the value for a nitrogen pressure of 124.5 mm. It is evident that for a constant mercury pressure ($10.7_8 \times 10^{-4}$ mm) the intensity of the band is proportional to the product of $[Hg^0]$ and $[N_2]$. From Fig. 4 it is also seen that at constant $[N_2]$ the intensity of the band is proportional to the product of $[Hg^0]$ and [Hg]. We conclude, therefore, that the 4850 Å band intensity is proportional to the product of $[Hg^0]$, [Hg], and $[N_2]$, at least in the range 20–125 mm of nitrogen.

Ratio of the Relative Intensities of the 4850 Å and 3350 Å Bands

The relative intensity data for the 3350 Å band are given in Table IV. To compare these directly with similar data on the 4850 Å band, the latter were interpolated graphically to give values of

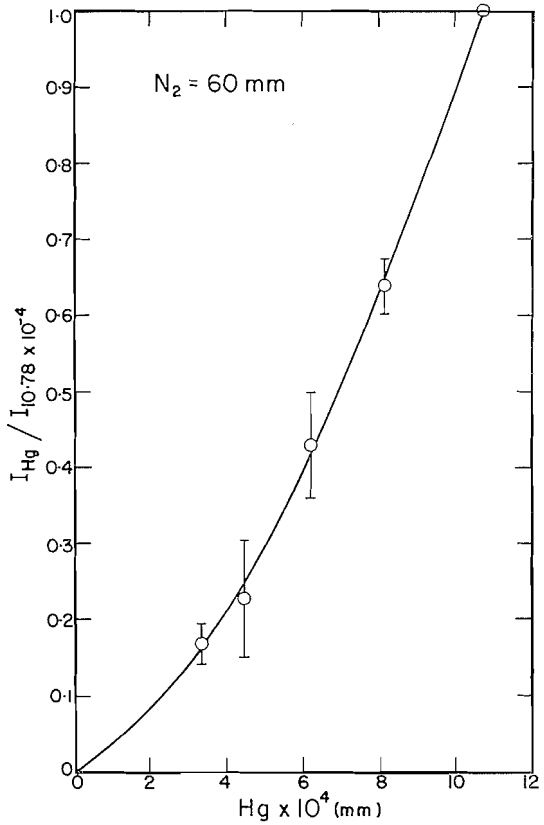

FIG. 2. Dependence of 4850 Å band intensity on [Hg] for $[N_2] = 60$ mm. The ordinate is the ratio of the intensity at [Hg] to the intensity at $[Hg] = 10.78 \times 10^{-4}$ mm.

Can. J. Chem. Downloaded from www.nrcresearchpress.com by 210.87.254.42 on 09/05/12
For personal use only.

TABLE II

Photometric intensity measurements at [Hg] = 10.78 × 10^{-4} mm (4850 Å band)

N_2 (mm)	$I_{5200\,Å}$	$I_{4660\,Å}$	$I_{4750Å}$	$I_{5030\,Å}$	$I_{5930\,Å}$	λ = 5200 Å, $I/I_{124.5}$	λ = 4660 Å, $I/I_{124.5}$	λ = 4750 Å, $I/I_{124.5}$	λ = 5030 Å, $I/I_{124.5}$	λ = 5930 Å, $I/I_{124.5}$	Ave. $I/I_{124.5}$
19.5	1.50	1.81	3.94	4.04	0.19_1	0.066	0.132	0.139	0.093	0.166	0.119 ± 0.035
34	4.45	3.22	7.48	9.33	0.28_3	0.196	0.235	0.264	0.214	0.246	0.231 ± 0.024
51	7.90	5.23	9.45	15.29	0.40_5	0.349	0.382	0.333	0.350	0.352	0.353 ± 0.016
60	9.70	6.64	11.81	18.17	0.45_8	0.428	0.485	0.417	0.416	0.398	0.429 ± 0.030
72	12.20	8.25	14.57	23.94	0.63_4	0.539	0.603	0.514	0.548	0.551	0.551 ± 0.029
96	17.00	11.27	21.26	33.56	0.87_9	0.751	0.824	0.750	0.769	0.764	0.772 ± 0.027
124.5	22.65	13.68	28.35	43.65	1.15	1.00	1.00	1.00	1.00	1.00	1.00

TABLE III

Photometric intensity measurements at [N_2] = 60 mm (4850 Å band)

Hg × 10^4 (mm)	$I_{4660\,Å}$	$I_{4750\,Å}$	$I_{5030\,Å}$	$I_{5930\,Å}$	λ = 4660 Å, $I/I_{10.78}$	λ = 4750 Å, $I/I_{10.78}$	λ = 5030 Å, $I/I_{10.78}$	λ = 5930 Å, $I/I_{10.78}$	Ave. $I/I_{10.78}$
10.78	6.64	11.81	18.17	0.46	1.00	1.00	1.00	1.00	1.00
8.18	4.02	7.09	12.02	0.31	0.60_5	0.60_0	0.66_2	0.68_3	$0.63_7\pm0.03_6$
6.25	3.62	4.33	7.69	0.18	0.54_5	0.36_7	0.42_3	0.38_4	$0.42_9\pm0.07_0$
4.46	2.21	2.76	4.13	0.05	0.33_3	0.23_4	0.22_7	0.11_6	$0.22_7\pm0.07_7$
3.31	1.41	1.97	2.60	0.07	0.21_2	0.16_7	0.14_3	0.15_1	$0.16_8\pm0.02_7$

Can. J. Chem. Downloaded from www.nrcresearchpress.com by 210.87.254.42 on 09/05/12
For personal use only.

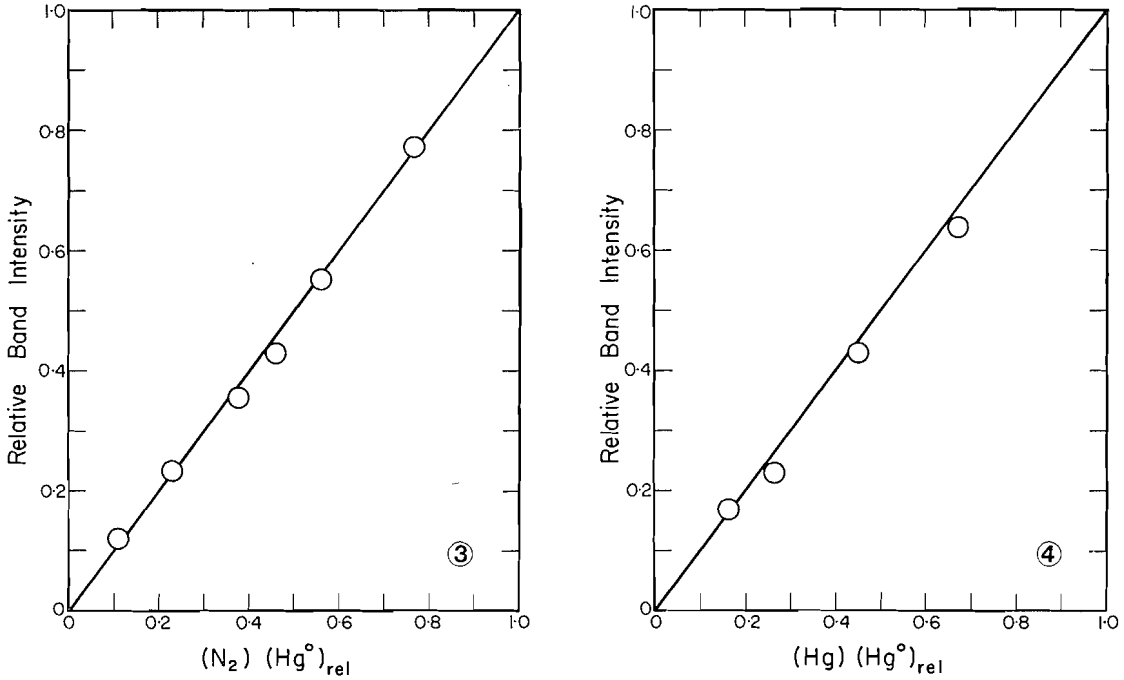

FIG. 3. Dependence of 4850 Å band intensity on the product of $[N_2]$ and $[Hg^0]$ for $[Hg] = 10.78 \times 10^{-4}$ mm. The abscissa is

$$\frac{K^0[Hg^0]L[N_2]}{[K^0[Hg^0]L[N_2]]_{N_2=124.5\text{ mm.}}}$$

FIG. 4. Dependence of 4850 Å band intensity on the product of [Hg] and $[Hg^0]$ for $[N_2] = 60$ mm. The abscissa is

$$\frac{K^0[Hg^0]L[Hg]}{[K^0[Hg^0]L[Hg]]_{[Hg]=10.78\times10^{-4}}}$$

TABLE IV

Relative intensities at $[Hg] = 9.30 \times 10^{-4}$ mm (3350 Å band)

N_2	Exposure (h)	$D^{\lambda=3400}$	$D^{N_2} - D^{N_2=97}$	$(D^{N_2} - D^{N_2=97})/\gamma$	$I_\lambda^{N_2}/I_\lambda^{N_2=97}$
35	3	5.4_5	−0.80	−0.09	0.813
42	3	5.9_5	−0.30	-0.03_4	0.925
55	3	5.9_5	−0.30	-0.03_4	0.925
72.5	3	5.8_5	−0.40	-0.04_5	0.90_2
80	3	5.2_5	−1.00	-0.11_2	0.77_2
95	3	6.4_0	0.15	0.01_7	1.04
116	3	7.2_0	0.95	0.10_7	1.28
97	3	6.2_5	0	0	1.00

$I_{4850}^{N_2}/I_{4850}^{N_2=97\text{ mm}}$ at the same nitrogen pressures at which the intensities of the 3350 Å band were determined. For each of these nitrogen pressures the ratio of the intensities of the two bands was then calculated as the ratio of the corresponding relative intensities. As shown in Fig. 5, the ratio of the intensity of the 4850 Å to that of the 3350 Å band is linear in $[N_2]$. The 4850 Å and 3350 Å band intensities were measured at slightly different mercury concentrations (10.78×10^{-4} mm and 9.30×10^{-4} mm respectively), but as relative intensities were used to calculate the ratio I_{4850}/I_{3350}, differences in the absolute intensities will tend to cancel in the present treatment. A least-squares analysis of the data gave the values of the slope and intercept as $(1.01 \pm 0.05) \times 10^{-2}$ mm^{-1} and (0.017 ± 0.032) respectively. In this calculation the two points

Can. J. Chem. Downloaded from www.nrcresearchpress.com by 210.87.254.42 on 09/05/12
For personal use only.

that have very large deviations from the straight line in Fig. 5 have been neglected.

While the standard deviation of the slope of Fig. 5 is small enough to warrant some confidence in the value quoted, the errors inherent in photographic spectrophotometry, used in the case of the 3350 Å band, are such that the reality of a finite intercept is doubtful.

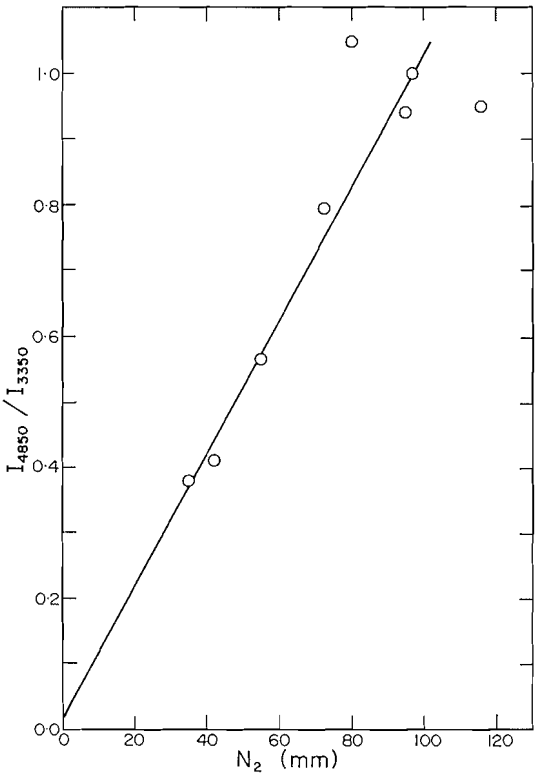

FIG. 5. Ratio of the intensities of the 4850 Å and 3350 Å bands as a function of the nitrogen pressure.

Discussion

In Part III of this series (1) we reported on the results of an investigation of the reactions of Hg 6^3P_0 atoms in systems containing from 2.34×10^{-4} to $12.6_3 \times 10^{-4}$ mm of mercury and from 0.075 to 7.95 mm of nitrogen. Relative concentrations of 6^3P_0 atoms were calculated from the optical densities for the absorption of an analysis beam of 4047 Å radiation, $K^0[Hg^0]L$, where K^0 is the decadic extinction coefficient for the absorption and L is the path length of the analysis beam. As before we will use Hg, Hg*, and Hg^0 to designate the 6^1S_0, the 6^3P_1, and the 6^3P_0 states of mercury; $Hg_2^0\dagger$ and Hg_2^0 represent nascent and stabilized $A^3\Sigma_u^+$ states.

The following mechanism was proposed (1).

[1] $Hg + h\nu^* = Hg^*$

[2] $Hg^* = Hg + h\nu^*$

[4] $Hg^* + N_2 = Hg^0 + N_2$

[5] $Hg^0 = Hg$ (on the wall)

[6] $Hg^0 = Hg + h\nu^0$

[7] $Hg^0 + N_2 = Hg + N_2$

[8] $Hg^0 + N_2 = Hg^* + N_2$

[10] $Hg^0 + Hg = Hg_2^0\dagger$

[12] $Hg_2^0\dagger = Hg^0 + Hg$

[13] $Hg_2^0\dagger + N_2 = Hg_2^0 + N_2$

Callear and Williams (10) found no evidence for third order removal of Hg^0 at nitrogen pressures of the order of 500 mm or more and were able to interpret their results in terms of two bimolecular reactions, one between Hg^0 and Hg, the other between Hg^0 and N_2. On the other hand, it was found in our laboratory that at nitrogen pressures of 8 mm or less, Hg^0 atoms are removed by a third order process involving Hg^0, Hg, and N_2, as well as by the bimolecular processes suggested by Callear and Williams (10). The apparent discrepancy between the observations at low and high pressures was resolved by the mechanism quoted above, and in particular by reactions [10], [12], and [13].

However, it is impossible to reconcile this mechanism with the present observation that the intensity of the 4850 Å band is proportional to the product $[Hg][Hg^0][N_2]$ if we assume that the 4850 Å band arises by reaction [17],

[17] $Hg_2^0 = 2Hg + h\nu$ (4850 Å).

If Hg_2^0 molecules are formed by [13] and consumed by [17], then

$$[i] \quad I_{4850} = k_{17}[Hg_2^0] = k_{13}[Hg_2^0\dagger][N_2] = \frac{k_{10}[Hg][Hg^0][N_2]}{\frac{k_{12}}{k_{13}} + [N_2]}.$$

This expression will only predict a third order dependence for I_{4850} if k_{12}/k_{13} is appreciably greater than $[N_2]$ in the range 20–125 mm. However, the value of k_{12}/k_{13} consistent with Hg^0 consumption was found (1) to be only 6.4 mm.

Can. J. Chem. Downloaded from www.nrcresearchpress.com by 210.87.254.42 on 09/05/12
For personal use only.

If we accept the conclusion (10) that the only important reactions removing Hg^0 at high (500 – 1000 mm) pressures of nitrogen are the bimolecular processes [7] and [10*a*],

[7] $Hg^0 + N_2 = Hg + N_2$

[10*a*] $Hg^0 + Hg = 2Hg,$

the formation of Hg_2^0 by the third order process [11],

[11] $Hg^0 + Hg + N_2 = Hg_2^0 + N_2,$

would have to be of minor importance in the removal of Hg^0 to have escaped observation. However, McAlduff and Le Roy (1) found that if they interpreted their results in terms of [10*a*] and [11], rather than [10], [12], and [13], the value of k_{11} required was so large (4.8×10^{20} cm^6 $mole^{-2}$ s^{-1}) that the third order removal of Hg^0 would be predominant at high pressures of nitrogen. Quite aside from predicting a result at variance with the observations of Callear and Williams (10), the calculated value of k_{11} was unrealistically large.

In a recent study of the steady-state emission of the 4850 Å and 3350 Å bands in the presence of nitrogen, Penzes, Gunning, and Strausz (11) have postulated a third order process for the removal of Hg^0 atoms with a rate constant of 1.1×10^{18} cm^6 $mole^{-2}$ s^{-1}. While the assumed product of the reaction was not Hg_2^0, no subsequent reaction producing Hg^0 was postulated. Although the magnitude of their third order rate constant is more realistic than the value of k_{11} calculated by McAlduff and Le Roy (1), it is, nevertheless, large enough to cause an observable third order effect at the nitrogen pressures used by Callear and Williams (10).

In the light of this analysis we feel that a mechanism analogous to our original [10], [12], and [13] is required, and suggest the following modification.

[10] $Hg^0 + Hg = Hg_2{}^*\dagger$

[12] $Hg_2{}^*\dagger = Hg^0 + Hg$

[13] $Hg_2{}^*\dagger + N_2 = Hg_2{}^* + N_2$

[14] $Hg_2{}^*\dagger + N_2 = 2Hg + N_2$

[15] $Hg_2{}^* = 2Hg + h\nu$ (3350 Å)

[16] $Hg_2{}^* + N_2 = Hg_2^0 + N_2$

[17] $Hg_2^0 = 2Hg + h\nu$ (4850 Å)

The essential difference between this mechanism and that postulated by McAlduff and Le Roy (1) is that we now assume that the transient species $Hg_2{}^*\dagger$ (referred to as $Hg_2\dagger{}^*$ in ref. 1) gives rise to $Hg_2{}^*$ (i.e. the $A^3 1_u$ state) in reaction [13] rather than Hg_2^0 (the $A^3 0_u^-$ state). The assumption that $Hg_2{}^*$ is the precursor of Hg_2^0 has been suggested by Penzes, Gunning, and Strausz (11).

Insofar as Hg^0 removal is concerned, reactions [10], [12], [13], and [14] above are kinetically equivalent to the reactions [10], [12], and [13] postulated by McAlduff and Le Roy (1). Thus, the rate of consumption of Hg^0 atoms by [10], [12], [13], and [14] of the present mechanism is given by

$$[ii] \quad \frac{-d[Hg^0]}{dt} = \frac{k_{10}[Hg][Hg^0][N_2]}{k_{12}/(k_{13} + k_{14}) + [N_2]},$$

in which $k_{12}/(k_{13} + k_{14}) = 6.4$ mm at room temperature, and hence becomes second order, independent of $[N_2]$, at high nitrogen pressures. It is not possible, with any available data, to calculate the relative magnitudes of k_{13} and k_{14} and reaction [14] has been included on purely speculative grounds.

By assuming that stabilization of $Hg_2{}^*\dagger$ results in the formation of $Hg_2{}^*$ rather than Hg_2^0 it becomes possible to interpret all of the results of the present investigation. The predicted intensity of the 4850 Å band is given by the expression

$$[iii] \quad I_{4850} = \frac{k_{10}k_{13}/(k_{13} + k_{14})[Hg^0][Hg][N_2]^2}{[k_{15}/k_{16} + [N_2]][k_{12}/(k_{13} + k_{14}) + [N_2]]}.$$

The second term in the denominator of [*iii*] would approach $[N_2]$ in the range of nitrogen pressures used in the present experiments. Further, the radiative lifetime of $Hg_2{}^*$ is likely to be of the order of 10^{-7} s, so if k_{16} is less than about 3×10^4 mm^{-1} s^{-1} (or about 6×10^{11} cm^3 $mole^{-1}$ s^{-1}) the first term in the denominator will be approximately equal to k_{15}/k_{16} in the range of nitrogen pressures used in the present experiments. Equation [*iii*] will then take the form

$$[iv] \quad I_{4850} = \frac{k_{10}k_{13}k_{16}}{k_{15}(k_{13} + k_{14})}[Hg][Hg^0][N_2],$$

in agreement with our observations.

The proposed mechanism is also in agreement with our observations on the dependence of the ratio of the intensities of the two bands on nitrogen pressure, viz.

$$[v] \quad \frac{I_{4850}}{I_{3350}} = \frac{k_{17}[Hg_2^0]}{k_{15}[Hg_2{}^*]} = \frac{k_{16}}{k_{15}}[N_2].$$

Acknowledgments

The authors are pleased to acknowledge the financial support received from the National Research Council of Canada. One of us (J. E. M.) was the recipient of a University of Toronto Open Fellowship.

1. J. E. McAlduff and D. J. Le Roy. Can. J. Chem. **43**, 2279 (1965).
2. P. Pringsheim. Fluorescence and phosphorescence. Interscience Publishers, Inc., New York. 1949.
3. Lord Rayleigh. Proc. Roy. Soc. London, Ser. A, **132**, 650 (1931).
4. F. S. Phillips. Proc. Roy. Soc. London, Ser. A, **89**, 39 (1913).
5. Lord Rayleigh. Proc. Roy. Soc. London, Ser. A, **137**, 101 (1932).
6. A. O. McCoubrey. Phys. Rev. **93**, 1249 (1954).
7. S. Mrozowski. Z. Physik, **104**, 228 (1937).
8. J. A. Berberet and K. C. Clark. Phys. Rev. **100**, 506 (1955).
9. G. H. Kimbell and D. J. Le Roy. Can. J. Chem. **38**, 1714 (1960).
10. A. B. Callear and G. J. Williams. Trans. Faraday Soc. **60**, 2158 (1964).
11. S. Penzes, H. E. Gunning, and O. P. Strausz. Private communication.

Can. J. Chem. Downloaded from www.nrcresearchpress.com by 210.87.254.42 on 09/05/12
For personal use only.

Can. J. Chem. Downloaded from www.nrcresearchpress.com by 210.87.254.6 on 09/05/12
For personal use only.

Tumbling of methyl radicals adsorbed on a silica gel surface studied by electron spin resonance[1]

C. L. GARDNER[2] AND E. J. CASEY
Defence Chemical Biological and Radiation Establishment, Ottawa, Canada

Received July 12, 1967

The electron spin resonance spectra of CH_3 and CD_3 adsorbed on a silica gel surface at 77 °K are characterized by a marked dependence of the line width on nuclear spin quantum number. This dependence can be interpreted in terms of the tumbling of the radicals on the surface, anisotropies in the hyperfine and g tensors giving rise to a relaxation mechanism dependent on M_I. A quantitative comparison of the spectra with the theory of this relaxation mechanism developed by McConnell, Kivelson, and Freed and Fraenkel enables the tumbling frequencies, 2.0×10^7 s^{-1} and 1.3×10^7 s^{-1} for CH_3 and CD_3 respectively, to be determined.

Canadian Journal of Chemistry, **46**, 207 (1968)

Introduction

The electron spin resonance detection of methyl radicals adsorbed on various surfaces has been reported in recent years (1–4). Like VO^{2+}, for example (5), these spectra are often characterized by a marked dependence of the line width on the nuclear spin quantum number M_I. Although Kazanskii *et al.* (1) suggested that this dependence was due to a combination of spin-orbit relaxation and incomplete averaging of the anisotropic hyperfine interaction, this idea was not developed quantitatively.

McConnell (6) first proposed a mechanism which could explain this phenomenon. He showed that the tumbling of a system with anisotropies in the hyperfine interaction and g tensors provided a relaxation mechanism dependent on M_I. Refinements and extensions to McConnell's theory have been made by Kivelson (7) and more recently by Wilson and Kivelson (8). Freed and Fraenkel (9) have given a more general theory capable of treating systems with sets of equivalent nuclei. In this case the lines can consist of several degenerate components with possibly different widths.

In the present work we apply this theory to the electron spin resonance (e.s.r.) spectrum of methyl radicals adsorbed on a silica gel surface and quantitatively interpret the dependence of line width on M_I.

Experimental Results

Samples were prepared by adsorbing reagent grade methyl iodide (British Drug Houses) or methyl-d_3 iodide (Stohler Isotope Chemicals) onto silica gel (Fisher) which had been degassed at ~ 300 °C for several hours at a pressure $< 10^{-4}$ mm. The methyl iodide was allowed to adsorb at a pressure low enough that less than monolayer adsorption occurred (4*a*). The sample tubes were sealed, cooled to 77 °K, and irradiated with ultraviolet radiation from an unfiltered GE-UAZ mercury lamp. The e.s.r. spectra were recorded with a Varian V-4500 spectrometer. Figures 1 and 2 show e.s.r. spectra of CH_3 and CD_3 on silica gel at 77 °K.

The experimental line widths were determined, as has been done previously (5), by measuring the width of one of the lines and determining the widths of the other lines from the derivative heights from the expression

$$(\text{derivative height}) \times (\text{derivative width})^2 = \text{constant}.$$

Within experimental error, the above relation was found to hold for our spectra. Values are given in Figs. 3 and 4.

Discussion

Asymmetry

An unexplained feature of the spectra is the asymmetry of the lines with respect to the base line. It is possible that part of this may result from incomplete averaging of the g-tensor anisotropy as suggested by Kazanskii *et al.* (1). In this case, however, the broadening should depend on M_I^2, that is be symmetric about the center. This is not the case with our spectra. In addition the broadening produced by this mechanism should be more pronounced for CD_3 than CH_3 because of the slower tumbling rate. This is not in agreement with experiment either and indicates further that incomplete averaging of anisotropy of the g tensor is not the prime cause of the line width variation. A similar asymmetry has also been observed by Rogers and Pake (5) in the solution spectrum of VO^{2+}. In their case, as they explain, the tumbling rate is sufficiently rapid that complete averaging

[1]Presented at the 2nd Canadian Catalysis Symposium, Hamilton, Ontario, June 12, 1967. Issued as DCBRE Report No. 540.

[2]Present address: Department of Chemistry, University of Sheffield, Sheffield, England.

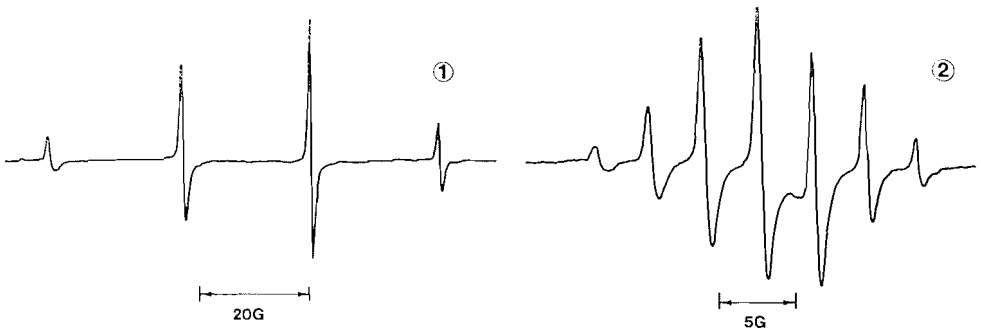

FIG. 1. Electron spin resonance spectrum of CH_3 on silica gel at 77 °K: $A_1 = 23.3 \pm 0.2$ G.
FIG. 2. Electron spin resonance spectrum of CD_3 on silica gel at 77 °K: $A_1 = 3.66 \pm 0.20$ G.

of the hyperfine and g-tensor anisotropies is expected. They suggested that in their studies the mixing of the real and imaginary parts of the resonant magnetic susceptibility could account for the asymmetry. (Asymmetry has been observed and discussed in certain n.m.r. studies (10).)

Analysis of Results

General equations for the secular, pseudosecular, and nonsecular contributions to the line width have been given by Freed and Fraenkel (9). Their equations (4.46 to 4.48), for the condition that only anisotropic hyperfine and g-tensor interactions are important, are given below for a single set of equivalent nuclei,

$$(T_2)^{-1} = (T_2)^{-1}_{\text{sec}} + (T_2)^{-1}_{\text{pseudosec}} + (T_2)^{-1}_{\text{nonsec}}$$

or in detail,

$$[1]\qquad \begin{cases} (T_2)^{-1}_{\text{sec}} = \frac{8}{3} j^{\text{D}}(0)M^2 + \frac{16}{3} j^{\text{DG}_2}(0)BM + \frac{8}{3} j^{\text{G}_2}(0)B^2 \\ (T_2)^{-1}_{\text{pseudosec}} = \frac{1}{2}\{j^{\text{D}}(w^+)[\langle J(J+1)\rangle - M^2] + j^{\text{D}}(w^-)[\langle J(J+1)\rangle - M^2]\} \\ (T_2)^{-1}_{\text{nonsec}} = \frac{1}{3} j^{\text{D}}(w_0)[7\langle J(J+1)\rangle - M^2] + 4j^{\text{DG}_2}(w_0)BM + 2j^{\text{G}_2}(w_0)B^2, \end{cases}$$

where $j(w)$ = spectral densities, B = static magnetic field, M = nuclear magnetic quantum number, and J = total nuclear spin quantum number.

In these equations an average line width has been assumed for the degenerate components of a single line and in this form they are identical with those given by Kivelson (7).

The quantity $\langle J(J+1)\rangle$ depends on the system and may be evaluated from Kivelson's equation 45.

For CH_3: $\langle J(J+1)\rangle = 3/2 + M^2$

For CD_3: $\langle J(J+1)\rangle = 12, 8, 5, (30/7)$

for $M = 3, 2, 1, 0$ respectively. An exact analytic expression for CD_3 is not easy to obtain, and we assume the approximate form $\langle J(J+1)\rangle = (30/7) + M^2$.

It is seen that the detailed eq. [1] can be written in the form

$$[2]\qquad (T_2)^{-1} = a_0 + a_1 M + a_2 M^2.$$

The spectral densities $j(w)$ are proportional to $\tau_c(1 + w^2\tau_c^2)^{-1}$, and the pseudosecular and nonsecular contributions to the line width will be negligible provided $w_0\,\tau_c \gg 1$ and $w \pm \tau_c \gg 1$. It can be readily verified that the nonsecular contribution to the line width is completely negligible by calculating correlation times from the experimental data, assuming both $w_0\,\tau_c \gg 1$ and $w_0\,\tau_c \ll 1$. The calculated correlation times are inconsistent with the condition $w_0\,\tau_c \ll 1$. To a fair approximation ($\backsim 10\%$) the pseudosecular contribution can also be neglected. For this case the constants in eq. [2] can be evaluated as

$$[3]\qquad \begin{cases} a_0 = \frac{4}{45}(\Delta\gamma B)^2\tau_c + K \\ a_1 = \frac{4}{15} b\Delta\gamma B\tau_c \\ a_2 = \frac{b^2}{5}\tau_c \end{cases}$$

Can. J. Chem. Downloaded from www.nrcresearchpress.com by 210.87.254.6 on 09/05/12
For personal use only.

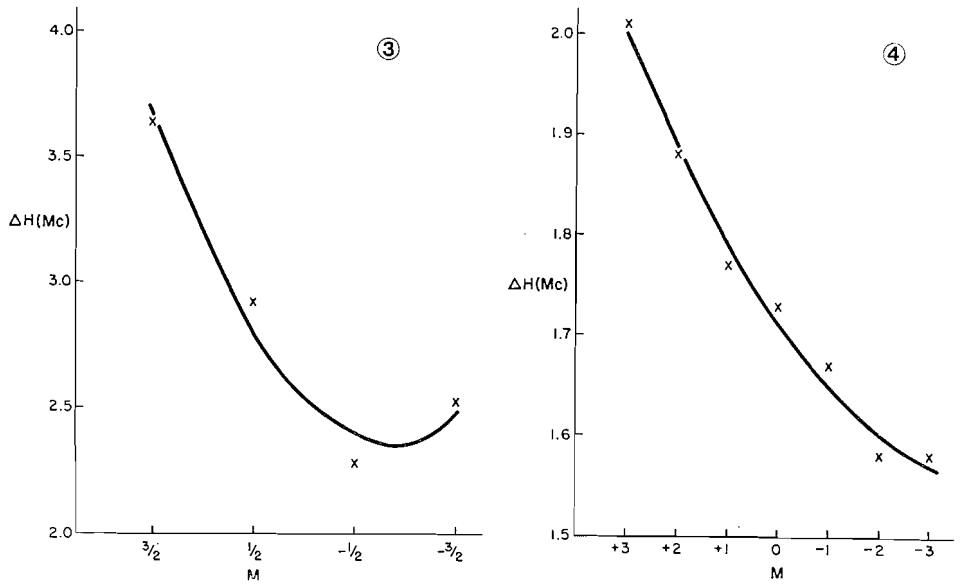

FIG. 3. Line widths as a function of nuclear magnetic quantum no. for CH_3 on silica gel. Fitted curve; experimental points.

FIG. 4. Line widths as a function of nuclear magnetic quantum no. for CD_3 on silica gel. Fitted curve; experimental points.

where τ_c = correlation time, b = hyperfine anisotropy = $\frac{2}{3}(A_\parallel - A_\perp)$, $\Delta\gamma$ = g-tensor anisotropy = $g_\parallel - g_\perp$, K = other unspecified contributions to the line width independent of M.

It should be pointed out that the constants a_1 and a_2 remain the same even if the small pseudo-secular contribution is included, since the M^2 dependence cancels out. It is also interesting to notice that the secular terms have no J dependence. This means that the degenerate components of a line will all have the same width, provided the pseudo- and non-secular contributions to the line width can be neglected. As has already been shown, in our case the above condition holds to a fair approximation. Therefore the detailed eqs. [1], which are based on the assumption of an average line width, should be nearly exact.

A least squares fit of the CH_3 line width data to eq. [2] yields

$$a_0 = 2.54 \pm 0.24 \text{ Mc s}^{-1}$$
$$a_1 = 0.400 \pm 0.133 \text{ Mc s}^{-1}$$
$$a_2 = 0.240 \pm 0.149 \text{ Mc s}^{-1}$$

Comparison of the data with the fitted curve is shown in Fig. 3.

Equation [3] should enable us to determine the correlation time τ_c, provided a value of b or $\Delta\gamma$ is known. As far as we are aware there is no experimental determination of either of these. However, if we use Heller's (11) value of $b = 4.5 \times 10^6 \text{ s}^{-1}$, obtained for the CH_3 group in the radical $CH_3C(COOH)_2$, as an estimate of b in the methyl radical, then from the ratio a_1/a_2 we obtain $\Delta\gamma = 1.20 \times 10^{-3}$. Using the value for b and an average $\Delta\gamma = 1.08 \times 10^{-3}$ from the CH_3 and CD_3 results, we obtain a value of $\tau_c = 5.0 \times 10^{-8}$ s from a_1.

In a similar manner, a least squares fit of the CD_3 line width data to eq. [2] yields

$$a_0 = 1.71 \pm 0.04 \text{ Mc s}^{-1}$$
$$a_1 = 0.071 \pm 0.012 \text{ Mc s}^{-1}$$
$$a_2 = 0.008 \pm 0.007 \text{ Mc s}^{-1}$$

A comparison of the data with the fitted curve is shown in Fig. 4.

The estimate of $b = 0.69 \times 10^6 \text{ s}^{-1}$ for CD_3 is now made by dividing the b for CH_3 by the ratio of the H:D nuclear moments, $\mu_H/\mu_D \simeq 6.5$. The ratio of a_1/a_2 gives $\Delta\gamma = 9.5 \times 10^{-4}$. As before, we use the average value of $\Delta\gamma$ and the value estimated for b to obtain an estimate of $\tau_c = 7.9 \times 10^{-8}$ s from the theoretical expression for a_1.

Can. J. Chem. Downloaded from www.nrcresearchpress.com by 210.87.254.6 on 09/05/12
For personal use only.

The values of $\Delta\gamma$ are somewhat larger than the value of 0.00053 calculated by Glarum (12). Fairly large g-value shifts can occur with change of environment (13), or even of surface preparation (4), however.

The correlation times of 5.0×10^{-8} s and 7.9×10^{-8} s for CH_3 and CD_3 radicals on the silica gel surface indicate tumbling frequencies of $2.0 \times 10^7\ s^{-1}$ and $1.3 \times 10^7\ s^{-1}$ respectively. Although rapid, these tumbling frequencies still indicate a considerable hindrance to the rotation by the surface, "free" rotational frequencies usually being of the order of 10^3 faster.

Since the methyl radical is symmetrical and planar, the lowest order non-vanishing electric multipole moment is the quadrupole moment. The most important first order contribution to the potential barrier to rotation would then be the interaction of this quadrupole moment with the field gradient at the surface. Previous experiments have shown this field gradient off the silica gel surface to be large (14). However, second order polarization effects, which could give rise to a non-vanishing dipole moment, might also be important. Although an independent estimate of the size of this barrier could not be made, from the experiments of Gutowsky *et al.* (15, 16), an estimate of the order of 1000 cm^{-1} seems to be reasonable. Although classical penetration of a barrier of this magnitude is very improbable at 77 °K, tunnelling at frequencies of the order of $10^7\ s^{-1}$ should be possible (14, 15). Because of the uncertainties, however, the exact nature of "tumbling" remains somewhat obscure.

Acknowledgment

The authors wish to thank the referee who pointed out the relevance of Freed and Fraenkel's work to us. The analysis is stronger because of his interest.

1. G. B. Pariiskii, G. M. Zhidomirov, and V. B Kazanskii. Zh. Strukt. Khim. **4**, 364 (1963).
2. V. B. Kazanskii and G. B. Pariiskii. Proc. Intern. Congr. Catalysis, 3rd, Amsterdam, 1964, **1**, 367 (1965).
3. J. Turkevich and Y. Fujita. Science, **152**, 1619 (1966).
4. (*a*) M. Fujimoto, H. D. Gesser, B. Garbutt, and A. Cohen. Science, **154**, 381 (1966).
   (*b*) M. Fujimoto, H. D. Gesser, B. Garbutt, and M. Shimizu. Science, **156**, 1105 (1967).
5. R. N. Rogers and G. E. Pake. J. Chem. Phys. **33**, 1107 (1960).
6. H. M. McConnell. J. Chem. Phys. **25**, 709 (1956).
7. D. Kivelson. J. Chem. Phys. **33**, 1094 (1960).
8. R. Wilson and D. Kivelson. J. Chem. Phys. **44**, 154 (1966).
9. J. H. Freed and G. K. Fraenkel. J. Chem. Phys. **39**, 326 (1963).
10. I. Solomon and J. Ezratty. Phys. Rev. **127**, 78 (1962).
11. C. Heller. J. Chem. Phys. **36**, 175 (1962).
12. S. H. Glarum. J. Chem. Phys. **39**, 3141 (1963).
13. C. K. Jen, S. N. Foner, E. L. Cochran, and V. A. Bowers. Phys. Rev. **112**, 1169 (1958).
14. C. L. Gardner. J. Chem. Phys. **46**, 2991 (1967).
15. J. G. Powles and H. S. Gutowsky. J. Chem. Phys. **23**, 1692 (1955).
16. E. D. Stejskal and H. S. Gutowsky. J. Chem. Phys. **28**, 388 (1958).

Can. J. Chem. Downloaded from www.nrcresearchpress.com by 210.87.254.6 on 09/05/12
For personal use only.

Can. J. Chem. Downloaded from www.nrcresearchpress.com by 210.87.254.40 on 09/05/12
For personal use only.

Preparation of some organotin compounds containing methylthio, phenylthio, and pentafluoro-phenylthio groups

M. E. PEACH[1]
Chemistry Department, Loughborough University of Technology, England
Received July 10, 1967

The new compounds n-Bu_3SnSR, n-$Bu_2Sn(SR)_2$, where R = Me, Ph, or C_6F_5, and $Ph_3SnSC_6F_5$ have been prepared and characterized. The fracture of the Sn—S bond with iodine has been examined and affords a quantitative method for analysis of compounds containing a Sn—S bond. The ^1H and ^{19}F n.m.r. have been studied; frequencies characteristic of the C_6F_5S— group in the infrared spectra have been tabulated.

Canadian Journal of Chemistry, 46, 211 (1968)

Alkyl- and aryl-thioorganotin compounds have recently been shown to be hydrolytically stable, and can be prepared in an aqueous media: previously this type of compound was prepared using carefully maintained anhydrous conditions (1). It has been postulated that organotin oxides and hydroxides are the reactive entities when alkyl- and aryl-thio compounds of tin are prepared in water from organotin halides and thiols (1). This paper describes the preparation of compounds of the type n-Bu_3SnSR and n-$Bu_2Sn(SR)_2$ from the corresponding organotin oxide and methanethiol, thiophenol, and pentafluorothiophenol. Some metal derivatives of pentafluorothiophenol are known: transition metal derivatives and complex ions have been formed in aqueous solution, i.e. $M(SC_6F_5)_4^{2-}$ (M = Co, Pd, Pt, Zn, Cd, Hg), $M(SC_6F_5)_2^-$ (M = Cu, Ag, Au), $Pd(SC_6F_5)_2$, and $AgSC_6F_5$ (2). (Pentafluorophenylthio)trimethyltin has been prepared by the reaction of pentafluorothiophenol with (n-butylthio)trimethyltin, n-butanethiol being evolved (3). The preparation of (pentafluorophenylthio)triphenyltin from triphenyltin chloride and pentafluorothiophenol in aqueous solution is described.

The fracture of the tin–sulfur bond with iodine has been studied in carbon tetrachloride solution: mono alkylthio- and arylthio-organotin compounds can be estimated by titration against iodine solution in carbon tetrachloride.

The proton, ^{19}F nuclear magnetic resonance, and infrared spectra of all the compounds prepared have been examined. Chemical shifts have been measured and frequencies characteristic of the pentafluorothiophenyl group have been found in the infrared spectra.

Discussion

The preparations using tri-n-butyltin oxide and di-n-butyltin oxide show that it is possible to prepare organo-sulfur derivatives of tin directly from stoichiometric amounts of the appropriate oxide and thiol.

$$(n\text{-}Bu_3Sn)_2O + 2MeSH \rightarrow 2n\text{-}Bu_3SnSMe + H_2O$$

This is a convenient preparation, but it cannot be applied to the preparation of the known tetra(phenylthio)tin from stannic oxide and thiophenol. Some (alkylthio)triethyltin compounds have been prepared similarly from triethyltin oxide and an excess of alkanethiol: the excess thiol and water were removed from the product by distillation (4). These reactions show the relatively acidic nature of the S—H hydrogens in thiols, and is in agreement with the observation that an —OR group can be displaced by the —SR group of thiols in organotin compounds (5).

The tin–sulfur bond in organotin sulfur derivatives can be fractured by bromine, forming an organotin bromide and a disulfide: a similar reaction has been reported as occurring with iodine, but no details are given (1). The fracture of the tin–sulfur bond is quantitative in carbon tetrachloride solution for derivatives of the type R_3SnSR'.

$$2n\text{-}Bu_3SnSPh + I_2 \rightarrow 2n\text{-}Bu_3SnI + Ph_2S_2.$$

For derivatives of the type $R_2Sn(SR')_2$ the results are not so good. This reaction probably

[1]Present address: Chemistry Department, Acadia University, Wolfville, Nova Scotia.

TABLE I

Infrared frequencies characteristic of the C_6F_5S— group (cm^{-1})

C_6F_5SH	$(C_6F_5S)_2NH$*	$CF_3SSC_6F_5$*	n-$Bu_3SnSC_6F_5$	n-$Bu_2Sn(SC_6F_5)_2$	$Ph_3SnSC_6F_5$
460 m	†	461 w			460 m
621 m					621 w
631 w	†	637 m	636 w	636 m	631 w
872 s	880 m	856 s	863 s	860 vs	860 vs
927 s	925 m	920 w	—	—	920 w
989 m	985 vs	983 vs	983 vs	981 vs	979 vs
1028 m	1025 m	1021 m	1017 m	1020 m	1018 m‡
1068 m	—	1072 m	—	—	—
1097 s	1090 s	1100 s‡	1090 s‡	1090 vs	1084 vs
1336 m	—	—	—	1320 m	1320 m
1360 m	—	1382 m	—	—	1360 m
1503 vs	1490 vs	1495 vs	1484 s	1485 vs	1488 vs
1518 vs	1515 vs	1517 vs	1512 s	1512 vs	1513 vs
1636 m				1628 w	1629 w
1640 m	1635 m	1640 s	1637 m	1640 m	1641 w
1646 m					

*See ref. 10.
†Only recorded 4000 – 650 cm^{-1}.
‡Exact assignment difficult, due to peaks from the other group in this region.

proceeds through the initial fracture of the Sn—S bond with the formation of an organotin iodide and an unstable sulfenyl iodide, RSI: the latter decomposes to the corresponding disulfide and iodine, which reacts further with the Sn—S bond. An unstable sulfur iodide is also formed in the reaction of a sulfur chloride with potassium iodide in aqueous solution: the resultant iodine formed can be estimated quantitatively, and hence the original sulfur chloride determined (6, 7). The transient red color observed in the titration of thiophenol derivatives must be due to the formation of unstable benzenesulfenyl iodide, PhSI.

Hexafluorobenzene is susceptible to nucleophilic attack: pentafluorothiophenol is prepared from hexafluorobenzene and sodium bisulfide (8). The sulfur in a sulfur–tin bond can act as a nucleophile, forming a sulfonium compound; (methylthio)-trimethyltin reacts with methyl iodide to form dimethyl(trimethylstannyl)sulfonium iodide (1). No sulfonium fluoride containing the pentafluorophenyl group attached to the sulfur could be prepared from hexafluorobenzene and (methylthio)tri-*n*-butyltin. This is probably due to the difficulty of breaking a C—F bond in hexafluorobenzene.

Infrared frequencies characteristic of the pentafluorophenylthio group have been deduced by comparison with similar non-sulfur containing compounds. These frequencies, other than the very weak ones, are shown in Table I. Assignment of these frequencies is difficult. Those at about 1500 cm^{-1} are due to carbon–carbon stretching in the fluorinated benzene ring. The C—S stretching frequency in pentafluorothiophenol metal derivatives has been claimed to be a weak band at 710 cm^{-1} (2), but in compounds containing the trifluoromethylthio group, CF_3S—, the C—S stretching frequency is stated to occur at about 490 cm^{-1} (9). The methylene carbon–tin stretching frequency has been calculated to occur at 551 cm^{-1}, and has been observed between 590 and 508 cm^{-1} (11). The following frequencies can be assigned to methylene carbon–tin stretching: 511 cm^{-1} (n-Bu_3SnSMe), 505 cm^{-1} (n-Bu_3SnSPh), 512 cm^{-1} (n-$Bu_3SnSC_6F_5$), 515 cm^{-1} (n-$Bu_2Sn(SMe)_2$), 512 cm^{-1} (n-$Bu_2Sn(SPh)_2$), 518 cm^{-1} (n-$Bu_2Sn(SC_6F_5)_2$).

The proton n.m.r. of the *n*-butyl compounds shows a sharp resonance corresponding to the methyl group and two overlapping envelopes for the methylene groups: the position of the resonances is slightly variable but there is no coupling when either an MeS— or PhS— group is attached to the tin. The methyl resonance of the MeS— group is sharp and shows no coupling. The ^{19}F chemical shifts are approximately the same as those for the C_6F_5— group in other compounds (12). The chemical shifts of the ortho and meta fluorine are complex multiplets. The para fluorine appears as a triplet, each of which may be a triplet, having weak shoulders on the main resonance. The coupling constants for the fluorines ortho to the para fluorine lie at

Can. J. Chem. Downloaded from www.nrcresearchpress.com by 210.87.254.40 on 09/05/12
For personal use only.

Can. J. Chem. Downloaded from www.nrcresearchpress.com by 210.87.254.40 on 09/05/12
For personal use only.

TABLE II

Products and analyses

Product	Color	Method	m.p. (°)	b.p. (°)/mm	n_D^{22}	Found (%)				Required (%)			
						C	H	F	S	C	H	F	S
n-Bu_3SnSMe	Colorless	A	—	104/0.2	1.5110	46.57	9.12	—	9.50	46.31	8.97	—	9.51
n-Bu_3SnSPh	Colorless	A	—	147/0.3	1.5479	54.79	8.66	—	7.73	54.15	8.80	—	8.05
n-$Bu_3SnSC_6F_5$	Colorless	A	—	118/0.03	1.5109	44.22	5.67	19.1	6.65	44.19	5.56	19.4	6.55
n-$Bu_2Sn(SMe)_2$	Colorless	B	—	94/0.02	1.5538	37.25	7.40	—	—	36.72	7.40	—	—
n-$Bu_2Sn(SPh)_2$	Colorless	B	—	162/0.05	1.6158	53.25	6.31	—	14.15	53.23	6.25	—	14.21
n-$Bu_2Sn(SC_6F_5)_2$	Yellow	B	30	139/0.02	—	38.51	2.75	29.8	—	38.06	2.87	30.1	—
$Ph_3SnSC_6F_5$	White	C	76	—	—	52.49	2.80	16.9	5.80	52.49	2.75	17.3	5.84

Can. J. Chem. Downloaded from www.nrcresearchpress.com by 210.87.254.40 on 09/05/12
For personal use only.

approximately 22.5 c/s (C_6F_5SH), 22.2 c/s (n-$Bu_3SnSC_6F_5$), 22.8 c/s (n-$Bu_2Sn(SC_6F_5)_2$), and 22.2 c/s ($Ph_3SnSC_6F_5$): these are somewhat higher than the quoted values 20.2–20.8 c/s (12). The coupling constants for the fluorines meta to the para fluorine are all less than 0.5 c/s: this is in agreement with the quoted value of 0–7 c/s (12).

Experimental

All reagents were available commercially. Microanalyses were performed by Mikroanalytisches Laboratorium Beller, Göttingen, Germany. Infrared spectra were recorded on a Perkin–Elmer 237B, 337, or 521, or on a Unicam SP 100 or SP 200G. N.m.r. spectra were recorded on a Perkin–Elmer R 10.

The new compounds prepared are shown in Table II, together with some physical properties and analyses. In method A approximately 2 mmoles of tri-n-butyltin oxide and 2 mmoles of the requisite thiol were shaken for 4–24 h; magnesium sulfate was added to dry the product, which was extracted with ether (ca. 20 ml). The product was purified by distillation after removal of the ether by fractionation. In method B approximately 1 mmole of di-n-butyltin oxide and 2 mmoles of the thiol in 20 ml of alcohol were stirred magnetically until the suspension of di-n-butyltin oxide disappeared (usually about 4 h): a clear colorless solution resulted. The alcohol plus water was fractionated off and the product purified by distillation; 2.11 mmoles of triphenyltin chloride and 2.11 mmoles of pentafluorothiophenol were dissolved on warming in a mixture of 20 ml water and 20 ml alcohol, and stirred magnetically overnight (method C). The acid produced was neutralized by the addition of an equivalent amount of 0.1 N caustic soda. A copious white precipitate formed which was filtered off, dried, and purified by vacuum sublimation.

No reaction was observed when stannic oxide and thiophenol were mixed as in method B.

Carbon tetrachloride solutions of various methylthio- and phenylthio-butyltins (ca. 0.05 M) were titrated against an approximately 0.05 M solution of iodine in carbon tetrachloride. An end point was observed when the iodine color remained for 2 min in a warm solution. The results are shown in Table III. During the titration with the thiophenol derivatives a deep-red color formed which disappeared within 2 min.

No reaction was observed when 3.55 mmoles of (methylthio)tri-n-butyltin and 3.54 mmoles of hexafluorobenzene were refluxed in alcohol or carbon tetrachloride for 3 h: on heating a similar mixture, without solvent, in a sealed evacuated tube at 250° for 24 h decomposition of the (methylthio)tri-n-butyltin occurred, forming tin and stannic sulfide.

TABLE III

Titration of compounds with iodine in CCl_4

Compound	Amount taken (mmoles)	Iodine used (mmoles)
n-Bu_3SnSMe	0.966	0.975
n-Bu_3SnSPh	1.003	0.998
n-$Bu_2Sn(SMe)_2$	0.7829	1.561
n-$Bu_2Sn(SPh)_2$	0.7331	1.518

Details of the ^1H and ^{19}F n.m.r. spectra are shown in Tables IV and V.

The infrared absorption peaks in the region 4000 to 400 cm^{-1} are:

n-Bu_3SnSMe: 2958 s, 2922 s, 2876 m, 2856 m, 1468 s, 1459 m, 1420 w, 1380 m, 1346 w, 1318 m, 1296 w, 1252 w, 1185 w, 1158 w, 1076 m, 1052 w, 1025 w, 1003 w, 963 m, 880 m, 871 m, 848 w, 695 s, 671 s, 602 m, 511 m, 454 w.

n-Bu_3SnSPh: 2960 s, 2928 s, 2875 m, 2855 m, 1582 m, 1478 s, 1465 m, 1460 sh, 1440 m, 1420 w, 1380 m, 1345 w, 1322 w, 1298 w, 1255 w, 1185 w, 1160 w, 1086 m, 1078 m, 1069 m, 1027 m, 1002 w, 962 m, 880 m, 870 m, 850 w, 743 vs, 697 sh, 692 vs, 666 m, 597 m, 505 m, 481 m, 445 w, 417 w.

n-$Bu_3SnSC_6F_5$: 2963 s, 2931 s, 2880 m, 2860 m, 1637 m, 1626 m, 1512 vs, 1484 vs, 1467 s, 1420 m, 1401 w, 1381 m, 1370 w, 1345 w, 1295 m, 1253 m, 1184 m, 1155 m, 1142 sh, 1100 sh, 1090 s, 1050 w, 1025 sh, 1017 m, 983 vs, 913 w, 875 m, 863 vs, 772 m, 748 m, 719 sh, 694 s, 674 s, 636 w, 606 m. 591 sh, 512 m, 450 m, 425 sh.

n-$Bu_2Sn(SMe)_2$: 2958 s, 2922 s, 2873 s, 2854 s, 1465 s, 1459 s, 1442 m, 1419 m, 1379 m, 1360 w, 1342 w, 1318 s, 1292 w, 1250 w, 1180 w, 1151 m, 1074 m, 1049 w,

TABLE IV

^1H n.m.r. relative to tetramethylsilane as internal standard (p.p.m.)

		n-Butyl group			
Compound	Solvent	—CH_3	Methylene group envelopes	—SMe	—SPh envelope
$(n$-$Bu_3Sn)_2O$	CCl_4	−0.90	−1.8 to −0.7	—	—
n-Bu_3SnSMe	CCl_4	−0.93	−1.7 to −0.7	−2.00	—
n-Bu_3SnSPh	CCl_4	−0.89	−1.7 to −0.8	—	−7.5 to −7.0
n-$Bu_3SnSC_6F_5$	CCl_4	−0.90	−1.8 to −0.7	—	—
n-$Bu_2Sn(SMe)_2$	None	−0.91	−1.8 to −0.7	−2.17	—
n-$Bu_2Sn(SPh)_2$	CCl_4	−0.92	−1.5 to −0.6	—	−7.5 to −7.0
n-$Bu_2Sn(SC_6F_5)_2$	CCl_4	−0.93	−1.8 to −0.8	—	—

TABLE V

^{19}F chemical shifts relative to $CFCl_3$ as internal standard (p.p.m.)

Compound	Solvent	δ(ortho)	δ(para)	δ(meta)
C_6F_5SH	None	138.1	159.6	162.9
n-$Bu_3SnSC_6F_5$	CCl_4	132.2	159.3	163.8
n-$Bu_2Sn(SC_6F_5)_2$	CCl_4	131.7	156.5	162.5
$Ph_3SnSC_6F_5$	CCl_4	130.5	158.1	163.7

1024 w, 1003 w, 961 s, 878 s, 868 s, 845 w, 771 w, 749 w, 696 s, 664 s, 602 m, 515 m, 458 w.

n-$Bu_2Sn(SPh)_2$: 3573 m, 3560 m, 3020 w, 3002 w, 2960 s, 2924 s, 2874 s, 2855 s, 1579 s, 1477 s, 1463 s, 1438 s, 1415 w, 1378 m, 1342 w, 1301 w, 1249 w, 1181 w, 1154 w, 1082 s, 1068 m, 1024 s, 1002 m, 961 m, 910 m, 879 m, 869 m, 745 vs, 691 vs, 665 m, 512 w, 485 m, 454 w, 423 m.

n-$Bu_2Sn(SC_6F_5)_2$: 2965 w, 2930 w, 2880 m, 2860 m, 1640 m, 1628 w, 1512 vs, 1485 vs, 1470 sh, 1463 sh, 1455 sh, 1420 w, 1402 w, 1382 w, 1320 m, 1295 m, 1252 w, 1194 w, 1152 w, 1146 w, 1090 vs, 1020 m, 981 vs, 960 sh, 880 sh, 860 vs, 830 sh, 775 w, 751 w, 717 m, 704 m, 681 s, 675 m, 650 vw, 636 m, 591 m, 575 sh, 518 m, 510 w, 445 w.

$Ph_3SnSC_6F_5$: 3065 w, 3050 w, 1641 w, 1629 w, 1513 vs, 1510 sh, 1495 sh, 1488 vs, 1472 sh, 1433 s, 1360 w, 1334 m, 1320 m, 1306 w, 1084 vs, 1075 vs, 1023 w, 1018 m, 999 m, 979 vs, 920 w, 860 vs, 729 vs, 722 sh, 697 vs, 661 w, 631 vw, 621 vw, 460 m, 450 m, 445 w.

Acknowledgments

The author wishes to thank Dr. H. Heaney for help with the interpretation of the n.m.r. spectra, and Albright and Wilson (Mfr.) Ltd., Oldbury, England, for the gift of butyltin oxides.

1. E. W. Abel and D. R. Brady. J. Chem. Soc. 1192 (1965).
2. W. Beck and K. Stetter. Inorg. Nucl. Chem. Letters, **2**, 383 (1966).
3. E. W. Abel, D. A. Armitage, and D. R. Brady. J. Organometal. Chem. Amsterdam, **5**, 130 (1966).
4. G. S. Sasin. J. Org. Chem. **18**, 1142 (1953).
5. R. K. Ingram, S. D. Rosenberg, and H. Gilman. Chem. Rev. **60**, 459 (1960).
6. H. Böhme and E. Schneider. Chem. Ber. **76B**, 483 (1943).
7. N. Kharasch and M. M. Wald. Anal. Chem. **27**, 996 (1955).
8. P. Robson, M. Stacey, R. Stephens, and J. C. Tatlow. J. Chem. Soc. 4754 (1960).
9. S. N. Nabi and N. Sheppard. J. Chem. Soc. 3439 (1959).
10. M. E. Peach. Can. J. Chem. **45**, 429 (1967).
11. P. Taimsalu and J. L. Wood. Trans. Faraday Soc. **59**, 1754 (1963).
12. J. W. Emsley, J. Feeney, and L. H. Sutcliffe. High resolution nuclear magnetic resonance spectroscopy. Pergamon, Oxford. 1966. pp. 903–905.

Can. J. Chem. Downloaded from www.nrcresearchpress.com by 210.87.254.40 on 09/05/12
For personal use only.

Can. J. Chem. Downloaded from www.nrcresearchpress.com by 210.87.254.42 on 09/05/12
For personal use only.

Kinetic study of iridium(I) complexes as homogeneous hydrogenation catalysts[1]

B. R. James and N. A. Memon
Department of Chemistry, University of British Columbia, Vancouver, British Columbia

Received July 25, 1967

A study is described of the kinetics of reactions in which the complexes *trans*-$IrX(CO)(PPh_3)_2$, where X = Cl, Br, and I, are used for the catalytic homogeneous hydrogenation of olefinic bonds. Catalytic activity is enhanced in coordinating solvents such as dimethylacetamide. The rate law is complex, showing between zero and first order in each of iridium, substrate, and hydrogen concentrations, and the mechanisms proposed show the importance of a dissociation step in making available a coordination site on the transition metal complex. The dependence of rate on the halogen followed the order I > Br > Cl. Quite remarkably, traces of oxygen in the system enhance the hydrogenation rate considerably.

Canadian Journal of Chemistry, 46, 217 (1968)

Introduction

In 1961 Vaska and Diluzio (1) had reported that the square planar complex $IrCl(CO)(PPh_3)_2$ reacted reversibly with molecular hydrogen to form an octahedral Ir(III) dihydride complex in which the hydrogen was present as anionic hydride ligands.

[1] $IrCl(CO)(PPh_3)_2 + H_2 \rightleftharpoons IrCl(CO)(PPh_3)_2H_2$

It seemed possible that in such a reaction the hydrogen molecule might be activated for chemical reaction. At the commencement of the present work in 1965, there were no reports of homogeneous hydrogenation by iridium complexes. Since then Vaska and co-workers (2, 3) have briefly reported that the complexes $IrX(CO)(PPh_3)_2$ and the five-coordinate species $IrH(CO)(PPh_3)_3$ do act as catalysts in benzene solution for the reduction of ethylene and acetylene. Detailed kinetics were not reported, however, and little could be said of the reaction mechanisms. Chock and Halpern (4) have recently studied the kinetics of oxidative–addition reactions such as [1] in benzene and dimethylformamide solutions and clearly these are of significance in the homogeneous catalytic reactions. We report here the results of the first detailed kinetic investigation of the catalytic hydrogenation reactions, particularly for the $IrCl(CO)(PPh_3)_2$ catalyzed hydrogenation of maleic acid in dimethylacetamide solution.

Experimental

Materials

Trans-$IrCl(CO)(PPh_3)_2$ was obtained from Johnson Matthey, the sample having properties identical with a sample prepared by the procedure of Vaska and Diluzio (1). Both samples were used. The corresponding bromo and iodo complexes were prepared according to the methods of Chock and Halpern (4).

Reagent grade maleic acid and fumaric acid were recrystallized before use. Prepurified H_2 and N_2 were obtained from Canadian Liquid Air Co.; the H_2 was passed through a Deoxo catalytic purifier to remove O_2 before use. Ethylene was obtained as C.P. grade (99.5%) from Matheson Co. Benzene and N,N-dimethylacetamide (DMA) were redistilled and dried over 5A molecular sieve. Prior to use, the solvents were deoxygenated with N_2. All other chemicals used were of reagent grade.

Gas Uptake Measurements

The kinetics of the hydrogenation reactions were studied by measuring the rate of uptake of gas at constant pressure using the apparatus and procedure described earlier (5). The systems were found to be extremely sensitive to the presence of traces of oxygen, and rigorous oxygen-free conditions were necessary in making up the reactant solutions of complex and substrate. The initial concentration of $IrX(CO)(PPh_3)_2$ in these experiments was in the range 5×10^{-4} to 6×10^{-3} *M* and the substrate concentration, for example maleic acid, was 10^{-2} to 10^{-1} *M*. The partial pressure of H_2 was varied from approximately 180 to 800 mm and the corresponding concentration in solution estimated from solubility data (6).

Spectrophotometric Measurements

The kinetics and equilibria of some reactions of the chloro complex have been studied using spectrophotometric techniques in the ultraviolet (u.v.)/visible range. Oxygen was rigorously excluded by using an optical cell fitted with an extended T-piece sidearm and stopcock arrangement for evacuating and filling with solutions and gases. Optical density measurements were made on a Cary model 14 spectrophotometer fitted with a thermostated cell compartment. Reaction rates could be investigated by following the disappearance of selected absorption peaks with time: $IrCl(CO)(PPh_3)_2$, λ_{max}, 340 mμ ($\epsilon = 3.1 \times 10^3$), λ_{max}, 387 mμ ($\epsilon = 3.8 \times 10^3$), λ_{max}, 439 mμ ($\epsilon = 7 \times 10^2$). A reflection spectrum of a powdered sample was measured over the range 320–750 mμ with a Bausch and Lomb Spectronic 600 spectrophotometer fitted with a diffuse reflection attachment and a magnesium carbonate reference disc.

[1]Presented at the 50th annual conference of the Chemical Institute of Canada, Toronto, June 1967.

Can. J. Chem. Downloaded from www.nrcresearchpress.com by 210.87.254.42 on 09/05/12
For personal use only.

Results

Gas Uptake Experiments

Hydrogenation of substrates such as hex-1-ene and cyclohexene using the $IrCl(CO)(PPh_3)_2/H_2$ system at 50° in benzene at 1 atm H_2 pressure was extremely slow and not practical for kinetic studies. Vaska and Rhodes (2) had found that ethylene could be catalytically hydrogenated in benzene solution, but the process was inefficient. With $[IrCl(CO)(PPh_3)_2] = 10^{-3}$ *M*, $H_2 \sim 1$ atm, and $C_2H_4 \sim 400$ mm at 60°, a 40% yield of ethane was obtained after 18 h; they also reported that the iridium complex reacted reversibly with the olefin as well as the H_2.

[2] $IrCl(CO)(PPh_3)_2 + C_2H_4 \rightleftharpoons IrCl(CO)(PPh_3)_2C_2H_4$

We observed no reduction of ethylene after 1 h under similar conditions but had observed the equilibrium [2].

Incompatibility in solubility problems and the knowledge that certain rhodium complexes showed enhanced catalytic activity in non-aqueous coordinating solvents such as dimethylacetamide (5) prompted us to investigate the activity of the iridium complexes in this medium. Slow gas uptake was observed from C_2H_4/H_2 mixtures ($\sim$ 1 atm) by a 5×10^{-3} *M* solution of $IrCl(CO)(PPh_3)_2$ at 80°, but a system using the solid substrates maleic or fumaric acid proved more amenable for a detailed study.

Rates of H_2 uptake were conveniently measured in the temperature range 65–80°. Figure 1 shows a complete uptake plot for the hydrogenation of maleic acid at 80°; in the absence of the chloro complex there is no measurable uptake. The initial rate increases for about 3000 s and then becomes linear almost up to the end-point, which corresponds to complete reduction to succinic acid (isolated and characterized by infrared and melting point). The rates in the linear region have been estimated from the uptake plots for series of experiments in which the reaction parameters have been varied. Figures 2, 3, and 4 show the variation of this linear rate with concentration of the iridium chloro complex, maleic acid, and hydrogen respectively. For each reactant the dependence is seen to be between zero and first order, being essentially first order at lower concentrations and tending to become zero order at higher concentrations when the rates approach a limiting value. Addition of 10^{-2} *M* triphenylphosphine to a system essentially stops hydrogenation altogether.

Much slower reactions were observed when fumaric acid was used as substrate; the rates were about 7 times slower than those for corresponding maleic acid systems. Uptake plots using dimethylsulfoxide as solvent were very similar to

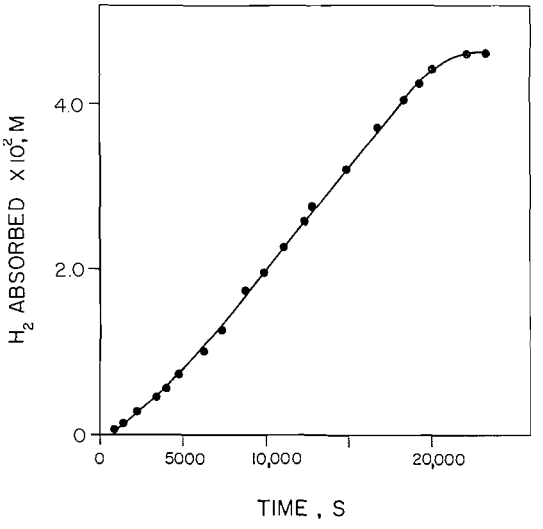

FIG. 1. Rate plot at 80°, 5.36×10^{-3} *M* $IrCl(CO)(PPh_3)_2$, 0.042 *M* maleic acid, 730 mm H_2, DMA solution.

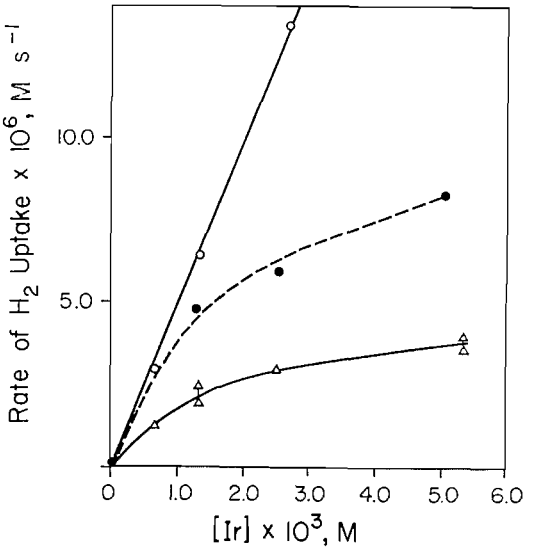

FIG. 2. Dependence of rate on $[IrX(CO)(PPh_3)_2]$, 80°, 0.07 *M* maleic acid, 730 mm H_2, DMA solution; (△) chloro complex; (●) bromo complex; (○) iodo complex.

Can. J. Chem. Downloaded from www.nrcresearchpress.com by 210.87.254.42 on 09/05/12
For personal use only.

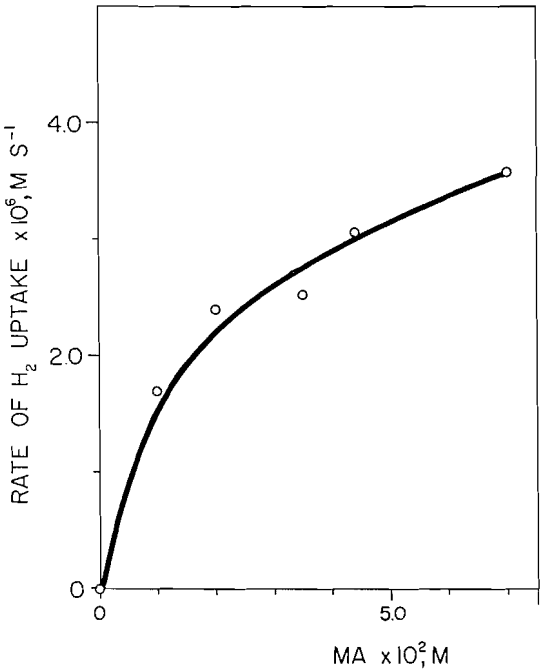

FIG. 3. Dependence of rate on maleic acid (MA) concentration, 80°, 5.36×10^{-3} *M* $IrCl(CO)(PPh_3)_2$, 730 mm H_2, DMA solution.

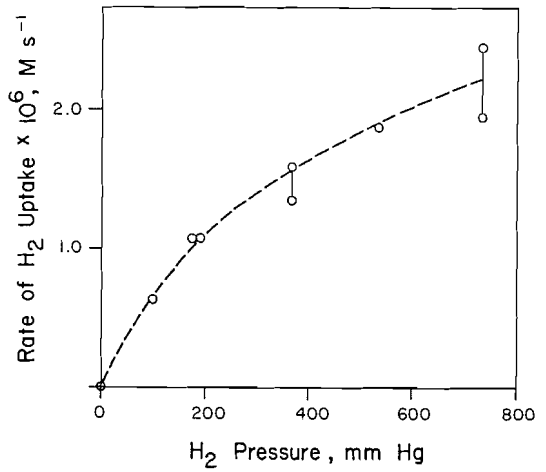

FIG. 4. Dependence of rate on H_2 pressure, 80°, 1.34×10^{-3} *M* $IrCl(CO)(PPh_3)_2$, 0.07 *M* maleic acid, DMA solution.

those observed in corresponding dimethylacetamide systems, but the initial autocatalysis region was more pronounced than in the latter. An extended linear region was again observed where the rates were about half those in dimethylacetamide solution; the initial rates were about 3 times slower in the dimethylsulfoxide system.

The catalytic hydrogenation of maleic acid has also been studied using the bromo and iodo iridium complexes. The uptake plots are similar to that shown in Fig. 1 for the chloro complex, but the rates in the linear region are about 2.5 times faster in the bromo systems and 4 times faster in the iodo systems. The dependences on maleic acid and hydrogen are similar to those in the chloro complex system. The dependence on $IrBr(CO)(PPh_3)_2$ concentration is again between zero and first order, but in the iodo complex system there is a first order dependence on iridium over the concentration range studied (Fig. 2).

The presence of a few percent of added oxygen in the gas phase increased the hydrogenation rate of maleic acid by a factor of about 100 for the $IrCl(CO)(PPh_3)_2$ catalyzed reaction.

Spectrophotometric Experiments

The gas uptake measurements clearly indicated that the hydrogenation reactions were not simple. Spectrophotometric studies were thus carried out to investigate separately the equilibrium between $IrCl(CO)(PPh_3)_2$ and H_2 (eq. [1]) and the possibility of complexing between this chloro species and maleic acid (cf. eq. [2]).

At temperatures above 30°, $IrCl(CO)(PPh_3)_2$ in DMA solution undergoes a quite rapid reversible reaction with H_2, the yellow color of the chloro complex fading; the spectrum of the dihydride shows a continuum below 400 mμ with slight absorption at 387 mμ ($\epsilon = 500$) compared with the chloro complex. The equilibrium constant expression $K_H[H_2](=[IrCl(CO)(PPh_3)_2H_2]/[IrCl(CO)(PPh_3)_2])$ is readily estimated (Table I).

TABLE I

Equilibrium constant for hydride formation

Temperature (°C)	40	50	60	70	80
$K_H[H_2]$	5.3	2.4	1.7	1.0	0.6

The spectrum of benzene solutions of $IrCl(CO)(PPh_3)_2$ remained unchanged in the absence of oxygen and exhibited the same absorption peaks as the reflection spectrum of a powdered sample at 340, 387, and 439 mμ. In DMA solutions, however, the optical density decreased slowly, as shown in Fig. 5, to a steady equilibrium value. No change in optical density was observed when 10^{-2} *M* triphenylphosphine was added. Conductivity measurements indicated no chloride

Can. J. Chem. Downloaded from www.nrcresearchpress.com by 210.87.254.42 on 09/05/12
For personal use only.

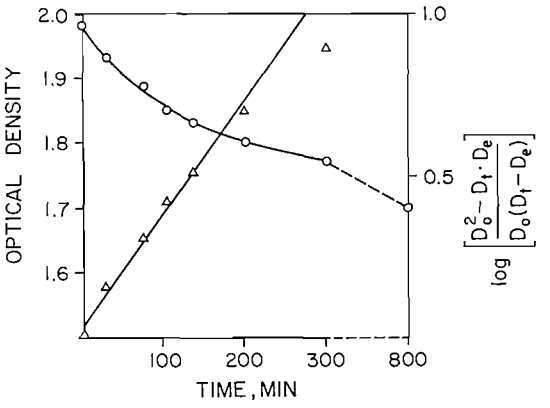

FIG. 5. Optical density plots at 387 mμ for dissociation of 1.10×10^{-4} M $IrCl(CO)(PPh_3)_2$ in DMA at 25°, 5 cm cell; (○) optical density; (△) corresponding log plot.

ion formation and the carbonyl group was not being evolved as gaseous carbon monoxide. It is concluded that the dissociation reaction

$$[3] \quad IrCl(CO)(PPh_3) \underset{k_{-1}}{\overset{k_1}{\leftrightharpoons}} IrCl(CO)(PPh_3)(S) + PPh_3$$

is occurring in DMA solution, a solvent molecule (S) presumably coordinating. This system can be analyzed by standard procedures (7) by the relationship

$$\log\left[\frac{D_0^2 - D_t D_e}{(D_t - D_e)D_0}\right] = \frac{k_1(D_0 + D_e)t}{2.3(D_0 - D_e)},$$

where D_t is the optical density at time t and subscripts 0 and e refer to initial and final equilibrium values. A plot of the log term against t is also shown in Fig. 5 and is reasonably linear. Absorption of the $IrCl(CO)(PPh_3)(S)$ species at 387 mμ was taken as zero; the slight curvature of the plot could result from a small contribution to the absorption by this species. The equilibrium constant K ($= k_1/k_{-1}$) is readily calculated from D_0 and D_e and the approximate data obtained are summarized in Table II.

TABLE II

Data for the dissociation reaction [3]

	k_1 (s^{-1})	k_{-1} (M^{-1} s^{-1})	K (M)
25°	10^{-5}	3.9	2.6×10^{-6}
80°	10^{-4}	75	1.3×10^{-6}

In the presence of maleic acid (MA) the decrease in optical density of $IrCl(CO)(PPh_3)_2$ in DMA is much greater than in a corresponding reaction without the acid, showing that complexing is occurring. Again an equilibrium is involved. Addition of triphenylphosphine completely inhibits complex formation, indicating that maleic acid forms a complex with the solvated species rather than the original $IrCl(CO)(PPh_3)_2$.

$$[4] \quad IrCl(CO)(PPh_3)(S) + \text{maleic acid} \overset{K_m}{\leftrightharpoons} \text{complex}$$

The kinetics of the complex formation are unaffected by variation in maleic acid concentration, showing that step [3] is rate determining followed by a relatively fast equilibrium [4]. The optical density curves can be analyzed by a procedure similar to that described for reaction [3] on its own. At 80° the data confirm that k_1 is about 10^{-4} s^{-1}; K_m is estimated to be about 1200 M^{-1}.

Discussion

The various equilibria and paths that could be involved in the hydrogenation reactions are summarized below.

$$IrCl(CO)P_2 + H_2 \overset{K_H}{\rightleftharpoons} IrCl(CO)P_2H_2$$

$$k_1 \downarrow\uparrow k_{-1}$$

$$P + IrCl(CO)P \overset{K'_H}{\rightleftharpoons} IrCl(CO)PH_2\,?$$

$$\begin{array}{ccc} + & H_2 & + \\ MA & & MA \\ \downarrow\uparrow K_m & k_2 \searrow & \downarrow k_3 \end{array}$$

$$IrCl(CO)P(MA) + H_2 \rightarrow IrCl(CO)P + \text{succinic acid (where } P = PPh_3)$$

The molecular hydride $IrCl(CO)(PPh_3)_2H_2$ is rapidly formed in the systems but is not directly involved in the main hydrogenation step; a reaction of this hydride with the olefin substrate would give an overall first order dependence on iridium and no initial autocatalysis would be expected in the uptake plot. Catalytic activity results from loss of a triphenylphosphine ligand from the original complex in a relatively slow step (k_1), giving rise to this autocatalytic region. The fourth coordination position of the $IrCl(CO)(PPh_3)$ species is probably occupied by a solvent molecule. This species forms a complex with maleic acid in a rapid equilibrium (K_m), which could then react with H_2 (k_2 path). Alternatively the hydride species IrCl(CO)-

Can. J. Chem. Downloaded from www.nrcresearchpress.com by 210.87.254.42 on 09/05/12
For personal use only.

$(PPh_3)H_2$ could be formed in a further equilibrium (K'_H), this then reacting with maleic acid (k_3 path). Either path, or reaction involving both, gives a rate law of the same form. Once the slow dissociation has been established, the rate law obtained for reaction by both paths is

$$\text{rate} = \frac{(k_2K_m + k_3K'_H)[H_2][MA][Ir_{total}]}{1 + K_m[MA] + K'_H[H_2] + [PPh_3](1 + K_H[H_2])/K},$$

where $K = k_1/k_{-1}$. The k_2K_m and $k_3K'_H$ terms refer respectively to the k_2 and k_3 paths; $k_3K'_H$ becomes zero if the k_2 path predominates and vice versa. Such a rate law agrees at least qualitatively with the data obtained. The reaction is between zero and first order in H_2 and maleic acid; addition of triphenylphosphine inhibits the reaction, and the reaction becomes less than first order in iridium, since with increasing total iridium concentration the extent of association back to $IrCl(CO)(PPh_3)_2$ increases (this is reflected in the $[PPh_3]/K$ term in the denominator).

Since we have no evidence for the existence of the K'_H equilibrium but have evidence and data for the maleic acid equilibrium, we tend to favor the k_2 path. The rate law simplifies to

$$[5] \quad \text{rate} = \frac{k_2K_m[H_2][MA][Ir_{total}]}{1 + K_m[MA] + [PPh_3](1 + K_H[H_2])/K}$$

and a somewhat more quantitative testing of the data can then be made. An expression such as [5] is normally analyzed by writing the inverse function (rate^{-1}) and plotting, for example, rate^{-1} against $[MA]^{-1}$ at constant $[H_2]$. However, remembering that

$$[PPh_3] = [IrCl(CO)(PPh_3)] + [IrCl(CO)(PPh_3)MA],$$

it is readily shown that the $[PPh_3]/K$ term also varies with both maleic acid and H_2 concentrations, and good linear inverse plots are not obtained. However, at sufficiently high maleic acid concentration the limiting rate will be given by $k_2[H_2][Ir_{total}]$; Fig. 3 indicates a limiting value of about 5×10^{-6} M s^{-1}, which gives $k_2[H_2] \simeq 1 \times 10^{-3}$ s^{-1}. Taking a value of 3.5×10^{-3} M atm^{-1} for the H_2 solubility (quoted for dimethylformamide (6)) gives $k_2 \simeq 0.3$ M^{-1} s^{-1} at 80°. For the initial autocatalytic part of the gas uptake plots, it can be shown that for relatively small values of time t, the total hydrogen uptake approximates to $k_1k_2K_m[H_2][MA][IrCl(CO)(PPh_3)_2]t^2/2$. Figure 6 shows a plot of H_2 uptake against t^2 for the data of Fig. 1; the initial linear slope is 7×10^{-10} M s^{-2}. Using the k_1, K_m, and K_H values determined spectroscopically gives $k_2 \simeq 0.1$ M^{-1} s^{-1} at 80°, which is considered in reasonable agreement with the value estimated from the limiting rate, particularly in view of the uncertainty associated with the equilibrium constants. Any absorption at 387 mμ by the $IrCl(CO)(PPh_3)$ or $IrCl(CO)(PPh_3)MA$ species (assumed to be negligible) could give considerable error in K and K_m and also the spectroscopic data are obtained at concentrations of about one tenth those used in the gas uptake measurements.

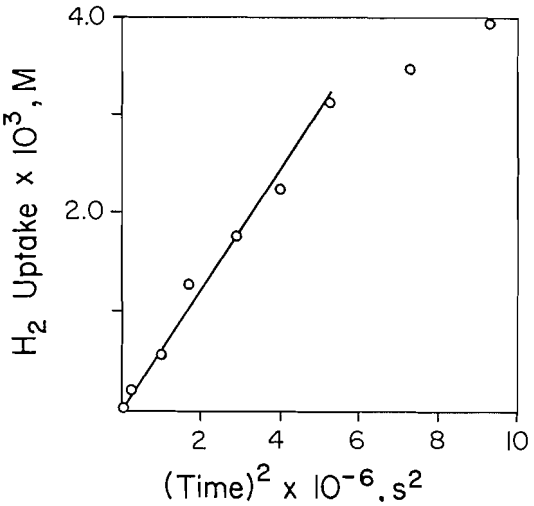

FIG. 6. Plot of total H_2 uptake vs. t^2 for the data of Fig. 1 (autocatalytic region).

To give the curved dependences shown in Figs. 2, 3, and 4 it is necessary that the three denominator terms $K_m[MA]$, $[PPh_3]/K$, and $K_H[PPh_3][H_2]/K$ be of comparable magnitude; that this is so can readily be shown by calculation over the range of concentrations used.

The kinetic and equilibrium data could be consistent therefore with a hydrogenation step involving reaction of molecular H_2 with an olefin complex formed from a slowly produced

intermediate $IrCl(CO)(PPh_3)$. However, the alternate path of reaction with the olefin with a corresponding H_2 complex cannot be completely ruled out.

Mechanisms of catalytic hydrogenation have been discussed in detail by several workers (3, 8–10). All systems must involve intermediate hydride species, but it is not known whether coordination of the olefin as a π-bonded ligand is a general feature. A plausible mechanism for the k_2 path suggested here is shown in the following scheme.

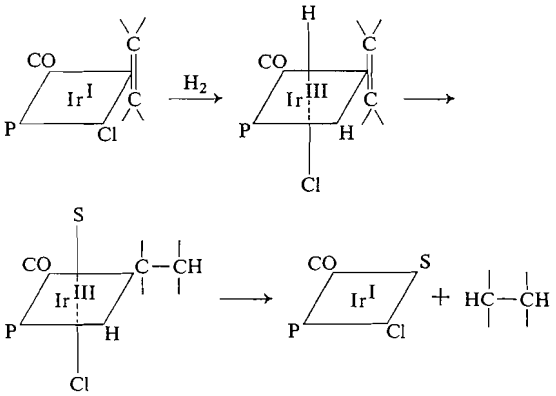

(where P = PPh_3 and S = solvent)

Hydride formation is accompanied by formal oxidation of the metal; hydrometallation of olefinic bonds (the second step) is well substantiated, being an example of a much wider class of insertion reactions.

A system much in common with the one described here is the recent one reported by Wilkinson and co-workers (10) on the hydrogenation catalyst $RhCl(PPh_3)_3$ in benzene solutions. This system is somewhat simpler in that the dissociation step

$$RhCl(PPh_3)_3 \rightleftharpoons RhCl(PPh_3)_2 + PPh_3$$

is rapid even at 25° and lies essentially to the right, giving a high catalytic activity. In this system, however, it seems that the k_3 path involving reaction of $RhCl(PPh_3)_2H_2$ with the olefin is dominant. Both studies show the importance of the dissociation step in making available a coordination site on the transition metal complex.

The efficiency of the catalyst is governed principally by the equilibrium constant K for the dissociation step; this is small (10^{-6} M at 80°) for the $IrCl(CO)(PPh_3)_2$ complex. The first order dependence on iridium concentration noted for the iodo complex indicates greater dissociation for this complex, which could give rise to the increased catalytic activity. Other workers (2, 4) have reported increasing chemical reactivity of the $IrX(CO)(PPh_3)_2$ complexes in the order I > Br > Cl in benzene solutions where there is no measurable dissociation.

A lower rate of reduction for fumaric acid is reasonable, since spectroscopic measurements indicate that the complexing with this substrate is weaker, corresponding to a smaller K_m value.

Catalytic activity of the $IrCl(CO)(PPh_3)_2$ species in the different solvents is seen to decrease in the order dimethylacetamide > dimethylsulfoxide $\gg$ benzene. Both the donor strength and solvating power of the solvents are likely to be important for this type of system. Good coordinating solvents enhance the solvent path for the associative trigonal-bipyramidal substitution mechanism of square planar d^8 complexes (11). Rates of hydrogen addition to $IrX(CO)(PPh_3)_2$ complexes and hydrogenation rates catalyzed by the $RhCl(PPh_3)_3$ complex are increased by the use of more polar solvents (4, 10) and these findings have been interpreted in terms of reaction through a highly polar transition state. Generally the donor strength and solvating power of dimethylacetamide and dimethylsulfoxide are thought to be very similar (12).

The reason for the marked increase in the hydrogenation rate in the presence of small amounts of O_2 is not understood. The known equilibrium

$$IrCl(CO)(PPh_3)_2 + O_2 \rightleftharpoons IrCl(CO)(PPh_3)_2O_2$$

is presumably involved, and the oxygen adduct is known to be light sensitive, giving as yet unidentified products (13). This oxygen effect is being further studied.

Acknowledgments

Grateful acknowledgment is made to the National Research Council of Canada for support of this research and we wish to thank Mr. A. C. McLaughlin for technical assistance.

1. L. Vaska and J. W. DiLuzio. J. Am. Chem. Soc. **83**, 2784 (1961); **84**, 679 (1962).
2. L. Vaska and R. E. Rhodes. J. Am. Chem. Soc. **87**, 4970 (1965).
3. L. Vaska. Inorg. Nucl. Chem. Letters, **1**, 89 (1965).
4. P. W. Chock and J. Halpern. J. Am. Chem. Soc. **88**, 3511 (1966).

Can. J. Chem. Downloaded from www.nrcresearchpress.com by 210.87.254.42 on 09/05/12
For personal use only.

5. B. R. JAMES and G. L. REMPEL. Can. J. Chem. **44**, 233 (1966).
6. DUPONT PRODUCT INFORMATION BULLETIN. A review of catalytic and synthetic applications for DMF and DMAC.
7. A. A. FROST and R. G. PEARSON. Kinetics and mechanism. Wiley, New York. 1963. p. 187.
8. J. HALPERN. Chem. Eng. News, **44**(45), 68 (1966).
9. J. HALPERN, J. F. HARROD, and B. R. JAMES. J. Am. Chem. Soc. **88**, 5150 (1966).
10. J. A. OSBORN, F. H. JARDINE, J. F. YOUNG, and G. WILKINSON. J. Chem. Soc. A, 1711 (1966).
11. H. B. GRAY and C. H. LANGFORD. Ligand substitution processes. Benjamin, New York. 1966. p. 39.
12. V. GUTMANN and R. S. DRAGO. Papers presented at Conference on Non-Aqueous Solvent Chemistry. Hamilton, Ontario. June 1967.
13. L. VASKA. Science, **140**, 809 (1963).

Can. J. Chem. Downloaded from www.nrcresearchpress.com by 210.87.254.42 on 09/05/12
For personal use only.

Intermolecular fluorine exchange between tetrabutylammonium hexafluorophosphate and BF_3 or PF_5[1]

S. BROWNSTEIN AND J. BORNAIS
Division of Applied Chemistry, National Research Council of Canada, Ottawa, Canada
Received August 4, 1967

A rapid exchange of fluorine between hexafluorophosphate ion and BF_3 or PF_5 in methylene chloride solution has been found to occur by a bimolecular mechanism. The exchange rates were determined by fluorine magnetic resonance spectroscopy and the apparent Arrhenius activation energies were obtained.

Canadian Journal of Chemistry, **46**, 225 (1968)

Can. J. Chem. Downloaded from www.nrcresearchpress.com by 210.87.254.5 on 09/05/12
For personal use only.

Introduction

The phenomenon of fluorine bridge bonding in Lewis acid fluorides and their anions has been found to occur frequently (1–5). It has also been observed that on the nuclear magnetic resonance (n.m.r.) time scale there is often rapid intra- and inter-molecular fluorine exchange. The purpose of this investigation was to attempt a quantitative determination of exchange rates in order to find the mechanism of some of the exchange reactions and the participation, if any, of fluorine bridge bonding in the fluorine exchange process. The hexafluorophosphate anion is an ideal system for magnetic resonance exchange rate investigations, since it has two narrow, well-separated resonance lines and contains only spin 1/2 nuclei. There have been two previous reports that it will readily undergo fluorine exchange (6, 7).

Numerous discussions of the measurement of exchange rates by changes in nuclear magnetic resonance line shapes have been published (8–11). Only in the simplest cases have analytic functions for the line shapes been determined. Even in these cases calculation of the line shapes is so tedious that a computer is normally used. For the present study a computer was programmed for a general N site case using the stochastic approach of Kubo (12, 13). At the limits of fast and very slow exchange this reduces to the usual simple approximations of a change in line widths alone.

Experimental

Commercially obtained boron trifluoride and phosphorus pentafluoride were distilled at low temperature into storage bulbs of the vacuum line and kept over phosphorus pentoxide. No signal from POF_3 could be detected in the fluorine resonance spectrum of the PF_5. The solvent, methylene chloride, and the tetrabutylammonium hexafluorophosphate were purified as before (7). Tetrabutylammonium perchlorate was synthesized and purified according to Fuoss *et al.* (14). Fluorotrichloromethane, used as an internal fluorine resonance reference, was distilled at room temperature into a storage container of the vacuum system and transferred as the vapor to the n.m.r. sample tubes. Tetrabutylammonium hexafluorophosphate was vacuum dried in the sample container and the other components added by standard vacuum line techniques. The n.m.r. sample tubes were sealed before removal from the vacuum system and kept in liquid nitrogen at all times except when their spectra were being obtained. For those samples with a very low concentration of BF_3 or PF_5 it was necessary to prepare several milliliters of solution in order to use a sufficient quantity of gas for accurate measurement. In these cases the entire sample container was kept at "Dry Ice" temperature and then tilted to introduce some of the sample into the n.m.r. tube. The tube was then sealed while its contents and that of the main sample container were kept at "Dry Ice" temperature. At this temperature essentially all of the BF_3 or PF_5 will be in solution. This procedure was adopted to insure that no changes in concentration would occur between the bulk sample and that in the n.m.r. tube. Despite all these precautions the principal error in this work is probably the value for the concentration of BF_3 or PF_5. There was no independent method of checking that the entire amount of BF_3 or PF_5 was transferred to the n.m.r. tube. The variation in τ values for almost identical samples was greater than the deviation from Arrhenius plots for individual samples. All concentrations are reported as molalities (m) assuming complete solution of the gas in the solvent.

Fluorine resonance spectra were obtained at 94.1 MHz on a Varian spectrometer modified to operate by a "time division" scheme. The pulsing frequency of 10 KHz was generated by a crystal oscillator. For very wide lines the spectra were calibrated with the side bands of the pulsing frequency. Narrower lines were measured by conventional side band techniques and referred via a frequency counter to the same crystal oscillator used for the pulsing. The probe temperature was controlled by a Varian controller using a platinum resistance thermometer and calibrated against a copper–constantan thermocouple in a dummy sample tube. The sample temperatures should be accurate within 1 °C.

All the data were correlated by least square procedures and any errors quoted are standard deviations.

[1]Issued as NRCC No. 9783.

Can. J. Chem. Downloaded from www.nrcresearchpress.com by 210.87.254.5 on 09/05/12
For personal use only.

Results and Discussion

The spin coupling constant of the hexafluorophosphate ion was found to be independent of temperature in the interval of this study. The chemical shifts of all the fluorine containing species moved slightly to low field with lower temperature. Theoretical spectra were calculated for chemical shift values in the middle of the temperature range studied. Since the theoretical spectra only depend on the difference in chemical shift of the exchanging species there should be no appreciable effect of temperature dependent chemical shifts upon the theoretical spectra. Some typical theoretical spectra for the PF_6^- resonance regions of the system PF_6^- plus BF_3 with a population ratio of 12:1 are shown in Fig. 1. Throughout this study only the resonances in the PF_6^- region of the spectrum were measured. Normally, the other species was present in much lower concentration and accurate measurement of its resonance would be difficult. From a study of the slow exchange region of the theoretical spectra, i.e. where the separate peaks of the PF_6^- resonance are well resolved, it was found that provided the population ratio was greater than 5:1 the usual approximations for an exchange-broadened doublet were completely adequate to describe the spectra. For the system PF_6^- plus BF_3 measurements were made in the rate regions where both one and two lines occurred. Only in the two-line region were sufficiently narrow lines observed that corrections were required for the natural line width in the absence of exchange. Because of the uncertainty of the spectrum for PF_5 in the absence of exchange (5) it was not possible to calculate theoretical spectra for the system PF_6^- plus PF_5 over the entire range of exchange rates. Therefore measurements were only made in the slow exchange region and with population ratios where it had been shown that the exchange-broadened doublet approximation was adequate.

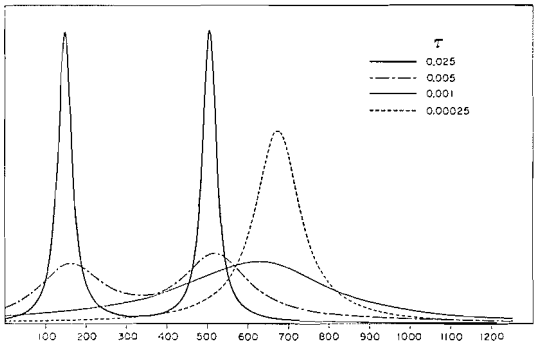

FIG. 1. Theoretical spectra of the PF_6^- region of the system $PF_6^- + BF_3$.

The technique of measuring exchange rates by nuclear magnetic resonance spectroscopy, as employed in this study, measures the lifetime, τ, of fluorine on a particular chemical species under equilibrium conditions. The relationship between this lifetime and the change in concentration with time measured in conventional chemical kinetics is

$$[1] \qquad \tau_x = [X]/(d[X]/dt).$$

The most general kinetic expression for the exchange of a fluorine on phosphorus in tetrabutylammonium hexafluorophosphate with a fluorine of BF_3 or PF_5 is

$$[2] \qquad \frac{d[(Bu)_4NPF_6]}{dt} = k[(Bu)_4NPF_6]^x[MF]^y,$$

where MF is either BF_3 or PF_5. Therefore

$$[3] \qquad k = 6\tau^{-1}[(Bu)_4NPF_6]^{1-x}[MF]^{-y}.$$

This implicitly assumes that only one fluorine atom is exchanged between the phosphorus fluoride species and MF on each effective encounter. If more than one is exchanged there will be no change in the form of eq. [3] but k will be multiplied by an appropriate constant.

It is assumed that the variation of rate constants with temperature will follow the usual Arrhenius dependence. It is then possible to directly compare the data for a given system at all temperatures and concentrations by a plot of log k versus the reciprocal temperature. This procedure is desirable when it is not possible to compare the rates at the same temperature for all concentrations. Such a plot for the system PF_6^- plus PF_5, where $x = 1/2$ and $y = 1$, is shown in Fig. 2. From this data the Arrhenius activation energy for this exchange is 1.5 ± 0.2 kcal mole^{-1}. Samples with concentrations of tetrabutylammonium hexafluorophosphate from 2.16×10^{-1} to 3.43×10^{-2} m and with PF_5 concentrations from 9.5×10^{-3} to 1.30×10^{-3} m were studied. Over this concentration range the exponents $x = 1/2$ and $y = 1$ fit the data much better than other simple numbers. For example, with $x = 1$ and $y = 1$, ΔE is found to

Can. J. Chem. Downloaded from www.nrcresearchpress.com by 210.87.254.5 on 09/05/12
For personal use only.

be 0.9 ± 0.5 kcal mole^{-1}. The raw data for this system are presented in Table I. Much more extensive data was obtained for the system PF_6^- plus BF_3. The Arrhenius activation energy for fluorine exchange was found to be 4.6 ± 0.2 kcal mole^{-1}. The tetrabutylammonium hexafluorophosphate concentration was varied from 8.70×10^{-1} to 3.47×10^{-2} *m* and the BF_3 concentration from 9.29×10^{-2} to 1.33×10^{-3} *m*. Again the exponents $x = 1/2$ and $y = 1$ were found to give the most satisfactory fit with the experimental results.

TABLE I

Lifetimes for fluorine exchange in the $PF_6^- + PF_5$ system

T(°K)	$[PF_6^-]$	$[PF_5]$	$\tau \times 10^3$
213	0.0343	0.00130	19.84
223	,,	,,	16.72
233	,,	,,	15.66
177	0.0822	0.0095	8.13
213	0.0806	0.00150	40.8
223	,,	,,	30.0
213	0.216	0.00147	57.5
223	,,	,,	47.2
233	,,	,,	40.7
243	,,	,,	30.8
253	,,	,,	29.0
263	,,	,,	23.2
273	,,	,,	20.5

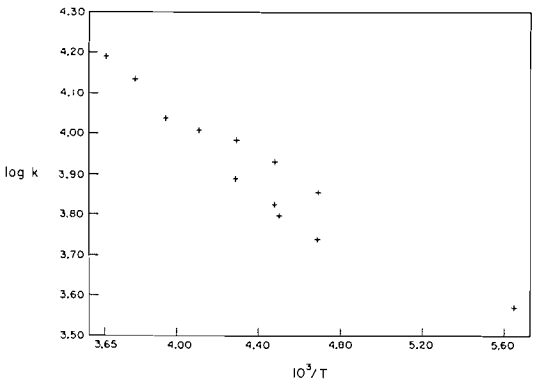

FIG. 2. Temperature dependence of the exchange rate in the system $PF_6^- + PF_5$.

The dependence of exchange rate upon the concentration of BF_3 or PF_5 to the first power is what would be expected for a normal bimolecular mechanism and rules out the possibility that the rate-controlling process is the dissociation of PF_6^- to PF_5 and fluoride ion. This is also consistent with the very low activation energies for the exchange reactions. A possible explanation of the half order dependence upon concentration of tetrabutylammonium hexafluorophosphate is its existence in methylene chloride solution as ion pairs. If the exchange reaction only occurs with the free PF_6^- ion and not when it is part of an ion pair the observed kinetics may be explained by the following scheme.

$$(Bu)_4NPF_6 \overset{\text{fast}}{\rightleftarrows} PF_6^- + (Bu)_4N^+$$

$$K = \frac{[PF_6^-]^2}{[(Bu)_4NPF_6]},$$

provided that the dissociation occurs to only a slight extent. Substituting this into eq. [2] with $x = 1/2$ and $y = 1$ yields

$$[4] \quad \frac{d[(Bu)_4NPF_6]}{dt} = \frac{k}{\sqrt{K}}[PF_6^-][MF],$$

which is of the usual form for a bimolecular rate process.

Such a scheme is also consistent with the very low Arrhenius activation energies which were measured. Since both the rate constant for exchange and the equilibrium constant for dissociation will decrease with decreasing temperature, the temperature dependence of their ratio will be less than the variation of either alone. According to the above scheme it is the temperature dependence of this ratio which determines the apparent activation energy.

Some support for the existence of the aggregate species is derived from molecular weight determinations. The molecular weights of tetrabutylammonium hexafluorophosphate and the homologous compound tetrabutylammonium hexafluoroarsenate were determined by vapor pressure osmometry on 2×10^{-2} *M* solutions in methylene chloride. In both cases the apparent molecular weight was about 5% greater than the formula weight. This suggests that both these compounds exist in solution primarily as ion pairs with the possibility of some association to higher aggregates. Conductivity studies on similar compounds in nonpolar solvents suggest that ion pairs predominate until quite low concentrations (14).

If the proposed mechanism is correct, one would predict a reduction in the rate of exchange upon addition of another tetrabutylammonium salt, since this would reduce the concentration

of PF_6^- by a common ion effect. Unfortunately, it was not possible to test this hypothesis, since no anion could be found which did not react with BF_3. Even tetrabutylammonium perchlorate was found to complex with boron trifluoride under the conditions used to study the exchange reaction.

A bimolecular mechanism for fluorine exchange requires PF_6^- and either BF_3 or PF_5 to form an intermediate species or transition state. It is possible that the two fluorine-containing species are joined together by fluorine bridge bonding in this reactive intermediate. This would be consistent with the interactions observed with other nonmetallic fluorides.

Conclusions

Boron trifluoride and phosphorus pentafluoride were found to readily exchange fluorine, by a bimolecular mechanism, with tetrabutylammonium hexafluorophosphate. The very low apparent Arrhenius activation energies may arise from a combination of dissociation and exchange processes. It is possible that tetrabutylammonium hexafluorophosphate exists primarily as ion pairs in CH_2Cl_2 solution but that fluorine exchange only occurs with the free PF_6^- ion.

Acknowledgments

The authors wish to thank Prof. M. Saunders for his computer program and Mr. F. Farrel for producing the theoretical spectra. Many helpful discussions were held with Dr. A. M. Eastham. Dr. B. Cernicki was involved in the experimental work.

1. C. J. Hoffman, B. E. Holder, and W. L. Jolly. J. Phys. Chem. **62**, 364 (1958).
2. S. Brownstein and J. Paasivirta. Can. J. Chem. **43**, 1645 (1965).
3. R. J. Gillespie and K. C. Moss. J. Chem. Soc. A, 1170 (1966).
4. P. J. Burchill, S. Brownstein, and A. M. Eastham. Can. J. Chem. **45**, 17 (1967).
5. S. Brownstein. Can. J. Chem. **45**, 1711 (1967).
6. F. N. Tebbe and E. L. Muetterties. Inorg. Chem. **6**, 129 (1967).
7. S. Brownstein. Can. J. Chem. **45**, 2403 (1967).
8. H. S. Gutowsky and C. H. Holm. J. Chem. Phys. **25**, 1228 (1956).
9. H. M. McConnell. J. Chem. Phys. **28**, 430 (1958).
10. S. Alexander. J. Chem. Phys. **37**, 967 (1962).
11. C. S. Johnson, Jr. *In* Advances in magnetic resonance. Vol. 1. *Edited by* J. S. Waugh. Academic Press, New York. 1965.
12. R. Kubo. Nuovo Cimento Suppl. **6**, 1063 (1957).
13. R. A. Sack. Mol. Phys. **1**, 163 (1958).
14. W. F. Luder, P. B. Kraus, C. A. Kraus, and R. M. Fuoss. J. Am. Chem. Soc. **58**, 255 (1936).

Can. J. Chem. Downloaded from www.nrcresearchpress.com by 210.87.254.5 on 09/05/12
For personal use only.

Infrared and Raman spectral studies of KNO_2–KNO_3 solutions[1]

M. H. Brooker and D. E. Irish
Department of Chemistry, University of Waterloo, Waterloo, Ontario
Received July 27, 1967

Potassium nitrite frequently contains significant nitrate impurity, detectable by vibration spectroscopy. Analyses based independently on infrared and Raman band intensities permit a quantitative determination of the nitrate impurity. Reassignment of some previously reported vibrational frequencies is discussed.

Canadian Journal of Chemistry, 46, 229 (1968)

Can. J. Chem. Downloaded from www.nrcresearchpress.com by 210.87.254.5 on 09/05/12
For personal use only.

For many years the accurate measurement of physical chemical properties of potassium nitrite has been hampered by its lack of purity. In 1937 Bureau (1) reported nitrate, chloride, and carbonate as the major impurities. Improved preparations have eliminated all but the nitrate. Rapoport (2) found 0.3 to 1% nitrate impurity in G.P.R. KNO_2 listed at 97% nitrite minimum. The assay of commercial reagent grade KNO_2 varies from 89 to 97% nitrite. Much of the remaining weight is water. Since drying transforms the crystals to an unmanageable plastic the salt is commonly shipped moist. Recrystallization of KNO_2 does not remove the nitrate impurity. This difficulty was explained by Bureau (1) who found that the solid formed in equilibrium with its saturated solution was a solid solution of KNO_3 and KNO_2, with composition almost identical with the solution composition. Ray (3) was able to purify KNO_2 by an ion exchange method; however, this achievement has not yet received the attention it deserves.

The development of a procedure for purification has probably been hindered by the lack of a suitable analytical method for the determination of small amounts of nitrate in nitrite. The failure to find nitrate listed as an impurity on the label of reagent grade nitrites illustrates the analysis problem and has probably led to considerable incorrect data in the literature. The usual difference techniques involve a nitrite analysis followed by either oxidation or reduction procedures and subsequent analysis for nitrate or total nitrogen. These procedures can be found in most analytical chemistry texts but are of little use if the nitrate is less than 2% of the nitrate–nitrite mixture, in part because of the instability of the nitrite ion in acid media. The resulting nitrous acid disproportionates into nitrate and gaseous oxides (4). A nonaqueous titration proposed by Cundiff and Markunas (5) is also incapable of providing valid data when the nitrate concentration is low. The overlap of ultraviolet absorption bands hinders the use of electronic spectra (6). A semimicro analysis of Leithe (7) is reported to determine nitrate to 0.05% in nitrate–nitrite mixtures. This method is far from routine and has two major drawbacks; the instability of the standard solutions and possibility of producing more nitrate during the nitrite reduction with sulfamic acid.

The infrared spectrum of the nitrite ion is well documented (8–10). Raman spectra have been recorded by photographic methods (11), but to our knowledge have not been studied with modern photoelectric instruments. For the nitrite ion with C_{2v} symmetry the predicted spectrum consists of three coincident infrared and Raman lines (Fig. 1). The frequencies given in the figure are those observed from a 14.0 M aqueous solution of KNO_2. The ν_2 frequency is sensitive to the cation and solution concentration. The assignments are consistent with qualitative observed degrees of depolarization of the Raman bands.

The predicted spectrum for the unperturbed nitrate ion of D_{3h} symmetry is also shown in Fig. 1. Differences from this idealized spectrum have been described elsewhere (12).

For both solid KNO_2 and the concentrated aqueous solution, variations from the simple three line infrared spectrum have been reported (8, 13, 14). Weston and Brodasky (8) have attributed the spectral variations to changes in the nitrite environment. This explanation aroused our interest since in this laboratory infrared and Raman spectroscopy are being used

[1]Presented in part at the 50th Canadian Chemical Conference, Toronto, Ontario, June 4–7, 1967.

Can. J. Chem. Downloaded from www.nrcresearchpress.com by 210.87.254.5 on 09/05/12
For personal use only.

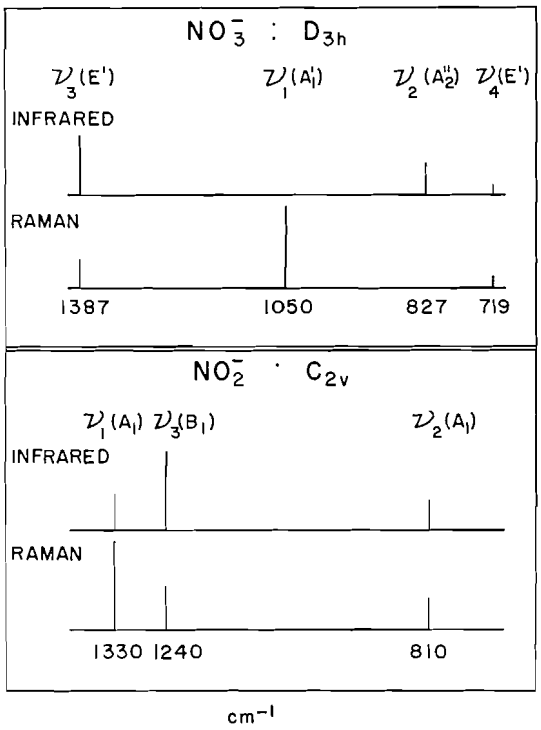

FIG. 1. Infrared and Raman spectra of unperturbed NO_3^- and NO_2^-.

to study ionic interactions in aqueous solutions.

In this paper we will show that the anomalies in the infrared spectrum of KNO_2 are due to nitrate impurities. Experiments involved in characterizing the nitrate impurity have led to development of simple quantitative infrared and Raman analyses for small quantities of nitrate in potassium nitrite. Previous infrared studies of nitrate–nitrite mixtures have been qualitative (15) or of little value for low nitrate: nitrite ratios (16). To our knowledge no previous Raman work has been done on nitrate–nitrite mixtures.

Experimental

Chemicals were the highest purity commercially available. KNO_2 and $NaNO_2$ were Baker and Adamson reagent grade with 95 and 98% minimum nitrite assay respectively. $Ba(NO_2)_2$ was supplied by Alfa Chemicals and listed at from 97 to 99% nitrite. KNO_3 was Analar 99% pure and used without further purification. $NaNO_2$ and $Ba(NO_2)_2$ were easily purified by recrystallization from aqueous solution. KNO_2 was purified by the ion exchange method of Ray (3), using Dowex 2-X8, 50–100 mesh anion exchange resin.

Pure KNO_2 was also prepared by mixing solutions of purified K_2SO_4 and $Ba(NO_2)_2$ and filtering off the $BaSO_4$. The purity of the nitrites was verified by absence of the ν_1 nitrate frequency at high Raman sensitivity. The ν_1 nitrate line could be observed from the KNO_2 before purification. It could also be seen in the effluent of the $NaNO_2$ regenerant from the ion exchange purification of the KNO_2.

Nitrate–nitrite mixtures for the quantitative analyses were prepared by addition of KNO_3 to a known volume of concentrated KNO_2 purified by ion exchange. The small volume change on mixing did not measurably change the nitrite concentration. A series of solutions was prepared in D_2O for aqueous infrared studies. All solutions were filtered through fine porosity sintered glass filters and although yellow were free from turbidity.

Solid mixtures were prepared by two methods. Aliquots of aqueous solutions containing KNO_2 and KNO_3 were dehydrated by evaporation to dryness followed by vacuum drying at 100 °C. A second series of solid samples was prepared by crystallization from the aqueous solutions.

Raman spectra obtained with a Cary 81 Raman spectrophotometer were excited by the 4358 Å mercury line. A slit width of 10 cm^{-1} was used. Aqueous solutions were contained in a 5 ml thermostated glass Raman cell. Infrared spectra were obtained with the Beckman IR-9 spectrophotometer operated on "three times standard" slits. Aqueous solutions were contained between silver chloride plates separated by a 0.025 mm Teflon gasket. Spectra of the solid mixtures were obtained for Nujol mulls between AgCl plates or solid powders pressed against an AgBr prism in the Wilks model 9 M.A.T.R. attachment. The latter method has the advantage of giving a clear spectrum in the region usually obscured by organic mulling agents. The infrared and Raman spectra for the aqueous mixtures were run at a constant temperature of 25 ± 0.2 °C controlled by a Haake constant temperature circulator. The solid samples were not thermostated.

The relative integrated Raman intensities were obtained by measurement of the band areas with a standard planimeter. The relative absorbances of the infrared bands were measured from peak heights. For the solids these proved to be less base-line sensitive.

Results

The observed spectral lines for high purity commercial KNO_2 are given in Table I. Band positions are expected to be accurate to ±1 cm^{-1}. The change in frequency for the bands in the 800 cm^{-1} region is as expected for the change from solid to solution. If the bands at 1330, 810, and 1240 cm^{-1} are assigned to ν_1, ν_2, and ν_3 respectively for the nitrite ion, three bands remain. Reference to Fig. 1 shows that the 833 or 837, 1055, and 1387 cm^{-1} bands can be assigned to nitrate present as impurity. The 1055 cm^{-1} band is Raman active but not infrared active. The 833 or 837 cm^{-1} band is infrared active but not Raman active. The 1387 cm^{-1}

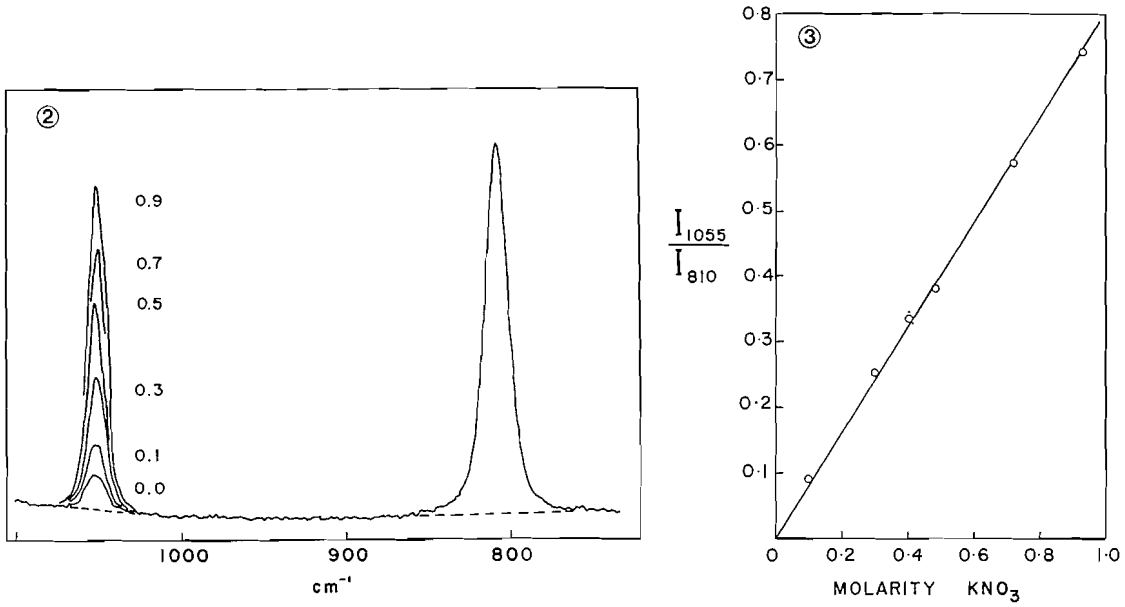

FIG. 2. Portion of the Raman spectrum of 14.0 *M* KNO_2 and solutions with increased nitrate concentration from 0.1 to 0.9 *M*.
Fig. 3. The Raman intensity ratio I_{1055}/I_{810} versus concentration of KNO_3.

band is seen for the solid by M.A.T.R. but is not seen for Nujol mulls or aqueous solutions. For Nujol mulls the 1387 cm^{-1} band is masked by absorption of the oil. In both the Raman and infrared spectra of aqueous solutions the broad envelope from the ν_1–ν_3 nitrite region prevents its detection. ν_4 of nitrate at 719 cm^{-1} is not observed due to its inherent weakness. In all cases the bands assigned to the nitrate impurity exhibit enhancement on addition of nitrate.

A portion of the Raman spectrum of 14.0 *M* KNO_2 as purchased and with increasing nitrate is shown in Fig. 2. The 1055 cm^{-1} band attributed to nitrate can be seen in the spectrum of unadulterated commercial KNO_2 and increases with added nitrate. The 810 cm^{-1} nitrite band is invariant. The ratio I_{1055}/I_{810} is directly proportional to concentration (Fig. 3). Since the nitrite

TABLE I

Vibrational spectrum of high purity commercial KNO_2

Observed frequencies		
Raman*	Infrared	Assignment
810	810*, 806†‡	ν_2 NO_2^-
	833*, 837†‡	ν_2 NO_3^-
1055		ν_1 NO_3^-
1240	1240*‡	ν_3 NO_2^-
1330	1330*‡	ν_1 NO_2^-
	1387‡	ν_3 NO_3^-

*Aqueous solution.
†Nujol mull.
‡Solid M.A.T.R.

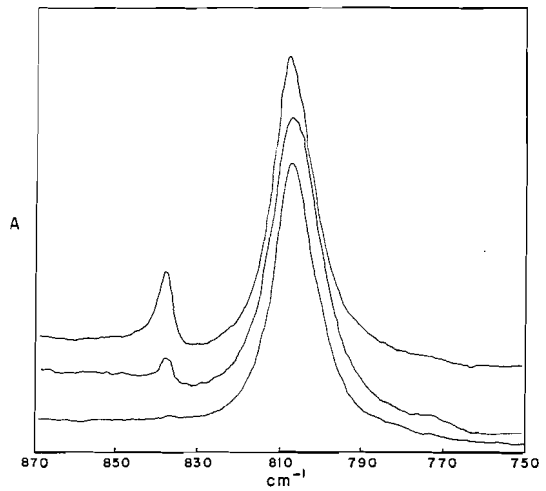

FIG. 4. Portion of infrared spectrum of solid KNO_2. Lower trace: purified; middle trace: commercial salt; upper trace: crystallized from solution containing 0.3 *M* KNO_3.

Can. J. Chem. Downloaded from www.nrcresearchpress.com by 210.87.254.5 on 09/05/12
For personal use only.

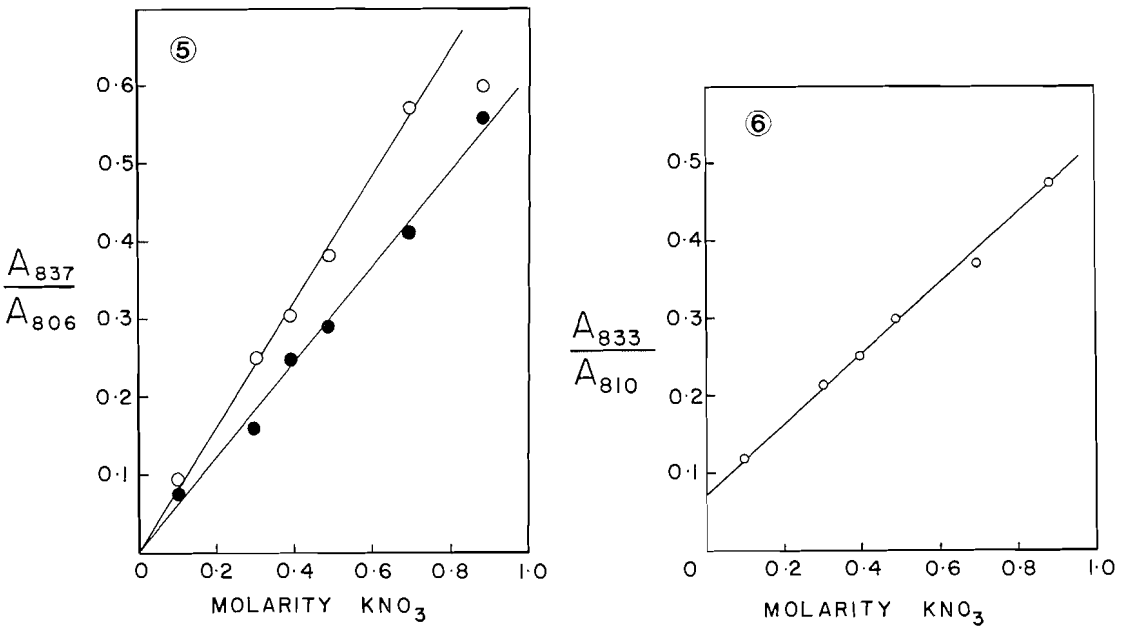

FIG. 5. The infrared absorbance ratio A_{837}/A_{806} from Nujol mulls versus the concentration of KNO_3 in solutions from which the solids were obtained: (○) dehydrated, (●) crystallized.

FIG. 6. The infrared absorbance ratio A_{833}/A_{810} for the KNO_3–KNO_2 mixture in D_2O solution versus concentration of KNO_3.

concentration is constant the ratio is independent of refractive index or color changes. The intensity ratio from the commercial salt corresponds to a nitrate molarity of 0.094, i.e. 0.49 wt. % impurity.

A portion of the infrared spectrum of solid KNO_2 purified by ion exchange is shown in Fig. 4 together with the spectrum of the commercial salt and a solid formed from a nitrate–nitrite solution. The linearity of A_{837}/A_{806} versus concentration of added nitrate is shown in Fig. 5. Division by A_{806} compensates for variation in sample thickness. The linearity, obtained for solid samples, indicates their homogeneity and is consistent with the solid solution nature of the mixture. The slight decrease of slope in the graph for the crystallized solid indicates that only slight removal of nitrate occurs on crystallization.

The intensity ratio, A_{833}/A_{810}, is plotted versus concentration of added nitrate (Fig. 6) for the KNO_3–KNO_2 mixture in D_2O solution. The line does not pass through the origin because the intense 810 cm^{-1} band contributes intensity at 833 cm^{-1}. In each of the above procedures nitrate concentrations could be obtained with 5% accuracy. The concordance of the three analytical methods confirms the above interpretation and indicates a 0.5% nitrate impurity in the commercial Baker and Adamson salt.

Discussion

The weak band at 833 cm^{-1} in the infrared spectrum of concentrated aqueous KNO_2 has previously been attributed to a split of the ν_2 nitrite band by ionic interactions in solution (8). The band at 837 cm^{-1} from the crystal was attributed to ν_2 of nitrite, split by crystal forces or lattice interactions (8, 13). These are curious explanations, since the nitrite bending mode is a totally symmetric A_1 species. Anbar *et al.* (13) observed a similar split in $AgNO_2$, i.e. bands at 846 and 829 cm^{-1}. We have prepared pure $AgNO_2$ as a precipitate from $AgClO_4$ and $NaNO_2$ solutions and observed only one band at 846 cm^{-1}, in agreement with the single band observed by Weston and Brodasky (8). The band at 829 cm^{-1} observed by Anbar *et al.* could be nitrate impurity or free nitrite.

The ν_1 nitrate band at 1055 cm^{-1} has not been reported before for reagent grade KNO_2. The shift of the band maximum from 1049 cm^{-1} where it occurs in a dilute solution of

Can. J. Chem. Downloaded from www.nrcresearchpress.com by 210.87.254.5 on 09/05/12
For personal use only.

KNO_3 (17) can be attributed to cation interactions. The magnitude and direction of the shift are as expected from a 14 *M* potassium ion concentration (17, 18). The 10 wavenumber shift for ν_2 of nitrate ion from 827 cm^{-1} in solid KNO_3 to 837 cm^{-1} in the KNO_3–KNO_2 solid solution may also be attributed to changes in the environment.

The band at 1387 cm^{-1} has been seen previously in the infrared spectrum of KNO_2 run as a KBr disc (8) and as a deposit on a fluorite plate (19). Weston and Brodasky (8) assigned the band (1384 cm^{-1}) to ν_1 nitrite shifted by an orientation effect that changed the coupling between lattice and internal vibrations. Failure to observe ν_1 of nitrite probably prompted this explanation. However, ν_1 is very weak in the infrared and often is completely masked in the solid by the strong broad ν_3. In our opinion the 837 cm^{-1} and 1384 cm^{-1} bands observed by Weston and Brodasky (8) arise from nitrate impurity in the KNO_2 salt. The only bands attributable to pure KNO_2 crystal are 806 cm^{-1}, 1240 cm^{-1}, and 1330 cm^{-1}.

In our estimation the quantitative infrared analysis will detect as low as 0.2 wt. % nitrate impurity in nitrite. The infrared methods are primarily useful for the potassium salt, due to the solid solution properties of the KNO_3–KNO_2 mixtures. The Raman method probably permits detection of even lower concentrations of nitrate impurity. The M.A.T.R. solid samples were not used for quantitative analysis because an order break in the IR-9 at 1200 cm^{-1} causes a discontinuity in the spectrum and prevents the drawing of an accurate base line.

Acknowledgments

This work was supported by a grant from the National Research Council of Canada and by the Government of Ontario in the form of an Ontario Graduate Fellowship award to one of us (M. H. B.).

1. J. Bureau. Ann. Chim. Paris, [11], **8**, 5 (1937).
2. E. Rapoport. J. Chem. Phys. **45**, 2721 (1966).
3. J. D. Ray. J. Inorg. Nucl. Chem. **15**, 290 (1960).
4. M. J. N. Pourbaix. Atlas of electrochemical equilibrium in aqueous solutions. Pergamon Press, New York. 1966. p. 501.
5. R. H. Cundiff and P. C. Markunas. Anal. Chim. Acta, **21**, 68 (1959).
6. G. Meerman. Ph.D. Thesis, University of Illinois, Urbana, Illinois. 1960. Dissertation Abstr. **20**, 4507 (1960).
7. W. Leithe. Mikrochim. Acta, 962 (1960).
8. R. E. Weston, Jr. and T. F. Brodasky. J. Chem. Phys. **27**, 683 (1957).
9. J. W. Sidman. J. Am. Chem. Soc. **79**, 2675 (1957).
10. B. M. Gatehouse. J. Inorg. Nucl. Chem. **8**, 79 (1958).
11. A. Langseth and E. Walles. Z. Physik. Chem. Leipzig, **B27**, 209 (1934).
12. D. E. Irish. *In* Raman spectroscopy theory and practice. *Edited by* H. A. Szymanski. Plenum Press, New York. 1967. Chap. 7. p. 224.
13. M. Anbar, M. Holman, and S. Pinchos. J. Chem. Soc. 1242 (1960).
14. J. Greenburg and L. J. Hallgren. J. Chem. Phys. **33**, 900 (1960).
15. F. Vratny and F. Gugliotta. J. Inorg. Nucl. Chem. **20**, 252 (1961).
16. A. L. Underwood, M. W. Millar, and L. H. Howe. Anal. Chim. Acta, **29**, 79 (1963).
17. P. M. Vollmar. J. Chem. Phys. **39**, 2236 (1963).
18. A. R. Davis. Ph.D. Thesis, University of Waterloo, Waterloo, Ontario. 1967. D. E. Irish and A. R. Davis. Can. J. Chem. In press. 1968.
19. I. Maslakowez. Z. Physik, **51**, 696 (1928).

Can. J. Chem. Downloaded from www.nrcresearchpress.com by 210.87.254.5 on 09/05/12
For personal use only.

Can. J. Chem. Downloaded from www.nrcresearchpress.com by 210.87.254.6 on 09/05/12
For personal use only.

Reactions of oxygen atoms with 2-propanol and methanol[1]

A. KATO[2] AND R. J. CVETANOVIĆ
Division of Applied Chemistry, National Research Council of Canada, Ottawa, Canada

Received June 12, 1967

An investigation of the reaction of 2-propanol at 25 °C with oxygen atoms in the ground electronic state, $O(^3P)$, and, as a corollary, with the excited mercury atoms, Hg $6(^3P_1)$, has been carried out. The reaction of oxygen atoms with methanol at 25 °C has also been briefly studied. The general mechanism of reaction of $O(^3P)$ atoms with simple alcohols is discussed.

Canadian Journal of Chemistry, 46, 235 (1968)

Introduction

In our recent study (1) of the reaction of oxygen atoms in their ground electronic state, $O(^3P)$, with ethanol it has been established that abstraction of an alpha-hydrogen atom from ethanol to give the alpha-ethanol radicals, $CH_3\dot{C}HOH$, takes place in the primary step. The radicals form predominantly acetaldehyde and 2,3-butanediol, by mutual disproportionation and combination, respectively. To test the generality of this finding, we have now extended the study of the reactions of oxygen atoms with alcohols to 2-propanol and, briefly, to methanol. The major initial organic reaction products observed with the three alcohols studied so far, methanol, ethanol, and 2-propanol, can be explained as resulting from the disproportionation and combination of the corresponding alpha-alcohol radicals, $\dot{C}H_2OH$, $CH_3\dot{C}HOH$, and $(CH_3)_2\dot{C}OH$. In the present article the results obtained with 2-propanol and methanol are reported and their implications are discussed.

Experimental

Oxygen atoms in their ground electronic state, $O(^3P)$, were produced by the mercury-photosensitized decomposition of nitrous oxide. The cylindrical quartz reaction vessel, reactor A of the previous study (1), was 5 cm in diameter, 10 cm long, and had a total volume of 240 ml. The mercury resonance radiation was supplied from a low-pressure mercury lamp placed at a distance of 11 cm from the reaction vessel window.

Anachemia Chemicals Ltd. reagent grade 2-propanol was used after repeated bulb-to-bulb distillation *in vacuo* and thorough degassing at −78 °C. It was further degassed at −196 °C before each run. No impurities could be detected in the purified 2-propanol on a 300 ft dinonylphthalate capillary column with a flame ionization detector. Analytical reagent methanol was obtained from Mallinckrodt Chemical Works Ltd. Nitrous oxide was obtained from Matheson Company and was purified by repeated bulb-to-bulb distillation *in vacuo* at −196 °C.

The reactions were carried out at room temperature, 25 ± 0.5 °C.

2-Propanol + $O(^3P)$ Atoms

Analysis of the products was similar to that used in the previous study (1). After irradiation, the reactant mixture was condensed by liquid nitrogen and the noncondensable gas was collected by means of a Töpler pump and analyzed for N_2, CO, CH_4, and H_2. The condensable product was transferred into a LeRoy still and about 80% of the unreacted nitrous oxide was distilled off at −160 °C. The nitrous oxide distillate, analyzed on the 300 ft dinonylphthalate capillary column with flame ionization detector, contained no detectable amount of acetone although there was a trace of acetaldehyde, which was not determined quantitatively. The residue from the LeRoy still, which contained the remainder of nitrous oxide together with the unreacted 2-propanol and the reaction products, was analyzed for acetone by gas chromatograph on a composite column of 4 m dinonylphthalate and 4.5 m Carbowax (1). No products other than acetone and a trace of acetaldehyde were detected on this column.

Qualitative analysis for the less volatile "liquid" products was done separately using samples subjected to long reaction times. After the removal of the noncondensable gases at −196 °C, the reaction vessel was washed with acetone and the solution was analyzed at 120 °C on the trimer acid column (1). Pinacol was found to be the major liquid product. A quantitative determination of pinacol was made on a sample obtained by trapping the liquid products in a known amount of *n*-propanol and analyzing on the trimer acid column. The chromatograms also showed the presence of two unknown products, at shorter retention times and in much smaller amounts than pinacol.

2-Propanol + Hg $6(^3P_1)$ Atoms

The experimental procedure was essentially the same as used in the study of the reaction of oxygen atoms, except for the simplified separation of the products because of the absence of nitrous oxide.

Methanol + $O(^3P)$ Atoms

Since it has been reported that methanol reacts with borosilicate (Pyrex) glass to form methyl borate and that

---

[1]Issued as NRCC No. 9697.

[2]NRCC Postdoctorate Fellow. Present address: Department of Applied Chemistry, Faculty of Engineering, Kyushu University, Fukuoka, Japan.

Can. J. Chem. Downloaded from www.nrcresearchpress.com by 210.87.254.6 on 09/05/12
For personal use only.

the formation of the borate is suppressed to an undetectable amount when a small amount of water is present (2), we have used a 90 mole % aqueous solution of methanol as the source of methanol vapor. Over such a solution the partial vapor pressures of methanol and water are 114 and 3.0 Torr at 25 °C, respectively (3). It is most unlikely that the presence of less than 3% water vapor would affect in any way the reaction of $O(^3P)$ atoms with methanol. In the analogous reaction of $O(^3P)$ atoms with ethanol it was found that up to 5% water vapor had no appreciable effect on the yields of reaction products. The aqueous methanol solution was degassed repeatedly at −78 °C and its vapor showed no organic impurity in detectable amounts on the 300 ft dinonylphthalate capillary column with flame ionization detector.

The noncondensable gas was analyzed in the same manner as in the study of the oxygen atom reaction with 2-propanol. The analysis of the liquid products for ethylene glycol was carried out as follows. After the removal of the noncondensables, the residue, which contained the unreacted nitrous oxide and methanol together with water and other reaction products, was washed out with water. In other cases the liquid products were trapped into a known amount of *n*-propanol after the removal of compounds volatile at −78 °C. Both the aqueous and the *n*-propanol extract were examined on a 7 ft Porapak Q column at 150 °C to determine the amount of ethylene glycol. The chromatograms showed no products other than ethylene glycol.

Results and Discussion

Quenching Cross Section of 2-Propanol

The quenching cross section of 2-propanol for the Hg $6(^3P_1)$ atoms, $\sigma^2_{2\text{-P}}$, was determined by the same competitive method as was used in the case of ethanol (1) and a large number of other substances (4). The reciprocal rate of nitrogen production is plotted in Fig. 1 against the 2-propanol to nitrous oxide ratio in agreement with the simple linear relationship between the two derived and discussed earlier (4). The plot gives a value of 6.4 Å^2 for $\sigma^2_{2\text{-P}}$ based on 18 Å^2 for $\sigma^2_{N_2O}$ (4). This value appears reasonable when compared with 3.5 Å^2 obtained similarly for ethanol (1).

Reaction of 2-Propanol with $O(^3P)$ Atoms

The reaction was studied using 500 Torr nitrous oxide with, alternatively, 10 and 40 Torr of 2-propanol. The volatile products were found to consist of a large amount of acetone and of small amounts of H_2, CO, CH_4, and acetaldehyde. Pinacol was also found to be a reaction product. The quantitative analyses were directed mainly towards a determination of the initial yield of acetone. The yields of acetone relative to that of nitrogen at finite reaction times are

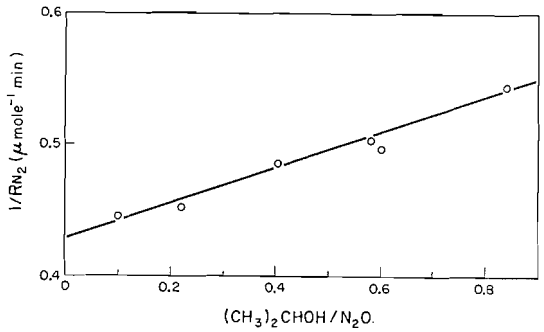

FIG. 1. Plot of the reciprocal rates of nitrogen production against the ratio of the partial pressures of 2-propanol and nitrous oxide (25 °C; light intensity equivalent to 2.60 μmoles N_2 per min; irradiation time 2 min; 50 Torr N_2O; 4.9 to 42 Torr 2-propanol).

plotted in Fig. 2 as a function of the extent of the reaction. The very small change in the relative yield of acetone with reaction time at both pressures of 2-propanol shows that acetone reacts considerably slower than 2-propanol with $O(^3P)$ atoms and therefore suffers very little secondary attack. The initial yields of acetone and of the minor products, obtained by extrapolating to zero reaction time, are shown in Table I. At 40 Torr 2-propanol, it is also found that the relative yield of pinacol is 0.11 (after 40 min irradiation, N_2 = 96 μmoles). The overall reaction of 2-propanol with $O(^3P)$ atoms can therefore be represented by the following stoichiometric equations.

[1] $(CH_3)_2CHOH + O = (CH_3)_2CO + H_2O$

[2] $2(CH_3)_2CHOH + O = (CH_3)_2C(OH)C(OH)(CH_3)_2 + H_2O$

The oxygen atom material balance requires that the sum of the relative yields of acetone and pinacol should be unity and this is seen to be so within the experimental error.

Reaction of 2-Propanol with Hg $6(^3P_1)$ Atoms

The mercury-photosensitized reaction was studied using 40 Torr of 2-propanol. Acetone and H_2 were found to be the major products, together with small amounts of CH_4, CO, and acetaldehyde. Formation of pinacol was confirmed qualitatively. The quantum yields of volatile products are shown as a function of reaction time in Fig. 3. The decrease in the quantum yield of acetone with increasing irradiation time shows its secondary reaction with the Hg $6(^3P_1)$ atoms, which is under-

TABLE I

Initial yields of products of the reactions of $O(^3P)$ and of Hg $6(^3P_1)$ atoms with 2-propanol at 25 °C

Products	2-Propanol + $O(^3P)$, yields relative to N_2		2-Propanol (40 Torr) + Hg $6(^3P_1)$, initial quantum yields, ϕ_0		
	(10 Torr)	(40 Torr)	(*a*)	(*b*)	(*c*)
$(CH_3)_2CO$	0.73	0.85	0.60	0.25	0.38
H_2	0.03–0.04	0.03–0.04	0.77	0.72	0.98
CO	0.007	0.005	~0.005	~0.000	
CH_4	0.004	0.004	<0.01	~0.000	
CH_3CHO			<0.005	~0.000	

(*a*) Present work.
(*b*) Reference 5, continuous illumination.
(*c*) Reference 5, intermittent illumination.

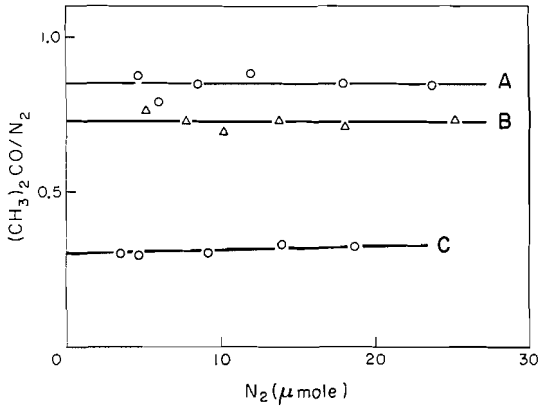

FIG. 2. Relative yields of acetone in the reaction of $O(^3P)$ atoms with 2-propanol (25 °C; light intensity equivalent to 2.60 μmoles N_2 per min): (A) 500 Torr N_2O, 40 Torr 2-propanol; (B) 500 Torr N_2O, 10 Torr 2-propanol; (C) 500 Torr N_2O, 40 Torr 2-propanol, 3.4 Torr butene-1.

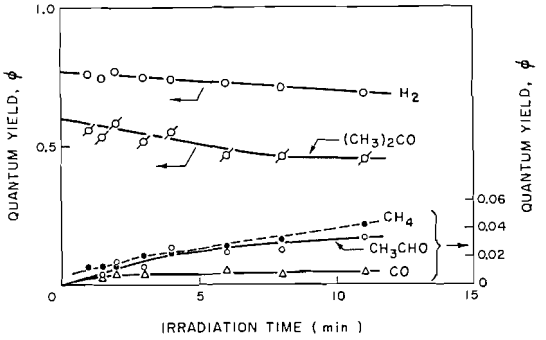

FIG. 3. Quantum yields of products in the reaction of 2-propanol with Hg $6(^3P_1)$ atoms (25 °C; light intensity equivalent to 2.60 μmoles N_2 per min; 40 Torr 2-propanol).

standable in view of its large quenching cross section ($\sigma^2 = 53$ Å^2 (4)). The minor products CH_4, CO, and acetaldehyde are most likely formed in secondary reactions. The initial quantum yields, obtained by extrapolations to zero reaction time, are shown in Table I, with the results of Knight and Gunning (5) shown also, for comparison. There is a large difference between the quantum yields of acetone obtained in the two studies, while the yields of hydrogen are in good agreement.

Rate of Reaction of 2-Propanol with $O(^3P)$ Atoms

The reaction rate was measured by the competitive method using butene-1 as the reference substance. The relative yield of acetone in 2-propanol/butene-1 mixtures is plotted against the extent of reaction in Fig. 2(C). For the conditions employed, the extrapolated value of $[(CH_3)_2CO/N_2]_{B\text{-}1}$ at zero reaction time is 0.30. With this value and the corresponding value of 0.85 in the absence of butene-1, a calculation similar to that used in the case of ethanol (1) gives 9.6×10^{10} cc mole^{-1} s^{-1} for the reaction rate of 2-propanol with oxygen atoms at 25 °C (Table I). The rate constant for 2-propanol is therefore 1.5 times larger than the value of 6.2×10^{10} cc mole^{-1} s^{-1} for ethanol (1), which is in agreement with the trends observed in the reactivity of alcohols towards OH radicals (1.1–3.5) (6, 7), CH_3 radicals (1.3–1.6) (8, 9), H atoms (2.3–3.1) (9, 10), and excited quinone (2.1) (11). The strength of the alpha-CH bond in 2-propanol has been reported as 90.3 kcal/mole (12), a value which is almost the same as that in ethanol (1). On the basis of the approximate parallelism between the reaction rates toward oxygen atoms and the strength of the

Can. J. Chem. Downloaded from www.nrcresearchpress.com by 210.87.254.6 on 09/05/12
For personal use only.

TABLE II

The yields of products in the reaction of $O(^3P)$ atoms with methanol at 25 °C

N_2O (Torr)	CH_3OH (Torr)	Irradiation (min)	N_2 (μmole)	Relative yields ($N_2 = 1$)				HCHO test†
				$C_2H_6O_2$*	H_2	CO	CH_4	
501	97.6	10	23.6	n.d.	0.037	0.033	None	
505	98.8	10	24.5	0.43 (A)	0.047	0.027	None	
501	98.4	20	49.0	0.53 (A)	0.037	0.031	None	
505	98.2	30	74.7	n.d.	0.032	0.027	None	
501	98.1	63	158.7	n.d.	0.024	0.026	None	
507	98.0	100	248.8	0.34 (B)	0.031	0.027	None	Negative

*n.d. = not determined; (A) = products collected by trapping in *n*-propanol; (B) = products collected by washing the reaction vessel with water.
†Chromotropic acid test (19); "negative" signifies $HCHO/N_2 < 0.04$.

bonds attacked (1), the difference in the reaction rate between 2-propanol and ethanol can be accounted for by a small difference of about 0.5 kcal/mole between the alpha-CH bond strengths in the two alcohols, which is well within the uncertainty of the thermochemical data.

Major Processes in the Reaction of 2-Propanol with $O(^3P)$ and Hg $6(^3P_1)$ Atoms

The following reactions have been postulated (5) to explain the reaction of 2-propanol with Hg $6(^3P_1)$ atoms.

[3] $(CH_3)_2CHOH + Hg\ 6(^3P_1) \rightarrow (CH_3)_2\dot{C}HO + H + Hg\ 6(^1S_0)$

[4] $(CH_3)_2CHOH + H \rightarrow (CH_3)_2\dot{C}OH + H_2$

[5] $(CH_3)_2CHOH + (CH_3)_2\dot{C}HO \rightarrow (CH_3)_2\dot{C}OH + (CH_3)_2CHOH$

[6] $2(CH_3)_2\dot{C}OH \rightarrow (CH_3)_2CO + (CH_3)_2CHOH$

[7] $2(CH_3)_2\dot{C}OH \rightarrow (CH_3)_2C(OH)C(OH)(CH_3)_2$

Reactions analogous to [3]–[5] could also be postulated as the primary reactions in the attack of $O(^3P)$ atoms on 2-propanol. However, electron spin resonance studies of the reaction of OH radicals with solid, liquid, and aqueous 2-propanol show selective abstraction of an alpha-hydrogen (13–16) and a similar result has been obtained in the photolysis of iodine/2-propanol mixtures (17). Also, hydrogen atoms abstract an alpha-hydrogen 105 times faster than a beta-hydrogen from 2-propanol in aqueous solution (18). The formation of pinacol as a major product and the value of the reaction rate of 2-propanol with $O(^3P)$ atoms determined in the present work also support selective abstraction of alpha-hydrogen by oxygen atoms. It appears likely therefore that the primary reactions in the attack of $O(^3P)$ atoms on 2-propanol are

[8] $(CH_3)_2CHOH + O(^3P) \rightarrow (CH_3)_2\dot{C}OH + OH$ and

[9] $(CH_3)_2CHOH + OH \rightarrow (CH_3)_2\dot{C}OH + H_2O$,

followed by reactions [6] and [7], as above. At the same time, reactions analogous to [3]–[5] cannot be ruled out.

If the predominant fate of $(CH_3)_2\dot{C}OH$ radicals were only disproportionation and combination in reactions [6] and [7], the initial values of $(CH_3)_2CO/N_2$ and $(CH_3)_2CO/H_2$ in the reactions of 2-propanol with oxygen atoms and with mercury atoms, respectively, would be expected to be the same or very similar. The observed values in Table I show a reasonably good agreement among the two reaction systems, in contrast to the fairly large difference between the analogous quantities in the case of ethanol (1). The one-step formation of acetone,

[10] $(CH_3)_2CHOH + O(^3P) \rightarrow (CH_3)_2CO + H_2O$,

is therefore not important under present conditions.

The somewhat smaller yield of acetone at the lower pressure of 2-propanol (10 Torr), following a similar trend in the yield of acetaldehyde observed in the reaction of ethanol with oxygen atoms (1), is difficult to explain quantitatively on the basis of the experimental information available at present. It is unlikely to be due to appreciable secondary reactions of acetone since the results in Fig. 2 show that the secondary reactions probably take place only to a very small extent. Similarly, the slight increase in quenching by 2-propanol at the higher pressure (40 Torr) is too small to explain the difference in the yield of acetone.

Can. J. Chem. Downloaded from www.nrcresearchpress.com by 210.87.254.6 on 09/05/12
For personal use only.

TABLE III

The initial yields of the carbonyl compounds and of glycols in the reactions of alcohols with $O(^3P)$ and Hg $6(^3P_1)$ atoms at 25 °C

Alcohol	Pressure of alcohol (Torr)	Source of data	Relative yields* Carbonyl compound $O(^3P)$	Carbonyl compound Hg $6(^3P_1)$	Glycol $O(^3P)$	Glycol Hg $6(^3P_1)$
Methanol	40	Ref. 23		0.02		
	98	Present	<0.04†		>0.53	
	100	Ref. 24		0.05‡		
Ethanol	40	Ref. 25		0.15		
	50	Ref. 1	0.55	0.32	0.37	0.53
2-Propanol	40	Ref. 5		0.35		
	40	Present	0.85	0.78	⩽0.15§	⩽0.22§

*The yields in the reaction with $O(^3P)$ atoms are relative to nitrogen and in the reaction with Hg $6(^3P_1)$ atoms relative to hydrogen taken as unity.
†After 100 min illumination.
‡After 120 min illumination.
§Estimated from the yield of acetone as a difference from unity.

Reaction of Methanol with $O(^3P)$ Atoms

Several experiments were carried out with 98 Torr methanol in the presence of 500 Torr nitrous oxide. Ethylene glycol was found to be a major product. The experimental results are summarized in Table II. As mentioned in the previous paper on ethanol (1), the recovery of such volatile products as ethylene glycol by trapping in *n*-propanol is not complete. The actual initial yield of ethylene glycol can therefore be expected to be appreciably higher than 0.53, the highest value observed. This can also be deduced from the fact that formaldehyde was not formed in detectable amounts and that no products other than ethylene glycol could be found by gas chromatography.

In the reaction of methanol with Hg $6(^3P_1)$ atoms the following primary reactions are generally accepted,

[11] $CH_3OH + Hg\ 6(^3P_1) \rightarrow CH_3O\cdot + H + Hg\ 6(^1S_0)$

[12] $H + CH_3OH \rightarrow \cdot CH_2OH + H$

[13] $CH_3O\cdot + CH_3OH \rightarrow \cdot CH_2OH + CH_3OH,$

and the reaction product consists almost entirely of hydrogen and ethylene glycol (4). In the reaction of $O(^3P)$ atoms with methanol, on the other hand, the primary reactions are likely to be reactions [14] and [15] in view of the relative strengths of the relevant bonds in methanol.

[14] $CH_3OH + O(^3P) \rightarrow \cdot CH_2OH + OH$

[15] $CH_3OH + OH \rightarrow \cdot CH_2OH + H_2O$

The $\cdot CH_2OH$ radicals may be expected to combine predominantly to form ethylene glycol,

[16] $\cdot CH_2OH + \cdot CH_2OH \rightarrow CH_2(OH)CH_2(OH),$

and to disproportionate into formaldehyde and methanol only to a very minor extent

[17] $\cdot CH_2OH + \cdot CH_2OH \rightarrow HCHO + CH_3OH.$

Disproportionation and Combination of Alpha-Alcohol Radicals

The relative yields of the major organic products of the reactions of alcohols with $O(^3P)$ and Hg $6(^3P_1)$ atoms, the glycols and the carbonyl compounds, are summarized in Table III. The yields of the glycols decrease and those of the carbonyl compounds increase in the order CH_3OH, C_2H_5OH, $(CH_3)_2CHOH$. This trend can be understood in terms of the number of beta-hydrogen atoms in the respective alpha-alcohol radicals, which may be expected to determine the disproportionation to combination ratio by analogy with alkyl radicals (20). The data in Table III are therefore consistent with the usual assumption that the glycols and the carbonyl compounds are formed, respectively, by combination and disproportionation of alpha-alcohol radicals. The ratio of disproportionation to combination of the alpha-alcohol radicals is about an order of magnitude larger than that of the corresponding alkyl radicals with the same number of beta-hydrogen atoms (0.12–0.14 for C_2H_5 and 0.5–0.63 for i-C_3H_7). The increased ease of disproportionation relative

Can. J. Chem. Downloaded from www.nrcresearchpress.com by 210.87.254.6 on 09/05/12
For personal use only.

Can. J. Chem. Downloaded from www.nrcresearchpress.com by 210.87.254.6 on 09/05/12
For personal use only.

to combination is apparently due to the presence of the electron-withdrawing OH groups in the alpha-alcohol radicals.

Mechanism of Reaction of $O(^3P)$ Atoms with Alcohols

The results of the present and our earlier (1) study show that $O(^3P)$ atoms react with methanol, ethanol, and 2-propanol, and presumably with other simple alcohols, by abstracting the most weakly bound hydrogen atoms in the alcohol molecules. In contrast to this, Avramenko, Kolesnikova, and Kuznetsova (21) have recently studied the reaction of oxygen atoms with methanol in the presence of molecular oxygen and concluded that the one-step formation of formaldehyde, reaction [18], is the major primary process.

[18] $$CH_3OH + O \rightarrow HCHO + H_2O \quad \text{or}$$
$$CH_3OH + O \rightarrow (\text{complex}) \rightarrow HCHO + H_2O$$

They used a flow system, producing oxygen atoms by electrical discharge in a stream of molecular oxygen, and observed formaldehyde as essentially the exclusive carbon-containing product. They considered the possibility that formaldehyde could be formed in the secondary reaction of the methoxy radicals with O_2,

[19] $$\cdot CH_2OH + O_2 \rightarrow O_2CH_2OH \rightarrow HCHO + HO_2,$$

but rejected it on the basis of their experiments with H atoms and methanol in the presence of O_2.

Evidently the conclusions of Avramenko and co-workers (21) and the experimental results with methanol in the present work are mutually inconsistent. Under conditions of our experiments formaldehyde is at best a very insignificant product, while the yield of ethylene glycol is equivalent to at least 53% of the oxygen atoms consumed in the process and probably to appreciably more than that. This indicates that the major process is the abstraction of one hydrogen atom from methanol in the primary step. In qualitative agreement with this view is the observation of strong emission of the OH band in the study of the reaction of oxygen atoms with methanol by Harteck and Kopsch (22). Nevertheless, it is necessary to point out the existence of these two radically different points of view, which are not confined to the reaction of oxygen atoms with methanol but extend to other reactions of oxygen atoms as well. Elsewhere (26) we have briefly discussed some of the features inherent in the flow system – electrical discharge technique, which in our opinion may complicate mechanistic studies and perhaps be responsible for the apparent discrepancies.

Acknowledgments

The authors are grateful to Dr. R. F. Pottie and Mr. R. L. Sander for the mass spectrometric analyses.

1. A. Kato and R. J. Cvetanović. Can. J. Chem. **45**, 1845 (1967).
2. R. P. Porter. J. Phys. Chem. **61**, 1260 (1957).
3. J. Timmermans. The physico-chemical constants of binary systems in concentrated solution. Vol. 4. Interscience Pub. Inc., New York. 1960.
4. R. J. Cvetanović. Progr. Reaction Kinetics, **2**, 41 (1964).
5. A. R. Knight and H. E. Gunning. Can. J. Chem. **40**, 1134 (1962).
6. M. Anbar, D. Meyerstein, and P. Neta. J. Chem. Soc. B, 742 (1966).
7. G. E. Adams, J. W. Boag, J. Currant, and B. D. Michael. *In* Pulse radiolysis. *Edited by* J. H. Baxendale, M. Ebert, J. P. Keene, and A. J. Swallow. Academic Press, London and New York. 1965. p. 131.
8. A. F. Trotman-Dickenson. Quart. Rev. **7**, 198 (1953).
9. G. A. Adams, J. H. Baxendale, and R. D. Sedgwick. J. Phys. Chem. **63**, 854 (1959).
10. A. Appleby, G. Scholes, and M. Simic. J. Am. Chem. Soc. **85**, 3891 (1963).
11. C. F. Wells. Trans. Faraday Soc. **57**, 1719 (1961).
12. R. Walsh and S. W. Benson. J. Am. Chem. Soc. **88**, 3480 (1966).
13. M. Fujimoto and D. J. E. Ingram. Trans. Faraday Soc. **54**, 1304 (1958).
14. J. F. Gibson, M. C. R. Symons, and M. G. Townsend. J. Chem. Soc. 269 (1959).
15. W. T. Dixon and R. O. C. Norman. J. Chem. Soc. 3119 (1963).
16. R. Livingston and H. Zeldes. J. Chem. Phys. **44**, 1245 (1966).
17. S. V. Filseth and J. E. Willard. J. Am. Chem. Soc. **84**, 3806 (1962).
18. M. Anbar and D. Meyerstein. J. Phys. Chem. **68**, 3184 (1964).
19. F. Feigl. Spot tests. Vol. 2. 4th Eng. ed. Elsevier Publ. Co., New York. 1954. p. 240.
20. J. N. Bradley. J. Chem. Phys. **35**, 748 (1961).
21. L. I. Avramenko, R. V Kolesnikova, and N. L. Kuznetsova. Izv. Akad. Nauk SSSR, Otd. Khim. Nauk, 599 (1961).
22. P. Harteck and U. Kopsch. Z. Physik Chem. B, **12**, 327 (1931).
23. A. R. Knight and H. E. Gunning. Can. J. Chem. **39**, 1231 (1961).
24. M. K. Phibbs and B. deB. Darwent. J. Chem. Phys. **18**, 495 (1950).
25. A. R. Knight and H. E. Gunning. Can. J. Chem. **39**, 2466 (1961).
26. H. E. Avery and R. J. Cvetanović. J. Chem. Phys. **43**, 3727 (1965); **44**, 3150 (1966).

Acid strengths of some substituted picric acids

P. J. PEARCE AND R. J. J. SIMKINS

Explosives Research and Development Establishment, Ministry of Technology, Waltham Abbey, Essex, England

Received May 9, 1967

The aqueous dissociation constants for a number of substituted picric acids and related compounds have been determined spectrophotometrically, and the values obtained correlated with the mid-equivalence potentials obtained by half-neutralization in acetone solution. Analysis of these results together with those obtained similarly for substituted benzoic acids shows that while the mid-equivalence potential method affords a rapid and convenient means of making a good estimate of the acid strength of a compound, it has its limitations and is only strictly applicable within the confines of a series of closely similar compounds. The observed pK_a values of a large series of polysubstituted phenols were correlated with the predicted values obtained from the Hammett relation, and good agreement obtained, even with substituted picric acids; styphnic acids appear to behave anomalously.

Canadian Journal of Chemistry, 46, 241 (1968)

It has recently been suggested (1) that the aqueous dissociation constant of an acid may be rapidly estimated by measuring the glass electrode potential of a half-neutralized solution of the acid in acetone solution. The discrepancy between the dissociation constant of styphnic acid (2,4,6-trinitroresorcinol) inferred from such a mid-equivalence potential and the value we had obtained by spectrophotometric measurement led us to investigate the method in more detail. Experimental work consisted of (*a*) the determination of the dissociation constant in water of a large number of picric acids and related compounds and (*b*) the parallel measurement of the mid-equivalence potentials of the picric acids, and also of a large number of benzoic acids, the aqueous dissociation constants of which were known. An analysis was then made of the relationship between the mid-equivalence potential, the solvent in which it was determined, and the aqueous dissociation constant of the acid involved.

Discussion

Although it has long been recognized that picric acid is a very strong acid, there has been no common agreement as to what its exact dissociation constant is; the following values for the pK_a have been recorded: 0.29 (2), 0.33 (3), and 0.96 (4). For the related acids methylpicric and dimethylpicric pK_a values of 0.81 and 1.38 respectively have been found (5, 6). It has been accepted that the picric acids are too strong for the usual electrolyte methods to give good results, and the best values are based on spectrophotometric measurements. These are rather tedious and suffer from a lack of precision in the values assigned for the extinction coefficient of the undissociated acid.

Elder and Mariella (1) found that the mid-equivalence potential (the electromotive force (e.m.f.) as measured with a glass electrode/modified calomel electrode pair in a standard acetone solution of acid half-neutralized with tetrabutylammonium hydroxide) gave a measure of the relative acidity of a wide series of acids. These authors pointed out that there was a linear relationship between the relative acidities so determined and such aqueous dissociation constants (expressed as pK) as had been determined. This rapid and convenient method is in effect a simplified version of the potentiometric microtitration technique developed by Simon *et al.* (7–9). Simon has used this method extensively, working on the premise that the apparent pH of a solution at half-neutralization of the functional group to be determined is equivalent to pK'_{Solvent}, where K'_{Solvent} is the apparent dissociation constant for a given solvent system. Such apparent dissociation constants are functions of the nature of the solvent, the structure of the acid involved, concentration, and determination procedure. However, rigid standardization of the technique employed can give pK'_{Solvent} values dependent only on the structure of the acid being investigated and the solvent system used. It has been shown (10, 11) that such pK'_{Solvent} values may justifiably be interpreted in analogous fashion to thermodynamic pK values; however, it must be borne in mind that

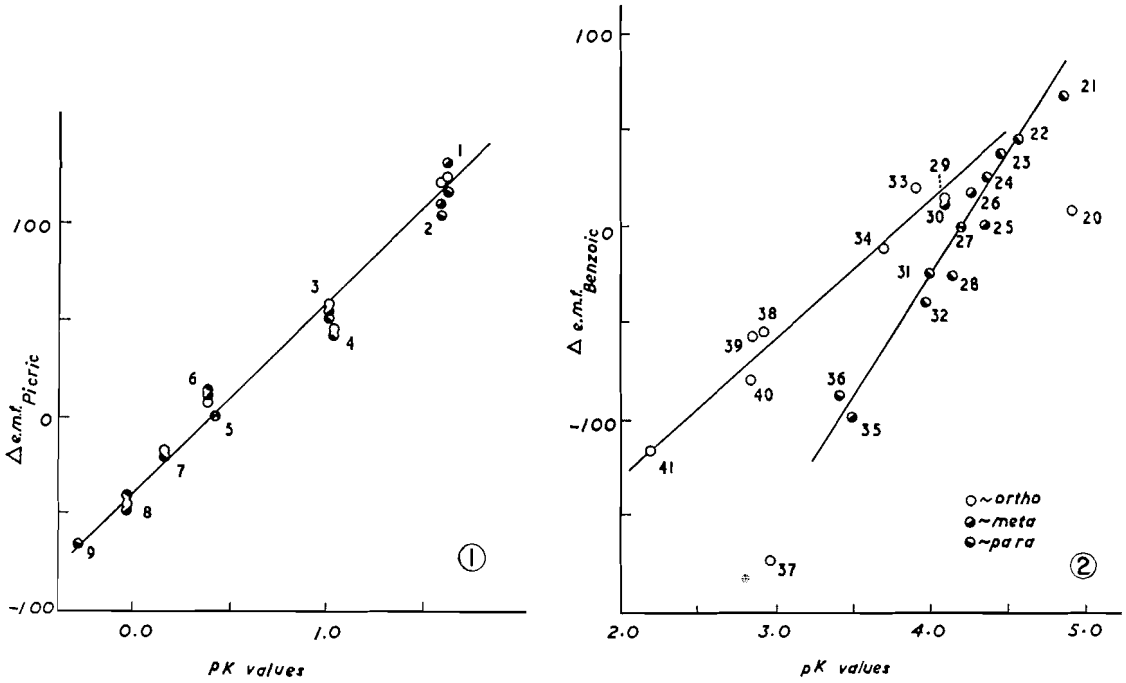

FIG. 1. Plot of mid-equivalence potential versus pK for substituted picric acids (in acetone solution).
FIG. 2. Plot of mid-equivalence potential versus pK for substituted benzoic acids (in acetone solution).

such values are specific to a given system, and that extensive extrapolation may not be warranted.

It is possible to derive an expression

$$pK'_{Solvent} = Q pK_a + \text{constant},$$

where Q is a term covering the various factors such as solvation energy inherent in the determination of $pK'_{Solvent}$. Since the mid-equivalence potential, $(e.m.f.)_{1/2}$, and the apparent dissociation constant are merely different scale readings of the same galvanometer deflection, one may write $(e.m.f.)_{1/2} = Q pK_a + C$ as the expression for the linear relationship that Elder and Mariella found. This relationship will only be general providing that the term Q remains constant; our results indicate that this is not so, and that while one given class of compounds (e.g. picric acids) have a certain linear relationship, this is not directly extensible to another class of acids (e.g. benzoic acids). Thus we conclude that while the mid-equivalence potential method affords a rapid means of making a good approximation of the pK_a value of an acid, it is really only valid within the confines of a series of closely related compounds, and that casual interpolation may give misleading results.

The relationship between mid-equivalence potential and dissociation constant for 8 picric acids is plotted in Fig. 1; a good straight line can be drawn through the plot. The results are also given in Table I, and from this it can be seen that the actual mid-equivalence potential recorded varied with the electrode system used. If, however, one takes the differences, Δ(e.m.f.), between the mid-equivalence potential of the test acid and that of a standard acid, in this case picric acid, both measured with the same electrode system, then consistent results are obtained.

The relationship between mid-equivalence potential and dissociation constant for 22 benzoic acids in two different solvent systems is plotted in Figs. 2 and 3 (cf. Table II). These plots show that, for a given solvent, one straight line cannot be drawn, but that two are necessary, one for the ortho-substituted benzoic acids and the other for the meta/para-substituted. As might be expected the slope of the plots is different in the

TABLE I

Mid-equivalence potentials of picric acids in acetone solution*

No.	Acid	pK_a	(e.m.f.)$_{1/2}$ observed			Δ(e.m.f.)$_{Picric}$		
			A	B	C	A	B	C
1	*t*-Butylpicric	1.593	152	111	215	125	133	119
2	Dimethylpicric	1.215	150	90	202	123	112	106
3	Methylpicric	1.000	85	39	142	58	51	46
4	Ethylpicric	1.002	74	—	138	47	—	42
5	Picric	0.402	27	−12	96	0	0	0
6	Methoxypicric	0.367	35	2	107	8	10	11
7	Iodopicric	0.152	8	—	79	−19	—	−17
8	Bromopicric	−0.050	−18	−53	48	−45	−41	−48
9	Chloropicric	—	—	−58	37	—	−46	−59
10	Dichloropicric	—	—	—	30 to −9†	—	—	−66 to −105

*Electrode system: A = glass electrode/acetone solution/agar bridge/aqueous KCl/calomel electrode; B = glass electrode/acetone solution/methanolic KCl/calomel electrode; C = as B, but with different glass electrode.
†The initial reading was 30 mV, but this decreased slowly to −9.

TABLE II

Mid-equivalence potentials of benzoic acids

No.	Acid	pK_a*	Acetone solution		Ethanol solution	
			(e.m.f.)$_{1/2}$	Δ(e.m.f.)$_{Benzoic}$ (mV)	(e.m.f.)$_{1/2}$	Δ(e.m.f.)$_{Benzoic}$ (mV)
20	2-Aminobenzoic	4.91	581	9	470	22
21	4-Aminobenzoic	4.86	640	68	488	40
22	4-Hydroxybenzoic	4.57	617	45	471	23
23	4-Methoxybenzoic	4.47	610	38	458	10
24	4-Methylbenzoic	4.37	598	26	452	4
25	3-Aminobenzoic	4.36	572	0		
26	3-Methylbenzoic	4.27	590	18	445	−3
27	Benzoic	4.20	572	0	448	0
28	4-Fluorobenzoic	4.14	546	−26		
29	2-Methoxybenzoic	4.09	586	14		
30	3-Hydroxybenzoic	4.08	585	13	451	3
31	4-Chlorobenzoic	3.98	547	−25	423	−25
32	4-Bromobenzoic	3.97	532	−40		
33	2-Methylbenzoic	3.91	592	20	438	−10
34	1-Naphthoic	3.70	567	−5	421	−27
35	3-Nitrobenzoic	3.49	472	−100	392	−56
36	4-Nitrobenzoic	3.42	485	−87	377	−71
37	2-Hydroxybenzoic	2.97	399	−173	351	−97
38	2-Chlorobenzoic	2.92	518	−54	385	−63
39	2-Iodobenzoic	2.86	516	−56		
40	2-Bromobenzoic	2.85	494	−78		
41	2-Nitrobenzoic	2.17	457	−115	353	−95

*pK_a values taken from McDaniell and Brown (27).

two solvents. These results indicate how the Q term may not only vary from solvent to solvent, but also how it may vary between different types of acid. It should be noted that in both solvents the 2-hydroxybenzoic acid and to a lesser extent the 2-aminobenzoic acid do not fit the ortho relationship. This deviation, which is probably the result of powerful intermolecular hydrogen bonding, illustrates the dangers of casual interpolation.

A check on the objectivity of the results is given by Fig. 4, where our mid-equivalence potentials determined in acetone solution are plotted against the apparent dissociation constants determined by Simon in a methylcellosolve/water system (9). The data for both ortho and meta/para acids group onto the same line, suggesting that the variation of the Q term as a function of the structure of the acid involved is similar in both solvent systems.

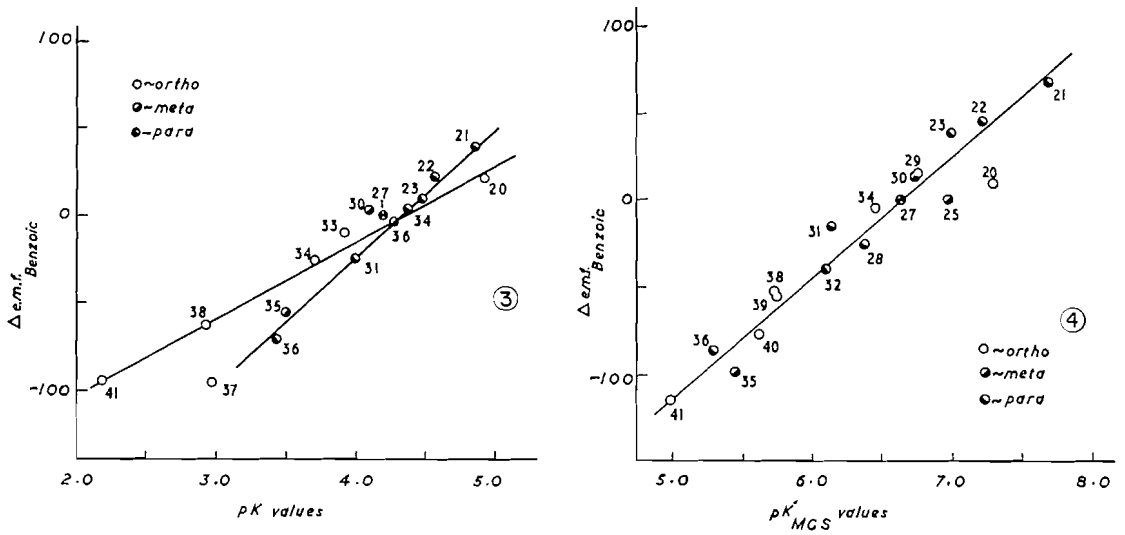

FIG. 3. Plot of mid-equivalence potential versus pK for substituted benzoic acids (in ethanol solution).
FIG. 4. Plot of mid-equivalence potential (in acetone) versus pK'_{MCS} (in 80% methylcellosolve/20% water) for substituted benzoic acids.

When the results for the picric acids and for the benzoic acids are combined into a single plot (cf. Fig. 5), it can clearly be seen that there is no unique relationship between the mid-equivalence potential and aqueous dissociation constant for all acids, but rather a family of lines, one for each class of acids. It is possible that this concept of a strictly limited relationship explains why a simple interpolation of the observed mid-equivalence potentials of styphnic acid and of trinitrophloroglucinol suggests dissociation constants markedly different from those we determined spectrophotometrically. The mid-equivalence potentials of 4 styphnic acids, 5 dinitrophenols, and 8 picric acids are plotted against pK_a values in Fig. 6 (cf. Table III). Examination prompts the following suggestions. (1) Our determination of the primary dissociation constants of styphnic acid and trinitrophloroglucinol would have to be reduced by two orders of magnitude for them to fall on the picric acid line. (2) It seems probable that with the removal of one ortho-nitro group the dinitrophenols no longer fall on the picric acid line, but form another family with a lower Q value. As with the benzoic acids the ortho-amino compound does not conform. (3) It is possible that the styphnic acids constitute another family, with a line of steeper slope.

Some calculations were made to see whether the experimentally determined acid strengths checked with those predicted by the Hammett relation $\log K = \rho\sigma \log K_0$ (12). Barlin and Perrin (13) have shown that pK values may be predicted for polysubstituted phenols provided that appropriate σ constants are used. The values suggested by these authors are satisfactory except for ortho-methoxy (where 0.04 gives better results than the suggested 0.00) and ortho-nitro. The results from polynitrophenols indicate that a value of 1.40 is the correct one for ortho-nitro substitution, even though for 2-nitrophenol itself this predicts a lower pK than is actually observed. Using a least mean square analysis for a series of 86 phenols it was found that the pK could be predicted by the relation: $pK = 9.94 - 2.26\,\Sigma\sigma$, with a relative deviation of 0.18. The observed and calculated results and σ constants used are given in Tables IV and V. Examination of the predicted values shows that serious deviation from the observed values normally only occurs when there are substituents on both sides of a nitro group. The effect of such grouping would be to hinder the coplanarity of the nitro group with the benzene ring, and by thus reducing the resonance effect give an observed pK value higher than that predicted. A single very bulky substituent between two nitro groups will produce the same effect. Such deviation can be noticed for 3,5-dimethyl-4-

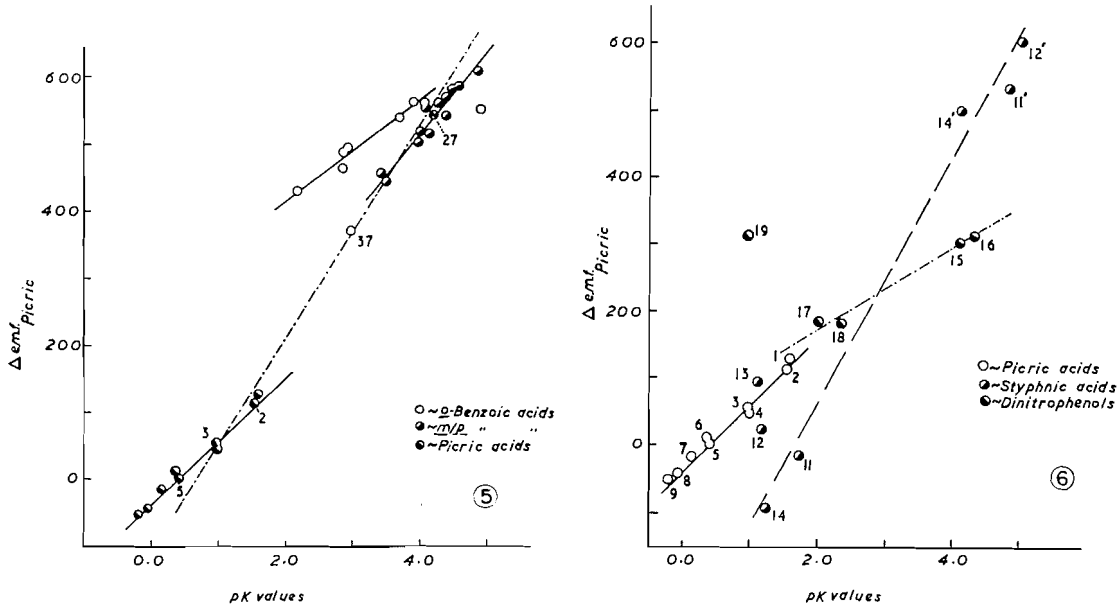

FIG. 5. Plot of mid-equivalence potential versus pK for three series of acids. (The numbered acids and pecke line indicate the relationship originally described.)
FIG. 6. Plot of mid-equivalence potential versus pK for various di- and tri-nitrophenols.

TABLE III

Mid-equivalence potentials of styphnic acids and dinitrophenols in acetone solution

No.	Compound	pK_a	$(e.m.f.)_{1/2}$	$\Delta(e.m.f.)_{Picric}$ (mV)
11	Styphnic acid	1.74	10	−17
		4.86	561	534
12	Methylstyphnic acid (Trinitroorcinol)	1.17	48	21
		5.04	632	605
13	Chlorostyphnic acid	1.13	122	95
		—	640	613
14	Hydroxystyphnic acid (Trinitrophloroglucinol)	1.26	−71	−98
		4.16	528	501
		7.66	791	764
15	2,4-Dinitrophenol*	4.13	329	302
16	6-Methyl-2,4-dinitrophenol*	4.35	339	312
17	6-Chloro-2,4-dinitrophenol	2.01	210	183
18	6-Bromo-2,4-dinitrophenol	2.35	209	182
19	6-Amino-2,4-dinitrophenol	1.00	343	316

*pK value taken from literature (28, 29), the others were determined in this laboratory.

nitro-, 3,5-dimethyl-2,4,6-trinitro-, and 3-*t*-butyl-2,4,6-trinitro-phenol. Allowing for this effect the predicted strength of the picric acids agrees well with the experimentally determined values. The Hammett relationship can be extended to the di- and tri-hydroxyphenols, with a good measure of agreement for simple substitution (the discrepancy for 2-methyl-*p*-hydroquinone is quite exceptional), but it breaks down with the introduction of a third nitro group.

One might expect a correlation between the pK_a value and the OH stretching frequency for the picric acids, and indeed Fig. 7 (cf. Table VI) shows the normal type of plot. It should be noted that the styphnic acid values do not fall on this plot. A similar form of correlation, though over

TABLE IV

Experimental and predicted pK values for phenols*

Substituent	pK Found	pK Calcd.	Substituent	pK Found	pK Calcd.
2-Me	10.28	10.23	2-Br	8.39	8.36
3-Me	10.09	10.10	3-Br	9.03	9.06
4-Me	10.26	10.32	4-Br	9.34	9.33
2,3-Me_2	10.42	10.39	2-I	8.46	8.52
2,4-Me_2	10.61	10.62	3-I	9.06	9.15
2,5-Me_2	10.22	10.39	4-I	9.31	9.26
2,6-Me_2	10.59	10.53	2-NO_2	7.21	6.78
3,4-Me_2	10.42	10.48	3-NO_2	8.35	8.34
3,5-Me_2	10.15	10.25	4-NO_2	7.15	7.14
2,4,5-Me_3	10.57	10.78	2,6-Me_2-4-NO_2	7.22	7.73
2,4,6-Me_3	10.88	10.91	3,5-Me_2-4-NO_2	8.24	7.45
2-Et	10.2	10.23	2,4,6-Me_3-3-NO_2	8.98	9.31
3-Et	9.9	10.10	2,4-$(NO_2)_2$	4.09	3.97
4-Et	10.0	10.28	2,5-$(NO_2)_2$	5.22	5.17
3-Et-5-Me	10.1	10.25	2,6-$(NO_2)_2$	3.71	3.61
2-Ph	9.97	9.94	3,4-$(NO_2)_2$	5.42	5.53
3-Ph	9.64	9.80	2,4-$(NO_2)_2$-6-Me	4.35	4.27
4-Ph	9.55	9.60	2,4-$(NO_2)_2$-6-Cl	2.01	2.44
2-CH_2OH	9.92	9.85	2,4-$(NO_2)_2$-6-Br	2.35	2.39
3-CH_2OH	9.83	9.76	2,6-$(NO_2)_2$-4-Cl	2.97	3.09
4-CH_2OH	9.82	9.76	2,4,6-$(NO_2)_3$	0.40	0.81
2-CH_2OH-4-Me	10.15	10.23	2,4,6-$(NO_2)_3$-3-Me	1.00	0.97
2,4-$(CH_2OH)_2$	9.77	9.67	2,4,6-$(NO_2)_3$-3-Et	1.00	0.97
2,6-$(CH_2OH)_2$	9.66	9.76	2,4,6-$(NO_2)_3$-3,5-Me_2	1.57	1.13
2,6-$(CH_2OH)_2$-4-Me	9.92	10.14	2,4,6-$(NO_2)_3$-3-tBu	1.59	1.04
2,4,6-$(CH_2OH)_3$	9.66	9.58	2,4,6-$(NO_2)_3$-3-MeO	0.37	0.63
2-MeO	9.98	9.85	2,4,6-$(NO_2)_3$-3-Cl	−0.20	−0.03
3-MeO	9.65	9.76	2,4,6-$(NO_2)_3$-3-Br	−0.05	−0.07
4-MeO	10.21	10.19	2,4,6-$(NO_2)_3$-3-I	0.15	0.02
2-MeO-4-CHO	7.40	7.52	2,4,6-$(NO_2)_3$-3,5-Cl_2	−0.7	−0.86
2-MeO-5-CHO	8.89	9.04			
2-MeO-6-CHO	7.91	8.15			
3-Ac	9.19	9.08			
4-Ac	8.05	8.04	2-OH	9.85	9.85
3-MeS	9.53	9.60	3-OH	9.15	9.17
4-MeS	9.53	9.47	4-OH	10.85	10.78
3-$MeSO_2$	8.40	8.40	2-Me-4-OH	10.20	11.07
4-$MeSO_2$	7.83	7.86	2,3,5,6-Me_4-4-OH	11.51	11.68
3,5-Me_2-4-$MeSO_2$	8.13	8.18	2,6-Cl_2-4-OH	7.33	7.70
3-CN	8.57	8.56	2-NO_2-4-OH	7.63	7.61
4-CN	7.95	7.95	2,6-$(NO_2)_2$-4-OH	4.42	4.45
2,6-Me_2-4-CN	8.27	8.54	2-NO_2-6-OH	6.70	6.69
3,5-Me_2-4-CN	8.21	8.27	2,3-$(OH)_2$	9.01	9.08
2-F	8.81	8.72	3,5-$(OH)_2$	8.45	8.40
3-F	9.28	9.17	2,4,6-$(NO_2)_3$-3-OH	1.74	0.04
4-F	9.81	9.80	2,4,6-$(NO_2)_3$-3-OH-5-Me	1.17	0.20
2-Cl	8.48	8.40	2,4,6-$(NO_2)_3$-3-OH-5-Cl	1.13	−0.79
3-Cl	9.08	9.10	2,4,6-$(NO_2)_3$-3,5-$(OH)_2$	1.26	−0.73
4-Cl	9.42	9.42			
2,3-Cl_2	7.70	7.57			
2,4-Cl_2	7.85	7.88			
2,5-Cl_2	7.51	7.57			
2,6-Cl_2	6.79	6.87			
3,4-Cl_2	8.59	8.58			
3,5-Cl_2	8.19	8.27			

*Experimental pK values taken from literature (29) unless determined in this laboratory.

TABLE V

Apparent σ constants for substituents in phenols* ($pK = 9.94 - 2.26\,\Sigma\sigma$)

Substituent	σ_{ortho}	σ_{meta}	σ_{para}
Methyl	−0.13	−0.07	−0.17
Ethyl	−0.13	−0.07	−0.15
t-Butyl		−0.10	
Phenyl	0.00	0.06	0.15
Methylol	0.04	0.08	0.08
Methoxy	0.04′	0.08	−0.11
Methylthio		0.15	0.21
Methylsulfonyl		0.68	0.92
Formyl	0.75	0.36	1.03
Acetyl		0.38	0.84
Fluoro	0.54	0.34	0.06
Chloro	0.68	0.37	0.23
Bromo	0.70	0.39	0.27
Iodo	0.63	0.35	0.30
Cyano		0.61	0.88
Nitro	1.40′	0.71	1.24
Hydroxy	0.04′	0.34′	−0.37

*Constants marked ′ differ from those previously proposed (13).

a much smaller range of wavenumbers, is found for the OH bending frequency. An interesting observation is that aminostyphnic acid has no peak in the 3100–3200 cm^{-1} range; the peak at 3410 cm^{-1} is undoubtedly NH stretching, and so probably is the less intense peak at 3290 cm^{-1}.

Experimental

All but one (no. 10) of the picric acids were prepared by mixed acid nitration of the corresponding phenol; they were purified by recrystallization from ethanol or acetone to constant melting point, and the purity then checked by thin layer chromatography on silica gel using a variety of solvent mixtures, of which methylene chloride/acetic acid 20/1 was typical. Trinitroorcinol was prepared by mixed acid nitration of orcinol, trinitrophloroglucinol by treatment of triacetoxybenzene with cold 98% nitric acid. The monopyridinium salt of trinitrophloroglucinol was treated with phosphorus oxychloride to give chlorostyphnic acid, m.p. 117 °C (Found: C, 24.5; H, 1.5; N, 14.0. $C_6H_2ClN_3O_8.H_2O$ requires C, 24.2; H, 1.3; N, 14.1), and this was converted via 5-ethoxytrinitroresorcinol to aminostyphnic acid, which was identical with that prepared by alkaline hydrolysis of pentanitroaniline. The pyridinium salt of chlorostyphnic acid was treated with phosphorus oxychloride to give dichloropicric acid. Melting points were determined on a Kofler hot-stage microscope; the melting points observed (and corresponding previous references) were: *t*-butylpicric acid 171° (14), dimethylpicric 108° (15), methylpicric 109° (16), ethylpicric 88° (4), picric 122° (17), methoxypicric 86° (18), iodopicric 196° (19), bromopicric 147° (20), chloropicric 114° (21), dichloropicric 138° (22), 2,4,6-trinitroresorcinol 174° (23), 5-methyltrinitroresorcinol 164° (23), 5-chlorotrinitroresorcinol 117°, 5-aminotrinitroresorcinol 240° (24), trinitrophloroglucinol 167° (25).

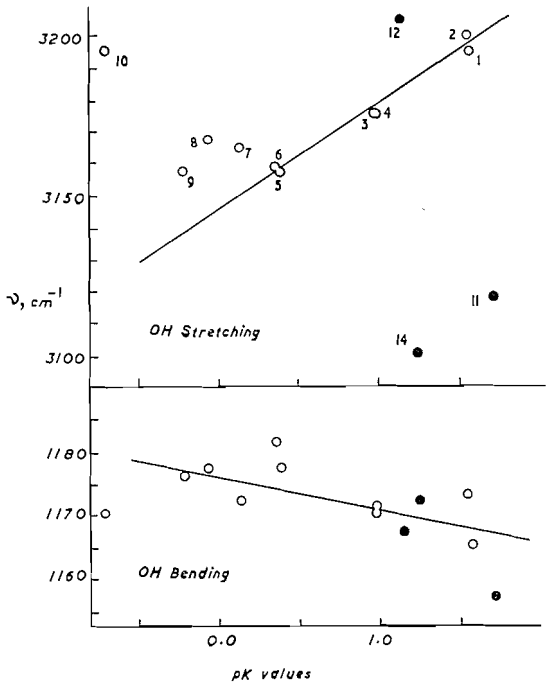

FIG. 7. Plot of infrared frequencies for (○) picric and (●) styphnic acid series.

Spectrophotometric Determination of pK Values

The method used was that of Richard and Sykes (26), which does not require a knowledge of the extinction coefficients involved. If an acid dissociates according to the expression

$$HA \overset{K}{\rightleftharpoons} H^+ + A',$$

then assuming that both the undissociated acid and the anion absorb light in the wavelength range studied, one may write

$$d(K + c) = E_{HA}ca + E_{A'}Ka,$$

where d is the optical density per unit cell length, c is the hydrogen ion concentration, E is the appropriate extinction coefficient, and a is the initial concentration of acid. If at a standard acid concentration c_0 one obtains an optical density d_0 for any given wavelength, then one may write

$$\frac{c - c_0}{d - d_0} = \frac{(K + c_0)(K + c)}{a(E_{A'} - E_{HA})}.$$

It follows that a plot of $(c - c_0)/(d - d_0)$ versus c at constant wavelength should be linear, with slope $= (K + c_0)/a(E_{A'} - E_{HA})$ and intercept $= K(K + c_0)/a(E_{A'} - E_{HA})$, and that intercept/slope should equal K.

Mixtures of varying proportions of 5 N perchloric acid and 5 N sodium perchlorate (total volume 4.8 ml) were made up to 50 ml with 0.003 M solutions of the picric acids, the resultant ionic product being 0.5. The optical density was measured over the range 340–430 mμ, and then $(c - c_0)/(d - d_0)$ plotted against the hydrogen ion

TABLE VI

Correlation of pK_a with OH stretching and bending frequencies

No.	Acid	pK_a	OH stretching (cm^{-1})	OH bending (cm^{-1})
1	*tert*-Butylpicric	1.59	3195	1165
2	Dimethylpicric	1.57	3200	1173
3	Methylpicric	1.00	3175	1170
4	Ethylpicric	1.00	3175	1171
5	Picric	0.40	3157	1177
6	Methoxypicric	0.37	3158	1181
7	Iodopicric	0.15	3165	1172
8	Bromopicric	−0.05	3167	1177
9	Chloropicric	−0.20	3157	1176
10	Dichloropicric	−0.7	3195	1170
11	Styphnic	1.74	3118	1157
14	Hydroxystyphnic	1.26	3100	1172
12	Methylstyphnic	1.17	3205	1167

concentration for various wavelengths. Under the best conditions the intercept/slope ratio was the same for all wavelengths; with acids stronger than picric the plots tended to be curved, and thus the ratios were less precise. The mass dissociation constants obtained in this were transformed, approximately, into thermodynamic aqueous dissociation constants by applying the Debye–Huckel expression. For simplicity it was assumed that the second ionization of the styphnic acids did not start until the first was complete. The average difference of three units between pK_I and pK_{II} makes this a fair assumption, but our failure to get a satisfactory differential plot for pK_{II} of chlorostyphnic acid suggests that it is not an inviolate one.

Determination of Mid-Equivalence Potential

The preparation of tetrabutylammonium hydroxide solution and the general conditions for determining the mid-equivalence potential followed those of Elder and Mariella (1). An Electronic Instruments Ltd. (E.I.L.) Model 23 direct reading pH meter was used, with an E.I.L. or a Cambridge Instruments Ltd. wide-range glass electrode. It was found that the use of an agar bridge with a normal calomel electrode (electrode system A) gave quicker and more reproducible results than did a modified calomel electrode (electrode systems B and C). In the case of polybasic acids after the initial reading a further 1/3 mmole of alkali was added to determine the second mid-equivalence potential.

Infrared spectra were determined in carbon tetrachloride solution, using 4 cm Infrasil cells for the 4000–2500 cm^{-1} region, and as Nujol and Florube mulls, using a Perkin–Elmer 237 instrument.

1. J. W. Elder and R. P. Mariella. Can. J. Chem. **42**, 1106 (1964).
2. R. G. Bates and G. Schwarzenbach. Experientia, **10**, 482 (1954).
3. M. M. Davis and M. Paabo. J. Res. Natl. Bur. Std. A, **67**, 241 (1963).
4. C. E. Moore and R. Peck. J. Org. Chem. **20**, 673 (1955).
5. M. M. Davis and M. Paabo. J. Res. Natl. Bur. Std. A, **64**, 533 (1960).
6. M. M. Davis, M. Paabo, and R. A. Robinson. J. Res. Natl. Bur. Std. A, **64**, 531 (1960).
7. W. Simon, E. Kováts, L. H. Chopard-dit-Jean, and E. Heilbronner. Helv. Chim. Acta, **37**, 1872 (1954).
8. W. Simon and E. Heilbronner. Helv. Chim. Acta, **40**, 210 (1957).
9. W. Simon. Angew. Chem. Intern. Ed. Engl. **3**, 661 (1964).
10. W. Simon, A. Mörikofer, and E. Heilbronner. Helv. Chim. Acta, **40**, 1919 (1957).
11. W. Simon, D. Meuche, and E. Heilbronner. Helv. Chim. Acta, **39**, 290 (1956).
12. L. P. Hammett. Physical organic chemistry. McGraw-Hill Book Co., New York. 1940.
13. G. B. Barlin and D. D. Perrin. Quart. Rev. London, **20**, 75 (1966).
14. M. S. Carpenter, W. M. Easter, and T. F. Wood. J. Org. Chem. **16**, 586 (1951).
15. F. M. Rowe, S. H. Bonnister, R. R. Seth, and R. C. Storey. J. Soc. Chem. Ind. London, **49**, 469T (1930).
16. F. H. Westheimer, E. Segel, and R. Schramm. J. Am. Chem. Soc. **69**, 773 (1947).
17. F. G. Badder and H. Mikhail. J. Chem. Soc. 2927 (1949).
18. H. H. Schlubach and F. Mergenthaler. Ber. **58**, 2732 (1925).
19. H. H. Hodgson and F. H. Moore. J. Chem. Soc. 630 (1927).
20. H. H. Hodgson and F. H. Moore. J. Chem. Soc. 155 (1926).
21. H. H. Hodgson and F. H. Moore. J. Chem. Soc. 1599 (1925).
22. R. Willstatter and G. Schudel. Ber. **51**, 782 (1918).
23. V. Merz and G. Zetter. Ber. **12**, 2035 (1879).
24. B. Flurscheim and E. L. Holmes. J. Chem. Soc. 3041 (1928).
25. S. V. Dubiel and S. Zuffonti. J. Org. Chem. **19**, 1359 (1954).
26. D. H. Richards and K. W. Sykes. J. Chem. Soc. 3626 (1960).
27. D. H. McDaniell and H. C. Brown. J. Org. Chem. **23**, 420 (1958).
28. S. Kertes. J. Chem. Soc. 1386 (1955).
29. G. Kortüm, W. Vogel, and K. Andrussow. Dissociation constants of organic acids in aqueous solution. Butterworths, London. 1961.

Note on the thermodynamic state of laminar flow and on the viscosity of liquids[1]

E. A. FLOOD AND R. F. BARTHOLOMEW[2]
Division of Pure Chemistry, National Research Council of Canada, Ottawa, Canada

Received January 20, 1967

Fluids in a steady state of laminar flow (shear) are not in their thermodynamic equilibrium states. They have more energy and (or) less entropy than their corresponding static states.

Phenomenological considèrations suggest that in the case of 'ideal' liquids, shear states involve dilational energy increases, while in the case of ideal gases shear states involve entropy decreases associated with distortions of momentum fluxes.

It is shown that the viscosities of some liquids (metals, hydrocarbons, water, etc.) can be described approximately by the equation

[*a*] $$\eta = \frac{F^2}{2\beta D}\left(\frac{M}{\rho N_v}\right)^{2/3},$$

where η is the viscosity, β the compressibility, D the coefficient of self-diffusion, M the molecular weight, ρ the density, and N_v Avogadro's number. F measures the strain or effective dilation necessary for a 'layer' to flow over an adjacent 'layer'. Ideally F should be about 0.06 but varies from about 0.05 for metals to 0.14 for water.

Equation [*a*] implies that liquids in a state of laminar flow are somewhat dilated compared with the static state at the same temperature and pressure. The density change as a function of the velocity gradient u' is given by

[*b*] $$\frac{\partial\rho}{\rho} \approx -\frac{F}{D}\left(\frac{M}{\rho N_v}\right)^{2/3} u'.$$

Canadian Journal of Chemistry, **46**, 249 (1968)

Introduction

In this paper we present a simple pseudo-thermodynamic description of fluids in a laminar flow state.

The description implies that under certain conditions a liquid in a state of laminar flow will be somewhat dilated, compared with the normal liquid at the same temperature and hydrostatic pressure. This implication is capable of experimental verification and hence the validity of some of the phenomenological aspects of the description can be tested experimentally.

The description also implies that the 'activation energy' of liquid viscosity is not primarily associated with the heat of evaporation, but is rather more a combination of the fluid shear strain potential and the activation energy of self-diffusion.

Some Ideal Laminar Flow States

Let N be the probable number of molecules per unit volume of a fluid 'layer' having a mean or 'mass' velocity u in, say, the $+x$ direction. Let P be the mean value of any reasonably definite additive molecular property of the fluid. The net property transported per second through unit area perpendicular to the $+x$ direction by the flowing fluid can be written

[1] $$\Gamma_P = cNuP,$$

where Γ_P is the net flux in the $+x$ direction of the property P and c is a dimensionless statistical correlation factor between the means N, P, and u.

Let the 'flux' be the ideal flux equivalent to moving an imaginary plane at a velocity u through a static fluid which is in reversible equilibrium with externally applied forces. Let A_0 be the mean Helmholtz free energy or Helmholtz potential per molecule of the fluid, then ignoring any kinetic energy effects (i.e. ignoring Helmholtz potentials relative to a moving frame of reference) the ideal flux of Helmholtz potential is given by

[2] $$\Gamma_{A_0} = NuA_0.$$

Since we shall consider N as virtually constant, c is unity for the ideal case.

This ideal 'process' is thermodynamically reversible in the sense that there is no creation of entropy or other energetically dissipative effects.

If, however, the velocity u is that of a fluid layer relative to an adjacent, say, lower layer

[1]NRCC No. 9767.
[2]NRCC Postdoctorate Fellow.

Can. J. Chem. Downloaded from www.nrcresearchpress.com by 210.87.254.5 on 09/05/12
For personal use only.

Can. J. Chem. Downloaded from www.nrcresearchpress.com by 210.87.254.5 on 09/05/12
For personal use only.

whose velocity is taken arbitrarily as zero, this 'process' will, in general, not be reversible. Work must be done on the system and (or) entropy created per second within the system to maintain the relative motion. The 'moving' layer and the adjacent 'stationary' reference layer will not in general correspond to a system whose thermodynamic properties lie on what Gibbs calls 'the surface of dissipated energy'. Such a system will have either too much energy to be in equilibrium with its entropy or too little entropy to be consistent with its energy in the state of 'dissipated energy'. In either case the Helmholtz potential A or $E - TS$, if we can use these terms in such cases, will be larger than that of a static system containing the same matter at the same temperature and either having the same volume or at the same hydrostatic pressure as measured remote from any shearing stresses.

If for the relative flux of Helmholtz potential carried by the moving layer we write

$$[3] \qquad \Gamma_{Au'} = cNuA_{u'},$$

this potential flux will be larger than the ideal flux of eq. [2] and must involve some irreversibility. While $\Gamma_{Au'}$ has the dimensions of work per second flowing through unit area it is not, of course, a measure of the actual work done per second. However, we can write,

$$[4] \qquad \Gamma_{Au'} = \Gamma'_{Au'} + \Gamma''_{Au'} = \dot{W} + \Gamma''_{Au'},$$

where $\dot{W}$ is the actual work done per second (or its equivalent) to maintain the total flux. Thus $\Gamma'_{Au'}$ or $\dot{W}$ represents the irreversible part of the potential flux and $\Gamma''_{Au'}$ the 'reversible' flux.

We assume that in a simple fluid in a laminar flow state a fraction of the molecules will be statistically indistinguishable from those in the corresponding equilibrium or bulk state and that the remainder will have either too much energy and (or) too little 'entropy' to correspond to the equilibrium state. Thus we assume that it is meaningful to write

$$[5] \qquad A_{u'} = \phi_u A + (1 - \phi_u)A_0 = \phi_u(A - A_0) + A_0,$$

where A and A_0 are independent of the relative velocity u (or of the velocity gradient u') while ϕ_u is of course dependent on u, i.e. when $u \rightarrow 0$, $\phi_u \rightarrow 0$. Accordingly, $A - A_0$ or A^+ is assumed a characteristic of the fluid in the laminar flow state.

If the external forces which maintain the flow are suddenly eliminated the relative motion of the two layers and hence the excess potential $\phi_u A^+$ will decrease due to diffusive interchange of molecules between the two layers. Hence the instantaneous rate of loss of potential should be proportional to $\phi_u A^+ D'$, where D' is the 'velocity' of molecular interchange between the layers. Also the rate of gain of potential should be proportional to $(1 - \phi_u)A^+ u$. In the steady state of flow these rates must be equal and we write

$$[6] \qquad \phi_u A^+ D' = K(1 - \phi_u)A^+ u,$$

where K is a proportionality constant for a given fluid.

Evidently,

$$[7] \qquad \phi_u = Ku/(Ku + D').$$

Hence also,

$$[8] \qquad \Gamma_{Au'} = c'Nu\phi_u A^+ + NuA_0 = \dot{W} + \Gamma''_{Au'},$$

where NuA_0 and $\Gamma''_{Au'}$ represent the reversible part of the potential flux and we assume that we can equate $c'Nu\phi_u A^+$ to the irreversible work done per second (and (or) to the rate of creation of any entropy at the temperature T of the system which may be carried along with the flux) to maintain the flow.

Let the volume per molecule of the layers in relative motion be as shown in the following sketch.

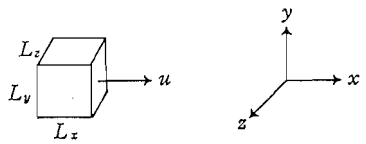

Since L_y is also the distance between layers, $u = L_y(\mathrm{d}u/\mathrm{d}y) = L_y u'$, where u' is the velocity gradient.

The irreversible Helmholtz potential flow through the molecular volume is

$$[9] \qquad L_y L_z \Gamma'_{Au'} = c'L_y L_z Nu\phi_{u'} A^+ = \frac{c'\phi_{u'}[A^+]u}{L_x}.$$

If $\dot{W}$ is the isothermal irreversible work done per second (or its entropy equivalent) by the shearing stresses or by the pressure gradient against the viscous forces we can write for the isothermal flow through the cell, L_x, L_y, L_z,

$$[10] \qquad \dot{W} = L_y L_z L_x \frac{\mathrm{d}p_u}{\mathrm{d}x} = L_z L_x \eta u' u = \frac{c'\phi_{u'}[A^+]u}{L_x},$$

Can. J. Chem. Downloaded from www.nrcresearchpress.com by 210.87.254.5 on 09/05/12
For personal use only.

where η is the viscosity, and u' is the velocity gradient. Therefore

$$[11] \qquad \eta = \frac{c'\phi_{u'}[A^+]}{u'L_zL_x^2}.$$

Inserting the value of $\phi_{u'}$ from eq. [7] and putting $u' = u/L_y$,

$$[12] \qquad \eta = \frac{c''L_y[A^+]}{(Ku + D')L_zL_x^2},$$

where c'' includes the proportionality 'constant' of eq. [6] as well as statistical correlation coefficients, i.e. $c'' = c'K$.

Ideal Values of A^+ and D'

For a Newtonian viscous fluid in a state of laminar flow the stress tensor is equivalent to a shear stress, the shear stress being proportional to the rate of change of 'deformation'. Accordingly, principal stresses on small volumes of the viscous flowing fluid are not equal and the fluid behaves as though it had a transient modulus of rigidity.

In dilute gases, the shear stress deformation involves no work against intermolecular forces but only a deformation of the velocity distributions $f(v_x)$, $f(v_y)$, etc., and the corresponding momentum fluxes. Hence compared with layers having the same kinetic energy but no relative velocity, A^+ must be largely a measure of an entropy decrease.

However, in the case of liquids having considerable tensile strengths, the deformation involves displacements from the time average equilibrium positions of molecules with respect to their considerable intermolecular forces, i.e. involves work against the net intermolecular and stress forces of the corresponding bulk state.

Referring to the two layers, where the upper layer flows over the stationary reference layer, if the state of stress results from shearing stresses only, i.e. little or no hydrostatic pressure but only such couples as are necessary to maintain the laminar flow and to prevent rotation, we might expect that the molecules of the upper layer would tend to rise over the repulsive fields of the lower layer since the repulsive fields are much steeper than the attractive. In regions where molecules 'rise' in passing from one equilibrium position to another, there would be local dilations and we might expect A^+ to include a work of dilation. Of course in the gradient free state, thermal fluctuations would also lead to local dilations and compressions, but in the laminar flow state the statistical weights of the local dilations should be increased when the hydrostatic pressure is small. When the attractive and repulsive fields balance, any appreciable compression will require a much larger δA than a corresponding dilation.

Hence we write

$$[13] \qquad A^+ = \delta A_B + \delta A',$$

where δA_B is the Helmholtz potential of the corresponding dilation of the bulk liquid and $\delta A'$ provides for the difference in thermodynamic properties of the bulk fluid and that of an equal volume of the same fluid having velocity gradients.

For the bulk liquid we assume Hooke's law in the form $(v - v_0)/v_0 = -\beta(p - p_0)$, where β is the compressibility and p_0 the initial hydrostatic pressure. Hence,

$$[14] \qquad \delta A_B = -\int_{v_0}^{v_0+\delta v} p\,dv = \frac{v_0F^2}{2\beta} - v_0p_0F,$$

where $F = \delta v/v_0$.

When F is appreciable and p_0 small,

$$[15] \qquad \delta A_B \simeq v_0F^2/2\bar{\beta},$$

where $\bar{\beta}$ replaces β to provide for variation of compressibility with dilation.

In the bulk state of given volume and temperature the entropy, S, will be a maximum and S' for the flowing fluid of equal volume and temperature will be equal to or less than S. Thus we can write

$$[16] \qquad \delta A' = -kT \log\frac{\Omega - \delta\Omega}{\Omega} = kT\delta\Omega/\Omega,$$

where k is the Boltzman constant, T the temperature, and Ω the appropriate partition function for the bulk fluid.

Putting $\delta\Omega/\Omega = F_\Omega$ in eq. [16], we get from eqs. [13] and [15]

$$[17] \qquad A^+ = v_0F^2/2 + kTF_\Omega.$$

Dense liquids just above their freezing temperatures have been described as 'random close-packed' structures. In close-packed (c-p) structures of spheres no sphere can move appreciably from its mean position. The closest packed regular structure having planes of spheres which can move through the structure is the tetragonal-sphenoid (t-s) structure. In a c-p bulk liquid at 'rest' thermal fluctuations will

Can. J. Chem. Downloaded from www.nrcresearchpress.com by 210.87.254.5 on 09/05/12
For personal use only.

probably produce structures of a variety of forms including pseudo t-s structures. We shall assume that in the laminar flow of more or less c-p spherical-molecule liquids the statistical weight of the pseudo t-s structures are increased, the increases being proportional to velocity gradients. The t-s structure has a 6% greater volume than the corresponding c-p structure. The minimal rise of a molecule lying in the well formed by three others when it rolls over any two is also 6%. Accordingly, we shall assume that under ideal conditions F in eq. [17] should be of the order of 0.06. Since at high temperatures and low densities F should approach zero and F_Ω approach that for an ideal gas, we can write empirically

$$[18] \qquad A^+ = av_0F_c^2/2\bar{\beta} + bkTF_{\Omega g},$$

when F_c refers to the ideal dilation (6%) of a close-packed liquid and $F_{\Omega g}$ to the change in partition function per unit gradient of the ideal gas.

The empirical parameters a and b are assumed to be functions of the temperature, critical temperature, liquid structures, etc. At temperatures well above the critical and at low densities, $a \rightarrow 0$ and $b \rightarrow 1$. At low temperatures and high densities of liquids of considerable tensile strengths $F^2/2\bar{\beta}$ should control A^+, i.e. a should be of the order of unity and b should be considerably less than unity in many cases.

If the volume of the liquid is kept constant during the flow A^+ should have about the same value as that of the low constant pressure A^+ but will be the result of a combination of compressions and dilations. Consequently the entropy term in A^+ will probably be somewhat larger. The δA of compression of condensed systems at room temperature consists of an energy decrease but a greater decrease in TS. The δA_B we have used is the equivalent dilational potential of the bulk fluid at near zero initial pressure. The actual value of A^+ consists of shear strain potential against a transient modulus of rigidity. It is only when the hydrostatic pressure is near zero that a unidirectional dilational potential of a bulk fluid resembles a shear strain potential of an elastic solid. At high pressures of bulk fluids the δA of dilation is of course negative. The value of A^+ for flow must always be positive. If the initial hydrostatic pressure of the flowing fluid is high, the dilation for flow will probably be about the same as at lower pressures, but the "distortional" or shear strain potential probably somewhat greater, since one would expect the "transient modulus of rigidity" to increase with increasing pressure. Evidently the term p_0v_0F in eq. [14] is not to be taken as a measure of the variation of A^+ with pressure.

Hence putting in the value of A^+ from eq. [18] and assuming $D' \gg Ku$, i.e. at low rates of shear,

$$[19] \qquad \eta = \frac{c''L_y[av_0F_c^2/2\bar{\beta} + bkTF_{\Omega g}]}{D'L_zL_x^2}.$$

For the ideal gas of simple kinetic theory (step lengths statistically independent of velocities) D' will be considerably less than the mean speed, $\bar{v}$. Most of the molecules emanating from the upper layer will pass through the lower 'layer'. D' should be of the order of DL_0/λ^2, where D is the self-diffusion coefficient $\bar{v}\lambda/3$, $L_0 = N^{-1/3}$, and λ the mean free path.

In the case of a more or less close-packed liquid, however, practically all molecules emanating from the upper layer which reach the lower layer will become statistically part of the lower layer and D' should be of the order D/L_y.

Putting in the appropriate values of D' we get for ideal gases and ideal liquids the following.

Ideal gases,

$$[20] \qquad \eta = c'''F_{\Omega g}Nm\bar{v}\lambda.$$

Ideal liquids,

$$[21] \qquad \eta = \frac{c^{IV}L_y^2[av_0F_c^2/2\bar{\beta} + bkTF_{\Omega g}]}{DL_zL_x^2}.$$

Putting $L_y = L_0(1 + F)$, $L_x = L_z = L_0$, $v_0 = L_0^3 = M/\rho N_v$, where M is gram molecular weight, ρ the liquid density, and N_v Avogadro's number,

$$[22] \qquad \eta = [c^{IV}(1 + F)^2/D][M/\rho N_v]^{2/3} \times [aF_c^2/2\bar{\beta} + bkTF_{\Omega g}].$$

Neglecting F compared with unity and assuming b small,

$$[23] \qquad \eta \approx \frac{c^{IV}F_c^2}{2\bar{\beta}D}\left(\frac{M}{\rho N_v}\right)^{2/3}$$

$$[24] \qquad \eta \approx \frac{F^2}{2\beta D}\left(\frac{M}{\rho N_v}\right)^{2/3}.$$

If the physical ideas underlying eqs. [23] and [24] have any validity, F_c should be of the order of

Can. J. Chem. Downloaded from www.nrcresearchpress.com by 210.87.254.5 on 09/05/12
For personal use only.

TABLE I

Apparent dilations, F, for laminar flow of various liquids

Liquid	T (°K)	η (cP)	$\beta \times 10^{11}$ (c.g.s.)	ρ (g/cc)	$D \times 10^5$ (cm^2 s^{-1})	F
H_2O	298.2	0.8937	4.57	0.9970_4	2.44	0.1421
CH_3OH	298.2	0.544[a]	12.55	0.7866[a]	2.27	0.1366
C_2H_5OH	298.2	1.078[a]	11.46	0.785[a]	1.01	0.1086
CH_4	102.6	0.1440[e]	18.15[d]	0.4372[e]	3.01[j]	0.1008
C_6H_6	298.2	0.596[a]	9.67	0.8737[a]	2.21	0.0970
A	85	0.272[f]	20.50[d]	1.41[d]	1.53[k]	0.1148
CCl_4	293.2	0.969	10.40	1.5940[a]	1.30[l]	0.0944
C_2H_5Br	295.7	0.389[b]	13.23	1.44	4.06	0.1291
C_2H_5I	292.55	0.596[b]	9.77	1.934[b]	1.212	0.0734
Hg	313.2	1.450	0.412	13.4973	1.69[m]	0.0488
Ga	303.7	1.96[g]	0.24[c]	6.095[g]	1.67	0.0460
Na	371.2	0.7264[h]	2.10[c]	0.93[h]	4.2	0.1038
In	492.2	1.94[i]	0.32[c]	7.05[o]	1.67[n]	0.0480
Sn	505.2	2.14[i]	0.31[c]	6.98[h]	2.60[n]	0.0610

*All values quoted for viscosity, density, and isothermal compressibility are taken from ref. 1, except where marked by superscript. All values of D are from ref. 2, except where marked.
[a]Ref. 3. [b]Ref. 4. [c]Ref. 5. [d]Ref. 6. [e]Ref. 7. [f]Ref. 8. [g]Ref. 9. [h]Ref. 10. [i]Ref. 11. [j]Ref. 12. [k]Ref. 13. [l]Ref. 14. [m]Ref.15. [n]Ref. 16. [o]Ref. 17.

TABLE II

Variation of F with temperature

T (°K)	η (cP)[a]	$\beta \times 10^{11}$[b]	ρ (g/u)[a]	$D \times 10^5$[c]	F
		Methane			
94.9	0.1765	15.12	0.4481	2.31	0.0900
102.6	0.1440	18.15	0.4372	3.01	0.1008
105.6	0.1348	18.84	0.4328	3.31	0.1039
111.4	0.1190	20.30	0.4241	3.91	0.1094
T (°K)	η (cP)[d]	$\beta \times 10^{11}$[d]	ρ (g/u)[e]	$D \times 10^5$[f]	F
		Carbon tetrachloride			
293.2	0.969	10.40	1.5940	1.30	0.0944
303.2	0.843	11.14	1.5748	1.57	0.996
313.2	0.739	12.19	1.5557	1.87	0.1061
323.2	0.651	13.29	1.5361	2.21	0.1124
T (°K)	η (cP)[d]	$\beta \times 10^{11}$[d]	ρ[d]	$D \times 10^5$[g]	F
		Mercury			
0	1.685	0.400	13.5955	1.33	0.0461
40	1.450	0.412	13.4973	1.69	0.0488
80	1.298	0.426	13.4003	2.04	0.0515

[a]Ref. 7. [b]Ref. 6. [c]Ref. 12. [d]Ref. 1. [e]Ref. 3. [f]Ref. 14. [g]Ref. 15.

0.06 and the numerical values of c^{IV} for liquids of similar structures should be about the same.

Values of F calculated by eq. [24] from known values of β, D, η, etc. appear in Table I.

Evidently η is roughly inversely proportional to βD and F is of the order of 0.06, varying from about 0.05 to 0.15. In the table βD varies by more than a 100-fold while the variations of F are comparatively small. If the 'deformation' involves 'breaking' of hydrogen bonds the apparent value of F will be larger than the actual value.

In Table II some variations of F with temperature are calculated on the same basis. The

Can. J. Chem. Downloaded from www.nrcresearchpress.com by 210.87.254.5 on 09/05/12
For personal use only.

apparent increase in F with temperature suggests that the entropy term is not negligible.

Equation [24] implies that a Newtonian liquid well below its critical temperature must be somewhat dilated when in a state of laminar flow at constant external hydrostatic pressure.

From eqs. [8] and [24]

$$[25] \qquad v_{u'} - v_0 = u' L_y^2 v_0 F/D,$$

where $v_{u'}$ is the specific volume of the layer having the relative velocity $u = u'L_y$ with respect to an adjacent layer; v_0 is the specific volume of normal liquid. Hence in terms of the density change,

$$[26] \qquad \delta\rho/\rho_0 \approx -\frac{F}{D}\left(\frac{M}{\rho N_v}\right)^{2/3} u'.$$

For liquid water at room temperature using the values of D, F, etc. from Table I,

$$[27] \quad \delta\rho/\rho_0 \approx -[5 \times 10^{-12}\,(\text{second})]\,u'\,(\text{per second}).$$

Assuming that one can detect a density change of the order of 10^{-9} by interferometry, u' will have to be of the order of 10^3 per second, or more, in order that the predicted dilation be detectable. The temperature difference required to permit the flow of heat equivalent to the work of shear is readily calculated and will be small if the thermal conductivity of the vessel walls is high and the fluid layer very thin. The temperature control, however, will have to be very good. For water at room temperature $d\rho/dT \approx -2\times10^{-4}$. Hence variations in temperature greater than 10^{-6} °C will mask dilations due to shear at velocity gradients of the order of 10^3 per second. However, when the velocity gradient varies with distance from the walls, in a steady state of shear, one should be able to distinguish between thermal and velocity gradient dilations. In viscometers of the inner rotating cylinder type it is easily shown that at appreciable distances from the surface of the rotating cylinder, under ordinary laboratory conditions, dilations associated with thermal gradients (i.e. those necessary to dissipate the work done per second as heat flow) will be much larger than the "viscosity dilation" of eq. [27]. However, very near to the surface of the rotating cylinder the viscosity dilation will be the larger. The combined effects will lead to an intercept in the density vs. distance plot, the intercept being a measure of the viscosity dilation.

Discussion

The description of the ideal gas viscosity sketched above is intended to illustrate the possible effect that an entropy in A^+ could have on the temperature coefficient of viscosity. The detailed molecular momentum scattering methods of calculating gas viscosities, such as those involving sophisticated tensor statistics, even those of simple classical kinetic theory, are of course much more direct than our pseudo-thermodynamic method.

Practically all theoretical descriptions of both gas and liquid viscosities involve a modification of the equilibrium state distribution laws, partition functions, etc. However, it is seldom emphasized that such modifications imply positive A^+ values in the laminar flow state. If the thermodynamic properties of a fluid in the laminar flow state were identical with those in the corresponding static state it would seem that there could be no viscous force.

While the physical nature of the viscous forces of gases and gas-like liquids are reasonably well understood, the situation concerning liquids is not so clear. It might help the theorist considerably, if experimental information concerning the nature of A^+ were available.

If it can be shown experimentally that Newtonian liquids, well below their critical temperatures, in the state of laminar flow are in fact dilated more or less as indicated by eq. [26], it might contribute a good deal to our knowledge of the mechanisms of liquid viscosities. The experimental determination of the temperature and pressure coefficients of F might prove particularly illuminating.

1. R. C. Weast and S. M. Selby (*Editors*). Handbook of chemistry and physics. 44th ed. The Chemical Rubber Co., Cleveland, Ohio. 1962–63.
2. H. J. V. Tyrrell. Diffusion and heat flow in liquids. Butterworths, London. 1961.
3. J. Timmermans. Physico-chemical constants of pure organic compounds. Elsevier Publishing Co., Inc., New York. 1950.
4. N. A. Lange. Handbook of chemistry. 10th ed. McGraw-Hill Book Co., Inc., New York. 1961.
5. O. J. Kleppa. J. Chem. Phys. **18**, 1335 (1950).
6. A. Van Itterbeek and L. Verhaegen. Proc. Phys. Soc. London, **62B**, 800 (1949).
7. F. D. Rossini *et al.* Selected values of physical and thermodynamic properties of hydrocarbons and related compounds. American Petroleum Institute Research Project 44, Carnegie Press, Pittsburgh. 1953.

8. E. McLAUGHLIN. Trans. Faraday Soc. **55**, 28 (1959).
9. K. E. SPELLS. Proc. Phys. Soc. London, **48**, 299 (1936).
10. J. W. MELLOR. A comprehensive treatise on inorganic and theoretical chemistry. Longmans, Green and Co., New York. 1947.
11. E. A. DA C. ANDRADE. Proc. Roy. Soc. London, Ser. A, **215**, 36 (1952).
12. J. V. GAVIN, JR., J. S. WAUGH, and W. H. STOCKMAYER. J. Chem. Phys. **38**, 287 (1963).
13. G. CINI-CASTAGNOLI and F. P. RICCI. J. Chem. Phys. **32**, 19 (1960).
14. H. WATTS, B. J. ALDER, and J. H. HILDEBRAND. J. Chem. Phys. **23**, 659 (1955).
15. N. H. NACHTRIEB and J. PETIT. J. Chem. Phys. **24**, 746 (1956).
16. VON A. LODDING. Z. Naturforsch. **11a**, 200 (1956).
17. D. D. WILLIAMS and R. R. MILLER. J. Am. Chem. Soc. **72**, 3821 (1950).

Can. J. Chem. Downloaded from www.nrcresearchpress.com by 210.87.254.5 on 09/05/12
For personal use only.

Can. J. Chem. Downloaded from www.nrcresearchpress.com by 210.87.254.105 on 09/05/12
For personal use only.

Infrared spectra and thermal decompositions of metal acetates and dicarboxylates[1]

K. C. Patil, G. V. Chandrashekhar, M. V. George, and C. N. R. Rao[2]
Department of Chemistry, Indian Institute of Technology, Kanpur, India

Received June 1, 1967

The infrared spectra of rare earth acetates have been studied to examine the metal-acetate bonding. The thermal decomposition of rare earth acetates as well as lead and copper acetates have been investigated in detail by employing thermogravimetric analysis and differential thermal analysis. Thermal decomposition of calcium dicarboxylates (malonate to sebacate) have been studied employing t.g.a. and d.t.a. Infrared spectra of the dicarboxylates have also been studied. Preliminary results on the products of decomposition of dicarboxylates have been reported.

Canadian Journal of Chemistry, 46, 257 (1968)

Introduction

The thermal decomposition of calcium acetate to acetone and calcium carbonate is a well-known reaction. There is, however, little or no information on the thermal decomposition of other metal acetates in the literature. In the present study, the thermal decompositions of copper acetate, lead di- and tetra-acetates, as well as of a few rare earth acetates, have been investigated employing differential thermal analysis (d.t.a.), thermogravimetric analysis (t.g.a.), and infrared spectroscopy. In addition, the infrared spectra of rare earth acetates have been examined in order to study the nature of the metal-acetate bonding in the rare earth series.

The thermal decompositions of several metal oxalates, particularly those of rare earths, have been studied exhaustively in the past few years (1, 2 and references cited therein, 3, 4). Preparation of ketones by the decarboxylation of the metal salts of long chain dicarboxylic acids has long been known to organic chemists. While this method was found to be somewhat useful for the preparation of some ketones, the pyrolysis of many of the salts are found to give rise to a variety of products, many of which have not been identified. It was therefore considered interesting to examine the thermal decomposition of the calcium salts of a few dicarboxylic acids (malonic to sebacic) employing t.g.a. and d.t.a. Such a study would throw light on the mode of decomposition and indicate, at least, the main inorganic residue left over after the removal of the organic part. Results of a preliminary study of the decomposition products have also been presented.

Experimental

All the rare earth acetates were prepared by dissolving the oxides in boiling 50% acetic acid and evaporating the solutions to dryness, as reported by Witt and Onstott (5). The resulting compounds were recrystallized from water and heated to ~ 220 °C in vacuum to obtain anhydrous acetates (5). Both lead and copper acetates were available commercially.

All the dicarboxylic acids used were commercial samples. The calcium salts were prepared by the reaction of calcium carbonate with the acid solutions in water. Calcium malonate and succinate were obtained as insoluble salts, whereas calcium glutarate, adipate, and pimelate were obtained by the evaporation of the resulting solutions, after completely neutralizing the acids. Dysprosium sebacate was prepared by the interaction of the sodium salt of the acid with the chloride solution.

The t.g.a. curves were recorded with an Aminco thermobalance. The heating rate employed was 10 °C/min and the ambient pressure was $\sim 3 \times 10^{-2}$ mm Hg. The d.t.a. curves were obtained by employing an Aminco thermoanalyzer with a temperature-programmed furnace (fitted with a voltage stabilizer), differential amplifier, and an X–Y recorder. Alumina was used as the reference. The heating rate employed was 16 °C/min. The enthalpy changes, ΔH, for the different reactions were obtained by measurement of peak areas with respect to a standard transformation. Dehydration of $CuSO_4.5H_2O$ and decomposition of $CaCO_3$ were employed as standards. Uncertainties in the ΔH values were of the order of $\pm 15\%$.

The infrared spectra of all the acetates and the dicarboxylates were recorded on a Perkin–Elmer model-521 double-grating spectrometer. Samples were prepared as KBr pellets or mulls in Nujol. The vapor phase spectra were taken using 10 cm gas cells (NaCl).

Vapor phase chromatographic (v.p.c.) analysis was done using F and M 700 (thermal conductivity detector) chromatograph fitted with 12 ft. $\times$ 1/8 in. stainless steel column packed with fire brick powder. The temperature

[1]Forms part of the Ph.D. Thesis of K. C. P.
[2]To whom all correspondence should be addressed.

TABLE I

Infrared frequencies of metal acetates (cm^{-1})*

Acetates	$\nu_{asym}(COO^-)$	$\nu_{sym}(COO^-)$	$\delta_{asym}(CH_3)$	$\delta_{sym}(CH_3)$	$\rho(CH_3)$	ν(C—C)	δ(OCO)	$\pi(COO^-)$ or π(CH)
Na	1575	1422 (153)	1438	1341	1046, 1014	923	650	620
La	1545	1440 (105)	1460	1335	1050, 1030, 1015	965, 952, 940	674, 660, 640	610, 604
Pr	1550	1440 (110)	1455	1345, 1315	1052, 1024	955, 948	675	610
Nd	1569	1439 (130)	1464	1341	1048, 1016	940	675	610
Sm	1550	1420 (130)	1458	1342	1050, 1018, 1008	960, 945	660, 645	608
Gd	1546	1420 (126)	1465	1341	1050, 1017	952, 943	675	608
Dy	1545	1418 (127)	1460	1341	1047, 1017	963, 941	675	606
Lu	1551	1412 (139)	1462	1348	1049, 1022	954	684	606

*Nomenclature of the bands is similar to that of Nakamoto (9). Values in parenthesis in the ν_{sym} column are the $\Delta\nu(\nu_{asym}(COO^-) - \nu_{sym}(COO^-))$ values.

of the column was maintained at 58 or 98 °C. Hydrogen was used as the carrier gas (at 35 cc/min).

Results and Discussion

Infrared Spectra of Rare Earth Acetates

The free acetate ion has 15 infrared active fundamentals of which the asymmetric and symmetric stretching modes of the CO_2^- group have been employed for structural studies. The various characteristic frequencies of the acetate ion in a number of metal acetates have been reported in the literature (6–8). Since the symmetry of the free ion is C_{2v}, no major differences in the spectra are expected for the different coordinated structures of the acetate ion (9). Nakamoto and co-workers (10) have shown that the separation $\Delta\nu$ between the asymmetric and the symmetric frequencies of the CO_2^- group is an indication of the nature of the coordination in a related group of acetates. The major frequencies of rare earth acetates characteristic of the acetate ion are shown in Table I along with the data on sodium acetate. It can be seen that the separation ($\Delta\nu$) in the rare earth acetates varies between 105 and 140 cm^{-1}, the largest separation being in the case of lutetium acetate. These separations are smaller than the $\Delta\nu$ in sodium acetate. Further, ν_{asym} and ν_{sym} are both lower than in sodium acetate, just as in the case of nickel acetate (9). It is possible that the acetate ion in rare earth acetates is present as a unidentate ligand, as in the case of nickel acetate, rather than as the symmetrical bridged structure (11). The bidentate structure proposed by Nakamoto (9) cannot also be ruled out, since all the rare earth acetates were anhydrous. Since $\Delta\nu$ in rare earth acetates does not vary much with the rare earth ion, it appears likely that the metal–oxygen bonds in all these cases are nearly of the same strength. The relatively high $\Delta\nu$ in lutetium acetate could be taken as indicative of the slightly stronger metal–oxygen bonding in the heavier rare earth acetates.

TABLE II

Thermogravimetric analysis data on the thermal decomposition of rare earth acetates, $Ln(CH_3CO_2)_3$

Ln	Oxycarbonate formation temperature $Ln_2O_3.CO_2$ (°C)	Minimum oxide formation temperature Ln_2O_3 (°C)
La	450	910
Pr	450	720 (Pr_6O_{11})
Nd	420	820
Sm	460	750
Gd	450	740
Dy	450	650
Lu	430	600

Thermal Decomposition of Rare Earth Acetates

All the rare earth acetates prepared were hydrates and the number of water molecules varied from 1 to 4. The water molecules were lost on heating the hydrates to 200–220 °C in all cases. For the tetrahydrates of gadolonium, dysprosium, and lutetium acetates, the d.t.a. curves showed that dehydration took place in two stages at $\sim$ 120 °C and $\sim$ 220 °C, indicating two types of water molecules bound differently.

The anhydrous acetates prepared from the decomposition of the hydrated rare earth acetates were stable and decomposed only above 400 °C.

Can. J. Chem. Downloaded from www.nrcresearchpress.com by 210.87.254.105 on 09/05/12
For personal use only.

Can. J. Chem. Downloaded from www.nrcresearchpress.com by 210.87.254.105 on 09/05/12
For personal use only.

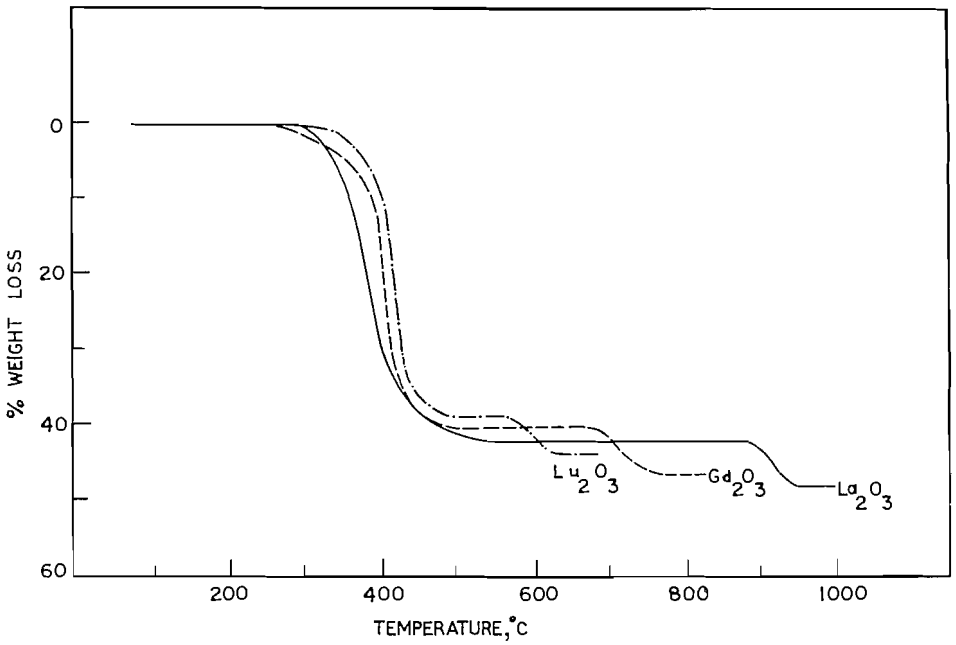

FIG. 1. The t.g.a. curves of anhydrous rare earth acetates (heating rate 10 °C/min).

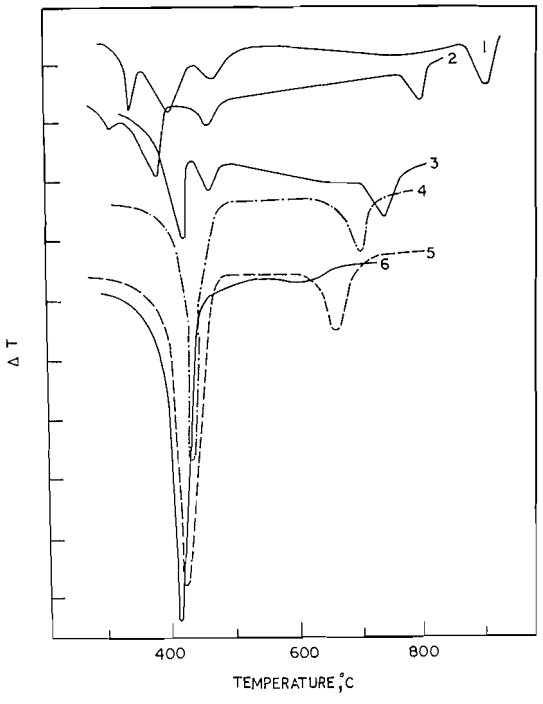

FIG. 2. The d.t.a. curves (in air) of anhydrous rare earth acetates $Ln(CH_3CO_2)_3$. Curve 1, La; 2, Nd; 3, Sm; 4, Gd; 5, Dy; and 6, Lu.

The results from the t.g.a. and d.t.a. of the anhydrous rare earth acetates are shown in Tables II and III. Typical t.g.a. and d.t.a. curves are shown in Figs. 1 and 2 respectively. The t.g.a. curves of all the rare earth acetates showed evidence for only two stages of decomposition: the first stage between 420–460 °C corresponding to the decomposition of the anhydrous acetate, $Ln(CH_3CO_2)_3$, to the oxycarbonate, $Ln_2O_3.CO_2$ and the second stage corresponding to the formation of the sesquioxide, Ln_2O_3 (with the exception of praseodymium acetate where the end product is the non-stoichiometric Pr_6O_{11})[3].

[1] $2Ln(CH_3CO_2)_3 \rightarrow Ln_2O_3.CO_2 + 2CO_2 + 3CH_3COCH_3$

[2] $Ln_2O_3.CO_2 \rightarrow Ln_2O_3 + CO_2$

There is no evidence for the formation of the normal carbonate, $Ln_2(CO_3)_3$, in the t.g.a. curves. The formation of the oxycarbonate, $Ln_2O_3.CO_2$, has been found to be the first stage

[3] Pr_6O_{11} is found to be the final product of decomposition of praseodymium salts. Oxidation of Pr^{3+} accompanies the last stage of decomposition.

TABLE III

Differential thermal analysis data on the thermal decompositions of rare earth acetates, $Ln(CH_3CO_2)_3$

Ln	Anhyd. acetate to carbonate T (°C)	ΔH (kcal mole^{-1})	Carbonate to oxycarbonate T (°C)	ΔH (kcal mole^{-1})	Oxycarbonate to oxide T (°C)	ΔH (kcal mole^{-1})
La	335, 405	70	465	40	900	77
Nd	300, 370	17	450	12	790	12
Sm	435	16	475	8	750	25
			Anhyd. acetate to oxycarbonate T (°C)	ΔH (kcal mole^{-1})	Oxycarbonate to oxide T (°C)	ΔH (kcal mole^{-1})
Gd			435	38	700	20
Dy			425	54	660	15
Lu			420	80	590	11

in the decomposition of normal rare earth carbonates (12, 13). The decomposition temperatures of rare earth carbonates are summarized in Table IV for purposes of comparison.

TABLE IV

Decomposition temperatures of rare earth carbonates from d.t.a. data

Ln	Decomposition of $Ln_2(CO_3)_3$ to $Ln_2O_3.CO_2$ (peak temperature (°C))	Decomposition of $Ln_2O_3.CO_2$ to Ln_2O_3 (peak temperature (°C))
La	530	900
Pr	485	615 (Pr_6O_{11})
Nd	510	730
Sm	450	700
Gd	420	600

The d.t.a. curves of lanthanum, neodymium, and samarium acetates showed evidence for the initial formation of the normal carbonate, $Ln_2(CO_3)_3$, prior to its decomposition to $Ln_2O_3.CO_2$.

[3] $2Ln(CH_3CO_2)_3 \rightarrow Ln_2(CO_3)_3 + 3CH_3COCH_3$,

where Ln = La, Nd, or Sm. Further, formation of the normal carbonate in the case of lanthanum and neodymium was found to take place in two stages, as can be seen from the d.t.a. curves (Fig. 2). The first of these two stages is unlikely to arise from the formation of oxyacetates, since oxyacetates cannot yield normal carbonates as the decomposition products. It should be noted that the decomposition temperatures of lanthanum, neodymium, and samarium carbonates are appreciably higher than the temperatures for these two stages (Table IV). The reactions for the two stages[4] of formation of the normal carbonates may be written as

[4] $Ln(CH_3CO_2)_3 \rightarrow LnCO_3(CH_3CO_2) + CH_3COCH_3$

[5] $LnCO_3(CH_3CO_2) \rightarrow \frac{1}{2}Ln_2(CO_3)_3 + \frac{1}{2}CH_3COCH_3$,

where Ln = La, Nd, or Sm. The lanthanum, neodymium, and samarium carbonates then decompose to the $Ln_2O_3.CO_2$, finally yielding Ln_2O_3 (Tables III and IV).

The d.t.a. curves of all the other rare earth acetates showed only two peaks corresponding to the decomposition of the acetate directly to the oxycarbonate and the subsequent decomposition of the basic salt to the oxide.[5] The decomposition temperatures of the carbonates agree well with those reported in the literature (12, 13). The formation of the oxycarbonate was also confirmed by infrared spectroscopy (Table V). The infrared data show that the carbonate ion is strongly coordinated to the metal ion, possibly as a unidentate ligand (9). The temperature of formation of the basic carbonate does not vary much with the rare earth ion. Apparently, the coordination between with acetate and the metal ion does not vary appreciably in the rare earth series (as already inferred from infrared spectra). The minimum oxide formation temperature (from the basic carbonate), however,

[4]These stages could not be seen in the t.g.a. curves. The differences in the t.g.a. and the d.t.a. results are not due to the different rates of heating employed.

[5]These results are in conformity with the known data on the stabilities of rare earth carbonates (12). The normal carbonates are found to be stable only in the case of the more basic (lighter) rare earths, while the heavier rare earths generally form the oxycarbonates.

Can. J. Chem. Downloaded from www.nrcresearchpress.com by 210.87.254.105 on 09/05/12
For personal use only.

TABLE V

Infrared frequencies of oxycarbonates (cm^{-1}), $Ln_2O_3.CO_2$

Ln	ν_{CO}			*	δ_{CO_3}	
La	1506	1442	1355	1048	870	845
Pr	1526	1462	1355	1050	870	841
Nd	1534	1460	1352	1053	873	840
Sm	1524	1459	1370	1055	873	844
Dy	1512	1449	1394	1055	870	844
Gd	1504	1440	1389, 1333	1053	860	844

*Assignment not clear.

decreases markedly as one goes down the rare earth series, possibly indicating that the coordination of carbonate ion to the metal ion becomes stronger as one goes to heavier rare earths. The variation in the enthalpies of the various reactions (Table III) are, however, difficult to interpret.

Thermal Decomposition of Lead and Copper Acetates

The t.g.a. curve of lead tetraacetate (Fig. 3) shows three distinct stages corresponding to the formation of the diacetate, carbonate, and oxide (PbO), the last two stages being confirmed by an independent t.g.a. curve of lead diacetate. The formation of lead diacetate from the tetraacetate will involve reactions of the acetoxy radical. The d.t.a. curve (Fig. 3) shows two exothermic peaks[6] at $\sim$ 150 °C and 190 °C, probably corresponding to the formation of diacetate as well as the products from the acetoxy radical. However, the d.t.a. results are difficult to understand. The products from the acetoxy radical were found to be mainly CO_2 and methyl acetate by vapor phase infrared spectroscopy. Ethane, if formed, must be present in small proportions. Thus, the different reactions in the decomposition of $Pb(CH_3CO_2)_4$ are:

[6] $Pb(CH_3CO_2)_4 \rightarrow Pb(CH_3CO_2)_2 + 2CH_3CO_2\cdot$

[7] $2CH_3CO_2\cdot \rightarrow CH_3CO_2CH_3 + CO_2$

[8] $Pb(CH_3CO_2)_2 \rightarrow PbCO_3 + CH_3COCH_3$

[9] $PbCO_3 \rightarrow PbO + CO_2$.

The t.g.a. curve of copper acetate, $Cu_2(CH_3CO_2)_4.2H_2O$, showed the first stage due to the dehydration at $\sim$ 180 °C. After the dehydration, there was only one rapid stage of decomposition. The decomposition was complete by $\sim$ 310 °C, but the t.g.a. curve showed a slight mass increase up to 550 °C. The mass increase indicated that some oxidation of Cu or Cu_2O formed in the decomposition may be taking place above $\sim$ 350 °C. The composition of the final product at 550 °C is CuO. The t.g.a. results from the present study agree with the d.t.a. studies of Hill and co-workers (14), who have also reported the product analysis by mass

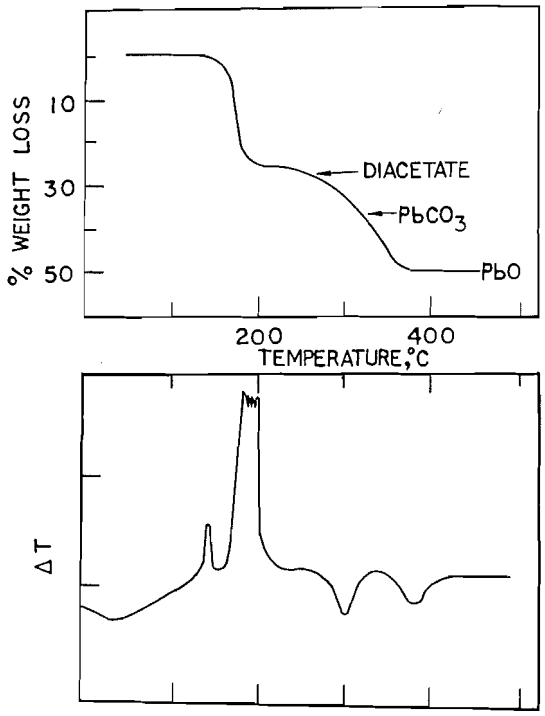

FIG. 3. The t.g.a. (3×10^{-2} mm Hg) and d.t.a. (in air) curves of lead tetraacetate. The heating rate was 10 °C/min in the t.g.a. and 16 °C/min in the d.t.a.

[6]The t.g.a. and d.t.a. curves may not be exactly comparable, particularly with respect to the reaction temperatures, since the heating rates are not identical. Further, the t.g.a. was in vacuum (3×10^{-2} mm Hg) while d.t.a. was in air.

Can. J. Chem. Downloaded from www.nrcresearchpress.com by 210.87.254.105 on 09/05/12
For personal use only.

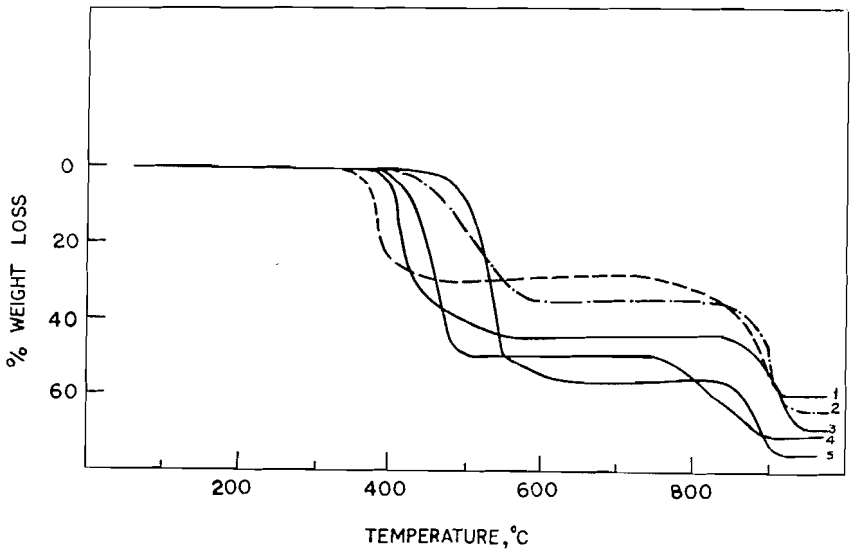

FIG. 4. The t.g.a. curves of anhydrous calcium dicarboxylates: (1) malonate, (2) succinate, (3) adipate, (4) pimelate, and (5) sebacate (heating rate 10 °C/min).

spectrometry. Considering water, acetone, and CO_2 to be the main products, the following reactions can be written for the decomposition of $Cu_2(CH_3CO_2)_4.2H_2O$.

[10] $Cu_2(CH_3CO_2)_4.2H_2O \rightarrow Cu_2(CH_3CO_2)_4 + 2H_2O$

[11] $Cu_2(CH_3CO_2)_4 \rightarrow 2CuO + 2CH_3COCH_3 + 2CO_2$

Methane and acetic acid, which have been found as (minor) products (14), are possibly formed from ketene (produced by the pyrolysis of acetone).

Infrared Spectra of Dicarboxylates

Infrared spectra of calcium dicarboxylates were studied with a view to examining the metal-carboxylate bonding. It has been shown that the magnitude of covalency of the metal–oxygen bonding in metal dicarboxylates can be inferred from the separation between the symmetric and asymmetric stretching frequencies of carboxylate ion (9). The separation between the symmetric and asymmetric stretching frequencies of the carboxylate ion in the various calcium dicarboxylates (malonate to sebacate) was nearly the same ($\sim 140\ cm^{-1}$), indicating that the metal–oxygen bonding is about the same in all these calcium salts.

Results from T.G.A. and D.T.A. of Dicarboxylates

The t.g.a. data of a number of calcium dicarboxylates are summarized in Table VI and typical t.g.a. curves are shown in Fig. 4. It can be seen that all the dicarboxylates (from malonate to sebacate) give $CaCO_3$ as the residue[7] by losing elements of the ketone in one step.

TABLE VI

Thermogravimetric analysis data on the thermal decomposition of calcium salts of dicarboxylic acids

	Formation of anhyd. salt (°C)	Formation of $CaCO_3$ (°C)	Formation of CaO (°C)
Oxalate.H_2O	250	530	910
Malonate.$2H_2O$	250	400	910
Succinate.$2H_2O$	200	580	920
Glutarate.$4H_2O$	290	550	940
Adipate.H_2O	200	550	950
Pimelate.H_2O	220	490	870
Sebacate.$3H_2O$	200	550	900

[12] $\left[O-\overset{O}{\overset{\|}{C}}-(CH_2)_n-\overset{O}{\overset{\|}{C}}-O\right]^{2-} Ca^{2+} \rightarrow [(CH_2)_nC{=}O] + CaCO_3$

The decomposition temperatures of the various calcium dicarboxylates do not seem to vary widely, confirming that the metal–oxygen bonding in these carboxylates does not vary with the

[7]The $CaCO_3$ formed decomposes to CaO at ~ 900 °C (see Table VI and Fig. 4).

Can. J. Chem. Downloaded from www.nrcresearchpress.com by 210.87.254.105 on 09/05/12
For personal use only.

Can. J. Chem. Downloaded from www.nrcresearchpress.com by 210.87.254.105 on 09/05/12
For personal use only.

anion. Further, the formation of $CaCO_3$ as the solid residue precludes the formation of anhydrides as the initial products of decomposition.[8]

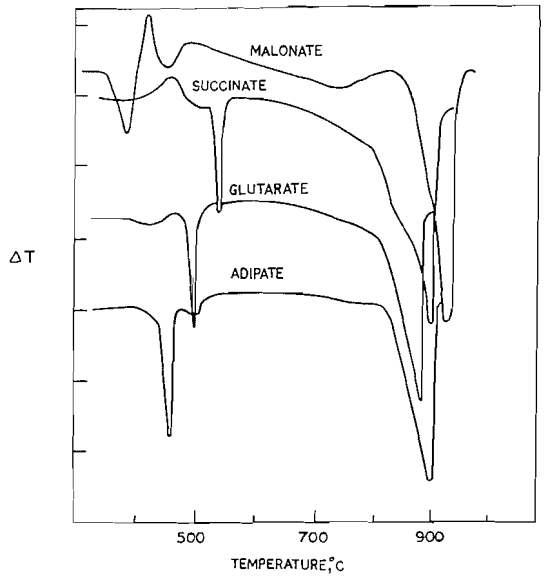

FIG. 5. The d.t.a. curves in air of anhydrous calcium dicarboxylates (heating rate 10 °C/min).

TABLE VII

Differential thermal analysis data on the thermal decomposition of calcium dicarboxylates (peak temperatures in °C)

	Dehydration	Decomposition to $CaCO_3$*	Decomposition to CaO
Malonate.$2H_2O$	190, 240	385	930
Succinate.$2H_2O$	185	540	910
Glutarate.$4H_2O$	190, 300	500	880
Adipate.H_2O	190	460	900
Pimelate.H_2O	100, 160, 320	410	840
Sebacate.$3H_2O$	190	340	840

*Better agreement with t.g.a. data is found if the temperatures (at the base line) after the peaks are considered.

The d.t.a. curves (Fig. 5) of calcium dicarboxylates showed several endothermic peaks (below 320 °C) due to dehydration. After the dehydration, the major peak in the curves corresponds to the endothermic decomposition of the dicarboxylate to $CaCO_3$ and there is fair agreement between the results from d.t.a. (Table VII) and t.g.a. (Table VI). In the case of calcium malonate, there seems to be some evidence for an exothermic reaction after the decomposition. All the d.t.a. curves show the decomposition of $CaCO_3$ to CaO in the 840–910 °C range, again showing that $CaCO_3$ is the only residue left after the decomposition of calcium dicarboxylates. The decomposition temperature of $CaCO_3$ varies slightly from one carboxylate to another.

The t.g.a. curve of dysprosium sebacate showed that the decomposition proceeded through the formation of the oxycarbonate. There was, however, clear evidence for the loss of the elements of nonanone in the first stage of decomposition.

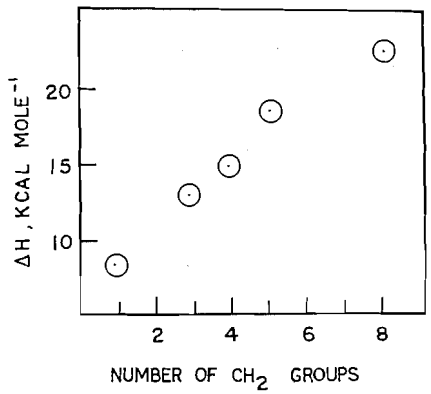

FIG. 6. Variation of ΔH of the decomposition of dicarboxylates with the number of CH_2 groups in the dicarboxylate.

By employing the endothermic decomposition peak of $CaCO_3$ as the internal standard ($\Delta H \sim 40$ kcal mole^{-1}), the enthalpies for the decomposition of calcium dicarboxylates to $CaCO_3$ were estimated by measuring the areas of the endothermic peaks. The ΔH values thus obtained show an interesting trend in the series of metal dicarboxylates (Fig. 6). The ΔH for the decomposition of dicarboxylates varies linearly with the number of methylene groups, showing an increment of $\sim$ 2 kcal per methylene group. Apparently, the enthalpy of decomposition of dicarboxylates is a thermomolecular property. This finding indicates that the organic products obtained in the decompositions of dicarboxylates are produced by the vapor phase decompositions of the elements of the ketones.

[8]Anhydrides have been found to be initially formed in the thermal decompositions of dicarboxylic acids (15).

TABLE VIII

Characterization of the products obtained by the thermal decomposition of calcium dicarboxylates

		Positions of important infrared bands, particularly in the $\nu_{C=O}$ region* (cm^{-1})			No. of peaks in v.p.c.	Some of the likely products	References†
Malonate[a]	(V)	2310 (w) 2115 (w)	1720 (m)	1640 (s)	—	Ketene[b]	
	(L)	2105 (w)	1695 (s)	1640 (s)	—	Acetic acid[b]	
Succinate[a,c]	(M)	3270 (m)	1700 (s)	1600 (s)	2[d]	1,4-Cyclohexane dione[b]	(21)
Glutarate[a]	(L)		1780 (m)	1720 (m) 1709 (s)	6–7[e]	Cyclohexanone cyclobutanone[b] acetone	(19)
Adipate	(L)		1750 (m)	1710 (s) 1646 (m)	6[f]	Cyclopentanone	(16, 20)
Pimelate[a]	(L)		1709 (s)		7[g]	Cyclohexanone	(16)
Sebacate[a]	(L)		1702 (s)		3[g,h]	[i]	

*V = vapor; L = pure liquid; M = mull in Nujol.
†Reference to the earlier literature on the thermal decomposition of calcium dicarboxylates.
[a]Also broad absorption in the OH region ($\sim$ 3200–3400 cm^{-1}). [b]Likely to be one of the products, but not very certain. [c]Semi-solid. [d]V.p.c. in diethyl ether solution. [e]V.p.c. in diethyl ether solution, some high boiling liquid insoluble in ether was left over. [f]Major fraction was cyclopentanone. [g]Major fraction was cyclohexanone. [h]More components likely to be present in the high boiling fraction. [i]Present studies cannot establish the identity of any of the compounds.

Preliminary Studies on the Characterization of the Decomposition Products

Results of a preliminary examination of the decomposition products of a few metal dicarboxylates by employing infrared spectroscopy and vapor phase chromatography are presented below.

Sufficient quantities of the products obtained by the distillation of the calcium dicarboxylates were collected and their infrared spectra were recorded; in the case of calcium malonate the spectrum of the vapors was recorded. The products were also passed through a firebrick column in a gas chromatograph. The findings from the infrared and vapor phase chromatographic experiments are summarized in Table VIII.

From the data in Table VIII it can be seen that thermal decompositions of calcium dicarboxylates give a number of products. The major components have been identified in the decomposition of some of the dicarboxylates: acetic acid from malonate, cyclopentanone from adipate, and cyclohexanone from pimelate.The formation of these products is in conformity with the early literature (16–21) on the subject and lends support to the observation that the elements of ketones are removed in the decarboxylation reaction. The variety of products formed in the decomposition, however, results from the fragmentation and subsequent reactions of the elements of ketone, many of which are likely to involve free radical mechanisms. It appears that a thorough study of the decomposition products will yield interesting results.

1. C. DUVAL. Inorganic thermogravimetric analysis. 2nd ed. Elsevier, Amsterdam. 1963.
2. A. GLASNER and M. STEINBERG. J. Inorg. Nucl. Chem. **22**, 39 (1961).
3. A. GLASNER, E. LEVY, and M. STEINBERG. J. Inorg. Nucl. Chem. **25**, 1415 (1963).
4. W. W. WENDLANDT. Thermal methods of analysis. Interscience Publishers, John Wiley and Sons, New York. 1964.
5. J. R. WITT and E. I. ONSTOTT. J. Inorg. Nucl. Chem. **24**, 637 (1962).
6. (*a*) K. ITO and H. J. BERNSTEIN. Can. J. Chem. **34**, 170 (1956). (*b*) F. VRATNY, C. N. R. RAO, and M. DILLING. Anal. Chem. **33**, 1455 (1961).
7. C. N. R. RAO. Chemical applications of infrared spectroscopy. Academic Press, New York. 1963.
8. K. NAKAMURA. J. Chem. Soc. Japan, **79**, 1411, 1420 (1958).
9. K. NAKAMOTO. Infrared spectra of inorganic and coordination compounds. John Wiley and Sons, New York. 1963.
10. K. NAKAMOTO, F. FUJITA, S. TANAKA, and M. KOBAYASHI. J. Am. Chem. Soc. **79**, 4904 (1957).
11. K. NAKAMOTO, Y. MORIMOTO, and A. E. MARTELL. J. Am. Chem. Soc. **83**, 4528 (1961).
12. (*a*) R. L. N. SASTRY, S. R. YOGANARASIMHAN, P. N. MEHROTRA, and C. N. R. RAO. J. Inorg. Nucl. Chem. **28**, 1165 (1966). (*b*) P. N. MEHROTRA. Ph.D. Thesis, Indian Institute of Technology, Kanpur, India. 1967.
13. W. W. WENDLANDT and T. D. GEORGE. Texas J. Sci. **13**, 316 (1961).
14. J. A. HILL, C. B. MURPHY, and G. P. SCHACHER. Anal. Chim. Acta, **24**, 496 (1961).

Can. J. Chem. Downloaded from www.nrcresearchpress.com by 210.87.254.105 on 09/05/12
For personal use only.

15. W. W. WENDLANDT and J. A. HOIBERG. Anal. Chim. Acta, **28**, 506 (1963); **29**, 539 (1963).
16. L. RUZICKA, W. BRUGGER, M. PFEIFFER, H. SCHINZ, and M. STOLL. Helv. Chim. Acta, **9**, 499 (1926).
17. L. RUZICKA, W. BRUGGER, C. F. SLIDEL, and H. SCHINZ. Helv. Chim. Acta, **11**, 496 (1928).
18. L. RUZICKA, M. STOLL, and H. SCHINZ. Helv. Chim. Acta, **11**, 670 (1928).
19. G. A. ROBERTSON. J. Chem. Soc. **119**, 810 (1921).
20. J. F. THORPE and G. A. R. KON. Organic synthesis. Coll. Vol. I. 2nd ed. 1941. p. 192.
21. F. FEIST. Ber. **28**, 739 (1898).

Can. J. Chem. Downloaded from www.nrcresearchpress.com by 210.87.254.105 on 09/05/12
For personal use only.

Can. J. Chem. Downloaded from www.nrcresearchpress.com by 210.87.254.6 on 09/05/12
For personal use only.

Recoil studies of the reaction $^{12}C(p,pn)^{11}C$ from threshold to 85 MeV

S. HONTZEAS[1]

Radiochemistry Laboratory, Department of Chemistry, McGill University, Montreal, Quebec

Received June 7, 1966[2]

In order to survey the features of the simple $^{12}C(p,pn)^{11}C$ reaction from threshold to 85 MeV, data were obtained for average projected ranges of ^{11}C along and perpendicular to the beam direction. The data from threshold to 45 MeV provide evidence for a large momentum transfer mechanism of the compound nucleus type. In the 45–85 MeV energy region the data were analyzed in terms of a vector model consistent with the cascade–evaporation mechanism. More detailed information regarding differential ranges and angular distributions are needed if the recoil parameters are to provide conclusive results.

Canadian Journal of Chemistry, 46, 267 (1968)

Introduction

The present study was undertaken as an initial survey of some features of the recoil properties of (p,pn) reactions in the energy range from threshold to 85 MeV. The very simple thick target – thick catcher technique was used. Similar experiments using the $^{12}C(p,pn)^{11}C$ reaction have been done by Hintz (1) in the same energy region and by Singh and Alexander (2) in the energy range between 0.25 and 6 GeV. Merz and Caretto (3) have studied the $^{65}Cu(p,pn)^{64}Cu$ reaction in the energy range 100–400 MeV by a similar technique.

The reaction $^{12}C(p,pn)^{11}C$ was chosen because, under the conditions of the experiment, ^{11}C should be the only detectable radioactive product. The identity of the ^{11}C recoil product uniquely determines the other nucleons emitted from the reaction but leaves unanswered the query as to whether these are emitted singly, as deuterons, or both.

Experimental Procedure and Results

A foil stack (Fig. 1*a*) of polyethylene targets and thick beryllium catcher foils was irradiated at various positions in the circulating beam of the McGill synchrocyclotron. In the 'forward–backward' experiments the direction of the proton beam was perpendicular to the target plane. In the 'perpendicular' experiments the direction of the proton beam was at an angle of 10° to the target plane.

Before irradiation, the catcher foils were cleaned by repeated washings in alcohol and acetone. The target foils were ~ 0.75 cm^2 in area. The catcher foils were larger (~ 1.20 cm^2 in area) and protruded in order to minimize losses from the very active leading edge of the target. While this experimental arrangement minimized these losses, account had to be taken of the fact that, in the Panontin–Sugarman equation (4) used in this work, these losses are normally neglected. Correction factors, as suggested by Panontin and Sugarman (4), were

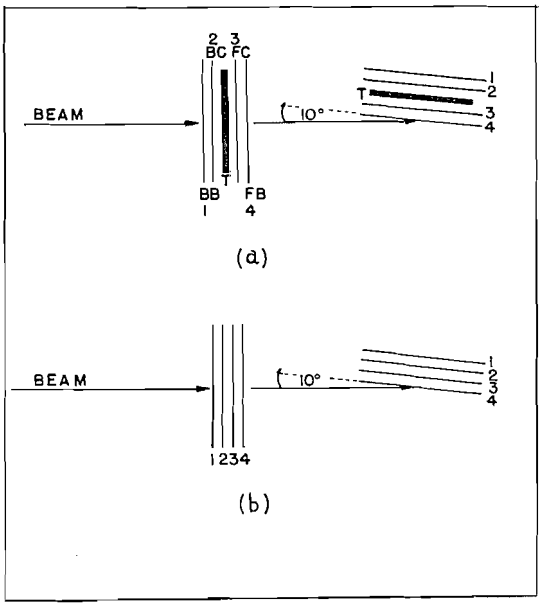

FIG. 1. Target assembly. (*a*) Experiment with target: Target assembly for bombardments that were along the beam and perpendicular to the beam direction. (*b*) Experiment without target: Be foils assembly for bombardments that were along the beam and perpendicular to the beam direction.

[1]Present address: Division of Natural Sciences, University of Saskatchewan, Regina Campus, Regina, Saskatchewan.

[2]Revised manuscript received July 25, 1967.

Can. J. Chem. Downloaded from www.nrcresearchpress.com by 210.87.254.6 on 09/05/12
For personal use only.

TABLE I

Activation correction in a typical ^{11}C recoil experiment

Bombarding energy in MeV (lab)	Sample	Order number	Type	Count rate at end of bombardment (c.p.m.)	Count rate corrected for activation (c.p.m.)	F (%)	B (%)	FW ($\mu g/cm^2$)	BW ($\mu g/cm^2$)	Count rate corrected for activation using exp. without target (c.p.m.)	F (%)	B (%)	FW ($\mu g/cm^2$)	BW ($\mu g/cm^2$)
Experiment with Target														
	Backward Blank	1	Be	4.3×10^3										
35	Backward Catcher	2	Be	7.6×10^3	3.3×10^3		0.14		11.50	3.66×10^3		0.143		11.90
	Target	3	P*	2.4×10^6										
35	Forward Catcher	4	Be	1.5×10^5	1.44×10^5	5.65		466		1.43×10^5	5.60		462	
	Forward Blank	5	Be	6×10^3										
Experiment without Target														
	Backward Blank	1	Be	4.2×10^4										
35	Backward Catcher	2	Be	3.85×10^4										
	Forward Catcher	3	Be	5.40×10^4										
	Forward Blank	4	Be	8.10×10^4										
Experiment with Target														
	Backward Blank	1	Be	1.43×10^4										
	Backward Catcher	2	Be	2.40×10^4	9.7×10^3		0.26		21.5	1.08×10^4		0.29		24.5
75	Target	3	P*	3.5×10^6										
	Forward Catcher	4	Be	1.53×10^5	1.34×10^5	3.7		305		1.35×10^5	3.6		297	
	Forward Blank	5	Be	1.9×10^4										
Experiment without Target														
	Backward Blank	1	Be	1.90×10^4										
75	Backward Catcher	2	Be	1.75×10^4										
	Forward Catcher	3	Be	1.66×10^4										
	Forward Blank	4	Be	2.5×10^4										

*P = polyethylene.

Can. J. Chem. Downloaded from www.nrcresearchpress.com by 210.87.254.6 on 09/05/12
For personal use only.

determined at bombarding energies of 24, 55, and 85 MeV and a correction factor of 0.984 ± 0.001 was used to correct for this effect.

After irradiation, the targets and catcher foils were separately mounted on cardboard cards and covered with thin (0.00025 in.) plastic sheet. The most active areas of the foils were centered on the cardboard trays and the side of the beryllium catcher foils that faced the target was mounted towards the counters. The relative activities of the polyethylene targets and beryllium catcher foils were determined with the aid of two end-window proportional β-counters. The relative efficiencies of these two counters were found to differ by less than 2% and day-to-day performance was normalized with a standard source of ^{36}Cl.

In the polyethylene samples, activity attributable only to ^{11}C was found. In the beryllium samples, additional activities with a 3–4 h half-life were found. These were small ($\sim$ 1% of the initial ^{11}C activity) and the decay curves were easily resolvable. The ^{11}C decay curves were extrapolated and the activities in the target and catchers determined at the end of bombardment. The relative counting efficiency of ^{11}C in the plastic targets and beryllium catchers was determined with a positron coincidence counter (calibrated with a ^{22}Na source). The relative efficiency of the plastic targets to the catchers was found to be 1.026 ± 0.044.

A correction had to be made for 'hot-atom' loss (2, 5) of ^{11}C from the plastic targets. The Brookhaven group had found (5) that the loss from polyethylene of 7–10 mg/cm^2 superficial density was 14 ± 3%. Since the same type of polyethylene was used in this experiment the above value was employed, giving a correction factor of 0.86 ± 0.03.

The correction factors for counting efficiency, edge effect, and hot-atom loss were combined to give an overall correction factor of 0.87 ± 0.05.

Although the beryllium was said to be free of traces of carbon, this was found not to be the case. During the progress of the experiment two different qualities of beryllium foils were used. The first quality of foil was found to be richer in C traces than the second one. This is indicated in Table I by the difference in the counting rates in the blanks at 75 and 35 MeV where the two different sets of beryllium foils were used. In general, the fraction of the total activity collected in the backward catcher becomes smaller as the bombarding energy decreases to the reaction threshold. Thus at low energies the correction for activation is extremely important. Table I shows a typical forward–backward experiment with and without target at bombarding energies of 35 and 75 MeV. In the experiment with the target, it can be seen that the fractions of the total activity collected in the forward catchers are 5.6% and 3.7% at 35 and 75 MeV respectively. The fractions of the total activity collected in the backward catchers are only 0.14% and 0.26% at 35 and 75 MeV respectively. It can also be seen that the ratios of activities found in the backward catchers to the backward blanks (inserted for activation correction for carbon impurities in the beryllium) were 1.76 and 1.66 at 35 and 75 MeV respectively. The fact that the activation correction was such a large fraction of the total activity would have introduced very large errors and the following technique was adopted to improve the situation.

A preliminary experiment was performed at each bombarding energy with no plastic target and only the four beryllium foils in place (Fig. 1*b*). Subsequent irradiations were carried out at each energy with the beryllium foils in the same position in the target stack but with a polythene target introduced between the second and third foils (Fig. 1*a*). The two experiments were normalized for variations in beam intensity with respect to the first beryllium foil. It can be seen from Table I, in the blank experiment, that the activity of ^{11}C fluctuates from foil to foil, showing a strong dependence on the position of the foil in the target stack. That this difference is associated with secondary effects, determined by the foil position, was clearly shown by reversing the order of the foils. To compensate for this effect after normalization of the beam intensity, the normalized count rate for the second foil in the blank experiment was used for the activation correction. This method of correction has the effect of slightly increasing the values of the backward fraction B.

The effective forward range is defined (2) as the sum of the projections along the beam axis of the ranges of the nuclei recoiling forward, divided by the total number of recoils. It is given by the product FW where F is the fraction of the ^{11}C activity observed in the forward catcher and W is the target thickness. Similarly the backward

TABLE II

Corrected recoil data for edge effect, hot-atom loss, and relative counting efficiency

Bombarding energy in MeV (lab)	FW (μg/cm^2)	BW (μg/cm^2)	$2PW$ (μg/cm^2)	FW/BW
25	260±9	8.5±2.0	105±7	30.5±.5
35	311±18	12.05±1.50	129±9	25.9±1.0
45	350±15	19.8±4.0	162±9	17.6±.5
55	323±27	16.25±2.50	221±22*	19.8±1.1
65	279±15	21.9±2.0	210±13	12.7±.4
75	251±9	21.9±2.0	232±19	11.4±.3
85	249±1	21.9±2.0	263±18	11.3±.2
Spread ±2%				

*Large error due to counter difficulties.

effective range is given by BW. The effective perpendicular range is expressed by $2PW$, where P is the average fraction of the total ^{11}C activity observed in the two beryllium catchers (front and back) for irradiations with the target plane at 10° to the beam direction.

At each bombarding energy four to eight experiments were performed for the forward–backward experiments, four at 25 and 45 MeV and two at each other energy, for those experiments designed to give the perpendicular effective ranges. The data with the estimated errors are shown in Table II and plotted in Fig. 2. At higher bombarding energies, the data of Singh and Alexander (2) are shown for purposes of comparison and extrapolate well from the present data.

Analysis of the Recoil Data

To analyze the data, it is necessary to know the effects of scattering of the recoil atoms and the relationship between range and energy.

Very little quantitative information is available (6, 7) about scattering effects which, in the present experiments, are not negligible. Alexander and Gazdik (7) have shown that scattering effects in fission experiments cause errors in the effective ranges as high as 5%. Singh and Alexander (2) pointed out that these errors are caused by preferential scattering of recoils out of a target of heavy atoms into a catcher of much lighter atoms. In the present experiment, as in ref. 2, scattering effects are much greater because the average recoil velocity is much less than that of fission products (6, 7). However, the number of recoils scattered into and out of the target foil should be similar because the masses of the target and catcher are almost similar. In such a case, if it is assumed that the recoils followed a straight path, the deviations from this path are identical.

Recently Lindhard *et al.* (8) developed a theory of energy loss from electronic and nuclear stopping. They defined the dimensionless quantities

$$[1]\quad \rho = \frac{4\pi a^2 NRA_1A_2}{(A_1+A_2)^2} \text{ and } \epsilon = \frac{aEA_2}{Z_1Z_2e^2(A_1+A_2)},$$

where the subscripts 1 and 2 refer to the recoiling particle and stopping material respectively, and A = mass number, Z = atomic number, N = number of atoms per cc of stopping material, and $a = 0.8853a_0(Z_1^{2/3}+Z_2^{2/3})^{-1/2}$, where a_0 = Bohr radius, E = energy of the recoiling particle, R = range of the recoiling particle, and e = electronic charge.

The total energy loss is given by

$$[2]\qquad \left(\frac{d\epsilon}{d\rho}\right)_{\text{Total}} = \left(\frac{d\epsilon}{d\rho}\right)_n + \left(\frac{d\epsilon}{d\rho}\right)_e,$$

where $(d\epsilon/d\rho)_n$ is the energy loss from nuclear stopping and $(d\epsilon/d\rho)_e$ is the energy loss from electronic stopping. The concept of extrapolated electronic range for large values of E, where electronic stopping is dominant, is introduced by Lindhard *et al.* (8) and is given by

$$\rho_e(\epsilon) = \rho(\epsilon) + \Delta(k,\epsilon) = (2/k)\epsilon^{1/2},$$

where $\Delta(k,\epsilon)$ is the reduction of range due to nuclear stopping and $\rho(\epsilon)$ is the true range.

In the system under consideration the constant $k = 0.11$ is determined by the theory of Lindhard *et al.*

Can. J. Chem. Downloaded from www.nrcresearchpress.com by 210.87.254.6 on 09/05/12
For personal use only.

Can. J. Chem. Downloaded from www.nrcresearchpress.com by 210.87.254.6 on 09/05/12
For personal use only.

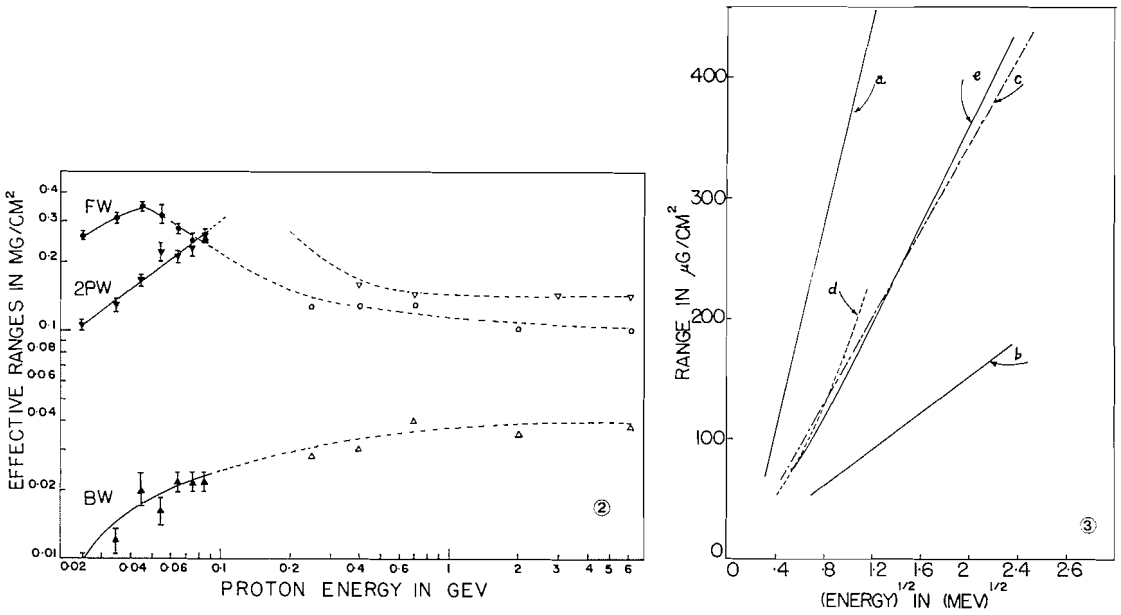

FIG. 2. Effective ranges vs. proton energy: *FW* (●) this work, (○) Singh and Alexander (2); *2PW* (▼) this work, (▽) Singh and Alexander (2); *BW* (▲) this work, (△) Singh and Alexander.

FIG. 3. Theoretical and semi-empirical range–energy relationships: (*a*) ^{11}C ranges in ^{12}C calculated using theory of Lindhard *et al.* (8); (*b*) ^{11}C ranges in H_2 calculated using theory of Lindhard *et al.* (8); (*c*) ^{11}C ranges in $-(CH_2)_n-$ calculated from (*a*) and (*b*) using the equation of Domeij *et al.* (9); (*d*) ^{11}C ranges in $-(CH_2)_n-$ calculated with the help of the semi-empirical equation of Singh and Alexander (2), $R = 0.176E^{0.8}$; (*e*) ^{11}C ranges in $-(CH_2)_n-$ calculated from the equation $R = 0.156E^{0.6}$.

The values of $\rho(\epsilon)$ obtained need a correction (8) which amounts to $\sim 10\%$ in the energy region of interest if they are to be compared with the projected ranges.

Ranges of ^{11}C in ^{12}C and ^{11}C in hydrogen were calculated for the energy region of interest and are presented in Figs. 3*a* and 3*b* respectively. Ranges of ^{11}C in polyethylene were estimated from curves *a* and *b*, using the equations proposed by Domeij *et al.* (9), and are given in Fig. 3*c*.

In analyzing the data a range–energy relationship is required in which the range is expressed as proportional to the *N*th power of the velocity of the recoil product, i.e.

$$[4] \qquad R = KV^N_{\text{lab}} = K'E^{N/2}.$$

The constants K' and N may be determined from experimental data, but experimental values of ^{11}C ranges in polyethylene are not yet available in the energy region of interest.

Singh and Alexander (2) determined experimentally the range–energy relationship

$$R = 0.213E^{0.8}$$

for ^{11}C recoils in polystyrene for values of E up to 0.6 MeV. The same authors also measured the ratio of ranges of ^{11}C in polystyrene and polyethylene and found a value of 0.83. On this basis a range–energy equation

$$[5] \qquad R = 0.176E^{0.8}$$

was determined for ^{11}C in polyethylene for values of E up to 0.6 MeV. Values of ^{11}C ranges in polyethylene predicted by eq. [5] are plotted in Fig. 3*d*.

Extrapolation of the curve resulting from eq. [5] up to 1 MeV gives results in very good agreement with the theoretical curve 3*c*. Discrepancies with the theory (8) of 20–30% are reported by Panontin *et al.* (10) for ^{11}C ranges in aluminium for values of E in the region of ~ 0.65–1.65 MeV.

The most probable explanation of discrepancies with the theory found by Panontin may be obtained from the results of Ormrod *et al.* (11). These authors have shown that the dependence of electronic stopping power on the atomic

Can. J. Chem. Downloaded from www.nrcresearchpress.com by 210.87.254.6 on 09/05/12
For personal use only.

number of the projectile oscillates on either side of the theoretically predicted curve by as much as 30%.

In the absence of experimental ^{11}C ranges in polyethylene in the region 1–5 MeV the range–energy equation

$$[6] \qquad R = 0.156E^{0.6}$$

was determined from the curve in Fig. 3*c* and used in the analysis of the data with the understanding that values for ranges are predicted with an error of the order of 30%, as the data of Panontin *et al.* (10) have indicated.

The range–energy equation [6] is plotted in Fig. 3*e*. The data are now analyzed by considering the following.

A. Compound Nucleus Mechanism for the Reaction $^{12}C(p,pn)^{11}C$

The experimental ranges are compared with values expected, assuming complete momentum transfer of the incident particle to the struck nucleus.

In such a case, in the center-of-mass system, the outgoing particles are emitted symmetrically about 90° to the beam direction. Since in the bombarding energy region of interest the amount of recoils in the backward direction is very small compared with that in the forward direction, FW is a measure of v, the velocity along the beam direction imparted to the recoil by the incident particle.

Winsberg and Alexander (12) pointed out that a correction due to the velocity imparted to the recoil by particle evaporation is important where the range is not proportional to velocity.

For $N = 1.2$ the Winsberg and Alexander expression becomes

$$[7] \qquad FW = R_0\left(1 + 0.12\frac{E_e}{E_{cn}}\right),$$

where E_e is the average kinetic energy imparted to the recoil in the evaporation system due to evaporation, E_{cn} is the energy that the recoil product would have after complete momentum transfer, and R_0 is the range which corresponds to v only.

The values of E_e and E_{cn} are obtained from the equations given by Winsberg and Alexander (12)

$$[8] \quad E_e = \left[\frac{E_b A_t}{A_{cn}} + Q\right]\frac{\bar{n}}{A_R} \qquad \text{and}$$

$$E_{cn} = \frac{E_b A_b A_R}{(A_b + A_t)^2},$$

where E_b is the energy of the bombarding particle, A_b, A_R, A_{cn}, and A_t are the mass numbers for the bombarding particle, recoil product, compound nucleus, and target respectively, Q is the energy released in the reaction and $\bar{n}$ is the average number of nucleons per evaporating particle.

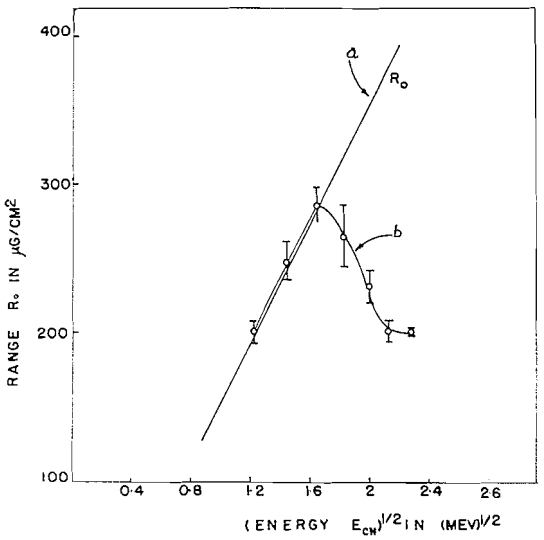

FIG. 4. Average range R_0 vs. $(E_{cn})^{1/2}$: (*a*) Range energy curve expressing R_0 corresponding to $v_{||}$ only and calculated from the equation $R_0 = 0.156E^{0.6}$. (*b*) Average range R_0 of ^{11}C in —$(CH_2)_n$— after being corrected for the effect of the recoil due to evaporation. R_0 values are plotted vs. $(E_{cn})^{1/2}$ where E_{cn} is the kinetic energy the recoil would have assuming full momentum transfer.

In the present experiment, it was assumed that a single nucleon is evaporated ($\bar{n} = 1$).

The values of R_0, calculated from the data after corrections were made according to eq. [7], are plotted in Fig. 4 and compare with R_0 estimated from eq. [6] using the E_{cn} values for energy.

If the assumption for compound nucleus formation is correct, the R_0 values calculated from the data should fall on the energy–range curve. As can be seen in Fig. 4, the agreement up to a bombarding energy of 45 MeV is very good. This of course is not indubitable evidence that the range–energy curve for ^{11}C in polyethylene is the correct one and only an experimentally determined range–energy curve could clarify this matter. However, the above analysis does show that, from the threshold to 45 MeV, ^{11}C is produced mainly by a compound nucleus type of reaction (large momentum transfer).

TABLE III

Recoil data for $W(\theta) = 1$ and $v_\perp = 0$

Bomb. energy (MeV)	$n_\parallel = (v_\parallel/V)$	$v_\parallel$, impact velocity (MeV/c)(a.m.u.)$^{-1}$	Forward–backward exp.		Perpendicular exp.	
			V (MeV)$^{1/2}$	R (μg/cm^2)	V (MeV)$^{1/2}$	R (μg/cm^2)
55	0.726	2.17	2.70	422	3.25	431
65	0.651	1.83	2.49	390	3.14	411
75	0.414	1.55	3.55	555	3.49	468
85	0.158	1.31	9.23	1440	3.80	568

TABLE IV

Recoil parameters for $W(\theta) = a + b\cos^2\theta$ and $v_\perp = 0$

Bomb. energy (MeV)	$n_\parallel = (v_\parallel/V)$	$v_\parallel$ (MeV/c)(a.m.u.)$^{-1}$	b/a	$W(90°)/W(0°)$	Forward–backward exp.		Perpendicular exp.	
					V (MeV)$^{1/2}$	R (μg/cm^2)	V (MeV)$^{1/2}$	R (μg/cm^2)
25	0.705	1.79	4.02	0.20		320		
35	0.720	2.08	4.23	0.19		373		
45	0.630	2.23	2.76	0.26	3.55	477	2.95	374
55	0.504	2.06	0.65	0.60	4.10	566	2.96	379
65	0.490	1.76	0.46	0.68	3.60	488	2.95	375
75	0.430	1.58	−0.26	1.35	3.68	498	2.75	350
85	0.425	1.57	−0.88	8.35	3.71	503		

B. Vector Analysis

In order to account for the possible mechanism at energies higher than 45 MeV, an attempt is made to fit the data to a set of vectors shown in Fig. 5.

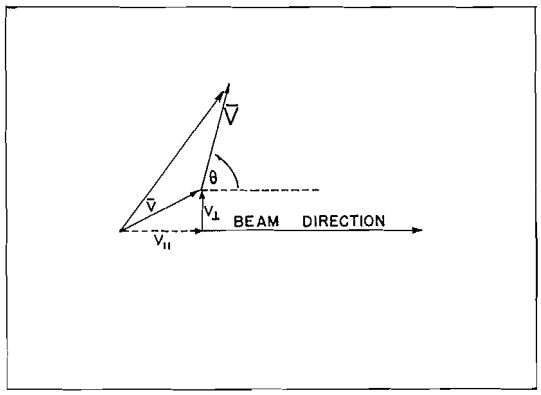

FIG. 5. Diagram of vectors used in the analysis of the data: **v** represents the knock-on kick with components $v_\parallel$ parallel and $v_\perp$ perpendicular to the beam direction; **V** represents the evaporation kick, and θ the angle of the recoil with respect to the beam direction, in the system of the struck nucleus. V accidently lies in the $v_\parallel$–$v_\perp$ plane.

This set of vectors is consistent with the basic cascade–evaporation model. The vector **v** represents the average velocity of the struck nucleus as a result of the knock-on cascade. The components $v_\parallel$ and $v_\perp$ of **v** are parallel and perpendicular to the beam direction respectively. In the moving system, the excited struck nucleus evaporates neutrons. The angle θ is the angle of the recoil with respect to the beam in the system of the struck nucleus. The average velocity imparted to the recoil in the system of the struck nucleus is represented by the vector **V**, which may have an isotropic ($W(\theta) = 1$) or an anisotropic ($W(\theta) = a + b\cos^2\theta$) distribution.

Since we are not dealing with a compound type of reaction, the struck nucleus is not the center of mass. Therefore the parameters used in the analysis are **v**, the knock-on kick, and b/a the anisotropy of the evaporation kick. These parameters may be calculated from the data using the Sugarman equations quoted in ref. 13. The equations assume straight recoil paths, and the range R is proportional to the Nth power of velocity. For the value $N = 1.2$ used in this paper, the equations in ref. 13 are reduced to

$$[9a]\quad FW + BW = R[0.5 + b/12a + n_\parallel^2(0.615 - 0.155b/a) + n_\perp^2(0.03 + 0.01b/a)]$$

$$[9b]\quad FW - BW = R[1.07n_\parallel + 0.01b/an_\parallel]$$

$$[9c]\quad FW + BW - 2PW = R[b/8a + n_\parallel^2(0.585 - 0.145b/a) - n_\perp^2(0.295 + 0.03b/a)],$$

Can. J. Chem. Downloaded from www.nrcresearchpress.com by 210.87.254.6 on 09/05/12
For personal use only.

TABLE V

Recoil parameters for $(b/a) = 0$ and $(b/a) = -0.26$

Bomb. energy (MeV)	$(v_\parallel/V) = n_\parallel$	$(v_\perp/V) = n_\perp$	$v_\parallel$ impact velocity (MeV/c) (a.m.u.)$^{-1}$	V (MeV)$^{1/2}$	R (μg/cm^2) corresponding to V only
			$(b/a) = 0$		
75	0.602	0.570	1.69	2.81	356
85	0.572	0.715	1.67	2.92	372
			$(b/a) = -0.26$		
75	0.537	0.470	1.70	3.17	398
85	0.544	0.710	1.65	3.04	380

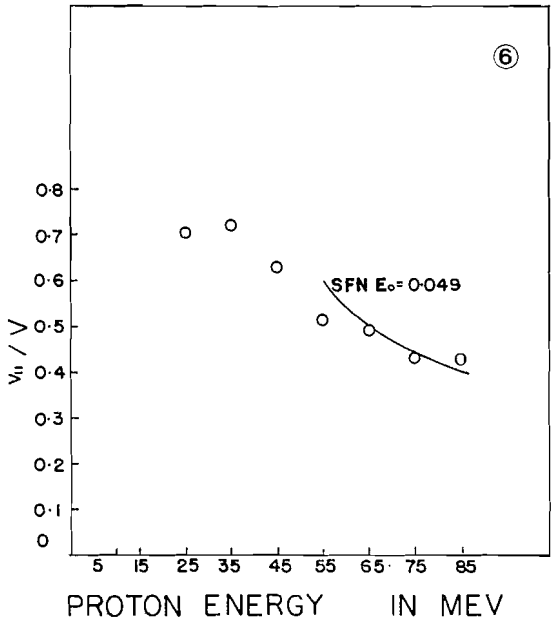

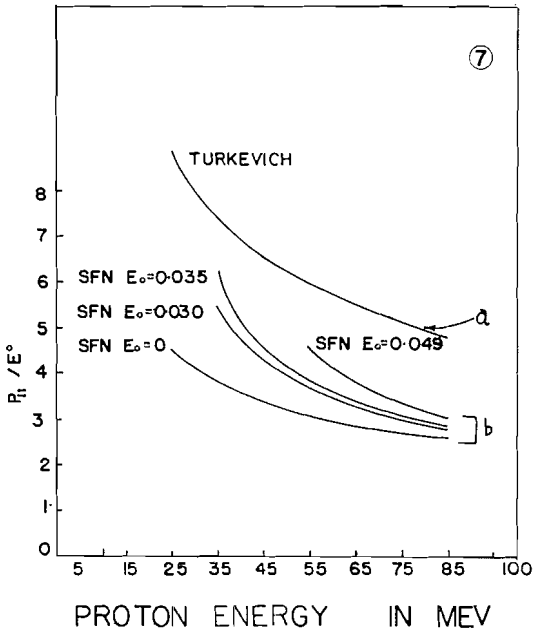

FIG. 6. Recoil parameter $n_\parallel$ vs. proton energy: (○) represents $n_\parallel = (v_\parallel/V)$ values calculated from the data (Table II) using eq. [9] and assuming $v_\perp = 0$, $W(\theta) = a + b\cos^2\theta$. The solid line was calculated from eq. [10a] and fits the data for $E_0 = 0.049$ nucleon units.

FIG. 7. $p_\parallel/E_0$ parameter vs. proton energy. (*a*) Curve obtained using eq. [11a] (Turkevich mechanism). (*b*) Calculated s.f.n. curves from eq. [10a] for different values of E_0.

where $n = v_\parallel/V$, $n = v_\perp/V$, and R = range in the target. This set of equations relate the experimental data to the two normalized parameters $n_\parallel = v_\parallel/V$ and $n_\perp = v_\perp/V$ and leaves one of the parameters undetermined, unless detailed experiments provide values for R or b/a.

The values of FW, BW, and $2PW$ from Table II are used, and eqs. [9] were solved assuming $n_\perp = 0$ for cases in which $W(\theta) = 1$ and $W(\theta) = a + b\cos^2\theta$. The results are shown in Tables III and IV respectively.

In the present experiment, the parameter $n_\parallel = v_\parallel/V$ is weighted according to R and, since N is closed to unity, $(N = 1.2)$, $\langle n_\parallel R\rangle/\langle R\rangle = \langle v_\parallel\rangle/\langle V\rangle$. In Table IV it is shown that R is not sensitive to energy in the bombarding region of interest (55–85 MeV) and is essentially constant. (At 55 MeV, R appears to be about 10% higher, but this is certainly due to the large experimental error which was introduced by counter difficulties (see Table II).

An average range $\langle R\rangle \sim 491$ μg/cm^2 is esti-

Can. J. Chem. Downloaded from www.nrcresearchpress.com by 210.87.254.6 on 09/05/12
For personal use only.

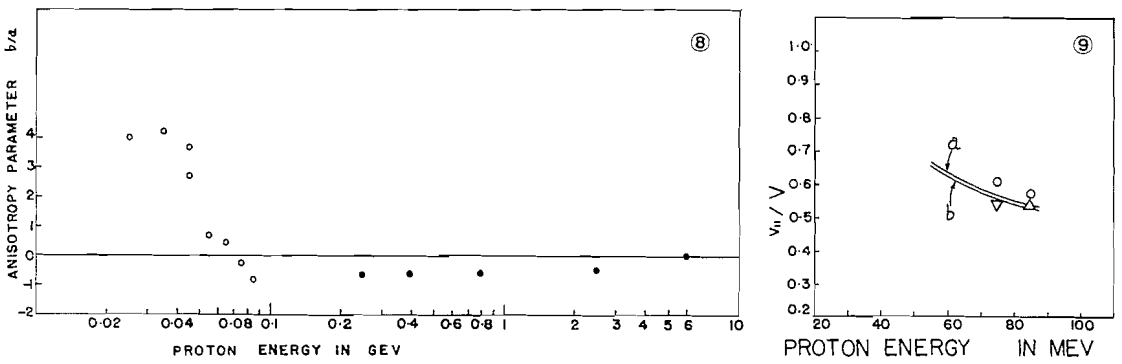

FIG. 8. Calculated from the data anisotropy parameter b/a vs. proton energy: (●) present work, (○) Singh and Alexander (2).

FIG. 9. Recoil parameter $n_{\parallel} = (v_{\parallel}/V)$ vs. proton energy: Solid line *a*, calculated values of $n_{\parallel}$ using eq. [11*a*] [$k = 0.117$]. (△) Data from Table V [$(b/a) = -0.26$]. Solid line *b*, calculated values of $n_{\parallel}$ using eq. [11*a*] [$k = 0.109$]. (○) Data from Table V [$(b/a) = 0$].

mated for the 55–85 MeV energy region corresponding to $\langle V \rangle$ only (evaporation kick), where $\langle V \rangle \sim 2.58$ MeV$^{1/2}$.

(a) Single Fast Nucleon Mechanism

A simple mechanism which is consistent with these features is the single fast nucleon mechanism (14) (s.f.n.). This mechanism assumes that the incident nucleon passes through the nucleus undeviated, but deposits energy E_0.

The s.f.n. mechanism is stated analytically (14, 15) in terms of the momentum imparted to the recoil.

$$[10a] \qquad p_{\parallel} = \frac{2EE_0}{p + (p - 2EE_0)^{1/2}}$$

$$[10b] \qquad p_{\perp} = 0,$$

where p and E are the momentum and total energy of the incident particle in m_0c and m_0c^2 natural units respectively.

Since V is a constant [$\langle V \rangle = 3.70$ MeV$^{1/2}$ ~ 0.034 c units, Table V], the quantity $n_{\parallel} = v_{\parallel}/V$ is a measure of $p_{\parallel}$ in the energy region of interest (55–85 MeV). The second equation of set [10] is consistent with the assumption $v_{\perp} = 0$ used to solve the set of eqs. [9]. The $v_{\parallel}/V$ values from Table IV are plotted in Fig. 6. The ratio $p_{\parallel}/E_0$, calculated from eq. [10*a*] for various values of E_0 ($E_0 = 0$, $E_0 = 0.03$, $E_0 = 0.049$), is plotted in Fig. 7.

The curve in Fig. 6 which fits the $v_{\parallel}/V$ data was calculated from eq. [10*a*] for $E_0 = 0.049 m_0c^2 = 45.90$ MeV.

Thus, according to the s.f.n. mechanism, the forward momentum of the recoil was explained in terms of constant deposition of energy for those knock-on cascades that would lead to ^{11}C at bombarding energies of 65–85 MeV. The reason for constant deposition energy is that the forward deposition momentum decreases initially as $E^{-1/2}(\Delta p \propto E^{-1/2}\Delta E)$ with increasing bombarding energy, while the backward deposition momentum increases. In these terms the falloff of the *FW* curve in Fig. 2 is explained, as well as the rise of the *BW* curve. The relativistic extension of the $p^2 = 2mE$ equation predicts the flattening out at higher energies, in agreement with experiment (Fig. 2). The rising of the *2PW* curve may be explained as indicating the importance of the cascade–evaporation mechanism in the energy region of interest.

The anisotropy parameter b/a decreases as energy increases (see data of Table IV plotted in Fig. 8) and assumes negative values at 75 MeV bombarding energy. The magnitude of the b/a values obtained from the analysis of the data in Fig. 8 is rather high. The s.f.n. mechanism cannot account for the negative values of b/a and will be discussed later.

This mechanism also does not take into account the effect of Fermi motion (because collisions with stationary nucleons in the nucleus are considered), although this effect will cause a distribution in the momentum of the recoil which may add to the deposition of energy unless the struck particle is subsequently captured (15).

(b) Turkevich Mechanism

In order to complete the survey of the features of the reaction at the energy region of interest,

Can. J. Chem. Downloaded from www.nrcresearchpress.com by 210.87.254.6 on 09/05/12
For personal use only.

Can. J. Chem. Downloaded from www.nrcresearchpress.com by 210.87.254.6 on 09/05/12
For personal use only.

the application of the mechanism proposed by Turkevich (quoted in refs. 15 and 16) was attempted.

This mechanism assumes that the incident nucleon scatters elastically off one nucleon in the nucleus and escapes from the nucleus, giving a (p,p′) knock-on cascade. The struck nucleon is captured by the nucleus converting its kinetic energy E_0 into deposition energy $E_0\,(A-1)/A$ and recoil, and momentum p into recoil momentum p.

The deposition of momentum parallel and perpendicular to the beam is given by

$$[11a] \qquad p_{\parallel} = \left[1 + \frac{2}{E}\right]^{1/2} E_0$$

$$[11b] \qquad p_{\perp} = \left[(2/E_0) - \left(1 + \frac{2}{E}\right)\right]^{1/2} E_0$$

where E is the bombarding energy in nucleon units. The components of the deposition momentum are related with the quantities $n_{\parallel} = v_{\parallel}/V$ and $n_{\perp} = v_{\perp}/V$ respectively (provided V is constant), which can be calculated from the data in Table II using eqs. [9].

In this respect, for $W(\theta) = 1$, eqs. [9] are applicable at bombarding energies of 75 and 85 MeV only. Although the estimated b/a values in Table V are rather high, the value $b/a = -0.26$ was used to solve eqs. [9] for $W(\theta) = a + b \cos^2 \theta$.

It is interesting that the inclusion of a negative anisotropy of such magnitude has no appreciable effect on the results, as indicated in Table V.

Only an average value of $\langle R \rangle$ corresponding to $\langle V \rangle$ can be extracted from the data in Table V. This value amounts to 0.39 mg/cm^2 and 0.36 mg/cm^2 for $b/a = 0$ and $b/a = -0.26$ respectively. The inclusion of anisotropy lowers the average value of $\langle R \rangle$ by 10%. Equation [11a] is plotted in Fig. 7a, and the curve obtained is very different from the calculated curve, using the s.f.n. mechanism. The parameters $n_{\parallel}$ and $n_{\perp}$ from Table V are plotted in Fig. 9 (for $b/a = 0$ and $b/a = -0.26$). The same value for both cases is obtained for $E_0 \propto \langle V \rangle = 30.9$ MeV.

If the kinetic energy acquired by the struck nucleus is taken into account, 28.30 MeV is left as deposition energy.[3] This low energy transfer predicted by the Turkevich mechanism may be due to the fact that only elastic collisions are considered. Low energy transfer is consistent with the assumed negative anisotropy (17), but it is not consistent with a situation where $W(\theta) = 1$.

Halpern (17) has proposed a mechanism to explain the negative anisotropy observed in fission experiments induced by high energy particles. This mechanism, as Poskanzer *et al.* (15) pointed out, may be considered an extension of the Turkevich mechanism. The negative anisotropy observed is explained if the collisions occur preferentially in a region of the nucleus where the struck nucleon is moving preferably perpendicular to the beam. With the calculated value of E_0, eq. [11b] predicts values of 0.62 and 0.65 for $\langle n_{\perp} \rangle = v_{\perp}/V$ at 75 and 85 MeV respectively. This means that the Turkevich mechanism predicts the recoil should travel at a very large angle to the incident beam (but less than 90°). The shape of the $2PW$ curve (Fig. 2) and the $n_{\perp}$ [for $W(\theta) = a + b \cos^2 \theta$] values of Table V are in fair agreement with this prediction of the Turkevich mechanism. However, it should be borne in mind that the analysis of the data, assuming $W(\theta) = 1$, leads to the same results. Thus the Turkevich mechanism does not give a unique answer and the situation cannot really be dissolved unless the thick-target data are reanalyzed in the light of experimental values obtained for R and b/a from differential range and angular distribution experiments.

Acknowledgments

The author wishes to thank Prof. N. T. Porile for suggesting this work and for encouragement during the course of it, Prof. L. Yaffe for continuous interest and support and for reading and correcting the manuscript, and Prof. R. E. Bell, Director of the Foster Radiation Laboratory at McGill University, for permission to use the cyclotron facilities.

1. N. M. Hintz. Phys. Rev. **86**, 1042 (1952).
2. J. Singh and J. M. Alexander. Phys. Rev. **128**, 711 (1962).
3. E. R. Merz and A. A. Caretto, Jr. Phys. Rev. **126**, 1173 (1962).
4. J. A. Panontin and N. Sugarman. J. Inorg. Nucl. Chem. **25**, 132 (1963).
5. J. B. Cumming, A. M. Poskanzer, and J. Hudis. Phys. Rev. Letters, **6**, 484 (1961).
6. J. Niday. Phys. Rev. **121**, 1471 (1961).

[3]The separation energy of a neutron from ^{12}C is about 18.3 MeV. This leaves an amount of about 10 MeV for γ-deexcitation ($\sim$ 5 MeV) and only about 5 MeV for the kinetic energy of one particle and recoil energy.

7. J. M. ALEXANDER and M. GAZDIK. Phys. Rev. **120**, 874 (1960).
8. J. LINDHARD, M. SCHARFF, and H. E. SCHIOTT. Kgl. Danske Videnskab. Selskab Mat. Phys. Medd. **33**, No. 14 (1963).
9. B. DOMEIJ, F. BROWN, J. A. DAVIES, and M. MCCARGO. Can. J. Phys. **42**, 1624 (1964).
10. J. A. PANONTIN, L. L. SCHWARTZ, A. F. STEHNEY, E. P. STEINBERG, and L. WINSBERG. Phys. Rev. **140**, A151 (1965).
11. J. H. ORMROD, J. R. MACDONALD, and A. E. DUCKWORTH. Can. J. Phys. **43**, 275 (1965).
12. L. WINSBERG and J. M. ALEXANDER. Phys. Rev. **121**, 518 (1961).
13. J. A. PANONTIN. Ph.D. Thesis, Part II, University of Chicago, Chicago, Illinois.
14. S. C. FUNG and I. PERLMAN. Phys. Rev. **87**, 622 (1952).
15. A. M. POSKANZER, J. B. CUMMING, and R. WOLFGANG. Phys. Rev. **129**, 374 (1963).
16. N. T. PORILE and N. SUGARMAN. Phys. Rev. **107**, 1410 (1957).
17. I. HALPERN. Nucl. Phys. **11**, 522 (1959).

Can. J. Chem. Downloaded from www.nrcresearchpress.com by 210.87.254.6 on 09/05/12
For personal use only.

Reaction between iodine and sodium bromate

D. E. C. KING AND M. W. LISTER
Department of Chemistry, University of Toronto, Toronto, Ontario

Received July 18, 1967

The mechanism of the reaction: $I_2 + 2BrO_3^- \rightarrow Br_2 + 2IO_3^-$ in aqueous solution (pH 1.5 to 2.5) at 25 °C has been investigated. It is found to go in four stages. Firstly, there is an induction period during which the acidified bromate produces a catalyst (probably HOBr) for the next stage. However, iodide ions, if present, destroy this catalyst. Secondly, iodine reacts by the overall equation, $I_2 + BrO_3^- \rightarrow IBr + IO_3^-$, at a rate proportional to $[H^+]^2[BrO_3^-]^2$. Thirdly, the iodine bromide reacts by the overall equation, $3IBr + 2BrO_3^- + 3H_2O \rightarrow 5Br^- + 3IO_3^- + 6H^+$, at a rate proportional to $[Br]^2[BrO_3^-]^2$. Finally bromide and bromate ions react to give bromine. Mechanisms are suggested for the various stages, and some of the rate constants are evaluated.

Canadian Journal of Chemistry, **46**, 279 (1968)

Can. J. Chem. Downloaded from www.nrcresearchpress.com by 210.87.254.42 on 09/05/12
For personal use only.

Iodine is known (1) to displace bromine from aqueous bromate solutions, although, of course, the displacement is the other way around in halide solutions. The total reaction, which is

$$I_2 + 2BrO_3^- \rightarrow Br_2 + 2IO_3^-,$$

can be expected to go in a number of steps, since it is unlikely that so many oxygen atoms would be transferred in a single stage. It seemed therefore to be of interest to investigate the mechanism of this reaction, especially as it might be expected to yield more information on oxy-halogen reactions in general. As will be seen in what follows, the reaction did indeed prove to be complicated, and although the mechanism has been elucidated to a considerable extent, only rather speculative proposals can be put forward for certain parts of the reaction.

Experimental

The experiments in general consisted of mixing aqueous solutions of iodine and sodium bromate, with added phosphoric acid and sodium dihydrogen phosphate as a pH buffer. The pH of the reaction mixture was in the range of 1.5 to 2.5; and was measured on a Beckman 101900 Research pH meter using a glass electrode, Beckman 40498, in the usual way. The pH reading was calibrated by means of a potassium tetroxalate buffer (pH 1.68) but various dilute HCl solutions of pH about 1.0 to 1.5 were checked against this buffer. It was assumed that the HCl was completely ionized, and consequently these measurements gave a correction which enabled pH readings to be converted to hydrogen ion concentrations. Sodium nitrate was also added to the reaction mixtures to control the ionic strength, which was always close to 0.15. The reacting solutions were kept in a thermostat at 25.0 ± 0.1 °C. The reaction was chiefly followed by measurements of optical density on a Beckman DU. spectrophotometer. In some cases spectra over the range 200 to 500 mμ were measured on a Bausch and Lomb Spectronic 505. The other analytical methods consisted of extracting the reacting mixture with carbon tetrachloride, and estimating the halogen extracted either spectrophotometrically, or by addition of aqueous potassium iodide and titration with sodium thiosulfate. Iodine–thiosulfate titrations were also used to standardize the stock solutions of iodine and sodium bromate. The substances used were all of analytical reagent grade, usually dried overnight at 115 °C, and made up by weight in standardized volumetric glassware.

The stock iodine solution might be mentioned in a little more detail. British Drug Houses Analar reagent iodine was shaken with doubly distilled water 10 to 15 times, and these solutions were discarded. In this way it was hoped to remove impurities such as traces of iodides or of lower halogens. The final solution was made up by shaking a few small crystals of iodine, which had been treated in this way, with fresh water. The saturated solution so produced, which is about 10^{-3} *M*, was poured off, standardized, and used as the stock solution.

In a typical run various amounts of the reacting solutions, the buffer, and sodium nitrate, initially at 25 °C, were rapidly mixed, and the reaction followed as described above. In almost all mixtures the bromate was in considerable excess, typical initial concentrations being: $[I_2] = 6 \times 10^{-4}$ *M*, $[BrO_3^-] = 2 \times 10^{-2}$ *M*.

Results

The reaction was found to occur in four well-defined stages.

(*i*) An induction period, during which very little, if any, iodine reacted. The length of this period depended on the concentrations, but was typically 20 to 30 min.

(*ii*) Iodine disappearance. This lasted usually 1 to 2 min, and during this time iodine was replaced by iodine bromide.

(*iii*) Iodine bromide disappearance. This lasted usually 2 to 5 min. At the end the solution was colorless, and contained sodium bromide.

(*iv*) Bromine appearance. This lasted several

TABLE I

Values of the slope, $s = \text{d log } [I^-]/dt_1$, for various concentrations

Series	$[H^+]$ (M)	$[BrO_3^-]$ (M)	Slope	K_1 (min^{-1} M^{-3})
1	2.43×10^{-2}	2.00×10^{-2}	0.070	1.95×10^4
2	4.60×10^{-2}	1.00×10^{-2}	0.118	1.84
3	2.60×10^{-2}	1.00×10^{-2}	0.037	1.81

hours, and eventually gave a bromine concentration equal to the initial iodine concentration.

These stages will now be considered in detail.

1. Induction Period

Initially the color of the solution, as estimated by eye, stays constant for some time, and then suddenly fades. It was found that the length of this induction period could be estimated visually to within a few seconds (roughly 0.05 min). Spectrophotometric measurements at 460 mμ, which detect iodine with very little interference from iodine bromide, also gave constant absorbances during this period. Experiments were also made in which the reacting solutions were shaken with carbon tetrachloride, and the iodine so extracted was estimated, either from the absorbance of the CCl_4 layer at 510 mμ or by shaking the separated CCl_4 layer with aqueous potassium iodide and titrating with sodium thiosulfate. These experiments showed no loss of iodine within experimental error during the induction period.

The existence of an induction period was attributed to the following mechanism. The acidified bromate ions are believed to decompose slowly producing a product which catalyzes the reaction of iodine and bromate ion. This catalyst, however, reacts with traces of iodide ions which are present, and it is only when virtually all the iodide has been used up that the iodine reaction can begin. The evidence for these statements will now be given.

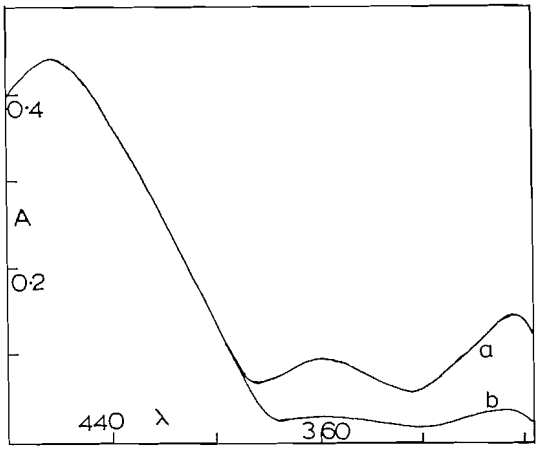

FIG. 1. Absorbance during the induction period of a solution initially containing 2.0×10^{-2} M $NaBrO_3$ and 6.0×10^{-4} M I_2 at pH 1.70.

The absorption spectrum of a reaction mixture was found to be as shown in Fig. 1. Initially the absorbance followed curve (*a*) with maxima at 460, 355, and 290 mμ. The peak at 460 mμ is due to iodine, and the two other peaks are attributed to triiodide ions, which are reported (2) to have maxima with extinction coefficients of 26 400 at 355 mμ, and 40 000 at 290 mμ. These last two maxima slowly diminished giving curve (*b*) after some minutes. If a trace of potassium iodide was then added, it restored the absorption curve approximately to curve (*a*). On further standing the triiodide peaks disappeared again at the same rate as before.

The induction period was, as might be expected, lengthened by added potassium iodide, and the extent of this lengthening was investigated. If T_1 is the induction time, a plot of log (added iodide concentration) against T_1 was linear for larger amounts of added iodide. This linearity could be extended to all the measurements if it was assumed that the concentration of iodide ion present as an impurity was 1.5×10^{-5} M (in 6×10^{-4} M iodine), and log (total iodide) was plotted against T_1. The concentrations of added potassium iodide varied up to 2×10^{-4} M. The slope, $\text{d log } [I^-]/dT_1$, was measured at various pH and bromate ion concentrations with the results in Table I. These results can be explained by supposing that the slow stage is the reaction

$$I^- + BrO_3^- + 2H^+ \rightarrow \text{products},$$

and that the induction period ends when $[I^-]$ has fallen to some critical value. The above equation requires that

$$\frac{-\text{d ln } [I^-]}{dt} = k_1[H^+]^2[BrO_3^-]$$

Can. J. Chem. Downloaded from www.nrcresearchpress.com by 210.87.254.42 on 09/05/12
For personal use only.

Can. J. Chem. Downloaded from www.nrcresearchpress.com by 210.87.254.42 on 09/05/12
For personal use only.

where k_1 is the rate constant. To relate k_1 to the slope, s, in Table I, a correction must be made for the fact that much of the iodide ion is combined as I_3^-. The equilibrium constant for

$$I_2 + I^- \rightleftharpoons I_3^-$$

is reported (3) to be 725 M^{-1}, and as $[I_2]$ was 6.0×10^{-4} M in these runs, this means that 69.7% of the total iodide was free I^-. Hence the relation of s and k_1 should be

$$\frac{2.303s}{0.697} = k_1[H^+]^2[BrO_3^-].$$

Values of k_1 obtained from this equation are given in the last column of Table I. The mean value of k_1 is 1.87×10^4 min^{-1} M^{-3}. Earlier workers on this reaction find the same rate law as given above, with values of k_1 of 2.9×10^4 min^{-1} M^{-3} (4), or 3.5×10^4 min^{-1} M^{-3} (5). These values were for somewhat different ionic strength, but if we consider the rather indirect way in which k_1 is obtained in the present work, the agreement is sufficiently good that there can be little doubt that removal of iodide is responsible for the induction period. Extrapolation of the results to zero induction time suggests that this would correspond to a concentration of iodide ions of about 4×10^{-6} M, which is presumably the concentration at which iodide ions cease to compete effectively with 6×10^{-4} M iodine for the decomposition product of the acidified sodium bromate.

Various other substances were added in order to find their effect on the induction period. Sodium bromide had no effect, though it did on the next stage of the reaction. Sodium iodate reduced, but did not totally remove, the induction period. This is somewhat surprising in view of the explanation offered above, but perhaps the reason is that though iodate and iodide ions react at pH 2, iodate ions do not help to produce the catalyst required in the next stage of the reaction. It might be added that kinetic data on the reaction of iodate and iodide ions, measured by Abel and Stadler (15), show that the explanation of our observations is not that the reaction is quite slow at the low iodide concentrations in the present experiments.

Sodium bromite, prepared as in ref. 16, at a concentration in the reaction mixture of 1.5×10^{-4} M, reduced the induction period to about 2 min. Hypobromous acid solution (prepared from aqueous bromine and silver nitrate) at about 10^{-4} M removed the induction period completely. In this preparation, bromine was in a slight excess, so bromine as well as hypobromous acid was added: however, it was found that small amounts of bromine alone did not greatly reduce the induction period. The bromine would presumably mostly react to give iodine bromide. Hypoiodous acid (prepared from aqueous iodine and silver nitrate and very rapidly filtered into the reaction mixture) at about 10^{-4} M reduced the induction period to less than a minute. Solutions of hypoiodous acid, though unstable, can exist long enough to have the kinetics of their decomposition studied (6); and it can be seen that hypoiodous acid behaves differently from its decomposition products, iodine and iodic acid. The hypobromous and hypoiodous acid solutions are saturated with silver bromide and iodide respectively; however, these silver salts, by themselves, did not reduce the induction time.

It was suggested earlier that acidified sodium bromate slowly produces a catalyst for its subsequent reaction with iodine. The effect on the induction period of various substances described above suggests that this catalyst is either bromous or hypobromous acid, more probably the latter, since bromous acid produces hypobromous acid during the course of its decomposition (7). Possibly both are active, though there is some balance in favor of hypobromous acid, since this removed the induction period most strikingly.

Another set of experiments was made in which the sodium bromate was acidified and allowed to stand for some time before the iodine solution was added. It was found that the triiodide ion absorption peaks, mentioned above, were immediately reduced after the addition, showing that some material was accumulating in the sodium bromate, which oxidized iodide ions rapidly. If T_0 is this "pre-acidification" period, and T_1 the induction period, it was found that a plot of $\log T_1$ against T_0 was approximately linear, provided T_0 was not too long. Thus we can write

$$\log T_1 = a - bT_0,$$

where a and b are constants. The values of the slope, b, each of which was obtained from a number of experiments, are given in Table II. It can be seen that b depends on pH and $[BrO_3^-]$. Both the sodium bromate and iodine solutions

TABLE II

Variation of the slope, $b = -\mathrm{d} \log T_1/\mathrm{d}T_0$ with pH and $[BrO_3^-]$

Run	pH	$[BrO_3^-]$ (M)	b*	$b/[H^+]^2[BrO_3^-]^2$
1	1.59	4.0×10^{-2}	23.0×10^{-3}	1.28×10^{4}
2	1.59	3.0	12.8	1.27
3	1.59	2.0	4.68	1.04
4	1.59	1.0	0.68	0.61
5	1.71	2.0	4.13	1.60
6	1.71	4.0	13.4	1.30
7	1.45	2.0	12.3	1.44
8	1.45	1.0	1.37	0.64
9	1.41	1.0	2.04	0.79
10	1.35	1.0	2.56	0.76
11	1.79	3.0	5.44	1.35

*Time in minutes.

were brought to the pH values given in Table II, before mixing, so the pH was constant throughout the experiment. The results in Table II show that at any bromate concentration, b is roughly proportional to $[H^+]^2$. The bromate concentrations in Table II are for the "pre-acidification" period, and these were halved on adding the iodine. Between 4 and 2×10^{-2} M bromate, b is proportional to $[BrO_3^-]^2$, but b is lower than would be expected on this basis for 1×10^{-2} M sodium bromate. The last column in Table II gives values of $b/[H^+]^2[BrO_3^-]^2$, obtained with the help of the correction to the pH (0.115 to get $-\log [H^+]$) mentioned above.

These observations are tentatively explained by the following proposals.

(i) The catalyst, X, is produced at a constant rate in any one run, though this rate may depend on pH and $[BrO_3^-]$, and it also decomposes so that its concentration is always low.

(ii) When the iodine is added, the catalyst rapidly reacts with some of the iodide ions present, and is thereby destroyed.

(iii) The remaining iodide ions then react with the acidified bromate during the induction period, by the usual iodide–bromate reaction. When the iodide concentration is low enough, the catalyst builds up again.

(iv) The dependence of b above on the concentrations probably indicates that the production of catalyst involves two hydrogen and two bromate ions, perhaps by the reaction (as a first slow stage)

$$2H^+ + 2BrO_3^- \rightleftharpoons 2HBrO_2 + O_2.$$

It is not possible to put these proposals into mathematical form with any confidence, since, in particular, the mode of decomposition of the catalyst is unknown. Either a first or second order decomposition gives a curve of T_1 against T_0 of the right general shape, and the extent of the reduction of T_1 for not too large values of T_0 depends on the rate of production of the catalyst, not on its decomposition.

2. Disappearance of Iodine

At the end of the induction period the rate of disappearance of iodine increased rapidly. As the iodine absorption peak vanished it was replaced by new peaks at 390 mμ and 255 mμ. The absorption at 410 mμ remained constant for a considerable part of the time of disappearance of the iodine, so that it behaved rather like an isosbestic point. This presumably indicates that there is a constant ratio between the amount of iodine disappearing and the amount of the new colored compound appearing.

The rate of disappearance of iodine was followed at 500 mμ, where there was very little absorption by the new colored intermediate. The rate of decrease of absorbance accelerated rapidly at first, but then stayed constant until the iodine had almost all disappeared. This constant rate was measured for different conditions with the results in Table III. The slope in Column 2 of this table is $-\mathrm{d}A/\mathrm{d}t$, where A is the absorbance at 500 mμ. Column 5 shows that the slope divided by $[H^+]^2[BrO_3^-]^2$ is reasonably constant, with an average value of 1.20×10^7 min^{-1} M^{-4} (average deviation 0.11×10^7). This means that

$$\frac{-\mathrm{d}[I_2]}{\mathrm{d}t} = k_2[H^+]^2[BrO_3^-]^2$$

Can. J. Chem. Downloaded from www.nrcresearchpress.com by 210.87.254.42 on 09/05/12
For personal use only.

TABLE III

Run	Slope (min^{-1})	$[H^+]$ (M)	$[BrO_3^-]$ (M)	Slope / $[H^+]^2[BrO_3^-]^2$
1	0.0324	4.90×10^{-3}	1.00×10^{-2}	1.35×10^{7}
2	0.0554	6.47	1.00	1.32
3	0.0813	8.22	1.00	1.20
4	0.0919	9.23	1.00	1.08
5	0.1065	6.61	1.60	0.95
6	0.0378	6.95	0.80	1.22
7	0.075	21.04	0.40	1.06
8	0.084	22.54	0.40	1.03
9	0.050	15.96	0.40	1.23
10	0.020	10.07	0.40	1.23
11	0.300	15.96	1.00	1.18
12	0.136	10.30	1.00	1.28
13	0.186	12.68	1.00	1.16
14	0.046	5.66	1.00	1.44
15	0.170	12.68	1.00	1.06
16	0.115	10.07	1.00	1.13
17	0.088	8.19	1.00	1.31
18	0.050	6.07	1.00	1.36
			Mean	1.20

and as the light path was 1 cm, and the extinction coefficient of iodine at 500 mμ is 466, it follows that k_2 is 2.6($\pm$ 0.2) $\times$ 10^4 min^{-1} M^{-3}.

The colored intermediate was found to be iodine bromide, the evidence for this being as follows. Firstly, the solution was shaken with carbon tetrachloride, approximately at the instant when the iodine had disappeared, and gave a red solution (in CCl_4) with an absorption peak at 496 mμ, which agrees with a peak previously reported for iodine bromide (8). The concentration of the iodine bromide was determined by shaking the carbon tetrachloride solution with aqueous potassium iodide, and titrating with sodium thiosulfate. From this the extinction coefficient at the maximum was calculated to be 394; the literature value is 390.

Aqueous iodine bromide was prepared by mixing equimolar amounts of iodine and bromine solutions. As the equilibrium constant for

$$I_2 + Br_2 \rightleftharpoons 2IBr$$

is 8.3×10^4, from free energy data (9), the formation of IBr is nearly complete. The extinction coefficients of aqueous iodine bromide were obtained from this solution, after corrections were made, firstly for hydrolysis by the reaction

$$5IBr + 3H_2O \rightleftharpoons 5Br^- + IO_3^- + 2I_2 + 6H^+$$

and secondly for the reaction

$$IBr + Br^- \rightleftharpoons IBr_2^-.$$

Data from ref. 9 make the equilibrium constant of the first reaction 10^{-20} M[9], and of the second 370 M^{-1} (10). The pH of the solutions were measured after adjustment to somewhere in the range of pH 1.0 to 2.0 by addition of a little nitric acid, and the concentrations of all the species present were calculated. The extinction coefficients of IBr_2^- were obtained by adding sodium bromide at a concentration of 0.05 M, when most of the iodine bromide is converted to IBr_2^-. The results are given in Table IV, together with those for iodine. The curves for iodine and iodine bromide cross at 412 mμ, close to the point where the absorbance stayed constant during most of the disappearance of iodine. This indicates that at this stage of the reaction one iodine molecule is being replaced by one iodine bromide. This was confirmed by the observation that the amount of iodine bromide extracted into carbon tetrachloride was sometimes as high as 83% of the maximum amount calculated from the equation

$$I_2 + BrO_3^- \rightarrow IBr + IO_3^-.$$

It was also found that addition of sodium bromide (about 0.045 M) to the reaction mixtures when the iodine had just disappeared gave the characteristic absorption peak of IBr_2^- at 375 mμ. The reported (11) extinction coefficient at 375 mμ is 590, in agreement with our results, and this was used to calculate the concentration

Can. J. Chem. Downloaded from www.nrcresearchpress.com by 210.87.254.42 on 09/05/12
For personal use only.

TABLE IV

Extinction coefficients (E) of various species

Wavelength (mμ)	380	390	400	410	420	440
E of IBr	310	346	370	360	338	246
E of IBr_2^-	580	500	378	250	179	96
E of I_2	157	176	245	341	450	650

TABLE V

Run	$d[IBr]^{-1}/dt$ (M^{-1} min^{-1})	$[H^+]$ (M)	$[BrO_3^-]$ (M)	$s/[BrO_3^-]^2$
1	10.2×10^3	27.9×10^{-3}	9.5×10^{-3}	1.13×10^8
2	2.66	24.3	4.5	1.31
3	6.99	23.2	7.5	1.24
4	11.6	21.9	9.5	1.28
5	1.74	21.0	3.5	1.42
6	20.7	12.7	9.5	2.29
7	13.9	7.75	7.5	2.47
8	93.1	7.67	19.5	2.45

of IBr in the reaction mixtures. These were about 90% of the maximum amount calculated from the equation above. Presumably a little iodine bromide has reacted before all the iodine has disappeared.

The mechanism of this stage of the reaction will be considered briefly later.

3. Disappearance of Iodine Bromide

The disappearance of iodine bromide was followed by its absorption at 390 mμ. It was found that a plot of (absorbance)$^{-1}$ against time was linear. As the extinction coefficient of IBr is 346 at this wavelength, the slopes of these lines could be converted to values of $d[IBr]^{-1}/dt$, and these are collected in Table V for experiments under different conditions. The bromate ion concentrations given in Table V allow for the amount of bromate consumed by the reaction

$$I_2 + BrO_3^- \rightarrow IBr + IO_3^-,$$

the initial iodine concentrations being about 5×10^{-4} M. The results in Table V show that $d[IBr]^{-1}/dt$ is proportional to $[BrO_3^-]^2$ and the last column gives the slope $d[IBr]^{-1}/dt$ divided by $[BrO_3^-]^2$. There is also probably some dependence on pH, since the last column increases as $[H^+]$ decreases, but it does not seem to depend on a simple power of $[H^+]$. However, the pH reading fell a little during this stage of the reaction, as would be expected since the reaction produces hydrogen ions.

$$3IBr + 2BrO_3^- + 3H_2O \rightarrow 5Br^- + 3IO_3^- + 6H^+$$

The phosphate buffer limited the change of pH to about 0.02. Consequently we may write

$$\frac{-d[IBr]}{dt} = k'[IBr]^2[BrO_3^-]^2$$

with k' about 1.5×10^8 min^{-1} M^{-3}, but somewhat dependent on pH. As before, the mechanism will be discussed later.

4. Appearance of Bromine

The equation for the removal of iodine bromide was given above, but so far the only evidence for it has been the observation that the pH fell somewhat during that stage of the reaction. Further evidence comes firstly from the observation that when the iodine bromide had disappeared the solution was colorless to the eye, and secondly from the data on the last stage of the reaction which will now be described.

The appearance of bromine was followed by its absorption at 390 mμ, and it was found (as was already known (1)) that the final concentration of bromine agreed within experimental error with the overall equation

$$I_2 + 2BrO_3^- \rightarrow Br_2 + 2IO_3^-.$$

The measured absorbances were found to be consistent with the following explanation. The total reaction up to the start of this final stage is

$$3I_2 + 5BrO_3^- + 3H_2O \rightarrow 5Br^- + 6IO_3^- + 6H^+.$$

It was assumed that the concentration of bromide ions at the beginning of this final step in the

Can. J. Chem. Downloaded from www.nrcresearchpress.com by 210.87.254.42 on 09/05/12
For personal use only.

TABLE VI

Values of $-\mathrm{d}\log[Br^-]/dt$ for various conditions

Run	$-\mathrm{d}\log[Br^-]/dt$ (min^{-1})	$[H^+]$ (M)	$[BrO_3^-]$ (M)	k_3
1	6.49×10^{-3}	2.37×10^{-2}	2.00×10^{-2}	1.33×10^3
2	12.9	3.41	2.00	1.28
3	3.66	2.66	1.00	1.19
4	9.03	3.94	1.00	1.34
5	20.0	5.50	1.00	1.52

Run with added sodium bromide

Part	Added $[Br^-]$ (M)	$-\mathrm{d}\log[Br^-]/dt$ (min^{-1})
a	0.0×10^{-3}	1.55×10^{-3}
b	0.25	1.55
c	0.50	1.49
d	0.75	1.50

reaction was determined by this equation, and that their subsequent concentrations could be calculated from the amount of bromine present in accordance with the equation

$$5Br^- + BrO_3^- + 6H^+ \rightarrow 3Br_2 + 3H_2O.$$

Hence $[Br^-]$ could be calculated at various times, and it was found that a plot of log $[Br^-]$ against time was linear. Experiments were carried out at various pH and $[BrO_3^-]$, and in addition some runs were made in which known amounts of sodium bromide were added to the reacting mixture. In the latter case it was found that log $[Br^-]$ against time was still linear, with the expected slope, thus confirming that the calculated amount of bromide, formed by reaction of the iodine, was indeed correct. Table VI gives values of the slope $-\mathrm{d}\log[Br^-]/dt$ for various conditions, and it can be seen that the slope divided by $[H^+]^2[BrO_3^-]$ is approximately constant, as shown in Column 5. This column gives the calculated rate constant of the reaction, defined by

$$\frac{-\mathrm{d}\ln[Br^-]}{dt} = k_3[H^+]^2[BrO_3^-].$$

In the run with added sodium bromide, the calculated $[Br^-]$ at the beginning of part (*a*) was 1.16×10^{-3} M, the bromate concentration was 2.0×10^{-2} M, and hydrogen ion concentration about 3.6×10^{-3} M. It can be seen that the calculated d log $[Br^-]/dt$ stayed constant. The results in Table VI make $k_3 = 1.33\times10^3$ min^{-1} M^{-3} with an average deviation of 0.08×10^3, at 25 °C and an ionic strength of 0.14. Literature values are 0.58×10^3 (5) at an ionic strength of 0.5, 1.5×10^3 at 0.013, 0.95×10^3 (12) at 0.21, and 0.65×10^3 min^{-1} M^{-3} (13) at 0.26. These are a little lower than our results, but Young and Bray (12) extrapolate k_3 to 2.7×10^3 min^{-1} M^{-3} at zero ionic strength. It may be noted that earlier values of the rate constant are generally reported in terms of $\mathrm{d}[BrO_3^-]/dt$, which is one fifth of $\mathrm{d}[Br^-]/dt$. The agreement between our rate constant and these earlier values is sufficiently good that they support the view that this is the same reaction.

Discussion of Results

This section will be an attempt to explain the results given above by mechanisms for the various stages of the reaction, and will be necessarily rather speculative in places. The various stages will be considered separately.

1. Induction Period

The experiments seem to establish the fact that the induction is due to reaction of iodide ions, partly with bromate ions, and partly with a species which develops in the acidified sodium bromate and which catalyzes the next stage of the reaction. The kinetics of the reaction of bromate ions with either bromide or iodide suggest that the slow stage of the reaction is

$$X^- + BrO_3^- + 2H^+ \rightarrow XBrO_2 + H_2O$$

(where X^- is bromide or iodide), with a reactive intermediate $XBrO_2$ of the sort proposed by Taube and Dodgen (14). This type of intermediate will be suggested for later stages of the present reaction.

Can. J. Chem. Downloaded from www.nrcresearchpress.com by 210.87.254.42 on 09/05/12
For personal use only.

Can. J. Chem. Downloaded from www.nrcresearchpress.com by 210.87.254.42 on 09/05/12
For personal use only.

The initial stage of the production of the catalyst mentioned above is probably

$$2H^+ + 2BrO_3^- \rightarrow 2HBrO_2 + O_2,$$

in agreement with the kinetic data, but as bromous acid would decompose further (7),

$$2HBrO_2 \rightarrow HOBr + BrO_3^- + H^+,$$

it is possible that either bromous or hypobromous acid could be the catalyst.

2. Removal of Iodine

The overall reaction in this period is

$$I_2 + BrO_3^- \rightarrow IBr + IO_3^-,$$

which proceeds over most of its range at a constant rate (in buffered solutions with a large excess of bromate ion) proportional to $[H^+]^2[BrO_3^-]^2$. It is difficult to suggest a mechanism which does not require the rate to tail off at the end more than is observed. However, the following proposal

	Rate constants
$2H^+ + 2BrO_3^- \rightarrow 2HBrO_2 + O_2$	k_a
$2HBrO_2 \rightarrow HOBr + H^+ + BrO_3^-$	k_b
$HOBr + I_2 \rightarrow HOI + IBr$	k_c
$HOI + BrO_3^- \rightarrow HIO_2 + BrO_2^-$	Fast
$HIO_2 + BrO_3^- \rightarrow IO_3^- + BrO_2^- + H^+$	Fast

leads to the equations

$$\frac{-dx}{dt} = k_c xz$$

$$\frac{dz}{dt} = k_b(Rt - 2z)^2 - k_c xz,$$

where $x = [I_2]$, $z = [HOBr]$, and R is the rate, assumed constant, of the first reaction. These equations were integrated numerically, and give curves of different shapes depending on the ratio of k_c to k_b. If k_c is much the same as k_b, a curve of $[I_2]$ against time with marked tailing off is obtained; if k_c is very much greater than k_b a curve is obtained in which the rate of disappearance of iodine increases continuously. If k_c is about $100k_b$, a curve with a long nearly linear portion and very little tailing off is obtained, approximately what is observed. It is not possible from the present data to evaluate k_b, and all that can be said about k_c, therefore, is that it must be at least $100k_b$.

3. Removal of Iodine Bromide

Since this stage was apparently fourth order in the reagents, it seems reasonable to suppose that a rapid pre-equilibrium occurs,

$$IBr + BrO_3^- \rightleftharpoons BrIOBrO_2^-,$$

to give a species rather like a polyhalide ion, and that two of these react slowly to give further intermediates, which in turn react rapidly to give eventually the final products. The slow stage is perhaps a transfer of oxygen, which is in effect a disproportionation.

$$2BrIOBrO_2^- \rightarrow BrI(O)OBrO_2^- + BrIOBrO^-$$

then

$$BrI(O)OBrO_2^- + IBr \rightarrow BrIO_2 + BrIOBrO^-$$

$$BrIOBrO^- \rightarrow Br^- + BrIO_2$$

$$BrIO_2 + H_2O \rightarrow Br^- + IO_3^- + 2H^+.$$

This mechanism is, of course, only a suggestion to show that the final products can be reached by a fairly simple scheme. The species $BrIO_2$ is formally similar to other XYO_2 intermediates proposed for halide–halate reactions (14).

4. Appearance of Bromine

This is believed to be the usual bromide–bromate reaction with the slow stage

$$Br^- + BrO_3^- + 2H^+ \rightarrow Br.BrO_2 + H_2O$$

followed by

$$Br^- + BrBrO_2 \rightarrow Br_2 + BrO_2^-$$

and other rapid steps which give bromine as the final product.

1. R. Lyden. Finska Kemistsamfundets Medd. **37**, 20 (1928).
2. A. D. Autrey and R. E. Connick. J. Am. Chem. Soc. **73**, 1842 (1953).
3. G. Daniele. Gazz. Chim. Ital. **90**, 1068 (1960).
4. R. H. Clarke. J. Phys. Chem. **10**, 679 (1906).
5. A. Skrabal and H. Schreiner. Monatsh. **65**, 213 (1935).
6. M. L. Josien. Bull. Soc. Chim. France, 301, 814 (1948).
7. P. Engel, A. Oplatka, and B. Perlmutter-Hayman. J. Am. Chem. Soc. **76**, 2010 (1954); B. Perlmutter-Hayman and G. Stein. J. Phys. Chem. **63**, 734 (1959).
8. A. E. Gillam and R. E. Morton. Proc. Roy. Soc. London, Ser. A, **124**, 604 (1929).
9. W. M. Latimer. Oxidation potentials. 2nd ed. Prentice-Hall, Inc., New York. 1952. p. 59.
10. J. H. Faull. J. Am. Chem. Soc. **56**, 522 (1934).
11. A. E. Gillam. Trans. Faraday Soc. **29**, 1132 (1933).
12. H. A. Young and W. C. Bray. J. Am. Chem. Soc. **54**, 4284 (1932).
13. J. Sigalla. J. Chim. Phys. **55**, 758 (1958).
14. H. Taube and H. Dodgen. J. Am. Chem. Soc. **71**, 3330 (1949).
15. E. Abel and F. Stadler. Z. Physik. Chem. Leipzig, **A122**, 49 (1926).
16. Societe d'Etudes Chimiques pour L'Industrie et L'Agriculture. Brit. Patent No. 843,558 (Aug. 4, 1960).

Can. J. Chem. Downloaded from www.nrcresearchpress.com by 210.87.254.105 on 09/05/12
For personal use only.

Molar excess volumes of binary *n*-alcohol systems at 25 °C[1]

H. D. PFLUG[2] AND G. C. BENSON
Division of Pure Chemistry, National Research Council of Canada, Ottawa, Canada

Received August 22, 1967

A dilatometer suitable for measuring small changes in volume associated with the mixing of liquids is described. The apparatus was used to measure the excess volumes of 11 binary *n*-alcohol systems at 25 °C.

Canadian Journal of Chemistry, 46, 287 (1968)

I. Introduction

Excess enthalpies at 25 °C for the 11 binary systems formed from the normal alcohols methanol (MeOH), ethanol (EtOH), propanol (PrOH), butanol (BuOH), hexanol (HxOH), octanol (OcOH), and decanol (DeOH), and containing either BuOH or OcOH as one component, were reported in a previous paper (1). The data were used to examine the applicability of the principle of congruence. Earlier work by Díaz Peña and Fernández Martín (2) indicated that the heats of mixing of binary alcohol systems containing MeOH conformed to the principle fairly well; however, it was found that the principle provided only a rough correlation of the enthalpy data for the more extensive set of systems.

The present paper continues our study of alcohol mixtures by describing measurements of the excess volumes for the same 11 systems at 25 °C. The experimental technique is outlined in the next Section; the results are summarized and discussed in Section III.

II. Experimental

All the alcohols used for the present measurements were the same as employed in our previous calorimetric studies (1). Reference should be made to the report of that investigation for information about the component liquids. The changes in volume occurring when binary mixtures were formed by successive additions of one component to a known amount of the other were measured in the dilatometer shown schematically in Fig. 1. The apparatus is basically similar to the dilatometer used by Geffcken, Kruis, and Solana (3), but the differences in detail of design and operation are sufficient to warrant description.

The mixing process is carried out in cell A (capacity approximately 200 cc) which can be joined at its top and bottom by two three-way stopcocks B and C to a tru-bore tube D (capacity approximately 10 cc). Angular bores in

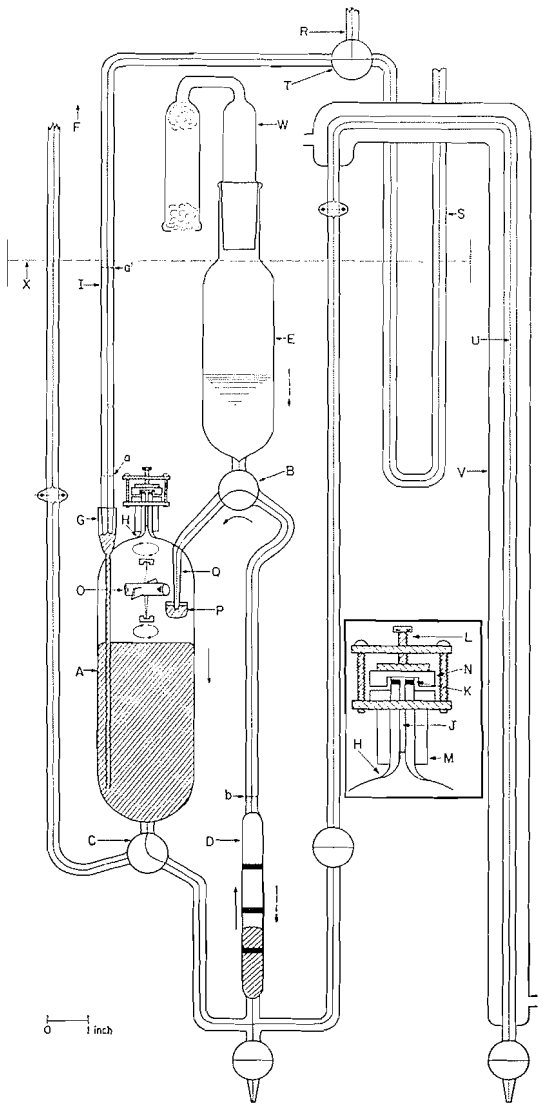

FIG. 1. Schematic diagram of the dilatometer.

[1]Issued as NRCC No. 9810.
[2]NRCC Postdoctorate Fellow, 1965–1967.

Can. J. Chem. Downloaded from www.nrcresearchpress.com by 210.87.254.105 on 09/05/12
For personal use only.

the three-way stopcocks also allow the upper and lower ends of the cell to be joined to a solvent reservoir E and to a mercury container F, respectively. The cell has two openings. One of them, G, is a standard taper joint which connects to a calibrated tru-bore capillary tube I, and has an extension reaching to the bottom of the cell. The other opening H is used for filling the cell; it is closed by a teflon plug J (see inset to Fig. 1) which is machined to fit the narrow aperture precisely and carries a latex washer K under its head. A brass screw-clamp L, slipped over a teflon collar M, makes it possible to pull a teflon cover N tightly against the plug, compressing the washer and providing an efficient seal. The cell is fitted with an externally driven magnetic stirrer O, the axle of which rotates with very little friction in the indentations in two supporting glass rods. The contents of the cell are separated from the solvent to be added by a cup P which contains sufficient mercury to cover the end of the inlet tube Q. In order to adjust the pressure on the liquid in the cell, the capillary I can be connected via a stopcock T to a vacuum line R and a U-tube manometer S containing mercury and having one arm open to the atmosphere.

The cell and solvent reservoir are immersed to level X in a water bath operated at 25.00 ± 0.01 °C, and controlled to ±0.001 °C during a run. The capillary extension U, attached to the dilatometer and kept at bath temperature by a water jacket V, makes it possible to remove mercury when the apparatus is immersed in the bath. Initially, the cell contains about 50 cc of one component (A) resting on the mercury which is in contact with the capillary I. Depending on whether expansion or contraction is expected on mixing, the meniscus in I is adjusted to be near either the lower (a) or upper (a′) reference mark. The pressure above the meniscus is reduced until the solvent in the cell is effectively at atmospheric pressure. Reservoir E, protected from atmospheric moisture by a drying tube W, holds component (B) which also fills the capillary from tube D to the cell. The part of this capillary containing reference mark (b) is made from calibrated tru-bore tubing (nominal i.d. 1.7 mm). Before mixing, the desired quantity of component (B) is dropped from the reservoir into D, displacing mercury which is drawn off through U and subsequently weighed. Stopcocks C and B are then turned joining D and the cell in a loop (as shown in Fig. 1); mercury from the cell then forces component (B) from tube D into the cell. The amount of (B) added is calculated from the weight of the mercury removed via tube U and the change in the level of the mercury relative to mark (b) determined with a cathetometer before and after the addition. After readjusting the pressure in the cell, the volume change accompanying the mixing is obtained from differences in cathetometer measurements of the level of the mercury in tube I. It was convenient to have several different capillaries for I (nominal i.d. values 1.7, 1.0, and 0.5 mm); the size used for a particular system was selected on the basis of the volume change expected. Runs using different capillaries were carried out for several systems; the results agreed within the estimated experimental uncertainty.

The procedure of drawing mercury from D and displacing component (B) into the cell was repeated 10–12 times with increasing increments (calculated to give approximately equal changes in mole fraction of the solution) until the liquid volume in the cell was more than doubled. The measurements yielded the volumes of mixing for a series of solutions predominantly rich in (A). To cover the whole concentration range, another run was carried out with the positions of the two components interchanged.

During the filling of the dilatometer, it is important to avoid trapping air bubbles in the mercury and the component liquids. A few runs were carried out with solvents from which dissolved air was partially removed by equilibrating them at a reduced pressure. However, no difference was observed in the results obtained with these materials and in general the solvents used were not degassed.

In our work, Apiezon N was used as a lubricant for stopcock B and care was taken to keep contact with the solvent to a minimum. The same lubricant was also used on C and G, both of which were always separated from the solvents by mercury. No effects attributable to contamination were detected.[3]

Estimates of the overall error of the volume measurement vary from ±0.5% in cases where the volume change per addition was of the order of 0.02 cc to ±5% where the change was only 0.0002 cc. (These correspond to excess volumes at a mole fraction of 0.5 ranging from 0.2 to 0.002 cm^3 $mole^{-1}$ respectively.) The performance of the dilatometer was investigated by comparison of the results for several systems with values measured by two different techniques:

(i) Determinations of the densities of the pure components and of a series of their solutions were carried out for the system MeOH–OcOH in a 10 cc twin-stem pycnometer.

(ii) A banana-shaped dilatometer similar to that described by Duncan, Sheridan, and Swinton (4) was used for a number of individual measurements of the volume changes on mixing PrOH with OcOH.

III. Results and Discussion

The experimental results for the excess volumes (V^E) of 11 binary *n*-alcohol systems at 25 °C, measured with the new dilatometer, are given in Table I. The data for two of the systems are plotted in Figs. 2 and 3, along with values obtained by methods (i) and (ii) mentioned above. The latter agree quite well with the data from Table I and provide a check on the performance of the new dilatometer. It is inherent in the continuous dilution method that the results show less scatter than methods (i) or (ii). We have found that the new dilatometer facilitates the collection of data and that the accuracy is as good or better than that obtained by the other methods.

The excess volumes are positive for all of the systems studied with the exception of PrOH–BuOH for which small contractions were ob-

[3]For aromatic hydrocarbons, a Dow Corning silicone base grease has proved satisfactory.

Can. J. Chem. Downloaded from www.nrcresearchpress.com by 210.87.254.105 on 09/05/12
For personal use only.

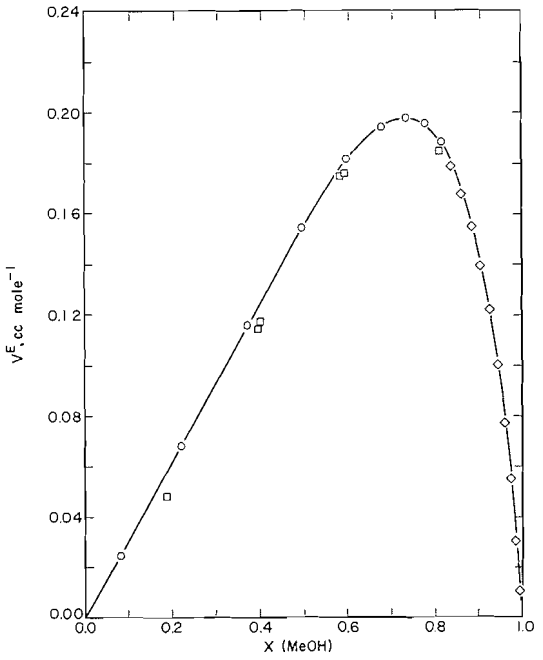

FIG. 2. Volumes of mixing for system MeOH–OcOH at 25 °C. (○) and (◇) results obtained with dilatometer; (□) values derived from density measurements (method (i) in Section II).

served over most of the concentration range. In general there is a rough correlation between the present excess volumes and the heat effects reported for the same systems in ref. 1, in the sense that systems which have relatively large excess enthalpies also exhibit relatively large volumes of mixing. However, within this pattern, the excess volumes of systems containing MeOH are unusually large when compared with the behavior of the corresponding heats of mixing.

Analysis of the experimental data follows lines similar to those already described for the excess enthalpies (1). The excess volumes for each system were fitted with an equation of the form

$$[1] \qquad V^E = x_1 x_2 \sum_{r=0}^{q} C_r (x_2 - x_1)^r$$

where x_1 and x_2 are mole fractions of the shorter and longer chain length components respectively. Values of the coefficients C_r determined by a least squares procedure are summarized in Table II along with values of σ_v, the standard deviation between the experimental and calculated values of V^E. In each case the number of coefficients was varied from 2 to 6 and the minimum number needed to represent the data adequately was adopted. It will be noted that as the difference in chain length of the components increases the curves become more asymmetric and correspondingly more coefficients are needed to fit the results. Although as many as 6 coefficients are not generally used in representing data by means of eq. [1], their use for some of the present systems seems justified. Thus in the case of MeOH–OcOH the standard deviation is reduced by a factor of nearly 2 when the number of coefficients is increased from 5 to 6. It is clear that eq. [1] is not particularly appropriate for the representation of data corresponding to fairly highly skewed curves. Similar difficulties have been encountered in representing the excess enthalpies (H^E) of alcohol–aromatic systems (5) and the use of polynomial fits of the reciprocal function x_1x_2/H^E has been recommended (6, 7). However, we have adopted eq. [1] since it is the traditional form and is more convenient for interpolation.

According to Brønsted's principle of congruence (8) the properties of solutions of *n*-alkanes at constant temperature and pressure

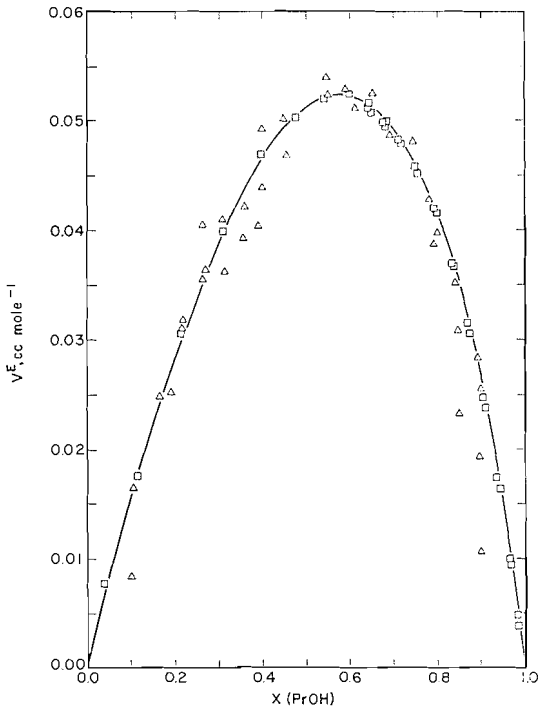

FIG. 3. Volumes of mixing for system PrOH–OcOH at 25 °C. (□) Results obtained with dilatometer; (△) values measured by method (ii) (see Section II).

Can. J. Chem. Downloaded from www.nrcresearchpress.com by 210.87.254.105 on 09/05/12
For personal use only.

TABLE I

Excess volumes of some binary *n*-alcohol systems at 25.00 °C (x_1 mole fraction of component with shorter chain length; V^E cm^3 mole^{-1})

MeOH–BuOH		EtOH–BuOH		PrOH–BuOH		BuOH–OcOH		BuOH–HxOH		BuOH–DeOH	
x_1	V^E	x_1	V^E	x_1	V^E	x_1	V^E	x_1	V^E	x_1	V^E
0.0631	0.0110	0.0438	0.0010	0.0357	0.0002	0.0480	0.0066	0.0372	0.0018	0.0430	0.0119
0.1338	0.0232	0.0968	0.0023	0.0784	−0.0001	0.1040	0.0151	0.0844	0.0039	0.1188	0.0310
0.2257	0.0381	0.1685	0.0039	0.1370	−0.0004	0.1794	0.0237	0.1505	0.0060	0.2109	0.0493
0.3214	0.0527	0.2486	0.0059	0.2046	−0.0007	0.2610	0.0305	0.2216	0.0077	0.3062	0.0631
0.4064	0.0640	0.3239	0.0079	0.2705	−0.0010	0.3381	0.0360	0.2919	0.0091	0.3956	0.0725
0.4866	0.0729	0.3985	0.0098	0.3388	−0.0012	0.4130	0.0395	0.3553	0.0102	0.4739	0.0770
0.5537	0.0779	0.4645	0.0114	0.4017	−0.0017	0.4783	0.0412	0.4207	0.0108	0.5426	0.0781
0.6116	0.0805	0.5211	0.0125	0.4580	−0.0018	0.5336	0.0417	0.4794	0.0113	0.5990	0.0769
0.6579	0.0808	0.5711	0.0132	0.5079	−0.0019	0.5822	0.0411	0.5296	0.0111	0.6511	0.0754
0.6675	0.0799	0.5721	0.0132	0.5212	−0.0020	0.6044	0.0400	0.5345	0.0123	0.6840	0.0727
0.6950	0.0798	0.6082	0.0135	0.5506	−0.0018	0.6231	0.0402	0.5719	0.0123	0.7203	0.0687
0.7003	0.0790	0.6124	0.0137	0.5593	−0.0019	0.6406	0.0388	0.5722	0.0111	0.7587	0.0638
0.7261	0.0781	0.6474	0.0137	0.5881	−0.0018	0.7221	0.0363	0.6094	0.0110	0.7983	0.0577
0.7350	0.0768	0.6478	0.0140	0.6018	−0.0017	0.7663	0.0331	0.6138	0.0121	0.8385	0.0499
0.7713	0.0732	0.6898	0.0137	0.6489	−0.0015	0.8131	0.0278	0.6596	0.0117	0.8742	0.0416
0.8090	0.0675	0.7398	0.0133	0.6988	−0.0014	0.8539	0.0233	0.7085	0.0111	0.9096	0.0321
0.8472	0.0598	0.7886	0.0123	0.7525	−0.0010	0.8947	0.0186	0.7608	0.0100	0.9418	0.0228
0.8846	0.0500	0.8359	0.0108	0.8073	−0.0009	0.9321	0.0130	0.8135	0.0085	0.9686	0.0132
0.9176	0.0388	0.8816	0.0086	0.8578	−0.0005	0.9631	0.0076	0.8637	0.0069	0.9859	0.0065
0.9474	0.0270	0.9235	0.0061	0.9072	−0.0001	0.9844	0.0036	0.9106	0.0050		
0.9715	0.0158	0.9583	0.0035	0.9496	0.0001			0.9506	0.0031		
0.9876	0.0070	0.9824	0.0015	0.9781	0.0001			0.9785	0.0015		

Can. J. Chem. Downloaded from www.nrcresearchpress.com by 210.87.254.105 on 09/05/12
For personal use only.

TABLE I (*Concluded*)

MeOH–OcOH		EtOH–OcOH		PrOH–OcOH		HxOH–OcOH		OcOH–DeOH	
x_1	V^E	x_1	V^E	x_1	V^E	x_1	V^E	x_1	V^E
0.0853	0.0248	0.0525	0.0064	0.0421	0.0078	0.0371	0.0011	0.0348	0.0006
0.2226	0.0683	0.1409	0.0181	0.1159	0.0176	0.0824	0.0025	0.0770	0.0022
0.3716	0.1161	0.2474	0.0314	0.2157	0.0306	0.1456	0.0043	0.1376	0.0038
0.4958	0.1547	0.3540	0.0444	0.3123	0.0400	0.2152	0.0060	0.2041	0.0053
0.5980	0.1815	0.4464	0.0545	0.3996	0.0470	0.2834	0.0076	0.2716	0.0059
0.6764	0.1947	0.5269	0.0624	0.4774	0.0503	0.3507	0.0086	0.3384	0.0069
0.7357	0.1982	0.5950	0.0672	0.5459	0.0521	0.4139	0.0091	0.4005	0.0075
0.7784	0.1959	0.6482	0.0700	0.6020	0.0525	0.4689	0.0094	0.4558	0.0076
0.8161	0.1885	0.6883	0.0705	0.6435	0.0513	0.5185	0.0095	0.5017	0.0076
0.8353	0.1790	0.6917	0.0710	0.6478	0.0517	0.5188	0.0103	0.5449	0.0075
0.8606	0.1686	0.7005	0.0703	0.6501	0.0508	0.5567	0.0102	0.6860	0.0068
0.8843	0.1555	0.7245	0.0706	0.6775	0.0499	0.5613	0.0095	0.7409	0.0062
0.9055	0.1401	0.7312	0.0704	0.6840	0.0495	0.5985	0.0100	0.7971	0.0058
0.9242	0.1225	0.7625	0.0694	0.6862	0.0500	0.6451	0.0097	0.8492	0.0049
0.9435	0.1004	0.7633	0.0696	0.7140	0.0483	0.6941	0.0090	0.9000	0.0038
0.9599	0.0777	0.7968	0.0677	0.7199	0.0479	0.7479	0.0080	0.9438	0.0025
0.9732	0.0553	0.8006	0.0671	0.7525	0.0458	0.8027	0.0070	0.9730	0.0016
0.9861	0.0306	0.8316	0.0636	0.7588	0.0452	0.8558	0.0057		
0.9952	0.0109	0.8664	0.0577	0.7932	0.0420	0.9057	0.0040		
		0.8971	0.0504	0.7985	0.0415	0.9492	0.0027		
		0.9119	0.0467	0.8354	0.0370	0.9779	0.0016		
		0.9299	0.0392	0.8384	0.0367				
		0.9437	0.0345	0.8714	0.0316				
		0.9566	0.0273	0.8780	0.0306				
		0.9691	0.0210	0.9083	0.0248				
		0.9776	0.0156	0.9133	0.0238				
		0.9891	0.0081	0.9411	0.0174				
		0.9915	0.0063	0.9454	0.0165				
				0.9683	0.0100				
				0.9716	0.0095				
				0.9867	0.0049				
				0.9887	0.0039				

TABLE II

Coefficients for least squares fit of data by eq. [1]

Component 1	Component 2	C_0	C_1	C_2	C_3	C_4	C_5	$10^4\sigma_v$
MeOH	BuOH	0.2952	−0.1700	0.0778	−0.0358			3.0
EtOH	BuOH	0.0483	−0.0390	0.0105	0.0038			0.8
PrOH	BuOH	−0.00748	0.00086	0.0087				1.1
BuOH	HxOH	0.0461	−0.0095	0.0136				3.6
BuOH	OcOH	0.1651	−0.0167	0.0197	−0.0129			4.5
BuOH	DeOH	0.3112	−0.0463	0.0356	−0.0205	0.022		3.8
MeOH	OcOH	0.6251	−0.6060	0.3560	−0.0190	0.280	−0.446	10.8
EtOH	OcOH	0.2398	−0.1849	0.1006	−0.0515	0.105	−0.098	2.9
PrOH	OcOH	0.2053	−0.0556	0.0206	−0.0287	0.043		2.6
HxOH	OcOH	0.0392	−0.0078	0.0029				2.7
OcOH	DeOH	0.0302	0.0021	0.0095	−0.0156			1.9

can be expressed as functions of the mean chain length,

$$[2] \qquad n = n_1x_1 + n_2x_2,$$

where n_1 and n_2 are chain lengths of the pure components. The excess volume can then be written in the form

$$[3] \quad V^E(n_1, n_2, x_1) = f(n) - x_1f(n_1) - x_2f(n_2),$$

where $f(n)$ is a suitable function. The excess volumes of *n*-alkane mixtures obey the principle quite closely (9–12). The extent to which the excess volumes of *n*-alcohol mixtures are congruent was investigated using the function

$$[4] \qquad f(n) = \sum_{r=0}^{p} B_r n^{-(r+1)}.$$

This form was employed by Díaz Peña and Fernández Martín (2) in analyzing data for the heats of mixing of methanol with other *n*-alcohols and was also used in our similar study (1).

Analogous to our treatment of the enthalpy data, the coefficients in eq. [4] were determined to minimize

$$[5] \qquad \sigma^2 = \frac{1}{N}\sum_{s=1}^{N} (\sigma^s)^2,$$

where

$$[6] \quad (\sigma^s)^2 = \int_0^1 (V^E_{calc}(n_1^s, n_2^s, x_1) - V^E_{obs})^2 dx_1.$$

$V^E_{calc}(n_1^s, n_2^s, x_1)$ is the value calculated for system *s* from the principle of congruence using eqs. [3] and [4], and V^E_{obs} is the experimental result given at mole fraction x_1 by eq. [1] with the coefficients C_r from Table II. The sum in eq. [5] extends over a set of N systems.

TABLE III

Coefficients for least squares fit of eq. [4]

	Set (a) (11 systems)	Set (b) (9 systems)
B_0	−6.75	−15.57
B_1	14.48	44.90
B_2	−15.04	−63.06
B_3	5.74	33.93

TABLE IV

Standard deviations σ^s and σ

	Set (a) (11 systems)	Set (b) (9 systems)
MeOH–BuOH	0.0100	
EtOH–BuOH	0.0039	0.0014
PrOH–BuOH	0.0026	0.0015
BuOH–HxOH	0.0020	0.0030
BuOH–OcOH	0.0072	0.0051
BuOH–DeOH	0.0145	0.0045
MeOH–OcOH	0.0212	
EtOH–OcOH	0.0173	0.0168
PrOH–OcOH	0.0035	0.0075
HxOH–OcOH	0.0025	0.0009
OcOH–DeOH	0.0028	0.0010
σ	0.0103	0.0067

Two sets of systems were considered: (a) the complete set of 11 systems, and (b) the 9 systems exclusive of methanol. Calculations carried out with an increasing number of constants B_r indicated that there was no significant improvement in fit when more than 4 were used. Values of B_r for the two sets of systems are listed in Table III. The standard deviations (σ) for each set are given in Table IV along with the standard deviations σ^s for each system of the set. As in the case of the excess enthalpies, the excess volumes

Can. J. Chem. Downloaded from www.nrcresearchpress.com by 210.87.254.105 on 09/05/12
For personal use only.

Can. J. Chem. Downloaded from www.nrcresearchpress.com by 210.87.254.105 on 09/05/12
For personal use only.

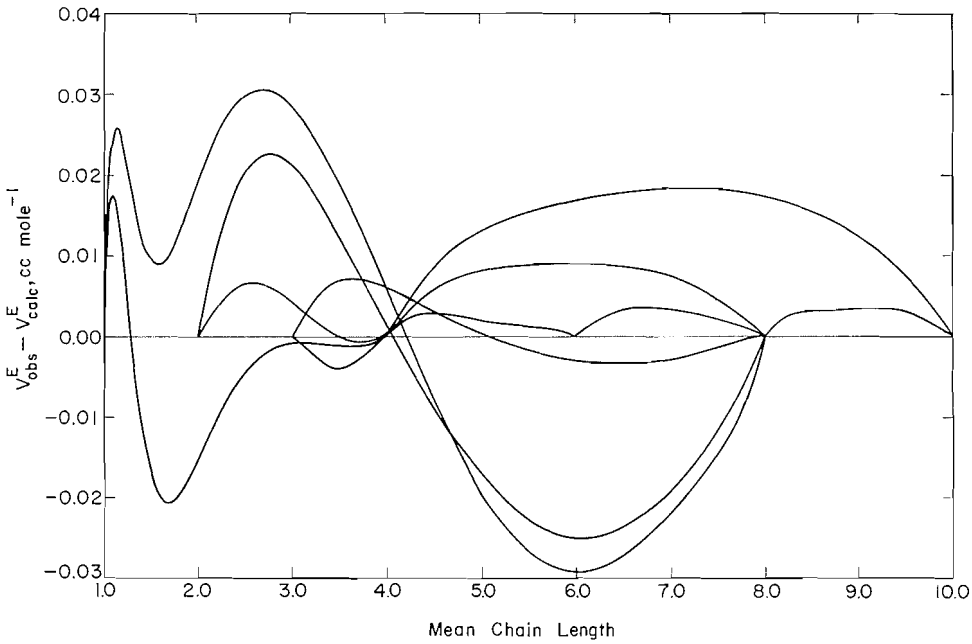

FIG. 4. Plot of deviations of V^E from congruence for 11 binary *n*-alcohol systems. The curves can be identified by the chain lengths corresponding to their termini.

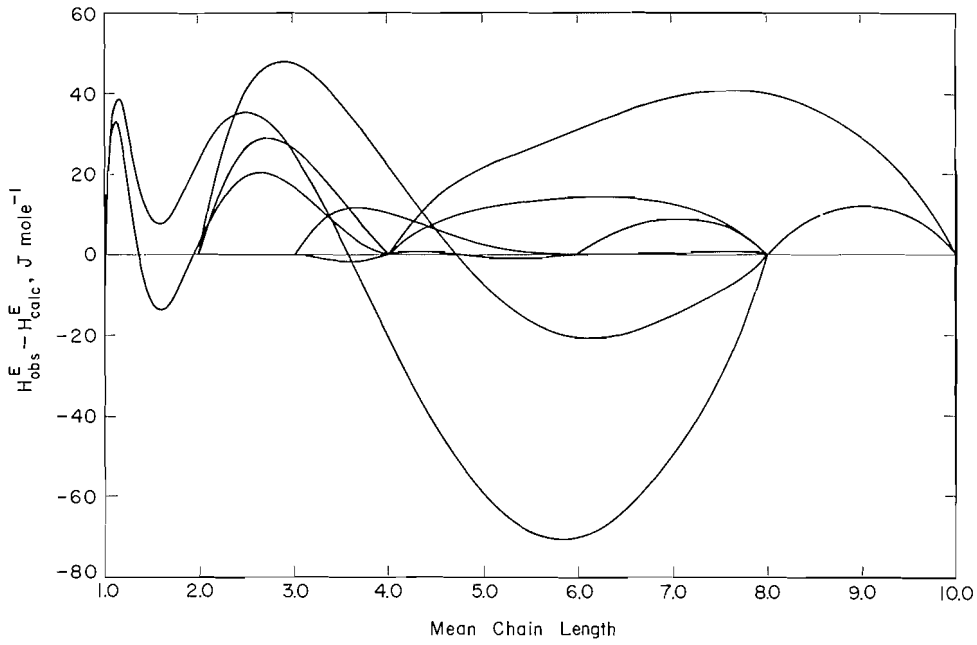

FIG. 5. Plot of deviations of H^E from congruence for 11 binary *n*-alcohol systems. The curves can be identified by the chain lengths corresponding to their termini.

of these binary alcohol systems are only approximately congruent. Omission of the two MeOH systems leads to an improved representation of the remaining data but the deviations are still relatively large.

One interesting feature of the analysis of the data is the close parallel between the deviations from congruence exhibited by the excess volumes and the excess enthalpies. In Fig. 4 the difference between the experimental excess volume and the value calculated from eqs. [3] and [4] with coefficients for set (a) taken from Table III has been plotted against mean chain length. Figure 5 is a similar plot of $H^{E}_{obs} - H^{E}_{calc}$ constructed from data in ref. 1. Comparison of Figs. 4 and 5 reveals many features in common and illustrates the correlation between the excess volumes and excess enthalpies of these systems.

IV. Acknowledgments

We are indebted to Mr. M. Ihnat for carrying out pycnometric measurements on the system MeOH–OcOH, the results of which are presented in Fig. 2. We also wish to thank Mr. C. J. Halpin for purifying the alcohols and Mr. J. M. C. van den Hoff for glass-blowing assistance. Most of the experimental measurements were carried out by Mr. P. J. D'Arcy who contributed many valuable ideas during the development of the dilatometer.

1. A. E. Pope, H. D. Pflug, B. Dacre, and G. C. Benson. Can. J. Chem. **45**, 2665 (1967).
2. M. Díaz Peña and F. Fernández Martín. Anales Real Soc. Espan. Fis. Quim. Madrid, Ser. B, **60**, 9 (1964).
3. W. Geffcken, A. Kruis, and L. Solana. Z. Physik. Chem. Leipzig, **35B**, 317 (1937).
4. W. A. Duncan, J. P. Sheridan, and F. L. Swinton. Trans. Faraday Soc. **62**, 1090 (1966).
5. H. W. Schnaible, H. C. Van Ness, and J. M. Smith. A.I.Ch.E. J. **3**, 147 (1957).
6. H. C. Van Ness and R. V. Mrazek. A.I.Ch.E. J. **5**, 209 (1959).
7. R. V. Mrazek and H. C. Van Ness. A.I.Ch.E. J. **7**, 190 (1961).
8. J. N. Brønsted and J. Koefoed. Kgl. Danske Videnskab. Selskab., Mat.-Fys. Medd. **22**, No. 17 (1946).
9. A. Desmyter and J. H. van der Waals. Rec. Trav. Chim. 77, 53 (1958).
10. J. Hijmans. Mol. Phys. **1**, 307 (1958).
11. M. L. McGlashan. Mol. Phys. **4**, 87 (1961).
12. Th. Holleman. Physica, **29**, 585 (1963).

Can. J. Chem. Downloaded from www.nrcresearchpress.com by 210.87.254.105 on 09/05/12
For personal use only.

Can. J. Chem. Downloaded from www.nrcresearchpress.com by 210.87.254.40 on 09/05/12
For personal use only.

Quantum yields and primary processes in the photolysis of HNCO vapor at 2062 Å[1]

W. D. WOOLLEY[2] AND R. A. BACK
Division of Pure Chemistry, National Research Council of Canada, Ottawa, Canada

Received August 11, 1967

Quantum yields of CO, N_2, and H_2 have been measured in the photolysis of HNCO vapor (2–23 Torr, 25 °C) at 2062 Å. Extrapolated values at zero pressure of HNCO were about 1.0, 0.40, and 0.13 respectively. $\Phi(CO)$ and $\Phi(N_2)$ increased with increasing HNCO pressure and became approximately constant at values of 1.5 and 0.6 respectively between 10 and 20 Torr. From these and other data it was concluded that two primary processes, each with a quantum yield of about 0.5, occur.

$$\mathrm{HNCO} + h\nu \begin{cases} \nearrow \mathrm{NH} + \mathrm{CO} \\ \searrow \mathrm{H} + \mathrm{NCO} \end{cases}$$

The abstraction of H from HNCO by methyl radicals was found to be slow, even at 250 °C, and it was concluded that abstraction of H from HNCO plays no part in the photolysis mechanism, contrary to previous conclusions. A mechanism is suggested, based on radical–radical reactions at low HNCO pressure or high intensity, with radical reactions with HNCO becoming important at higher pressures or low intensity. It is concluded that H_2 was formed in the system by reactions of H atoms.

Canadian Journal of Chemistry, **46**, 295 (1968)

Introduction

The photolysis of HNCO vapor was first studied in detail in this laboratory a few years ago (1). The results were interpreted in terms of a single primary process,

[1A] $$\mathrm{HNCO} + h\nu \rightarrow \mathrm{NH} + \mathrm{CO},$$

followed by rapid abstraction of hydrogen from HNCO,

[2] $$\mathrm{NH} + \mathrm{HNCO} \rightarrow \mathrm{NH_2} + \mathrm{NCO}$$

[3] $$\mathrm{NH_2} + \mathrm{HNCO} \rightarrow \mathrm{NH_3} + \mathrm{NCO},$$

and combination of NCO radicals,

[4] $$2\mathrm{NCO} \rightarrow \mathrm{N_2} + 2\mathrm{CO},$$

with the combination of NH radicals,

[5] $$2\mathrm{NH} \rightarrow \mathrm{N_2} + \mathrm{H_2},$$

becoming important at low HNCO pressures, low temperatures, and high light intensities.

Subsequent work has cast some doubt on this mechanism (2–4). The production of hydrogen in the presence of alkanes suggested that a second primary process,

[1B] $$\mathrm{HNCO} + h\nu \rightarrow \mathrm{NCO} + \mathrm{H},$$

might be occurring (3). This was also suggested to account for differences in the products formed when HN_3 and HNCO were photolyzed in the presence of olefins (4). The present experiments were undertaken to obtain further information about the mechanism of the HNCO photolysis.

One feature of the previously suggested mechanism was the very ready abstraction of hydrogen from HNCO (reactions [2] and [3]). Similar rapid abstraction by hydrogen atoms,

[6] $$\mathrm{H} + \mathrm{HNCO} \rightarrow \mathrm{H_2} + \mathrm{NCO},$$

was also required to account for the isotopic composition of the hydrogen from the photolysis of HNCO–C_3D_8 and DNCO–C_3H_8 mixtures in terms of reaction [1A] as the exclusive primary process (3). Because nothing was known directly about the ease of abstraction of H from HNCO, we undertook a study of the reaction of methyl radicals with HNCO to obtain such information.

In previous studies of the photolysis, no quantum yields were measured, as there was no convenient monochromatic light source in the wavelength region (2000–2400 Å) in which HNCO absorbs. The development of the iodine lamp (5) seemed to offer a useful monochromatic source at 2062 Å, and measurements of quantum yields were therefore undertaken.

Other experiments described in the present

---

[1]Issued as NRCC No. 9806.

[2]NRCC Postdoctorate Fellow, 1964–1966. Present address: Fire Research Station, Boreham Wood, Herts., England.

Can. J. Chem. Downloaded from www.nrcresearchpress.com by 210.87.254.40 on 09/05/12
For personal use only.

paper include a study of the intensity dependence, and a reinvestigation of the effects of ethylene on the photolysis.

Experimental

Apparatus

The conventional cylindrical quartz photolysis vessel was 5 cm in diameter and 10 cm long and equipped with a plane Suprasil window at each end. The vessel was connected, by a small sidearm at each end, in series with an all-glass piston-type circulating pump and a small U-trap, and joined to the vacuum line by a mercury cutoff. Reagents were condensed in the U-trap, the cutoff closed, the trap warmed, and the reagents thoroughly mixed by the circulating pump. As before (1, 3), the vessel was baked under vacuum at 200 °C before each experiment in order to remove small amounts of solid material (probably cyanuric acid) deposited on the windows during the previous photolysis.

Light Sources

Two light sources were employed: a Hanovia S-500 medium pressure mercury lamp and the iodine lamp. The latter was basically similar to that described by Harteck *et al.* (5), but considerably modified to suit our purposes. Argon (Linde, commercial grade) at a pressure of a few tenths of a Torr was pumped continuously through a trap containing iodine crystals at 25 °C, and thence through the lamp, a 13 mm o.d. Suprasil quartz tube which passed through a cylindrical tuned cavity powered by a Raytheon PG-10 85-watt 2450 Mc microwave generator. Light from the discharge emerged through a hole of about 1 cm diameter in one side of the wave guide, which was cooled by water and by a stream of air. A Suprasil quartz lens, mounted with the discharge at its focus, yielded a roughly parallel beam of light. Because the lamp generated objectionable amounts of ozone when operated in the open, the entire unit was enclosed in a box which was flushed continuously with a stream of air vented to a fume hood.

When the flow rate and pressure of argon were carefully adjusted to the minima required for a stable discharge, the only emission lines below 3500 Å were those of atomic iodine at 2062, 1876, 1845, and 1830 Å. About 90% of the light was in the 2062 line, but the shorter wavelengths caused serious actinometry problems because they were very much more strongly absorbed by the azomethane actinometer (Fig. 1). They were virtually completely removed by a liquid water filter 45 mm thick, leaving a light source with 95% of its intensity in the 2062 Å line. The remaining 5% was mostly in a very weak continuum ranging from about 2400 to 3500 Å. It was necessary to flow fresh nonaerated distilled water continuously through the water filter because strongly absorbing substances built up rapidly upon irradiation (perhaps H_2O_2) or upon exposure to air with the lamp off (perhaps H_2CO_3 or CO_3^-). The use of Suprasil quartz in the lens and in all windows in the light path greatly enhanced the available intensity of the 2062 Å light. The light transmitted and absorbed by the photolysis vessel was measured continuously during all experiments, using either the photomultiplier signal from a grating spectrometer set at 2062 Å, or, after the chromatic purity of the source had been established, by a phototube with a platinum cathode treated by baking with H_2 until it was sensitive only to light of wavelength below about 2200 Å.

Analysis

Gases noncondensable at −196 °C (CO, N_2, H_2, and CH_4) were collected by a Toepler pump, measured in a gas burette, and analyzed by gas chromatography, using a molecular sieve column, 1.5 m long, at 25 °C. In experiments with added ethylene these gases were removed from a solid nitrogen trap (−210 °C). Ethane, ethylene, and residual methane were removed from a trap at −155 °C and analyzed on a silica gel column, 1.5 m long, at 25 °C. Other columns used were di-nonyl phthalate (15%) on firebrick, 1 m long, at 50 °C (for HCN and to check the purity of the HNCO), and Poropak Q, 1.5 m long, at 100 °C (for C_2H_6, C_3H_8, C_4H_{10}, HCN, CH_3NCO, C_2H_5NCO, and HNCO). All columns were of 6 mm o.d. Pyrex tubing, as metal columns appear to interfere with the analysis of some of the nitrogen compounds.

Materials

Initially, HNCO was prepared by pyrolysis of cyanuric acid vapor, and purified, as described previously (1). A more convenient preparation, from the reaction of saturated aqueous KNCO solution with 95% H_3PO_4 at 25 °C (6), gave much purer HNCO and was used in the later stages of the work. Azomethane was obtained from Merck, Sharp and Dohme of Canada, Ltd. It was rigorously degassed to remove traces of N_2 and C_2H_6, distilled from bulb to bulb under vacuum, and stored in the dark. Ethylene was Phillips research grade.

Results

The Reaction of CH_3 with HNCO

Azomethane (6.6 Torr) was photolyzed with light from an S-500 medium-pressure mercury arc modified by a Corning glass filter No. 774 (which removes light of wavelength below 2800 Å), from 25 to 250 °C, with and without HNCO added. Blank experiments showed that HNCO by itself was not decomposed, as was expected from its absorption spectrum (Fig. 1). Products of the azomethane photolysis detected and measured were N_2, C_2H_6, and CH_4. At temperatures below 250 °C, the yields of these products were virtually unchanged by the presence of HNCO. Relative yields of the three products were in good accord with previous studies of the azomethane photolysis (7–9). At 250 °C, with 100 Torr HNCO present, the CH_4 yield was marginally enhanced, while that of C_2H_6 was raised by about 30% (Table I). The latter effect can be attributed to the action of HNCO as a third body for the combination of methyl radicals (8); this would have reduced the concentration of methyl radicals somewhat, so that in fact there

Can. J. Chem. Downloaded from www.nrcresearchpress.com by 210.87.254.40 on 09/05/12
For personal use only.

was more abstraction from HNCO than appears at first sight. Taking this into account, it may be estimated that between 14 and 30% of the CH_4 in the experiments at 250 °C with added HNCO came from the reaction

[7] $$CH_3 + HNCO \rightarrow CH_4 + NCO,$$

which is thus between 40 and 100 times slower than the corresponding abstraction from azomethane. The failure to observe reaction [7] at lower temperatures indicates an activation energy considerably higher than that of the latter reaction. Small amounts of CO, not detected at the lower temperatures, were observed at 250 °C, perhaps arising from subsequent reactions of NCO radicals from reaction [7].

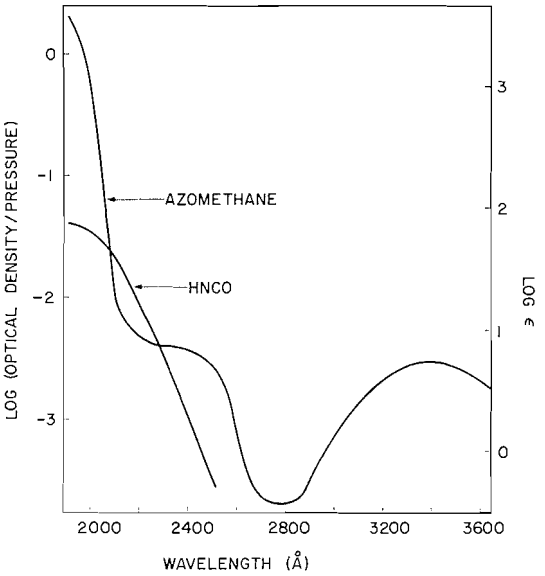

FIG. 1. The absorption spectra of HNCO and azomethane vapors. The left-hand scale shows $\log_{10}$ of the optical density of the photolysis vessel at a pressure of 1 Torr.

TABLE I

Photolysis of azomethane (6.6 Torr) at 250 °C with and without HNCO

	Rates of product formation (μmole/h)			
	N_2	CH_4	C_2H_6	CH_3 loss
Azomethane alone	8.68	4.78	1.39	9.78
Azomethane with HNCO (100 Torr)	9.00	5.16	1.86	9.12

As observed in previous studies of the azomethane photolysis (7–9), there was considerable loss of methyl radicals to give products other than ethane and methane at the higher temperatures (Table I). There was a marginally greater loss in the presence of HNCO, approximately independent of temperature, suggesting an addition reaction of CH_3 with HNCO yielding higher products which were not detected. The rate of this reaction may be very roughly estimated to be about 100 times slower than the corresponding addition to azomethane.

Relative Product Yields from the Photolysis of HNCO at 2062 Å

As in the earlier studies, the noncondensable gases, CO, N_2, and H_2, were the only products detected and measured. As before, the elemental balance of these products implies that NH_3 or its stoichiometric equivalent is also produced. Blank experiments showed that NH_3 was rapidly removed by reaction with HNCO in the gas phase, forming a nonvolatile solid (probably NH_4NCO or urea), which rendered analysis of micromolar quantities of NH_3 impossible, especially since small amounts are formed, together with CO_2, by hydrolysis of HNCO.

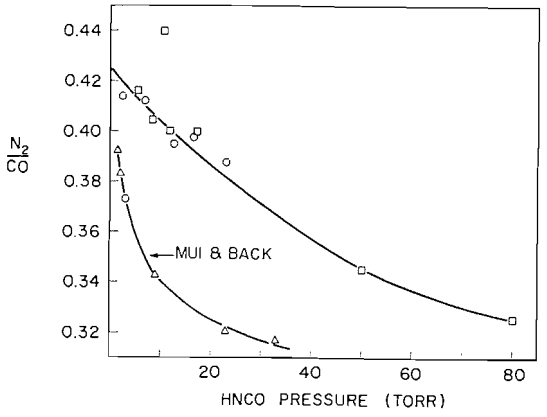

FIG. 2. The product ratio N_2/CO vs. HNCO pressure. Circles represent experiments with the iodine lamp, the squares those with an unfiltered S500 mercury arc. Triangles are from Mui and Back (1).

Figures 2 and 3 show yields of N_2 and H_2 respectively, relative to that of CO, as a function of HNCO pressure. These data obtained at 25 °C lie substantially higher than those of Back and Mui at 37 °C (plotted for comparison) obtained with an unfiltered S-500 medium-pressure mercury lamp (1). It was suspected

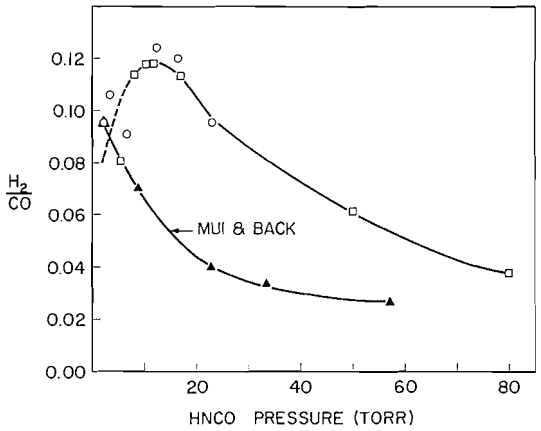

FIG. 3. The product ratio H_2/CO vs. HNCO pressure. Circles represent experiments with the iodine lamp, the squares those with an unfiltered S500 mercury lamp. Triangles are from Mui and Back (1).

(vide infra) that this difference was largely an effect of light intensity rather than of wavelength, so some experiments were made with an S-500 lamp arranged in such a way as to approximately match the effective intensity of the iodine lamp. The results also plotted in Figs. 2 and 3 agree well with the 2062 Å data, confirming the suspected intensity effect; the difference in temperature may also have played a small part.

The trend of N_2/CO with HNCO pressure is similar to that observed previously (1), apparently increasing towards a value of 0.42 or 0.43 as the pressure decreases towards zero. The value of H_2/CO on the other hand shows a levelling out or even a hint of a decrease at the lowest pressures, although the experimental uncertainty is considerable because the amounts of products became very small. The previous experiments (1) showed no such effect, but did not extend to as low pressures and are not incompatible with the present data (Fig. 3).

Quantum Yield Measurements in the Photolysis of HNCO at 2062 Å

To measure quantum yields, the photolysis of azomethane at 25 °C was used as an actinometer, assuming $\Phi(N_2) = 1$. While the photolysis has not been studied at 2062 Å, the trend of observations at longer wavelengths suggest that this assumption is reasonably safe (7–9). It is supported by the observations that N_2 and C_2H_6 (in equal amounts) were the only products observed, and that the yield of N_2 was linearly proportional to the light absorbed but otherwise independent of pressure (Fig. 4).

Some photolysis of azomethane was observed with a Corning 7910 glass filter in front of the cell, which cut off the 2062 Å line completely but transmitted light above 2200 Å. This photolysis, which was thus due to light not absorbed by HNCO, amounted to about 9% of the total, and was corrected for in the actinometry.

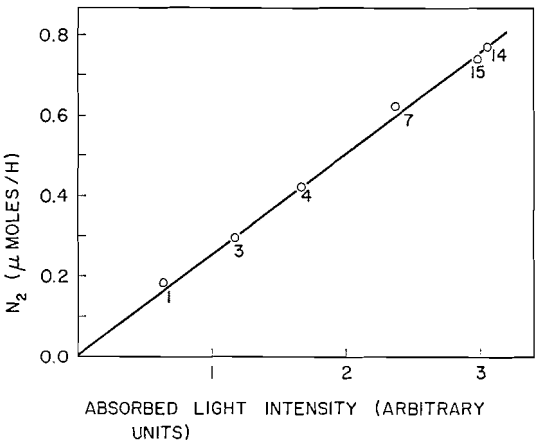

FIG. 4. Nitrogen yields from the azomethane actinometry experiments. Numbers give the azomethane pressure in Torr.

Relative amounts of light absorbed in both azomethane and HNCO were measured by the platinum photocell, which proved very stable and reliable over a period of months. With HNCO the light transmitted by the vessel decreased measurably during the course of a photolysis experiment (30 to 60 min) because of the deposition of a solid compound (presumably the HNCO trimer, cyanuric acid) on the windows. Upon baking under vacuum at 200 °C for a few hours, the solid sublimed off the windows and the cell transmission was restored to its original value. This was done after each photolysis experiment and was quite reproducible. To correct for the loss of intensity during the course of a photolysis, the photocell output was monitored on a chart recorder and a simple correction made, assuming a linear dependence of product yields on intensity and assuming that deposition of solid on front and rear windows was equal. The correction was higher at the higher HNCO pressures but rarely exceeded 10%.

Can. J. Chem. Downloaded from www.nrcresearchpress.com by 210.87.254.40 on 09/05/12
For personal use only.

Can. J. Chem. Downloaded from www.nrcresearchpress.com by 210.87.254.40 on 09/05/12
For personal use only.

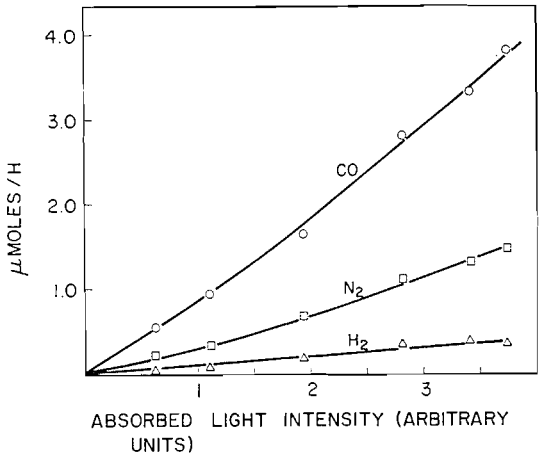

FIG. 5. Product yields from the HNCO actinometry experiments.

In Fig. 5 are shown the rates of production of CO, N_2, and H_2 plotted against the light absorbed. From a correlation of these data with those of Fig. 4, quantum yields were calculated, using the smoothed curves rather than the experimental points, and are shown in Fig. 6.

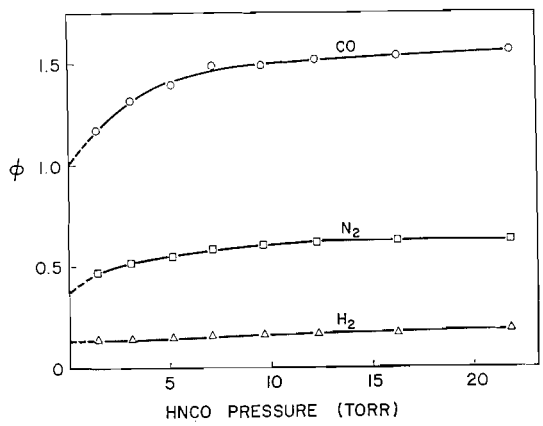

FIG. 6. Quantum yields from the photolysis of HNCO. The points shown do not represent individual experiments, but are derived from the smooth curves in Fig. 5.

A few experiments were made in a special reaction vessel cooled to −60 °C with 2.5 Torr HNCO. Quantum yields of N_2 and CO were essentially unchanged from the values at 25 °; that of H_2 was substantially lower, although the error in the measurements was fairly large.

The Intensity Dependence of the Photolysis of HNCO

These experiments were done with an unfiltered S-500 medium-pressure mercury lamp. In one set of experiments the relative light intensity was varied by inserting in the light path wire gauzes of known transmission. Pressure of HNCO was constant at 4.5 Torr and the temperature was 37 °C. In Fig. 7 the yield of CO is shown as a function of relative intensity. In Fig. 8 are shown yields of N_2 and H_2 relative to that of CO for a much wider range of intensities. These are plotted against the rate of CO production, taken as a measure (not linear) of the light intensity, as relative light intensities were not known in this series of experiments.[3]

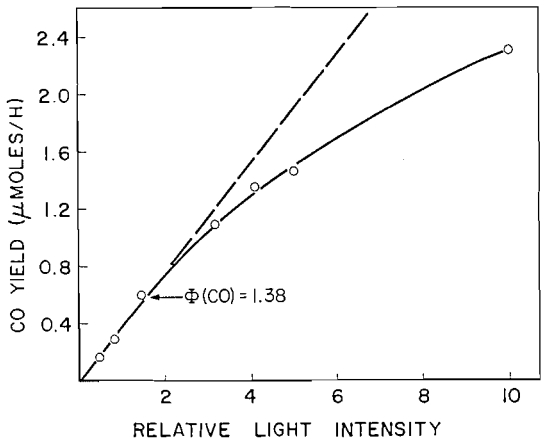

FIG. 7. Yield of CO vs. relative light intensity. HNCO = 4.5 Torr.

The intensity dependence was studied partly to determine whether at high intensity and low HNCO pressure the product ratios would approach those of the flash photolysis (2). In the high-intensity plateaux in Fig. 8, N_2/CO was indeed approximately equal to the flash photolysis value of 0.42; H_2/CO was somewhat lower than in the flash photolysis. If the earlier interpretation of the flash photolysis data were correct, and could be applied in these experiments, the CO at high intensity should have been a primary product only and hence unaffected by the addition of ethylene. In fact, upon the addition of 100 Torr of ethylene, the CO yield

[3]The authors are grateful to Mr. R. Ketcheson, formerly of these laboratories, for performing the experiments shown in Figs. 7 and 8.

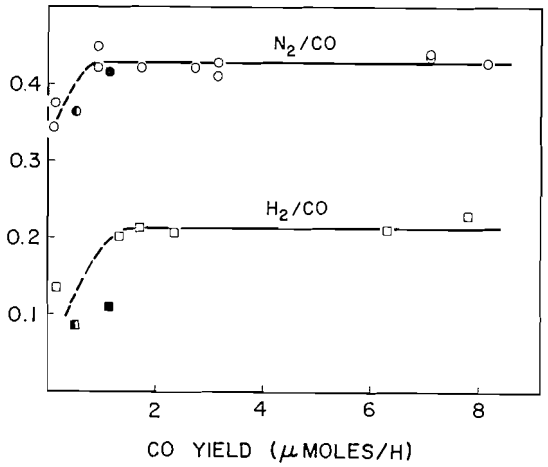

FIG. 8. Product ratios vs. absorbed light intensity, taking the rate of CO production as a (nonlinear) measure of the latter. HNCO = 4.5 Torr. The points ● and ■ are derived from Figs. 2 and 3, ◐ and ◧ taken from Mui and Back (1).

decreased by about a factor of 2. To ensure that competitive absorption of light by ethylene was not contributing to this decrease (as it apparently did in the flash photolysis (2)), a filter cell filled with ethylene was placed in the light path during these experiments.

Photolysis of HNCO at 2062 Å in the Presence of Ethylene

These experiments had a double purpose, first, to examine the effect of ethylene as a radical scavenger on the yields of the normal products, and second, from the new products formed to obtain evidence about the radicals present. The pressure of HNCO was 10 Torr and the temperature 25 °C. The addition of ethylene at pressures of 100 Torr and above reduced the CO production to about half its original value and almost completely suppressed formation of N_2 and H_2. Measurements of the transmitted light showed that even at 600 Torr, ethylene absorbed a quite negligible fraction of the light; this had been a point of uncertainty in earlier experiments (1–3). The suppression of N_2 and H_2 is in agreement with previous observations, while it will be seen that the reduction of CO by a factor of 2 rather than 3 can be attributed to differences in pressure and intensity.

The effect of relatively low pressures of ethylene was also studied in some detail (Fig. 9). It is noteworthy that the hydrogen was reduced almost to zero at pressures of ethylene (0.3 Torr) which left the CO and N_2 almost unaffected. As

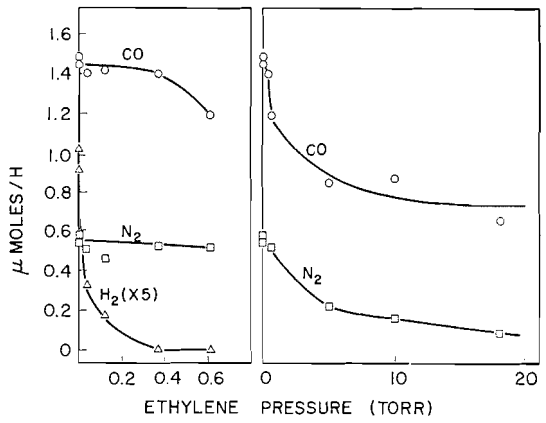

FIG. 9. Product yields from the photolysis of HNCO (10 Torr) in the presence of ethylene.

the ethylene pressure was further increased, CO and N_2 were reduced towards their limiting high-pressure values.

A number of relatively minor new products were observed in the HNCO–ethylene system. These were CH_4, C_2H_6, C_3H_8, n-C_4H_{10}, shown in Fig. 10, and HCN and C_2H_5NCO, shown in Fig. 11.

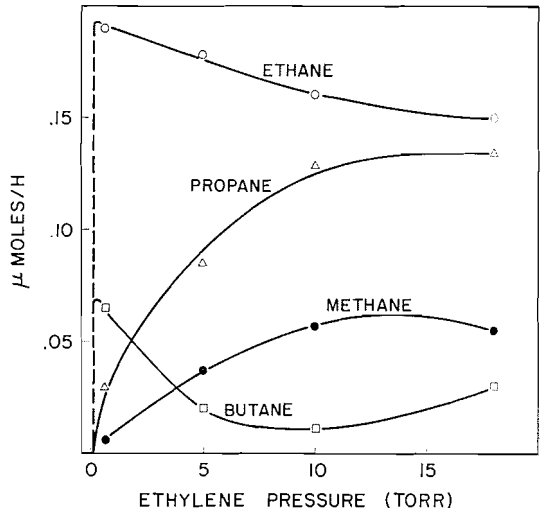

FIG. 10. Hydrocarbon products from the photolysis of HNCO (10 Torr) in the presence of ethylene.

The Co-photolysis of Azomethane and HNCO

These experiments, done at 25 °C, were designed as an attempt to trap NCO radicals by combination with CH_3. With about 5 Torr of each gas and an unfiltered S-500 lamp, the extent of photolysis of azomethane was about 6 times that of HNCO. No CH_3NCO could be detected in any of a number of experiments

Can. J. Chem. Downloaded from www.nrcresearchpress.com by 210.87.254.40 on 09/05/12
For personal use only.

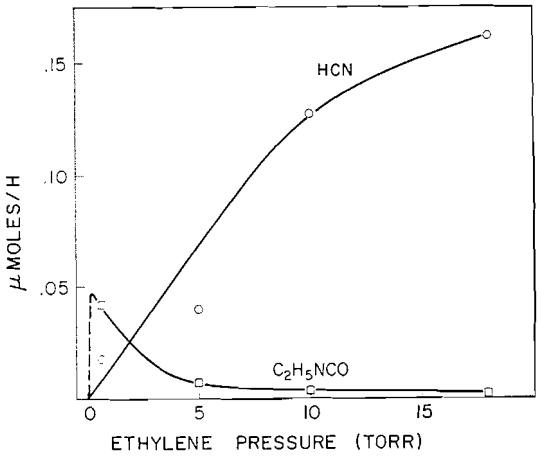

FIG. 11. HCN and C_2H_5NCO from the photolysis of HNCO (10 Torr) in the presence of ethylene.

including several with inert gases added (650 Torr CH_4, 310 Torr N_2, 600 Torr C_2F_6) in an attempt to stabilize CH_3NCO formed in a vibrationally excited state. Blank experiments showed that about 0.1 μmole of CH_3NCO could have been detected by gas chromatography, using a glass column packed with Poropak Q. There was an appreciable loss of CH_3 radicals in the system, and since our earlier experiments showed that this did not occur when only azomethane was photolyzed in a mixture with HNCO, this suggests reactions of CH_3 with NCO not yielding CH_3NCO, or with NH.

Discussion

Primary Processes in the Photolysis of HNCO

It is quite clear from the present results that the simple mechanism (reactions [1]–[5]) based on the single primary process, [1A], is untenable. The very slow rate of abstraction of hydrogen by CH_3 from HNCO (reaction [7]) indicates that the H—NCO bond is relatively strong with a dissociation energy probably in excess of 100 kcal. The relatively large value of the N—H stretching force constant in HNCO lends some support to this conclusion (10). The reactivity of NH_2 in reaction [3] should be similar to that of CH_3 in reaction [7], while reaction [2] is almost certainly endothermic if NH is in its ground state.[4] It seems impossible that reactions [2] and [3] should be quantitative at a pressure of a few Torr of HNCO at room temperature, as required by the simple mechanism.

The interpretation of the isotopic composition of the hydrogen formed from DNCO–propane and HNCO–propane-d_8 experiments (3) in terms of the single primary process [1A] required that the reactions

[8] $$D + HNCO \rightarrow HD + NCO$$

[9] $$H + DNCO \rightarrow HD + NCO$$

be at least 100 times faster than the corresponding abstraction from propane. This also now seems most unlikely.

The observed quantum yields are also not in accord with the simple mechanism based on [1A] as the only primary process, which would predict $\Phi(CO) = 3$.

From this and other evidence it appears quite certain that HNCO decomposes in two ways on photolysis:

[1A] $$HNCO + h\nu \rightarrow NH + CO$$

[1B] $$HNCO + h\nu \rightarrow H + NCO$$

There is no evidence from the absorption spectrum or from the photochemistry to suggest that any intermediate excited state has anything but a transient existence or takes part in processes other than dissociation. This is not surprising for such a simple molecule absorbing 139 kcal of energy (at 2062 Å), far in excess of that required to dissociate either the H—NCO or the HN—CO bond.

The direct evidence for each of the primary processes may be summarized. Evidence for [1A] is the persistence of CO as a product in the presence of high pressures of hydrocarbons (1, 3); the observation of NH by absorption spectroscopy following flash photolysis (13, 14) and the production of CO in the matrix photolysis (15). Evidence for [1B] is the formation of H_2 in the photolysis in the presence of alkanes (3), which was shown by isotopic experiments to contain one H atom from the alkane and one from HNCO, and presumably was formed by reaction of H with the alkane; the observation of NCO by absorption spectroscopy following flash photolysis (13, 14); the formation of *n*-butane, propane, and ethyl isocyanate in the photolysis of HNCO in the presence of ethylene (Figs. 10 and 11), which almost certainly were formed from combination reactions of ethyl

[4]The bond energies for successive removal of H from NH_3 are estimated to be about 102, 93, and 85 kcal/mole (11). A recent estimate of D(N—H) = 74 kcal, if substantiated, would make D(H—NH) = 105 kcal, and change this conclusion (12).

Can. J. Chem. Downloaded from www.nrcresearchpress.com by 210.87.254.40 on 09/05/12
For personal use only.

Can. J. Chem. Downloaded from www.nrcresearchpress.com by 210.87.254.40 on 09/05/12
For personal use only.

radicals generated by the addition of H atoms to ethylene, with the last product, C_2H_5NCO, also providing evidence for the presence of NCO radicals; the elimination of H_2 as a product by the addition of very small pressures of ethylene (Fig. 9), NO, or O_2 (16), strongly suggesting that it was formed from reactions of H atoms.

The relative extents of processes [1A] and [1B] respectively can be estimated from the limiting yields of CO with high pressures of alkanes or alkenes added, and from the yield of H_2 in the presence of alkanes (3). From these data and the quantum yield measurements, it appears that the two processes are of approximately equal importance, each with a quantum yield of about 0.5.

Secondary Reactions at Low HNCO Pressure or High Light Intensity

Secondary reactions must follow [1A] and [1B] to produce the ultimate products of the photolysis, CO, N_2, H_2, and NH_3 (or its equivalent). At HNCO pressures approaching zero, or at high light intensities, radical–radical reactions should predominate, and all the possible interactions of NH, NCO, H, and N (from reaction [13], below) must be considered. Atom–atom reactions requiring a third body would be relatively slow and can be neglected, together with several spin-forbidden or endothermic processes. The following reactions remain and are probably important.

[10] $2NH \rightarrow N_2 + 2H$

[11] $2NH \xrightarrow{M} N_2H_2$

[12] $NH + NCO \rightarrow N_2 + CO + H$

[13] $NH + H \rightarrow H_2 + N$

[14] $NH + N \rightarrow N_2 + H$

[4] $2NCO \rightarrow N_2 + 2CO$

[15] $H + NCO \rightarrow NH + CO$

This set of reactions can account for the extrapolated value of $\Phi(CO) = 1$ at zero pressure, as each NCO is converted to CO and reaction [1A] of course yields CO directly. This suggests that in the zero pressure limit there is no radical attack on HNCO leading to CO formation.

If the nitrogen in NH and NCO were all converted to N_2, an extrapolated zero-pressure value of $\Phi(N_2) = 0.5$ would be expected. In fact the data indicate a lower value than this, with the N_2/CO ratio (and hence $\Phi(N_2)$ if $\Phi(CO) = 1$) approaching 0.42–0.43 at zero pressure (Fig. 2). The same limiting value was observed at high light intensity (Fig. 8) and in the flash photolysis (2), and is accompanied by a larger loss of hydrogen which in the flash photolysis approximately corresponded to the formation of NH_3 or its stoichiometric equivalent. Reaction [11] seems to be the only reaction in the scheme above likely to lead to loss of N_2 and H_2 through ammonia formation. To account for the same behavior in the flash photolysis, it was suggested previously (2) that N_2H_2 formed in reaction [11] decomposed in such a way as to form $N_2 + NH_3$ rather than $N_2 + H_2$ or $N_2 + 2H$,

[16] $N_2H_2 \rightarrow 2/3(N_2 + NH_3)$,

perhaps at the vessel wall, or by reaction with NH,

[17] $NH + N_2H_2 \rightarrow N_2 + NH_3$.

The relative extents of reactions [10] to [15] are difficult to estimate, but it seems possible that about half the NH radicals could have reacted via reactions [11], [16], and [17] as required by the observed deficit of about half the H_2 and one sixth of the N_2. The occurrence of reaction [15] would favor NH combination, and it is probably necessary that reaction [10] be much slower than [11]. This last requirement is the major weak point in the reaction scheme, as reaction [11] should be at least partly pressure dependent at low pressure and there is no reason to think that reaction [10] should not be very fast.

An alternative and perhaps more attractive mechanism for the photolysis at low pressure or high intensity can be based on the assumption that even under these conditions the reaction

[18] $H + HNCO \rightarrow NH_2CO$

is very fast, and together with

[19] $H + NH_2CO \rightarrow NH_3 + CO$

and

[20] $H + NH_2CO \rightarrow H_2 + HNCO$

consumes most of the H atoms. With reduced H-atom concentration, reactions [10], [12], and [4], and perhaps

[21] $NH + NH_2CO \rightarrow NH_2 + HNCO$

[22] $NCO + NH_2CO \rightarrow 2HNCO$

[23] $2NH_2CO \rightarrow HNCO + NH_3 + CO$,

would become the only ones of importance.

Can. J. Chem. Downloaded from www.nrcresearchpress.com by 210.87.254.40 on 09/05/12
For personal use only.

There are two difficulties with this mechanism. The first involves the stability of the NH_2CO radical formed in reaction [18], which by analogy with acetyl might be expected to decompose into $NH_2 + CO$ before the energy of formation of the N—H bond could be dissipated. There is some evidence, however, that $D(NH_2—CO)$ is considerably higher than $D(CH_3—CO)$ (17); and that in fact the weakest bond in the radical is H—NH.CO; this would remove the difficulty. The second problem is that reactions [19] and [23] produce one extra CO for each NH_3, leading to $\Phi(CO) = 1.15$ instead of 1.0. Related to this, removal of H atoms by ethylene should have decreased the yield of CO somewhat (Fig. 9). Loss of NCO (and hence ultimately of CO) in reaction [22] may, however, have approximately compensated for the extra CO. Taking account of the uncertainty in the experimental data, this would seem to resolve this problem also.

The mechanism of hydrogen formation and of hydrogen loss has an important bearing on the reaction mechanism. The complete suppression of H_2 by low pressures of ethylene (Fig. 9), oxygen, or nitric oxide (16), virtually without affecting the yields of CO and N_2, strongly suggests that reactions of hydrogen atoms, rather than the combination of NH radicals (reaction [5]) previously suggested, are the source of H_2, since scavenging of NH by these additives would have suppressed the reactions of NH leading to formation of N_2 and CO (vide infra). Reaction [10], proceeding through diimide,

[10] $2NH \rightarrow [HNNH]^* \rightarrow [NNH] + H \rightarrow N_2 + 2H,$

seems rather more likely than reaction [5] by analogy with the decomposition of azoalkanes, especially in view of the very large exothermicity of both reactions (157 and 55 kcal for reactions [5] and [10] respectively).

The chain sequence of reactions [13] and [14], or reaction [20], are the most probable sources of H_2. Both involve radical–radical reactions which would be favored at high light intensity and low HNCO pressure, as observed. Several facts suggest that reaction [20] is the more likely, and that the reaction sequence [18]–[23] rather than [11]–[17] is predominant. This would offer the simplest explanation of the sharp reduction in H_2 with increasing temperature (1) which could be attributed to the thermal decomposition of the NH_2CO radical. Reaction [21], and perhaps the thermal decomposition of NH_2CO, are sources of the NH_2 radicals observed in the flash photolysis (13, 14). The [18]–[23] sequence can also explain the fact that while the N_2/CO ratio in the zero-pressure limit approaches the high-intensity value, H_2/CO does not (Figs. 2, 3, and 8). At high intensity, both in the flash photolysis (2) and the present experiments, the H_2/CO and N_2/CO ratios were such that the missing N_2 and H_2 roughly corresponded to NH_3 or its equivalent. At low pressure (Figs. 2 and 3) this was not so, as H_2/CO is much too low, and in fact shows a tendency to go through a maximum and decrease again with decreasing pressure. Thus hydrogen must be lost by reactions not forming NH_3 and not affecting the N_2 yield, which seems unlikely if reaction [5] or the [13] + [13] sequence were the source of H_2. Combination of NH_2CO radicals, however,

[24] $2NH_2CO \rightarrow NH_2CO.CONH_2$ (biuret),

or some other reaction of NH_2CO leading to higher products, could account for the loss of H_2 without affecting CO or N_2. It seems possible that the [13] + [14] sequence might still be important at high intensity. The dependence of the photolysis on pressure and on intensity are interrelated, and with probably six radicals present (NH, H, NCO, N, NH_2CO, NH_2), the system is too complex to permit a more precise delineation of the low-pressure and high-intensity mechanisms at the present time.

Secondary Reactions at Higher HNCO Pressures

As the HNCO pressure was increased, quantum yields of CO and N_2 rose, and by about 10 Torr had approximately levelled out at about 1.5 times their extrapolated zero-pressure values (Fig. 6). The magnitude of this increase suggests that either NH, or NCO, or H (each having $\Phi = 0.5$) had reacted quantitatively with HNCO at this pressure, yielding CO and N_2 in about the same proportions as the low-pressure photolysis (note that N_2/CO changed very little (Fig. 2)). Because H_2 could be completely suppressed by the addition of amounts of ethylene, NO, or O_2 too small to affect N_2 appreciably, reaction of H atoms with HNCO can be ruled out as a source of the extra CO and N_2 at 10 Torr pressure of HNCO. The most probable source would seem to be

[25] $NH + HNCO \rightarrow N_2H_2 + CO$

followed by reaction [16]. The reaction

[26] $NCO + HNCO \rightarrow N_2 + 2CO + H$

appears less likely than [25] on the general principle that diradicals are more reactive than monoradicals, and by analogy with the very fast reaction of CH_2 with ketene (18). Reaction [26] on the other hand would presumably proceed through addition of NCO to the N atom of HNCO, and would require considerable energy release from incipient formation of N_2 and CO before the strong NH bond could be broken, which suggests an appreciable activation energy.

The slight increase in $\Phi(H_2)$ observed with increasing pressure probably arises from effects of pressure and intensity on the reactions forming H_2, unrelated to the production of extra CO and N_2.

When the HNCO pressure was increased further, above 10 Torr, the N_2/CO and H_2/CO ratios fell steadily, as observed by Mui and Back (1). Quantum yield measurements were not extended beyond 23 Torr because polymer formation on the cell windows began to interfere seriously with the actinometry. There is a suggestion in the data in Fig. 6 that the decrease in these ratios was chiefly due to an increase in $\Phi(CO)$. The ratio H_2/CO fell off rather faster than N_2/CO, which might be attributed to reaction [23] or [24] becoming the predominant mode of disappearance of NH_2CO. Possible reactions, perhaps of NCO, leading to extra CO have been discussed previously (1) and will not be considered further, as the present results offer no new information about them.

The dependence of the CO yield on relative light intensity (Fig. 7) requires some comment. The pressure of HNCO was 4.5 Torr in these experiments, and from Fig. 6 $\Phi(CO)$ at this pressure was about 1.4 with a CO yield of about 1.1 μmoles/h. This fixes the absolute value of $\Phi(CO)$ at one point in Fig. 7, as shown, and on this basis the falloff in the CO yield with increasing intensity in Fig. 7 corresponds to a change in $\Phi(CO)$ from about 1.5 at low intensity to 1.0 at the highest intensity employed. This illustrates the interrelated dependence of the photolysis on both pressure and light intensity. Thus, increasing the intensity at constant pressure has the same general effect as decreasing the pressure at constant incident light intensity. This is compatible with our suggested mechanism in which radical–radical reactions, favored at high intensity and low pressure, are in competition with reactions of radicals with HNCO, favored at low intensity and high HNCO pressure. The variables themselves, pressure and (absorbed) intensity, are of course themselves related, as the local absorbed intensity (with fixed incident intensity) varies directly with HNCO pressure.

Reactions in the Photolysis of HNCO in the Presence of Ethylene

The reduction of the H_2 yield to zero at relatively low pressures of ethylene has already been discussed and almost certainly is caused by removal of H in the reaction

[27] $H + C_2H_4 \rightarrow C_2H_5.$

The reduction of the CO yield to about half its original value, and the N_2 yield to zero, at high pressures of ethylene can be attributed to removal of NH and NCO radicals by reaction with ethylene. At an HNCO pressure of 10 Torr, $\Phi(CO)$ was 1.5, and according to our mechanism complete scavenging of NH and NCO should have reduced $\Phi(CO)$ to 0.5, one third rather than one half its original value. This suggests that CO formation from NCO was not completely suppressed, perhaps because the CH_2CH_2NCO radical formed in the reaction

[28] $NCO + C_2H_4 \rightarrow CH_2CH_2NCO$

decomposed part of the time by the reaction

[29] $CH_2CH_2NCO \rightarrow CO + [C_2H_4N] \rightarrow$ products

or by some other reaction that released CO. Mui and Back (1) did observe a reduction in CO by a factor of about 3 at high pressures of ethylene, with 22 Torr HNCO and about one half the present incident light intensity. The precise cause of the difference is not clear, but is probably related to the differences in pressure and intensity.

The hydrocarbon products (Fig. 10), overlooked in previous studies (1–3), are of considerable interest. At the lowest ethylene pressure ethane and butane are the main hydrocarbons formed, almost certainly from reactions of ethyl radicals from reaction [27], with butane produced by

[30] $2C_2H_5 \rightarrow C_4H_{10}.$

Can. J. Chem. Downloaded from www.nrcresearchpress.com by 210.87.254.40 on 09/05/12
For personal use only.

Can. J. Chem. Downloaded from www.nrcresearchpress.com by 210.87.254.40 on 09/05/12
For personal use only.

Attempts to explain the large yield of ethane by the reaction

[31] $$H + C_2H_5 \rightarrow C_2H_6$$

are not successful, as at these pressures the cracking reaction

[32] $$H + C_2H_5 \rightarrow [C_2H_6]^* \rightarrow 2CH_3$$

should have been at least as important as reaction [31] (19). Propane would then have arisen by the reaction

[33] $$CH_3 + C_2H_5 \rightarrow C_3H_8.$$

With rising pressure, reaction [31] should have tended to replace [32], propane should have decreased and ethane and butane increased. In fact the reverse was observed, with propane tending towards zero at zero ethylene pressure, while ethane and butane decreased with increasing ethylene. Formation of ethane by reactions of vibrationally excited ethyl radicals formed in reaction [27], either by abstraction of H from HNCO or by enhanced disproportionation, also seems unlikely. The most probable explanation of the high initial yield of ethane is that at low ethylene pressure, reaction [18] was still competing with reaction [27], and ethane arose by

[34] $$C_2H_5 + NH_2CO \rightarrow C_2H_6 + HNCO.$$

The behavior of the yields of ethane, propane, and butane with rising ethylene pressure suggests that CH_3 radicals are being produced. It has been seen that their formation by reaction [32] does not fit the observed data. The most probable source of CH_3 appears to be the decomposition of C_2H_4N formed in reaction [29],

[35] $$C_2H_4N \rightarrow HCN + CH_3.$$

Reaction [35] has been postulated to occur in the reaction of nitrogen atoms with ethylene (20, 21). The parallel rise of propane and HCN (Figs. 10 and 11) offers some support to the idea that it occurs in the present system. With increasing ethylene pressure, reactions [18] and [34] would decrease sharply. Ethane formation thus would decrease but this would be partly compensated by the reaction

[36] $$2CH_3 \rightarrow C_2H_6$$

as more CH_3 radicals were formed, and propane formation by reaction [33] would increase. The decrease and subsequent slight rise in butane production can be explained by the removal of C_2H_5 in reaction [33] and its enhanced formation as reaction [27] replaced [18]. This general picture is supported by the observation that with 18 Torr of ethylene present, the ratio (propane)2/ (butane $\times$ ethane) has risen to 3.93, approaching the value of about 4 expected if these products arose solely by reactions [30], [33], and 36. The same ratio with 0.6 Torr of ethylene was equal to 0.073.

The production of CH_4 parallels that of propane, suggesting that it may have come from CH_3 radicals. Disproportionation of CH_3 with C_2H_5, NH, or NH_2CO may have produced some CH_4, but it seems probable that most of it came from the reaction (4)

[37] $$NH + C_2H_4 \rightarrow HCN + CH_4.$$

This and reaction [35] can account for the observed yield of HCN. It is of interest that $CH_3CN + H_2$, alternate products of reaction [37] observed by Cornell *et al.* (4), were not detected in the present experiments.

The C_2H_5NCO almost certainly arose from combination of C_2H_5 with NCO. The yield relative to butane is rather low if (as postulated) NCO and H were produced in equal amounts. An efficient disproportionation reaction reforming C_2H_4 and HNCO, together with reaction [29], may be responsible. The rapid fall of C_2H_5NCO towards zero with increasing ethylene pressure reflects the loss of NCO radicals in reaction [28]. It is noteworthy that no CH_3NCO was observed although CH_3 radicals were evidently present. The mixed photolysis of azomethane and HNCO also failed to yield CH_3NCO although CH_3 radicals were consumed, and it appears that this combination product is not formed under the conditions of the present experiments. The reaction

[38] $$CH_3 + NCO \rightarrow CH_3NCO \rightarrow HCN + 2H + CO \text{ (or } CH_3N + CO)$$

may account for this behavior, and could also account for some of the CO formed from NCO in the presence of ethylene at high intensity, discussed earlier.

In the photolysis of HNCO with 0.6 Torr of ethylene present, our suggested mechanism predicts that the yield of H atoms in the system should

be given approximately by the sum, $(2 \times C_2H_6) + C_3H_8 + (2 \times C_4H_{10}) + C_2H_5NCO$, which was equal to 0.58 μmole/h. The yield of CO at the same pressure of HNCO alone was 1.48 μmoles/h and Φ(CO) was 1.5, from which $\Phi(H) = 0.59$. Considering the uncertainties in the product yields this is in reasonable agreement with the suggested value of about 0.5.

Summary and Conclusions

The main conclusions of the present study can be summarized.

(1) There is strong cumulative evidence from these and other experiments that there are two primary processes (reactions [1A] and [1B]) in the photolysis of HNCO, each with a quantum yield of about 0.5.

(2) The H—NCO bond appears to be rather strong with a dissociation energy probably in excess of 100 kcal. Abstraction of H from HNCO by free radicals is unlikely to play a part in the photolysis mechanism, and a previous mechanism which assumed rapid abstraction from HNCO is untenable.

(3) Hydrogen arises in the photolysis from reactions of H atoms, probably with NH_2CO or NH (reactions [13] and [20]). It appears that H atoms add rapidly to HNCO even at low pressures to form NH_2CO.

(4) The mechanism of the photolysis is complex as it may involve as many as 6 free radicals: NH, NCO, H, NH_2CO, NH_2, and N. The details of the mechanism are by no means certain, but a general pattern of radical–radical reactions at low pressure or high light intensity, and reactions of radicals with HNCO at higher HNCO pressures or lower intensities, appears to account for most of the experimental observations.

1. J. Y. P. Mui and R. A. Back. Can. J. Chem. **41**, 826 (1963).
2. R. A. Back. J. Chem. Phys. **40**, 3493 (1964).
3. J. L. Brash and R. A. Back. Can. J. Chem. **43**, 1778 (1965).
4. D. W. Cornell, R. S. Berry, and W. Lwowski. J. Am. Chem. Soc. **88**, 544 (1966).
5. P. Harteck, R. R. Reeves, and B. A. Thompson. Z. Naturforsch. **19a**, 2 (1964).
6. R. A. Ashby and R. L. Werner. J. Mol. Spectr. **18**, 184 (1965); Spectrochim. Acta, **22**, 1345 (1966).
7. J. G. Calvert and J. N. Pitts. Photochemistry. Wiley, New York. 1966.
8. S. Toby and B. H. Weiss. J. Phys. Chem. **68**, 2492 (1964).
9. P. Gray and J. C. J. Thynne. Trans. Faraday Soc. **59**, 2277 (1963).
10. W. J. Orville Thomas. Trans. Faraday Soc. **49**, 855 (1953).
11. T. L. Cottrell. The strengths of chemical bonds. 2nd ed. Butterworths, London. 1958.
12. K. E. Seal and A. G. Gaydon. Proc. Phys. Soc. London, **89**, 459 (1966).
13. R. Holland, D. W. G. Style, R. N. Nixon, and D. A. Ramsay. Nature, **182**, 336 (1958).
14. R. N. Nixon. Can. J. Phys. **37**, 1171 (1959).
15. M. E. Jacox and D. E. Milligan. J. Chem. Phys. **40**, 2457 (1964).
16. R. A. Back and R. Ketcheson. Can. J. Chem. In press. February 1968.
17. B. C. Spall and E. W. R. Steacie. Proc. Roy. Soc. London, Ser. A, **239**, 1 (1957).
18. G. B. Kistiakowsky and K. Sauer. J. Am. Chem. Soc. **80**, 1066 (1958).
19. R. A. Back and D. W. L. Griffiths. J. Chem. Phys. **46**, 4839 (1967).
20. H. G. V. Evans, G. R. Freeman, and C. A. Winkler. Can. J. Chem. **34**, 1271 (1956).
21. J. T. Herron. J. Phys. Chem. **70**, 2803 (1966).

Can. J. Chem. Downloaded from www.nrcresearchpress.com by 210.87.254.40 on 09/05/12
For personal use only.

Calculations on the rate of photodissociation of hexafluoroacetone

P. G. BOWERS[1]

Department of Chemistry, The University of British Columbia, Vancouver, British Columbia

Received May 30, 1967

The dissociation of hexafluoroacetone from high vibrational levels of its first excited singlet state is treated by the methods of RRKM unimolecular theory. Predictions of the relative photodissociation rates for various exciting wavelengths are in reasonable accord with the observed rates and indicate a critical predissociation energy of about 6 kcal/mole. The calculated temperature dependence is less satisfactory and somewhat lower than the experimental variation.

Canadian Journal of Chemistry, 46, 307 (1968)

Can. J. Chem. Downloaded from www.nrcresearchpress.com by 210.87.254.105 on 09/05/12
For personal use only.

Introduction

In a recent paper (1), we have shown how rate constants for the dissociation of ketene from its first excited singlet state may be adequately understood in terms of RRKM (Rice–Kassel–Ramsberger–Marcus) unimolecular theory. The photodissociation was assumed to be a predissociation, rate controlled by the rate at which sufficient vibrational energy accumulates in a suitable internal mode.

This paper reports similar calculations for hexafluoroacetone (HFA), where data for the primary dissociation rates can be extracted from conventional measurements of the decomposition quantum yields.

Extensive studies of the photochemistry of HFA (2–5) have led to a generally accepted mechanism for the overall kinetics, which invokes reactions from three excited species, $^1A^*$, a vibrationally excited singlet state, and $^1A^0$ and $^3A^0$, vibrationally equilibrated singlet and triplet states respectively.

[1] $A + h\nu \rightarrow {}^1A^*$

[2] $^1A^* \rightarrow CF_3CO + CF_3$

[3] $A + {}^1A^* \rightarrow A + {}^1A^0$

[4] $^1A^0 \rightarrow A(+ h\nu)$

[5] $^1A^0 \rightarrow CF_3CO + CF_3$

[6] $^1A^0 \rightarrow {}^3A^0$

[7] $^3A^0 \rightarrow CF_3CO + CF_3$

[8] $^3A^0(+ Hg) \rightarrow A(+ h\nu)$

Steady-state treatment leads to several equations relating the primary quantum yield ϕ to concentration. A particularly useful form is

$$[i] \quad \frac{\phi}{1-\phi} = \frac{\phi^\infty}{1-\phi^\infty} + \frac{k_2}{k_3[A](1-\phi^\infty)},$$

where

$$\phi^\infty = \frac{k_5(k_7+k_8)+k_6k_7}{(k_4+k_5+k_6)(k_7+k_8)}.$$

Kutschke and his co-workers (7, 8) have recently shown that the discrepancy in the ϕ^∞ values obtained in various laboratories is due to quenching of the triplet state by mercury vapor. Reaction [8] includes such quenching, as well as phosphorescence and true radiationless conversion. Dissociation of $^1A^0$ (reaction [5]) has not previously been included in the analysis, but the detailed energetic considerations presented below indicate that it may occur. In principle, eq. [*i*] may be used to obtain values for k_2/k_3 regardless of whether ϕ^∞ is determined by reaction [5] or reaction [7], and regardless of whether mercury vapor is present or not. In practice, however, the function $\phi/(1-\phi)$ plotted against $1/[A]$ deviates considerably from linearity at low pressure. Part of the discrepancy arises from large random scatter when ϕ is close to unity, but examination of the data of Ayscough and Steacie (2) shows that there is in addition a systematic deviation at some temperatures, even when the quantum yield is moderately low. Such behavior could be indicative of a complex deactivation mechanism, or it might arise because the value of k_2, averaged over all energies, decreases at low pressure (1). For our present purposes, we have considered dissociation data taken at higher pressures (>10 mm), which do correlate reasonably well with eq. [*i*].[2] The values of k_2 were obtained using a strong

[1]Present address: Department of Chemistry, Boston University, Boston, Mass. 02215.

[2]In their original analysis, Ayscough and Steacie reduced the random scatter by taking points from a smoothed plot of ϕ vs. log [A]. The k_2 values quoted by these authors are incorrect because their mechanism, while still predicting a linear relationship of the form of eq. [*i*], did not include triplet dissociation.

collision model (9) with the collision diameter of HFA equal to 6.0 Å, independent of temperature. These are listed in Table I.

TABLE I

Rate constants for the dissociation of $^1A^*$

λ (Å)	T (°C)	$10^{-7}k_2$ (s^{-1})	Ref.
3130	−78	0.47	4
3130	25	3.4	4
3130	27	2.9	2
3130	53	5.4	2
3130	78	8.8	2
3130	108	9.4	2
3020	25	6.0	4
2804	25	17.0	4
2652	25	23.0	4
2652	27	30.0	3

Calculation of the Dissociation Rate Constants

Detailed energetics for the dissociation of a vibrationally excited singlet state have been discussed in our previous paper (1). The rate constant k_2 is calculated using the expression

$$[ii] \quad \langle k_2 \rangle = \frac{1}{Q}\int_{E>0} k_2(E_x + E)N(E)e^{-E/kT}dE,$$

where Q and E are the vibrational partition function and total vibrational energy respectively, for the ground state molecule, and E_x is the difference in energy between the exciting wavelength and the zero–zero energy, E_{00}. The specific rate constant for dissociation of a $^1A^*$ molecule with total internal energy E^* is given, according to the Marcus theory (6), by

$$[iii] \quad k_2(E^*) = \frac{1}{h} \times \frac{Z^+}{Z^*} \times \frac{S^+(E^+)}{N^*(E^*)},$$

where $E^* = E_x + E$

and $E^+ = E_x - E_{min} + E$.

Here, Z^+/Z^* is the ratio of the partition functions for adiabatic degrees of freedom of the activated complex and excited molecule respectively, and E_{min} is the critical dissociation energy. $S^+(E^+)$ is the sum of all energy states for the active vibration–rotation degrees of freedom of the activated complex up to its energy E^+, while $N^*(E^*)$ is the corresponding density of states for the excited molecule. In Fig. 1, which summarizes the energetics, the function $f(E)$ is equal

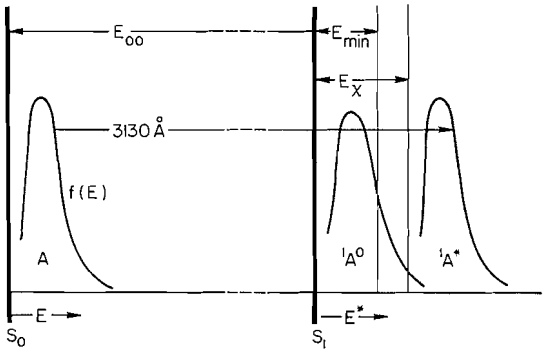

FIG. 1. Energy diagram for photodissociation.

to $N(E)\,e^{-E/kT}$, the Boltzmann distribution function for the ground state.

Evaluation of Energy Level Densities and Sums

The vibrational analysis of Berney (10) was used to calculate the function $N(E)$. For ease of computation, the 24 frequencies were grouped into 11 degenerate sets as follows: 1807 cm^{-1}(1), 1241(6), 972(1), 748(2), 633(1), 506(4), 343(2), 256(3), 168(2), 66(1), 48(1). The density of vibrational states up to 3000 cm^{-1} was found by direct count. For higher energies, the Whitten–Rabinovitch (11) approximation was employed, and this gave good agreement with the direct count to within a few per cent at energies above 2000 cm^{-1}.

The absorption spectrum of HFA has been studied only in the gas phase and gives no information about the excited singlet state frequencies. Hence these had to be estimated. The 16 modes associated with non-torsional motions of the CF_3 groups are remote from the region of $n\pi^*$ excitation and were assigned frequencies 10% less than the corresponding ground state values. The C—C, C—O, and skeletal modes were reduced by 20%, by comparison with the work of Sidman and McClure (13) on biacetyl. The two CF_3 torsions, 66 and 48 cm^{-1} in the ground state, were treated as free internal rotations in the excited state. This will almost certainly be the case at the excess energies (3000 cm^{-1} or more) possessed by the excited molecule. The overall assignment was as follows: 1450 cm^{-1}(1), 1120(6), 780(1), 635(2), 572(1), 460(4), 309(2), 232(3), 150(2). Vibrational frequencies for the activated complex were taken to be the same as those for the excited molecule, omitting the asymmetric C—C

Can. J. Chem. Downloaded from www.nrcresearchpress.com by 210.87.254.105 on 09/05/12
For personal use only.

TABLE II

Comparison between the calculated and observed rate constant ratios

	Calculated								Observed
	Model I				Model II				
E_{00} (Å)	3395	3454	3500	3500	3500	3340	3500	3700	3500
E_{min} (cm^{-1})	2000	2000	2000	2500	3000	1800	2500	3500	1000
Relative k_2									
3130 Å; −78°	0.18	0.26	0.41	0.23	0.12	0.42	0.34	0.35	0.15
3130 Å; 25°	1.0	1.0	1.0	1.0	1.0	1.0	1.0	1.0	1.0
3130 Å; 53°	1.4	1.2	1.2	1.3	1.5	1.3	1.3	1.3	1.7
3130 Å; 78°	1.7	1.4	1.3	1.6	1.9	1.6	1.5	1.6	2.7
3130 Å; 108°	2.1	1.7	1.5	1.9	2.5	2.0	1.9	2.0	2.9
3020 Å; 25°	2.4	1.9	1.6	2.2	3.0	2.3	2.2	2.2	1.9
2804 Å; 25°	7.7	6.1	5.1	8.5	14.7	6.1	6.0	7.2	5.3
2652 Å; 25°	15.0	11.2	9.0	17.6	36.0	8.3	8.8	12.0	8.5

stretching mode, which becomes the reaction coordinate as the molecule decomposes into CF_3CO and CF_3. Two models for the activated complex were investigated. In model I, only the two torsional CF_3 motions were treated as free rotors, while in model II, eight free internal rotations were allowed, three for each CF_3 group, and two for the carbonyl group, and appropriate vibrations omitted. It was felt that these two extremes should bracket the actual behavior. The modified Whitten–Rabinovitch formula (11) was used in calculating the vibration–rotation functions $N^*(E^*)$ and $S^+(E^+)$ in each case. All the calculations involved either a number of low vibrational frequencies and (or) rotations, so the density and sum functions could be regarded as continuous for energy regions of interest.

Relative Rate Constants

In order to calculate $\langle k_2 \rangle$ according to eqs. [*ii*] and [*iii*], values have to be assigned to E_{00} and E_{min}. From the overlap of the fluorescence and absorption spectra, E_{00} is approximately 3500 Å (28 570 cm^{-1}) (3). The apparent "activation" energy for reaction [2], judged from the k_2 values in Table I, is 1000 cm^{-1}, and as we have previously indicated, E_{min} must be greater than this. Furthermore, ϕ^0, the extrapolated zero-pressure quantum yield, is unity for wavelength 3130 Å or shorter (i.e. every molecule has enough energy to decompose in the absence of collisions), and hence $E_x(3130\text{ Å}) > E_{min}$.

With these points in mind, relative values for $\langle k_2 \rangle$ were calculated for each of the two complex models, and the comparison is shown in Table II.

Discussion

Results of the calculations for the wavelength dependence of k_2 at 25° are in good agreement with experiment using $E_{00} = 3500$ Å, and $E_{min} = 2000$ cm^{-1} (model I) or 2500 cm^{-1} (model II). However, using these same parameters, or indeed using any reasonable parameters, the calculated temperature variation is significantly too small. The discrepancy is less serious when the loose complex (model II) is considered. This is so because of the behavior of the function $S^+(E^+)$, which increases very sharply at low energies when many internal rotations are included.

The experimental variation of k_2 at elevated temperature would be somewhat smaller than indicated, if the effective collision diameter of HFA were subjected to a Sutherland correction, but the adjustment is unlikely to be more than 10–15%.

Calculation of the absolute rate constants required further assumptions about the geometry of the excited molecule and complex and was not investigated in any detail. Approximate values for k_2(3130 Å, 25°) using model I were 10^9 s^{-1}, about two orders of magnitude too high.

Treatment of the photodissociation process according to RRKM unimolecular theory is severely limited at present by lack of any detailed knowledge about the excited states involved. In particular, two important factors have been necessarily neglected in our calculations. The first concerns the probability of

Can. J. Chem. Downloaded from www.nrcresearchpress.com by 210.87.254.105 on 09/05/12
For personal use only.

crossover from the excited singlet state to the predissociating state. We have assumed that a molecule which accumulates any energy above E_{min} in the reaction coordinate always dissociates, but this may not be so. A molecule which suddenly gathers a *large* excess energy in the C—C mode might possibly remain on the singlet potential energy surface, i.e. by analogy with the reappearance of fine structure above the predissociation limit in some diatomic molecule spectra. This effect would decrease the absolute rate constant, particularly at short wavelength excitation.

A second point is that the electronic transition probability will vary with ground state vibrational energy, depending on Franck–Condon and symmetry factors, whereas we have taken the energy profile $f(E)$ to be retained in the excited state. The error introduced here might be quite large, particularly in the calculated temperature variation of photodissociation.

Dissociation of $^1A^0$

The Boltzmann distribution of excited singlet molecules ($^1A^0$) is sketched in Fig. 1, and has a maximum at around 1000 cm^{-1} at 25°, and 2000 cm^{-1} at 108°. If E_{min} is between 2000 – 3000 cm^{-1}, then a significant thermal dissociation of $^1A^0$ is possible, particularly at higher temperatures. For this reason, reaction [5] was included in the overall scheme. It may be the origin of the small (but reproducible) values of ϕ^∞ in the presence of mercury vapor.

Dissociation via the Ground State

It has been periodically suggested that dissociations such as reaction [2] could occur by fast internal conversion to high vibrational levels of the ground state, which then dissociates. A few calculations were made using this model, taking E_{min} to be 18 000 cm^{-1}, the value given by Batey and Trenwith (12) for the thermal dissociation of HFA into CO and C_2F_6. Relative to the rate at 3130 Å, 25°, the rates at 3130 Å, 108° and 2652 Å, 25° were found to be 1.4 and 4.9 respectively, which compare with the experimental ratios of 2.9 and 8.5. This reaction path therefore appears unlikely in HFA, and would indeed be difficult to reconcile with the rest of the kinetics.

1. P. G. Bowers. J. Chem. Soc. A, 466 (1967).
2. P. B. Ayscough and E. W. R. Steacie. Proc. Roy. Soc. London, Ser. A, **234**, 476 (1956).
3. G. Giacometti, H. Okabe, and E. W. R. Steacie. Proc. Roy. Soc. London, Ser. A, **250**, 287 (1959).
4. P. G. Bowers and G. B. Porter. J. Phys. Chem. **68**, 2982 (1964); **70**, 1622 (1966).
5. A. N. Strachan, R. K. Boyd, and K. O. Kutschke. Can. J. Chem. **43**, 1345 (1964).
6. R. A. Marcus. J. Chem. Phys. **20**, 352 (1952).
7. A. Gandini and K. O. Kutschke. Can. J. Chem. **44**, 1720 (1965).
8. K. O. Kutschke and D. Whytock. Unpublished results.
9. G. B. Porter and K. Uchida. J. Phys. Chem. **70**, 4079 (1966).
10. C. V. Berney. Spectrochim. Acta, **21**, 1809 (1965).
11. G. Z. Whitten and B. S. Rabinovitch. J. Chem. Phys. **38**, 2466 (1963); **41**, 1883 (1964).
12. W. Batey and A. B. Trenwith. J. Chem. Soc. 1388 (1961).
13. J. W. Sidman and D. S. McClure. J. Am. Chem. Soc. **77**, 6471 (1955).

Can. J. Chem. Downloaded from www.nrcresearchpress.com by 210.87.254.105 on 09/05/12
For personal use only.

Potentiometric and conductometric studies on the composition and stability of zinc complexes of thiomalic acid

R. S. SAXENA, K. C. GUPTA, AND M. L. MITTAL
Department of Chemistry, Malaviya Regional Engineering College, Jaipur, India

Received May 19, 1967

The precise nature of the reaction between zinc and thiomalic acid in aqueous 0.1 *M* KNO_3 has been investigated potentiometrically and conductometrically. The formation of two complexes, one predominating at pH 5.5–7 and another at pH 8–9.5, was found. The stability constants of the complexes formed have been determined by applying Calvin and Melchior's extension of Bjerrum's method at three different temperatures. The log *K* values for 1:1 and 1:2 complexes computed by alternative methods at 25, 30, and 35 °C have been found to be 8.75, 8.85, 8.86, and 6.82, 6.75, 6.93, respectively. The values of the overall changes in ΔG, ΔH, and ΔS accompanying the reaction have also been evaluated at 30 °C and found to be −21.61 kcal/mole, −5.3 kcal/mole, and +53.8 cal/deg respectively.

Canadian Journal of Chemistry, **46**, 311 (1968)

Can. J. Chem. Downloaded from www.nrcresearchpress.com by 210.87.254.105 on 09/05/12
For personal use only.

Introduction

A survey of the literature shows that though the metal complexes of thiomalic acid (TMA)

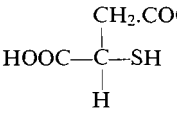

containing an active —SH group have been studied by many authors, the stability constants and their refinement by alternative methods have not been reported. No exhaustive study of the Zn–TMA system has been done. The present investigation has, therefore, been carried out to make a detailed study of the system involving the computation of true stability constants by alternative methods (method of successive approximation, least-square treatment, correction term method, convergence formulas of successive approximation, and the effect of temperature variation on the stabilities of complexes together with the determination of overall changes in free energy, enthalpy, and entropy accompanying the reaction.

Experimental

Thiomalic acid (99.8%, Evan's Chemetics, Inc., New York) and Anal-R (B.D.H.) reagents $ZnSO_4$, KNO_3, NaOH, etc. were used and their solutions were prepared in doubly distilled air-free conductivity water. Freshly prepared solutions of the reagents were always used to avoid the effects of age and hydrolysis. Zinc contents in $ZnSO_4$ solutions were checked by estimating it as zinc pyrophosphate.

A cambridge bench pattern (null-deflection type) pH meter, manufactured by Cambridge Instrument Co. Ltd., 13, Grosvenor Place, London, S.W.1., was used for pH measurements. A glass electrode of 0–14 pH range, calibrated frequently by using buffer solutions of different pH values, was used in conjunction with a saturated calomel electrode connected to the cell by a low resistance salt bridge. All the pH titrations were carried out in aqueous 0.1 *M* KNO_3. The temperatures were controlled by an electrically maintained thermostat.

The conductance measurements were carried out with an electronic eye type conductometer (Leitfahigkeits-meBgerat type LBR Wissenschafflich Technische Werkstaffen, G.m.b.H. Weilheim/obb, Germany).

The experimental procedure consists in performing a series of pH and conductometric titrations of thiomalic acid with standard NaOH in the absence and presence of Zn^{2+} at various ligand to metal ratios, viz. 1:1, 2:1, 3:1, etc. The Calvin and Melchior's (1) extension of Bjerrum's (2) method was used to calculate the stability constants of the complexes formed and were further refined by alternative methods.

Results and Discussion

Stoichiometry

To establish the stoichiometry of the complex species formed during the interaction of $ZnSO_4$ and TMA, the magnitude of proton displacement was determined by titrating solutions containing TMA and $ZnSO_4$ in different ratios against standard alkali.

Figure 1 represents the pH and conductometric titrations of solutions 3.33×10^{-3} *M* in TMA (curves 1 and 5), 3.33×10^{-3} *M* in TMA and 3.33×10^{-3} *M* in $ZnSO_4$ (curves 2 and 6), 6.66×10^{-3} *M* in TMA and 3.33×10^{-3} *M* in $ZnSO_4$ (curves 3 and 7), 10.0×10^{-3} *M* in TMA and 3.33×10^{-3} *M* in $ZnSO_4$ (curve 4) with 0.1 *M* NaOH. The abscissa represents the moles of NaOH added per mole of ligand, *m*.

The appearance of only one inflection (Fig. 1, curve 1) after 2 moles of base per mole of ligand

Can. J. Chem. Downloaded from www.nrcresearchpress.com by 210.87.254.105 on 09/05/12
For personal use only.

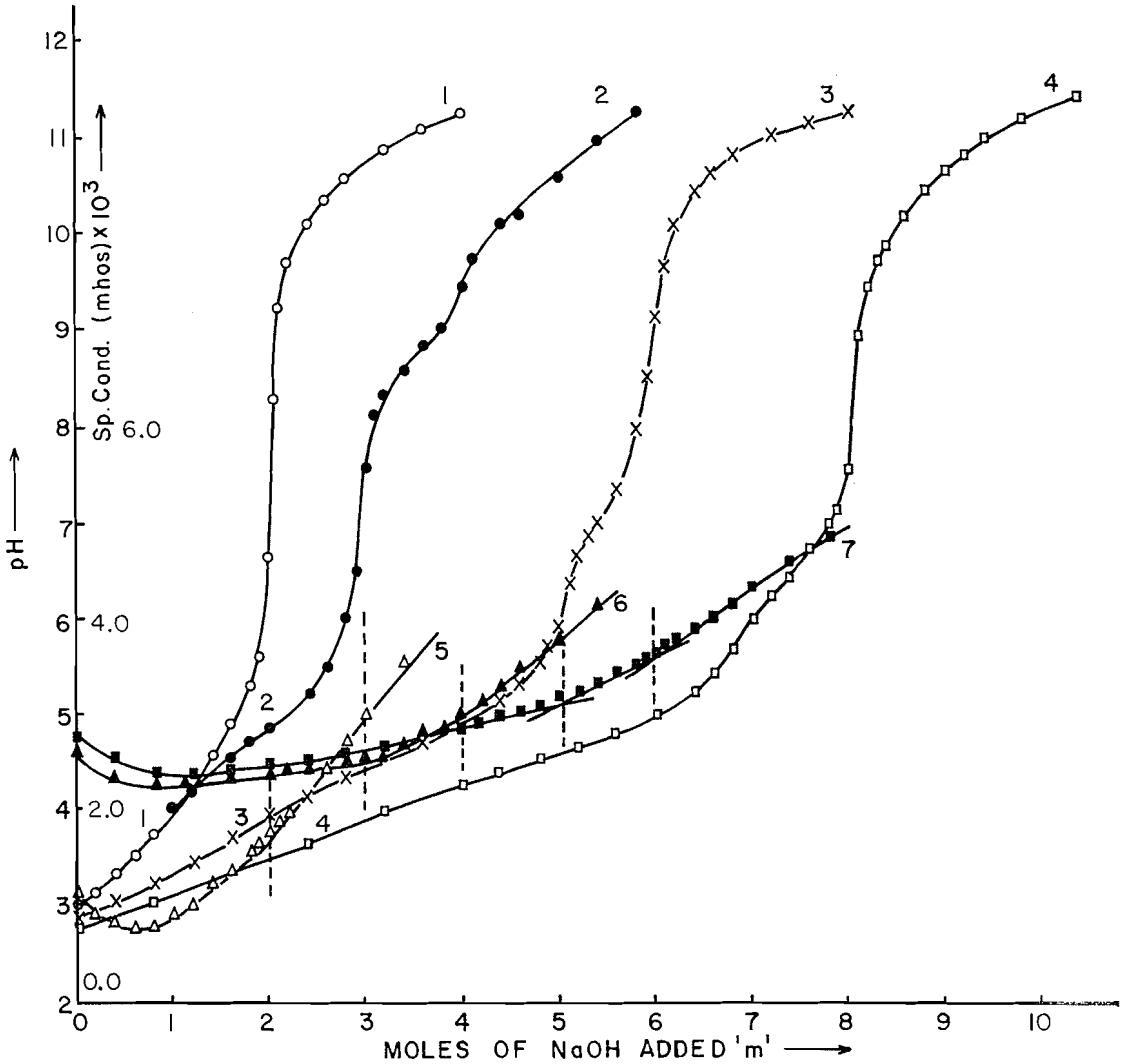

FIG. 1. Potentiometric and conductometric titrations of TMA in the absence and presence of Zn^{2+} with 0.1 *M* NaOH: curves 1 and 5, 3.33×10^{-3} *M* TMA; curves 2 and 6, 3.33×10^{-3} *M* TMA + 3.33×10^{-3} *M* $ZnSO_4$; curves 3 and 7, 6.66×10^{-3} *M* TMA + 3.33×10^{-3} *M* $ZnSO_4$; and curve 4, 10.0×10^{-3} *M* TMA + 3.33×10^{-3} *M* $ZnSO_4$.

was added, corresponds to the complete neutralization of two carboxyl hydrogens in a single step. Hence if free TMA, having three replaceable hydrogen ions, is denoted as H_3SA, the reaction between the *m* interval of 0–2 may be represented in single step by the equation

[1] $$H_3SA + 2OH^- \rightarrow HSA^{2-} + 2H_2O.$$

The absence of an inflection at $m = 1$ (Fig. 1, curve 1) indicates that the acidities of both the hydrogens are fairly comparable in magnitude and that the three ligand species H_3SA, H_2SA^-, and HSA^{2-} exist in equilibrium in the pH range corresponding to the values of *m* from 0–2. Addition of an equimolar concentration of Zn^{2+} ions (Fig. 1, curve 2) greatly alters the shape of the free ligand titration curve as a result of complex formation and consequently a considerable shift in the position of the end point is indicated. Since the extent of the proton displacement depends on the relative affinities of the ligand for hydrogen ions and the metal ions, it is obvious from the curve that the affinity of Zn^{2+} for the ligand is not great

Can. J. Chem. Downloaded from www.nrcresearchpress.com by 210.87.254.105 on 09/05/12
For personal use only.

enough to compete with the relatively high concentration of hydrogen ions in the pH range 3–4, and consequently Zn complex is not appreciably formed in this pH range. Beyond pH 4, the affinity of ligand for Zn^{2+} ions increases, as a result of which a considerable lowering in buffer region starts, showing finally two inflections at 3 and 4 moles of NaOH per mole of metal. The first inflection at 3 moles of NaOH per mole of metal suggests the formation of $ZnSA^-$, which may be given by the equation

[2] $$Zn^{2+} + H_3SA + 3OH^- \rightleftharpoons ZnSA^- + 3H_2O.$$

This 1:1 complex then changes to a relatively more stable 1:2 complex above pH 8, as a result of disproportionation of 1:1 complex with simultaneous precipitation of half of the metal in the form of its hydroxide in accordance with the equation

[3] $$2ZnSA^- + 2OH^- \rightleftharpoons Zn(SA)_2^{4-} + Zn(OH)_2,$$

justifying the inflection at $m \approx 4$.

When 2 moles of ligand are added to zinc sulfate (Fig. 1, curve 3) the curve shows only two inflections, the first at 5 and the second at 6 moles of NaOH per mole of metal, which correspond to the stepwise formation of $ZnSA^-$ and $Zn(SA)_2^{4-}$ respectively. The reaction equilibria may be expressed as

[4] $$Zn^{2+} + 2H_3SA + 5OH^- \rightleftharpoons ZnSA^- + HSA^{2-} + 5H_2O$$

[5] $$ZnSA^- + HSA^{2-} + OH^- \rightleftharpoons Zn(SA)_2^{4-} + H_2O.$$

The stepwise formation of these two complexes have been further confirmed by the inflections at 7 and 8 moles of NaOH per mole of metal (Fig. 1, curve 4) even when the ratio of ligand to metal has increased to 3:1.

Conductometric Studies

Figure 1, curves 5, 6, and 7, represents the changes in conductance when TMA solutions were titrated against NaOH in the absence and presence of Zn^{2+}. In such conductometric titrations, where the weak acid was neutralized by a strong base, the shape of the titration curves depends on the concentrations and dissociation constants of the acid. The curves show a minima, because when NaOH was added progressively to a solution of TMA, the salt formed during the first part of the reaction tends to repress the ionization of the acid still present, so that its conductance decreases. The rising salt concentration will, however, tend to increase the conductance; owing to these opposing influences, the titration curves show a minima. As the titration proceeds, a break at $m = 2$ (Fig. 1, curve 5) was obtained, beyond which the graph becomes linear. Figure 1, curve 6, for a solution containing TMA and zinc sulfate in the ratio of 1:1 shows two breaks at 3 and 4 moles of NaOH per mole of metal, corresponding to the formation of $ZnSA^-$ and the formation of $Zn(SA)_2^{4-}$ and $Zn(OH)_2$ respectively in accordance with eqs. [2] and [3].

Figure 1, curve 7, for a solution containing a 2:1 ratio of TMA to $ZnSO_4$ shows two breaks at 5 and 6 moles of NaOH per mole of Zn^{2+}, which corresponds to the formation of $ZnSA^-$ and $Zn(SA)_2^{4-}$ (eqs. [4] and [5]).

These results are similar to those obtained by potentiometric methods, demonstrating the stepwise formation of 1:1 and 1:2 complexes.

It may be particularly pointed out that the possible polynuclear complex Zn_2SA^+ is not formed because the $\bar{n}$ is a function of $[SA^{3-}]$ only (which has been tested by obtaining measurements at various metal ion concentrations) and is independent of the total metal ion concentration.

Stability Constants

The Calvin and Melchior's (1) extension of Bjerrum's (2) method was used to calculate the stability constants of the complexes formed from potentiometric titration data. The two successive reactions of the complex formation may be represented by eqs. [6] and [7].

[6] $$Zn^{2+} + SA^{3-} \rightleftharpoons ZnSA^-$$

[7] $$ZnSA^- + SA^{3-} \rightleftharpoons Zn(SA)_2^{4-}$$

The overall stability constant β is given by

[8] $$\beta = \frac{[Zn(SA)_2^{4-}]}{[Zn^{2+}][SA^{3-}]^2} = K_1K_2,$$

where K_1 and K_2 are the formation constants of reactions [6] and [7].

The evaluation of $\bar{n}$ values, which may be defined as the average number of ligand molecules bound per mole of metal, were made from Fig. 2, which represents the potentiometric titrations of TMA with standard alkali in the absence and presence of Zn^{2+} at three different temperatures. No precipitation of zinc was observed during any of these titrations. At any pH, the horizontal distances between curves 1–2, 3–4, and 5–6 (corresponding to 25, 30, and

Can. J. Chem. Downloaded from www.nrcresearchpress.com by 210.87.254.105 on 09/05/12
For personal use only.

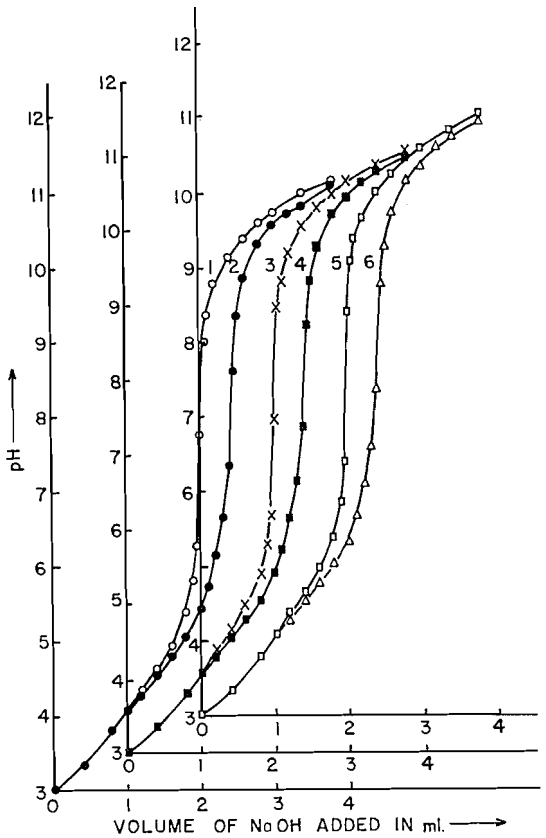

FIG. 2. Potentiometric titrations of TMA in the absence and presence of Zn^{2+} with 0.1 *M* NaOH at three different temperatures: curves 1, 3, and 5, 3.0 ml *M* KNO_3 + 5.0 ml *M*/50 TMA (total volume 30.0 ml) at 25, 30, and 35 °C respectively; and curves 2, 4, and 6, 3.0 ml *M* KNO_3 + 5.0 ml *M*/50 TMA + 1.0 ml *M*/50 $ZnSO_4$ (total volume 30.0 ml) at 25, 30, and 35 °C respectively.

35 °C respectively) measures quite accurately the additional base consumed or the total number of SA^{3-} complexed. This number divided by total Zn^{2+} is $\bar{n}$. At any pH, $[SA^{3-}]$ was calculated as

$$[9]\quad [SA^{3-}] = \frac{[H_3SA]_{total} - [ZnSA^-] + 2[Zn(SA)_2^{4-}]}{\frac{[H^+]^3}{K_{a1}K_{a2}K_{a3}} + \frac{[H^+]^2}{K_{a2}K_{a3}} + \frac{[H^+]}{K_{a3}} + 1},$$

where K_{a1}, K_{a2}, and K_{a3} are the first, second, and third dissociation constants of the acid. The pK_{a1}, pK_{a2}, and pK_{a3} values determined are 3.30, 4.94, and 10.64 respectively. All quantities in eq. [9] are known and thus a series of $\bar{n}$ and $[SA^{3-}]$ values at various pH were obtained at different temperatures and formation curves were plotted. Curves 1, 2, and 3 of Fig. 3 are the plots of $\bar{n}$ against $-\log [SA^{3-}]$ at 25, 30, and 35 °C respectively. The values of $\log K_1$ and $\log K_2$ were read directly from the graph at $\bar{n}$ values of 0.5 and 1.5 respectively and their refinement was made using the following methods: (i) method of successive approximation (m.s.a.) (2), (ii) convergence formulas of Schroder for successive approximation (3), (iii) least-square treatment (4), and (iv) correction term method (4).

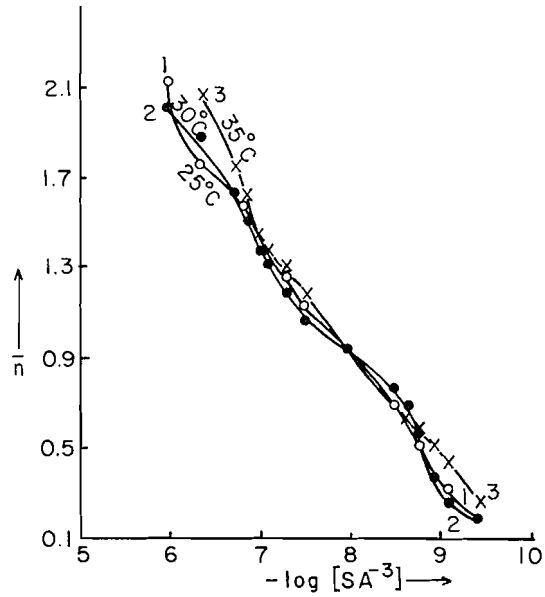

FIG. 3. Plot of $\bar{n}$ as a function of $-\log [SA^{3-}]$ at three different temperatures: curve 1, at 25 °C; curve 2, at 30 °C; curve 3, at 35 °C.

Table I illustrates the comparative statement of the refined values of $\log K_1$, $\log K_2$, and $\log \beta$ obtained from various methods.

It is apparent from the table that the direct expressions

$$[10]\quad K_1 = \frac{1}{[L]_{\bar{n}=1/2}} - \frac{3}{[L]_{\bar{n}=3/2}}$$

$$[11]\quad K_2 = \frac{1}{[L]_{\bar{n}=3/2} - 3[L]_{\bar{n}=1/2}},$$

given by Schroder (3) for the convergence values of successive approximation as a modification of m.s.a., are strictly followed by our data and no divergence of the convergence formula is noted. This method is, however, recent and

TABLE I

No.	Methods	25 °C			30 °C			35 °C		
		Log K_1	Log K_2	Log β	Log K_1	Log K_2	Log β	Log K_1	Log K_2	Log β
1	Extension of Bjerrum's method	8.74	6.88	15.62	8.80	6.79	15.59	8.91	6.91	15.82
2	Method of successive approximation	8.72	6.89	15.61	8.88	6.80	15.68	8.89	6.92	15.81
3	Convergence formulas	8.72	6.89	15.61	8.88	6.80	15.68	8.89	6.92	15.81
4	Least square	8.86	6.53	15.39	8.95	6.50	15.45	8.76	6.93	15.69
5	Correction term	8.73	6.88	15.61	8.76	6.87	15.63	8.87	6.98	15.85
Mean		8.75	6.82	15.57	8.85	6.75	15.60	8.86	6.93	15.79

directly gives the true values of successive stability constants.

Thermodynamic Functions

The values of the overall changes in free energy (ΔG), enthalpy (ΔH), and entropy (ΔS) on complex formation have been determined at 30 °C. The expression (5)

$$[12] \qquad \Delta G = -RT \ln \beta,$$

relating overall stability constant β to the total free energy change of reaction was employed for evaluating the value of ΔG, which was found to be −21.61 kcal/mole. The value of ΔH was determined with the help of an isobar equation (5)

$$[13] \qquad \mathrm{d} \ln \beta / \mathrm{d}T = \Delta H / RT^2,$$

where T is the absolute temperature and R is the gas constant and may be conveniently written in the form

$$[14] \qquad \mathrm{d} \log \beta / \mathrm{d}(1/T) = \Delta H / 4.57.$$

The values of $\log \beta$ obtained at different temperatures were plotted as a function of $1/T$. The gradient of the tangent drawn at the point corresponding to 30 °C was determined and equated with $-\Delta H/4.57$. The value of ΔH thus obtained was found to be −5.3 kcal/mole.

The overall entropy change (ΔS) of the reaction was calculated from the equation $\Delta S = (\Delta H - \Delta G)/T$ and found to be +53.8 cal/deg.

The present investigation clearly reveals the formation of two complex species, ZnA^- and $Zn(SA)_2^{4-}$. The logarithm values of the successive stability constants were found to be 8.75 and 6.82 (at 25 °C), 8.85 and 6.79 (at 30 °C), and 8.86 and 6.93 (at 35 °C) respectively. The values of ΔG, ΔH, and ΔS, evaluated at 30 °C, were found to be −21.61 kcal/mole, −5.3 kcal/mole, and +53.8 cal/deg respectively.

Acknowledgments

The authors wish to express their sincere thanks to The Ministry of Education, Government of India, for the grant of Research Scholarship to one of us (K.C.G.) and to Evan's Chemetics, Inc., N.Y., for supplying TMA as a gift. We are also indebted to Prof. R. M. Advani, Principal, M.R. Engineering College, Jaipur, for providing research facilities.

1. M. Calvin and N. C. Melchior. J. Am. Chem. Soc. **70**, 3270 (1948).
2. J. Bjerrum. Metal amine formation in aqueous solutions. P. Haase and Son, Copenhagen. 1941.
3. K. H. Schroder. Acta Chem. Scand. **20**, 1401 (1966).
4. H. Irving and H. S. Rossotti. J. Chem. Soc. 3397 (1953).
5. K. B. Yatsimirskii and V. P. Vasil'Ev. Instability constants of complex compounds. Pergamon Press, London. 1960.

Can. J. Chem. Downloaded from www.nrcresearchpress.com by 210.87.254.105 on 09/05/12
For personal use only.

Organic and biological spectrochemical studies. XXV. Properties of the *p*-bis(methylthio)benzene and *p*-bis(ethylthio)benzene cation radicals[1]

W. F. FORBES AND P. D. SULLIVAN[2]

Department of Chemistry, University of Waterloo, Waterloo, Ontario, and Department of Biochemistry, University of Rochester, Rochester, New York

Received May 16, 1967

The electron spin resonance spectra of the sulfur analogs of the *p*-dimethoxy and *p*-diethoxy benzene cation radicals, i.e. the cation radicals of *p*-bis(methylthio)benzene (**1**) and *p*-bis(ethylthio)benzene (**2**), were investigated in aluminium chloride – nitromethane. The spectra are interpreted in terms of *cis–trans* isomerism. Empirical molecular orbital calculations support this assignment and yield qualitatively correct spin densities at the ring positions. Comparison of the spectral properties of these species with corresponding compounds containing oxygen atoms indicates changes which can be associated with the greater tendency of the sulfur atom to attract spin density. There is also evidence from the β-alkyl proton splitting constants that the conformation of the radical of **2** differs from that of its oxygen analog. Slightly different *g* values are again observed for the *cis* and *trans* isomers, as previously noted for related compounds.

Canadian Journal of Chemistry, 46, 317 (1968)

Introduction

The electron spin resonance (e.s.r.) spectra in aluminium chloride – nitromethane for a number of *p*-dialkoxybenzenes (1) and of hydroquinone (2) have recently been interpreted, assuming rotational isomerism. As an extension of this work, it seemed of interest to study some of the sulfur analogs, partly because of the known ability of sulfur atoms, under certain conditions, to attract unpaired electrons. For example, it is well known that on irradiation of proteins, peptides, and amino acids, there is a tendency for the unpaired electron to be located predominantly on the sulfur atoms (3).

The compounds investigated were the *p*-bis(methylthio)benzene cation radical (**1**) and the *p*-bis(ethylthio)benzene cation radical (**2**); the former compound has previously been studied by Zweig *et al.* (4), who were unable to resolve the spectrum completely, but who postulated rotational isomerism to account for the observed spectral complexity.

Experimental and Results

Generous samples of the parent compounds **1** and **2** were obtained from Dr. A. Zweig and Professor Roger Adams, respectively. Radicals were produced, and their e.s.r. spectra recorded, as described previously (1, 2, 5, 6). E.s.r. spectra were determined in sulfuric acid and in aluminium chloride – nitromethane; they were generally better resolved in the latter system. The computer programs used were also those previously described (2, 6), except that a Benson–Lehner Corp. plotter was used to trace out simulated spectra.

*E.S.R. Spectra of the Cation Radicals of p-Bis(methylthio)benzene (**1**) and p-Bis(ethylthio)benzene (**2**)*

The spectrum of radical **1** is shown in Fig. 1*a*. The experimental spectrum can be simulated (see Fig. 1*b*), assuming the presence of two isomers, with their centers displaced by ca. 30 mG, and using the splitting constants shown in Table I with a line width of 140 mG.

A similar spectrum was obtained in sulfuric acid at +12 °C; this could be simulated using the splitting constants shown (Table I), but assuming slightly larger line widths (170 mG) than those used for the spectrum in aluminium chloride – nitromethane.

The spectrum of **2** (Fig. 2*a*) could again be simulated (Fig. 2*b*), assuming rotational isomerism with splitting constants as shown in Table I, a displacement of centers of ca. 40 mG, and a line width of 150 mG. It may be noted that splittings due to the β-methyl groups could not be detected and, also, that the SCH_2 splittings afforded no temperature dependence within the experimental error (cf. ref. 1).

Since the data for **1** (Table I) show six equivalent proton splittings, assigned to the two

[1]Part XXIV; ref. 2.

[2]Present address: Department of Chemistry, University of Minnesota, Minneapolis, Minnesota, 55455.

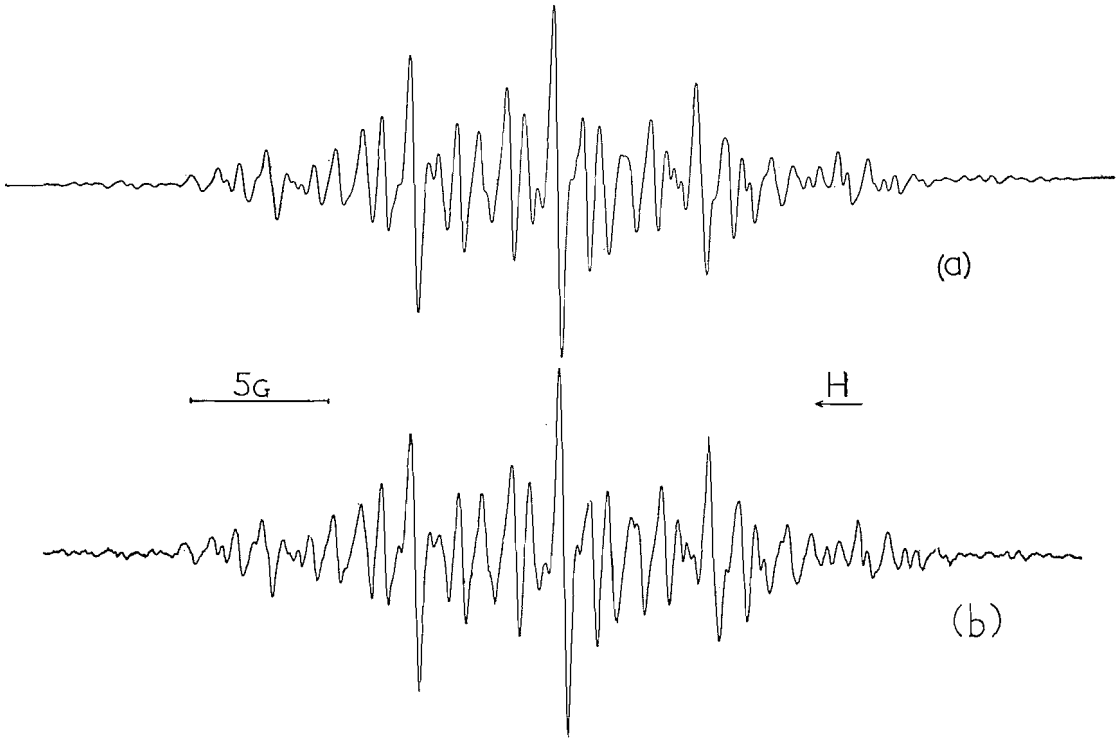

FIG. 1. (*a*) E.s.r. spectrum of the cation radical of **1** in aluminium chloride – nitromethane at −21°C. (*b*) Simulated spectrum using parameters shown in Table I.

—SCH_3 groups, the smaller splitting constants are associated with the ring protons. By analogy, the smaller splittings for **2** are also ascribed to ring splittings.

Molecular Orbital Calculations

The self-consistent field theory of McLachlan (7) was utilized to calculate spin densities and the sulfur atom was treated in terms of the p-orbital model (8). The Coulomb and resonance integrals are defined as $\alpha_S = \alpha + h_S\beta$, $\beta_{CS} = k_{CS}\beta$. A variety of h_S and k_{CS} values afforded the experimentally obtained spin densities for the ring positions of radical **1** (dotted line connecting the circled points in Fig. 3*a*) and these parameters were also plotted against different values of Q_{SCH_3}, calculated from the relationship $a_{SCH_3} = \rho_S Q_{SCH_3}$ (Fig. 3*b*).[3]

Similar calculations were made for the cation radical of 1,2,4,5-tetrakis(methylthio)benzene (**3**), for which experimentally obtained splitting constants are available (9). These calculations gave a series of points, shown as dotted lines in Fig. 3*b*. For radical **3**, however, negative spin densities are obtained at the unsubstituted ring positions, which are larger than those found from experimental splitting constants and which were found to be insensitive to changes in the h_S and k_{CS} parameters. There is therefore no unique set of h_S and k_{CS} parameters giving good agreement for both **2** and **3**. However, decreasing h_S and increasing k_{CS} tends to give better agreement.

In selecting a set of parameters, previous molecular orbital calculations for sulfur-containing compounds were also considered. For systems of type —CH=CH—S—CH=CH—, h_S values of between 1.0 and 1.1 give good results for a number of correlations (10). Using the intermediate value of $h_S = 1.05$, calculated spin densities at the ring positions for radical **1** agree with experiment, if $k_{CS} = 0.97$ (Fig. 3). This value is larger than previously used values

[3] Q_{SCH_3} refers to the constant relating spin density on the sulfur atom to the methyl proton splittings; following some methods of nomenclature, it could be written as $Q^{H}{}_{SCH_3}$.

TABLE I

Proton splitting constants (in gauss) for the radicals **1** and **2**

Assignment	Number of protons	Rotational isomer*	Radical cations		
			1 (g value $2.0087_4 + 0.00002$)		**2** (g value $2.0087_2 + 0.00002$)
			$AlCl_3$–CH_3NO_2 (−38 °C)	H_2SO_4 (+12 °C)	$AlCl_3$–CH_3NO_2 (−38 °C)
$a_{CH}(A)$	2	T	1.03_3	1.00_8	1.02_4
$a_{CH}(B)$	2	T	1.79_3	1.79_5	1.79_1
a_{SCH_3}	6	T	5.44_4	5.40_3	—
a_{SCH_2}	4	T	—	—	4.46_6
$a_{CH}(A)$	2	C	1.12_4	1.12_5	1.13_0
$a_{CH}(B)$	2	C	1.69_5	1.69_2	1.67_2
a_{SCH_3}	6	C	5.30_9	5.25_3	—
a_{SCH_2}	4	C	—	—	4.36_8

*See text.

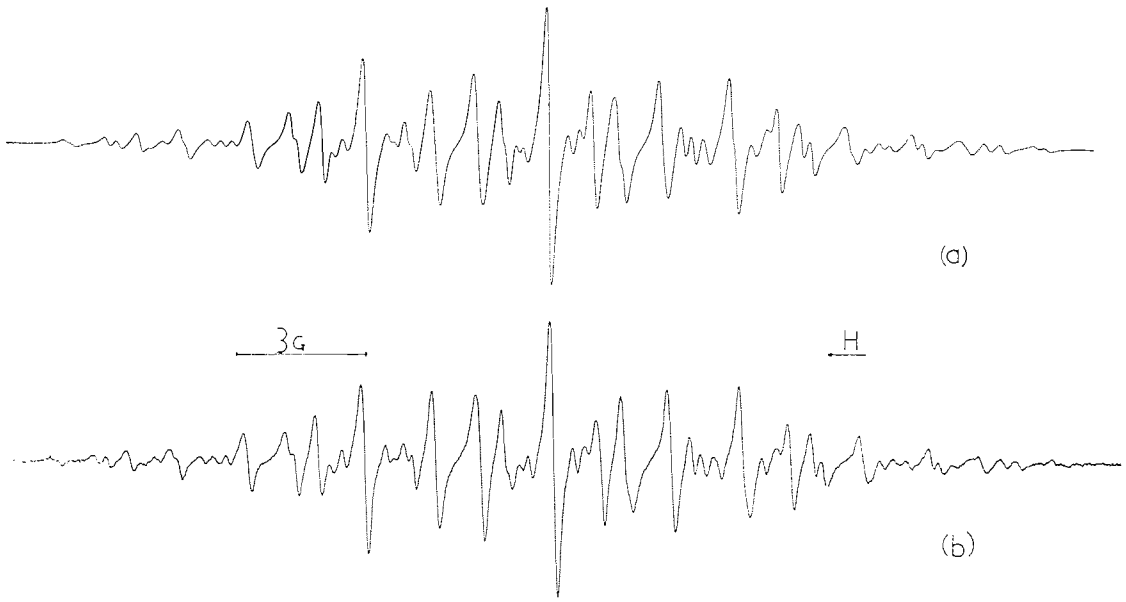

FIG. 2. (*a*) E.s.r. spectrum of the cation radical of **2** in aluminium chloride – nitromethane at −38°C. (*b*) Simulated spectrum using parameters shown in Table II.

(10), possibly because of the different environment of the sulfur atom in compounds such as 1,4-dithiin, containing the chromophore —CH=CH—S—CH=CH—, and in species such as **1** and **2**, which contain the system Ph—SR. Using values of $h_S = 1.05$ and $k_{CS} = 0.97$, the relevant spin densities for **1** and **3** are shown in Table II. The agreement between the experimental and calculated proton splittings (0.71 and 1.18) for **3** is not good but the McLachlan method is known to overestimate negative spin densities (11, 12). Nevertheless, the h_S and k_{CS} values chosen must be regarded as tentative, until additional experimental data for related sulfur compounds are available.

Assignment of Splitting Constants

It remains to assign the pairs of ring splitting constants, A and B, to the appropriate ring positions, and also to assign each isomer to the *cis* or *trans* conformation (see Table I). This can be done using the empirical approach of Stone and Maki (13), which has been applied previously to the cation radicals of *p*-dimethoxybenzene (6) and hydroquinone (2). Neglecting the β effect as a first approximation, and considering only

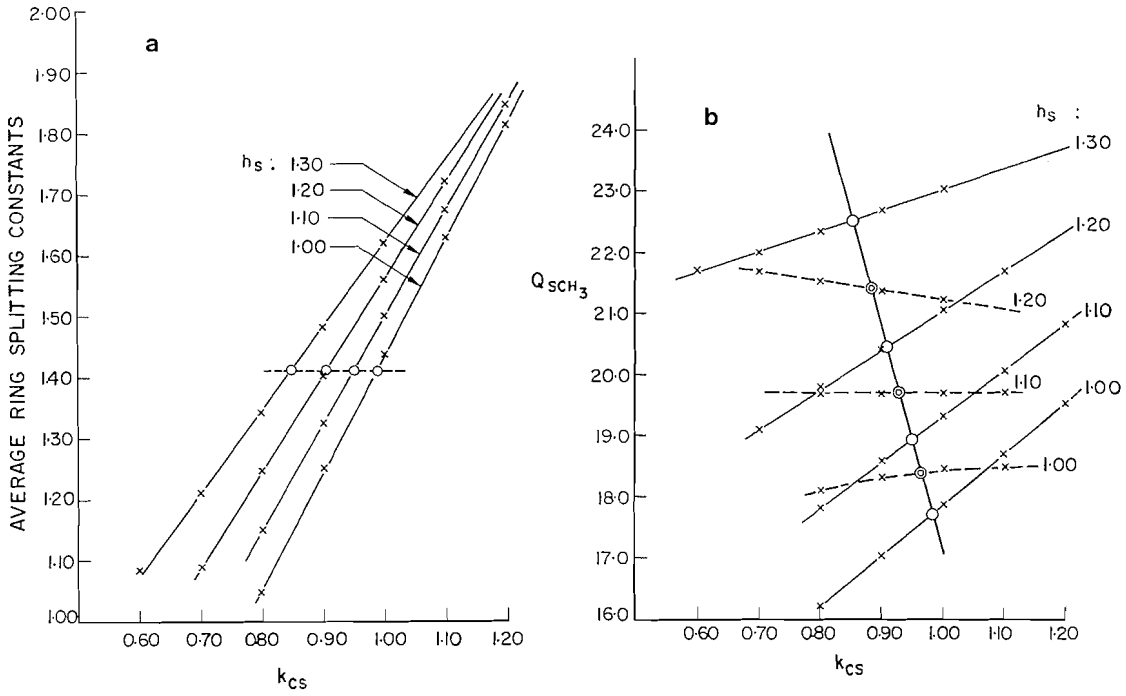

FIG. 3. (*a*) A plot of different k_{CS} parameters against average ring splitting constants, a_{CH}, of radical **1** (obtained from the relation $a_{CH} = \rho_C Q_{CH}$; Q_{CH} assumed to be -24) for values of $h_S = 1.00$, 1.10, 1.20, and 1.30. The circles lying on these lines correspond to the experimentally obtained average ring splitting constants (1.41). (*b*) A plot of different k_{CS} parameters against Q_{SCH_3} values for radical **1** (assuming different values of ρ_S calculated from $a_{SCH_3} = \rho_S Q_{SCH_3}$) for values of $h_S = 1.00$, 1.10, 1.20, and 1.30 (full lines). The circles lying on the thin full lines, thus obtained, correspond to the circles in Fig. 3*a*. Similar calculations plotting Q_{SCH_3} (from a_{SCH_3}(exp.) = ρ_S(calcd.) Q_{SCH_3}) against various combinations of h_S and k_{CS} values for radical **3** are shown in dotted lines.

TABLE II

Calculated spin densities for radicals **1** and **3**

Compound	Position	ρ(calcd.)*	a(calcd.)	a(exp.)
p-Bis(methylthio)benzene (**1**)	1	0.074_7		
	2	0.058_9	−1.41†	1.41
	7	0.293_3	5.43‡	5.38
1,2,4,5-Tetrakis(methylthio)benzene (**3**)	1	0.130		
	3	-0.049_4	1.18†	0.71
	7	0.138_2	2.56‡	2.63

*Parameters used were $h_S = 1.05$, $k_{CS} = 0.97$ (see text), $h_{CH_3} = 3.0$, $k_{CCH_3} = 0.70$ (6).
†Calculated from $a_{CH} = \rho Q_{CH}$, where Q_{CH} is taken, somewhat arbitrarily, as -24; values ranging between ca. 22 and 30 have been reported in the literature.
‡Calculated from $a_{SCH_3} = \rho_S Q_{SCH_3}$, where $Q_{SCH_3} = 18.5$.

the electrostatic effect of the SR group on the carbon atoms of the ring (the α effect), the data in Table I can be rationalized (see Table III). That is, assuming parameters as shown, the differences between the pairs of ring splitting constants can be approximately simulated. Moreover, the isomers can be identified, since differences between the two pairs of ring splitting constants are greater in the *trans* than in the *cis* isomer (see assignments in Table I, where T = *trans* and C = *cis*). These assignments are further confirmed by studying the cation radicals

of the 2,3- and 2,5-dimethylhydroquinones which exist predominantly in the *cis* and *trans* conformations, respectively (14).

Comparison between Sulfur and Oxygen Analogs

The relevant splitting constants, in aluminium chloride – nitromethane, for the radical ions investigated and for the corresponding oxygen analogs are as shown

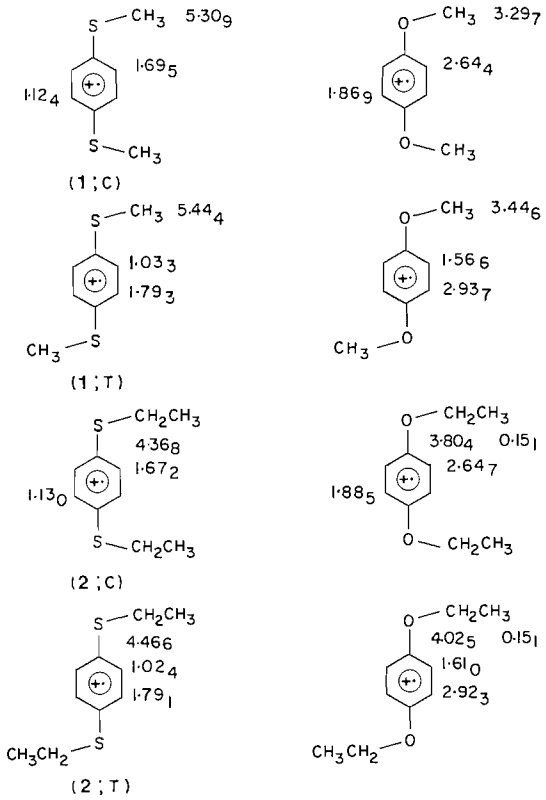

The data indicate that for these compounds, the sulfur atom has a greater tendency than oxygen to concentrate spin density in areas away from the benzene ring (cf. refs. 15, 16). This tendency is also of interest because of the observation that sulfur-containing proteins and amino acids on irradiation frequently give rise to an e.s.r. signal associated predominantly with the sulfur atom (3, 17). Since there is no evidence that the unpaired electron is *initially* located on the sulfur atom and since it is believed that the unpaired electron site is able to migrate both intra- and inter-molecularly towards the sulfur atom, the formation of —S· radicals in proteins is probably determined, at least partly, by the ability of the sulfur atom to attract spin density. It may also be noted that the present data are in qualitative agreement with the relative electron-releasing abilities of the OCH_3— and SCH_3— groups, attached to substituted benzene rings, as deduced from acid and base dissociation data (18).

The data further show that for the dimethoxy and diethoxy compounds, the β-alkoxy proton splittings increase in the latter, whereas a decrease is observed for the corresponding sulfur analogs. The change in β-alkoxy splitting constants has been discussed in terms of preferred conformations (1), following Stone and Maki (19). Recently, McKinney and Geske (20, 21) have examined some alkyl-substituted nitrobenzenes in a similar manner. These authors defined a parameter R as the ratio of the β-proton[4] splitting constant to that of the corresponding methyl proton constant (20, 21). For radicals of type $RCH_2Ar\cdot$, two equilibrium conformations similar to Fig. 4*a* and 4*b* were considered, where the angle (θ) between the CH bonds and the pπ orbitals was 60° and 30° respectively. Since $R \approx 2\langle\cos^2\theta\rangle$, the corresponding R values are 0.5 and 1.5 respectively.

For reasons discussed elsewhere (1), the *p*-diethoxybenzene cation radical is believed to possess the conformation in Fig. 4*b*, and the lower (1.16) than predicted (1.5) R value can be ascribed to torsional oscillations about the equilibrium conformation. However, the R value of 0.83 for radical **2** suggests that the equilibrium conformation of radical **2** differs from that of the *p*-diethoxybenzene radical and is consistent with $\theta = 60°$. Possibly, it exists as shown in Fig. 4*a*, because of the increased length of the C(aryl)—S compared with the C(aryl)—O bond, which results in decreased steric interactions between the β-alkyl protons and the ortho-ring protons, and (or) because the increased sulfur lone-pair – R group interactions favor the conformation shown in Fig. 4*a* rather than that in Fig. 4*b*. If the form in Fig. 4*a* is indeed preferred for radical **2**, examination of the appropriate molecular models shows that the C—H bond of the methyl group is at an angle of 60° with the pπ orbitals, whereas it is at an angle of 30° for the conformation shown in

[4] β protons are defined as the protons on an sp^3 carbon which is itself bonded to a π system.

TABLE III

Experimental and calculated parameters for the cation radical of **1**

Species	Position	ρ_i(calcd.)*	a_i(calcd.)	a_i(exp.)† (G)
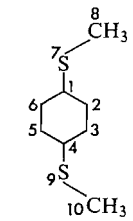	1	0.063_3		
	2	0.073_4	−1.76‡	1.69
	5	0.049_5	−1.18‡	1.12
	7	0.299_2	5.53§	5.28
	8	0.014_6		
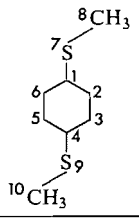	1	0.068_4		
	2	0.044_2	−1.06	1.02
	3	0.076_5	−1.83	1.79
	7	0.296_3	5.48	5.42
	8	0.014_3		

*Parameters used were $h_S = 1.05$, $k_{CS} = 0.97$, $h_{C(2)} = h_{C(3)} = 0.17$ for *cis*; $h_{C(2)} = h_{C(5)} = 0.10$ for *trans*.
†Average values from Table I.
‡Calculated from $a_{CH} = \rho_C Q_{CH}$, where $Q_{CH} = -24$.
§Calculated from a_{SCH_3} (experimentally obtained values for the methyl group) $= \rho_S Q_{SCH_3}$, where $Q_{SCH_3} = 18.5$.

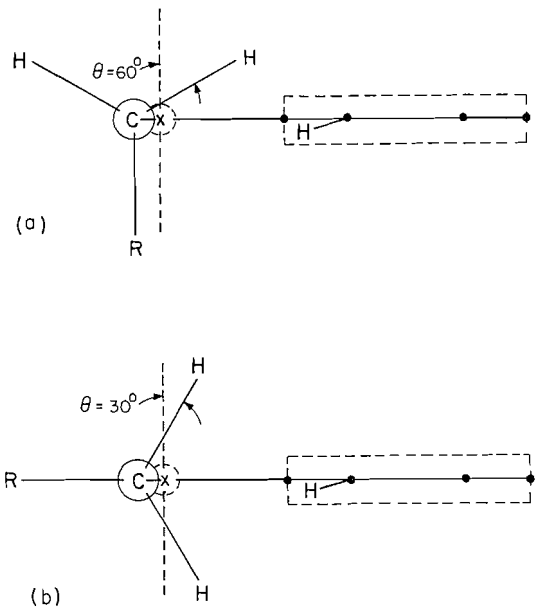

FIG. 4. Possible conformations for radicals **1** and **2** and for the corresponding oxygen analogs (X = S or O).

Fig. 4*b*. This may account for the absence of detectable splittings, due to the β-methyl group, in radical **2**. This different conformation may also explain the temperature independence of the β-alkylthio protons in radical **2**, but the reason for this independence cannot be ascribed with certainty to any particular electronic interaction.

Lastly, for both the sulfur and oxygen compounds studied the experimental data indicate a slightly different g value for the *cis* and *trans* isomers. Consistently, g_{trans} is greater than g_{cis} by ca. 2.0×10^{-5}. Since the first report (6) of this g value displacement between stereoisomers, several other examples have been noted (1, 22–24) and the effect, therefore, appears to represent a general phenomenon.

Acknowledgments

The authors are indebted to the late Mr. A. B. Barabas for excellent technical assistance and to the National Research Council of Canada for a studentship (to P. D. S.) and financial assistance. This research was also supported, in part, by the National Cancer Institute of Canada, by the Defence Research Board of Canada, grant number 1675-04, and by the U.S. Public Health Service Research Grant RH00392, National Center for Radiological Health.

1. W. F. FORBES, P. D. SULLIVAN, and H. M. WANG. J. Am. Chem. Soc. **89**, 2705 (1967).
2. A. B. BARABAS, W. F. FORBES, and P. D. SULLIVAN. Can. J. Chem. **45**, 267 (1967).

3. W. GORDY, W. B. ARD, and H. SHIELDS. Proc. Natl. Acad. Sci. U.S. **41**, 983 (1955).
4. A. ZWEIG, W. G. HODGSON, W. H. JURA, and D. L. MARICLE. Tetrahedron Letters, No. 26, 1821 (1963).
5. W. F. FORBES and P. D. SULLIVAN. J. Am. Chem. Soc. **88**, 2862 (1966).
6. W. F. FORBES and P. D. SULLIVAN. Can. J. Chem. **44**, 1501 (1966).
7. A. D. MCLACHLAN. Mol. Phys. **3**, 233 (1960).
8. E. A. C. LUCKEN. Theoret. Chim. Acta, **1**, 397 (1963).
9. A. ZWEIG and W. G. HODGSON. Proc. Chem. Soc. 417 (1964).
10. R. ZAHRADNIK. Advan. Heterocyclic Chem. **5**, 1 (1965).
11. I. BERNAL, P. H. RIEGER, and G. K. FRAENKEL. J. Chem. Phys. **37**, 1489 (1962).
12. A. CARRINGTON and I. C. P. SMITH. Mol. Phys. **9**, 140 (1965).
13. E. W. STONE and A. H. MAKI. J. Chem. Phys. **38**, 1999 (1963).
14. P. D. SULLIVAN. Unpublished information.
15. E. T. STROM and G. A. RUSSELL. J. Am. Chem. Soc. **87**, 3326 (1965).
16. A. ZWEIG and J. E. LEHNSEN. J. Am. Chem. Soc. **87**, 2647 (1965).
17. W. GORDY and H. SHIELDS. Proc. Natl. Acad. Sci. U.S. **46**, 1124 (1960).
18. C. C. PRICE and S. OAE. Sulfur bonding. Ronald Press Co., New York. 1962. pp. 13–16.
19. E. W. STONE and A. H. MAKI. J. Chem. Phys. **37**, 1326 (1962); **38**, 1254 (1963).
20. T. M. MCKINNEY and D. H. GESKE. J. Am. Chem. Soc. **89**, 2806 (1967).
21. D. H. GESKE. Progr. Phys. Org. Chem. **4**, 125 (1967).
22. J. V. RAMSBOTTOM and W. A. WATERS. J. Chem. Soc. B, 220 (1966).
23. H. C. HELLER and H. C. YAO. R61, Abstracts, 153rd ACS Meeting, April 1967.
24. C. CORVAJA, P. L. NORDIO, and G. GIACOMETTI. J. Am. Chem. Soc. **89**, 1751 (1967).

Can. J. Chem. Downloaded from www.nrcresearchpress.com by 210.87.254.40 on 09/05/12
For personal use only.

Organic and biological spectrochemical studies. XXVI. E.s.r. spectra of the 4,4′-dimethoxybiphenyl cation radical[1]

W. F. FORBES AND P. D. SULLIVAN[2]

Department of Chemistry, University of Waterloo, Waterloo, Ontario, and Department of Biochemistry, University of Rochester, Rochester, N.Y.

Received July 26, 1967

The electron spin resonance (e.s.r.) spectrum of 4,4′-dimethoxybiphenyl in aluminium chloride – nitromethane is remarkably temperature dependent. The changes are explained by postulating the rapid interconversion of conformational isomers, leading to line-width alternation.

Canadian Journal of Chemistry, **46**, 325 (1968)

The electron spin resonance (e.s.r.) spectrum of the cation radical of 4,4′-dimethoxybiphenyl has previously been reported (1, 2), but the spectra were not resolved completely. Further investigation of this radical in aluminium chloride – nitromethane at different temperatures afforded spectra as shown (Fig. 1(*a–c*)). The spectra at −20 °C and −60 °C (Figs. 1*a* and 1*c*) could be analyzed in terms of 12 interacting protons (Table I), suggesting the presence of a species other than the 4,4′-dimethoxybiphenyl radical cation, which would be expected to give 14 proton splittings. It is difficult to postulate a likely species having 12 interacting protons. However, the spectra can be explained by assuming that the splitting constants are modified as shown in Table I. That is, it is assumed that at −20 °C, 4 equivalent protons (predicted five lines with splitting constants 1.89 G) give rise to only three lines (splitting 3.78 (2 × 1.89) G), and at −60 °C, instead of four equivalent splittings of 0.79 G, three lines with splittings of 1.58 (2 × 0.79) G are observed.

This phenomenon of five lines with splitting constant *a* reducing to three lines with splitting constant 2*a* is ascribed to line-width alternation and the effect is confirmed by the observed change in the intensities of the five lines separated by 0.79 G. That is, at −36 °C, instead of a quintet of relative intensity 1:4:6:4:1, the lines of relative intensity 4 have decreased, whereas those of relative intensity 1 have increased, relative to the central line (see Fig. 1*b*). Since *cis–trans* isomers have previously been postulated for related molecules, such as *p*-dimethoxybenzene (3), and can account for line-width

TABLE I

Predicted and actual splitting constants (in gauss) for the 4,4′-dimethoxybiphenyl cation radical. (Apparent number of equivalent protons in parentheses)

		Ring splittings	
	OMe- splittings	*o*-	*m*-
Predicted*:	1.78 (6)	1.89 (4)	0.79 (4)
Actual†: −20°C	1.78_3 (6)	3.78_1 (2)	0.79_1 (4) (g=2.0030_6)
−60°C	1.78_3 (6)	1.58_2 (2) 2.19_2 (2)	1.58_2 (2) (g=2.0030_6)

*The "predicted" spectrum would be expected to be observed at higher temperatures.
†The spectrum at −20 °C was completely analyzed through careful analysis of the wing lines and by computed simulation. The agreement at −60 °C was less satisfactory, but the main lines are well accounted for by the values given.

[1]For Part XXV in this series, see ref. 7.
[2]Present address: Department of Chemistry, University of Minnesota, Minneapolis, Minn.

Can. J. Chem. Downloaded from www.nrcresearchpress.com by 210.87.254.40 on 09/05/12
For personal use only.

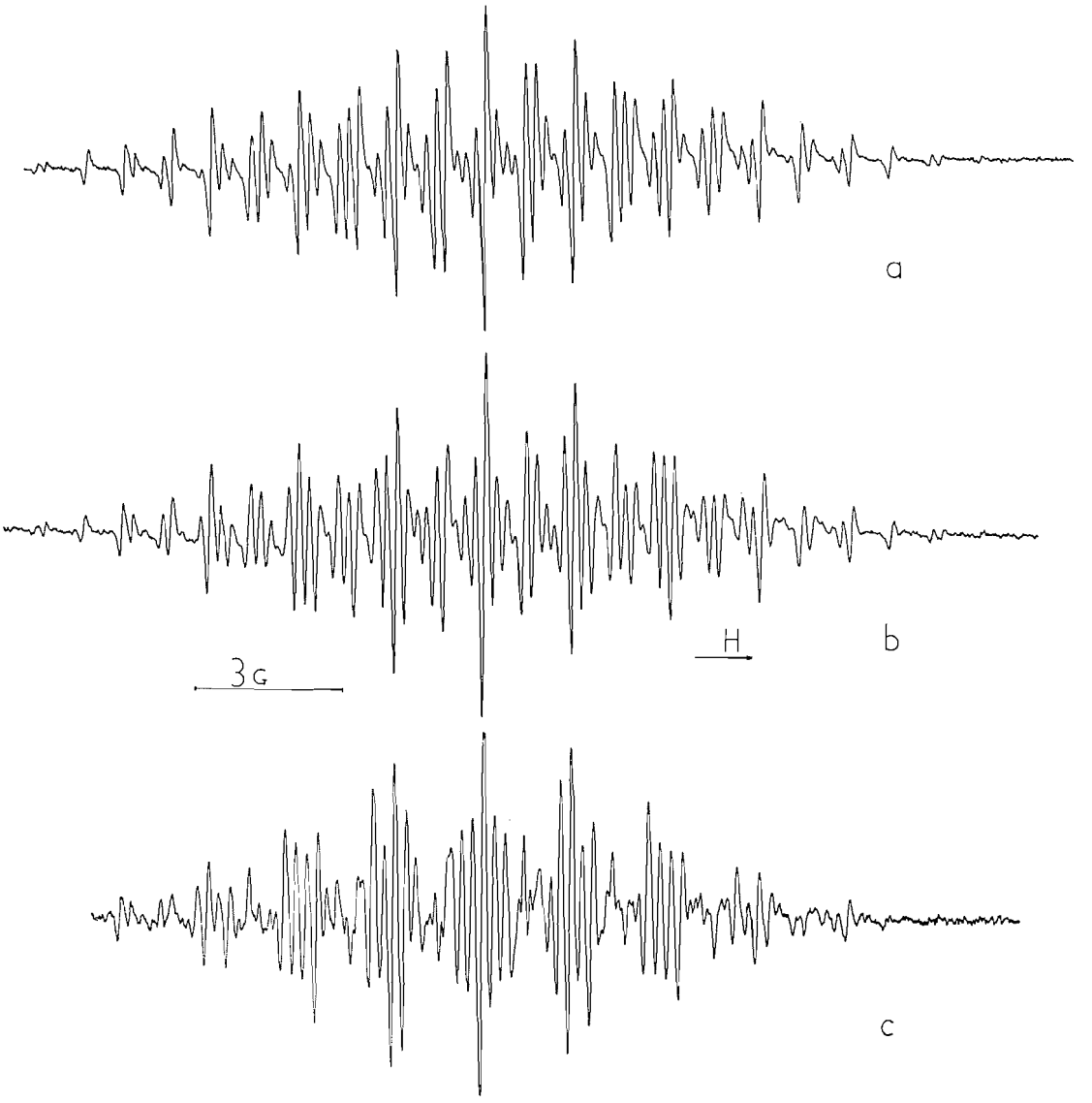

FIG. 1. Electron spin resonance spectrum of 4,4′-dimethoxybiphenyl in aluminium chloride – nitromethane at (*a*) −20 °C, (*b*) −36 °C, and (*c*) −60 °C.

alternation, the present alternation also suggests the presence of conformational isomers. More specifically, a four-jump model (4) is postulated in which the spin densities on the ring hydrogens in the *cis* and *trans* isomers are equal. This implies that the *cis* and *trans* forms are of comparable stability and that the conformation of the methoxy groups does not affect the spin density in the opposite ring.

An alternative explanation of the temperature effect is to assume localization of unpaired spin density on only one ring at low temperatures (5). However, this explanation is rejected because the methyl proton splittings remain constant within the investigated temperature range (see Table I) and the observed maximal ultraviolet absorptions near 810 and 740 mμ at +20 °C do not indicate locally excited states (cf. the absorption maxima at 440 and 460 mμ for the *p*-dimethoxybenzene cation radical under similar conditions).

It remains to assign the two sets of four ring splittings given in Table I to the *o*- and *m*-posi-

tions (relative to the central C—C bond) respectively. This is done by comparison with the e.s.r. spectrum of the 3,3′,5,5′-tetramethyl-4,4′-biphenol cation radical which shows four equivalent splittings of 1.83 G, indicating that the splittings of 1.89 G should be associated with the *o*-positions. An interesting feature is that molecular orbital calculations using normal parameters (3) do not afford the experimentally observed greater splittings for the *o*-hydrogens. However, if a bond order of $>$ ca. 1.6 (which seems high, although a bond order of > 1 is necessary to rationalize the observed *cis–trans* isomerism) is ascribed to the central C—C bond, the ratio of the ring splitting constants reverts to that experimentally observed.

Similar effects have also been obtained for 4,4′-biphenol and 4,4′-diethoxybiphenyl.

Experimental

The dialkoxybiphenyls were prepared by the Ullmann method and purified by recrystallization. E.s.r. spectra were determined, and computer programs used, as described previously (3, 6).

Acknowledgments

This research was supported by the National Research Council of Canada, the National Cancer Institute of Canada, the Defence Research Board of Canada, grant number 1675-04, and the U.S. Public Health Service, research grant RH00392, National Center for Radiological Health.

1. H. M. Buck, W. Bloemhoff, and L. J. Oosterhoff. Tetrahedron Letters, No. 9, 5 (1960).
2. D. L. Allara, B. C. Gilbert, and R. O. C. Norman. Chem. Commun. **1**, 319 (1965).
3. W. F. Forbes and P. D. Sullivan. Can. J. Chem. **44**, 1501 (1966).
4. A. Carrington. Mol. Phys. **5**, 425 (1962).
5. J. E. Harriman and A. H. Maki. J. Chem. Phys. **39**, 778 (1963).
6. W. F. Forbes and P. D. Sullivan. J. Am. Chem. Soc. **88**, 2862 (1966).
7. W. F. Forbes and P. D. Sullivan. Can. J. Chem. This issue.

Disubstituted hydroxamic acids and the determination of vanadium[1]

R. M. Cassidy and D. E. Ryan
Department of Chemistry, Dalhousie University, Halifax, Nova Scotia

Received August 2, 1967

A number of disubstituted hydroxamic acids were investigated as possible replacements for benzoylphenylhydroxylamine in the determination of vanadium; none is superior. At 378 mμ, *p*-phenylazobenzoylphenylhydroxylamine shows a marked sensitivity increase but selectivity is poor. In the visible region, there is an increase in molecular extinction coefficient as the reagent π system is extended; however, complete coplanarity of the aromatic and metal chelate rings is not possible and the increase is not large enough to be of much practical value.

Canadian Journal of Chemistry, 46, 327 (1968)

A disubstituted hydroxamic acid, N-benzoylphenylhydroxylamine (BPHA), provides a rapid and selective method for the determination of vanadium (1); it is extremely valuable for the direct determination of small amounts of vanadium in ores, alloys, petroleum products, and biological materials (2). In strong hydrochloric acid medium vanadium(V) reacts with BPHA to form a 1:2 species (3), $(C_{13}H_{10}O_2N)_2VO_2H_2Cl$, which is extracted by chloroform; the purple-colored extract has a maximum absorption at 530 mμ and a molecular extinction coefficient of 4.5×10^3 l/mole cm. A number of similar disubstituted hydroxamic acids have been recommended for the determination of vanadium (4–8), but, apart from some increase in sensitivity of reaction, they do not show any particular advantage over BPHA.

Transition metals are capable of forming π bonds with complexing ligands and can act as links in extending π systems from one chelating molecule to another. If the absorption band of the complex formed from the reaction of vanadium with BPHA is influenced by π bonding, changes in the aromaticity of the organic molecule might significantly affect sensitivity. The molecular extinction coefficient of a molecule can be quite simply related to the probability of

[1]Abstracted from the M.Sc. Thesis of R. M. Cassidy.

Can. J. Chem. Downloaded from www.nrcresearchpress.com by 210.87.254.40 on 09/05/12
For personal use only.

tions (relative to the central C—C bond) respectively. This is done by comparison with the e.s.r. spectrum of the 3,3′,5,5′-tetramethyl-4,4′-biphenol cation radical which shows four equivalent splittings of 1.83 G, indicating that the splittings of 1.89 G should be associated with the *o*-positions. An interesting feature is that molecular orbital calculations using normal parameters (3) do not afford the experimentally observed greater splittings for the *o*-hydrogens. However, if a bond order of $>$ ca. 1.6 (which seems high, although a bond order of > 1 is necessary to rationalize the observed *cis–trans* isomerism) is ascribed to the central C—C bond, the ratio of the ring splitting constants reverts to that experimentally observed.

Similar effects have also been obtained for 4,4′-biphenol and 4,4′-diethoxybiphenyl.

Experimental

The dialkoxybiphenyls were prepared by the Ullmann method and purified by recrystallization. E.s.r. spectra were determined, and computer programs used, as described previously (3, 6).

Acknowledgments

This research was supported by the National Research Council of Canada, the National Cancer Institute of Canada, the Defence Research Board of Canada, grant number 1675-04, and the U.S. Public Health Service, research grant RH00392, National Center for Radiological Health.

1. H. M. Buck, W. Bloemhoff, and L. J. Oosterhoff. Tetrahedron Letters, No. 9, 5 (1960).
2. D. L. Allara, B. C. Gilbert, and R. O. C. Norman. Chem. Commun. **1**, 319 (1965).
3. W. F. Forbes and P. D. Sullivan. Can. J. Chem. **44**, 1501 (1966).
4. A. Carrington. Mol. Phys. **5**, 425 (1962).
5. J. E. Harriman and A. H. Maki. J. Chem. Phys. **39**, 778 (1963).
6. W. F. Forbes and P. D. Sullivan. J. Am. Chem. Soc. **88**, 2862 (1966).
7. W. F. Forbes and P. D. Sullivan. Can. J. Chem. This issue.

Disubstituted hydroxamic acids and the determination of vanadium[1]

R. M. Cassidy and D. E. Ryan
Department of Chemistry, Dalhousie University, Halifax, Nova Scotia

Received August 2, 1967

A number of disubstituted hydroxamic acids were investigated as possible replacements for benzoylphenylhydroxylamine in the determination of vanadium; none is superior. At 378 mμ, *p*-phenylazobenzoylphenylhydroxylamine shows a marked sensitivity increase but selectivity is poor. In the visible region, there is an increase in molecular extinction coefficient as the reagent π system is extended; however, complete coplanarity of the aromatic and metal chelate rings is not possible and the increase is not large enough to be of much practical value.

Canadian Journal of Chemistry, 46, 327 (1968)

A disubstituted hydroxamic acid, N-benzoylphenylhydroxylamine (BPHA), provides a rapid and selective method for the determination of vanadium (1); it is extremely valuable for the direct determination of small amounts of vanadium in ores, alloys, petroleum products, and biological materials (2). In strong hydrochloric acid medium vanadium(V) reacts with BPHA to form a 1:2 species (3), $(C_{13}H_{10}O_2N)_2VO_2H_2Cl$, which is extracted by chloroform; the purple-colored extract has a maximum absorption at 530 mμ and a molecular extinction coefficient of 4.5×10^3 l/mole cm. A number of similar disubstituted hydroxamic acids have been recommended for the determination of vanadium (4–8), but, apart from some increase in sensitivity of reaction, they do not show any particular advantage over BPHA.

Transition metals are capable of forming π bonds with complexing ligands and can act as links in extending π systems from one chelating molecule to another. If the absorption band of the complex formed from the reaction of vanadium with BPHA is influenced by π bonding, changes in the aromaticity of the organic molecule might significantly affect sensitivity. The molecular extinction coefficient of a molecule can be quite simply related to the probability of

[1]Abstracted from the M.Sc. Thesis of R. M. Cassidy.

Can. J. Chem. Downloaded from www.nrcresearchpress.com by 210.87.254.6 on 09/05/12
For personal use only.

TABLE I
Analytical results

	Compound	Melting point (°C)	λ_{max} in mμ for vanadium complex	Molecular extinction coefficient $\times 10^{-3}$ for vanadium complex
(1)	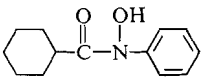	124	520	4.2
(2)	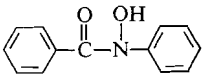	120–121	530	4.5
(3)	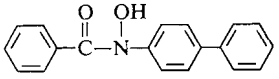	150 (decomposes slowly)	545	4.9
(4)	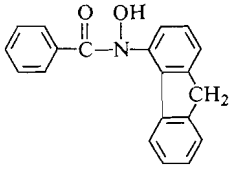	147 (decomposes slowly)	548	5.1
(5)	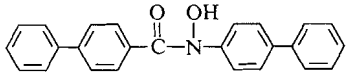	200 (decomposes slowly)	553	5.6
(6)	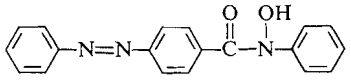	178–179 (melts with decomposition)	550 378	6.4 12.0

transition, a statistical factor, and the molecular dimensions of the absorbing species (9). If changes are made in the aromaticity and thus also the size of the BPHA molecule, significant changes in the molecular extinction coefficient may result; no alteration of selectivity should occur since basic structural characteristics would remain unaltered. With these ideas in mind, a number of disubstituted hydroxamic acids were prepared in the hope of developing a reagent that would show a large increase in sensitivity over BPHA in its reaction with vanadium.

Experimental

Preparation of Reagents

The following compounds were prepared and purified by procedures previously described (10, 11): cyclohexanoylphenylhydroxylamine (**1**), benzoylphenylhydroxylamine (**2**), benzoyl-4-biphenylhydroxylamine (**3**), benzoyl-4-fluorylhydroxylamine (**4**), 4-phenylbenzoyl-4-biphenylhydroxylamine (**5**), and *p*-phenylazobenzoylphenylhydroxylamine (**6**). Compound **6**, when recrystallized from an ethanol–water mixture, forms flaky red-orange crystals which melt at 178–179 °C with decomposition. The nuclear magnetic resonance (n.m.r.) spectrum shows a complex structure at 2.8 τ (phenyl hydrogens) and a single peak at -0.5 τ (oxime hydrogen); integration is in the expected ratio of 14:1. Attempts to prepare *o*-phenylbenzoyl-2-biphenylhydroxylamine, α-naphthoyl-α-naphthylhydroxylamine, and 9-anthroyl-9-anthrylhydroxylamine were not very successful; the crude reaction products would react with vanadium in certain instances but purified compounds were not obtained. Except for compound **6**, these hydroxamic acids are white and their chloroform solutions show little or no absorption in the visible region of the spectrum.

Procedure for Determination of Vanadium

Five milliliters of solution containing a known amount of vanadium (~0.2 mg) were added to a separatory funnel and an equal volume of concentrated hydrochloric acid was added. Four milliliters of a 0.5% solution of the reagent in chloroform were added and the organic layer diluted to about 10 ml with chloroform. The funnel was shaken vigorously, the phases allowed to separate, and the organic phase transferred to a 50 ml volumetric flask. The aqueous layer was extracted again with 10 ml of chloroform. The combined extracts were diluted to the mark with chloroform and the spectrum

Can. J. Chem. Downloaded from www.nrcresearchpress.com by 210.87.254.6 on 09/05/12
For personal use only.

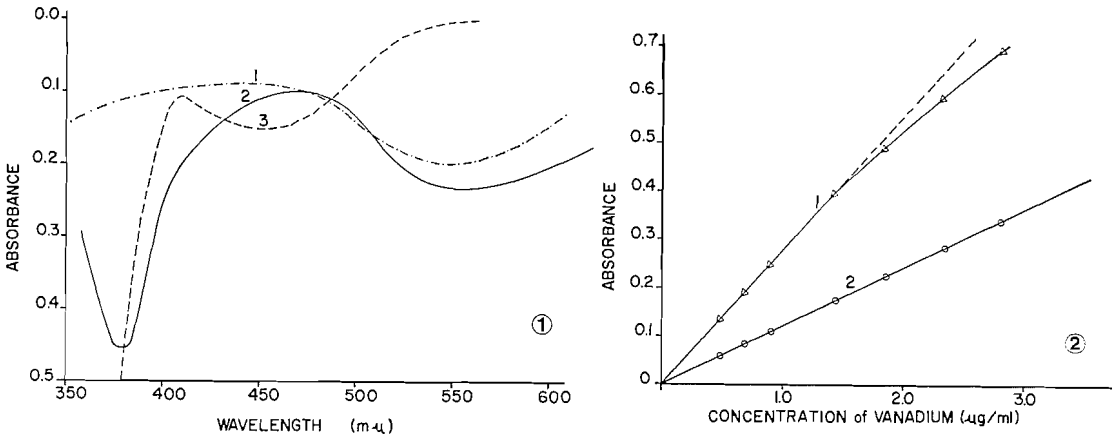

FIG. 1. Absorption spectra: (1) 4.6×10^{-3} *M* vanadium–BPHA complex; (2) 3.68×10^{-5} *M* vanadium–**6** complex; (3) 2.0×10^{-4} *M* **6**.

FIG. 2. Beer's law plots for vanadium–**6** complexes: (1) at 378 mμ; (2) at 550 mμ.

recorded in a 1 cm cell, using a Bausch and Lomb Spectronic 505 recording spectrophotometer; chloroform served as a blank except for compound **6** where a reagent blank was necessary. The results are shown in Table I.

Results and Discussion

Although there is an increase in the molecular extinction coefficient as the reagent π system is extended, there is no large increase in the sensitivity of reaction for vanadium in the visible region of the spectrum; complete coplanarity of the aromatic rings with the metal chelate ring is no more possible with these compounds than with BPHA and there is no large increase in molecular extinction coefficient as a result of a π system extending over the entire chelate molecule. However, the *p*-phenylazobenzoylphenylhydroxylamine (**6**) complex exhibits a strong absorption at 378 mμ in addition to that at 550 mμ, and the molecular extinction coefficient is almost three times that with BPHA. This high sensitivity prompted further investigation of the possible use of this compound for the practical determination of vanadium.

Figure 1 shows the absorption spectrum of **6** and its vanadium complex in chloroform; a typical spectrum for complexes of the other compounds is shown for comparison. If measurements are made at 550 mμ, **6** is similar to BPHA in its reaction with vanadium and is subject to the same limited number of interferences; there is a 40–45% increase in sensitivity of reaction.

At 378 mμ there is a sharp absorption peak, the sensitivity is increased by almost a factor of three, and vanadium can be determined with an accuracy of 1%. However, selectivity at 378 mμ is very poor and apparent deviations from Beer's law occur at high vanadium concentrations. At this wavelength the titanium, zirconium, and niobium complexes that are extracted interfere seriously by absorption of light, although no interference occurs, except at high metal concentrations, at 550 mμ. Deviations from ideality for absorbance–concentration plots are caused by overcompensation by reagent blank for reagent in sample. Compound **6** absorbs light at 378 mμ and the amount of **6** reacting, with the concentrations used, is no longer negligible compared with the total amount of reagent added; the linear plot obtained from measurements made at 550 mμ on these solutions shows that deviation is not caused by incomplete reaction.

Despite increased sensitivity, *p*-phenylazobenzoylphenylhydroxylamine cannot be recommended over BPHA. At 378 mμ, where there is a worthwhile increase in sensitivity, the selectivity is poor. At 540 mμ, where selectivity is good, the small sensitivity increase of 45% does not make the use of **6** much more attractive, particularly in view of the ready availability and ease of preparation and purification of BPHA.

Conclusions

None of the compounds prepared can be reasonably recommended as superior to BPHA

Can. J. Chem. Downloaded from www.nrcresearchpress.com by 210.87.254.6 on 09/05/12
For personal use only.

for determining vanadium and similar reservations must be held for other disubstituted hydroxamic acids reported in the literature (4–8). One of these compounds, N-cinnamoylphenylhydroxylamine (5), is of interest; it is a pale-green solid whose vanadium complex has a molecular extinction coefficient ($\epsilon = 6.3 \times 10^3$ l/mole cm) similar to **6**. Here, however, the increase in ϵ can be attributed to the presence of the HC=CH group which permits greater coplanarity of the aromatic rings with the metal chelate rings. It is probable that a more sensitive reagent for vanadium would result if a second HC=CH group could be introduced, so that both aromatic rings were coplanar with the chelate ring; a compound such as

$$C_6H_5{-}CH{=}CH{-}\underset{\underset{O}{\|}}{C}{-}\underset{\underset{OH}{|}}{N}{-}CH{=}CH{-}C_6H_5$$

could replace BPHA as a colorimetric reagent for metals if it could be easily prepared and purified. BPHA, at the moment, remains the most practical and useful reagent for determining trace amounts of vanadium.

Acknowledgment

This work was supported by a grant from the National Research Council of Canada.

1. D. E. Ryan. Analyst, **85**, 569 (1960).
2. U. Priyadarshini and S. G. Tandon. Anal. Chem. **33**, 435 (1961).
3. R. Montequi. Anales Real Soc. Espan. Fis. Quim. Madrid, Ser. B, **60** (4), 325 (1964).
4. S. G. Tandon and S. C. Bhattacharyya. Anal. Chem. **33**, 1267 (1961).
5. U. Priyadarshini and S. G. Tandon. Analyst, **86**, 544 (1961).
6. A. K. Majumdar and G. Das. Anal. Chim. Acta, **31**, 147 (1964).
7. A. K. Majumdar and G. Das. J. Indian Chem. Soc. **42**, 189 (1965).
8. A. K. Majumdar and G. Das. Anal. Chim. Acta, **36**, 454 (1966).
9. E. A. Braude. J. Chem. Soc. 379 (1950).
10. G. D. Lutwick and D. E. Ryan. Can. J. Chem. **32**, 949 (1954).
11. C. A. Armour and D. E. Ryan. Can. J. Chem. **35**, 1454 (1957).

Concerning the preparation of anhydrous hydrogen peroxide

J. E. Dove and J. Riddick
Department of Chemistry, University of Toronto, Toronto, Ontario

Received June 13, 1967

Preparation of pure anhydrous hydrogen peroxide has been attempted by a literature method which involves extraction of the aqueous solution with diethyl ether, followed by fractional distillation under vacuum. Mass spectrometric analysis shows that the product is seriously impure, and indicates that a reaction has occurred between the ether and hydrogen peroxide.

Canadian Journal of Chemistry, 46, 330 (1968)

Schmidt and Bornmann (1) have recently described an attractively simple procedure for preparing anhydrous hydrogen peroxide in small quantities. The procedure involves adding 100 cc of pure diethyl ether to 10 g of a 90% to 98% aqueous solution of hydrogen peroxide and drying the separated ether layer by gently shaking for several minutes with granular calcium chloride. Dehydration of the ethereal solution is completed by two successive treatments with phosphorus pentoxide, and anhydrous hydrogen peroxide is then recovered by distillation under vacuum.

We have attempted to make small quantities of water-free hydrogen peroxide by this method. The procedure adopted was identical with that recommended by Schmidt and Bornmann except for the following minor modifications: (i) we found it necessary to dry the ethereal solution over calcium chloride for at least 1 h to prevent an over-vigorous evolution of heat on treatment with phosphorus pentoxide and (ii) the treatment with phosphorus pentoxide was carried out three times. The diethyl ether was removed on a water pump, and the residue distilled at 45–50 °C under a good rotary pump vacuum, only the middle 50% of the distillate being collected. (Schmidt and Bornmann state that 80–90% can be collected.) The ether used was taken from a freshly opened sealed can of Eastman Organic Chemicals Spectro grade diethyl ether. This is a highly purified grade with

Can. J. Chem. Downloaded from www.nrcresearchpress.com by 210.87.254.6 on 09/05/12
For personal use only.

for determining vanadium and similar reservations must be held for other disubstituted hydroxamic acids reported in the literature (4–8). One of these compounds, N-cinnamoylphenylhydroxylamine (5), is of interest; it is a pale-green solid whose vanadium complex has a molecular extinction coefficient ($\epsilon = 6.3 \times 10^3$ l/mole cm) similar to **6**. Here, however, the increase in ϵ can be attributed to the presence of the HC=CH group which permits greater coplanarity of the aromatic rings with the metal chelate rings. It is probable that a more sensitive reagent for vanadium would result if a second HC=CH group could be introduced, so that both aromatic rings were coplanar with the chelate ring; a compound such as

$$C_6H_5{-}CH{=}CH{-}\underset{\underset{O}{\|}}{C}{-}\underset{\underset{OH}{|}}{N}{-}CH{=}CH{-}C_6H_5$$

could replace BPHA as a colorimetric reagent for metals if it could be easily prepared and purified. BPHA, at the moment, remains the most practical and useful reagent for determining trace amounts of vanadium.

Acknowledgment

This work was supported by a grant from the National Research Council of Canada.

1. D. E. Ryan. Analyst, **85**, 569 (1960).
2. U. Priyadarshini and S. G. Tandon. Anal. Chem. **33**, 435 (1961).
3. R. Montequi. Anales Real Soc. Espan. Fis. Quim. Madrid, Ser. B, **60** (4), 325 (1964).
4. S. G. Tandon and S. C. Bhattacharyya. Anal. Chem. **33**, 1267 (1961).
5. U. Priyadarshini and S. G. Tandon. Analyst, **86**, 544 (1961).
6. A. K. Majumdar and G. Das. Anal. Chim. Acta, **31**, 147 (1964).
7. A. K. Majumdar and G. Das. J. Indian Chem. Soc. **42**, 189 (1965).
8. A. K. Majumdar and G. Das. Anal. Chim. Acta, **36**, 454 (1966).
9. E. A. Braude. J. Chem. Soc. 379 (1950).
10. G. D. Lutwick and D. E. Ryan. Can. J. Chem. **32**, 949 (1954).
11. C. A. Armour and D. E. Ryan. Can. J. Chem. **35**, 1454 (1957).

Concerning the preparation of anhydrous hydrogen peroxide

J. E. Dove and J. Riddick
Department of Chemistry, University of Toronto, Toronto, Ontario

Received June 13, 1967

Preparation of pure anhydrous hydrogen peroxide has been attempted by a literature method which involves extraction of the aqueous solution with diethyl ether, followed by fractional distillation under vacuum. Mass spectrometric analysis shows that the product is seriously impure, and indicates that a reaction has occurred between the ether and hydrogen peroxide.

Canadian Journal of Chemistry, 46, 330 (1968)

Schmidt and Bornmann (1) have recently described an attractively simple procedure for preparing anhydrous hydrogen peroxide in small quantities. The procedure involves adding 100 cc of pure diethyl ether to 10 g of a 90% to 98% aqueous solution of hydrogen peroxide and drying the separated ether layer by gently shaking for several minutes with granular calcium chloride. Dehydration of the ethereal solution is completed by two successive treatments with phosphorus pentoxide, and anhydrous hydrogen peroxide is then recovered by distillation under vacuum.

We have attempted to make small quantities of water-free hydrogen peroxide by this method. The procedure adopted was identical with that recommended by Schmidt and Bornmann except for the following minor modifications: (i) we found it necessary to dry the ethereal solution over calcium chloride for at least 1 h to prevent an over-vigorous evolution of heat on treatment with phosphorus pentoxide and (ii) the treatment with phosphorus pentoxide was carried out three times. The diethyl ether was removed on a water pump, and the residue distilled at 45–50 °C under a good rotary pump vacuum, only the middle 50% of the distillate being collected. (Schmidt and Bornmann state that 80–90% can be collected.) The ether used was taken from a freshly opened sealed can of Eastman Organic Chemicals Spectro grade diethyl ether. This is a highly purified grade with

Can. J. Chem. Downloaded from www.nrcresearchpress.com by 210.87.254.6 on 09/05/12
For personal use only.

TABLE I

Mass spectra of distillate, diethyl ether solvent, and 98% hydrogen peroxide

	Relative peak height				
	Distillate		Diethyl ether		Hydrogen peroxide
m/e	50 volts	20 volts	50 volts	20 volts	50 volts
12	1.5				
13	4.1				
14	11.8		1.3		
15	44.5	6.5	7.2		
16	4.4	1.0			8.7
17	6.1				32.2
18	11.2	3.5			100
19	1.9		2.7		1.3
25	1.3				
26	6.2		5.4		
27	20.3	1.0	29.9		
28	8.7	1.8	11.0	1.7	
29	4.5	10.8	58.1	15.2	
30	3.8	1.0	3.9	1.3	
31	49.0	11.6	100	9.4	
32	5.2	4.6	2.9	2.8	48.8
34	—				4.4
41	5.3		5.1	5.3	
42	10.4	1.3	2.3		
43	100	100	11.4	1.0	
44	9.3	6.2	3.3		
45	42.0	22.8	39.0	31.0	
46	4.2	5.2	1.1	1.0	
59	11.2	5.7	55.9	100	
60	11.4		2.8	4.3	
61	1.9				
70	2.4	0.5			
73	2.0		2.8	5.8	
74	5.5	0.5	27.2	88.8	
75	—		1.8	5.3	
87	3.7	0.5			

stated impurity levels below 0.01%. All glassware was cleaned by soaking for 24 h in concentrated nitric acid and then thoroughly leached with distilled water.

The collected distillate was analyzed mass spectrometrically on a Bendix time-of-flight mass spectrometer. The relative heights of the main peaks in the mass spectrum at two settings of the energy of the ionizing electrons are given in Table I, together with the corresponding figures for the diethyl ether solvent. It is apparent that the vapor from the "anhydrous hydrogen peroxide" contains a large proportion of some organic impurity, and that the impurity is not ether solvent. Hydrogen peroxide vapor decomposes fairly rapidly in the stainless steel inlet of the mass spectrometer and, indeed, an attempt to analyze the original hydrogen peroxide gave a spectrum (Table I) which indicated considerable decomposition to H_2O and O_2 in the inlet system. This, however, in no way explains the mass spectrum of the distillate.

We have not attempted additional experiments to identify the impurity, but the results quoted above strongly suggest that it is formed in a chemical reaction involving the ethyl ether and hydrogen peroxide. Although the physical properties of this system have been studied in some detail (2), there does not appear to be any previous record of a reaction between these two compounds. However, hydrogen peroxide has been found to react with certain substituted ethers and unsaturated ethers (3). Moreover, the $-CH_2-$ groups of ethyl ether are known to be relatively susceptible to oxidative attack (4, 5).

Comparison of the mass spectrum of the distillate with standard mass spectra (6, 7) did not yield any positive identification. However, the main features of the spectrum, including large peaks at $m/e = 31$ (CH_3O^+), 43 (CH_3CO^+), and 45 ($C_2H_5O^+$ or HCO_2^+) suggest a fairly complex oxygenated compound or mixture of compounds. The highest mass observed, $m/e = 87$, is almost certainly a fragment, so that the

Can. J. Chem. Downloaded from www.nrcresearchpress.com by 210.87.254.6 on 09/05/12
For personal use only.

corresponding heavier parent ion is presumably unstable and hence does not appear in the mass spectrum.

We conclude that the preparation of anhydrous hydrogen peroxide by this method can produce a seriously impure sample, and that all such samples should be carefully analyzed. Ether extraction has in fact been used for hydrogen peroxide purification by a number of previous workers (8) and can lead to serious explosions (9). It is therefore imperative to employ the appropriate safety precautions (1, 8, 10). This is particularly the case since our work indicates that organic peroxides may be formed, and many of these are known to be highly sensitive and dangerous explosives (10, 11). We therefore suggest that the alternative method of fractional crystallization (12), which does not require the use of other chemicals, may be more reliable in yielding a highly pure product. The improvements to the crystallization method suggested by Giguère (13) appear to have made it relatively straightforward.

Acknowledgments

This work was supported by the National Research Council of Canada and by Imperial Oil Limited. We wish to thank Professor P. A. Giguère for a helpful discussion.

1. M. SCHMIDT and P. BORNMANN. Z. Anorg. Allgem. Chem. **330**, 309 (1964).
2. W. C. SCHUMB, C. N. SATTERFIELD, and R. L. WENTWORTH. Hydrogen peroxide. Reinhold Publishing Corp., New York. 1955. Chap. 5.
3. A. G. DAVIES. Organic peroxides. Butterworths, London. 1961. pp. 4, 78.
4. A. G. DAVIES. Organic peroxides. Butterworths, London. 1961. p. 79.
5. W. E. CASS. J. Am. Chem. Soc. **69**, 500 (1947).
6. MASS SPECTRAL DATA. American Petroleum Institute Research Project 44, Texas A & M University, College Station, Texas.
7. MASS SPECTRAL DATA. Manufacturing Chemists Association Research Project, Texas A & M University, College Station, Texas.
8. W. C. SCHUMB, C. N. SATTERFIELD, and R. L. WENTWORTH. Hydrogen peroxide. Reinhold Publishing Corp., New York. 1955. Chap. 4.
9. W. SPRING. Z. Anorg. Allgem. Chem. **8**, 424 (1895).
10. W. C. SCHUMB, C. N. SATTERFIELD, and R. L. WENTWORTH. Hydrogen peroxide. Reinhold Publishing Corp., New York. 1955. Chap. 14.
11. A. RIECHE and R. MEISTER. Angew. Chem. **49**, 101 (1936).
12. G. BRAUER (*Editor*). (R. F. Riley (*Translation Editor*)). Handbook of preparative inorganic chemistry. 2nd ed. Vol. 1. Academic Press Inc., New York. 1963. p. 140.
13. P. A. GIGUÈRE. Bull. Soc. Chim. France, 720 (1954)

Can. J. Chem. Downloaded from www.nrcresearchpress.com by 210.87.254.6 on 09/05/12
For personal use only.

Trifluoromethylfluoroformate

TIMOTHY JOHNSTON, JULIAN HEICKLEN,[1] AND WAYNE STUCKEY
Aerospace Corporation, El Segundo, California

Received July 11, 1967

Trifluoromethylfluoroformate (CF_3OCFO) was produced as a secondary product in the mercury-photosensitized oxidation of 2-C_4F_8. It was identified by its mass, infrared, and fluorine n.m.r. spectra, as well as by vapor density and physical property determinations.

Canadian Journal of Chemistry, **46**, 332 (1968)

The only published report of CF_3OCFO was by Aymonino (1), who produced it from the photolysis of a mixture of CF_3OF and CO, listed some of its physical properties, and reported its infrared spectrum. We wish to report the formation of CF_3OCFO as a secondary product in the mercury-sensitized oxidation of 2-C_4F_8. In addition to the properties reported by Aymonino, we have also obtained the mass and fluorine nuclear magnetic resonance (n.m.r.) spectra.

In the mercury-photosensitized oxidation of 2-C_4F_8, it was observed (2) that the rate of formation of CF_3CFO decreased as the exposure time was lengthened. Simultaneously, a secondary product was formed. Thus, it appeared that CF_3CFO decomposed (presumably by mercury sensitization) to ultimately yield the secondary product. To check this hypothesis,

[1]Present address: Department of Chemistry, Penn State University, University Park, Pennsylvania 16802.

corresponding heavier parent ion is presumably unstable and hence does not appear in the mass spectrum.

We conclude that the preparation of anhydrous hydrogen peroxide by this method can produce a seriously impure sample, and that all such samples should be carefully analyzed. Ether extraction has in fact been used for hydrogen peroxide purification by a number of previous workers (8) and can lead to serious explosions (9). It is therefore imperative to employ the appropriate safety precautions (1, 8, 10). This is particularly the case since our work indicates that organic peroxides may be formed, and many of these are known to be highly sensitive and dangerous explosives (10, 11). We therefore suggest that the alternative method of fractional crystallization (12), which does not require the use of other chemicals, may be more reliable in yielding a highly pure product. The improvements to the crystallization method suggested by Giguère (13) appear to have made it relatively straightforward.

Acknowledgments

This work was supported by the National Research Council of Canada and by Imperial Oil Limited. We wish to thank Professor P. A. Giguère for a helpful discussion.

1. M. SCHMIDT and P. BORNMANN. Z. Anorg. Allgem. Chem. **330**, 309 (1964).
2. W. C. SCHUMB, C. N. SATTERFIELD, and R. L. WENTWORTH. Hydrogen peroxide. Reinhold Publishing Corp., New York. 1955. Chap. 5.
3. A. G. DAVIES. Organic peroxides. Butterworths, London. 1961. pp. 4, 78.
4. A. G. DAVIES. Organic peroxides. Butterworths, London. 1961. p. 79.
5. W. E. CASS. J. Am. Chem. Soc. **69**, 500 (1947).
6. MASS SPECTRAL DATA. American Petroleum Institute Research Project 44, Texas A & M University, College Station, Texas.
7. MASS SPECTRAL DATA. Manufacturing Chemists Association Research Project, Texas A & M University, College Station, Texas.
8. W. C. SCHUMB, C. N. SATTERFIELD, and R. L. WENTWORTH. Hydrogen peroxide. Reinhold Publishing Corp., New York. 1955. Chap. 4.
9. W. SPRING. Z. Anorg. Allgem. Chem. **8**, 424 (1895).
10. W. C. SCHUMB, C. N. SATTERFIELD, and R. L. WENTWORTH. Hydrogen peroxide. Reinhold Publishing Corp., New York. 1955. Chap. 14.
11. A. RIECHE and R. MEISTER. Angew. Chem. **49**, 101 (1936).
12. G. BRAUER (*Editor*). (R. F. Riley (*Translation Editor*)). Handbook of preparative inorganic chemistry. 2nd ed. Vol. 1. Academic Press Inc., New York. 1963. p. 140.
13. P. A. GIGUÈRE. Bull. Soc. Chim. France, 720 (1954)

Can. J. Chem. Downloaded from www.nrcresearchpress.com by 210.87.254.6 on 09/05/12
For personal use only.

Trifluoromethylfluoroformate

TIMOTHY JOHNSTON, JULIAN HEICKLEN,[1] AND WAYNE STUCKEY
Aerospace Corporation, El Segundo, California

Received July 11, 1967

Trifluoromethylfluoroformate (CF_3OCFO) was produced as a secondary product in the mercury-photosensitized oxidation of 2-C_4F_8. It was identified by its mass, infrared, and fluorine n.m.r. spectra, as well as by vapor density and physical property determinations.

Canadian Journal of Chemistry, **46**, 332 (1968)

The only published report of CF_3OCFO was by Aymonino (1), who produced it from the photolysis of a mixture of CF_3OF and CO, listed some of its physical properties, and reported its infrared spectrum. We wish to report the formation of CF_3OCFO as a secondary product in the mercury-sensitized oxidation of 2-C_4F_8. In addition to the properties reported by Aymonino, we have also obtained the mass and fluorine nuclear magnetic resonance (n.m.r.) spectra.

In the mercury-photosensitized oxidation of 2-C_4F_8, it was observed (2) that the rate of formation of CF_3CFO decreased as the exposure time was lengthened. Simultaneously, a secondary product was formed. Thus, it appeared that CF_3CFO decomposed (presumably by mercury sensitization) to ultimately yield the secondary product. To check this hypothesis,

[1]Present address: Department of Chemistry, Penn State University, University Park, Pennsylvania 16802.

we examined the mercury-sensitized oxidation of C_3F_6 for lengthy exposures, where CF_3CFO is also produced, and observed the same results.

The secondary product was isolated by gas chromatography, utilizing a 20 ft column composed of 20% fluorolube FS-5 on firebrick at 0 °C. The retention time of the secondary product was identical with that for perfluoropropyleneoxide, another product in the C_3F_6 system. Since with 2-C_4F_8, perfluoropropyleneoxide is not produced, a clean separation could be effected in this system. Gas density measurements of the secondary product gave a molecular weight of 131 compared with the expected value of 132 for CF_3OCFO.

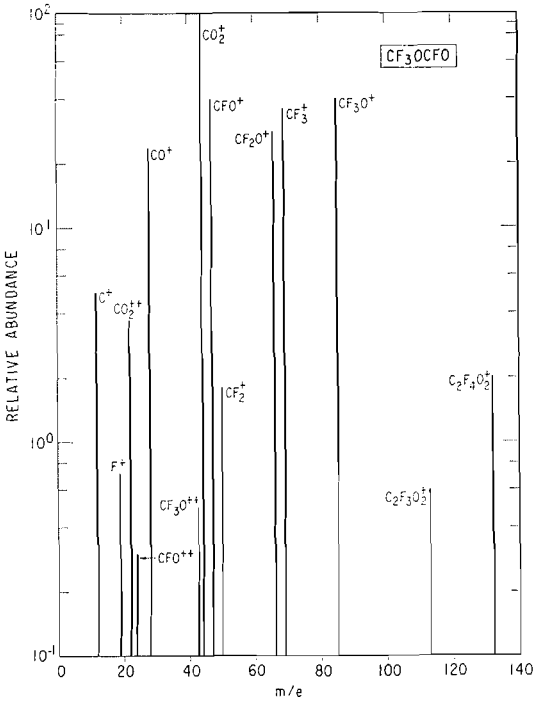

FIG. 1. Mass spectrum of CF_3OCFO at an ionizing voltage of 70 eV.

The mass spectrum of the product is summarized in Fig. 1. In order to compensate for any material bleeding from the column, a sample was collected at the appropriate retention time from an unexposed mixture of 2-C_4F_8 and O_2. This background mass spectrum indicated small amounts of fluorocarbons containing no oxygen. The sample from the photolyzed mixture gave intense peaks at *m/e* 28(CO^+), 44(CO_2^+), 47(FCO^+), 66(CF_2O^+), 69(CF_3^+), and 85(CF_3O^+). The peak of highest *m/e* is at 132 and must correspond to the parent molecule ion. The low intensity of the parent ion is a common feature of fluorocarbon mass spectra. Significantly, there are no peaks suggesting a carbon–carbon bond. The mass spectrum clearly indicates that the molecule is CF_3OCFO.

The infrared spectrum, shown in Fig. 2, supports the identification as CF_3OCFO. The spectrum is simple with bands at 5.28, 7.70, 7.93, 8.50, 9.80, 11.20, 13.05, and 15.0 μ. The prominent band at 5.28 μ, characteristic of the —CFO group, is slightly shifted from the value of 5.25 μ reported by Aymonino (1). The bands at 7.7 to 8.5 μ can easily be associated with the intense C—F bond stretching vibrations. Except for the band 5.28 μ and the weak band at 11.20 μ not reported by Aymonino, the frequencies of all the other bands correspond to those previously reported (1). The extinction coefficient (to base 10) for the 5.28 μ band was found to be 512 $\pm$ 28 l/mole cm.

Final confirmation of the identification of CF_3OCFO comes from the fluorine n.m.r. spectrum which showed a doublet with a chemical shift centered at 14.20 p.p.m. and a quartet with a chemical shift centered at 59.68 p.p.m., both downfield and with respect to CF_3COOH. The integrated area of the doublet was three times that of the quartet. Thus the spectrum indicates two sets of fluorine atoms; one consisting of one fluorine atom, and the other consisting of three equivalent fluorine atoms. The relatively weak splitting of the bands of 10.3 cycles/s infers that the two sets of fluorine atoms are not bonded to adjacent atoms in the molecule.

The vapor pressure curve of CF_3OCFO yielded a heat of vaporization of 6.1 kcal/mole between 169 and 238 °K. The boiling point was at 238 °K, which gives a value of 25.5 for Trouton's constant. Our values correspond favorably to the values of 6.3 kcal/mole and 237 °K reported by Aymonino for the heat of vaporization and the extrapolated boiling point respectively.

It is interesting to speculate on the formation of CF_3OCFO. Presumably the initial step is [1].

[1] $Hg^* + CF_3CFO \rightarrow Hg + CF_3 + FCO$

Can. J. Chem. Downloaded from www.nrcresearchpress.com by 210.87.254.6 on 09/05/12
For personal use only.

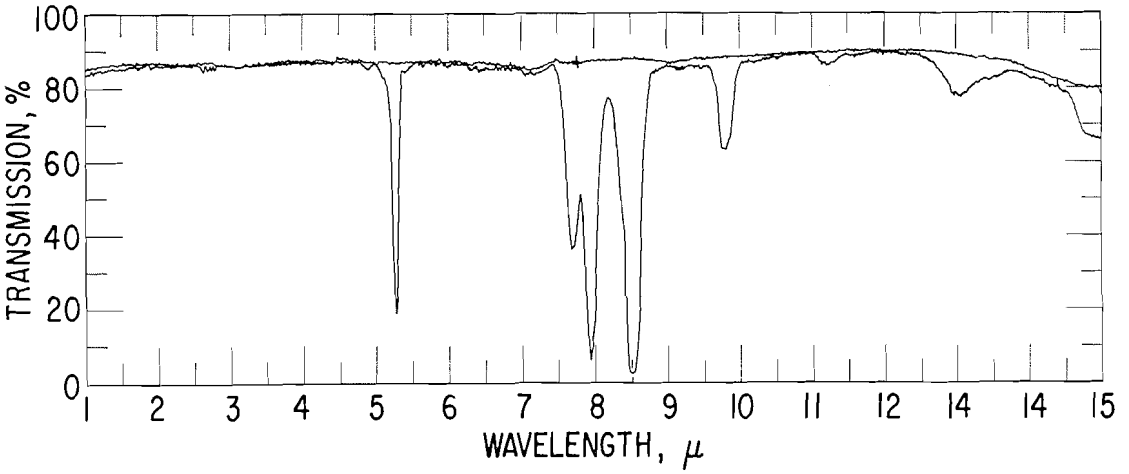

Fig. 2. Infrared spectrum of 2.57 Torr CF_3OCFO.

The radicals can then oxidize, possibly forming CF_3O and FCO_2. There are four reactions involving these radicals which could produce CF_3OCFO.

[2] $$CF_3O + FCO \rightarrow CF_3OCFO$$

[3] $$CF_3 + FCO_2 \rightarrow CF_3OCFO$$

[4] $$CF_3O + CF_3CFO \rightarrow CF_3OCFO + CF_3$$

[5] $$FCO_2 + CF_3CFO \rightarrow CF_3OCFO + FCO$$

The last two reactions are chain steps. It did not appear that a long chain was involved. Thus for reactions [4] and [5] to be important, the chain length should be small.

Acknowledgments

The authors wish to thank Professor Robert Taft for providing the facilities for the fluorine n.m.r. spectrum and Mr. Vester Knight for aid in preparing the samples.

1. P. J. Aymonino. Chem. Commun. 241 (1965).
2. T. H. Johnston and J. Heicklen. Aerospace Report No. TR-1001 (2250-40)-8. Aerospace Corporation, El Segundo, California (1967).

Mixed ligand complexes of cadmium(II)

B. Paul and D. V. Ramana Rao
Department of Chemistry, Regional Engineering College, Rourkela-8 (Orissa), India

Received May 18, 1967

Trichloro or tetrachloro cadmium(II) compounds were reacted with thiourea in ethanolic medium and mixed ligand anionic complexes having the formula $M^+(CdCl_3.tu)^-$, where M is tetraethyl ammonium, tetraphenyl arsonium, and tetraphenyl phosphonium, have been characterized. The infrared spectra indicate the presence of both the quaternary halide and thiourea.

Canadian Journal of Chemistry, 46, 334 (1968)

Previous work (1–4) in our laboratories revealed that d^{10} metal ions like Zn(II), Cd(II), and Hg(II) form stable four-coordinated complexes with a variety of ligands containing different donor atoms. The relative affinities of ligand atoms for different acceptors have been summarized by Chatt *et al.* (5). It was thought worthwhile to investigate whether a stable complex can be formed containing heterogeneous ligand atoms. Earlier, several thiourea complexes of cadmium(II) obtained by the *direct reaction* of cadmium chloride or nitrate

Can. J. Chem. Downloaded from www.nrcresearchpress.com by 210.87.254.6 on 09/05/12
For personal use only.

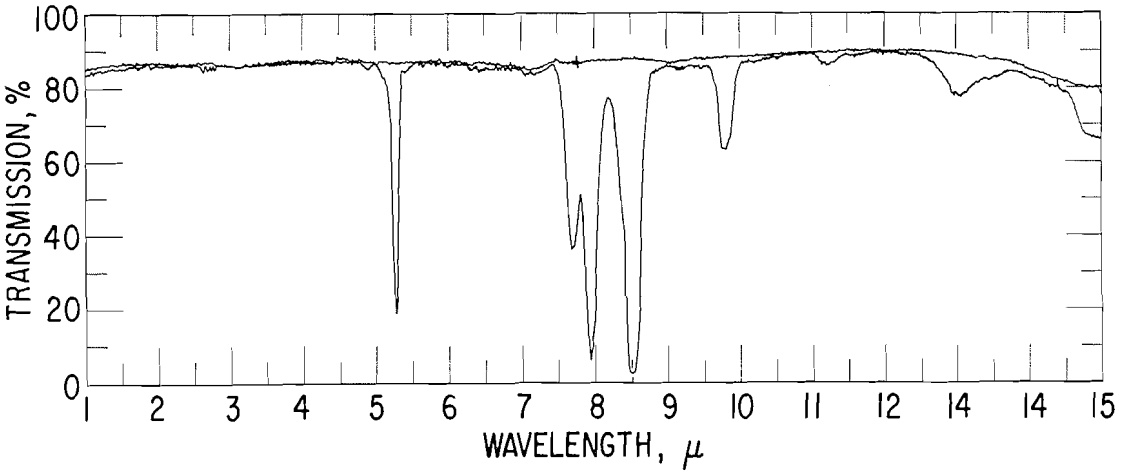

Fig. 2. Infrared spectrum of 2.57 Torr CF_3OCFO.

The radicals can then oxidize, possibly forming CF_3O and FCO_2. There are four reactions involving these radicals which could produce CF_3OCFO.

[2] $$CF_3O + FCO \rightarrow CF_3OCFO$$

[3] $$CF_3 + FCO_2 \rightarrow CF_3OCFO$$

[4] $$CF_3O + CF_3CFO \rightarrow CF_3OCFO + CF_3$$

[5] $$FCO_2 + CF_3CFO \rightarrow CF_3OCFO + FCO$$

The last two reactions are chain steps. It did not appear that a long chain was involved. Thus for reactions [4] and [5] to be important, the chain length should be small.

Acknowledgments

The authors wish to thank Professor Robert Taft for providing the facilities for the fluorine n.m.r. spectrum and Mr. Vester Knight for aid in preparing the samples.

1. P. J. Aymonino. Chem. Commun. 241 (1965).
2. T. H. Johnston and J. Heicklen. Aerospace Report No. TR-1001 (2250-40)-8. Aerospace Corporation, El Segundo, California (1967).

Mixed ligand complexes of cadmium(II)

B. Paul and D. V. Ramana Rao
Department of Chemistry, Regional Engineering College, Rourkela-8 (Orissa), India

Received May 18, 1967

Trichloro or tetrachloro cadmium(II) compounds were reacted with thiourea in ethanolic medium and mixed ligand anionic complexes having the formula $M^+(CdCl_3.tu)^-$, where M is tetraethyl ammonium, tetraphenyl arsonium, and tetraphenyl phosphonium, have been characterized. The infrared spectra indicate the presence of both the quaternary halide and thiourea.

Canadian Journal of Chemistry, 46, 334 (1968)

Previous work (1–4) in our laboratories revealed that d^{10} metal ions like Zn(II), Cd(II), and Hg(II) form stable four-coordinated complexes with a variety of ligands containing different donor atoms. The relative affinities of ligand atoms for different acceptors have been summarized by Chatt *et al.* (5). It was thought worthwhile to investigate whether a stable complex can be formed containing heterogeneous ligand atoms. Earlier, several thiourea complexes of cadmium(II) obtained by the *direct reaction* of cadmium chloride or nitrate

Can. J. Chem. Downloaded from www.nrcresearchpress.com by 210.87.254.105 on 09/05/12
For personal use only.

TABLE I

Analysis, melting point, and molar conductance of mixed ligand complexes of cadmium(II)

Complex	Melting point (°C)	% cadmium		% halogen		Λ_M (mhos)
		Found	Reqd.	Found	Reqd.	
$[Et_4N][CdCl_3.tu]$	110	25.6	26.5	25.0	25.0	125
$[Ph_4As][CdCl_3.tu]$	177	15.5	16.6	15.2	15.7	101
$[Ph_4P][CdCl_3.tu]$	210	16.8	17.7	16.7	16.8	109

TABLE II

Infrared spectra of the mixed ligand complexes of cadmium(II) (cm^{-1})

Et_4N^+	Ph_4As^+	Ph_4P^+	tu	$[Et_4N][CdCl_3.tu]$	$[Ph_4As][CdCl_3.tu]$	$[Ph_4P][CdCl_3.tu]$
740 (br)	705 w	710 s	740 s	758 vs	745 vs	690 vs
800 vs	760 br	742 vs	1 095 s	763 w	762 s	747 s
1 020 vs	1 015 w	778 w	1 420 s	798 vs	772 vs	763 vs
1 070 w	1 095 s	1 018 w	1 476 w	1 016 vs	1 000 vs	775 sw
1 180 vs		1 122 vs	1 610 s	1 100 w	1 025 sw	780 sw
				1 180 vs	1 090 vs	1 000 s
				1 630 vs	1 630 vs	1 115 vs
				1 640 s		1 420 w
						1 630 vs

ABBREVIATIONS: s, sharp; vs, very sharp; w, weak; br, broad.

with thiourea were reported (6–10) in the literature. In this communication, we report mixed ligand *anionic* complexes obtained by reacting trihalo or tetrahalo cadmium(II) compounds with thiourea in ethanolic medium. They have the formula $M^+[CdCl_3.tu]^-$ where M is tetraethyl ammonium, tetraphenyl arsonium, or tetraphenyl phosphonium cation.

Experimental

Tetraethyl Amnonium Trichloro Monothiourea Cadmium(II)

To a suspension of freshly prepared tetraethyl ammonium trichloro cadmium(II), $[Et_4N][CdCl_3]$, in alcohol was added thiourea in 1:2 ratio. No change took place immediately but on refluxing for 3 h a clear solution was obtained. When this was cooled overnight, a shining crystalline compound separated and was washed with ethanol followed by ether and dried *in vacuo*. Alternatively, a suspension of dichloro bis-thiourea cadmium-(II), $Cdtu_2Cl_2$, was reacted with tetraethyl ammonium chloride in 1:1 ratio. This process also resulted in a similar compound.

Tetraphenyl Arsonium Trichloro Monothiourea Cadmium(II)

This compound was prepared as above by reacting a suspension of $[Ph_4As][CdCl_3]$ with thiourea in 1:2 ratio. On cooling overnight, a needle-shaped crystalline compound separated and was washed with ether and dried *in vacuo*.

Tetraphenyl Phosphonium Trichloro Monothiourea Cadmium(II)

This compound, prepared as above, was obtained as beautiful shining long needles and dried *in vacuo*.

Physical Measurements

All the complexes are fairly soluble in acetone. The conductance measurements were carried out in acetone medium. The analytical and conductance data are recorded in Table I.

The magnetic susceptibility measurements made at room temperature over solid specimens using the Gouy method indicate that all the complexes are diamagnetic. The infrared spectra (i.r.) were recorded on Nujol mulls using a Karl-Zeiss UR-10 spectrophotometer, and the absorption bands in the region 5000–650 cm^{-1} are recorded in Table II.

Results and Discussion

Usually cadmium(II) ion favors the formation of four-coordinated tetrahedral complexes involving the use of $5s5p^3$ bonding orbitals. We had earlier reported (11) complexes containing the $[CdCl_3]^-$ anion, presumably having a dimeric structure to increase the coordination number to four. We have now observed that this dimeric anion breaks down to a monomeric form $[CdCl_4]^{2-}$ on refluxing. When either of these two complexes was refluxed with thiourea, a mixed anionic complex $[CdCl_3.tu]^-$ was

Can. J. Chem. Downloaded from www.nrcresearchpress.com by 210.87.254.105 on 09/05/12
For personal use only.

obtained. The i.r. spectra (Table II) indicate the presence of both the quaternary halide and thiourea. In acetone medium, these complexes are 1:1 electrolytes as indicated by their Λ_M values, which is in conformity with their formulae. The compounds isolated are therefore definitely mixed ligand anionic complexes of cadmium(II). Similar mixed ligand complexes of cobalt(II) having the formula $[Et_4N][CoBr_3 . Benzimidazole]$ and $[MePh_3As][CoI_3 . Benzimidazole]$ were reported earlier (12).

Acknowledgments

Thanks are due to the Ministry of Education, Government of India, for the award of a Research Training Scholarship (to B.P.) and Professor C. C. Patel, Indian Institute of Science, Bangalore, for recording the spectra.

1. K. C. Dash and D. V. R. Rao. J. Indian Chem. Soc. **41**, 600 (1964).
2. M. Ali and D. V. R. Rao. J. Indian Chem. Soc. **43**, 583 (1966).
3. S. Guru and D. V. R. Rao. J. Indian Chem. Soc. **44**, 594 (1967).
4. B. Paul and D. V. R. Rao. J. Indian Chem. Soc. **44**, 532 (1967).
5. S. Ahrland, J. Chatt, and N. R. Davies. Quart. Rev. **12**, 265 (1958).
6. M. Nardelli, L. Cavalca, and A. Braibanti. Gazz. Chim. Ital. **86**, 867 (1956).
7. M. Nardelli and I. Chierici. Ric. Sci. **28**, 1016 (1958).
8. M. Nardelli, A. Braibanti, and I. Chierici. Gazz. Chim. Ital. **87**, 1226 (1957).
9. T. J. Lane, J. A. Ryan, and E. F. Britton. J. Am. Chem. Soc. **80**, 315 (1958).
10. P. K. Migal and V. A. Tsiplyakova. Zh. Neorgan. Khim. **9**, 601 (1964).
11. B. Paul and D. V. R. Rao. Current Sci. India, **36**, 291 (1967).
12. D. M. L. Goodgame and F. A. Cotton. J. Am. Chem. Soc. **84**, 1543 (1962).

γ-Radiolysis of cyclohexane with electron scavengers. IV. CO_2 as an electron scavenger[1]

N. H. Sagert

Research Chemistry Branch, Chalk River Nuclear Laboratories, Chalk River, Ontario

Received September 13, 1967

The room temperature liquid phase radiolysis of cyclohexane has been examined in the presence of CO_2 and of CO_2 with N_2O. CO_2 decreases the yields of all major products by scavenging electrons. It is concluded that the CO_2 anion does not dissociate and that no precursors of cyclohexyl radicals are formed when it is finally neutralized by a hydrocarbon cation. No evidence that CO_2 acts as an efficient O^- scavenger in liquid phase cyclohexane was found. Its rate of reaction with O^- appears comparable to its rate of reaction with electrons.

Canadian Journal of Chemistry, **46**, 336 (1968)

Introduction

Warman has recently suggested (1) that CO_2 acts as an O^- scavenger in the gas phase radiolysis of the propane–N_2O system according to reaction [1].

[1] $$O^- + CO_2 \rightarrow CO_3^-.$$

He further suggests that with sufficient CO_2 present, the nitrogen yield is a measure of the yield of electrons (reaction [2]),

[2] $$e^- + N_2O \rightarrow [N_2O^-] \rightarrow N_2 + O^-,$$

and no nitrogen is then produced by reaction [3], which Johnson and Warman (2) proposed earlier to explain nitrogen yields from the gas phase propane–N_2O system.

[3] $$O^- + N_2O \rightarrow N_2 + O_2^-$$

Yields of nitrogen which are larger than the normally accepted value of $G(e^-)$ are obtained from the liquid phase radiolysis of the cyclohexane–N_2O system (3–6). The origin of this extra nitrogen yield is uncertain, although the suggestion has been made that reaction [3] is responsible (1, 5). Yields of the major liquid products, bicyclohexyl and cyclohexene, are larger than when N_2O is absent (4). We have suggested that the increase in liquid product yields represents that yield of electrons which, in the absence of electron scavengers, does not give hydrogen

[1]Issued as A.E.C.L. No. ~~2893~~. 2983

Can. J. Chem. Downloaded from www.nrcresearchpress.com by 210.87.254.105 on 09/05/12
For personal use only.

obtained. The i.r. spectra (Table II) indicate the presence of both the quaternary halide and thiourea. In acetone medium, these complexes are 1:1 electrolytes as indicated by their Λ_M values, which is in conformity with their formulae. The compounds isolated are therefore definitely mixed ligand anionic complexes of cadmium(II). Similar mixed ligand complexes of cobalt(II) having the formula $[Et_4N][CoBr_3 . Benzimidazole]$ and $[MePh_3As][CoI_3 . Benzimidazole]$ were reported earlier (12).

Acknowledgments

Thanks are due to the Ministry of Education, Government of India, for the award of a Research Training Scholarship (to B.P.) and Professor C. C. Patel, Indian Institute of Science, Bangalore, for recording the spectra.

1. K. C. Dash and D. V. R. Rao. J. Indian Chem. Soc. **41**, 600 (1964).
2. M. Ali and D. V. R. Rao. J. Indian Chem. Soc. **43**, 583 (1966).
3. S. Guru and D. V. R. Rao. J. Indian Chem. Soc. **44**, 594 (1967).
4. B. Paul and D. V. R. Rao. J. Indian Chem. Soc. **44**, 532 (1967).
5. S. Ahrland, J. Chatt, and N. R. Davies. Quart. Rev. **12**, 265 (1958).
6. M. Nardelli, L. Cavalca, and A. Braibanti. Gazz. Chim. Ital. **86**, 867 (1956).
7. M. Nardelli and I. Chierici. Ric. Sci. **28**, 1016 (1958).
8. M. Nardelli, A. Braibanti, and I. Chierici. Gazz. Chim. Ital. **87**, 1226 (1957).
9. T. J. Lane, J. A. Ryan, and E. F. Britton. J. Am. Chem. Soc. **80**, 315 (1958).
10. P. K. Migal and V. A. Tsiplyakova. Zh. Neorgan. Khim. **9**, 601 (1964).
11. B. Paul and D. V. R. Rao. Current Sci. India, **36**, 291 (1967).
12. D. M. L. Goodgame and F. A. Cotton. J. Am. Chem. Soc. **84**, 1543 (1962).

γ-Radiolysis of cyclohexane with electron scavengers. IV. CO_2 as an electron scavenger[1]

N. H. Sagert

Research Chemistry Branch, Chalk River Nuclear Laboratories, Chalk River, Ontario

Received September 13, 1967

The room temperature liquid phase radiolysis of cyclohexane has been examined in the presence of CO_2 and of CO_2 with N_2O. CO_2 decreases the yields of all major products by scavenging electrons. It is concluded that the CO_2 anion does not dissociate and that no precursors of cyclohexyl radicals are formed when it is finally neutralized by a hydrocarbon cation. No evidence that CO_2 acts as an efficient O^- scavenger in liquid phase cyclohexane was found. Its rate of reaction with O^- appears comparable to its rate of reaction with electrons.

Canadian Journal of Chemistry, **46**, 336 (1968)

Introduction

Warman has recently suggested (1) that CO_2 acts as an O^- scavenger in the gas phase radiolysis of the propane–N_2O system according to reaction [1].

[1] $$O^- + CO_2 \rightarrow CO_3^-.$$

He further suggests that with sufficient CO_2 present, the nitrogen yield is a measure of the yield of electrons (reaction [2]),

[2] $$e^- + N_2O \rightarrow [N_2O^-] \rightarrow N_2 + O^-,$$

and no nitrogen is then produced by reaction [3], which Johnson and Warman (2) proposed earlier to explain nitrogen yields from the gas phase propane–N_2O system.

[3] $$O^- + N_2O \rightarrow N_2 + O_2^-$$

Yields of nitrogen which are larger than the normally accepted value of $G(e^-)$ are obtained from the liquid phase radiolysis of the cyclohexane–N_2O system (3–6). The origin of this extra nitrogen yield is uncertain, although the suggestion has been made that reaction [3] is responsible (1, 5). Yields of the major liquid products, bicyclohexyl and cyclohexene, are larger than when N_2O is absent (4). We have suggested that the increase in liquid product yields represents that yield of electrons which, in the absence of electron scavengers, does not give hydrogen

[1]Issued as A.E.C.L. No. ~~2893~~. 2983

Can. J. Chem. Downloaded from www.nrcresearchpress.com by 210.87.254.42 on 09/05/12
For personal use only.

Can. J. Chem. Downloaded from www.nrcresearchpress.com by 210.87.254.42 on 09/05/12
For personal use only.

precursors when neutralized (4). It was therefore of interest to examine the radiolysis of the liquid phase cyclohexane–N_2O system in the presence of CO_2 to see if a limiting yield of nitrogen could be obtained which could be equated with $G(e^-)$, and also to see if an O^- scavenger could eliminate part of the extra yields of cyclohexene and bicyclohexyl.

The radiolysis of the liquid phase cyclohexane–CO_2 system was examined as well. Although yields of gaseous products from this system have been reported recently by Sato *et al.* (7), bicyclohexyl and cyclohexene yields do not appear to have been given previously.

Experimental

The experimental procedures and sources of N_2O and cyclohexane have been described (4). CO_2 (Matheson) was used as received after removing permanent gases by the freeze–thaw technique. The solubility of CO_2 in cyclohexane used to calculate CO_2 concentrations was taken from the results of Dymond (8).

Results and Discussion

The major products from the radiolysis of cyclohexane are hydrogen, cyclohexene, and bicyclohexyl (9). Yields of these products in the presence of up to 0.9 mole of CO_2 per liter are shown in Fig. 1. These yields are independent of dose up to 7×10^{22} eV/l. All G values are molecules produced for every 100 eV of energy absorbed in the entire system. The yields of major products are reduced simultaneously in a manner similar to that observed when SF_6 is used as an electron scavenger (4), except that over five times as much CO_2 is required. This is in direct contrast to the results of Sato *et al.* (7), who found SF_6 and CO_2 to have about the same scavenging efficiency. At least part of this discrepancy lies in the values of the gas solubilities used. There is a small yield of CO which increases with increasing CO_2 concentration, but it is only 0.18 G unit at 0.84_5 mole/l of CO_2.

Carbon dioxide is known to be inert to attack by atoms and has often been used as inert gas in systems containing H atoms (10). Hence it is improbable that CO_2 is acting as an atom scavenger in this system. The high ionization potential of CO_2 (11) indicates that charge transfer from the solvent to the solute is improbable. The direct observation of CO_2^- in the solid 3-methylpentane–CO_2 system by Johnson and Albrecht using electron spin resonance (e.s.r.) methods (12) indicates that CO_2 may act as an electron scavenger in the liquid cyclohexane–CO_2 system.

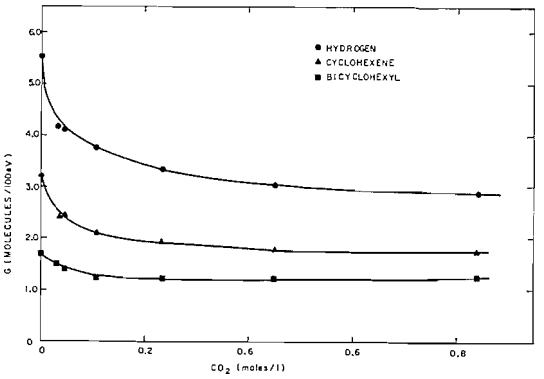

FIG. 1. Yields of hydrogen, cyclohexene, and bicyclohexyl from the cyclohexane–CO_2 system. Dose = 2.90×10^{22} eV/l.

[4] $$e^- + CO_2 \rightarrow CO_2^-$$

All yields are reduced simultaneously and no large yields of CO are observed. Thus CO_2^- does not dissociate to any appreciable extent.

[5] $$CO_2^- \rightarrow CO + O^-$$

As reaction [5] is endothermic by more than 3.6 eV in the gas phase (13, 14), this is not surprising. The CO_2^- ion will eventually be neutralized by a hydrocarbon cation. As all yields are reduced simultaneously, no precursors of hydrogen or cyclohexyl radicals are formed by this neutralization.

Yields of nitrogen, cyclohexene, and bicyclohexyl when CO_2 is added to a 0.28 M solution of

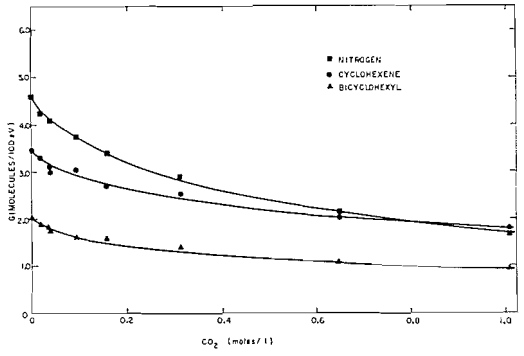

FIG. 2. Yields of nitrogen, cyclohexene, and bicyclohexyl from the cyclohexane–N_2O–CO_2 system. [N_2O] = 0.28 mole/l. Dose = 2.90×10^{22} eV/l.

Can. J. Chem. Downloaded from www.nrcresearchpress.com by 210.87.254.42 on 09/05/12
For personal use only.

N_2O in cyclohexane are shown in Fig. 2. Hydrogen yields are reduced slightly from 2.7 to 2.4 *G* units when the maximum amount of CO_2 is added (1 mole/l). All yields are independent of dose to 7×10^{22} eV/l. The nitrogen yield is reduced smoothly to a value below the assumed total electron yield (4 *G* units) and the liquid product yields are reduced well below the yields from pure cyclohexane. Hence the action of CO_2 in this system is to scavenge electrons as well as O^-. Asmus and Warman (15) have reached a similar conclusion based on hydrogen and nitrogen yields alone.

At the largest concentration of CO_2 the nitrogen yield is still appreciable and the sum of the cyclohexene and bicyclohexyl yields (2.8 *G* units) is still larger than the hydrogen yield (2.4 *G* units), so that N_2O is scavenging some of the electrons. A plot of $(G(N_2)_0 - G(N_2))^{-1}$ against $[N_2O]/[CO_2]$, where $G(N_2)_0$ is the yield of nitrogen in the absence of CO_2, is curved, indicating that there are at least two ways in which the nitrogen yield is reduced. One of these processes is undoubtedly the competition of CO_2 and N_2O for O^- as suggested by Warman (1) for the gas phase, or with some chain process of a type similar to that proposed by Holtslander and Freeman (16) for the gas phase N_2O–methylcyclohexane system.

These results have shown that CO_2 in irradiated liquid cyclohexane probably acts as a well-behaved electron scavenger which does not initiate secondary reactions. They have also shown that CO_2 cannot be used as a simple O^- scavenger. Its rate of reaction with electrons is comparable to or greater than its rate of reaction with O^-.

Acknowledgments

I wish to thank Dr. J. M. Warman for discussion of his unpublished results and Dr. A. W. Boyd for helpful advice.

1. J. M. WARMAN. Nature, **213**, 381 (1967).
2. G. R. A. JOHNSON and J. M. WARMAN. Trans. Faraday Soc. **61**, 1709 (1965).
3. G. SCHOLES and M. SIMIC. Nature, **202**, 895 (1964).
4. N. H. SAGERT and A. S. BLAIR. Can. J. Chem. **45**, 1351 (1967).
5. S. SATO, R. YUGETA, K. SHINSAKA, and T. TERAO. Bull. Chem. Soc. Japan, **39**, 156 (1966).
6. W. V. SHERMAN. J. Chem. Soc. A, 599 (1966).
7. S. SATO, T. TERAO, M. KONO, and S. SHIDA. Bull. Chem. Soc. Japan, **40**, 1818 (1967).
8. J. H. DYMOND. J. Phys. Chem. **71**, 1829 (1967).
9. P. J. DYNE and J. A. STONE. Can. J. Chem. **39**, 2381 (1961).
10. B. A. THRUSH. Progr. Reaction Kinetics, **3**, 63 (1965).
11. V. I. VEDENEYEV, L. V. GURVICH, V. N. KONDRAT'YEV, V. A. MEDVEDEV, and YE. L. FRANKEVICH. Bond energies, ionization potentials and electron affinities. Edward Arnold (Publishers) Ltd., London. 1966.
12. P. M. JOHNSON and A. C. ALBRECHT. J. Chem. Phys. **44**, 1845 (1966).
13. R. K. ASUNDI, J. D. CRAGGS, and V. M. KUREPA. Proc. Phys. Soc. London, **82**, 967 (1963).
14. D. RAPP and D. D. BRIGLIA. J. Chem. Phys. **43**, 1480 (1965).
15. K.-D. ASMUS and J. M. WARMAN. Private communication.
16. W. J. HOLTSLANDER and G. R. FREEMAN. Can. J. Chem. **45**, 1661 (1967).

Far ultraviolet photolysis of carbon dioxide

J. Y. YANG[1] AND F. M. SERVEDIO
North American Aviation Science Center, Thousand Oaks, California

Received July 18, 1967

Carbon dioxide in the pressure range of 50–600 Torr has been photolyzed at 1470 Å. An initial quantum yield of $\Phi(CO) = 1.0$ was observed. The O_2/CO ratio was 0.35 ± 0.02. While the O_2/CO ratio remained constant, the rate of CO formation decreased significantly with an increase in the photolysis time. Such a lowering of the conversion rate is attributed to a light attenuation due to solid deposit being formed on the lamp window.

Canadian Journal of Chemistry, 46, 338 (1968)

The far ultraviolet photolysis of carbon dioxide is of importance toward our understanding of the upper atmosphere photochemistry as well as that of the Mars and Venus atmospheres. In addition, the measurement of CO yields from carbon dioxide photolysis is widely used as an actinometer for light sources emitting at short wavelengths. Thus, both a detailed understanding of the reaction mechan-

[1]Present address: Western New York Nuclear Research Center, State University of New York at Buffalo, Buffalo, New York 14214.

N_2O in cyclohexane are shown in Fig. 2. Hydrogen yields are reduced slightly from 2.7 to 2.4 G units when the maximum amount of CO_2 is added (1 mole/l). All yields are independent of dose to 7×10^{22} eV/l. The nitrogen yield is reduced smoothly to a value below the assumed total electron yield (4 G units) and the liquid product yields are reduced well below the yields from pure cyclohexane. Hence the action of CO_2 in this system is to scavenge electrons as well as O^-. Asmus and Warman (15) have reached a similar conclusion based on hydrogen and nitrogen yields alone.

At the largest concentration of CO_2 the nitrogen yield is still appreciable and the sum of the cyclohexene and bicyclohexyl yields (2.8 G units) is still larger than the hydrogen yield (2.4 G units), so that N_2O is scavenging some of the electrons. A plot of $(G(N_2)_0 - G(N_2))^{-1}$ against $[N_2O]/[CO_2]$, where $G(N_2)_0$ is the yield of nitrogen in the absence of CO_2, is curved, indicating that there are at least two ways in which the nitrogen yield is reduced. One of these processes is undoubtedly the competition of CO_2 and N_2O for O^- as suggested by Warman (1) for the gas phase, or with some chain process of a type similar to that proposed by Holtslander and Freeman (16) for the gas phase N_2O–methylcyclohexane system.

These results have shown that CO_2 in irradiated liquid cyclohexane probably acts as a well-behaved electron scavenger which does not initiate secondary reactions. They have also shown that CO_2 cannot be used as a simple O^- scavenger. Its rate of reaction with electrons is comparable to or greater than its rate of reaction with O^-.

Acknowledgments

I wish to thank Dr. J. M. Warman for discussion of his unpublished results and Dr. A. W. Boyd for helpful advice.

1. J. M. WARMAN. Nature, **213**, 381 (1967).
2. G. R. A. JOHNSON and J. M. WARMAN. Trans. Faraday Soc. **61**, 1709 (1965).
3. G. SCHOLES and M. SIMIC. Nature, **202**, 895 (1964).
4. N. H. SAGERT and A. S. BLAIR. Can. J. Chem. **45**, 1351 (1967).
5. S. SATO, R. YUGETA, K. SHINSAKA, and T. TERAO. Bull. Chem. Soc. Japan, **39**, 156 (1966).
6. W. V. SHERMAN. J. Chem. Soc. A, 599 (1966).
7. S. SATO, T. TERAO, M. KONO, and S. SHIDA. Bull. Chem. Soc. Japan, **40**, 1818 (1967).
8. J. H. DYMOND. J. Phys. Chem. **71**, 1829 (1967).
9. P. J. DYNE and J. A. STONE. Can. J. Chem. **39**, 2381 (1961).
10. B. A. THRUSH. Progr. Reaction Kinetics, **3**, 63 (1965).
11. V. I. VEDENEYEV, L. V. GURVICH, V. N. KONDRAT'YEV, V. A. MEDVEDEV, and YE. L. FRANKEVICH. Bond energies, ionization potentials and electron affinities. Edward Arnold (Publishers) Ltd., London. 1966.
12. P. M. JOHNSON and A. C. ALBRECHT. J. Chem. Phys. **44**, 1845 (1966).
13. R. K. ASUNDI, J. D. CRAGGS, and V. M. KUREPA. Proc. Phys. Soc. London, **82**, 967 (1963).
14. D. RAPP and D. D. BRIGLIA. J. Chem. Phys. **43**, 1480 (1965).
15. K.-D. ASMUS and J. M. WARMAN. Private communication.
16. W. J. HOLTSLANDER and G. R. FREEMAN. Can. J. Chem. **45**, 1661 (1967).

Far ultraviolet photolysis of carbon dioxide

J. Y. YANG[1] AND F. M. SERVEDIO
North American Aviation Science Center, Thousand Oaks, California

Received July 18, 1967

Carbon dioxide in the pressure range of 50–600 Torr has been photolyzed at 1470 Å. An initial quantum yield of $\Phi(CO) = 1.0$ was observed. The O_2/CO ratio was 0.35 ± 0.02. While the O_2/CO ratio remained constant, the rate of CO formation decreased significantly with an increase in the photolysis time. Such a lowering of the conversion rate is attributed to a light attenuation due to solid deposit being formed on the lamp window.

Canadian Journal of Chemistry, 46, 338 (1968)

The far ultraviolet photolysis of carbon dioxide is of importance toward our understanding of the upper atmosphere photochemistry as well as that of the Mars and Venus atmospheres. In addition, the measurement of CO yields from carbon dioxide photolysis is widely used as an actinometer for light sources emitting at short wavelengths. Thus, both a detailed understanding of the reaction mechan-

[1]Present address: Western New York Nuclear Research Center, State University of New York at Buffalo, Buffalo, New York 14214.

Can. J. Chem. Downloaded from www.nrcresearchpress.com by 210.87.254.5 on 09/05/12
For personal use only.

Can. J. Chem. Downloaded from www.nrcresearchpress.com by 210.87.254.5 on 09/05/12
For personal use only.

ism and a knowledge of the product quantum yields are highly essential. Recent mechanistic studies on this subject have yielded significant findings to enable a reasonably complete understanding of the major reaction processes (1–6). However, serious disagreement on the quantum yield of CO remains unresolved. In particular, a value of $\Phi(CO) = 0.25$ for photolysis at 1470 Å was reported by Ung and Schiff (7). Such a value is greatly different from the heretofore accepted value of near unity (1, 2, 8). It appears rather urgent to reexamine the CO quantum yield and to seek out possible causes for discrepancies in the reported findings.

To achieve fairly precise and reproducible product analysis, a closed system was chosen for our experiments. The photolysis cell, as illustrated in Fig. 1, consisted of a spherical section (10 cm dia.) to allow for divergence of the light source and a magnetic stirrer to eliminate possible inner filter effects. The 25 mm dia. $\times$ 1 mm thick sapphire window was sealed to the Pyrex body through a graded seal. The lamp assembly was baked at 400 °C for 24 h while being evacuated to less than 1×10^{-6} Torr. The barium getter was deposited as a black mirror by flaming the quartz side arm to 800 °C. The lamp was filled to 0.9 Torr with research grade xenon (Air Reduction Company). The discharge was powered by a Raytheon Model PGM-10 microwave power generator (2 450 mc) operating at a power input of 100 W through an Ophthus Evenson type cavity (9) tuned to less than 1% power reflection. The emission spectra of the discharge lamps were examined with a McPherson Model 230 S one meter vacuum UV scanning monochromator up to 3000 Å, and in every case only the 1470 Å line was observed. During photolysis the getter arm of the lamp was immersed in a dry ice mixture and the lamp body was cooled by air blast from a ring-shaped source.

The carbon dioxide was Air Products Company C.P. grade and was further purified by bulb to bulb distillations first at 77 °K to remove air and then at 196 °K to eliminate water and mercury. The photolysis products CO and O_2 were transferred through cold traps at 77 °K by means of a Toepler pump, measured in a gas buret, and then analyzed by gas chromatography using a 2 m Linde 5A molecular sieve column at 50 °C. The yield was found to decrease with each successive photolysis. In order to reproduce the initial rates, it was necessary to clean the cells by photolysis of water vapor followed by photolysis of oxygen at atmospheric pressure, each for a period of about half an hour. The products from water vapor photolysis were separated into fractions noncondensable at 77 and at 195 °K, and then analyzed gas chromatographically through Linde 5A molecular sieve and Porapak "Q" columns respectively.

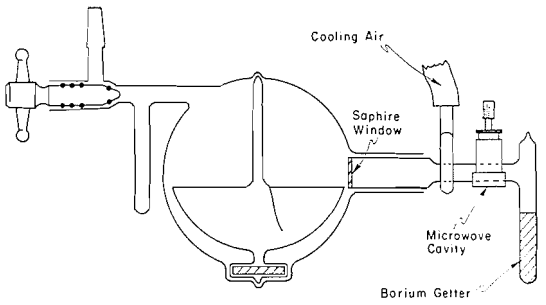

FIG. 1. Photolysis cell.

Two xenon discharge lamps were used, and their 1470 Å light intensities were found to be 2.1×10^{16} and 1.8×10^{16} quanta/s respectively. These values were determined by measuring the yield of nitrogen ($\Phi_{N_2} = 1.4$) (11, 12) from nitrous oxide photolysis. Stability of the output intensities is indicated by a constant rate of nitrogen formation even with the lamps having been operated continuously up to half an hour. The nitrogen yield was independent of the nitrous oxide pressure when the pressure was greater than 2 Torr. Since the absorption cross section for N_2O is about 10 times that for CO_2, possible effects of radiation divergence may be eliminated by photolysis of CO_2 at pressures greater than 20 Torr.

Carbon dioxide photolysis was carried out with total conversion not to exceed 1% in each run. The O_2 and CO yields were found to be independent of carbon dioxide pressure in the range of 50 to 600 Torr, and the O_2/CO ratio was 0.35 ± 0.02. Carbon monoxide yields as functions of photolysis time are shown in Fig. 2 for two separate light sources. In contrast to the reported findings of earlier investigations (1, 2, 7), the rate of CO formation decreased significantly with increasing photolysis time. However, in earlier studies the maximum conversion was only 4 micromoles and up to that extent of reaction our data also appear to be

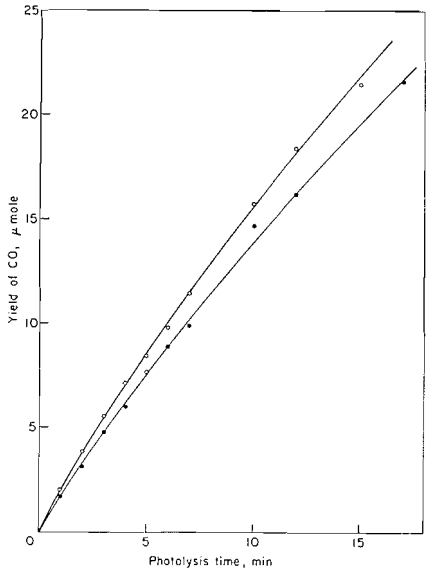

FIG. 2. Yield of CO as function of time: (○) Xe lamp No. 1, (●) Xe lamp No. 2.

linear. In addition, the intensities of our light sources are considerably higher than those used in previous studies. A similar nonlinearity at relatively high light intensities has been reported by Mahan (1) for carbon dioxide photolysis at 1236 Å. We have further observed that, for a given photolysis time, the CO yield from a single run is always the same as the sum of products from successive runs of shorter durations. Thus, the observed lowering of the rate of CO formation cannot be accounted for by either back reactions or a possible inner filter effect. Another significant observation is that the initial rates can be reproduced by rigorous cleaning of the photolysis cells. Slanger (5) has suggested recently that solid products may result from wall reactions involving a CO_3 intermediate. Under our experimental conditions, such a transient intermediate would be concentrated within a few millimeters of the lamp window, and the solid products will be deposited mainly on the window surface. Therefore, we attribute the observed lowering of the CO yield to an attenuation of the photo-intensity by impurities deposited on the window, which has been noted earlier by Jucker and Rideal (10).

It may be assumed that the deposit is formed by photo-initiated reactions near the lamp window and it is decomposed by absorption of the light within the layer. Thus, the growth of the deposit thickness is given by eq. [1],

$$[1] \qquad \frac{dl}{dt} = k_1 I_0 e^{-\epsilon l} - k_2 I_0 (1 - e^{-\epsilon l}),$$

where k_1 and k_2 may be functions of the light intensity. When the fraction of the light absorbed in the layer is small, i.e. $\epsilon l \ll 1$, eq. [1] is reduced by an approximation as follows,

$$[2] \qquad \frac{dl}{dt} = k_1 I_0 - k_2 I_0 \epsilon l,$$

and a simple integration ($l = 0$, at $t = 0$) gives eq. [3]

$$[3] \qquad l = \frac{k_1}{k_2 \epsilon} (1 - e^{-k_2 I_0 \epsilon t});$$

since the CO yield is proportional to the light quanta transmitted through such a layer, the rate of CO formation should decrease initially as a logarithmic function of the photolysis time and gradually reach a constant value. The instantaneous rates are taken from the slopes of the curves in Fig. 2, and these are plotted in Fig. 3. An initial quantum yield of $\Phi(CO) = 1.0$ is obtained.

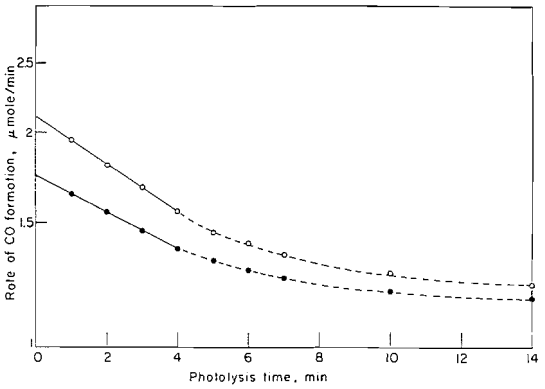

FIG. 3. Rate of CO formation: (○) Xe lamp No. 1, (●) Xe lamp No. 2.

The observed CO quantum yield of unity is in good agreement with findings by Groth (8), Mahan (1), and Warneck (2). The value of 2 reported by Jucker and Rideal (10) may be dismissed for uncertainties in their actinometry. It is possible that their thermocouple output may show significant spectral dependence and thus lead to an erroneous calibration of their source intensity. The low value of 0.25 by Ung

Can. J. Chem. Downloaded from www.nrcresearchpress.com by 210.87.254.5 on 09/05/12
For personal use only.

and Schiff (7), however, is more difficult to dispute. Low CO yields may result from decreased transparency of the lamp window, but such a source of error would be compensated by correspondingly lower values in actinometric measurements. Reeves and co-workers (13) demonstrated recently that the presence of traces of H_2O or H_2 will catalyze back reactions so as to inhibit the dissociation of CO_2. Since Ung and Schiff (7) found that CO yields were not affected by the addition of H_2, their results may have been influenced by the presence of moisture in their photolysis systems.

Acknowledgment

The photolysis cells used in this study were constructed by George Andry and Ernest Eisel. Their valuable assistance is gratefully acknowledged.

1. B. H. MAHAN. J. Chem. Phys. **33**, 959 (1960).
2. P. WARNECK. Discussions Faraday Soc. **37**, 57 (1964).
3. P. WARNECK. J. Chem. Phys. **43**, 1849 (1965).
4. N. G. MOLL, D. R. CLUTTER, and W. E. THOMPSON. J. Chem. Phys. **45**, 4469 (1966).
5. T. G. SLANGER. J. Chem. Phys. **45**, 4127 (1966).
6. M. CLERC and F. BARAT. J. Chem. Phys. **46**, 107 (1967).
7. A. Y. UNG and H. I. SCHIFF. Can. J. Chem. **44**, 1981 (1966).
8. W. E. GROTH. Z. Physik. Chem. Leipzig, **B37**, 307 (1937).
9. F. C. FEHSENFELD, K. M. EVENSON, and H. P. BROIDA. Rev. Sci. Instr. **36**, 294 (1965).
10. H. JUCKER and E. K. RIDEAL. J. Chem. Soc. London, 1058 (1957).
11. M. ZELIKOFF and L. M. ASCHENBRAND. J. Chem. Phys. **22**, 1680 (1954).
12. W. E. GROTH and H. SCHIERHOLZ. Planetary Space Sci. **1**, 333 (1959).
13. R. R. REEVES, JR., P. HARTECK, B. A. THOMPSON, and R. W. WALDRON. J. Phys. Chem. **70**, 1637 (1966).

Vibrational energy transfer. Collisional quenching of competitive unimolecular reactions[1]

D. C. TARDY,[2] C. W. LARSON,[3] AND B. S. RABINOVITCH
Department of Chemistry, University of Washington, Seattle, Washington

Received August 9, 1967

A technique is described for the study of collisional deexcitation of highly vibrationally excited polyatomic molecules by use of externally activated competitive unimolecular reaction systems. This method has some advantages and is illustrated by the decomposition of chemically activated hexyl-3 radicals in the presence of H_2 and CF_4 as heat bath molecules. The former removes ~ 1.2 kcal mole^{-1} per successful collision; while for the latter a value in excess of 4.6 kcal is found so that CF_4 behaves operationally like a strong collider.

Canadian Journal of Chemistry, **46**, 341 (1968)

We report on a technique for study of collisional vibrational energy transfer in a chemically activated *competitive* unimolecular reaction system which promises greater experimental accuracy and facility than has been possible heretofore (1, 2). (Reference 2 gives a summary of the literature.) The method appears quite useful in the light of analysis and experimental results given recently for competitive unimolecular systems (3). The technique can extend to any type of external activation system.

Molecules may be inserted directly into high levels of vibrational excitation by "external" activation methods, in contrast with internal excitation by thermal collisional transport. In chemical activation, the substrate is simultaneously formed and excited. If the excitation level exceeds a reaction threshold energy E_0, unimolecular reaction may occur. Collisional quenching of excited molecules to levels below E_0 results in stabilization. Earlier work (1, 2) has shown how the relative amounts of collisional cascade, leading to stabilization (S), and of reaction, say decomposition (D), can yield information about the average amount of energy, $\langle \Delta E \rangle$, transferred to a bath molecule on collision, and about the transition probabilities, p_{mn}.

[1]Work supported by the U.S. Air Force Office of Scientific Research, Contract No. AF 49(638)-1633.
[2]NASA predoctoral fellow. Present address, University of Toronto, Toronto, Ont.
[3]NSF predoctoral trainee.

Can. J. Chem. Downloaded from www.nrcresearchpress.com by 210.87.254.5 on 09/05/12
For personal use only.

and Schiff (7), however, is more difficult to dispute. Low CO yields may result from decreased transparency of the lamp window, but such a source of error would be compensated by correspondingly lower values in actinometric measurements. Reeves and co-workers (13) demonstrated recently that the presence of traces of H_2O or H_2 will catalyze back reactions so as to inhibit the dissociation of CO_2. Since Ung and Schiff (7) found that CO yields were not affected by the addition of H_2, their results may have been influenced by the presence of moisture in their photolysis systems.

Acknowledgment

The photolysis cells used in this study were constructed by George Andry and Ernest Eisel. Their valuable assistance is gratefully acknowledged.

1. B. H. MAHAN. J. Chem. Phys. **33**, 959 (1960).
2. P. WARNECK. Discussions Faraday Soc. **37**, 57 (1964).
3. P. WARNECK. J. Chem. Phys. **43**, 1849 (1965).
4. N. G. MOLL, D. R. CLUTTER, and W. E. THOMPSON. J. Chem. Phys. **45**, 4469 (1966).
5. T. G. SLANGER. J. Chem. Phys. **45**, 4127 (1966).
6. M. CLERC and F. BARAT. J. Chem. Phys. **46**, 107 (1967).
7. A. Y. UNG and H. I. SCHIFF. Can. J. Chem. **44**, 1981 (1966).
8. W. E. GROTH. Z. Physik. Chem. Leipzig, **B37**, 307 (1937).
9. F. C. FEHSENFELD, K. M. EVENSON, and H. P. BROIDA. Rev. Sci. Instr. **36**, 294 (1965).
10. H. JUCKER and E. K. RIDEAL. J. Chem. Soc. London, 1058 (1957).
11. M. ZELIKOFF and L. M. ASCHENBRAND. J. Chem. Phys. **22**, 1680 (1954).
12. W. E. GROTH and H. SCHIERHOLZ. Planetary Space Sci. **1**, 333 (1959).
13. R. R. REEVES, JR., P. HARTECK, B. A. THOMPSON, and R. W. WALDRON. J. Phys. Chem. **70**, 1637 (1966).

Vibrational energy transfer. Collisional quenching of competitive unimolecular reactions[1]

D. C. TARDY,[2] C. W. LARSON,[3] AND B. S. RABINOVITCH
Department of Chemistry, University of Washington, Seattle, Washington

Received August 9, 1967

A technique is described for the study of collisional deexcitation of highly vibrationally excited polyatomic molecules by use of externally activated competitive unimolecular reaction systems. This method has some advantages and is illustrated by the decomposition of chemically activated hexyl-3 radicals in the presence of H_2 and CF_4 as heat bath molecules. The former removes ~ 1.2 kcal mole^{-1} per successful collision; while for the latter a value in excess of 4.6 kcal is found so that CF_4 behaves operationally like a strong collider.

Canadian Journal of Chemistry, **46**, 341 (1968)

We report on a technique for study of collisional vibrational energy transfer in a chemically activated *competitive* unimolecular reaction system which promises greater experimental accuracy and facility than has been possible heretofore (1, 2). (Reference 2 gives a summary of the literature.) The method appears quite useful in the light of analysis and experimental results given recently for competitive unimolecular systems (3). The technique can extend to any type of external activation system.

Molecules may be inserted directly into high levels of vibrational excitation by "external" activation methods, in contrast with internal excitation by thermal collisional transport. In chemical activation, the substrate is simultaneously formed and excited. If the excitation level exceeds a reaction threshold energy E_0, unimolecular reaction may occur. Collisional quenching of excited molecules to levels below E_0 results in stabilization. Earlier work (1, 2) has shown how the relative amounts of collisional cascade, leading to stabilization (S), and of reaction, say decomposition (D), can yield information about the average amount of energy, $\langle \Delta E \rangle$, transferred to a bath molecule on collision, and about the transition probabilities, p_{mn}.

[1]Work supported by the U.S. Air Force Office of Scientific Research, Contract No. AF 49(638)-1633.
[2]NASA predoctoral fellow. Present address, University of Toronto, Toronto, Ont.
[3]NSF predoctoral trainee.

Can. J. Chem. Downloaded from www.nrcresearchpress.com by 210.87.254.40 on 09/05/12
For personal use only.

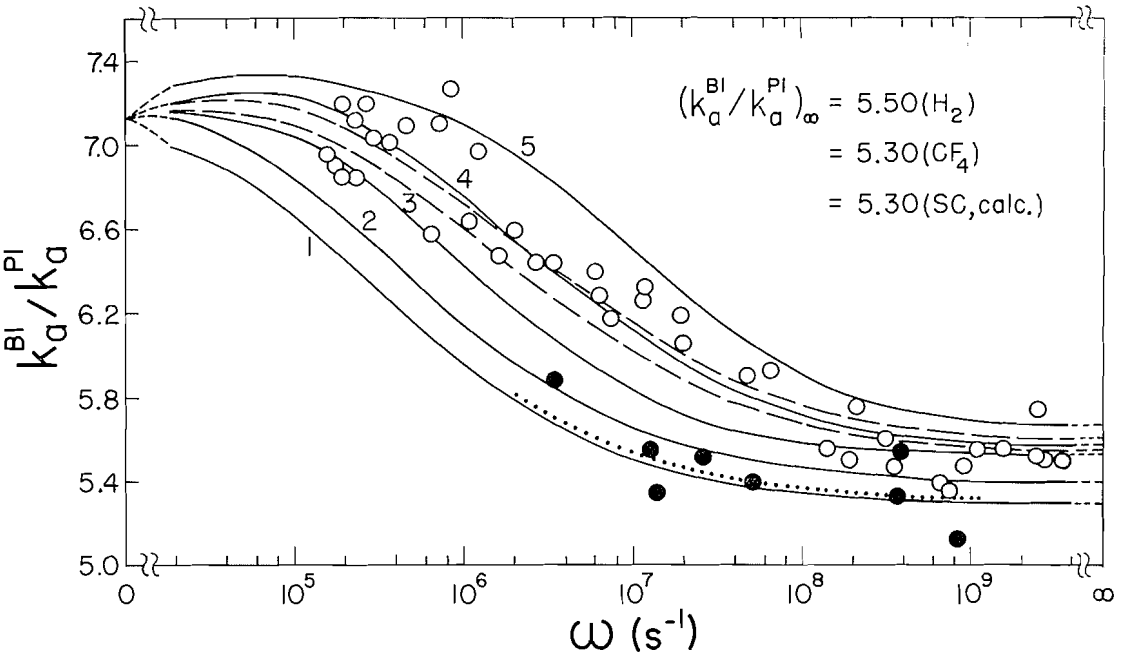

FIG. 1. Plots of the competitive rate ratio, k_a^{BI}/k_a^{PI} vs. the specific collision rate of hexyl-3 radicals, ω. Experimental points: (○) H_2; (●) 91% CF_4 + 9% H_2. Calculated values: solid curves: (curve 1) strong collider (SC); stepladder model (SL), ΔE (cm^{-1}) = 1600 (curve 2), 800, (curve 3); 400, (curve 4); 200, (curve 5); dashed curves: exponential model (Exp), ΔE (cm^{-1}) = 800 and 400, lower and upper curves, respectively. Dotted curve is for a bath mixture that simulates the CF_4 system in composition and is 83% SC + 17% SL (400 cm^{-1}). Collision rate calculated for σ_{H3,H_2} = 4.76 Å, σ_{H3,CF_4} = 6.38 Å, so $\omega_{H_2} = 3.95 \times 10^7$ s^{-1} mm^{-1} H_2 and $\omega_{CF_4} = 1.56 \times 10^7$ s^{-1} mm^{-1} CF_4; the collision diameters were calculated in the manner of σ^{L-J} in ref. 2. It may be noted that for other than a strong collider a maximum exists in the curves, which is more pronounced and moved to higher pressures the lower is $\langle \Delta E \rangle$.

Information about p_{mn} is best obtained at low pressures (low specific collision rates, ω), where $S/D \ll 1$, and is independent of the collision cross sections of the species concerned; by contrast, in the more convenient high pressure region where $S/D \gg 1$, only $\langle \Delta E \rangle$ can be deduced, and its magnitude depends on the cross sections adopted and on the transition probability model assumed.

In this communication we consider a substrate system which reacts concurrently by several channels, each characterized by a threshold energy, $E_0{}^i$. Such a system provides a considerable improvement in experimental accuracy, since relative rates within a system can be determined more accurately than can absolute values of individual rates (3). In addition, the competition confers independence from cross-sectional information upon deductions regarding energy transfer, even at high pressures where $S/\Sigma_i D_i \gg 1$; D_t represents decomposition by the ith channel; S is the amount of substrate quenched by collision to levels below the *lowest* threshold, $E_0{}^i$. Consider a molecule in the nth vibrational level having excess energies, $E_n{}^{+i} = E_n - E_0{}^i$, and specific microscopic reaction rates, $k_n{}^i$. A collisional decrement ΔE reduces the excess energies to $E_m{}^{+i}$, with corresponding rates, $k_m{}^i$. The decomposition ratios $D_1{:}D_2{:}D_t$ are

$$\sum_{j=E_0{}^1}^{\infty} k_j{}^1 N_j{}^s : \sum_{j=E_0{}^2}^{\infty} k_j{}^2 N_j{}^s : \sum_{j=E_0{}^i}^{\infty} k_j{}^i N_j{}^s,$$

where the $N_j{}^s$ are the steady state populations whose ratios are independent of ω at high pressure. The magnitudes of these ratios are peculiar to the particular scheme of transition probabilities involved in the energy cascade. When the index i is restricted to 1 or 2, only the average, $\langle \Delta E \rangle$, can be determined from the high pressure ratio; as i rises above 2, increasingly refined information about p_{mn} may be obtained;

Can. J. Chem. Downloaded from www.nrcresearchpress.com by 210.87.254.40 on 09/05/12
For personal use only.

systems have been described (3*b*) where *i* might equal 18, and this technique could take on the aspect of chemical reaction "spectroscopy".

We have restudied the hexyl-3 radical (H3) system (3*a*)[4]

$$C{-}C{-}C{-}\dot{C}{-}C{-}C^*$$

$$\xrightarrow{k_j^{B1}} C{-}C\cdot + C{=}C{-}C{-}C \text{ (butene-1)}$$

$$\xrightarrow{k_j^{P1}} C\cdot + C{=}C{-}C{-}C{-}C \text{ (pentene-1)}$$

$$\xrightarrow{\omega} C{-}C{-}C{-}\dot{C}{-}C{-}C,$$

which, although not an optimum example,[5] can be used to illustrate the method. Rate ratio measurements were made with H_2 and CF_4 as bath molecules (Fig. 1). Analytical difficulties limited the lowest pressure accessible for CF_4.

Theoretical rate calculations were made for a stochastic model[6] with use of the known input activation function and specific decomposition rates (2, 3). Step ladder and exponential transition probability models were employed.[7] The calculations are compared with experiment in Fig. 1. As expected (3*a*), the average rate ratios k_a^{B1}/k_a^{P1} increase as $\omega \to 0$. At $\omega = 0$, all collision models give, of course, the same limiting ratio. At $\omega = \infty$, the limiting rate ratio increases as $\langle \Delta E \rangle$ decreases, and the data can be fitted to $\langle \Delta E \rangle$ for a particular assumed transition model; the lower pressure data enhance the accuracy of fit and, for a system with more optimal energetics, could provide the form of p_{mn} even when *i* is limited to 2.

For this system, the best fit for H_2 is $\langle \Delta E \rangle_{SL} \simeq \langle \Delta E \rangle_{Exp} \simeq 1.2$ kcal (400 cm^{-1}); for CF_4, $\langle \Delta E \rangle >$ 4.6 kcal (1 600 cm^{-1}) and approaches the strong collision value ($\gtrsim$ 10 kcal) (2) without regard to model. These results give general agreement with earlier work (2).

Further work is being done along these lines.

[4]For a description of the system and the experimental method see ref. 3*a*.

[5]Here *i* assumes the values 1 or 2, only. Ideally, also, the difference in critical energies, $\Delta E_0 = E_0^2 - E_0^1$, should be large. For H3, $\Delta E_0 = 2.1$ kcal with $E_{min}^{+B1} = 7.2$ and $E_{min}^{+P1} = 5.1$ kcal mole^{-1}. See ref. 3 for the potential energy reaction profile and other details.

[6]Determination of the set of p_{mn} that fit the data by simultaneous solution of the coupled set of differential equations involved for reaction and collisional transfer at each level is not practical for several reasons.

[7]The calculations were analogous to those given by Tardy and Rabinovitch (4) with an appropriate input function. The step ladder and exponential models represent two markedly contrasting functional forms of the p_{mn} and are discussed in this reference in some detail.

1. R. E. Harrington, B. S. Rabinovitch, and M. R. Hoare. J. Chem. Phys. **33**, 744 (1960). D. W. Setser, J. W. Simons, and B. S. Rabinovitch. Bull. Soc. Chim. Belges, **71**, 662 (1962).
2. G. Kohlmaier and B. S. Rabinovitch. J. Chem. Phys. **38**, 1692, 1709 (1963).
3. (*a*) D. C. Tardy, B. S. Rabinovitch, and C. W. Larson. J. Chem. Phys. **45**, 1163 (1966). (*b*) C. W. Larson, B. S. Rabinovitch, and D. C. Tardy. J. Chem. Phys. In press.
4. D. C. Tardy and B. S. Rabinovitch. J. Chem. Phys. **45**, 3720 (1965); J. Chem. Phys. In press.

Erratum: Radiation chemical data in water using nitrous oxide

D. A. Head and D. C. Walker

Chemistry Department, University of British Columbia, Vancouver, British Columbia

Received September 28, 1967

(Ref. Can. J. Chem. **45**, 2051 (1967))

Canadian Journal of Chemistry, **46**, 343 (1968)

On page 2056, line 4 of second column should read: $k_9 \gg k_{-8}$ not $k_9 \gg k_8$.

On page 2057, line 21 of first column should read: pH 4.8 not pH 4.

Can. J. Chem. Downloaded from www.nrcresearchpress.com by 210.87.254.40 on 09/05/12
For personal use only.

Can. J. Chem. Downloaded from www.nrcresearchpress.com by 210.87.254.105 on 09/05/12
For personal use only.

Canadian Journal of Chemistry

Published by THE NATIONAL RESEARCH COUNCIL OF CANADA

VOLUME 46 FEBRUARY 1, 1968 NUMBER 3

A new hydroxy fatty acid sophoroside from *Candida bogoriensis*[1]

A. P. TULLOCH AND J. F. T. SPENCER
National Research Council of Canada, Prairie Regional Laboratory, Saskatoon, Saskatchewan

AND

M. H. DEINEMA
Agricultural University, Wageningen, The Netherlands

Received September 22, 1967

When cultured in stirred fermentors the yeast *Candida bogoriensis* produces extracellular glycolipids in yields of 0.5 to 1 g/l. The principal component of these is a crystalline sophorosyl hydroxy fatty acid, the structure of which has been established as 13-[(2′-*O*-β-D-glucopyranosyl-β-D-glucopyranosyl)-oxy]docosanoic acid 6′,6″-diacetate. The hydroxy acid portion of the molecule probably has the L-configuration. A monoacetyl glycolipid is also present as a minor component.

Canadian Journal of Chemistry, 46, 345 (1968)

Deinema (1) discovered that the yeast *Candida bogoriensis*, which had been isolated from the leaf surface of the shrub *Randia malleifera* in Indonesia, produced insoluble extracellular acidic glycolipids when grown on a glucose-yeast extract medium. Sometimes the product appeared as crystals but on other occasions it separated as viscous droplets from which, however, crystalline material could usually be isolated. The crystalline glycolipid is now shown to be 13-[(2′-*O*-β-D-glucopyranosyl-β-D-glucopyranosyl)oxy]docosanoic acid 6′,6″-diacetate (**1**). The total yield of crystalline glycolipid varied from a half to one tenth of this. However, chromatography of the crude glycolipid as methyl esters showed that, in fact, it contained about 50% of the diacetyl sophoroside, 10–15% of the remainder appeared to be a monoacetyl sophoroside, and the rest consisted of unsaturated 18-carbon fatty acids.

Alkaline hydrolysis of the glycolipid gave about two moles of acetic acid per mole of glycolipid; acid methanolysis yielded about one mole of methyl 13-hydroxydocosanoate and about two moles of methyl αβ-D-glucopyranosides. Reduction of the fatty acid ester gave methyl docosanoate. Oxidative cleavage gave two dicarboxylic acids, dodecanedioic and tridecanedioic acids, indicating that the hydroxyl group was at carbon-13. Methyl 13-oxodocosanoate, indistinguishable from material synthesized by the 12-carbon chain extension method of Hünig and Buysch (2), was obtained by mild oxidation.

The hydroxy docosanoate from the glycolipid has a very low optical rotation at the D line, but optical rotatory dispersion (o.r.d.) measurements show that it has a positive plain dispersion curve. Since 9-D-, 10-D-, and 12-D-hydroxyoctadecanoates have negative dispersion curves (3), the present acid probably has the L-configuration. The other hydroxy acid isolated from extracellular yeast lipids, 17-hydroxyoctadecanoic acid from *Torulopsis apicola* (4), also has the L-configuration suggesting that hydroxy acids from yeasts have configurations opposite to those from plants. Monohydroxydocosanoic acids, substituted near the center of the chain, do not appear to have been found previously, though it is of interest that an unidentified species of yeast produces the triacetate of 8,9,13-trihydroxydocosanoic acid (5).

Complete methylation of the glycolipid (4) yielded a hepta-*O*-methyl methyl ester which on

[1]NRCC No. 9862.

TABLE I

Assignments in the n.m.r. spectrum of **2** in dimethyl sulfoxide-d_6

Group	CH_3	CH_2	CH_3CO_2	αCH_2	Glucose ring protons and H-13	OCH_3	H-6	H-1	OH
Chemical shift (p.p.m.)	0.87	1.25	1.99	2.27	3.0–3.6	3.61	4.14	4.26–4.46	5.01 5.09 5.23 5.37 5.58
Protons observed	3.0	34.8	5.5	2.3	7.8	3.3		6.0	4.8
Protons calculated	3	36	6	2	9	3		6	5

acid methanolysis gave methyl 3,4,6-tri-*O*-methyl- and methyl 2,3,4,6-tetra-*O*-methylglucosides indicating a 1→2 linkage. This was confirmed when acetobrominolysis of the fully acetylated glycoside methyl ester gave α-acetobromosophorose. On periodate oxidation **1** consumed 2.9 molar equivalents of oxidant as would be expected from the presence of the 3,4-diol and 2,3,4-triol groupings in the sophorose portion of the molecule. This result also indicates that the secondary hydroxyl groups are not acylated and therefore the two acetate groups must be at the 6′- and 6″-positions.

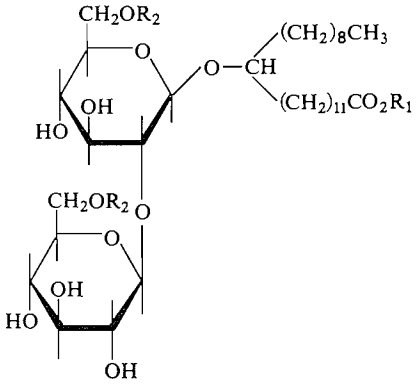

1 $R_1 = H$, $R_2 = CH_3CO$
2 $R_1 = CH_3$, $R_2 = CH_3CO$
3 $R_1 = CH_3$, $R_2 = H$

The positions of these groups were confirmed by the nuclear magnetic resonance (n.m.r.) spectrum (in dimethyl sulfoxide-d_6) of the methyl ester (**2**), prepared by treating **1** with diazomethane. Comparison of the spectrum of **2** with that of **1** showed that both compounds have the same number of acetate groups. Table I shows the chemical shifts of the signals and the observed and calculated number of protons. The chemical shift attributed to the H-6 protons (center at 4.14 p.p.m.) is that expected for acylated glucosides (in the spectrum of methyl 6-*O*-acetyl-β-D-glucopyranoside, in this solvent, the center of the H-6 signal is at 4.10 p.p.m.). Also, low field triplets for secondary acyl groupings (6) are absent. In addition 5 doublets due to the 5 secondary hydroxyl protons are present at relatively low field.

In the spectrum of **2** the signals due to the anomeric protons overlap each other and also those of H-6, but H-1 signals can be easily seen in the spectra of the deacetylated ester **3** and the hepta-*O*-methyl derivative. The spacing of the H-1 doublets is 7–7.5 c.p.s. showing that both glycosidic linkages have the β-configuration (7). The negative molecular rotation of the glycolipid (−11 500°) agrees with this conclusion (8).

Thus the glycolipid (**1**) is quite similar to the sophoroside of 17-hydroxyoctadecanoic acid produced by *Torulopsis apicola* (4); it has since been shown that the latter compound also has two acetate groups at the 6′- and 6″-positions ((5), and A. P. Tulloch, unpublished work).

Experimental

Nuclear magnetic resonance (n.m.r.) spectra were measured using a Varian HA-100 spectrometer. Silicic acid (Bio-Sil A from Bio-Rad Laboratories, California) was used for column chromatography. Optical rotatory dispersion measurements were made with a Jasco model ORD/UV-5 spectropolarimeter. Gas–liquid chromatography (g.l.c.) was carried out as described previously (4, 9) using an apparatus of conventional design with thermal conductivity detectors.

Method of Glycolipid Production

The strain of *Candida bogoriensis* was that isolated by Deinema (1). The medium was: glucose (8%), dialyzed yeast extract (0.4%), KH_2PO_4 (0.1%), and $MgSO_4 \cdot 7H_2O$ (0.02%). Medium (20 l) was inoculated with 500 ml of 3 day old shaken culture and agitated, at 350 r.p.m. for 11 days at 25° with an air flow rate of 8 l/min, in 305 fermentors.

Isolation of Glycolipid (1)

The culture medium was centrifuged and insoluble

Can. J. Chem. Downloaded from www.nrcresearchpress.com by 210.87.254.105 on 09/05/12
For personal use only.

Can. J. Chem. Downloaded from www.nrcresearchpress.com by 210.87.254.105 on 09/05/12
For personal use only.

extracellular gum, which was mixed with cells, was extracted with ethyl acetate. Crystalline glycolipid (**1**) was obtained by dissolving the gum in acetone containing 5% water and cooling at 0°; the yield varied from 10–50% of the weight of gum. **1** had m.p. 74–77° and $[\alpha]_D^{24}$ −15° (*c*, 3.1 in chloroform).

Anal. Calcd. for $C_{38}H_{68}O_{15}$: C, 59.66; H, 8.96. Found: C, 59.43; H, 8.75.

The neutralization equivalent was 766.6 (calcd. 764.92) and the saponification equivalent was 255.6 (calcd. 254.97); 2.1 moles of acetic acid were obtained per mole of glycolipid.

Mother liquors (2.1 g), from which 10% of solid glycoside had been removed, were converted to methyl esters by the procedure given below and chromatographed on a silicic acid column (57 g). Elution with chloroform gave a mixture of methyl esters of mono- and di-unsaturated C-18 fatty acids (0.58 g). Elution with chloroform containing 1–2% methanol gave the glycolipid methyl ester (**2**) (1.11 g), and elution with chloroform containing 5% methanol gave a gum (0.32 g). This material was examined by thin-layer chromatography (t.l.c.) in chloroform–methanol (4:1) and had an R_f close to that expected for a monoacetyl sophoroside methyl ester. The relative intensity of the acetoxyl signal in the n.m.r. spectrum also indicated that only one acetate group was present.

Glycolipid Methyl Ester (2)

Crystalline **1** (1 g) was dissolved in dry acetone, cooled to 0°, and a solution of diazomethane in methylene chloride added with stirring until a faint yellow color persisted. Just sufficient glacial acetic acid to react with excess reagent was then added. The solvent was removed leaving the ester as a clear gum (0.97 g) which crystallized from benzene–hexane (1:1) as leaflets (0.47 g) with m.p. 58–59°, $[\alpha]_D^{27}$ −22° (*c*, 1.2 in chloroform).

Anal. Calcd. for $C_{39}H_{70}O_{15}$: C, 60.13; H, 9.06. Found: C, 60.27; H, 9.06.

Both the ester (**2**) and the acid (**1**) were difficult to recrystallize in reasonable yields even when they had been chromatographed more than once; however, examination of the mother liquors by n.m.r. spectroscopy and t.l.c. showed them to be homogeneous and almost indistinguishable from the crystalline material.

Deacetylated methyl ester (**3**) (0.81 g) was prepared by treatment of **2** (1.00 g) with methanolic sodium methoxide. The solution was neutralized with acetic acid and the solvent removed. The residue was taken up in benzene and washed with water, the benzene was removed leaving a brittle resinous product which could not be induced to crystallize. The melting point was 110–115° and $[\alpha]_D^{25}$ was −22.5° (*c*, 2.6 in chloroform).

Anal. Calcd. for $C_{35}H_{66}O_{13}$: C, 60.49; H, 9.57. Found: C, 60.43; H, 9.85.

The n.m.r. spectrum (in pyridine) showed signals for H-1′ at 4.86 p.p.m. ($J_{1,2}$ = 7.5 c.p.s.) and H-1″ at 5.16 p.p.m. ($J_{1,2}$ = 7 c.p.s.).

Determination of Structure of Fatty Acid Portion of 1

Crystalline **1** (1 g) was refluxed for 18 h with methanol containing 4% HCl, the acid was neutralized with silver carbonate and solvent removed leaving a semisolid residue (0.94 g). Fatty acid ester (0.53 g) was extracted with hexane leaving methyl αβ-D-glucopyranosides (0.46 g) which were crystallized from ethanol giving methyl α-D-glucopyranoside (0.35 g) with melting point and mixed melting point 169–171° and $[\alpha]_D^{27}$ +161° (*c*, 1.8 in H_2O). Crystallization of the hexane extract from methanol gave methyl 13-hydroxydocosanoate (0.37 g) with m.p. 69–70°, $[\alpha]_D^{25}$ +0.07°, $[\alpha]_{500}$ +0.09°, $[\alpha]_{400}$ +0.14°, $[\alpha]_{300}$ +0.21°, $[\alpha]_{250}$ +0.28°, (*c*, 20 in chloroform).

Anal. Calcd. for $C_{23}H_{46}O_3$: C, 74.54; H, 12.51. Found: C, 74.74; H, 12.30.

Saponification gave 13-hydroxydocosanoic acid which was crystallized from acetone and had m.p. 86°.

Anal. Calcd. for $C_{22}H_{44}O_3$: C, 74.10; H, 12.44. Found: C, 74.08; H, 12.32.

Reduction of the hydroxy ester with hydrogen iodide and red phosphorus followed by zinc and hydrochloric acid (9) gave methyl docosanoate, identified by gas–liquid chromatography (g.l.c.). Oxidation with chromic acid at 100° (9) gave dodecanedioic and tridecanedioic acids which were identified by g.l.c. Oxidation with chromic acid in acetic acid at 25° (9) gave methyl 13-oxodocosanoate, which crystallized from acetone with m.p. 61–62.5°, and did not depress the m.p. of an authentic sample.

Synthesis of Racemic 13-Hydroxydocosanoic Acid

1-Morpholino-1-cyclododecene (2) (17.5 g) and triethylamine (7.1 g) were allowed to react with decanoyl chloride (9.5 g) in chloroform (10 ml) and the product hydrolyzed and worked up by the general method of Buysch (2). The yield of crude 2-decanoylcyclododecanone, b.p. 155–185/0.1 mm, was 15 g. This product in ethanol (10 ml) was hydrolyzed with sodium hydroxide (6 g) in ethanol (70 ml) as described previously (2). After heating on a steam bath for 2 h the suspended sodium salt was poured into water (250 ml) and the hot solution acidified with hydrochloric acid giving insoluble 13-oxodocosanoic acid (12.5 g). The acid was converted to the methyl ester which had m.p. 60–61° (lit. (10) gives 61–62°). The ester was hydrogenated over Raney nickel (11) to give methyl 13-hydroxydocosanoate which was crystallized from hexane and had m.p. 63–64°.

Anal. Calcd. for $C_{23}H_{46}O_3$: C, 74.54; H, 12.51. Found: C, 74.49; H, 12.23.

13-Hydroxydocosanoic acid was prepared by hydrolysis and crystallized from acetone and had m.p. 87°.

Anal. Calcd. for $C_{22}H_{44}O_3$: C, 74.10; H, 12.44. Found: C, 73.90; H, 12.16.

Determination of the Structure of Sugar Portion of 1

Periodate Oxidation of 1

1 (21.7m g) was dissolved in *t*-butanol (3 ml) and water (3 ml) and 0.1 *M* sodium periodate (4 ml) was added. The rate of oxidation was followed by the method of Neumüller and Vasseur (12). One mole of **1** consumed 2.9 moles of oxidant in 48 h. Under the same conditions methyl β-D-glucopyranoside consumed 1.9 moles oxidant in 24 h.

Methylation of 1

1 (1 g) was fully methylated as described previously (4) to give a hepta-*O*-methyl methyl ester (0.67 g). The n.m.r. spectrum (in benzene) showed eight $-OCH_3$ signals at 3.24, 3.34, 3.36 (methyl ester), 3.38, 3.41, 3.55, 3.58, and 3.62 p.p.m. and two signals for anomeric

protons at 4.30 and 4.82 p.p.m. (both had splittings of about 7 c.p.s.). A portion of this material was refluxed overnight with 4% methanolic hydrogen chloride. The resulting mixture was shown by g.l.c., using an ethylene glycol phthalate column (13), to consist of methyl 3,4,6-tri-*O*-methyl- and methyl 2,3,4,6-tetra-*O*-methyl-D-gluco-pyranosides.

Isolation of α-Acetobromosophorose and β-Sophorose Octaacetate

2 (1.9 g) was acetylated with acetic anhydride and pyridine, chromatography on silicic acid (elution with chloroform–hexane 1:1) gave a syrupy heptaacetate methyl ester (1.61 g) which could not be induced to crystallize.

Anal. Calcd. for $C_{49}H_{80}O_{20}$: C, 59.50; H, 8.15. Found: C, 59.83; H, 8.14.

The n.m.r. spectrum (in deuteriochloroform) showed acetoxyl signals at 1.97, 1.99, 2.00, 2.02, 2.05, and 2.08 (for 6 protons probably due to overlap of the signals due to acetoxyl at C6′ and C6″) and H-1′ at 4.43 ($J_{1,2} = 7.5$ c.p.s.) and H-1″ at 4.69 p.p.m. ($J_{1,2} = 7$ c.p.s.). Its $[\alpha]_D^{25}$ was −16° (*c*, 4.7 in acetic acid). The heptaacetate (1 g) was then dissolved in acetic acid (18 ml) and acetic acid containing 33% hydrogen bromide (2 ml) was added (14). After 6 days at room temperature methylene chloride (300 ml) was added, acid removed by washing with aqueous sodium bicarbonate and then with water and the solution dried over sodium sulfate. Solvent was removed, the residue dissolved in methylene chloride (4 ml), and hexane (10 ml) added. α-Acetobromosophorose (0.13 g, 18%) crystallized at 0°, after recrystallization from methylene chloride – hexane (1:1) it had m.p. 193–195° and $[\alpha]_D^{25}$ +94° (*c*, 2.5 in chloroform) (lit. (14) gives m.p. 195–197° and $[\alpha]_D$ +94.2°). Treatment with silver acetate in acetic acid gave β-octaacetylsophorose which crystallized from ethanol in long needles with m.p. 194–196° and which did not depress the m.p. of authentic material (4, 14).

Acknowledgments

The authors wish to thank Dr. P. A. J. Gorin for helpful discussions, Mr. L. L. Hoffman, and Mr. N. R. Gardner for experimental assistance, Mr. M. Mazurek for n.m.r. measurements and Mr. W. Haid for microanalyses and o.r.d. measurements.

1. M. H. Deinema. Ph.D. Thesis. Agricultural University, Wageningen, The Netherlands. 1961.
2. H-J. Buysch. Ph.D. Thesis. Julius-Maximilian University, Würzburg, Germany. 1963.
3. T. H. Applewhite, R. G. Binder, and W. Gaffield. J. Org. Chem. **32**, 1173 (1967).
4. P. A. J. Gorin, J. F. T. Spencer, and A. P. Tulloch. Can. J. Chem. **39**, 846 (1961).
5. F. H. Stodola, R. F. Vesonder, and L. J. Wickerham. Biochemistry, **4**, 1390 (1965).
6. A. P. Tulloch, A. Hill, and J. F. T. Spencer. Chem. Comm. 584 (1967).
7. R. U. Lemieux, R. K. Kullnig, H. J. Bernstein, and W. G. Schneider. J. Am. Chem. Soc. **80**, 6098 (1958).
8. R. U. Lemieux and M. L. Wolfrom. *In* Advances in carbohydrate chemistry. Vol. 3. *Edited by* W. W. Pigman and M. L. Wolfrom. Academic Press, Inc., New York. 1948. p. 375.
9. A. P. Tulloch. Can. J. Chem. **43**, 415 (1965).
10. F. L. Breusch and A. Kirkali. Fette, Seifen, Anstrichmittel, **67**, 4 (1965).
11. M. Skogh. Acta Chem. Scand. **6**, 809 (1952).
12. G. Neumüller and E. Vasseur. Arkiv Kemi, Mineral. Geol. **5**, 235 (1935).
13. B. M. Craig. Chem. Ind. (London) 1442 (1960).
14. E. Vis and H. G. Fletcher. J. Am. Chem. Soc. **78**, 4709 (1956).

Can. J. Chem. Downloaded from www.nrcresearchpress.com by 210.87.254.105 on 09/05/12
For personal use only.

Can. J. Chem. Downloaded from www.nrcresearchpress.com by 210.87.254.6 on 09/05/12
For personal use only.

Steroids. CCCIX.[1] Synthesis of new steroids with unnatural configuration

PIERRE CRABBÉ, ALICIA CRUZ, AND JOSÉ IRIARTE
Research Laboratories, Syntex, S.A., Apartado Postal 2679, Mexico

Received August 22, 1967

The preparation of several new estrane, androstane, and 19-norpregnane derivatives with unnatural configuration is discussed. A synthesis of both enantiomers (**16***b*) and (**18**) from estrone is described. The structure and configuration of the compounds reported are established on the basis of their physical properties.

Canadian Journal of Chemistry, 46, 349 (1968)

When reporting the multistage transformation of the cardiac aglycone strophanthidin (**1**) to 14β,17α-19-norprogesterone (**2***a*), Ehrenstein (2) opened the field of steroid chemistry to new horizons. The bis-iso-19-norprogesterone (**2***a*) resembled the natural hormone progesterone (**3**) but lacked the angular methyl grouping at position-10, and the stereochemistry at C-14, as well as at C-17 was different. Because the 14β,17α-19-norprogesterone (**2***a*) was shown to exhibit higher biological activity (3) than progesterone (**3**), several research groups decided to undertake the synthesis of steroids with abnormal configuration (4). Hence, since Ehrenstein's early observation, numerous similar steroids, among which the 14β,17α-progesterone (**2***b*) and 19-norsteroids (4, 5), have been prepared. Related work was also undertaken in the Syntex Laboratories (4*d*, 6). In the present study the preparation of several other new steroids with unnatural configuration, belonging to the estrane, androstane, and 19-norpregnane series is reported.

Treatment of the enol acetate (**5**) (7, 8) of estrone methyl ether (**4***a*) with bromine affords the 16α-bromo derivative, (**4***b*) (7), as the main compound. The 16α-configuration[2] is assigned to the bromine atom on the basis of the optical properties exhibited by this compound (**4***b*), since the Cotton effect associated with the 17-keto chromophore is less intense than in **4***a*, in agreement with the octant rule (10). Conversion of the bromo-ketone (**4***b*) into its cycloethylene ketal followed by dehydrobromination (7, 11) and mild acid hydrolysis provides the known Δ^{15}-17-ketone (**6***a*) (7, 11), typified by a *negative* Cotton effect in the 350 mμ region. On treatment

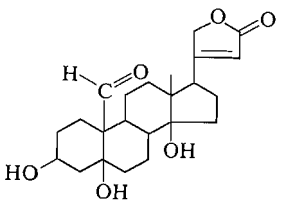

1

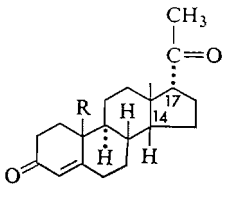

2*a*, R = H
b, R = CH_3

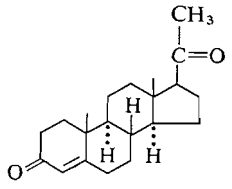

3

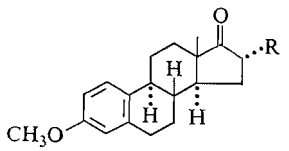

4*a*, R = H
b, R = Br

with acid, the α,β-unsaturated ketone (**6***a*) affords a mixture of three isomeric compounds separable by column chromatography. The first substance is the 14β-isomer (**6***b*) (7), characterized by its nuclear magnetic resonance (n.m.r.) spectrum which shows olefinic resonance as a doublet at 374 c.p.s. ($J_{15,16} = 6$ c.p.s.) (C-16H) and a further doublet of doublets ($J_{15,16} = 5$ c.p.s.; $J_{14,15} = 8$ c.p.s.) at 427 c.p.s. (C-15H). Its ultraviolet (u.v.) absorption spectrum and the *positive* Cotton effect for the n–π^* transition of the α,β-unsaturated ketone, at ca. 340 mμ are also characteristic of compound (**6***b*). The second isomer is the β,γ-ethylenic ketone (**6***c*) (7). Although the u.v. spectrum of this compound is reminiscent of (but less intense than) that of compound (**6***b*), its n.m.r. spectrum is characteristic in having only *one* olefinic proton (338 c.p.s.). Moreover, compound (**6***c*) exhibits a relatively strong *positive* Cotton effect in the 300 mμ region, as expected for such a chromophore (12).

[1]For Steroids. CCCVIII, see ref. 1.
[2]For the stereochemistry of enolization of 17-keto steroids, see ref. 9.

Can. J. Chem. Downloaded from www.nrcresearchpress.com by 210.87.254.6 on 09/05/12
For personal use only.

At equilibrium the isomers (**6***b*) and (**6***c*) are obtained in the 2:3 ratio, when the isomerization of **6***a* is performed under mild acidic conditions. The predominance of the β,γ-unsaturated ketone (**6***c*) in the mixture is attributable to conformational factors (13), interpretable by consideration of dihedral angles (14) at the C/D ring junction.

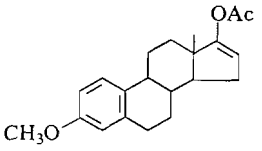

5

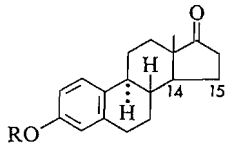

6*a*, R = CH_3; 14αH; Δ^{15}
b, R = CH_3; 14βH; Δ^{15}
c, R = CH_3; Δ^{14}
d, R = CH_3; 14βH
e, R = H; 14βH
f, R = THP; 14βH

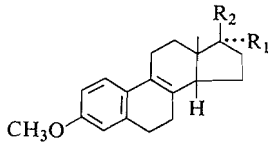

7*a*, R_1, R_2 = ketone
b, R_1 = OH; R_2 = C≡CH

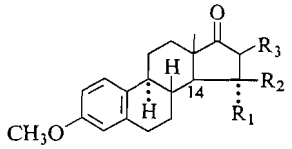

8*a*, 14αH; R_1 = OCH_3; R_2 = R_3 = H
b, 14αH; R_1 = R_3 = H; R_2 = OCH_3
c, 14βH; R_1 = R_3 = H; R_2 = OCH_3
d, 14βH; R_1 = H; R_2, R_3 = epoxy

The third compound isolated is the steroid (**7***a*) (7). The u.v. absorption spectrum presents the styrene chromophore at ca. 273 mμ and the n.m.r. spectrum does not show any olefinic proton. Furthermore, this compund (**7***a*) exhibits two Cotton effects. The weakly positive Cotton effect associated with the 17-ketone in the 300 mμ region is in agreement with the *cis* C/D ring junction (12); whereas the strong positive Cotton effect at ca. 270 mμ is due to the styrene chromophore (15) ($a = +601$). The steroid (**7***a*) is obtained exclusively when **6***a* is submitted to relatively vigorous acidic conditions. This is worth noting, since it is known that the double bond of a ring A aromatic Δ^8-steroid with the 14αH-stereochemistry is readily isomerized to the $\Delta^{9(11)}$-position. Although a 9,(11)-dehydro 14-iso-compound is a known product of the isomerization of equilin (16), it appears that with the 14β-configuration, the 8,9-double bond is energetically preferred over the 9(11)-position. This also can be interpreted by the dihedral angle theory (14).

Reaction of **7***a* with ethinylmagnesium bromide (17) furnishes the corresponding ethinyl derivative (**7***b*) (for stereochemistry see below).

Worth mentioning here is the earlier attempt (7) to effect a base-catalyzed isomerization of **6***a* with methanolic potassium hydroxide. When repeated, this reaction leads to the isolation of various substances, depending on the experimental conditions (18). Indeed, it has been observed that base treatment of **6***a* in methanol solution gives, besides the isomers (**6***b*) and (**6***c*), addition of methoxyl to the α,β-unsaturated chromophore.

When **6***a* is treated with methanolic potassium hydroxide, under rather mild conditions, its 14β-isomer (**6***b*) and the Δ^{14}-derivative (**6***c*) are obtained. Furthermore, two new methoxylated compounds are also isolated. To the first substance, structure (**8***a*) is assigned. The new methoxyl group gives a three proton signal at 200 c.p.s. in the n.m.r. Since the positive Cotton effect associated with the 17-carbonyl of the steroid (**8***a*) is rather intense ($a = +103$), and because of the position of the 18-methyl group is normal for a 14α-17-keto steroid, the 14αH, 15$\alpha$$OCH_3$-stereochemistry is assigned to this substance. The second methoxyl derivative appears to be the 15β-isomer (**8***b*). The Cotton effect associated with the 17-carbonyl chromophore in **8***b* is in agreement (12) with the 14α-configuration. Moreover, the β-configuration at C-15 is assigned on the basis of the chemical shift of the C-18 methyl protons in the n.m.r. (67 c.p.s.). This shift is attributed to interactions in space between the 15β-methoxyl and the 18-methyl groups.

The reversibility of the Michael addition of methoxyl to the Δ^{15}-17-keto system is deduced from the following observation. When **8***a* is heated in 2% methanolic potassium hydroxide solution, besides some starting material, ca. 50% of compound (**6***c*) and 20% of its double bond isomer (**6***b*) are obtained.

Base treatment of **6***b* under mild conditions affords mainly unchanged starting material, the Δ^{14}-17-ketone (**6***c*), and some of the 14β,15β-

Can. J. Chem. Downloaded from www.nrcresearchpress.com by 210.87.254.6 on 09/05/12
For personal use only.

methoxylated steroid (**8***c*). The configuration at C-14 in **8***c* is assigned on the basis of the chemical shift of the C-18 methyl protons (68 c.p.s.). The resonance signal is similar to that of the 18-methyl group in 14β-compounds, eg. (**6***d*, **6***e*, **6***f*), and (**7***a*), showing some 16 c.p.s. downfield shift of the corresponding resonance in the 14α-analogue (**4***a*). Further confirmation of the 14βH-stereochemistry is obtained from the circular dichroism (c.d.) molecular ellipticity exhibited by **8***c* ($[\Theta]_{291} = +4\,720$), which is reminiscent of the Cotton effect of saturated 14β-17-keto steroids (12). Using the same reasoning as before (19), the β-configuration is assigned to the methoxyl at C-15 since addition from the hindered α-side is not favored in C/D-*cis*-β-steroids.

When the Δ^{14}-isomer (**6***c*) is submitted to similar basic reaction conditions, one recovers some unchanged product and obtains as major compound the 14β-derivative (**6***b*), as well as a small amount of the methoxylated steroid (**8***c*).

Base treatment of 15-dehydro-14β-estrone methyl ether (**6***b*) in a mixture of methanol and tetrahydrofuran (containing peroxides), in the presence of air, gave the 15,16β-oxido derivative (**8***d*). The physical properties (see Experimental) support the structure and stereochemistry assigned to this compound (**8***d*).[3]

This indicates that under acidic or basic conditions, compound (**6***a*) is isomerized into **6***b* and **6***c*, the last two ones existing in equilibrium. Furthermore, in methanolic alkaline conditions, addition of methoxyl can take place to the α,β-unsaturated system of **6***a* and **6***b*.

Catalytic hydrogenation of **6***b* or **6***c*, in presence of palladium on carbon, gives 14-isoestrone methyl ether (**6***d*) (7). The 14β-configuration in **6***d* is confirmed by the 18-methyl resonance signal (67 c.p.s.) and the weakly positive Cotton effect ($a = +34$), typifying the 17-keto chromophore in such a *cis*-hydrindanone system (12, 21). Treatment of the 3-methyl ether (**6***d*) with hydrogen bromide (22) affords the free phenol (**6***e*), from which the corresponding tetrahydropyranyl ether (**6***f*) is obtained by reaction with dihydropyrane (23). When **6***d* is reduced with lithium in liquid ammonia (24)[4] followed by mild acid treatment, the 14β,17α-19-nortestosterone (**9***a*) is obtained. The α-configuration of the secondary alcohol grouping at C-17 is established by Horeau's method (25).[5]

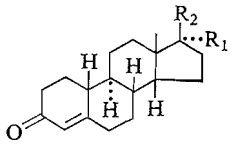

9*a*, R_1 = OH; R_2 = H
b, R_1 = OH; R_2 = C≡CH
c, R_1 = OTHP; R_2 = C≡CH
d, R_1 = —CHOH—CH_3; R_2 = H

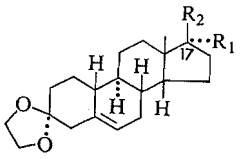

10*a*, R_1 = OH; R_2 = H
b, R_1, R_2 = ketone
c, R_1 = OH; R_2 = C≡CH

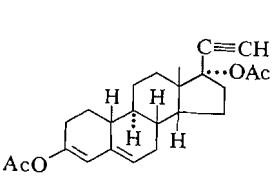

11

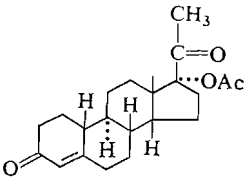

12

Protection of the 3-keto group of **9***a* as the cycloethylene ketal (**10***a*), followed by oxidation (26) at C-17 provides the ketone (**10***b*). Addition of ethinylmagnesium bromide (17) at C-17, affords the 17β-ethinyl derivative (**10***c*), characterized by the resonance signal (153 c.p.s.) corresponding to an acetylenic proton. Acid hydrolysis of the ketal at C-3 and isomerization of the double bond to C-4 gives the nor-steroid (**9***b*). The structure of this compound results from its physical and spectroscopic properties, ie. the typical u.v. absorption for the Δ^4-3-keto chromophore, an hydroxyl band in the infrared (i.r.) spectrum and the acetylenic proton detected by i.r. and n.m.r. spectroscopy (see Experimental). The 17α-tetrahydropyranyl derivative (**9***c*) is also prepared (23). The β-configuration for the ethinyl side chain is deduced from the observations which follow.

Treatment of compound (**9***b*) with acetic anhydride in presence of *p*-toluenesulfonic acid

[3]For a similar example of epoxidation of Δ^{15}-17-ketone with alkaline hydrogen peroxide, see ref. 20.

[4]For a review on reduction with metal–ammonia reagents, see ref. 24*d*.

[5]We are indebted to Professor A. Horeau and Dr. H. Kagan, Collège de France, Paris, for this determination.

Can. J. Chem. Downloaded from www.nrcresearchpress.com by 210.87.254.6 on 09/05/12
For personal use only.

gives the enol acetate (**11**). This bis-acetate (**11**) is characterized by a u.v. absorption band at 234 mμ and its n.m.r. spectrum which shows two lowfield methyl signals (121 and 127 c.p.s.), ascribed to acetoxy groupings, an acetylenic proton signal (156 c.p.s.), and two olefinic proton signals (C-4: 340 and C-6: 330 c.p.s.) respectively. When the triple bond of **11** is reacted with mercuric sulfate in ethanol solution, in the presence of dilute sulfuric acid,[6] 17α-acetoxy-14β-19-norprogesterone (**12**) is obtained. The physical properties support structure (**12**) proposed for this compound. Its c.d. curve exhibits a multiple negative Cotton effect in the 330 mμ region, due to the n–π^* transition of the Δ^4-3-keto chromophore (12). Moreover, a mild positive Cotton effect appears at 285 mμ ([θ] = +2 050), which is in agreement with the 17β-stereochemistry of the methyl ketone side chain (12). The positive molecular ellipticity of the acetyl side chain in **12** is weaker than in normal 17β-acetyl steroids, such as in progesterone (3; [θ] = +11 000) (12). This is due to the *cis*-β-C/D-ring juncture (12, and see, for example 28) and the 17α-acetoxy grouping (29), both factors being known to reduce the positive Cotton effect of a 20-keto grouping (12).

Since hydration of the triple bond in **11** occurs with retention of configuration,[6] this necessarily implies the stereochemistry for the ethinyl side chain to be β in compounds (**10***c*), (**9***b*,*c*) and (**11**), as well as in (**7***b*).

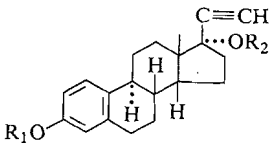

13*a*, $R_1 = CH_3$; $R_2 = H$
b, $R_1 = CH_3$; $R_2 = Ac$
c, $R_1 = R_2 = H$
d, $R_1 = THP$; $R_2 = H$
e, $R_1 = CH_3$; $R_2 = THP$

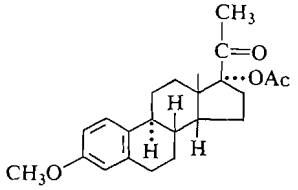

14

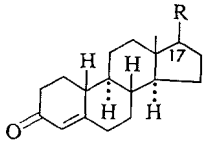

15*a*, R = ξOH
b, R = ketone
c, R = βOH

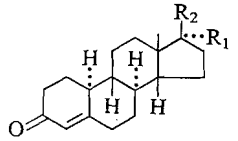

16*a*, R_1 = OH; R_2 = H
b, R_1, R_2 = ketone

[6]Private communication from Dr. J. Fried, Institute of Steroid Chemistry, Syntex Research, Palo Alto, Calif. See ref. 27.

The 14-isoestrone derivative (**6***d*) is converted into the 17-substituted steroid (**14**) *via* the intermediates (**13***a*) and (**13***b*) by the above mentioned reaction sequence. The physical properties of these compounds support the proposed structure and stereochemistry. Reduction of compound (**14**) under Birch's conditions (24) simultaneously reduces ring A and the 20-ketone, with concurrent removal of the 17α-acetoxy grouping and inversion of the acetyl side chain (30). After mild acid treatment, a mixture of alcohols stereoisomeric at C-20 (**9***d*) is obtained. Chromic acid oxidation (31) of this mixture of alcohols furnishes 14β,17α-19-norprogesterone (**2***a*), the physical properties of which are identical with the reported data (2). Furthermore, the negative c.d. maximum at ca. 300 mμ clearly indicates (12) the configuration of the acetyl side chain to be α.

Lithium in ammonia reduction (24) of Δ^8-isoestrone-3-methyl ether (**7***a*) followed by subsequent acid hydrolysis leads to a mixture of compounds separated by thin-layer chromatography. To the main isomers, the 8β,9α,10β,14α (**15***a*) and 8α,9β,10α,14β (**16***a*) configuration is suggested from the data mentioned below. Since the steroid (**15***a*) could not be obtained in crystalline form (being presumably a complex mixture of 17α- and 17β-alcohols, as well as some 14β-derivative), the crude product was oxidized (31) to afford the diketone (**15***b*) which exhibited physical properties identical with those of the known compound (24*b*). The multiple Cotton effect of the Δ^4-3-keto chromophore in **15***b* is *negative*, in agreement (12) with the 9α,10β "natural" stereochemistry. Conversely, the optical rotatory dispersion (o.r.d.) and c.d. curves show that the multiple Cotton effect of the n–π^* transition of the unsaturated chromophore in the nor-steroid (**16***a*) is *positive*. This is in keeping with the "retro" configuration (9β, 10α), since Δ^4-3-keto retrosteroids are known to exhibit a positive multiple Cotton effect in the 330 mμ region (12, 32).

The formation of compound (**15***a*) by reduction of **7***a* implies an inversion of the configuration at C-14, presumably through double bond migration from position-8,9 to -8,14, prior to reduction.

The optical properties of compound (**16***a*) establish its stereochemistry at C-9 and C-10, but no definite conclusion can be drawn for the configuration of the hydrogen atom at C-8. If the configuration at C-8 is α, then the stereochemistry of **16***a* should be the opposite of 19-

Can. J. Chem. Downloaded from www.nrcresearchpress.com by 210.87.254.6 on 09/05/12
For personal use only.

nortestosterone (**15***c*) (5a) at all asymmetric centers, with the exception of the methyl grouping at C-13. This point is confirmed as follows.

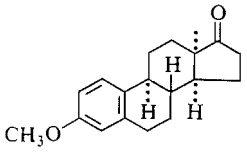

17

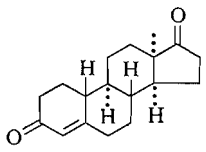

18

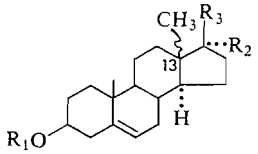

19*a*, R_1 = THP; 13βCH_3; R_2, R_3 = ketone
b, R_1 = THP; 13αCH_3; R_2, R_3 = ketone
c, R_1 = THP; 13αCH_3; R_2 = OH; R_3 = C≡CH
d, R_1 = H; 13αCH_3; R_2 = OH; R_3 = C≡CH

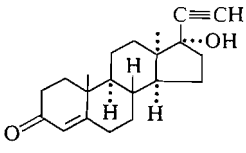

20

Irradiation of estrone 3-methyl ether (**4***a*) with ultraviolet light gives its 13α-isomer (**17**) (33). The *cis*-α-stereochemistry at the C/D ring junction in **17** is established by the weakly negative Cotton effect exhibited by the 17-keto chromophore ($[\theta]_{307} = -1\,980$) (12, 29, 34). The methyl ether of lumiestrone (**17**) (33, 35) is then reduced with lithium in liquid ammonia (24) and treated with acid to provide a mixture of epimers at C-17. Chromic acid oxidation (31) of this mixture of secondary alcohols affords the 19-nor diketo steroid (**18**). Similarly, the keto alcohol (**16***a*) is oxidized to the diketo steroid (**16***b*). The isomeric compounds (**16***b*) and (**18**) exhibit superimposable i.r. curves, identical n.m.r. and u.v. spectra, as well as other physical properties except for the sign of the specific rotation which is opposite (see Experimental). Worth noting is the identity of the fragmentation pattern of the antipodes (**16***b*) and (**18**) under electron impact, (see Experimental).[7]

The enantiomeric relationship characterizing these steroids is further confirmed by their o.r.d. and c.d. curves. As shown in Fig. 1, the o.r.d. and c.d. curves of **16***b* and **18** are mirror images, confirming the stereochemistry at all asymmetric centers, particularly the 8αH-configuration in **16***b* and hence in its precursor **16***a*. The o.r.d. and c.d. curves of the enantiomers (**16***b*) and (**18**) reproduced in Fig. 1 clearly show that the multiple Cotton effect at ca. 330 mμ associated with the n–π^* transition of the Δ^4-3-keto chromophore is negative in compound (**18**) and positive in **16***b*. Conversely, the π–π^* transition of the same chromophore, appearing in the 235 mμ region, is positive for **18** and negative for its enantiomer (**16***b*). The n–π^* transition of the saturated 17-keto chromophore at ca. 300 mμ is hardly observed in these curves, even in the c.d. curves. This is due to the very intense Cotton effect associated with the π–π^* transition of the unsaturated ketone (12, 37).

A 1:1 mixture of the enantiomers (**16***b*) and (**18**) provides the racemate devoid of optical activity (see Experimental).

While the 14β-estradiol derivatives (**13***c*–**13***e*) are also prepared by conventional methods (see Experimental), ultraviolet irradiation (33, 34b, 35, 38) of the 17-keto androstane derivative (**19***a*) affords the 13α-steroid (**19***b*). Nucleophilic addition of acetylene (17) to the carbonyl gives a mixture of ethinyl derivatives. The main constituent is considered (39, see also 34*b*) to be the 17β-ethinyl compound (**19***c*). Mild acid hydrolysis gives the 3-alcohol (**19***d*). Oxidation (31) then leads to the iso-ethinyl testosterone derivative (**20**).

Experimental

Microanalyses were done by Dr. A. Bernhardt, Mülheim, Germany. Melting points (m.p.) were determined in capillary tubes with a "Mel-temp" apparatus; they are corrected. Rotations were taken between 16° and 22° with a 1 dm tube at sodium D-line, in chloroform solution. Optical rotatory dispersion (o.r.d.) curves were taken with an automatic recording JASCO/UV-5 spectropolarimeter. Circular dichroism (c.d.) curves have been obtained with a Jouan dichrograph at the University of Strasbourg, through the kind cooperation of Professor G. Ourisson. The o.r.d. and c.d. curves of enantiomers (**16***b*) and (**18**) (Fig. 1) are due to the courtesy of Dr. H. Wolf, Institute für Organische Chemie der Technischen Hochschule, Braunschweig, Germany, to whom we express our sincere gratitude. Infrared spectra were taken with a Perkin–Elmer, model 21, NaCl prism in KBr pellets. Unless stated otherwise, u.v. absorption spectra were obtained in 95% ethyl alcohol, with a Beckman model DU spectrophotometer. Nuclear magnetic resonance spectra were recorded at 60 Mc.p.s. using 5–8% w/v solutions of steroid in chloroform containing tetramethylsilane (TMS) as an internal reference. Resonance frequencies, ν, are quoted as c.p.s. downfield from the TMS reference (0.0 c.p.s.) and are accurate to ±1 c.p.s. Coupling constants,

[7]A similar case has been reported recently (36).

Can. J. Chem. Downloaded from www.nrcresearchpress.com by 210.87.254.6 on 09/05/12
For personal use only.

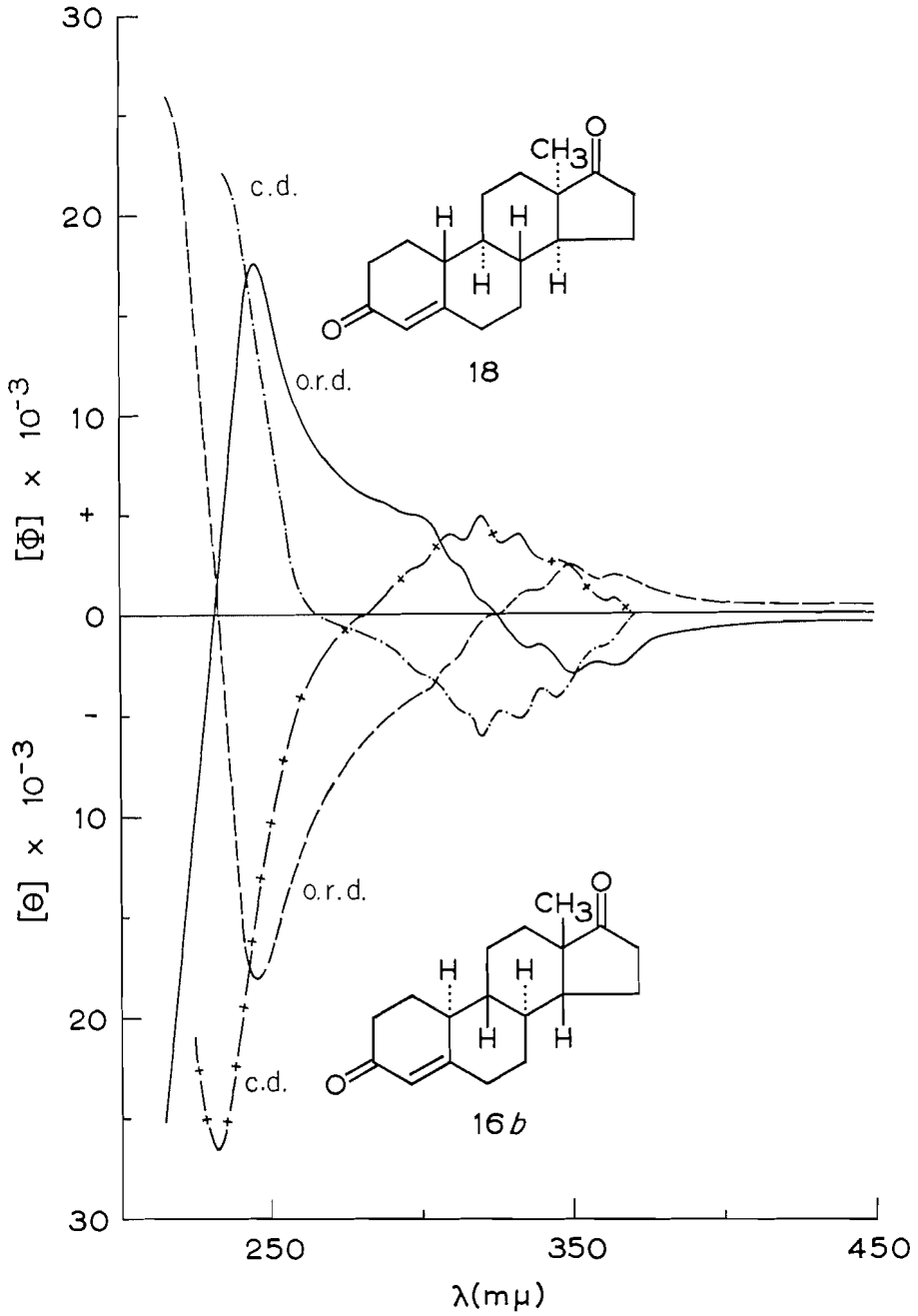

FIG. 1. Optical rotatory dispersion and circular dichroism curves of the enantiomeric steroids (**16***b*) and (**18**).

Can. J. Chem. Downloaded from www.nrcresearchpress.com by 210.87.254.6 on 09/05/12
For personal use only.

J, also expressed in c.p.s. units, are accurate to ±0.5 c.p.s. We are indebted to Dr. L. Throop and his staff, Syntex Research, Palo Alto, California, for o.r.d. and n.m.r. measurements. Silica gel G (Merck) and neutral alumina were used for preparative thin-layer and column chromatography.

Estrone 3-Methyl Ether (4a)

Optical rotatory dispersion (*c*, 0.0003; dioxane): $[\Phi]_{600}$ +539°; $[\Phi]_{350}$ +2938°; $[\Phi]_{319}$ +8814°; $[\Phi]_{297}$ ±0°; $[\Phi]_{278}$ −5190°; $[\Phi]_{246}$ ±0°; $[\Phi]_{234}$ +3526°; c.d. (*c*, 0.0003; dioxane): $[\Theta]_{332}$ ±0; $[\Theta]_{300}$ +11 080; $[\Theta]_{268-271}$ +9400.

16α-Bromo-3-hydroxyestra-1,3,5(10)-trien-17-one-3-methyl Ether (4b) (7)

Optical rotatory dispersion (*c*, 0.001; dioxane): $[\Phi]_{600}$ +436°; $[\Phi]_{380}$ +2327°; $[\Phi]_{341}$ +5743°; $[\Phi]_{314}$ ±0°; $[\Phi]_{292}$ −5080°; $[\Phi]_{258}$ +0°; $[\Phi]_{234}$ +8228°; $[\Phi]_{229}$ ±0°; $[\Phi]_{225}$ −16 333°; c.d. (*c*, 0.009; dioxane): $[\Theta]_{362}$ ±0; $[\Theta]_{317}$ +7890; $[\Theta]_{186}$ +3200.

3-Hydroxyestra-1,3,5(10),-15-tetraen-17-one-3-methyl Ether (6a) (7)

Melting point 180–181°; $[\alpha]_D$ −56°; c.d. (*c*, 0.001; dioxane): $[\Theta]_{400}$ ±0; $[\Theta]_{357}$ −1350; $[\Theta]_{298}$ −120; u.v. λ_{max} 224, 278, 287 mμ (log ε 4.16, 3.37, 3.32); i.r. ν_{max} 1720 cm^{-1}; n.m.r. 66 (18-H), 176 (benzylic H), 227 (3-methoxyl), 360, 363, 366, 369 (quartet, 16-vinyl H split by 15H, J = 6 c.p.s.) and by 14αH (J = 3 c.p.s.); 400, 404 (C-2 and C-4 aromatic H), 429, 437 (doublet J = 8, C-1 aromatic H); 456, 462 c.p.s. (15-vinyl H, doublet).

3-Hydroxy-14β-estra-1,3,5(10),15-tetraen-17-one-3-methyl Ether (6b) and 3-Hydroxyestra-1,3,5(10),14-tetraen-17-one-3-methyl Ether (6c) (7)

A mixture of 15-dehydroestrone 3-methyl ether (**6***a*) (3.5 g) and *p*-toluenesulfonic acid monohydrate (2.28 g) in 175 ml of benzene was heated under reflux for 15 min. A saturated solution of sodium bicarbonate was added, the mixture was extracted with methylene chloride, and washed with water until neutral. The solution was dried over anhydrous sodium sulfate, filtered, and evaporated to dryness *in vacuo*. The residue appeared to be a mixture of two components in the 2:3 ratio. Chromatography on silica gel followed by crystallization from methylene chloride – methanol of the fractions eluted with hexane – ethyl acetate (95:5) afforded 1.85 g of 14-dehydroestrone-3-methyl ether (**6***c*) exhibiting: m.p. 102–103°; $[\alpha]_D$ +287°; c.d. (*c*, 0.001; dioxane): $[\Theta]_{320}$ +3470; $[\Theta]_{315}$ +4650; $[\Theta]_{306}$ +6800; $[\Theta]_{297}$ +7000; u.v. λ_{max} 221–222, 280, 287 mμ (log ε 3.94, 3.31, 3.29); i.r. ν_{max} 1750, 1650, 1640, 1610 cm^{-1}; n.m.r. 70 (18-H), 180 (benzylic H), 227 (methoxyl H), 338 (15-vinyl H), 401 (C-4 aromatic H), 401, 408 (C-2 H), 430, 437 (C-1 H).

Further elution of the column with the same solvent system, followed by crystallization from methylene chloride – methanol, gave 1.04 g of 15-dehydro-14β-estrone-3-methyl ether (**6***b*) showing: m.p. 100–101°; $[\alpha]_D$ +476°; c.d. (*c*, 0.0014; dioxane): $[\Theta]_{349}$ +2840; $[\Theta]_{337}$ +3660; $[\Theta]_{326}$ +3465; u.v. λ_{max} 220–221, 277–278, 286–287 mμ (log ε 4.22, 3.40, 3.35); i.r. ν_{max} 1700, 1615, 1575 cm^{-1}; n.m.r. 70 (18-H), 172 (benzylic H), 226 (methoxyl H), 371, 377 (C-16 H, doublet J = 6), 398 (C-4 H), 398, 407, 423, 431 (C-15 H, doublet J = 8). 456, 462, c.p.s.

Anal. Calcd. for $C_{19}H_{22}O_2$: C, 80.81; H, 7.85. Found: C, 80.46; H, 7.94.

Acid Isomerization of 15-Dehydroestrone-3-methyl Ether (6a)

A solution of 50 mg of pure 15-dehydroestrone methyl ether (**6***a*) and 33 mg of *p*-toluenesulfonic acid monohydrate in 2.5 ml of anhydrous benzene was allowed to reflux for 3 min. The reaction mixture was then poured into a saturated sodium bicarbonate solution. Extraction with methylene chloride gave a residue which was purified by chromatography on silica gel. The fractions eluted with hexane – ethyl acetate (95:5) afforded 30 mg of starting material. Further elution gave 10 mg of 14-dehydroestrone methyl ether (**6***c*) with m.p. 100–101°; $[\alpha]_D$ +290°; u.v. λ_{max} 219–221, 280, 287 mμ (log ε 3.95, 3,31, 3.29), identified by thin-layer chromatography (t.l.c.) infrared spectra and mixture melting point with an authentic specimen.

Alkaline Isomerization of 15-Dehydroestrone Methyl Ether (6a)

A solution of 1 g 15-dehydroestrone methyl ether (**6***a*) in 200 ml of 2% methanolic potassium hydroxide was heated to reflux for 30 min under nitrogen. Extraction with methylene chloride, washing to neutrality with water, and evaporation of the solvent gave 970 mg of an amorphous product. This mixture was chromatographed on fluorescent, preparative silica gel chromatoplates. The following products were isolated. First, 200 mg of 14-dehydroestrone methyl ether (**6***c*); m.p. 99–100°; $[\alpha]_D$ +288°; undepressed on admixture with an authentic sample. Then a semicrystalline material with $[\alpha]_D$ +377° which after recrystallization from methylene chloride – methanol gave 295 mg of 14β-15-dehydroestrone methyl ether (**6***b*); m.p. 99–100°; $[\alpha]_D$ +470°, identified by t.l.c., i.r., and mixture m.p. (undepressed) with an authentic sample. A third compound (220 mg) was obtained. Its physical properties agree with the 15α-hydroxyestrone dimethyl ether (**8***a*) structure. Recrystallization from methylene chloride – methanol afforded the analytical sample of **8***a*: m.p. 126–127°; $[\alpha]_D$ +227°; o.r.d. (*c*, 0.0006; dioxane): $[\Phi]_{600}$ +625°; $[\Phi]_{589}$ +729°; $[\Phi]_{318}$ +8547°; $[\Phi]_{288}$ ±0°; $[\Phi]_{279}$ −1772°; $[\Phi]_{270}$ −1563°; $[\Phi]_{262}$ ±0°; $[\Phi]_{240}$ +7558°; $[\Phi]_{234}$ +9902°; $[\Phi]_{224}$ ±0; $[\Phi]_{223}$ +1954°; $[\Phi]_{222}$ ±0°; $[\Phi]_{216}$ +5081°; c.d. (*c*, 0.0005; dioxane): $[\Theta]_{326}$ +0; $[\Theta]_{299}$ +9970; $[\Theta]_{286}$ +7500; u.v. λ_{max} 219–220, 278, 287 mμ (log ε 3.94, 3.34, 3.31); i.r. ν_{max} 1745, 1613 cm^{-1}; n.m.r. 55 (18-H), 200 (15-methoxyl), 224 (3-methoxyl), ~240 (15-H), 396 (C-4 H), 404, 406 (C-2 H), 426, 434 (C-1 H) c.p.s.

Anal. Calcd. for $C_{20}H_{26}O_3$: C, 76.40; H, 8.34. Found: C, 76.91; H, 8.37.[8]

Finally chromatography of the residue on silica gel gave by elution with hexane – ethyl acetate (4:1), followed by crystallization from methanol 15β-hydroxyestrone dimethyl ether (**8***b*) (75 mg) as needles: m.p. 125–127°;

[8]This compound (**8***a*) is the 15-methyl ether of 3,15α-dihydroxyestra-1,3,5(10)-trien-17-one obtained previously by microbiological hydroxylation of estrone, followed by methylation; see ref. 40.

Can. J. Chem. Downloaded from www.nrcresearchpress.com by 210.87.254.6 on 09/05/12
For personal use only.

$[\alpha]_D$ +92°; o.r.d. (*c*, 0.0007; dioxane): $[\Phi]_{600}$ +476°; $[\Phi]_{350}$ +2474°; $[\Phi]_{321}$ +6613°; $[\Phi]_{297}$ ±0°; $[\Phi]_{275}$ −3425°; $[\Phi]_{250}$ ±0°; $[\Phi]_{237}$ +3045°; $[\Phi]_{230}$ ±0°; $[\Phi]_{223}$ −3093°; c.d. (*c*, 0.0016; dioxane): $[\Theta]_{337}$ ±0; $[\Theta]_{303}$ +8750; $[\Theta]_{299}$ +7900; u.v. λ_{max} 279, 288 mμ (log ε 3.33, 3.31); i.r. ν_{max} 1735, 1613 cm^{-1}; n.m.r. 67 (18-H), 197 (15-methoxyl), 224 (3-methoxyl), ~242 (15-H), 398 (C-4 H), 398, 405, 408 (C-2 H), 426, 436 c.p.s. (C-1 H).

Anal. Calcd. for $C_{20}H_{26}O_3$: C, 76.40; H, 8.34; O, 15.27. Found: C, 76.57; H, 8.10; O, 15.43.

Acid Isomerization of 14-Dehydroestrone-3-methyl Ether (6c)

A solution containing 50 mg of 14-dehydroestrone-3-methyl ether (**6***c*), 33 mg of *p*-toluenesulfonic acid monohydrate, and 2.5 ml of anhydrous benzene was heated at reflux temperature for 3 min. Neutralization, followed by extraction with methylene chloride and chromatography on silica gave, after elution with hexane – ethyl acetate (95:9) and crystallization from methylene chloride – methanol, 12.5 mg of starting material (m.p. 101–102°), and 7.5 mg of 15-dehydroestrone-3-methyl ether (**6***b*), with m.p. 99–100°, $[\alpha]_D$ +456°; u.v. λ_{max} 220–222, 278, 287 mμ (log ε 4.15, 3.38, 3.32), identified by direct comparison (mixture melting point, t.l.c., and infrared spectra) with an authentic specimen.

Alkaline Isomerization of 14-Dehydroestrone-3-methyl Ether (6c)

A solution of 14-dehydroestrone methyl ether (**6***c*) (540 mg) in 100 ml of 2% methanolic potassium hydroxide was heated to reflux, under nitrogen, for 30 min. Extraction with methylene chloride, washing to neutrality, furnished an amorphous residue which was chromatographed on fluorescent silica gel chromatoplates. Two compounds were isolated besides 170 mg of unchanged starting material with: m.p. 99–100°; $[\alpha]_D$ +291°; undepressed by mixture m.p. with an authentic sample. The 14β-15-dehydroestrone derivative (**6***b*) (310 mg) was also isolated; m.p. 99–100°; $[\alpha]_D$ +434°; t.l.c., i.r., and mixture melting point identical with an authentic sample. Finally, 40 mg of an homogenous product were obtained, which provided, after crystallization from methylene chloride – methanol, pure 15β-hydroxy-14β-estrone dimethyl ether (**8***c*); m.p. 87–89°; $[\alpha]_D$ +137°; c.d. (*c*, 0.0006; dioxane): $[\Theta]_{320}$ ±0; $[\Theta]_{291}$ +4720; $[\Theta]_{286}$ +3600; u.v. λ_{max} 220–221, 278, 287 mμ (log ε 3.92, 3.28, 3.27); i.r. ν_{max} 1740, 1610 cm^{-1}; n.m.r. 68 (18-H), 197 (15-methoxyl), 225 (3-methoxyl), 242, 250 (15-H), 398 (C-4 H), 398, 405, 408 (C-2 H), 428, 435 c.p.s. (C-1 H).

Anal. Calcd. for $C_{20}H_{26}O_3$: C, 76.40; H, 8.34. Found: C, 76.44; H, 8.33.

Acid Isomerization of 15-Dehydro-14β-estrone-3-methyl Ether (6b)

A solution of 200 mg of 15-dehydro-14β-estrone-3-methyl ether (**6***b*) and 120 mg of *p*-toluenesulfonic acid monohydrate in 10 ml of anhydrous benzene, was heated under reflux for 3 min. Neutralization with a sodium bicarbonate solution followed by extraction with methylene chloride, gave a product which was chromatographed on silica gel. Elution with 5% ethyl acetate in hexane and subsequent crystallization from methylene chloride–methanol afforded 14-dehydroestrone methyl ether (**6***c*) (100 mg); m.p. 101–102°, $[\alpha]_D$ +250°, u.v. λ_{max} 220–221, 278, 287 mμ (log ε 3.96, 3.32, 3.31). A second crop gave impure starting material (**6***b*) (60 mg); m.p. 97–99°, $[\alpha]_D$ +448°; u.v. λ_{max} 220–222, 278, 287 mμ (log ε 4.2, 3.4, 3.34).

Alkaline Treatment of 3,15α-Dihydroxyestrone-3-methyl Ether (8a)

A solution containing 50 mg of **8***a*, and 50 mg of potassium hydroxide in 25 ml methanol was gently refluxed for 4 h under nitrogen. After cooling and extraction by usual procedure a crude mixture (50 mg) was obtained. Preparative thin-layer chromatography allowed the isolation of 25 mg of the 14-dehydro compound (**6***c*): m.p. 95–97°; $[\alpha]_D$ +286°, identical in every respect (t.l.c., i.r., and m.p.) with an authentic sample. Moreover, 10 mg of 15-dehydro-14β-estrone-3-methyl ether (**8***b*) were also obtained; m.p. 96–97°; $[\alpha]_D$ +408°, and shown, by usual criteria (t.l.c., mixture melting point, i.r.), to be identical with a pure sample of **6***b*.

3-Hydroxy-14β-estra-1,3,5(10), 8-tetraen-17-one-3-methyl Ether (7a)

A mixture of 15-dehydroestrone-3-methyl ether (**6***a*) (2.33 g), *p*-toluenesulfonic acid monohydrate (1.5 g) and toluene (120 ml) was heated at reflux temperature for 16 h. This solution was then washed thoroughly with saturated sodium bicarbonate solution, and with water until neutral. Removal of the solvent *in vacuo* and subsequent crystallization from methanol afforded Δ^8-14β-estrone-3-methyl ether (**7***a*) (1.4 g); m.p. 121–122°, $[\alpha]_D$ +213°; o.r.d. (*c*, 0.001; dioxane): $[\Phi]_{600}$ +590°; $[\Phi]_{500}$ +1000°; $[\Phi]_{400}$ +1290°; $[\Phi]_{321}$ +3270°; $[\Phi]_{310}$ +2440°; $[\Phi]_{299}$ +4150°; $[\Phi]_{276}$ +30 500°; $[\Phi]_{248}$ −29 600°; $[\Phi]_{228}$ −23 000°; c.d. (*c*, 0.001; dioxane): $[\Theta]_{356}$ ±0; $[\Theta]_{322}$ + 3170; $[\Theta]_{300}$ −6500; u.v. λ_{max} 273–274 mμ (log ε 4.22); i.r. ν_{max} 1730, 1650, 1610 cm^{-1}; n.m.r. 65 (18-H), 164 (benzylic H), 228 c.p.s. (methoxyl H).

Alkaline Isomerization of 15-Dehydro-14β-estrone-3-methyl Ether (6b)

A solution of 550 mg of **6***b* and 2 g of potassium hydroxide in 100 ml methanol was heated to reflux under nitrogen for 30 min. By extraction with methylene chloride, washing with water until neutral, and removal of the solvent an amorphous residue (540 mg) was obtained. By chromatography on silica gel preparative fluorescent chromatoplates there were isolated three substances. First, 170 mg of 14-dehydroestrone methyl ether (**6***c*) were obtained. Recrystallization from methylene chloride – methanol provided the pure isomer (**6***c*); m.p. 102–103°; $[\alpha]_D$ +284°, identical in all respects with an authentic sample. Moreover 310 mg of unchanged starting material (**6***b*) with m.p. 96–97°; $[\alpha]_D$ +448° were recovered. Finally, 45 mg of an homogeneous substance were obtained which crystallized from methylene chloride – methanol, to give the analytical sample of 15β-hydroxy-14β-estrone dimethyl ether (**8***c*); m.p. 87–89°; $[\alpha]_D$ +137°; u.v. λ_{max} 219–221, 278, 287 mμ (log ε 3.95, 3.31, 3.28); i.r. ν_{max} 1738, 1610 cm^{-1}, shown to be identical (mixture melting point, t.l.c., i.r.) with an authentic sample.

3-Hydroxy-15, 16β-oxido-14β-estra-1,3,5(10)-trien-17-one-3-methyl Ether (8d)

A solution of 15-dehydro-14β-estrone methyl ether (**6***b*) (880 mg) in undistilled tetrahydrofuran (10 ml) was

Can. J. Chem. Downloaded from www.nrcresearchpress.com by 210.87.254.6 on 09/05/12
For personal use only.

treated with 50 ml of a 3% solution of potassium hydroxide in aqueous methanol. The mixture was heated for 30 min at reflux temperature. Subsequent neutralization, addition into water, extraction with methylene chloride, and chromatography of the residue on fluorescent silica gel plates, gave 200 mg of unchanged starting material, as well as 286 mg of a compound with m.p. 100–101°, without defined absorption maximum around 220 mμ. Further crystallization of this product from methanol gave 205 mg of pure 15,16β-oxido-14β-estrone methyl ether (**8***d*): m.p. 100–111°; $[\alpha]_D$ +311°; c.d. (*c*, 0.001; dioxane): $[\Theta]_{350}$ ±0; $[\Theta]_{326}$ −3300; $[\Theta]_{320}$ −3470; $[\Theta]_{297}$ ±0; u.v. λ_{max} 278, 287 mμ (log ε 3.34, 3.32); i.r. ν_{max} 1740, 1610 cm^{-1}; n.m.r. 68 (18-H), 207, 209, 227, 230 (2-epoxide-H), 225 (C-3 methoxyl H), 398 (C-4 H), 398, 406, 409 (C-2 H), 421, 429 c.p.s. (C-1 H).

Anal. Calcd. for $C_{19}H_{22}O_3$: C, 76.48; H, 7.43. Found: C, 77.09; H, 7.49.

3,17α-Dihydroxy-17β-ethinyl-14β-estra-1,3,5(10),8-tetraene-3-methyl Ether (7b)

A stream of purified acetylene was bubbled through 200 ml of tetrahydrofuran for 2 h. A 3 *N* solution of methylmagnesium bromide in ether (5 ml) was then added slowly and the stream of acetylene was maintained for 5 h. A solution of dehydro-14β-estrone 3-methyl ether (**7***a*) (500 mg) in a few ml of tetrahydrofuran was added and the mixture was heated at reflux temperature for 1.5 h. The reaction mixture was then added to a cold saturated ammonium chloride solution and extracted with methylene chloride. Crystallization of the crude extract from ether–hexane afforded 125 mg (25%) of the 17β-ethinyl derivative (**7***b*); m.p. 91–92°; $[\alpha]_D$ +65°; u.v. λ_{max} 272–273 mμ (log ε 4.08); i.r. ν_{max} 3540, 3225, 1640, 1605 cm^{-1}; n.m.r. 67 (18-H), 130 (hydroxyl), 154 (—C≡CH), 226 c.p.s. (methoxyl).

Anal. Calcd. for $C_{21}H_{24}O_2 \cdot 1/2\ H_2O$: C, 79.46; H, 7.94; O, 12.60. Found: C, 79.52; H, 7.95; O, 12.34.

14β-Estrone-3-methyl Ether (6d)

(a) From 15-Dehydro-14β-estrone-3-methyl Ether (6b)

A solution of **6***b* (5.8 g) in ethyl acetate (125 ml) was shaken with 10% palladium on charcoal (1 g) in an atmosphere of hydrogen at 50 pounds per square inch (p.s.i.). Crystallization of the product from methanol afforded 5.5 g of 14β-estrone-3-methyl ether (**6***d*); m.p. 112–113°; $[\alpha]_D$ +179°; o.r.d. (*c*, 0.0004; dioxane): $[\Phi]_{600}$ +530°; $[\Phi]_{350}$ +2159°; $[\Phi]_{306}$ +4998°; $[\Phi]_{227}$ +1590°; $[\Phi]_{240}$ +7573°; $[\Phi]_{218}$ +22 421°; c.d. (*c*, 0.0003; dioxane): $[\Theta]_{320}$ ±0; $[\Theta]_{290}$ +4420; $[\Theta]_{280}$ +1400; u.v. λ_{max} 278, 287 mμ (log ε 3.33, 3.30); i.r. ν_{max} 1730, 1613 cm^{-1}; n.m.r. 67 (18-H); 223 (C-3 methoxyl); (lit. (7) m.p. 114–115°, $[\alpha]_D$ +156°).

(b) From 14-Dehydroestrone-3-methyl Ether (6c)

Hydrogenation of **6***c* (2.1 g) in ethyl acetate (100 ml) with 10% palladium on charcoal (0.5 g) at 50 p.s.i. afforded, after crystallization from methanol, 14β-estrone-3-methyl ether (**6***d*) (1.77 g); m.p. 110–111°; $[\alpha]_D$ +177°; u.v. λ_{max} 278, 287 mμ (log ε 3.33, 3.30). This compound was identical by i.r., t.l.c., and mixture melting point comparison with the product obtained in the previous experiment (*a*).

14β-Estrone (6e)

14β-Estrone 3-methyl ether (**6***d*) (1.7 g) was added to a saturated solution of hydrogen bromide in acetic acid (25 ml) (22). The mixture was left at room temperature for 16 h and then poured into ice-water to give a precipitate. The solid material was separated by filtration, washed with water, redissolved in methanol (36 ml), and heated to reflux with aqueous potassium hydroxide (10%, 6 ml) for 1 h. Addition to ice-water, acidification with 5% aqueous hydrogen chloride and extraction with methylene chloride gave a semicrystalline residue, which after crystallization from methylene chloride–methanol furnished 14β-estrone (**6***e*) (1.42 g). The analytical sample exhibited; m.p. 210–211°; $[\alpha]_D$ +183°; u.v. λ_{max} 280–281 mμ (log ε 3.30); i.r. ν_{max} 3250, 1715, 1613 cm^{-1}; n.m.r. 67 (18-H), ~ 324 (hydroxyl), ~ 396 (C-4 H), ~ 405 (C-2 H), 425, 435 (C-1 H) c.p.s.

Anal. Calcd. for $C_{18}H_{22}O_2$: C, 79.96; H, 8.20. Found: C, 79.14; H, 8.21.

14β-Estrone-3-tetrahydropyranyl Ether (6f)

A solution containing 14β-estrone (**6***e*) (1.3 g), anhydrous benzene (20 ml), anhydrous tetrahydrofuran (10 ml), dihydropyrane, and 50 mg of *p*-toluenesulfonic acid monohydrate was stirred at room temperature for 1 h (23). The reaction mixture was then poured into a saturated aqueous sodium bicarbonate solution and extracted with methylene chloride. After alumina chromatography the material eluted with hexane–ether (9:1) was crystallized from ether–methanol to give 14β-estrone tetrahydropyranyl ether (**6***f*) (800 mg); m.p. 102–103°; $[\alpha]_D$ +148°; u.v. λ_{max} 277, 284 mμ (log ε 3.18, 3.13); i.r. ν_{max} 1730, 1610 cm^{-1}; n.m.r. 65 (18-H), 172 (benzylic H), 200–250 (—CH_2—O—), 321 (—O—CH—O—), 407 (C-4 H) ~ 415 (C-2 H), 427–436 (C-1 H) c.p.s.

Anal. Calcd. for $C_{23}H_{30}O_3$: C, 77.93; H, 8.53; O, 13.54. Found: C, 78.32; H, 8.43; O, 13.40.

3,17α-Dihydroxy-17β-ethinyl-14β-estra-1,3,5(10)-triene-3-methyl Ether (13a)

Purified acetylene was bubbled through 200 ml of anhydrous tetrahydrofuran for 2 h. Without stopping the acetylene stream, 21.3 ml of 3 *N* solution of methylmagnesium bromide in ether were slowly added and the acetylene was allowed to pass through the solution for a further 5 h. 14β-Estrone-3-methyl ether (**6***d*) (1.7 g) in a few milliliters of anhydrous tetrahydrofuran was then added and the mixture was refluxed for 1.5 h. Addition of this solution to an ice-cold saturated solution of ammonium chloride in water and extraction with methylene chloride furnished a semicrystalline product which after recrystallization from methanol–hexane gave 900 mg of 17β-ethinyl-14β,17α-estradiol 3-methyl ether (**13***a*). Further purification by crystallization afforded the analytical sample; m.p. 112–113°; $[\alpha]_D$ +140°; u.v. λ_{max} 219–221, 278–279, 287 mμ (log ε 3.94, 3.30, 3.27); i.r. ν_{max} 3500, 3300, 3200, 3160, 1625, 1600 cm^{-1}; n.m.r. 70 (18-H), 153 (acetylenic H), 171 (benzylic H), 227 (methoxyl H), 399 (C-4 H), 408 (C-2 H), 432, 441 c.p.s. (C-1 H).

Anal. Calcd. for $C_{21}H_{26}O_2 \cdot 1/2\ H_2O$: C, 79.02; H, 8.52. Found: C, 79.43; H, 8.69.

3,17α-Dihydroxy-17β-ethinyl-14β-estra-1,3,5(10)-triene-3-methyl Ether 17-Tetrahydropyranyl Ether (13e)

A solution containing 17β-ethinyl-14β-estradiol-3-methyl ether (**13***a*) (300 mg), anhydrous benzene (30 ml),

Can. J. Chem. Downloaded from www.nrcresearchpress.com by 210.87.254.6 on 09/05/12
For personal use only.

dihydropyrane (0.3 ml) and *p*-toluenesulfonic acid monohydrate (15 mg), was stirred at room temperature for 1 h (23). It was then poured into a saturated aqueous sodium bicarbonate solution and extracted with methylene chloride. The amorphous residue was purified by chromatography on alumina. Concentration of the hexane – methylene chloride (9:1) eluates and subsequent crystallization from ether–methanol afforded 140 mg of the tetrahydropyranyl ether derivative (**13***e*); m.p. 89–90°; $[\alpha]_D$ +144°; u.v. λ_{max} 279, 287 mμ (log ε 3.29, 3.26); i.r. ν_{max} 3200, 2090, 1610 cm^{-1}; n.m.r. 69 (18-H), 151 (—C≡CH), 200–250 (—CH_2—O—), 223 (CH_3—O—), ~ 314 (—O—CH—O—), 395 (C-4 H), 405 (C-2 H), 428, 437 c.p.s. (C-1 H).

Anal. Calcd. for $C_{26}H_{34}O_3$: C, 79.15; H, 8.69; O, 12.17. Found: C, 79.01; H, 8.77; O, 12.13.

*3,17α-Dihydroxy-17β-ethinyl-14β-estra-1,3,5(10)-triene 3-methyl Ether 17-Acetate (**13***b*)*

The ethinyl steroid (**13***a*) (400 mg) was treated with acetic anhydride (4 ml) and *p*-toluenesulfonic acid monohydrate (120 mg) at room temperature for 20 h. The reaction mixture was poured into water and extracted with methylene chloride. This extract was washed successively with saturated aqueous sodium bicarbonate solution and water, dried, and concentrated *in vacuo* to give a residue which crystallized from methylene chloride – methanol to give the 17β-ethinyl-14β-estratriene acetate (**13***b*) (310 mg); m.p. 129–130°; $[\alpha]_D$ +110°; u.v. λ_{max} 278–279, 287 mμ (log ε 3.29, 3.26); i.r. ν_{max} 3225, 1750, 1615, 1255 cm^{-1}; n.m.r. 73 (18-H), 122 (—OAc), 154 (—C≡CH), 224 (CH_3O—), 397 (C-4 H), ~ 407 (C-2 H, C-1 H), 437, 429 c.p.s. (C-1 H).

Anal. Calcd. for $C_{23}H_{28}O_3$: C, 78.37; H, 8.01; O, 13.62. Found: C, 78.76; H, 8.04; O, 13.49.

*3,17α-Dihydroxy-17β-ethinyl-14β-estra-1,3,5(10)-triene-3-tetrahydropyranyl Ether (**13***d*)*

A solution of methylmagnesium bromide in ether (10 ml of 3 *N*) was slowly added to a saturated solution of purified acetylene in anhydrous tetrahydrofuran (200 ml). A stream of acetylene was passed through this mixture for 4 h. 14β-Estrone tetrahydropyranyl ether (**6***f*) (700 mg) in a few ml of anhydrous tetrahydrofuran was then added and the mixture was refluxed for 1.5 h. Addition to an ice-cold saturated aqueous solution of ammonium chloride and extraction with methylene chloride gave an amorphous residue which crystallized from methylene chloride – ether, to give 750 mg of 17β-ethinyl-14β, 17α-estradiol-3-tetrahydropyranyl ether (**13***d*); m.p. 147–148°. Recrystallization afforded a pure sample; m.p. 157–158.5°; $[\alpha]_D$ +72°; u.v. λ_{max} 284 mμ (log ε 3.16); i.r. ν_{max} 3200, 3150, 2075, 1610 cm^{-1}; n.m.r. 68 (18-H), 142 (hydroxyl), 151 (—C≡CH), 200–250 (—CH_2—O—), 322 (—O—CH—O—), 406 (C-4 H), 415 (C-2 H), 428, 437 c.p.s. (C-1 H).

Anal. Calcd. for $C_{25}H_{32}O_3$: C, 78.91; H, 8.48; O, 12.61. Found: C, 78.34; H, 8.37; O, 12.79.

*3,17α-Dihydroxy-17β-ethinyl-14β-estra-1,3,5(10)-triene (**13***c*)*

A solution of 800 mg of 17β-ethinyl-14β,17α-estradiol-3-monotetrahydropyranyl ether (**13***d*) in 50 ml methanol was treated with a saturated solution of oxalic acid in 50% aqueous methanol (10 ml) at room temperature for 16 h. The reaction mixture was then poured into a saturated solution of sodium bicarbonate and extracted with methylene chloride. The residue crystallized from acetone–ether to give 600 mg of 17β-ethinyl-14β,17α-estradiol (**13***c*); m.p. 184–185°; $[\alpha]_D$ +118°; u.v. λ_{max} 281 mμ (log ε 3.29); i.r. ν_{max} 3300, 3220, 2080, 1610 cm^{-1}; n.m.r. 70 (18-H), 94 (hydroxyl), 153 (—C≡CH), 278 (hydroxyl), ~ 395 (C-4 H), ~ 404 c.p.s. (C-2 H).

Anal. Calcd. for $C_{20}H_{24}O_2 \cdot 1/2\ H_2O$: C, 78.65; H, 8.25. Found: C, 78.09; H, 8.23.

*3,17α-Dihydroxy-19-norpregna-1,3,5 (10)-triene-20-one 3-methyl Ether 17-Acetate (**14**)*

The acetate (**13***b*) (1.4 g) was added to a refluxing mixture of 20% aqueous sulfuric acid (50 ml), mercuric sulfate (1.26 g) and ethanol (300 ml). The resulting solution was allowed to reflux under nitrogen for 1.5 h (27). The solution was cooled, neutralized with saturated aqueous sodium bicarbonate, and then extracted with ethyl acetate. Working-up as usual and crystallization of the residue from methylene chloride – methanol gave 750 mg of 3,17α-dihydroxy-19-norpregna-1,3,5(10)-trien-20-one 3-methyl ether 17-acetate (**14**); m.p. 140–141°; $[\alpha]_D$ +74°; c.d. (*c*, 0.0009; dioxane): $[\theta]_{380}$ ±0; $[\theta]_{293}$ +2360; $[\theta]_{260}$ +100; u.v. λ_{max} 278, 287 mμ (log ε 3.33, 3.31); i.r. ν_{max} 1730, 1708, 1610, 1250 cm^{-1}; n.m.r. 58 (18-H), 125, 127 (21-H plus an acetate grouping), ~ 168 (benzylic H), ~ 224 (methoxyl), ~ 397 (C-4 H), 397, 405, 408 (C-2 H), 428, 436 c.p.s. (C-1 H).

Anal. Calcd. for $C_{20}H_{30}O_4$: C, 74.56; H, 8.16. Found: C, 74.21; H, 8.10.

*14β,17α-19-Norpregn-4-ene-3,20-dione (**2***a*)*

A solution of compound (**14**) (780 mg) in anhydrous dioxane (100 ml) was added to a stirred solution of lithium metal (1.46 g) in 300 ml liquid ammonia – anhydrous dioxane (2:1). After stirring for 2 h, methanol was carefully added until the blue color had disappeared. The ammonia was then allowed to evaporate and the mixture was poured into saturated aqueous ammonium chloride solution, extracted with methylene chloride, and washed with water to neutrality. The residue was then dissolved in a mixture of 65 ml of methanol and 5 ml of methylene chloride, 50% aqueous hydrochloric acid (31 ml) was added, and the solution was stirred at room temperature for 1 h. Extraction with methylene chloride and chromatography on silica gel afforded 380 mg of an amorphous epimeric mixture of 20-hydroxy-14β,17α-19-norpregn-4-en-3-one (**9***d*), showing: u.v. λ_{max} 240 mμ (log ε 4.18); i.r. ν_{max} 3350, 1665, 1613 cm^{-1}. One pure isomer, presumably the 20β-compound (**9***d*) exhibited; m.p. 145–146°; $[\alpha]_D$ +86°; u.v. λ_{max} 240 mμ (log ε 4.21); i.r. ν_{max} 3400, 1655, 1625, 1605 cm^{-1}; n.m.r. 66, 72 (21–H, doublet), 74 (18-H), ~ 102 (—OH), ~ 210–235 (20-H), 349 (C-4 H), This material was dissolved in acetone (4 ml) and treated with 8 *N* chromic acid (31) (0.4 ml) at 0–5° for 10 min. Ice and water were added and the mixture was extracted with methylene chloride. This extract was washed with saturated aqueous sodium bisulfite and with water, then dried and concentrated to give an amorphous residue. Crystallization of the product from methanol–water gave 14β,17α-19-norprogesterone (**2***a*) (225 mg); m.p. 87–88°; $[\alpha]_D$ +54°; c.d. (*c*, 0.001: dioxane): $[\theta]_{376}$

Can. J. Chem. Downloaded from www.nrcresearchpress.com by 210.87.254.6 on 09/05/12
For personal use only.

±0; $[\Theta]_{356}$ −1520; $[\Theta]_{342}$ −3630; $[\Theta]_{330}$ −4620; $[\Theta]_{316}$ −4520; $[\Theta]_{304}$ −4690; $[\Theta]_{286}$ −4690; $[\Theta]_{260}$ −610; u.v. λ_{max} 240 mμ (log ε 4.22); i.r. ν_{max} 1705, 1660, 1605 cm^{-1} (in agreement with the published constants (2)); n.m.r. 77 (18-H), 128 (21-H), 348 c.p.s. (C-4 H).

17α-Hydroxy 14β-Estr-4-en-3-one (9a)

A solution of 3.2 g of 15-dehydro-14β-estrone-3-methyl ether *(6b)* in 100 ml of anhydrous dioxane was added with stirring to 4 g of lithium in 900 ml liquid ammonia – anhydrous dioxane (2:1). After stirring for 2 h, methanol was carefully added until the blue color had disappeared. After allowing the ammonia to evaporate the mixture was poured into saturated aqueous ammonium chloride solution, extracted with methylene chloride, and the extract was washed with water to neutrality. The residue after removal of solvent was dissolved in 70 ml of methanol, and stirred with 5 *N* hydrochloric acid (125 ml) at room temperature for 1.5 h. Isolation of the product with methylene chloride and chromatography of the residue on silica gel gave 1.74 g (56%) of homogeneous amorphous material. Upon crystallization from ether–pentane, 1.1 g of 14β,17α-19-nortestosterone (**9***a*) was obtained; m.p. 105–106°; $[\alpha]_D$ +69°; u.v. λ_{max} 240, 310–316 mμ (log ε 4.21, 2.0); i.r. ν_{max} 3500, 1660, 1613 cm^{-1}; n.m.r. 64 (18-H), 157 (hydroxyl), 210–240 (17β-H), ~ 349 c.p.s. (C-4 H).

Anal. Calcd. for $C_{18}H_{26}O_2$: C, 78.79; H, 9.55; O, 11.66. Found: C, 78.75; H, 9.44; O, 11.91.

17α-Hydroxy-14β-estr-5-en-3-one Cycloethylene Ketal (10a)

A solution of 1.1 g of **9***a*, 375 mg of *p*-toluenesulfonic acid, 73 ml ethylene glycol, and 500 ml of benzene was allowed to reflux for 19 h. After cooling, the reaction mixture was poured into a saturated solution of sodium bicarbonate, and extracted with benzene. The organic layer was washed, dried, and evaporated *in vacuo*, furnishing 1.19 g of the crude ketal (**10***a*). Crystallization from ether afforded the analytical sample; m.p. 136–138°; $[\alpha]_D$ +98°; i.r. ν_{max} 3475 cm^{-1}; n.m.r. 61 (18-H), 134 (OH), ~ 225 (17β-H), 237 (—O—CH—), 328 c.p.s. (C-6 vinyl H).

Anal. Calcd. for $C_{20}H_{30}O_3$: C, 75.43; H, 9.50; O, 15.07. Found: C, 75.02; H, 9.58; O, 15.16.

14β-Estr-5-ene-3,17-dione 3-Cycloethylene Ketal (10b)

14β,17α-19-Nortestosterone cycloethylene ketal (**10***a*) (1.27 g) in 65 ml of pyridine was added to a cold pyridinium chromate solution, (prepared from 1.3 g of chromium trioxide and 65 ml anhydrous pyridine) (26). After stirring for 15 h at room temperature, ethyl acetate was added and the suspension was filtered through alumina. The filtrate was evaporated to dryness under vacuum to give a residue which crystallized from ether, to yield 1.0 g of 14β-estr-5-ene-3,17-dione 3-cycloethyleneketal (**10***b*); m.p. 114–115°; $[\alpha]_D$ +17°; i.r. ν_{max} 1735 cm^{-1}; n.m.r. 64 (18-H), 237 c.p.s. (cycloethylene ketal H).

Anal. Calcd. for $C_{20}H_{28}O_3$: C, 75.91; H, 8.92; O, 15.17. Found: C, 75.75; H, 8.97; O, 15.50.

17β-Ethinyl 17α-Hydroxy-14β-estr-5-en-3-one Cycloethylene Ketal (10c)

A stream of purified acetylene was bubbled through 200 ml of anhydrous tetrahydrofuran until complete saturation was achieved. A 3 *N* solution of methylmagnesium bromide in ether (10 ml) was added slowly and the stream of acetylene was maintained during 4 h. A solution of 750 mg of 14β-estr-5-ene-3,17-dione 3-cycloethylene ketal (**10***b*) in 150 ml of anhydrous tetrahydrofuran was then added and the mixture was heated at reflux temperature for 1.5 h. The product was isolated after addition of the reaction mixture to an ice-cold saturated aqueous solution of ammonium chloride, followed by extraction with methylene chloride, and washing with water to neutrality. The colored extract was dissolved in ethyl acetate, treated with charcoal, and filtered through alumina. Evaporation of the solvent and crystallization from ether gave 635 mg of 17β-ethinyl-14β,17α-19-nortestosterone cycloethylene ketal (**10***c*) the analytical sample of which exhibited; m.p. 177–179°; $[\alpha]_D$ +127°; i.r. ν_{max} 3450, 3400, 3250 cm^{-1}; n.m.r. 68 (18-H), 152 (ethinyl H), 239 c.p.s. (cycloethylene ketal H).

Anal. Calcd. for $C_{22}H_{30}O_3$: C, 77.15; H, 8.83. Found: C, 76.98; H, 8.79.

17β-Ethinyl 17α-Hydroxy-14β-estr-4-en-3-one (9b)

Perchloric acid (3 *N*, 28.2 ml) was added to a solution of the 17β-ethinyl derivative (**10***c*) (2.35 g) in tetrahydrofuran (33 ml), and the mixture was stirred at room temperature for 48 h. After addition of ice-water and extraction with methylene chloride, the organic layer was washed with sodium bicarbonate, then with water. Crystallization of the residue from methylene chloride – methanol furnished 826 mg of **9***b*. The mother liquors gave 610 mg of additional impure material. Recrystallization from the same solvents afforded the analytical sample of **9***b*; m.p. 214–215°; $[\alpha]_D$ +59°; c.d. (*c*, 0.001; dioxane): $[\Theta]_{356}$ −1620; $[\Theta]_{343}$ −4060; $[\Theta]_{330}$ −5050; $[\Theta]_{320}$ −4060; $[\Theta]_{308}$ −2670; u.v. λ_{max} 240–241 mμ (log ε 4.24); i.r. ν_{max} 3370, 3200, 2070, 1660, 1610 cm^{-1}; n.m.r. 70 (18-H), 153 (ethinyl H), 351 c.p.s. (C-4 H).

Anal. Calcd. for $C_{20}H_{26}O_2$: C, 80.49; H, 8.78. Found: C, 80.64; H, 8.76.

17β-Ethinyl 17α-Hydroxy-14β-estr-4-en-3-one Tetrahydropyranyl Ether (9c)

17β-Ethinyl-14β,17α-19-nortestosterone (**9***b*) (290 mg), 20 ml of anhydrous benzene, 0.2 ml of dihydropyrane, and 5 mg of *p*-toluenesulfonic acid monohydrate were stirred at room temperature for 1 h. The reaction mixture was then poured into a saturated aqueous solution of sodium bicarbonate and the product was isolated by extraction with methylene chloride. The organic extracts were washed until neutral, dried, and evaporated to give an amorphous residue which was crystallized from methylene chloride – methanol to yield 200 mg of 17β-ethinyl-14β,17α-19-nortestosterone tetrahydropyranyl ether (**9***c*); m.p. 160–161°; $[\alpha]_D$ +102°; u.v. λ_{max} 238 mμ (log ε 4.22); i.r. ν_{max} 3150, 2070, 1670, 1620 cm^{-1}; n.m.r. 69 (18-H), 153 (ethinyl H), 200–245 (—CH_2—O—), ~312 (—O—CH—O—); 350 c.p.s. (C-4 H).

Anal. Calcd. for $C_{25}H_{36}O_3$: C, 78.08; H, 9.44. Found: C, 78.09; H, 8.89.

3,17α-Dihydroxy 17β-Ethinyl-14β-estra-3,5-diene Diacetate (11)

A solution of 400 mg of the 19-nortestosterone derivative (**9***b*) and *p*-toluenesulfonic acid monohydrate (120

Can. J. Chem. Downloaded from www.nrcresearchpress.com by 210.87.254.6 on 09/05/12
For personal use only.

mg) in acetic anhydride (4 ml) was left at room temperature for 16 h. This solution was poured into ice-water and extracted with methylene chloride. The organic phase was first washed with sodium bicarbonate and then with water until neutral. The amorphous residue obtained after evaporation of the solvent, crystallized from methanol, to yield 200 mg of diacetate (**11**); m.p. 166–168°; $[\alpha]_D$ −39°; u.v. λ_{max} 234 mμ (log ε 4.23); i.r. ν_{max} 3200, 2125, 1755, 1745, 1660, 1630, 1245, 1205 cm^{-1}; n.m.r. 72 (18-H), 121, 127 (2-acetate methyls), 156 (ethinyl H), 330 (C-6 H), ~ 340 c.p.s. (C-4 H).

Anal. Calcd. for $C_{24}H_{30}O_4 \cdot 1/2\,H_2O$: C, 73.67; H, 7.98; O, 18.35. Found: C, 74.31; H, 7.80; O, 17.89.

17α-Hydroxy-14β-19-norpregn-4-ene-3,20-dione Acetate (12)

Mercuric sulfate (390 mg) and 15.4 ml of aqueous 20% sulfuric acid were added to a refluxing solution of 3,17α-dihydroxy 17β-ethinyl-14β-estra-3,5-diene diacetate (**11**) (440 mg) in ethanol (92.4 ml), and the mixture was heated at reflux temperature under nitrogen for 1.5 h. The cooled solution was poured into ice-water, extracted with ethyl acetate, washed with sodium bicarbonate solution, and finally with water until neutral. The residue appeared practically homogeneous on a chromatoplate. Crystallization from ether afforded the pure sample of 17α-hydroxy-14β-19-norprogesterone acetate (**12**) (250 mg); m.p. 159–161°; $[\alpha]_D$ +43°; c.d. (*c*, 0.001; dioxane): $[\Theta]_{370}$ ±0; $[\Theta]_{359}$ −1490; $[\Theta]_{343}$ −3930; $[\Theta]_{331}$ −4880; $[\Theta]_{321}$ −3660; $[\Theta]_{289}$ +1910; $[\Theta]_{285}$ +2050; $[\Theta]_{260}$ +520; u.v. λ_{max} 240 mμ (log ε 4.33); i.r. ν_{max} 1735, 1710, 1670, 1625, 1258 cm^{-1}; n.m.r. 60 (18-H); 125, 126 (21-H and 17α-acetate), ~ 349 c.p.s. (C-4 vinylic H).

Anal. Calcd. for $C_{22}H_{30}O_4$: C, 73.71; H, 8.44; O, 17.85. Found: C, 73.62; H, 8.74; O, 17.74.

13α-Estrone 3-Methyl Ether (17)

A solution of estrone methyl ether (**4***a*) (10 g) in 500 ml of tetrahydrofuran was irradiated, under nitrogen, with a Hanau Q-81 high pressure ultraviolet lamp for 12 h in a centrally illuminating apparatus, provided with a water cooled quartz filter and magnetic stirring. Evaporation of the solvent left a residue which was chromatographed on silica gel to give 2.71 g of lumiestrone methyl ether (**17**) from the hexane eluates. A pure sample, obtained by crystallization from methanol, showed; m.p. 126–128°; $[\alpha]_D$ −30°; c.d. (*c*, 0.001; dioxane): $[\Theta]_{340}$ ±0; $[\Theta]_{319}$ −1520; $[\Theta]_{307}$ −1980; $[\Theta]_{298-300}$ −1155; $[\Theta]_{285}$ −300; u.v. λ_{max} 278, 287 mμ (log ε 3.31, 3.28); i.r. ν_{max} 1725, 1613 cm^{-1}; n.m.r. 61 (18-H), 224 (methoxyl H), 397 (C-4 H), ~ 406 (C-2 H), ~ 436, ~ 427 c.p.s. (C-1 H) (in agreement with the published data).

13α-Estr-4-ene-3,17-dione (18)

A solution of pure 13α-estrone methyl ether (**17**) (1.08 g) in anhydrous dioxane (100 ml) was added with vigorous stirring to a mixture of lithium (2 g) in liquid ammonia and anhydrous dioxane (2:1, 300 ml). The reaction mixture was stirred for 2 h and then methanol was carefully added until the blue color had disappeared. The ammonia was allowed to evaporate, an excess of cold saturated ammonium chloride solution was added, and the product was extracted with methylene chloride. The amorphous residue thus obtained was dissolved in methanol (50 ml) and stirred with 50% aqueous hydrochloric acid (45 ml) for 1 h at room temperature. The product was again extracted with methylene chloride and purified by chromatography on silica. An amorphous fraction, corresponding to the mixture of alcohols at C-17 (39): u.v. λ_{max} 240 (log ε 3.94); i.r. ν_{max} 3400, 1715, 1645, 1620 cm^{-1}, was obtained by elution with hexane–ethyl acetate (4:1). This material was dissolved in 3 ml acetone and oxidized by treatment with 8 *N* chromic acid (31) (0.25 ml) for 10 min at 0–5°. Isolation of the product by addition of water and extraction with methylene chloride, followed by washing with sodium bisulfite solution gave an homogeneous material. Recrystallization from methanol furnished the analytical sample of 13α-estr-4-ene-3,17-dione (**18**); m.p. 160–162°; $[\alpha]_D$ −45°; o.r.d. (*c*, 0.001; dioxane): $[\Phi]_{600}$ −326°; $[\Phi]_{363}$ −2550°; $[\Phi]_{358}$ −2400°; $[\Phi]_{350}$ −2950°; $[\Phi]_{340}$ −1500°; $[\Phi]_{336}$ −1600° $[\Phi]_{326}$ ±0°; $[\Phi]_{324}$ +200°; $[\Phi]_{300}$ +4900°; $[\Phi]_{285}$ +5700°; $[\Phi]_{246}$ +17 500°; $[\Phi]_{232}$ ±0°; $[\Phi]_{215}$ +25 250°; c.d. (*c*, 0.001; dioxane): $[\Theta]_{372}$ ±0; $[\Theta]_{360}$ −1650; $[\Theta]_{346}$ −4100; $[\Theta]_{340}$ −3700; $[\Theta]_{333}$ −5050; $[\Theta]_{327}$ −4800; $[\Theta]_{321}$ −6000; $[\Theta]_{315}$ −4900; $[\Theta]_{301}$ −2900; $[\Theta]_{274}$ ±0; $[\Theta]_{261}$ ±0; $[\Theta]_{234}$ +24 500; u.v. λ_{max} 240 mμ (log ε 4.23); i.r. ν_{max} 1740, 1670, 1615 cm^{-1}; n.m.r. 60 (18-H), 352 c.p.s. (C-4 H).

Anal. Calcd. for $C_{18}H_{24}O_2$: C, 79.37; H, 8.88. Found: C, 79.33; H, 9.00.

Birch Reduction of 3-Hydroxy-14β-estra-1,3,5(10),8-tetraen-17-one 3-Methyl Ether (7a)

The 8(9)-dehydro steroid (**7***a*) (1.87 g) was added to a stirred solution of 2.5 g lithium in 200 ml liquid ammonia and 200 ml anhydrous dioxane (24). After stirring for 2 h, methanol was carefully dropped into the mixture until the blue color had disappeared. The ammonia was allowed to evaporate, and excess of an ice cold saturated ammonium chloride solution was added. The product was extracted with methylene chloride. The amorphous residue obtained (1.75 g) was treated with 75 ml of methanol and 75 ml of 50% aqueous hydrochloric acid and stirred for 1 h at room temperature. The product was isolated by extraction with methylene chloride and the residue [λ_{max} 240 mμ (log ε 3.97)], was chromatographed on fluorescent silica gel preparative chromatoplates. Development with hexane–ethyl acetate (4:1) and elution of zones with ethyl acetate furnished starting material (490 mg) (λ_{max} 272, log ε 3.79), an amorphous by-product without specific u.v. absorption (60 mg), the retrosteroid (**16***a*): m.p. 138–140° (150 mg), and an epimeric mixture of 17ζ-19-nortestosterone (**15***a*) (350 mg) which could not be induced to crystallize. An analytical sample of the retrosteroid (**16***a*) ,was prepared by recrystallization from ether; m.p. 140–141°; $[\alpha]_D$ −46°, o.r.d. (*c*, 0.001; dioxane): $[\Phi]_{700}$ −119°; $[\Phi]_{400}$ −260°; $[\Phi]_{390}$ −61°; $[\Phi]_{385}$ +39°; $[\Phi]_{380}$ +182°; $[\Phi]_{360}$ +1379°; $[\Phi]_{355}$ +1233°; $[\Phi]_{348}$ +1625°; $[\Phi]_{345}$ +1030°; $[\Phi]_{343}$ +284°; $[\Phi]_{340}$ −171°; $[\Phi]_{330}$ −1295°; $[\Phi]_{325}$ −2760°; $[\Phi]_{315}$ −4000°; $[\Phi]_{313}$ −4150°; c.d. (*c*, 0.001; dioxane): $[\Theta]_{370}$ ±0; $[\Theta]_{357}$ +1350; $[\Theta]_{342}$ +3630; $[\Theta]_{329}$ +4360; $[\Theta]_{318}$ +3300; $[\Theta]_{280}$ ±0; u.v. λ_{max} 242 mμ (log ε 4.2); i.r. ν_{max} 3400, 1660, 1615 cm^{-1}; n.m.r. 51 (18-H), ~ 139 (—OH), 227, 231 (17β-H), ~ 350 c.p.s. (C-4 H).

Anal. Calcd. for $C_{18}H_{26}O_2$: C, 78.79; H, 9.55; O, 11.66. Found: C, 78.85; H, 9.50; O, 12.04.

Can. J. Chem. Downloaded from www.nrcresearchpress.com by 210.87.254.6 on 09/05/12
For personal use only.

Estr-4-ene-3,17-dione (15b)

The C-17 epimeric mixture (**15a**) (235 mg) obtained in the above experiment was dissolved in 20 ml acetone and treated with 8 *N* chromic acid (0.23 ml) at 0–5° with stirring for 12 min (31). Addition to a saturated sodium bisulfite solution and extraction with methylene chloride gave 220 mg of a crystalline residue which was purified by recrystallization from methanol–ether and identified, by mixture melting point, t.l.c., and i.r. spectra, as the known estr-4-ene-3,17-dione (**15b**) (24*b*); m.p. 160–162°; $[\alpha]_D$ +140°; u.v. λ_{max} 240 mμ (log ε 4.24); i.r. ν_{max} 1740, 1670, 1620 cm^{-1}; n.m.r. 57 (18-H), 352 c.p.s. (C-4 H).

Anal. Calcd. for $C_{18}H_{24}O_2$: C, 78.33; H, 9.00. Found: C, 78.80; H, 8.59.

8α,9β,10α,14β-Estr-4-ene-3,17-dione (16b)

A solution of the retrosteroid (**16a**) (99 mg) in acetone (10 ml) was treated with 8 *N* chromic acid at 0–5° (0.1 ml) with stirring, for 10 min (31). The reaction mixture was added to ice-water, extracted with ethyl acetate, and the extract was washed with sodium bisulfite solution and then with water until neutral. The residue (88 mg) appeared homogeneous on a chromatoplate and was crystallized readily from ether to furnish a pure sample of the diketone (**16b**); m.p. 160–161°; $[\alpha]_D$ +44°; o.r.d. (*c*, 0.001; dioxane): $[\Phi]_{600}$ +169°; $[\Phi]_{450}$ +300°; $[\Phi]_{363}$ +2000°; $[\Phi]_{358}$ +1900°; $[\Phi]_{350}$ +2450°; $[\Phi]_{340}$ +1200°; $[\Phi]_{335}$ +1200°; $[\Phi]_{324}$ ±0°; $[\Phi]_{312}$ −2200°; $[\Phi]_{310}$ −2400°; $[\Phi]_{302}$ −3800°; $[\Phi]_{244}$ −1855°; $[\Phi]_{233}$ ±0°; $[\Phi]_{217}$ +26 000°; c.d. (*c*, 0.001; dioxane: $[\Theta]_{371}$ ±0; $[\Theta]_{365}$ +800; $[\Theta]_{361}$ +750; $[\Theta]_{348}$ +2600; $[\Theta]_{338}$ +2800; $[\Theta]_{333}$ +4000; $[\Theta]_{327}$ +3700; $[\Theta]_{320}$ +4900; $[\Theta]_{315}$ +3800; $[\Theta]_{310}$ +4000; $[\Theta]_{300}$ +2400; $[\Theta]_{282}$ ±0; $[\Theta]_{259}$ ±0; $[\Theta]_{232}$ −26 500; $[\Theta]_{225}$ −21 000; u.v. λ_{max} 240 mμ (log ε 4.24); i.r. ν_{max} 1740, 1670, 1615 cm^{-1}; n.m.r. 60 (18-H), 352 c.p.s. (C-4 H).

Anal. Calcd. for $C_{18}H_{24}O_2$: C, 79.37; H, 8.88. Found: C, 79.14; H, 8.76.

D,L-13-Isoestr-4-ene-3,17-dione (18 + 16b)

A mixture of 10 mg **18** and 10 mg **16***b* was recrystallized from acetone–ether to afford sharp melting crystals: m.p. 149–150°; $[\alpha]_D$ ±0°, with u.v. and i.r. spectra identical with these of the enantiomers (**18**) and (**16***b*).

3β-Hydroxy-13α-androst-5-en-17-one Tetrahydropyranyl Ether (19b)

A solution of 3β-hydroxy-androst-5-en-17-one tetrahydropyranyl ether (**19***a*) (m.p. 171–174°) (23.5 g) in anhydrous tetrahydrofuran (1 550 ml) was irradiated with a Hanau Q-81 high pressure ultraviolet lamp, under nitrogen, for 9 h, in an apparatus designed for central illumination, water cooled quartz filtering and magnetic stirring. Evaporation of the solvent and chromatography of the residue on neutral alumina gave by elution with hexane–benzene (7:3) and crystallization from methanol 3β-hydroxy-13α-androst-5-en-17-one tetrahydropyranyl ether (**19***b*) (7.5 g). The analytical sample was obtained by recrystallization from ether and showed; m.p. 133–135°; $[\alpha]_D$ −124°; o.r.d. (*c*, 0.005; dioxane): $[\Phi]_{600}$ −597°; $[\Phi]_{340}$ −2420°; $[\Phi]_{325}$ −3871°; $[\Phi]_{317}$ −2821°; $[\Phi]_{313}$ −3023°; $[\Phi]_{304}$ −1705°; $[\Phi]_{300}$ −1976°; $[\Phi]_{295}$ −1570°; $[\Phi]_{240}$ −6588°; $[\Phi]_{213}$ −13 098°; c.d. (*c*, 0.001; dioxane): $[\Theta]_{340}$ ±0; $[\Theta]_{318}$ −2010; $[\Theta]_{309}$ −2570; $[\Theta]_{298-302}$ −1680; $[\Theta]_{280}$ ±0; i.r. ν_{max} 1735 cm^{-1}; n.m.r. 51 (18-H), 59 (19-H), ~ 210–230 (—CH_2— O—), 286(—O—CH—O—), 325 c.p.s. (C-5 H).

Anal. Calcd. for $C_{24}H_{35}O_3$: C, 77.58; H, 9.49. Found: C, 77.51; H, 9.80.

3β,17α-Dihydroxy-17β-ethinyl-13α-androst-5-ene (19d)

A stream of purified acetylene was bubbled through 1250 ml of anhydrous tetrahydrofuran at room temperature for 1 h. Without interrupting the acetylene stream, methylmagnesium bromide in ether (3 *N*, 55 ml) was then slowly added and the passage of acetylene was continued for 5 h. A solution of pure 3β-hydroxy-13α-androst-5-en-17-one tetrahydropyranyl ether (**19***b*) (7.5 g) in anhydrous tetrahydrofuran (250 ml) was added and the mixture was heated at reflux temperature for 6.5 h. The product was isolated by addition to a cold saturated aqueous ammonium chloride solution, followed by extraction with methylene chloride, and chromatography of the residue on silica. Elution with hexane–ethyl acetate (9:1) provided 1.5 g of an homogeneous amorphous material (**19***c*) which was redissolved in 50 ml of aqueous methanol. Oxalic acid (3 g) in methanol (50 ml) was added and this acid solution (pH 3) was stirred at room temperature for 16 h. Addition to a saturated sodium bicarbonate solution and extraction with methylene chloride gave 3β,17α-dihydroxy-17β-ethinyl-13α-androst-5-ene (**19***d*) (1.2 g), which after crystallization from ether gave the pure sample; m.p. 239–241°; $[\alpha]_D$ −143°; i.r. ν_{max} 3400, 3220 cm^{-1}; n.m.r. (DMSO solution) 44 (18-H), 58 (19-H), 194 (ethinyl H), 188–202 (3α-H), 242 (doublet, J = 3 c.p.s., secondary —OH) 313 (tertiary OH), 325 c.p.s. (vinyl H).

Anal. Calcd. for $C_{21}H_{30}O_2$: C, 80.21; H, 9.62. Found: C, 80.14; H, 9.68.

17β-Ethinyl 17α-Hydroxy-13α-androst-4-en-3-one (20)

A solution of 3β,17α-dihydroxy-17β-ethinyl-13α-androst-5-ene (**19***d*) (1 g), 2 g of aluminium isopropoxide and 50 ml cyclohexanone in 300 ml toluene was heated to boiling until about 100 ml of solvent had distilled off. Then the reaction mixture was refluxed for 3 h. The solution was cooled and a saturated solution of sodium–potassium tartrate (excess) was added. The volatile materials were removed by steam distillation and the residue was extracted with ethyl acetate. The amorphous extract thus obtained (0.7 g) showed; λ_{max} 242 mμ (log ε 3.89). Preparative thin-layer chromatography allowed to divide the mixture into three fractions of different polarity. The intermediate fraction (0.3 g) was further purified on fluorescent silica gel chromatoplates until an homogeneous product (110 mg, λ_{max} 240 mμ, (log ε 4.10) was obtained. Recrystallization from methylene chloride – methanol furnished a pure sample of compound (**20**); m.p. 188–189°; $[\alpha]_D$ +117°; u.v. λ_{max} 242 mμ (log ε 4.29); i.r. λ_{max} 3300, 3200, 2160, 1660, 1610 cm^{-1}; n.m.r. 60 (18-H), 68 (19-H), 142 (hydroxyl), 154 (ethinyl H), 344 (C-4 H) c.p.s.

Anal. Calcd. for $C_{21}H_{28}O_2$: C, 80.73; H, 9.03; O, 10.24. Found: C, 80.72; H, 9.06; O, 10.45.

Acknowledgments

We should like to thank Prof. M. Ehrenstein, Prof. F. Sondheimer, and Prof. G. Stork for

their interest in this work, as well as for valuable suggestions.

1. G. TARZIA, N. H. DYSON, I. T. HARRISON, J. A. EDWARDS, and J. H. FRIED. Steroids **9**, 487 (1967).
2. M. EHRENSTEIN. J. Org. Chem. **9**, 435 (1944).
3. (*a*) W. M. ALLEN and M. EHRENSTEIN. Science, **100**, 251 (1944).
   (*b*) G. W. BARBER and M. EHRENSTEIN. Ann. Chem. **603**, 89 (1957).
   (*c*) C. DJERASSI, M. EHRENSTEIN, and G. W. BARBER. Ann. Chem. **612**, 93 (1958).
   (*d*) M. EHRENSTEIN, G. W. BARBER, and R. HERTZ. Endocrinology, **60**, 681 (1957).
4. [9] (*a*) L. F. FIESER and M. FIESER. Steroids. Reinhold Publ. Co., New York. 1959.
   (*b*) L. F. FIESER and M. FIESER. Topics in organic chemistry. Reinhold Publ. Co., New York. 1963.
   (*c*) P. A. PLATTNER, H. HEUSSER, and A. SEGRE. Helv. Chim. Acta, **31**, 249 (1948), and related papers.
   (*d*) C. DJERASSI, G. ROSENKRANZ, J. IRIARTE, J. BERLIN, and J. ROMO. J. Am. Chem. Soc. **73**, 1523 (1951); L. MIRAMONTES, G. ROSENKRANZ, and C. DJERASSI. J. Am. Chem. Soc. **73**, 3540 (1951); C. DJERASSI, L. MIRAMONTES, and G. ROSENKRANZ. J. Am. Chem. Soc. **75**, 4440 (1953).
   (*e*) L. VELLUZ, J. MATHIEU, and G. NOMINÉ. Tetrahedron, Suppl. 8, Part II, 495 (1966), and references therein.
5. [9] (*a*) A. J. BIRCH. J. Chem. Soc. 367 (1950).
   (*b*) A. J. BIRCH. Ann. Rept. Progr. Chem. Chem. Soc. London, **47**, 210 (1950).
   (*c*) C. DJERASSI, R. RINIKER, and B. RINIKER. J. Am. Chem. Soc. **78**, 6362 (1956).
   (*d*) E. FARKAS, J. M. OWEN, M. DEBONO, R. M. MOLLOY, and M. M. MARSH. Tetrahedron Letters, No. 10, 1023 (1966).
   (*e*) R. BUCOURT, J. TESSIER, and G. NOMINÉ. Bull. Soc. Chim. France, 1923 (1963).
   (*f*) H. SMITH. Trans. N.Y. Acad. Sci. **27**, 546 (1965).
   (*g*) C. DJERASSI. Science, **151**, 1055 (1966), and references cited therein.
   (*h*) J. A. WATERS and B. WITKOP. J. Am. Chem. Soc. **89**, 1022 (1967).
6. (*a*) J. A. EDWARDS, P. CRABBÉ, and A. BOWERS. J. Am. Chem. Soc. **85**, 3313 (1963).
   (*b*) J. A. EDWARDS, H. CARPIO, and A. D. CROSS. Tetrahedron Letters, No. 45, 3299 (1964).
   (*c*) R. GINSIG and A. D. CROSS. J. Am. Chem. Soc. **87**, 4629 (1965).
   (*d*) R. GINSIG and A. D. CROSS. J. Org. Chem. **31**, 1761 (1966).
   (*e*) J. P. TURNBULL and J. H. FRIED. Tetrahedron Letters No. 8, 801 (1966).
7. W. S. JOHNSON and W. F. JOHNS. J. Am. Chem. Soc. **79**, 2005 (1957), and references cited therein; see also W. S. JOHNSON, R. G. CHRISTIANSEN, and R. E. IRELAND. J. Am. Chem. Soc. **79**, 1995 (1957).
8. F. S. ALVAREZ and M. ARREGUIN. Chem. Ind., London, 720 (1960).
9. J. FISHMAN. J. Org. Chem. **31**, 520 (1966).
10. W. MOFFITT, R. B. WOODWARD, A. MOSCOWITZ, W. KLYNE, and C. DJERASSI. J. Am. Chem. Soc. **83**, 4013 (1961).
11. F. SONDHEIMER, S. BURSTEIN, and R. MECHOULAM. J. Am. Chem. Soc. **82**, 3209 (1960).
12. P. CRABBÉ. Applications de la dispersion rotatoire optique et du dichroisme circulaire optique en chimie organique. Gauthier–Villars, Paris, 1968.
13. M. FÉTIZON and M. GOLFIER. Bull. Soc. Chim. France, 859 (1966).
14. [9] (*a*) J. S. E. HOLKER and W. B. WHALLEY. Proc. Chem. Soc. 464 (1961).
   (*b*) M. J. T. ROBINSON and W. B. WHALLEY. Tetrahedron, **19**, 2123 (1963).
   (*c*) W. D. COTTERILL and M. J. T. ROBINSON. Tetrahedron, **20**, 765, 777 (1964).
   (*d*) R. BUCOURT and G. NOMINÉ. Bull. Soc. Chim. France, 1537 (1966); and earlier work by Bucourt *et al.* cited therein.
   (*e*) H. CHRISTOL and Y. PIETRASANTA. Bull. Soc. Chim. France, 1034 (1967); and earlier papers.
15. P. CRABBÉ and W. KLYNE. Tetrahedron, **23**, 3449 (1967).
16. (*a*) H. HIRSCHMANN and O. WINTERSTEINER. J. Biol. Chem. **126**, 737 (1938).
   (*b*) D. BANES, J. CAROL, and E. O. HAENNI. J. Biol. Chem. **187**, 557 (1950).
   (*c*) D. BANES and J. CAROL. J. Biol. Chem. **204**, 509 (1953).
17. (*a*) E. R. H. JONES, L. SKATTEBÖL, and M. C. WHITING. J. Chem. Soc. 4765 (1956).
   (*b*) H. E. STAVELY. J. Am. Chem. Soc. **61**, 79 (1939).
18. J. FAJKŐS. Collection Czech. Chem. Commun. **23**, 2155 (1958).
19. (*a*) D. K. FUKUSHIMA and T. F. GALLAGHER. J. Am. Chem. Soc. **73**, 196 (1951).
   (*b*) H. HIRSCHMANN, F. B. HIRSCHMANN, and M. A. DAUS. J. Am. Chem. Soc. **74**, 539 (1952).
   (*c*) P. CRABBÉ, L. M. GUERRERO, J. ROMO, and F. SÁNCHEZ-VIESCA. Tetrahedron, **19**, 25 (1963); and references therein.
20. C. DJERASSI, G. VON MUTZENBECHER, J. FAJKŐS, D. H. WILLIAMS and H. BUDZIKIEWICZ. J. Am. Chem. Soc. **87**, 817 (1965).
21. (*a*) W. KLYNE. Anales. Real. Soc. Espan. Fis. Quim. Madrid, Ser. B, **62**, 371 (1966).
   (*b*) A. R. VAN HORN and C. DJERASSI. J. Am. Chem. Soc. **89**, 651 (1967); and references cited.
22. [9] (*a*) E. C. KORNFELD. J. Am. Chem. Soc, **70**, 1373 (1948).
   (*b*) J. LEVINE, T. E. EBLE, and H. FISCHBACH. J. Am. Chem. Soc. **70**, 1930 (1948).
   (*c*) G. STORK, S. D. DARLING, I. T. HARRISON, and P. S. WHARTON. J. Am. Chem. Soc. **84**, 2018 (1962).
23. A. D. CROSS, E. DENOT, H. CARPIO, R. ACEVEDO, and P. CRABBÉ. Steroids, **5**, 557 (1965).
24. (*a*) A. J. BIRCH. Quart. Rev. London, **4**, 69 (1950); see also ref. 5*a*.
   (*b*) A. L. WILDS and N. A. NELSON. J. Am. Chem. Soc. **75**, 5366 (1963).
   (*c*) W. HÜCKEL, S. GUPTÉ, and M. WARTINI. Chem. Ber. **99**, 1388 (1966); and references cited.
   (*d*) H. SMITH. Organic reactions in liquid ammonia. *In* Chemistry in nonaqueous ionizing solvents. *Edited by* G. Jander. Vol. I. Part 2. Interscience Publ., New York. 1963.
25. A. HOREAU. Tetrahedron Letters, No. 15, 506 (1961); No. 21, 965 (1962); A. HOREAU and H. B. KAGAN. Tetrahedron, **20**, 2431 (1964); A. MARQUET and A. HOREAU. Bull. Soc. Chim. France, 124 (1967).
26. G. I. POOS, G. E. ARTH, R. E. BEYLER, and L. H. SARETT. J. Am. Chem. Soc. **75**, 422 (1953).
27. D. GREEN, J. P. TURNBULL, and J. H. FRIED. Intern. Congr. on Hormonal Steroids. 2nd Intern. Congr. Ser. No. 111, 124 Excerpta Med, (1966).
28. [9] (*a*) H. MITSUHASHI and T. NOMURA. Steroids, **3**, 271 (1964).
   (*b*) H. MITSUHASHI, T. NOMURA, and M. FUKUOKA. Steroids, **4**, 483 (1964).

[9]This reference should not be considered as representing *all* the pertinent literature.

Can. J. Chem. Downloaded from www.nrcresearchpress.com by 210.87.254.6 on 09/05/12
For personal use only.

(*c*) H. MITSUHASHI, T. SATO, T. NOMURA, and I. TAKEMORI. Chem. Pharm. Bull. Tokyo, **12**, 981, 1523 (1964).
(*d*) R. TSCHESCHE, G. BRUGMANN, and G. SNATZKE. Tetrahedron Letters, No. 9, 473 (1964).
(*e*) M. MITSUHASHI and T. NOMURA. Chem. Pharm. Bull. Tokyo, **13**, 274, 1332 (1965).
(*f*) H. MITSUHASHI, T. NOMURA, and M. FUKUOKA. Chem. Pharm. Bull. Tokyo, **14**, 726 (1966).
(*g*) H. MISUHASHI and M. FUKUOKA. Chem. Pharm. Bull. Tokyo, **14**, 809 (1966).
(*h*) U. EPPENBERGER, W. VETTER, and T. REICHSTEIN Helv. Chim. Acta, **49**, 1505 (1966).
(*i*) H. H. SAUER, E. WEISS, and T. REICHSTEIN. Helv. Chim. Acta, **49**, 1632 (1966).
(*j*) N. DANIELI, Y. MAZUR, and F. SONDHEIMER. Tetrahedron, **22**, 3189 (1966); and **23**, 715 (1967).
(*k*) T. TSCHESCHE, M. BAUMGARTH, and P. WELZEL. Tetrahedron, **23**, 249 (1967).
(*l*) T. TSCHESCHE and E. SCHWINUM. Chem. Ber. **100**, 464 (1967).
29. L. VELLUZ, M. LEGRAND, and M. GROSJEAN. Optical circular dichroism, principles, measurements, and applications. Verlag Chemie, Weinheim 1965. pp. 105–110.
30. (*a*) J. S. MILLS, H. J. RINGOLD, and C. DJERASSI. J. Am. Chem. Soc. **80**, 6118 (1958); and references therein.
(*b*) M. J. WEISS, R. E. SCHAUB, G. R. ALLEN, J. F. POLETTO, C. PIDACKS, R. B. CONROW, and C. J. COSCIA. Tetrahedron, **20**, 357 (1964).
31. K. BOWDEN, I. M. HEILBRON, E. R. H. JONES, and B. C. L. WEEDON. J. Chem. Soc. 39 (1946).
32. P. CRABBÉ and A. BOWERS. J. Org. Chem. **32**, 2921 (1967).
33. (*a*) A. BUTENANDT, A. WOLFF, and P. KARLSON. Chem. Ber. **74**, 1308 (1941).
(*b*) A. BUTENANDT, W. FRIEDRICH, and L. POSCHMANN. Chem. Ber. **75**, 1931 (1942).
(*c*) A. BUTENANDT and L. POSCHMANN. Chem. Ber. **77**, 392, 394 (1944).
(*d*) A. WOLFF. Angew. Chem. **52**, 514 (1939).
(*e*) H. WEHRLI and K. SCHAFFNER. Helv. Chim. Acta, **45**, 385 (1962).
34. (*a*) J. D. CHANLEY, T. MEZZETTI, and H. SOBOTKA. Tetrahedron, **22**, 1857 (1966).
(*b*) M. FÉTIZON and J. C. GRAMAIN. Bull. Soc. Chim. France, 1003 (1967).
35. (*a*) J. HEER and K. MIESCHER. Helv. Chim. Acta, **29**, 1895 (1946).
(*b*) H. GIBIAN, K. KIESLICH, H. J. KOCH, H. KOSMOL, C. RUFER, E. SCHRÖDER, and R. VÖSSING. Tetrahedron Letters, No. 21, 2321 (1966).
(*c*) H. KOSMOL, K. KIESLICH, R. VÖSSING, H. J. KOCH, K. PETZOLDT, and H. GIBIAN. Ann. Chem. **701**, 198, 206 (1967).
36. E. SANTOS, J. PADILLA, and P. CRABBÉ. Can. J. Chem. **45**, 2275 (1967).
37. (*a*) C. DJERASSI, R. RECORDS, E. BUNNENBERG, K. MISLOW, and A. MOSCOWITZ. J. Am. Chem. Soc. **84**, 870 (1962).
(*b*) L. VELLUZ, M. LEGRAND, and R. VIENNET. Compt. Rend. **261**, 1687 (1965).
38. J. P. L. BOTS. Rec. Trav. Chim. **77**, 1010 (1958).
39. L. J. CHINN. J. Org. Chem. **40**, 4165 (1965).
40. P. CRABBÉ and C. CASAS-CAMPILLO. J. Org. Chem. **29**, 2731 (1964).

Can. J. Chem. Downloaded from www.nrcresearchpress.com by 210.87.254.6 on 09/05/12
For personal use only.

Can. J. Chem. Downloaded from www.nrcresearchpress.com by 210.87.254.42 on 09/05/12
For personal use only.

Mass spectral studies of some desaurins and related 3,5-bismethylene-1,2,4-trithiolanes

PETER YATES AND THOMAS R. LYNCH[1]
Lash Miller Chemical Laboratories, University of Toronto, Toronto, Ontario

AND

L. S. WEILER
Department of Chemistry, Harvard University, Cambridge, Massachusetts

Received August 16, 1967

The mass spectra of three desaurins and four related 3,5-bismethylene-1,2,4-trithiolanes have been interpreted with the aid of metastable peak assignments and accurate mass measurements. Strong molecular ion peaks are observed in the case of the aryl desaurins but not in that of their trithiolane counterparts. A variety of fragmentation pathways are postulated for the molecular ions, including cleavage on either side of a carbonyl group and elimination of a molecule of acylthioketene. In the case of the desaurins the latter process results in the formation of acylthioketene molecular ions, which could be distinguished from the doubly charged desaurin molecular ions. In the case of two of the trithiolanes, it is proposed that the ions resulting from loss of acylthioketene from the molecular ions undergo a novel type of McLafferty rearrangement and loss of carbon suboxysulfide to give aryl mercaptan molecular ions.

Canadian Journal of Chemistry, 46, 365 (1968)

Introduction

The desaurins, heterocylic sulfur compounds of type **1**, have been known for eighty years (1), but their structures have been established only recently (2, 3). The structures of the analogous 3,5-bismethylene-1,2,4-trithiolane derivatives, **2**, have also been established recently (4, 5). We discuss here the mass spectra of the three desaurins, **1***a–c*, and the four related 3,5-bismethylene-1,2,4-trithiolanes, **2***a–d*.

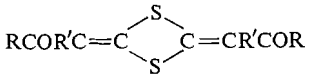

1*a*, R = C_6H_5, R′ = H
1*b*, R = C_6H_5, R′ = C_6H_5
1*c*, R = $(CH_3)_3C$, R′ = H

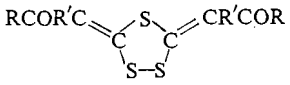

2*a*, R = C_6H_5, R′ = H
2*b*, R = *p*-$CH_3C_6H_4$, R′ = H
2*c*, R = C_6H_5, R′ = C_6H_5
2*d*, R = $(CH_3)_3C$, R′ = H

The desaurins can each exist as pairs of geometrical isomers; the samples used in the present study are considered to be single isomers, but the stereochemistry is known only in the case of **1***a*, where an x-ray structure determination has shown it to be *trans* (3). The 3,5-bismethylene-1,2,4-trithiolanes can exist in three stereoisomeric forms, two *cis* and one *trans*. In the case of **2***b*, two of the three stereoisomers have been isolated and examined, although their stereochemistry has not been established (5); they were found to give very similar mass spectra, perhaps resulting from formation of a common molecular ion. In the case of each of the other trithiolanes, a single stereoisomer was examined; again, the stereochemistry is undefined, although the nuclear magnetic resonance (n.m.r.) spectrum of **2***d* suggests that it is one of the two *cis* isomers (5).

[1]Holder of a NRCC Studentship, 1963–1966.

Experimental

The desaurins **1***a–c* and 3,5-bismethylene-1,2,4-trithiolanes **2***a–d* were prepared by known methods (1, 4); their characterization is described elsewhere (5). The solvents used for their recrystallization and their melting points are listed in Table I.

The mass spectra, which are shown in Figs. 1–3, were recorded with an Associated Electrical Industries model MS-9 double-focussing high resolution spectrometer with an ionization energy of 70 eV, an emission current of 94 μA, and a source temperature of 170–200°. Relative abundances are given as percentages of the strongest peak (the base peak) in each spectrum.

Discussion

Desaurins

In the case of each of the desaurins derived from aromatic ketones, *ie.*, compounds **1***a* and

TABLE I

Recrystallization solvents and melting points of desaurins and 3,5-bismethylene-1,2,4-trithiolanes

Compound	Melting point	Recrystallization solvent
1*a*	270–272.5° (decomp.)	Toluene
1*b*	300.5–302.5° (decomp.)	Nitrobenzene
1*c*	259.5–260°	Chloroform–Hexane
2*a*	235–237° (decomp.)	Toluene
2*b* (Isomer A)	251–252°	Toluene
(Isomer B)	213.5–214.5°	Benzene
2*c*	277–278° (decomp.)	Toluene
2*d*	211.5–212.5°	Chloroform–Hexane

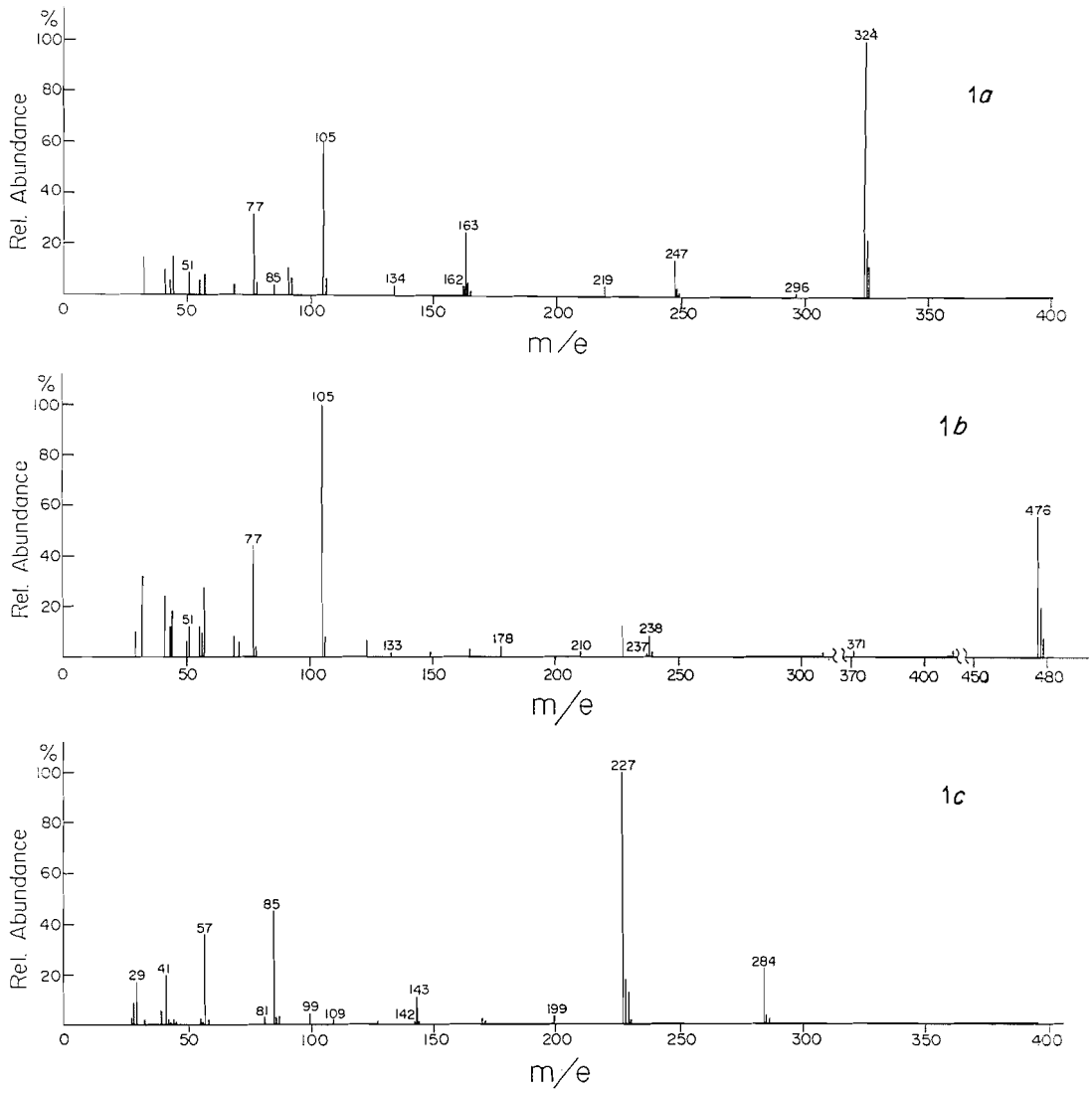

FIG. 1. The mass spectra of the desaurins **1***a–c*.

Can. J. Chem. Downloaded from www.nrcresearchpress.com by 210.87.254.42 on 09/05/12
For personal use only.

Can. J. Chem. Downloaded from www.nrcresearchpress.com by 210.87.254.42 on 09/05/12
For personal use only.

1*b*, the molecular ion peak is remarkably intense, constituting the base peak in the spectrum of **1***a* and corresponding to 56% of the base peak in the spectrum of **1***b*. These large relative abundances must reflect a considerable stability of the radical–ions derived from **1***a* and **1***b*. Not unexpectedly, the relative abundance of the molecular ion from **1***c* is only 22%; the reduced relative abundance can be attributed to poorer electron delocalization and/or the availability of more facile fragmentation pathways.

$[RCOR'C{=}C{=}S]\cdot^+$

3*a*, R = C_6H_5, R′ = H
3*b*, R = C_6H_5, R′ = C_6H_5
3*c*, R = $(CH_3)_3C$, R′ = H

The spectrum of each of the three desaurins exhibits a small peak (0.25–8.0%) at *m/e* M/2 which could be due to the dipositive molecular ion, or to the corresponding acyl thioketene molecular ion (**3***a–c*),[2] or to both of these ions. A means of distinguishing between these interpretations is provided by comparison of the ratios of the intensities of the M and M + 1 peaks and of the M/2 and (M + 1)/2 peaks. If these ratios are identical, then the peak at M/2 must be due solely to the dipositive molecular ion, if non-identical, the percentage contribution of the dipositive molecular ion to the peak at M/2 can be calculated (7). It was thus found that in the spectra of **1***a* and **1***b* the peaks at M/2 are due in part to the dipositive molecular ion (ca. 40% and 10%, respectively), while in the spectrum of **1***c* the dipositive molecular ion makes no contribution to the peak at M/2. In the spectrum of **1***b*, a metastable peak was observed at *m/e* 119.0 (calcd., 119.0) corresponding to the formation of the benzoylphenylthioketene molecular ion, **3***b*, from the molecular ion of **1***b*.

The major fragmentation path of the molecular ions of all three desaurins involves cleavage of a C—CO bond. The molecular ions of compounds **1***a* and **1***b* fragment by loss of the benzoyl ion (*m/e* 105), a type of fragment well known to be formed by electron impact upon aryl ketones (8) (see Schemes 1 and 3). A metastable peak corresponding to this process was observed in the spectrum of **1***b* only at *m/e* 23.2 (calcd., 23.2). The benzoyl ion decomposes by successive loss of carbon monoxide and acetylene, leading to the ions $[C_6H_5]^+$ (*m/e* 77) and $[C_4H_3]^+$ (*m/e* 51), respectively (8). Metastable peaks corresponding to these two fragmentation processes with *m/e* 56.5 (calcd., 56.5) and 33.8 (calcd., 33.8) are observed in the case of both **1***a* and **1***b*.

Another path in the decomposition of the molecular ion from **1***a* involves the alternative cleavage α to a carbonyl group, with loss of a phenyl radical and formation of an ion with *m/e* 247 of relative abundance 14%, which is considered to be **4**[3] (see Scheme 1). Loss of a molecule of carbon monoxide from **4** or of the benzoyl radical from the molecular ion leads to an ion with *m/e* 219 (4%), which is formulated as **5**. The view that **5** arises from both the molecular ion and the ion **4** is corroborated by the presence of metastable peaks with *m/e* 148.0 (calcd., 148.0) and *m/e* 194.0 (calcd., 194.2), respectively.

Metastable peaks with *m/e* 82.0 (calcd., 82.0) and *m/e* 107.7 (calcd., 107.6) in the spectrum of **1***a* indicate that an ion with *m/e* 163 of 25% relative abundance arises from both the molecular ion, and the ion **4**. A possible structure for this daughter ion is **6** (see Scheme 1), formed by loss of the benzoylthioketene radical, PhCOC≡C—S·, from the molecular ion, or of the species carbon suboxysulfide, C_3OS, from **4**. The transient existence of the latter species has recently been inferred from spectroscopic studies of electric discharges through carbonyl sulfide (9). An ion analogous to **6** is also observed in the spectrum of the desaurin **1***c*. The route for the formation of **6** could involve transfer of hydrogen via a six-membered transition state as in Scheme 2.

A peak at *m/e* 85 of relative abundance 4% in the spectrum of **1***a* may be due to the ion **7** (see Scheme 1). No metastable peak related to its formation was observed, but a possible precursor is the ion **4** which could lead to **7** by loss of benzoylthioketene. A peak attributable to the $[C_3HOS]^+$ ion, **7**, is observed in the spectrum of **1***c* where its formation from an ion analogous to **4** is indicated by an appropriate metastable peak; in the case of **1***c* the constitution of the ion has been confirmed by an accurate mass determination (*vide infra*). The spectra of the

[2]The preparation of bis(trifluoromethyl)thioketene by pyrolysis of 2,4-bis-(hexafluoroisopropylidene)-2,4-dithetane has recently been reported (6).

[3]In the case of this and related ions discussed subsequently, the structural assignment must be considered as tentative since the possibility of ring cleavage or rearrangement cannot be excluded.

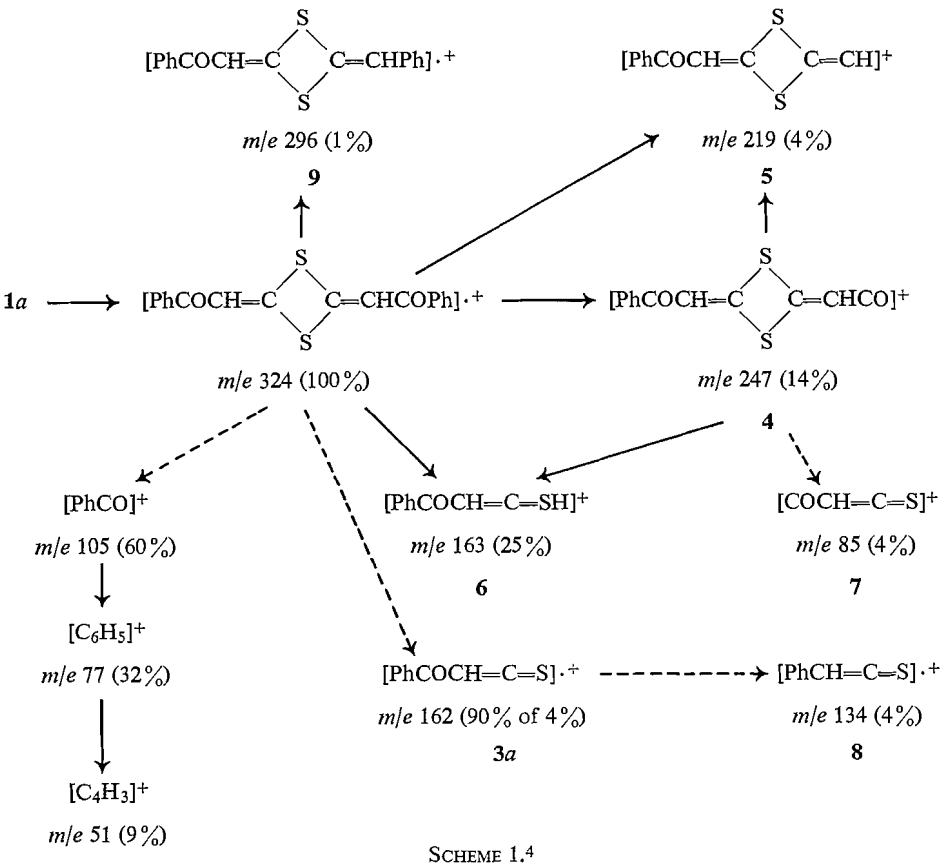

SCHEME 1.[4]

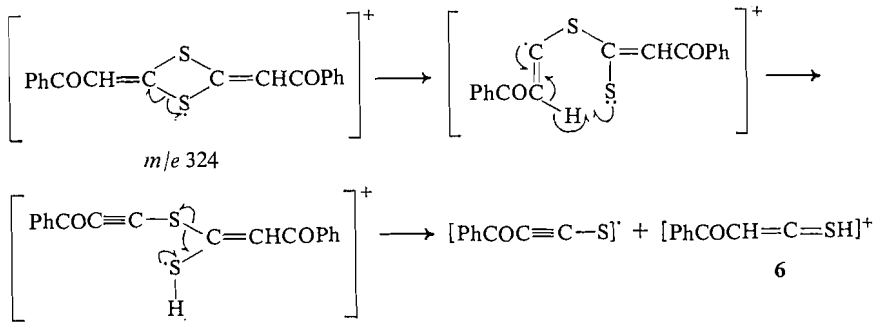

SCHEME 2.

trithiolanes **2***a*, **2***b*, and **2***d* also show peaks which appear to be due to the ion **7**.[5]

Loss of carbon monoxide from the benzoylthioketene molecular ion, **3***a*, to give the phenylthioketene molecular ion **8** accounts for the presence of a peak with *m/e* 134 of relative abundance 4%, although no corresponding metastable peak was observed. Loss of carbon monoxide from the molecular ion from **1***a* also accounts for the presence of a weak peak with *m/e* 296 (1%), due to an ion formulable as **9**.

[4]In this and similar Schemes, unbroken arrows indicate fragmentations for which metastable peaks were observed. Broken arrows indicate fragmentations for which no metastable peaks were observed, but which are analogous to processes whose occurrence in related cases is corroborated by the observation of metastable peaks.

[5]An analogous $[C_3HO_2]^+$ ion has recently been observed in the mass spectra of hydroxy- and methoxy-*p*-benzoquinones (10).

Can. J. Chem. Downloaded from www.nrcresearchpress.com by 210.87.254.42 on 09/05/12
For personal use only.

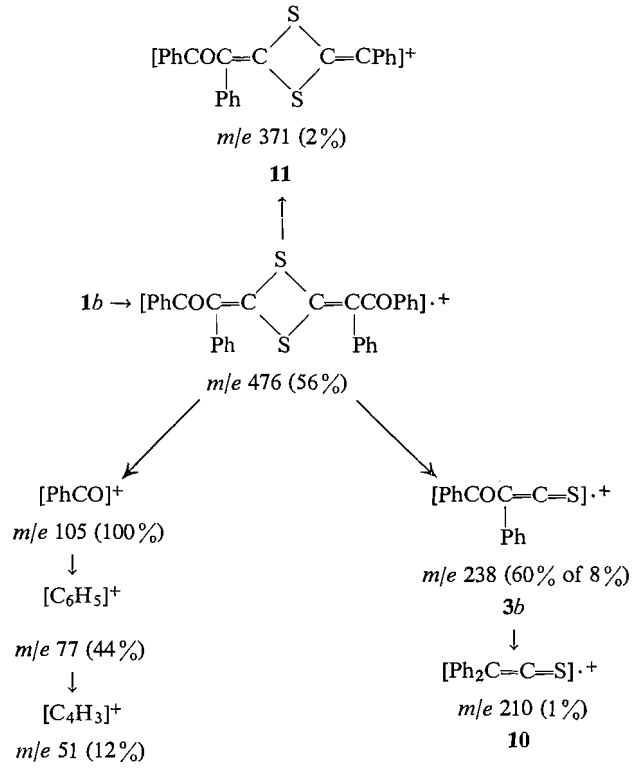

SCHEME 3.

A metastable peak at *m/e* 270.0 (calcd., 270.4) indicates this origin.

As mentioned previously, a significant fragmentation path for the molecular ion from **1***b*, in addition to the major one leading to the formation of the benzoyl ion, is that leading to the benzoylphenylthioketene molecular ion, **3***b*, whose relative abundance is 5% (60% of 8%) (see Scheme 3). A small peak at *m/e* 210 (1%), may correspond to structure **10** and arise from the ion **3***b* (Scheme 3), as indicated by a metastable peak at *m/e* 185.2 (calcd., 185.6).

A peak at *m/e* 371 of relative abundance 2% in the spectrum of **1***b* may arise by loss of the benzoyl radical from the molecular ion to give **11**, to which interpretation a metastable peak at *m/e* 289–290 (calcd., 289.2) lends support, as does analogy with the formation of **5** from the molecular ion of **1***a*. A trace of nitrobenzene, from which **1***b* was crystallized, is considered to give rise to a peak at *m/e* 123 (6%).

Proposed fragmentation paths in the case of the desaurin **1***c* are shown in Scheme 4, together with possible structures for the ions formed. The base peak in the spectrum of **1***c* is considered to arise from cleavage α to the carbonyl group with loss of the elements of a *t*-butyl radical to give an ion formulable as **12** (cf. the formation of **4** from **1***a*). A metastable peak at *m/e* 181 (calcd., 181.4) corroborates this view. The presence of a metastable peak at *m/e* 90.0 (calcd., 90.1) indicates that **12** decomposes to an ion with *m/e* 143 (11%); this is formulable as **13**. The formula $C_7H_{11}OS$ for **13** was confirmed by an accurate mass measurement. (Calcd. for $C_7H_{11}OS$: 143.0531. Found: 143.0527). The formation of **13** from **12** can be rationalized in terms of a route similar to that invoked for the formation of the ion **6** from the molecular ion of **1***a*, ie., by loss of carbon suboxysulfide and migration of hydrogen via a six-membered transition state (Scheme 2). In the case of **1***a*, metastable peaks indicated that **6**, the analogue of **13**, is formed both from **4**, the analogue of **12**, and also from the molecular ion of **1***a*. In the case of **1***c*, however, no metastable peak corresponding to the latter type of fragmentation was observed.

Decomposition of **13** via an ion with *m/e* 109 (2%) to one with *m/e* 81 (3%) is indicated by metastable peaks at *m/e* 83.1 (calcd., 83.1) and

Can. J. Chem. Downloaded from www.nrcresearchpress.com by 210.87.254.42 on 09/05/12
For personal use only.

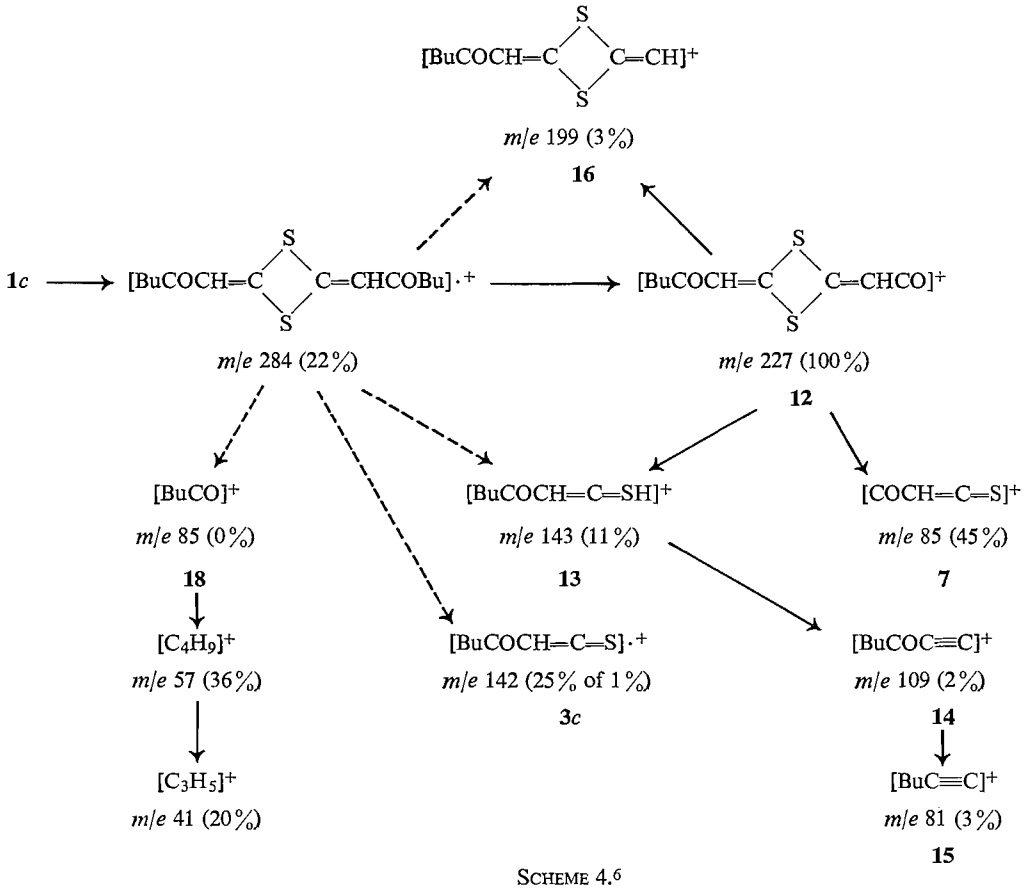

SCHEME 4.[6]

60.2 (calcd., 60.2). Possible structures for these daughter ions from **13** are **14** and **15**, respectively (Scheme 4).

Loss of carbon monoxide from **12** to give the ion **16** (*m/e* 199, 3%) accounts for the metastable peak at *m/e* 174–175 (calcd., 174.5) (cf. the formation of **5** from **4** in Scheme 1).

As discussed previously, the spectrum of **1***c* shows a peak at M/2 (*m/e* 142) which is not due to the doubly charged molecular ion. High resolution spectroscopy shows that this peak (1%) is a doublet. Accurate mass measurement of the minor component (25% of 1%) shows it to have the constitution $C_7H_{10}OS$ (calcd. for $C_7H_{10}OS$: 142.0452; found: 142.0460), and thus this peak most probably corresponds to the pivalylthioketene molecular ion **3***c*. Accurate mass measurement of the other component (75% of 1%) shows it to have the constitution $C_5H_2OS_2$. (Calcd. for $C_5H_2OS_2$: 141.9547. Found: 141.9547.) A possible structure for this ion is **17**.

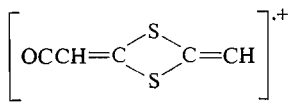

m/e 142 (75% of 1%)

17

The substantial peak at *m/e* 85 (45%) is shown by accurate mass measurement to be due to an ion C_3HOS (calcd. for C_3HOS: 84.97481; found: 84.97489); this is formulable as **7**, derived from **12** by loss of pivalylthioketen (see Scheme 4). A metastable peak at *m/e* 31.8 (calcd., 31.8) corroborates the occurrence of such a process. This ion is also observed in the spectra of **1***a* (*vide supra*) and the trithiolanes (with the exception of **2***c*, where the corresponding phenyl-substituted ion is observed).

The pivalyl cation, **18**, also has *m/e* 85, but

[6]Here, and subsequently, Bu = $(CH_3)_3C$.

Can. J. Chem. Downloaded from www.nrcresearchpress.com by 210.87.254.42 on 09/05/12
For personal use only.

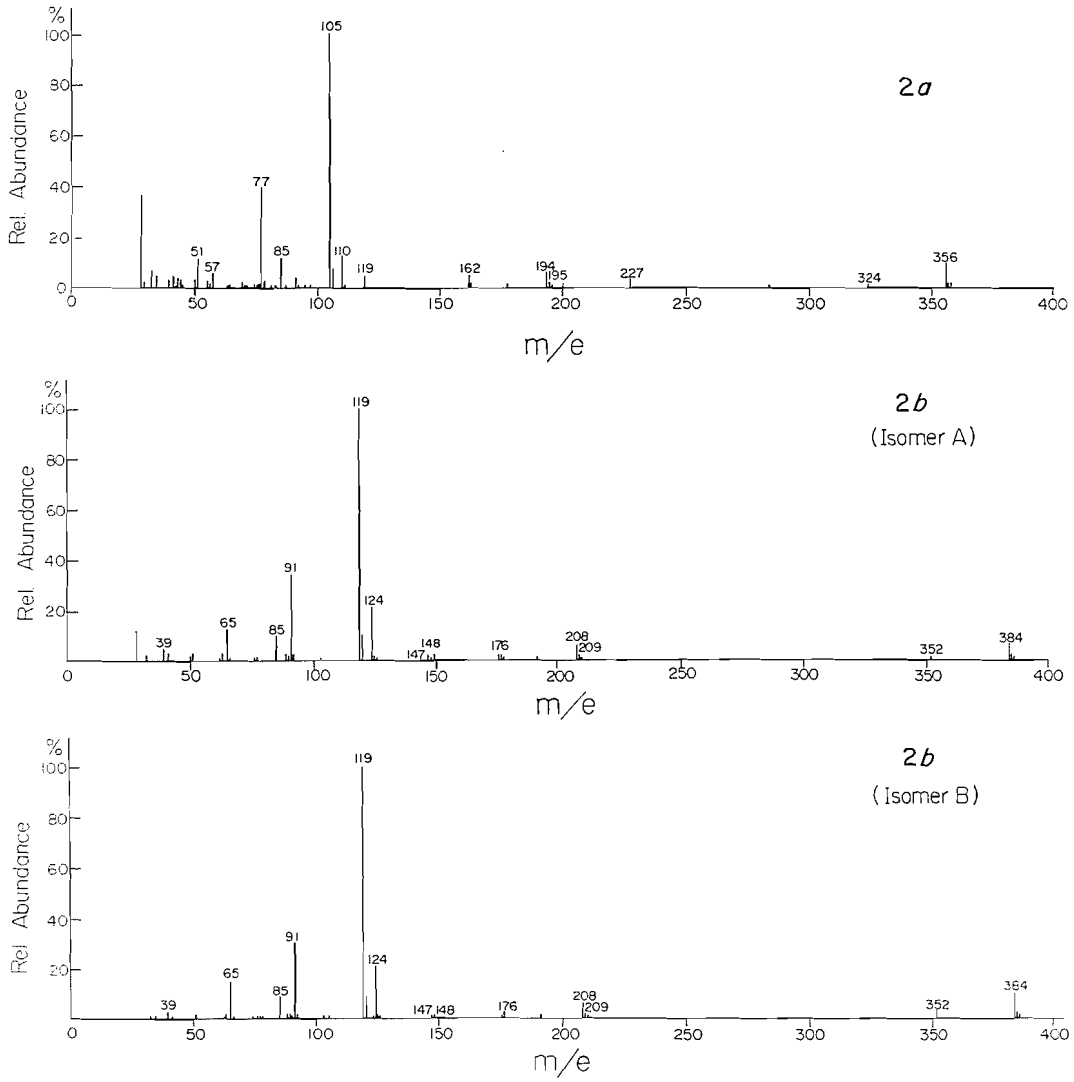

FIG. 2. The mass spectra of the trithiolanes **2***a* and **2***b* (Isomers A and B).

accurate mass measurement shows no peak corresponding to this ion. However, evidence for its formation and immediate decomposition exists. A metastable peak at *m/e* 38.2 (calcd., 38.2) indicates that **18** is formed and decomposes to an ion with *m/e* 57 (see Scheme 4). The ion with *m/e* 57 (36%) is probably the $[C_4H_9]^+$ ion, which may correspond to the methylated cyclopropane cation (*11*). Loss of methane from the $[C_4H_9]^+$ ion produces the $[C_3H_5]^+$ ion at *m/e* 41 (30%), as indicated by a metastable peak at *m/e* 29.5 (calcd., 29.5).

$[M—S]\cdot^+$ and $[M—2S]\cdot^+$ rearrangement ions have been observed recently in the mass spectra of certain sulfides and disulfides (*12*). No peaks corresponding to the rearrangement ions $[M—S]\cdot^+$ were observed in the spectra of the desaurins **1***a–c*, but a small peak (2%) corresponding to the ion $[M—2S]\cdot^+$ was observed in the spectrum of **1***b* although not in the spectra of **1***a* and **1***c*.

3,5-Bismethylene-1,2,4-trithiolanes

In the mass spectra of the trithiolanes **2***a–d*, the relative abundances of the molecular ions (6–29%) are considerably lower than in the

Can. J. Chem. Downloaded from www.nrcresearchpress.com by 210.87.254.42 on 09/05/12
For personal use only.

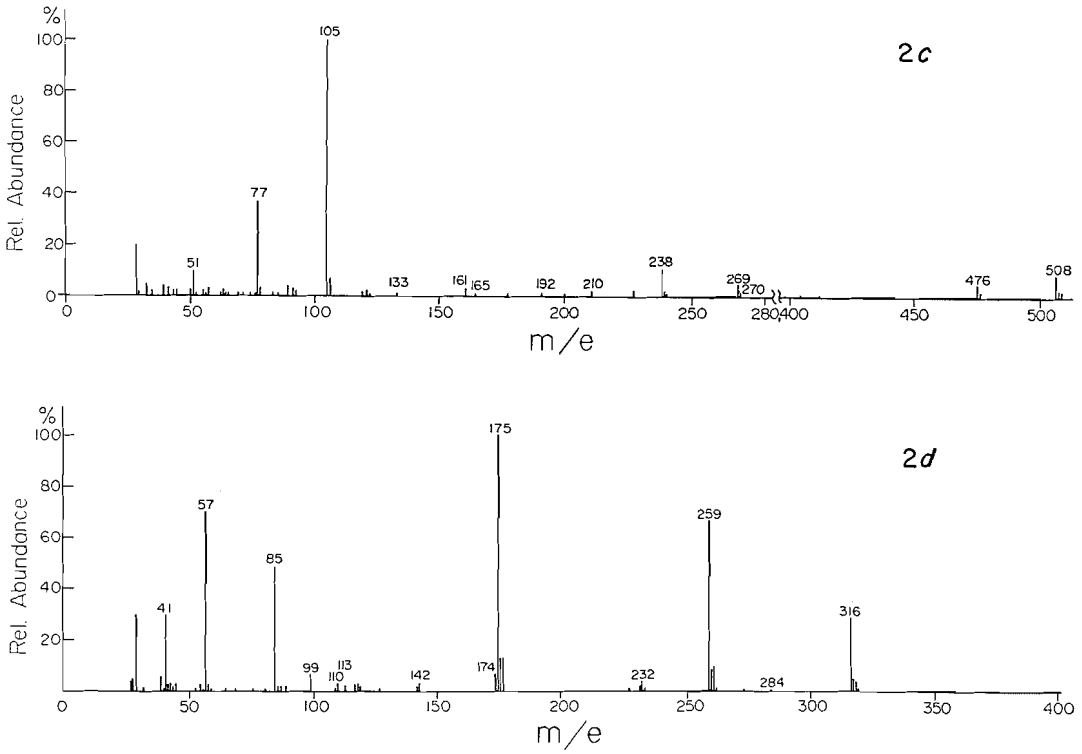

FIG. 3. The mass spectra of the trithiolanes **2***c* and **2***d*.

spectra of the corresponding desaurins (22–100%). Thus the stability of the radical ions of the trithiolanes must be lower and/or they must fragment more readily.

In Table II are shown ions formed upon electron impact on the trithiolanes. As in the case of the aryl desaurins, the formation of the base peak and the major decomposition pathway of the aryl trithiolanes involve cleavage α to the carbonyl group in the molecular ion with formation of $[ArCO]^+$ ions. The benzoyl ion fragments as previously described, while the *p*-toluyl ion (from **2***b*) decomposes by loss of carbon monoxide to give an ion with *m/e* 91 which is most probably the tropylium ion (13); a metastable peak corresponding to this fragmentation is observed at *m/e* 69.6 (calcd., 69.6). Stepwise loss of two molecules of acetylene from the tropylium ion accounts for peaks at *m/e* 65 and 39, and metastable peaks at *m/e* 46.4 (calcd., 46.4) and 23.4 (calcd., 23.4).

All the trithiolanes gave peaks with *m/e* corresponding to ions with the structure

$[RCOR'C{=}C\begin{smallmatrix}S\\S\end{smallmatrix}]^{\cdot+}$, eg., **19**, whose relative abundances vary from 2–7%; these ions probably arise by ejection of thioketene molecules from the molecular ions, but no metastable peaks indicating their origin were observed. In addition, all of the trithiolanes give peaks with *m/e* corresponding to ions with the structure

$[RCOR'C{=}C\begin{smallmatrix}S\\SH\end{smallmatrix}]^{+}$; the relative abundances of these are low in the case of the aryl trithiolanes (1–2%), but such an ion corresponds to the base peak in the case of **2***d* (*vide infra*).

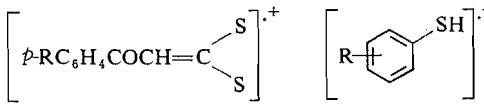

19, R = H [*m/e* 194 (6%)]
20, R = CH_3 [*m/e* 208 (6%)]

21, R = H [*m/e* 110 (13%)]
22, R = CH_3 [*m/e* 124 (21%)]

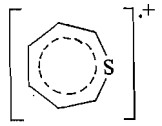

21*a*

Can. J. Chem. Downloaded from www.nrcresearchpress.com by 210.87.254.42 on 09/05/12
For personal use only.

TABLE II

Relative abundances of ions formed by electron impact upon the trithiolanes **2***a–d*

	Relative abundances			
	2*a*	**2***b* (Isomer A)	**2***c*	**2***d*
Ion	R,C_6H_5; R′,H	R,*p*-$CH_3C_6H_4$; R′,H	R,C_6H_5; R′,C_6H_5	R,$(CH_3)_3C$; R′,H
M	10	6	9	29
M—S	1	1	5	0.5
M—R	—	—	—	67
M—RCO	—	—	—	2
RCO	100	100	100	48
R	40	34	37	70
RCOR′C=C(S)S	6	6	2	7
RCOR′C=C(S)SH	2	2	1	90
RSH	13	21	—	—
RCOCHR′	5	—	—	7
RCOCR′=C=S	5	2	11	2
COCR′=C=S	12	10	3	48
R′C=C=S	6	—	1	—
RR′C=C=S	—	1	1	—
RC=C=S	—	2	1	2

Arising from the ion **19** in the spectrum of **2***a* is a significant ion with *m/e* 110 (13%) whose formula, C_6H_6S, was confirmed by an accurate mass measurement (calcd. for C_6H_6S: 110.0190; found: 110.0201), and whose origin from **19** is indicated by the presence of a metastable peak at 62.4 (calcd., 62.4). An analogous ion, C_7H_8S (calcd. for C_7H_8S: 124.0347; found: 124.0348), was observed in the spectrum of **2***b* (21%), and its formation from **20**, the analogue of **19**, was corroborated by a metastable peak at *m/e* 74.0 (calcd., 73.9). These two ions are considered to be the thiophenol and thiocresol molecular ions, **21** and **22**, respectively, formed by migration of the aryl group from carbon to sulfur. A rationale for the formation of the thiophenol ion is illustrated in Scheme 5. A similar scheme would account for the formation of the thiocresol molecular ion, **22**; such a scheme predicts the formation of the *m*-thiocresol ion.[7]

The formation of **21** and **22** entails the migration of an aryl group from carbon to sulfur, and is thus an example of a McLafferty rearrangement of a group other than hydrogen (15).

[7]These ions may possess seven-membered ring structures analogous to the tropylium ion, eg., **21***a* [cf. (14)].

A metastable peak at *m/e* 56.5 (calcd., 56.8) in the spectrum of **2***a* indicates that the ion **19** also decomposes to the benzoyl ion. In contrast, no metastable peak for the analogous fragmentation is observed in the spectrum of **2***b*.

The spectrum of **2***a* also exhibits a peak at *m/e* 119 (5%), which may be due to the phenacyl ion, $[PhCOCH_2]^+$ (*vide infra*). In addition, peaks which may be due to the ions **3***a* (5%) and **7** (12%), previously observed in the spectrum of the desaurin **1***a*, are observed in the spectrum of **2***a*. Metastable peaks for the formation of these ions were not observed, however. Ions analogous to **3***a* and **7** are observed in the spectra of all of the other trithiolanes.

The mass spectrum of the trithiolane **2***c* resembles the spectra of the trithiolanes **2***a* and **2***b* in that the same types of fragmentation pathways explain many of the peaks. Also a number of ions are common to the spectra of **2***c* and the related desuarin, **1***b*. Apart from the benzoyl and related ions formed by cleavage α to the carbonyl group in the molecular ion, loss of benzoylphenylthioketene leads to the ion **23**, *m/e* 270 (2%), the analogue of the ion **19**. A metastable peak at *m/e* 268.0 (calcd., 268.0) indicates that **23** loses a hydrogen atom to give an ion, *m/e* 269

Can. J. Chem. Downloaded from www.nrcresearchpress.com by 210.87.254.42 on 09/05/12
For personal use only.

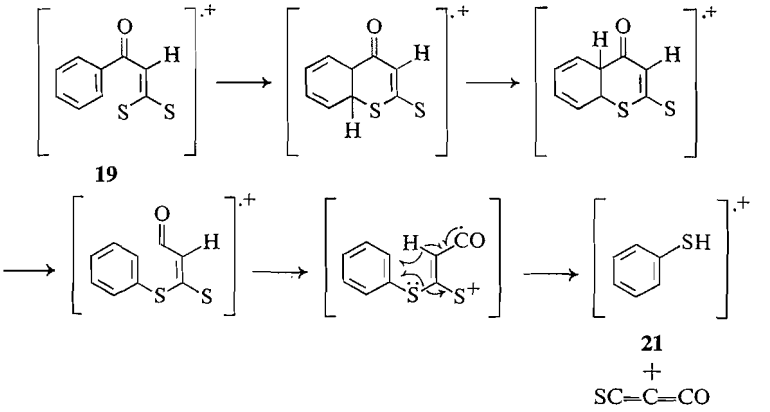

19 **21** + $SC{=}C{=}CO$

SCHEME 5.

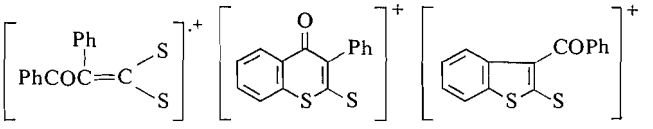

m/e 270 (2%) *m/e* 269 (5%)

23 **24***a* **24***b*

(5%), for which possible structures are **24***a* and **24***b*. A route for the formation of **24***a* is illustrated in Scheme 6. The similarity between this route and that suggested for the first steps in the formation of **21** from **19** (Scheme 5) is apparent. An ion at *m/e* 238 (11%) probably corresponds to **3***b*, previously observed in the spectrum of the desaurin **1***b*.

The fragmentation of the trithiolane **2***d* can be interpreted largely in terms of the processes previously observed in the spectra of the corresponding desaurin, **1***c*, and of the other trithiolanes. The formation of an ion with *m/e* 259 (67%) can be rationalized in terms of cleavage α to a carbonyl group of the molecular ion, with loss of the elements of a *t*-butyl radical, to give the ion **25**. A metastable peak at *m/e* 212.2 (calcd., 212.3) corroborates this view. Two further metastable peaks at *m/e* 118.2 (calcd., 118.2) and 206 (calcd., 206.0) indicate that **25** is the parent of ions which are formulable as **26** (*m/e* 175) and **27** (*m/e* 231, 2%) (see Scheme 7). Under high resolution, the peak at *m/e* 175 (100%) is found to be a doublet, of which the major component (90%) has the formula $C_7H_{11}OS_2$, as shown by accurate mass measurement (calcd. for $C_7H_{11}OS_2$: 175.0251; found: 175.0258) and with which structure **26** is in accord. As mentioned previously, ions formulable as analogues of **26** are observed in the

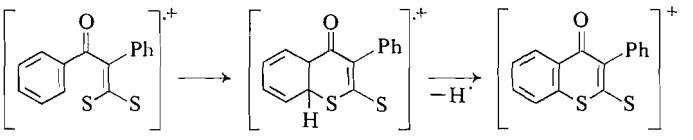

23 **24***a*

SCHEME 6.

Can. J. Chem. Downloaded from www.nrcresearchpress.com by 210.87.254.42 on 09/05/12
For personal use only.

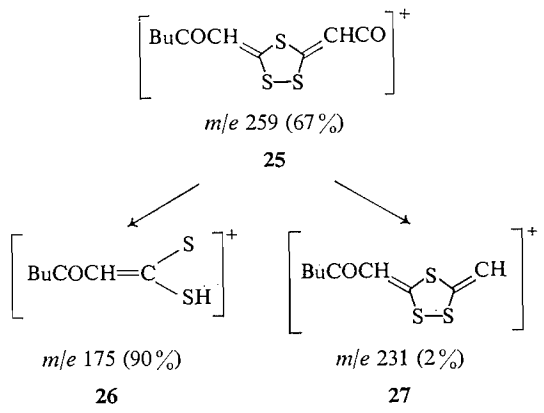

SCHEME 7.

spectra of all the trithiolanes examined, but only in the case of **26**, where it is in fact the base peak, is this ion of high abundance. Metastable peaks at *m/e* 56.2 (calcd., 56.0) and 69.1 (calcd., 69.1) indicate that **26** decomposes by two pathways to ions of *m/e* 110 (3%) and 99 (7%), for which possible structures are **28** and **29** (Scheme 8). The latter is analogous to the ion $(C_6H_5COCH_2]^+$ suggested to be formed from **2***a*.

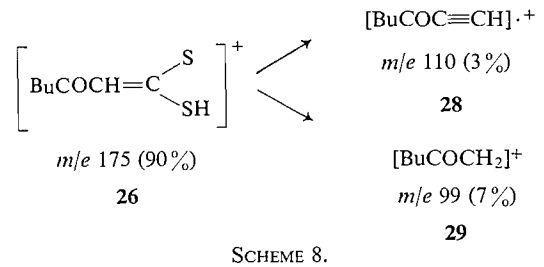

SCHEME 8.

The minor component (10%) of the doublet at *m/e* 175 has the formula $C_5H_3OS_3$ as shown by accurate mass measurement (calcd. for $C_5H_3OS_3$: 174.9346; found: 174.920); a reasonable path for the formation of this ion proceeds from the molecular ion via an ion with *m/e* 232, formulable as **30**, to **31**. That **30** arises from the molecular ion is indicated by a metastable peak at *m/e* 170.3 (calcd., 170.3).

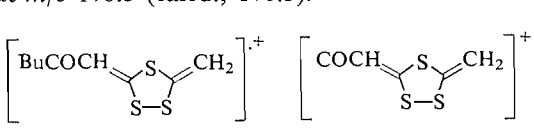

High resolution shows the peak at *m/e* 85 (48%) to be a doublet, 20% of which is probably due to the pivalyl ion, **18** (calcd. for C_5H_9O: 85.0653; found: 85.0651); a metastable peak at *m/e* 23.0 (calcd., 22.9) indicates that this may be formed from the molecular ion. The second component (80% of 48%) of the doublet may be due to the ion **7** (calcd. for C_3HOS: 84.9748; found: 84.9745).

The spectra of all of the trithiolanes show the formation of $[M—S]\cdot^+$ ions of relative abundances 0.5–5%. None had peaks corresponding to $[M—2S]\cdot^+$ ions. Finally, the spectra of **2***a* and **2***b* exhibited ions at half molecular weight (1%) which were shown to be doubly charged molecular ions by use of the isotope method previously described.

Acknowledgment

We thank the National Research Council of Canada for generous support of this work.

1. H. BERGREEN. Ber. **21**, 337 (1888). V. MEYER. Ber. **21**, 353 (1888); **23**, 1571 (1890). V. MEYER and H. WEGE. Ber. **24**, 3535 (1891). W. WACHTER. Ber. **25**, 1727 (1892). P. PETRENKO-KRITSCHENKO. Ber. **25**, 2239 (1892). C. KELBER. Ber. **43**, 1252 (1910). C. KELBER and A. SCHWARZ. Ber. **45**, 137 (1912).
2. P. YATES and D. R. MOORE. J. Am. Chem. Soc. **80**, 5577 (1958).
3. T. R. LYNCH, I. P. MELLOR, S. C. NYBURG, and P. YATES. Tetrahedron Letters, 373 (1967).
4. R. GOMPPER and W. TÖPFL. Ber. **95**, 2861 (1962).
5. T. R. LYNCH. Ph.D. Thesis, University of Toronto, Toronto, Ontario. 1967. P. YATES and T. R. LYNCH. To be published.
6. M. S. RAASCH. Chem. Commun. 577 (1966).
7. K. BIEMANN. Mass spectrometry. McGraw-Hill Book Co., Inc., New York. 1962. p. 158.
8. S. MEYERSON and P. N. RYLANDER. J. Am. Chem. Soc. **79**, 1058 (1957).
9. J. AKRICHE, L. HERMAN, and R. HERMAN. J. Quant. Spectry. Radiative Transfer, **4**, 863 (1964); Chem. Abstr. **62**, 12614a (1965).
10. J. H. BOWIE, D. W. CAMERON, R. G. F. GILES, and D. H. WILLIAMS. J. Chem. Soc. (B), 335 (1966).
11. H. M. GRUBB and S. MEYERSON. *In* Mass spectrometry of organic ions. *Edited by* F. W. McLafferty. Academic Press, Inc., New York. 1963. p. 517.
12. J. Ø. MADSEN, C. NOLDE, S.-O. LAWESSON, G. SCHROLL, J. H. BOWIE, and D. H. WILLIAMS. Tetrahedron Letters, 4377 (1965). R. G. GILLIS and J. L. OCCOLOWITZ. Tetrahedron Letters, 1997 (1966).
13. P. N. RYLANDER, S. MEYERSON, and H. M. GRUBB. J. Am. Chem. Soc. **79**, 842 (1957).
14. D. J. EARNSHAW, G. L. COOK, and G. U. DINEEN. J. Phys. Chem. **68**, 296 (1964),
15. B. R. WEBSTER. Chem. Commun. 124 (1966).

Can. J. Chem. Downloaded from www.nrcresearchpress.com by 210.87.254.42 on 09/05/12
For personal use only.

Can. J. Chem. Downloaded from www.nrcresearchpress.com by 210.87.254.40 on 09/05/12
For personal use only.

Conversion of (−)-α-santonin into (+)-α-cyperone

EDWARD PIERS AND KIN FAI CHENG
Department of Chemistry, University of British Columbia, Vancouver 8, British Columbia

Received September 11, 1967

An efficient, 8-step synthesis of (+)-α-cyperone (**1**) from (−)-α-santonin (**5**) is described. The key steps of the sequence involve the conversion of the keto ester **8** into the substituted octalone **9**, by hydrogenation of the former in the presence of the homogeneous catalyst tris(triphenylphosphine)-chlororhodium, and the pyrolysis of the keto carbonate **16**, which produces (+)-α-cyperone in good yield.

Canadian Journal of Chemistry, **46**, 377 (1968)

In connection with another problem in our laboratory (1), we required a relatively large quantity of the naturally occurring sesquiterpene (+)-α-cyperone (**1**). In addition, we were interested in preparing certain cross-conjugated cyclohexadienone systems of type **2** (R = CH_3-CHCOOH, CH_3CHCOOCH$_3$, CH_3CHCH$_2$OH, etc.).

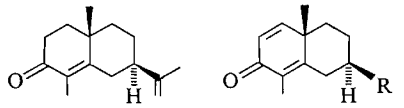

1

2

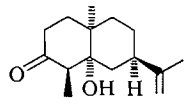

3

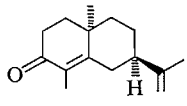

4

(+)-α-Cyperone (**1**) had been previously synthesized (2) by condensation of (+)-dihydrocarvone with 1-diethylamino-3-pentanone methiodide in the presence of sodium amide (Robinson annelation) (see ref. 3). However, from a preparative point of view, this method suffered from a low yield, since the major product of the reaction was the ketol **3**, accompanied by its dehydration product (−)-7-epi-α-cyperone (**4**). At best, only about 15–20% of the mixture of reaction products was (+)-α-cyperone (**1**). In addition, although the ketol **3** could be obtained relatively easily by direct crystallization of the distilled reaction product followed by column chromatography of the material from the mother liquors, it was very difficult to effect separation of the remaining epimeric products (**1** and **4**) in such a way as to maximize the quantity of (+)-α-cyperone (**1**) obtained. Thus, the isolated yield of **1** reported by Howe and McQuillin (2) was approximately only 4%. We have, therefore, considered alternative methods for the preparation of (+)-α-cyperone (**1**) and report in this paper its synthesis from the well-known and readily available sesquiterpene, (−)-α-santonin (**5**).

Conversion of (−)-α-santonin (**5**), of known absolute stereochemistry (4, 5), into the epimeric (−)-6-epi-α-santonin (**6**) was readily accomplished by a procedure similar to that described by Ishikawa (6). Treatment of compound **6** with zinc dust in glacial acetic acid – methanol (7) caused reductive cleavage of the *cis*-fused lactone ring and afforded a very good yield of the carboxylic acid **7**. Although the latter, which was isolated as a viscous yellow oil, was not purified further, the spectral properties of the crude material were in complete agreement with structure **7**. Of particular pertinence were the ultraviolet spectrum (λ_{max} 242 mμ) and the nuclear magnetic resonance (n.m.r.) spectrum, which exhibited a typical AB quartet for the protons at C-1 and C-2: τ 3.32 (doublet, —C^1H) and τ 3.79 (doublet, —C^2H, $J_{1,2}$ = 10 Hz). In addition, there appeared three 3-proton signals at τ 8.14 (singlet, —$C^{14}H_3$), τ 8.78 (doublet, —$C^{13}H_3$, $J_{11,13}$ = 7 Hz), and τ 8.82 (singlet, —$C^{15}H_3$). The acid was further characterized as its crystalline cyclohexylamine salt, m.p. 122–124°.

The crude carboxylic acid (**7**), upon treatment with excess ethereal diazomethane, was converted into the corresponding methyl ester (**8**). The latter was purified by distillation under reduced pressure (b.p. 164–167° at 0.25 mm) and exhibited the expected spectral characteristics.

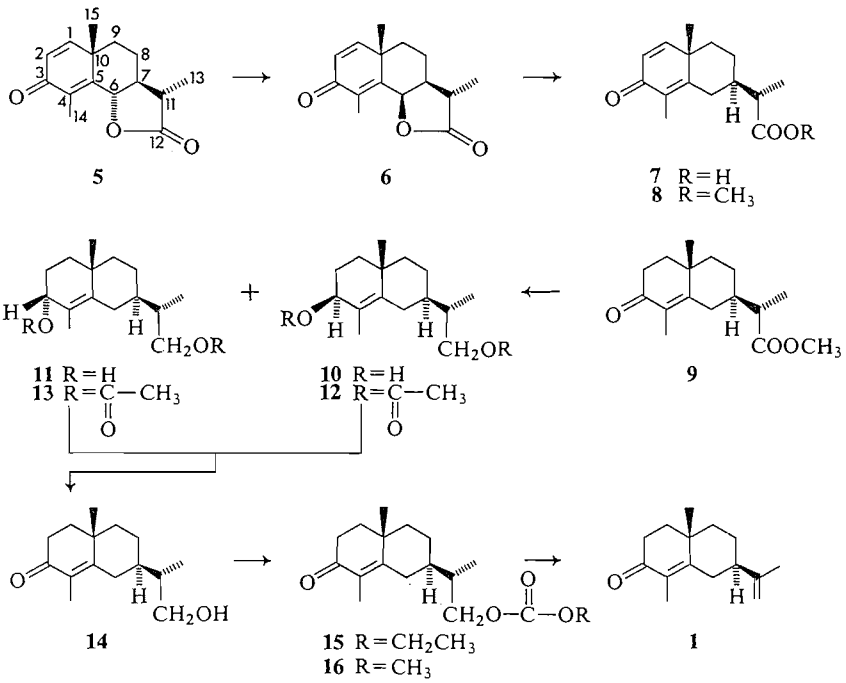

Of note was the appearance, in the n.m.r. spectrum, of a strong singlet at τ 6.32, due to the $-COOCH_3$ grouping.

At this point in the synthetic sequence, the selective removal of the C^1–C^2 olefinic double bond of keto ester **8** was desired. In this connection, it is pertinent to point out that the catalytic hydrogenation of (−)-α-santonin (**5**) and its derivatives has been studied in some detail (8). From the results of this work, it appeared unlikely that the use of usual heterogeneous catalytic hydrogenation would effect complete selective removal of the C^1–C^2 double bond in the presence of the C^4–C^5 double bond. Therefore, an alternative method was sought and it seemed probable that the use of the novel homogeneous hydrogenation catalyst tris(triphenylphosphine)chlororhodium (9–11) would prove fruitful. Indeed, two different groups (10, 11) have recently reported that hydrogenation of a number of $\Delta^{1,4}$-3-keto steroids in the presence of this catalyst resulted, in each case, in a highly selective reduction of the C^1–C^2 double bond.

Hydrogenation, at room temperature and atmospheric pressure, of a benzene solution of keto ester **8** and tris(triphenylphosphine)chlororhodium, gave an excellent yield (96%) of the desired substituted octalone **9**, b.p. 150° at 0.1 mm, $[\alpha]_D^{23}$ +115°. The ultraviolet spectrum of this material showed the expected absorption maximum (248 mμ), while the n.m.r. spectrum, which showed no peaks due to olefinic protons, exhibited pertinent signals at τ 6.34 (singlet, $-COOCH_3$), τ 8.27 (doublet, $-C^{14}H_3$, $J = 1$ Hz, splitting probably due to homoallyic coupling with the 6β-proton (12*a*)), τ 8.80 (singlet, $-C^{15}H_3$), and τ 8.81 (doublet,— $C^{13}H_3$, $J_{11,13} = 7$ Hz). The excellent success of this hydrogenation again emphasizes the potential use, in synthetic organic chemistry, of tris-(triphenylphosphine)chlororhodium as a homogeneous hydrogenation catalyst, particularly for selective hydrogenation of relatively non-hindered olefinic double bonds in the presence of those which are more hindered.

It is relevant to point out that the keto ester **9** had been previously prepared (13) by direct lithium – liquid ammonia reduction of (−)-α-santonin (**5**), followed by treatment of the crude product with diazomethane. However, this method, in addition to being experimentally laborious to carry out on a large scale, gave, in our hands, a mixture of compounds which proved difficult to separate into its individual components.

Reduction of the keto ester **9** with lithium aluminium hydride in ether afforded a high yield (97%) of a crystalline material. Examina-

Can. J. Chem. Downloaded from www.nrcresearchpress.com by 210.87.254.40 on 09/05/12
For personal use only.

Can. J. Chem. Downloaded from www.nrcresearchpress.com by 210.87.254.40 on 09/05/12
For personal use only.

tion of the latter by thin-layer chromatography indicated that it was a mixture of two different compounds. Indeed, it was subsequently shown (see below) that this material was an epimeric (at C-3) mixture (approximately 4:1) of two different diols,[1] the major component (**10**) having a 3β(pseudoequatorial) hydroxyl group and the minor component (**11**) having a 3α-(pseudoaxial) hydroxyl group.

Careful column chromatography of the crystalline material on activity II alumina effected separation of the two components. The diol which was eluted first (**10**) showed m.p. 127.5–129° and $[\alpha]_D^{25}$ +13°, while the more polar diol (**11**) exhibited m.p. 115–116° and $[\alpha]_D^{25}$ +105°. The spectral data for each compound fully corroborated the respective structural proposals. However, since the configurational assignments at C-3 were based entirely upon the n.m.r. spectra, these will be discussed in some detail.

The n.m.r. spectrum of the 3β-alcohol (**10**) exhibited the C-3 proton as a distorted, unsymmetrical triplet (overlapped pair of doublets), with the center peak at τ 6.01, the low-field peak at τ 5.95, and the high-field peak at τ 6.08. The total half-height width of the signal was 15 Hz. The unsymmetrical nature of this triplet will be commented upon later. It is also interesting to note that the methylene protons at C-12 of compound **10** appeared as a septet (AB part of an ABX system) centered at τ 6.46 (see Experimental for details). However, the magnetic nonequivalence of methylene protons immediately adjacent to an asymmetric center is a common phenomenon (14*a*), and this therefore deserves no further comment. Other pertinent signals appeared at τ 8.31 (singlet, $-C^{14}H_3$), τ 8.95 (singlet, $-C^{15}H_3$), and τ 9.06 (doublet, $-C^{13}H_3$).

In the n.m.r. spectrum of the 3α-alcohol (**11**), the C-3 proton was present as a broad, unresolved peak centered at τ 6.12, with a width at half-height of approximately 7 Hz. Other assignable signals were similar in chemical shift and multiplicity to the corresponding resonances of the 3β-alcohol (**10**).

On a first-order basis, the C-2 and C-3 protons of each of the diols **10** and **11** would be assigned as an $A(-C^2H_a)B(-C^2H_e)^2X(-C^3H)$ system. The coupling of X in an ABX system gives the sum of the two couplings, $J_{AX} + J_{BX}$. For the 3β-alcohol (**10**), the sum $J_{2a,3a} + J_{2e,3a}$ should be approximately 12–15 Hz, while for the 3α-alcohol (**11**), the sum $J_{2a,3e} + J_{2e,3e}$ should be approximately 5–8 Hz (12*b*). As noted above, the total half-height width of the $-C^3H$ resonance of compound **10** was found to be 15 Hz, which is clearly in good agreement with a compound having a 3β-configuration of the hydroxyl group. Further, the width at half-height of the $-C^3H$ signal for the diol **11** was, as noted above, approximately 7 Hz, indicating clearly that this compound has the hydroxyl group at C-3 in the α-configuration. The fact that the "three" lines of the $-C^3H$ resonance of the 3β-alcohol (**10**) were not symmetrical may reflect the fact that the system is not merely an ABX system, but is rather an $ABXC(-C^1H_a)$-$D(-C^1H_e)$ system. However, this does not invalidate the above *qualitative* argument.

Each of the diols **10** and **11** was converted, by treatment with acetic anhydride in pyridine, into the corresponding diacetate (**12** and **13**, respectively). The n.m.r. spectra of these compounds completely corroborated the above structural assignments. In the spectrum of diacetate **12**, the C-3 proton again appeared as an unsymmetrical triplet, with individual peaks at τ 4.70, τ 4.76, and τ 4.83 and a half-height width of 15 Hz. Further, an octet centered at τ 6.02 could be assigned to the methylene protons at C-12. Thus, acetylation of the hydroxyl groups produced the expected (14*b*) paramagnetic shifts of the $-C^3H$ and $-C^{12}H_2$ resonances, since, relative to the corresponding signals in the diol **10**, the $-C^3H$ resonance was moved downfield by 1.25 p.p.m. and the $-C^{12}H_2$ resonance was moved down-field by 0.44 p.p.m. Similarly, the n.m.r. spectrum of the diacetate **13** exhibited a broad signal at τ 4.90 ($-C^3H$, width at half-height = 7.5 Hz) and an octet centered at τ 6.00 ($-C^{12}H_2$).

Oxidation of the crystalline mixture of diols **10** and **11** (see above) with 2,3-dichloro-5,6-dicyanobenzoquinone (15) in dry dioxane gave an 81% yield (based on unrecovered starting material) of the keto alcohol **14**, m.p. 70.5–71°,[3] $[\alpha]_D^{25}$ +97°. In order to effect only oxidation of the allylic alcohol at C-3, it was important to

[1]This material had been prepared previously (ref. 13), although no physical data was reported and no comment was made regarding homogeneity.

[2]*a* = axial (or pseudoaxial), *e* = equatorial (or pseudoequatorial).

[3]This material was previously reported as an oil (ref. 13).

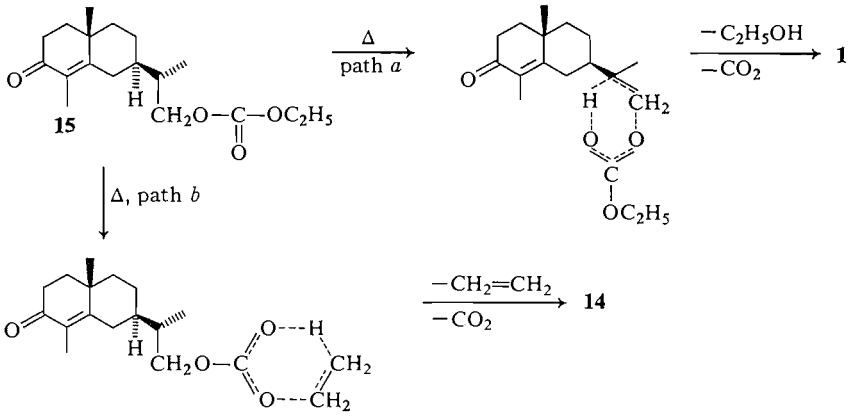

choose proper reaction conditions. Thus, if the reaction was allowed to proceed until all of the starting material had reacted, a significant amount of oxidation of the primary alcohol group to the corresponding aldehyde occurred. Therefore, conditions were adopted which gave only the keto alcohol **14**, along with starting materials **10** and **11**. The desired product **14** was readily obtained by column chromatography of the mixture, and the recovered diols (**10** and **11**) were then subjected to a second oxidation reaction.

Treatment of compound **14** with freshly distilled ethyl chloroformate in dry pyridine gave, in 75% yield, the corresponding keto carbonate **15**, b.p. 166° at 0.25 mm. Pyrolysis of the latter by passage through a heated (400°) helix-packed pyrex glass tube effected elimination of ethanol and carbon dioxide (see path *a* below) (ref 16) and gave, after column chromatography of the resulting pyrolysate, (+)-α-cyperone (**1**) in 61% yield. The latter was identical (infrared, n.m.r., optical rotation, gas–liquid chromatographic retention times) with an authentic sample of the sesquiterpene. Also obtained from this reaction was the keto alcohol **14** (32% yield), obviously formed by elimination, during pyrolysis, of ethylene and carbon dioxide, as shown below (path *b*).

In order to avoid this undesirable formation of compound **14** during pyrolysis, the keto alcohol **14** was converted into the corresponding methyl carbonate **16** (m.p. 51.5–52°), by treatment of the former with methyl chloroformate in dry pyridine. Pyrolysis of compound **16** under conditions identical with those used for **15** gave, as expected, only one product, the desired (+)-α-cyperone (**1**), in 84% yield.

The above described synthesis of (+)-α-cyperone (**1**) has several advantages over the previously reported (2) preparation of this compound. Although the former was somewhat lengthy (eight steps), the overall yield of the desired sesquiterpene, based on (−)-α-santonin (**5**), was approximately 20%. Additionally, each of the steps was readily adaptable to relatively large scale, and the preparation of moderately large amounts of pure (+)-α-cyperone was, therefore, easily accomplished.

Experimental

Melting points, which were determined on a Kofler block, and boiling points are uncorrected. Activity II alumina refers to Shawinigan reagent, deactivated with 10% aqueous acetic acid (3 ml per 100 g of alumina). Ultraviolet spectra were measured in methanol solution on a Cary spectrophotometer, model 14, and infrared spectra were recorded on Perkin–Elmer Infracord model 137 and Perkin–Elmer model 21 spectrophotometers. Nuclear magnetic resonance (n.m.r.) spectra were taken in deuterochloroform solution on either a JEOLCO C-60-H spectrometer or a Varian Associates model HA-100 spectrometer. Line positions are given in the Tiers τ scale, with tetramethylsilane as an internal standard; the multiplicity, integrated peak areas, and proton assignments are indicated in parentheses. Mass spectra were recorded on an AEI, type MS-9, mass spectrometer. Gas–liquid chromatography was carried out on an Aerograph Autoprep, model 700. Microanalyses were performed by Mr. P. Borda, Microanalytical Laboratory, University of British Columbia, Vancouver.

(−)-Epi-α-santonin (6)

This compound was prepared by a procedure similar to that described by Ishikawa (6). (−)-α-Santonin (100 g) was dissolved in 1 l of anhydrous dimethylformamide containing 5% anhydrous hydrogen chloride. The resulting solution was heated to 85–90° for 3.5 h, and then allowed to stand at room temperature overnight. The solution was diluted with 750 ml of water, and then extracted thoroughly with chloroform. The combined extracts were washed thrice with saturated brine, once

Can. J. Chem. Downloaded from www.nrcresearchpress.com by 210.87.254.40 on 09/05/12
For personal use only.

Can. J. Chem. Downloaded from www.nrcresearchpress.com by 210.87.254.40 on 09/05/12
For personal use only.

with saturated sodium bicarbonate solution, once with water, and then evaporated under reduced pressure. Removal of the dimethylformamide remaining in the residual material was effected by distillation under reduced pressure at 50°, and the viscous red oil thus obtained was purified by column chromatography on 750 g of activity II alumina. Elution with 3 l of benzene gave a crystalline solid which, upon recrystallization from ethyl acetate, afforded 63 g (63%) of light-yellow blocks. Recrystallization of a small amount of this material gave an analytical sample of (−)-6-epi-α-santonin, m.p., 103–104°, $[\alpha]_D^{23}$ −308° (*c*, 0.9 in methanol); lit. m.p. 102–105°, $[\alpha]_D^{10}$ −311° (*c*, 1.5 in ethanol) (7). Ultraviolet, λ_{max} 246 mμ (ε = 14 100); infrared (Nujol), λ_{max} 5.68, 6.04, 6.19, 6.25 μ; n.m.r., τ 3.26 (doublet, 1H, —C^1H), 3.80 (doublet, 1H, —C^2H, $J_{1,2}$ = 10 Hz), 4.46 (doublet, 1H, —C^6H, $J_{6,7}$ = 4.5 Hz), 7.45 (quartet, 1H, —C^{11}H, $J_{11,13}$ = 8 Hz), 7.96 (singlet, 3H, —$C^{14}H_3$), 8.62 (doublet, 3H, —$C^{13}H_3$, $J_{11,13}$ = 8 Hz), 8.72 (singlet, 3H, —$C^{15}H_3$).

Preparation of Keto Acid 7

This compound was prepared by a procedure similar to that used by Nakazaki and Naemura (7) for the hydrogenolysis of (−)-6-epi-β-santonin. To a solution of (−)-6-epi-α-santonin (**6**) (21 g) in 500 ml of methanol was added 25 ml of glacial acetic acid and 50 g of zinc dust. The resulting mixture was refluxed gently for 15 min under an atmosphere of nitrogen, cooled, and filtered. The filtrate was evaporated under reduced pressure to a volume of approximately 250 ml. Addition of ether (100 ml) caused the formation of a white precipitate, which was removed by filtration. The filtrate was made basic by addition of saturated sodium bicarbonate solution and extracted thoroughly with ether. The aqueous layer was acidified with 2 *N* hydrochloric acid and the resulting mixture was extracted thrice with ether. After the combined ether extracts had been washed with water and dried over anhydrous sodium sulfate, the ether was removed under reduced pressure, giving 18 g (85%) of a viscous yellow oil. This crude keto acid (7) was not purified further, but exhibited the following expected spectral properties: ultraviolet, λ_{max} 240 mμ; infrared (film), λ_{max} 2.95–3.95 (very broad), 5.85, 6.05, 6.24 μ; n.m.r., τ 3.32 (doublet, 1H, —C^1H), 3.79 (doublet, 1H, —C^2H, $J_{1,2}$ = 10 Hz), 8.14 (singlet, 3H, —$C^{14}H_3$), 8.78 (doublet, 3H, —$C^{13}H_3$, $J_{11,13}$ = 9 Hz), 8.82 (singlet, 3H, —$C^{15}H_3$).

A 0.5 g sample of the keto acid **7** was dissolved in ether and treated with an equivalent amount of cyclohexylamine. The precipitated salt was collected by filtration and recrystallized twice from acetone, giving 0.55 g of colorless crystals, m.p. 122–124°; ultraviolet, λ_{max} 241 (ε = 9800).

Anal. Calcd. for $C_{21}H_{33}O_3N$: C, 72.62; H, 9.51; N, 4.04. Found: C, 72.48; H, 9.72; N, 4.15.

Preparation of Keto Ester 8

The crude keto acid **7** (50 g), obtained as described above, was esterified by treatment with excess ethereal diazomethane at 0°. The crude material was purified by distillation under reduced pressure, affording 40 g (76%) of keto ester **8** as a clear, pale-yellow oil, b.p. 164–167° at 0.25 mm, n_D^{20} 1.5252, $[\alpha]_D^{23}$ −99° (*c*, 0.8 in methanol). Ultraviolet, λ_{max} 240 mμ (ε = 10 900); infrared (film), λ_{max} 5.84, 6.08, 6.18, 6.26 μ; n.m.r., τ 3.32 (doublet, 1H, —C^1H), 3.82 (doublet, 1H, —C^2H, $J_{1,2}$ = 10 Hz), 6.32 (singlet, 3H, —$COOCH_3$), 8.12 (singlet, 3H, —$C^{14}H_3$), 8.78 (doublet, 3H, —$C^{13}H_3$, $J_{11,13}$ = 7 Hz), 8.79 (singlet, 3H, —$C^{15}H_3$).

Anal. Calcd. for $C_{16}H_{22}O_3$ (mol. wt., 262): C, 73.25; H, 8.45. Found (mol. wt., 262, mass spectrometry): C, 73.21; H, 8.55.

Preparation of Keto Ester 9

To a solution of compound **8** (12 g) in 200 ml of dry benzene was added a solution of 2.4 g of tris(triphenylphosphine)chlororhodium (9–11) in 250 ml of dry benzene. The resulting solution was subjected to hydrogenation at room temperature and atmospheric pressure. After one equivalent of hydrogen had been absorbed (approximately 9 h) the rate of hydrogenation decreased markedly. The solution was filtered through a column of 450 g of activity II alumina, and the column was washed with 2 l of ether. Evaporation of the combined filtrate and washings afforded a reddish-brown oil which, upon distillation under reduced pressure, gave 11.6 g (96%) of keto ester **9** as a clear, colorless oil, b.p. 150° at 0.1 mm, n_D^{20} 1.5138, $[\alpha]_D^{23}$ +115° (*c*, 0.2 in methanol), lit. b.p. 135–140° (bath temperature) at 0.1 mm, $[\alpha]_D$ +90° (*c*, 1.04 in $CHCl_3$) (13). Ultraviolet, λ_{max} 248 (ε = 14 400); infrared (film), λ_{max} 5.84, 6.07, 6.24 μ; n.m.r., τ 6.34 (singlet, 3H, —$COOCH_3$), 8.27 (doublet, 3H, —$C^{14}H_3$, *J* = 1 Hz), 8.80 (singlet, 3H, —$C^{15}H_3$), 8.81 (doublet, 3H, —$C^{13}H_3$, $J_{11,13}$ = 7 Hz).

Anal. Calcd. for $C_{16}H_{24}O_3$ (mol. wt., 264): C, 72.69; H, 9.15. Found (mol. wt., 264, mass spectrometry): C, 72.80; H, 8.82.

Lithium Aluminium Hydride Reduction of Keto Ester 9

To a stirred mixture of lithium aluminium hydride (7.0 g) in 700 ml of anhydrous ether was added slowly a solution of keto ester **9** (11.0 g) in 300 ml of anhydrous ether. The resulting mixture was refluxed under an atmosphere of dry nitrogen for 4 h, and then cooled to 0°. After the excess lithium aluminium hydride had been destroyed by dropwise addition of 50 ml of acetone, ice-cold water (300 ml) was added and the resulting mixture was stirred for 30 min and then filtered. The inorganic salts were washed thoroughly with ether. The organic and aqueous layers of the filtrate were separated, and the aqueous layer was extracted twice with ether. After the combined ether layer and washings had been dried (anhydrous sodium sulfate), the solvent was removed under reduced pressure, giving 9.6 g (97%) of a white crystalline solid. Examination of this material by thin-layer chromatography (Woelm neutral alumina plates, developed with 2:1 ethyl acetate – chloroform) indicated that it was a mixture of two compounds.

A 1.0 g sample of the crystalline material was subjected to column chromatography on activity II alumina (50 g). Elution with 300 ml of benzene, 150 ml of 1:1 benzene–chloroform and 150 ml of chloroform gave 680 mg of the diol **10**. Recrystallization from methanol–ether gave material with m.p. 127.5–129°, $[\alpha]_D^{25}$ +13° (*c*, 0.8 in methanol); infrared (KBr), λ_{max} 3.08, 6.12 μ; n.m.r., τ 5.90–6.12 (unsymmetrical triplet with peaks at 5.95, 6.01, and 6.08, 1H, —C^3H, total width a half-height = 15 Hz), 6.27–6.70 (septet, 2H, —$C^{12}H_AH_B$ with H_A at τ 6.43 and H_B at τ 6.56, $J_{A,B}$ = 10.5 Hz, $J_{A,11}$ = 6.4 Hz, $J_{B,11}$ = 7.1 Hz), 8.31 (broad singlet, 3H, —$C^{14}H_3$), 8.95 (singlet, 3H, —$C^{15}H_3$), 9.08 (doublet, 3H, —$C^{13}H_3$, $J_{11,13}$ = 6.5 Hz).

Can. J. Chem. Downloaded from www.nrcresearchpress.com by 210.87.254.40 on 09/05/12
For personal use only.

Anal. Calcd. for $C_{15}H_{26}O_2$ (mol. wt., 238): C, 75.58; H, 10.99. Found (mol. wt., 238, mass spectrometry): C, 75.52; H, 10.85.

Further elution in the above chromatography with 150 ml of chloroform and 200 ml of ethyl acetate gave 160 mg of diol **11** as a white solid. Recrystallization from methanol–ether afforded colorless needles, m.p. 115–116°, $[\alpha]_D^{25}$ +105° (*c*, 0.2 in methanol); infrared, λ_{max} 3.11, 6.10 μ; n.m.r., τ 6.12 (broad signal, 1H, —C^3H, width at half-height = 7 Hz), 6.24–6.63 (septet, 2H, —$C^{12}H_AH_B$ with H_A at τ 6.37 and H_B at τ 6.48, $J_{A,B}$ = 10.8 Hz, $J_{A,11}$ = 5.9 Hz, $J_{B,11}$ = 6.5 Hz), 8.26 (broad singlet, 3H, —$C^{14}H_3$), 9.02 (singlet, 3H, —$C^{15}H_3$), 9.08 (doublet, 3H, —$C^{13}H_3$, $J_{11,13}$ = 6.5 Hz).

Anal. Calcd. for $C_{15}H_{26}O_2$ (mol. wt., 238): C, 75.58; H, 10.99. Found (mol. wt., 238, mass spectrometry): C, 75.37; H, 11.06.

Preparation of Diacetate ***12***

A solution of diol **10** (300 mg) and freshly distilled acetic anhydride (0.5 ml) in 2 ml of dry pyridine was allowed to stand at 0° for 15 h. Water (10 ml) was added and the resulting mixture extracted thoroughly with chloroform. The combined extracts were washed twice with 2 *N* hydrochloric acid, thrice with water, and dried over anhydrous magnesium sulfate. Removal of the solvent gave a yellow oil which was purified by chromatography on 15 g of activity II alumina. Elution with 50 ml of 1:1 petroleum ether (b.p. 30–60°) – benzene afforded 360 mg of diacetate **12** as a pale-yellow oil, n_D^{25} 1.4946; infrared (film), λ_{max} 5.81, 8.08, 9.90 μ; n.m.r., τ 4.65–4.87 (unsymmetrical triplet with peaks at 4.70, 4.76, and 4.83, 1H, —C^3H, total width at half-height = 15 Hz), 5.84–6.20 (octet, 2H, —$C^{12}H_AH_B$ with H_A at τ 5.94 and H_B at τ 6.05, $J_{A,B}$ = 11.0 Hz, $J_{A,11}$ = 6.0 Hz, $J_{B,11}$ = 6.3 Hz), 7.96 and 7.97 (two singlets, 6H, two —$COCH_3$), 8.43 (singlet, 3H, —$C^{14}H_3$), 8.92 (singlet, 3H, —$C^{15}H_3$), 9.06 (doublet, 3H, —$C^{13}H_3$, $J_{11,13}$ = 7.0 Hz).

Anal. Calcd. for $C_{19}H_{30}O_4$: C, 70.80; H, 9.38. Found: C, 71.00; H, 9.51.

Preparation of Diacetate ***13***

The diol **11** was converted into the corresponding diacetate **13** by a procedure identical with that described above. From 120 mg of **11** there was obtained 127 mg of **13**, as a clear oil, n_D^{25} 1.4918; infrared (film), λ_{max} 5.82, 8.06, 9.71, 9.90 μ; n.m.r., τ 4.90 (broad signal, 1H, —C^3H, width at half-height 7.5 Hz), 5.82–6.17 (octet, 2H, —$C^{12}H_AH_B$ with H_A at τ 5.93 and H_B at τ 6.02, $J_{A,B}$ = 11 Hz, $J_{A,11}$ = 5.8 Hz, $J_{B,11}$ = 6.9 Hz), 7.96 (singlet, 6H, two —$COCH_3$), 8.40 (singlet, 3H, —$C^{14}H_3$), 9.01 (singlet, 3H, —$C^{15}H_3$), 9.06 (doublet, 3H, —$C^{13}H_3$, $J_{11,13}$ = 7 Hz).

Anal. Calcd. for $C_{19}H_{30}O_4$: C, 70.80; H, 9.38. Found: C, 70.62; H, 9.12.

Preparation of Keto Alcohol ***14***

To a solution of 8.8 g of the mixture of diols **10** and **11** (see above) in 1 l of dry dioxane was added 10 g of 2,3-dichloro-5,6-dicyanobenzoquinone (15) in 500 ml of dry dioxane. The resulting solution was stirred at room temperature for 4 h, and filtered. The filtrate was diluted with 1 l of ether and then passed through a column of 200 g of activity II alumina. The column was washed with 2 l of ether and 1 l of chloroform, and the total eluant was evaporated under reduced pressure. The residual orange gummy material was subjected to column chromatography on activity II alumina (550 g). Elution with 3 l of benzene gave 4.6 g of keto alcohol **14** as an oily, semicrystalline material. Crystallization of a small sample from ether at 0° gave colorless plates, m.p. 70.5–71°, $[\alpha]_D^{20}$ +97° (*c*, 0.26 in methanol). Ultraviolet, λ_{max} 249 mμ (ε = 13 600); infrared (Nujol), λ_{max} 3.00, 6.09, 6.27, 9.78 μ; n.m.r., τ 6.28–6.62 (octet, 2H, —$C^{12}H_AH_B$ with H_A at τ 6.41 and H_B at τ 6.49, $J_{A,B}$ = 10.3 Hz, $J_{A,11}$ = $J_{B,11}$ = 6.0 Hz), 7.32 (broad singlet, 1H, —OH), 8.26 (broad singlet, 3H, —$C^{14}H_3$), 8.83 (singlet, 3H, —$C^{15}H_3$), 9.06 (doublet, 3H, —$C^{13}H_3$, $J_{11,13}$ = 6.5 Hz).

Anal. Calcd. for $C_{15}H_{24}O_2$ (mol. wt., 236): C, 76.20; H, 10.23. Found (mol. wt., 236, mass spectrometry): C, 76.19; H, 10.03.

Continued elution in the above chromatography with 1.5 l of 1:1 benzene–chloroform and 1 l of chloroform gave 2.5 g of diol **10**, as shown by m.p., and by its infrared spectrum. Finally, elution with 2 l of chloroform and 1 l of ethyl acetate afforded 0.6 g of diol **12**, again identified by m.p. and infrared spectrum. Thus, in the above oxidation, the yield of keto alcohol **14**, based on unrecovered starting material, was 81%.

Preparation of Keto Carbonate ***15***

A solution of the keto alcohol **14** (13.9 g) in 310 ml of dry pyridine was cooled to 0°, and freshly distilled ethyl chloroformate (134 ml) was added dropwise, over a period of 3 h. The reactants were allowed to stand at room temperature, under an atmosphere of nitrogen, for 20 h, during which time a white precipitate had formed. The reaction mixture was poured into cold (0°) 50% aqueous acetic acid (600 ml) and the resulting mixture was extracted thoroughly with ether. The combined ether extracts were washed several times with water and evaporated. The residue was dissolved in benzene and the resulting solution was dried over anhydrous sodium sulfate. Removal of the benzene gave a clear oil which, upon distillation under reduced pressure, afforded 13.4 g (75%) of the keto carbonate **15** as a clear, pale-yellow liquid, b.p. 166° at 0.25 mm, n_D^{20} 1.5078, $[\alpha]_D^{23}$ + 75° (*c*, 0.25 in methanol). Ultraviolet, λ_{max} 249 mμ (ε = 13 600); infrared (film), λ_{max} 5.81, 6.06, 6.25, 8.01, 9.98 μ; n.m.r., τ 5.73–6.12 (complex pattern of lines, 4H, —$C^{12}H_AH_B$ and —OCH_2CH_3), 8.31 (broad singlet, 3H, —$C^{14}H_3$), 8.76 (triplet, 3H, —OCH_2CH_3, *J* = 7.1 Hz), 8.86 (singlet, 3H, —$C^{15}H_3$), 9.03 (doublet, 3H, —$C^{13}H_3$, $J_{11,13}$ = 6.7 Hz).

Anal. Calcd. for $C_{18}H_{28}O_4$: C, 70.10; H, 9.15. Found: C, 69.87; H, 8.98.

Preparation of Keto Carbonate ***16***

This compound was prepared by reaction of keto alcohol **14** with methyl chloroformate, using a procedure identical with that described above. The crude product obtained from 8.5 g of keto alcohol **14** was purified by distillation under reduced pressure and gave 8.5 g (81%) of a pale-yellow oil (b.p. 154° at 0.03 mm) which crystallized on standing. Recrystallization of a small sample from ether–petroleum ether (b.p. 30–60°) gave colorless blocks, m.p. 51.5–52°, $[\alpha]_D^{23}$ +98° (*c*, 0.8 in methanol)

Can. J. Chem. Downloaded from www.nrcresearchpress.com by 210.87.254.40 on 09/05/12
For personal use only.

Ultraviolet, λ_{max} 249 mμ (ε = 13 700); infrared (Nujol), λ_{max} 5.78, 6.05, 6.26, 7.92 μ; n.m.r., τ 5.75–6.09 (octet, 2H, $-C^{12}H_AH_B$ with H_A at τ 5.84 and H_B at τ 5.90, $J_{A,B}$ = 10.5 Hz, $J_{A,11}$ = 6.3 Hz, $J_{B,11}$ = 6.0 Hz), 6.28 (singlet, 3H, $-OCH_3$), 8.28 (broad singlet, 3H, $-C^{14}H_3$), 8.82 (singlet, 3H, $-C^{15}H_3$), 9.01 (doublet, 3H, $-C^{13}H_3$, $J_{11,13}$ = 7.0 Hz).

Anal. Calcd. for $C_{17}H_{26}O_4$: C, 69.36; H, 8.90. Found: C, 69.52: H, 8.68.

(+)-α-Cyperone (1)

(a) By Pyrolysis of Keto Carbonate 15

Compound **15** (2.80 g) was introduced dropwise onto a vertical pyrex glass column (1.5 cm × 40 cm) packed with glass helices and heated to approximately 400° by a vertical furnace. During the pyrolysis, nitrogen was passed slowly through the column from the top to the bottom, and the pyrolysate was collected in a receiving tube cooled in an ice-water bath. The contact time of pyrolysis was approximately 2 min. When the ester had been subjected to this procedure, the product still contained some starting material and it was therefore necessary to pass the first pyrolysate through the heated column a second time. The crude product (2.10 g) thus obtained was subjected to column chromatography on 150 g of activity II alumina. Elution with 400 ml of petroleum ether (b.p. 30–60°), 1200 ml of 1:1 petroleum ether – benzene, 800 ml of benzene, and 60 ml of 1:1 benzene–chloroform gave 1.2 g (61%) of (+)-α-cyperone (**1**), which was identical (infrared, n.m.r., optical rotation, gas–liquid chromatographic retention time on two different columns[4]) with an authentic sample.

Further elution with 1 l of chloroform gave 0.7 g (32%) of the keto alcohol **14**, identified by m.p., mixture m.p., and infrared comparison with compound **14** prepared previously.

(b) By Pyrolysis of Keto Carbonate 16

Compound **16** was subjected to pyrolysis under conditions identical with those described above. The crude pyrolysate obtained from 7.4 g of **16** gave, upon distillation under reduced pressure, 4.6 g (84%) of pure (+)-α-cyperone, b.p. 101° at 0.04 mm.

[4]The following gas–liquid chromatography columns (10 ft × ¼ in.) were used: 20% FFAP on 60/80 mesh Chromosorb W, 208°; 20% SE30 on 60/80 mesh Chromosorb W, 190°. The flow-rate in each case was approximately 80 ml/min.

Acknowledgments

We thank the National Research Council of Canada and the University of British Columbia Committee on Research for financial support, and the Canadian Commonwealth Scholarship and Fellowship Committee for a scholarship (to K.F.C.). We are grateful to Dr. Sukh Dev for a generous sample of natural (+)-α-cyperone.

1. E. Piers and K. F. Cheng. Can. J. Chem. **45**, 1591 (1967).
2. R. Howe and F. J. McQuillin. J. Chem. Soc. 2423 (1955).
3. E. D. Bergmann, D. Ginsberg, and R. Pappo. Organic reactions. Vol. 10. John Wiley & Sons, Inc., New York. 1959. p. 179.
4. W. Cocker and T. B. H. McMurry. Tetrahedron, **8**, 181 (1961).
5. D. H. R. Barton, J. E. D. Levisalles, and J. T. Pinhey. J. Chem. Soc. 3472 (1962).
6. H. Ishikawa. Yakugaku Zasshi, **76**, 504 (1956).
7. M. Nakazaki and K. Naemura. Bull. Chem. Soc. Japan, **37**, 1842 (1964).
8. W. Cocker, H. Gobinsingh, T. B. H. McMurry, and M. A. Nisbet. J. Chem. Soc. 1432 (1962), and references therein.
9. F. H. Jardine and G. Wilkinson. J. Chem. Soc. (C), 270 (1967), and references therein.
10. A. J. Birch and K. A. M. Walker. Tetrahedron Letters, 1935 (1967), and references therein.
11. C. Djerassi and J. Gutzwiller. J. Am. Chem. Soc. **88**, 4537 (1966).
12. N. S. Bhacca and D. H. Williams. Applications of nuclear magnetic resonance spectroscopy in organic chemistry. Holden-Day, Inc., San Francisco. 1964. (*a*) p. 110. (*b*) pp. 49–52.
13. H. Bruderer, D. Arigoni, and O. Jeger. Helv. Chim. Acta, **39**, 858 (1956).
14. L. M. Jackman. Applications of nuclear magnetic resonance spectroscopy in organic chemistry. The Pergamon Press, Ltd. Oxford. 1959. (*a*) pp. 99–103. (*b*) p. 55.
15. D. Walker and J. D. Hiebert. Chem. Rev. **67**, 153 (1967).
16. E. L. Eliel, N. L. Allinger, S. J. Angyal, and G. A. Morrison. Conformational analysis. Interscience Publishers, New York. 1965. p. 102.

Can. J. Chem. Downloaded from www.nrcresearchpress.com by 210.87.254.5 on 09/05/12
For personal use only.

Reinvestigation of the Polonovski reaction. Synthesis of deuterated dimethylamine and formaldehyde[1]

R. N. Renaud and L. C. Leitch
Division of Pure Chemistry, National Research Council of Canada, Ottawa, Canada

Received September 18, 1967

Dimethylaminomethyl acetate, a postulated intermediate in the Polonovski reaction, has been isolated for the first time in 80% yield from the reaction between trimethylamine *N*-oxide and one equivalent of acetic anhydride. With more acetic anhydride the dimethylaminomethyl ester gave *N,N*-dimethyl acetamide and two other products which have been identified as 2-(dimethylaminomethyl)acrylic acid and 2,2-bis(acetoxymethyl)-3-(dimethylamino)propionic acid. The manner of formation of these two products has been clarified by using deuterium and ^{13}C labelled reagents.

Hydrolysis of deuterated dimethylaminomethyl acetate prepared from trimethyl-d_9 amine *N*-oxide and acetic anhydride gave satisfactory yields of dimethyl-d_6 amine and formaldehyde-d_2.

L'acétate de diméthylaminométhyle, considéré comme produit intermédiaire de la réaction de Polonovski, a été isolé avec un rendement de 80% par l'action de l'anhydride acétique sur l'oxyde de triméthylamine. Lorsque l'anhydride acétique est employé en excès, on obtient, en plus de la diméthyl-*N,N* acétamide, l'acide diméthylaminométhyl-2 acrylique et l'acide diacétoxyméthyl-2,2 diméthylamino-3 propionique. Le processus de formation de ces acides a été étudié à partir de réactifs marqués au deutérium ou au ^{13}C.

La dideutérioformaldéhyde et la hexadeutériodiméthylamine ont donc été préparées avec un bon rendement par l'hydrolyze de l'acétate de diméthylaminométhyl deutérié correspondant.

Canadian Journal of Chemistry, 46, 385 (1968)

Introduction

Deuterated trimethylamine can now be conveniently prepared in good yield by the equilibration of tetramethylammonium hydroxide with deuterium oxide at 130° and subsequent pyrolysis of the exchanged quaternary base (1). It seemed of interest to try to utilize such a readily accessible compound in the preparation of other deuterated substances which are now difficult to obtain. The Polonovski reaction which is the conversion of amine oxides with at least one methyl group into an *N*-substituted amide and formaldehyde might be successfully exploited for this purpose. For example, Huisgen, Bayerlein, and Heydkamp (2), prepared *N,N*-dimethylacetamide from trimethylamine *N*-oxide and acetic anhydride in 82% yield by the Polonovski reaction. However, formaldehyde could only be isolated in 3% yield. It was mainly to obtain increased yields of formaldehyde that the mechanism of the reaction was reexamined in this work.

After having considered mechanisms proposed earlier for the reaction, Huisgen and coworkers (2) advanced the following:

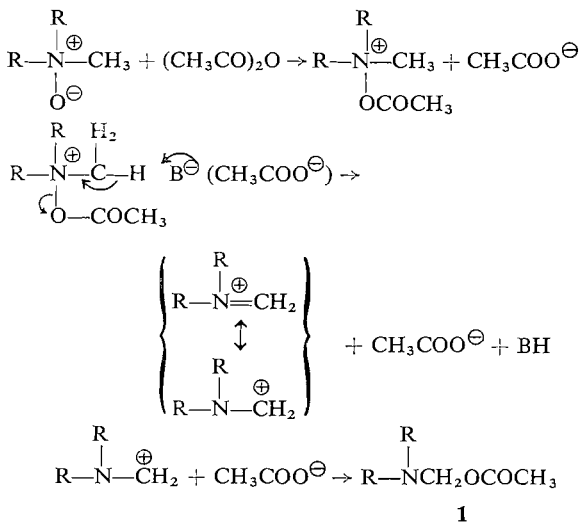

Alternatively, the aminoester **1** could arise by rearrangement of an ylide type of intermediate.

According to the same authors the ultimate products of the reaction, *N*-substituted amides and formaldehyde, could be formed from the aminoester **1** in two ways.

Route *a* seems unlikely since the ester is stable under anhydrous conditions but route *b* appears to be plausible.

[1]Issued as NRCC No. 9859.

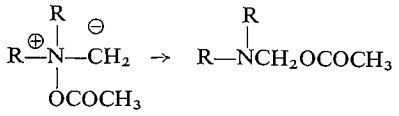

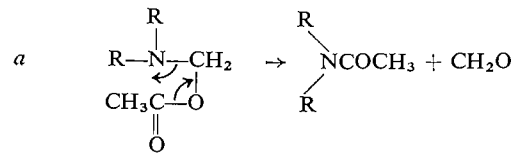

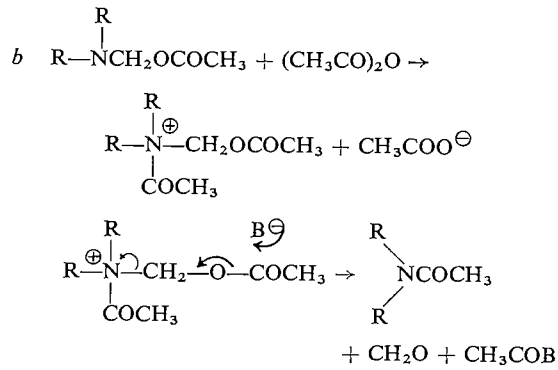

This mechanism, and others before it, all postulate the formation of an aminoester as an intermediate although no one has yet succeeded in isolating such a substance. Two reasons motivated our attempts to isolate the dimethylaminoester: firstly, to prove its actual formation during the Polonovski reaction, and, secondly, to prepare dimethyl-d_6 amine and formaldehyde-d_2 in improved yield by hydrolysis of its deuterated analogue. In the present work the acetate salt of the aminoester where R=CH_3 was isolated in up to 80% yield using *equimolar* amounts of trimethylamine *N*-oxide and acetic anhydride in chloroform while keeping the temperature below 15°. The structure of this aminoester was proved by comparison of its nuclear magnetic resonance (n.m.r.) spectrum with that of dimethylaminomethyl acetate prepared by the method described by Böhme, Bohn, Köhler, and Roehr (3). It seems therefore that dialkylaminomethyl acetate is in fact an intermediate in the Polonovski reaction as assumed by earlier workers.

With a molar equivalent of acetic anhydride, the aminoester in boiling chloroform gives a high yield of *N*,*N*-dimethylacetamide as reported by Huisgen *et al.* (2) but no formaldehyde. However, when the volatile materials such as acetic acid and dimethylacetamide were removed in a vacuum manifold, a rather brown residue remained. When heated in a vacuum sublimator at 120°, this residue decomposed into carbon dioxide and a colorless liquid which were collected in a Stock trap kept in liquid nitrogen, and a white solid sublimate. The sublimate was identified by mass spectrometry and its n.m.r. spectrum as 2-(dimethylaminomethyl)-acrylic acid and was identical with the compound reported by Pelletier and Franz (4). One of the products collected in the Stock trap was identified as 2-(acetoxymethyl)allyl acetate by comparison of its n.m.r. spectrum with the compound reported by Nerbel, Heymons, and Croon (5).

The same crude gummy brown solid material obtained from another run was also examined after recrystallization from alcohol. Micro analysis, nuclear magnetic resonance, infrared, and ultraviolet spectra of this material indicated it was 2,2-bis(acetoxymethyl)-3-(dimethylamino)-propionic acid. This substituted propionic acid decomposed thermally into carbon dioxide, dimethylamine, acetic acid, and 2-(acetoxymethyl)-allyl acetate but gave no 2-(dimethylaminomethyl)acrylic acid. The same type of thermal decomposition had been observed by Nerbel *et al.* (5) with triacetoxypivalic acid.

We have observed that the nonvolatile residue obtained from the Polonovski reaction carried out at the boiling point of chloroform gives more substituted acrylic than substituted propionic acid. On the other hand, a higher yield of substituted propionic than substituted acrylic acid is obtained if the residue is heated for a short time at 85°. This result would seem to indicate that the acrylic acid is the precursor of the propionic acid.

In dilute acetic acid the aminoester was hydrolyzed to dimethylamine which was isolated in 51% yield as the hydrochloride, and formaldehyde which was recovered in 62% yield as polyoxymethylene (72% yield as the dimedone derivative from aqueous solution). From the deuterated aminoester, deuterated polyoxymethylene and dimethylamine can therefore be obtained in moderate yields.

Can. J. Chem. Downloaded from www.nrcresearchpress.com by 210.87.254.5 on 09/05/12
For personal use only.

Can. J. Chem. Downloaded from www.nrcresearchpress.com by 210.87.254.5 on 09/05/12
For personal use only.

Discussion

The most plausible mechanism to account for the formation of the acrylic acid is illustrated below.

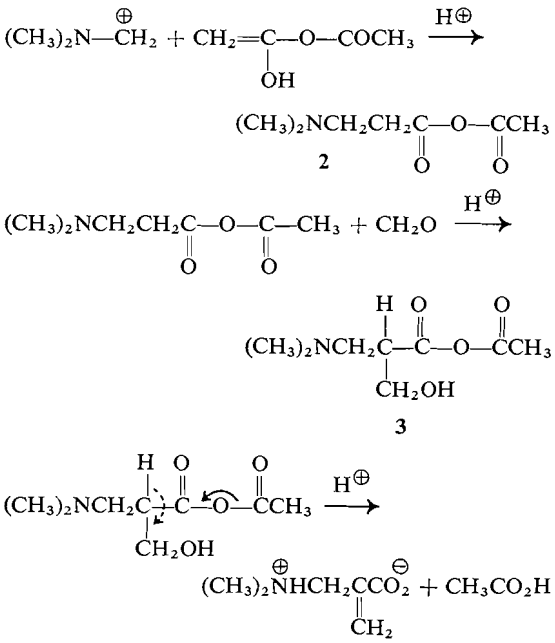

The first step consists in the attack of acetic anhydride on the aminoester by a nucleophilic displacement to give 2-(dimethylaminomethyl)-acetic anhydride **2** which can then form **3** by reaction with formaldehyde. Finally this substituted anhydride decomposes to the acrylic acid as shown. In order to verify this tentative mechanism the Polonovski reaction was conducted with trimethylamine-d_9 *N*-oxide and acetic anhydride in the presence of normal formaldehyde. The n.m.r. spectrum of the substituted acrylic acid showed two sharp doublets at τ 3.74 and 4.50, each having a coupling constant of 1.3 c.p.s., and a sharp singlet at τ 6.47. The only possible explanation of the n.m.r. spectrum observed is that a mixture of two compounds is obtained, one through path *a* with hydrogen on the terminal methylene group and the other through path *b* with hydrogen on the methylene group attached to nitrogen. It can be concluded from these results that formaldehyde has taken part in the formation of 2-(dimethylaminomethyl)acrylic acid. Whenever the same

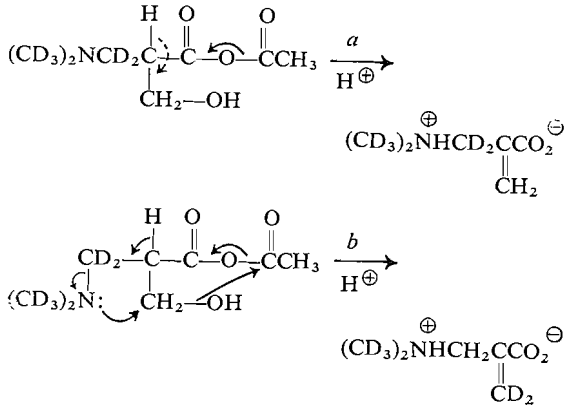

reaction was conducted without normal formaldehyde, only completely deuterated 2-(dimethylaminomethyl)acrylic acid was obtained.

In order to determine the origin of the 2-carbon atom in the substituted acrylic acid, the Polonovski reaction was carried out with acetic anhydride labelled with ^{13}C in the methyl group. The resulting substituted acrylic acid should now be labelled with ^{13}C in the 2-position according to the mechanism proposed for this reaction. Since the band width of the two methylene groups is of the order of 6 c.p.s. and the satellites corresponding to the long-range coupling of the methylene protons with ^{13}C are expected to be of the order of 4 c.p.s., the proton resonance spectrum for the presence of ^{13}C in the 2-position of the acrylic acid was inconclusive. A platinum catalyzed reduction of the substituted acrylic acid gave isobutyric acid and dimethylamine by hydrogenation and hydrogenolysis of the molecule. There is no reason to believe that the carbon in the 2-position in the acrylic acid should not be the carbon in the 2-position in the isobutyric acid. The proton resonance spectrum after six scannings using a CAT (computer of average transients; Varian C-1024 model) shows the satellites of the seven bands corresponding to the proton attached to a ^{13}C in the 2-position in the isobutyric acid. Therefore, ^{13}C from the acetic anhydride was introduced only in the 2-position of the acrylic acid which further supports the mechanism proposed in the present work for the formation of 2-(dimethylaminomethyl)acrylic acid during the Polonovski reaction.

A possible mechanism for the formation of

2,2-bis(acetoxymethyl)-3-(dimethylamino)propionic acid is shown below.

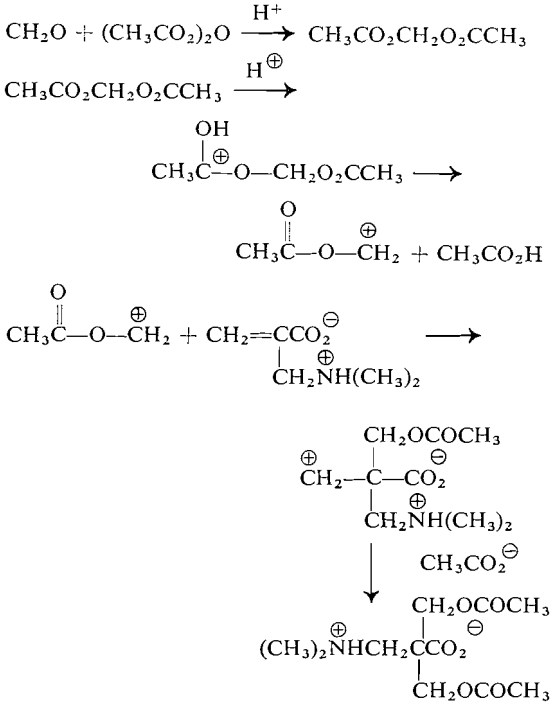

Experimental

Tetramethylammonium Hydroxide

The quaternary base was prepared from the bromide or the iodide by treating a solution of the dry salt in deuterium oxide with freshly prepared silver oxide washed with deuterium oxide. Reaction of the chloride was much slower and invariably gave a solution which still contained chloride ions even after stirring on the steam bath overnight. Alternatively, commercial 10% tetramethylammonium hydroxide was concentrated under reduced pressure and the residue was dissolved in deuterium oxide.

Tris(trideuteriomethyl)amine

A solution of 50 g (0.55 mole) of tetramethylammonium hydroxide in 200 ml of 99.87% deuterium oxide was poured into a stainless steel tube 32 cm × 5 cm (OD). The tube was closed with a screw cap and heated for 24 h at 130 °C in an oven. At the end of this period the content of the cold tube was poured into a 500 ml round bottomed flask. The solvent was then removed on the vacuum line, collecting the distillate which contained partly deuterated trimethylamine in a trap cooled to −78° with dry ice. The residue was redissolved in 200 ml of fresh deuterium oxide and heated as before. After eight exchanges the deuterium content of a sample of deuterated trimethylamine was 98.5 mole %. The infrared spectra of trimethylamine and deuteriotrimethylamine in the gas phase are shown in Figs. 1 and 2 respectively.

The distillate recovered after each exchange was neutralized with *N* deuterium chloride in deuterium oxide and the solution was evaporated to dryness in a rotary evaporator. The residue of partly deuterated trimethylamine hydrochloride was weighed and analyzed by n.m.r. using a solution of normal trimethylamine hydrochloride as standard.

The quaternary base obtained after eight exchanges was decomposed by pyrolysis to deuterated trimethylamine which was absorbed in *N* hydrochloric acid. The yield of hydrochloride was 36.1 g (63% of the theoretical amount).

The partly deuterated trimethylamine hydrochloride recovered after each exchange was combined to give 17.7 g (31%) and converted into quaternary base for reuse in another exchange. The overall loss was thus only 6.0%.

Anhydrous Trimethylamine N-Oxide

Trimethylamine *N*-oxide dihydrate (44.5 g, 0.4 mole), prepared from an aqueous solution of trimethylamine and hydrogen peroxide (6, 7), was placed in a 500 ml round-bottomed flask connected in series with a wide necked glass tube, a Stock trap and a vacuum pump. The amine oxide was heated slowly to 100° in an oil bath under a pressure of less than 1 mm. Only half of the flask was immersed in the oil. At that temperature the solid mass first liquified and then later resolidified. The temperature was raised slowly to 150° and kept at that temperature until all the solid had sublimed in the upper part of the flask. Then the flask was totally immersed in the oil bath and the white solid was resublimed onto the wide tube. The hard film of amine oxide was scraped off the wall of the tube into a dry flask by means of a stainless steel rod. The salt was protected from moisture by plugging the neck of the tube with absorbent cotton and by circulating a current of dry nitrogen during this operation. The yield of dry trimethylamine *N*-oxide was nearly quantitative. The n.m.r. spectrum of the oxide dissolved in D_2O showed only one band.

Dimethylaminomethyl Acetate

To a solution of 20.7 g (0.277 mole) of dry trimethylamine *N*-oxide in 100 ml of ethanol-free chloroform at 15° was added dropwise with stirring 29.1 g (0.277 mole) of 97% acetic anhydride during 3 h. Stirring was continued for an additional 3 h and the solution was allowed to stand for 12 h at 15°. The solution was fractionated in a vacuum manifold at room temperature. The fraction with a vapor pressure of 5 mm and less was collected separately. 33 g of a colorless liquid were obtained; n.m.r. ($CDCl_3$) 7.92(s), 7.52(s), 5.05(s), and −1.68 τ, corresponding to dimethylaminomethyl acetate containing 23% by weight acetic acid. The net yield of the acetate was thus 79%.

Formaldehyde and Dimethylamine

To dimethylaminomethyl acetate (8.2 g) was added a solution of 15 ml of acetic acid in 100 ml of water. The solution was heated to boiling and the formaldehyde was distilled over with the water vapor through a Vigreux column. The addition of water containing acetic acid was continued through a separatory funnel at the same rate as the distillation until a volume of 300 ml had been collected. Then the distillate was evaporated under a pressure of 15 mm. The white solid residue which was nearly pure polyoxymethylene weighed 1.3 g (62%).

Can. J. Chem. Downloaded from www.nrcresearchpress.com by 210.87.254.5 on 09/05/12
For personal use only.

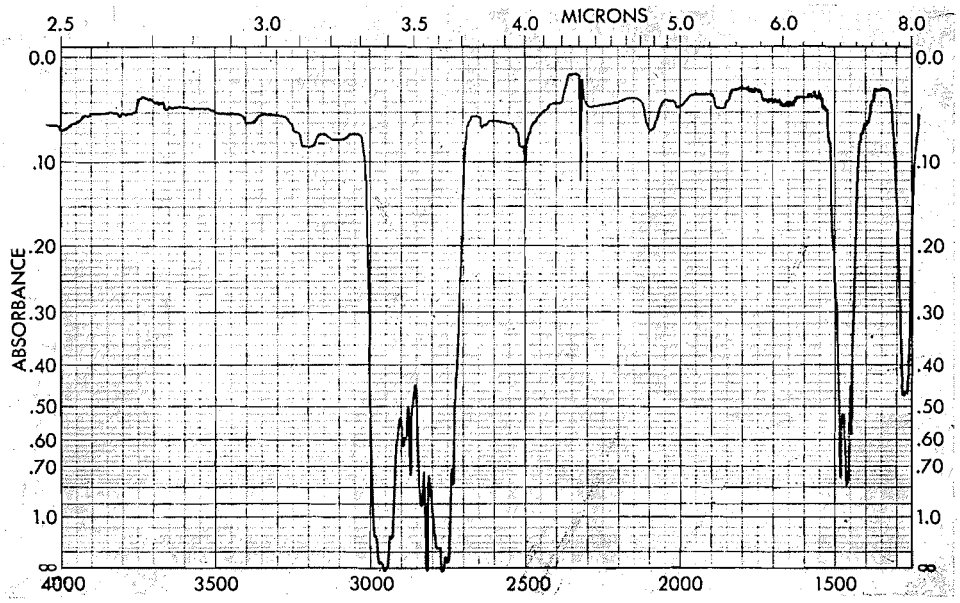

FIG. 1. The infrared spectrum of trimethylamine.

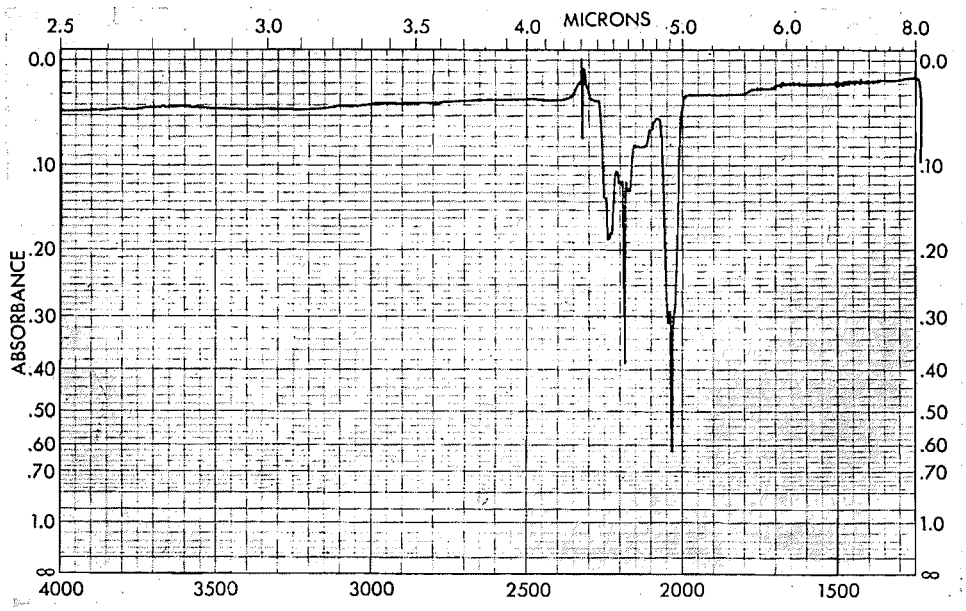

FIG. 2. The infrared spectrum of deuteriotrimethylamine.

Concentrated hydrochloric acid (7 ml) was added to the aqueous residue and the solvent was removed under reduced pressure. The residue was sublimed at 60° in a vacuum sublimator. The yield of dimethylamine-HCl (m.p. 172–173.5°) was 2.9 g (51%).

Deuterated formaldehyde and deuterated dimethylamine were obtained with the same yields starting with nonadeuteriotrimethylamine *N*-oxide, prepared from deuteriotrimethylamine.

2-(Dimethylaminomethyl)acrylic Acid and 2,2-Bis-(acetoxymethyl)-3-(dimethylamino)propionic Acid

(*a*) A solution of dimethylaminomethyl acetate, prepared from 10 g of trimethylamine *N*-oxide, and acetic anhydride (13.0 ml) in ethanol-free chloroform (100 ml) was heated under reflux for 3 h. Then the volatile material was distilled *in vacuo* into a Stock trap cooled in dry ice and acetone. The residue (1 g) was heated to 110° in a vacuum sublimator. A white sublimate was obtained

Can. J. Chem. Downloaded from www.nrcresearchpress.com by 210.87.254.5 on 09/05/12
For personal use only.

along with a very small quantity of CO_2 and a liquid with a low vapor pressure which was identified as mostly 2-(acetoxymethyl)allyl acetate (5) after purification. The solid was resublimed at 80° under a pressure of 0.1 mm. The yield of sublimed 2-(dimethylaminomethyl)acrylic acid melting at 115–116°, HCl salt m.p. 144–146°, (lit. m.p. 117.7–119.7°, HCl salt m.p. 143.9–145.7° (4)) was 0.7 g.

Mass spectral analysis: parent peak at *m/e* 129; n.m.r. (in $CDCl_3$) signals at 7.37 (6H, s, $(CH_3)_2N$), 6.43 (2H, m), 4.48 (1H, m), 3.78 (1H, m), and -2.72 τ (1H, s).

The n.m.r. spectrum of the distillate indicated it was a mixture of dimethylaminomethyl acetate (9.0 g), dimethylacetamide, acetic anhydride, and acetic acid in chloroform. This mixture was distilled at atmospheric pressure until the temperature of the reaction mixture reached 85°. Then the remaining volatiles were removed under a pressure of 0.1 mm. The distillate consisted only of dimethylacetamide and acetic acid. A brown solid residue weighing 5.3 g, which crystallized from ethanol as a white solid (4.8 g, m.p. 155–155.5°), was obtained. Thermal decomposition of the white solid gave mainly carbon dioxide and 2-(acetoxymethyl)allyl acetate.

Nuclear magnetic resonance (in $CDCl_3$) signals at 7.92 (6H, s, CH_3COO), 7.20 (6H, s, $(CH_3)_2N$), 6.92 (2H, s), 5.64 (4H, s), and -0.50 τ (1H, s); ν_{max} 1745 (ester), 1625 (acid), and 1040 cm^{-1} (C—N); $\lambda_{max}(H_2O)$ 217 mμ(ϵ 450).

Anal. Calcd. for $C_{11}H_{19}NO_6$ (2,2-bis(acetoxymethyl)-3-(dimethylamino)propionic acid): C, 50.57; H, 7.28; N, 5.36. Found: C, 50.38; H, 7.47; N, 5.32.

The compound recovered from the ethanol mother liquor (0.4 g) was nearly pure 2-(dimethylaminomethyl)-acrylic acid.

(*b*) To a solution of trimethylamine *N*-oxide (10 g) in ethanol-free chloroform (75 ml) at 15°, was added dropwise during 4 h acetic anhydride (13 ml) in chloroform (25 ml). The solution was kept at 0° for 24 h. Then acetic anhydride (18 ml) was added all at once at room temperature. The mixture was heated to reflux for 4 h and the solvent was removed by distillation until the temperature of the distilling flask reached 85°. The volatiles were distilled in a Stock trap at −78° at a pressure of 0.1 mm and the gummy residue was heated for 2 h at 100°. The light brown solid (11.6 g) which was obtained was 2,2-bis(acetoxymethyl)-3-(dimethylamino)-propionic acid contaminated with a very small quantity of 2-(dimethylaminomethyl)acrylic acid.

(*c*) A solution of dimethylaminomethyl acetate, prepared as in *b*, and acetic anhydride (18 ml) in 100 ml of ethanol-free chloroform was heated to boiling for 24 h. Then the volatiles from the cold solution were removed at reduced pressure. Dimethylacetamide (8.5 g, 73.3%) was isolated from the distillate. The residue was heated at 100° in a vacuum sublimator. A yield of 2.4 g of 2-(dimethylaminomethyl)acrylic acid was obtained.

Partially Protonated Deuterated 2-(Dimethylaminomethyl)-acrylic Acid

To a solution of octadeuteriodimethylaminomethyl acetate, $CH_3COOCD_2N(CD_3)_2$, prepared from 6.7 g of deuteriotrimethylamine *N*-oxide and 8.2 g of acetic anhydride in chloroform (75 ml), was added a mixture of acetic anhydride (11 ml) and polyoxymethylene (0.5 g) previously dried over P_2O_5 and allowed to stand in acetic anhydride for 19 h. The solution was heated under reflux with stirring for 18 h. Then the volatiles were removed under reduced pressure as described in *a* above. The residue, heated at 120° in a vacuum sublimator, gave a white sublimate which was resublimed at 80°.

Two doublets (τ 4.50 and 3.74, $J = 1.3$ c.p.s.) corresponding to the acid $CH_2{=}C(CO_2H)CD_2N(CD_3)_2$ and 1 singlet (τ 6.49) corresponding to the acid $CD_2{=}C(CO_2H)CH_2N(CD_3)_2$ were present in its n.m.r. spectrum in $CDCl_3$, indicating that normal formaldehyde had taken part in the reaction between the ester and the anhydride.

2-(Dimethylaminomethyl)acrylic Acid-2-^{13}C and Isobutyric Acid-2-^{13}C

2-(Dimethylaminomethyl)acrylic acid-2-^{13}C was isolated as described above by reacting trimethylamine *N*-oxide (3.7 g) with acetic anhydride containing 33% ^{13}C in the methyl group. 2-(Dimethylaminomethyl)-acrylic acid-2-^{13}C (0.3 g) and Adam's catalyst (0.02 g) in ethanol were shaken under an atmosphere of hydrogen for ¾ h. The catalyst was removed by filtration and the filtrate was distilled on a vacuum manifold. The low vapor pressure liquid was collected separately. The n.m.r. spectrum of this liquid in $CDCl_3$ showed the expected septet at τ 7.38 ($J = 6.5$ c.p.s.) corresponding to the proton on the 2-carbon in isobutyric acid and also two series of septets at τ 8.47 and 6.31 ($J = 6.5$ c.p.s.) corresponding to the proton attached to the carbon-13 atom in the acid.

1. J. C. Stephens, R. N. Renaud, and L. C. Leitch. Proc. Conf. Methods of Preparing and Storing Marked Molecules. Brussels. Euratom. In preparation. 1966.
2. R. Huisgen, F. Bayerlein, and W. Heydkamp. Chem. Ber. **92**, 3223 (1959).
3. H. Böhme, H. J. Bohn, E. Köhler, and J. Roehr. Ann. **664**, 130 (1963).
4. S. W. Pelletier and J. E. Franz. J. Org. Chem. **17**, 855 (1952).
5. F. Nerbel, A. Heymons, and H. Croon. Chem. Ber. **91**, 938 (1958).
6. W. R. Dunstan and E. Goulding. J. Chem. Soc. **75**, 792 (1899).
7. J. Meisenheimer and K. Brating. Ann. **397**, 284 (1913).

Can. J. Chem. Downloaded from www.nrcresearchpress.com by 210.87.254.5 on 09/05/12
For personal use only.

Hydrogen isotopic exchange in biphenylene and the preparation of biphenylene-d_8[1]

BRUNO LUNELLI AND CESARE PECILE
Institute of Physical Chemistry, University of Padua, Padua, Italy

Received July 25, 1967

The hydrogen isotopic exchange with basic and acidic agents has been widely investigated with the aim of preparing fully deuterated biphenylene. It has been noted that the very strong base KOD completely decomposes the hydrocarbon, while the strong base NaOD leads to random exchange, and the medium strength base $Ca(OD)_2$ gives preferential exchange in α-position. Since the stability of biphenylene is less in acid mixtures than in basic ones, only acids of medium strength, which give preferential exchange in β-position, can be used.

Good results in preparing fully deuterated biphenylene are obtained from two methods. The first of these consists of two exchanges which occur successively; one with an acid mixture and the other with a base. Both agents are of medium strength. The second method entails repeated exchanges with the strong base NaOD supported on $Ca(OD)_2$. The latter method gives the highest isotopic purity and the best yield, as well as being much easier to carry out.

Canadian Journal of Chemistry, 46, 391 (1968)

Can. J. Chem. Downloaded from www.nrcresearchpress.com by 210.87.254.105 on 09/05/12
For personal use only.

The study of the vibrational spectrum of biphenylene (BPH), which is in progress in this laboratory,[2] has required the availability of the corresponding fully deuterated compound (BPH-d_8). Since the reported syntheses of BPH, which give reasonable yields (1–3), did not appear to be conveniently adaptable[3] to the preparation of BPH-d_8, the hydrogen isotopic exchange method was chosen, since it gives good results with aromatic compounds (5, 6).

The reactivity of the hydrogen atoms of BPH has been the object of both theoretical and experimental research (7–11). Kinetic data for hydrogen isotopic exchange in trifluoroacetic acid and trifluoroacetic acid – 70% $HClO_4$ are also available (12, 13) and the β-position has been shown to be more reactive than the α one, which has almost the same reactivity as the β-position in naphthalene (13). Since each of the hydrogen atoms of naphthalene exchange with 50% D_2SO_4 (14), the first exchange experiments attempted were with 30–70% D_2SO_4 (runs 1–3, Table I). In these reaction mixtures, the D/H atom ratio was 10:1 and therefore BPH with 90% deuterium content could be expected if a random distribution of hydrogen isotopes were obtained. The results (Table I) show that an increase of acid concentration results in an increase in deuterium content of the product but a poorer yield of recovered BPH is obtained. The 60% D_2SO_4 gives an acceptable yield but the percentage of deuterium is too far below 90%; the 70% D_2SO_4 (5 h at 110 °C) produces nearly complete decomposition.

Results obtained with other acids were not useful. Gaseous DCl (15) bubbled through a 5% solution of BPH in benzene or in carbon disulfide in the presence of $AlCl_3$ gave unexchanged BPH and 30% decomposition products. Liquid anhydrous DBr (12 h at room temperature in a stainless steel bomb), which is a very efficient exchange agent (16), led to a tarry product from which no BPH could be recovered.

The above mentioned studies on the exchange of BPH with trifluoroacetic acid (12, 13) do not provide information on the amount of decomposition, a factor which is important in preparation of the fully deuterated compound in reasonable yield. On the other hand the reported kinetic data (12), despite referring to a somewhat different exchange (17), satisfactorily account for the deuterium percentage obtained in run 4 (Table I); the same experiment also shows that the decomposition rate prevails for exchange in the α-position. In an attempt to find a better exchange medium, D_2SO_4 (18) or D_3PO_4 (19) was added to CF_3COOD, thus increasing the value of the acidity function (20) (and hence the exchange rate in the α-position (21)) of the exchange agent, which still remains a sufficiently good solvent for BPH. A series of experiments (runs 5–10, Table I) was carried out to find the

[1]This investigation was supported by the National Research Council of Italy, Chemistry Committee.

[2]C. Pecile and B. Lunelli. J. Chem. Phys. In preparation.

[3]A new method, which may be adaptable, was reported briefly (4) when the present work was in an advanced stage.

TABLE I

Hydrogen isotopic exchange in biphenylene

Run No.	Exchange agents	D:H atom ratio	Temp (°C)	Time (h)	Biphenylene recovered	
					%yield	% D
1	D_2SO_4 30% in D_2O	10	110	10	75	15
2	D_2SO_4 40%	10	110	10	75	18
3	D_2SO_4 60%	10	110	5	67	50
4	CF_3COOD	10	80	24	73	62
5	D_3PO_4 and CF_3COOD (3:1) by weight	10	75	5	73	60
6	D_2SO_4 60% and CF_3COOD (1:1)	10	115	4	40	79
7	D_2SO_4 60% and CCl_3COOD (1:1)	10	120	2	40	58
8	D_2SO_4 50% and CF_3COOD (1:1)	20	115	5	63	63
9	D_2SO_4 50% and CF_3COOD (1:1)	20	115	10	57	67
10	D_2SO_4 50% and CF_3COOD (3:1)	20	115	10	75	66
11	$Ca(OD)_2$	20	300	48	72	60
12	$Ca(OD)_2$	20	300	72	60	61
13	$Ca(OD)_2$	20	350	24	50	75
14	$Ca(OD)_2$	20	350	48	40	83
15	NaOD on $Ca(OD)_2$	10	300	48	90	90

composition and the exchange conditions from which the best compromise between good yield and high deuterium content might be achieved. Such a compromise is satisfactorily obtained in run 10. When the exchange was repeated under the same conditions, the deuterium content reached a maximum of 70%. Even when the acidity was increased and extensive decomposition tolerated, the deuterium content could not be raised above 80%.

We then turned to high temperature exchange with $Ca(OD)_2$, a method which has been used successfully to prepare the corresponding deuterated compounds of some aromatic hydrocarbons (22–25). We found a satisfactory degree of exchange at temperatures of 300 °C or higher. The thermal instability of BPH (26), however, prevents the use of temperatures higher than 350 °C. A suitable choice of temperature and time is that of run 11, since longer exchange times lead to poorer yield without appreciable increase in deuterium content. When exchange was repeated twice in the conditions of run 11, BPH obtained had only about 70% deuterium; however, this percentage never exceeded 85%, even when more drastic conditions were used and lower yields were accepted.

It is possible to understand the ease with which deuterium content of ∽50% is reached in exchange in acid media if we assume behavior similar to that known for trifluoroacetic acid (12, 13) where the reversible exchange in the β-position is fast and that in the α-position is slow. The difficulty encountered in our attempts to exceed the limit of 80% deuterium is due to the sensitivity of BPH to acids. This causes the irreversible decomposition reaction to prevail over the exchange reaction in the α-position.

As reported above, the deuterium content and yield in exchange with $Ca(OD)_2$ follow a pattern similar to that observed with acids. The behavior with $Ca(OD)_2$ can be explained by assuming the decomposition rate to be intermediate between the substitution rates of the α- and β-positions, each of which is very different from the other. In this case, however, it is not known whether the more rapidly exchanging hydrogen atoms are the α or the β ones.[4] The infrared spectra of ∽50% deuterated BPH prepared by exchange with $Ca(OD)_2$ are significantly different from spectra of ∼50% deuterated BPH prepared by exchange with acids, and suggest that the exchange reactions follow different routes. In the absence of studies on the mechanism of the heterogeneous hydrogen isotopic exchanges with deuteroxides, it is useful to note that alkaline hydroxides at room temperature metalate some aromatic hydrocarbons giving the corresponding anion (27). Therefore, it seems reasonable to assume that $Ca(OD)_2$ behaves analogously at high temperature, the hydrocarbon anion reacting successively with the D_2O coming from the reversible decomposition of the deuteroxide.

[4]In naphthalene both electrophilic and nucleophilic substitution of hydrogen with deuterium occurs more easily in the α-position (28).

Can. J. Chem. Downloaded from www.nrcresearchpress.com by 210.87.254.105 on 09/05/12
For personal use only.

Can. J. Chem. Downloaded from www.nrcresearchpress.com by 210.87.254.105 on 09/05/12
For personal use only.

Since metalation of BPH takes place preferentially in the α-position (11), the hydrogen atoms which exchange more rapidly with $Ca(OD)_2$ are probably the α ones.

The results of our experiments together with the interpretations given above allow us to suppose that the amount of decomposition should be reduced if, in exchanging the β-hydrogens, we use an acid solution and for the α ones, we use $Ca(OD)_2$. By this process it should be possible to obtain BPH in acceptable yield and with a high deuterium content. Two successive exchanges, one with $CF_3COOD - D_2SO_4 - D_2O$ and the other with $Ca(OD)_2$ (under the conditions of runs 10 and 11 respectively) gave BPH in 35% yield with deuterium content of 96.21%.[5] This result confirms the accuracy of the hypothesis stated above, but the percentage of BPH-d_8 is not completely satisfactory for spectroscopic work.

To achieve better results we investigated the influence of basicity on the heterogeneous hydrogen exchange with hydroxides.[6] Though very little is known on this topic (22), extensive data are reported on the basicity of hydroxides at high temperatures. Barium and strontium hydroxides as well as all the alkaline hydroxides are bases stronger than calcium hydroxide ($K > Na > Li$) (29, 30); hence, presumably (31), more efficient exchange agents. The strongest base, anhydrous potassium hydroxide, cannot be used as a liquid because it melts at a temperature which is too high for the thermal stability of BPH; it was therefore used on a $Ca(OD)_2$ support in experiments analogous to those performed with pure $Ca(OD)_2$. Even at relatively low temperature (250 °C) it led to complete decomposition of BPH. A similar experiment with NaOD gave BPH in 90% yield and a deuterium percentage which corresponded to one involving almost random distribution of hydrogen atoms of the reagents. Random distribution in exchange with NaOD as opposed to selective exchange with $Ca(OD)_2$ may well be a consequence of the higher basicity of the former—a behavior which parallels that of acidic agents (21). After three successive exchanges using the same procedure, BPH-d_8 of high deuterium content[7] was obtained in good yield (70%).

[5]Spectrometric mass analysis by Merck, Sharp, and Dohme of Canada Ltd., gave: BPH-d_8, 73.13%; BPH-d_7, 23.45%; BPH-d_6, 3.42%.

[6]Mixing was shown to be unimportant by an experiment performed under the conditions of run 11 in which glass balls were introduced into the Pyrex bulb which was then rotated at 70 r.p.m.

Experimental

Starting Materials

Biphenylene was prepared as described by Baker *et al.* (1). Two steam distillations and two crystallizations from methanol gave a product of m.p. 112 °C (corrected).

Trifluoroacetic acid-*d*, trichloroacetic acid-*d*, and orthophosphoric acid-d_3 were obtained by using an all-glass apparatus and allowing the pure anhydride to distil slowly over D_2O, held at 0 °C, or vice versa.

Deuterium chloride (or bromide) was prepared from deuterium oxide and phosphorous trichloride (or tribromide) in the presence of CCl_3COCl (or CCl_3COBr).

Calcium Deuteroxide

Calcium oxide was prepared by heating $CaCO_3$ at 900 °C in a refractory vessel for 24 h. The partially sintered mass was finely ground (under nitrogen) and heated at 900 °C for another 24 h. The hydroxide was prepared (under nitrogen) from deuterium oxide and an excess (15%) of calcium oxide in the same Pyrex tube to be used in the exchange. The tube was allowed to stand 24 h before introducing it into the furnace; this proved to be a useful precaution to avoid explosions.

Potassium (or sodium) hydroxide on calcium hydroxide was obtained analogously to $Ca(OD)_2$ by using, instead of deuterium oxide, a solution of KOD (or NaOD) in deuterium oxide prepared by careful addition of a calculated quantity of D_2O to a weighed amount of the metal.

Hydrogen Exchanges with Acids

The exchanges with D_2O–D_2SO_4, CF_3COOD, and CF_3COOD–D_3PO_4 were carried out by stirring the reagents under nitrogen in a flask immersed in a thermostatically controlled bath. With the mixtures $D_2O - D_2SO_4 - CF_3COOD$ we used an apparatus made from borosilicate glass tubing as shown in Fig. 1. Resistance wires (covered with asbestos) wound on tubes A, B, and C provided electrical heating and gave the maximum temperature at the bottom of A. Here the mixture boiled vigorously and separated into a liquid, which flowed down tube B, and a vapor (rich in trifluoroacetic acid) which condensed in E (air cooled) and flowed down tube C. The very rapid circulation of the mixture produced good mixing and this was found to substantially improve the exchange. The reagents were introduced under nitrogen and the apparatus was then cooled in liquid nitrogen, evacuated, and sealed in G. The input current was chosen so that a temperature higher than the melting point of BPH would be obtained at all points in contact with the liquids. Once a steady state was reached the apparatus did not require control and could be left in operation overnight.

Hydrogen Exchange with Bases

Exchanges with calcium deuteroxide, with potassium deuteroxide on $Ca(OD)_2$, and with sodium deuteroxide

[7]Mass spectrometric analysis gave: BPH-d_8, 86.39%; BPH-d_7, 13.61%; overall deuterium content, 98.30%.

Can. J. Chem. Downloaded from www.nrcresearchpress.com by 210.87.254.105 on 09/05/12
For personal use only.

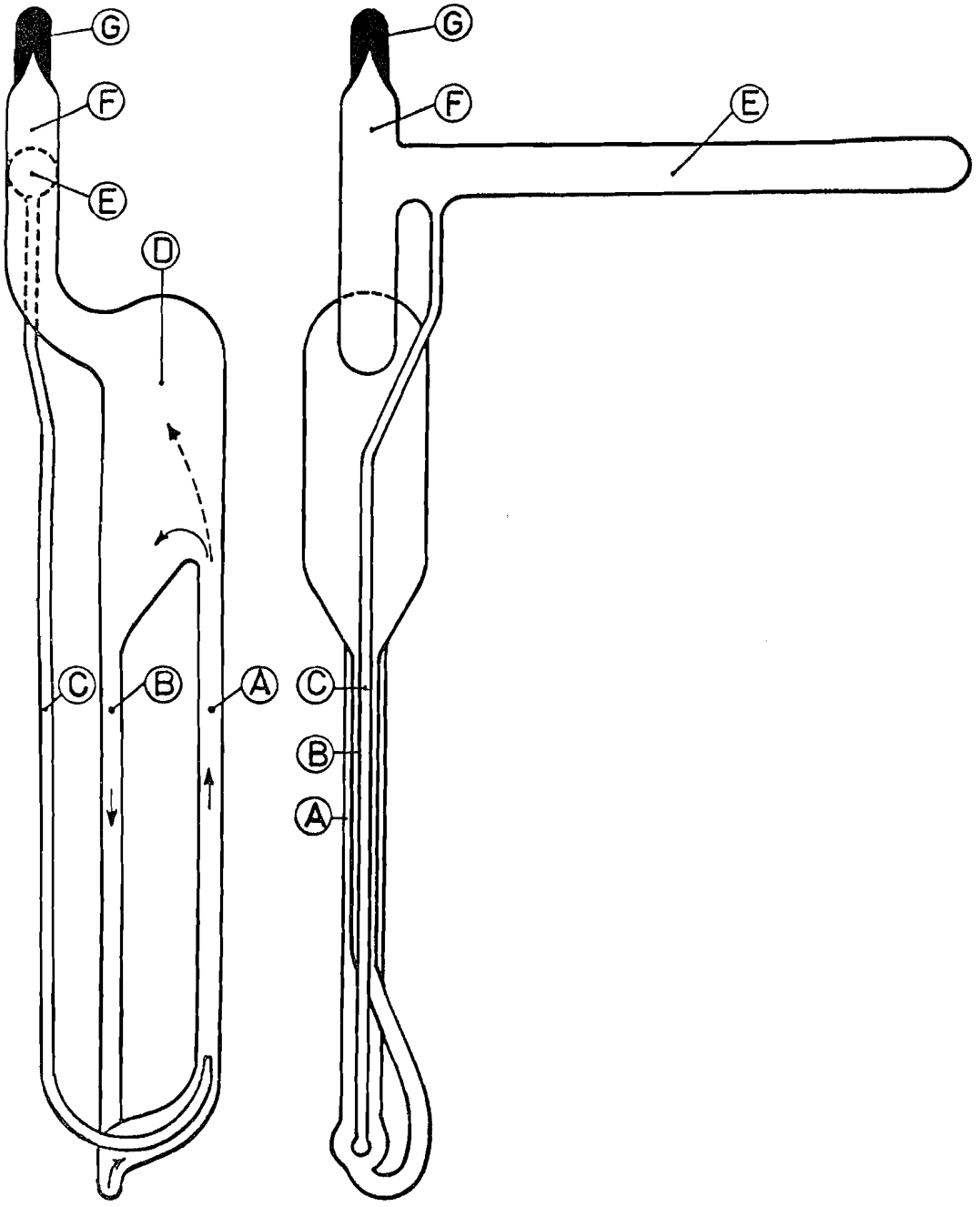

FIG. 1. An apparatus for the exchange of biphenylene with liquid acid mixtures.

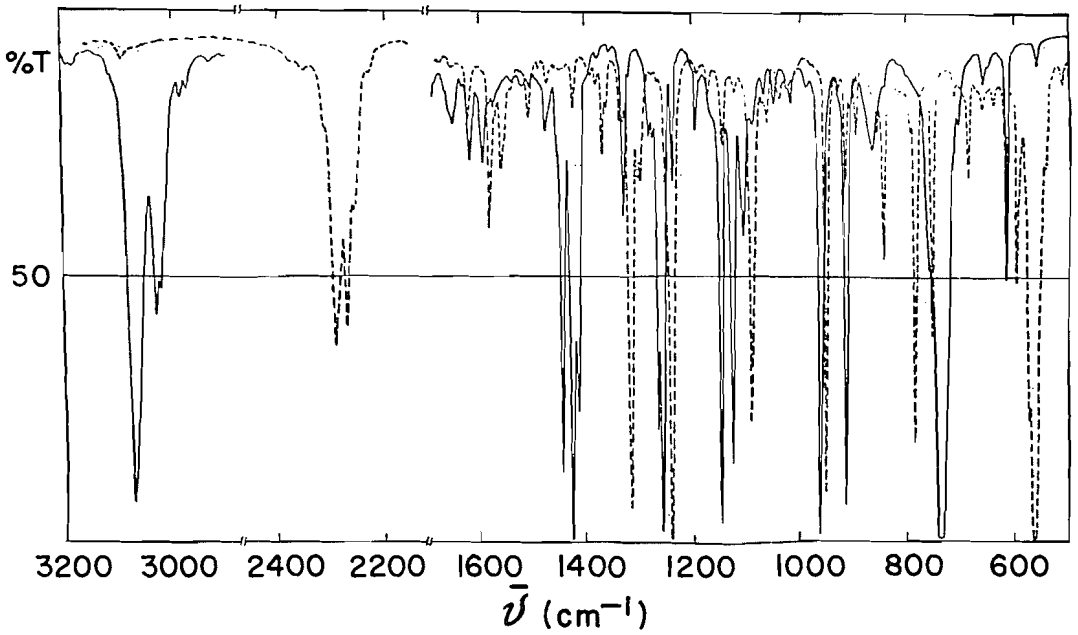

FIG. 2. Infrared spectra of biphenylene (solid line) and biphenylene-d_8 (broken line) in CCl_4, C_2Cl_4, or CS_2 solution (20 mg in 1 ml; cell thickness 1 mm). The spectra were measured with a Beckman IR9 spectrometer.

on $Ca(OD)_2$ were carried out by heating a vacuum sealed Pyrex tube containing the BPH and the base in a thermostatically controlled (±5 °C) furnace. At the end of the exchange period, BPH was extracted with CH_2Cl_2 and purified as reported above for the light compound.

Preparation of Biphenylene-d_8

BPH (200 mg), calcium oxide (8 g), and a solution of sodium deuteroxide in D_2O (prepared from deuterium oxide (2.5 ml) and sodium (280 mg)) were introduced in a 50 ml Pyrex tube in which the temperature was held at 20 °C. After 24 h, the tube was cooled in liquid nitrogen, evacuated, and sealed; it was then heated at 300 ± 5 °C for 48 h. The BPH was extracted with CH_2Cl_2 and purified as reported above. The procedure was repeated twice for the same BPH so that 140 mg of the pure compound was obtained, m.p. 112 °C (corrected). Its infrared spectrum is shown in Fig. 2 together with that for the light compound. The intensities of ν(CH) and ν(CD) stretching bands indicate 98% deuterium content; mass spectrometric analysis gave 98.30%.[7]

Acknowledgment

The technical aid of Miss Miranda Zanetti is gratefully acknowledged.

1. W. BAKER, M. P. V. BOARLAND, and J. F. W. MCOMIE. J. Chem. Soc. 1476 (1954).
2. G. WITTIG and W. HERWIG. Chem. Ber. **87**, 1511 (1954).
3. G. WITTIG and L. POHMER. Chem. Ber. **89**, 1334 (1956).
4. R. F. C. BROWN, D. V. GARDNER, J. F. W. MCOMIE, and R. K. SOLLY. Chem. Commun. 407 (1966).
5. A. I. SHATENSHTEIN. Isotopic exchange and the replacement of hydrogen in organic compounds. Consultants Bureau. New York. 1962.
6. B. LUNELLI and C. PECILE. Can. J. Chem. **44**, 1633 (1966).
7. W. BAKER, J. W. BARTON, and J. F. W. MCOMIE. J. Chem. Soc. 2666 (1958).
8. A. STREITWIESER, JR., J. I. BRAUMAN, and J. B. BUSH. Tetrahedron, **19**, Suppl. 2, 379 (1963).
9. J. W. BARTON, D. E. HENN, K. A. MCLAUGHLAN, and J. F. W. MCOMIE. J. Chem. Soc. 1622 (1964).
10. J. M. BLATCHLY, A. J. BOULTON, and J. F. W. MCOMIE. J. Chem. Soc. 4930 (1965).
11. W. BAKER, A. J. BOULTON, C. R. HARRISON, and J. F. W. MCOMIE. Proc. Chem. Soc. 414 (1964).
12. J. M. BLATCHLY and R. TAYLOR. J. Chem. Soc. 4641 (1964).
13. A. STREITWIESER, JR. and I. SCHWAGER. J. Am. Chem. Soc. **85**, 2855 (1963).
14. W. B. PERSON, G. C. PIMENTEL, and O. SCHNEPP. J. Chem. Phys. **23**, 230 (1955).
15. M. BRULLMANN, H. J. GERBER, and D. MEYER. Helv. Chim. Acta, **41**, 1831 (1958).
16. A. I. SHATENSHTEIN. Isotopic exchange and the replacement of hydrogen in organic compounds. Consultants Bureau. New York. 1962. pp. 167 and 303.
17. C. EABORN, P. M. JACKSON, and R. TAYLOR. J. Chem. Soc. (B), 613 (1966).
18. G. DALLINGA, A. A. VERRIJN STUART, P. J. SMITH, and E. L. MACKOR. Z. Elektrochem. **61**, 1019 (1957).
19. V. GOLD and D. P. N. SATCHELL. J. Chem. Soc. 3622 (1955).
20. A. I. SHATENSHTEIN. Isotopic exchange and the

Can. J. Chem. Downloaded from www.nrcresearchpress.com by 210.87.254.105 on 09/05/12
For personal use only.

replacement of hydrogen in organic compounds. Consultants Bureau. New York. 1962. p. 53.
21. R. BAKER, R. W. BOTT, and C. EABORN. J. Chem. Soc. 2136 (1963).
22. L. H. P. WELDON and C. WILSON. J. Chem. Soc. 244 (1946).
23. E. R. LIPPINCOTT and E. J. O'REILLY. J. Chem. Phys. **23**, 238 (1955).
24. J. E. KATON and E. R. LIPPINCOTT. Spectrochim. Acta, **15**, 627 (1959).
25. S. CALIFANO. J. Chem. Phys. **36**, 903 (1962).
26. D. F. LINDOW and L. FRIEDMAN. J. Am. Chem. Soc. **89**, 1271 (1967).
27. A. I. SHATENSHTEIN. Isotopic exchange and the replacement of hydrogen in organic compounds. Consultants Bureau. New York. 1962. p. 84.
28. A. I. SHATENSHTEIN. Isotopic exchange and the replacement of hydrogen in organic compounds. Consultants Bureau. New York. 1962. p. 105.
29. J. GORET. Bull. Soc. Chim. France, 1074 (1964).
30. J. GORET and B. TREMILLON. Bull. Soc. Chim. France, 2872 (1966).
31. A. I. SHATENSHTEIN. Isotopic exchange and the replacement of hydrogen in organic compounds. Consultants Bureau. New York. 1962. Sect. III.

Can. J. Chem. Downloaded from www.nrcresearchpress.com by 210.87.254.105 on 09/05/12
For personal use only.

Can. J. Chem. Downloaded from www.nrcresearchpress.com by 210.87.254.105 on 09/05/12
For personal use only.

Hydrogenation of alkyl 2-oximino-α-D-*arabino*-hexopyranosides[1]

R. U. LEMIEUX AND S. W. GUNNER
Department of Chemistry, University of Alberta, Edmonton, Alberta

Received August 9, 1967

Hydrogenation of alkyl 2-oximino-α-D-*arabino*-hexopyranosides in the presence of palladium on charcoal and hydrochloric acid gave mixtures of the alkyl 2-amino-2-deoxy-α-D-hexopyranoside hydrochlorides with the *gluco* and *manno* configurations in about 90% yields. The fraction of *gluco* compound varied substantially with the nature of the alkyl group; viz., methyl, 71%; ethyl or *n*-propyl, 62%; isopropyl, 80%. More of the *manno* compound is formed, viz., isopropyl, 50%, when the 3,4,6-triacetate of the oximinoglycoside is hydrogenated. Hydrogenation of methyl 6-*O*-(2-oximino-α-D-*arabino*-hexopyranosyl)-β-D-glucopyranoside gave an about equimolar mixture of the two configurations.

Canadian Journal of Chemistry, **46**, 397 (1968)

The occurrence of 2-amino-2-deoxy-α-glycopyranosyl groups in a wide variety of antibiotics (1) has rendered the synthesis of such glycosides (α-glycosaminides) a leading problem in carbohydrate chemistry. β-Glycosaminides in which the aglycon is either the residue of a simple alcohol or a more complex carbohydrate structure can normally be obtained via the Koenigs–Knorr reaction or its modifications (2). The yield depends strongly on the complexity of the potential aglycon. To date there exists no controlled synthesis of complex α-glycosaminides in appreciable yield. Of the various methods employed, alcoholysis of the parent sugar or derivative in the presence of acid proceeds in best yield (3). However this method is inherently limited to simple acid-resistant alcohols. For more complex alcohols, for example appropriately blocked carbohydrate structures, only low yields of α-glycosaminides are available usually via Koenigs–Knorr type reactions (4). The reduction of the 2-oximino-α-hexopyranosides, which are formed in high yield on reaction of alcohols with the nitrosyl chloride adduct of acetylated glycals (5, 6), offered a new approach to these compounds and is the subject of this paper. The work is concerned mainly with the preparation of alkyl glycopyranosaminides from simple alkyl (methyl, ethyl, *n*-propyl, and isopropyl) alcohols which are normally best prepared by alcoholysis of the aminosugars. Nevertheless, the data provide an insight to the factors which affect the stereochemical routes of the reductions. Also, the result obtained in the preparation of a mixture of methyl 6-*O*-(2-amino-2-deoxy-α-D-glucopyranosyl)-β-D-glucopyranoside with the corresponding α-D-*manno* isomer is described as an illustration of an α-linked disaccharide synthesis.

The alkyl 2-amino-2-deoxy-α-D-glucopyranosides formed in the reductions were identified by direct comparisons with authentic samples prepared from D-glucosamine and this comprises proof of the α-D-configuration for the parent *oximino*-glycosides.[2] The formation of alkyl 2-amino-2-deoxy-α-D-mannopyranosides was based on this fact together with nuclear magnetic resonance (n.m.r.) data for these compounds and the demonstration by gas–liquid partition chromatographic (g.l.p.c.) analysis that D-mannosamine is liberated on hydrolysis.

A study of the hydrogenation of the alkyl tri-*O*-acetyl-2-oximino-α-D-*arabino*-hexopyranosides (**1**) using palladium on charcoal as catalyst was first undertaken. The isopropyl oximino glycoside in methanol proved highly resistant to hydrogenation at 60 p.s.i. and room

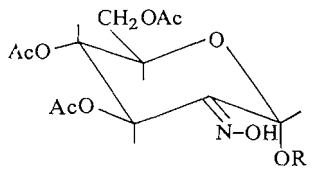

1

[1]Presented at the Symposium on Synthesis, Organic Division, Chemical Institute of Canada, Banff, Alberta, August 31 – September 2, 1966.

[2]T. L. Nagabhushan (Ph.D. Thesis, University of Alberta, Edmonton, (1966)) provided a proof of this point of configuration by gas–liquid partition chromatography and n.m.r. comparisons of the product from the reduction of methyl tri-*O*-acetyl-2-oximino-α-D-*arabino*-hexopyranoside with authentic samples of the methyl glycosides in the *gluco* and *manno* series.

Can. J. Chem. Downloaded from www.nrcresearchpress.com by 210.87.254.105 on 09/05/12
For personal use only.

temperature. However, when the hydrogenation was carried out in the presence of 1.1 equivalents of hydrochloric acid, reduction was complete within 18 h at room temperature. The product was *N*-acetylated, then de-*O*-acetylated for trimethylsilylation (7) prior to g.l.p.c. analysis employing an internal standard. It was found that a virtually quantitative yield of the isopropyl α-D-*gluco* and α-D-*manno* glycopyranosaminides was obtained in a near 1:1 mixture. These compounds were obtained in the same ratio but in lower yield when higher pressures were used for the hydrogenation. When **1** (R = isopropyl) was deacetylated prior to hydrogenation in water containing an equivalent amount of hydrochloric acid, the ratio of glucosaminide to mannosaminide was 3.9:1. Thus, the stereospecificity was appreciably greater. However, the ratio of the *gluco* to *manno* diastereoisomers formed on hydrogenation of the deacetylated oximinoglycosides proved sensitive to the nature of the aglycon. When the methyl group was the aglycon, the ratio was 2.5:1 and the ratio decreased to 1.6:1 when either the ethyl or *n*-propyl group was the aglycon.

In the absence of steric effects from the aglycon, equatorial approach by the hydrogenated catalyst to yield axial amine would be expected to provide the more stable transition state as is normally observed in the reduction of simple oximinocyclohexanes (8). Evidently, the presence of the axial aglycon renders axial approach by the hydrogenated catalyst to the oximino group the more favorable route for these α-D-oximinoglycosides. That this route is most favorable for the isopropyl α-D-oximinoglycosides likely is related to the strain in the orientation shown in **2** for the isopropyl group (6)—the orientation which should allow the most facile equatorial approach by the catalyst. Since axial attack is on the same side of the pyranose ring as is situated the 3-substituent it is not surprising that this route became less favorable when the 3-substituent was changed from hydroxyl to the bulkier acetoxy group.

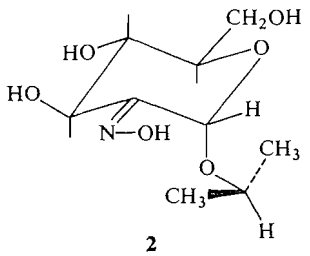

2

As expected from the stereochemical routes of the reductions of the ethyl and *n*-propyl oximinoglycosides, the hydrogenation of methyl 6-*O*-(2-oximino-α-D-*arabino*-hexopyranosyl)-β-D-glucopyranoside gave an about equimolar mixture of the two amino compounds.

It may be noted that a generally stereospecific reduction to equatorial amine has been achieved by way of the corresponding hydrazones (9).

Experimental

Methods and Reference Compounds

Unless otherwise stated, optical rotations were measured in 1 dm tubes using a Perkin–Elmer 141 automatic polarimeter. The nuclear magnetic resonance (n.m.r.) spectra were determined using Varian A60 and HA100 spectrometers and the solvents are mentioned where pertinent. Melting points were determined on a microstage and are uncorrected.

The alkyl tri-*O*-acetyl-2-oximino-α-D-*arabino*-hexopyranosides were previously described (6). The hydrogenation catalyst, about 1 part to 2 parts of the oxime, was 5% palladium on charcoal. All hydrogenations were carried out in a Parr apparatus at 60 p.s.i. and room temperature.

Authentic samples of alkyl 2-acetamido-2-deoxy-α-D-glucopyranoside were prepared by alcoholysis of *N*-acetyl-D-glucosamine in the presence of alcohol-washed Amberlite IR-120 resin in the proton form (10). After reaction at the reflux temperature was complete, the resin was removed by filtration and washed with the alcohol. The combined filtrates were evaporated to dryness *in vacuo* and the solid residue recrystallized to purity in the case of the ethyl, *n*-propyl, and isopropyl 2-acetamido-2-deoxy-α-D-glucopyranosides. In the case of the methyl compound, the crystalline product (68% yield), m.p. 185–187°, $[\alpha]_D^{23}$ +105° (water), was a mixture of the α and β forms. This was evident from the presence of signals for methoxy groups at τ 6.58 (α-form) and 6.46 (β-form) in the n.m.r. spectrum (D_2O as solvent.) The H-1 proton of the α-form gave its signal at τ 5.21. The composition of the product was found to be 9:1 (α:β) by g.l.p.c. analysis as described below. Methanolysis of *N*-acetyl-D-mannosamine provided a syrupy product which appeared to be a mixture of the α and β forms of the methyl 2-acetamido-2-deoxy-D-mannopyranosides in 4:1 ratio both by g.l.p.c. analysis and n.m.r. The spectrum of the product in D_2O showed signals for methoxy groups at τ 6.61 and 6.56 assigned to the α and β anomers, respectively. The ethyl, *n*-propyl, and isopropyl 2-acetamido-2-deoxy-α-D-glucopyranosides were obtained in pure crystalline condition (11).

Ethyl 2-acetamido-2-deoxy-α-D-glucopyranoside, recrystallized from methanol – ethyl acetate, m.p. 175–176°, $[\alpha]_D^{25}$ +144° (*c*, 1 in water). Literature (12) m.p. 177–178°, $[\alpha]_D^{25}$ +134°. The 60 Mc.p.s. n.m.r. spectrum in D_2O exhibited the H-1 doublet at τ 5.15 with a spacing of 2.9 c.p.s.

n-Propyl 2-acetamido-2-deoxy-α-D-glucopyranoside, recrystallized from methanol – ethyl acetate, m.p. 172–

Can. J. Chem. Downloaded from www.nrcresearchpress.com by 210.87.254.105 on 09/05/12
For personal use only.

174°, $[\alpha]_D^{25}$ +139° (*c*, 0.74 in water). Literature (12) m.p. 170–171°, $[\alpha]_D^{25}$ +140.2°. The 60 Mc.p.s. n.m.r. spectrum in D_2O exhibited the H-1 doublet at τ 5.11 with a spacing of 2.9 c.p.s.

Isopropyl 2-acetamido-2-deoxy-α-D-glucopyranoside, recrystallized from methanol – ethyl acetate, m.p. 187–189°, $[\alpha]_D^{25}$ +150° (*c*, 1.3 in water). The product of hydrolysis in refluxing 1.5 *N* hydrochloric acid for 12 h had an infrared spectrum identical to D-glucosamine hydrochloride. The 60 Mc.p.s. n.m.r. spectrum in D_2O exhibited the H-1 doublet at τ 5.03 with a spacing of 2.9 c.p.s.

Anal. Calcd. for $C_{11}H_{21}O_6N$: C, 50.18; H, 8.04; N, 5.32. Found: C, 50.03; H, 8.13; N, 5.26.

Gas–Liquid Partition Chromatographic Analysis and Characterization of Alkyl 2-Acetamido-2-deoxyhexopyranosides

The product formed on hydrogenation of an alkyl oximinoglycoside was analyzed as in the following example using ethyl 2-oximino-α-D-*arabino*-hexopyranoside.

Ethyl tri-*O*-acetyl-2-oximino-α-D-*arabino*-hexopyranoside (347 mg, 1 mole) and tetra-*O*-acetylpentaerythritol (368 mg, 1 mole) were dissolved in methanol (6 ml) and water (6 ml) followed by triethylamine (0.7 ml) were added. The solution was left at room temperature for 5 h after which time it was stirred with washed Amberlite IR 120 H^+ resin (4 ml) until neutral to pH paper. The mixture was filtered, the resin washed with methanol–water (4 × 10 ml, 1:1) and the combined filtrate and washings were reduced to a volume of 1 ml. This was transferred to the hydrogenation flask with water (10 ml) followed by concentrated hydrochloric acid (0.09 ml, 1.1 equivalent) and the palladium on charcoal. After hydrogenation, the catalyst was removed by filtration through Celite, washed with water (4 × 5 ml) and the aqueous solution was freeze-dried to yield an amorphous mass in near quantitatitve yield (400 mg). Nuclear magnetic resonance spectral examination at 60 Mc.p.s. in D_2O showed virtually no acetyl absorptions and revealed the anomeric protons as overlapping doublets at τ 4.84. A sample of the crude hydrogenation product (100 mg) was exchanged with D_2O, freeze-dried, and examined at 100 Mc.p.s. in the same solvent. The anomeric signals were resolved into two sets of doublets with spacings of 3.8 c.p.s. and 1.5. c.p.s. The doublets, which were attributed to the H-1 protons of the α-D-glucosaminyl and α-D-mannosaminyl glycosides respectively, had a relative intensity of 1.8:1.

The crude hydrogenation product (100 mg) was dissolved in water (15 ml) containing methanol (1 ml). Dowex 1X2, 200–400 mesh, carbonate form (3.0 g), and acetic anhydride (1.5 ml) were added. The mixture was stirred for 1.5 h at room temperature after which time the resin was removed by filtration, washed with water (5 × 10 ml), and the combined aqueous solution was freeze-dried to yield an amorphous mass (90 mg). A portion (30–40 mg) of this product was taken up in dry pyridine (1 ml) and treated in a glass-stoppered vial with hexamethyldisilazane (0.5 ml) and trimethylsilyl chloride (0.5 ml). The mixture was shaken for 15 min, centrifuged, and the clear supernatant was taken to dryness at 35°. The resultant pale-brown syrup was taken up in dry methylene chloride (0.3 ml) and examined gas-chromatographically. The chromatograms were obtained with an apparatus equipped with a thermal conductivity detector using a 6 ft (¼ in. O.D.) copper tube packed with 5% SE-GE30 silicone rubber on nonacid-washed 30–60 mesh Chromosorb W. The temperature was first programmed at 4° per min from 100° to 200° and then kept constant at 200°. The flow rate of helium was 100 ml per min. Control experiments indicated an accuracy of ±2% in the estimation of the amount of a trimethylsilylated glycoside relative to the amount of the internal standard (tetra-*O*-trimethylsilylpentaerythritol).

Three main peaks were observed corresponding to the internal standard and to the two α-glycosaminides. Integration by the method of triangulation indicated an about 90% yield of the glycosides with the *gluco–manno* ratio 1.6:1. The *gluco* isomer, retention time 2.4 relative to the internal standard, was identified by direct comparison with authentic samples. The *manno* isomer, retention time 2.0, was identified from the correspondence of the ratio determined with that determined by n.m.r. Several unidentified peaks corresponding to less than 10% of the total product were observed.

Hydrogenation of the methyl oximinoglycoside followed by conversion to the *N*-acetates of the methyl glycosaminides gave a syrupy product which was exchanged with deuterium oxide for n.m.r. analysis at 100 Mc.p.s. and 55°. Doublets were present at τ 4.71 and 4.80 (using pyrazine as an internal standard) with spacings of 3.0 and 1.5 c.p.s., respectively. These signals, assigned to the anomeric protons of methyl *N*-acetyl-α-D-glucosaminide and methyl *N*-acetyl-α-D-mannosaminide, respectively, had relative intensities of 2.7:1. Gas–liquid partition chromatographic analysis showed the presence of two main components in the ratio of 2.5:1. The major component had a retention time identical to that of an authentic sample prepared from methyl *N*-acetyl-α-D-glucosaminide.

In the case of the *n*-propyl and isopropyl glycosides, the relative amounts of α-D-*gluco* to α-D-*manno* products were 1.6:1 (1.6:1 by n.m.r.) and 3.9:1 (3.7:1 by n.m.r.), respectively.

The hydrogenation of the isopropyl oxime gave a sufficiently high yield of isopropyl 2-amino-2-deoxy-α-D-glucopyranoside hydrochloride to allow the direct isolation and purification of this compound (see below). However, the corresponding experiments starting from the ethyl and *n*-propyl oximes required purification of the hydrochlorides by column chromatography on microcrystalline cellulose (13) followed by *N*-acetylation (10) to obtain a pure crystalline product. The yields were 25–35% in each case and the products were identified by direct comparison with authentic samples.

A portion of the products from the catalytic hydrogenation of the ethyl, *n*-propyl, and isopropyl oximes was passed through basic ion exchange resin (Dowex 1X2, OH^- form) to remove reducing sugars (4). The material (20 mg) was hydrolyzed for 12 h in 2 *N* hydrochloric acid (1 ml), and after workup in the usual manner was *N*-acetylated (10), trimethylsilylated and (7), examined by g.l.p.c. using the conditions previously mentioned. In all cases glucosamine and mannosamine were shown to be present by direct chromatographic comparison with authentic samples.

Hydrogenation of isopropyl tri-*O*-acetyl-2-oximino-α-D-*arabino*-hexopyranoside in methanol and in the pres-

Can. J. Chem. Downloaded from www.nrcresearchpress.com by 210.87.254.105 on 09/05/12
For personal use only.

ence of 1.1 equivalents of hydrogen chloride was found by g.l.p.c. analysis to give a near quantitative yield of the α-D-*gluco* and α-D-*manno* products in 1:1 ratio. The only variation in the analytical procedure was to fully acetylate the product with pyridine and acetic anhydride and then to de-*O*-acetylate prior to trimethylsilylation. The yield was only 50% when the hydrogenation was conducted at 1000 p.s.i.

Isopropyl 2-Amino-2-deoxy-α-D-glucopyranoside Hydrochloride

Deacetylation of 1.44 g of crystalline isopropyl tri-*O*-acetyl-2-oximino-α-D-*arabino*-hexopyranoside followed by hydrogenation as described above but in the absence of the internal standard gave, on freeze-drying the aqueous solution, 0.87 g of a product which crystallized from 95% ethanol on the addition of ethyl acetate. The yield was 35%, m.p. 209–211° (decomp.), $[\alpha]_D^{25}$ +156° (*c*, 1 in water).

Anal. Calcd. for $C_9H_{20}O_5NCl$: C, 41.94; H, 7.82; N, 5.44. Found: C, 42.04; H, 8.08; N, 5.40.

N-Acetylation following the method of Roseman and Ludowieg (10) gave a product identical to isopropyl 2-acetamido-2-deoxy-α-D-glucopyranoside.

Methyl 6-O-(2-Amino-2-deoxy-α-D-glucopyranosyl)-β-D-glucopyranoside and Methyl 6-O-(2-Amino-2-deoxy-α-D-mannopyranosyl)-β-D-glucopyranoside Hydrochlorides

The crude condensation product (6) (4.9 g) was dissolved in methanol (20 ml) with water added to turbidity and deacetylated using triethylamine (3 ml) as described above. The deacetylated material was hydrogenated at 60 p.s.i. in the presence of one equivalent of hydrochloric acid and 5% palladium on charcoal (1 g) for 24 h at room temperature. The freeze-dried product was a pale-yellow syrup which was shown by paper chromatography in *n*-butanol – pyridine – water – acetic acid (6:4:3:1) to contain one major ninhydrin positive component (R_{gNH_3Cl} = 0.70), methyl β-D-glucopyranoside (R_{gNH_3Cl} = 2.2), as well as several unidentified minor components which appeared as streaks. The mixture was chromatographed on microcrystalline cellulose (13) using the above solvent system and a column of dimensions 60 × 5 cm. A flow rate of 20 ml/h was employed and 5 ml fractions were collected and analyzed polarimetrically. The observed rotations were plotted graphically and the pertinent fractions were combined. Methyl β-D-glucopyranoside (550 mg) was obtained crystalline on evaporation of the levorotatory fractions. The methyl 6-*O*-(α-D-glucosaminyl and α-D-mannosaminyl)-β-D-glucoside hydrochlorides (750 mg, 24% based on the nitrosyl chloride dimeric adduct), although separated from other materials, were not resolved and were obtained as a pale-yellow amorphous solid, $[\alpha]_D$ +18.3° (*c*, 2.4 in water).

The disaccharide fraction appeared as a homogeneous spot on paper chromatographic analysis in several solvent systems. However, the use of electrophoresis (borate buffer, pH 8.6, sodium borate 8.8 g/l, boric acid 4.65 g/l) at a constant voltage of 400 V for 4 h indicated the presence of two close-moving, ninhydrin-positive components.

Nuclear magnetic resonance analysis at 100 Mc.p.s. in D_2O at 55° indicated the presence of the four expected anomeric doublets. Two overlapping H-1 doublets were observed at approximately τ 5.5 with spacings of 7.5 c.p.s. as expected for the two axial H-1 protons of the methyl β-glucosidic residues. Two doublets at about τ 4.90, which could not be resolved at 60 Mc.p.s., had spacings at 100 Mc.p.s. of 3.5 c.p.s. and less than 1 c.p.s. and these were attributed to the α-glucosaminyl and α-mannosaminyl groups, respectively. The ratio of the intensities of the latter doublets was 1.1/1 with the glucosaminyl isomer predominating.

Acknowledgments

The authors are indebted to the Corn Industries Research Foundation and the National Research Council of Canada for grants in aid of this research. The n.m.r. and microanalyses were determined in this department. The methanolyses of *N*-acetyl-D-mannosamine were carried out by T. L. Nagabhushan.

1. J. D. Dutcher. Advan. Carbohydrate Chem. **18**, 259 (1963).
2. J. Staněk, M. Černý, J. Kocourek, and J. Pacák. The monosaccharides. Publishing House of the Czechoslovak Academy of Sciences, Prague. 1963. pp. 267 and 514.
3. S. A. Barker, M. Stacey, and D. J. Tipper. Nature, **184**, 1718 (1959); J. Hoshimura, H. Ando, Y. Takahashi, M. Ono, and T. Sato. Nippon Kagaku Zasshi, **85** (2), 142 (1964); Chem. Abstr. **62**, 623 (1965); Y. Matsushima and T. Miyazaki. Bull. Chem. Soc. Japan, **38**, 1325 (1965).
4. F. E. Hardy, J. G. Buchanan, and J. Baddiley. J. Chem. Soc. 3360 (1963); F. E. Hardy. J. Chem. Soc. 375 (1965); P. F. Lloyd and G. P. Roberts. J. Chem. Soc. 6910 (1965); S. Umezawa and S. Koto. J. Antibiotics Tokyo, Ser. A, **17**, No. 5, 186 (1964); **19**, No. 2, 88 (1966).
5. R. U. Lemieux, S. W. Gunner, and T. L. Nagabhushan. Tetrahedron Letters, No. 26, 2149 (1965).
6. R. U. Lemieux, S. W. Gunner, and T. L. Nagabhushan. Can. J. Chem. **46**. This issue.
7. M. B. Perry. Can. J. Biochem. **42**, 451 (1964).
8. E. L. Eliel, N. L. Allinger, S. J. Angyal, and G. A. Morrison. Conformational analysis. Interscience Publishers, New York. 1965. p. 119. *See also* P. M. Collins and W. G. Overend. J. Chem. Soc. 1912 (1965); 3448 (1965).
9. R. U. Lemieux, S. W. Gunner, Y. Ito, and M. E. Evans. 154th meeting, American Chemical Society, Chicago, Sept. 11–14, 1967. Abstr. papers D 18.
10. S. Roseman and J. Ludowieg. J. Am. Chem. Soc. Soc. **76**, 301 (1954).
11. D. Horton. Advan. Carbohydrate Chem. **15**, 159 (1960).
12. F. Zilliken, C. S. Rose, G. A. Braun, and P. György. Arch. Biochem. Biophys. **54**, 392 (1955).
13. M. L. Wolfrom, D. H. Busch, R. M. de Lederkremer, S. C. Vergez, and J. R. Vercellotti. J. Chromatog. **18**, 42 (1965).

Can. J. Chem. Downloaded from www.nrcresearchpress.com by 210.87.254.105 on 09/05/12
For personal use only.

The synthesis of 2-amino-2-deoxyhexoses: D-glucosamine, D-mannosamine, D-galactosamine, and D-talosamine[1]

R. U. LEMIEUX AND T. L. NAGABHUSHAN
Department of Chemistry, University of Alberta, Edmonton, Alberta

Received August 9, 1967

Methods for the preparation of the hydrochlorides of 2-amino-2-deoxy-D-glucose (D-glucosamine) and 2-amino-2-deoxy-D-mannose (D-mannosamine) from tri-*O*-acetyl-D-glucal and of 2-amino-2-deoxy-D-galactose (D-galactosamine) and 2-amino-2-deoxy-D-talose (D-talosamine) from tri-*O*-acetyl-D-galactal are described. The reactions involve addition of nitrosyl chloride to the acetylated glycal followed by conversion of the adduct to acetylated derivative of the 2-oximinohexose and reduction of the oxime to amine.

Canadian Journal of Chemistry, **46**, 401 (1968)

Although 2-amino-2-deoxy-D-glucose (D-glucosamine) is readily available from natural sources (1), other naturally occurring 2-amino-2-deoxyhexoses such as D-galactosamine (2), D-mannosamine (3–5), and D-talosamine (6, 7) can only be obtained through multi-step chemical syntheses in low overall yield. Thus, D-galactosamine hydrochloride was prepared from D-lyxose by way of 2-amino-2-deoxy-D-galactononitrile in 33–38% overall yield (8). Another method proceeds from 1,6:2,3-dianhydro-β-D-talopyranose (9). Several methods for the preparation of D-mannosamine have been reported (10–14). Of these, the modified synthesis (12) of Sowden and Oftedahl (11) seems most practical. The general epimerization procedure (13) has been applied to the preparation of D-talosamine from D-galactosamine (15). Jeanloz and co-workers (16) have reported a multi-step synthesis of D-talosamine from D-galactose.

The purpose of this publication is to report in further detail the procedures outlined in a preliminary communication (17) for the synthesis of either D-glucosamine or D-mannosamine from tri-*O*-acetyl-D-glucal and of either D-galactosamine or D-talosamine from tri-*O*-acetyl-D-galactal. In the first step, nitrosyl chloride is added to the acetylated glycal to yield the dimeric tri-*O*-acetyl-2-deoxy-2-nitroso-α-D-hexopyranosyl chloride—a reaction which yields well defined crystalline products in near quantitative yield (18–20). Acetolysis of this glycosyl halide yields the tetra-*O*-acetyl-2-oximinosugar (**1***a* or **1***b*) and reduction of the oxime with zinc – copper couple in glacial acetic acid followed by acetylation provides, as expected, the acetylated derivative of the 2-amino-2-deoxyhexose with the amino group in equatorial orientation, e.g., either D-glucosamine or D-galactosamine, which after deacetylation provides the crystalline hydrochloride (**2***a* or **2***b*). On the other hand, treatment of the glycosyl chloride with acetic anhydride and a base (for example, sodium acetate or triethylamine) provides the penta-*O*-acetyl derivative of the 2-oximinohexose (**3***a* or **3***b*) (20) and catalytic hydrogenation of this compound using palladium on carbon affords, after deacetylation of the product, the 2-amino-2-deoxyhexose as the hydrochloride (**4***a* or **4***b*) with the amino group in axial orientation, e.g., either D-mannosamine or D-talosamine. The yields are in the range 70–80% from the acetylated glycal and the method should prove of general application for the synthesis of 2-amino-2-deoxysugars from glycals. Serfontein, Jordaan, and White (18) have identified D-glucosamine by paper and thin-layer chromatography as a product from the zinc – copper couple in glacial acetic acid reduction of tri-*O*-acetyl-2-deoxy-2-nitroso-α-D-glucopyranosyl chloride followed by deacetylation.

Experimental

D-*Glucosamine Hydrochloride*

Zinc–copper couple (0.7 g, Ventron Corporation, Congress Street, Beverly, Massachusetts) was added to a stirred solution of dimeric tri-*O*-acetyl-2-deoxy-2-nitroso-α-D-glucopyranosyl chloride (20) (0.38 g) in glacial acetic acid (3.5 ml) and acetic anhydride (0.5 ml). The mixture was stirred efficiently for two days at room temperature, after which time the same amounts of zinc–copper couple,

[1]This research was presented in a thesis by T. L. Nagabhushan in partial fulfillment of the requirements for the Ph.D. degree, 1966. Presented at the 150th Meeting of the American Chemical Society, Atlantic City, New Jersey, September 13–17, 1965. Abstract of papers, p. 21D.

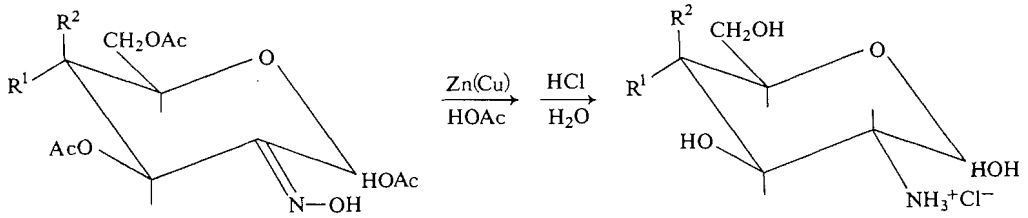

1*a*, R^1 = OAc, R^2 = H
1*b*, R^1 = H, R^2 = OAc

2*a*, R^1 = OH, R^2 = H
2*b*, R^1 = H, R^2 = OH

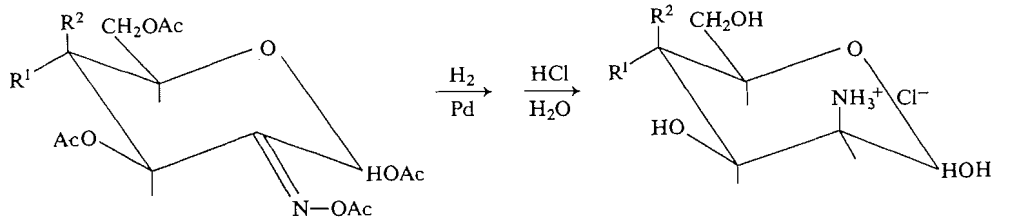

3*a*, R^1 = OAc, R^2 = H
3*b*, R^1 = H, R^2 = OAc

4*a*, R^1 = OH, R^2 = H
4*b*, R^1 = H, R^2 = OH

acetic acid, and acetic anhydride were introduced and the stirring continued for an additional two days. The solids were collected by filtration and washed with chloroform. The combined filtrates were diluted with chloroform (20 ml) and the chloroform solution was washed successively with water, saturated aqueous sodium bicarbonate solution, and again water. The resulting chloroform solution was dried over sodium sulfate and taken to dryness. The syrupy residue was heated with stirring on a steam bath for 70 min with 1.5 ml of 4 *N* hydrochloric acid. The light-brown solution was decolorized with active charcoal, filtered through Celite, and taken to dryness *in vacuo*. The residual syrup was dehydrated by adding 2-propanol and its removal *in vacuo*. The white solid material was dried and crystallized from ethanol–acetone. A 0.171 g yield (80%) of a crystalline precipitate was deposited which gave infrared and nuclear magnetic resonance (n.m.r.) spectra identical to those of a commercial sample of D-glucosamine hydrochloride and which possessed the expected specific rotation (1). Furthermore, when examined by high voltage paper electrophoresis, under conditions which separated D-glucosamine (mobility, 17.5 cm) and D-mannosamine (mobility, 20.4 cm) (3 kV, 35 min; pyridine, acetic acid, water buffer of pH 6.5) the compound showed a single spot (mobility, 17.5 cm) after development with the cadmium acetate – ninhydrin reagent (21).

In a separate experiment, the residue (1.15 g) from the chloroform extraction was dissolved in 15 ml of 70% aqueous methanol and 4 ml of triethylamine was added. After standing overnight at room temperature, the solution was taken to dryness *in vacuo*, the residue dissolved in water, and the aqueous extract decolorized. The solution was then neutralized with a small amount of Amberlite IR-120 ion-exchange resin in the proton form. Removal of the water left a syrup which crystallized from a mixture of ethanol and ether. The yield was 0.51 g (70%) of a compound, m.p. 186–190°, $[\alpha]_D^{23}$ +40° (*c*, 1 in water), with the same n.m.r. and infrared spectra as those for an authentic sample of *N*-acetyl-D-glucosamine (22), m.p. 186–189°, $[\alpha]_D^{23}$ +42° (*c*, 1 in water), prepared by *N*-acetylation of D-glucosamine hydrochloride following the procedure of Roseman and Ludowieg (23).

Reduction of 1,3,4,6-Tetra-O-acetyl-2-oximino-α-D-arabino-hexopyranose (24)

A solution of the 1,3,4,6-tetra-*O*-acetyl-2-oximino-α-D-*arabino*-hexopyranose (0.722 g, 2 mmoles) in glacial acetic acid (7 ml) and acetic anhydride (1 ml) was reduced with zinc – copper couple (1.4 g) as described above and worked-up in the usual manner afforded a syrupy product which was chromatographed on a silicic acid column (1 × 30 cm) using ethyl acetate as the solvent. Evaporation of the solvent left a white solid residue which was crystallized from ethanol. The yield of the compound, m.p. 136–138°, $[\alpha]_D^{24}$ +90° (*c*, 2 in chloroform), was 0.4 g (52%) (reported in the literature (25) for α-D-glucosamine pentaacetate, m.p. 139°, $[\alpha]_D$ +92°).

D-Galactosamine Hydrochloride

Dimeric tri-*O*-acetyl-2-deoxy-2-nitroso-α-D-galactopyranosyl chloride (20) (0.34 g) was reduced with the zinc – copper couple described above and the product isolated and deacetylated as described above for the preparation of D-glucosamine hydrochloride. The yield, after one recrystallization from ethanol–ether was 0.175 g (82%), m.p. 180° (decomp.), $[\alpha]_D^{23}$ +91.4° (*c*, 2 in water, final). D-Galactosamine hydrochloride is reported (26) to melt at 178° with $[\alpha]_D$ +93° (*c*, 0.75 in water). The n.m.r. and infrared spectra of the compound were identical to those of an authentic commercial sample of D-galactosamine hydrochloride. The high voltage paper electrophoresis of the synthetic compound (see section under D-Glucosamine Hydrochloride) showed a single spot (mobility, 18.2 cm).

Can. J. Chem. Downloaded from www.nrcresearchpress.com by 210.87.254.105 on 09/05/12
For personal use only.

Can. J. Chem. Downloaded from www.nrcresearchpress.com by 210.87.254.105 on 09/05/12
For personal use only.

D-*Mannosamine Hydrochloride*

A solution of syrupy penta-*O*-acetyl-2-oximino-D-*arabino*-hexopyranose (20) (2.5 g) in glacial acetic acid (25 ml) and acetic anhydride (10 ml) was hydrogenated in the presence of 5% palladium on carbon (0.75 g) at room temperature and an initial pressure of 60 p.s.i. for 48 h. The catalyst was removed by filtration through Celite. The filter cake was washed with glacial acetic acid and the combined filtrates were evaporated to a syrup at diminished pressure. The syrupy product was heated with 4 *N* hydrochloric acid (30 ml) on a steam bath, within initial swirling in order to obtain a homogenous solution, for 50 min. The light-brown colored solution was treated with charcoal and the solids were removed by filtration. The filter cake was washed with water and the combined filtrates evaporated to a syrup at reduced pressure. The syrup was dehydrated by the addition of isopropyl alcohol followed by its removal by evaporation *in vacuo*. The residual white crystals, gathered by filtration with the aid of ice-cold isopropyl alcohol, were washed with ether and dried. Recrystallization of the crude product from ethanol–acetone mixture gave 1.04 g (80%) of a compound, m.p. 178–180°, $[\alpha]_D^{23}$ −3.0° (*c*, 2 in water, no mutarotation), literature (11) m.p. not given, $[\alpha]_D^{25}$ −3.2°, (*c*, 10 in water, no mutarotation). Ninhydrin degradation (27) of the compound afforded D-arabinose which was identified by paper chromatography.

Anal. Calcd. for $C_6H_{14}NO_5Cl$: C, 33.40; H, 6.49; N, 6.49. Found: C, 33.38; H, 6.51; N, 6.49.

Although the *x*-ray powder diagram was identical to that of an authentic sample of D-mannosamine hydrochloride prepared following the procedure of Satoh and Kiyomoto (12), a high-voltage paper electrophoresis examination showed the presence of a trace of D-glucosamine.

The compound was *N*-acetylated following the procedure of Roseman and Ludowieg (23) to yield a product which crystallized from 70% aqueous ethanol on the addition of ether to the point of turbidity. A 76% yield of substance, m.p. 107–108°, $[\alpha]_D^{23}$ +10° (*c*, 2.5 in water, final) was obtained with physical constants in close agreement with those reported for *N*-acetyl-D-mannosamine (12).

D-*Talosamine Hydrochloride*

Penta-*O*-acetyl-2-oximino-D-*lyxo*-hexopyranose (20) (2.5 g) was reduced in a mixture of glacial acetic acid (25 ml) and acetic anhydride (10 ml) using the procedure described above for the reduction of the *arabino* isomer. The syrupy product was hydrolyzed with 4 *N* hydrochloric acid (30 ml) for 80 min at 100° and the residue, on solvent removal, was recrystallized from a mixture of hot ethanol and acetone. The yield was 1.03 g (80%) of a compound, m.p. 152–153° with decomposition, $[\alpha]_D^{23}$ −5.8° (*c*, 1 in water). D-Talosamine hydrochloride is reported (16) to melt at 150–151° with $[\alpha]_D^{23}$ +3° (3 min) to −6° (final) (*c*, 0.9 in water). Ninhydrin oxidation gave D-lyxose as identified by paper chromatography (27).

Acknowledgments

The authors are grateful for a grant to R.U.L. from the National Research Council of Canada (T-172) in aid of this research. We wish to thank Dr. C. Campbell for the *x*-ray powder diagram and Dr. L. B. Smillie for the use of the high-voltage electrophorator.

1. M. Stacey and J. M. Webber. *In* Methods in carbohydrate chemistry. Vol. I. Academic Press, Inc., New York. 1962. p. 228.
2. S. Suzuki and J. L. Strominger. J. Biol. Chem. **235**, 2768 (1960).
3. R. Kuhn and R. Brossmer. Ann. **616**, 222 (1958).
4. D. G. Comb and S. Roseman. J. Am. Chem. Soc. **80**, 498, 3166 (1958).
5. J. Brug and G. B. Paerels. Nature, **182**, 1159 (1958).
6. H. Muir. Biochem. J. **62**, 26 (1956); **65**, 33 (1957).
7. M. J. Crumpton. Nature. **180**, 605 (1957).
8. R. Brossmer. *In* Methods in carbohydrate chemistry. Vol. I. Academic Press, Inc., New York. 1962. p. 216.
9. R. W. Jeanloz and P. J. Stoffyn. *In* Methods in carbohydrate chemistry. Vol. I. Academic Press, Inc., New York. 1962. p. 221.
10. W. Roth and W. Pigman. J. Org. Chem. **26**, 2455 (1961).
11. J. C. Sowden and M. L. Oftedahl. J. Am. Chem. Soc. **82**, 2303 (1960).
12. C. Satoh and A. Kiyomoto. Chem. Pharm. Bull. Tokyo. **12**, No. 5, 615 (1964).
13. C. T. Spivak and S. Roseman. J. Am. Chem. Soc. **81**, 2403 (1959).
14. R. Kuhn and W. Bister. Ann. **602**, 217 (1957).
15. S. Fujii and H. Kushida. Biochim. Biophys. Acta, **69**, 572 (1963).
16. R. W. Jeanloz, Z. Tarasiejska-Glazer, and D. A. Jeanloz. J. Org. Chem. **26**, 532 (1961).
17. R. U. Lemieux and T. L. Nagabhushan. Tetrahedron Letters, No. 26, 2143 (1965).
18. W. J. Serfontein, J. H. Jordaan, and J. White. Tetrahedron Letters, No. 18, 1069 (1964).
19. R. U. Lemieux, T. L. Nagabhushan, and I. K. O'Neill. Tetrahedron Letters, No. 29, 1909 (1964).
20. R. U. Lemieux, T. L. Nagabhushan, and I. K. O'Neill. Can. J. Chem. This issue.
21. J. Heilmann, J. Barollier, and E. Watzke. Z. Physiol. Chem. **309**, 219 (1957).
22. P. Kasser and A. Hoffmann. Helv. Chim. Acta, **12**, 616 (1929).
23. S. Roseman and J. Ludowieg. J. Am. Chem. Soc. **76**, 301 (1954).
24. R. U. Lemieux, T. L. Nagabhushan, and S. W. Gunner. Can. J. Chem. This issue.
25. O. Westphal and H. Holzmann. Ber. **75**, 1274 (1942).
26. R. Kuhn and W. Kirschenlohr. Ann. **600**, 126 (1956).
27. S. Gardell, F. Heykenskjold, and A. Roch-Norlund. Acta Chem. Scand. **4**, 970 (1950).

Synthesis of 3,4,6-Tri-*O*-acetyl-2-oximino-α-D-hexopyranosides[1]

R. U. LEMIEUX, T. L. NAGABHUSHAN, AND S. W. GUNNER[2]
Department of Chemistry, University of Alberta, Edmonton, Alberta
Received August 9, 1967

The reaction of the dimeric nitrosyl chloride adducts of tri-*O*-acetyl-D-glucal and tri-*O*-acetyl-D-galactal with alcohols and phenols in dimethylformamide at room temperature provides the corresponding tri-*O*-acetyl-2-oximino-α-D-hexopyranosides in good to excellent yields. The condensation can also be carried out in tetrahydrofuran in the presence of pyridine or simply in refluxing methylene chloride for the simple alkyl alcohols. The stereospecificity of the reaction is extreme; only products of one configuration for both glycosidic linkage and the oximino group were detected. This result is rationalized on the basis of a *cis*-configuration for a tri-*O*-acetyl-2-nitroso-D-glycal intermediate in the H1 half-chair conformation. The introduction of methyl groups on the carbon of the methoxy group of methyl α-D-glucopyranosides causes a progressive deshielding of the anomeric proton. The data indicate that isopropyl α-D-glycopyranosides avoid the orientation for the aglycon which has the anomeric hydrogen projecting between the two methyl groups of the aglycon. Methyl tri-*O*-acetyl-6-*O*-(tri-*O*-acetyl-2-oximino-α-D-*arabino*-hexopyranosyl)-β-D-glucopyranoside was prepared in 70% yield to illustrate the use of the method for the preparation of an α-linked disaccharide.

Canadian Journal of Chemistry, 46, 405 (1968)

The presence of the α-linkage between a variety of 2-amino-2-deoxysugar residues and the aglycon in several antibiotics has rendered important the development of reliable methods for the synthesis of 2-amino-2-deoxy-α-glycopyranosides. Although the 2-amino group in most of these antibiotics (1), e.g. streptomycin, kanamycin B, neomycins, and paromomycins, is in equatorial orientation, in at least one case, e.g. kasugamycin (2), the group is oriented axially. The purpose of this communication is to report a general synthesis of 2-oximino-α-glucopyranosides which can serve, through reduction, as precursors of the corresponding 2-amino-2-deoxy-α-glucopyranosides (3). Also, through hydrolysis followed by reduction the oximes can serve as precursors of α-D-glucopyranosides (4). The preparations of the α-oximinoglycosides are highly stereospecific and the yields are good even with highly hindered alcohols. Preliminary reports of this work were published (5, 6).

As previously shown (5), reaction of tri-*O*-acetyl-D-glucal with nitrosyl chloride yields tri-*O*-acetyl-2-deoxy-2-nitroso-α-D-glucopyranosyl chloride (**1**) as a dimer in over 90% yield. Compound **1** is extremely prone to dehydrochlorination. This is demonstrated by the fact that addition of triethylamine to the compound dissolved in tetrahydrofuran at −15° results in the immediate precipitation of triethylamine hydrochloride and the formation of an intensely blue solution. The product isolated was an amorphous colorless substance which was not characterized. The colored intermediate in this reaction is considered to be 2-nitroso-D-glucal triacetate (**2**). The postulation of this compound as an intermediate in the reaction provides a basis for the rationalization of the retention of configuration obtained in the overall reaction. Indeed, recently, Collin and Pritzkow (7, 8) have shown several dimeric nitroso–chloro adducts of olefins to undergo nucleophilic substitution by way of highly reactive conjugated nitroso-olefins to give α-substituted oximes. It was expected then, that the intermediate **2** would be strongly electrophilic especially in view of its enolic ether structure and readily undergo reaction with a wide variety of nucleophiles. This has proven to be the case.

Initially, it was thought necessary to perform the condensation of the nitrosyl chloride adduct (**1**) with an alcohol in the presence of a base to carry out the dehydrochlorination reaction and release the acetylated 2-nitroso-D-glucal (**2**). Indeed, using 4 moles of alcohol per mole of the dimer (**1**) and 4 mole equivalents of pyridine

---

[1]Presented in part by T. L. Nagabhushan in partial fulfillment of the requirements for the Ph.D. degree, 1966. Presented in part at the 150th Meeting of the American Chemical Society, Atlantic City, N.J., September 13–17, 1965. Abstract of Papers, p. 21D.

[2]University of Alberta Postdoctorate Fellow, 1964–1965. Corn Industries Research Foundation Research Associate, 1965–1967. Present address: Food and Drug Directorate, Department of Health and Welfare, Ottawa, Canada.

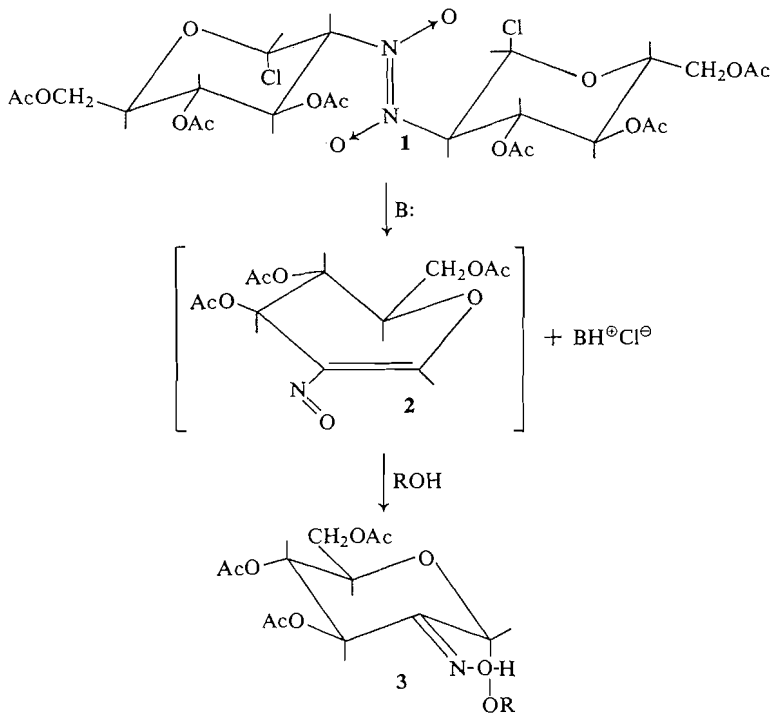

in tetrahydrofuran, excellent yields (over 80%) of the oximino-α-D-hexopyranoside (**3**) were obtained (see Table I). In the absence of the alcohol, acetylated pyridinium oximinoglycoside was the product of the reaction. The compound was highly unstable and could not be purified. It was subsequently found that the nitrosyl chloride adduct (**1**) underwent dehydrochlorination with sufficient ease that a base, such as pyridine, was not required in the reaction medium. Thus, for example, the variety of alkyl tri-*O*-acetyl-2-oximino-α-D-*arabino*-hexopyranosides (see Table I) were prepared in excellent yield simply by refluxing for a few hours a solution of the nitrosyl chloride adduct (**1**) in methylene chloride containing about 1.2 mole equivalents of the alkyl alcohol. The products of these reactions were the same as those obtained in the presence of the pyridine. It was found that the glycosidation reaction proceeded well at room temperature using dimethylformamide as solvent. This fact renders this reaction useful for the α-glycosidation of virtually any alcohol. To illustrate this fact, the preparation of methyl tri-*O*-acetyl-6-*O*-(3,4,6-tri-*O*-acetyl-2-oximino-α-D-*arabino*-hexopyranosyl)-β-D-glucopyranoside in 70% yield is reported herein. This and other similar condensations did not proceed in acceptable yields by simply refluxing a solution of the reactants in methylene chloride. The

TABLE I

3,4,6-Tri-*O*-acetyl-2-oximinohexopyranosides

Aglycon	Method*	Yield, %	Melting point, °C	$[\alpha]_D^{25}$ (chloroform)
α-D-*Arabino*				
Methyl	A	81†	145–146	+48°
	B	88		
Ethyl	B	75†	154–157	+72
n-Propyl	B	75†	61.5–62	+74
n-Butyl	B	80‡	—	+61
Isobutyl	B	83‡	—	+63
Isopropyl	A	85†	94–96	+79
	B	89†	94–96	+79
	C	80†	94–96	+79
t-Butyl	B	80‡	—	+77
Phenyl	C	67†	165–167	+94
α-Naphthyl	C	42†	155–158	+131
Acetyl	—	31†	138–139	+44
α-D-*Lyxo*				
n-Propyl	A	—‡	—	+51
Isopropyl	A	—‡	—	+66

*See Experimental section.
†After purification by recrystallization.
‡Crude syrupy product.

TABLE II

Nuclear magnetic resonance parameters for alkyl, aryl, and acetyl 3,4,6-tri-*O*-acetyl-2-oximino-α-D-*arabino*-hexopyranosides[1]

Aglycon	Chemical shifts, τ values			
	H-1	H-3	H-4	OH
Deuteriochloroform as solvent				
Methyl	4.08	4.18	4.79	—
Ethyl	3.95	4.14	4.78	—
n-Propyl	3.97	4.15	4.81	—
n-Butyl	3.99	4.16	4.82	—
Isobutyl	4.01	4.17	4.81	—
Isopropyl	3.86	4.13	4.81	—
Isopropyl, *O*-acetyl	3.93	4.08	4.71	—
trans-4-*t*-Butylcyclohexyl	3.83	4.13	4.82	—
t-Butyl	3.65	4.11	4.83	—
Phenyl	3.50	4.06	4.87	—
α-Naphthyl	3.32	4.04	4.81	—
Acetyl	2.71	4.18	4.75	—
Perdeuteriodimethyl sulfoxide as solvent				
Methyl	4.18	4.43	4.96	−1.75
Ethyl	4.12	4.45	5.02	—
n-Propyl	4.13	4.46	5.02	—
n-Butyl	4.10	4.45	4.98	−1.68
Isobutyl	4.12	4.44	4.98	−1.68
Isopropyl	4.01	4.47	5.02	—
trans-4-*t*-Butylcyclohexyl	4.00	4.50	5.04	—
t-Butyl	3.78	4.43	5.01	−1.52

[1]The spacings arising from $J_{3,4}$ and $J_{4,5}$ were 9.5 c.p.s. in deuteriochloroform and 10.0 c.p.s. in perdeuteriodimethyl sulfoxide.

phenyl and α-naphthyl oximinoglycosides were obtained readily using dimethylformamide as solvent. Inspection of the nuclear magnetic resonance (n.m.r.) and optical rotational data in Tables I and II indicates that the reaction products are configurationally and conformationally related. The values of the coupling constants $J_{3,4}$ and $J_{4,5}$, reported in Table II require the compounds to exist in solution in the C1 conformation. That these compounds were in fact oximes was established by the presence of a signal at τ 0.28–0.75 in deuteriochloroform which was attributable to oximino-hydroxyl and which disappeared on exchange with deuterium oxide. Further evidence for the oximino group in the title compounds was provided by the infrared absorption for the hydroxyl group at 3450 cm^{-1} and the preparation of isopropyl tetra-*O*-acetyl-2-oximino-α-D-*arabino*-hexopyranoside with n.m.r. parameters similar to the parent triacetate. The α-configurations for the *O*-acetyl-oximinoglucosides were in several cases established by reduction to known 2-amino-2-deoxy-α-D-glucopyranosides (3). In the cases of the isopropyl and phenyl oximinoglucosides, each compound was converted to the known α-D-glucopyranoside tetraacetate by hydrolysis of the oxime followed by borohydride reduction and reacetylation (4).

Reaction of the nitrosyl chloride adduct **1** with sodium acetate in acetic acid gave crystalline 1,3,4,6-tetra-*O*-acetyl-2-oximino-α-D-*arabino*-hexopyranose. The α-configuration was established by reduction with zinc–copper couple in glacial acetic acid followed by *N*-acetylation to the known 2-acetamido-tetra-*O*-acetyl-2-deoxy-α-D-glucopyranose (5).

Table I reports the syrupy products obtained on reaction of dimeric tri-*O*-acetyl-2-deoxy-2-nitroso-α-D-galactopyranosyl chloride with *n*-propyl and isopropyl alcohol. The n.m.r. spectra of these products left no doubt as to their virtual purity and structure. The α-D-anomeric configurations are assigned on the basis of the rotational and n.m.r. data.

The yields given in Table I relate in most cases to the amount of material obtained in pure form after crystallization of the crude product. In these instances, the n.m.r. spectrum of the purified substance was virtually identical to that of the initially isolated syrupy product. It was evident, therefore, that the reactions proceeded in near quantitative yield and that the reaction was of extreme stereospecificity. Collins (9) has shown that the oximation of ketoglycosides normally provides mixtures of the expected *syn* and *anti* forms. Efforts are at present underway to determine the configuration of β-chloroethyl tri-*O*-acetyl-2-oximino-α-D-*arabino*-hexopyranoside by *x*-ray crystallography.

Nuclear magnetic resonance parameters for a number of oximinoglycosides using both deuteriochloroform and perdeuterated dimethylsulfoxide as solvents are presented in Table II. The data indicate that all the oximes have the same configuration since the range in chemical shifts for the anomeric protons is less than would be expected if these occurred as *syn* and *anti* forms (9). In this regard, it is to be noted that the trend observed for the chemical shift of the anomeric proton on changing the aglycon from methyl to ethyl to isopropyl to *t*-butyl is the same as that for the corresponding alkyl α-D-glucopyranosides listed in Table III and consequently is not related to the presence of the oximino group. Also, the chemical shift for H-1

TABLE III

Nuclear magnetic resonance parameters for the anomeric proton of alkyl α-D-glucopyranosides in deuterium oxide

Aglycon	Chemical shifts, τ values	Spacing, c.p.s.
Methyl	5.13	3.0
Ethyl	5.08	3.0
Isopropyl	4.95	3.0
t-Butyl	4.78	3.5

of *t*-butyl 2-deoxy-α-D-glucopyranoside is 0.46 τ-values to lower field than that of H-1 for the corresponding methyl glycoside (10). The magnitudes of the shifts for H-1 as methyl groups are introduced into the aglycon of the methyl oximinoglycoside suggest that the aglycons are oriented as shown in **4** with the anomeric hydrogen (H-1) projecting between the R^1 and R^2 substituents. On this basis, the chemical shift difference of H-1 for the methyl and *t*-butyl glycosides using deuteriochloroform as solvent indicates a deshielding effect amounting to 0.22 τ-values per methyl group. It would follow, for the isopropyl group, that the conformation where both R^1 and R^2 are methyl groups is of very low abundance. Indeed, a consideration of molecular models indicates a strong interaction between R^1 and R^2 and the anomeric proton which is to be expected in view of the relatively short C—O bonds. The chemical shift of H-1 for the isopropyl glycoside would then require an about equal abundance of the two conformations with a methyl group at the position of R^3. These considerations are of obvious interest relative to the orientation of the aglycons in α-glucopyranosides.

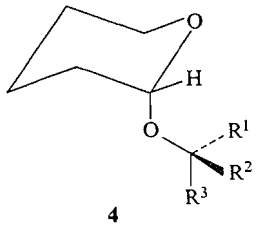

4

The precise mechanism of the nucleophilic attack of the alcohol at the anomeric center of the tri-*O*-acetyl-2-nitroso-D-glucal (**2**) was not determined. Nevertheless, the high degree of stereospecificity of the glycosidation reaction can readily be appreciated since carbon-2 must retain a trigonal configuration throughout the course of the reaction and the compound must be expected to undergo reaction in the H1 half-chair conformation shown. This latter expectation follows from the fact that the triacetates of 2-acetoxy and 2-chloro-D-glucal exist in H1 conformations (11) and the non-bonded interaction between the 3-acetoxy group and the 2-substituent in these compounds [$A^{(1,3)}$ effect (12, 13)] can be expected to be at least as great as that between the nitroso group and the 3-acetoxy group in **2** if, indeed, the nitrosoolefinic system is in the *cis*-configuration as shown. *p*-Iodonitrosobenzene exists as a planar molecule in the monomeric form presumably because of conjugation (14). Therefore, the nitroso group of a 2-nitrosoglycal must be conjugated with vinylic ether system as indicated by the extreme canonical partial structures **5** and **6**. A powerful $A^{(1,3)}$ interaction between the nitroso group and the 3-acetoxy group would be expected should the nitrosoglucal possess a *trans* arrangement of the nitrosoolefinic system (as in **7**) since in the structurally closely related tri-*O*-acetyl-2-nitro-D-glucal (**9**) this interaction is sufficiently strong to require the 1H half-chair conformation (**10**) for this compound (11). Because of this conformation, this nitroglucal undergoes nucleophilic attack at the anomeric center primarily by way of axial approach from the β-side of the pyranoid ring (15). Therefore, if the nitrosoglucal possessed the *trans* configuration, it would, in all likelihood, exist in the 1H conformation (**8**) and also provide β-glucoside on nucleophilic attack. However, the reaction is, in fact, highly preferential for the formation of α-glucoside. The inference then is clear that the nitrosoglucal exists in the *cis* configuration and in the H1 conformation as shown in **2** and **5**. The preference of the compound for axial nucleophilic attack at the anomeric center is then readily appreciated on both steric and electronic grounds regardless of whether or not nucleophilic attack precedes or follows protonation of the nitroso group or, indeed, whether or not these are synchronous (bi- or trimolecular) or not. By making an axial attack, the alcohol both provides maximum orbital overlap in the transition state and avoids a strong destabilizing nonbonded interaction with the developing oximino group. In all likelihood, therefore, the oximes prepared in this research have the configuration wherein the hydroxyl group points in the direction of the anomeric center as shown in **3**. Fur-

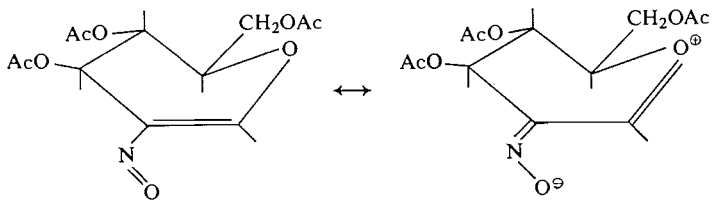

5 6

thermore, this isomer must be considerably more stable than the other possible geometrical isomer which was never detected in the reaction products. In this regard, prolonged heating in methanol did not give rise to a second oxime as detectable by n.m.r. spectroscopy.

Experimental

Unless otherwise stated, optical rotations were measured in 1 dm tubes using a Perkin–Elmer 141 automatic polarimeter. The nuclear magnetic resonance (n.m.r.) spectra were determined using Varian A60 and HA100 spectrometers, and the solvents are mentioned where pertinent. Melting points were determined on a microstage and are uncorrected.

Dimeric 3,4,6-tri-*O*-acetyl-2-deoxy-2-nitroso-α-D-glucopyranosyl chloride (**1**), m.p. 129–130° (decomp.), $[\alpha]_D^{23}$ +149° (*c*, 2.2 in chloroform) and dimeric 3,4,6-tri-*O*-acetyl-2-deoxy-2-nitroso-α-D-galactopyranosyl chloride, m.p. 128–131°, $[\alpha]_D^{23}$ +128° (*c*, 2.2 in chloroform) were prepared as described previously (5).

Methyl 3,4,6-Tri-O-acetyl-2-oximino-α-D-arabino-hexopyranoside (Method A)

Dry pyridine (0.316 g, 4 mmoles) was added with stirring to a solution of dimeric 3,4,6-tri-*O*-acetyl-2-deoxy-2-nitroso-α-D-glucopyranosyl chloride (0.675 g, 1 mmole) in anhydrous tetrahydrofuran (15 ml) containing anhydrous methanol (0.128 g, 4 mmoles). The resultant mixture was heated under reflux for 1.5 h with the exclusion of moisture and then taken to dryness *in vacuo*. The resultant syrup was taken up in chloroform (200 ml) and washed with water. The chloroform solution was dried over anhydrous sodium sulfate and the solvent was removed *in vacuo* to yield a syrup. Crystallization from ether–hexane gave material (0.54 g) with m.p. 145–146°, $[\alpha]_D^{24}$ +48° (*c*, 1.24 in chloroform) in 81% yield.

Anal. Calcd. for $C_{13}H_{19}O_9N$: C, 46.85; H, 5.75; N, 4.20. Found: C, 46.82; H, 5.46; N, 3.84.

The n.m.r. spectrum of the crude syrup was essentially the same as that for the crystalline product (see Table II).

N-(3,4,6-Tri-O-acetyl-2-oximino-D-arabino- hexopyranosyl) pyridinium Chloride

To a solution of dimeric 3,4,6-tri-*O*-acetyl-2-deoxy-2-nitroso-α-D-glucopyranosyl chloride (**1**, 0.675 g) in dry tetrahydrofuran (3 ml) was added dry benzene until it appeared that further addition of benzene to the solution would cause turbidity. Anhydrous pyridine (0.16 g) was then introduced into the mixture with swirling of the flask and then the mixture was set aside at room temperature. Soon the solution turned turbid and the mixture was shaken for 5 h. The precipitated white crystalline mass was filtered, washed with benzene, and dried in a high vacuum. The yield of the compound, m.p. 82–84°, $[\alpha]_D^{23}$ +54° (*c*, 0.5 in water) was 0.7 g (84%). The n.m.r. spectrum was in general agreement with the assigned structure. Attempts to purify the substance by recrystallization led to extensive decomposition.

Isopropyl 3,4,6-Tri-O-acetyl-2-oximino-α-D-arabino-hexopyranoside (Method B)

Tri-*O*-acetyl-2-deoxy-2-nitroso-α-D-glucopyranosyl

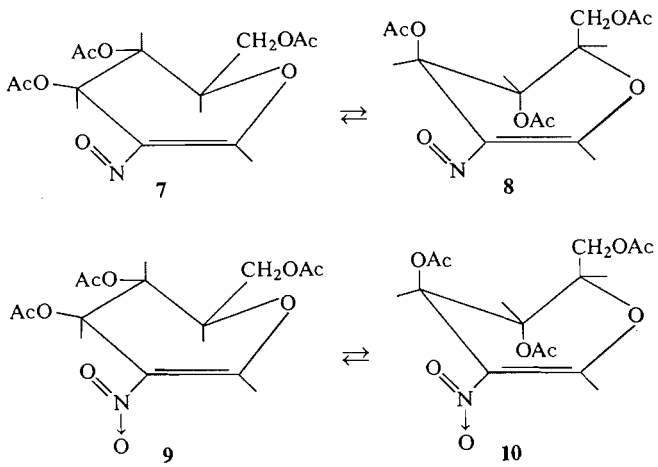

7 8 9 10

chloride dimer (**1**) (3.37 g, 5 mmoles) was added to a solution of dry isopropyl alcohol (0.72 g, 12 mmoles) in anhydrous methylene chloride (5 ml) contained in a 10 ml flask. The resultant solution was heated under very gentle reflux for 3–4 h with the exclusion of moisture, cooled, and after dilution with methylene chloride (100 ml), was passed through a small pad of neutral alumina (2 g). The pale-green solution was taken to dryness *in vacuo* to yield a syrup in near quantitative yield. Crystallization from dry isopropyl alcohol (20 ml) afforded the purified material (yields varying from 80 to 89% in a large number of experiments) with m.p. 85–87°. This could be raised to 94–96° on successive recrystallizations from the same solvent; $[\alpha]_D^{25}$ +79° (*c*, 3 in chloroform).

Anal. Calcd. for $C_{15}H_{23}O_9N$: C, 49.86; H, 6.42; N, 3.88. Found: C, 50.63; H, 6.91; N, 3.87.

The n.m.r. spectrum (see Table II) of the compound was in accord with the assigned structure.

This material could also be prepared in comparable yield using the conditions described for the preparation of the corresponding methyl oximino glycoside (Method A). Reaction of 1.35 g of **1** with 0.3 g of isopropyl alcohol in 4 ml of dimethylformamide (Method C) for 76 h at room temperature followed by isolation of the product in the usual manner (see below), gave, after recrystallization, 1.15 g (80% yield) of this compound.

Isopropyl Tetra-O-acetyl-2-oximino-α-D-arabino-hexopyranoside

Isopropyl 3,4,6-tri-*O*-acetyl-2-oximino-α-D-*arabino*-hexopyranoside (1.0 g) was dissolved in dry acetic anhydride (10 ml) containing fused sodium acetate (1 g) and heated at 50° for 20 h. Workup in the usual manner yielded a syrup in near quantitative yield which crystallized *in vacuo*. Recrystallization from ethanol–water yielded the fully acetylated oximinoglycoside as plates, m.p. 83.5–84.5°, $[\alpha]_D^{25}$ +76° (*c*, 3.2 in chloroform). The n.m.r. spectrum of the compound in deuteriochloroform showed the presence of four acetyl groups per isopropyl moiety and the pertinent data are given in Table II.

Anal. Calcd. for $C_{17}H_{25}O_{10}N$: C, 50.61; H, 6.25; N, 3.47. Found: C, 50.98; H, 6.33; N, 3.44.

n-Propyl 3,4,6-Tri-O-acetyl-2-oximino-α-D-arabino-hexopyranoside

Method B was employed. The pale-green syrup which was obtained in near quantitative yield gave an n.m.r. spectrum identical with that of the material after crystallization from *n*-propanol – *n*-hexane in 75% yield with m.p. 61.5–62°, $[\alpha]_D^{25}$ +74° (*c*, 0.8 in chloroform).

Anal. Calcd. for $C_{15}H_{23}O_9N$: C, 49.86; H, 6.42; N, 3.88. Found: C, 49.81; H, 6.36; N, 3.85.

Ethyl 3,4,6-Tri-O-acetyl-2-oximino-α-D-arabino-hexopyranoside

This compound was obtained as a pale-green syrup in near quantitative yield using Method B. Crystallization from methylene chloride – petroleum ether gave small needles in 75% yield, m.p. 154–157°, $[\alpha]_D$ +72° (*c*, 0.8 in chloroform). Nuclear magnetic resonance data are given in Table II.

Anal. Calcd. for $C_{14}H_{21}O_9N$: C, 48.41; H, 6.09; N, 4.03. Found: C, 48.61; H, 6.11; N, 4.15.

4-t-Butylcyclohexyl 3,4,6-Tri-O-acetyl-2-oximino-α-D-arabino-hexopyranoside

This compound was prepared as described previously (Method B) using commercial *trans*-4-*t*-butylcyclohexanol except that a reaction time of 18 h was necessary. The resultant pale-green syrup was taken up in carbon tetrachloride (25 ml) and *n*-hexane was added to turbidity. After standing at 0° for 12 h the precipitated material was filtered to yield an amorphous solid in 38% yield, $[\alpha]_D^{25}$ +74° (*c*, 0.59 in chloroform). Attempts at crystallization were unsuccessful. Nuclear magnetic resonance data are given in Table II.

Anal. Calcd. for $C_{22}H_{35}O_9N$: C, 57.75; H, 7.71; N, 3.06; Found: C, 57.82; H, 7.43; N, 3.22.

n-Butyl, Isobutyl and t-Butyl 3,4,6-Tri-O-acetyl-2-oximino-α-D-arabino-hexopyranosides

These compounds were obtained using Method B as syrups which could not be induced to crystallize. The physical constants are reported in Tables I and II. The n.m.r. spectra required in each case a high degree of purity.

Phenyl 3,4,6-Tri-O-acetyl-2-oximino-α-D-arabino-hexopyranoside (Method C)

Dimeric 3,4,6-tri-*O*-acetyl-2-deoxy-2-nitroso-α-D-glucopyranosyl chloride (3.375 g, 5 mmoles) and phenol (1.50 g, 15 mmoles) were dissolved in dry dimethylformamide (10 ml) and kept for 66 h at room temperature. The resultant light-brown solution was diluted with methylene chloride (100 ml) and washed with 0.01 *N* sodium hydroxide (5 × 25 ml). The organic layer was dried and yielded a yellow syrup which crystallized on standing. Recrystallization from aqueous ethanol gave 2.65 g (67% yield), m.p. 165–167°, $[\alpha]_D^{25}$ +94° (*c*, 2.0 in chloroform).

Anal. Calcd. for $C_{18}H_{21}O_9N$: C, 54.68; H, 5.35; N, 3.54. Found: C, 54.57; H, 5.20; N, 3.57.

Nuclear magnetic resonance data are presented in Table II.

A somewhat lower yield (51%) was obtained when the reaction was carried out at 35° for 18 h.

α-Naphthyl 3,4,6-Tri-O-acetyl-2-oximino-α-D-arabino-hexopyranoside

Dimeric 3,4,6-tri-*O*-acetyl-2-deoxy-2-nitroso-α-D-glucopyranosyl chloride (2.03 g, 3 mmole) and α-napthol (1.3 g, 9 mmoles) were dissolved in dry dimethylformamide (10 ml) and the procedure described for the preparation of the corresponding phenyl oximinoglycoside was followed. The crude brown syrup was then taken up in aqueous ethanol and afforded shiny plates; 1.2 g (42% yield), m.p. 155–158°, $[\alpha]_D^{25}$ +131° (*c*, 2 in chloroform).

Anal. Calcd. for $C_{24}H_{23}O_9N$: C, 61.40; H, 4.94; N, 2.98. Found: C, 60.35; H, 5.08; N, 2.72.

Nuclear magnetic resonance data are presented in Table II.

Methyl 2,3,4-Tri-O-acetyl-6-O-(3,4,6-tri-O-acetyl-2-oximino-α-D-arabino-hexopyranosyl)-β-D-glucoside (Method C)

Methyl 2,3,4-tri-*O*-acetyl-β-D-glucopyranoside was prepared by standard procedures and had physical constants identical to those reported in the literature (16).

The compound (2.56 g, 8 mmoles), m.p. 134–137°, $[\alpha]_D^{25}$ −10.9° (*c*, 1.12 in $CHCl_3$), and dimeric 3,4,6-tri-*O*-acetyl-2-deoxy-2-nitroso-α-D-glucopyranosyl chloride (2.70 g, 4 mmoles) were placed in a 25 ml flask and dry dimethylformamide (8 ml) was added. The flask was flushed with a stream of dry nitrogen, stoppered with a serum cap, and kept at 40° for 24 h. The resultant light-brown solution was diluted with methylene chloride (120 ml) and repeatedly washed with water (6 × 25 ml) until the aqueous layer was near colorless. The organic layer was dried over anhydrous sodium sulfate and then taken to dryness *in vacuo* at 40° to yield a yellow foam (5.12 g), $[\alpha]_D^{25}$ +23° (*c*, 0.77 in chloroform). The n.m.r. spectrum of the crude product in deuteriochloroform was similar to those of the acetylated alkyl oximinoglycosides in that a sharp singlet attributable to H-1, was present at τ 3.99. The expected H-3′ doublet was noted at τ 4.23 with a spacing of 9.5 c.p.s. The signal due to the oximino proton (τ ~ 1) disappeared on exchange with deuterium oxide. The H-4′, triplet could not be seen due to overlapping of the other signals. A comparison of the integrated H-1′, H-3′ signals and the acetoxy and methoxy signals showed that the α-oximino disaccharide had formed to an extent of 70% in the condensation reaction.

The same yield of crude product could also be obtained if the reaction was carried out in dry dimethylformamide at room temperature for 96 h. However, no isolable product was obtained when the reaction was carried out for 24 h in methylene chloride as previously described for the alkyl glycoside derivatives (Method B).

1,3,4,6-Tetra-O-acetyl-2-oximino-α-D-arabino-hexopyranose

A solution of the dimeric nitrosyl chloride adduct (**1**) (6.75 g, 10 mmoles) in glacial acetic acid (55 ml) was stirred with anhydrous sodium acetate (1.64 g, 20 mmoles) at 60° for 30 min under anhydrous conditions. The solvent was removed *in vacuo* at 35° and the residual syrup was taken up in chloroform (100 ml). The chloroform solution was washed successively with water (30 ml), saturated sodium bicarbonate solution (30 ml), and water (30 ml). The organic phase was dried over anhydrous sodium sulfate and the solvent removed *in vacuo*. The residual foamy white solid was dried and crystallized from ether – *n*-hexane. The yield was 2.2 g (31%), m.p. 138–139°, $[\alpha]_D^{24}$ +44.39° (*c*, 1.2 in chloroform).

Anal. Calcd. for $C_{14}H_{19}O_{10}N$: C, 46.54; H, 5.30; N, 3.88. Found: C, 46.60; H, 5.04; N, 3.64.

In the absence of sodium acetate and at room temperature the reaction was much slower.

n-Propyl and Isopropyl 3,4,6-Tri-O-acetyl-2-oximino-α-D-lyxo-hexopyranosides

These compounds were prepared from dimeric tri-*O*-acetyl-deoxy-2-nitroso-α-D-galactopyranosyl chloride using Method A. The syrupy crude products were obtained in near quantitative yields. Although some purification was effected by passing a solution in benzene through a small column of silica gel and elution with benzene, the compounds failed to crystallize. Nevertheless, the n.m.r. spectra were in agreement with the assigned structures. The chemical shifts for H-1, H-3, and H-4 were τ 3.90, 4.10, and 4.48, respectively, for the *n*-propyl compound and τ 3.76, 4.08, and 4.50, respectively, for the isopropyl compound. In both cases, spacings of 3.5 and <1 c.p.s. were present arising from the $J_{3,4}$ and $J_{4,5}$ interactions, respectively. The optical rotations are reported in Table I.

Acknowledgments

The authors are grateful for grants to R.U.L. from the National Research Council of Canada (T-172) and the Corn Industries Research Foundation in aid of this research. The microanalyses and n.m.r. spectra were determined in this department.

1. J. D. DUTCHER. Advan. Carbohydrate Chem. **18**, 259 (1963).
2. T. IKEKAWA, H. UMEZAWA, and Y. IITAKA. J. Antibiotics Tokyo, Ser. A, **19**, 49 (1966).
3. R. U. LEMIEUX and S. W. GUNNER. Can. J. Chem. This issue.
4. R. U. LEMIEUX, R. SUEMITSU, and S. W. GUNNER. Can. J. Chem. In preparation.
5. R. U. LEMIEUX, T. L. NAGABHUSHAN, and I. K. O'NEILL. Tetrahedron Letters, No. 29, 1909 (1964); Can. J. Chem. This issue,
6. R. U. LEMIEUX, S. W. GUNNER, and T. L. NAGABHUSHAN. Tetrahedron Letters, No. 26, 2149 (1965).
7. G. COLLIN and W. PRITZKOW. Tetrahedron Letters, No. 29, 3493 (1966).
8. W. PRITZKOW, H. SCHAEFER, P. PABST, A. EBENROTH, and J. BEGER. J. Prakt. Chem. [4], **29**, 123 (1965).
9. P. M. COLLINS. Chem. Commun. No. 6, 164 (1966).
10. R. U. LEMIEUX and S. LEVINE. Can. J. Chem. **42**, 1473 (1964).
11. R. U. LEMIEUX and I. K. O'NEILL. In preparation.
12. F. JOHNSON and S. K. MALHOTRA. J. Am. Chem. Soc. **87**, 5492, 5493 (1965).
13. R. CAPLE and W. V. VAUGHAN. Tetrahedron Letters, No. 34, 4067 (1966).
14. M. S. WEBSTER. J. Chem. Soc. 2841 (1956).
15. R. U. LEMIEUX and I. K. O'NEILL. In preparation.
16. G. ZEMPLÉN and Z. CSÜRÖS. Ber. **62**, 993 (1929).

The reactions of nitrosyl chloride and dinitrogen tetroxide with acetylated glycals. Acetylated 2-deoxy-2-nitroso-α-D-hexopyranosyl chlorides and nitrates and acetylated 2-nitroglycals[1]

R. U. LEMIEUX, T. L. NAGABHUSHAN,[2] AND I. K. O'NEILL
Department of Chemistry, University of Alberta, Edmonton, Alberta

Received August 9, 1967

Reaction of nitrosyl chloride with acetylated glycals affords, with a high degree of stereospecificity, dimeric acetylated 1,2-*cis*-2-deoxy-2-nitroso-α-D-aldopyranosyl chlorides. Reaction of acetylated glycals with dinitrogen tetroxide, depending on the reaction conditions, can give either acetylated 2-deoxy-2-nitroso-α-D-aldopyranosyl nitrates as dimers or acetylated 2-nitroglycals. The mechanisms of these reactions are discussed.

Canadian Journal of Chemistry, 46, 413 (1968)

Can. J. Chem. Downloaded from www.nrcresearchpress.com by 210.87.254.5 on 09/05/12
For personal use only.

Although nitrosyl chloride has been used extensively since its early introduction into organic chemistry (1), the mechanism and stereochemical route of the addition of nitrosyl chloride to olefinic double bonds has received attention only in recent years (2, 3). The kinetic studies by Beier and co-workers (2) led to the conclusion that the reaction proceeds by way of a moderately polar and highly ordered transition state. Meinwald, Meinwald, and Baker (3) concluded that the *cis*-addition to strained olefins involves a four-centered addition mechanism. Although no reference could be found to addition of nitrosyl chloride to vinyl ethers, it could be anticipated at the debut of this investigation that nitrosyl chloride would add readily to acetylated glycals in a *cis*-addition as previously noted for the chlorination of the triacetates of D-glucal and D-galactal (4). In the course of this research a publication by Serfontein, Jordaan, and White (5) appeared in which the nitrosyl chloride adducts of the acetates of D-glucal and D-arabinal were described as 3,4,6-tri-*O*-acetyl-2-nitroso-2-deoxy-α-D-glucopyranosyl chloride and 3,4-di-*O*-acetyl-2-nitroso-2-deoxy-β-D-arabinopyranosyl chloride, respectively. We accordingly communicated (6) the results of our own investigation. The purpose of this communication is to report the details of this research together with the addition of dinitrogen tetroxide to acetylated glycals.

The addition of dinitrogen tetroxide to alkenes has received much attention (7) and is known to provide a variety of products. The path of the reaction is strongly dependent on such factors as the solvent (7), the temperature (8), and the nature of the alkene (9). These characteristics are also exhibited in the reactions of dinitrogen tetroxide with alcohols and amines (10). Thus, although the reaction with alcohols and secondary amines gave nitrites and nitrosoamines at 0° with ether as solvent, nitrates, and nitramines were produced at −80° using methylene chloride as solvent. These observations could be rationalized on the basis that dinitrogen tetroxide exhibits the properties of nitrosyl nitrate (**2**) and can undergo nucleophilic attack at either the nitro or the nitroso group depending on the nature of its activation by the environmental factors. However, physical measurements at very low temperatures indicate the dinitro structure (**1**) (11, 12). Thus, as suggested by Schaarschmidt (13) in 1924, dinitrogen tetroxide is an equilibrium mixture of structural isomers. The isomerization may involve homolysis to the monomeric nitrogen dioxide. However, in view of the powerful electrophilic nature of the reagent, heterolysis to nitronium and nitrite ions by way of intimate ion pairs can be envisaged. In nitric acid the compound exists as ionic nitronium nitrite (14). Certainly, nucleophilic attack on the dinitro form (**1**) can be expected to yield nitration with nitrite ion as leaving group. On the other hand, nucleophilic attack on the nitrosyl nitrate form (**2**) should lead to nitrosylation

[1]This research was presented in theses by T. L. Nagabhushan and I. K. O'Neill in partial fulfillment of the requirements for the Ph.D. degree, 1966, and also at the 150th Meeting of the American Chemical Society, Atlantic City, N.J., September 13–17, 1965. Abstract of Papers, p. 21D.

[2]Present address: R & L Molecular Research Ltd., 8045 Argyll Road, Edmonton, Alberta.

Can. J. Chem. Downloaded from www.nrcresearchpress.com by 210.87.254.5 on 09/05/12
For personal use only.

with nitrate ion as leaving group in the manner observed for nitrosyl chloride. Indeed, the results of this investigation are in agreement with these contentions.

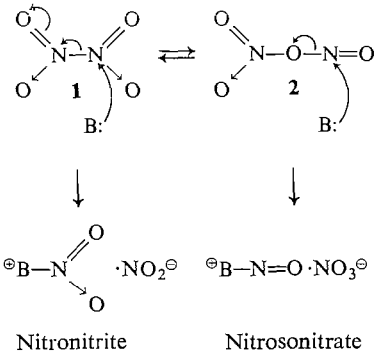

Reaction of tri-*O*-acetyl-D-glucal (**3**) at −40° in ethyl acetate and a nitrogen atmosphere with nitrosyl chloride resulted in a product (**5**) readily isolated in near quantitative yield with the composition expected for addition across the double bond. No evidence for the formation of more than one isomer was obtained and it is assumed that the compound has the *trans* configuration shown. The molecular weight was in agreement with the dimeric structure shown and this was confirmed by hydrogenation to a substance characterized as the corresponding azoxy compound. Thus, the intermediate adduct (**4**) did not tautomerize to the chlorooxime. Solutions of (**5**) were only a very light blue-green indicating a highly stable dimer. The monomeric form appeared to be a deep blue-green since this was the color of the first product of the reaction. The spacing of the doublet for the anomeric protons of 3.5 c.p.s. together with the spacings, 9.0 and 3.5 c.p.s. of the quartet for the 2-protons require the configuration of the compound to be a α-D-*gluco* on both moieties. The nuclear magnetic resonance (n.m.r.) parameters for **5** and related compounds are given in Table I.

TABLE I

Nuclear magnetic resonance parameters for dimeric acetylated 2-deoxy-2-nitrosoaldopyranosyl chlorides and nitrates*

	Chemical shifts (τ) H-1	H-2	H-3	Spacings (c.p.s.) $J_{1,2}$	$J_{2,3}$	$J_{3,4}$
Chlorides						
α-D-*gluco* (**5**)	3.33	4.54	3.95	3.5	9.0	9.5
α-D-*galacto* (**7**)	3.31	4.47	4.08	3.7	11.1	3.6
α-D-*xylo* (**8**)	3.39	4.62	3.98	3.8	11.0	9.8
Nitrates						
α-D-*gluco* (**9**)	3.23	4.49	4.06	4.2	11.1	9.4
α-D-*galacto* (**11**)	3.26	—†	—†	3.7	—	—

*In each case, the signals for the other protons (acetyl, C-5, and C-6 positions) were in the normal positions.
†Part of a multiplet in the τ 4–5 region.

The *cis*-addition of nitrosyl chloride to tri-*O*-acetyl-D-glucal (**3**) is in keeping with the facts that the initial electrophilic attack provides a relatively stable carbonium (oxocarbonium) ion and that the solvent is of relatively low polarity. Thus, both bridging of the double bond in the cation and separation of the ions are not to be expected and addition by way of an intermediate (probably with considerable intimate ion-pair character) as depicted in (**6**) is both sterically and electronically favorable. It is noteworthy in this

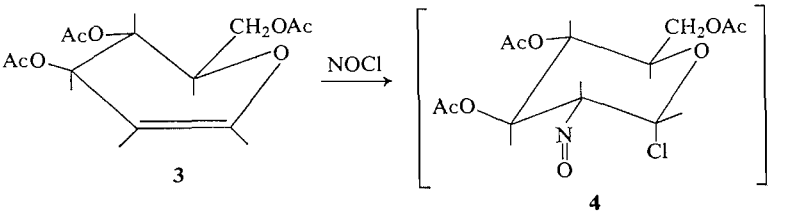

3 4

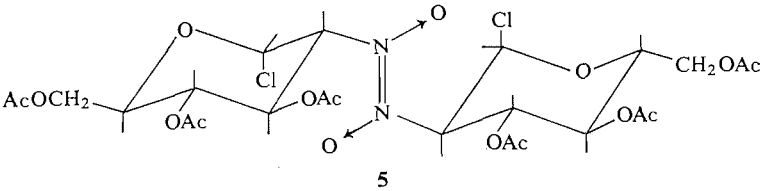

5

Can. J. Chem. Downloaded from www.nrcresearchpress.com by 210.87.254.5 on 09/05/12
For personal use only.

regard that Ohno, Okamoto, and Nukada (15) have found the addition of nitrosyl chloride to cyclohexene to give the *trans* dimeric adduct in liquid sulfur dioxide and the *cis* isomer in methylene chloride, chloroform, and trichloroethylene. The preference of the route to the *α-gluco* rather than the *β-manno* configuration in the addition to (**3**) is considered likely as a result of the stereoelectronic considerations advanced by Lemieux and Fraser-Reid (4) to explain the *cis*-addition of chlorine to (**3**) to yield the *α-gluco* dichloride.

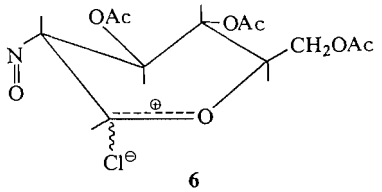

6

Dimeric tri-*O*-acetyl-2-deoxy-2-nitroso-α-D-galactopyranosyl chloride (**7**) was readily prepared in the manner described for the preparation of **5**. A lower temperature and the use of methylene chloride as solvent seemed desirable for the preparation of dimeric di-*O*-acetyl-2-deoxy-2-nitroso-α-D-xylopyranosyl chloride (**8**). Attempts to purify this substance led to its conversion to di-*O*-acetyl-2-nitro-D-xylal (**15**) in low yield. This latter compound, as will be seen below, is readily obtained by reaction of di-*O*-acetyl-D-xylal with dinitrogen tetroxide.

The reaction of acetylated glycals with dinitrogen tetroxide could be made to yield either dimeric acetylated 2-deoxy-2-nitrosoglycosyl nitrates or acetylated 2-nitroglycals depending on the reaction conditions used. In all experiments, an approximately equimolar mixture of dinitrogen tetroxide and oxygen was passed through the solution of the acetylated glycal in order to suppress the formation of dinitrogen trioxide (8). When the reactions were carried out at 0° using diethyl ether as solvent, the nitrosyl nitrate adducts were readily isolated in crystalline form. Thus, tri-*O*-acetyl-D-glucal was converted to dimeric tri-*O*-acetyl-2-deoxy-2-nitroso-α-D-glucopyranosyl nitrate (**9**) in 91% yield. The structure of this compound was evident from its composition, molecular weight, and n.m.r. spectrum (see Table I). Furthermore, treatment of (**9**) with acetic anhydride and sodium acetate was found to yield the same penta-*O*-acetyl-2-oximino-D-*arabino*-hexose (**10**) as was formed on a similar treatment of the nitrosyl chloride adduct (**5**). The inorganic residue from this reaction was found to contain nitrate but not nitrite ion. The yield of nitrosyl nitrate adduct (**11**) from tri-*O*-acetyl-D-galactal was only 58%. These compounds, particularly the latter, were extremely prone to decomposition. The product expected to be dimeric di-*O*-acetyl-2-deoxy-2-nitroso-α-D-xylopyranosyl nitrate was too unstable to allow its isolation. In all these decompositions, as for that noted above for the decomposition of dimeric di-*O*-acetyl-2-deoxy-2-nitroso-α-D-xylopyranosyl chloride, the main product was the acetylated 2-nitroglycal.

When the acetylated glycal was reacted at −70° in methylene chloride, no evidence for the formation of the nitrosyl nitrate adduct was obtained. On work-up, gases were evolved and virtually pure acetylated 2-nitroglycal was obtained directly. In the case of the reaction with tri-*O*-acetyl-D-glucal, it was evident that the nitrosyl nitrate adduct (**9**) was not an intermediate since its treatment with dinitrogen tetroxide under the same conditions resulted in less than 10% change to tri-*O*-acetyl-2-nitro-D-glucal (**12**). In view of this result and the fact that the reactions of dinitrogen tetroxide are known to be strongly solvent and temperature dependent, it seems likely that the initial attack by the dinitrogen tetroxide introduced a nitro group at the 2-position. Such an event could conceivably lead to dinitro or nitronitrite intermediates (7). However, it is also possible that the only intermediate was a dipolar ion which suffered loss of the 2-proton perhaps in a concerted mechanism as depicted in (**13**.)

The acetylated 2-nitroglycals are highly prone to nucleophilic attack at the anomeric center and enter into a multistage reaction sequence with, for example, alcohols. The stereochemical routes of these reactions are primarily set by the conformation of the acetylated nitroglycal through operation of the $A^{1,3}$ effect (16, 17) involving strong interaction between the nitro group, in conjugation with the olefinic double bond, and the 3-acetoxy group. Thus, tri-*O*-acetyl-2-nitro-D-glucal has the conformation shown in (**12**). These matters will be considered in detail in separate communications (18, 19). The nitrosyl chloride adduct (**5**) provides a highly

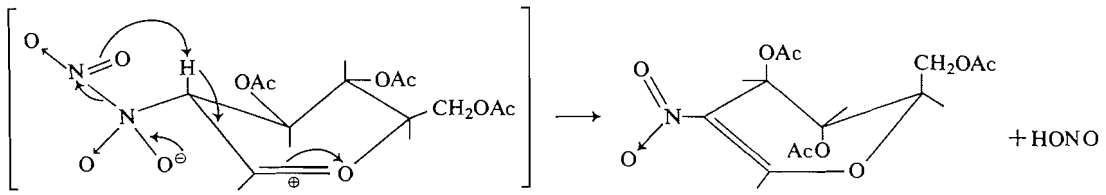

13 12

stereospecific synthesis of 2-oximino-α-D-*arabino*-hexopyranosides which in turn can be converted in high yield to either 2-amino-2-deoxy-α-D-glucopyranosides (20) or to α-D-glucopyranosides (21). The nitrosyl chloride or nitrosyl nitrate adducts can be used to synthesize 2-amino-2-deoxysugars (22). Thus, it is considered that this research has opened a number of important synthetic approaches in carbohydrate chemistry.

Experimental

The melting points were determined on a heating stage and are uncorrected. Unless otherwise stated, the n.m.r. spectra were obtained with a Varian Associates A-60 spectrometer using deuteriochloroform as solvent and tetramethylsilane as internal standard.

The nitrosyl chloride (93%) and dinitrogen tetroxide was supplied by the Matheson Co., Inc., East Rutherford, New Jersey.

The acetylated glycals were prepared following standard procedures (23). It was necessary to distill the crude products in the preparations of di-*O*-acetyl-D-xylal (24) (b.p. 95–105° at 0.3 mm) and tri-*O*-acetyl-D-galactal (b.p. 140–145° at 0.3 mm) in order to achieve crystalline materials. Highly pure preparations of the latter compound, m.p. 30°, were not necessary to obtain excellent yields of the nitrosyl chloride adduct. Preparations which were syrups at room temperature but which appeared better than 95% pure by n.m.r. spectroscopy were used.

Dimeric Tri-O-acetyl-2-deoxy-2-nitroso-α-D-glucopyranosyl Chloride (5)

Dry tri-*O*-acetyl-D-glucal (12 g) was dissolved in reagent grade ethyl acetate (100 ml) in a 250 ml 3-neck flask equipped with a low temperature thermometer, gas inlet, and outlet tubes. Nitrogen was passed through the magnetically-stirred solution while it was cooled to −40° in a dry ice – acetone mixture. The gas was then changed from nitrogen to a *slow* stream of nitrosyl chloride (see below). After 10 min, the gas stream was reverted to nitrogen and the stirring was continued for 15 min while the solution was allowed to warm to 0°. The solution was then rapidly evaporated *in vacuo* at room temperature to a residue using a rotatory evaporator. The residue was normally a near white crystalline product. However, on occasions a blue-green syrup was obtained which soon crystallized. Recrystallization from chloroform – *n*-hexane gave colorless needles (11.9 g, 80% yield) m.p. 129–130°, $[\alpha]_D^{23}$ +149° (*c*, 2.15 in chloroform). The n.m.r. parameters are given in Table I. Thin-layer chromatography on silica gel using 10% methanol in benzene as the mobile phase showed a single spot of R_f 0.67 on spraying with 25% sulfuric acid.

Anal. Calcd. for $C_{24}H_{32}N_2O_{16}Cl_2$ (mol. wt., 675): C, 42.67; H, 4.74; N, 4.15; Cl, 10.52. Found (mol. wt., 600, osmometric): C, 42.50; H, 4.71; N, 4.10; Cl, 10.49.

On occasions, the product of the reaction was tri-*O*-acetyl-2-nitro-D-glucal (**12**). The formation of this compound appeared related to the rate of addition of the nitrosyl chloride.

Dimeric Tri-O-acetyl-2-deoxy-2-nitroso-α-D-galactopyranosyl Chloride (7)

The procedure described above for the preparation of the *gluco* isomer was applied to syrupy tri-*O*-acetyl-D-galactal (47.5 g) and gave 49.5 g (84%) of compound, m.p. 128–131°, $[\alpha]_D^{23}$ +128° (*c*, 2.2 in chloroform). The n.m.r. parameters are given in Table I. Thin-layer chromatography as above detected only one component.

Anal. Calcd. for $C_{24}H_{32}N_2O_{16}Cl_2$ (mol. wt., 675): C, 42.67; H, 4.74; N, 4.15%. Found (mol. wt., 674, osmometric):C, 42.44; H, 4.78; N, 4.16.

Dimeric Di-O-acetyl-2-deoxy-2-nitroso-α-D-xylopyranosyl Chloride (8)

Di-*O*-acetyl-D-xylal (4.9 g) was reacted with nitrosyl chloride under the conditions described above except that dry methylene chloride (15 ml) was used as solvent and the reaction was conducted initially at about −80°. The blue syrup obtained on solvent removal *in vacuo* below 30° crystallized from a methylene chloride – hexane mixture. The yield was 5.85 g (90%). After one recrystallization, the very labile compound, $[\alpha]_D^{23}$ +164° (*c*, 3 in chloroform), melted in the range 102–106°. Although satisfactory elementary analyses could not be obtained, the n.m.r. parameters for the compound listed in Table I are taken as unequivocal evidence for its identity. Also, the n.m.r. spectrum required the compound to be of high purity. Attempts to further purify the substance by recrystallization from methylene chloride – hexane gave a partially crystalline material from which a 29% overall yield of solid di-*O*-acetyl-2-nitro-D-xylal (**15**) was isolated. Recrystallization of this product from ethyl acetate gave a colorless compound, m.p. 128–129°, $[\alpha]_D^{23}$ −319° (*c*, 2.1 in chloroform), identical to that prepared in high yield by reaction of di-*O*-acetyl-D-xylal with dinitrogen tetroxide.

Hydrogenation of (5) to an Azoxy Compound

Dimeric tri-*O*-acetyl-2-deoxy-2-nitroso-α-D-glucopyranosyl chloride (**5**) (2 g) in 20 ml of dioxane containing

Can. J. Chem. Downloaded from www.nrcresearchpress.com by 210.87.254.5 on 09/05/12
For personal use only.

Can. J. Chem. Downloaded from www.nrcresearchpress.com by 210.87.254.5 on 09/05/12
For personal use only.

five drops of acetic acid was hydrogenated over 0.5 g of 5% palladium on carbon at atmospheric pressure and room temperature. Within 1 h, one mole-equivalent of hydrogen was consumed. The catalyst was removed by filtration through Celite and the filtrate was evaporated to about 10 ml. Addition of water caused precipitation and the precipitate was collected, dried, and recrystallized from ether. The yield was 1.17 g (60%) of a compound, m.p. 201–202°, $[\alpha]_D^{23}$ +204° (*c*, 1.8 in chloroform). The infrared spectrum exhibited characteristic ester carbonyl absorptions at 1725 cm^{-1}, 1740 cm^{-1}, and 1750 cm^{-1}. In addition, bands at 1635 cm^{-1} and 1295 cm^{-1} attributable to N=N and N→O absorptions, respectively, were present. The n.m.r. spectrum showed the presence of six acetyl groups and two doublets at τ 3.43 and 3.47 each with a spacing of 3.5 c.p.s. attributable to two nonequivalent anomeric protons.

Anal. Calcd. for $C_{24}H_{32}N_2O_{15}Cl_2$ (mol. wt., 658.8): C, 43.71; H, 4.85; N, 4.25. Found (mol. wt., 654, osmometric): C, 43.85; H, 4.95; N, 4.24.

*Penta-O-acetyl-2-oximino-*D*-arabino-hexopyranose (**10**)*

Anhydrous sodium acetate (2.44 g) was added to a solution of dimeric tri-*O*-acetyl-2-deoxy-2-nitroso-α-D-glucopyranosyl chloride (**5**) (5 g) in acetic anhydride (50 ml). The mixture was stirred vigorously for 30 min at 60°. The product, 5.80 g (near quantitative yield), isolated in the usual manner, was a colorless syrup, $[\alpha]_D^{23}$ +31.7° (*c*, 3.15 in chloroform).

The infrared and n.m.r. spectra were identical to those of the product from the same reaction starting from dimeric tri-*O*-acetyl-2-deoxy-2-nitroso-α-D-glucopyranosyl nitrate (**9**) (see below).

The same product was obtained when triethylamine was used as base and the reaction conducted at 0° during the addition of the base and then at room temperature for 30 min.

*Penta-O-acetyl-2-oximino-*D*-lyxo-hexopyranose*

Treatment of tri-*O*-acetyl-2-deoxy-2-nitroso-α-D-galactopyranosyl chloride (**7**) with acetic anhydride containing either sodium acetate or triethylamine as indicated above for the *gluco* isomer gave a colorless syrup, $[\alpha]_D^{23}$ +18° (*c*, 2.76 in chloroform), with the same characteristic infrared absorption bands as reported below for compound (**10**). In this case, however, the n.m.r. spectrum of the syrup showed it to be an about 1:2 mixture of two isomeric compounds. The minor component produced a singlet at τ 2.91 (anomeric proton) and a doublet with spacing of 3.5 c.p.s. at τ 3.99 (3-proton). The major component had these signals at τ 3.33 and 3.87, respectively.

*Dimeric Tri-O-acetyl-2-deoxy-2-nitroso-α-*D*-glucopyranosyl Nitrate (**9**)*

The cylinder of dinitrogen tetroxide was kept in a water bath to ensure a constant stream of the gas. The gas was blended with a stream of dry oxygen to provide an about equimolar mixture. Tri-*O*-acetyl-D-glucal (4.00 g) was dissolved in ether (50 ml) in an apparatus similar to that described for its reaction with nitrosyl chloride. The flask was cooled to 0° in an ice-water bath and oxygen was briefly passed through the solution. The mixture of dinitrogen tetroxide and oxygen was then introduced to the stirred solution until a slight excess of the dinitrogen tetroxide had been added (about 4 h). This amount was estimated by prior calibration of the flow rate. At this point, the gas stream was changed to a rapid stream of oxygen until most of the ether had evaporated. The semisolid residue was dissolved in the minimum amount of methylene chloride and this solution was added to *n*-hexane kept at 0°. The crystalline precipitate was collected, washed with *n*-hexane, and dried. The yield was 4.91 g (91%), m.p. 120–121°, $[\alpha]_D^{27}$ +165° (*c*, 1.7 in chloroform). The infrared spectrum contained a broad nitrate absorption band centered at 1680 cm^{-1}. The n.m.r. parameters are given in Table I.

Anal. Calcd. for $C_{24}H_{32}N_4O_{22}$ (mol. wt., 728.6): C, 39.56; H, 4.43; N, 7.69. Found (mol. wt., 701, osmometric in chloroform): C, 39.63; H, 4.53; N, 7.33.

Attempts to concentrate the ethereal solution to a solvent-free syrup led to extensive decomposition with the formation of tri-*O*-acetyl-2-nitro-D-glucal (**12**).

Reaction of (**9**) with sodium acetate in acetic anhydride as described above for the preparation of penta-*O*-acetyl-2-oximino-D-*arabino*-hexopyranose (**10**) gave an identical product. The configuration of the anomeric center is not known but is most likely α-D in view of the high degree of stereospecificity in the reactions of the corresponding nitrosyl chloride adduct (**5**) with alcohols and phenols (25). The n.m.r. spectrum of compound (**10**) showed signals for H-1 (singlet), H-3 (doublet), and H-4 (quartet) at τ 3.35, 3.84, and 4.46, respectively. The spacings indicated approximate coupling constants of $J_{3,4} = 7.5$ and $J_{4,5} = 8$ c.p.s. H-5 and the two H-6's gave their signals in the region τ 5.5–6.1. Acetyl group signals were at τ 7.84 (two), 7.87 (one), and 7.93 (two). The infrared spectrum contained a broad, weak C=N stretching at 1645 cm^{-1}, and C=N—OAc at 1780 cm^{-1} (26) but no absorptions characteristic of the nitro group.

Anal. Calcd. for $C_{16}H_{21}NO_{11}$ (mol. wt., 403.3): C, 47.64; H, 5.25; N, 3.47. Found (mol. wt., 385, osmometric): C, 47.94; H, 5.29; N, 3.55.

Dilution of the reaction mixture in the above preparation with ether caused the precipitation of salts. The solid gave no liberation of iodine on adding to acidified aqueous sodium iodide solution but a dark blue coloration was produced on adding the material to diphenylamine in concentrated sulfuric acid (27). Therefore, nitrate but not nitrite was a product of the reaction.

*Dimeric Tri-O-acetyl-2-deoxy-2-nitroso-α-*D*-galactopyranosyl Nitrate (**11**)*

Tri-*O*-acetyl-D-galactal (1.72 g) in anhydrous ether (30 ml) was allowed to react with dinitrogen tetroxide as described above for 1.5 h. The yield of crystalline product was 1.18 g, m.p. 123–124° (decomp.), $[\alpha]_D^{27}$ +187° (*c*, 2.6 in chloroform). The infrared spectrum contained a broad band centered at 1680 cm^{-1} assigned to the nitrate group. The n.m.r. parameters are given in Table I.

Anal. Calcd. for $C_{24}H_{32}N_4O_{22}$ (mol. wt., 728.6): C, 39.56; H, 4.43; N, 7.69. Found (mol. wt., 725, osmometric): C, 39.55; H, 4.56; N, 7.83.

*Tri-O-acetyl-2-nitro-*D*-glucal (**12**)*

Tri-*O*-acetyl-D-glucal (3.00 g) was dissolved in dry methylene chloride (50 ml) in the apparatus described

Can. J. Chem. Downloaded from www.nrcresearchpress.com by 210.87.254.5 on 09/05/12
For personal use only.

above. With the oxygen stream on, the solution was cooled to approximately −80° in a dry ice – acetone bath. The dinitrogen tetroxide stream was then admixed with the oxygen stream. At this point, the temperature of the solution rose by about 10° and there developed a very pale-blue coloration. After 10 min, the stream of dinitrogen tetroxide was turned off and the stream of oxygen continued for a further 10 min. The resulting solution was then evaporated below 25° to a green syrup which evolved gases. Carbon tetrachloride was repeatedly evaporated *in vacuo* from this syrup until gases were no longer evolved. After thorough drying in a high vacuum, the hard colorless glassy material weighed 3.46 g (99% yield). The n.m.r. spectrum allowed the presence of only one compound, $[\alpha]_D^6$ −20° (*c*, 3 in chloroform) which resisted crystallization. The infrared spectrum contained strong absorptions for olefinic bond and nitro group asymmetric stretching at 1645 and 1510 cm^{-1}, respectively. The n.m.r. spectrum at 100 Mc.p.s. showed signals at τ 1.67, 4.01, 4.73, 5.26, 5.52, and 5.80 assigned to H-1, H-3, H-4, H-5, H-6, and H-6′, respectively. The following coupling constants were estimated, $J_{3,4} = 2.9$, $J_{4,5} = 2.0$, $J_{6,6'} = 12.0$, $J_{1,3} = 0.3$, $J_{3,5} = 1.8$ c.p.s. An interpretation of these data is reserved for a forthcoming publication (18). The acetyl-group signals were at τ 7.89 (two) and 7.90 (one).

Anal. Calcd. for $C_{12}H_{15}NO_9$ (mol. wt., 317.3): C, 45.43; H, 4.77; N, 4.42. Found (mol. wt., 337, osmometric in benzene): C, 45.37; H, 4.85; N, 4.12.

*Tri-O-acetyl-2-nitro-*D*-galactal (**14**)*

Tri-*O*-acetyl-D-galactal (6.41 g) was treated with dinitrogen tetroxide and oxygen as described above. The yield was 7.07 g (94%) of a hard glass, $[\alpha]_D^{23}$ +68° (*c*, 3 in chloroform), which could not be crystallized. The n.m.r. spectrum at 100 Mc.p.s. required a high degree of purity. The signals at τ 1.77, 3.68, 4.52, 5.35, 5.46, and 5.63 were assigned to H-1, H-3, H-4, H-5, H-6, and H-6′, respectively. The following coupling constants were estimated, $J_{3,4} = 5.1$, $J_{4,5} = 4.1$, $J_{5,6} = 3.5$, $J_{5,6'} = 4.1$, $J_{6,6'} = 12.1$, $J_{1,3} \leq 0.3$, $J_{3,5} = 0.4$ c.p.s. The acetyl-group signals were at τ 7.89 (two) and 7.92 (one).

*Di-O-acetyl-2-nitro-*D*-xylal (**15**)*

Di-*O*-acetyl-D-xylal (4.13 g) was treated with dinitrogen tetroxide and oxygen as described above. The yield was 5.0 g of a crude crystalline product which was purified by sublimation at 100° and 0.3 mm. The yield was 3.91 g (77%) of material, m.p. 128–129°, $[\alpha]_D^{23}$ −319° (*c*, 2.1 in chloroform). The n.m.r. spectrum at 100 Mc.p.s. had signals at τ 1.61, 4.02, 4.90, 5.46, and 5.92 which were assigned to the H-1, H-3, H-4, H-5, and H-5′ protons, respectively. The following coupling constants were estimated, $J_{3,4} = 3.0$, $J_{4,5} = 2.1$, $J_{4,5'} = 1.5$, $J_{5,5'} = 12.8$, $J_{1,3} \leq 0.3$, $J_{3,5} = 1.8$, $J_{3,5'} = 0.6$, and $J_{1,5'} = 0.9$.

Anal. Calcd. for $C_9H_{11}NO_7$ (mol. wt., 245.2): C, 44.08; H, 4.52; N, 5.71. Found (mol. wt., 237, osmometric): C, 44.19; H, 4.54; N, 5.69.

Acknowledgments

The authors are indebted to the National Research Council of Canada for grants (T-172) in aid of this research. The spectra and microanalyses were provided by the service laboratories of this department.

1. W. A. TILDEN and W. A. SHENSTONE. J. Chem. Soc. **31**, 554 (1877).
2. T. BEIER, H. G. HAUTHAL, and W. PRITZKOW. J. Prakt. Chem. **26**, 4, 304 (1964).
3. J. MEINWALD, Y. C. MEINWALD, and T. N. BAKER. J. Am. Chem. Soc. **85**, 2513 (1963).
4. R. U. LEMIEUX and B. FRASER-REID. Can. J. Chem. **43**, 1460 (1965).
5. W. J. SERFONTEIN, J. H. JORDAAN, and J. WHITE. Tetrahedron Letters, No. 18, 1069 (1964).
6. R. U. LEMIEUX, T. L. NAGABHUSHAN, and I. K. O'NEILL. Tetrahedron Letters, No. 29, 1909 (1964).
7. H. SHECHTER. Record Chem. Progr. Kresge-Hooker Sci. Lib. **25**, 55 (1964).
8. N. LEVY and C. W. SCAIFE. J. Chem. Soc. 1100 (1946); N. LEVY, C. W. SCAIFE, and A. E. WILDER-SMITH. J. Chem. Soc. 52 (1948); H. BALDOCK, N. LEVY, and C. W. SCAIFE. J. Chem. Soc. 2627 (1949).
9. N. THORNE. J. Chem. Soc. 4271 (1956).
10. E. H. WHITE and W. R. FELDMAN. J. Am. Chem. Soc. **79**, 5832 (1957).
11. B. S. CARTWRIGHT and J. H. ROBERTSON. Chem. Commun. No. 3, 82 (1966).
12. R. V. ST. LOUIS and B. CRAWFORD, JR. J. Chem. Phys. **42**, 857 (1965).
13. A. SCHAARSCHMIDT. Z. Angew. Chem. **37**, 933 (1924).
14. J. D. S. GOULDEN and D. J. MILLEN. J. Chem. Soc. 2620 (1950).
15. M. OHNO, M. OKAMOTO, and K. NUKADA. Tetrahedron Letters, No. 45, 4047 (1965).
16. F. JOHNSON and S. K. MALHOTRA. J. Am. Chem. Soc. **87**, 5492, 5493 (1965).
17. R. CAPLE and W. V. VAUGHAN. Tetrahedron Letters, No. 34, 4067 (1966).
18. R. U. LEMIEUX and I. K. O'NEILL. Can. J. Chem. In preparation.
19. R. U. LEMIEUX and I. K. O'NEILL. Can. J. Chem. In preparation.
20. R. U. LEMIEUX, S. W. GUNNER, and Y. ITO. Can. J. Chem. To be published.
21. R. U. LEMIEUX, R. SUEMITSU, and S. W. GUNNER. Can. J. Chem. To be published.
22. R. U. LEMIEUX and T. L. NAGABHUSHAN. Can. J. Chem. This issue.
23. W. ROTH and W. PIGMAN. *In* Methods in carbohydrate chemistry. *Edited by* R. L. Whistler and M. L. Wolfrom. Vol. II. Academic Press, Inc., New York. 1963. p. 405. *See also* F. Shafizadeh. p. 409.
24. P. A. LEVENE and T. MORI. J. Biol. Chem. **83**, 803 (1929).
25. R. U. LEMIEUX, T. L. NAGABHUSHAN, and S. W. GUNNER. Can. J. Chem. This issue.
26. A. HASSNER and I. H. POMERANTZ. J. Org. Chem. **27**, 1760 (1962).
27. J. W. H. OLDHAM. J. Chem. Soc. 2840 (1925).

The synthesis of some 9-furfuryl-6-substituted purines as potential antimetabolites[1,2]

H. C. HAMANN, V. T. SPAZIANO, T. C. CHOU, C. C. PRICE, AND H. H. LIN

Department of Chemistry, Saint Joseph's College and Department of Chemistry, University of Pennsylvania, Philadelphia, Pennsylvania

Received April 28, 1967

Several 9-furfuryl-6-substituted purines were synthesized by reacting 9-furfuryl-6-chloropurine (**5**) with the corresponding nucleophilic reagent. The mother compound (**5**) was prepared by direct cyclization of 4-furfurylamino-5-amino-6-chloropyrimidine (**4**) with a mixture of ethyl orthoformate and acetic anhydride. The diaminopyrimidine (**5**) was prepared by treatment of 4,6-dichloro-5-aminopyrimidine with furfurylamine in boiling water.

Canadian Journal of Chemistry, 46, 419 (1968)

Can. J. Chem. Downloaded from www.nrcresearchpress.com by 210.87.254.40 on 09/05/12
For personal use only.

In the synthesis of various potential antagonists of the natural purines 9-methyl-6-chloropurine (1) has shown the same order of activity against Adenocarcinoma 755 in C-57 black mice as 6-chloropurine[3] (2), while two other 9-methyl-6-substituted purines have shown less activity against this tumor. 9-Ethyl-6-chloropurine (3) and 9-propyl-6-chloropurine (4), synthesized by Montgomery and Temple, have also shown the same kind of activity.

Due to the structural similarity between naturally occurring metabolic purine ribonucleosides, deoxyribonucleosides, and 9-furfuryl-6-substituted purines, the investigation of the biological activity of 9-furfuryl-6-substituted purines could be of some interest. A comparison of the biological activity of 9-furfuryl-6-chloropurine with that of 9-methyl-, 9-ethyl-, 9-propyl-, and 9-phenyl-6-chloropurine (5) would be especially desirable.

Thirteen such derivatives of purine were synthesized through the method devised by Robins and Lin (1) and sent to the Cancer Chemotherapy National Service Center, National Institutes of Health, Bethesda, Maryland, for screening their biological activities. The mother compound 9-furfuryl-6-chloropurine (**5**) was prepared in good yield by direct cyclization of 4-furfurylamino-5-amino-6-chloropyrimidine (**4**) with a mixture of ethyl orthoformate and acetic anhydride.

Treatment of several aliphatic and aromatic amines with **5** in boiling amyl alcohol yielded corresponding amino derivatives in fairly good yield. Cyclization of 4-furfurylamino-5-amino-6-chloropyrimidine by refluxing with 97% formic acid failed to yield 9-furfuryl-6-hydroxypurine (**6**). A black sticky polymeric residue was the only product that could be isolated. The ring cleavage of furfuryl ring in the boiling formic acid could cause the formation of this polymeric residue. 9-Furfuryl-6-hydroxypurine (**6**) was prepared easily by treatment of the mother compound (**5**) with 1 *N* sodium hydroxide in good yield. 9-Furfuryl-6-methoxypurine (**9**) was prepared by treatment of **5** with sodium methoxide. 9-Furfuryl-6-aminopurine (9-furfuryladenine) (**8**) was prepared by heating **5** with excess concentrated ammonium hydroxide at 130° in a steel Parr bomb. 9-Furfuryl-6-mercaptopurine (**7**) was prepared in high yield by treatment of **5** with thiourea. The ultraviolet absorption spectra of the 9-furfuryl-6-substituted purines are in general very similar to that of 9-methyl-6-substituted purines.

Biological Activities

9-Furfuryl-6-mercaptopurine (**7**) was found to be active at 112 mg/Kg (T/C, 31%) against Adenocarcinoma 755. 4,6-Difurfurylamino-5-nitropyrimidine (**1**) was found to be non-toxic and inactive at 125 mg/Kg in the cell culture and cell line SA. 9-Furfuryl-6-chloropurine (**5**) and 9-furfuryl-6-hydroxypurine (**6**) were found to be inactive at 100 mg/Kg against Adenocarcinoma

[1]This investigation was supported by the fund from the National Cancer Institute, National Institutes of Health, the United States Public Health Service, Bethesda, Maryland under grant No. CA-06492.

[2]The data published here is taken from the theses submitted by H. C. Hamann and V. T. Spaziano in partial fulfillment for the degree of Master of Science at Saint Joseph's College, Philadelphia, Pennsylvania.

[3]H. E. Skipper, J. R. Thompson, and R. K. Robins. The Southern Research Institute, Birmingham, Alabama. Unpublished data.

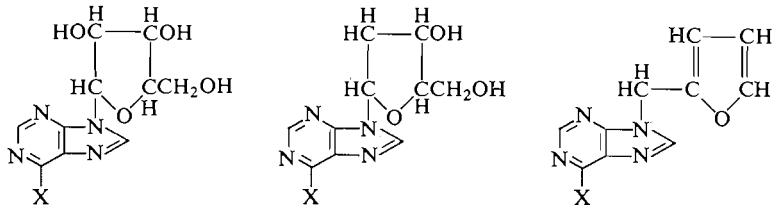

Ribonucleoside
X = —OH, —NH_2

Deoxyribonucleoside
X = —OH, —NH_2

9-Furfuryl-6-substituted purine
X = —OH, —NH_2

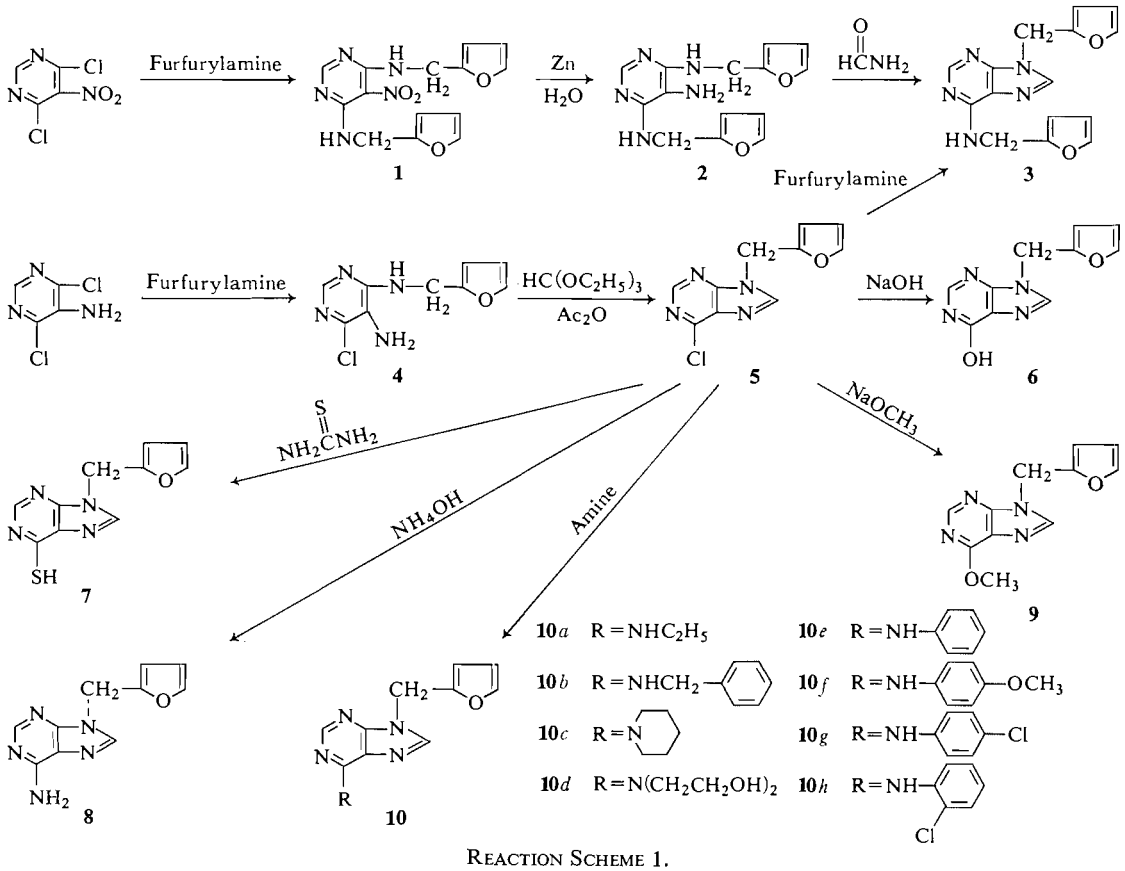

REACTION SCHEME 1.

755. 9-Furfuryl-6-ethylaminopurine (**10***a*) and 9-furfuryl-6-methoxyanilinopurine (**10***f*) were found to be inactive at 10^{-3} mg/ml against the Leukemia L1210 and Walker 256 tumors.

Experimental

4,6-Difurfurylamino-5-nitropyrimidine (1)

A mixture of 5.8 g of 4,6-dichloro-5-nitropyrimidine and 11.6 g of furfurylamine in 150 ml of absolute ethanol was refluxed for 1 h. Upon cooling the reaction mixture in the refrigerator, yellow crystalline needles separated out. The crystals were filtered with suction and dried, yield 5.4 g. Upon evaporation of filtrate to half its original volume, further crystals (1.8 g) were collected, m.p. 128–131°. A small portion of crude product was recrystallized from a mixture of ethanol and water to yield yellow needles, m.p. 131–132°; total yield was 77%.

Anal. Calcd. for $C_{14}H_{13}N_5O_4$: C, 53.33; H, 4.17; N, 22.21. Found: C, 53.61; H, 4.31; N, 22.13.

4,6-Difurfurylamino-5-aminopyrimidine (2)

To constantly stirred boiling water (500 ml) containing 200 g of zinc dust was added in small portions 4 g of 4,6-difurfurylamino-5-nitropyrimidine. The reaction mixture was digested for an additional 10 min.

Can. J. Chem. Downloaded from www.nrcresearchpress.com by 210.87.254.40 on 09/05/12
For personal use only.

Can. J. Chem. Downloaded from www.nrcresearchpress.com by 210.87.254.40 on 09/05/12
For personal use only.

After the addition, the mixture was filtered with suction while still hot. Slightly tan needles separated out upon cooling. The crystals were collected and dried, gave a crude product of 1.1 g, m.p. 114–117°. A small amount of crude product was recrystallized from water to give white crystals, m.p. 116–117°, yield 31%.

Anal. Calcd. for $C_{14}H_{15}N_5O_2$: C, 58.94; H, 5.29; N, 24.55. Found: C, 59.02; H, 5.16; N, 24.40.

9-Furfuryl-6-furfurylaminopurine (3)

Method A

4,6-Difurfurylamino-5-aminopyrimidine (2 g) was added to 6 ml of formamide. The mixture was then heated to boiling on a hot plate for 15 min. As the triaminopyrimidine dissolved in the hot formamide, the resultant solution became dark and viscous. The liquid was then extracted with 150 ml of hot boiling benzene. The benzene solution was then treated with activated charcoal and filtered. The filtrate was then evaporated to half its original volume and *n*-heptane was added until it became cloudy. Upon cooling, tan solid separated out, m.p. 123–126°, yield 1.2 g. A portion of the crude product was recrystallized from a mixture of ethanol and water to give m.p. 127–128°, yield 57%.

Anal. Calcd. for $C_{15}H_{13}N_5O_2$: C, 61.02; H, 4.43; N, 23.72. Found: C, 61.04; H, 4.42; N, 23.60.

Method B

A mixture of 9-furfuryl-6-chloropurine (0.59 g) and furfurylamine (0.49 g) in 20 ml of 2-ethoxyethanol was refluxed for 3 h. The residue was then distilled to dryness *in vacuo* and recrystallized from a mixture of water and ethanol to give tan crystals, m.p. 120–124°, yield, 0.42 g. Further recrystallization gave m.p. 127–128°. A mixture melting point showed that it is identical with the product prepared from Method A, yield 74%.

4-Furfurylamino-5-amino-6-chloropyrimidine (4)

A mixture of 3.28 g of 4,6-dichloro-5-aminopyrimidine and 4.0 g of furfurylamine in 60 ml water was heated on a steam bath for 4 h. The dark-brown oil separated and crystallized upon cooling the reaction mixture in the refrigerator. The crude product was collected and dried, m.p. 126–129°, yield 4.1 g. A small portion of the crude product was recrystallized from a mixture of water and ethanol to give tan prisms of m.p. 130–131°, yield 91%.

Anal. Calcd. for $C_9H_9N_4ClO$: C, 48.11; H, 4.04; N, 24.94; Cl, 15.78. Found: C, 48.43; H, 4.20; N, 25.15; Cl, 15.59.

9-Furfuryl-6-chloropurine (5)

4-Furfurylamino-5-amino-6-chloropyrimidine (6 g) was added to a mixture of 60 ml of triethylorthoformate and 60 ml of acetic anhydride. The mixture was refluxed for 3 h and distilled to near dryness *in vacuo*. The viscous black residue was then dissolved in 200 ml of hot benzene, and charcoal was added. The mixture was filtered and the filtrate was evaporated to half of its original volume. To the hot solution, *n*-hexane was added until the mixture became slightly cloudy. Upon cooling of the solution, a sticky brownish-yellow solid crystallized out. Further scratching of the sticky semicrystalline mass yielded more crystalline solid. The crude product was collected, m.p. 105–109°, yield 4.5 g. A portion of the sticky solid was recrystallized again from a mixture of benzene and hexane, m.p. 109–112°, yield 72%.

Anal. Calcd. for $C_{10}H_7N_4ClO$: C, 51.18; H, 3.00; N, 23.87; Cl, 15.11. Found: C, 51.02; H, 2.80; N, 23.81; Cl, 15.68.

9-Furfuryl-6-hydroxypurine(9-furfurylhypoxanthine) (6)

9-Furfuryl-6-chloropurine was added to 40 ml of 1 *N* NaOH. The mixture was heated on a steam bath for ½ h. The chloropurine dissolved completely into the alkaline solution at the end of heating. The dark-brown solution was treated with charcoal and filtered. The filtrate was acidified with glacial acetic acid. Light-tan solids precipitated, were collected, and dried, m.p. 260–264°, yield 0.6 g. A small portion of the crude product was recrystallized from water, m.p. 265° (decomp.), yield 65%.

Anal. Calcd. for $C_{10}H_8N_4O_2$: C, 55.55; H, 3.73; N, 25.92. Found: C, 55.81; H, 3.92; N, 25.59.

9-Furfuryl-6-mercaptorpurine (7)

A mixture of 9-furfuryl-6-chloropurine (2.35 g) and thiourea (0.8 g) in 60 ml of 2-ethoxyethanol was refluxed for 3 h. A light-tan solid separated and was filtered. The filtrate was distilled to dryness *in vacuo*. The residue was combined with the light-tan solid and dissolved in 50 ml of 5% hot NaOH solution. The solution was treated with activated charcoal and filtered. The filtrate was acidified with glacial acetic acid to yield 2.1 g of light-tan solid, which became pale-yellow upon drying, m.p. 315° (decomp.). A small portion of the product was suspended in hot water with a minimum amount of NaOH to ensure complete dissolution. The solution was filtered and acidified with glacial acetic acid. White crystalline solids separated, were collected, and dried, m.p. 315° (decomp.), yield 90%.

Anal. Calcd. for $C_{10}H_8N_4SO$: C, 51.72; H, 3.44; N, 24.13; S, 13.79. Found: C, 51.52; H, 3.64; N, 24.18; S, 13.59.

9-Furfuryl-6-aminopurine(9-furfuryladenine) (8)

A mixture of 9-furfuryl-6-chloropurine (1.0 g) and 20 ml of concentrated NH_4OH was sealed in a steel Parr bomb (40 ml). The bomb was heated to 130° in a steel high pressure bomb (500 ml) for 3 h. The mixture was taken out from the bomb upon cooling to room temperature. White crystalline prisms separated and were filtered, m.p 195–201°, yield 0.6 g. A small portion of the crude product was recrystallized from hot water to give m.p. 202–205°, yield 65%.

Anal. Calcd. for $C_{10}H_9N_5O$: C, 55.81; H, 4.22; N, 32.54. Found: C, 55.90; H, 4.41; N, 32.25.

9-Furfuryl-6-methoxypurine (9)

9-Furfuryl-6-chloropurine (1.4 g) was added to 100 ml of absolute methanol in which 0.13 g of sodium metal was dissolved. The mixture was refluxed on the steam bath for ½ h. A small amount of sodium chloride which precipitated was filtered off. The filtrate was then evaporated to about 25 ml, then allowed to cool. Colorless crystalline needles separated, were collected, and were dried, m.p. 100–103°, yield 0.8 g. A small portion of the crude product was recrystallized from water (0.7 g), m.p. 103–104°, yield 58%.

Anal. Calcd. for $C_{11}H_{10}N_4O_2$: C, 57.38; H, 4.37; N, 24.33. Found: C, 57.64; H, 4.15; N, 24.38.

Can. J. Chem. Downloaded from www.nrcresearchpress.com by 210.87.254.40 on 09/05/12
For personal use only.

TABLE I

9-Furfuryl-6-anilinopurines

Compound	Yield %	Melting point °C	Formula	Recrystallization solvent	Analysis							
					Calculated, %				Found, %			
					C	H	N	Cl	C	H	N	Cl
10*a*	55	125–127	$C_{12}H_{13}N_5O$	water	59.25	5.39	28.79		59.02	5.27	28.75	
10*b*	76	124–125	$C_{17}H_{15}N_5O$	water and ethanol mixture	66.88	4.95	22.94		67.26	5.36	22.75	
10*c*	52	151–153	$C_{15}H_{18}N_5OCl$	ethanol	56.33	5.67	21.89	11.09	56.37	5.94	22.18	11.06
10*d*	59	109–110	$C_{14}H_{17}N_5O_3$	ethyl acetate	55.43	5.65	23.08		55.36	5.43	23.18	
10*e*	53	151–152	$C_{16}H_{13}N_5O$	water and ethanol mixture	65.95	4.49	24.08		66.11	4.47	24.08	
10*f*	31	137–139	$C_{17}H_{15}N_5O_2$	water and ethanol mixture	63.54	4.70	21.79		63.53	4.79	21.99	
10*g*	62	155–158	$C_{16}H_{12}N_5OCl$	water and ethanol mixture	58.99	3.71	21.49	10.88	59.08	3.79	21.61	10.60
10*h*	73	143–144	$C_{16}H_{12}N_5OCl$	water and ethanol mixture	58.99	3.71	21.49	10.88	59.06	3.73	21.28	10.50

TABLE II

The ultraviolet absorption maxima of 9-furfuryl-6-substituted purines*

R	0.1 *N* HCl, λ_{max} mμ	ε	0.1 *N* NaOH, λ_{max} mμ	ε
OH	248	1.5×10^4	254	1.7×10^4
SH	insoluble		311	2.0×10^4
Cl	264	1.0×10^4	264	1.1×10^4
OCH_3	264	1.5×10^4	255	1.2×10^4
$-NHCH_2CH_3$	266	1.7×10^4	270	1.9×10^4
$-NHCH_2C_6H_5$	268	1.9×10^4	270	2.0×10^4
$-NC_5H_{10}$	279	0.69×10^4	282	2.4×10^4
$-N(CH_2CH_2OH)_2$	276	2.5×10^4	280	2.5×10^4
p-$C_6H_4-OCH_3$	277	2.5×10^4	286	2.3×10^4
$-NHCH_2$-furyl	267	1.5×10^4	268	2.0×10^4

*Compounds of structure 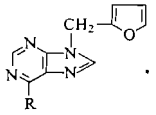 .

9-Furfuryl-6-ethylaminopurine (10a)

A mixture of 9-furfuryl-6-chloropurine (1.4 g) and 20 ml of aqueous ethylamine (70%) was heated in a steel Parr bomb at 120° for 3 h. The mixture was then evaporated to dryness on a steam bath. The brown residue was recrystallized from water to give analytically pure product.

9-Furfuryl-6-benzylaminopurine (10b), 9-Furfuryl-6-piperidinopurine Monohydrochloride (10c), 9-Furfuryl-6-N,N-bis(2-hydroxyethyl)amino Purine (10d), 9-Furfuryl-6-anilinopurine(10e), 9-Furfuryl-6-p-methoxyanilinopurine (10f), 9-Furfuryl-6-p-chloroanilinopurine (10g), and 9-Furfuryl-6-o-chloroanilinopurine (10h)

A mixture of 9-furfuryl-6-chloropurine (0.005 mole) and corresponding aniline (0.01 mole) in 50 ml of *n*-amyl alcohol was refluxed for 3 h. The solution was distilled to dryness under reduced pressure. The residue was then recrystallized from a mixture of water and ethanol to give light-tan crystals. The crude products were further purified to analytically pure compounds. The data for each compound are tabulated in Table I.

Acknowledgments

The authors would like to thank Dr. George J. Beichl for his active interest and support. Financial support from the National Cancer Institute, National Institutes of Health, the United States Public Health Service, Bethesda, Maryland, is gratefully acknowledged.

1. R. K. Robins and H. H. Lin. J. Am. Chem. Soc. **79**, 490 (1957).
2. A. Bendich, P. J. Russell, Jr., and J. J. Fox. J. Am. Chem. Soc. **76**, 6073 (1954).
3. J. A. Montgomery and C. Temple, Jr. J. Am. Chem. Soc. **79**, 5238 (1957).
4. J. A. Montgomery and C. Temple, Jr. J. Am. Chem. Soc. **80**, 409 (1958).
5. S. M. Greenberg, L. O. Ross, and R. K. Robins. J. Org. Chem. **24**, 1314 (1959).

Can. J. Chem. Downloaded from www.nrcresearchpress.com by 210.87.254.40 on 09/05/12
For personal use only.

Can. J. Chem. Downloaded from www.nrcresearchpress.com by 210.87.254.6 on 09/05/12
For personal use only.

Synthesis of derivatives of 4-acetamido-4-deoxy-D- and L-arabinose

A. J. DICK[1] and J. K. N. JONES
Department of Chemistry, Queen's University, Kingston, Ontario

Received September 13, 1967

4-Acetamido-4-deoxy-D- and L-arabinose have been synthesized from methyl 4-azido-4-deoxy-D- and L-arabinopyranoside, respectively. In contrast to other 4-acetamido-4-deoxypentoses, the arabinose derivatives in aqueous solution at tautomeric equilibrium exist both in the pyranose and in the furanose forms. The presence of the furanose form (containing nitrogen as the hetero atom in the ring) has been demonstrated by paper chromatography and infrared and nuclear magnetic resonance (n.m.r.) spectroscopy. Acetolysis of methyl 4-amino-4-deoxy-α-D-arabinopyranoside hydrochloride and of the *N*-acetyl derivative gave 4-acetamido-4-deoxy-D-arabinofuranose tetraacetates whose anomeric configurations were assigned by n.m.r. spectroscopy. Treatment of the 4-acetamido-4-deoxy-D-arabinofuranose tetraacetates with a cation exchange resin in methanol solution and subsequent de-*O*-acetylation, gave the anomeric methyl 4-acetamido-4-deoxy-D-arabinofuranosides, whose n.m.r. spectra in D_2O exhibited the phenomenon of hindered internal rotation.

Canadian Journal of Chemistry, **46**, 425 (1968)

There has been considerable interest recently in the synthesis of sugar derivatives in which the ring oxygen atom is replaced by other hetero atoms, notably nitrogen or sulfur. The subject has been comprehensively reviewed by Paulsen (1). Of the 4-acetamido-4-deoxypentoses, in which the possibility exists for the formation of a furanose ring containing nitrogen, the D-ribose (2), L-xylose (3, 4), 5-deoxy-D-xylose (5), and 5-deoxy-L-xylose (5, 6) derivatives have been synthesized. More recently, derivatives of 4-amino-4-deoxy-D-xylose (7, 8) have been prepared from methyl 2,3-di-*O*-benzoyl-4-*O*-*p*-(toluenesulfonyl)-β-L-arabinopyranoside by nucleophilic displacement of the tosylate by azide ion. Facile substitution at C-4 of certain methyl pyranoside sulfonates by azide ion is well known (2, 9–13). In previous communications, we reported the saponification of the methanesulfonyl ester groups of methyl 4-azido-4-deoxy-2,3-di-*O*-methanesulfonylpentopyranosides of the *xylo* and *arabino* configuration (9) and epoxide ring cleavage of methyl 2,3-anhydro-4-azido-4-deoxypentopyranosides which gave methyl 4-azido-4-deoxypentopyranosides (14). These 4-azido sugar derivatives are readily converted into acetamido deoxypentoses of which those of the D- and L-*arabino* configurations are herein described.

*4-Acetamido-4-deoxy-*D*-arabinose*

Reduction of methyl 4-azido-4-deoxy-α-D-arabinopyranoside (**1**) over 10% palladium on carbon gave syrupy methyl 4-amino-4-deoxy-α-D-arabinopyranoside (**2**) which was characterized as its crystalline hydrochloride (**3**). *N*-Acetylation of **2** gave methyl 4-acetamido-4-deoxy-α-D-arabinopyranoside (**4**) in crystalline form.

Pyrrolidine derivatives of 4-acetamido-4-deoxy-D-arabinose were obtained by acetolysis of **3** and **4**. Acetolysis of acetamido derivative, **4**, gave a mixture of the anomeric 4-acetamido-4-deoxy-D-arabinofuranose tetraacetates. Acetolysis of the amine hydrochloride, **3**, and work-up of the reaction shortly after cleavage of the glycosidic methoxyl group was complete gave a pyranose tetraacetate as well as the furanoses. Fractionation of the mixture by adsorption chromatography on silica gel gave 4-acetamido-4-deoxy-1,2,3,5-tetra-*O*-acetyl-α-D-arabinofuranose (**5**), 4-acetamido-4-deoxy-1,2,3,5-tetra-*O*-acetyl-β-D-arabinofuranose (**6**), and 4-acetamido 4-deoxy-1,2,3-tri-*O*-acetyl-D-arabinopyranose (**7**). The furanose derivatives, **5** and **6**, were obtained in a relative yield of 1:5, respectively, and their ring size was inferred from the infrared spectra which showed amide I absorption but not an amide II band. The infrared spectrum of **7** showed amide I and II bands. The elemental analyses supported these structural assignments as did the nuclear magnetic resonance (n.m.r.) spectra.

The n.m.r. spectrum of **5** in chloroform-*d* (Fig. 1) showed a doublet at τ 3.53 ($J_{1,2} < 1$ c.p.s.) which was assigned to H-1. The small coupling constant indicated the α-configuration for the

[1]Present Address: Division of Biosciences, National Research Council of Canada, Ottawa, Canada.

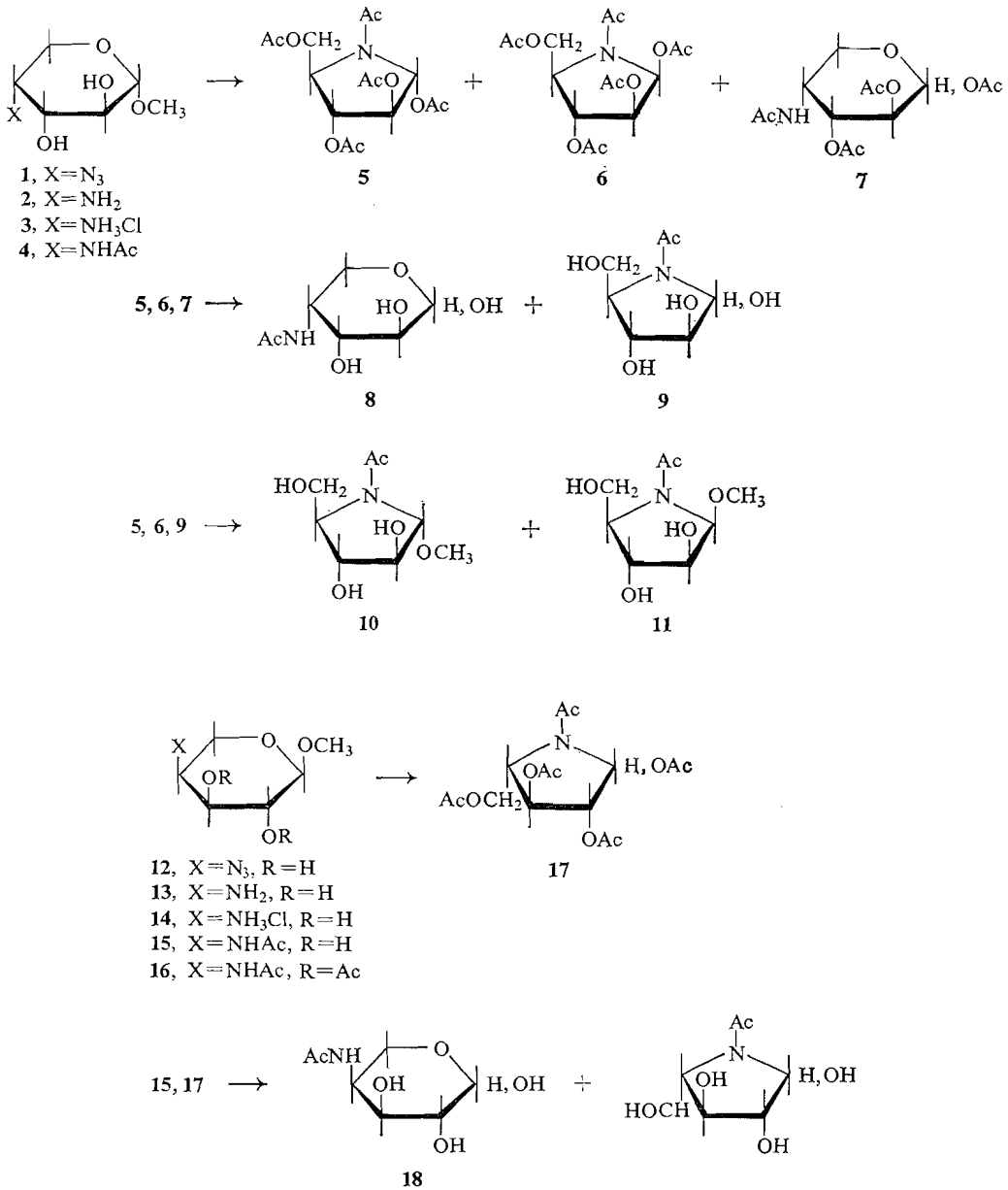

acetoxy group at C-1 (15, 16). Two broad singlets at τ 4.70 and 4.77, corresponding in intensity to approximately one proton each, were assigned to H-2 and H-3. The small coupling is indicative of a dihedral angle of close to 90° which is possible only if H-1, H-2, H-3, and H-4 are all *trans* in a five-membered ring as in the α-D-arabino configuration. The n.m.r. spectrum of **6** (Fig. 2) showed a doublet at τ 3.28 ($J_{1,2}$ 5 c.p.s.) for H-1 which indicates that **6** has the β-D-furanose configuration.

De-*O*-acetylation of a mixture of **5**, **6**, and **7** and trituration of the syrupy product with ethanol – ethyl acetate gave crystalline 4-acetamido-4-deoxy-D-arabinopyranose (**8**). The infrared spectrum showed absorption for N—H and N—Ac and the n.m.r. spectrum (Fig. 3) was quite similar to that of L-arabinose (17). A

Can. J. Chem. Downloaded from www.nrcresearchpress.com by 210.87.254.6 on 09/05/12
For personal use only.

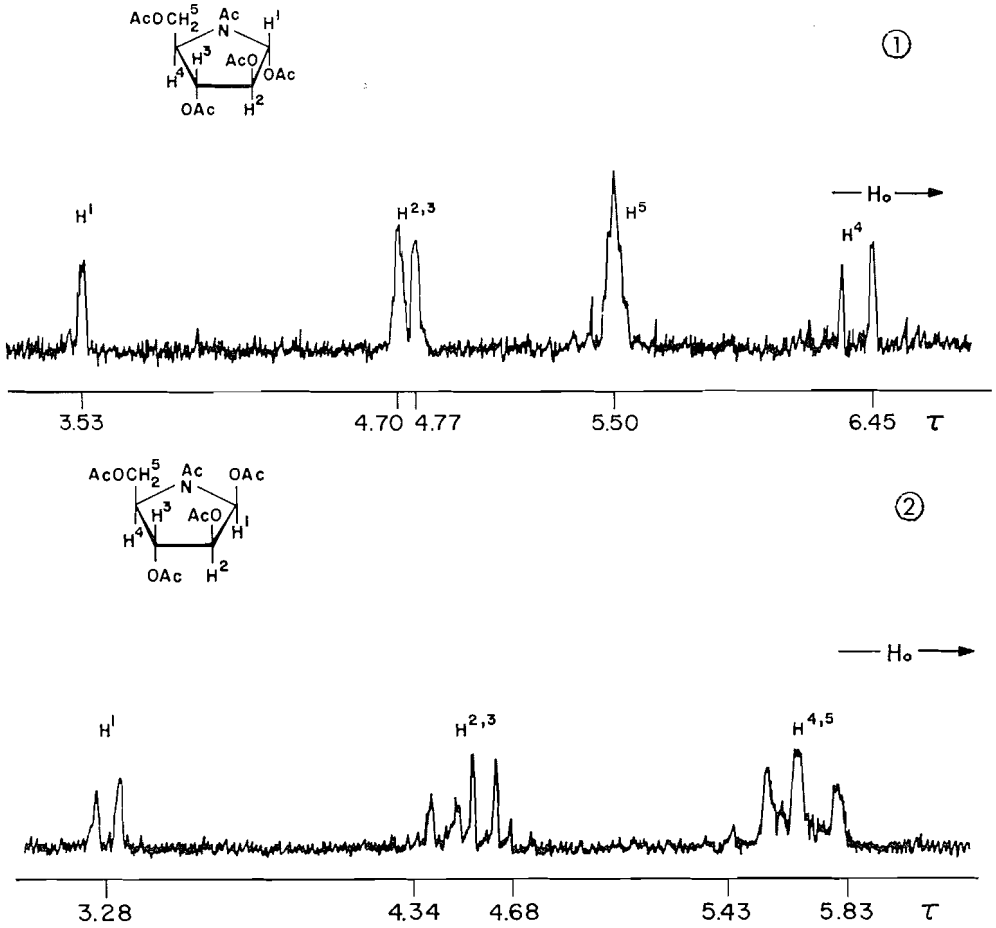

FIG. 1. Partial n.m.r. spectrum of 4-acetamido-4-deoxy-1,2,3,5-tetra-*O*-acetyl-α-D-arabinofuranose (**5**) in chloroform-*d*.

FIG. 2. Partial n.m.r. spectrum of 4-acetamido-4-deoxy-1,2,3,5-tetra-*O*-acetyl-β-D-arabinofuranose (**6**) in chloroform-*d*.

solution of **8** at the ambient probe temperature showed a doublet at τ 4.78 ($J_{1,2} \sim 2.7$ c.p.s.) which was assigned to H-1 of the β anomer and a doublet at τ 5.42 ($J_{1,2}$ 7.5 c.p.s.) for H-1 of the α anomer in the ratio of approximately 2:3. The acetyl protons were seen as a singlet at τ 7.93.

In the n.m.r. spectrum of **8** at 83°, the HOD signal was shifted upfield from the α H-1 proton resonance which made that signal more readily discernible but, also, additional lines appeared between τ 4.5–4.7 and another acetyl proton resonance at τ 7.81. These additional lines were thought to be due to 4-acetamido-4-deoxy-D-arabinofuranose (**9**), its appearance being caused by pyranose–furanose interconversion of **8** in the hot aqueous solution. Indeed, examination of the syrupy product obtained from de-*O*-acetylation of **5**, **6**, and **7** by paper chromatography revealed, besides a relatively intense spot at R_{rh} 0.71 for **8**, a faint spot at R_{rh} 0.90. This minor component (R_{rh} 0.90) was not observed upon chromatography of a freshly prepared aqueous solution of crystalline **8** but reappeared upon heating the solution. Although isolation of **9** was not achieved by preparative paper chromatography, a syrup rich in **9** was obtained from the mother liquors of several preparations of 4-acetamido-4-deoxy-D-arabinose from which most of the pyranose form (**8**) had been removed by

Can. J. Chem. Downloaded from www.nrcresearchpress.com by 210.87.254.6 on 09/05/12
For personal use only.

Can. J. Chem. Downloaded from www.nrcresearchpress.com by 210.87.254.6 on 09/05/12
For personal use only.

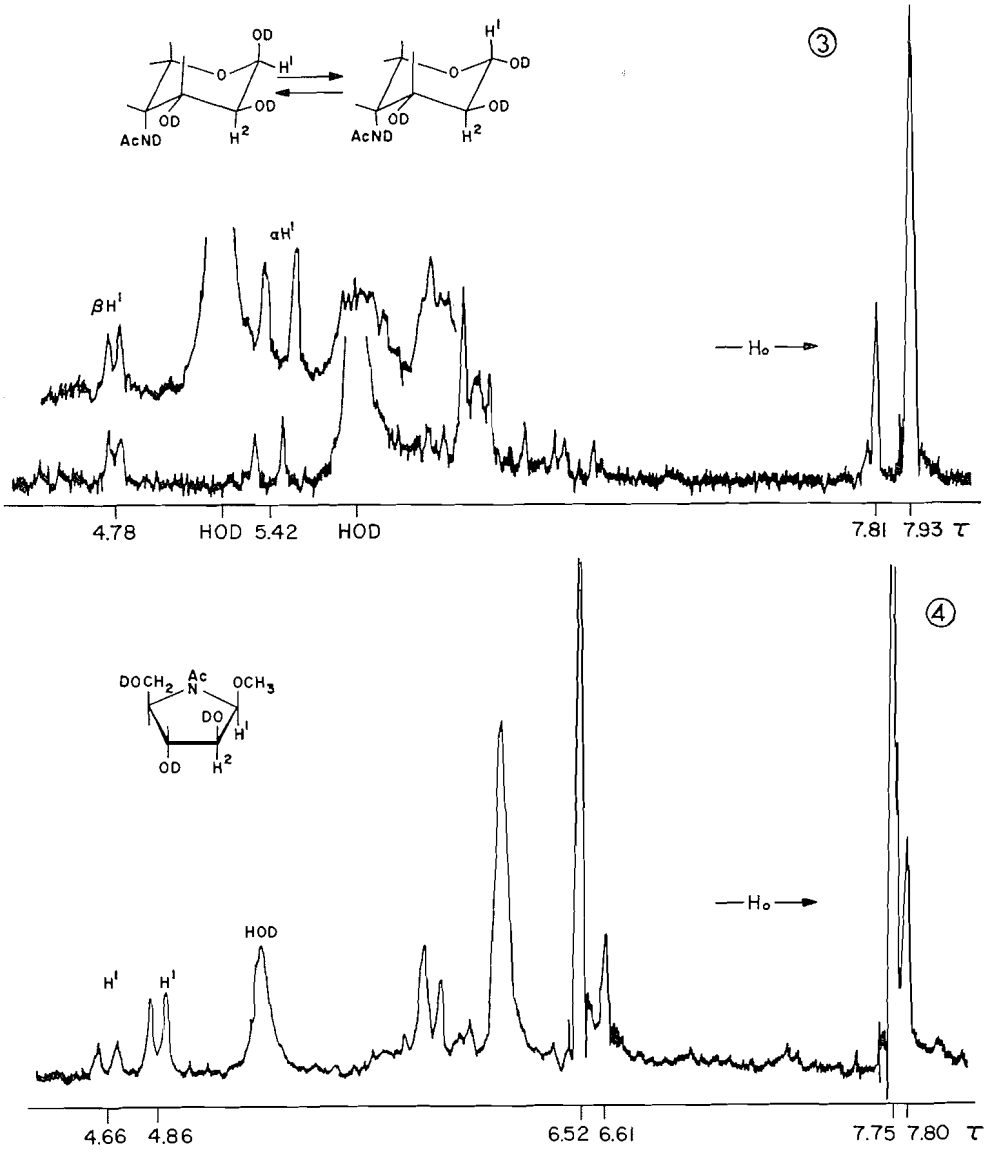

FIG. 3. Nuclear magnetic resonance spectrum of 4-acetamido-4-deoxy-D-arabinopyranose (**8**) in D_2O at 83°. Insert shows partial n.m.r. spectrum of **8** at the ambient probe temperature.

FIG. 4. Nuclear magnetic resonance spectrum of methyl 4-acetamido-4-deoxy-β-D-arabinofuranoside (**9**) in D_2O at the ambient probe temperature.

crystallization. An infrared spectrum of this syrupy mixture showed intense absorption at 1640 cm^{-1} (amide I) but only weak absorption at 1550 cm^{-1} (amide II) suggesting that **9** had a furanose structure. The n.m.r. spectrum of the mixture in D_2O (at the ambient probe temperature) showed, in addition to the signals for **8**, a complexity of signals between τ 4.5–4.7 the pattern of which showed a temperature dependence exemplary of hindered internal rotation (18). At 90°, the spectrum showed a broad singlet at τ 5.10 assigned to H-1 of the α anomer of 4-acetamido-4-deoxy-D-arabinofuranose (**9**) and a poorly resolved doublet at τ 4.54 assigned

Can. J. Chem. Downloaded from www.nrcresearchpress.com by 210.87.254.6 on 09/05/12
For personal use only.

to H-1 of the β anomer. The acetyl protons gave peaks at τ 7.75, 7.79, and 7.93, which collapsed to two at τ 7.78 and 7.93 at 90°. These latter lines correspond to those in the spectrum of **8** at 83°.

4-Acetamido-4-deoxyarabinose is the only 4-acetamidopentose reported which contains detectable amounts of the furanose form containing nitrogen as the hetero atom in the ring in equilibrium with the pyranose form. 4-Acetamido-4-deoxy-L-xylose (3, 4) has been described only in the pyranose form. This result is surprising when it is considered that arabinose itself, in aqueous solution, is detected only in the pyranose form at tautomeric equilibrium (17) and that the acetamido group is a much weaker nucleophile than the hydroxyl group.

It has been shown that the interconversion of the pyranose and furanose forms of 5-acetamido-5-deoxypentoses in methanolic hydrogen chloride solution occurs at a much slower rate than glycoside formation (22). Thus, support for the furanose formulation for **9** was obtained by treating the syrupy mixture containing an enrichment of **9** in dry methanol with a cation exchange resin. Examination of the syrupy product of this reaction by paper chromatography revealed two components (R_{rh} 1.37 and 1.88) when sprayed with *p*-anisidine hydrochloride. These substances are subsequently shown to be the β and α anomers of methyl 4-acetamido-4-deoxy-D-arabinofuranoside, respectively. The methyl pyranoside, **4**, is not detected by this spray reagent on paper chromatograms. These methyl furanosides were considered to have been formed from **9** before conversion to **8** took place.

The methyl 4-acetamido-4-deoxy-D-arabinofuranosides were readily prepared from the furanose pentaacetates. Treatment of the acetolysis product of **3** (containing **5**, **6**, and **7**) in methanol solution with a cation exchange resin and subsequent de-*O*-acetylation gave, after preparative paper chromatography, methyl 4-acetamido-4-deoxy-β-D-arabinofuranoside (**11**, R_{rh} 1.37) and methyl 4-acetamido-4-deoxy-α-D-arabinofuranoside (**10**, R_{rh} 1.88). The former was obtained as a syrup and the latter in a crystalline state. They were collected in the ratio 8:1. The infrared spectra of both showed the amide I band at 1640 cm^{-1} but no absorption at 1550 cm^{-1} (amide II). Compounds **10** and **11** were easily hydrolyzed by acid since they were detected by the *p*-anisidine hydrochloride spray reagent. Also, warming an aqueous solution of them containing a cation exchange resin at 40° led to complete hydrolysis in 2 h.

The n.m.r. spectra of **10** and **11** showed all the characteristics expected of compounds containing an acetamido group in a five-membered ring (18). The n.m.r. spectrum of **11** in D_2O at the ambient probe temperature (Fig. 4) showed H-1 as two doublets at τ 4.66 and 4.86 ($J_{1,2}$ 4.5 c.p.s.). The methoxyl protons appeared as two peaks at τ 6.52 and 6.61 with a relative intensity of 4:1. The acetyl proton resonance was also split, appearing at τ 7.75 and 7.80 with a similar relative intensity as for the methoxyl resonances. At 90° (Fig. 5), H-1 appeared as an ill-resolved doublet at τ 4.78. The methoxyl proton resonance had collapsed to a singlet at τ 6.52 and the acetyl protons were seen as a singlet at τ 7.75. The original pattern was restored upon cooling the solution. At 80°, the H-1 doublets had not completely coalesced and the methoxyl and acetyl protons still exhibited a doublet pattern.

The n.m.r. spectrum of **10** in D_2O at the ambient probe temperature (Fig. 6) showed a narrow doublet at τ 5.11 ($J_{1,2} < 1$ c.p.s.) which was assigned to H-1. A very weak signal at τ 5.00 which was more clearly seen at higher gain but was not well resolved was also assigned to H-1. That this was indeed a manifestation of hindered rotation was substantiated by measuring the spectrum at 80° when the two signals coalesced to a broad line centered at τ 5.10.

4-Acetamido-4-deoxy-L-arabinose

Reduction of methyl 4-azido-4-deoxy-α-L-arabinopyranoside (**12**; 9) over 5% palladium on carbon gave methyl 4-amino-4-deoxy-α-L-arabinopyranoside (**13**) as a syrup which was characterized as its crystalline hydrochloride (**14**). Crystalline methyl 4-acetamido-4-deoxy-α-L-arabinopyranoside (**15**) and the syrupy 2,3-di-*O*-acetyl derivative (**16**) of **15** were prepared in the usual manner.

Acetolysis of methyl 4-acetamido-4-deoxy-α-L-arabinopyranoside (**15**) and of its 2,3-diacetate (**16**) gave the same syrupy acetate, as shown by thin-layer chromatography, probably 4-acetamido-4-deoxy-1,2,3,5-tetra-*O*-acetyl-L-arabinofuranose (**17**). Infrared spectra of the syrups showed ester and amide I absorptions but negligible absorption for *N*—*H* (amide II).

De-*O*-acetylation of **17** gave a syrupy product which was shown by paper chromatography to contain two reducing components (R_{rh} 0.71 and

Can. J. Chem. Downloaded from www.nrcresearchpress.com by 210.87.254.6 on 09/05/12
For personal use only.

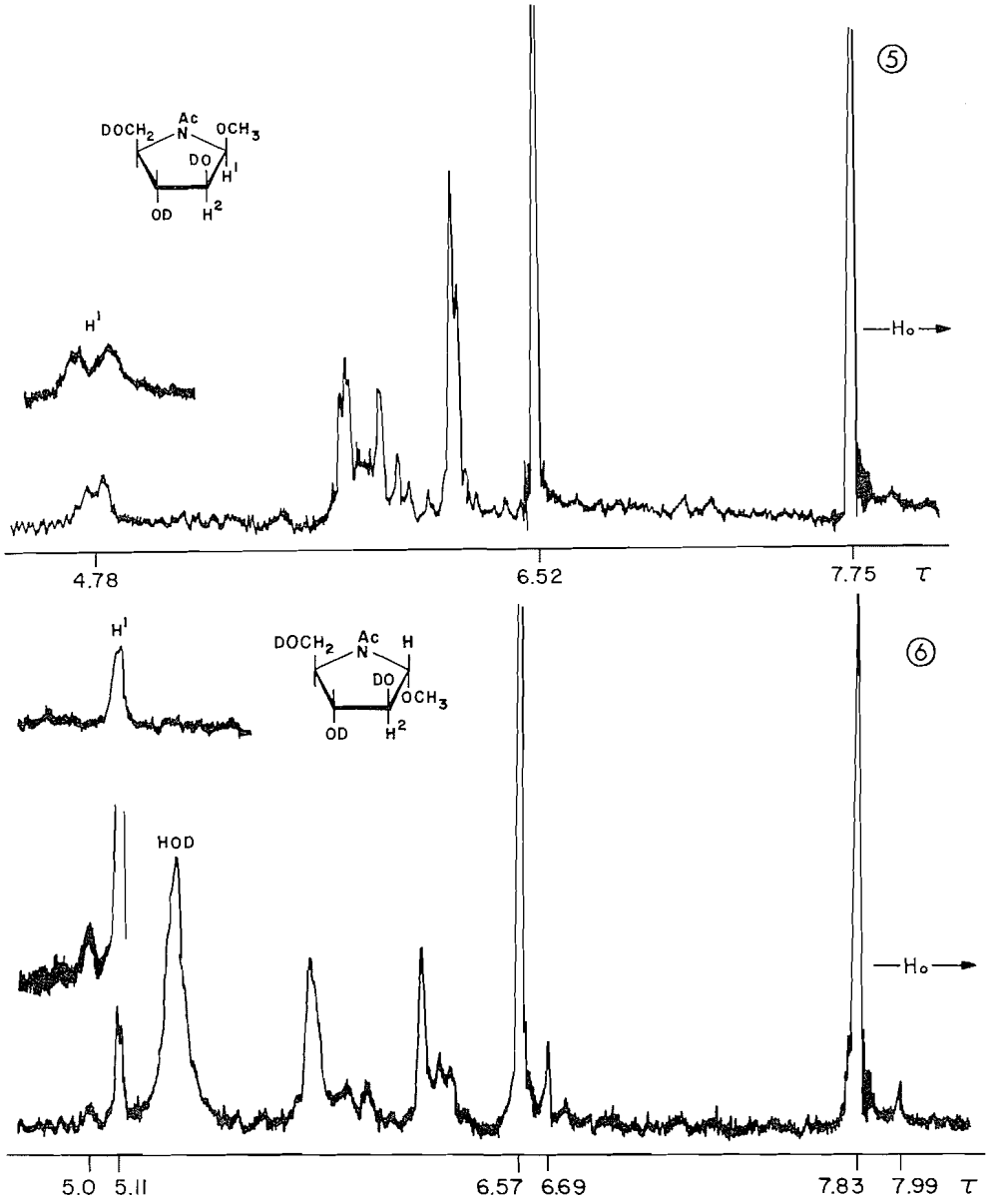

FIG. 5. Nuclear magnetic resonance spectrum of methyl 4-acetamido-4-deoxy-β-D-arabinofuranoside (**9**) in D_2O at 90°. Insert shows anomeric proton signal at a sweep width of 250 c.p.s.

FIG. 6. Nuclear magnetic resonance spectrum of methyl 4-acetamido-4-deoxy-α-D-arabinofuranoside (**10**) in D_2O at the ambient probe temperature. Center insert shows anomeric proton signal at increased gain. Top insert shows anomeric proton signal of **10** at 80°.

0.90). Treatment of the syrup with ethanol – ethyl acetate gave crystalline 4-acetamido-4-deoxy-L-arabinopyranose (**18**, R_{rh} 0.71) whose physical properties were identical in all respects with those of the D-enantiomer (**8**) except for a specific rotation of opposite sign. The component with R_{rh} 0.90 was probably 4-acetamido-4-deoxy-L-arabinofuranose (**19**) by analogy with the D-enantiomer.

Acid hydrolysis of methyl 4-acetamido-4-deoxy-α-L-arabinopyranoside with a cation exchange resin gave the same products (**18** and **19**)

Can. J. Chem. Downloaded from www.nrcresearchpress.com by 210.87.254.6 on 09/05/12
For personal use only.

but in a very low yield and the product required purification by preparative paper chromatography before crystallization of **18** could be induced.

Experimental

Solutions were concentrated under reduced pressure below 50° with a rotating-type evaporator. Melting points were determined on a Fisher–Johns melting point apparatus and are uncorrected. Optical rotations were measured at 23 ± 3° with a Hilger standard polarimeter. Infrared spectra were measured with a Beckman IR 5A spectrophotometer. Nuclear magnetic resonance spectra were determined with a Varian A 60 nuclear magnetic resonance (n.m.r.) spectrometer; chemical shifts were measured using 6% tetramethylsilane in chloroform as an external standard. Paper chromatography was carried out by the descending method at room temperature on Whatman No. 1 filter paper for qualitative purposes or Whatman 3MM filter paper for preparative purposes in butan-1-ol – ethanol – water, 3:1:1 (v/v). Sugars were detected on paper chromatograms by the p-anisidine hydrochloride spray reagent (19) (spray *i*) or the sodium metaperiodate – potassium permanganate spray reagent (20) (spray *ii*). Rates of movement of sugars on paper chromatograms are given relative to that of rhamnose (R_{rh}). Thin-layer chromatography (t.l.c.) was carried out on silica gel (supplied for that purpose); after irrigation, the plates were air-dried, and the spots located by spraying the chromatograms with a 5% solution of sulfuric acid in ethanol and heating the plates at 120°. Column chromatography on silica gel was carried out using Davison silica gel grade 950, mesh size 60-200.

Methyl 4-Amino-4-deoxy-α-D-arabinopyranoside Hydrochloride (3)

Methyl 4-azido-4-deoxy-α-D-arabinopyranoside (**1** (14), 2.3 g) was hydrogenated over 10% palladium on carbon in methanol solution containing 1 mole of hydrochloric acid. The catalyst was removed by filtration and the filtrate concentrated to a clear syrup. The syrupy product was crystallized by treatment with ethanol and afforded methyl 4-amino-4-deoxy-α-D-arabinopyranoside hydrochloride (**3**). **3** was recrystallized twice from ethanol and melted at 180–183° (decomp.) and had $[\alpha]_D$ +3° (*c*, 1.75 in water).

Anal. Calcd. for $C_6H_{14}ClNO_4$: C, 36.1; H, 7.0; Cl, 17.8; N, 7.0. Found: C, 35.8; H, 7.2; Cl, 17.8; N, 6.8.

Methyl 4-Acetamido-4-deoxy-α-D-arabinopyranoside (4)

Methyl 4-azido-4-deoxy-α-D-arabinopyranoside (**1**; 0.4 g) was hydrogenated over 10% palladium on carbon in methanol solution and worked up as above. The syrupy amine (**2**, 0.35 g) was *N*-acetylated according to the procedure of Roseman and Ludowieg (21). The syrup was dissolved in water (7 ml) and methanol (3 ml) and Amberlite IR 400 anion exchange resin (carbonate form; 5 g wet) was added. Acetic anhydride (1.5 moles) was added dropwise to the stirred mixture and the mixture was then stirred at room temperature for 90 min. The resin was removed by filtration and the filtrate passed through Amberlite IR 120 cation exchange resin (H^+ form). The eluate and washings were concentrated to a syrup which crystallized on standing. Recrystallization from ethanol gave methyl 4-acetamido-4-deoxy-α-D-arabinopyranoside (**4**) which melted at 129–130° and had $[\alpha]_D$ +1.6° (*c*, 1.83 in water); λ_{max} (Nujol); 1660 cm^{-1} and 1540 cm^{-1} (NHAc).

Anal. Calcd. for $C_8H_{15}NO_5$: C, 46.8; H, 7.3; N, 6.8. Found: C, 46.9; H, 7.8; N, 7.1.

Acetolysis of Methyl 4-Amino-4-deoxy-α-D-arabinopyranoside Hydrochloride (3)

3 (0.3 g) was dissolved in a mixture of acetic anhydride (5 ml) and acetic acid (5 ml). The solution was cooled in an ice bath and concentrated sulfuric acid (0.2 ml) was added. This solution was gently shaken for 48 h at room temperature. It was then poured into an excess of sodium bicarbonate in water and the aqueous mixture was extracted with chloroform. The chloroform extract was washed with water, dried ($MgSO_4$), filtered, and the filtrate concentrated to a dull-yellow syrup (0.5 g). Examination of this syrup by t.l.c. (irrigant: diethyl ether) revealed three components, the slower-moving one being only slightly displaced from the origin and being preponderant. An infrared spectrum (smear on NaCl) showed absorption at 3300 cm^{-1} (*N*—*H*), 1750 cm^{-1} (*O*—Ac), 1660, and 1540 cm^{-1} (*NH*Ac). The syrup was combined with the product from the following experiment and then fractionated.

Acetolysis of Methyl 4-Acetamido-4-deoxy-α-D-arabinopyranoside (4)

4 (1.0 g) was acetolyzed (acetic anhydride, 15 ml; acetic acid, 15 ml; sulfuric acid, 0.3 ml) for 24 h at room temperature and the product was worked up as described above. The product which was a brown syrup (0.8 g) contained two components, as indicated by t.l.c. (irrigant: diethyl ether), which corresponded to the two faster-moving components from the foregoing experiment. An infrared spectrum showed absorption at 1750 cm^{-1} (*O*—Ac) and at 1660 cm^{-1} (*N*—Ac) but no absorption for *N*—*H*.

Fractionation of Acetolysis Products of 3 and 4

The combined acetate syrups (1.3 g) from the foregoing two experiments were fractionated by column chromatography on silica gel (irrigant: diethyl ether). Three fractions were collected in order of elution:

(a) 4-Acetamido-4-deoxy-1,2,3,5-tetra-O-acetyl-α-D-arabinofuranose (5)

5 was obtained as a syrup (0.1 g) which was homogeneous by t.l.c. (irrigant: diethyl ether and ether acetate) and was vacuum distilled. It has $[\alpha]_D$ −31° (*c*, 0.45 in chloroform); λ_{max} (smear on NaCl): 1750 cm^{-1} (*O*Ac), 1660 cm^{-1} (*N*—Ac); n.m.r. data in chloroform-*d*: τ 3.53 (1 proton doublet, $J_{1,2} < 1$ c.p.s., *H*-1), τ 4.67–4.8 (2 proton multiplet, *H*-2,3); τ 5.50 (center of 2 proton multiplet, *H*-5), τ 6.2–6.6 (1 proton multiplet, *H*-4); τ 7.72, 7.78 (acetyl protons).

Anal. Calcd. for $C_{15}H_{21}NO_9$: C, 50.2; H, 5.85; N, 3.9; acetyl, 60.0. Found: C, 50.4; H, 5.9; N, 4.0; acetyl 56.9.

(b) 4-Acetamido-4-deoxy-1,2,3,5-tetra-O-acetyl-β-D-arabinofuranose (6)

6 was obtained as a syrup (ca. 0.5 g) which was homogeneous by t.l.c. (irrigants: diethyl ether and ethyl acetate) and was vacuum distilled. It had $[\alpha]_D$ −70° (*c*, 1.35

Can. J. Chem. Downloaded from www.nrcresearchpress.com by 210.87.254.6 on 09/05/12
For personal use only.

in chloroform); λ_{max} (smear on NaCl): 1750 cm^{-1} (*O*—Ac); 1660 cm^{-1} (*N*Ac); n.m.r. data in chloroform-*d*: τ 3.28 (1 proton doublet, $J_{1,2}$ 5 c.p.s., *H*-1), τ 4.35–4.7 (2 proton multiplet, *H*-2, 3), τ 5.45–5.85 (3 proton multiplet, *H*-4,5), τ 7.85 (acetyl protons).

Anal. Calcd. for $C_{15}H_{21}NO_9$: C, 50.2; H, 5.9; N, 3.9; acetyl, 60.0. Found: C, 50.4; H, 6.2; N, 4.1; acetyl, 57.8.

*(c) 4-Acetamido-4-deoxy-1,2,3-tri-O-acetyl-*D*-arabinopyranose (7)*

7 was obtained from the column, by irrigation with ethyl acetate, as a syrup (ca. 0.4 g) which was homogeneous by t.l.c. (irrigants:diethyl ether and ethyl acetate) and was vacuum distilled. It had $[\alpha]_D$ −10° (*c*, 1.15 in chloroform; λ_{max} (smear on NaCl): 3300 cm^{-1} (broad, *N*—*H*), 1725 cm^{-1} (*O*–Ac), 1640, and 1520 cm^{-1} (*NH*—Ac).

Anal. Calcd. for $C_{13}H_{19}NO_8$: C, 49.2; H, 6.0; N, 4.4; acetyl, 54.3. Found: C, 49.0; H, 6.2; N, 4.0; acetyl, 57.3.

*4-Acetamido-4-deoxy-*D*-arabinopyranose (8)*

A syrupy mixture (0.4 g) of acetolysis products, obtained as described from **3**, was de-*O*-acetylated with sodium methoxide in methanol. The solution was neutralized with Amberlite IR 120 cation exchange resin (H^+), filtered, and the filtrate concentrated to a clear syrup (0.16 g). Examination of the syrup by paper chromatography revealed two reducing components which had R_{rh} 0.71 and 0.90 (spray *i*), the former greatly preponderating. Trituration of the syrup with ethanol – ethyl acetate gave a crystalline reducing compound (0.13 g). Recrystallization from methanol–ether gave 4-acetamido-4-deoxy-D-arabinopyranose (**8**) which melted at 157.5–158.5 and had $[\alpha]_D$ −65° (5 min after solution) mutarotating to −73° (*c*, 2.53 in water); R_{rh} 0.71 (spray *i*); λ_{max} (Nujol): 1640 and 1550 cm^{-1} (*NH*Ac); n.m.r. data in D_2O (at ambient temperature): τ 4.78 and τ 5.42 (1 proton, 2 doublets, $J_{1,2} \sim 2.7$ c.p.s. and 7.5. c.p.s., *H*-1, β and α anomers respectively), τ 5.2 (HOD), τ 5.6–6.7 (5 protons, complex multiplet, *H*-2,3,4,5), τ 7.93 (3 proton singlet, acetyl protons); (at 83° and tautomeric equilibrium): τ 4.5 (apparent doublet, probably due to β *H*-1 of furanose form) and τ 4.81 (doublet, $J_{1,2}$ 3 c.p.s., *H*-1 of β anomer) and τ 5.42 (doublet, $J_{1,2}$ 7 c.p.s., *H*-1 of α anomer) (total integral approximately 1 proton), τ 5.6–6.7 (HOD, H-2,3,4,5), τ 7.81 and 7.95 (singlets, total integral 3 protons, relative integral ca. 1:4, acetyl protons of furanose and pyranose forms respectively).

Anal. Calcd. for $C_7H_{13}NO_5$: C, 44.0; H, 6.8; N, 7.3. Found: C, 44.0; H, 7.2; N, 7.3.

*4-Acetamido-4-deoxy-*D*-arabinofuranose (9)*

The mother liquors from several preparations of **8** were pooled and concentrated to a syrup. Most of the 4-acetamido-4-deoxy-D-arabinopyranose (**8**) was removed by dissolving the syrup in ethanol and adding ethyl acetate to a faint turbidity. Seeding with **8** caused its crystallization and it was collected as gummy crystals by filtration. The filtrate was concentrated to a brown syrup (0.12 g). A paper chromatogram of the syrup showed two components (R_{rh} 0.71, 0.90 (spray *i*)), the second preponderating. An infrared spectrum (smear on NaCl) showed the amide II band at greatly reduced intensity compared with the amide I band. The component with R_{rh} 0.90 was thus considered to be 4-acetamido-4-deoxy-D-arabinofuranose (**9**). The n.m.r. spectrum of the mixture in D_2O at ambient temperature showed the two doublets due to H-1 of the anomeric pyranose forms but, in addition, a number of signals in the anomeric region which were difficult to assign. The acetyl protons also showed complexity in that maxima were observed at τ 7.75, 7.79, and 7.93. At 90°, the n.m.r. spectrum showed besides the pyranose resonances, signals at τ 4.54 (diffuse doublet, $J_{1,2}$ 3–4 c.p.s., H-1 of β anomer of **9**) τ 5.10 (broad singlet, H-1 of α anomer of **9**), τ 7.78 and 7.93 (singlets, acetyl protons).

The aqueous solution used for n.m.r. analysis was concentrated to a syrup. The syrup was dissolved in dry methanol and Amberlite IR 120 cation exchange resin (H^+; washed with methanol) was added. The mixture was shaken for 6 h and then poured onto a column of Amberlite IR 400 anion exchange resin (carbonate form). The effluent was concentrated and examined on paper chromatograms. Two spots were observed which had R_{rh} 1.37 and 1.88 (spray *i*). A third with R_{rh} 0.71 was present in trace amounts. The components with R_{rh} 1.37 and 1.88 were the methyl 4-acetamido-4-deoxy-D-arabinofuranosides. The methyl pyranosides of **8** are not detected by the *p*-anisidine hydrochloride reagent.

*The Methyl 4-Acetamido-4-deoxy-*D*-arabinofuranosides (**10** and **11**)*

Methyl 4-amino-4-deoxy-α-D-arabinopyranoside (**2**, syrup, 2.1 g) was dissolved in a mixture of acetic anhydride (25 ml) and glacial acetic acid (25 ml). This was cooled in an ice bath and concentrated sulfuric acid (1.0 ml) was added dropwise. The solution was shaken at room temperature for 72 h and was then worked up as previously described to give a syrupy acetate (3.9 g). Examination of the syrup by t.l.c. showed that the major components were the anomeric 4-acetamido-4-deoxy-1,2,3,5-tetra-*O*-acetyl-D-arabinofuranoses (**5** and **6**) and 4-acetamido-4-deoxy-1,2,3-tri-*O*-acetyl-D-arabinopyranose (7).

This syrupy mixture (3.9 g) was dissolved in dry methanol (50 ml) and Amberlite IR 120 cation exchange resin (H^+; pre-washed with methanol) was added. The mixture was stirred for 6 h at room temperature. It was then filtered and the filtrate concentrated to a clear syrupy acetate.

This acetate was dissolved in dry methanol (100 ml) and de-*O*-acetylated with sodium methoxide according to the Zemplén procedure. The solution was then neutralized by passage through columns of Amberlite IR 120 cation exchange resin (H^+) and Amberlite IR 400 anion exchange resin (carbonate state). The effluent was concentrated to a clear syrup (1.5 g). Examination of this syrup by paper chromatography revealed 4 components with R_{rh} 0.71, 0.90, 1.37, and 1.88 (sprays *i*, *ii*). Treatment of the syrup with ethanol – chloroform – ethyl acetate gave crystalline 4-acetamido-4-deoxy-D-arabinopyranose (**8**, 0.23 g). The mother liquors were concentrated to a syrup (1.2 g). An infrared spectrum of this syrup (smear on NaCl) showed intense absorption at 1640 cm^{-1} (amide I) and weak absorption at 1550 cm^{-1} (amide II).

A portion (1.0 g) of the syrupy mixture was fractionated by preparative paper chromatography and fractions were collected according to their mobility on paper.

Fraction 1 with R_{rh} 0.71 was 4-acetamido-4-deoxy-D-arabinopyranose (**8**, 0.08 g).

Can. J. Chem. Downloaded from www.nrcresearchpress.com by 210.87.254.6 on 09/05/12
For personal use only.

Fraction 2 was made up of two components which had R_{rh} 0.71 and 0.90 in similar proportion.

Methyl 4-Acetamido-4-deoxy-β-D-arabinofuranoside (11)

Fraction 3, with R_{rh} 1.37, was obtained as a syrup (0.38 g) and was homogeneous on paper. It was methyl 4-acetamido-4-deoxy-β-D-arabinofuranoside (**11**) which had $[\alpha]_D$ −68° (*c*, 0.50 in water); λ_{max} (smear on NaCl): 1640 cm^{-1} (N—Ac); n.m.r. data in D_2O (at ambient temperature): τ 4.66 and 4.86 (1 proton: 2 doublets, $J_{1,2}$ 4–4.5 c.p.s., H-1), τ 5.7–6.3 (5 protons, H-2,3,4,5), τ 6.52 and 6.61 (3 protons, two singlets, methoxyl protons), τ 7.75 and 7.80 (3 protons, 2 singlets, acetyl protons); (at 90°); τ 4.78 (1 proton, diffuse doublet, $J_{1,2}$ 4–4.5 c.p.s., H-1), τ 5.7–6.3 (HOD, H-2,3,4,5), τ 6.52 (singlet, 3 protons, OCH_3), τ 7.75 (singlet, 3 protons, acetyl protons).

Anal. Calcd. for $C_8H_{15}NO_5$: N, 6.8. Found: N, 6.6

Methyl 4-Acetamido-4-deoxy-α-D-arabinofuranoside (10)

Fraction 4 with R_{rh} 1.88 was obtained as a syrup (0.06 g) which crystallized on standing. Recrystallization from methanol – diethyl ether – heptane gave methyl 4-acetamido-4-deoxy-α-D-arabinofuranoside (**10**) which melted at 145.5–146.5° and had $[\alpha]_D$ −44° (*c*, 1.00 in water); λ_{max} (smear on NaCl): 1640 cm^{-1} (NAc); n.m.r. data in D_2O (at ambient temperature): τ 5.0 and 5.11 (1 proton, possibly doublets, $J_{1,2}$ 1 c.p.s., H-1), τ 5.7–6.4 (H-2,3,4,5), τ 6.57 and 6.69 (2 singlets, OCH_3), τ 7.83 and 7.99 (2 singlets, acetyl protons), (at 80°); τ 5.10 (1 proton, broad singlet, H-1), τ 5.7–6.4 (HOD H-2,3,4,5), τ 6.58 and 6.68 (2 singlets, OCH_3), τ 7.84 and 8.0 (2 singlets, acetyl protons).

Anal. Calcd. for $C_8H_{15}NO_5$: C, 46.8; H, 7.3; N, 6.8. Found: C, 47.0; H, 7.5; N, 6.9.

A portion (0.2 g) of the unfractionated syrup (containing **8**, **9**, **10**, and **11**) was dissolved in water (20 ml) and Amberlite IR 120 cation exchange resin (H^+) was added. This mixture was stirred at 40° for 2 h. It was then filtered, the filtrate treated with Amberlite IR 400 anion exchange resin (carbonate form), filtered, and the filtrate concentrated to a clear syrup. Examination of this product by paper chromatography revealed only those components with R_{rh} 0.71 and 0.90 (**8** and **9**). Trituration of the syrup with ethanol – ethyl acetate gave 4-acetamido-4-deoxy-D-arabinopyranose (**8**) (0.12 g).

Methyl 4-Amino-4-deoxy-α-L-arabinopyranoside Hydrochloride (14)

Methyl 4-azido-4-deoxy-α-L-arabinopyranoside (**12** (14), 0.20 g) was reduced over 5% palladium on carbon as usual. The syrupy product (0.18 g) was dissolved in ethanol (15 ml) and ethyl acetate (15 ml) and concentrated hydrochloric acid (0.04 ml) was added. Upon cooling, the solution provided crystals of methyl 4-amino-4-deoxy-α-L-arabinopyranoside hydrochloride (**14**, 0.10 g) which melted at 184.5–185° (decomp.) and had $[\alpha]_D$ −3° (*c*, 0.98 in water).

Anal. Calcd. for $C_6H_{14}ClNO_4$: C, 36.1; H, 7.0; Cl, 17.8; N, 7.0. Found: C, 36.4; H, 6.8; Cl, 18.0; N, 7.2.

Methyl 4-Acetamido-4-deoxy-α-L-arabinopyranoside (15)

Syrupy methyl 4-amino-4-deoxy-α-L-arabinopyranoside (**13**, 0.9 g) was treated with aqueous acetic anhydride according to the procedure of Roseman and Ludowieg (21). The colorless syrupy product (0.9 g) crystallized on standing and gave methyl 4-acetamido-4-deoxy-α-L-arabinopyranoside (**15**, 0.6 g) which melted at 129–130° and had $[\alpha]_D$ −1.8° (*c*, 3.43 in water).

Anal. Calcd. for $C_8H_{15}NO_5$: C, 46.8; H, 7.3; N, 6.8. Found: C, 46.7; H, 7.3; N, 6.5.

Methyl 4-Acetamido-4-deoxy-2,3-di-O-acetyl-α-L-arabinopyranoside (16)

Syrupy methyl 4-acetamido-4-deoxy-α-L-arabinopyranoside (**15**, 0.4 g) was dissolved in pyridine and acetylated as usual with acetic anhydride (2 moles). The syrupy product (0.65 g) was homogeneous by t.l.c. Methyl 4-acetamido-4-deoxy-2,3-di-*O*-acetyl-α-L-arabinopyranoside (**16**) was purified by vacuum distillation and was obtained as a hard glass. It has $[\alpha]_D$ −34° (*c*, 1.35 in chloroform).

Anal. Calcd. for $C_{12}H_{19}NO_7$: C, 49.8; H, 6.6; N, 4.8. Found: C, 50.1; H, 6.5; N, 4.6.

Acetolysis of Methyl 4-Acetamido-4-deoxy-α-L-arabinopyranoside

Methyl 4-acetamido-4-deoxy-α-L-arabinopyranoside (**15**, 0.45 g) was dissolved in an acetolysis solution (10 ml; as described for **4**). The mixture was shaken for 24 h and was then poured into an excess of sodium bicarbonate in water; the aqueous solution was extracted with chloroform. Examination of the chloroform extract by t.l.c. (irrigant: ethyl acetate) revealed one major component. Evaporation of the chloroform gave a syrupy product whose n.m.r. spectrum in chloroform-*d* showed a doublet at τ 3.28 ($J_{1,2}$ 5 c.p.s.) similar to the H-1 resonance of 4-acetamido-4-deoxy-1,2,3,5-tetra-*O*-acetyl-β-D-arabinofuranose. The product was purified by passage through a column of silica gel (irrigant: ethyl acetate) and gave a syrup (0.3 g) whose infrared spectrum showed absorption at 1750 cm^{-1} (*O*Ac) and at 1680 cm^{-1} (*N*Ac) but no absorption for *N*—*H* (amide II). Thus, it was probably 4-acetamido-4-deoxy-1,2,3,5-tetra-*O*-acetyl-L-arabinofuranose (**17**).

4-Acetamido-4-deoxy-L-arabinopyranose (18)

(a) From Methyl 4-Acetamido-4-deoxy-α-L-arabinopyranoside (15)

15 (1.3 g) was dissolved in water (20 ml) and Amberlite IR 120 cation exchange resin (H^+; 7 g wet) was added. The mixture was heated with stirring in a boiling water bath for 1.5 h. It was then cooled, filtered, the filtrate treated with Dowex 1 × 8 anion exchange resin (carbonate state), filtered again, and the filtrate concentrated to a colorless syrup (0.55 g). The syrup was reducing to Fehling's solution. Examination of the syrup by paper chromatography showed three spots: R_{rh} 1.5 (spray *ii*; corresponded to starting material), R_{rh} 0.90 (faintly detected), and R_{rh} 0.71 (sprays *i* and *ii*). The syrup was fractionated by preparative paper chromatography. The bands corresponding to R_{rh} 0.90 and R_{rh} 0.71 were eluted separately with ethanol and the ethanol was evaporated at room temperature.

The substances which had R_{rh} 0.90 was obtained as a syrup (less than 10 mg) whose infrared spectrum (smear on NaCl) showed absorption at 1620 cm^{-1} for NAc but negligible absorption for N—H. By analogy with the D-enantiomer, this substance was probably 4-acetamido-4-deoxy-L-arabinofuranose (**19**). Examination of it, after it

had been kept for several weeks, by paper chromatography showed that it now contained mostly that component with R_{rh} 0.71 with a smaller amount of that with R_{rh} 0.90.

The substance which had R_{rh} 0.71 was also obtained as a syrup (90 mg) which crystallized on standing. Recrystallization from methanol – diethyl ether afforded 4-acetamido-4-deoxy-L-arabinopyranose (**18**; 45 mg) which melted at 156.5–157.5° and had R_{rh} 0.71; $[\alpha]_D$ +66 (5 min after solution) mutarotating to +73° (*c*, 0.98 in water); λ_{max} (Nujol): 1640 cm^{-1} and 1550 cm^{-1} (NHAc).

Anal. Calcd. for $C_7H_{13}NO_5$: C, 44.0; H, 6.8; N, 7.3. Found: C, 44.1; H, 7.1; N, 7.5.

(b) From 4-Acetamido-1,2,3,5-tetra-O-acetyl-4-deoxy-L-arabinofuranose (17)

4-Acetamido-1,2,3,5-tetra-*O*-acetyl-4-deoxy-L-arabinofuranose (**17**, 0.3 g) was dissolved in dry methanol (30 ml) and de-*O*-acetylated with sodium methoxide according to the Zemplén method. The methanolic solution was neutralized with Amberlite IR 120 cation exchange resin (H^+ form), filtered, the filtrate treated with Amberlite IR 400 anion exchange resin (carbonate form), filtered, and the filtrate concentrated to a clear colorless syrup (ca. 70 mg). Crystallization with ethanol – ethyl acetate gave 4-acetamido-4-deoxy-L-arabinopyranose (60 mg). After recrystallization from methanol – diethyl ether, **18** melted at 156.5–157.5° undepressed upon admixture with a specimen from the foregoing experiment.

1. H. PAULSEN. Angew. Chem. **48,** 501 (1966); Angew. Chem. Intern. Ed. Engl. **5,** 495 (1966).
2. E. J. REIST, D. E. GEOFFROY, R. W. BLACKFORD, and L. GOODMAN. J. Org. Chem. **31,** 4025 (1965).
3. A. J. DICK and J. K. N. JONES. Can. J. Chem. **43,** 977 (1965).
4. D. HORTON and A. E. EL-ASHMAWY. Carbohydrate Res. **3,** 191 (1966).
5. S. HANESSIAN. Carbohydrate Res. **1,** 178 (1965).
6. M. L. WOLFROM, J. L. MINOR, and W. A. SZAREK. Carbohydrate Res. **1,** 156 (1965).
7. E. J. REIST, L. V. FISHER, and L. GOODMAN. J. Org. Chem. **32,** 2541 (1967).
8. A. J. DICK. Ph.D. Thesis. Queen's University, Kingston, Ontario. February, 1967.
9. A. J. DICK and J. K. N. JONES. Can. J. Chem. **44,** 79 (1966).
10. J. HILL, L. HOUGH, and A. C. RICHARDSON. Proc. Chem. Soc. 346 (1963).
11. E. J. REIST, R. R. SPENCER, B. R. BAKER, and L. GOODMAN. Chem. Ind. London, 1794 (1962).
12. E. J. REIST, R. R. SPENCER, D. F. CALKINS, B. R. BAKER, and L. GOODMAN. J. Org. Chem. **30,** 2312 (1965).
13. C. L. STEVENS, P. BLUMBERGS, and D. H. OTTERBACH. J. Org. Chem. **31,** 2817 (1966).
14. A. J. DICK and J. K. N. JONES. Can. J. Chem. **45,** 2879 (1967).
15. L. D. HALL. Advan. Carbohydrate Chem. **19,** 51 (1964).
16. B. CAPON and D. THACKER. Proc. Chem. Soc. 369 (1964).
17. R. U. LEMIEUX and R. O. STEVENS. Can. J. Chem. **44,** 249 (1966).
18. W. A. SZAREK, S. WOLFE, and J. K. N. JONES. Tetrahedron Letters, 2743 (1964).
19. L. HOUGH, J. K. N. JONES, and W. H. WADMAN. J. Chem. Soc. 1702 (1950).
20. R. U. LEMIEUX and H. F. BAUER. Anal. Chem. **26,** 920 (1954).
21. S. ROSEMAN and J. LUDOWIEG. J. Am. Chem. Soc. **76,** 301 (1954).
22. J. K. N. JONES and W. A. SZAREK. Can. J. Chem. **41,** 636 (1964).

Can. J. Chem. Downloaded from www.nrcresearchpress.com by 210.87.254.6 on 09/05/12
For personal use only.

Can. J. Chem. Downloaded from www.nrcresearchpress.com by 210.87.254.5 on 09/05/12
For personal use only.

Synthesis and chemistry of 1-methyl-3-hydroxy-3-phenyl-6-chloro-1,2,3,4-tetrahydroquinoline-2,4-dione

C. PODESVA, C. SOLOMON, AND K. VAGI
Delmar Chemicals Limited, Lasalle, Quebec

Received April 21, 1967

Treatment of 2-(*N*-methyl)-dichloroacetamido-5-chlorobenzophenone with an aqueous–alcoholic solution of sodium acetate yields 1-methyl-3-hydroxy-3-phenyl-6-chloro-1,2,3,4-tetrahydroquinoline-2,4-dione. Some transformation products of this compound are described.

Canadian Journal of Chemistry, 46, 435 (1968)

In an attempt to prepare 2-(*N*-methyl)-glyoxylylamido-5-chlorobenzophenone by heating a solution of 2-(*N*-methyl)-dichloroacetamido-5-chlorobenzophenone in aqueous ethanol in the presence of sodium acetate, 1-methyl-3-phenyl-3-hydroxy-6-chloro-1,2,3,4-tetrahydroquinoline-2,4-dione (**1**) was obtained in 41.5% yield. The structure of this product was established on the basis of its infrared and nuclear magnetic resonance (n.m.r.) spectra, its chemical reactions as well as on the basis of an unambiguous synthesis of one of its transformation products.

The product was obtained in two crystalline forms of which one exhibited infrared maxima in KBr or Nujol at 3275 (OH), 1715 (ketone), 1670 (amide), and 1605 cm^{-1} (aromatic), whereas the other crystalline modification showed bands at 3465, 1720, 1680, and 1605 cm^{-1}. Both crystalline forms melted at 170–172° individually and as a mixture. Their chemical identity was established by the infrared spectra in chloroform solution, which were superimposable, containing maxima at 3520, 1720, 1670, and 1605 cm^{-1}. The n.m.r. spectrum (in $CDCl_3$ with tetramethylsilane as internal reference standard) showed singlets at τ 6.45 and at 5.60 (N—CH_3 and OH respectively) and a multiplet containing 8 protons at τ 2.20–2.96 with the strongest peak appearing at τ 2.65.

The presence of the keto group was further substantiated by an easy formation of oxime **2** and by formation of the diol **3** (ν_{max} (Nujol) 3485, 3425 (inflection), 3345, 1660, and 1605 cm^{-1}) on reduction with sodium borohydride. An attempt to accomplish a Beckmann rearrangement on the oxime **2** using phosphorus pentachloride resulted in formation of nitrile **13** (ν_{max} (KBr) 2230, 1685, 1660, and 1595 cm^{-1}) by an obvious mechanism, presupposing a vicinal position of the oxime with respect to the hydroxyl. Oxidation of diol **3** with periodic acid yielded the ketoaldehyde **14**, showing in its n.m.r. spectrum an aldehyde proton singlet at τ 0.0 (in $CDCl_3$ with tetramethylsilane as internal reference standard). The position of the aldehyde carbonyl in the infrared spectrum at 1695 cm^{-1}, which is characteristic for an aromatic aldehyde, compelled us to assign structure **1** to the ketol, which up to that point could also be considered to be 1-methyl-4-hydroxy-4-phenyl-6-chloro-1,2,3,4-tetrahydroquinoline-2,3-dione, the functionalities of these two compounds being identical. The aldehyde carbonyl resulting from the periodic acid oxidation of this latter compound would be expected to absorb well over 1700 cm^{-1}, as is generally the case for α-dicarbonyl compounds (1).

A surprisingly good yield of ketimine **4** (ν_{max} (Nujol) 3275 (sharp,=NH), 1695 (amide), 1640 (C=N), and 1605 cm^{-1} (aromatic)) was obtained by allowing to react **1** with ammonia in methanolic solution. This substance was found to be quite stable to alcoholic and aqueous alkalis, but was readily reconverted to the starting ketone even by treatment with aqueous acetic acid at room temperature.

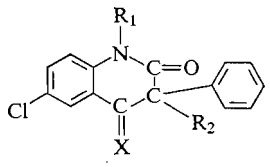

1	$R_1 = CH_3$,	$R_2 = OH$,	X = O
2	$R_1 = CH_3$,	$R_2 = OH$,	X = N—OH
4	$R_1 = CH_3$,	$R_2 = OH$,	X = NH
6	$R_1 = CH_3$,	$R_2 = OAc$,	X = O
7	$R_1 = CH_3$,	$R_2 = Cl$,	X = O
11	$R_1 = H$,	$R_2 = OH$,	X = O
12	$R_1 = H$,	$R_2 = OH$,	X = NH

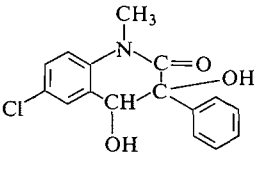

3

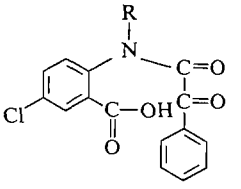

8*a*, R = CH_3
8*b*, R = H

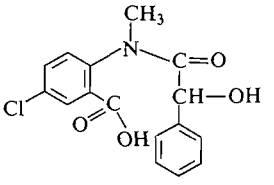

9

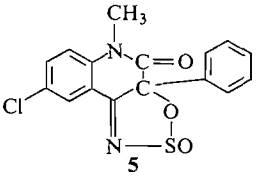

5

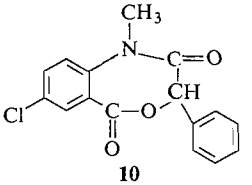

10

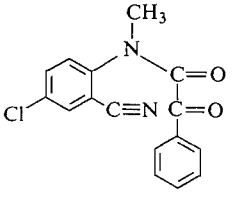

13

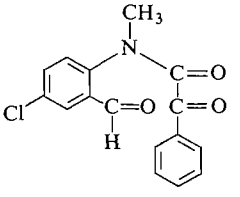

14

Treatment of the ketimine **4** with thionyl chloride produced thiaoxazole-2-oxide **5**, which constitutes a heretofore undescribed ring system. Its infrared spectrum in Nujol did not show any absorption in the hydroxyl and amine region, whereas the amide I band appeared at an unusually high frequency of 1723 cm^{-1}. The only other band was the aromatic absorption at 1605 cm^{-1}. The formation of this last product thus confirmed the relative position of the hydroxyl with respect to the ketimine as well as to the original ketone. Aqueous or alcoholic alkali hydroxides at room temperature recovered the starting ketimine **4**.

Evidence for the presence of hydroxyl was further obtained by acetylation of **1**, whereby the ketoester **6** was readily formed (ν_{max} (KBr) 1740 (ester), 1710 (ketone), 1675 (amide), and 1600 cm^{-1} (aromatic)). Ammonolysis of the ketoester with methanolic ammonia produced the previously mentioned ketimine **4**.

By allowing **1** to react with thionyl chloride the expected chloro compound **7** was readily obtained, whereas oxidation with periodic acid yielded the keto acid **8***a* (ν_{max} 1710 (carboxyl), 1675 (ketone), 1650 (amide), and 1600 cm^{-1} (aromatic)). This could be reduced with sodium borohydride to a salt of the corresponding hydroxy acid, which on acidification produced a mixture of the free hydroxy acid **9** (ν_{max} (KBr) 3350 (OH), 1700 (carboxyl), and 1680 cm^{-1} (amide)), and of the corresponding lactone **10**. This mixture when refluxed in toluene in presence of *p*-toluenesulfonic acid with azeotropic removal of water produced pure lactone (ν_{max} (KBr) 1725 (lactone), 1680 (amide), and 1600 cm^{-1} (aromatic)).

When 2-dichloroacetamido-5-chlorobenzophenone was refluxed with a solution of sodium acetate, 3-phenyl-3-hydroxy-6-chloro-1,2,3,4-tetrahydroquinoline-2,4-dione **11** was obtained in substantially lower yield than when the *N*-methyl derivative was used. A good yield of the imine **12**, however, was obtained from this substance on treatment with methanolic ammonia. Oxidation of **11** with periodic acid yielded the corresponding keto acid **8***b* (ν_{max} (KBr) 3275, 1700, 1680, and 1670 cm^{-1}). We have also prepared this last substance by unambiguous synthesis from 5-chloroanthranilic acid and the chloride of benzoylformic acid, whereby the structure of **1** as well as the structures of its transformation products are rigorously established. Further proof was obtained by condensation of 2-methylamino-5-chlorobenzoic acid with the chloride of benzoylformic acid, which yielded the above mentioned keto acid **8***a*.

Formation of **1** by a reaction of 2-(*N*-methyl)-dichloroacetamido-5-chlorobenzophenone with an aqueous base merits some comment. The product results obviously from a ketol rearrangement of its isomer precursor, namely 1-methyl-4-hydroxy-4-phenyl-6-chloro-1,2,3,4-tetrahydroquinoline-2,3-dione. This intermediate could not possibly be formed from the aldehyde resulting from the hydrolysis of the starting dichloroacetamide. However, the vicinal position of aldehyde and amide carbonyls would be expected to favor hydration of the aldehyde in order to remove one of the neighboring partial positive charges. Such hydrated form then can easily produce the anion necessary for the attack on the phenone carbonyl in order to accomplish the cyclization. The reaction mechanism can then be visualized as follows.

Can. J. Chem. Downloaded from www.nrcresearchpress.com by 210.87.254.5 on 09/05/12
For personal use only.

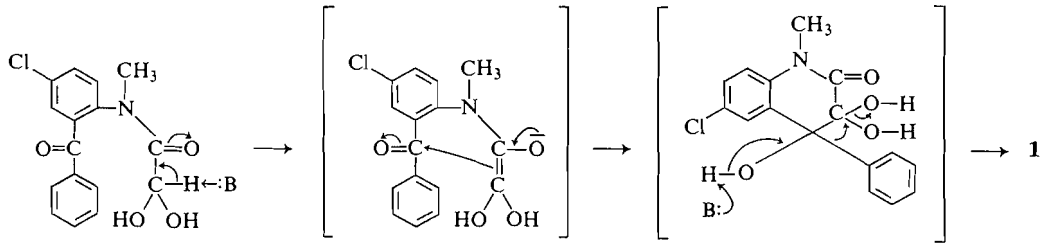

It might be argued that the anion may also be produced on the dichloroacetamide, which then would cyclize to an intermediate 3,3-dichloro derivative. As, however, we were unable to isolate any chloro intermediate even in small quantities, we favor the former mechanism.

Experimental

The infrared spectra were recorded on a Perkin–Elmer 237 apparatus. The nuclear magnetic resonance spectra were obtained on Varian model HR-60 spectrometer. The melting points were determined in capillaries on a Mel-Temp apparatus and are uncorrected. Microanalyses were performed by Organic Microanalysis, Dr. C. Daesle, Montreal. The molecular weights were taken in chloroform solution on Mechrolab Osmometer model 301.

2-Methylamino-5-chlorobenzophenone

To a solution of commercially available 2-amino-5-chlorobenzophenone (10 g) in glacial acetic acid (50 ml) was added dimethyl sulfate (4.2 ml) and the mixture was heated under reflux for 2 h. After standing another 2 h at room temperature the reaction mixture was poured into cold water (200 ml) and extracted with chloroform (3 × 50 ml). After washing with water the extract was evaporated to dryness *in vacuo* and the residue dissolved in hot methanol (15 ml). After standing overnight at room temperature the crystalline 2-methylamino-5-chlorobenzophenone (3.9 g) was collected by filtration and washed with cold methanol. The combined filtrate and washings were taken to dryness, redissolved in glacial acetic acid (50 ml) containing dimethyl sulfate (4 ml), and the whole operation was repeated. A second crop (1.2 g) of the product was so obtained, bringing the total yield to 48%, m.p. 93–95° (lit. m.p. 94–95° (2)) without any further purification.

2-(N-Methyl)-dichloroacetamido-5-chlorobenzophenone

A solution of 2-methylamino-5-chlorobenzophenone (98.28 g, 0.4 mole) and dichloroacetyl chloride (59 g, 0.4 mole) in dry chloroform (300 ml) was heated under reflux for 3 h. The solvent was removed *in vacuo* and the residue was triturated with methanol. The product (107 g, 75% yield) was further purified for analysis by crystallization from methanol, m.p. 130–131°.

Anal. Calcd. for $C_{16}H_{12}Cl_3NO_2$: C, 53.89; H, 3.39; Cl, 29.82; N, 3.93. Found: C, 54.01; H, 3.65; Cl, 29.74; N, 3.96.

2-Dichloroacetamido-5-chlorobenzophenone

A mixture of 2-amino-5-chlorobenzophenone (23 g, 0.1 mole) and dichloroacetyl chloride (14.75 g, 0.1 mole) in dry chloroform (150 ml) was kept under reflux for 3 h. The solvent was removed by distillation *in vacuo* and the residue was purified by crystallization from methanol. Twenty-six grams (76%) of the product melting at 89–90° were obtained.

Anal. Calcd. for $C_{15}H_{10}Cl_3NO_2$: C, 52.58; H, 2.94; Cl, 31.05; N, 4.09. Found: C, 52.40; H, 2.71; Cl, 30.92; N, 4.08.

1-Methyl-3-hydroxy-3-phenyl-6-chloro-1,2,3,4-tetrahydroquinoline-2,4-dione (1)

To a solution of 2-(*N*-methyl)-dichloroacetamido-5-chlorobenzophenone (30 g, 0.0825 mole) in ethanol (300 ml) was added a solution of sodium acetate (82.9 g on anhydrous basis, 1.01 mole) in water (300 ml) and the mixture refluxed overnight. After cooling to room temperature the unreacted starting material (10 g) was recovered by filtration, the filtrate was diluted with more water and exhaustively extracted with chloroform. The solvent was removed by distillation *in vacuo* and the residue triturated with ether. The crystalline product (10.5 g, 41.5%) was purified for analysis by recrystallization from methanol–water, m.p. 170–172°.

Anal. Calcd. for $C_{16}H_{12}ClNO_3$ (mol. wt., 301.73): C, 63.69; H, 4.01; Cl, 11.75; N, 4.64. Found (mol. wt., 277.4): C, 63.91; H, 4.30; Cl, 12.25; N, 5.00.

3-Hydroxy-3-phenyl-6-chloro-1,2,3,4-tetrahydroquinoline-2,4-dione (11)

To a solution of 2-dichloroacetamido-5-chlorobenzophenone (30 g, 0.0878 mole) in ethanol (300 ml) was added a solution of sodium acetate (86.4 g on anhydrous basis) in water (300 ml) and the mixture refluxed overnight. After cooling the reaction mixture was diluted with water and extracted with chloroform. The solvent was removed *in vacuo* and the residue was purified by crystallization first from ether, then from methanol; yield 7 g (26%), m.p. 244–245°.

Anal. Calcd. for $C_{15}H_{10}ClNO_3$: C, 62.62; H, 3.50; Cl, 12.33; N, 4.87. Found: C, 62.31; H, 3.60; Cl, 12.38; N, 5.09.

1-Methyl-4-isonitroso-3-hydroxy-3-phenyl-6-chloro-1,2,3,4-tetrahydroquinoline-2-one (2)

A mixture of **1** (3 g, 0.01 mole), hydroxylamine hydrochloride (0.695 g, 0.01 mole) and triethylamine (1.01 g, 0.01 mole) in toluene (50 ml) was refluxed for 7 h with azeotropic removal of water. After cooling to room temperature the precipitated triethylamine hydrochloride was collected by filtration, the filtrate evaporated to dryness *in vacuo*, and the residue was crystallized from acetone. The pure product (1.42 g, 45%) had a m.p. of 230–232°.

Can. J. Chem. Downloaded from www.nrcresearchpress.com by 210.87.254.5 on 09/05/12
For personal use only.

Can. J. Chem. Downloaded from www.nrcresearchpress.com by 210.87.254.5 on 09/05/12
For personal use only.

Anal. Calcd. for $C_{16}H_{13}ClN_2O_3$: C, 60.67; H, 4.14; Cl, 11.19; N, 8.85. Found: C, 61.02; H, 4.36; Cl, 10.90; N, 8.87.

*2-(N-Methyl)-benzoylformamido-5-chlorobenzonitrile (**13**)*

A solution of the oxime **2** (5.5 g) in dry toluene (190 ml) was refluxed for 5 h in presence of a few milligrams of phosphorus pentachloride. After cooling to room temperature the solution was decanted from a small amount of a tarry material which settled at the bottom and the solvent was removed by distillation *in vacuo*. The residue was crystallized by treatment with methanol and purified by recrystallization from aqueous methanol; 4 g (76%) of product melting at 99° were obtained.

Anal. Calcd. for $C_{16}H_{11}ClN_2O_2$: C, 64.33; H, 3.71; Cl, 11.87; N, 9.38. Found: C, 64.41; H, 3.47; Cl, 12.10; N, 8.96.

1-Methyl-3,4-dihydroxy-3-phenyl-6-chloro-1,2,3,4-tetrahydroquinoline-2-one (3)

To a solution of **1** (3 g, 0.01 mole) in methanol (100 ml) was added a solution of sodium borohydride (0.2 g, 0.005 mole) in water (10 ml) and the mixture was left standing overnight at room temperature. After dilution with water the reaction product was extracted into chloroform, the solvent was removed by distillation *in vacuo*, and the residue was crystallized from methanol–ether mixture. The pure product (2 g, 66%) had a m.p. of 194°.

Anal. Calcd. for $C_{16}H_{14}ClNO_3$: C, 63.27; H, 4.65; Cl, 11.67; N, 4.61. Found: C, 63.09; H, 4.21; Cl, 11.73; N, 4.63.

*2-(N-Methyl)-benzoylformamido-5-chlorobenzaldehyde (**14**)*

A solution of **3** (5 g, 0.0164 mole) and periodic acid (3.8 g, 0.0166 mole) in 90% ethanol (110 ml) was stirred at room temperature overnight. After dilution with water, the reaction mixture was extracted with chloroform, the solvent was distilled off *in vacuo*, the residue was treated with decolorizing carbon in boiling acetone solution, filtered, acetone removed by distillation *in vacuo* and the product crystallized from ether–hexane mixture. The yield was 2.85 g (57%), m.p. 80–82°.

Anal. Calcd. for $C_{16}H_{12}ClNO_3$: C, 63.69; H, 4.01; Cl, 11.75; N, 4.64. Found: C, 63.77; H, 3.98; Cl, 11.88; N, 4.59.

*1-Methyl-3-hydroxy-3-phenyl-4-imino-1,2,3,4-tetrahydroquinoline-2-one (**4**)*

A solution of **1** (5 g, 0.0167 mole) in a mixture of methanol (200 ml) and dimethylformamide (25 ml), containing a few drops of triethylamine was saturated with ammonia gas and left standing overnight at room temperature. The product separated in crystalline form and was collected by filtration (3 g). The filtrate was evaporated to dryness *in vacuo* and a second crop (1 g) was collected, giving a total yield of 80%. The analytical sample had a m.p. of 220–221° after recrystallization from dimethylformamide–ether mixture.

Anal. Calcd. for $C_{16}H_{13}ClN_2O_2$: C, 63.90; H, 4.35; Cl, 11.79; N, 9.32. Found: C, 63.66; H, 4.31; Cl, 11.86; N, 9.35.

*3-Hydroxy-3-phenyl-6-chloro-4-imino-1,2,3,4-tetrahydroquinoline-2-one (**12**)*

A solution of **11** (2 g, 0.69 mole) in methanol (200 ml) containing a few drops of triethylamine was saturated with ammonia gas and left standing at room temperature overnight. The solvent was removed by distillation *in vacuo* and the residue triturated with ether. The crystalline product was purified by crystallization from dimethylformamide–ether to a m.p. of 190–192° (decomp.); yield, 1.4 g (70%).

Anal. Calcd. for $C_{15}H_{11}ClN_2O_2$: C, 62.83; H, 3.87; Cl, 12.37; N, 9.77. Found: C, 62.81; H, 3.91; Cl, 12.51; N, 9.63.

Thiaoxazole 5

A solution of **4** (0.75 g, 0.0025 mole) and thionyl chloride (6 ml) in dry benzene (50 ml) was kept under reflux for 3 h. The solvent was removed by distillation *in vacuo* and the residue triturated with ether. The crystalline product was collected by filtration and purified by crystallization from benzene, m.p. 229–230°, yield 0.7 g (81%).

Anal. Calcd. for $C_{16}H_{11}ClN_2O_3S$ (mol. wt., 346.79): C, 55.42; H, 3.20; Cl, 10.22; N, 8.08; S, 9.24. Found (mol. wt., 301.5): C, 55.33; H, 3.46; Cl, 9.92; N, 8.08; S, 9.20.

*1-Methyl-3-acetoxy-3-phenyl-6-chloro-1,2,3,4-tetrahydroquinoline-2,4-dione (**6**)*

A solution of **1** (2 g, 0.00665 mole) in acetic anhydride (10 ml) containing anhydrous sodium acetate (1 g) was refluxed for 1 h. After cooling to room temperature some methanol was added in order to destroy the unreacted anhydride, the reaction mixture was diluted with water and the crystalline precipitate collected by filtration. The product was purified for analysis by crystallization from ether, m.p. 150–152°, yield 2 g (88%).

Anal. Calcd. for $C_{18}H_{14}ClNO_4$: C, 62.89; H, 4.10; Cl, 10.31; N, 4.08. Found: C, 63.11; H, 4.29; Cl, 10.27; N, 3.95.

*1-Methyl-3,6-dichloro-3-phenyl-1,2,3,4-tetrahydroquinoline-2,4-dione (**7**)*

A mixture of **1** (1.5 g, 0.005 mole) and thionyl chloride (6 ml) in dry benzene (30 ml) was kept under reflux for 3 h. The solvent and the excess of thionyl chloride were distilled *in vacuo* and the residue was purified by crystallization from ether, then from methanol–ether mixture; yield 0.7 g (43%), m.p. 228°.

Anal. Calcd. for $C_{16}H_{11}Cl_2NO_2$: C, 60.02; H, 3.46; Cl, 22.15; N, 4.37. Found: C, 59.84; H, 3.49; Cl, 22.36; N, 4.22.

*2-(N-Methyl)benzoylformamido-5-chlorobenzoic Acid (**8a**)*

To a solution of **1** (5 g, 0.0167 mole) in ethanol (150 ml) was added a solution of periodic acid (3.8 g, 0.0167 mole) in water (10 ml) and the reaction mixture stirred at room temperature overnight. The product precipitated in crystalline form after dilution with water. It was collected by filtration and purified by crystallization from acetone–benzene mixture; yield 5 g (96%), m.p. 204°.

Anal. Calcd. for $C_{16}H_{12}ClNO_4$: C, 60.48; H, 3.80; Cl, 11.16; N, 4.41. Found: C, 60.50; H, 4.08; Cl, 11.20; N, 4.14.

The same product was also obtained by condensation of 2-methylamino-5-chlorobenzoic acid with the chloride of benzoylformic acid in the following way.

A solution of 5-chloroanthranilic acid (0.6 g, 0.0035 mole) in glacial acetic acid (10 ml) containing dimethyl sulfate (0.54 g, 0.0043 mole) was heated under reflux for 4 h. The acetic acid was removed by distillation *in vacuo* and the oily residue treated with water. The crystalline

Can. J. Chem. Downloaded from www.nrcresearchpress.com by 210.87.254.5 on 09/05/12
For personal use only.

2-methylamino-5-chlorobenzoic acid, which precipitated after some time, was collected by filtration and recrystallized from aqueous ethanol; yield 0.25 g (38.5%), m.p. 172° (lit. m.p. 173° (3)).

The above product (0.0013 mole) was dissolved in dry chloroform (20 ml) containing the chloride of benzoylformic acid (0.23 g, 0.0013 mole) and the solution heated under reflux overnight. The solvent was removed by distillation *in vacuo*, the oily residue was dissolved in dilute aqueous sodium hydroxide, the insolubles were removed by filtration, and the filtrate acidified with dilute hydrochloric acid. The crystalline precipitate was collected by filtration and purified by crystallization from acetone–benzene mixture. The yield was 0.05 g (11.6%), m.p. 204 °C. This melting point was not depressed on admixture of **8***a* and infrared spectra of these two products were superimposable.

2-Benzoylformamido-5-chlorobenzoic Acid (8b)

A solution of **11** (10 g, 0.033 mole) and periodic acid (8 g, 0.035 mole) in 90% ethanol (400 ml) was stirred at room temperature overnight. The product which separated as a crystalline precipitate was collected by filtration and the filtrate was diluted with water, whereby more of the product precipitated. The combined crops were purified by crystallization from acetone. The yield was 9.5 g (95%), m.p. 259–261°.

Anal. Calcd. for $C_{15}H_{10}ClNO_4$: C, 59.31; H, 3.32; Cl, 11.68; N, 4.61. Found: C, 59.14; H, 3.50; Cl, 11.80; N, 4.86.

The same product was also obtained in the following way. A mixture of 5-chloroanthranilic acid (2.57 g, 0.015 mole) and benzoylformyl chloride (2.52 g, 0.015 mole) in chloroform–dimethylformamide (50 ml and 25 ml respectively) was kept refluxing for 4 h. Some undissolved material was removed by filtration, chloroform was distilled from the filtrate *in vacuo*, and the remaining solution was diluted with water. The crystalline precipitate was collected by filtration and recrystallized from acetone. The yield was 0.95 g (21%). This product was found identical with **8***b* by determination of its m.p., mixture m.p., and by comparison of infrared spectra.

2-(N-Methyl)-phenylglycolylamido-5-chlorobenzoic Acid (9)

To a solution of **8***a* (5 g, 0.0157 mole) in methanol (200 ml) was added some sodium bicarbonate and then a solution of sodium borohydride (0.32 g, 0.008 mole) in water (20 ml). After 3 h standing at room temperature the reaction mixture was diluted with water, acidified with hydrochloric acid, and extracted with chloroform. The solvent was distilled *in vacuo* and the residue was dissolved in toluene. After a few hours refluxing the solution was cooled to room temperature, whereby the acid separated in crystalline form. It was collected by filtration and purified by crystallization from acetone–benzene mixture; yield 2 g (40%), m.p. 187–189°.

Anal. Calcd. for $C_{16}H_{14}ClNO_4$: C, 60.10; H, 4.41; Cl, 11.09; N, 4.38. Found: C, 59.91; H, 4.30; Cl, 11.20; N, 4.45.

1-Methyl-3-phenyl-7-chloro-4,1-benzoxazepine-2,5-dione (10)

The toluene filtrate from the above experiment was evaporated to dryness *in vacuo* and the residue was triturated with benzene. The crystalline product was collected by filtration and purified by crystallization from acetone–benzene mixture; yield 1 g (21.4%), m.p. 220–222°.

Anal. Calcd. for $C_{16}H_{12}ClNO_3$ (mol. wt., 301.73): C, 63.69; H, 4.01; Cl, 11.75; N, 4.64. Found (mol. wt., 276.4): C, 63.89; H, 4.29; Cl, 12.13; N, 4.83.

The same lactone was obtained in 73% yield when **9** (13 g, 0.046 mole) was refluxed overnight in toluene (150 ml) in the presence of *p*-toluenesulfonic acid (3 g) with azeotropic removal of water. The identity was established on the basis of m.p., mixture m.p., and infrared spectra.

Acknowledgments

The authors thank Professor Z. Valenta from the University of New Brunswick for helpful discussions and for the nuclear magnetic resonance spectra. The skillful technical assistance of Miss Lise Lacasse is also gratefully acknowledged.

1. L. J. Bellamy. The infrared spectra of complex molecules. John Wiley & Sons, Inc., New York. 1960.
2. L. H. Sternbach, R. I. Fryer, W. Methlesics, G. Sach, and A. Stempel. J. Org. Chem. **27**, 3781 (1962).
3. O. Keller. Arch. Pharm. **246**, 37 (1908).

Kinetics of the chromic acid oxidation of alcohols in aqueous acetone solutions

DONALD G. LEE,[1] WILLIAM L. DOWNEY, AND R. MICHAEL MAASS
Department of Chemistry, Pacific Lutheran University, Tacoma, Washington, 98447

Received September 8, 1967

The rate law for oxidation of 2-propanol by chromic acid in aqueous acetone solutions has been found to be $V = k_3$ [Cr(VI)][2-propanol]h_0, with the magnitude of k_3 being over 700 times as great in 93.3% acetone as it is in water. In other respects (primary deuterium isotope effect, Hammett "rho" value, and salt effects) the general features of the reaction strongly resemble those observed in aqueous acetic acid solutions.

Canadian Journal of Chemistry, 46, 441 (1968)

Can. J. Chem. Downloaded from www.nrcresearchpress.com by 210.87.254.42 on 09/05/12
For personal use only.

Introduction

Acetone was first used as a solvent for chromic acid oxidations by Jones and his co-workers in the preparation of unsaturated ketones from the corresponding unsaturated secondary alcohols (1). Since then this reaction, which is now commonly referred to as the Jones oxidation, has also been used in the preparation of cyclic (2), bicyclic (3), and, steroidal ketones (4). Part of the success of the reaction lies in the rapidity with which chromium(VI) reacts under these conditions. In fact, the reaction is so facile that alcohols can often be titrated by dropwise addition of a solution of chromium trioxide in aqueous sulfuric acid to an acetone solution of the alcohol.

Despite the extensive use that has been made of this procedure and the apparent unanimity that the reaction is particularly fast, a search of the literature revealed that no kinetic or mechanism studies had been conducted for chromic acid oxidations in aqueous acetone solutions. Moreover, it appeared as if a kinetic study in this solvent might prove helpful in arriving at a more thorough understanding of the accelerated rates which are also obtained when chromic acid oxidations are carried out in aqueous acetic acid solutions. This latter reaction has been extensively studied and is known to proceed via the following sequence (5).

[1] $HCrO_4^- + H_3O^+ \rightleftharpoons H_2CrO_4 + H_2O$

[2] $H_2CrO_4 + R_2CHOH \rightleftharpoons R_2CHOCrO_3H + H_2O$

[3] $R_2CHOCrO_3H \rightarrow R_2CO + Cr(IV)$

[4] $Cr(IV) + Cr(VI) \rightarrow 2\,Cr(V)$

[5] $2\,Cr(V) + 2R_2CHOH \rightarrow 2\,Cr(III) + 2R_2CO$

[1]Author to whom inquiries should be sent at the Department of Chemistry, University of Saskatchewan, Regina Campus, Regina, Saskatchewan.

The observation of a kinetic isotope effect, $k_H/k_D = 7$, for the oxidation of 2-propanol-2-*d* in aqueous and acetic acid solutions has established that decomposition of the chromate ester (step [3]) is rate determining. However some uncertainty still exists as to the exact details of this step. Both an open chain mechanism in which the carbon–hydrogen bond is cleaved by transfer of a proton to a base such as water and a cyclic mechanism with internal transfer of hydrogen have been suggested. Stewart and Wiberg have discussed the relative merits of the two mechanisms (6).

In 86.5% acetic acid the rate of oxidation of 2-propanol is 250 times as fast as in aqueous solutions of the same acidity (5*a*). However it has not been possible to determine definitely if this acceleration is due to a shift to the right in equilibria [1] and [2], or to formation of an acetylchromate species ($AcOCrO_3H$) which would presumably be a more vigorous oxidant (7). In acetone solutions the formation of such an acetylchromate species is precluded and any rate enhancement observed must be attributed to other causes.

Experimental

Acetone was purified by refluxing over potassium permanganate for one week followed by distillation from anhydrous potassium carbonate through a 45-cm Vigreaux column (8). The fraction boiling at 55.8–56.0° was collected and stored in a glass vessel until used.

Perchloric acid (Baker analyzed reagent, 70–72%) was diluted with distilled water, standardized with 1 *M* NaOH, and used without further purification.

Chromium(VI) solutions were prepared by dissolving weighed amounts of potassium dichromate (Baker analyzed reagent, primary standard) in distilled water.

Solutions of sodium chloride, sodium perchlorate, sodium nitrate, and chromium(III) perchlorate were prepared by dissolving weighed amounts of these commercially available compounds in distilled water.

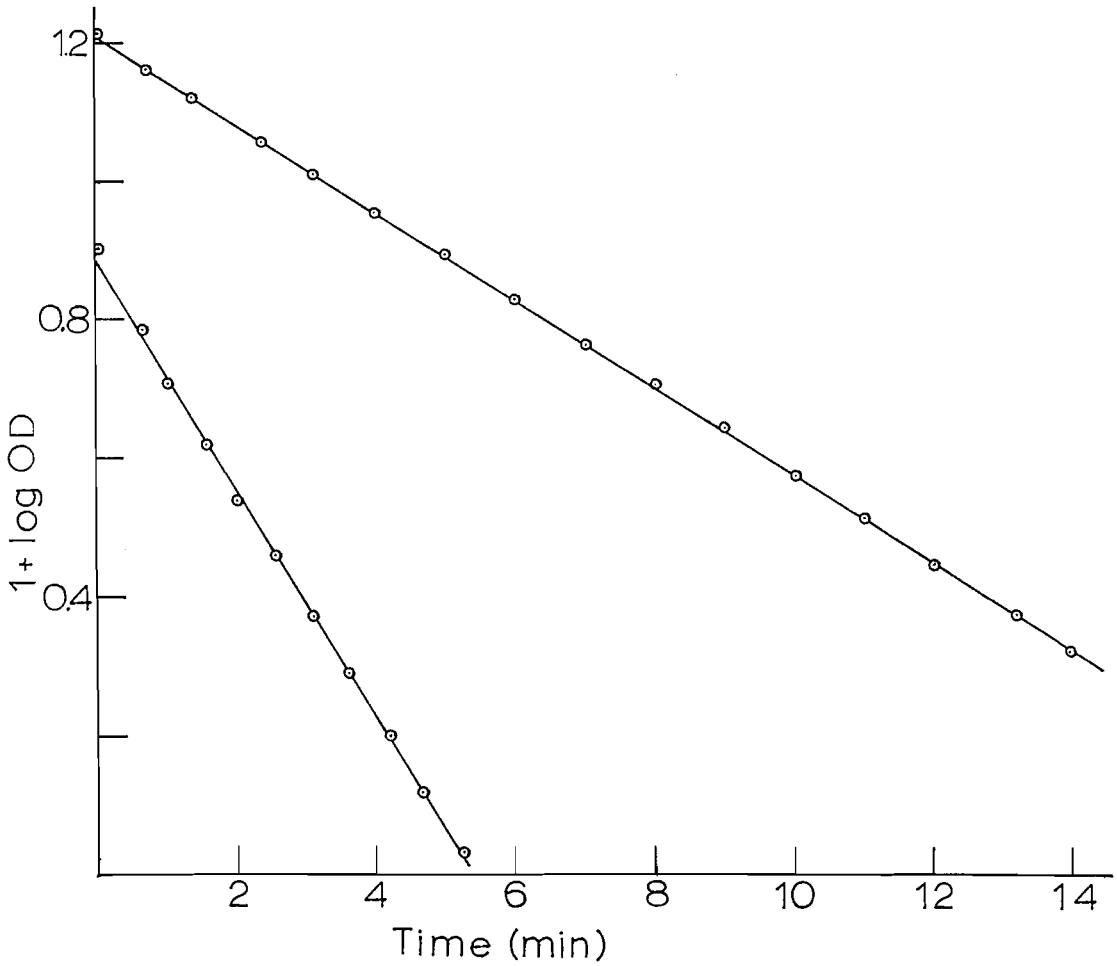

FIG. 1. Typical pseudo first order rate plots for oxidation in 15.2% acetone (top) and 61.7% acetone (bottom).

2-Propanol was distilled from calcium oxide through a 45-cm Vigreaux column and a small middle fraction boiling at 82.0–82.1° was collected for use in the kinetic runs.

2-Propanol-2-*d* was prepared by the method of Leo and Westheimer from acetone and lithium aluminium deuteride and was purified by use of vapor-phase chromatography (9).

4-Chloro-2-nitroaniline and *o*-nitroaniline were obtained commercially and recrystallized repeatedly from ethanol until constant melting points, in agreement with the literature values, were obtained (10*a*, *b*).

Phenylmethylcarbinol was purified by column chromatography (neutral alumina) in order to eliminate traces of a carbonyl impurity that could be detected spectrometrically in the commercially available material. The column was eluted in turn with petroleum ether, 50% benzene – petroleum ether, and pure benzene. Evaporation of the benzene eluant gave a product which distilled at 104.0°/18 mm (lit.; 100° at 18 mm (10*c*)) and which showed no carbonyl absorption in its infrared spectrum.

p-Tolylmethylcarbinol was prepared by lithium aluminium hydride reduction of the corresponding ketone, *p*-methylacetophenone, giving 80% of impure *p*-tolylmethylcarbinol boiling at 116–119° at 19 mm (lit.; 120°/19 mm (10*d*)). This material, after purification by column chromatography on alumina as for the phenylmethylcarbinol, gave a carbonyl-free product distilling at 104.0–104.2° at 8 mm (lit.; 102° at 8 mm (11)).

p-Methoxyphenylmethylcarbinol was also prepared by lithium aluminium hydride reduction of the corresponding ketone, *p*-methoxyacetophenone. The yield was 74% of crude material boiling at 104–105° at 2.7 mm. Chromatographic purification gave a carbonyl-free product distilling at 106.8–107.0° at 3 mm (lit.; 104° at 3 mm (11)).

p-Chlorophenylmethylcarbinol was prepared by reacting methylmagnesium iodide with *p*-chlorobenzaldehyde in a typical Grignard synthesis. After hydrolysis with dilute HCl and thorough washing with aqueous sodium bisulfite, the reaction mixture gave a 70% yield of crude

Can. J. Chem. Downloaded from www.nrcresearchpress.com by 210.87.254.42 on 09/05/12
For personal use only.

Can. J. Chem. Downloaded from www.nrcresearchpress.com by 210.87.254.42 on 09/05/12
For personal use only.

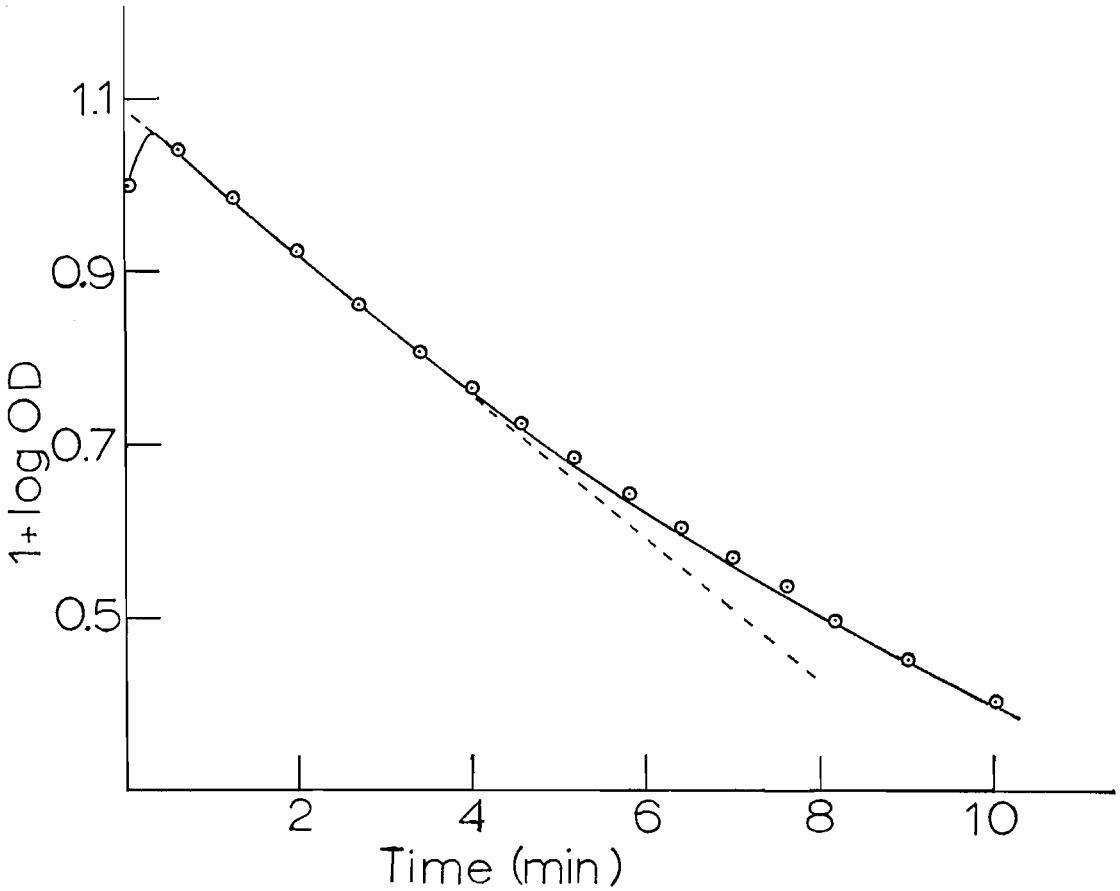

FIG. 2. Typical pseudo first order rate plot for oxidation in 92.2% acetone.

material which could be purified by distillation at reduced pressure; b.p. 64.0–64.1° at 0.3 mm (lit.; 90° at 2.5 mm and 81–86° at 1 mm (11, 12)).

p-Nitrophenylmethylcarbinol was prepared from the corresponding ketone, *p*-nitroacetophenone, by Meerwein – Pondorf – Verley reduction using the procedure of Wilds (13). The yield was 15% of material boiling at 106–108°/0.3 mm. Chromatographic purification gave a ketone-free product which distilled at 110.6° at 0.4 mm (lit.; 161–163° at 4 mm and 158° at 16 mm (14, 10*e*)).

β-Naphthylmethylcarbinol was also prepared from the corresponding ketone, 2-acetonaphthone, by Meerwein – Pondorf – Verley reduction. Recrystallization of the product from aqueous ethanol gave a 96% yield of material with m.p. 71.0–71.5° (lit.; 71–72° (10*f*)).

Kinetic Methods

All kinetic measurements were made, as previously described, using a Beckman model DU spectrophotometer fitted with a thermostated cell compartment (15). Since chromic acid is known to attack slowly ketones the rate of disappearance of chromium(VI) due to solvent oxidation was routinely determined for each set of conditions used and the rate constants were corrected for these blanks. In the majority of runs these corrections were small (0–5%) and in no instance were they greater than 13%.

As indicated in Fig. 1, those solutions containing 0–70% acetone gave good pseudo first order rate plots up to at least 80% completion of the reaction. However, the plots obtained from solutions containing greater than 70% acetone and in particular those with greater than 90% acetone exhibited a slight upward curvature, i.e. the rate of reaction appeared to decrease slightly as the reaction proceeded. (See Fig. 2.) This decrease was not associated with a depletion of oxygen in the cell as the reaction proceeded; solutions flushed with nitrogen exhibited the same curvature and gave the same rates within about 3% as those solutions not flushed. Some of the rate decrease probably can be attributed to formation of a chromium(III) oxy anion which could complex chromium(VI) as many other anions do (15). A slight decrease in rate was, in fact, observed when the reaction was carried out in the presence of chromium(III) perchlorate, but the curvature of the rate plot remained about the same even in the presence of an excess of this salt. It is, however, possible

Can. J. Chem. Downloaded from www.nrcresearchpress.com by 210.87.254.42 on 09/05/12
For personal use only.

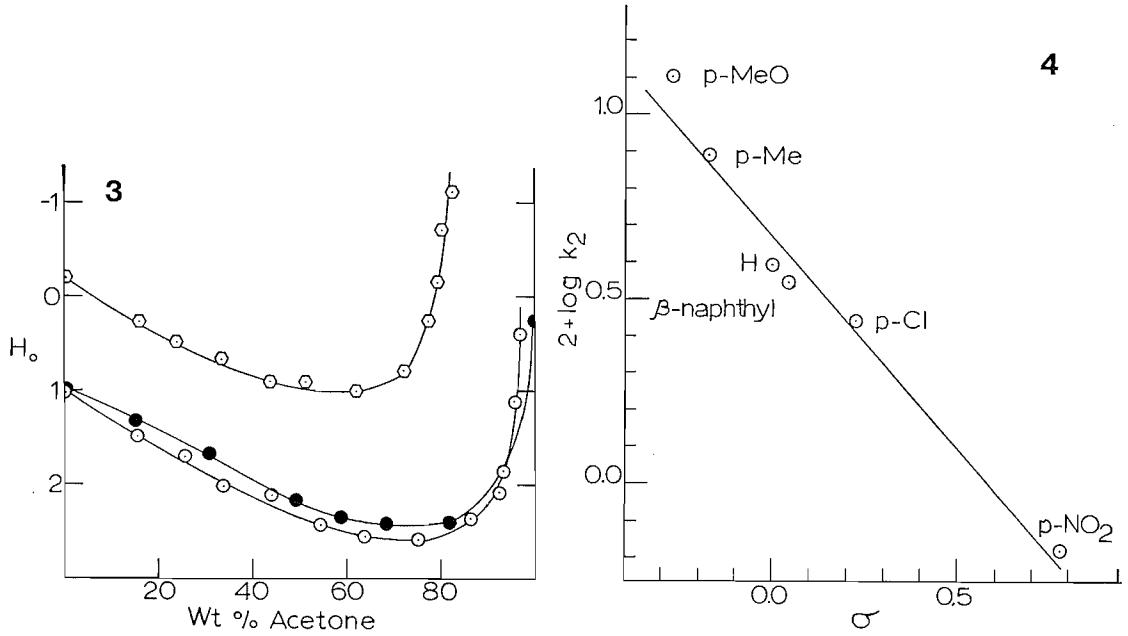

FIG. 3. Acidities of aqueous acetone solutions: ⟨·⟩, 0.883 *M* $HClO_4$; ⊙, 0.0883 *M* $HClO_4$; ●, 0.1 *M* HCl (18).
FIG. 4. Hammett plot for the oxidation of substituted phenylmethylcarbinols in 93% acetone. $\rho = -1.16$, $r = -0.984$, $s = 0.0862$.

that the decrease in rate might be caused by complexing between chromium(VI) and one of the intermediate chromium(IV) or chromium(V) species. In any event, the effect of this phenomenon on the rate constants reported in this paper was minimized by consistently drawing the best straight line through the first half-life of the reaction. In this way the rate constants could be reproduced with good precision. All rate constants reported in this paper, except those in Tables I and II, are the average of two or more determinations with a deviation from the mean of less than ±3 %.

As Fig. 2 also illustrates, the plots obtained in greater than 70% acetone failed to extrapolate back through the initial point corresponding to the optical density of the solution before alcohol was added. In all probability this is due to formation of an intermediate chromate ester with a higher extinction coefficient than chromic acid. Such observations have previously been made during chromic acid oxidations in 97% acetic acid and in concentrated aqueous sulfuric acid solutions, and have been thoroughly discussed elsewhere (5*d*, 16).

TABLE I

Variation in rate with changes in the concentration* of chromium(VI)

[Cr(VI)](*M*)	k_1 (s^{-1})
2.48×10^{-3}	2.48×10^{-3}
1.24×10^{-3}	2.68×10^{-3}
0.62×10^{-3}	2.56×10^{-3}

*$[HClO_4] = 8.83 \times 10^{-2}$ *M*, [2-Propanol] = 0.216 *M*, 93.4% acetone, $T = 25°$.

Acidity Measurements

Acidities of the aqueous acetone solutions were determined by use of the indicators, *o*-nitroaniline, and 4-chloro-2-nitroaniline, (17). A plot of acidity against solvent composition at two concentrations of perchloric acid (0.883 *M* and 0.0883 *M*) is given in Fig. 3. For the purposes of comparison the plot for 0.1 *M* HCl, which had previously been determined by Braude and Stern, is also included (18).

Results and Discussion

Rate Law

In establishing the rate law for this reaction it was necessary to determine the order with respect to the acidity of the solution and with respect to the concentrations of chromium(VI) and 2-propanol. This was done by changing in turn each of the three variables while holding the other two constant. The results obtained from these experiments are presented in Tables I, II, and III. As indicated by the constancy of the values given in the last column of each table, the reaction is first order in chromium(VI), 2-propanol, and acidity, and hence the rate law is $V = k_3[\text{Cr(VI)}][\text{2-propanol}]ho$.

Isotope Effects

A comparison of the rate of oxidation of 2-propanol and 2-propanol-2-*d* at two different

TABLE II

Variation in rate with changes in the concentration* of 2-propanol

[2-Propanol] (M)	% acetone	$k_1(s^{-1})$	$k_2 = \frac{k_1}{[2\text{-Propanol}]}$ (1/mole s)
1.22×10^{-2}	76.0	7.70×10^{-6}	6.31×10^{-4}
2.22×10^{-2}	76.0	1.40×10^{-5}	6.30×10^{-4}
10.0×10^{-2}	76.0	6.27×10^{-5}	6.27×10^{-4}
18.4×10^{-2}	76.0	1.18×10^{-4}	6.42×10^{-4}
2.18×10^{-2}	93.4	2.28×10^{-4}	1.04×10^{-2}
4.36×10^{-2}	93.4	4.47×10^{-4}	1.02×10^{-2}
8.68×10^{-2}	93.4	1.03×10^{-3}	1.20×10^{-2}
21.6×10^{-2}	93.4	1.94×10^{-3}	9.08×10^{-3}

*$[Cr(VI)] = 9.77 \times 10^{-4}$ M, $[HClO_4] = 8.83 \times 10^{-2}$ M, T=25°.

TABLE III

Variation in rate with changes in acidity*

$[HClO_4]$ (M)	Ho	% acetone	$k_1(s^{-1})$	$\log k_2 = \log k_1 + Ho$
0.177	2.38	75.5	2.12×10^{-4}	−1.29
0.353	1.86	74.7	6.99×10^{-4}	−1.29
0.530	1.46	73.1	1.92×10^{-3}	−1.26
0.705	1.10	73.1	4.33×10^{-3}	−1.26
0.883	0.68	72.3	1.11×10^{-2}	−1.27

*$[Cr(VI)] = 9.77 \times 10^{-4}$ M, [2-Propanol] = 0.132 M, T = 25°.

solvent compositions (65.2 and 92.4% acetone) indicated, in agreement with the results obtained in aqueous and acetic acid solutions, that the rate-determining step is cleavage of the α-carbon–hydrogen bond. The results are presented in Table IV.

TABLE IV

Primary deuterium isotope effects*

% acetone	k_2(H) (1/mole s)	k_2(D) (1/mole s)	$\frac{k_2(H)}{k_2(D)}$
65.2	3.68×10^{-4}	4.82×10^{-5}	7.6
92.4	9.55×10^{-3}	1.46×10^{-3}	6.5

*$[HClO_4] = 8.82 \times 10^{-2}$ M, [2-Propanol] = 0.216 M, T = 25°.

Substituent Effects

The effect of substituents on the rate of oxidation in 93% acetone was determined by the use of a series of substituted α-phenylethanols. The results are given in Table V, and Fig. 4 shows a Hammett plot for the reaction. The "rho" value, −1.16, obtained by drawing the best straight line as determined by the least squares method, is similar to that reported for this reaction in aqueous acetic acid solutions, −1.01 (*5b*, *d*), and since a normal primary deuterium isotope effect was also obtained in both solvents, it is very probable that the mechanism is the same in both media.

TABLE V

Oxidation of phenylmethylcarbinols in 93% acetone*

Alcohol	[Alcohol] (M)	k_2(1/mole s)
p-Methoxyphenylmethylcarbinol	3.55×10^{-2}	1.28×10^{-1}
p-Tolylmethylcarbinol	5.86×10^{-2}	7.76×10^{-2}
Phenylmethylcarbinol	6.82×10^{-2}	3.94×10^{-2}
β-Naphthylmethylcarbinol	6.50×10^{-2}	3.54×10^{-2}
p-Chlorophenylmethylcarbinol	6.00×10^{-2}	2.79×10^{-2}
p-Nitrophenylmethylcarbinol	1.23×10^{-1}	6.62×10^{-3}

*$[HClO_4] = 8.83 \times 10^{-2}$ M, T = 25°.

Effect of Solvent Composition on Rates

The rate constants obtained for oxidation of 2-propanol in aqueous acetone solvents varying from 0 to 95.7% (by weight) acetone are presented in Table VI. A plot of $k_2(k_2 = k_1/[2\text{-propanol}])$ against solvent composition indicates that the rates increase markedly in solvents composed largely of acetone (see Fig. 5). However the acidities of solutions containing high percentages of acetone also increase sharply

Can. J. Chem. Downloaded from www.nrcresearchpress.com by 210.87.254.42 on 09/05/12
For personal use only.

Can. J. Chem. Downloaded from www.nrcresearchpress.com by 210.87.254.42 on 09/05/12
For personal use only.

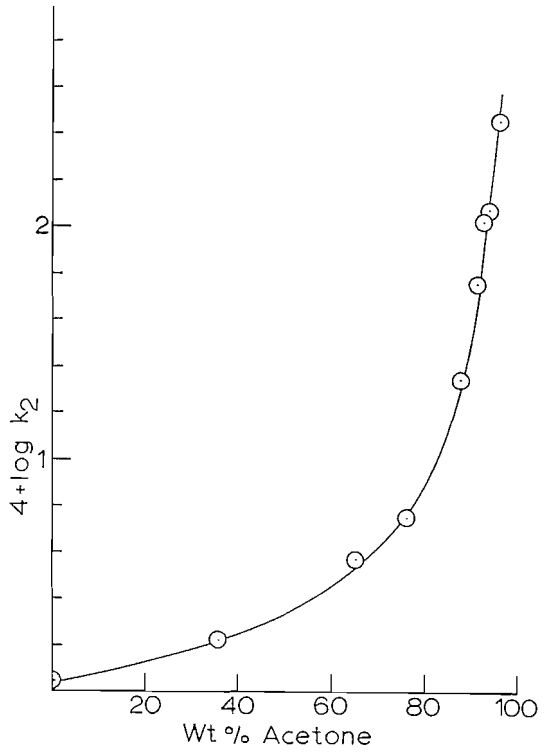

FIG. 5. Variation in k_2 with solvent composition.

(Fig. 3), and at least part of the rate increase is a consequence of the higher acidities. As indicated in Fig. 6, a plot of log $k_3(k_3 = k_2/ho)$ against acetone concentration is approximately linear.

TABLE VI

Effect of solvent composition on rate constants*

% acetone	*Ho*	k_2(1/mole s)†	3 + log k_3‡
0	1.03	1.16×10^{-4}	0.09
35.5	1.98	1.67×10^{-4}	1.20
64.9	2.60	3.69×10^{-4}	2.17
75.9	2.59	5.83×10^{-4}	2.36
87.2	2.34	2.22×10^{-3}	2.69
90.7	2.16	5.60×10^{-3}	2.91
92.2	2.04	1.06×10^{-2}	3.07
93.3	1.91	1.18×10^{-2}	2.98
95.7	1.18	2.86×10^{-2}	2.64

*[2-Propanol] = 0.216 *M*, [$HClO_4$] = 8.82×10^{-2} *M*, *T* = 25°.
†$k_2 = k_1$/[2-Propanol].
‡$k_3' = k_2/ho$.

The third order rate constants are over 700-fold greater in 93.3% acetone than those obtained in aqueous solutions. This is a rate increase comparable to that observed in 86.5% acetic acid solutions (*5a*). Moreover the rate increase in acetone solutions cannot be attributed to formation of a more reactive acetylchromate species, as is possible in acetic acid solutions (7). In light of the results previously presented, which have all tended to indicate that the reaction mechanisms are similar, it follows that the rate increase observed in both solvents as the water content decreases is likely due to a shift in equilibria [1] and [2], and perhaps to an increase in the rate of decomposition of the chromate ester if this step takes place via a cyclic transition state. Decomposition by a transfer of a proton to an external base would be more difficult in nonpolar solutions since it results in the formation of ions, i.e.

$$R_2\underset{H}{C}OCrO_3H + B \rightarrow BH^+ + R_2CO + HCrO_3^-$$

On the other hand, an internal cyclic transfer of electrons would not be retarded by use of a less polar solvent since no ionic products are formed and a large charge separation need not develop in the transition state.

Effect of Added Salts

The rates of reaction were also determined in 92.2% acetone solutions containing variable amounts of potassium chloride, sodium nitrate, sodium perchlorate, and chromium(III) perchlorate. The results are presented graphically in Fig. 7. The near constancy of the rates obtained in the presence of sodium perchlorate indicates that the reaction is not sensitive to changes in the ionic strength of the solvent, while the small but definite decrease in the presence of chromium(III) perchlorate indicates that chromium(III) ions retard the rate of reaction under these conditions. This may at least partly explain, as described in the Experimental section of this paper, the decrease detectable when the rates are followed until nearly all of the chromium(VI) has reacted.

It remains then to explain the opposite effects

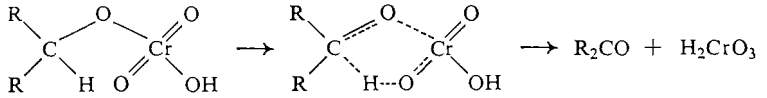

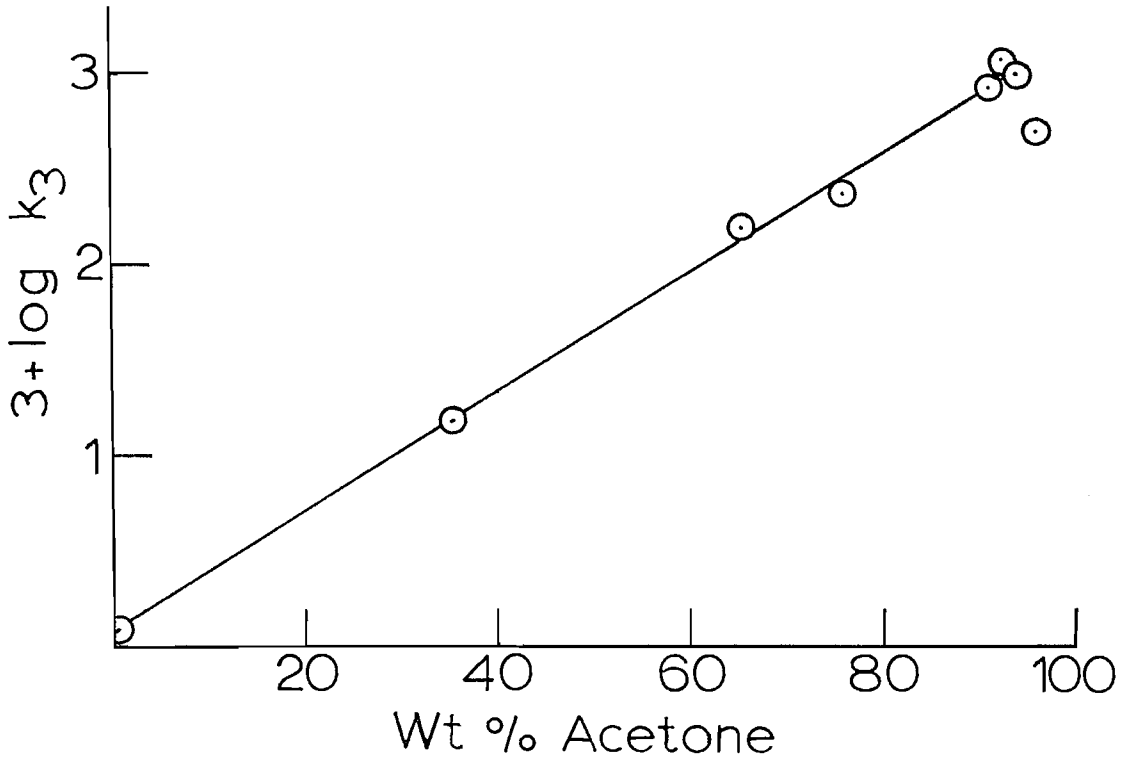

FIG. 6. Variation in k_3 with solvent composition.

of chloride and nitrate ion on the rates of reaction. Retardation of the reaction rates in the presence of chloride ion has also been observed in acetic acid and trifluoroacetic acid solutions, and spectroscopic evidence has indicated the formation, in both solvents, of a new chromium(VI) species produced by incorporation of a chloride ligand (5*a*, 19). In acidic aqueous solutions both kinetic and spectroscopic evidence indicates that chromium(VI) combines with anions to form compounds of the type $HOCrO_2A$, where A is an anion ligand (15). Thus in the presence of chloride ion the active oxidant becomes $HO\overset{\overset{\displaystyle O}{\|}}{\underset{\underset{\displaystyle O}{\|}}{Cr}}Cl$, while in the presence of nitrate ion it is $HO\overset{\overset{\displaystyle O}{\|}}{\underset{\underset{\displaystyle O}{\|}}{Cr}}ONO_2$. Since similar spectral and rate changes were obtained in the present work when chloride ion was added to a dilute solution of chromium(VI) in 92.2% acetone, it is likely that the same species are formed in this solvent.

The lower rate of reaction caused by attachment of a chloride atom to the chromium suggests that it acts as an electron donating ligand, i.e. chromium(VI) is partly reduced by transfer of electronic charge from one of the nonbonding orbitals of chlorine.

$$HO\overset{\overset{\displaystyle O}{\|}}{\underset{\underset{\displaystyle O}{\|}}{Cr}}-Cl : \longleftrightarrow HO\overset{\overset{\displaystyle O}{\|}}{\underset{\underset{\displaystyle O}{\|}}{Cr}}\overset{\delta-}{\cdots}\overset{\delta+}{Cl}$$

The nitrate ligand could, however, withdraw electrons from the chromium, thus creating a more active oxidant.

$$HO\overset{\overset{\displaystyle O}{\|}}{\underset{\underset{\displaystyle O}{\|}}{Cr}}-O-N\begin{matrix}\nearrow O\\ \searrow O\end{matrix} \longleftrightarrow HO\overset{\overset{\displaystyle O}{\|}}{\underset{\underset{\displaystyle O}{\|}}{Cr}}-O-\overset{+}{N}\begin{matrix}\nearrow \bar{O}\\ \searrow O\end{matrix}$$

Can. J. Chem. Downloaded from www.nrcresearchpress.com by 210.87.254.42 on 09/05/12
For personal use only.

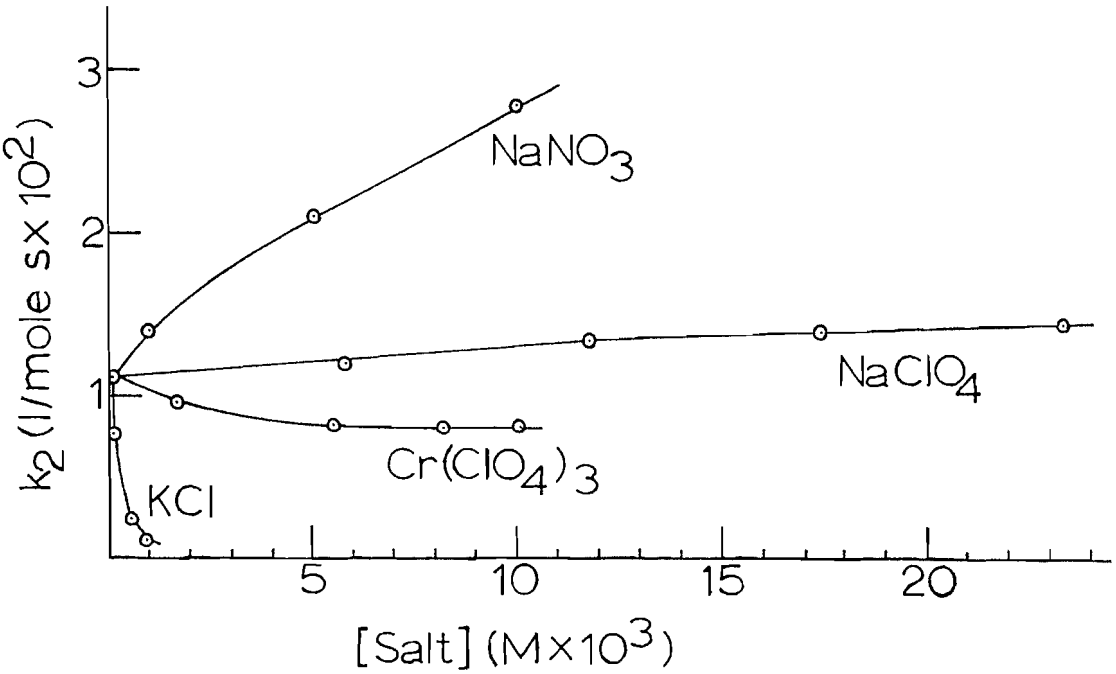

FIG. 7. Salt effects in 92.2% acetone solutions.

Acknowledgment

The authors gratefully acknowledge support from the United States National Science Foundation in the form of an Undergraduate Research Participation Grant.

1. K. BOWDEN, I. M. HEILBRON, E. R. H. JONES, and B. C. L. WEEDON. J. Chem. Soc. 39 (1946); E. A. BRAUDE, E. R. H. JONES, F. SONDHEIMER, and J. B. TOOGOOD. J. Chem. Soc. 607 (1949).
2. R. E. IRELAND and P. W. SCHIESS. Tetrahedron Letters, 37 (1960); R. F. CHURCH and R. E. IRELAND. Tetrahedron Letters, 493 (1961); E. J. EISENBRAUN. Org. Syn. **45**, 28 (1965).
3. J. MEINWALD, J. CRANDALL, and W. E. HYMANS. Org. Syn. **45**, 77 (1965).
4. P. BLADON, J. M. FABIAN, H. B. HENBEST, H. P. KOCH, and G. W. WOOD. J. Chem. Soc. 2402 (1951); R. G. CURTIS, I. HEILBRON, E. R. H. JONES, and G. F. WOODS. J. Chem. Soc. 457 (1953); A. BOWERS, T. G. HALSALL, E. R. H. JONES, and A. J. LEMIN. J. Chem. Soc. 2548 (1953); T. G. HALSALL, R. HODGES, and E. R. H. JONES. J. Chem. Soc. 3019 (1953); C. DJERASSI, R. R. ENGLE, and A. BOWERS. J. Org. Chem. **21**, 1547 (1956); E. S. ROTHMAN and M. E. WALL. J. Am. Chem. Soc. **81**, 411 (1959); A. BOWERS, E. DENOT, M. B. SÁNCHEZ, L. M. SÁNCHEZ-HIDALGO, and H. J. RINGOLD. J. Am. Chem. Soc. **81**, 5233 (1959); W. S. JOHNSON, W. A. UREDENBURGH, and J. E. PIKE. J. Am. Chem. Soc. **82**, 3409 (1960); P. A. MAYOR and G. D. MEAKINS. J. Chem. Soc. 2792 (1960); K. HEUSLER, J. KALVODA, CH. MEYSTRE, P. WIELAND, G. ANNER, A. WETTSTEIN, G. CAINELLI, D. ARIGONI, and O. JEGER. Helv. Chim. Acta. **44**, 502 (1961); J. IRIARTE, J. N. SHOOLERY, and C. DJERASSI. J. Org. Chem. **27**, 1139 (1962).
5. (*a*) M. COHEN and F. H. WESTHEIMER. J. Am. Chem. Soc. **74**, 4387 (1952). (*b*) H. KWART and P. S. FRANCIS. J. Am. Chem. Soc. **77**, 4907 (1955). (*c*) J. ROCEK, F. H. WESTHEIMER, A. ESCHENMOSER, L. MOLDOVÁNYI, and J. SCHREIBER. Helv. Chim. Acta. **45**, 2554 (1962). (*d*) R. STEWART and D. G. LEE. Can. J. Chem. **42**, 439 (1964). (*e*) K. B. WIBERG and H. SCHÄFER. J. Am. Chem. Soc. **89**, 455 (1967).
6. R. STEWART. Oxidation mechanisms. W. A. Benjamin, New York. 1964. pp. 37–42; K. B. WIBERG. *In* Oxidation in organic chemistry. Part A. *Edited by* K. B. Wiberg. Academic Press, Inc., New York. 1965. pp. 166–167.
7. U. KLÄNING and M. C. R. SYMONS. J. Chem. Soc. 3204 (1961); M. C. R. SYMONS. J. Chem. Soc. 4331 (1963).
8. J. A. RIDDICK and E. E. TOUPS, JR. Technique of organic chemistry. *Edited by* A. Weissberger. Vol. VII. Organic solvents. Revised 2nd ed. Interscience Publishers, Inc., New York. 1955. p. 381.
9. A. LEO and F. H. WESTHEIMER. J. Am. Chem. Soc. **74**, 4383 (1952).
10. I. HEIBRON and H. M. BUNBURY. Dictionary of organic compounds. Oxford University Press. New York. 1953. (*a*) Vol. III. p. 628. (*b*) Vol. I. p. 532. (*c*) Vol. III. p. 478. (*d*) Vol. III. p. 518. (*e*) Vol. III. p. 462. (*f*) Vol. III. p. 459.
11. J. GRUNDY. J. Chem. Soc. 5087 (1957).
12. C. S. MARVEL and G. L. SCHERTZ. J. Am. Chem. Soc. **65**, 2054 (1943).
13. A. L. WILDS. Org. Reactions, **2**, 178 (1944).

Can. J. Chem. Downloaded from www.nrcresearchpress.com by 210.87.254.42 on 09/05/12
For personal use only.

14. A. H. FORD-MOORE and H. N. RYDON. J. Chem. Soc. 679 (1946).
15. D. G. LEE and R. STEWART. J. Am. Chem. Soc. **86**, 3051 (1964).
16. D. G. LEE and R. STEWART. J. Org. Chem. **32**, 2868 (1967).
17. M. A. PAUL and F. A. LONG. Chem. Rev. **57**, 1 (1967).
18. E. A. BRAUDE and E. S. STERN. J. Chem. Soc. 1976 (1948).
19. D. G. LEE and D. T. JOHNSON. Can. J. Chem. **43**, 1952 (1965).

Can. J. Chem. Downloaded from www.nrcresearchpress.com by 210.87.254.42 on 09/05/12
For personal use only.

Can. J. Chem. Downloaded from www.nrcresearchpress.com by 210.87.254.40 on 09/05/12
For personal use only.

Reagent effects on distribution of methylsulfonylethyl substituents in the D-glucopyranosyl unit of cotton cellulose[1]

STANLEY P. ROWLAND, AUSTIN L. BULLOCK, VIDABELLE O. CIRINO, AND CLINTON P. WADE
Southern Regional Research Laboratory, Southern Utilization Research and Development Division, Agricultural Research Service, United States Department of Agriculture, New Orleans, Louisiana

Received September 25, 1967

The distribution of methylsulfonylethyl substituents at the 2-*O*-, 3-*O*-, and 6-*O*-positions of the monosubstituted D-glucopyranosyl unit of cotton cellulose was found to be a function of the specific reagent and the reaction conditions. The distribution is dependent upon the extent to which rate or equilibrium of reaction at the individual hydroxyl groups is the controlling factor. Under conditions which approach equilibrium in the reaction of methyl vinyl sulfone with cotton cellulose, the ratio of 2-*O*- to 6-*O*-substitution is 0.14:1.0. A variety of precursors for methyl vinyl sulfone (i.e., 2-(methylsulfonyl)-ethanol, [2-(methylsulfonyl)ethyl]pyridinium chloride, 2-bromoethyl methyl sulfone, and *bis*-[2-(methylsulfonyl)ethyl]ether) react with cotton cellulose under non-equilibrium conditions to generate ratios of 2-*O*- to 6-*O*-substitutions as high as 0.44:1.0. The effect of diffusion of reagents into the cotton fiber upon the distribution of substituents is clearly evident in these reactions. Specific modifications of the process of reaction of methyl vinyl sulfone or 2-(methylsulfonyl)ethanol with cotton cellulose yield ratios of substituents in the 2-*O*- to 6-*O*-positions as high as 0.8:1.0; this ratio is similar to those which characterize certain rate-controlled Williamson etherification reactions with cotton cellulose.

Canadian Journal of Chemistry, 46, 451 (1968)

Introduction

An interest in the chemistry of the crosslinking of cotton cellulose led us to an investigation of the effect of the specific reagent employed for introducing the methylsulfonylethyl group upon the distribution of these substituents in the D-glucopyranosyl unit of cotton cellulose. Methyl vinyl sulfone and a variety of precursors for methyl vinyl sulfone were employed as analogues of crosslinking agents (1, 2).

Several studies (3–5) of the modification of cotton cellulose have been conducted with a variety of activated vinyl compounds (and their saturated analogues), including vinyl sulfones and their precursors that differ from those employed in this study only in polyfunctionality. However, it is only recently (6) that techniques have been established for determining accurately the distribution of these substituents that are present at low degrees of substitution in chemically modified cotton celluloses. In that study, the distribution of methylsulfonylethyl substituents in the 2-*O*-, 3-*O*-, and 6-*O*-positions of the monosubstituted D-glucopyranosyl unit of cotton (from reaction of methyl vinyl sulfone catalyzed by aqueous base to a degree of substitution of 0.11) was indicated to be in the ratio of 0.20:0.03:1.00.

Touzinsky (7) using a closely related system allowed acrylamide to react with cotton linters in the presence of sodium hydroxide to a degree of substitution of 0.8. From analysis of the mole fractions of unsubstituted, mono-, di-, and trisubstituted glucose units, he deduced mathematically the relative equilibrium constants to be 9:1:19 (i.e., 0.47:0.05:1.00) for reactions at the 2-*O*-, 3-*O*-, and 6-*O*-positions.

Results and Discussion

The Reaction of Methyl Vinyl Sulfone with Cotton Cellulose

In this study, major interest lies in reactions carried to degrees of substitution in cotton cellulose that are generally encountered with crosslinking agents. At conventional levels of various polyfunctional agents (2–15% add-on), the apparent maximum degree of substitution could be as high as 0.5. In view of the multitude of structures that can develop in addition to the "simple" crosslink, it is likely that the maximum degree of substitution does not exceed 0.2. As a result of reactions of methyl vinyl sulfone **(1)** with cotton cellulose to degrees of substitution of 0.11 and 0.33, the mono-*O*-(methylsulfonylethyl)-D-glucopyranose fraction constituted 95 and 81 mole percentages, respectively, of the substituted glucoses. Thus, the major portion of the product can be assessed by the distribution

[1]Presented in part at the 153rd meeting of the American Chemical Society, April 1967, Miami Beach, Florida.

TABLE I

Methylsulfonylethyl celluloses

No.	Reagent system[a] Sulfone	Catalyst	Reaction conditions[b]	Degree of substitution[c]	Distribution of substituents[d] 2-*O*-	3-*O*-	Crystallinity index[e]
1	**1** (20)	OH^- (10S)	25°, 1 h	0.11	0.22	0.05	—
2	**1** (20)	OH^- (10S)	as #1: triple treatment	0.33	0.22	0.04	84
3	**1** (20)	OH^- (23S)	25°, 1 h	0.09	0.18	0.03	(0.75)
4	**1** (20)	OH^- (23S)	as #3: double treatment	0.17	0.17	0.04	(0.94)
5	**1** (20)	OH^- (23S)	as #3: triple treatment	0.35	0.17	0.03	(1.15)
6	**1** (20)	OH^- (10S)	25°, 24 h	0.09	0.14	0.05	—
7	**1** (20)	OH^- (10S)	140°, 5 min	0.14	0.28	0.10	—
8	**1** (100)	OH^- (10S)	25°, 1 min	0.16	0.22	0.05	86
9	**1** (100)	OH^- (10S)	25°, 7.5 min	0.30	0.25	0.04	83
10	**1** (100)	OH^- (10S)	25°, 15 min	0.35	0.27	0.04	81
11	**1** (100)	OH^- (10S)	25°, 30 min	0.38	0.29	0.05	79
12	**1** (100)	OH^- (10S)	25°, 60 min	0.38	0.28	0.04	81
13	**1** (100)	OH^- (10S)	25°, 24 h	0.32	0.20	0.04	86
14	**1** (100)	OH^- (10S)	25°, 72 h	0.16	0.15	0.04	88
15	**2** (12) (single solution)	$CO_3^=$ (2)	148°, 3 min	0.04	0.26	0.10	—
16	**2** (20) (single solution)	OH^- (2)	148°, 3 min	0.06	0.27	0.11	—
17	**2** (12) (single solution)	OH^- (2)	148°, 3 min	0.09	0.27	0.08	—
18	**2** (12)	OH^- (10S)	140°, 5 min	0.07	0.27	0.13	—
19	**2** (20) (single solution)	OH^- (5)	140°, 5 min	0.12	0.28	0.11	88
20	**3** (50)[f]	OH^- (5)	25°, 1 min	0.005	0.17	0.06	—
21	**3** (50)[f]	OH^- (5)	25°, 30 min	0.037	0.24	0.05	—
22	**3** (50)[f]	OH^- (5)	25°, 60 min	0.033	0.26	0.05	—
23	**3** (50)[f]	OH^- (5)	25°, 17 h	0.090	0.44	0.03	—
24	**4** (20) (single solution)	$CO_3^=$ (5)[g]	140°, 5 min	0.08	0.42	0.06	—
25	**5** (20) (single solution)	OH^- (5)	140°, 5 min	0.11	0.34	0.08	—
26	**5** (20) (single solution)	$CO_3^=$ (5)	140°, 5 min	0.05	0.27	0.07	—
27	**1** (20)[h]	OH^- (10S)	140°, 5 min	0.08	0.75	0.00	—
28	**2** (20)[i] (single solution)	OH^- (5)	140°, 5 min	0.15	0.80	0.00	—

[a] **1** = methyl vinyl sulfone; **2** = 2-(methylsulfonyl)ethanol; **3** = [2-(methylsulfonyl)ethyl]pyridinium chloride; **4** = 2-bromoethyl methyl sulfone; **5** = *bis*-[2-(methylsulfonyl)ethyl]ether. Numbers in parentheses following the sulfone are the % concentrations of the reagent in the aqueous solutions. Catalysts were sodium hydroxide (OH^-) or sodium carbonate ($CO_3^=$) and the numbers in parentheses following these designations indicate the % concentrations of the base. The sulfone and catalyst solutions were separate except where it is indicated that a "single solution" was employed. "S" indicates that the solution of catalyst was saturated with sodium sulfate (to minimize extraction of the sulfone from the cotton cellulose).

[b] "Double" or "triple" treatments started with the air-equilibrated fabric in each case.

[c] Average number of substituent groups per D-glucopyranosyl unit of the cotton cellulose based on sulfur content of the modified cotton.

[d] Distributions of methylsulfonylethyl substituents at the 2-*O*- and 3-*O*-positions of the D-glucopyranosyl unit relative to unity at the 6-*O*-position for the mono-substituted glucose fraction.

[e] Crystallinity Indices (CI) measured by X-ray diffraction and calculated by the method of Segal *et al.* (8). The CI of unmodified cotton cellulose = 91. The values in parentheses are the ratios of the intensities of the $10\bar{1}$ and the 002 peaks of the X-ray diffractogram. The former peak appears and this ratio increases as the crystalline lattice structure of the cellulose is modified by mercerization from lattice I to lattice II type. The small but regular changes in CI of cotton cellulose during the course of one of these reactions is shown in curve CC of Fig. 2.

[f] The cotton fabric impregnated with **3** was dried prior to contact with ca. 70% of the stoichiometric requirement of base in a minimum volume of solution.

[g] Potassium bicarbonate was employed and the solution was warmed to maintain both the sulfone and the bicarbonate in solution.

[h] Time elapsed between the individual steps (impregnation with the solution of sulfone, squeeze through rolls, impregnation with the solution of base, squeeze through the rolls, and cure in the oven) was reduced to the minimum in these "piece operations."

[i] The solutions of base and sulfone were mixed immediately prior to the impregnation of the fabric; subsequent steps of squeezing through rolls and inserting into the curing oven were conducted as rapidly as possible.

Can. J. Chem. Downloaded from www.nrcresearchpress.com by 210.87.254.40 on 09/05/12
For personal use only.

Can. J. Chem. Downloaded from www.nrcresearchpress.com by 210.87.254.40 on 09/05/12
For personal use only.

of isomers in the monosubstituted glucose fraction (6).

Higher levels of methylsulfonylethyl substitution in cotton obtained by repeated reactions in the conventional treatment of fabric (i.e., impregnation with the sulfone, impregnation with alkali, followed by cure) caused no change in distribution of substituents in the mono-*O*-(methylsulfonylethyl)-D-glucopyranose fraction (Table I: nos. 1 vs. 2, and 3 vs. 4 vs. 5). An increase in the concentration of the sodium hydroxide catalyst from 10% (nos. 1 and 2) to 23% (nos. 3–5) changed the average ratio of substituents at the 2-*O*-, 3-*O*-, and 6-*O*-position from 0.22:0.04:1.00 to 0.17:0.03:1.00. This difference in relative substitution at the 2-*O*-position is beyond the range of experimental variation: the maximum variation in reproducibility of the ratio of isomers in the monosubstituted glucose fraction, as measured by gas–liquid chromatography and expressed in the usual terms, was ± 0.02:± 0.02:0.00; the average variation was less than ± 0.01:± 0.01:0.00.

A notable difference between distributions of substituents from equilibrium-controlled Michael-type addition reactions and those from rate-controlled Williamson reactions is the higher proportion of substitution in the 2-*O*-position for the latter. Ratios of distribution of substituents in the 2-*O*- and 6-*O*-positions from Williamson reactions have been reported to range from ca. 0.7–0.8:1.0 for etherifications of cellulose involving sodium chloroacetate (9) or sodium allyl sulfate (10) to 2.5:1.0 for the methylation reaction with methyl chloride (9). Data already cited (6) indicate a ratio of 0.20:1.00 for the corresponding distribution of substituents resulting from the reversible reaction of methyl vinyl sulfone with cellulose; therefore, the substitution at the 2-*O*-position (relative to that at the 6-*O*-position) for the reversible reaction of methyl vinyl sulfone with cellulose is 0.08 to 0.29 of that for the irreversible (rate-controlled) reactions. If this is a characteristic difference between equilibrium- and rate-controlled reactions of cellulose, then a higher relative level of reaction of methyl vinyl sulfone at the 2-*O*-position may reflect changes from equilibrium control toward rate control of the reaction.

The product of reaction of cotton with methyl vinyl sulfone in a 24 h reaction period (no. 6) showed a small but distinct difference from that product formed in a 1 h reaction period (no. 1). Thus, the former is a closer approach to equilibrium distribution of substituents: i.e., 0.14:0.05:1.00.

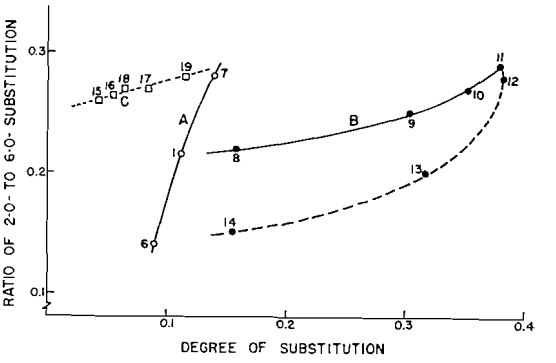

FIG. 1. The relationship between the ratio of 2-*O*- to 6-*O*-substitution in the mono-*O*-(methylsulfonylethyl)-D-glucopyranose fraction to the degree of substitution of the chemically modified cellulose. The numbers refer to experiments listed in Table I.

An attempt toward rate control in this reaction was made by shortening the reaction period to 5 min and raising the temperature to 140°.[2] The measured distribution of substituents (no. 7) was 0.28:0.10:1.00, showing significant increases at both the 2-*O*- and 3-*O*-positions. The differences in distribution of substituents at 2-*O*-position that result from different opportunities for the reaction to reach equilibrium are illustrated in the points connected by curve A of Fig. 1. The behavior noted thus far is indicative of a $K_2/K_6 \cong 0.14$ (where K's denote equilibrium constants and the subscripts refer to the specific hydroxyl groups), but the results suggest that $k_2/k_6 \gg 0.28$[3] (where k's denote forward rate constants for the reactions).

In view of the foregoing results, products obtained in the earliest stage of reaction of methyl vinyl sulfone with the D-glucopyranosyl

[2]The objective was to achieve, in a short reaction period, a degree of substitution sufficient for accurate measurement of the distribution of the methylsulfonylethyl substituents.

[3]The K_2/K_6 is the ratio of 2-*O*- to 6-*O*-substitution at apparent equilibrium (no. 6). The k_2/k_6 is considered to be reflected in the ratio of 2-*O*- to 6-*O*-substitution to increasing extents as reaction conditions deviate the farther from equilibrium toward rate control. Thus, the 2-*O*- to 6-*O*-substituent ratio of 0.28:1.00 (no. 7) reflects a degree of rate control and indicates that k_2/k_6 is at least as high as 0.28.

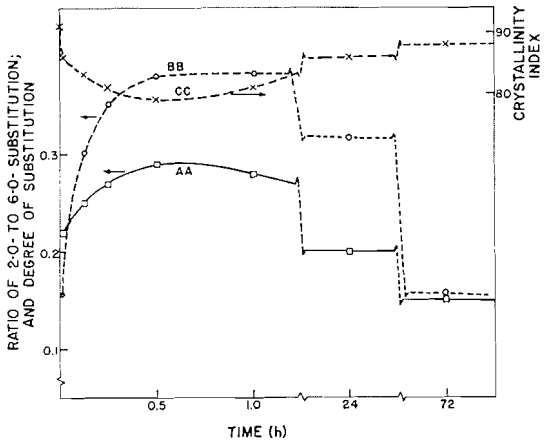

FIG. 2. The effects of duration of reaction of methyl vinyl sulfone with cotton cellulose (nos. 8–14, Table I) upon the ratio of 2-*O*- to 6-*O*-substitution (curve AA), the degree of substitution (curve BB), and the crystallinity index (curve CC).

unit would be expected to reflect the greatest extent of rate-controlled distributions of substituents. The products actually obtained from cotton cellulose and methyl vinyl sulfone in reactions of 1–30 min duration (nos. 8–11) show progressive increase in the ratio of 2-*O*- to 6-*O*-substituents from 0.22 at 1 min to a maximum of 0.29 at 30 min (Fig. 1, curve B). Although the slight drop in this ratio at 60 min (no. 12) is within the experimental variability, it may indicate the beginning of progression toward the equilibrium distribution. As seen in Fig. 1, curve B, there is a relationship between the degree of substitution and the ratio of 2-*O*- to 6-*O*-substitution. This relationship is further illustrated in Fig.2, curves AA and BB: non-equilibrium conditions of reaction result in a high degree of substitution *and* a high ratio of 2-*O*- to 6-*O*-substitution, whereas subsequent progression toward equilibrium is accompanied by decreases in both.

The peak in the ratio of 2-*O*- to 6-*O*-substitution in Fig. 2 is interpreted to be a consequence of diffusion-controlled penetration of the chemical agents into the cotton cellulose during the course of the reaction. In the initial phase of reaction (no. 8), the most accessible D-glucopyranosyl units of the fibrous microstructure of cotton cellulose undergo reaction and the ratio of the 2-*O*- to 6-*O*-substitution in these units approaches the equilibrium distribution. In the next phase (for example, no. 11), reagent diffuses to and reacts with additional D-glucopyranosyl units. The spectrum of distributions of substituents at the 2-*O*-, 3-*O*-, and 6-*O*-positions ranges from near equilibrium distribution for the most accessible D-glucopyranosyl units to near rate-controlled distribution for the least accessible units; however, this intermediate phase reflects greater rate control than does the initial phase of the reaction. In the final phase of reaction (no. 14), all accessible regions of the polymer are reached by the reagents and equilibrium distribution of substituents results in all of the D-glucopyranosyl units.

The average distribution of substituents in the incremental product formed between 1 and 30 min of reaction is calculated to be 0.34:0.05:1.00 (without correction for progression of the product formed during the 0–1 min period further toward an equilibrium distribution). Thus, the ratio of 2-*O*- to 6-*O*-substituents in the D-glucopyranosyl units which are least equilibrated is estimated to be substantially higher than 0.34:1.00.

The Reactions of Precursors of Methyl Vinyl Sulfone with Cotton Cellulose

2-Hydroxyethyl sulfones undergo the Michael-type addition reactions at elevated temperatures in the presence of base with the elimination of water (11, 12). 2-(Methylsulfonyl)ethanol (**2**), upon reaction with cotton cellulose at 140° via sodium carbonate or sodium hydroxide catalysis, yielded higher proportions of substitution in the 2-*O*- and 3-*O*-positions than those that are characteristic of the equilibrium distribution (nos. 15–19 vs. 6 and 14). In the former cases, the distribution of substituents appears independent of the amount and strength of the base catalyst, but a relationship is evident between ratio of 2-*O*- to 6-*O*-substitution and the degree of substitution (Fig. 1: curve C). The result from the reaction of methyl vinyl sulfone with cellulose at elevated temperature (no. 7) lies close to curve C. The relationship shown in curve C of Fig. 1 is similar to that previously noted for the products formed from the reaction of methyl vinyl sulfone in various periods at room temperature (Fig. 1: curve B).

[2-(Methylsulfonyl)ethyl]pyridinium chloride (**3**) reacted with cotton cellulose at 25° in the presence of less than a stoichiometric amount

Can. J. Chem. Downloaded from www.nrcresearchpress.com by 210.87.254.40 on 09/05/12
For personal use only.

Can. J. Chem. Downloaded from www.nrcresearchpress.com by 210.87.254.40 on 09/05/12
For personal use only.

of base (ca. 70%) to yield a distribution of methylsulfonylethyl substituents in the 2-*O*-, 3-*O*-, and 6-*O*-positions in the ratio of 0.44:0.03:1.00 (no. 23). This reaction proceeds through elimination of pyridine hydrochloride, requiring an equivalent of base per 2-pyridiniumethyl sulfone unit for generation of the vinyl sulfone (13, 14). The latter undergoes conventional Michael-type addition in the presence of catalytic amounts of strong base. In this specific reaction with cotton cellulose, the equilibration of distribution of the methylsulfonylethyl groups was arrested at a relatively high ratio of 2-*O*- to 6-*O*-substitution: i.e., more characteristic of a rate-controlled distribution throughout the fibrous cotton than achieved in the foregoing experiments. An insight into this reaction is gained from an examination of the course of the distribution of substituents in the cotton fiber as a function of time (nos. 20–23). As the solution of strong base contacts and diffuses into the cotton that is impregnated with [2-(methylsulfonyl)ethyl]pyridinium chloride, reaction occurs at the surface and equilibrium is reached rapidly in the presence of the local excess of free base (no. 20). With progression of the base to the less accessible regions of the fibers, the rate-controlled disposition of methylsulfonylethyl groups is equilibrated less rapidly (nos. 20 and 21); and toward the innermost regions of the fibers, even less equilibration of the distribution of substituents occurs as the base, present in less than stoichiometric amounts, is neutralized by the excess of the substituted pyridinium chloride (no. 23). The average distribution of substituents in the incremental product formed between 1 and 17 h is calculated on the same basis as in the preceding section to be 0.54:0.02:1.00.

2-Bromoethyl methyl sulfone (**4**), when reacted with cotton cellulose at elevated temperature in a conventional procedure (but with bicarbonate catalysis to minimize premature dehydrobromination), yielded a distribution of substituents in the 2-*O*-, 3-*O*-, and 6-*O*-positions in the ratio of 0.42:0.06:1.00 (no. 24). This shows evidence of higher degrees of rate control than the products from generally similar reactions involving 2-(methylsulfonyl)ethanol (or methyl vinyl sulfone).

bis-[2-(Methylsulfonyl)ethyl]ether (**5**) underwent reaction with cotton cellulose at elevated temperature, when catalyzed with either sodium hydroxide or sodium carbonate, with the development of distributions of substituents (nos. 25 and 26) similar to those realized from reactions of 2-(methylsulfonyl)ethanol.

The Effect of a Variation in Process of Reaction

The conditions under which methyl vinyl sulfone and 2-(methylsulfonyl)ethanol were reacted with cotton cellulose in the preceding section were generally similar to the processes that were employed with corresponding difunctional sulfones (1, 2) for the crosslinking of cotton to develop wrinkle-resistant characteristics in the fabric. Reactions of [2-(methylsulfonyl)-ethyl]pyridinium chloride, 2-bromoethyl methyl sulfone, and *bis*-[2-(methylsulfonyl)ethyl]ether were carried out in much the same manner but with modifications aimed toward rate-controlled distributions of substituents. In the reactions of methyl vinyl sulfone and 2-(methylsulfonyl)-ethanol, an unconventional process variation (i.e., abbreviated duration of contact of the reagent with the strong base catalyst and the cotton prior to cure at elevated temperature) produced a substantially different distribution of substituents than those noted from preceding experiments. In this case, the ratio of methylsulfonylethyl groups at the 2-*O*- and 6-*O*-positions was raised to approximately 0.8:1.0 from the previous range of approximately 0.3:1.0 (no. 27 vs. 7 and 28 vs. 19). The higher ratio of 2-*O*- to 6-*O*-substitution is believed to result from a higher degree of rate control in these reactions. The 0.8:1.0 ratio of 2-*O*- to 6-*O*-substitution is approximately the same as those reported for sodium carboxymethyl substituents (9) and for allyl substituents (10) introduced by the rate-controlled Williamson reactions. Thus, distributions of substituents that are characteristic of equilibrium-controlled or rate-controlled reactions have been achieved with a single reagent.

Experimental

Materials

Reagents were used as received from the following sources: methyl vinyl sulfone, K & K Laboratories, Inc.;[4] 2-(methylthio)ethanol, Pennsalt Chemicals Corp.; trimethylchlorosilane, General Electric Co.; hexamethyldisilazane, Peninsular ChemResearch; grade 923 silica

[4]Mention of a company and (or) product by the United States Department of Agriculture does not imply approval or recommendation of the product to the exclusion of others which may also be suitable.

Can. J. Chem. Downloaded from www.nrcresearchpress.com by 210.87.254.40 on 09/05/12
For personal use only.

gel of 100–200 mesh, W. R. Grace & Co.; acid-washed dimethyldichlorosilane-treated Chromosorb W of 80–100 mesh, and acid-washed dimethyldichlorosilane-treated Chromosorb G of 100–200 mesh, Johns-Manville Corp.; QF-1 and SE-52 liquid phases, Wilkens Instrument and Research, Inc.

Gas–Liquid Chromatography

The chromatograph was an F & M model 1609 unit equipped with hydrogen flame ionization detector. Columns were prepared in $\frac{1}{4}$ in. outside diameter tubing and were (*a*) 3% SE-52 on Chromosorb W, 6 ft (*b*) 3% QF-1 on Chromosorb W, 5.5 ft and (*c*) 3% QF-1 on Chromosorb G, 5.5 ft.

2-(Methylsulfonyl)ethanol

To 138.2 g (1.5 mole) of 2-(methylthio)ethanol containing 3.3 g of phosphoric acid and 100 ml of water and warmed to 40° was added 168 g of 30.6% hydrogen peroxide at a dropwise rate with cooling to maintain the temperature at 40–50° (15, 16). When the starch-iodide test on the reaction mixture became negative, a 200 g portion of hydrogen peroxide was introduced slowly to the reaction mixture at reflux. After 2 h at reflux and 16 h at room temperature, the phosphoric acid was removed with a weak base ion exchange resin, the excess hydrogen peroxide was destroyed with sodium bisulfite, and the mixture was concentrated under vacuum below 40°. The semicrystalline residue was taken up in anhydrous acetone, filtered, and the solvent removed under vacuum. The product was dissolved in water, decolorized with carbon, and the water removed under vacuum. The colorless syrup crystallized to yield 155 g of product: yield 83%, m.p. 25–28°.

Anal. Calcd. for $C_3H_8O_3S$: C, 29.02; H, 6.50; S, 25.83. Found: C, 28.83; H, 6.40; S, 25.79.

[2-(Methylsulfonyl)ethyl]pyridinium Chloride

To 7 g (0.06 mole) of pyridine hydrochloride (m.p. 144–147 °C) in 25 ml of absolute ethanol was added 6 ml of pyridine, 100 ml of acetone, 2 drops of triethylamine, and 6 g (0.06 mole) of methyl vinyl sulfone (13). After 48 h at room temperature, the crystalline product was removed by filtration, recrystallized from methanol–acetone, and dried *in vacuo* at 85°: yield 4.6 g, 36%, m.p. 230° (decomp.). Additional product crystallized from the mother liquor.

Anal. Calcd. for $C_8H_{12}O_2SNCl$: C, 43.34; H, 5.46; S, 14.46; N, 6.32; Cl, 15.99. Found: C, 43.24; H, 5.32; S, 14.11; N, 6.26; Cl, 15.88.

2-Bromoethyl Methyl Sulfone

To 25 g (0.2 mole) of 2-(methylsulfonyl)ethanol was added 20 g (0.74 mole) of phosphorus tribromide, dropwise, with agitation over a period of 1.5 h (17). The reaction mixture was warmed to 50° and allowed to remain at room temperature for 4 days prior to being poured into an equal volume of water, from which the product crystallized on cooling: ca. 50% yield, white crystals, m.p. 36°.

Anal. Calcd. for $C_3H_7O_2BrS$: C, 19.26; H, 3.78; Br, 42.72; S, 17.14. Found: C, 19.44; H, 3.57; Br, 42.58; S, 17.23.

bis-[2-(Methylsulfonyl)ethyl]ether

Methyl vinyl sulfone (10 g) was stirred into a 6.25% solution (40 g) of sodium hydroxide. Crystals, which began to form after 5 min, were removed at the end of 45 min. This product was recrystallized twice from water: 62% yield, white needles, m.p. 78° (lit. (18) 78°). Gas–liquid chromatograms (injection port 225°, column *c*, programmed 160–240°) of this product showed two peaks, one having a retention time identical to that of methyl vinyl sulfone and the other having a retention time identical to that of 2-(methylsulfonyl)ethanol, indicating that the sulfonylethyl ether dissociates under these conditions. The nuclear magnetic resonance spectra of the product showed a singlet, δ 3.05; a triplet, δ 3.34; and a second triplet, δ 4.07. The ratio of the protons was 6:4:4, respectively.

Anal. Calcd. for $C_6H_{14}O_5S_2$: C, 31.29; H, 6.13; S, 27.85. Found: C, 31.06; H, 6.05; S, 27.98.

Methylsulfonylethyl Cellulose

Cotton cellulose in the form of desized, scoured, bleached, 80 × 80 print cloth (3.3 oz/ yd^2) was immersed in the reagent bath and squeezed through rolls to a specific level of wet pickup (19). With the exceptions noted in Table I, the initial immersion involved the sulfone reagent for a 100% wet pickup and the second immersion involved the aqueous alkali for an additional 50% wet pickup. Time was measured from the immersion in the second reagent. In the case of reactions at elevated temperature, the fabric was placed in a forced-draft oven preset at the desired temperature. Impregnated fabrics that were allowed to react at room temperature were placed in polyethylene bags to retard evaporation. After the reactions, all samples were rinsed vigorously for 15 min in running tap water, then in 1% acetic acid, and finally, three times in distilled water. The extent of incorporation of methylsulfonylethyl groups was determined by sulfur analysis on the dry fabric and checked by weight gain on the air-equilibrated sample.

Hydrolysis of Methylsulfonylethyl Celluloses and Estimation of Distribution of Substituents

One-gram samples of methylsulfonylethyl celluloses were dissolved in sulfuric acid (15 g, 72%, 25–30°, 8 h) and hydrolyzed in subsequent dilutions (to 7.7 *N*, 25–30°, 16–20 h, and 1.5 *N*, reflux, 6 h) under an atmosphere of nitrogen (6). The acid was neutralized with barium hydroxide and the filtrate was freeze-dried to a solid mixture of glucose and *O*-methylsulfonylethyl-D-glucopyranoses.

Trimethylsilyl ethers (20) of the dry hydrolyzates were prepared and analyzed for the ratio of the 2-*O*-, 3-*O*-, and 6-*O*-mono(methylsulfonylethyl)-D-glucopyranoses by gas–liquid chromatography on QF-1 columns: isothermal at 200° and 30 psig on column *b*; isothermal at 218° and 40 psig on column *c*. These procedures have been described in detail in an earlier publication (6). Results (Table I) of ratios of peak areas from triangulation or from the product of peak height and retention time were identical for the two columns. Polysubstitution of methylsulfonylethyl groups in the D-glucopyranosyl unit was measured on thin-layer sheets of silica gel, by elution with methyl ethyl ketone–water (30 + 2, v/v) with a travel of 20 cm and color development with aniline phosphate spray reagent (21). Spot densities were measured with a densitometer (Photovolt Corp.), values were plotted, and the areas under the peaks were inte-

grated. This technique will be described in detail elsewhere.

1. G. C. TESORO, P. LINDEN, and S. B. SELLO. Textile Research J. **31**, 283 (1961).
2. G. C. TESORO. Textile Research J. **32**, 189 (1962).
3. K. WARD, JR. and A. J. MORAK. Reactions of cellulose. *In* High polymers XIX. *Edited by* E. M. Fettes, Interscience Publishers, New York. 1964. Chap. V.
4. G. C. TESORO and S. B. SELLO. Textile Research J. **36**, 158 (1966).
5. J. G. FRICK, JR., W. A. REEVES, and J. G. GUTHRIE. Textile Research J. **27**, 92 (1957).
6. S. P. ROWLAND, V. O. CIRINO, and A. L. BULLOCK. Can. J. Chem. **44**, 1051 (1966).
7. G. F. TOUZINSKY. J. Org. Chem. **30**, 426 (1965).
8. L. SEGAL, J. J. CREELY, A. E. MARTIN, and C. M. CONRAD. Textile Research J. **29**, 76 (1959).
9. I. CROON. Svensk. Papperstidn. **63**, 247 (1960).
10. D. E. HOINESS, C. P. WADE, and S. P. ROWLAND. Can. J. Chem. To be published.
11. H. B. FREYERMUTH and R. L. MAYHEW. Belg. Pat. 600,667. To General Analine and Film Corp. (June, 1961).
12. R. STEELE and C. HUGGETT. Can. Pat. 625,790 To Rohm and Haas Company (August, 1961).
13. M. A. STAHMANN, C. GOLUMBIC, W. H. STEIN, and J. S. FRUTON. J. Org. Chem. **11**, 719 (1946).
14. G. C. TESORO. J. Appl. Polymer Sci. **5**, 721 (1961).
15. I. TASHLICK. U.S. Pat. 3,069,471 to Monsanto Chemical Company (December 1962).
16. E. I. VALKO, B. BITTER, and R. S. PERRY. Textile Research J. **34**, 849 (1964).
17. G. C. HARRISON and H. DIEHL. Org. Syn. Col. Vol. 3. John Wiley and Sons, Inc., New York. 1960. p. 370.
18. P. MAMALIS and H. M. RYDON. J. Chem. Soc. 1062 (1955).
19. G. C. TESORO and A. OROSZLAN. Textile Research J. **33**, 93 (1963).
20. C. C. SWEELEY, R. BENTLEY, M. MAKETA, and W. W. WELLS. J. Am. Chem. Soc. **85**, 2497 (1963).
21. L. HOUGH, J. K. N. JONES, and W. H. WADMAN. J. Chem. Soc. 1702 (1950).

Can. J. Chem. Downloaded from www.nrcresearchpress.com by 210.87.254.40 on 09/05/12
For personal use only.

Can. J. Chem. Downloaded from www.nrcresearchpress.com by 210.87.254.40 on 09/05/12
For personal use only.

Two general intermediates for the synthesis of anhydropenicillins

SAUL WOLFE[1]
Department of Chemistry, Queen's University, Kingston, Ontario

Received September 27, 1967

A procedure is given for the preparation of the hydrated potassium salt of 6-*N*-tritylaminopenicillanic acid (**1**). Conversion of **1** to the acid chloride followed by treatment with triethylamine produced the anhydro derivative **2**. Reaction of **2** with *p*-toluenesulfonic acid monohydrate gave the *p*-toluenesulfonic acid salt **3** of anhydro 6-aminopenicillanic acid. The free base **4** was generated with sodium bicarbonate; acylation with phenylacetic acid by the carbodiimide method afforded anhydropenicillin G.

Canadian Journal of Chemistry, 46, 459 (1968)

Anhydropenicillins are stable organic compounds which are derived from penicillins by a rearrangement of the thiazolidine ring (1). Although they have negligible antibacterial activity, the anhydropenicillins do induce the formation of penicillinase.[2] Mercuric acetate converts anhydro-α-phenoxyethylpenicillin to an antibacterial agent (2) which does not induce the formation of penicillinase.[2] Since the activity of a penicillin (3) or cephalosporin (4) depends on the nature of the acyl side chain it seems reasonable to expect that the biological activity of a substance derived from an anhydropenicillin will also depend on the nature of the side chain. A general procedure for the routine replacement of the side chain of an anhydropenicillin would, therefore, seem to be desirable. One obvious route involves acylation of 6-aminopenicillanic acid and rearrangement of the resulting penicillin; this has the disadvantage that in every case conditions would have to be worked out for both the acylation and the rearrangement.

The purpose of this note is to report that detritylation of the anhydro derivative (**2**) of 6-*N*-tritylaminopenicillanic acid (**1**) can be achieved in high yield by Koe's procedure (5) and that the resulting base can be acylated by the carbodiimide method to produce an anhydropenicillin. Reaction of **2** with an equivalent of *p*-toluenesulfonic acid monohydrate in dry acetone (5) gave in 81% yield the the crystalline *p*-toluenesulfonic acid salt (**3**) of anhydro-6-aminopenicillanic acid. The infrared spectra of **2** and **3** are shown in Fig. 1; both compounds have the characteristic peaks at 5.5, 5.9, and 6.1μ (1). Treatment of **3** with sodium bicarbonate generated the free base **4** which, with phenylacetic acid and diisopropylcarbodiimide, gave in 50% yield anhydrobenzylpenicillin, identical with the compound prepared from Penicillin G. The reaction sequence is shown below.

Both **2** and **3** are stable at room temperature for at least two years. Since the carbodiimide method is a general one for the synthesis of an amide (6) the route from **2** or **3** to an anhydropenicillin should have general applicability.

Experimental

Infrared spectra were obtained as pressed KBr discs on a Beckmann 5A spectrophotometer. Melting points were taken on a Fisher–Johns block, and are uncorrected.

6-N-Tritylaminopenicillanic Acid (1) (See also reference 7)

6-Aminopenicillanic acid (21.6 g, 0.1 mole) was dissolved in a mixture of water (40 ml) and isopropyl alcohol (80 ml) containing diethylamine (30 ml, 0.3 mole). Finely powdered trityl chloride (36 g, 0.13 mole) was added in portions during 90 min with vigorous stirring. Halfway through the addition more water (40 ml) and isopropyl alcohol (100 ml) were added. The mixture was stirred for 24 h and some triphenylcarbinol was then separated by filtration. Dilution of the filtrate with water precipitated additional triphenylcarbinol. After removal of this solid, addition of 25 ml of glacial acetic acid precipitated 6-tritylaminopenicillanic acid as a viscous mass. This did not dissolve in ether alone but did dissolve in ether containing acetone. The acetone was removed by washing with water. The dried ether solution was treated with 36 ml (0.1 mole) of 50% potassium 2-ethylhexanoate

[1]Part of the work described in this note was performed by the author in the laboratories of the Organic Research Division, Bristol Laboratories, Division of Bristol–Myers Inc., Syracuse, New York.

[2]J. F. Collins. Unpublished results.

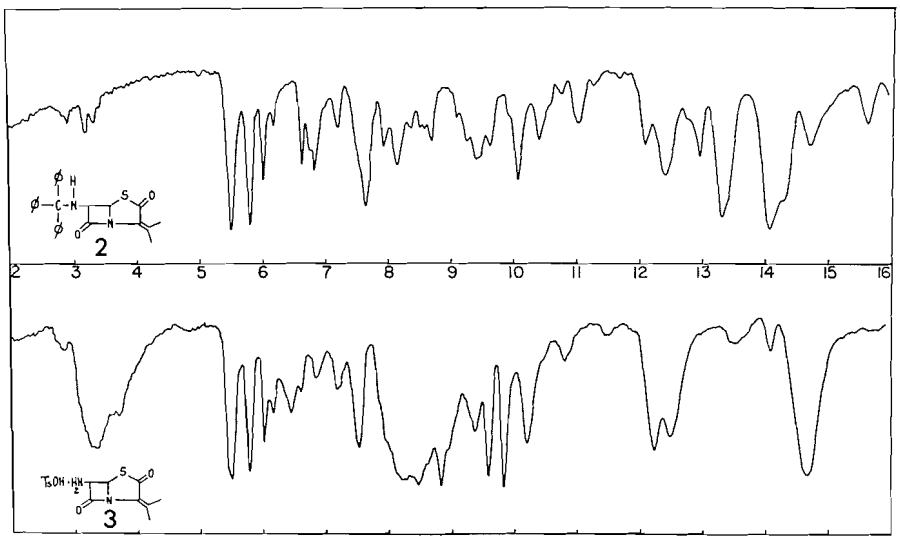

FIG. 1. The infrared spectra of **2** and **3**.

in *n*-butanol. The crystalline potassium 6-tritylaminopenicillanate was collected, washed with ether, and dried *in vacuo* over P_2O_5. The yield was 12.7 g (25%).

Anal. Calcd. for $C_{27}H_{25}N_2O_3SK \cdot H_2O$: C, 63.2; H, 5.4. Found: C, 63.03; H, 5.67.

Anhydro-6-tritylaminopenicillanic Acid (2)

A suspension of potassium 6-tritylaminopenicillanate monohydrate (25.7 g, 0.05 mole) in methylene chloride (340 ml) containing pyridine (20.1 ml, 0.25 mole) was cooled to −40°, stirred, and treated with thionyl chloride (9.05 ml, 0.125 mole). The mixture was maintained at −40° for 3 h and was then treated dropwise with a solution of triethylamine (30.3 g, 0.3 mole) in 100 ml of methylene chloride. After the addition was complete an additional 7.0 ml (0.05 mole) of triethylamine was added, the cooling bath was removed, and stirring was continued for 90 min. The reaction mixture was concentrated and the product plus pyridine were separated from salts by extraction into ether. The ether and pyridine were removed under reduced pressure and the residue was treated with isopropyl alcohol (300 ml). Cooling of this solution precipitated 1.5 g of **2**. Slow concentration of the mother liquor gave an additional 3.57 g of **2**. The combined material (5.07 g, 22%) was purified by trituration with cold glacial acetic acid. This procedure gave thick rods, m.p. 165–166°.

Anal. Calcd. for $C_{27}H_{24}N_2O_2S$: C, 73.60; H, 5.45; N, 6.35; S, 7.28. Found: C, 73.55; H, 5.57; N, 6.00; S, 7.00.

Further concentration of the isopropyl alcohol mother liquors gave a hydrated form of **2**. This material melted initially at 134–135°; after resolidification the melting point was 162–165°.

Anal. Calcd. for $C_{27}H_{24}N_2O_2S \cdot 0.5\ H_2O$: C, 72.3; H, 5.58; N, 6.25. Found: C, 72.30; H, 5.61; N, 5.88.

p-Toluenesulfonic Acid Salt of Anhydro-6-aminopenicillanic Acid (3)

The anhydro compound **2** (0.2 g, 0.5 mmoles) was dissolved in 1.0 ml of dry acetone and *p*-toluenesulfonic acid monohydrate (0.095 g, 0.5 mmoles) was added. The acid dissolved and after 20 s the reaction mixture set to a crystalline mass. This was triturated with ether and the solid was collected and washed with ether. The yield of

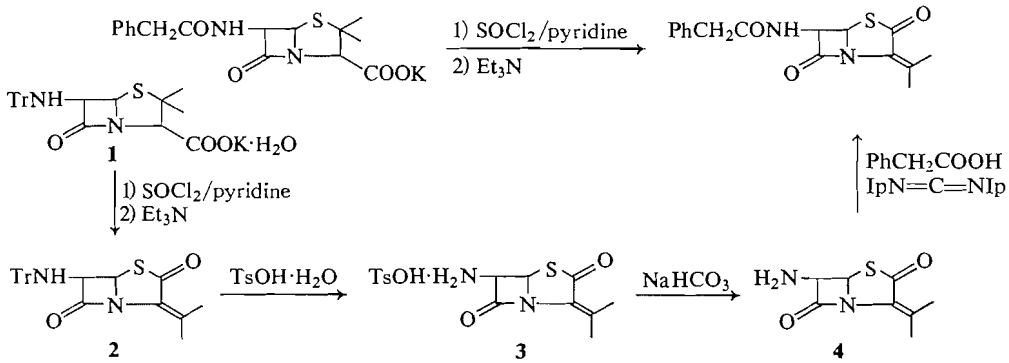

Can. J. Chem. Downloaded from www.nrcresearchpress.com by 210.87.254.40 on 09/05/12
For personal use only.

analytically pure material was 0.15 g (81%), m.p. 153–154° (decomp.).

Anal. Calcd. for $C_{15}H_{18}N_2O_5S_2$: C, 48.65; H, 4.86. Found: C, 48.52; H, 5.02.

Conversion of the Toluenesulfonic Acid Salt to Anhydrobenzylpenicillin

The salt **3** (100 mg, 0.27 mmoles) was suspended in methylene chloride (2 ml) and an ice-cold saturated sodium bicarbonate solution (2 ml) was added. The salt dissolved when this mixture was shaken. The yellowish aqueous layer was removed and the methylene chloride layer was passed through a short column of anhydrous sodium sulfate. The column was washed with methylene chloride and the dry solution of the base **4** (volume, 3 ml) was treated with a solution of phenylacetic acid (37 mg, 0.27 mmole) in methylene chloride (1 ml) and then with a solution of diisopropylcarbodiimide (34 mg, 0.27 mmole) in methylene chloride (1 ml). The reaction mixture was left for 20 h at room temperature and the solvent was then removed. The crystalline residue was triturated with ether and the ether-insoluble material was recrystallized twice from isopropyl alcohol, giving 43 mg (52% from **3**) of anhydrobenzylpenicillin, m.p. 148–150°, identical with the compound prepared from Penicillin G on the basis of its infrared spectrum and an undepressed mixture melting point.

1. S. WOLFE, J. C. GODFREY, C. T. HOLDREGE, and Y. G. PERRON. J. Am. Chem. Soc. **85**, 643 (1963).
2. S. WOLFE. U.S. Patent No. 3,311,638 (1967) to Bristol-Myers Co. Ltd.; S. WOLFE, C. FERRARI, and W. S. LEE. 49th Canadian Chemical Conference, Saskatoon, Saskatchewan, June, 1966. Abstr. p. 65.
3. A. GOUREVITCH, G. A. HUNT, and J. LEIN. Antibiot. Chemotherapy, **10**, 121 (1960).
4. R. R. CHAUVETTE, E. H. FLYNN, B. G. JACKSON, E. R. LAVAGNINO, R. B. MORIN, R. A. MEULLER, R. P. PIOCH, R. W. ROESKE, C. W. RYAN, J. L. SPENCER, and E. V. HEYNINGEN. J. Am. Chem. Soc. **84**, 3401 (1962).
5. B. K. KOE. Nature, **195**, 1200 (1962).
6. J. C. SHEEHAN. U.S. Patent No. 2,938,892 (1960).
7. J. C. SHEEHAN and K. R. HENERY-LOGAN. J. Am. Chem. Soc. **84**, 2983 (1962).

The chemistry of ylids. XVI.[1] The acidifying effects of 'onium groups

A. WILLIAM JOHNSON[2] AND RONALD T. AMEL

Division of Natural Sciences, University of Saskatchewan, Regina, Saskatchewan

Received September 1, 1967

An examination of the pK_a's of a series of phenacyl 'onium salts has indicated that the acidifying effects of the 'onium groups increase in the order arsonium < phosphonium < sulfonium. The acidifying effects of the 'onium atom substituents increase in the order methyl < *n*-butyl < phenyl. These observations have been accounted for in terms of $p\pi$–$d\pi$ overlap between the carbanion and the heteroatom of the 'onium group.

Canadian Journal of Chemistry, **46**, 461 (1968)

The discovery and use of ylids containing a variety of heteroatom groups has given rise to questions regarding the relative effectiveness with which the different 'onium groups (X in **2**) provide stabilization for the adjacent carbanion.

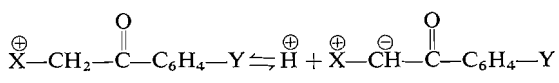

1 **2**

3 Y = H **4** Y = H

It is well recognized, especially on the basis of infrared (1) and x-ray crystallographic (2) evidence on phenacylides (**4**), that considerable stabilization is afforded the carbanion by delocalization of the negative charge through the carbon portion of the ylids (i.e. through the carbonyl group in **2**). However, it also appears that the 'onium group (X in **2**) must provide conjugative stabilization of the carbanion in order for such ylids to have any finite existence. The stabilization probably is via $p\pi - d\pi$ overlap between the carbanion and the 'onium group if the latter has available empty, low-energy *d*-orbitals (3). Such is the case with arsonium, phosphonium, and sulfonium ylids.

We wish to report some recent pK_a determinations which indicate the relative effectiveness of the groups X in increasing the acidity of the 'onium salts (**3**) or in stabilizing the corresponding ylids (**4**). We view these two characteristics as being complementary, if not synonymous.

[1]For part XV in this series, see A. W. Johnson and S. C. K. Wong, Can. J. Chem. **44**, 2793 (1966).

[2]Author to whom inquiries should be addressed at The Chemistry Department, University of North Dakota, Grand Forks, North Dakota, U.S.A.

Can. J. Chem. Downloaded from www.nrcresearchpress.com by 210.87.254.40 on 09/05/12
For personal use only.

analytically pure material was 0.15 g (81%), m.p. 153–154° (decomp.).

Anal. Calcd. for $C_{15}H_{18}N_2O_5S_2$: C, 48.65; H, 4.86. Found: C, 48.52; H, 5.02.

Conversion of the Toluenesulfonic Acid Salt to Anhydrobenzylpenicillin

The salt **3** (100 mg, 0.27 mmoles) was suspended in methylene chloride (2 ml) and an ice-cold saturated sodium bicarbonate solution (2 ml) was added. The salt dissolved when this mixture was shaken. The yellowish aqueous layer was removed and the methylene chloride layer was passed through a short column of anhydrous sodium sulfate. The column was washed with methylene chloride and the dry solution of the base **4** (volume, 3 ml) was treated with a solution of phenylacetic acid (37 mg, 0.27 mmole) in methylene chloride (1 ml) and then with a solution of diisopropylcarbodiimide (34 mg, 0.27 mmole) in methylene chloride (1 ml). The reaction mixture was left for 20 h at room temperature and the solvent was then removed. The crystalline residue was triturated with ether and the ether-insoluble material was recrystallized twice from isopropyl alcohol, giving 43 mg (52% from **3**) of anhydrobenzylpenicillin, m.p. 148–150°, identical with the compound prepared from Penicillin G on the basis of its infrared spectrum and an undepressed mixture melting point.

1. S. WOLFE, J. C. GODFREY, C. T. HOLDREGE, and Y. G. PERRON. J. Am. Chem. Soc. **85**, 643 (1963).
2. S. WOLFE. U.S. Patent No. 3,311,638 (1967) to Bristol-Myers Co. Ltd.; S. WOLFE, C. FERRARI, and W. S. LEE. 49th Canadian Chemical Conference, Saskatoon, Saskatchewan, June, 1966. Abstr. p. 65.
3. A. GOUREVITCH, G. A. HUNT, and J. LEIN. Antibiot. Chemotherapy, **10**, 121 (1960).
4. R. R. CHAUVETTE, E. H. FLYNN, B. G. JACKSON, E. R. LAVAGNINO, R. B. MORIN, R. A. MEULLER, R. P. PIOCH, R. W. ROESKE, C. W. RYAN, J. L. SPENCER, and E. V. HEYNINGEN. J. Am. Chem. Soc. **84**, 3401 (1962).
5. B. K. KOE. Nature, **195**, 1200 (1962).
6. J. C. SHEEHAN. U.S. Patent No. 2,938,892 (1960).
7. J. C. SHEEHAN and K. R. HENERY-LOGAN. J. Am. Chem. Soc. **84**, 2983 (1962).

The chemistry of ylids. XVI.[1] The acidifying effects of 'onium groups

A. WILLIAM JOHNSON[2] AND RONALD T. AMEL

Division of Natural Sciences, University of Saskatchewan, Regina, Saskatchewan

Received September 1, 1967

An examination of the pK_a's of a series of phenacyl 'onium salts has indicated that the acidifying effects of the 'onium groups increase in the order arsonium < phosphonium < sulfonium. The acidifying effects of the 'onium atom substituents increase in the order methyl < *n*-butyl < phenyl. These observations have been accounted for in terms of $p\pi$–$d\pi$ overlap between the carbanion and the heteroatom of the 'onium group.

Canadian Journal of Chemistry, **46**, 461 (1968)

The discovery and use of ylids containing a variety of heteroatom groups has given rise to questions regarding the relative effectiveness with which the different 'onium groups (X in **2**) provide stabilization for the adjacent carbanion.

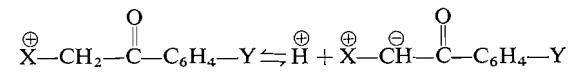

1 **2**

3 Y = H **4** Y = H

It is well recognized, especially on the basis of infrared (1) and x-ray crystallographic (2) evidence on phenacylides (**4**), that considerable stabilization is afforded the carbanion by delocalization of the negative charge through the carbon portion of the ylids (i.e. through the carbonyl group in **2**). However, it also appears that the 'onium group (X in **2**) must provide conjugative stabilization of the carbanion in order for such ylids to have any finite existence. The stabilization probably is via $p\pi - d\pi$ overlap between the carbanion and the 'onium group if the latter has available empty, low-energy *d*-orbitals (3). Such is the case with arsonium, phosphonium, and sulfonium ylids.

We wish to report some recent pK_a determinations which indicate the relative effectiveness of the groups X in increasing the acidity of the 'onium salts (**3**) or in stabilizing the corresponding ylids (**4**). We view these two characteristics as being complementary, if not synonymous.

[1]For part XV in this series, see A. W. Johnson and S. C. K. Wong, Can. J. Chem. **44**, 2793 (1966).

[2]Author to whom inquiries should be addressed at The Chemistry Department, University of North Dakota, Grand Forks, North Dakota, U.S.A.

Can. J. Chem. Downloaded from www.nrcresearchpress.com by 210.87.254.42 on 09/05/12
For personal use only.

Can. J. Chem. Downloaded from www.nrcresearchpress.com by 210.87.254.42 on 09/05/12
For personal use only.

Doering and Hoffmann (4), as a result of studying the deuteroxide-catalyzed exchange of D_2O with several permethyl 'onium salts, including $(CH_3)_4As^+$, $(CH_3)_4P^+$, and $(CH_3)_3S^+$, concluded that a sulfonium group was more effective than a phosphonium group, and that a phosphonium group was more effective than an arsonium group in providing stabilization for an adjacent carbanion via *d*-orbital overlap. Recently, Ratts and Yao (5) determined the pK_a's of a series of *p*-Y-phenacyldimethylsulfonium salts (**1**, X = $(CH_3)_2S$). A plot of the pK_a's versus σ for the groups Y afforded a straight line with a negative slope as expected. However, this line was parallel to, *but above*, a straight line obtained much earlier by Fliszar, Hudson, and Salvadori (6) from a plot of σ versus pK_a for a similar series of *p*-Y-phenacyltriphenylphosphonium salts (**1**, X = $(C_6H_5)_3P$). Therefore, in this comparison the triphenylphosphonium salts were more acidic than the dimethylsulfonium salts, implying that the phosphonium group was more effective than the sulfonium group in providing delocalization for the carbanion of the resulting ylids. However, Ratts and Yao did surmise that the different substituents on the heteroatom affected the acidity relationships.

Following up our recently published work on the acidities of fluorenylphosphonium salts (7), we have examined the acidities of a series of similarly substituted phenacylphosphonium and phenacylsulfonium salts (3). We believe that our results clarify the superficial conflict between the work cited in refs. 4 and 5. The acidities of our salts were obtained in 95% ethanol solution by the spectrophotometric method of Flexser *et al.* (8) as previously adapted by us (7). The physical data on these salts are in accord with their proposed structure and will be reported in a full paper. The pK_a's obtained, together with some pertinent data already published, are listed in Table I.

TABLE I

pK_a's of Phenacyl 'onium salts (**3**)

Compound	X	pK_a	Reference
3*a*	$(CH_3)_2S$	7.68	This work
3*b*	$(C_4H_9)_2S$	6.65	This work
3*c*	$CH_3SC_6H_5$	6.66	This work
3*d*	$(C_6H_5)_2S$	5.36	This work
3*e*	$(CH_3)_3P$	8.60[1]	Ref. 9
3*f*	$(C_4H_9)_3P$	7.49	This work
3*g*	$(CH_3)_2PC_6H_5$	7.75[1]	Ref. 9
3*h*	$CH_3P(C_6H_5)_2$	6.51	This work
3*i*	$(C_6H_5)_3P$	5.60	This work
3*j*	$(CH_3)_3As$	9.80[1]	Ref. 9
3*k*	$(CH_3)_2AsC_6H_5$	9.45[1]	Ref. 9
3*l*	$(C_6H_5)_3As$	8.25[1]	Ref. 9

[1]These values have been adjusted downward by 0.40 pK units from those reported in ref. 9 to account for the difference in solvent. The data reported above are in 95% ethanol solvent.

The results reported herein clearly indicate that in structurally parallel cases *a sulfonium group is more effective than a phosphonium group, and the latter is more effective than an arsonium group in acidifying the alpha hydrogens of the methylene group in* **3**. This relationship holds true for the permethylphenacyl 'onium salts (**3***a*, **3***e*, and **3***j*), the perphenylphenacyl 'onium salts (**3***d*, **3***i*, and **3***l*) and the per-*n*-butylphenacyl 'onium salts (**3***b* and **3***f*). Accordingly, it seems warranted to conclude that when the heteroatoms in question carry the same substituents, the effectiveness of $p\pi - d\pi$ overlap for ylid (**4**) stabilization is in the order S > P > As.

An examination of our results indicates that it is dangerous to compare the properties of 'onium salts or ylids when the heteroatoms involved do not carry the same substituents. We previously fell into this trap when comparing dimethylsulfoniumfluorenylide and triphenylphosphoniumfluorenylide (10).[3] The superficial implication of the comparison by Ratts and Yao (5) between dimethylsulfoniumphenacylides and triphenylphosphoniumphenacylides is misleading for the same reasons. Such comparisons were made in both instances due to the unavailability of the requisite similarly substituted ylids. In addition, tri-*n*-butylphosphonium–fluorenylide has been used for comparisons in place of trimethylphosphoniumfluorenylide due to the relative instability of the latter (10). Obviously, it was not a valid assumption that the electronic characteristics of the two heteroatom groups, trimethyl- and tri-*n*-butylphosphonium were virtually identical, especially when related to ylids carrying other heteroatoms.

The effect of altering the nature of the substituents on the heteroatom in **3** or **4** is consistent in all cases studied, irrespective of whether the heteroatom was arsenic, phosphorus, or sulfur. In every instance replacement of methyl

[3]In ref. 10 we reported 9-fluorenyldimethylsulfonium bromide (**5**) to be slightly more acidic than 9-fluorenyltriphenylphosphonium bromide (**6**). Using our new solvent system (7) and checking these results we have now found that the pK_a of **5** is 11.4 while that of **6** is 8.9, the latter as reported in ref. 7.

by phenyl (i.e. **3***a* to **3***c*, **3***e* to **3***g*, **3***j* to **3***k*) led to a decrease in the pK_a of the salt, usually by about one pK_a unit. Thereby were provided additional examples of an effect first noted by us in 1960 (10) and subsequently amplified in our more recent work (7). This increase in acidity has been attributed by us (7) to the powerful inductive withdrawal effect of the phenyl group (relative to alkyl) which decreases the electron density on the heteroatom. The lowered electron density on the heteroatom results in better $p\pi - d\pi$ overlap, in other words, better stabilization of the ylid by the heteroatom group.

The replacement of methyl by *n*-butyl also led to a decrease in the pK_a of the 'onium salts (**3**). This implies that *n*-butyl is electron-withdrawing (or less electron-donating) with respect to methyl. It is worth noting that the same effect has been noted by Grim *et al.* (11) in comparing the effect of methyl and *n*-butyl on the shielding of phosphorus in phosphonium salts as detected by ^{31}P nuclear magnetic resonance spectra. These authors attributed the effect to hyperconjugation differences between the two alkyl groups. We intend to explore this phenomenon further.

Although there is no exact quantitative data available, it appears that 'onium ylids with similar substitution follow a reactivity sequence of As > P > S, at least as measured by reaction with carbonyl compounds. From the pK_a data in Table I it is apparent that a basicity sequence for the same ylids is As > P > S. Thus, for similarly substituted ylids, but with different heteroatoms, nucleophilicity seems to parallel basicity. Fliszar *et al.* (6) have demonstrated such a quantitative relationship, but only within the triphenylphosphoniumphenacylide series (**2**, $X = (C_6H_5)_3P$). However, for some as yet unknown reason, this kind of relationship seems not to hold between dimethylsulfoniumfluorenylide and triphenylphosphoniumfluorenylide in light of their new pK_a values (10). We are exploring this aspect further.

Acknowledgment

The work described herein was generously supported by the National Research Council of Canada and the Petroleum Research Fund, administered by the American Chemical Society.

1. A. Wm. Johnson. Ylid chemistry. Academic Press, Inc., New York. 1966. pp. 68, 317.
2. F. S. Stephens. J. Chem. Soc. 5640, 5658 (1965).
3. A. Wm. Johnson. Ylid chemistry. Academic Press, Inc., New York. 1966. pp. 7–14, 304–308.
4. W. von E. Doering and A. K. Hoffmann. J. Am. Chem. Soc. 77, 521 (1955).
5. K. W. Ratts and A. N. Yao. J. Org. Chem. **31**, 1185 (1966).
6. S. Fliszar, R. F. Hudson, and G. Salvadori. Helv. Chem. Acta, **46**, 1580 (1963).
7. A. Wm. Johnson, S. Y. Lee, R. A. Swor, and L. D. Royer. J. Am. Chem. Soc. **88**, 1953 (1966).
8. L. A. Flexser, L. P. Hammett, and A. Dingwall. J. Am. Chem. Soc. **57**, 2103 (1935).
9. G. Aksnes and J. Songstad. Acta Chem. Scand. **18**, 655 (1964).
10. A. Wm. Johnson and R. B. LaCount. Tetrahedron, **9**, 130 (1960).
11. S. O. Grim, W. McFarlane, E. F. Davidoff, and T. J. Marks. J. Phys. Chem. **70**, 581 (1966).

Fluoranthene studies. III. A synthesis of 3-bromo-6-nitrofluorenone

E. H. Charlesworth and P. Mathiaparanam
Department of Chemistry, The University of Manitoba, Winnipeg, Manitoba

Received July 20, 1967

A synthesis of 3-bromo-6-nitrofluorenone has been accomplished by the diazotization and Pschorr cyclization of 2-amino-4-bromo-4′-nitrobenzophenone, the synthesis of which is described. The identity of the above bromonitrofluorenone with the degradative oxidation product of 9-bromo-2-nitrofluoranthene establishes unequivocally the structure of the latter substance.

Canadian Journal of Chemistry, **46**, 463 (1968)

By degradative oxidation of what was presumably 9-bromo-2-nitrofluoranthene (**1**), Charlesworth and Dolenko (1) obtained a previously unrecorded bromonitrofluorenone. Other evidence suggested that the bromine was in the 9-position of the fluoranthene nucleus and thus

Can. J. Chem. Downloaded from www.nrcresearchpress.com by 210.87.254.42 on 09/05/12
For personal use only.

by phenyl (i.e. 3*a* to 3*c*, 3*e* to 3*g*, 3*j* to 3*k*) led to a decrease in the pK_a of the salt, usually by about one pK_a unit. Thereby were provided additional examples of an effect first noted by us in 1960 (10) and subsequently amplified in our more recent work (7). This increase in acidity has been attributed by us (7) to the powerful inductive withdrawal effect of the phenyl group (relative to alkyl) which decreases the electron density on the heteroatom. The lowered electron density on the heteroatom results in better $p\pi - d\pi$ overlap, in other words, better stabilization of the ylid by the heteroatom group.

The replacement of methyl by *n*-butyl also led to a decrease in the pK_a of the 'onium salts (3). This implies that *n*-butyl is electron-withdrawing (or less electron-donating) with respect to methyl. It is worth noting that the same effect has been noted by Grim *et al.* (11) in comparing the effect of methyl and *n*-butyl on the shielding of phosphorus in phosphonium salts as detected by ^{31}P nuclear magnetic resonance spectra. These authors attributed the effect to hyperconjugation differences between the two alkyl groups. We intend to explore this phenomenon further.

Although there is no exact quantitative data available, it appears that 'onium ylids with similar substitution follow a reactivity sequence of As > P > S, at least as measured by reaction with carbonyl compounds. From the pK_a data in Table I it is apparent that a basicity sequence for the same ylids is As > P > S. Thus, for similarly substituted ylids, but with different heteroatoms, nucleophilicity seems to parallel basicity. Fliszar *et al.* (6) have demonstrated such a quantitative relationship, but only within the triphenylphosphoniumphenacylide series (2, $X = (C_6H_5)_3P$). However, for some as yet unknown reason, this kind of relationship seems not to hold between dimethylsulfoniumfluorenylide and triphenylphosphoniumfluorenylide in light of their new pK_a values (10). We are exploring this aspect further.

Acknowledgment

The work described herein was generously supported by the National Research Council of Canada and the Petroleum Research Fund, administered by the American Chemical Society.

1. A. Wm. Johnson. Ylid chemistry. Academic Press, Inc., New York. 1966. pp. 68, 317.
2. F. S. Stephens. J. Chem. Soc. 5640, 5658 (1965).
3. A. Wm. Johnson. Ylid chemistry. Academic Press, Inc., New York. 1966. pp. 7–14, 304–308.
4. W. von E. Doering and A. K. Hoffmann. J. Am. Chem. Soc. 77, 521 (1955).
5. K. W. Ratts and A. N. Yao. J. Org. Chem. **31**, 1185 (1966).
6. S. Fliszar, R. F. Hudson, and G. Salvadori. Helv. Chem. Acta, **46**, 1580 (1963).
7. A. Wm. Johnson, S. Y. Lee, R. A. Swor, and L. D. Royer. J. Am. Chem. Soc. **88**, 1953 (1966).
8. L. A. Flexser, L. P. Hammett, and A. Dingwall. J. Am. Chem. Soc. **57**, 2103 (1935).
9. G. Aksnes and J. Songstad. Acta Chem. Scand. **18**, 655 (1964).
10. A. Wm. Johnson and R. B. LaCount. Tetrahedron, **9**, 130 (1960).
11. S. O. Grim, W. McFarlane, E. F. Davidoff, and T. J. Marks. J. Phys. Chem. **70**, 581 (1966).

Fluoranthene studies. III. A synthesis of 3-bromo-6-nitrofluorenone

E. H. Charlesworth and P. Mathiaparanam
Department of Chemistry, The University of Manitoba, Winnipeg, Manitoba

Received July 20, 1967

A synthesis of 3-bromo-6-nitrofluorenone has been accomplished by the diazotization and Pschorr cyclization of 2-amino-4-bromo-4′-nitrobenzophenone, the synthesis of which is described. The identity of the above bromonitrofluorenone with the degradative oxidation product of 9-bromo-2-nitrofluoranthene establishes unequivocally the structure of the latter substance.

Canadian Journal of Chemistry, **46**, 463 (1968)

By degradative oxidation of what was presumably 9-bromo-2-nitrofluoranthene (**1**), Charlesworth and Dolenko (1) obtained a previously unrecorded bromonitrofluorenone. Other evidence suggested that the bromine was in the 9-position of the fluoranthene nucleus and thus

Can. J. Chem. Downloaded from www.nrcresearchpress.com by 210.87.254.5 on 09/05/12
For personal use only.

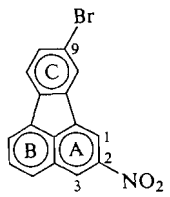

1

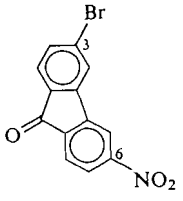

2

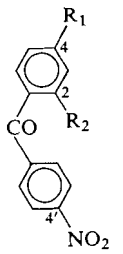

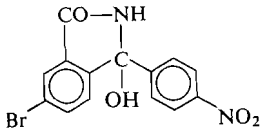

10

3 $R_1 = NH_2$, $R_2 = CH_3$
4 $R_1 = Br$, $R_2 = CH_3$
5 $R_1 = Br$, $R_2 = COOH$
6 $R_1 = Br$, $R_2 = COCl$
7 $R_1 = Br$, $R_2 = CONH_2$
8 $R_1 = Br$, $R_2 = NH_2$
9 $R_1 = Br$, $R_2 = OH$

that the degradation product was 3-bromo-6-nitrofluorenone (**2**). It seemed desirable to synthesize this substance by an unambiguous method which would leave no doubt as to its structure and that of the 9-bromo-2-nitrofluoranthene.

From the variety of methods in the literature for the synthesis of substituted fluorenones, the most hopeful seemed to be the general method of Miller and Bachman (2) which involves a Pschorr cyclization of 2-aminobenzophenones. Two variations of the scheme were attempted. 4-Nitroanthranilic acid was tosylated and converted to its acid chloride. The tosylated acid chloride, however, failed to go into a Friedel–Crafts reaction with bromobenzene. The second variation was successful. 4-Amino-2-methyl-4′-nitrobenzophenone (**3**) was prepared by a Friedel–Crafts reaction following the directions of Mehta, Sacha, and Patel (3). By a Sandmeyer reaction the amino group was replaced by bromine (**4**). The methyl group was oxidized to carboxyl (**5**) and then by means of a Curtius degradation the 2-amino compound **8** was finally obtained. Diazotization of **8** and Pschorr cyclization yielded the 3-bromo-6-nitrofluorenone (**2**), somewhat purer than that obtained by Charlesworth and Dolenko (1). No depression in melting point occurred on mixing and both samples gave identical infrared spectra.

We were unable to obtain the amine **8** by the Hofmann degradation of the amide **7**. An acidic compound was produced which might possess the pseudo structure **10**, as suggested for similar compounds by Bhatt (4).

Experimental

A supply of 4-amino-2-methyl-4′-nitrobenzophenone (**3**) was prepared by a Friedel–Crafts reaction between *p*-nitrobenzoyl chloride and *m*-acetotoluidide according to the directions of Mehta, Sacha, and Patel (3). This product was obtained as red, elongated prisms which melted at 164–166 °C. The original authors reported a melting point of 159–161 °C.

Anal. Calcd. for $C_{14}H_{12}O_3N_2$: N, 10.93. Found: N, 10.98.

4-Bromo-2-methyl-4′-nitrobenzophenone (*4*)

4-Amino-2-methyl-4′-nitrobenzophenone (16 g) was dissolved in hot hydrobromic acid (75 ml, 48%) and cooled to 0 °C by the addition of ice. The amino compound was diazotized by the slow addition of a solution of sodium nitrite (6.0 g) in water (30 ml). After standing at 0 °C for 15 min, the diazonium salt solution was poured into a boiling solution of cuprous bromide (92 g) in hydrobromic acid (200 ml, 48%) at such a rate that the boiling was not interrupted. The boiling was continued for a further 30 min. After cooling and dilution with water, a reddish-white solid precipitated, which was filtered, dried, and extracted with benzene. The benzene solution was washed successively with solutions of sodium sulfite (5%) and sodium hydroxide (10%) and finally with water. After drying with calcium chloride and removal of the benzene, the crude residue was crystallized from acetone. The 4-bromo-2-methyl-4′-nitrobenzophenone (17.2 g) melted at 110–111 °C.

Anal. Calcd. for $C_{14}H_{10}O_3N$ Br: N, 4.38; Br, 25.0. Found: N, 4.27; Br, 25.1.

2-(p-Nitrobenzoyl)-5-bromobenzoic acid (*5*)

4-Bromo-2-methyl-4′-nitrobenzophenone (15.6 g) was dissolved under reflux in hot acetic acid (45 ml). An oxidizing solution of chromium trioxide (13.2 g), acetic acid (45 ml), concentrated sulfuric acid (15 ml), and water (30 ml) was added to the ketone at such a rate that the temperature was kept just below the boiling point. The mixture was refluxed for 3 h, cooled, and diluted with water. The precipitated solid was filtered and washed with water until white. It was suspended in hot water and potassium hydroxide solution added to dissolve as much of the acid as possible. The mixture was filtered and acidified with concentrated hydrochloric acid. The precipitated acid was collected and recrystallized from ethanol. It (13.2 g) melted at 194–196 °C.

Can. J. Chem. Downloaded from www.nrcresearchpress.com by 210.87.254.5 on 09/05/12
For personal use only.

Can. J. Chem. Downloaded from www.nrcresearchpress.com by 210.87.254.5 on 09/05/12
For personal use only.

Anal. Calcd. for $C_{14}H_8O_5N$ Br: N, 4.00; Br, 22.8. Found: N, 3.96; Br, 23.0.

5-Bromo-2-(p-nitrobenzoyl)benzoyl Chloride (6)

The acid chloride was prepared from the acid (5.5 g) by treatment with thionyl chloride (10 ml) in the usual manner in benzene (40 ml) as solvent. 5-Bromo-2-(*p*-nitrobenzoyl)benzoyl chloride (4.2 g) melted at 124–126 °C.

Anal. Calcd. for $C_{14}H_7O_4NClBr$: N, 3.80; Cl, 9.62; Br, 21.7. Found: N, 3.68; Cl, 9.37; Br, 21.9.

5-Bromo-2-(p-nitrobenzoyl)benzamide (7)

The above acid chloride (8.5 g) was dissolved in benzene and with cooling slowly treated with ammonia solution (100 ml, *d* 0.88). The crude pasty mass of amide was filtered and washed several times with hot water. It was recrystallized from ethanol. 5-Bromo-2-(*p*-nitrobenzoyl)-benzamide (8.0 g) melted at 239–240 °C.

Anal. Calcd. for $C_{14}H_9O_4N_2Br$: C, 48.2; H, 2.60; N, 8.03; Br, 22.9. Found: C, 47.9; H, 2.55; N, 8.04; Br, 22.9.

2-Amino-4-bromo-4′-nitrobenzophenone (8)

(a) By the Curtius Method

Sodium azide (0.75 g) activated as described (6) was dissolved in water (2.0 ml) and added to a cold solution of 5-bromo-2-(*p*-nitrobenzoyl)benzoyl chloride (1.5 g) in acetone (20 ml). The reaction mixture was stirred for 15 min and the solid which had precipitated was filtered and dried *in vacuo*. The acid azide (1.5 g) thus obtained melted at 99–101 °C.

The dry azide was dissolved by refluxing for 2 h with benzene (25 ml). After cooling, potassium hydroxide solution (15 ml, 50%) was added and the mixture was warmed on a water bath during which time a yellow solid separated. The benzene was removed by vacuum distillation and the suspension cooled and filtered. The solid was treated with hot concentrated hydrochloric acid and the hot solution filtered through a sintered glass funnel. After cooling the amine was precipitated by the addition of 10% sodium hydroxide solution, collected, and dried. It was recrystallized from pyridine as bright-yellow needles (1.2 g) which melted at 213–214 °C.

Anal. Calcd. for $C_{13}H_9O_3N_2Br$: N, 8.73; Br, 24.9. Found: N, 8.71; Br, 24.4.

(b) By the Hofmann Method

A number of attempts to obtain the amine **8** by the Hofmann degradation of the amide **7** with sodium hypobromite or sodium hypochlorite were unsuccessful. Acidification at the end of the treatment gave a substantial yield of a product which crystallized from alcohol as yellow plates, m.p. 232–233 °C. This substance has not been identified. Color, melting point depression on mixing, and its greater solubility in sodium hydroxide solution indicate it is not the original amide. It is acidic (soluble in sodium hydroxide) and not identical with the amine obtained by the Curtius method. It might have the tautomeric pseudo structure **10** as suggested for similar compounds by Bhatt (4).

Anal. Calcd. for $C_{14}H_9O_4N_2Br$ (amide or ψ-amide): C, 48.2; H, 2.60; N, 8.03; Br, 22.9. Found: C, 48.3; H, 2.77; N, 7.99; Br, 23.1.

3-Bromo-6-nitrofluorenone (2)

2-Amino-4-bromo-4′-nitrobenzophenone (0.8 g) was dissolved in concentrated sulfuric acid (2.0 ml) and a few drops of water were added. The amine sulfate separated as a fine suspension which was cooled to 0 °C. An ice-cold solution of sodium nitrite (0.2 g) in water (2.0 ml) was added. The amine sulfate first dissolved and a solid compound separated. On warming, this product dissolved and then a yellow solid separated which was collected by filtration and washed with sodium hydroxide solution (10%) and then with water. The dried 3-bromo-6-nitrofluorenone crystallized from nitrobenzene as bright-yellow plates (0.3 g) which melted at 339–341 °C.

Anal. Calcd. for $C_{13}H_6O_3NBr$: N, 4.61; Br, 26.3. Found: N, 4.72; Br, 26.2.

There was no depression of melting point of this product on the addition of a little of the sample produced by Charlesworth and Dolenko (1). Comparison of the infrared spectra of the two specimens also confirmed their identity.

The oxime of 3-bromo-6-nitrofluorenone was prepared by refluxing the ketone with a solution of hydroxylamine hydrochloride in ethanol for 2 h. On cooling a pale-yellow product separated. After recrystallization from ethanol it melted at 269–270 °C.

Anal. Calcd. for $C_{13}H_7O_3N_2Br$: N, 8.78; Br, 25.0. Found: N, 8.70; Br, 25.4.

Acidification of the sodium hydroxide washings from the preparation of the ketone mentioned above gave a yellow product (0.26 g) which crystallized from aqueous ethanol in light-yellow needles. These melted at 150–151 °C and were presumably 2-hydroxy-4-bromo-4′-nitrobenzophenone (**9**) produced in a side reaction.

Anal. Calcd. for $C_{13}H_8O_4N$ Br: N, 4.35; Br, 24.8. Found: N, 4.55; Br, 24.9.

4-Nitro-2-(p-toluenesulphonamido)benzoic Acid (4-Nitro-p-tosylanthranilic acid)

This previously unreported derivative was made from 4-nitroanthranilic acid and *p*-toluene sulfonyl chloride following the directions of Scheifele and DeTar (5). The crude product crystallized from ethanol in pale-yellow plates, m.p. 225–226 °C.

Anal. Calcd. for $C_{14}H_{12}O_6N_2S$: N, 8.33; S, 9.52. Found: N, 8.35; S, 9.46.

Friedel–Crafts reactions with phosphorus pentachloride, aluminium chloride, and bromobenzene failed to give any 2-amino-4-bromo-4′-nitrobenzophenone (**8**).

Acknowledgments

The authors are grateful to the National Research Council of Canada for a grant-in-aid of this research and to the Canadian Commonwealth Scholarship and Fellowship Committee for the award of a Scholarship to one of us (P.M.).

1. E. H. Charlesworth and A. J. Dolenko. Can. J. Chem. **45**, 96 (1967).
2. H. F. Miller and G. B. Bachman. J. Am. Chem. Soc. **57**, 2443 (1935).
3. V. K. Mehta, M. J. Sacha, and S. R. Patel. J. Indian Chem. Soc. **33**, 867 (1956).
4. M. V. Bhatt. Tetrahedron, **20**, 803 (1964).
5. H. J. Scheifele and D. F. DeTar. Organic Syntheses. Collective Vol. IV. John Wiley and Sons, Inc., New York. 1963. p. 34.
6. P. A. Smith. Org. Reactions, **3**, 382 (1946).

Preparation of *cis*-crotonyl chloride[1]

M. B. HOCKING
Exploratory Research Laboratory, Dow Chemical of Canada, Limited, Sarnia, Ontario

Received August 18, 1967

Published methods for the preparation of *cis*-crotonyl chloride were found to give a product contaminated with appreciable proportions of the *trans* isomer. Separation of these two isomers was found to be impossible because of the small boiling point difference and the readiness with which the *cis* acid chloride isomerizes to the *trans*. Herein are outlined the precautions necessary to obtain pure *cis*-crotonyl chloride contaminated only with the free acid, from which it is readily separated by cold distillation.

Canadian Journal of Chemistry, 46, 466 (1968)

Can. J. Chem. Downloaded from www.nrcresearchpress.com by 210.87.254.40 on 09/05/12
For personal use only.

The preparation of *cis*-crotonyl chloride has been given cursory description in the literature (1–3) but in our hands, perhaps because of the paucity of experimental detail in the earlier reports, these preparations consistently gave large proportions of *trans*. The recent publication by Lee (4) of a fairly general route to the acid chlorides of sensitive acids using postulated phosphonium salt intermediates prompted experiments along these lines with little success. However, in the course of this work a procedure using neat thionyl chloride was evolved by which high purity *cis* chloride can be obtained.

$$Ph_3\overset{\oplus}{P}CCl_3\overset{\ominus}{Cl} + RCOOH \rightarrow Ph_3\overset{\oplus}{P}(Cl^{\ominus})(O{=}C{-}R) + CHCl_3$$

$$Ph_3\overset{\oplus}{P}(Cl^{\ominus})(O{=}C{-}R) \rightarrow Ph_3PO + RCOCl$$

When Lee's method was tried a 30% conversion of the *cis* acid was obtained but examination of the product by nuclear magnetic resonance showed that it was mainly (80%) *trans*. An oil which separated during the reaction analyzed as a mixture of triphenylphosphine – carbon tetrachloride complex and crotonyl triphenylphosphonium chloride. Either of these salts may have catalyzed the isomerization of *cis* acid or acid chloride (5) to the *trans*, or it might have been a purely thermal process. In any case, neither of the latter conditions could be avoided, and despite the likelihood of improvement with a trialkylphosphine in place of the triarylphosphine (6), this approach to *cis*-crotonyl chloride was discontinued.

[1]Contribution No. 151 from the Dow Chemical of Canada Exploratory Research Laboratory, Sarnia, Ontario.

Even with dimethylformamide (7) or sodium chloride (8) catalysis, reaction of the *cis* acid with thionyl chloride in boiling ether was very slow. Neat thionyl chloride under relatively mild conditions gave a rapid reaction but the product was largely *trans*. To avoid acid catalysis of isomerization (5) pyridine was employed, but unfortunately the simultaneous catalytic effect of pyridine (9) resulted in vigorous reaction and extensive charring.

It appears that successful preparations of *cis*-crotonyl chloride are possible using neat thionyl chloride if it is carried out as a rapid low temperature conversion, with immediate purification. Fast isolation of the *cis* acid chloride when formed was necessary to avoid its rapid isomerization from reaction by-products present, and was only possible by distillation at low temperatures. The crude *cis* acid chloride obtained, containing some unreacted *cis* acid, sulfur dioxide, and HCl, possessed only reasonable geometrical stability on cold storage. However, the distilled product, 97% *cis*-crotonyl chloride, was still 93.5% *cis* after two months at −20°.

Experimental

Melting points and boiling points are uncorrected. Infrared spectra were obtained on a Perkin–Elmer model 337 grating spectrometer on thin films between rock salt plates. Nuclear magnetic resonance (n.m.r.) spectra were obtained on a Varian A60 instrument fitted with a phase detector integrator. Sweep width calibration was by the side band technique using the combination of a wide range oscillator and an electronic counter (Hewlett–Packard models 200CD, and 5212A respectively). All n.m.r. data were obtained at room temperature on deuteriochloroform solutions. Shifts are reported on the centers of spin–spin multiplets in c.p.s. downfield from internal tetramethylsilane. Crotonic acid used was 97% *cis* checked by n.m.r.

TABLE I

Nuclear magnetic resonance data* for *cis*- and *trans*-crotonyl chloride†

Protons	Multiplicity	*Trans* chloride		*Cis* chloride	
		Shifts	Coupling	Shifts	Coupling
δ_a	Double doublet	124.2	$J_{a,b} = 7.1$ $J_{a,c} = 1.8$	128.2	$J_{a,b} = 6.8$ $J_{a,c} = 1.4$
δ_b	Overlapping quartet pair	448.8	$J_{b,a} = 7.1$ $J_{b,c} = 15.2$	393.0	$J_{b,a} = 6.8$ $J_{b,c} = 11.0$
δ_c	Well-differentiated quartet pair	376.0	$J_{c,a} = 1.8$ $J_{c,b} = 15.2$	368.3	$J_{c,a} = 1.4$ $J_{c,b} = 11.0$

*Couplings measured on appropriate portions of the spectra expanded to 100 c.p.s. sweep width, given in c.p.s.
†CH_3—CH=CHCOCl; where CH_3 protons are H_a, CH—Me protons are H_b, and COCH= protons are H_c.

Preparation of Cis-crotonyl Chloride

(a) Triphenylphosphine Method

Cis-crotonic acid (4.3 g, 0.05 mole) and triphenylphosphine (13.1 g, 0.05 mole) dissolved in cold dry carbon tetrachloride (125 ml) was left to stand at room temperature with protection from atmospheric moisture for 2 h. No detectable (by the relative intensities of acid chloride carbonyl to acid carbonyl frequencies in the infrared) acid chloride formed during this time. The solution was then boiled under reflux for 2½ h, which converted about 30% of the acid to acid chloride; an upper yellow viscous phase was formed. The two phases were allowed to cool to room temperature and the solution was decanted from the viscous gum (12.6 g). Cold hexane (125 ml) added to the decanted solution precipitated 5.1 g of triphenylphosphine oxide (m.p. and mixture m.p. of a small recrystallized portion; 153–155°). Solvent removal from the mother liquor and distillation, both under reduced pressure, yielded 0.4 ml (9%) of crotonyl chloride (b.p. 60–70°/100 mm) which n.m.r. analysis showed was 80% *trans*, 20% *cis*. The gum (infrared maxima at 1440 (P—Ph), 1710 (C=O), and broad bands with fine structure centered at 2550 and 2850 cm^{-1}) was soluble in water, insoluble in benzene, and the analysis was intermediate between those calculated for the salts of triphenylphosphine with carbon tetrachloride and with crotonyl chloride.

Anal. Calcd. for $C_{19}H_{15}Cl_4P$ (gum formed by triphenylphosphine and carbon tetrachloride): C, 54.8; H, 3.6; Cl, 33.9. Anal. Calcd. for $C_{22}H_{20}ClP$ (gum formed by triphenylphosphine and crotonyl chloride): C, 69.5; H, 5.5; Cl, 9.7. Found: C, 53.8; H, 4.3; Cl, 26.3.

Elemental analysis of a portion of the gum which had been evacuated (100° at 14 mm) for 1 h had changed considerably, but the infrared was unaffected, both probably due to the loss of dissolved CCl_4.

Found: C, 60.2; H, 4.9; Cl, 17.8.

(b) Thionyl Chloride Method

Equimolar amounts of thionyl chloride and the *cis* acid in boiling ether had only achieved about 50% conversion in 16 h. The addition of a few drops of dimethylformamide to the reaction carried out in methylene chloride – ether (50:50) still took 28 h for completion; similar results were found on addition of NaCl in place of the dimethylformamide. Stirred equimolar proportions of pyridine and thionyl chloride in cold ether (salt separates) to which *cis* acid in cold ether was added gave very vigorous reactions resulting in black tars.

The following method resulted in no geometrical isomerization. Freshly redistilled thionyl chloride (40 ml; 0.56 mole) cooled to 0° was added over 1 min to gently swirled *cis*-crotonic acid (52 g, 0.62 mole) in an ice bath. A few carbon boiling chips were added, a drying tube ($CaSO_4$) was fitted, and the reaction flask kept in the ice bath with occasional swirling for 1½ h. Then, with the flask still in the ice bath, aspirator vacuum (about 14 mm) was applied for 1 h. Analysis of the crude reaction mixture (68 g) by n.m.r. showed 14% was unreacted acid, but of the acid chloride present 97% was *cis*. Distillation of this material using a 30 cm Widmer column water-jacketed to +5°, a condenser brine-cooled to −10°, and a vacuum-jacketed head yielded 35 g (56%) of 97% *cis*-crotonyl chloride (b.p. <23.5°/10 mm, pot 10 to 25°) containing no free acid.

Identification and Analysis of Mixtures

The geometry of the acid chloride obtained was confirmed by conversion to the amide. Dry ammonia gas was passed over the surface of a stirred, ice-bath cooled, ethereal solution of *cis*-crotonyl chloride. The ether was evaporated off in a stream of air and the residual white solid extracted with hot benzene, filtered, and the benzene solution concentrated and cooled yielding fluffy white needles (m.p. 105–108°). The literature quotes 102° (2) for the *cis* and 160° (10) for the *trans* amides.

Easy analyses of mixtures of *cis* and *trans* acid chlorides with no chance of fractionation or isomerization were carried out by integration of the methyl region of n.m.r. spectra expanded to 100 cycles sweep width. Data found for each isomer on its own are given in Table I. The presence of unreacted *cis* acid, n.m.r. data on which have appeared earlier (11), was also readily determined by integration of the n.m.r. spectrum.

Acknowledgments

The author thanks Mr. H. D. Mak of this laboratory for the n.m.r. spectra required for this work and one of his referees for suggesting the inclusion of the "In Press" publication of ref. 6.

1. J. P. MASON. Ph.D. Thesis, Princeton University, Princeton, N.J. 1927. p. 12; L. W. JONES and J. P. MASON. J. Am. Chem. Soc. **49**, 2534 (1927).

Can. J. Chem. Downloaded from www.nrcresearchpress.com by 210.87.254.40 on 09/05/12
For personal use only.

2. R. STOERMER and E. ROBERT. Ber. **55**, I, 1030 (1922).
3. W. AUTENREITH and P. SPIESS. Ber. **34**, 191 (1901).
4. J. B. LEE. J. Am. Chem. Soc. **88**, 3440 (1966).
5. W. HUCKEL. Theoretical principles of organic chemistry. Vol. I. Elsevier Publishing Co., New York. 1955. p. 522.
6. S. S. H. GILANI and J. HOOZ. Personal communication; I. M. DOWNIE and J. B. LEE. Tetrahedron, in press. 1967.
7. H. H. BOSSHARD, R. MORY, M. SCHMID, and H. ZOLLINGER. Helv. Chim. Acta, **42**, 1653 (1959).
8. M. YA. KRAFT and V. V. KATYSHKINA. Dokl. Akad. Nauk S.S.S.R., **109**, 312 (1956); Chem. Abstr. **51**, 1832 (1957).
9. J. F. NORRIS and A. E. BEARSE. J. Am. Chem. Soc. **62**, 953 (1940).
10. R. KUHN, F. KÖHLER, and L. KÖHLER. Z. Physiol. Chem. **247**, 206 (1937).
11. C. RAPPE. Acta Chem. Scand. **17**, 2766 (1963); V. J. KOWALEWSKI and D. G. DEKOWALEWSKI. J. Chem. Phys. **33**, 1794 (1960).

Can. J. Chem. Downloaded from www.nrcresearchpress.com by 210.87.254.40 on 09/05/12
For personal use only.

Erratum: Desert plant constituents. II. Ocotillol: An intermediate in the oxidation of hydroxy isooctenyl side chains

E. W. WARNHOFF AND C. M. M. HALLS
Department of Chemistry, University of Western Ontario, London, Ontario

Received October 27, 1967

(Ref.: Can. J. Chem. **43**, 3311 (1965))

Canadian Journal of Chemistry, **46**, 468 (1968)

On p. 3317, the eleventh line of the first paragraph should read as follows:

. . . "Further extraction of this bark with methanol gave . . . etc."

Erratum: Mechanism of the ninhydrin reaction. II. Preparation and spectral properties of reaction products from primary aromatic amines and ninhydrin hydrate

MENDEL FRIEDMAN
Northern Regional Research Laboratory, Northern Utilization Research and Development Division, Agriculture Research Service, U.S. Department of Agriculture, Peoria, Illinois

Received October 27, 1967

(Ref.: Can. J. Chem. **45**, 2271 (1967))

Canadian Journal of Chemistry, **46**, 468 (1968)

On p. 2271, lines 4 and 5 in the second column, should read:
. . . "from *p*- and *o*-aminophenol (IV and IV*b*) . . ." etc.

On p. 2272, structure IV should be

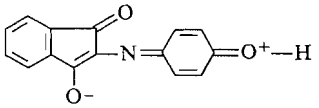

and not

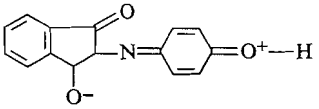

and structure IV*b* should be

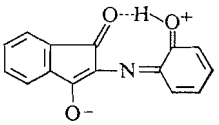

and not

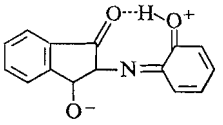

Can. J. Chem. Downloaded from www.nrcresearchpress.com by 210.87.254.6 on 09/05/12
For personal use only.

Fixation of atmospheric nitrogen by ruthenium compounds

A. D. ALLEN AND F. BOTTOMLEY
Lash Miller Chemistry Laboratories, University of Toronto, Toronto, Ontario

Received January 17, 1968

Allen and Senoff's ion $[Ru(NH_3)_5N_2]^{2+}$, prepared from gaseous nitrogen by Harrison and Taube, has now been prepared from the nitrogen in the atmosphere.

Canadian Journal of Chemistry, 46, 469 (1968)

Following Harrison and Taube's successful preparation (1) of Allen and Senoff's ion $[Ru(NH_3)_5N_2]^{2+}$ (2) from gaseous nitrogen, we now report its preparation from the nitrogen in the atmosphere.

A solution about 0.1 *M* in $[Ru^{III}(NH_3)_5Cl]Cl_2$ in 0.1 *M* H_2SO_4 was reduced with amalgamated zinc under argon until the solution became neutral. A stream of air was then drawn through the solution until a pink color developed (presumably due to $[Ru^{III}(NH_3)_5OH]^{2+}$). The air was replaced by argon and, after the air had been expelled from the flask, a further portion of acid was added. Reduction was allowed to proceed under argon until the solution was again neutral, at which time the argon was again replaced by air. These steps were repeated for 5–7 h, until no pink color developed on passing air through the solution for 45 min. A final portion of acid was then added under argon, to reduce any remaining ruthenium(III) and dissolve any zinc hydroxide. At this stage the electronic spectrum of the solution showed a strong band at 263 mμ and a weak band at 221 mμ. Addition of a filtered solution of sodium fluoborate to the filtered reaction solution gave a yellow precipitate. The infrared and electronic spectrum of this precipitate showed that it was mainly $[(NH_3)_5Ru{-}N_2{-}Ru(NH_3)_5]^{4+}$ (3), with some $[Ru(NH_3)_5N_2]^{2+}$. On warming with concentrated aqueous ammonia it was converted into $[Ru(NH_3)_5N_2]^{2+}$, which was precipitated as the fluoborate salt and identified by its electronic and infrared spectrum (4). A control experiment in which argon was used throughout gave no indication of the formation of a nitrogen compound.

This preparation is a very important development in the story of nitrogen – transition metal complexes, since it is the first time it has been demonstrated that it is possible to prepare such compounds from atmospheric nitrogen. It appears, from these experiments, that N_2 is an effective nucleophile for ruthenium(II), even in competition with oxidation by O_2. This opens up new possibilities for the direct utilization of atmospheric nitrogen and is an important step towards our understanding of biological nitrogen fixation.

1. D. E. HARRISON and H. TAUBE. J. Am. Chem. Soc. **89**, 5706 (1967).
2. A. D. ALLEN and C. V. SENOFF. Chem. Commun. 621 (1965).
3. D. E. HARRISON, E. WEISSBERGER, and H. TAUBE. Private communication. To be published.
4. A. D. ALLEN, F. BOTTOMLEY, R. O. HARRIS, V. P. REINSALU, and C. V. SENOFF. J. Am. Chem. Soc. **89**, 5595 (1967).

Can. J. Chem. Downloaded from www.nrcresearchpress.com by 210.87.254.40 on 09/05/12
For personal use only.

Canadian Journal of Chemistry

Published by THE NATIONAL RESEARCH COUNCIL OF CANADA

VOLUME 46 FEBRUARY 15, 1968 NUMBER 4

Crystal and molecular structure of the pyridine solvate of bis(8-hydroxyquinoline)silver(I)

J. E. FLEMING[1] AND H. LYNTON[2]

Department of Chemistry, University of Victoria, Victoria, British Columbia

Received June 20, 1967

Crystals of the pyridine solvate of bis(8-hydroxyquinoline)silver(I), $Ag(C_9H_6NO)C_9H_6NOH.C_5H_5N$, are monoclinic, space group $P2_1/a$, with cell dimensions $a = 10.87 \pm 0.01$ Å, $b = 10.65 \pm 0.01$ Å, $c = 16.70 \pm 0.01$ Å, $\beta = 92.6 \pm 0.2°$, $Z = 4$. Atomic parameters have been determined from a three-dimensional analysis using 2163 independent intensities to which no absorption corrections were applied. Refinement was by observed and calculated differential syntheses using isotropic temperature factors. The final discrepancy index is $R = 0.116$.

The coordination of the silver atom is distorted tetrahedral, with bonds to the phenolic oxygen and ring nitrogen atoms of both 8-hydroxyquinoline molecules. Adjacent bis(8-hydroxyquinoline)silver molecules are linked by a hydrogen bond between two oxygen atoms. The pyridine molecules are held in the lattice by van der Waals' forces.

Canadian Journal of Chemistry, **46**, 471 (1968)

Introduction

The reaction of 8-hydroxyquinoline with silver(I) ion to give a metal chelate is well established (1, 2). Both a yellow and a green form have been prepared and it has been shown that the two are identical, with the green form containing a small amount of free silver (3). The chelate has the structure $Ag(C_9H_6NO)C_9H_6NOH$, and is diamagnetic, as expected for a silver(I) compound (2). Thermal decomposition curves show that it is not possible to remove one of the 8-hydroxyquinoline molecules to leave the 1:1 chelate $Ag(C_6H_9NO)$ (4). This indicates that both 8-hydroxyquinoline molecules are bonded directly to the central silver atom.

In a recent study of the extraction into chloroform of Ag(I) ion with 8-hydroxyquinoline, measurement of stability constants led Hala (5) to conclude that the 8-hydroxyquinoline molecules act as bidentate ligands and that the structure is tetrahedral. A literature survey shows that evidence for a tetrahedral arrangement around the silver atom in Ag(I) compounds with coordination number four has been reported in several papers. Preliminary X-ray investigations of tetrakisthioacetamide-argentous chloride (6), tetrakis(monoiodotrialkylphosphinesilver), and tetrakis(monoiodotrialkylarsinesilver) (7), and the completed structure determinations by Brink *et al.* of Cs_2AgCl_3, Cs_2AgI_3, Rb_2AgI_3, K_2AgI_3, $(NH_4)_2AgI_3$, and $CsAg_2I_3$ (8–10) support this view, as do the studies of Hall, Plowman, and Preston on the infrared spectra and conductivities in nitrobenzene of some complexes of Ag(I) (11).

Crystallographic Data

A specimen of the compound was prepared by the method of Nakatsuka (1), and recrystallized from pyridine to give thin yellow needles of the adduct $Ag(C_6H_9NO)C_6H_9NOH.C_5H_5N$. Magnetic susceptibility measurements showed the compound to be diamagnetic as expected.

The space group was established as $P2_1/a$, and precise cell dimensions were determined using Weissenberg photographs calibrated with aluminium powder. The crystal data are given in Table I.

Intensity Data

The crystal chosen for intensity data collection was about 0.25 mm long and had a roughly

[1]Present address: Christ's Hospital, Hertford, Herts., England.

[2]Present address: Department of Chemistry, University of New Brunswick, Fredericton, New Brunswick.

square cross section with an average thickness of 0.17 mm. The long direction corresponded to the a crystallographic axis. The calculated optimum thickness, $2/\mu$, was 0.23 mm. No absorption corrections were applied to the data.

TABLE I

Crystal data for $Ag(C_9H_6NO)C_9H_6NOH.C_5H_5N$

System	Monoclinic
Molecular weight	476.3
Space group	$P2_1/a$
a	10.87±0.01 Å
b	10.65±0.01 Å
c	16.70±0.01 Å
β	92.6±0.2°
V	1 931 Å^3
D_m (by flotation)	1.63 g cm^{-3}
Z	4
D_c	1.64 g cm^{-3}
μ, absorption coefficient for Cu Kα	87.4 cm^{-1}
Systematic absences	$h0l$: $h = 2n + 1$ $0k0$: $k = 2n + 1$

Using the multiple filmpack technique, equi-inclination Weissenberg photographs were taken of the $h0l$, $hk0$, and $0kl$–$8kl$ layers. There were calculated to be 4510 permitted independent reflections within the range of the Cu Kα radiation; 3555 reflections were within the range covered by the photographs, and 2163 of these were above the minimum intensity limit for observation.

The intensities of all reflections were estimated by visual comparison with a calibration strip prepared using a suitable reflection from the intensity crystal. Lorentz-polarization factors were then applied to all intensity data.

Structure Analysis

Patterson syntheses[3] were computed for the $hk0$, $h0l$, and $0kl$ zones and from these syntheses the positions of the silver atoms were found unambiguously.

A three-dimensional Fourier synthesis was computed and from this, the coordinates of all other atoms in the structure were derived. It was noted that, whilst the electron density distribution in the region of the two 8-hydroxyquinoline rings was well shaped, the electron density distribution in the pyridine ring was somewhat irregular.

[3]All computations were carried out on an I.B.M. 1620 computer using the programs of Ahmed, Gabe, Mair, and Pippy (12).

The atomic coordinates were refined by means of observed and calculated differential syntheses. Initially all atoms of the same element were given the same isotropic temperature factor. Temperature factors were then adjusted individually during the refinement.

No difficulty was experienced in refining the positions of the atoms in the 8-hydroxyquinoline molecules, and after several cycles had reduced the shifts to small values, the atomic arrangement in these molecules was in good agreement with that found in other metal chelates containing 8-hydroxyquinoline. In the pyridine molecule, however, the two atoms designated C(11) and C(12) had positions which would have given interatomic distances incompatible with what is known of the geometry of the pyridine ring (13–15). The nitrogen atom could not be identified at this stage, so all pyridine atoms were given carbon scattering factors.

All high intensity reflections in the range $\sin^2\theta < 0.100$ were examined to see if any appeared to show extinction. There were 22 reflections for which $|F_o| \ll |F_c|$. The $|F_o|$ values of these reflections were modified by adding either 1/4, 1/2, or 3/4 $|\Delta F|$ depending on the magnitude of $|F_c|$, $\sin^2\theta$, and $|\Delta F|/|F_o|$ for that particular reflection. Initially, the scaling of the intensities had used only reflections common to two or more photographs. The progress of the analysis now permitted each layer of reflections to be scaled directly with the model.

Refinement was continued. The 8-hydroxyquinoline molecules had large shifts indicated on the first cycle only, and their refinement appeared to be near completion. The positions of atoms C(11) and C(12) were still improbable. The remaining four atoms refined sufficiently for tentative identification of the nitrogen atom, and the appropriate scattering curve was applied to this atom.

Assuming a planar symmetric ring for the pyridine molecule and carbon–carbon distances of the order of 1.4 Å (13–15), possible positions for C(11) and C(12) were calculated. These were found to be positions of appreciable electron density (see Table III). These coordinates were used in the calculation of the final set of structure factors. The temperature factors assigned to C(11) and C(12) were an average of those used for the other pyridine ring atoms.

The refinement was stopped when the atomic coordinates of all the atoms undergoing refine-

Can. J. Chem. Downloaded from www.nrcresearchpress.com by 210.87.254.40 on 09/05/12
For personal use only.

Can. J. Chem. Downloaded from www.nrcresearchpress.com by 210.87.254.40 on 09/05/12
For personal use only.

ment began to oscillate, and when the adjustment of the temperature factors had given good agreement between observed and calculated values of the electron densities, slopes, and curvatures. At this stage the average coordinate shift indicated for the 8-hydroxyquinoline atoms was 0.001 Å (less than one fifth of the e.s.d.) for the atoms in the pyridine molecule 0.01 Å.

Results

The final coordinates are listed in Table II, and the electron densities, mean curvatures, and isotropic temperature parameters in Table III. The arrangement of the atoms in the bis(8-hydroxyquinoline)silver molecule is shown in Fig. 1.

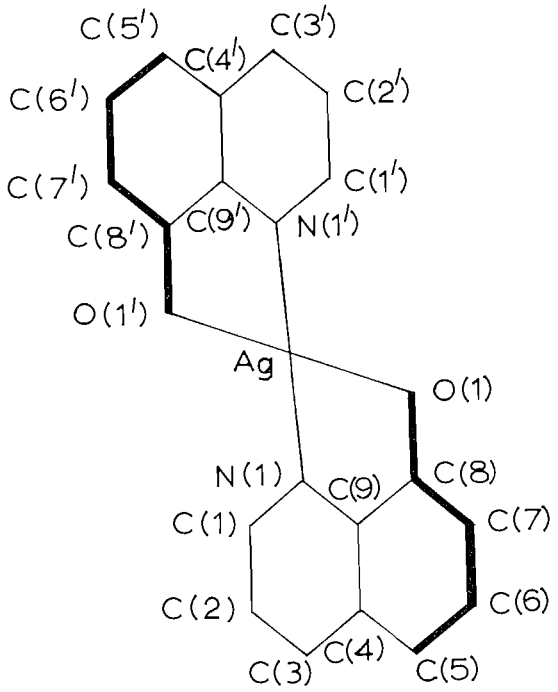

FIG. 1. The arrangement of the atoms in the bis(8-hydroxyquinoline)silver(I) molecule.

A final set of structure factors[4] was computed; these gave a discrepancy index of $R = 0.116$. A detailed analysis (16) of the agreement of individual reflections is summarized in Table IV. Only 15 observed reflections showed relatively high discrepancies, whilst 46 unobserved reflections were in poor agreement.

TABLE II

Fractional atomic coordinates, and e.s.d.'s (Å). All values have been multiplied by 10^4

Atom	x	y	z	$\sigma(x)$	$\sigma(y)$	$\sigma(z)$
Ag	2081	583	2420	5	5	4
O(1)	4142	1526	2784	51	52	46
N(1)	2463	303	3679	50	48	34
C(1)	1720	−310	4142	71	61	83
C(2)	1827	−321	4988	87	80	60
C(3)	2756	300	5360	79	72	62
C(4)	3637	970	4904	67	56	54
C(5)	4628	1614	5278	73	72	67
C(6)	5451	2206	4783	67	63	73
C(7)	5306	2154	3959	58	61	71
C(8)	4300	1553	3570	61	62	70
C(9)	3444	947	4066	65	59	71
O(1′)	609	2243	2029	42	41	41
N(1′)	1683	434	1148	53	53	40
C(1′)	2164	−463	688	69	62	96
C(2′)	2095	−468	−150	62	66	66
C(3′)	1490	471	−540	78	89	64
C(4′)	922	1445	−90	57	75	62
C(5′)	234	2443	−476	77	87	72
C(6′)	−287	3296	−14	70	67	70
C(7′)	−184	3245	831	70	74	86
C(8′)	491	2317	1237	55	58	56
C(9′)	1062	1379	755	58	61	60
N(2)	927	1281	7132	90	87	130
C(10)	1316	128	7274	104	84	68
C(11)*	2457	−203	7545			
C(12)*	3484	629	7432			
C(13)	3022	1853	7443	67	126	88
C(14)	1818	2116	7246	115	99	121

*Denotes calculated atomic positions for which no e.s.d.'s can be quoted.

The e.s.d.'s (estimated standard deviations) for the atomic parameters were calculated according to the expression of Cruickshank and Robertson (17), using the observed data only. The results are included in Table II. No e.s.d.'s can be quoted for C(11) and C(12) as those atoms had been placed by calculation.

Table V gives the intramolecular distances in the structure together with their e.s.d.'s which were estimated for atomic coordinate errors using the expression of Ahmed and Cruickshank (18). No corrections were applied for errors in the cell dimensions. Once again, no e.s.d.'s can be quoted for bonds to the atoms C(11) and C(12). Table VI gives the bond angles and their e.s.d.'s calculated according to the equation given in ref. 19. Table VII gives some of the intermolecular distances shorter than 4.0 Å.

[4]These data have been placed in the Depository of Unpublished Data. Photocopies may be obtained upon request to: Depository of Unpublished Data, National Science Library, National Research Council of Canada, Ottawa, Canada.

Can. J. Chem. Downloaded from www.nrcresearchpress.com by 210.87.254.40 on 09/05/12
For personal use only.

TABLE III

Electron densities (e Å^{-3}), mean curvatures (e Å^{-5}), and isotropic temperature parameters (Å^2)

Atom	ρ_o	ρ_c	ρ_o''	ρ_c''	B_{iso}
Ag	96.5	96.2	825	826	3.11
O(1)	10.4	10.6	79	80	3.65
N(1)	11.0	10.9	93	93	2.41
C(1)	7.6	7.5	55	57	3.28
C(2)	7.3	7.3	54	54	3.00
C(3)	7.6	7.5	56	57	2.93
C(4)	8.3	8.3	68	68	2.72
C(5)	7.4	7.3	56	56	3.45
C(6)	7.3	7.3	58	59	3.70
C(7)	8.0	7.9	62	62	3.40
C(8)	8.0	8.1	61	62	2.80
C(9)	7.8	8.0	61	61	2.80
O(1′)	12.3	12.4	95	95	2.95
N(1′)	10.7	10.6	82	84	2.65
C(1′)	7.3	7.2	53	54	3.80
C(2′)	7.9	7.7	60	61	4.00
C(3′)	7.3	7.2	52	53	3.15
C(4′)	8.1	8.1	61	61	2.80
C(5′)	7.2	7.2	50	51	3.15
C(6′)	7.5	7.3	57	57	3.75
C(7′)	7.4	7.2	51	52	3.05
C(8′)	8.4	8.5	69	70	2.90
C(9′)	8.8	8.5	65	64	2.70
N(2)	6.9	7.0	39	39	5.00
C(10)	6.4	6.4	48	50	4.80
C(11)*	4.1	4.0	25	22	5.25
C(12)*	3.2	5.3	39	27	5.25
C(13)	5.8	5.8	43	43	5.90
C(14)	5.4	5.4	35	36	5.25

*Atoms with calculated atomic positions.

Least squares planes through each of the 8-hydroxyquinoline molecules were calculated (Table VIII). Distances of atoms from these planes are given in Table IX.

Discussion

The silver atom is bonded to both 8-hydroxyquinoline molecules through the phenolic oxygen and the ring nitrogen atoms. The arrangement about the silver atom is distorted tetrahedral, the angles being: O(1)—Ag—N(1) = 71.7°; O(1′)—Ag—N(1′) = 72.0°; O(1)—Ag—N(1′) = 113.9°; O(1′)—Ag—N(1) = 117.2°.

The Ag—O bond lengths of 2.451 Å and 2.505 Å are significantly different ($t = 8.31$) according to Cruickshank's criterion (17). Summaries of Ag—O distances in a number of compounds are given by Britton and Dunitz (20, 21) and Dickens (22). Consideration of these bond lengths show that they fall into three main groups. The first contains lengths in the range 2.0 to 2.1 Å found in covalent silver compounds such as Ag_2O and Ag_2PbO_2; the second contains lengths in the range 2.4 to 2.6 Å found in compounds such as $AgClO_3$, $AgClO_4$, $KAgCO_3$, $AgClO_2$, $AgNO_2$, which are said to be partially

TABLE IV

Agreement summary
(overall discrepancy index $R = 0.116$)

Category	Limits	Number
2163 observed reflections ($6.5 \leqslant \lvert F_o \rvert \leqslant 298.6$)		
1	$\lvert \Delta F \rvert \leqslant 1.0 \lvert F_{th} \rvert$*, or $\lvert \Delta F \rvert / \lvert F_o \rvert \leqslant 2R$	2031
2	$1.0F_{th} < \lvert \Delta F \rvert \leqslant 2.0 \lvert F_{th} \rvert$, or $2R < \lvert \Delta F \rvert / \lvert F_o \rvert \leqslant 3R$	117
3	$2.0F_{th} < \lvert \Delta F \rvert \leqslant 3.0 \lvert F_{th} \rvert$, or $3R < \lvert \Delta F \rvert / \lvert F_o \rvert \leqslant 4R$	9
4	$3.0F_{th} < \lvert \Delta F \rvert \leqslant 5.0 \lvert F_{th} \rvert$, or $4R < \lvert \Delta F \rvert / \lvert F_o \rvert \leqslant 6R$	6
1392 unobserved reflections ($\lvert F_c \rvert_{max} = 21.6$)		
1	$\lvert F_c \rvert \leqslant 1.0 \lvert F_{th} \rvert$	1146
2	$1.0 \lvert F_{th} \rvert < \lvert F_c \rvert \leqslant 2.0 \lvert F_{th} \rvert$	200
3	$2.0 \lvert F_{th} \rvert < \lvert F_o \rvert \leqslant 3.0 \lvert F_{th} \rvert$	40
4	$3.0 \lvert F_{th} \rvert < \lvert F_c \rvert \leqslant 4.0 \lvert F_{th} \rvert$	6

*$\lvert F_{th} \rvert$ = threshold amplitude = 1.4 to 10.7.

TABLE V

Intramolecular distances with their e.s.d.'s in parentheses (Å)

Interatomic distance	Length	
The bis(8-hydroxyquinoline)silver molecule		
	A*	B*
Ag—N(1)	2.145 (0.004)	2.155 (0.004)
Ag—O(1)	2.505 (0.005)	2.451 (0.004)
O(1)—C(8)	1.316 (0.008)	1.325 (0.007)
N(1)—C(1)	1.319 (0.009)	1.348 (0.009)
C(1)—C(2)	1.411 (0.010)	1.396 (0.012)
C(2)—C(3)	1.337 (0.011)	1.351 (0.010)
C(3)—C(4)	1.440 (0.010)	1.439 (0.011)
C(4)—C(5)	1.400 (0.010)	1.433 (0.011)
C(5)—C(6)	1.396 (0.010)	1.340 (0.011)
C(6)—C(7)	1.379 (0.010)	1.408 (0.011)
C(7)—C(8)	1.403 (0.009)	1.389 (0.009)
C(8)—C(9)	1.429 (0.009)	1.442 (0.008)
C(9)—C(4)	1.404 (0.009)	1.412 (0.009)
C(9)—N(1)	1.401 (0.008)	1.365 (0.008)
The pyridine molecule		
N(2)—C(10)	1.29 (0.01)	
C(10)—C(11)	1.37†	
C(11)—C(12)	1.44†	
C(12)—C(13)	1.40†	
C(13)—C(14)	1.37 (0.01)	
C(14)—N(2)	1.32 (0.01)	

*A refers to the unprimed coordinates in Table II, B to the primed coordinates.
†These lengths involve atoms with calculated atomic positions.

Can. J. Chem. Downloaded from www.nrcresearchpress.com by 210.87.254.40 on 09/05/12
For personal use only.

TABLE VI

Angles with their e.s.d.'s in parentheses (°)

Angle	Measure	
The bis(8-hydroxyquinoline)silver molecule		
	A*	B*
O(1)—Ag—N(1)	71.7 (0.2)	72.0 (0.2)
N(1)—C(1)—C(2)	124.4 (0.7)	124.7 (0.7)
C(1)—C(2)—C(3)	119.3 (0.7)	119.0 (0.7)
C(2)—C(3)—C(4)	120.4 (0.7)	119.5 (0.7)
C(3)—C(4)—C(5)	121.5 (0.6)	121.6 (0.6)
C(4)—C(5)—C(6)	117.1 (0.6)	117.9 (0.7)
C(5)—C(6)—C(7)	121.7 (0.6)	122.4 (0.7)
C(6)—C(7)—C(8)	122.3 (0.6)	122.1 (0.7)
C(7)—C(8)—C(9)	116.8 (0.6)	116.8 (0.6)
N(1)—C(9)—C(4)	123.2 (0.6)	123.1 (0.6)
C(8)—C(9)—C(4)	119.9 (0.6)	119.6 (0.5)
C(1)—N(1)—Ag	123.3 (0.4)	123.4 (0.5)
C(9)—N(1)—Ag	119.7 (0.4)	119.5 (0.4)
C(9)—C(8)—O(1)	120.8 (0.6)	119.4 (0.5)
C(7)—C(8)—O(1)	122.4 (0.6)	123.8 (0.6)
C(8)—O(1)—Ag	108.9 (0.4)	110.1 (0.3)
C(3)—C(4)—C(9)	116.3 (0.6)	117.2 (0.6)
C(9)—N(1)—C(1)	116.3 (0.5)	116.5 (0.5)
C(9)—C(4)—C(5)	122.2 (0.6)	121.2 (0.6)
N(1)—C(9)—C(8)	116.9 (0.6)	117.4 (0.5)
O(1′)—Ag—N(1)	117.2 (0.2)	
O(1)—Ag—N(1′)	113.9 (0.2)	
O(1′)—Ag—O(1)	109.9 (0.2)	
N(1)—Ag—N(1′)	167.9 (0.2)	
The pyridine molecule		
N(2)—C(10)—C(11)	125†	
C(10)—C(11)—C(12)	120†	
C(11)—C(12)—C(13)	107†	
C(12)—C(13)—C(14)	121 (2)	
C(13)—C(14)—N(2)	125 (1)	
C(14)—N(2)—C(10)	113†	

*A refers to unprimed coordinates in Table II, B to primed coordinates.
†These angles involve atoms with calculated atomic positions.

TABLE VII

Some intermolecular distances

X*	Y*	Distance
Between two bis(8-hydroxyquinoline)silver molecules		
O(1′)	O(1) (D)	2.457
C(8)	O(1′) (D)	3.260
C(8′)	O(1) (D)	3.267
C(7)	O(1′) (D)	3.319
C(7′)	O(1) (D)	3.383
C(6)	C(3) (B)	3.322
C(5)	C(4) (B)	3.356
C(5′)	C(1′) (B)	3.358
C(9′)	C(3′) (B)	3.404
C(4′)	C(2′) (B)	3.480
C(5′)	C(2′) (B)	3.490
C(7)	C(3) (B)	3.514
C(4′)	C(3′) (B)	3.519
C(7)	N(1) (D)	3.627
C(3′)	N(1′) (B)	3.678
Between a bis(8-hydroxyquinoline)silver molecule and a pyridine molecule		
C(11)	C(3′) (A)	3.48
C(12)	O(1) (B)	3.48
C(11)	O(1′) (C)	3.49
C(10)	O(1′) (B)	3.50
C(12)	C(3) (X)	3.53
C(10)	C(3) (X)	3.63
N(2)	C(1) (B)	3.66
C(10)	C(3′) (A)	3.66
C(10)	Ag (B)	3.81
C(14)	Ag (C)	3.92
N(2)	Ag (B)	3.92
Between two pyridine molecules		
C(13)	N(2) (D)	3.79

*Atom X is in the molecule specified by the parameters given in Table II and Y is in the molecule specified by the letter in parentheses. These molecules are located as follows.
(A) x, y, z (adjacent cell), (B) $\bar{x}, \bar{y}, \bar{z}$ (same cell), (C) $\frac{1}{2} - x, \frac{1}{2} + y, \bar{z}$ (same cell), (D) $\frac{1}{2} + x, \frac{1}{2} - y, z$ (same cell).

ionic. Finally, a value of 2.78 Å is quoted for a covalent-type bond found in silver fulminate. The lengths found in the present investigation thus lie within the range of values associated with partially ionic Ag—O bonds.

The distance between atom O(1) in one molecule and atom O(1′) in an adjacent molecule (see Table VII) is 2.457 Å and is the shortest intermolecular distance in the structure. Comparison of this bond length with those found in hydrogen-bonded cases (23) shows that it is at the low end of the range of values listed, indicating that the phenolic hydrogen is contained between the two oxygen atoms forming a strong hydrogen bond. There is some controversy as to whether a hydrogen bond of this length is or is not expected to have the hydrogen atom centrally located. The non-equivalence of the Ag—O bonds in this structure would seem to favor the idea of a nonsymmetric hydrogen bond between the oxygen atoms.

The Ag—N bond distances of 2.145 Å and 2.155 Å are not significantly different. There are few precise values available for comparison, but distances of 2.115 Å and 2.223 Å have been reported for silver cyanate (20) and silver thiocyanate (24). The bond in silver cyanate is said to be strongly covalent. The Ag—N bond lengths found in this structure would appear to be compatible with covalent bonding. It is noted that the metal–oxygen distance is about 0.3 Å longer than the metal–nitrogen distance.

TABLE VIII

Least squares planes

Plane	Direction cosines × 10^4 with respect to directions			Distance to origin	Description of plane
	a	*b*	*c**		
I	5583	−8290	−0309	0.907	8 hydroxyquinoline molecule, atoms O(1)—C(9)
II	8383	5450	−0174	1.668	8 hydroxyquinoline molecule, atoms O(1′)—C(9′)

The calculation of the least squares planes (see Tables VIII and IX) shows that each 8-hydroxyquinoline molecule is substantially planar. The mean distance of an atom from the best plane is 0.018 Å for the molecule O(1)—C(9) and 0.015 Å for the molecule O(1′)—C(9′). The angle between the two best planes is 89°. The Ag atom is displaced by a distance of 0.386 Å from the first plane and 0.335 Å from the second plane. Figures 2 and 3 show the structure as viewed along the *c** and *b* axes.

TABLE IX

Deviations (Å) from least squares planes.
All values multiplied by 10^3

Atom	Plane I	Atom	Plane II
O(1)	−4	O(1′)	2
N(1)	−23	N(1′)	13
C(1)	27	C(1′)	10
C(2)	23	C(2′)	−17
C(3)	−1	C(3′)	10
C(4)	−16	C(4′)	19
C(5)	−19	C(5′)	8
C(6)	2	C(6′)	−15
C(7)	38	C(7′)	−30
C(8)	−7	C(8′)	8
C(9)	−35	C(9′)	30
Ag	−386	Ag	335

Corresponding distances in the two 8-hydroxyquinoline rings in the molecule were compared (see Table V). The average difference between corresponding distances is 0.022 Å, and the largest difference is 0.056 Å. This difference is significant ($t = 3.81$) according to Cruickshank's criterion (17) and there are three more differences on the border of significance. However, there are no other distinguishing features about these particular bonds, so it is not possible to conclude from this alone whether the two groups are really not chemically equivalent or whether the method of calculation of the e.s.d.'s used in the analysis has given too low a value for the coordinate errors.

A literature survey shows that there are a number of recent reports of the structures of 8-hydroxyquinoline metal chelates (25–34). Accurate values are quoted for the bis(8-hydroxyquinoline)zinc(II) complex (33), and the α and β forms of anhydrous bis(8-hydroxyquinoline)-copper(II) (32, 34). The molecules of the zinc and α-copper complexes are essentially planar, whilst the β-copper complex has a distorted planar arrangement. There is good agreement shown between equivalent bond distances in these structures, and a comparison with the bond distances found in the present structure shows no major differences. It would thus appear that

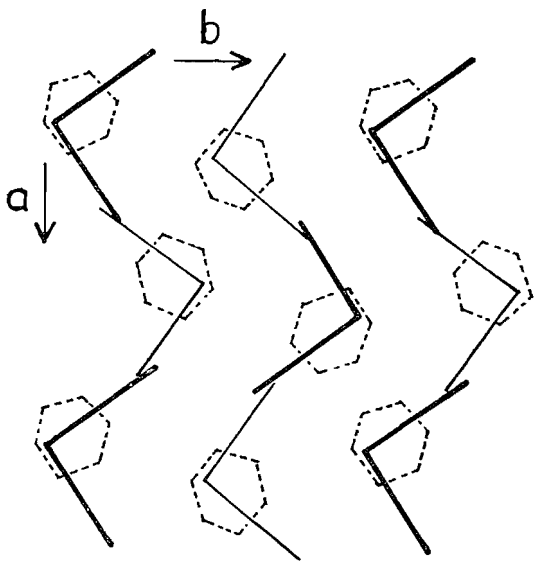

FIG. 2. The structure of the pyridine adduct of bis(8-hydroxyquinoline)silver(I) viewed along the *c** axis. Solid lines indicate the edges of the best planes through the 8-hydroxyquinoline molecules. The pyridine rings are shown by broken lines.

Can. J. Chem. Downloaded from www.nrcresearchpress.com by 210.87.254.40 on 09/05/12
For personal use only.

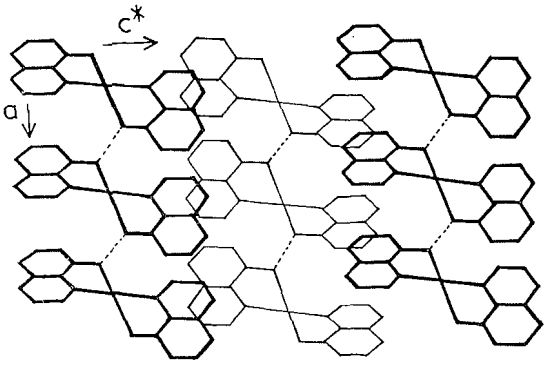

FIG. 3. The structure of the pyridine adduct of bis(8-hydroxyquinoline)silver(I) viewed along the *b* axis. Solid lines show the bis(8-hydroxyquinoline)silver molecules, with broken lines indicating the hydrogen bonds. The pyridine molecules are omitted for clarity.

the 8-hydroxyquinoline groups are not significantly affected by the nature of the central metal atom.

It was not possible to refine two atoms in the pyridine molecule and for the four other atoms the positional accuracy is low. The identification of the nitrogen atom is not certain. Examination of the nearest intermolecular approach distances (see Table VII) shows there are no short distances between atoms in a pyridine molecule and a bis(8-hydroxyquinoline)silver molecule. This indicates that the pyridine molecule is held in the lattice by van der Waals forces only. The isotropic temperature factors for the pyridine atoms are larger than for similar atoms in the 8-hydroxyquinoline rings. This, coupled with drawn out electron density of at least two pyridine atoms, suggests considerable thermal motion, as might be expected for a molecule subject only to van der Waals forces. The pyridine positions given in Table II, at best, represent a fit of a reasonable model.

This structure analysis gives definite evidence for the existence of tetrahedral bonding in a four-coordinated silver(I) complex, in agreement with the predictions of other workers.

Acknowledgments

We acknowledge the financial support of the National Research Council of Canada for this work, and we thank H. Lynne Dougan for estimating the intensity data used in the analysis, and Malcolm J. R. Clark for measurement of the magnetic susceptibility of the compound.

1. Y. NAKATSUKA. Bull. Chem. Soc. Japan, **11**, 45 (1936).
2. B. P. BLOCK, J. C. BAILAR, JR., and D. W. PEARCE. J. Am. Chem. Soc. **73**, 4971 (1951).
3. W. W. WENDLANDT and J. HASCHKE. Nature, **193**, 1174 (1962).
4. W. W. WENDLANDT and J. H. VAN TASSEL. Science, **127**, 242 (1958).
5. J. HALA. J. Inorg. Nucl. Chem. **27**, 2659 (1965).
6. E. G. COX, W. WARDLAW, and K. C. WEBSTER. J. Chem. Soc. 775 (1936).
7. F. G. MANN, A. F. WELLS, and D. PURDIE. J. Chem. Soc. 1828 (1937).
8. C. BRINK and C. H. MACGILLAVRY. Acta Cryst. **2**, 158 (1949).
9. C. BRINK and H. A. S. KROESE. Acta Cryst. **5**, 433 (1952).
10. C. BRINK, N. F. BINNENDIJK, and J. VAN DE LINDE. Acta Cryst. **7**, 176 (1954).
11. J. R. HALL, R. A. PLOWMAN, and H. S. PRESTON. Australian J. Chem. **18**, 1345 (1965).
12. F. R. AHMED, E. J. GABE, G. A. MAIR, and M. E. PIPPY. A unified set of crystallographic programs for the I.B.M. 1620 computer. Divisions of Pure Physics and Pure Chemistry, National Research Council, Ottawa, Canada.
13. K. E. MCCULLOH and G. F. POLLNOW. J. Chem. Phys. **22**, 681 (1954).
14. B. B. DEMORE, W. S. WILCOX, and J. H. GOLDSTEIN. J. Chem. Phys. **22**, 876 (1954).
15. B. BAK, L. HANSEN, and J. RASTRUP-ANDERSEN. J. Chem. Phys. **22**, 2013 (1954).
16. F. R. AHMED and W. H. BARNES. Acta Cryst. **16**, 1249 (1963).
17. D. W. J. CRUICKSHANK and A. P. ROBERTSON. Acta Cryst. **6**, 698 (1953).
18. F. R. AHMED and D. W. J. CRUICKSHANK. Acta Cryst. **6**, 385 (1953).
19. International Tables for X-ray Crystallography. Vol. II. The Kynoch Press, Birmingham, England. 1959. 6.4.3.3.(17).
20. D. BRITTON and J. D. DUNITZ. Acta Cryst. **18**, 424 (1965).
21. D. BRITTON and J. D. DUNITZ. Acta Cryst. **19**, 662 (1965).
22. B. DICKENS. J. Inorg. Nucl. Chem. **28**, 2793 (1966).
23. G. C. PIMENTEL and A. L. MCCLELLAN. The hydrogen bond. W. H. Freeman and Co., San Francisco. 1960. p. 259.
24. I. LINDQUIST. Acta Cryst. **10**, 29 (1957).
25. B. KAMENAR, C. K. PROUT, and J. D. WRIGHT. J. Chem. Soc. 4851 (1965).
26. A. S. BAILEY and C. K. PROUT. J. Chem. Soc. 4867 (1965).
27. C. K. PROUT and H. M. POWELL. J. Chem. Soc. 4882 (1965).
28. B. KAMENAR, C. K. PROUT, and J. D. WRIGHT. J. Chem. Soc. A, 661 (1966).
29. C. K. PROUT and A. G. WHEELER. J. Chem. Soc. A, 1286 (1966).
30. C. K. PROUT and A. G. WHEELER. J. Chem. Soc. A, 469 (1967).
31. J. E. LYDON and M. R. TRUTER. J. Chem. Soc. 6899 (1965).
32. G. J. PALENIK. Acta Cryst. **17**, 687 (1964).
33. G. J. PALENIK. Acta Cryst. **17**, 696 (1964).
34. R. C. HOY and R. H. MORRISS. Acta Cryst. **22**, 476 (1967).

Can. J. Chem. Downloaded from www.nrcresearchpress.com by 210.87.254.40 on 09/05/12
For personal use only.

Elementary processes in the acetaldehyde pyrolysis

MICHAEL T. H. LIU[1] AND K. J. LAIDLER
Department of Chemistry, University of Ottawa, Ottawa, Canada

Received September 12, 1967

The acetaldehyde pyrolysis has been studied over the 480–540 °C temperature range, and at pressures from 1 to 560 mm Hg. Measurements were made of the rates of production of the major product methane and of the minor products hydrogen, ethane, acetone, and propionaldehyde. The kinetic effects of adding carbon dioxide, of changing the surface:volume ratio, and of coating the vessel have been determined. The elementary processes are found to occur largely in the gas phase. The dissociation of CH_3CHO into $CH_3 + CHO$ is deduced from the rates of hydrogen and ethane formation; there is significant falling off of the rate constants at lower pressures. The kinetic parameters for the reaction $CH_3 + CH_3CHO \rightarrow CH_4 + CH_3CO$ are obtained, and it is suggested that quantum-mechanical tunnelling plays a role. Acetone production has an activation energy of 12.4 kcal/mole and it is concluded that its formation involves the participation of the isopropoxy radical, the activation energies being as indicated:

$$CH_3 + CH_3CHO \underset{17.3}{\overset{10.6}{\rightleftharpoons}} (CH_3)_2CHO \overset{19.1}{\rightarrow} CH_3COCH_3 + H.$$

Canadian Journal of Chemistry, 46, 479 (1968)

In a recent paper (1) we have described a reinvestigation, at 523 °C, of the pyrolysis of acetaldehyde. The acetaldehyde used was prepared from paraldehyde, and was shown to be free from traces of impurity. Measurements were made of the rates of formation of the major products (methane and carbon monoxide) and of the minor products (hydrogen, ethane, acetone, and propionaldehyde). On the basis of this work a specific mechanism was proposed.

The present paper describes a more detailed investigation of the problem, at temperatures from 480 to 540 °C, and pressures from 1 to 560 mm. Studies have been made of the effects of added inert gas and of changing the surface: volume ratio and the nature of the surface. The results confirm the mechanism previously proposed and lead to a number of kinetic parameters for the elementary processes.

Experimental

The apparatus was that described in the previous paper (1) and the procedures were essentially the same. The following additional points may be noted.

For the experiments in which the pressure of acetaldehyde was low (20–50 mm) a small bulb was used for the expansion. Since low pressures of acetaldehyde could not be read accurately on the manometer, it was necessary to have a calibration curve for this purpose. This was achieved by expanding a certain amount of inert gas into the reaction vessel using a 3 cc tube on the manifold so that the initial pressure was always greater than 20 mm Hg. The concentration of the inert gas after expansion was measured by means of a gas burette, and the pressure in the vessel could then be calculated.

Attempts were made to detect ketene in the system, but it was not found. However, ketene polymerizes with acetaldehyde to a small extent at low temperatures. A transparent polymer was noted in the −130 and −150 °C traps after each run. When acetaldehyde was pyrolyzed together with small amounts of ketene at 450 °C, 80% of the ketene was found to be consumed.

Rates of formation of the products CO, CH_4, H_2, CH_3COCH_3, C_2H_6, and C_2H_5CHO were measured at 480, 500, 523, and 540 °C.

Results and Analysis

Initial rates of formation of the products were obtained by extrapolating rates to zero time. The rates of formation of hydrogen and acetone were, at all temperatures, roughly three orders of magnitude less than those of the major products; those of ethane were roughly one fifth of those of hydrogen, and those of propionaldehyde about one quarter of those of ethane. (Rates at 523 °C were tabulated in the previous paper (1) and the general pattern is similar at the other temperatures.)

To explain these results, especially the products obtained, we suggest the following mechanism, which is the Rice–Herzfeld scheme to which a number of reactions have been added:

[1] $$CH_3CHO \rightarrow CH_3 + CHO$$

[2] $$CHO \rightarrow CO + H$$

[3] $$H + CH_3CHO \rightarrow H_2 + CH_3CO$$

[1]Present address: Department of Chemistry, The University, Reading, England.

[4] $CH_3 + CH_3CHO \rightarrow CH_4 + CH_3CO$

[5] $CH_3CO \rightarrow CH_3 + CO$

[6] $CH_3 + CH_3CHO \rightarrow CH_4 + CH_2CHO$

[7a] $CH_2CHO \rightarrow CH_2CO + H$

[7b] $CH_2CHO + CH_3CHO \rightarrow CH_3CHO + CH_3CO$

[8] $CH_3 + CH_3CHO \rightarrow CH_3COCH_3 + H$

[9] $CH_3 + CH_3 \rightarrow C_2H_6$

[10] $CH_3 + CH_2CHO \rightarrow CH_3CH_2CHO$

If the minor termination step [10] is ignored the rate of disappearance of acetaldehyde, approximately equal to the rates of formation of carbon monoxide and methane, is found to be

$$[1] \quad \frac{-d[CH_3CHO]}{dt} = k_4\left(\frac{k_1}{k_9}\right)^{1/2}[CH_3CHO]^{3/2}.$$

Since earlier work (1) indicated that there was a slight falling off of the overall rate constant at low pressures, it was decided that further work should be done to confirm this effect. Rates of production of methane were measured at 540 °C at pressures from 0.8 to 558 mm Hg. Some results are shown in Fig. 1, and there is seen to be a significant falling off of the overall 3/2-order rate constant. The order of methane formation is exactly 1.5 at high pressures (> 100 mm Hg) and is about 1.7 when the initial pressures have gone below 20 mm Hg. As k is also a measure of the square root of the ratio k_1/k_9, it is concluded that k_1 is falling off faster than k_9; this is understandable since acetaldehyde has three vibrational degrees of freedom less than ethane.

The overall rate constant is given by

$$\log k(\text{cc}^{\frac{1}{2}}\,\text{mole}^{-\frac{1}{2}}\,\text{s}^{-1}) = (13.5 \pm 0.2) - \frac{49100 \pm 1000}{2.303RT}.$$

The activation energy agrees satisfactorily with the value of 48.0 kcal/mole obtained by Boyer, Niclause, and Letort (2) and of 47.6 kcal/mole obtained by Eusuf and Laidler (3).

According to eq. [1] k is identified with $k_4(k_1/k_9)^{\frac{1}{2}}$ so that $E = E_4 + \frac{1}{2}E_1 - \frac{1}{2}E_9$. As shown later, E_4 is found to be 8.4 kcal/mole, and it is assumed that $E_9 \simeq 0$ for the recombination of methyl radicals. The average value for the activation energy of 80.3 kcal/mole for reaction [1] (see later) gives 48.6 kcal/mole for the experimental activation energy, in excellent agreement with the directly observed value of 49.1 kcal. In the same manner, the frequency factor can be calculated to be 2.6×10^{13} s^{-1}, also in agreement with the value obtained (2.8×10^{13}).

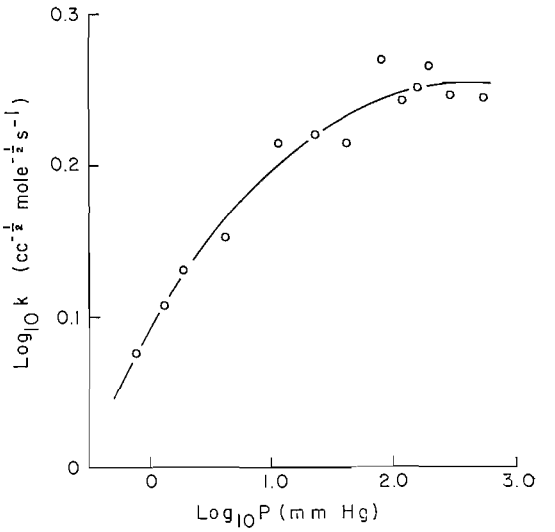

FIG. 1. Double logarithmic plot of the 3/2-order overall rate constant against the pressure. Temperature = 540 °C.

Ethane Production

The order of ethane production is approximately 1.1 at higher pressures, but there is a significant falling off at pressures below 80 mm Hg. The formation of methane can result from reactions [4] and [6]. The low rate of propionaldehyde formation suggests that the ratio v_6/v_4 or k_6/k_4 may be as low as 10^{-2} under the experimental conditions, and hence the methane production due to reaction [6] is extremely small compared with reaction [4]; it can therefore be neglected. If reaction [4] is the only source of methane, and reaction [9] the only source of ethane,

$$[2] \quad \frac{k_9}{k_4^2} = \frac{v_{C_2H_6}}{v_{CH_4}^2}[CH_3CHO]^2.$$

Figure 2 shows a plot of the logarithm of the right-hand side of this equation against the logarithm of the acetaldehyde pressure; again the falling off of k_9 at low pressures is observed. The falloff of k_9 has been observed at various pressure regions in different systems. Dodd and Steacie (4) found a significant decrease of k_9 at about 10 mm of acetone at 247 °C. In the ethane pyrolysis at 550 °C Lin and Back (5) have observed a falloff of the rate coefficient for

methyl radical combination below about 200 mm Hg pressure, while in the mercury-photosensitized decomposition of dimethyl ether at 200 to 300 °C Loucks and Laidler (6) observed a falloff at 100 mm Hg pressure. From the photolysis of azomethane at temperatures from 25 to 180 °C, Toby and Weiss (7) have shown an appreciable decrease of the coefficient at about 15 mm of azomethane:

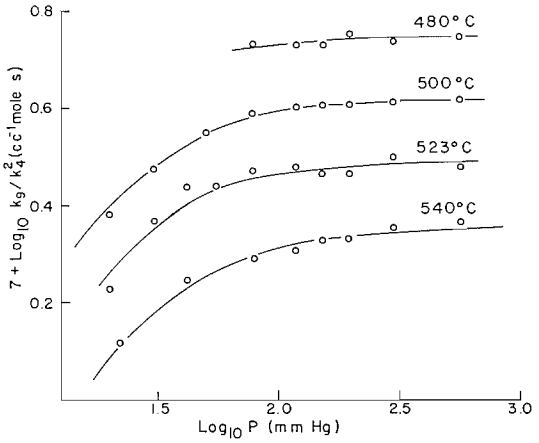

FIG. 2. Plots of $\log k_9/k_4^2$ against $\log P$.

The value of k_4 can be calculated from eq. [2] from the rates of formation of methane and ethane at a particular pressure and using Shepp's value of k_9 (8).

The rate constant k_4 obtained from extrapolation to high pressures is expressed by the equation

$$\log k_4(\text{cc mole}^{-1}\,\text{s}^{-1}) = (12.24 \pm 0.06) - \frac{8440 \pm 210}{2.303RT}.$$

Côme, Dzierzynski, Martin, and Niclause (9, 10) have recently studied the decomposition of acetaldehyde at 500 °C with initial pressures from 50 to 400 mm Hg and reported that the order of ethane formation was 1.2, in agreement with our finding.

Acetone Production

The acetone production was found to be exactly of 3/2 order. The mechanism leads to the following expression for the rate of acetone production:

$$[3] \qquad v_{CH_3COCH_3} = k_8\left(\frac{k_1}{k_9}\right)^{\frac{1}{2}}[CH_3CHO]^{3/2}.$$

Also,

$$[4] \qquad \frac{v_{CH_3COCH_3}}{v_{CH_4}} = \frac{k_8}{k_4},$$

and k_8, and its parameters, can therefore be deduced from the rates of formation of acetone and methane, and the k_4 values; the result is

$$\log k_8(\text{cc mole}^{-1}\,\text{s}^{-1}) = 10.22 \pm 0.07 - \frac{12400 \pm 300}{2.303RT}.$$

Reasons for concluding that acetone is produced in reaction [8] and not in a chain-termination step $CH_3 + CH_3CO \rightarrow CH_3COCH_3$ were given in the previous paper (1). Reaction [8] is considered to occur in two stages, the details of which are discussed later.

Hydrogen Production

In our earlier paper we reported that we did not find the induction period for hydrogen production that was observed by Trenwith (11). The order of hydrogen production, at all four temperatures, is 1.4. Our results have been recently confirmed by Côme *et al.* (9, 10). The mechanism leads to the following expression for hydrogen production.

$$[5] \qquad v_{H_2} = k_1[CH_3CHO] + \left(\frac{k_1}{k_9}\right)^{\frac{1}{2}}\left[\frac{k_{7a}k_6}{k_{7a} + k_{7b}[CH_3CHO]} + k_8\right] \times [CH_3CHO]^{3/2}$$

According to this expression the order of hydrogen production should be between 1 and 3/2 in agreement with the experimental observation of 1.4. Figure 5 of the previous paper showed a plot of $v_{H_2}/[CH_3CHO]$ against $[CH_3CHO]^{\frac{1}{2}}$; a straight line was obtained. The plot still shows a linear relationship at a fairly low pressure, and this is attributed to the fact that k_1 and k_9 largely compensate each other; the result is little net change in the ratio k_1/k_9 although each rate constant is in its pressure-dependent region. In fact, the ratio k_1/k_9 falls off when the pressure is below 20 mm Hg (see Fig. 3 below, with reference to inert-gas effects). The k_1 values obtained by extrapolation on the basis of eq. [5] are represented by

$$\log k_1(\text{s}^{-1}) = 16.12 - \frac{81500 \pm 4500}{2.303RT}.$$

The value of $\Delta S_1^{\ddagger}$ is 11.3 e.u. at 783 °K. The corresponding equation for k_1 obtained from rates of ethane and propionaldehyde production is

$$\log k_1(s^{-1}) = 15.3 - \frac{79000 \pm 2000}{2.303RT}.$$

The second equation is considered to be more reliable, the values obtained on the basis of eq. [5] being slightly pressure dependent. Also, the term $k_{7b}[CH_3CHO]$ is not unimportant compared with k_{7a} and cannot be completely neglected.

The CO_2 and C_2H_4 Production

The initial rates of formation of both CO_2 and C_2H_4 are non-zero, so that these substances are primary products. The order of C_2H_4 formation is 1.5 at 540 °C, which suggests that the C_2H_4 production is resulting from the reaction between a methyl radical and a CH_3CHO molecule:

$$CH_3 + CH_3CHO \rightleftharpoons CH_3{-}O{-}\overset{\displaystyle H}{\underset{\displaystyle |}{\overset{|}{C}}}{-}CH_3$$

$$CH_3{-}O{-}\overset{\displaystyle H}{\underset{\displaystyle |}{\overset{|}{C}}}{-}CH_3 \rightarrow CH_3O + C_2H_4.$$

Other products such as CH_3OH or $CH_3OCH{=}CH_2$, which may be produced from the above reactions, were not detected. The time-course studies of CO_2 (1) show a sharp increase in its production at high conversion, indicating that both primary and secondary reactions are occurring. The initial formation of CO_2 may be due to the reaction of the acetyl radical with acetaldehyde,

$$CH_3CO + CH_3CHO \rightarrow CO_2 + C_3H_7,$$

and the secondary contribution of CO_2 can be attributed to the following exothermic reactions:

$$CH_2CO + CH_3CHO \rightarrow CO_2 + C_3H_6$$

$$CH_3O + CO \rightarrow CO_2 + CH_3$$

$$(CH_3)_2CHO + CO \rightarrow CO_2 + C_3H_7.$$

The oxidation of carbon monoxide to carbon dioxide is quite likely in this system. On pyrolyzing a mixture of *t*-butyl peroxide and formaldehyde, Lin (12) has found a large amount of CO_2, which is probably due to

$$(CH_3)_3CO + CO \rightarrow CO_2 + (CH_3)_3C.$$

The reaction of carbon monoxide with itself,

$$CO + CO \rightarrow CO_2 + C,$$

was also studied but was found not to occur at 523 °C.

Inert-Gas Effects

The effects of inert gas on the rates of methane, ethane, acetone, and hydrogen production were examined at 540 °C with different initial pressures of acetaldehyde.

The rate of methane formation is given by eq. [1], and k_1/k_9 values were calculated from this rate. Figure 3 shows how this ratio falls off at

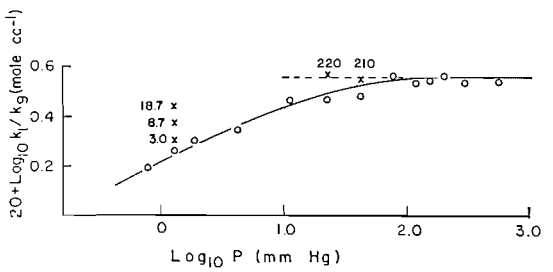

FIG. 3. Plot of log k_1/k_9 against log P at 540 °C, showing the effects of added CO_2, whose pressures in mm are indicated.

540 °C when the acetaldehyde pressure is reduced below 60 mm. In this lower pressure range the k_1/k_9 ratio was increased by addition of CO_2, as shown by the crosses in Fig. 3. The results are consistent with the view that CO_2 is about half as efficient as acetaldehyde in the transfer of energy.

The effects of added CO_2 on the rates of formation of ethane, acetone, and hydrogen were also studied. Figures 4, 5, and 6 show some results, and it is seen that there are significant increases in rates. The effects are similar with methane and acetone, and greater for ethane and hydrogen. These results are consistent with the proposed mechanism. The rates of methane and acetone formation involve the ratio k_1/k_9, so that the inert-gas effects partly compensate one another. Ethane and hydrogen formation involve largely k_1.

The results of Dexter and Trenwith (13) can be explained on the same basis. When 250 mm of acetaldehyde was pyrolyzed in the presence of 200 mm CO_2, they found that the yields of acetone and methane remain unchanged and the rates of formation of hydrogen and of ethane increase.

Surface Effects

(a) Packing

Experiments were made at 500 °C with a

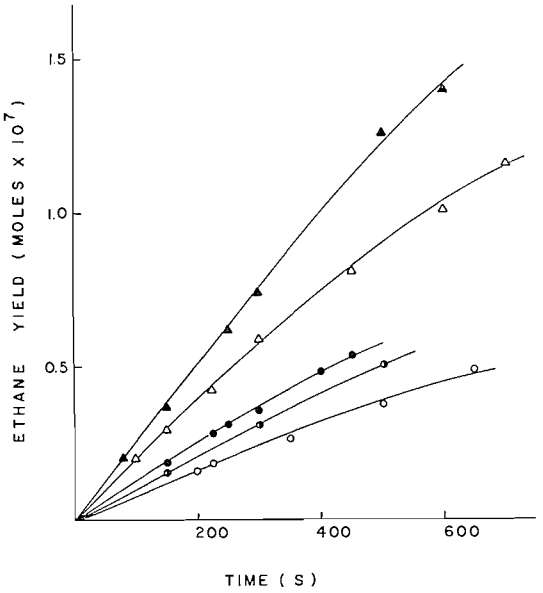

FIG. 4. Typical yield–time plots for ethane formation in the presence of CO_2, $T = 540$ °C: (△) 42 mm CH_3CHO, (▲) 42 mm CH_3CHO + 210 mm CO_2, (○) 22 mm CH_3CHO, (◑) 22 mm CH_3CHO + 110 mm CO_2, (●) 22 mm CH_3CHO + 220 mm CO_2.

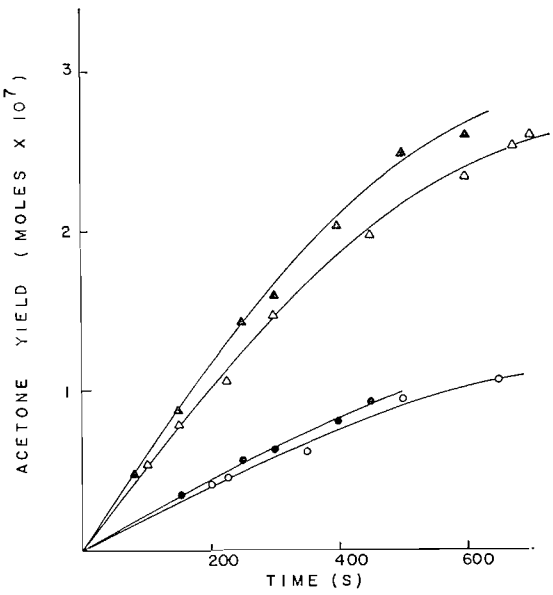

FIG. 5. Typical yield–time plots for acetone formation in the presence of CO_2, $T = 540$ °C: (△) 42 mm CH_3CHO, (▲) 42 mm CH_3CHO + 210 CO_2, (○) 22 mm CH_3CHO, (●) 22 mm CH_3CHO + 220 mm CO_2.

packed vessel in which the S/V ratio was increased 16-fold from 0.6 to 9.38 cm^{-1}. All the products show a small increase in rate. Some initial rates of formation are given in Table I. The increases in the rates of formation of CH_4, CH_3COCH_3, H_2, and C_2H_6 are about 10, 10–15, 20, and1 5–20% respectively. The ratios $v_{C_2H_6}^{1/2}/v_{CH_4}$ at 118 mm pressure of CH_3CHO at 500 °C are equal to 8.4×10^{-5} and 8.3×10^{-5} for the packed and unpacked vessels. These results suggest that the small increase in rate can be attributed to a surface initiation reaction. As soon as the chain is initiated, the rest of the products will increase proportionally according to eqs. [2] and [4]. The ratio $v_{acetone}/v_{CH_4}$ can be explained on similar grounds.

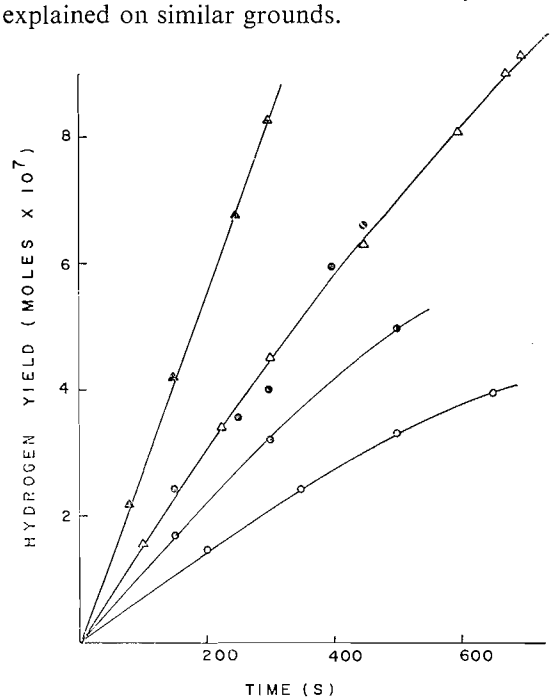

FIG. 6. Typical yield–time plots for hydrogen formation in the presence of CO_2, $T = 540$ °C: (△) 42 mm CH_3CHO, (▲) 42 mm CH_3CHO + 210 mm CO_2, (○) 22 mm CH_3CHO, (◑) 22 mm CH_3CHO + 110 mm CO_2, (●) 22 mm CH_3CHO + 220 mm CO_2.

It has been shown by Lin and Back (5) that the process $C_2H_6 \rightarrow 2CH_3$ is not affected by changing the surface:volume ratio, and from the principle of microscopic reversibility, $CH_3 + CH_3 \rightarrow C_2H_6$ should not be influenced by the nature of the surface. The rates at zero S/V ratio, obtained by extrapolation, have essentially the same values as for the unpacked vessel. The initiation on the surface may be of the type proposed by Wojciechowski and Laidler (14), in which initiation may occur as

$$CH_3CHO + S \rightarrow CH_3CO + S\text{—}H,$$

TABLE I

Initial rates of formation in mole cc^{-1} s^{-1}, for various products at 500 °C in packed and unpacked vessels

P_{CH_3CHO} (mm Hg)	$v_{CH_4} \times 10^{10}$		$v_{H_2} \times 10^{13}$		$v_{acetone} \times 10^{13}$		$v_{C_2H_6} \times 10^{13}$	
	Packed	Unp.	Packed	Unp.	Packed	Unp.	Packed	Unp.
81	9.35	8.52	15.8	13.8	7.05	6.50	1.25	1.05
118	16.2	14.80	25.0	21.8	12.3	11.0	1.86	1.49
181	31.2	29.1	45.2	40.8	22.34	21.0	2.82	2.34
325	76.6	71.0	105.0	91.3	—	—	5.13	4.27
452	129.0	116.0	166.0	145.0	—	—	—	—
520	155.0	142.0	200.0	174.0	—	—	—	—

followed by

$$S—H \rightarrow S + H$$

or

$$CH_3 + HS \rightarrow CH_4 + S.$$

If the latter reaction dominates, i.e. surface is equally involved in both initiation and termination, there will be no net effect of surface on the overall kinetics. There is no direct evidence as to whether the termination occurs on the surface or not, but it is clear that the initiation is more sensitive to surface than the termination reaction.

(b) Carbon Coating

In kinetic studies of the gas phase pyrolysis of alkyl halides it has proved necessary to "season" the reaction vessel in order that reproducible kinetics may be obtained (15). "Seasoning" may be achieved by prolonged treatment of the vessel with the compound under investigation until a carbonaceous deposit is observed. It was believed that this coating covers active sites in the polar glass surface so that heterogeneous reactions were eliminated. Holbrook (16) found, however, that the carbon deposit from the gas-phase pyrolysis of allyl bromide showed a strong e.s.r. signal and that it had an odd electron content of 10^{18} per g. He proposed that such carbons might therefore be *reactive* rather than *inactive* as previously believed. Holmes (17) found that allyl-bromide carbon catalyzes the HI decomposition and olefin isomerizations. The activation energies for these heterogeneous reactions are lower than those of the corresponding homogeneous reactions. In the present work, it was found that the rate of the acetaldehyde decomposition was almost doubled when the reaction vessel was coated with allyl-bromide carbon. These results are shown in Fig. 7. The order of methane production is 3/2 in both the uncoated and coated vessels. The processes responsible for the surface-initiation reactions are suggested to be either

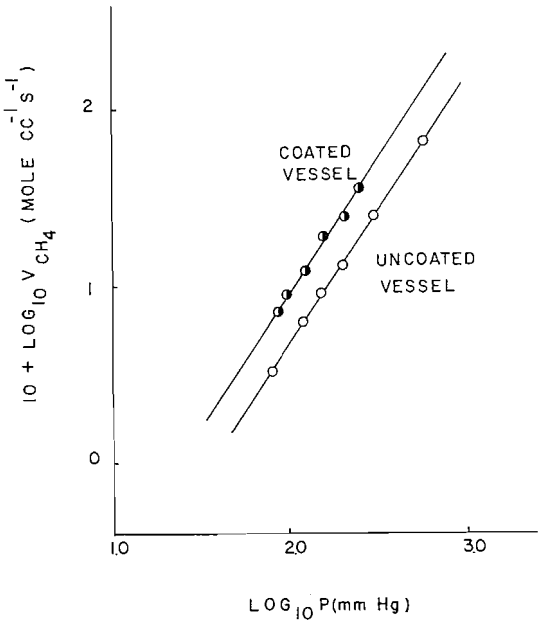

FIG. 7. Plots showing the effect of carbon coating on the rates of methane production, $T = 480$ °C.

[*i*] $$CH_3CHO + S \rightarrow SH + CH_3CO$$

or

[*ii*] $$CH_3CHO + S \rightarrow CH_3CHO^*$$

$$CH_3CHO^* + CH_3CHO \rightarrow CH_3CHOH + CH_3CO,$$

where CH_3CHO^* represents an excited species. If reaction [*ii*] is significant in the initiation process the steady-state treatment leads to an overall order which is higher than 3/2; this is not observed. Reaction [*i*], the abstraction of the hydrogen atom of the aldehyde group by the surface, therefore, seems more probable. These observations show that a pyrolytic carbon with

a high odd-electron content is capable of initiating free-radical reactions, as postulated by Wojciechowski and Laidler (14).

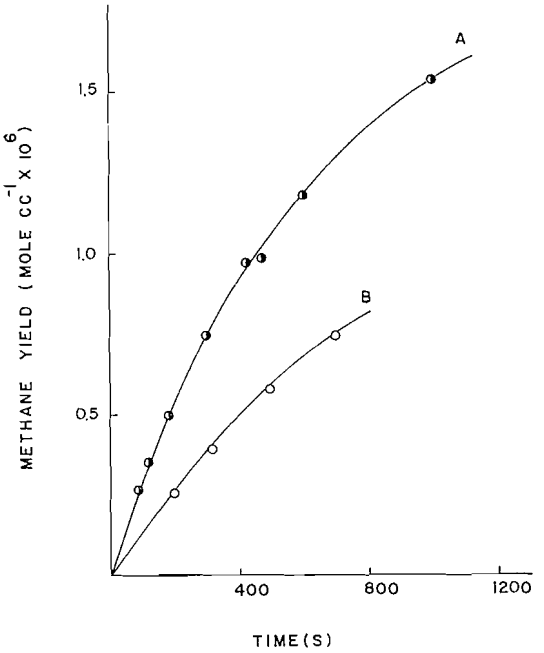

FIG. 8. Comparison of calculated yield–time curves with experimental results for methane production. The solid curves are calculated from eqs. [6] and [7]; the circles are experimental values. (A) 523 °C, 117 mm Hg; (B) 500 °C, 118 mm Hg.

Time-Course Studies

Equations have been derived to fit the experimental time-course data. The integrated equation for 3/2-order kinetics is

$$[6] \qquad [\mathrm{M}] = \left[\frac{2[\mathrm{M}]_0^{\frac{1}{2}}}{kt[\mathrm{M}]_0^{\frac{1}{2}} + 2}\right]^2,$$

where $[\mathrm{M}]_0$ is the initial concentration of acetaldehyde, and [M] that at time t. The concentration of methane as a function of $[\mathrm{M}]_0$, t, and k can be expressed using

$$[7] \qquad [\mathrm{CH_4}] = [\mathrm{M}]_0 - [\mathrm{M}].$$

Comparison of calculated yield-time curves with experimental results for methane production is shown in Fig. 8. The calculated curve agrees well with the experimental results even to very high conversion (70%), indicating that the bending of the curve is due to the disappearance of acetaldehyde only. Figure 9 shows alternative plots; Curve A is based on

$$[8] \qquad \frac{[\mathrm{CH_4}]}{t} = [\mathrm{M}]_0 - \left[\frac{2[\mathrm{M}]_0^{\frac{1}{2}}}{kt[\mathrm{M}]_0^{\frac{1}{2}} + 2}\right]^3 \Big/ t$$

and Curve B on

$$[9] \qquad \frac{\mathrm{d}[\mathrm{CH_4}]}{\mathrm{d}t} = k\left[\frac{2[\mathrm{M}]_0^{\frac{1}{2}}}{kt[\mathrm{M}]_0^{\frac{1}{2}} + 2}\right]^3,$$

which follows from eq. [6]. It is to be noted that the differential equation deviates from linearity at a much earlier stage (at about 20% conversion as compared with 50%); the integration method (eq. [8]), used in the present work, is therefore more reliable for obtaining initial rates.

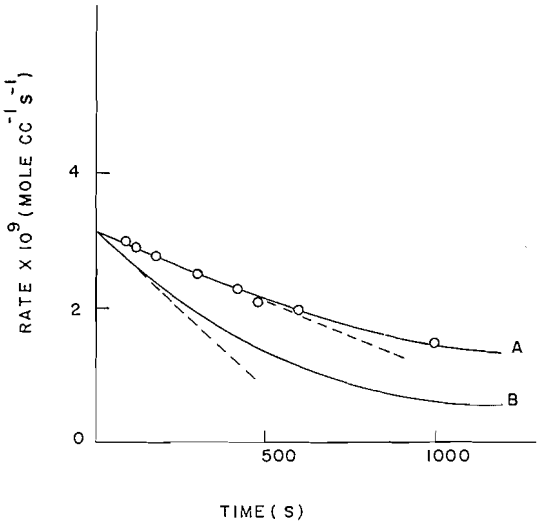

FIG. 9. Theoretical yield–time curves based on eq. [8] (Curve A) and eq. [9] (Curve B). The points are experimental values.

According to the proposed mechanism, the rate of formation of acetone is

$$[10] \qquad \frac{\mathrm{d}[\mathrm{CH_3COCH_3}]}{\mathrm{d}t} = k_8\left(\frac{k_1}{k_9}\right)^{\frac{1}{2}}[\mathrm{M}]^{3/2},$$

and hence

$$[11] \qquad [\mathrm{CH_3COCH_3}] = k_8\left(\frac{k_1}{k_9}\right)^{\frac{1}{2}}[\mathrm{M}]_0^{3/2} \times \frac{4}{k[\mathrm{M}]_0^{\frac{1}{2}}}\left[\frac{1}{4} - \frac{1}{(kt[\mathrm{M}]_0^{\frac{1}{2}} + 2)^2}\right].$$

The calculated yields of acetone calculated from eq. [11] agree with the experimental yields up to 50% conversion, as shown in Fig. 10. Again, the curvature in the plot is due to the disappearance of acetaldehyde alone.

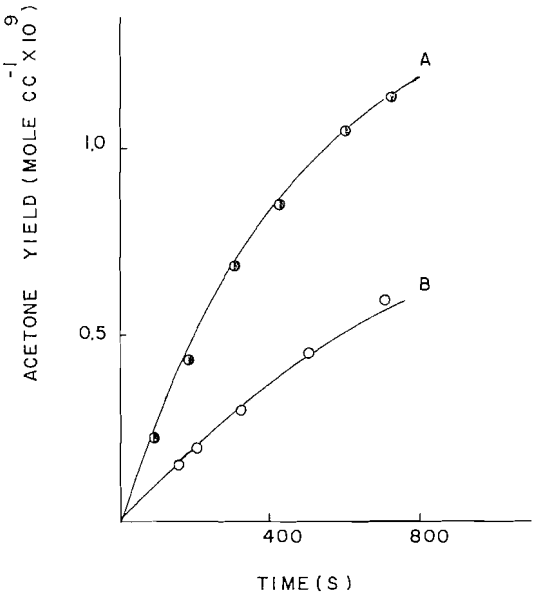

FIG. 10. Comparison of calculated yield–time curves with experimental results for acetone production. Solid curve calculated from eq. [*ii*]; the circles are experimental values. (A) 532 °C, 117 mm Hg; (B) 500 °C, 118 mm Hg.

Similarly, the yield of ethane production can be derived using the equation

$$[12]\quad [C_2H_6] = k_9\left(\frac{k_1}{k_9}\right) \times \frac{4}{k}[M]_0^{\frac{1}{2}}\left[\frac{1}{2} - \frac{1}{(kt[M]_0^{\frac{1}{2}}+2)}\right].$$

Figure 11 shows the calculated curves and the experimental points.

The rate of hydrogen production is given by eq. [5] and hence

$$[13]\quad \frac{[H_2]}{t} = \frac{4k_1}{k}[M]_0^{\frac{1}{2}}\left[\frac{1}{2t} - \frac{1}{(kt[M]_0^{\frac{1}{2}}+2)t}\right] + 4(k_6' + k_8)\left(\frac{k_1}{k_9}\right)^{\frac{1}{2}}\frac{[M]_0}{k} \times \left[\frac{1}{4t} - \frac{1}{(kt[M]_0^{\frac{1}{2}}+2)^2 t}\right]$$

or

$$[14]\quad \frac{[H_2]}{t} - f(t) = y.g(t).$$

The plot of $[H_2]/t - f(t)$ vs. $g(t)$ is given in Fig. 12; a linear relationship is obtained.

It is concluded that the production of CH_4, CH_3COCH_3, C_2H_6, and H_2 is consistent with the proposed mechanism, and that there is no loss or gain of these products resulting from other secondary processes.

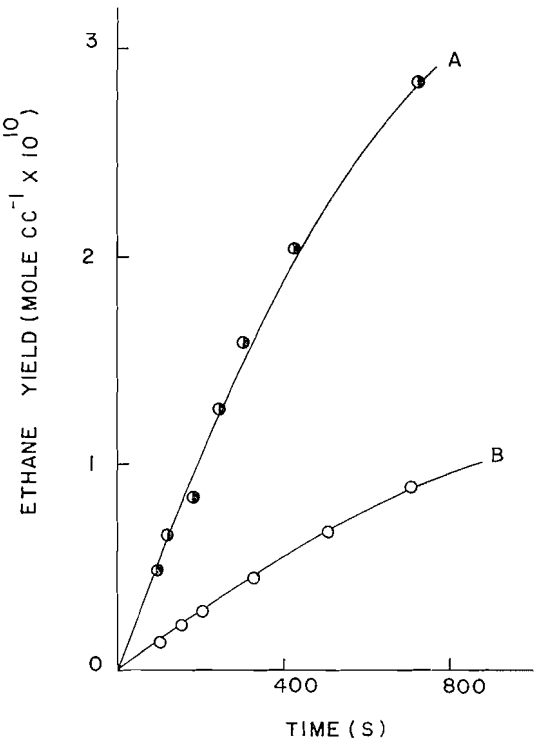

FIG. 11. Comparison of calculated yield–time curves with experimental results for ethane production. Solid curve calculated from eq. [12]; the circles are experimental values. (A) 523 °C, 117 mm Hg; (B) 500 °C, 118 mm Hg.

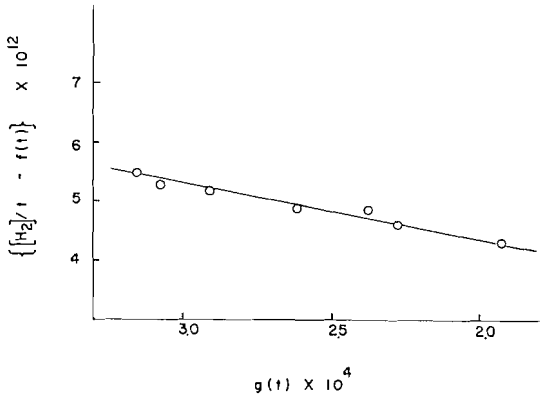

FIG. 12. Plot of $[H_2]/t - f(t)$ against $g(t)$ [cf. eqs. [13] and [14]], $T = 523$ °C.

General Discussion

In this section, additional discussion is made on a few special topics which previously have not been described in detail.

Unimolecular Decomposition of Acetaldehyde

It has been seen (Fig. 3) that the ratio k_1/k_9 at 540 °C becomes pressure dependent below 20 mm Hg. On the other hand, the rate constant k_9 shows a strong pressure dependence below 80 mm Hg (see Fig. 2). At lower pressures, k_1 must be falling off faster than k_9 so that an overall decrease in the ratio k_1/k_9 is noted. Since the rate of initiation must be equal to the rate of termination,

$$[15] \qquad v_1 = v_{C_2H_6} + v_{C_2H_5CHO}$$

$$[16] \quad k_1[CH_3CHO] = k_1'[CH_3CHO] + v_{C_2H_5CHO}$$

$$[17] \qquad k_1 = k_1' + \frac{v_{C_2H_5CHO}}{[CH_3CHO]}.$$

The values of k_1' at different pressures can be calculated from the rate of formation of ethane. Figure 13 depicts the falling off of this rate constant k_1' as a function of pressure. The effect is very pronounced at lower pressures and still noticeable in the high-pressure region. The extrapolated value of k_1' is obtained by plotting $[CH_3CHO]/v_{C_2H_6}$ against the reciprocal of the square root of the acetaldehyde pressure. The resulting equation is

$$\log k_1' \ (s^{-1}) = 16.25 \pm 0.45 - \frac{82700 \pm 1500}{2.303RT}.$$

In order to obtain k_1, the term $v_{C_2H_5CHO}/[CH_3CHO]$ must be added to k_1' according to eq. [17]. The resulting rate equation is

$$\log k_1 \ (s^{-1}) = 15.30 - \frac{79000 \pm 2000}{2.303RT}.$$

It is of interest to contrast the acetaldehyde pyrolysis with that of ethane (5). The rate expression for the latter reaction under ordinary conditions contains pressure-dependent terms in the numerator only, so that the compensation effect found with acetaldehyde is not found with ethane.

Szwarc (18) has shown that for a reaction such as the acetaldehyde dissociation the activation energy is related to the bond dissociation energy in the following way:

$$D + RT > E_{exp} > D.$$

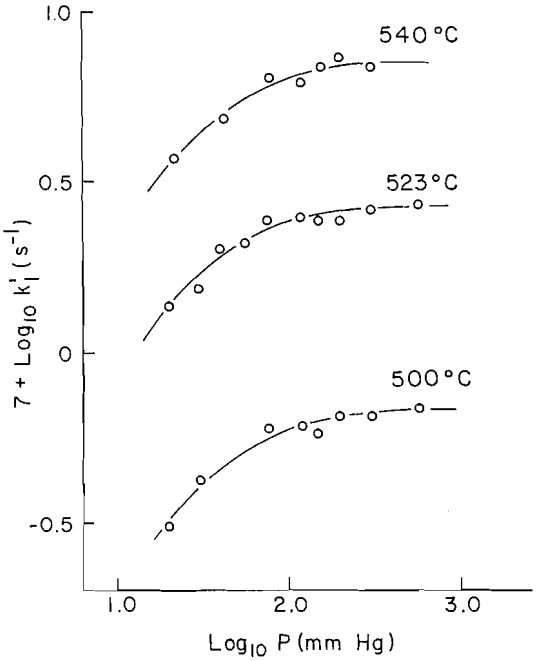

FIG. 13. Plots of log k_1' against log P.

In the case of the acetaldehyde decomposition,

$$D(CH_3—CHO) = E_1 - \tfrac{1}{2}RT = 78.2 \pm 2 \text{ kcal/mole}.$$

This value leads to

$$\Delta H_f^0(CHO) \simeq 7 \text{ kcal/mole}$$

and

$$D(H—CHO) \simeq 87 \text{ kcal/mole},$$

in good agreement with the recent determination of Walsh and Benson (19). The recent value of $D(CH_3CO—H)$ in CH_3CHO is 88 kcal/mole (20) and the present estimates appear to support the view that $D(H—CHO) \simeq D(CH_3CO—H)$, as suggested by several other authors (21–23). Using the above value, we get

$$D(H—CO) = \Delta H_f^0(CO) + \Delta H_f^0(H) - \Delta H_f^0(HCO) \simeq 19 \text{ kcal}.$$

This value is consistent with that of ~ 15 kcal suggested by Calvert (23, 26), but not with the high value of ~ 27 kcal favored by Klein and Schoen (24, 25).

The Decomposition of the Isopropoxy Radical

The rate constant k_8 is not a simple rate

constant but an apparent rate coefficient involving two elementary steps, as follows:

$$[11] \quad CH_3 + CH_3CHO \rightleftharpoons (CH_3)_2\dot{C}H\,(i\text{-PrO})$$

$$[12] \quad (CH_3)_2\dot{C}H \rightarrow CH_3COCH_3 + H\,.$$

Application of the steady-state treatment to these reactions leads to

$$[18] \quad k_8 = \frac{k_{11}k_{12}}{k_{-11} + k_{12}}\,.$$

In normal molecules, the carbon–hydrogen bond is stronger than the carbon–carbon bond, and this relation is also true for radicals (27). If on this basis one assumes that $k_{-11} \gg k_{12}$, eq. [15] reduces to $k_8 = k_{11}k_{12}/k_{-11}$. It is possible to estimate k_{12} since $K_{11} = k_{11}/k_{-11}$ can be calculated from the enthalpy and entropy changes, ΔH_{11} and ΔS_{11}. Use of values from ref. 28 leads to

$$K_{11} = 10^{2.33} \text{ cc mole}^{-1} \text{ at } 298.2\ ^\circ\text{K}.$$

Extrapolation of our value of k_8 to 298.2 °K leads to

$$k_{12}(298.2\ ^\circ\text{K}) = 6.82 \times 10^{-2}\ \text{s}^{-1}.$$

Taking $E_{12} = 19.1$ kcal/mole (see below), the Arrhenius equation for k_{12} is

$$\log k_{12}\ (\text{s}^{-1}) = 12.83 - \frac{19100}{2.303RT}\,.$$

The only value available in the literature for the decomposition of the isopropoxy radical by carbon–carbon fission is by Cox, Livermore, and Phillips (29). Their result is that at 298.2 °K, $k_{-11} = 1.3 \times 10^{-1}\ \text{s}^{-1}$, which is slightly greater than k_{12}.

Reaction [11] is exothermic by 7.3 kcal. The heat of activation can be related to the experimental activation energy by the relationship (30)

$$[19] \quad \Delta H^{\ddagger} = E_{\text{exp}} + (\Delta n^{\ddagger} - 1)RT,$$

where $\Delta n^{\ddagger}$ is the increase in the number of molecules from reactants to activated complex. This gives the value of 6.7 kcal for ΔE_{11} at 298.2 °K. If E_{-11} is taken to be 17.3 kcal/mole (29) at 298.2 °K, E_{11} and E_{12} will be 10.6 and 19.1 kcal/mole. With the use of the ΔH_f^0 values of the species involved in reaction [12], the heat of reaction turns out to be 15.4 kcal/mole which leads to $\Delta E_{12} = 14.8$ kcal/mole at 298.2 °K; hence $E_{-12} = 4.3$ kcal/mole.

Although the activation energy is low for reaction [−12], this reaction is not important in the present system as the concentration of hydrogen atoms is small. The activation energy diagram at 298.2 °K for these processes is given in Fig. 14.

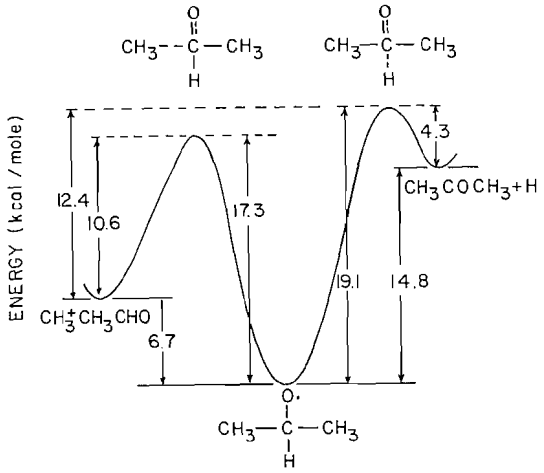

FIG. 14. Activation energy diagram for reactions of the $(CH_3)_2CHO$ radical at 298.2 °K.

It is seen from the diagram that not only is E_{12} greater than E_{-11}, but also the endothermicity of reaction [12] is much greater than that of [11]. This would favor an alkyl elimination and seems to support our earlier assumption that $k_{-11} \gg k_{12}$.

Since the isopropoxy radical is an intermediate of reaction [8] the possibility of other reaction products such as isopropyl alcohol and isopropyl methyl ether was not overlooked. These were not detected in our system. The steady-state concentration of isopropoxy radicals can be estimated; the ratio of $[i\text{-PrO}]/[CH_3]$ is about 10^{-7}–10^{-8} and that of $[CH_3CO]/[CH_3]$ is 10^{-2}–10^{-3}. Since the recombination of methyl and acetyl radicals to produce acetone is negligible, it is likely that $CH_3 + i\text{-PrO} \rightarrow i\text{-PrOCH}_3$ or $i\text{-PrO} + CH_3CHO \rightarrow i\text{-PrOH} + CH_3CO$ is not important. The concentration of the isopropoxy radical is of the order 10^{-20} mole/cc.

Possible Tunnelling in the Reaction $CH_3 + CH_3CHO \rightarrow CH_4 + CH_3CO$

The abstraction by the methyl radical of a hydrogen atom from acetaldehyde has been studied by many workers and by various methods; the results are tabulated in Table II.

TABLE II

Hydrogen atom abstraction reaction by a methyl radical from acetaldehyde

Reference	Method	Temperature (°C)	Rate constant (cc mole^{-1} s^{-1})	
This work	Pyrolysis of acetaldehyde	480–540	$10^{12.2}$	$10^{-8400/4.57T}$
Dodd (31)	Photolysis of acetaldehyde	117.8–266.8	$10^{12.3}$	$10^{-8000/4.57T}$
Birrell and Trotman-Dickenson (32)	Thermal decomposition of di-*t*-butyl peroxide in presence of acetaldehyde	121.4–174.1	$10^{11.9}$	$10^{-7500/4.57T}$
Ausloos and Steacie (33)	Photolysis of azomethane in presence of acetaldehyde	27–165	$10^{11.2}$	$10^{-6800/4.57T}$
Volman and Brinton (34, 35)	Thermal decomposition of di-*t*-butyl peroxide in presence of acetaldehyde	124.4–155.8	$10^{11.9}$	$10^{-7500/4.57T}$
Kerr and Calvert (20)	Photolysis of azomethane in presence of acetaldehyde	32–121.4	$10^{11.5}$	$10^{-6800/4.57T}$

The Arrhenius plot for different values of $k_4/k_9^{1/2}$ is shown in Fig. 15. Our results agree very well with Dodd's results and, in fact, a straight line can be drawn to link up his and our set of points in the Arrhenius plot; his temperature range is the next highest to ours. Taken all together the results seem to suggest a slight increase in activation energy over the range of temperatures investigated. There are several possible explanations for this:

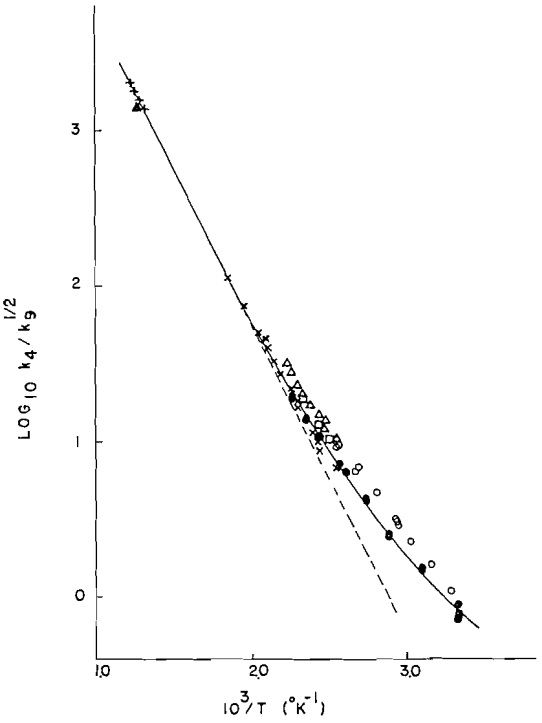

FIG. 15. Arrhenius plot of $k_4/k_9^{1/2}$. (+) Present work, (×) Dodd, (○) Kerr and Calvert, (△) Birrell and Trotman-Dickenson, (●) Ausloos and Steacie, (□) Volman and Brinton, (▲) Côme *et al.*

(1) Some of the methane in our experiments might have arisen from another source, such as

[6] $$CH_3 + CH_3CHO \rightarrow CH_4 + CH_2CHO.$$

The indications, however, are that the rate of this process is negligible.

(2) The pyrolysis experiments may give somewhat high results for $k_4/k_9^{1/2}$, because of pressure effects on k_9; this, however, has been taken into account in the present work.

(3) The low-temperature work may produce results which are too high because of reactions such as the disproportionation of CH_3 and CH_3CO.

(4) The curvature may be due to the occurrence of hot-radical reactions. This, however, seems unlikely since some of the work involved photosensitized production of radicals and showed similar results to those obtained in photolysis experiments.

(5) There may be quantum-mechanical tunnelling. Johnston (36, 37) has concluded that the similar processes

$$CH_3 + CH_3COCH_3 \rightarrow CH_4 + CH_2COCH_3$$

and

$$CD_3 + C_2H_6 \rightarrow CD_3H + C_2H_5$$

are best interpreted in terms of tunnelling. Further work is required to test this possibility; work with deuterated compounds would be of value.

Chain Lengths

On the basis of the mechanism the chain length is given by

[19] $$\Phi = k_4\left(\frac{1}{k_1k_9}\right)^{1/2}[CH_3CHO]^{1/2}.$$

Table III gives chain lengths calculated using the

values of k_1, k_4, and k_9 given earlier in this paper.

TABLE III

Chain lengths Φ as functions of pressure and temperature

	Pressure		
T (°C)	77 mm	118 mm	559 mm
480	9850	12160	26540
500	5570	6890	15030
523	3110	3850	8430
540	1920	2340	5080

Acknowledgments

The authors are grateful to Drs. M. H. Back, J. L. Holmes, and M. C. Lin for their valuable aid and constructive suggestions. M. T. H. L. thanks the National Research Council of Canada and Canadian Industries Limited for the award of research fellowships.

1. K. J. Laidler and M. T. H. Liu. Proc. Roy. Soc. London, Ser. A, **297**, 365 (1967).
2. A. Boyer, M. Niclause, and M. Letort. J. Chim. Phys. **49**, 337 (1952).
3. M. Eusuf and K. J. Laidler. Can. J. Chem. **42**, 1851 (1964).
4. R. E. Dodd and E. W. R. Steacie. Proc. Roy. Soc. London, Ser. A, **223**, 283 (1954).
5. M. C. Lin and M. H. Back. Can. J. Chem. **44**, 505 (1966).
6. L. F. Loucks and K. J. Laidler. Can. J. Chem. **45**, 2767 (1967).
7. S. Toby and B. H. Weiss. J. Phys. Chem. **68**, 2492 (1964).
8. A. J. Shepp. J. Chem. Phys. **24**, 939 (1956).
9. G. M. Côme, M. Dzierzynski, R. Martin, and M. Niclause. Compt. Rend. **264**, Ser. C, 548 (1967).
10. G. M. Côme, M. Dzierzynski, R. Martin, and M. Niclause. Compt. Rend. **264**, Ser. C, 836 (1967).
11. A. B. Trenwith. J. Chem. Soc. 4426 (1963).
12. M. C. Lin. Private communication
13. R. W. Dexter and A. B. Trenwith. J. Chem. Soc. 5459 (1964).
14. B. W. Wojciechowski and K. J. Laidler. Trans. Faraday Soc. **59**, 369 (1963).
15. A. Maccoll and P. J. Thomas. J. Chem. Soc. 979 (1955).
16. K. A. Holbrook. Proc. Chem. Soc. 418 (1964).
17. J. L. Holmes. Private communication.
18. M. Szwarc. Chem. Rev. **67**, 75 (1950).
19. R. Walsh and S. W. Benson. J. Am. Chem. Soc. **88**, 4570 (1966).
20. J. A. Kerr and J. G. Calvert. J. Phys. Chem. **69**, 1022 (1965).
21. E. O'Neal and S. W. Benson. J. Chem. Phys. **36**, 2196 (1962).
22. A. F. Trotman-Dickenson. Gas kinetics. Butterworths Scientific Publications, London. 1955.
23. J. G. Calvert. J. Chem. Phys. **29**, 954 (1958).
24. R. Klein and L. J. Schoen. J. Chem. Phys. **29**, 953 (1958).
25. R. Klein and L. J. Schoen. J. Chem. Phys. **24**, 1094 (1956).
26. J. G. Calvert. J. Phys. Chem. **61**, 1206 (1957).
27. M. C. Lin and K. J. Laidler. Can. J. Chem. **44**, 2927 (1966).
28. J. G. Calvert and J. N. Pitts, Jr. Photochemistry. John Wiley and Sons, New York. 1966. pp. 815–820.
29. D. L. Cox, R. A. Livermore, and L. Phillips. J. Chem. Soc. 245 (1966).
30. S. Glasstone, K. J. Laidler, and H. Eyring. The theory of rate processes. McGraw-Hill Book Company, New York. 1941.
31. R. E. Dodd. Can. J. Chem. **33**, 699 (1955).
32. R. N. Birrell and A. F. Trotman-Dickenson. J. Chem. Soc. 2059 (1960).
33. P. Ausloos and E. W. R. Steacie. Can. J. Chem. **33**, 31 (1955).
34. D. H. Volman and R. K. Brinton. J. Chem. Phys. **20**, 1053 (1952).
35. D. H. Volman and R. K. Brinton. J. Chem. Phys. **20**, 1764 (1952).
36. H. S. Johnston. Advan. Chem. Phys. **3**, 131 (1961).
37. H. S. Johnston. Gas phase reaction rate theory. Ronald Press Co., New York. 1966.

Can. J. Chem. Downloaded from www.nrcresearchpress.com by 210.87.254.40 on 09/05/12
For personal use only.

Study of phase changes in some iodides by the Hahn emanation technique[1]

V. P. NARANG[2] AND L. YAFFE
Radiochemistry Laboratory, Department of Chemistry, McGill University, Montreal, Quebec

Received July 18, 1967

^{135}I was incorporated into TlI, AgI, HgI_2, CuI, and PbI_2 and phase changes in the solid were studied by the Hahn emanation technique of following the emanation of the ^{135}Xe daughter. Good agreement was obtained with results previously obtained by conventional techniques.

Canadian Journal of Chemistry, **46**, 491 (1968)

Introduction

The Hahn emanation technique, i.e. the rate of evolution of a noble gas (1), has served as a useful qualitative indicator system in the study of reaction mechanisms (2) and thermal behavior of solids. Early workers (2–6) extensively made use of only those naturally occurring isotopes of radium and thorium which decay to form radon and thoron and thus their work had only limited application.

In order to derive useful information from these techniques the rate of emanation has to be known accurately. This requires uniform incorporation of the radioactive parent of the emanating substance into the system under investigation. It is also preferable that the half-life of the parent should be longer than the emanating daughter, in order to avoid possible errors introduced by the decay of parent during the period of experiment. However, if the duration of the experiment is small compared with the half-life of the parent, the results are not seriously affected (7).

In the present study the system

$$^{135}I \xrightarrow[6.7\ h]{\beta^-} {}^{135}Xe \xrightarrow[9.2\ h]{\beta^-}$$

was selected. This same system had previously been used by Zimens (8) to study the behavior of silver iodide. The present study was limited to an investigation of the thermal behavior of the iodides. No attempt was made to determine the "emanating power" as proposed by Flügge and Zimens (9), since an accurate knowledge of the diffusion coefficient and recoil ranges of ^{135}Xe in the various iodides is required.

[1]This research was assisted financially by the National Research Council of Canada.

[2]Present address: International Atomic Energy Agency, 11 Karntnerring, Vienna 1010, Austria.

Experimental

^{135}I was produced by the proton-induced fission of uranium oxide, U_3O_8, in the McGill synchrocyclotron at low energies (20–23 MeV).

Iodine was separated by the standard radiochemical procedure described by Glendenin and Metcalf (10). The purified iodine in the form of iodide was then mixed with

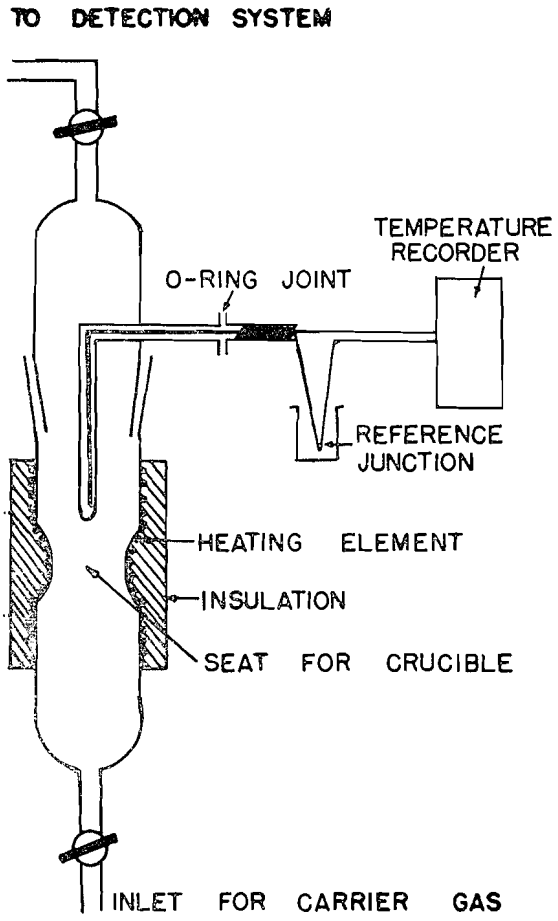

FIG. 1. Diagram of apparatus.

Can. J. Chem. Downloaded from www.nrcresearchpress.com by 210.87.254.40 on 09/05/12
For personal use only.

20 ml of 0.1 *M* potassium iodide solution. The mixing was carried out mechanically for 30 min to ensure uniform distribution of active and inactive iodine.

The iodides of Pb, Cu, Ag, Hg, and Tl were precipitated from this mixture by classical methods, care being taken to ensure that maximum specific activity was obtained in the samples. The iodide precipitates were subsequently transferred directly to sintered porcelain microcrucibles specially designed for this work. The microcrucibles containing the iodides were placed in a vacuum desiccator, left for about 6 to 7 h to allow some of the ^{135}Xe to be formed, dried, and then transferred to the heating system, details of which are shown in Fig. 1.

The temperature of the heating system was measured by a copper–constantan thermocouple and was controlled by a precision variable transformer.

Freon-12 (difluorodichloromethane) was used as a carrier gas for ^{135}Xe since many of its physical properties such as density, viscosity, and thermal conductivity are very similar to xenon. Each experiment lasted 15–25 min.

The ^{135}Xe activity was measured continuously by gamma-ray scintillation techniques with a NaI(Tl) Harshaw-type AF crystal with a through side-hole. The crystal was mounted on a Dumont, type 6292 photomultiplier tube whose output was fed to a preamplifier, a linear amplifier, and a single channel pulse height analyzer. The analyzer, gated to accept the 250-keV γ ray of ^{135}Xe (branching ratio 97%), was connected to a counting-rate meter and a strip chart recorder.

Results and Discussion

The number of runs performed for each compound varied from 3 to 5 and the results are quoted along with the standard deviation.

1. Thallous Iodide

A sharp peak was observed in the ^{135}Xe activity at 166 ± 0.8 °C as shown in Fig. 2. Three runs were performed. A visual observation at 168 °C showed that the color of the thallous iodide, yellow at room temperature, had changed to red. It is well known (11) that the yellow layer lattice form of TlI changes into red rhombic at 170 °C. The present observations confirm the studies of Schulz (12, 13) on the polymorphism of thallous iodide.

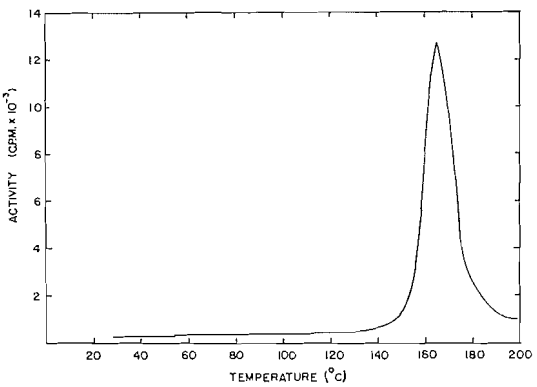

FIG. 2. ^{135}Xe activity vs. temperature — TlI.

2. Silver Iodide

A broad peak was observed at 143 ± 2 °C as shown in Fig. 3.

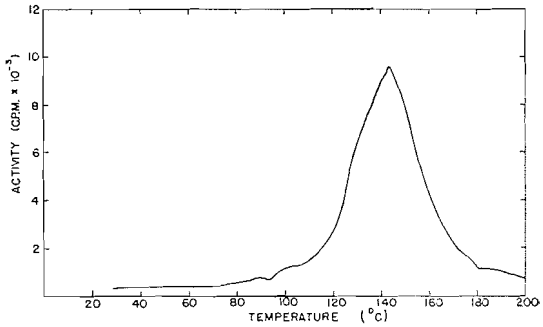

FIG. 3. ^{135}Xe activity vs. temperature — AgI.

According to Wells (14), there appears to be some confusion in the literature concerning the polymorphism of AgI. This compound occurs as a hexagonal mineral with wurzite structure. On being powdered the hexagonal crystals are converted into the cubic form. A mixture of the two is obtained if silver iodide is precipitated from a silver nitrate solution by potassium iodide. The form, stable at room temperature, is apparently the cubic (γ) form which on heating at 137 °C changes to the hexagonal (β) form, and at 145.8 °C changes to the α form.

Our method of obtaining AgI was similar to that described above, and the broadening of the peak is due to the changes in various modifications of the AgI.

Zimens (8) also studied AgI and he obtained a single broad peak at 145 °C.

3. Mercuric Iodide

In this case a sharp rise in ^{135}Xe activity was observed at 125.8 ± 0.1 °C as shown in Fig. 4. It was also noticed that the color of the HgI_2 changed from red to yellow at 126 °C.

It has been reported (15) that at 127.4 ± 0.4 °C the crystalline form of HgI_2 changes from tetragonal to rhombic.

4. Cuprous Iodide

In this case as shown in Fig. 5, the ^{135}Xe activity starts increasing at 80 °C and reaches a maximum at 138 ± 2 °C. There are two more humps at 163.5 ± 2 °C and 179 ± 2 °C. Miyake

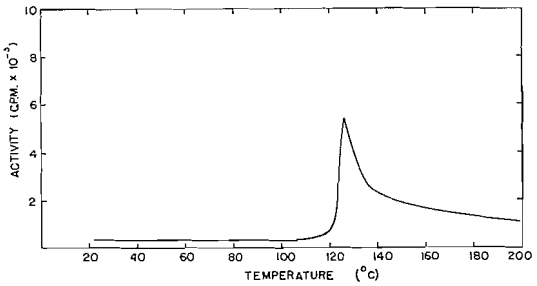

FIG. 4. ^{135}Xe activity vs. temperature — HgI_2.

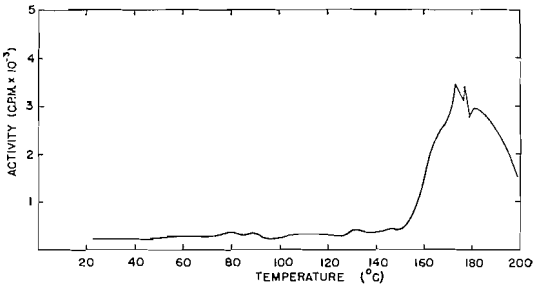

FIG. 6. ^{135}Xe activity vs. temperature — PbI.

et al. (16) reported that CuI, which has normally the zinc blende type (γ) structure at room temperature, changes completely to the hexagonal wurzite (β) at 369 °C. However, anomalous changes in the crystal structure were said to begin at about 200 °C. From the present results one would say that the anomalous behavior of CuI starts at 138 °C. Three runs were performed and identical results were obtained.

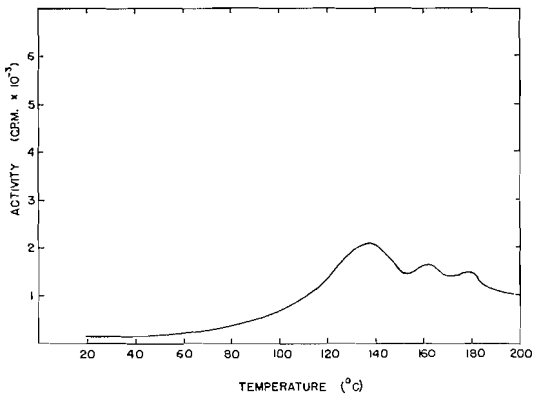

FIG. 5. ^{135}Xe activity vs. temperature — CuI.

5. Lead Iodide

In the case of PbI_2, the increase in the ^{135}Xe activity starts at 150 °C. Two very closely placed small peaks at 172 ± 0.7 °C and 176.1 ± 0.7 °C, as shown in Fig. 6, were observed in the region of maximum activity. These occurred reproducibly in each of the three trials. Pinsker *et al.* (17) reported a hexagonal-type structure for PbI_2 of which two modifications exist. When PbI_2 is crystallized from water (as was done in the present work), the form that results depends upon the velocity of crystallization and both or either of the two forms may be prepared. No other data exist about the temperature dependence of the phases.

Yet another possibility could be phase changes in $KPbI_3$, formed by the reaction of any potassium iodide adsorbed on the surface of the PbI_2 with the lead iodide (18).

The present work shows that the results obtained by the emanation method, using the ^{135}I–^{135}Xe system, are in close agreement with those obtained by the conventional crystallographic techniques, particularly in the cases of AgI, HgI_2, and TlI. This method enables one to obtain a very good qualitative indication of the phase changes.

1. O. HAHN and O. MULLER. Z. Elektrochem. **29**, 189 (1923).
2. R. JAGITSCH. Z. Physik. Chem. Leipzig, **B35**, 196 (1936).
3. O. ERBACHER. Z. Physik. Chem. Leipzig, **B33**, 47 (1936).
4. O. HAHN. Applied radiochemistry. Cornell University Press, Ithaca, New York. 1936.
5. G. GRAUE. Kolloidchem. Beih. **32**, 403 (1931).
6. K. ZIMENS. Z. Physik. Chem. Leipzig, **B37**, 23 (1937).
7. G. B. COOK and E. W. PROUT. J. Inorg. Nucl. Chem. **3**, 225 (1956).
8. K. ZIMENS. Z. Physik. Chem. Leipzig, **A191**, 1 (1942).
9. S. FLÜGGE and K. ZIMENS. Z. Physik. Chem. Leipzig, **B42**, 179 (1939).
10. L. E. GLENDENIN and R. D. METCALF. Radiochemical studies: the fission products. Book II. *Edited by* C. D. Coryell and N. Sugarman. McGraw-Hill Book Co., New York. 1951. Paper 278. p. 1625.
11. N. V. SIDGWICK. The chemical elements and their compounds. Oxford University Press, London. 1950. p. 486.
12. L. G. SCHULZ. J. Chem. Phys. **18**, 996 (1950).
13. L. G. SCHULZ. Acta Cryst. **4**, 487 (1951).
14. A. F. WELLS. Structural inorganic chemistry. Oxford University Press, London. 1950. p. 271.
15. INTERNATIONAL CRITICAL TABLES. Vol. 4. McGraw-Hill Publ. Co., New York, N.Y. 1928. p. 7.
16. S. MIYAKE, S. HOSHINO, and T. TAKENAKA. J. Phys. Soc. Japan, **7**, 19 (1952).
17. Z. G. PINSKER, L. I. TATRINOVA, and V. A. NOVIKOVA. Acta Physicochim. URSS, **18**, 378 (1943).
18. C. A. JACOBSON (*Editor*). Encyclopedia of chemical reactions. Vol. V. Reinhold Publishing Corporation, New York. 1951. p. 235.

Can. J. Chem. Downloaded from www.nrcresearchpress.com by 210.87.254.40 on 09/05/12
For personal use only.

Can. J. Chem. Downloaded from www.nrcresearchpress.com by 210.87.254.6 on 09/05/12
For personal use only.

Properties of the solutions of the alkali-chlorozirconate compounds in alkali-chloride melts

S. N. FLENGAS, J. E. DUTRIZAC,[1] AND R. L. LISTER[2]
Department of Metallurgy and Materials Science, University of Toronto, Toronto, Ontario

Received May 23, 1967

The activities of Li_2ZrCl_6, Na_2ZrCl_6, and K_2ZrCl_6 in the systems LiCl–Li_2ZrCl_6, NaCl–Na_2ZrCl_6, and KCl–K_2ZrCl_6, respectively, were calculated from available pressure data using a modified form of the Gibbs–Duhem relationship. The calculations indicate positive deviations from ideality that decrease with increasing size of the alkali metal cation.

Canadian Journal of Chemistry, 46, 495 (1968)

Introduction

Recent work from this laboratory (1, 2) has shown that the pressures of zirconium tetrachloride vapor in equilibrium with the systems LiCl–Li_2ZrCl_6, NaCl–Na_2ZrCl_6, and KCl–K_2ZrCl_6, are directly related to the corresponding phase diagrams. The phase diagrams for the three systems were also determined and were of the simple eutectic type with no evidence of solid solubility.

The thermal decomposition of the chlorozirconates is represented by the reaction

$$[1] \quad \underset{\text{solid or in solution}}{M_2ZrCl_6} = \underset{\text{solid or in solution}}{2MCl} + \underset{\text{vapor}}{ZrCl_4},$$

where M is either Li^+, Na^+, or K^+.

The equilibrium vapor pressures of zirconium tetrachloride have been measured using various MCl–M_2ZrCl_6 mixtures over the permissible composition and temperature range for each binary system. The data indicated eutectic and liquidus melting, and were used to compare the thermal stability of the chlorozirconate compounds and to evaluate their potential use as electrolytes for the recovery of zirconium metal by fused salt electrolysis.

In the present investigation, a method has been applied whereby isothermal activities in the liquid solutions are calculated from the available pressure data (1, 2).

Calculation of Activities from Pressure Data in a Reactive System

Considering the all-liquid temperature–composition region in the phase diagram of the binary system MCl–M_2ZrCl_6, the equilibrium constant for reaction [1] is written as

$$[2] \quad K = \frac{a^2_{MCl} \cdot P_{ZrCl_4}}{a_{M_2ZrCl_6}}.$$

For the purpose of this treatment, the states of reference for MCl and M_2ZrCl_6 are chosen as the pure liquids at all temperatures and, for zirconium tetrachloride vapor, the pure vapor at 1 atm pressure.

Equation [2] may be written in a differential form as

$$[3] \quad d \ln K = 2\, d \ln a_{MCl} + d \ln P_{ZrCl_4} - d \ln a_{M_2ZrCl_6}.$$

Considering any isotherm in the all-liquid range, K is constant and

$$d \ln K = 0.$$

Hence, at constant temperature,

$$[4] \quad 2\, d \ln a_{MCl} + d \ln P_{ZrCl_4} - d \ln a_{M_2ZrCl_6} = 0.$$

Furthermore, the activities a_{MCl} and $a_{M_2ZrCl_6}$ in the liquid solutions are related by the Gibbs–Duhem expression in the form (see Appendix A)

$$[5] \quad d \ln a_{MCl} = -\frac{X_{M_2ZrCl_6}}{X_{MCl}}\, d \ln a_{M_2ZrCl_6}.$$

If it is assumed that the pressure dependence of the activities is negligibly small for pressures not exceeding 1 or 2 atm (3), then eq. [5] may be introduced into eq. [4]. Upon rearrangement of the terms, the following relationship is readily obtained.

$$[6] \quad d \ln a_{M_2ZrCl_6} = \frac{X_{MCl}}{1 + X_{M_2ZrCl_6}}\, d \ln P_{ZrCl_4}$$

The activities of M_2ZrCl_6 may be calculated by integration along any given isotherm from available pressure data. The integration of eq. [6] is

[1]Present address: Noranda Research Centre, Pointe Claire, Quebec, Canada.

[2]Present address: National Lead Company, Research Laboratory, P.O. Box 58, South Amboy, New Jersey 08879, U.S.A.

TABLE I

Activity calculations from vapor pressure data

(a) System: $LiCl–Li_2ZrCl_6$

$X_{Li_2ZrCl_6}$	$\frac{X_{LiCl}}{1 + X_{Li_2ZrCl_6}}$	Log P_{ZrCl_4} (Torr) at 808 °K (±0.02)	$a_{Li_2ZrCl_6}$ (±0.02)
1	0	3.234	1.0
0.400	0.428	2.895	0.86
0.302	0.536	2.715	0.71
0.199	0.668	2.543	0.57
0.100	0.818	2.452	0.46

(b) System: $NaCl–Na_2ZrCl_6$

$X_{Na_2ZrCl_6}$	$\frac{X_{NaCl}}{1 + X_{Na_2ZrCl_6}}$	Log P_{ZrCl_4} (Torr) (±0.01)		$a_{Na_2ZrCl_6}$ (±0.01)	
		919 °K	1023 °K	919 °K	1023 °K
1.0	0	3.029	4.085*	1.0	1.0
0.873	0.0678	2.860	3.302*	0.97	0.95
0.784	0.1204	2.686	3.149*	0.93	0.92
0.710	0.1696	2.519	3.058*	0.89	0.89
0.627	0.2292	2.420	3.024*	0.86	0.87
0.576	0.2690	2.312	2.913*	0.81	0.82
0.507	0.3271	2.233	2.817	0.75	0.76
0.254	0.5949	1.844*	2.442	0.49	0.53
0.104	0.8099	1.367*	1.966	0.23	0.23

(c) System: $KCl–K_2ZrCl_6$

$X_{K_2ZrCl_6}$	$\frac{X_{KCl}}{1 + X_{K_2ZrCl_6}}$	Log P_{ZrCl_4} (Torr) (±0.005)		$a_{K_2ZrCl_6}$ (±0.01)	
		1072 °K	1173 °K	1072 °K	1173 °K
1.0	0	2.750	3.127*	1.0	1.0
0.888	0.0593	2.558	2.980*	0.99	0.98
0.819	0.0995	2.398	2.894	0.97	0.96
0.588	0.2594	1.775	2.405	0.75	0.80
0.513	0.3219	1.599	2.203	0.66	0.70
0.295	0.5444	1.144	1.747	0.46	0.45
0.168	0.7123	1.005	1.584	0.34	0.35
0.109	0.8034	0.851	1.446	0.25	0.28

*Extrapolated from pressures measured in a different temperature range.

conducted graphically by plotting the concentration parameter $Q = X_{MCl}/(1 + X_{M_2ZrCl_6})$ against the logarithm of pressure from pure liquid M_2ZrCl_6 to any given composition. For the pure liquid chlorozirconate, $a_{M_2ZrCl_6} = 1$ and $Q = 0$. Hence,

$$[7] \qquad \ln a_{M_2ZrCl_6} = \int_{Q=0}^{Q} Q \, d \ln P_{ZrCl_4}.$$

Results

The pressures of zirconium tetrachloride in equilibrium with liquid solutions at various compositions were available (1, 2) in the form of logarithmic equations, linear with respect to temperature, obtained by the least squares method. For the systems $NaCl–Na_2ZrCl_6$ and $KCl–K_2ZrCl_6$, the accuracy of the results corresponded to a standard deviation of 0.005 to 0.01 in the log p values. For the $LiCl–Li_2ZrCl_6$ system, the results were less accurate, and the standard deviations in the log p values were of the order of 0.02. The pressure data at various compositions calculated from these expressions at the temperatures selected for the activity calculation are given in Table I.

For pure Na_2ZrCl_6, pressures at temperatures higher than the melting point were not available. These were computed using the expression

$$[8] \qquad \Delta G_{F(T)} = RT \ln \frac{P_L}{P_s},$$

where $\Delta G_{F(T)}$ is the free energy of fusion of Na_2ZrCl_6 at a temperature T and, P_L and P_s, respectively, are the pressures of zirconium tetrachloride in equilibrium with pure liquid

Can. J. Chem. Downloaded from www.nrcresearchpress.com by 210.87.254.6 on 09/05/12
For personal use only.

Can. J. Chem. Downloaded from www.nrcresearchpress.com by 210.87.254.6 on 09/05/12
For personal use only.

and pure solid Na_2ZrCl_6 at the same temperature. The necessary thermal data for calculating the free energy of fusion as a function of temperature were also available from previous calorimetric work (4) and are given in Table II.

TABLE II

Activities at the liquidus temperatures from cryoscopic calculations*

$X_{Li_2ZrCl_6}$	T_L (°C)	$a_{Li_2ZrCl_6}$ at T_L
System: $LiCl$–Li_2ZrCl_6		
1.0	535	1.0
0.9	533	0.985±0.001
0.8	530	0.965±0.005
0.7	526	0.930±0.015
0.6	519	0.890±0.025
0.5	506	0.805±0.030
$X_{Na_2ZrCl_6}$	T_L (°C)	$a_{Na_2ZrCl_6}$
System: $NaCl$–Na_2ZrCl_6		
1.0	646	1.0
0.9	630	0.960±0.002
0.8	604	0.900±0.020
0.7	575	0.830±0.040
$X_{K_2ZrCl_6}$	T_L (°C)	$a_{K_2ZrCl_6}$
System: KCl–K_2ZrCl_6		
1.0	799	1.0
0.9	788	0.985±0.005
0.8	770	0.930±0.025
0.7	750	0.885±0.035
0.6	720	0.845±0.060
0.5	676	0.770±0.095

*The thermal data for this calculation are (3):
For Li_2ZrCl_6: ΔH_F at T_F = 9300 ± 1600 (cal/mole), C_p(solid) = 42.5 + 5.02 × 10^{-2} T(cal/deg mole), C_p(liquid) = 76.9 (cal/deg mole).
For Na_2ZrCl_6: ΔH_F at T_F = 4000 ± 1300 (cal/mole), C_p(solid) = 63.7 (cal/deg mole), C_p(liquid) = 61.7 (cal/deg mole).
For K_2ZrCl_6: ΔH_F at T_F = 5500 ± 2000 (cal/mole), C_p(solid) = 64.9, C_p(liquid) = 78.0.

For compositions close to pure chlorozirconate, the reaction pressures at the melting temperature of the chlorozirconate exceeded 1 atm, and these had to be obtained by extrapolating data available at lower temperatures. For this reason, the activities of Na_2ZrCl_6 and K_2ZrCl_6 were calculated at two temperatures only, e.g. at the melting point of the pure compounds and at a temperature higher than the melting point by about 100 °C. For the $LiCl$–Li_2ZrCl_6 system, the available pressures for pure Li_2ZrCl_6 represented part of the Li_2ZrCl_6 liquidus tie line and had to be extrapolated to the melting point of pure Li_2ZrCl_6. Hence, for this system, activity calculations were performed only at the melting temperature of Li_2ZrCl_6.

For graphical integration, the parameter Q was plotted against log p and the activities were obtained at the various compositions from the corresponding areas under the curves.

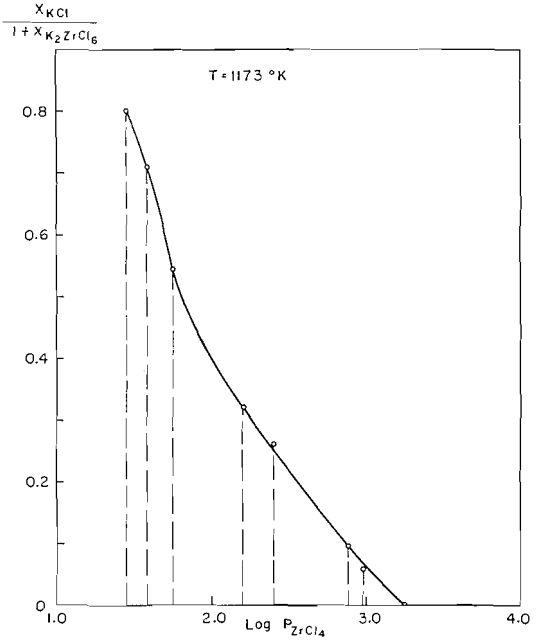

FIG. 1. Q vs. log P_{ZrCl_4} integration curve for K_2ZrCl_6 at 1173 °K.

A typical integration curve for K_2ZrCl_6 at 1173 °K is shown in Fig. 1. The results of these calculations for the three systems at the specified temperatures are given in Figs. 2, 3, and 4.

The activities of the hexachlorozirconate compounds at the corresponding liquidus temperatures, calculated from the phase diagrams (1, 2) using the expanded form of the well-known Van't Hoff equation,

$$[9] \qquad \frac{d \ln a}{d\left(\frac{1}{T}\right)} = -\frac{\Delta H_F}{R},$$

are also shown for comparison.

The width of the arrows on the curves reflects the uncertainty which appears in the cryoscopic calculations because of the error limits in the heats of fusion. The data is also given in detail in Table II. In spite of such large uncertainties,

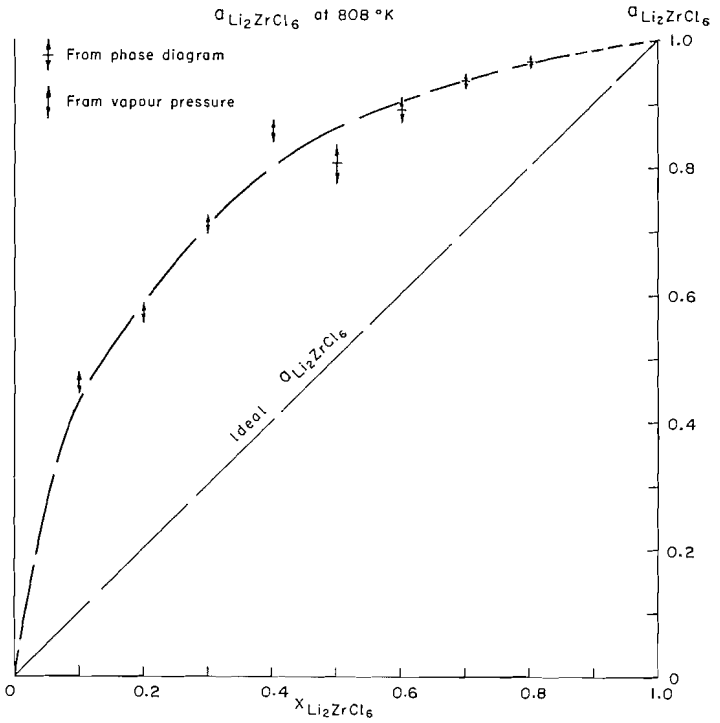

FIG. 2. Activity isotherms in the LiCl-Li_2ZrCl_6 system.

it is evident that the cryoscopic and the vapor pressure methods are in substantial agreement. For the latter, the error limits are readily calculated from the standard deviations in the log p values, and are also given in Table I.

The activities of the alkali metal chlorides in the NaCl–Na_2ZrCl_6 and KCl–K_2ZrCl_6 systems were then calculated from the activity isotherms for the chlorozirconates, using the Gibbs–Duhem eq. [5] and are included in Figs. 3 and 4. For the integration, it is taken as self-evident that Raoult's law is applicable to the MCl component, irrespective of the method of expressing concentrations (Appendix A). However, in the vicinity of the M_2ZrCl_6 component, Henry's law is not valid as at $X_{MCl} = 0$ the activity of MCl acquires a finite value corresponding to that in a liquid of the M_2ZrCl_6 composition.

The activity of M_2ZrCl_6 becomes equal to unity only at $X_{M_2ZrCl_6} = 1$ and, hence, Raoult's law is not expected to hold for this component.

An approximate numerical value for the activity of MCl may be obtained from the data as follows:

The equilibrium constants for reaction [1] may be evaluated from the pressure and activity data given in Table I, and in Figs. 3 and 4 at corresponding compositions. For Na_2ZrCl_6 and K_2ZrCl_6, these have the average values of 87.0 ± 7.0 and 76.0 ± 6, respectively, when the pressures are given in Torr. Using these values at $X_{M_2ZrCl_6} = 1$, the activities for NaCl and KCl are found to be 0.28 ± 0.04 and 0.24 ± 0.03, respectively. Thus, the activity curves in Figs. 3 and 4 approach the nominal composition $X_{MCl} = 0$ in the manner shown on the graphs.

Discussion

If the "ideal" activity line is defined to represent the overall MCl–$ZrCl_4$ system, then the activities of NaCl and KCl show negative deviations from ideality, as expected for a system where compound formation occurs. However, considering the MCl–M_2ZrCl_6 subsystem, the "ideal" solution may also be described as consisting of M^+ cations, $ZrCl_6^{2-}$ anions, and the stoichiometric balance of "free" Cl^- anions. In this model, the measured activities show positive deviations from the new "ideal"

Can. J. Chem. Downloaded from www.nrcresearchpress.com by 210.87.254.6 on 09/05/12
For personal use only.

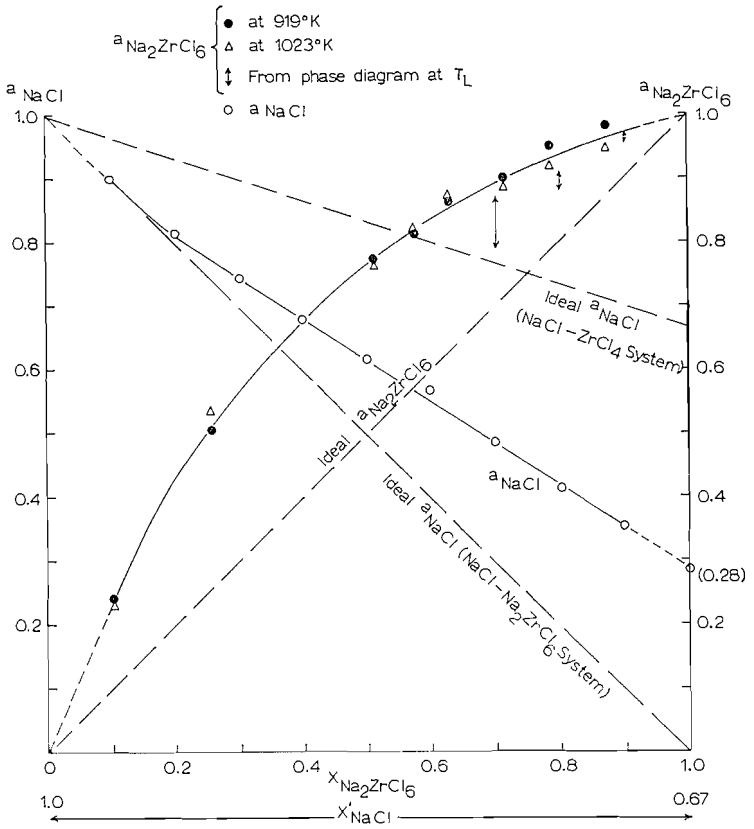

FIG. 3. Activity isotherms in the $NaCl–Na_2ZrCl_6$ system. X'_{NaCl} represents concentrations in the $NaCl–ZrCl_4$ system.

line. This behavior could be interpreted as indicating a decrease in the chemical stability of the chlorozirconate compounds from the hypothetical "ideal" solution of undissociated and non-interacting $ZrCl_6^{2-}$ species.

For a binary system with a common cation, the mole fractions are numerically equal to the ionic fractions and, hence, the observed positive deviations from ideality imply deviations from Temkin's (5) model for the ideal ionic solution. The equivalent fraction model (6) is similarly non-applicable, as it predicts negative deviations from ideality.

The activity isotherms in Figs. 3 and 4 indicate that, for the systems $NaCl–Na_2ZrCl_6$ and $KCl–K_2ZrCl_6$, the temperature dependence of the activity should be negligibly small. Over the 100 °C temperature range investigated, a consistent temperature dependence cannot be predicted and, if such dependence exists, it should be well within the accuracy limits of the measurements.

This observation is in qualitative agreement with the few available data on the general behavior of other binary systems with common cation. For example, the systems Li(Cl–Br), Na(Cl–Br) and K(Cl–Br), investigated by Kleppa, Hersh, and Toguri (7), were found to have very small positive heats of mixing. Flood and Muan (8) found that in the melts $Na_2(CrO_4–Cr_2O_7)$ and $K_2(CrO_4–Cr_2O_7)$ of equimolar composition the heats were only 150 and 250 cal respectively. However, the $Na_2(CO_3–S)$ system, investigated by Rosen and Sillen (9), was found to have heats of mixing as high as 950 cal, while the $Na_2(CO_3–SO_4)$ system, investigated by Flood, Forland, and Motzfeldt (10), was found to be ideal.

Activities and partial molar heats of mixing for the two systems $Na_2ZrCl_6–NaCl$ and $K_2ZrCl_6–KCl$ have also been reported in a

Can. J. Chem. Downloaded from www.nrcresearchpress.com by 210.87.254.6 on 09/05/12
For personal use only.

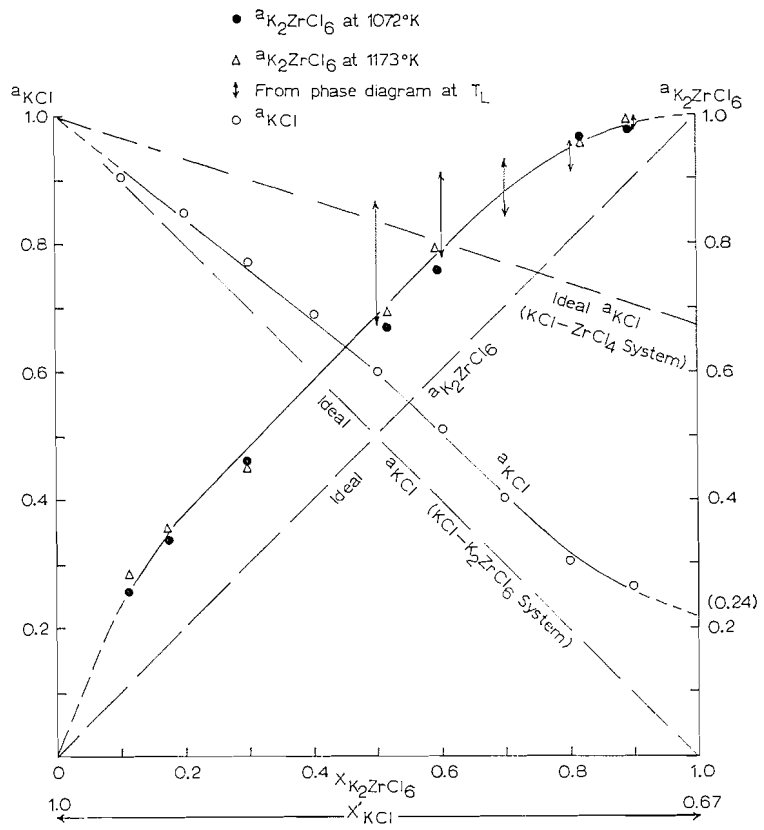

FIG. 4. Activity isotherms in the KCl–K_2ZrCl_6 system. X'_{KCl} represents concentrations in the KCl–$ZrCl_4$ system.

previous publication (1) from this laboratory, using the heat terms calculated from the log p against $1/T$ curves, for pressure data obtained at temperatures above and below the liquidus. This method is now known (11) to be incorrect as it ignores the concentration dependence of activity along a liquidus tie line. Accordingly, the previously reported partial molar properties for these two systems should be disregarded.

The method employed in the present investigation yields data which are consistent with cryoscopic calculations. The method should be particularly useful with reactive systems, for which other methods like calorimetry or e.m.f. measurements cannot be readily applied owing to the thermal instability of the solutions.

The activity coefficients of M_2ZrCl_6 for the three systems investigated in the concentration range 0.2 to 0.8 mole fraction may be expressed by empirical equations of the general form

$$[11] \quad \log \gamma_{M_2ZrCl_6} = \frac{a}{2.3RT} + X^2_{MCl}\frac{b}{2.3RT}.$$

The plots of log $\gamma_{M_2ZrCl_6}$ against X^2_{MCl} are given in Fig. 5*a*. The b constants calculated from the slope of the curves are also given in the graph. It is significant that the b parameters decrease with increasing ionic size in proportion to the square of the ionic radius of the alkali metal cation, as shown in Fig. 5*b*. Hence, the b parameters appear to be related to anion to anion next neighbor repulsions that are expected to be predominant in solutions of this type. If the distance separating the two anions is assumed to be proportional to the size of the common alkali metal cation, then it should also be expected that the repulsive forces between anions should decrease in proportion to the square of the cation radius, thus justifying the observed empirical relationships.

However, the solutions cannot be described as "regular" either, on the basis of eq. [11]. If the entropy of mixing is wholly configurational, then the quasichemical theory (6, 12, 13) applied to interactions between nearest neighbors pre-

Can. J. Chem. Downloaded from www.nrcresearchpress.com by 210.87.254.6 on 09/05/12
For personal use only.

Can. J. Chem. Downloaded from www.nrcresearchpress.com by 210.87.254.6 on 09/05/12
For personal use only.

dicts that the concentration dependence of the activity coefficient should be given by simple expressions of the form

[12] $$RT \ln \gamma_{M_2ZrCl_6} = X^2{}_{MCl} b.$$

Hence, the a parameter in eq. [11], which is almost constant and independent of the cation size, could be associated with slight deviations from random mixing. The assumption is justified because of the significant differences in the electrical charge and in the molar volumes of the $ZrCl_6^{2-}$ and Cl^- anions.

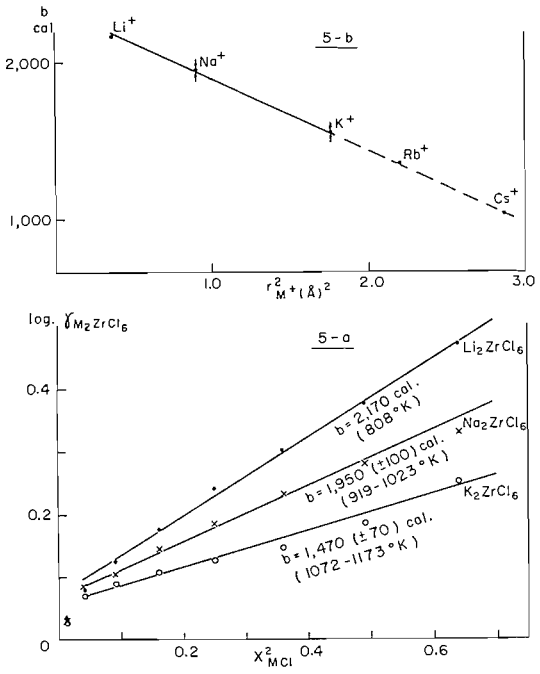

FIG. 5. Regular solution model. (*a*) Plot of log $\gamma_{M_2ZrCl_6}$ against $X^2{}_{MCl}$. (*b*) Plot of the interaction parameter b against the square of the ionic radii of the alkali metal cations.

It is significant that the size of the cation in an alkali metal chloride plays a predominant role in stabilizing zirconium tetrachloride as the hexachlorozirconate and also in providing further stabilization when the M_2ZrCl_6 compound is dissolved in a MCl melt. It may be predicted that the solutions of zirconium tetrachloride in rubidium and caesium chlorides should be the most stable of the entire family of the chlorozirconates.

Acknowledgments

The authors are indebted to the Defence Research Board of Canada for its financial aid in support of this investigation. Many helpful discussions with Dr. J. P. Valleau of the Department of Chemistry of the University of Toronto are also gratefully acknowledged.

Appendix A

Let us consider a series of solutions in the all-liquid region of the phase diagram of the binary system MCl–$ZrCl_4$ at constant temperature and pressure. This phase diagram is described by one congruently melting compound of the type M_2ZrCl_6 and the corresponding two eutectics (1, 2). The obvious components in this case are MCl and $ZrCl_4$ respectively, and the standard form of the Gibbs–Duhem expression for this system is

[1] $$X'_{MCl} \, d \ln a_{MCl} + X_{ZrCl_4} \, d \ln a_{ZrCl_4} = 0,$$

where X'_{MCl} and X_{ZrCl_4} are the mole fractions of MCl and $ZrCl_4$ respectively in the binary system MCl–$ZrCl_4$.

The same series of solutions, between compositions corresponding to pure MCl and M_2ZrCl_6, may also be described by the components MCl and M_2ZrCl_6.

The mole fractions are now redefined as X_{MCl} and $X_{M_2ZrCl_6}$ respectively, where X_{MCl} is different from X'_{MCl}.

From the stoichiometry of the reaction, it is readily shown that

[2] $$X'_{MCl} = \frac{1 + X_{M_2ZrCl_6}}{1 + 2X_{M_2ZrCl_6}}$$

and

[3] $$X_{ZrCl_4} = \frac{X_{M_2ZrCl_6}}{1 + 2X_{M_2ZrCl_6}}.$$

For the equilibrium, we may also write

[4] $$a_{M_2ZrCl_6} = K a^2{}_{MCl} \cdot a_{ZrCl_4},$$

where all activities are independent of the mode of expressing compositions. At constant temperature and pressure, eq. [4] is also written as

[5] $$d \ln a_{ZrCl_4} = d \ln a_{M_2ZrCl_6} - 2 \, d \ln a_{MCl}.$$

Substituting X'_{MCl} and X_{ZrCl_4} from [2], [3] and $d \ln a_{ZrCl_4}$ from [5] into eq. [1], we find that

$$X_{MCl} \, d \ln a_{MCl} + X_{M_2ZrCl_6} \, d \ln a_{M_2ZrCl_6} = 0.$$

It is significant that the Gibbs–Duhem equation is applicable for any "arbitrary sub-system" within the phase diagram describing the primary binary system.

1. R. L. LISTER and S. N. FLENGAS. Can. J. Chem. **43**, 2947 (1965).
2. J. E. DUTRIZAC and S. N. FLENGAS. Symposium on Advances in Extractive Metallurgy. Institute of Mining and Metallurgy, London. April, 1967. Paper 24.
3. L. S. DARKEN and R. W. GURRY. Physical chemistry of metals. McGraw-Hill Book Co. Inc., New York and London. 1953. p. 342.
4. J. E. DUTRIZAC and S. N. FLENGAS. Can. J. Chem. **45**, 2313 (1967).
5. M. TEMKIN. Acta Physicochim. URSS, **20**, 411 (1945).
6. H. FLOOD, T. FORLAND, and K. GRJOTHEIM. The physical chemistry of melts. The Institute of Mining and Metallurgy, London. 1953. p. 46.
7. O. J. KLEPPA, L. S. HERSH, and J. M. TOGURI. Symposium on Thermodynamics and Thermochemistry, Lund, Sweden. 1963.
8. H. FLOOD and A. MUAN. Acta Chem. Scand. **4**, 359, 364 (1950).
9. E. ROSEN and L. G. SILLEN. Acta Chem. Scand. **14**, 692 (1960).
10. H. FLOOD, T. FORLAND, and K. MOTZFELDT. Acta Chem. Scand. **6**, 257 (1952).
11. J. E. DUTRIZAC. Ph.D. Thesis, University of Toronto, Toronto, Ont. 1967.
12. J. H. HILDEBRAND and E. J. SALSTROM. J. Am. Chem. Soc. **54**, 4237 (1932).
13. B. R. SUNDHEIM (*Editor*). Fused salts. McGraw-Hill Book Co., New York. 1964. p. 76.

Can. J. Chem. Downloaded from www.nrcresearchpress.com by 210.87.254.6 on 09/05/12
For personal use only.

Can. J. Chem. Downloaded from www.nrcresearchpress.com by 210.87.254.42 on 09/05/12
For personal use only.

Analysis of the n.m.r. spectrum of pentafluorobenzene[1]

K. SCHAUMBURG, D. GILLIES, AND H. J. BERNSTEIN
Division of Pure Chemistry, National Research Council of Canada, Ottawa, Canada

Received August 31, 1967

The ^1H and ^{19}F spectra of pentafluorobenzene (PFB) have been analyzed, and spectral parameters obtained by iteration using least squares criterion. A number of solutions were found by this procedure. The physical solution was selected by "tickling" experiments.

Canadian Journal of Chemistry, **46**, 503 (1968)

Introduction

Investigation of many spin systems has become possible through the use of computers. The normal procedure in analysis of a spectrum starts with a tentative assignment of values for the parameters involved by transfer of data from related molecules. The final result is then often obtained by iterative improvement of the parameters using least squares criterion for the iteration. In most cases where many spin systems have been studied, only a fraction of the experimental lines are used in the iteration. This has been justified by limitations in computer time and capacity and by the ambiguity involved in extracting reliable data from large numbers of overlapping lines likely to be present in such spectra.

In principle it is possible to extract all necessary information from a reduced subspectrum (1). It is nevertheless important to remember that in such an analysis one depends heavily on the accuracy of the measurement of a small number of lines. Since all data are determined with limited accuracy, the "best" solution will still be found using a maximum number of lines in the analysis. The use of iterative minimization procedures does not in general assure a unique final result. Dependent on the initial data several local minima or 'best fits' can be obtained. No automatic selection of the best solution has been developed, and careful verification of the proposed solution using spin tickling, isotopic substitution, e.g., is therefore necessary.

As an example showing a multiplicity of possible solutions we have studied the spectra of PFB (see Fig. 1). Studies of the spectrum of PFB has been reported by several authors (1–3). Recent improvements in experimental techniques and computational facilities have made it possible to obtain more accurate data, thus providing the basis for a new investigation.

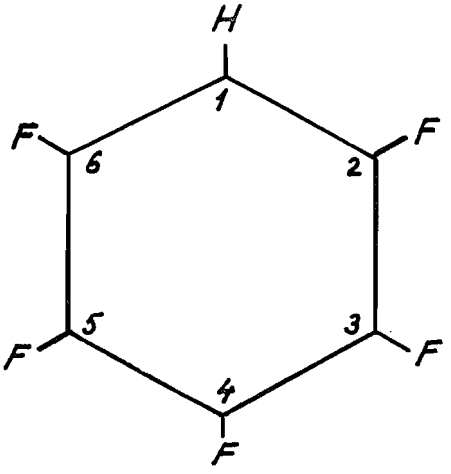

FIG. 1.

The literature data for the ^{19}F chemical shifts are listed in Table I. Analysis of the spin–spin splittings have been done in various approximations, the results of which are given in Table II. Boden *et al.* (2) found, in a first order approximation, values for the F—F coupling constants. As a result of the approximation only the sign relation between the ortho and meta coupling constants could be found. A complete set of parameters were given by Lawrenson (3), still using a first order approximation. No signs were indicated and like Boden, the question of relative magnitude of J_{26} and J_{35} was not solved. Recently Lustig and Diehl (1) reviewed the information available for coupling constants in fluorobenzene with regard to signs. They applied a second order perturbation calculation to the para fluoro spectrum of PFB to obtain a value for J_{14} as given in Table II.

[1]Issued as NRCC No. 9830.

Can. J. Chem. Downloaded from www.nrcresearchpress.com by 210.87.254.42 on 09/05/12
For personal use only.

TABLE I

^{19}F chemical shift in PFB

^{19}F chemical shift (p.p.m.)			
Ortho	Meta[a]	Para	Reference
23.39	0.22	8.78	2
23.05	0.44	8.92	4
23.8	0.30	8.90	3
23.67	0.22[b]	8.70	This work

[a]Measured relative to C_6F_6.
[b]$\delta_{CF_3COOH} - \delta_{C_6F_6} = 82.3$.

TABLE II

Coupling constants in PFB

	Reference			
J	3	2	1	This work
12 16	10.2			$+9.9_8$[b]
13 15	6.9			$+6.7_9$
14	2.7		−2.65	-2.6_4
23 56	20.6	±21.0		$+21.1_9$[b]
24 46	1.3	1.3	1.3	$+1.2_9$
34 45	18.8	±18.7	18.9	19.5_1
26	$\binom{1.2}{2.4}$[a]	$\binom{1.2}{2.2}$[a]		-2.2_8
25 36	8.8	±8.9		-8.8_5
35	$\binom{2.4}{1.2}$[a]	$\binom{2.2}{1.2}$[a]		-1.1_5

[a]Relative magnitude not known.
[b]Sign assumed to be positive.

Experimental

PFB was obtained from Columbia Organic Chemicals and purified by distillation. Samples were prepared on a vacuum line to assure proper degassing of the sample. PFB and CCl_4 were distilled into the sample tube containing a capillary standard of CF_3COOH. The concentration of PFB was approximately 10%. The proton spectra were recorded at 60 MHz on a Varian A60A spectrometer using precalibrated charts. ^{19}F spectra were recorded at 56.4 MHz using a Varian HA60 spectrometer. On this spectrometer all spectra were recorded using internal lock and frequency sweep. Both spectrometers were operated at 30 ± 2 °C. Data used in the calculation of spectral parameters were the average of 3–5 spectra. As reported elsewhere (5) a modified sweep arrangement allowed an expanded recording 0.3 Hz/cm at a sweep rate of 0.02 Hz/s combined with a continuously variable manual oscillator in the range 0.5–10 KHz. For tickling experiments a Wavetek 111 voltage-controlled oscillator of high frequency stability was used (5).

For calculation of the spectra and subsequent iterative improvement a modified Laocoon II program including optional weighting of individual lines and dampening of the iteration was used.

Results

The final results of the analysis are given in Tables I and II. The chemical shifts are in agreement with the literature data as far as it can be expected when solvent effects are considered. The coupling constants are all within 1 Hz from the values given by Lawrenson (3).

To obtain the final parameter set iteration was initiated in two points with $J_{26} > J_{35}$ and $J_{26} < J_{35}$ using the data of Lawrenson (3). From the calculations two solutions were obtained corresponding to 2 local minima for the iteration. The root mean square (r.m.s.) error was, in both cases, less than 0.2 Hz. This is comparable to the experimental error estimated to be ±0.1 Hz. The r.m.s. error is, in this case, not a sensitive measure of the reliability of a parameter set.

If the ortho HF and FF coupling constants are taken as positive, it immediately follows that HF meta is positive and FF para negative. The FF meta coupling constant J_{24} is reported to be positive, which is also found as the result of our calculations. The relative signs have not been established previously for the remaining three coupling constants J_{14}, J_{26}, and J_{35}. By combination of the 8 possible permutations of signs, 16 possible parameter sets were obtained which were used to start the iteration procedure.

As a result of the calculations we obtained a total of 16 local minima for the iteration. The solutions all corresponded to the same numerical set of parameters, within experimental error, but the sign relations reflected the different starting points. The r.m.s. error was in all cases between 0.1 and 0.2 Hz, which does not permit exclusion of any of the solutions.

To decide which, if any, of the obtained solutions is physically acceptable, a selection must be made by additional experimental information. Spin tickling (6) proved in this case to be particularly useful. By this method it is, in principle, possible to deduce the energy diagram for the spin system. Since the energy diagram is different for all 16 cases under investigation, it is sufficient to construct such a part of the energy diagram that only one parameter set is left possible.

In all the 16 energy diagrams a transition is found for the meta fluorine at[2] 4757.9 Hz corresponding to $F_z - 2 \rightarrow -1$. This transition is connected progressively to one in the para fluorine spectrum at either 4281.6 Hz or 4278.9 Hz, depending on the sign of J_{14}. As concluded

[2]The frequencies are given relative to CF_3COOH in a capillary. δ(F ortho) − $\delta(CF_3COOH) = 3414.0$ Hz.

Can. J. Chem. Downloaded from www.nrcresearchpress.com by 210.87.254.42 on 09/05/12
For personal use only.

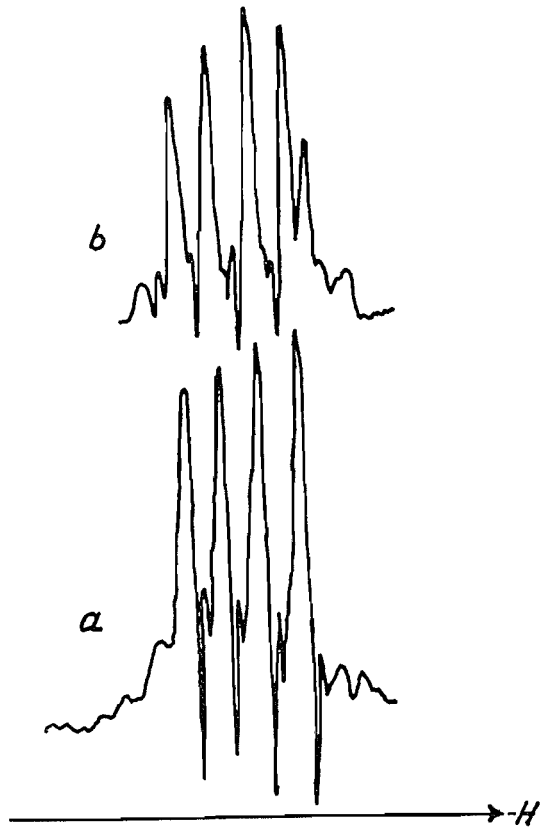

FIG. 2. Part of the spectrum of meta fluorine in PFB between 1760–1765 Hz: (*a*) normal; (*b*) tickling at 423.7 Hz in the ortho spectrum.

earlier by Lustig and Diehl (1) J_{14} was found to be negative.

Of the remaining 8 possibilities a group of 2 can be selected by tickling of a line in the ortho fluorine spectrum at 3427.7 Hz common to the 8 cases. Connected regressively to this transition is a line in the 4764–4769 Hz region of the meta fluorine spectrum. As shown in Fig. 2 the spectrum consists of a quartet where each of the lines will be affected only in two cases. The experimentally observed splitting of the low field line corresponds to the cases where both J_{26} and J_{35} are negative.

To find the relative magnitude of the two coupling constants a tickling of the meta fluorine transition at 4765.5 Hz corresponding to $F_z + 1 \rightarrow +2$ was performed. The line affected in the para fluorine spectrum at 4275.4 Hz is only connected to the transition tickled, in the case where $|J_{26}| > |J_{35}|$.

Discussion

To confirm the results obtained above, several other tickling experiments were done, all of which could be explained in terms of the energy diagram selected. This does not only confirm the values of the coupling constants but it also assures that the chemical shifts calculated cannot be more than approximately 0.2 Hz from the exact value. A comparison of the r.m.s. error shows that the selected set of parameters corresponds to the second lowest r.m.s. error 0.11 Hz.

The sign relations given in Table II are only to be taken as relative within the group of HF or FF couplings respectively. The relation between signs in these two groups can be established in studies at low field strength or by studies in nematic solvents.

1. E. LUSTIG and P. DIEHL. J. Chem. Phys. **44**, 2974 (1966).
2. N. BODEN, J. W. EMSLEY, J. FEENEY, and L. H. SUTCLIFFE. Mol. Phys. **8**, 133 (1964).
3. I. J. LAWRENSON. J. Chem. Soc. 1117 (1965).
4. G. L. CALDOW. Mol. Phys. **11**, 71 (1966).
5. D. GILLIES and K. SCHAUMBURG. To be published.
6. R. A. HOFFMAN and S. FORSEN. Progress in nuclear magnetic resonance spectroscopy. Vol. 1. Pergamon Press, London. 1966. pp. 14–205.

Dipole moments of glycerol, isopropyl alcohol, and isobutyl alcohol

H. A. RIZK AND I. M. ELANWAR

Department of Chemistry, Faculty of Science, University of Cairo, Cairo, Egypt, U.A.R.

Received May 29, 1967

By the application of a modified form of Onsager's equation to dilute solutions of glycerol in isopropyl alcohol and isobutyl alcohol, and conversely to dilute solutions of each of the latter two alcohols in glycerol, it is found that the apparent solution moments of these alcohols, at the condition of infinite dilution, are 2.68, 1.61, and 1.66 D respectively over the temperature range 30 to 50 °C.

Canadian Journal of Chemistry, **46**, 507 (1968)

Can. J. Chem. Downloaded from www.nrcresearchpress.com by 210.87.254.105 on 09/05/12
For personal use only.

The dipole moment of glycerol in dioxane, as determined by Wang (1), is 2.67 and 2.66 ± 0.02 D at 15 and 30 °C respectively. Using the same solvent, Darmois and Mouradoff (2) obtained the value 2.56 D for the dipole moment of glycerol. Debye (3), Lange (4), Stranathan (5), Ghosh (6), and Donle (7) measured the dipole moment of isopropyl alcohol in benzene, the values obtained being 1.66, 1.53, 1.74, 1.78, and 1.72–1.69 ± 0.04 D respectively. According to Higasi (8), the apparent solution moment of isopropyl alcohol, as well as that of isobutyl alcohol, using benzene as a solvent, is equal to 1.70 D. His measurements (8) in carbon disulfide gave for those two alcohols the moments 1.48 and 1.41 D respectively. The dipole moments of isopropyl and isobutyl alcohol were also measured in benzene by Maryott (9), the values obtained being 1.66 and 1.70 D respectively. On the other hand, the dipole moments of isopropyl alcohol and isobutyl alcohol in the gaseous state, as measured by Kubo (10) and by Smyth (11), are 1.63 and 1.65 D respectively. Also, a value equal to 1.67 D was obtained by Stranathan (12) for the vapor moment of isobutyl alcohol.

The differing results, as obtained by various authors, concerning the dipole moments of the above alcohols suggested a redetermination of their moments with the help of Onsager's equation (13) applicable to dilute solutions of a polar solute in a polar solvent. Thus in the case of glycerol, isopropyl alcohol and isobutyl alcohol were alternately chosen as the polar solvent, and conversely in the case of each of the latter two alcohols, glycerol was used as the solvent.

Experimental

Glycerol, isopropyl alcohol, and isobutyl alcohol were purified according to recommended procedures (14). Measurements of dielectric constant, density, and refractive index were carried out as described in an earlier investigation (15). Calculations with regard to the infinite dilution condition were made using eq. [A]. This equation was derived from Onsager's equation (13), as shown in the Appendix.

Results and Discussion

It will be seen from Tables I and II that over the temperature range 30 to 50 °C the apparent solution moment of glycerol is equal to 2.67 D when isopropyl alcohol is used as a solvent, and equal to 2.69 D when isobutyl alcohol is used. Although the former value is slightly lower than the latter, the difference is within the limits of experimental error. Thus an average value, namely 2.68 D, may be taken to represent the dipole moment of glycerol in isopropyl or isobutyl alcohol. This value, which is evidently in good agreement with the value, 2.66 D, obtained by Wang (1) for the dipole moment of glycerol at 30 °C using dioxane and applying the usual Debye equation (17), may suggest, when compared with the moment, 2.8 D, calculated for glycerol from Girard's formula (18), that in pure glycerol there is unequal distribution of the six dipoles among the potential troughs that exist when dipole rotation takes place around a bond; in other words, in pure glycerol there is incomplete random orientation of the dipoles relative to one another.

The apparent solution moment of isopropyl alcohol in glycerol, namely 1.61 D (Table III), is slightly lower than the solution value in benzene, 1.66 D, which was obtained by Debye (3) and Maryott (9), and is in agreement with the vapor value, 1.63 D, as determined by Kubo (10) and Smyth (11). Similarly, the solution moment of isobutyl alcohol in glycerol, 1.66 D (Table IV), is slightly lower than the solution value in benzene, 1.70 D (8, 9), and in agreement with the vapor value, 1.65 D (10, 11).

Can. J. Chem. Downloaded from www.nrcresearchpress.com by 210.87.254.105 on 09/05/12
For personal use only.

TABLE I

Glycerol in isopropyl alcohol

W_2	t (°C)	ϵ_{12}	d_{12}	C_2
	30	17.38	0.7769	
0	40	16.23	0.7687	0
	50	15.06	0.7605	
	30	17.54	0.7852	0.2174
0.02550	40	16.40	0.7768	0.2151
	50	15.22	0.7684	0.2128
	30	17.71	0.7949	0.4192
0.04857	40	16.56	0.7866	0.4149
	50	15.37	0.7783	0.4106
	30	17.89	0.8077	0.6203
0.07073	40	16.72	0.7995	0.6140
	50	15.53	0.7913	0.6077
	30	18.09	0.8130	0.8751
0.09955	40	16.94	0.8034	0.8648
	50	15.74	0.7963	0.8571

t (°C)	n^2_{1-D}	$\mu_1 \times 10^{18}$	$C_1{}^0$	$(d\epsilon_{12}/dC_2)_{C_2\to 0}$	$(F)_{C_2\to 0}$	$\mu_2 \times 10^{18}$*
30	1.8882	1.63	12.925	0.810	0.976	2.65
40	1.8789	1.63	12.788	0.807	0.973	2.68
50	1.8706	1.63	12.650	0.784	0.971	2.68

*μ_2 = 2.67 D.

TABLE II

Glycerol in isobutyl alcohol

W_2	t (°C)	ϵ_{12}	d_{12}	C_2
	30	15.27	0.7944	
0	40	14.00	0.7869	0
	50	12.83	0.7793	
	30	15.46	0.8065	0.2247
0.02552	40	14.18	0.7989	0.2226
	50	12.99	0.7913	0.2205
	30	15.67	0.8124	0.4702
0.05331	40	14.38	0.8049	0.4659
	50	13.19	0.7974	0.4616
	30	15.84	0.8204	0.6565
0.07370	40	14.54	0.8131	0.6507
	50	13.35	0.8058	0.6449
	30	16.26	0.8314	0.8949
0.09913	40	15.02	0.8223	0.8851
	50	13.81	0.8144	0.8766

	n^2_{1-D}	$\mu_1 \times 10^{18}$	$C_1{}^0$	$(d\epsilon_{12}/dC_2)_{C_2\to 0}$	$(F)_{C_2\to 0}$	$\mu_2 \times 10^{18}$*
30	1.9386	1.65	10.720	0.859	0.971	2.70
40	1.9264	1.65	10.616	0.823	0.967	2.69
50	1.9159	1.65	10.512	0.791	0.964	2.69

*μ_2 = 2.69 D.

Can. J. Chem. Downloaded from www.nrcresearchpress.com by 210.87.254.105 on 09/05/12
For personal use only.

TABLE III

Isopropyl alcohol in glycerol

W_2	t (°C)	ϵ_{12}	d_{12}	C_2
	30	41.49	1.2552	
0	40	39.55	1.2423	0
	50	37.70	1.2359	
	30	41.00	1.2376	0.5431
0.02637	40	39.05	1.2293	0.5394
	50	37.22	1.2210	0.5357
	30	40.78	1.2312	0.7525
0.03673	40	38.89	1.2230	0.7475
	50	37.07	1.2148	0.7426
	30	40.50	1.2251	0.9422
0.04622	40	38.69	1.2172	0.9361
	50	36.87	1.2092	0.9300
	30	40.15	1.2208	1.0858
0.05345	40	38.36	1.2131	1.0789
	50	36.65	1.2054	1.0720
	30	35.83	1.1929	1.9975
0.10063	40	33.97	1.1856	1.9853
	50	32.35	1.1783	1.9731

	n^2_{1-D}	$\mu_1 \times 10^{18}$	$C_1{}^0$	$(d\epsilon_{12}/dC_2)_{C_2\to 0}$	$(F)_{C_2\to 0}$	$\mu_2 \times 10^{18}$*
30	2.1677	2.68	13.559	−0.933	0.983	1.60
40	2.1612	2.68	13.489	−0.913	0.983	1.60
50	2.1549	2.68	13.420	−0.881	0.981	1.62

*μ_2 = 1.61 D.

TABLE IV

Isobutyl alcohol in glycerol

W_2	t (°C)	ϵ_{12}	d_{12}	C_2
	30	41.49	1.2552	
0	40	39.55	1.2423	0
	50	37.70	1.2359	
	30	40.99	1.2397	0.4415
0.02640	40	39.06	1.2314	0.4386
	50	37.23	1.2231	0.4357
	30	40.76	1.2353	0.6201
0.03721	40	38.85	1.2271	0.6160
	50	37.06	1.2189	0.6119
	30	40.65	1.2318	0.7046
0.04239	40	38.75	1.2237	0.7000
	50	36.92	1.2156	0.6954
	30	40.42	1.2240	0.8987
0.05442	40	38.51	1.2161	0.8929
	50	36.73	1.2081	0.8873
	30	35.66	1.2004	1.6836
0.10400	40	33.85	1.1940	1.6746
	50	32.41	1.1888	1.6673

	n^2_{1-D}	$\mu_1 \times 10^{18}$	$C_1{}^0$	$(d\epsilon_{12}/dC_2)_{C_2\to 0}$	$(F)_{C_2\to 0}$	$\mu_2 \times 10^{18}$
30	2.1677	2.68	13.559	−1.162	0.983	1.65
40	2.1612	2.68	13.489	−1.135	0.983	1.65
50	2.1549	2.68	13.420	−1.092	0.981	1.67

*μ_2 = 1.66 D.

TABLE V

Dipole moments ($\times 10^{18}$) of glycerol, isopropyl alcohol, and isobutyl alcohol

	Glycerol			Isopropyl alcohol			Isobutyl alcohol		
	30 °C	40 °C	50 °C	30 °C	40 °C	50 °C	30 °C	40 °C	50 °C
ϵ	41.49	39.55	37.70	17.38	16.23	15.06	15.27	14.00	12.83
$n^2 - D$	2.1677	2.1612	2.1549	1.8882	1.8789	1.8706	1.9386	1.9264	1.9159
d_4^t	1.2552	1.2423	1.2359	0.7769	0.7687	0.7605	0.7944	0.7869	0.7793
μ_0 (Debye)	1.52	1.57	1.60	1.53	1.56	1.58	1.68	1.71	1.74
$S^{1/2}\mu_0$ (Onsager)	4.12	4.08	4.04	2.88	2.84	2.80	3.15	3.14	3.13
$g^{1/2}\mu$ (Kirkwood)	5.66	5.66	5.54	3.69	3.62	3.55	4.06	4.04	4.00
$g^{1/2}\mu_0$ (Kirkwood)	4.13	4.10	4.06	2.91	2.88	2.83	3.17	3.17	3.15
μ solution		2.68			1.61			1.66	

It will be evident from the above that there exists a good agreement between the solution moments of glycerol, isopropyl alcohol, and isobutyl alcohol, as obtained by applying Onsager's equation at the condition of infinite dilution of a polar solute in a polar solvent, and those which are obtained with the aid of usual methods. This result may suggest that it is possible to use Onsager's equation (with the assumption of ideality) to get reasonable dipole moments of alcohols dissolved in alcohols. Although there is no conclusive evidence that this method could generally be recommended for the determination of dipole moments of different types of molecules, nevertheless the simple model of a spherical cavity of a homogeneous dielectric used by Onsager (13) is more accurate than would be expected on first consideration.

From measurements of the static dielectric constants, refractive indices for the sodium D line, and densities of glycerol, isopropyl alcohol, and isobutyl alcohol at 30, 40, and 50 °C, the dipole moments of these alcohols, as calculated from the Debye (17), Onsager (13), and Kirkwood (19) equations applied to the pure liquids, are shown in Table V.

It will be seen from this table that Debye's equation (17), which is inapplicable to pure polar liquids, gives in the case of glycerol a dipole moment value which is much lower than the measured apparent solution moment, whereas it gives a moment value in the case of isopropyl alcohol, or isobutyl alcohol, which is more or less in fortuitous agreement with that obtained from solution measurements. The apparent increase in the moment of each alcohol calculated from Onsager's equation (13), $S^{1/2}\mu_0$, as compared with the measured solution moment (Table V), may be qualitatively accounted for by complex formation in each liquid. On the other hand, hindered relative molecular rotation arising from short-range intermolecular forces in each liquid would account for the higher dipole moment calculated from Kirkwood's equation (19), $g^{1/2}\mu$, or $g^{1/2}\mu_0$, as compared with the measured solution moment, μ being the actual dipole moment of the molecule in the liquid and μ_0 the vapor moment. According to Kirkwood (19), the correlation parameter g of hindered molecular rotation is equal to unity in Onsager's model, since in this model only the effect of electrostatic forces on hindered rotation was considered. The discrepancies between the dielectric constants calculated for highly polar liquids from Onsager's equation, in which there is no contribution to the local field from the material in the interior of the cavity, and those measured were accounted for by introducing in this equation a factor based on the formation of complex molecules, namely the association factor S. The meaning and the derivation of this factor are different from the Kirkwood correlation parameter g. Thus while the value of S helps in the prediction of the probable types of aggregates in pure polar liquids, the value of g measures by its departure from unity the degree of hindered relative molecular rotation. Further, the deviation of g from unity may be either positive when short-range hindering torques favor parallel orientation of the dipole moments of neighboring molecules or negative when the hindering torques favor antiparallel orientation.

Following Fröhlich (20), Kirkwood's equation would be very useful in the presence of strong short-range forces, since it is identical with a formula which one would obtain if the dipoles are assumed to associate. Suppose that on an average $\bar{\mu}/\mu$ dipoles associate forming a group

Can. J. Chem. Downloaded from www.nrcresearchpress.com by 210.87.254.105 on 09/05/12
For personal use only.

Can. J. Chem. Downloaded from www.nrcresearchpress.com by 210.87.254.105 on 09/05/12
For personal use only.

of dipoles with moment $\bar{\mu}$. Here μ is the molecular dipole moment in the liquid and $\bar{\mu}$ the total moment of the content of a Lorentz cavity (19) centered on a molecule of fixed orientation in the absence of an external field, $\mu \times \bar{\mu}$ being equal to $g\mu^2$. The number of such groups per unit volume is equal to $1/(\bar{\mu}/\mu)$ of the original volume, n, i.e. equal to $n\mu/\bar{\mu}$, which on multiplying by the square of the moment of each group gives $n\mu\bar{\mu} = ng\mu^2$. Thus, applying Onsager's formula to these groups leads, as was pointed out by Fröhlich (20), to Kirkwood's equation.

From a knowledge of the vapor phase dipole moments of isopropyl alcohol and isobutyl alcohol, which are 1.63 and 1.65 D respectively (10, 11), an estimate was made of S and g for these two alcohols, the molecules of which are of the type R—OH. The results obtained are shown in Table VI.

TABLE VI

Estimates of S and g for isopropyl alcohol and isobutyl alcohol

	Isopropyl alcohol		Isobutyl alcohol	
t (°C)	S	g	S	g
30	3.12	3.19	3.65	3.69
40	3.03	3.12	3.61	3.69
50	2.95	3.02	3.61	3.65

It will be seen that for each alcohol the association factor S, or the correlation parameter g, decreases with increasing temperature, this being presumably due to decrease in association or in the degree of hindered relative molecular rotation arising from short-range intermolecular forces. Also, it can be seen that for each alcohol the value of the correlation parameter g, which departs significantly from unity, is slightly higher than the value of the association factor S. And that the association factor S, as well as the correlation parameter g, is smaller in the case of isopropyl alcohol than in the case of isobutyl alcohol. Therefore, it can be inferred that there is more association, or more hindrance to relative molecular rotation, in liquid isobutyl alcohol than in liquid isopropyl alcohol. This may be ascribed in part to the location of the hydroxyl group. Being more remote from the branch in the chain of the molecule in the case of isobutyl alcohol than in the case of isopropyl alcohol, the hydroxyl group is less screened in the former case than in the latter. This in turn results in stronger dipole–dipole interactions between a central dipole and surrounding dipoles, thus giving rise to more coordination through hydrogen bonds in liquid isobutyl alcohol than in liquid isopropyl alcohol. It may be noted here that the coordination which exists in these alcohols, as has been concluded from X-ray scattering data, is chainwise (19). On the other hand, when the association factor S of isobutyl alcohol, 3.65, at 30 °C is compared with that of n-butyl alcohol, 3.16, at 25 °C, which was determined by Huyskens and Cracco (21), it can be deduced that the former alcohol is more associated than the latter. That the relative molecular rotation is more strongly hindered in liquid isobutyl alcohol than in liquid n-butyl alcohol is revealed by comparing the correlation parameter value, 3.69, which we obtained for the former alcohol at 30 °C with the value, 3.21, which was observed for the latter alcohol at 20 °C by Oster and Kirkwood (22) and by Oster (23).

Appendix

Onsager's equation (13) in a modified form, without taking association into consideration, may be written in Böttcher's expression (16) as

$$[1] \quad \epsilon_{12} - 1 = 4\pi \sum_i N_i \left[\frac{\mu_i^2}{9kT} \times \frac{(\epsilon_{\infty i} + 2)^2 \epsilon_{12}(2\epsilon_{12} + 1)}{(2\epsilon_{12} + \epsilon_{\infty i})^2} + a_i^3 \frac{\epsilon_{12}(\epsilon_{\infty i} - 1)}{(2\epsilon_{12} + \epsilon_{\infty i})} \right],$$

where N_i is the number of molecules of type i per cc of the solution, $\epsilon_{\infty i}$ square of refractive index of component i, μ_i dipole moment of type i in the vapor state, and a_i radius of the hypothetical spherical molecule containing the point dipole, μ_i, the subscript 12 being for the solution. N_i is related to C_i, which is the number of gram-molecules of component i per liter of solution, by the equation

$$[2] \quad N_i = \frac{C_i}{1000} N_a,$$

where N_a is Avogadro's number.

Assuming that the hypothetical volume of N_a spherical molecules in a gram-molecule of

Can. J. Chem. Downloaded from www.nrcresearchpress.com by 210.87.254.105 on 09/05/12
For personal use only.

component i is equal to the molar volume, V_i, we have

$$[3] \qquad 4\pi \sum_i a_i^3 N_i = 3 \sum_i V_i C_i.$$

Substituting for N_i in eq. [1] from eqs. [2] and [3], and putting

$$[4] \qquad \frac{4\pi N_a}{9000kT} \cdot \frac{(\epsilon_{\infty i} + 2)^2 \epsilon_{12}(2\epsilon_{12} + 1)}{(2\epsilon_{12} + \epsilon_{\infty i})^2} = A_i,$$

and

$$[5] \qquad 3V_i \frac{\epsilon_{12}(\epsilon_{\infty i} - 1)}{(2\epsilon_{12} + \epsilon_{\infty i})} = B_i,$$

one gets

$$[6] \qquad \epsilon_{12} - 1 = \sum_i (A_i C_i \mu_i^2 + B_i C_i) = \sum_i (A_i \mu_i^2 + B_i) C_i.$$

Assuming an ideal solution of two components, and designating the polar solute by the subscript 2 and the polar solvent by the subscript 1, the volume additivity is given by

$$[7] \qquad 1000 = \frac{M_1 C_1}{d_1} + \frac{M_2 C_2}{d_2}.$$

Substitution of $C_1^0 = 1000 \times (d_1/M_1)$ for the molar concentration of pure solvent and $V_2 = M_2/(1000 \times d_2)$ for the molar volume (in liters) of pure solute gives

$$[8] \qquad C_1 = C_1^0(1 - C_2 V_2).$$

Equation [8] expresses the solvent concentration in gram-molecules per liter of solution, C_1, in terms of that of the solute, C_2, provided that the solution is ideal.

For a binary mixture, eq. [6] can be written as

$$[9] \qquad \epsilon_{12} - 1 = (A_1\mu_1^2 + B_1)C_1 + (A_2\mu_2^2 + B_2)C_2.$$

Substituting in eq. [9] for C_1 from eq. [8] and taking the derivative of ϵ_{12} with respect to C_2, we obtain

$$\frac{d\epsilon_{12}}{dC_2} = -A_1\mu_1^2 C_1^0 V_2 - B_1 C_1^0 V_2 + A_1'\mu_1^2 C_1^0 + B_1' C_1^0 - C_1^0 C_2 V_2 B_1' + A_2\mu_2^2 + B_2 + C_2\mu_2^2 A_2' + C_2 B_2' - C_1^0 C_2 V_2 \mu_1^2 A_1'.$$

Therefore

$$[10] \qquad \mu_2^2 = \frac{1}{A_2} \cdot \frac{d\epsilon_{12}}{dC_2} + \frac{(A_1\mu_1^2 C_1^0 V_2 + B_1 C_1^0 V_2 - B_2)}{A_2} - \frac{C_2\mu_2^2 A_2' + C_2 B_2' + C_1^0 B_1' + C_1^0 \mu_1^2 A_1'}{A_2} + \frac{C_1^0 C_2 V_2(\mu_1^2 A_1' + B_1')}{A_2},$$

where A' and B' are the derivatives of A and B with respect to C_2, that is

$$[11] \qquad A_1' = \frac{(\epsilon_{\infty 1} + 4\epsilon_{12}\epsilon_{\infty 1} - 2\epsilon_{12})}{\epsilon_{12}(2\epsilon_{12} + 1)(2\epsilon_{12} + \epsilon_{\infty 1})} A_1 \frac{d\epsilon_{12}}{dC_2},$$

$$A_2' = \frac{(\epsilon_{\infty 2} + 4\epsilon_{12}\epsilon_{\infty 2} - 2\epsilon_{12})}{\epsilon_{12}(2\epsilon_{12} + 1)(2\epsilon_{12} + \epsilon_{\infty 2})} A_2 \frac{d\epsilon_{12}}{dC_2},$$

$$B_1' = \frac{\epsilon_{\infty 1}}{\epsilon_{12}(2\epsilon_{12} + 1)} B_1 \frac{d\epsilon_{12}}{dC_2}, \quad \text{and}$$

$$B_2' = \frac{\epsilon_{\infty 2}}{\epsilon_{12}(2\epsilon_{12} + \epsilon_{\infty 2})} B_2 \frac{d\epsilon_{12}}{dC_2}.$$

Substituting for A_1', A_2', B_1', and B_2' from eq. [11] in eq. [10], and putting

$$[12] \qquad F = 1 - C_2\mu_2^2 A_2 \frac{(\epsilon_{\infty 2} + 4\epsilon_{12}\epsilon_{\infty 2} - 2\epsilon_{12})}{\epsilon_{12}(2\epsilon_{12} + 1)(2\epsilon_{12} + \epsilon_{\infty 2})} - C_1\mu_1^2 A_1 \frac{(\epsilon_{\infty 1} + 4\epsilon_{12}\epsilon_{\infty 1} - 2\epsilon_{12})}{\epsilon_{12}(2\epsilon_{12} + 1)(2\epsilon_{12} + \epsilon_{\infty 1})} - C_2 B_2 \frac{\epsilon_{\infty 2}}{\epsilon_{12}(2\epsilon_{12} + \epsilon_{2\infty})} - C_1 B_1 \frac{\epsilon_{\infty 1}}{\epsilon_{12}(2\epsilon_{12} + \epsilon_{\infty 1})},$$

we finally obtain

$$[A] \qquad \mu_2^2 = F \frac{d\epsilon_{12}}{dC_2} \cdot \frac{1}{A_2} + \frac{(A_1\mu_1^2 C_1^0 V_2 + B_1 C_1^0 V_2 - B_2)}{A_2}.$$

Taking the slope, $d\epsilon_{12}/dC_2$, in the limit as C_2 approaches zero, the terms A_1, A_2, B_1, and B_2 can be calculated using the dielectric constant of the solvent, ϵ_1, instead of that of the solution, ϵ_{12}. Similarly, in deriving the numerical value of the factor F for the condition of infinite

dilution, the second and fourth terms of F involving $C_2\mu_2^2$ and C_2 respectively disappear, C_1 becomes equal to C_1^0, and then ϵ_{12} becomes equal to ϵ_1.

1. Y. L. WANG. Z. Physik. Chem. Leipzig, **B45**, 323 (1940).
2. M. E. DARMOIS and L. MOURADOFF. Bull. Soc. Chim. France, **16**, 446 D (1949).
3. P. DEBYE. Hand. Radiol. (Marx), Akademische Nerlagsgesellschaft m.b.H., Leipzig. **6**, 597 (1925).
4. L. LANGE. Z. Physik, **33**, 169 (1925).
5. J. D. STRANATHAN. Phys. Rev. **31**, 156, 653 (1928).
6. P. N. GHOSH. Nature, **123**, 413 (1929).
7. H. L. DONLE. Z. Physik. Chem. Leipzig, **B14**, 362 (1931).
8. K. HIGASI. Bull. Inst. Phys. Chem. Res. Tokyo, **15**, 766 (1936).
9. A. A. MARYOTT. J. Am. Chem. Soc. **63**, 3079 (1941).
10. M. KUBO. Sci. Papers Inst. Phys. Chem. Res. Tokyo, **26**, 242 (1935).
11. C. P. SMYTH. J. Am. Chem. Soc. **63**, 57 (1941).
12. J. D. STRANATHAN. J. Chem. Phys. **5**, 828 (1937).
13. L. ONSAGER. J. Am. Chem. Soc. **58**, 1486 (1936).
14. A. WEISSBERGER and E. PROSKAUER. Organic solvents, physical constants and methods of purification. Clarendon Press, Oxford. 1935. pp. 125, 127, 133.
15. A. R. TOURKY, H. A. RIZK, and Y. M. GIRGIS. J. Phys. Chem. **64**, 565 (1960).
16. C. J. F. BÖTTCHER. Rec. Trav. Chim. **62**, 119 (1943).
17. P. DEBYE. Physik. Z. **13**, 97 (1912); Polar molecules. Chemical Catalog, New York. 1929. Chap. III.
18. P. GIRARD. Trans. Faraday Soc. **30**, 763 (1934).
19. J. G. KIRKWOOD. J. Chem. Phys. **7**, 911 (1939); Ann. N.Y. Acad. Sci. **40**, 315 (1940); Trans. Faraday Soc. A, **42**, 7 (1946).
20. H. FRÖHLICH. Trans. Faraday Soc. A, **42**, 3 (1946).
21. P. HUYSKENS and F. CRACCO. Bull. Soc. Chim. Belges, **69**, 422 (1960).
22. G. OSTER and J. G. KIRKWOOD. J. Chem. Phys. **11**, 175 (1943).
23. G. OSTER. J. Am. Chem. Soc. **68**, 2036 (1946).

Can. J. Chem. Downloaded from www.nrcresearchpress.com by 210.87.254.105 on 09/05/12
For personal use only.

Can. J. Chem. Downloaded from www.nrcresearchpress.com by 210.87.254.105 on 09/05/12
For personal use only.

Nuclear magnetic resonance study of arene metal tricarbonyl complexes[1]

J. T. PRICE AND T. S. SORENSEN
The Department of Chemistry, The University of Calgary, Calgary, Alberta

Received May 9, 1967

The n.m.r. spectra of all the methyl-substituted benzene complexes of chromium tricarbonyl, molybdenum tricarbonyl, and tungsten tricarbonyl have been obtained. The unusual features include a large upfield shift of alkene proton chemical shifts on complex formation, but within the metals the order of increasing shift is Cr > W > Mo, a non-periodic trend. It has also been observed that the individual alkene proton chemical shifts in an unsymmetrical methyl benzene become markedly different on complex formation, in contrast to the behavior found in the free arene. Symmetrical methyl-substituted benzene metal complexes, on the other hand, show the same symmetry characteristics as the free arenes, and hence, on an n.m.r. time scale, there is no permanent distortion of the ring. A theory is presented, invoking partial three-point bonding of the $M(CO)_3$ moiety to the arene ring. This bonding is postulated to occur most strongly at arene carbon atoms bearing methyl groups and, as a consequence, results in an abnormally strong electron withdrawal from carbon positions meta to this carbon, even though this meta position may be unsubstituted.

Canadian Journal of Chemistry, **46**, 515 (1968)

Introduction

Overwhelming evidence has now been presented (1–6) to show that three-fold distortion of the arene ring does not occur in dibenzene chromium.

Arene tricarbonyl metal complexes have not been as rigorously investigated regarding a possible three-fold distortion. However, an X-ray structural determination of benzene chromium tricarbonyl (7) provides no evidence for bond alteration. Curiously, hexamethylbenzene chromium tricarbonyl shows an anomalous two-fold distortion (8), which may be caused by crystal-packing forces.

In spite of the lack of evidence for any bond alteration, it might still be considered that some alteration of the π-electron cloud of the benzene ring could occur without being manifest in significant bond distortions. The metal tricarbonyl benzene complexes, in contrast to dibenzene chromium, have at best only three-fold symmetry overall and it might be naively supposed that the metal octahedral bonding directions, as determined by the carbonyl group directions, might lead to bonding which is strongest at three specific points of the arene ligand. These three points *could* coincide with the midpoint of three $\rangle C{=}{=}C\langle$ bonds, in which case bond alteration *might* also result, but it is equally possible that the three points could correspond to three carbon atoms, in which case *no* bond alteration would occur in ligands like benzene, although bond lengths might change. These two possibilities are shown in Fig. 1.

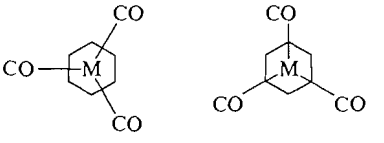

FIG. 1. Two possible conformations for arene metal tricarbonyl complexes.

X-ray evidence on this matter is equivocal. In benzene chromium tricarbonyl, the carbonyl bonds project through the center of $\rangle C{=}{=}C\langle$ bonds (7), while in anisole chromium tricarbonyl, an eclipsed form is adopted in which the octahedral bonds would point towards the positions ortho and para to the methoxyl group (9). Indeed, the latter workers discuss this orientation in terms of an octahedral disposition of ligands in which the electron-rich ortho and para positions are to be preferred as bonding centers. X-ray structural studies using *o*-toluidine chromium tricarbonyl (9) further suggest that steric factors are not responsible for this structural preference. It is of course possible that these structural features are due to crystal forces and one cannot extrapolate to the solution state with any great confidence.

An examination of the possibility of three-fold arene distortion has been made for a number of methoxy-substituted benzene chromium tricarbonyl complexes using an n.m.r. method (6).

[1]Taken in part from M.Sc. Thesis of J. T. P.

Can. J. Chem. Downloaded from www.nrcresearchpress.com by 210.87.254.105 on 09/05/12
For personal use only.

The conclusions from this study can be summarized as follows: (1) there is no evidence for localization of the π-electron cloud and (2) relative to benzene and benzene chromium tricarbonyl, the ability of the aromatic nucleus to transmit mesomeric effects (of the methoxyl group) is little affected by association with the $Cr(CO)_3$ group, whereas there is a considerable change in inductive effects on complex formation.

The authors of a recent communication (10) have offered n.m.r. evidence for restricted rotation in isopropylbenzene and *t*-butylbenzene chromium tricarbonyl complexes, the former compound reported to exhibit a temperature dependent alkene proton n.m.r. spectrum, the latter a complex alkene proton spectrum unchanged by temperature changes.

The n.m.r. spectra of a number of individual arene metal tricarbonyl compounds have been measured (11). It has been shown that the arene protons of the chromium complexes resonate at the highest field with tungsten next and molybdenum the lowest (11). It has also been noted that the coupling constant of ortho-protons decreases from a value of 7.8–8.8 c.p.s. in the free arene to 6.4–6.8 c.p.s. in the complexes (11).

Results

In order to simplify the presentation we have adopted a procedure similar to that used by McFarlane and Grim (6), in which individual proton positions are given a number, which can then be portrayed by graphical representation for showing variations in chemical shifts between different protons etc. The numbering system is given below.

The n.m.r. spectra of the free arene compounds at 60 Mc show in almost all cases (the exception is *m*-xylene) a relatively sharp signal for all of the alkene protons, even where these protons are not equivalent (12). Thus, methyl groups on a benzene ring do not cause ortho, meta, and para protons to have different chemical shifts, in contrast to the effect exerted by more strongly electron donating and attracting groups.

It was surprising to note, therefore, that in all cases where the arene protons are not symmetry equivalent, the n.m.r. spectrum of the arene metal compound showed a complex series of peaks in the alkene region. However, in all cases where the arene protons are equivalent, only a single sharp signal was observed, indicating that on an n.m.r. time scale, no permanent

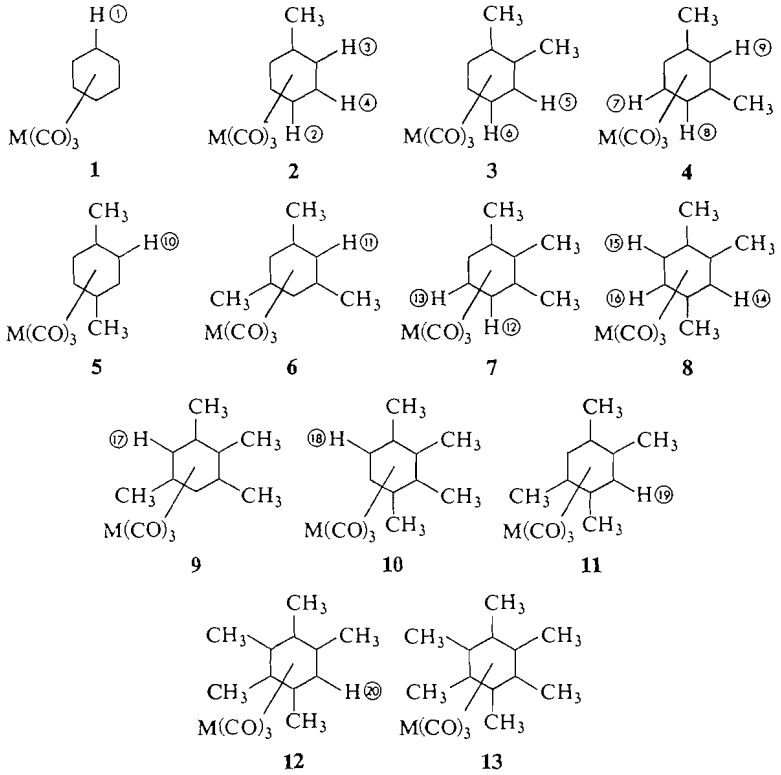

Can. J. Chem. Downloaded from www.nrcresearchpress.com by 210.87.254.105 on 09/05/12
For personal use only.

asymmetry is being introduced by complex formation. Furthermore, the n.m.r. non-equivalence of protons varies from compound to compound. For example, in ortho-xylene, protons 5 and 6 (all these numbers refer to our numbering system) have very similar n.m.r. chemical shifts, while in meta-xylene, protons 7 and 8 have quite large chemical shift differences. The difference in the n.m.r. spectrum between the complexes and the free ligand for 1,2,4-trimethylbenzene is shown in Fig. 2. By matching computer-calculated curves and the experimental curves, it has been possible to successfully analyze the alkene region n.m.r. spectra of all of the complexes with the exception of those from toluene and *o*-xylene. For these arene complexes the total separation of peaks is not sufficient to allow a reliable analysis; however, estimates were made even for these.

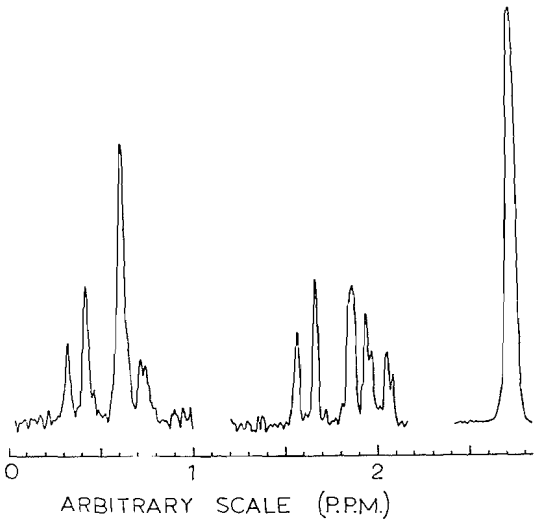

FIG. 2. The n.m.r. spectrum of the alkene region of: left, 1,2,4-trimethylbenzene $Cr(CO)_3$; center, 1,2,4-trimethylbenzene $Mo(CO)_3$, and right, 1,2,4-trimethylbenzene.

The coupling constant between adjacent protons in *m*-xylene, 1,2,3-trimethylbenzene, and 1,2,4-trimethylbenzene complexes of chromium, molybdenum, and tungsten are all between 6.2 and 6.6 c.p.s., in agreement with previous findings (11) on other metal arene complexes. In the 1,2,4-trimethylbenzene complexes, the small meta coupling is easily observed (see Fig. 2).

In Fig. 3, we have plotted the chemical shift data for each proton for the chromium, molybdenum, and tungsten derivatives of all of the arenes. The abscissa represents the proton number using our numbering system and the ordinate represents the chemical shift (Δ) between a proton in the complex and in the free arene. In Fig. 4, a similar plot shows the average chemical shift for the methyl groups numbered by compound number, also relative to their chemical shift value in the free arenes. The individual methyl group protons show of course a single peak, with non-equivalent methyl groups often showing differing chemical shifts. Since it is not always possible to specifically identify these peaks for a polymethylbenzene, we have plotted the weighted median chemical shift for these methyl resonances.

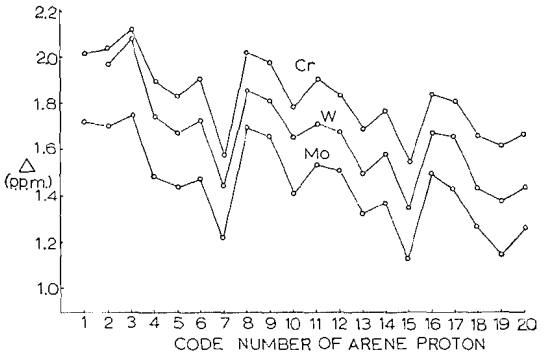

FIG. 3. Plot of the difference (Δ) between the chemical shift of alkene protons in the complexes and the same protons in the free arenes for all of the different protons coded under Results.

It will be noticed that the order in magnitude of Δ for arene protons is Cr > W > Mo, while that for the methyl groups is Cr > Mo > W. The order for arene protons is clearly out of line with the periodic occurrence Cr, Mo, W. The correlation of individual protons in all three metal complexes is, however, excellent.

In order to rationalize the variation in chemical shifts observed for the alkene protons of the complexes, both within a given complex and in comparisons between various complexes, we have attempted to measure the effect on the chemical shift of individual protons caused by an ortho, meta, or para methyl substituent, again using a procedure similar to that used by McFarlane and Grim (6) for methoxy-substituted benzenes. The chemical shift value for the six equivalent protons of the benzene complex was taken as the reference point, the addition of methyl groups to the ring causing a comparative decrease, no change, or an increase to the chemical shift value of the protons. The method involves a least squares type of analysis in which

Can. J. Chem. Downloaded from www.nrcresearchpress.com by 210.87.254.105 on 09/05/12
For personal use only.

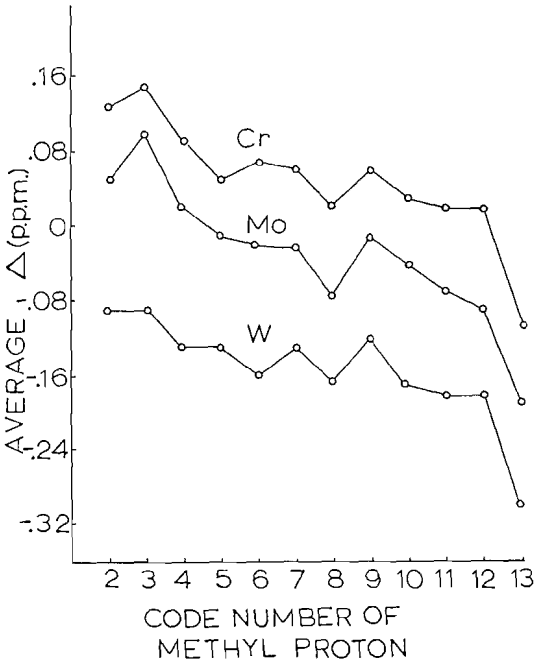

FIG. 4. Plot of the difference (Δ) between the chemical shift of methyl protons in the complexes and the same protons in the free arenes coded for all of the complexes by compound number.

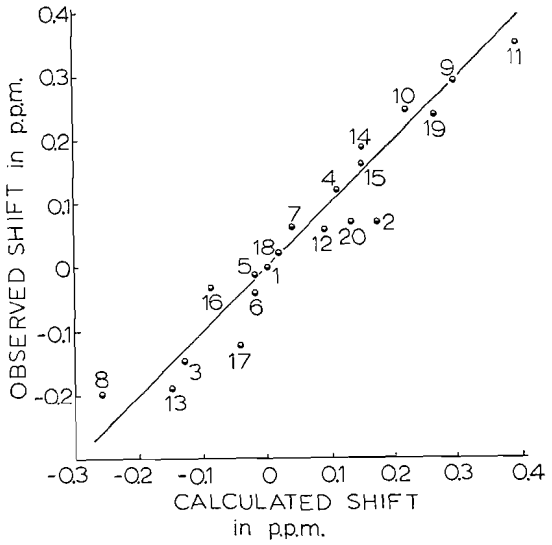

FIG. 5. Plot of the observed shift, relative to benzene chromium tricarbonyl, caused by methyl groups ortho, meta, and para to the alkene proton (code numbered as under Results) versus the calculated shift using ortho = +0.14 p.p.m., meta = −0.08 p.p.m., and para = +0.15 p.p.m.

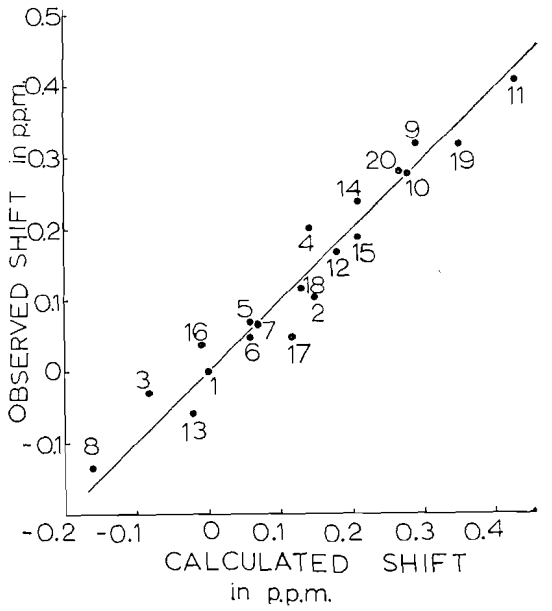

FIG. 6. Plot of the observed shift, relative to benzene molybdenum tricarbonyl, caused by methyl groups ortho, meta, and para to the alkene proton (code numbered as under Results) versus the calculated shift using ortho = +0.08 p.p.m., meta = −0.12 p.p.m., and para = +0.14 p.p.m.

the value for the chemical shift increment caused by ortho, meta, and para methyl groups is assumed to be additive and internally self-consistent within the complete series. For the chromium complexes, the best set of values are: ortho = +0.14 p.p.m., meta = −0.08 p.p.m., and para = +0.15 p.p.m. Using these values, the agreement between the calculated and the observed chemical shift differences for the individual protons, relative to the protons in benzene chromium tricarbonyl, are plotted in Fig. 5. A similar plot for the molybdenum complexes is given in Fig. 6, using ortho = +0.11 p.p.m., meta = −0.13 p.p.m., and para = 0.17 p.p.m. For the tungsten case, a reasonably consistent set of values are: ortho = +0.08 p.p.m., meta = −0.12 p.p.m., and para = +0.14 p.p.m.

In comparison, adding methyl groups to the free ligands serves only to increase (or at best leave unchanged) the chemical shift value for all alkene protons. While there is obviously no satisfactory correlation of the type used above,[2] a reasonable set of values is: ortho = para ≈ 0.15 p.p.m. and meta ~ 0 p.p.m. (relative to the chemical shift value for benzene). For ex-

[2]Linear correlations of n.m.r. proton shifts in benzene compounds due to ortho, meta, and para substituents in mono-, di-, and poly-substituted benzenes have been shown by a number of workers (see ref. 13 for a discussion). The values given for ortho and para methyl are similar to ours but the value for meta methyl is even more positive (+0.13 p.p.m.).

Can. J. Chem. Downloaded from www.nrcresearchpress.com by 210.87.254.105 on 09/05/12
For personal use only.

ample, comparisons of the alkene proton chemical shifts of mesitylene (τ 3.22), isodurene (τ 3.21), and pentamethylbenzene (τ 3.20) suggest that added meta methyl groups have almost no effect.

The previously mentioned results suggest, therefore, that the electron-enriching mesomeric effect, which is presumed to account for the higher chemical shift values found for protons ortho and para to a methyl group, does not change appreciably on complex formation, but that on complex formation a methyl group appears to *decrease* the electron density at positions meta to itself.

The n.m.r. spectrum of toluene chromium tricarbonyl was measured at 35 and 52 °C with no change observed. The spectra of both *m*- and *p*-xylene chromium tricarbonyl were measured at −30 and 35 °C with again no change detected. There is no reason to believe, in fact, that any of the spectra are changing over the temperature range −30 to 50 °C.

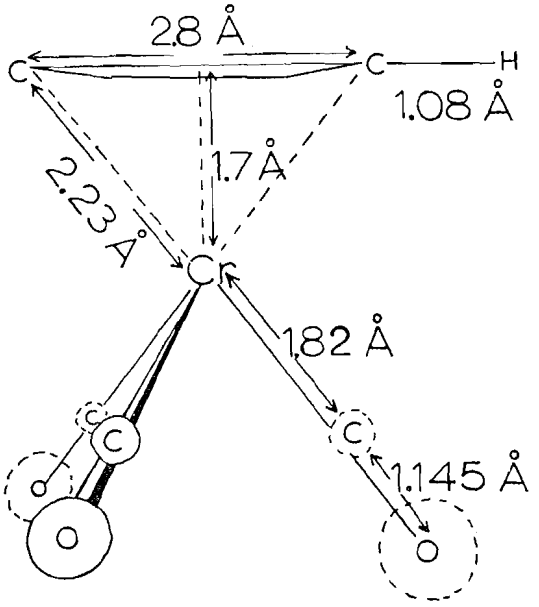

FIG. 7. Scale drawing of the benzene chromium tricarbonyl complex.

Discussion

Three observations merit discussion:

(1) The large upfield shift of arene protons observed for all of the metal complexes (relative to the free arene).

(2) The variation of these chemical shifts depending on the particular metal.

(3) The variation of individual proton chemical shifts within a given unsymmetrical arene metal complex.

The large upfield shift of the alkene arene proton n.m.r. resonances on complex formation is assumed to be due to a shielding of the protons by the metal atom and/or a return to normal alkene proton positions resulting from a decreased or altered "ring current" (14). In addition, however, the $M(CO)_3$ fragments (M = Cr, Mo) have been shown to be quite strongly electron withdrawing (15, 16), and this would be expected to cause shifts to *lower* fields. There are indications based on dipole moment data (17, 18) that variations occur among the metals in this regard. It is possible to invoke suitable combinations of these opposing effects and to thereby provide a reasonable rationale for points 1 and 2 above.

At least two, essentially unrelated, explanations are possible for the third point. In a recent communication, Gracey *et al.* (10) have reported a complex alkene region n.m.r. spectrum for *t*-butylbenzene chromium tricarbonyl, and they have explained the result on the basis of a preferred conformation in which the three carbonyl groups are assumed to deshield the ortho and para proton positions relative to the meta. In Fig. 7, a scale drawing of benzene chromium tricarbonyl is presented, based on the X-ray structure of Bailey and Dahl (7). A significant deshielding of specific alkene protons by the C≡O or M—C bonds seems unlikely, partly because of the distance involved, but more importantly because of the particular disposition of these groups relative to the alkene protons. The observation that the lowest values of Δ (see Fig. 3) occur in the molybdenum complexes, where the carbonyl – alkene proton distances are *increased* relative to the chromium analogs, is also at variance with this explanation.

We prefer to explain the chemical shift differences of ring protons, in for example toluene molybdenum tricarbonyl,[3] as due to differences in the π-electron density of the arene ring carbon atoms. The carbon π-electron density is then assumed to be reflected in the n.m.r. chemical shifts of the corresponding proton resonances (19).

One is then left with the fact that, in the complexes, protons meta to a methyl group have

[3]Since *both* toluene and *t*-butylbenzene chromium tricarbonyl have complex alkene proton n.m.r. spectra and since restricted rotation of the type proposed by Gracey *et al.* seems improbable for the toluene case, the necessity for invoking restricted rotation, as an explanation of the n.m.r. spectrum in the *t*-butyl case, should be reconsidered.

Can. J. Chem. Downloaded from www.nrcresearchpress.com by 210.87.254.105 on 09/05/12
For personal use only.

decreased chemical shifts and, from the previous discussion, an assumed decreased electron density, relative to the benzene analogs. This observation can be rationalized, however, if we postulate, as was discussed in the Introduction, that $M(CO)_3$ bonding is concentrated at three 120° positions on the arene ring; these positions occurring at carbon atoms and corresponding to octahedral bonding sites as determined by the M—CO bond orientations. Since the $M(CO)_3$ groups are electron withdrawing, this bonding would be expected at the most electron-rich carbon atoms. In alkyl benzenes, where inductive effects are dominant, the bonding would be "strongest" at those carbon atoms to which methyl groups are directly bonded. This would then also result in abnormal electron withdrawal from the positions 120° to this carbon, in fact corresponding to positions meta to the alkyl group.[4]

In arenes like anisole and aniline, where mesomeric effects are dominant, the positions ortho and para to the functional group are those most electron rich and it is these positions to which one might expect the strongest octahedral bonding. Such a postulate has in fact been proposed, on the basis of X-ray evidence (see Introduction) (9). The n.m.r. results of McFarlane and Grim, on the methoxy-substituted benzene chromium tricarbonyl complexes, do not support, nor do they rule out, this hypothesis.

The rotation of the $M(CO)_3$ group relative to the arene ring would have to be fast on the n.m.r. time scale since no permanent distortion is noted in complexes like *p*-xylene $M(CO)_3$. The two rotamers possible for this complex are shown in Fig. 8 (octahedral points are indicated by arrows). The two rotamers are of equal energy, Fig. 8, and hence have equal populations, giving only one averaged n.m.r. alkene proton peak. With two unequal energy rotamers, as for example in *m*-xylene $M(CO)_3$, the population of one form is much greater than that of the other (Fig. 8). While proton averaging occurs, the actual n.m.r. chemical shift positions of the individual protons will be mainly due to those of

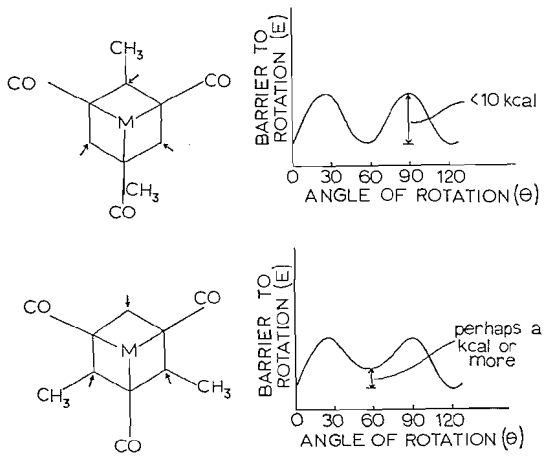

FIG. 8. *Top*, one of the two equivalent conformations proposed for the *p*-xylene metal tricarbonyl complex, showing on the right the proposed energy variation (the value of 10 kcal is based on the observation of only averaged spectra at −30 °C) on rotation of the $M(CO)_3$ group. *Bottom*, the proposed most stable conformation of the meta-xylene metal tricarbonyl complex, showing on the right the proposed energy variation on rotation of the $M(CO)_3$ group and the energy difference between the two conformations. (Estimated at 1 kcal or more ($K > 5$) on the basis that a linear correlation of the type shown in Figs. 5 and 6 would be invalid if both isomers were present in substantial amounts.)

the most stable conformer. Modest cooling of the solution has no effect on the shape of the spectra although a Boltzmann distribution plot of the chemical shift might ideally be expected.

A good inverse correlation exists between the order observed for Δ (Fig. 3), Cr > W > Mo, and the magnitude of the negative meta proton chemical shift increment, Cr < W < Mo. This is entirely consistent with the supposition that the former order is due partially to differing electron-withdrawing effects among the metals.

The above analysis satisfactorily accounts for the observation that n.m.r. equivalent protons in the free arenes are also equivalent in the metal complexes. This analysis also accounts for the increased chemical shift separation observed for the n.m.r. non-equivalent protons in the unsymmetrical arene metal complexes.

Experimental

The complexes required for this study were synthesized using standard procedures already described in the literature (20, 22). The crude reaction products were purified by sublimation and in some cases, where an oily product was initially obtained, by chromatography on alumina. The chromium and tungsten complexes, once

[4]This three-fold distortion does not change the n.m.r. analysis of the toluene, *m*-xylene, 1,2,3-, and 1,2,4-trimethylbenzene metal tricarbonyl compounds. In *o*-xylene, the symmetry changes from AA′BB′ to ABCD but in this case a reliable analysis is impossible for either type.

TABLE I
Analytical results

Ligand	Metal	Ref. to prev. lit.	Melting point of new complex[7] (°C)	Yield (%)	Analyses Calcd. C	Calcd. H	Found C	Found H
Benzene	Cr	20						
	Mo	21						
	W	21						
Toluene	Cr	21						
	Mo	22						
	W	23						
o-Xylene[1]	Cr	21						
	Mo		100–105	54	46.2	3.5	46.1	3.7
	W[8]		120–121	11				
m-Xylene[1]	Cr	21						
	Mo		126–130	46	46.2	3.5	46.5	3.8
	W	24						
p-Xylene[1]	Cr	21						
	Mo	22						
	W	23						
Mesitylene[2]	Cr	21						
	Mo	21						
	W	21						
1,2,3-Trimethylbenzene[3]	Cr	25						
	Mo		138–139	45	48.0	4.0	49.1	4.6
	W		125–130	6	37.1	3.1	39.9	4.3
1,2,4-Trimethylbenzene[3]	Cr	26						
	Mo		84–85	40	48.0	4.0	48.3	4.2
	W		96–97	6	37.1	3.1	37.0	3.5
1,2,3,4-Tetramethylbenzene[4]	Cr		115–117	32	57.8	5.2	58.1	5.3
	Mo		142–144	40	49.7	4.5	50.4	4.9
	W		134–137	8	38.8	3.5	41.8	4.1
1,2,3,5-Tetramethylbenzene[5]	Cr		124–126	52	57.8	5.2	58.3	5.7
	Mo		135–136	55	49.7	4.5	49.5	4.9
	W		165–169	10				
Durene	Cr	18						
	Mo		90–98	51	49.7	4.5	49.7	5.0
	W		150–155	15	38.8	3.5	39.5	3.7
Pentamethylbenzene[6]	Cr		101–102	43	59.2	5.6	59.8	6.1
	Mo		140–142	47	51.2	4.9	51.2	5.5
	W		148 (decomp.)	10	40.4	3.9	42.9	4.9
Hexamethylbenzene	Cr	21						
	Mo	27						
	W	28						

[1]Matheson, Coleman and Bell "chromatographically pure".
[2]Aldrich Chem. Co. "puriss. grade".
[3]Purified by distillation.
[4]Chemical Procurement Laboratories.
[5]Aldrich Chem. Co.
[6]Recrystallized to remove hexamethylbenzene impurity.
[7]Uncorrected.
[8]Considerable difficulty was encountered in trying to get acceptable analyses on some of the tungsten compounds. The residue was high as were carbon and hydrogen values.

obtained, were thermally more stable than the molybdenum analogs, but were in general not as easily prepared. The melting points reported for the molybdenum and tungsten compounds are probably decomposition points in most cases and are very variable and unreproducible. The melting points of the known chromium complexes were in good agreement with those reported. The infrared spectra of many of the complexes were obtained and, for known compounds, were found to agree well with the literature values. Table I lists the complete series, for the compounds synthesized in this work, with a reference to those compounds previously reported in the chemical literature.

N.M.R. Spectral Measurements

All measurements were made using a Varian Assoc. A-60 equipped with a variable temperature probe. The measurements reported in Figs. 3 and 4 are for 7% w/v solutions of the metal complex in deuterochloroform solvent except in a few cases where the solubility was too low. In these cases, a saturated or supersaturated solution was used. Tetramethylsilane was used as the internal reference in all cases. The n.m.r. spectra of the free arenes have been previously measured (12, 29). However, in order to get the maximum consistency, these spectra were remeasured as 7% w/v solutions in deuterochloroform and we have used these values to obtain Δ. The results, where

Can. J. Chem. Downloaded from www.nrcresearchpress.com by 210.87.254.105 on 09/05/12
For personal use only.

comparable, agree well with the published spectra. The effect of concentration on the n.m.r. chemical shift values was investigated in several instances. Over the range 3–10% there is very little change. Many of the complexes were also measured in chloroform and carbon disulfide solutions. The chemical shift values are consistently 0.02–0.04 p.p.m. higher field in chloroform solvent and up to 0.2 p.p.m. higher field in carbon disulfide solvent, compared with deuterochloroform. The shape of the n.m.r. curves are identical, however. The molybdenum complexes, in particular, are not very stable in chloroform solutions and measurements must be made reasonably soon after dissolution. All peak areas showed the correct relative intensities. The actual chemical shift values are not tabulated as such in this paper (see Thesis of J. T. P.) but one can obtain these from Figs. 3 and 4 by adding Δ to the known values for the chemical shifts of the free arene compounds. The possible error in Δ is approximately ± 0.02 p.p.m., representing approximately ± 0.01 p.p.m. error in each measurement contributing to Δ.

In cases where a complex alkene region was observed, the curve was reproduced a number of times at 100 c.p.s. sweep width. The curves were analyzed by standard procedures, i.e. matching with computer-calculated curves (30).

Acknowledgments

The authors wish to thank Mrs. V. Boon for many of the n.m.r. spectral measurements and Mr. P. Campbell and Mr. G. Aikenhead for technical assistance. We also wish to thank the National Research Council of Canada for generous financial support.

1. E. Weiss and E. O. Fischer. Z. Anorg. Allgem. Chem. **286**, 142 (1956).
2. F. Jellinek. J. Organometal. Chem. Amsterdam, **1**, 43 (1963). E. Keulen and F. Jellinek. J. Organometal. Chem. Amsterdam, **5**, 490 (1966).
3. F. A. Cotton, W. A. Dollase, and J. S. Wood. J. Am. Chem. Soc. **85**, 1543 (1963).
4. A. Haaland. Acta Chem. Scand. **19**, 41 (1965).
5. H. P. Fritz. *In* Advances in organometallic chemistry. Vol. I. *Edited by* F. G. A. Stone and R. West. Academic Press, New York. 1964. pp. 240–315.
6. W. McFarlane and S. O. Grim. J. Organometal. Chem. Amsterdam, **5**, 147 (1966).
7. M. F. Bailey and L. F. Dahl. Inorg. Chem. **4**, 1314 (1965).
8. M. F. Bailey and L. F. Dahl. Inorg. Chem. **4**, 1298 (1965).
9. O. L. Carter, A. T. McPhail, and G. A. Sim. Chem. Commun. 212 (1966).
10. D. E. F. Gracey, W. R. Jackson, W. B. Jennings, S. C. Rennison, and R. Spratt. Chem. Commun. 231 (1966).
11. H. Zeiss, P. J. Wheatley, and H. J. S. Winkler. Benzenoid–metal complexes. Ronald Press Co., New York. 1966. H. P. Fritz and C. G. Kreiter. J. Organometal. Chem. Amsterdam, 7, 427 (1967).
12. J. A. Pople, W. G. Schneider, and H. J. Bernstein. High-resolution nuclear magnetic resonance. McGraw-Hill, New York. 1959.
13. J. W. Emsley, J. Feeney, and L. H. Sutcliffe. High resolution nuclear magnetic resonance spectroscopy. Vol. II. Pergamon Press, Oxford. 1966.
14. W. Strohmeier and H. Hellmann. Chem. Ber. **97**, 1877 (1964).
15. E. O. Fischer, K. Öfele, H. Essler, W. Frohlich, J. P. Mortensen, and W. Semmlinger. Chem. Ber. **91**, 2763 (1958).
16. B. Nicholls and M. C. Whiting. J. Chem. Soc. 551 (1959).
17. E. O. Fischer and S. Schreiner. Chem. Ber. **92**, 938 (1959).
18. E. W. Randall and L. E. Sutton. Proc. Chem. Soc. 93 (1959).
19. G. Fraenkel, R. E. Carter, A. McLachlan, and J. H. Richards. J. Am. Chem. Soc. **82**, 5846 (1960). T. Schaefer and W. G. Schneider. Can. J. Chem. **41**, 966 (1963). T. S. Sorensen. J. Am. Chem. Soc. **87**, 5075 (1965).
20. E. O. Fischer and K. Öfele. Chem. Ber. **90**, 2532 (1957).
21. E. O. Fischer, K. Öfele, H. Essler, W. Frohlich, J. P. Mortensen, and W. Semmlinger. Z. Naturforsch. **13b**, 458 (1958).
22. W. Strohmeier. Chem. Ber. **94**, 3337 (1961).
23. W. Strohmeier. Z. Naturforsch. **17b**, 566 (1962).
24. Ethyl Corporation. Brit. Patent No. 856,354; Chem. Abstr. **55**, 16483*a* (1961).
25. G. G. Ecke. U.S. Patent No. 3,135,776; Chem. Abstr. **61**, 13344*g* (1964).
26. C. N. Matthews. U.S. Patent No. 3,117,983; Chem. Abstr. **60**, 6870*f* (1964).
27. D. H. Antonsen. U.S. Patent No. 3,010,978; Chem. Abstr. **56**, 11620*b* (1962).
28. T. A. Manuel and F. G. A. Stone. Chem. Ind. London, 1349 (1959).
29. Varian Associates. High resolution NMR spectra catalog. Vol. I and II. Varian Associates, Palo Alto, California. 1962 and 1963.
30. K. B. Wiberg and B. J. Nist. The interpretation of NMR spectra. W. A. Benjamin, Inc., New York. 1962.

Can. J. Chem. Downloaded from www.nrcresearchpress.com by 210.87.254.105 on 09/05/12
For personal use only.

Can. J. Chem. Downloaded from www.nrcresearchpress.com by 210.87.254.105 on 09/05/12
For personal use only.

Dipole moments of some molecules in dilute benzene solutions

E. Bock and D. Iwacha
Parker Chemistry Laboratory, University of Manitoba, Winnipeg, Manitoba

Received August 9, 1967

The dipole moments of bromochloromethane, bromodichloromethane, bromotrichloromethane, dimethylcarbamyl chloride, dimethylcarbamyl fluoride, vinyl formate, phenyl chlorothiolformate, γ-valerolactone, and 2-iodopropene were determined in dilute benzene solutions at 25 °C. The observed magnitudes of the dipole moments are rationalized in terms of molecular electronic charge distributions.

Canadian Journal of Chemistry, 46, 523 (1968)

Introduction

Over the past several years, the nuclear magnetic resonance (n.m.r.) group of the Parker Chemistry Laboratory, University of Manitoba, has investigated the solvent effects on the proton spectra of different molecules (1–4). As is well known, the solvent effect on the proton chemical shift in molecules may be roughly divided into four main contributions, viz. dispersion forces, electric field forces, and magnetic anisotropy and bulk susceptibility effects. Of these, the electric field effect is strongly dependent on the molecular dipole moment. In order to theoretically calculate the effect of the reaction field, and from the latter, the electric field contribution to the solvent effect, it is necessary to know the dipole moment of the solute molecule. It was for this reason that we measured the dipole moments of the above-mentioned molecules. We report our findings here in the hope that they will be of some use to other workers in related or different research fields.

Experimental

Solvent

Fisher Certified reagent benzene was used as solvent. The benzene was dried by repeated shaking with Linde Molecular Sieve 4A.

Solute

The bromochloromethanes and γ-valerolactone, obtained from Aldrich Chemical Co., were used without further purification. The vinyl formate, phenyl chlorothiolformate, and dimethylcarbamyl chloride, also obtained from Aldrich Chemical Co., were further purified by fractional distillation, under reduced pressure. The dimethylcarbamyl fluoride was prepared from dimethylcarbamyl chloride by reacting the latter with SbF_3 after the method of Schrader (5). The product was subjected to fractional distillation under reduced pressure and was further purified using a Varian 1520 gas chromatograph. The 2-iodopropene, obtained from Columbia Chemical Co., was also purified by gas chromatography. The apparatus and experimental procedure have been described elsewhere (6).

Results

The experimental results are summarized in Table I. In Table II the dipole moments obtained by us are compared with the results of earlier dipole moments determinations recorded in the literature. The following comments may be in order regarding the entries in Table II. The dipole moment of bromotrichloromethane determined by us, i.e. 0.59 D, is significantly larger than the value found by Miller and Smyth (7) for this molecule, viz. 0.21 D. We believe that this discrepancy is due in part to the fact that the above authors used the Onsager equation in deriving the dipole moment for the molecule. It is well known that the application of the Onsager equation to dielectric constant data derived from pure liquids does not yield even approximately correct dipole moment values for many molecules (8). However, it is only proper to also note that our treatment of the experimental data (the modified Guggenheim treatment of Smith (9)) lacks in precision especially for molecules with low dipole moments. The *true* dipole moment of the molecule may therefore lie between 0.21 D and 0.59 D respectively.

The dipole moments of dimethylcarbamyl fluoride and dimethylcarbamyl chloride are almost equal, viz. 4.02 D and 4.08 D respectively, but are considerably larger than the dipole moments of methylchloroformate, 2.38 D (10), and methylfluoroformate 2.61 D.[1] Now the chief structural difference between these two types of molecules consists in a nitrogen atom being situated between the halocarbonyl group and the alkyl radical in the former molecules and an oxygen atom in the latter molecules, respectively. The very much larger dipole moments of the

[1]Unpublished results determined in this laboratory.

Can. J. Chem. Downloaded from www.nrcresearchpress.com by 210.87.254.105 on 09/05/12
For personal use only.

TABLE I

Weight fractions (W), dielectric constants (ϵ), and densities (d) of solutions in benzene at 25 °C

$W \times 10^3$	ϵ	d
Bromochloromethane		
1.169	2.2755	0.8742
2.7666	2.2789	0.8750
4.177	2.2813	0.8756
6.603	2.2861	0.8768
7.73	2.2884	0.8774
Bromodichloromethane		
1.103	2.2741	0.8743
2.557	2.2752	0.8749
4.191	2.2768	0.8758
6.0997	2.2787	0.8767
8.457	2.2804	0.8778
Bromotrichloromethane		
1.0559	2.2727	0.8742
2.548	2.2729	0.8749
4.084	2.2730	0.8757
6.095	2.2732	0.8768
7.783	2.2734	0.8775
Dimethylcarbamyl (fluoride)		
8.957	2.2897	0.8738
2.764	2.3248	0.8741
4.489	2.3574	0.8744
6.105	2.3887	0.8746
Dimethylcarbamyl (chloride)		
1.273	2.2941	0.8739
2.648	2.3168	0.8742
4.491	2.3476	0.8748
6.622	2.3822	0.8753
8.663	2.4164	0.8757
Vinyl formate		
1.058	2.2767	0.8737
2.731	2.2829	0.8738
4.4156	2.2887	0.8738
6.462	2.2962	0.8739
7.9025	2.3016	0.8740
Phenyl thiochloroformate		
1.419	2.2805	0.8740
3.414	2.2908	0.8746
5.05	2.3000	0.8752
7.025	2.3101	0.8756
9.227	2.3222	0.8762
γ-Valerolactone		
1.078	2.2945	0.8738
2.42	2.3203	0.8739
4.119	2.3541	0.8743
6.473	2.4007	0.8746
7.584	2.4227	0.8748
2-Iodopropene		
1.28	2.2754	0.8742
1.947	2.2758	0.8744
2.903	2.2773	0.8750
4.438	2.2797	0.8757

carbamyl molecules suggest that the nitrogen atom must act as an electron donor in these molecules by, perhaps, forming a double bond with the carbon atom; i.e.

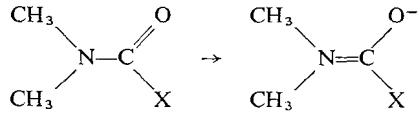

The resulting shift of electronic charge towards the oxygen would in turn result in an enhanced value of the dipole moment.

TABLE II

Comparison of dipole moments from dilute benzene solutions obtained in this work with earlier reported values

Compound	μ (D)	μ (D)
CH_2BrCl	1.66*	—
$CHBrCl_2$	1.31*	—
$CBrCl_3$	0.59*	0.21 (7)
$(CH_3)_2NCOCl$	4.08*	—
$(CH_3)_2NCOF$	4.02*	—
$CH_2CHOCOH$	1.66*	1.48 (12)
C_6H_5SCOCl	2.91*	—
$CH_3(CH_2)_2OCO$	4.30*	—
CH_3ClCH_2	1.57*	—

*Values obtained in this work.

The phenyl chlorothiolformate presents a particularly interesting case. Its dipole moment, in dilute benzene solution, is 2.91 D, whereas that of phenyl chloroformate in the same solvent is 2.39 D (10). This is a rather surprising result. One would expect that because of its larger size and hence greater polarizability, the sulfur atom would concentrate less electronic charge than an oxygen atom and would therefore lead to a smaller molecular dipole moment than an oxygen atom in a corresponding molecule. It is equally surprising to find that the dipole moments of all thioethers which have been measured to date are larger than the dipole moments of the corresponding oxygen ethers; yet the water molecule, which may be regarded as a special kind of ether, has a much higher dipole moment, 1.85 D, than the hydrogen sulfide molecule, 1.0 D. (See Table III.) From Table III it is apparent that the enhanced dipole moment of the thioethers is not due to a change in the bond angle; the carbon–sulfur bond moments in all molecules listed in Table III are either equal to or larger than the corresponding carbon–oxygen bond moments. The observed facts may be interpreted in terms of a number of different mechanisms. Thus Gibbs suggested that the reason for the observed magnitudes of the dipole moments of the group VI element

TABLE III

Comparison of dipole moments and molecular parameters of normal ethers with the dipole moments and corresponding molecular parameters of thioethers

Compound	μ (B) (D)	μ (V) (D)	<COC or <HOH	<CSC or <HSH	μ(C—O) (B) or μ(H—O) (B)	μ(C—O) (V) or μ(H—O) (V)	μ(C—S) (B) or μ(H—S) (B)	μ(C—S) (V) or μ(H—S) (V)
Water	1.71–1.85	1.82	105°		1.52	1.49		
Hydrogen sulfide	0.85–0.97	0.974 (15)		93°			0.69	0.69
Dimethyl ether	1.25	1.31 (16)	111° (16)		1.12	1.16		
Dimethyl sulfide	1.45 (17)	1.50 (18)		99° (18)			1.11	1.16
Diethyl ether	1.30	1.17	108°		1.11	1.0		
Diethyl sulfide	1.161 (17)	1.52		112°			1.44	1.34
							1.25 (*a*)	1.17 (*a*)
Dipropyl ether	1.13–1.31	1.03–1.21	—		1.11 (*b*)	1.03 (*b*)		
Dipropyl sulfide	1.60 (17)	—		—			1.24 (*a*)	—
Dibutyl ether	1.09–1.26	1.18	—		1.08 (*b*)	1.0 (*b*)		
Dibutyl sulfide	1.60 (17)	—		—			1.24 (*a*)	—
Diphenyl ether	1.11	1.0–1.36			0.95 (*b*)	1.1 (*b*)		
Diphenyl sulfide	1.55 (19)	—		—			1.13 (*a*)	—

(B) Benzene solution, (V) vapor, (L) liquid dipole moment values from ref. 11 or as indicated. Bond angles from ref. 21 or as indicated.

(*a*) Bond moment calculated on the assumption that the bond angle $\widehat{CSC} = 99°$.

(*b*) Bond moment calculated on the assumption that the bond angle $\widehat{COC} = 108°$.

dihydrides and dialkyls, viz: $\mu(H_2O) > \mu(H_2S)$, but $\mu((CH_3)_2O) < \mu(CH_3)_2S$, is to be found in the lone-pair electron charge cloud distribution (20). The latter being more concentrated "behind" the atom the greater the degree of sp^3 hybridization of the group VI element orbitals. By making the usual assumption that the bonding orbital axes coincide with the bond axes and using the then available bond angle data, Gibbs concluded that the sulfur atom in dimethyl sulfide retains a considerable degree of sp^3 hybridization and that it was this effect coupled with the increase in the size of the atomic orbital that accounted for the observed dipole moment relationship, viz. $\mu((CH_3)_2O) < \mu((CH_3)_2S)$. However, more recent work on the structure of dimethyl sulfide (17) shows that the C—S bond angle in that molecule is 99° rather than 104°, as assumed by Gibbs. This suggests that the degree of hybridization in the two molecules H_2S and $(CH_3)_2S$ is of the same order of magnitude, and that an explanation of the observed dipole moments magnitudes in the two molecules in terms of differences in the degree of hybridization only is inadequate. Moreover, if the O—H, S—H, O—C, and S—C bond moments in H_2O, H_2S, $(CH_3)_2O$, and $(CH_3)_2S$, calculated in terms of a vector model using the latest available structure data, are divided by the respective bond length one obtains in each case a measure for the apparent charge residing on the oxygen and sulfur atom respectively. Such calculations yield the following values for the apparent charge: H_2O, 1.59×10^{-10} e.s.u., H_2S, 0.52×10^{-10} e.s.u., $(CH_3)_2O$, 0.82×10^{-10} e.s.u., and $(CH_3)_2S$, 0.64×10^{-10} e.s.u. From these numbers it is apparent that a substitution of the two hydrogen atoms by two methyl groups results in a larger concentration of charge on the sulfur atom in $(CH_3)_2S$ than in H_2S. And the larger dipole moment of the former molecule is seen to be due to the combined effect of a larger bond length and a larger charge concentration on the sulfur atom in $(CH_3)_2S$. The enhanced concentration of charge may be rationalized in terms of a hyperconjugation mechanism and a partial overlap of the d orbitals of sulfur with the carbon orbitals. Hyperconjugation will tend to concentrate excess negative charge on the methyl carbon. This excess concentration of charge may be removed to some extent by the d orbitals of sulfur. Both effects will enhance each other and will result in a higher dipole moment for the dimethyl sulfide molecule as compared with the dimethyl ether molecule, where the former effect, viz. expansion of the octet of electrons, is impossible. If this explanation is true, then one should expect that the increase in the dipole moment in the higher homologues should diminish with increase in the chain length of the hydrocarbon radical and should, finally, tend to a limiting value. That this is indeed the case is borne out by Table III.

Can. J. Chem. Downloaded from www.nrcresearchpress.com by 210.87.254.105 on 09/05/12
For personal use only.

Can. J. Chem. Downloaded from www.nrcresearchpress.com by 210.87.254.105 on 09/05/12
For personal use only.

A similar mechanism, i.e. the participation of the sulfur d orbitals, may be used to explain the higher dipole moment of the phenyl chlorothiolformate molecule compared with the phenyl chloroformate molecule. In an earlier paper (10), it was noted that the dipole moment of phenyl chloroformate was lower than the dipole moments of the higher homologues of the aliphatic chloroformate series. It was suggested there that the smaller value of the dipole moment for the phenyl chloroformate molecule resulted from the mesomeric transfer of electronic charge into the benzene ring. In the case of the phenyl chlorothiolformate molecule the sulfur atom, by virtue of its ability to expand its octet of electrons (use of d orbitals), will retain more electronic charge than the oxygen atom in the corresponding position in the phenyl chloroformate molecule. Since the benzene ring is at the positive end of the molecular dipole, concentration of electronic charge on the sulfur, roughly at the midpoint of the molecular dipole, will result in a higher dipole moment for the phenyl chlorothiolformate molecule. Such a mechanism is supported by the observation, made in this laboratory, that the C=O stretching frequency in phenyl chlorothiolformate molecule is shifted by about 8 cm^{-1} towards longer wavelength compared with the phenyl chloroformate molecule. This suggests that there is a lower charge concentration in the C=O bond in the phenyl chlorothiolformate molecule compared with the corresponding bond in the phenyl chloroformate molecule.

The dipole moment for vinyl formate determined by us, 1.66 D, is larger than the value found by Rao and Curl 1.48 D (12). This discrepancy is surprising and we are at a loss to explain it. Normally one would expect that the dipole moment derived from solution measurements in benzene would be lower than the vapor phase value. Thus the dipole moment for methyl formate determined earlier in this laboratory (13) in benzene and carbon disulfide solution was lower than the corresponding vapor phase value found by Curl (14), viz. 1.75 D, 1.52 D, and 1.77 D respectively. This is usually the case; the so-called solvent effect in benzene solution is negative for the majority of molecules. In this case, however, the solvent effect seems to be positive.

The dipole moment of γ-valerolactone is, as expected, of the same order as the dipole moments of β- and γ-butyrolactone, 418, 415, and 4.30 D respectively.

Acknowledgments

We thank Dr. A. Queen for the synthesis of dimethylcarbamyl fluoride. We also thank Dr. D. W. McBride for helpful discussions. The financial assistance of the National Research Council of Canada is deeply appreciated.

1. F. Hruska, E. Bock, and T. Schaefer. Can. J. Chem. **41**, 3034 (1963).
2. F. Hruska, H. M. Hutton, and T. Schaefer. Can. J. Chem. **43**, 2392 (1965).
3. F. Hruska, D. W. McBride, and T. Schaefer. Can. J. Chem. **45**, 1081 (1967).
4. H. M. Hutton and T. Schaefer. Can. J. Chem. **45**, 1111 (1967).
5. Schrader. British Intelligence Objectives Subcommittee Final Rept. No. 714, 39 (1947).
6. E. Bock and E. F. Dojack. Can. J. Chem. **45**, 1097 (1967).
7. R. C. Miller and C. P. Smyth. J. Chem. Phys. **24**, 814 (1956).
8. J. W. Smith. Electric dipole moments. Butterworths Scientific Publications, London. 1955. p. 149.
9. J. W. Smith. Trans. Faraday Soc. **46**, 394 (1950).
10. E. Bock and D. Iwacha. Can. J. Chem. **45**, 3177 (1967).
11. A. L. McClellan. Tables of experimental dipole moments. W. H. Freeman and Co., San Francisco and London. 1963.
12. V. M. Rao and R. F. Curl, Jr. J. Chem. Phys. **40**, 3688 (1964).
13. E. Bock. Can. J. Chem. **45**, 2761 (1967).
14. R. F. Curl, Jr. J. Chem. Phys. **30**, 1529 (1959).
15. C. Huizoon and D. Dymanns. Physica, **31**, 1049 (1965).
16. U. Bulkis, P. H. Kasai, and R. J. Myers. J. Chem. Phys. **38**, 2753 (1963).
17. C. W. N. Cumper, J. F. Read, and A. I. Vogel. J. Chem. Soc. 5323 (1965).
18. L. Pierre and M. Hayashi. J. Chem. Phys. **35**, 479 (1961).
19. C. W. N. Cumper, J. F. Read, and A. I. Vogel. J. Chem. Soc. 5860 (1965).
20. J. H. Gibbs. J. Chem. Phys. **22**, 1460 (1954).
21. The Chemical Society, London. Tables of interatomic distances and configuration in molecules and ions. Special Publication No. 11 (1958); Special Publication No. 18 (1965).

$Hg(6^3P_1)$-sensitized decomposition of HNCO vapor and HNCO–H_2 mixtures; the reaction of hydrogen atoms with HNCO[1]

N. J. FRISWELL[2] AND R. A. BACK

Division of Pure Chemistry, National Research Council of Canada, Ottawa, Canada

Received September 1, 1967

The $Hg(6^3P_1)$-sensitized decomposition of HNCO vapor has been briefly studied at 26 °C with HNCO pressures from about 3 to 30 Torr. The products detected were the same as in the direct photolysis, CO, N_2, and H_2. The quantum yield of CO was appreciably less than unity, compared with a value of 1.5 in the direct photolysis under similar conditions. From this and other observations it is tentatively concluded that a single primary process occurs:

[1] $$Hg(6^3P_1) + HNCO \rightarrow Hg(6^1S_0) + H + NCO.$$

From a study of the mercury-photosensitized reactions in mixtures of HNCO with H_2, it was concluded that hydrogen atoms react with HNCO to form CO but not N_2. The initial step is probably addition to form NH_2CO. From the competition between reaction [1] and the corresponding quenching by H_2, the cross section for reaction [1] was estimated to be 2.3 times that of hydrogen.

Canadian Journal of Chemistry, 46, 527 (1968)

Introduction

The photolysis of HNCO vapor has been investigated in some detail in this laboratory (1–4). The mercury-photosensitized decomposition, which apparently has not been studied before, is of obvious interest for comparison with the photolysis. At the same time it was convenient and of interest to examine the mercury-photosensitized decomposition of H_2–HNCO mixtures, in which hydrogen atoms will be formed by the decomposition of H_2, since hydrogen atoms are thought to play an important part in the photolysis mechanism.

Experimental

The apparatus, the preparation of HNCO, and the product analysis were all essentially as described by Woolley and Back (4). Gases were circulated through the reaction vessel and through a U-trap held at 0 °C during the irradiation to control the pressure of mercury vapor. The mercury resonance lamp was a flat spiral (5), water cooled (25 °C), and operated at 50 mA. A Vycor filter (Corning 7910) removed the 1849 Å emission. All irradiations were done at 26 °C and were of 1 h duration.

Quantum yields were determined by comparison with the decomposition of propane at 300 Torr. The hydrogen yield from the latter at conversions below 0.03% was linear with time and was assumed to be unity (6, 7). In the quantum yield measurements, the light absorbed in the photolysis vessel at 2537 Å was measured and small corrections were made for the observed differences in absorption, which are due to the effects of pressure on the profile of the resonance line. Complete quenching of $Hg(6^3P_1)$ by propane, HNCO, or H_2 was assumed.

[1]NRCC No. 9839.

[2]NRCC Postdoctorate Fellow, 1966–68.

Results

The Decomposition of HNCO Alone

As in the direct photolysis, CO, N_2, and H_2 were the only products observed and measured. Table I shows quantum yields of CO, and yields of N_2 and H_2 expressed as fractions of the CO yield. The values of $\Phi(CO)$ are badly scattered, reflecting an irreproducibility that plagued all the present experiments with HNCO (actinometry experiments with propane were very much better in this respect). It is thought to have arisen from variation of the partial pressure of mercury vapor in the photolysis cell, caused by occlusion of mercury in the HNCO trimer which was deposited in various parts of the circulatory system, and its irregular release to the gas phase. Mercury removal by chemical reaction, perhaps via HgNCO formation, is also a possibility.

TABLE I

Product yields in the $Hg(6^3P_1)$-sensitized decomposition of HNCO

HNCO pressure (Torr)	$\Phi(CO)$	N_2/CO	H_2/CO
2.9	0.70	0.36	0.11
8.2	0.52	0.36	0.090
12.4	0.53	0.36	0.075
19.2	0.80	—	0.062
25.6	0.63	0.35	0.046
29.3	0.94	0.37	—

Within the considerable scatter, $\Phi(CO)$ shows no trend with HNCO pressure, and the average value appears to be significantly less than unity. This is in contrast to the direct photolysis at

Can. J. Chem. Downloaded from www.nrcresearchpress.com by 210.87.254.6 on 09/05/12
For personal use only.

2062 Å in which Φ(CO) was about 1.5 at HNCO pressures above 10 Torr and decreased towards an extrapolated value of 1.0 at zero pressure.

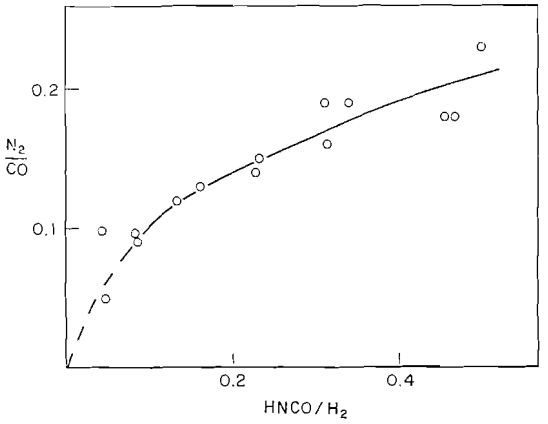

FIG. 1. The dependence of the product ratio, N_2/CO, on the ratio $HNCO/H_2$ in the mercury-photosensitized decomposition of $HNCO–H_2$ mixtures.

The product ratios were much more reproducible than the absolute yields. The ratio N_2/CO was somewhat lower in the present experiments than in the photolysis and did not decrease with increasing pressure. Values of H_2/CO below about 10 Torr were close to those found in the photolysis, but decreased more rapidly with increasing HNCO pressure.

The Decomposition of $HNCO–H_2$ Mixtures

Table II shows values of Φ(CO) and N_2/CO for various pressures of H_2 and HNCO, with ratios of $H_2/HNCO$ ranging from 0 to 23. Any H_2 produced could not of course be measured. Again values of Φ(CO) are badly scattered, but within the scatter show no trend with pressure of H_2 or HNCO, or with the $H_2/HNCO$ ratio; again, Φ(CO) appears to be significantly less than one. The N_2/CO ratio, on the other hand, decreased markedly with increasing values of $H_2/HNCO$; this is shown more clearly in a plot of N_2/CO vs. $HNCO/H_2$ (Fig. 1) which includes additional data not shown in Table II.

TABLE II

Product yields in the $Hg(6^3P_1)$-sensitized decomposition of $HNCO–H_2$ mixtures

p(HNCO) (Torr)	$p(H_2)$ (Torr)	$H_2/HNCO$	Φ(CO)	N_2/CO
3 to 30	0.0	0.00	0.69*	0.36
8.2	16.4	2.00	0.88	0.23
4.3	9.2	2.12	0.39	0.18
2.7	8.0	2.96	0.42	0.19
15.6	49.7	3.19	0.95	0.16
4.2	49.7	11.85	0.54	0.096
2.2	49.9	22.70	0.57	0.098

*Average value.

Discussion

A comparison between the mercury-photosensitized decomposition and the direct photolysis is complicated by the dependence of the latter on HNCO pressure and light intensity (4). These effects are interrelated in the photolysis because the local absorbed light intensity (einsteins cc^{-1} s^{-1}) is roughly linearly dependent on HNCO pressure. This is not so in the sensitized decomposition in which the light is absorbed by mercury vapor, so that the rate of decomposition of HNCO, if quenching is complete, is approximately independent of HNCO pressure. The rate of production of CO in the present experiments was about 2 μmoles/h, independent of pressure. The same rate was obtained in recent photolysis experiments (4) at an HNCO pressure of about 8 Torr, so that the two systems may be compared at this pressure (Table III). The values of Φ(CO) and the product ratios appear to be significantly lower in the sensitized decomposition. In the photolysis, it was thought that the increase in Φ(CO), and probably the decrease in N_2/CO, with increasing HNCO pressure, was due to reaction of NH with HNCO. The lower value of Φ(CO) and the independence of Φ(CO) and N_2/CO on HNCO pressure in the present experiments suggests that NH was not present, and that a single primary process,

[1] $$Hg^* + HNCO \rightarrow Hg + H + NCO,$$

occurs in the mercury-photosensitized decomposition. In the photolysis, H_2 was thought to arise from reactions of hydrogen atoms and NH_2CO radicals, which would be approximately the same in the present system, thus accounting for the roughly similar values of H_2/CO. The slight reduction in both H_2/CO and N_2/CO could be explained by the absence of the reactions

[2] $$H + NH \rightarrow H_2 + N$$

[3] $$N + NH \rightarrow N_2 + H,$$

Can. J. Chem. Downloaded from www.nrcresearchpress.com by 210.87.254.6 on 09/05/12
For personal use only.

Can. J. Chem. Downloaded from www.nrcresearchpress.com by 210.87.254.6 on 09/05/12
For personal use only.

thought to occur to some extent in the photolysis. Because of the large uncertainties in some of the present data, these conclusions about the mechanism of the sensitized decomposition must remain speculative.

TABLE III

A comparison of the mercury-photosensitized decomposition of HNCO with the photolysis at an HNCO pressure of 8 Torr and rate of CO production of 10 μmoles/l h

	Φ(CO)	N_2/CO	H_2/CO
Hg-photosensitized	0.69 (av.)	0.36	0.09
Photolysis at 2 062 Å	1.48	0.41	0.11

The conclusions to be drawn from the experiments with HNCO–H_2 mixtures are more clear-cut. The ratio N_2/CO fell towards zero or close to zero at HNCO/H_2 = 0 (Fig. 1), while Φ(CO), within the rather large scatter, remained constant and approximately equal to its value in pure HNCO. As H_2/HNCO was increased, the reaction

[4] $$Hg^* + H_2 \rightarrow Hg + 2H$$

should have replaced reaction [1], and our observations suggest that hydrogen atoms must have reacted with HNCO, forming CO but not N_2. It was concluded previously (4) that hydrogen atoms probably added to HNCO rather than abstracting hydrogen.

[5] $$H + HNCO \rightarrow NH_2.CO$$

The subsequent reactions

[6] $$H + NH_2CO \rightarrow NH_3 + CO$$

[7] $$2NH_2CO \rightarrow NH_3 + CO + HNCO,$$

also suggested previously (4), seem the most probable sources of CO in the present system. This mechanism would lead to Φ(CO) = 1; the competing reaction

[8] $$H + NH_2CO \rightarrow H_2 + HNCO$$

could account for the somewhat lower value observed. A similar reaction sequence, together with

[9] $$2NCO \rightarrow N_2 + 2CO,$$

can also explain the products observed in the sensitized decomposition of HNCO alone.

If it is assumed that all the NCO radicals formed in reaction [1] form N_2 via reaction [9], and that Φ(CO) was the same with and without H_2 present, then N_2/CO should be given by

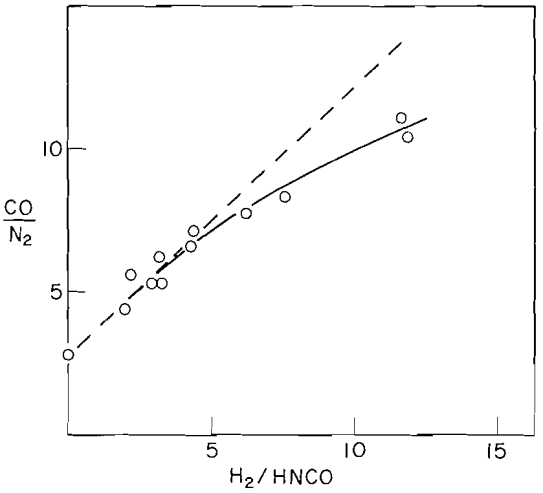

FIG. 2. A plot of CO/N_2 vs. H_2/HNCO for the mercury-photosensitized decomposition of HNCO–H_2 mixtures, based on eq. [11].

[10] $$N_2/CO = 0.36\sigma_1 [HNCO] / (\sigma_1[HNCO] + \sigma_4[H_2])$$

in which σ_1 and σ_4 are cross sections for reactive quenching. Equation [10] may be rearranged,

[11] $$CO/N_2 = 2.78 (1 + \sigma_4 [H_2] / \sigma_1 [HNCO]),$$

and a plot of CO/N_2 vs. H_2/HNCO should be linear (Fig. 2). From the initial slope it may be estimated that $\sigma_1/\sigma_4 = 2.3$. The relatively slight effect of H_2 on the HNCO photolysis at 37 °C (1) suggests that the assumption that N_2/CO depends only on competitive quenching of Hg* and not on other reactions (NCO + H_2 → HNCO + H, for example) is reasonably safe, at low H_2 pressures at least. The deviation from linearity in Fig. 2 could have arisen from a decrease in Φ(CO) with increasing H_2/HNCO, or from other secondary effects; the formation of a small amount of N_2 even at very high values of H_2/HNCO, which cannot be ruled out from the data in Fig. 1, could explain the deviation. The relatively small value of σ_1 compared with other carbonyl compounds (8) lends some support to hydrogen removal in the primary process (reaction [1]) rather than an excitation transfer which might be expected to yield NH + CO at least part of the time (9).

1. J. Y. P. Mui and R. A. Back. Can. J. Chem. **41,** 826 (1963).
2. R. A. Back. J. Chem. Phys. **40**, 3493 (1964).
3. J. L. Brash and R. A. Back. Can. J. Chem. **43**, 1778 (1965).
4. W. D. Woolley and R. A. Back. Can. J. Chem. **46**, 295 (1968).
5. R. A. Back and D. van der Auwera. Can. J. Chem. **40**, 2339 (1962).
6. R. A. Back. Can. J. Chem. **37**, 1834 (1959).
7. K. Yang. J. Am. Chem. Soc. **86**, 3941 (1964).
8. R. J. Cvetanović. Progr. Reaction Kinetics, **2**, 39 (1964).
9. A. Jones and F. P. Lossing. Can. J. Chem. **45,** 1685 (1967).

Can. J. Chem. Downloaded from www.nrcresearchpress.com by 210.87.254.6 on 09/05/12
For personal use only.

Can. J. Chem. Downloaded from www.nrcresearchpress.com by 210.87.254.6 on 09/05/12
For personal use only.

Photolysis of HNCO vapor in the presence of NO and O_2[1]

R. A. Back and R. Ketcheson[2]
Division of Pure Chemistry, National Research Council of Canada, Ottawa, Canada

Received August 17, 1967

The effect of NO at pressures up to 380 Torr on the photolysis of HNCO vapor (4.5 Torr) by light from an unfiltered medium-pressure mercury lamp has been studied at 37 °C. The yield of CO was reduced to about half its original value, which is attributed to reactions of NH and NCO with NO. The yield of N_2 showed a steady increase with increasing NO pressure, probably due to reactions of $NO(A^2\Sigma^+)$ excited by absorption of light. The hydrogen yield fell rapidly to zero as the NO pressure was increased.

Added oxygen at pressures up to 5 Torr had no effect on the CO and N_2 production at 37 °C; at 110 °C the CO yield decreased somewhat while the N_2 remained unaffected. These observations suggest that NH and NCO do not react readily with O_2. The production of H_2 fell rapidly to zero with increasing O_2 pressure at both temperatures. The suppression of H_2 formation by both NO and O_2 supports the belief that it is formed by reactions of hydrogen atoms.

Canadian Journal of Chemistry, 46, 531 (1968)

Introduction

The photolysis of HNCO has been studied extensively in this laboratory (1–5). It is believed that two primary processes, of about equal importance, occur.

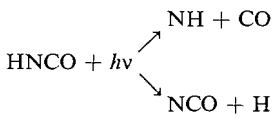

Nitric oxide and oxygen are known to react rapidly with hydrogen atoms, and reactions with NH and NCO might be expected. The present experiments were undertaken to obtain further information about the photolysis mechanism, and about reactions of NH and NCO with NO and O_2.

Experimental

Apparatus and techniques were similar to those described previously (1–5). The light source was an unfiltered Hanovia S-500 medium-pressure mercury lamp. In the experiments with NO, noncondensable gases (H_2, N_2, and CO) were removed through a solid-nitrogen trap at −210 °C which retained the NO, measured in a gas burette, and analyzed by gas chromatography. With O_2 present, O_2 and noncondensable products were removed through a trap at −196 °C and analyzed as before.

Results and Discussion

HNCO + NO

All experiments were done at 37 °C. Figures 1 to 3 show the effect of added NO on the yields of CO, H_2, and N_2 with a constant pressure of HNCO of 4.5 Torr, irradiation time of 1 h, and constant light intensity. The reduction in the yields of CO and H_2 can be readily explained in terms of the photolysis mechanism suggested previously (4). The residual yield of CO at high pressures of NO, which was somewhat less than half its value in pure HNCO, can be ascribed to reaction [1*a*], while the "scavengable" CO can be attributed to subsequent reactions of NH and NCO formed in [1*a*] and [1*b*]. In the presence of NO, the plausible reactions[3]

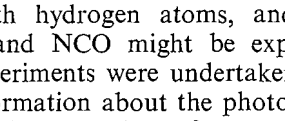

would remove NH and NCO, thus suppressing secondary formation of CO. The complete suppression of hydrogen production by low pressures of NO which left the CO and N_2 relatively unaffected resembles the behavior observed with added ethylene (4), and supports the contention that hydrogen atoms are necessary precursors of H_2 in the photolysis. The well-established (7) reaction

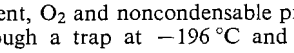

would remove hydrogen atoms fairly quickly from the system.

The striking increase in the nitrogen yield with increasing NO pressure was unexpected, and is not so easily explained. It was first ascertained by careful blank experiments that the linear increase in N_2 was real and not due

[1]NRCC No. 9838.

[2]Present address: Department of Chemistry, York University, Toronto, Ontario.

[3]Reaction [4] was postulated by Bamford and Bamford (6).

Can. J. Chem. Downloaded from www.nrcresearchpress.com by 210.87.254.6 on 09/05/12
For personal use only.

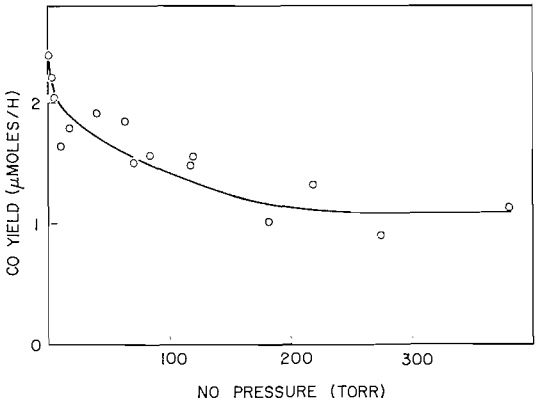

FIG. 1. Yield of CO vs. added NO in the photolysis of HNCO at 4.5 Torr and 37 °C.

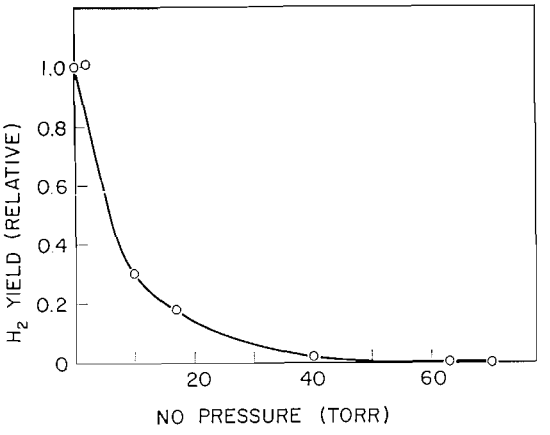

FIG. 2. Yield of H_2, relative to that in pure HNCO, vs. added NO in the photolysis of HNCO at 4.5 Torr and 37 °C.

to the last traces of N_2 impurity in the NO, which are difficult to remove. In the experiments shown in Fig. 3, such impurity was always less than 5% of the observed yield of N_2. Most convincing also was a series of experiments with 63 Torr NO and irradiation times from 15 min to 3 h, in which the yields of both CO and N_2 were linear functions of time, passing through the origin. To shed further light on the source of the extra nitrogen, two experiments were made using ^{15}NO, at pressures of 17 and 32 Torr (Table I). The sharp decline in $^{14}N^{14}N$ with increasing ^{15}NO pressure parallels the decrease in CO production (Fig. 1), and supports the suggestion that NCO and NH, the precursors of N_2 in pure HNCO, were removed by reactions

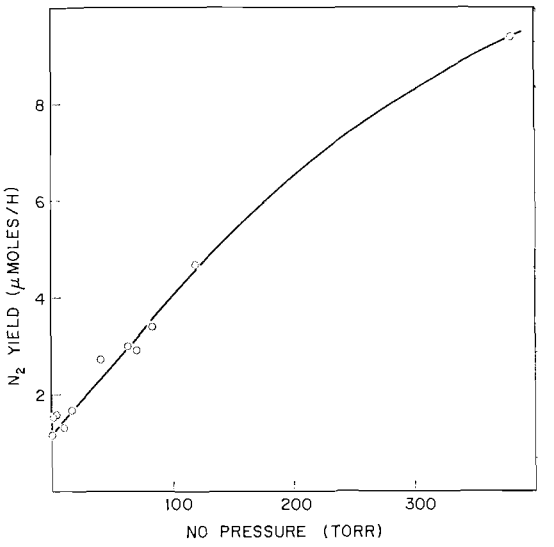

FIG. 3. Yield of N_2 vs. added NO in the photolysis of HNCO at 4.5 Torr and 37 °C.

such as [2] and [4]. There appear to be two possible mechanisms to account for the extra N_2 formed in the presence of NO, which from the data in Table I consisted of $^{14}N^{15}N$ and $^{15}N^{15}N$ in a 3:1 ratio. One possibility is a chain reaction initiated by radicals formed by the photolysis of HNCO, and involving both HNCO and NO in such a way that the production of N_2 depended linearly on NO pressure and gave the observed isotopic composition; a further requirement is that neither CO nor H_2 should be produced. We have, however, been unable to devise a plausible chain mechanism having these properties.

The second possibility is that reactions of $NO(A^2\Sigma^+)$, formed by direct excitation of NO by absorption of light[4] between 2000 and 2300 Å, are responsible for N_2 formation (7). This could lead to an approximately linear increase in N_2; the reaction

$$[6] \qquad NO^* + HNCO \rightarrow N_2 + CO_2 + H$$

(where $NO^* = NO(A^2\Sigma^+)$ could account for the $^{14}N^{15}N$ in the experiments with ^{15}NO,

[4]The light absorbed by NO and HNCO in these experiments cannot be estimated precisely because of the banded nature of the absorption spectra and the non-monochromatic character of the light source, but would appear (1, 7) to be compatible with the suggested mechanism.

Can. J. Chem. Downloaded from www.nrcresearchpress.com by 210.87.254.6 on 09/05/12
For personal use only.

while the $^{15}N^{15}N$ could come from the reaction

$$[7]\quad NO^* + NO \rightarrow N_2 + O_2 \xrightarrow{+4NO} N_2 + 2N_2O_3,$$

which has been postulated in the photolysis of NO (7). Irradiation of NO alone did yield some N_2, although appreciably less than the $^{15}N^{15}N$ observed with HNCO present.

TABLE I

Isotopic composition of N_2 from photolysis of $H^{14}NCO$–^{15}NO mixtures

	17 Torr ^{15}NO		32 Torr ^{15}NO	
	%	μmoles/h	%	μmoles/h
$^{14}N^{14}N$	51	0.88	14	0.30
$^{14}N^{15}N$	37	0.64	64	1.37
$^{15}N^{15}N$	12	0.21	22	0.47

No correction has been made for 5% ^{14}NO present in the NO and 0.4% $H^{15}NCO$ in the HNCO.

One difficulty with this mechanism is that reaction [7] should have been favored over reaction [6] with increasing NO pressure, whereas the ratio $^{14}N^{15}N/^{15}N^{15}N$ in fact decreased only very slightly (from 3.05 to 2.92) in going from 17 to 32 Torr of ^{15}NO. At these relatively low pressures, however, the scavenging reactions, [2] and [4], would still have been contributing an appreciable fraction of the $^{14}N^{15}N$, which may have affected the trend in these ratios.

An alternative and perhaps more probable source of $^{14}N^{15}N$ which would lead to a $^{14}N^{15}N/^{15}N^{15}N$ ratio independent of NO pressure is the reaction

$$[8]\quad NO^* + NO \rightarrow N_2O + O$$

also postulated in the NO photolysis (7), followed by

$$[9]\quad O + HNCO \rightarrow CO_2 + NH,$$

followed in turn by reactions [2], [3], and [4]. Heicklen and Cohen (7) note that reaction [7] may in fact occur via

$$[10]\quad NO^* + NO \rightarrow NO_2 + N$$

$$[11]\quad N + NO \rightarrow N_2 + O.$$

It has also been estimated (7) that reaction [7] (or [10]) is twice as fast as reaction [8], and it can be shown that reactions [8], [10], and [11], followed by [9], [2], [3], and [4], would then result in $^{14}N^{15}N/^{15}N^{15}N = 3$, as observed.

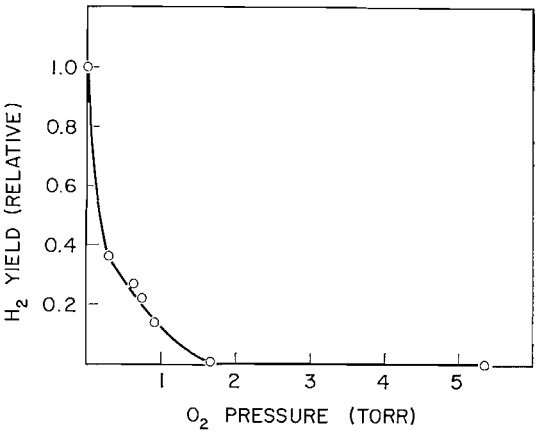

FIG. 4. Yield of H_2, relative to that in pure HNCO, vs. added O_2 in the photolysis of HNCO at 4.5 Torr and 110 °C.

Analysis of condensable products would obviously be useful in determining the reaction mechanism, and this was undertaken. It was established that CO_2 and N_2O were formed in the reaction, but quantitative estimates of these products were rendered impossible by their presence in small but rather variable amounts as impurities in the HNCO and NO reagents respectively. No other products were detected. Both CO_2 and N_2O are expected from the suggested mechanisms, and N_2O may also have come from combination of HNO radicals.

HNCO + O_2

This system was studied in much less detail, and the pressure of O_2 added was limited by analytical problems to about 5 Torr. Preliminary experiments at 37 °C showed no effect of oxygen except the rapid and complete suppression of H_2 production. All subsequent experiments were made at 110 °C. Figure 4 shows the yield of H_2 and Fig. 5 those of N_2 and CO, as a function of added O_2.

The complete suppression of H_2 formation at 37 °C by pressures of O_2 which left the yields of CO and N_2 unchanged is similar to the behavior observed with NO and with ethylene (4), and further supports the belief that hydrogen atoms, known to react readily with O_2, are the precursors of H_2 in the HNCO photolysis (4). From the present and previous (4) data, the relative efficiencies of NO (at 37 °C), O_2 (at 110 °C), and ethylene (at 25 °C), in suppressing H_2 formation, are in the ratio 1:2:33 (based on

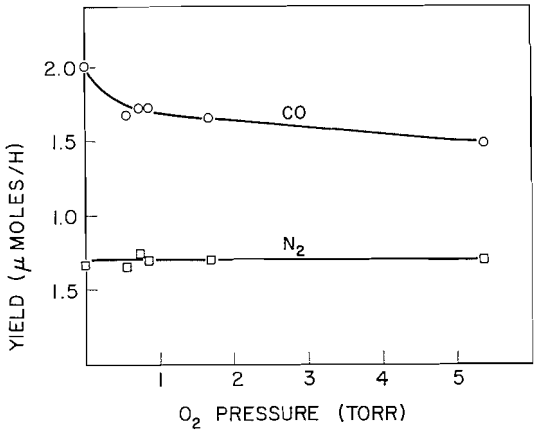

FIG. 5. Yields of CO and N_2 vs. added O_2 in the photolysis of HNCO at 4.5 Torr and 110 °C.

the pressure required for suppression of 80% of the H_2, and in the case of ethylene corrected for a higher HNCO pressure (10 Torr)). These relative efficiencies are in reasonable accord with published values of the relevant rate constants for reactions of hydrogen atoms (7–9).

At 110 °C, the CO yield was reduced somewhat by O_2, while N_2 was unaffected. The decrease in CO roughly paralleled that of H_2, and suggests that at this temperature some CO might arise from decomposition of NH_2CO radicals formed by addition of H to HNCO, which would be suppressed by O_2. The lack of effect of O_2 on CO and N_2 at 37 °C, and the slight effect at 110 °C, indicates that reactions of NH and NCO with O_2 are relatively slow and did not occur to any extent in the present system.

1. J. Y. P. MUI and R. A. BACK. Can. J. Chem. **41**, 826 (1963).
2. R. A. BACK. J. Chem. Phys. **40**, 3493 (1964).
3. J. L. BRASH and R. A. BACK. Can. J. Chem. **43**, 1778 (1965).
4. W. D. WOOLLEY and R. A. BACK. Can. J. Chem. **46**, 295 (1968).
5. N. J. FRISWELL and R. A. BACK. Can. J. Chem. This issue.
6. D. A. BAMFORD and C. H. BAMFORD. J. Chem. Soc. 30 (1941).
7. J. HEICKLEN and N. COHEN. The role of nitric oxide in photochemistry. Advan. Photochem. **5**. To be published.
8. J. M. BROWN and B. A. THRUSH. Trans. Faraday Soc. **63**, 630 (1967).
9. M. A. A. CLYNE and B. A. THRUSH. Proc. Roy. Soc. London, Ser. A, **275**, 559 (1963).

Can. J. Chem. Downloaded from www.nrcresearchpress.com by 210.87.254.6 on 09/05/12
For personal use only.

Can. J. Chem. Downloaded from www.nrcresearchpress.com by 210.87.254.5 on 09/05/12
For personal use only.

High field kinetic processes in anodic oxide films on aluminium. I. Current transients for linearly changing electric field strength

M. J. DIGNAM AND P. J. RYAN[1]

Department of Chemistry, University of Toronto, Toronto, Ontario

Received June 26, 1967

Anodic oxide films were formed on high purity aluminium (99.996%) under steady-state conditions (current and field strength constant) in a glycol–borate electrolyte until the film reached a predetermined thickness at which point the anodic overpotential was changed rapidly and in a linear manner. As little film growth occurred during these linear sweeps, the conditions corresponded to linearly changing field strength. From these data, the transient differential field coefficient, β_1, defined by

$$\beta_1 = \underset{\dot{E}\text{ large}}{\text{Limit}} \left[\frac{\partial(\ln i)}{\partial E}\right]_{E=E_s},$$

where i and E are the ion current density and electric field strength and E_s the steady-state formation field strength, was determined. β_1 was found to vary linearly with E_s in the manner $\beta_1 = (\mu_1^*/kT)[1 - 2(\mu_s^*/C\phi)E_s]$, with $\mu_1^* = 13.2$ eÅ $\pm$ 9%, $\mu_s^*/C\phi = 4.16$ ÅV^{-1} $\pm$ 16%. A recent theory proposed by one of us (M. J. D.) predicts that the parameter $\mu_s^*/C\phi$ should have the same value as that deduced from the field dependence of the steady-state differential field coefficient,

$$\beta_s = \underset{\dot{E}\to 0}{\text{Limit}} \frac{\partial(\ln i)}{\partial E} = (\mu_s^*/kT)[1 - 2(\mu_s^*/C\phi)E_s].$$

Such agreement was indeed found, two independently determined 'steady-state' values of $\mu_s^*/C\phi$ being 3.53 $\pm$ 11% and 3.11 $\pm$ 14% ÅV^{-1}. A direct comparison of the present results with previous steady-state results gave $\beta_s/\beta_1 = \mu_s/\mu_1 = 3.0_9$. More complex features of the transients were also found to be in accord with the above theory, but could be accounted for almost as well by an earlier theory, the so-called high field Frenkel defect theory.

Dielectric constant values determined from the current discontinuity appearing upon application of the linearly increasing field gave $K_1 = 8.35 \pm .1$ for transients commencing from steady-state conditions and $K_1 = 8.8_5 \pm .2$ for films formed then 'aged' at $E = 0$ before measurement. Certain anomalies with regard to the charging current were apparent.

Canadian Journal of Chemistry, **46**, 535 (1968)

Introduction

A number of theories (1) have been proposed over the past years to explain the observed features for the anodic oxidation of the valve metals (principally aluminium, niobium, and tantalum). The name valve metal stresses the rectifying action of the oxide-coated electrode; however, a more fundamental characteristic property of the group is the tendency to form a protective, very high resistance oxide film on anodic polarization to the exclusion of other electrode processes. All of the theories relating to the kinetics of growth of these films are concerned with ionic transport within the film and/or at the interfaces, and furthermore, all lead to essentially the same relationship between the average field strength in the film, E, and the current density under steady-state conditions, i_s, namely

$$[1] \qquad i_s = \alpha \exp \beta' E,$$

where α and β' are temperature dependent positive constants. A recent theoretical consideration of high field ion transport processes (2) has led to the replacement of eq. [1] by an equation of the form

$$[2] \qquad i_s = \alpha \exp(\beta' E - \gamma E^2),$$

where β' and γ are temperature dependent positive constants. The very rapid variation of i_s with E both predicted and found experimentally makes it difficult to detect the quadratic variation of $\log i_s$ with E. Recent measurements, however, definitely indicate the existence of such a quadratic term for the anodic oxidation of tantalum, niobium, and aluminium (3–5). Once again, however, the various theories cannot be distinguished on the basis of eq. [2], as on modification in accord with the ideas published previously (2) by one of us (M. J. D.), they should all give rise to steady-state equations of essentially the same form.

It is clear that steady-state measurements of current density as a function of field strength and

[1]Present address: J. Roy Gordon Research Laboratories, Sheridan Park, Clarkson, Ontario, Canada.

Can. J. Chem. Downloaded from www.nrcresearchpress.com by 210.87.254.5 on 09/05/12
For personal use only.

temperature, however accurate, can provide little basis for choosing between alternative mechanisms or theories. In order to distinguish between the theories, non steady-state or transient conduction measurement and transport number measurements must be made. The present investigation concerns the former.

At the outset of this investigation it was felt that a detailed and critical investigation of transient effects in the anodic oxidation of a typical valve metal (aluminium) would serve to test the postulates of the Frenkel defect theory (6, 7), the only theory at the time able to account for transient conduction phenomena. A note (8) published earlier on this work is concerned solely with this matter. Since publishing the note, however, a new theory has been proposed by one of us (M. J. D.), so that experiments were subsequently designed to test the two models.

In the present study, electropolished samples of aluminium were anodically oxidized at room temperature at a linear rate of voltage rise (i.e. constant current density), the steady-state current being observed on a recorder. When the anodic overpotential had risen to a predetermined value, the linear rate of overpotential rise was suddenly increased by means of an automatic switching circuit. The ensuing current transients were displayed on a cathode-ray oscilloscope and photographed with a Polaroid camera. These transients were recorded for a very short time, typically of the order of 100 ms from start to finish. So little charge is passed in this time that the growth of the film during the transient measuring period may be neglected. For these experiments, therefore, a linear rate of overpotential rise corresponds essentially to a linear field rise.

It is important, when describing the properties of such an oxide film, to state its previous history. Alternating current impedance measurements on these systems have shown that the capacity of the oxide film varies with time after formation (9–12). Moreover, the conduction properties of the film change with time (13, 14) and the extent of annealing (15, 16). As the method of measuring the kinetic phenomena involves a very short time, it allows the properties of the oxide film to be determined "in situ".

Experimental

Apparatus

Figure 1 is a block diagram of the apparatus. It consists of several d.c. operational amplifiers which maintain an anodic overpotential varying in some set fashion, the electrochemical cell, and current-measuring instruments. Setting aside for the moment any discussion of the function of the switches $O_1 \ldots O_3$, the mode of operation is as follows. Fixed potentials e_1 and e_2 are led through precision resistance selector switches R_1 and R_2 to the inputs of amplifiers 1 and 2, which are connected as integrators. With the circuit as shown, the output of amplifier 1 rises linearly with time, the rate of voltage rise being determined by the values of e_1, R_1, and C_1. Amplifier 1 was employed to produce slow rates of voltage rise of the order of 10^{-3} V/s to 1 V/s, suitable for steady-state film formation at current densities from 2×10^{-6} to 2×10^{-3} A/cm^2. By changing C_1 from 10 μF to 0.5 μF, rates of voltage rise up to 200 V/s could be produced at the output of amplifier 1. Amplifier 2 is similarly employed to produce rates of voltage rise from 10^1 to 10^4 V/s. When on "stand-by", this amplifier is stabilized by a 10 kΩ resistor in the feed-back circuit in order to minimize output drift. The output of this amplifier was employed to initiate the current transients associated with the high rates of change of anodic overpotential. The outputs of amplifiers 1 and 2 are fed through a summing amplifier 3 to the aluminium anode in the cell. The working cathode is connected to ground via two sets of precision resistors. Current passing through the cell, as detected by the potential difference across each resistor, is displayed as desired on a strip-chart record and/or oscilloscope. A reference electrode, placed close to the anode, is connected through a cathode follower back to the input of the adder amplifier. The cathode follower circuit automatically adjusts the potential of the anode to compensate for all potential drop from the reference electrode to ground. The potential difference between the aluminium anode and the reference electrode is then given simply by the negative of the sum of the outputs of amplifiers 1 and 2.

The switches $O_1 \ldots O_3$ represent the poles of electromagnetic relays. During steady-state formation of the oxide film (e_1 switched on), the output of amplifier 1 rises linearly with time. When V_1 reaches a preset value, one of the relays is activated automatically and hence one of the switches $O_1 \ldots O_3$ is opened or closed depending on the particular application. Figure 2 shows the form of anodic overpotential versus time curves attainable with this apparatus. In the present paper, we are concerned primarily with the use of the apparatus in the manner indicated in Fig. 2(*a*).

Materials

99.996% aluminium sheet (0.04 in. thick) was formed into paddle-shaped electrodes of dimensions 1 in. $\times$ 0.25 in. for the paddle, 1 in. $\times$ 0.06 in. for the tab. Following routine cleaning procedures, the electrodes were electropolished at about 0.2 A/cm^2 and 25 °C in 5 parts ethyl alcohol to 1 part 70% perchloric acid by volume (17). The electrodes were rinsed briefly in ethyl alcohol, then for 1 min in running distilled water, being dried in a clean air jet and stored in a desiccator over activated alumina.

The electrolysis cell, constructed of Lucite, is shown diagramatically in Fig. 1. The electrolyte used was a 30% solution of ammonium pentaborate in ethylene glycol. The cathodes were cut from a 1/10 in. sheet of commercial grade nickel.

The reference electrode ($Zn/Zn(NO_3)_2$ (1.0 *M*)//KNO_3 (2 *M*) agar–agar//) was chosen despite its rather poor

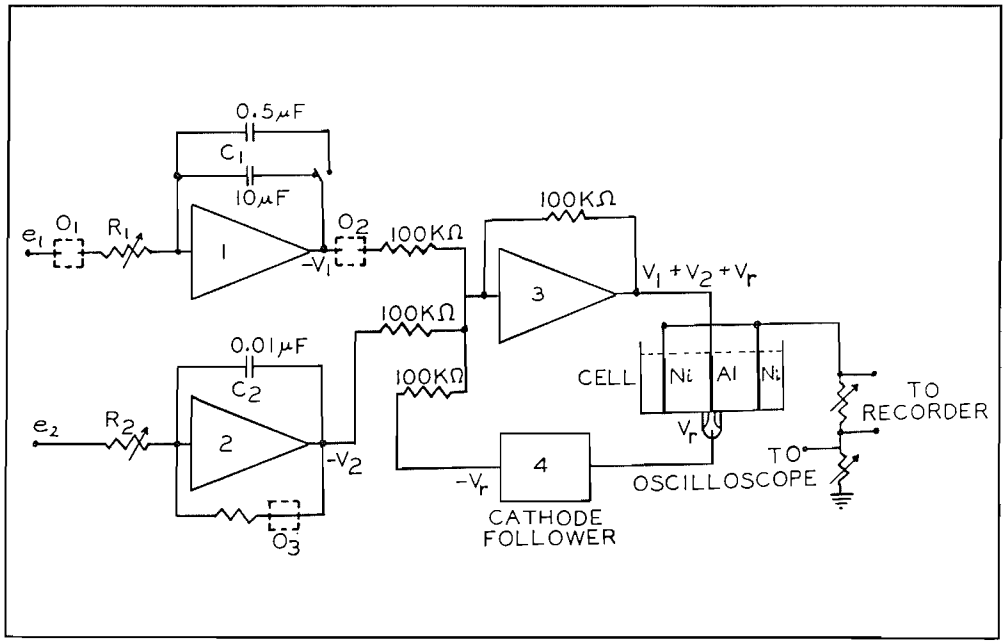

FIG. 1. Schematic diagram of the apparatus.

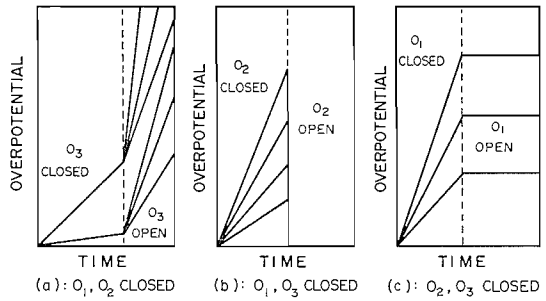

FIG. 2. Overpotential–time curves generated by the electronic apparatus.

reproducibility (±30 mV) in order to achieve low electrode impedance and avoid introducing either mercury or chloride ion. It was found that the frequency response of the reference electrode amplifier system fell off rapidly for an electrode impedance in excess of 10 kΩ, and it is well known that mercury and halides have very deleterious effects on the oxide film on aluminium. In the present experiments where overpotentials of the order of 40 V were employed, the uncertainty in the potential of this electrode system was of no great consequence. The reference electrode was found by measurement to have a potential of -0.30_8 V at 25 °C against a hydrogen electrode in the glycol electrolyte (which contains water).

Oxide films on valve metals such as aluminium and tantalum may be formed in a large variety of "wet" solutions, both aqueous and nonaqueous, and also gaseous and solid electrolytes (18–20). Care must be taken, however, to ensure that the electrolyte does not dissolve the oxide, no oxygen evolution is initiated, and the electrolyte material is not incorporated into the film. For example, films formed on aluminium in phosphate solutions contain appreciable amounts of $AlPO_4$ (21), while sulfate is incorporated into the material formed on tantalum in 100% H_2SO_4 (22). The electrolyte employed for these measurements, a 30% solution of ammonium pentaborate, $(NH_4)_2B_{10}O_{16}.8H_2O$, in ethylene glycol, has been found by Bernard and Cook (23) to be characterized by 100% current efficiency of formation up to 150 V. Moreover these authors found that there was no apparent oxygen evolution during formation, the presence of borates in the film could not be detected by chemical analysis, and heating the oxide to 600 °C resulted in no change of weight, indicating that the film contained neither water nor glycol. This electrolyte was probably first used (24) to increase the shelf life of aluminium electrolytic capacitors.

Various aqueous electrolytes were initially examined and compared to the performance of the glycol electrolyte. These included boric acid, tartaric acid (both buffered to about pH 6 with ammonia), aqueous ammonium pentaborate, and sodium potassium tartrate. For a given sample anodized at a slow rate of voltage rise (e.g. 0.1 V/s) successively in the glycol electrolyte, and then in one of the above aqueous solutions, it was found that the steady-state current density depended markedly on the particular electrolyte chosen. For example the current density was lowest for the glycol solution, approximately 10% higher in an aqueous boric acid solution, and 20% higher in an aqueous tartaric acid solution. At the time this was taken to indicate a rather low current efficiency of formation for the aqueous electrolytes, the nonaqueous electrolyte being therefore favored. Cheseldine (25) has

Can. J. Chem. Downloaded from www.nrcresearchpress.com by 210.87.254.5 on 09/05/12
For personal use only.

Can. J. Chem. Downloaded from www.nrcresearchpress.com by 210.87.254.5 on 09/05/12
For personal use only.

shown that tantalum oxide films formed from a non-aqueous electrolyte require less coulombs for formation than films formed in aqueous electrolytes.

Methods

Determination of Field Strength and Current Density

Field strength and current density in the oxide film were calculated from the current–voltage measurements in the following manner. For the majority of the experiments, oxide films were formed to the same thickness, and all experiments reported herein were performed at room temperature. The samples were all oxidized initially at the rate of voltage rise of 1.000×10^{-1} V/s and the corresponding current observed. Subsequent film formation (Fig. 3) was carried out at one of the following values for the rate of voltage rise, 1.000×10^{-3}; 1.000×10^{-2}; 1.000×10^{-1}; and 9.78×10^{-1} V/s, corresponding to steady-state current densities varying in factors of 10 from about 2×10^{-6} to 2×10^{-3} A/cm^2. From the data of Bernard and Cook (23), at 25 °C, the field and current density in the oxide corresponding to a rate of voltage rise for formation of 1.000×10^{-1} V/s were calculated to be 0.0856 V/Å and 2.095×10^{-4} A/cm^2 respectively (4). Using the current measured during a run for formation conditions of 1.000×10^{-1} V/s rate of voltage rise in conjunction with the known current density enabled the electrode area, and hence the current density during subsequent measurements, to be calculated. For films formed entirely at the rate of voltage rise of 1.000×10^{-1} V/s to an overpotential value, V, the film thickness was assumed to be given by V divided by the above field value. In making this assumption, interfacial potentials and space charge effects are ignored (4, 26). However, this neglect will not lead to serious error in the present case.

For films formed initially at 1.000×10^{-1} V/s and subsequently at a different rate of voltage rise the film thickness formed at the initial rate of voltage rise was calculated as above with the subsequent increase in film thickness being determined from the charge passed and a knowledge of the surface area of the electrode and the oxide density (23). The film thicknesses determined in this way have subsequently been checked using the more recent steady-state data obtained in this laboratory (4), and satisfactory agreement obtained.

The potential drop across the oxide film, assumed to be given by the anode overpotential, V, was determined as follows.

It is clear that

$$V = V_{\text{app}} + \epsilon_{\text{ref}} - \epsilon_{\text{rev}},$$

where V_{app} is the applied potential from the driving circuit (output of amplifiers 1 and 2), ϵ_{ref} is the potential of the reference electrode with respect to a hydrogen electrode in the glycol–borate electrolyte, and ϵ_{rev} is the reversible e.m.f. for the reaction:

$$2Al + 3H_2O \text{ (in glycol–borate electrolyte)} \rightarrow Al_2O_3 + 3H_2.$$

ϵ_{rev} was calculated from the following data at 25 °C:

$$2Al + \tfrac{3}{2}O_2 \rightarrow Al_2O_3 \qquad \Delta G_1{}^0 = -365.901 \text{ kcal}$$

$$H_2 + \tfrac{1}{2}O_2 \rightarrow H_2O(g) \qquad \Delta G_2{}^0 = -54.638 \text{ kcal}$$

$$H_2O(l) \rightarrow H_2O(g) \qquad \Delta G_3{}^0 = 2.053 \text{ kcal}$$

and

$$H_2O(l) \rightarrow H_2O \text{ (in glycol–borate electrolyte) } \Delta G_4.$$

The free energy change ΔG_4 may be calculated from the measured vapor pressure of the electrolyte. When a borate salt is dissolved in a polyalcohol such as ethylene glycol, the following reaction takes place (27).

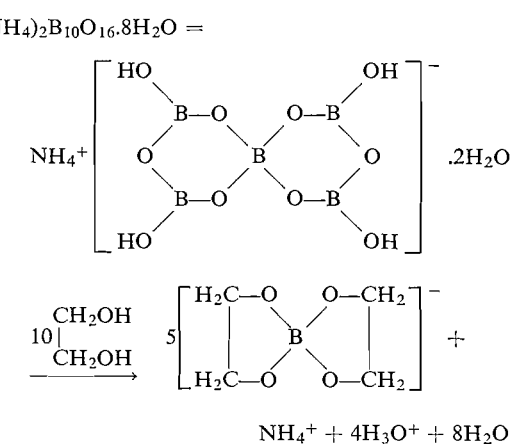

One may calculate that a 30% by weight solution of ammonium pentaborate in ethylene glycol is very nearly the stoichiometric amount for the above reaction. Therefore there is likely very little ethylene glycol in solution. In any event the vapor pressure of pure $(CH_2OH)_2$ at 25 °C, 0.14 Torr (28), is too low to affect the following calculation.

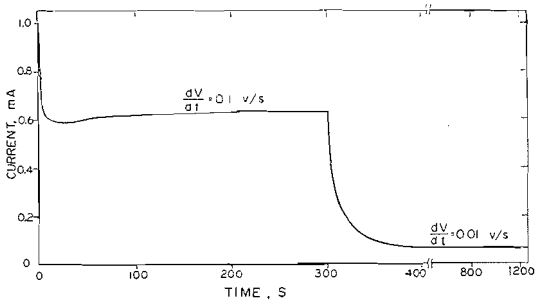

FIG. 3. Current versus time for film formation under conditions of linearly increasing anodic overpotential.

The mole fraction of water in the above solution is about 0.5 so that it should have an appreciable vapor pressure. Assuming ideal thermodynamic behavior for the vapor, $\Delta G_4 = RT \ln P_1/P_0$, where P_1 is the partial pressure of water vapor which can exist in equilibrium with the electrolyte, and P_0 is the vapor pressure of pure H_2O. The vapor pressure of the electrolyte, measured directly on a dibutyl phthalate (DBP) differential manometer, was 2.56 Torr at 26.8 °C. Combining this with $P_0 = 26.43$ Torr (29), ΔG_4 is calculated to be

$$\Delta G_4 = RT \ln P_1/P_0 = -1.384 \text{ kcal.}$$

Therefore, $\Delta G = \Delta G_1^0 - 3\Delta G_2^0 + 3\Delta G_3^0 - 3\Delta G_4 = -191.676$ kcal from which $\epsilon_{rev} = 1.38_6$ V.

The potential of the reference electrode with respect to a hydrogen electrode in the glycol–borate electrolyte ϵ_{ref} was measured to be $\epsilon_{ref} = -0.308$ V, and thus

$$V = V_{app} + \epsilon_{ref} - \epsilon_{rev} = V_{app} + 1.07_8 \text{ V.}$$

Figure 3 represents a typical curve of current versus time for a film formed initially at 0.1 V/s and subsequently at a lower rate of voltage rise. There is an initial nonreproducible peak in the current which rapidly gives way to a current minimum. The current then rises slowly and levels off at an applied potential of about 25 to 30 V, this rise being due presumably to the effects of space charge in the relatively thin film (26).

Procedure and Results for a Typical Run

A typical experimental run was carried out as follows. The cell was filled to just above the shoulders of the paddle-shaped aluminium electrode and was then connected into the circuit with the relays O_1, O_2, and O_3 set to produce overpotential–time curves of the form indicated in Fig. 2*a*. The current during the initial slow rate of voltage rise portion of the run was measured with a recording potentiometer. For the fast rate of voltage rise portion of the run a Tektronix oscilloscope model 532-S7 in conjunction with a Polaroid camera was used to measure the current transients. The oscilloscope was modified to permit triggering of the instrument into a continuous sweep mode. Also, the appropriate circuit components were adjusted to minimize the hold-off time between sweeps. The horizontal and vertical axis of the oscilloscope were calibrated in terms of current and time as follows. A square wave generator synchronized by a Tektronix incorporated type 181 time mark generator was used to modulate the beam intensity of the oscilloscope, thus providing an accurate time scale on the signal trace itself. Following a run, current calibration lines were photographed on the same negative, prior to developing. The readings were made on 8 in. by 10 in. enlargements of the photographs.

A number of runs were performed using a specially designed preamplifier for the oscilloscope which permitted current measurements to be made with precision over three decades in the current. This preamplifier operated at high gain for the initial portion of the transient, switching automatically to successively lower gains as the current increased. In this manner a precision of approximately 1% in the current density was maintained for all experimental measurements.

Because of the short times in which the current transients are measured (1 ms to 1 s) negligible charge is passed compared with the total charge required to form the films. The actual increase in film thickness as determined from the incremental charge passed was about 0.003% for a fast rate of voltage rise of 1076 V/s, 0.02% for 107.6 V/s, and less than 0.1% for 10.76 V/s. The error arising in neglecting these is only significant in the last case where it is equivalent to about a 2% error in the current at the end of the run. For constant film thickness, therefore, the field rises linearly with time, the field at any given time being assumed to be given by V/X, where X is the film thickness calculated as indicated previously.

Figure 4 is a multiple sweep oscilloscope photograph of a typical current transient showing the time base, the horizontal current calibration lines, and the initial current jump due to

Can. J. Chem. Downloaded from www.nrcresearchpress.com by 210.87.254.5 on 09/05/12
For personal use only.

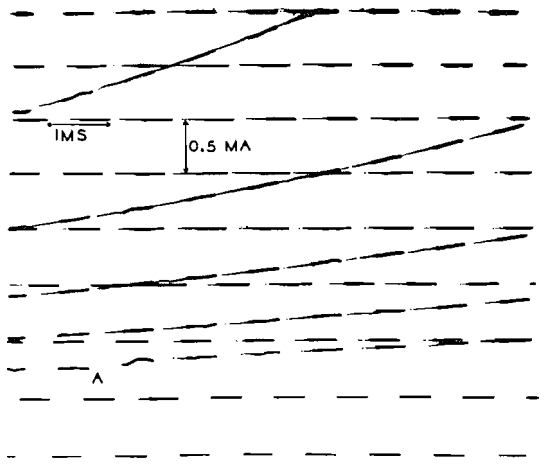

FIG. 4. Typical photograph of oscilloscope trace (current versus time) for film formed at 0.1 V/s and transients measured at 107.6 V/s. Sensitivity, 0.5 mA/cm.

capacitor charging. Figure 5 is a run done under identical conditions with a 10 times greater sensitivity so that the total current displayed (0.4 mA) is only 1/10 that shown in Fig. 4. In both these photographs the transient is initiated from the steady-state formation at point A.

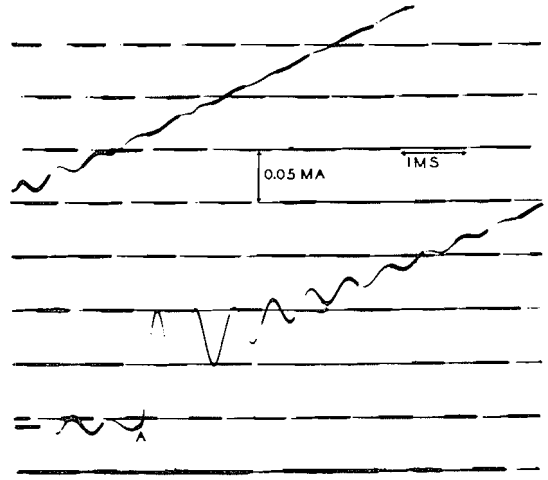

FIG. 5. Typical photograph of oscilloscope trace for film formed and measured as in Fig. 4. Sensitivity, 0.05 mA/cm.

Superimposed on the d.c. transient is a rapidly decaying a.c. oscillation, the amplitude of which depended markedly on the fast rate of voltage rise employed. This extra signal probably arises as a result of the positive feedback of the cathode follower circuit in the potentiostat. For runs done at a fast sweep rate of 10.76 V/s the oscillation was undetectable, while the amplitude was appreciable (0.5 divisions on the photograph for a sensitivity of 0.5 mA per division) at a fast sweep rate of 1076 V/s. The transient component was read from the recorded trace by taking the vertical mean position of the upper and lower envelope to the oscillations, this being the correct procedure if the oscillations are damped harmonic in nature.

Figure 6 is a multiple sweep oscilloscope photograph of a typical current transient obtained with the aid of the multiple gain preamplifier described earlier. The data illustrated were obtained from a sample formed at 0.001 V/s, the transient measurements being made at 10.76 V/s. The three sets of multiple sweeps recorded corresponding to amplification varying from approximately 1 to 100 in factors of 10 may clearly be

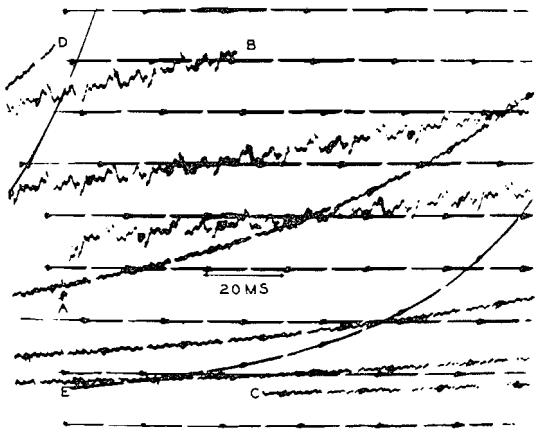

FIG. 6. Typical photograph of oscilloscope trace for film formed at 0.001 V/s and transients measured at 10.76 V/s. The data were obtained using the automatically switching, multiple gain, preamplifier; sensitivity 5, 55, and 555 μA/cm.

distinguished by the extent of 60 cycle a.c. noise superimposed on the transient. The noise level is highest for the initial set of sweeps (starting from Point A) where the current amplification is 100 times that of the third and final set of sweeps. At Point B, the gain of the multiple gain preamplifier is decreased automatically by a factor of about 10, hence the beam deflection of the oscilloscope drops to Point C whence the next set of sweeps (with a consequently lower a.c. noise level) start. Similarly at Point D, the amplification is further

Can. J. Chem. Downloaded from www.nrcresearchpress.com by 210.87.254.5 on 09/05/12
For personal use only.

Can. J. Chem. Downloaded from www.nrcresearchpress.com by 210.87.254.5 on 09/05/12
For personal use only.

reduced and the beam deflection drops to Point E. From this point on the beam deflection rises continuously and goes off scale at the top of the photograph.

The charging current, i_c, associated with charging up the dielectric film must be subtracted from the measured current density I in order to obtain the ion current density i. The charging current was determined as follows. Poisson's equation, combined with the equation of continuity for a medium of dielectric constant K_1, yields

$$i_c = (I - i) = \epsilon_0 K_1 \frac{dE}{dt} = \text{constant}$$

for these experimental conditions. Measurement of the charging current therefore allows the dielectric constant to be calculated, and vice versa. Several runs were carried out in which the current sensitivity was adjusted so that the charging current was displayed as a deflection of at least one-half full scale in the photograph. These were carried out at both 1076 and 2704 V/s. From these runs the dielectric constant was calculated to be 8.35 ± 0.1 in good agreement with the value 8.4 ± 0.2 obtained by Bernard and Cook (23) from capacity measurements on films formed in the same electrolyte as used here.

Several samples were formed under steady-state conditions at 0.1 V per second to $V = 41.78$ V at which point the anode potential was automatically switched to 0. The samples were then either annealed in mineral oil at 60 °C for 2 h followed by a thorough washing in a succession of solvents (cyclohexane, acetone) and dried in a stream of air or simply annealed at room temperature for 10 or more minutes. The samples were then returned to the anodizing cell and the anode potential reapplied at a rate of 209.4 V/s. Analysis of the initial current jump as above gave $K_1 = 8.8 \pm 0.2$ for the samples annealed at 60 °C and $K_1 = 8.9 \pm 0.2$ for those annealed at room temperature. These two values are in good accord with one another but are notably higher than the value determined commencing from steady-state formation conditions. It appears probable that K_1 is a function either of the extent to which the system departs from steady-state formation conditions, or of the field strength.

In Fig. 7 typical results for films formed at the same slow rate of voltage rise, namely 0.1 V/s, with the transient measurements taken at various fast

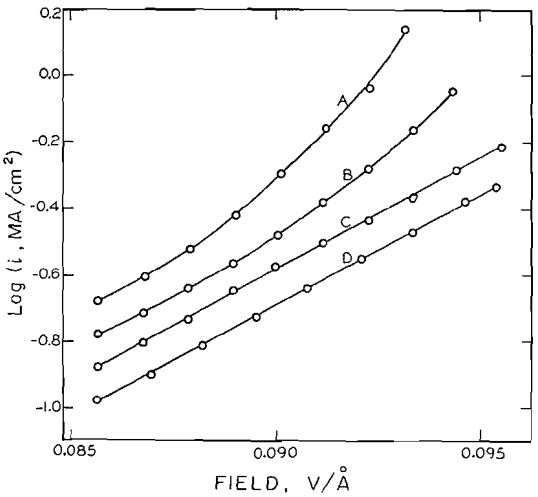

FIG. 7. Ion current transients for films formed at 0.1 V/s and transients measured at A, 10.76 V/s; B, 107.6 V/s; C, 1076 V/s; D, 2704 V/s.

rates of voltage rise, are illustrated. The curves in this graph have been displaced from one another (by an amount 0.1 in log i) for the sake of clarity, curve A giving the correct scale. Figure 8 shows results for films formed at different formation rates of voltage rise, the transients being measured in all cases at 10.76 V/s. Curve B in Fig. 7 is a plot of the data obtained from the photograph shown in Fig. 5. Curve A in Fig. 8 is a plot of the data obtained from the photograph shown in Fig. 6. The maximum current density for all the curves of Figs. 7 and 8 is about 1 mA/cm². Current densities in excess of about 1 mA/cm² were avoided, as it has been shown (30) that heating effects become of importance at such current densities.

Curves similar to those illustrated in Figs. 7 and 8 were analyzed for the initial features of the transient by taking the slope of the cord, $(\ln i/i_s)/\Delta E$, over the linear portion of the ln i versus E plot, ΔE being the change in field over this portion, i the ion current density, and i_s the steady-state ion current density just before initiating the transient. This slope was evaluated for runs carried out under various combinations of formation rate of voltage rise and measurement rate of voltage rise. The current sensitivity was always chosen to obtain accurately the slope of the initial straight line portion of the curve. The results are given graphically in Fig. 9, in the form $kT(\ln i/i_s)/\Delta E$ plotted against the steady-state formation field, E_s, for a wide range of transient

Can. J. Chem. Downloaded from www.nrcresearchpress.com by 210.87.254.5 on 09/05/12
For personal use only.

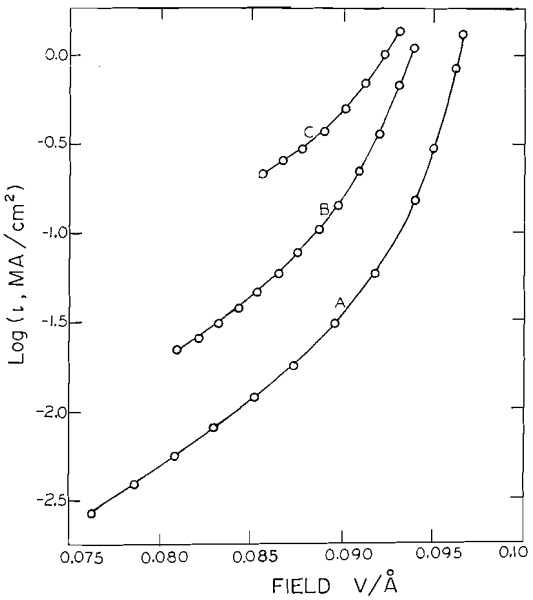

FIG. 8. Ion current transients measured at 10.76 V/s for films formed at A, 0.001 V/s; B, 0.01 V/s; C, 0.1 V/s.

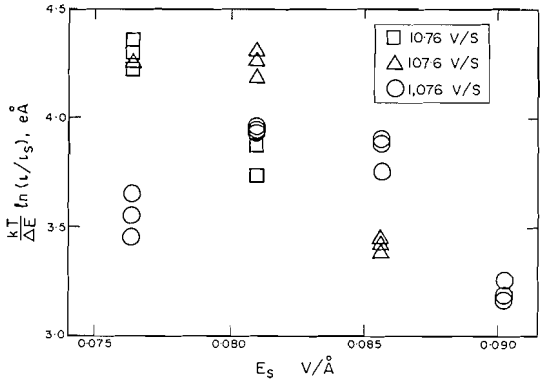

FIG. 9. Values of $kT(\ln i/i_s)/\Delta E$ obtained from linear field rise transients, versus formation field strength, E_s. The transients were measured at (□) 10.76 V/s, (△) 107.6 V/s, (○) 1076 V/s.

sweep rates and formation current densities. It is seen that the initial slopes vary by as much as 30% from the highest formation current density to the lowest even though any given run is reproduced to within 1 or 2%. Moreover the initial slopes measured for samples which had been formed at the same steady-state current density differ greatly depending on the fast sweep rate employed to initiate the transient. A detailed analysis of these results in terms of theoretical models will be presented in a subsequent section.

Theory

As the data obtained were analyzed in terms of the high field Frenkel defect theory and the new theory proposed by one of us (M. J. D.) a brief outline of these is presented here. Detailed developments can be found elsewhere (1, 31).

High Field Frenkel Defect Theory

According to this theory, interstitial metal ions are transported through the oxide film in accord with the following equations:

$$[3] \qquad i = 2qa\nu n \exp -(U - Eaq)/kT,$$

where i = ion current density in the film; q = charge on the cation; ν = vibrational frequency of an interstitial cation; n = concentration of interstitial cations; U = activation energy for the migration of interstitial cations in the absence of an electric field; a = activation distance corresponding to U; E = electric field strength in the oxide.

To account for transient conduction phenomena, the concentration of interstitial cations is assumed to be a function of the electric field strength and time. The simplest specific model is that suggested by Bean, Fisher, and Vermilyea (6) and by Dewald (7). They proposed that interstitial cation–cation vacancy pairs (i.e. Frenkel defects) are produced by the action of the field on lattice cations, and destroyed by their recombination. The net rate of formation of interstitials and vacancies is given by

$$[4] \qquad \frac{\partial n}{\partial t} = \frac{\partial m}{\partial t} = (N - m)\nu_0 \exp - (W - E\lambda q)/kT - i\sigma m/q,$$

where N = concentration of cation lattice sites; m = concentration of cation vacancies; t = time; ν_0 = vibrational frequency of a lattice cation; W = activation energy for formation of a Frenkel defect in the absence of an external electric field; λ = activation distance corresponding to W; σ = capture cross section of a vacancy for an interstitial cation.

Equation [4] is usually further simplified by assuming that the oxide film is sufficiently thick so that space charge effects may be neglected (26). For these conditions n and m are equal and independent of position in the oxide. Furthermore it is usually assumed that only a small percentage of the cations contribute to the

Can. J. Chem. Downloaded from www.nrcresearchpress.com by 210.87.254.5 on 09/05/12
For personal use only.

ionic conduction, so that $N - m \approx N$. Equation [4] therefore becomes

$$[5]\quad \frac{dn}{dt} = N\nu_0 \exp\left[-(W - E\lambda q)/kT\right] - i\sigma n/q.$$

The solution of [3] and [5] for steady-state conditions (i.e. $dn/dt = 0$) takes the form of [1] with α and β' given by

$$\alpha = q(\nu_0 \nu 2Na/\sigma)^{1/2} \exp\left[-(W + U)/2kT\right],$$
$$\beta' = q(\lambda + a)/2kT.$$

For the purpose of comparing the experimental data with the predictions of the Frenkel defect theory, n may be eliminated from [3] and [5] to yield

$$[6]\quad \frac{d \ln i}{dE} = \frac{\sigma}{q\,dE/dt} \times \left[\frac{(\alpha \exp \beta' E)^2 - i^2}{i}\right] + \frac{qa}{kT},$$

where α and β' are given above. Integration of [6] gives

$$[7]\quad \frac{1}{\Delta E} \ln \frac{i}{i_s} = \frac{qa}{kT} + \frac{\sigma}{q\Delta E} \int_0^Q \frac{(i_s \exp \beta'\, \Delta E)^2 - i^2}{i^2}\, dQ,$$

where $Q = \int_0^t i\,dt$ and i_s and E_s are the initial steady-state current density and field respectively, and ΔE the change in field during the transient.

A recent theoretical consideration of high field ion transport processes (2) by one of us (M. J. D.) when applied to the present model leads to the following modified equations in place of [3] and [5].

$$[8]\quad i = 2qa\nu n \exp\left\{-[U - qaE \times (1 - qaE/C_1U)]/kT\right\}$$

$$[9]\quad \frac{dn}{dt} = N_0\nu_0 \exp\left\{-[W - q\lambda E \times (1 - q\lambda E/C_2W)]/kT\right\} - i\sigma n/q,$$

where C_1 and C_2 are dimensionless parameters whose values depend on the shape of the potential energy surface in question. Elimination of n from eqs. [8] and [9] leads to

$$[10]\quad \frac{d \ln i}{dE} = \frac{qa}{kT}\left[1 - \frac{2qaE}{C_1U}\right] + \frac{\sigma/q}{dE/dt}\left[\frac{[\alpha \exp(\beta' E - \gamma E^2)]^2 - i^2}{i}\right],$$

with α and β' given as before, and $\gamma = q^2(\lambda^2/C_2W + a^2/C_1U)/2kT$. Integrating [10], the analogue of [7] is obtained as

$$[11]\quad \frac{1}{\Delta E} \ln \frac{i}{i_s} = \frac{qa}{kT}\left[1 - \frac{2qaE_s}{C_1U}\left(1 + \frac{\Delta E}{2E_s}\right)\right] + g,$$

where

$$[12]\quad g = \frac{\sigma}{q\Delta E} \times \int_0^Q \frac{[\alpha \exp(\beta' E - \gamma E^2)]^2 - i^2}{i^2}\, dQ.$$

In the limit, as $dE/dt \to \infty$, it is clear that $g \to 0$. For the rapid linear field transients reported herein, g may be regarded therefore as a correction term which goes to zero as $dE/dt \to \infty$.

For steady-state conditions (i.e. $di/dt = 0 = dE/dt$) [8] and [9] lead to [2] with α, β', and γ given above.

Outline of New Theory

The principal features of the new theory may be summarized as follows.

It is assumed that the polarization of the medium makes a substantial contribution to the local field assisting defect migration. The main consequence of this assumption is that dielectric relaxation phenomena will lead to ionic conduction transients. The overall polarization of the oxide is considered to arise as a result of ordinary polarization processes, which are assumed to have small relaxation times, and in addition abnormal processes which are associated with a fairly major structural reorganization. These latter polarization processes will have large relaxation times. Thus transient conduction phenomena will arise as a result of the time dependence of the slow polarization process.

For sufficiently high current densities, it is assumed that the motion of the defects themselves assists in bringing about equilibrium polarization conditions. In fact, this is assumed to be the dominant process by which slow polarization proceeds for measurable current densities at normal temperatures. At sufficiently low ion current densities, however, thermal activation must make a substantial contribution. For the purposes of the present paper, the thermally activated polarization processes will be neglected. The relevant equations are recorded

Can. J. Chem. Downloaded from www.nrcresearchpress.com by 210.87.254.5 on 09/05/12
For personal use only.

below and are obtained from eqs. [13] to [37] and [38] of the original publication concerning this theory (31). Since publishing this paper, some changes in the model have been proposed (32). The above description, however, applies equally to the old as well as the revised model. Furthermore, relevant kinetic equations are not changed.

$$[13]\quad i = i_0 \exp\left[-[\phi - \mu^* E_e(1 - \mu^* E_e/C\phi)]/kT\right]$$

$$[14]\quad \mu^* \frac{dE_e}{dt} + Bi\mu^* E_e = \mu_1^* \frac{dE}{dt} + Bi\mu_s^* E,$$

where

$$[15]\quad i_c \approx \epsilon_0 K_1 \left[dE/dt + Bi\left(\frac{\mu_s^* E - \mu^* E_e}{\mu_1^*}\right)\right]$$

and i_0 and B are constants. The remaining symbols have the following meanings: ϕ, zero field activation energy for the overall conduction process. μ^*, charge-activation distance product, or "activation dipole". E_e, effective field assisting ion transport given by $E + \delta P/\epsilon_0$, where P is the polarization of the medium, δ a geometric factor, and ϵ_0 the permittivity of free space. C, dimensionless parameter, the value for which depends on the shape of the potential energy surfaces involved. μ_1^* and μ_s^*, the dynamic and static "effective activation dipoles", given by $(1 + \delta\chi_1)\mu^*$ and $(1 + \delta\chi_s)\mu^*$ respectively where χ_1 and χ_s are the dynamic and static electric susceptibilities of the oxide. i_c, total charging current made up of the "normal" charging current, $\epsilon_0 K_1$ (dE/dt), plus a contribution from the slow polarization process. K_1, dynamic dielectric constant of the oxide, $= 1 + \chi_1$.

For steady-state conditions (i.e. $dE/dt = 0 = di/dt$), it follows from [13] to [15] that $\mu^* E_e = \mu_s^* E$ and $i_c = 0$; hence

$$[16]\quad i_s = i_0 \exp\{-[\phi - \mu_s^* E(1 - \mu_s^* E/C\phi)]/kT\}.$$

This equation is formally identical with [2], with $\alpha = i_0 \exp(-\phi/kT)$, $\beta' = \mu_s^*/kT$, and $\gamma = \mu_s^{*2}/C\phi kT$.

Since the total current density is given by $I = i + i_c$, eq. [15] can be written

$$[17]\quad I' = I - \epsilon_0 K_1 \frac{dE}{dt} = i\left[1 + B\epsilon_0 K_1 \left(\frac{\mu_s^* E - \mu^* E_e}{\mu_1^*}\right)\right].$$

Since the term in B is at most only a few percent of unity (33), we have to a satisfactory approximation, $I' \approx i$. As K_1 is easily determined, I' is a directly measurable quantity.

Equation [14] is a first order, first degree linear differential equation in E_e which may be solved for E_e using standard procedures to give

$$[18]\quad \mu^* E_e = \mu_s^* E_s + \mu_1^*(1 + \Delta)\Delta E,$$

where

$$[19]\quad \Delta = (\mu_s^*/\mu_1^* - 1) \times \left[\int_{Q=0}^{Q=Q} \Delta E \, d(e^{BQ})\right]/\Delta E \, e^{BQ}$$

and $Q = \int_0^t i dt$ as before. The boundary conditions $\Delta E = 0$, $\mu^* E_e = \mu_s^* E_s$ at $t = 0 = Q$ were used to obtain [18] and [19].

Upon obtaining an expression for $\ln i/i_s$ from [13] and eliminating $\mu^* E_e$ noting that when $i = i_s$, $\mu^* E_e = \mu_s^* E_s$, we get

$$[20]\quad \frac{\ln (i/i_s)}{\Delta E(1 + \Delta)} = \frac{\mu_1^*}{kT} \times \left[1 - \frac{2\mu_s^*}{C\phi}\left(E_s + \frac{(1 + \Delta)}{2(\mu_s^*/\mu_1^*)}\Delta E\right)\right].$$

As with eq. [11], we see that for the rapid linear field transients reported herein, Δ may be regarded as a correction term which goes to zero as $dE/dt \to \infty$. Indeed, the similarity between eqs. [11] and [20] is striking, the only difference apart from the correction term being a slight difference in the coefficient of ΔE for the two. As the terms in ΔE will both be small compared with unity for realizable experimental conditions, it is clear that experimental data will only distinguish between [11] and [20] for conditions in which the terms g and Δ dominate.

For Δ sufficiently small, it may be evaluated in the following way for transient experiments of the kind conducted herein; that is for experiments for which dE/dt is a constant. For Δ small, $\ln i$ is very nearly a linear function of E. (See e.g. curves C and D, Fig. 7). For these conditions, therefore, we may set

$$[21]\quad i \approx i_s \exp \beta_1' \Delta E,$$

where β_1' is the slope of the linear portion of the $\ln i$ vs. E graph. Noting that $i = [dQ/d(\Delta E)][(dE/dt)]$, [21] may be integrated and rearranged to give

$$[22]\quad \Delta E = (1/\beta_1') \ln (BQ/b + 1),$$

Can. J. Chem. Downloaded from www.nrcresearchpress.com by 210.87.254.5 on 09/05/12
For personal use only.

where

$$[23] \qquad b = Bi_s/\beta_1'(\mathrm{d}E/\mathrm{d}t).$$

Substituting [22] in [19] and evaluating the integral leads to the following result,

$$[24] \quad \Delta = \left[\frac{\mu_s^*}{\mu_1^*} - 1\right] \times \left[1 - \frac{\exp(-by)}{\ln y}(E_1(by) - E_1(b))\right]$$

where $y = \exp(\beta_1'\Delta E) = i/i_s = BQ/b + 1$ and $E_1(x) = \int_{-\infty}^{x}(\exp(u)/u)\,\mathrm{d}u$ is the first degree exponential integral, tabulated values for which are readily available (29).

For by and $b \ll 1$ (i.e. $\Delta \ll 1$) the exponential functions may be replaced by the first two terms in their expansion which on simplifying gives

$$[25] \qquad \Delta = \left[\frac{\mu_s^*}{\mu_1^*} - 1\right] b\left[\frac{1-y}{\ln y} + y\right].$$

Setting $I \simeq i + \epsilon_0 K_1 \mathrm{d}E/\mathrm{d}t$, [20] can be written in the form

$$[26] \quad I = \epsilon_0 K_1(\mathrm{d}E/\mathrm{d}t) + i_s \exp\left[\beta_1(E_s).\Delta E' - \frac{(\mu_1^*\Delta E')^2}{C\phi kT}\right],$$

where $\Delta E' = \Delta E(1 + \Delta)$ and $\beta_1(E_s)$ is the transient differential field coefficient evaluated at $E = E_s$. The transient differential field coefficient may be defined through the relation

$$[27] \quad \beta_1(E_s) = \underset{\dot{E}\ \text{large}}{\text{Limit}}\left(\frac{\mathrm{d}\ln i}{\mathrm{d}E}\right)_{E=Es} = \frac{\mu_1^*}{kT}\left(1 - \frac{2\mu_s^* E_s}{C\phi}\right).$$

Analysis and Discussion of Results

The data similar to those illustrated in Figs. 7 and 8 were analyzed according to the dielectric polarization theory using the following procedure. The experimental data consist of current density versus ΔE, the fixed parameters for any given run being E_s and $\mathrm{d}E/\mathrm{d}t$. Referring to eq. [26], to a first approximation the term in $\Delta E'^2$ may be neglected compared to the term in $\Delta E'$, which in turn is nearly equal to ΔE. Given a first approximation value for the ratio μ_s^* to μ_1^* the correction term, Δ, may be calculated with sufficient accuracy from [25]. Again given a first approximation value for μ_1^* and $C\phi$, the term in $\Delta E'^2$ may be calculated with sufficient accuracy. In this way, $\beta_1(E_s)$ was calculated from [26] using a nonlinear least squares program which selected values of β_1 and $\epsilon_0 K_1(\mathrm{d}E/\mathrm{d}t)$ which minimized the variance in I. The resulting values of β_1 are presented graphically in Fig. 10. The following values were used in calculating the correction terms: $B = 1.32 \times 10^4$ cm^2 per coulomb (Part II); $\mu_s^*/\mu_1^* = 3.09$; $K_1 = 8.35$, $C\phi = 7.37$ eV (33), $\mu_s^* = 24.4$ eÅ (33). The calculated values of β_1 are only very weakly dependent on the particular choice of values for the above parameters. Thus a successive approximation approach to the calculation was unnecessary.

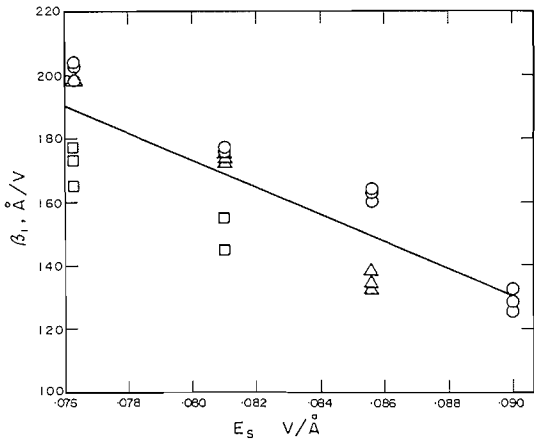

FIG. 10. Transient field coefficient, β_1, calculated from transient data and eq. [26], versus formation field strength, E_s. The transients were measured at (□) 10.76 V/s, (△) 107.6 V/s, (○) 1076 V/s.

From Fig. 10 it can be seen that the values for β_1 versus E_s fall reasonably well on a straight line. It is clear, however, that the values for β_1 calculated from runs done under identical conditions agree much more closely with one another than do those involving the same value for E_s but measured at different rates of voltage rise. A further anomaly was observed for those runs in which the charging current represented a very substantial fraction of the total measured current. For these runs a plot of log $[I - \epsilon_0 K_1(\mathrm{d}E/\mathrm{d}t)]$ versus ΔE produced an initial straight line portion which did not extrapolate to the point log i_s (see eq. [26]), in fact in the extreme case involving an electrode formed at 10^{-3} V/s

Can. J. Chem. Downloaded from www.nrcresearchpress.com by 210.87.254.5 on 09/05/12
For personal use only.

($i_s = 2.6 \times 10^{-6}$ A/cm^2) with the transient measurement being made at 1076 V/s, extrapolation gave a value for the current density a factor of 4 higher than i_s. The curves in Figs. 7 and 8 do not show this anomaly since the charging currents for these runs represented only a small portion of the total current.

Two possible explanations for this anomaly are offered. The first and most obvious explanation is that the charging current varies in a complex manner with displacement from steady-state conditions and rate of change of potential. A further possibility exists, however. It has been assumed that the extra potential, $\dot{V}\,\Delta t$, applied to the anode during the transient, increases the field by $\dot{V}\Delta t/X$. However, the current density is changing rapidly during the transient. If the potential differences due to interface phenomena are current dependent (4), then the potential drop across the oxide film during the transient will not increase as $\dot{V}\Delta t/X$. It is clear that any error introduced by such a current dependence of interfacial potentials will decrease with increasing film thickness. To assess the possible importance of such an effect, two sets of films were formed at the same current density (i.e. that corresponding to 0.1 V/s), the first set being formed to $V = 10.25$ V, the second to $V = 41.78$ V. Transient measurements were then made at 270.4 V/s and 1076 V/s, respectively, for the two sets. These were chosen in order to give essentially the same rate of change of field with time for the two sets of measurements. In the absence of current dependent interfacial phenomena, the two sets of runs should therefore give identical results. In order to obtain identical values for β'_1, however, it was necessary to assume that the film thicknesses for the two sets were not given by a proportionality relationship with V but rather with $V + 1.66$ V. It is difficult to assess either the importance or the source of this additional potential term. Interpreted simply as a constant error in the film thickness values, its effect would be to lead to values of β_1 in Fig. 10 which are 4% too small. This follows from the fact that all the measurements leading to the results in Fig. 10 were made for specimens having the same film thickness as those for set 2 above. Such an assumption, however, will account neither for the intercept anomaly nor for the systematic scatter of β_1 values in Fig. 10. Perhaps the 15% or so discrepancy found for β_1 values determined at different rates of voltage rise is brought about by a current and/or time dependence of the interfacial potentials. Further experiments would have to be performed in order to test this possibility. It seems more likely, however, that the effect is related in some way to the charging current, since the intercept anomaly mentioned previously occurs only for runs in which the charging current makes an appreciable contribution to the total current.

The least squares regression analysis for the data in Fig. 10 leads to the following values for the parameters and their standard deviations.

$$\mu_1^* = 13.2 \text{ eÅ}, \ \sigma = 9\%$$
$$\mu_s^*/C\phi = 4.16 \text{ ÅV}^{-1}, \ \sigma = 16\%$$

The value of $\mu_s^*/C\phi$ may be compared with the same quantity determined from the field dependence of the steady-state Tafel slope, namely

$$\mu_s^*/C\phi = 3.53 \text{ ÅV}^{-1}, \ \sigma = 11\% \ (33)$$
$$\mu_s^*/C\phi = 3.11 \text{ ÅV}^{-1}, \ \sigma = 14\% \ (4).$$

Within experimental uncertainty the results are seen to be in accord with the polarization theory. As noted in a previous publication (34) the high field Frenkel defect theory does not predict any simple relationship between the field dependence of the transient and steady-state Tafel slopes. This result may be regarded as further support for the polarization theory, but by no means conclusive support.

In the following section, an attempt is made to reproduce the experimental log i versus E curve which showed the most curvature (Curve A, Fig. 8). That is, the appropriate equations were solved for selected values of the parameters to obtain calculated log i versus E curves which were compared with the data. For the Frenkel defect theory, theoretical curves were generated from the solution of eq. [10] by a finite difference method using an IBM 7090 digital computer. The measured value of the initial slope gave $qa = 4.28$ eÅ. ΔE was obtained from $\Delta E = E - E_s$, with i_s and E_s being the steady-state current density and field respectively. The theoretical curves were generated for various sets of values for the parameters β' and σ ($1/C_1$ and γ were set equal to 0, which is equivalent to neglecting the field dependence of the Tafel slopes). Figure 11 shows a comparison between the theoretical curves generated in this way and the experimental data. It is apparent that in no case do the

Can. J. Chem. Downloaded from www.nrcresearchpress.com by 210.87.254.5 on 09/05/12
For personal use only.

calculated curves rise fast enough in the non-linear region, most of them in fact showing an inflection point at about $E = 0.095$ V/Å, a feature which is totally absent from the experimental data. The best fit (middle line, family B in Fig. 11) differs from the experimental data by about 20% in the current at the end of the run. Inclusion of the terms in the square of the field (i.e. $1/C_1$ and γ) would result in the calculated curves rising less steeply than shown by an estimated 5 to 10% at the end of the run, thus increasing further the discrepancy between theory and experiment. The best fit, neglecting the quadratic terms, gave $\beta' = 380$ Å/V and $\sigma = 1.6$ Å^2. Steady-state data for this system (23) give $\beta' = 490 \pm 40$ Å/V.

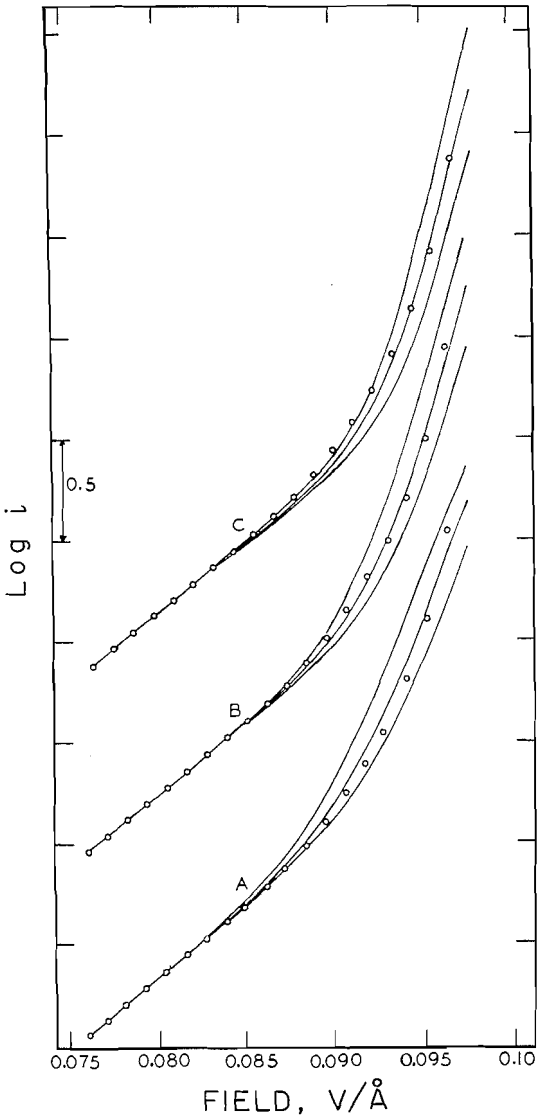

FIG. 11. Comparison of data (open circles) for a film formed at 0.001 V/s and transients measured at 10.76 V/s with curves calculated according to high field Frenkel defect theory (eq. [10] with $1/C_1 = 0 = \gamma$). (Curves A, $\beta' = 321$ Å/V; curves B, $\beta' = 380$ Å/V; curves C, $\beta' = 434$ Å/V).

The data for this run have also been fitted to the dielectric polarization theory. In this case, values for log i as a function of ΔE were calculated using eqs. [13] to [15] and the following values for the parameters: $\mu_s^* = 24$ eÅ (4), $C\phi = 7.65$ eV (4), $\mu_1^* = 8.28$ eÅ. This value for μ_1^* was determined from the initial slope of log i versus ΔE in conjunction with the aforementioned value of $\mu_s^*/C\phi$ obtained from steady-state measurements. It differs somewhat from the value determined from the regression line of Fig. 10 (13.2 eÅ), a result perhaps due in part to the systematic deviation of the data of Fig. 10. As the steady-state data are free from charging current anomalies, the smaller value for μ_1^* is regarded as more reliable. Since i_s and E_s as well as K_1 are known, the only unknown parameter in the calculation was B. Theoretical curves calculated in this way are shown along with the experimental data in Fig. 12. The calculated curves represent a one-parameter fit to the data insofar as the curved portion of the graph is concerned. The best fit differs from the data by about 20% in the current at the end of the run. For this one-parameter trial solution the best fit gave $B = 1.52 \times 10^4$ cm^2/C, in excellent agreement with a value obtained from constant field transient experiments (to be described in Part II of this paper), that value being 1.48×10^4 cm^2/C.

It would appear that the equations derived on the basis of the polarization theory give an appreciably better fit to these data than do those derived on the basis of the high field Frenkel defect theory. One must admit, however, that in relation to the present data the decision between the two theories is not a particularly convincing one.

Summary

Analysis of linear field transients following steady-state formation of oxide films on aluminium are in accord with the predictions of the polarization theory, although they cannot be said to provide a convincing basis upon which to

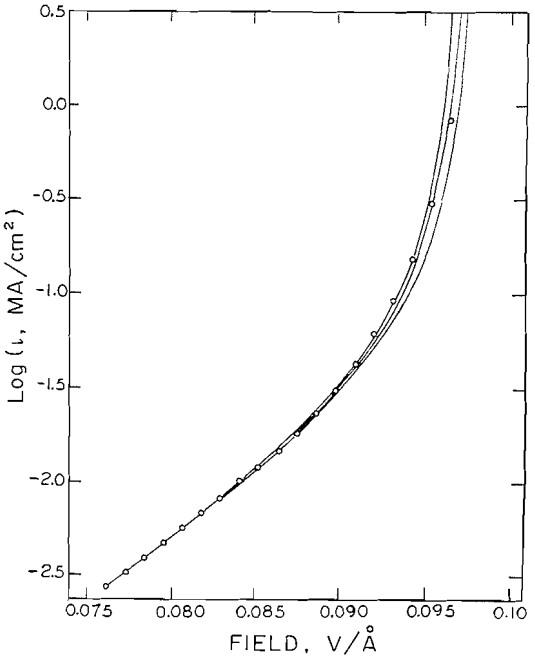

FIG. 12. Comparison of data (open circles) as described in Fig. 11, with curves calculated according to polarization theory (eqs. [13] to [15]), for three closely spaced values of the parameter B.

decide between the polarization and high field Frenkel defect theories. Assuming the polarization theory to be valid, then $\beta_s/\beta_1 = \mu_s^*/\mu_1^* = 3.09$ on combining the present results with those published previously (4). The value for the kinetic parameter $B = 1.52 \times 10^4$ cm²/C was determined for films formed at .001 V/s (about 2×10^{-6} A/cm²).

It is believed that the first in situ measurement of the dynamic dielectric constant ($K_1 = 8.3_5 \pm 0.1$) determined during the steady-state anodic formation of Al_2O_3 has been obtained. A notably higher value for the dielectric constant ($8.8_5 \pm 0.2$) was obtained at $E = 0$ for films which had been either 'annealed' at 60 °C or allowed to stand for 10 min after formation. It is evident from both the above results and the apparent anomaly relating to linear field transient measurements involving large charging currents that a detailed analysis of the interaction of the dielectric constant with formation conditions, field strength, and departure from steady-state conditions is required. We are at present embarked upon such a study.

Acknowledgments

The authors are grateful to the National Research Council of Canada for supporting this research and for a scholarship (P. J. R.).

1. L. YOUNG. Anodic oxide films. Academic Press, New York. 1961.
2. M. J. DIGNAM. Can. J. Chem. **42**, 1155 (1964).
3. L. YOUNG. Proc. Roy. Soc. London, Ser. A, **258**, 496 (1960).
4. M. J. DIGNAM, D. GOAD, and M. SOLE. Can. J. Chem. **43**, 800 (1965).
5. A. YA. SHATALOV and T. P. BONDAREVA. Russ. J. Phys. Chem. English Transl. **37**, 450 (1963).
6. C. P. BEAN, J. C. FISHER, and D. A. VERMILYEA. Phys. Rev. **101**, 551 (1956).
7. J. F. DEWALD. J. Phys. Chem. Solids, **2**, 55 (1957).
8. P. J. RYAN and M. J. DIGNAM. Can. J. Chem. **40**, 1875 (1962).
9. A. CHARLESBY. Proc. Phys. Soc. London, **B66**, 317 (1953).
10. L. YOUNG. Trans. Faraday Soc. **51**, 1250 (1955); **52**, 5002 (1956); **55**, 632 (1959).
11. L. MASING and L. YOUNG. Can. J. Chem. **40**, 903 (1962).
12. M. A. HEINE and M. J. PRYOR. J. Electrochem. Soc. **110**, 1205 (1963).
13. R. K. HART. Proc. Roy. Soc. London, Ser. A, **236**, 68 (1956).
14. M. J. DIGNAM. Can. J. Chem. **41**, 537 (1963).
15. D. A. VERMILYEA. J. Electrochem. Soc. **104**, 140 (1957).
16. M. J. DIGNAM. J. Electrochem. Soc. **109**, 184 (1962).
17. P. A. JACQUET. Met. Rev. **1**, 157 (1956).
18. J. L. MILES and P. H. SMITH. J. Electrochem. Soc. **110**, 1240 (1963).
19. O. M. SMYTH. J. Electrochem. Soc. **113**, 19 (1966).
20. G. J. TIBOL and R. W. HULL. J. Electrochem. Soc. **111**, 1368 (1964).
21. R. C. PLUMB. J. Electrochem. Soc. **105**, 498 (1958).
22. P. H. G. DRAPER. Acta Met. **11**, 1061 (1963).
23. W. J. BERNARD and J. W. COOK. J. Electrochem. Soc. **106**, 643 (1959).
24. P. ROBINSON and J. BURNHAM. Trans. Electrochem. Soc. **83**, 125 (1943).
25. O. M. CHESELDINE. J. Electrochem. Soc. **111**, 1128 (1964).
26. M. J. DIGNAM and P. J. RYAN. Can. J. Chem. **41**, 3108 (1963).
27. F. A. COTTON and G. WILKINSON. Advanced inorganic chemistry. Interscience, New York. 1962.
28. E. W. WASHBURN (*Editor-in-Chief*). International critical tables. Vol. III. 1st ed. McGraw-Hill Book Co., Inc., New York. 1928. p. 217.
29. R. C. WEAST and S. M. SELBY (*Editors*). Handbook of chemistry and physics. 47th ed. Chemical Rubber Publishing Co., Cleveland, Ohio. 1966–67.
30. L. YOUNG. Trans. Faraday Soc. **53**, 229 (1957).
31. M. J. DIGNAM. J. Electrochem. Soc. **112**, 722 (1965).
32. M. J. DIGNAM. Paper presented at meeting of American Electrochemical Society, Dallas, May 1967; J. Electrochem. Soc. **114**, 56C (1967), Abstr. No. 36.
33. M. J. DIGNAM and D. GOAD. J. Electrochem. Soc. **113**, 381 (1966).
34. M. J. DIGNAM. J. Electrochem. Soc. **112**, 729 (1965).

Can. J. Chem. Downloaded from www.nrcresearchpress.com by 210.87.254.5 on 09/05/12
For personal use only.

Can. J. Chem. Downloaded from www.nrcresearchpress.com by 210.87.254.5 on 09/05/12
For personal use only.

High field kinetic processes in anodic oxide films on aluminium. II. Current transients for constant field conditions

M. J. DIGNAM AND P. J. RYAN[1]
Department of Chemistry, University of Toronto, Toronto, Ontario

Received June 26, 1967

Anodic oxide films were formed on high purity aluminium (99.996%) in a glycol–borate electrolyte. Following aging of the films under zero field conditions either at room temperature or 60 °C the electrodes were returned to the electrolysis cell where the anodic overpotential was increased rapidly until a predetermined value was reached, then maintained constant. The ensuing current transients were recorded and analyzed. As little film growth occurred during these measurements the conditions correspond closely to constant field strength. For sufficiently low field strengths the observed current decreased monotonically with increasing time. No single empirical equation could be found to represent these data, although they appear to be in the nature of charging currents rather than ion currents. For somewhat higher applied fields the current is observed to decrease initially, reach a minimum, and then increase approaching ultimately the steady-state ion current for the applied field strength. These data can be accounted for satisfactorily by only the polarization theory of ionic current transients.[2]

Canadian Journal of Chemistry, **46**, 549 (1968)

Introduction

In Part I, current transients under conditions of linearly increasing field strength were examined for the anodic oxidation of aluminium in a glycol–borate electrolyte. On the basis of these studies, it was not possible to make a definitive choice between the two theories which have to date been proposed to explain the transient phenomena, the high field Frenkel defect theory (1, 2) and the dielectric polarization theory (3). In the present paper, the same electronic apparatus was employed to measure the time dependence of the current under conditions approximating those of constant field strength. The results of these experiments provide an unambiguous choice between these two models while at the same time raising a number of questions concerning the nature of the slow polarization processes.

Experimental

The apparatus and materials used in this study are described in Part I (4).

Procedure and Results

Aluminium electrodes were first formed to a fixed potential under steady-state conditions. The anode overpotential was then dropped automatically to zero, the electrodes removed and annealed in mineral oil at 60 °C for 2 h, washed in a succession of solvents (cyclohexane, acetone), and finally dried in a stream of air. They were then replaced in the cell and the anode potential reapplied at a linear rate until a potential a few volts below the formation voltage was reached, at which point it was held constant. The results for a typical run of this kind are shown in Fig. 1. This electrode was first formed at 0.1 V/s to $V = 99.7$ V, annealed, and the potential reapplied at 10.76 V/s to $V = 91.7$ V. Upon initiating the voltage rise, there is a very rapid jump in current to Point A, thence a slower accelerated rise to Point B as the applied potential is increased to its maximum value. At B the anode potential is held constant and the current falls rapidly, then more slowly to a minimum at C. From this point the current rises through an inflection point, reaching at D the steady-state value for the applied field.

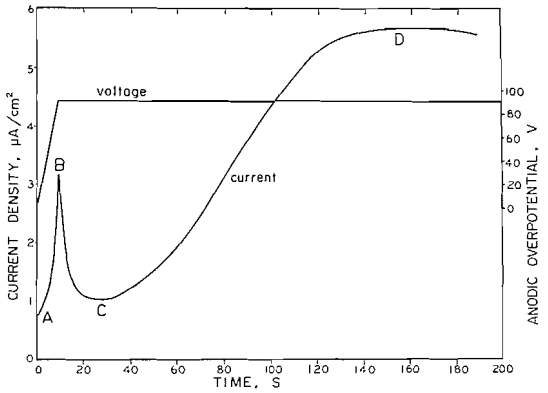

FIG. 1. Current as a function of time upon reapplication of potential, as illustrated, to an electrode formed initially at 0.1 V/s to $V = 99.7$ V then annealed at 60 °C.

Little film growth occurs during these measurements compared with the total thickness impressed during formation, so that for the part of the curve where the anode potential is held constant, the field E is approximately constant. In fact, however, the formation of new oxide results in a slow decrease in field strength and hence in current density.

[1]Present address: J. Roy Gordon Research Laboratories, Sheridan Park, Clarkson, Ontario.

[2]Reference 3.

The general features of Fig. 1 were reproduced irrespective of the value of the limiting potential reapplied to the anode, provided that it was not so far below the formation voltage that no ion current would result. Moreover, annealing was not essential in producing these effects since electrodes treated essentially as above, but omitting the annealing procedure, gave results displaying the same features.

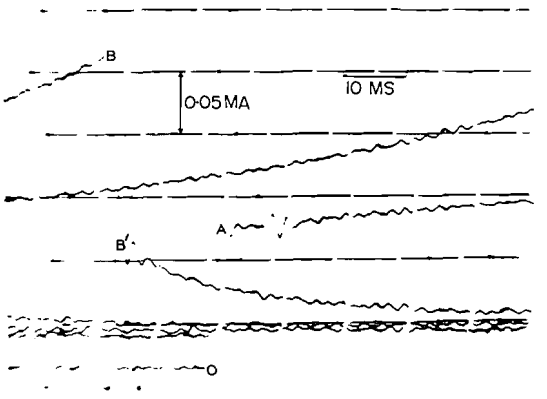

FIG. 2. Typical photograph of oscilloscope trace for films formed at 0.1 V/s to $V = 41.8$ V, annealed at 60 °C, and current transients measured during and following the reapplication of potential at 209.4 V/s to 35.8 V.

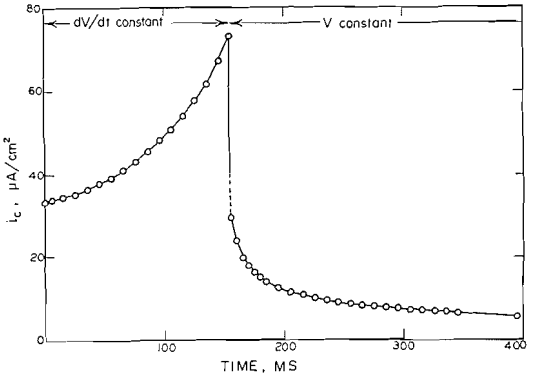

FIG. 3. Current transients upon reapplication of potential at 209.4 V/s to $V = 33.8$ V. The data are for an electrode formed at 0.1 V/s to $V = 41.8$ V.

In a further series of experiments, specimens were formed at 0.1 V/s to $V = 41.8$ V, at which point the anode potential was switched to zero. Following annealing and washing as above, the potential was reapplied at 209.4 V/s to a value in the range 30 to 35 V, which is sufficiently below that to which the sample was formed so that theoretically no detectable ion current should result. Similar runs were also performed on samples for which the annealing treatment was omitted. For these runs the potential was reapplied following about 10 min at room temperature.

In these experiments the current transients during the initial period were displayed and photographed on an oscilloscope, the longer period transients being recorded on a strip chart recorder. A typical photograph of a multiple sweep oscillograph trace is shown in Fig. 2. In Fig. 3 the data are represented in the form of current, i_c, versus time for a sample formed at 0.1 V/s to 41.8 V, the anode potential dropped to zero and reapplied after a delay of 10 min at 209.4 V/s to 33.8 V. All of the data for the decay in the charging current at constant potential is not shown on the graph. Typically, $i_c \sim 0.1$ μA/cm² after about 1 h at constant potential.

Theory

The data obtained were analyzed in terms of the high field Frenkel defect theory (1, 2) and the polarization theory (3) outlined in Part I. Further equations required for interpreting the present data are developed herein.

High Field Frenkel Defect Theory

The expected form for constant field ion current transients can be obtained most easily from eq. [10] of the previous paper, recorded below for convenience.

$$[1]\quad \frac{\mathrm{d}\ln i}{\mathrm{d}E} = \frac{qa}{kT}\left[1 - \frac{2qaE}{C_1U}\right] + \frac{\sigma/q}{\mathrm{d}E/\mathrm{d}t}\left[\frac{[\alpha \exp(\beta'E - \gamma E^2)]^2 - i^2}{i}\right]$$

Multiplying by $\mathrm{d}E/\mathrm{d}t$ and setting $\mathrm{d}E = 0$, eq. [1] reduces to

$$[2]\quad \frac{\mathrm{d}i}{\mathrm{d}t} = (\sigma/q)(i_s^2 - i^2),$$

where $i_s = \alpha \exp(\beta'E - \gamma E^2)$ and is the steady-state current density corresponding to the constant applied field E (refer to Part I). Equation [2] may be integrated to yield

$$[3]\quad i = i_s \frac{D \exp(2i_s\sigma t/q) - 1}{D \exp(2i_s\sigma t/q) + 1},$$

where $D = (i_s + i_{t=0})/(i_s - i_{t=0})$.

For the constant field experiments described herein, $i \ll i_s$. From [2], therefore, $\mathrm{d}i/\mathrm{d}t$ is always positive so that i increases monotonically with t. Furthermore it follows that $\mathrm{d}i/\mathrm{d}t$ is maximum at $t = 0$, decreasing monotonically to zero for large times. The predicted form of the graph of i versus t is therefore one in which i increases monotonically with t, the curve being concave downwards.

Can. J. Chem. Downloaded from www.nrcresearchpress.com by 210.87.254.5 on 09/05/12
For personal use only.

Can. J. Chem. Downloaded from www.nrcresearchpress.com by 210.87.254.5 on 09/05/12
For personal use only.

Dielectric Polarization Theory

The expected form for ion current transients under conditions of constant field strength have been derived in some detail in a previous publication (3). A much simpler, though somewhat approximate, derivation is presented here. Setting $dE/dt = 0$, eq. [14] of Part I reduces to

$$[4] \qquad \mu^*(dE_e/dt) = Bi(\mu_s^*E - \mu^*E_e).$$

Defining the differential field coefficients β and β_s as follows

$$[5] \qquad \beta = \frac{d \ln i}{dE_e}, \quad \beta_s = \lim_{\dot{E}\to 0}\left(\frac{d \ln i}{dE}\right),$$

then the ratio β_s/β is clearly equal to the ratio of the effective field under steady-state conditions to the applied field, which in turn is equal to $(1 + \delta\chi_s) = \mu_s^*/\mu^*$. On multiplying by β/μ^*, eq. [4] therefore becomes

$$[6] \qquad \beta(dE_e/dt) = Bi(\beta_s E - \beta E_e).$$

Neglecting to a first approximation the field dependence of β and β_s (that is treating β and β_s as constants), eq. [5] for β can be integrated to yield

$$[7] \qquad \ln (i_s/i) \simeq \beta(E_e)_{\text{steady state}} - \beta E_e,$$

which reduces to

$$[8] \qquad \ln (i_s/i) \simeq \beta_s E - \beta E_e,$$

since βE_e at steady state $= \beta_s E$. Eliminating βdE_e from eqs. [6] and [5] and $\beta_s E - \beta E_e$ from [6] and [8] leads to

$$[9] \qquad (di/dt) = Bi^2 \ln (i_s/i).$$

Integration of [9] gives the desired relationship

$$[10] \qquad \frac{1}{i} = \frac{1}{i_{t=0}} - B\int_0^t \ln (i_s/i)dt.$$

Once again, for the experimental conditions used herein, i is always $\leqslant i_s$. From [9] it follows, therefore, that i is a monotonically increasing function of time. In contrast with the Frenkel defect theory, however, it can be shown that i versus t will be concave upward for $\ln (i_s/i) > \frac{1}{2}$ and concave downward for $\ln (i_s/i) < \frac{1}{2}$.

In Part I, the contribution of the slow polarization process to the measured current was neglected, since in all cases the ion current was dominant. In the present set of experiments, however, several runs were carried out under conditions where the contribution of the ion current to the total measured current should be negligible. For such cases, the current contributed by the slow polarization process will be important. Furthermore, the dominant process leading to attainment of equilibrium polarization conditions cannot be that induced by ion transport but rather must arise from thermal activation. In the original paper in which this theory was presented (3), the field assisting the rate of change of the slow polarization process was assumed to be proportional to the displacement of the effective field from its steady-state value. The polarization current was then represented as a hyperbolic sine function of the effective field displacement multiplied by the usual kinetic parameters. In writing such an expression, it is assumed implicitly that the slow polarization process may be described in terms of a single activation energy and single activation dipole. That this should be the case, however, seems improbable. Nevertheless we might expect to achieve qualitative agreement with data on the basis of such an assumption, provided of course the basic model is appropriate.

On including the contribution of thermal activation to the rate of change for the slow polarization process, in the manner outlined above, eqs. [14] and [15] of Part I of this paper take the forms

$$[11] \qquad \mu^*\frac{dE_e}{dt} + Bi\mu^*E_e \simeq \mu_1^*\frac{dE}{dt} + Bi\mu_s^*E + \left(\frac{\mu_1^*}{\epsilon_0 K_1}\right)\alpha_e \sinh\left[\frac{\omega_e^*}{kT}\left(\frac{\mu_s^*E - \mu^*E_e}{\mu_s^*}\right)\right]$$

$$[12] \qquad i_e \simeq \epsilon_0 K_1\left[\frac{dE}{dt} + Bi\left(\frac{\mu_s^*E - \mu^*E_e}{\mu_1^*}\right)\right] + \alpha_e \sinh\left[\frac{\omega_e^*}{kT}\left(\frac{\mu_s^*E - \mu^*E_e}{\mu_s^*}\right)\right],$$

where α_e is a temperature dependent constant and ω_e^* is of the order of the activation dipole for the slow polarization process. (Equations [11] and [12] follow from eqs. [31] and [33] of ref. 3, certain substitutions and one approximation, however, having been made, the nature of which are apparent on referring to the original paper.) From eq. [12] we can see that the additional polarization process takes the form of a thermally activated charging current which goes to zero for steady-state conditions (i.e. when

Can. J. Chem. Downloaded from www.nrcresearchpress.com by 210.87.254.5 on 09/05/12
For personal use only.

$\mu_s^* E = \mu^* E_e$). As this thermally activated polarization process also contributes to the time variation of E_e, essentially the same term appears in eq. [11]. For conditions in which i is negligible compared with i_c, a useful form of eq. [12] can be written as follows.

$$[13] \quad i_{c_2} \simeq \alpha_c \sinh\left[\frac{\omega_e^*}{kT}\left(\frac{\mu_s^* - \mu_1^*}{\mu_s^*}E - \frac{\mu_1^*}{\mu_s^*}\frac{P_2}{\epsilon_0 K_1}\right)\right], \quad i_{c_2} \gg i,$$

where $i_{c_2} = i_c - \epsilon_0 K_1 (dE/dt)$ and P_2 is the polarization of the medium arising from the slow polarization process and is related to i_{c_2} by the equation

$$[14] \qquad i_{c_2} = (dP_2/dt).$$

Equation [13] is obtained by setting $i = 0$ and substituting $E_e = E + \delta P/\epsilon_0 = E(1 + \delta\chi_1) + \delta P_2/\epsilon_0$, where P is the total polarization of the medium. In addition, an approximation is required in which $(1/\delta + \chi_1)$ is replaced by K_1.

For conditions in which i is negligible and furthermore the external field is held constant, eq. [12] may be transformed to give

$$[15] \quad \ln\left[\frac{|i_c/\alpha_c|}{(1 + i_c^2/\alpha_c^2)^{1/2} - 1}\right] = gt - \ln|D|$$

(see eq. [64] of ref. 3), where

$$g \simeq \omega_e^* \alpha_c \mu_1^* / \mu_s \epsilon_0 K_1 kT \quad \text{and}$$

$$D = \tanh\left[\frac{\omega_e^*}{2kT}\left(\frac{\mu_s^* - \mu_1^*}{\mu_s^*}\right)\left(E - \frac{P_2(t=0)}{\epsilon_0}\right)\right].$$

For conditions in which the charging current, i_c, may be approximated by an exponential function of the effective field displacement (i.e. $i_c \gg \alpha_c$), [15] may be approximated by

$$[16] \quad (\alpha_c/i_c) - 1/6(\alpha_c/i_c)^3 + \ldots = gt - \ln|D|$$

or

$$\ln i_c \doteq \mathscr{K} - \ln[t + t_0],$$

where

$$\mathscr{K} = \ln(\alpha_c/g) = \ln(\mu_s^* \epsilon_0 kT/\omega_e^* \mu_1^*)$$

and

$$t_0 = \alpha_c/g i_c(t=0) = \frac{\mu_s^* \epsilon_0 kT}{\mu_1^* \omega_e^* i_c(t=0)}.$$

Analysis and Discussion of Results

The features of the constant field transients displayed in Fig. 1 may be interpreted qualitatively in terms of the dielectric polarization theory. During the initial linear increase in potential the ion current will be negligible, the total current being given therefore by eq. [13]. Thus the initial rapid rise in current, equal to $\epsilon_0 K_1 dE/dt$, is seen to be followed by a slow buildup in current which from [13] should be approximately a hyperbolic sine function in E or t. During this period the effective field strength, E_e, whose time dependence is given by eq. [11], lags far behind its steady-state value since the slow polarization process does not 'follow' the change in applied field. Once the potential (and hence the field) is held constant (Point B, Fig. 1) $dE/dt = 0$ so that the component of the charging current, $\epsilon_0 K_1 dE/dt$, should drop rapidly to zero followed by a slow decay in the component of the charging current arising from the slow polarization process. This decay should be approximately in accord with eqs. [15] or [16] (i.e. approximately a negative exponential decay with time). The decay in charging current will continue in accord with eq. [15] until the polarization of the medium, and hence E_e, becomes sufficiently large so that the ion current may no longer be neglected. At this point (presumably in the neighborhood of C) the total observed current begins to increase as the contribution of the ion current increases, and furthermore the rate of increase in current increases initially as a result of the contribution of the ion current to the rate of change of the polarization of the medium and hence to the rate of change of the effective field strength (see eq. [11]). From Point C on the ion current presumably makes the dominant contribution to the observed current so that in region CD the variation of current with time should be given to a good approximation by eq. [10]. Beyond D the current falls off slightly as a result of the slow decrease in field strength arising from film growth.

With reference to the high field Frenkel defect theory, we note that the results of Fig. 1 are qualitatively discrepant with the theoretical predictions. In particular, the rate of increase in current from C to D is initially accelerating (i.e. the curve is initially concave upward) in direct conflict with the predictions of this

Can. J. Chem. Downloaded from www.nrcresearchpress.com by 210.87.254.5 on 09/05/12
For personal use only.

theory. In addition, of course, the initial features of the transient (i.e. regions AB and BC) are not accounted for in any manner whatsoever. It is clear, therefore, that no satisfactory explanation of these data is forthcoming from the high field Frenkel defect theory. We shall therefore concentrate our attention on the dielectric polarization theory.

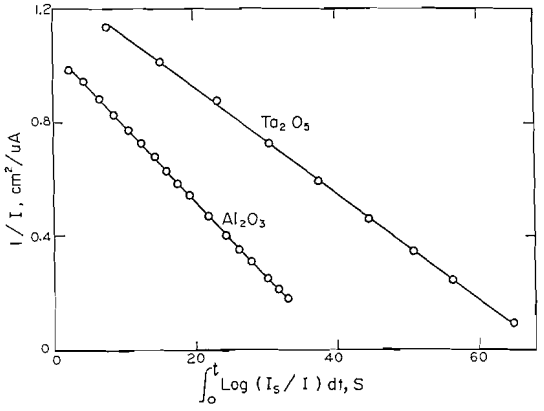

FIG. 4. Analysis of constant field ion current transients (Fig. 1) according to eq. [10]. Similar data obtained by Young for tantalum (5) are also presented for comparison.

As the ion current transients falling in the region CD of Fig. 1 are readily analyzed, we shall tackle this first. Making the approximation that the field is essentially constant for this portion of the transient, and furthermore that the total observed current I is approximately equal to i, the ion current, the data in this region were plotted in the form suggested by eq. [10], the results being given in Fig. 4. It can be seen that the data, covering the range 30 to 150 s, conform extremely well to a linear plot. As eq. [10] involves only a single unknown parameter B, Fig. 4 represents a significant confirmation of the dielectric polarization theory. For comparison purposes, similar constant field ionic transient measurements made by Young on tantalum (5) are also presented in Fig. 4. These also conform extremely well to a straight line.

Two different sets of constant field transient runs were carried out for aluminium. In one set the films were formed initially at 0.1 V/s rate of voltage rise. Five different runs of this kind yielded a mean value for B of $(1.22 \pm 0.07) \times 10^4$ cm²/C. In the other set of measurements the films were formed at 10^{-3} V/s rate of voltage rise, these runs giving a mean value for B of $(1.46 \pm 0.04) \times 10^4$ cm²/C. From these results it would appear that B depends to some extent on the formation conditions of the film. The value for B determined in Part I was for films formed at 10^{-3} V/s and hence should be compared with the second value quoted above. The values to be compared $(1.46 \pm .04) \times 10^4$ and 1.52×10^4 cm²/C are seen to be in excellent agreement.

The theoretical significance of the parameter B is discussed elsewhere (3, 6) and will not be repeated here.

Before attempting to fit the initial features of the data in Fig. 1 to the polarization theory we shall examine first the data illustrated in Fig. 3 since for these runs the ion current may presumably be neglected throughout the entire transient, thus simplifying the interpretation. The features of these charging current transients are essentially the same as those of Fig. 1 except that there is no minimum and subsequent increase in total current, since for these runs the potential reapplied was sufficiently low so that the ion current should remain indefinitely immeasurable.

The data up to the maximum in Fig. 3 were fitted to eq. [13] in the following manner. For convenience of computation eq. [13] may be rearranged to give

$$[17] \qquad Y = mX + G,$$

where

$$Y = E - [\mu_1^*/(\mu_s^* - \mu_1^*)\epsilon_0 K_1] \int_0^t i_{c_2} dt$$

$$X = \sinh^{-1}(i_{c_2}/\alpha_c)$$

$$m = kT\mu_s^*/\omega_e^*(\mu_s^* - \mu_1^*)$$

$$G = [\mu_1^*/(\mu_s^* - \mu_1^*)\epsilon_0 K_1] P_{2(t=0)}.$$

The data were then fitted to eq. [17] using a 7090 digital computer which carried out linear regression analyses of Y against X for a number of assumed values of α_c, the value of α_c which minimized the variance being accepted. The values of μ_s^*/μ_1^* and K_1 used in calculating Y were obtained from Part I (i.e. $\mu_s^*/\mu_1^* = 3.09$, $K_1 = 8.35$). The results are plotted in Fig. 5 in the form Y versus X. The data can be seen to conform very well to a straight line relationship. It must be remembered, however, that three

disposable constants are involved in the fit: m, G, and α_c. Three different runs of this kind gave the following values for the relevant parameters: $\alpha_c = 3.0 \times 10^{-6}$ A/cm^2, $\omega_e^* = 2.22$ eÅ; $\alpha_c = 5.4 \times 10^{-6}$ A/cm^2, $\omega_e^* = 1.75$ eÅ; $\alpha_c = 7.6 \times 10^{-6}$ A/cm^2, $\omega_e^* = 1.34$ eÅ. The results appear to give a value for the effective activation dipole ω_e^* which is of the correct order of magnitude. No independent estimate of α_c, however, can be made.

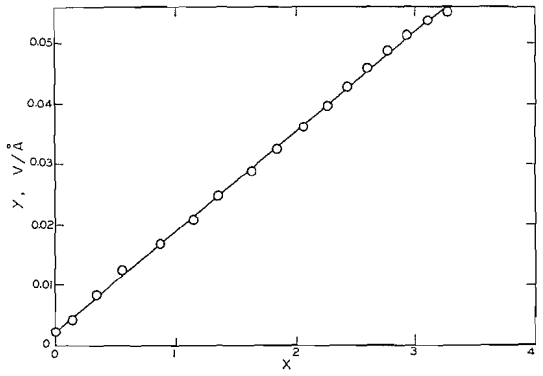

FIG. 5. Data of Fig. 3 (dV/dt constant) plotted according to eq. [13] (or [17]).

The latter portion of the data presented in Fig. 3, commencing from the peak current onward, should be in accord with eq. [15], since the data presumably represent the decay in the slow polarization process under conditions of constant applied field. In Fig. 6 the data are plotted in accordance with eq. [15] using the value of α_c determined from the foregoing analysis. As can be seen the data do not conform well to a straight line, the form predicted from [15]. The straight line included in the graph has been drawn with slope g calculated using the parameters deduced from the foregoing analysis. Although the experimental data conform more or less to this slope over a fair range it must be concluded that the fit is at best qualitative.

In a further attempt to account for the results, the above data were plotted in a form suggested by eq. [16]. For the present data, we may calculate $t_0 \leqslant 10^{-2}$ s for $\omega_e^* \geqslant 2$ eÅ. Thus for nearly all the data points t_0 should be negligible compared with t. Accordingly, the data have been plotted in Fig. 7 in the form log i_c versus log t. It is clear that this form of plot represents

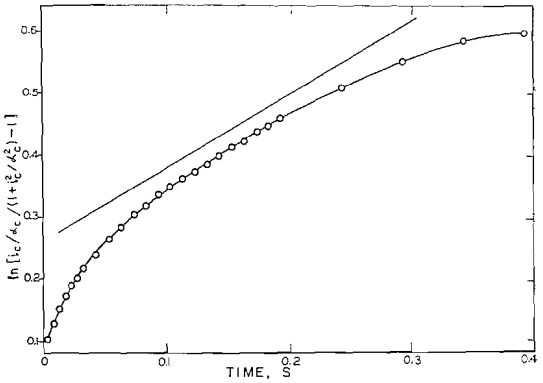

FIG. 6. Data of Fig. 3 (V constant) plotted according to eq. [15]. The solid line is drawn with the slope expected from the analysis illustrated in Fig. 5.

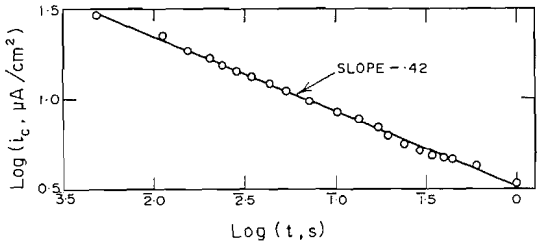

FIG. 7. Data of Fig. 3 (V constant) plotted in a form suggested by eq. [16].

the data extremely well. However, the slope of the plot is $-.42$ rather than -1 as predicted by eq. [16]. Another set of constant field charging current measurements, in which the current decay was followed by means of an electrometer amplifier and strip chart recorder for a period of about 10 min, was also obtained. These data are plotted in Fig. 8 in the same form as the previous set of results. Although the initial slope is close to that found in Fig. 8 (i.e. $-.42$) as the time elapsed increases the slope decreases, apparently approaching a limiting value close to -1.

If one makes allowance for a possible range or distribution of activation energies and activation dipoles for the polarization processes, then it is possible to derive an equation formally the same as [16] except that the slope is given not by -1 but rather by $-1/(1 + \epsilon^2)$ where the parameter ϵ is connected with the breadth of the distributions. Details of the analysis will be presented elsewhere. The point we wish to make here is simply that it is likely that the discrepancy observed between the predicted form for the charging currents and that found experimentally

Can. J. Chem. Downloaded from www.nrcresearchpress.com by 210.87.254.5 on 09/05/12
For personal use only.

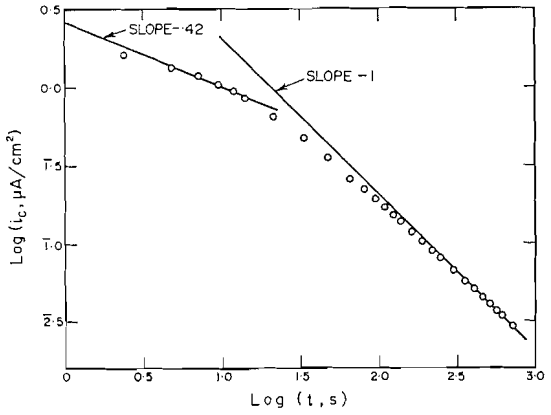

FIG. 8. Charging current data similar to that of Fig. 3 (V constant) plotted in a form suggested by eq. [16].

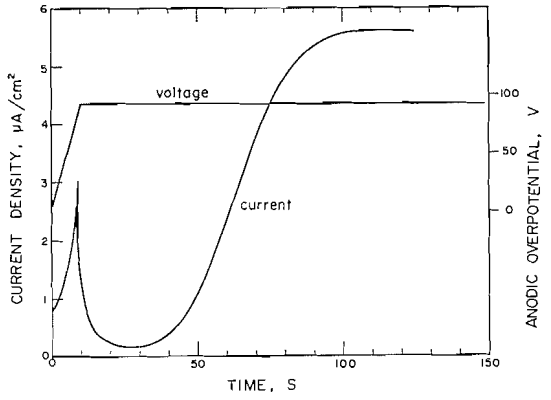

FIG. 9. Current as a function of time calculated according to the polarization theory of current transients for an electrode treated in the same manner as that giving rise to the data of Fig. 1.

can be reconciled by taking into account the distribution of the kinetic parameters and the expected time variation of the distribution. The time variation of the distributions will arise because the distributions are being depopulated in an asymmetric manner as a result of the kinetics of the polarization process. In fact, one would expect the distributions to become narrower with elapsed time (i.e. $\epsilon \rightarrow 0$ as $t \rightarrow \infty$) so that the slope would be expected to approach -1 for large times as observed. It must be admitted, however, that arguments such as these should be treated with some skepticism, since by careful choice of the form of the distribution functions almost any desired result may be obtained.

We return now to Fig. 1, and the problem of reconstructing the entire curve from the full set of kinetic equations. Since the equations relating to the thermally activated polarization process have been found to be in only qualitative agreement with the experimental data, the equations presented herein can only be expected to yield qualitative agreement with the data of Fig. 1. It is nevertheless worthwhile showing that the present set of equations do indeed give rise to all of the features found in the experimental data. In Fig. 9 the form of the curve $I = i + i_c$ versus time has been calculated for an experiment carried out in the manner of that represented in Fig. 1. Equations [11] and [12] of this paper in conjunction with the equations recorded below were solved by a finite difference method using an IBM 7094 digital computer.

$$[18] \quad i = i_0 \exp\left[-[\phi - \mu^* E_e(1 - \mu^* E_e/C\phi)]/kT\right]$$

$$I = i + i_c$$

$$[19] \quad \mu^* E_e = \mu^*(E + \delta P/\epsilon_0) = \mu_1^* E + \delta\mu^* P_2/\epsilon_0,$$

which on making the approximation $\mu_1^* \approx \delta K_1 \mu^*$ becomes

$$[20] \quad \mu^* E_e \simeq \mu_1^*(E + P_2/K_1\epsilon_0)$$

$$[21] \quad P_2 \simeq \int_0^t i_{c_2} dt = \int_0^t i_c dt - \epsilon_0 K_1 E.$$

Equation [18] is eq. [13] of Part I reproduced. Equations [19] to [21] follow from the definitions of the parameters involved, in the manner indicated. In carrying out this calculation μ_1^*, μ_s^*, and K_1 were given the values determined in Part I of this paper. The remaining three parameters were given the following values: $B = 10^4$ cm²/C, $\omega_e^* = 2$ eÅ, and $\alpha_e = 0.14$ μA/cm². No attempt was made to vary the parameters in order to obtain the best possible fit as such an exercise did not seem to be worthwhile.

It is apparent that the calculated curve does indeed reproduce all the features of the experimental curve in Fig. 1. The agreement is rather better than qualitative but certainly not quantitative. It remains to be seen whether quantitative agreement can be achieved by modifying the equations to allow for a range of values for the kinetic parameters for the slow polarization process.

Can. J. Chem. Downloaded from www.nrcresearchpress.com by 210.87.254.5 on 09/05/12
For personal use only.

Can. J. Chem. Downloaded from www.nrcresearchpress.com by 210.87.254.5 on 09/05/12
For personal use only.

Summary and Conclusions

In Part I it was shown that both the high field Frenkel defect model and the dielectric polarization model could account satisfactorily for transient phenomena occurring during rapid changes in the field strength. The polarization theory gave a slightly better account of the data but not sufficiently so to enable one to choose between the models. In the present paper, in which transients were investigated under conditions of approximately constant field strength, the data presented enable one to make a clear choice between the two models. Thus the polarization theory was able to account quantitatively for constant field transients under conditions where the anomalous charging current could be neglected. On the other hand, the predictions based on the high field Frenkel defect theory are qualitatively discrepant with these same data. Again, the dielectric polarization theory was able to account semiquantitatively for the form of the anomalous charging current transients for measurements made under conditions where the ion current could be neglected. The discrepancy between the data and the predictions has been tentatively ascribed to the invalid assumption of a single activation energy and activation dipole for the slow polarization process. It seems highly probable that a range of such parameters would be present. The high field Frenkel defect theory contains no features to account for these anomalous charging currents though it does not specifically preclude their existence.

Perhaps the greatest achievement of the polarization theory concerns its semiquantitative reproduction of the complex transient behavior observed under conditions where the anomalous charging current and ion current are comparable (Figs. 1 and 9). It is clear from the above that the high field Frenkel defect theory cannot account even qualitatively for such behavior.

Acknowledgments

The authors are grateful to the National Research Council of Canada for supporting this research and for a scholarship (P. J. R.). They also wish to express their thanks to Mr. M. Moskovitz and Mr. P. Dalziel for assistance in carrying out some of the calculations.

1. C. P. Bean, J. C. Fisher, and D. A. Vermilyea. Phys. Rev. **101**, 551 (1956).
2. J. F. Dewald. J. Phys. Chem. Solids, **2**, 55 (1957).
3. M. J. Dignam. J. Electrochem. Soc. **112**, 722 (1965).
4. M. J. Dignam and P. J. Ryan. Can. J. Chem. This issue.
5. L. Young. Proc. Roy. Soc. London, Ser. A, **263**, 395 (1961).
6. M. J. Dignam. J. Electrochem. Soc. **112**, 729 (1965).

Can. J. Chem. Downloaded from www.nrcresearchpress.com by 210.87.254.40 on 09/05/12
For personal use only.

Magnetic properties of pyridine copper(II) chlorobenzoates

Y. C. Lin and R. C. Thompson
Department of Chemistry, University of British Columbia, Vancouver, British Columbia

Received July 11, 1967

Magnetic susceptibility studies have been made on the bispyridine adducts of copper(II) *m*-chlorobenzoate and copper(II) *p*-chlorobenzoate and on samples of composition $Cu(ClC_6H_4CO_2)_2(C_5H_5N)_x$, where $2 > x \geq 0$. Results show that whereas the bispyridine adducts are essentially magnetically dilute the monopyridine and hemipyridine adducts of these copper chlorobenzoates are antiferromagnetic, exhibiting magnetic properties typical of binuclear molecules.

Canadian Journal of Chemistry, 46, 557 (1968)

Introduction

Magnetic susceptibility measurements have been used extensively in the study of copper(II) carboxylates and related compounds (1). Copper(II) acetate monohydrate, which has a binuclear structure with pairs of copper atoms bonded together by four bridging carboxylate groups and water molecules occupying terminal positions on the copper atoms (2), exhibits typical antiferromagnetic behavior. Figgis and Martin (3) have shown that the magnetic susceptibility – temperature behavior of this compound agrees well with eq. [1], the theoretical expression for the case of two paramagnetic centers interacting in such a way as to form lower singlet and upper triplet electronic states.

$$[1]\quad \chi'_M = \frac{g^2N\beta^2}{3kT}\left[1 + \tfrac{1}{3}\exp\left(2J/kT\right)\right]^{-1} + N\alpha$$

In equation [1] χ'_M is the molar magnetic susceptibility based on monomeric formula weights, g is the Landé spectroscopic splitting factor, N is Avogadro's number, β is the Bohr magneton, k is the Boltzmann constant, T is the temperature (°K), J is the exchange coupling constant, and $N\alpha$ is the temperature-independent paramagnetic contribution for copper(II). A number of other copper(II) carboxylates have magnetic properties similar to those of copper(II) acetate monohydrate and it has been generally accepted that, provided agreement with eq. [1] is observed, these compounds have analogous binuclear structures (4–8).

A considerable amount of published work has been concerned with the preparation and study of Lewis-base adducts of binuclear copper(II) carboxylates in order to determine what effect the presence of the base has on the magnetic interaction between the contiguous copper atoms. Of particular interest are the monopyridine adducts which are prepared by the elimination of all but one molecule of pyridine per copper atom from compounds which originally had two or more pyridine molecules per copper. Magnetic susceptibility studies have shown that whereas the monopyridine derivatives are binuclear, the starting materials are not, and hence considerable molecular rearrangement must be taking place as the pyridine molecules are removed (5–8). To investigate this phenomenon more fully we have studied the magnetic properties of material of composition $Cu(ClC_6H_4CO_2)_2(C_5H_5N)_x$, where $2 > x \geq 0$, prepared by heating under reduced pressure the bispyridine adducts of copper(II) *m*-chlorobenzoate and copper(II) *p*-chlorobenzoate.

Experimental

Preparations

The bispyridine adducts of copper(II) *m*-chlorobenzoate and copper(II) *p*-chlorobenzoate were prepared as follows. The anhydrous copper(II) chlorobenzoate was dissolved in boiling, freshly distilled pyridine, yielding a blue solution which was filtered hot and allowed to cool to room temperature. The blue precipitate which formed on cooling was recovered and dried in a desiccator over calcium chloride.

Anal. Calcd. for $Cu(ClC_6H_4CO_2)_2(C_5H_5N)_2$: C, 54.1; H, 3.40; Cu, 11.9; N, 5.26. Found for *m*-chloro-: C, 54.4; H, 3.83; Cu, 12.0; N, 5.08. Found for *p*-chloro-: C, 54.7; H, 3.92; Cu, 11.7; N, 5.21.

Attempts to prepare monopyridine derivatives by methods analogous to those used in the preparation of the monopyridine adducts of copper(II) benzoate (7), *o*-chlorobenzoate (5), and acetate (6) were unsuccessful.

When the bispyridine derivatives were heated under reduced pressure (about 10 mm), pyridine was evolved. We attempted to obtain samples of composition corresponding to the monopyridine derivatives by this method but were not able to do so. In two experiments with bispyridine copper(II) *p*-chlorobenzoate for example, we

TABLE I

Room-temperature magnetic properties

Sample [a]	Temp. (°K)	$10^6\chi_g$	$-10^6\chi$	$10^6\chi'_M$	μ_{eff} (B.M.)
$Cu(m\text{-}ClC_6H_4CO_2)_2\cdot py_2$	297	2.24	281	1475	1.84
$Cu(m\text{-}ClC_6H_4CO_2)_2\cdot py_{0.8}$	296	1.61	222	927	1.43
$Cu(m\text{-}ClC_6H_4CO_2)_2\cdot py_{0.5}$	295	1.82	208	962	1.46
$Cu(m\text{-}ClC_6H_4CO_2)_2$	296	2.87	183	1259	1.69
$Cu(p\text{-}ClC_6H_4CO_2)_2\cdot py_2$	295	2.21	281	1459	1.82
$Cu(p\text{-}ClC_6H_4CO_2)_2\cdot py_{1.2}$	300	1.60	242	993	1.50
$Cu(p\text{-}ClC_6H_4CO_2)_2\cdot py_{0.8}$	297	1.67	222	953	1.46
$Cu(p\text{-}ClC_6H_4CO_2)_2\cdot py_{0.5}$	297	2.03	208	1049	1.53
$Cu(p\text{-}ClC_6H_4CO_2)_2$	293	2.08	183	963	1.46

[a] py = pyridine.

obtained samples of composition close to that expected for the monopyridine derivative, but in fact corresponding to $Cu(ClC_6H_4CO_2)_2(C_5H_5N)_x$, where x is 0.8 and 1.2. As will be shown in the discussion to follow, the magnetic properties of the samples assuming these compositions may be readily understood. The values of x may be considered significant to approximately ± 0.05.

All of the samples listed below were obtained by heating the corresponding bispyridine adduct and the highest temperature to which the sample was heated is recorded in parenthesis.

$Cu(m\text{-}ClC_6H_4CO_2)_2(C_5H_5N)_{0.8}$ (126°). Found: C, 49.4; H, 2.87; N, 2.65; Cu, 14.3. Calcd.: C, 49.4; H, 2.76; N, 2.56; Cu, 14.5.

$Cu(m\text{-}ClC_6H_4CO_2)_2(C_5H_5N)_{0.5}$ (126°). Found: C, 47.7; H, 2.75; N, 1.70; Cu, 15.3. Calcd.: C, 47.8; H, 2.55; N, 1.69; Cu, 15.3.

$Cu(m\text{-}ClC_6H_4CO_2)_2$ (156°). Found: C, 44.8; H, 2.40; Cu, 16.9. Calcd.: C, 44.9; H, 2.15; Cu, 17.0.

$Cu(p\text{-}ClC_6H_4CO_2)_2(C_5H_5N)_{1.2}$ (77°). Found: C, 51.2; H, 3.16; N, 3.64; Cu, 13.8. Calcd.: C, 51.2; H, 3.00; N, 3.58; Cu, 13.5.

$Cu(p\text{-}ClC_6H_4CO_2)_2(C_5H_5N)_{0.8}$ (126°). Found: C, 49.4; H, 2.89; N, 2.50; Cu, 14.4.

$Cu(p\text{-}ClC_6H_4CO_2)_2(C_5H_5N)_{0.5}$ (111°). Found: C, 47.9; H, 2.69; N, 1.71; Cu, 15.4.

$Cu(p\text{-}ClC_6H_4CO_2)_2$ (156°). Found: C, 44.7; H, 2.29; Cu, 16.4.

Analyses

Copper was determined iodometrically and carbon, hydrogen, and nitrogen analyses were obtained by standard techniques in the microanalytical laboratory of the University of British Columbia.

Magnetic-Susceptibility Measurements

Susceptibilities on powdered samples were obtained by the Gouy method. For all compounds studied the room-temperature results reported are the average of at least three separate determinations (each involving repacking of the Gouy tube). The apparatus used to study magnetic-susceptibility temperature dependences was described previously (9). Data reported were obtained at a field strength of about 8000 G; room-temperature measurements at about 4000, 6000, and 8000 G gave no evidence for the dependence of the susceptibility of the samples studied upon the strength of the magnetic field. Diamagnetic corrections were estimated as described previously (5). Calibration was achieved using a gravimetrically analyzed nickel(II) chloride solution (10). The value 60×10^{-6} c.g.s., e.m.u. was taken as the temperature-independent paramagnetic contribution for copper(II).

Electronic Spectra

Diffuse reflectance spectra on powdered samples were obtained using a Bausch and Lomb Spectronic 600 spectrophotometer.

Results and Discussion

Magnetic Studies on Copper(II) p-Chlorobenzoate Derivatives

Magnetic-susceptibility data on all of the samples studied are given in Tables I and II. The magnetic susceptibility of bispyridine copper(II) *p*-chlorobenzoate obeys the Curie–Weiss law, $\chi'_M = C/(T - \Theta) + N\alpha$ with $C = 0.4314$ and $\Theta = -10.6°$. It is possible that the compound has a monomeric structure with the carboxylate groups acting as chelating ligands. However, as Martin and Waterman point out

TABLE II

Cryomagnetic data

$Cu(m\text{-}ClC_6H_4CO_2)_2\cdot py_2$		$Cu(p\text{-}ClC_6H_4CO_2)\cdot py_2$	
T (°K)	$10^6\chi'_M$	T (°K)	$10^6\chi'_M$
297	1475	295	1459
283	1507	288	1497
267	1598	276	1550
249	1705	260	1641
232	1801	242	1774
212	1950	225	1886
191	2147	206	2051
169	2504	187	2227
150	2803	166	2600
129	3150	152	2814
108	3288	135	3102
91	4056	113	3464
		100	3741
		83	4419

Can. J. Chem. Downloaded from www.nrcresearchpress.com by 210.87.254.40 on 09/05/12
For personal use only.

Can. J. Chem. Downloaded from www.nrcresearchpress.com by 210.87.254.40 on 09/05/12
For personal use only.

TABLE II (*Continued*)

$Cu(m\text{-}ClC_6H_4CO_2)_2\cdot py_{0.5}$		$Cu(p\text{-}ClC_6H_4CO_2)_2\cdot py_{0.5}$	
T (°K)	$10^6\chi'_M$	T (°K)	$10^6\chi'_M$
348	904	345	954
332	933	329	1008
320	942	315	1025
304	971	297	1049
295	962	288	1041
284	950	280	1033
270	962	274	1045
258	954	265	1049
246	942	251	1045
233	942	239	1062
222	925	224	1049
196	867	215	1062
178	821	211	1054
168	759	199	1045
159	689	196	1041
139	613	181	1008
126	530	164	946
115	458	154	892
101	419	142	842
84	332	129	776
		119	738
		107	676
		86	565
		77	455

$Cu(m\text{-}ClC_6H_4CO_2)_2\cdot py_{0.8}$		$Cu(p\text{-}ClC_6H_4CO_2)_2\cdot py_{0.8}$	
T (°K)	$10^6\chi'_M$	T (°K)	$10^6\chi'_M$
314	888	297	953
305	892	291	953
298	901	277	958
296	927	263	958
293	910	246	945
277	901	229	936
262	901	214	910
251	888	199	888
236	870	179	826
222	857	163	748
208	826	148	664
193	778	131	569
175	717	109	452
161	631	92	297
145	540	77	267
129	432		
106	331		
93	191		

$Cu(p\text{-}ClC_6H_4CO_2)_2\cdot py_{1.2}$		
T (°K)	$10^6\chi'_M$	$10^6\chi'_M$*
324	960	863
312	984	880
300	993	879
288	1012	888
272	1026	885
255	1050	893
236	1064	878
218	1083	866
198	1073	809
179	1064	745
158	1059	671
140	1045	576
120	1031	449
98	1092	358
77	1200	253

TABLE II (*Concluded*)

$Cu(m\text{-}ClC_6H_4CO_2)_2$		$Cu(p\text{-}ClC_6H_4CO_2)_2$	
T (°K)	$10^6\chi'_M$	T (°K)	$10^6\chi'_M$
296	1259	293	963
289	1274	283	967
276	1308	269	974
263	1353	256	978
250	1387	241	986
237	1432	226	1001
223	1477	213	1008
211	1526	195	1019
194	1574	163	1019
176	1624	150	993
161	1671	133	971
144	1712	112	918
125	1730	93	896
108	1717	79	787
98	1698		
88	1638		
81	1612		

(4), the formation of a four-membered chelate ring is structurally unfavorable and as a result a polymeric structure in which each carboxylate group forms a bridge between two copper atoms (as for example in copper(II) formate tetrahydrate (11)) seems more favorable. The small negative Weiss constant which is observed could be due to weak antiferromagnetic coupling between adjacent copper atoms, occurring via the bridging carboxylate groups. However, such small Weiss constants have questionable significance.

The susceptibility–temperature behavior of $Cu(p\text{-}ClC_6H_4CO_2)_2(C_5H_5N)_{1.2}$ exhibits both a maximum and a minimum over the range studied, typical behavior for a mixture of two magnetically distinct forms (5). It seems likely that this sample is a 20/80 mixture of the bispyridine adduct and the monopyridine adduct of copper(II) *p*-chlorobenzoate. From a knowledge of the magnetic behavior of the bispyridine derivative it is possible to subtract its contribution from the results for the compound where x is 1.2 and so calculate the molar susceptibility contribution from the monopyridine adduct. This has been done and the results are tabulated under the column headed χ'^{*}_M in Table II and plotted in Fig. 1. These χ'^{*}_M results for the monopyridine derivative agree with eq. [1] with $g = 2.185$ and $2J = 300\ cm^{-1}$. The theoretical curve is shown in the figure and the agreement between experiment and theory supports the formulation of the monopyridine derivative as a binuclear molecule.

From the magnetic-susceptibility data it is clear that for values of x equal to unity or less

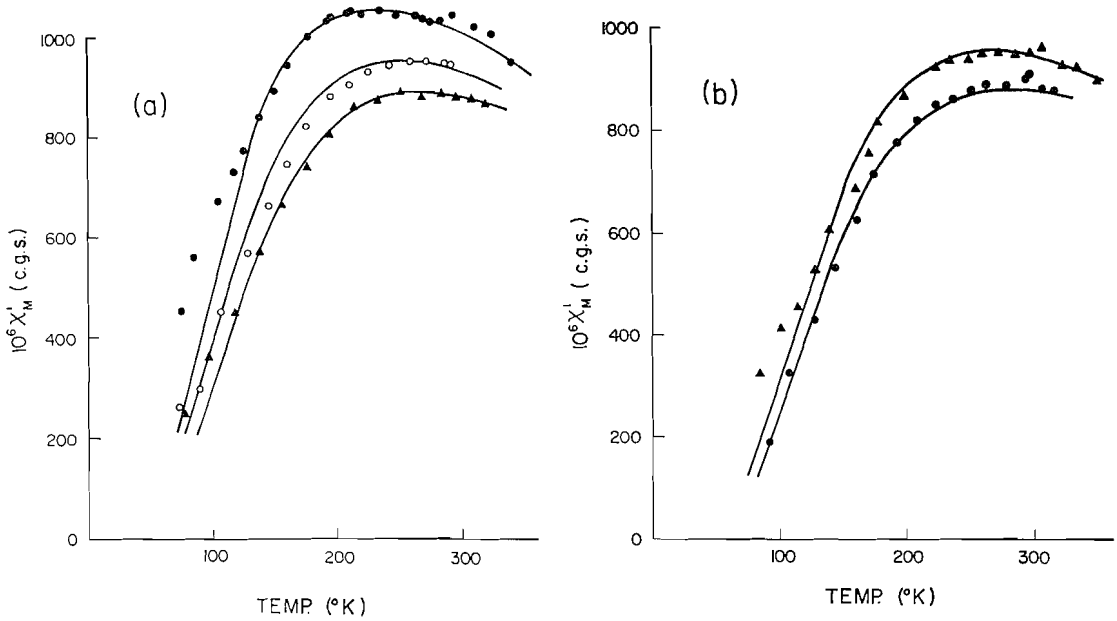

FIG. 1. Observed and calculated χ'_M vs. T curves. (*a*) $Cu(p\text{-}ClC_6H_4CO_2)_2(C_5H_5N)_x$: (●) $x = 0.5$; (○) $x = 0.8$; (▲) $x = 1$ (see text). The solid lines are calculated curves. (*b*) $Cu(m\text{-}ClC_6H_4CO_2)_2(C_5H_5N)_x$: (▲) $x = 0.5$; (●) $x = 0.8$. The solid lines are calculated curves.

the magnitude of the magnetic interaction decreases as x decreases. It is difficult to be certain of the composition of the sample, $Cu(p\text{-}ClC_6H_4CO_2)_2(C_5H_5N)_{0.5}$. The magnetic properties are not consistent with it being a 50/50 mixture of the monopyridine derivative and copper(II) *p*-chlorobenzoate and we suggest that this sample is largely in the form of the hemipyridine derivative with a structure analogous to that of the monopyridine adduct modified, however, in that only one copper atom of the dimeric unit has a pyridine molecule bonded to it. This conclusion is supported by the agreement between the experimental results and the theoretical curve calculated using eq. [1] with $g = 2.21$ and $2J = 225\ cm^{-1}$ (see Fig. 1). It is possible, however, that part of this sample is in the form of the 50/50 mixture mentioned above. The sample $Cu(p\text{-}ClC_6H_4CO_2)_2(C_5H_5N)_{0.8}$ exhibits magnetic properties intermediate between those of the hemipyridine and monopyridine derivatives and is probably a 40/60 mixture of these. The agreement between the experimental susceptibility values for this sample and the middle curve in Fig. 1, calculated from a 40/60 mixture of the theoretical curves for the hemipyridine and monopyridine derivatives, is good.

Although the magnetic susceptibility – temperature behavior of copper(II) *p*-chlorobenzoate exhibits a maximum, it was not possible to fit the results for this compound to eq. [1]. It seems likely that a mixture of dimeric and more highly polymeric species are present here, a result not too surprising in view of earlier work on this compound (5).

In summary, bispyridine copper(II) *p*-chlorobenzoate is a magnetically dilute compound which probably has a highly polymeric structure with two pyridine molecules bonded to each copper atom and carboxylate groups bridging the copper atoms. As pyridine molecules are removed to give samples in which the ratio of pyridine to copper is greater than 1, appropriate mixtures of the bispyridine adduct and the binuclear monopyridine adduct are obtained. The binuclear structure is maintained at ratios of pyridine to copper down to 0.5 (the hemipyridine adduct having pyridine molecules bonded to one copper atom only of the dimeric unit). Complete removal of pyridine molecules results in at

Can. J. Chem. Downloaded from www.nrcresearchpress.com by 210.87.254.40 on 09/05/12
For personal use only.

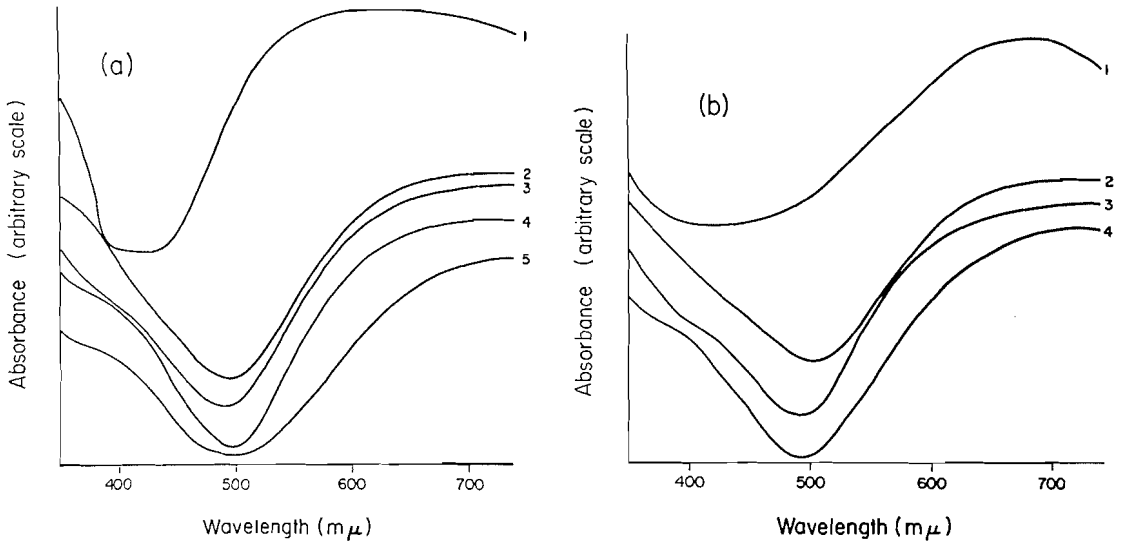

FIG. 2. Diffuse-reflectance spectra. (*a*) $Cu(p\text{-}ClC_6H_4CO_2)_2(C_5H_5N)_x$: (1) $x = 2$; (2) $x = 0$; (3) $x = 0.5$; (4) $x = 0.8$; (5) $x = 1.2$. (*b*) $Cu(m\text{-}ClC_6H_4CO_2)_2(C_5H_5N)_x$: (1) $x = 2$; (2) $x = 0$; (3) $x = 0.5$; (4) $x = 0.8$.

least partial breakdown of the binuclear structure. This latter result demonstrates the ability of pyridine molecules to "condition" copper(II) *p*-chlorobenzoate to a binuclear structure. Attention should be drawn to the fact that the terminal pyridine molecules affect the singlet–triplet energy separation; the value of $2J$ is greater for the monopyridine derivative than for the hemipyridine derivative.

Magnetic Studies on Copper(II) m-Chlorobenzoate Derivatives

The results for this group of compounds parallel very closely those outlined above for the *p*-chloro derivatives. Bispyridine copper(II) *m*-chlorobenzoate obeys the Curie–Weiss law with $C = 0.4308$ and $\Theta = -12°$. The hemipyridine adduct, $Cu(m\text{-}ClC_6H_4CO_2)_2(C_5H_5N)_{0.5}$, exhibits magnetic properties typical of a binuclear molecule. Good agreement is obtained between experiment and theory (eq. [1]) for values of $g = 2.25$ and $2J = 294$ cm^{-1} (see Fig. 1). Again it is reasonable to assume that the sample of composition $Cu(m\text{-}ClC_6H_4CO_2)_2(C_5H_5N)_{0.8}$ is a 40/60 mixture of binuclear hemipyridine and monopyridine derivatives. By arbitrarily choosing values of g and $2J$ for the monopyridine derivative it is possible to obtain theoretical susceptibility versus temperature curves for this compound and then calculate theoretical curves for the sample of composition $x = 0.8$ as described above. The best agreement between experiment and theory (Fig. 1) was obtained with $g = 2.21$ and $2J = 327$ cm^{-1} for the monopyridine derivative.

The susceptibility–temperature behavior of copper(II) *m*-chlorobenzoate shows a single maximum around 120 °K. A comparison of the magnetic properties of this compound with the properties of an authentic sample of binuclear copper(II) *m*-chlorobenzoate (reported previously (5)) shows that the antiferromagnetic interaction in the latter compound is considerably greater. We conclude that the compound prepared in this work is not binuclear but probably has a highly polymeric structure with magnetic interaction occurring via bridging carboxylate groups.

A consideration of the curves in Fig. 1 shows that at low temperatures the experimental susceptibilities are often higher than those predicted by theory. Similar discrepancies were observed in the earlier work on copper(II) carboxylates (5) and could be explained by incomplete conversion of, for example, the monopyridine derivative, into the binuclear structure. It has been suggested (12) that heating samples of copper(II) carboxylates as we have done in this

Can. J. Chem. Downloaded from www.nrcresearchpress.com by 210.87.254.40 on 09/05/12
For personal use only.

work will lead to decarboxylation with the formation of CuO and the loss of volatile organic decomposition products. The presence of trace amounts of CuO could account for the observed discrepancies; however, our analytical results show that if such decomposition is occurring it must be very slight.

Electronic Spectra

The diffuse reflectance spectra of all the samples studied in this work are given in Fig. 2. The spectra of binuclear copper(II) carboxylates are characterized by two bands in the visible region: about 7000 Å (band I) and about 3750 Å (band II). Of the compounds studied, all of the pyridine derivatives, except the bispyridine adducts, have bands I and II. It is difficult to say whether band II is present in the spectra of copper(II) *p*-chlorobenzoate and copper(II) *m*-chlorobenzoate, as they could be of relatively low intensity and hidden under the tail of the high energy charge-transfer band.

Acknowledgment

Financial support of this work by the National Research Council of Canada is gratefully acknowledged.

1. M. KATO, H. B. JONASSEN, and J. C. FANNING. Chem. Rev. **64**, 99 (1964).
2. J. N. VAN NIERKIRK and R. F. L. SCHOENING. Acta Cryst. **6**, 227 (1953).
3. B. N. FIGGIS and R. L. MARTIN. J. Chem. Soc. 3837 (1956).
4. R. L. MARTIN and H. WATERMAN. J. Chem. Soc. 2545 (1957).
5. J. LEWIS, Y. C. LIN, L. K. ROYSTON, and R. C. THOMPSON. J. Chem. Soc. 6464 (1965).
6. E. KOKOT and R. L. MARTIN. Inorg. Chem. **3**, 1306 (1964).
7. J. LEWIS and F. MABBS. J. Chem. Soc. 3894 (1965).
8. W. E. HATFIELD, C. S. FOUNTAIN, and R. WHYMAN. Inorg. Chem. **5**, 1855 (1966).
9. H. C. CLARK and R. J. O'BRIEN. Can. J. Chem. **39**, 1030 (1961).
10. H. R. NETTLETON and S. SUGDEN. Proc. Roy. Soc. London, Ser. A, **173**, 313 (1939).
11. R. KIRIYAMA, H. IBAMOTO, and K. MATSUO. Acta Cryst. **7**, 482 (1954).
12. C. S. FOUNTAIN and W. E. HATFIELD. Inorg. Chem. **4**, 1368 (1965).

Can. J. Chem. Downloaded from www.nrcresearchpress.com by 210.87.254.40 on 09/05/12
For personal use only.

Can. J. Chem. Downloaded from www.nrcresearchpress.com by 210.87.254.42 on 09/05/12
For personal use only.

Effect of changing pH upon the kinetic ^{13}C-isotope effect in the decarboxylation of 4-methoxyanthranilic acid

G. E. Dunn and John Buccini
Chemistry Department, University of Manitoba, Winnipeg, Manitoba

Received April 25, 1967

The ^{13}C-carboxyl kinetic isotope effect on decarboxylation of 4-methoxyanthranilic acid has been determined in aqueous solutions of ionic strength 0.50 at 60 °C. The isotope effect, $100(k_{12}/k_{13} - 1)$, is found to be 4.2% at pH −0.3, 1.4% at pH 1.3, and zero at pH 4.0. This information makes it possible to decide between two mechanisms previously proposed in favor of the one in which both anion and neutral acid are protonated at carbon-1 of the aromatic ring but only the protonated anion decarboxylates.

Canadian Journal of Chemistry, **46**, 563 (1968)

Kinetic studies of the decarboxylation of aromatic aminoacids are complicated by the existence of the acid in four forms all in equilibrium with hydrogen ion (1). These are shown below with hydrogen ions omitted.

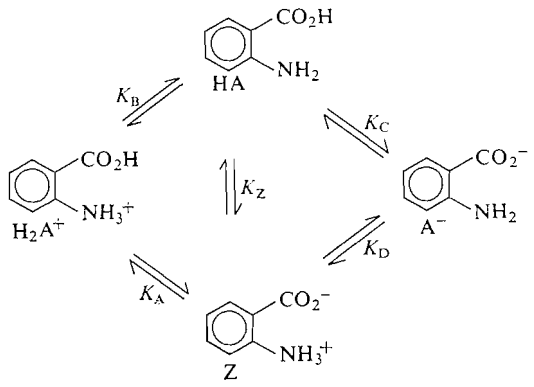

The concentrations of the various species present at equilibrium depend upon the acidity of the solution, except for the ratio $[Z]/[HA] = K_Z$ which varies with ionic strength but not with pH. Consequently, for most purposes the ampholyte may be treated as a single species $[N] = [Z] + [HA]$. The equilibrium constants which relate the four species are difficult to evaluate (2) but they can be related to the measurable ionization constants, K_1 and K_2, of the equilibria

$$H_2A^+ \overset{K_1}{\rightleftharpoons} H^+ + N$$

$$N \overset{K_2}{\rightleftharpoons} H^+ + A^-,$$

by the equations

$$K_1 = K_A + K_B$$

$$1/K_2 = 1/K_C + 1/K_D.$$

In a solution of concentration [C] with respect to total aminoacid, $[H_2A^+]$ and $[A^-]$ approach [C] at low and high pH respectively, and it is easily shown (1) that [N] is a maximum at the isoelectric point, $pH = (pK_1 + pK_2)/2$.

In principle, any of the four forms of aminoacid could decarboxylate, and the rate of decarboxylation should be greatest at the pH where the concentration of that form is greatest. However, it has been shown in a preceding publication (3) that the rate of decarboxylation of 4-methoxyanthranilic acid at 60 °C and ionic strength 0.50 is a maximum at pH = 1.38, whereas the isoelectric pH under these conditions is 3.32.

It was shown (3) that this behavior can be accounted for by postulating that the anion, A^-, and the neutral species, HA and (or) Z, are both protonated to form transient intermediates, HA* and H_2A^*, which are in equilibrium with each other, and that these intermediates may either deprotonate to regenerate starting materials or decarboxylate to form products. This is the first demonstration by a kinetic method that acid-catalyzed decarboxylation is not a concerted process. It had previously been demonstrated by an ingenious isotopic method for 2,4-dihydroxybenzoic acid by Lynn and Bourns (5). The mechanism was formulated in ref. 3 using both HA and Z as neutral species but either may be omitted without changing the form of the kinetic expression, so in eq. [1] it has been written using only HA.

Assuming that the equilibrium concentration of intermediates in eq. [1] maintains a steady state during the bulk of the decarboxylation, the following rate equation (eq. [2]) is obtained.

[1]

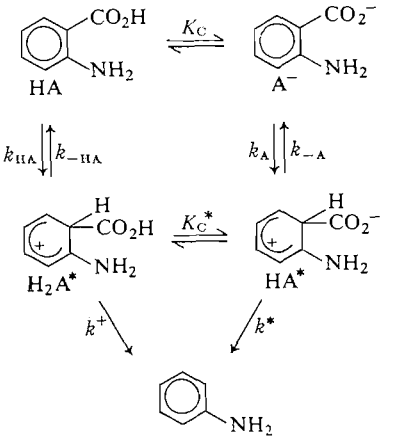

$$[2]\quad \frac{-d[C]}{dt} = k[C] = [N] \times \frac{(k_A K_2 + [H^+]k_{HA}K_B/K_1)(k^* + [H^+]k^+/K_{C^*})}{k^* + k_{-A} + [H^+](k^+ + k_{-HA})/K_{C^*}}$$

This is eq. [8] of ref. 3 with the terms referring to Z omitted. It was shown (3) that the rates of decarboxylation could be fitted to this equation if either (but not both) of the terms containing $[H^+]$ is omitted from the numerator, which is equivalent to assuming that either HA is not protonated at a significant rate (mechanism I) or that after protonation it does not decarboxylate (mechanism II).

It was also shown (3) that mechanism I requires a ^{13}C-carboxyl kinetic isotope effect at all pH's but mechanism II need not have one except at very low pH. It was therefore the object of the present investigation to study the ^{13}C-carboxyl isotope effect in the decarboxylation of 4-methoxyanthranilic acid as a function of pH.

Experimental

4-Methoxyanthranilic acid was prepared and decarboxylated at 60° and ionic strength 0.50 as previously described (3), except that the carbon dioxide produced in the reaction was swept from the reaction vessel by a stream of nitrogen gas and collected in a liquid nitrogen trap. It was then transferred to a high-vacuum line, sublimed 10 times from liquid nitrogen, and its volume, temperature, and pressure were measured. The fraction of acid reacted, f, was calculated from the weight of 4-methoxyanthranilic acid used and the volume of gas collected. Mass-spectrometric analyses of the $^{13}CO_2/^{12}CO_2$ ratio were performed by Mr. Jan Monster of the Chemistry Department, McMaster University. The isotope effect, $100((k_{12}/k_{13}) - 1)$, was calculated (8) from the equation

$$\frac{k_{12}}{k_{13}} = \frac{\log(1-f)}{\log\left(1 - f\frac{R_f}{R_0}\right)},$$

where R_f is the ratio $^{13}CO_2/^{12}CO_2$ when the fraction of acid decarboxylated is f, and R_0 is the same ratio when decarboxylation is complete. The results are shown in Table I.

Discussion

Table I shows clearly that there is a ^{13}C-isotope effect in the decarboxylation at pH −0.3 and that it decreases to the limit of reproducibility of the method at pH 4.0. The decarboxylation therefore can not take place by mechanism I. This leaves mechanism II as the most probable one.

However, a referee has suggested that the kinetic data of ref. 3 might in principle be fitted to eq. [2] without dropping any terms; that is, that there is no real distinction between mechanisms I and II. This approach may be examined as follows. Equation [3] of ref. 3 is

$$[3]\quad [N] = \frac{[C]}{[H^+]/K_1 + 1 + K_2/[H^+]},$$

but since $K_2 = 2.27 \times 10^{-5}$ (3) the last term in the denominator is negligible throughout the pH range 0–4 in which rate measurements were made. Hence, eq. [3] becomes

$$[N] = \frac{K_1[C]}{K_1 + [H^+]}$$

and eq. [2] can be rewritten

$$[4]\quad k = \frac{k_A K_1 K_2 + k_{HA}K_B[H^+]}{K_1 + [H^+]} \times \frac{k^*K_{C^*} + k^+[H^+]}{(k^* + k_{-A})K_{C^*} + (k^+ + k_{-HA})[H^+]}.$$

The two fractions separated by the multiplication sign in eq. [4] are of the same form with respect to $[H^+]$; as $[H^+]$ increases, the first fraction increases (or decreases) monotonically from $k_A K_2$ to $k_{HA}K_B$, and the second increases (or decreases) from $k^*/(k^* + k_{-A})$ to $k^+/(k^+ + k_{-HA})$. Hence, if one fraction increases with increasing $[H^+]$ and the other decreases, k could have the maximum at intermediate $[H^+]$ that was observed in the data.

k^* and k^+ are the rate constants for decarboxylation steps, so the second fraction would govern the ^{13}C-carboxyl isotope effect. In

Can. J. Chem. Downloaded from www.nrcresearchpress.com by 210.87.254.42 on 09/05/12
For personal use only.

TABLE I

Decarboxylation of 4-methoxyanthranilic acid at 60 °C and $\mu = 0.50$

Buffer	Vol. (ml)	pH	Acid (mg)	Reaction time (min)	f	R	$100(\frac{k_{12}}{k_{13}} - 1)$
HCl–KCl	100	1.3	37.78	2250	0.9792	0.010825	
HCl–KCl	100	1.3	40.51	2355	0.9806	0.010825	
2 *N* HCl	200	−0.3	349.3	80	0.0801	0.010412	4.14
2 *N* HCl	200	−0.3	350.2	87	0.09105	0.010409	4.20
HCl–KCl	200	1.3	350.1	20	0.1197	0.010680	1.45
HCl–KCl	200	1.3	350.2	18	0.1008	0.010694	1.27
HCl–KCl	225	1.3	354.2	17	0.09136	0.010672	1.49
Formate	400	4.0	322.4	85	0.08165	0.010804	0.19
Formate	425	4.0	318.5	95	0.08453	0.010798	0.24

order to have no isotope effect at low $[H^+]$ this second fraction must disappear, which is possible only if $k^* > k_{-A}$; that is, if the protonated anion, HA*, decarboxylates much faster than it deprotonates. If the second fraction disappears at low $[H^+]$ then the first fraction must govern the rate at low $[H^+]$ according to

$$[5] \qquad k = \frac{k_A K_1 K_2 + k_{HA} K_B [H^+]}{K_1 + [H^+]},$$

and the second fraction must govern the rate at high $[H^+]$ according to

$$[6] \quad k = k_{HA} K_B \frac{k^* K_{C^*} + k^+ [H^+]}{k^* K_{C^*} + (k^+ + k_{-HA})[H^+]}.$$

Figure 3, ref. 3, shows that the rate data at low $[H^+]$ do indeed fit eq. [5] and from the slope and intercept of the plot it follows that $k_A = 1.05\ s^{-1}$ and $k_{HA} K_B = 2.63 \times 10^{-4}\ s^{-1}$. Since K_B is of the order of 10^{-2} it follows that this mechanism requires the rate constant for ring protonation of the anion, A^-, to be about 100 times greater than that for protonation of the neutral acid, HA (or Z).

Since there is a large kinetic isotope effect at high $[H^+]$, eq. [6], which governs in this region, shows that k_{-HA} must be much larger than k^+; that is, that the protonated acid H_2A^* deprotonates much faster than it decarboxylates. In the region of hydrogen ion concentration where $k^+[H^+]$ is of the same order of magnitude as $k^* K_{C^*}$, eq. [6] becomes

$$[7] \qquad k = k_{HA} K_B \left(\frac{k^* K_{C^*}}{k_{-HA}[H^+]} + \frac{k^+}{k_{-HA}} \right)$$

and at $[H^+]$ where $k_{-HA}[H^+]$ approaches $k^* K_{C^*}$, so that $k^+[H^+]$ is negligible, eq. [6] becomes

$$[8] \qquad \frac{1}{K} = \frac{1}{k_{HA} K_B} + \frac{k_{-HA}[H^+]}{k_{HA} K_B k^* K_{C^*}}.$$

Figure 1 shows the rate data in the pH range 1 to −0.3 plotted according to eqs. [7] and [8] and it is clear that the latter is the better fit. The intercept gives $k_{HA} K_B = 2.7 \times 10^{-4}\ s^{-1}$, in excellent agreement with the value obtained from eq. [5] at low $[H^+]$, and the slope gives $k_{-HA}/k^* K_{C^*} = 0.78$. It follows that, in the pH range of this study, decarboxylation of the protonated acid, H_2A^*, does not compete detectably with decarboxylation of the protonated anion, HA*. That is, the reaction follows mechanism II.

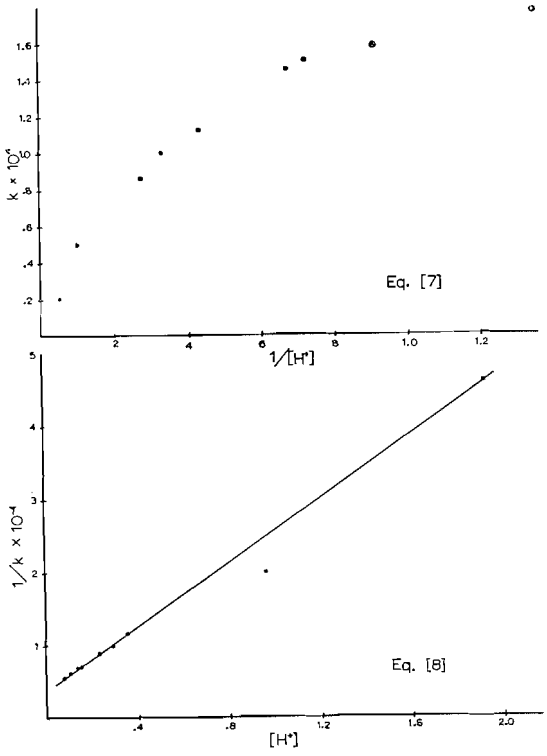

FIG. 1. Test of eq. [7] and eq. [8].

Can. J. Chem. Downloaded from www.nrcresearchpress.com by 210.87.254.42 on 09/05/12
For personal use only.

There are several interesting points which arise in connection with this conclusion. First, the results obtained with 4-methoxyanthranilic acid should be compared with those reported by Stevens, Pepper, and Lounsbury (4) for decarboxylation of anthranilic acid. They found very small ^{13}C-isotope effects in sulfuric acid concentrations up to 1 *N*, which shows that the ^{13}C-isotope effect becomes apparent at lower acidities for 4-methoxyanthranilic acid than for anthranilic acid itself. This is perhaps not surprising, since the rates of decarboxylation of anthranilic acids have been shown to be sensitive to substituent, pH, and ionic strength (3).

Second, a pH dependence of ^{13}C-carboxyl kinetic isotope effect similar to the one reported here has been observed by Bourns in the decarboxylations of 2,4-dihydroxybenzoic (6) and 2,4,6-trihydroxybenzoic acids (7). For these acids there was an isotope effect of about 4% in 8 *M* perchloric acid but none in perchloric acid solutions 0.1 *M* or less. This suggests that the mechanism of acid-catalyzed decarboxylation of other aromatic acids may be similar to that of 4-methoxyanthranilic acid.

Finally, it is interesting to note that decarboxylation of 4-methoxyanthranilic acid occurs only from that intermediate in which the carboxyl group is present in its anionic form. This is commonly observed in decarboxylations of those acids which contain electron-withdrawing groups (9), but the present report is the first in which it has been demonstrated for acid-catalyzed decarboxylation. Evidently the $-CO_2^-$ group has a greater advantage over $-CO_2H$ as a leaving group than has previously been supposed (6, 10).

Acknowledgments

The authors are grateful to the National Research Council of Canada for financial support of this project, to Shell Oil (Canada) for a fellowship, to Mr. Jan Monster for the mass-spectrometric analyses, and especially to Dr. A. N. Bourns for discussions and for communicating his results in advance of publication.

1. N. Bjerrum. Z. Physik. Chem. Leipzig, **104**, 147 (1923).
2. P. Leggate and G. E. Dunn. Can. J. Chem. **43**, 1158 (1965).
3. G. E. Dunn, P. Leggate, and I. E. Scheffler. Can. J. Chem. **43**, 3080 (1965).
4. W. H. Stevens, J. M. Pepper, and M. Lounsbury. Can. J. Chem. **30**, 529 (1952).
5. K. R. Lynn and A. N. Bourns. Chem. Ind. London, 782 (1963).
6. A. N. Bourns. Trans. Roy. Soc. Can. Sect. III, [4], **2**, 277 (1964).
7. A. N. Bourns. *Quoted in* A. V. Willi. Saeurekatalytische Reactionen der organischen Chemie, Kinetik und Mechanismen. F. Vieweg, Brunswick, Germany. 1965.
8. J. Bigeleisen and M. Wolfsberg. Advan. Chem. Phys. **1**, 15 (1958).
9. B. R. Brown. Quart. Rev. London, **5**, 131 (1951).
10. A. V. Willi and J. F. Stocker. Helv. Chim. Acta, **37**, 1113 (1954). A. V. Willi. Helv. Chim. Acta, **40**, 1053 (1957); Trans. Faraday Soc. **55**, 433 (1959); Z. Physik. Chem. Frankfurt, **27**, 221 (1961).

Can. J. Chem. Downloaded from www.nrcresearchpress.com by 210.87.254.42 on 09/05/12
For personal use only.

Can. J. Chem. Downloaded from www.nrcresearchpress.com by 210.87.254.42 on 09/05/12
For personal use only.

Infrared study of the self-association of water dissolved in 1,2-dichloroethane

C. JOLICOEUR AND A. CABANA
Département de Chimie, Université de Sherbrooke, Sherbrooke, Québec

Received April 21, 1967

The infrared spectra, in the 3 micron region, of H_2O or HDO dissolved in 1,2-dichloroethane are presented. Self-association of the solute molecules is revealed by the appearance of a shoulder on the low frequency side of the OH stretching bands of monomeric H_2O or HDO. From the linear increase of the intensity of the shoulder with the third power of the solute concentration, it is inferred that trimers constitute the main polymeric species present in these solutions. The small frequency shifts of the OH stretching mode of trimeric water favors a cyclic rather than an open-chain structure. The observation of a single band for the trimer correlates with this last assertion.

Les spectres infrarouges de H_2O ou HDO, en solution dans le 1,2-dichloroéthane, sont étudiés dans la région de 3 microns. L'épaulement qui apparaît sur les bandes de vibration de valence OH des monomères H_2O ou HDO révèle l'association des molécules du soluté. L'augmentation linéaire de l'intensité de l'épaulement selon le cube de la concentration en soluté nous permet de conclure que les espèces polymériques présentes en solution sont surtout des trimères. Les faibles déplacements de fréquence des modes d'élongation OH du trimère indiquent une structure cyclique plutôt qu'une chaîne linéaire. L'observation d'une seule bande pour le trimère vient confirmer cette dernière suggestion.

Canadian Journal of Chemistry, **46**, 567 (1968)

Introduction

Recent investigations of the relationship between the activity and the solubility of water in 1,2-dichloroethane (1, 2) provided strong evidence for the self-association of water in this solvent. Johnson *et al.* (1) could account for the deviations from Henry's law occurring at the higher water activities by assuming either a monomer–trimer or monomer–tetramer equilibrium; their solubility data could not be fitted on the assumption that dimers were the main polymeric species. Lin *et al.* (3) have shown that the concentration dependence of the proton chemical shift of water in 1,2-dichloroethane is consistent with the monomer – cyclic trimer model. More recently, from isopiestic measurements similar to those reported in ref. 1, Masterton and Gendrano (2) concluded that a monomer–dimer or a monomer–trimer equilibrium could equally well be responsible for their findings. The vibrational frequencies and the integrated intensities of the water bands are very sensitive to the size and structure of the polymeric species involved. Therefore an investigation of these physical properties will be undertaken in order to obtain more information on the state of aggregation of H_2O or HDO dissolved in 1,2-dichloroethane.

Experimental

The spectra were recorded with a Perkin–Elmer 125 spectrometer. Factory calibrations were "spot checked" against vibration–rotation lines of gases using I.U.P.A.C. (4) standards. The spectral slit widths were smaller than 2 cm^{-1} and the frequency accuracy, limited mainly by the broadness of the observed peaks, was ± 3 cm^{-1}; side bands have an approximate uncertainty of ± 5 cm^{-1}. Sapphire was used as window material; it is highly insoluble in water and perfectly transparent in the infrared region investigated. Compensation for absorption by the solvent is necessary, since 1,2-dichloroethane absorbs to an appreciable extent. Furthermore, when concentrated water solutions are studied, the quantity of solvent in the sample cell is less than that in the reference cell since both cells have an equal thickness. To overcome this problem, carbon tetrachloride was added to the reference cell until good compensation was achieved. 1,2-$C_2H_4Cl_2$ was carefully purified and dried over a column of activated alumina until the addition of D_2O to one of two matched 1 mm thick samples of solvent caused no OH stretching absorption. Doubly distilled H_2O and D_2O from Merck, Sharp and Dohme Canada Ltd. were used. The solutions were prepared in 50 ml calibrated flasks from dry 1,2-$C_2H_4Cl_2$. The water content was adjusted with a micrometer type syringe graduated to 0.1 μl; thus the concentrations are reliable to better than 1%. The manipulations required to dry the solvent and to prepare quantitative solutions were carried out in an atmosphere of dry nitrogen. To ensure that no absorption resulted from water droplets in suspension, the most concentrated solutions studied were saturated at 25 °C and the spectra recorded at 30 °C.

Results and Discussion

Figures 1 and 2 show the OH stretching vibration bands of H_2O and HDO respectively at various concentrations in 1,2-dichloroethane. On the spectra of the most concentrated solutions, a shoulder appears on the low frequency side of the main peaks (3530 cm^{-1} for HDO and 3525 cm^{-1} for H_2O, with a ± 5 cm^{-1} uncertainty.) No other absorption is detected down

to 3200 cm^{-1}, the practical transmission limit of the solvent. The integrated intensity of the shoulder increases with concentration (Figs. 1 and 2), but decreases with temperature (Fig. 2). Both observations support the assignment of these spectral features to polymeric water species.

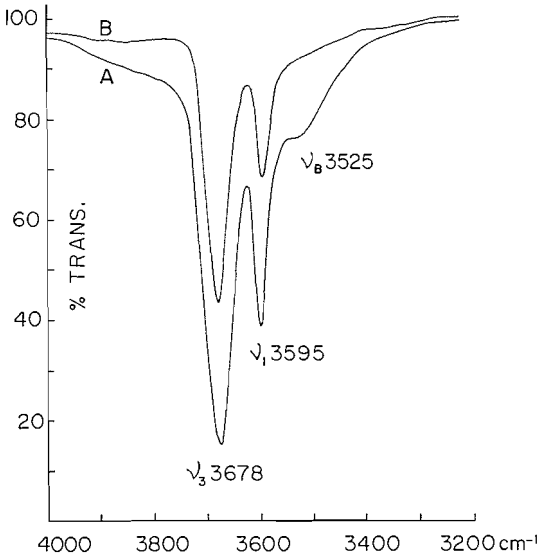

FIG. 1. Stretching vibrations of H_2O dissolved in 1,2-dichloroethane. The spectra were recorded at 30 °C with a cell thickness of 1 mm. (A) concentration 0.126 *M*, (B) concentration 0.05 *M* (υ_B refers to the bonded species).

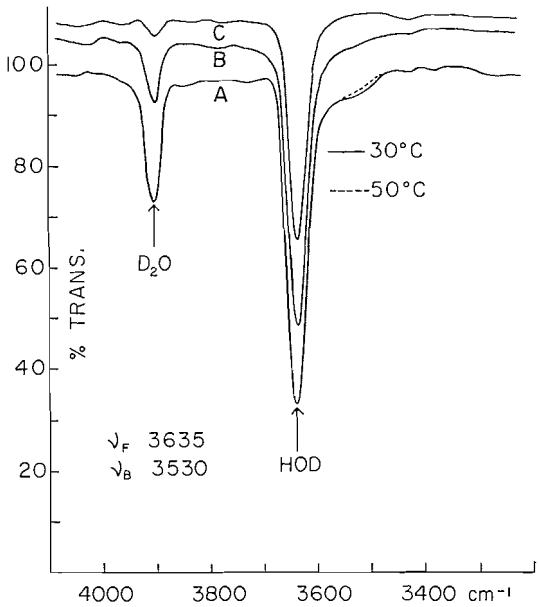

FIG. 2. The OH stretching vibration of HDO dissolved in 1,2-dichloroethane at several concentrations. The spectra were recorded at 30 °C (except 2A which was also recorded at 50 °C) with a cell thickness of 5 mm. (A) concentration 0.126 *M*, (B) concentration 0.06 *M*, (C) concentration 0.02 *M*. The water concentration quoted is the sum of the H_2O and D_2O content (95% D_2O and 5% H_2O). υ_F and υ_B refer to free and bonded species respectively.

Some information on the nature of the aggregates can be gained from the measurement of the OH frequency shifts occurring upon polymerization. However, a complete elucidation of the polymer structure requires, in addition, a quantitative investigation of the concentration dependence of the band intensities. Unfortunately, the limited solubility of water in 1,2-dichloroethane and the excessive solvent absorption does not allow sufficiently accurate intensity measurements on the HDO–1,2-$C_2H_4Cl_2$ system, where the spectra are more easily interpreted than in the H_2O–1,2-$C_2H_4Cl_2$ solutions. In spite of strong band overlapping, the effect of concentration on the polymeric H_2O band is easily followed, as can be seen from Fig. 3. After correction for the overlapping with the monomeric H_2O bands, the area under the side bands was measured. The results are plotted against second and third power of water concentration (Fig. 4). The integrated intensity of the polymeric band is seen to vary linearly with $C^3_{H_2O}$. It can easily be shown that this linear dependence on $C^3_{H_2O}$ implies that the aggregates responsible for this absorption are trimers. In the occurrence of dimers the integrated intensity would vary linearly with $C^2_{H_2O}$, contrary to what is observed (Fig. 4).

The measured OH frequency shifts occurring upon the self-association of water in 1,2-dichloroethane can be compared to those observed by Van Thiel and collaborators (5) for the polymerization of water in a solid nitrogen matrix at 20 °K. Obviously, the hydrogen bonding condition of water in the H_2O–1,2-$C_2H_4Cl_2$ liquid solution are completely different from those prevailing in the H_2O–N_2 matrix; however, the results of the matrix studies are unique in ascribing frequencies to small polymeric water units. In the latter investigation, dimers were identified with absorption bands at 3691 cm^{-1} (uncoupled free OH in the dimer) and 3546 cm^{-1}; the bands that could be assigned to trimers appeared at 3510 and 3355 cm^{-1} and

Can. J. Chem. Downloaded from www.nrcresearchpress.com by 210.87.254.42 on 09/05/12
For personal use only.

Can. J. Chem. Downloaded from www.nrcresearchpress.com by 210.87.254.42 on 09/05/12
For personal use only.

still lower frequencies were attributed to tetramers and higher polymers. Relative to monomeric water, frequency displacements were given as follows: dimers +15 and −130 cm^{-1} and trimers −166 and −311 cm^{-1}. These shifts were measured from the average of υ_1 and υ_3 (symmetric and antisymmetric stretching frequencies) of monomeric H_2O. This procedure is justified since hydrogen bonding of the H_2O molecule through one hydrogen atom partially destroys the mechanical coupling between the two OH oscillators; the stretching frequency of the uncoupled free OH should fall at a position intermediate between υ_1 and υ_3, i.e. close to the free OH frequency of HDO. For the self-association of HDO dissolved in 1,2-dichloroethane a 105 cm^{-1} shift from the free OH frequency is directly measured. Under similar conditions H_2O exhibits a 110 cm^{-1} shift from the uncoupled free OH frequency. These shifts, compared with those reported in the low temperature investigation of Van Thiel *et al.* (5), exclude the presence of large aggregates as well as that of tetramers. Trimers having a structure similar to those existing in a solid nitrogen matrix (5) may also be ruled out.

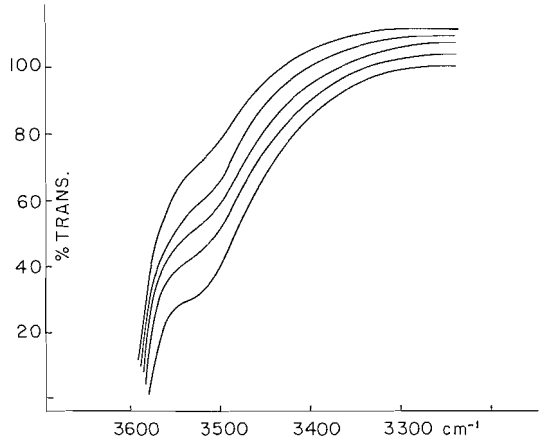

FIG. 3. Polymeric absorption band of H_2O dissolved in 1,2-dichloroethane. The spectra were recorded at 30 °C with a cell thickness of 5 mm. (A) concentration 0.126 *M*, (B) concentration 0.110 *M*, (C) concentration 0.100 *M*, (D) concentration 0.085 *M*, (E) concentration 0.070 *M*.

From the shift comparison alone, one may propose that the species yielding the shoulder in 1,2-dichloroethane are dimers, but the results of our intensity measurements preclude this assertion. However, the observation of small shifts can be reconciled with our intensity data if a cyclic trimer is postulated. In cyclic structures small shifts occur because of the nonlinearity of the hydrogen bonds involved.

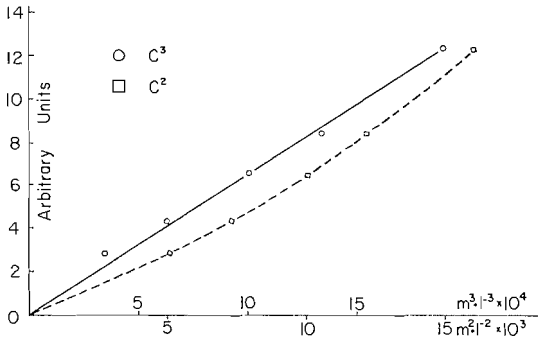

FIG. 4. Integrated intensities (*A*) of the polymeric water band vs. concentration. Full line curve: *A* vs. the third power of the water concentration. Dashed line curve: *A* vs. the square of the water concentration.

Additional support for the cyclic structure may be gained from a discussion of the expected number of bands in cyclic and linear trimers. In the first instance two bands may be found: one for the uncoupled free OH (type I band, assigned to the OH in which the hydrogen atom is not engaged in hydrogen bonding) and one for the OH whose hydrogen is bonded (type II). The type I band should fall at an intermediate frequency between υ_3 and υ_1 of monomeric water. This band is not seen in the present study because of severe overlapping with the bands of monomeric water; thus the only observed feature corresponds to the type II band. For open-chain trimers three bands are possible, two of which should fall outside the free OH features and should be observed, i.e. two non-equivalent type II bands. The single type II band found in the present study thus points to a cyclic structure, in agreement with the conclusions drawn from the small observed shifts.

Conclusion

The deduction that the aggregates of water dissolved in 1,2-dichloroethane are cyclic trimers is in complete agreement with independent conclusions drawn from n.m.r. spectra (3). In a solid nitrogen matrix the trimers take up different geometries (5). Additional studies on small polymeric water species are certainly desirable

since they should help in the elucidation of the structure of liquid water.

Acknowledgment

The authors gratefully acknowledge financial support from the National Research Council of Canada.

1. J. R. JOHNSON, S. D. CHRISTIAN, and H. E. AFFSPRUNG. J. Chem. Soc. 77 (1966).
2. W. L. MASTERTON and M. G. GENDRANO. J. Phys. Chem. **70**, 2895 (1966).
3. T. F. LIN, S. D. CHRISTIAN, and H. E. AFFSPRUNG. J. Phys. Chem. **69**, 2980 (1965).
4. INTERNATIONAL UNION OF PURE AND APPLIED CHEMISTRY. Tables for the calibration of infrared spectrometers. Butterworths Scientific Publications, London. 1960.
5. M. VAN THIEL, E. D. BECKER, and G. C. PIMENTEL. J. Chem. Phys. **27**, 486 (1957).

Can. J. Chem. Downloaded from www.nrcresearchpress.com by 210.87.254.42 on 09/05/12
For personal use only.

Can. J. Chem. Downloaded from www.nrcresearchpress.com by 210.87.254.40 on 09/05/12
For personal use only.

Kinetics and mechanism of the ethylene reduction of rhodium(III) chloride in dimethylacetamide solution

B. R. James and G. L. Rempel
Department of Chemistry, University of British Columbia, Vancouver, British Columbia

Received September 27, 1967

The kinetics of the ethylene reduction of rhodium(III) trichloride to a rhodium(I) ethylene complex in dimethylacetamide solution have been examined over a range of temperatures and of concentrations of rhodium(III), ethylene, hydrogen ion, and chloride ion. The results suggest that the reaction proceeds through an initial dissociation of a chloro rhodium(III) species. A resulting intermediate rhodium(III) ethylene complex decomposes to rhodium(I) which is stabilized by rapid reaction with further ethylene as an olefin complex.

Canadian Journal of Chemistry, **46**, 571 (1968)

Introduction

Reaction between metal ions and olefins in solution is of much current interest particularly because the complexes formed are possible intermediates in transition metal catalyzed reactions of the olefins such as hydrogenation, isomerization, and polymerization and in the oxidation of the olefin (1). Rhodium salts seem to be particularly effective for such catalytic reactions and a number of these have been studied kinetically (2). Kinetic studies of formation of the olefin complex are usually complicated by subsequent rearrangement or decomposition of the complex. Cramer (3) has reported an important paper on the rhodium trichloride catalyzed dimerization of ethylene to linear butenes in ethanolic HCl solutions; the first stage involves production of a rhodium(I) ethylene complex but the kinetics of this step were not studied. During our studies on rhodium(III) catalyzed hydrogenation of olefins in dimethylacetamide solution (4), we became involved in the reaction between rhodium trichloride and ethylene, and this paper describes results on the kinetics and mechanism of formation of a rhodium(I) ethylene complex and some observations on its catalytic properties.

Experimental and Results

The experimental procedure has been described previously (4, 5) and involves measurement of ethylene uptake at constant pressure. The solubility of ethylene in dimethylacetamide (DMA) was determined as 0.044 M atm^{-1} at 80°, Henry's law being obeyed at least up to 1 atm; the solubility was unaffected by addition of 0.05 M LiCl or $LiClO_4$ and varied little over the temperature range 70–85°. Solutions of rhodium trichloride trihydrate in DMA absorb ethylene at measurable rates from 70–85° and give uptake plots of the kind shown in Fig. 1. Ethylene consumption is practically linear for the first 1000 s and then slowly decreases with time; for the reaction shown using 0.02 M rhodium the gas consumption after 8 h corresponds to greater than a 5:1 mole ratio of C_2H_4:Rh and reaction is still proceeding slowly. The original red solution ($\lambda_{max} = 448$ mμ, $\varepsilon = 360$; $\lambda_{max} = 530$ mμ, $\varepsilon = 100$) soon became yellow, indicating likely reduction to the Rh(I) state (6), and on standing in air this reverted slowly back to the original red solution. Analysis for reaction products in solution gave acetaldehyde (about 1 mole for each mole of Rh^{III}) and a small amount of acetone. Gas phase analysis by mass spectrometry showed the presence of acetaldehyde, butene-1, butene-2, and unconsumed ethylene.

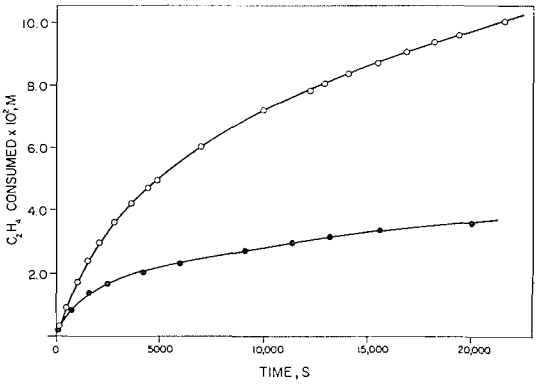

FIG. 1. Ethylene uptake plots at 80°, 730 mm C_2H_4: (○) 0.02 M Rh; (●) 0.01 M Rh.

Can. J. Chem. Downloaded from www.nrcresearchpress.com by 210.87.254.40 on 09/05/12
For personal use only.

Kinetics

The ethylene consumption plots did not analyze for simple first or second order reactions but the initial slopes could be measured with reasonable accuracy and these are summarized in Table I for experiments in which concentrations of Rh^{III}, ethylene, and added chloride, perchlorate, and acid were varied. The results show a good first order dependence on Rh^{III} at least up to 0.02 *M* but the dependence on ethylene is less than one, the order decreasing with increasing ethylene concentration and the rate tending to approach a limiting value. A marked inverse dependence on added chloride concentration was noted over the range 0–0.05 *M* when the total salt strength was kept constant by addition of perchlorate. Addition of 0.05 *M* benzene sulfonic acid (a strong acid) had essentially no effect on the initial rate.

TABLE I

Summary of kinetic data at 80°

$[Rh^{III}] \times 10^2$ (*M*)	C_2H_4 (mm)	$[C_2H_4] \times 10^2$ (*M*)	Initial rate of uptake $\times 10^5$ ($M\ s^{-1}$)	$k' \times 10^4$ (s^{-1})
0.25	730	4.0	0.17	6.9
0.75	730	4.0	0.46	6.2
1.00	730	4.0	0.69	6.9
1.50	730	4.0	1.12	7.4
2.00	730	4.0	1.58	7.9
1.00	83	0.45	0.15	1.5
1.00	112	0.61	0.22	2.2
1.00	128	0.70	0.22	2.2
1.00	142	0.78	0.24	2.4
1.00	160	0.88	0.33	3.3
1.00	216	1.2	0.40	4.0
1.00	369	2.0	0.49	4.9
1.00	473	2.6	0.54	5.4
1.00	602	3.3	0.63	6.3
1.00	796	4.3	0.64	6.4
1.00	730	4.0	0.16	1.6[a]
1.00	730	4.0	0.27	2.7[b]
1.00	730	4.0	0.42	4.2[c]
1.00	730	4.0	0.73	7.3[d]
1.00	730	4.0	1.02	10.2[e]
1.00	730	4.0	1.06	10.6[f]

[a]0.05 *M* LiCl. [b]0.03 *M* LiCl, 0.02 *M* $LiClO_4$. [c]0.02 *M* LiCl, 0.03 *M* $LiClO_4$. [d]0.01 *M* LiCl, 0.04 *M* $LiClO_4$. [e]0.05 *M* $LiClO_4$. [f]0.05 *M* benzene sulfonic acid.

If the previously mentioned yellow solution was subjected to an ethylene/hydrogen atmosphere, a much more rapid gas uptake was observed and ethane was produced. This homogeneous catalytic hydrogenation could be studied more conveniently at lower temperatures where the dimerization reaction is extremely slow, and this is described in more detail elsewhere (7).

Discussion

The results clearly indicate that the ethylene initially reduces Rh(III) to the univalent state, acetaldehyde being the other product of the redox process. The olefin must then complex rapidly with Rh(I) to prevent disproportionation of this to metal (4).

The kinetics of the initial region are similar to those observed previously for the formation of a ruthenium(II) olefin complex in aqueous HCl solution (5) and suggest that formation of the rhodium(I) ethylene complex proceeds through a two-step dissociation mechanism of the type,

$$[1] \qquad Rh^{III}Cl_n \underset{k_{-1}}{\overset{k_1}{\rightleftharpoons}} Rh^{III}Cl_{n-1} + Cl^-$$

$$[2] \qquad Rh^{III}Cl_{n-1} + C_2H_4 \overset{k_2}{\rightarrow} [Rh^{III}Cl_{n-1}(C_2H_4)]^{(4-n)+}. \qquad (1)$$

These steps could then be followed by faster steps such as

$$[3] \qquad (1) \overset{H_2O}{\rightarrow} Rh^{I}Cl_{n-1} + CH_3CHO + 2H^+$$

$$[4] \qquad Rh^{I}Cl_{n-1} + C_2H_4 \rightarrow \text{complex}.$$

Assuming the steady state approximation for the $Rh^{III}Cl_{n-1}$ species this mechanism yields the rate law

$$[5] \qquad -\frac{d[C_2H_4]}{dt} = \frac{k_1k_2[Rh^{III}Cl_n][C_2H_4]}{k_{-1}[Cl^-] + k_2[C_2H_4]}.$$

At constant $[C_2H_4]$ and $[Cl^-]$ (the latter determined by the solution equilibria of the $RhCl_3 \cdot 3H_2O$ in DMA), this becomes

$$[6] \qquad -\frac{d[C_2H_4]}{dt} = k'[Rh^{III}Cl_n],$$

where $k' = k_1k_2[C_2H_4]/k_{-1}[Cl^-] + k_2[C_2H_4]$. Values of k' are calculated from the initial slope using eq. [6] and these are listed in Table I. The expression for k' can be rewritten as

$$[7] \qquad \frac{1}{k'} = \frac{1}{k_1} + \frac{k_{-1}[Cl^-]}{k_1k_2[C_2H_4]}.$$

Considering the uncertainty in measuring initial slopes the plot of $1/k'$ versus $1/[C_2H_4]$ shown in Fig. 2 is reasonable and yields the values $k_1 \approx 10^{-3}\ s^{-1}$ and $k_{-1}[Cl^-]/k_2 \approx 0.025$ *M*. A plot of $1/k'$ versus added $[Cl^-]$ is shown in Fig. 3 and the straight line drawn gives k_1

Can. J. Chem. Downloaded from www.nrcresearchpress.com by 210.87.254.40 on 09/05/12
For personal use only.

$\approx 1.35 \times 10^{-3}$ s^{-1} and $k_{-1}/k_2 \approx 5.4$. Combining with the $k_{-1}[Cl^-]/k_2$ value above indicates that the free $[Cl^-]$ at the start of these experiments using 10^{-2} M $RhCl_3 \cdot 3H_2O$ is about 5×10^{-3} M. Thus n in eqs. [1] to [6] is likely to be 3 or 2, which is also indicated by the spectrum of the original red solutions (6). k' and k_1 must be considered as composite constants reflecting contribution from several species present.

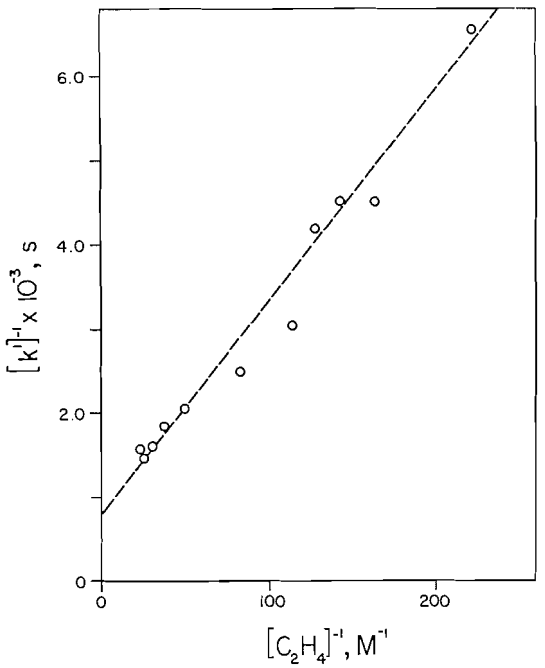

FIG. 2. Dependence of initial rate on the ethylene concentration plotted in accord with eq. [7] (80°, 0.01 M Rh).

The oxygen of the acetaldehyde must presumably come from the trihydrate and the H_2O molecule required for reaction (3) may be coordinated in the Rh^{III} intermediate (**1**) along with coordinated DMA solvent molecules to make a coordination number of 6 for octahedral configuration (anhydrous $RhCl_3$ was found to be insoluble in DMA). **1** could dissociate to give a hydroxo species, this then decomposing via a σ-bonded complex to product as in the ethylene reduction of other metal ions (8),

[8] $\mathbf{1} + H_2O \rightarrow [RhCl_{n-1}(OH)(C_2H_4)]^{(3-n)+} + H^+$
(2)

[9] $\mathbf{2} \rightarrow [Cl_{n-1}\text{—}Rh\text{—}CH_2\text{—}CH_2\text{—}OH]$
(3)

[10] $\mathbf{3} \rightarrow Cl_{n-1}Rh^I + CH_3CHO + H^+$.

It is of interest that in the corresponding palladium(II) system in aqueous solution (8), reaction [9] is postulated as rate determining, the π-complex formation being a rapid equilibrium; reaction [8] was also written as an equilibrium, this giving rise to an inverse acid dependence in the rate law. A mechanism such as

[11] $Rh^{III}Cl_n + C_2H_4 \overset{K}{\rightleftharpoons} Rh^{III}Cl_{n-1}(C_2H_4) + Cl^-$

[12] $Rh^{III}Cl_{n-1}(C_2H_4) \xrightarrow[H_2O]{k_3} Rh^ICl_{n-1} + CH_3CHO + 2H^+$

would give a rate law

$$-\frac{d[C_2H_4]}{dt} = \frac{k_3K[Rh^{III}{}_{total}][C_2H_4]}{[Cl^-] + K[C_2H_4]},$$

which is the same form as the rate law of eq. [5]. However, we have no spectral or gas uptake evidence to indicate any equilibrium such as [11] and for this reason as well as the parallel with the Ru^{II}–C_2H_4 system, the dissociation mechanism is strongly favored.

The extent of solvent participation in reaction [1] is of course uncertain. Recent reports (9) indicate that aquation reactions of rhodium(III) complexes show considerably more S_N2 character

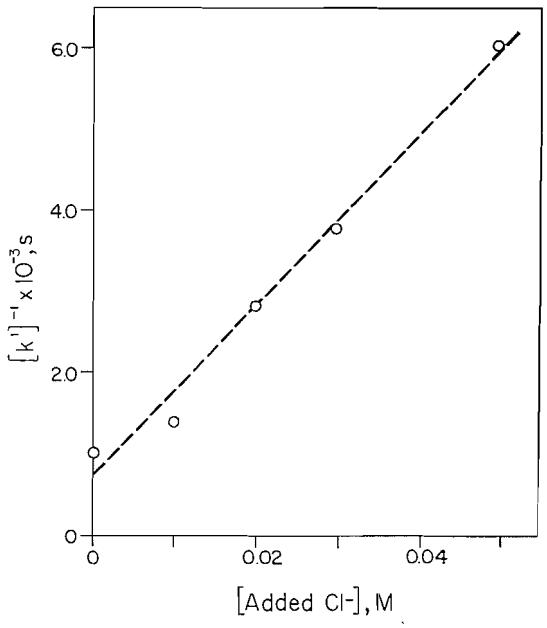

FIG. 3. Dependence of initial rate on the chloride concentration plotted in accord with eq. [7] (80°, 0.01 M Rh, 730 mm C_2H_4, $[Cl^-] + [ClO_4^-] = 0.05$ M).

Can. J. Chem. Downloaded from www.nrcresearchpress.com by 210.87.254.40 on 09/05/12
For personal use only.

than the corresponding well-studied cobalt(III) reactions. Studies of substitution reactions of rhodium(III) complexes in nonaqueous solvents have not been reported previously.

TABLE II

Temperature dependence of k'

Temp. (°C)	$k' \times 10^4$ (s^{-1})
70	4.5
75	6.5
80	6.9
85	8.5

Determined for 10^{-2} M Rh^{III}, 4.0 $\times$ 10^{-2} M C_2H_4.

Measurements on the temperature dependence of k' over the range of 70–85° (Table II) at an essentially constant ethylene concentration sufficiently high that $k' \approx k_1$ yield the activation parameters $\Delta H^{\ddagger} = 9.5$ kcal and $\Delta S^{\ddagger} = -46$ e.u. Large negative entropies of activation such as this are found for ionization reactions in solvents of moderate polarity and are explained by the freezing of solvent molecules around the incipient ions on going to the activated state (10).

The nature of the rhodium(I) ethylene complex resulting from the fast reaction [4] has not been elucidated. Many fruitless attempts were made to isolate this rhodium complex. Cramer has reported a reaction between rhodium trichloride hydrate and ethylene in aqueous methanol solution at 25° when the dimer complex $(C_2H_4)_4Rh_2Cl_2$ eventually precipitates (11); we have prepared this compound but its solution in DMA has quite different properties from our yellow solutions. The ultraviolet and visible spectra are quite different and a solution of the dimer complex was rapidly converted to metal at 80° even under an ethylene atmosphere. The dimer is clearly not the catalytically active species either for dimerization (as concluded also by Cramer (3)) or hydrogenation. Cramer suggests that the anion $[Cl_2Rh(C_2H_4)_2]^-$ is the most likely active catalyst for dimerization and such a species may well be present in our system. The mechanism postulated involves the following features: (i) the reversible oxidation of Rh^I by a proton acid to give a Rh^{III} hydride, (ii) a rate-determining insertion of coordinated olefin between an alkyl group and the metal ion to which it is attached, (iii) the lability of hydrogen in Rh^{III} alkyl and olefin complexes. Both proton and halide essential for dimerization will also be present in our system.

Acknowledgment

Grateful acknowledgment is made to the National Research Council of Canada for support of this research.

1. J. HALPERN. Ann. Rev. Phys. Chem. **16**, 103 (1965).
2. B. R. JAMES. Coord. Chem. Rev. **1**, 505 (1966).
3. R. CRAMER. J. Am. Chem. Soc. **87**, 4717 (1965).
4. B. R. JAMES and G. L. REMPEL. Can. J. Chem. **44**, 233 (1966).
5. B. R. JAMES and J. HALPERN. Can. J. Chem. **44**, 495 (1966).
6. C. K. JORGENSEN. Acta Chem. Scand. **10**, 500 (1956).
7. B. R. JAMES and G. L. REMPEL. To be published.
8. P. M. HENRY. J. Am. Chem. Soc. **86**, 3246 (1964).
9. G. M. HARRIS. Inorg. Chem. **6**, 616 (1967).
10. A. A. FROST and R. G. PEARSON. Kinetics and mechanism. Wiley, New York. 1963. p. 137.
11. R. CRAMER. Inorg. Chem. **1**, 722 (1962).

Orthobaric data of certain pure liquids in the neighborhood of the critical point

A. N. CAMPBELL AND R. M. CHATTERJEE
Department of Chemistry, The University of Manitoba, Winnipeg, Manitoba

Received July 18, 1967

The orthobaric densities of liquid and vapor, and the vapor pressure, have been determined for the three pure liquids, acetone, chloroform, and benzene. It is shown that the nose of the curve, representing orthobaric densities (or volumes) as a function of temperature, though very flat, is probably not a horizontal straight line. Nevertheless, critical phenomena can be observed over a range of total volume, at the critical temperature.

Canadian Journal of Chemistry, 46, 575 (1968)

Can. J. Chem. Downloaded from www.nrcresearchpress.com by 210.87.254.105 on 09/05/12
For personal use only.

Mayer and Mayer (1) and Harrison and Mayer (2) have propounded a statistical theory of the critical point which has aroused considerable controversy. In the past, the critical temperature, T_c, has always been identified with the temperature of disappearance of the meniscus, T_m, but according to Mayer and Harrison, these temperatures are not identical. T_m is the temperature at which the refractive indices of the two phases become identical but the critical temperature is the temperature at which all orthobaric properties, notably volume, become identical. A schematic representation of the Mayer and Harrison theory implies that at T_m (previously identified with T_c) a difference in orthobaric volumes still exists, in other words, that there is a horizontal on the P–V plot, at T_m.

The point in which the present authors are interested is whether or not such a horizontal really exists at T_m. It would mean experimentally that, at the temperature of disappearance of the meniscus, there is a demonstrable difference in the orthobaric volumes of liquid and vapor.

Rice (3) treats the process of condensation of vapor to liquid from the point of view of associating molecules. He also arrives at the conclusion that the area of heterogeneity is bounded at the top by a horizontal straight line at T_c (identified by him with T_m), i.e. there is no such thing as a critical volume but discrete orthobaric volumes of liquid and vapor exist, even at the critical temperature. This means that critical phenomena (fluctuating striae, sharp disappearance of the meniscus, etc.) will be observed over a range of total volume of the system. It is notorious among workers in this field that this is so, although this does not necessarily establish Rice's theory. An important difference between the two theories consists in that, while Mayer and Harrison predict horizontal P–V plots, over a range of total volume, in the region lying between T_m and T_c, Rice concludes that these curves will have continuous, though slight, curvature, immediately above T_m. We are not, however, concerned with this point here.

Maass and his co-workers (4) appear to have confirmed the predictions of Mayer and Harrison, in that they showed that the disappearance of the meniscus in a closed tube could be observed (at constant temperature) with varying total volumes of material in the tube. They also claimed to have observed differences in density at different heights in the tube, at temperatures slightly above T_m. These results have frequently been confirmed since (5–8), but these effects are now explained as due to a gravitational potential in a fluid of great compressibility. This means that at, or just below, the critical temperature, the critical pressure can only prevail at the meniscus, as was first pointed out by Gouy (9).

More recently, it has been suggested that orthobaric properties should be plotted against $(T_c - T)^{1/3}$ (T_c being identified with T_m) (10). It is found that when this is done, two straight lines are frequently obtained. One would expect these straight lines to intersect at the critical volume, at the critical temperature. Work by Campbell and Kartzmark (11) on the analogous critical phenomenon, $L_1 \rightleftarrows L_2$, indicates that this is not always the case. When, however, the $(T_c - T)^{1/3}$ relation is obeyed, the slope of the P versus V curve, in the neighborhood of T_c, will be very slight. The crux of the problem therefore is: is the slope of the curve, near T_c, less than that predicted by the $(T_c - T)^{1/3}$ relation? If it is, the existence of a horizontal might be conceded. To settle the point experimentally,

TABLE I
Most recent critical data

Year	t_c (°C)	P_c (atm)	d_c (g/cc)	
			A. Acetone	
1902	233.7	46.78	—	Kuenan and Robson (12)
1923	235.6	—	0.252	Herz and Neukirch (13)
1943	235.8	—	—	Fischer and Reichel (14)
1951	235.5	46.6	0.273	Rosenbaum (15)
			B. Chloroform	
1902	262.9	53.8	—	Kuenan and Robson (12)
1923	262.5	—	0.496	Herz and Neukirch (13)
1934	263.4	—	—	Harand (16)
1943	263.5	—	—	Fischer and Reichel (14)
			C. Benzene	
1910	288.5	47.9	0.3045	Young (17)
1934	290.8	—	—	Harand (16)
1941	289.45	48.9	—	Esso Laboratories, quoted in ref. 18
1943	291.2	—	—	Fischer and Reichel (14)
1947	289.5	48.7	0.297	Gornowski, Amick, and Hixson (18)
1952	288.94	48.34	0.308	Bender, Furukawa, and Hyndman (19)

materials of the highest purity must be used and the temperature controlled with great accuracy, say to $\pm 0.001°$. Our temperature control was only good to $\pm 0.05°$ and therefore our conclusions are only valid to this extent. Thus, for example, while we are in a position to say that, while at a temperature of $T_c - 0.05°$ two different phases of distinctly different orthobaric volumes are detectable, at a temperature 0.05° higher no meniscus is detectable in an ordinary telescope: an interferometer technique might, and probably would, reveal differences in refractive index with differences in height. In the case of the $L \rightleftarrows V$ critical point, certain characteristic phenomena, such as the occurrence of fluctuating striae, are usually considered peculiar to the critical volume. This has never been proved, however, and even if it is found that such phenomena can be observed over a range of volume, their occurrence proves nothing. The validity of the cubical relation has frequently been confirmed, e.g. by Weinberger and Schneider (8), despite the lack of rigidity in its deduction. Others have proposed a power other than 1/3 but we have found no need in this work for such a relationship.

Experimental

Acetone, chloroform, and benzene, respectively, were used as the three pure liquids. Objection might be made to the choice of chloroform since it decomposes very readily in the neighborhood of the critical point. A slight yellow color was always observable in the chloroform, after an experiment. In view of the well-known effect of traces of impurity on the critical constants, this is a serious matter but it cannot be avoided. Any determination of the critical constants of chloroform, however carefully made, must be subject to this criticism.

We determined critical temperature, critical pressure, equilibrium pressures (vapor pressures) at temperatures below the critical temperature, and orthobaric volumes. The literature data on orthobaric volumes, even of well known liquids, are surprisingly limited. Table I gives a resume of the most recent data.

Purity of Materials

Because of the well-known effect of slight traces of impurity on critical phenomena, considerable care was devoted to purification. The details are given in a previous publication (20).

Experimental Methods

Because of the importance of the results, these are described in some detail.

Orthobaric Densities

Two tubes of heavy walled annealed glass, 15 cm in length and 2 mm internal diameter, were used, for each temperature. The volumes of each tube up to calibration marks were determined, using mercury as calibrating liquid. Widely different quantities of the compound under investigation were distilled into each tube and the tube evacuated after freezing the liquid in liquid nitrogen. Dissolved air was removed by the usual technique of freezing, pumping, and thawing. After sealing, the tubes were weighed. They were then placed in a thermostat and the difference in height from the meniscus to the nearest calibration mark measured with a cathetometer. The equilibrium vapor and liquid volumes thus became known; correction was applied for the expansion of the glass. Temperature of the thermostat was measured with a copper–constantan multiple junction thermocouple. Up to 250 °C, the thermostat liquid was Silicone fluid 550. Above

Can. J. Chem. Downloaded from www.nrcresearchpress.com by 210.87.254.105 on 09/05/12
For personal use only.

TABLE II

Vapor pressure and orthobaric densities of acetone (t_c = 235.0 °C)

Temp. (°C)	Pressure (cm of Hg at 0 °C)	Density of vapor	Density of liquid	$(t_c - t)^{1/3}$
101.5	284.2	0.0081	0.6904	
107.4	331.8	0.0086	0.6816	
115.1	403.5	0.0092	0.6710	
117.5	428.0	0.0098	0.6678	
124.1	500.2	0.0110	0.6583	
127.4	532.4	0.0118	0.6536	
132.5	604.3	0.0124	0.6460	
135.4	646.7	0.0131	0.6419	
140.1	712.3	0.0160	0.6343	
145.8	805.6	0.0172	0.6250	
149.9	872.3	0.0186	0.6182	
151.2	896.7	0.0191	0.6168	
155.9	939.5	0.0209	0.6095	
159.9	1052.1	0.0236	0.6032	
164.3	1140.9	0.0261	0.5962	
171.2	1292.3	0.0314	0.5840	
180.1	1518.6	0.0393	0.5679	3.800
187.2	1716.0	0.0488	0.5508	3.629
189.7	1799.3	0.0496	0.5421	3.565
198.3	2051.1	0.0632	0.5212	3.323
202.6	2201.6	0.0704	0.5108	3.188
207.5	2392.5	0.0794	0.4952	3.018
211.7	2541.0	0.0885	0.4802	2.856
216.4	2738.8	0.1002	0.4608	2.651
219.8	2877.1	0.1097	0.4436	2.477
223.8	3053.3	0.1248	0.4238	2.238
225.3	3118.7	0.1290	0.4134	2.133
228.7	3271.1	0.1450	0.3959	1.847
230.2	3330.8	0.1521	0.3880	1.687
231.2	—	—	0.3627	1.563
232.1	3432.1	0.1723	0.3542	1.426
232.5	—	0.1820	—	1.357
233.5	—	—	0.3356	1.145
233.7	—	0.2024	—	1.091
233.9	—	—	0.3273	1.032
235.0	—	—	—	—

Critical data: t_c = 235.0 °C; p_c = 46.96 atm; d_c = 0.234.
Critical phenomena were observed, at a constant temperature of 235.0 °C, at the following total densities: 0.2160, 0.2356, 0.2362, 0.2372, 0.2536, 0.2693, 0.3067.

250°, the eutectic mixture of potassium, sodium, and lithium nitrates was used. This fused salt bath functioned perfectly. The accuracy of temperature control was somewhat better than ±0.05°. The following equations allow the determination of the orthobaric densities,

$$w' = v_l' d_l + v_g' d_g$$

$$w'' = v_l'' d_l + v_g'' d_g,$$

where w' and w'' are the weights of the two fillings. From the orthobaric densities, the orthobaric volumes are obtained. This method was not applicable in the immediate neighborhood of the critical temperature because slight fluctuations of temperature caused too great fluctuations in the level. Therefore, over a temperature range of 2° below the critical temperature, we made use of the method of "total exhaustion". For this method, tubes of known total volume were charged with known weights of liquid and the temperatures noted at which the meniscus disappeared "by exhaustion", i.e. when the meniscus either rose just to the upper extremity of the tube, when the tube was entirely filled with liquid, or sank to the bottom of the tube, when it was entirely filled with vapor. Congruent densities were therefore not obtained directly, in this region, but each determination gave a point on one side or the other of the orthobaric curve. Experience taught us how to choose the fillings so that all temperatures were within the desired narrow region of temperature.

Critical Temperature

This was determined in the classical manner, using different fillings of a sealed tube. As the temperature is raised, the surface tension between the two phases approaches zero, the dividing meniscus becomes faint and hazy, and the measurement of the exact temperature of its disappearance is to some extent subjective. Nevertheless, the phenomenon is clearly distinguished as "critical" since the meniscus disappears in the body of the tube and not "by exhaustion" at the top or bottom end. It must be confessed, however, that the determination of critical temperature (temperature of disappearance of the meniscus) by this method is the least satisfactory of the critical determinations.

Can. J. Chem. Downloaded from www.nrcresearchpress.com by 210.87.254.105 on 09/05/12
For personal use only.

TABLE III

Vapor pressure and orthobaric densities of benzene ($t_c = 288.95$ °C)

	Temp. (°C)	Pressure (cm of Hg at 0 °C)	Density of vapor	Density of liquid	$(t_c - t)^{1/3}$
1.	105.65		0.0060	0.7860	
2.	106.25	173.7	0.0060	0.7858	
3.	109.00		0.0058	0.7825	
4.	109.40	189.5	0.0057	0.7831	
5.	111.55		0.0067	0.7792	
6.	113.75	206.7	0.0072	0.7764	
7.	116.20		0.0076	0.7738	
8.	117.05	222.5	0.0079	0.7726	
9.	120.85	241.2	0.0080	0.7679	
10.	122.80	255.5	0.0083	0.7657	
11.	125.80	270.5	0.0088	0.7618	
12.	126.85		0.0090	0.7621	
13.	128.70		0.0096	0.7586	
14.	131.80	298.7	0.0106	0.7550	
15.	132.55		0.0102	0.7539	
16.	138.15	343.6	0.0110	0.7464	
17.	139.85	354.6	0.0118	0.7441	
18.	146.25	410.8	0.0121	0.7371	
19.	147.60	421.7	0.0123	0.7350	
20.	152.25	461.6	0.0140	0.7290	
21.	154.90	487.8	0.0144	0.7248	
22.	160.35	537.7	0.0163	0.7181	
23.	163.60	573.8	0.0179	0.7136	
24.	170.45	651.7	0.0203	0.7041	
25.	171.50	662.6	0.0208	0.7020	
26.	177.55	739.1	0.0237	0.6932	
27.	178.50	748.0	0.0240	0.6919	
28.	183.20	810.1	0.0261	0.6850	
29.	185.70	844.3	0.0278	0.6812	
30.	190.00	909.9	0.0300	0.6746	
31.	194.50	987.2	0.0326	0.6670	
32.	196.40	1015.8	0.0338	0.6647	
33.	204.15	1151.5	0.0372	0.6571	4.393
34.	210.95	1279.9	0.0438	0.6408	4.273
35.	219.95	1472.8	0.0508	0.6257	4.101
36.	228.05	1652.3	0.0581	0.6100	3.934
37.	235.25	1829.6	0.0658	0.5960	3.773
38.	242.65	2021.4	0.0739	0.5790	3.591
39.	252.85	2320.5	0.0900	0.5521	3.306
40.	262.25	2624.7	0.1101	0.5244	2.989
41.	267.75	2827.6	0.1239	0.5070	2.768
42.	272.80	3006.8	0.1400	0.4868	2.528
43.	277.20	3175.5	0.1556	0.4660	2.273
44.	280.00	3282.4	0.1661	0.4508	2.077
45.	284.05			0.4199	1.698
46.	285.30	3521.5			
47.	286.30		0.2144		
48.	286.65			0.3844	1.320
49.	287.15			0.3737	1.216
50.	288.40			0.3360	
51.	288.50	3636.7		0.2625	

Critical data: $t_c = 288.95$ °C; $p_c = 48.22$ atm; $d_c = 0.275$.
Critical phenomena were observed, at a constant temperature of 288.95 °C, at the following total densities: 0.3257, 0.3109, 0.2914, 0.2900.

Vapor Pressures

Vapor pressures were determined in the apparatus of Fig. 1, which is essentially a closed manometer containing air. The closed manometer was calibrated for volume as a function of length. The sample was poured at room temperature into bulb A, over mercury which filled B and part of C. The liquid was then frozen and the vacuum applied simultaneously at both A and C. The process of freezing, pumping, and thawing was continued until all dissolved air was expelled from the liquid. The open end of A was then sealed off, keeping the liquid frozen. The liquid was then allowed to melt and air allowed to enter C, with the result that liquid, followed by mercury, was pushed completely to the end of A. The open end of C was then sealed off, under atmospheric pressure. C was then enclosed in a glass mantle, through which water at 25° was circulated. Atmospheric pressure was recorded at the moment of sealing. The volume of

Can. J. Chem. Downloaded from www.nrcresearchpress.com by 210.87.254.105 on 09/05/12
For personal use only.

Can. J. Chem. Downloaded from www.nrcresearchpress.com by 210.87.254.105 on 09/05/12
For personal use only.

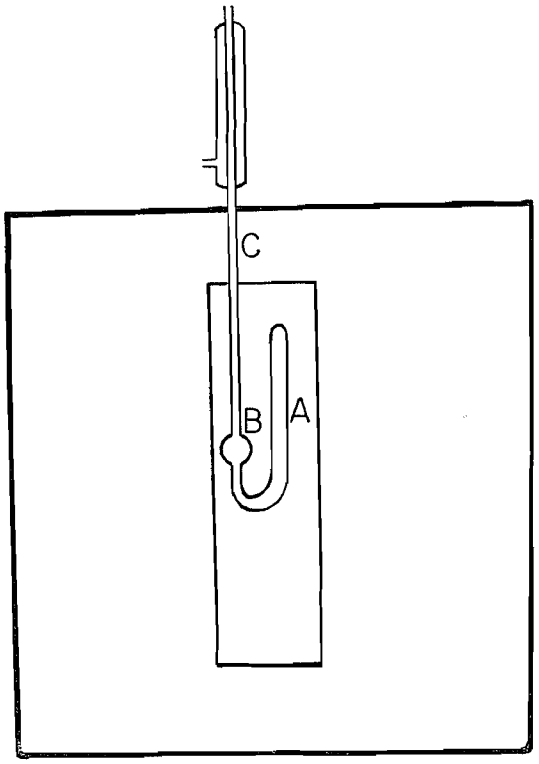

FIG. 1. Diagram showing mercury–air manometer in bath.

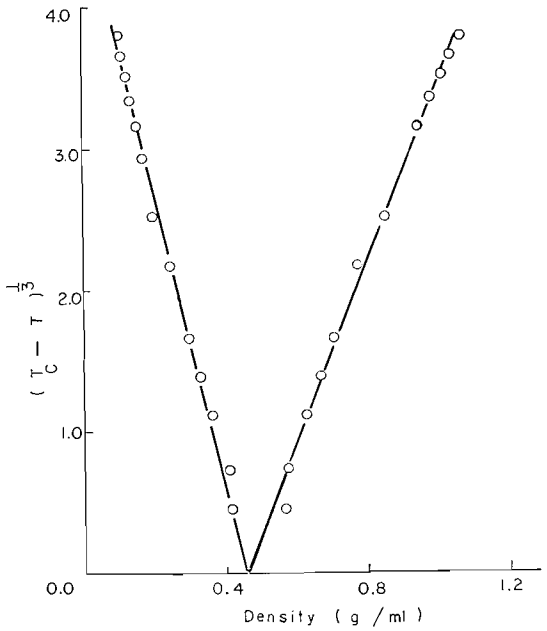

FIG. 2. Plot of d_l and d_v vs. $(t_c - t)^{1/3}$ for $CHCl_3$.

air in C, under atmospheric pressure, was then obtained by means of a cathetometer reading.

Bulbs A and B were then immersed in a thermostat at the desired high temperature, that is, at a temperature at which the vapor pressure of the liquid was greater than 1 atm. Vapor formed in bulb A and the vapor pressure was automatically established. From the equilibrium volume of air in C, the pressure was calculated, using van der Waals' equation. Other equations of state gave variations within the experimental error. Thus, using the Beattie–Bridgman equation, at 288.50°, i.e. 0.45° below the critical temperature of benzene, the pressure calculated by van der Waals was 3636.7 cm Hg, by Beattie–Bridgman 3651.2 cm Hg, while the experimental figure of Bender, Furukawa, and Hyndman (much the best figure) is 3641.0. The maximum error of 0.3% is about that of our experimental work.

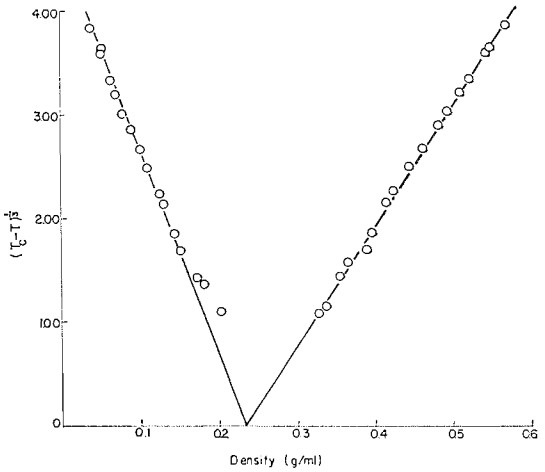

FIG. 3. Plot of d_l and d_v vs. $(t_c - t)^{1/3}$ for acetone.

For the reason previously given, namely that in the neighborhood of the critical temperature slight fluctuations of temperature caused great fluctuations in level, it was not found possible to make pressure measurements by this method to temperatures higher than about 3° below the critical temperature. The critical pressures were therefore obtained from the plot of log P versus $1/T$: the agreement with the latest figures is good.

Results

The experimental results are expressed in Tables II to IV. For all three substances, when orthobaric densities are plotted against $(T_c - T)^{1/3}$ two straight lines are obtained, intersecting at the critical temperature (Figs. 2, 3, and 4). The values of critical density thus obtained are

Acetone, $d_c = 0.234$ g/cc
Chloroform, $d_c = 0.458$ g/cc
Benzene, $d_c = 0.275$ g/cc.

Can. J. Chem. Downloaded from www.nrcresearchpress.com by 210.87.254.105 on 09/05/12
For personal use only.

TABLE IV

Vapor pressure and orthobaric densities of chloroform ($t_c = 262.9$ °C)

Temp. (°C)	Pressure (cm of Hg at 0 °C)	Density (vap.)	Density (liq.)	$(t_c - t)^{1/3}$
101.4	245.7	0.0136	1.4884	
111.7	313.2	0.0182	1.4510	
119.2	371.4	0.0224	1.4230	
127.5	450.8	0.0278	1.3914	
135.7	537.6	0.0320	1.3612	
144.7	642.5	0.0389	1.3259	
151.3	739.8	0.0440	1.3000	
160.0	865.4	0.0512	1.2652	
167.6	989.6	0.0578	1.2346	
173.2	1093.5	0.0621	1.2127	
180.5	1250.1	0.0684	1.1832	
187.1	1401.3	0.0756	1.1552	
196.3	1628.6	0.0871	1.1149	
207.4	1963.2	0.1038	1.0628	3.814
213.7	2177.3	0.1132	1.0336	3.664
219.6	2388.5	0.1236	1.0044	3.512
225.3	2592.7	0.1360	0.9740	3.350
231.2	2815.1	0.1504	0.9410	3.164
237.5	3040.3	0.1690	0.9024	2.940
244.9	3313.6	0.1998	0.8482	2.523
252.7	3609.7	0.2446	0.7788	2.169
258.3	3818.9	0.3008	0.7052	1.663
260.2	3890.8	0.3301	0.6699	1.393
261.5		0.3642	0.6314	1.119
262.5		0.4138	0.5786	0.737
262.8		0.4201		0.464
262.8			0.5662	0.464

Critical data: $t_c = 262.9$ °C; $p_c = 52.59$ atm; $d_c = 0.458$.
Critical phenomena were observed, at a constant temperature of 262.9 °C, at the following total densities: 0.4279, 0.4697, 0.4872, 0.5120, 0.5381, 0.5610.

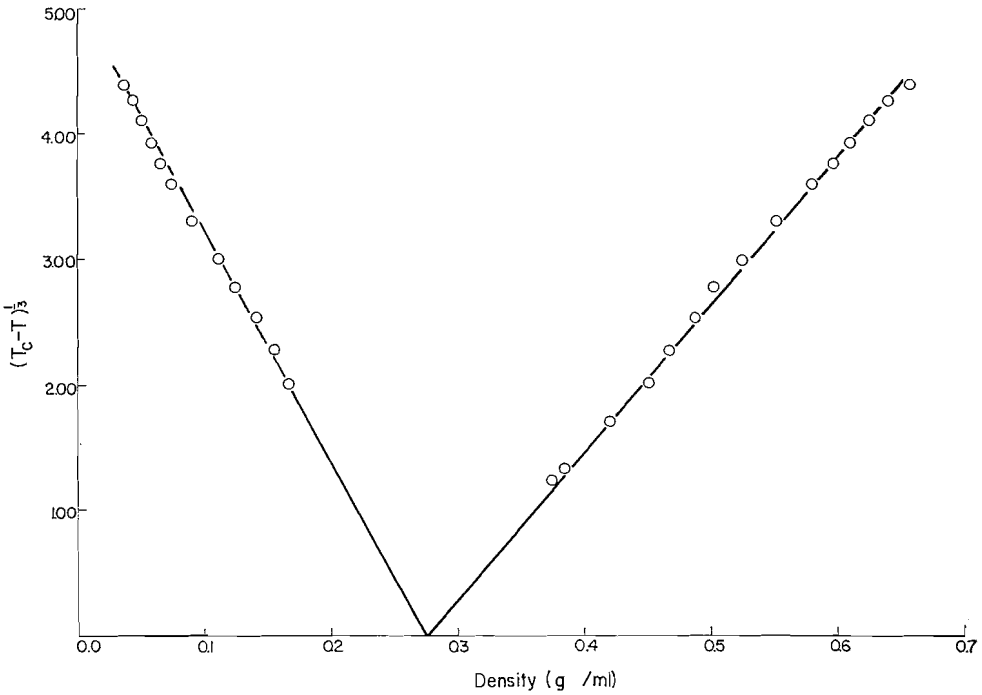

FIG. 4. Plot of d_l and d_v vs. $(t_c - t)^{1/3}$ for benzene.

On the basis of this criterion it appears that the nose of the curve of orthobaric densities versus temperature, though very flat, is not a horizontal straight line. Nevertheless, the fact remains that, at the critical temperature, the meniscus disappears sharply in the body of the liquid, with accompanying phenomena usually described as "critical", over a rather extensive range of total density (or volume). It is an old observation, however, which has recently been reaffirmed by Lorentzen (7) that the disappearance in the body of the tube (and not by "moving out", as Lorentzen calls it) can be observed over a range of total volume and is not confined to the critical volume. This is due to the existence of a density gradient and does not necessarily prove that the nose of the curve is horizontal.

1. J. E. MAYER and M. G. MAYER. Statistical mechanics. Wiley, N.Y. 1940. p. 312.
2. B. F. HARRISON and J. E. MAYER. J. Chem. Phys. **6**, 101 (1938).
3. O. K. RICE. Chem. Rev. **44**, 69 (1949).
4. J. S. TAPP, E. W. R. STEACIE, and O. MAASS. Can. J. Res. **9**, 217 (1933); J. R. DACEY, R. L. MACINTOSH, and O. MAASS. Can. J. Res. **B17**, 206 (1939); R. L. MACINTOSH, J. R. DACEY, and O. MAASS. Can. J. Res. **B18**, 241 (1939); S. N. NALDRETT and O. MAASS. Can. J. Res. **B18**, 118 (1940).
5. E. H. W. SCHMIDT. Critical phenomena. Natl. Bur. Std. U.S. Misc. Publ. No. 273, 13 (1966).
6. H. L. LORENTZEN and B. B. HANSEN. Critical phenomena. Natl. Bur. Std. U.S. Misc. Publ. No. 273, 213 (1966).
7. H. L. LORENTZEN. Acta Chem. Scand. **7**, 1335 (1953).
8. M. A. WEINBERGER and W. G. SCHNEIDER. Can. J. Chem. **30**, 422 (1952).
9. R. GOUY. Compt. Rend. **115**, 720 (1892).
10. E. A. GUGGENHEIM. J. Chem. Phys. **13**, 253 (1945).
11. A. N. CAMPBELL and E. M. KARTZMARK. Can. J. Chem. **45**, 2433 (1967).
12. J. P. KUENAN and W. G. ROBSON. Phil. Mag. **3**, 628 (1902).
13. W. HERZ and E. NEUKIRCH. Z. Physik. Chem. Leipzig, **104**, 433 (1923).
14. M. FISCHER and H. P. REICHEL. Mikrochemie ver. Mikrochim. Acta, **31**, 102 (1943).
15. F. B. ROSENBAUM. M.S. Thesis, University of Texas, Austin, Tex. August 1951.
16. J. HARAND. Monatsh. **65**, 153 (1935).
17. S. YOUNG. Sci. Proc. Roy. Dublin Soc. **12**, 374 (1909–10).
18. E. J. GORNOWSKI, E. H. AMICK, and A. N. HIXSON. Ind. Eng. Chem. **39**, 1348 (1947).
19. P. BENDER, G. T. FURUKAWA, and J. R. HYNDMAN. Ind. Eng. Chem. **44**, 387 (1952).
20. A. N. CAMPBELL, E. M. KARTZMARK, and R. M. CHATTERJEE. Can. J. Chem. **44**, 1183 (1966).

Can. J. Chem. Downloaded from www.nrcresearchpress.com by 210.87.254.105 on 09/05/12
For personal use only.

Can. J. Chem. Downloaded from www.nrcresearchpress.com by 210.87.254.105 on 09/05/12
For personal use only.

Tellurium isotope fractionation study

R. M. SMITHERS[1] AND H. R. KROUSE
Department of Physics, University of Alberta, Edmonton, Alberta

Received June 19, 1967

"Normal vibration equations" have been solved to yield vibrational frequencies for isotopic compounds of tellurium. These frequencies were used to evaluate "partition function ratios" for ^{122}Te- and ^{130}Te-containing compounds. Theoretical "isotopic equilibrium exchange constants" and estimates of "kinetic isotope effects" were derived from these ratios. The results suggest that the ^{122}Te/^{130}Te abundance may be altered significantly in laboratory reactions and terrestrial processes.

Preliminary experiments have realized kinetic isotope effects of 0.7 and 0.6% in inorganic and microbiological reductions respectively of tellurite to elemental tellurium. These results are interpreted in terms of the isotope effect in Te—O bond breakage.

The maximum variation in the ^{130}Te/^{122}Te abundance ratio of six natural tellurides and two commercial preparations of TeO_3^{2-} was found to be 0.4%.

The results are compared with those found in analogous selenium and sulfur isotope investigations.

Canadian Journal of Chemistry, **46**, 583 (1968)

Introduction

It is well known that isotopes of an element differ in their natural abundances and behavior in laboratory processes. This is explained theoretically by the dependence of many thermodynamic properties of molecules upon their vibrational frequencies which, in turn, depend upon the masses of the atoms in the molecule.

Earlier studies were carried out with lighter elements. Here the mass difference between the isotopes is significant and isotopic compounds of these elements are capable of undergoing physical, chemical, and microbiological processes at markedly different rates. In contrast to the lighter elements, many of the heavier elements possess large numbers of isotopes. In many cases, the percentage mass difference between the heaviest and lightest isotope is quite comparable to that of lighter elements. Therefore "isotopic exchange equilibrium constants" and "kinetic isotope effects" of the same order are expected with these heavier elements. Tellurium, element 52, has 8 stable isotopes with mass numbers 120, 122, 123, 124, 125, 126, 128, and 130. Their abundances as determined by White and Cameron (1) and Hollander *et al.* (2) are (dropping one significant figure from the data) 0.1, 2.5, 0.9, 4.6, 7.0, 18.7, 31.8, and 34.5% respectively. Although ^{120}Te is the lightest isotope, it has the disadvantage of being low in abundance. Therefore ^{122}Te and ^{130}Te were selected for experimental study to facilitate the mass spectrometry, but yet provide a significant percentage mass difference ($> 6\%$).

The chemical group VIA elements are interesting to study isotopically because of the range of valence states and chemical forms in which they exist in nature. Since the initial findings in 1949 of variations in the terrestrial ^{34}S/^{32}S abundance ratio by Thode *et al.* (3), sulfur isotope investigations have been carried out with natural samples and laboratory reactions by several researchers. Motivated by the usefulness of sulfur isotope studies in chemical, geological, and biological investigations, Krouse and Thode (4) carried out an initial investigation of the thermodynamic properties and geochemistry of isotopic compounds of selenium. Significant natural variations were found in the ^{76}Se/^{82}Se ratio and a kinetic isotope effect of 1.5% was found in the chemical reduction of $^{76}SeO_3^{2-}$ and $^{82}SeO_3^{2-}$. Subsequent investigations by Rees and Thode (5) have revealed further interesting alterations to the ^{76}Se/^{82}Se ratio in chemical reactions. These successful studies with sulfur and selenium further prompted the present investigation of tellurium isotope fractionation.

Theory

Isotopic Equilibrium Exchange Reactions

A typical isotope exchange reaction may be written as

$$[1] \qquad aA_1 + bB_2 \overset{k}{\rightleftharpoons} aA_2 + bB_1,$$

where the subscripts 1 and 2 refer to the light

[1]Present address: Physics Department, Selkirk College, Castlegar, British Columbia.

TABLE I

Diatomic molecular frequencies (cm^{-1}) (with anharmonicity corrections)

	Molecule						
	^{74}GeTe	^{208}PbTe	^{120}SnTe	Te^{16}O	^{28}SiTe	^{130}TeTe	HTe
ω_{130}	321.4	211.6	258.5	789.0	478.0	250.4	2167.4
ω_{122}	325.2	215.8	262.5	791.8	480.8	254.5	2167.9

and heavy isotopes respectively while A and B are molecules having the element under consideration as a common constituent. The equilibrium constant for this exchange can be shown to be equal to the following ratio of the total partition functions of the participating isotopic molecules.

$$[2] \qquad K = \frac{[Q_{A_2}/Q_{A_1}]^a}{[Q_{B_2}/Q_{B_1}]^b}$$

Urey (6) and Bigeleisen and Mayer (7) have shown that with few exceptions (e.g. H_2 at room temperature where the rotational partition function cannot be expressed by the classical limit), K can be expressed in terms of isotopic partition function ratios Q_2'/Q_1' which depend only on the vibrational frequencies of the participating molecules.

The exact expression for Q_2'/Q_1' in the simple harmonic oscillator approximation is

$$[3] \qquad \frac{Q_2'}{Q_1'} = \prod_i^N \frac{u_{2_i}}{u_{1_i}} \frac{e^{-u_{2i}/2}}{e^{-u_{1i}/2}} \frac{1 - e^{-u_{1i}}}{1 - e^{-u_{2i}}},$$

where $u_i = h\upsilon_i/kT$ and υ_i is the ith fundamental vibrational frequency of the molecule. $N = 3n - 6$ for nonlinear and $3n - 5$ for linear molecules where n is the number of atoms. Other terms which would appear in the numerator and denominator of K (e.g. symmetry numbers) are omitted in the above expression since they are not required in the present study.

Urey (6) and Bigeleisen and Mayer (7) have made approximations to simplify the expression for manual calculations. In our studies, however, I.B.M. 7040 programming was used to evaluate Q_2'/Q_1' ratios according to the exact expression [3].

Kinetic Isotope Effects

Theoretical predictions of kinetic isotope effects are based on the theory of absolute reaction rates as developed by Eyring (8) and Evans and Polanyi (9). Competing isotopic reactions may be written

$$[4] \qquad \begin{aligned} A_1 + B + \text{---} &\xrightarrow{k_1} P_1 \\ A_2 + B + \text{---} &\xrightarrow{k_2} P_2, \end{aligned}$$

where k_1 and k_2 express the rates at which A_1 and A_2 form products P_1 and P_2. Although the calculations of isotopic rate constants can be very sophisticated, only the initial expressions derived by Bigeleisen (10) will be considered in this study. Bigeleisen's expression can be written

$$[5] \qquad \frac{k_1}{k_2} = \frac{\upsilon_{1L}^{\ddagger}}{\upsilon_{2L}^{\ddagger}} \left(\frac{Q_2}{Q_1}\right) \Big/ \left(\frac{Q_2^{\ddagger}}{Q_1^{\ddagger}}\right).$$

This form omits the transmission coefficient and Wigner tunnelling corrections which are assumed independent of isotopic substitution in this investigation; $\ddagger$ refers to the activated complex of reaction rate theory. As before, the partition function ratios depend only on vibrational motions and expression [3] may be used for their calculation. The summation for the activated complex is over $3n - 7$ rather than $3n - 6$ since one of the vibrational degrees of freedom becomes a translational one along the reaction coordinate during the bond cleavage. The term $\upsilon_{1L}^{\ddagger}/\upsilon_{2L}^{\ddagger}$ is the ratio of the "imaginary" frequencies of the isotopic bonds being broken and gives the ratio of the number of light and heavy molecules which decompose in unit time from the transition state. According to Slater (11), this term is

$$[6] \qquad \frac{\upsilon_{1L}^{\ddagger}}{\upsilon_{2L}^{\ddagger}} = \left(\frac{\mu_2^{\ddagger}}{\mu_1^{\ddagger}}\right)^{1/2},$$

where μ refers to the reduced mass of the atoms across the bond being broken. Bigeleisen and Wolfsberg (12) have suggested that the two fragments being separated, rather than the two atoms, be used in expression [6]. The effective mass will depend on the strength of the bond being broken relative to the other interatomic

Can. J. Chem. Downloaded from www.nrcresearchpress.com by 210.87.254.105 on 09/05/12
For personal use only.

TABLE II

Polyatomic molecular frequencies (cm^{-1}) (degeneracy is denoted by number in parenthesis)

Molecule	ω_1	ω_2	ω_3	ω_4	ω_5	ω_6	References
$^{130}TeF_6$	701	674(2)	751(3)	327(3)	313(3)	164(3)	15, 16, 17
$^{122}TeF_6$	701	674(2)	756.9(3)	329.4(3)	313(3)	164(3)	
$^{130}TeBr_4$	190	51(2)	209(3)	64(3)			18, 19, 20
$^{122}TeBr_4$	190	51(2)	212.1(3)	64.5(3)			
$^{130}TeO_3^{2-}$	758	364	703(2)	326(2)			
$^{122}TeO_3^{2-}$	761.1	364.8	705.5(2)	326.9(2)			Appendix
$SC^{130}Te$	1347	337(2)	423				
$SC^{122}Te$	1347.4	340.0(2)	426.4				21
$H_2{}^{130}Te$	2047	860.8	2133				
$H_2{}^{122}Te$	2047.4	861.4	2133.5				Appendix

bonds as discussed by Wolfsberg (13). If the bond being broken is comparatively strong, then the case is closer to that of Slater whereas if the bond being ruptured is comparatively weak, then the mass fragments should be more representative. In any case, lack of knowledge about the activated complex forbids an exact expression for $\upsilon_{1L}{}^{\ddagger}/\upsilon_{2L}{}^{\ddagger}$. Similarly, data is not available for evaluating the activated state isotopic partition function ratio. In practice, certain limiting cases can be considered and compared with the experimental results.

Results of Theoretical Calculations

All of the numerical calculations were carried out on an I.B.M. 7040 computer using Fortran IV programming. Checks were made by also calculating analogous expressions for Se-containing compounds and checking with published results (4, 5). In each program, observed vibrational frequencies were identified with the most abundant ^{130}Te species.

Calculation of Isotopic Vibrational Frequencies

Table I summarizes the vibrational frequencies for ^{122}Te- and ^{130}Te-diatomic species. The spectroscopic data and method of calculation are given in Herzberg (14). Anharmonicity corrections were made. It is interesting to note in the case of HTe, the vibrational frequency is not very sensitive to Te isotope substitution. This results because the Te atom is so much heavier than the H that the reduced mass is not altered much by altering the Te mass.

Table II summarizes the fundamental vibrational frequencies calculated for ^{122}Te- and ^{130}Te-containing polyatomic molecules. References are given in the table for spectroscopic data and the normal vibrational force equations used in the calculations. With the exception of H_2Te and TeO_3^{2-}, the calculations were straightforward. The H_2Te and TeO_3^{2-} treatments were more involved because of lack of data in the literature. The derivation of their force constants is treated in the Appendix of this paper.

Table III summarizes the isotopic partition function ratios and equilibrium constants for hypothetical $^{122}Te \leftrightarrow {}^{130}Te$ exchange reactions. The method of tabulation is that used by Urey (6). The partition function ratios are listed in the first row under their respective compounds for the temperatures in the right column. The main body of the table contains the equilibrium constants at the intersection of the column and row of interest. K values of greater than unity mean that the ^{130}Te is favored in the compound listed in the left column. For example, the value 1.0096 underlined in the table means that $K = 1.0096$ at 20 °C for the hypothetical exchange

$$^{122}TeO_3^{2-} + H_2{}^{130}Te \overset{K}{\rightleftharpoons} H_2{}^{122}Te + {}^{130}TeO_3^{2-}.$$

Although calculations were made for several compounds and hypothetical exchanges up to 1000 °C, only the results of a few selected exchanges at four lower temperatures are reported here.

Experimental

All samples were converted to elemental Te. The tellurium was then fluorinated at 200 °C with excess F_2 in a stainless steel F_2 line to produce TeF_6 gas for mass spectrometric analyses.

Natural Samples

Tellurium was extracted in the elemental form by following essentially the procedure of Reed (22). In

Can. J. Chem. Downloaded from www.nrcresearchpress.com by 210.87.254.105 on 09/05/12
For personal use only.

TABLE III

Equilibrium constants for ^{130}Te–^{122}Te exchange reactions

	$\frac{^{130}TeF_6}{^{122}TeF_6}$	$\frac{^{130}TeO_3^{2-}}{^{122}TeO_3^{2-}}$	$\frac{SC^{130}Te}{SC^{122}Te}$	$\frac{^{130}TeBr_4}{^{122}TeBr_4}$	$\frac{^{130}TeO}{^{122}TeO}$	$\frac{H_2{}^{130}Te}{H_2{}^{122}Te}$	$\frac{^{130}Te^{130}Te}{^{130}Te^{122}Te}$	$\frac{Pb^{130}Te}{Pb^{122}Te}$	$\frac{H^{130}Te}{H^{122}Te}$	T (°C)
Q_2'/Q_1'	1.0307	1.0133	1.0083	1.0047	1.0041	1.0024	1.0023	1.0021	1.0011	0
	1.0271	1.0118	1.0073	1.0041	1.0036	1.0022	1.0020	1.0018	1.0011	20
	1.0229	1.0100	1.0061	1.0034	1.0031	1.0019	1.0017	1.0015	1.0009	50
	1.0176	1.0077	1.0046	1.0025	1.0024	1.0016	1.0013	1.0011	1.0008	100
$\frac{^{130}TeF_6}{^{122}TeF_6}$	1.0000	1.0171	1.0222	1.0259	1.0265	1.0281	1.0283	1.0286	1.0294	0
		1.0152	1.0197	1.0230	1.0234	1.0249	1.0251	1.0253	1.0261	20
		1.0128	1.0167	1.0194	1.0197	1.0209	1.0212	1.0213	1.0219	50
		1.0099	1.0129	1.0151	1.0152	1.0160	1.0164	1.0165	1.0169	100
$\frac{^{130}TeO_3^{2-}}{^{122}TeO_3^{2-}}$		1.0000	1.0049	1.0086	1.0092	1.0109	1.0110	1.0112	1.0122	0
			1.0044	1.0077	1.0081	1.0096	1.0098	1.0100	1.0107	20
			1.0038	1.0066	1.0068	1.0080	1.0083	1.0084	1.0090	50
			1.0030	1.0051	1.0052	1.0061	1.0064	1.0066	1.0069	100
$\frac{SC^{130}Te}{SC^{122}Te}$			1.0000	1.0036	1.0042	1.0059	1.0060	1.0063	1.0072	0
				1.0032	1.0037	1.0051	1.0053	1.0055	1.0063	20
				1.0027	1.0030	1.0042	1.0044	1.0046	1.0052	50
				1.0021	1.0022	1.0030	1.0034	1.0035	1.0039	100
$\frac{^{130}TeBr_4}{^{122}TeBr_4}$				1.0000	1.0006	1.0023	1.0024	1.0026	1.0035	0
					1.0004	1.0019	1.0020	1.0023	1.0030	20
					1.0003	1.0014	1.0017	1.0019	1.0024	50
					1.0001	1.0009	1.0013	1.0014	1.0017	100
$\frac{^{130}TeO}{^{122}TeO}$					1.0000	1.0017	1.0018	1.0020	1.0029	0
						1.0014	1.0016	1.0019	1.0026	20
						1.0012	1.0014	1.0016	1.0022	50
						1.0008	1.0012	1.0013	1.0016	100
$\frac{H_2{}^{130}Te}{H_2{}^{122}Te}$						1.0000	1.0004	1.0004	1.0013	0
							1.0002	1.0004	1.0011	20
							1.0003	1.0005	1.0010	50
							1.0003	1.0005	1.0003	100
$\frac{^{130}Te^{130}Te}{^{130}Te^{122}Te}$							1.0000	1.0002	1.0012	0
								1.0002	1.0010	20
								1.0002	1.0007	50
								1.0001	1.0005	100
$\frac{Pb^{130}Te}{Pb^{122}Te}$								1.0000	1.0009	0
									1.0007	20
									1.0005	50
									1.0003	100

this method, Se can be separated from Te by using H_2SO_3 as a reducing agent and altering the pH by varying the addition of HCl. Extractions with artificial mixtures recovered over 98% of the Te.

Chemical Reduction of TeO_3^{2-}

K_2TeO_3 was reduced to elemental Te using H_2SO_3 as the reducing agent. Yields appeared consistent with the reaction

$$K_2TeO_3 + 2H_2SO_3 \rightarrow K_2SO_4 + H_2SO_4 + Te\downarrow + H_2O.$$

In order to measure a kinetic isotope effect, products and/or reactants must be separated after a known percentage of reaction. In our experiments, 5 to 20% reductions were effected by adding the corresponding insufficient amount of reducing agent. The precipitated Te was separated from the supernatant solution by alternately centrifuging and washing.

Reduction of TeO_3^{2-} by Scopulariopsis brevicaulis

Bird and Challenger (23) reported that *Scopulariopsis brevicaulis* (penicillium brevicaule) reduced K_2TeO_3 to elemental Te and gaseous $(CH_3)_2Te$. Our cultures were grown in an aerated medium of Trypticase Soy Broth (Baltimore Biological Co.). The air was filtered by passage through H_2SO_4 and 1:1000 solution of $HgCl_2$. After 12 days, 1.5 g of K_2TeO_3 in solution were introduced into the medium. The air stream was exhausted through an alcoholic iodine solution to trap any $(CH_3)_2Te$ as $(CH_3)_2TeI_2$ (24). Every 6 h, 10 cc samples of the medium were taken. The samples were filtered and washed to separate the unreduced TeO_3^{2-} from biological material and reduced Te. The TeO_3^{2-} was chemically reduced to Te for mass spectrometric analysis.

Mass Spectrometry

Although TeF_6 poses certain chemical disadvantages as a gas for analysis, there is the advantage that ^{19}F

Can. J. Chem. Downloaded from www.nrcresearchpress.com by 210.87.254.105 on 09/05/12
For personal use only.

TABLE IV

Variations of $^{130}Te/^{122}Te$ in natural samples

Sample No.	Description	δ_{130}
1	Refined Te from Coppercliff, Ontario	0
2	Sylvanite; Grant Co., New Mexico	−1.5±0.3
3	Sylvanite; Cripple Creek, Colorado	0.0±0.2
4	Sylvanite; Boulder Co., Colorado	−2.3±0.3
5	Tellurium; Boulder Co., Colorado	−1.8±0.3
6	Tetradymite; Precambrian Mines, Okanagan, B.C.	−4.0±0.5
7	Same as 6, but different hand specimen	−3.7±0.3
8	Commercial K_2TeO_3 (Fisher Scientific)	−3.5±0.3
9	Commercial K_2TeO_3 (British Drug Houses)	0.0±0.2

TABLE V

Fractionation in chemical reduction of $K_2TeO_3^{2-}$ to Te

Sample No.	Description	R
1	10% reduction of #9, Table IV	1.0071±0.0003
2	18% reduction of #9, Table IV	1.0044±0.0003
3	10% reduction of #8, Table IV	1.0071±0.0003
4	10–20% fraction of #8, Table IV	1.0070±0.0003

$$R = \frac{^{122}Te/^{130}Te_{\text{product Te}}}{^{122}Te/^{130}Te_{\text{initial } TeO_3^{2-}}}$$

$$k_{122}/k_{130} = 1.0065 \pm 0.0008$$

is the only stable isotope. Therefore any ion species reveals the Te isotope abundances directly. When TeF_6 undergoes electron bombardment in a conventional gas source mass spectrometer, TeF_5^+ is the most abundant species formed. In our case, 6 singly charged and 5 doubly charged ion species were identified while TeF_5^+ formed over 58% of the total ions present. The mass spectrometer was a 12″ radius, 90° magnetic analyzer equipped to simultaneously collect $^{130}TeF_5^+$ and $^{122}TeF_5^+$. The ratio of these ions was digitally recorded (25). The mass resolution was ~ 1/350 for the lighter mass and 1/200 for the heavier mass. The wider collector slit (corresponding to 1/200 resolution) provided ample resolution for the $^{130}TeF_5^+$ ions since the nearest ion current is two mass units away ($^{128}TeF_5^+$). This wider slit permitted easier alignment for simultaneous collection. A standard and an unknown sample could be introduced alternately into the mass spectrometer source. Five minutes were required between sample switches in order to obtain a stable ratio. This appeared to be due to short time memory effects. The standard deviation within a set of comparisons and between sets run on different days for samples prepared from the same specimens was ±0.04% or better.

Results and Discussion

Theoretical Calculations

It is seen in Table III that alterations of up to 3% in the $^{130}Te/^{122}Te$ ratio are predicted in $^{130}Te \leftrightarrow {}^{122}Te$ exchange processes, provided that mechanisms exist to effect these exchanges.

Natural Samples

Table IV summarizes the tellurium isotope abundance data for 8 natural and commercial samples. δ_{130}, the enrichment in ^{130}Te in parts per thousand is defined in terms of the coppercliff sample as

$$\delta_{130} = \left(\frac{^{130}Te/^{122}Te_{\text{sample}}}{^{130}Te/^{122}Te_{\text{coppercliff}}} - 1 \right) \times 1000$$

It is seen that the overall variation in the natural and commercial samples is 4 δ units. Although no extensive conclusions can be drawn from this survey, most of the samples represent natural tellurides which presumably have not undergone chemical valence change. Therefore, isotope fractionation would most likely result from fairly high temperature physical processes, in which case, little variation in the $^{130}Te/^{122}Te$ ratio is expected. This compares to the $^{76}Se/^{82}Se$ ratio which showed very little variation in natural selenides. It was surprising to see 3.5 δ units difference between the two commercial TeO_3^{2-} samples. This difference may reflect different natural sources of supply or it may have resulted during processing.

Kinetic Isotope Effects

Table V shows the results of fractionation

Can. J. Chem. Downloaded from www.nrcresearchpress.com by 210.87.254.105 on 09/05/12
For personal use only.

TABLE VI

Theoretical values of k_{122}/k_{130} in TeO_3^{2-} reduction

	k_{122}/k_{130}					
	Low		Intermediate		High	
T (°C)	Mass	Atom	Mass	Atom	Mass	Atom
0	1.002	1.004	1.0054	1.0069	1.0153	1.0169
20	1.002	1.004	1.0050	1.0065	1.0138	1.0153
50	1.002	1.004	1.0046	1.0061	1.0120	1.0135

during chemical reduction of K_2TeO_3 to elemental Te. If it is assumed that the measured effect is purely kinetic, then for small percentage reactions, R can be related to the ratio of the isotopic rate constants k_{122}/k_{130} where

$$^{122}TeO_3^{2-} \xrightarrow{k_{122}} {}^{122}Te$$

$$^{130}TeO_3^{2-} \xrightarrow{k_{130}} {}^{130}Te.$$

For larger percentages of reaction, the depletion in ^{122}Te in the TeO_3^{2-} solution must be considered in evaluating k_{122}/k_{130} (5). The average k_{122}/k_{130} was found to be 1.0065 ± 0.0008.

In the microbiological reduction, some difficulty was experienced in obtaining suitable material for analyses. Some $(CH_3)_2Te$ was obtained, but it was judged insufficient in quantity. One problem inherent in both the chemical and microbiological study is the separation of all unreduced TeO_3^{2-} from the precipitated Te. This was more difficult in the microbiological reduction where the Te was entrapped in biological material. Further, one cannot recover all the Te at any percentage reaction because of this entrapment. Therefore observations on the depletion of ^{122}Te in the unreduced TeO_3^{2-} are the most reliable. It is necessary, however, to carry out a significant percentage conversion in order to noticeably alter the isotopic composition of the remaining TeO_3^{2-}. In our experiments, microbiological conversions in excess of 50% were possible. Preliminary measurements and the use of suitable equations (see Rees and Thode (5)), gave $k_{122}/k_{130} = 1.0060 \pm 0.0005$ at room temperature.

Discussion

Table VI summarizes theoretical kinetic isotope effects assuming various models for the reduction.

The lowest values (and also the high temperature limit) result from setting the partition function ratio of the activated complex equal to that of the reactant so that

$$\frac{k_1}{k_2} = \left(\frac{\mu_2^{\ddagger}}{\mu_1^{\ddagger}}\right)^{1/2}.$$

k_1/k_2 is evaluated using mass and atom fragments.

The upper limit to k_1/k_2 is obtained by setting $Q_{130}^{\ddagger}/Q_{122}^{\ddagger} = 1$. Physically, this would correspond to an activated complex whose vibrational partition function is insensitive to isotopic substitution.

An intermediate value for k_1/k_2 results by assuming that the activated complex differs from the reactant only by the missing frequency associated with bond rupture. In this case, k_1/k_2 is that consistent with the rupture of a diatomic bond which possesses the missing frequency.

$$\frac{k_1}{k_2} = \frac{Q(\upsilon_{2L})}{Q(\upsilon_{1L})}\left(\frac{\upsilon_{1L}^{\ddagger}}{\upsilon_{2L}^{\ddagger}}\right)$$

where $Q(\upsilon_{L2})$ is the partition function associated with missing frequency υ_{L2}, etc. The missing vibrational mode was assumed to be one of the doubly degenerate E type asymmetric stretching ω_3 vibrations.

It is seen that the intermediate case, using the reduced mass ratio of the atoms involved in the bond rupture, agrees most closely with the experimental value. Rees and Thode (5) found a similar agreement between the theoretical and experimental results in the analogous SeO_3^{2-} reduction.

The microbiological experiment realized a kinetic isotope effect of the same order as the inorganic reduction. This suggests that the fractionation in both studies may be due to the same step in the reduction, namely the breaking

Can. J. Chem. Downloaded from www.nrcresearchpress.com by 210.87.254.105 on 09/05/12
For personal use only.

TABLE VII

Theoretical equilibrium exchange constants between highest and lowest valence states of S, Se, and Te existing in nature

$^{32}SO_4^{2-}$	+	$H_2{}^{34}S$	$\rightleftharpoons H_2{}^{32}S$	+	$^{34}SO_4^{2-}$	$K = 1.074$ (25 °C)
$^{76}SeO_4^{2-}$	+	$H_2{}^{82}Se$	$\rightleftharpoons H_2{}^{76}Se$	+	$^{82}SeO_4^{2-}$	$K = 1.043$ (20 °C) (?)
$^{76}SeO_3^{2-}$	+	$H_2{}^{82}Se$	$\rightleftharpoons H_2{}^{76}Se$	+	$^{82}SeO_3^{2-}$	$K = 1.020$ (20 °C)
$^{122}TeO_3^{2-}$	+	$H_2{}^{130}Te$	$\rightleftharpoons H_2{}^{122}Te$	+	$^{130}TeO_3^{2-}$	$K = 1.010$ (20 °C)

of the initial Te—O bond. This result is consistent with those found by Harrison and Thode (26, 27) with chemical and microbiological reduction of SO_4^{2-}. It should be mentioned, however, that under some conditions microbiological isotope fractionation may encompass more than the initial bond rupture.

One may estimate the relative fractionations of sulfur, selenium, and tellurium isotopes in nature by considering theoretical equilibrium exchanges of the elements between their lowest and highest natural valence states. These are summarized in Table VII. Sulfur exists in valence states ranging from +6 to −2. The equilibrium constant for isotopic exchange of ^{32}S and ^{34}S between SO_4^{2-} and H_2S at 25 °C is 1.074. It is interesting that the overall terrestrial $^{32}S/^{34}S$ variation is of this same order. It is questionable whether Se exists in the +6 valence state in nature because of the oxidation potential involved. It certainly exists in the +4 state and one sees that K for exchange between SeO_3^{2-} and H_2Se is much smaller than that for exchange involving SeO_4^{2-} and H_2Se. Therefore, the smaller range of natural valence states of Se and Te lowers their expected isotope fractionation when compared with that of sulfur. It should be emphasized that Table VII is for the purpose of theoretical estimation. Further interpretation will require many experimental studies.

With sulfur and selenium isotope studies, the isotope fractionation found in high temperature ore deposits is small. The present study has shown the same relationship with Te isotopes. Numerous sulfur isotope investigations have verified that microbiological conversions are responsible for large terrestrial $^{32}S/^{34}S$ variations. Consistent with this, Krouse and Thode (4) found that plants and soil samples displayed relatively large $^{76}Se/^{82}Se$ variations. However, microbiological selenium isotope fractionation in a controlled laboratory reaction has not yet been reported. The laboratory microbiological fractionation of Te isotopes in this report, coupled with the S and Se studies to date, suggest that all three elements may undergo a number of analogous biological isotope fractionation processes in nature.

Acknowledgments

The authors wish to thank the National Research Council of Canada for financial support of this project. Dr. J. W. Carmichael of the Provincial Laboratory of Public Health, University of Alberta, kindly supplied us with a culture for the microbiological study. Mineral specimens were obtained from Dr. R. E. Folinsbee of the Geology Department, University of Alberta.

Appendix

Calculation of Force Constants for TeO_3^{2-} and H_2Te

Tellurite Ion (TeO_3^{2-})

The fundamental vibrational frequencies for TeO_3^{2-} have been reported by Siebert (28) as follows (in cm^{-1}): ω_1, 758; ω_2, 364; ω_3, 703; ω_4, 326. The tellurite ion has a pyramidal XY_3 structure and a force constant analysis must consider the apex angle of the pyramid. The following expression from Herzberg (29) was used to compute the angle,

$$\cos^2 \beta = \frac{1}{4\dfrac{\omega_3^2\omega_4^2}{\omega_1^2\omega_2^2} + \dfrac{3M_y - M_x}{3M_y + M_x}},$$

where $\sin \beta = 2/\sqrt{3}$ $(\sin \alpha/2)$, where α is the apex angle, $\omega_i = i$th vibrational frequency, M_y = mass of the Y atoms, M_x = mass of the X atom.

It is noted from the expression that the angle is dependent on the mass of the tellurium atom and varies from 81.23° for $^{130}TeO_3^{2-}$ to 81.65° for $^{122}TeO_3^{2-}$. The former value was used since ^{130}Te is the most abundant isotope.

The Wilson F–G matrix method, as discussed by Nakamoto (30), was used to determine the force constants. The A_1 modes consist of two

Can. J. Chem. Downloaded from www.nrcresearchpress.com by 210.87.254.105 on 09/05/12
For personal use only.

TABLE VIII

Force constants for XY_2 nonlinear molecules ($\times 10^5$ dyn/cm)

	$C_1(k_1)$	$C_2(k_\alpha/r^2)$	$C_3(k_{1\alpha}/r)$	$C_4(k_{11})$
H_2O (11)	8.36	0.75	0.20	−0.10
H_2S (11)	4.4±0.2	0.55±0.05	0.2±0.2	−0.15±0.5
H_2Se (11)	3.4±0.1	0.38±0.06	0.15±0.03	−0.15±0.15
H_2Te (this work)	2.54±0.01	0.23±0.01	0.13±0.05	−0.12±0.01

Notation in brackets follows Smith and Linnett (38).

non-degenerate vibrations ω_1 and ω_2, and the E modes consist of the doubly degenerate ω_3 and ω_4 vibrations. The secular equation for both A_1 and E vibrations is

$$\lambda^2 - \lambda(F_{11}G_{11} + 2F_{12}G_{12} + F_{22}G_{22}) + (F_{11}F_{22} - F_{12}^2)(G_{11}G_{22} - G_{12}^2) = 0.$$

Six force constants arise, but only four distinguishable frequencies. Therefore, $F_{r\alpha}$ and $F_{r\alpha'}$ which represent interaction between the stretching and bending modes are neglected, while the stretching constants f_r and f_{rr} and the bending constants f_α and $f_{\alpha\alpha}$ are determined. Since the matrix F_{ij} is always multiplied by G_{ij} in the secular equation, the Te—O bond distance "r" is absorbed into the bending constants and is therefore not required in the calculations. The force constants, using the apex angle as calculated above, were evaluated as follows.

$$f_r = 4.361 \times 10^5 \text{ dyn cm}^{-1}$$
$$f_\alpha = 0.503 \times 10^5 \text{ dyn cm}^{-1}$$
$$f_{rr} = 0.140 \times 10^5 \text{ dyn cm}^{-1}$$
$$f_{\alpha\alpha} = 0.156 \times 10^5 \text{ dyn cm}^{-1}$$

The accuracy of this approach may be checked by considering available data on SeO_3^{2-}. Wells and Bailey (31) obtained a mean apex angle of 100.6° in their determination of the SeO_3^{2-} groups in crystals of selenious acid. The angle calculated by the Herzberg expression and observed frequencies (32, 33) is 80.54°. If the same discrepancy existed between the calculated and actual apex angle for TeO_3^{2-}, then $\alpha_{actual} \approx 101°$. For comparison, the force constants were recalculated using $\alpha = 101°$ in which case,

$$f_r = 4.377 \times 10^5 \text{ dyn cm}^{-1}$$
$$f_\alpha = 0.493 \times 10^5 \text{ dyn cm}^{-1}$$
$$f_{rr} = 0.321 \times 10^5 \text{ dyn cm}^{-1}$$
$$f_{\alpha\alpha} = 0.078 \times 10^5 \text{ dyn cm}^{-1}.$$

Although f_{rr} and $f_{\alpha\alpha}$ are significantly different for the two values of α, this was not a limitation in our study. The calculated isotopic frequencies and partition function ratios agreed to better than 0.1% for either value of α. This verifies the well-known axiom that isotopic shifts in vibrational frequencies can be determined much more accurately than the frequencies themselves.

Hydrogen Telluride (H_2Te)

Due to the chemical instability of this gas, high resolution spectroscopy has been limited and the vibrational frequencies used are peak values for bands of unresolved spectral lines. The two observed symmetric frequencies were 2047 cm^{-1} and 2133 cm^{-1} and the antisymmetric frequency observed was 860.79 cm^{-1} (34). Rossman and Straley (35) report 89°30′ as a value for the apex angle.

Triatomic nonlinear XY_2 molecules have been studied by Glockler and Tung (36) with the assumption of general force fields. Three equations with four force constants arise so that it is impossible to determine the force constants uniquely. However, a non-imaginary solution exists for only a limited range of C_4. Therefore, values of the constants C_1, C_2, and C_3 were computed in terms of permissible values of C_4 using increments of 0.01×10^5 dyn cm^{-1} from C_{4min} to C_{4max}. Figure 1 shows the relationships between the constants. The constants have the following ranges: $-1.11 < C_4 < -0.11$; $-0.50 < C_3 < 0.50$; $0.22 < C_2 < 1.22$; $1.55 < C_1 < 2.55$ (all $\times 10^5$ dyn cm^{-1}). To find a unique set of force constants requires that one constant be estimated by other means. If ω_3 is approximated by a simple diatomic H—Te bond, then the value observed (2250 cm^{-1}) by Lippincott and Dayhoff (37) may be used with a simple harmonic oscillator approximation to obtain a value of $C_1 = 2.66 \times 10^5$ dyn cm^{-1}. This suggests that C_1 is close to the maximum permitted value of 2.55×10^5 dyn cm^{-1} in Fig. 1.

Another approach is to examine the values obtained by Smith and Linnett (38) for the force constants of other members of the group VIA elements as shown in Table VIII. It is noted that

Can. J. Chem. Downloaded from www.nrcresearchpress.com by 210.87.254.105 on 09/05/12
For personal use only.

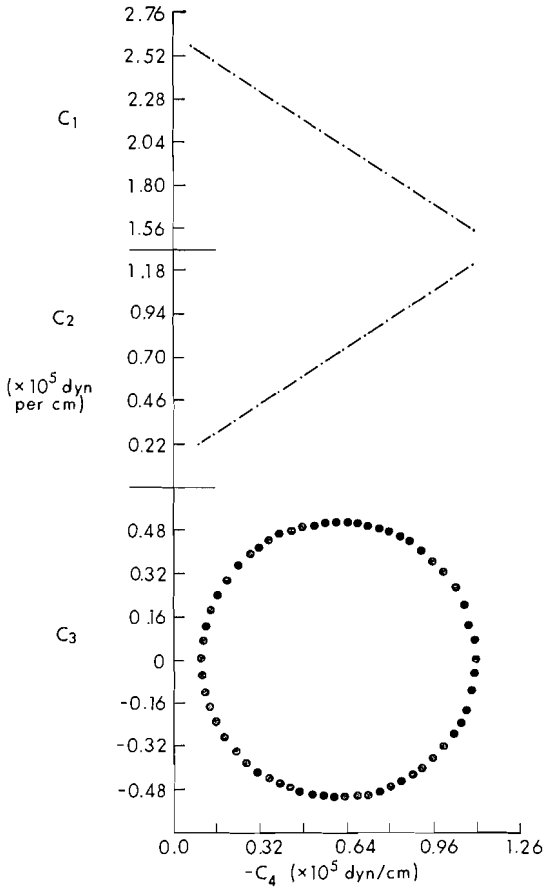

FIG. 1. Relationships between constants for H_2Te.

C_3 for H_2Se is given as $0.15 \pm 0.03 \times 10^5$ dyn cm^{-1}. Considering the trend, C_3 for H_2Te should be smaller. If, however, C_3 were taken as equal to 0.18×10^5 dyn cm^{-1} for H_2Te, this would imply that $C_2 < 0.25$; $C_1 > 2.52$; and $C_4 > -0.14$. C_3 must be also positive. Returning now to C_1, its maximum and minimum permitted values are confined to $\pm 0.01 \times 10^5$ dyn cm^{-1} and the following assignments of the force constants result.

$$C_1 = 2.54 \pm 0.01 \times 10^5 \text{ dyn cm}^{-1}$$
$$C_2 = 0.23 \pm 0.01 \times 10^5 \text{ dyn cm}^{-1}$$
$$C_3 = 0.13 \pm 0.05 \times 10^5 \text{ dyn cm}^{-1}$$
$$C_4 = -0.12 \pm 0.01 \times 10^5 \text{ dyn cm}^{-1}$$

Table VIII compares the results for H_2Te with the previous results of Smith and Linnett (38) for H_2O, H_2S, H_2Se. The deviations quoted represent mathematical limits and bear no relation to observational errors which would be much larger. The smaller deviations arise with H_2Te because of the tighter restrictions that could be placed on C_1.

1. J. R. WHITE and A. CAMERON. Phys. Rev. **74**, 991 (1948).
2. J. M. HOLLANDER, I. PERLMAN, and G. T. SEABORG. Rev. Mod. Phys. **25**, 469 (1953).
3. H. G. THODE, J. MACNAMARA, and C. B. COLLINS. Can. J. Res. B, **27**, 361 (1949).
4. H. R. KROUSE and H. G. THODE. Can. J. Chem. **40**, 367 (1962).
5. C. E. REES and H. G. THODE. Can. J. Chem. **44**, 419 (1966).
6. H. C. UREY. J. Chem. Soc. 562 (1947).
7. J. BIGELEISEN and M. G. MAYER. J. Chem. Phys. **15**, 261 (1947).
8. H. EYRING. J. Chem. Phys. **3**, 107 (1935).
9. M. G. EVANS and M. POLANYI. Trans. Faraday Soc. **31**, 875 (1935).
10. J. BIGELEISEN. J. Chem. Phys. **17**, 675 (1949).
11. N. B. SLATER. The theory of unimolecular reactions. Cornell Univ. Press, Ithaca, N.Y. 1959.
12. J. BIGELEISEN and M. WOLFSBERG. Advances in chemical physics. Vol. 1. Interscience Publishers Inc., New York. 1958. p. 15.
13. M. WOLFSBERG. J. Chem. Phys. **33**, 21 (1960).
14. G. HERZBERG. Spectra of diatomic molecules. Van Nostrand, Princeton, N.J. 1950.
15. D. F. HEATH and J. W. LINNETT. Trans. Faraday Soc. **45**, 264 (1949).
16. J. GAUNT. Trans. Faraday Soc. **50**, 546 (1954).
17. J. W. LINNETT and C. J. S. M. SIMPSON. Trans. Faraday Soc. **55**, 857 (1959).
18. C. W. F. T. Pistorius. J. Chem. Phys. **27**, 965 (1957).
19. D. F. HEATH and J. W. LINNETT. Trans. Faraday Soc. **44**, 878 (1948).
20. R. THANALAKSHMI. Current Sci. India, **31**, 374 (1962).
21. T. WENTINK, JR. J. Chem. Phys. **30**, 105 (1959).
22. J. F. REED. Anal. Chem. **32**, 662 (1960).
23. M. L. BIRD and F. CHALLENGER. J. Chem. Soc. 163 (1939).
24. F. CARR and T. G. PEARSON. J. Chem. Soc. 282 (1938).
25. H. MCCULLOUGH and H. R. KROUSE. Rev. Sci. Instr. **36**, 1132 (1965).
26. A. G. HARRISON and H. G. THODE. Trans. Faraday Soc. **53**, 1648 (1957).
27. A. G. HARRISON and H. G. THODE. Trans. Faraday Soc. **54**, 84 (1958).
28. H. SIEBERT. Z. Anorg. Allgem. Chem. **275**, 225 (1955).
29. G. HERZBERG. Infrared and Raman spectra. Van Nostrand, Princeton. 1956.
30. K. NAKAMOTO. Infrared spectra of inorganic and co-ordination compounds. Wiley, New York. 1963.
31. A. F. WELLS and M. BAILEY. J. Chem. Soc. 1282 (1949).
32. C. ROCCHICCIOLI. Compt. Rend. **247**, 1108 (1958); Ann. Chim. Paris, **5**, 999 (1960).
33. G. E. WALRAFEN. J. Chem. Phys. **39**, 1479 (1963).
34. R. A. HILL, T. H. EDWARDS, K. ROSSMAN, K. HARAHARI RAO, and H. H. NIELSEN. J. Mol. Spectry. **14**, 221 (1964).
35. K. ROSSMAN and J. W. STRALEY. J. Chem. Phys. **24**, 1276 (1956).
36. G. GLOCKLER and J. Y. TUNG. J. Chem. Phys. **13**, 338 (1945).
37. E. R. LIPPINCOTT and M. O. DAYHOFF. Spectrochim. Acta, **16**, 807 (1960).
38. S. SMITH and J. W. LINNETT. Trans. Faraday Soc. **52**, 891 (1956).

Can. J. Chem. Downloaded from www.nrcresearchpress.com by 210.87.254.105 on 09/05/12
For personal use only.

Can. J. Chem. Downloaded from www.nrcresearchpress.com by 210.87.254.40 on 09/05/12
For personal use only.

Radiolysis of *n*-hexenes

J. L. BRASH AND M. A. GOLUB
Polymer Chemistry Department, Stanford Research Institute, Menlo Park, California

Received April 28, 1967

The radiolysis of hexene-1, hexene-2, and hexene-3 at room temperature was studied with particular emphasis on the mechanisms leading to dimer formation. The structures of the hexene dimers were investigated by means of infrared and n.m.r. spectroscopy. The dimers from hexene-1, -2, and -3 had average unsaturations of 1.0, 1.2, and 1.2 double bonds/molecule, respectively, and were formed with G values of 4.6, 4.6, and 4.1 respectively. The dimerization of hexene-1 could be interpreted as proceeding, in part, through an ionic mechanism leading exclusively to monoolefinic structures, and in part through another ionic mechanism leading to a mixture of saturated, monoolefinic, and diolefinic structures. Hexene-2 and hexene-3 were found not to dimerize by the first of these ionic mechanisms, but largely by the second mechanism, along with some contribution from an exclusively radical process. The hexene-1 results are in qualitative accord with those previously reported for this olefin, while the differences noted here between this terminal olefin and the nonterminal olefins, hexene-2 and hexene-3, are qualitatively similar to the differences reported previously for butene-1 and butene-2.

Canadian Journal of Chemistry, 46, 593 (1968)

Introduction

In contrast to the saturated hydrocarbons, relatively little work has been carried out on the radiolysis of olefins, and most of that work has been concerned with terminal olefins. There is consequently a need for additional work on the radiation-induced effects in various nonterminal olefins. In view of the current interest in the role of ion–molecule processes in the radiolysis of olefins (1–5), comparative studies dealing with the relative importance of ion–molecule and free radical processes in isomeric *n*-olefins (where the double bond is in either a terminal or nonterminal position) are particularly desirable. Such a study was reported recently by Kaufman (5) for butene-1 and butene-2 in which it was shown that the position of the double bond has a pronounced effect on the relative extents of two competing ion–molecule processes in the overall mechanism. One process (involving molecule–ion condensation with a parent molecule, designated [I*a*] below) yields exclusively monoolefinic dimers, and the other process (involving hydrogen transfer to the molecule–ion to form a carbonium ion and an alkenyl radical, designated [I*b*] below) yields mixtures of saturated, monoolefinic, and diolefinic dimers, but having an average unsaturation of 1.00 double bond per dimer molecule. Any radical processes (designated [R]) occurring concomitantly yield additional diolefinic dimers (6). Kaufman concluded that butene-1, in common with hexene-1 studied earlier (1), undergoes mainly ion–molecule process [I*a*], some [I*b*], and negligible radical process [R], while butene-2 undergoes mainly [I*b*], some [I*a*], and a small but definite amount of [R].

It appeared of interest to follow up Kaufman's work with a study of another olefin system, namely, hexene-1, hexene-2, and hexene-3, and from a microstructural analysis of the dimers formed in the radiolysis, to determine how the relative extents of processes [I*a*], [I*b*], and [R] may be influenced by the double bond being at the carbon-1, -2, or -3 position.

Experimental

Hexene-1 (Phillips research grade) was chromatographically pure and used as received. Hexene-2 (Phillips pure grade, 82.6% *cis*, 17.4% *trans*) was subjected to bulb-to-bulb distillation on the vacuum line prior to use. Hexene-3 (100% *cis*) was obtained from the American Petroleum Institute. Resublimed iodine crystals were obtained from Mallinckrodt Chemicals.

Irradiation of the pure liquid hexenes up to 300 Mrads (and up to 700 Mrads in some cases to achieve the conversion necessary for identification of certain products) was carried out at $\sim$ 20 °C using 1-MeV electrons from a G.E. resonant transformer (and also using ^{60}Co γ rays in the case of hexene-1). Standard thin-wall-glass n.m.r. vials were used as reaction vessels; ceric ion dosimetry was used.

Hexene samples of about 1 g were distilled into the vials from a reservoir on the vacuum line, taken through several degassing cycles, and pumped at -196 °C to a pressure not exceeding 10^{-5} Torr. In scavenging experiments, resublimed crystalline iodine was dissolved in the hexene prior to degassing, and irradiation carried out as above.

For gas analysis the vials were broken under vacuum and noncondensable gas determined by Toepler pumping

Can. J. Chem. Downloaded from www.nrcresearchpress.com by 210.87.254.40 on 09/05/12
For personal use only.

through two liquid nitrogen traps to a gas burette. The liquid was taken through several thaw–freeze–pump degassing cycles to ensure complete removal of dissolved gas. The analysis for hydrogen and methane was done by gas chromatography using a 20 ft Linde molecular sieve 5A column at room temperature, and in a few cases by mass spectrometry.

The *cis–trans* isomerization was determined by gas–liquid chromatography (g.l.c.) using a 20 ft β,β'-oxydipropionitrile column at 30 °C, which gave complete resolution of the geometric isomers of both hexene-2 and hexene-3.

The formation of dimers from all three hexenes was established by isolation of a peak from the g.l.c. of each irradiated olefin on a 3 ft silicone column (G.E. SF-96) at 150 °C, and confirmed by mass spectrometry. Apart from unreacted hexene, dimer was by far the major feature of the silicone g.l.c.; some minor peaks appeared at intermediate retention times indicating likely side reactions involving parent hexene and radiolysis fragments. The chromatograph was calibrated by reinjection of measured volumes of g.l.c.-purified dimer under conditions identical with those used in the analysis. G(dimer) values were obtained for irradiations in the range 0–300 Mrads.

The dimers (and various dimer components as described in the results) were collected as they emerged from the g.l.c. and further characterized by n.m.r. (Varian HA-100 spectrometer) and infrared (Perkin–Elmer model 221) spectroscopy.

Results and Discussion

Gas Evolution

The radiation-induced evolution of gas in the different *n*-hexenes was linear with dose in the range 0–300 Mrads; the G values are given in Table I. The $G(\text{gas}) = 0.92$ for hexene-1, obtained for both γ rays and electrons, is in good agreement with the values of 0.8–0.9 reported by Chang *et al.* (1). As expected, the gas produced by the internal olefins consisted of a relatively higher methane content ($\sim$ 6–8% CH_4) than the gas from hexene-1, which was nearly all hydrogen (> 97% H_2, 2% CH_4). That the G(gas) for hexene-2 is higher than for hexene-1 is in line with the observation (5) that $G(H_2 + CH_4)$ for liquid butene-2 at room temperature (1.12–1.16) is higher than the corresponding value for liquid butene-1 (0.60–0.69). The finding that the gas yield from hexene-3 is higher than that from hexene-2 is surprising, however, and it suggests the desirability of examining a series of *n*-octenes or *n*-decenes to see if this apparent trend of increasing G(gas) with approach of the double bond towards the center of the molecule is a general one.

TABLE I

Radiolysis of *n*-hexenes

Compound	$G(H_2)$	$G(CH_4)$	G(isom.)	G(dimer)
Hexene-1	0.90	0.02	—	4.6
Hexene-2	1.17	0.08	2.13	4.6
Hexene-3	1.61	0.14	2.86	4.1

Most of the gas evolved in the radiolysis of hexene-2 (and probably also in the other *n*-hexenes) arises from some nonradical process as indicated by the fact that the G(gas) for this olefin in the presence of 2% iodine (1.07) is more than 80% of the G value in the absence of this free-radical scavenger (1.25). This situation is similar to that encountered in polyisoprene (7, 8), where only 10% of the hydrogen produced radiolytically arises from a radical source. It is also similar to that noted for the radiolysis of butene-2 in which, according to some work (9),[1] less than $\sim$ 20% of the hydrogen yield is radical in origin, while according to other work (10), the nonradical production of hydrogen is negligible.

Isomerization

The G(isom.) values given in Table I were obtained from the initial slopes of the plots of % *trans* isomer formed vs. dose. The value for hexene-2 fits a regular pattern of decreasing G(isom.) with length of the molecule for a series of 2-olefins, as indicated previously (11). The higher G(isom.) value obtained for hexene-3 compared with that for hexene-2 finds a parallel in early work by Charlesby (12) in which *cis*-octadecene-7 had a somewhat higher yield of radiation-induced isomerization than *cis*-octadecene-2.

Dimerization

As shown in Table I, the G(dimer) values for the various *n*-hexenes (determined over the dose range 0–300 Mrads) were substantially the same. For hexene-1, the value of 4.6 is considerably higher than the values of 1.9 and 1.0 reported by Chang *et al.* (1) for γ rays and electrons respectively.[2] It is difficult to account for this difference, especially since the G(gas)

[1]The estimate of 20% is based on a $G(H_2) \sim 1.0$ for liquid *cis*-butene-2 (5, 10) and a corresponding G(H atom) < 0.4 (9).

[2]Private discussion with Dr. C. D. Wagner has not disclosed the source of this discrepancy.

Can. J. Chem. Downloaded from www.nrcresearchpress.com by 210.87.254.40 on 09/05/12
For personal use only.

yields for hexene-1 reported in this work and by Chang *et al.* are in rather close agreement. There are no prior data in the literature for *G*(dimer) for hexene-2 and -3.

Further g.l.c. analysis of the dimeric fractions on the same silicone column at lower temperature (100 °C) showed them to consist of groups of several peaks rather than a single peak. Attempts were made to resolve these components both for quantitation and for identification. The results are reported below for each *n*-hexene with some speculation as to possible modes of dimerization.

(a) Hexene-1

The dimeric product showed three distinct peaks in the molar ratio 2.5:1.5:1.0, which ratio did not change with dose up to 300 Mrads. These components were well resolved and could be collected separately as they emerged from the column. The infrared and n.m.r. spectra of the largest peak (H-1*a*) showed it to be a pure straight chain, nonterminal monoolefin. Such a product, according to Chang *et al.* (1), could arise only by the ion–molecule process [I*a*]

[I*a*] $CH_2{=}CH(CH_2)_3CH_3 \rightsquigarrow$

$$CH_2{=}\overset{+}{C}H(CH_2)_3CH_3 \rightarrow \left[\dot{C}H_2{-}\overset{+}{C}H(CH_2)_3CH_3 \leftrightarrow \overset{+}{C}H_2{-}\dot{C}H(CH_2)_3CH_3\right]$$

$$\overset{+}{C}H_2{-}\dot{C}H(CH_2)_3CH_3 + CH_2{=}CH(CH_2)_3CH_3 \rightarrow CH_2{-}\dot{C}H(CH_2)_3CH_3 \,|\, CH{-}\overset{+}{C}H(CH_2)_3CH_3 \rightarrow$$

$$\overset{+}{C}H{-}\dot{C}H(CH_2)_3CH_3 \,|\, CH_2{-}CH_2(CH_2)_3CH_3 \xrightarrow{e^-} CH{=}CH(CH_2)_3CH_3 \,|\, CH_2{-}(CH_2)_4CH_3$$

1

The formation of substantial nonterminal monoolefinic dimer (presumably *n*-dodecene-5 (**1**)), amounting to 50% of the dimer yield from hexene-1, is in line with that indicated by Chang *et al.*, who reported as much as 80% of such a product. It is therefore reasonable to suggest that at least half of the dimer formed from hexene-1 in this study (i.e. H-1*a* peak) was formed via ion–molecule process [I*a*].

Based on the n.m.r. spectra, the average unsaturation of the whole hexene-1 dimer was seen to be 1.00 double bond/molecule, in agreement with Chang *et al.* This degree of unsaturation indicates that an exclusively radical process [R] (i.e. one *not* involving any coparticipation of ions) is probably not implicated, since such a process characteristically yields diolefinic dimer (6).

[R] $CH_2{=}CHCH_2(CH_2)_2CH_3 \rightsquigarrow$

$CH_2{=}CH\dot{C}H(CH_2)_2CH_3 \rightarrow$ diolefinic dimers

Unfortunately, the structures of the various dimer components present in the other g.l.c. peaks, H-1*b* and H-1*c*, could not be determined with sufficient precision to establish the mechanism responsible for their formation. However, infrared analysis of the intermediate peak H-1*b* indicated the presence of —CH=CH— (at 10.4 μ) and $CH_2{=}CH$— (at 11.0 μ) double bonds in the ratio of about 2:1, with a very minor amount of $CH_2{=}C<$ (at 11.3 μ), while the n.m.r. spectrum showed the presence of 34% "saturated" methyl protons (at 9.0–9.1 τ), and 47% "saturated" methylene protons (8.5–8.9 τ range), along with 12% "unsaturated" methylene protons (at 8.0 τ), 4.4% —CH= protons (at 4.7 τ), and 1.9% —CH=CH_2 protons (at 5.1 τ). These spectroscopic data indicate the formation of both saturated dimer structures as well as unsaturated dimer, with an *average* saturation of 0.7 double bond per dimer molecule in H-1*b*. The smallest peak (H-1*c*) was not obtained in sufficient quantity to give useful spectra, but on a material balance basis it may be considered to have an unsaturation approaching 1.5 double bonds/molecule.

Although the results on H-1*b* and H-1*c* do not point to any specific mechanism, they are

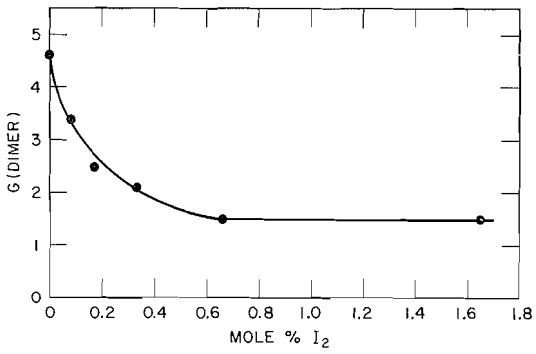

FIG. 1. The effect of iodine on the dimer yield in the radiolysis of hexene-2.

[*Ib*] $CH_2{=}\overset{+}{C}H(CH_2)_3CH_3 + C_6H_{12} \rightarrow CH_3{-}\overset{+}{C}H(CH_2)_3CH_3 +$ [$CH_2{=}CH\dot{C}H(CH_2)_2CH_3 \leftrightarrow \cdot CH_2{-}CH{=}CH(CH_2)_2CH_3$] (*a*, *b*)

$CH_3\overset{+}{C}H(CH_2)_3CH_3 + CH_2{=}CH(CH_2)_3CH_3 \longrightarrow CH_3{-}CH(CH_2)_3CH_3$ (at $CH_2{-}\overset{+}{C}H(CH_2)_3CH_3$) $\xrightarrow{C_6H_{12}}$ $CH_3{-}CH(CH_2)_3CH_3$ (at $CH_2{-}CH_2(CH_2)_3CH_3$) $+ C_6H_{11}^+$

2

$C_6H_{11}^+ \xrightarrow{e^-} a$ (or *b*)

2*a* (or *b*) → diolefinic dimers

compatible with a second kind of ion–molecule process [*Ib*] indicated by Chang *et al.* for hexene-1 dimerization. This process is considered (1, 5) to yield saturated dimers (such as **2**) and diolefinic dimers in essentially equal amounts, and hence, quite apart from [*Ia*], to yield an average unsaturation of one double bond per dimer molecule.

A possible competing reaction involving the carbonium ion $C_6H_{13}^+$ in [*Ib*], although not specifically identified in Kaufman's mechanism (5), is that yielding monoolefinic dimer,

$$CH_3\overset{+}{C}H(CH_2)_3CH_3 \xrightarrow{e^-} CH_3\dot{C}H(CH_2)_3CH_3$$

a (or *b*) + $CH_3\dot{C}H(CH_2)_3CH_3$ → monoolefinic dimers,

a reaction which would not affect, of course, the net monoolefinic character of the dimer formed by [*Ib*].[3]

(b) Hexene-2

The silicone chromatogram for hexene-2 dimer showed seven peaks which could not be separated under even the most favorable practical conditions; thus we report data only on the spectra of the total dimeric product. The infrared spectrum showed a *trans* vinylene/vinyl ratio of 3.2 and a vinyl/vinylidene ratio of ~ 8, while the n.m.r. spectrum showed 7.3% of the protons as $CH_3{-}\dot{C}{=}$, 42.4% as $CH_3{-}\dot{C}{-}$, 8.3% as —CH=CH— (*cis* and *trans*), and 1.3% as —CH=CH_2, the remaining protons being found in "saturated" and "unsaturated" methylene groups. From these spectroscopic data, the hexene-2 dimer was seen to have an *average* unsaturation of 1.2 double bonds/molecule, consisting of 1.0 vinylene, 0.2 vinyl, and negligible vinylidene units.

Significantly, no trisubstituted double bonds (>C=CH—) were found in the hexene-2 dimer as attested by the absence of both the characteristic infrared absorption at 12.0–12.4 μ and n.m.r. peak at 5.0 τ. The lack of trisubstituted double bonds definitely ruled out the contribution of ion–molecule mechanism [*Ia*] to the dimerization of hexene-2 since that mechanism would yield structures *c* and *d*

$[CH_3\overset{+}{C}H{-}\dot{C}HCH_2CH_2CH_3 \leftrightarrow CH_3\dot{C}H{-}\overset{+}{C}HCH_2CH_2CH_3]$ (*c*, *d*)

which on condensation with parent molecules, would lead to various monoolefin dimers (typified by structure **3**) containing just that type of double bond.

$CH_3{-}C{=}CH(CH_2)_2CH_3$ (at $CH_3CH_2CH{-}(CH_2)_2CH_3$)

3

Evidence that ionic (or molecular) species nevertheless probably take part in the dimerization of hexene-2 was obtained from experi-

[3]This variation in [*Ib*] is necessary to account for the fact that the monoolefinic dimers are produced in excess of the amount indicated by mechanism [*Ia*] alone. Thus, for example, out of the 60% monoolefinic dimer formed in the radiolysis of butene-2 (5), only 25–30% was attributed to mechanism [*Ia*], the balance presumably coming from [*Ib*].

Can. J. Chem. Downloaded from www.nrcresearchpress.com by 210.87.254.40 on 09/05/12
For personal use only.

Can. J. Chem. Downloaded from www.nrcresearchpress.com by 210.87.254.40 on 09/05/12
For personal use only.

ments involving iodine as free radical scavenger (13). Figure 1 shows that the scavenging effect reached a maximum at about 0.6 mole % iodine when the dimer yield dropped to about one third its value in the absence of iodine, and remained constant thereafter. These results signify that the precursors to about two thirds of the dimer produced from hexene-2 are free radical in nature while the remainder are ionic (or molecular). It is quite possible that the unscavengeable precursors are of the carbonium ion type depicted in mechanism [I*b*]. That mechanism would lead to equimolar amounts of ionic and radical precursors, so that scavenging of the latter would reduce the dimer yield by half. The remaining scavengeable precursors of dimer (to make up the total of two thirds scavenged) could be those radicals arising from process [R]. On this basis, we could imagine about 68% of the dimerization proceeding through [I*b*] and 32% through [R].

This general picture is qualitatively supported by the fact that the average unsaturation of the hexene-2 dimer is 1.2 double bonds/molecule. Mechanism [I*b*] yields an average unsaturation of one double bond, and mechanism [R] yields two double bonds, per dimer molecule, while both processes occurring at the same time would be expected to yield some intermediate unsaturation. The average unsaturation of 1.2 double bonds/dimer molecule can be taken, therefore, as suggesting that about 80% of the dimerization proceeds through [I*b*] and 20% through [R], values which are not far off from those indicated by the scavenging experiments. At any rate, as noted earlier, mechanism [I*a*] is definitely excluded as a route to hexene-2 dimer.

(c) Hexene-3

The silicone chromatogram for hexene-3 dimer showed five peaks, four of which could not be separated. The fifth peak, representing about 7% of the dimer mixture, provided little information beyond the fact that it was completely saturated. The observations on the hexene-3 dimerization were, therefore, based on the infrared and n.m.r. spectra of the whole dimeric product.

The spectral data can be summarized by stating that the infrared showed only vinylene (—CH=CH—) unsaturation and apparently no vinyl or vinylidene double bonds, while the n.m.r. indicated an average of 1.2 double bonds/dimer molecule (based on the olefinic proton peak at 4.7 τ). These results indicate that the dimerization of hexene-3 is similar to that of hexene-2. Thus, as with hexene-2, the ion–molecule mechanism [I*a*] can be ruled out since the spectra show no evidence for the trisubstituted double bonds of structure **4** required by that process. Moreover, the *average* unsaturation of 1.2 double bonds/dimer molecule implies, just as with hexene-2, that the hexene-3 dimer may be formed to a considerable extent (perhaps as much as 80%) by the ion–molecule process [I*b*], and also to some extent (~ 20%) by the radical process [R].

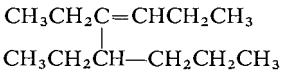

4

To sum up the dimerization of the *n*-hexenes, we see that the nonterminal olefins (hexene-2 and -3) differ in their overall behavior from the terminal olefin (hexene-1) in that the latter probably dimerize by the ionic processes [I*a*] and [I*b*], with little or no contribution from [R], whereas the former probably dimerize by [I*b*] and [R] with *no* contribution from [I*a*]. This trend towards a much higher contribution of [I*b*] compared with [I*a*] as the double bond is moved from a terminal to a carbon-2 or -3 position, exhibited by the *n*-hexenes, is in keeping with the findings of Kaufman for the radiolysis of butene-1 and butene-2 (5). In that work the analog of [I*a*] is considered to occur to the extent of about 70–80% in the dimerization of butene-1 and to about 25–30% in butene-2. It is interesting to note that according to recent work of Howton and Wu (14), when the double bond is located near the center of a rather long olefin molecule, ionic processes no longer contribute and the dimerization proceeds mainly by process [R]: thus, the dimeric hydrocarbon obtained from the radiolysis of oleic acid ($C_8H_{17}CH{=}CHC_7H_{14}COOH$) is largely, if not entirely, diolefinic.

Acknowledgments

This research was supported in part by the Air Force Materials Laboratory, Wright-Patterson Air Force Base, Ohio, and in part by Stanford Research Institute.

1. P. C. CHANG, N. C. YANG, and C. D. WAGNER. J. Am. Chem. Soc. **81**, 2060 (1959).
2. C. D. WAGNER. Tetrahedron, **14**, 164 (1961).
3. E. COLLINSON, F. S. DAINTON, and D. C. WALKER. Trans. Faraday Soc. **57**, 1732 (1961).
4. C. D. WAGNER. J. Phys. Chem. **66**, 1158 (1962).
5. P. C. KAUFMAN. J. Phys. Chem. **67**, 1671 (1963).
6. M. S. KHARASCH, D. SCHWARTZ, and W. NUDENBERG. J. Org. Chem. **18**, 337 (1953).
7. D. T. TURNER. Polymer, **1**, 27 (1960).
8. D. T. TURNER. J. Polymer Sci. Pt. B, **1**, 93, 97 (1963).
9. R. A. HOLROYD and G. W. KLEIN. J. Phys. Chem. **69**, 194 (1965).
10. Y. HATANO, S. SHIDA, and S. SATO. Bull. Chem. Soc. Japan, **37**, 1854 (1964).
11. M. A. GOLUB, C. L. STEPHENS, and J. L. BRASH. J. Chem. Phys. **45**, 1503 (1966).
12. A. CHARLESBY. Radiation Res. **2**, 96 (1955).
13. R. H. SCHULER. J. Phys. Chem. **62**, 37 (1958).
14. D. R. HOWTON and G.-S. WU. J. Am. Chem. Soc. **89**, 516 (1967).

Can. J. Chem. Downloaded from www.nrcresearchpress.com by 210.87.254.40 on 09/05/12
For personal use only.

Can. J. Chem. Downloaded from www.nrcresearchpress.com by 210.87.254.5 on 09/05/12
For personal use only.

Hameka theory of optical rotation

D. A. HUTCHINSON
Department of Chemistry, Queen's University, Kingston, Ontario

Received August 4, 1967

Rosenfeld's formula, for off-resonance optical rotation, is derived by an alternative approach. The scattering amplitudes are determined for the scattering of right circularly polarized light and left circularly polarized light by a molecule. The calculation is carried out to the order of approximation which includes electric quadrupole and magnetic dipole terms. From the real parts of the forward scattering amplitudes the corresponding indices of refraction are determined for left and right circularly polarized light. Rosenfeld's formula then follows from the difference between the two refractive indices.

Canadian Journal of Chemistry, **46**, 599 (1968)

Introduction

The first quantum mechanical discussion of optical rotation was provided by Rosenfeld (1); Rosenfeld's calculation used the semi-classical method where the molecules were treated by quantum mechanics and the radiation field was treated by classical electromagnetic theory. The review article by Condon (2) describes a calculation which is equivalent to Rosenfeld's.

An optically active medium is one for which the respective indices of refraction $n_R(k,+)$ and $n_R(k,-)$, for left and right circularly polarized light, are different. This is referred to as circular double refraction. In terms of the difference between the refractive indices, the optical rotation (angle of rotation per unit length, $\phi(k)/l$) is

$$[1] \qquad \phi(k)/l = \tfrac{1}{2}k\{n_R(k,+) - n_R(k,-)\}.$$

$\boldsymbol{k}$ is the propagation vector for the light; $k = 2\pi/\lambda$, where λ is the wavelength.

Condon's (2) calculation leads to the final result

$$[2] \qquad \frac{\phi(k)}{l} = \frac{4\pi N\alpha k^2}{3mc}\sum_{n''}\frac{Im(\langle g|\hat{\boldsymbol{R}}|n''\rangle\cdot\langle n''|\hat{\boldsymbol{L}}|g\rangle)}{k^2_{n''g} - k^2}$$

for dilute systems where the mean index of refraction is nearly unity. In the above equation, N is the number of molecules per unit volume, $\alpha = e^2/\hbar c = 1/137$ is the fine structure constant, m is the electron mass, c is the velocity of light *in vacuo*, and $k_{n''g}$ is related to the energy difference between an excited molecular state $|n''\rangle$ and the ground state $|g\rangle$ by

$$E_{n''} - E_g = \hbar c k_{n''g}.$$

Finally $\hat{\boldsymbol{R}}$ and $\hat{\boldsymbol{L}}$ are respectively the coordinate and orbital angular momentum operators for the molecule. Throughout this paper the discussion is restricted to molecules whose ground state $|g\rangle$ is a singlet.

If for no other purpose than an academic exercise, a calculation of optical rotation which treats both the molecules and radiation field quantum mechanically would be of interest. Hameka has performed such calculations for both optical rotation (3) and magnetic optical rotation (4). In these calculations, Hameka was primarily interested in the rotation spectra; the calculations employed the Heitler–Ma (5) perturbation method. In his calculations, Hameka concluded that optical rotation is not physically meaningful at resonance.

The work in this paper presents a different deduction of Rosenfeld's formula, eq. [2]; the description is limited to the off-resonance situation where optical rotation is physically meaningful. The forward scattering amplitudes are determined for the scattering of right and left circularly polarized light by a molecule. The methods used are essentially those given in Dirac's book (6) for the theory of dispersive scattering. In fact only two refinements are required. Firstly the method is made applicable to circularly polarized light and second it is extended to the approximation where $e^{i\boldsymbol{k}\cdot\boldsymbol{r}}$ is replaced by $1 + i\boldsymbol{k}\cdot\boldsymbol{r}$ rather than simply unity.

From the real parts of the forward scattering amplitudes $f_R(k,\pm,g)$ for left and right circularly polarized light, the corresponding indices of refraction $n_R(k,\pm)$ follow readily from the relation (7)

$$[3] \qquad n_R(k,\pm) - 1 = 2\pi N k^{-2} f_R(k,\pm,g).$$

A subscript R is used to indicate the real part of a quantity which in general can be complex; similarly a subscript I indicates the imaginary

Can. J. Chem. Downloaded from www.nrcresearchpress.com by 210.87.254.5 on 09/05/12
For personal use only.

part. An outline of a derivation of eq. [3], based on dispersion relations, is given in the appendix.

Once the refractive indices $n_R(k,\pm)$ have been determined, Rosenfeld's formula can be obtained with the use of eq. [1]. The determinations of the forward scattering amplitudes, refractive indices, and Rosenfeld's formula are discussed in the next section.

Scattering Amplitudes, Refractive Indices, and Rosenfeld's Formula

An appropriate starting point for a discussion of scattering amplitudes is to consider a scattering process for which the incident particle has momentum $\hbar\boldsymbol{k}$, the scattered particle has momentum $\hbar\boldsymbol{k}'$, the scatterer is initially in its ground state $|g\rangle$ and finally in a state $|n'\rangle$. The relevant scattering amplitude $f(\boldsymbol{k}'n', \boldsymbol{k}g)$ is defined by

$$f(\boldsymbol{k}'n', \boldsymbol{k}g) = -(2\pi/\hbar c)^2 W' \langle \boldsymbol{k}'n'|\hat{V}^1|\boldsymbol{k}g^{(+)}\rangle,$$

W' is the kinetic energy corresponding to momentum $\hbar\boldsymbol{k}'$, $|\boldsymbol{k}'n'\rangle$ is the state where the particle has momentum $\hbar\boldsymbol{k}'$ and the scatterer is in the state $|n'\rangle$. $|\boldsymbol{k}g^{(+)}\rangle$ is an outgoing solution of the Schrödinger equation describing the scatterer plus the particle plus the interaction $\hat{V}^1$; $|\boldsymbol{k}g^{(+)}\rangle$ reduces to the state $|\boldsymbol{k}g\rangle$ as $\hat{V}^1$ tends to zero.

The situation of interest is one where the scatterer is capable of emitting or absorbing particles. If the first Born approximation is used, and if matrix elements of $\hat{V}^1$ involving a change of one particle are of first order whereas those involving a change of two particles are of second order, the scattering amplitude to second order is

$$[4] \quad f(\boldsymbol{k}'n', \boldsymbol{k}g) = -(2\pi/\hbar c)^2 W' \left\{ \langle \boldsymbol{k}'n'|\hat{V}^1|\boldsymbol{k}g\rangle + \sum_{n''} \left(\frac{\langle \boldsymbol{k}'n'|\hat{V}^1|On''\rangle\langle On''|\hat{V}^1|\boldsymbol{k}g\rangle}{W - (E_{n''} - E_g)} - \frac{\langle \boldsymbol{k}'n'|\hat{V}^1|\boldsymbol{k}\boldsymbol{k}'n''\rangle\langle \boldsymbol{k}\boldsymbol{k}'n''|\hat{V}^1|\boldsymbol{k}g\rangle}{W' + (E_{n''} - E_g)} \right) \right\}.$$

This result is valid for the off-resonance situation

$$W \neq E_{n''} - E_g \quad \text{for all } n''.$$

All that is required in order to make eq. [4] applicable to photon scattering is to include the polarization σ in the state vector and to substitute the appropriate expression for the interaction $\hat{V}^1$.

The gauge chosen for the radiation field is the one for which the magnetic vector potential $\boldsymbol{A}$ and the electrostatic potential ϕ satisfy the equations

$$\left(\frac{1}{c^2}\frac{\partial^2}{\partial t^2} - \nabla^2\right)\boldsymbol{A} = 0, \quad \text{div } \boldsymbol{A} = 0, \quad \phi = 0.$$

In this gauge, the interaction between an electron of momentum $\boldsymbol{p}$ and the radiation field is

$$\hat{V}^1 = \frac{e}{mc}\hat{\boldsymbol{A}}\cdot\hat{\boldsymbol{p}} + \frac{e^2}{2mc^2}\hat{A}^2.$$

If the vector potential operator $\hat{\boldsymbol{A}}$ is expressed in terms of the photon creation and annihilation operators $\hat{s}_\sigma(\boldsymbol{k})$ and $\hat{s}_\sigma\dagger(\boldsymbol{k})$, $\hat{V}^1$ in Schrödinger representation is

$$[5] \quad \hat{V}^1 = (\alpha^{\frac{1}{2}}\hbar/2\pi m)\sum_\sigma \sum_{\boldsymbol{k}} k^{-\frac{1}{2}}\{\hat{s}_\sigma(\boldsymbol{k})e^{-i\boldsymbol{k}\cdot\hat{\boldsymbol{r}}}\hat{p}_\sigma{}^\dagger + \hat{s}_\sigma\dagger(\boldsymbol{k})e^{i\boldsymbol{k}\cdot\hat{\boldsymbol{r}}}\hat{p}_\sigma\}\rho_\sigma^{-\frac{1}{2}}(\boldsymbol{k}) +$$
$$(\alpha\hbar^2/8\pi^2 m)\sum_\sigma \sum_{\boldsymbol{k}} \sum_{\sigma'} \sum_{\boldsymbol{k}'} k^{-\frac{1}{2}}k'^{-\frac{1}{2}}\{\hat{s}_\sigma(\boldsymbol{k})e^{-i\boldsymbol{k}\cdot\hat{\boldsymbol{r}}}\hat{s}_{\sigma'}(\boldsymbol{k}')e^{-i\boldsymbol{k}'\cdot\hat{\boldsymbol{r}}}\boldsymbol{e}_\sigma\cdot\boldsymbol{e}_{\sigma'} +$$
$$\hat{s}_\sigma(\boldsymbol{k})e^{-i\boldsymbol{k}\cdot\hat{\boldsymbol{r}}}\hat{s}_{\sigma'}\dagger(\boldsymbol{k}')e^{i\boldsymbol{k}'\cdot\hat{\boldsymbol{r}}}\boldsymbol{e}_\sigma\cdot\boldsymbol{e}_{\sigma'}{}^* + \hat{s}_\sigma\dagger(\boldsymbol{k})e^{i\boldsymbol{k}\cdot\hat{\boldsymbol{r}}}\hat{s}_{\sigma'}(\boldsymbol{k}')e^{-i\boldsymbol{k}'\cdot\hat{\boldsymbol{r}}}\boldsymbol{e}_\sigma{}^*\cdot\boldsymbol{e}_{\sigma'} +$$
$$\hat{s}_\sigma\dagger(\boldsymbol{k})e^{i\boldsymbol{k}\cdot\hat{\boldsymbol{r}}}\hat{s}_{\sigma'}\dagger(\boldsymbol{k}')e^{i\boldsymbol{k}'\cdot\hat{\boldsymbol{r}}}\boldsymbol{e}_\sigma{}^*\cdot\boldsymbol{e}_{\sigma'}{}^*\}\rho_\sigma{}^{-\frac{1}{2}}(\boldsymbol{k})\rho_{\sigma'}{}^{-\frac{1}{2}}(\boldsymbol{k}').$$

In the above equation, the adjoint of an operator is indicated by a dagger and $\rho_\sigma(\boldsymbol{k})$ represents the density of states which is involved in the replacing of a summation by an integration. $\boldsymbol{e}_\sigma = \boldsymbol{e}_\sigma(\boldsymbol{k})$ is a unit vector which describes the polarization. For left circularly polarized light

$$\boldsymbol{e}_+ = 2^{-\frac{1}{2}}(\boldsymbol{e}_1 - i\boldsymbol{e}_2)$$

and for right circularly polarized light

$$\boldsymbol{e}_- = 2^{-\frac{1}{2}}(\boldsymbol{e}_1 + i\boldsymbol{e}_2);$$

the unit vectors $\boldsymbol{e}_1$, $\boldsymbol{e}_2$ and the propagation vector $\boldsymbol{k}$ are mutually perpendicular.

If eq. [5] is substituted into eq. [4], and terms up to first order in $\boldsymbol{k}\cdot\hat{\boldsymbol{r}}$ are retained, then

$$[6] \quad f(\boldsymbol{k}'\sigma'n', \boldsymbol{k}\sigma g) = f_0(\boldsymbol{k}'\sigma'n', \boldsymbol{k}\sigma g) + f_1(\boldsymbol{k}'\sigma'n', \boldsymbol{k}\sigma g),$$

Can. J. Chem. Downloaded from www.nrcresearchpress.com by 210.87.254.5 on 09/05/12
For personal use only.

where

$$f_O(\boldsymbol{k}'\sigma'n',\ \boldsymbol{k}\sigma g) = -\alpha(mc)^{-2}k'^{\frac{1}{2}}k^{-\frac{1}{2}}\Big\{mc\hbar\delta_{n'g}\boldsymbol{e}_{\sigma'}\cdot\boldsymbol{e}_\sigma^* + \sum_{n''}\left(\frac{\langle n'|\hat{p}_{\sigma'}\dagger|n''\rangle\langle n''|\hat{p}_\sigma|g\rangle}{k - k_{n''g}} - \frac{\langle n'|\hat{p}_\sigma|n''\rangle\langle n''|\hat{p}_{\sigma'}\dagger|g\rangle}{k' + k_{n''g}}\right)\Big\}$$

and

$$f_1(\boldsymbol{k}'\sigma'n',\ \boldsymbol{k}\sigma g) = -\alpha(mc)^{-2}k'^{\frac{1}{2}}k^{-\frac{1}{2}}\Big\{imc\hbar\langle n'| - k'\hat{x}_{k'} + k\hat{x}_k|g\rangle\boldsymbol{e}_{\sigma'}\cdot\boldsymbol{e}_\sigma^* + \sum_{n''}\left(\frac{-ik'\langle n'|\hat{x}_{k'}\hat{p}_{\sigma'}\dagger|n''\rangle\langle n''|\hat{p}_\sigma|g\rangle + ik\langle n'|\hat{p}_{\sigma'}\dagger|n''\rangle\langle n''|\hat{x}_k\hat{p}_\sigma|g\rangle}{k - k_{n''g}} + \frac{-ik\langle n'|\hat{x}_k\hat{p}_\sigma|n''\rangle\langle n''|\hat{p}_{\sigma'}\dagger|g\rangle + ik'\langle n'|\hat{p}_\sigma|n''\rangle\langle n''|\hat{x}_{k'}\hat{p}_{\sigma'}\dagger|g\rangle}{k' + k_{n''g}}\right)\Big\},$$

in which $\hat{x}_k = k^{-1}\boldsymbol{k}\cdot\hat{\boldsymbol{r}}$, etc.

Now, in scattering problems the vector $\boldsymbol{k}'$ is restricted to a vector $\boldsymbol{k}(n'g)$ whose magnitude is

$$k(n'g) = k - k_{n'g}; \tag{7}$$

this restriction is essentially a consequence of the law of conservation of energy. From this point onward, it shall be understood that

$$\boldsymbol{k}' = \boldsymbol{k}(n'g),$$

but in formulae the simpler symbol $\boldsymbol{k}'$ shall be retained so that the notation does not become too cumbersome. The restriction eq. [7] allows $f_O(\boldsymbol{k}'\sigma'n',\ \boldsymbol{k}\sigma g)$ to be simplified to

$$f_O(\boldsymbol{k}'\sigma'n',\ \boldsymbol{k}\sigma g) = -\alpha k'^{\frac{3}{2}}k^{\frac{1}{2}}\sum_{n''}\left(\frac{\langle n'|\hat{x}_{\sigma'}\dagger|n''\rangle\langle n''|\hat{x}_\sigma|g\rangle}{k - k_{n''g}} - \frac{\langle n'|\hat{x}_\sigma|n''\rangle\langle n''|\hat{x}_{\sigma'}\dagger|g\rangle}{k' + k_{n''g}}\right). \tag{8}$$

Since the details of this simplification are given by Dirac (6) in a derivation of the Kramers–Heisenberg dispersion formula, there is no need to repeat them here. Also, the methods are quite similar to those involved in the simplification of $f_1(\boldsymbol{k}'\sigma'n', \boldsymbol{k}\sigma g)$. If the restriction eq. [7] is imposed on $\boldsymbol{k}'$, $f_1(\boldsymbol{k}'\sigma'n', \boldsymbol{k}\sigma g)$ can be simplified as follows.

First of all the result

$$\langle n'|\hat{p}_{\sigma'}\dagger|n''\rangle = imck_{n'n''}\langle n'|\hat{x}_{\sigma'}\dagger|n''\rangle$$

is applied to those matrix elements which only contain a single component of the momentum operator; this yields the equation

$$f_1(\boldsymbol{k}'\sigma'n',\ \boldsymbol{k}\sigma g) = -\alpha(mc)^{-1}k'^{\frac{1}{2}}k^{-\frac{1}{2}}\Big\{i\hbar\langle n'| - k'\hat{x}_{k'} + k\hat{x}_k|g\rangle\boldsymbol{e}_{\sigma'}\cdot\boldsymbol{e}_\sigma^* + \sum_{n''}\left(\frac{k'k_{n''g}\langle n'|\hat{x}_{k'}\hat{p}_{\sigma'}\dagger|n''\rangle\langle n''|\hat{x}_\sigma|g\rangle - kk_{n'n''}\langle n'|\hat{x}_{\sigma'}\dagger|n''\rangle\langle n''|\hat{x}_k\hat{p}_\sigma|g\rangle}{k - k_{n''g}} + \frac{kk_{n''g}\langle n'|\hat{x}_k\hat{p}_\sigma|n''\rangle\langle n''|\hat{x}_{\sigma'}\dagger|g\rangle - k'k_{n'n''}\langle n'|\hat{x}_\sigma|n''\rangle\langle n''|\hat{x}_{k'}\hat{p}_{\sigma'}\dagger|g\rangle}{k' + k_{n''g}}\right)\Big\}.$$

Next, the commutators

$$[\hat{x}_{k'}\hat{p}_{\sigma'}\dagger,\ \hat{x}_\sigma] = \hat{x}_{k'}[\hat{p}_{\sigma'}\dagger\hat{x}_\sigma] = -i\hbar\hat{x}_{k'}\boldsymbol{e}_{\sigma'}\cdot\boldsymbol{e}_\sigma^*$$

$$[\hat{x}_k\hat{p}_\sigma,\ \hat{x}_{\sigma'}\dagger] = \hat{x}_k[\hat{p}_\sigma\hat{x}_{\sigma'}\dagger] = -i\hbar\hat{x}_k\boldsymbol{e}_{\sigma'}\cdot\boldsymbol{e}_\sigma^*$$

yield the identities

$$\sum_{n''}\left(\langle n'|\hat{x}_{k'}\hat{p}_{\sigma'}\dagger|n''\rangle\langle n''|\hat{x}_\sigma|g\rangle - \langle n'|\hat{x}_\sigma|n''\rangle\langle n''|\hat{x}_{k'}\hat{p}_{\sigma'}\dagger|g\rangle\right) = -i\hbar\langle n'|\hat{x}_{k'}|g\rangle\boldsymbol{e}_{\sigma'}\cdot\boldsymbol{e}_\sigma^*$$

$$\sum_{n''}\left(\langle n'|\hat{x}_k\hat{p}_\sigma|n''\rangle\langle n''|\hat{x}_{\sigma'}\dagger|g\rangle - \langle n'|\hat{x}_{\sigma'}\dagger|n''\rangle\langle n''|\hat{x}_k\hat{p}_\sigma|g\rangle\right) = -i\hbar\langle n'|\hat{x}_k|g\rangle\boldsymbol{e}_{\sigma'}\cdot\boldsymbol{e}_\sigma^*,$$

which in turn lead to the following result for $f_1(\boldsymbol{k}'\sigma'n', \boldsymbol{k}\sigma g)$

$$f_1(\boldsymbol{k}'\sigma'n', \boldsymbol{k}\sigma g) = -\alpha(mc)^{-1}k'^{\frac{3}{2}}k^{\frac{1}{2}} \sum_{n''}\left(\frac{\langle n'|\hat{x}_{k'}\hat{p}_{\sigma'}\dagger|n''\rangle\langle n''|\hat{x}_\sigma|g\rangle + \langle n'|\hat{x}_{\sigma'}\dagger|n''\rangle\langle n''|\hat{x}_k\hat{p}_\sigma|g\rangle}{k - k_{n''g}} - \frac{\langle n'|\hat{x}_k\hat{p}_\sigma|n''\rangle\langle n''|\hat{x}_{\sigma'}\dagger|g\rangle + \langle n'|\hat{x}_\sigma|n''\rangle\langle n''|\hat{x}_{k'}\hat{p}_{\sigma'}\dagger|g\rangle}{k' + k_{n''g}}\right).$$

Finally, the identities

$$\langle n'|\hat{x}_{k'}\hat{p}_{\sigma'}\dagger|n''\rangle = \tfrac{1}{2}imck_{n'n''}\langle n'|\hat{x}_{k'}\hat{x}_{\sigma'}\dagger|n''\rangle + \tfrac{1}{2}(k'^{-1}\boldsymbol{k}'\times\boldsymbol{e}_{\sigma'})\cdot\langle n'|\hat{\boldsymbol{l}}|n''\rangle$$

$$\langle n'|\hat{x}_k\hat{p}_\sigma|n''\rangle = \tfrac{1}{2}imck_{n'n''}\langle n'|\hat{x}_k\hat{x}_\sigma|n''\rangle + \tfrac{1}{2}(k^{-1}\boldsymbol{k}\times\boldsymbol{e}_\sigma^*)\cdot\langle n'|\hat{\boldsymbol{l}}|n''\rangle$$

are used to express matrix elements of the form $\langle n'|\hat{x}_{k'}\hat{p}_{\sigma'}\dagger|n''\rangle$ in terms of matrix elements of the electric quadrupole and magnetic dipole operators. For left (+) and right (−) circularly polarized light, $f_1(\boldsymbol{k}'\sigma'n', \boldsymbol{k}\sigma g)$ becomes

[9] $$f_1(\boldsymbol{k}'\sigma'n', \boldsymbol{k}\sigma g) = -\tfrac{1}{2}i\alpha k'^{\frac{3}{2}}k^{\frac{1}{2}} \left\{\sum_{n''}\left(\frac{k_{n'n''}\langle n'|\hat{x}_{k'}\hat{x}_{\sigma'}\dagger|n''\rangle\langle n''|\hat{x}_\sigma|g\rangle + k_{n''g}\langle n'|\hat{x}_{\sigma'}\dagger|n''\rangle\langle n''|\hat{x}_k\hat{x}_\sigma|g\rangle}{k - k_{n''g}} - \frac{k_{n'n''}\langle n'|\hat{x}_k\hat{x}_\sigma|n''\rangle\langle n''|\hat{x}_{\sigma'}\dagger|g\rangle + k_{n''g}\langle n'|\hat{x}_\sigma|n''\rangle\langle n''|\hat{x}_{k'}\hat{x}_{\sigma'}\dagger|g\rangle}{k' + k_{n''g}}\right) \pm \frac{1}{mc}\sum_{n''}\left(\frac{\langle n'|\hat{l}_{\sigma'}\dagger|n''\rangle\langle n''|\hat{x}_\sigma|g\rangle - \langle n'|\hat{x}_{\sigma'}\dagger|n''\rangle\langle n''|\hat{l}_\sigma|g\rangle}{k - k_{n''g}} + \frac{\langle n'|\hat{l}_\sigma|n''\rangle\langle n''|\hat{x}_{\sigma'}\dagger|g\rangle - \langle n'|\hat{x}_\sigma|n''\rangle\langle n''|\hat{l}_{\sigma'}\dagger|g\rangle}{k' + k_{n''g}}\right)\right\}.$$

For the purpose of determining refractive indices, only the forward scattering amplitudes

$$f(k\pm g) = f(\boldsymbol{k}\pm g, \boldsymbol{k}\pm g)$$

are required. Substitution of eqs. [8] and [9] into eq. [6] yields the following expression for the forward scattering amplitudes

[10] $$f(k\pm g) = -\alpha k^2\left\{\sum_{n''}\left(\frac{\langle g|\hat{x}_\mp|n''\rangle\langle n''|\hat{x}_\pm|g\rangle}{k - k_{n''g}} - \frac{\langle g|\hat{x}_\pm|n''\rangle\langle n''|\hat{x}_\mp|g\rangle}{k + k_{n''g}}\right) + \frac{1}{2}i\sum_{n''}k_{n''g}\left(\frac{-\langle g|\hat{x}_k\hat{x}_\mp|n''\rangle\langle n''|\hat{x}_\pm|g\rangle + \langle g|\hat{x}_\mp|n''\rangle\langle n''|\hat{x}_k\hat{x}_\pm|g\rangle}{k - k_{n''g}} + \frac{\langle g|\hat{x}_k\hat{x}_\pm|n''\rangle\langle n''|\hat{x}_\mp|g\rangle - \langle g|\hat{x}_\pm|n''\rangle\langle n''|\hat{x}_k\hat{x}_\mp|g\rangle}{k + k_{n''g}}\right) \pm \frac{i}{2mc}\sum_{n''}\left(\frac{\langle g|\hat{l}_\mp|n''\rangle\langle n''|\hat{x}_\pm|g\rangle - \langle g|\hat{x}_\mp|n''\rangle\langle n''|\hat{l}_\pm|g\rangle}{k - k_{n''g}} + \frac{\langle g|\hat{l}_\pm|n''\rangle\langle n''|\hat{x}_\mp|g\rangle - \langle g|\hat{x}_\pm|n''\rangle\langle n''|\hat{l}_\mp|g\rangle}{k + k_{n''g}}\right)\right\}.$$

Can. J. Chem. Downloaded from www.nrcresearchpress.com by 210.87.254.5 on 09/05/12
For personal use only.

Can. J. Chem. Downloaded from www.nrcresearchpress.com by 210.87.254.5 on 09/05/12
For personal use only.

In eq. [10] and a number of the preceding equations the components of vector operators, which appear in the various matrix elements, are defined with respect to an external coordinate system. The components $\hat{a}_i$ of a vector operator, with respect to an external coordinate system, are related to the components $\hat{a}_r'$, with respect to a molecular coordinate system, as follows

$$[11] \qquad \hat{a}_i = \sum_r \hat{D}_{ir}\hat{a}_r'.$$

The operators $\hat{D}_{ir}$ act on the rotational part of the molecular state vector. The matrix elements of the operators $\hat{D}_{ir}$ are derived by group theoretic methods in a paper by Casimir (8). Also the matrix elements of $\hat{D}_{ir}$ can be worked out by employing the $\hat{\boldsymbol{T}}$ type vector operator method of Condon and Shortley (9).

Through the use of eq. [11], it is possible in eq. [10] to sum over all the rotational states for each vibronic state so that one is left with just a sum over the vibronic states. For spherical top and symmetric top molecules, this procedure is not too difficult. However, asymmetric top molecules are a different matter, and it is the asymmetric top molecules which are of interest in optical rotation. For an asymmetric top molecule, it is convenient to use the less rigorous but more straightforward treatment: this is to replace a summation over the rotational states by an average over the Euler angles $\theta\phi\chi$ which orient the molecular coordinate system $\boldsymbol{e}_r'$ with respect to the external coordinate system $\boldsymbol{e}_i$.

Only two results are required in order to average eq. [10] over the Euler angles. Firstly, the Euler angle average of a product of two vector components $a_\pm b_\mp$, defined with respect to the external axes, is

$$(a_\pm b_\mp)_{\text{avg}} = \tfrac{1}{3}\boldsymbol{a}\cdot\boldsymbol{b}.$$

Second, the Euler angle average of a product of three vector components $a_+b_-c_0$ is

$$(a_+b_-c_0)_{\text{avg}} = -\frac{i}{6}(\boldsymbol{a}\times\boldsymbol{b})\cdot\boldsymbol{c}.$$

If two or more of the vectors $\boldsymbol{a}$, $\boldsymbol{b}$, $\boldsymbol{c}$ are identical, the scalar triple product vanishes. Consequently, the Euler angle average of the electric dipole – electric quadrupole terms of eq. [10] is zero. After averaging over the Euler angles, eq. [10] becomes

$$[12] \quad f(k\pm g) = \frac{2}{3}\alpha k^2\left\{\sum_{n''}\frac{k_{n''g}\langle g|\hat{\boldsymbol{R}}|n''\rangle\cdot\langle n''|\hat{\boldsymbol{R}}|g\rangle}{k^2_{n''g}-k^2} \pm \frac{k}{mc}\sum_{n''}\frac{Im(\langle g|\hat{\boldsymbol{R}}|n''\rangle\cdot\langle n''|\hat{\boldsymbol{L}}|g\rangle)}{k^2_{n''g}-k^2}\right\}.$$

Capital letters are now used for the vector operators $\hat{\boldsymbol{R}}$ and $\hat{\boldsymbol{L}}$ to indicate that the Euler angle average has been carried out; in other words the summation is now over the vibronic states alone.

Substitution of eq. [12] into eq. [3] gives the refractive indices; if the refractive indices are then substituted into eq. [1], Rosenfeld's formula, eq. [2], then follows.

Discussion

The preceding calculations demonstrate that it is possible to obtain the Rosenfeld formula by a direct calculation of the refractive indices $n_R(k+)$ and $n_R(k-)$ in eq. [1]. The main advantage of this procedure is that the mathematical manipulations are not too far removed from the physics of the situation. The refractive indices for left and right circularly polarized light are required and thus the corresponding forward scattering amplitudes are determined. In addition, it is interesting to derive a well known result by an alternative method.

The derivation of Rosenfeld's formula presented in this paper, like the earlier derivations, shows up some of its limitations. Firstly, the independent particle model is used; the derivation of eq. [3] is based on the independent particle model (details are in the Appendix). Consequently Rosenfeld's formula is only applicable to low density gases and dilute solutions. The second limitation of Rosenfeld's formula is that the procedure of averaging over the Euler angles limits its applicability to situations where fine details, depending on the rotational states, are not important. Finally, the Rosenfeld formula is not valid at resonance. However, this is not a serious limitation as Hameka (3, 4) has pointed out that optical rotation is not a physically meaningful concept at resonance.

Acknowledgments

The author is grateful to the National Research Council of Canada for the opportunity to spend

3 weeks in Ottawa in June of 1967. During this time some useful information was gained from informal conversations with various people. In particular, the author expresses his thanks to Dr. C. Z. Mavroyannis and Prof. H. F. Hameka for some stimulating discussions.

Appendix

One means of deducing eq. [3] is by the dispersion relations for the real and imaginary parts of both the forward scattering amplitude and the complex index of refraction. The real and imaginary parts of the refractive index satisfy the dispersion relations

$$[A1] \quad n_R(k) - 1 = \frac{1}{\pi} P \int_{-\infty}^{\infty} \frac{x n_I(x)}{x^2 - k^2} dx$$

$$n_I(k) = -\frac{k}{\pi} P \int_{-\infty}^{\infty} \frac{n_R(x) - 1}{x^2 - k^2} dx,$$

where P stands for the principal value of the integrals, and the real and imaginary parts of the forward scattering amplitude satisfy

$$[A2] \quad f_R(k) - f_R(0) = \frac{k^2}{\pi} P \int_{-\infty}^{\infty} \frac{f_I(x)}{x(x^2 - k^2)} dx$$

$$f_I(k) = -\frac{k}{\pi} P \int_{-\infty}^{\infty} \frac{f_R(x)}{x^2 - k^2} dx.$$

The optical theorem (10), a consequence of the unitary property of the scattering matrix, relates the total scattering cross section $\sigma_T(k)$ to the imaginary part of the forward scattering amplitude as follows

$$\sigma_T(k) = \frac{4\pi}{k} f_I(k).$$

For the situation in which the decrease in the intensity of light passing through a sample is due entirely to scattering, the extinction coefficient $\epsilon(k)$ is related to $\sigma_T(k)$ and $n_I(k)$ by

$$\epsilon(k) = 2k n_I(k) = N\sigma_T(k),$$

thus

$$[A3] \quad n_I(k) = 2\pi N k^{-2} f_I(k).$$

This result depends on the independent particle model for which it is assumed that the total scattering cross section for N molecules is equal to N times the total scattering cross section for one molecule.

Now, substitution of eq. [A3] into eq. [A1] gives

$$n_R(k) - 1 = 2NP \int_{-\infty}^{\infty} \frac{f_I(x)}{x(x^2 - k^2)} dx,$$

from which eq. [3] follows with the aid of eq. [A2]. It is assumed that $f_R(0) = 0$ for photon scattering.

1. L. Rosenfeld. Z. Physik, **52**, 161 (1928).
2. E. U. Condon. Rev. Mod. Phys. **9**, 432 (1937).
3. H. F. Hameka. Ann. Phys. N.Y. **26**, 122 (1964).
4. H. F. Hameka. J. Chem. Phys. **36**, 2540 (1962).
5. W. Heitler and S. T. Ma. Proc. Roy. Irish Acad. **52**, 109 (1949).
6. P. A. M. Dirac. The principles of quantum mechanics. 4th ed. Oxford University Press. 1958. pp. 199–201 and 244–248.
7. P. Roman. Advanced quantum theory. Addison-Wesley, Reading, Mass. 1965. p. 203.
8. H. B. G. Casimir. Z. Physik, **59**, 623 (1930).
9. E. U. Condon and G. H. Shortley. The theory of atomic spectra. Cambridge University Press. 1935. Chap. 3.
10. E. Merzbacher. Quantum mechanics. Wiley, New York. 1961. p. 499.

Can. J. Chem. Downloaded from www.nrcresearchpress.com by 210.87.254.5 on 09/05/12
For personal use only.

Can. J. Chem. Downloaded from www.nrcresearchpress.com by 210.87.254.105 on 09/05/12
For personal use only.

Crystal structure of β-$Cu_2P_2O_7$

B. E. ROBERTSON[1] AND C. CALVO
Department of Physics, McMaster University, Hamilton, Ontario

Received July 21, 1967

The crystal structure of β-$Cu_2P_2O_7$ has been determined by X-ray methods. The crystals are monoclinic with $a = 6.827(8)$ Å, $b = 8.118(10)$ Å, $c = 4.576(6)$ Å, $\beta = 108.85(10)°$, $Z = 2$, and space group $C2/m$. This structure is analogous to that of the mineral thortveitite and the high temperature forms of the pyrophosphates of Zn, Mg, and Mn. The cations are octahedrally coordinated to oxygen atoms with equatorial Cu—O bonds of 2.00 Å and 1.94 Å while the axial bond lengths are 2.58 Å. The anion has inner P—O bonds of 1.542 Å and average terminal bonds of 1.509 Å. In addition to the usual refinement with anisotropic thermal parameters, the structure has been refined in terms of a disordered structure generated from the low temperature α form of $Cu_2P_2O_7$. This disordered model agrees as well with the data ($R = 0.12$) as the structure based on the thortveitite structure with large anisotropic motion assigned to the atoms.

Canadian Journal of Chemistry, **46**, 605 (1968)

Introduction

A number of pyrophosphates, $Mn_2P_2O_7$ (1), $Zn_2P_2O_7$ (2), and $Mg_2P_2O_7$ (3), are known to have the thortveitite structure (4) as their high temperature modifications. These compounds show linear P—O—P groups in the $P_2O_7^{4-}$ anion with cations having irregular octahedral coordination. The low temperature structures of this series have bent P—O—P bonds with some fraction of the cations lying in fivefold coordinate sites while the remainder are in sixfold coordinate sites. In α-$Cu_2P_2O_7$ (5), the P—O—P bond angle is 157° with average equatorial cation – oxygen atom bond distances of 1.95 ± 0.04 Å and axial bond distances of 2.322(6) Å and 2.947(6) Å. In α-$Mg_2P_2O_7$ (6) the P—O—P bond angle is 144° with half the cations having fivefold coordination and the remainder showing sixfold coordination. $Co_2P_2O_7$ (7) and $Ni_2P_2O_7$ (8) at room temperature apparently are isostructures of α-$Mg_2P_2O_7$. Three unique anions are found in α-$Zn_2P_2O_7$ (9) all with bent P—O—P groups and only 1/3 of the cations show sixfold coordination. The pertinent features of these structures are summarized in Table I.

All the pyrophosphates mentioned above, except for $Mn_2P_2O_7$, have been shown to manifest solid state phase transitions (10–12). α-$Cu_2P_2O_7$ disorders by a mechanism involving a random distribution of stacking faults of 1/2 c in the packing of adjacent layers in the a^* direction (5). This can be seen by the appearance of diffuse streaks through those non-extinct reflections with l odd which appears at about 71 °C and gradually fades into the background (9). Thus it was deemed advisable to obtain an accurate resolution of the high temperature structure of $Cu_2P_2O_7$ to determine, if possible, whether β-$Cu_2P_2O_7$ could be described as simply a disordered α-$Cu_2P_2O_7$ structure. Since the transformation mechanism of $Cu_2P_2O_7$ seems to be the simplest, an understanding of it may provide a basis for the description of the transitions of the remainder of the series.

Experimental

Crystals of $Cu_2P_2O_7$ were prepared from a melt of the product obtained by the reaction, in aqueous solution, of $Na_4P_2O_7$ and Cu_2SO_4. Small green crystals were selected for use in single crystal studies and the remainder was ground into a powder and used to determine accurate lattice parameters. These together with the observed extinction conditions and other pertinent crystal data are found in Table II.

Data of the type hnl with $n = 0$, 1, 2, 3, 4, 5 and $hk0$ were collected using MoKα radiation at 100 ± 3 °C. The former data was obtained from a crystal with dimensions 0.10 × 0.10 × 0.05 mm³ and the shortest axis parallel to the axis of the Weissenberg camera. The data were recorded on film and the intensities were visually estimated. The $hk0$ data were obtained from a crystal of dimensions 0.08 × 0.08 × 0.40 mm³ with the long axis parallel to the c axis. These data were measured with a manual diffractometer using a Geiger–Müller tube detector. Dead time corrections were determined and applied where necessary.

As with the other structural analogues of thortveitite the X-ray extinctions limit the space group to one among $C2$, Cm, and $C2/m$. Electron paramagnetic resonance techniques have been used to show that the space groups in thortveitite (13), β-$Zn_2P_2O_7$ (11), and β-$Mg_2P_2O_7$ (14)

[1]Present address: Department of Chemistry, Cornell University, Ithaca, New York.

Can. J. Chem. Downloaded from www.nrcresearchpress.com by 210.87.254.105 on 09/05/12
For personal use only.

TABLE I

Summary of data on pyrophosphate analogues of thortveitite

Compound	Transition temperature (°K)	a (Å)	b (Å)	c (Å)	$\beta°$	Space group	<P—O(P)>(Å)	Terminal <P—O>(Å)	P—O—P
β-$Cu_2P_2O_7$	348–373	6.827	8.118	4.576	108.85	$C2/m$	1.544	1.510	180°
α-$Cu_2P_2O_7$[a]		6.876	8.113	9.162	109.54	$C2/c$	1.58	1.53	157°
β-$Mg_2P_2O_7$[b]	333–343	6.494	8.28	4.522	103.8	$C2/m$	1.557	1.538	180°
α-$Mg_2P_2O_7$[c]		13.198	8.295	9.072	104.9	$B2_1/c$[i]	1.591	1.516	144°
β-$Zn_2P_2O_7$[d]	405–428	6.61	8.29	4.51	105.4	$C2/m$	1.569	1.556	180°
α-$Zn_2P_2O_7$[e]		20.068	8.259	9.099	106.35	Ic[i]	1.57	1.52	147° 150°, 139°
$Mn_2P_2O_7$[f,g]		6.63	8.58	4.54	102.7	$C2/m$	1.571	1.531	180°
α-$Ni_2P_2O_7$[h]	847	13.172	8.290	9.053	105.18	$B2_1/c$[i]	1.602	1.539	137°
α-$Co_2P_2O_7$[g]	561	13.23	8.32	8.98	104.4	$B2_1/c$[i]	1.57	1.52	143°

[a]Reference 5. [b]Reference 3. [c]Reference 6. [d]Reference 2. [e]Reference 9. [f]Reference 1. [g]Reference 7. [h]Referenee 8.
[i]Non-standard unit cells have been chosen to preserve a simple relationship between the unit cell parameters of the high and low temperature forms.

Can. J. Chem. Downloaded from www.nrcresearchpress.com by 210.87.254.105 on 09/05/12
For personal use only.

TABLE II

Crystal data

a 6.827(8) Å	
b 8.118(10) Å	
c 4.576(6) Å	
β 108.85(10)	
Z 2*	
Systematic extinction	hkl: $h + k$ odd
Space group	$C2/m$, Cm, or $C2$
Linear absorption coefficient	$\mu = 100$ cm^{-1}
Number of reflections	613
Number measurable	371

*This number is approximate since it is based upon the room temperature density value.

are $C2/m$ by doping at low concentrations with paramagnetic ions. The nuclear magnetic resonance (n.m.r.) of P in α-$Cu_2P_2O_7$ (5) has established the space group to be $C2/c$. This experiment in the temperature range where the β phase is stable shows only one resonance line with no angular anisotropy. This result is inconsistent with space group $C2$ and Cm because of the lack of anisotropy as the direction of the magnetic field is changed relative to the crystalline axes and because only one site appears. The $C2/m$ space group has been chosen for this refinement because of the n.m.r. results and because thortveitite and its analogues have been shown to have this space group.

The atomic coordinates found for β-$Zn_2P_2O_7$ (2) were used as trial coordinates in a full matrix least squares refinement. The refinement was begun with individual isotropic temperature factors but the final cycles allowed full anisotropic variation of the thermal parameters. The program used was prepared at McMaster University for use with an IBM 7040 by J. S. Stephens. Weights, W, were chosen so that $W\Delta F^2$ was independent of the magnitude of the observed structure factor, F_o (15). Since data was taken by two different techniques separate coefficients in the equation $W^{-1} = C_o + C_1F_o + C_2F_o^2 + C_3F_o^3$ were used for each set of data and are listed on Table III. Only 371 of a possible 613 independent reflections were observed. The unobserved reflections were assigned zero weight in the least square refinement if their calculated value was less than the minimum observable value in that area of reciprocal space. The atomic scattering factors were taken from Volume III of the International Tables (16). The final

$$R_1 = \frac{\sum||F_o| - |F_c||}{\sum|F_o|}$$

value for the atomic parameters reported in Table III and thermal parameters in Table IV is 0.149 and the residual

$$R_2 = \left\{\frac{\sum\omega||F_o|^2 - |F_c|^2|}{\sum\omega F_o^2}\right\}^{1/2}$$

is 0.120. The observed and calculated structure factors can be found in Table V.

The structure consists of close packed double layers of oxygen atoms with cations distributed in 2/3 of the octahedral holes in a psuedo-hexagonal arrangement. These $(CuO_3)_\infty$ sheets run parallel to the ab plane and adjacent sheets are separated by P—O—P groups which lie above the empty octahedral site. Each side of the anion shares one oxygen atom with one sheet and two additional ones with the adjacent sheet. The cations are on a twofold axis,

TABLE III

Atomic positions (estimated standard deviations in parenthesis)

	Point symmetry	x/a	y/b	z/c
Cu	2	0	0.3122(2)	$\frac{1}{2}$
P	m	0.1998(4)	0	−0.0883(6)
O_I	$2/m$	0	0	0
O_{II}	m	0.3759(9)	0	0.2161(17)
O_{III}	1	0.2035(10)	0.1533(7)	−0.2708(15)

These parameters have been determined by least squares refinement where $W^{-1} = 3.708 + 0.320F - 0.0356F^2 + 0.00065F^3$ for the data taken with the counter and $W^{-1} = 32.75 - 2.943F + 0.0688F^2 + 0.00013F^3$ for the remainder of the data.

TABLE IV

Mean square atomic displacements (Å^2) × 10^4 (estimated standard deviations in parenthesis)

	U_{11}†	U_{22}	U_{33}	U_{12}	U_{13}	U_{23}
Cu	185(5)	65(4)	92(6)	—	−73(4)	—
P	84(7)	92(7)	62(8)	—	18(7)	—
O_I	104(35)	1 197(226)	292(78)	—	126(50)	—
O_{II}	75(15)	87(16)	71(20)	—	10(18)	—
*O_{III}	296(24)	91(12)	121(19)	45(17)	23(20)	126(35)

*Non-positive definite.
†These values were obtained from $\beta_{ij} = 2\pi^2 b_i b_j U_{ij}$ where β_{ij}'s appear as a temperature effect through exp $[-(\beta_{11}h^2 + 2\beta_{12}hk \ldots)]$ in the structure factor expression and b_i are the reciprocal lattice vectors.

TABLE V

Observed and calculated structure factors (×10)
FC(A) are calculated using the parameters of Tables III and IV while FC(D) are calculated using the parameters of the disordered structure shown in Table VII. (Unobserved reflections are designated with an asterisk.)

H	L	IFØI	FC(A)	FC(D)
				K = 0
0	2	545	550	555
0	3	647	-626	-625
0	4	587	583	590
0	5	600	-556	-558
0	6	*118	57	60
0	-7	267	-285	-283
0	-8	156	163	164
0	-9	*119	-111	-103
0	-10	*108	141	142
0	-11	* 87	-28	-22
2	-11	* 96	-115	-109
2	-10	*113	70	60
2	-9	*120	-42	-34
2	-8	226	212	218
2	-7	*108	-65	-64
2	-6	623	454	467
2	-5	219	-228	-232
2	-4	480	411	429
2	-3	564	-564	-585
2	-2	1058	823	843
2	-1	1277	-1706	-1727
2	0	284	288	286
2	1	427	-458	-458
2	2	1124	1102	1107
2	3	554	-615	-607
2	4	532	582	582
2	5	100	-53	-38
2	6	481	447	446
2	7	264	-256	-249
-2	-8	*120	121	113
-2	-9	135	-162	-155
-2	-10	* 99	79	75
-2	-11	95	-119	-111
4	-10	*115	-3	-19
4	-9	196	-166	-159
4	-8	*116	64	56
4	-7	199	-221	-221
4	-6	* 79	79	77
4	-5	262	-241	-258
4	-4	623	601	625
4	-3	242	-227	-249
4	-2	1014	948	966
4	-1	120	-139	-161
4	0	754	796	815
4	1	784	-871	-887
4	2	388	472	466
4	3	464	-488	-481
4	4	125	176	164
4	5	604	-507	-496
4	6	260	284	278
4	7	*120	-99	-78
-4	-8	203	215	206
-4	-9	105	-135	-124
-4	-10	161	155	145
6	-10	*115	130	108
6	-9	*120	-1	30
6	-8	*117	99	80
6	-7	*110	-7	9
6	-6	214	216	212
6	-5	295	-317	-330
6	-4	* 68	-0	-14
6	-3	483	-453	-487
6	-2	266	295	303
6	-1	432	-460	-501
6	0	504	563	544
6	1	150	-181	-182
6	2	466	528	539
6	3	187	-178	-171
6	4	520	457	455
6	5	221	-231	-219
-6	-6	*119	117	99
-6	-7	269	-255	-241
-6	-8	142	162	150
-6	-9	170	-158	-143
8	-10	*113	-17	-73
8	-9	*119	-37	2
8	-8	*119	30	-12
8	-7	114	-96	-69
8	-6	169	183	155
8	-5	158	139	166
8	-4	379	357	354
8	-3	135	-128	-136
8	-2	742	255	253
8	-1	185	-211	-232
8	0	153	154	144
8	1	561	-414	-446
8	2	122	134	129
8	3	313	-283	-285
8	4	225	217	214
8	5	*120	-121	-107
-8	-6	298	250	244
-8	-7	119	-137	-121
-8	-8	171	156	142
10	-9	*116	-1	59
10	-8	*120	49	-17
10	-7	*118	-67	-24
10	-6	*115	-72	-143
10	-5	184	-183	-175
10	-4	* 87	92	42
10	-3	* 85	-35	-26
10	-2	163	157	141
10	-1	*105	-59	-56
10	0	323	321	316
10	1	*112	-1	2
10	2	201	195	195
10	3	218	-178	-184
10	4	*119	109	102
10	5	233	-181	-180
-10	-6	*102	106	94
-10	-7	181	-145	-135
12	-8	*116	65	-9
12	-7	*120	74	149
12	-6	*120	124	64
12	-5	*118	0	57
12	-4	*117	31	-31
12	-3	*116	-58	-44
12	-2	*116	55	5
12	-1	163	-155	-163
12	0	24	-12	-42
12	1	123	-103	-106
12	2	195	154	155
12	3	*116	-49	-43
12	4	123	122	123
12	5	* 94	-72	-63
-12	-6	134	126	125
14	-6	*116	22	-76
14	-5	*118	14	74
14	-4	*119	59	-2
14	-3	*119	17	71
14	-2	*119	114	76
14	-1	*118	44	78
14	0	*116	73	50
14	1	*112	-86	-80
14	2	*105	23	2
16	-4	*106	-0	-95
16	-3	*106	-48	-8
16	-2	*105	-12	-80
16	-1	*101	-16	15
16	D	* 46	61	27
H	L			K = 1
1	-8	*169	-18	-15
1	-7	168	193	195
1	-6	*115	-34	-26
1	-5	*101	-54	-45
1	-4	591	-517	-509
1	-3	147	130	130
1	-2	491	-303	-296
1	0	193	-196	-187
1	1	997	862	845
1	2	85	63	70
1	3	454	571	565
1	4	116	47	50
1	5	134	137	132
-1	-6	246	-237	-228
-1	-7	*163	14	17
-1	-8	*172	-92	-85
3	-8	*136	-95	-92
3	-7	*126	31	30
3	-6	*112	71	69
3	-5	546	473	473
3	-4	114	86	86
3	-3	329	224	227
3	-2	90	-86	-97
3	-1	959	576	566
3	0	470	-533	-516
3	1	153	-139	-141
3	2	384	-450	-438
3	3	119	140	139
3	4	103	-132	-118
-3	-5	251	244	241
-3	-6	*129	13	20
-3	-7	138	146	142
-3	-8	*140	-8	0
5	-7	*127	-35	-39
5	-6	262	-268	-270
5	-5	106	-87	-95
5	-4	104	-90	-104
5	-3	267	226	224
5	-2	236	-193	-203
5	-1	525	415	411
5	0	290	301	286
5	1	497	522	517
5	2	132	-140	-138
5	3	*129	105	98
5	4	143	-174	-166
5	5	*157	23	18
5	6	*168	-181	-171
7	-7	*131	171	164
7	-6	121	101	112
7	-5	118	126	123
7	-4	*104	-75	-83
7	-3	* 98	92	75
7	-2	206	-187	-207
7	-1	133	-139	-151
7	0	362	-346	-352
7	1	135	141	136
7	2	*137	11	14
7	3	157	178	177
7	4	*160	-32	-24
9	-6	*159	-43	-44
9	-5	*151	57	36
9	-4	*144	39	46
9	-3	187	201	195
9	-2	119	153	151
9	-1	233	258	257
9	0	* 48	-33	-36
9	1	*150	-0	-8
11	-5	*165	2	-37
11	-4	*162	-108	-119
11	-3	*159	-78	-113
11	-2	*159	-96	-108
11	-1	*161	57	37
11	0	*164	32	31
H	L			K = 2
0	2	471	-384	-373
0	3	380	383	382
0	4	453	-464	-457
0	5	113	157	163
0	-6	378	-320	-315
0	-7	*132	13	12
0	-8	*141	-156	-149
2	-8	*139	41	48
2	-7	293	265	272
2	-6	115	-95	-95
2	-5	327	346	353
2	-4	146	-159	-158
2	-3	574	388	401
2	-2	589	-945	-949
2	-1	212	163	172
2	0	692	-729	-716
2	1	513	643	641
2	2	425	-417	-405
2	3	564	571	569
2	4	111	-113	-101
-2	-5	500	428	423
-2	-6	*127	-70	-58
-2	-7	172	195	190
-2	-8	177	-170	-166
-2	-9	*136	32	27
4	-8	172	-176	-173
4	-7	*128	57	53
4	-6	189	-165	-165
4	-5	146	137	143
4	-4	170	-164	-178
4	-3	698	732	745
4	-2	143	114	105
4	-1	928	641	648
4	0	455	-479	-468
4	1	436	446	448
4	2	354	-420	-414
4	3	105	134	125
4	4	397	-461	-449
4	5	*125	126	119
-4	-6	144	-172	-156
-4	-7	187	203	198
6	-8	*140	4	24
6	-7	*131	111	102
6	-6	*120	-60	-58
6	-5	110	90	84
6	-4	381	-380	-393
6	-3	80	-68	-75
6	-2	356	-346	-374
6	-1	394	395	400
6	0	178	-186	-187
6	1	428	364	368
6	2	*106	-67	-60
6	3	510	463	466
6	4	*127	-92	-82
6	5	136	150	138
6	6	233	-216	-206
8	-7	*136	54	29
8	-6	128	25	46
8	-5	235	266	254
8	-4	109	114	124
8	-3	225	251	253
8	-2	114	-156	-165
8	-1	113	120	110
8	0	231	-218	-230
8	1	*116	63	55
8	2	391	-333	-345
8	3	*132	77	71
8	4	*139	-101	-91
8	5	275	218	217
10	-5	*132	-45	-92
10	-4	*127	-83	-83
10	-3	*125	113	85
10	-2	*124	-15	-9
10	-1	194	184	188
10	0	60	23	27
10	1	288	246	251
10	2	*138	-35	-33
10	3	*142	77	73
10	4	197	-169	-173
12	-4	*140	-28	-3
12	-3	*139	34	-9
12	-2	*139	-79	-86
12	-1	*140	-23	-57
12	0	149	-135	-142
12	1	*142	42	31
H	L			K = 3
1	-8	209	225	229
1	-7	195	-150	-143
1	-6	320	233	241
1	-5	338	-335	-334
1	-4	198	158	173
1	-3	1335	-1021	-1020
1	-2	725	672	681
1	0	645	760	740
1	1	1396	-930	-916
1	2	1838	1211	1217
1	3	* 93	-14	-4
-1	-4	539	474	472
-1	-5	546	-421	-413
-1	-6	242	235	235
-1	-7	213	-227	-220
-1	-8	*200	55	54
3	-8	*196	48	41
3	-7	*181	-83	-83
3	-6	414	332	345
3	-5	*144	-96	-102
3	-4	784	656	673
3	-3	225	-192	-197
3	-2	552	484	508
3	-1	733	-783	-798
3	0	666	778	754
3	1	1113	-826	-818
3	2	* 93	87	86
3	3	499	-578	-562
3	4	625	546	545
3	5	169	-183	-168
-3	-6	322	249	241
-3	-7	*198	-117	-104
-3	-8	325	272	266
5	-8	*196	60	53
5	-7	240	-258	-257
5	-6	*166	12	5
5	-5	312	-279	-285
5	-4	145	145	151
5	-3	395	-367	-393
5	-2	638	596	619
5	-1	207	-192	-198
5	0	689	672	685
5	1	107	-132	-135
5	2	494	580	585
5	3	433	-426	-419
5	4	*169	147	135
5	5	243	-284	-269
-5	-6	*197	182	170
-5	-7	262	-280	-268
7	-7	*188	83	115
7	-6	175	165	154
7	-5	*162	-85	-78
7	-4	252	262	263
7	-3	225	-225	-240
7	-2	*113	36	26
7	-1	498	-477	-505
7	0	172	173	173
7	1	345	-328	-338
7	2	297	309	310
7	3	*175	-120	-110
7	4	309	316	317
7	5	*198	-151	-137
7	6	210	245	236
9	-5	*178	-81	-60
9	-4	*170	120	100
9	-3	*165	53	69
9	-2	393	386	396
9	-1	*165	-36	-38
9	0	170	170	170
9	1	192	-195	-203
9	2	*186	130	127
9	3	218	-240	-250
9	4	*200	91	82
11	-5	*194	-38	-10
11	-4	*190	-16	-69
11	-3	198	-206	-206
11	-2	*187	8	-27
11	-1	*189	-42	-38
11	0	165	165	155
11	1	*197	-71	-67
H	L			K = 4
0	0	332	325	331
0	-2	300	242	240
0	-3	148	-139	-128
0	-4	197	-147	-134
0	-5	*104	-44	-38
0	-6	155	-113	-110
0	-7	162	-168	-161
0	-8	*137	-30	-24
2	-8	151	139	139
2	-7	149	156	158
2	-6	*114	39	46
2	-5	* 82	60	63
2	-4	212	193	193
2	-3	63	-42	-29
2	-2	688	-465	-442
2	-1	429	-342	-328
2	0	17	-21	-11
2	1	83	-87	-70
2	2	* 58	33	44
2	3	142	210	210
2	4	147	177	177
-2	-5	147	112	118
-2	-6	132	139	142
-2	-7	*135	62	60
4	-7	*126	-57	-58
4	-6	*114	9	9
4	-5	83	-51	-46
4	-4	* 74	20	23
4	-3	446	373	369
4	-2	624	480	480
4	-1	87	89	97
4	0	* 58	-39	-33
4	1	63	61	63
4	2	* 71	-67	-62
4	3	183	-222	-214
4	4	117	-153	-149
4	5	*123	-69	-65
6	-7	*128	29	33
6	-6	*118	3	2
6	-5	*108	-25	-28
6	-4	195	-176	-177
6	-3	331	-303	-305
6	-2	95	-103	-110
6	-1	93	126	123
6	0	* 74	69	73
6	1	* 78	35	40
6	2	174	200	204
6	3	197	222	226
6	4	*124	73	76
8	-6	125	85	89
8	-5	155	146	148
8	-4	204	193	196
8	-3	119	125	131
8	-2	*105	-25	-24
8	-1	*105	-68	-76
8	0	24	-24	-32
8	1	114	-103	-109
8	2	160	-175	-180
8	3	*129	-76	-77
10	-5	*129	-80	-92
10	-4	*125	-33	-47
10	-3	*123	23	13
10	-2	*122	70	72
10	-1	*123	76	84
10	0	111	100	102
H	L			K = 5
1	-7	*346	263	267
1	-6	314	-215	-204
1	-5	*277	141	147
1	-4	619	-595	-587
1	-3	268	247	265
1	-2	677	-665	-648
1	0	912	-643	-604
1	1	753	819	824
1	2	266	-219	-211
1	3	782	740	728
1	4	275	-258	-244
1	5	309	290	284
1	6	338	-301	-294
3	-7	*341	127	124
3	-6	*309	-26	-29
3	-5	432	478	490
3	-4	*196	-135	-139
3	-3	508	485	494
3	-2	489	-422	-420
3	-1	520	566	583
3	0	699	-684	-677
3	1	170	202	206
3	2	779	-735	-708
3	3	353	351	348
3	4	300	-268	-252
3	5	356	338	329
3	6	*349	-152	-137
5	-7	*343	-4	-7
5	-6	*315	-322	-320
5	-5	*285	62	61
5	-4	235	-252	-257
5	-3	297	289	305
5	-2	308	-310	-320
5	-1	467	549	561
5	0	80	-76	-73
5	1	614	647	650
5	2	238	-291	-286
5	3	298	227	221
5	4	337	-336	-318
5	5	*348	196	184
7	-6	*331	9	32
7	-5	*307	149	147
7	-4	*287	-140	-140
7	-3	*272	174	172
7	-2	283	-338	-347
7	-1	*215	22	28
7	0	424	-429	-429
7	1	287	229	234
7	2	*308	-150	-145
7	3	*331	309	307
9	-4	*322	-52	-29
9	-3	*313	235	232
9	-2	*310	52	59
9	-1	330	280	286
9	0	134	-138	-134
9	1	*334	104	104
H	K			L = 0
0	6	857	1084	1052
0	8	80	-155	-167
0	10	384	385	376
0	12	212	213	201
0	14	37	17	-9
0	16	229	213	214
0	18	23	-33	-47
0	20	42	80	70
1	7	286	288	284
1	9	141	143	141
1	11	316	-293	-296
1	13	270	255	253
1	15	92	-80	-91
1	17	44	-68	-75
1	19	70	118	128
1	21	59	-91	-108
2	6	77	65	75
2	8	612	-633	-607
2	10	217	203	203
2	12	149	-143	-143
2	14	253	-244	-243
2	16	185	161	172
2	18	77	-135	-148
2	20	11	-41	-35
3	7	45	-39	-25
3	9	97	88	93
3	11	323	-302	-310
3	13	117	101	110
3	15	100	-99	-100
3	17	* 56	-43	-51
3	19	32	70	83
3	21	51	-101	-110
4	6	356	373	376
4	8	383	-369	-367
4	10	179	169	171
4	12	14	10	8
4	14	74	-127	-140
4	16	70	118	126
4	18	55	-86	-97
4	20	* 42	3	0
5	7	436	468	460
5	9	233	235	228
5	11	46	-86	-96
5	13	345	331	330
5	15	* 58	9	-7
5	17	73	-10	-18
5	19	87	152	160
6	6	296	294	294
6	8	208	-198	-201
6	10	178	179	183
6	12	36	18	14
6	14	* 58	-65	-76
7	7	109	-101	-96
7	9	* 52	-11	-4
7	11	249	-236	-245
7	13	* 58	19	26
7	15	* 56	-89	-91
7	17	* 50	-59	-65
8	6	* 49	58	55
8	8	242	-232	-238
8	10	98	98	99
8	12	* 58	-33	-38
8	14	103	-105	-114
8	16	* 52	90	98
8	18	* 42	-53	-62
9	7	40	76	80
9	9	* 56	31	31
9	11	55	-102	-105
9	13	* 57	97	102
9	15	* 52	-46	-51
9	17	* 44	-28	-32
10	6	223	212	217
10	8	* 57	-21	-15
10	10	59	115	117
10	12	* 57	59	62
10	14	* 52	1	-0
10	16	* 44	78	80
11	5	* 56	-38	-32
11	7	* 57	87	85
11	9	* 57	72	72
11	11	* 56	-38	-37
11	13	* 51	85	83
11	15	* 44	4	4
12	4	14	-70	-77
12	6	12	-36	-51
12	8	71	-137	-130
12	10	* 55	-5	-12
12	12	* 50	-55	-59
12	14	* 43	-73	-72
12	16	* 31	14	11
13	1	29	-44	-53
13	3	* 57	43	14
13	5	* 57	-72	-66
13	7	* 56	-2	-16
13	9	* 53	4	-5
13	11	* 48	-48	-42
13	13	* 41	22	9
14	2	* 56	-13	-1
14	4	* 55	15	13
14	6	* 53	46	34
14	8	* 50	-29	-10
14	10	* 45	30	18
14	12	* 38	8	10
15	1	* 52	23	38
15	3	* 51	58	37
15	5	* 49	-3	27
15	7	* 46	36	35
15	9	* 41	25	23
16	2	* 34	18	38
16	4	* 44	32	31
16	6	* 40	43	24
17	1	* 38	-35	-32
17	3	* 37	-10	-49
17	5	* 34	-43	-19
18	0	* 24	0	-46

Can. J. Chem. Downloaded from www.nrcresearchpress.com by 210.87.254.105 on 09/05/12
For personal use only.

Can. J. Chem. Downloaded from www.nrcresearchpress.com by 210.87.254.105 on 09/05/12
For personal use only.

TABLE VI

Bond distances and angles in β-$Cu_2P_2O_7$ (estimated standard deviations in parenthesis)

Distances (Å)			
P—O_I	1.542(4)	O_I—O_{II}	2.43(3)
P—O_{II}	1.516(15)	O_I—O_{III}	2.47(3)
P—O_{III}	1.503(15)	O_{II}—O_{III}	2.49(3)
		O_{III}—O_{III}	2.49(3)
Cu—O_{II}	2.003(15)		
Cu—O_{III}	1.937(15)		
Cu—O_{III}	2.577(15)		
Angles (°)			
O_I—P—O_{II}	105.5		
O_I—P—O_{III}	108.7		
O_{II}—P—O_{III}	111.0		
O_{III}—P—O'_{III}*	111.8		
Angles subtended at terminal oxygen atoms by ligands (°)			
Cu(1)—O_{II}—Cu(1′)	99	Cu(1)—O_{III}—Cu(1′)	103
Cu(1)—O_{II}—P	130	Cu(1)—O_{III}—P	136
Cu(1[1])—O_{II}—P	130	Cu(1[1])—O_{III}—P	118
Sum	359	Sum	357

*Atom A′ is related to atom A by the mirror plane through the origin.

the central oxygen atoms at the intersection of a twofold and the mirror plane. The anion possesses a mirror plane containing the two phosphorus atoms and two oxygen atoms in addition to the central oxygen atom.

As has been found in β-$Mg_2P_2O_7$ (3) and β-$Zn_2P_2O_7$ (2) the central oxygen atom which lies at the intersection of the mirror plane and the twofold axis shows enhanced thermal activity in the plane perpendicular to the P—P vector. In β-$Cu_2P_2O_7$ the major component of vibration of this oxygen atom is along the *b* axis and of a magnitude of 0.3 Å. The bond distances and angles found for this structure are listed in Table VI.

X-ray photographs of $Cu_2P_2O_7$ taken in the temperature range of 70 to 100 °C showed diffuse streaks emanating from those reflections characterizing the low temperature phase. Since the essential difference between the α and β unit cells is a doubled *c* axis in the α phase, these are the *l* odd reflections of this phase. These streaks, discussed previously (5), were directed along a^* and gradually faded into the background upon raising the temperature of the crystal. This implies a one dimensional disorder describable as a stacking fault of $\frac{1}{2}$ *c* in adjacent layers along *a*. The effect of disorders can be reproduced by minor relative rearrangements of the atom in adjacent layers and naturally leads to model for the β-phase where there is no correlation in the directions of these displacements between adjacent layers. In Fig. 1 the effect of one disordered layer in α-$Cu_2P_2O_7$ is shown and this structure is compared with the β-$Cu_2P_2O_7$ structure.

In order to test this model each atom was replaced by two half atoms, one half arising from the normal α-$Cu_2P_2O_7$ structure and the other half from the α-$Cu_2P_2O_7$ structure with the origin translated by $\frac{1}{2}$ *c*. The position of each pair of atoms was described by a vector to their center of mass and the displacement of one of them from this center of mass. The vectors were chosen so as to maintain the space group symmetry. Both halves of an atom were constrained to have the same isotropic temperature factor. When all the atoms were described in this manner it was found that the attempted refinement would not converge. The terminal oxygen atoms were then replaced by single atoms with an anisotropic thermal ellipsoid and this model refined easily. The weight functions used are reported in Table VI. The final value of R_1 is 0.150 and the R_2 value is 0.121. The final atomic parameters for the Cu, P, and O_I atoms are compared with their positions in the α phase in Table VII. The origin of the α-$Cu_2P_2O_7$ cell has been shifted to coincide with that chosen for β-$Cu_2P_2O_7$ and the former structure refined with individual isotropic temperature factors.

Discussion

The structural features of β-$Cu_2P_2O_7$ are similar to those found in the other analogues of thortveitite. The inner P—O bond distance of 1.542 Å with an e.s.d. of 0.004 is slightly longer than the terminal P—O bond distances, 1.516 Å and 1.503 Å with e.s.d.'s of 0.015 Å, but these differ by less than two standard deviations. If thermal corrections are applied the inner P—O bond distance will be increased by at least 0.02 Å whereas the average terminal bond distances would be increased by at least 0.003 Å. The three terminal oxygen atoms are related by an approximate threefold axis passing through the phosphorus atom to which they are bonded and nearly parallels the central P—O(—P) bond. The central oxygen atom shows high thermal activity, a feature common to these β phase pyrophosphates. In this case the major component of thermal motion is the *b* axis. The amplitude of this component is 0.35 Å compared with a value of 0.39 Å found for the displacement of

Can. J. Chem. Downloaded from www.nrcresearchpress.com by 210.87.254.105 on 09/05/12
For personal use only.

TABLE VII

Atomic coordinates in disordered β-$Cu_2P_2O_7$ compared with α-$Cu_2P_2O_7$ (α-$Cu_2P_2O_7$ are coordinates in brackets)

				Isotropic temp. factor	Anisotropic temp. factors (Å^2) × 10^4					
	x/a	y/c	z/c	B	U_{11}	U_{22}	U_{33}	U_{12}	U_{13}	U_{23}
Cu	−0.0162(2)	0.3122(1)	0.5144(5)	0.40(2)						
	[−0.0183(2)	0.3133(2)	0.5138(3)	0.39(2)]						
P	0.1997(3)	0.0073(8)	−0.0886(6)	0.48(4)						
	[0.1978(4)	0.0086(4)	−0.0878(5)	0.13(3)]						
O_I	0	0.0256(23)	0	1.69(24)						
	[0	0.0480(24)	0	1.19(19)]						
O_{II}	0.3760(8)	0	0.2165(17)		60(8)	44(7)	102(22)	—	4(13)	—
	[0.3768(11)	−0.0019(15)	0.2254(18)		12(15)	180(48)	86(21)	−1(32)	−52(16)	41(44)]
O_{III}	0.2043(10)	0.1544(7)	−0.2714(15)		149(12)	44(6)	168(20)	16(8)	15(14)	68(18)
	[0.2223(11)	0.1556(12)	−0.2714(15)		84(20)	−2(28)	72(21)	−6(12)	3(17)	64(40)]
	[0.1782(13)	0.1530(10)	−0.2634(10)		164(30)	41(38)	83(24)	−3(38)	−45(22)	6(46)]

These parameters have been determined by least squares where $W^{-1} = 4.996 + 0.0333F - 0.0208F^2 + 0.00041F^3$ for the data taken with the counter and $W^{-1} = 28.15 - 2.384F + 0.0513F^2 + 0.00027F^3$ for the remainder of the data.

Can. J. Chem. Downloaded from www.nrcresearchpress.com by 210.87.254.105 on 09/05/12
For personal use only.

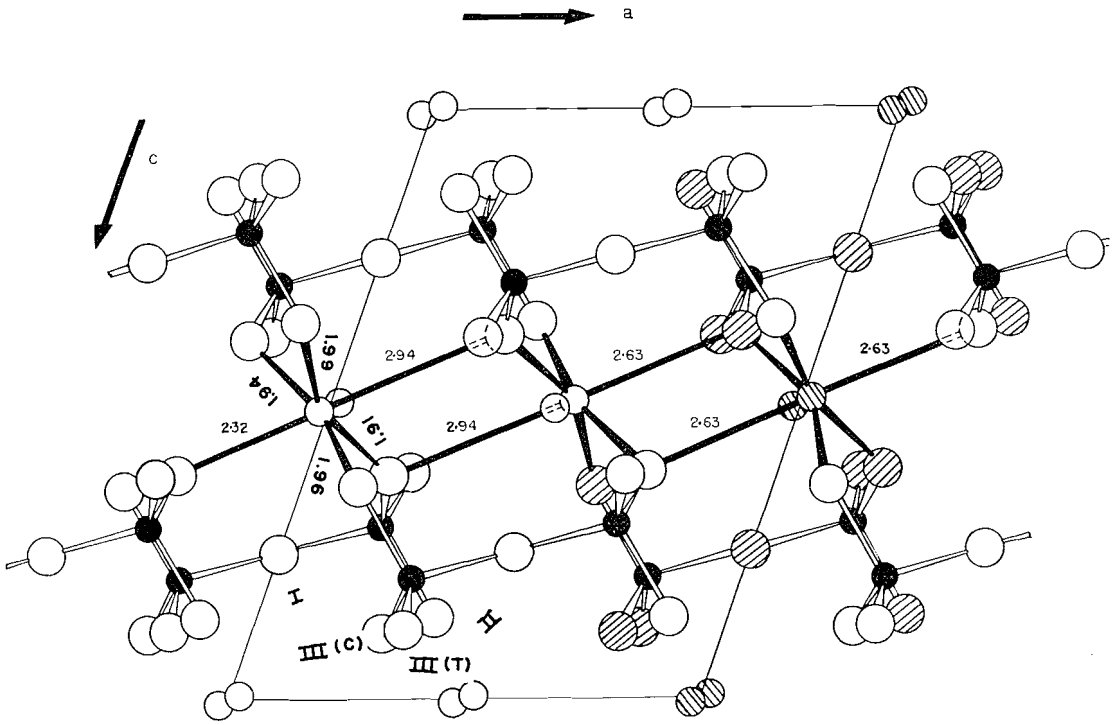

FIG. 1*a*. Three layers of the α-$Cu_2P_2O_7$ are shown in projection onto the *a*–*c* plane. The layer containing cross-hatched atoms has been disordered by introducing a stacking fault of $\frac{1}{2}$ *c*. The disordered β-$Cu_2P_2O_7$ is obtained by superimposing an order and disorder layer giving each atom a weight of $\frac{1}{2}$.

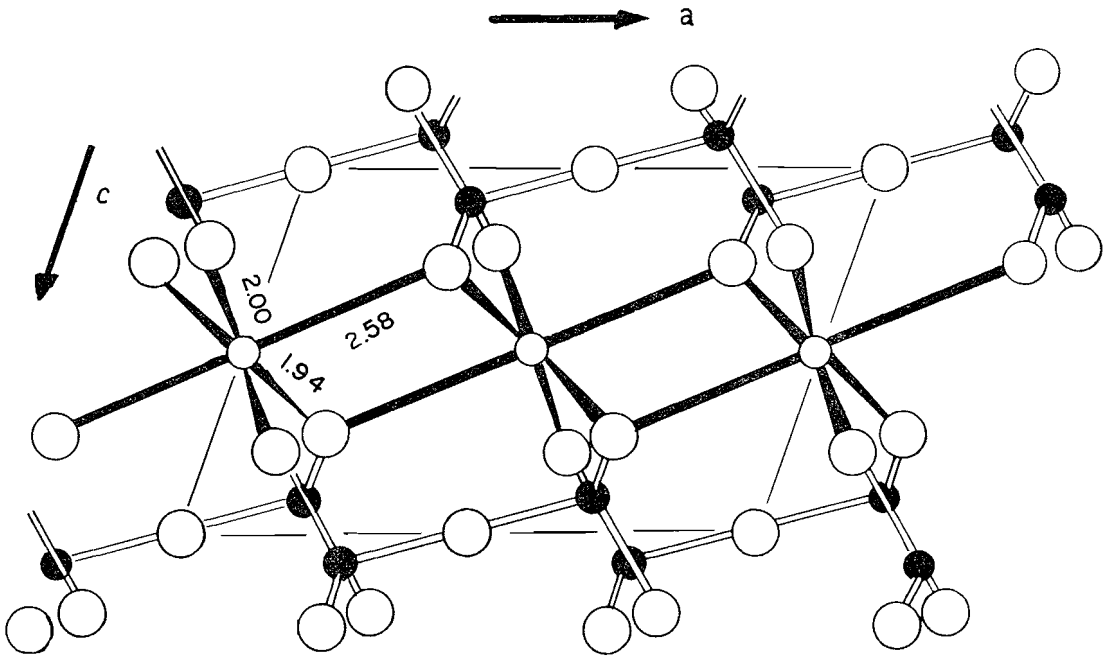

FIG. 1*b*. The atomic arrangement of β-$Cu_2P_2O_7$ is shown projected onto the *a*–*c* plane. The filled circles represent phosphorus atoms whereas the large and small non-filled circles represent oxygen atoms and Cu ions respectively.

this atom from the glide plane in α-$Cu_2P_2O_7$. The temperature factor of O_{III} is non-positive definite but not significantly so since U_{23} is just barely larger than U_{22} and U_{33}.

The Cu—O_6 groups show large axial distortions in directions perpendicular to the b axis. The average equatorial Cu—O bond distance is 1.97 ± 0.03 Å compared with 1.95 ± 0.04 Å in α-$Cu_2P_2O_7$. The axial Cu—O bond distance is 2.58 Å which is roughly the mean of the α phase bond distances of 2.322(6) Å and 2.940(6) Å. As can be seen in Table VI the terminal oxygen atoms nearly lie in the plane generated by the phosphorus atom and two cations to which they are ligated. This feature has been noted previously (5).

The structure refinement based upon the disordered model presents an interesting problem. Since the model with anisotropic thermal motion attributed to each atom yields slightly better R_1 and R_2 values than does the disorder model, we can ask to what degree does this better agreement reflect the additional variables in the former model. Hamilton (17) has shown that one can answer this question by examining the ratio of the R values for the two models. In the case at hand using the R_2 values for observed reflections only, the anisotropic model cannot be rejected as being the better model even at the 0.5% level of confidence. If the R_1 were used the anisotropic model can be rejected at the 10% level of confidence. The unobserved reflections were not used in this analysis because it is not clear how they should be treated. An additional and perhaps somewhat more significant test of the disorder model is how well the coordinates found correlate with those of α-$Cu_2P_2O_7$. In general the coordinates are found to lie within three times the sum of the e.s.d. found for the atom parameters compared. The y coordinate of O_I is one of the few parameters which fall outside the range of this criterion and this would suggest that disordered pyrophosphate ion in the β phase has a slightly larger P—O—P angle than that found in α-$Cu_2P_2O_7$. Of course there is no way of estimating the extent by which the molecular geometry deviates from its room temperature form disordering. It is unfortunate that the rather large errors as indicated by an R_2 near 0.12 prevents a more minute examination of the model.

Acknowledgments

This work was supported by a grant from the National Research Council of Canada. Special thanks are extended to C. V. Stager and R. Atkinson for providing their n.m.r. results on $Cu_2P_2O_7$.

1. K. Tukaszewicz and R. Smajkioewicz. Roczniki Chem. **35**, 741 (1961).
2. C. Calvo. Can. J. Chem. **43**, 1147 (1965).
3. C. Calvo. Can. J. Chem. **43**, 1139 (1965).
4. D. W. J. Cruickshank, H. Lynton, and G. A. Barclay. Acta Cryst. **15**, 491 (1962).
5. B. E. Robertson and C. Calvo. Acta Cryst. **22**, 665 (1967).
6. C. Calvo. Acta Cryst. **23**, 289 (1967).
7. C. Calvo. Unpublished results.
8. K. Tukaszewicz. Bull. Acad. Polon. Sci. Ser. Sci. Chim. **15**, 47 (1967).
9. B. E. Robertson. Ph.D. Dissertation, McMaster University, Hamilton, Ontario. 1967.
10. Z. Melkvi, C. V. Stager, and C. Calvo. Can. J. Phys. **45**, 83 (1967).
11. J. G. Chambers, W. R. Datars, and C. Calvo. J. Chem. Phys. **41**, 806 (1964).
12. R. Roy, E. T. Middlewarth, and F. A. Hummel. Am. Mineralogist, **33**, 458 (1948).
13. W. R. Datars and C. Calvo. J. Chem. Phys. In press.
14. C. Calvo, J. S. Leung, and W. R. Datars. J. Chem. Phys. **46**, 796 (1967).
15. D. W. J. Cruickshank, D. E. Pilling, A. Bujosa, F. M. Lovell, and M. R. Truter. *In* Computing methods and the phase problem in X-ray crystal analysis. *Edited by* R. Pepinsky, J. M. Robertson, and J. C. Speakman. Pergamon Press, New York. 1961.
16. International tables for crystallography. Vol. III. Kynock Press, Birmingham. 1962.
17. W. C. Hamilton. Acta Cryst. **18**, 502 (1965).

Can. J. Chem. Downloaded from www.nrcresearchpress.com by 210.87.254.105 on 09/05/12
For personal use only.

Can. J. Chem. Downloaded from www.nrcresearchpress.com by 210.87.254.5 on 09/05/12
For personal use only.

Chemistry of phosphorus fluorides. Part III. The reaction of thiophosphoryl-fluoride with dimethylamine and some properties of the dimethylaminothio-phosphoryl fluorides[1]

R. G. CAVELL
Department of Chemistry, University of Alberta, Edmonton, Alberta

Received April 6, 1967

Dimethylamine reacts with thiophosphoryl fluoride with non-integral stoichiometry to yield the volatile compound dimethylaminothiophosphoryldifluoride and the solid products contained hexafluoro-phosphate and difluorodithiophosphate ions, and an unstable complex ion containing phosphorus and fluorine. The reaction of dimethylaminothiophosphoryldifluoride with dimethylamine to form bis-(dimethylamino)thiophosphorylfluoride has also been studied. The solid residues of this reaction contained hexafluorophosphate and difluorodithiophosphate ions and an unidentified phosphorus-fluoride salt. Dimethylaminothiophosphoryldifluoride did not complex with boron trifluoride but reacted with hydrogen halides to yield the halogenothiophosphoryldifluorides. Physical and spectroscopic data on the alkylaminothiophosphoryl fluorides are reported.

Canadian Journal of Chemistry, **46**, 613 (1968)

Introduction

A variety of alkyl- and aryl-aminothiophos-phoryl fluorides have been prepared from the appropriate amine and either thiophosphoryl-fluoride or monochlorothiophosphoryldifluoride (2, 3). In all cases the reactions were done in a solvent and were presumed to follow the equation

$$[I]\quad SPF_3 + 2R_2NH \rightarrow SPF_2{\cdot}NR_2 + R_2NH_2^+F^-,$$

analogous to the behavior of phosphorus chlorides (4). Our previous studies have shown that the aminolysis reactions of phosphorus fluorides are not simple analogues of the chloride reactions; for example dimethylamine reacts with phosphorus trifluoride to yield the *bifluoride* rather than the fluoride salt (5),

$$[II]\quad 2PF_3 + 3(CH_3)_2NH \rightarrow 2(CH_3)_2NPF_2 + (CH_3)_2\overset{+}{N}H_2{\cdot}H\bar{F}_2,$$

and with phosphoryl fluoride (1) to yield the hexafluorophosphate and difluorophosphate salts according to the equation

$$[III]\quad 4POF_3 + 4(CH_3)_2NH \rightarrow 2(CH_3)_2NP(O)F_2 + (CH_3)_2\overset{+}{N}H_2{\cdot}P\bar{F}_6 + (CH_3)_2\overset{+}{N}H_2{\cdot}PO_2\bar{F}_2.$$

The reaction of thiophosphoryl fluoride with dimethylamine is also complex.

Results and Discussion

The Aminolysis of Thiophosphoryl Fluoride

In accord with the behavior of phosphoryl fluoride, gaseous thiophosphoryl fluoride reacted immediately and exothermally on contact with dimethylamine to form a white solid and volatile dimethylaminothiophosphoryldifluoride. Instead of the equimolar stoichiometry observed (1) in the case of phosphoryl fluoride however, 1.3 moles of dimethylamine reacted with each mole of thiophosphoryl fluoride. Although this stoich-iometry is close to that expected for the forma-tion of bifluoride ion according to eq. [IV],

$$[IV]\quad 2SPF_3 + 3(CH_3)_2NH \rightarrow 2SPF_2{\cdot}N(CH_3)_2 + (CH_3)_2\overset{+}{N}H_2{\cdot}H\bar{F}_2,$$

the reaction is considerably more complicated. Small amounts of hydrogen sulfide were also recovered in the volatile products.

In the simplest case (illustrated in Fig. 1*b*) the residues were found to contain the difluorodi-thiophosphate (A) and hexafluorophosphate (C) ions, identified by comparison of the measured fluorine nuclear magnetic resonance (n.m.r.) parameters (Table I) with the literature (6, 7). Also present in the spectra were two broad singlets (E, G) which may be due to fluoride or bifluoride ions or both.

The principal reaction therefore appears to be the analogue of the aminolysis of phosphoryl fluoride (1).

$$[V]\quad 4(CH_3)_2NH + 4SPF_3 \rightarrow 2(CH_3)_2NP(S)F_2 + (CH_3)_2\overset{+}{N}H_2{\cdot}P\bar{F}_6 + (CH_3)_2\overset{+}{N}H_2{\cdot}PS_2\bar{F}_2.$$

Secondary reactions and decompositions may account for the observed non-integral stoichiom-etry. For example, the observed hydrogen sulfide

[1]Part II: ref. 1.

Can. J. Chem. Downloaded from www.nrcresearchpress.com by 210.87.254.5 on 09/05/12
For personal use only.

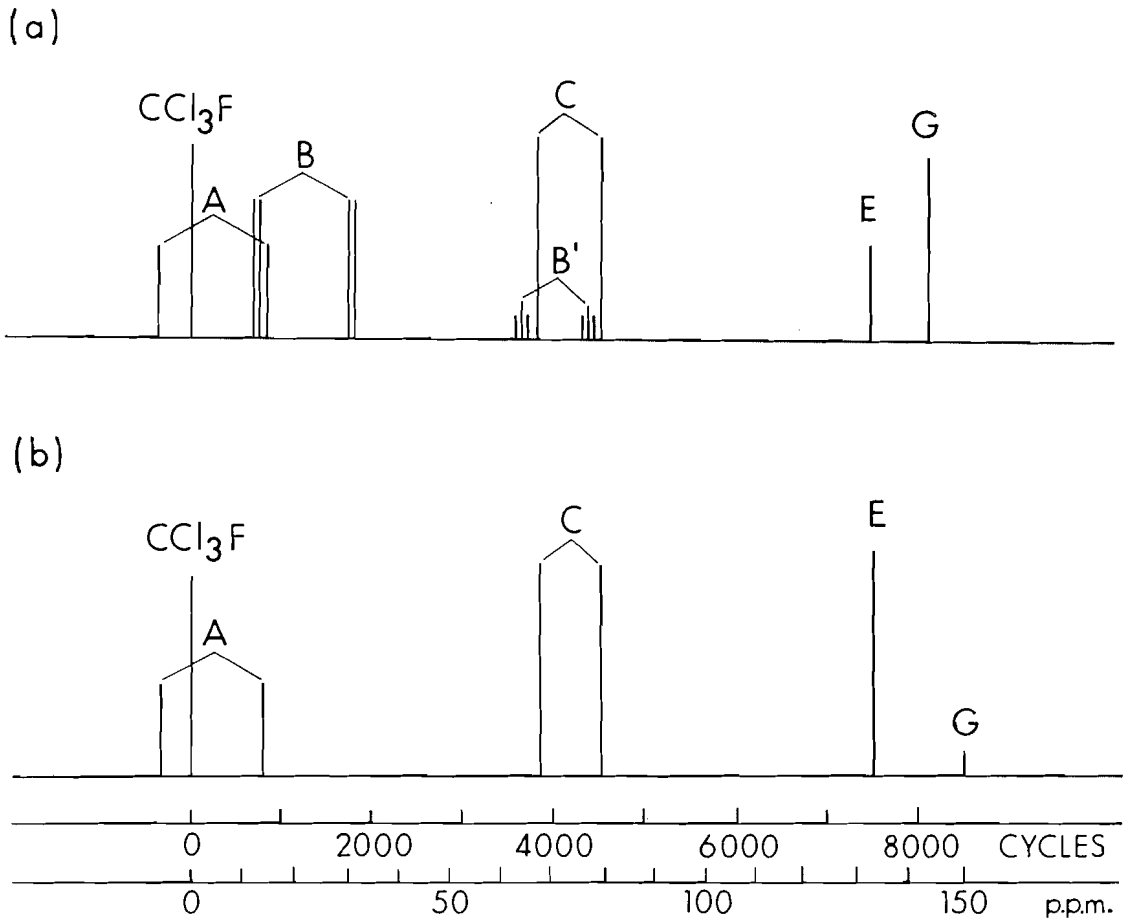

FIG. 1. Fluorine nuclear magnetic resonance spectra of acetonitrile solutions of the solid reaction residues from the reaction of dimethylamine with thiophosphorylfluoride. Spectra were measured at 56.4 Mcycles/s against an external (capillary) CCl_3F standard. (*a*) Freshly prepared solution of the residues of a low concentration reaction. (*b*) Freshly prepared solution of the residues from high concentration reactions or solution (*a*) after 24 h at room temperature. Parameters are given in Table I.

TABLE I

Fluorine n.m.r. data for solid residues from aminolysis of thiophosphoryl fluoride[a]

Line	Description	Chemical shift ϕ (p.p.m. vs. CCl_3F)	Coupling constants (cycles) J_{P-F}	J_{FF}
A	Doublet	+4.3	1146[c]	—
B	Pair of doublets	+22.0	909	48
B′	Pair of quintets[b]	+71.0	718	47
C	Doublet	+73.0	707[d]	—
E	Singlet	+132	—	—
G	Singlet	+148 (±5)	—	—

[a]Spectra illustrated in Fig. 1.
[b]Only three central lines of quintet (intensity 1:1.5:1) observed.
[c]$S_2PF_2^-$, see ref. 7.
[d]PF_6^-, see ref. 6.

may arise from aminolysis of the P=S unit. The presence of fluoride or bifluoride ion in the salt residues, in contrast to the aminolysis of phosphoryl fluoride where only the fluorophosphorus ions were observed in the salt products (1), may indicate incomplete formation of the phosphorus-fluoride complex ions or decomposition.

If the reaction was done under conditions of low reagent concentration, the residues contained, as illustrated in Fig. 1*a*, another species in addition to those already identified above. The multiplet patterns (B, B′) are assigned to a single species because of the similarity of the small splitting within the individual parts of the multiplet and because the whole multiplet disappears simultaneously when the solution is aged. The

Can. J. Chem. Downloaded from www.nrcresearchpress.com by 210.87.254.5 on 09/05/12
For personal use only.

spectrum of the solution reverted to that illustrated in Fig. 1*b* upon aging and a black precipitate was formed. The species appears to be decomposing rather than reacting with the solvent because dry reaction residues, which initially gave the spectrum shown in Fig. 1*a*, decomposed slowly at room temperatures to form hydrogen sulfide and dimethylamine and the residues remaining after decomposition gave the simple spectrum shown in Fig. 1*b*. The observed n.m.r. parameters of the B–B′ multiplet are not consistent with any known phosphorus-fluorine species. They cannot be assigned to any species containing P—H or P—$N(CH_3)_2$ functions because the hydrogen n.m.r. spectra showed only the resonances of the dimethylammonium cation. All of the line spacings are regular so the spectrum is probably first order. The B′ component is best regarded as a doublet of quintets in view of the 1:1.5:1 intensity ratio of the three lines in each half, which is in better agreement with the expected 4:6:4 intensity ratio for the three central lines of a quintet than with the 1:2:1 intensity ratio expected for a triplet. We suggest that the spectrum arises from the hexacoordinate SPF_5^{2-} ion with the structure

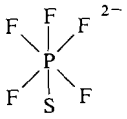

in which the doublet of doublets (B) is due to the equatorial fluorine atoms (F_e) split into a doublet by the phosphorus (J(P—F_e) = 909 cycles) further split by the single axial fluorine atom (F_a) (J(F_a—F_e) = 48 cycles) and the pair of quintets (B′) is due to the resonance of the single axial fluorine atom split by phosphorus (J(P—F_a) = 718 cycles) further split into a quintet by four equivalent equatorial fluorine atoms (J(F_a—F_e) = 47 cycles). These values of axial–equatorial fluorine coupling and the two P—F coupling constants are similar to those reported (8) for the substituted fluorophosphates $CH_3PF_5^-$ and $C_6H_5PF_5^-$. Conclusive assignment of the spectrum is not possible in view of the approximate nature of our intensity data. The pentacoordinate SPF_4^- ion is a likely alternative although recent studies suggest that this would probably show only a simple doublet due to the 'pseudorotation' averaging process (9) rather than a resolved multiplet.

The unstable complex fluorophosphorus anion was obtained only under conditions of low reagent concentration probably because the exothermicity of the reaction can be dissipated effectively under these conditions. The complex ion may be a thermally unstable intermediate which eventually decomposes to hexafluorophosphate and difluorodithiophosphate ions.

[VI] $$2SPF_5^{2-} \rightarrow S_2PF_2^- + PF_6^- + 2F^-$$

It seems reasonable to suggest that the aminolysis reaction proceeds through the formation of dimethylammonium fluoride or bifluoride by means of an initial acid–base association of thiophosphoryl fluoride with dimethylamine followed by elimination of hydrogen fluoride from the complex. The complex fluorophosphate ions may be formed in a second step involving reaction between the fluorophosphorus compound and fluoride or bifluoride ion. In the former case the SPF_4^- ion would be a likely intermediate analogous to our previous suggestion (1) of the POF_4^- ion as the intermediate ion in the aminolysis of phosphoryl fluoride. The latter case could lead to an ion such as SPF_5^{2-}, e.g.

[VII] $$SPF_3{\cdot}(CH_3)_2NH + (CH_3)_2\overset{+}{N}H_2{\cdot}HF_2^- \rightarrow [(CH_3)_2NH_2]_2{\cdot}SPF_5^{2-}.$$

Fluoride salts have been reported to react with thiophosphoryl fluoride (see footnote in ref. 10) to yield the difluorodithiophosphate and hexafluorophosphate ions but the intermediates are unknown. In the present case the intermediate *may* have been identified by the n.m.r. spectrum but further studies must be undertaken before a definite conclusion can be reached.

The aminolysis of dimethylaminothiophosphoryldifluoride proceeds slowly, with *equimolar* stoichiometry, in contrast to the rapid spontaneous reaction of thiophosphoryl fluoride. Similar behavior has been observed in the aminolysis of dimethylamino-phosphoryldifluoride (1) and -difluorophosphine (5) and can be attributed to the increased basicity of the dimethylamino derivatives which inhibits the reaction by retarding the formation of the primary acid–base adduct of the phosphorus fluoride with the amine.

The stoichiometry of the aminolysis is equimolar as in the case of the phosphoryl analogue (1) and the principal residual ions, identified by comparison of the fluorine n.m.r. parameters

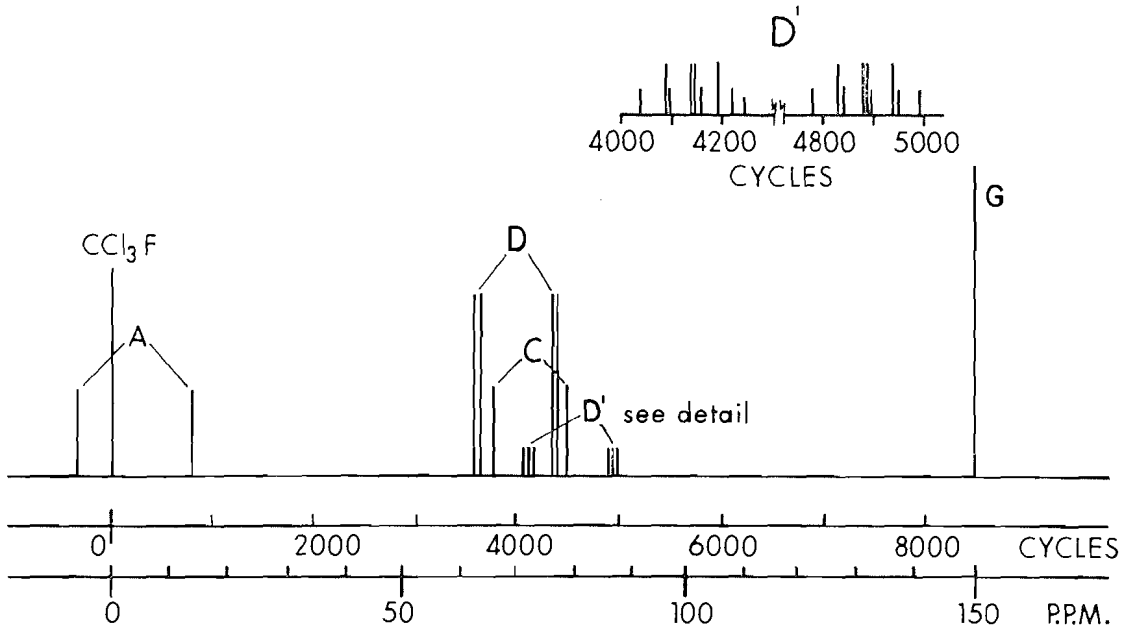

FIG. 2. Fluorine nuclear magnetic resonance spectrum, measured at 56.4 Mcycles/s, of an acetonitrile solution of the solid residues resulting from the reaction of dimethylamine with dimethylaminothiophosphoryldifluoride. Parameters are given in Table III.

obtained on the residues (Fig. 2 and Table II) with the literature (6, 7), are the analogous difluorodithiophosphate (A), hexafluorophosphate (C), and either fluoride or bifluoride (G) ions. In addition, however, a complex multiplet (D, D′) was observed which did not decompose over an extended period of time. As before the hydrogen n.m.r. spectra show only the resonances due to the dimethylammonium cation so species containing P—$N(CH_3)_2$ and P—H functions can be excluded as well as all known fluorophosphorus anions. Since the spectrum appears to be second order we cannot assign a structure to the multiplet without additional information although the line spacing is reminiscent of the hexacoordinate RPF_5^- ions (8).

It is somewhat surprising that unusual complex ions have been observed only in the aminolysis of the thiophosphoryl compounds and not the phosphoryl compounds, suggesting that species formed in the thiophosphoryl system are more stable. Conclusive identification of the species which give rise to the B–B′ and D–D′ multiplets is necessary before complete understanding of this system can be achieved.

TABLE II

Fluorine n.m.r. data for solid residues from aminolysis of dimethylaminophosphoryl fluoride[a]

Line	Description	Chemical shift ϕ (p.p.m. vs. CCl_3F)	Coupling constants (cycles) J_{P-F}	J_{FF}
A	Doublet	+4.0	1150[b]	—
C	Doublet	+73.0	708[c]	—
D	Pair of doublets	+70.9	796	52
D′	Complex multiplet[d]	+79.0	740?[e]	?[d]
G	Broad, single line	+150	—	—

[a]Spectrum illustrated in Fig. 2.
[b]$S_2PF_2^-$, see ref. 7.
[c]PF_6^-, see ref. 6.
[d]Apparently second order since the spacing between adjacent lines is irregular.
[e]A constant separation of 740 cycles is observed between each corresponding line in the two halves of the D′ doublet.

Properties of the Alkylaminothiophosphoryl-fluorides

Dimethylaminothiophosphoryldifluoride is a clear liquid with a foul odor. Its vapor pressure obeys the equation

$$\log_{10} P \text{ (mm)} = 8.213 - \frac{2082}{T},$$

giving an extrapolated boiling point of 117°, heat

Can. J. Chem. Downloaded from www.nrcresearchpress.com by 210.87.254.5 on 09/05/12
For personal use only.

Can. J. Chem. Downloaded from www.nrcresearchpress.com by 210.87.254.5 on 09/05/12
For personal use only.

of evaporation of 9530 cal/mole and a Trouton constant of 24.4.

Dimethylaminothiophosphoryldifluoride has also been prepared by fluorination of dimethylaminothiophosphoryldichloride with antimony trifluoride at 70–80°. Fluorination of the P=S group was not observed in contrast to the facile conversion of alkylphosphine sulfides to the fluorophosphoranes by antimony trifluoride under similar conditions (10). The difference in fluorination reactions can be attributed to the substitution of electron-withdrawing substituents such as chlorine or fluorine for alkyl groups on the phosphorus (11). Various other fluorinating agents were also tried: potassium fluorosulfinate produced a mixture of the phosphoryl and thiophosphoryl fluoride compounds and zinc fluoride gave a very low yield of impure dimethylaminothiophosphoryldifluoride and no other volatile products.

Hydrogen chloride and hydrogen bromide react slowly at room temperatures with dimethylaminothiophosphoryldifluoride (in contrast to the rapid reaction with dimethylaminodifluorophosphine (5)) to yield the halogenothiophosphoryl difluorides in high yield according to the equation

$$[\text{VIII}]\quad (CH_3)_2NP(S)F_2 + 2HX \rightarrow XP(S)F_2 + (CH_3)_2\overset{+}{N}H_2\overset{-}{X}.$$

Previous reports of low yields from the analogous reaction with the diethylamino derivatives may be due to the higher reaction temperatures used (3).

Thiophosphoryl fluoride does not complex with boron trifluoride (12). We suggested above that the increase in basicity of the molecule upon substitution of a dimethylamino group for a fluoride results in much slower reaction of the substituted molecule with basic reagents. It was of interest therefore to see if the increased basicity of dimethylaminothiophosphoryldifluoride was sufficient to permit formation of a complex with boron trifluoride as has been demonstrated for dimethylaminodifluorophosphine (5, 13). Boron trifluoride did not complex with dimethylaminothiophosphoryldifluoride, even at −78 °C, so neither the sulfur nor the nitrogen atom appears to be an effective donor. The lack of basicity associated with the nitrogen atom, which appears to be the effective donor in dimethylaminodifluorophosphine (13), suggests that the lone pair is delocalized onto the phosphorus, although we cannot exclude the possibility that stable complex formation is prevented by steric considerations.

TABLE III

Nuclear magnetic resonance parameters for methylaminothiophosphoryl fluorides

	$(CH_3)_2NP(S)F_2$	$[(CH_3)_2N]_2PSF$
Chemical shift		
τ ^1H vs. TMS (τ = 10.0)	6.67	7.42
ϕ ^{19}F p.p.m. vs. CCl_3F	+51.6	+62.3
Coupling constant (cycles)		
J(P—F)	1079	1016
J(P—H)	12.2	12.6
J(F—H)	2.1	1.70

Partial mass spectra of the mono- and disubstituted alkylaminothiophosphoryl fluorides are given in Table IV and the n.m.r. parameters are given in Table III. The hydrogen and fluorine n.m.r. spectra of dimethylaminothiophosphoryldifluoride show a pair of triplets and a doublet of septets respectively as expected for first order spin coupling interaction of six equivalent hydrogens and two equivalent fluorine atoms with phosphorus. The hydrogen spectrum of bis(dimethylamino)thiophosphorylfluoride showed the expected pair of doublets but the fluorine spectrum showed only a pair of fairly broad lines with unresolved fluorine–hydrogen coupling.

The infrared spectra of the two compounds, given in Table V, are similar to each other and to the phosphoryl analogues. The assignments are based on the analysis of the vibrational spectrum of dimethylaminodifluorophosphine (14) and the available data on alkylaminophosphorylhalides (1, 15) and alkylaminothiophosphorylhalides (15, 16).

Dimethylaminothiophosphoryldifluoride does not have the absorption band at 1365 cm^{-1} which was assigned to the P=O stretch of the phosphoryl compound (1) and instead of two bands in the 950–700 cm^{-1} region there are three. There are four vibrational modes to be assigned; the symmetric and antisymmetric PF stretch, the P=S, and the P—N stretch. Since these vibrations may be mixed, particularly the last named which has been reported as a weak, easily mixed band (14), we can only make a tentative assignment at present. The 910 cm^{-1} band is

TABLE IV

Mass spectra of methylaminothiophosphoryl fluorides[a]

$(CH_3)_2NP(S)F_2$			$[(CH_3)_2N]_2P(S)F$		
m/e	Rel. int.	Assignment	*m/e*	Rel. int.	Assignment
146	3.5	M + 1 isotope of parent	171	3	M + 1 isotope of parent
145	74	$C_2H_6NPSF_2$	170	52	$C_4H_{12}N_2PSF$
144	13	$C_2H_5NPSF_2$			
143	tr[b]	$C_2H_4NPSF_2$	137	8	$C_4H_{11}N_2PSF$
142	tr	$C_2H_3NPSF_2$	128	1	M + 2 isotope of 126
130	1	CH_3NSPF_2	127	2	C_2H_7NPSF or M + 1 isotope of 126
129	tr	CH_2NSPF_2			
128	1	$CHNSPF_2$	126	18	C_2H_6NSPF
126	2.8	C_2H_6NPSF, $CNPSF_2$			
116	1	?	95	3	M + 1 isotope of 94
115	tr	$NSPF_2$	94	100	C_2H_6NPF
113	4	$C_2H_6NPF_2$	93	1	C_2H_5NPF
112	100	$C_2H_5NPF_2$	83	2	SPFH
110	1.5	$C_2H_3NPF_2$			
103	1	M + 2 isotope of 101	78	3	CH_2NPF, N_2PF
102	2	SPF_2H			
101	11	SPF_2	65	2	NHPF
98	1.5	CH_3NPF_2, C_2NPF			
96	1.5	NPSF	63	1.3	SP
94	1.5	C_2H_6NPF			
93	tr	C_2H_5NPF	60	1.3	CH_3NP
83	1	NPF_2, SPFH			
82	1	SPF	51	1	PFH
78	1	H_2CNPF	50	0.5	PF
75	1	C_2H_6NP	45	4	C_2H_7N, NP
69	14	PF_2	44	91	C_2H_6N
63	tr	PS	43	5	C_2H_5N
61	1.4		42	16	C_2H_4N
60	1.4	CH_3NP	41	1	C_2H_3N
51	1				
50	1.5	PF			
45	1.5	C_2H_7N, NP			
44	3	C_2H_6N			
43	18	C_2H_5N			
42	53	C_2H_4N			
41	3	C_2H_3N			
40	1.5	C_2H_2N			
32	1.5	S			

[a]Only ^{32}S mass assignments indicated.
[b]tr = trace.

therefore assigned to the antisymmetric and the 858 cm^{-1} band to the symmetric P—F stretching motions leaving the 790 cm^{-1} band to be assigned to a vibration which is principally P=S stretching, noting, however, that the last two are probably mixed with the P—N stretch.

The spectrum of the monofluorothiophosphoryl compound is similar to that of the difluoro analogue except for doubling of the 1000 cm^{-1} absorption band into two strong absorption bands at 975 and 995 cm^{-1} respectively. The band observed at 910 cm^{-1} in the difluoro compound is not observed in the monofluoro derivative. Instead absorption bands are found at 820 cm^{-1}, 765 cm^{-1}, and 745 cm^{-1}. The first is probably the PF stretching vibration and the second the N_2P valence vibration characteristic of N_2P compounds. Comparison of the spectra of bis(dimethylamino)thiophosphorylfluoride with the phosphoryl analogue (1) indicates that the medium intensity band at 745 cm^{-1} is unique to the thiophosphoryl compound and hence is reasonably assigned to the P=S stretch. Considerable mixing of vibrations may occur, however, which may require modification of these assignments (14).

Experimental

Standard vacuum techniques were used throughout. Infrared spectra were measured with Perkin-Elmer 421 or

Can. J. Chem. Downloaded from www.nrcresearchpress.com by 210.87.254.5 on 09/05/12
For personal use only.

TABLE V

Infrared spectra of alkylaminothiophosphoryl fluorides*

$(CH_3)_2NPSF_2$ (gas)	$[(CH_3)_2N]_2PSF$ (film)	Assignment
3000 (w)	3000 (w)	
2940 (s)	2940 (s)	CH_3 antisymmetric stretch
2910 (sh)	2890 (m)	
2865 (m)	2850 (m)	CH_3 symmetric stretch
2820 (m)	2810 (m)	
	1473 (sh)	
1460 (m,br)	1458 (s)	CH_3 deformation
	1410 (w)	
1313 (s)	1302 (s)	CH_3 symmetric deformation
	1278 (sh)	
1182 (s)	1180 (s)	Antisymmetric C—N stretch
	1160 (s)	
1070 (w)	1060 (m)	CH_3 rocking
1005 (s)	1000 (vs)	Symmetric C_2NP stretch
	978 (vs)	
910 (vs)	825 (vs)	P—F stretch
858 (s)	—	See text
790 (sh)	—	
782 (s)		
—	765 (vs)	PN_2 skeletal vibration
—	745 (m)	P=S stretch
620 (w)	—	
425 (m)	—	Symmetric PF_2 deformation

*All values given in cm^{-1}. br = broad, w = weak, m = medium, s = strong, sh = shoulder, v = very.

337 spectrophotometers covering the ranges 5000–600 and 4000–400 cm^{-1} respectively. Hydrogen nuclear magnetic resonance spectra were measured with Varian HA100 or A60 instruments and compared with the tetramethylsilane ($\tau = 10.0$) reference. All fluorine n.m.r. were measured at 56.4 Mc/s with a Varian HA60 instrument. Mass spectra were measured with A.E.I. MS-9 double focussing spectrometer. Thiophosphoryl fluoride was prepared from zinc fluoride and thiophosphoryl chloride (10*a*, 17).

The Reaction of Thiophosphoryl Fluoride with Dimethylamine

(*a*) Dimethylamine (0.518 g, 11.7 mmoles) was added slowly to an equimolar quantity of gaseous thiophosphoryl fluoride (1.404 g, 11.7 mmoles) at room temperature in a 1 l reaction vessel similar to that described previously (5). A white solid precipitated immediately on mixing the gaseous reactants and a volatile liquid was also formed in the reaction. The reagents were allowed to mix thoroughly for approximately 1 h and then the volatile materials were withdrawn from the reaction vessel and fractionated to yield, in the most volatile fraction, an inseparable mixture of unreacted thiophosphoryl fluoride (0.337 g, 2.8 mmoles), identified by its infrared spectrum, and hydrogen sulfide (0.3 mmole), identified by its n.m.r. chemical shift (6). The consumption of thiophosphoryl fluoride by 11.7 mmoles dimethylamine was thus 8.9 mmoles for a reacting ratio of amine/SPF_3 of 1.3/1. The least volatile fraction, collected at −78°, contained dimethylaminothiophosphoryldifluoride, identified by molecular weight (M) (Found: M, 145. Calcd. for $C_2H_6F_2NPS$: M, 145), analysis (Found: P, 21.10; S, 22.15; F, 26.41; N, 9.63. Calcd. for $C_2H_6F_2NPS$: P, 21.34; S, 22.05; F, 26.2; N, 9.65%), and by measurement of the accurate mass of the molecular ion at 145 atomic mass units with the MS-9 spectrometer (Found: *m/e*, 144.9934. Calcd. for $C_2H_6F_2NP^{32}S$: *m/e*, 144.9926).

(*b*) In a second experiment, about 30 mmoles of thiophosphoryl fluoride was combined with a 1.30 molar ratio of dimethylamine in the same reaction vessel. No unreacted thiophosphoryl fluoride was recovered; the most volatile reaction product was identified as impure hydrogen sulfide (0.028 g, about 0.6 mmoles). The only other volatile product obtained was dimethylaminothiophosphoryldifluoride, identified by comparison with an authentic sample prepared earlier.

The residual solid remaining in the reaction bulb after removal of the volatile reaction products was kept at room temperature for 4 weeks in the evacuated bulb. After this period of time it was found that the reaction bulb contained impure hydrogen sulfide, identified by molecular weight (Found: M, 38. Calcd. for H_2S: M, 34.0) and accurate mass measurement by mass spectrometry (Found: *m/e*, 34.9875. Calcd. for $H_2{}^{32}S$: *m/e*, 34.9877). Dimethylamine was also identified as a minor constituent of the volatile products by its mass spectrum.

(*c*) Several small scale experiments were done to provide samples of the solid reaction products for nuclear magnetic resonance studies. Gaseous dimethylamine and thiophosphoryl fluoride were combined in an equimolar ratio in a 100 cc reaction vessel. In each case unreacted thiophosphoryl fluoride was recovered (contaminated with hydrogen sulfide) in sufficient quantity to yield a reacting ratio of amine/SPF_3 of 1.3/1. A 0.57/1 molar ratio of dimethylaminothiophosphoryldifluoride relative

Can. J. Chem. Downloaded from www.nrcresearchpress.com by 210.87.254.5 on 09/05/12
For personal use only.

Can. J. Chem. Downloaded from www.nrcresearchpress.com by 210.87.254.5 on 09/05/12
For personal use only.

to the amount of amine taken was recovered in each case. Reactions done on a 1 mmole scale in the 100 cc vessel and those done in the 1 l vessel described above (section *a*) yielded solid residues with the fluorine n.m.r. spectrum illustrated in Fig. 1*a*. Reactions done on a 5 mmoles scale in the 100 cc vessel gave solid residues with the n.m.r. spectrum shown in Fig. 1*b*.

The solid residues were dissolved in carefully dried acetonitrile or deuterated acetonitrile in vacuum by distilling 0.5 ml of the solvent into the reaction vessel after removal of the volatile products. The residues appeared to dissolve quickly and completely in acetonitrile. The reaction vessel was then opened to a nitrogen atmosphere and the solution pipetted quickly into a n.m.r. tube containing a reference CCl_3F capillary, degassed, and sealed. The initial n.m.r. spectra were run within 2 h of the sample preparation. The results are given in Fig. 1 and Table I. Rigorous exclusion of moisture from the solvent and apparatus was necessary during preparation of the residue solutions for n.m.r. studies otherwise additional doublet resonances due to the $PO(S)F_2^-$ (18) and $PO_2F_2^-$ (6*a*) ions were observed in the spectrum.

The Vapor Pressure of Dimethylaminothiophosphoryldifluoride

The vapor pressure was measured with a glass spiral microtensimeter over the range 0 to 68 °C. The data are given in the following table (*descending temperature).

t (°C)	0.1	0.1*	7.2	10.7*	13.0
P (mm)	4.2	4.1	6.1	7.1	7.9
t (°C)	20.5	26.8*	29.5	43.1	50.95
P (mm)	13.0	18.3	22.3	43.5	62.2
t (°C)	51.4*	58.3	67.9		
P (mm)	62.9	85.3	123.6		

The Reaction of Dimethylamine with Dimethylaminothiophosphoryldifluoride

(*a*) A mixture of dimethylaminothiophosphoryldifluoride (0.76 g, 5.23 mmoles) and 0.32 g (7.06 mmoles) dimethylamine was heated to 80° for 6 h. Fractionation of the volatile products yielded, in the most volatile fraction, unreacted dimethylamine (0.074 g, 1.65 mmole) thus indicating a ratio of amine consumed to dimethylaminothiophosphoryldifluoride taken of nearly 1:1. The least volatile fraction was bis(dimethylamino)thiophosphorylfluoride, identified by analysis (Found: P, 17.74; S, 18.30; F, 10.56; N, 16.29. Calcd. for $C_4H_{12}FN_2PS$: P, 18.2; S, 18.6; F, 11.2; N, 16.48) and mass measurement of the molecular ion with the MS-9 mass spectrometer (Found: *m/e*, 170.0438. Calcd. for $C_4H_{12}FN_2P^{32}S$: *m/e*, 170.0442). Bis(dimethylamino)thiophosphoryl fluoride was not very volatile and appeared to react with mercury, thus the vapor pressure could not be determined accurately. The compound has a vapor pressure of approximately 1.4 mm at 27 °C.

The white solid residue which remained in the reaction vessel was dissolved in acetonitrile in vacuum and transferred, in an atmosphere of nitrogen, to a nuclear magnetic resonance tube which was then degassed and sealed in vacuum. The spectrum was obtained within a few hours of preparing the sample and again after several weeks at room temperatures. The results are given in Fig. 2 and Table II.

Fluorination of Dimethylaminothiophosphoryldichloride

Dimethylaminothiophosphoryldichloride was prepared as described in the literature (4) and characterized by n.m.r. spectroscopy (19).

(a) With Potassium Fluorosulfinate

Dimethylaminothiophosphoryldichloride (25 g) was heated with 60 g KSO_2F. Reaction began at 60°. The products were collected and identified by infrared and n.m.r. spectroscopy as sulfur dioxide, thiophosphoryl fluoride, dimethylaminothiophosphoryldifluoride, and dimethylaminophosphoryldifluoride, as well as traces of dimethylaminothiophosphorylchlorofluoride.

(b) With Zinc Fluoride

Dimethylaminothiophosphoryldichloride (20 g) was heated to 80° for 3 h with zinc fluoride (50 g) in a sealed evacuated vessel. Fractionation of the volatile products yielded silicon tetrafluoride, thiophosphoryl fluoride, and a material of low volatility which could not be identified, but was not the desired dimethylaminothiophosphoryldifluoride. The products were identified by n.m.r. and infrared spectroscopy.

(c) With Antimony Trifluoride

Antimony trifluoride (10 g) was slowly added to 5 g of dimethylaminothiophosphoryldichloride in an evacuated flask with stirring. No reaction was observed until the vessel was warmed to 70–80°, whereupon the reaction proceeded smoothly. Fractionation of the products in the vacuum system yielded mainly dimethylaminothiophosphoryldifluoride plus a small amount of thiophosphoryl fluoride impurity, both identified by infrared and n.m.r. spectroscopy.

The Reaction of Dimethylaminothiophosphoryldifluoride with Hydrogen Chloride

Dimethylaminothiophosphoryldifluoride (0.200 g, 1.37 mmoles) was combined with hydrogen chloride (0.101 g; 2.78 mmoles) in a large bulb. No visible signs of reaction were observed at room temperature even after several hours, so the contents of the reaction vessel were transferred to a smaller sealed tube whereupon visible signs of reaction appeared within 1/2 h at room temperature (probably because of the greater hydrogen halide pressure). Separation of the volatile products from the white crystalline solid yielded a trace of hydrogen chloride and 0.173 g of chlorothiophosphoryldifluoride, identified by molecular weight (Found: M, 139. Calcd. for ClF_2PS: M, 136.5) and mass spectrometric measurement of the accurate mass of the parent ion (Found: *m/e*, 135.9110. Calcd. for $^{35}ClF_2P^{32}S$: *m/e*, 135.9116). The yield was 1.27 mmoles or 93% of theoretical (eq. [VIII]).

The Reaction of Dimethylaminothiophosphoryldifluoride with Hydrogen Bromide

Dimethylaminothiophosphoryldifluoride (0.391 g, 2.7 mmoles) was combined with excess hydrogen bromide (0.484 g, 6.0 mmoles) in a sealed glass ampoule. Long white needle-like crystals formed within 15 min of warming the vessel to room temperature and the reaction was complete after 1 h. Separation of the volatile products yielded unreacted hydrogen bromide (0.042 g, 0.55 mmole) corresponding to a consumption of 2.1 moles of hydrogen bromide by each mole of dimethylaminothiophosphoryldifluoride. The least volatile fraction was identified as monbromothiophosphoryldifluoride by molecular weight

(Found: M, 178. Calcd. for BrF_2PS: M, 181) and mass spectrometry (Found: *m/e*, 179.8609. Calcd. for $^{79}BrF_2P^{32}S$: *m/e*, 179.8611).

The Reaction of Dimethylaminothiophosphoryldifluoride with Boron Trifluoride

Dimethylaminothiophosphoryldifluoride (0.134 g, 0.94 mmole) was combined with boron trifluoride (0.134 g, 1.98 mmole) in a sealed glass ampoule and allowed to react at room temperature for 2 days. Fractionation of the volatile materials through a −78 trap led to nearly quantitative (98%) recovery of each of the starting materials. The purity of the recovered reactants was verified by molecular weight and infrared measurements.

Acknowledgments

The author thanks Mr. G. Bigam and Mr. M. Hogben for their assistance in measuring the nuclear magnetic resonance spectra, Mr. A. I. Budd for measurement of the mass spectra, and the National Research Council of Canada (Ottawa) for financial support.

1. R. G. CAVELL. Can. J. Chem. **45**, 1309 (1967).
2. G. A. OLAH, A. A. OSWALD, and S. KUHN. Ann. Chem. **625**, 88 (1959).
3. A. MULLER, H.-G. HORN, and O. GLEMSER. Z. Naturforsch. **21b**, 1150 (1965).
4. G. M. KOSOLAPOFF. Organophosphorus compounds. Wiley, New York. 1958.
5. R. G. CAVELL. J. Chem. Soc. 1992 (1964).
6. (*a*) E. FLUCK. Die kernmagnetische Resonanz und ihre Anwendung in der anorganischen Chemie. Springer Verlag, Berlin. 1963. (*b*) E. L. MUETTERTIES and W. D. PHILLIPS. Advan. Inorg. Chem. Radiochem. **4**, 231 (1962).
7. H. W. ROESKY, F. N. TEBBE, and E. L. MUETTERTIES. J. Am. Chem. Soc. **89**, 1272 (1967).
8. R. SCHMUTZLER. J. Am. Chem. Soc. **86**, 4500 (1964); Inorg. Chem. **5**, 164 (1966); J. Chem. Soc. 5630 (1965).
9. E. L. MUETTERTIES, W. MAHLER, and R. SCHMUTZLER. Inorg. Chem. **2**, 613 (1963).
10. R. SCHMUTZLER. (*a*) Advan. Fluorine Chem. **5**, 31 (1965); (*b*) Inorg. Chem. **3**, 421 (1964).
11. J. F. NIXON. Chem. Ind. London, 1555 (1963).
12. H. S. BOOTH and J. H. WALKUP. J. Am. Chem. Soc. **65**, 2334 (1943).
13. M. A. FLEMING. Thesis, University of Michigan, Ann Arbor, Mich. 1963. Quoted in ref. 10*a*, p. 57.
14. M. A. FLEMING, R. J. WYMA, and R. C. TAYLOR. Spectrochim. Acta, **21**, 1189 (1965).
15. R. B. HARVEY and J. E. MAYHOOD. Can. J. Chem. **33**, 1552 (1955).
16. F. N. HOOGE and P. J. CHRISTEN. Rec. Trav. Chim. **77**, 911 (1958).
17. R. G. CAVELL. Unpublished work.
18. H. W. ROESKY. Chem. Ber. **100**, 950 (1967).
19. A. H. COWLEY and R. P. PINNELL. J. Am. Chem. Soc. **87**, 4454 (1965).

Can. J. Chem. Downloaded from www.nrcresearchpress.com by 210.87.254.5 on 09/05/12
For personal use only.

Can. J. Chem. Downloaded from www.nrcresearchpress.com by 210.87.254.5 on 09/05/12
For personal use only.

Hydrogenation of methylacetylene. III. The reaction of methylacetylene with hydrogen catalyzed by nickel, copper, and their alloys[1]

R. S. Mann and K. C. Khulbe
Department of Chemical Engineering, University of Ottawa, Ottawa, Canada

Received June 27, 1967

The reaction between methylacetylene and hydrogen over unsupported nickel, copper, and their alloys has been investigated in a static constant volume system between 20 and 220 °C for a wide range of reactant ratios. The order of reaction with respect to hydrogen was one and nearly independent of temperature. While the order of reaction with respect to methylacetylene over nickel catalyst was slightly negative and temperature dependent, it was always positive and nearly independent of temperature for copper and copper-rich alloys. Selectivity was independent of initial hydrogen pressure for nickel and copper only; for others it decreased rapidly with increasing hydrogen pressure. The overall activation energy varied between 9 and 21.2 kcal/g mole. Selectivity and extent of polymerization increased with increasing amount of copper in the alloy.

Canadian Journal of Chemistry, **46**, 623 (1968)

Introduction

Though recently several papers (1) have appeared describing the kinetics of catalytic hydrogenation of acetylene, very little has been reported about the kinetics of methylacetylene hydrogenation. Bond and Sheridan (2) studied the reaction of methylacetylene and hydrogen over pumice-supported nickel, platinum, and palladium metals. Recently, the kinetics of methylacetylene hydrogenation over supported and unsupported nickel have been reported by Mann and Naik (3) and over unsupported nickel, iron, and cobalt by Mann and Khulbe (4). In the present study, we have examined the hydrogenation of methylacetylene over nickel, copper, and their alloys. Here we report the kinetics of the reaction and the yields of propylene and propane over a wide range of conditions.

Experimental

The apparatus and experimental procedure were essentially the same as described by Mann and Naik (3). Homogeneous nickel–copper alloys, pure nickel and copper powders, were prepared by the method of Best and Russell (5). The mixed basic carbonates (in case of alloys) or basic carbonates (for nickel and copper) precipitated by ammonium bicarbonate from their nitrate solutions (copper nitrate solution contained some acetic acid to avoid hydrolysis), containing the appropriate quantities of the nitrates, were dried at 105 °C overnight. The basic carbonates were decomposed to the oxides by calcination at 600 °C in a muffle furnace, and then reduced in a hydrogen stream for 24 h at 400 °C. Methylacetylene and hydrogen were purified as described previously (4). Quantitative analysis of the products was carried out by means of a Fisher gas partitioner as described by Mann and Naik (3) and slightly modified by Mann and Khulbe (4).

X-ray analysis of the reduced nickel–copper oxides showed that solid solutions closely corresponding to the expected composition were indeed formed. All the alloys contained no detectable free metal, and had face-centered cubic structure. The lattice constants and calculated compositions of these are given in Table I. These checked very well with the expected values within a reasonable accuracy. Surface areas of these catalysts as determined by B.E.T. method were less than 1 sq. m/g of catalyst.

Results and Discussion

(a) Pressure–Time Curves

Bond (6) has classified the observed pressure–time curves for acetylene hydrogenation over nickel pumice. The kinetic form of these curves depended on (i) initial hydrogen/acetylene ratio, (ii) the order of admission of reactants, if added separately, and (iii) the pretreatment of the catalyst, if both the reactants added together. The pressure–time curves obtained in methylacetylene hydrogenation over pumice-supported and unsupported nickel catalyst have been discussed in detail by Mann and Naik (3). In agreement with their findings for methylacetylene hydrogenation over nickel, supported and unsupported, the pressure–time curves observed over nickel powders in the present investigations consisted of two linear portions of different rates (Fig. 1, curve AFG, type IIA). In case of copper-catalyzed hydrogenation, the rate was nearly constant up to a pressure fall about equal to the initial methylacetylene pressure (Fig. 1, curve AB) for all hydrogen/methylacetylene

[1]Based on the paper presented at the Second Symposium on Catalysis of the Canadian Institute of Chemistry, Hamilton, June 14–16, 1967.

TABLE I

Orders of reaction and activation energies for catalysts

Catalyst wt. % Ni in alloy	Wt. of catalyst (g)	a, lattice parameter (A)	Calculated composition of copper in alloy	Temp. range (°C)	Specific* reaction rate ($k \times 10^2$) min^{-1}	Activation energy (kcal/mole)	Average order†	
							m	n
100	0.15	3.516	0	72–111	0.69	12.2±0.2	−0.11±.11	1.1±.1
90	0.15	3.522	5	26–55	6.61	11.2±0.2	0.03±.03	1.06±.03
80	0.15	3.538	25	29–52	13.18	10.4±0.2	0.01±.01	1.09±.09
65	0.15	3.550	35	30–50	10.05	10.3±0.2	0.01±.01	1.05±.05
50	0.15	3.557	45	35–55	6.56	9.8±0.2	0.00±.00	1.03±.03
40	0.15	3.579	65	73–92	1.11	9.10±0.2	−0.04±.03	1.05±.05
25	0.30	3.584	70	64–90	1.00	10.1±0.2	0.02±.03	1.0±.03
10	0.40	3.602	90	131–166	~0.00	16.2±0.2	0.53±.02	1.01±.02
0	0.50	3.610	100	181–220	~0.00	21.2±0.2	0.49±.02	0.97±.04

*k is specific reaction rate at 60 °C.
†m and n are order of reaction with respect to methylacetylene and hydrogen respectively.

ratios between 0.5 and 6. With nickel–copper alloys, for hydrogen/methylacetylene ratios of about one and less, the rate of pressure fall during the course of reaction was approximately proportional to the first power of the remaining hydrogen pressure until about 90% of the reaction has taken place (Fig. 1, curve ADE). When the initial hydrogen/methylacetylene ratio was more than one, a different form of pressure–time (Fig. 1, curve ABC) relation was observed. Curve ABC was comprised of two linear regions, region AB in which the reaction was of first order, and region BC in which the rate of pressure fall accelerated. The acceleration point ($-\Delta p_a$) is defined as the pressure obtained by extrapolating the linear portion of the first and second stage of the reaction. Recently similar type of behavior was observed by Bond and Wells (7) while investigating the kinetics of acetylene hydrogenation, over alumina-supported platinum catalysts. In the region AB, the main product of the reaction was propylene with little amount of propane, whereas after the rapid acceleration (region BC) the main process occurring was the further hydrogenation of propylene to propane. At higher concentrations of copper, the region BC was considerably reduced. The total pressure fall, observed for complete reaction, was about 6% more than extrapolated from the stoichiometric equation $C_3H_4 + 2H_2 = C_3H_8$ on account of hydropolymerization of methylacetylene to higher hydrocarbons.

(b) The Dependence of Activity on Composition of Nickel–Copper Alloys

The hydrogenation of methylacetylene has been studied over seven different nickel–copper alloys. The results are summarized in Table I. The striking feature of these results is that the catalytic activity rapidly increases with the slight increase of copper content (up to 25% Cu) in the alloy, and then decreases with the increasing copper content. Similar behavior was observed by Best and Russell (5), in the hydrogenation of ethylene over nickel–copper alloys, in the copper-rich region.

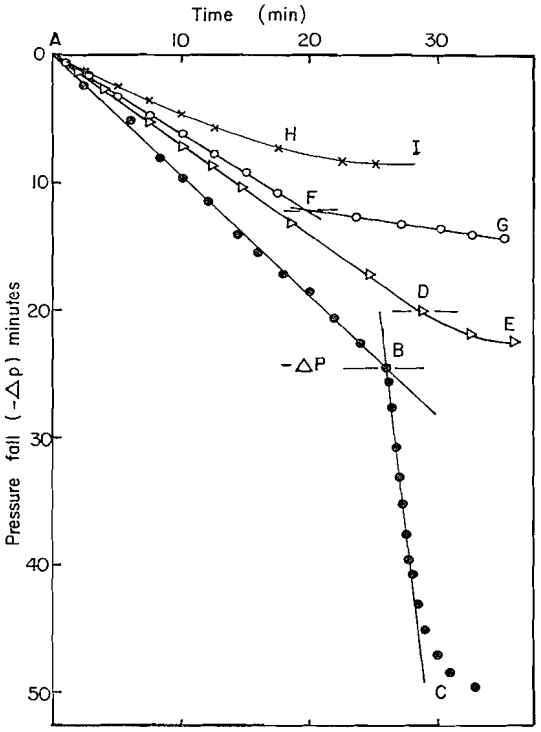

FIG. 1. Pressure–time curve.

Can. J. Chem. Downloaded from www.nrcresearchpress.com by 210.87.254.5 on 09/05/12
For personal use only.

Can. J. Chem. Downloaded from www.nrcresearchpress.com by 210.87.254.5 on 09/05/12
For personal use only.

(c) Orders of Reaction by the Initial Rate Method

Using a fixed methylacetylene pressure (30 mm) and a wide range of hydrogen pressures (15–180 mm) order of reaction with respect to hydrogen (n) was determined at several temperatures. The order of reaction with respect to hydrogen over nickel–copper alloy in the region AB (Fig. 1) was always one (Table I) and independent of temperature. The reaction order with respect to methylacetylene (m) over nickel, copper, and their alloys was determined for a constant hydrogen pressure at 60 mm. The order of reaction with respect to methylacetylene was temperature dependent and became slightly negative with increased temperature. For pure copper and nickel–copper alloy (90% Cu), the order with respect to methylacetylene was half and nearly independent of temperature. Table II shows the order of reaction with respect to methylacetylene for nickel and copper at different temperatures.

TABLE II

Order of reaction with respect to C_3H_4 (m)

Catalyst			
Nickel		Copper	
Temp. (°C)	m	Temp. (°C)	m
72	0	181	0.47
82	0	190	0.51
90	−0.12	200	0.47
100	−0.20	210	0.50
111	−0.22	220	0.46

The positive order with respect to methylacetylene for copper, and the alloy containing 90% copper, is due to the weaker adsorption of methylacetylene on the surface of the catalyst as compared with hydrogen. Recently Campbell and Emmett (8) studied the hydrogenation of ethylene on copper and found that the order with respect to ethylene was one and temperature independent between 140 and 200 °C, supporting the results of Pease and Harris (9). A half order with respect to methylacetylene as compared to first order with respect to ethylene on copper suggests that the former is more strongly adsorbed on the surface than the latter.

In the case of nickel–copper alloys for the region BC, where rate accelerates, when the rate of pressure fall ($\Delta p_\alpha/t$) was plotted against hydrogen pressure (Fig. 2), for several temperatures, straight lines intercepting the x-axis at approximately 30 mm of hydrogen were obtained, showing that for hydrogen/methylacetylene ratios of one or less than one, second region BC would not be observed.

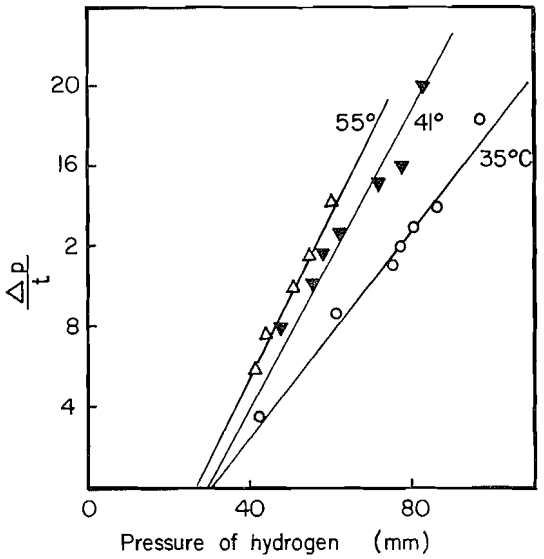

FIG. 2. $\Delta p_\alpha/t$ vs. P_{H_2}, Ni:Cu = 50:50. $P_{C_3H_6}$ = 30 mm Hg.

(d) Dependence of Acceleration Point ($-\Delta p_\alpha$) upon Experimental Variables

The acceleration point ($-\Delta p_\alpha$) decreased linearly with increasing hydrogen pressures (Fig. 3). Since methylacetylene is more strongly adsorbed than propylene, any increase in the partial pressure of hydrogen or propylene would serve to secure the entry of propylene into the reactive layer, thereby accelerating the reaction (propylene to propane) much earlier. In the temperature range 31–55 °C, the acceleration point showed a fairly linear relationship with increasing temperature and was given by the expression

$$(-\Delta p_\alpha) = 42.7 - 0.57T,$$

where T is in °C.

(e) Temperature Dependence of Rate Constants

Plots of $\log_{10}$ of specific rates against the reciprocal of absolute temperature were good straight lines over a wide range of temperature for all catalysts satisfying the Arrhenius equation. The derived apparent activation energy is plotted against alloy composition in Fig. 4. The activation energy at first decreased with increasing copper content, passed through a minimum

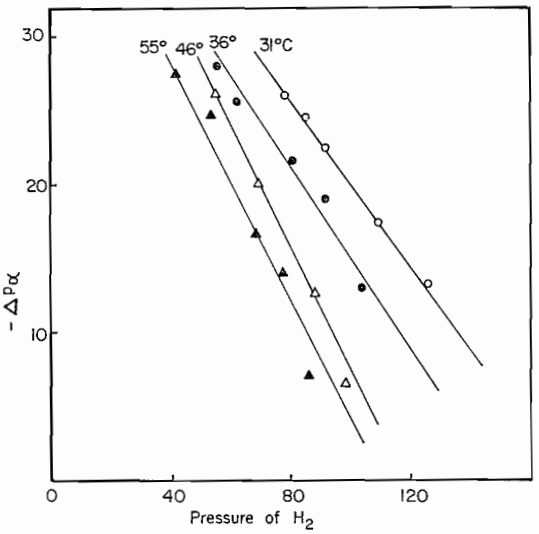

FIG. 3. $-\Delta p_\alpha$ vs. P_{H_2}, Ni:Cu = 90:10. $P_{C_3H_4} = 30$ mm Hg.

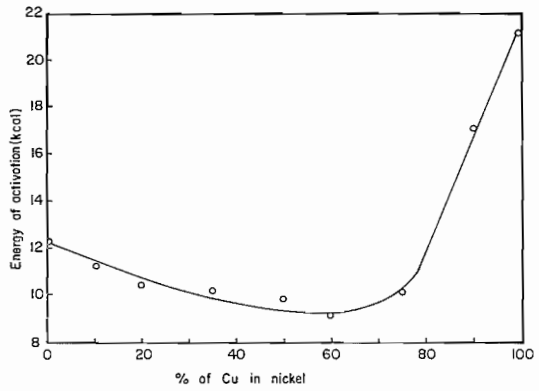

FIG. 4. Energy of activation vs. % of copper.

of about 9 kcal/g mole at about 60% copper, and then subsequently steadily increased to 21.2 kcal/g mole for pure copper.

(f) Dependence of Selectivity upon the Composition of Nickel–Copper Alloys

The dependence of selectivity *S*(propylene/(propylene + propane)) upon the composition of copper was studied at 85 °C, keeping the concentration of both the reactants constant, that is 50 mm of pressure each. The products were analyzed at a total pressure fall of 20 mm. The results are given in Table III. While over nickel, the main products were propylene and propane, over pure copper, the products were propylene and some polymers. The yellow-colored polymers formed were highly viscous in nature and deposited on the walls of the reaction vessel. Sheridan (10) also obtained a similar type of highly viscous liquid while hydrogenating acetylene over pumice-supported copper catalysts. In case of alloys, the main products were propylene and propane (traces for 80–90% copper). The selectivity thus increased with increasing copper content.

TABLE III

Effect of alloy composition on selectivity at 85 °C

Catalyst Ni–Cu	Selectivity
100–0	0.864
90–10	0.985
50–50	0.987
25–75	0.989
0–100*	1.00

*At 173 °C.

(g) Dependence of Selectivity upon Pressure Fall

The dependency of selectivity upon pressure fall was studied by analyzing the reaction products of a 1:1 hydrogen–methylacetylene mixture (50 mm each) for various falls in pressure. The selectivity appeared to be independent of pressure fall (Fig. 5).

(h) Dependency of Selectivity upon Temperature

The selectivity increased in a linear manner with increasing temperature for pure nickel and a nickel–copper alloy containing 10% copper. Similar phenomenon has been observed by Bond *et al.* in ethylene exchange (11) and

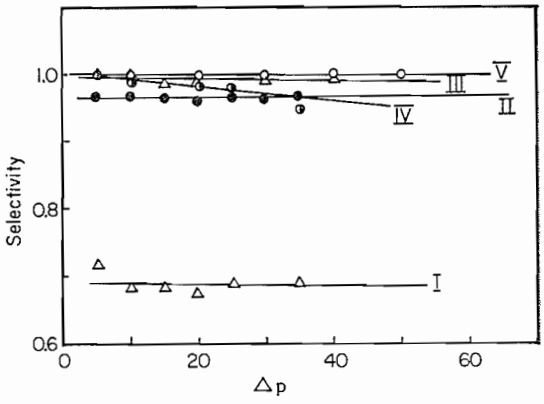

FIG. 5. Selectivity vs. Δp, $P_{C_3H_4} = P_{H_2} = 50$ mm Hg. I, 0% Cu (67 °C); II, 10% Cu (44 °C); III, 20% Cu (53 °C); IV, 50% Cu (51 °C); V, 100% Cu (173 °C).

Can. J. Chem. Downloaded from www.nrcresearchpress.com by 210.87.254.5 on 09/05/12
For personal use only.

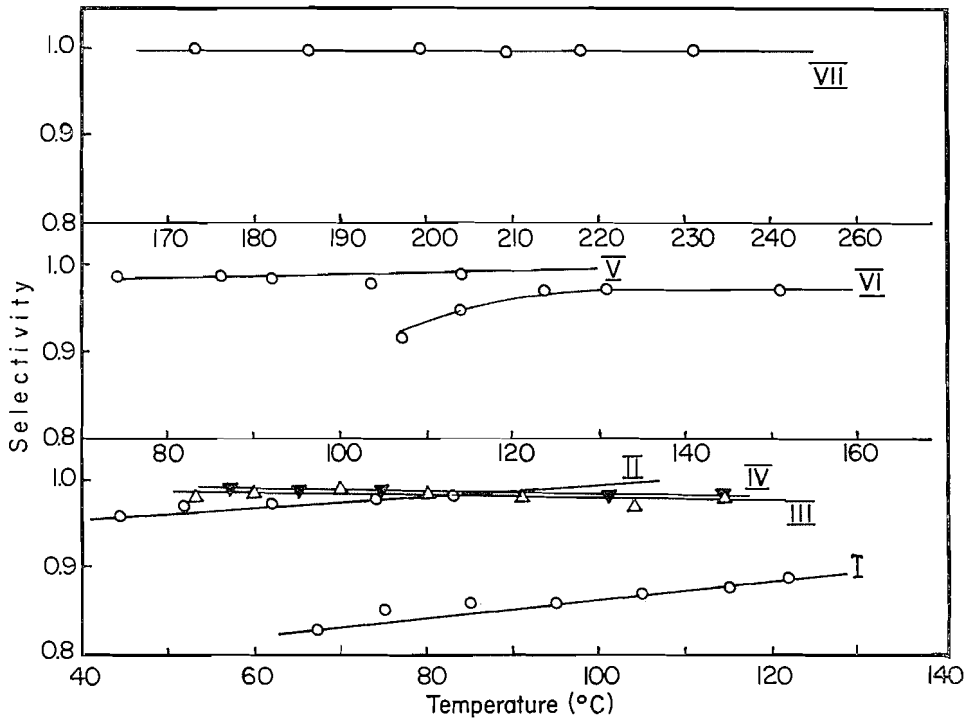

FIG. 6. Selectivity vs. Temp. (°C). $P_{C_3H_4} = P_{H_2} = 50$ mm Hg. I, 0% Cu; II, 10% Cu; III, 20% Cu; IV, 50% Cu; V, 75% Cu; VI, 90% Cu; VII, 100% Cu.

acetylene hydrogenation (7) over alumina-supported platinum catalyst. However, it is not clear whether this is due to a decrease in the surface coverage of hydrogen as the temperature is raised or to a genuinely higher activation energy for propylene desorption relative to hydrogen. For other alloys and pure copper, no appreciable amount of propane was formed, and the selectivity was independent of temperature (Fig. 6).

(i) Dependence of Selectivity upon the Initial Pressures of Hydrogen and Methylacetylene

Measurements were made of selectivity as a function of initial hydrogen pressure for a fixed initial pressure of methylacetylene (50 mm). Products were analyzed when the total pressure fall was equal to 20 mm. The variation of selectivity against initial hydrogen pressure is shown in Fig. 7. The selectivity was independent of initial hydrogen pressure for nickel, copper, and the alloy containing 10% nickel. For other alloys, the selectivity remained constant up to a certain pressure of hydrogen, beyond which it rapidly decreased with increasing hydrogen pressure. Similarly the variation of selectivity with methylacetylene pressure (Fig. 8) was determined for a fixed hydrogen pressure (50 mm). Though the selectivity slightly increased with increasing methylacetylene pressure for nickel, it was independent of methylacetylene pressures for copper and nickel–copper alloy containing 90% copper. For other alloys, the selectivity rapidly increased with increasing methylacetylene pressure up to pressures equal to the hydrogen pressure and then leveled off.

(j) Polymerization

The extent of polymerization increased as the copper concentration of the alloys was increased (Table IV).

(k) Comparison with the Results of Previous Investigators and General Discussions

The kinetic study of Bond and Sheridan (2) for methylacetylene hydrogenation is limited to pumice-supported nickel, platinum, and palladium catalysts, and that of Mann and Naik (3)

Can. J. Chem. Downloaded from www.nrcresearchpress.com by 210.87.254.5 on 09/05/12
For personal use only.

Can. J. Chem. Downloaded from www.nrcresearchpress.com by 210.87.254.5 on 09/05/12
For personal use only.

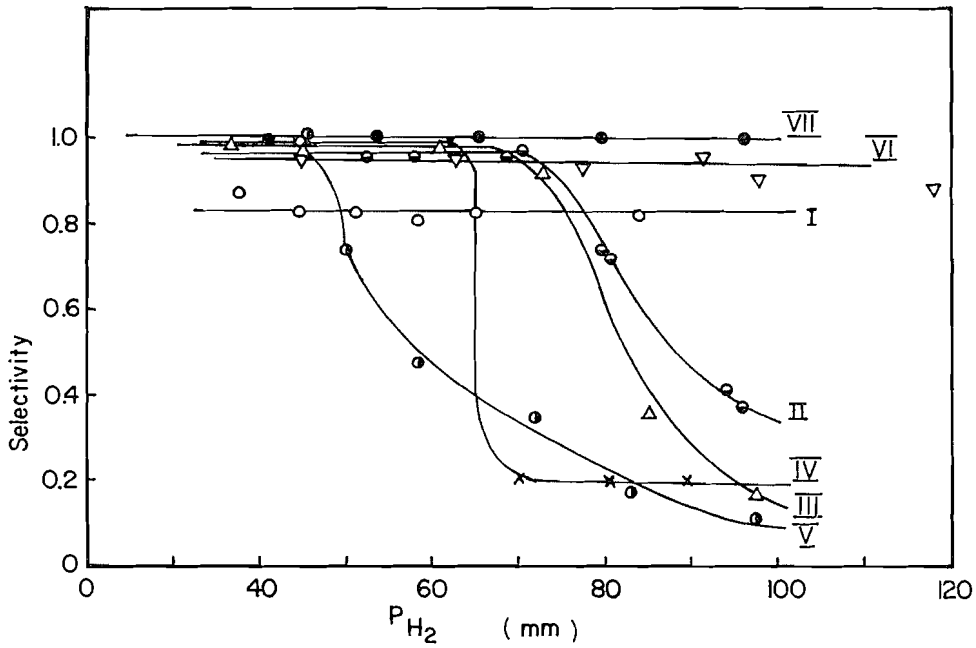

FIG. 7. Selectivity vs. P_{H_2}. I, 0% Cu (67 °C); II, 10% Cu (51 °C); III, 20% Cu (60 °C); IV, 50% Cu (57 °C); V, 75% Cu (74 °C); VI, 90% Cu (114 °C); VII, 100% Cu (173 °C).

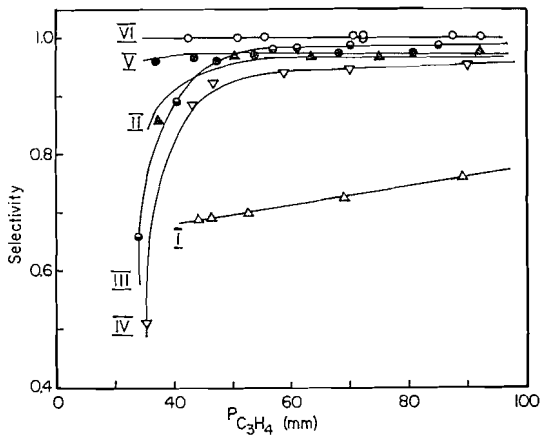

FIG. 8. Selectivity vs. $P_{C_3H_4}$, P_{H_2} = 60 mm Hg. I, 0% Cu (95 °C); II, 10% Cu (85 °C); III, 50% Cu (65 °C); IV, 75% Cu (74 °C); V, 90% Cu (124 °C); VI, 100% Cu (173 °C).

to pumice-supported and unsupported nickel and supported metals of the eighth group only. Though Bond (6) has studied the pressure–time curves in detail for acetylene hydrogenation over different supported metals, no such curves are reported for methylacetylene hydrogenation. Hence no direct comparison of this work can be made to Bond's or other published work.

The kinetic form of the pressure–time curve depends on the nature and especially on the concentration of species in the reactive layer on the surface of the catalyst at the moment the massive reaction begins. In case of nickel catalyst, which had been previously reduced for about 24 h in a stream of hydrogen, the species of reactive layer were richer in hydrogen and the admission of hydrogen or methylacetylene was not enough to nullify the effect of pretreatment of the catalyst. Hence pressure–time curve AFG (Fig. 1) similar to that obtained by Bond for acetylene hydrogenation (both reactants added together) over nickel was observed. In case of methylacetylene hydrogenation over copper and alloys, the curve ABC (Fig. 1) similar to the one obtained by Bond and Wells (7) for acetylene hydrogenation over platinum–alumina was observed. The acceleration in the rate (region BC) is due to the inability of methylacetylene to maintain full coverage of the surface and actual competition by propylene becoming important as well. In this case, methylacetylene and propylene both are cohydrogenating.

A sudden increase in the activity of the nickel catalyst was observed on the addition of small amounts of copper. The activity seemed to increase with small additions of copper (Fig. 9), pass

TABLE IV

Effect of copper concentration on polymerization (hydrogen = 46 mm, methylacetylene = 46 mm (room temp.), temperature = 83 °C)

% copper in alloy	Pressure of products (mm Hg)			% Polymers
	Propane	Propylene	Methylacetylene	
0	3.25	18	23.5	2.72
10	0.25	17	20.5	17.93
50	0.15	12	24	21.41
75	0.10	9.5	22.5	30.21
100*	0.00	2.25	17	46.88

*Temperature = 173 °C, initial pressure hydrogen = methylaeetylene = 40 mm at room temperature.

through a maximum for about 25% copper, and then decrease on further additions of copper. Several investigators (5, 12, 13) have observed a similar phenomenon. Bond and Mann (14) studied acetylene hydrogenation over nickel–cobalt and nickel–copper alloys. In case of nickel–copper alloys, they found that the energy of activation increased markedly with increasing copper concentration in the range 0–60%, reaching a maximum at about 60%, but thereafter it did not change very much. Activity patterns were temperature sensitive, and indicated that at high temperatures d-band hole concentration determined the activity, but at low temperatures the situation was more complex. Recently Campbell and Emmett (8), while hydrogenating ethylene on nickel–copper films, observed a minima in the activity–composition curve for an alloy containing approximately 25–35% nickel.

According to Beeck's (15) correlation between the catalytic activity of the metals and their lattice parameters, the activity of the series of the alloys would be expected to increase markedly between pure nickel and copper. Hall and Emmett (13), Gharpurey and Emmett (16), and Lyubarskii *et al.* (17) also observed marked increase in the catalytic activity in ethylene hydrogenation on nickel being alloyed with small amounts of copper. They attributed this to hydrogen exerting a poisoning effect on pure nickel. Takeuchi *et al.* (18) also observed that the catalytic activity of the metals in hydrogenation was directly related to their ability in absorbing hydrogen. Takai and Yamanaka (19) observed that the ability of nickel metal to absorb hydrogen increased with increasing amounts of copper with a maximum for an alloy containing about 80% copper. It then decreased rapidly with further amounts of copper. However, they did not observe any simple relation between the catalytic activity for the hydrogenation of maleic acid, acetone, and allyl alcohol and the hydrogen content of nickel–copper alloys.

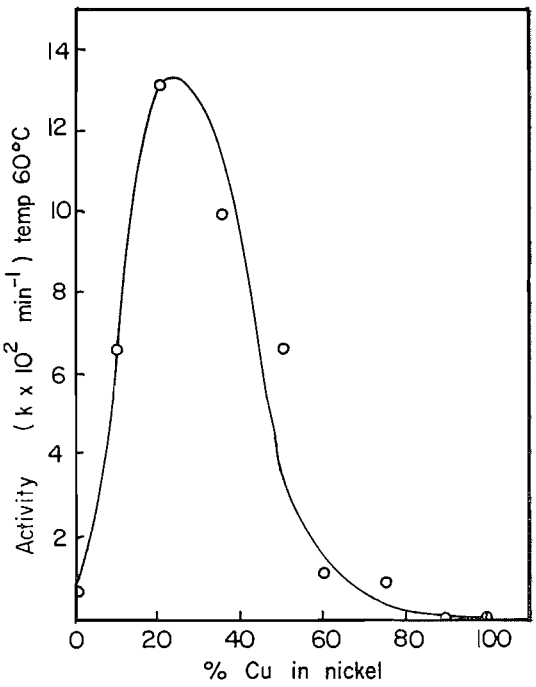

FIG. 9. Activity vs. % copper in alloy.

Sachtler and Dorgelo (20) and Sachtler and Jongepier (21) studied the surface of nickel–copper alloy films prepared by evaporation, and subsequent annealing at 200 °C under ultrahigh vacuum. They measured work function and the phase compositions. They concluded that all the alloys of intermediate compositions, between 3% and 80% copper, if equilibrated at 200 °C, will produce solids exposing the high copper phase of a given composition at the surface of the catalyst. The second phase (low copper concentration) does not appear on the surface. They also found that whereas nickel and copper had a

Can. J. Chem. Downloaded from www.nrcresearchpress.com by 210.87.254.5 on 09/05/12
For personal use only.

Can. J. Chem. Downloaded from www.nrcresearchpress.com by 210.87.254.5 on 09/05/12
For personal use only.

work function of 5.1 and 4.66 eV respectively, the nickel–copper alloys containing 3 to 80% copper had a work function of only 4.61 eV. Sachtler and Jongepier (21) appear to conclude a general similarity between the work function of their alloy films and the catalytic activity. The work of Best and Russell (5), Campbell and Emmett (8), Alexander and Russell (22), and our own observations cast doubt on the general validity of the conclusions of Sachtler and Jongepier. Recently Toyosaburo (23) studied a number of nickel–copper catalysts prepared by different methods and suggested that this activity factor is due to the imperfection of the crystal.

However, on the basis of the correlation of the activity with Pauling's (24) % δ-character, the activity would be expected to decrease as copper is alloyed with nickel. As the d band is filled, the binding strength would decrease although a maximum would be attained before the d band is completely filled.

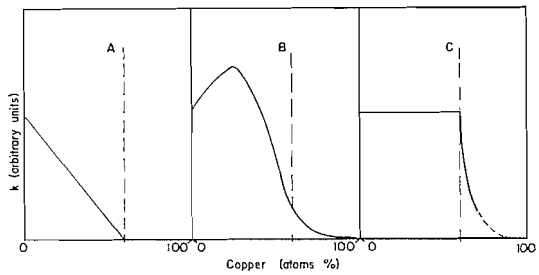

FIG. 10. Idealized possible forms for the dependence of activity on composition for nickel–copper alloys.

Theoretically, there can be three possible forms of activity pattern, represented in an idealized manner in Fig. 10. In case of A (Fig. 10A) there is a progressive decrease in the activity as the concentration of holes in the d band [h_d] falls until it becomes zero at 60% copper. Hydrogenation of styrene on nickel–copper alloys by Dowden and Reynolds (25) conforms to this pattern. In case B (Fig. 10B), it is suggested that as the d band is filled, the binding strength decreases and the activity increases, reaching a maximum before the band is completely filled. This type of pattern has been observed by Couper and Eley (26) in the para hydrogen conversion on palladium–gold alloys, and in the present study. However, there may be several other factors present. These opposing effects may lead to an earlier maximum than expected (at 60% copper). Case C (Fig. 10C) shows the effect if $n(E)$ determines the activity, or if the activity is independent of the hole concentrations so long as there are some holes in the d band. The results of Rienacker and Bommer (27) for the hydrogenation of ethylene on nickel–copper foils at 500 °C conforms to this pattern.

Several other factors, besides those discussed in this paper, may also affect the catalytic activity of nickel–copper alloys. Although a theoretical interpretation of these results has not been completely established, it seems certain that changes observed in the activities of the alloys in the present investigations might be related to the hydrogen preadsorbed (or dissolved) on them. It has been observed that while the nickel–copper alloys reversibly adsorbed many monolayers of hydrogen, pure copper and nickel were found to take up hydrogen hardly sufficient for two and one monolayers respectively.

A detailed study of some factors, such as structure of alloys, method of preparation of the catalyst, chemisorption on the surface of the alloys, are necessary to establish any firm interpretation for the maximum activity being at 25% copper. There appears to be no direct relationship between electronic parameters and energy of activation.

Acknowledgments

The authors are grateful to the National Research Council of Canada for financial aid and to Mr. John F. Rowland, of Mines, Energy and Resources Department, for X-ray analysis of the nickel–copper alloys.

1. G. C. BOND and P. B. WELLS. Advan. Catalysis, **15**, 91 (1965).
2. G. C. BOND and J. SHERIDAN. Trans. Faraday Soc. **48**, 651 (1952).
3. R. S. MANN and S. C. NAIK. Can. J. Chem. **45**, 1023 (1967).
4. R. S. MANN and K. C. KHULBE. Can. J. Chem. **45**, 2755 (1967).
5. R. J. BEST and W. W. RUSSELL. J. Am. Chem. Soc. **76**, 838 (1954).
6. G. C. BOND. J. Chem. Soc. 2705 (1958).
7. G. C. BOND and P. B. WELLS. J. Catalysis, **4**, 211 (1965).
8. J. B. CAMPBELL and P. H. EMMETT. J. Catalysis, **7**, 252 (1967).
9. R. N. PEASE and C. A. HARRIS. J. Am. Chem. Soc. **49**, 2503 (1927).
10. J. SHERIDAN. J. Chem. Soc. 470 (1945).
11. G. C. BOND, J. J. PHILIPSON, P. B. WELLS, and J. M. WINTERBOTTOM. Trans. Faraday Soc. **62**, 443 (1966).

12. G. M. SCHWAB and W. BRENNECKE. Z. Physik. Chem. Leipzig, **B24**, 393 (1933).
13. W. K. HALL and P. H. EMMETT. J. Phys. Chem. **63**, 1102 (1959).
14. G. C. BOND and R. S. MANN. J. Chem. Soc. 3566 (1959).
15. O. BEECK. Rev. Mod. Phys. **17**, 61 (1945).
16. M. K. GHARPUREY and P. H. EMMETT. J. Phys. Chem. **65**, 1182 (1961).
17. G. D. LYUBARSKII, E. I. ERZERIKHIM, and A. A. SLUKI. Kinetika i Kataliz, **5**, 311 (1964).
18. T. TAKEUCHI, M. SAKAKAGUCHI, and I. MIYOSHI. Bull. Chem. Soc. Japan, **35**, 1390 (1962).
19. E. TAKAI and T. YAMANAKA. Sci. Papers Inst. Phys. Chem. Res. Tokyo, **55**, 194 (1962).
20. W. M. H. SACHTLER and G. J. H. DORGELO. J. Catalysis, **4**, 654 (1965).
21. W. M. H. SACHTLER and R. JONGEPIER. J. Catalysis, **4**, 665 (1965).
22. E. G. ALEXANDER and W. W. RUSSELL. J. Catalysis, **4**, 184 (1965).
23. T. TOYOSABURO. Nippon Kagaku Zasshi, **88**, 381 (1967).
24. L. PAULING. Phys. Rev. **54**, 899 (1938); Proc. Roy. Soc. London, Ser. A, **196**, 343 (1949).
25. D. A. DOWDEN and P. W. REYNOLDS. Discussions Faraday Soc. **8**, 184 (1950).
26. A. COUPER and D. D. ELEY. Discussions Faraday Soc. **8**, 172 (1950).
27. G. RIENACKER and Z. BOMMER. Z. Anorg. Allgem. Chem. **242**, 302 (1939).

Can. J. Chem. Downloaded from www.nrcresearchpress.com by 210.87.254.5 on 09/05/12
For personal use only.

Can. J. Chem. Downloaded from www.nrcresearchpress.com by 210.87.254.5 on 09/05/12
For personal use only.

Can. J. Chem. Downloaded from www.nrcresearchpress.com by 210.87.254.5 on 09/05/12
For personal use only.

Reactions of organotin compounds. VIII. The reactions of tin hydrides with perfluorovinyl silicon compounds

M. AKHTAR AND H. C. CLARK
Department of Chemistry, University of Western Ontario, London, Ontario
Received September 18, 1967

The reactions of trimethyltin hydride and dimethyltin dihydride with $(CH_3)_3SiCF{=}CF_2$ and $(CH_3)_2Si(CF{=}CF_2)_2$ respectively have been investigated. Under thermal conditions, reaction led to organotin fluorides and fluorovinyl-silanes. However, under ultraviolet irradiation at 25°, addition products were isolated of which $(CH_3)_3SiCFHCF_2Sn(CH_3)_3$ and $(CH_3)_3SiCF[Sn(CH_3)_3]CF_2H$ were fully characterized. Evidence is presented which shows that these addition products are formed by a free radical process and that their decomposition to organotin fluorides and fluorovinyl-silanes proceeds *via* a β-fluorine elimination. Spectroscopic data are presented for a number of new organo-silanes.

Canadian Journal of Chemistry, 46, 633 (1968)

Introduction

In previous papers (1–4), we have described the behavior of organotin hydrides with unsaturated fluorocarbon derivatives of two types, firstly fluoro-olefins and secondly perfluorovinyl tin compounds. For the reactions with fluoro-olefins convincing arguments were presented (1–3) that a free radical mechanism is involved in which the formation of radicals from the tin hydride is probably the rate-determining step. This is in agreement with other studies of tin hydride addition reactions (e.g. ref. 5), although it has been established (6, 7) that, under other circumstances, reactions of tin hydrides may occur *via* a polar mechanism. The process by which perfluorovinyltin compounds are converted by tin hydrides to derivatives containing $-CF{=}CFH$, $-CH{=}CF_2$, and $-C_2H_2F$ groups (4) is even less fully understood. A free radical type behavior may well be involved either directly or alternatively though the addition of the hydride across the vinylic C=C bond, followed immediately by elimination of trimethyltin fluoride or dimethyltin difluoride. The present study was undertaken in order to obtain further information on this process. By using perfluorovinyl silanes subtle changes can be made in the nature of the vinylic C=C bond, not only because of differences between the inductive effects of, say, R_3Si and R_3Sn groups, but also because of variations in $d\pi$–$p\pi$ interactions in the M—C=C group (8, 9) when M is changed from Sn to Si.

Discussion

The conversion of perfluorovinyl to fluorovinyl groups with the accompanying formation of R_3SnF or R_2SnF_2 results from the reaction of organotin hydrides with perfluorovinyltin derivatives (4). There was no evidence that addition compounds were formed, even as transient intermediates, even though such addition has been observed (9) in the reaction of triphenyltin hydride and triphenylvinyltin to give 1,2-bis-(triphenyltin) ethane. Similarly, triphenyltin hydride adds across the C=C bond of vinyl-silanes very readily (9).

$$(C_6H_5)_3SnH + CH_2{=}CHSi(C_6H_5)_3 \rightarrow (C_6H_5)_3SnCH_2CH_2Si(C_6H_5)_3$$

However, no evidence was provided which would distinguish between the two possible isomers, that above and $(C_6H_5)_3SiCH[Sn(C_6H_5)_3]$-$CH_3$. Addition reactions of perfluorovinyl-silanes are also known, although frequently the elimination of a fluoride occurs readily. Thus triphenylsilyllithium adds to $(C_2H_5)_3SiCF{=}CF_2$ and the resulting adduct loses lithium fluoride (10).

$$(C_2H_5)_3SiCF{=}CF_2 + (C_6H_5)_3SiLi \rightarrow (C_2H_5)_3SiCF{=}CFSi(C_6H_5)_3 + LiF$$

These are also the features of the reactions of organotin hydrides with perfluorovinyl-silanes.

Trimethyltin hydride did not react with $(CH_3)_3SiCF{=}CF_2$ at room temperature, even over a long period, but at 55° reaction occurs readily with the deposition of trimethyltin fluoride and formation of fluorovinyl-silanes, notably $(CH_3)_3SiCH{=}CF_2$, *cis*-$CFH{=}CFSi(CH_3)_3$, *trans*-$CFH{=}CFSi(CH_3)_3$, and $(CH_3)_3SiC_2H_2F$, these being listed in the order of decreasing yield. This may be compared with the analogous reaction of the hydride with $(CH_3)_3SnCF{=}CF_2$ (4) where very little reaction

Can. J. Chem. Downloaded from www.nrcresearchpress.com by 210.87.254.5 on 09/05/12
For personal use only.

Reactions of organotin compounds. VIII. The reactions of tin hydrides with perfluorovinyl silicon compounds

M. AKHTAR AND H. C. CLARK
Department of Chemistry, University of Western Ontario, London, Ontario
Received September 18, 1967

The reactions of trimethyltin hydride and dimethyltin dihydride with $(CH_3)_3SiCF{=}CF_2$ and $(CH_3)_2Si(CF{=}CF_2)_2$ respectively have been investigated. Under thermal conditions, reaction led to organotin fluorides and fluorovinyl-silanes. However, under ultraviolet irradiation at 25°, addition products were isolated of which $(CH_3)_3SiCFHCF_2Sn(CH_3)_3$ and $(CH_3)_3SiCF[Sn(CH_3)_3]CF_2H$ were fully characterized. Evidence is presented which shows that these addition products are formed by a free radical process and that their decomposition to organotin fluorides and fluorovinyl-silanes proceeds *via* a β-fluorine elimination. Spectroscopic data are presented for a number of new organo-silanes.

Canadian Journal of Chemistry, 46, 633 (1968)

Introduction

In previous papers (1–4), we have described the behavior of organotin hydrides with unsaturated fluorocarbon derivatives of two types, firstly fluoro-olefins and secondly perfluorovinyl tin compounds. For the reactions with fluoro-olefins convincing arguments were presented (1–3) that a free radical mechanism is involved in which the formation of radicals from the tin hydride is probably the rate-determining step. This is in agreement with other studies of tin hydride addition reactions (e.g. ref. 5), although it has been established (6, 7) that, under other circumstances, reactions of tin hydrides may occur *via* a polar mechanism. The process by which perfluorovinyltin compounds are converted by tin hydrides to derivatives containing $-CF{=}CFH$, $-CH{=}CF_2$, and $-C_2H_2F$ groups (4) is even less fully understood. A free radical type behavior may well be involved either directly or alternatively though the addition of the hydride across the vinylic C=C bond, followed immediately by elimination of trimethyltin fluoride or dimethyltin difluoride. The present study was undertaken in order to obtain further information on this process. By using perfluorovinyl silanes subtle changes can be made in the nature of the vinylic C=C bond, not only because of differences between the inductive effects of, say, R_3Si and R_3Sn groups, but also because of variations in $d\pi$–$p\pi$ interactions in the M—C=C group (8, 9) when M is changed from Sn to Si.

Discussion

The conversion of perfluorovinyl to fluorovinyl groups with the accompanying formation of R_3SnF or R_2SnF_2 results from the reaction of organotin hydrides with perfluorovinyltin derivatives (4). There was no evidence that addition compounds were formed, even as transient intermediates, even though such addition has been observed (9) in the reaction of triphenyltin hydride and triphenylvinyltin to give 1,2-bis-(triphenyltin) ethane. Similarly, triphenyltin hydride adds across the C=C bond of vinyl-silanes very readily (9).

$$(C_6H_5)_3SnH + CH_2{=}CHSi(C_6H_5)_3 \rightarrow (C_6H_5)_3SnCH_2CH_2Si(C_6H_5)_3$$

However, no evidence was provided which would distinguish between the two possible isomers, that above and $(C_6H_5)_3SiCH[Sn(C_6H_5)_3]$-$CH_3$. Addition reactions of perfluorovinyl-silanes are also known, although frequently the elimination of a fluoride occurs readily. Thus triphenylsilyllithium adds to $(C_2H_5)_3SiCF{=}CF_2$ and the resulting adduct loses lithium fluoride (10).

$$(C_2H_5)_3SiCF{=}CF_2 + (C_6H_5)_3SiLi \rightarrow (C_2H_5)_3SiCF{=}CFSi(C_6H_5)_3 + LiF$$

These are also the features of the reactions of organotin hydrides with perfluorovinyl-silanes.

Trimethyltin hydride did not react with $(CH_3)_3SiCF{=}CF_2$ at room temperature, even over a long period, but at 55° reaction occurs readily with the deposition of trimethyltin fluoride and formation of fluorovinyl-silanes, notably $(CH_3)_3SiCH{=}CF_2$, *cis*-$CFH{=}CFSi(CH_3)_3$, *trans*-$CFH{=}CFSi(CH_3)_3$, and $(CH_3)_3SiC_2H_2F$, these being listed in the order of decreasing yield. This may be compared with the analogous reaction of the hydride with $(CH_3)_3SnCF{=}CF_2$ (4) where very little reaction

occurred after 18 h at 70°. When the hydride and the perfluorovinyl-silane were irradiated at room temperature, a high yield of the two possible addition products, $(CH_3)_3SiCFHCF_2Sn(CH_3)_3$ and $(CH_3)_3SiCF[Sn(CH_3)_3]CF_2H$, in the ratio 3:2 was obtained, with virtually no formation of trimethyltin fluoride. Although this mixture is stable at room temperature for a short period, trimethyltin fluoride is rapidly deposited to leave $(CH_3)_3SiCH{=}CF_2$ and *cis*-$CFH{=}CFSi(CH_3)_3$ in a 2:1 ratio. This latter ratio, together with the above ratio of the addition products, clearly indicates that $(CH_3)_3SiCH{=}CF_2$ has been formed from the adduct $(CH_3)_3SiCFHCF_2Sn(CH_3)_3$, and *cis*-$CFH{=}CFSi(CH_3)_3$ from the other adduct $(CH_3)_3SiCF[Sn(CH_3)_3]CF_2H$, in both cases by a β-fluorine elimination leading to the formation of trimethyltin fluoride. The reasonable nature of this type of elimination can be readily established by the use of molecular models, from which it can be seen that the p orbitals of the β-fluorine are directed more toward the tin than are the p orbitals of the α-fluorine, and that the $Sn{-}F_\beta$ distance is the smaller. This evidence for β-elimination is particularly significant with respect to the addition of fluoro-olefins across metal–metal bonds. We have previously shown, for example, that trifluoroethylene (11) reacts with $(CH_3)_3SnMn(CO)_5$ to give trimethyltin fluoride and *cis*- and *trans*-$CFH{=}CFMn(CO)_5$. The similarity of the hypothetical addition product $(CH_3)_3SnCFHCF_2Mn(CO)_5$ to the present addition compounds, and the above evidence for β-elimination, strongly suggest that the same type of process is involved in all these reactions, as has been suggested by Booth (12). The alternative process would be an α-elimination followed by a fluoride ion migration (13), which seems much less likely from energetic grounds alone.

The isolation of these addition products under ultraviolet irradiation can be compared with the products formed in the irradiation of trimethyltin hydride with trimethyl (perfluorovinyl) tin (4). In the latter case, no addition compounds were isolated, only the fluoroalkyl derivatives, *cis*- and *trans*-$CFH{=}CFSn(CH_3)_3$, $(CH_3)_3SnCH{=}CF_2$, and $(CH_3)_3SnC_2H_2F$, and trimethyltin fluoride, but it now seems very probable that these resulted from a β-fluorine elimination of trimethyltin fluoride from unstable addition products. Moreover, the fact that in this latter case the principal product was *cis*-$CFH{=}CFSn(CH_3)_3$, in contrast to $(CH_3)_3SiCH{=}CF_2$ for the silane reaction, is further support for the β-fluorine elimination process. The hypothetical products $(CH_3)_3SnCFHCF_2Sn(CH_3)_3$ and $[(CH_3)_3Sn]_2CFCF_2H$ can *both* give *cis*-$CFH{=}CFSn(CH_3)_3$ by such an elimination, while for the silane only β-fluorine elimination from $(CH_3)_3SiCF[Sn(CH_3)_3]CF_2H$ can give *cis*-$CFH{=}CFSi(CH_3)_3$.

There remains the question of the mechanism by which the tin hydride adds across the vinylic C=C bond. As mentioned above, there is good evidence that tin hydride additions to olefins proceed via a free radical mechanism (4, 5). One argument supporting this is the fact that free radical sources readily initiate these additions at room temperature (5). In the present case, therefore, the addition of trimethyltin hydride to $(CH_3)_3SiCF{=}CF_2$ in the presence of azobisisobutyronitrile as a free radical source (5) was studied. The same mixture of addition products was isolated, in approximately the same ratio, although for extensive reaction, a temperature of 50° was necessary so that reasonable yields of the fluorovinyl decomposition products were also obtained. It seems that azobisisobutyronitrile certainly initiates the addition process although less effectively than for other olefins (5). This is consistent with the generally lower reactivity of the perfluorovinylic C=C bond. A similar reaction in which the effect of hydroquinone on the formation of the addition product was studied likewise led to a high yield of the addition products. This supports earlier statements (14, 15) that hydroquinone does not inhibit addition reactions of tin hydrides. A more effective inhibitor was found to be "galvinoxyl" (16) which, even in the presence of azobisisobutyronitrile, completely quenched the addition reaction. This contrasts with other reactions of tin hydrides (7, 17) where "galvinoxyl" had no effect on the rate of the addition reaction, but leaves no doubt that these additions to C=C bonds are indeed free radical processes.

The behavior of dimethyltin dihydride with $(CH_3)_3SiCF{=}CF_2$ was next investigated. At 60°, little reaction occurred, but under ultraviolet irradiation at 25°, there was extensive conversion to dimethyltin difluoride and the fluorovinyl-silanes, with $(CH_3)_3SiCH{=}CF_2$ again

Can. J. Chem. Downloaded from www.nrcresearchpress.com by 210.87.254.5 on 09/05/12
For personal use only.

Can. J. Chem. Downloaded from www.nrcresearchpress.com by 210.87.254.5 on 09/05/12
For personal use only.

being the major volatile product. In view of the greater reactivity of dimethyltin dihydride compared with trimethyltin hydride, and also of their probable structures, it is not too surprising that the addition compounds were not isolated. A further obvious extension was to examine the reactions of dimethylbis(perfluorovinyl)silane with organotin hydrides, particularly since with dihydrides cyclic compounds might result similar to that obtained (18) from diphenyltin dihydride and phenylacetylene. Trimethyltin hydride and $(CH_3)_2Si(CF{=}CF_2)_2$ did not react at room temperature and only very slowly at 55°. Ultraviolet irradiation at 25° gave as the major product an involatile liquid identified spectroscopically as a mixture of the addition products **1**, **2**, and **3**.

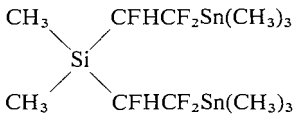

1

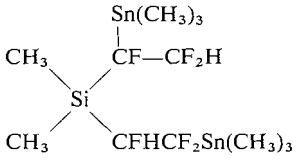

2

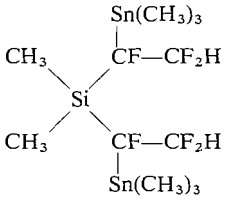

3

The mixture was unstable at room temperature, slowly depositing trimethyltin fluoride; nor was it possible to separate individual compounds from the mixture chromatographically due to this instability.

In the presence of azobisisobutyronitrile, trimethyltin hydride and $(CH_3)_2Si(CF{=}CF_2)_2$ at 55° gave more of the above addition products although some trimethyltin fluoride and volatile silanes containing —CF=CFH (*cis* and *trans*), —CH=CF_2, and —C_2H_2F groups were formed in low yield. Similarly, dimethyltin dihydride and $(CH_3)_2Si(CF{=}CF_2)_2$ did not react extensively at room temperature, but at 55° or under ultraviolet irradiation at 25°, considerable amounts of dimethyltin difluoride and volatile silanes containing —CF=CFH, —CH=CF_2, and —C_2H_2F groups were formed. In neither case could any addition product be separated or detected.

As in our previous study (4), considerable use was made of spectroscopic methods in characterizing new products, since fluorovinyl compounds have very characteristic infrared and nuclear magnetic resonance (n.m.r.) features. The trimethyl- and dimethyl-fluorovinyl silanes are completely analogous to the fluorovinyltin compounds described previously (4) and it is only necessary to list the data in Tables I and II. The characterization of the addition products of trimethyltin hydride and $(CH_3)_3SiCF{=}CF_2$ is based on the n.m.r. spectra which are shown in Fig. 1 (proton spectrum) with the numerical data tabulated in Tables III and IV. The proton spectrum clearly shows the presence of two compounds, each of which gives a complex pattern of eight lines in addition to signals from the methyl-Si and methyl-Sn protons. The two sets of eight lines can be attributed to the two ethane protons of $AC^{\alpha}F_2C^{\beta}FHB$ and $ABC^{\beta}FC^{\alpha}F_2H$ molecules, where the non-equivalence of the two α-fluorine atoms arises from the fact that there are three different substituents on the β-carbon atom. Hence the proton spectrum for each proton is of the ABX pattern. The spectra of closely related compounds have been discussed in considerable detail (19, 20), and hence a full analysis of the proton and ^{19}F spectra is not given here. Each set of eight lines in the proton spectrum could be attributed to the signal of the ethane proton, split successively three times into doublets by coupling with the three non-equivalent fluorine nuclei. For one molecule, the coupling constants, J_{H-F}, were 62, 56, and 10 c.p.s. respectively and for the other 37, 44, and 10 respectively. For the proton of a —CF_2H group, where the two fluorines are not equivalent, coupling constants of 55–65 c.p.s. are normally observed (e.g. ref. 21) while the second set of values is consistent (19) with the group —CFHCF_2—. The proton spectrum is thus interpreted in terms of a mixture of $(CH_3)_3SiCFHCF_2Sn(CH_3)_3$ and $(CH_3)_3SiCF[Sn(CH_3)_3]CF_2H$ in a ratio of 3:2. From closely coincident values of H—F coupling constants it

TABLE I

Proton n.m.r. assignments for perfluorovinyl and fluorovinyl silanes

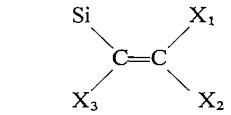	δ_{CH_3}	δ_{vinyl}	J_{12}	J_{23}	J_{13}
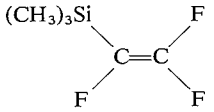	−0.10	—	—	—	—
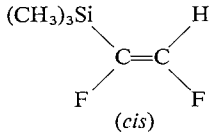 (*cis*)	−0.18	−6.18 quartet	75	—	22
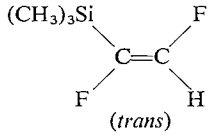 (*trans*)	−0.32	−6.88 quartet	78	12	—
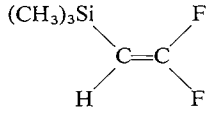	−0.04	−3.18 quartet	—	7	40
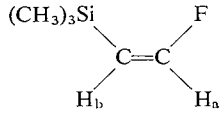	Not distinguished	−6.2 quartet −5.4 quartet	82	6	96
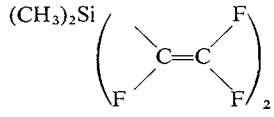	−0.45	—	—	—	—
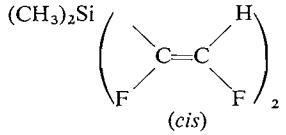 (*cis*)	−0.14	−5.95 quartet	74	—	21
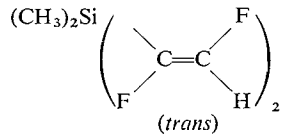 (*trans*)	−0.21	−6.14 quartet	74	15	—
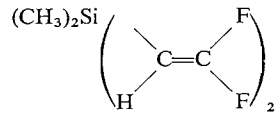	−0.05	−3.39 quartet	—	7	30
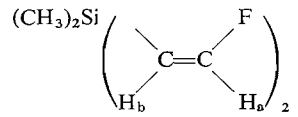	Not distinguished	−6.2 quartet −5.81 quartet	76	5	95

Chemical shifts (p.p.m.) are with respect to external TMS for trimethyl derivatives and to external $CHCl_3$ for dimethyl derivatives. Coupling constants are in c.p.s.

Can. J. Chem. Downloaded from www.nrcresearchpress.com by 210.87.254.5 on 09/05/12
For personal use only.

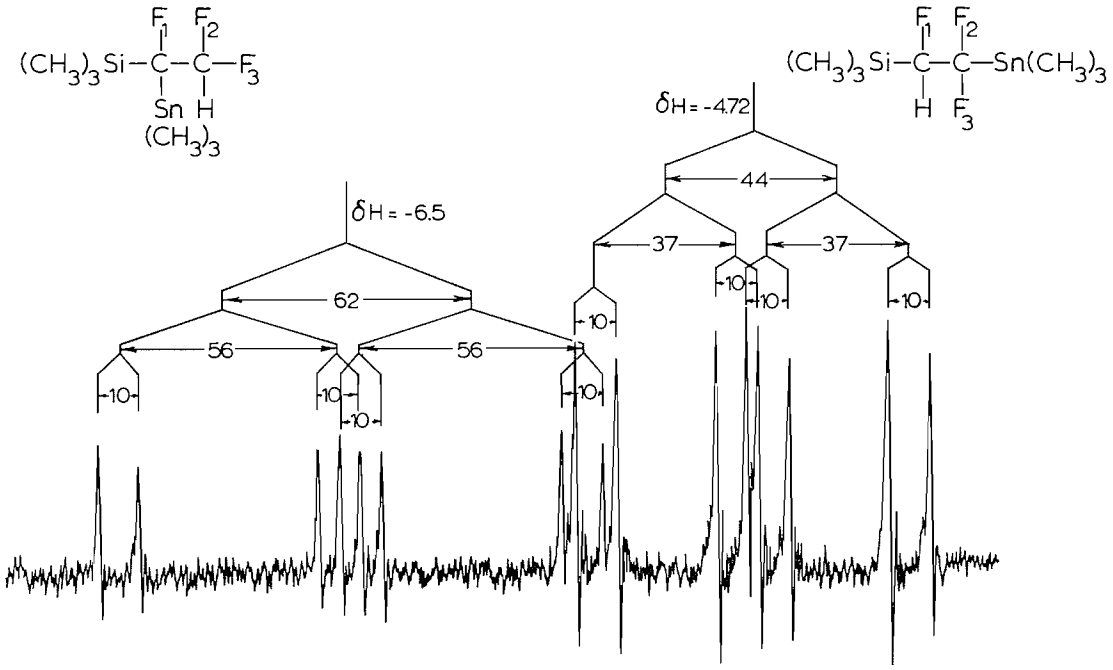

FIG. 1

TABLE II

Characteristic C=C stretching and C—F frequencies observed in trimethyl and dimethyl perfluorovinyl and fluorovinyl silanes [gas phase – KBr windows]

Compound	C=C region (± 2 cm^{-1})	C—F region (± 2 cm^{-1})
$Me_3SiCF{=}CF_2$	1725 s	1290 vs, 1265 vs, 1135 vs, 1045 vs
$Me_3SiCF{=}CFH$ (*cis*)	1695 s	1290 s, 1255 vs, 1135 s, 1075 s, 920 s
$Me_3SiCF{=}CFH$ (*trans*)	1665 s	1258 w, 1125 s, 1010 w
$Me_3SiCH{=}CF_2$	1720 s	1295 s, 1260 vs, 1065 s
$Me_3SiC_2H_2F$	1625 s	1070 m, 1000 w, 950 s,b
$Me_2Si(CF{=}CF_2)_2$	1730 s	1305 vs, 1265 vs, 1150 s, 1110 m, 1055 m
$Me_2Si(CF{=}CFH)_2$ (*cis*)	1700 s	1295 s, 1270 s, 1145 m, 900 s
$Me_2Si(CF{=}CFH)_2$ (*trans*)	1665 s	1130 vs, 1000 vw
$Me_2Si(CH{=}CF_2)_2$	1722 s	1300 vs, 1262 s, 1175 m, 1050 s
$Me_2Si(C_2H_2F)_2$	1625 s	1140 s,b 905 m

was then possible to match the proton and ^{19}F spectra (Fig. 2), thus showing the latter to consist of two sets of 24 lines each, the ratio of the species producing the sets being 3:2 respectively. The normal first-order analysis then gave the values shown in Table III.

The involatile liquid obtained from the ultraviolet irradiation of trimethyltin hydride and $(CH_3)_2Si(CF{=}CF_2)_2$ was quickly shown from spectroscopic evidence to be a mixture containing both $-SiCFHCF_2Sn(CH_3)_3$ and $-SiCF[Sn(CH_3)_3]CF_2H$ groups, but it was not possible to distinguish between the three possible molecular species **1**, **2**, and **3**. The proton n.m.r. spectrum, however, although complex, was completely consistent with the data for other addition products above and assignments to the above two types of ethane protons could be made on the same basis. The data are given in Table V.

Experimental

All reactions were carried out using standard high vacuum techniques. Reactions under thermal conditions were performed in pyrex Carius tubes, whereas those

Can. J. Chem. Downloaded from www.nrcresearchpress.com by 210.87.254.5 on 09/05/12
For personal use only.

Can. J. Chem. Downloaded from www.nrcresearchpress.com by 210.87.254.5 on 09/05/12
For personal use only.

TABLE III

N.m.r. data* for the addition products of $(CH_3)_3SnH$ with $(CH_3)_3SiCF{=}CF_2$

	$(CH_3)_3Si-C(F_1)(Sn(CH_3)_3)-C(F_2)(H)-F_3$		$(CH_3)_3Si-C(F_1)(H)-C(F_2)(F_3)-Sn(CH_3)_3$	
	^1H spectrum	^{19}F spectrum	^1H spectrum	^{19}F spectrum
δ_{Si-CH_3}	−0.08		−0.08	
δ_H	−6.5		−4.72	
δ_{Sn-CH_3}	−0.15		−0.15	
$J^{119}{}_{Sn-CH_3}$	57		57	
$J^{117}{}_{Sn-CH_3}$	55		55	
δ_{F_1}		220.9		233.3
δ_{F_2}		205.9		216.6
δ_{F_3}		192.7		203.7
J_{H-F_1}	10	10.9	44	43.1
J_{H-F_2}	62	58.5	37	36
J_{H-F_3}	56	57.6	10	9.6
$J_{F_1-F_2}$		20		8.4
$J_{F_1-F_3}$		27		9.6
$J_{F_2-F_3}$		290		312

*Chemical shifts are in p.p.m. and coupling constants in c.p.s. Neat liquid samples were used with external CCl_3F and external $CHCl_3$ as references.

TABLE IV

Infrared spectra of the addition products as liquid films

$(CH_3)_3SnH$ + $(CH_3)_3SiCF{=}CF_2$	$(CH_3)_3SnH$ + $(CH_3)_2Si(CF{=}CF_2)_2$	Assignment
510 (s)	505 (s)	Sn—C stretch
535 (vs)	525 (vs)	
620 (w)		
700 (m)	675 (sh,m)	
	715 (s)	CH_3—Sn and CH_3—Si rock
770 (s,b)	770 (vs,b)	
845 (vs)	830 (s,b)	
860 (sh,s)	860 (sh,m)	
875 (sh,m)		
950 (vs)	945 (vs)	
985 (s)	982 (vs)	
1030 (s)	1030 (vs)	C—F stretch
1040 (s)		
1065 (m)	1060 (s,sh)	
1110 (sh,m)	1110 (sh,s)	
1130 (s)	1125 (vs)	
1190 (w)	1190 (w)	CH_3 deform.
1225 (m)	1225 (m)	C—F stretch
1255 (vs)	1250 (vs)	CH_3—Si
1300 (w)	1300 (m)	
1335 (m)	1330 (m)	
1360 (w)	1360 (m)	
1415 (w)	1405 (m)	
2360 (w)	2360 (w)	
2810 (w)	2795 (w)	C—H stretch
2920 (s)	2910 (s)	
2970 (s)	2995 (s)	

Can. J. Chem. Downloaded from www.nrcresearchpress.com by 210.87.254.5 on 09/05/12
For personal use only.

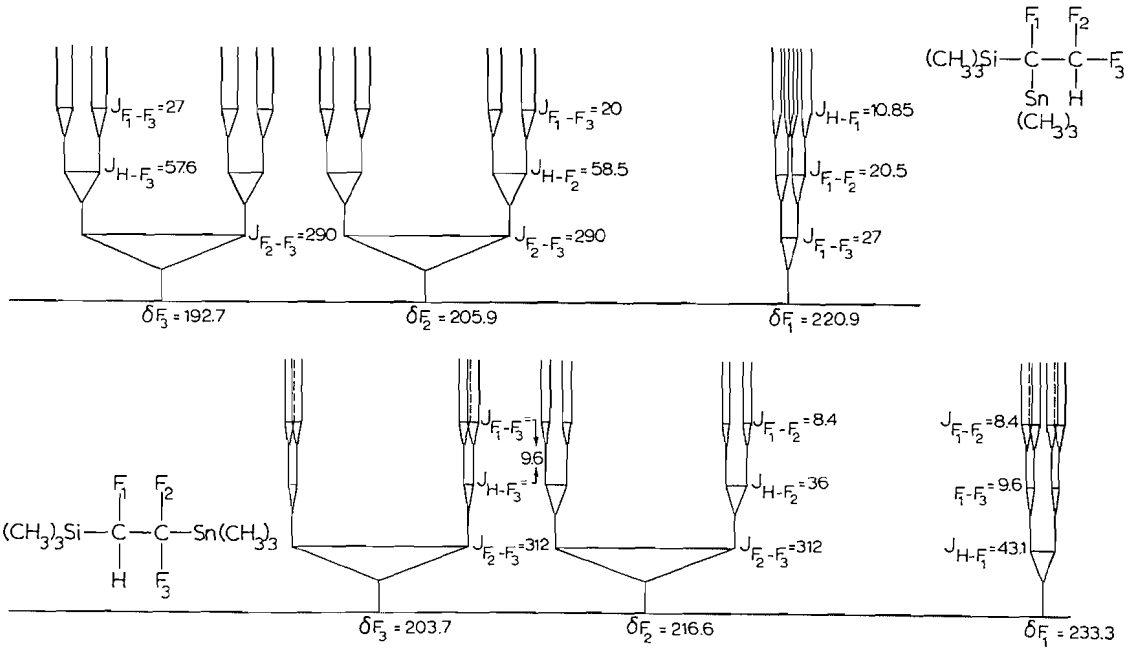

FIG. 2

TABLE V

Proton n.m.r. data for the product of $(CH_3)_3SnH$ and $(CH_3)_2Si(CF{=}CF_2)_2$ in cyclohexane

	$-Si-C(Sn(CH_3)_3)(F_1)-C(H)(F_2)-F_3$	$-Si-C(F_1)-C(H)(F_3)-Sn(CH_3)_3$
δ_{Si-CH_3}	−0.18	−0.18
δ_H	−6.06	−4.46
δ_{Sn-CH_3}	−0.15	−0.15
$J^{119}{}_{Sn-CH_3}$	56	56
$J^{117}{}_{Sn-CH_3}$	55	55
J_{H-F_1}	10	44
J_{H-F_2}	61	38
J_{H-F_3}	55	8

Chemical shifts (p.p.m.) are relative to internal cyclohexane. Coupling constants in c.p.s.

involving ultraviolet irradiation were conducted in silica tubes. Infrared spectra were recorded with a Beckman IR 10 double beam spectrophotometer using a 10 cm cell for vapor samples, and liquid films for the spectra of liquids. Proton n.m.r. spectra were obtained with a Varian A60 spectrometer, and ^{19}F spectra with a Varian DP-60 spectrometer operating at 56.4 Mc s^{-1}. Molecular weight measurements were performed on a Hewlett-Packard vapor pressure osmometer. Gas chromatographic separations were carried out on an Aerograph model A-700 Autoprep instrument with helium as carrier gas.

Trimethyltin hydride and dimethyltin dihydride were prepared by the procedure of Finholt *et al.* (22), using *n*-butyl ether as solvent. Trimethyl(perfluorovinyl)silane and dimethylbis(perfluorovinyl)silane were prepared by the method of Tarrant and Oliver (23) in 50 and 44% yields respectively.

In all of the reactions described below, the reaction mixture was worked up as follows. The reaction tube was opened to the vacuum system and all volatile components were separated by conventional trap-to-trap fractionation. Further purification was achieved by gas chromatography and each fraction was identified from its infrared spectrum, and for pure compounds ultimately by their n.m.r spectra. Any involatile material remaining in the reaction tube was examined spectroscopically.

Can. J. Chem. Downloaded from www.nrcresearchpress.com by 210.87.254.5 on 09/05/12
For personal use only.

Reactions of Trimethyl(perfluorovinyl)silane with Organotin Hydrides

(*a*) Trimethyltin hydride (0.24 g, 1.4 mmoles) and $(CH_3)_3SiCF{=}CF_2$ (0.204 g, 1.3 mmoles) were allowed to react at 25° for 24 h. There was no visible reaction and vacuum fractionation gave the starting materials quantitatively. In a similar experiment using identical quantities, the reaction mixture was allowed to stand at 25° for 2 weeks. A trace of white solid was deposited but recovery of the reactants was essentially quantitative.

(*b*) Trimethyltin hydride (0.40 g, 2.4 mmoles) and $(CH_3)_3SiCF{=}CF_2$ (0.40 g, 2.4 mmoles) were heated at 55° for 60 h. A white solid was deposited, which was identified spectroscopically as trimethyltin fluoride (0.228 g, ca. 50% yield). Vacuum fractionation gave incomplete separation, but an examination of the infrared spectrum of the gas phase mixture showed the presence of both reactants and at least four reaction products. Gas chromatography on a silicone QF-1 column at 170° gave pure products which were identified by their characteristic infrared and proton n.m.r. spectra (Tables I and II). From the peak areas of the latter spectra the percentage of each component in the total reaction mixture could be determined. The products were *cis*-$CFH{=}CFSi(CH_3)_3$ (36%), *trans*-$CFH{=}CFSi(CH_3)_3$ (5%), $CF_2{=}CHSi(CH_3)_3$ (41%), and $(CH_3)_3SiC_2H_2F$ (18%).

(*c*) Trimethyltin hydride (0.54 g, 3.3 mmoles) and $(CH_3)_3SiCF{=}CF_2$ (0.51 g, 3.3 mmoles) were exposed to ultraviolet irradiation at 25° for 10 h. A trace of trimethyltin fluoride, identified spectroscopically, was deposited, as well as a small amount of metallic tin. Vacuum fractionation gave, at −78°, a negligible amount of the two reactants, and a high yield (0.773 g) of a very involatile liquid at −23°. This was identified unambiguously from infrared and n.m.r. studies (Tables III and IV) as a mixture of the two addition compounds $(CH_3)_3SiCFHCF_2Sn(CH_3)_3$ and $(CH_3)_3SiCF[Sn(CH_3)_3]CF_2H$ in the ratio 3:2. The total yield of addition products was 77%.

The addition products are stable under vacuum at 25° for about 4 h, after which white crystals are slowly deposited. After 1 week, all liquid had disappeared and only a white solid remained. At this stage, the volatile products were removed and identified spectroscopically (Tables I and II) as $(CH_3)_3SiCH{=}CF_2$ and *cis*-$(CH_3)_3SiCF{=}CFH$, formed in the ratio 2:1. The remaining white solid was shown to be pure trimethyltin fluoride. The addition products are stable at 80° for only a few minutes, while at 100° decomposition is very rapid to give trimethyltin fluoride and a complex mixture of volatile products. Because of the instability of the addition products, completely satisfactory analytical data could not be obtained.

Anal. Calcd. for $C_8H_{19}F_3SiSn$: C, 30.12; H, 5.95; molecular weight, 319. Found: C, 31.21; H, 6.50; molecular weight (in benzene osmometrically), 368. Further characterization was obtained by alkaline hydrolysis of the products. A sample (0.110 g, 0.344 mmole) was hydrolyzed with 20% sodium hydroxide solution at 25°. The only volatile product was trifluoroethylene (0.028 g, 0.34 mmole) characterized spectroscopically (24).

(*d*) Trimethyltin hydride (0.24 g, 1.4 mmoles) and $(CH_3)_3SiCF{=}CF_2$ (0.204 g, 1.3 mmoles) were sealed with 80 mg of azobisisobutyronitrile and allowed to react at 35° for 10 h. Examination of the reaction mixture then showed only the starting materials, which were accordingly resealed with a further sample (80 mg) of azobisisobutyronitrile and kept at 50° for a further 10 h. Vacuum fractionation gave a trace of noncondensable gas, presumably a mixture of hydrogen nitrogen, but the bulk of the material (0.221 g, 54% yield) condensed at −23°. It was spectroscopically identified (Tables III and IV) as a mixture of the two addition products, $(CH_3)_3SiCFHCF_2Sn(CH_3)_3$ and $(CH_3)_3SiCF[Sn(CH_3)_3]CF_2H$, in a 3:2 ratio.

The fractions which condensed at −78 and −196° were shown spectroscopically to be mixtures of $(CH_3)_3SiCH{=}CF_2$, *cis*- and *trans*-$(CH_3)_3SiCF{=}CFH$, and $(CH_3)_3SiC_2H_2F$, with the first two compounds being the major components. A mixture of metallic tin, trimethyltin fluoride, and azobisisobutyronitrile remained in the reaction tube.

(*e*) Trimethyltin hydride (0.247 g, 1.5 mmoles) and $(CH_3)_3SiCF{=}CF_2$ (0.23 g, 1.5 mmoles) were sealed with hydroquinone (0.157 g) and irradiated for 10 h at 25–50°. A small amount of hydrogen was obtained, but the bulk of material condensed in the −23° trap, with very small amounts in the −78 and −196° traps. The −23° fraction (0.287 g) was spectroscopically identical with the mixture of addition products obtained previously, and corresponded to a 62% yield. The infrared spectra of the −78 and −196° fraction showed $(CH_3)_3SiCF{=}CF_2$ and its reduced products such as $(CH_3)_3SiC_2F_2H$ to be present, but the yields were insufficient for full characterization. Trimethyltin fluoride, some metallic tin, and hydroquinone remained in the reaction tube.

(*f*) Galvinoxyl (421 mg) prepared by the method of Bartlett and Funahashi (16) and azobisisobutyronitrile (82 mg) with 2 ml of dry benzene were taken in a pyrex Carius tube, and trimethyltin hydride (0.265 g, 1.6 mmoles) and $(CH_3)_3SiCF{=}CF_2$ (0.247 g, 1.6 mmoles) were then added under vacuum. The reaction mixture was heated at 50° for 10 h. On opening the tube, a small amount of noncondensable gas was first pumped off and all volatile materials were removed to leave a dark-red solid as described by Bartlett and Funahashi (16). Vacuum fractionation of the volatiles gave $(CH_3)_3SiCF{=}CF_2$ (0.192 g) and trimethyltin hydride (0.260 g). No other compound was present.

(*g*) Dimethyltin dihydride (0.225 g, 1.5 mmoles) and $(CH_3)_3SiCF{=}CF_2$ (0.462 g, 3.0 mmoles) were allowed to react at 60° for 24 h. The infrared spectrum (gas phase) of the volatile products showed a band at 1695 cm^{-1} (C=C stretch) characteristic of *cis*-$CFH{=}CFSi(CH_3)_3$, with a shoulder at 1720 cm^{-1} characteristic of $(CH_3)_3SiCH{=}CF_2$, but the amounts were so small that the proton n.m.r. spectrum showed only $(CH_3)_2SnH_2$ and $(CH_3)_3SiCF{=}CF_2$. From the reaction tube, a trace of dimethyltin difluoride (0.002 g) was recovered, from which it could be calculated that the reaction was only about 1% complete.

(*h*) Dimethyltin dihydride (0.225 g, 1.5 mmoles) and $(CH_3)_3SiCF{=}CF_2$ (0.462 g, 3.0 mmoles) were irradiated at 25° for 16 h, leading to the extensive formation of a white solid. A mixture of methane and hydrogen (total pressure 4 mm) was present in the tube on opening, and was pumped off. The infrared spectrum (gas phase) of the

Can. J. Chem. Downloaded from www.nrcresearchpress.com by 210.87.254.5 on 09/05/12
For personal use only.

volatiles showed the presence of *cis*- and *trans*-CFH $=$CFSi$(CH_3)_3$, $(CH_3)_3$SiCH$=CF_2$, and $(CH_3)_3SiC_2H_2F$, based on the observed C$=$C stretching frequencies. Confirmation was obtained from the proton n.m.r. spectrum, which on integration showed the percentage composition to be *cis*-CFH$=$CFSi$(CH_3)_3$ 29%, *trans*-CFH$=$CFSi$(CH_3)_3$ 5.5%, $(CH_3)_3$SiCH$=CF_2$ 49%, and $(CH_3)_3SiC_2H_2F$ 16.5%. From the reaction tube, dimethyltin difluoride (0.223 g) was recovered, corresponding to 80% complete reaction.

Reactions of Dimethylbis(perfluorovinyl)silane with Organotin Hydrides

(*a*) Trimethyltin hydride (0.72 g, 4.5 mmoles) and $(CH_3)_2Si(CF{=}CF_2)_2$ (0.48 g, 2.18 mmoles) were allowed to react at 25° for 1 week. There was no visible reaction, and no noncondensable gas was formed. Vacuum fractionation lead to complete recovery of the reactants.

(*b*) In a similar reaction, the mixture was heated at 55° for 45 h. A small amount of solid was deposited and a trace of a noncondensable gas was pumped off. Satisfactory separation by vacuum fractionation could not be achieved although infrared spectra and proton n.m.r spectra showed the presence in small and decreasing amounts of $(CH_3)_2Si(CH{=}CF_2)_2$, *cis*- and *trans*-(CFH $=$CF$)_2$Si$(CH_3)_2$, and $(CH_3)_2Si(C_2H_2F)_2$ with characteristic infrared C$=$C stretching frequencies at 1700, 1665, 1722, and 1625 cm^{-1} respectively, in addition to the starting materials. However, the amounts of these products were too small to determine quantitatively even by integration of the n.m.r. spectrum, and the quantity of trimethyltin fluoride (0.012 g) recovered from the reaction tube showed that the reaction was only 1.5% complete.

(*c*) Trimethyltin hydride (0.72 g, 4.5 mmoles) and $(CH_3)_2Si(CF{=}CF_2)_2$ (0.48 g, 2.18 mmoles) were irradiated for 4 h at 25°, at the end of which time a small amount of white solid had been deposited. Other than some noncondensable gas, the volatile products were identified as trimethyltin hydride (0.02 g) and $(CH_3)_2Si(CF{=}CF_2)_2$ (0.082 g). There remained in the reaction tube an involatile liquid which was washed out with cyclohexane, and examined spectroscopically after removal of the solvent. The infrared and proton n.m.r. spectra (Tables IV and V) showed the material to be a mixture of the addition products of $(CH_3)_3$SnH and $(CH_3)_2Si(CF{=}CF_2)_2$, which could not be separated chromatographically because of instability. On standing at 25°, decomposition occurred slowly with the deposition of trimethyltin fluoride. The yield (0.417 g) was 34.7%.

(*d*) Trimethyltin hydride (0.36 g, 2.25 mmoles) and $(CH_3)_2Si(CF{=}CF_2)_2$ (0.24 g, 1.1 mmoles) with azobisisobutyronitrile (50 mg) were heated at 55° for 45 h. The infrared spectrum (gas phase) of the volatile products showed, from the C$=$C stretching frequencies, the presence of —CF$=$CFH, —C_2H_2F, and —CH$=CF_2$ groups, but separation of this complex mixture was not attempted. The reaction tube contained some trimethyltin fluoride and azobisisobutyronitrile, but none of the involatile liquid addition products.

(*e*) Dimethyltin dihydride (0.127 g, 0.85 mmole) and $(CH_3)_2Si(CF{=}CF_2)_2$ (0.186 g, 0.85 mmole) were allowed to react at room temperature. After 2 days, a white solid had appeared and this became grey in color after another 15 days. The infrared spectrum (gas phase) of the volatile reaction products showed the presence of —CF$=$CFH and —CH$=CF_2$ groups in addition to considerable amounts of the starting material. The grey solid (0.026 g) was washed out of the tube, examined, and found to be mainly metallic tin with a little dimethyltin difluoride.

(*f*) Dimethyltin dihydride (0.161 g, 1.07 mmoles) and $(CH_3)_2Si(CF{=}CF_2)_2$ (0.235 g, 1.07 mmoles) were allowed to react at 55° for 8 h. White to yellow solid was deposited and a small amount of noncondensable gas was pumped off. Spectroscopic examination (infrared and proton n.m.r.) showed the presence of *cis*- and *trans*-HCF$=$CF—, —CH$=CF_2$, and —C_2H_2F groups, with *cis*-HCF$=$CF— and —CH$=CF_2$ being the most abundant. Only traces of the original reactants were still present. From the residue in the reaction tube, dimethyltin difluoride (0.158 g) was extracted, corresponding to a 79% yield.

(*g*) Dimethyltin dihydride (0.323 g, 2.17 mmoles) and $(CH_3)_2Si(CF{=}CF_2)_2$ (0.475 g, 2.16 mmoles) were irradiated for 30 min at 25°. Treatment of the reaction mixture as in the last experiment showed the volatiles to consist of $(CH_3)_2Si$ derivatives containing *cis*- and *trans*-CFH$=$CF—, —CH$=CF_2$, and —C_2H_2F groups, with those containing *cis*-CFH$=$CF— and —CH$=CF_2$ being the major products. Some of the original reactants were also present. From the residue in the tube, dimethyltin difluoride (0.165 g, 41% yield) was extracted.

Acknowledgments

The financial support of the National Research Council of Canada is greatly appreciated.

1. H. C. Clark, S. G. Furnival, and J. T. Kwon. Can. J. Chem. **41**, 2889 (1963).
2. C. Barnetson, H. C. Clark, and J. T. Kwon. Chem. Ind. London, 458 (1964).
3. H. C. Clark and J. T. Kwon. Can. J. Chem. **42**, 1288 (1964).
4. A. D. Beveridge, H. C. Clark, and J. T. Kwon. Can. J. Chem. **44**, 179 (1966).
5. W. P. Neumann and E. Heymann. Ann. Chem. **683**, 11 (1965).
6. A. J. Leusink and J. G. Noltes. Rec. Trav. Chim. **84**, 585 (1965).
7. H. M. J. C. Creemers and J. G. Noltes. Rec. Trav. Chim. **84**, 590 (1965).
8. D. Seyferth. *In* Progress in inorganic chemistry. Vol. III. *Edited by* F. A. Cotton. Interscience Publishers, New York. 1962. pp. 129–180.
9. M. C. Henry and J. C. Noltes. J. Am. Chem. Soc. **82**, 558 (1960).
10. D. Seyferth and T. Wada. Inorg. Chem. **1**, 78 (1962).
11. H. C. Clark and J. H. Tsai. Inorg. Chem. **5**, 1407 (1966).
12. M. R. Booth. Ph.D. Thesis, University of Western Ontario, London, Ont. 1967.
13. R. N. Haszeldine and J. C. Young. Proc. Chem. Soc. 394 (1959).
14. J. G. Noltes and G. J. M. van der Kerk. Functionally substituted organotin compounds. Tin

Research Institute, Greenford, Middlesex, England. 1958.
15. H. G. KUIVILA. *In* Advances in organometallic chemistry. *Edited by* F. G. A. Stone and R. West. Vol. 1. Academic Press Inc., New York. 1964.
16. P. D. BARTLETT and T. FUNAHASHI. J. Am. Chem. Soc. **84**, 2596 (1962).
17. H. M. J. C. CREEMERS, F. VERBEEK, and J. G. NOLTES. J. Organometal. Chem. **8**, 469 (1967).
18. M. C. HENRY and J. G. NOLTES. J. Am. Chem. Soc. **82**, 561 (1960).
19. D. SEYFERTH, T. WADA, and G. E. MACIEL. Inorg. Chem. **1**, 232 (1962).
20. H. C. CLARK, N. CYR, and J. H. TSAI. Can. J. Chem. **45**, 1073 (1967).
21. H. C. CLARK, J. T. KWON, L. W. REEVES, and E. J. WELLS. Can. J. Chem. **41**, 3005 (1963).
22. A. E. FINHOLT, A. C. BOND, JR., K. E. WILZBACH, and H. I. SCHLESINGER. J. Am. Chem. Soc. **69**, 2692 (1947).
23. P. TARRANT and W. H. OLIVER. J. Org. Chem. **31**, 1143 (1966).
24. D. G. WEIBLEN. *In* Fluorine chemistry. *Edited by* J. H. Simons. Vol. 2. Academic Press Inc., New York. 1954.

Can. J. Chem. Downloaded from www.nrcresearchpress.com by 210.87.254.5 on 09/05/12
For personal use only.

Can. J. Chem. Downloaded from www.nrcresearchpress.com by 210.87.254.5 on 09/05/12
For personal use only.

Reactivity of metal–metal bonds. IV. The reaction of sulfur dioxide with compounds containing Sn—Sn and Sn—Mn bonds

N. A. D. Carey and H. C. Clark
Department of Chemistry, University of Western Ontario, London, Ontario

Received June 13, 1967

The reactions of sulfur dioxide with the compounds R_6Sn_2 and $R_3SnMn(CO)_5$ (R = CH_3 or C_6H_5) have been studied. In all cases the evidence indicates that the metal–metal bond has been cleaved. With the ditins the new compounds $R_3Sn.SO_2$ (R = CH_3 or C_6H_5) and $R_3Sn.2SO_2$ (R = C_6H_5) were obtained, while the mixed bimetallic compounds gave $R_3SnMn(CO)_5.2.5SO_2$ (R = CH_3 or C_6H_5) and $R_3SnMn(CO)_5.1.5SO_2$ (R = CH_3). The possible structures of these derivatives are discussed.

Canadian Journal of Chemistry, **46**, 643 (1968)

Introduction

We have previously examined the reactivity of several metal–metal bonded compounds towards unsaturated systems, notably those containing C=C and C≡C bonds (1–4). As an extension of this study, we have carried out some reactions between sulfur dioxide and compounds containing Sn—Sn and Sn—Mn bonds. The results imply that the type of ligand attached to tin appreciably affects the course of the reaction, although in all cases, interaction occurs readily with the multiple sulfur–oxygen bond. These reactions may therefore be related to those investigated by Wojcicki (5–7) who has shown that sulfur dioxide can cleave the alkyl–manganese bond of $CH_3Mn(CO)_5$ to give the sulfone, with no displacement of carbon monoxide.

Experimental

Elemental analysis was carried out by Dr. A. B. Gygli, Microanalyses Laboratory, Toronto, and by Dr. Alfred Bernhardt, Mikroanalytisches Laboratorium, Mulheim. Molecular weight determinations were carried out using a Mechrolab osmometer 301A. Infrared spectra were recorded on a Beckmann IR10 spectrometer using Nujol and halocarbon oil as dispersion media. The instrument was calibrated using the reference spectra of polystyrene film. The carbonyl stretching region was recorded on a Beckmann IR7 spectrometer, using the water line at 1946.5 cm^{-1} as reference. The spectra were recorded as solutions in chloroform using 0.1 mm NaCl solution cells. The proton nuclear magnetic resonance (n.m.r.) spectrum was recorded on a Varian Associates A-60 n.m.r. spectrometer, using methanol as internal standard.

Preparation of Starting Materials

Hexaphenylditin was purchased from K and K Labs. Inc. Its melting point and infrared spectrum compared favorably with the literature and the material was used without further purification. Hexamethylditin was prepared by the addition of trimethyltin chloride to a solution of sodium in liquid ammonia (8). The procedure for its purification was identical with that given by Tsai (9), and its purity was checked by comparison with the infrared spectrum of hexamethylditin (10). Triphenyltinmanganesepentacarbonyl was prepared by the addition of the sodium salt of dimanganese decarbonyl in anhydrous tetrahydrofuran to a solution of triphenyltinchloride in tetrahydrofuran (11). Similarly, trimethyltinmanganesepentacarbonyl was prepared, but using trimethyltinchloride (9). Anhydrous sulfur dioxide from Matheson Ltd. (Canada) was used; it was distilled *in vacuo* before use.

Wojcicki (6) has reported that reactions involving sulfur dioxide proceed more readily in the absence of solvent. A similar observation has been made in the course of this investigation, whereby the reaction of triphenyltinmanganesepentacarbonyl proceeded very slowly in the presence of benzene, whereas it had gone to completion within 15 h if the carbonyl was simply dissolved in liquid sulfur dioxide. Unless stated to the contrary, the reactions were carried out as follows: an approximate 5% by weight solution of the compound in sulfur dioxide was initially allowed to react for at least 15 h at room temperature, with continuous shaking. The reactions were carried out in thick-walled pyrex glass carius tubes. The sulfur dioxide was added, and removed under vacuum, and all handling operations were performed in a N_2-filled drybag.

Reaction with Hexamethylditin

This reacted instantly with sulfur dioxide to form a deep-yellow solution. The reaction was apparently complete within an hour. On removing the sulfur dioxide, the color began to leave the solid, so that finally, having removed all the sulfur dioxide (which in fact proved to be a lengthy operation involving continuous pumping for 24 h *in vacuo* at room temperature), a white, free-flowing solid remained. If sulfur dioxide was added to this solid, a yellow solution was obtained, which suggests that an equilibrium is set up between the product, and a sulfur dioxide adduct of the product. This would explain the difficulty associated with removing the final traces of sulfur dioxide. The white solid proved to be soluble only in methanol.

The compound analyzed for an empirical formula $(CH_3)_3Sn.SO_2$.

Can. J. Chem. Downloaded from www.nrcresearchpress.com by 210.87.254.5 on 09/05/12
For personal use only.

Anal. Calcd. for $C_3H_9SnSO_2$: C, 15.9; H, 3.86; S, 14.1. Found: C, 15.4; H, 3.86; S, 13.5.

The compound possessed no melting point, decomposition setting in above 110 °C. The proton n.m.r. spectrum of the compound, as a 10% by weight solution in methanol, gave a single sharp line at τ 9.55 with $J(^{117}Sn—C—H)$ of 78.6 c/s and $J(^{119}Sn—C—H)$ of 85.9 c/s. The infrared spectrum, shown in Fig. 1 for the region 1300–300 cm^{-1}, has absorption maxima at: 1290 (vw), 1195 (vw), 1100 (sb), 1040 (w), 990 (sb), 930 (m), 870 (w), 770 (s,b), 720 (m,sh), 630 (m), 550 (s), 520 (m), 430 (w), 400 (w) cm^{-1}.

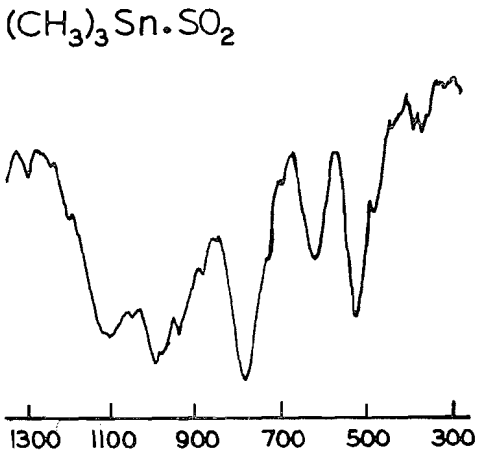

FIG. 1. Spectrum of hexamethylditin with sulfur dioxide.

Reaction with Trimethyltinmanganesepentacarbonyl

The colorless solution of trimethyltinmanganesepentacarbonyl in sulfur dioxide turned first yellow, then claret colored, and finally began to deposit a yellow solid, so that within an hour of starting the reaction at room temperature, a yellow precipitate had formed, draining the color out of the solution. On removing the sulfur dioxide, the last traces of which were removed by warming the contents of the carius tube under vacuum with a hair dryer, a red-yellow residue was left that proved to be insoluble in diethylether. However, a dark-red compound was extracted with methylene chloride, leaving behind a pale-yellow residue. The latter decomposed at 150 °C to evolve sulfur dioxide, carbon dioxide, and $(CH_3)_4Sn$. Elemental analysis of this compound suggested an adduct of sulfur dioxide with $(CH_3)_3SnMn(CO)_5$.

Anal. Calcd. for $CH_3SnMn(CO)_5.2.5SO_2$: C, 18.49; H, 1.73. Found: C, 18.78; H, 2.76.

No molecular weight was obtained. The infrared spectrum of the pale-yellow residue differed from the red compound only in the absence of two bands of medium intensity at 1160 cm^{-1} and 1115 cm^{-1}.

The red compound analyzed for an empirical formula $(CH_3)_3SnMn(CO)_5.1.5SO_2$.

Anal. Calcd. for $C_3H_9SnMn(CO)_5.1.5SO_2$: C, 20.77; H, 2.00; S, 10.5. Found: C, 20.57; H, 2.03; S, 10.22.

The compound decomposed above 200 °C. The molecular weight (m.w.) in chloroform suggested that the compound was a dimer. Calcd. m.w. for dimer, 910. Found: m.w., 960 ± 20. The infrared spectrum is shown in Fig. 2 for the region 1300–300 cm^{-1} and has bands at 1300 (vw), 1160 (m), 1115 (m), 1010 (s,b), 970 (s,b), 770 (s), 720 (m), 640 (s), 615 (s), 550 (m), 520 (mw,sh), 440 (w), 410 (w), and 260 (m) cm^{-1}. The proton n.m.r. spectrum of a 10% w/w solution in methylene chloride gave a broad line, centered at τ of 9.3. The red compound formed between 60 and 70% of the total product of this reaction, the pale-yellow compound making up the difference.

Reaction with Hexaphenylditin

Hexaphenylditin (1.5 g) was allowed to react with about 5 ml of sulfur dioxide for 75 h at room temperature. On opening up, only sulfur dioxide was recovered as volatile material. The white residue contained two compounds, one of which was soluble in diethylether, methylene chloride, or benzene, whilst the second proved to be insoluble in all the usual organic solvents.

The soluble compound, a white crystalline material, analyzed for an empirical formula $Ph_3Sn.SO_2$.

Anal. Calcd. for $C_{18}H_{15}SnSO_2$: C, 52.1; H, 3.60; S, 7.75. Found: C, 51.6; H, 3.65; S, 7.7. m.p. 153 ± 1° (uncorr.). Calcd. m.w. for dimer, 826. Found: m.w., 815 ± 15 (benzene solution).

The infrared spectrum for the region 1300–300 cm^{-1} showed bands at 1325 (w), 1300 (w), 1260 (w), 1175 (w,b), 1150 (w), 1070 (ms) (with shoulders at 1075 and 1065), 1010 (m), 990, 957 (vs), 925 (vs), 745 (s), 720 (s), 685 (s), 610 (w), 555 (s), 470 (s), 435 (s), 355 (w), and 305 (m) cm^{-1}.

The insoluble compound, a white powder, analyzed for an empirical formula $Ph_3Sn.2SO_2$.

Anal. Calcd. for $C_{18}H_{15}SnS_2O_4$: C, 45.3; H, 3.15; S, 12.9. Found: C, 45.2; H, 3.12; S, 13.4.

It decomposed sharply at 201°. No molecular weight was obtained. The infrared spectrum for the region 1300–300 cm^{-1} showed bands at 1300 (vs), 1175 (vw,b), 1150 (vw), 1110 (mw), 1080 (m), 1070 (mw), 1015 (mw), 995

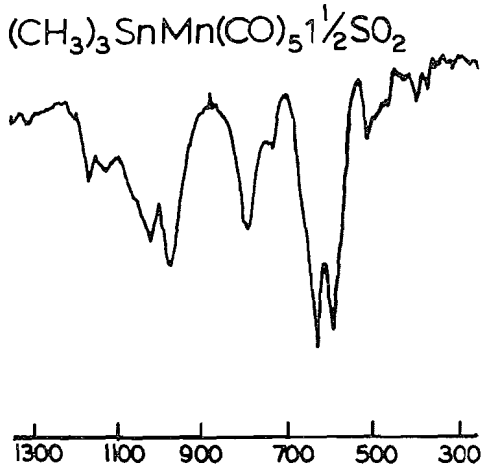

FIG. 2. Spectrum of trimethyltinmanganesepentacarbonyl with sulfur dioxide.

Can. J. Chem. Downloaded from www.nrcresearchpress.com by 210.87.254.5 on 09/05/12
For personal use only.

(mw,sh), 948 (vs,b), 750 (s), 730 (s), 695 (s), 685 (s), 590 (s), 450 (ms), 410 (w), 320 (mw), 290 (mw) cm^{-1}.

On reacting the soluble compound, $Ph_3Sn.SO_2$, with an excess of sulfur dioxide for a further 48 h at room temperature, a compound was obtained whose infrared spectrum was identical with that of the insoluble compound, $Ph_3Sn.2SO_2$.

Reaction with Triphenyltinmanganesepentacarbonyl

The colorless solution of triphenyltinmanganesepentacarbonyl in sulfur dioxide turned yellow overnight at room temperature. After 15 h, the sulfur dioxide was removed to leave a white residue in the carius tube. A white crystalline compound was obtained on extraction with diethylether and subsequent evaporation. (A small quantity of material, insoluble in diethylether, representing about 5% w/w of the total product, was also formed. This has not been examined in any detail since it proved insoluble in all the solvents used; its infrared spectrum would suggest that it was a mixed oxide of tin and manganese).

On heating the white compound *in vacuo* at 100 °C, sulfur dioxide was evolved and the compound gradually turned yellow. After half an hour, evolution of sulfur dioxide had ceased (as measured by the manometer). The infrared spectra of the two compounds differ only by the presence in the yellow compound of a medium intense band at 1155 cm^{-1}. The same yellow compound was also formed, in the presence of starting material, by stopping the reaction after 5 h. The white compound represents an adduct of sulfur dioxide with the yellow compound.

Anal. Calcd. for $C_{18}H_{15}SnMnC_5O_5.B.25SO_2$: C, 36.7; H, 1.99; S, 13.9. Found: C, 36.1; H, 2.53; S, 13.6.

Further support for this hypothesis comes from the observation that some conversion to the white compound occurred after allowing the yellow compound to react with sulfur dioxide for a further 2 h at room temperature.

The yellow crystalline solid analyzed for an empirical formula $Ph_3SnMn(CO)_5.2.5SO_2$.

Anal. Calcd. for $C_{23}H_{15}SnMnS_{2.5}O_{10}$: C, 39.3; H, 2.24; S, 11.3. Found: C, 39.5; H, 2.24; S, 10.3.

The compound began to decompose above 200 °C. Calcd. m.w. for dimer, 1410. Found: m.w., 1370 ± 30 (in chloroform). The infrared spectrum showed bands at 1300 (vw), 1155 (m), 1080 (m), 1070 (m), 1025 (mw,sh), 970 (s,b), 935 (s,b), 750 (m), 725 (m), 695 (m), 685 (m), 695 (m), 645 (vs), 615 (mw), 585 (m), 530 (mw), 475 (m), 460 (m), 445 (m) cm^{-1}.

Discussion

It is clear that the reactions of sulfur dioxide with these metal–metal bonded compounds give chemically discrete products, but to elucidate their structure is very difficult. The proton n.m.r. spectrum of the white, air-stable compound of empirical formula $C_3H_9SnSO_2$ gave a single sharp line at $\tau = 9.55$. The methyl groups are therefore equivalent and the chemical shift suggests that they are bonded to the metal rather than to oxygen or sulfur. Hence, the sulfur dioxide must have cleaved the Sn—Sn bond. The $J^{117}_{Sn-CH_3}$ and $J^{119}_{Sn-CH_3}$ values of 78.6 c.p.s. and 85.4 c.p.s. respectively are of the same order of magnitude as those observed in the proton n.m.r. spectrum of trimethyltin fluoride (13), whilst the corresponding coupling constants in $(CH_3)_3SnX$, where X is Cl, Br, or I, are about 20 c.p.s. smaller (14). Since the coupling constant is related to the type of bond through which the coupling is being induced (15), the CH_3 groups are apparently in an environment similar to that in $(CH_3)_3SnF$. In addition, the Sn—C infrared stretching vibration in $(CH_3)_3SnF$ is observed at 550 cm^{-1}, whilst in pyramidal $(CH_3)_3Sn$— compounds, the Sn—C symmetrical stretching vibrations are at 500 ± 10 cm^{-1} (16). From Fig. 1, it can be seen that whilst there are no bands at 500 cm^{-1}, a band is observed at 550 cm^{-1}. Accordingly it is believed that the tin is five coordinate, with the three methyl groups in the equatorial plane, by analogy with the structure of $(CH_3)_3SnF$ (17). The antisymmetric (Sn—O) stretching vibration in compounds of the type $(R_3Sn)_2O$ comes in the range 740–790 cm^{-1} (18), whilst the symmetric (Sn—O) stretching vibration comes between 395–415 cm^{-1} (18). In compounds containing Sn—O—Si, the (Sn—O) stretch is between 960–980 cm^{-1} (18). It seems reasonable therefore to associate one of the bands, either at 930 cm^{-1} or 720 cm^{-1}, with the (Sn—O) stretching vibration. Similarly, one of the two weak bands occurring at 430 or 400 cm^{-1} might be associated with the symmetric (Sn—O) stretching vibration. There is some chemical evidence that in related compounds (20) Sn—O—S groups are formed in preference to Sn—S—O. The strong, broad band at 990 cm^{-1} can be assigned to the S—O stretching vibration (19), whilst the band at 770 cm^{-1} is characteristic of the methyl tin rock (16). The strong, broad band at 1100 cm^{-1} suggests the presence of a terminal >S=O which is not participating in coordination of the type >S=O → Sn, since Cotton *et al.* (21, 22) have shown that in complexes of dimethylsulfoxide with transition metals in which coordination is occurring through the oxygen, the (S=O) stretching vibration is shifted ca. 100 cm^{-1} to lower frequencies.

While there are three possible monomeric structures, **1–3**, none agrees with the above spectroscopic data.

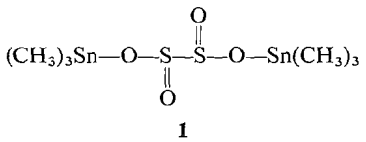

1

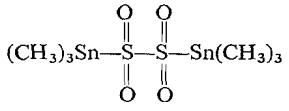

2

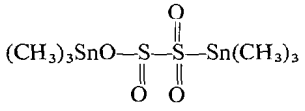

3

In order to maintain the equivalence of the $(CH_3)_3Sn$ groups, and to be consistent with the infrared spectrum, the occurrence of coordination through S → Sn in structure **1**, O → Sn in structure **2**, and both S → Sn and O → Sn in structure **3** can be proposed. In this way, all three of the above structures reduce to the same polymeric system, consisting of five coordinate tin units best described as

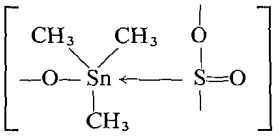

or

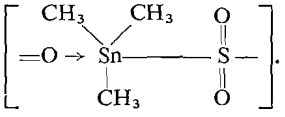

This polymeric structure is consistent with the poor solubility of the compound.

With sulfur dioxide, trimethyltinmanganesepentacarbonyl gave a rust-colored product of empirical formula $C_{16}H_{18}O_{16}S_3Mn_2Sn_2$. The infrared spectrum (Fig. 2) is similar to the spectrum obtained for $[(CH_3)_3SnSO_2]_n$, apart from bands due to the —$Mn(CO)_5$ group. The strong band at 770 cm^{-1}, together with the band at 550 cm^{-1}, show that the methyls are attached to the tin, and that the tin is five coordinate. Certainly, the shift of ca. 50 cm^{-1} to higher frequencies for the Sn—C stretching vibrations is consistent with cleavage of the Sn—Mn bond. Similarly the bands at 720, 440, and 410 cm^{-1} correspond to the (Sn—O) stretching vibrations and the (S—S) stretching vibrations. The band at 260 cm^{-1} is in the region associated with the (Mn—S) stretching vibration (7).

Wojcicki *et al.* (7) analyzed the carbonyl stretching region for $(CO)_5Mn—SO_2—$ and showed that the degeneracy was removed, causing all five modes to become infrared active, and that the absorption region was shifted to higher frequencies. We have similarly observed a more complex spectrum in the carbonyl stretching region than that observed for a compound such as $(CH_3)_3SnMn(CO)_5$ and with values shifted to higher frequencies. These are given in Table I. However, the spectrum cannot be analyzed fully, although it does seem likely that the degeneracy has been removed to some extent. The presence of the medium intensity bands at 1100 cm^{-1} suggest the presence of S=O, although the bands are less intense than those usually encountered for *terminal* S=O groups (19). These results suggest that the group

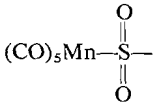

is probably present. It also seems likely from similarities in the infrared spectra that the group

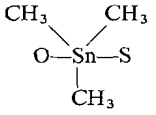

is occurring, as in $[(CH_3)_3SnSO_2]_n$.

Hexaphenylditin and sulfur dioxide gave two products of which one was a soluble, white crystalline solid of empirical formula $C_{18}H_{15}O_2SSn$. Its infrared spectrum does not exclude the possibility of C_6H_5—S groups being present (23), and does not allow any firm structural conclusions to be reached, although the structure may well be identical to that of $[(CH_3)_3SnSO_2]_n$. The second product of empirical formula $(C_6H_5)_3Sn.2SO_2$ was insoluble and hence presumably polymeric. If one excludes the possibility of sulfur dioxide acting as a bidentate Lewis base, then either insertion into the phenyl–tin bond must be occurring to give this stoichiometry, or the species $(C_6H_5)_3Sn(SO_2)_4Sn(C_6H_5)_3$ must be postulated. However, it is not clear why, in the latter species, such multiinsertion should stop at four SO_2, or why its solubility should be so low. Again, however, the complexity of the bands associated with the

Can. J. Chem. Downloaded from www.nrcresearchpress.com by 210.87.254.5 on 09/05/12
For personal use only.

TABLE I

Carbonyl stretching region (as solutions in $CHCl_3$)

$Mn(CO)_5.Sn(CH_3)_3$[b]	$Mn(CO)_5.1\frac{1}{2}SO_2.Sn(CH_3)_3$	$Mn(CO_5.2\frac{1}{2}SO_2.Sn(C_6H_5)_3$	$Mn(CO)_5.SO_2CH_3$[a]
2091 (m)	2114 (mw)	2106 (mw)	2142 (mw)
1995 (m)	2106 (w)	2094 (w)	2095 (w)
1989 (vs)	2062 (s)	2047 (s)	2055 (s)
1957 (w)	2032 (s)	2019 (s)	2037 (m,sh)
	2016 (sh)		

[a]Reference 5.
[b]Reference 12, as a solution in cyclohexane.

$(C_6H_5)_3Sn$ group prevents any conclusion concerning structure being reached, on the basis of the available spectroscopic data.

Similar difficulties arise in discussing the nature of the product obtained from triphenyltinmanganesepentacarbonyl and sulfur dioxide. This was a yellow crystalline compound, $[(C_6H_5)_3SnMn(CO)_5]_2.5SO_2$. Its infrared spectrum does not exclude the presence of C_6H_5—S groups, although the carbonyl stretching absorptions (Table I) are similar to those observed for the $[(CH_3)_3SnMn(CO)_5]_2.3SO_2$. By analogy with the latter compound, it seems reasonable to postulate the existence of the group

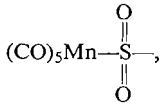

in that the band at 260 cm^{-1} might be associated with the (Mn—S) stretching vibration, and in addition the band at 1155 cm^{-1} is in the region associated with the (S=O) stretching vibrations. It is interesting that whilst a 2:1 ratio of sulfur dioxide to R_3Sn is required for the ditins to form a polymer when R is phenyl, a 1:1 ratio is required if R is methyl. This order is reproduced when a $Mn(CO)_5$ group is present. This appears to be related to the fact that polymerization can occur through the R_3Sn moiety, either by expanding its coordination number from 4 to 5 in the case of $(CH_3)_3Sn$ or perhaps by cleavage of the C—Sn bond, in the case of $(C_6H_5)_3Sn$—.

There is thus reasonable spectroscopic evidence that reaction of sulfur dioxide with such metal–metal bonded compounds leads to cleavage of the metal–metal bond. However, the products are frequently complex polymers, whose structure can only be determined conclusively by diffraction studies, rather than by infrared and n.m.r. spectroscopic investigations.

Acknowledgments

This work was supported by a grant awarded under the Research Grants Programme of the North Atlantic Treaty Organization.

1. H. C. Clark, J. D. Cotton, and J. H. Tsai. Can. J. Chem. **44**, 903 (1966).
2. H. C. Clark and J. H. Tsai. Inorg. Chem. **5**, 1407 (1966).
3. H. C. Clark, J. D. Cotton, and J. H. Tsai. Inorg. Chem. **5**, 1583 (1966).
4. R. E. J. Bichler, M. R. Booth, and H. C. Clark. Inorg. Nucl. Chem. Letters, **3**, 71 (1967).
5. F. A. Hartman and A. Wojcicki. J. Am. Chem. Soc. **88**, 844 (1966).
6. J. P. Bibler and A. Wojcicki. J. Am. Chem. Soc. **88**, 4862 (1966).
7. F. A. Hartman, P. J. Pollick, and A. Wojcicki. Abstracts 152nd A.C.S. Meeting, New York. September 1966. p. O91.
8. H. C. Clark and C. J. Willis. J. Am. Chem. Soc. **82**, 1888 (1960).
9. J. H. Tsai. Ph.D. Thesis, University of British Columbia, Vancouver, B.C. 1966.
10. T. L. Brown and G. L. Morgan. Inorg. Chem. **2**, 736 (1963).
11. R. D. Gorsich. J. Am. Chem. Soc. **84**, 2486 (1962).
12. M. R. Booth. Ph.D. Thesis, University of Western Ontario, London, Ont. 1967.
13. R. J. O'Brien. Ph.D. Thesis, University of British Columbia, Vancouver, B.C. 1963.
14. H. Schmidbaur and I. Ruidisch. Inorg. Chem. **3**, 599 (1964).
15. J. A. Pople, W. G. Schneider, and H. J. Bernstein. High resolution nuclear magnetic resonance. McGraw-Hill, New York. 1959.
16. R. Okawara, D. E. Webster, and E. G. Rochow. J. Am. Chem. Soc. **82**, 3287 (1960).
17. H. C. Clark, R. J. O'Brien, and J. Trotter. J. Chem. Soc. 2332 (1964).
18. M. Onyszchuk. Private communication.
19. J. L. Bellamy. *In* Organic sulfur compounds. *Edited by* N. Kharasch. Pergamon Press, London. 1961. pp. 47–57.
20. M. Pang and E. I. Becker. J. Org. Chem. **29**, 1948 (1964).
21. F. A. Cotton, R. Francis, and W. D. Horrocks. J. Phys. Chem. **64**, 1534 (1960).
22. R. Francis and F. A. Cotton. J. Chem. Soc. 2078 (1961).
23. N. S. Ham, A. N. Hambly, and R. H. Laby. Australian J. Chem. **13**, 451 (1960).

Can. J. Chem. Downloaded from www.nrcresearchpress.com by 210.87.254.5 on 09/05/12
For personal use only.

Can. J. Chem. Downloaded from www.nrcresearchpress.com by 210.87.254.105 on 09/05/12
For personal use only.

Reaction of sulfur dioxide with dimethylzinc and dimethylmercury

N. A. D. CAREY AND H. C. CLARK
Department of Chemistry, University of Western Ontario, London, Ontario

Received June 13, 1967

Dimethylzinc and sulfur dioxide give the products $(CH_3)_2Zn.SO_2$ and $(CH_3)_2Zn.2SO_2$ for which the formulations $CH_3ZnO.SO.CH_3$ and $(CH_3SO.O)_2Zn$ are proposed. With dimethylmercury, sulfur dioxide gives products best formulated as $(CH_3Hg)_2SO_2$ and $CH_3HgSO.OCH_3$.

Canadian Journal of Chemistry, 46, 649 (1968)

The cleavage of alkyl–metal bonds by sulfur dioxide has been demonstrated for a variety of different systems (1–3). In some cases, the sulfone is formed; thus, Hartman and Wojcicki (1) have shown that $CH_3Mn(CO)_5$ gives CH_3-$SO_2Mn(CO)_5$. Alternatively, the ester may be formed, a probable example being the formation of tris(ethylsulfinato)aluminium, $(C_2H_5SO_2)_3Al$, from the reaction of triethylaluminium with sulfur dioxide (2). Surprisingly, the reactions of sulfur dioxide with other organometallic compounds have not been studied in detail, and we describe here the behavior of dimethylzinc and dimethylmercury with sulfur dioxide. Incomplete reports have been published (4) of related reactions with diphenyl, diethyl, and dibenzyl mercurials.

Experimental

All reactions were carried out *in vacuo*, using conventional vacuum techniques and all-glass apparatus. Involatile products were handled in a nitrogen-filled drybag. Dimethylmercury, a commercial sample from Alfa Inorganics Ltd., was distilled *in vacuo* before use. Dimethylzinc was prepared from the reaction of methyl iodide with zinc powder in the presence of copper (5). Its purity was checked from its infrared spectrum and molecular weight (m.w.) (Calcd. for C_2H_6Zn: m.w., 95.3. Found: m.w., 95.0).

Dimethylzinc and Sulfur Dioxide

In a typical experiment, sulfur dioxide (1.0 mmole) was condensed on to $(CH_3)_2Zn$ (1.0 mmole) and the vessel sealed off. A white solid was formed as the contents warmed up. No volatiles were observed on opening up the vessel and the weight of solid produced corresponded exactly to the weight of SO_2 and $(CH_3)_2Zn$ added. The compound proved to be insoluble in all the more familiar solvents (e.g. carbon disulfide, pentane, diethylether, methylene chloride, acetone), but it reacted rapidly with water to form a white precipitate. The compound analyzed approximately for an empirical formula $C_2H_6SO_2Zn$.

Anal. Calcd. for $C_2H_6SO_2Zn$: C, 15.0; H, 3.75; S, 20.6. Found: C, 14.4; H, 4.12; S, 18.7.

The infrared spectrum (Fig. 1) showed absorption at 1300 (m), 1150 (m), 1005 (s), 955 (m), 940 (m), 890 (s), 715 (w), 700 (m), 670 (m), 535 (s), 445 (m), 375 (m), 255 (m) cm^{-1}.

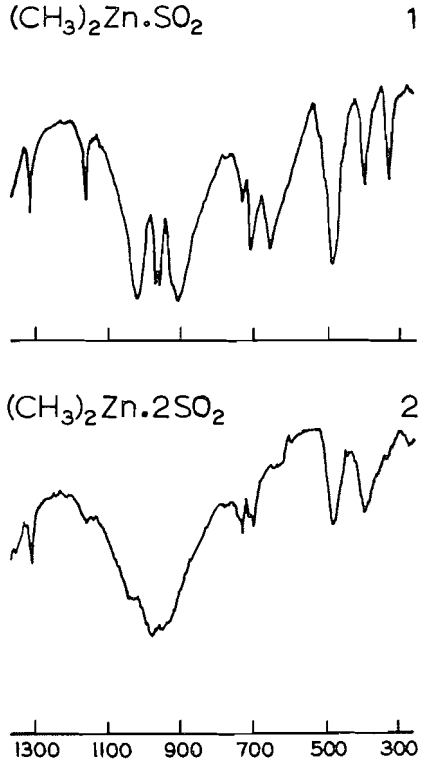

FIG. 1. Spectra of dimethylzinc with sulfur dioxide 1:1 complex.
FIG. 2. Spectra of dimethylzinc with sulfur dioxide 1:2 complex.

The compound proved to be very air sensitive, taking up water rapidly from the atmosphere. A further experiment demonstrated that this product can take up a further mole of sulfur dioxide to give a compound which analyzed for an empirical formula $C_2H_6O_4S_2Zn$.

Can. J. Chem. Downloaded from www.nrcresearchpress.com by 210.87.254.105 on 09/05/12
For personal use only.

Anal. Calcd. for $C_2H_6O_4S_2Zn$: C, 10.7; H, 2.68; S, 27.9. Found: C, 10.5; H, 2.80; S, 27.5. The infrared spectrum (Fig. 2) was as follows: 1295 (m), 1150 (w), 1025 (sh, m), 960 (s), 930 (s), 715 (m), 690 (m), 530 (ms), 440 (ms), 380 (w), 310 (vw) cm^{-1}.

The same compound was also obtained by reacting $(CH_3)_2Zn$ with an excess of sulfur dioxide.

Dimethylmercury and Sulfur Dioxide

In a typical experiment, an excess quantity of sulfur dioxide (~15 mmoles) was allowed to react with dimethylmercury (1 mmole) for 150 h at room temperature. During this time, a white crystalline solid was formed. No noncondensable products (with respect to liquid N_2) were formed. On removing the sulfur dioxide, together with a trace of dimethylmercury, by vacuum distillation, an involatile oil, together with the solid residue, remained in the reaction vessel. The involatile oil, which possessed an obnoxious smell, was soluble in methylene chloride and air sensitive, and its infrared and nuclear magnetic resonance (n.m.r.) spectra suggested the presence of $CH_3—\overset{\overset{O}{\|}}{S}—$ and $CH_3—O—S$ groups. The white crystalline solid which proved to be insoluble in all the common solvents, was air stable and did not begin to decompose until 225 °C. The compound analyzed for an empirical formula $C_2H_6Hg_2O_2S$.

Anal. Calcd. for $C_2H_6Hg_2O_2S$: C, 4.8; H, 1.2; S, 6.46. Found: C, 4.5; H, 1.3; S, 6.48.

The infrared spectrum (Fig. 3) showed absorption at 1250 (s), 1085 (vs), 940 (vs), 800 (m), 715 (w), 670 (m), 590 (s), 578 (m), 547 (m), 525 (w) cm^{-1}. A single, sharp line was observed in the proton n.m.r. spectrum of a dilute solution in dimethylsulfoxide, at τ 9.2. The reaction was also carried out at 65 °C, and was completed in 2 h.

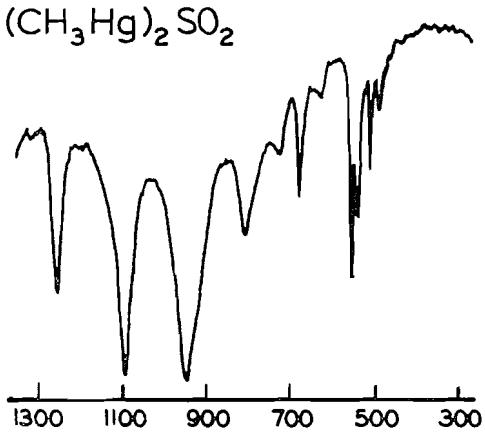

FIG. 3. Spectra of dimethylmercury with sulfur dioxide $CH_3Hg.SO_2$ compound.

On repeating the reaction, using equimolar quantities of dimethylmercury and sulfur dioxide, for 11 days at room temperature, two products were isolated in the ratio of approximately 3:1, accounting for 70% of the dimethylmercury. The product obtained in higher yield possessed an infrared and n.m.r. spectrum identical with the compound shown above to be $(CH_3)_2HgSO_2$, while the other which was obtained by extraction from the reaction mixture with methylene chloride, followed by recrystallization, gave an infrared spectrum of (as a mull in Nujol) 1320 (w), 1290 (w), 1230 (m), 1180 (s), 1115 (m, b), 1030 (m), 980 (m), 950 (m), 800 (m), 765 (m), 710 (m), 565 (s), 545 (s), 505 (s), 470 (sh), 445 (sh), 390 (m), 330 (w). Its n.m.r. spectrum, as a solution in $CHCl_3$, consisted of two peaks of equal intensity at τ values 7.01 and 8.68. The compound melted quite sharply at 148 °C and analyzed for $C_2H_6O_2SHg$.

Anal. Calcd. for $C_2H_6O_2SHg$: C, 8.15; H, 2.04. Found: C, 7.80; H, 2.27.

For this particular compound, no satisfactory sulfur analysis could be obtained to confirm its identity.

Discussion

Coates and Ridley (6) have assigned the band at 670 cm^{-1}, occurring in the infrared spectra of compounds containing the CH_3—Zn group, to the methylzinc rocking mode. It is significant that this band is present in the infrared spectrum of the 1:1 complex (Fig. 1), $(CH_3)_2Zn.SO_2$, whilst it disappears in the infrared spectrum (Fig. 2) of the 1:2 complex, $(CH_3)_2Zn.2SO_2$. By analogy with the infrared spectra of dimethylsulfoxide (7) and dimethylsulfone (8), the bands around 700 cm^{-1} can be assigned to the (S—C) stretching vibrations, and the band at 890 cm^{-1} to the methylsulfur rock. Finally, it is significant that there is no strong band in the region (ca. 1100 cm^{-1}) associated with the S=O stretching vibration (9) for either of the two zinc-containing compounds. Accordingly it is believed that SO_2 reacts with $(CH_3)_2Zn$ in the following manner.

$$CH_3—ZnCH_3 + SO_2 \rightarrow \underset{\mathbf{1}}{CH_3—ZnO.SO.CH_3} \xrightarrow{+SO_2} \underset{\mathbf{2}}{(CH_3.SO.O)_2Zn}$$

Both compounds **1** and **2** must exist in a highly associated state through coordination of the type $>S—O \rightarrow Zn$, by analogy with dimethylsulfoxide (10, 11).

The reaction with dimethylmercury is different. The compound, analyzing for $C_2H_6O_2SHg_2$, which was always obtained in the predominant amount, probably has the structure

$$CH_3—Hg—\overset{\overset{O}{\|}}{\underset{\underset{O}{\|}}{S}}—Hg—CH_3,$$

since both the infrared and n.m.r. spectra of this compound suggest the presence of CH_3—Hg in

Can. J. Chem. Downloaded from www.nrcresearchpress.com by 210.87.254.105 on 09/05/12
For personal use only.

that the band at 800 cm^{-1} can best be assigned to the CH_3—Hg rocking made by analogy with the infrared spectrum of $(CH_3)_2Hg$ (12), while the two sharp bands at 547 and 525 cm^{-1} can be assigned to the Hg—C stretching vibrations (12). Moreover, there are present the strong bands at 1245 and 1085 cm^{-1} that can be assigned to the (S=O) stretching vibrations (8). The lack of solubility and its stability to temperature would suggest a polymeric structure in which association is occurring, either through S → Hg coordination, or through >S=O → Hg, since the band at 940 cm^{-1} is consistent with the latter type of association (9, 10). This would also be consistent with the n.m.r. spectrum, since the methyl groups are equivalent in such a structure, and are bonded to the metal.

The compound analyzing as $C_2H_6O_2SHg$ is interesting. By analogy with Wojcicki's work (1) with diethylmercury and sulfur dioxide one would expect the sulfone to be formed, namely CH_3—Hg.SO_2.CH_3. However, the presence of the strong bands at 980 and 950 cm^{-1} do imply S—O, either as >S=O → or as S—O—, while the bands at 1230 and 1115 cm^{-1} suggest

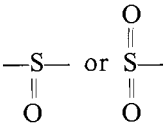

—S— or —S—. The n.m.r. spectrum would not be

inconsistent with either CH_3—Hg—S—O—CH_3

or

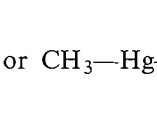

where the low field absorption would be due to either —O—CH_3 or —S—CH_3. However, the considerable difference in chemical shift between CH_3—Hg in the compound $(CH_3Hg)_2SO_2$ and the high field line in the spectrum of this compound would suggest that the sulfur atom is having a markedly different effect on the mercury. So much so that we would favor the structure CH_3—Hg—S—

O—CH_3 as being the most plausible.

Acknowledgments

We are most grateful for the award of a research grant under the NATO Scientific Grant Programme.

1. F. A. Hartman and A. Wojcicki. J. Am. Chem. Soc. **88**, 844 (1966).
2. E. B. Baker and H. H. Sisler. J. Am. Chem. Soc. **75**, 5193 (1953).
3. R. Gelius. Z. Anorg. Allgem. Chem. **349**, 22 (1967).
4. M. F. Lappert and B. Prokai. *In* Advances in organometallic chemistry. Vol. 5. Academic Press Inc., New York. 1967.
5. N. Hota and D. J. Willis. J. Organometal. Chem. Amsterdam, **9**, 169 (1967).
6. G. E. Coates and D. Ridley. J. Chem. Soc. 1870 (1965).
7. W. D. Horrocks and F. A. Cotton. Spectrochim. Acta, **17**, 134 (1961).
8. K. Fujimori. Bull. Chem. Soc. Japan, **32**, 1376 (1959).
9. J. L. Bellamy. *In* Organic sulfur compounds. *Edited by* N. Kharasch. Pergamon Press, London. 1961. pp. 47–57.
10. F. A. Cotton, R. Francis, and W. D. Horrocks. J. Phys. Chem. **64**, 1534 (1960).
11. R. Francis and F. A. Cotton. J. Chem. Soc. 2078 (1961).
12. H. S. Gutowsky. J. Chem. Phys. **17**, 128 (1949).

Signs of long-range proton–fluorine spin–spin coupling constants in 2-amino-5-bromobenzotrifluoride[1]

D. J. BLEARS, S. S. DANYLUK, AND T. SCHAEFER[2]
Division of Biological and Medical Research, Argonne National Laboratory, Argonne, Illinois

Received September 8, 1967

The signs of the spin–spin coupling constants between the fluorine nuclei in the trifluoromethyl group and the ring protons in 2-amino-5-bromobenzotrifluoride are reported. J_o^{H,CF_3} and J_p^{H,CF_3} are negative while J_m^{H,CF_3} is positive. These signs are in agreement with fluorine contact shifts in certain Ni(II) chelates and therefore provide evidence for hyperconjugation of the CF_3 group with the ring. The magnitude of J_m^{H,CF_3} is rather larger than expected on the basis of a relationship between the square of the bond order between the relevant ring carbons and the size of the coupling.

Canadian Journal of Chemistry, **46**, 652 (1968)

Can. J. Chem. Downloaded from www.nrcresearchpress.com by 210.87.254.105 on 09/05/12
For personal use only.

It has been established recently that the signs of the long-range methyl proton – ring proton coupling constants in substituted toluenes, J_o^{H,CH_3}, J_m^{H,CH_3}, and J_p^{H,CH_3} are negative, positive, and negative respectively (1, 2). These couplings are primarily determined by π contributions (3–9), the sign and variation in magnitude of which can be qualitatively interpreted on the basis of a σ–π mechanism involving negative (Q_{C_1H}) and positive ($Q_{C_1C_2H}$) hyperfine interactions (5–9).

More recently it has been shown (10) that in fluorotoluene derivatives J_o^{F,CH_3}, J_m^{F,CH_3}, and J_p^{F,CH_3} have the opposite sign sequence to that found for the corresponding proton–methyl group couplings. In this case the results have been interpreted on the basis of a positive hyperfine interaction Q_{CF}, a consequence of two competing σ–π mechanisms in the C—F bond and involving double bond character of this bond. This interpretation is in qualitative agreement with the observed contact shifts in the fluorine resonance spectra of a variety of Ni(II) chelates (11). In this note we report the signs of J_o^{H,CF_3}, J_m^{H,CF_3}, and J_p^{H,CF_3} in 2-amino-5-bromobenzotrifluoride.

Experimental

The 2-amino-5-bromobenzotrifluoride was obtained from K and K Laboratories while the 4-chloro-3-iodobenzotrifluoride was obtained from the Aldrich Chemical Company. These compounds were dissolved in carbon disulfide containing about 20 vol. % tetramethylsilane (TMS) and the solutions were degassed by the freeze–pump–thaw technique. Proton resonance spectra were measured on an HA-60I spectrometer locked to internal TMS. Double resonance experiments were carried out in the usual way (12).

Results

The 60 Mc/s proton resonance spectrum of 2-amino-5-bromobenzotrifluoride corresponds to a loosely coupled ABC part of an $ABCX_3$ spectrum. The proton–fluorine coupling magnitudes were obtained to an accuracy of 0.1 c/s or better from the ABC region.

A stick diagram showing an idealized first order spectrum for protons 3 and 4 is shown in the upper part of Fig. 1 (see the figure for the structural formula and numbering). For proton 3 the individual peaks of the two quartets are split by a small para coupling to proton 6. The four quartets, each of which arises from the coupling to the three equivalent fluorine nuclei, are indicated for proton 4.

The spin states of the nuclei coupled to protons 3 and 4 are given below the stick diagram with the convention that a positive sign under a low-field peak of the proton denotes a positive coupling to the nucleus in question. The spin states are labelled in accordance with the signs found experimentally. The ring proton couplings are positive (13–16) and since the proton–fluorine couplings are found relative to them, the absolute signs of the latter are determined.

As an illustration of one of the many experiments which were performed, the single resonance spectrum of the two low-field quartets of proton 4 is shown in the lower part of Fig. 1. The same spectrum, repeated while tickling transition 8 of proton 3, is also shown in the

[1]Work supported under the auspices of the U.S. Atomic Energy Commission.

[2]Visiting summer scientist, 1967. Permanent address: Department of Chemistry, University of Manitoba, Winnipeg, Manitoba.

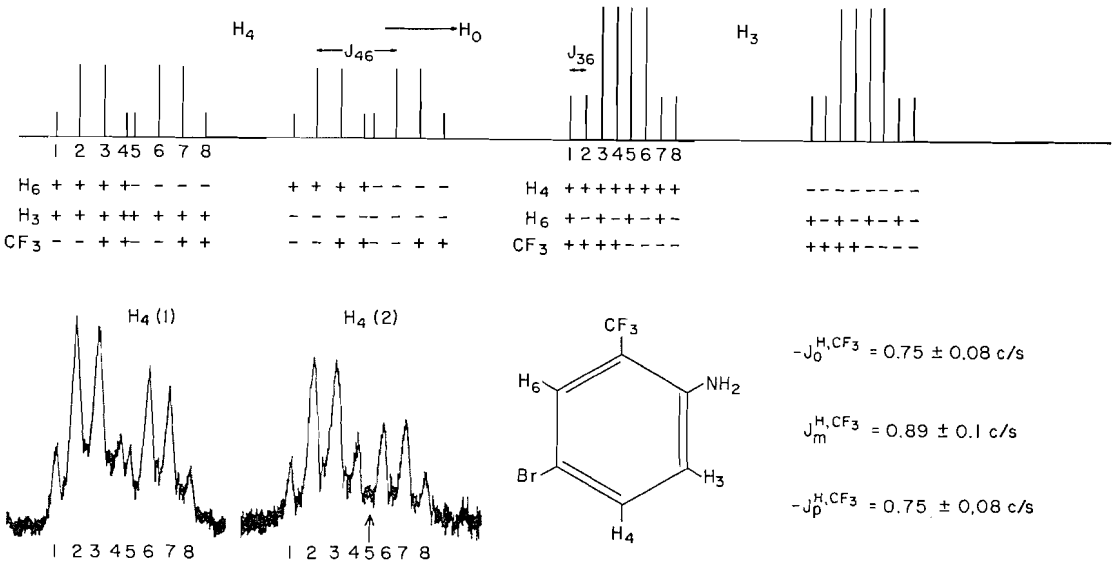

FIG. 1. In the upper part a stick diagram is given of the magnetic resonance spectrum of protons 3 and 4 in 2-amino-5-bromobenzotrifluoride, whose structural formula is also given. The transitions are labelled with the spin states of the coupled nuclei as discussed in the text (see Results). In the lower part is given the single resonance spectrum of the low-field pair of quartets of proton 4. The same spectrum recorded while transition 8 of proton 3 is being tickled is also shown. The arrow indicates that transition 5 of proton 4 is being perturbed. See the text for a full discussion.

adjacent trace. An arrow indicates the transition (peak 5) whose intensity has been affected. It follows therefore that $J_m^{H,CF_3}/J_p^{H,CF_3} < 0$ and $J_p^{HH}/J_m^{HH} > 0$. Other tickling experiments confirmed these results and also gave the signs of $J_{o,m,p}^{H,CF_3}$ relative to J_o^{HH} indicated in the figure.

The proton spectrum of 4-chloro-3-iodobenzotrifluoride in carbon disulfide solution is effectively an AMM′ part of an AMM′X_3 system. The equal chemical shift of the 5 and 6 protons ensures that the observed coupling of these protons to the fluorine nuclei of the trifluoromethyl group is equal to $|J_o^{H,CF_3} + J_m^{H,CF_3}|/2$. The width at half height of the doublet from the 5,6 protons is 0.6 c/s with no discernible fine structure, indicating that the two couplings are of opposite sign and nearly equal in magnitude (the magnitude of the coupling between proton 2 and the fluorine nuclei is 0.7 ± 0.1 c/s). These results confirm the opposite sign of J_o^{H,CF_3} and J_m^{H,CF_3} found in the double resonance experiments on 2-amino-5-bromobenzotrifluoride.

Discussion

J_o^{H,CF_3} and J_p^{H,CF_3} are negative and J_m^{H,CF_3} is positive. The signs of the para and meta couplings are in qualitative agreement with the contact shifts measured for fluorine in the Ni(II) chelates of N,N′-(*p*- and *m*-trifluoromethylphenyl) aminotroponeimines (17). From the observed contact shifts it has been inferred that hyperconjugation of the CF_3 group with the ring is comparable to that of the CH_3 group.[3] Although a spin polarization mechanism (rather than the spin delocalization mechanism) would also account for the determined sign sequence this interpretation would not be in accord with the magnitude of the contact shifts (17).

It is interesting to note that although the magnitude of J_m^{H,CH_3} is usually about half that of $J_{o,p}^{H,CH_3}$ couplings (1, 10), in the present compounds $J_m^{H,CF_3} \approx J_{o,p}^{H,CF_3}$. On the basis of the relationship between these couplings and the square of the bond order between the relevant ring carbon atoms (6), $J_m^{H,CF_3} < J_{o,p}^{H,CF_3}$ is expected. In view of these considerations it is

[3]The observed $Q_{C_1C_2H}$ values associated with the interpretation of the proton–methyl group couplings are usually interpreted in terms of a predominant hyperconjugation mechanism (18). It may be noted that there is only a tenuous connection between the n.m.r. and e.s.r. evidence for hyperconjugation and that adduced from chemical reactivity data (10).

Can. J. Chem. Downloaded from www.nrcresearchpress.com by 210.87.254.105 on 09/05/12
For personal use only.

tempting to ascribe a positive σ contribution to J_m^{H,CF_3} and perhaps to J_o^{H,CF_3} also. A positive σ contribution would not conflict with the Dirac vector model (19), but there are no theoretical estimates of such a contribution. In the case of J_o^{H,CF_3} it may be possible to rely on an analogy to the calculations of Barfield (20) on four-bond proton–proton couplings which indicate either positive or negative contributions depending on the conformation of the coupled fragment. In this connection it may be noted that temperature dependent J_o^{F,CF_3} values in benzotrifluoride derivatives have been explained as arising from barriers of about 1 kcal/mole (21) to the internal rotation of the CF_3 group. Experiments designed to clarify these questions are in progress.

1. G. KOTOWYCZ and T. SCHAEFER. Can. J. Chem. **44**, 2743 (1966).
2. D. GAGNAIRE and TRINH-HUU-ICH. Bull. Chem. Soc. France, 3763 (1966).
3. H. M. MCCONNELL. J. Mol. Spectry. **1**, 11 (1957).
4. H. M. MCCONNELL. J. Chem. Phys. **30**, 126 (1959).
5. J. ACRIVOS. Mol. Phys. **5**, 1 (1962).
6. M. J. S. DEWAR and R. C. FAHEY. J. Am. Chem. Soc. **85**, 2703 (1963).
7. A. D. MCLACHLAN. Mol. Phys. **1**, 233 (1958).
8. A. FORMAN, J. N. MURRELL, and L. E. ORGEL. J. Chem. Phys. **31**, 1129 (1960).
9. R. A. HOFFMAN. Arkiv Kemi, **17**, 1 (1961).
10. D. J. BLEARS, S. S. DANYLUK, and T. SCHAEFER. To be published.
11. D. R. EATON, A. D. JOSEY, W. D. PHILLIPS, and R. E. BENSON. Mol. Phys. **5**, 407 (1962).
12. W. A. ANDERSON and R. FREEMAN. J. Chem. Phys. **37**, 2053 (1962); **39**, 806 (1963).
13. R. FREEMAN. J. Chem. Phys. **43**, 3087 (1965).
14. C. N. BANWELL, A. D. COHEN, N. SHEPPARD, and J. J. TURNER. Proc. Chem. Soc. 266 (1959).
15. J. S. MARTIN and B. P. DAILEY. J. Chem. Phys. **37**, 2593 (1962).
16. A. SAUPE. Z. Naturforsch. **20a**, 572 (1965).
17. D. R. EATON, A. D. JOSEY, and W. A. SHEPPARD. J. Am. Chem. Soc. **85**, 2689 (1963).
18. E. DE BOER and C. MACLEAN. J. Chem. Phys. **44**, 1334 (1966).
19. H. M. MCCONNELL. J. Chem. Phys. **23**, 2454 (1955).
20. M. BARFIELD. J. Chem. Phys. **41**, 3825 (1964).
21. J. JONAS and H. S. GUTOWSKY. J. Chem. Phys. **42**, 140 (1965).

Concerning a relationship between long-range ring proton – methyl proton coupling constants and mobile bond order[1]

D. J. BLEARS, S. S. DANYLUK, AND T. SCHAEFER[2]

Division of Biological and Medical Research, Argonne National Laboratory, Argonne, Illinois

Received September 8, 1967

Long-range proton – methyl proton coupling constants in propene, mesitylene, 9-methylphenanthrene, and acenaphthene appear to be linearly related to the square of the mobile bond order between the carbon atoms bonded to the methyl group and the proton. However, substituent-induced changes in the charge on and hybridization state of the carbon atoms, in excitation parameters and in potential barriers to rotation of the methyl group, may also affect the coupling. Such changes must be considered in the application of a possible linear relationship.

Canadian Journal of Chemistry, **46**, 654 (1968)

The simple molecular orbital theory (1) of the π contribution to the spin–spin coupling of protons in aromatic systems has been extended to long-range ring proton – methyl proton couplings by replacing (2–5) one of the (negative) hyperfine interaction terms Q_{CH} by a (positive) term Q_{CCH} to give eq. [1].

$$[1] \qquad J_\pi \propto Q_{CH}Q_{CCH}\rho_{NN'}^2/\Delta E,$$

where $\rho_{NN'}$ is the mobile bond order between the carbon atoms bonded to the methyl group and the proton, and ΔE is an average excitation energy to low-lying triplet states. Equation [1] predicts that the coupling J_π in a given molecule will be proportional to the square of the mobile bond order, $\rho_{NN'}^2$. A useful test of the validity of this equation (and hence its applicability to long-range couplings) could be achieved by demonstration of such a relationship. Its establishment would additionally permit a convenient estimation of unknown bond orders by measurement of the coupling constant involved. Although tentative suggestions of this relationship have been made (7–9), especially for J_0^{H,CH_3}, no conclusive scheme has been determined. In this

[1]Work supported under the auspices of the U.S. Atomic Energy Commission.

[2]Visiting summer scientist, 1967. Permanent address: Department of Chemistry, University of Manitoba, Winnipeg, Manitoba.

Can. J. Chem. Downloaded from www.nrcresearchpress.com by 210.87.254.105 on 09/05/12
For personal use only.

tempting to ascribe a positive σ contribution to J_m^{H,CF_3} and perhaps to J_o^{H,CF_3} also. A positive σ contribution would not conflict with the Dirac vector model (19), but there are no theoretical estimates of such a contribution. In the case of J_o^{H,CF_3} it may be possible to rely on an analogy to the calculations of Barfield (20) on four-bond proton–proton couplings which indicate either positive or negative contributions depending on the conformation of the coupled fragment. In this connection it may be noted that temperature dependent J_o^{F,CF_3} values in benzotrifluoride derivatives have been explained as arising from barriers of about 1 kcal/mole (21) to the internal rotation of the CF_3 group. Experiments designed to clarify these questions are in progress.

1. G. KOTOWYCZ and T. SCHAEFER. Can. J. Chem. **44**, 2743 (1966).
2. D. GAGNAIRE and TRINH-HUU-ICH. Bull. Chem. Soc. France, 3763 (1966).
3. H. M. MCCONNELL. J. Mol. Spectry. **1**, 11 (1957).
4. H. M. MCCONNELL. J. Chem. Phys. **30**, 126 (1959).
5. J. ACRIVOS. Mol. Phys. **5**, 1 (1962).
6. M. J. S. DEWAR and R. C. FAHEY. J. Am. Chem. Soc. **85**, 2703 (1963).
7. A. D. MCLACHLAN. Mol. Phys. **1**, 233 (1958).
8. A. FORMAN, J. N. MURRELL, and L. E. ORGEL. J. Chem. Phys. **31**, 1129 (1960).
9. R. A. HOFFMAN. Arkiv Kemi, **17**, 1 (1961).
10. D. J. BLEARS, S. S. DANYLUK, and T. SCHAEFER. To be published.
11. D. R. EATON, A. D. JOSEY, W. D. PHILLIPS, and R. E. BENSON. Mol. Phys. **5**, 407 (1962).
12. W. A. ANDERSON and R. FREEMAN. J. Chem. Phys. **37**, 2053 (1962); **39**, 806 (1963).
13. R. FREEMAN. J. Chem. Phys. **43**, 3087 (1965).
14. C. N. BANWELL, A. D. COHEN, N. SHEPPARD, and J. J. TURNER. Proc. Chem. Soc. 266 (1959).
15. J. S. MARTIN and B. P. DAILEY. J. Chem. Phys. **37**, 2593 (1962).
16. A. SAUPE. Z. Naturforsch. **20a**, 572 (1965).
17. D. R. EATON, A. D. JOSEY, and W. A. SHEPPARD. J. Am. Chem. Soc. **85**, 2689 (1963).
18. E. DE BOER and C. MACLEAN. J. Chem. Phys. **44**, 1334 (1966).
19. H. M. MCCONNELL. J. Chem. Phys. **23**, 2454 (1955).
20. M. BARFIELD. J. Chem. Phys. **41**, 3825 (1964).
21. J. JONAS and H. S. GUTOWSKY. J. Chem. Phys. **42**, 140 (1965).

Concerning a relationship between long-range ring proton – methyl proton coupling constants and mobile bond order[1]

D. J. BLEARS, S. S. DANYLUK, AND T. SCHAEFER[2]
Division of Biological and Medical Research, Argonne National Laboratory, Argonne, Illinois

Received September 8, 1967

Long-range proton – methyl proton coupling constants in propene, mesitylene, 9-methylphenanthrene, and acenaphthene appear to be linearly related to the square of the mobile bond order between the carbon atoms bonded to the methyl group and the proton. However, substituent-induced changes in the charge on and hybridization state of the carbon atoms, in excitation parameters and in potential barriers to rotation of the methyl group, may also affect the coupling. Such changes must be considered in the application of a possible linear relationship.

Canadian Journal of Chemistry, **46**, 654 (1968)

The simple molecular orbital theory (1) of the π contribution to the spin–spin coupling of protons in aromatic systems has been extended to long-range ring proton – methyl proton couplings by replacing (2–5) one of the (negative) hyperfine interaction terms Q_{CH} by a (positive) term Q_{CCH} to give eq. [1].

$$[1] \qquad J_\pi \propto Q_{CH}Q_{CCH}\rho_{NN'}{}^2/\Delta E,$$

where $\rho_{NN'}$ is the mobile bond order between the carbon atoms bonded to the methyl group and the proton, and ΔE is an average excitation energy to low-lying triplet states. Equation [1] predicts that the coupling J_π in a given molecule will be proportional to the square of the mobile bond order, $\rho_{NN'}{}^2$. A useful test of the validity of this equation (and hence its applicability to long-range couplings) could be achieved by demonstration of such a relationship. Its establishment would additionally permit a convenient estimation of unknown bond orders by measurement of the coupling constant involved. Although tentative suggestions of this relationship have been made (7–9), especially for J_0^{H,CH_3}, no conclusive scheme has been determined. In this

[1]Work supported under the auspices of the U.S. Atomic Energy Commission.
[2]Visiting summer scientist, 1967. Permanent address: Department of Chemistry, University of Manitoba, Winnipeg, Manitoba.

Can. J. Chem. Downloaded from www.nrcresearchpress.com by 210.87.254.5 on 09/05/12
For personal use only.

TABLE I

Long-range ring proton – methyl proton coupling constants[1] and mobile bond orders in some hydrocarbons

	Molecule	$\rho_{NN'}$	$\rho_{NN'}{}^2$	J^{H,CH_3}	Type	Reference
1.	Propene	1.00	1.00	-1.75 ± 0.1	*Cis*	10
2.	Mesitylene	0.667	0.444	-0.87 ± 0.1	Ortho	6
3.	9-Methyl phenanthrene	0.760	0.578	-1.1 ± 0.1	Ortho	9
4.	Acenaphthene[2]	0.725	0.526	-0.9 ± 0.1	Ortho	5
		0.362	0.131	-0.3 ± 0.1	Para	

[1]Only in propene is the sign of J^{H,CH_3} actually known (10), but in view of the work of Kotowycz and Schaefer (25) it can be assumed that the signs are all negative.
[2]The measured coupling constants are multiplied by 25/41 to convert to values appropriate to a freely rotating methyl group (5).

note we review the available evidence and point out the dangers of an uncritical application of the persuant ideas.

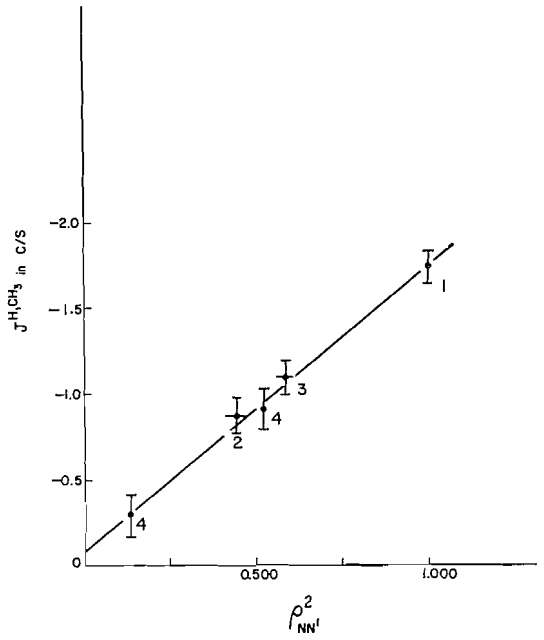

FIG. 1. The long-range couplings, J^{H,CH_3}, in the molecules of Table I are plotted versus the squares of the mobile bond orders between the relevant carbon atoms. See the text for a full discussion.

Hydrocarbons for which both bond orders and coupling constants are known with any precision are propene (10), acenaphthene (5), mesitylene (6), and 9-methylphenanthrene (9). In Table I the bond orders and J^{H,CH_3} values are given and in Fig. 1 the coupling constants are plotted against $\rho_{NN'}{}^2$. A straight line is drawn through the point for propene and through $J = -0.1$ c/s at $\rho_{NN'} = 0$, establishing in these hydrocarbons a relationship between coupling constant and bond order. The line can be represented by J (c/s) $= -0.1-1.6\rho_{NN'}{}^2$. In view of the possible errors in the two quantities a line through $J = 0$ c/s at $\rho_{NN'} = 0$ may be just as reasonable.

Although a straight line plot of J^{H,CH_3} versus $\rho_{NN'}{}^2$ is obtained, prediction of bond orders from J values by direct interpolation of Fig. 1 is subject to a number of difficulties. Q_{CH} is dependent upon both the charge on the carbon atom (11, 12) and its hybridization state (13). Substituents are known to affect the former (14) and measurements of $J(^{13}C—H)$ indicate the latter changes on substitution also (15). Consequently a substituent-induced change in Q_{CH} is likely. A change in Q_{CH} on substitution of up to 10% can be estimated from the known charge densities (14) and $J(^{13}C—H)$ values (15) in representative compounds. Similar considerations also apply to Q_{CCH}.[3] Additionally Q_{CCH} is a function of the angle between the C—C—H plane and the pπ orbitals of the aromatic ring (17). In toluene and some of its para derivatives (18–20) the rotation of the methyl group is essentially free. In ortho-substituted toluenes the threefold potential barrier is no longer zero (21) and may approach 1 to 2 kcal/mole, as observed in propene and its derivatives (22–24). A temperature dependence of J_π in ortho-substituted toluenes is therefore a possibility and would have to be considered in any application of eq. [1]. Finally, in view of the effect of substituents on electronic spectra, ΔE variations are also to be anticipated.

Experimentally, $J_0{}^{H,CH_3}$ in substituted toluenes ranges from -0.60 to 0.87 c/s (25–31), a range which could adequately be attributed to a 20% variation in $\rho_{NN'}{}^2$. Thus, on the basis of the preceding remarks, it is apparent that variations in coupling constants can be related to variations

[3]See refs. 12, 16, 17 for recent discussions of these points.

Can. J. Chem. Downloaded from www.nrcresearchpress.com by 210.87.254.5 on 09/05/12
For personal use only.

in bond order, provided consideration of the concomitant substituent-induced changes in the other parameters of eq. [1] is included.

1. H. M. McConnell. J. Mol. Spectry. **1**, 11 (1957).
2. R. A. Hoffman. Arkiv Kemi, **17**, 1 (1961).
3. A. D. McLachlan. Mol. Phys. **1**, 233 (1958).
4. A. Forman, J. N. Murrell, and L. E. Orgel. J. Chem. Phys. **31**, 1129 (1960).
5. M. J. S. Dewar and R. C. Fahey. J. Am. Chem. Soc. **85**, 2704 (1963).
6. J. V. Acrivos. Mol. Phys. **5**, 1 (1962).
7. S. Sternhell. Rev. Pure Appl. Chem. **14**, 15 (1964).
8. P. M. Nair and G. Gopakumar. Tetrahedron Letters, 708 (1964).
9. K. D. Bartle and J. A. S. Smith. Spectrochim. Acta, **23A**, 1689 (1967).
10. A. A. Bothner-By and C. Naar-Colin. J. Am. Chem. Soc. **83**, 231 (1961).
11. J. P. Colpa and J. S. Bolton. Mol. Phys. **6**, 273 (1963).
12. M. E. Carter and G. Vincow. J. Chem. Phys. **47**, 292 (1967).
13. M. Karplus and G. K. Fraenkel. J. Chem. Phys. **35**, 1312 (1961).
14. T. K. Wu and B. P. Dailey. J. Chem. Phys. **41**, 2796 (1964).
15. H. M. Hutton, W. F. Reynolds, and T. Schaefer. Can. J. Chem. **40**, 1758 (1962).
16. M. E. Carter and G. Vincow. J. Chem. Phys. **47**, 302 (1967).
17. T. M. McKinney and T. H. Geske. J. Am. Chem. Soc. **89**, 2806 (1967).
18. H. C. Rudolph, H. Dreizler, A. Jaeschke, and P. Wendling. Z. Naturforsch. **22a**, 940 (1967).
19. H. D. Rudolph and H. Seiler. Z. Naturforsch. **20a**, 1682 (1965).
20. G. E. Herberich. Z. Naturforsch. **22a**, 761 (1967).
21. J. Jonás and H. S. Gutowsky. J. Chem. Phys. **42**, 140 (1965).
22. D. R. Lide and D. E. Mann. J. Chem. Phys. **27**, 868 (1957).
23. L. Pierce and J. M. O'Reilly. J. Mol. Spectry. **3**, 356 (1959).
24. M. L. Unland, V. Weiss, and W. H. Flygare. J. Chem. Phys. **42**, 2138 (1965).
25. G. Kotowycz and T. Schaefer. Can. J. Chem. **44**, 2743 (1966).
26. W. G. Ripka and D. E. Applequist. J. Am. Chem. Soc. **89**, 4035 (1967).
27. D. Gagnaire and Trinh-Huu-Ich. Bull. Chem. Soc. France, 3763 (1966).
28. D. T. Witiak, D. D. Patel, and Y. Lin. J. Am. Chem. Soc. **89**, 1908 (1967).
29. H. Rottendorf and S. Sternhell. Australian J. Chem. **17**, 1315 (1964).
30. R. Freeman. Mol. Phys. **6**, 535 (1963).
31. G. Kotowycz. Private communication.

Line-width effects in the electron spin resonance spectra of ion-pairs of 2,3- and 2,5-dimethyl-*p*-benzosemiquinones

P. S. Gill and T. E. Gough

Department of Chemistry, University of Waterloo, Waterloo, Ontario

Received October 6, 1967

Electron spin resonance spectra of ion-pairs of 2,3- and 2,5-dimethyl-*p*-benzosemiquinone are reported. Numerical relationships between the various splitting constants suggest the equality of Q_{C-Me} and Q_{C-H}. Unexpected sharp lines in the spectra recorded under conditions of line-width alternation are interpreted in terms of these numerical relationships.

Canadian Journal of Chemistry, **46**, 656 (1968)

Intramolecular migration of alkali metal cations within ion-pairs of *p*-benzosemiquinone (1, 2) and durosemiquinone (3, 4) has been shown to give rise to an alternating line-width effect in a manner analogous to that observed for the pyracene radical anion dissolved in tetrahydrofuran (5). Similar effects should be observable for the ion-pairs of 2,3- and 2,5-dimethyl-*p*-benzosemiquinone, since the two sub-spectra arising from interaction of the unpaired electron with the two methyl or the two C—H groups should each exhibit line-width alternation. Because sharp lines in the complete spectrum can only arise from combination of the sharp components of the sub-spectra, at suitable rates of exchange, the combined spectrum should be a doublet of quartets, the intensity distribution within each quartet being 1:9:9:1. The observed splittings will be twice the appropriate time-averaged splittings, obtainable from the fast exchange spectrum, or alternatively the sums of the appropriate splittings obtained from the slow exchange spectrum.

The electron spin resonance spectrum of 2,3-dimethyl-*p*-benzosemiquinone associated with potassium ions in 1,2-dimethoxyethane is reproduced in Fig. 1. The temperature, −14 °C, has been chosen to give the maximum amount of

Can. J. Chem. Downloaded from www.nrcresearchpress.com by 210.87.254.5 on 09/05/12
For personal use only.

in bond order, provided consideration of the concomitant substituent-induced changes in the other parameters of eq. [1] is included.

1. H. M. McConnell. J. Mol. Spectry. **1**, 11 (1957).
2. R. A. Hoffman. Arkiv Kemi, **17**, 1 (1961).
3. A. D. McLachlan. Mol. Phys. **1**, 233 (1958).
4. A. Forman, J. N. Murrell, and L. E. Orgel. J. Chem. Phys. **31**, 1129 (1960).
5. M. J. S. Dewar and R. C. Fahey. J. Am. Chem. Soc. **85**, 2704 (1963).
6. J. V. Acrivos. Mol. Phys. **5**, 1 (1962).
7. S. Sternhell. Rev. Pure Appl. Chem. **14**, 15 (1964).
8. P. M. Nair and G. Gopakumar. Tetrahedron Letters, 708 (1964).
9. K. D. Bartle and J. A. S. Smith. Spectrochim. Acta, **23A**, 1689 (1967).
10. A. A. Bothner-By and C. Naar-Colin. J. Am. Chem. Soc. **83**, 231 (1961).
11. J. P. Colpa and J. S. Bolton. Mol. Phys. **6**, 273 (1963).
12. M. E. Carter and G. Vincow. J. Chem. Phys. **47**, 292 (1967).
13. M. Karplus and G. K. Fraenkel. J. Chem. Phys. **35**, 1312 (1961).
14. T. K. Wu and B. P. Dailey. J. Chem. Phys. **41**, 2796 (1964).
15. H. M. Hutton, W. F. Reynolds, and T. Schaefer. Can. J. Chem. **40**, 1758 (1962).
16. M. E. Carter and G. Vincow. J. Chem. Phys. **47**, 302 (1967).
17. T. M. McKinney and T. H. Geske. J. Am. Chem. Soc. **89**, 2806 (1967).
18. H. C. Rudolph, H. Dreizler, A. Jaeschke, and P. Wendling. Z. Naturforsch. **22a**, 940 (1967).
19. H. D. Rudolph and H. Seiler. Z. Naturforsch. **20a**, 1682 (1965).
20. G. E. Herberich. Z. Naturforsch. **22a**, 761 (1967).
21. J. Jonás and H. S. Gutowsky. J. Chem. Phys. **42**, 140 (1965).
22. D. R. Lide and D. E. Mann. J. Chem. Phys. **27**, 868 (1957).
23. L. Pierce and J. M. O'Reilly. J. Mol. Spectry. **3**, 356 (1959).
24. M. L. Unland, V. Weiss, and W. H. Flygare. J. Chem. Phys. **42**, 2138 (1965).
25. G. Kotowycz and T. Schaefer. Can. J. Chem. **44**, 2743 (1966).
26. W. G. Ripka and D. E. Applequist. J. Am. Chem. Soc. **89**, 4035 (1967).
27. D. Gagnaire and Trinh-Huu-Ich. Bull. Chem. Soc. France, 3763 (1966).
28. D. T. Witiak, D. D. Patel, and Y. Lin. J. Am. Chem. Soc. **89**, 1908 (1967).
29. H. Rottendorf and S. Sternhell. Australian J. Chem. **17**, 1315 (1964).
30. R. Freeman. Mol. Phys. **6**, 535 (1963).
31. G. Kotowycz. Private communication.

Line-width effects in the electron spin resonance spectra of ion-pairs of 2,3- and 2,5-dimethyl-*p*-benzosemiquinones

P. S. Gill and T. E. Gough

Department of Chemistry, University of Waterloo, Waterloo, Ontario

Received October 6, 1967

Electron spin resonance spectra of ion-pairs of 2,3- and 2,5-dimethyl-*p*-benzosemiquinone are reported. Numerical relationships between the various splitting constants suggest the equality of Q_{C-Me} and Q_{C-H}. Unexpected sharp lines in the spectra recorded under conditions of line-width alternation are interpreted in terms of these numerical relationships.

Canadian Journal of Chemistry, **46**, 656 (1968)

Intramolecular migration of alkali metal cations within ion-pairs of *p*-benzosemiquinone (1, 2) and durosemiquinone (3, 4) has been shown to give rise to an alternating line-width effect in a manner analogous to that observed for the pyracene radical anion dissolved in tetrahydrofuran (5). Similar effects should be observable for the ion-pairs of 2,3- and 2,5-dimethyl-*p*-benzosemiquinone, since the two sub-spectra arising from interaction of the unpaired electron with the two methyl or the two C—H groups should each exhibit line-width alternation. Because sharp lines in the complete spectrum can only arise from combination of the sharp components of the sub-spectra, at suitable rates of exchange, the combined spectrum should be a doublet of quartets, the intensity distribution within each quartet being 1:9:9:1. The observed splittings will be twice the appropriate time-averaged splittings, obtainable from the fast exchange spectrum, or alternatively the sums of the appropriate splittings obtained from the slow exchange spectrum.

The electron spin resonance spectrum of 2,3-dimethyl-*p*-benzosemiquinone associated with potassium ions in 1,2-dimethoxyethane is reproduced in Fig. 1. The temperature, −14 °C, has been chosen to give the maximum amount of

Can. J. Chem. Downloaded from www.nrcresearchpress.com by 210.87.254.5 on 09/05/12
For personal use only.

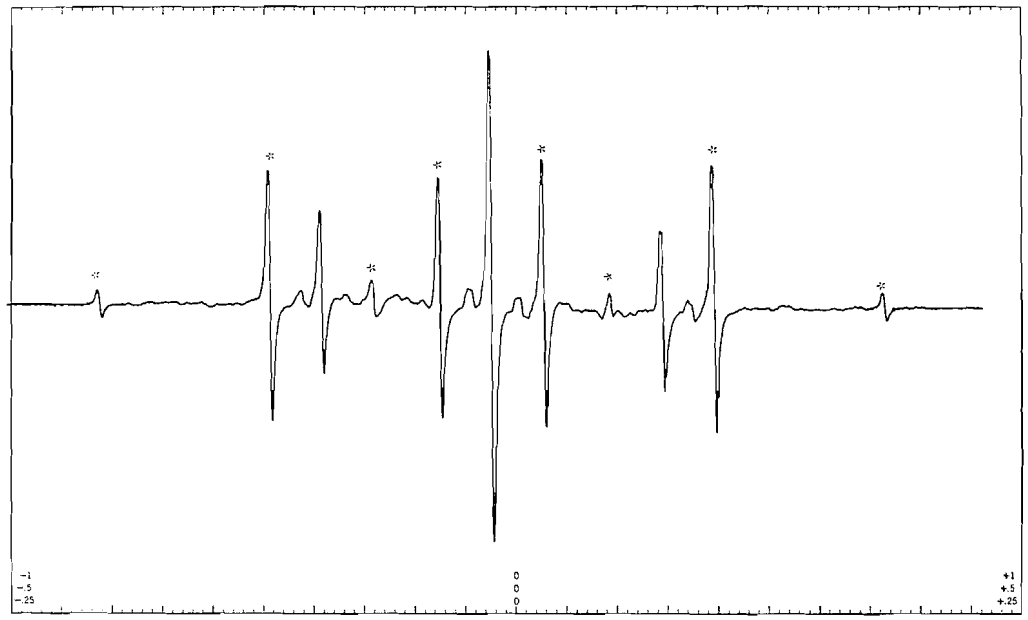

FIG. 1. The electron spin resonance spectrum of the ion-pair potassium – 2,3-dimethyl-*p*-benzosemiquinone dissolved in 1,2-dimethoxyethane at −14 °C.

line-width alternation, and the eight lines described above are indicated by asterisks. Weak lines due to the free ion are also present; these are readily distinguishable because of a difference in g value between the ion-pair and free ion. The apparent C—H and methyl splitting constants were found to be 5.42 and 3.38 G respectively; these values should be compared with the fast-exchange values of 2.74 and 1.71 G and with the slow-exchange values reported in Table I. The fast-exchange values are very close to those reported for the unassociated anion (6). In addition to the eight expected lines, three further sharp lines were observed; these lines occur at the center of the spectrum, and at distances from the center of plus or minus twice the time-averaged methyl splitting constant.

Since the spacing between these lines does not involve the C—H splitting constants, it may be concluded that the radicals giving rise to these lines have combined C—H spin quantum numbers of zero. Furthermore, for the outer two of the three extra lines, a combined methyl quantum number of 2 can only arise by combination of spin quantum numbers of $+1/2$ and $+3/2$ or of $-1/2$ and $-3/2$.

Table II lists all those spin states for 2,3-dimethyl-*p*-benzosemiquinone which are characterized by combined spin quantum numbers for the methyl groups of $+2$ and for the C—H groups of zero. If the slow-exchange methyl and C—H hyperfine splitting constants are denoted by x, $x + a$ and y, $y + b$ respectively, the position of the line generated by each spin state may be found by suitable combination of the appropriate quantum numbers and splitting constants. The results in Table II under the column heading "Line position I" were obtained by assigning the splitting constants x and y to sites 2 and 6; the results under the column heading "Line position II" were obtained by assigning these constants to sites 3 and 5. This procedure involves no loss of generality, since the signs of a and b have not been specified. These two columns, therefore, simulate the ion-pair locked into each of the two configurations between which exchange can occur under suitable conditions. The exact nature of the configurations remains in doubt, though it is convenient to regard them as association of the cation with either of the two oxygen atoms.

When the exchange process occurs, the line position will be modulated by an amount equal to the difference between the columns "Line position I" and "Line position II". For a sharp line to be observed this modulation should equal

Can. J. Chem. Downloaded from www.nrcresearchpress.com by 210.87.254.5 on 09/05/12
For personal use only.

TABLE I

Hyperfine splitting constants, in gauss, of semiquinone ion-pairs dissolved in 1,2-dimethoxyethane at −85 °C. Splitting constants are accurate to ±0.02

Anion	Cation	A_{Me}		A_H			
		x*	$x+a$	y	$y+b$	a	b
2,3-Dimethyl-*p*-benzosemiquinone	K^+	1.22	2.20	2.25	3.23	0.98	0.98
2,5-Dimethyl-*p*-benzosemiquinone	Na^+	1.54	2.74	1.40	2.60	1.20	1.20
2,5-Dimethyl-*p*-benzosemiquinone	K^+	1.65	2.63	1.55	2.52	0.98	0.97

*x, y, a, b are defined in the text.

TABLE II

Spin states of 2,3-dimethyl-*p*-benzosemiquinone which may give rise to a sharp line at a distance from the center of $+2\langle A_{Me}\rangle$*

Spin state			Line position I	Line position II	Modulation	Conditions for sharp line
2-Me	3-Me	5-H—6-H				
ααβ, αβα, βαα	ααα	β α	$2x+\frac{1}{2}(3a-b)$	$2x+\frac{1}{2}(a+b)$	$\lvert a-b\rvert$	$a=b$
ααα	ααβ, αβα, βαα	α β	$2x+\frac{1}{2}(a+b)$	$2x+\frac{1}{2}(3a-b)$	$\lvert a-b\rvert$	$a=b$
ααβ, αβα, βαα	ααα	α β	$2x+\frac{1}{2}(3a+b)$	$2x+\frac{1}{2}(a-b)$	$\lvert a+b\rvert$	$a=-b$
ααα	ααβ, αβα, βαα	β α	$2x+\frac{1}{2}(a-b)$	$2x+\frac{1}{2}(3a+b)$	$\lvert a+b\rvert$	$a=-b$

*x, a, b are defined in the text.

zero, and hence it may be concluded that for the system under consideration $a=\pm b$. Valence bond (7) and molecular orbital (8) calculations indicate that $a=+b$ is the physically significant result indicating that the anion experiences an end to end rather than a diagonal perturbation. Therefore, if $a=b$, a sharp line of intensity 6 (the number of suitable spin states) should occur at a position $2(x+\frac{1}{2}a)$ i.e. at a distance from the center of twice the time-averaged methyl splitting constant. There will, likewise, be a line of intensity 6 at $-2(x+\frac{1}{2}a)$. If it is accepted that $a=b$, the spin states giving rise to a sharp line at the center of the spectrum may be enumerated: these states will have combined quantum numbers for both the methyl and C—H groups of zero. Rather than reproduce a table similar to Table II, we simply state that 18 spin states meet our requirements. Experimentally the measured intensities and positions of the three lines are in excellent agreement with these expectations.

These three further sharp lines have also been observed in the spectra of 2,5-dimethyl-*p*-benzosemiquinone associated with sodium or with potassium ions, and similar reasoning predicts that $a=b$ for both of these systems. In Table I are listed the results of the analyses of the slow-exchange spectra, recorded at −85 °C, of the three systems; the criterion $a=b$ is met surprisingly well. The sodium ion-pair of 2,3-dimethyl-*p*-benzosemiquinone could not be obtained in detectable concentrations, while the caesium ion-pair, although it exhibited the extra sharp lines, could never be "frozen" into one configuration.

The correlation between a and b is unexpected, especially since the Q values of the C—Me and C—H fragments are generally accepted as being different. Since all the perturbations are rather similar, it is possible that a coincidental relationship exists between the various spin densities and Q values. Alternatively, the equality of a and b may indicate that the Q values of the C—Me and C—H fragments are equal for these com-

Can. J. Chem. Downloaded from www.nrcresearchpress.com by 210.87.254.5 on 09/05/12
For personal use only.

pounds. We are at present looking for further examples of this effect before attempting to distinguish between these alternatives.

Since submission of this note, equality of Q_{C-Me} and Q_{C-H} has been postulated to interpret the electron spin resonance spectrum of monoprotonated 2,6-dimethyl-*p*-benzosemiquinone (9).

Acknowledgments

This work received financial support from the National Research Council of Canada and the Ontario Department of University Affairs.

1. E. A. C. LUCKEN. J. Chem. Soc. 4234 (1964).
2. E. WARHURST. Private communication.
3. T. E. GOUGH and M. C. R. SYMONS. Trans. Faraday Soc. **62**, 269 (1966).
4. P. S. GILL and T. E. GOUGH. Can. J. Chem. **45**, 2112 (1967).
5. E. DEBOER and E. L. MACKOR. J. Am. Chem. Soc. **86**, 1513 (1964).
6. B. VENKATARAMAN, B. G. SEGAL, and G. K. FRAENKEL. J. Chem. Phys. **30**, 1006 (1959).
7. T. A. CLAXTON, T. E. GOUGH, and M. C. R. SYMONS. Trans. Faraday Soc. **62**, 279 (1966).
8. P. S. GILL. Unpublished results.
9. T. A. CLAXTON, J. OAKES, and M. C. R. SYMONS. Trans. Faraday Soc. **63**, 2125 (1967).

Phenolysis of 1-menthyl borate

J.-M. LALANCETTE AND Y. BEAUREGARD

Département de Chimie, Faculté des Sciences, Université de Sherbrooke, Sherbrooke, Québec

Received August 9, 1967

The phenolysis of 1-menthyl borate has been made by a variety of phenols, the kinetics of the reaction being followed by polarimetry. The behavior of the system can be related to the acidity of the phenol. With phenols of $pK_a < 10.0$, the course of the reaction indicates a phenolysis proceeding normally towards an equilibrium. With phenols of $pK_a > 10.0$, the rotatory power of the reaction mixture increases and in the case of phenols of $pK_a \cong 10.0$, an intermediate type of curves is obtained. Hydrolysis and solvent effects are reported.

Canadian Journal of Chemistry, **46**, 659 (1968)

The facile hydrolysis of alkyl and aryl orthoborates has been noted by the first authors who reported the preparation of these esters (1). Subsequent observations of the hydrolysis are numerous but the first attempt to a quantitative treatment of the reaction has been made by Scattergood *et al.* (2), who report the time of apparation of boric acid when a borate is treated by a small amount of water. This work indicates that the speed of hydrolysis is a function of the steric hindrance of the substituents on the orthoester. If the steric hindrance of the substituents becomes important (such as with the 2,6-di-*t*-butylphenyl group) the speed of hydrolysis becomes almost negligible (3). More recently, Steinberg (4) has extended the evaluation of the role of steric factors and his work confirms the early report of Scattergood. If steric influences are well understood, the appreciation of electronic factors in the course of the hydrolysis remains speculative because of lack of experimental backing.

The initial object of the present study was to evaluate the role of electronic factors in the course of hydrolysis. The necessity of having a constant steric environment around the boron atom and a speed of hydrolysis not too fast led us to consider unsymmetric borates as substrate for the reaction. Contrary to the literature (5, 6), it has been impossible to obtain pure unsymmetric borates, without disproportionation.

An alternate approach was then used in order to appreciate the role of electronic factors. A symmetrical, sterically hindered borate was used as substrate and the variations of electronic densities were made on the attacking species instead of the substrate. 1-Menthyl borate (**1**) was used, and the attacking reagents were phenols bearing appropriate substituents in meta or para positions.

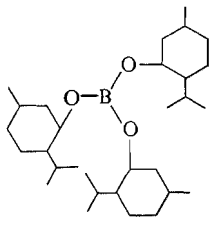

1

Can. J. Chem. Downloaded from www.nrcresearchpress.com by 210.87.254.5 on 09/05/12
For personal use only.

pounds. We are at present looking for further examples of this effect before attempting to distinguish between these alternatives.

Since submission of this note, equality of Q_{C-Me} and Q_{C-H} has been postulated to interpret the electron spin resonance spectrum of monoprotonated 2,6-dimethyl-*p*-benzosemiquinone (9).

Acknowledgments

This work received financial support from the National Research Council of Canada and the Ontario Department of University Affairs.

1. E. A. C. LUCKEN. J. Chem. Soc. 4234 (1964).
2. E. WARHURST. Private communication.
3. T. E. GOUGH and M. C. R. SYMONS. Trans. Faraday Soc. **62**, 269 (1966).
4. P. S. GILL and T. E. GOUGH. Can. J. Chem. **45**, 2112 (1967).
5. E. DEBOER and E. L. MACKOR. J. Am. Chem. Soc. **86**, 1513 (1964).
6. B. VENKATARAMAN, B. G. SEGAL, and G. K. FRAENKEL. J. Chem. Phys. **30**, 1006 (1959).
7. T. A. CLAXTON, T. E. GOUGH, and M. C. R. SYMONS. Trans. Faraday Soc. **62**, 279 (1966).
8. P. S. GILL. Unpublished results.
9. T. A. CLAXTON, J. OAKES, and M. C. R. SYMONS. Trans. Faraday Soc. **63**, 2125 (1967).

Phenolysis of 1-menthyl borate

J.-M. LALANCETTE AND Y. BEAUREGARD

Département de Chimie, Faculté des Sciences, Université de Sherbrooke, Sherbrooke, Québec

Received August 9, 1967

The phenolysis of 1-menthyl borate has been made by a variety of phenols, the kinetics of the reaction being followed by polarimetry. The behavior of the system can be related to the acidity of the phenol. With phenols of $pK_a < 10.0$, the course of the reaction indicates a phenolysis proceeding normally towards an equilibrium. With phenols of $pK_a > 10.0$, the rotatory power of the reaction mixture increases and in the case of phenols of $pK_a \cong 10.0$, an intermediate type of curves is obtained. Hydrolysis and solvent effects are reported.

Canadian Journal of Chemistry, **46**, 659 (1968)

The facile hydrolysis of alkyl and aryl orthoborates has been noted by the first authors who reported the preparation of these esters (1). Subsequent observations of the hydrolysis are numerous but the first attempt to a quantitative treatment of the reaction has been made by Scattergood *et al.* (2), who report the time of apparation of boric acid when a borate is treated by a small amount of water. This work indicates that the speed of hydrolysis is a function of the steric hindrance of the substituents on the orthoester. If the steric hindrance of the substituents becomes important (such as with the 2,6-di-*t*-butylphenyl group) the speed of hydrolysis becomes almost negligible (3). More recently, Steinberg (4) has extended the evaluation of the role of steric factors and his work confirms the early report of Scattergood. If steric influences are well understood, the appreciation of electronic factors in the course of the hydrolysis remains speculative because of lack of experimental backing.

The initial object of the present study was to evaluate the role of electronic factors in the course of hydrolysis. The necessity of having a constant steric environment around the boron atom and a speed of hydrolysis not too fast led us to consider unsymmetric borates as substrate for the reaction. Contrary to the literature (5, 6), it has been impossible to obtain pure unsymmetric borates, without disproportionation.

An alternate approach was then used in order to appreciate the role of electronic factors. A symmetrical, sterically hindered borate was used as substrate and the variations of electronic densities were made on the attacking species instead of the substrate. 1-Menthyl borate (**1**) was used, and the attacking reagents were phenols bearing appropriate substituents in meta or para positions.

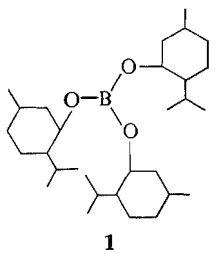

1

Can. J. Chem. Downloaded from www.nrcresearchpress.com by 210.87.254.42 on 09/05/12
For personal use only.

TABLE I

Variation of optical activity of a solution of 1-menthol in CCl_4 in presence of various concentrations of phenol. Concentration of phenol expressed as weight per volume of solution: g/100 ml

C_6H_5OH	0%	5%	10%	15%	20%
$[\alpha]_D^{22}$	−46.478	−46.480	−46.488	−46.497	−46.508

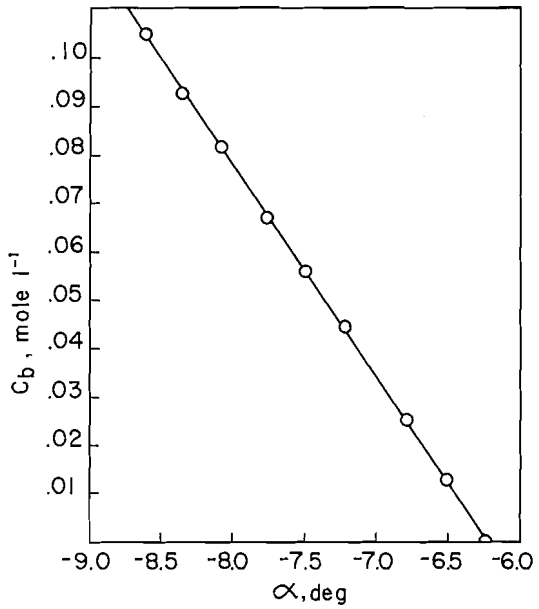

FIG. 1. Variation of rotatory power of 1-menthol with 1-menthol concentration (C_b). Solvent: dimethoxyethane/CCl_4, 70/30. Temp. 25.00°.

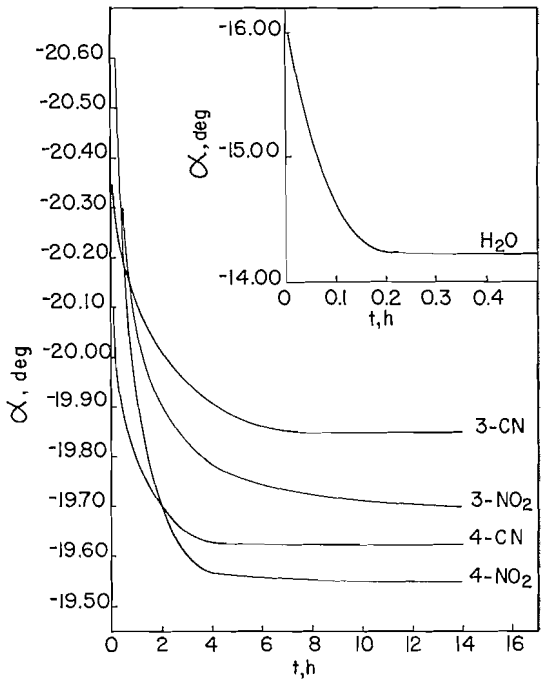

FIG. 2. Phenolysis of 1-menthol borate (0.148 *M*) by phenols (0.446 *M*) of $pK_a < 10.0$. Hydrolysis of 1-menthyl borate (0.131 *M*) by water (0.393 *M*); measured in a 2 dm tube. Solvent: dimethoxyethane/CCl_4, 70/30. Temp. 25.00°.

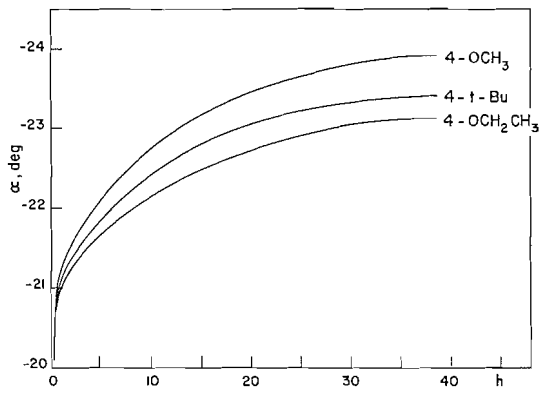

FIG. 3. Phenolysis of 1-menthyl borate by phenols of $pK_a > 10.0$. Molar ratio of 3 to 1 between the phenol and the borate (0.130 *M*). Solvent: dimethoxyethane/CCl_4, 70/30. Temp. 25.00°.

Results

The kinetics of the phenolysis were followed by polarimetry, taking advantage of the difference in optical activity between the 1-menthol and its borate. It can be seen from Table I that the presence of phenol does not affect appreciably the rotatory power of 1-menthol and Fig. 1 indicates that the optical activity of 1-menthyl borate varies linearly with the concentration of the ester. It has been verified that the phenols could not racemize 1-menthol under the experimental conditions used. The course of the phenolysis is shown in Figs. 2, 3, and 4. Three types of curves are obtained. The first type (Fig. 2), observed with substituted phenols which are more acid than phenol ($pK_a < 10.0$), shows that the phenolysis follows its course until an equilibrium composition is reached. This result is in accordance with the works of Bradley (7), who reports the hydrolysis of borates with a stoichio-

Can. J. Chem. Downloaded from www.nrcresearchpress.com by 210.87.254.42 on 09/05/12
For personal use only.

Can. J. Chem. Downloaded from www.nrcresearchpress.com by 210.87.254.42 on 09/05/12
For personal use only.

metric amount of water as a reversible reaction. The second type of curve (Fig. 3) groups the substituted phenols less acid than phenol ($pK_a > 10.0$). As can be seen, the reaction is accompanied by an increase (in absolute value) of the optical activity of the reaction mixture. With phenols of intermediate acidity ($pK_a \cong 10.0$), the curve observed (Fig. 4) is a composite of the two previous types: the optical activity increases first and then decreases. As can be seen from Fig. 5, the nature of the solvent has a definite effect on the course of the reaction.

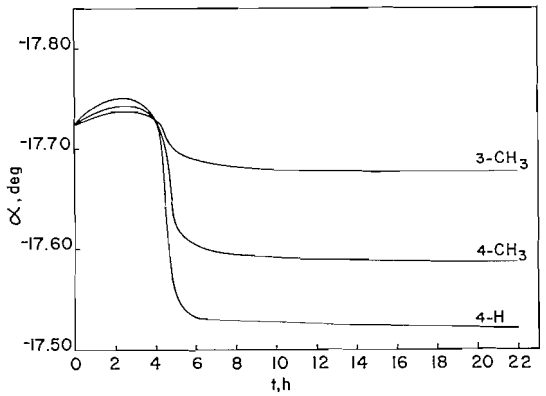

FIG. 4. Phenolysis of 1-menthyl borate by phenols of $pK_a \cong 10.0$. Molar ratio of 3 to 1 between the phenol and the borate (0.126 *M*). Solvent: dimethoxyethane/CCl_4, 70/30. Temp. 25.00°.

Experimental

Nuclear magnetic resonance (n.m.r.) measurements were made with a Varian, A-60 apparatus. Phenols were obtained commercially and purified by distillation or crystallization (8). The absence of position isomers in the phenols was verified by melting points and by thin layer chromatography. Solvents were dried over magnesium sulfate and redistilled. Rotatory power measurements were made with a "Rudolph, model 80" polarimeter, using 4.00 dm tubes kept at 25.000 ± 0.005° by water circulation in a jacket around the tube.

1-Menthyl Orthoborate

1-Menthol (122.8 g, $[\alpha]_D^{22}$: −46.478°, CCl_4) was treated with 16.2 g of boric acid, the water produced in the course of the reaction being eliminated by azeotropic distillation with benzene. After removal of the calculated amount of water the solvent was evaporated under vacuum and the white residual mass recrystallized in ethyl acetate/acetone mixture (1/1). Yield: 80%; $[\alpha]_D^{25}$: −73.950°, CCl_4.

Phenolysis of 1-Menthyl Borate by p-t-Butyl Phenol

A solution of 11.741 g (0.079 mole) of *p*-*t*-butyl phenol in 100 ml of a mixture dimethoxyethane/CCl_4 (70/30 in volume) was prepared and thermostated at 25.000 ± 0.005°. A second solution of 12.500 g (0.026 mole) of 1-menthyl borate in 100 ml of the same mixture of solvents was prepared and thermostated at the same temperature. Equal volumes (20 ml) of these two solutions were mixed at 25.000° and the variation of rotatory power was noted. A similar procedure was used for all phenolysis or hydrolysis reported.

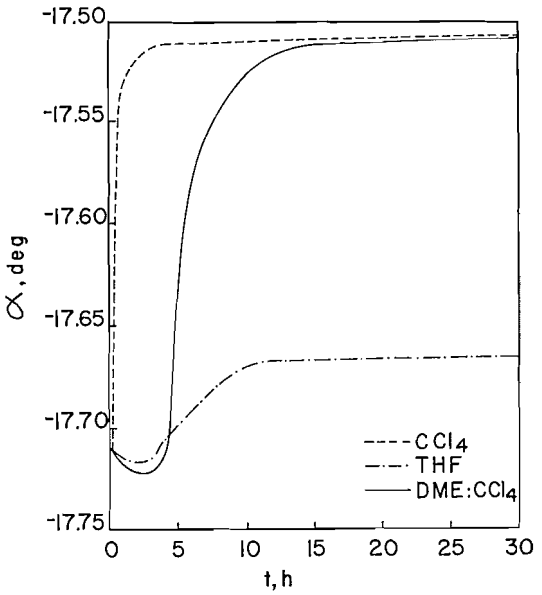

FIG. 5. Solvent effect for the phenolysis of 1-menthyl borate (0.131 *M*) by phenol (0.393 *M*). Temp. 25.00°.

Attempt to Prepare Unsymmetrical Orthoborates

To a solution of 20.6 g (0.10 mole) of 2,6-di-*t*-butyl phenol in methylene chloride cooled to −78° was added a solution of 11.7 g (0.10 mole) of BCl_3 in the same solvent. After the evolution of HCl had stopped, 21.6 g (0.20 mole) of *p*-cresol was added and the reaction mixture was kept at room temperature overnight. After removal of the solvent the residue was distilled under vacuum, the main product being a yellow oil boiling at 206–213° and 0.03 mm Hg. Even after repeated distillation or keeping under vacuum in a desiccator containing KOH pellets the compound retained traces of HCl, rendering it unusable for kinetic measurements. Between each of these distillations, a n.m.r. spectra of the main fraction was taken. From these measurements, it could be seen that the $CH_3/(CH_3)_3C$ ratio (at 2.3 and 1.4 p.p.m.) varied for each distillation, strongly suggesting disproportionation.

Racemization of 1-Menthol

A solution of 10.00 g of 1-menthol in 100 ml dimethoxyethane/CCl_4, 70/30 mixture, was treated by 5.00 g of *p*-*t*-butyl phenol. The rotatory power of the solution remained constant, at −9.437°, during 3 days. These results are in accordance with earlier reports on the stability of 1-menthol towards racemization (9).

Acknowledgment

The financial support of the Defence Research Board of Canada (grant No. 9530-30) is gratefully acknowledged.

1. J. J. EBELMEN and M. BOUQUET. Ann. Chim. Phys. **17**, 54 (1846).
2. A. SCATTERGOOD, W. H. MILLER, and J. GAMMON. J. Am. Chem. Soc. **67**, 2150 (1945).
3. H. STEINBERG. Organoboron chemistry. Vol. I. Interscience Publishers, New York. 1964. p. 852.
4. H. STEINBERG and D. L. HUNTER. Ind. Eng. Chem. **49**, 174 (1957).
5. H. STEINBERG, D. L. HUNTER, and A. L. MCCLOSKEY. 133rd Meeting, Am. Chem. Soc. 1959. Abstract of Papers, p. 41-O.
6. R. F. PRESCOTT, R. C. DOSSER, and J. J. SCULATI. U.S. Patent No. 2,260,336 (1941).
7. J. A. BRADLEY and P. M. CHRISTOPHER. 129th Meeting, Am. Chem. Soc. 1956. Abstracts of Papers, p. 39-N.
8. A. I. VOGEL. Practical organic chemistry. 3rd ed. Longmans, London. 1957. p. 664.
9. M. P. DE ALMEIDA. Chem. Abstr. **39**, 1403 (1945).

Co-extraction of phosphoric and tetrachloroferric acids

ROBERT H. MCCORKELL[1] AND JOHN W. IRVINE, JR.

Department of Chemistry and Laboratory for Nuclear Science, Massachusetts Institute of Technology, Cambridge, Massachusetts

Received August 9, 1967

The presence of an extracting strong acid greatly enhances the extraction of phosphoric acid from aqueous solutions into organic solvents, but no type of compound forms between the phosphoric acid and the other extracted species. Only the alteration of the solvent properties when an ionic species and water are added to it can account for the increase in $D_{H_3PO_4}$.

Canadian Journal of Chemistry, **46**, 662 (1968)

The co-extraction of H_3PO_4 with $HFeCl_4$ from hydrochloric acid solutions into isopropyl ether has been noted before (1, 2), but no attempts have been made to learn what phenomena are involved. Former studies have shown only that H_3PO_4 is little extracted in the absence of iron. This raised the possibilities that a mixed chloride–phosphate complex of iron is extracted, that H_3PO_4 replaces some of the water of the extracted hydrated proton, or that a species such as $H_4PO_4^+FeCl_4^-$ is extracted. These possibilities led us to a study of the HCl–$FeCl_3$–H_3PO_4 – isopropyl ether and similar systems, which has shown only that phosphoric acid will extract when the organic phase contains a strong acid.

Typical data[2] for the isopropyl ether system are shown in Table I. The ratio $[PO_4]$:$[Fe^{3+}]$ in the organic phase varies continuously, showing no indication of the formation of a compound of fixed composition. The "excess chloride" in the organic phase, $[Cl^-]$–$4[Fe^{3+}]$, shows no relation to the concentration of H_3PO_4 in the organic phase as it should if phosphoric acid extracts as a compound of the sort $H_4PO_4^+Cl^-$. Clearly, though, the presence of $HFeCl_4$ in the organic phase greatly enhances the extraction of phosphoric acid.

Two organic phases sometimes form in the isopropyl ether extraction system. We designate the lighter of these phase 3, the heavier phase 2, and the aqueous phase 1. $D_{2/3}$ for any species then is

$$\frac{\text{conc. of species in phase 2}}{\text{conc. of species in phase 3}}, \text{ etc.}$$

It is found that the presence of H_3PO_4 in the isopropyl ether layer increases $D_{2/3}$ for iron. It has been shown (3) that the extracted iron species in the heavy phase is $HFeCl_4 \cdot 4H_2O$, while that in the light phase is $HFeCl_4 \cdot 5H_2O$. Thus the H_3PO_4 may increase $D_{2/3}$ for iron by dehydrating the extracted tetrachloroferric acid.

The extracted iron and phosphoric acid are both concentrated in the heavy phase, and $D_{2/3}$ is similar for both.

The same phenomena are noted in the extraction of $HFeCl_4$ and H_3PO_4 with butyl ether, pentyl ether, and nitrobenzene. In these, however, only one organic phase forms. At the same

[1]Present address: Smithsonian Institution Astrophysical Observatory, 60 Garden St., Cambridge, Mass. 02138, USA.

[2]Complete data for this and other systems have been placed in the Depository for Unpublished Data. Photocopies may be obtained upon request to: The Depository of Unpublished Data, National Science Library, National Research Council of Canada, Ottawa, Canada.

Can. J. Chem. Downloaded from www.nrcresearchpress.com by 210.87.254.42 on 09/05/12
For personal use only.

Acknowledgment

The financial support of the Defence Research Board of Canada (grant No. 9530-30) is gratefully acknowledged.

1. J. J. EBELMEN and M. BOUQUET. Ann. Chim. Phys. **17**, 54 (1846).
2. A. SCATTERGOOD, W. H. MILLER, and J. GAMMON. J. Am. Chem. Soc. **67**, 2150 (1945).
3. H. STEINBERG. Organoboron chemistry. Vol. I. Interscience Publishers, New York. 1964. p. 852.
4. H. STEINBERG and D. L. HUNTER. Ind. Eng. Chem. **49**, 174 (1957).
5. H. STEINBERG, D. L. HUNTER, and A. L. MCCLOSKEY. 133rd Meeting, Am. Chem. Soc. 1959. Abstract of Papers, p. 41-O.
6. R. F. PRESCOTT, R. C. DOSSER, and J. J. SCULATI. U.S. Patent No. 2,260,336 (1941).
7. J. A. BRADLEY and P. M. CHRISTOPHER. 129th Meeting, Am. Chem. Soc. 1956. Abstracts of Papers, p. 39-N.
8. A. I. VOGEL. Practical organic chemistry. 3rd ed. Longmans, London. 1957. p. 664.
9. M. P. DE ALMEIDA. Chem. Abstr. **39**, 1403 (1945).

Co-extraction of phosphoric and tetrachloroferric acids

ROBERT H. MCCORKELL[1] AND JOHN W. IRVINE, JR.

Department of Chemistry and Laboratory for Nuclear Science, Massachusetts Institute of Technology, Cambridge, Massachusetts

Received August 9, 1967

The presence of an extracting strong acid greatly enhances the extraction of phosphoric acid from aqueous solutions into organic solvents, but no type of compound forms between the phosphoric acid and the other extracted species. Only the alteration of the solvent properties when an ionic species and water are added to it can account for the increase in $D_{H_3PO_4}$.

Canadian Journal of Chemistry, **46**, 662 (1968)

The co-extraction of H_3PO_4 with $HFeCl_4$ from hydrochloric acid solutions into isopropyl ether has been noted before (1, 2), but no attempts have been made to learn what phenomena are involved. Former studies have shown only that H_3PO_4 is little extracted in the absence of iron. This raised the possibilities that a mixed chloride–phosphate complex of iron is extracted, that H_3PO_4 replaces some of the water of the extracted hydrated proton, or that a species such as $H_4PO_4^+FeCl_4^-$ is extracted. These possibilities led us to a study of the HCl–$FeCl_3$–H_3PO_4 – isopropyl ether and similar systems, which has shown only that phosphoric acid will extract when the organic phase contains a strong acid.

Typical data[2] for the isopropyl ether system are shown in Table I. The ratio $[PO_4]$:$[Fe^{3+}]$ in the organic phase varies continuously, showing no indication of the formation of a compound of fixed composition. The "excess chloride" in the organic phase, $[Cl^-]$–$4[Fe^{3+}]$, shows no relation to the concentration of H_3PO_4 in the organic phase as it should if phosphoric acid extracts as a compound of the sort $H_4PO_4^+Cl^-$. Clearly, though, the presence of $HFeCl_4$ in the organic phase greatly enhances the extraction of phosphoric acid.

Two organic phases sometimes form in the isopropyl ether extraction system. We designate the lighter of these phase 3, the heavier phase 2, and the aqueous phase 1. $D_{2/3}$ for any species then is

$$\frac{\text{conc. of species in phase 2}}{\text{conc. of species in phase 3}}, \text{ etc.}$$

It is found that the presence of H_3PO_4 in the isopropyl ether layer increases $D_{2/3}$ for iron. It has been shown (3) that the extracted iron species in the heavy phase is $HFeCl_4 \cdot 4H_2O$, while that in the light phase is $HFeCl_4 \cdot 5H_2O$. Thus the H_3PO_4 may increase $D_{2/3}$ for iron by dehydrating the extracted tetrachloroferric acid.

The extracted iron and phosphoric acid are both concentrated in the heavy phase, and $D_{2/3}$ is similar for both.

The same phenomena are noted in the extraction of $HFeCl_4$ and H_3PO_4 with butyl ether, pentyl ether, and nitrobenzene. In these, however, only one organic phase forms. At the same

[1]Present address: Smithsonian Institution Astrophysical Observatory, 60 Garden St., Cambridge, Mass. 02138, USA.

[2]Complete data for this and other systems have been placed in the Depository for Unpublished Data. Photocopies may be obtained upon request to: The Depository of Unpublished Data, National Science Library, National Research Council of Canada, Ottawa, Canada.

Can. J. Chem. Downloaded from www.nrcresearchpress.com by 210.87.254.40 on 09/05/12
For personal use only.

TABLE I

Extraction of $HFeCl_4$ and H_3PO_4 from HCl by isopropyl ether (Initial aqueous $[Fe^{3+}] = 0.18$ *M*. Symbols: phase 1, aqueous; phase 2, lower (heavy) organic (or organic where only two phases form); phase 3, light organic)

Initial aqueous		$[Fe^{3+}]$		$[H_3PO_4]$		$[Cl^-]-4[Fe^{3+}]$		$D_{H_3PO_4}$ ($\times 10^3$)	
[HCl]	$[H_3PO_4]$	Phase 2	Phase 3	Phase 2	Phase 3	Phase 2	Phase 3	Fe^{3+} present	Fe^{3+} absent
6.00	0.00	0.176	—	0.00	—	0.004	—	—	—
6.00	0.50	0.180	—	0.020	—	0.030	—	0.044	
6.00	2.00	0.268	0.088	0.250	0.060	0.210	0.00	0.092	
6.00	3.00	0.348	0.029	0.573	0.041	0.526	0.022	0.13	
6.00	4.00	0.278	0.010	1.05	0.0307	1.42	0.046	0.24	
6.00	5.00	0.135	—	2.02	—	2.66	—	0.53	
7.75	0.00	0.406	0.073	0.00	0.00	0.239	0.00	—	—
7.75	0.04	0.420	0.056	0.006	0.0007			74	1.1
7.75	0.08	0.426	0.058	0.012	0.00093			67	1.0
7.75	0.20	0.420	0.055	0.045	0.0030			110	1.0
7.75	0.59	0.416	0.046	0.081	0.0071			82	1.2
7.75	1.50	0.485	0.025	0.349	0.0056	0.437	0.052	108	2.3
7.75	2.00	0.401	0.0017	0.557	0.0053	1.01	0.143	174	2.8
7.75	2.50	0.380	0.018	0.728	0.016	1.25	0.069	240	
7.75	3.00	0.299	0.014	0.948	0.023	1.89	0.127	330	

concentrations of HCl_{aq} and $HFeCl_{4org}$, $D_{H_3PO_4}$ varies with the solvent:

isopropyl ether > butyl ether
> pentyl ether > nitrobenzene.

This is also the order of D_{HFeCl_4} with solvent.

In the absence of HCl no measurable extraction of iron from H_3PO_4 solutions takes place into any of these solvents. However, H_3PO_4 also co-extracts with $HClO_4$ into nitrobenzene. Ratios of $H_3PO_4/HClO_4$ in the organic phase vary continuously with the concentration of these acids in the aqueous phase.

Changes in the volume of phases during equilibration are considerable in all these systems except those in which the organic phase is nitrobenzene.

Near infrared (visible to 2 000 mμ) absorption spectra were obtained of extracts of HCl, $HClO_4$, $HFeCl_4$, H_3PO_4, and combinations of these in isopropyl ether and nitrobenzene. These showed only bands attributable to water, i.e. to the hydrated proton. The intensities of these absorption bands show that the water content of $HFeCl_4$ or $HClO_4$ extracts increases with the addition of H_3PO_4. This indicates that H_3PO_4 is itself hydrated. If $H_4PO_4^+$ is formed it carries more water of hydration than the original H^+ does.

In conclusion, we have found no evidence of association of H_3PO_4 with $HFeCl_4$ or $HClO_4$ in the organic phase. It is probable that the strong acid and its associated water in the organic phase acts to increase $D_{H_3PO_4}$ not by associating with the phosphoric acid but by altering the properties of the solvent.

Experimental

Solutions were made up from reagent grade HCl, H_3PO_4, $HClO_4$, and $FeCl_3$. Standard analytical techniques were used in measuring their concentrations. Solvents were purified by fractional distillation. Equal volumes of solution and solvent were pipetted to graduated centrifuge tubes and suitable activities of ^{59}Fe and ^{32}P (as $FeCl_3$ and H_3PO_4) were added. The tubes were closed with disposable polyethylene caps and equilibrated at 26 ± 2 °C. Equilibrium was shown to be attained in < 1 min but equilibration times of 5 min were used.

After equilibration the tubes were centrifuged and the phase volumes read. Samples for gamma counting for ^{59}Fe were withdrawn into counting vials using disposable 1 ml pipettes. For β counting of ^{32}P 0.1 ml samples were withdrawn and dried on circles of filter paper.

A scintillation counter with a well-type NaI (Tl) crystal was used for gamma counting. ^{32}P activity was measured with a thin window proportional counter and absorbers to cut out the weaker ^{59}Fe β rays.

Sample preparation methods were checked for reproducibility by preparing duplicate samples.

Near infrared absorption spectra were obtained with a Cary No. 14 recording spectrophotometer.

Acknowledgment

This work was supported by A.E.C. contract No. AT(30-1)-905.

1. R. W. Dodson, G. J. Forney, and E. H. Swift. J. Am. Chem. Soc. **58**, 2573 (1936).
2. N. Haberman. Anal. Chem. **36**, 1876 (1964).
3. A. H. Laurene, D. E. Campbell, S. E. Weberly, and H. M. Clark. J. Phys. Chem. **60**, 901 (1956).

Can. J. Chem. Downloaded from www.nrcresearchpress.com by 210.87.254.40 on 09/05/12
For personal use only.

Reaction of ethyl with isobutyl and *t*-butyl free radicals

J. O. TERRY AND J. H. FUTRELL[1]

Chemistry Research Laboratory, Aerospace Research Laboratories, Wright-Patterson Air Force Base, Ohio

Received July 26, 1967

1,1′-Azoisobutane, 2,2′-azoisobutane, 1-isobutyl azoethane, and mixtures of azoethane with 2,2′-azoisobutane were photolyzed under high intensity conditions in order to study the disproportionation of isobutyl and *t*-butyl free radicals and their cross reactions with ethyl radicals. The relative rates of disproportionation to combination which were determined for the various radical interactions are as follows: $\Delta(i\text{-}C_4H_9,\ i\text{-}C_4H_9)$, 0.078; $\Delta(t\text{-}C_4H_9,\ t\text{-}C_4H_9)$, 2.32; $\Delta(C_2H_5,\ i\text{-}C_4H_9)$, 0.04; $\Delta(C_2H_5,\ t\text{-}C_4H_9)$, 0.498; $\Delta(i\text{-}C_4H_9,\ C_2H_5)$, 0.04; $\Delta(t\text{-}C_4H_9,\ C_2H_5)$, 0.283.

Canadian Journal of Chemistry, 46, 664 (1968)

A general mechanism for the high intensity photolysis of azoalkanes and of asymmetric azoalkanes was presented in a recent paper from this laboratory (1). For the asymmetric azoalkane an adequate mechanism is:

$$R_1\text{—N=N—}R_2 + h\nu \xrightarrow{k_0} R_1\text{—N=N—}R_2^*$$

$$R_1\text{—N=N—}R_2^* \xrightarrow{k_1} N_2 + R_1 + R_2$$

$$R_1\text{—N=N—}R_2^* + \text{Azo} \xrightarrow{k_2} 2R_1\text{—N=N—}R_2$$

$$R_1 + R_1 \xrightarrow{k_3} \text{alkane}_1 + \text{alkene}_1$$

$$\xrightarrow{k_4} \text{alkane}_{1,1}$$

$$R_2 + R_2 \xrightarrow{k_5} \text{alkane}_2 + \text{alkene}_2$$

$$\xrightarrow{k_6} \text{alkane}_{2,2}$$

$$R_1 + R_2 \xrightarrow{k_7} \text{alkane}_1 + \text{alkene}_2$$

$$\xrightarrow{k_8} \text{alkane}_2 + \text{alkene}_1$$

$$\xrightarrow{k_9} \text{alkane}_{1,2}$$

The extension of this mechanism to the photolysis of mixtures of azoalkanes is obvious.

A quantity of interest for describing free radical reactions is the cross-combination ratio, $k_9/(k_4 \times k_6)^{1/2}$, often termed the ϕ factor (2, 3). As an alternative we discussed the cross-reaction ratio

$$[1] \qquad \phi' = \frac{1 + (k_7 + k_8)/k_9}{[(1 + k_3/k_4)(1 + k_5/k_6)]^{1/2}}\,\phi,$$

which, as first pointed out by Blake, Henderson, and Kutschke (4), is the correct statistical formulation. Derivation of this ratio assumes that each radical–radical collision results in either disproportionation or combination, and the steric factor for the sum of mutual disproportionation plus combination reactions is near unity. If the sum of the steric factors for these reactions differ significantly from unity, there is no theoretical relationship relating the various free radical reaction pairs.

For the various free radicals investigated in the earlier study, both ϕ and ϕ' were close to the statistical factor 2. An examination of the literature suggested, however, that for butyl radical systems ϕ and ϕ' might differ significantly and, in particular, that ϕ', appeared not to equal the statistical factor 2. If true, this result is an argument against the hypothesis of a common transition state for disproportionation and combination reaction (5, 6), or an argument that the sum of steric factors is not equal to unity. Accordingly the present study was initiated to obtain quantitative data on the disproportionation of isobutyl and *t*-butyl free radicals and their cross reactions with ethyl radicals.

Experimental

The symmetric azoisobutanes were obtained from Merck, Sharp and Dohme of Canada, Ltd. and the unsymmetrical one was prepared as described by Spialter and co-workers (7). These compounds were purified by gas chromatography and stored under vacuum in a blackened cold finger. The high intensity photolysis apparatus and the gas chromatographic techniques used were described earlier (1). In this series of experiments, 10 ft of 1/4 o.d. tubing filled with 10% polyphenyl ether on chromsorb P was used to analyze the photolysis products from 1,1′-azoisobutane and that of 2,2′-azoisobutane. For the unsymmetric case, 1-isobutyl azoethane, the total C_2 concentration, isobutane, *n*-butane, isobutene, and 2-methyl pentane were obtained on a 12 ft, 20%

[1]Present address: Department of Chemistry, University of Utah, Salt Lake City, Utah, 84112.

Can. J. Chem. Downloaded from www.nrcresearchpress.com by 210.87.254.42 on 09/05/12
For personal use only.

TABLE I

Relative rates for disproportionation and combination reactions

Reactants[a]	Literature	This research
(1) i-C_4H_9+i-C_4H_9	0.42 (8), 0.17 (9), 0.075 (17)	0.078± .005
(2) t-C_4H_9+t-C_4H_9	4.5 (10), 7.4 (11) 4.38 (12), 3.19 (13)	2.32± .05
(3) C_2H_5[b]+i-C_4H_9	0.02± .02 (14)	0.04± .005
(4) C_2H_5+t-C_4H_9	0.53 (13), 0.54 (15)	0.498± .02
(5) i-C_4H_9+C_2H_5		0.04± .005
(6) t-C_4H_9+C_2H_5	1.7 (16), 0.31 (13)	0.283±0.2

[a]The alkane product of the disproportionation reaction corresponds to the first reactant listed; i.e. in reaction [4] ethane and isobutene are products, while in reaction [6] isobutane and ethylene are products.
[b] $k_d/k_c(C_2H_5 + C_2H_5) = 0.135$[1].

β-β'-oxydipropionitrile column maintained at 15 °C. The ratios of 2-methyl pentane to 2,5-dimethyl hexane and ethylene to ethane were obtained on the polyphenyl ether column maintained at 60° and a 25 ft section of 1/4 o.d. tubing filled with 25% squalane on chromsorb P. For the mixture experiment (azoethane plus 2,2′-azoisobutane) a series column consisting of 6 ft of the β-β'-oxydipropionitrile plus 6 ft of the polyphenyl ether was used to determine all the decomposition products except the ratio of ethylene to ethane. This ratio was obtained on the squalane column.

Results and Discussion

The results of some 30 experiments are summarized in Table I. The experimental precision of these experiments compares favorably with our previous report (1). As before, the concentration of alkene from reactions [3], [5], [7], and [8] equalled the concentration of alkane produced by the same reactions within experimental error. No products other than those predicted by the mechanism were detected. The agreement with previous literature values is quite good for the cross reaction of ethyl with t-butyl radicals but is poor for the mutual reactions of isobutyl and t-butyl radicals. No reasons can be advanced for the poor agreement in the latter cases.

The cross-combination and cross-reaction ratios ϕ and ϕ' for the reactions of ethyl with isobutyl radicals are 1.86 and 1.81 and for the reactions of ethyl with t-butyl radicals are 1.93 and 1.78, respectively. In agreement with Blake, Henderson, and Kutschke (4), we find that the factor

$$\frac{1 + (k_7 + k_8)/k_9}{[(1 + k_3/k_4)(1 + k_5/k_6)]^{1/2}}$$

of eq. [1] is close to unity. This was also true for our previously reported study of the cross-disproportionation and combination reactions of methyl, ethyl, n-propyl, and isopropyl radicals (1). It is not obvious why this factor should equal unity, but the equality does appear useful as a tentative cross-check on experimental k_d/k_c ratios for mixed alkyl free-radical systems. The concept of a common transition state is consistent with the present results, although they do not provide definitive support for this idea.

1. J. O. Terry and J. H. Futrell. Can. J. Chem. **45**, 2327 (1967).
2. J. A. Kerr and A. F. Trotman-Dickenson. Chem. Ind. London, 125 (1959).
3. R. Bowles, J. R. Majer, and J. C. Robb. Trans. Faraday Soc. **58**, 2394 (1962).
4. A. R. Blake, J. F. Henderson, and K. O. Kutschke. Can. J. Chem. **39**, 1920 (1961).
5. J. N. Bradley. J. Chem. Phys. **35**, 748 (1961).
6. J. N. Bradley and B. S. Rabinovitch. J. Chem. Phys. **36**, 3498 (1962).
7. L. Spialter, D. H. O'Brien, G. L. Untereiner, and W. A. Rush. J. Org. Chem. **30**, 3278 (1965).
8. J. W. Kraus and J. G. Calvert. J. Am. Chem. Soc. **79**, 5921 (1957).
9. E. L. Metcalfe and A. F. Trotman-Dickenson. J. Chem. Soc. 5072 (1960).
10. W. J. Moore and L. A. Wall. J. Chem. Phys. **17**, 1325 (1949).
11. H. M. Frey. Proc. Chem. Soc. 385 (1959).
12. R. N. Birrell and A. F. Trotman-Dickenson. J. Chem. Soc. 4218 (1960).
13. J. A. Garcia Dominguez, J. A. Kerr, and A. F. Trotman-Dickenson. J. Chem. Soc. 3357 (1962).
14. R. A. Holroyd and T. E. Pierce. J. Phys. Chem. **68**, 1392 (1964).
15. R. A. Holroyd and G. W. Klein. J. Phys. Chem. **67**, 2273 (1963).
16. P. J. Boddy and J. C. Robb. Proc. Roy. Soc. London, Ser. A, **249**, 547 (1959).
17. D. H. Slater, S. S. Collier, and J. G. Calvert. J. Am. Chem. Soc. To be published.

Can. J. Chem. Downloaded from www.nrcresearchpress.com by 210.87.254.42 on 09/05/12
For personal use only.

Erratum: Spontaneous decarboxylation of oxalacetic acid

C. S. TSAI
Department of Chemistry, Carleton University, Ottawa, Canada

Received October 6, 1967

(Ref.: Can. J. Chem. **45**, 873 (1967))

Canadian Journal of Chemistry, **46**, 666 (1968)

The heading-row of Tables I (page 875), III (page 876), and IV (page 877) under $k_{obs} \times 10^3$ and $k_{Zn^{2+}} \times 10^3$ should read (min^{-1}) instead of (s^{-1}).

Erratum: γ-Radiolysis of cyclohexane with electron scavengers. IV. CO_2 as an electron scavenger

N. H. SAGERT
Research Chemistry Branch, Chalk River Nuclear Laboratories, Chalk River, Ontario

Received January 29, 1968

(Ref.: Can. J. Chem. **46**, 336 (1968))

Canadian Journal of Chemistry, **46**, 666 (1968)

The footnote at the bottom of page 336 should read: "Issued as A.E.C.L. No. 2983".

Can. J. Chem. Downloaded from www.nrcresearchpress.com by 210.87.254.40 on 09/05/12
For personal use only.

Can. J. Chem. Downloaded from www.nrcresearchpress.com by 210.87.254.105 on 09/05/12
For personal use only.

Canadian Journal of Chemistry

Published by THE NATIONAL RESEARCH COUNCIL OF CANADA

VOLUME 46 MARCH 1, 1968 NUMBER 5

The synthesis and identification of allyl ethers of glucose and cellulose[1]

D. E. HOINESS,[2] C. P. WADE, AND S. P. ROWLAND[3]

Southern Regional Research Laboratory, Southern Utilization Research and Development Division, Agricultural Research Service, United States Department of Agriculture, New Orleans, Louisiana

Received August 23, 1967

Substituent group distribution in allyl cellulose, resulting from the base-catalyzed condensation of sodium allyl sulfate with cotton cellulose and having a degree of substitution of 0.07, was found to be 0.7:0.2:1.0 in the 2-*O*-, 3-*O*-, and 6-*O*-positions of the anhydroglucose units. Several new glucose derivatives were prepared in the syntheses of the 2-*O*-, 3-*O*-, and 6-*O*-allyl-D-glucoses.

Canadian Journal of Chemistry, 46, 667 (1968)

Introduction

As a part of a program to characterize the reactivities of the hydroxyl groups of the D-glucopyranosyl units of cotton cellulose toward mono- and polyfunctional reagents, we have studied the substituent group distribution resulting from the base-catalyzed condensation of sodium allyl sulfate with cotton cellulose. In order to identify the 2-*O*-, 3-*O*-, and 6-*O*-allyl-D-glucoses obtained from the hydrolytic cleavage of the molecular chain of the modified cotton cellulose, it has been necessary to synthesize and characterize several new derivatives of glucose. These were prepared by the nucleophilic substitution reaction on allyl bromide with the alkoxide group of a selected glucose derivative.

Substituent groups on glucose hydroxyls which were stable to the conditions of the reactions, yet easily removed by acid hydrolysis after introduction of the allyl group, were employed to block all the hydroxyl groups which were to be free in the final product. The requirement of stable blocking groups in basic reaction media for the preparation of 2-*O*-, 3-*O*-, and 6-*O*-substituted glucoses has been discussed by Bullock, Cirino, and Rowland (1).

The allyl ether group, itself, has recently been used as a protective group in carbohydrate chemistry. Gigg and Cunningham (2, 3) and Montgomery and Thomas (4) discussed the removal of this group. Bullock and co-workers (1) indicated that this group was more satisfactory than the benzyl group, since it was more readily removed after the condensation reaction was complete.

Experimental

Gas–Liquid Chromatography

The gas–liquid chromatographic unit was an F & M model 1609 (hydrogen flame ionization detector).[4] Columns were based on a solid phase of acid-washed silanized Chromosorb W of 80–100 mesh (Johns–Manville Corporation) and liquid phases consisting of SE-52, XE-60, QF-1, Apiezon M, ECNSS-M, and SE-30 (Applied Science, Inc.). The columns were prepared in $\frac{1}{4}$-in. O.D. aluminium tubing. The most effective columns were: (*a*) 19% w/w SE-52 on Chromosorb W, 6 ft, and (*b*) 8.5% w/w XE-60 on Chromosorb W, 2 ft. Trimethylsilyl ether derivatives of the saccharides were prepared for gas–liquid chromatographic analyses by the method of Sweeley *et al.* (5).

Steps in Synthesis of 3-O-Allyl-D-glucose

3-O-Allyl-1,2:5,6-di-O-isopropylidene-α-D-glucofuranose (1)

1,2:5,6-Di-*O*-isopropylidene-α-D-glucofuranose (13 g,

[1]Presented, in part, at the 151st National Meeting of the American Chemical Society, March 1966, Pittsburgh, Pennsylvania.

[2]Postdoctoral Resident Research Associate, November 1964 to November 1966. Present address: Pioneering Research Laboratory, Textile Fiber Division, E. I. du Pont de Nemours & Co., Wilmington, Delaware.

[3]To whom correspondence should be addressed.

[4]Mention of a company and/or product by the U.S. Department of Agriculture does not imply approval or recommendation of the product to the exclusion of others which may also be suitable.

Can. J. Chem. Downloaded from www.nrcresearchpress.com by 210.87.254.105 on 09/05/12
For personal use only.

50 mmoles) was dissolved in ca. 50 ml of anhydrous liquid ammonia and 1.95 g (50 mmoles) of potassium metal was added slowly. The system was flushed with argon and warmed gently to remove the ammonia. Anhydrous ethyl ether (20 ml) was added to flush any remaining ammonia from the reaction mixture. Excess allyl bromide (35 g, 289 mmoles) was then added and the reaction mixture was refluxed briefly. After standing at room temperature overnight the reaction mixture was evaporated to dryness under reduced pressure, the residue was extracted with ethyl ether, and the extract was washed with water. The ether was evaporated and the residue was distilled under reduced pressure. The product was a colorless liquid weighing 6.6 g (51%); b.p. 80–83° at 0.004 mm, n_D^{23} 1.4574 (lit. (6) n_D^{24} 1.4570).

Anal. Calcd. for $C_{15}H_{24}O_6$: C, 59.98; H, 8.05. Found: C, 59.66; H, 7.83.

*3-O-Allyl-*D*-glucose (2)*

Compound **1** (0.51 g, 1.7 mmoles) was dissolved in 17.5 g of 7.6 *N* sulfuric acid and subjected to mild agitation at reflux temperature under an atmosphere of argon for 2 h. The solution was cooled, diluted to 1.5 *N* with 60 ml of water, and stirred for 16 h under argon. The pH of the solution was adjusted to 6.0–6.5 with barium hydroxide, the barium sulfate was removed, the filtrate was concentrated under vacuum below 40°, and the concentrate was freeze-dried to a solid product (yield >90%). Gas–liquid chromatogram of the trimethylsilyl ether of this product on SE-52 column showed only two peaks (α and β anomers) (curve A, Fig. 1).

Anal. Calcd. for $C_9H_{16}O_6$: C, 49.10; H, 7.32. Found: C, 49.02; H, 7.42.

*Steps in Synthesis of 6-O-Allyl-*D*-glucose*

*6-O-Allyl-3,5-O-benzylidene-1,2-O-isopropylidene-α-*D*-glucofuranose (3)*

3,5-*O*-Benzylidene-1,2-*O*-isopropylidene-α-D-glucofuranose (7) (1.07 g, 3.3 mmoles) was added to a dispersion of sodium hydroxide (0.34 g, 8.5 mmoles) in 35 ml of anhydrous dioxane. The mixture was warmed gently and then allyl bromide (5 g, 42 mmoles), dissolved in 10 ml of anhydrous dioxane, was added dropwise. The mixture was refluxed for 3 h, cooled, filtered, and the remaining solvent was evaporated under reduced pressure. The syrupy residue was shaken with ethyl ether and water and the ether layer separated. The organic layer was washed with water, dried with anhydrous sodium sulfate, and the solvent was evaporated under vacuum. The residue was then dried under high vacuum for several hours to a viscous liquid. Gas–liquid chromatography of this material, following treatment to silylate the free hydroxyl group of any unconverted starting material, showed only a small amount (estimated 1%) of starting material to be present in addition to the desired product. The viscous liquid was dissolved in cyclohexane and crystallized to yield a white crystalline solid, m.p. 67–67.8°, 53% yield.

Anal. Calcd. for $C_{19}H_{24}O_6$: C, 65.50; H, 6.94. Found: C, 65.50; H, 6.86.

*6-O-Allyl-1,2:3,5-di-O-benzylidene-α-*D*-glucofuranose*

1,2:3,5-Di-*O*-benzylidene-α-D-glucofuranose (8) (4.20 g, 13 mmoles), which had been recrystallized several times from ethanol, was added to a dispersion of sodium hydroxide (1.04 g, 26 mmoles) in 50 ml of anhydrous dioxane. The mixture was warmed gently and then allyl bromide (3.13 g, 26 mmoles), dissolved in 10 ml of anhydrous dioxane, was added dropwise. The mixture was refluxed for several hours. A product which proved to be a mixture and which could not be separated into pure components was isolated by the procedure of the preceding preparation. The hydrolyzate of this product (by the procedure described below for **4**) was shown by gas–liquid chromatography to be predominantly 6-*O*-allyl-D-glucose together with glucose, 3-*O*-allyl-D-glucose, and an unidentified component. Due to the difficulty of purification of the product, this route was abandoned.

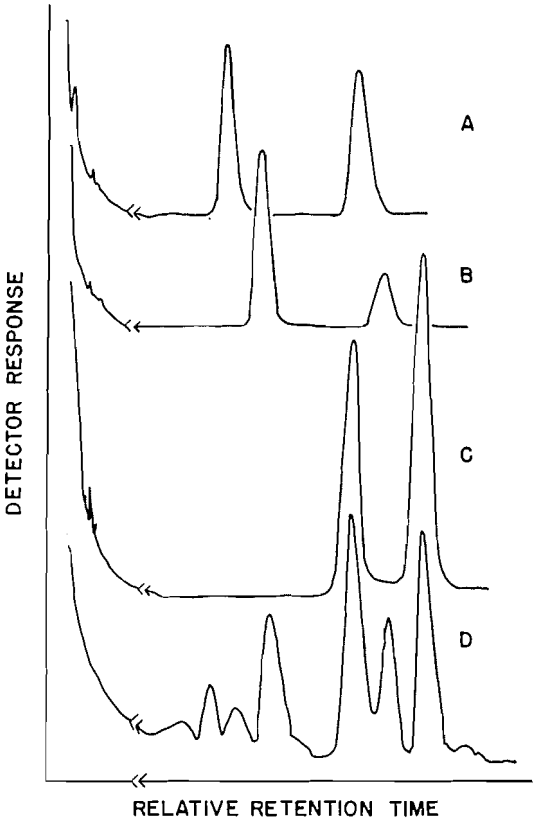

FIG. 1. Chromatograms of trimethylsilyl derivatives on SE-52 column programmed from 180–220° at 0.5° per min. Curve A is 3-*O*-allyl-D-glucose; curve B is 2-*O*-allyl-D-glucose; curve C is 6-*O*-allyl-D-glucose; curve D is the fermented hydrolyzate of allyl cellulose.

*6-O-Allyl-*D*-glucose (4)*

Recrystallized compound **3** (0.20 g, 0.9 mmole) was dissolved in 7.0 g of cold 7.6 *N* sulfuric acid and refluxed under an atmosphere of argon for 2 h. The solution was diluted to 1.5 *N* with 24 ml of water and stirred for 16 to 18 h. The solution was then adjusted with barium hydroxide to a pH of 6.0–6.5, the barium sulfate was removed, the filtrate was concentrated under vacuum below 40°, and the concentrate was freeze-dried to a solid product (yield >90%); m.p. 112–114°. A gas–liquid chromatogram of the trimethylsilyl ether of this product

Can. J. Chem. Downloaded from www.nrcresearchpress.com by 210.87.254.105 on 09/05/12
For personal use only.

on SE-52 column showed only two peaks (α and β anomers) (curve C, Fig. 1).

Anal. Calcd. for $C_9H_{16}O_6$: C, 49.10; H, 7.32. Found: C, 48.70; H, 6.94.

Steps in Synthesis of 2-O-Allyl-D-glucose. Route A

N-(2-O-Allyl-3,4,6-tri-O-acetyl-D-glucosyl)-piperidine (6)

N-(3,4,6-Tri-*O*-acetyl-D-glucosyl)piperidine (9) (20.2 g, 54 mmoles) was suspended in allyl bromide (60.5 g, 500 mmoles) and the mixture was allowed to stand for 20 min. Freshly prepared moist silver oxide (15 g, 64 mmoles) was then added in portions with constant stirring. Toward the end of the addition (30 min), the viscosity of the slurry decreased noticeably and the mixture became warm. The mixture was stirred in a closed flask for 48 h. The mixture was filtered and the filtrate concentrated under reduced pressure to yield a crystalline solid. This product (18 g) was recrystallized from *n*-butyl ether, yielding 15 g (68%) of colorless crystals; m.p. 107.5–108°.

Anal. Calcd. for $C_{20}H_{31}O_8N$: C, 58.09; H, 7.56; N, 3.39. Found: C, 57.79; H, 7.55; N, 3.33.

N-(2-O-Allyl-D-glucosyl)piperidine (7)

Compound **6** (4 g, 3.7 mmoles) dissolved in 20 ml of absolute methanol, was added to a saturated, anhydrous solution of ammonia in methanol (25 ml) prepared at 0°. The solution was held at 0° while dry ammonia gas was bubbled through for 1 h and subsequently was concentrated *in vacuo* to a light-yellow syrup. The syrup was decolorized in ethyl ether with Darco G-60 and upon concentration of the solution, white crystals formed. Recrystallization from ether yielded 1.5 g (54%) of white needles; m.p. 118–119°.

Anal. Calcd. for $C_{14}H_{25}O_5N$: C, 58.51; H, 8.77; N, 4.88. Found: C, 58.32; H, 8.67; N, 4.90.

2-O-Allyl-D-glucose (5)

Compound **7** (0.5 g, 1.7 mmoles) was dissolved in 25 ml of 1.0 *N* sulfuric acid and the solution heated (97°) for 1½ h. The acid solution was cooled and neutralized with an excess of barium carbonate, then filtered. The neutral filtrate was concentrated to a semisolid. A portion of this material was recrystallized from 1-hexanol to yield white crystals (0.05 g); m.p. 146°. In addition, 0.1 g of oil was recovered which gas–liquid chromatography indicated to be >90% 2-*O*-allyl-D-glucose.

Anal. Calcd. for $C_9H_{16}O_6$: C, 49.08; H, 7.32. Found: C, 49.86; H, 7.34.

Steps in Synthesis of 2-O-Allyl-D-glucose. Route B

3,5,6-Tri-O-allyl-1,2-O-isopropylidene-α-D-glucofuranose (8)

1,2-*O*-Isopropylidene-α-D-glucofuranose (6.03 g, 27 mmoles) dissolved in 10 ml of anhydrous dioxane was added to 20 ml of dioxane containing finely dispersed potassium hydroxide (2.1 g). The rapidly stirred mixture was heated to about 40° while an excess of allyl bromide (20.0 g, 165 mmoles) was added dropwise over a period of about 30 min. The temperature was raised to reflux and maintained there for about 4 h. The reaction mixture was cooled, filtered, and the solvent and unreacted allyl bromide were removed by evaporation under reduced pressure. The viscous residue was shaken with ethyl ether and water. The ethyl ether layer was separated, washed with water. dried with anhydrous sodium sulfate, filtered, and the filtrate was concentrated under reduced pressure. Distillation resulted in a colorless liquid; b.p. 116–118° at 0.002 mm (yield 82%). An infrared spectrum showed no absorption band at 2.85 μ, confirming the absence of free hydroxyl groups. Absorption bands at 6.04 and 10.85 μ were characteristic of the allyl group (10).

Anal. Calcd. for $C_{18}H_{28}O_6$: C, 63.51; H, 8.29. Found: C, 63.19; H, 8.13.

Methyl 3,5,6-Tri-O-allyl-D-glucofuranoside (9)

Compound **8** (15 g) was dissolved in 200 ml of absolute methyl alcohol and percolated through a bed of Dowex 50-X8 in the acid form at the boiling point of methanol (11). The product isolated after removal of the solvent showed two peaks on gas–liquid chromatography; these are attributed to the α and β anomers (yield 99%). The peak characteristic of compound **8** was absent from the chromatogram. Gas–liquid chromatographic analysis of the trimethylsilyl ether of this product indicated shorter retention times for both peaks, indicative of a free hydroxl group in product **9**. An infrared spectrum showed strong hydroxyl absorption (2.85 μ) and absorption bands (6.05 and 10.83 μ) characteristic of the allyl group (10).

Anal. Calcd. for $C_{16}H_{26}O_6$: C, 61.12; H, 8.34. Found: C, 60.3; H, 8.05.

Methyl 3,5,6-Tri-O-(1-propenyl)-D-glucofuranoside (10)

Product **9** (1.3 g, 3.8 mmoles), potassium *t*-butoxide (1.5 g, 13 mmoles), and dry dimethyl sulfoxide (10 ml) were heated (100°) together for 2 h. Gas–liquid chromatographic analyses of samples taken at ½ h intervals showed that the two peaks present initially and characteristic of **9** gradually diminished in size and finally disappeared, while two new peaks appeared and gradually enlarged. The appearance of new infrared bands at 5.98, 7.8, and 13.8 μ as well as the disappearance of allylic bands at 6.06 and 10.8 μ were evidence for the completeness of the allylic rearrangement.

Methyl 2-O-Allyl-3,5,6-tri-O-(1-propenyl)-D-glucofuranoside (11)

Compound **10** (0.5 g, 1.6 mmoles) was dissolved in 15 ml of dioxane and added to a suspension of sodium hydroxide (2.0 g, 50 mmoles) in 10 ml of dioxane. The mixture was warmed gently and allyl bromide (0.6 g, 5 mmoles) dissolved in 10 ml of dioxane was added dropwise over a period of 20 min. The mixture was refluxed for 3 h, cooled, and stirred overnight. After filtration and concentration *in vacuo*, gas–liquid chromatographic analyses of the viscous product indicated no movement of the single major peak when the product was treated with trimethylchlorosilane, thus indicating that the hydroxyl groups of this product were substituted.

2-O-Allyl-D-glucose (5)

The product from the previous preparation (**11**) was dissolved in 27 ml of 7.6 *N* sulfuric acid and refluxed for 2 h under an argon atmosphere. The solution was then diluted to 1.5 *N* with distilled water and stirred for 6 h at room temperature. The solution was neutralized with barium hydroxide, filtered, and concentrated under vacuum while maintaining the temperature below 40°. The trimethylsilyl ether derivative was prepared from a portion of this sample. Gas–liquid chromatograms yielded

Can. J. Chem. Downloaded from www.nrcresearchpress.com by 210.87.254.105 on 09/05/12
For personal use only.

retention times in agreement with those previously found for 2-*O*-allyl-D-glucose. Several byproduct peaks also appeared in the chromatograms, and separation of these materials from the desired 2-*O*-allyl-D-glucose anomers was not realized.

Allyl Cellulose

The cotton cellulose in the form of desized, scoured, and bleached 80 × 80 print cloth weighing 3.3 oz per yd was immersed in a solution of sodium allyl sulfate (15.5%), sodium hydroxide (20.7%), and wetting agent (Alkamerse, 1.7%). The wet fabric was squeezed through rollers to obtain a 135% wet pickup (12). Cure was carried out at 127° for 70 min. The fabric was washed thoroughly and dried. The extent of reaction of the cellulose with sodium allyl sulfate was measured by weight gain and by bromine number determination. The allyl groups were present at a degree of substitution of 0.07.

Hydrolysis of Allyl Cellulose to Glucose and Allyl Glucoses

Cotton cellulose and allyl cellulose were hydrolyzed with sulfuric acid by the general procedure described by Rowland *et al.* (13). One gram of fabric, homogenized as small (ca. 0.25 cm^2) squares, was covered with 15 g of 72% sulfuric acid and subjected to mild agitation at room temperature under an atmosphere of argon for 8 h. The solution was diluted to 7.6 *N* with 20 ml of distilled water and mild agitation was continued for 16 h. The solution was then diluted to 1.5 *N* with 120 ml of water and refluxed for 6 h. Barium hydroxide was utilized to adjust the acidity to a pH of 6.0–7.0, barium sulfate was removed by filtration, the filtrate was concentrated under vacuum below 40°, and the concentrate was freeze-dried to yield a solid hygroscopic product.

Removal of Glucose from Chemically Modified Glucoses

A 1.0 g sample of the hydrolyzate of the cotton fabric or allyl cotton was dissolved in 20 ml of water and 0.2 g of dried yeast was added. Fermentation was allowed to proceed at 80° F until no more microbubbles appeared (2 to 3 days). The solution was filtered (Millepore 0.4 μ) and freeze-dried to a solid product. The hydrolyzed cotton or glucose yielded less than 0.1 g of residual nonvolatile product; allyl cellulose yielded 0.4 g of residue.

Glucose was shown to be absent in the concentrate from allyl cellulose by the absence of a peak in the area of β-D-glucopyranose in gas chromatographic analysis. Further evidence for the absence of glucose was obtained by fermenting a sample of dextrose under the same experimental conditions as were used for the allyl cotton hydrolyzates. Gas–liquid chromatographic analysis of this material showed the absence of all peaks for glucose and showed only a single peak corresponding to glycerol.

Results and Discussion

The preparation of 3-*O*-allyl-D-glucose (**2**) was carried out by reacting 1,2:5,6-di-*O*-isopropylidene-α-D-glucofuranose with allyl bromide followed by hydrolysis of the blocking isopropylidene groups. The reaction proceeded well with either potassium metal in liquid ammonia or a suspension of potassium hydroxide in anhydrous dioxane. After hydrolysis of the blocking groups, **2** was obtained as a crystalline solid in ca. 45% overall yield. The trimethylsilyl ether derivative of this product was shown by gas–liquid chromatography to consist of two anomers (curve A, Fig. 1) which are assumed to be the α and β anomers.

6-*O*-Allyl-D-glucose (**4**) was prepared through 1,2:3,5-di-*O*-benzylidene-α-D-glucofuranose and through 3,5-*O*-benzylidene-1,2-*O*-isopropylidene-α-D-glucofuranose. Potassium hydroxide suspended in anhydrous dioxane proved to be the preferred reagent in both cases. The latter starting material yielded the purer product due to the difficulty in removing a byproduct, 1,2-*O*-benzylidene-α-D-glucopyranose from the former. Compound **4** was obtained in ca. 50% overall yield as a hygroscopic white solid upon hydrolysis of the intermediate.

Synthesis of 2-*O*-allyl-D-glucose (**5**) was achieved through *N*-(3,4,6-tri-*O*-acetyl-D-glucosyl)piperidine which was prepared from penta-*O*-acetyl-β-D-glucopyranose by the method of Hodge and Rist (9). The condensation of this intermediate with allyl bromide in the presence of moist silver oxide resulted in a 68% yield of *N*-(2-*O*-allyl-3,4,6-tri-*O*-acetyl-D-glucosyl)-piperidine (**6**). This product was then hydrolyzed in two steps to the white crystalline **5** in ca. 7% overall yield.

Another route to the 2-*O*-allyl isomer was attempted initially. This method made use of the allyl group as a protective group (1) as well as the reactant. Allyl bromide was condensed with 1,2-*O*-isopropylidene-α-D-glucofuranose using potassium hydroxide suspended in dioxane. The resulting 3,5,6-tri-*O*-allyl-1,2-*O*-isopropylidene-α-D-glucofuranose was subjected to methanolysis for removal of the isopropylidene group and introduction of a methyl group on the hydroxyl at C-1. The three allyl groups were then isomerized to propenyl substituents with potassium *t*-butoxide in dimethyl sulfoxide by the method of Gigg and Cunningham (2, 3). The rearrangement was followed by gas–liquid chromatography and showed the disappearance of the two original peaks and the simultaneous appearance of two new peaks. The completeness of the allylic rearrangement was further substantiated by infrared analysis which indicated the appearance of bands, at 5.98, 7.8, and 13.8 μ,

TABLE I

Relative retention values for trimethylsilyl ethers of allyl-D-glucoses*

Compound	Columns			
	SE-52-19%†	XE-60-8.5%‡	SE-52-19%§	XE-60-8.5%‖
Glucose	1.00	1.00	1.00	1.00
	1.29	1.40	1.54	1.95
2-*O*-Allyl-D-glucose	1.08	1.06	1.05	1.10
	1.30	1.22	1.38	2.50
3-*O*-Allyl-D-glucose	0.92	0.92	0.88	0.77
	1.24	1.16	1.36	1.39
6-*O*-Allyl-D-glucose	1.25	1.28	1.29	1.98
	1.39	1.45	1.50	2.82

*The first anomer of glucose was employed as an internal standard and was assigned a relative retention value of 1.00.
†Temperature 180–220 °C; rate 0.5°/min.
‡Temperature 80–140 °C; rate 0.5°/min.
§Temperature 200 °C; isothermal.
‖Temperature 125 °C; isothermal.

due to the propenyl linkage. Methyl 3,5,6-tri-*O*-(1-propenyl)-D-glucofuranoside (**10**) was condensed with allyl bromide in dioxane containing finely divided potassium hydroxide to produce a compound which is believed to be methyl 2-*O*-allyl-3,5,6-tri-*O*-(1-propenyl)-D-glucofuranoside (**11**). This product, obtained as a yellow viscous liquid, was hydrolyzed without further purification. Gas–liquid chromatographic analysis showed two primary peaks representing the two anomeric forms of 2-*O*-allyl-D-glucose. The impurity was glucose together with small amounts of unidentified material which showed much greater retention times on gas–liquid chromatograms than those of the desired product.

Preliminary to the determination of the identities and relative ratios of mono-*O*-allyl-D-glucoses obtained from the hydrolytic degradation of the molecular chain of allyl cellulose, the 2-*O*-, 3-*O*-, and 6-*O*-allyl-D-glucoses were characterized thoroughly by gas–liquid chromatography. Among the variety of columns examined (see Experimental section), SE-52 and XE-60 columns proved most effective in separating the trimethylsilyl ethers of the isomeric allyl-D-glucoses into separate peaks; the relative retention times for the two anomers for each isomer are summarized in Table I. We have found, as have Bullock and co-workers (1), Roberts and Rowland (14), and Willard and co-workers (15), that each isomer appears as two anomers and that the order of elution in gas–liquid chromatography is 3-*O*-isomer, 2-*O*-isomer, and 6-*O*-isomer. There is in these cases considerable variation, however, in the overlap which the anomers of the 2-*O*-isomer develop with the anomers of the 3-*O*- or 6-*O*-isomers.

Allyl cellulose was hydrolyzed with 72% sulfuric acid to glucose and allyl-D-glucoses and the latter were concentrated by the procedure of Rowland, Cirino, and Bullock (13). Chromatograms of the concentrate appeared to be free of interference in the region in which the mono-*O*-allyl-D-glucoses appeared. Peaks corresponding to glycerol and other components appeared near the solvent front.

Chromatograms of the concentrate of allyl-D-glucoses from allyl cellulose are reproduced in curve D of Fig. 1. The identities of the peaks were verified on SE-52 and XE-60 columns by relative retention times and by introducing small amounts of the authentic derivatives to the fermented hydrolyzate mixture and noting the increase in size of the corresponding peaks.

On a gas chromatographic column based on a liquid phase of 19% SE-52, both anomers of the 2-*O*-allyl-D-glucose and one anomer of each of the 3-*O*- and 6-*O*-allyl-D-glucoses were resolved separately (curve D, Fig. 1). The ratio of peak areas on this column, isothermal or programmed, for the 2-*O*-, 3-*O*-, and 6-*O*-isomers was 0.7:0.2:1.0 for an allyl cotton cellulose of a degree of substitution of 0.07. The variability of results from triangulation of various chromatograms was ± 0.05:± 0.05:0.0.

The ratio of the areas calculated on XE-60 column verified the ratio for the 3-*O*-allyl-D-glucose to the 6-*O*-allyl-D-glucose (0.25:1.0). The ratio of 2-*O*- to the 6-*O*-isomer (ca. 0.4:1.0)

Can. J. Chem. Downloaded from www.nrcresearchpress.com by 210.87.254.105 on 09/05/12
For personal use only.

could not be calculated with accuracy due to peak interference in the area of the first 2-*O*-anomer and to lack of resolution between the second anomer of 2-*O*-allyl-D-glucose and the first anomer of the 6-*O*-allyl-D-glucose.

The proportion of allyl groups distributed in the 2-*O*- and 3-*O*-positions of the monosubstituted D-glucopyranosyl residues is approximately 40% of the values which Croon reported (16) (i.e., 1.75:0.50:1.0) for the relative rate constants for these hydroxyl groups in the heterogeneous reaction with dimethyl sulfate. Although several factors (e.g., mechanism, media, specific availability of the different hydroxyl groups) may prove to have a bearing on the relative distribution of substituents from Williamson-type reactions of cellulose in heterogeneous systems, the only relationship which is currently evident in the literature (14) is the relationship between increasing molecular size of the reagent and decreasing proportion of substitution in the 2-*O*- and 3-*O*-positions.

1. A. L. BULLOCK, V. O. CIRINO, and S. P. ROWLAND. Can. J. Chem. **45**, 255 (1967).
2. J. CUNNINGHAM, R. GIGG, and C. D. WARREN. Tetrahedron Letters, No. **19**, 1191 (1964).
3. J. GIGG and R. GIGG. J. Chem. Soc. (C), 82 (1966).
4. J. MONTGOMERY and H. THOMAS. J. Org. Chem. **30**, 3235 (1965).
5. C. C. SWEELEY, R. BENTLEY, M. MAKITA, and W. W. WELLS. J. Am. Chem. Soc. **85**, 2497 (1963).
6. W. CORBETT and J. MCKAY. J. Chem. Soc. 2930 (1961).
7. P. BRIGL and H. GRUNER. Chem. Ber. **65**, 1428 (1932).
8. H. B. WOOD, H. W. DIEHL, and H. G. FLETCHER, JR. J. Am. Chem. Soc. **79**, 3863 (1957).
9. J. E. HODGE and C. RIST. J. Am. Chem. Soc. **74**, 1498 (1952).
10. T. J. PROSSER. J. Am. Chem. Soc. **83**, 1701 (1961).
11. J. E. CADOTTE, F. SMITH, and D. SPRIESTERSBACH. J. Am. Chem. Soc. **74**, 1501 (1952).
12. E. D. PARKER and J. D. GUTHRIE. U.S. Patent No. 2,727,805 to United States Secretary of Agriculture (December 20, 1955).
13. S. P. ROWLAND, V. O. CIRINO, and A. L. BULLOCK. Can. J. Chem. **44**, 1051 (1966).
14. E. J. ROBERTS and S. P. ROWLAND. Can. J. Chem. **45**, 261 (1967).
15. J. WILLARD, R. TURNER, and R. SCHWENKER, JR. Textile Res. J. **35**, 565 (1965).
16. I. CROON and B. LINDBERG. Svensk Papperstid. **60**, 843 (1957).

Can. J. Chem. Downloaded from www.nrcresearchpress.com by 210.87.254.105 on 09/05/12
For personal use only.

Can. J. Chem. Downloaded from www.nrcresearchpress.com by 210.87.254.40 on 09/05/12
For personal use only.

Methods for the synthesis of L-lactyl-L-valine-1-^{14}C[1]

G. P. SLATER AND H. SPENCER[2]

Prairie Regional Laboratory, National Research Council of Canada, Saskatoon, Saskatchewan

Received October 4, 1967

The preparation of L-lactyl-L-valine from L-lactic acid and L-valine, by methods used for the synthesis of peptides, was investigated. Initial experiments with *O*-benzoyl-DL-lactic acid and DL-valine benzyl ester unexpectedly gave *N*-benzoyl-DL-valine benzyl ester. However, coupling between *O*-benzyloxycarbonyl-DL-lactic acid and either DL-valine, or DL-valine benzyl ester, occurred in good yield. A simpler method, which was reported to give a 39% yield of L-lactyl-L-valine, gave only 10% of product but was modified to give L-lactyl-L-valine-1-^{14}C in 90% yield.

Canadian Journal of Chemistry, 46, 673 (1968)

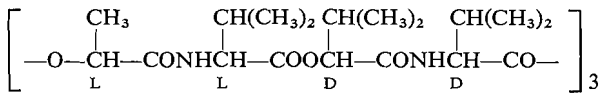

1

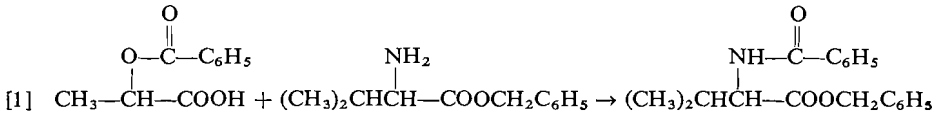

2

Previous studies (1) on the biosynthesis of valinomycin (**1**) have shown that L-valine-1-^{14}C is distributed equally between the L- and D-valine moieties and that D-valine is not incorporated. In view of these results, the preparation of L-lactyl-L-valine-1-^{14}C was undertaken so that this compound could be used for further investigation of the biosynthesis of valinomycin.

As the essential step in the synthesis required the formation of an amide bond between L-lactic acid and L-valine, a number of methods of peptide synthesis, for which good retention of optical purity has been reported (2), were investigated. The intended method envisaged the condensation of *O*-benzyloxycarbonyl-L-lactic acid and L-valine benzyl ester since the protecting groups on these two compounds are easily removed by hydrogenolysis (2). However, because *O*-benzyloxycarbonyl-DL-lactic acid was not readily obtainable in crystalline form the corresponding *O*-benzoyl derivative was used for the initial investigations on racemic compounds.

The condensation reactions were performed using the substituted phosphite ester technique (2), ethoxyacetylene (3), or benzenesulfonyl chloride (4); however, these methods gave (See eq. [1]) a new and unexpected product, which was shown to be *N*-benzoyl-DL-valine benzyl ester (**2**).

The acid chloride method of peptide synthesis (2) was no more successful than the foregoing procedures, and *N*-benzoyl-DL-valine benzyl ester (**2**) was obtained whether phosphorus pentachloride or thionyl chloride was used to generate the acid chloride.

These results were difficult to explain until the reactions were reinvestigated. It was then found that *O*-benzoyl-DL-lactic acid reacted with phosphorus pentachloride and benzenesulfonyl chloride to give benzoyl chloride and benzoic anhydride, respectively. The effects of the substituted phosphite esters and of ethoxyacetylene were not reexamined. However, it seems probable that the result would be production of benzoic anhydride, since ethoxyacetylene reacts with carboxylic acids to give anhydrides (5,6), as does benzenesulfonyl chloride (4), and the phosphite esters produce mixed anhydrides with acyl amino acids (2).

Phosphorus pentachloride did not react with

---

[1]Issued as NRCC No. 9886.

[2]NRCC Postdoctorate Fellow, 1965–1966. Present address: Chemistry Department, University of Saskatchewan, Saskatoon, Saskatchewan.

Can. J. Chem. Downloaded from www.nrcresearchpress.com by 210.87.254.40 on 09/05/12
For personal use only.

O-benzyloxycarbonyl-DL-lactic acid to give benzyloxycarbonyl chloride. The nuclear magnetic resonance (n.m.r.) spectrum indicated that the main product was *O*-benzyloxycarbonyl-DL-lactyl chloride together with impurities. When DL-valine benzyl ester was treated with this crude product the result was an oil whose elemental analysis did not indicate *O*-benzyloxycarbonyl-DL-lactyl-DL-valine benzyl ester. However, this compound appears to have been produced, since hydrogenolysis (2) gave DL-lactyl-DL-valine which was characterized as the dicyclohexylamine salt (7).

The required compound was also obtained using a method of peptide synthesis introduced by Birkofer and Ritter (8). In this procedure, *O*-benzyloxycarbonyl-DL-lactic acid *p*-nitrophenyl ester and DL-valine were fused with *N*-trimethylsilylacetamide (9). The product was again an oil which did not give a satisfactory elemental analysis. However, hydrogenolysis (2) gave DL-lactyl-DL-valine identical with the previously obtained compound.

While this work was in progress the synthesis of L-lactyl-L-valine was reported by Shemyakin and co-workers (7). The Russian group first resolved DL-lactic acid and the L-isomer was then converted in turn to the benzyl ester, the hydrazide, and the azide. The azide, in ethyl acetate, was added to an aqueous solution of L-valine and triethylamine. The reported yield of L-lactyl-L-valine was 39% but this could not be duplicated in our laboratory, the best yield being 10% of product which was always contaminated with benzyl alcohol.

The foregoing method involved a two-phase system and was complicated by the precipitation of L-valine during the reaction. A homogeneous reaction in which L-valine benzyl ester was treated with L-lactic azide, using ethyl acetate as the common solvent, was therefore examined. Using equimolar quantities of L-lactic hydrazide and L-valine benzyl ester good yields (60–70%) of L-lactyl-L-valine benzyl ester were obtained together with unreacted L-valine benzyl ester (40–30%). In order to achieve a high conversion of benzyl-L-valine to L-lactyl-L-valine benzyl ester it was necessary to use a 2.5 mole excess of L-lactic hydrazide. This resulted in a 95% yield of the desired product, or 100% based on benzyl-L-valine used.

The L-lactyl-L-valine benzyl ester thus obtained was always contaminated with solvent and occasionally with a small amount of compound absorbing at 2150 cm^{-1}, corresponding to an azide (10). The solvent could be removed by prolonged heating at 50° under vacuum (0.05 mm) and if the other contaminant was present it would sublime out of the flask. The infrared spectrum (KBr) of the sublimate showed an intense band at 2150 cm^{-1}. This impurity could be removed by washing an ether solution of the product several times with water or by warming the reaction mixture to 40–45° for 2 h prior to isolating the product. L-Lactyl-L-valine benzyl ester obtained in this way had n.m.r. and infrared spectra consistent with the expected structure.

The hydrogenolysis step proved to be very rapid and gave a quantitative yield of L-lactyl-L-valine. Again, the product was always contaminated with solvent, as indicated by the yield (105%). Complete removal of solvent by warming under vacuum was not feasible due to the tendency of L-lactyl-L-valine to form a lactone (11). The L-lactyl-L-valine, however, could be characterized as the dicyclohexylamine salt (7).

The specific rotations of L-lactyl-L-valine and its dicyclohexylamine salt are given (7) as +8.5° and —13°, respectively. The corresponding products synthesized in this laboratory from commercially available L-lactic acid and L-valine had specific rotations of +9.5° and —8.9°, respectively. There is reasonable agreement on the specific rotation of L-lactyl-L-valine but this is not the case for the dicyclohexylamine salt. In order to resolve this discrepancy, valinomycin was hydrolyzed with dilute methanolic sodium hydroxide (12) to give D-α-hydroxyisovaleryl-D-valine and L-lactyl-L-valine. The specific rotation of D-α-hydroxyisovaleryl-D-valine dicyclohexylamine salt (+25.9°) was in good agreement with the value (+24°) for the product synthesized by Shemyakin *et al.* (7). However, the specific rotation of the L-lactyl-L-valine dicyclohexylamine salt (—8.7°) was close to the value (—8.9°) obtained for the synthetic product from this laboratory.

As an alternative to benzyl L-valine, the use of L-valine *t*-butyl ester was investigated. This had the advantage that the L-lactyl-L-valine *t*-butyl ester was a solid readily purified by crystallization. However, the yield of L-valine *t*-butyl ester

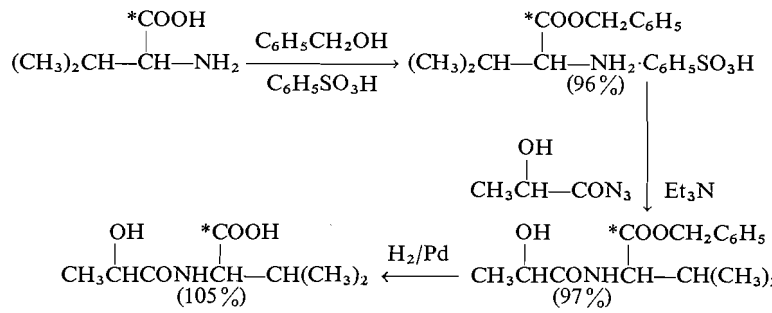

(53%) was considerably lower than that (96%) of L-valine benzyl ester benzenesulfonate.

The best method of preparing L-lactyl-L-valine-1-^{14}C appeared to be by formation of the amide bond between L-lactic azide and L-valine-1-^{14}C benzyl ester. The desired compound was therefore synthesized according to the following scheme (yield of each step in brackets) in an overall yield of 90% based on the L-valine used and on the L-lactyl-L-valine theoretically obtainable from the L-lactyl-L-valine benzyl ester.

The specific activity of the product of each step is shown in Table I. It is seen that the specific activities of the crystalline products are very similar while those of non-crystalline products are somewhat lower. Using the values in Table I, the purity of L-lactyl-L-valine, compared to the L-valine, is 90%.

TABLE I

Specific activity of products

Compound	Specific activity (μc/mmole)
L-Valine	2.57
Benzyl-L-valine benzenesulfonate	2.53
Benzyl L-lactyl-L-valine	2.39
L-Lactyl-L-valine	2.31
L-Lactyl-L-valine dicyclohexylammonium salt	2.50

Experimental

Melting points are uncorrected and were determined on a Fisher–Johns or Thomas–Hoover apparatus (latter for sealed capillaries). Petroleum ether (Skelly F.) had b.p. 30–60°. Infrared spectra were recorded on a Perkin–Elmer 257 grating spectrophotometer, and nuclear magnetic resonance spectra on a Varian H-100 instrument. Optical rotations were measured on a Rudolph polarimeter.

*O-Benzoyl-*DL*-lactic Acid*

A commercially available solution of DL-lactic acid (20 ml, 85%) was extracted with ether overnight and the dried ($MgSO_4$) extract evaporated at 30° under reduced pressure. The residue (5.5 g, 0.061 mole) was dissolved in pyridine (100 ml), cooled in ice, and freshly distilled benzoyl chloride (9.4 g, 0.067 mole) was added slowly with stirring. After standing at room temperature overnight the mixture was poured onto crushed ice, acidified with concentrated HCl and extracted with ether. Evaporation of the washed (H_2O) and dried ($MgSO_4$) extract gave a colorless gum (9.6 g) which crystallized from ether – petroleum ether to give *O*-benzoyl-DL-lactic acid (7.5 g, 63%), m.p. 111–113° (lit. (13) m.p. 111.5°).

DL-*Valine Benzyl Ester Benzenesulfonate*

DL-Valine (4.68 g, 0.04 mole), benzenesulfonic acid monohydrate (7.74 g, 0.044 mole), and benzyl alcohol (28 ml, 0.27 mole) in carbon tetrachloride (100 ml) were heated under reflux for 16 h and the condensate dried by passage through silica gel (14). A white crust, which adhered to the wall of the reaction flask, formed rapidly and did not dissolve during the reaction. The mixture was filtered hot and the white solid washed with hot carbon tetrachloride. Dilution of the filtrate with ether and cooling (0°) gave DL-valine benzyl ester benzenesulfonate (12.9 g, 88%), m.p. 152–154°. Recrystallization from ethanol–ether raised the m.p. to 156–157°.

Anal. Calcd. for $C_{18}H_{23}NO_5S$: C, 59.2; H, 6.3; N, 3.8; S, 8.8. Found: C, 59.1; H, 6.6; N, 4.0; S, 9.0.

The white precipitate (0.94 g, 8.5%) had m.p. 167–169°, raised to 170–171° by crystallization from ethanol–ether.

Anal. Calcd. for $C_{11}H_{17}NO_5S$: C, 47.9; H, 6.2; N, 5.1; S, 11.6. Found: C, 47.7; H, 6.4; N, 4.8; S, 11.7.

DL-*Valine Benzenesulfonate*

DL-Valine (117 mg, 1.0 mmole) and benzenesulfonic acid monohydrate (194 mg, 1.1 mmole) were dissolved in water (5 ml) and evaporated to dryness under reduced pressure at 60°. The residue was crystallized from ethanol–ether to give white crystals, m.p. 167–169°. A mixture m.p. with the foregoing product was not depressed and the infrared spectra (KBr) of the two compounds were identical.

DL-*Valine Benzyl Ester*

DL-Valine benzyl ester benzenesulfonate (3.65 g, 0.01 mole) in 5% aqueous potassium bicarbonate (100 ml) was shaken at room temperature for 30 min. Extraction of the aqueous mixture with ether and evaporation of the washed and dried extract gave a pale-yellow oil (1.93 g)

Can. J. Chem. Downloaded from www.nrcresearchpress.com by 210.87.254.40 on 09/05/12
For personal use only.

Can. J. Chem. Downloaded from www.nrcresearchpress.com by 210.87.254.40 on 09/05/12
For personal use only.

which was distilled to give DL-valine benzyl ester (1.73 g, 84%), b.p. 113–115° at 2mm.

Anal. Calcd. for $C_{12}H_{17}NO_2$: C, 69.5; H, 8.3; N, 6.8. Found: C, 69.5; H, 8.1; N, 6.5.

*Reaction of O-Benzoyl-*DL*-lactic Acid and Benzyl-*DL*-valine with Tetraethylpyrophosphite*

A mixture of benzyl-DL-valine (207 mg, 1.0 mmole), *O*-benzoyl-DL-lactic acid (199 mg, 1.0 mmole), diethylphosphite (680 mg, 5.0 mmole), and tetraethylpyrophosphite (290 mg, 1.1 mmole), was heated on a steam bath for 30 min (15). The mixture was cooled in ice, diluted with cold (0°) water, and extracted with ether. The ether extract was washed with water, 5% potassium bicarbonate solution, and water. Neutralization of the bicarbonate extract with 2 *N* HCl gave *O*-benzoyl-DL-lactic acid (109 mg, 58%), m.p. 108–110° while evaporation of the dried ether extract gave a yellow oil (199 mg) which could not be induced to crystallize. The product in benzene – petroleum ether (1:3) was chromatographed on deactivated (16) Spence type 'H' alumina (6 g) to give *N*-benzoyl-DL-valine benzyl ester (90 mg, 28%), m.p. 73–74° from diisopropyl ether – petroleum ether.

Anal. Calcd. for $C_{19}H_{21}NO_5$: C, 73.3; H, 6.8; N, 4.5. Found: C, 73.2; H, 7.0; N, 4.6.

Benzoylation of DL*-Valine Benzyl Ester*

DL-Valine benzyl ester (1 g, 0.0048 mole) in pyridine (10 ml) was cooled in ice and freshly distilled benzoyl chloride (0.63 ml, 0.0053 mole) added. After standing at room temperature overnight the mixture was poured on to crushed ice, acidified with 2 *N* HCl, and extracted with ether. Evaporation of the washed (H_2O, 5% $KHCO_3$, H_2O) and dried extract gave an oil which solidified on standing. Crystallization from diisopropyl ether – petroleum ether gave *N*-benzoyl-DL-valine benzyl ester (1.21 g, 80%), m.p. 73–74°. A mixture m.p. with the product from the previous reaction was not depressed and the infrared spectra (KBr) of the two products were identical.

*Reaction of O-Benzoyl-*DL*-lactic Acid and Benzyl-*DL*-valine with Diethylchlorophosphite*

A mixture of DL-valine benzyl ester (1.22 g, 0.0059 mole), triethylamine (0.6 g, 0.0059 mole), and diethylchlorophosphite (2) (0.93 g, 0.0059 mole) in dry ether (30 ml) was shaken at room temperature for 17 h, filtered, and evaporated under reduced pressure to give a pale-green oil (17). *O*-Benzoyl-DL-lactic acid (1.15 g, 0.0059 mole) in dry toluene (30 ml) was added and the mixture boiled under reflux for 6 h. After standing overnight (16 h) at room temperature, the mixture was washed with water, 5% potassium bicarbonate solution, and water. Evaporation of the dried toluene solution gave a pale-brown gum (1.45 g), which was chromatographed as before to give *N*-benzoyl-DL-valine benzyl ester, m.p. 73–74° (0.69 g, 37%). Acidification of the bicarbonate extract with 2 *N* HCl gave *O*-benzoyl-DL-lactic acid (0.61 g, 52%).

*Reaction of O-Benzoyl-*DL*-lactic Acid and* DL*-Valine Benzyl Ester with Ethoxyacetylene*

A mixture of DL-valine benzyl ester (2.92 g, 0.014 mole), *O*-benzoyl-DL-lactic acid (2.75 g, 0.014 mole), and ethoxyacetylene (4.1 g, 0.06 mole) in ethyl acetate (70 ml) containing 0.5% water (3), was boiled under reflux for 5 h. After standing at room temperature overnight, the mixture was washed with water, 5% potassium bicarbonate solution, water, 2 *N* HCl, and water. Evaporation of the dried ethyl acetate solution gave a pale-brown gum (5.23 g) which was chromatographed as before to give *N*-benzoyl-DL-valine benzyl ester (3.72 g, 71%). Neutralization of the bicarbonate washings gave *O*-benzoyl-DL-lactic acid (0.57 g, 21%), while neutralization of the acid wash and extraction with ether gave a pale-yellow oil (25 mg) whose infrared spectrum was identical with that of DL-valine benzyl ester.

*Reaction of O-Benzoyl-*DL*-lactic Acid and* DL*-Valine Benzyl Ester with Benzenesulfonyl Chloride*

A solution of benzyl DL-valine (168 mg, 0.8 mmole) in toluene (10 ml) was added over 2 h to a boiling solution of *O*-benzoyl DL-lactic acid (194 mg, 1.0 mmole), triethylamine (130 mg, 1.3 mmole), and benzenesulfonyl chloride (88 mg, 0.5 mmole) in toluene (10 ml). Boiling was continued overnight (17 h) and the mixture evaporated under reduced pressure. The residue was dissolved in ether and the solution washed with water, 4 *N* HCl, water, saturated $NaHCO_3$ solution, and water. Evaporation of the dried ether solution gave a colorless gum (157 mg, 50%) whose infrared spectrum was identical with that of *N*-benzoyl-DL-valine benzyl ester. (When the reaction was repeated without benzyl-DL-valine the product was benzoic anhydride, identified by comparison with an authentic sample).

*Reaction of O-Benzoyl-*DL*-lactic Acid and* DL*-Valine Benzyl Ester Benzenesulfonate by the Acid Chloride Method*

(*a*) *With* PCl_5

Phosphorus pentachloride (720 mg, 3.5 mmole) was added over 5 min to a solution of *O*-benzoyl-DL-lactic acid (560 mg, 2.9 mmole) in cold (0°) ether (20 ml). The mixture was stirred at 0° for 1 h and at room temperature for 1 h before pouring the mixture onto crushed ice and extracting with ether. The ether extract was washed (H_2O, 5% $NaHCO_3$, H_2O), dried, and evaporated to give a colorless oil which was dissolved in dry tetrahydrofuran (10 ml). (In a separate experiment the oil was identified as benzoyl chloride by comparison with an authentic sample).

While the above reaction was proceeding, DL-valine benzyl ester benzenesulfonate (1.06 g, 2.9 mmole) and triethylamine (0.92 ml, 6.5 mmole) in tetrahydrofuran (10 ml) were stirred at room temperature for 2 h. The mixture was cooled to −30° and the product from the previous reaction added over 5 min. After stirring at −30° for 1 h, the mixture was stirred at room temperature for 2 h before removing the solvent under reduced pressure at 50°. The residue was acidified with 1 *N* HCl and extracted with ether, and the extract washed with water, saturated potassium bicarbonate solution, and water. Evaporation of the dried extract gave a pale-yellow oil (0.96 g) which solidified on standing. Crystallization from ether – petroleum ether gave *N*-benzoyl-DL-valine benzyl ester (0.76 g, 85%), m.p. 73–74°.

(*b*) *With* $SOCl_2$

O-Benzoyl-DL-lactic acid (560 mg, 2.9 mmole) in thionyl chloride (5 ml) was boiled under reflux for 2 h and allowed to stand overnight (16 h) at room temperature. Excess thionyl chloride was removed at 50° under reduced pressure to give a dark-brown oil. The residue

Can. J. Chem. Downloaded from www.nrcresearchpress.com by 210.87.254.40 on 09/05/12
For personal use only.

was dissolved in tetrahydrofuran and added to a mixture of DL-valine benzyl ester benzenesulfonate and triethylamine as in (*a*). The product from the reaction was obtained as a brown gum (0.98 g, 108%) which did not solidify on standing. However, the infrared spectrum was identical with that of the crude product obtained in (*a*).

*O-Benzyloxycarbonyl-*DL*-lactyl-*DL*-valine Benzyl Ester*

O-Benzyloxycarbonyl-DL-lactic acid (18) (1.14 g, 0.0051 mole) in tetrahydrofuran (10 ml) at −5° was treated over 5 min with PCl_5 (1.32 g, 0.0064 mole). The solution was stirred at −5° for 1 h and at room temperature for a further hour before adding it to the following mixture.

DL-Valine benzyl ester benzenesulfonate (1.86 g, 0.0051 mole) and triethylamine (4 ml, 0.029 mole) in tetrahydrofuran (20 ml) were stirred at room temperature for 2 h and then cooled to −30° before adding the above solution over 15 min. The mixture was stirred at −30° for 1 h and at room temperature for 4 h before removing solvent at 50° under reduced pressure. The residue was acidified with 1 *N* HCl and extracted with ether. The ether extract was washed with water, 5% sodium bicarbonate solution, and water. Evaporation of the dried extract gave a brown gum (2.2 g, 104%) which could not be induced to crystallize.

DL-*Lactyl-*DL*-valine*

The foregoing product (2.2 g) in methanol – acetic acid (249:1 v/v, 50 ml) was hydrogenolyzed over palladium oxide (250 mg) for 7 h. The mixture was filtered and evaporated to dryness to give DL-lactyl-DL-valine as a pale-brown gum (0.89 g, 88%). Part of the product (100 mg) was dissolved in ethyl acetate (5 ml) and treated with freshly distilled dicyclohexylamine until no further precipitation occurred. The DL-lactyl-DL-valine dicyclohexylamine salt was recrystallized from ethanol–ether and had m.p. 162–163°.

Anal. Calcd. for $C_{20}H_{38}N_2O_4$: C, 64.8; H, 10.3. Found: C, 65.1; H, 10.2.

*O-Benzyloxycarbonyl-*DL*-lactyl-*DL*-valine*

To a cold (0°) solution of benzyloxycarbonyl-DL-lactic acid (896 mg, 4.0 mmole) in anhydrous tetrahydrofuran (10 ml) was added ethylchloroformate (432 mg, 4.0 mmole) and triethylamine (404 mg, 4.0 mmole). After standing at 0° for 8 min, *p*-nitrophenol (556 mg, 4.0 mmole) was added and the mixture boiled for 3–4 min and then evaporated under reduced pressure. The residual oil was dissolved in ether, washed with 2 *N* HCl and water and the dried solution evaporated under reduced pressure. The *O*-benzyloxycarbonyl-DL-lactic acid *p*-nitrophenyl ester (1.44 g, 4.6 mmole) so obtained was mixed with DL-valine (490 mg, 4.2 mmole) and trimethylsilyl acetamide (9) (1.36 g, 10 mmole) and fused at 80° (8). After stirring at 80° for 22 h the cooled (25°) mixture was treated with saturated potassium bicarbonate solution and extracted with ether. The aqueous phase was acidified with concentrated sulfuric acid and extracted with ether in the usual manner to give a mixture of carboxylic acids (0.99 g). Chromatography on silicic acid using chloroform – benzene – acetic acid (4:1:1 v/v) gave the major component (892 mg, 67%). Further elution with chloroform – methanol – acetic acid (8:1:1) gave a second fraction (82 mg).

The major component was heated at 90° under vacuum (0.1 mm) to remove acetic acid. The product, which could not be induced to crystallize, was hydrogenolyzed over palladium oxide (157 mg) as for the *O*-benzyloxycarbonyl-DL-lactyl-DL-valine benzyl ester. The DL-lactyl-DL-valine obtained was identical (infrared spectrum) with the previously obtained product and gave an identical dicyclohexylamine salt (258 mg). The yield of DL-lactyl-DL-valine dicyclohexylamine salt, based on the DL-valine used, was 22%.

Hydrolysis of Valinomycin

Valinomycin (200 mg) was hydrolyzed in dilute methanolic NaOH according to the procedure of Vining and Taber (12). The crude product (277 mg) was chromatographed on silica gel using Neish's method (19) to give D-α-hydroxyisovaleryl-D-valine (120 mg, 103%) and L-lactyl-L-valine (93 mg, 91%), which were characterized as the dicyclohexylamine salts. D-α-Hydroxyisovaleryl-D-valine dicyclohexylamine salt, m.p. 196–197° (sealed capillary), $[\alpha]_D^{23}$ +25.9° (*c*, 1.45 EtOH) (lit. (7) m.p. 197–198°, $[\alpha]_D^{20}$ +24°). L-Lactyl-L-valine dicyclohexylammonium salt, m.p. 174–176° (sealed capillary), $[\alpha]_D^{23}$ −8.7° (*c*, 2.23 EtOH) (lit. (7) m.p. 174–175°, $[\alpha]_D^{20}$ −13°).

L-*Valine-1-*^{14}*C Benzyl Ester Benzenesulfonate*

L-Valine-1-^{14}C (approximately 20 μc) was added to L-valine (881 mg), $[\alpha]_D^{25}$ +26.5° (*c*, 2.07 5 *N* HCl) and the whole dissolved in water and evaporated to dryness to give L-valine-1-^{14}C (891 mg) specific activity 2.57 μc/mmole. This product (888 mg, 0.0076 mole) together with benzenesulfonic acid monohydrate (1.47 g, 0.0084 mole) and benzyl alcohol (8.1 ml, 0.079 mole) in carbon tetrachloride (22 ml) was boiled under reflux for 26 h and the condensate dried with silica gel (14). After standing at room temperature overnight the product was filtered and washed with ether until the smell of benzyl alcohol could no longer be detected. The L-valine benzyl ester benzenesulfonate (2.67 g, 96%) had m.p. 180–182° and specific activity 2.53 μc/mmole, (lit. (14) m.p. 177–180°).

L-*Lactyl-*L*-valine-1-*^{14}*C Benzyl Ester*

Ethyl L-lactate (20) (3.10 g, 0.026 mole) and hydrazine hydrate (5.8 ml, 0.12 mole) in ethanol (30 ml) was boiled for 7 h and then evaporated under reduced pressure on a boiling water bath. The residue was stored over concentrated sulfuric acid in a vacuum desiccator to give L-lactic hydrazide (2.75 g, 101%) as a brown gum.

The hydrazide (0.027 mole) was dissolved in 1 *N* HCl (33 ml), cooled to −5°, and treated with sodium nitrite solution (7.6 ml, 0.028 mole). After 5 min the test for nitrite was negative and more sodium nitrite solution (1 ml) was added. After stirring at −5° for 30 min the mixture was extracted with ethyl acetate and the washed (H_2O, 2% $NaHCO_3$, H_2O) extract added to the following mixture.

L-Valine-1-^{14}C benzyl ester benzenesulfonate (2.67 g, 0.0073 mole) in ethyl acetate (60 ml) containing triethylamine (1.2 ml, 0.0085 mole) was stirred in a cold room at 12° for 3 h and then cooled in ice for 15 min prior to adding triethylamine (1.2 ml) and the solution of L-lactic azide in ethyl acetate. The mixture was stirred at 0° for 7 h, at 12° for 14 h, and at 40–45° for 2 h. The reaction mixture was washed with 1 *N* HCl and water, and the

dried solution evaporated to give L-lactyl-L-valine-1-^{14}C benzyl ester as a pale-yellow oil (1.97 g, 97%), $[\alpha]_D^{25}$ −25.1° (*c*, 1.98 EtOH), specific activity 2.39 μc/mmole.

The acid wash on neutralization and extraction with ether gave L-valine-1-^{14}C benzyl ester (0.05 g, 2%).

L-Lactyl-L-valine-1-^{14}C

The benzyl L-lactyl-L-valine-1-^{14}C (1.92 g, 0.0069 mole) in methanol – acetic acid (50 ml, 249:1 v/v) was hydrogenolyzed over palladium oxide (347 mg). The mixture was filtered and evaporated under reduced pressure to give L-lactyl-L-valine-1-^{14}C (1.37 g, 105%), $[\alpha]^{25}$ +9.1° (*c*, 1.46 EtOH) (lit. (7) $[\alpha]^{20}$ +8.5°), specific activity 2.31 μc/mmole.

A sample of the above product was converted to the dicyclohexylammonium salt, m.p. 175–176° (sealed capillary) (lit. (7) m.p. 174–175°), specific activity 2.50 μc/mmole.

L-Lactyl-L-valine t-Butyl Ester

Ethyl L-lactate (3.36 g, 0.0285 mole) and hydrazine hydrate (5.5 ml, 0.113 mole) in ethanol (30 ml) was boiled for 7 h and worked up as before to give L-lactic hydrazide (2.90 g, 98%). The hydrazide (0.028 mole) in 1 *N* HCl (35 ml) was cooled to −5° and treated with sodium nitrite solution (8 ml, 0.029 mole). After 5 min more sodium nitrite (1 ml) was required to give a positive test. The mixture was worked up after 30 min and the azide solution added to L-valine *t*-butyl ester (21) (1.57 g, 0.009 mole) and triethylamine (1.5 ml, 0.011 mole) in ethyl acetate (60 ml) at 0°. The mixture was stirred at 0° for 6 h, 12° for 16 h, and at 40–45° for 2 h. The mixture was worked up in the same way as for the lactylvaline benzyl ester to give L-lactyl-L-valine *t*-butyl ester as a pale-yellow solid (1.77 g, 80%). Recrystallization from ether – petroleum ether gave colorless crystals m.p. 83°, $[\alpha]_D^{25}$ −13.9° (*c*, 2.43 EtOH).

Anal. Calcd. for $C_{12}H_{23}NO_4$: C, 58.8; H, 9.5; N, 5.7. Found: C, 58.9; H, 9.5; N, 5.9.

Acknowledgments

Elemental analyses and nuclear magnetic resonance spectra were determined by Mr. W. C. Haid and Mr. M. Mazurek, respectively. Radioisotope analyses were performed by Mr. J. Dyck. The authors thank Dr. J. C. MacDonald of these laboratories for a generous gift of valinomycin.

1. J. C. MacDonald. Can. J. Microbiol. **6**, 27 (1960).
2. J. P. Greenstein and M. Winitz. *In* Chemistry of the amino acids. Vol. II. J. Wiley and Sons, Inc., New York. 1961. Chap. 10.
3. G. Tadema, E. Harryvan, H. J. Panneman, and J. F. Arens. Rec. Trav. Chim. **83**, 345 (1964), and references therein.
4. J. H. Brewster and C. J. Ciotti. J. Am. Chem. Soc. **77**, 6214 (1955).
5. G. Eglinton, E. R. H. Jones, B. L. Shaw, and M. C. Whiting. J. Chem. Soc. 1860 (1954).
6. J. F. Arens and T. Doornbos. Rec. Trav. Chim. **74**, 79 (1955).
7. M. M. Shemyakin, E. I. Vinogradova, M. Yu. Feigina, N. A. Aldanova, Yu. A. Ovchinnikov, and A. A. Keryushkin. Zh. Obshch. Khim. **34**, 1782 (1964).
8. L. Birkofer and A. Ritter. Angew. Chem. Intern. Ed. Engl. **4**, 417 (1965).
9. L. Birkofer, A. Ritter, and H. Dickopp. Ber. **96**, 1473 (1963).
10. L. J. Bellamy. *In* The infrared spectra of complex molecules. John Wiley and Sons, Inc., New York. 1962. p. 263.
11. H. Brockmann and H. Geeren. Ann. **603**, 216 (1957).
12. L. C. Vining and W. A. Taber. Can. J. Chem. **35**, 1109 (1957).
13. J. Wislicenus. Ann. **133** 257 (1865).
14. J. E. Shields, W. H. McGregor, and F. H. Carpenter. J. Org. Chem. **26**, 1491 (1961).
15. G. W. Anderson, J. Blodinger, and A. P. Welcher. J. Am. Chem. Soc. **74**, 5309 (1952).
16. K. R. Farrer, J. C. Hamlet, H. B. Henbest, and E. R. H. Jones. J. Chem. Soc. 2657 (1952).
17. H. K. Miller and H. Waelsch. Arch. Biochem. Biophys. **35**, 176 (1952).
18. G. Losse and G. Bachmann. Ber. **97**, 2671 (1964).
19. A. C. Neish. National Research Council of Canada, Report No. 46-8-3. Second revision 1952. p.27.
20. E. R. Gonzalez. Ciencia (Mex.) **8**, 175 (1947); Chem. Abst. **43**, 127 (1949).
21. R. W. Roeske. Chem. Ind. London, 1121 (1959).

Can. J. Chem. Downloaded from www.nrcresearchpress.com by 210.87.254.40 on 09/05/12
For personal use only.

Can. J. Chem. Downloaded from www.nrcresearchpress.com by 210.87.254.42 on 09/05/12
For personal use only.

Gas-liquid chromatography of terpenes. Part XVI. The volatile oil of the leaves of *Juniperus ashei* Buchholz[1]

E. VON RUDLOFF

National Research Council of Canada, Prairie Regional Laboratory, Saskatoon, Saskatchewan

Received August 17, 1967

The major components of the leaf oil of the Ashe juniper were found to be *d*-camphor (42.1%), *d*-bornyl acetate (22.5%), *d*-limonene (8.4%), tricyclene (4.8%), *d*-camphene (4.4%), *d*-borneol (2.9%), *p*-cymene (2.8%), *d*-myrcene (1.8%), *d*-α-pinene (1.7%), and *d*-camphene hydrate (1.5%). This appears to be the first time that the latter alcohol has been isolated from a natural source. Smaller amounts of linalool, carvone, elemol, and traces of *trans*-2-methyl-6-methylene-3,7-octadien-2-ol were also identified. Several alcohols having terminal methylene groups were isolated in trace amounts.

The monoterpenes found in this oil are not typical for the genus *Juniperus* and this result offers a unique chemical approach to the study of introgression of the Ashe juniper with other juniper species.

Canadian Journal of Chemistry, **46**, 679 (1968)

Introduction

The Ashe juniper, *Juniperus ashei* Buchholz, is a member of the section Sabina of the genus *Juniperus* which occurs in a rather limited area of Texas and Oklahoma (1). Its distribution, morphology, and introgression with adjacent juniper species, including *J. virginiana*, *J. monosperma*, and *J. pinchoti*, were studied by Hall (2). It has been shown in recent years that chemical components found in related or supposedly related plants may give information which supplements classical taxonomic data (3, 4). Von Rudloff has shown that the distribution pattern of the terpenes found in the leaf oils of spruce species (5, 6), and possibly also of juniper species (7, 8), may be a useful tool in chemosystematic studies. To carry out such a chemosystematic investigation of the Ashe juniper, and its introgression with *J. virginiana* (9), the chemical composition of its leaf oil was required. A search of the literature failed to yield any reference to chemical analyses of this species, although its wood oil is used in the production of cedarwood oil in areas where the red cedar, *J. virginiana*, is scarce or absent (10).

The analysis of the leaf oils of several juniper species by means of gas–liquid chromatography (g.l.c.) was described earlier (7, 8, 11). However, it has since become apparent that quantitative differences may be significant in studies of introgression or hybridization (5, 12). Hence, improvement of the quantitative results would be desirable as determination of peak areas by the triangulation method or similar techniques can be subject to comparatively large errors (13), especially in partially resolved or minor peaks. A digital computer was employed in this study to obtain such improvement.

It was found that in spruce there exists considerable variation in the quantitative leaf oil composition from one leaf to another, and that several branches had to be collected at different heights of a tree to give a representative leaf oil sample (5). Hence, the direct injection technique (14) was employed to determine what variation, if any, may be encountered in going from one leaf to another and from the green to the brown portions of the scaly leaves of the Ashe juniper.

Experimental

The g.l.c. analyses were carried out with an F & M model 500 instrument (linear temperature programming, thermal conductivity detector: F & M Scientific Instrument Inc.) and a unit of conventional design (isothermal operation). An Aerograph model A-700 gas chromatograph (Wilkens Instrument and Research Inc.) was used for preparative g.l.c. and the experiments employing direct injection (14) were carried out with an Aerograph model 695 inductor and an Aerograph model 600-D gas chromatograph (flame-ionization detector). Integration and summation of the area under each peak was achieved by means of an Aerograph model 471 digital integrator. Helium was used as carrier gas and flow rates were measured by the soap bubble method. Retention times were measured from the time of injection to the initial emergence of the peaks (15). The packing of the g.l.c. columns was prepared by the tray method and columns were packed by means of mild mechanical vibration (excessive stirring and vibration was avoided to minimize fracture of the solid support). The following liquid phases were employed: polyethylene glycol (Carbowax 20M, PEG; 5% and 15% on Gaschrom P, 60–80 mesh); silicone gum polymer (SE-30, 5% on silanized Anakrom ABS,

[1]Issued as NRCC No. 9890. For Part XV, see Can. J. Chem. **44**, 2015 (1966).

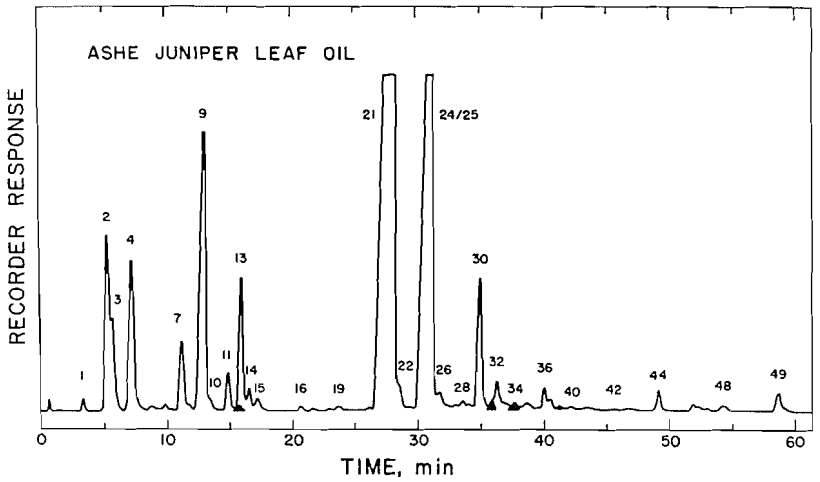

FIG. 1. Gas chromatogram of the leaf oil of *Juniperus ashei* Buchholz. (5% Polyethylene glycol 350 × 0.4 cm column, 50° to 215° at 2.9°/min). Identities of the individual peaks are shown in Table I.

70–80 mesh); fluorinated silicone polymer (QF-1, 5% on Anakrom ABS and 15% on Gaschrom P); rapeseed oil (10% on Gaschrom P); ethylene glycol *bis*propionitrile (15% on Gaschrom P); and a C-modified polyphenyl ether (Monsanto type MCS-562, Monsanto Company, St. Louis, Missouri, 15% on Gaschrom P).

Figure 1 shows a typical gas chromatogram of the leaf oil as obtained in a temperature programmed run (50 to 215° at 2.9° at min) on the 5% PEG (350 × 0.4 cm O.D.) column. The peak numbering used throughout this study is the sequence of elution on this column. In the fractionation procedures the composition of the resulting fractions was determined on this column. The purity of individual components was checked on this, as well as the other analytical columns.

Individual components were isolated by hand collection in glass or teflon tubes (externally cooled with ice or solid carbon dioxide) or in the special collectors of the Aerograph A-700 unit. Fractions which were submitted to nuclear magnetic resonance analysis (n.m.r.) were collected in carbon tetrachloride (0.5 ml). The n.m.r. spectra were recorded with the aid of a Varian HA-100 (100 Hz) spectrometer, using tetramethylsilane as internal standard. Infrared spectra (i.r.) were recorded as films on sodium chloride plates with a Perkin–Elmer model 21 double beam spectrophotometer.

Plant Material and Recovery of Leaf Oil

The foliage (20 kg) of *J. ashei* collected near Austin, Texas, by R. Irving and identified by Prof. B. L. Turner, was steam-distilled in a conventional apparatus. The distillate was extracted with methylene chloride and, after drying, the solvent was removed by distillation; yield 1.1%, $[\alpha]_D^{22}$ +37.3° (*c*, 12.7; $CHCl_3$), n_D^{22} 1.4687. Leaf samples of 15 to 30 g were sent in polyethylene bags from Austin and small scale distillation was carried out as described earlier (12). During the steam-distillation camphor, m.p. 160–175° (sealed tube), $[\alpha]_D^{23}$ +38.0 (*c*, 5.3; $CHCl_3$), crystallized in the condenser of the distillation apparatus. Its identity was confirmed by comparison of the i.r. and n.m.r. spectra with those of an authentic specimen.

Prefractionation

Aliquots of the oil (10 g) were chromatographed on modified silicic acid (120 g) as described previously (3, 5). Elution with petrol (b.p. 40–50°; 500 ml) gave a hydrocarbon fraction *a* (2.4 g, after distilling the solvent (12)) free of oxygenated terpenes (i.r., g.l.c.). A mid-fraction *b* (5.5 g) was obtained by subsequent elution with methylene chloride (400 ml) and a more polar fraction *c* (2.1 g) by elution with methanol (400 ml). The first two fractions could be used as such in preparative g.l.c., but the polar fraction was too complex. It was further fractionated on a 200 × 0.9 cm O.D. QF-1 (15%) column (nonlinear temperature programming from 80 to 200°, 100 µl aliquots) into an alcohol fraction, a mixed fraction, and 3 carbonyl fractions. Final separation of these fractions, as well as the hydrocarbon and mid-fraction, was carried out on 200 × 0.6 O.D. PEG (15%) or MCS-562 columns. The purity of each fraction isolated was tested on analytical g.l.c. columns after recording their i.r. and n.m.r. spectra, and when sufficient material could be isolated the refractive index and optical rotation were determined.

Individual Components

Fractionation of the hydrocarbon fraction *a* on a 200 × 0.6 cm O.D. MCS-562 column operated at 100° resulted in the isolation of fairly pure tricyclene (peak 2), α-pinene (peak 3), camphene (peak 4), myrcene (peak 7), limonene (peak 9), and *p*-cymene (peak 13). The optical rotations of the isolated fractions are shown in Table I. The identity of peaks 5, 6, 8, 10, 11, and 14 could be established only tentatively as β-pinene, 3-carene, α-phellandrene, β-phellandrene, γ-terpinene, and terpinolene respectively by comparison of retention data. Peak 1 appeared to be residual methylene chloride from the extractions of the steam-distilled oil. No sesquiterpene hydrocarbons could be isolated, but trace amounts of peaks 31, 34, and 38 were recorded. Retention times

Can. J. Chem. Downloaded from www.nrcresearchpress.com by 210.87.254.42 on 09/05/12
For personal use only.

Can. J. Chem. Downloaded from www.nrcresearchpress.com by 210.87.254.42 on 09/05/12
For personal use only.

TABLE I

Percentage composition of the leaf oil of *Juniperus ashei* Buchholz.

Peak No.	Compound*	$[\alpha]_D^{25}$	%
1	(Methylene chloride)	—	0.2
2	Tricyclene	(+1.0°)	4.8
3	α-Pinene	+49.2°	1.7
4	Camphene	+21.0°	4.4
5	(β-Pinene)	—	0.1
6	(3-Carene)	—	0.1
7	Myrcene	+4.8°	1.8
8	(α-Phellandrene)	—	0.1
9	Limonene	+94.9°	8.4
10	(β-Phellandrene)	—	0.2
11	(γ-Terpinene)	—	0.8
12	Unidentified	—	0.1
13	*p*-Cymene	0°	2.8
14	(Terpinolene)	—	0.4
15	Unidentified	—	0.2
16	Unidentified	—	0.1
17	Unidentified	—	trace
18	Unidentified	—	trace
19	Unidentified	—	0.1
20	(Methyl nonanone)	—	trace
21	Camphor	+38.0°	42.1
22	Linalool	—	0.4
23	Unidentified	—	trace
24	Bornyl acetate	+35.0°	22.5
25	Camphene hydrate	+ve	1.5
26	*trans*-2-methyl-6-methylene-3,7-octadien-2-ol	—	0.4
27	Unidentified	—	trace
28	Alcohol B	—	0.1
29	Unidentified	—	trace
30	Borneol	+34.0°	2.9
31	(Bisabolene)	—	0.1
32	Carvone	+ve	0.6
33	Unidentified acetate		0.1
34	(δ-Cadinene)		0.1
35	Alcohol C		0.1
36	Alcohol D		0.4
37	Aromatic alcohol		0.2
38	(Calamenene)		trace
39–43	Unidentified		traces
44	Elemol		0.5
45	Unidentified		0.2
46	Unidentified		0.1
47	Unidentified		trace
48	Unknown ester		0.8

*Names in parentheses refer to tentatively identified compounds.

suggest that these could be bisabolene, a cadinene isomer, and calamenene (16).

The mid-fraction *b* contained only two major and one minor component. Camphor (peak 21), m.p. 160–170°, $[\alpha]_D^{23}$ +35.05° (*c*, 5.1; $CHCl_3$) and bornyl acetate (peak 24), n_D^{25} 1.4619, $[\alpha]_D^{25}$ +34.0° (*c*, 4.8; $CHCl_3$) were readily isolated by fractionation on a 150 × 0.9 cm O.D. QF-1 (15%) column (100 to 200°). The third component, peak 49, was obtained in low yield after many repetitive injections. Its i.r. spectrum had absorption bands at 1735 cm^{-1} (m) ($\rangle C{=}O$); 3100 (w), 1640 (w), and 912 cm^{-1} (m) with inflexion near 895 cm^{-1} ($\rangle C{=}CH_2$), and a multiplet in the 1390–1365 cm^{-1} which permitted no conclusion about the presence of isopropyl or gem dimethyl groups. Strong bands were also recorded at 2940, 2880, 1262, 1208, 1120, 1095, 1074, and 1025 cm^{-1} and bands of medium intensity at 1420–1395, 1041, 990, 965, 955, 835, and 795 cm^{-1}. The n.m.r. spectrum showed four single proton signals, viz. three quartets centered near τ5.22, 4.98, and 4.25 with couplings of δ2 and 11, 2 and 17.5, and 17.5 and 11 Hz respectively ($-CH{=}CH_2$), and a quartet centered near τ6.65 with couplings of δ6.5 and 13 Hz ($\rangle CHOR$). Five three-proton signals occurred at τ8.74, 8.79, 9.11, 9.18, and 9.20 and less well defined signals in the τ8.0 to 9.1 range. The latter made the integration of the three-proton signals somewhat inaccurate.

The various oxygenated fractions obtained in the pre-fractionation (see above) were resolved on a 180 × 0.6 cm O.D. PEG (15%) column operated either isothermally (120 and 140°) or programmed from 120 to 200° at 4°/min. The alcohol fraction was resolved into 5 components which had spectral properties corresponding to linalool (peak 22), camphene hydrate (peak 25), *trans*-2-methyl-6-methylene-3,7-octadien-2-ol (peak 26) (17), and unknown alcohol (*a*), with a terminal methylene group (peak 28) and borneol (peak 30). Terpinen-4-ol, α-terpineol, and isoborneol were not present. The identity of camphene hydrate (m.p. 145–149°) was confirmed by synthesis (18) (m.p. 147–149°) and co-injection on all analytical columns, when identical retention times were recorded.

The mixed fraction was found to contain a trace of a methyl ketone (possible methyl nonanone; peak 20), camphor (peak 21), camphene hydrate (peak 25), the unidentified alcohol *a* (peak 28), borneol (peak 30), three unidentified alcohols (*b*, *c*, and *d*; peaks 33, 35, and 36), and an unknown aromatic alcohol (peak 37). The methyl ketone (peak 20) had the retention time of 2-decanone, but the weak infrared spectrum did not show the band near 700 cm^{-1} expected for an aliphatic chain of more than four carbon atoms. Only alcohol *d* (peak 36) was obtained in sufficient amount to record a satisfactory i.r. spectrum with strong bands near 3360, 2980–2880, 1642, 1450–1440, 1375, 1255, 1163, 1151, 1050, 1025, 955, 937, 880 (inflexion near 898), and 810 (inflexion near 803) cm^{-1} and weaker ones near 3090, 1212, 1110, 1090, 858–850, and 715 cm^{-1}. Only a weak n.m.r. spectrum with signals near τ8.30, 8.73, 8.78, 9.00, 9.12, and 9.18 and very weak ones near τ4.2, 5.0, and 5.2 could be recognized. The infrared spectrum of component 37 showed absorption bands characteristic of a hydroxyl group (3370 cm^{-1}) and an aromatic ring (1515 cm^{-1}). The other alcohols were not obtained in sufficient amount for further characterization. The i.r. spectrum of the aromatic alcohol differed from those of *p*-cuminyl alcohol, carvacrol, thymol, and the common ethers of the eugenol type. The three carbonyl fractions consisted mainly of camphor, bornyl acetate, and carvone respectively. Each compound was purified by g.l.c. on the 150 × 0.6 cm O.D. PEG (15%) column. The amount of purified carvone isolated was not sufficient for accurate determination of the optical rotation. The values for camphor (m.p. 165–175°) and bornyl acetate were +37.6° and +35.0° respectively. The third carbonyl fraction contained some higher boiling

components in small amounts, but these could not be obtained in sufficient amount for further identification.

Single Leaf Injection

Leaf portions (5–20 mg) were placed into the boat-shaped cavity of the Aerograph inductor and were injected for 15 to 30 s into the pyro-oven (at 250°) with the helium flow turned on 5 s after the injection. The released volatiles were analyzed on a 180 × 0.3 cm O.D. SE-30 (5% on Anakron ABS) column. For comparative purposes the leaf oil (0.1 μl) was enclosed in indium tubing (0.02 in. I.D.) and injected in the same manner. The green and brown portions of the same leaf stalks from the same and neighboring branchlets gave the same qualitative chromatogram. The quantitative differences were relatively small in the monoterpene range (±1 to 5%), but were more pronounced in the sesquiterpene range (±5 to 20%). When the bark from a branchlet was injected in the same manner, virtually the same chromatograms were obtained, but the amount of sequiterpenes was invariably low.

Results and Discussion

The quantitative data, as calculated from the gas chromatograms obtained with the PEG, SE-30, and MCS-562 columns are shown in Table I. The peak numbering is that of the sequence of elution on the PEG column, which provided the best overall resolution (see Fig. 1). The accuracy of determining the percentage composition with the digital integrator was ±0.1 unit % on well resolved peaks and ±0.1 to 0.5 unit % on poorly resolved peaks or when comparing data obtained on different columns. This is a noticeable improvement over the accuracy obtained previously (6, 7) by the triangulation method (13).

The identification of the major components *d*-camphor (peak 21) and *d*-bornyl acetate presented no difficulties and tricyclene (peak 2), *d*-α-pinene (peak 3), *d*-camphene (peak 4), *d*-myrcene (peak 7), *d*-limonene (peak 9), *p*-cymene (peak 13), linalool (peak 22), *d*-borneol (peak 30), carvone (peak 32), and elemol (peak 44), were also obtained in sufficient amounts to permit positive identification. Camphene hydrate (peak 25) was only identified after synthesizing this tertiary alcohol (18) and comparing g.l.c. and spectral properties. Under all g.l.c. conditions normally employed in conifer leaf analysis this labile alcohol was found to form from 10 to 30% camphene. This facile dehydration was already observed by Ashan (18) and may account for camphene hydrate not having been found in nature before. The dehydration during g.l.c. leads to a single peak with the retention time of camphene and this may serve as a convenient means of detecting camphene hydrate. The retention time of camphene hydrate is similar to that of 4-terpinenol (PEG, MCS-562, QF-1, polyester columns) except on the SE-30 column, where it coincides with isoborneol. In oils which contain these two alcohols it is difficult to distinguish camphene hydrate. Thus, alcohol **1** of red and black spruce leaf oil (6), was found to be a mixture of camphene hydrate and 4-terpinenol. If camphor is present in large amounts, it is not clearly resolved from camphene hydrate on the latter column.

Noteworthy is the finding of small amounts of alcohols all having terminal methylene groups (peaks 27, 29, 35, and 36). Of these, alcohol *a* (peak 27) had the same spectral properties of *trans*-2-methyl-6-methylene-3,7-octadien-2-ol, which was recently isolated from the frass produced by *Ips confucus* feeding on ponderosa pine (17). Silverstein *et al.* (17) report this alcohol as well as 2-methyl-6-methylene-7-octen-4-ol, to attract this beetle to the pine. Hence the alcohols found in the leaf oil of *J. ashei* may also be insect attractants. Component 36 had the retention time and spectral properties expected for *cis*- or *trans*-carveol, but neither isomer was available for comparison.

The most interesting unidentified compound from a chemical point of view appears to be component 49. The i.r. suggest it is an acetate or ester (1735, 1262 cm^{-1}) with a terminal methylene group of the type —CH=CH_2 (3100, 1640, 912–895, and possibly 990 cm^{-1}). This is confirmed by the n.m.r. spectrum. The single proton signals (quartets) near τ 5.22, 4.98, and 4.25 are typical of the ABX system in —CH_2—C(CH_3)OH—CH=CH_2 as found in nerolidol and manool (19). The presence of a secondary alkoxy group is confirmed by the single proton signal near τ6.65 and since this is a quartet it must have an adjacent methyl group (—CH(CH_3)—OCOR). The five methyl signals in the range τ 8.74 to 9.19 are more difficult to interpret but these signals as well as the fingerprint region of the i.r. spectrum differed markedly from those of nerolidol, nerolidyl acetate, manool (19), mannoyl oxide, and 13-epimanoyl oxide (20). Hence, component 49 must have a structure different from the terpenes normally found in the volatile oils of conifers.

The separation and isolation of the trace com-

Can. J. Chem. Downloaded from www.nrcresearchpress.com by 210.87.254.42 on 09/05/12
For personal use only.

ponents of the oil of *J. ashei* presented difficulties owing to overlaps which could not be resolved and some of these components could only be identified tentatively by comparison of retention data. Thus, the three trace components 31, 34, and 38 which are obtained in the hydrocarbon fraction may be bisabolene, a candinene isomer, and calamenene respectively. The former two sesquiterpenes were identified in the leaf oils of spruces (6), with which the leaf oil of *J. ashei* shows remarkable similarities. In fact, all of the components except elemol of this oil are not typical of the members of the genus *Juniperus* as well as other members of the family Cupressaceae. This finding makes the leaf oil of the Ashe juniper well suited for chemosystematic studies, especially with regard to introgression with related juniper species. The results obtained with direct injection of small portions of the leaves of *J. ashei* indicate that no significant differences exist between the green and brown portions of the leaf stalks. Hence, for chemosystematic studies the branchlets may be steam-distilled without danger of contamination of the leaf oil. These findings are being employed in a detailed investigation of the introgression of *J. ashei* with *J. virginiana* (9).

Acknowledgments

The author wishes to thank Prof. B. L. Turner, University of Texas, Austin, for discussing the various aspects of chemosystematics of the genus *Juniperus* and R. Irving for carrying out the large-scale steam-distillation. The technical assistance of Mr. M. Granat is also gratefully acknowledged. Infrared and nuclear magnetic resonance spectra were recorded by Mr. W. C. Haid and M. Mazurek.

1. S. ENDLICHER. Generum plantarum supplementum quartum pars, Vol. II, p. 2 (1847).
2. M. T. HALL. Ann. Missouri Botan. Garden, **39** (1), 1 (1952).
3. R. E. ALSTON and B. L. TURNER. Biochemical systematics. Prentice Hall, Inc., Englewood Cliffs, New Jersey. 1963.
4. T. SWAIN. Chemical plant taxonomy. Academic Press, Inc., New York. 1963.
5. E. VON RUDLOFF. Can. J. Botany, **45**, 891 (1967).
6. E. VON RUDLOFF. Phytochemistry, **5**, 331 (1966).
7. F. M. COUCHMAN and E. VON RUDLOFF. Can. J. Chem. **43**, 1017 (1965).
8. E. VON RUDLOFF and F. M. COUCHMAN. Can. J. Chem. **42**, 1890 (1964).
9. R. IRVING, B. L. TURNER, and E. VON RUDLOFF. Annual Meeting Am. Inst. Biol. Sci., College Station, Texas, August 27–September 1, 1967.
10. E. GILDEMEISTER and F. HOFFMANN. Die ätherischen öle. Vol. 4. *Edited by* W. Treibs and K. Bournot. 4th ed. Akademie Verlag, Berlin. 1956.
11. E. VON RUDLOFF. Can. J. Chem. **41**, 2876 (1963).
12. E. VON RUDLOFF and M. HOLST. Can. J. Botany. In preparation.
13. J. JANÁK. J. Chromatog. **3**, 308 (1960).
14. E. VON RUDLOFF. J. Gas Chromatog. **3**, 390 (1965).
15. E. VON RUDLOFF. Can. J. Chem. **39**, 1190 (1961).
16. V. LUKES and R. KOMERS. Collection Czech. Chem. Commun. **29**, 1598 (1964).
17. R. M. SILVERSTEIN, J. O. RODIN, D. L. WOOD, and L. E. BROWNE. Tetrahedron, **22**, 1929 (1966).
18. O. ASHAN. Chem. Ber. **41**, 1092 (1908).
19. VARIAN AEROGRAPH ASSOCIATES. High resolution nuclear magnetic resonance spectra catalog. Vol. II. 1963. No. 685.
20. J. A. GILES, J. N. SCHUMACHER, S. S. MIMS, and E. BERNASEK. Tetrahedron, **18**, 169 (1962).

Can. J. Chem. Downloaded from www.nrcresearchpress.com by 210.87.254.42 on 09/05/12
For personal use only.

Can. J. Chem. Downloaded from www.nrcresearchpress.com by 210.87.254.42 on 09/05/12
For personal use only.

Phosphinohydrazines. Reactions of hydrazine and alkylhydrazines with substituted phosphines[1]

L. K. Peterson and G. L. Wilson
Department of Chemistry, Simon Fraser University, Burnaby 2, British Columbia

Received October 11, 1967

Reactions between hydrazine or *N,N*-dimethylhydrazine and $(CF_3)_2PI$, $(CF_3)_2PCl$, $(CF_3)_3P$, and $(CF_3)_2PNMe_2$ have been further investigated as synthetic routes to phosphinohydrazine compounds. The new compound *N,N*-dimethyl,*N'*-bis(trifluoromethyl)phosphinohydrazine (m.p. 40.45°, b.p. 112° extrapolated) is described, and instability of $[(CF_3)_2P]_xN_2H_{4-x}$ systems with respect to elimination of fluoroform is inferred.

Canadian Journal of Chemistry, 46, 685 (1968)

Discussion

Hydrazines and substituted hydrazines present a number of interesting chemical and stereochemical features which have been discussed in the current literature. The decrease (1) in base strength with increasing alkyl substitution, relative to hydrazine, is in contrast to the amine series (2) $Me_2NH > MeNH_2 > Me_3N \simeq NH_3$, and contradicts other reports that alkylhydrazines are more basic than hydrazine (3). Tetrasilylhydrazine (4) and trisilylamine (5) are analogous with regard to non-basic character and skeletal planarity. In substituted hydrazines $R_aR_bNNR_cR_d$ ($R's$ = H, methyl) (6, 7), $(CF_3)_2NN(CF_3)_2$ (8), and F_2NNF_2 (9), the N—N bond energy is sensitive to substituents in a complex and imperfectly understood fashion which has been related to steric and electrical forces (8), enhanced π-bonding (10), and radical stability (11). Although there has been no systematic study of trends in the properties of compounds based on the covalently bonded skeletal arrangements A—N—N and A—N—N—A, where A represents a metalloidal atom, and N—N the hydrazine moiety, a substantial number of such compounds are now known, viz. hydrazino boranes (12–14), alanes (15, 16), silanes (17), phosphines (18), phosphine oxides (19, 20), and arsines (21).

As part of an investigation of systems based on hydrazine, we report here our studies of reactions between selected hydrazines and tris(trifluoromethyl)phosphine or bis(trifluoromethyl)halophosphine. The new compound *N,N*-dimethyl,*N'*-bis(trifluoromethyl)phosphinohydrazine, $Me_2NNHP(CF_3)_2$(**1**), was isolated and characterized. Like $Me_2NNHAs(CF_3)_2$ (21), compound **1** is a potential bifunctional chelating agent, with one site simply σ-donating (terminal nitrogen), and the second site (phosphorous) able to serve as σ-donor and π-acceptor. Under the influence of the electronegative CF_3 groups on phosphorous, we anticipate that intramolecular $N(p_\pi) - P(d_\pi)$ dative bonding (22) may determine the skeletal structure of the molecule and hence modify both its chelating ability and the properties of the N—N bond.

Compound **1** was obtained in high yield by the action of bis(trifluoromethyl)iodophosphine or chlorophosphine on anhydrous dimethylhydrazine in ether solution, according to the reaction stoichiometry. Compound **1** was

[1] $(CF_3)_2PX + 2Me_2NNH_2 \rightarrow Me_2N—NHP(CF_3)_2 + Me_2NNH_2HX$

characterized by vapor-phase molecular weight measurements, and by the quantitative cleavage of the P—N bond with HCl. In addition, the

[2] $Me_2N—NHP(CF_3)_2 + 2HCl \rightarrow (CF_3)_2PCl + Me_2NNH_3Cl$

^1H and ^{19}F nuclear magnetic resonance (n.m.r.) and the infrared spectra confirmed this formulation. The proton n.m.r. spectrum consisted of two resonance absorptions in approximately 6:1 ratio, corresponding to six equivalent protons on the two methyl groups [at τ 7.50, reference internal $Si(Me_3)_4$] and one proton on the nitrogen atom [τ 5.95]. The ^{19}F resonance was a doublet, [δ, midpoint, +63.5 p.p.m., reference external $CFCl_3$] which remained unchanged over the temperature range

[1]Presented in part at the Annual Conference, Chemical Institute of Canada, Toronto, Ontario, June, 1967.

TABLE I

Infrared spectrum[1] of $Me_2NNHP(CF_3)_2$

cm^{-1} Intensity	cm^{-1} Intensity	cm^{-1} Intensity	cm^{-1} Intensity
423 (26)	902 (24)	1285 (9)	2790 (33)
447 (21)	1019 (12)	1386 (12)	2835 (30)
476 shoulder	1069 shoulder	1455 (19)	2865 (20)
491 (21)	1109 (80)	1460 (20)	2912 (11)
541 (11)	1151 (99)	1470 (22)	2939 (8)
562 (18)	1155 (100)	2250 (4)	2975 (32)
739 (2)	1160 (98)	2272 (4)	3008 (27)
744 (2)	1167 (98)	2295 (3)	3300 (15)
798 (2)	1206 (93)	2310 (2)	3422 (5)

[1]Intensities are quoted relative to the strongest band, at 1155 cm^{-1}, with a value of 100 arbitrary units.

$-50°$ to $+60$ °C. This pattern is consistent with splitting of the absorption due to six equivalent fluorines, on two CF_3 groups, by coupling with the spin $+\frac{1}{2}$ ^{31}P nucleus [JP–CF_3, 84 c.p.s.]. Thus, the n.m.r. measurements suggest essentially free rotation about the N—P bond, at least at temperatures down to $-50°$. Lower temperatures would be needed to separate bands due to possible rotational isomers, to enable the rotation barrier to be evaluated. Together with the infrared evidence for the secondary amino (>N—H) grouping and bands due to methyl, CF_3, and N—N, the ^1H and ^{19}F n.m.r. spectra preclude alternative formulations that could arise as the result of methyl, H, or CF_3 migration or molecular rearrangement during the synthesis. The main features of the infrared spectrum (see Table I) show six peaks in the region 1109–1206 cm^{-1}, all of similar intensity, and attributable to C—F stretching modes of two independent CF_3 groups. Of the seven peaks, of varying intensity, in the region 2790–3008 cm^{-1}, no more than six may be due to C—H stretching, leaving one as an overtone or combination band. The spectrum is consistent with that expected for a molecule lacking in symmetry features (C_1). We attribute the bands at 3300 cm^{-1} and 3422 cm^{-1} to N—H stretching in associated and free species, respectively.[2] The mechanism of association may be hydrogen-bonding and/or N → P dative σ-bonding, either of which would lead to differing environments for the free and the associated molecules.

A number of other features suggest fairly strong intermolecular forces of attraction, such as the relatively high melting point (40.45°), the high latent heat of sublimation (15 500 cal $mole^{-1}$), the higher than normal Trouton constant (22.2 cal deg^{-1} $mole^{-1}$), and high values for vapor-phase molecular weight measurements (M_{obs}, 231; M_{calcd}, 228). Polymerization or cyclization in the solid state is possible, via intermolecular N → P σ-bonding. A similar interaction was postulated for dimethylsilylamine (23), which was shown to possess a pentameric, ten-membered ring structure in the crystalline state (24). Related alanes $Me_2NNRAlMe_2$ (R = H, Me) are known to be dimeric in solution (16*b*).

In the absence of ether, the action of $(CF_2)_2PI$ on neat Me_2NNH_2 gave compound **1** in very low yield, together with unresolved volatile by-products and involatile residues. Nor was the action of Me_2NNH_2 on $(CF_3)_3P$ a practical route to compound **1**. Whereas the ammonolysis of $(CF_3)_3P$ with ammonia affords a convenient synthesis of $(CF_3)_2PNH_2$ (25), the corresponding solvolysis with Me_2NNH_2 occurs only to a minor extent, giving extremely low yields of $Me_2NNHP(CF_3)_2$. The diminished solvolyzing power of Me_2NNH_2 relative to ammonia is in accord with its smaller basicity in aqueous solution (pK'_a (Me_2NNH_2), 7.21 (1); $pK'_a(NH_3)$, 9.25 (26)). In the nonaqueous system, conditions favoring hydrogen-bonded dimerization (27) of the hydrazine molecules, rather than nucleophilic attack at phosphorus centers, would also account for the absence of reaction.

Reactions using hydrazine failed to yield recognizable products. With $(CF_3)_2PX$ (X = I, Cl), two immiscible layers were formed, and even at 100° the disproportionation of the iodophosphine (28) was the only observable change.

[2]One of the referees has suggested that the missing N—H bending mode could appear as a Fermi-resonance enhanced overtone at 3300–3400 cm^{-1}, thus giving rise to the two bands observed in the N—H stretch region.

Can. J. Chem. Downloaded from www.nrcresearchpress.com by 210.87.254.42 on 09/05/12
For personal use only.

TABLE II

Saturated vapor pressure data* for solid $Me_2NNHP(CF_3)_2$

T °C	P_{mm} (obs)	P_{mm} (calcd)	T °C	P_{mm} (obs)	P_{mm} (calcd)
20.6	9.90	9.51	31.6	24.1	24.8
22.6	11.8	11.4	34.2	30.2	30.8
25.8	15.4	15.1	36.2	36.3	36.3
29.1	20.2	20.1	39.4	46.8	47.0

*Log $P_{mm} = 12.51 - 3388/T$.

Though slightly more basic (1) than Me_2NNH_2, hydrazine is unable to cleave fluoroform from $(CF_3)_3P$. Transamination between N_2H_4 and $(CF_3)_2PNMe_2$ did not occur at temperatures up to 100°, consistent with the greater basicity of Me_2NH relative to N_2H_4. In the presence of trimethylamine, however, reaction between N_2H_4 and $(CF_3)_2PI$ or $(CF_3)_3P$ occurred readily, presumably forming, in the first instance, one or more of a possible series of phosphinohydrazines.

[3] $$N_2H_4 + (CF_3)_3P \rightarrow [(CF_3)_2P]_nN_2H_{4-n} + CF_3H$$

[4] $$N_2H_4 + (CF_3)_2PI \xrightarrow{Me_3N} [(CF_3)_2P]_nN_2H_{4-n} + Me_3NHI$$

During manipulation, these unstable intermediates condensed, among themselves or with excess hydrazine, with elimination of additional quantities of CF_3H, forming intractable waxy materials for which a variety of polymeric and cross-linked structures may be postulated.

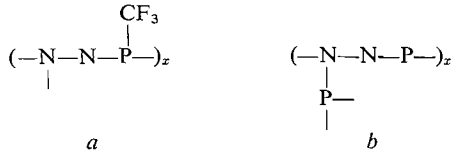

a *b*

Attempts to replace both amino protons of Me_2NNH_2 with phosphino groups did not succeed, although models show the bis(phosphino)-hydrazine to be sterically possible. When $(CF_3)_2PX$ and Me_2NNH_2 were mixed in ether in a 2:3 molar ratio, and when an excess of $(CF_3)_2PX$ was used, compound **1** was the sole derivative obtained. Steric factors, and a lowering of the basicity (22) of the secondary nitrogen atom through internal $N(p_\pi) - P(d_\pi)$ dative bonding of its lone pair, would account for this inactivity, the formation of an intermediate complex via nucleophilic attack by nitrogen being mechanistically unfavorable.

Experimental

Volatile materials were handled in a vacuum system. Reactions were carried out in sealed Pyrex tubes. Nuclear magnetic resonance (n.m.r.) spectra were determined with a Varian A56/60 instrument.

Bis(trifluoromethyl)iodophosphine was prepared by the method of Bennett *et al.* (28). The chlorophosphine $(CF_3)_2PCl$ was obtained by reaction between $(CF_3)_2PI$ and $HgCl_2$. These compounds were purified by low temperature column distillation under vacuum. Dimethylhydrazine and hydrazine were dried over anhydrous barium hydroxide; both were distilled under nitrogen, the latter at reduced pressure. Diethyl ether and toluene were dried over sodium and distilled under nitrogen from lithium aluminium hydride.

Reaction of $(CF_3)_2PX$ with Me_2NNH_2, in Ether

In a typical synthesis, a mixture of Me_2NNH_2 (0.9663 g) and $(CF_3)_2PI$ (1.8849 g) in ether (3.8672 g) reacted at about −70 °C, as shown by the formation of a white precipitate of Me_2NNH_2HI. After 60 h, the products were separated into ether (3.8600 g), unused Me_2NNH_2 (0.2897), Me_2NNH_2HI (1.1879 g), and the new compound $Me_2NNHP(CF_3)_2$, (**1**), (1.3655 g, 94%). The latter product was identified by its molecular weight (M_{obs}, 231; M_{calcd}, 228) and by infrared and n.m.r. spectra. Reactions with $(CF_3)_2PCl$ were similar, affording compound **1** in high yields.

Reaction of $(CF_3)_2PI$ with Me_2NNH_2 in Absence of Solvent

A mixture of $(CF_3)_2PI$ and Me_2NNH_2 gave two immiscible layers at −63°, but did not react. At room temperature, a white solid was produced. After several days, most of the $(CF_3)_2PI$ was recovered, together with a minor amount of material with the infrared spectrum of compound **1**, and other unstable products which decomposed during vacuum distillation, forming nonvolatile, waxy deposits on the walls of the apparatus.

Reaction of $(CF_3)_3P$ with Me_2NNH_2

At room temperature, mixtures of $(CF_3)P$ and Me_2NNH_2 gave colored products. After several hours at −10°, no coloration was observed; most of the reactants were recovered, together with fluoroform and a small fraction showing the infrared spectrum of compound (**1**).

Reaction of $Me_2NNHP(CF_3)_2$ with Anhydrous Hydrogen Chloride

Compound (**1**) (0.1774 g) reacted readily with an excess of hydrogen chloride (0.0850 g), yielding $(CF_3)_2$-PCl (0.1548 g), Me_2NNH_2HCl (0.0645 g), and unused

Can. J. Chem. Downloaded from www.nrcresearchpress.com by 210.87.254.42 on 09/05/12
For personal use only.

TABLE III

Saturated vapor pressure data* for liquid $Me_2NNHP(CF_3)_3$

T °C	P_{mm} (obs)	P_{mm} (calcd)	T °C	P_{mm} (obs)	P_{mm} (calcd)
41.1	52.1	52.0	79.8	267	266
50.6	81.5	81.1	89.6	377	376
60.6	125.7	125.5	100.1	536	531
73.4	208.6	209.7	111.9	749	755

*Log $P_{mm} = 6.6638 - 0.005465\,T + 1.75\,T - 2389/T$.

HCl (0.0243 g). Thus the yield of $(CF_3)_2PCl$ was essentially quantitative, while the minor discrepancies in the HCl recovery and Me_2NNH_2HCl yield were almost certainly due to formation of some $Me_2NNH_4Cl_2$.

Reaction of N_2H_4 with $(CF_3)_2PI$ and $(CF_3)_2PCl$

Initial runs indicated that neat mixtures of N_2H_4 and $(CF_3)_2PI$ did not react at room temperature or when heated to 100°. At the higher temperature, disproportionation products of $(CF_3)_2PI$ (iodine, CF_3PI_2, and other compounds) were observed. No N_2H_4HI was formed. On warming (from −196°) a mixture of $(CF_3)_2PI$ (3.6590 g), hydrazine (0.0755 g), and trimethylamine (0.6490 g), reaction occurred well below room temperature as shown by the formation of a white smoke of N_2H_4HI. After 48 h the products were separated into $(CF_3)_2PI$ (1.2068 g), CF_3H (0.1400 g), and products of low volatility held in traps at −45° and −63°, as needle-like crystals and a yellow oil. During trap-to-trap distillation these compounds evolved fluoroform, becoming less volatile, and forming a waxy layer on the walls of the apparatus.

Similar results were obtained with $(CF_3)_2PCl$ in place of $(CF_3)_2PI$.

Reaction of N_2H_4 with $(CF_3)_3P$

A mixture of $(CF_3)_3P$ and hydrazine yielded trace amounts of CF_3H when heated at 100° for 36 h. On adding trimethylamine to the mixture, at room temperature, fluoroform was produced in increased yield, together with a range of products condensing in traps at −23°, −45°, −63°, −96°, and −120°, and decomposing during distillation into involatile residues and fluoroform.

Reaction of N_2H_4 with $(CF_3)_2PNMe_2$

Dimethylaminobis(trifluoromethyl)phosphine was prepared (25) from dimethylamine and bis(trifluoromethyl)-chlorophosphine. A mixture of this compound and hydrazine was kept at room temperature for 72 h. The starting materials were recovered quantitatively. After heating the same mixture at 85 °C for 6 h, no evidence of reaction was found.

Physical Properties of $Me_2NNHP(CF_3)_2$

The melting point of $Me_2NNHP(CF_3)_2$, determined on samples sealed under vacuum into capillary tubes, was 40.45 ± 0.15°.

Saturated vapor pressures were measured with a mercury tensimeter. The compound was stable at 120°, as shown by reproducible vapor pressures. Representative data for solid–vapor equilibria are given in Table II, and in Table III for liquid–vapor equilibria. The calculated latent heat of sublimation is 15 500 cal. mole^{-1}, the extrapolated boiling point is 112°, the latent heat of vaporisation at the boiling point is 8570 cal mole^{-1}, and the Trouton constant is 22.2 cal deg^{-1}. From the two curves, the theoretical melting point is 40.0°, in good agreement with the experimental value. The calculated latent heat of fusion at the melting point is 5940 cal mole^{-1}.

The infrared spectrum over the range 400 to 4000 cm^{-1}, measured in the gas phase (10 cm cell, KBr windows) with a Beckmann I.R. 12 spectrophotometer, is given in Table I.

Acknowledgments

The authors gratefully acknowledge financial support from the National Research Council of Canada, and from the President's Research Fund of Simon Fraser University. Stimulating discussions with Dr. E. J. Wells and Dr. N. Flitcroft were of considerable value.

1. R. L. Hinman. J. Org. Chem. **23**, 1587 (1959).
2. H. C. Brown, H. Batholomay, and M. D. Taylor. J. Am. Chem. Soc. **66**, 435 (1944).
3. H. H. Sisler, G. M. Omietanski, and B. Rudner, Chem. Rev. **57**, 1027 (1957).
4. B. J. Aylett. J. Inorg. Nucl. Chem. **2**, 325 (1956).
5. K. Hedberg. J. Am. Chem. Soc. **77**, 6491 (1955).
6. J. A. Kerr, R. C. Sekhar, and A. F. Trotman-Dickenson. J. Chem. Soc. 3217 (1963).
7. B. G. Gowenlock, P. P. Jones, and J. R. Majer. Trans. Faraday Soc. **57**, 23 (1961).
8. L. S. Bartell and H. K. Higginbotham. Inorg. Chem. **4**, 1346 (1965).
9. C. B. Colburn and F. A. Johnson. J. Chem. Phys. **33**, 1869 (1960). J. A. Young and R. D. Dresdner. J. Org. Chem. **28**, 833 (1963).
10. K. A. Jensen, A. Holm, B. Kägi, and C. T. Pedersen. Acta Chem. Scand. **19**, 772 (1965).
11. J. Kaufmann. Chem. Eng. News, **4**, 1342 (1965).
12. H. Noeth. Z. Naturforsch. **16b**, 471 (1961).
13. C. Belinski, G. Francais, C. Horney, and F. X. Lalan-Keraly. Compt. Rend. **259**, 3737 (1964).
14. M. S. Bains. Can. J. Chem. **44**, 534 (1966).
15. N. R. Fetter, B. Bartocha, F. E. Brinckman, and D. W. Moore. Can. J. Chem. **41**, 1359 (1963). N. R. Fetter and B. Bartocha. Can. J. Chem. **39**, 2001 (1961).
16. (*a*) D. F. Clemens, W. S. Brey, and H. H. Sisler. Inorg. Chem. **2**, 1251 (1963). (*b*) R. P. Nielsen and H. H. Sisler. J. Chem. Soc. 3818 (1962).
17. U. Wannagat and F. Höfler. Monatsh. Chem. **97**, 976 (1966), and references therein.
18. H. H. Sisler and J. Weiss. Inorg. Chem. **4**, 1514 (1965).

Can. J. Chem. Downloaded from www.nrcresearchpress.com by 210.87.254.42 on 09/05/12
For personal use only.

19. M. BECKE-GOEHRING and W. WEBER. Z. Anorg. Allgem. Chem. **333**, 128 (1964).
20. H. BOCK and G. RUDOLPH. Chem. Ber. **98**, 2273 (1965).
21. L. K. PETERSON and K. I. THÉ. Chem. Commun. 1056 (1956).
22. A. B. BURG and J. HENERS. J. Am. Chem. Soc. **87**, 3092 (1965).
23. S. SUJISHI and S. WITZ. J. Am. Chem. Soc. **76**, 4631 (1954).
24. R. RUDMAN, W. C. HAMILTON, S. NOVICK, and T. D. HOLDFARB. J. Am. Chem. Soc. **89**, 5157 (1967).
25. G. S. HARRIS. J. Chem. Soc. 512 (1958).
26. R. C. WEAST (*Editor*). Handbook of chemistry and physics. 47th ed. The Chemical Rubber Co., Cleveland, Ohio. 1966–1967. p. D85.
27. J. R. COOK and K. SCHUG. J. Am. Chem. Soc. **86**, 4271 (1964).
28. F. W. BENNETT, H. J. EMELÉUS, and R. N. HASZELDINE. J. Chem. Soc. 1565 (1953).

Can. J. Chem. Downloaded from www.nrcresearchpress.com by 210.87.254.42 on 09/05/12
For personal use only.

Can. J. Chem. Downloaded from www.nrcresearchpress.com by 210.87.254.40 on 09/05/12
For personal use only.

Thiazoloisoquinolines. III. Structure and methylation of 2-hydroxythiazolo[4,5-*c*]- and -[5,4-*c*]isoquinolines[1,2]

CATHERINE E. HALL[3] AND ALFRED TAURINS
Department of Chemistry, McGill University, Montreal, Quebec
Received October 2, 1967

2-Hydroxythiazolo[4,5-*c*]isoquinoline (**1**) and 2-hydroxythiazolo[5,4-*c*]isoquinoline (**2**) were both found to exist predominantly in the lactam form (**1***b* and **2***b* respectively) from infrared, nuclear magnetic resonance, and ultraviolet spectral evidence. Various methylating agents methylated compound **1** exclusively on the N-3 atom in the thiazole ring. Compound **2** on the other hand, gave a mixture of O- and N-3 methylated products with diazomethane and a mixture of N-1 and N-4 methylated products with either methyl iodide or dimethyl sulfate.

Canadian Journal of Chemistry, 46, 691 (1968)

The synthesis of 2-hydroxythiazolo[4,5-*c*]isoquinoline (**1**) and 2-hydroxythiazolo[5,4-*c*]isoquinoline (**2**) have been described in earlier papers of this series (1,2). Three tautomeric structures are possible for each of these compounds (**1***a*, **1***b*, **1***c*, and **2***a*, **2***b*, **2***c*), and the subject of this paper is to describe evidence showing the predominant form present in each series and also to discuss the reaction of **1** and **2** with various methylating agents.

From infrared evidence, the hydroxyl forms, **1***a* and **2***a*, do not appear to be present in detectable amounts in either **1** or **2** since a strong band is observed in the carbonyl stretching region at 1700 cm^{-1} in each case. Furthermore, the nuclear magnetic resonance (n.m.r.) spectra of both compounds showed a broad singlet at τ −2.58 to −2.60 for the N—H proton.

Additional evidence about the structure of **1** and **2** was obtained by comparison of the ultraviolet spectra of **1** and **2** with the spectra of their methyl derivatives **3***a*, **3***b* and **4***a*, **4***b*, **4***c* (Tables I and II). In this way it was proved conclusively that compound **1** exists predominantly in the tautomeric form **1***b* and compound **2** in the form **2***b*.

Methylation of 2-hydroxythiazolo[4,5-*c*]isoquinoline (**1**) with methyl iodide in the presence of sodium hydroxide gave a monomethylderivative **3**. The same compound was obtained using diazomethane as the methylating agent. Compound **3** was not the *O*-methyl derivative **3***a* since it was different from authentic 2-methoxythiazolo[4,5-*c*]isoquinoline (**3***a*) prepared by treatment of 2-chlorothiazolo[4,5-*c*]isoquinoline with sodium methoxide (1). Structure **3***b* rather than **3***c* is assigned to compound **3** on the basis of the following evidence. It showed a carbonyl stretching band in the infrared at 1680 cm^{-1}. The positions of ultraviolet absorption maxima of 2-hydroxy[4,5-*c*]-isoquinoline (**1***b*) and **3***b* were exactly at the same wavelength but in the longer wavelength region the band positions of **3***a* were different (Table I). The n.m.r. spectrum of **3***b* ($DCCl_3$) showed a singlet at τ 1.15 for H-5, an ABCX pattern for the four remaining aromatic protons (a doublet centered at τ 2.08 assigned to H-9, and a multiplet at τ 2.33 to 2.74 assigned to H-6, H-7, and H-8) and a sharp singlet at τ 6.41 for the N—CH_3 protons. If **3***c* were the correct structure instead of **3***b*, H-5 would be expected to absorb at higher field (τ 1.6 to 1.8) (3).

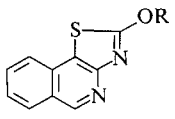

1*a*, R = H
3*a*, R = CH_3

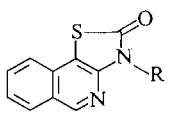

1*b*, R = H
3*b*, R = CH_3

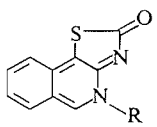

1*c*, R = H
3*c*, R = CH_3

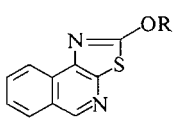

2*a*, R = H
4*a*, R = CH_3

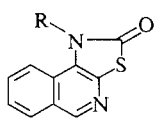

2*b*, R = H
4*b*, R = CH_3

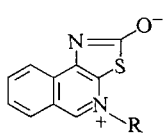

2*c*, R = H
4*c*, R = CH_3

[1]This work received financial assistance from the National Research Council of Canada.
[2]For Part I, see C. E. Hall and A. Taurins, Can. J. Chem. **44**, 2465 (1966). For Part II, see C. E. Hall and A. Taurins, Can. J. Chem. **44**, 2473 (1966).
[3]Holder of a NRCC Studentship, 1962–1963 and 1963–1964.

TABLE I

Ultraviolet absorption maxima and log ε values of some thiazolo[4,5-*c*]isoquinoline derivatives (solvent: ethanol)

Compound	α-Band		*p*-Band		β-Band	
	mμ	log ε	mμ	log ε	mμ	log ε
2-Methoxythiazolo-[4,5-*c*]isoquinoline (**3***a*)	345	3.61	301	3.73	247	4.63
	335	3.61	289	3.79		
			278	3.71		
2-Hydroxythiazolo-[4,5-*c*]isoquinoline (**1***b*)	350	3.66	301	3.55	246.5	4.45
			288	3.60		
			278	3.56		
3-Methylthiazolo-[4,5-*c*]isoquinolin-2(3*H*)-one (**3***b*)	350	3.83	302	3.72	247	4.60
			290	3.78		
			282	3.67		

Basic hydrolysis of **3***b* ruptured the thiazole ring and produced a base soluble, acetic acid insoluble compound which proved to be very unstable and was believed to be 3-*N*-methylaminoisoquinoline-4-thiol (**5**). The only useful solvent for the n.m.r. analysis of **5** was dimethyl sulfoxide-d_6. However, this solvent acted as oxidizing agent and **5** was transformed into a compound **6** which was no longer soluble in base after recovery from solvent.[4] The n.m.r. spectrum of compound **6** was in agreement with the structure of di-(3-*N*-methylaminoisoquinolyl)-4,4^1-disulfide. It shows a singlet at τ 1.25 (2H) (H-1 and H-1′), a complex multiplet at τ 2.39 to 3.29 (8H) (carbocyclic ring protons), a quartet centered at τ 3.58 ($J = 4.6$ c.p.s.) (2H) (N—H), and a doublet centered at τ 3.58 ($J = 4.6$ c.p.s.) (6H) (N—CH_3). Thus, there appears to be coupling between the N—H and N—CH_3 protons.[5] This coupling is further evidence that the compound is a relatively non-basic *N*-monosubstituted methylamine (**7**).

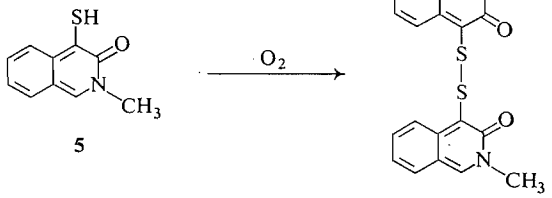

5 **6**

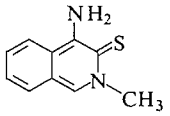

7

Methylation of 2-hydroxythiazolo[5,4-*c*]isoquinoline (**2**) with either methyl iodide or dimethyl sulfate in the presence of sodium hydroxide gave a mixture of two *N*-methyl derivatives in about the same ratio in each case. The major product was proven to have structure **4***c* on the basis of the following evidence. It was yellow, soluble in hot water, and exhibited a carbonyl stretching band in the infrared at 1655 cm^{-1}. Its n.m.r. spectrum showed a singlet at τ 0.96 for H-5, a complex multiplet at τ 1.74 to 2.37 for the carbocyclic ring protons and a sharp singlet at τ 5.85 for the N—CH_3 protons. Basic hydrolysis produced a red base-insoluble compound (**7**) whose infrared spectrum showed a primary amino group with bands at 3250, 3345, and 1625 cm^{-1}. Its n.m.r. spectrum exhibited a singlet at τ 1.81 (1H, C-1 H), a multiplet at τ 2.23 to 3.00 (4H, carbocyclic ring protons), a broad singlet at τ 3.65 (2H, NH_2) and a sharp singlet at τ 5.73 (3H, N—CH_3). Its visible and ultraviolet spectrum showed bands at 482 mμ (log ε 3.77), 379 mμ (3.86), 283 mμ (3.99), and 244 mμ (4.13).

[4]The oxidation of various thiols by dimethyl sulfoxide has been reported by other workers (4–6).

[5]Coupling has previously been observed between NH or NH_2 protons and adjacent CH protons in such compounds as pyrrole (8), formamide (9), and uracil (10).

FOR ERRATA SEE
V.47 ... 1969 ... P. 2490

Can. J. Chem. Downloaded from www.nrcresearchpress.com by 210.87.254.40 on 09/05/12
For personal use only.

Erratum: Thiazoloisoquinolines. III. Structure and methylation of 2-hydroxythiazolo[4,5-*c*]- and -[5,4-*c*]isoquinolines

CATHERINE E. HALL AND ALFRED TAURINS
Department of Chemistry, McGill University, Montreal, Quebec

Received January 27, 1969
(Ref.: Can. J. Chem. 46, 691 (1968))

Canadian Journal of Chemistry 47, 2490 (1969)

On page 692, the structures **5** and **6** should be and not

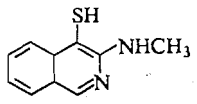

5

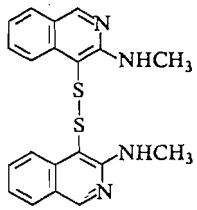

6

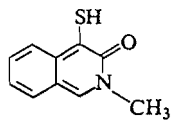

5

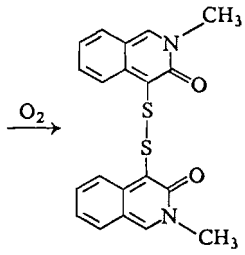

6

Can. J. Chem. Downloaded from www.nrcresearchpress.com by 210.87.254.40 on 09/05/12
For personal use only.

Can. J. Chem. Downloaded from www.nrcresearchpress.com by 210.87.254.40 on 09/05/12
For personal use only.

TABLE II

Ultraviolet absorption maxima and log ε values of some thiazolo[5,4-*c*]isoquinoline derivatives (solvent: ethanol)

Compound	α-Band		*p*-Band		β-Band	
	mμ	log ε	mμ	log ε	mμ	log ε
2-Hydroxythiazolo[5,4-*c*]-isoquinoline (**2***b*)	346	3.82	304 293	3.59 3.58	240	4.51
1-Methylthiazolo[5,4-*c*]-isoquinolin-2(1*H*)-one (**4***b*)	348	3.83	307 296	3.59 3.55	242	4.54
2-Methoxythizaolo[5,4-*c*]-isoquinoline (**4***a*)	338 330	3.85 3.80	299 287.5	3.66 3.69	263(sh) 237.5	3.52 4.73
2-Hydroxy-4-methylthiazolo-[5,4-*c*]isoquinolinium hydroxide, betaine (**2***c*)	417 345	4.27 3.39	285(sh) 266	3.81 4.01	234.5 229	4.48 4.48

These results show unequivocally that the hydrolysis product must be 4-amino-2-methylisoquinoline-3(2*H*)-thione (**7**), and therefore, the major product from the methylation of **2** with methyl iodide or dimethyl sulfate must have structure **4***c*.

The minor product from the methylation of **2** with either methyl iodide or dimethyl sulfate in the presence of sodium hydroxide was also an *N*-methyl derivative since it showed a strong carbonyl stretching band in the infrared at 1684 cm^{-1}. In addition, it was different from authentic 2-methoxythiazolo[5,4-*c*]isoquinoline (**4***a*) prepared by reaction of 2-chlorothiazolo[5,4-*c*]isoquinoline with sodium methoxide (2). Therefore this compound must have structure **4***b*. The frequency of the carbonyl absorption in the infrared was higher for **4***b* than for **4***c* as expected, since **4***b* has a true C—O double bond whereas the C—O bond in the zwitterionic **4***c* possesses much more single bond character. Comparison of the ultraviolet spectra of **2**, **4***b*, and **4***c* (Table II) shows that **2** exists mainly as thiazolo[5,4-*c*] isoquinolin-2(1*H*)-one (**2***b*). The spectrum of 2-methoxy derivative (**4***a*) is also different from that of **2**.

Methylation of 2-hydroxythiazolo[5,4-*c*]isoquinoline (**2**) with ethereal diazomethane gave a mixture of the O- and N-1 methyl derivatives (**4***a* and **4***b* respectively) in a ratio of about 1 to 2.

Experimental

Melting points were determined on a Gallenkamp melting point apparatus and are corrected. Infrared spectra were recorded on a Perkin–Elmer model 421 grating spectrophotometer as KBr discs. Ultraviolet spectra were obtained on a Perkin–Elmer model 350 spectrophotometer with absolute ethanol as solvent. Nuclear magnetic resonance (n.m.r.) spectra were determined on Varian high-resolution n.m.r. spectrometers, model HR-60 or model A60. Solvents used were chloroform-*d*, dimethyl sulfoxide, and dimethyl sulfoxide-d_6. Tetramethylsilane was used as an internal standard. Elemental analyses were carried out by A. Bernhardt, Mülheim, Germany.

Methylation of 2-Hydroxythiazolo[4,5-c]isoquinoline (1)

(a) With Methyl Iodide and Sodium Hydroxide

Methyl iodide (0.25 ml, 4.0 mmoles) in 15 ml of absolute methanol was added to a solution of 0.25 g (1.4 mmoles) of 2-hydroxythiazolo[4,5-*c*]isoquinoline in 0.5 ml of 10% sodium hydroxide. The resulting clear yellow solution was allowed to stand with occasional swirling at room temperature for 23 h. During this time 0.17 g (57% yield) of 3-methylthiazolo[4,5-*c*]isoquinolin-2(3*H*)-one (**3***b*) precipitated. Crystallization from methanol gave pale-yellow needles, m.p. 182.5–183.5°; ν(KBr) 1680 cm^{-1}; τ($CDCl_3$) 1.15 (singlet, H-5), 2.08 (doublet, J = 8.7 c.p.s., H-9), 2.33–2.74 (multiplet, H-6, H-7, H-8) and τ 6.41 (singlet, N—CH_3).

Anal. Calcd. for $C_{11}N_2OS$: C_7, 61.09; H, 3.73; N, 12.96; S, 14.83. Found: C, 60.99; H, 3.51; N, 18.09; S, 14.73.

This compound (**3***b*) (152 mg, 0.70 mmole) was hydrolyzed by refluxing in a mixture of 3.1 ml of 1 *N* sodium hydroxide and 2–3 drops of ethanol and refluxed for 3 h. The reaction mixture was filtered while hot, the filtrate was cooled and then acidified with acetic acid. An orange solid, (**5**) m.p. 70–90°, was obtained by filtration.

(b) With Diazomethane

Diazomethane was prepared according to McKay (11). One gram (6.8 mmoles) of *N*-methyl-*N*-nitroso-*N'*-nitroguanidine was added in small portions to a solution of 1 g of potassium hydroxide in 2 ml of water covered with 20 ml of ether and cooled to −5°. The yellow ether layer was decanted after the addition was complete and 8 ml was

Can. J. Chem. Downloaded from www.nrcresearchpress.com by 210.87.254.40 on 09/05/12
For personal use only.

Can. J. Chem. Downloaded from www.nrcresearchpress.com by 210.87.254.40 on 09/05/12
For personal use only.

used for this experiment. 2-Hydroxythiazolo[4,5-*c*]isoquinoline (65 mg, 0.32 mmole) was suspended in 10 ml of ether and the diazomethane solution added all at once. The resulting mixture was left to stand at room temperature with occasional swirling for 3 h. Then 2 ml of absolute methanol was added and the resulting mixture left to stand overnight. The yellow solution was filtered and the filtrate evaporated leaving 58 mg (84% yield) of 3-methylthiazolo[4,5-*c*]isoquinolin-2(3*H*)-one (**3***b*), m.p. 181–183°. The infrared spectrum was superimposable on that of the product obtained by methylation of **1** with methyl iodide and sodium hydroxide and the melting point of a mixture of the two compounds showed no depression.

Methylation of 2-Hydroxythiazolo[5,4-c]isoquinoline (2)

(a) With Dimethyl Sulfate and Sodium Hydroxide

2-Hydroxythiazolo[5,4-*c*]isoquinoline (0.40 g, 2.0 mmoles) was dissolved in 12 ml of 2% sodium hydroxide solution and filtered. To the filtrate in a 50 ml round-bottomed flask was added 0.30 ml (0.40 g, 3.0 mmoles) of dimethyl sulfate. The flask was stoppered and the reaction mixture stirred magnetically at room temperature for 2 h. The precipitate which had formed was filtered off to give 0.20 g of yellow solid. After extraction with boiling benzene, 0.13 g (30% yield) of insoluble yellow 2-hydroxy-4-methylthiazolo[5,4-*c*]isoquinolinium hydroxide, betaine (**4***c*) remained, m.p. 276–279°. Evaporation of the benzene left a few milligrams of brown solid which showed an infrared band in the carbonyl region at 1690 cm^{-1}. Crystallization of the benzene insoluble product from ethanol gave yellow needles of **4***c*, m.p. 277.5–278.5°; ν(KBr) 1655 cm^{-1}; τ ($CDCl_3$/DMSO) 0.96 (singlet, H-5), 1.74–2.37 (multiplet, H-6, H-7, H-8, H-9), and τ 5.85 (singlet, N—CH_3).

Anal. Calcd. for $C_{11}H_8N_2OS$: C, 61.09; H, 3.37; N, 12.96; S, 14.83. Found: C, 61.13; H, 3.88; N, 12.80; S, 14.76.

This compound (**4***c*) (125 mg, 0.6 mmole) was hydrolyzed by refluxing in a mixture of 2.5 ml of 1 *N* sodium hydroxide and 1–2 drops of ethanol for 30 min. The reaction mixture was cooled and filtered to give 85 mg (75% yield) of orange solid. Crystallization from water gave shining orange needles of 4-amino-2-methylisoquinoline-2-(3*H*)-thione (**7**), m.p. 194–196°; ν(KBr) 3250, 3345, and 1625 cm^{-1} (NH_2); λ_{max} (ethanol) 482 (log ε 3.77), 370 (3.86), 283 (3.99), and 244 mμ (4.13); τ ($CDCl_3$/DMSO-d_6) 1.81 (singlet, H-1), 2.23–3.00 (multiplet, H-5, H-6, H-7, H-8) 3.65 (broad singlet, NH_2) and τ 5.73 (singlet, N—CH_3).

Anal. Calcd. for $C_{10}H_{10}N_2S$: C, 63.12; H, 5.30; N, 14.73. Found: C, 63.09; H, 5.29; N, 14.65.

(b) With Methyl Iodide and Sodium Hydroxide

2-Hydroxythiazolo[5,4-*c*]isoquinoline (0.20 g, 1.0 mmole) was dissolved in 0.5 ml of 10% sodium hydroxide and 0.80 ml (11.0 mmoles) of methyl iodide in 12 ml of absolute methanol was added and the reaction mixture allowed to stand at room temperature for 3 days. The orange needles which precipitated were filtered and extracted with boiling benzene leaving 0.06 g (28% yield) of insoluble yellow needles, the infrared spectrum of which was identical to **4***c*.

The benzene soluble material was sublimed *in vacuo* to give 14 mg (7% yield) of pale-yellow solid, m.p. 238–241°. From infrared analysis and mixture melting point determination, this material was found to be identical to the *N*-methyl derivative (**4***b*) obtained by methylation of **2** with diazomethane.

(c) With Diazomethane

2-Hydroxythiazolo[5,4-*c*]isoquinoline (96 mg, 0.47 mmole) was suspended in 15 ml of ether and 12 ml of diazomethane solution added all at once. After standing at room temperature for 3 h, 3 ml of absolute methanol was added and the resulting mixture allowed to stand overnight at room temperature. The yellow solution was filtered and the solvent evaporated from the filtrate leaving 66 mg of yellow solid which was crystallized from methanol to give 19 mg of 1-methylthiazolo[5,4-*c*]isoquinolin-2(1*H*)-one (**4***b*) as pale-yellow needles, m.p. 243.5–245°. The precipitate from the reaction mixture (10 mg) was also **4***b* thus giving a total yield of 29 mg (28%). Vacuum sublimation of the crystallized material raised the melting point to 246–247°; ν (KBr) 1684 cm^{-1} (C═O); τ (DMSO-d_6) 1.00 (singlet, H-5), 1.52 (doublet, J = 8.0 c.p.s., H-9), 1.78–2.37 (multiplet, H-6, H-7, H-8), and τ 5.94 (singlet, N—CH_3).

Anal. Calcd. for $C_{11}H_8N_2OS$: C, 61.09; H, 3.73; N, 12.96. Found: C, 60.98, H, 3.71; N, 12.81.

The mother liquor from the crystallization above was evaporated and the residue sublimed *in vacuo* to give 16 mg (15% yield) of 2-methoxythiazolo[5,4-*c*]isoquinoline (**4***a*), m.p. 101–103°. This material was identical to authentic **4***a* by mixture melting point and infrared spectra.

1. C. E. HALL and A. TAURINS. Can. J. Chem. **44**, 2465 (1966).
2. C. E. HALL and A. TAURINS. Can. J. Chem. **44**, 2473 (1966).
3. G. R. BEDFORD, H. DORN, G. HILGETAG, and A. R. KATRITZKY. Rec. Trav. Chim. **83**, 189 (1964).
4. T. J. WALLACE and H. A. WEISS. Chem. Ind. London 1558. (1966).
5. T. J. WALLACE. Chem. Ind. London, 501 (1964).
6. T. J. WALLACE. J. Am. Chem. Soc. **86**, 2018 (1964).
7. M. FREIFELDER, R. W. MATTOON, and R. KRIESE. J. Phys. Chem. **69**, 3645 (1965).
8. R. J. ABRAHAM and H. J. BERNSTEIN. Can. J. Chem. **37**, 1056 (1959).
9. L. H. PIETTE, J. D. RAY, and R. A. OGG, JR. J. Mol. Spectry. **2**, 66 (1958).
10. J. P. KOKKO, J. H. GOLDSTEIN, and L. MANDELL. J. Am. Chem. Soc. **83**, 2909 (1961).
11. A. F. MCKAY. J. Am. Chem. Soc. **70**, 1974 (1948).

Can. J. Chem. Downloaded from www.nrcresearchpress.com by 210.87.254.5 on 09/05/12
For personal use only.

Pyrone studies. Linear α-pyrone route to protected β-polyketones

J. L. Douglas and T. Money
Chemistry Department, University of British Columbia, Vancouver 8, British Columbia

Received October 5, 1967

Preliminary studies on an alternative polypyrone route to protected β-polyketo acid chains are reported. The synthesis of the basic pyrone units involved and their conversion to C-3 acylated compounds are described.

Canadian Journal of Chemistry, 46, 695 (1968)

In previous reports (1–6) we have shown the value of using condensed polypyrone structures (e.g. **1**) as suitable substitutes for synthetically inaccessible β-polyketo acid chains. We have also shown that these complex pyrones can be converted to phenolic compounds possessing carbon skeletons identical to those which occur naturally. The latter transformations were performed under a variety of basic conditions and some degree of control over the mode of cyclization was made possible by the suitable choice of basic reagent (3–6).

In parallel with these studies we have recently investigated the possibility of using polypyrone structures which could be constructed by the linear condensation of suitable α-pyrone units. The particular α-pyrone chosen for this study is represented by the general formula **2** and possesses important structural features. As shown, **2** (R′ = OH or OAlkyl; R = H) may be regarded as the "tail" of a masked β-polyketo acid chain. The absent starter unit (RCO—) is potentially available since 4-hydroxy-2-pyrones are readily acylated at the C-3 position. Alternatively compound **2** (R′ = Cl; R = Me) could be employed as a chain propagating entity (e.g. **2** → **3** or **4**) and would allow entry into linearly condensed polypyrone compounds. The possible advantage of such a process over our previous use of pyrones is that it could provide a more efficient method of constructing long-chain β-polyketones in protected form. This report describes the snythesis of the basic pyrone units, **7**, **8**, and **9**, and some pertinent acylation studies.

Triacetic acid lactone methyl ether **5** (R = CH_3)(7) was converted to its ethoxyalyl derivative **6** (R = C_2H_5) by treatment with diethyl oxalate in the presence of metallic sodium. Acid hydrolysis, followed by treatment with alkaline hydrogen peroxide, gave 6-carboxymethyl-4-methoxy-2-pyrone **7** (R_1' = H). Esterification

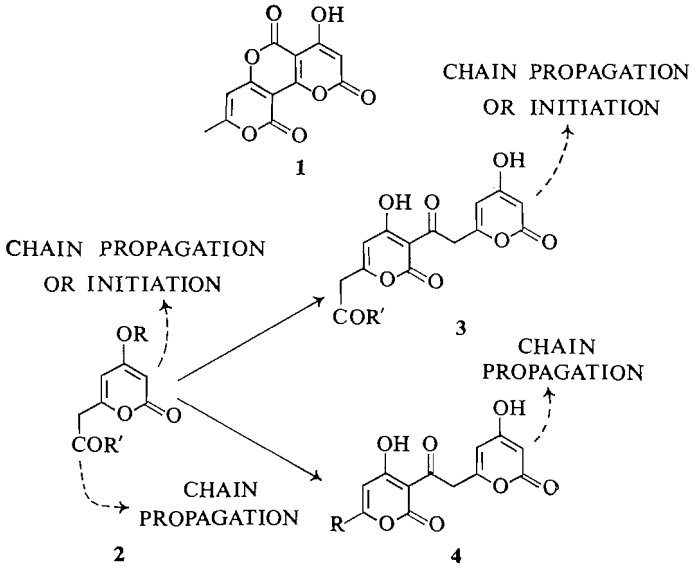

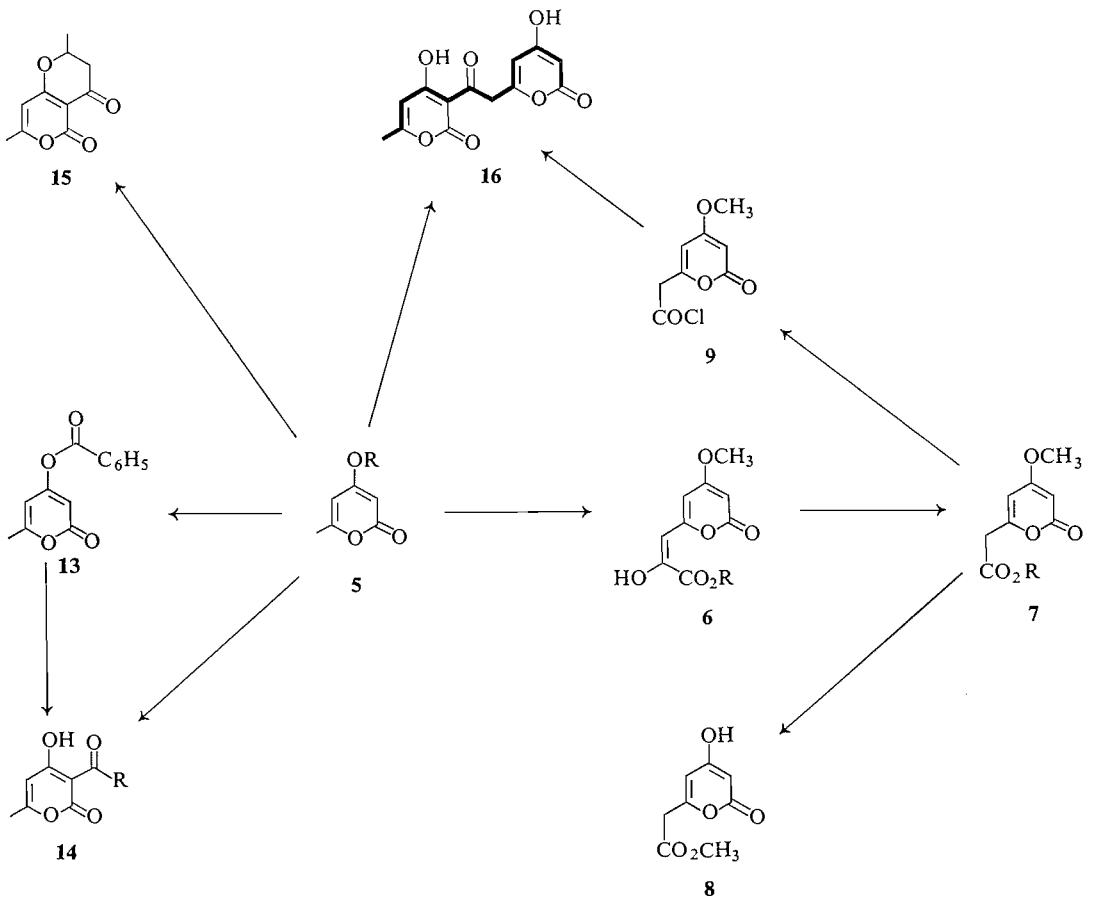

yielded the methyl ester **7** (R = CH_3) which was converted to 6-carbomethoxymethyl-4-hydroxy-2-pyrone **8** by demethylation with anhydrous aluminium chloride. The required acid chloride **9** was obtained from the corresponding acid **7** (R = H) by treatment with oxalyl chloride (thionyl chloride was ineffective in this reaction) and was reconvertible to the ester **7** (R = CH_3).

The successful synthesis of **7**, **8**, and **9** provided us with an opportunity to study other aspects of our speculative proposals. Thus the reaction of **8** with acetyl chloride in the presence of trifluoroacetic acid (8) resulted in smooth conversion to the 3-acetyl derivative **10** (R = CH_3). This compound is potentially equivalent to a β-polyketo acid chain containing eight carbon atoms (four acetate units) and, by analogy with our previous results (1–6) should be convertible to simple phenolic compounds. A similar reaction with cinnamoyl chloride yielded the expected product **12** which is potentially equivalent to the β-polyketo acid precursor of the flavonoids and stilbenes (9). Previous acylation studies (10) with triacetic acid lactone **5** (R = H) indicated that crotonyl chloride in the presence of trifluoroacetic acid yielded the bicyclic product **15**. In contrast to these results the reaction of benzoyl chloride with **8** gave the *O*-benzoyl derivative **11** (R = C_6H_5). Model studies with triacetic acid lactone **5** (R = H) indicated that *O*-benzoylation is the preferred mode of reaction under these conditions (trifluoroacetic acid) and that rearrangement **13** → **14** (R = C_6H_5) to the *C*-benzoyl derivative can be accomplished with anhydrous aluminium chloride (cf. 11). Unfortunately repeated attempts to rearrange (**11**; R = C_6H_5) to **10** (R = C_6H_5) under these conditions failed. The use of propionyl chloride yielded a mixture of *O*- and *C*-acylated com-

[1]We are grateful to Dr. T. A. Neilson for his expert experimental assistance.

Can. J. Chem. Downloaded from www.nrcresearchpress.com by 210.87.254.5 on 09/05/12
For personal use only.

Can. J. Chem. Downloaded from www.nrcresearchpress.com by 210.87.254.5 on 09/05/12
For personal use only.

pounds, **10** (R = C_2H_5) and **11** (R = C_2H_5), which were separable by preparative thin-layer chromatography.

Because of the ambiguity encountered in the benzoyl and propionyl examples we investigated other condensation conditions. As a result of this we have found that when triacetic acid lactone **5** (R = H) is treated with benzoyl or propionyl chloride in the presence of aluminium chloride *C*-acylation is achieved and the required C-3 acylated products **14** (R = C_6H_5 or C_2H_5) are obtained directly. The pyrone **8** however was extensively degraded under these conditions and did not yield the corresponding *C*-benzoyl derivative (**10**; R = C_6H_5). It is of interest to note that reaction of monopyrone **8** with malonyl dichloride (cf. 12) produced the expected dipyrone structure **17**. The latter compound provides us with an entry into a combined fused-linear pyrone route to protected β-polyketones and this variant is being evaluated.

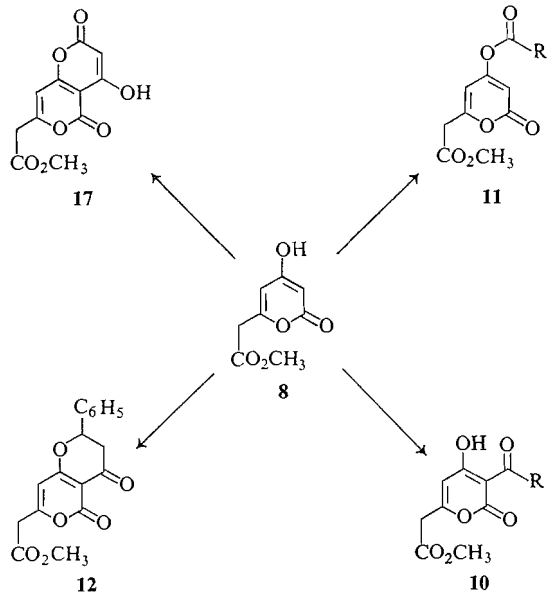

As a result of the acylation studies outlined above we proceeded with the projected synthesis of the extended pyrone system **16**. Treatment of triacetic acid lactone **5** (R = H) with the acid chloride **9** in the presence of aluminium chloride at 100 °C yielded a crystalline product m.p. 186–188 ° (decomp.) whose structure **16** was assigned on the basis of spectroscopic and analytical evidence: λ_{max} (MeOH) 227, 302, 410 mμ (ε 11 900, 11 600, 2700); nuclear magnetic resonance (n.m.r.) (trifluoroacetic acid) τ3.50 (1H, doublet J = 2 c.p.s.), 3.73 (1H, doublet J = 2 c.p.s.), 3.78 (1H), 5.53 (2H), 7.66 (3H). It was indeed fortunate but not surprising (see above) that concomitant demethylation had occurred during the acylation reaction since this step would have been necessary before further extensions of the theme could be investigated.

The results described in this report indicate that this alternative route to protected β-polyketo acid chains is feasible and the synthesis of **16** (equivalent to a C-12 polyacetate chain) allows us to examine some obvious extensions of this theme. Preliminary studies also indicate that compounds of the type described in this paper can be converted to aromatic compounds and we are presently investigating the scope of these reactions.

Experimental

Unless otherwise noted, the following are implied. Melting points were determined on a Kofler apparatus and are not corrected. The infrared spectra were recorded on Perkin–Elmer models 137-b or 237 spectrophotometers as Nujol mulls. The ultraviolet spectra were recorded on a Cary model 14 or a Unicam model S.P. 800 spectrophotometer in methanol solutions. The nuclear magnetic resonance (n.m.r.) spectra were recorded on Varian Associates models A-60 or HA-100 spectrometers with tetramethylsilane as an internal reference. Peak positions are recorded in the tau scale (tetramethylsilane = 10τ). Mass spectra were determined on an Atlas model CH-4 or an AEI model MS-9 mass spectrometer. All molecular weights were determined by mass spectrometry. Thin-layer chromatography (t.l.c.) results were obtained using silica gel plates (containing fluorescent indicator) 0.25 mm thick developed with chloroform – acetic acid 9:1 (solvent *a*) or carbon tetrachloride – chloroform – acetic acid 10:9:1 (solvent *b*).

Methyl Triacetic Lactone α-Keto Ester (6, R = CH_2CH_3)

The methyl ether of triacetic lactone (**5**, R = CH_3) (42 g, 0.3 moles) in benzene (1000 ml) and diethyl oxalate (50 ml) in benzene (800 ml) were added to a slurry of atomized sodium (9.2 g) in benzene (200 ml). The mixture was stirred and heated under reflux during which hydrogen was evolved vigorously. After the sodium had all reacted (about 15 min), the solution was cooled and added to chloroform (6 l) and the chloroform solution washed with 1 *N* hydrochloric acid (2 × 4 l) and water (4 l). The aqueous layers were extracted with chloroform (4 l) and the combined chloroform layers dried (anhydrous magnesium sulfate) and evaporated under reduced pressure to a mixture of a brown oil and a solid. The product was triturated with ether (the ether discarded) to yield 4-methoxy 6-(2′-hydroxy 2′-carbethoxyvinyl)-2-pyrone (**6**, R = CH_2CH_3) (31 g, 43%). Recrystallization from ethylacetate gave pale-yellow crystals, m.p. 171–173°; ultraviolet spectrum, λ_{max} (ε) 250 (3400), 280 (4400), 339 (13 800), and 400 (shoulder, 2900) mμ; infrared spectrum, 3300, 1725 (shoulder), 1700, 1660

Can. J. Chem. Downloaded from www.nrcresearchpress.com by 210.87.254.5 on 09/05/12
For personal use only.

(weak), 1620 and 1550 cm^{-1}; n.m.r. spectrum (in trifluoroacetic acid), 8.50 (t, 3H, $J = 7$ c.p.s.), 5.93 (s, 3H), 5.44 (q, 2H, $J = 7$ c.p.s.), 3.90 (d, 1H, $J = 2$ c.p.s.), 3.58 (s, 1H), and 2.77 (d, 1H, $J = 2$ c.p.s.); t.l.c. results solvent *a* R_f 0.44, solvent *b* R_f 0.11.

Anal. Calcd. for $C_{11}H_{12}O_6$ (mol. wt., 240): C, 55.00 H, 5.04. Found (mol. wt., 240): C, 55.08; H, 4.95.

*Methyl Triacetic Lactone α-Hydroxy Acid (**6**, R = H)*

Methyl triacetic lactone α-hydroxy ester (**6**, R = CH_2-CH_3) (7.5 g) was added to 0.1 *N* hydrochloric acid (600 ml) and the mixture was stirred and heated under reflux for 1 h. The reaction mixture was evaporated to 150 ml volume under reduced pressure, cooled in ice, and the precipitate collected and washed with cold water. The product was added to refluxing ethanol containing 10% water (250 ml) and evaporated under reduced pressure to 100 ml volume, cooled in ice and 4-methoxy-6-(2′-hydroxy 2′-carboxyvinyl)-2-pyrone (**6**, R = H) collected (4.2 g, 63%). Recrystallization from ethanol gave a pale-yellow, microcrystalline solid, m.p. 242–249° (decomp.); ultraviolet spectrum, λ_{max} (ε) 251 (9000), 280 (shoulder, 4900), and 337 (16 000) mμ; infrared spectrum, 3380, 3100 (weak), 1725, 1680, 1615, and 1555 cm^{-1}; n.m.r. spectrum (in trifluoroacetic acid), 5.98 (s, 3H), 3.95 (d, 1H, $J = 1.5$ c.p.s.), 3.50 (s, 1H), and 2.95 (d, 1H, $J = 1.5$ c.p.s.); t.l.c. results, solvent *a* R_f 0.

Anal. Calcd. for $C_9H_8O_6$ (mol. wt., 212): C, 50.95; H, 3.80. Found (mol. wt., 212): C, 51.42; H, 3.88.

*Methyl Triacetic Lactone Acid (**7**, R = H)*

Methyl triacetic lactone α-hydroxy acid (**6**, R = H) (8.0 g) was dissolved in an ice-cold solution of sodium hydroxide (4.0 g) in water (125 ml) and 30% hydrogen peroxide (13.5 ml) was added dropwise (cf. 14)). Stirring and cooling of the solution was continued for 15 min and then the solution was acidified carefully with 2 *N* hydrochloric acid. The solution was evaporated under reduced pressure to 80 ml and left at 0° overnight. The resulting crystals were collected, washed with water, and recrystallized from ethyl acetate to yield 4-methoxy-6-methylenecarboxy-2-pyrone (**7**, R = H) (4.0 g, 57%). Further recrystallization from ethyl acetate gave fine colorless needles, m.p. 178–180° (decomp.); ultraviolet spectrum, λ_{max} (ε) 280 (7300) mμ; infrared spectrum, 3080 (weak), 2680, 2590, 2500 (shoulder), 1730, 1680, 1640, and 1560 cm^{-1}; n.m.r. spectrum (in trifluoroacetic acid), 6.15 (s, 2H), 5.96 (s, 3H), 3.93 (d, 1H, $J = 2$ c.p.s.) and 3.50 (d, 1H, $J = 2$ c.p.s.); t.l.c. results, solvent *a* R_f 0.15.

Anal. Calcd. for $C_8H_8O_5$ (mol. wt., 184, 184 with loss of CO_2 gives 140): C, 52.18; H, 4.38. Found (mol. wt. 140): C, 52.05; H, 4.42.

*Methyl Triacetic Lactone Ester (**7**, R = CH_3)*

Methyl triacetic lactone acid (**7**, R = H) (6 g) was dissolved in methanol (120 ml) and concentrated sulfuric acid (1.4 ml) was added. The solution was heated under reflux for one h, evaporated under reduced pressure to 20 ml volume and cold water (200 ml) added. On standing, a precipitate formed. The pH of the mixture was adjusted to 8 by addition of 10% sodium bicarbonate solution. The mixture was extracted with ethyl acetate and the ethyl acetate was washed, dried (anhydrous magnesium sulfate and decolorizing charcoal), and evaporated under reduced pressure to yield crystalline 4-methoxy-6-methylenecarbomethoxy-2-pyrone (**7**, R = CH_3) (6.0 g, 93%). The product was recrystallized from benzene–cyclohexane 1:1 to give colorless crystals, m.p. 93.5–95°; ultraviolet spectrum; λ_{max} (ε) 279 (6100) mμ; infrared spectrum, 3100 (weak), 1750, 1700, 1650, and 1560 cm^{-1}; n.m.r. spectrum (in deuteriochloroform), 6.52 (s, 2H), 6.26 (s, 3H), 6.20 (s, 3H), 4.53 (d, 1H, $J = 2$ c.p.s.), and 4.03 (d, 1H, $J = 2$ c.p.s.); t.l.c. results, solvent *a* R_f 0.60, solvent *b* R_f 0.20.

Anal. Calcd. for $C_9H_{10}O_5$ (mol. wt., 198): C, 54.54; H, 5.09. Found (mol. wt., 198); C, 54.61; H, 5.27.

*Triacetic Lactone Ester (**8**)*

Methyl triacetic lactone ester (**7**, R = CH_3) (3 g) was dissolved in warm benzene (75 ml) and powdered anhydrous aluminium chloride (12 g) was added (cf. 15). The mixture was stirred and heated under reflux for 75 min and then the benzene was evaporated under reduced pressure. The resulting oil was cooled thoroughly in an ice-salt bath and partially frozen 3 *N* hydrochloric acid (20 ml) was added with stirring and breaking up of the residue over a period of 20 min. A further 60 ml of cold 3 *N* hydrochloric acid was added over a period of 10 min. With the cooling continued, powdered sodium bicarbonate was added slowly until the mixture was of pH 2. Water (150 ml) was added and the mixture was extracted with ethyl acetate and the ethyl acetate solution was washed, dried (anhydrous magnesium sulfate), and evaporated under reduced pressure to give a brown solid. The solid was triturated with a small amount of ether (the ether discarded) to yield crystalline 4-hydroxy-6-methylenecarbomethoxy-2-pyrone (**7**) (2.0 g, 73%). Recrystallization from ethyl acetate gave colorless, cubic crystals, m.p. 138.5–140°; ultraviolet spectrum, λ_{max} (ε) 284 (6700) mμ; infrared spectrum, 3100 (weak), 2700, 2600, 1750, 1700, 1660, 1620, 1560, and 1525 cm^{-1}; n.m.r. spectrum (in trifluoroacetic acid), 6.17 (s, 2H), 6.06 (s, 3H), 3.78 (d, 1H, $J = 2$ c.p.s.), and 3.48 (d, 1H, $J = 2$ c.p.s.); t.l.c. results, solvent *a* R_f 0.10.

Anal. Calcd. for $C_8H_8O_5$ (mol. wt., 184): C, 52.18; H, 4.38. Found (mol. wt., 184): C, 52.48; H, 4.43.

Acylation Studies using Trifluoroacetic Acid

To the pyrone (triacetic lactone (**5**, R = H) or triacetic lactone ester (**8**) (0.005 moles) was added trifluoroacetic acid (3 ml) and the appropriate acid chloride (0.01 mole) (8). The mixture was stirred and heated under reflux for 3 h, then cooled and poured into ice-water (15 ml). In the experiments in which triacetic lactone ester was treated with acetyl or propionyl chloride, sodium bicarbonate was added to adjust the mixture to pH 2 and the mixture was extracted with ethyl acetate. The ethyl acetate was washed, dried (anhydrous magnesium sulfate), and evaporated to give a crystalline solid. In the other experiments, a crystalline solid precipitated which was collected, washed with water, and dried.

*C-Acetyl Triacetic Lactone (**14**, R = CH_3) (Dehydroacetic Acid)*

The product was recrystallized from methanol to yield colorless crystals of 3-acetyl-4-hydroxy-6-methyl-2-pyrone (dehydroacetic acid) (0.48 g, 55%), m.p. and

Can. J. Chem. Downloaded from www.nrcresearchpress.com by 210.87.254.5 on 09/05/12
For personal use only.

mixture m.p. with authentic dehydroacetic acid 109–111.5°; with identical ultraviolet, infrared, and t.l.c. behavior to authentic dehydroacetic acid.

*O-Benzoyl Triacetic Lactone (**13**)*

The product was mixed with a solution of sodium bicarbonate in water (20 ml, pH 8) and the resulting mixture was extracted with chloroform. The chloroform was washed, dried (anhydrous magnesium sulfate), and evaporated under reduced pressure to yield 4-*O*-benzoyl-6-methyl-2-pyrone (**13**) (0.66 g, 95%) which was recrystallized from cyclohexane–benzene 1:1 to give large colorless rectangular prisms, m.p. 89–90° (lit. m.p. 90° (13);[2] ultraviolet spectrum, λ_{max} (ε) 238 (24 000) and 286 (8200) mμ; infrared spectrum, 1745, 1715, 1640, 1600 (weak), and 1560 cm^{-1}; n.m.r. spectrum (in deuteriochloroform), 7.71 (s, 3H), 3.83 (slightly broadened, 2H), 2.40 (m, 3H), and 1.90 (m, 2H); t.l.c. results, solvent *a* R_f 0.72, solvent *b* R_f 0.34.

Anal. Calcd. for $C_{13}H_{10}O_4$ (mol. wt., 230): C, 67.82; H, 4.38. Found (mol. wt., 230): C, 68.12; H, 4.59.

*C-Acetyl Triacetic Lactone Ester (**10**, R = CH_3)*

The product was dissolved in ethyl acetate and extracted with 5% sodium bicarbonate solution. The basic solution was acidified to pH 1.5 with dilute hydrochloric acid, extracted with ethyl acetate, and the ethyl acetate solution was dried (anhydrous magnesium sulfate and charcoal) and evaporated under reduced pressure to yield 3-acetyl-4-hydroxy-6-methylenecarbomethoxy-2-pyrone (**10**, R = CH_3) (0.54 g, 48%). Recrystallization from methanol gave colorless crystals, m.p. 100–101.5°; ultraviolet spectrum, λ_{max} (ε) 224 (14 100) and 310 (12 900) mμ; infrared spectrum, 1730, 1660, 1610, and 1550 cm^{-1}; n.m.r. spectrum (in deuteriochloroform), 7.31 (s, 3H) (6.41 s, 2H) 6.20 (s, 3H), 3.86 (s, 1H), and −7.00 (s, 1H); t.l.c. results, solvent *a* R_f 0.63.

Anal. Calcd. for $C_{10}H_{10}O_6$ (mol. wt., 226): C, 53.10; H, 4.46. Found (mol. wt., 226): C, 52.89; H, 4.70.

*Cinnamoyl Triacetic Lactone Ester (**12**)*

The product was triturated with ethyl acetate and the ethyl acetate discarded to yield 2-phenyl-7-methylenecarbomethoxy-4,5-diketo-1,6-dioxy-2,3-dihydronaphthalene (**12**) (0.20 g, 13%). Recrystallization from acetonitrile gave colorless leaflets, m.p. 211–213°; ultraviolet spectrum, $\lambda_{max}(CH_3CN)$ (ε) 250 (shoulder, 4200), 309 (10 400), 382 (shoulder, 1600), and 400 (2100) mμ; infrared spectrum, 3080 (weak), 1745, 1660, 1650, and 1540 cm^{-1}; n.m.r. spectrum (in trifluoroacetic acid), 6.70 (m, 2H, AB portion of ABX system, J_{AB} = 19 c.p.s., J_{AX} = 10.5 c.p.s., J_{BX} = 5.4 c.p.s.), 6.13 (s, 2H), 6.05 (s, 3H), 4.10 (m, 1H, X portion of ABX system, $J_{AX} + J_{BX}$ = 16 c.p.s.), 3.43 (s, 1H), and 2.50 (s, 5H); t.l.c. results, solvent *a* R_f 0.16.

Anal. Calcd. for $C_{17}H_{14}O_6$ (mol. wt., 314): C, 64.96; H, 4.49. Found (mol. wt., 314): C, 64.83; H, 4.83.

*O-Benzoyl Triacetic Lactone Ester (**11**, R = C_6H_5)*

The product was recrystallized from ethyl acetate to yield (0.74 g, 51%) colorless, thick needles of 4-*O*-benzoyl-6-methylenecarbomethoxy-2-pyrone, (**11**), R = C_6H_5) m.p. 127.5–128°; ultraviolet spectrum, λ_{max} (ε) 239 (23 200) and 296 (8300) mμ; infrared spectrum, 1750, 1715, 1650, 1600 (weak), and 1570 cm^{-1}; n.m.r. spectrum (in deuteriochloroform), 6.43 (s, 2H); 6.24 (s, 3H), 3.71 (d, 1H, J = 2 c.p.s.), 3.66 (d, 1H, J = 2 c.p.s.), 2.40 (m, 3H), and 1.85 (m, 2H); t.l.c. results, solvent *a* R_f 0.71; solvent *b* R_f 0.20.

Anal. Calcd. for $C_{15}H_{12}O_6$ (mol. wt., 288): C, 62.50; H, 4.20. Found (mol. wt., 288) C, 62.58; H, 4.01.

*Proprionyl Triacetic Lactone Esters (**10** and **11**, R = CH_2CH_3)*

A portion of the product was dissolved in acetone and streaked on several 20 × 60 × 0.01 cm preparative t.l.c. plates which were developed with solvent *b*. Extraction of the two main bands gave *O*- and *C*- propionyl triaceticlactone esters in approximately equal quantities.

*C-Propionyl Triacetic Lactone Ester (**10**, R = CH_2CH_3)*

3-propionyl-4-hydroxy-6-methylenecarbomethoxy-2-pyrone (**10**, R = CH_2CH_3) was further purified by short-path sublimation (70° at 0.2 mm Hg) to give a colorless microcrystalline solid, m.p. 69–70°; ultraviolet spectrum, λ_{max} (ε) 224 (10 200) and 309 (12 000 mμ; infrared spectrum, 1750, 1720 (shoulder) 1645, 1615, and 1580 cm^{-1}; n.m.r. spectrum (in deuteriochloroform), 8.82 (t, 3H, J = 7 c.p.s.), 6.86 (q, 2H, J = 7 c.p.s.), 6.43 (s, 2H), 6.20 (s, 3H), 3.81 (s, 1H), and −6.87 (s, 1H); t.l.c. results, solvent *a* R_f 0.68, solvent *b* R_f 0.34.

Anal. Calcd. for $C_{11}H_{12}O_6$ (mol. wt., 240): C, 55.00; H, 5.04. Found (mol. wt., 240): C, 54.79; H, 4.94.

*O-Propionyl Triacetic Lactone Ester (**11**, R = CH_2CH_3)*

4-*O*-propinyl-6-methylenecarbomethoxy-2-pyrone (**11**, R = CH_2CH_3) was further purified by recrystallization at −23° from cyclohexene to give colorless leaflets, m.p. 65–67°; ultraviolet spectrum, λ_{max} (ε) 292 (6400) mμ; infrared spectrum, 1770, 1725, 1645 (weak), and 1580 cm^{-1}; n.m.r. spectrum (in deuteriochloroform); 8.79 (t, 3H, J = 7.5 c.p.s.) 7.42 (q, 2H, J = 7.5 c.p.s.), 6.45 (s, 2H), 6.25 (s, 3H,) and 3.83 slightly broadened, 2H); t.l.c. results, solvent *a* R_f 0.60. solvent *b* R_f 0.25.

Anal. Calcd. for $C_{11}H_{12}O_6$ (mol. wt., 240): C, 55.00; H, 5.04. Found (mol. wt., 240): C, 55.24; H, 5.11.

*Methylene Carbomethoxy Dipyrone (**17**)*

To triacetic lactone ester (**8**) (0.30 g) was added trifluoroacetic acid (1.2 ml) and malonyl dichloride (0.6 ml). The solution was stirred and heated under reflux for 4 h, then cooled and cold ethyl acetate (1 ml) added. After 30 min, the precipitate was collected and washed with ethyl acetate. The precipitate was dissolved in chloroform and placed on a silica gel column (2 g) which was then eluted with chloroform. The first fraction (0.20 g) was dissolved in benzene and placed on a silica gel column (6 g) which was eluted with benzene–chloroform 9:1. The first main fraction was evaporated to yield (47 mg, 11%) crystalline 7-methylenecarbomethoxy-2,5-diketo-4-hydroxy-1,6-dioxanaphthalene (**17**) which was recrystallized from benzene–cyclohexane 5:2 to give colorless needles, m.p. 159–161° (decomp.); ultraviolet spectrum, λ_{max} (ε) 215 (15 200), 269 (14 100), and 328 (7500) mμ; infrared spectrum, 3200 (weak), 3090 (weak), 1735, 1720,

[2]The m.p. and other physical data given in this paper are erroneously ascribed to the *C*-benzoyl derivative (**14**, R = C_6H_5).

1640, 1620 (weak), and 1565 cm^{-1}; n.m.r. spectrum (in deuteriochloroform), 6.36 (s, 2H), 6.24 (s, 3H), 4.41 (s, 1H), 3.47 (s, 1H), and −0.35 (broad, 1H); t.l.c. results, solvent *a* R_f 0.37, solvent *b* R_f 0.09.

Anal. Calcd. for $C_{11}H_8O_7$ (mol. wt., 252): C, 52.39; H, 3.20. Found (mol. wt., 252): C, 52.26; H, 3.06.

Methyl Triacetic Lactone Acid Chloride (9)

To methyl triacetic lactone acid (**9**, R = H) (1 g) was added oxalyl chloride (10 ml) and the mixture was cooled to 10°, stirred, and one drop of dimethyl formamide added. After 2.5 h, the excess oxalyl chloride was distilled off under reduced pressure at 10°. The tarry product was extracted with boiling cyclohexane which on cooling deposited colorless needles of 4-methoxy-6-methylene-carboxylchloride-2-pyrone (**9**), infrared spectrum: 3080 (weak), 1795, 1710, 1655, and 1565 cm^{-1}. A small portion of the acid chloride was treated with methanol and the methanol evaporated. The resulting solid was recrystallized from benzene–cyclohexane 1:1 to give methyltriacetic lactone ester (**7**, R = CH_3), with identical t.l.c. behavior to that of previously prepared methyl triacetic lactone ester, and mixture m.p. with methyl triacetic lactone ester, 90–93°.

Acylation Studies using Aluminium Chloride

Powdered triacetic lactone (**5**, R = H) (0.6 g, 0.005 moles), powdered aluminium chloride (4 g) and the appropriate acid chloride (0.006 moles) were mixed very thoroughly and fused at 100–120° for 1 h. (In the experiment which methyl triacetic lactone acid chloride was used, half quantities were used and the acid chloride was used unpurified.) The resulting tarry mass was cooled in ice-salt and cold 3 *N* hydrochloric acid (30 ml) was slowly added with breaking up of the residue. The mixture was adjusted to pH 2 with sodium bicarbonate and extracted with ethyl acetate. The ethyl acetate was filtered and evaporated under reduced pressure to give a brown solid which was dissolved in trifluoroacetic acid (6 ml) and 12 *N* hydrochloric acid (0.5 ml). After 14 h, the acid solution was poured into water (30 ml) and after a day the resulting precipitate was collected.

*Propionyl Triacetic Lactone (**14**, R = CH_2CH_3)*

The crystalline product (0.57 g, 63%) (3-propionyl-4-hydroxy-6-methyl-2-pyrone) was recrystallized from methanol to give colorless needles. m.p. 103–105° (lit. m.p. 104° (13)); ultraviolet spectrum; λ_{max} (ε) 225 (12 600) and 307 (11 800) mμ; infrared spectrum, 3080 (weak) 1715, 1640, 1600, and 1540 cm^{-1}; n.m.r. spectrum (in deuteriochloroform), 8.88 (t, 3H, $J = 7$ c.p.s.), 7.79 (s, 3H), 6.95 (q, 2H, $J = 2$ c.p.s.), 4.12 (s, 1H), and −6.69 (s, 1H); t.l.c. results, solvent *b*, R_f 0.43; mol. wt., 182, $C_9H_{10}O_4$ requires mol. wt., 182.

*C-benzoyl Triacetic Lactone (**14**, R = C_6H_5)*

The product was recrystallized from methanol to give colorless, short needles of 3-benzoyl-4-hydroxy-6-methyl-2-pyrone (**14**, R = C_6H_5) m.p. 107–109°; ultraviolet spectrum, λ_{max} (ε) 239 (9600) and 325 (11 900) mμ; infrared spectrum, 3100 (weak), 1750, 1640, 1590 (shoulder), and 1560 cm^{-1}; n.m.r. spectrum (in deuteriochloroform), 7.77 (s, 3H), 4.02 (s, 1H), 2.50 (m, 5H), and −5.95 (s, 1H); t.l.c. results, solvent *b* R_f 0.28.

Anal. Calcd. for $C_{13}H_{10}O_4$ (mol. wt., 230): C, 67.82: H, 4.38. Found (mol. wt., 230): C, 67.79; H, 4.76.

Condensation of Triacetic Lactone with (9). Formation of (16)

The product (70 mg, 10%) (3-[4′-hydroxy-6′-methyl-eneacyl-2′-pyrone]-4′-hydroxy-6-methyl-2-pyrone) (**16**) was recrystallized from methanol–ethyl acetate 1:1 to give a faintly-yellow microcrystalline powder, m.p. 186–188° (decomp.); ultraviolet spectrum, λ_{max} (ε) 228 (11 900), 302 (11 600), and 410 (2700) mμ; infrared spectrum, 3150 (broad), 3100, 1710, 1675, 1650 (shoulder), and 1560 cm^{-1}; n.m.r. spectrum (in trifluoroacetic acid), 7.66 (s, 3H), 5.53 (s, 2H), 3.78 (s, 1H, 3.73 (d, 1H, $J = 2$ c.p.s.), and 3.50 (d, 1H, $J = 2$ c.p.s.); t.l.c. results, solvent *a*, R_f 0.06.

Anal. Calcd. for $C_{13}H_{10}O_7$ (mol. wt., 278): C, 56.12; H. 3.62. Found (mol. wt., 278): C, 56.45; H. 3.81.

Acknowledgment

We are grateful to the National Research Council of Canada for a research grant (NRCC A2267) and a research studentship to one of us (J. L. D.).

1. T. Money, I. H. Qureshi, G. R. B. Webster, and A. I. Scott. J. Am. Chem. Soc. **87**, 3004 (1965).
2. T. Money, F. W. Comer, G. R. B. Webster, I. G. Wright, and A. I. Scott. Tetrahedron, **23**, 3435 (1967).
3. T. Money, J. L. Douglas, and A. I. Scott. J. Am. Chem. Soc. **88**, 624 (1966).
4. J. L. Douglas and T. Money. Tetrahedron, **23**, 3545 (1967).
5. J. L. Douglas and T. Money. Can. J. Chem. **45**, 1990 (1967).
6. F. W. Comer, T. Money, and A. I. Scott. Chem. Commun. 231 (1967).
7. J. D. Bu'Lock and H. G. Smith. J. Chem. Soc. 502 (1960).
8. L. L. Woods and P. A. Dix. J. Org. Chem. **26**, 2588 (1961).
9. A. J. Birch. Proc. Chem. Soc. **3**, (1962).
10. H. Hanni and T. Money. Unpublished observations.
11. C. Goetschel and C. Mentzer. Bull. Soc. Chim. France, 365 (1962).
12. M. A. Butt and J. A. Elvidge. J. Chem. Soc. 4483 (1963).
13. K. Kiyaki and S. Yamazishi. Yakugaku Zasshi, **75**, 43 (1955).
14. Org. Syn. Coll. Vol. II, p. 333. (1943).
15. F. King, N. Clark, and P. Davis. J. Chem. Soc. 3012 (1949).

Can. J. Chem. Downloaded from www.nrcresearchpress.com by 210.87.254.5 on 09/05/12
For personal use only.

Can. J. Chem. Downloaded from www.nrcresearchpress.com by 210.87.254.5 on 09/05/12
For personal use only.

Carbodihydrazones and oxalyl dihydrazones[1]

D. M. WILES AND T. SUPRUNCHUK
Division of Applied Chemistry, National Research Council of Canada, Ottawa, Canada

Received September 13, 1967

Carbodihydrazones and oxalyl dihydrazones have been prepared using the reaction between aldehydes and carbohydrazide and oxalyl dihydrazide, respectively. The structures of these new series of compounds have been established by comparing their infrared absorption spectra with those of related compounds. The potential scope of the synthetic method has been indicated by the preparation of analogous derivatives from two aromatic aldehydes and from two simple ketones.

Canadian Journal of Chemistry, 46, 701 (1968)

Introduction

Reactions of carbonyl-containing compounds with hydrazides and semicarbazides have been extensively investigated both as versatile methods of synthesis and for specific use in structural elucidation by infrared spectroscopy. It has been suggested, for example, that semicarbazones are suitable derivatives for identifying and characterizing liquid ketones (1). The semicarbazones (1, 2) and hydrazones (2, 3) have been prepared (and their infrared spectra reported) for a wide variety of aldehydes and ketones.

The condensation reaction referred to above,

$$\text{i.e., } \rangle C{=}O + NH_2NHC(=O)-,$$

has been utilized in the present work to synthesize two new series of compounds. Seven aliphatic aldehydes have been used to prepare oxalyl dihydrazones and to prepare carbodihydrazones from oxalyl dihydrazide and carbohydrazide, respectively. Dihydrazones of both types were also prepared from two substituted benzaldehydes and from two low molecular weight ketones.

Experimental

Oxalyl dihydrazide, carbohydrazide, and the aldehydes and ketones used in the syntheses described below were the purest grade obtainable from commercial sources. Melting points were obtained with a Fisher–Johns apparatus and are corrected. Elemental analyses were performed at the microanalytical laboratory of Drs. Weiler and Strauss in Oxford. Infrared spectra were obtained with a model 21 Perkin–Elmer double-beam spectrophotometer (NaCl prism) using KBr pellets.

General Procedure for Preparing Oxalyl Dihydrazones

Aldehyde (20 ml) was added to oxalyl dihydrazide (0.016 mole) and the mixture was heated until the latter dissolved. The white precipitate which formed during subsequent cooling was collected by filtration, washed with *n*-hexane until all excess aldehyde was removed, and dried. Yields, melting points, solvents used for recrystallization, and analyses for the 7 dihydrazones prepared in this way are listed in Table I.

General Procedure for Preparing Carbodihydrazones

Carbohydrazide (0.01 mole) was dissolved in warm water (25 ml). To this was slowly added a solution of aldehyde (0.02 mole) in 25 ml ethanol containing a few drops of glacial acetic acid. The mixture was heated on the steam bath for 15 min, then cooled. The precipitate which formed was collected by filtration, washed repeatedly with cold 50% aqueous ethanol solution, and dried. Data for the compounds prepared by this method are given in Table II.

In order to investigate the scope of this reaction between carbonyl-containing compounds and the difunctional hydrazides, two aromatic aldehydes and two ketones were used. The oxalyl dihydrazones and carbodihydrazones of *o*-chlorobenzaldehyde, anisaldehyde, acetone, and methyl ethyl ketone were prepared by methods similar to those described above. The relevant data are as follows:

Oxalyl di(*o*-chlorobenzaldehyde)hydrazone, m.p. 271°C.
Anal. Calcd. for $C_{16}H_{12}Cl_2N_4O_2$: C, 53.04; H, 3.31; Cl, 19.34; N, 15.47. Found: C, 52.84; H, 3.36; Cl, 19.20; N, 15.50.

Oxalyl di(anisaldehyde)hydrazone, m.p. > 300 °C.
Anal. Calcd. for $C_{18}H_{18}N_4O_4$: C, 61.02; H, 5.08; N, 15.82. Found: C, 60.95; H, 4.95; N, 15.80.

Oxalyl di(acetone)hydrazone, m.p. 225 °C.
Anal. Calcd. for $C_8H_{14}N_4O_2$: C, 48.48; H, 7.07; N, 28.28. Found: C, 48.43; H, 6.98; N, 28.20.

Oxalyl di(methyl ethyl ketone)hydrazone, m.p. 168 °C.
Anal. Calcd. for $C_{10}H_{18}N_4O_2$: C, 53.09; H, 7.96; N, 24.78. Found: C, 53.46; H, 8.01; N, 25.01.

Carbodi(*o*-chlorobenzaldehyde)hydrazone, m.p. 225 °C.
Anal. Calcd. for $C_{15}H_{12}Cl_2N_4O$: C, 53.73; H, 3.58; Cl, 21.19; N, 16.72. Found: C, 53.86; H, 3.58; Cl, 20.99; N, 16.91.

Carbodi(anisaldehyde)hydrazone, m.p. 218 °C.
Anal. Calcd. for $C_{17}H_{18}N_4O_3$: C, 62.58; H, 5.52; N, 17.17. Found: C, 62.28; H, 5.54; N, 17.25.

Carbodi(acetone)hydrazone, m.p. 165 °C.
Anal. Calcd. for $C_7H_{14}N_4O$: C, 49.41; H, 8.24; N, 32.94. Found: C, 49.06; H, 8.36; N, 32.60.

[1]Issued as NRCC No. 9907.

Can. J. Chem. Downloaded from www.nrcresearchpress.com by 210.87.254.5 on 09/05/12
For personal use only.

TABLE I

Oxalyl dihydrazones*

No.	Aldehyde	Melting point °C	Yield %	Formula	Calculated %	Found %
1	Heptanal	236	98†	$C_{16}H_{30}N_4O_2$	C, 61.94 H, 9.68 N, 18.06	C, 61.75 H, 9.86 N, 17.90
2	Octanal	221	97†	$C_{18}H_{34}N_4O_2$	C, 63.91 H, 10.06 N, 16.57	C, 63.81 H, 10.18 N, 16.35
3	Nonanal	217	97†	$C_{20}H_{38}N_4O_2$	C, 65.57 H, 10.38 N, 15.30	C, 65.28 H, 10.48 N, 15.05
4	Decanal	212	91‡	$C_{22}H_{42}N_4O_2$	C, 67.01 H, 10.66 N, 14.21	C, 67.02 H, 10.46 N, 14.00
5	Undecanal	205	96§	$C_{24}H_{46}N_4O_2$	C, 68.25 H, 10.90 N, 13.27	C, 68.33 H, 11.02 N, 13.38
6	9-Undecenal	203	95§	$C_{24}H_{42}N_4O_2$	C, 68.89 H, 10.05 N, 13.39	C, 69.08 H, 9.88 N, 13.49
7	Dodecanal	204	91§	$C_{26}H_{50}N_4O_2$	C, 69.33 H, 11.11 N, 12.44	C, 69.51 H, 11.18 N, 12.42

*Oxalyl dihydrazones of aldehydes have the structure 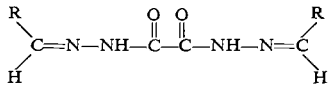 .

†Recrystallized from methanol.
‡Recrystallized from ethanol.
§Recrystallized from chloroform.

TABLE II

Carbodihydrazones*

No.	Aldehyde	Melting point °C	Yield† %	Formula	Calculated %	Found %
8	Heptanal	121	80	$C_{15}H_{30}N_4O$	C, 63.83 H, 10.64 N, 19.86	C, 64.00 H, 10.40 N, 19.92
9	Octanal	127	79	$C_{17}H_{34}N_4O$	C, 65.81 H, 10.97 N, 18.06	C, 65.44 H, 10.83 N, 18.25
10	Nonanal	126	85	$C_{19}H_{38}N_4O$	C, 67.46 H, 11.24 N, 16.57	C, 67.28 H, 11.24 N, 16.65
11	Decanal	126	95	$C_{21}H_{42}N_4O$	C, 68.85 H, 11.48 N, 15.30	C, 68.88 H, 11.60 N, 15.18
12	Undecanal	121	77	$C_{23}H_{46}N_4O$	C, 70.05 H, 11.67 N, 14.21	C, 70.25 H, 11.64 N, 14.06
13	9-Undecenal	118	81	$C_{23}H_{42}N_4O$	C, 70.77 H, 10.77 N, 14.36	C, 70.65 H, 10.71 N, 14.43
14	Dodecanal	109	87	$C_{25}H_{50}N_4O$	C, 71.09 H, 11.85 N, 13.27	C, 71.08 H, 11.80 N, 13.50

*Carbodihydrazones of aldehydes have the structure 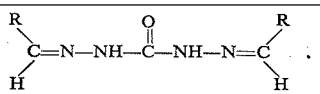 .

†All products recrystallized from 50% aqueous ethanol solution.

Carbodi(methyl ethyl ketone)hydrazone, m.p. 111 °C. Anal. Calcd. for $C_9H_{18}N_4O$: C, 54.54; H, 9.09; N, 28.28. Found: C, 54.54; H, 9.03; N, 28.30.

The ratio of aldehyde (or ketone) to (di)hydrazide used in the preparations described above was varied in some cases to improve the yields of the desired dihydrazone products over the monosubstituted products. For example, high yields (Table II) of dihydrazones were obtained from aliphatic aldehydes and carbohydrazide with a 2:1 ratio of reagents but a greater excess of aliphatic aldehyde was required in the reactions involving oxalyl dihydrazide. Similarly, the dihydrazones from the substituted benzaldehydes were obtained in high yield in 50% aqueous ethanol solution with a 2:1 ratio whereas the ketones were used in greater excess.

Results and Discussion

Evidence that the structures, proposed (Tables I and II) for the new compounds reported here, are correct was obtained by measuring their infrared absorption spectra in the 4000 to 700 cm^{-1} frequency range. These data, presented in Tables III and IV, are discussed below in terms of the bands characteristic of the functional groups involved. In addition, some comparisons are made with the previously published spectra of compounds having related structural entities.

Absorptions arising from NH stretching vibrations occur in the 3240 to 3200 cm^{-1} region of the spectra of the oxalyl dihydrazones (Table III), i.e., there is a single medium to strong band in this region for each of these compounds. The much weaker band in the 3070 to 3060 cm^{-1} region of each spectrum is almost certainly an overtone of the 1535 cm^{-1} band (4) (see below). As expected, the same pattern is observed in this region of the spectra of the carbodihydrazones (Table IV). The absorption due to ν (NH) occurs between 3260 and 3240 cm^{-1} and the weaker CNH overtone (4) is found between 3100 and 3090 cm^{-1}. The absorptions for both series of compounds correspond closely to those reported (4) for simple secondary amides. In this connection, it is worth noting that Mashima (5) ascribes the band at 3250 cm^{-1} in the spectrum of oxamide acid hydrazide to ν (NH), and that the corresponding absorption for the hydrazone prepared from isoniazid and *p*-hydroxybenzaldehyde occurs (3) at 3200 cm^{-1}.

The "double-bond region", 1700 to 1500 cm^{-1}, is of particular importance in characterizing the compounds prepared in this work. In the case of the oxalyl dihydrazones the absorptions seem to fit a clear-cut pattern, i.e., the strong carbonyl band at 1665 cm^{-1}, the medium intensity band at 1630 cm^{-1} due to ν (C═N), and the strong band at 1535 cm^{-1} arising from CNH vibration (involving both NH bending and CN stretching (6)). These assignments appear to be unambiguous (4) and exhibit the expected degree of correlation with those proposed for semicarbazones (1), and for some hydrazones (3) and hydrazides (5).

The interpretation of the absorptions which occur in this region of the carbodihydrazone spectra is more difficult, however, since four bands are observed. It is probable that the very strong band at 1670 to 1660 cm^{-1} should be attributed to C═O stretching vibrations. It is likely that the band at 1560 to 1550 cm^{-1} represents the CNH vibration. Of the remaining two bands, the one at lower frequency (1610 to 1600 cm^{-1}) would seem, on the basis of relative intensity, to result from ν (C═N). It is tempting to speculate, on the basis of this assumption, concerning the origin of the remaining weak band in the 1635 cm^{-1} region. Since it appears invariably in the spectra of the carbodihydrazones but never in the spectra of the oxalyl dihydrazones, an assignment based on the only structural difference between the two series of compounds would appear to have some merit. The 1635 cm^{-1} band could therefore be tentatively attributed to N—C—N stretching vibrations if it is assumed that there is considerable double bond character to the bonds of this group. At this frequency it could presumably be the asymmetric stretching mode (7, 8), but this is only one of several possible assignments. Davison and Christie (1), for example, have suggested that two bands in the 1665 cm^{-1} region of the spectra of some semicarbazones should be attributed to ν (C═N).

There are characteristic absorptions in three other regions for which assignments may be proposed. The bands at 1225 to 1220 cm^{-1} and 1240 to 1235 cm^{-1} in the spectra of the oxalyl dihydrazones and the carbodihydrazones, respectively, may be due to the lower frequency CNH vibration (where the N and H atoms move in the same direction relative to the carbon) referred to by Colthup *et al.* (4). The bands observed in the 725 cm^{-1} region in both sets of spectra could arise from out-of-plane NH wagging vibrations (4). Finally, the absorption in the 805 cm^{-1} region of the oxalyl dihydrazone

Can. J. Chem. Downloaded from www.nrcresearchpress.com by 210.87.254.5 on 09/05/12
For personal use only.

Can. J. Chem. Downloaded from www.nrcresearchpress.com by 210.87.254.5 on 09/05/12
For personal use only.

TABLE III

Infrared absorption bands for oxalyl dihydrazones

1	3240	3070	2940	2860	1665	1630	1535	1465	1430	1360	1220	1155	1040		950	885		810	725
	m	w	m	w	vs	m	s	w,m	w	m	m	vw	m		w	w		m	m,s
2	3210	3060	2930	2860	1665	1630	1535	1470	1435	1370	1225	1155	1040		950	890	835	805	725
	s	w	s	w	vs	m	s	w,m	w	m	m	w	m		w	w	sh	m	m,s
3	3210	3060	2920	2860	1665	1630	1535	1470	1425	1365	1220	1155	1040	965			850	805	720
	s	vw	s	vw	vs	m	s	m	w	m	w	vw	m	w			vw	m	m,s
4	3200	3060	2920	2850	1665	1630	1535	1470	1435	1370	1225	1155	1035	960	940	885	830	805	720
	s	w	s	w	vs	m	vs	m	w	s	m	w	m	vw	w	w	sh	m	s
5	3220	3060	2930	2850	1665	1630	1535	1475	1425	1370	1220	1155	1040	960		875		805	720
	m	vw	m	w	vs	m	s	m	w	m	w	vw	m	vw		vw		m	m
6	3230	3060	2920	2850	1665	1630	1535	1475	1425	1370	1220	1155	1040	960	910			810	715
	s	w	s	w	vs	m	s	m	w	m	m	w	m	w	m			m	m,s
7	3220	3060	2920	2850	1665	1630	1535	1475	1425	1370	1220	1155	1035		950	875		805	720
	s	w	s	w	vs	m	s	m	w	s	m	vw	m		w	vw		m	m,s

TABLE IV

Infrared absorption bands for carbodihydrazones

8	3260	3100	2960	2880	1670	1637	1600	1560	1475	1435	1390	1360	1235	1200	1165	1076	920		725
	m	w	m	vw	vs	sh	m	m	m	w	w	vw	m	w	m	m	m		w
9	3240	3100	2940	2880	1660	1635	1600	1560	1470	1435	1380	1350	1235	1190	1165	1080	920	770	725
	m	w	m	w	vs	sh	s	m	m	w	m	vw	s	w	w,m	m	m	w	w
10	3240	3100	2940	2880	1660	1635	1610	1555	1470	1440	1377	1355	1240	1190	1165	1080	925	770	725
	m	w	m	vw	vs	w	s	sh	m	vw	m	vw	s	w	w,m	m	w	vw	w
11	3240	3100	2940	2880	1665	1635	1600	1550	1475	1440	1380	1350	1240	1180	1165	1080	935	770	725
	br	w	m	vw	vs	w	s	m	m	vw	m	vw	s	w	w	m	m	vw	w
12	3240	3095	2940	2880	1665	1635	1610	1560	1475	1440	1380	1355	1240	1180	1165	1075	935	770	725
	br	w	m	w	vs	w	s	m	m	w	m	vw	m	w	m	m	m	vw	m
13	3240	3090	2940	2860	1665	1635	1605	1555	1475	1440	1380	1355	1240	1180	1165	1077	935	770	725
	br	w	w	vw	vs	w	s	m	m	vw	m	w	s	vw	m	m	w	vw	m
14	3240	3090	2940	2860	1665	1635	1605	1560	1470	1440	1380		1240		1165	1075	920	770	725
	br	vw	w	vw	vs	vw	s	sh	m	vw	m		s		w	m	m	vw	w

spectra may be tentatively assigned to the out-of-plane —CO—CO— wag which is observed at 802 cm^{-1} in the spectrum of glyoxal vapor (9).

The evidence presented above, both analytical (Tables I and II) and spectroscopic (Tables III and IV), clearly supports the structures proposed for the new compounds reported here. It follows, therefore, that the general synthetic method used is as effective in this application as it is in the preparation of semicarbazones and hydrazones.

The infrared spectra of the dihydrazones of aromatic aldehydes and simple ketones show the same characteristic features as are given in Tables III and IV and described above. The following minor differences are noted relative to the bands listed in the tables: (*a*) the carbonyl group absorption occurs at a frequency 35 cm^{-1} higher in the spectra of the carbodihydrazones; (*b*) the band arising from CNH vibrations is lower by 20 to 30 cm^{-1} in the spectra of oxalyl dihydrazones prepared from the ketones and in those of the carbodihydrazones made from both the aromatic aldehydes and the ketones. The same types of chemical structures are involved in all cases. This limited investigation of the preparation of dihydrazones from aromatic aldehydes and simple ketones indicates the potentially wide applicability of the method of synthesis used.

Acknowledgments

The authors wish to thank Dr. R. Norman Jones for helpful discussions and are grateful to Mr. R. Ironside for making the infrared measurements.

1. W. H. T. Davison and P. E. Christie. J. Chem. Soc. 3389 (1955).
2. D. Hadzi and J. Jan. Spectrochim. Acta, **23A**, 571 (1967).
3. N. E. Alexandrou and G. S. Vasilikiotis. Spectrochim. Acta, **23A**, 677 (1967).
4. N. B. Colthup, L. H. Daly, and S. E. Wiberley. Introduction to infrared and Raman spectroscopy. Academic Press, New York. 1964. pp. 264, 383, and references therein.
5. M. Mashima. Bull. Chem. Soc. Japan, **35**, 2020 (1962).
6. N. B. Colthup, L. H. Daly, and S. E. Wiberley. Introduction to infrared and Raman spectroscopy. Academic Press, New York. 1964. pp. 181 and 264.
7. E. Spinner. Spectrochim. Acta, **15**, 95 (1959).
8. N. B. Colthup, L. H. Daly, and S. E. Wiberley. Introduction to infrared and Raman spectroscopy. Academic Press, New York. 1964. pp. 389 and 390.
9. R. K. Harris. Spectrochim. Acta, **20**, 1129 (1964).

Can. J. Chem. Downloaded from www.nrcresearchpress.com by 210.87.254.5 on 09/05/12
For personal use only.

Can. J. Chem. Downloaded from www.nrcresearchpress.com by 210.87.254.5 on 09/05/12
For personal use only.

Stereochemical vs. polar control in the preparation and $LiAlH_4$ reduction of *cis*- and *trans*-2-alkoxy-3,4-epoxytetrahydropyrans[1]

F. SWEET AND R. K. BROWN
Department of Chemistry, University of Alberta, Edmonton, Alberta

Received August 11, 1967

2-Methoxy- and 2-*t*-butoxy-5,6-dihydro-2*H*-pyran react with *m*-chloroperoxybenzoic acid to give mixtures of *trans*- and *cis*-2-alkoxy-3,4-epoxytetrahydropyrans in which the *trans* to *cis* ratio is 3:1 and 9:1 for the 2-methoxy and 2-*t*-butoxy homologues respectively. This selectivity is attributed to the steric effect of the 2-alkoxy group.

Lithium aluminium hydride attacks the ring in these *cis* and *trans* compounds exclusively at the epoxide carbon remote from the alkoxy substituent to form only 2-alkoxy-3-hydroxytetrahydropyrans. This selectivity of hydride attack is attributed to the polar influence of the two geminal oxygen atoms. Steric factors in this hydride reduction are apparently completely submerged by this polar effect.

Canadian Journal of Chemistry, 46, 707 (1968)

Introduction

It is known that in systems containing the cyclohexene ring, the C-3 substituent controls the direction of peroxy acid epoxidation of the double bond. If the C-3 substituent is an hydroxyl group the peroxy acid attacks the double bond on the side *cis* to the hydroxyl substituent (1, 2). This is attributed to hydrogen bonding between the hydroxyl group and the incoming peroxy acid (1). If the C-3 substituent is alkoxy, acetoxy, or alkyl, epoxidation occurs preferentially *trans* to the C-3 substituent (1, 3), presumably because of steric hindrance to approach by the peroxy acid.

We wish to report the results of the epoxidation of some 2-alkoxy-5,6-dihydro-2*H*-pyrans and the $LiAlH_4$ redution of the epoxides so obtained.

Results and Discussion

In ether solution, at 30–35°, the reaction between *m*-chloroperoxybenzoic acid and either 2-methoxy- or 2-*t*-butoxy-5,6-dihydro-2*H*-pyran produced in each case an 80–85% yield of a mixture of *cis*- and *trans*-2-alkoxy-3,4-epoxytetrahydropyrans in which the *trans* isomer predominated to the extent of 75% and ~90% for the 2-methoxy and 2-*t*-butoxy compounds respectively (Chart I).

The *cis* and *trans* isomers of the 2-methoxy compound could be separated quite readily by gas–liquid chromatography and the physical characteristics determined (see Experimental and Table I). The *cis* and *trans* isomeric mixture of the 2-*t*-butoxy homologue, however, gave on a column of Carbowax 20M on Gas-Chrom P, two peaks in the ratio of 9:1 which overlapped slightly. Gas–liquid chromatographic (g.l.c.) separation of the isomer present in larger amount was readily accomplished, but isolation by the same method of the second (minor) isomer in a pure state from this reaction mixture was difficult, hence abandoned. The nuclear magnetic resonance (n.m.r.) spectrum of the isomeric mixture of the 2-*t*-butoxy homologue also showed their presence in the approximate ratio of 9:1.

The configurational assignment was obtained from the $LiAlH_4$ reduction of the epoxides. Reduction of the 3,4-epoxy-2-methoxytetrahydropyran isomer obtained in major proportion gave a nearly quantitative yield of a compound identical in every respect to *trans*-3-hydroxy-2-methoxytetrahydropyran previously prepared by another route (4). From the known reactions of epoxides with nucleophilic reagents (5) it follows that this 3,4-epoxy-2-methoxytetrahydropyran must be the *trans* isomer. Both gas–liquid chromatography and the n.m.r. spectrum of the mixture obtained from the hydride reduction showed no detectable amount of the *cis* isomer or any other isomer to be present.[2]

Similarly, reduction of the major isomer of the *cis–trans* mixture of 2-*t*-butoxy-3,4-epoxytetrahydropyran gave exclusively, in ~90% yield, *trans*-2-*t*-butoxy-3-hydroxytetrahydropyran[2] identical in retention time with an authentic

[1]Taken from the thesis of F. Sweet to be submitted to the Faculty of Graduate Studies, University of Alberta, Edmonton, Alberta, in partial fulfilment of the requirements for the degree of Doctor of Philosophy.

[2]*Cis*- and *trans*-4-hydroxy-2-methoxytetrahydropyran, prepared by a different route in our laboratory have retention times clearly greater than those of *cis*- and *trans*-3-hydroxy-2-methoxytetrahydropyran hence they could easily have been detected had they been present in significant quantity.

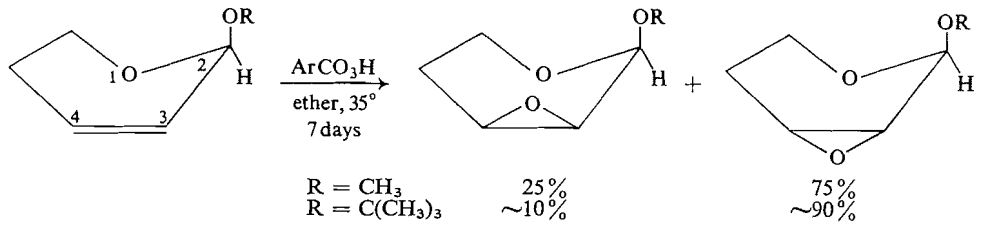

(Ar = *m*-Chlorophenyl)

Chart I

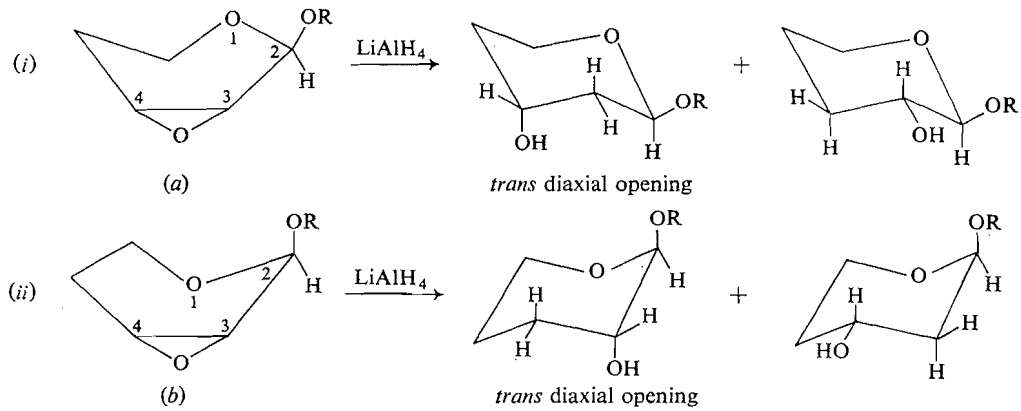

(R = CH_3 or $C(CH_3)_3$)

Chart II

specimen (4). Accordingly the 3,4-epoxy precursor was *trans*-2-*t*-butoxy-3,4-epoxytetrahydropyran.

Hydride redution of the 3,4-epoxy-2-methoxytetrahydropyran isomer obtained in minor amount from the epoxidation reaction gave only *cis*-3-hydroxy-2-methoxytetrahydropyran. Gas–liquid chromatography of the reaction mixture showed no sign of the *trans* isomer or any other isomer. It followed then that this 3,4-epoxy-2-methoxytetrahydropyran must have been the *cis* isomer.

Finally lithium aluminium hydride reduction of the 9:1 mixture of the two isomeric 2-*t*-butoxy-3,4-epoxytetrahydropyrans gave, according to g.l.c., a 9:1 mixture of *trans*- and *cis*-2-*t*-butoxy-3-hydroxytetrahydropyrans respectively with retention times identical to those found for authentic *trans*-2-*t*-butoxy-3-hydroxytetrahydropyran and its contaminating (2–3%) *cis* isomer (4). A n.m.r. spectrum of this reduced mixture, showed a ratio of ~9:1 for the *trans* to *cis* isomer. Neither the gas–liquid chromatogram nor the n.m.r. spectrum showed evidence for the presence of any other compound which might indicate that hydride reduction had produced as well some of the isomeric 2-*t*-butoxy-4-hydroxytetrahydropyrans.

On the basis of the above information it is clear that epoxidation of the 2-alkoxy-5,6-dihydro-2*H*-pyrans is strongly subject to steric influences since the larger group R produces the greater proportion of *trans* epoxy isomer (Chart I).

The highly selective attack of the lithium aluminium hydride on the epoxy carbon remote from the C-2 substituent is interesting. It is known that the reaction of anions with the epoxide ring produces predominantly that compound resulting from *trans* diaxial opening of the ring (1, 6, 7). The flexibility of the 2-alkoxy-3,4-epoxytetrahydropyran ring would permit *trans* diaxial epoxide ring opening in either of the two half-chair conformers *a* and *b* (Chart II) and thus both *trans*-4-hydroxy-2-alkoxytetrahydropyran and *trans*-3-hydroxy-2-alkoxytetrahydropyran could be formed. Experimentally, however, attack by $LiAlH_4$ appears to occur practi-

Can. J. Chem. Downloaded from www.nrcresearchpress.com by 210.87.254.5 on 09/05/12
For personal use only.

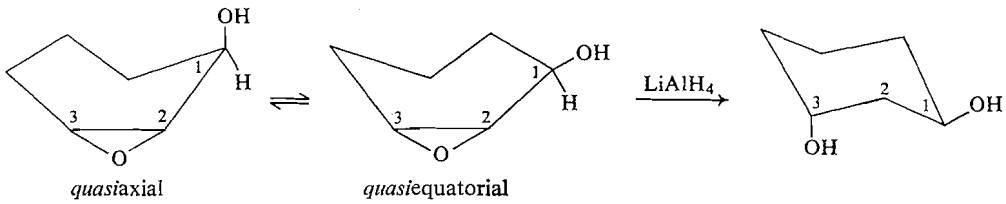

Chart III

cally completely on the carbon of the epoxide ring remote from the C-2 alkoxy group (Chart II, route *ii*).

Such a directive influence could be due to either steric or polar factors or a combination of both. The flexibility of the *trans*-2-alkoxy-3,4-epoxytetrahydropyran ring may be limited due to the anomeric effect (8, 9) which would favor the conformer *b* (Chart II). In this conformation, the steric hindrance caused by the *quasi* axial 2-alkoxy group to the approach of the $LiAlH_4$ to position-3 would be considerably greater and thus lead to the observed hydride attack at position-4 yielding only the *trans*-2-alkoxy-3-hydroxytetrahydropyran. But the observation that $LiAlH_4$ reduction of *trans*-2,3-epoxycyclohexanol occurs via preferential attack on the C-2 carbon (Chart III) to give predominantly the *trans*-1,3-cyclohexanediol (1) indicates at first glance that attack by $LiAlH_4$ on the epoxide ring carbon, C-2, is not seriously hindered by the C-1 hydroxyl group. The absence of an anomeric effect permits ready formation of the half-chair conformer in which the OH group is *quasi*-equatorial and this may be a factor in allowing approach by the $LiAlH_4$ to C-2. However, in our view, there is no apparent reason why one conformer should be preferred over the other and thus provide the selectivity of hydride attack that is observed (1). A more likely explanation of the selective formation of this *trans*-1,3-cyclohexanediol involves the expected rapid initial reaction of $LiAlH_4$ with the free hydroxyl group of *trans*-2,3-epoxycyclohexanol to form the alkoxyaluminium hydride *a* which could, by an intramolecular process, readily attack the epoxy carbon closest to the aluminooxy substituent via a 5-membered ring system.[3] It has been shown (10) that the reaction of *trans*-2,3-epoxy-1-methoxycyclohexane with $LiAlH_4$ produces preferentially the *trans*-2-methoxycyclohexanol while with aqueous NaOH the same epoxide gives selectively 3α-methoxy-1α,2β-cyclohexanediol (Chart IV, *a*). The reaction of *cis*-2,3-epoxy-1-methoxycyclohexane with aqueous NaOH produces primarily the 3α-methoxy-1β,2α-cyclohexane-1,2-diol (Chart IV, *b*). This selective attack on the epoxide carbon remote from the C-3 methoxy substituent in *both cis* and *trans* isomers was considered to be due to the inductive effect of the 3-alkoxy group directing the course of ring opening (10). But the presence as well of a steric effect was thought to be likely in the case of the *trans*-2,3-epoxy-1-methoxycyclohexane. For the *trans*-2-alkoxy-3,4-epoxytetrahydropyrans, both steric and polar factors could contribute to the apparently exclusive attack by hydride on the epoxide carbon remote from the alkoxy group. The presence of *two* oxygen atoms on the anomeric carbon (C-2, Charts I and II). would no doubt enhance the importance of the inductive effect in promoting attack by hydride at position-4 (Chart II). It is significant that the *cis*-2-alkoxy-3,4-epoxytetrahydropyrans, wherein the steric interference by the 2-alkoxy group to attack by lithium aluminium hydride on the epoxy group is minimal or nonexistent, still gives exclusively *cis*-2-alkoxy-3-hydroxytetrahydropyrans. This strongly suggests that a steric effect, considered to be

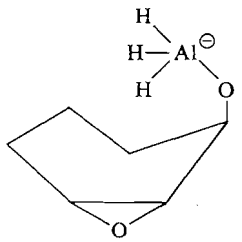

a

[3]Henbest and Wilson (1) have explained the selective formation of *trans*-1,3-cyclohexanediol from $LiAlH_4$ reduction of *trans*-2,3-epoxycyclohexanol on the basis of the preferred *trans* diaxial opening of the epoxide ring by anionic reagents. This requires a preference for the conformer in which the hydroxyl group is *quasi* equatorial (Chart III). They explain the formation of some 1,2-cyclohexanediol as occurring by an intramolecular reaction in a structure such as *a*, involving hydride attack at C-3 rather than at C-2.

Can. J. Chem. Downloaded from www.nrcresearchpress.com by 210.87.254.5 on 09/05/12
For personal use only.

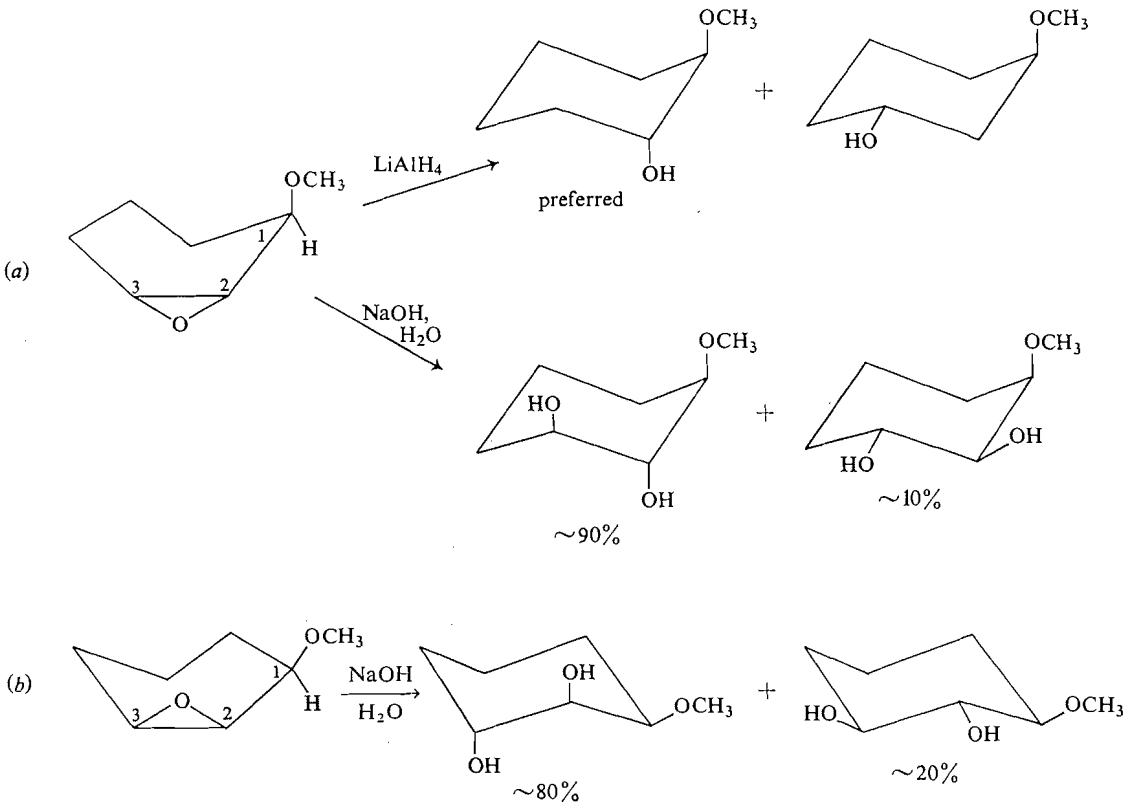

Chart IV

possible in the *trans*-2-alkoxy-3,4-epoxytetrahydropyrans, is in fact completely submerged by the polar effect of the two oxygen atoms attached to C-2 in the tetrahydropyrans above. The combined inductive effect of the two oxygen atoms would destabilize the incipient carbonium ion formed by partial C_3—O epoxide ring cleavage according to route *i* (Chart II) more than that formed by C_4—O epoxide cleavage by route *ii*.

Experimental

Analytical and physical data for all compounds prepared below are shown in Table I.

Trans 3-Bromo-2-methoxytetrahydropyran

A modification of the published procedure (11, 12) permitted a greater stereoselectivity than that previously obtained (11, 12). The whole synthesis was done in an efficient fume hood.

A solution of 3,4-dihydro-2-*H*-pyran (84 g, 1 mole) in a mixture of 100 ml of anhydrous liquid ammonia and 1 l of methanol was cooled to −60° with a dry ice – acetone bath. To the stirred solution, kept between −60° and −55°, was added dropwise, over a 2 h period, a solution of 160 g of bromine in 200 ml of carbon tetrachloride. A precipitate of ammonium bromide appeared when half of the bromine had been added. When the bromine addition was completed, the cooling bath was removed and the reaction mixture was stirred overnight and thus came to room temperature. The residual ammonia and methanol were removed in a rotary evaporator (bath temperature 50°) under reduced pressure attained by a water pump. To the remaining material was added 500 ml of dry ether. The precipitated ammonium bromide was removed by filtration at reduced pressure, the solid subsequently washed with ether, and the combined ether washings and filtrate washed with water (2 × 100 ml). The ether layer was dried (Na_2SO_4) and freed from solvent by rotary evaporator. The residue was distilled under reduced pressure and afforded 165 g (85%) of *trans* 3-bromo-2-methoxytetrahydropyran whose integrated 100 Mc.p.s. nuclear magnetic resonance (n.m.r.) spectrum in $CDCl_3$ agreed with the structure and showed evidence (at high amplitude) for only a small amount (<5%) of the *cis* isomer. Gas–liquid chromatography showed the *cis* isomer to be present in ~1%.

The use of 2 moles of sodium methoxide rather than ammonia in the above reaction gave equally good results.

The preparation of *trans 3-bromo-2-t-butoxytetrahydropyran* followed the same procedure. However, in this case a 40% solution of *t*-butyl alcohol in ether, rather than pure *t*-butyl alcohol, was used as solvent to avoid

Can. J. Chem. Downloaded from www.nrcresearchpress.com by 210.87.254.5 on 09/05/12
For personal use only.

Can. J. Chem. Downloaded from www.nrcresearchpress.com by 210.87.254.5 on 09/05/12
For personal use only.

solidification of the alcohol when the mixture was cooled and diluted with liquid ammonia.

Note:—This *trans* 3-bromo-2-*t*-butoxytetrahydropyran could be distilled successfully only under vacuum and at a pressure which required the heating bath temperature to be no higher than 95°. Higher bath temperatures caused violent decomposition of the distilling liquid. The 3-bromo-2-alkoxytetrahydropyrans generally are subject to considerable decomposition during distillation, particularly at higher distillation temperatures.

2-Methoxy-5,6-dihydro-2H-pyran

Dehydrohalogenation of *trans* 3-bromo-2-methoxytetrahydropyran to form 2-methoxy-5,6-dihydro-2*H*-pyran was accomplished by the procedure of Woods and Sanders (11). The small amount of *cis* isomer present offered no complication since it apparently dehydrohalogenated to the 2-methoxy-5,6-dihydro-2*H*-pyran.

2-t-Butoxy-5,6-dihydro-2H-pyran

This compound was prepared by a procedure similar to that employed for the methyl homologue above but modified as follows.

Sodium hydride (Metal Hydrides Corp.) was added slowly to dry *t*-butyl alcohol (kept between 30° and 40°) to form sodium *t*-butoxide. To a solution of 3 molar equivalents of sodium *t*-butoxide in *t*-butyl alcohol (about 8 times the weight of the bromo compound) was added, gradually, one molar equivalent of 3-bromo-2-*t*-butoxytetrahydropyran (neat). The solution temperature rose to 60°. When the initial exothermic reaction had subsided, the solution was heated under reflux overnight, then reduced to half its volume by fractional distillation at atmospheric pressure. To the residue was added an equal volume of dry ether to complete the precipitation of the sodium bromide. The solid, removed by filtration under suction, was washed once with ether. The combined ethereal washings and filtrate were washed once with water and dried (Na_2SO_4). After separation of the solid, the solvents were removed by fractional distillation at atmospheric pressure and then the residual oil was distilled under vacuum, giving pure 2-*t*-butoxy-5,6-dihydro-2*H*-pyran. Gas–liquid chromatography showed the presence of only one compound.

3,4-Epoxy-2-methoxytetrahydropyran

To 27 g (0.24 mole) of 2-methoxy-5,6-dihydro-2*H*-pyran in 275 ml of dry ether contained in a 500 ml, 3-neck flask equipped with a magnetic stirrer, condenser, and thermometer, was added 60 g (0.27 mole) of 80% *m*-chloroperoxybenzoic acid. Cautious addition of the oxidizing agent was found to be unnecessary since epoxidation in this system occurs very slowly. The peroxy acid dissolved readily. The mixture was stirred at ~35° for several days. Gas–liquid chromatography (g.l.c.) of an aliquot showed that little reaction had occurred in the first 24 h. In 2.5 days a precipitate of the slightly soluble *m*-chlorobenzoic acid appeared and accumulated with time. Seven days later the mixture was cooled in a refrigerator for 2 h, then filtered by suction. The solid *m*-chlorobenzoic acid was washed with cold ether. The combined ether solutions from the washings and filtrate were extracted with saturated aqueous sodium carbonate (3 × 25 ml) and the sodium carbonate solutions in turn extracted with ether. The combined ether solutions were dried (Na_2SO_4) and filtered. Removal of the ether by rotary evaporator at atmospheric pressure left an oil which was distilled under vacuum giving 25 g (80%; a second run gave 85%) of 3,4-epoxy-2-methoxytetrahydopyran. Nuclear magnetic resonance and gas–liquid chromatography analysis showed this to be a mixture of *cis* and *trans* isomers in the ratio of 25:75. These were separated by g.l.c. using an Aerograph autoprep, model A-700 with a 20 ft × ¼ in. (I.D.) column packed with 25% Carbowax 20M on Gas-Chrom P (60–80 mesh) and helium as the carrier gas at a flow rate of 110 ml/min. Column, injector, and detector temperatures were 175°, 190°, and 190° respectively.

2-t-Butoxy-3,4-epoxytetrahydropyran

This compound was prepared in the same manner as described immediately above, starting with 2-*t*-butoxy-5,6-dihydro-2*H*-pyran. According to the n.m.r. spectrum and g.l.c. analysis, the product was a mixture of *cis* and *trans* isomers in the ratio *cis*/*trans* = <10%/>90%. The *trans* isomer was separated by g.l.c. (via an Aerograph 700; Carbowax 20M column at 170°; helium flow, 60 ml/min) under the same conditions as for the 2-methoxy homologue. The separation of the *cis* isomer was abandoned due to its presence in <10% concentration and the partial overlapping of the peaks for the *cis* and *trans* isomers.

$LiAlH_4$ Reduction of 3,4-Epoxy-2-methoxytetrahydropyran

A solution of *trans*-3,4-epoxy-2-methoxytetrahydropyran (80 mg, 6×10^{-4} mole) in 20 ml of dry ether was added slowly and dropwise to a stirred solution of $LiAlH_4$ (0.03 g, 8×10^{-4} mole) in 25 ml of dry ether at room temperature. Each drop caused a vigorous reaction. After the addition was complete, the reaction mixture was stirred and left overnight at room temperature. The aluminium complex was then decomposed by gradual addition of 15 ml of ether saturated with water, followed by 1 ml of 15% aqueous sodium hydroxide. The granular precipitate was filtered by gravity and the colorless solid washed with ether (5 × 10 ml). The combined ether solution from the washings and filtrate was dried (Na_2SO_4) and freed from solvent at room temperature under vacuum (20 mm) using a rotary evaporator. Analysis of the residual colorless oil by g.l.c. on a 20 ft column of 20% butanediol succinate on Chromosorb P (60–80 mesh) showed that it consisted of one major product to the extent of 95%. No evidence was obtained for the *cis* isomer or other isomeric products. The contaminant present proved to be diethyl ether. The n.m.r. and infrared spectra of the oil were identical in all respects with those obtained from authentic *trans*-3-hydroxy-2-methoxytetrahydropyran (4). The retention time on the gas–liquid chromatogram was identical to that of an authentic sample of *trans*-3-hydroxy-2-methoxytetrahydropyran (4).

A solution of *cis*-3,4-epoxy-2-methoxytetrahydropyran (120 mg, 9×10^{-4} mole) in 5 ml of anhydrous ether was added to 0.45 g of lithium aluminium hydride in 35 ml of ether. The mixture was stirred overnight at room temperature, then diluted with 20 ml of ether, and cooled to 0°. The complex was destroyed by cautious addition of 1 ml of water, then 1 ml of 15% aqueous sodium hydroxide followed by 1 ml of water. The mixture was stirred for 30 min at room temperature then filtered. The granular

Can. J. Chem. Downloaded from www.nrcresearchpress.com by 210.87.254.5 on 09/05/12
For personal use only.

TABLE I

Analyses and physical data for the pyranyl ethers

Compound	Substituent R	Boiling point, °C	Refractive index, n_D^{25}	% yield	Anomeric H*		Analysis, %					
							Calc'd			Found		
					τ	$J_{2,3}$ c.p.s.	C	H	Br	C	H	Br
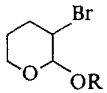	CH_3 *trans* (with ~1% *cis*)	87 at 12 mm	1.4843	85	5.50(d)	3.9						
		88–89 at 18 mm (11)‡	1.4838 (11)									
		78 at 10 mm (12)§	1.4841 (23°) (12)		5.54(d) (12)	3.9 (12)						
	CH_3 *cis*				5.42(d)	2.8						
					5.45(d) (12)	2.7 (12)						
	$C(CH_3)_3$ *trans*	75 at 1.5 mm	1.4726		5.27(d)	5.5	45.58	7.23	33.70	45.64	7.05	33.85
	CH_3	134 at 705 mm	1.4420		5.30(s) (broad)	$w/2 = 5$						
		136–138 (11)	1.4425 (11)									
	$C(CH_3)_3$	80 at 45 mm	1.4397	70	4.88(s) (broad)	$w/2 = 5$	69.19	10.32		68.99	9.90	
		103 at 100 mm										
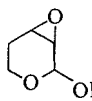	CH_3 *trans*	88 at 100 mm	1.4450	80–85†	5.22(s)	~0	55.37	7.74		55.04	7.52	(*cis*, *trans* mixture)
	CH_3 *cis*	84 at 100 mm	1.4415		5.13(d)	2.5				55.28	8.00	(pure *trans*)
										55.65	7.59	(pure *cis*)
	$C(CH_3)_3$ *trans*	72–74 at 4 mm	1.4480 *cis trans mixture* (1:9)	82	4.90(s)	~0	62.76	9.36		63.16	8.87	(pure *trans*)
										62.35	8.94	(*cis*, *trans* mixture)
	$C(CH_3)_3$ *cis*	65 at 2.75 mm	1.4475 (*trans*)		4.82(d)	~3						

*s, Singlet; d, doublet; $w/2$, width at half height. Spectra obtained in $CDCL_3$ referred to tetramethylsilane.
†A yield of 80–85% was obtained for the 1:3 = *cis*/*trans* mixture which boiled at 86–88° at 100 mm.
‡Probably for a mixture of *cis* and *trans* isomers.
§For a 2:3 mixture of *cis* and *trans* isomers.

Can. J. Chem. Downloaded from www.nrcresearchpress.com by 210.87.254.5 on 09/05/12
For personal use only.

residue was washed with ether (3 × 15 ml). The combined ether solutions were dried (Na_2SO_4) and freed from solvent at atmospheric pressure. The residual oil (110 mg, 83%) contained only one component when analyzed by g.l.c. on an F and M model 700 laboratory chromatograph using 20 ft × ¼ in. column packed with 20% butanediol succinate on Gas Chrom P (60–80 mesh) at 175°, and helium flow rate of 100 ml/min. This had a retention time and a n.m.r. spectrum identical to those for authentic *cis*-3-hydroxy-2-methoxytetrahydropyran (4). The 3,5-dinitrobenzoate of this oil melted at 87–88° (crystallized from methyl alcohol – water) and was identical (n.m.r. spectrum) with the 3,5-dinitrobenzoate of authentic *cis*-3-hydroxy-2-methoxytetrahydropyran (4).

$LiAlH_4$ Reduction of Cis–Trans 2-t-Butoxy-3,4-epoxytetrahydropyran

The 9:1 isomeric mixture (1.72 g, 0.01 mole) of *cis–trans* 2-*t*-butoxy-3,4-epoxytetrahydropyran in dry ether (25 ml) was slowly added over a 5 min period to a mixture of 500 mg of lithium aluminium hydride in 35 ml of anhydrous ether. The reaction flask (250 ml) was equipped with a magnetic stirrer, thermometer, and condenser with a drying tube. The mixture was stirred at 30–35° overnight (heated only by the stirring motor) and then diluted with 25 ml of ether and cooled with an acetone – dry ice bath kept between −10° and −5°. To the reaction mixture (at ~0°) was added, carefully, 1 ml of water, then 1 ml of 15% aqueous sodium hydroxide, and finally 1 ml of water. The contents of the flask were stirred for 30 min to complete the formation of a granular precipitate. The supernatant ether was decanted and the residue extracted successively with ether (3 × 20 ml) and chloroform (1 × 20 ml). The combined organic extracts were dried with anhydrous sodium sulfate containing a small amount of dry sodium carbonate to prevent any acid-catalyzed isomerizations. After separation of the solid, the filtrate was freed from solvent at atmospheric pressure. Residual solvent was removed under reduced pressure with a rotary evaporator. In the last two steps some dry sodium carbonate was added to prevent acid-catalyzed isomerization. Analysis of the residual oil (1.65 g, 86%) after subtraction of ~5% of remaining solvent by gas–liquid chromatography (F and M chromatograph, model 700; 20 ft × ¼ in. column of 20% Carbowax 20 M on Gas Chrom P, 60–80 mesh; column temperature, 175°; helium flow, 60 ml/min) showed the presence of only two compounds in the ratio 9:1, plus ~5% of solvent. The retention times of these two compounds (ratio 9:1) were identical to those of authentic *trans*-2-*t*-butoxy-3-hydroxytetrahydropyran and its 2–3% contaminant of *cis*-2-*t*-butoxy-3-hydroxytetrahydropyran (4).

A n.m.r. spectrum of the residual oil above showed, by integration of the signals for the anomeric protons, a ratio of *trans* to *cis* isomers of about 9:1. This spectrum was superimposable on that of authentic *trans*-2-*t*-butoxy-3-hydroxytetrahydropyran containing 2–3% of the *cis* isomer (4).

Acknowledgment

The authors wish to thank the National Research Council of Canada for the financial support throughout the course of this work.

1. H. B. Henbest and R. A. L. Wilson. J. Chem. Soc. 1958 (1957).
2. H. B. Wood, Jr. and H. G. Fletcher, Jr. J. Am. Chem. Soc. **79**, 3234 (1957).
3. P. A. Levene and R. S. Tipson. J. Biol. Chem. **93**, 631 (1931).
4. F. Sweet and R. K. Brown. Can. J. Chem. **44**, 1571 (1966).
5. R. E. Parker and N. S. Isaacs. Chem. Rev. **59**, 737 (1959).
6. A. Furst and Pl. A. Plattner. Intern. Congr. Pure and Appl. Chem. 12th Congr. New York (1951). Abstr. of Papers, p. 405.
7. A. S. Hallsworth and H. B. Henbest. J. Chem. Soc. 3571 (1960).
8. J. T. Edward and J. Puskas. Can. J. Chem. **40**, 711 (1962).
9. E. L. Eliel, N. L. Allinger, S. F. Angyal, and G. A. Morrison, Conformational analysis. Interscience Publishers, Inc., New York. 1965. Pp. 375–377.
10. R. U. Lemieux, R. K. Kullnig, and R. Y. Moir. J. Am. Chem. Soc. **80**, 2237 (1958).
11. G. F. Woods and H. Sanders. J. Am. Chem. Soc. **68**, 2483 (1946).
12. R. U. Lemieux and B. Fraser-Reid. Can. J. Chem. **43**, 1460 (1965).

The preparation of C-1 and C-2 methylated acenaphthenes[1]

A. Bosch[2] and R. K. Brown
Department of Chemistry, University of Alberta, Edmonton, Alberta
Received July 26, 1967

The syntheses of 1-methyl-, 1,1-dimethyl-, *cis*(?)-1,2-dimethyl-, 1,1,2-trimethyl-, and 1,1,2,2-tetramethylacenaphthene have been accomplished by standard reactions from the two compounds 1-acenaphthenone and 2-methyl-1-acenaphthenone. These two ketones were in turn obtained from 1-naphthaleneacetic acid.

Canadian Journal of Chemistry, 46, 715 (1968)

Can. J. Chem. Downloaded from www.nrcresearchpress.com by 210.87.254.5 on 09/05/12
For personal use only.

Introduction

Required as reference substances for a study currently in progress in this laboratory was the series of compounds 1-methyl-, 1,1-dimethyl-, 1,2-dimethyl-, 1,1,2-trimethyl-, and 1,1,2,2-tetramethylacenaphthene (A). Up to the time of this work, only 1-methylacenaphthene was known (1). This paper describes the synthesis of these C-1 and C-2 methylated acenaphthenes.

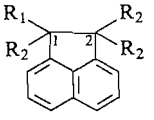

A $R_1 = CH_3$
$R_2 = CH_3$ or H

Results and Discussion

All of the C-1 and C-2 methylated acenaphthenes were prepared from the two ketones 1-acenaphthenone, **1**, and 2-methyl-1-acenaphthenone, **2**. The former has been made by lead tetraacetate oxidation of acenaphthene to 1-acenaphthenol followed by chromic acid oxidation to the ketone (2, 3). In a repetition of the published procedure it was found that the tedious steam distillation required to separate the ketone from the chromium salts (2, 3) could be avoided by facile removal of these salts by a cold alkaline aqueous wash of the benzene solution, resulting in 46% overall yield of the ketone. A more convenient preparation, giving ketone **1** in at least 60–70% yield, involved intramolecular cyclization of α-naphthylacetyl chloride according to general directions available in the literature (4) (Scheme 1, *a*).

To make the ketone **2**, ethyl α-naphthylacetate was alkylated with excess methyl iodide and sodium hydride (5). Such conditions gave only monomethylation, as had been shown previously for analogous alkylations with methyl iodide in the presence of potassium *t*-butoxide (6). Intramolecular cyclization of α-(1-naphthyl)propionyl chloride, obtained from the above ester, gave **2** in 47% overall yield.[3] The broad melting point of the oxime (of **2**), (126–140°), its elemental analysis and its nuclear magnetic resonance (n.m.r.) spectrum showing two overlapping methinyl hydrogen quartets centered at τ 5.6 and two overlapping methyl doublets centered at τ 8.3, indicated the presence of equal amounts of the *syn* and *anti* isomers of the oxime.

Reaction of **1** with methylmagnesium iodide, followed by dehydration of the resulting alcohol with picric acid to the olefin, 1-methylacenaphthylene, and its subsequent reduction with platinum oxide and hydrogen, according to published directions (1, 7) (Scheme 2) gave 1-methylacenaphthene, **3** of 95–96% purity according to gas–liquid chromatographic analysis. All efforts to remove this impurity failed. Pure **3**, however, was obtained in 70% yield by Wolff–Kishner reduction (8) of 2-methyl-1-acenaphthenone, **2** (Scheme 2).

1,1-Dimethylacenaphthene, **4** (yield, 41%) was prepared by sodium hydride – methyl iodide alkylation (5) of 1-acenaphthenone, **1**, followed by Wolff–Kishner reduction (8) of the resulting 2,2-dimethyl-1-acenaphthenone (Scheme 2). Here again, elemental analysis and the presence of two methyl singlets at τ 8.15 and τ 8.38 (area ratio,

[1]Taken from the thesis submitted by A. Bosch to the Faculty of Graduate Studies, University of Alberta, Edmonton, Alberta, in partial fulfilment of the requirements for the degree of Doctor of Philosophy.

[2]Presently at R. and L. Molecular Research, 8045 Argyle Road, Edmonton, Alberta.

[3]The low yield in the cyclization step was no doubt due to poor quality $AlCl_3$ available at the time.

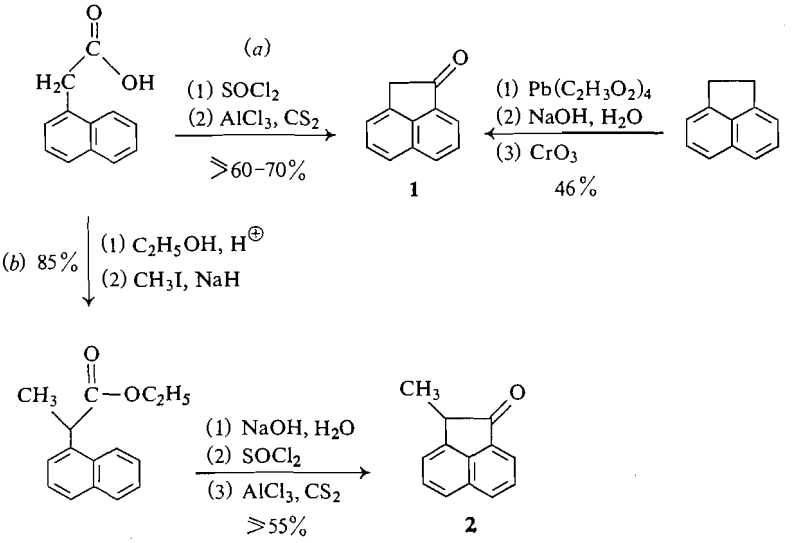

SCHEME 1.

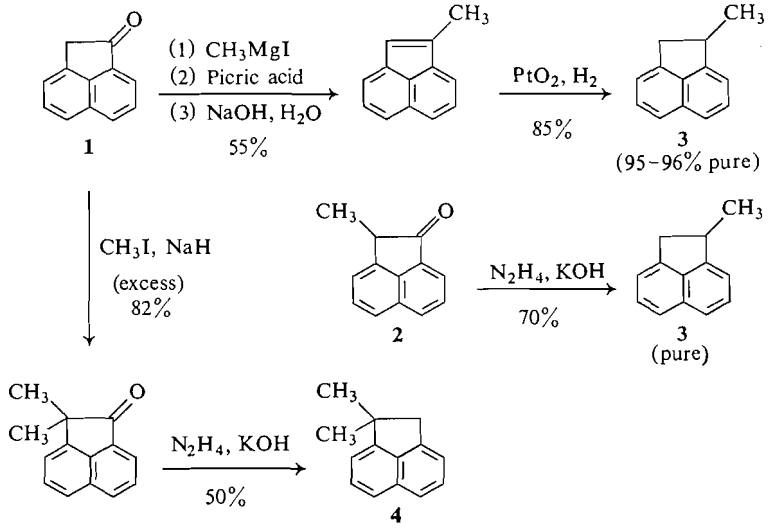

SCHEME 2.

4:21) in the n.m.r. spectrum of 2,2-dimethyl-1-acenaphthenone oxime indicated this to be a mixture of two isomers.

The reaction of methylmagnesium iodide with 2-methyl-1-acenaphthenone (Scheme 3) gave, in 93% yield, a mixture of two alcohols in the ratio 54:46 according to the n.m.r. spectrum (Fig. 1). The nearly equal proportions of these two alcohols (*cis* and *trans*) indicates that the methyl group of 2-methyl-1-acenaphthenone provides little or no directive influence in the reaction of methylmagnesium iodide with the carbonyl group. Separation of these isomeric alcohols and assignment of structure has not been done as yet since this was not required at the time. Picric acid dehydration (1) of this *cis–trans* mixture of the alcohols gave an excellent yield of 1,2-dimethylacenaphthylene. Diimide reduction (9–11), in an attempt to prepare the *cis*-1,2-dimethylacenaphthene, was unsuccessful. In one week of

Can. J. Chem. Downloaded from www.nrcresearchpress.com by 210.87.254.5 on 09/05/12
For personal use only.

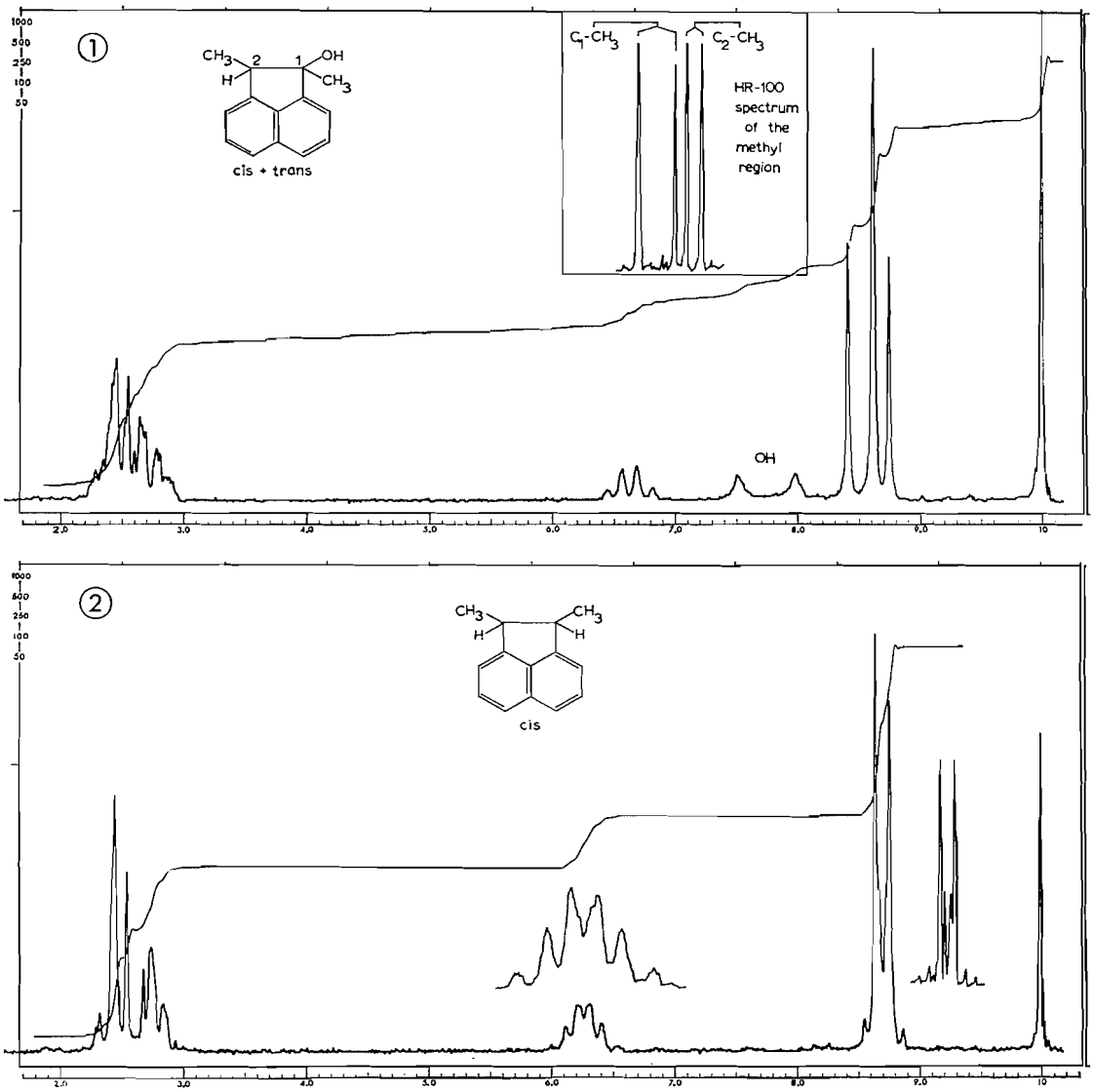

FIG. 1. The 100 Mcycle/s n.m.r. spectrum of the *cis* and *trans* alcohols resulting from the reaction between methylmagnesium iodide and 2-methyl-1-acenaphthenone (solvent $CDCl_3$).
FIG. 2. The n.m.r. spectrum of 1,2-dimethylacenaphthene (solvent $CDCl_3$).

reaction, 43% of the original olefin was still present, as shown by gas–liquid chromatography along with an unidentified higher boiling substance present in 13% yield. However, catalytic reduction with platinum oxide and hydrogen occurred readily giving a 95% yield of 1,2-dimethylacenaphthene, **5**, which after crystallization from ethanol to remove the 5% impurity, gave colorless needles melting at 53–54°. The sharpness of the melting point as well as the recorded experience of other investigators in catalytic hydrogenation of olefins (12–14) leads us to believe that this 1,2-dimethylacenaphthene is the *cis* isomer. Of this, however, we are not certain. The n.m.r. spectrum (Fig. 2) is not inconsistent with the assignment of the structure as *cis*. The two methinyl protons appear as a sextet centered at τ 6.26, but coupling values between the peaks are not identical. The two methyl groups do not show up as a simple

Can. J. Chem. Downloaded from www.nrcresearchpress.com by 210.87.254.5 on 09/05/12
For personal use only.

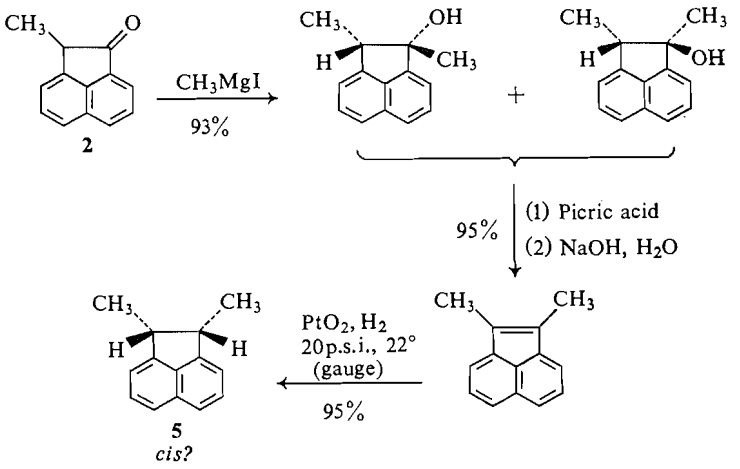

SCHEME 3.

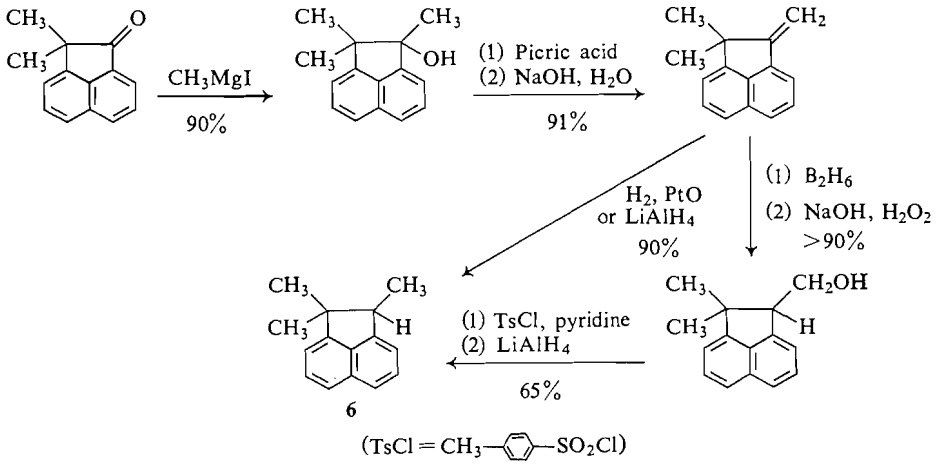

SCHEME 4.

doublet. Instead there are six peaks, all of which are real. Obviously first order analysis is not applicable. This problem is still under examination.

The unambiguous preparation of the *trans*-1,2-dimethylacenaphthene has not yet been achieved.

1,1,2-Trimethylacenaphthene, **6**, was prepared by reduction of 2,2-dimethyl-1-methyleneacenaphthene, the latter having been obtained by picric acid dehydration of the product provided by the reaction of methylmagnesium iodide with 2,2-dimethyl-1-acenaphthenone (Scheme 4). Catalytic hydrogenation yielded a product of 95% purity as shown by gas–liquid chromatography, whereas reduction by lithium aluminium hydride in tetrahydrofuran gave 1,1,2-trimethylacenaphthene of greater than 98% purity. In both cases gas–liquid chromatography permitted separation of the trimethyl compound from its impurity. An indirect route to 1,1,2-trimethylacenaphthene involved conversion, in good yield, of 2,2-dimethyl-1-methyleneacenaphthene to 2,2-dimethyl-1-hydroxymethylacenaphthene (n.m.r. spectrum, Fig. 3) via hydroboration and subsequent alkaline oxidation (15). The *p*-toluenesulfonate ester of this alcohol was then reduced nearly quantitatively by lithium aluminium hydride (16) to **6**.

Preparation of 1,1,2,2-tetramethylacenaphthene, **7**, required the precursor 2,2-dimethyl-1-acenaphthenecarboxaldehyde. One route

Can. J. Chem. Downloaded from www.nrcresearchpress.com by 210.87.254.5 on 09/05/12
For personal use only.

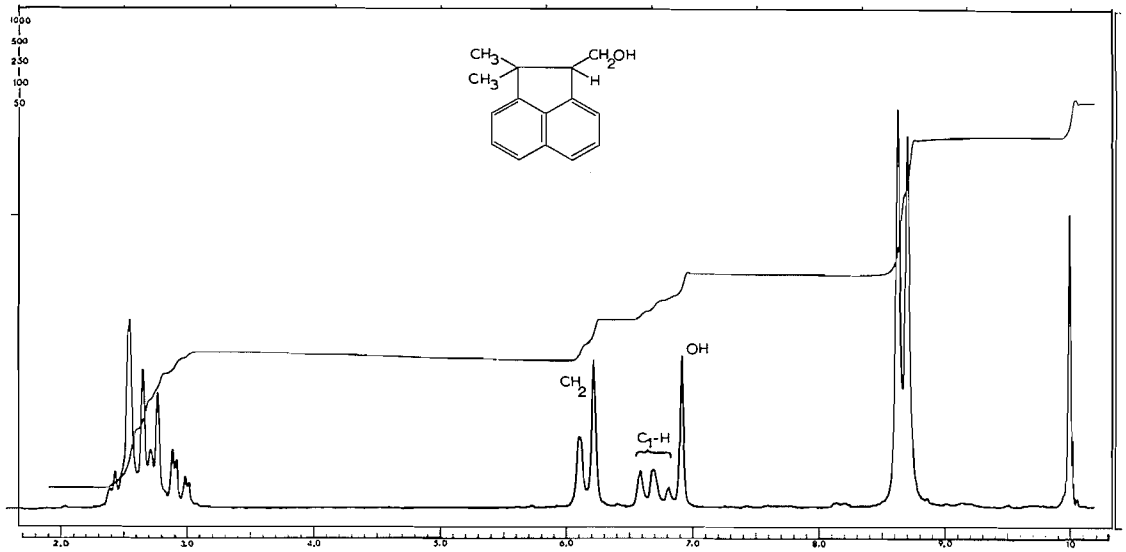

FIG. 3. The n.m.r. spectrum of 2,2-dimethyl-1-hydroxymethylacenaphthene (solvent CCl_4).

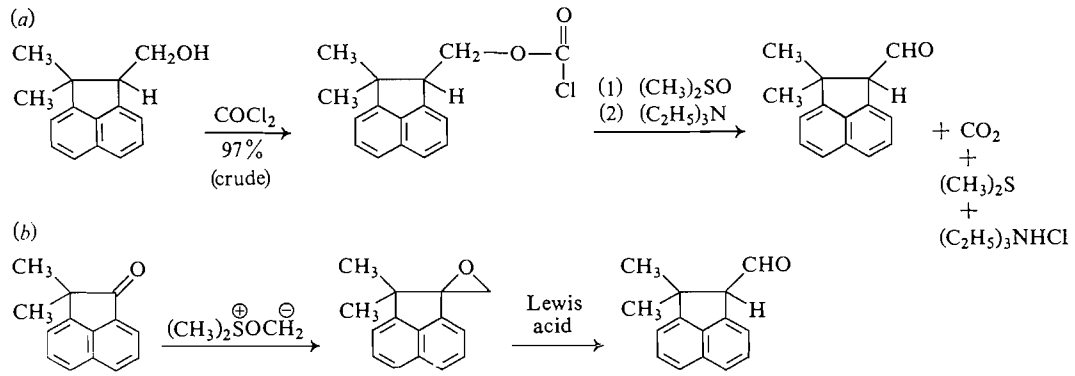

SCHEME 5.

(Scheme 5, *a*) to this aldehyde employed dimethyl sulfoxide oxidation of 2,2-dimethyl-1-hydroxymethylacenaphthene via its chloroformate ester according to Barton's procedure (17). The oil so obtained was found to contain the aldehyde in 75–80% concentration. The aldehyde could not be separated by chromatography or by sodium bisulfite addition. However, purification in small batches[4] by use of Girard's T reagent[5] (18) gave a 50% yield of the aldehyde still containing about 5% impurity.

A second route to the aldehyde utilized dimethyloxosulfonium methylide (19) to form the oxirane from 2,2-dimethyl-1-acenaphthenone (Scheme 5, *b*) which could be rearranged to the aldehyde under acidic conditions. The oil which was obtained from the first step, using excess ylid, was found by its n.m.r. spectrum (Fig. 4) to be a 4:1 mixture of the desired oxirane and starting ketone. The former's presence could be readily discerned by the characteristic signals of the methylene protons of the oxirane ring, appearing as a quartet centered at τ 6.78, the two small outer peaks separated by 12 c.p.s., and the two large inner peaks separated by 1.5 c.p.s. This is in agreement with the general observation

[4]Large scale reaction gave considerable tarry decomposition.

[5]Fisher Scientific Girard's T reagent (reagent grade) was far superior to the BDH product.

Can. J. Chem. Downloaded from www.nrcresearchpress.com by 210.87.254.5 on 09/05/12
For personal use only.

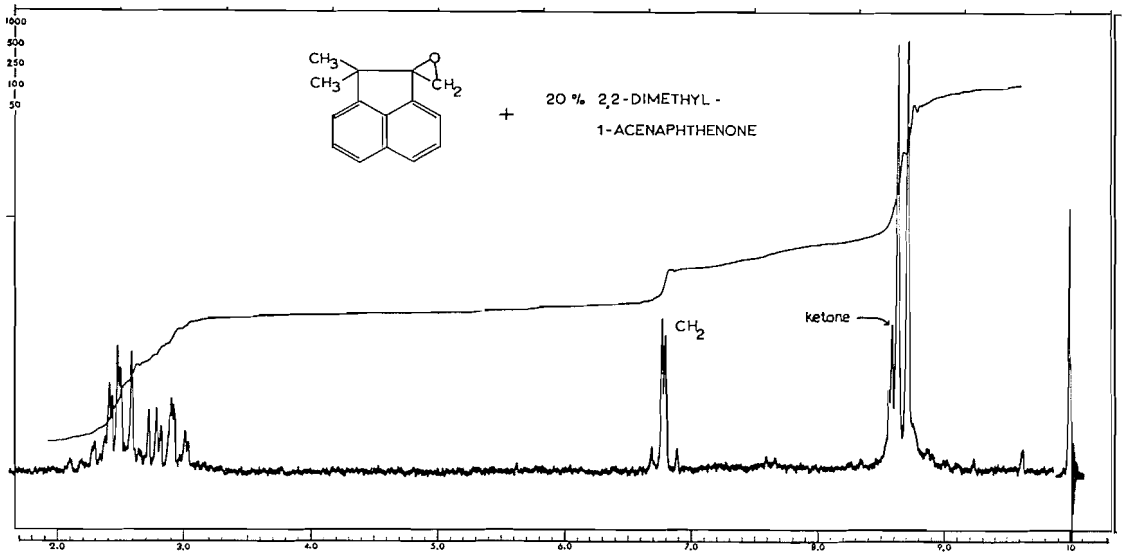

FIG. 4. The n.m.r. spectrum of the oxirane from 2,2-dimethyl-1-acenaphthenone and 20% 2,2-dimethyl-1-acenaphthenone (solvent CCl_4).

that protons of a methylene group adjacent to an asymmetric center are non-equivalent (20). Signals at τ 8.64 and τ 8.72 showed that the two methyl groups were in different environments. Chromatography on neutral alumina readily separated the starting ketone but no oxirane was obtained. Instead, elution with methanol gave a material which proved to be mainly the aldehyde. Apparently rearrangement of the oxirane had occurred on the column. A second chromatographic separation gave pure aldehyde but the yield was low ($\sim$ 30% based on the ketone).

Formation of the oxirane from 2,2-dimethyl-1-methyleneacenaphthene with peroxybenzoic acid or *m*-chloroperoxy benzoic acid was unsuccessful. The original olefin was recovered in high yield. No evidence of oxirane formation was observed.

Sodium hydride – methyl iodide alkylation of 2,2 - dimethyl - 1 - acenaphthenecarboxaldehyde, followed by chromatography of the crude product, gave nearly pure 1,2,2-trimethyl-1-acenaphthenecarboxaldehyde in 80% yield (Scheme 6). Further purification could be achieved by use of Girard's T reagent. This trimethyl aldehyde was converted into 1,1,2,2-tetramethylacenaphthene **7** by two methods. In the first method a Wolff–Kishner reduction of the aldehyde gave a mixture of two substances in the ratio of 85:15 from which the tetramethylacenaphthene was obtained (72% yield). The identity of the second component was not determined. The second route utilized the method of Caglioti and Grasselli (21) of hydride reduction of the *p*-toluenesulfonylhydrazones of aldehydes or ketones to the corresponding hydrocarbons. Lithium aluminium hydride reduction of 1,2,2-trimethyl-1-acenaphthenecarboxaldehyde *p*-toluenesulfonylhydrazone gave a 75% yield of a mixture which contained essentially two products in about equal amounts (Scheme 6). One other substance (unknown) was also present in about 5% concentration. Comparison of retention times with those of authentic samples revealed that the two major products were 1,1,2-trimethylacenaphthene, **6**, and 1,1,2,2-tetramethylacenaphthene, **7**. These were not separated.

The formation of 1,1,2-trimethylacenaphthene, involving loss of one carbon, might conceivably have occurred by a route such as shown in Scheme 7. Tautomerization of the *p*-toluenesulfonylhydrazone followed by loss of the *p*-toluenesulfonyl group would give the structure which contains a diazomethyl group. This, by loss of nitrogen and subsequent reduction, would provide **7**, whereas loss of diazomethane

Can. J. Chem. Downloaded from www.nrcresearchpress.com by 210.87.254.5 on 09/05/12
For personal use only.

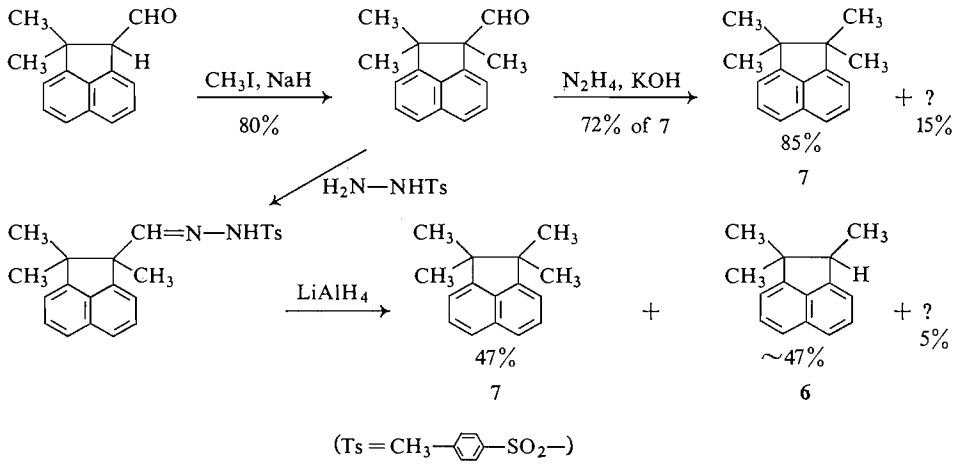

SCHEME 6.

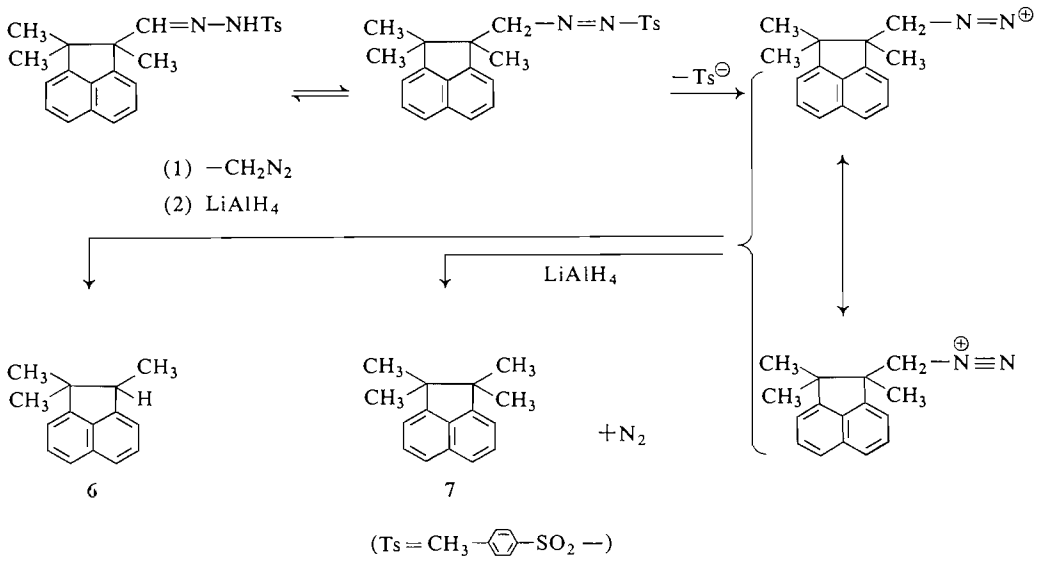

SCHEME 7.

followed by hydride reduction would lead to the trimethylacenaphthene, **6**, The loss of diazomethane is reasonable both on the basis of its own stability and the simultaneous relief of strong steric interaction present in the tetra substituted structure.

Experimental

All melting points and boiling points are uncorrected.

Microanalyses were performed by Mrs. D. Mahlow of the Microanalytical Section, Department of Chemistry, University of Alberta, Edmonton, and by C. Daesslé, Organic Microanalysis, 5757 Decelles Avenue, Montreal.

Infrared spectra were recorded with a Perkin–Elmer model 421 spectrophotometer. Nuclear magnetic resonance (n.m.r.) spectra were obtained with Varian A-60 and HR-100 spectrometers by Mr. R. N. Swindlehurst and Mr. Glen Bigam, Department of Chemistry, University of Alberta, Edmonton.

Analysis by gas–liquid chromatography and product identification was made with a Burrell model K-2 Kromo-Tog equipped with an integrator. Columns, 2.5 m in length, were packed with silicone rubber, neopentylglycol succinate or Apiezon L, each 25% by weight on Gas–Chrom P (60–80 mesh). For complete separation of products of alkylation it was sometimes necessary to change from one column to another. Helium at a flow rate of 100 ml/min. was the carrier gas. Column temperatures, generally 175–210°, varied with the different packings but were adjusted to give maximum separation

Can. J. Chem. Downloaded from www.nrcresearchpress.com by 210.87.254.5 on 09/05/12
For personal use only.

Can. J. Chem. Downloaded from www.nrcresearchpress.com by 210.87.254.5 on 09/05/12
For personal use only.

of products. Products were identified by comparison of their retention times with those of authentic samples, as well as by their isolation via gas–liquid chromatography and subsequent identification by n.m.r. and infrared spectral determinations. The paper areas of the various product peaks were measured by an integrator. Analyses of carefully weighed authentic mixtures of reaction products showed that these paper areas could be used as direct measures of molar compositions of the reaction mixtures.

1-Acenaphthenone, ***1***

Two methods were used for the preparation of 1-acenaphthenone.

Method A

This method employed published directions (2, 3) with the following modifications. Rather than utilizing steam distillation to purify the ketone from the chromium salts, the latter were removed by washing a solution of the crude oxidation product (50 g) in 500 ml of benzene first with 400 ml of ice cold 0.5 *N* sodium hydroxide, then with 300 ml of cold, 1 *N* hydrochloric acid, then with water. The dried ($MgSO_4$) benzene layer was freed from solvent. The residual solid, after two crystallizations from 95% ethanol and one from benzene – Skellysolve B[6] (1:4) melted at 119–121°, lit. m.p., 121–121.5° (2), yield, 55%.

Method B

This method followed in part the general directions of Wenham and Whitehurst for analogous cyclizations (4). An excess (130 g, 1.09 moles) of thionyl chloride was added in portions to a solution of 100 g (0.54 mole) of 1-naphthaleneacetic acid (Eastman Kodak Co.) in 300 ml of dry benzene. The mixture was stirred under reflux for 3 h, then the excess thionyl chloride and the benzene were removed by distillation. The residual oil was distilled under reduced pressure giving a nearly quantitative yield of 1-naphthaleneacetyl chloride as a yellow oil; b.p., 149–150° at 3.4 mm; lit. b.p., 188° at 23 mm (22).

A solution of the acid chloride (59 g, 0.29 mole) in 60 ml of carbon disulfide was added dropwise, during 30–40 min, to a stirred suspension of 56 g (0.42 mole) of anhydrous, powdered aluminium chloride in 175 ml of carbon disulfide maintained at room temperature. The mixture was then stirred overnight (12 h) and the resulting green material poured into ice water. The solid ketone, contaminated with aluminium salts, was removed by filtration. When the carbon disulfide was removed from the filtrate by means of a water aspirator additional ketone was obtained. The combined dried solids were extracted with 750 ml of hot benzene – Skellysolve B (1:4) and the hot solution filtered, then chilled. The precipitated ketone (41 g, 84%) when air dried, melted at 119–121°. A small sample, further purified by steam distillation and crystallization from benzene – Skellysolve B (1:4) melted at 121–123°.

2-Methyl-1-acenaphthenone, ***2***

A solution of 1-naphthaleneacetic acid (400 g, 2.15 moles) in 950 ml of 98% ethanol containing 100 ml of concentrated sulfuric acid was refluxed for 2 h. The cooled mixture was poured into 1 l of water and extracted twice with ether. The ether layer was washed repeatedly with 5% aqueous sodium bicarbonate until starting material no longer could be recovered upon acidification of the bicarbonate extracts. The ether solution was dried ($MgSO_4$) and distilled. The *ethyl 1-naphthaleneacetate* so obtained boiled at 139–141° at 2.1 mm, lit. b.p., 134–141° at 0.8 mm (6); yield, 428 g, 98% allowing for recovered starting material.

In a flame-dried, 3-neck flask, fitted with a magnetic stirrer, condenser, and a thermometer to measure the solution temperature, were placed 130 g (0.61 mole) of the above ester, 800 ml of dry benzene and 140 g (1 mole) of methyl iodide. An Erlenmeyer flask, attached to one neck of the reaction vessel by means of a short piece of large diameter Tygon Tubing, contained 46 g (1 mole) of a 56% sodium hydride dispersion in paraffin oil (Metal Hydrides, Inc.). The hydride was added to the reaction vessel in small portions during a period of 1.5 h while the temperature was maintained at 20–25° by external cooling. After the addition was complete, stirring was continued for 1.5 h at room temperature then for 18 h with the solution under reflux. The cooled mixture was carefully decomposed by the slow addition of 200 ml of glacial acetic acid followed by 500 ml of water. The mixture was extracted twice with ether and the extracts washed with water and then 5% aqueous sodium bicarbonate until free of acetic acid. The dried ($MgSO_4$) solution was then distilled, affording 130 g (94%) of *ethyl α-(1-naphthyl)-propionate*; b.p., 136–138° at 1.8 mm; lit. b.p., 144–148° at 0.8 mm (6).

A mixture of the above ester (430 g, 1.89 moles) and 100 g (2.5 moles) of sodium hydroxide in 750 ml of water was refluxed for 4 h. The resulting colorless solution was cooled and extracted with ether to remove unreacted ester, and the aqueous layer acidified with hydrochloric acid. The colorless solid, collected by suction filtration, was crystallized from aqueous ethyl alcohol giving *α-(1-naphthyl)propionic acid* (334 g, 91%) melting at 152–153°; lit. m.p., 148–149° (23).

The solution of α-(1-naphthyl)propionic acid (163 g) and thionyl chloride (150 g) in 450 ml of benzene was refluxed for 3 h. The solvent and excess thionyl chloride was removed and the crude *α-(1-naphthyl)propionyl chloride* was used directly in the following cyclization step.

The crude α-(1-naphthyl)propionyl chloride (350 g, ~1.6 moles) in 300 ml of carbon disulfide was added dropwise over a period of 2 h to a well-stirred mixture of 325 g (2.4 moles) of granular aluminium chloride (BDH) in 1 l of carbon disulfide kept at room temperature. The mixture which turned dark green and then black, was stirred overnight, then decomposed carefully with ice and water. The dark, sticky organic fraction could not be distilled, hence was subjected to steam distillation. A yellow oil came over very slowly (5 g per 3 l of distillate). An ether extract of this oil was dried ($MgSO_4$) and distilled, affording 2-methyl-1-acenaphthenone as a colorless oil (137.5 g, 47%) boiling at 152–153° at 4.3 mm; n_D^{25}, 1.6385. The low yield is attributed to the granular aluminium chloride used. When chilled, the oil solidified. Crystallization once from ethyl alcohol and twice from benzene – Skellysolve B (1:4), gave solid *2-methyl-1-acenaphthenone* **2** melting at 33–34°.

The infrared spectrum in CCl_4 showed absorption at 1715 cm^{-1} (C=O). The n.m.r. spectrum (CCl_4, with

[6]Skellysolve B is commercial hexane.

Can. J. Chem. Downloaded from www.nrcresearchpress.com by 210.87.254.5 on 09/05/12
For personal use only.

tetramethylsilane as reference) was consistent with the structure and showed a quartet centered at τ 6.45 ($J = 7.5$ c.p.s.) and a doublet at τ 8.51 ($J = 7.5$ c.p.s.) along with aromatic protons between τ 2 and τ 3 in the area ratio of 1:3:6 respectively.

Anal. Calcd. for $C_{13}H_{10}O$: C, 85.69; H, 5.53. Found: C, 85.82; H, 5.60.

2-Methyl-1-acenaphthenone Oxime

This compound melted at 126–140° (from water–ethanol). The infrared spectrum showed free and bonded hydroxyl at 3600 cm^{-1} and 3265 cm^{-1} respectively as well as absorption at 1620 cm^{-1} for C=N. The n.m.r. spectrum referred to tetramethylsilane indicated a 1:1 mixture of *syn* and *anti* isomers; — hydroxyl proton doublets at τ 1.42 ($J = 1$ c.p.s.) and τ 1.52 ($J = 1$ c.p.s.); two overlapping methinyl proton quartets centered at τ 5.43 ($J = 7$ c.p.s.) and τ 5.75 ($J = 7$ c.p.s.); two overlapping methyl proton doublets at τ 8.28 ($J = 7$ c.p.s.) and τ 8.32 ($J = 7$ c.p.s.); 6 aromatic protons between τ 2.0 and τ 3.0.

Anal. Calcd. for $C_{13}H_{11}NO$: C, 79.16; H, 5.62; N, 7.10. Found: C, 79.17; H, 5.92; N, 7.25.

2,2-Dimethyl-1-acenaphthenone

This compound was prepared by exhaustive methylation of 1-acenaphthenone as described above for the preparation of ethyl α-(1-naphthyl)propionate from ethyl 1-naphthaleneacetate. From a dry benzene solution (400 ml) of 50 g (0.3 mole) of 1-acenaphthenone, **1**, 100 g (0.75 mole) of methyl iodide and 44 g (0.91 mole) of sodium hydride dispersion (49%), was obtained a dark yellow oil boiling at 106–106.5° at 0.6 mm. The oil was remethylated with 30 g of methyl iodide and 10 g of sodium hydride dispersion in 250 ml of benzene. After work-up and complete removal of benzene and ether solvents, the oil solidified, and after crystallization from 95% ethyl alcohol gave 48 g (82%) of pale-yellow 2,2-dimethyl-1-acenaphthenone. An analytical sample, prepared by steam distillation and four crystallizations (charcoal) from ethyl alcohol, gave colorless plates melting at 72–73°.

The infrared spectrum (in CCl_4) showed a strong band at 1718 cm^{-1} (C=O). The n.m.r. spectrum in $CDCl_3$ referred to tetramethylsilane, showed a sharp singlet at τ 8.55 (methyl protons) and aromatic protons at τ 1.8–τ 2.75 in the ratio of 1:1.

Anal. Calcd. for $C_{14}H_{12}O$: C, 85.68; H, 6.17. Found: C, 85.52; H, 6.09.

2,2-Dimethyl-1-acenaphthenone Oxime

This compound melted at 130–141° (from water–ethanol). The n.m.r. spectrum (in $CDCl_3$, with tetramethylsilane as reference) indicated the presence of two isomers in the ratio of 16:84, — two hydroxyl proton doublets at τ 1.38 ($J = 1$ c.p.s.) and τ 1.50 ($J = 1$ c.p.s.), two methyl singlets at τ 8.15 and τ 8.37; aromatic protons at τ 2 to τ 3. The infrared spectrum (CCl_4) showed free and bonded hydroxyl at 3595 cm^{-1} and 3270 cm^{-1} respectively as well as absorption 1618 cm^{-1} for C=N.

Anal. Calcd. for $C_{14}H_{13}NO$: C, 79.59; H, 6.20; N, 6.63. Found: C, 79.15; H, 6.20; N, 6.33.

1-Methylacenaphthene, 3

Method A

1-Acenaphthenone was converted to *1-methylacenaphthylene* by the procedure of Brown and Hammick (1) as modified by Lozac'h and Mollier (7). The picrate of this olefin melted at 187–188° (from ethyl alcohol); lit. m.p., 178–179° (1). Decomposition of the picrate with sodium hydroxide solution (7) gave the known *1-methylacenaphthylene* as a dark-orange liquid. The n.m.r. spectrum in $CDCl_3$ (reference, tetramethylsilane) agreed with the structure, — one vinyl proton at τ 3.42 as a narrowly spaced quartet ($J = 1.5$ c.p.s.); a doublet at τ 7.75 ($J = 1.5$ c.p.s.) for the three methyl protons; six aromatic protons between τ 2.2 and τ 2.9.

The 1-methylacenaphthylene in ethyl alcohol was reduced at room temperature with platinum oxide and hydrogen at 50 p.s.i. giving a colorless oil (85% yield) boiling at 92–94° at 0.9 mm; lit. b.p., 145–155° at 28 mm (1). Gas–liquid chromatography indicated this to be of 95–96% purity.

Further purification was unsuccessful.

Method B

2-Methyl-1-acenaphthenone was subjected to Wolff–Kishner reduction following the modified method of Anderson and Wade (8)

A mixture of 20 g (0.11 mole) of 2-methyl-1-acenaphthenone in 70 ml of 95% ethyl alcohol and 100 ml of 85% hydrazine hydrate was refluxed for 1.5 h. To this was added 100 ml of diethylene glycol, and then the ethyl alcohol, water and excess hydrazine were removed by distillation until a temperature of 160–165° was reached. Subsequent addition of 14 g (0.25 mole) of potassium hydroxide to the cooled solution was followed by a reflux period of 4 h after which 100 ml of water was added to the cooled solution. The three successive ether extracts were combined and washed with water, dried ($MgSO_4$) and distilled, giving 13 g (70%) of pure 1-methylacenaphthene boiling sharply at 94° at 1.2 mm; n_D^{24}, 1.6180. The n.m.r. spectrum (neat) is consistent with the assigned structure; — three methyl protons as a doublet at τ 8.93 ($J = 6.5$ c.p.s.); a multiplet between τ 6.5 and τ 7.7 for three protons on carbon atoms α to the aromatic nucleus and 6 aromatic protons between τ 2.2 and τ 3.3.

1,1-Dimethylacenaphthene, 4

Wolff–Kishner reduction of 2,2-dimethyl-1-acenaphthenone was carried out as above for the reduction of 2-methyl-1-acenaphthenone to 1-methylacenaphthene. From 25 g (0.128 mole) of 2,2-dimethyl-1-acenaphthenone and 125 ml of 85% hydrazine hydrate there was obtained 11.5 g (50%) of 1,1-dimethylacenaphthene as a clear yellow liquid boiling at 97–98° at 1.5 mm; n_D^{23}, 1.6001. The n.m.r spectrum (neat, tetramethylsilane as internal reference) showed singlets at τ 7.11 (CH_2) and τ 8.85 (CH_3) and aromatic protons at τ 2.4 to τ 3.2 in the ratio 2:6:6 respectively.

Anal. Calcd. for $C_{14}H_{14}$: C, 92.26; H, 7.74. Found: C, 92.51; H, 7.44.

The *picrate* was obtained as orange needles from a small amount of ethyl alcohol. It decomposed readily in solvents such as ether and hexane or when dried at 72° at 2 mm; m.p., 112–112.5°.

Anal. Calcd. for $C_{20}H_{17}N_3O_7$: C, 58.39; H, 4.17; N, 10.21. Found: C, 58.41; H, 4.44; N, 10.11.

Cis- and Trans-1,2-dimethyl-1-acenaphthenol

2-Methyl-1-acenaphthenone (25 g, 0.138 mole) in dry benzene (250 ml) was added slowly to methylmagnesium

Can. J. Chem. Downloaded from www.nrcresearchpress.com by 210.87.254.5 on 09/05/12
For personal use only.

bromide (from 5.1 g, 0.21 mole, of magnesium and 45 g of methyl iodide in 200 ml of ether). The mixture was then refluxed for 2 h, cooled, and decomposed with ice and saturated aqueous ammonium chloride. The aqueous layer was extracted with ether, and the resulting ether–benzene solution dried ($MgSO_4$) and freed from solvent. The pale-yellow solid (25.4 g, 93%) so obtained was crystallized once from ethyl alcohol (charcoal) and thrice from Skellysolve B giving colorless crystals which yellowed slightly on standing at room temperature. The broad melting point, 88–101°, and the analysis indicated a mixture of isomers. The n.m.r. spectrum (Fig. 1) in $CDCl_3$ (tetramethylsilane as reference) supported the presence of two isomers in the ratio of 54:46, and showed two different methyl proton signals at τ 8.40 and τ 8.62 in addition to the expected methyl doublet at τ 8.68 (J = 7.5 c.p.s.). As well there was present a quartet for the methinyl proton at τ 6.62 (J = 7.5 c.p.s.), two hydroxyl proton signals at τ 7.51 and τ 7.98 and six aromatic protons at τ 2.2 to τ 3.0. Resolution at 100 megacycles led to clear separation of signals (inset, Fig. 1). Peak identification was achieved by use of spin coupling values as well as irradiation at τ 6.6 which caused collapse of the methyl doublet at τ 8.68 to a singlet.

Anal. Calcd. for $C_{14}H_{14}O$: C, 84.81; H, 7.12. Found: C, 84.46; H, 6.87.

1,2-Dimethylacenaphthylene

A quantity (20.7 g, 0.105 mole) of *cis-trans*-1,2-dimethyl-1-acenaphthenol was dissolved in a minimum amount of hot 95% ethyl alcohol and this was added immediately to a hot solution of 24 g (0.105 mole) of picric acid in 250 ml of ethyl alcohol. The *picrate of 1,2-dimethylacenaphthylene* precipitated immediately from the hot solution and was collected and thrice crystallized from ethyl alcohol. The orange needles (41 g, 92%) melted at 194–195° with decomposition.

Anal. Calcd. for $C_{20}H_{15}N_3O_7$: C, 58.68; H, 3.69; N, 10.27. Found: C, 58.63; H, 3.85; N, 10.38.

Decomposition of 40 g of the above picrate with excess aqueous sodium hydroxide (in a large quantity of water to permit solution of the picrate) was followed by ether extraction of the precipitated yellow solid. The extract was washed thoroughly with water, dried ($MgSO_4$) and freed from solvent affording crude 1,2-dimethylacenaphthylene in 97% yield. Three crystallizations from ethyl alcohol gave yellow plates melting at 71.5–72°. The n.m.r. spectrum in $CDCl_3$ (reference, tetramethylsilane) showed only a singlet for the methyl protons at τ 7.84 and the aromatic proton multiplet between τ 2.3 and τ 2.8 in the ratio 1:1. The infrared spectrum showed a sharp band at 1620 cm^{-1} (unsaturation).

Anal. Calcd. for $C_{14}H_{12}$: C, 93.29; H, 6.71. Found: C, 93.48; H, 6.65.

1,2-Dimethylacenaphthene

(a) Attempted Reduction by Diimide (9–11)

A continuous stream of air was bubbled through a mixture of 5 g of 1,2-dimethylacenaphthylene in 65 ml of methanol containing 6.5 g of 85% hydrazine hydrate and a small amount of cupric sulfate catalyst, while the mixture was stirred at 45–50° for 1 week. Small quantities of hydrazine hydrate along with fresh catalyst was added every 12 h. As well, methyl alcohol was added, as required, to offset losses due to evaporation. The reaction mixture was filtered, the solvent removed and the residue taken up in ether. The ether solution was washed with dilute aqueous hydrochloric acid, water and dried ($MgSO_4$), then concentrated to a small volume and analyzed by gas–liquid chromatography. The mixture of products contained unreduced 1,2-dimethylacenaphthylene (43%) along with 13% of an unidentified higher boiling impurity.

(b) Catalytic Hydrogenation

Catalytic hydrogenation at room temperature of 1,2-dimethylacenaphthylene (5 g) in 100 ml of ethyl alcohol was carried out in the presence of platinum oxide and hydrogen at an initial pressure of 20 p.s.i. When hydrogen uptake was completed, the solution was filtered and the solvent removed, leaving a crude grey solid in nearly quantitative yield and of 96% purity. Three crystallizations from ethyl alcohol (charcoal) gave colorless needles of *cis* (?)-1,2-dimethylacenaphthene, **5**, melting sharply at 53–54°. The n.m.r. spectrum in $CDCl_3$ with tetramethylsilane as reference, shown in Fig. 2, agrees with the assignment of the structure as 1,2-dimethylacenaphthene.

Anal. Calcd. for $C_{14}H_{14}$: C, 92.26; H, 7.74. Found: C, 92.38; H, 7.63.

Cis(?)-1,2-dimethylacenaphthene picrate (from alcohol) was obtained as fine orange needles, melting at 116–117°.

Anal. Calcd. for $C_{20}H_{17}N_3O_7$: C, 58.39; H, 4.17; N, 10.21. Found: C, 58.27; H, 4.27; N, 10.41.

1,2,2-Trimethyl-1-acenaphthenol

This compound was prepared by dropwise addition of 10 g (0.051 mole) of 2,2-dimethyl-1-acenaphthenone in 100 ml of dry benzene to a Grignard solution made from magnesium (2 g, 0.082 mole) and methyl iodide (15 g, 0.105 mole) in 80 ml of dry ether. The mixture was then refluxed for 1 h and subsequently decomposed with ice and saturated aqueous ammonium chloride. The organic layer was washed with water, dried ($MgSO_4$), and freed from solvent. A quantitative yield of crude 1,2,2-trimethyl-1-acenaphthenol was obtained as a pale-yellow solid. Three crystallizations from 95% ethyl alcohol (charcoal) gave colorless crystals melting at 101–102°. The carbinol decomposed slowly on standing.

The n.m.r. spectrum in $CDCl_3$ (tetramethylsilane as reference) was consistent with the structure assigned showing one hydroxyl proton singlet at τ 8.0, three different methyl groups at τ 8.49, τ 8.67, and τ 8.74 and aromatic protons at τ 2.2 to τ 3.0 in the ratio 1:3:3:3:6. The infrared spectrum (CCl_4) showed a narrow band at 3620 cm^{-1} (free hydroxyl).

Anal. Calcd. for $C_{15}H_{16}O$: C, 84.86; H, 7.60. Found: C, 84.89; H, 7.40.

2,2-Dimethyl-1-methyleneacenaphthene

Dehydration of 1,2,2-trimethyl-1-acenaphthenol (50 g, 0.236 mole) was accomplished with picric acid following the same procedure used for the conversion of *cis, trans*-1,2-dimethyl-1-acenaphthenol to 1,2-dimethylacenaphthylene above. Decomposition of the picrate with base, followed by ether extraction and distillation of the dried ether solution, afforded 41.5 g (91%) of 2,2-dimethyl-1-methyleneacenaphthene as a pale-yellow oil boiling at 101.5–102° at 0.9 mm; n_D^{25}, 1.6315.

The n.m.r. spectrum (neat, reference tetramethylsilane) showed a singlet at τ 8.72 for the six methyl protons, two

Can. J. Chem. Downloaded from www.nrcresearchpress.com by 210.87.254.5 on 09/05/12
For personal use only.

geminal methylene proton singlets at τ 4.32 and τ 4.91 and 6 aromatic protons at τ 2.3 to τ 3.2.

Anal. Calcd. for $C_{15}H_{14}$: C, 92.74; H, 7.26. Found: C, 92.61; H, 7.26.

The 2,2-dimethyl-1-methyleneacenaphthene picrate, obtained from cold ethyl alcohol solution, melted initially at 62–63° (decomp.) and then at 85–100° with further decomposition.

Anal. Calcd. for $C_{21}H_{17}N_3O_7$: C, 59.57; H, 4.05: N, 9.93. Found: C, 59.22; H, 4.21; N, 10.13.

1,1,2-Trimethylacenaphthene, 6

Method A

2,2-Dimethyl-1-methyleneacenaphthene was reduced catalytically according to the procedure described above for the hydrogenation of 1,2-dimethylacenaphthylene. The yield of colorless product, after distillation, was 90%; b.p. 98–99° at 1.0 mm. A 5% impurity was present but this could be removed by gas–liquid chromatography on a 20-ft preparative column of 20% butanediol succinate on Gas-Chrom W at 200 °C. Pure *1,1,2-trimethylacenaphthene*, **6**, boiled at 108° at 1.5 mm; n_D^{25}, 1.5932.

The n.m.r. spectrum agreed with the structure, showing one methinyl proton as a quartet at τ 6.9 (J = 7 c.p.s.), one methyl proton doublet at τ 8.67 (J = 7 c.p.s.) and singlets for two methyl group protons at τ 8.6 and τ 8.82. A multiplet between τ 2.3 and τ 3.0 is due to 6 aromatic protons.

Anal. Calcd. for $C_{15}H_{16}$: C, 91.78; H, 8.22. Found: C, 91.65; H, 7.98.

1,1,2-Trimethylacenaphthene picrate, from ethanol, melted at 71–72° (decomp.) with further decomposition up to 105°.

Anal. Calcd. for $C_{21}H_{19}N_3O_7$: C, 59.29; H, 4.50; N, 9.88. Found: C, 59.28; H, 4.72; N, 9.86.

Method B

To 2,2-dimethyl-1-methyleneacenaphthene (5 g) in 40 ml of dry tetrahydrofuran was added 2 g of lithium aluminium hydride (two-fold excess) and the mixture then heated under reflux for 20 h. The cooled solution was decomposed cautiously with water and dilute hydrochloric acid. The ether extract was washed with water, dried ($MgSO_4$), and freed from solvent. The residue, when purified by chromatography on neutral alumina with Skellysolve B as eluant, gave 4 g of colorless liquid of better than 98% purity which was identical, as shown by its n.m.r. spectrum, to 1,1,2-trimethylacenaphthene.

Method C

To 1 g (0.026 mole) of lithium aluminium hydride in 50 ml of dry ether was added, dropwise, over a period of 1 h (16), an ether solution of 4.4 g (0.012 mole) of 2,2-dimethyl-1-hydroxymethylacenaphthene *p*-toluenesulfonate (see below). The reaction mixture was then stirred at room temperature for 1 h, then under reflux for 16 h. The cooled solution was decomposed with ethyl acetate and water. An ether extract was filtered and dried ($MgSO_4$). Removal of the solvent left 2.4 g of pale-yellow oil which was purified by chromatography on neutral alumina with Skellysolve B as eluant. A colorless oil was obtained (2.3 g, 97%) which was shown to be 1,1,2-trimethylacenaphthene by its n.m.r. spectrum.

2,2-Dimethyl-1-hydroxymethylacenaphthene

The hydroboration–oxidation procedure (15) for conversion of olefins to alcohols was employed. In a 1 l, 3-neck flask equipped with a magnetic stirrer, dropping funnel, thermometer, condenser, and nitrogen inlet, were placed 110 ml of a 1.0 *M* solution of sodium borohydride in diglyme, and 50 g (0.258 mole) of 2,2-dimethyl-1-methyleneacenaphthene in 30 ml of diglyme. The flask was immersed in water at 20° and flushed with nitrogen. Subsequently, throughout the reaction, a static nitrogen atmosphere was maintained. From the dropping funnel, 18 ml of freshly distilled boron trifluoride etherate was added dropwise, while the temperature of the reaction mixture was maintained at 20–25°. After the etherate had been added, the solution was stirred for 1 h, then the excess hydride was destroyed cautiously by dropwise addition of 30 ml of water. The organoborane was oxidized at 40–50° by addition first of 28 ml of 3 *N* aqueous sodium hydroxide, the solution stirred for a short time at this temperature, then 28 ml of 30% hydrogen peroxide added dropwise. The mixture was then stirred at room temperature for 1 h, extracted with ether and the ether layer washed five times with water to remove the diglyme. The ether solution was dried ($MgSO_4$) and the solvent removed, leaving 53 g (97%) of a pale-yellow, viscous oil. Distillation under reduced pressure of a small amount of the product, using steam to heat the condenser, gave 2,2-dimethyl-1-hydroxymethylacenaphthene as an extremely viscous, nearly colorless oil of 97–98% purity as shown by gas–liquid chromatography, b.p. 140–141° at 0.75 mm; $n_D^{24.5°}$, 1.6149.

The n.m.r. spectrum (Fig. 3) in CCl_4 (referred to tetramethylsilane) agreed with the assigned structure. Two sharp singlets appeared for the two methyl groups at τ 8.62 and τ 8.70 as well as a singlet for the hydroxyl proton at τ 6.91. The two methylene protons along with the one methine proton gave rise to an AB type spectrum with multiplets centered at τ 6.16 and τ 6.69. Aromatic protons appeared between τ 2.3 and τ 3.1.

Anal. Calcd. for $C_{15}H_{16}O$: C, 84.86; H, 7.60. Found: C, 84.55; H, 7.60.

The *3,5-dinitrobenzoate of 2,2-dimethyl-1-hydroxymethylacenaphthene* was a yellow solid (from chloroform) melting at 200–201°. The n.m.r. spectrum in $CDCl_3$ agreed fully with the structure assigned.

Anal. Calcd. for $C_{22}H_{18}N_2O_6$: C, 65.02; H, 4.46; N, 6.90. Found: C, 65.25; H, 4.61; N, 6.66.

2,2-Dimethyl-1-hydroxymethylacenaphthene p-Toluenesulfonate

This compound was prepared by the addition of a solution of *p*-toluenesulfonyl chloride (10 g, 0.053 mole) in 30 ml of pyridine to 8 g (0.038 mole) of 2,2-dimethyl-1-hydroxymethylacenaphthene in 30 ml of pyridine. The mixture was kept at room temperature for 2 days and then poured into 400 ml of ice water and extracted twice with chloroform. The combined chloroform extracts were washed three times with 200 ml quantities of cold, 6 *N* hydrochloric acid, twice with 200 ml quantities of cold saturated aqueous sodium bicarbonate and then twice with water. The solution, when dried ($CaCl_2$) and freed from solvent, gave 13.3 g of crude ester as a thick yellow oil. This oil was dissolved in excess hot 98% ethanol. The cooled solution deposited 9.8 g (70%) of grey crystals. Two crystallizations from ethanol gave colorless crystals melting at 72–73°.

The n.m.r. spectrum agreed with the assigned structure.

Can. J. Chem. Downloaded from www.nrcresearchpress.com by 210.87.254.5 on 09/05/12
For personal use only.

Anal. Calcd. for $C_{22}H_{22}O_3S$: C, 72.10; H, 6.05; S, 8.75. Found: C, 71.94; H, 6.06; S, 9.00.

2,2-Dimethyl-1-acenaphthenecarboxaldehyde

Method A

By oxidation of 2,2-dimethyl-1-hydroxymethylacenaphthene according to Barton's procedure (17).

Phosgene was bubbled into a stirred solution of 400 ml of dry ether for 1 h. To the resulting solution was added 50 g (0.236 mole) of 2,2-dimethyl-1-hydroxymethylacenaphthene in 100 ml of ether. Stirring was then continued for 2 h, while phosgene was passed continuously into the solution. This procedure was repeated until, after evaporation of the solvent from a sample of the solution, the product so obtained showed no hydroxyl absorption in the infrared spectrum. In this manner 63 g (97%) of the chloroformate ester was obtained as a viscous, pale-yellow oil boiling at 150–151° at 0.8 mm. This formate ester darkened to a black color on standing at room temperature for a prolonged period, hence should be used soon after its preparation.

The crude ester, in a 1 l flask, was treated with dimethyl sulfoxide (previously dried by passage through a column of molecular sieves and then distilled from calcium hydride under reduced pressure) and the mixture stirred at 15° for several minutes. A vigorous evolution of carbon dioxide took place. When gas evolution had ceased, the solution was stirred at room temperature for 15–20 min and then dry, distilled triethylamine (120 ml) was added dropwise during a 20–30 min period while the reaction mixture was kept cool in an ice water bath. This cooling caused some of the dimethyl sulfoxide to solidify, but solution was attained by slight warming of the reaction vessel after all the amine had been added.

The mixture was stirred at room temperature for 1 h and then 200 ml of water was added followed by sufficient 2 *N* hydrochloric acid to acidify the solution (about 450–500 ml). The solution was extracted twice with ether, and the combined ether extracts washed twice with water and dried ($MgSO_4$). Removal of the solvent gave 54 g of oil which consisted of two components in the ratio 4:1 as shown by gas–liquid chromatography on a silicone rubber column. The main fraction was the desired aldehyde while the smaller fraction was mainly starting material.

Purification of the reaction product by chromatography on neutral alumina or via bisulfite addition was unsuccessful. However, the aldehyde was separated by mixing 5 g quantities of the oil with 12.5 ml of ethyl alcohol and 4 g of Girard's T reagent (Fisher Scientific Co.) and 1.25 ml of glacial acetic acid and heating this mixture under reflux for 1 h (18). To the cooled solution was added 50 ml of water and the mixture then thoroughly extracted with 3 portions of ether. From these ether extracts, first washed with aqueous bicarbonate and then with water, small quantities of starting alcohol could be recovered. To the aqueous layer was added 2.5 ml of concentrated hydrochloric acid along with 25 ml of benzene and the whole warmed gently on a steam bath for 30 min. An ether extract of this mixture was dried ($MgSO_4$) and freed from solvent, leaving 2.75 g of dark oil which gas–liquid chromatography showed to be the aldehyde of 95% purity. Benzene elution of this contaminated aldehyde on neutral alumina gave a clear yellow liquid of similar purity (~ 95%) but about 40% of the aldehyde was lost in this last step.

No analysis was performed on the 95% pure aldehyde. However the n.m.r. spectrum in CCl_4 (referred to tetramethylsilane) agreed well with the assigned structure and showed two singlets at τ 8.52 and τ 8.58 for the two methyl groups, a doublet at τ 6.13 ($J = 4$ c.p.s.) for the methine proton and a doublet at τ 0.45 ($J = 4$ c.p.s.) for the aldehyde proton. Aromatic protons were found between τ 2.2 and τ 3.0. The spectrum was devoid of any other significant signals.

Method B — via reaction of 2,2-dimethyl-1-acenaphthenone with dimethyloxosulfonium methylide (19).

Trimethyloxosulfonium Iodide

This compound was prepared by refluxing a solution of 32 g (0.41 mole) of dry dimethyl sulfoxide in 60 ml of methyl iodide under nitrogen for 3 days, during which time the solution turned yellow and a colorless solid precipitated. The colorless solid, removed by filtration, washed with chloroform and dried, weighed 27 g (30%). Crystallization from 150 ml of water gave 24.3 g of large colorless prisms. These were crushed and then dried in a vacuum desiccator over phosphorus pentoxide.

Dimethyloxosulfonium Methylide

Sodium hydride (6.45 g, 0.15 mole), as a 56% dispersion in mineral oil, was placed in a 3-neck, round bottom flask equipped with a magnetic stirrer. The hydride was washed three times with Skellysolve B, by swirling and decanting the liquid portion, to remove the mineral oil. The flask was fitted immediately with a reflux condenser and the system stoppered and evacuated. Immersion of the vessel in warm water (~ 50°) for 10 min permitted removal of the last traces of Skellysolve B. The vacuum was released and 33 g (0.15 mole) of powdered trimethyloxosulfonium iodide was introduced through one of the side arms. The system was put under nitrogen by repeatedly evacuating the flask and filling it with nitrogen. Thereafter the system was opened to atmospheric pressure and a slow influx of nitrogen maintained. Dry dimethyl sulfoxide (100 ml) was introduced slowly over a 30 min period via a dropping funnel, to the stirred solution. A vigorous evolution of hydrogen ensued and a milky-white mixture formed. This was stirred for an additional 20 min.

To the above stirred solution of the ylid was added, over a period of 20 min, a solution of 16 g (0.082 mole) of 2,2-dimethyl-1-acenaphthenone in 50 ml of dimethyl sulfoxide. The mixture was then heated at 50–60° for 4.5 h, then cooled and diluted with 250 ml of water. The mixture was extracted twice with ether, the combined ether extracts washed twice with water, then dried ($MgSO_4$), and freed from solvent. The residual yellow oil was shown by its n.m.r. spectrum (Fig. 4) to be a 4:1 mixture of the oxirane (Scheme 5, *b*) and starting ketone respectively. When only a 10% excess of methylide was used, and the mixture heated at 50–60° for 1 h, a 3:2 ratio of oxirane to ketone was obtained. This ratio was raised to 2:1 when the reactants were stirred at room temperature overnight and then heated at 50–60° for 5 h. A 10-h heating period caused decomposition of the products and the products in this case showed the presence of very little oxirane (by n.m.r.).

The yellow oil (above), containing a mixture of oxirane and ketone 4:1, was dissolved in Skellysolve B and subjected to chromatography on neutral alumina (250 g). The column temperature increased when this mixture was added. The original ketone was removed with ether.

Can. J. Chem. Downloaded from www.nrcresearchpress.com by 210.87.254.5 on 09/05/12
For personal use only.

Elution with methanol gave 10.4 g of crude 2,2-dimethyl-1-acenaphthenone carboxaldehyde as an orange oil. A second chromatography on neutral alumina, with benzene as eluant gave 4 g (~30%) of nearly pure aldehyde as a pale-yellow oil. Both the infrared and n.m.r. spectra supported the structure.

Attempted Reaction between 2,2-Dimethyl-1-methyleneacenaphthene and Peroxybenzoic Acid

To 3 g (0.0155 mole) of 2,2-dimethyl-1-methyleneacenaphthene in 100 ml of chloroform at 0–5° was added, over a period of 1 h, a solution of peroxybenzoic acid (0.0183 mole) in chloroform (35 ml of a solution containing 0.072 g of acid per ml of solvent diluted with an additional 40 ml of chloroform). The reaction mixture was stirred at ice bath temperature for 6 h and then at room temperature for 10 h. The solution was washed with saturated aqueous bisulfite, then twice with 5% aqueous sodium bicarbonate, and dried ($MgSO_4$). Removal of the chloroform gave a dark brown oil which became viscous and black on standing. The n.m.r. spectrum showed this to be chiefly starting material. No oxirane signals at τ 6.8 were evident.

Similar results were obtained with *m*-chloroperoxybenzoic acid.

1,2,2-Trimethyl-1-acenaphthenecarboxaldehyde

This compound was prepared in 84% yield by alkylation of the above compound, 2,2-dimethyl-1-acenaphthenecarboxaldehyde using methyl iodide and sodium hydride in benzene following the procedure employed for the methylation of 1-acenaphthenone above. The product was obtained by chromatography on neutral alumina. Elution with Skellysolve B removed the paraffin oil. Elution with benzene and finally with ether gave the trimethyl aldehyde as a nearly pure yellow oil. When cooled, the oil solidified and then was crystallized twice from ethyl alcohol. The nearly colorless crystals melted at 53–54°. The infrared spectrum in CCl_4 showed strong absorption at 1720 cm^{-1} (C=O). The n.m.r. spectrum in CCl_4 (reference, tetramethylsilane) showed three singlets for the three methyl groups at τ 8.56, τ 8.59, and τ 8.82, as well as a singlet at τ 0.80, for the aldehyde proton. Aromatic proton signals appeared as a multiplet between τ 2.2 and τ 3.0.

Anal. Calcd. for $C_{16}H_{16}O$: C, 85.67; H, 7.19. Found: C, 86.02; H, 6.98.

1,2,2-Trimethyl-1-acenaphthenecarboxaldehyde p-Toluenesulfonylhydrazone

This compound was synthesized by heating under reflux a solution of 5.6 g (0.025 mole) of 1,2,2-trimethyl-1-acenaphthenecarboxaldehyde with a slight excess of *p*-toluenesulfonylhydrazine in 100 ml of methanol for 4–5 h. The reaction mixture, cooled in a refrigerator, deposited 5 g of nearly colorless crystals which were collected and washed with ether. The filtrate was evaporated to a small oily residue from which an additional 2.4 g of solid was obtained by scratching, seeding, and chilling. The combined crude hydrazone was washed with cold, 10% aqueous sulfuric acid to remove unreacted hydrazine. The solid was then dissolved in a minimum quantity of hot methanol, and water was added dropwise until a faint cloudiness appeared. Subsequent cooling gave crystals which were collected and subjected to a second crystallization by the same procedure. The small, glistening white plates melted at 163.5–164.5°.

The n.m.r. spectrum in $CDCl_3$ showed the following peaks, — τ 8.51, τ 8.78, and τ 8.95 for 3 aliphatic methyl groups; τ 7.58 for the aromatic methyl group. Both the N—H proton and vinylic proton were found buried in the aromatic proton region between τ 2.0 and τ 3.2, an observation reported elsewhere (24).

1,1,2,2-Tetramethylacenaphthene, 7

Method A

Wolff–Kishner reduction (8) of 1.25 g of 1,2,2-trimethyl-1-acenaphthenecarboxaldehyde by the method used for the reduction of 2-methyl-1-acenaphthenone to 1-methyl-acenaphthene above gave, after evaporation of the solvent from the ether extract, a light-brown oil (1.02 g) which consisted of two components in the ratio 15:85 as indicated by gas–liquid chromatography on a silicone rubber column. When cooled and scratched, the oil solidified. Crystallization from ethyl alcohol (charcoal) gave 500 mg of a yellow solid which gas–liquid chromatography showed to be ~98% pure, m.p., 43.5–44.5°. Sublimation at 0.5 mm pressure and oil bath temperature of 90–100° produced a white solid better than 99.5% pure; m.p., 57–58°.

The n.m.r. spectrum in CCl_4 (reference, tetramethylsilane) showed aromatic protons at τ 2.6 to τ 3.1 and a sharp singlet at τ 8.75 for the four methyl groups, in the ratio 1:2.

Anal. Calcd. for $C_{16}H_{18}$: C, 91.37; H, 8.63. Found: C, 91.10; H, 8.51.

A pure picrate of the tetramethylacenaphthene could not be obtained.

The 15% impurity was not identified.

Method B

By a modification of the procedure of Caglioti and Grasselli (21), a mixture of 6.1 g (0.0156 mole) of 1,2,2-trimethyl - 1 - acenaphthenecarboxaldehyde *p* - toluene - sulfonylhydrazone in 150 ml of dry tetrahydrofuran (distilled from lithium aluminium hydride) and 6 g (0.16 mole) of lithium aluminium hydride was heated under reflux for 8 h. The cooled solution was poured cautiously into moist ether. To this was added water and 10% aqueous sulfuric acid to complete the decomposition of excess hydride. After the ether solution was washed successively with 10% aqueous sulfuric acid, 10% aqueous sodium hydroxide, and water, the organic layer was dried ($MgSO_4$) and freed of solvent to give 2.3 g of yellow-brown oil. Gas–liquid chromatography, using three different columns, showed the presence of only three products, one in 5% concentration and the other two in approximately equal amounts (~47.5%). Comparison of retention times with those of known compounds identified the latter two as 1,1,2-trimethylacenaphthene and 1,1,2,2-tetramethylacenaphthene. The n.m.r. spectrum corroborated such a mixture. The mixture was not separated.

Acknowledgments

The authors are grateful for financial support obtained from the National Research Council of Canada. One of us, A. Bosch, wishes to thank the University of Alberta, Edmonton for a Dissertation Fellowship which permitted him to complete this work.

1. B. R. BROWN and D. L. HAMMICK. J. Chem. Soc. 1395 (1948).
2. L. F. FIESER and J. CARSON. J. Am. Chem. Soc. **62**, 432 (1940).
3. J. CASON. Org. Syn. Coll. Vol. **III**, 3 (1955).
4. A. J. M. WENHAM and J. S. WHITEHURST. J. Chem. Soc. 3857 (1956).
5. M. D. SOFFER, R. A. STEWART, J. C. CAVAGNOL, H. E. GELLERSON, and E. A. BOWLER. J. Am. Chem. Soc. **72**, 3704 (1950).
6. M. JULIA and M. BAILLARGÉ. Bull. Soc. Chim. France, 928 (1957).
7. N. LOZAC'H and Y. MOLLIER. Bull. Soc. Chim. France, 1243 (1950).
8. A. G. ANDERSON, JR. and R. H. WADE. J. Am. Chem. Soc. **74**, 2274 (1952).
9. E. J. COREY, D. J. PASTO, and W. L. MOCK. J. Am. Chem. Soc. **83**, 2957 (1961).
10. E. J. COREY, W. L. MOCK, and D. J. PASTO. Tetrahedron Letters, 347 (1961).
11. H. ROTTENDORF and S. STERNHELL. Australian J. Chem. **16**, 647 (1963).
12. E. E. VAN TAMELEN and R. J. TIMMONS. J. Am. Chem. Soc. **84**, 1067 (1962).
13. S. SIEGEL, M. DUNKEL, G. V. SMITH, W. HALPERN, and J. COZORT. J. Org. Chem. **31**, 2802 (1966).
14. I. JARDINE and F. J. MCQUILLIN. J. Chem. Soc. 458 (1966).
15. G. ZWEIFEL and H. C. BROWN. J. Am. Chem. Soc. **86**, 393 (1964).
16. N. G. GAYLORD. Reduction with complex metal hydrides. Interscience Publishers, Inc., New York. 1956. p. 855.
17. D. H. R. BARTON, B. J. GARNER, and R. H. WIGHTMAN. J. Chem. Soc. 1855 (1964).
18. L. F. FIESER. Organic experiments. D. C. Heath and Co., Boston. 1964. p. 99.
19. E. J. COREY and M. CHAYKOVSKY. J. Am. Chem. Soc. **87**, 1345, 1353 (1965).
20. J. D. ROBERTS. Nuclear magnetic resonance. McGraw-Hill Book Co., Inc., New York. 1959. pp. 58–60.
21. L. CAGLIOTI and P. GRASSELLI. Chem. Ind. London, 153 (1964).
22. I. M. HEILBRON and H. M. BUNBURY. Dictionary of organic compounds. Eyre and Spottiswoode. London. 1953.
23. F. F. BLICKE and R. F. FELDKAMP. J. Am. Chem. Soc. **66**, 1087 (1966).
24. HIGH RESOLUTION NMR SPECTRA CATALOG. Vol. I and II. Varian Associates, Instrument Division, Palo Alto, California. 1963. Spectra Nos. 20, 443, 485, and 562.

Can. J. Chem. Downloaded from www.nrcresearchpress.com by 210.87.254.5 on 09/05/12
For personal use only.

Ranunculin

M. H. Benn and Lois Jean Yelland
Department of Chemistry, The University, Calgary, Alberta
Received September 26, 1967

A reinvestigation of the structure of ranunculin, the glucosidic precursor of the vesicant principle of many *Ranunculus* species, protoanemonin, supported the gross structure proposed by Hill and van Heyningen and led to the stereochemistry at the asymmetric center of the aglucone.

Canadian Journal of Chemistry, **46**, 729 (1968)

Can. J. Chem. Downloaded from www.nrcresearchpress.com by 210.87.254.105 on 09/05/12
For personal use only.

When chewed, the leaves of many plants of the family Ranunculaceae rapidly produce an intense burning or tingling sensation on the tip of the tongue. In some cases, the bruised plants are also capable of producing erythema or in severe cases blistering of the skin. The chemical agent responsible for these effects has been identified (1) as protoanemonin (**2**), an unstable compound which dimerizes to give anemonin (**3**) (2), which is non-vesicant.

In 1951, Hill and van Heyningen reported (3) the isolation of a glucosidic precursor of protoanemonin, to which they assigned the name Ranunculin and the provisional structure **1**.

The results of subsequent studies by Hellström (4) and by Bredenberg (5) supported this structure, and Hellström inferred, from an analysis of the infrared spectrum of ranunculin, that the glucosidic linkage most probably had the β-D-configuration. This conclusion was supported by the observation (4) that ranunculin was cleaved by almond emulsin, to give D-glucose and an apparently levorotatory aglucone, presumably **4**.

We describe here the results of a new study of ranunculin which further corroborate Hill and van Heyningen's structure and which also establish the configuration at the asymmetric center in the aglucone.

Ranunculin was isolated from a number of sources, including *Ranunculus cardiophyllus* Hook and *Anemone patens* L. var *wolfgangiana* (Bess.) Koch, which represent additions to the list (6) of ranunculin-containing plants. The physical properties of the glucoside were in excellent agreement with those previously reported.

The proton magnetic resonance (p.m.r.) spectrum[1] of ranunculin is also consistent with structure **1**. Prominent features of the spectrum are three low field signals, each corresponding in area to one hydrogen atom, at τ 2.17 (dd, $J = 6$ and 1.8 c.p.s.), 3.66 (dd, $J = 6$ and 2.4 c.p.s.), and 4.49 (complex 8 line multiplet, width 12 c.p.s.). The first two signals we ascribe to the hydrogens in positions 3-2 and 4-3 of the lactone ring respectively and the last to the proton at position-4. (These signals are not present in the p.m.r. spectrum of dihydroranunculin tetraacetate.) Furthermore, a doublet, with area corresponding to one hydrogen atom, at τ 5.47 ($J = 8$ c.p.s.) corresponds, both in position and coupling constant to a proton at an anomeric center with the (C-1) β-D-glucosidic configuration (7).[2]

We determined the configuration at C-4 of the lactone ring as follows. Hydrogenation of ranunculin over palladium–charcoal resulted in the smooth uptake of one mole of hydrogen and the formation of dihydroranunculin (**6**) which we did not obtain crystalline, but which gave a nicely crystalline tetraacetate. The p.m.r. and infrared spectra of this tetraacetate revealed that, as expected, the conjugated carbon–carbon double bond present in ranunculin had been reduced. Periodate oxidation of the dihydroranunculin resulted in a clean-cut consumption of two moles of periodate, and the initial product (**7**) was then further oxidized with bromine (9). Acid hydrolysis of this oxidation product followed by reoxidation with bromine (9) and removal of acidic products yielded a syrup which showed infrared absorption in the γ-lactone region and was presumably mainly **8**. This syrup was then reduced with lithium aluminium hydride to give

[1]Measured using a solution of ranunculin in D_2O, after repeated hydrogen–deuterium exchange, at 60 Mcycles/s, with tetramethylsilane as external, and tetramethyl ammonium chloride as internal standard.

[2]The anomeric proton signal is frequently more complex (ABX system) (8), but the absence of a signal in the τ 4.6–5.2 region, where the signal for a hydrogen atom at an anomeric center with the (C-1) (11) α-D-configuration is to be expected (7) provides some additional support for our assignment.

FOR ERRATA SEE
Vol. 46, No. 19, 1968 P. 3118

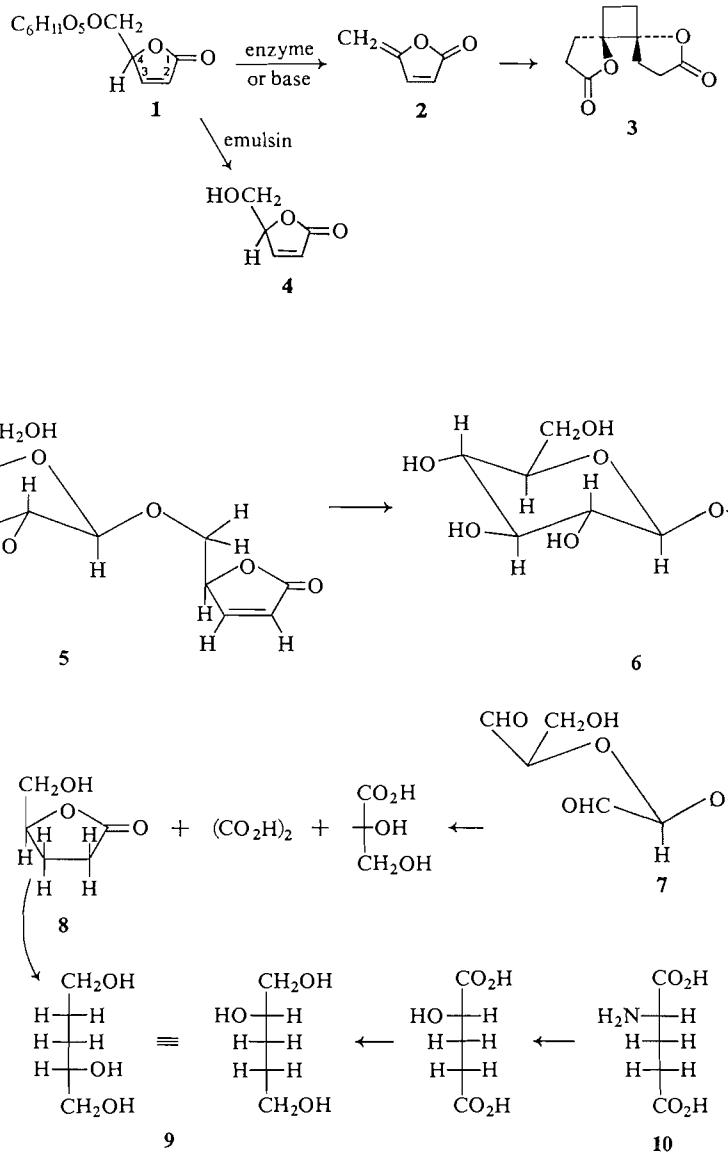

an oily triol with $[\alpha]_D$ −13° and an infrared spectrum virtually identical with that of authentic L-1,2,5-pentanetriol (**9**), $[\alpha]_D$ −15.5°, prepared from L-glutamic acid (**10**). The identity of the two triols was confirmed by comparison of their tri-*p*-nitrobenzoates, which were identical in all respects.

Thus the absolute configuration at C-4 of the lactone moiety of ranunculin is S (or D), the aglucone (**4**) is (S) 5-hydroxy-2-penten-4-olide; and ranunculin itself is as **5**.

Various biogeneses may be suggested for ranunculin; attractive are those which involve modification of a disaccharide, such as 6-*O*-β-D-glucopyranosyl-2-deoxy-D-ribonolactone; alternatively the aglucone may be derived from L-glutamic acid.

Experimental

Ranunculin (4)

Ranunculin was isolated from *Ranunculus acris* L., *R. cardiophyllus* Hook. and *Anemone patens* L. var. *wolfgangiana* (Bess.) Koch by a slight modification of Hill and van Heyningen's procedure.

Freshly collected plants (2 kg) were macerated, in portions, in a Waring blendor with dilute hydrochloric

Can. J. Chem. Downloaded from www.nrcresearchpress.com by 210.87.254.105 on 09/05/12
For personal use only.

Can. J. Chem. Downloaded from www.nrcresearchpress.com by 210.87.254.105 on 09/05/12
For personal use only.

acid (40 ml concentrated acid in a l of water) to which sufficient crushed ice was added to keep the temperature below 30°. The pulp was strained through cheese-cloth and the turbid liquid so obtained was then filtered (suction) through a pad of Celite to give a clear, rosé-colored solution. This solution (ca. 2.5 l) was stirred with "degassed" active charcoal (100 g) for 1 h and then filtered through a thick pad of Celite. The filtrate was colorless. The filter pad was washed with distilled water until the washings were almost neutral (pH ca. 6.5) and the filtrate and washings were rejected. Aqueous ethanol (1:1, v/v) (2 l) was slowly sucked through the pad and the filtrate was evaporated to a small volume (ca. 50 ml) initially in a cyclone evaporator and finally on a rotatory evaporator, maintaining the solution temperature below 40°. The concentrated solution was diluted with methanol (100 ml) and, after having been allowed to stand at room temperature for 10 min, the solution was filtered through a pad of Celite. The filter pad was washed with methanol (50 ml) and the combined, clear, pale-yellow filtrate and washings were evaporated, initially on a rotatory evaporator and finally under an air jet, to a yellow syrup. Crystals slowly separated from the syrup and were collected and washed with ethanol. Further crops of crystals were obtained upon refrigerating the combined mother liquor and washings. Recrystallization of the crystals from methanol gave ranunculin (9–10 g) as colorless crystals, m.p. 140–141° (capillary); $[\alpha]_D^{24}$ $-77(\pm 3°)$ (*c*, 2 in H_2O); $\lambda_{max}(H_2O)$ 208 mμ, ε 10 650; lit. m.p. 141–142° (3), 140–141° (5), 140–143° (4); $[\alpha]_D^{17.5}$ −80.7 (3), $[\alpha]_D^{24}$ −80° (4); λ_{max} 205 mμ, ε 9800 (5), 210 mμ, ε 14 000 (4). The infrared spectrum of the crystals (in KBr disc) was also identical with the spectra given for ranunculin by Hellström (4) and Bredenberg (5).

Dihydroranunculin (6)

A solution of ranunculin (2.76 g, 0.01 mole) in methanol (250 ml) was added to prereduced 5% palladium on charcoal (2 g) in methanol (50 ml) and the mixture was hydrogenated at atmospheric pressure. (CAUTION. The palladium catalyst sometimes caught fire when it was first suspended in methanol prior to prereduction!) Hydrogen uptake ceased after 0.01 mole had been taken up. The suspension was filtered through a pad of Celite and the filter pad washed with methanol (150 ml). The combined filtrate and washings were evaporated under reduced pressure to yield a colorless gum which refused to crystallize.

The *tetraacetate* of the reduction product was prepared by acetylation with pyridine – acetic anhydride, and was obtained as fine colorless needles, from ethanol, (3.0 g) m.p. 134–136°, $[\alpha]_D^{27}$ $+6.1 \pm 0.6°$ (*c*, 6 in $CHCl_3$).

Anal. Calcd. for $C_{19}H_{26}O_{12}$: C, 51.12; H, 5.87. Found: C, 51.01; H, 5.88.

Degradation of Ranunculin

Ranunculin (4.4 g, 14.9 mmoles) was converted to dihydroranunculin, as described above. The total product from the hydrogenation was taken up in water (ca. 50 ml) and transferred to a 250 ml graduated flask. A solution of sodium metaperiodate (40 g in 350 ml) (80.0 g) was added and the reaction mixture made up to the mark and stored in the dark, at room temperature. Aliquots (1 ml) of the reaction mixture were withdrawn periodically, quenched in 0.02 *N* sodium arsenite solution to which 10% aqueous potassium iodide (1 ml) had been added, and the excess of arsenite titrated with standard iodine solution. The results were compared to those obtained with a "blank" reaction mixture, prepared by diluting the metaperiodate solution (80.0 g) to 250 ml with water alone. The uptake of periodate was essentially complete (30.1 mmoles) in 1 h. After 24 h the uptake of periodate was practically unchanged (30.5 mmole) and the iodate and excess periodate were then precipitated by the addition of a solution of barium chloride dihydrate (11.0 g) in water (100 ml). The precipitated salts were filtered off and washed with water (100 ml). Barium carbonate (60 g) and bromine (5 ml) were added to the combined filtrate and washings and the reaction mixture was stored at room temperature, in the dark, overnight. Excess bromine was removed by aeration and the reaction mixture was filtered and the filter cake washed well with warm water (ca. 100 ml). The combined filtrate and washings were concentrated under reduced pressure to about half-volume and 6 *N* aqueous sulfuric acid was added until there was no further precipitation of barium sulfate (ca. 20 ml required). The barium sulfate was centrifuged down and washed by resuspension in warm water and re-centrifugation. The combined supernatants were heated on a steam bath overnight (internal temperature 80°) and then adjusted to pH 4–5 with a hot 10% aqueous solution of barium hydroxide. The reaction mixture was filtered and the filter cake washed with water (100 ml). Barium carbonate (30 g) and bromine (5 ml) were added to the combined filtrate and washings (total volume ca. 750 ml) and the reaction mixture again kept at room temperature in the dark, overnight, then aerated to remove excess bromine and filtered. As before, the filter cake was washed with water (250 ml). Silver carbonate (300 g) was added to the combined filtrate and washings and the suspension was stirred at room temperature, with exclusion of light, until a halide test on the solution was negative. The reaction mixture was once again filtered and the filter cake washed with water (250 ml) and the combined filtrate and washings were evaporated under reduced pressure to a small volume (ca. 100 ml). This solution was then passed through a column (2.5 cm × 30 cm) of Dowex-50 ion-exchange resin (H-form) and the column washed with water until the eluates were neutral. Evaporation of the eluates under reduced pressure (bath $\gtrsim$40°) yielded a pale-yellow oil, smelling of nitric acid. Barium carbonate (ca. 5 g) and ethanol (20 ml) were added to this oil (some effervescence); the suspension was filtered and the filter cake washed with ethanol. Evaporation of the filtrate and washings left a residual yellow oil (1.62 g).

The oil was taken up in dry dioxane (20 ml) and added, dropwise over 1 h to a stirred and boiling suspension of lithium aluminium hydride (1.5 g) in dry dioxane (35 ml). The reaction mixture was cooled in ice and ethyl acetate (5 ml) added, followed by saturated aqueous sodium sulfate solution (5 ml). The reaction mixture was stirred and refluxed for 15 min, then cooled and anhydrous magnesium sulfate (9 g) was added. After stirring for a further 10 min, the mixture was filtered and the filter cake washed well with warm dioxane (50 ml). Evaporation of the combined filtrate and washings gave a very pale-yellow oil (410 mg). Further extraction of the filter cake with dioxane and ethanol gave an additional

amount of oil (809 mg). The combined oils were distilled under reduced pressure to give a pale-yellow oil, b.p. 150–160° at 3–5 mm (438 mg), $[\alpha]_D^{25}$ −13.3 ± 0.5° (*c*, 4 in ethanol) with an infrared spectrum (liquid film) that was virtually identical to that of authentic L-1,2,5-pentanetriol.

A *p*-nitrobenzoate was prepared by heating the oil (115 mg) and *p*-nitrobenzoyl chloride (600 mg) in pyridine (5 ml), on the steam bath for 20 min, and was obtained as very pale-yellow needles, from solution in acetone–ethanol, m.p. 135–136° (264 mg), $[\alpha]_D^{24}$ +7.7 ± 0.3° (*c*, 6 in dichloromethane); lit. m.p. for L-1,2,5-pentanetriol tri-*p*-nitrobenzoate, 130–132°, $[\alpha]_D^{24}$ +8.6 (*c*, 5 in dichloromethane) (10*b*). A mixture m.p. with authentic L-1,2,5-pentanetriol tri-*p*-nitrobenzoate (see below) was undepressed and the infrared spectra of the two materials were superimposable upon one another.

L-1,2,5-Pentanetriol

L-Glutamic acid (50 g) was converted to dimethyl L-α-hydroxyglutarate as described by Hartman and Barker (10*b*). The ester was obtained (36.6 g) as a colorless oil b.p. 97–98° at 0.2 mm, n_D^{23} 1.4463, $[\alpha]_D^{24}$ −1.3° (*c*, 9 in ethanol), the optical rotatory dispersion curve shows a peak $[\Phi]_{215}^{24}$ ~1525; lit. b.p. 85–92° at 0.1 mm (10*b*), 82–90° at 0.13 mm (10*a*).

The ester (10.4 g) was dissolved in dry dioxane (100 ml) and the solution was added to a stirred and refluxing suspension of lithium aluminium hydride (9 g) in dioxane (150 ml), over 30 min. The reaction mixture was stirred and refluxed for 30 min, then cooled in ice and ethyl acetate (20 ml) added, followed by saturated aqueous sodium sulfate solution (25 ml). The mixture was stirred and boiled for 30 min, during which time the color of the suspended solids changed from grey to white. The reaction mixture was allowed to cool somewhat and anhydrous magnesium sulfate (45 g) was then added. After stirring the mixture for a further 5 min, it was filtered, hot. The filter cake was washed with hot dioxane (200 ml) and the combined filtrate and washings were evaporated to yield a residual pale-yellow oil (5.7 g). Distillation of the oil gave pure L-1,2,5-pentanetriol, b.p. 135–136° at 1–2 mm, n_D^{23} 1.4752, $[\alpha]_D^{25}$ −15.5 ± 0.3° (*c*, 5 in ethanol); lit., $[\alpha]_D^{24}$ −19.6° (10*b*), $[\alpha]_D^{29}$ −11.6° (in ethanol) (10*a*).

The tri-*p*-nitrobenzoate was prepared, as described above, m.p. 133–134°, $[\alpha]_D^{24}$ +7.5 ± 0.4° (*c*, 4 in dichloromethane).

Acknowledgment

This work was supported by Grant A4547 of the National Research Council of Canada.

1. Y. ASAHINA and A. FUJITA. Acta Phytochim. Japan, **1**, 1 (1922); Chem. Zent. **3**, 712 (1922). F. B. KIPPING. J. Chem. Soc. 1145 (1935).
2. R. M. MORIARTY, C. R. ROMAIN, I. L. KARLE, and J. KARLE. J. Am. Chem. Soc. **87**, 3251 (1965), and references therein.
3. R. HILL and R. VAN HEYNINGEN. Biochem. J. **49**, 332 (1951).
4. N. HELLSTRÖM. Kgl. Lantbruks-Högskol. Ann. **25**, 171 (1959).
5. B. B. BREDENBERG. Suomen Kemistilehti, **B34**, 80 (1961).
6. H. W. L. RUIJGROK. *In* Comparative phytochemistry. *Edited by* T. Swain. Academic Press, Inc., New York. 1966. p. 175.
7. J. M. VAN DER VEEN. J. Org. Chem. **28**, 564 (1963).
8. L. D. HALL. Advan. Carbohydrate Chem. **19**, 51 (1964).
9. L. C. STEWART and N. K. RICHTMEYER. J. Am. Chem. Soc. 77, 1021 (1955); J. W. PRATT and N. K. RICHTMEYER. J. Am. Chem. Soc. 77, 1906 (1955).
10. (*a*) H. KATSURA. Nippon Kagaku Zasshi, 77, 1789 (1956); Chem. Abstr. **53**, 5126 (1959). (*b*) F. C. HARTMAN and R. BARKER. J. Org. Chem. **29**, 873 (1964).
11. R. E. REEVES. Advan. Carbohydrate Chem. **6**, 107 (1951).

Can. J. Chem. Downloaded from www.nrcresearchpress.com by 210.87.254.105 on 09/05/12
For personal use only.

Can. J. Chem. Downloaded from www.nrcresearchpress.com by 210.87.254.105 on 09/05/12
For personal use only.

Steroids and related products. XXV.[1] Cardiotonic steroids. II.[2] The synthesis of 17β-substituted 14(15)-unsaturated steroids of the A/B-cis series. Part I[3]

G. BACH, J. CAPITAINE, and CH. R. ENGEL
Department of Chemistry, Laval University, Quebec, Quebec

Received August 3, 1967

The synthesis, from smilagenin, progesterone, and pregnenolone, of Δ^{14}-3β-hydroxy-5β-etienic acid and some of its ester derivatives, as well as of β-anhydrodigitoxigenin acetate, is described. Since these 14-unsaturated products have served as starting materials for our previously published syntheses of 3β,14β-dihydroxy-5β-etianic acid and of digitoxigenin, the present work establishes that these 17β-substituted 14β-hydroxylated products are available from readily accessible materials and that the syntheses of these 14β-hydroxylated products must be regarded, from a formal point of view, as total syntheses. We have thus elaborated a general pathway from common steroids—also available by total synthesis—to 14β-hydroxylated derivatives, in particular to steroid cardiotonics.

Canadian Journal of Chemistry, **46**, 733 (1968)

It is well known that one of the major problems of the synthesis of cardiotonic steroids is that of the preparation of 14β-hydroxylated products with a 17β-side chain—an arrangement which is thermodynamically not favored. Whereas another important problem of cardiotonic synthesis, the elaboration of a butenolide ring system attached to position 17 had been solved in various ways and for some time,[4] and whereas Sondheimer and his collaborators (4) had more recently succeeded in solving the delicate problem of elaborating the butenolide structure of cardenolides in the presence of a labile 14β-hydroxyl group, without epimerization in position 17, no general and truly useful method for the introduction of the 14β-hydroxy function into 17β-substituted steroids was known until the development of such a procedure in our laboratory (2).[5] It is well known that the previously described method (7) is lengthy, that its yields are unsatisfactory, and that it cannot be applied to the introduction of a 14β-hydroxy function into a steroid already bearing a 17β-butenolide or α-pyrone substituent.

In our general method for the introduction of the 14β-hydroxy group into 17β-substituted steroids, 14,15-unsaturated products serve as starting materials. In our previous paper on cardiotonic steroids (2), we described, as examples of our procedure, the synthesis of digitoxigenin (**2**) from β-anhydrodigitoxigenin acetate (**1***a*), and of methyl 3β-acetoxy-14β-hydroxy-5β-etianate (**4***c*) —which can be converted by Sondheimer's method (4) to digitoxigenin (**2**)—from methyl $\Delta^{14(15)}$-3β-acetoxy-5β-etianate (**3***c*). The 14-unsaturated products which we had used as the

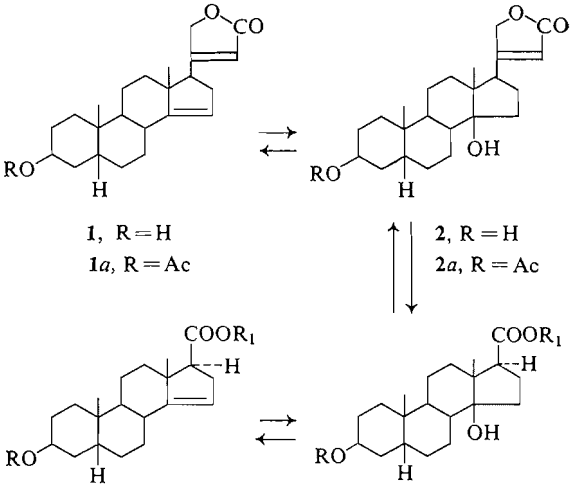

1, R = H
1*a*, R = Ac
2, R = H
2*a*, R = Ac

3, R = R₁ = H
3*a*, R = Ac, R₁ = H
3*b*, R = H, R₁ = CH_3
3*c*, R = Ac, R₁ = CH_3

4, R = R₁ = H
4*a*, R = Ac, R₁ = H
4*b*, R = H, R₁ = CH_3
4*c*, R = Ac, R₁ = CH_3

[1]For the previous paper of this series see ref. 1.
[2]For the communication: "Cardiotonic Steroids. I", see ref. 2.
[3]The results reported in this paper are part of the D.Sc. thesis of G. Bach, accepted by the School of Graduate Studies of Laval University, in September 1965; they were presented at the 49th Annual Conference of the Chemical Institute of Canada, in Saskatoon, June 1966.
[4]For general literature references concerning syntheses in the field of cardiotonics we refer to the quotations contained in ref. 2 of this paper. Very recently, Ferland *et al.* (3) have reported a new and interesting approach to the construction of the butenolide ring of cardenolides.
[5]The first report on this procedure and on our synthesis of digitoxigenin was given at the 46th Annual Conference of the Chemical Institute of Canada, June 1963 (compare ref. 5). The synthesis of periplogenin by Deghenghi *et al.* (6), also started from a 14-unsaturated steroid with a 17β-side chain.

Can. J. Chem. Downloaded from www.nrcresearchpress.com by 210.87.254.105 on 09/05/12
For personal use only.

starting materials had been prepared previously from natural cardiotonics (8, 9) and we indicated in our publication (2), in a summary fashion, possible pathways to these products from abundant steroids. In the present paper, we wish to report in detail their synthesis from such readily available steroids as pregnenolone (**9**), progesterone (**10**), and smilagenin (**5**), products which themselves are available also by total synthesis.

Although a number of routes to the desired 14-unsaturated steroids can be envisaged, we limit ourselves in this paper to the description of syntheses using for the introduction of the unsaturation in positions-14,15 the general method elaborated by Heusser and his collaborators (10) in which a 14,16-dien-20-one of type *i* is converted by dissolving metal reduction to a 14-unsaturated 20-alcohol, or a mixture of epimeric 14-unsaturated 20-alcohols of type *ii*, which is then reoxidized to a 14-unsaturated 20-ketone of type *iii*.

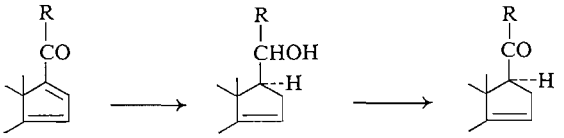

i *ii* *iii*

We chose for our first synthesis of β-anhydrodigitogenin (**1**) a pathway in which the other 14-unsaturated steroids which we wished to synthesize—Δ^{14}-3β-acetoxy-5β-etianic acid (**3***a*) and its methyl ester **3***c*—could be used as intermediates. At a later date we shall describe a more direct route.

Since $\Delta^{14,16}$-diunsaturated 20-ketones of type *i* are conveniently prepared from the corresponding 16-mono-unsaturated 20-ketones (see below), Δ^{16}-3β-acetoxy-5β-pregnen-20-one (**6***a*) seemed a logical intermediate in the proposed synthesis. In one series of experiments we prepared this product in 61% yield from smilagenin (**5**) by the use of Marker's sapogenin degradation procedure (11), as modified by Dr. M. E. Wall.[6] In this procedure, as in one published earlier by Hewett (12), methylamine hydrochloride is used as catalyst for the preparation of the pseudosapogenin.[7] In another series of experiments, we prepared the 16-unsaturated 20-ketone **6***a* in 81% yield from 3β-acetoxy-5β-pregnan-20-one (**7***a*) by bromination with *N*-bromosuccinimide (14, *cf.* also 15, 16) and dehydrobromination of the resulting 17α-bromide **8**[8] with lithium chloride in dimethylformamide (17, cf. also 16).

The 3β-acetoxy-5β-pregnan-20-one (**7***a*) used in this reaction was synthesized from Δ^5-pregnenolone (**9**) and progesterone (**10**). We transformed the 20-ethylene ketal **9***b* of pregnenolone (18) by Oppenauer oxidation with tertiary aluminium butylate and cyclohexanone to the 20-ethylene ketal **10***a* of progesterone (18). Reduction with palladium on calcium carbonate gave in 93% yield the 20-ethylene ketal **12***a* of 5β-pregnane-3,20-dione, which can be readily converted to the free 3,20-dione **12**. The reduction with the same reagents of free progesterone (**10**) was less stereoselective: the 5β-pregnane-3,20-dione (**12**) could be isolated only in 65% yield and 16% of the pure 5α-isomer **11** was obtained.

Since in our hands—in contrast to an earlier report by Butenandt and Müller (19)—the catalytic reduction of 3-ketones of the 5β-series led, even in acid media, predominantly to the equatorial 3α-alcohols (20), we investigated in one series the deliberate formation of the 3α-alcohol and its "inversion", *via* its tosylate, to the 3β-alcohol.

Lithium aluminium hydride reduction of the keto acetal **12***a* gave indeed in 74% yield the 3α-hydroxy 20-ketal **14** and in less than 10% yield the 3β-epimer **13**. Also, the formation of the tosylate **14***a* was almost quantitative but treatment of this product with dimethyl formamide (21), followed by saponification of the intermediate formate with methanolic potassium hydroxide, gave the desired 3β-hydroxy-5β-pregnan-20-one (**7**) in only 18% yield; the 3α-hydroxy derivative **15** was isolated in 13% yield. The deketalization had occurred during the formylation reaction.

The application of Djerassi's method (22) for

[6]We express our sincerest thanks to Dr. M. E. Wall for very kindly communicating the details of the procedure to us, and also for providing us with smilagenin.

[7]Recently, Pettit and Piatak (13) reported the degradation of smilagenin, using one of Dr. Wall's earlier methods (11*f*), but without recording the yields.

[8]It is known that a free-radical bromination of a 20-ketone affords the same stereoisomer as an acid-catalyzed bromination (cf. ref. 16, p. 706, and the references quoted in that publication).

Can. J. Chem. Downloaded from www.nrcresearchpress.com by 210.87.254.105 on 09/05/12
For personal use only.

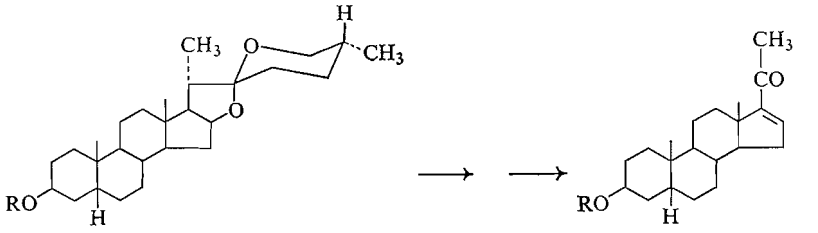

5, R = H
5*a*, R = Ac

6, R = H
6*a*, R = Ac

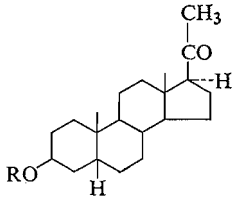

7, R = H
7*a*, R = Ac

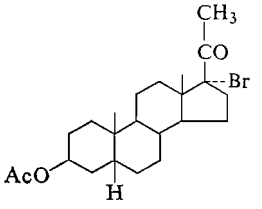

8

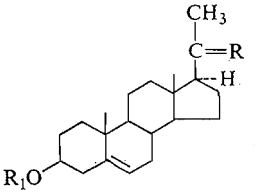

9, R = O, R_1 = H
9*a*, R = O, R_1 = Ac
9*b*, R = ethylenedioxy, R_1 = H
9*c*, R = ethylenedioxy, R_1 = Ac

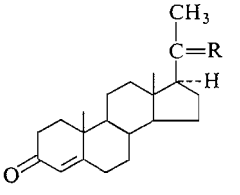

10, R = O
10*a*, R = ethylenedioxy

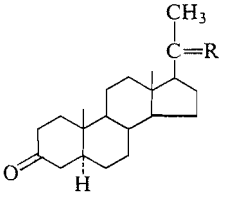

11, R = O
11*a*, R = ethylenedioxy

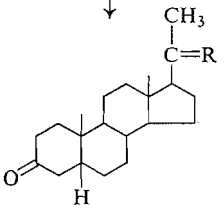

12, R = O
12*a*, R = ethylenedioxy

the preferential reduction of steroid ketones to axial alcohols with aged Raney nickel (cf. also 23) to the reduction of the 20-ketal **12***a* represented an improvement, but in that case the equatorial alcohol (**14**) still predominated: it was obtained in 62% yield while the 3β-alcohol **13** could be isolated only in 32% yield.

The most satisfactory results were obtained by the use of a method developed in our laboratory (24), by which the axial 3β-alcohols of the 5β-pregnane series are obtained as the major reaction products from the corresponding 3-keto derivatives by a Meerwein–Pondorf reduction, the salient feature of the procedure being the limitation of the reaction time to very short periods. The reaction of the ethylenedioxy ketone **12***a* with *sec*-butanol and aluminium *t*-butoxide for 20 min gave, after deketalization with acetone and *p*-toluenesulfonic acid (25), the desired 3β-hydroxy-5β-pregnan-20-one (**7**) in 52% yield and its epimer **15** in 40% yield. A single recyclization of the still ketalized 3α-hydroxy derivative (**14**) by oxidation with Jones' reagent (26) and another Meerwein–Pondorf reduction raises the yield of the 3β-epimer to 75%.[9]

[9]This experiment was carried out in collaboration with Mr. R. Bouchard of this laboratory.

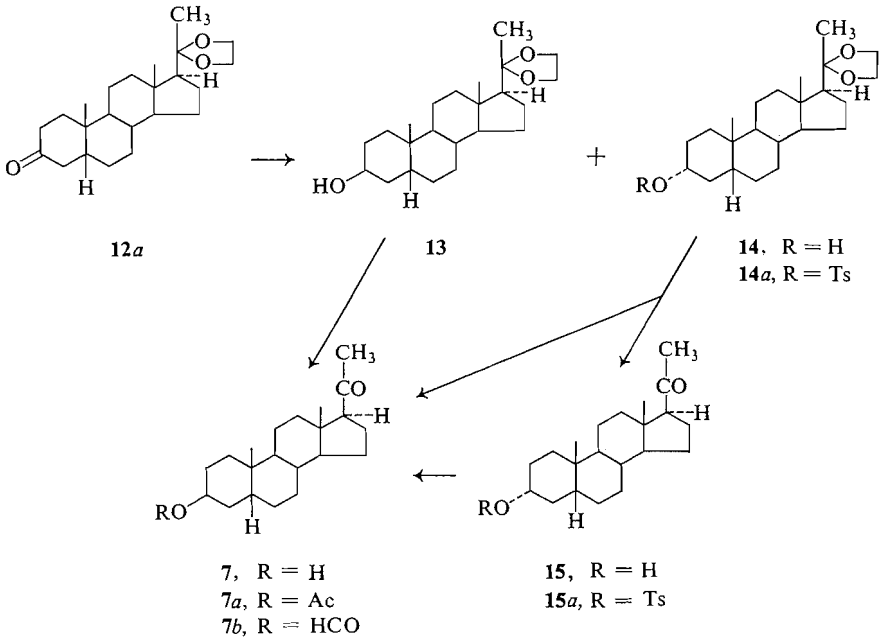

For the reduction of 5β-pregnane-3,20-dione (**12**), unprotected in position-20, this method can, of course, not be used. In this case the best method remained reduction with Raney nickel which gave a 39% yield of the desired 3β-hydroxy derivative **7** and a 32% yield of its epimer **15**.[10]

We have thus prepared, as well from smilagenin (**5**) as from pregnenolone (**9**) and progesterone (**10**), the 16-unsaturated ketone ***6a*** which had now to be transformed into a 14,16-dien-20-one and hence to a 14-mono-unsaturated 20-oxygenated derivative. For the introduction of the unsaturation in position-14, we followed essentially the general pathway elaborated by Ruzicka, Plattner, Heusser, and their co-workers (27–30), which consists in allylic bromination with *N*-bromosuccinimide and dehydrobromination of the mixture of allylic bromides (compare **16**) (cf. also 31) which contains, as already pointed out by the Swiss authors, some dienone (compare ***17a***). The dehydrobromination was performed in our case with dimethyl formamide and lithium chloride (17). As already observed by the Swiss workers (cf. 29, 30, and also 32), the isolation of pure pregnadienones of type ***17a*** presents considerable difficulties because of the contamination of the products with starting material and secondary reaction products (cf. 31). Very recently, Pettit and Piatak (13) prepared the dienone ***17a*** from the mono-unsaturated ketone, following also essentially the method of the Swiss workers but using sodium iodide in acetone for the dehydrobromination reaction; they were able to isolate the pure product only in minute yields (approximately 5%), after complicated, lengthy, and from a preparative point of view, not satisfactory purification procedures. We found that the dienone could be isolated advantageously in the form of the free hydroxydienone **17**, which we used, as will be shown, in any event for the following reactions and which was obtained by treatment of the crude reaction product with methanolic perchloric acid (33).[11] However, we found it more useful not to purify the hydroxy dienone at all and to subject the crude product to the following reduction.

We obtained the best results in the preferential reduction of the 16-double bond of the 14,16-

[10]It may be noted that the inversion of the 3α-hydroxy 20-ketone **15** to the 3β-hydroxy ketone **7** *via* the tosylate ***15a*** and the formate ***7b*** proceeded in a somewhat better yield (29%) than the analogous series of reactions applied to the ethylenedioxy derivative **14**; this sequence of reactions is, however, still less attractive than the Raney nickel reduction.

[11]Although this compound was, according to spectral analysis, free from the mono-unsaturated starting material, the results of its microanalysis did not reach our usual standards.

Can. J. Chem. Downloaded from www.nrcresearchpress.com by 210.87.254.105 on 09/05/12
For personal use only.

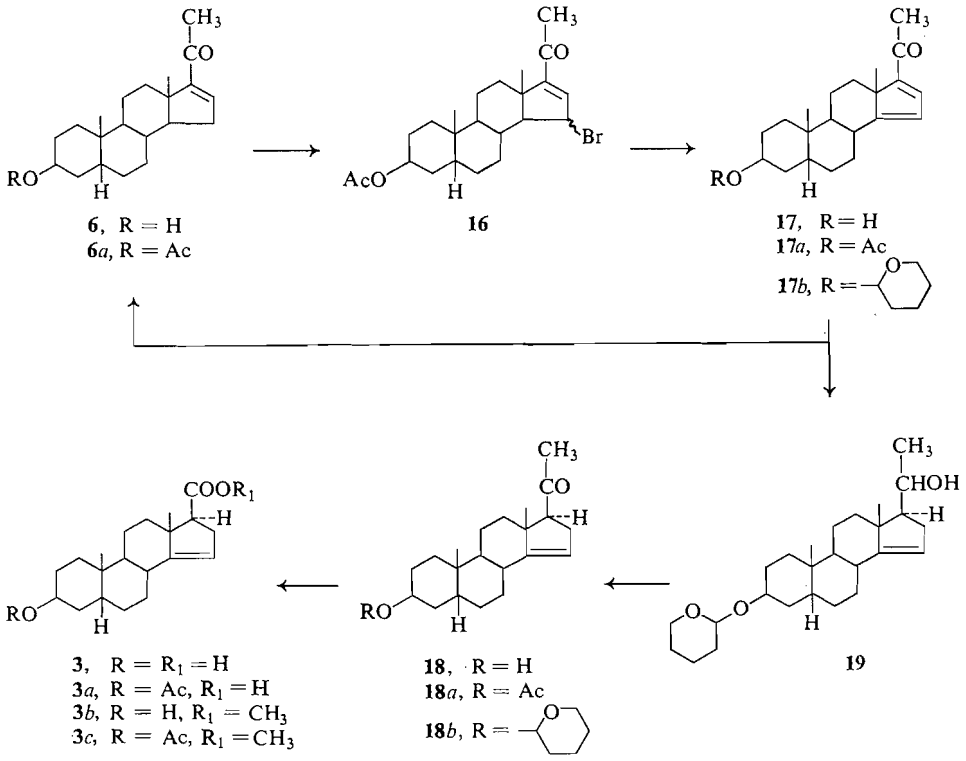

dien-20-one system with sodium and *n*-propanol, as recommended by Heusser *et al.* (10). Since the reaction results also in the reduction of the 20-keto group and would be accompanied by hydrolysis of an ester group in position-3, the 3-hydroxy group of the free dienone **17** was protected prior to reduction by the formation (in 97% yield) of the tetrahydropyranyl ether **17***b* (cf. 34–38, in particular 36), so that the reduction product (**19**) could be re-oxidized with Jones' reagent (26) to the keto ether **18***b*, which gave with *p*-toluenesulfonic acid in ethanol (34) Δ^{14}-3β-hydroxy-5β-pregnen-20-one (**18**). The yield from the hydroxydienone **17** amounted to 31% and the yield from the 16-unsaturated ketone **6** to 8%. As intimated, a considerable improvement in yields was achieved when none of the intermediates between the Δ^{16}-3β-hydroxy-5β-pregnen-20-one (**6**) and the Δ^{14}-3β-hydroxy-5β-pregnen-20-one (**18**) was purified; thus, the total yield of compound **18** from ketone **6** was raised from 8 to 33%.

We also investigated the Birch reduction of the hydroxydienone **17** with lithium in liquid ammonia, in the absence of an alcohol, but in the presence of ammonium chloride as a proton source. Using such a system, described by Stork and co-workers (39), Schaub and Weiss (40) had reduced 6-dehydrotestosterone to the 5-mono-unsaturated 3-ketone, whereas the Birch reduction of this product under classical conditions (lithium in liquid ammonia in the presence of ether and ethanol) gives the α,β-unsaturated Δ^4-3-ketone (41). We considered that in our case the reduction under Schaub's conditions could possibly lead also to the γ,δ-unsaturated Δ^{14}-20-ketone **18**. This was indeed the case[12] but the product could be obtained only in 26% yield and was accompanied by unreacted starting material (**17**) and by a further product which was not completely purified but to which we may assign, according to its spectral characteristics, the structure of the α,β-unsaturated Δ^{16}-20-ketone **6**.[13]

[12]Ether was used as solvent, as described by Barton (42).

[13]The structure of the mono-unsaturated ketone **18** thus prepared was not only confirmed by its comparison with the product obtained by reduction with sodium and *n*-propanol but also by its transformation into authentic methyl Δ^{14}-3β-hydroxy-5β-etianate (**3***b*) obtained from digitoxigenin (**2**) (see below).

Can. J. Chem. Downloaded from www.nrcresearchpress.com by 210.87.254.105 on 09/05/12
For personal use only.

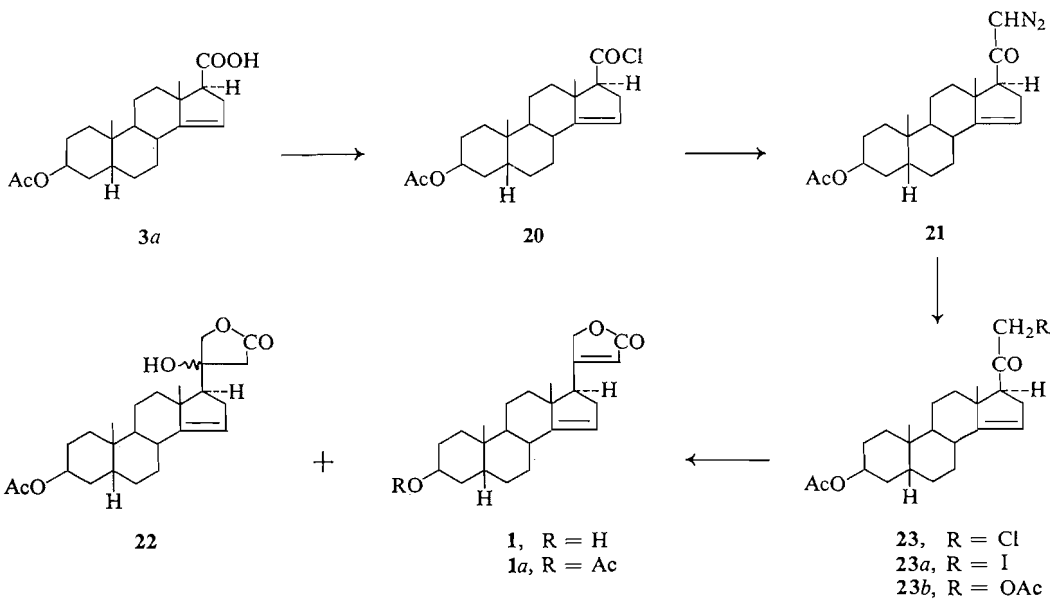

The transformation of the 14-unsaturated 20-ketone **18** to Δ^{14}-3β-hydroxy-5β-etienic acid (**3**), and its ester derivatives and thence to β-anhydrodigitoxigenin (**1**), followed classical lines. A haloform degradation of the 3-acetylated 20-ketone **18***a*, according to the procedure of Djerassi and Staunton (43), gave in approximately 85% yield the desired 14-unsaturated 3β-hydroxy acid **3** which was readily acetylated to the acetoxy acid **3***a* (cf. 43), and methylated with diazomethane to the methyl ester **3***b*, which in turn gave under the usual conditions the acetoxy ester **3***c*. The structure of ester **3***c* was not only confirmed by microanalysis, the determination of the usual physical constants, and by ultraviolet and infrared spectroscopy, but also by comparison with an authentic sample prepared from natural digitoxigenin (**2**)[14]. For that purpose, digitoxigenin acetate (**2***a*) was transformed in 85% yield, according to Reichstein's method (44), by ozonolysis and hydrolysis of the resulting glyoxylic ester, into the 21-hydroxy 20-ketone and thence by periodic acid degradation, followed by methylation, to the 14β-hydroxyetianate **4***c* which was dehydrated in 85% yield with thionyl chloride, using Darzens' method (45, compare also 8*d*), to methyl Δ^{14}-3β-acetoxy-5β-etienate (**3***c*) (9). This product proved in every respect identical with the one prepared from smilagenin (**5**), progesterone (**10**), and pregnenolone (**9**), as described above.

The conversion of the 14-unsaturated etioester **3***c* to the 3β,14β-dihydroxyetianic acid **4** and its ester derivatives **4***a–c* was previously described by us (2). The conversion of methyl ester **4***c* to digitoxigenin was reported, as already mentioned, by Sondheimer and his collaborators (4).

For the transformation of the 14-unsaturated acid **3** into β-anhydrodigitoxigenin (**1**) we prepared, according to Reichstein's modification (46) of the method of Adams–Wilds (47), from the acetoxy acid **3***a* the acid chloride **20** which we converted with diazomethane to the diazoketone **21**. In one series of experiments the crude diazoketone was directly transformed into the 21-acetoxy derivative **23***b* with acetic acid (cf. 47*b*, 48, 49), in another, *via* the chloride **23** and the iodide **23***a*, prepared according to the experimental conditions usually employed in this laboratory (50), the replacement of the iodine substituent by an acetoxy group being carried out with potassium bicarbonate and glacial acetic acid (51). The yields of both pathways amounted to 68%, calculated from acid **3***a*. Finally, the diacetoxy ketone **23***b* was subjected to the classical Reformatsky reaction (cf. 52, 53); this led in 26% yield to the desired β-anhydrodigitoxigenin acetate (**1***a*) (8), accompanied by a secondary reaction product which was not fur-

[14]We sincerely thank Dr. J. Renz from Sandoz S.A., Basle, for kindly providing us with this valuable material.

Can. J. Chem. Downloaded from www.nrcresearchpress.com by 210.87.254.105 on 09/05/12
For personal use only.

Can. J. Chem. Downloaded from www.nrcresearchpress.com by 210.87.254.105 on 09/05/12
For personal use only.

ther investigated but which probably represents the 20-hydroxycardenolide **22**. The structure of β-anhydrodigitoxigenin acetate (**1***a*) was established by the determination of the usual physical constants, microanalysis, ultraviolet and infrared spectroscopy, and by comparison with an authentic sample prepared by dehydration with thionyl chloride in pyridine (45, 8*d*) of digitoxigenin acetate (**2***a*) from natural sources.

This synthesis of the 14-unsaturated 5β-etienic acid **3** and of the 14-unsaturated cardadienolide **1***a* from smilagenin (**5**), progesterone (**10**), and pregnenolone (**9**), establishes the accessibility from readily available materials of 3β,14β-dihydroxyetianic acid and digitoxigenin—previously synthesized in our laboratory from the 14-unsaturated precursors (2). Furthermore, our previously described syntheses of the 14β-hydroxylated products can now be considered to represent—from a formal point of view—total syntheses.

Experimental[15–17]

3β-Hydroxy-20-ethylenedioxy-5-pregnene (9b)

(a) From Pregnenolone Acetate (9a)

Following the procedure of Allen *et al.* (54), 5.003 g of 3β-acetoxy-5-pregnen-20-one (**9***a*) was heated for 8 h at reduced pressure (2–3 mm Hg) with 202 mg of *p*-toluenesulfonic acid in 210 ml of ethylene glycol until 85 ml of the solvent was removed by distillation. The usual working-up gave 5.589 g (99.5% yield) of crystalline *3β-acetoxy-20-ethylenedioxy-5-pregnene* (**9***c*), m.p. 153–156°. One recrystallization from methanol gave 4.85 g (86.3%) of pure ketal **9***c*. The identity of this product with an authentic sample, previously prepared in this laboratory (16), was established by the determination of a mixture melting point and the comparison of the infrared spectra.

The solution of the product in 853 ml of methanol was refluxed for 4 h with a solution of 20.5 g of potassium carbonate in 153 ml of water. After cooling, the product was poured into 800 ml of cold water and the mixture was extracted with ether. The organic solution was washed with water and dried over sodium sulfate. Removal of the solvent gave 4.431 g of an amorphous residue which gave, upon crystallization from methanol, 4.337 g (99.8% yield) of *3β-hydroxy-20-ethylenedioxy-5-pregnene* (**9***b*), m.p. 165–167° [lit. (18), m.p. 163–166°]. The identity with an authentic sample previously prepared in this laboratory was established by the determination of a mixture melting point and the comparison of the infrared spectra.

(b) From Pregnenolone (9)

A quantity of 999 mg of 3β-hydroxy-5-pregnen-20-one (**9**) was added to 45 ml of freshly distilled ethylene glycol, containing 40 mg of *p*-toluenesulfonic acid. From this mixture ethylene glycol was removed by slow distillation in the course of 8 h under a vacuum of 0.5–1 mm Hg, the temperature of the oil bath being maintained at approximately 80°. Agitation was provided with a magnetic stirrer. After cooling, the reaction mixture was poured into 700 ml of a saturated potassium bicarbonate solution at 0°. The crystalline precipitate was filtered and the filtrate was washed with water until neutral and dried. Thus there was obtained 1.16 g (quantitative yield) of 3β-hydroxy-20-ethylenedioxy-5-pregnene (**9***b*), m.p. 160–163°. The product was purified by chromatography on aluminium oxide to give 918 mg (80%) of pure ketal **9***b*, eluted with a benzene–ether mixture (9:1), m.p. 163–166°, and 52 mg (4.5%) of a product of lesser purity, eluted with a benzene–ether mixture (4:1), m.p. 158–161°. The material was found in every respect identical to the one described under *(a)*.

20-Ethylenedioxy-4-pregnen-3-one (10a)

A mixture of 46.845 g of 3β-hydroxy-20-ethylenedioxy-5-pregnene (**9***b*), m.p. 158–163°, 47.164 g of aluminium *t*-butylate and 115 ml of absolute cyclohexanone in 910 ml of absolute benzene was refluxed for 18 h with exclusion of moisture. After cooling, the product was extracted with ether and the organic phase was washed with a cold dilute sulfuric acid solution, with an iced potassium bicarbonate solution, and with water and was dried over sodium sulfate. Removal of the solvent left 123.466 g of an amorphous residue which was chromatographed on 1.82 kg of aluminium oxide. Elutions with petroleum ether – benzene mixtures (9:1, 4:1, and 1:1), with pure benzene and with a (9:1) benzene–ether mixture gave 37.271 g (80% yield) of *20-ethylenedioxy-4-pregnen-3-one* (**10***a*), m.p. 170–192°. Recrystallization from methanol gave 28.141 g (60.3% yield) of the pure progesterone ketal **10***a*, m.p. 187–192.5° [lit. (18), m.p. 189–190°]. A sample was recrystallized twice from methanol and once from ether–hexane for analysis; m.p. 194.5–195°; $[\alpha]_D^{22}$ +112.6° (*c*, 1.000 in $CHCl_3$).

Anal. Calcd. for $C_{23}H_{34}O_3$: C, 77.05; H, 9.56. Found: C, 77.14; H, 9.52.

20-Ethylenedioxy-5β-pregnan-3-one (12a)

A quantity of 26.32 g of 20-ethylenedioxy-4-pregnen-3-one (**10***a*), m.p. 187–194°, was dissolved in 1.644 l of dioxane and 1.25 l of ethanol and hydrogenated at atmospheric pressure with 2.362 g of a 4% palladium on calcium carbonate catalyst in the presence of 4.73 g of potassium hydroxide in 5 ml of water. Within 40 min, 1.8 l of hydrogen was taken up (theoretical quantity: 1.79 l). The catalyst was removed by filtration and washed with methylene chloride. The filtrate and the washings were combined and reduced *in vacuo* and the product was precipitated in ice water. The organic material was extracted with ether, the ethereal solution was washed with water and dried over sodium sulfate. The evaporation of the solvent left 26.43 g of a crystalline product, m.p. 162–165°. Recrystallization from methylene chloride – hexane

[15]The melting points were taken in evacuated capillaries and the temperatures were corrected.

[16]If not otherwise stated, Woelm's non-alkaline aluminium oxide, activity III, and Davison's silica gel No. 923 were used for chromatography.

[17]The microanalyses were performed by Dr. C. Daesslé, Montreal, and Mr. A. Bernhardt, Max Planck Institute for Coal Research, in Mülheim, Germany. We express to them and their associates our sincere appreciation.

Can. J. Chem. Downloaded from www.nrcresearchpress.com by 210.87.254.105 on 09/05/12
For personal use only.

gave 25.26 g (95.4% yield) of *20-ethylenedioxy-5β-pregnan-3-one* (**12***a*), m.p. 168–173°, and 996 mg of the same substance of lesser purity, melting between 154 and 158° (total yield 99.1%). A sample was recrystallized twice from methylene chloride – hexane for analysis; m.p. 172.5–173°; $[\alpha]_D^{27}$ +37.1° (*c* 1.124 in $CHCl_3$) [lit. (55), m.p. 169.8–172.8°; $[\alpha]_D$+32.0°]; ν_{max} (KBr) 1722 cm^{-1} (3-ketone), 1069 and 1052 cm^{-1} (ketal doublet).

Anal. Calcd. for $C_{23}H_{36}O_3$: C, 76.62; H, 10.07. Found: C, 76.81; H, 10.12.

5β-Pregnane-3,20-dione (12)

A quantity of 1 g of progesterone (**10**), m.p. 127.5–128°, was dissolved in 110 ml of dioxane and 100 ml of ethanol and hydrogenated at atmospheric pressure with 100 mg of a 4% palladium on calcium carbonate catalyst, in the presence of 150 mg of potassium hydroxide in 0.4 ml of water. After 25 min, 76 ml of hydrogen was taken up (theoretical quantity: 77 ml). The catalyst was removed by filtration and washed with methylene chloride. The filtrate was combined with the washings and concentrated at reduced pressure. The mixture was poured into ice water and the precipitate was extracted with ether. The organic solution was washed with water and dried over sodium sulfate. The evaporation of the solvent gave 1.01 g of a partly crystalline product which was chromatographed on 30 g of aluminium oxide. Elutions with petroleum ether and with mixtures of petroleum ether – benzene (4:1 and 1:1) gave a crystalline material which was recrystallized from acetone – hexane. Thus there was obtained 645 mg of *5β-pregnane-3,20-dione* (**12**), m.p. 112–116° (64.1% yield). A sample was recrystallized 3 times from acetone–hexane for analysis; m.p. 118–119° [lit. (56*a*), 123°, (56*b*), 120–122°]; $[\alpha]_D^{26}$ +118° (*c*, 1.063 in $CHCl_3$) [lit. (56*b*), 111°]; ν_{max} (KBr) 1722 cm^{-1} (3-ketone), 1705 cm^{-1} (shoulder, 20-ketone).

Anal. Calcd. for $C_{21}H_{32}O_2$: C, 79.98; H, 10.19. Found: C, 79.73; H, 10.09.

Two of the first petroleum ether chromatogram fractions gave by recrystallization from acetone–hexane 160 mg (16%) of *5α-pregnane-3,20-dione* (**11**), m.p. 194–198°; a sample was recrystallized from acetone–hexane for analysis; m.p. 197–198° [lit. 200.5° (57*a*), 203–205° (57*b*)]; $[\alpha]_D^{28}$ +121° (*c*, 1.038 in $CHCl_3$) [lit. 126.9° (57*a*), 108.5 ± 4° (57*b*), 121° (57*c*)]; ν_{max} (KBr) 1719 cm^{-1} (3-ketone), 1700 cm^{-1} (shoulder, 20-ketone).

Anal. Calcd. for $C_{21}H_{32}O_2$: C, 79.98; H, 10.19. Found: C, 79.91; H, 10.15.

Reduction of 20-Ethylenedioxy-5β-pregnan-3-one (12a) with Lithium Aluminium Hydride

In the course of 30 min, a solution of 15.2 g of 20-ethylenedioxy-5β-pregnan-3-one (**12***a*), m.p. 168–173°, in 500 ml of tetrahydrofuran, was added with stirring to a suspension of 17.2 g of lithium aluminium hydride in 1.25 l of tetrahydrofuran. The mixture was refluxed with stirring for 1 h and then left for 16 h at room temperature. The excess reagent was decomposed in the cold with 80 ml of ethyl acetate and with ice and there was added 20 ml of a 10% ammonium chloride solution. The mixture was extracted with ether, the organic phase was washed with a dilute ammonium chloride solution and with water, and was dried over sodium sulfate. The evaporation of the solvent gave 15 g of an amorphous product. Crystallization from methanol yielded 6.8 g (44.5%) of *3α-hydroxy-20-ethylenedioxy-5β-pregnane* (**14**), m.p. 146–147°. A sample was recrystallized twice from methanol for analysis; needles, m.p. 150–151° [lit. 147–149° (55), 149–151° (58)]; $[\alpha]_D^{22}$ +27.0° (*c*, 1.04 in $CHCl_3$) [lit. (55), +28.5°]; ν_{max} (KBr) 3300 cm^{-1} (3α-hydroxyl), 1069 cm^{-1} (doublet), and 1046 cm^{-1} (large band) (ethylenedioxy bands).

Anal. Calcd. for $C_{23}H_{38}O_3$: C, 76.19; H, 10.57. Found: C, 76.14; H, 10.48.

The mother liquors (8.2 g) of the crystallization which had yielded the 3α-hydroxy ketal **14** were chromatographed on 225 g of aluminium oxide. Elutions with petroleum ether – benzene (4:1) gave 975 mg (6.4%) of *3β-hydroxy-20-ethylenedioxy-5β-pregnane* (**13**), m.p. 149–157°. A sample was recrystallized twice from methanol for analysis; colorless plates; m.p. 160–161°; $[\alpha]_D^{22}$ +58° (*c*, 1.00 in $CHCl_3$); ν_{max} (KBr) 3420 cm^{-1} (3β-hydroxyl), 1049, and 1035 cm^{-1} (doublet, ethylenedioxy absorption).

Anal. Calcd. for $C_{23}H_{38}O_3$: C, 76.19; H, 10.57. Found: C, 76.34; H, 10.47.

Further elutions in the above-described chromatogram with pure benzene and with a benzene – ether mixture (9:1) gave another 4.52 g (29.6%) of the 3α-hydroxy ketal **14**, m.p. 137–150° (total yield of the 3α-hydroxy derivative **14**: 74%).

Reduction of 20-Ethylenedioxy-5β-pregnan-3-one (12a) with Raney Nickel

(a) A quantity of 1 g of 20-ethylenedioxy-5β-pregnan-3-one (**12***a*), m.p. 164–165°, was dissolved in 150 ml of dioxan and reduced at atmospheric pressure with hydrogen in the presence of 5 g of three-year-old "sponge nickel catalyst" from Davison & Co., for a period of 20 h. The catalyst was removed by filtration and was washed with methylene chloride. Evaporation of the solvent from the filtrate and the washings gave 1.01 g of an amorphous reaction product which was chromatographed on 30 g of aluminium oxide. The first fractions, eluted with pure petroleum ether and with a petroleum ether – benzene mixture (9:1), gave 245 mg of starting material **12***a*, m.p. 164–172°. The following fractions, eluted with petroleum ether – benzene mixtures (9:1, 4:1, and 1:1), gave 244 mg of *3β-hydroxy-20-ethylenedioxy-5β-pregnane* (**13**), m.p. 145–156° (32.2% yield). The product was identified by comparison with an authentic sample (see above) through a mixture melting point determination and infrared analysis.

Further elutions with petroleum ether – benzene (1:1 and 1:4) gave 475 mg of *3α-hydroxy-20-ethylenedioxy-5β-pregnane* (**14**), m.p. 144–148° (62.2% yield). The product was identified by comparison with an authentic sample (see above) through a mixture melting point determination and infrared analysis.

(*b*) In another experiment, 6.6 g of the keto ketal **12***a* was reduced under the conditions described under (*a*) for 2 h. No starting material was isolated. The yield of the 3β-hydroxy ketal **13**, m.p. 141–158°, was 2.017 g (30.4%), that of the 3α-hydroxy epimer **14**, m.p. 133–148°, 4.5 g (67.8%).

(*c*) In a third experiment, 1 g of the keto ketal **12***a* was reduced with Raney nickel, freshly prepared from a nickel–aluminium alloy. The reduction time was 1 h. Chromatography of the reaction product afforded 187

Can. J. Chem. Downloaded from www.nrcresearchpress.com by 210.87.254.105 on 09/05/12
For personal use only.

mg (18.7%) of 3β-hydroxy-20-ethylenedioxy-5β-pregnane (**13**), m.p. 146–154°, and 769 mg (76.8%) of the 3α-hydroxy derivative **14**, m.p. 144–148°.

Reduction of 5β-Pregnane-3,20-dione (12) with Raney Nickel

A quantity of 450 mg of 5β-pregnane-3,20-dione (**12**), m.p. 113–115°, was dissolved in 75 ml of dioxane and hydrogenated at atmospheric pressure in the presence of 2.5 g of aged Raney nickel (see above). After 11 min, 35 ml of hydrogen was absorbed (theoretical quantity: 34.7 ml). The product was worked up as described before in the case of the reduction of the keto ketal **12***a*. The crude product (460 mg) was amorphous and was chromatographed on 15 g of aluminium oxide. The first fractions eluted with pure petroleum ether and with petroleum ether – benzene mixtures (9:1 and 4:1) gave 254 mg (56.6%) of starting material **12**, m.p. 109–119°. The following fractions, eluted with a petroleum ether – benzene mixture (1:1), gave 112 mg of a crystalline product, m.p. 108–139°. Recrystallization from ether–hexane and rechromatography of the mother liquors gave 60 mg (30.5%) of *3β-hydroxy-5β-pregnan-20-one* (**7**), m.p. 132–135°, as well as 16 mg of the same product of lesser purity, m.p. 110–116° (total yield: 38.6%). Three recrystallizations for analysis from ether–hexane gave fine needles, m.p. 143–143.5° [lit. (19), 142–143°]; $[\alpha]_D^{24}$ +100.6° (*c* 0.976 in $CHCl_3$) [lit. (19), 101° (EtOH)]; ν_{max} (KBr) 3350 cm^{-1} (3β-hydroxyl), 1707 cm^{-1} (20-ketone), 1031 cm^{-1} (alcohol).

Anal. Calcd. for $C_{21}H_{34}O_2$: C, 79.19; H, 10.76. Found: C, 79.15; H, 10.63.

Further elutions in the first chromatogram described above (which had yielded the crude 3β-hydroxy 20-ketone **7**) with pure benzene and with a mixture of benzene and ether (4:1) gave 63 mg (32%) of *3α-hydroxy-5β-pregnan-20-one* (**15**), m.p. 135–149°. A sample was recrystallized from dichloromethane–hexane for analysis; needles, m.p. 150–151° [lit. (19), 148–149°]; $[\alpha]_D^{23}$ +104.6° (*c* 1.000 in $CHCl_3$) [lit. (57*b*), +109.5° ±4°]; ν_{max} (KBr) 3380 cm^{-1} (3α-hydroxyl), 1706 cm^{-1} (20-ketone), 1038 cm^{-1} (hydroxyl).

Anal. Calcd. for $C_{21}H_{34}O_2$: C, 79.19; H, 10.76. Found: C, 79.22; H, 10.77.

3α-Hydroxy-5β-pregnan-20-one (15) from 3α-Hydroxy-20-ethylenedioxy-5β-pregnane (14)

A solution of 520 mg of 3α-hydroxy-20-ethylenedioxy-5β-pregnane (**14**), m.p. 136–138°, and of 60 mg of *p*-toluenesulfonic acid in 50 ml of absolute acetone was kept at room temperature for 48 h. The mixture was poured into ice water and the precipitate was extracted with ether. The organic phase was washed with water and dried over sodium sulfate. The evaporation of the solvent gave 450 mg of crystalline *3α-hydroxy-5β-pregnan-20-one* (**15**), m.p. 146–148° (98.6% yield). The identity of the product with an authentic sample (see above) was established by the determination of a mixture melting point and the comparison of the infrared spectra.

3β-Hydroxy-5β-pregnan-20-one (7) from 3β-Hydroxy-20-ethylenedioxy-5β-pregnane (13)

A quantity of 9.9 g of 3β-hydroxy-20-ethylenedioxy-5β-pregnane (**13**), m.p. 155–161°, was treated with 1 l of absolute acetone and 1.24 g of *p*-toluenesulfonic acid and the reaction mixture was worked up as described above for the analogous reaction of the 3α-hydroxy derivative (**14**). The crude crystalline 3β-hydroxy-5β-pregnan-20-one (**7**), m.p. 135–137°, was obtained in 98% yield (8.45 g). Recrystallization from ether gave the following batches of pure product: 3.39 g, m.p. 143–143.5°; 2.809 g, m.p. 142–143°; 1.421 g, m.p. 141–142°; and 236 mg, m.p. 140–141° (yield of purified product: 90%). The identity of the product with the one prepared from 5β-pregnane-3,20-dione (**12**) (see above) was established by the determination of a mixture melting point and by infrared analysis.

3β-Hydroxy-5β-pregnan-20-one (7) from 3α-Hydroxy-20-ethylenedioxy-5β-pregnane (14)

A solution of 1.5 g of 3α-hydroxy-20-ethylenedioxy-5β-pregnane (**14**), m.p. 150–151°, in 25 ml of pyridine was treated for 20 h with 1.6 g of *p*-toluenesulfonyl chloride which had previously been dissolved in 6.4 ml of pyridine. The mixture was poured into ice water and the precipitate was extracted with ether. The ethereal solution was washed with water, iced dilute hydrochloric acid, a cold sodium bicarbonate solution, and with water and was dried over sodium sulfate. Evaporation of the solvent gave 2.13 g (99.6%) of *3α-tosyloxy-20-ethylenedioxy-5β-pregnane* (**14***a*), m.p. 160–161°. A sample was recrystallized five times from methylene chloride – ether for analysis; needles, m.p. 162.5–163°, $[\alpha]_D^{25}$ +37.7° (*c* 0.937 in $CHCl_3$); λ_{max} (EtOH) 200 mμ (log ε 3.88), 224 mμ (log ε 4.05), 262 mμ (log ε 2.84); ν_{max} (KBr) 1600 cm^{-1} (aromatic substituent), 1054 and 1034 cm^{-1} (ketal).

Anal. Calcd. for $C_{30}H_{44}O_5S$: C, 69.73; H, 8.58; S, 6.21. Found: C, 69.92; H, 8.63; S, 6.44.

A portion of 1.48 g of the above-described 3α-tosyloxy-20-ethylenedioxy-5β-pregnane (**14***a*), m.p. 158–161°, was dissolved in 86 ml of dimethyl formamide and the solution was refluxed for 105 h, cooled and poured into ice water. The precipitate was extracted with ether and the ethereal solution was washed with water and dried over sodium sulfate. Removal of the solvent gave 1.02 g of crude amorphous *3β-formoxy-5β-pregnan-20-one* (**7***b*), ν_{max} ($CHCl_3$) 1720 cm^{-1} (shoulder) (formate), 1708 cm^{-1} (20-ketone), 1198 cm^{-1} (large band) (formate); this product showed in the ultraviolet no maximum in the region of 222–230 mμ typical of a tosylate function (59). This crude product was treated for 24 h with a solution of 9 g of potassium hydroxide in 175 ml of methanol and 2 ml of water. The solution was concentrated under reduced pressure and poured into ice water. The ethereal extract was washed with water and dried over sodium sulfate. Evaporation of the solvent gave 900 mg of an oil, ν_{max} ($CHCl_3$) 3420 cm^{-1} (large band) (hydroxyl), 1708 cm^{-1} (20-ketone), 1670 cm^{-1} (weak absorption) (double bond), 1032 cm^{-1} (hydroxyl). The product was chromatographed on 28 g of aluminium oxide. Elutions with petroleum ether gave 345 mg of a crystalline unsaturated material, m.p. 114–128°, ν_{max} (KBr) 1707 cm^{-1} (20-ketone), 1672 cm^{-1} (double bond); this material, the formation of which must be due to an elimination reaction, was not further investigated. Elutions with petroleum ether – benzene (1:1) gave 168 mg (18.4%) of *3β-hydroxy-5β-pregnan-20-one* (**7**), m.p. 127–139°. Recrystallization from ether–hexane raised the melting point to 143–143.5°. The identification of the material with an authentic

Can. J. Chem. Downloaded from www.nrcresearchpress.com by 210.87.254.105 on 09/05/12
For personal use only.

product, the preparation of which was described above, was effected by a mixture melting point determination and by infrared analysis.

Further elutions in the above-described chromatogram with pure benzene and with a benzene–ether mixture (4:1) gave 122 mg (13.4%) of *3α-hydroxy-5β-pregnan-20-one* (**15**), m.p. 127–138°. Recrystallization from dichloromethane–hexane raised the melting point to 150–151°. The product was identified by a mixture melting point determination and by infrared analysis with authentic material, the preparation of which was described above.

3β-Hydroxy-5β-pregnan-20-one (7) from 3α-Hydroxy-5β-pregnan-20-one (15)

To a solution of 450 mg of 3α-hydroxy-5β-pregnan-20-one (**15**), m.p. 146–148°, in 4.5 ml of pyridine was added 480 mg of *p*-toluenesulfonyl chloride in 2 ml of pyridine and the mixture was stored for 20 h at room temperature, cooled and poured into ice water. Extraction with ether and the usual working-up (see above) gave 670 mg of a partly crystalline product which was recrystallized from methylene chloride – ether to give 528 mg (79.2%) of *3α-tosyloxy-5β-pregnan-20-one* (**15***a*), m.p. 143–151°; recrystallization of the mother liquors gave another 82 mg of the same product of lesser purity, m.p. 137–138° (total yield: 91.3%). A sample was recrystallized 3 times from methylene chloride – ether for analysis; fine needles, m.p. 154–154.5°; $[\alpha]_D^{24}$ +100.1° (*c*, 0.950 in $CHCl_3$); λ_{max} (EtOH) 206 mμ (log ε 3.88), 224 mμ (log ε 4.07), 262 mμ (log ε 2.80); ν_{max} (KBr) 1700 cm^{-1} (20-ketone), 1600 cm^{-1} (aromatic absorption).

Anal. Calcd. for $C_{28}H_{44}O_5S$: C, 71.15; H, 8.53; S, 6.78. Found: C, 71.07; H, 8.47; S, 6.62.

A portion of 450 mg of the above-described 3α-tosyloxy-5β-pregnan-20-one (**15***a*), m.p. 143–151°, was dissolved in 26 ml of dimethyl formamide. The solution was refluxed for four days, cooled and poured into ice water. Extraction with ether and the usual working-up (see above) gave 310 mg of an amorphous product which yielded upon crystallization from methanol–hexane 133 mg (40.3%) of *3β-formoxy-5β-pregnan-20-one* (7*b*), m.p. 107–114°. A sample was recrystallized twice from methanol–hexane for analysis; prisms, m.p. 126–126.5°; $[\alpha]_D^{24}$ +104.1° (*c* 1.038 in $CHCl_3$); ν_{max} (KBr) 1730 cm^{-1} (formate), 1708 cm^{-1} (shoulder) (20-ketone), 1119 cm^{-1} (formate). The product showed no ultraviolet maximum between 222–230 mμ.

Anal. Calcd. for $C_{22}H_{34}O_3$: C, 76.26; H, 9.89. Found: C, 76.38; H, 9.77.

The filtration of the mother liquors (160 mg) from the crystallization of the formate **7***b* through an aluminium oxide column with an ether–hexane mixture gave 31 mg (10.2%) of *3α-hydroxy-5β-pregnan-20-one* (**15**), m.p. 142–143°, identified by a mixture melting point determination with an authentic sample and by infrared analysis.

A portion of 118 mg of the above-described formate **7***b*, m.p. 107–114°, and of 132 mg of mother liquors representing the same formate, were treated for 16 h at room temperature with 2.5 g of potassium hydroxide in 50 ml of methanol and 2 ml of water. The usual working-up (see above) gave 222 mg of an oil; ν_{max} ($CHCl_3$) 3600 cm^{-1} (sharp band) and 3400 cm^{-1} (wide band) (hydroxyl), 1704 cm^{-1} (20-ketone), 1030 cm^{-1} (hydroxyl). This product was chromatographed on 8 g of aluminium oxide. Elutions with petroleum ether gave 46 mg of the dehydration product, crystallizing in prisms, m.p. 119–128°; ν_{max} (KBr) 2970 cm^{-1} (vinylic hydrogens), 1699 cm^{-1} (20-ketone), 1658 cm^{-1} (double bond), 679 and 665 cm^{-1} (vinylic hydrogen doublet). Elutions with petroleum ether – benzene (9:1, 4:1, and 1:1) gave 93 mg (30.7%) of *3β-hydroxy-5β-pregnan-20-one* (7), m.p. 130–141°, identified by a mixture melting point determination with an authentic sample and by infrared analysis. Elutions with a benzene–ether mixture (4:1) gave 10 mg (3.3%) of *3α-hydroxy-5β-pregnan-20-one* (**15**), m.p. 142–146°, identified in the usual way by comparison with an authentic sample. Taking into account the recovery of starting material, the yield of 3β-hydroxy-5β-pregnan-20-one (**7**) from 3α-hydroxy-5β-pregnan-20-one (**15**) amounted to 22.7%.

3β-Hydroxy-5β-pregnan-20-one (7) by Meerwein–Pondorf Reduction of 20-Ethylenedioxy-5β-pregnan-3-one (12a) and Subsequent Deketalization

To a solution of 136 mg of 20-ethylenedioxy-5β-pregnan-3-one (**12***a*) in 0.75 ml of absolute benzene, 3.8 ml of *sec*-butyl alcohol and 136 mg of aluminium *t*-butylate were added at room temperature. The mixture was refluxed for 20 min and during that time 0.5 ml of absolute benzene was added. Subsequently the product was poured into ice water and the precipitate was extracted with a (3:1) ether – methylene chloride mixture. The organic solution was washed with an iced ammonium chloride solution and was dried over sodium sulfate. Removal of the solvent gave a crystalline product (146 mg), representing a crude mixture of *3β-hydroxy-20-ethylenedioxy-5β-pregnane* (**13**) and of *3α-hydroxy-20-ethylenedioxy-5β-pregnane* (**14**) which was dissolved in 15 ml of absolute acetone. The solution was treated with 18 mg of *p*-toluenesulfonic acid at room temperature for 48 h and poured into ice water. The precipitate was extracted with ether, the ethereal solution was washed with water and dried over sodium sulfate. The removal of the solvent gave 148 mg of a partly crystalline product which was chromatographed on 9 g of aluminium oxide. Elutions with petroleum ether – benzene mixtures (4:1 and 1:1) gave 58 mg (53%) of *3β-hydroxy-5β-pregnan-20-one* (7), m.p. 143.5–144.5°, identified by infrared analysis and by a mixture melting point determination with an authentic sample. Elutions with a (1:4) petroleum ether – benzene mixture, pure benzene, and a (4:1) benzene – ether mixture gave 49 mg (45% yield) of *3α-hydroxy-5β-pregnan-20-one* (**15**), m.p. 146–147°, identified by spectral analysis and by the determination of a mixture melting point with an authentic sample.

17α-Bromo-3β-acetoxy-5β-pregnan-20-one (8)

A quantity of 7.8 g of 3β-hydroxy-5β-pregnan-20-one (7), m.p. 140–143°, was acetylated in the usual fashion, at room temperature, with 35 ml of acetic anhydride in 70 ml of pyridine. The usual working-up gave 8.788 g (99.4%) of crystalline *3β-acetoxy-5β-pregnan-20-one* (7*a*), m.p. 114.5–115°. Two recrystallizations from ether–hexane raised the melting point of the crystalline pellets to 116–117° [lit. (19), 116.5°]; $[\alpha]_D^{24}$ +79.2° (*c*, 0.963 in $CHCl_3$), [lit. (19), +68° (EtOH)]; ν_{max} (KBr) 1743 cm^{-1} (acetate), 1704 cm^{-1} (20-ketone), 1251 and 1230 cm^{-1} (acetate).

A portion of 6.9 g of the above-described 3β-acetoxy-5β-pregnan-20-one (7*a*), m.p. 114–115°, was dissolved in

Can. J. Chem. Downloaded from www.nrcresearchpress.com by 210.87.254.105 on 09/05/12
For personal use only.

70 ml of absolute carbon tetrachloride. To this solution was added under vigorous stirring and at reflux temperature 4.25 g of *N*-bromosuccinimide and the mixture was irradiated for 8 min with a 660 W lamp. As the reaction proceeded, the bromosuccinimide at the bottom of the flask disappeared and a light flocculating material was raised to the surface of the yellow solution. The cooled solution was filtered, the precipitate was rinsed with carbon tetrachloride, and the combined solutions were washed with a dilute sodium bisulfite solution and with water, and dried over sodium sulfate. Evaporation of the solvent at reduced pressure gave 8.41 g of foamy material, representing crude *17α-bromo-3β-acetoxy-5β-pregnan-20-one* (**8**), ν_{max} (KBr) 1742 cm^{-1} (acetate), 1706 cm^{-1} (20-ketone), 1251 and 1236 cm^{-1} (acetate), 670 cm^{-1} (17α-bromine substituent). A sample of the crude product was analyzed for bromine.

Anal. Calcd. for $C_{23}H_{35}O_3Br$: Br, 18.19. Found: Br, 18.57.

Crystallization of the crude product from ether–hexane gave 7.668 g (91% yield) of crystalline *17α-bromo-3β-acetoxy-5β-pregnan-20-one* (**8**), m.p. (decomp.) 144–157°. A sample was recrystallized twice from ether–hexane for analysis; prisms, m.p. (decomp.) 158–159°, $[\alpha]_D^{24}$ −46.7° (*c*, 1.200 in $CHCl_3$); ν_{max} (KBr) 1745 cm^{-1} (acetate), 1708 cm^{-1} (20-ketone), 1251 and 1239 cm^{-1} (acetate).

Anal. Calcd. for $C_{23}H_{35}O_3Br$: C, 62.86; H, 8.03; Br, 18.19. Found: C, 62.57; H, 7.97; Br, 18.33.

Δ^{16}-3β-Acetoxy-5β-pregnen-20-one (6a)

(a) From 17α-Bromo-3β-acetoxy-5β-pregnan-20-one (8)

A solution of 2.06 g of 17α-bromo-3β-acetoxy-5β-pregnan-20-one (**8**), m.p. (decomp.) 155–157°, and of 420 mg of lithium chloride in 520 ml of dimethyl formamide was refluxed in a nitrogen atmosphere for 1 h. The mixture was cooled and poured into ice water and the precipitate was extracted with ether. The ethereal solution was washed with an iced dilute hydrochloric acid solution, with a cold sodium bicarbonate solution, and with water and was dried over sodium sulfate. Evaporation of the solvent gave 1.68 g of *Δ^{16}-3β-acetoxy-5β-pregnen-20-one* (*6a*), m.p. 135–136° (quantitative yield). One recrystallization from ether–hexane gave 1.405 g (88%) of pure Δ^{16}-pregnenolone acetate (*6a*), m.p. 136–141°. A sample was recrystallized twice from ether–hexane for analysis; prisms, m.p. 144–144.5°, $[\alpha]_D^{22}$ −48.6° (*c*, 1.000 in $CHCl_3$); λ_{max} (EtOH) 239 mμ (log ε 3.97); ν_{max} (KBr) 3010 cm^{-1} (vinylic hydrogen), 1740 cm^{-1} (acetate), 1658 and 1583 cm^{-1} (Δ^{16}-20-keto doublet), 1252 and 1231 cm^{-1} (acetate).

Anal. Calcd. for $C_{23}H_{34}O_3$: C, 77.05; H, 9.56. Found: C, 77.32; H, 9.40.

(b) From Smilagenin Acetate (5a)[18]

To a warm solution of 25 g of smilagenin acetate (25-iso-sarsasapogenin acetate) (*5a*), m.p. 136–142°, in 50 ml of acetic anhydride and 25 ml of pyridine, 8.5 g of methylamine hydrochloride was added, the mixture was refluxed for 2 h, cooled, and poured into ice water. The precipitate was extracted with methylene chloride, the organic solution was washed with water and dried over sodium sulfate. Removal of the solvent at reduced pressure gave 25.6 g of *pseudosmilagenin acetate* which was used without further purification. The product was dissolved in 125 ml of acetic acid and 125 ml of dichloroethane and cooled to −8°. There was added, under vigorous stirring, a cold solution of 12.5 g of chromic acid in 125 ml of acetic acid. Subsequently, there was added slowly to the stirred mixture, at −5°, a solution of 12.5 g of sodium metabisulfite in 38 ml of water. The product was extracted with ether and the organic phase was washed with cold water, an iced sodium bicarbonate solution and with water and was dried over sodium sulfate. Evaporation of the solvent at reduced pressure gave 24.8 g of *3β-acetoxy-16β-hydroxy-5β-pregnan-20-one 16-(δ-acetoxy-γ-methylvalerate)* in the crude state. This product was dissolved in 150 ml of glacial acetic acid and the solution was refluxed for 2 h, cooled, and poured into ice water. The precipitate was extracted with methylene chloride, the organic solution was washed with an iced sodium bicarbonate solution and with water, and was dried over sodium sulfate. The removal of the solvent left 26.2 g of an amorphous product which was chromatographed on 700 g of aluminium oxide. Elutions with petroleum ether and with petroleum ether – benzene mixtures (9:1 and 4:1) gave 12.6 g (64.4%) of *Δ^{16}-3β-acetoxy-5β-pregnen-20-one* (*6a*), m.p. 121–138°. Recrystallization from ether–hexane gave 11.883 g (60.7%) of the pure pregnenolone acetate *6a*, m.p. 139–140°, the identity of which with the product prepared as described under (*a*) was established by the determination of a mixture melting point and by the comparison of the infrared spectra.

$\Delta^{14,16}$-3β-Hydroxy-5β-pregnadien-20-one (17)

A quantity of 5.4 g of Δ^{16}-3β-acetoxy-5β-pregnen-20-one (*6a*), m.p. 137–140°, was brominated in 54 ml of carbon tetrachloride with 3.24 g of *N*-bromosuccinimide as described above for the preparation of the 17-bromide **8**. The usual working-up (see above) gave 6.66 g of an amorphous product, representing crude *Δ^{16}-3β-acetoxy-15ξ-bromo-5β-pregnen-20-one* (**16**); λ_{max} (EtOH) 237 mμ (log ε 3.61), 308 mμ (log ε 2.96); ν_{max} (KBr) 1740 cm^{-1} (acetate), 1678 cm^{-1} (γ-halogenated α,β-unsaturated 20-ketone), 1655 cm^{-1} (α,β,γ,δ-unsaturated 20-ketone), 1585 and 1525 cm^{-1} (weak bands due to the presence of diene **17***a*), 1251 and 1235 cm^{-1} (acetate). A sample of the crude product was analyzed for its bromine contents.

Anal. Calcd. for $C_{23}H_{33}O_3Br$: Br, 18.27. Found: Br, 18.37.

The majority of the crude product (6.63 g) which, according to the spectral data, already contained some diene **17***a*, was dissolved with 1.32 g of lithium chloride in 1.5 l of dimethylformamide and dehydrobrominated as described above for the preparation of the pregnenolone acetate *6a*. There was obtained 5.1 g of a product which, according to the ultraviolet spectrum, represented an approximate (2:3) mixture of the unsaturated bromoketone **16** and the dienone **17***a*; λ_{max} (EtOH) 238 mμ (log ε 3.6), 308 mμ (log ε 3.8); ν_{max} (KBr) 3040 cm^{-1} (shoulder, vinylic hydrogen), 1742 cm^{-1} (acetate), 1670 cm^{-1} (α,β-unsaturated 20-ketone), 1653 cm^{-1}(α,β,γ, δ di-unsaturated 20-ketone), 1590 and 1530 cm^{-1} (weak band) (conjugated double bond), 1252 and 1234 cm^{-1} (acetate). The isolation of pure $\Delta^{14,16}$-3β-acetoxy-5β-pregnadien-20-one

[18]According to a procedure kindly provided by Dr. M. E. Wall.

Can. J. Chem. Downloaded from www.nrcresearchpress.com by 210.87.254.105 on 09/05/12
For personal use only.

(**17***a*) by chromatography on aluminium oxide was unsuccessful. The purest fractions obtained, eluted with petroleum ether – benzene (1:1) (459 mg), m.p. 116–119°, still contained some mono-unsaturated product (approximately 10%); λ_{max} (EtOH) 237 mμ (log ε 2.9), 308 mμ (log ε 4.1); ν_{max} (KBr) 3040 cm^{-1} (vinylic hydrogen), 1741 cm^{-1} (acetate), 1642 cm^{-1} (14,16-di-unsaturated 20-ketone), 1526 cm^{-1} (conjugated double bond), 1252 and 1238 cm^{-1} (acetate). No further purification could be achieved by crystallization and sublimation under high vacuum.

A portion of 5.05 g of crude dehydrobromination product was dissolved in 800 ml of methanol containing 2.5% of perchloric acid. The solution was kept for 22 h at room temperature and poured into ice water. The precipitate was extracted with ether, the ethereal solution was washed with a saturated sodium bicarbonate solution and with water, and was dried over sodium sulfate. Removal of the solvent left 4.5 g of an amorphous product which was absorbed on 290 g of aluminium oxide. Elutions with a petroleum ether – benzene mixture (1:1) gave 924 mg of crystalline material, m.p. 135–139°, still containing 30% of mono-unsaturated product, 720 mg of material melting between 142 and 150°, containing approximately 20% of mono-unsaturated material, and 1.205 g melting between 150 and 163°, containing approximately 10% of mono-unsaturated product. Recrystallization of the various fractions in methanol–hexane gave 1.255 g of $\Delta^{14,16}$-3β-*hydroxy-5β-pregnadien-20-one* (**17**), m.p. 152–160°, the ultraviolet spectrum of which showed no mono-unsaturated product (yield from pregnenolone acetate **6***a*: 23.4%). A sample was recrystallized four times from methanol–hexane and sublimed twice in high *vacuo* at 105–110°; pellets, m.p. 173–174°; $[\alpha]_D^{21}$ +453° (*c*, 1.010 in $CHCl_3$); λ_{max} (EtOH) 308 mμ (log ε 4.04); ν_{max} (KBr) 3440 cm^{-1} (hydroxyl), 3040 cm^{-1} (vinylic hydrogen), 1630 and 1523 cm^{-1} ($\Delta^{14,16}$-20-keto doublet), 1034 cm^{-1} (hydroxyl).

Anal. Calcd. for $C_{21}H_{30}O_2$: C, 80.21; H, 9.62. Found: C, 80.98; H, 9.16.[19]

For the following reaction, crystalline material melting between 152 and 161° was used.

*Δ^{14}-3β-Hydroxy-5β-pregnen-20-one (**18**)*

*(a) From $\Delta^{14,16}$-3β-Hydroxy-5β-pregnadien-20-one (**17**) by Reduction with Lithium and Ammonia*

In the course of 4 min, a solution of 100 mg of $\Delta^{14,16}$-3β-hydroxy-5β-pregnadien-20-one (**17**), m.p. 158–161°, in 6.7 ml of absolute ether was added to a well-stirred solution of 100 mg of lithium and 50 ml of ammonia at −70°. After a further 4 min of stirring, the dark-blue color started to fade and 500 mg of ammonium chloride was added which resulted in complete discoloration. In the course of 3.6 h, the ammonia was evaporated in a nitrogen current and the volume of the liquid was maintained by addition of absolute ether. The mixture was poured into ice water and the precipitate was extracted with ether. The ethereal solution was washed with water and dried over sodium sulfate. Evaporation of the solvent gave 99 mg of an amorphous product which was chromatographed on 4 g of aluminium oxide. The petroleum ether – benzene fractions (4:1 and 1:1) gave 26 mg of Δ^{14}-3β-*hydroxy-5β-pregnen-20-one* (**18**), m.p. 140–159° (25.8% yield). The product was recrystallized three times from ether–hexane for analysis; needles, m.p. 164–164.5°; $[\alpha]_D^{26}$ +66.5° (*c*, 1.000 in $CHCl_3$); λ_{max} (cyclohexane) 194 mμ (log ε 2.17); ν_{max} (KBr) 3485 cm^{-1} (hydroxyl), 3040 cm^{-1} (vinylic hydrogen), 1702 cm^{-1} (20-ketone), 1649 cm^{-1} (double bond), 1135 cm^{-1} (hydroxyl).

Anal. Calcd. for $C_{21}H_{32}O_2$: C, 79.64; H, 10.19. Found: C, 79.46; H, 10.02.

Elutions with petroleum ether – benzene (1:1) gave 10 mg of $\Delta^{14,16}$-3β-*hydroxy-5β-pregnadien-20-one* (**17**), m.p. 151–154°, identified by a mixture melting point, and thin-layer, ultraviolet, and infrared analyses. Taking the recovery of this material into consideration, the yield of the Δ^{14}-pregnenolone **18** amounted to 28.7%.

Benzene and a benzene–ether mixture (4:1) eluted 40 mg of a partly crystalline product, m.p. 148–167°; λ_{max} (EtOH) 231 mμ (log ε ~ 4); ν_{max} (KBr) 3480 cm^{-1} (hydroxyl), 1685 and 1610 cm^{-1} (α,β-unsaturated keto doublet). This product was not further investigated.

*(b) From $\Delta^{14,16}$-3β-Hydroxy-5β-pregnadien-20-one (**17**) by Reduction with Sodium and n-Propanol and Subsequent Oxidation*

From a solution of 800 mg of $\Delta^{14,16}$-3β-hydroxy-5β-pregnadien-20-one (**17**), m.p. 152–160°, in 50 ml of absolute benzene and 1.68 ml of dihydropyran, 25 ml of benzene was removed by distillation, and 32 mg of *p*-toluenesulfonic acid was added at room temperature. After 3.5 days, the mixture was poured into ice water and the precipitate was extracted with ether. The organic phase was washed with a saturated sodium bicarbonate solution and with water, and was dried over sodium sulfate. Evaporation of the solvent gave 1.06 g of an amorphous product which was chromatographed on 50 g of aluminium oxide. Elutions with petroleum ether and with petroleum ether – benzene mixtures (9:1 and 4:1) gave 987 mg (97.4%) of $\Delta^{14,16}$-3β-*(2′-tetrahydropyranyloxy)-5β-pregnadien-20-one* (**17***b*), m.p. 110–132°; λ_{max} (EtOH) 309 mμ (log ε 4.13); ν_{max} (KBr) 3040 cm^{-1} (vinylic hydrogen), 1644 and 1521 cm^{-1} ($\Delta^{14,16}$-20-keto doublet), 1129, 1110, 1015, and 990 cm^{-1} (tetrahydropyranyl ether). This product was employed without further purification in the next step.

A portion of 480 mg of the crude $\Delta^{14,16}$-di-unsaturated tetrahydropyranyl ether **17***b*, m.p. 114–136°, was dissolved in 100 ml of absolute *n*-propanol. At reflux temperature, in the course of 30 min, 1.5 g of metallic sodium was added portionwise to this solution; after 1 h, the sodium was completely dissolved. The crude mixture was diluted with water and neutralized with a 2 *N* hydrochloric acid solution, concentrated at reduced pressure and extracted with ether. The ethereal solution was washed with a sodium bicarbonate solution and with water, and was dried over sodium sulfate. Removal of the solvent gave 500 mg of amorphous Δ^{14}-3β-*(2′-tetrahydropyranyloxy)-20ξ-hydroxy-5β-pregnene* (**19**); ν_{max} ($CHCl_3$) 3620, 3470 cm^{-1} (20-hydroxyl), 3040 cm^{-1} (vinylic hydrogen), 1652 cm^{-1} (double bond), 1131, 1111, 1021, and 997 cm^{-1} (tetrahydropyranyl ether). This product was used without further purification in the next step.

The 14-unsaturated 20-hydroxy ether **19** (500 mg) was dissolved in 50 ml of absolute acetone and the solution

[19]No better analytical results could be obtained.

Can. J. Chem. Downloaded from www.nrcresearchpress.com by 210.87.254.105 on 09/05/12
For personal use only.

was cooled to 0°. To this solution was added 0.5 ml of Jones' reagent, prepared by dissolving 267 g of chromic acid in 230 ml of concentrated sulfuric acid and 770 ml of water. After 8 min, the product was poured into ice water and extracted with ether. The organic solution was washed with a saturated sodium bicarbonate solution and with water, and dried over sodium sulfate. The removal of the solvent left 505 mg of an amorphous product, representing crude Δ^{14}-*3β-(2'-tetrahydropyranyloxy)-5β-pregnen-20-one* (**18***b*); ν_{max} (CCl_4) 3040 cm^{-1} (vinylic hydrogen), 1712 cm^{-1} (20-ketone), 1651 cm^{-1} (double bond), 1132, 1112, 1022, and 998 cm^{-1} (tetrahydropyranyl ether). This product was used without purification in the next step.

A portion of 500 mg of the above-described Δ^{14}-pregnenolone ether **18***b* was dissolved in 5 ml of ethanol and heated at reflux temperature for 1 h with 29 mg of *p*-toluenesulfonic acid. The solution was concentrated to half of its volume and extracted with ether. The ethereal solution was washed with a saturated potassium bicarbonate solution and with water, and was dried over sodium sulfate. Removal of the solvent gave 376 mg of a crude product which was chromatographed on 15 g of aluminium oxide. Elutions with petroleum ether – benzene (3:2 and 1:1) gave 123 mg of Δ^{14}-*3β-hydroxy-5β-pregnen-20-one* (**18**), m.p. 150–158° (yield from the tetrahydropyranyloxy diene **17***b*: 32.2%). The identity of the product with the one prepared as described under (*a*) was established by the comparison of the infrared spectra and the determination of a mixture melting point.

(c) From Δ^{16}-3β-Acetoxy-5β-pregnen-20-one (6a) without Isolation of Intermediates

A quantity of 14.9 g of Δ^{16}-3β-acetoxy-5β-pregnen-20-one (**6***a*), m.p. 139–142°, was treated with 8.55 g of *N*-bromosuccinimide in 150 ml of carbon tetrachloride as described above. The amorphous halogenated reaction product (19.2 g) (compare **16**) was dissolved in 4 l of dimethylformamide and the solution was refluxed for 1 h under nitrogen with 3.85 g of lithium chloride. The usual working-up gave 12.5 g of crude dienone **17***a* which was treated for 22 h with 1.6 l of methanol and 40 ml of perchloric acid as described above. The crude reaction product (11.6 g) was filtered through a column of 350 g of aluminium oxide to yield 10.8 g of a clear oil. This product was treated for 110 h in 338 ml of benzene with 21 ml of dihydropyran and 410 mg of *p*-toluenesulfonic acid at room temperature. The resulting product was filtered through a column of 380 g of aluminium oxide and thus gave 14.5 g of crude tetrahydropyranyl ether **17***b* which was treated with 43.5 g of sodium in 2.9 l of *n*-propanol for 2.25 h, as described above. This gave 13.2 g of the crude 14-unsaturated 20-hydroxy ether **19** which was oxidized with 11.5 ml of Jones' reagent. The resulting 20-keto tetrahydropyranyl ether **18***b* (13.46 g) was dissolved in 1.35 l of ethanol and the solution was refluxed for 1 h with 758 mg of *p*-toluenesulfonic acid. The usual working-up gave 12.83 g of amorphous product which was chromatographed on 350 g of aluminium oxide. Petroleum ether – benzene mixtures (4:1 and 1:1) gave 4.371 g of Δ^{14}-*3β-hydroxy-5β-pregnen-20-one* (**18**), m.p. 138–147° (yield from the Δ^{16}-pregnenolone acetate **6***a*: 33.2%). The identity of the material with the products prepared as described under (*a*) and (*b*) was determined by infrared analysis and the determination of mixture melting points.

Δ^{14}-3β-Hydroxy-5β-etianic Acid (3) from Δ^{14}-3β-Hydroxy-5β-pregnen-20-one (18)

A quantity of 3.11 g of Δ^{14}-3β-hydroxy-5β-pregnen-20-one (**18**), m.p. 138–147°, was acetylated in the usual fashion with 18 ml of acetic anhydride in 36 ml of pyridine. Thus was obtained 3.52 g of crude Δ^{14}-*3β-acetoxy-5β-pregnen-20-one* (**18***a*); ν_{max} (CCl_4) 3040 cm^{-1} (vinylic hydrogen), 1740 cm^{-1} (acetate), 1713 cm^{-1} (20-ketone), 1651 cm^{-1} (double bond), 1246 and 1233 cm^{-1} (acetate). This product was dissolved in 130 ml of dioxane and 36.5 ml of water. To this solution was added, in the course of 45 min, with stirring, a sodium hypobromite solution prepared by adding at first 6.64 g of bromine and then 28 ml of dioxane to a cold solution of 4.85 g of sodium hydroxide in 41.6 ml of water. The reaction mixture containing the oxidizing solution and the steroid was stirred at room temperature until the yellow color disappeared, which took 3 h. A few drops of a sodium bisulfite solution was added and the mixture was acidified to pH 3 and poured into ice water. By filtration, 543 mg (17%) of Δ^{14}-*3β-hydroxy-5β-etianic acid* (**3**), m.p. 170–172°, was isolated; $[\alpha]_D^{25}$ +32.7° (*c*, 1.025 in $CHCl_3$); ν_{max} (KBr) 3400 cm^{-1} (large, associated hydroxyl band), 3025 cm^{-1} (vinylic hydrogen), 1707 cm^{-1} (carboxyl), 1646 cm^{-1} (double bond). The mother liquors were extracted with ether and the ethereal solution was washed with a dilute sodium bisulfite solution, with a dilute sulfuric acid solution and with water, and was dried over sodium sulfate. The solvent was evaporated, the residue was dissolved in a few ml of methanol and precipitated with ice water. Thus, another 2.1 g of the 3β-hydroxy Δ^{14}-acid **3**, m.p. 162–174°, was obtained (total yield: 84.4%). The product was characterized completely in the form of its 3-acetoxy methyl ester (see below).

Methyl Δ^{14}-3β-Acetoxy-5β-etianate (3c) (7a, 9, 60)

(a) From the Hydroxyetianic Acid 3 Prepared from Pregnenolone (9), Progesterone (10), and Smilagenin (5)

A quantity of 19 mg of the above-described Δ^{14}-3β-hydroxy-5β-etianic acid (**3**), m.p. 169–170°, was dissolved in 3 ml of absolute methanol and 1.5 ml of absolute ether and treated at 0° with 3.3 ml of a 0.8% ethereal diazomethane solution. After 16 h the product was worked up in the usual way and 20 mg of crude *methyl Δ^{14}-3β-hydroxy-5β-etianate* (**3***b*) was isolated. This product was dissolved without further purification in 0.2 ml of pyridine and acetylated in the usual fashion at room temperature with 0.1 ml of acetic anhydride. Thus, 22 mg of *methyl Δ^{14}-3β-acetoxy-5β-etianate* (**3***c*), m.p. 115–116°, was obtained (yield from the hydroxy acid **3**: 98.4%). A sample was recrystallized once from methanol for analysis; small plates, m.p. 126–126.5°, $[\alpha]_D^{27}$ +37.5° (*c* 1.000 in $CHCl_3$) [lit. (9), m.p. 116–119°, $[\alpha]_D^{24}$ +34.7° ±2° ($CHCl_3$)]; λ_{max} (cyclohexane) 180 mμ (log ε 2.72); ν_{max} (KBr) 3040 cm^{-1} (vinylic hydrogen), 1729 cm^{-1} (acetate), 1722 cm^{-1} (methyl ester), 1648 cm^{-1} (double bond), 1259 and 1234 cm^{-1} (acetate), 1154 cm^{-1} (methyl ester).

Anal. Calcd. for $C_{23}H_{34}O_4$: C, 73.76; H, 9.15. Found: C, 73.82; H, 9.30.

Can. J. Chem. Downloaded from www.nrcresearchpress.com by 210.87.254.105 on 09/05/12
For personal use only.

(b) From Digitoxigenin (2)

A quantity of 1 g of digitoxigenin (**2**), m.p. 249–250°, was acetylated in the usual fashion at room temperature with 4.4 ml of acetic anhydride in 8.8 ml of pyridine. There was obtained 1.11 g (99.8%) of *digitoxigenin acetate* (**2***a*), m.p. 219–220°. One recrystallization from acetone–hexane gave 1.08 g (97.2%) of a product melting between 232 and 235°. A sample was recrystallized three times from acetone–hexane for analysis; prisms, m.p. 224–225°; $[\alpha]_D^{26}$ +21.1° (*c*, 0.991 in $CHCl_3$) [lit. (61), m.p. 222/227°; $[\alpha]_D^{17}$ +19.2°, 21.4° ($CHCl_3$)]; λ_{max} (EtOH) 216 mμ (log ε 4.05); ν_{max} (KBr) 3500 cm^{-1} (14-hydroxyl), 1780 and 1752 cm^{-1} (butenolide), 1740 cm^{-1} (acetate), 1625 cm^{-1} (20(22)-double bond), 1258 and 1238 cm^{-1} (acetate).

Anal. Calcd. for $C_{25}H_{36}O_5$: C, 72.08; H, 8.71. Found: C, 71.92; H, 8.85.

Through a solution of 2.2 g of digitoxigenin acetate (**2***a*), m.p. 224–226°, in 120 ml of ethyl acetate, there was passed, at −80°, in the course of 62 min, an oxygen current containing 4.5% of ozone at a rate of 71.3 ml per min. The pale-blue solution was left for 20 min at −80°. The solvent was removed at reduced pressure and the residue dissolved in 18 ml of glacial acetic acid; zinc dust was added portionwise until the solution showed no more reaction with starch and potassium iodide. The mixture was filtered and the residue was washed with chloroform, the filtrate and washings were diluted with chloroform, washed with an iced potassium bicarbonate solution and with water, and dried over sodium sulfate. Evaporation of the solvent gave 2.7 g of amorphous *3β-acetoxy-14β-hydroxy-21-glyoxyloxy-5β-pregnan-20-one*, which was treated in 130 ml of methanol for 20 h at room temperature with a solution 1.75 g of potassium bicarbonate in 55 ml of water. After concentration, the product was extracted with a mixture of chloroform and ether (1:3). The organic solution was washed with water, dried over sodium sulfate, and taken to dryness. There was obtained 2.1 g of crude *3β-acetoxy-14β,21-dihydroxy-5β-pregnan-20-one*; ν_{max} (KBr) 3450 cm^{-1} (hydroxyls), 1742 cm^{-1} (acetate), 1718 cm^{-1} (shoulder) (20-ketone), 1259 and 1238 cm^{-1} (acetate). A quantity of 1.98 g of this product was treated at room temperature for 20 h in 56 ml of methanol with a solution of 3.3 g of periodic acid in 11.2 ml of water. The chloroform extract of the product was washed with water, an iced sodium bicarbonate solution, and with water, and was dried over sodium sulfate. Evaporation of the solvent gave 1.125 g of a *neutral product*. The bicarbonate washings were acidified with sulfuric acid and extracted with chloroform to give 880 mg of an *acid fraction*.

The *neutral fraction* was acetylated in the usual way with 5.25 ml of acetic anhydride in 10.5 ml of pyridine to give 1.064 g of an amorphous product which, upon crystallization from methylene chloride – ether, gave 259 mg of *methyl 3β-acetoxy-14β-hydroxy-5β-etianate* (**4***c*), m.p. 150–153°. The mother liquors of the crystallization were filtered through an aluminium oxide column and thus gave another 559 mg of hydroxyetianate **4***c*, m.p. 150–153° (yield of product from the neutral fraction: 41.9%). A sample was recrystallized three times from ether–hexane; m.p. 155–156°, $[\alpha]_D^{27}$ +38.0° (*c* 1.000 in $CHCl_3$) [lit. (9); m.p. 154–157°; $[\alpha]_D^{25}$ +30.7° ±2° (in $CHCl_3$)]. The product proved identical in every respect with the one prepared in this laboratory from methyl Δ^{14}-3β-acetoxy-5β-etienate (**3***c*) (2).

The *acid fraction* (880 mg) was methylated in the usual fashion in 25 ml of absolute methanol and 7 ml of absolute ether with 54 ml of a 0.7% ethereal diazomethane solution to give 850 mg (43.5%) of *methyl 3β-acetoxy-14β-hydroxy-5β-etianate* (**4***c*), m.p. 147–150° (total yield of this product from digitoxigenin acetate (**2***a*): 85.4%).

A portion of 600 mg of this product, m.p. 148–154°, was dissolved in 6 ml of absolute pyridine; the solution was cooled to 0° and there was added 0.6 ml of thionyl chloride. The mixture was sealed and left for 11 h at 0° and for 1 h at 20°, and was then poured into ice water. The precipitate was extracted with a mixture of chloroform and ether (1:3). The organic layer was washed with iced dilute hydrochloric acid, with a cold potassium bicarbonate solution and with water, and was dried over sodium sulfate. Evaporation of the solvent gave 700 mg of an amorphous product which was chromatographed on 10 g of aluminium oxide (activity II). Elutions with petroleum ether gave 492 mg of *methyl Δ^{14}-3β-acetoxy-5β-etianate* (**3***c*), m.p. 115–120° (yield from the hydroxy ester **4***c*: 85.9%). A sample was recrystallized three times from methanol; m.p. 126–126.5°. The product was found identical with that prepared as described under (*a*) by the comparison of the infrared and ultraviolet spectra and by the determination of a mixture melting point.

Δ^{14}-21-Diazo-3β-acetoxy-5β-pregnen-20-one (21)

A quantity of 810 mg of Δ^{14}-3β-hydroxy-5β-etianic acid (**3**), m.p. 170–172°, was dissolved in 4 ml of pyridine and treated for 16 h with 1.5 ml of acetic anhydride. Subsequently, 1.5 ml of water was added and the mixture was refluxed for 1 h. After cooling, 25 ml of ice water was added and the precipitate was filtered, washed with an iced dilute hydrochloric acid solution and with water, and was dried *in vacuo*. Thus, 800 mg (87.3%) of crude *Δ^{14}-3β-acetoxy-5β-etianic acid* (**3***a*), m.p. 163–164°, was obtained; ν_{max} (KBr) 3400 cm^{-1} (large, associated hydroxyl band), 1738 cm^{-1} (acetate), 1704 cm^{-1} (carboxylic acid), 1648 cm^{-1} (double bond), 1255 (shoulder) and 1234 cm^{-1} (acetate). This product was used without further purification in the following reaction.

A suspension of this product in 42 ml of absolute benzene was cooled to 5°. With repeated shaking, 5.6 ml of oxalyl chloride in 20 ml of absolute benzene was added in the course of 2 min. The mixture was shaken repeatedly and allowed to reach room temperature. After 30 min, the acid was completely dissolved. The solvent was evaporated 1.3 h after the end of the addition of the oxalyl chloride, the product was dried by being dissolved in absolute benzene and by being taken to dryness repeatedly, with exclusion of moisture. There was obtained 822 mg of partly crystalline *Δ^{14}-3β-acetoxy-5β-etianic acid chloride* (**20**), which was used without further purification in the next step.

The acid chloride **20** was dissolved in 30 ml of absolute benzene. To this solution was added at −10°, in the course of 3 min, 20 ml of a 2.9% ethereal diazomethane solution and the mixture was left at 0° for 18 h and at 25° for 25 min. The evaporation of the solvent under reduced pressure, at 22°, gave 890 mg of crude, amorphous *Δ^{14}-21-diazo-3β-acetoxy-5β-pregnen-20-one* (**21**); ν_{max} (CCl_4)

Can. J. Chem. Downloaded from www.nrcresearchpress.com by 210.87.254.105 on 09/05/12
For personal use only.

3080 cm^{-1} (vinylic hydrogen), 2100 cm^{-1} (sharp diazo band), 1742 cm^{-1} (acetate), 1650 cm^{-1} (large diazo band), 1260 and 1238 cm^{-1} (acetate). This product was used without purification in the following reaction (see below).

β-*Anhydrodigitoxigenin Acetate (1a)*

(a) From Δ^{14}*-21-Diazo-3β-acetoxy-5β-pregnen-20-one (21) through* Δ^{14}*-21-Chloro-3β-acetoxy-5β-pregnen-20-one(23) and* Δ^{14}*-3β,21-Diacetoxy-5β-pregnen-20-one (23b)*

To a solution of 890 mg of crude Δ^{14}-21-diazo-3β-acetoxy-5β-pregnen-20-one (**21**) in 30 ml of absolute benzene there was added in the course of 4 min, dropwise and with stirring, a solution of 435 mg of anhydrous hydrogen chloride in 5.5 ml of absolute ether. The mixture was stirred for another 40 min at room temperature, poured into ice water and extracted with ether. The organic solution was washed repeatedly with water and was dried over sodium sulfate. The evaporation of the solvent under reduced pressure gave 906 mg of crude, amorphous Δ^{14}*-21-chloro-3β-acetoxy-5β-pregnen-20-one* (**23**); ν_{max} (KBr) 1738 cm^{-1} (acetate), 1651 cm^{-1} (double bond), 1258 and 1234 cm^{-1} (acetate) which gave a positive Beilstein test and which was used without further purification in the next step.

A solution of the crude chloride **23** (904 mg) in 35 ml of absolute acetone was refluxed under nitrogen with 703 mg of sodium iodide for 45 min. The product was extracted with ether and the ethereal solution was washed with water, a small quantity of iced 0.8% sodium hydroxide solution, again with water, and was dried over sodium sulfate. The evaporation of the solvent gave 937 mg of an oil, representing crude Δ^{14}*-21-iodo-3β-acetoxy-5β-pregnen-20-one* (**23a**), which was dissolved in 37 ml of absolute acetone and refluxed for 12 h with 4.3 g of potassium bicarbonate in 2.4 ml of glacial acetic acid. The mixture was diluted with ice water and the precipitate was filtered, washed and dried *in vacuo* to give 809 mg of a partly crystalline product. Recrystallization from methanol gave 625 mg of crude crystalline Δ^{14}*-3β,21-diacetoxy-5β-pregnen-20-one* (**23b**), m.p. 98–106°; ν_{max} (KBr) 1745 cm^{-1} (shoulder, 20-oxo-21-acetate and 3β-acetate), 1728 cm^{-1} (21-acetoxy-20-ketone); (yield from Δ^{14}-3β-hydroxy-5β-etianic acid (**3**): 68.3%). This product which is recrystallized only with difficulty was used without further purification in the next reaction.

A portion of 495 mg of the above-described Δ^{14}-diacetoxypregnenone **23b**, m.p. 98–106°, was dried with absolute benzene and dissolved in 15 ml of absolute benzene and 15 ml of absolute ether. There was added 1.2 g of granulated zinc, activated with iodine, and 17 ml of solvent was removed by distillation. Freshly distilled ethyl bromoacetate (1.64 ml) was added and 1 ml of solvent was again removed by distillation. The thus initiated vigorous reaction lost its intensity after 3 min and the mixture was heated to ebullition for another 15 min. Absolute dioxane (2.1 ml) was added and the mixture was heated for 30 min, cooled, and acidified with iced dilute hydrochloric acid. The product was extracted with ether, the organic layer was washed with an iced saturated potassium bicarbonate solution and with water and was dried over sodium sulfate. Evaporation of the solvent gave 850 mg of an oil which was acetylated in the usual fashion with 3 ml of acetic anhydride in 6 ml of pyridine to give 640 mg of an amorphous residue which was chromatographed on 30 g of aluminium oxide. Elutions with petroleum ether – benzene (1:1) gave 121 mg 25.5% yield from Δ^{14}-3β,21-diacetoxypregnenone **23b** of 3β-acetoxy-5β-carda-14(15),20(22)-dienolide (β-anhydrodigitoxigenin acetate) (**1a**), m.p. 179–185° (yield from the Δ^{14}-3β-hydroxyetianic acid **3**: 17.4%). A sample was recrystallized three times from acetone–hexane for analysis; needles, m.p. 190–192°; $[\alpha]_D^{26}$ −18.2° (*c*, 0.810 in $CHCl_3$) [lit. (*8b*, *8c*, *62a*, *62b*); m.p. 185°; $[\alpha]_D$ −18° ($CHCl_3$)]; λ_{max} (EtOH) 212 mμ (log ε 4.11); ν_{max} (KBr) 1783 and 1752 cm^{-1} (butenolide), 1738 cm^{-1} (acetate), 1645 cm^{-1} (shoulder, 14-double bond), 1630 cm^{-1} (20(22)-double bond), 1250 and 1234 cm^{-1} (large acetate band).

Anal. Calcd. for $C_{25}H_{34}O_4$: C, 75.34; H, 8.60. Found: C, 75.02; H, 8.46.

Elutions in the above-mentioned chromatogram with benzene–ether (9:1) gave 100 mg (20%) of an amorphous product; ν_{max} (KBr) 3430 cm^{-1} (20-hydroxyl), 1782 cm^{-1} (γ-lactone), 1740 cm^{-1} (acetate), 1663 cm^{-1} (double bond), 1245 cm^{-1} (large acetate band), which was not further investigated but to which we assign tentatively the structure of Δ^{14}*-3β-acetoxy-20ξ-hydroxy-5β-cardenolide* (**22**).

(b) From Δ^{14}*-21-Diazo-3β-acetoxy-5β-pregnen-20-one (21) Directly through* Δ^{14}*-3β,21-Diacetoxy-5β-pregnen-20-one (23b)*

A solution of 1.342 g of crude Δ^{14}-21-diazo-3β-acetoxy-5β-pregnen-20-one (**21**) in 90 ml of glacial acetic acid was placed in an oil bath preheated to 135° and was heated for 10 min (total reaction time: 20 min). The acetic acid was removed *in vacuo* and the residue was dried repeatedly with absolute ethanol and absolute ether. The product, representing crude Δ^{14}*-3β,21-diacetoxy-5β-pregnen-20-one* (**23b**), was purified as described above to give 989 mg of crystalline diacetate **23b** (68.3%) and 88 mg (6%) of a less pure, only partly crystalline material.

Both purified fractions of the diacetate **23b** (1.077 g) were subjected under the conditions described above to the Reformatsky reaction to give, after chromatography of the crude reaction product, 258 mg (25.7% from the diacetate **23b**) of β-*anhydrodigitoxigenin acetate* (**1a**), m.p. 181–184°. The identity of the product with the one described under (*a*) was established by comparison of the ultraviolet and infrared spectra and by the determination of a mixture melting point.

(c) From Digitoxigenin Acetate (2a)

To a solution of 500 mg of digitoxigenin acetate (**2a**), m.p. 224–225°, in 5 ml of absolute pyridine, there was added at 0°, 0.5 ml of thionyl chloride and the mixture was transferred into an ampulla which was sealed. The product was kept for 16 h at 0° and for 1 h at room temperature and then poured into ice water. The precipitate was extracted with a mixture of chloroform and ether (1:3) and the organic layer was washed with cold dilute hydrochloric acid, with an iced saturated potassium bicarbonate solution, and with water and was dried over sodium sulfate. Evaporation of the solvent gave 500 mg of a product which was recrystallized from acetone–hexane to give 465 mg (97.2%) of *3β-acetoxy-5β-carda-14(15), 20-(22)-dienolide (β-anhydrodigitoxigenin acetate)* (**1a**), m.p. 180–183°. Two recrystallizations from dichloromethane–

ether raised the melting point to 190–192°. The identity of this product with the materials synthesized according to (*a*) and (*b*) was established by the comparison of the infrared and ultraviolet spectra and by the determination of mixture melting points.

Acknowledgments

We express our sincere appreciation to Mr. R. Bouchard of this laboratory for his cooperation in the Meerwein–Pondorf reduction experiments and to Mr. D. Capitaine and Mrs. G. Pelletier for their valuable assistance. We are most grateful to Dr. J. Renz from Sandoz S.A., Basle, Dr. E. B. Hershberg and Dr. H. Herzog from the Schering Corporation, Bloomfield, N.J., and to Dr. M. E. Wall from the Research Triangle Institute, Durham, North Carolina, for generous gifts of starting materials. One of us (G.B.) acknowledges with gratitude the award of a Shell of Canada Fellowship during the academic year 1963–1964. We are greatly indebted to the National Research Council of Canada and the Quebec Heart Foundation for financial support of this project.

1. F. Winternitz and Ch. R. Engel. Steroids, **6,** 805 (1965).
2. Ch. R. Engel and G. Bach. Steroids, **3,** 593 (1964).
3. J. M. Ferland, Y. Lefebvre, R. Deghenghi, and K. Wiesner. Tetrahedron Letters, 3617 (1966).
4. N. Danieli, Y. Mazur, and F. Sondheimer. J. Am. Chem. Soc. **84,** 875 (1962); Tetrahedron, **22,** 3189 (1966).
5. Ch. R. Engel and G. Bach. Chem. Can. IV, 35 (1963).
6. R. Deghenghi, A. Philipp, and R. Gaudry. Tetrahedron Letters, 2045 (1963).
7. (*a*) Pl. A. Plattner, L. Ruzicka, H. Heusser, J. Pataki, and Kd. Meier. Helv. Chim. Acta, **29,** 942 (1946); (*b*) Pl. A. Plattner, L. Ruzicka, H. Heusser, and E. Angliker. Helv. Chim. Acta, **30,** 385 (1947); (*c*) Pl. A. Plattner, L. Ruzicka, H. Heusser, and E. Angliker. Helv. Chim. Acta, **30,** 395 (1947); (*d*) L. Ruzicka, Pl. A. Plattner, H. Heusser, and Kd. Meier. Helv. Chim. Acta, **30,** 1342 (1947).
8. (*a*) S. Smith. J. Chem. Soc. 2478 (1930); (*b*) S. Smith. J. Chem. Soc. 1050 (1935); (*c*) H. M. E. Cardwell and S. Smith. J. Chem. Soc. 2012 (1954); (*d*) O. Schindler. Helv. Chim. Acta, **39,** 375 (1956).
9. F. Hunziker and T. Reichstein. Helv. Chim. Acta, **28,** 1472 (1945).
10. H. Heusser, M. Roth, O. Rohr, and R. Anliker. Helv. Chim. Acta, **38,** 1178 (1955).
11. (*a*) R. E. Marker and E. Rohrmann. J. Am. Chem. Soc. **62,** 518 (1940); (*b*) R. E. Marker. J. Am. Chem. Soc. **62,** 3350 (1940); (*c*) R. E. Marker, R. B. Wagner, P. R. Ulshafer, E. L. Wittbecker, D. P. J. Goldsmith, and C. H. Ruof. J. Am. Chem. Soc. **69,** 2167 (1947); (*d*) D. H. Gould, H. Staeudle, and E. B. Hershberg. J. Am. Chem. Soc. **74,** 3685 (1952); (*e*) W. G. Dauben and G. J. Fonken. J. Am. Chem. Soc. **76,** 4618 (1954); (*f*) M. E. Wall, H. E. Kenney, and E. S. Rothman. J. Am. Chem. Soc. **77,** 5665 (1955); (*g*) M. E. Wall and E. S. Serota. Tetrahedron, **10,** 238 (1960).
12. C. L. Hewett. Brit. Patent 749,697 (1954).
13. G. R. Pettit and D. M. Piatak. Can. J. Chem. **44,** 844 (1966).
14. R. U. Schock and W. J. Karpel. U.S. Patent No. 2,684,963 to Abbott Laboratories, North Chicago. (1954).
15. Ch. R. Engel and R. Deghenghi. Can. J. Chem. **38,** 452 (1960).
16. S. Rakhit, R. Deghenghi, and Ch. R. Engel. Can. J. Chem. **41,** 703 (1963).
17. P. P. Holysz. J. Am. Chem. Soc. **75,** 4432 (1953).
18. M. Gut. J. Org. Chem. **21,** 1327 (1956).
19. A. Butenandt and G. Müller. Ber. **71,** 191 (1938).
20. Ch. R. Engel, J. Lessard, and R. Bouchard. Unpublished results.
21. F. C. Chang and R. T. Blickenstaff. J. Am. Chem. Soc. **80,** 2906 (1958).
22. C. Djerassi, A. J. Manson, and M. Gorman. J. Am. Chem. Soc. **77,** 4925 (1955).
23. M. Harnik. Steroids, **3,** 359 (1964).
24. R. Bouchard and Ch. R. Engel. 49th Conf. Chem. Inst. Can. Saskatoon, 1966. Abstr. p. 72. R. Bouchard and Ch. R. Engel. Can. J. Chem. To be published.
25. H. Schinz and G. Schäppi. Helv. Chim. Acta, **30,** 1483 (1947).
26. K. Bowden, J. Heilbron, E. R. H. Jones, and B. C. L. Weedon. J. Chem. Soc. 39 (1946).
27. Pl. A. Plattner and H. Heusser. Helv. Chim. Acta, **29,** 727 (1946).
28. L. Ruzicka, Pl. A. Plattner, H. Heusser, and J. Pataki. Helv. Chim. Acta, **29,** 936 (1946).
29. Pl. A. Plattner, Kd. Meier, and H. Heusser. Helv. Chim. Acta, **30,** 905 (1947).
30. Pl. A. Plattner, H. Heusser, and A. Segre. Helv. Chim. Acta, **31,** 249 (1948).
31. R. Tschesche, F. Riemhofer, and G. Snatzke. Chem. Ber. **98,** 1188 (1965).
32. J. Press and T. Reichstein. Helv. Chim. Acta, **30,** 2127 (1947).
33. J. Fried and F. Sabo. J. Am. Chem. Soc. **79,** 1130 (1957).
34. W. G. Dauben and H. L. Bradlow. J. Am. Chem. Soc. **74,** 559 (1952).
35. A. C. Ott, M. F. Murray, and R. L. Pederson. J. Am. Chem. Soc. **74,** 1239 (1952).
36. F. Sondheimer, M. Velasco, and G. Rosenkranz. J. Am. Chem. Soc. **77,** 5673 (1955).
37. F. Sondheimer, N. Stjernström, and D. Rosenthal. J. Org. Chem. **24,** 1280 (1959).
38. L. Lábler and F. Šorm. Collection Czech. Chem. Commun. **25,** 2855 (1960).
39. (*a*) G. Stork and J. Tsuji. J. Am. Chem. Soc. **83,** 2783 (1961); (*b*) G. Stork, P. Rosen, and N. L. Goldman. J. Am. Chem. Soc. **83,** 2965 (1961).
40. R. E. Schaub and M. J. Weiss. Chem. Ind. London, 2003 (1961).
41. (*a*) F. Johnson, G. T. Newbold, and F. S. Spring. J. Chem. Soc. 1302 (1954); (*b*) A. F. Daglish, J. Green, and V. D. Poole. J. Chem. Soc. 2627 (1954); (*c*) R. Wiechert and E. Kaspar. Chem. Ber. **93,** 1710 (1960).
42. D. H. R. Barton and C. H. Robinson. J. Chem. Soc. 3045 (1954).
43. C. Djerassi and J. Staunton. J. Am. Chem. Soc. **83,** 736 (1961).
44. K. Meyer and T. Reichstein. Helv. Chim. Acta, **30,** 1508 (1947).

Can. J. Chem. Downloaded from www.nrcresearchpress.com by 210.87.254.105 on 09/05/12
For personal use only.

45. G. DARZENS. Compt. Rend. **152,** 1601 (1911).
46. (*a*) F. REBER, A. LARDON, and T. REICHSTEIN. Helv. Chim. Acta, **37,** 45 (1954); (*b*) A. LARDON and T. REICHSTEIN. Helv. Chim. Acta, **37,** 388, 443 (1954).
47. (*a*) R. ADAMS and L. H. ULICH. J. Am. Chem. Soc. **42,** 599 (1920); (*b*) A. L. WILDS and C. H. SHUNK. J. Am. Chem. Soc. **70,** 2427 (1948).
48. (*a*) M. STEIGER and T. REICHSTEIN. Helv. Chim. Acta, **20,** 1164 (1937); (*b*) T. REICHSTEIN and J. VON EUW. Helv. Chim. Acta, **23,** 136 (1940).
49. K. OTTO and M. EHRENSTEIN. J. Org. Chem. **26,** 2871 (1948).
50. CH. R. ENGEL. J. Am. Chem. Soc. **78,** 4727 (1956).
51. (*a*) R. B. MOFFETT and D. I. WEISBLAT. J. Am. Chem. Soc. **74,** 2183 (1952); (*b*) C. DJERASSI and C. T. LENK. J. Am. Chem. Soc. **75,** 3493 (1953).
52. (*a*) L. RUZICKA, T. REICHSTEIN, and A. FÜRST. Helv. Chim. Acta, **24,** 76 (1941); (*b*) L. RUZICKA, PL. A. PLATTNER, and A. FÜRST. Helv. Chim. Acta, **24,** 716 (1941).
53. J. FRIED, R. A. LINVILLE, and C. ELDERFIELD. J. Org. Chem. **7,** 362 (1942).
54. W. S. ALLEN, S. BERNSTEIN, and R. LITTELL. J. Am. Chem. Soc. **76,** 6116 (1954).
55. R. O. CLINTON, R. L. CLARKE, F. W. STONNER, A. J. MANSON, K. F. JENNINGS, and D. K. PHILLIPS. J. Org. Chem. **27,** 2800 (1962).
56. (*a*) A. BUTENANDT. Ber. **63,** 659 (1930); (*b*) G. SLOMP, JR., Y. F. SHEALY, J. L. JOHNSON, R. A. DONIA, B. A. JOHNSON, R. P. HOLYSZ, R. L. PEDERSON, A. O. JENSEN, and O. OTT. J. Am. Chem. Soc. **77,** 1216 (1955).
57. (*a*) A. BUTENANDT and L. MAMOLI. Ber. **68,** 1847 (1935); (*b*) CH. MEYSTRE and K. MIESCHER. Helv. Chim. Acta, **29,** 33 (1946); (*c*) D. H. R. BARTON. *Quoted by* C. W. Shoppee. J. Chem. Soc. 1671 (1949).
58. GLIDDEN CO. Brit. Patent 736,817 (1955).
59. CH. R. ENGEL, K. F. JENNINGS, and G. JUST. J. Am. Chem. Soc. **78,** 6153 (1956).
60. A. LARDON and T. REICHSTEIN. Helv. Chim. Acta, **46,** 392 (1963).
61. S. RANGASWAMI and T. REICHSTEIN. Helv. Chim. Acta, **32,** 939 (1949).
62. (*a*) H. HELFENBERGER and T. REICHSTEIN. Helv. Chim. Acta, **31,** 1470 (1948); (*b*) A. RHEINER, A. HUNGER, and T. REICHSTEIN. Helv. Chim. Acta, **35,** 687 (1952).

Can. J. Chem. Downloaded from www.nrcresearchpress.com by 210.87.254.105 on 09/05/12
For personal use only.

Can. J. Chem. Downloaded from www.nrcresearchpress.com by 210.87.254.40 on 09/05/12
For personal use only.

Spirocyclic tetrahydropyrimidines derived from pentaerythritol

ROMANO L. SALVADOR and MICHEL SAUCIER
Medicinal Chemistry Laboratory, Faculty of Pharmacy, University of Montreal, Montreal, Quebec
Received October 2, 1967

A series of seven spirocyclic compounds bearing the newly synthesized 6,8-diaza-2-oxaspiro[3·5]nonane ring system are reported. Their preparation consists in the condensation of 3,3-bis(aminomethyl)oxetane monohydrate, obtained via pentaerythritol tribromide and, 3,3-bis(bromomethyl)oxetane, with certain amidines and guanidines.

Canadian Journal of Chemistry, 46, 751 (1968)

The focus of attention in the field of hypotensive drugs has been placed for some years on certain guanidines (1–3) and amidines (4) which produce their effect by preventing the release of the adrenergic transmitter substance at sympathetic nerve endings. The series of amidines and guanidines presented in this paper were prepared as potential sympathetic blocking agents. These constitute a departure from the recognized chemical pattern of such drugs in that the amidine or guanidine moieties are part of a new spirocyclic structure, i.e., 6,8-diaza-2-oxaspiro[3·5]nonane. The spirocyclic compounds were obtained in five or six steps from pentaerythritol (**1**) according to Scheme 1.

Pentaerythritol (**1**) was first converted into 2,2-bis(bromomethyl)-3-bromo-propanol (**2**) in high yields (90%) with anhydrous hydrobromic acid in acetic acid (5). The tribromo derivative **2** was then converted to 3,3-bis(aminomethyl)-oxetane dihydrobromide as described previously (6) and as illustrated in Scheme 1. Attempts to isolate base **5** by the steam distillation method of Beyaert and Govaert (6) and by the salting out process described by Campbell (7) were unsuccessful in our hands. However, good recovery (ca. 70%) of 3,3-bis(aminomethyl)oxetane monohydrate (**5**) was obtained when the dihydrobromide salt (**4**) was treated with a theoretical amount of solid potassium hydroxide and the free base was extracted with absolute alcohol.

The syntheses of structures **8** *a*, *b*, *c*, and *d*,

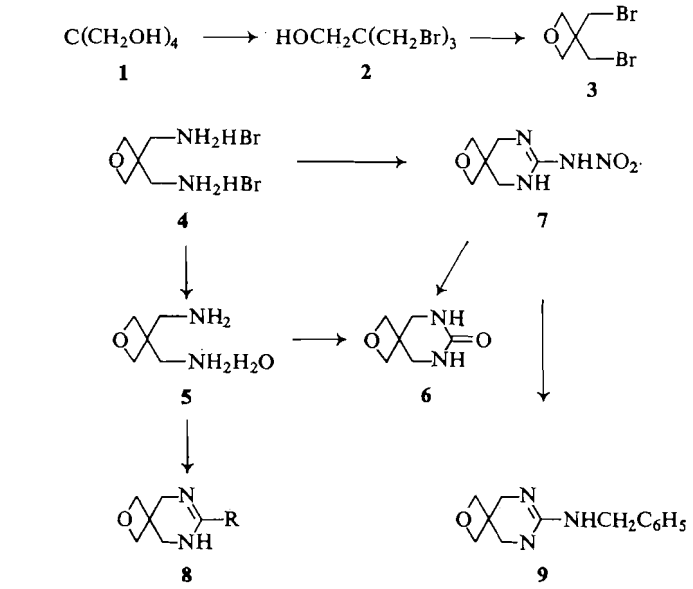

1 **2** **3** **4** **5** **6** **7** **8** **9**

8*a* R = CH_3
8*b* R = C_6H_5
8*c* R = $CH_2C_6H_5$
8*d* R = NH_2

Scheme 1

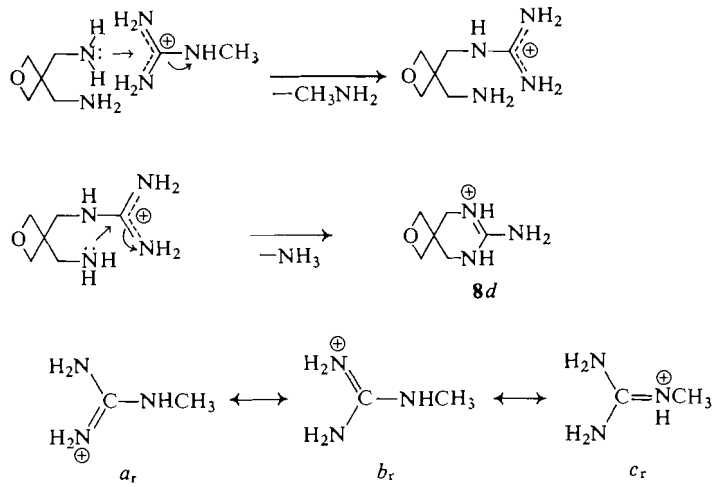

Scheme 2

were performed by a general method for the preparation of 2-substituted-1,4,5,6-tetrahydropyrimidines devised by Brown and Evans (8). Accordingly, acetamidine hydrochloride, benzamidine hydrochloride, phenylacetamidine hydrochloride, and guanidine hydrochloride were condensed with 3,3-bis(aminomethyl)oxetane monohydrate (**5**) yielding the hydrochloride salts of the new spiro structures **8** *a*, *b*, *c*, *d*. These reactions proceeded smoothly at low temperatures with the evolution of two moles of ammonia.

The synthesis of compound **9** was attempted by direct condensation of benzylguanidine hydrochloride with diamine **5**, but this reaction failed to give the expected product and gave instead product **8** *d* in 16% yield. A similar condensation was attempted between phenylguanidine hydrochloride and diamine **5** producing once again compound **8** *d* in 25% yield. Ammonia was collected in both cases and estimated. In order to ascertain the importance of recurring compound **8** *d* in these reactions it was decided to react methylguanidine hydrochloride with diamine **5** and collect the volatile bases thus produced. The expected *N*-methylcyclic guanidine could not be isolated from the reaction but instead compound **8** *d* was again produced in 31% yield. The gases evolved during this reaction were collected in an alcoholic solution of anhydrous hydrogen chloride and methylamine was isolated as its hydrochloride and characterized as its phenylthiourea derivative along with ammonium chloride. As the yield of compound **8** *d* produced by the condensation of guanidine hydrochloride and diamine **5** was found to be 44% (see Table I), this reaction was taken as a basis for comparison with the aforementioned condensations. It was then reasonable to assume that the elimination of methylamine as well as the likely elimination of benzylamine and aniline from the corresponding guanidines constitutes a preferred reaction course. These observations suggested the following reaction mechanism as a possible explanation for the production of compound **8** *d* (Scheme 2).

The methylguanidinium ion is a resonating hybrid of structures a_r, b_r, and c_r. Structures a_r and b_r are equivalent and contribute strongly to the stability of the resonating molecule whereas structure c_r offers little contribution to the stability of the hybrid inasmuch as the inductive effect of the methyl group does not favor this structure and for reasons of non equivalence. As a consequence, it is reasonable to assume that the $=N^+HCH_3$ entity is more labile than its well stabilized NH_2 counterparts resulting in the elimination of methylamine from the methylguanidine molecule under attack by a nucleophile. The reaction of 3,3-bis(aminomethyl) oxetane with methylguanidine hydrochloride would imply firstly a nucleophilic attack on the central carbon atom of methylguanidine by one of the NH_2 groups of the 1,3-diamine **5** with the elimination of methylamine, followed by a second nucleophilic attack on the same carbon atom by the second NH_2 group of the diamine

Can. J. Chem. Downloaded from www.nrcresearchpress.com by 210.87.254.40 on 09/05/12
For personal use only.

TABLE I

Data for *N*-substituted 6,8-diaza-2-oxaspiro[3·5]non-6-ene hydrochlorides

HCl Salt of compound	Reaction time	Temperature °C	Melting point °C	% yield	Formula	Analyses			
						%C	%H	%N	%Cl
8*a*	10 min	room temperature	241–251 d*	77	$C_7H_{13}ClN_2O$	Calcd. 47.59 Found 47.64	7.41 7.69	15.85 15.82	20.07 20.29
8*b*	2 h	75	230–231†	76	$C_{12}H_{15}ClN_2O$	Calcd. 60.37 Found 60.23	6.33 6.33	11.73 11.63	14.85 14.68
8*c*	1 h	50	231–231.5‡	77	$C_{13}H_{17}ClN_2O$	Calcd. 61.77 Found 61.51	6.77 6.73	11.08 11.28	14.02 13.95
8*d*	3 h	140	225–226§	44	$C_6H_{12}ClN_3O$	Calcd. 40.56 Found 40.55	6.80 6.80	23.65 23.40	19.95 19.50

*Recrystallized from absolute ethyl alcohol. Infrared cm^{-1}, C—O—C (split band) 970, 940; $HN{=}\overset{+}{C}{-}NH$ 1660 (Nujol mull).

†Recrystallized from dry isopropyl alcohol. Infrared cm^{-1}, C—O—C (split band) 975, 940; $HN{=}\overset{+}{C}{-}NH$ 1640 (Nujol mull).

‡Recrystallized from absolute ethyl alcohol. Infrared cm^{-1}, C—O—C (split band) 970, 940; $NH{=}\overset{+}{C}{-}NH$ 1650 (Nujol mull).

§Recrystallized from absolute ethyl alcohol. Infrared cm^{-1}, C—O—C (split band) 980, 950; $NH{=}\overset{+}{C}{-}NH$ 1670 (Nujol mull).

5 with subsequent evolution of ammonia and cyclization to produce compound **8** *d*.

Since a direct method of cyclization to compound **9** did not seem available, another synthetic pathway based on reactions described by McKay *et al.* (9, 10) was chosen. Compound **7** was thus prepared by reacting the dihydrobromide salt **4** with potassium hydroxide and nitroguanidine in aqueous solution according to these authors. This compound was then refluxed with an excess of anhydrous benzylamine to afford the cyclic guanidine **9**. The pyrimidone **6** was obtained incidentally by the hydrolysis of compound **7** with an aqueous solution of benzylamine. This reaction has been described by McKay *et al.* (10). The same pyrimidone was also prepared by the condensation of urea with the 1,3-diamine **5** according to a procedure described by Bradbury *et al.* (11).

Pharmacological testing of the above compounds is in its preliminary stage.

Experimental

The melting points reported in this work are uncorrected. The elemental analyses were performed by Dr. Daesslé, 5757 Decelles, Montreal. The infrared spectra were made on a Beckman IR 8 spectrophotometer. The hydrochloride salts were titrated potentiometrically with silver nitrate. Acetamidine hydrochloride, practical grade, was purchased from Eastman and used without further purification.

Non-cyclic Amidines and Guanidines

Benzamidine hydrochloride, phenylacetamidine hydrochloride, and nitroguanidine were prepared by methods described in the literature (12–14).

Guanidine hydrochloride was obtained by passing dry hydrochloric acid into an alcoholic suspension of guanidine carbonate (Matheson, Coleman, and Bell).

3,3-Bis(aminomethyl)oxetane Monohydrate (5)

3,3-Bis(aminomethyl)oxetane dihydrobromide (**4**) (20 g, 0.07 mole) was treated with potassium hydroxide pellets (9.4 g, 0.14 mole) while stirring rapidly. After a period of 5 min an exothermic reaction occurred. The stirring was continued until all the potassium hydroxide pellets were consumed. The liberated 1,3-diamine was taken up in 50 ml of absolute ethyl alcohol and the potassium bromide formed in the reaction eliminated by filtration. After evaporation of the alcohol, the residue was distilled under reduced pressure to afford 6.5 g (67%) of 3,3-bis(aminomethyl)oxetane monohydrate, b.p. 121° at 15 mm; lit. 121° at 15 mn (6).

7-Nitramino-6,8-diaza-2-oxaspiro[3·5]non-6-ene (7)

Nitroguanidine, 7.48 g (.07 mole) was dissolved in a solution of potassium hydroxide prepared from 9.4 g (0.14 mole) of KOH in 15 ml of water. 3,3-Bis(aminomethyl)oxetane dihydrobromide (**4**) (20 g, 0.07 mole) was then added to this solution which formed a thick paste. The mixture was heated and stirred for 20 min at 65°. At the end of the reaction, most of the solid material had dissolved. On cooling in an ice-salt bath, 4 g (31%) of a white solid precipitated out. This product was purified by several recrystallizations in a mixture of ethyl alcohol and water and identified as 7-nitramino-6,8-diaza-2-oxaspiro[3·5]non-6-ene, m.p. 254–255° (decomp.). Infrared cm^{-1}: C—O—C (split band) 968, 940; $HN{-}\overset{+}{C}{=}N$ 1620 (Nujol mull).

Anal. Calcd. for $C_6H_{10}N_4O_3$: C, 38.70; H, 5.41; N, 30.09. Found: C, 38.52; H, 5.47; N, 30.10.

7-Benzylamino-6,8-diaza-2-oxaspiro[3·5]non-6-ene (9)

7-Nitramino-6,8-diaza-2-oxaspiro[3·5]non-6-ene (**7**),

Can. J. Chem. Downloaded from www.nrcresearchpress.com by 210.87.254.40 on 09/05/12
For personal use only.

Can. J. Chem. Downloaded from www.nrcresearchpress.com by 210.87.254.40 on 09/05/12
For personal use only.

(2 g, 0.01 mole) and freshly distilled benzylamine (10 ml) were heated at 150° until the evolution of nitrous oxide had ceased which took approximately 20 min. The benzylamine in excess was then eliminated *in vacuo*. The residual yellow oil which amounted to 1.5 g (62%) was distilled, b.p. 210–213° at 0.08 mm. This product formed a salt with picric acid which was the picrate of 7-benzylamino-6,8-diaza-2-oxaspiro[3·5]non-6-ene, m.p. 165–165.5°. Infrared cm^{-1}: C—O—C (split band) 970, 950; HN=$\overset{+}{C}$— NH 1650 (Nujol mull).

Anal. Calcd. for $C_{19}H_{20}N_6O_8$: C, 49.56; H, 4.37; N, 18.25. Found: C, 49.77; H, 4.42; N, 18.25.

6,8-Diaza-2-oxaspiro[3·5]nonan-7-one (6)

A mixture of urea (2.6 g, 0.042 mole) and 3,3-bis-(aminomethyl)oxetane monohydrate (**5**) (5.7 g, 0.642 mole) was heated over a period of 1 h at 150°. At the end of the reaction, the contents of the flask turned into a solid mass. The solid material, after recrystallization from absolute ethyl alcohol, gave 3 g (50%) of a white crystalline product m.p. 277.5–278° C. This compound was identical with a sample obtained by the hydrolysis of 7-nitramino-6,8-diaza-2-oxaspiro[3·5]non-6-ene (**7**) with aqueous benzylamine as determined by mixture melting points and infrared spectra. The pyrimidone is very soluble in water and insoluble in most other organic solvents. Infrared cm^{-1}: C—O—C (split band) 970, 945; HN—CO—NH 1670 (Nujol mull).

Anal. Calcd. for $C_6H_{10}N_2O_2$: C, 50.69; H, 7.08; N, 19.70; Found: C, 50.07; H, 7.17; N, 19.54.

N-Substituted 6,8-Diaza-2-oxaspiro[3·5]non-6-enes (8)

These compounds were prepared by successively condensing **5** with the hydrochloride salts of acetamidine, benzamidine, phenylacetamidine, and guanidine as follows: the amidine or guanidine (0.025 mole) was added to 3,3-bis(aminomethyl)oxetane monohydrate (**5**) (0.025 mole) in a 25 ml flask with magnetic stirring. The reaction occurred at room temperature (**8** *a*) or was heated in an oil bath (**8** *b*, *c*, *d*) for a period of 10 min to 3 h after which the mixture solidified. The product of the reaction was then crystallized in absolute ethyl alcohol or dry isopropyl alcohol yielding the hydrochloride salt of the desired spiro compound. Data pertaining to these compounds are given in Table I.

Condensation of N-Substituted Guanidine Hydrochlorides with 3,3-Bis(aminomethyl)oxetane Monohydrate (5)

Condensation with Benzylguanidine Hydrochloride

A mixture of benzylguanidine hydrochloride (2.04 g, 0.011 mole), and 3,3-bis(aminomethyl)oxetane monohydrate **5** (1.5 g, 0.011 mole) was heated over a period of 3 h at 125°. The ammonia evolved was passed into a standardized aqueous solution of hydrochloric acid. After 2 h of heating almost all evolution of ammonia had ceased. The hydrochloric acid solution was then back-titrated with aqueous standardized sodium hydroxide and was found to correspond to 0.0078 mole of ammonia. To the viscous liquid remaining in the flask was added a minimum of hot isopropyl alcohol until solution was effected. Acetone was then added to incipient cloudiness and the solution permitted to crystallize in the cold for 2 days. The yield of compound **8** *d*, m.p. 225–226°, was 0.273 g (16%) verified by mixture melting point and infrared spectroscopy.

Condensation with Phenylguanidine Hydrochloride

A similar reaction was effected with phenylguanidine hydrochloride (1.88 g, 0.011 mole) and diamine **5** (1.5 g, 0.011 mole). The ammonia evolved was passed into hydrochloric acid solution as above and back-titrated with standard sodium hydroxide corresponding to 0.012 mole of NH_3. Compound **8** *d* isolated from the reaction weighed 0.505 g (25%).

Condensation with Methylguanidine Hydrochloride

Methylguanidine hydrochloride (2.46 g, 0.019 mole) and diamine **5** (2.64 g, 0.019 mole) were reacted in a similar way. The evolved gases were collected in an anhydrous alcoholic solution of hydrogen chloride and the solution was then evaporated to dryness *in vacuo*. The crystalline solid, which weighed 1.25 g, was evaluated at 0.010 mole each for methylamine and ammonia assuming equimolar evolution of these gases. A weighed sample of the crystalline solid in aqueous solution was analyzed by gas–liquid chromatography (Perkin–Elmer model 881 equipped with flame ionization detector). The sample was determined by comparing with a standard graph prepared from pure samples of methylamine hydrochloride. The value for this determination corresponded to 0.008 mole of methylamine which is in good accord with the above estimate. The remaining portion of the solid was placed in absolute alcohol, the ammonium chloride was removed by filtration, the methylamine hydrochloride was recrystallized several times from the same solvent, and was characterized as its phenylthiourea derivative, m.p. 114.5–115°, lit. 113° (15).

Acknowledgment

The authors wish to thank the National Research Council of Canada for financial assistance in carrying out this research project. Thanks must also be expressed to Mr. Claude Sauriol of our Analytical Section who performed the analyses by gas–liquid chromatography.

1. R. A. Maxwell, R. P. Mull, and A. J. Plummer. Experientia, **15**, 267 (1959).
2. W. B. Abrams, R. Pocelinko, M. Klausner, L. Hanauer, and E. N. Whitman. J. New Drugs, **4**, 268 (1964).
3. A. L. A. Boura, F. C. Copp, A. F. Green, H. F. Hodson, G. K. Ruffell, M. F. Sim, E. Walton, and E. M. Grivsky. Nature, **191**, 1312 (1961).
4. A. L. A. Boura, F. C. Copp, and A. F. Green. Nature, **195**, 1213 (1962).
5. M. Saucier, C. Sauriol, and R. L. Salvador. Can. J. Chem. **44**, 1599 (1966).
6. M. Beyaert and F. Govaert. Proc. Acad. Sci. Amsterdam, **42**, 776 (1939).
7. T. W. Campbell. J. Org. Chem. **22**, 1029 (1957).
8. D. J. Brown and R. F. Evans. J. Chem. Soc. 4039 (1962).
9. A. F. McKay and G. F. Wright. J. Am. Chem. Soc. **70**, 430 (1948).
10. A. F. McKay, M. N. Buchanan, and A. G. Gordon. J. Am. Chem. Soc. **71**, 766 (1949).

11. R. B. BRADBURY, N. C. HANCOX, and H. H. HATT. J. Chem. Soc. 1394 (1947).
12. A. W. DOX. *In* Organic syntheses. Coll. Vol. 1. *Edited by* H. Gilman and A. H. Blatt. John Wiley and Sons, Inc., New York. 1941. p. 5.
13. G. LUCKENBACH. Ber. deut. chem. Ges. **17**, 1421 (1884).
14. T. L. DAVIS. *In* Organic syntheses. Coll. Vol. 1. *Edited by* H. Gilman and A. H. Blatt. John Wiley and Sons, Inc., New York. 1941. p. 399.
15. R. L. SHRINER, R. C. FUSON, and D. Y. CURTIN. The systematic identification of organic compounds. 5th ed. John Wiley and Sons, New York. 1965. p. 326.

Can. J. Chem. Downloaded from www.nrcresearchpress.com by 210.87.254.40 on 09/05/12
For personal use only.

Can. J. Chem. Downloaded from www.nrcresearchpress.com by 210.87.254.6 on 09/05/12
For personal use only.

Concerning the mechanism of the reaction of methyllithium with methyl 2,3-anhydro-4,6-*O*-benzylidene-α-D-allopyranoside to form 4,6-*O*-benzylidene-1,2-didehydro-1,2-dideoxy-2-methyl-D-*ribo*-hexopyranose

M. SHARMA[1] AND R. K. BROWN
Department of Chemistry, University of Alberta, Edmonton, Alberta

Received August 17, 1967

Evidence supports the view that methyllithium, which contains no iodide or bromide ions as competitors, reacts with methyl 2,3-anhydro-4,6-*O*-benzylidene-α-D-allopyranoside to form, first, methyl 4,6-*O*-benzylidene-2-deoxy-2-methyl-α-D-altropyranoside. The latter compound then reacts with excess methyllithium to form 4,6-*O*-benzylidene-1,2-didehydro-1,2-dideoxy-2-methyl-D-*ribo*-hexopyranose by loss of methyl alcohol.

A synthesis of methyl 4,6-*O*-benzylidene-2-deoxy-2-methyl-α-D-altropyranoside is given.

The reactions of excess lithium iodide, bromide, and chloride with both methyl 2,3-anhydro-4,6-*O*-benzylidene-α-D-allopyranoside and methyl 2,3-anhydro-4,6-*O*-benzylidene-α-D-mannopyranoside are described.

Canadian Journal of Chemistry, **46**, 757 (1968)

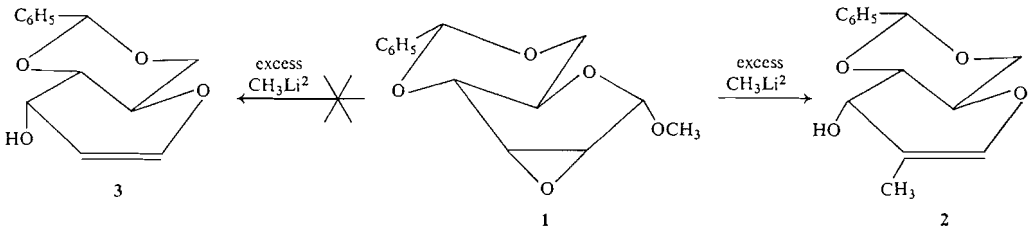

3 1 2

Scheme 1.

Introduction

In a previous report (1) it was shown that the reaction of excess commercial methyllithium[2] in ether with methyl 2,3-anhydro-4,6-*O*-benzylidene-α-D-allopyranoside (**1**) gave, in 22% yield, 4,6-*O*-benzylidene-1,2-didehydro-1,2-dideoxy-2-methyl-D-*ribo*-hexopyranose (**2**) rather than 4,6-*O*-benzylidene-1,2-didehydro-1,2-dideoxy-D-*ribo*-hexopyranose (**3**) (Scheme 1) as had been expected on the basis of published work (2). This paper presents information concerning the route by which methyllithium converts **1** to **2**.

Results and Discussion

The incorporation of the methyl group in **2** must have occurred via the well known epoxide ring opening by anionic reagents (3) such as methyllithium. An illustration of such a reaction is found in the treatment of methyl 2,3-anhydro-4,6-*O*-benzylidene-α-D-mannopyranoside (**7**, Scheme 6) with methyllithium to form methyl 4,6-*O*-benzylidene-3-deoxy-3-methyl-α-D-altropyranoside, **9** (2). It was therefore considered possible that the epoxide **1** is first converted to methyl 4,6-*O*-benzylidene-2-deoxy-2-methyl-α-D-altropyranoside (**4**) which in turn reacts with the excess methyllithium to form the olefin, **2** (Scheme 2). Accordingly, it was deemed necessary to determine whether **4** would indeed react with methyllithium to yield the olefin **2**.

A successful route to compound **4** was obtained by the reaction of methylsulfinyl carbanion (4) with epoxide **1**, which gave methyl 4,6-*O*-benzylidene-2-deoxy-2-methylsulfinylmethyl-α-D-altropyranoside, **5** (Scheme 3). Compound **5** crystallized well from benzene–ether to give a product of melting point 135–136° and whose

---

[1]Postdoctorate Fellow at the University of Alberta, Edmonton, Alberta.

[2]*Note*. The commercial methyllithium was obtained from Foote Mineral Co., Route 100, Exton, Pennsylvania, U.S.A. In our previous paper (1) it was erroneously reported that the methyllithium employed in that work was obtained from Alfa Inorganics, Inc., 8 Congress Street, Beverly, Massachusetts, U.S.A., when in fact it was the Foote Co. product. Foote methyllithium is prepared from methyl chloride and lithium and the ether solution of this material contains practically no chloride. Methyllithium from Alfa Inorganics is prepared from methyl bromide and lithium, and its ether solution contains much bromide ion.

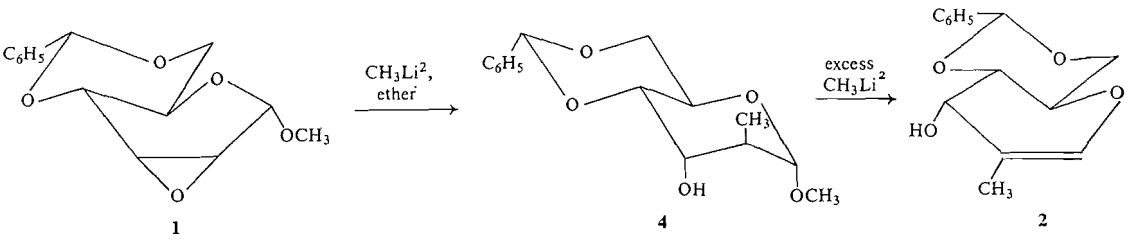

1 4 2

Scheme 2.

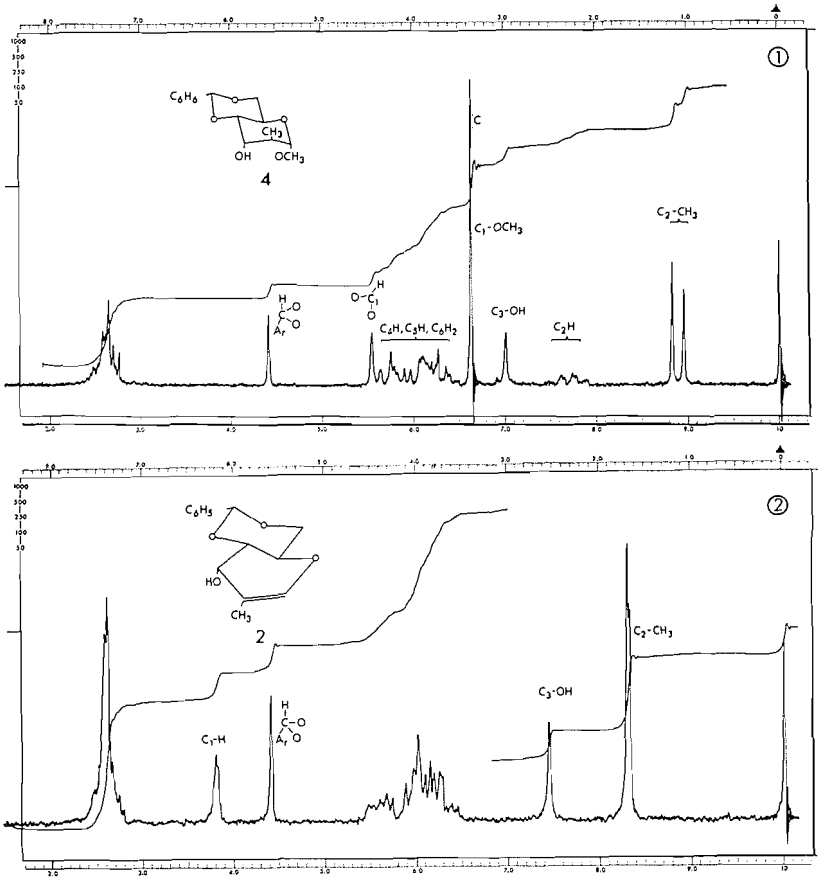

FIG. 1. The n.m.r. spectrum of methyl 4,6-*O*-benzylidene-2-deoxy-2-methyl-α-D-altropyranoside (**4**).
FIG. 2. The n.m.r. spectrum of 4,6-*O*-benzylidene-1,2-didehydro-1,2-dideoxy-2-methyl-D-*ribo*-hexopyranose (**2**).

elemental analysis was correct for structure **5**. But when **5** was crystallized from methanol it was obtained, according to the elemental analysis and the integrated nuclear magnetic resonance (n.m.r.) spectrum, as a 1:1 complex of methanol with **5**. The methanol of crystallization could be removed only by heating the complex above its melting point, 165–166°, and under vacuum for 6 h.

Crystallization of **5** from acetone gave back **5**, of melting point 136–137°, uncomplexed with acetone, as shown also by the absence of carbonyl absorption in the infrared spectrum.

Desulfurization of **5** by refluxing an acetone solution of **5** with Raney nickel (5) for 4 h removed the oxygen atom from the sulfur, giving methyl 4,6-*O*-benzylidene-2-deoxy-2-methylthiomethyl-α-D-altropyranoside (**6**). Compound **6**

Can. J. Chem. Downloaded from www.nrcresearchpress.com by 210.87.254.6 on 09/05/12
For personal use only.

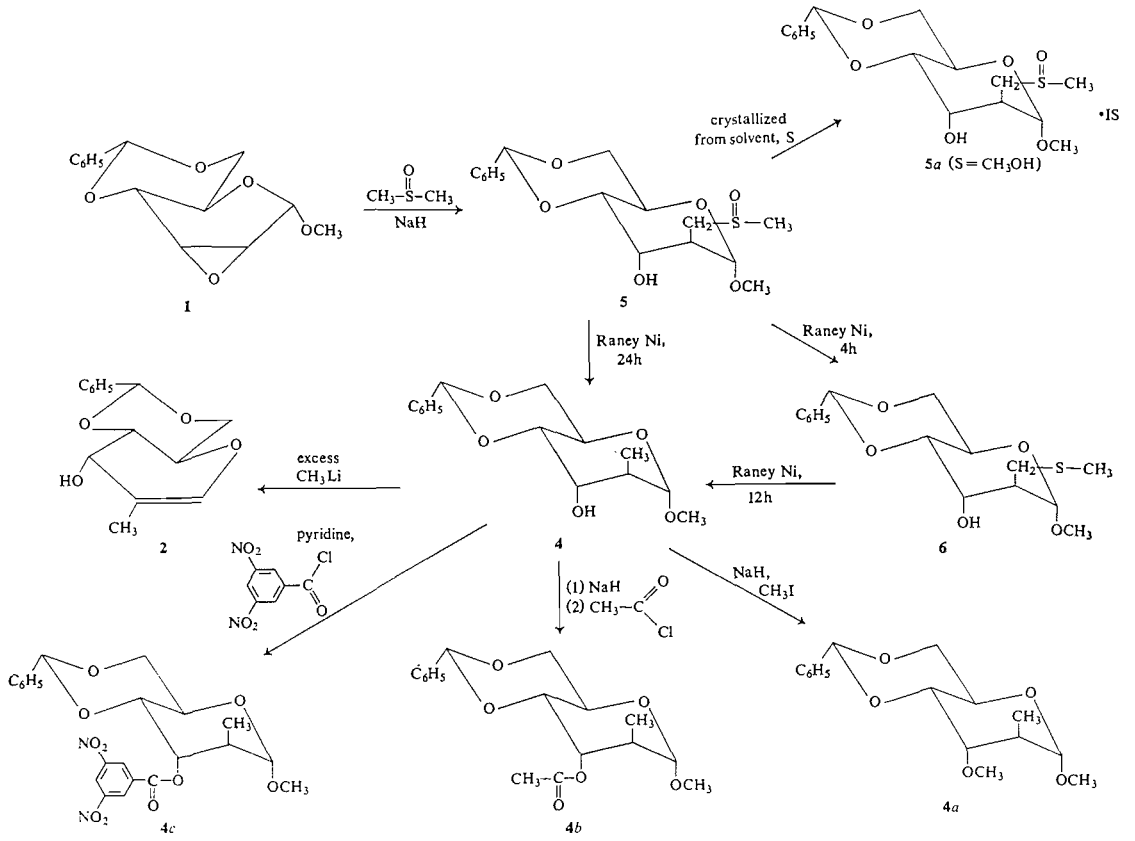

Scheme 3.

could be converted, by further reduction for a 12 h period under the same conditions as before, to methyl 4,6-*O*-benzylidene-2-deoxy-2-methyl-α-D-altropyranoside (**4**) (nuclear magnetic resonance (n.m.r.) spectrum, Fig. 1). Similarly, **5** was desulfurized, with Raney nickel, during a 24 h reflux period, to **4**.

When an ether solution of **4** was refluxed with *one equivalent* of methyllithium, the starting material was recovered intact, nearly quantitatively. However, when two or more equivalents of methyllithium were used, olefin **2** (n.m.r. spectrum, Fig. 2) was obtained in 78% yield.

The structural assignments of the products of the reaction of **1** with the methylsulfinyl carbanion and subsequent Raney nickel desulfurizations (**4**–**6**, Scheme 3) are as indicated, and follow from the known preferred *trans* diaxial opening of the epoxide ring in **1** (3, 6) as well as the eventual conversion to **2** in which the methyl group has been shown to be attached to C-2 (1).

Attempts to acetylate methyl 4,6-*O*-benzylidene-2-deoxy-2-methyl-α-D-altropyranoside (**4**) with acetic anhydride and pyridine were quite unsuccessful, probably due to the strong 1,3-diaxial interaction developed in the transition state. However *O*-acetylation to **4***b* was accomplished with pyridine and acetyl chloride or, more conveniently, by the reaction of **4** with sodium hydride followed by the addition of acetyl chloride. The reaction of **4** with a mixture of pyridine and 3,5-dinitrobenzoyl chloride according to published directions (7) readily provided the 3,5-dinitrobenzoate, **4***c*.

Treatment of **4** with sodium hydride and methyl iodide (8) gave methyl 4,6-*O*-benzylidene-2-deoxy-2-*C*,3-*O*-dimethyl-α-D-altropyranoside (**4***a*).

The reaction of methylsulfinyl carbanion with methyl 2,3-anhydro-4,6-*O*-benzylidene-α-D-mannopyranoside (**7**) gave an oil which crystallized from benzene–hexane to produce **8** (Scheme 4).

Can. J. Chem. Downloaded from www.nrcresearchpress.com by 210.87.254.6 on 09/05/12
For personal use only.

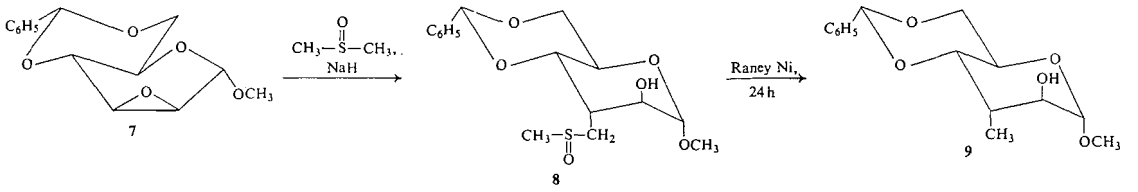

Scheme 4.

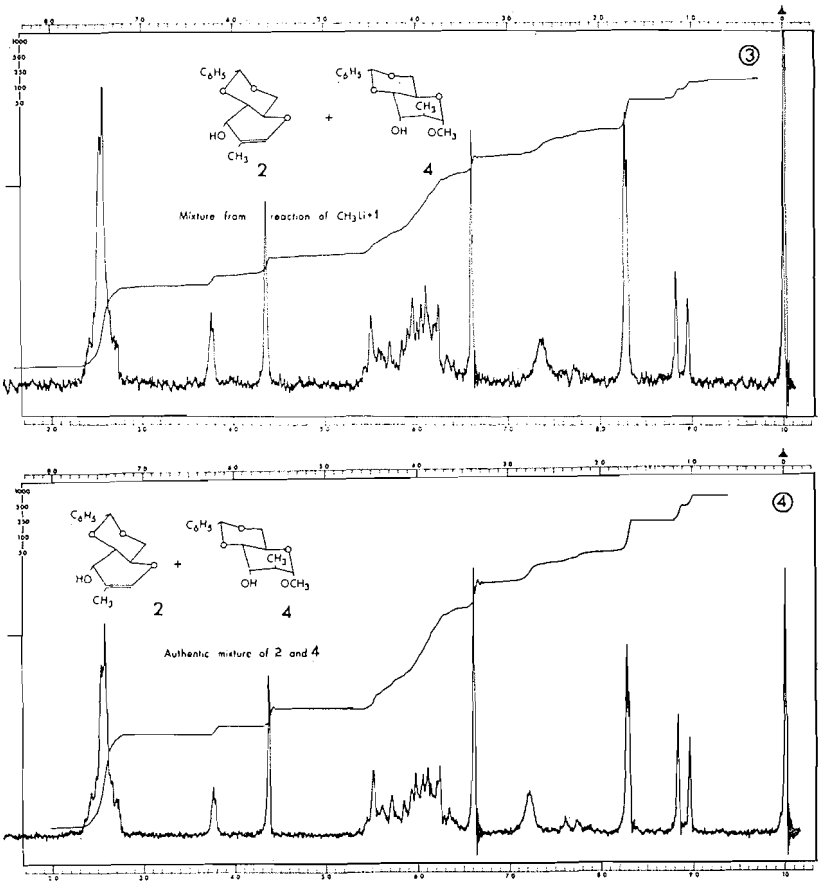

FIG. 3. The n.m.r. spectrum of the oily product (**2** and **4**) from the reaction of CH_3Li and methyl 2,3-anhydro-4,6-*O*-benzylidene-α-D-allopyranoside (**1**).
FIG. 4. The n.m.r. spectrum of an authentic mixture of **2** and **4**.

The elemental analysis of **8**, as well as the integrated n.m.r. spectrum, agreed with a 1:1 complex of **8** and benzene. Here again, only by heating this complex above its melting point (83–84°) for 6 h at 100° could the benzene be removed. The melting point of the product, obtained by removal of the benzene, was 80–81°. Elemental analysis as well as the n.m.r. spectrum supported structure **8**.

When methyl 4,6-*O*-benzylidene-3-deoxy-3-methylsulfinylmethyl-α-D-altropyranoside, **8**, was crystallized from acetone it formed a 1:1 complex with acetone melting at 76°. The elemental analysis, integrated nuclear magnetic resonance spectrum, as well as carbonyl absorption in the infrared spectrum supported the 1:1 complex of **8** and acetone. When this complex was heated at 110° under vacuum for 12 h a solid was obtained melting broadly at 130–135°. The infrared spectrum showed no absorption in the

Can. J. Chem. Downloaded from www.nrcresearchpress.com by 210.87.254.6 on 09/05/12
For personal use only.

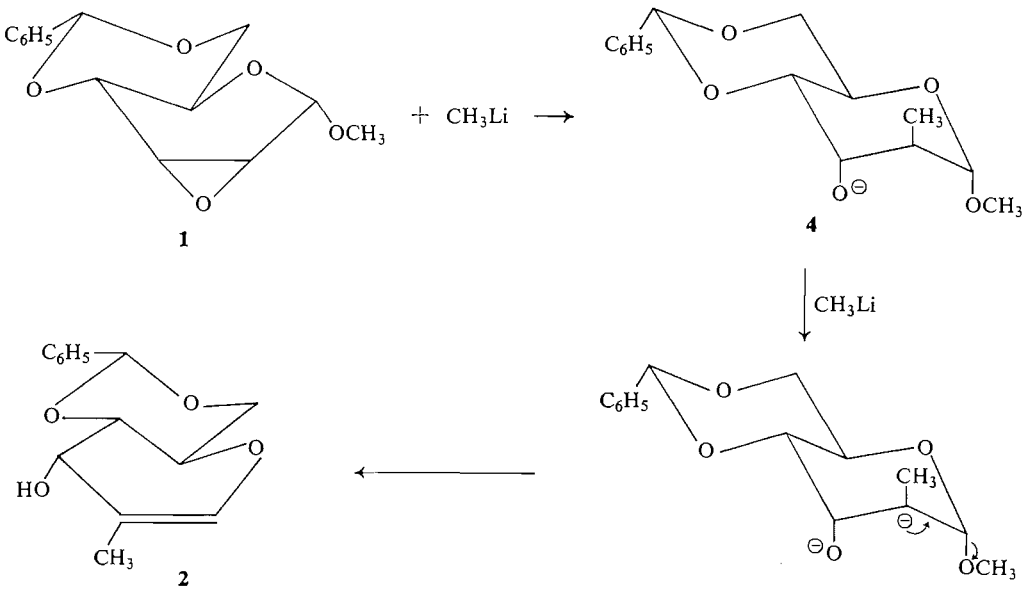

Scheme 5.

carbonyl region. The identity of this material is still unknown.

Treatment of **8**, as the 1:1 complex with benzene with Raney nickel in refluxing acetone for 24 h gave methyl 4,6-*O*-benzylidene-3-deoxy-3-methyl-α-D-altropyranoside (**9**) identical in every respect with an authentic sample prepared by the reaction of methyllithium with **7** (2).

The reaction of excess methyllithium with the epoxide **1**, as previously described (1), was now examined more closely. When an ether solution of equimolar proportions of methyllithium (Foote Mineral Co.) and **1** was allowed to stand at room temperature for 24 h, little if any reaction occurred since the epoxide was recovered nearly quantitatively. However, when this solution was refluxed for 3 h, the reaction mixture yielded nearly half of the original crystalline epoxide (**1**) plus crystalline olefin **2** (23% based on the epoxide consumed). Chromatography of the residue gave, upon elution with ether–hexane, an oil whose n.m.r. spectrum (Fig. 3) showed it to be essentially a mixture of **2** and **4** in the ratio of about 2:1 (compare Figs. 1–4). Final elution with ether gave 25 mg of pure **4**. The total yield of olefin **2** and intermediate **4** was 44% and 14% respectively based on the epoxide consumed.

The information above supports the view that the reaction of methyllithium with epoxide **1** involves first the expected opening of the epoxide ring to give **4** irreversibly. Any lithium chloride present would offer no competition. In the next step the powerful base methyllithium, in excess, then abstracts a proton from C-2 to provide a carbanion which rapidly is converted to the olefin **2** by loss of the methoxide ion as shown in Scheme 5.

That a proton on C-2, specifically, should be susceptible to removal by a strong base, in spite of the fact that here we are dealing with a tertiary hydrogen, is not unreasonable. It is well known that the C-2 hydroxyl group in glucopyranosides is somewhat more acidic than is the C-3 hydroxyl group, due to its position on the carbon α to the anomeric carbon which bears *two* electronegative oxygen atoms (9). The same inductive effect may be responsible for the phenomenon observed above.

Our previous report (1) suggested that the reaction of methyllithium (made from methyl iodide and lithium, hence containing lithium iodide) with the epoxide **1** to give **3** (Scheme 1) as had been described (2), was no doubt due to the preferred reaction of **1** with the iodide ion to give the iodohydrin **10** (Scheme 6, *a*) which then reacted with the base methyllithium to produce **3**.

Additional information has now been obtained concerning these reactions.

The reaction of an ether solution of methyllithium – lithium iodide with methyl 2,3-anhydro-4,6-*O*-benzylidene-α-D-mannopyranoside (**7**) did

Can. J. Chem. Downloaded from www.nrcresearchpress.com by 210.87.254.6 on 09/05/12
For personal use only.

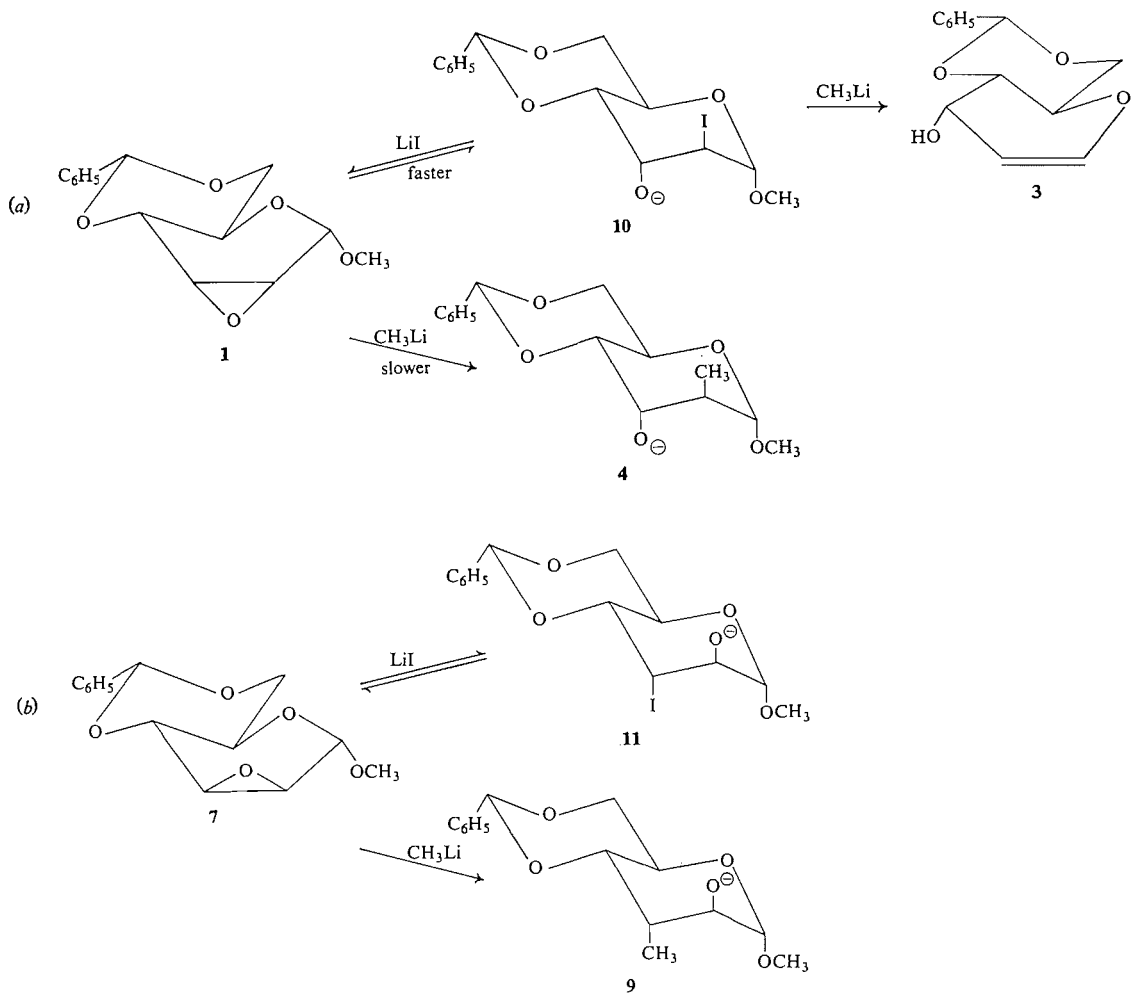

Scheme 6.

not give the iodohydrin **11** (Scheme 6, *b*) but instead gave **9** (2). This is no doubt due to the strong 1,3-diaxial interaction of the iodine atom and methoxy group in **11** which would force the equilibrium back to the epoxide **7** and thus favor the slower alternate (and non-reversible) reaction of methyllithium with the epoxide **7** to form **9**, as had been found (2).

Our attempts to prepare the iodohydrin **11** by reaction of **7** with excess lithium iodide, as had been possible (1) for the iodohydrin **10** (Scheme 6, *a*), were unsuccessful and only unchanged epoxide **7** was recovered quantitatively. The same negative results were obtained in attempts to form the bromohydrin by reaction of **7** with excess lithium bromide.

Lithium bromide was found to react with epoxide **1** to give the bromohydrin analogue of **10** in 71% yield as compared with 76% yield of the iodohydrin (1). Both epoxides, **1** and **7**, failed to react with lithium chloride to produce isolable chlorohydrin. This difference is no doubt due to the much lower nucleophilicity of the chloride ion.

Experimental

All melting points are uncorrected. Elemental analyses were done by Mrs. Darlene Mahlow and Mrs. Andrea Dunn of the Microanalytical Section in the Department of Chemistry, University of Alberta, Edmonton. Infrared spectra were obtained with a Perkin–Elmer model 337 grating Infracord and nuclear magnetic resonance (n.m.r.) spectra were obtained with a Varian A-60 spectrometer.

Can. J. Chem. Downloaded from www.nrcresearchpress.com by 210.87.254.6 on 09/05/12
For personal use only.

Can. J. Chem. Downloaded from www.nrcresearchpress.com by 210.87.254.6 on 09/05/12
For personal use only.

The latter spectra were obtained by R. N. Swindlehurst of the Chemistry Department. Rotations were obtained with a Perkin–Elmer model 141 polarimeter.

Methyl 4, 6-O-Benzylidene-2-deoxy-2-methylsulfinyl-methyl-α-D-altropyranoside, 5

Sodium hydride (400 mg of a 56% dispersion of the hydride in mineral oil) was washed with dry hexane and then added under an atmosphere of dry nitrogen to stirred dimethyl sulfoxide (30 ml) previously distilled from calcium hydride. The mixture was then warmed to 70° until evolution of hydrogen ceased. To the resulting greenish-yellow solution, cooled to 30°, was added methyl 2,3-anhydro-4,6-*O*-benzylidene-α-D-allopyranoside **1** (1.3 g). In 10 min the stirred yellow solution became homogeneous. Stirring was continued for 1 h at 30–35°. The solution was then poured into cold water. A chloroform extract was washed with water and dried (Na_2SO_4). Removal of the solvent gave an oil which solidified when triturated with ether. A solution of this solid in benzene, after addition of ether to faint turbidity, deposited 1.6 g (95%) of material melting at 135–136°; $[\alpha]_D^{25}$, +43.5° (*c*, 1 in $CHCl_3$).

Anal. Calcd. for $C_{16}H_{22}O_6S$: C, 56.14; H, 6.48; S, 9.35. Found: C, 56.13; H, 6.39; S, 9.45.

The infrared spectrum in nujol (reference, polystyrene) showed absorption at 3400 cm^{-1} (OH) and at 700 cm^{-1} (monosubstituted phenyl).

The n.m.r. spectrum in $CDCl_3$ showed a ratio of aromatic to total protons of 5:22. Significant signals, referred to tetramethylsilane, were at τ 2.5 to τ 2.8 (aromatic multiplet); τ 4.42 (singlet, benzylidene methinyl proton); τ 5.27 (doublet, anomeric proton, $J = 4$ c.p.s.); τ 6.62 (singlet, anomeric methyl group); τ 6.68 (closely spaced doublet, C_3OH); τ 7.28 (singlet, two methylene protons); τ 7.45 (singlet for S—CH_3).

Crystallization of **5** from methanol gave ***5a***, a 1:1 complex of methanol and **5**. The colorless needles melted at 165–166°.

Anal. Calcd. for $C_{17}H_{26}O_7S$: C, 54.58; H, 7.00; S, 8.55. Found: C, 54.52; H, 6.88; S, 8.75.

The n.m.r. spectrum in $CDCl_3$ (reference, tetramethylsilane) showed aromatic to total protons in the ratio 5:26. Significant signals were at τ 2.3 to τ 2.8 (aromatic multiplet); τ 4.3 (singlet for benzylidene methinyl proton); τ 5.26 (singlet, half width, 2.5 c.p.s., anomeric proton); τ 6.58 (singlet, anomeric methyl group); τ 6.73 (singlet for C_3OH); τ 7.22 (singlet, half width, 3 c.p.s., methylene protons); τ 7.41 (singlet for S—CH_3).

When the methanol complex with **5** was heated at 165° for 6 h under vacuum it lost methanol. The solid remaining melted at 136–137°. Admixture with **5** did not depress the melting point.

Crystallization of **5** from acetone gave a material whose melting point and mixed melting point (136–137°) and its infrared spectrum showed that it was **5**, uncomplexed with acetone.

Methyl 4,6-O-Benzylidene-2-deoxy-2-methylthiomethyl-α-D-altropyranoside, 6

A mixture of **5** (500 mg) in acetone (80 ml) was refluxed with Raney nickel (10 g) for 4 h. The nickel was separated by filtration of the cooled solution and washed with acetone. The combined acetone solutions were freed from solvent in a rotary evaporator. The residual thick oil was dissolved in ether. On standing this solution deposited crystals melting at 97–98° (300 mg, 61%); $[\alpha]_D^{25}$, +53.7° (*c*, 1 in $CHCl_3$).

Anal. Calcd. for $C_{16}H_{22}O_5S$: C, 58.84; H, 6.74; S, 9.80. Found: C, 58.64; H, 6.33; S, 10.29.

The infrared spectrum in nujol showed a band at 3490 cm^{-1} (OH) and at 710 cm^{-1} (monosubstituted phenyl). The n.m.r. spectrum in $CDCl_3$ (reference tetramethylsilane) agreed with the structure assigned.

Methyl 4,6-O-Benzylidene-2-deoxy-2-methyl-α-D-altropyranoside, 4

The desulfurization of **5** (342 mg) with Raney nickel (15 g) was carried out as above except that the acetone solution (60 ml) was refluxed for 24 h. Work-up followed the same procedure as above. The oily residue obtained after removal of the acetone was crystallized twice from ether–hexane giving 155 mg (55%) of solid melting at 110–111°; $[\alpha]_D^{25}$, +120.8° (*c*, 1 in $CHCl_3$).

Anal. Calcd. for $C_{15}H_{20}O_5$: C, 64.27; H, 7.19. Found: C, 64.34; H, 7.05.

The infrared spectrum in nujol showed absorption bands at 3503 cm^{-1} (OH) and 710 cm^{-1} and 760 cm^{-1} (benzylidene).

The n.m.r. spectrum in $CDCl_3$ (Fig. 1) referred to tetramethylsilane showed aromatic to total protons in the ratio 5:20. The significant signals were found at τ 2.4 to τ 2.8 (aromatic); τ 4.40 (sharp singlet, methine proton of the benzylidene); τ 5.52 (apparent singlet, anomeric proton); τ 6.63 (singlet, anomeric methyl group); τ 7.02 (singlet; OH), a complicated quartet centered at τ 7.70, $J \simeq 7.5$ c.p.s. (C_2H) and at τ 8.91 a doublet ($J = 7.5$ c.p.s., C_2—CH_3).

Compound **4** was also obtained by a 12-h reflux of an acetone solution of **6** in the presence of Raney nickel; m.p. and mixture m.p., 110–111°.

Methyl 3-O-Acetyl-4,6-O-benzylidene-2-deoxy-2-methyl-α-D-altropyranoside, 4b

Method 1

To a solution of **4** (280 mg) in 20 ml of 1,2-dimethoxyethane, previously distilled from calcium hydride, was added sodium hydride (36 mg, suspended in mineral oil). When the hydrogen evolution had ceased, the solution was cooled to 0° and acetyl chloride (1 ml) was added slowly. The reaction mixture was stirred at room temperature for 3 h, neutralized with cold glacial acetic acid, and then poured into water. The ether extract was washed first with 5% aqueous sodium bicarbonate, then with water and then dried (Na_2SO_4). Removal of the solvent gave an oily residue which was dissolved in hexane and added to a short column of neutral alumina. The acetylated derivative was eluted with hexane and subsequently crystallized from hexane; m.p., 65–66°; yield, 195 mg (61%); $[\alpha]_D^{25}$, +86.5°, (*c*, 1 in $CHCl_3$).

Anal. Calcd. for $C_{17}H_{22}O_6$: C, 63.34; H, 6.88. Found: C, 63.34; H, 6.79.

The infrared spectrum (Nujol) showed a band at 1750 cm^{-1} (C=O) and bands at 710 cm^{-1} and 770 cm^{-1} for the benzylidene group.

The n.m.r. spectrum in $CDCl_3$ referred to tetramethylsilane agreed with the structure. The C_3-acetoxy group did not shift the C_3—H proton signal sufficiently downfield for its identification.

Can. J. Chem. Downloaded from www.nrcresearchpress.com by 210.87.254.6 on 09/05/12
For personal use only.

Method 2

To a mixture of acetyl chloride (1 ml) and **4** (140 mg) in 10 ml of dry ether, cooled in an ice bath, was added with stirring a solution of pyridine (3 ml) in ether (10 ml). A white precipitate appeared immediately. The reaction mixture was stirred at room temperature for 2 h and then poured into cold water. An ether extract was washed with water and dried (Na_2SO_4). Removal of the solvent left an oil contaminated with pyridine. To this was added toluene (20 ml) to facilitate removal of the pyridine. Evaporation under reduced pressure removed both the toluene and pyridine. The residue in hexane was put onto a short column of neutral alumina. Elution with hexane and removal of the solvent gave a solid which was crystallized from hexane; yield, 80 mg (51%); m.p., 65–66°; $[\alpha]_D^{25}$, +85.4° (*c*, 1 in $CHCl_3$).

Methyl 4,6-O-Benzylidene-2-deoxy-2-C-methyl-3-O-(3,5-dinitrobenzoyl)-α-D-altropyranoside, 4c

A mixture of **4** (100 mg) and 100 mg of 3,5-dinitrobenzoyl chloride in pyridine (3 ml) was heated on a steam bath for 20 min. To the cooled solution was added 50 ml of toluene and then both the pyridine and toluene were removed under reduced pressure in a rotary evaporator. The thick yellow residue was dissolved in toluene (50 ml) and the solution washed with aqueous 5% sodium bicarbonate and then with water. The dried (Na_2SO_4) liquid was freed from solvent. The residue was crystallized twice from methanol; m.p., 165–166°; yield, 110 mg (65%); $[\alpha]_D^{25}$, +101.2° (*c*, 1 in $CHCl_3$).

Anal. Calcd. for $C_{22}H_{22}O_{10}N_2$: C, 55.7; H, 4.65; N, 5.90. Found: C, 55.38; H, 4.59; N, 5.88.

The n.m.r. spectrum in $CDCl_3$ (reference, tetramethylsilane) agreed with the assigned structure. The ratio of aromatic protons to total protons was 8:22. Significant signals appeared at τ 2.5 to τ 2.8 and τ 0.62 to τ 0.78 (two aromatic multiplets); τ 4.40 (sharp singlet, methine proton of benzylidene group); τ 5.43 (singlet for anomeric proton); τ 6.48 (singlet for anomeric methyl group); τ 8.72 (doublet for C_2—CH_3, $J = 7$ c.p.s.); τ 7.57 (quartet, $J = 7$ c.p.s., split again by C_3—H, $J_{C_2HC_3H} = 2.5$ c.p.s.); τ 4.54 (triplet for C_3H, $J_{C_2HC_3H} = 2.5$ c.p.s., $J_{C_3HC_4H} = \sim 2.5$ c.p.s.). This confirms the orientation of C_3OH in the parent compound.

Methyl 4,6-O-Benzylidene-2-deoxy-2-C,3-O-dimethyl-α-D-altropyranoside, 4a

The literature procedure (8) was employed to methylate **4**. By the addition of 60 mg of sodium hydride to a solution of 280 mg of **4** and 2 ml of methyl iodide in 25 ml of dry 1,2-dimethoxyethane there was obtained, after crystallization of the product from ether–hexane, 255 mg (86%) of the methyl 4,6-*O*-benzylidene-2-deoxy-2-*C*,3-*O*-dimethyl-α-D-altropyranoside, **4***a*; m.p., 132–133°; $[\alpha]_D^{25}$, +104.5° (*c*, 1 in $CHCl_3$).

Anal. Calcd. for $C_{16}H_{22}O_5$: C, 65.29; H, 7.53. Found: C, 65.02; H, 7.49.

Both the infrared and n.m.r. spectra agreed with the structure.

The Reaction of Methyl 4,6-O-Benzylidene-2-deoxy-2-methyl-α-altropyranoside (4) with Methyllithium

(*a*) To an ether (25 ml) solution of **4** (280 mg) was added an equimolar quantity of methyllithium in ether. Hydrogen was evolved. The solution was refluxed for 16 h, then poured into ice water. An ether extract was washed with water, dried (Na_2SO_4), and freed from solvent. The residual solid was crystallized from ether–hexane; yield, 260 mg (recovery of **4**, 93%); m.p., 110–111°.

(*b*) An ether solution of **4** (280 mg) and excess methyllithium (500 mg in ether) was refluxed for 16 h under nitrogen. The resulting cloudy light-yellow solution was filtered and the solid residue was washed with ether. The combined ether solutions were washed with water, dried (Na_2SO_4), and freed from solvent. The residue solidified when triturated with hexane. Crystallization from ether–hexane gave 212 mg (78%) of 4,6-*O*-benzylidene-1,2-didehydro-1,2-dideoxy-2-methyl-D-*ribo*-hexopyranose identical with an authentic sample (1); m.p. and mixture m.p., 125–126°; $[\alpha]_D^{25}$, +172.5° (*c*, 1 in $CHCl_3$); lit. m.p., 126–127°; $[\alpha]_D^{27}$, +175° (*c*, 1 in $CHCl_3$) (1).

The Reaction of Methyl 2,3-Anhydro-4,6-O-benzylidene-α-D-allopyranoside (1) with Methyllithium

To a stirred suspension of **1** (1.3 g) in dry ether (50 ml) under a nitrogen atmosphere, was added a solution of excess methyllithium in ether (2.5 ml). The mixture was refluxed for 5 h and then poured carefully into ice water. The organic layer was separated and the aqueous layer was extracted with ether. The combined ether extracts were washed with water, dried (Na_2SO_4) and freed from solvent. The semisolid residue when triturated with ether, gave 600 mg of crude unreacted **1** (m.p., 190–193°). Crystallization from chloroform–ether raised the melting point to 199°. The residual oil left after separation of the 600 mg of crude **1** was dissolved in ether and seeded with **2**. On standing, the solution deposited crystals melting at 115–118°. Recrystallization from ether–hexane gave 150 mg of material melting at 126–127° which was identical in every respect with the olefin **2** (1).

The mother liquor obtained after separation of **2** was freed from solvent and the oily residue (425 mg) was subjected to chromatography on 15 g of neutral alumina, grade 2 (containing 3% H_2O). A hexane eluate gave 100 mg of a colorless oil whose n.m.r. spectrum showed that it contained no carbohydrate species but only hydrocarbons. This was not investigated further. Subsequent elution with hexane–ether (3:2) gave 220 mg of solid melting at 95–100°. Its infrared spectrum in Nujol, and its n.m.r. spectrum in $CDCl_3$ (Fig. 3) indicated it to be a mixture of the olefin **2** and the intermediate **4** (cf. Scheme 2) in the proportion 2:1 respectively. Further elution with ether gave a colorless oil which crystallized from ether–hexane to give 25 mg of material melting at 109–110°; $[\alpha]_D^{25}$, +118° (*c*, 1 in $CHCl_3$). A mixture melting point showed it to be identical with methyl 4,6-*O*-benzylidene-2-deoxy-2-methyl-α-D-altropyranoside, **4**. Final yield of **2** and **4**, based on epoxide **1** consumed is 44% and 14% respectively.

The Reaction of Methyl 2,3-Anhydro-4,6-O-benzylidene-α-D-mannopyranoside (7) with Lithium Halides

A mixture of 1.3 g of **7** (11) and lithium iodide (2.6 g) in anhydrous ether (70 ml) was heated to reflux for 4 h. The cooled solution was washed with water, dried (Na_2SO_4), and freed from solvent. The solid residue was crystallized from acetone–hexane and gave 1.2 g (~92%) of material melting at 145–146° identical in all respects with starting material, **7**.

Can. J. Chem. Downloaded from www.nrcresearchpress.com by 210.87.254.6 on 09/05/12
For personal use only.

Similarly lithium bromide and lithium chloride failed to react with the 2,3-anhydromannoside (7) even after a 24 h and 48 h reflux period respectively.

Methyl 4,6-O-Benzylidene-2-bromo-2-deoxy-α-D-altropyranoside

A mixture of methyl 2,3-anhydro-4,6-*O*-benzylidene-α-D-allopyranoside (**1**) (1.3 g) and lithium bromide (2.6 g) in 80 ml of ether was heated under reflux for 24 h. After 6 h, all suspended epoxide had gone into solution. The mixture was poured into water, the organic layer separated, and the aqueous layer extracted with ether. The combined ether (organic) solutions were washed with water, dried (Na_2SO_4), and freed from solvent. The thick oily residue was taken up in ether. On standing, the solution deposited 200 mg of crystalline epoxide **1**. The addition of hexane to the mother liquor, to faint turbidity, caused a slow deposition of solid. This was crystallized first from hexane then from acetone–hexane. Yield of the water soluble bromohydrin was 1 g (71%); m.p., 117–118°; $[\alpha]_D^{25}$, +59.2° (*c*, 1 in $CHCl_3$).

Anal. Calcd. for $C_{14}H_{17}O_5Br$: C, 48.89; H, 4.64; Br, 23.25. Found: C, 49.05; H, 4.88; Br, 23.17.

The infrared spectrum in Nujol showed absorption bands at 3460 cm^{-1} (OH) and 765 cm^{-1} and 700 cm^{-1} (benzylidene).

The n.m.r. spectrum in $CDCl_3$ (reference, tetramethylsilane) agreed with the structure indicated.

Assignment of structure was based on the preferred *trans* diaxial opening of the epoxide ring in **1** and **7** by anionic reagents (3,6) and the fact that debromination with Raney nickel gave methyl 4,6-*O*-benzylidene-2-deoxy-α-D-allopyranoside (see below) identical with an authentic sample (10).

Debromination of Methyl 4,6-O-Benzylidene-2-bromo-2-deoxy-α-D-altropyranoside

A mixture of methyl 4,6-*O*-benzylidene-2-bromo-2-deoxy-α-D-altropyranoside (344 mg) and Raney nickel (15 g) in acetone (60 ml) was heated under reflux for 24 h. The catalyst was separated by filtration and the acetone removed under vacuum in a rotary evaporator. An ether solution of the semisolid residue was washed with water, dried (Na_2SO_4), and freed from solvent. The solid was crystallized from acetone–hexane; yield, 180 mg (68%); m.p., 128–129°; $[\alpha]_D^{25}$, ±154.7° (*c*, 0.65 in $CHCl_3$); lit. m.p., 128–129°; $[\alpha]_D^{19}$, +155.6° (*c*, 0.649 in $CHCl_3$) (10). A mixture melting point was undepressed.

Methyl 4,6-O-Benzylidene-3-deoxy-3-methylsulfinyl-methyl-α-D-altropyranoside, 8

To a stirred solution of methylsulfinyl carbanion at 30° (prepared as described in the synthesis of **5** above, by the reaction under nitrogen of 30 ml of dimethyl sulfoxide with 200 mg of sodium hydride) was added 1.3 g of methyl 2,3-anhydro-4,6-*O*-benzylidene-α-D-mannopyranoside (11). The mixture was stirred for 45 min at 30–35° and then poured into cold water. A chloroform extract was washed with water, dried (Na_2SO_4), and freed from solvent. The residual light yellow oil was crystallized from benzene–hexane as a 1:1 complex of **8** and benzene; yield, 1.5 g (74%); m.p., 83–84°; $[\alpha]_D^{25}$, +59.2° (*c*, 1 in $CHCl_3$).

Anal. Calcd. for $C_{22}H_{28}O_6S$: C, 62.85; H, 6.71; S, 7.6. Found: C, 62.25; H, 6.44; S, 7.92.

The infrared spectrum in Nujol showed absorption at 3375 cm^{-1} (OH) and at 755 cm^{-1} and 705 cm^{-1} (benzylidene).

The n.m.r. spectrum in $CDCl_3$ (reference, tetramethylsilane) showed a ratio of aromatic to total protons of 11:28 in agreement with a 1:1 complex of benzene and **8**. Significant signals appeared at τ 2.4 to τ 2.8 (aromatic multiplet); τ 4.48 (sharp singlet for methinyl proton of benzylidene); τ 5.14 (singlet, OH); τ 5.38 (broad singlet, anomeric proton, half width, 4 c.p.s.); τ 6.65 (singlet, anomeric CH_3); τ 6.8 to τ 7.0 (multiplet for C-3 methylene protons); τ 7.46 (singlet, S—CH_3).

When this 1:1 complex of benzene and **8** was heated under vacuum at 100° for 6 h, it lost benzene; m.p. of product, 80–81°; $[\alpha]_D^{25}$, +62.1° (*c*, 1 in $CHCl_3$).

Anal. Calcd. for $C_{16}H_{22}O_6S$: C, 56.14; H, 6.48; S, 9.35. Found: C, 55.58; H, 6.18; S, 9.34.

The n.m.r. spectrum in $CDCl_3$ (reference, tetramethylsilane) showed a ratio of aromatic to total protons of 5:22. Significant signals appeared at τ 2.3 to τ 2.7 (aromatic multiplet); τ 4.42 (singlet, methine proton of benzylidene); τ 5.33 (broad singlet, half width, 4 c.p.s., anomeric proton), τ 5.80 (singlet, OH), τ 6.60 (singlet, anomeric methyl), τ 7.41 (singlet, S—CH_3) and a multiplet centered at τ 6.9 for methylene protons adjacent to S).

Crystallization of **8** from acetone gave a 1:1 complex of acetone and **8** melting at 76°; $[\alpha]_D^{25}$, +51.2° (*c*, 1 in $CHCl_3$).

Anal. Calcd. for $C_{19}H_{28}O_7S$: C, 56.99; H, 7.05; S, 8.0. Found: C, 56.74; H, 6.98; S, 8.14.

The n.m.r. spectrum in $CDCl_3$ (reference, tetramethylsilane) showed a ratio of aromatic to total protons of 5:28. Significant signals appeared at τ 2.4 to τ 2.7 (aromatic multiplet); τ 4.41 (sharp singlet, methine proton of benzylidene); τ 5.12 (broad, OH); τ 5.33 (singlet, anomeric proton, half width, 3 c.p.s.); τ 6.60 (sharp singlet, anomeric methyl); τ 6.86 (multiplet, methylene protons adjacent to S); τ 7.40 (singlet, S—CH_3); τ 7.83 (singlet, acetone methyl groups).

When the 1:1 complex of **8** and acetone was heated for 12 h at 110°, a solid was obtained melting at 130–135°. This was obviously not **8**. This solid was not identified

Methyl 4,6-O-Benzylidene-3-deoxy-3-methyl-α-D-altropyranoside

Compound **8** (1 g of the 1:1 complex with benzene) was desulfurized with Raney nickel (20 g) by heating it in acetone for 24 h. The cooled solution was filtered and freed from solvent. The oily residue gave crystals from ether–hexane; yield, 425 mg (64%); m.p. 114–115° $[\alpha]_D$, +115.9° (*c*, 0.28 in ethanol) (4). A mixture melting point with authentic material (4) was undepressed.

Acknowledgments

The authors are grateful for financial assistance given by the National Research Council of Canada.

We wish to express our appreciation to the Defence Research Board of Canada for funds which enabled us to continue a portion of this work.

1. M. SHARMA and R. K. BROWN. Can. J. Chem. **44,** 2825 (1966).
2. A. A. J. FEAST, W. G. OVEREND, and N. R. WILLIAMS. J. Chem. Soc. 7378 (1965).
3. R. E. PARKER and N. S. ISAACS. Chem. Rev. **59,** 737 (1959).
4. E. J. COREY and M. CHAYKOVSKY. J. Am. Chem. Soc. **87,** 1345 (1965).
5. U. G. NAYAK, M. SHARMA, and R. K. BROWN. Can. J. Chem. **45,** 481 (1967).
6. F. H. NEWTH. Quart. Rev. London, **13,** 30 (1959).
7. F. SWEET and R. K. BROWN. Can. J. Chem. **44,** 1571 (1966).
8. U. E. DINER, F. SWEET, and R. K. BROWN. Can. J. Chem. **44,** 1591 (1966).
9. J. M. SUGIHARA. *In* Advances in carbohydrate chemistry. Academic Press Inc., New York. 1953. pp 16–22.
10. D. A. PRINS. J. Am. Chem. Soc. **70,** 3955 (1948).
11. G. J. ROBERTSON and C. F. GRIFFITH. J. Chem. Soc. 1193 (1935).

Can. J. Chem. Downloaded from www.nrcresearchpress.com by 210.87.254.6 on 09/05/12
For personal use only.

Zinniol: a major metabolite of *Alternaria zinniae*[1]

A. N. STARRATT

Research Institute, Research Branch, Canada Department of Agriculture, University Sub Post Office, London, Ontario

Received October 27, 1967

Zinniol, a compound recently obtained from the phytopathogenic fungus *Alternaria zinniae*, is shown to be 1,2-bis(hydroxymethyl)-5-(3′,3′-dimethylallyloxy)-3-methoxy-4-methylbenzene (**1**) by chemical and spectroscopic studies. Attempts to isolate other metabolites are described briefly.

Canadian Journal of Chemistry, 46, 767 (1968)

Can. J. Chem. Downloaded from www.nrcresearchpress.com by 210.87.254.5 on 09/05/12
For personal use only.

A recent investigation (1) of filtrates from stationary liquid cultures of the phytopathogenic fungus *Alternaria zinniae* resulted in the isolation of a major metabolite, $C_{15}H_{22}O_4$, which has been named zinniol. This compound, which is an oil, was characterized by the preparation of crystalline diacetyl (**2**) and dibenzoyl (**3**) derivatives. Zinniol (**1**) is now shown by chemical and spectroscopic evidence to be a novel penta-substituted benzene closely related to quadrilineatin (**4**) (3).

The nuclear magnetic resonance (n.m.r.) spectrum of zinniol exhibited bands attributable to the presence of one aromatic proton (δ 6.66, singlet), a methoxyl (δ 3.72), and a methyl group on an aromatic nucleus (δ 2.14). In addition there were bands assignable to the methylene protons of two $-CH_2OH$ groupings at δ 4.69 and 4.61 (singlets, 2 protons each) which appeared at δ 5.21 and 5.15 in the spectrum of the diacetate. The spectrum also showed signals attributable to a 3,3-dimethylallyloxy grouping (2).

When zinniol diacetate (**2**) was warmed with acetic anhydride containing a small amount of sulfuric acid, a triacetate (**5**) was formed. The n.m.r. spectrum of this compound showed the absence of bands due to the dimethylallyloxy side chain and the presence of an additional acetyl grouping. This indicated that solvolysis of the allylic ether function followed by acetylation of the resulting phenol had occurred. Zinniol, similarly treated, gave the same product, though in lower yield.

Chromic acid oxidation of zinniol (**1**) in acetone afforded two isomeric phthalides, **6** and **10**, which could be reduced to zinniol with lithium aluminium hydride. Phthalide **6** was also obtained during the chromatographic isolation of zinniol but it was probably an artifact since aqueous alkali soluble substances had been removed from the original culture extract at an earlier stage. Phthalide **6**, when warmed with acetic anhydride – sulfuric acid, gave an acetate (**7**) lacking the dimethylallyl grouping. Similarly, phthalide **10** gave the isomeric acetate **11**.

Hydrolysis of acetate **7** gave a phenol, needles, m.p. 234–236°, corresponding to 6-hydroxy-4-methoxy-5-methyl phthalide (**8**), m.p. 234–235°, obtained previously from quadrilineatin, a metabolic product of *Aspergillus quadrilineatus* (3). Methylation of this phenol gave a substance, m.p. 158–159°, identical with 4,6-dimethoxy-5-methyl phthalide (**9**) which was obtained synthetically (3).

The presence of the dimethylallyloxy substituent on the aromatic nucleus of zinniol was confirmed by reacting **8** with 1-chloro-3-methyl-2-butene to give phthalide **6**.

Hydrolysis of acetate **11** yielded a phenol, m.p. 234–235° (change in crystal form approximately 190–200°) which differed from the m.p. of 198° reported (3) for 5-hydroxy-7-methoxy-6-methyl phthalide (**12**). This discrepancy is probably due to the occurrence of different crystalline forms as suggested by the phase change noted during determination of the melting point. Methylation with diazomethane yielded a substance, m.p. 172–173°, corresponding to 5,7-dimethoxy-6-methyl phthalide (**13**), m.p. 172–172.5°, synthesized by Birkinshaw *et al.* (4).

The evidence so far adduced indicates that **1** represents the structure of zinniol. However, no direct proof other than melting point data has been introduced to exclude the possibility that the methoxy and dimethylallyloxy substituents may be interchanged. The following observations support the assigned structure. Phenol **12** did not give a color reaction with ferric chloride as would be expected for the alternative formulation,

---

[1]Contribution No. 359 from the Research Institute of the Canada Department of Agriculture.

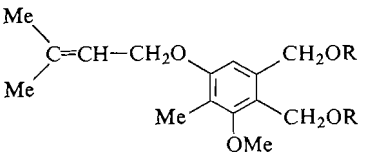

1 R = H
2 R = Ac
3 R = Bz

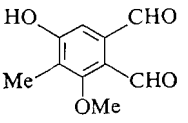

4

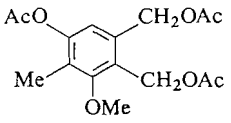

5

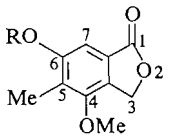

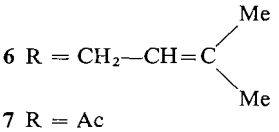

6 R = CH_2—CH=C(Me)(Me)

7 R = Ac
8 R = H
9 R = Me

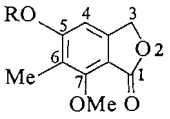

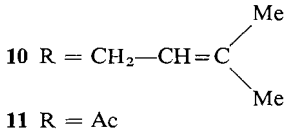

10 R = CH_2—CH=C(Me)(Me)

11 R = Ac
12 R = H
13 R = Me

7-hydroxy-5-methoxy-6-methyl phthalide (3, 7), and the shift in the ultraviolet spectrum of phenol **12** when measured in alkali corresponded to that anticipated for a *p*-hydroxybenzoic acid (5). Since this phenol must therefore have structure **12** it follows that structure **1** represents zinniol.

Only acetate **7** could be isolated from the acetylated phenolic fraction of the culture medium extract. It is not known whether this compound is a natural product or an artifact although a late stage in the biosynthesis of zinniol probably involves the alkylation of a phenolic precursor with 3,3-dimethylallyl pyrophosphate (6).

Mannitol was isolated from the mycelium of *A. zinniae*.

Experimental

Melting points were measured on a Kofler hot stage and are uncorrected. Ultraviolet spectra of substances dissolved in 95% ethanol were recorded using a Beckman DK spectrophotometer and infrared spectra were obtained on a Perkin-Elmer model 21 spectrometer. Neutral Woelm alumina standardized according to Brockmann was used for column chromatography. Kieselgel (Camag) containing fluorescent indicator was used for thin-layer chromatography (t.l.c.). Nuclear magnetic resonance spectra were obtained with Varian A-60 and A-60A spectrometers using $CDCl_3$ as solvent. Chemical shifts are reported in p.p.m. (δ) downfield from an internal tetramethylsilane reference. Microanalyses were performed by Dr. C. Daesslé, Montreal. Petrol refers to a light petroleum fraction of b.p. 60–80°.

Zinniol (1)

The isolation of this compound has been described (1). Nuclear magnetic resonance (n.m.r.) spectrum: δ 1.73 (6 protons, broad singlet, $=CMe_2$), 2.14 (3 protons, singlet, aromatic Me), 3.22 (2 protons, broad band, hydroxyl protons), 3.72 (3 protons, singlet, —OMe), 4.50 (2 protons, doublet, J = 7 c.p.s., $=C(H)-CH_2-O$), 4.61 and 4.69 (singlets of 2 protons each, $-CH_2OH$), 5.46 (1 proton, triplet, J = 7 c.p.s., =CH—) and 6.66 (1 proton, singlet, aromatic).

Zinniol Diacetate (2)

The preparation of this compound has been described (1). Nuclear magnetic resonance spectrum: δ 1.77 (6 protons, broad singlet, $=CMe_2$), 2.05, and 2.08 (singlets of 3 protons each, —OAc), 2.17 (3 protons, singlet, aromatic Me), 3.73 (3 protons, singlet, —OMe), 4.53 (2 protons, doublet, J = 7 c.p.s., $=C(H)-CH_2-O$), 5.15 and 5.21 (singlets of 2 protons each, $-CH_2OAc$), 5.47 (1 proton, triplet, J = 7 c.p.s., =CH—) and 6.71 (1 proton, singlet, aromatic).

Zinniol Dibenzoate (3)

A solution of zinniol (29 mg) in pyridine (10 drops) was treated for 18 h with freshly distilled benzoyl chloride (5 drops) at room temperature. After dilution with water, the product was extracted into ether. Removal of the ether afforded a gum which was separated by preparative t.l.c. (chloroform–benzene, 3:1). Isolation of material from the major band and recrystallization from ether–petrol gave zinniol dibenzoate (**3**), m.p. 79–80°; ν_{max} ($CHCl_3$) 1705, 1603, 1586 cm^{-1}.

Anal. Calcd. for $C_{29}H_{30}O_6$: C, 73.40; H, 6.37. Found: C, 73.75; H, 6.31.

Triacetate (5) from Zinniol Diacetate

Zinniol diacetate (50 mg) was heated on a steam bath

Can. J. Chem. Downloaded from www.nrcresearchpress.com by 210.87.254.5 on 09/05/12
For personal use only.

Can. J. Chem. Downloaded from www.nrcresearchpress.com by 210.87.254.5 on 09/05/12
For personal use only.

for 15 min in acetic anhydride (2 ml) containing 1 drop of concentrated sulfuric acid. The solution was diluted with water and extracted with chloroform. The product was chromatographed over alumina (Grade III; 5g). The material (34 mg) eluted with benzene was recrystallized from ether - isopropyl ether to give the triacetate m.p. 79–80°; ν_{max}(KBr) 1735 cm^{-1}; n.m.r. spectrum: δ 2.06 and 2.11 (singlets of 6 protons and 3 protons, —OAc) 2.31 (3 protons, singlet, aromatic Me), 3.74 (3 protons, singlet, —OMe), 5.13, and 5.23 (singlets of 2 protons each, —CH_2 OAc) and 6.88 (1 proton, singlet, aromatic).

Anal. Calcd. for $C_{16}H_{20}O_7$: C, 59.25; H, 6.22. Found: C, 59.15; H, 5.75.

Triacetate from Zinniol

Zinniol (77 mg) was treated with acetic anhydride containing a trace of sulfuric acid as described for zinniol diacetate. Chromatography of the product over alumina (Grade III; 5g) followed by separation by preparative t.l.c. (chloroform) yielded material (22 mg) which was recrystallized from ether - isopropyl ether to give the triacetate (**5**).

Oxidation of Zinniol

Zinniol (52 mg) in acetone (20 ml) was stirred at room temperature for 3 min with an excess of a stock chromic acid solution prepared from 11.0 g of chromium trioxide in 10 ml of concentrated sulfuric acid and diluted to 50 ml with water (8). The reaction solution was diluted with water and the product isolated by ether extraction. The product proved to be a mixture from which two isomeric crystalline compounds were obtained by preparative t.l.c. (chloroform). Recrystallization of the less polar component (13 mg) from ether–petrol gave phthalide **6**, m.p. 85–86°; ν_{max}($CHCl_3$) 1750 cm^{-1}; λ_{max} 253, 301 mμ (ε 7100, 3500); n.m.r. spectrum: δ 1.74 (6 protons, broad singlet, $=CMe_2$), 2.18 (3 protons, singlet, aromatic Me), 3.86 (3 protons, singlet, —OMe), 4.55 (2 protons, doublet, J = 7 c.p.s., $=C(-CH_2-O)$), 5.33 (2 protons, singlet, $-CH_2-O-C=O$), 5.46 (1 proton, triplet, J = 7 c.p.s., $=CH-$) and 7.03 (1 proton, singlet, aromatic).

Anal. Calcd. for $C_{15}H_{18}O_4$: C, 68.68; H, 6.92. Found: C, 68.60; H, 6.18.

The second component (23 mg) was recrystallized from ether - isopropyl ether to give phthalide **10** as needles, m.p. 106–108°; ν_{max}($CHCl_3$) 1743 cm^{-1}; λ_{max} 259 mμ (ε 15 200); n.m.r. spectrum: δ 1.77 (6 protons, broad singlet, $=CMe_2$), 2.13 (3 protons, singlet, aromatic Me), 4.02 (3 protons, singlet, —OMe), 4.56 (2 protons, doublet, J = 6.5 c.p.s., $=C(-CH_2-O)$), 5.13 (2 protons, singlet, $-CH_2-O-C=O$), 5.46 (1 proton, triplet, J = 6.5 c.p.s., $=CH-$) and 6.58 (1 proton, singlet, aromatic).

Anal. Calcd. for $C_{15}H_{18}O_4$: C, 68.68; H, 6.92. Found: C, 69.31; H, 7.19.

Reduction of the crude oxidation product in anhydrous ether with lithium aluminium hydride yielded zinniol. No other product was detected by t.l.c.

Phthalide 6 from Extract of Culture Filtrate

Early fractions eluted with petrol–benzene (1:1) during the chromatographic isolation of zinniol (1) gave crystalline material (85 mg) which, after recrystallization from ether–petrol, was found to be identical (t.l.c., mixture m.p., infrared) with phthalide **6**, m.p. 84–85°, obtained by oxidation of zinniol.

Acetate 7

Phthalide **6** (22 mg) was heated on a steam bath for 15 min in acetic anhydride (1 ml) containing 1 drop of concentrated sulfuric acid. The reaction solution was diluted with water and the product isolated by chloroform extraction. Removal of the chloroform gave a crystalline residue which was chromatographed over alumina (Grade III; 3g). Elution with benzene afforded a substance which was recrystallized from chloroform - isopropyl ether to give acetate **7**, m.p. 134–135°; ν_{max}(KBr) 1753 cm^{-1}; n.m.r. spectrum: δ 2.17 (3 protons, singlet, aromatic Me), 2.36 (3 protons, singlet, —OAc), 3.94 (3 protons, singlet, —OMe), 5.45 (2 protons, singlet, $—CH_2—O—C=O$), and 7.35 (1 proton, singlet, aromatic).

Anal. Calcd. for $C_{12}H_{12}O_5$: C, 61.01; H, 5.12. Found: C, 60.98; H, 5.51.

Acetate 11

Phthalide **10** (109 mg) was warmed with acetic anhydride (3 ml) containing a drop of sulfuric acid under the conditions described above. Isolation and chromatography of the product over alumina gave crystalline material (46 mg) which was recrystallized from chloroform – isopropyl ether to yield acetate **11** as plates, m.p. 100–101°; ν_{max}(KBr) 1755, 1739 cm^{-1}; n.m.r. spectrum: δ 2.18 (3 protons, singlet, aromatic Me), 2.36 (3 protons, singlet, —OAc), 3.95 (3 protons, singlet, —OMe), 5.46 (2 protons, singlet, $—CH_2—O—C=O$) and 7.36 (1 proton, singlet, aromatic).

Anal. Calcd. for $C_{12}H_{12}O_5$: C, 61.01; H, 5.12. Found: C, 61.49; H, 5.26.

Hydrolysis of Acetate 7

Acetate **7** (37 mg) in methanol (3.5 ml) was refluxed under nitrogen for 15 min with potassium hydroxide solution (0.5 ml; 16%). After dilution with water, the reaction mixture was neutralized with dilute hydrochloric acid and extracted with ether. Removal of the ether and recrystallization of the product from methanol–chloroform gave phenol **8** as needles, m.p. 233–235°; ν_{max}(KBr) 3350, 1738 cm^{-1}; λ_{max} 254, 304 mμ (ε 5840, 3200) and, after addition of 1 drop of 0.1 *N* NaOH, λ_{max} 338 mμ (ε 3880). Sublimation in high vacuum at 125° gave needles, m.p. 234–236°.

Methylation of Phenol 8

Phenol **8** (25 mg) in ether was treated overnight at room temperature with diazomethane in ether. The reaction mixture was evaporated to dryness and chromatographed over alumina (Grade III; 2g). Elution with benzene yielded material (21 mg) which was recrystallized from chloroform - isopropyl ether to give needles, m.p. 158–159°; ν_{max}($CHCl_3$) 1753 cm^{-1}; ν_{max}(KBr) 1755, 1735 cm^{-1}; n.m.r. spectrum: δ 2.22 (3 protons, singlet, aromatic Me), 3.90 (6 protons, singlet, —OMe), 5.38 (2 protons, singlet, $—CH_2—O—C=O$) and 7.11 (1 proton, singlet, aromatic). This substance was identical (m.p., mixture m.p., t.l.c., infrared) with 4,6-dimethoxy-5-methyl phthalide (***9***) obtained synthetically (3).

Phthalide 6 from Phenol 8

Phenol **8** (3.2 mg) in anhydrous acetone (3 ml) containing potassium carbonate (200 mg) was refluxed 6 h with 1-chloro-3-methyl-2-butene (0.05 ml). The potassium carbonate was removed and washed with acetone and the solvent evaporated *in vacuo*. The product was purified by t.l.c. (chloroform) and recrystallization from ether-petrol gave phthalide **6**, m.p. 85–86°, undepressed by mixture with phthalide **6** obtained by oxidation of zinniol. Thin-layer chromatography behavior and the infrared spectra further demonstrated these compounds to be identical.

Hydrolysis of Acetate 11

Acetate **11** (29 mg) was hydrolyzed in the same manner as described for acetate **7**. The product (23 mg) was recrystallized from methanol–chloroform to yield phenol **12**, m.p. 233–234° (change in crystal form approximately 190–200°); ν_{max}(KBr) 3280, 1717 cm^{-1}; λ_{max} 260 mμ (ε 11 700) and after addition of 1 drop of 0.1 *N* NaOH, $\lambda_{inflection}$ 234, λ_{max} 302 mμ, (ε 17 500, 26 800). Phenol **12** showed no color reaction with ferric chloride.

Anal. Calcd. for $C_{10}H_{10}O_4$: C, 61.85; H, 5.19. Found: C, 61.80; H, 5.19.

Methylation of Phenol 12

Phenol **12** (17 mg) in ether (4 ml) and methanol (0.5 ml) was treated overnight at room temperature with diazomethane in ether. The solvent was removed and the residue chromatographed over alumina (Grade III; 2 g). Elution with benzene yielded material which, after recrystallization from chloroform – isopropyl ether, gave **13** as needles, m.p. 172–173°; ν_{max}(KBr) 1738, 1608 cm^{-1}; n.m.r. spectrum: δ 2.15 (3 protons, singlet, aromatic Me), 3.92, 4.06 (singlets of 3 protons each, —OMe), 5.18 (2 protons, singlet, $—CH_2—O—C=O$), and 6.64 (1 proton, singlet, aromatic). Birkinshaw *et al.* (4) report m.p. 172–172.5° for 5,7-dimethoxy-6-methyl phthalide.

Anal. Calcd. for $C_{11}H_{12}O_4$: C, 63.45; H, 5.81. Found: C, 63.51; H, 5.88.

Phenol 8 from Alkaline Extract

Sodium hydroxide soluble material (900 mg) from the extraction of two batches of culture medium (1) was chromatographed over silica gel (British Drug Houses; 100 g). Benzene–ether (3:1) eluted a crystalline fraction (47 mg) which was acetylated (acetic anhydride – pyridine, overnight at room temperature). The product was purified by preparative t.l.c. (chloroform–methanol, 49:1) and recrystallized from chloroform – isopropyl ether to give a substance (12 mg) identified (m.p., mixture m.p., infrared) as the acetate of phenol **8**, m.p. 136–137°. No other compound could be isolated from the complex mixture.

Isolation of Mannitol from the Mycelium

Mycelium of *Alternaria zinniae* was continuously extracted in a Soxhlet apparatus with petrol (1 day), chloroform (4 days), and methanol (3 days). The methanol extract yielded material which was recrystallized from methanol to give needles, m.p. 165–166°, identical (m.p., mixture m.p., infrared) with authentic mannitol. Acetylation yielded mannitol hexaacetate, m.p. 123–124° (chloroform–methanol). No other crystalline substance could be obtained from the mycelial extracts.

Acknowledgments

Crude culture extracts were kindly provided by Dr. G. A. White. The technical assistance of Mrs. M. E. Stevens is gratefully acknowledged.

1. G. A. White and A. N. Starratt. Can. J. Botany, **45**, 2087 (1967).
2. E. Ritchie and W. C. Taylor. Tetrahedron Letters, 1431 (1964).
3. J. H. Birkinshaw, P. Chaplen, and R. Lahoz-Oliver. Biochem. J. **67**, 155 (1957).
4. J. H. Birkinshaw, H. Raistrick, D. J. Ross, and C. E. Stickings. Biochem. J. **50**, 610 (1952).
5. A. I. Scott. Interpretation of the ultraviolet spectra of natural products. The Macmillan Co., New York. 1964. p. 116.
6. J. D. Bu'Lock. The biosynthesis of natural products. McGraw-Hill Publishing Co. Ltd., London. 1965. p. 48.
7. J. F. Grove. Biochem. J. **50**, 648 (1952).
8. K. Bowden, I. M. Heilbron, E. R. H. Jones, and B. C. L. Weedon. J. Chem. Soc. 39 (1946).

Can. J. Chem. Downloaded from www.nrcresearchpress.com by 210.87.254.5 on 09/05/12
For personal use only.

Rates of reaction of *n*-butanethiol with some conjugated heteroenoid compounds

C. E. LOUGH, D. J. CURRIE, AND H. L. HOLMES
Chemistry Section, Defence Research Establishment Suffield, Ralston, Alberta

Received September 5, 1967

The reactions of substituted 3-benzal-2,4-pentanediones, ethyl benzalacetoacetates, diethyl benzalmalonates, benzalmalonamides, cinnamalmalononitriles, β-nitrostyrenes, and β-nitropropenylbenzenes with excess *n*-butanethiol go essentially to completion in 20% aqueous ethanolic solution buffered to pH 7. The second order rate constants derived from the reactions of meta- and para- substituted derivatives correlate well with Hammett σ constants. The nature and conformation of the functional group *cis* to the phenyl group determines the extent to which ortho substituents hinder the reaction.

Canadian Journal of Chemistry, 46, 771 (1968)

Introduction

Aliphatic and/or aromatic thiols have been added to benzalacetone (1), benzalacetophenone (2–10), β-nitrostyrene (11–13), 3-benzal-2,4-pentanedione (1), and ethyl benzalacetoacetate (1) but no attempt was made to demonstrate that the adducts of the latter two compounds arose by 1,4-addition to the conjugated system. Moreover, no record could be found of the isolation of an adduct arising from the addition of a thiol to the conjugated system of a cinnamonitrile with a second functional group on the α carbon atom. In some instances, reaction proceeds without a catalyst (3, 4, 9) but in general, catalysts such as dry hydrogen chloride (7, 8), piperidine (1, 2, 7, 8, 10), or sodium ethoxide are employed.

The 1,4-addition of thiophenol to β-nitrostyrene, in the presence of piperidine, has been demonstrated (12) by reduction of the nitro group of the adduct (**1**) to **2** and the preparation of the hydrochloride of **2** from thiophenol and **3**. At least in the case of the hydrogen chloride

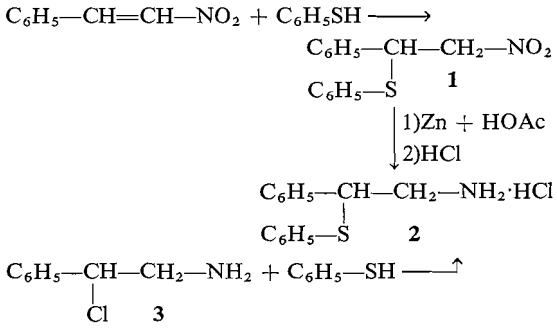

catalyzed reaction of ethanethiol and thiophenol to benzalacetophenone some 1,2- as well as 1,4-addition occurs (2, 7, 8).

This paper describes some related aqueous solution reactions and although excessive β eliminations occur when thiol adducts are treated with strong base (5), such eliminations are unlikely in solutions buffered to pH 7 when excess thiol is present.

Experimental

The preparation of the compounds used in this work and their purity have been described by Silver *et al.* (14). The butanethiol isomers and ethanol were purified by distillation and deionized water was used in the Sörensen phosphate buffer. The butanethiol addition reactions were run in 80% aqueous buffer (pH 7)- 20% ethanol (v/v) at 25 °C and followed by ultraviolet spectroscopy (15) and the insolubility of the adducts required that these reactions be run in very dilute solution.

The thiophenol and *n*-butanethiol adducts of 3-benzal-2,4-pentanedione were prepared by the method of Ruhemann (1). 3-Acetyl-4-phenyl-4-phenylthio-2-butanone melted at 116.0–117.0 °C and 3-acetyl-4,*n*-butylthio-4-phenyl-2-butanone at 62.0–62.5 °C.

Anal. Calcd. for $C_{16}H_{22}O_2S$: C, 69.02; H, 7.96; S, 11.51. Found: C, 69.06; H, 7.92; S, 11.43.

The former showed a weak absorption in ethanol at 286 mμ (ε = 2900) indicating that destruction of conjugation accompanied the addition. The spectrum of the latter in ethanol and that of the solution at the conclusion of the *n*-butanethiol reaction showed insignificant absorption from 250 to 350 mμ.

Results

The equilibrium reactions went virtually to completion and were pseudo first order with respect to the unsaturated compounds. Concentration change of the butanethiols [C_4H_9SH] present in excess, demonstrated that, within experimental error, the thiol exponent was unity and therefore second order rate constants, k_2 as defined by

$$\frac{d[C_6H_5 - CH{=}CAB]}{dt} = k_2\,[C_6H_5CH{=}CAB]\,[C_4H_9SH]$$

TABLE I

Rate constants for the reactions* of some conjugated heteroenoid compounds† with *n*-butanethiol in 20% ethanol – 80% pH 7 buffer‡ (v/v) at 25 °C

A	B	X	Y	$k_2(M^{-1}\ s^{-1})$	Exponent
$COCH_3$	$COCH_3$	H	H	2.0	0.93±0.05
		2-CH_3	H	0.19	0.93±0.07
		4-CH_3	H	1.1	0.94±0.17
		2-Cl	H	1.4	1.00±0.00
		3-Cl	H	6.4	0.98±0.04
		4-Cl	H	4.0	1.08±0.14
		2-CH_3O	H	0.34	0.91±0.10
		3-CH_3O	H	2.8	0.94±0.03
		4-CH_3O	H	0.83	0.90±0.08
		2-CH_3O	4-CH_3O	0.15	0.95±0.04
$COCH_3$	$CO_2C_2H_5$	H	H	1.5	0.99±0.02
		§2-CH_3	H	0.35	0.97±0.13
		§3-CH_3	H	1.3	1.16±0.01
		4-CH_3	H	0.95	1.11±0.09
		§3-F	H	3.8	1.16±0.02
		§2-Cl	H	1.3	1.04±0.01
		§3-Cl	H	5.3	1.14±0.02
		4-Cl	H	3.5	1.07±0.08
		§2-CH_3O	H	0.26	1.09±0.41
		3-CH_3O	H	1.9	0.92±0.08
		§4-CH_3O	H	0.57	1.02±0.07
		2-Cl	4-Cl	5.1	0.99±0.07
		3-Cl	4-Cl	23.	1.01±0.45
		§2-CH_3O	3-CH_3O	0.40	1.05±0.03
		§2-CH_3O	4-CH_3O	0.12	0.87±0.12
		3-CH_3O	4-CH_3O	0.75	1.08±0.12
		§3—O—CH_2—O—4		0.75	1.17±0.15
$CO_2C_2H_5$	$CO_2C_2H_5$	H	H	0.085	1.00±0.00
		2-F	H	0.24	1.13±0.10
		3-F	H	0.51	1.23±0.04
		2-Cl	H	0.18	1.04±0.08
		2-CH_3O	H	0.022	1.03±0.02
		4-CH_3O	H	0.048	1.20±0.08
		3-C_2H_5O	H	0.21	1.03±0.11
$CONH_2$	$CONH_2$	H	H	0.012	0.95±0.05
		3-CH_3	H	0.009_2	0.96±0.00
		3-Cl	H	0.048	0.90±0.22
		4-Cl	H	0.023	0.93±0.00
		3-CH_3O	H	0.014	0.92±0.04
NO_2	‖H	H	H	32.	1.09±0.00
NO_2	‖CH_3	H	H	5.6	1.02±0.06
		2-Cl	H	5.8	1.15±0.04
		3-Cl	H	11.	0.93±0.00
		4-Cl	H	11.	0.82±0.10
		2-CH_3O	H	2.5	1.14±0.00
		3-CH_3O	H	6.4	1.00±0.00
		4-CH_3O	H	5.9	0.89±0.04

*The reaction of 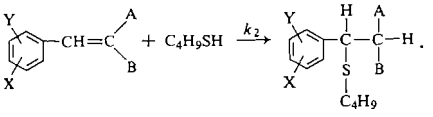 .

†Concentrations: 5×10^{-6} to 10^{-4} *M* heteroenoid, 2.5×10^{-5} to 5×10^{-3} *M* *n*-butanethiol.
‡*M*/15 Na_2HPO_4 (60%) and *M*/15 KH_2PO_4 (40%) (Sörensen).
§These compounds are geometrically nonhomogeneous (19).
‖For β-nitrostyrene and the β-nitropropenylbenzenes, only the initial 50% of the reaction was employed to calculate k_2.

TABLE II

Reaction constants and correlation data* for rate constants

A	B	ρ	k_H	Regression coefficient, r	Standard error	
					Δr	Δ estimate
$COCH_3$	$COCH_3$	1.39	1.94	1.00	0.02	0.01
$COCH_3$	$CO_2C_2H_5$	1.68	1.48	0.98	0.11	0.10
$CO_2C_2H_5$	$CO_2C_2H_5$	1.72	0.11_6	0.98	0.27	0.12
$CONH_2$	$CONH_2$	1.56	0.011_0	0.98	0.18	0.06
NO_2	CH_3	0.50	6.87	0.82	0.20	0.10

*Log $k_{xy} = \rho\sigma + \log k_H$.

were calculated. These k_2 values and the observed thiol exponents are given in Table I for *n*-butanethiol. The logarithms of the rate constants for meta- and para-substituted derivatives correlate well with Hammett σ constants (16) (Table II). The analogous compounds with C-2 substituents, are less reactive than their C-4 isomers and moreover the magnitude of the differences in k_2 for the C-2 and C-4 isomers vary from series to series.

The rate constants (k_2) have also been determined in this work for the addition of *sec*-butanethiol and *t*-butanethiol to 3-benzal-2,4-pentanedione, ethyl benzalacetoacetate, and diethyl benzalmalonate at 25 °C. For the former nucleophile the approximate values are 5×10^{-1}, 4×10^{-1}, and 5×10^{-2} M^{-1} s^{-1} respectively and for the latter, 2×10^{-2}, 1×10^{-2}, and 1×10^{-3} M^{-1} s^{-1}.

When the pH of the buffer component was 6.47, the rate constant, k_2, for the reaction of 3-benzal-2, 4-pentanedione with *n*-butanethiol, was 0.54 $M^{-1}s^{-1}$ indicating general base catalysis of the reaction.

These reactions are inherently reversible. The excess mercaptan forces the equilibrium to the right since in the absence of the appropriate mercaptan both 3-acetyl-4-phenyl-4-phenylthio-2-butanone and 3-acetyl-4-phenyl-4,*n*-butylthio-2-butanone in 20% ethanol – 80% buffer (pH 7) undergo β-elimination reactions to form 3-benzal-2,4-pentanedione.

By following the rate of formation of 3-benzal-2,4-pentanedione, the rate constant, k_r, for the reaction

$$C_6H_5CH(SC_4H_9)\ CH(COCH_3)_2 \rightarrow C_6H_5CH{=}C(COCH_3)_2 + C_4H_9SH$$

was found to be 1.35×10^{-4} s^{-1}. The calculated equilibrium constant, $K = k_2/k_r$, is therefore $1.48 \times 10^4 M^{-1}$; that measured was 1.81×10^4 M^{-1}.

An examination of phenyl substituent effects on this reverse reaction will be investigated.

Discussion

The conjugative power of the functional group in these *gem* difunctional compounds as gauged by relative k_2 values increases as anticipated (17, 18) in the order $CONH_2 < CO_2C_2H_5 < COCH_3$. As would be expected from the analysis of their absorption spectra (20), the rate constants for the ethyl benzalacetoacetates with dissimilar functional groups approximate those for the 3-benzal-2,4-pentanediones (Table I) more closely than they do those of the diethyl benzalmalonates. The nuclear magnetic resonance (n.m.r.) spectra (19) of these substituted ethyl benzalacetoacetates demonstrate that only about half of them are geometrically homogeneous. However, the log k_2 values for the geometrically homogeneous members (with the ketone *trans* and the ester *cis* to the phenyl group) in the Hammett σ plot fall on the same line as the nonhomogeneous members. Therefore, either the homogeneous members equilibrate prior to reaction, or the transition state of the nonhomogeneous members is the same as that for the homogeneous ones.

The ratio k_2 (para)/k_2 (ortho) decreases in the order $CH_3 > Cl > CH_3O$ and is less for the diethyl benzalmalonates and ethyl benzalacetoacetates than for the corresponding 3-benzal-2,4-pentanediones. The main factor contributing to the differences between series would appear to be the hindrance due to the functional group *cis* to the phenyl group. The n.m.r. spectra of the diethyl benzalmalonates and the 3-benzal-2,4-pentanediones indicate that on time average the

carbonyl is remote from the *cis* phenyl group (19) and so the oxygen of the *cis* ester ethoxyl facing the phenyl group provides more freedom of approach for the nucleophile to the reaction center than does the bulkier methyl group of the *cis* methylketone. The bulk of the ortho substituent accounts in part for differences within series. This is in accord with the steric increments assigned to these groups from absorption spectra maxima (20).

The lower ρ values for the *n*-butanethiol additions to the 3-benzal-2,4-pentanediones as compared with those for the diethyl benzalmalonates (Table II) indicate less dependence of the reaction rate of the former upon substitution in the phenyl ring. For conformational reasons similar to those given above, rotation of the phenyl group of the 3-benzal-2,4-pentanediones further out of the plane of the ethylene functional group system than in the corresponding diethyl benzalmalonates accommodates this observation. The ρ value for the addition of *n*-butanethiol to the analogous benzalmalonamides also indicates little interference between the phenyl group and the *cis* carboxyamide grouping. The interference of the methyl group with both the phenyl and nitro groups of β-nitropropenylbenzenes as deduced from their dipole moments (16) is reflected in the low ρ value for their *n*-butanethiol addition reactions as well as in the retardation of the addition reaction by ortho substituents.

Since the acidity constants, pK, of *n*-butanethiol and *t*-butanethiol are similar (12.4 and 12.7 respectively) (21), the rate constants determined for the addition of *sec*-butanethiol and of *t*-butanethiol to 3-benzal-2,4-pentanedione, ethyl benzalacetoacetate, and diethyl benzalmalonate indicate that steric hindrance in the attacking nucleophile can also result in significantly reduced reaction rates.

1. S. RUHEMANN. J. Chem. Soc. **87**, 17 (1905).
2. W. DAVEY and J. R. GWILT. J. Chem. Soc. 1015 (1957).
3. B. H. NICOLET. J. Am. Chem. Soc. **57**, 1098 (1935).
4. R. L. FRANK and P. V. SMITH. J. Am. Chem. Soc. **68**, 2104 (1946).
5. B. H. NICOLET. J. Am. Chem. Soc. **53**, 3066 (1931).
6. B. H. NICOLET. J. Am. Chem. Soc. **54**, 1998 (1932).
7. T. POSNER. Ber. **34**, 1395 (1901).
8. T. POSNER. Ber. **35**, 808 (1902).
9. F. KIPNIS and J. ORNFELT. J. Am. Chem. Soc. **71**, 3554 (1949).
10. S. RUHEMANN. J. Chem. Soc. **87**, 461 (1905).
11. R. L. HEATH and A. LAMBERT. J. Chem. Soc. 1477 (1947).
12. L. F. CASON and C. C. WANSER. J. Am. Chem. Soc. **73**, 142 (1951).
13. A. MUSTAFA, A. H. E. HARHASH, and M. KAMEL. J. Am. Chem. Soc. **77**, 3860 (1955).
14. R. F. SILVER, K. A. KERR, P. D. FRANDSEN, S. J. KELLEY, and H. L. HOLMES. Can. J. Chem. **45**, 1001 (1967).
15. C. E. LOUGH and D. J. CURRIE. Can. J. Chem. **44**, 1563 (1966).
16. R. W. TAFT. *In* Steric effects in organic chemistry. *Edited by* M. S. Newman. John Wiley and Sons, Inc., New York. 1956. pp. 571 and 619.
17. R. G. PEARSON and R. L. DILLON. J. Am. Chem. Soc. **75**, 2439 (1953).
18. U. EISNER and P. H. GORE. J. Chem. Soc. 922 (1958).
19. W. M. PHILLIPS, F. K. MCCLUSKY, and D. J. CURRIE. Unpublished work in this laboratory.
20. D. J. CURRIE, C. E. LOUGH, R. F. SILVER, and H. L. HOLMES. Can. J. Chem. **45**, 1567 (1967).
21. J. MAURIN and R. A. PÂRIS. Compt. Rend. **232**, 2428 (1951); Chem. Abstr. **45**, 8857 (1951).

Can. J. Chem. Downloaded from www.nrcresearchpress.com by 210.87.254.42 on 09/05/12
For personal use only.

Equilibrium reactions of *n*-butanethiol with some conjugated heteroenoid compounds

R. B. PRITCHARD,[1] C. E. LOUGH, D. J. CURRIE, AND H. L. HOLMES
Chemistry Section, Defence Research Establishment Suffield, Ralston, Alberta

Received September 5, 1967

The reactions of 2-benzal-1,3-indanediones and the cyano-containing benzalmalononitriles, ethyl benzalcyanoacetates, benzalcyanoacetamides, and benzalcyanoacetanilides with *n*-butanethiol at 25 °C in 20% ethanol – 80% pH 7 buffer attain equlibrium at a rate too fast to measure by standard methods. The equilibrium constants have been calculated and these in turn related to Hammett σ and Taft σ* constants. The differences in the reactions of these and other *gem* difunctional systems which react virtually completely with *n*-butanethiol under the same experimental conditions and at a measurable rate, are attributed to participation of the functional group *cis* to the phenyl group in the reverse reaction. It is shown that *n*-butanethiol adds to cinnamalacetophenone by a 1,4-mechanism and the reactions of this nucleophile with similar compounds having extended conjugated systems are discussed.

Canadian Journal of Chemistry, 46, 775 (1968)

Introduction

It was stated (1) that no report could be found of the isolation of an adduct arising from the addition of a thiol to the conjugated system of a cinnamonitrile with a second functional group on the α carbon. It has been demonstrated, however, that mercaptans react with the cyano grouping of acetonitrile (2) and that hydrogen sulfide reacts similarly with cinnamonitrile (3) and *p*-methoxybenzonitrile (4). Feniak *et al.* (5) have recently demonstrated that *n*-butanethiol adds to benzalmalononitrile in the presence of piperidine in chloroform solution but the rapid reversibility of the system precludes the isolation of this thiol adduct. This paper describes the related aqueous solution reactions of *n*-butanethiol with conjugated heteroenoid compounds containing a cyano group.

Extension of the conjugated system by the introduction of an additional ethylenic double bond into the conjugated system increases the number of possible modes of thiol addition. Addition can conceivably occur by 1,2-, 1,4-, or 1,6-mechanisms and in the latter case subsequent 1,4-addition to the derived α,β-unsaturated system is possible. Thiophenol and isoamyl mercaptan have been added to cinnamalacetophenone, and the same adducts result when the reactions are catalyzed by hydrogen chloride (6) or piperidine (7). Although no attempt was made to establish the structures of the adducts, only one molar equivalent of isoamyl mercaptan reacted with cinnamalacetophenone which suggests that addition occurred by a 1,4-mechanism.

[1]Summer student. Present address: Faculty of Medicine, Queen's University, Kingston, Ontario.

Experimental

Except for the 2-benzal-1,3-indanediones, the preparation and purity of all the unsaturated compounds used in this work are described by Silver *et al.* (8).

2-Benzal-1,3-indanediones

The benzaldehydes were condensed with 1,3-indanedione by the method of Geita and Vanags (9). The melting points of these 2-benzal-1,3-indanediones and the solvents from which they were crystallized are given in Table I while the analytical figures are listed in Table II.

2-(2-Thenylidene)-1,3-indanedione

This compound was prepared by the method of Buu-Hoï *et al.* (12). After three crystallizations from ethanol, it melted constantly at 175.0–175.5 °C.

n-Butanethiol – Cinnamalacetophenone Adduct

The addition of *n*-butanethiol to cinnamalacetophenone by the procedure of Ruhemann (7) in benzene solution and in the presence of two drops of piperidine gave an 88% yield of an equimolar adduct which when crystallized from ethanol gave white needles melting at 46.2–46.8 °C.

Anal. Calcd. for $C_{21}H_{24}OS$: C, 77.73; H, 7.45; S, 9.88. Found: C, 77.60; H, 7.36; S, 9.77.

Results

In general, in the very rapid equilibrium reactions of these conjugated heteroenoid compounds with *n*-butanethiol in 20% ethanol – 80% aqueous buffer (Sörensen, pH 7) (v/v) the approach to equilibrium could not be observed. The equilibrium concentration of the unsaturated compound was determined by ultraviolet spectroscopy (1).[2] Since in this solvent system many compounds of type **1** undergo reverse aldol

[2]The long wavelength absorption maxima in general were 2 to 5 mμ longer in the aqueous ethanol than those in ethanol (19).

Can. J. Chem. Downloaded from www.nrcresearchpress.com by 210.87.254.42 on 09/05/12
For personal use only.

TABLE I

The melting points* of some 2-benzal-1,3-indanediones†

X	Crystallization solvent	Melting point (°C) Found	Lit.	Reference
H	C_2H_5OH	152.0–153.0	152	9
2-CH_3	C_2H_5OH	152.5–153.0	—	—
4-CH_3	C_2H_5OH	151.0–151.5	154.5–155.0	10
2-F	C_2H_5OH	135.5–135.6	—	—
2-Cl	C_2H_5OH	132.0–133.0	—	—
4-Cl	C_2H_5OH	179.0–180.0	177–178	11
2-Br	C_2H_5OH	125.5–126.0	—	—
2-CH_3O	$CH_3—CO_2H$	167.8–168.2	167.5–168	10
4-CH_3O	C_2H_5OH	158.5–159.0	—	—

*All melting points were recorded in an apparatus designed by E. B. Hershberg (13) using Anschütz thermometers for complete immersion so the melting points are corrected.

†These compounds, of structure, 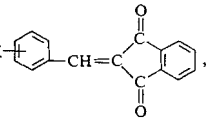 , were prepared by Mr. R. F. Silver.

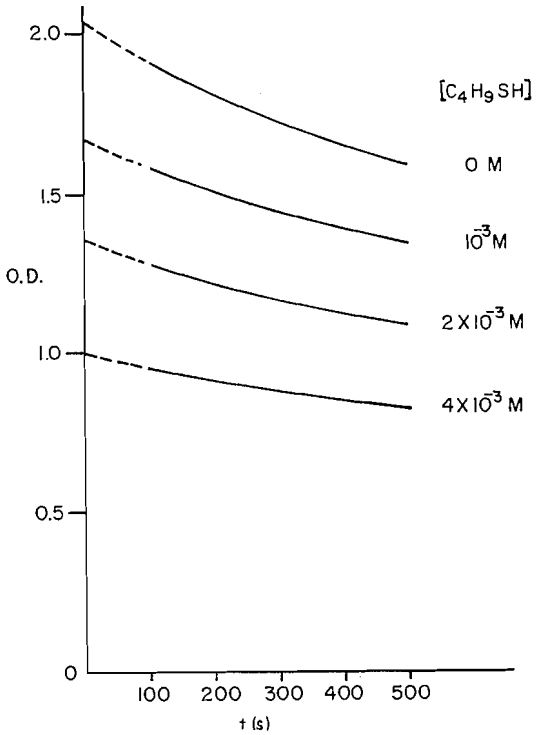

FIG. 1. The equilibrium reaction of *n*-butanethiol with a readily hydrolyzable compound. For example: when $[C_4H_9SH] = 2 \times 10^{-3}\ M$ and $[3—C_2H_5O—C_6H_4CH{=}C(CN)_2] = 4 \times 10^{-5}\ M$, then

$$K = \frac{(2.04 - 1.35)}{(1.35)(2 \times 10^{-3})}.$$

reactions (14) (Table III),[3] where necessary

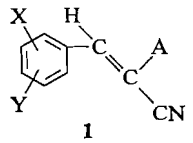

1

A = CN, $CO_2C_2H_5$, $CONH_2$, $CONHC_6H_5$

the optical densities of the solutions at equilibrium were determined by extrapolation of the optical density – time trace to zero time (Fig. 1). Assuming $C_6H_5—CH(SC_4H_9)—CH(A)CN$ to be the structure of the adduct, in analogy with that deduced for the analogous reaction with 3-benzal-2,4-pentanedione (1), equilibrium constants, $K(M^{-1})$, were calculated from the following expression. The values that are listed

$$K = \frac{[C_6H_5—CH(SC_4H_9)—CH(A)CN]}{[C_6H_5—CH{=}C(A)CN] \times [C_4H_9SH]}$$

in Table IV are the means, $\bar{K}$, of at least three separate determinations with initial *n*-butanethiol concentrations differing by at least a factor of five. The % deviation, $100(K - \bar{K})/\bar{K}$, is a measure of the maximum range of the experimental values from the mean and all results are consistent with the participation of only one

[3]For the hydrolysis of the 2-benzal-1,3-indanediones $\log k = 1.42\ \sigma - 2.71$; regression coefficient, r 0.89; and standard error of r, Δr 0.29 and standard error of the estimate, Δ estimate 0.16.

TABLE II

Analytical figures* for some 2-benzal-1,3-indanediones†

X	Calculated % C	Calculated % H	Found % C	Found % H
2-CH_3	82.23	4.87	82.12	4.60
2-F	76.18	3.51	76.15	3.22
2-Cl	71.51	3.37	71.35	3.25
2-Br	61.36	2.89	61.15	2.76
4-CH_3O	77.26	4.57	76.98	4.48

*These analyses were done in this laboratory by Mr. R. P. Hicken.

†Compounds of structure 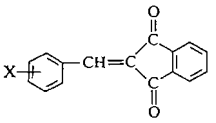 .

TABLE III

The reaction* of water with some conjugated heteroenoid compounds† in 20% ethanol – 80% pH 7 buffer‡ (v/v) at 25 °C

B	A	X	$k \times 10^3$ (s^{-1})
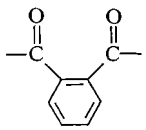		H	2.05
		2-CH_3	1.41
		4-CH_3	1.68
		2-Cl	4.63
		4-Cl	2.44
		2-F	4.34
		2-Br	4.67
		4-CH_3O	0.48
CN	CN	H	0.48
CN	$CO_2C_2H_5$	H	0.04_1
CN	$CONH_2$	H	0.00_3
$COCH_3$	$COCH_3$	H	0.00_2

*The reaction: 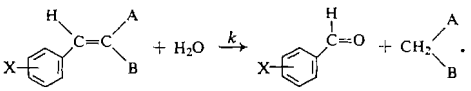 .

†Concentration from 5×10^{-6} to 2×10^{-5} *M* of heteroenoid compound.
‡*M*/15 Na_2PO_4 (60%) and *M*/15 KH_2PO_4 (40%) (Sörensen).

mole equivalent of *n*-butanethiol in the reaction. The *n*-butanethiol concentrations used with all the cinnamonitrile derivatives were the same (5×10^{-4} to 2.5×10^{-3} *M*), but to obtain measurable *K* values for the 2-benzal-1,3-indanedione series, the concentration of the butanethiol had to be reduced by an order of magnitude.

The logarithms of the equilibrium constants for the 2-benzal-1,3-indanedione series and for the cinnamonitriles with a second functional group on the α carbon correlate with Hammett σ constants and Taft σ* constants (Table V), but because of the values of the correlation coefficients, no particular significance can be attached to the variations in the ρ values. The equilibrium constants parallel the rate constants for the reaction of the benzalmalononitriles with water and cyanide ion (14) and, in addition, steric hindrance to nucleophilic attack apparently occurs with some C-2 alkyl derivatives.

The ultraviolet spectrum of the *n*-butanethiol adduct of cinnamalacetophenone in ethanol (λ, ε; 295 mμ, ~3000; ~286 mμ, —; 249 mμ, 27 000) is very similar to that of propenylbenzene or of cinnamyl alcohol (15) plus hexylphenyl ketone (λ, ε, 279.5 mμ, 1030; 242 mμ, 13 000) but does not resemble that of

Can. J. Chem. Downloaded from www.nrcresearchpress.com by 210.87.254.42 on 09/05/12
For personal use only.

TABLE IV

Equilibrium constants for the reactions* of some conjugated heteroenoid compounds† with *n*-butanethiol in 20% ethanol – 80% pH 7 buffer‡ (v/v) at 25 °C

B	A	X	Y	$K \times 10^{-2}$ (M^{-1})	% deviation
CN	$CO_2C_2H_5$	H	§H	0.92	27
		2-CH_3	H	0.71	23
		4-CH_3	H	0.47	49
		3-F	H	4.9	14
		2-Cl	H	7.6	1
		3-Cl	H	6.5	17
		4-Cl	H	3.4	15
		2-CH_3O	H	1.8	29
		3-CH_3O	H	2.8	5
		4-CH_3O	H	0.21	24
		4-CN	H	13	15
		3-NO_2	H	7.5	15
		2-Cl	4-Cl	9.6	3
		2-Cl	6-Cl	6.1	14
		2-CH_3O	4-CH_3O	0.17	17
		3-CH_3O	4-CH_3O	0.41	4
CN	$CONH_2$	H	H	4.7	33
		2-CH_3	H	2.7	7
		4-CH_3	H	2.3	20
		2-Cl	H	19	10
		4-Cl	H	6.9	2
		2-CH_3O	H	4.7	18
		3-CH_3O	H	7.8	13
		4-CH_3O	H	0.32	8
		3-CH_3O	4-CH_3O	1.0	22
CN	$CONHC_6H_5$	H	H	14	9
		2-CH_3	H	6.9	9
		4-CH_3	H	7.3	1
		2-Cl	H	44	6
		4-Cl	H	22	10
		2-CH_3O	H	19	6
		3-CH_3O	H	14	15
		4-CH_3O	H	3.1	12
		3—O—CH_2—O—4		4.7	16
CN	CN	H	‖H	1.7	17
		2-CH_3	H	0.90	10
		2-C_2H_5	H	¶0.44	12
		2-$C(CH_3)_3$	H	¶0.006	<1
		3-CH_3	H	1.4	7
		4-CH_3	H	0.55	16
		2-F	H	4.5	5
		3-F	H	5.5	4
		4-F	H	1.2	8
		2-Cl	H	7.0	9
		3-Cl	H	6.7	1
		4-Cl	H	2.5	8
		2-Br	H	8.2	7
		3-Br	H	4.6	8
		4-Br	H	2.6	13
		2-CH_3O	H	1.3	7
		3-CH_3O	H	2.5	4
		4-CH_3O	H	0.24	19
		2-C_2H_5O	H	1.2	16
		3-C_2H_5O	H	2.4	7
		4-C_2H_5O	H	0.13	40
		2-$CH(CH_3)_2O$	H	¶1.2	15
		3-HO	H	1.9	11
		4-HO	H	¶~0	—
		2-CO_2CH_3	H	¶1.6	7
		4-CO_2CH_3	H	¶8.9	10
		2-NO_2	H	¶1.6	11
		3-NO_2	H	9.9	22
		4-NO_2	H	12	11

Can. J. Chem. Downloaded from www.nrcresearchpress.com by 210.87.254.42 on 09/05/12
For personal use only.

TABLE IV (*Concluded*)

B	A	X	Y	$K \times 10^{-2}$ (M^{-1})	% deviation
		2-Cl	4-Cl	10	9
		2-Cl	6-Cl	7.7	4
		3-Cl	4-Cl	8.8	8
		2-CH_3O	4-CH_3O	0.16	17
		3-CH_3O	4-CH_3O	0.26	2
		3-CH_3O	4-HO	0.13	16
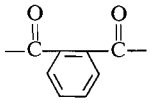		H	**H	620	28
		2-CH_3	H	410	9
		4-CH_3	H	180	9
		2-F	H	1600	5
		2-Cl	H	2500	9
		4-Cl	H	2000	26
		2-Br	H	2700	14
		2-CH_3O	H	130	18
		4-CH_3O	H	67	14

*The reaction: 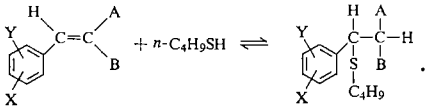

†Concentration from 5×10^{-6} to 4×10^{-5} M of heteroenoid compound.
‡M/15 Na_2PO_4 (60%) and M/15 KH_2PO_4 (40%) (Sörensen).
§The reactions of this compound with *sec*-butanethiol and *t*-butanethiol gave approximate equilibrium constants of 84 and 20 M^{-1} respectively.
‖The reactions of this compound with *sec*-butanethiol and *t*-butanethiol gave approximate equilibrium constants of 76 and 21 M^{-1} respectively.
¶These rate constants were not included in the correlations.

**The compound 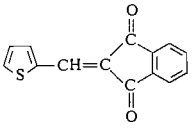 gave an equilibrium constant of 1600 ± 430 M^{-1}.

crotonophenone (16, 17) plus ethylbenzene. Furthermore from the spectrum run in CCl_4 solution the 1690 cm^{-1} ketone stretching band of the adduct differs markedly from that of crotonophenone (1673 cm^{-1}) (16). Hence it would appear that the *n*-butanethiol adduct has structure **2**.

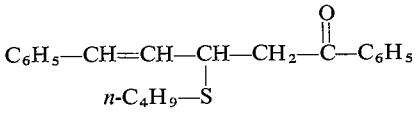

2

The reaction of 3-cinnamal-2,4-pentanedione occupies an intermediate position in the transition between the rapid reversible addition for the 2-benzal-1,3-indanediones and the slower virtually complete additions for the 3-benzal-2,4-pentanediones since, although no reliable rate constants could be determined, the approach to equilibrium could be followed ($K = 110 \pm 10$ M^{-1}).

The reactions of 2-cinnamal-1,3-indanedione and cinnamalmalononitrile contrast. The former is an equilibrium reaction ($K = 1800 \pm 200$ M^{-1}) while the latter goes virtually to completion ($k_2 = 3.6 \times 10^{-2}$ M^{-1} s^{-1}, thiol exponent 1.09 ± 0.03).

Discussion

Except for the 2,6-dichloro derivatives of 3-benzal-2,4-pentanedione and the appropriate geometric isomer of ethyl benzalacetoacetate[4] in all the 3-benzal-2,4-pentanediones, ethyl benzalacetoacetates, and the diethyl benzalmalonates studied in the previous paper, the *cis* carbonyl oxygen is remote from the styrene system (18). The reaction of excess *n*-butanethiol with the above mentioned compounds goes essentially to completion at a measurable rate (1). With the 2-benzal-1,3-indanediones on the

[4]The mixture of geometric isomers (2×10^{-5} M) failed to react with *n*-butanethiol (5×10^{-3} M).

Can. J. Chem. Downloaded from www.nrcresearchpress.com by 210.87.254.42 on 09/05/12
For personal use only.

TABLE V

Reaction constants and correlation data* for equilibrium constants taken from Table IV

B	A	ρ	K_H	Correlation coefficient r	Standard error Δr	Standard error Δ estimate
CN	$CO_2C_2H_5$	1.45	147	0.89	0.20	0.29
CN	$CONH_2$	1.63	424	0.67	0.69	0.42
CN	$CONHC_6H_5$	1.03	1310	0.62	0.50	0.30
CN	CN	1.53	137	0.87	0.17	0.31
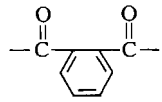		2 35	63400	0.95	0.30	0.21

*Log $K_{xy} = \rho\sigma + \log K_H$.

other hand, where the *cis* carbonyl oxygen of necessity is directed towards the benzene ring, reaction with excess *n*-butanethiol is rapid and reversible. The same is true for the benzalmalononitriles, ethyl benzalcyanoacetates, benzalcyanoacetamides, and benzalcyanoacetanilides in which the *cis* cyano group (19) lies in close juxtaposition to the benzene ring. Besides the rapid rate of the forward reaction in the addition of *n*-butanethiol to these cyano-containing compounds, increased reactivity of these systems relative to that of 3-benzal-2,4-pentanedione is reflected in their rates of hydrolysis (Table II). This increased reactivity may be explained in terms of inductive, resonance, and steric effects since the ultraviolet absorption maxima of these compounds are at wavelengths considerably longer than those for related compounds with angular functional groups (19). On the other hand, insertion of another ethylenic double bond into benzalmalononitrile as in cinnamalmalononitrile removes the *cis* cyano grouping from the benzene ring and now the *n*-butanethiol reaction goes virtually to completion.

The acidity of the α hydrogen in the *n*-butanethiol adducts of the cyano-containing compounds and of the 2-benzal-1,3-indanediones (21, 22) does not appear to be the sole or even dominant factor promoting β elimination in the reverse reaction. Even in the absence of rate constants for the forward and reverse reactions which will require stop flow techniques, we are prompted to suggest that elimination of the *n*-butyl mercaptide ion from the adduct may be promoted by interaction of the sulfur atom with the carbon atom of the polarized cyano group thus facilitating the withdrawal of the mercaptide ion by stabilizing the anion until it is solvated (20). The favorably oriented carbonyl groups of the 2-benzal-1,3-indanedione and 2-cinnamal-1,3-indanedione adducts could achieve the same effect but to a lesser extent by facilitating hydrogen transfer from a protonated or solvated carbonyl grouping to the leaving mercaptide ion.[5] It must be assumed from this, however, that the orientation of the carbonyl groups in the adducts of the 3-benzal-2,4-pentanediones, the ethyl benzalacetoacetates, the diethyl benzalmalonates, and the benzalmalonamides does not favor the reverse reaction. If the addition of *n*-butanethiol to 3-cinnamal-2,4-pentanedione goes by a 1,4-mechanism as has been shown in the case of cinnamalacetophenone[6] then reduced spatial congestion in the thiol adducts would allow a favorable orientation of the *cis* carbonyl so that the reversibility of this reaction perhaps is not surprising.

Acknowledgment

The authors thank Mr. N. Bannister and Mr. H. Lightfoot for computational assistance, and Mr. R. F. Silver for the compounds used in this study.

1. C. E. Lough, D. J. Currie, and H. L. Holmes. Can. J. Chem. This issue.
2. C. M. Himel. U.S. Patent No. 2 458075 (January 4, 1949); Chem. Abstr. **43**, 3444 (1949).
3. Beilstein. Vol. IX. p. 589.
4. A. E. S. Fairfull, J. L. Lowe, and D. A. Peak. J. Chem. Soc. 742 (1952).

[5]C-2 methoxyl, and to a lesser extent C-2 chloro (but not C-2 methyl) derivatives may assist in this process.

[6]The second order rate constant for this reaction is $< 7 \times 10^{-3}\ M^{-1}\ s^{-1}$.

Can. J. Chem. Downloaded from www.nrcresearchpress.com by 210.87.254.42 on 09/05/12
For personal use only.

5. G. FENIAK, H. L. HOLMES, and J. B. REESOR. Unpublished work done in this laboratory.
6. T. POSNER. Ber. **37**, 502 (1904).
7. S. RUHEMANN. J. Chem. Soc. **87**, 17 (1905).
8. R. F. SILVER, K. A. KERR, P. D. FRANDSEN, S. J. KELLEY, and H. L. HOLMES. Can. J. Chem. **45**, 1001 (1967).
9. L. S. GEITA and G. VANAGS. Zh. Obshch. Khim. **27**, 3109 (1957).
10. V. PETROW, J. SAPER, and B. STURGEON. J. Chem. Soc. 2134 (1949).
11. IONESCU. Bull. Soc. Chim. France, [4], **47**, 212 (1930); Beilstein. Vol. VII, 2nd Suppl. p. 752.
12. N. P. BUU-HOĪ, N. HOÁN, and D. LAVIT. J. Chem. Soc. 2130 (1950).
13. E. B. HERSHBERG. Ind. Eng. Chem. Anal. Ed. **8**, 312 (1936).
14. R. B. PRITCHARD, C. E. LOUGH, J. B. REESOR, H. L. HOLMES, and D. J. CURRIE. Can. J. Chem. **45**, 775 (1967).
15. T. W. CAMPBELL, S. LINDEN, S. GODSHALK, and W. G. YOUNG. J. Am. Chem. Soc. **69**, 880 (1947).
16. J. U. LOWE and L. N. FERGUSON. J. Org. Chem. **30**, 3000 (1965).
17. N. H. CROMWELL and W. R. WATSON. J. Org. Chem. **14**, 411 (1949).
18. W. M. PHILLIPS, F. K. MCCLUSKY, and D. J. CURRIE. Unpublished work done in this laboratory.
19. D. J. CURRIE, C. E. LOUGH, R. F. SILVER, and H. L. HOLMES. Can. J. Chem. **45**, 1567 (1967).
20. R. H. F. MANSKE and H. L. HOLMES. The alkaloids. Vol. II. Academic Press, New York. 1952. p. 517.
21. R. G. PEARSON and R. L. DILLON. J. Am. Chem. Soc. **75**, 2439 (1953).
22. E. GRENS and G. VANAGS. Zh. Organ. Khim. **1**, 3 (1965); Chem. Abstr. **62**, 14468 (1965).

Can. J. Chem. Downloaded from www.nrcresearchpress.com by 210.87.254.42 on 09/05/12
For personal use only.

Can. J. Chem. Downloaded from www.nrcresearchpress.com by 210.87.254.105 on 09/05/12
For personal use only.

Etude quantitative des réactions d'ozonolyse. VI. Sur la réduction du zwitterion de Criegee en composé carbonylé

S. FLISZÁR ET J. B. CHYLIŃSKA[1]
Département de Chimie, Université de Montréal, Montréal, Québec

Reçu le 31 octobre 1967

It is shown for a series of symmetric olefins that ca. 44% of the zwitterion which does not react to give ozonide yields open-chain peroxides. The latter, when formed of R—$\overset{+}{C}$HO$\overset{-}{O}$ units, decompose rapidly into aldehyde and O_2 (at room temperature), whereas such polymeric peroxides are relatively stable at 25° in CCl_4 when built of ketonic carbonyloxides.

Lors de l'ozonation des oléfines symétriques, environ 44% du zwitterion qui n'est pas engagé dans la production d'ozonide engendre des peroxydes polymères en chaîne ouverte. Ceux-ci, lorsqu'ils sont constitués d'unités R—$\overset{+}{C}$HO$\overset{-}{O}$, se décomposent rapidement (à la température ambiante) en aldéhyde et O_2; ces peroxydes sont, par contre, relativement stables à 25° (dans le CCl_4) lorsqu'ils sont constitués d'oxydes de carbonyle cétoniques.

Canadian Journal of Chemistry, **46**, 783 (1968)

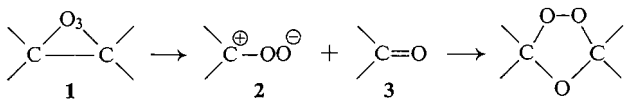

1 **2** **3** **4**

D'après la théorie de Criegee (1) sur le mécanisme de l'ozonolyse "normale" dans un solvant inerte, l'attaque de l'ozone sur une double liaison C=C engendre un ozonide primaire (**1**) qui se scinde en un zwitterion (**2**) plus un composé carbonylé (**3**) dans une proportion de 1:1; l'ozonide (**4**) serait ensuite engendré par la réaction de **2** avec **3**.[2]

Au cours d'études portant sur les bilans d'ozonation du stilbène (3) et du diphényl-1,4 butène-2 (4) nous nous sommes trouvés en apparente contradiction avec cette stoïchiométrie vu que nous avons observé (*i*) qu'il se forme plus qu'une mole d'aldéhyde par mole d'oléfine ozonée (en tenant compte de l'aldéhyde fixé sous forme d'ozonide) et (*ii*) que la quantité d'oxyde de carbonyle formée est inférieure à la quantité d'oléfine consommée.

Nous avons alors interpreté les observations faites, concernant les réactions du zwitterion **2**, en supposant deux modes de réaction: (*a*) formation d'un peroxyde dimère cyclique (**5**) et (*b*) polymérisation en chaîne ouverte, conduisant à une réduction du zwitterion en composé carbonylé plus oxygène. Le zwitterion polymère en chaîne ouverte est représenté ici par son dimère (**6**), sans pour autant présumer de la possibilité de polymérisation à un plus haut degré.

Par ailleurs nous sommes arrivés à des conclusions similaires en établissant les bilans d'ozonation du tétraphényléthylène (5). Dans ce cas il n'y a pas de formation d'ozonide vu qu'un groupement cétonique est, en général, moins susceptible à une attaque nucléophile qu'un groupement aldéhydique. On retrouve alors, à côté de la benzophénone et du peroxyde dimère de benzophénone cyclique, un composé peroxydique supposé en chaîne ouverte, du type **6**, suffisamment stable à la température ambiante (en solution dans du CCl_4) pour en permettre le dosage. La quantité de cétone formée est égale à la quantité d'oléfine consommée par la réaction.

L'intérêt croissant manifesté, en vue de discussions mécanistiques, pour des bilans d'ozonations précis nous a conduit à examiner plus en détail cet aspect particulier de la réaction entre

[1]Chercheur invité, en congé de l'Institut de Chimie Organique, Académie des Sciences de Pologne, Varsovie 10, Pologne.

[2]On n'exclut pas cependant de façon impérative les vues de Murray, Story *et al.* (2), qui proposent le clivage d'une liaison O—O de l'ozonide primaire et non pas de la liaison C—C. Relevons toutefois que la réaction étudiée par ces auteurs est celle d'un molozonide plus un aldéhyde à −70 °C, tandis que nous étudions le clivage de l'ozonide primaire dans des conditions de température (0–45 °C) qui favorisent la très rapide décomposition de celui-ci, en accord avec la théorie de Criegee (1).

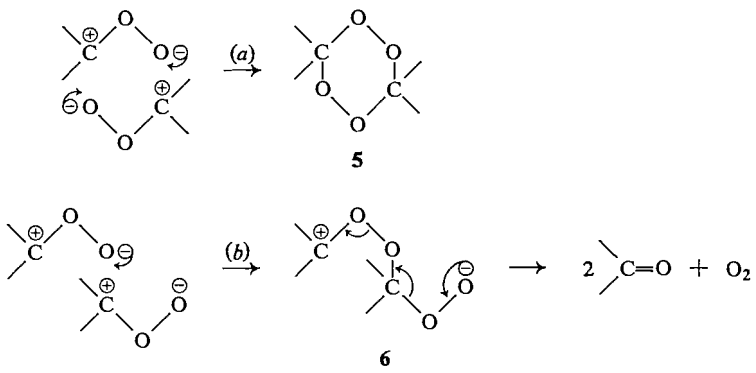

5

6

zwitterions. En effet, la formation d'aldéhyde par la réduction de ceux-ci peut modifier le cours des réactions, notamment dans le cas d'oléfines dissymétriques.

Ozonation des oléfines du type R—CH=CH—R

L'ozonation de ces oléfines dans le CCl_4 engendre des aldéhydes, des ozonides, à côté de produits peroxydiques. Il a déjà été montré (6, 7) que la production d'aldéhyde se manifeste dès le début de l'ozonation et qu'elle n'est pas due à une décomposition de l'ozonide. Pour mieux nous en assurer, nous avons mesuré les constantes de vitesse pour la décomposition[3] unimoléculaire de l'ozonide du fumarate d'éthyle, particulièrement instable par rapport aux autres ozonides étudiés dans ce travail: k (0 °C) = 0.44×10^{-3}, k (25°) = 2.1×10^{-3} et k (35°) = 3.4×10^{-3} (1/h); énergie d'activation = 9.8 ± 0.1 kcal/mole. Le temps requis pour effectuer les ozonations et les mesures rapportées plus loin (15–20 min) est donc bien inférieur au temps de demi-vie (330 h à 25°) mesuré pour cet ozonide relativement peu stable. Dans d'autres cas (par exemple avec l'ozonide du *trans*-stilbène) on n'observe pas de production d'aldéhyde après un reflux pendant 5 h de l'ozonide en solution dans du CCl_4.

Les bilans d'ozonation nous renseignent sur la proportion de zwitterion qui se décompose en aldéhyde plus oxygène par rapport à la quantité de zwitterion non engagé dans la production d'ozonide; cette proportion, f, peut être déterminée de deux façons:

(*a*) On mesure les quantités d'aldéhyde (A) et d'ozonide (Oz) engendrés par l'ozonation de S moles d'oléfine. Alors S—Oz = le nombre de moles de zwitterion non utilisé pour former l'ozonide = le nombre de moles d'aldéhyde devant donc normalement se retrouver. Ainsi le nombre de moles d'aldéhyde formé en excès, par la décomposition partielle de zwitterion, est égal à A − (S − Oz) et, par conséquent, $f = [A - (S - Oz)]/(S - Oz)$.

(*b*) On mesure les quantités de l'oléfine consommée (S), de l'ozonide engendré (Oz), ainsi que l'oxygène actif (O*a*) qui est une mesure de la quantité totale de zwitterion fixé soit sous forme d'ozonide, soit sous forme de peroxydes; alors S − O*a* mesure la quantité de zwitterion décomposé et $f = (S - Oa)/(S - Oz)$.

Il convient, en général, de se tenir à des ozonations modérées, ceci pour prévenir la formation de peracide par autoxydation de l'aldéhyde.[4] La reproductibilité satisfaisante de ces déterminations est illustrée par l'exemple suivant (Tableau I) se rapportant à l'ozonation du *trans* octène-4.

Des résultats analogues ont été obtenus lors de l'ozonation du dichloro-1,4 butène-2 (Tableau IV). On relève que le *trans* octène-4 se distingue des autres oléfines examinées principalement à deux points de vue: (*i*) le rendement en ozonide est, dans l'intervalle 15–25°, pratiquement indépendant de la température, tandis qu'avec d'autres oléfines (comme, par exemple, le *trans*-stilbène et le fumarate d'éthyle) on observe un effet de température très marqué. Ainsi avons-nous observé pour le fumarate d'éthyle des rendements de 80–85% en ozonide lors d'ozona-

[3]Les produits de décomposition de cet ozonide ont été étudiés lors d'un travail précédent (7).

[4]Une correction tenant compte de la formation de peracide a été faite lors de l'ozonation du diphényl-1,4 butène-2 (3).

Can. J. Chem. Downloaded from www.nrcresearchpress.com by 210.87.254.105 on 09/05/12
For personal use only.

TABLEAU I

Ozonation de 1 millimole de *trans* octène-4, en solution dans 10 ml de CCl_4

Température °C	Oléfine consommée (mmole)	Aldéhyde formé (mmole)	Ozonide formé (mmole)	Rendement (%) en ozonide	f
−15	0.468	0.360	0.185	39.5	0.272
	0.680	0.495	0.285	41.9	0.253
0	0.515	0.403	0.205	39.8	0.300
	0.616	0.470	0.255	41.4	0.302
	0.816	0.620	0.339	41.5	0.300
25	0.224	0.20	0.086	38.4	0.449
	0.49	0.42	0.202	40.8	0.458
	0.51	0.43	0.213	41.8	0.448
	0.72	0.58	0.32	44.4	0.450
	0.86	0.68	0.39	45.3	0.447
45	0.410	0.377	0.150	36.8	0.450
	0.425	0.392	0.152	35.8	0.436
	0.760	0.665	0.292	38.4	0.421

tions effectuées à 25 °C (dans le CCl_4), contre 10–20% de rendement obtenus à environ −15°. (*ii*) Deuxièment, f décroît de façon marquée avec la température décroissante. Cet effet peut être attribué à une meilleure stabilisation des peroxydes en chaîne ouverte dans le cas de l'octène (par comparaison avec le stilbène) ce qui favoriserait à froid la polymérisation ultérieure de ceux-ci, accompagnée d'un accroissement supplémentaire de leur stabilisation par l'augmentation de la distance entre les charges positive et négative du zwitterion polymère.[5]

Ozonation des oléfines du type $(R)_2C{=}C(R)_2$

Contrastant d'avec les oléfines du type R—CH=CH—R, les éthylènes tétrasubstitués étudiés ici engendrent des produits peroxydiques présumés du type **6** relativement plus stables, à la température ambiante, en solution dans du CCl_4. Ainsi est-il possible de doser ces composés, car ils libèrent rapidement l'iode à partir de solutions acétiques de NaI. Comme nous l'avons vérifié, la quantité de cétone engendrée est alors, aux erreurs expérimentales près, égale à la quantité d'oléfine consommée.

On définit f de manière similaire à celle déjà exposée: f représente ici la proportion de zwitterion ayant engendré un peroxyde à chaîne ouverte par rapport au zwitterion non engagé dans la production d'ozonide, c'est-à-dire la quantité totale de zwitterion formé. Lors de la détermination de f il faut tenir compte que les dosages des peroxydes en chaîne ouverte peuvent être faussés à la suite de la réaction d'une partie des peroxydes cycliques avec I^-.

En ce qui concerne la stabilité des peroxydes d'acétone cycliques, on cite dans la littérature (8) que le dimère cyclique (F 132–133 °C) libère assez rapidement l'iode à partir d'une solution acétique de NaI (environ 25% de réaction en 30 min). Dans nos conditions expérimentales cependant, dans un mélange 1:2 de CCl_4 et de CH_3-COOH, nous trouvons que seulement 5% du peroxyde dimère réagit en 30 min à 25°, tandis que l'on ne peut percevoir avec certitude une réaction du trimère (F 95 °C) dans ces mêmes conditions (<1% de réaction). Dans le cas du peroxyde dimère de la cyclohexanone, la proportion de peroxyde qui réagit avec I^- dans nos conditions expérimentales s'élève à environ 27%.

On a pu par ailleurs vérifier que l'oxydation de I^- par ces peroxydes suit une cinétique de premier ordre en peroxyde; dès lors, vu que l'on opère en présence d'un grand excès de I^-, on peut calculer f en apportant la correction suivante dans son évaluation. En absence de réaction du dimère cyclique avec I^- on aurait $f =$ (oxygène actif)/(cétone formée) $= Oa/S$, du fait que la quantité de cétone formée est égale à la quantité d'oléfine consommée. Par contre on trouve $f_{exp} > f$, vu que la proportion x du peroxyde cyclique libère de l'iode à partir de I^-, d'où $f_{exp} = f + x(1 - f)$ et $f = (f_{exp} - x)/(1 - x)$, avec $x = 0.05$ pour le peroxyde dimère d'acétone et $x = 0.27$ pour le peroxyde dimère de cyclohexanone.

Les Tableaux II et III résument les résultats

[5]On note un phénomène semblable lors de l'ozonation du *trans*-stilbène à −20°, mais le polymère se décompose rapidement en benzaldéhyde, à 25°.

Can. J. Chem. Downloaded from www.nrcresearchpress.com by 210.87.254.105 on 09/05/12
For personal use only.

TABLEAU II

Ozonation de 20 ml de solution de tétraméthyléthylène dans du CCl_4, à 0 °C [oléfine] = concentration initiale de l'oléfine (mole/l); le débit est indiqué en millimole O_3 par min. Les quantités O_3 consommé, peroxyde formé et acétone formée sont indiquées en millimoles

[Oléfine]	Débit O_3	O_3 consommé	Peroxyde formé	Acétone formée	Peroxyde / Acétone
0.05	0.078	0.30	0.14	0.30	0.47
	0.150	0.47	0.20	0.44	0.46
	0.079	0.60	0.30	0.62	0.48
	0.123	0.75	0.37	0.79	0.47
0.10	0.880	0.60	0.27	0.59	0.46
	0.043	0.78	0.38	0.83	0.46
	0.810	1.10	0.48	1.03	0.47
	0.130	1.20	0.66	1.38	0.48

obtenus lors de l'ozonation du tétraméthyléthylène et du biscyclohexylidène, oléfines auxquelles s'appliquent les calculs sus-mentionnés.

TABLEAU III

Ozonation de 10 ml de solution 0.1 *M* de bis-cyclohexylidène dans du CCl_4. Les quantités de peroxyde titré et de cyclohexanone sont indiquées en millimoles

Température °C	Peroxyde titré	Cyclohexanone formée	Peroxyde / cétone	*f*
0	0.26	0.45	0.578	0.44
	0.46	0.85	0.541	0.40
25	0.11	0.20	0.550	0.41
	0.17	0.31	0.548	0.41
	0.24	0.44	0.545	0.40
	0.34	0.64	0.531	0.38
	0.37	0.69	0.536	0.39

En ce qui touche l'ozonation du tétraméthyléthylène, mis à part nos conclusions quant à la formation de peroxydes en chaîne ouverte, nos observations rejoignent celles de Criegee et Lohaus (9) qui ont mis en évidence la formation des peroxydes d'acétone cycliques; ces auteurs ont également montré qu'à la suite du clivage du molozonide il se forme, en un premier temps, autant de zwitterion que d'acétone, ce qui confirme bien les bilans que nous proposons.[6]

[6]Nos méthodes d'analyse ne nous ont pas permis de déceler le peroxyhydroperoxyde récemment trouvé par Story (10) parmis les produits isolés par chromatographie en phase gazeuse, à partir de solutions de tétraméthyléthylène ozonées. La présence de ce dimère de zwitterion, issus de la réaction entre un zwitterion $(CH_3)_2\overset{+}{C}—\overset{-}{O}O$ avec son tautomère $CH_2=C(CH_3)—OOH$, ne modifierait pas sensiblement nos bilans, car l'oxygène actif de l'hydroperoxyde serait titré iodométriquement, tandis que les oxygènes du cycle du peroxyhydroperoxyde décrit par Story ne réagirait vraisemblablement que très peu (ou pas du tout) avec I^- dans nos conditions analytiques.

Quant à l'ozonation du biscyclohexylidène, nos observations sont également en accord avec les résultats de Criegee et Lohaus (9) qui démontrent la formation du peroxyde dimère de cyclohexanone lors de l'ozonation de cette oléfine. Notons encore qu'en laissant reposer pendant quelques heures, à la température du laboratoire, des solutions de biscyclohexylidène fraîchement ozonées, on observe une lente augmentation de la quantité de cyclohexanone; ceci confirme l'existence d'un peroxyde relativement peu stable (présumé en chaîne ouverte) car des solutions-témoin de peroxyde cyclique de cyclohexanone ne produisent pas, dans les mêmes conditions, de cyclohexanone. Des mesures de la vitesse de formation de cyclohexanone à partir des peroxydes en chaîne ouverte n'ont pas été concluantes; la cinétique de cette décomposition semble être fonction du pourcentage d'ozonation, donc, peut être, du degré de polymérisation du zwitterion en chaîne ouverte. Les augmentations de la quantité de cétone observées étaient de l'ordre de 20–25% après 24 h, pouvant aller jusqu'à 40% dans certains cas, après un repos de 7–10 jours.

Des essais effectués avec éthylènes substitués par 4 groupements tendant à déstabiliser les peroxydes polymères en chaîne ouverte, favorisant ainsi leur décomposition en cétone plus O_2, ont échoué: le tétracyanoéthylène n'est pas soluble dans le CCl_4 et l'éthylène tétracarboxylate d'éthyle n'absorbe pas l'ozone.

Conclusions

Les bilans d'ozonation des oléfines symétriques, résumés dans le Tableau IV, indiquent que dans tous les cas étudiés environ 44% du zwit-

Can. J. Chem. Downloaded from www.nrcresearchpress.com by 210.87.254.105 on 09/05/12
For personal use only.

TABLEAU IV

Résumé des résultats des ozonations dans le CCl_4

Oléfine ozonée	Température °C	Rendement (%) en ozonide (25°)	f
Tétraphényléthylène	0–45	0	0.43±0.02
Tétraméthyléthylène	0	0	0.44±0.01
Bis-cyclohexylidène	0–25	0	0.41±0.03
Diphényl-1,4 butène-2	0–25	41	0.44±0.01
Trans octène-4	25–45	46	0.45±0.01
Trans-stilbène	25–45	68	0.45±0.01
Trans dichloro-1,4 butène-2	0–25	73	0.43±0.03

TABLEAU V

Sens de clivage des molozonides de quelques oléfines dissymétriques*

Oléfine	Pourcentage de zwitterion formé
p-méthylstyrène	71±1% de p. $CH_3—C_6H_4—\overset{+}{C}H—O\bar{O}$
β-méthylstyrène	82±1% de $CH_3—\overset{+}{C}H—O\bar{O}$
Méthyl-4 pentène-2 *trans*	73±4% de $CH_3—\overset{+}{C}H—O\bar{O}$
Triphényléthylène	71±1% de $Ph_2\overset{+}{C}—O\bar{O}$

*Ces valeurs sont extraites d'une étude détaillée devant paraître ultérieurement.

terion non engagé dans la production d'ozonide se polymérise en chaîne ouverte lors des ozonations effectuées dans le CCl_4, aux températures voisines de 25 °C. La décomposition de ces polymères est très rapide et conduit à la formation d'aldéhyde et d'oxygène dans le cas des éthylènes 1,2-disubstitués, contrastant ainsi d'avec les éthylènes tétrasubstitués qui engendrent, lors de leur ozonation, des peroxydes en chaîne ouverte relativement stables. Il est intéressant d'observer que f est, dans les limites d'erreurs expérimentales, indépendant de la nature des substituants.

La réduction d'une partie du zwitterion a également été observée lors de l'ozonation d'oléfines dissymétriques, par exemple le styrène (11). C'est notamment lors de l'ozonation des oléfines dissymétriques que la production d'aldéhyde à partir de zwitterion peut modifier le cours de l'ozonation. Supposons, en effet, d'ozoner une oléfine $R_1—CH{=}CH—R_2$ qui engendre, à la suite du clivage du molozonide, 70% de $R_1\overset{+}{C}H—O\bar{O}$ et de R_2CHO, donc 30% de $R_2\overset{+}{C}H—O\bar{O}$ et de R_1CHO. Des cas semblables sont fréquemment rencontrés, comme le montrent les quelques exemples suivants (Tableau V).

Si les rendements en ozonide sont relativement faibles (de l'ordre de 40–50%, par exemple) on serait porté à conclure à une accumulation plus importante de R_2CHO que de R_1CHO si les réactions des deux zwitterions avec les deux aldéhydes sont à peu près également faciles. Or, la quantité de $R_1\overset{+}{C}H—O\bar{O}$ qui se forme étant bien supérieure à celle de $R_2\overset{+}{C}H—O\bar{O}$, la production de R_1CHO par réduction du zwitterion correspondant pourra, dans ces conditions, favoriser une accumulation plus rapide de R_1CHO. Dès lors le rapport des concentrations $[R_1CHO]/[R_2CHO]$ des aldéhydes qui s'accumulent pendant l'ozonation peut être considérablement modifié par rapport aux quantités attendues d'après les proportions des sens de clivage du molozonide, en modifiant ainsi les données cinétiques. Il en découle que des bilans d'ozonation ne tenant pas compte de la production d'aldéhyde à partir de zwitterion ne sauraient suffire à établir des conclusions mécanistiques précises.

Partie expérimentale

La technique d'ozonation et le dosage de l'ozone ont été décrits précédemment (5), de même que le dosage des composés peroxydiques à chaîne ouverte (5) et celui de l'oxygène actif (4). Les aldéhydes chloroacétique et butyrique, ainsi que l'acétone et la cyclohexanone ont été dosés par voie spectrographique infrarouge, d'après les densités optiques de la bande de vibration de leur groupement carbonyle dans la région de 1700 cm^{-1}. En prenant soin de ne pas surozoner les solutions on évite, dans cas ici étudiés, l'autoxydation d'aldéhyde en peracide, ce qui entraînerait également la formation d'acide;

Can. J. Chem. Downloaded from www.nrcresearchpress.com by 210.87.254.105 on 09/05/12
For personal use only.

Can. J. Chem. Downloaded from www.nrcresearchpress.com by 210.87.254.105 on 09/05/12
For personal use only.

la non-formation d'acide et de peracide est bien démontrée par les spectres infrarouges. Les oléfines ont été dosées par chromatographie en phase gazeuse, au moyen d'un appareil F et M, modèle 5750, avec détecteur à flamme ionisante, comprenant une colonne de Silicone Rubber UC W98 de 6 pieds.

Les mesures des constantes de vitesse de décomposition de l'ozonide du fumarate d'éthyle ont été faites à partir de solutions 0.1–0.05 *M* de cet ozonide dans le CCl_4 anhydre, maintenues à température constante, à l'obscurité; les proportions d'ozonide non consommé ont été déterminées en spectrographie infrarouge, à intervalles de temps connus, d'après les densités optiques de la forte bande de la liaison ozonique vers 1103 cm^{-1}. L'équation 2.3 log $C_0/C = kt$ est bien vérifiée jusqu'à 50–60% de réaction (C_0 et C représentent, respectivement, les concentrations initiale et au temps t en ozonide). Une courbe de calibration a été obtenue au moyen de solutions d'ozonide de fumarate d'éthyle fraîchement préparé et purifié: ε_{1103} = 580 (l/mole·cm).

Les produits suivants ont été préparés et purifiés selon les données de la littérature: les peroxydes dimère et trimère d'acétone (12), le peroxyde dimère de cyclohexanone (13), l'ozonide du *trans* octène-4 (14) et l'ozonide du fumarate d'éthyle (15); lors de la préparation des ozonides nous avons toutesfois préféré effectuer les ozonations à la température ambiante, dans le but d'obtenir de meilleurs rendements.

Ozonide du trans dichloro-1,4 butène-2

Une solution de 3.75 g (0.03 mole) d'oléfine dans 15 ml de CCl_4 a été ozonée à la température de 25° par la quantité théorique d'ozone. Après l'évaporation du solvant, le résidu (4.45 g) a été distillé. L'ozonide distille à 33° à la pression de 0.3 mm Hg (2.35 g) et se présente comme un liquide incolore, n_{25}^{D} = 1.4658, densité (25°) = 1.420 g/ml.

Anal. Calc. pour $C_4H_6O_3Cl_2$: C, 27.77; H, 3.50; Cl, 40.99. Trouvé: C, 27.56; H, 3.68; Cl, 40.60.

Les spectres infrarouges confirment la nature de ce produit: on reconnaît notamment la forte bande ozonique à 1102 cm^{-1} (épaulement à 1110 cm^{-1}) (ε = 302 l/mole·cm à 1102 cm^{-1}) ainsi qu'une bande vers 1037 cm^{-1}, environ de moitié moins intense. Le spectre du produit purifié ne montre pas de bande carbonyle dans la région de 1700 cm^{-1}. On note encore de faibles bandes vers 850, 970 et 990 cm^{-1}, ainsi que deux bandes moyennes, vers 1358 et 1428 cm^{-1}.

Les spectres de résonance magnétique nucléaire révèlent la présence de deux doublets (protons méthyléniques) à 6.40 τ (J = 0.08 c.p.s.) et à 6.47 τ (J = 0.08 c.p.s.) ainsi que deux triplets (protons tertiaires) à 4.45 τ (J = 0.08 c.p.s.) et à 4.55 τ (J = 0.08 c.p.s.). Un estimé des intensités des signaux semble indiquer que cet ozonide est constitué d'un mélange des isomères *cis-* et *trans-*, très approximativement en égale quantité.

Remerciements

Nous remercions le Conseil National de Recherches du Canada pour un octroi qui a permis le présent travail, ainsi que Mlle S. Horoupian de son assistance technique précieuse.

1. R. Criegee. Record Chem. Progr. Kresge-Hooker Sci. Lib. **18**, 111 (1957).
2. R. W. Murray, R. D. Youssefyeh et P. R. Story. J. Am. Chem. Soc. **88**, 3143 (1966). P. R. Story, R. W. Murray et R. D. Youssefyeh. J. Am. Chem. Soc. **88**, 3144 (1966). R. W. Murray, R. D. Youssefyeh, et P. R. Story. J. Am. Chem. Soc. **89**, 2429 (1967).
3. S. Fliszár, D. Gravel et E. Cavalieri. Can. J. Chem. **44**, 1013 (1966).
4. S. Fliszár et J. B. Chyliński. Can. J. Chem. **45**, 29 (1967).
5. S. Fliszár, D. Gravel, et E. Cavalieri. Can. J. Chem. **44**, 67 (1966).
6. E. Briner, S. Fliszár et G. P. Rossetti. Helv. Chim. Acta, **47**, 2041 (1964); **47**, 2387 (1964).
7. E. Briner, G. P. Rossetti, et S. Fliszár. Helv. Chim. Acta, **48**, 1076 (1965).
8. R. Criegee, W. Schnorrenberg, et J. Becke. Ann. **565**, 10 (1949).
9. R. Criegee et G. Lohaus. Ann. **583**, 6 (1953).
10. P. R. Story. J. Am. Chem. Soc. **89**, 5726 (1967).
11. S. Fliszár. Can. J. Chem. **44**, 2351 (1966).
12. A. Baeyer et V. Villiger. Ber. **32**, 3632 (1899); Ber. **33**, 858 (1900).
13. M. Stoll et W. Scherrer. Helv. Chim. Acta, **13**, 142 (1930).
14. R. Criegee, A. Kerckov, et H. Zinke. Ber. **88**, 1878 (1955).
15. S. M. Goodwin, N. M. Johnson et B. Witkop. J. Am. Chem. Soc. **75**, 4273 (1953).

Can. J. Chem. Downloaded from www.nrcresearchpress.com by 210.87.254.105 on 09/05/12
For personal use only.

2-Deoxy-D-*galacto*-heptose

M. B. PERRY and ANN C. WEBB
Division of Biosciences, National Research Council of Canada, Ottawa, Canada

Received October 18, 1967

Catalytic reduction of 3,4,5,6,7-pentaacetoxy-D-*galacto*-1-nitro-1-heptene afforded 3,4,5,6,7-penta-*O*-acetyl-1,2-dideoxy-1-nitro-D-*galacto*-heptitol which on treatment with acid gave 2-deoxy-D-*galacto*-heptose. The properties of 2-deoxy-D-*galacto*-heptose and the preparation of its derivatives 1,3,4,5,6,7-hexa-*O*-acetyl-2-deoxy-D-*galacto*-heptitol, 2-deoxy-D-*galacto*-heptose 2,5-dichlorophenylhydrazone and 2-deoxy-D-*galacto*-heptose methylphenylhydrazone are recorded.

Canadian Journal of Chemistry, 46, 789 (1968)

2-Deoxy-D-*galacto*-heptose, required for comparison with a degradation product of a synthetic 3-deoxyoctulosonic acid, was prepared by the general procedure developed by Sowden and Fischer (1). The synthesis together with the properties of the glycose and its derivatives are reported in this note.

3,4,5,6,7-Pentaacetoxy-D-*galacto*-1-nitro-1-heptene (2) was readily reduced by hydrogen in the presence of palladium black to give 3,4,5,6,7-penta-*O*-acetyl-1,2-dideoxy-1-nitro-D-*galacto*-heptitol which on treatment with aqueous alkali followed by strong sulfuric acid gave 2-deoxy-D-*galacto*-heptose in good overall yield (90%). The 2-deoxy-D-*galacto*-heptose was identified by paper and by gas–liquid partition chromatography, and by the preparation of the crystalline derivatives 1,3,4,5,6,7-hexa-*O*-acetyl-2-deoxy-D-*galacto*-heptitol, 2-deoxy-D-*galacto*-heptose 2,5-dichlorophenylhydrazone, and 2-deoxy-D-*galacto*-heptose methylphenylhydrazone.

Experimental

Paper chromatography was performed by the descending method (3) on Whatman No. 1 filter paper using pyridine – ethyl acetate – water (2:5:5 v/v, top layer) as the mobile phase. Glycoses were detected with (*a*) 1% silver nitrate in acetone followed by 2% sodium hydroxide in ethanol (4) and (*b*) 0.02 *M* aqueous sodium metaperiodate followed by ethylene glycol – acetone – sulfuric acid (50:50:0:3 v/v) and 6% aqueous sodium 2-thiobarbiturate (5). The rates of movement of the glycoses on the chromatograms are quoted relative to D-galactose (R_{Gal}).

Gas–liquid partition chromatography was carried out on a Pye argon chromatograph fitted with an ionization detector (^{90}Sr 20 μ Ci), using a straight glass column (120 × 0.5 cm I.D.) packed with 10% neopentylglycol sebacate polyester on 100–120 mesh Chromosorb W. Retention times of the compounds are quoted relative to methyl 2,3,4,6-tetra-*O*-methyl-α-D-glucoside (t_g) or penta-*O*-acetyl-L-arabinitol (t_a).

Melting points were determined on a hot stage and are corrected. The optical rotations were determined at 22° with a Perkin–Elmer 141 polarimeter. Solutions were concentrated in a rotary evaporator below 45°.

Preparation of 2-Deoxy-D-galacto-heptose

3,4,5,6,7-Penta-O-acetyl-1,2-dideoxy-1-nitro-D-galacto-heptitol

3,4,5,6,7-Pentaacetoxy-D-*galacto*-1-nitro-1-heptene (2) (10 g) dissolved in an ethanol (500 ml) and propan-2-ol (300 ml) mixture at 50° was shaken with hydrogen at atmospheric pressure in the presence of palladium black (0.5 g). One mole equivalent of hydrogen was absorbed in 28 min, and the rate of reduction then became very slow. At this point the reaction mixture was filtered, the filtrate was concentrated to a small bulk and, when cooled to 5°, gave crystalline 3,4,5,6,7-penta-*O*-acetyl-1,2-dideoxy-1-nitro-D-*galacto*-heptitol (9.1 g) having m.p. 161° and $[\alpha]_D$ +17° (*c*, 0.5 in chloroform). After two recrystallizations from ethanol, the product had m.p. 161° and $[\alpha]_D$ +17.2° (*c*, 0.5 in chloroform).

Anal. Calcd. for $C_{17}H_{25}O_{12}N$: C, 46.89; H, 5.79; N, 3.22. Found: C, 46.9; H, 5.65; N, 3.18.

2-Deoxy-D-galacto-heptose

3,4,5,6,7-Penta-*O*-acetyl-1,2-dideoxy-1-nitro-D-*galacto*-heptitol (8 g) was dissolved at 35° in *N* sodium hydroxide solution (102 ml) and the mixture, after being kept for 1 h at 20°, was added dropwise to a cooled, stirred solution of concentrated sulfuric acid (148 ml) and water (200 ml). The reaction mixture was adjusted in the cold to pH 5.7 by the addition of saturated aqueous barium hydroxide and then finally neutralized by the addition of barium carbonate. After centrifugation and filtration the solution was treated with acetic acid (2 ml) and then passed down columns of Rexyn 101(H^+) (180 ml) and RG6(OH^-) ion-exchange resins, and the eluate and washings were concentrated to a syrup (3.6 g). Paper chromatographic examination of the syrup showed it to contain 2-deoxy-D-*galacto*-heptose (ca. 95%) having R_{Gal} 1.45 (revealed by the silver nitrate spray, and as a

characteristic red spot with the periodate–thiobarbiturate spray) together with several minor components detectable with the silver nitrate spray only. The crude 2-deoxy-D-*galacto*-heptose (3.5 g) was fractionated chromatographically on a cellulose column (50 × 4 cm), using butan-1-ol half saturated with water as the mobile phase (6); concentration of the fractions containing only 2-deoxy-D-*galacto*-heptose yielded a colorless syrup (3.0 g) which after taking up in a propan-2-ol – ether mixture, on standing gave a semicrystalline, hygroscopic product which had an indefinite melting point; $[\alpha]_D$ −43.2° (*c*, 0.8 in water).

Anal. Calcd. for $C_7H_{14}O_6$: C, 43.30; H, 7.27. Found: C, 43.31; H, 7.2.

Gas–liquid partition chromatographic examination of the 2-deoxy-D-*galacto*-heptose, equilibrated in an aqueous solution, as its fully *O*-trimethylsilylated derivatives (7) at 162° gave two peaks having t_g 1.58 (56%) and t_g 2.15 (44%).

Derivatives of 2-Deoxy-D-galacto-heptose

1,3,4,5,6,7-Hexa-O-acetyl-2-deoxy-D-galacto-heptitol

2-Deoxy-D-*galacto*-heptose (0.2 g) in water (5 ml) was reduced at room temperature by the addition of sodium borohydride (0.15 g); after 2 h the excess borohydride was destroyed with acetic acid, and the concentrated reaction mixture was treated with acetic anhydride (5 ml) containing sulfuric acid (0.1 ml) at 35° for 4 h. The solution was poured into ice water containing pyridine (4 ml) and after 1 h the aqueous solution was extracted with chloroform (4 × 20 ml) and the combined chloroform extracts were washed with water, dilute sulfuric acid, dilute sodium bicarbonate, and water, and then dried over anhydrous sodium sulfate. The chloroform solution was concentrated to a syrup (0.26 g), the syrup was dissolved in methanol (15 ml) and on cooling to 5° gave crystalline 1,3,4,5,6,7-hexa-*O*-acetyl-2-deoxy-D-*galacto*-heptitol (0.17 g) which, after two further recrystallizations from methanol, had m.p. 118° and $[\alpha]_D$ +10.7° (*c*, 0.1 in methanol).

Anal. Calcd. for $C_{19}H_{28}O_{12}$: C, 50.89; H, 6.29. Found: C, 50.6; H, 6.0.

On gas–liquid partition chromatography (202°) the acetylated heptitol gave a single peak having t_a 4.43.

2-Deoxy-D-galacto-heptose 2,5-dichlorophenylhydrazone

2-Deoxy-D-*galacto*-heptose (0.15 g) in methanol (2 ml) was mixed with 2,5-dichlorophenylhydrazine (0.15 g); the solution was warmed to 40° for 10 min and on cooling to 5° gave the crystalline product (0.19 g). After two recrystallizations from ethanol, the pure 2-deoxy-D-*galacto*-heptose 2,5-dichlorophenylhydrazone was found to have m.p. 180° and $[\alpha]_D$ −12.5° → +13.5° (*c*, 0.1 in methanol).

Anal. Calcd. for $C_{13}H_{18}O_5N_2Cl_2$: C, 44.20; H, 5.14; N, 7.93. Found: C, 44.00; H, 5.14; N, 7.68.

2-Deoxy-D-galacto-heptose Methylphenylhydrazone

2-Deoxy-D-*galacto*-heptose (0.15 g) in methanol (2 ml) was treated with 1-methyl-1-phenylhydrazine (0.15 g) and after keeping at 40° for 1 h the mixture was cooled to 5° when the resulting crystalline product was collected. The product after two recrystallizations from ethanol gave pure 2-deoxy-D-*galacto*-heptose methylphenylhydrazone (0.11 g) which had m.p. 171–172° and $[\alpha]_D$ −28° → −21° (*c*, 0.08 in methanol).

Anal. Calcd. for $C_{14}H_{22}O_5N_2$: C, 56.36; H, 7.43; N, 9.39. Found: C, 56.0; H, 7.45; N, 9.6.

1. J. C. SOWDEN and H. O. L. FISCHER. J. Am. Chem. Soc. **69**, 1048 (1947).
2. J. C. SOWDEN and D. R. STROBACH. J. Am. Chem. Soc. **82**, 954 (1960).
3. S. M. PARTRIDGE. Biochem. J. **42**, 238 (1948).
4. W. E. TREVELYAN, D. D. PROCTER, and J. S. HARRISON. Nature, **166**, 444 (1950).
5. L. WARREN. Nature, **186**, 237 (1960).
6. L. HOUGH, J. K. N. JONES, and W. H. WADMAN. J. Chem. Soc. 2511 (1949).
7. C. C. SWEELEY, R. BENTLEY, M. MAKITA, and W. W. WELLS. J. Am. Chem. Soc. **85**, 2497 (1963).

Phenoxazinones by oxidative dimerization of aminophenols[1]

NANCY N. GERBER

Institute of Microbiology, Rutgers, The State University, New Brunswick, New Jersey, 08903

Received June 22, 1967

Several 2-amino-3*H*-phenoxazin-3-ones, including cinnabarin, were obtained from the appropriate *o*-aminophenols by oxidative dimerization on thin-layer plates in air. Shake-flask fermentation of *Pycnoporus cinnabarinus* also gave cinnabarin.

Canadian Journal of Chemistry, 46, 790 (1968)

The oxidative dimerization of certain *o*-aminophenols to the corresponding 2-amino-3*H*-phenoxazin-3-ones has been effected by the cytochrome-c-cytochrome oxidase system of mammalian mitochondria (1), by enzymes found in the soluble liver fraction from poikilothermic vertebrates (2), in the nuclear fraction of rat liver (3), in the leaves of *Tecoma stans* (4), in *Pycnoporus coccineus* (5) and *Streptomyces antibioticus* (6), as well as by tyrosinase in the presence of catechol and air (7). The same dimerization has been accomplished in certain cases by a variety of one-equivalent oxidizing agents (8), for

[1]Supported by the U.S. Public Health Service Grant AI 06230-03.

Can. J. Chem. Downloaded from www.nrcresearchpress.com by 210.87.254.105 on 09/05/12
For personal use only.

Can. J. Chem. Downloaded from www.nrcresearchpress.com by 210.87.254.40 on 09/05/12
For personal use only.

characteristic red spot with the periodate–thiobarbiturate spray) together with several minor components detectable with the silver nitrate spray only. The crude 2-deoxy-D-*galacto*-heptose (3.5 g) was fractionated chromatographically on a cellulose column (50 × 4 cm), using butan-1-ol half saturated with water as the mobile phase (6); concentration of the fractions containing only 2-deoxy-D-*galacto*-heptose yielded a colorless syrup (3.0 g) which after taking up in a propan-2-ol – ether mixture, on standing gave a semicrystalline, hygroscopic product which had an indefinite melting point; $[\alpha]_D$ −43.2° (*c*, 0.8 in water).

Anal. Calcd. for $C_7H_{14}O_6$: C, 43.30; H, 7.27. Found: C, 43.31; H, 7.2.

Gas–liquid partition chromatographic examination of the 2-deoxy-D-*galacto*-heptose, equilibrated in an aqueous solution, as its fully *O*-trimethylsilylated derivatives (7) at 162° gave two peaks having t_g 1.58 (56%) and t_g 2.15 (44%).

Derivatives of 2-Deoxy-D-galacto-heptose

1,3,4,5,6,7-Hexa-O-acetyl-2-deoxy-D-galacto-heptitol

2-Deoxy-D-*galacto*-heptose (0.2 g) in water (5 ml) was reduced at room temperature by the addition of sodium borohydride (0.15 g); after 2 h the excess borohydride was destroyed with acetic acid, and the concentrated reaction mixture was treated with acetic anhydride (5 ml) containing sulfuric acid (0.1 ml) at 35° for 4 h. The solution was poured into ice water containing pyridine (4 ml) and after 1 h the aqueous solution was extracted with chloroform (4 × 20 ml) and the combined chloroform extracts were washed with water, dilute sulfuric acid, dilute sodium bicarbonate, and water, and then dried over anhydrous sodium sulfate. The chloroform solution was concentrated to a syrup (0.26 g), the syrup was dissolved in methanol (15 ml) and on cooling to 5° gave crystalline 1,3,4,5,6,7-hexa-*O*-acetyl-2-deoxy-D-*galacto*-heptitol (0.17 g) which, after two further recrystallizations from methanol, had m.p. 118° and $[\alpha]_D$ +10.7° (*c*, 0.1 in methanol).

Anal. Calcd. for $C_{19}H_{28}O_{12}$: C, 50.89; H, 6.29. Found: C, 50.6; H, 6.0.

On gas–liquid partition chromatography (202°) the acetylated heptitol gave a single peak having t_a 4.43.

2-Deoxy-D-galacto-heptose 2,5-dichlorophenylhydrazone

2-Deoxy-D-*galacto*-heptose (0.15 g) in methanol (2 ml) was mixed with 2,5-dichlorophenylhydrazine (0.15 g); the solution was warmed to 40° for 10 min and on cooling to 5° gave the crystalline product (0.19 g). After two recrystallizations from ethanol, the pure 2-deoxy-D-*galacto*-heptose 2,5-dichlorophenylhydrazone was found to have m.p. 180° and $[\alpha]_D$ −12.5° → +13.5° (*c*, 0.1 in methanol).

Anal. Calcd. for $C_{13}H_{18}O_5N_2Cl_2$: C, 44.20; H, 5.14; N, 7.93. Found: C, 44.00; H, 5.14; N, 7.68.

2-Deoxy-D-galacto-heptose Methylphenylhydrazone

2-Deoxy-D-*galacto*-heptose (0.15 g) in methanol (2 ml) was treated with 1-methyl-1-phenylhydrazine (0.15 g) and after keeping at 40° for 1 h the mixture was cooled to 5° when the resulting crystalline product was collected. The product after two recrystallizations from ethanol gave pure 2-deoxy-D-*galacto*-heptose methylphenylhydrazone (0.11 g) which had m.p. 171–172° and $[\alpha]_D$ −28° → −21° (*c*, 0.08 in methanol).

Anal. Calcd. for $C_{14}H_{22}O_5N_2$: C, 56.36; H, 7.43; N, 9.39. Found: C, 56.0; H, 7.45; N, 9.6.

1. J. C. SOWDEN and H. O. L. FISCHER. J. Am. Chem. Soc. **69**, 1048 (1947).
2. J. C. SOWDEN and D. R. STROBACH. J. Am. Chem. Soc. **82**, 954 (1960).
3. S. M. PARTRIDGE. Biochem. J. **42**, 238 (1948).
4. W. E. TREVELYAN, D. D. PROCTER, and J. S. HARRISON. Nature, **166**, 444 (1950).
5. L. WARREN. Nature, **186**, 237 (1960).
6. L. HOUGH, J. K. N. JONES, and W. H. WADMAN. J. Chem. Soc. 2511 (1949).
7. C. C. SWEELEY, R. BENTLEY, M. MAKITA, and W. W. WELLS. J. Am. Chem. Soc. **85**, 2497 (1963).

Phenoxazinones by oxidative dimerization of aminophenols[1]

NANCY N. GERBER

Institute of Microbiology, Rutgers, The State University, New Brunswick, New Jersey, 08903

Received June 22, 1967

Several 2-amino-3*H*-phenoxazin-3-ones, including cinnabarin, were obtained from the appropriate *o*-aminophenols by oxidative dimerization on thin-layer plates in air. Shake-flask fermentation of *Pycnoporus cinnabarinus* also gave cinnabarin.

Canadian Journal of Chemistry, **46**, 790 (1968)

The oxidative dimerization of certain *o*-aminophenols to the corresponding 2-amino-3*H*-phenoxazin-3-ones has been effected by the cytochrome-c-cytochrome oxidase system of mammalian mitochondria (1), by enzymes found in the soluble liver fraction from poikilothermic vertebrates (2), in the nuclear fraction of rat liver (3), in the leaves of *Tecoma stans* (4), in *Pycnoporus coccineus* (5) and *Streptomyces antibioticus* (6), as well as by tyrosinase in the presence of catechol and air (7). The same dimerization has been accomplished in certain cases by a variety of one-equivalent oxidizing agents (8), for

[1]Supported by the U.S. Public Health Service Grant AI 06230-03.

Can. J. Chem. Downloaded from www.nrcresearchpress.com by 210.87.254.40 on 09/05/12
For personal use only.

example potassium ferricyanide (9), air in alkaline solution, yellow mercuric oxide (10, 11), lead dioxide (1), ferric chloride (12), and benzoquinone (13).

A new system for effecting such reactions is air acting on the *o*-aminophenols which are adsorbed and thus activated (14) on silica thin-layer plates. In this way **1** was prepared from *o*-aminophenol and **2** (cinnabarinic acid) from 3-hydroxyanthranilic acid. The method is convenient on a small scale since chromatographically homogeneous material can often be obtained by synthesis and purification on the same thin-layer chromatography (t.l.c.) plate. A mixture of *o*-aminophenol and 3-hydroxyanthranilic acid furnished the four expected products; **3** had been previously isolated from some novel *Nocardiaceae* (15), recently identified as *Nocardia dassonvillei* (16); the structure of **4** was proved by its conversion to 2-hydroxy-3-oxo-3*H*-phenoxazin-9-carboxylic acid (11). Compound **3** (40% yield, $R_f = 0.6$, carbonyl band at 6.05 μ) because of its stronger intramolecular hydrogen bonding was soluble in chloroform and not extracted by aqueous acid or bicarbonate; **4** (4% yield, $R_f = 0.25$, carbonyl band at 5.95 μ) crystallized from chloroform and was readily extracted into dilute acid or bicarbonate.

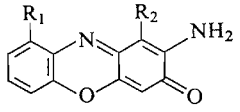

1 $R_1=R_2=H$
2 $R_1=R_2=COOH$
3 $R_1=H$, $R_2=COOH$
4 $R_1=COOH$, $R_2=H$
5 $R_1=CH_2OH$, $R_2=COOH$
6 $R_1=COOH$, $R_2=CH_2OH$

The same relative yields and differences in properties were observed for **5** (cinnabarin) and **6** prepared on t.l.c. plates or with potassium ferricyanide (15) from 3-hydroxyanthranilic acid and 2-amino-3-hydroxybenzyl alcohol (17). Cinnabarin was recently synthesized from these precursors using benzoquinone (13).

Since the natural **5** obtained from Professor Clezy contained some **2**, pure **5** was prepared by conventional shake flask fermentation using *Pycnoporus cinnabarinus*. (This fungus has been known by many synonyms including *Polyporus* (18).)

Experimental

The details of the methods are given in reference 15. Solvent *d* is chloroform – acetic acid 9:1; solvent *h* is ethyl acetate – acetic acid 9:1; solvent *j* is chloroform–ethyl acetate 9:1.

General Method

A solution of one or two *o*-aminophenols (0.2–1 mg total weight) was applied to the starting line of a 4 × 8 in. silica gel G t.l.c. plate. After 3 days at room temperature and in diffuse light the plate was activated 30 min at 50 °C then chromatographed in a suitable solvent such as *d* or *h*. The one or more yellow, orange, brown, or red-brown bands which resulted were scraped off, packed into micro columns, eluted, and assayed spectrophotometrically.

2-Amino-3-oxo-3H-phenoxazine-1-carboxylic Acid (3)

An ethanol solution of *o*-aminophenol (5 mg) and 3-hydroxyanthranilic acid (10 mg) was applied to the whole surface of a silica gel G plate which had been prepared using 8% ammonium acetate instead of water. After 3 days as above, the silica was packed in a small column and eluted with solvent *h* (200 ml). After evaporation of the ethyl acetate, the acetic acid solution was diluted with chloroform, and washed with water. The residue from the chloroform solution was applied to a 50 g silica column. Elution with solvent *j* furnished **3** (4.4 mg), then **1**.

2-Amino-3-oxo-3H-phenoxazine-9-carboxylic Acid (4)

A few mg of **4** were allowed to stand overnight in 1 ml of 1 *N* sodium hydroxide. Acidification gave a small amount of brown solid, λ_{max} (EtOH) 404, λ_{max} (EtOH—HCl) 404, λ_{max} (EtOH—NH_3) 435, 415, 312, 275, chromatographically identical in four solvent systems with authentic 2-hydroxy-3-oxo-3*H*-phenoxazin-9-carboxylic acid synthesized by the method in (11).

2-Amino-3-hydroxybenzyl Alcohol

A suspension of 3-hydroxyanthranilic acid (500 mg) in methanol was treated with excess ethereal diazomethane. The resulting solution was evaporated to dryness, dissolved in chloroform, and applied to a 20 g silica column. Elution with solvent *j* furnished 190 mg of methyl-3-hydroxyanthranilate, m.p. 94–98°. This ester was treated with lithium aluminium hydride (17) and after column chromatography on silica eluting with ethyl acetate gave 43 mg of white crystals m.p. 123–125°, λ_{max} (H_2O) 285, λ_{max} (acid) 274, λ_{max} (base) 298.

Cinnabarin (5) from Pycnoporus cinnabarinus (Jacq. ex Fr.) P. Karst.

The title organism was maintained on XSM slants (1.0 g Fisher malt extract, 1.0 g Difco yeast extract, 1.0 g Mann desiccated liver powder, 1.0 g corn steep, 5.0 g glucose, 2.0 g sucrose, 15.0 g agar/l, pH 7.8 before autoclaving) transferred every 4–6 weeks, incubated at 28° and when well grown stored at 5°. For production 7 day-old slants were used to inoculate XSM or PGB-2 broth (5.0 g of Wilsons Peptone #851, The Wilson Co., Chicago, Illinois, 5.0 g of BYF #50, a fraction of autolyzed brewers yeast sold by Amber Laboratories, Inc., Milwaukee, Wisconsin, 10 g of Cerelose/1, pH 7.5, before autoclaving, 100 ml/250 ml flask). After 4 days at 215 r.p.m. (Rotary action shaker, model V, New Brunswick Scientific Co., New Brunswick, New Jersey) at 28° the resulting whole broth was inoculated at 5% into PGB-2 broth (100 ml/250 ml flask). After 7 days shaking at 28° flasks containing

light-tan broth were discarded (t.l.c. disclosed negligible amount of **5**). Those with dark-brown broth were combined, filtered, and the air-dried mycelium, in a Soxhlet apparatus, extracted 18 h with hexane. The mycelium was then extracted 15–30 times with warm pyridine and the combined pyridine extracts assayed spectrophotometrically at 440 mμ. Products in the concentrated pyridine solution were separated by t.l.c. in solvent *d*. The orange bands, $R_f = 0.2$, from 30 plates were combined and eluted with solvent *h*. The residue from the eluate was dissolved in a small amount of pyridine and applied to a 20 g silica column which had been prepared in ethyl acetate. The column was eluted with ethyl acetate and the main orange fraction furnished crystals which did not melt under 330°. The crystals were identical with synthetic **5** and with the major component of natural **5** by chromatography in 6 solvent systems. The acetate derivatives were also identical. The yields varied from 2–6 g of dry mycelium and 2–10 mg of **5** from 4 l of whole broth.

Acknowledgments

The author wishes to thank Mrs. M. P. Lechevalier for invaluable guidance in fermentation procedures. The excellent technical assistance of Mrs. Eva M. Fekete is acknowledged. The author is grateful to Mrs. M. Semerdzieva and Dr. M. Podojil for the strain of *Pycnoporus cinnabarinus* and to Professor P. S. Clezy for a sample of cinnabarin.

1. H. T. NAGASAWA, H. R. GUTMANN, and M. A. MORGAN. J. Biol. Chem. **234,** 1600 (1959).
2. L. R. MORGAN, JR., D. M. WEIMORTS, and C. C. AUBERT. Biochim. Biophys. Acta, **100,** 393 (1965).
3. P. V. SUBBA RAO, N. S. JEGANNATHAN, and C. S. VAIDYANATHAN. Biochem. J. **95,** 628 (1965).
4. P. V. SUBBA RAO and C. S. VAIDYANATHAN. Arch. Biochem. Biophys. **115,** 27 (1966). P. M. NAIR and C. S. VAIDYANATHAN. Biochim. Biophys. Acta, **81,** 507 (1964).
5. P. M. NAIR and L. C. VINING. Can. J. Biochem. **42,** 1515 (1964).
6. E. KATZ and H. WEISSBACH. Develop. Ind. Microbiol. **8,** 67 (1967).
7. A. BUTENANDT, E. BIEKERT, and G. NEUBERT. Ann. **602,** 72 (1957).
8. R. STEWART. Oxidation mechanisms. W. A. Benjamin, Inc., New York. 1964. Chap. 2.
9. A. BUTENANDT, U. SCHIEDT, and E. BIEKERT. Ann. **588,** 106 (1954). H. BROCKMANN and H. LACHNER. Naturwiss. **51,** 384 (1964).
10. H. BROCKMANN and H. MUXFELDT. Chem. Ber. **91,** 1242 (1958).
11. A. BUTENANDTE, J. KECK, and G. NEUBERT. Ann. **602,** 61 (1957).
12. W. SCHÄFER. Progr. Org. Chem. **6,** 135 (1964).
13. B. WEINSTEIN and D. N. BRATTESANI. J. Heterocyclic Chem. **4,** 151 (1967).
14. K. RANDERATH. Thin-layer chromatography. Academic Press, Inc., New York. 1964. pp. 11–12.
15. N. N. GERBER. Biochemistry, **5,** 3824 (1966).
16. R. E. GORDON and A. C. HORAN. J. Gen. Microbiol. To be published.
17. J. GRIPENBERG. Acta Chem. Scand. **13,** 1305 (1959).
18. M. K. NOBLES and B. P. FREW. Can. J. Botany, **40,** 987 (1962).

N-alkyne-*N*-bis(2-chloroethyl)amines[1,2]

GEORGE R. PETTIT AND B. J. DANLEY
Department of Chemistry, Arizona State University, Tempe, Arizona, 85281

Received October 20, 1967

A reaction employing copper(II) chloride has been developed for condensing propargyl alcohol with formaldehyde and bis(2-chloroethyl)amine. The modified Mannich reaction was extended to include condensation of several other α-hydroxyacetylenes of the terminal alkyne class with bis(2-chloroethyl)-amine.

Canadian Journal of Chemistry, **46,** 792 (1968)

Preparation of actidione acetate and estrone nitrogen mustards (1) has been used to illustrate utility of the Mannich reaction as a mild route to bis(2-chloroethyl)amine derivatives of certain biologically important natural products. A series of model experiments preceding this study clearly emphasized that such reactions involving bis(2-chloroethyl)amine required carefully defined experimental conditions for each broad class of active-hydrogen component. At that time, procedures were developed for Mannich reactions between bis(2-chloroethyl)amine and various ketones (2*a*) or amides (2*b*).[3] Extension to acetylene derivatives of the propargyl alcohol type became the next objective. Encouraging results here should allow extension to several important ethynyl steroids.

[1]Antineoplastic Agents. XXI. For Part XX, see G. R. Pettit and S. K. Gupta, Can. J. Chem. **45,** 1561 (1967). The present contribution was abstracted in part from the M.S. thesis submitted by B. J. Danley to the Graduate School, Arizona State University, October 1967.

[2]This investigation was aided by Grant No. T-79G from the American Cancer Society and in part by a grant from the Ortho Research Foundation, Raritan, New Jersey.

[3]See also reference 3.

Can. J. Chem. Downloaded from www.nrcresearchpress.com by 210.87.254.40 on 09/05/12
For personal use only.

light-tan broth were discarded (t.l.c. disclosed negligible amount of **5**). Those with dark-brown broth were combined, filtered, and the air-dried mycelium, in a Soxhlet apparatus, extracted 18 h with hexane. The mycelium was then extracted 15–30 times with warm pyridine and the combined pyridine extracts assayed spectrophotometrically at 440 mμ. Products in the concentrated pyridine solution were separated by t.l.c. in solvent *d*. The orange bands, $R_f = 0.2$, from 30 plates were combined and eluted with solvent *h*. The residue from the eluate was dissolved in a small amount of pyridine and applied to a 20 g silica column which had been prepared in ethyl acetate. The column was eluted with ethyl acetate and the main orange fraction furnished crystals which did not melt under 330°. The crystals were identical with synthetic **5** and with the major component of natural **5** by chromatography in 6 solvent systems. The acetate derivatives were also identical. The yields varied from 2–6 g of dry mycelium and 2–10 mg of **5** from 4 l of whole broth.

Acknowledgments

The author wishes to thank Mrs. M. P. Lechevalier for invaluable guidance in fermentation procedures. The excellent technical assistance of Mrs. Eva M. Fekete is acknowledged. The author is grateful to Mrs. M. Semerdzieva and Dr. M. Podojil for the strain of *Pycnoporus cinnabarinus* and to Professor P. S. Clezy for a sample of cinnabarin.

1. H. T. NAGASAWA, H. R. GUTMANN, and M. A. MORGAN. J. Biol. Chem. **234,** 1600 (1959).
2. L. R. MORGAN, JR., D. M. WEIMORTS, and C. C. AUBERT. Biochim. Biophys. Acta, **100,** 393 (1965).
3. P. V. SUBBA RAO, N. S. JEGANNATHAN, and C. S. VAIDYANATHAN. Biochem. J. **95,** 628 (1965).
4. P. V. SUBBA RAO and C. S. VAIDYANATHAN. Arch. Biochem. Biophys. **115,** 27 (1966). P. M. NAIR and C. S. VAIDYANATHAN. Biochim. Biophys. Acta, **81,** 507 (1964).
5. P. M. NAIR and L. C. VINING. Can. J. Biochem. **42,** 1515 (1964).
6. E. KATZ and H. WEISSBACH. Develop. Ind. Microbiol. **8,** 67 (1967).
7. A. BUTENANDT, E. BIEKERT, and G. NEUBERT. Ann. **602,** 72 (1957).
8. R. STEWART. Oxidation mechanisms. W. A. Benjamin, Inc., New York. 1964. Chap. 2.
9. A. BUTENANDT, U. SCHIEDT, and E. BIEKERT. Ann. **588,** 106 (1954). H. BROCKMANN and H. LACHNER. Naturwiss. **51,** 384 (1964).
10. H. BROCKMANN and H. MUXFELDT. Chem. Ber. **91,** 1242 (1958).
11. A. BUTENANDTE, J. KECK, and G. NEUBERT. Ann. **602,** 61 (1957).
12. W. SCHÄFER. Progr. Org. Chem. **6,** 135 (1964).
13. B. WEINSTEIN and D. N. BRATTESANI. J. Heterocyclic Chem. **4,** 151 (1967).
14. K. RANDERATH. Thin-layer chromatography. Academic Press, Inc., New York. 1964. pp. 11–12.
15. N. N. GERBER. Biochemistry, **5,** 3824 (1966).
16. R. E. GORDON and A. C. HORAN. J. Gen. Microbiol. To be published.
17. J. GRIPENBERG. Acta Chem. Scand. **13,** 1305 (1959).
18. M. K. NOBLES and B. P. FREW. Can. J. Botany, **40,** 987 (1962).

N-alkyne-*N*-bis(2-chloroethyl)amines[1,2]

GEORGE R. PETTIT AND B. J. DANLEY
Department of Chemistry, Arizona State University, Tempe, Arizona, 85281

Received October 20, 1967

A reaction employing copper(II) chloride has been developed for condensing propargyl alcohol with formaldehyde and bis(2-chloroethyl)amine. The modified Mannich reaction was extended to include condensation of several other α-hydroxyacetylenes of the terminal alkyne class with bis(2-chloroethyl)-amine.

Canadian Journal of Chemistry, **46,** 792 (1968)

Preparation of actidione acetate and estrone nitrogen mustards (1) has been used to illustrate utility of the Mannich reaction as a mild route to bis(2-chloroethyl)amine derivatives of certain biologically important natural products. A series of model experiments preceding this study clearly emphasized that such reactions involving bis(2-chloroethyl)amine required carefully defined experimental conditions for each broad class of active-hydrogen component. At that time, procedures were developed for Mannich reactions between bis(2-chloroethyl)amine and various ketones (2*a*) or amides (2*b*).[3] Extension to acetylene derivatives of the propargyl alcohol type became the next objective. Encouraging results here should allow extension to several important ethynyl steroids.

[1]Antineoplastic Agents. XXI. For Part XX, see G. R. Pettit and S. K. Gupta, Can. J. Chem. **45,** 1561 (1967). The present contribution was abstracted in part from the M.S. thesis submitted by B. J. Danley to the Graduate School, Arizona State University, October 1967.

[2]This investigation was aided by Grant No. T-79G from the American Cancer Society and in part by a grant from the Ortho Research Foundation, Raritan, New Jersey.

[3]See also reference 3.

Can. J. Chem. Downloaded from www.nrcresearchpress.com by 210.87.254.40 on 09/05/12
For personal use only.

Can. J. Chem. Downloaded from www.nrcresearchpress.com by 210.87.254.40 on 09/05/12
For personal use only.

In 1933 Mannich and Chang (4) succeeded in condensing phenylacetylene with formaldehyde and diethyl amine in dioxane solution. Subsequently, a number of similar transformations were recorded (5). However, propargyl alcohol and related α-hydroxyacetylenes proved refractory in the usual Mannich reaction and could only be successfully employed as ester or ether derivatives (6). While I. G. Farbenindustrie patents in 1939 (7) disclosed a reaction between acetylene, formaldehyde, and secondary amines in acetic acid containing small amounts of cuprous acetate or cuprous chloride as catalyst, this modification of the Mannich reaction appears to have remained unexplored with α-hydroxyacetylenes until Libman and Kuznetsov (8) described successful Mannich reactions with α-hydroxyacetylenes in the presence of cuprous acetylide or cuprous chloride catalysts. The following year a patent (9) with similar observations was recorded. More recently a study of propargyl alcohol in the Mannich reaction with copper(II) sulfate as catalyst was summarized (10).[4]

No example of a Mannich reaction between bis(2-chloroethyl)amine and a terminal alkyne appears to have been described.[5] A considerable number of experiments (without addition of copper salts) directed at obtaining the Mannich base derived from propargyl alcohol (**1***a*), formaldehyde, and bis(2-chloroethyl)amine were without exception unsuccessful. Those reaction conditions commonly employed in Mannich reactions involving terminal alkynes which seemed feasible[6] with bis(2-chloroethyl)amine and those already known to be useful with this amine in similar condensation reactions (2,3) proved of no value.[7] Substitution of propargyl acetate gave no improvement.

The required transformation (**1** → **2**) was finally achieved as follows. An equimolar mixture of propargyl alcohol and cupric chloride dihydrate in ethyl alcohol was heated at reflux approximately 30 min. The reaction mixture changed in color from dark green to light yellow and a colorless solid separated.[8] Next, 37% formalin (1.25 mole) and bis(2-chloroethyl)amine hydrochloride (0.5 mole) were added and heating at reflux continued 1 h. An extended cooling period resulted in separation of amine **2***a* hydrochloride accompanied by copper containing products. Dissolution of the solid phase in ammonium hydroxide and subsequent reconversion of amine **2***a* to the hydrochloride salt provided 62% of the required Mannich base. Application of a similar (*t*-butyl alcohol as solvent) technique

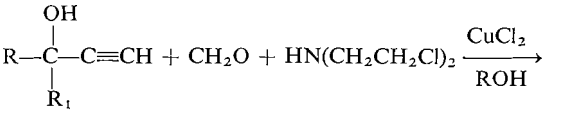

1

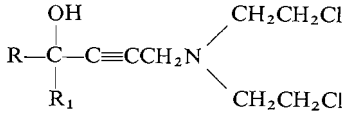

2*a*, R = R_1 = H
2*b*, R = R_1 = CH_3
2*c*, R = CH_3CH_2—, R_1 = CH_3

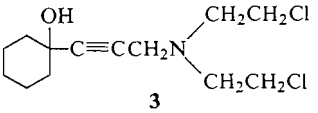

3

with three tertiary alcohols (eg., 1-ethynylcyclohexanol) provided Mannich base nitrogen mustards **2***b*, **2***c*, and **3** in 85, 75, and 49% conversion,

[4]A useful mechanistic interpretation of the Mannich reaction with propargyl alcohol and rationale for use of copper salts in such reactions is also summarized in ref. 10.

[5]However, one such amine (cf. *i*) has been obtained by chlorination of the diol derived from propargyl bromide and diethanol amine (11).

$$RC{\equiv}CCH_2N(CH_2CH_2Cl)_2$$

i

[6]For example, condensation of formaldehyde with bis-(2-chloroethyl)amine readily leads to 1,4-diazabicyclo-[2·2·1]heptane (*ii*) (12). Additional evidence for the structure of quarternary salt *ii* has recently been provided by Böhme and Orth (13).

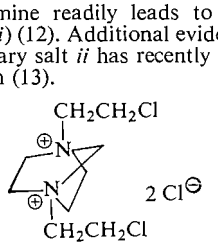

ii

[7]The same result was obtained by Dr. J. A. Settepani with 1-ethynylcyclohexanol.

[8]Reduction of copper(II) to copper(I) under similar conditions has been proposed previously (8). The Russian chemists (8) noted that when the Mannich reaction with α-hydroxyacetylenes was performed with the free amine, copper(I) or copper(II) gave similar yields of Mannich base but under acidic conditions, copper(II) resulted in smaller conversion. The latter observation suggested that before a Mannich reaction could occur, copper(I) was necessary. Although the carbanion derived from a cuprous acetylide seemed an attractive intermediate in the present study, a more elaborate mechanism involving a π-bonded copper complex (14) was not excluded.

Can. J. Chem. Downloaded from www.nrcresearchpress.com by 210.87.254.40 on 09/05/12
For personal use only.

respectively. Purity of the Mannich base hydrochlorides was ascertained by thin-layer chromatography. The assigned structures received support from elemental analyses and interpretation of their proton magnetic resonance spectra.

In summary, the copper salt modification of the Mannich reaction seems particularly suited to a 1-alkyne bearing electron releasing substituents at position-3.

Experimental

The acetylene intermediates with the exception of propargyl alcohol (from J. T. Baker) were supplied (we wish to thank Dr. R. Tedeschi) by Airco Chemical, Middlesex, New Jersey. Each reaction was performed with magnetic stirring under nitrogen. Solvent extracts of aqueous solutions were dried over magnesium sulfate. Analytical specimens were colorless and exhibited one spot on a thin-layer chromatogram (95:5 chloroform–ethanol mobile phase). The thin-layer chromatographic determinations were executed using microscrope slides coated with silica gel HF_{254} (E. Merck, A. G. Darmstadt, Germany). Plates used to detect bis(2-chloroethyl)amine hydrochloride were eluted with the upper phase from a mixture of 1:4:5 acetic acid–*n*-butyl alcohol–water and developed with iodine vapor.

Melting points were determined using a Thomas Hoover capillary melting point apparatus and are uncorrected. The proton magnetic resonance (Varian A-60 spectrometer, deuterium oxide as solvent and tetramethylsilane as external standard) and infrared (Beckman IR-12 spectrophotometer) spectra were recorded by Miss K. Reimer of these laboratories. The atomic absorption spectra (Perkin–Elmer model 303 instrument) were determined (sample dissolved in concentrated nitric acid) by David Nava of this Department. Elemental microanalyses were provided by Dr. A. Bernhardt, Max Planck Institut, Mülheim, Germany.

4-[Bis(2'-chloroethyl)amino]-2-butyn-1-ol (2a) Hydrochloride

A general study of the sequence of adding reactants, time and temperature, mole ratios of reactants, and 37% formalin vs. trioxymethylene led to the following choice of experimental conditions. A mixture of propargyl alcohol (9.0 g, 0.16 mole) and cupric chloride dihydrate (27.3 g, 0.16 mole) in absolute ethanol (120 ml) was heated at reflux approximately 30 min. During heating the solution changed from dark green to light yellow and a colorless solid separated. Next, 37% formalin (16.2 g, 0.20 mole) and bis(2-chloroethyl)amine hydrochloride (14.3 g, 0.08 mole, ref. 15) were added to the mixture. Following a 1 h period at reflux, the solution was placed in a refrigerator 14 days while the crude crystalline product (26.5 g) slowly separated. A 25.2 g portion of the solid was added to cold concentrated ammonium hydroxide (240 ml). The basic solution was extracted with diethyl ether (4 × 100 ml) and the extract was washed with water (100 ml). The dry ethereal extract was treated with hydrogen chloride and the oil which separated was crystallized from acetone–diethyl ether; yield 11.8 g, m.p. 86.0–88.5°. Based upon expected recovery of product from the original 26.5 g of crude solid, the yield was 62% from propargyl alcohol. Three recrystallizations from acetone gave a pure specimen melting at 88.2–88.9°. In another experiment an analytical sample[9] was recrystallized (4 times) from *n*-butyl alcohol to provide crystals melting at 88.5–89.0°; ν_{max} (KBr) 3310 cm^{-1}; p.m.r. response at δ 3.70–4.21 (multiplet, 8 CH_2CH_2 protons), 4.37 (singlet, 4 protons, O—CH_2—C and C—CH_2—N).

Anal. Calcd. for $C_8H_{14}Cl_3NO$: C, 38.96; H, 5.73; Cl, 43.14; N, 5.68. Found: C, 38.85; H, 5.64; Cl, 43.09; N, 5.57.

Examination of the amine components from the liquid phase of the original reaction mixture by thin-layer chromatography indicated that very little, if any, amine **2***a* remained in solution at end of the 14 day cooling period. However, a substantial amount of bis(2-chloroethyl)-amine was detected. A similar study of the solid reaction product indicated amine **2***a* hydrochloride as major nitrogen-containing component. The solid products which separated from four successive reaction mixtures were examined (atomic absorption spectroscopy), and found to contain 18.4, 18.7, 18.7, and 20.4% copper, respectively.

5-[Bis(2'-chloroethyl)amino]-2-methyl-3-pentyn-2-ol (2b) Hydrochloride

The following procedure was found satisfactory for the alkyne tertiary alcohols. A mixture composed of 2-methyl-3-butyn-2-ol (13.5 g, 0.16 mole), cupric chloride dihydrate (27.3 g, 0.16 mole), and *t*-butyl alcohol (120 ml) was heated at reflux 1 h. The solution changed from dark green to a medium yellow-green and a substantial amount of colorless solid separated. To the cooled mixture was added 37% formalin (16.2 g, 0.20 mole) and bis(2-chloroethyl)amine hydrochloride (14.3 g, 0.08 mole). Heating at reflux was continued 1 h and during this period a major portion of the colorless solid redissolved. The cool mixture was concentrated to dryness *in vacuo*. Water (100 ml) was added and evaporated (*in vacuo*). The residue was dissolved in cold concentrated ammonium hydroxide (240 ml) and the solution extracted with diethyl ether. The ethereal extract was washed with cold water, dried, and treated with hydrogen chloride. After cooling (2 days), the solid hydrochloride (18.7 g, 85% yield, m.p. 123.5–127.5°) was collected. Three recrystallizations from acetone provided an analytical sample as needles; m.p. 134.5–135°; ν_{max} (KBr) 3370 and 2570 cm^{-1}; and p.m.r. δ 1.54 (singlet, 6 methyl protons), 3.66–4.17 (multiplet, 8 CH_2CH_2 protons), and 4.32 (singlet, 2 protons, C—CH_2—N).

Anal. Calcd. for $C_{10}H_{18}Cl_3NO$: C, 43.73; H, 6.61; Cl, 38.73; N, 5.10. Found: C, 43.61; H, 6.53; Cl, 38.66; N, 5.30.

6-[Bis(2'-chloroethyl)amino]-3-methyl-4-hexyn-3-ol (2c) Hydrochloride

The preceding experiment was repeated employing 3-methyl-1-pentyn-3-ol (15.7 g, 0.16 mole). In this case the crude crystalline amine (**2***c*) hydrochloride weighed 17.3 g (75% yield) and melted at 114–118° (sintering from 112°). Three recrystallizations from acetone led to a pure sample

[9]The analytical sample was dried to constant weight.

of needles; m.p. 137–138.5°; ν_{max} (KBr) 3380 and 2550 cm^{-1}; and p.m.r. δ 1.01 [triplet, 3 methyl (C-1) protons], 1.47–2.00 (partially masked quartet, 2 protons, C-2 methylene, $J = 7$ c.p.s.), 1.51 [singlet, 3 methyl (C-3) protons], 3.64–4.18 (multiplet, 8 CH_2CH_2 protons), and 4.34 (singlet, 2 protons, C—CH_2N).

Anal. Calcd. for $C_{11}H_{20}Cl_3NO$: C, 45.77; H, 6.98; Cl, 36.85; N, 4.85. Found: C, 45.63; H, 6.99; Cl, 36.78; N, 5.05.

1-(1'-Hydroxycyclohexane)-3-[bis(2'-chloroethyl)amino]-1-propyne (3) Hydrochloride

Starting with 1-ethynylcyclohexanol (19.9 g, 0.16 mole) the preceding experiment was repeated. Crystallization of the crude oily amine (**3**) hydrochloride from acetone provided 12.3 g (49% yield) of needles melting at 116–117.5° (sintering from 114°). Four recrystallizations from ethyl acetate gave an analytical sample as needles; m.p. 129.7–130.6°. After drying at 80° (2 mm) for 48 h, the specimen melted at 125–128°; ν_{max} (KBr) 3370 and 2560 cm^{-1}; p.m.r., δ 1.2–2.2 (broad multiplet, 10 methylene protons), 3.67–4.21 [multiplet, 8 protons, $N(CH_2CH_2Cl)_2$], and 4.38 (singlet, 2 protons, C-CH_2-N).

Anal. Calcd. for $C_{13}H_{21}Cl_3NO$: C, 49.62; H, 7.05; Cl, 33.80; N, 4.45. Found: C, 49.47; H, 7.13; Cl, 33.70; N, 4.55.

1. G. R. Pettit and A. K. Das Gupta. Chem. Ind. London, 1016 (1962).
2. (*a*) G. R. Pettit and J. A. Settepani. J. Med. Pharm. Chem. **5,** 296 (1962). (*b*) G. R. Pettit and J. A. Settepani. J. Org. Chem. **27,** 1714 (1962).
3. R. C. Elderfield and A. C. Mehta. J. Med. Chem. **10,** 922 (1967). G. R. Revanker and S. Siddappa. Monatsh. Chem. **98,** 169 (1967). W. Werner. Arch. Pharm. **299,** 513 (1966). W. Werner and M. Mühlstädt. Ann. **693,** 197 (1966). W. J. Serfontein and H. H. E. Schröder. J. S. African Chem. Inst. **19,** 38 (1966).
4. C. Mannich and F. T. Chang. Ber. **66,** 418 (1933).
5. H. Hellmann and G. Opitz. Alpha-aminoalkylierung. Verlag Chemie, G.m.b.H., Weinheim, Germany. 1960. B. Reichert. Die Mannichreaktion. Springer-Verlag, Berlin. 1959. F. F. Blicke. The Mannich reaction. *In* Organic reactions. Vol. I. *Edited by* R. Adams. John Wiley and Sons, Inc., New York. 1942. p. 303.
6. D. Burn and V. Petrov. Tetrahedron, **20,** 2295 (1964). G. A. Shvekhgeĭmer. Izv. Akad. Nauk SSSR Otd. Khim. Nauk, 1265 (1957); Chem. Abstr. **52,** 6211 (1958), I. N. Nazarov and G. A. Shvekgheĭmer. Zh. Obshch. Khim. **26,** 813 (1956); Chem. Abstr. **50,** 13901 (1956). I. Marszak, R. Epsztein, and J. Jacob. Compt. Rend. **231,** 1578 (1950). H. P. W. Huggill and J. D. Rose. J. Chem. Soc. 335 (1950). I. Marszak, M. Diament, and J. P. Guermont. Mem. Serv. Chim. Etat Paris, **35,** 67 (1950); Chem. Abstr. **46,** 7045 (1952), E. R. H. Jones, I. Marszak, and H. Bader. J. Chem. Soc. 1578 (1947).
7. Brit. Patent No. 510, 904 to I. G. Farbenindustrie A.-G. (1939); Chem. Abstr. **34,** 5462 (1940). Fr. Patent No. 839, 875, to I. G. Farbenindustrie A.-G. (1939); Chem. Abstr. **33,** 7820 (1939).
8. N. M. Libman and S. G. Kuznetsov. J. Gen. Chem. USSR (English Transl.), **30,** 1218 (1960).
9. P. Dimroth, P. Duffner, R. Oster, and H. Pasedach. Ger. Patent No. 1 100 617 (1961); Chem. Abstr. **55,** 19960 (1961).
10. R. L. Salvador and D. Simon. Can. J. Chem. **44,** 2570 (1966).
11. S. Fujiki. Nippon Kagaku Zasshi, **87,** (2), 189 (1966); Chem. Abstr. **65,** 15215 (1966).
12. G. R. Pettit and J. A. Settepani. Chem. Ind. London, 1805 (1964).
13. H. Böhme and H. Orth. Arch. Pharm. **300,** 148 (1967).
14. O. A. Chaltykyan. *In* Copper-catalytic reactions. *Translated by* A. E. Stubbs. *Translation Editor* T. Gray. Consultants Bureau, New York. 1966. pp. 39–63.
15. F. G. Mann. J. Chem. Soc. 461 (1934).

The molecular structure of ryanodol-*p*-bromo benzyl ether[1]

Surendra Nath Srivastava and Maria Przybylska

Division of Pure Chemistry, National Research Council of Canada, Ottawa, Canada

Received October 20, 1967

The molecular structure of ryanodol-*p*-bromo benzyl ether was solved without any chemical assumptions, using three dimensional data obtained by the heavy atom technique. It was found to be identical with the structure proposed by Dr. K. Wiesner, except that the configuration was reversed at one carbon atom. The refinement of atomic parameters with a least-squares method is still in progress. The *R* factor is at present 0.12.

Canadian Journal of Chemistry, **46,** 795 (1968)

The structure of ryanodine, isolated from *Ryania speciosa* Vahl, has been deduced from extensive chemical study by Wiesner, Valenta, and Findlay (1). Ryanodine is an ester of pyrrole-α-carboxylic acid with ryanodol. Since this alkaloid has heavy oxygen substitution and complex structure, Dr. K. Wiesner suggested an *x*-ray analysis be done and he supplied authentic crystals of ryanodol-*p*-bromo benzyl ether, $C_{27}H_{37}O_8Br$.

[1]Issued as NRCC no. 9895.

Can. J. Chem. Downloaded from www.nrcresearchpress.com by 210.87.254.40 on 09/05/12
For personal use only.

of needles; m.p. 137–138.5°; ν_{max} (KBr) 3380 and 2550 cm^{-1}; and p.m.r. δ 1.01 [triplet, 3 methyl (C-1) protons], 1.47–2.00 (partially masked quartet, 2 protons, C-2 methylene, $J = 7$ c.p.s.), 1.51 [singlet, 3 methyl (C-3) protons], 3.64–4.18 (multiplet, 8 CH_2CH_2 protons), and 4.34 (singlet, 2 protons, C—CH_2N).

Anal. Calcd. for $C_{11}H_{20}Cl_3NO$: C, 45.77; H, 6.98; Cl, 36.85; N, 4.85. Found: C, 45.63; H, 6.99; Cl, 36.78; N, 5.05.

1-(1'-Hydroxycyclohexane)-3-[bis(2'-chloroethyl)amino]-1-propyne (3) Hydrochloride

Starting with 1-ethynylcyclohexanol (19.9 g, 0.16 mole) the preceding experiment was repeated. Crystallization of the crude oily amine (**3**) hydrochloride from acetone provided 12.3 g (49% yield) of needles melting at 116–117.5° (sintering from 114°). Four recrystallizations from ethyl acetate gave an analytical sample as needles; m.p. 129.7–130.6°. After drying at 80° (2 mm) for 48 h, the specimen melted at 125–128°; ν_{max} (KBr) 3370 and 2560 cm^{-1}; p.m.r., δ 1.2–2.2 (broad multiplet, 10 methylene protons), 3.67–4.21 [multiplet, 8 protons, $N(CH_2CH_2Cl)_2$], and 4.38 (singlet, 2 protons, C-CH_2-N).

Anal. Calcd. for $C_{13}H_{21}Cl_3NO$: C, 49.62; H, 7.05; Cl, 33.80; N, 4.45. Found: C, 49.47; H, 7.13; Cl, 33.70; N, 4.55.

1. G. R. Pettit and A. K. Das Gupta. Chem. Ind. London, 1016 (1962).
2. (*a*) G. R. Pettit and J. A. Settepani. J. Med. Pharm. Chem. **5,** 296 (1962). (*b*) G. R. Pettit and J. A. Settepani. J. Org. Chem. **27,** 1714 (1962).
3. R. C. Elderfield and A. C. Mehta. J. Med. Chem. **10,** 922 (1967). G. R. Revanker and S. Siddappa. Monatsh. Chem. **98,** 169 (1967). W. Werner. Arch. Pharm. **299,** 513 (1966). W. Werner and M. Mühlstädt. Ann. **693,** 197 (1966). W. J. Serfontein and H. H. E. Schröder. J. S. African Chem. Inst. **19,** 38 (1966).
4. C. Mannich and F. T. Chang. Ber. **66,** 418 (1933).
5. H. Hellmann and G. Opitz. Alpha-aminoalkylierung. Verlag Chemie, G.m.b.H., Weinheim, Germany. 1960. B. Reichert. Die Mannichreaktion. Springer-Verlag, Berlin. 1959. F. F. Blicke. The Mannich reaction. *In* Organic reactions. Vol. I. *Edited by* R. Adams. John Wiley and Sons, Inc., New York. 1942. p. 303.
6. D. Burn and V. Petrov. Tetrahedron, **20,** 2295 (1964). G. A. Shvekhgeĭmer. Izv. Akad. Nauk SSSR Otd. Khim. Nauk, 1265 (1957); Chem. Abstr. **52,** 6211 (1958), I. N. Nazarov and G. A. Shvekgheĭmer. Zh. Obshch. Khim. **26,** 813 (1956); Chem. Abstr. **50,** 13901 (1956). I. Marszak, R. Epsztein, and J. Jacob. Compt. Rend. **231,** 1578 (1950). H. P. W. Huggill and J. D. Rose. J. Chem. Soc. 335 (1950). I. Marszak, M. Diament, and J. P. Guermont. Mem. Serv. Chim. Etat Paris, **35,** 67 (1950); Chem. Abstr. **46,** 7045 (1952), E. R. H. Jones, I. Marszak, and H. Bader. J. Chem. Soc. 1578 (1947).
7. Brit. Patent No. 510, 904 to I. G. Farbenindustrie A.-G. (1939); Chem. Abstr. **34,** 5462 (1940). Fr. Patent No. 839, 875, to I. G. Farbenindustrie A.-G. (1939); Chem. Abstr. **33,** 7820 (1939).
8. N. M. Libman and S. G. Kuznetsov. J. Gen. Chem. USSR (English Transl.), **30,** 1218 (1960).
9. P. Dimroth, P. Duffner, R. Oster, and H. Pasedach. Ger. Patent No. 1 100 617 (1961); Chem. Abstr. **55,** 19960 (1961).
10. R. L. Salvador and D. Simon. Can. J. Chem. **44,** 2570 (1966).
11. S. Fujiki. Nippon Kagaku Zasshi, **87,** (2), 189 (1966); Chem. Abstr. **65,** 15215 (1966).
12. G. R. Pettit and J. A. Settepani. Chem. Ind. London, 1805 (1964).
13. H. Böhme and H. Orth. Arch. Pharm. **300,** 148 (1967).
14. O. A. Chaltykyan. *In* Copper-catalytic reactions. *Translated by* A. E. Stubbs. *Translation Editor* T. Gray. Consultants Bureau, New York. 1966. pp. 39–63.
15. F. G. Mann. J. Chem. Soc. 461 (1934).

The molecular structure of ryanodol-*p*-bromo benzyl ether[1]

Surendra Nath Srivastava and Maria Przybylska

Division of Pure Chemistry, National Research Council of Canada, Ottawa, Canada

Received October 20, 1967

The molecular structure of ryanodol-*p*-bromo benzyl ether was solved without any chemical assumptions, using three dimensional data obtained by the heavy atom technique. It was found to be identical with the structure proposed by Dr. K. Wiesner, except that the configuration was reversed at one carbon atom. The refinement of atomic parameters with a least-squares method is still in progress. The *R* factor is at present 0.12.

Canadian Journal of Chemistry, **46,** 795 (1968)

The structure of ryanodine, isolated from *Ryania speciosa* Vahl, has been deduced from extensive chemical study by Wiesner, Valenta, and Findlay (1). Ryanodine is an ester of pyrrole-α-carboxylic acid with ryanodol. Since this alkaloid has heavy oxygen substitution and complex structure, Dr. K. Wiesner suggested an *x*-ray analysis be done and he supplied authentic crystals of ryanodol-*p*-bromo benzyl ether, $C_{27}H_{37}O_8Br$.

[1]Issued as NRCC no. 9895.

Can. J. Chem. Downloaded from www.nrcresearchpress.com by 210.87.254.42 on 09/05/12
For personal use only.

Can. J. Chem. Downloaded from www.nrcresearchpress.com by 210.87.254.42 on 09/05/12
For personal use only.

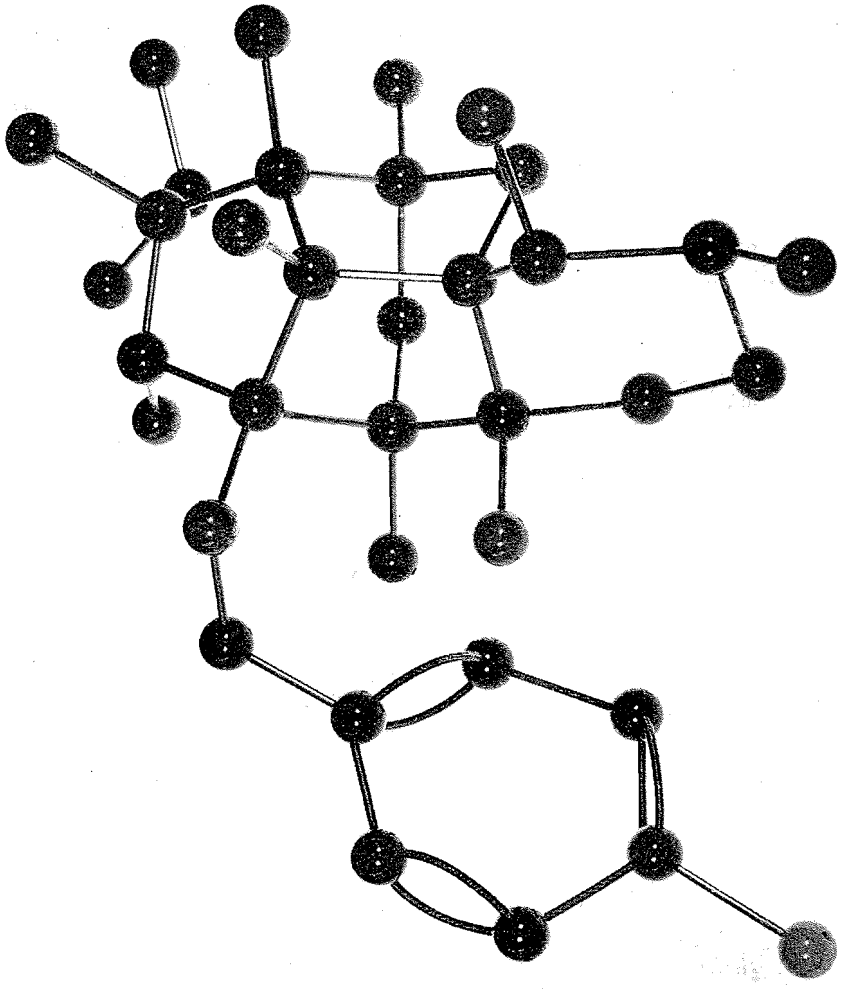

FIG. 1. The stereochemical configuration of ryanodol-*p*-bromo benzyl ether represented in model form.

The space group was found to be $P2_12_12_1$ with four molecules per unit cell of the dimensions: $a = 17.68 \pm 0.03$, $b = 14.45 \pm 0.02$, and $c = 10.13 \pm 0.02$ Å. About 2400 reflections were measured from Weissenberg films. The bromine atom was located by means of a three dimensional Patterson synthesis and the first Fourier synthesis based on phases calculated only for the heavy atom gave the positions of nine atoms of the molecule. Three subsequent Fourier cycles yielded the remaining atoms. The oxygen atoms were distinguished from those of carbon from two additional $\rho_o-\rho_c$ syntheses. The molecular structure was solved without any chemical assumptions. The photograph of its model is shown in Fig. 1 and the structural formula is represented in Fig. 2. The refinement of atomic parameters is still in progress using a least-squares method with anisotropic temperature factors for the bromine atom. All other atoms are refined isotropically. The reliability factor, R, is now about 0.12 for observed reflections; therefore, there is no doubt that the structure is correct.

Wiesner's proposed structure for ryanodol was found to be identical with the molecular model which resulted from this investigation,

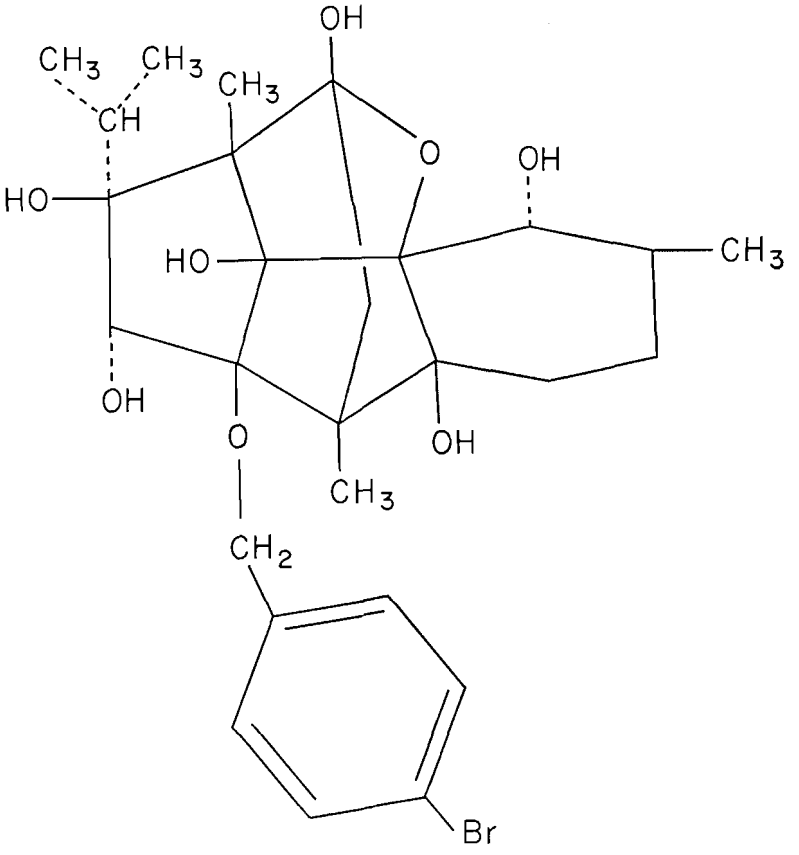

FIG. 2. The stereochemical configuration of ryanodol-*p*-bromo benzyl ether represented in structural formula form.

except that the configuration of the carbon atom carrying the isopropyl group in the five-membered ring is reversed.

The absolute configuration of this compound has not been determined since the anomalous dispersion effects of the Cu Kα radiation caused by the bromine atom are not very marked. The model represented in Fig. 1 conforms with the absolute configuration derived by Wiesner (2) from the nuclear magnetic resonance study of ryanodine degradation products.

Acknowledgment

We wish to thank Dr. F. R. Ahmed and Mrs. M. E. Pippy for computational assistance and Dr. C. P. Huber and Dr. G. I. Birnbaum for helpful discussions. We are indebted to Dr. K. Wiesner for suggesting this investigation and for providing the crystals.

1. K. WIESNER, Z. VALENTA, and J. A. FINDLAY. Tetrahedron Letters, **3**, 221 (1967).
2. K. WIESNER. Pure Appl. Chem. **7**, 285 (1963).

Can. J. Chem. Downloaded from www.nrcresearchpress.com by 210.87.254.42 on 09/05/12
For personal use only.

Pyrrole chemistry. VIII. By-products in the synthesis of 2-pyrrolecarbonitrile

HUGH J. ANDERSON
Memorial University of Newfoundland, St. John's, Newfoundland

Received October 13, 1967

Two by-products are formed when 2-pyrrolecarbonitrile is prepared by the acetic anhydride dehydration of 2-pyrrolecarbaldoxime. These have been proved to be 2-acetamidocarbonylpyrrole and 1-acetyl-2-pyrrolecarbonitrile. The latter acts as an acetylating agent.

Canadian Journal of Chemistry, 46, 798 (1968)

Can. J. Chem. Downloaded from www.nrcresearchpress.com by 210.87.254.105 on 09/05/12
For personal use only.

An earlier paper in this series (1) reported the synthesis of 2-pyrrolecarbonitrile by the dehydration of 2-pyrrolecarbaldoxime using hot acetic anhydride. Subsequently, in the course of large scale preparations of the nitrile, we obtained two by-products. One of these, a high-melting solid from the residue after vacuum distillation, was also reported by Fournari and Tirouflet (2) who prepared the nitrile by the same method. On the basis of the elemental analysis and polarographic behavior they suggested it to be the acetylated oxime. The second by-product was a solid whose much lower melting point was close to that reported by Fischer and Orth (3) for a compound which they obtained by heating the 2-aldoxime with acetic anhydride and sodium acetate. These authors assigned to it the structure 5-acetyl-2-pyrrolecarbonitrile (α-acetyl-α′-cyanopyrrole) but advanced no evidence other than elemental analysis.

The nuclear magnetic resonance (n.m.r.) and infrared spectra of our lower-melting nitrile by-product suggested it to be 1-acetyl-2-pyrrolecarbonitrile. It could be prepared very easily by the action of acetic anhydride on the 2-nitrile in the presence of triethylamine. The synthesis of Fischer and Orth was then repeated and found to give only this same compound. However, it seemed possible that those authors might have obtained the 5-acetyl compound, not otherwise recorded in the literature, and that it could possibly have nearly the same melting point as the 1-acetyl-2-nitrile.

It had been shown earlier (4) that the Friedel–Crafts acetylation of 2-pyrrolecarbonitrile gave only the 4-acetyl-2-nitrile. However, the action of a catalytic amount of perchloric acid on a solution of the 2-nitrile in acetic anhydride and acetic acid gave a mixture of the 4-acetyl and 5-acetyl derivatives from which the much more soluble 5-acetyl-2-nitrile was separated by extraction. The structure of this isomer was confirmed by elemental analysis, n.m.r., and infrared spectra. It was quite different from the low-melting 1-acetyl derivative obtained above and consequently could not have been the compound obtained by Fischer and Orth.

From the ease of formation it appeared likely that 1-acetyl-2-pyrrolecarbonitrile would act as an acetylating agent. It was found that refluxing this compound in benzene with an equimolar quantity of aniline produced a 33% conversion to acetanilide. No attempt has yet been made to find the best conditions for this reaction.

The n.m.r. spectrum of the high-melting by-product appeared consistent with the acetylated oxime structure suggested by Tirouflet and Fournari while the infrared spectrum was not conclusive. It seemed possible that the product was the acetylated *syn* oxime arising from the difference in the ease of dehydration of the *syn* and *anti* forms. The presence of a small amount of the *syn* oxime, which should not dehydrate as easily as the *anti* (5), might result in some surviving the reaction in the acetylated form. However, a purified sample of the more easily obtained *anti* form was acetylated in the cold to the rather unstable *O*-acetyl-2-oxime and the infrared spectrum was found to be quite different from that of the high-melting by-product. In addition, this acetylated oxime decomposed very easily. These observations excluded the possibility that the structure could be that of an acetylated oxime in either form.

The n.m.r. splittings of the aromatic protons of the high-melting by-product indicated only a single attachment at the 2-position of the pyrrole ring, an acetyl group, and another acidic proton of the NH type.

This evidence suggested a —CO—NH—CO—CH_3 side chain, consistent with the infrared

Can. J. Chem. Downloaded from www.nrcresearchpress.com by 210.87.254.105 on 09/05/12
For personal use only.

spectrum which showed two carbonyl bands. It did not seem likely that acetylation of 2-pyrrolecarboxamide, formed by partial hydrolysis of the nitrile, could have occurred. Acetylation of the pyrrole nitrogen of that compound would be much more likely than attack on the amide nitrogen. An attempted synthesis of 2-acetamidocarbonylpyrrole by acetylation of the amide failed to give the desired product. A possible mode of formation of the suggested side chain would be a Beckmann rearrangement in which the *O*-acetylated oxime rearranged to the *N*-acetylated amide. There appears to be general agreement that both the dehydration of aldoximes and the Beckmann rearrangement proceed through *O*-acetylated oxime intermediates (6). However, while nitriles generally arise in the Beckmann rearrangement of aldoximes, the normal conditions for nitrile formation do not appear to produce amides as by-products (7). There are a few examples where *O*-acyloximes have been rearranged to *N*-acylamides (8); however, none was an aldoxime rearrangement.

A possible approach to the synthesis of substituted amides is through the attack of isocyanates on the pyrrole ring (9). This would require the use of acetyl isocyanate, first prepared by Billeter (10). That reagent was prepared in benzene solution and pyrrole was added directly to it. The product, when purified, was found to be identical to the high-melting by-product through comparison of its infrared spectrum and a mixture melting point.

Thus the two by-products from the acetic anhydride dehydration of 2-pyrrolecarbaldoxime are 1-acetyl-2-pyrrolecarbonitrile and 2-acetamidocarbonylpyrrole.

Experimental

General

Melting points are uncorrected. Elemental analyses were determined by Alfred Bernhardt, Mülheim (Ruhr), Germany.

Infrared spectra were recorded on a Perkin–Elmer 237B spectrophotometer by the potassium chloride disc, solution (chloroform, 0.5 mm NaCl cell), or paraffin mull techniques.

The nuclear magnetic resonance spectra were determined on a Varian A-60 spectrometer at 60 Mc.p.s. The chemical shifts are in parts per million from tetramethylsilane as internal reference and are recorded on the δ scale. The proton on the pyrrole ring nitrogen was decoupled by the addition of a few drops of deuterium oxide.

Isolation of the By-products

2-Pyrrolecarbaldoxime (22 g, 0.24 moles) was heated with acetic anhydride (60 ml) and the product worked up in the usual manner (1). The vacuum distillate was then fractionated several times until the nitrile, b.p. 80–82° at 1 mm, was shown to be pure by gas–liquid chromatography. The higher boiling material, 111–135° at 4 mm, partly crystallized on standing and was recrystallized from ethanol–water and then water to give about 200 mg 1-acetyl-2-pyrrolecarbonitrile, m.p. 74–74.5°. (Fischer and Orth (3) reported m.p. 74–75° for their α-acetyl-α′-cyanopyrrole.) Infrared carbonyl 1740 cm^{-1} and nitrile 2220 cm^{-1} (chloroform). Nuclear magnetic resonance: H-3, 7.02; H-4, 6.36; H-5, 7.42; $J_{3,5}$ 1.46; $J_{3,4}$ 3.45; $J_{4,5}$ 3.24 c.p.s. (chloroform-*d*).

Anal. Calcd. for $C_7H_6N_2O$: C, 62.67; H, 4.51; N, 20.88. Found: C, 62.56; H, 4.52; N, 21.07.

A solid was recovered by successive extraction with boiling water of the black residue after vacuum distillation. Several recrystallizations, with decolorizing, from water and then from isopropyl alcohol gave about 750 mg of 2-acetamidocarbonylpyrrole, m.p. 219–219.5°; (lit. m.p. 218° (2)). Infrared carbonyls 1700 cm^{-1} and 1650 cm^{-1} (paraffin mull). Nuclear magnetic resonance: H-3, 7.08; H-4, 6.16; H-5, 7.22 (dimethyl sulfoxide-d_6). Sample solubility too low to determine coupling constants.

Anal. Calcd. for $C_7H_8N_2O_2$: C, 55.26; H, 5.30; N, 18.41. Found: C, 55.18; H, 5.25; N, 18.28.

1-Acetyl-2-pyrrolecarbonitrile

This compound was synthesized in nearly quantitative yield by the action of acetic anhydride on 2-pyrrolecarbonitrile in the presence of triethylamine. It was the only product when the 2-nitrile was refluxed in acetic anhydride – acetic acid. It formed in about 60% yield when 2-pyrrolecarbaldoxime was treated with acetic anhydride and triethylamine. No heat was necessary for this reaction beyond that which it developed. The synthesis of Fischer and Orth (3) was repeated and the product isolated according to their directions. The yield was about 35%. It was established that the same compound was produced from each of these reactions and that it was identical to the lower-melting by-product obtained above through the identity of infrared spectra in KCl discs and in chloroform solution as well as through a series of mixture melting points.

Acetylation of Aniline

A solution of 1-acetyl-2-pyrrolecarbonitrile (0.83 g) and aniline (0.57 g) in 10 ml benzene was refluxed for 5 h. The cold product was washed with 3 ml 6 *N* hydrochloric acid, 3 ml 10% sodium hydroxide, and with 3 ml water. After evaporation the oily solid was dissolved in ether and again washed with 10% sodium hydroxide solution, dried, and evaporated. The solid was recrystallized from benzene–cyclohexane to give 0.27 g (33%) acetanilide. The identity of the product was confirmed by the infrared spectrum and mixture melting point with an authentic sample.

The C-Acetylation of 2-Pyrrolecarbonitrile

2-Pyrrolecarbonitrile (0.5 g) was dissolved in a mixture of acetic acid (4 ml) and acetic anhydride (2 ml). To this

solution 5–6 drops of perchloric acid (70%) was added and the mixture swirled. After the reaction ceased the solution was poured into about 50 g of ice and water with stirring and allowed to hydrolyze. The buff solid was filtered (0.33 g) and the mother liquor saturated with salt and extracted three times with ether. When all the solvent was removed by flash evaporation a further 0.22 g was obtained. Finally, by making the mother liquor basic and extracting again, 0.13 g was obtained. The total crude product recovered was about 94% of theory, assuming monoacetylation. Extraction of the crude solid with cold ether, evaporation, then extraction of the recovered solid with cold chloroform and evaporation gave about 0.15 g (20%) of 5-acetyl-2-pyrrolecarbonitrile, m.p. 154.5–155.5° from benzene–cyclohexane. Infrared carbonyl 1655 cm^{-1} and nitrile 2220 cm^{-1} (chloroform). Nuclear magnetic resonance: H-3, 7.08; H-4, 7.00; $J_{3,4}$ 3.80 c.p.s. (dimethyl sulfoxide-d_6).

Anal. Calcd. for $C_7H_6N_2O$: C, 62.67; H, 4.51; N, 20.88. Found: C, 62.76; H, 4.65; N, 21.03.

The very much less soluble isomer was identified, through mixture melting point and infrared spectrum of a purified sample, as the known (4) 4-acetyl-2-pyrrolecarbonitrile.

The O-Acetyl Derivative of Anti-2-pyrrolecarbaldoxime

A pure sample of the *anti* form of 2-pyrrolecarbaldoxime, (20 mg) m.p. 165–167° (lit. m.p. 165–166° (11)) was prepared. Infrared NH at 3440 cm^{-1}, OH at 3560 cm^{-1}, C=N at 1640 cm^{-1} (chloroform). Nuclear magnetic resonance[1]: H-3, 6.57; H-4, 6.12; H-5, 6.90; —CH= 7.26; —OH, 11.12 (dimethyl sulfoxide); $J_{3,4}$ 3.62; $J_{3,5}$ 1.50; $J_{4,5}$ 2.62 c.p.s.

It was covered with 1–2 ml of acetic anhydride and shaken until a clear yellow solution was obtained. Ice was added and, after hydrolysis was complete, the solution was neutralized with solid sodium carbonate. After extraction with ether and evaporation the solid was recrystallized from water. The oxime acetate decomposed on attempted purification. Infrared on crude product: NH at 3445, 3460; carbonyl 1765 cm^{-1} and C=N at 1630 cm^{-1} (chloroform).

2-Acetamidocarbonylpyrrole

In a 3-necked flask was placed 6.75 g silver isocyanate (13) in 5 ml dry benzene. To this was added, with stirring, a solution of acetyl chloride (3 g) in 5 ml benzene. The reaction mixture became quite hot and the color darkened somewhat. It was stirred and refluxed for 20 min and cooled to room temperature. Then pyrrole (2.5 g) in 5 ml benzene was added and the mixture refluxed for about an hour, giving a deep green solution. After cooling, the mixture was suction filtered, and the solid washed thoroughly with acetone. All the organic solvent was removed by flash evaporation giving a greenish-black solid. The solid was continuously extracted with boiling water which was then saturated with salt, cooled, and extracted with ether. Evaporation gave a yellow-brown solid which was sublimed and recrystallized to give 0.6 g white crystals m.p. 219–219.5° (11%). This solid was proved to be identical with the high-melting by-product obtained above through the infrared spectrum and mixture melting point.

[1]The difference between the chemical shifts of —CH= and —OH protons ($\Delta \simeq 3.8$) was in agreement with the range suggested for *anti* aldoximes by Kleinspehn *et al.* (12), i.e. about 3.8.

Acknowledgments

The author is pleased to acknowledge the continued financial support of the National Research Council of Canada. He is also indebted to Professor E. Bullock for useful discussions and to Mr. L. C. Hopkins who first isolated the two by-products.

1. H. J. Anderson. Can. J. Chem. **37**, 2053 (1959).
2. P. Fournari and J. Tirouflet. Bull. Soc. Chim. France, 484 (1963).
3. H. Fischer and H. Orth. Ann. **502**, 237 (1933).
4. H. J. Anderson and C. W. Huang. Can. J. Chem. **45**, 897 (1967).
5. L. F. Fieser and M. Fieser. Advanced organic chemistry. Reinhold Publishing Corp., New York. 1961. p. 438.
6. P. A. S. Smith. Open chain nitrogen compounds. W. A. Benjamin, Inc., New York. 1966. pp. 49, 52.
7. L. G. Donoruma and W. Z. Heldt. *In* Organic reactions. Vol. XI. *Edited by* A. C. Cope. John Wiley & Sons, Inc., New York. 1960. p. 41.
8. M. Kuhara, K. Matsumija, and N. Matsunami. Mem. Coll. Sci. Kyoto Imp. Univ. **1**, 105 (1914); Chem. Abstr. **9**, 1613 (1915).
9. A. Treibs and W. Ott. Ann. **577**, 119 (1952).
10. O. Billeter. Ber. **36**, 3213 (1903).
11. R. M. Silverstein, E. E. Ryskiewicz, and S. W. Chaiken. J. Am. Chem. Soc. **76**, 4485 (1954).
12. G. G. Kleinspehn, J. A. Jung, and S. A. Studniarz. J. Org. Chem. **32**, 460 (1967).
13. D. L. Williams and A. R. Ronzio. J. Am. Chem. Soc. **74**, 240 (1952).

Can. J. Chem. Downloaded from www.nrcresearchpress.com by 210.87.254.105 on 09/05/12
For personal use only.

Addition of *C*-phenyl-*N*-methyl nitrone to norbornene and norbornadiene

ROBERT R. FRASER AND Y. S. LIN
Department of Chemistry, University of Ottawa, Ottawa, Canada

Received November 16, 1967

The reaction of *C*-phenyl-*N*-methyl nitrone with norbornene gave two 1:1 cycloadducts in a ratio of 9:1. Both adducts have been shown to possess an *exo-cis* isoxazolidine ring by nuclear magnetic resonance and to be diastereomeric at the benzylic carbon of the isoxazolidine ring by chemical degradation of both adducts to 3-*exo*-benzyl-2-*exo*-hydroxybicyclo[2·2·1]heptane. The reaction of the same nitrone with norbornadiene gave a 1:1 and a 2:1 adduct. The stereochemistry of the 1:1 adduct was shown to be the same as that of the major norbornene adduct which it gave on hydrogenation of the double bond. The structure of the 2:1 adduct was not investigated.

Canadian Journal of Chemistry, **46**, 801 (1968)

Can. J. Chem. Downloaded from www.nrcresearchpress.com by 210.87.254.105 on 09/05/12
For personal use only.

The addition of a nitrone to a double bond to form an isoxazolidine ring is a reaction which belongs to the general category of 1,3-dipolar cycloadditions. Both the scope and the mechanistic aspects of these cycloadditions have been reviewed by Huisgen (1, 2). One of the many reactions studied by Huisgen and co-workers was the addition of *C*,*N*-diphenyl nitrone to norbornene which they reported gave two 1:1 adducts, "presumably epimeric at the atom bearing the phenyl substituent" (1). Details regarding the proof of structure of these adducts have not yet been published. Grashey, Huisgen, and Leitermann (3) have reported that *C*-phenyl-*N*-methyl nitrone adds to norbornene to give a 100% yield of product and adds to norbornadiene to give a 98% yield of product although no further data was given in this preliminary communication. We have independently studied the reaction of *C*-phenyl-*N*-methyl nitrone with norbornadiene and norbornene and wish to report the proof of structure and stereochemistry of the 1:1 cycloadducts obtained.

The reaction of *C*-phenyl-*N*-methyl nitrone with norbornene was carried out for 12 h in toluene at 110°. After removal of the solvent, a compound (**1**) was obtained in 79% yield by crystallization of the reaction mixture. A second compound (**2**) was isolated in 9% yield by chromatography of the mother liquors. When a solution of *C*-phenyl-*N*-methyl nitrone in norbornadiene was heated under reflux for 4 h, two products were produced. Compound **3** was isolated in 82% yield and compound (**4**) in 3% yield. Compound **3** absorbed one mole of hydrogen in the presence of platinum to give compound **1**. Elemental analysis of **1**, **2**, and **3** showed that they were all 1:1 adducts. Compound **4** had an elemental composition consistent with its being a 2:1 adduct. Its structure was not further investigated. The above findings are summarized in Scheme I.

We then subjected compounds **1** and **2** to a chemical degradation in order to establish their stereochemical interrelation. Compounds **1** and **2** were each methylated with methyl iodide, then reduced by zinc in acetic acid to produce two isomeric amino alcohols, **5** and **7** respectively. Repetition of methylation and reduction converted both **5** and **7** into the same compound, **6**. These reactions, which are shown in Scheme II, prove that **1** and **2** are indeed epimeric at the benzylic carbon of the isoxazolidine ring.

Both the gross structural features and the stereochemistry of the ring fusion in **3** and thus, in all the compounds related to it by the reactions in Schemes I and II, can be determined by an examination of the nuclear magnetic resonance (n.m.r.) spectrum of **3**. The spectrum of **3** is shown in Fig. 1 (*a*). The multiplet centered at τ 3.9 can only result from olefinic protons. Their presence immediately rules out the possibility of nortricyclene structure for **3**. The doublet at τ 5.63 (spacing 6.1 c.p.s.) is assigned to the proton on the carbon bearing the oxygen atom. The splitting of 6.1 c.p.s. is attributed to a vicinal interaction[1] with the adjacent *endo* hydrogen. Davis and Van Auken (4) reported a

[1]We are purposefully avoiding the use of the word coupling constant in this instance as the spectra are not completely first order in character. Anet, Lee, and Sudmeier (5) have recently shown that some of the spacings reported by Davis and Van Auken as coupling constants for the compound 2-carbomethoxynorbornene are in error by more than 5 c.p.s. So the spacing of 6.1 c.p.s. in **3** does not necessarily represent the true coupling constant.

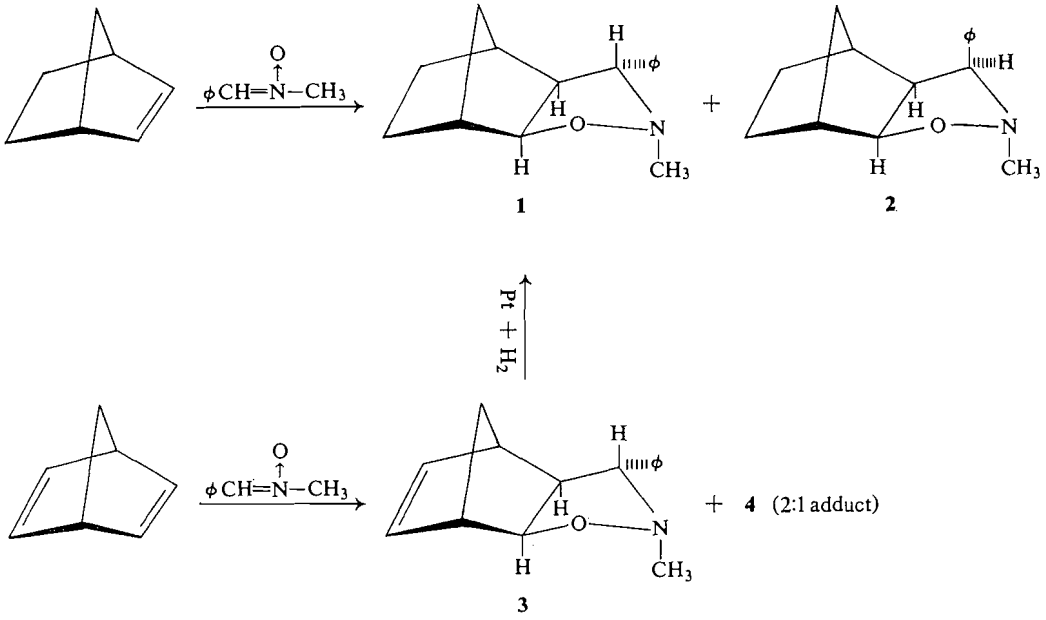

SCHEME I.

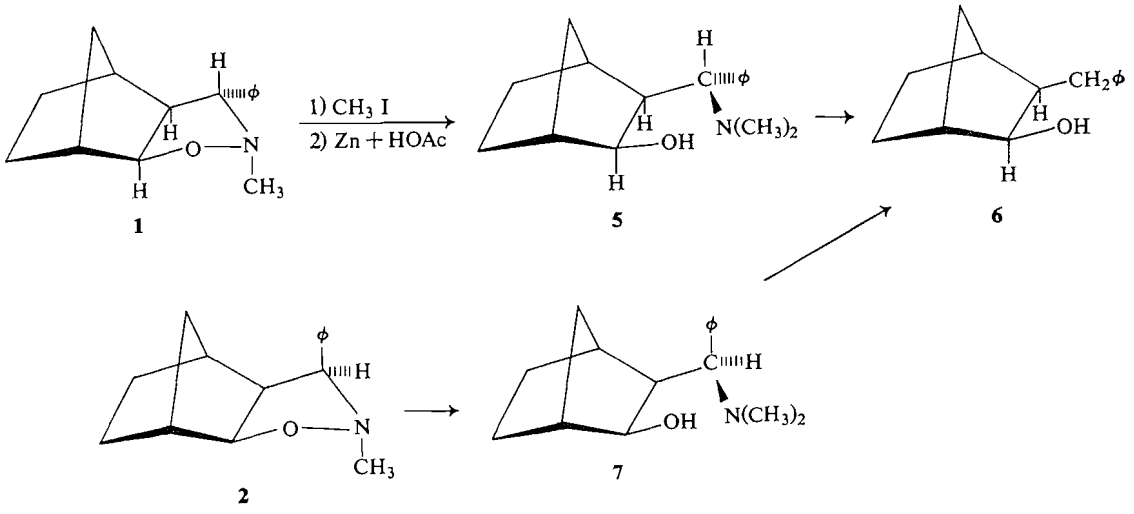

SCHEME II.

splitting of 5.6 c.p.s. for the *endo–endo* interaction in *exo*-2-hydroxynorbornene, 8.1 c.p.s. for the *exo–exo* splitting in the *endo* isomer and 3.0 c.p.s. for the *exo–endo* splitting. Thus the splitting of 6.1 c.p.s. indicates an *endo–endo* relation or possibly an *exo–exo* relation of the protons. That the proton in question is *endo* is conclusively established by the lack of any observable splitting with the adjacent bridgehead hydrogen. It has been established previously that the vicinal coupling constant J between a bridgehead proton and an *endo* proton is < 1 c.p.s., while J between a bridgehead and an *exo* proton is 3–5 c.p.s. (3, 4, and references therein). The lack of further observable splitting of the absorption at τ 5.63 establishes the orientation of the proton as *endo*. Thus the adducts **3**, **1**, and **2** are all *exo* adducts.

Can. J. Chem. Downloaded from www.nrcresearchpress.com by 210.87.254.105 on 09/05/12
For personal use only.

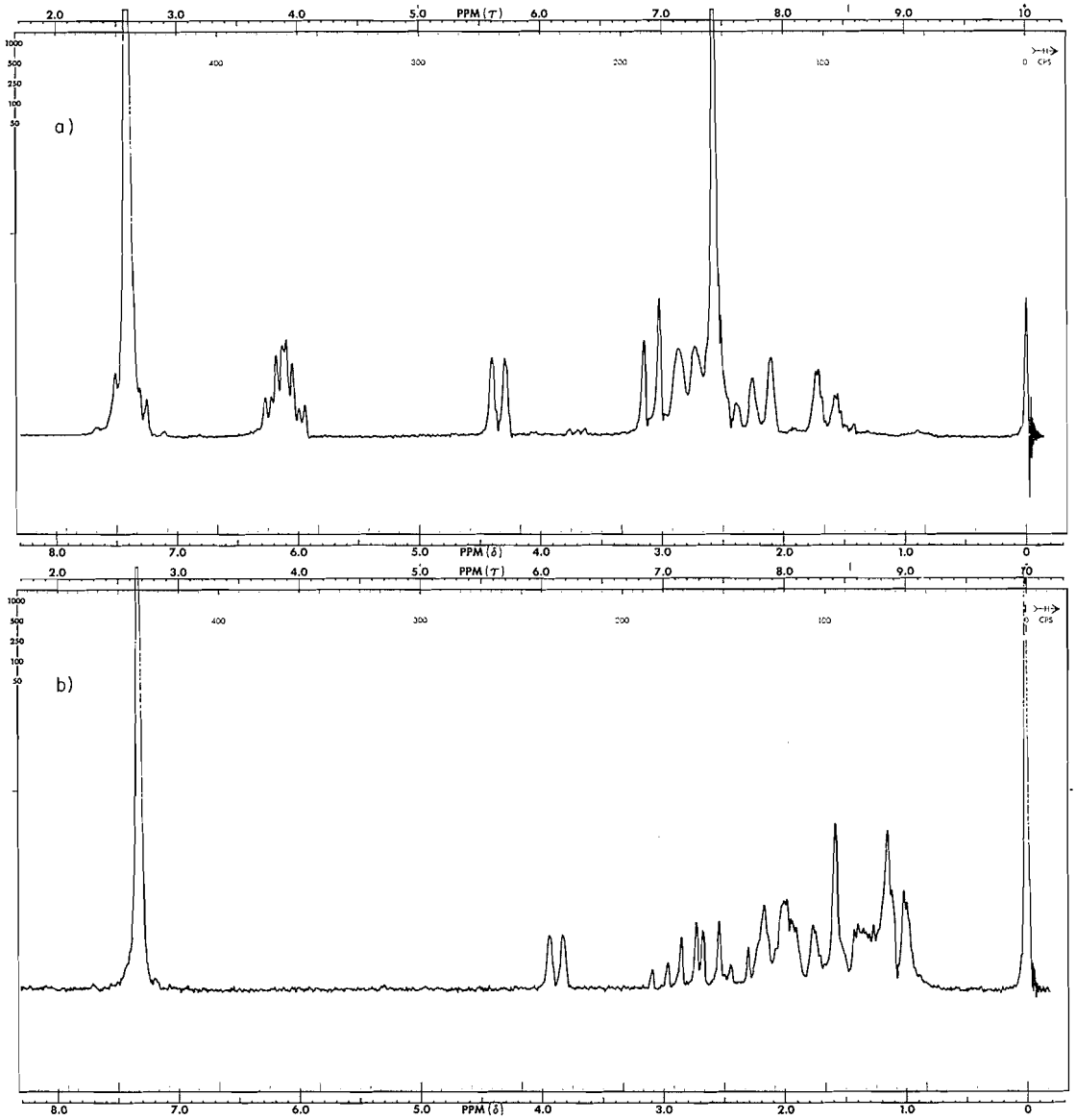

FIG. 1. (*a*) The 60 Mcycles spectrum of **3**, the 1:1 adduct of norbornadiene and *C*-phenyl-*N*-methyl nitrone in CCl_4. (*b*) The 60 Mcycles spectrum of **6**, 3-benzyl-2-hydroxybicyclo[2·2·1]heptane in CCl_4.

Similarly, the proton on carbon-2 of compounds **1**, **2**, **5**, **6**, and **7** always appeared as a doublet of spacing 6.1–6.5 c.p.s. which confirms the *exo* stereochemistry of these compounds. The spectrum of the final conversion product **6** serves to illustrate this behavior in Fig. 1*b*. Further support for the reliability of the above conclusions is provided by a recent paper of Huisgen and co-workers (6). They prepared the *endo* and *exo* adducts of diphenyl nitrile imine and norbornene. The n.m.r. spectra of these adducts provide model examples of the above correlation between *J* and the *exo–endo* relationship.

One final point of stereochemistry remains to be assigned, ie. the configuration at the benzylic carbon of adducts **1** and **2**. Unfortunately n.m.r. does not provide any definite evidence on this point; however, one fact does provide a clue.

Can. J. Chem. Downloaded from www.nrcresearchpress.com by 210.87.254.105 on 09/05/12
For personal use only.

Can. J. Chem. Downloaded from www.nrcresearchpress.com by 210.87.254.105 on 09/05/12
For personal use only.

Compound **1** is thermally stable whereas **2** is not. If **1** and **2** have the stereochemistry denoted in Schemes I and II this finding can be explained. An examination of molecular models of **1** and **2** reveals the presence of a serious non-bonded interaction between the phenyl substituent and the methylene bridge in **2** but not in **1**. This interaction would be expected to make **2** less stable than **1**. It is on this basis that the assignment of relative stereochemistry to the diastereoisomers **1** and **2** in Scheme I has been made.

In conclusion, we have established that *C*-phenyl-*N*-methyl nitrone adds to norbornene producing two *exo–cis* adducts. This nitrone also adds to norbornadiene to give an *exo–cis* adduct. Recently several papers have reported that the additions of diphenyl nitrile imine (6), thiobenzoyl isocyanate (7), and fulminic acid (8) all occur in the same *exo–cis* manner. In another paper, Huisgen and co-workers (9) discuss the mechanism of cycloaddition of diphenyl nitrile imine in considerable detail. Since our results provide no further evidence about this mechanism, they need not be discussed in this context.

Experimental

All melting points and boiling points are uncorrected. The nuclear magnetic resonance (n.m.r.) spectra were measured on a Varian V-4302 HA-60 spectrometer using tetramethylsilane as an internal standard. All infrared spectra were measured on a Beckman IR-8 spectrometer. Elemental analyses were performed by Alfred Bernhardt, Mülheim, W. Germany and H. Seguin, NRCC, Ottawa.

Reaction of C-Phenyl-N-methyl Nitrone with Norbornadiene

By following the procedure of Brady *et al.* (10), *C*-phenyl-*N*-methyl nitrone was prepared in 80% yield. A solution of *C*-phenyl-*N*-methyl nitrone (10.1 g, 0.075 mole) in norbornadiene (150 ml) was heated under reflux for 4 h. The excess of norbornadiene was removed by evaporation under reduced pressure. The residue was dissolved in ether (450 ml), and the ether solution was extracted with water (4 × 100 ml) to remove the unreacted nitrone. Concentration of the ether solution to dryness gave crude product (14 g, 82%). A solution of a portion of the crude product (4.5 g) in hexane (10 ml) was applied to a column of neutral grade alumina (200 g, Fisher reagent). The column was eluted with hexane (1000 ml), hexane–chloroform (2:1, v/v, 1200 ml), and hexane–chloroform (1:1, v/v, 1000 ml). Concentration of the hexane–chloroform (2:1, v/v) eluant under reduced pressure and recrystallization of the residue from hexane gave **3**,*N*-methyl-5-phenyl-3-oxa-4-azatricyclo-[5·2·1·$0^{2,6}$]dec-8-ene (4.1 g) as colorless crystals, m.p. 67–68°.

Anal. Calcd. for $C_{15}H_{17}NO$: C, 79.26; H, 7.55; N, 6.16. Found: C, 79.47; H, 7.43; N, 6.10.

Concentration of the hexane–chloroform (1:1, v/v) eluant to dryness under reduced pressure and recrystallization of the residue from methanol gave the di-adduct **4**, possibly 4,10-dimethyl-5,11-diphenyl-3,9-dioxa-4,10-diazatetracyclo[5·5·1·$0^{2,6}$,$0^{8,12}$]tridecane (0.15 g) as colorless crystals, m.p. 214–216° (decomp.).

Anal. Calcd. for $C_{23}H_{26}N_2O_2$: C, 76.21; H, 7.23; N, 7.73. Found: C, 76.42; H, 7.17; N, 7.59.

Catalytic Hydrogenation of N-Methyl-5-phenyl-3-oxa-4-azatricyclo[5·2·1·$0^{2,6}$]dec-8-ene (3)

A solution of **3** (0.22 g, 0.001 mole) in anhydrous methanol (25 ml) was shaken in a hydrogen atmosphere with prereduced Adam's catalyst at room temperature and atmospheric pressure. The hydrogen uptake corresponded to 0.001 mole. The reaction mixture was filtered and the filtrate was concentrated to dryness. Bulb-to-bulb sublimation of the residue under reduced pressure (0.02 mm) gave *N*-methyl-5-phenyl-3-oxa-4-azatricyclo[5·2·1·$0^{2,6}$]decane, isomer **1** (0.21 g, 96%), m.p. 64–65°.

Reaction of C-Phenyl-N-methyl Nitrone with Norbornene

A solution of *C*-phenyl-*N*-methyl nitrone (27.1 g, 0.2 mole) and norbornene (18.8 g, 0.2 mole) in toluene (250 ml) was heated under reflux for 12 h. After every 2 h of reflux a further portion of norbornene (4.7 g, 0.05 mole) was added. The reaction mixture was concentrated to dryness under reduced pressure, and the residue was dissolved in ether (700 ml). The ether solution was extracted with water (3 × 75 ml) to remove unreacted nitrone and was concentrated to dryness. Recrystallization of the residue from dioxane gave yellow *N*-methyl-5-phenyl-3-oxa-4-azatricyclo[5·2·1·$0^{2,6}$]decane, isomer **1** (36.2 g, 79%), which was purified further by bulb-to-bulb sublimation under reduced pressure. The sublimation gave a colorless needle-like crystalline compound, which melted at 65–66°. The mixture melting point with the material prepared in the previous experiment was 64–65°.

Anal. Calcd. for $C_{15}H_{19}NO$: C, 78.57; H, 8.35; N, 6.12. Found: C, 78.65; H, 8.28; N, 6.08.

The infrared and n.m.r. spectra of the present product were identical to those of the compound prepared in the previous experiment.

The mother liquors from the recrystallization described above were concentrated to dryness and the residue was dissolved in hexane (15 ml). The solution was poured onto a column of basic grade alumina (250 g, Shawinigan reagent). The column was eluted with hexane (1500 ml), hexane–chloroform (2:1, v/v, 1000 ml), and hexane–chloroform (1:1, v/v, 1000 ml). Concentration of the hexane eluant gave *N*-methyl-5-phenyl-3-oxa-4-azatricyclo[5·2·1·$0^{2,6}$]decane, isomer **2** (4.2 g, 9%) as colorless needle-like crystals, m.p. 62–64°. This compound slowly decomposed at room temperature. Its infrared and n.m.r. spectra were strikingly different from those of isomer **1**. For example, the proton on the benzylic carbon in **2** gives rise to an n.m.r. signal at τ 6.53 (doublet of spacing 7.6 c.p.s.) while that in **1** appears at τ 7.18 (doublet of spacing 8.0 c.p.s.). The instability of **2** prevented us from obtaining accurate combustion analyses.

3-(α-Dimethylaminobenzyl)-2-hydroxybicyclo[2·2·1]-heptane (5)

A mixture of isomer **1** (2.75 g, 0.012 mole) and methyl iodide (7 ml) was heated under reflux on an oil bath for 96 h. The reaction mixture was concentrated to dryness

Can. J. Chem. Downloaded from www.nrcresearchpress.com by 210.87.254.105 on 09/05/12
For personal use only.

and the residue was used for the next step without further purification. Reductive cleavage of the isoxazolidine ring of the residue (3.7 g) with zinc dust (13 g), as described by Rayburn *et al.* (11), gave **5**, 3-(α-dimethylaminobenzyl)-2-hydroxybicyclo[2·2·1]heptane (2.45 g, 83%) as colorless crystals, m.p. 114–116 °C (recrystallization from hexane).

Anal. Calcd. for $C_{16}H_{23}NO$: C, 78.32; H, 9.45; N, 5.71. Found: C, 78.91; H, 9.75; N, 5.64.

Methylation of 5 by Methyl Iodide and Reductive Cleavage of the Product by Zinc Dust

A mixture of **5** (0.73 g, 0.003 mole) and methyl iodide (10 ml) was heated under reflux on an oil bath for 96 h, after which the reaction mixture was concentrated to dryness. The residue (1.0 g) was used for the next step without further purification. Zinc dust (15 g) was added in small portions to a vigorously stirred solution of the above residue (0.97 g) in 20% acetic acid (100 ml). The reaction mixture was heated under reflux for 86 h on an oil bath and then was filtered. The filtrate was extracted with ether (5 × 50 ml). The ethereal extracts were washed with water (2 × 30 ml), with 10% hydrochloric acid solution (3 × 30 ml), with 10% sodium hydroxide solution (3 × 30 ml), and with water (3 × 30 ml) again. Concentration of the ethereal solution to dryness and bulb-to-bulb distillation of the residue under reduced pressure gave **7**, 3-benzyl-2-hydroxybicyclo-[2·2·1]heptane (0.6 g, 92%) as colorless crystals, m.p. 41–42°.

Anal. Calcd. for $C_{14}H_{18}O$: C, 83.12; H, 8.97. Found: C, 83.21; H, 8.95.

The alcohol was converted to a crystalline phenyl urethane, m.p. 132–133°.

Anal. Calcd. for $C_{21}H_{23}NO_2$: C, 78.47; H, 7.21; N, 4.36. Found: C, 78.32; H, 7.11; N, 4.52.

Degradation of Isomer 2 to 3-Benzyl-2-hydroxybicyclo-[2·2·1]heptane

Methylation of isomer **2** (4.1 g, 0.018 mole) with methyl iodide (10 ml) and reductive cleavage of isoxazolidine ring of the product with zinc dust (20 g), as described above for **1**, gave **7**, 3-(α-dimethylaminobenzyl)-2-hydroxybicyclo[2·2·1]heptane (3.9 g, 85%). The infrared and n.m.r. spectra of this product showed it to be slightly impure, yet different from **5**. For example the *N*-methyl singlet appeared at τ 7.87 in **5** and at τ 7.77 in **7**. Further methylation of **7** with methyl iodide (12 ml) then reductive cleavage of the carbon–nitrogen bond with zinc dust (15 g) gave **6**, 3-benzyl-2-hydroxybicyclo[2·2·1]-heptane (2.36 g, 64%). This sample of **6** was found to have a melting point of 40–41°. The melting point of this sample when mixed with that prepared from **1** was also 40–41°. The infrared and n.m.r. spectra of the product of the present experiment were indistinguishable from those of the compound prepared in the previous experiment.

Acknowledgments

The authors thank the National Research Council of Canada for their financial support. We also wish to thank Mr. Hector Seguin for his analysis of the phenyl urethane of compound **6**.

1. R. Huisgen. Angew. Chem. Intern. Ed. Engl. **2**, 565 (1963).
2. R. Huisgen. Angew. Chem. Intern. Ed. Engl. **2**, 633 (1963).
3. R. Grashey, R. Huisgen, and H. Leitermann. Tetrahedron Letters, **12**, 9 (1960).
4. J. C. Davis, Jr. and T. V. Van Auken. J. Am. Chem. Soc. **87**, 3900 (1965).
5. F. A. L. Anet, H. H. Lee, and J. L. Sudmeier. J. Am. Chem. Soc. **89**, 4431 (1967).
6. R. Huisgen, H. Knupfer, R. Sustmann, G. Wallbillich, and V. Weberndörfer. Chem. Ber. **100**, 1580 (1967).
7. R. Weiss. Chem. Ber. **100**, 655 (1967).
8. R. Huisgen and M. Christl. Angew. Chem. Intern. Ed. Engl. **6**, 456 (1967).
9. A. Eckell, R. Huisgen, R. Sustmann, G. Wallbillich, D. Grashey, and E. Spindler. Chem. Ber. **100**, 2192 (1967).
10. O. L. Brady, F. P. Dunn, and R. F. Goldstein. J. Chem. Soc. 2390 (1926).
11. C. H. Rayburn, W. R. Harlan, and H. R. Hanmer. J. Am. Chem. Soc. **72**, 1721 (1950).

Reductive elimination of 1,2-dibromides with sodium borohydrides

J. F. King, A. D. Allbutt, and R. G. Pews
Department of Chemistry, University of Western Ontario, London, Ontario

Received October 2, 1967

Sodium trimethoxyborohydride or a 1:3 mixture of sodium borohydride and sodium tetramethylborate reacts with a number of vicinal dibromides to form the corresponding olefin. Variable (sometimes good) yields were obtained when the bromine atoms were on secondary or tertiary carbons, but little or no olefin was detected when one bromine was primary.

Canadian Journal of Chemistry, **46**, 805 (1968)

We have previously reported (1) on our study of the reductive elimination of 1,2-dibromides and related species with lithium aluminium hydride. In that account we mentioned that sodium trimethoxyborohydride reduced 2β,3α-dibromo-5α-cholestane to 5α-cholest-2-ene in good yield. In the hope of casting some light on the mechanism of reductive elimination we have further investigated the reaction of sodium borohydride and related reagents on some of the same compounds. We find that these reagents effect reductive elimination in fairly good yield with

and the residue was used for the next step without further purification. Reductive cleavage of the isoxazolidine ring of the residue (3.7 g) with zinc dust (13 g), as described by Rayburn *et al.* (11), gave **5**, 3-(α-dimethylaminobenzyl)-2-hydroxybicyclo[2·2·1]heptane (2.45 g, 83%) as colorless crystals, m.p. 114–116 °C (recrystallization from hexane).

Anal. Calcd. for $C_{16}H_{23}NO$: C, 78.32; H, 9.45; N, 5.71. Found: C, 78.91; H, 9.75; N, 5.64.

Methylation of 5 by Methyl Iodide and Reductive Cleavage of the Product by Zinc Dust

A mixture of **5** (0.73 g, 0.003 mole) and methyl iodide (10 ml) was heated under reflux on an oil bath for 96 h, after which the reaction mixture was concentrated to dryness. The residue (1.0 g) was used for the next step without further purification. Zinc dust (15 g) was added in small portions to a vigorously stirred solution of the above residue (0.97 g) in 20% acetic acid (100 ml). The reaction mixture was heated under reflux for 86 h on an oil bath and then was filtered. The filtrate was extracted with ether (5 × 50 ml). The ethereal extracts were washed with water (2 × 30 ml), with 10% hydrochloric acid solution (3 × 30 ml), with 10% sodium hydroxide solution (3 × 30 ml), and with water (3 × 30 ml) again. Concentration of the ethereal solution to dryness and bulb-to-bulb distillation of the residue under reduced pressure gave **7**, 3-benzyl-2-hydroxybicyclo-[2·2·1]heptane (0.6 g, 92%) as colorless crystals, m.p. 41–42°.

Anal. Calcd. for $C_{14}H_{18}O$: C, 83.12; H, 8.97. Found: C, 83.21; H, 8.95.

The alcohol was converted to a crystalline phenyl urethane, m.p. 132–133°.

Anal. Calcd. for $C_{21}H_{23}NO_2$: C, 78.47; H, 7.21; N, 4.36. Found: C, 78.32; H, 7.11; N, 4.52.

Degradation of Isomer 2 to 3-Benzyl-2-hydroxybicyclo-[2·2·1]heptane

Methylation of isomer **2** (4.1 g, 0.018 mole) with methyl iodide (10 ml) and reductive cleavage of isoxazolidine ring of the product with zinc dust (20 g), as described above for **1**, gave **7**, 3-(α-dimethylaminobenzyl)-2-hydroxybicyclo[2·2·1]heptane (3.9 g, 85%). The infrared and n.m.r. spectra of this product showed it to be slightly impure, yet different from **5**. For example the *N*-methyl singlet appeared at τ 7.87 in **5** and at τ 7.77 in **7**. Further methylation of **7** with methyl iodide (12 ml) then reductive cleavage of the carbon–nitrogen bond with zinc dust (15 g) gave **6**, 3-benzyl-2-hydroxybicyclo[2·2·1]-heptane (2.36 g, 64%). This sample of **6** was found to have a melting point of 40–41°. The melting point of this sample when mixed with that prepared from **1** was also 40–41°. The infrared and n.m.r. spectra of the product of the present experiment were indistinguishable from those of the compound prepared in the previous experiment.

Acknowledgments

The authors thank the National Research Council of Canada for their financial support. We also wish to thank Mr. Hector Seguin for his analysis of the phenyl urethane of compound **6**.

1. R. Huisgen. Angew. Chem. Intern. Ed. Engl. **2**, 565 (1963).
2. R. Huisgen. Angew. Chem. Intern. Ed. Engl. **2**, 633 (1963).
3. R. Grashey, R. Huisgen, and H. Leitermann. Tetrahedron Letters, **12**, 9 (1960).
4. J. C. Davis, Jr. and T. V. Van Auken. J. Am. Chem. Soc. **87**, 3900 (1965).
5. F. A. L. Anet, H. H. Lee, and J. L. Sudmeier. J. Am. Chem. Soc. **89**, 4431 (1967).
6. R. Huisgen, H. Knupfer, R. Sustmann, G. Wallbillich, and V. Weberndörfer. Chem. Ber. **100**, 1580 (1967).
7. R. Weiss. Chem. Ber. **100**, 655 (1967).
8. R. Huisgen and M. Christl. Angew. Chem. Intern. Ed. Engl. **6**, 456 (1967).
9. A. Eckell, R. Huisgen, R. Sustmann, G. Wallbillich, D. Grashey, and E. Spindler. Chem. Ber. **100**, 2192 (1967).
10. O. L. Brady, F. P. Dunn, and R. F. Goldstein. J. Chem. Soc. 2390 (1926).
11. C. H. Rayburn, W. R. Harlan, and H. R. Hanmer. J. Am. Chem. Soc. **72**, 1721 (1950).

Reductive elimination of 1,2-dibromides with sodium borohydrides

J. F. King, A. D. Allbutt, and R. G. Pews
Department of Chemistry, University of Western Ontario, London, Ontario

Received October 2, 1967

Sodium trimethoxyborohydride or a 1:3 mixture of sodium borohydride and sodium tetramethylborate reacts with a number of vicinal dibromides to form the corresponding olefin. Variable (sometimes good) yields were obtained when the bromine atoms were on secondary or tertiary carbons, but little or no olefin was detected when one bromine was primary.

Canadian Journal of Chemistry, **46**, 805 (1968)

We have previously reported (1) on our study of the reductive elimination of 1,2-dibromides and related species with lithium aluminium hydride. In that account we mentioned that sodium trimethoxyborohydride reduced 2β,3α-dibromo-5α-cholestane to 5α-cholest-2-ene in good yield. In the hope of casting some light on the mechanism of reductive elimination we have further investigated the reaction of sodium borohydride and related reagents on some of the same compounds. We find that these reagents effect reductive elimination in fairly good yield with

Can. J. Chem. Downloaded from www.nrcresearchpress.com by 210.87.254.5 on 09/05/12
For personal use only.

Can. J. Chem. Downloaded from www.nrcresearchpress.com by 210.87.254.5 on 09/05/12
For personal use only.

some substrates, but only in poor yield or not at all with others. For reasons which will be apparent from this account, the results are of only limited value for the purposes of our mechanistic study, but since our observations may perhaps have some application in organic synthesis, we hereby offer a brief summary of our findings.

Our study of this reaction under a variety of conditions and reagents is summarized in Table I. No particular attempt has been made to find the best reaction conditions. It is apparent that the stilbene dibromides reduce very readily and the *trans* cyclic dibromides fairly readily with sodium trimethoxyborohydride, but the aliphatic secondary dibromides only in poor yield. If one of the bromine atoms is primary virtually no reductive elimination is observed at all.

Brown (3) has suggested that sodium trimethoxyborohydride in solution readily establishes the following equilibrium:

$$4NaBH(OCH_3)_3 \rightleftharpoons NaBH_4 + 3NaB(OCH_3)_4.$$

On this basis the same reducing agent would be obtained if one were to mix the appropriate portions of sodium borohydride and sodium tetramethylborate. In a qualitative sense, at least, this was in fact found to be the case, as may be seen from Table I. The table also lists a few experiments with sodium borohydride by itself, in order to demonstrate the effect of adding sodium tetramethylborate. In general, sodium borohydride by itself does not effect the reductive elimination, though stilbene dibromide (which is readily reduced by a number of reducing agents) is converted to stilbene in good yield.

It should perhaps be pointed out that in many of the experiments listed in Table I, the low yields are not simply due to insufficient reaction time. In the reaction of the sodium borohydride – sodium tetramethylborate mixture with 1,2-dibromooctane, for example, the dibromide was entirely consumed and no 1-octene was formed. The fate of most of the material is not known. In order to check the possibility that some of it may have been converted to alkylboranes, the crude product from one run was treated with alkaline hydrogen peroxide. Only a small amount of 1-octanol (equivalent to about 11% of the starting material) was obtained; the mixture was not examined further.

For the purposes of mechanistic study we attempted to determine the kinetic order of these reductive eliminations. Using a 20-fold excess of sodium trimethoxyborohydride, the reaction did not show simple pseudo first-order kinetics, decelerating too quickly for such a system. With the sodium borohydride – sodium tetramethylborate mixture on the other hand, the reverse was observed; in at least one set of experiments the rate appeared to be *zero* order with respect to the dibromide. Unfortunately with both reducing agents, the results varied considerably from one batch of reducing agent to the next, though showing internally consistent results for each lot. Faced with both the somewhat narrow scope of the reaction and the difficulty of reproducing the kinetic results, we discontinued further rate studies.

Experimental

Unless specifically described below, the general techniques and methods of purification of solvents and preparation of compounds, were as described previously (1). Commercial diglyme (diethylene glycol dimethyl ether, supplied under the trade name Ansul Ether 141 by the Ansul Chemical Company) was distilled under reduced pressure first from sodium and then from lithium aluminium hydride. Woelm, grade I, neutral alumina was used for column chromatography. Commercial sodium borohydride (Metal Hydrides Inc.) on analysis by the method of Lyttle, *et al.* (4) gave assays of 84–88% $NaBH_4$. Recrystallization from diglyme as described by Brown, *et al.* (5) gave a material analyzing for 99% $NaBH_4$. Sodium trimethoxyborohydride was prepared from sodium hydride and methyl borate (6) and purified by dissolving in isopropylamine, filtering the solution through sintered glass and evaporating the solvent; analysis indicated 85–90% $NaBH(OMe)_3$. Sodium tetramethylborate was prepared from methyl borate (supplied by Anderson Chemical Co.) and sodium methoxide (7).

1,2-Dibromooctane was prepared as follows. 1-Octene (15.9 g) in carbon tetrachloride (100 ml) was maintained at −10 to −20° while a solution of bromine (22.5 g) in carbon tetrachloride (150 ml) was added over a period of 2 h. The resulting solution was washed with dilute $NaHSO_3$, dilute KOH, and water, and then dried, and the solvent removed. Distillation under reduced pressure gave 1,2-dibromooctane, b.p. 48–50° (2 mm), n_D^{25} 1.4950. Similarly prepared were 2,3-dibromo-2-methylbutane (b.p. 48–50° at 15 mm, n_D^{25} 1.5100) and 2,3-dibromo-2,3-dimethylbutane (m.p. 175–176° in a sealed capillary tube). *trans*-2-Bromocyclohexyl tosylate was prepared from the reaction of the alcohol and *p*-toluenesulfonyl chloride in pyridine, m.p. 44–46°, reported m.p. 44–45° (8). 5α,6β-Dibromocholestane was prepared from cholest-5-ene by the method of Grob and Winstein (9). After recrystallization from ether–methanol it melted at 94–95°, $[\alpha]_D$ −36°; the reported melting points are 95–96° and 109.5°, $[\alpha]_D$ −40° (9).

The experimental procedures for the reactions summarized in Table I are illustrated by the specific examples described below. Much more detailed descriptions of the other experiments are given elsewhere (10, 11).

Can. J. Chem. Downloaded from www.nrcresearchpress.com by 210.87.254.5 on 09/05/12
For personal use only.

TABLE I

Reaction of sodium trimethoxyborohydride and related reducing agents on vicinal dibromides

Substrate	Reducing agent	Olefinic product	Percentage yield	Reaction conditions
meso-Stilbene dibromide	$NaBH(OMe)_3$	*trans*-Stilbene	72	Diglyme, 15 min at 25°
dl-Stilbene dibromide	$NaBH(OMe)_3$	*trans*-Stilbene	70	Diglyme, 1 h at 25°
meso-Stilbene dibromide	$NaBH_4$	*trans*-Stilbene	95	Diglyme, 15 min at 25°
dl-Stilbene dibromide	$NaBH_4$	*cis*-Stilbene, *trans*-Stilbene (1:3)	39	Diglyme, 30 min at 25°
2β,3α-Dibromo-5α-cholestane	$NaBH(OMe)_3$	5α-Cholest-2-ene	81	Diglyme, 2.75 h at 100°
2β,3α-Dibromo-5α-cholestane	$NaBH(OMe)_3$	5α-Cholest-2-ene*	45	Dioxane, 30 min at 135°
2β,3α-Dibromo-5α-cholestane	$NaBH_4$	5α-Cholest-2-ene	10	Diglyme, 11 h at 85°
2β,3α-Dibromo-5α-cholestane	$NaBH_4$:$NaB(OMe)_4$–1:3	5α-Cholest-2-ene	73	Diglyme, 2 h at 100°
2α,3β-Dibromo-5α-cholestane	$NaBH(OMe)_3$	5α-Cholest-2-ene†	50	Dioxane, 20 h at 135°
2β-Bromo-5α-cholestan-3α-yl tosylate	$NaBH(OMe)_3$	5α-Cholest-2-ene‡	15	Dioxane, 11 h at 135°
5α,6β-Dibromocholestan-3β-ol	$NaBH(OMe)_3$	Cholesterol	80	Diglyme, 24 h at 25°
5α,6β-Dibromocholestane	$NaBH(OMe)_3$	Cholest-5-ene	80	Diglyme, 24 h at 25°
trans-1,2-Dibromocyclohexane	$NaBH(OMe)_3$	Cyclohexene	79	Diglyme, 24 h at 100°
trans-1,2-Dibromocyclohexane	$NaBH(OMe)_3$	Cyclohexene	56	Tetrahydrofuran, 24 h at 75°
trans-1,2-Dibromocyclohexane	$NaBH(OMe)_3$	Cyclohexene	30	Dioxane, 24 h at 100°
trans-1,2-Dibromocyclohexane	$NaBH_4$	Cyclohexene	0	Diglyme, 12 h at 110°
trans-1,2-Dibromocyclohexane	$NaBH_4$:$NaB(OMe)_4$–1:3	Cyclohexene	71	Diglyme, 24 h at 100°
trans-1,2-Dibromocyclohexane	$NaBH_4$:$NaB(OMe)_4$–1:3	Cyclohexene	55	Diglyme, 2 h at 110°
trans-2-Bromocyclohexyl tosylate	$NaBH(OMe)_3$	Cyclohexene	10	Tetrahydrofuran, 24 h at 75°
meso-2,3-Dibromobutane	$NaBH(OMe)_3$	*trans*-2-Butene, *cis*-2-Butene (9:1)	12	Tetrahydrofuran, 24 h at 100°
meso-2,3-Dibromobutane	$NaBH(OMe)_3$	*trans*-2-Butene	21	Dioxane, 10.5 h at 100°
dl-2,3-Dibromobutane	$NaBH(OMe)_3$	*cis*-2-Butene, *trans*-2-Butene (58:42)	5	Tetrahydrofuran, 24 h at 100°
dl-2,3-Dibromobutane	$NaBH(OMe)_3$	*cis*-2-Butene, *trans*-2-Butene (56:44)	8	Dioxane, 10.5 h at 100°
2,3-Dibromo-2-methylbutane	$NaBH(OMe)_3$	2-Methyl-2-butene	23	Diglyme, 24 h at 90°
1,2-Dibromooctane	$NaBH(OMe)_3$	1-Octene	Trace	Dioxane, 48 h at 100°
1,2-Dibromooctane	$NaBH_4$:$NaB(OMe)_4$–1:3	1-Octene	0	Diglyme, 30 min at 110°
Ethylene dibromide	$NaBH(OMe)_3$	Ethylene	0	Dioxane, 47 h at 100°
Ethylene dibromide	$NaBH_4$	Ethylene	0	Diglyme, 1.5 h at 60°
2,3-Dimethyl-2,3-dibromo butane	$NaBH_4$:$NaB(OMe)_4$–1:3	Tetramethylethylene	60	Diglyme, 20 min at 110°

*Reaction product contained ~30% unreacted starting material and ~25% 2α,3β-dibromo-5α-cholestane, the diaxial → diequatorial rearrangement product (cf. reference 2).
†Reaction product contained about 50% unreacted starting material.
‡Remainder of product appeared from the infrared spectrum to be 3β-bromo-5α-cholestan-2α-yl tosylate, the diaxial → diequatorial rearrangement product (cf. reference 2).

Reduction of 2β,3α-Dibromo-5α-cholestane with Sodium Trimethoxyborohydride

The dibromide (57 mg) was heated with sodium trimethoxyborohydride (50 mg) in diglyme (5 ml) at 100° in a sealed tube for 2¾ h. The reaction mixture was poured into acidified water and extracted with ether; the ether extracts were washed with dilute sodium bicarbonate solution and water, dried, and the solvent evaporated. Thin-layer chromatography (t.l.c.) using petroleum ether as the developing solvent showed the product to consist mainly of cholest-2-ene together with small amounts of starting material and of the corresponding diequatorial dibromide. Column chromatography on alumina, eluting with petroleum ether, gave cholest-2-ene (32 mg), crystallized from ether–methanol, m.p. 72°.

Reduction of trans-1,2-Dibromocyclohexane with Sodium Trimethoxyborohydride

A solution of the dibromide (0.97 g) and the hydride (2.6 g) in diglyme (25 ml) was heated at 100 °C for 24 h. Benzene (10 ml) was added to the reaction solution which was then distilled in a stream of nitrogen at 100°, to distil off the volatile components. The resulting distillate was made up to 25 ml in a graduated flask and analyzed by vapor-phase chromatography. Comparison of the peak area of cyclohexene in the product solution to the peak areas of standard solutions of cyclohexene in benzene showed a yield of 79% of cyclohexene.

Reduction of 2β,3α-Dibromo-5α-cholestane with Sodium Borohydride – Sodium Tetramethylborate Mixture

The dibromide (52 mg) was heated for 2 h, at 100°, in a sealed tube with a mixture of sodium borohydride (10 mg) and sodium tetramethylborate (40 mg) in diglyme (5 ml). Thin-layer chromatography (developing with petroleum ether) showed the product (35 mg) to be mainly cholest-2-ene together with traces of starting material and 2α:3β-dibromo-5α-cholestane. Column chromatography on alumina, eluting with petroleum ether, gave cholest-2-ene (27 mg), which on recrystallization from ether–methanol melted at 71–73°.

Reaction of 1,2-Dibromooctane with Sodium Borohydride – Sodium Tetramethylborate Mixture

The dibromide (2.24 g) together with sodium borohydride (0.4 g) and sodium tetramethylborate (4.8 g) in diglyme (100 ml) was heated at 110°, in a sealed tube, for 2½ h. The contents of the tube were transferred to a round-bottomed flask equipped with a reflux condenser and dropping funnel. Water (20 ml), and when reaction ceased, 50 ml of 3 *N* sodium hydroxide solution were added followed by 25 ml of 30% hydrogen peroxide. The reaction mixture was stirred for 1 h at room temperature, and then sodium hydroxide pellets were added. Addition of ether resulted in the separation of two layers; the ether layer was removed, washed with water, dried, and made up to 100 ml in a graduated flask. This solution was analyzed by vapor-phase chromatography on propylene carbonate at 50°. 1-Octanol to the extent of 11.5% was detected, but no dibromide or 1-octene was found.

Acknowledgments

This work was supported by grants-in-aid and a studentship from the National Research Council of Canada, and by a Province of Ontario graduate fellowship.

1. J. F. KING and R. G. PEWS. Can. J. Chem. **42**, 1294 (1964).
2. J. F. KING and R. G. PEWS. Can. J. Chem. **43**, 847 (1965).
3. H. C. BROWN, E. J. MEAD, and P. A. TIERNEY. J. Am. Chem. Soc. **79**, 5400 (1957).
4. D. A. LYTTLE, E. H. JENSEN, and W. A. STRUCK. Anal. Chem. **24**, 1843 (1952).
5. H. C. BROWN, E. J. MEAD, and B. C. SUBBA RAO. J. Am. Chem. Soc. **77**, 6209 (1955).
6. H. C. BROWN, H. I. SCHLESINGER, I. SHEFT, and D. M. RITTER. J. Am. Chem. Soc. **75**, 192 (1953).
7. H. C. BROWN and E. J. MEAD. J. Am. Chem. Soc. **78**, 3614 (1956).
8. S. J. CRISTOL, J. Q. WEBER, and M. C. BRINDELL. J. Am. Chem. Soc. **78**, 598 (1956).
9. C. A. GROB and S. WINSTEIN. Helv. Chim. Acta, **35**, 782 (1952).
10. A. D. ALLBUTT. Ph.D. Thesis. University of Western Ontario, London, Ontario. 1967. pp. 152–202.
11. R. G. PEWS. Ph.D. Thesis, University of Western Ontario, London, Ontario. 1963. pp. 51–56 and 113–117.

The measurement of angles and distances in molecular models. II.[1] A device for the benzene ring

J. W. APSIMON

Department of Chemistry, Carleton University, Ottawa, Canada

Received October 19, 1967

A measuring device which is useful for attachment to the benzene ring unit of Dreiding models and which could be useful for the location of distant groups is described.

Canadian Journal of Chemistry, **46**, 808 (1968)

During our work on the long range shielding effects of anisotropic groups in the nuclear magnetic resonance spectra of terpenes and steroids (1–4), it became necessary to develop a method of locating distant groups reproducibly from the anisotropic group in Dreiding molecular models (5).

I wish to report here the extension of our

[1]For Part I, see J. W. ApSimon, P. V. Demarco, and A. Raffler. Chem. Ind. London, 1792 (1966).

Can. J. Chem. Downloaded from www.nrcresearchpress.com by 210.87.254.5 on 09/05/12
For personal use only.

Reduction of 2β,3α-Dibromo-5α-cholestane with Sodium Trimethoxyborohydride

The dibromide (57 mg) was heated with sodium trimethoxyborohydride (50 mg) in diglyme (5 ml) at 100° in a sealed tube for 2¾ h. The reaction mixture was poured into acidified water and extracted with ether; the ether extracts were washed with dilute sodium bicarbonate solution and water, dried, and the solvent evaporated. Thin-layer chromatography (t.l.c.) using petroleum ether as the developing solvent showed the product to consist mainly of cholest-2-ene together with small amounts of starting material and of the corresponding diequatorial dibromide. Column chromatography on alumina, eluting with petroleum ether, gave cholest-2-ene (32 mg), crystallized from ether–methanol, m.p. 72°.

Reduction of trans-1,2-Dibromocyclohexane with Sodium Trimethoxyborohydride

A solution of the dibromide (0.97 g) and the hydride (2.6 g) in diglyme (25 ml) was heated at 100 °C for 24 h. Benzene (10 ml) was added to the reaction solution which was then distilled in a stream of nitrogen at 100°, to distil off the volatile components. The resulting distillate was made up to 25 ml in a graduated flask and analyzed by vapor-phase chromatography. Comparison of the peak area of cyclohexene in the product solution to the peak areas of standard solutions of cyclohexene in benzene showed a yield of 79% of cyclohexene.

Reduction of 2β,3α-Dibromo-5α-cholestane with Sodium Borohydride – Sodium Tetramethylborate Mixture

The dibromide (52 mg) was heated for 2 h, at 100°, in a sealed tube with a mixture of sodium borohydride (10 mg) and sodium tetramethylborate (40 mg) in diglyme (5 ml). Thin-layer chromatography (developing with petroleum ether) showed the product (35 mg) to be mainly cholest-2-ene together with traces of starting material and 2α:3β-dibromo-5α-cholestane. Column chromatography on alumina, eluting with petroleum ether, gave cholest-2-ene (27 mg), which on recrystallization from ether–methanol melted at 71–73°.

Reaction of 1,2-Dibromooctane with Sodium Borohydride – Sodium Tetramethylborate Mixture

The dibromide (2.24 g) together with sodium borohydride (0.4 g) and sodium tetramethylborate (4.8 g) in diglyme (100 ml) was heated at 110°, in a sealed tube, for 2½ h. The contents of the tube were transferred to a round-bottomed flask equipped with a reflux condenser and dropping funnel. Water (20 ml), and when reaction ceased, 50 ml of 3 *N* sodium hydroxide solution were added followed by 25 ml of 30% hydrogen peroxide. The reaction mixture was stirred for 1 h at room temperature, and then sodium hydroxide pellets were added. Addition of ether resulted in the separation of two layers; the ether layer was removed, washed with water, dried, and made up to 100 ml in a graduated flask. This solution was analyzed by vapor-phase chromatography on propylene carbonate at 50°. 1-Octanol to the extent of 11.5% was detected, but no dibromide or 1-octene was found.

Acknowledgments

This work was supported by grants-in-aid and a studentship from the National Research Council of Canada, and by a Province of Ontario graduate fellowship.

1. J. F. King and R. G. Pews. Can. J. Chem. **42**, 1294 (1964).
2. J. F. King and R. G. Pews. Can. J. Chem. **43**, 847 (1965).
3. H. C. Brown, E. J. Mead, and P. A. Tierney. J. Am. Chem. Soc. **79**, 5400 (1957).
4. D. A. Lyttle, E. H. Jensen, and W. A. Struck. Anal. Chem. **24**, 1843 (1952).
5. H. C. Brown, E. J. Mead, and B. C. Subba Rao. J. Am. Chem. Soc. **77**, 6209 (1955).
6. H. C. Brown, H. I. Schlesinger, I. Sheft, and D. M. Ritter. J. Am. Chem. Soc. **75**, 192 (1953).
7. H. C. Brown and E. J. Mead. J. Am. Chem. Soc. **78**, 3614 (1956).
8. S. J. Cristol, J. Q. Weber, and M. C. Brindell. J. Am. Chem. Soc. **78**, 598 (1956).
9. C. A. Grob and S. Winstein. Helv. Chim. Acta, **35**, 782 (1952).
10. A. D. Allbutt. Ph.D. Thesis. University of Western Ontario, London, Ontario. 1967. pp. 152–202.
11. R. G. Pews. Ph.D. Thesis, University of Western Ontario, London, Ontario. 1963. pp. 51–56 and 113–117.

The measurement of angles and distances in molecular models. II.[1] A device for the benzene ring

J. W. ApSimon

Department of Chemistry, Carleton University, Ottawa, Canada

Received October 19, 1967

A measuring device which is useful for attachment to the benzene ring unit of Dreiding models and which could be useful for the location of distant groups is described.

Canadian Journal of Chemistry, **46**, 808 (1968)

During our work on the long range shielding effects of anisotropic groups in the nuclear magnetic resonance spectra of terpenes and steroids (1–4), it became necessary to develop a method of locating distant groups reproducibly from the anisotropic group in Dreiding molecular models (5).

I wish to report here the extension of our

[1]For Part I, see J. W. ApSimon, P. V. Demarco, and A. Raffler. Chem. Ind. London, 1792 (1966).

Can. J. Chem. Downloaded from www.nrcresearchpress.com by 210.87.254.6 on 09/05/12
For personal use only.

Can. J. Chem. Downloaded from www.nrcresearchpress.com by 210.87.254.6 on 09/05/12
For personal use only.

PLATE I

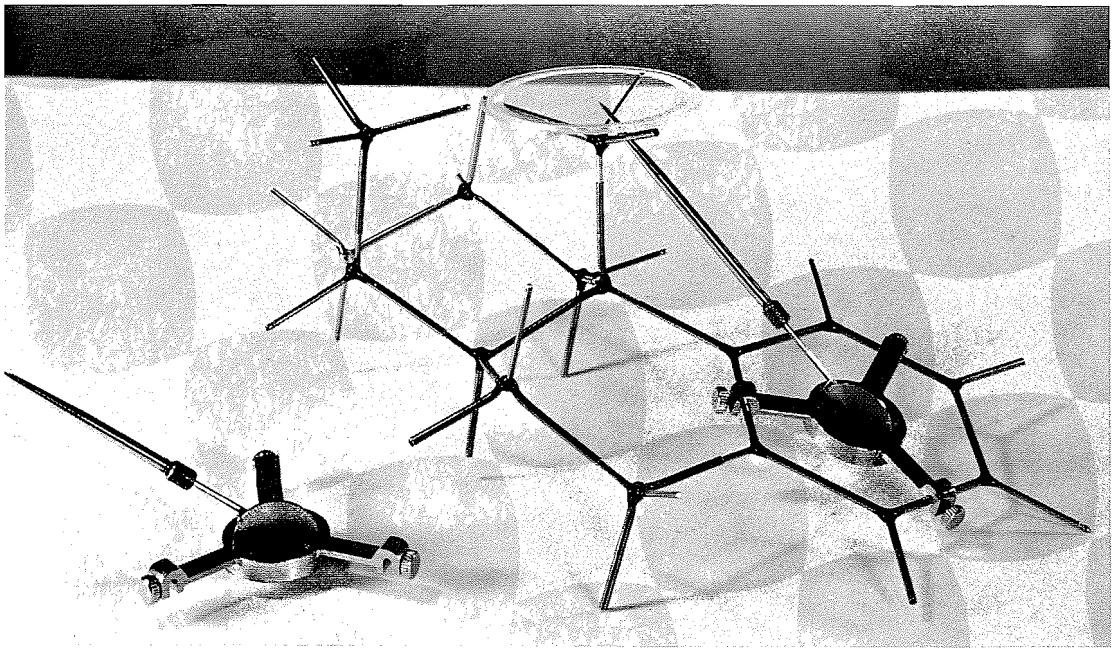

Can. J. Chem. Downloaded from www.nrcresearchpress.com by 210.87.254.6 on 09/05/12
For personal use only.

PLATE I

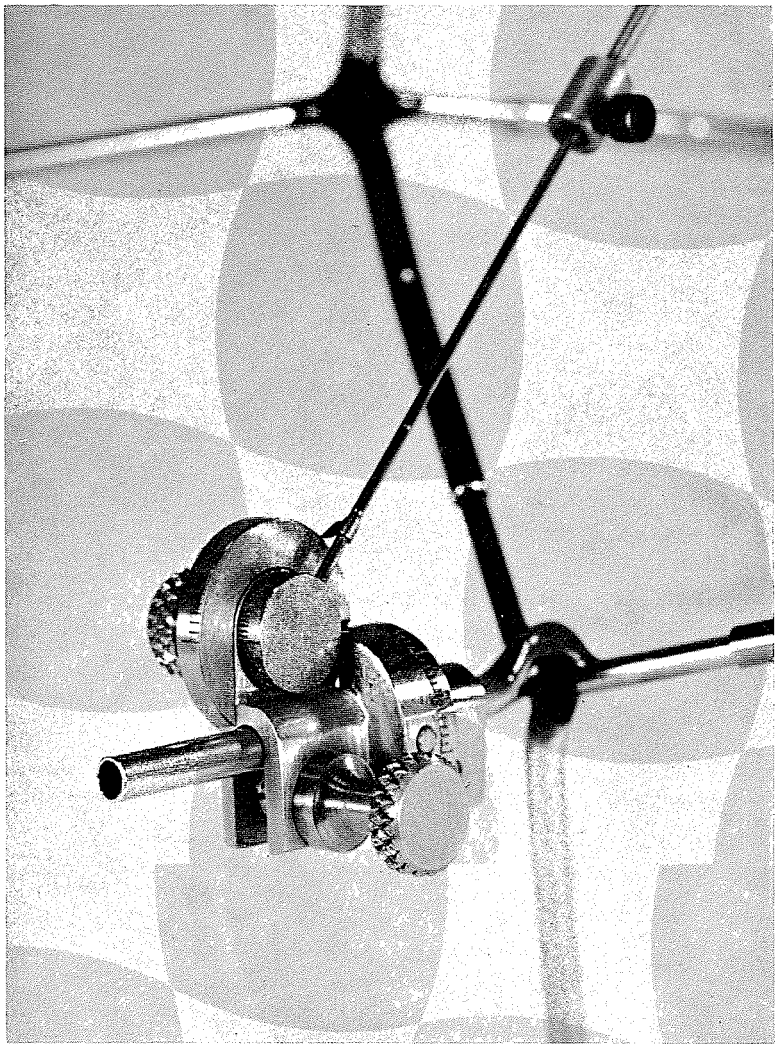

Can. J. Chem. Downloaded from www.nrcresearchpress.com by 210.87.254.6 on 09/05/12
For personal use only.

Can. J. Chem. Downloaded from www.nrcresearchpress.com by 210.87.254.6 on 09/05/12
For personal use only.

PLATE II

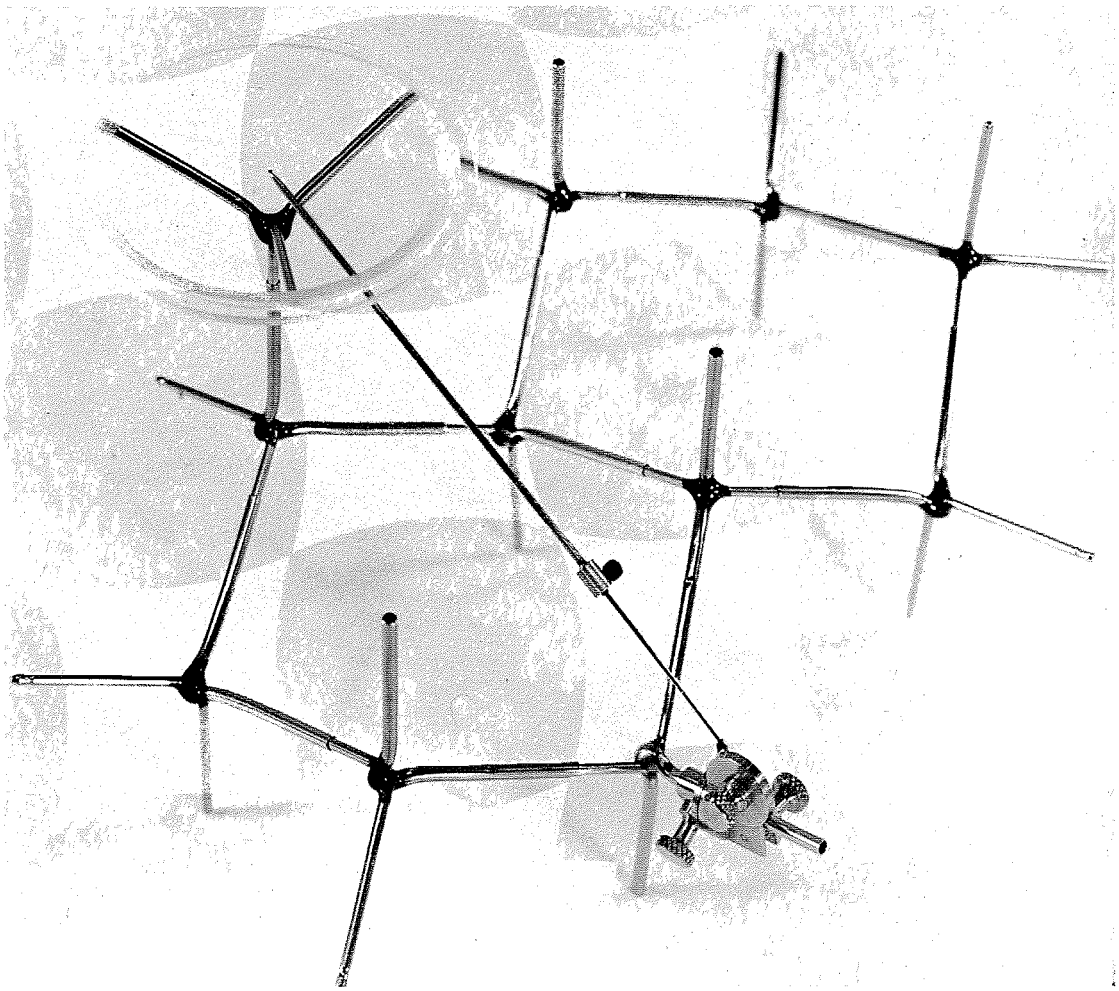

earlier idea (6) to the benzene ring. The protractor and distance measuring device has the same basic design as described before (6) except that three locating arms form part of the base plate of the unit. These arms are arranged so that the unit is automatically centered in the benzene ring on tightening set screws at the ends. The center of the benzene ring then corresponds to the pivot point of the measuring arm. Plate I illustrates the complete device both separately and installed in a model of a ring-C aromatic diterpene. The location of a distant methyl group is then a simple matter; the angles and distance required (6) are readily obtained.

This device can be used readily in the application of Johnson and Bovey's (7) approach to the shielding effects of aromatic systems, and could possibly be of use in the study of solvent effects in nuclear magnetic resonance spectra (8, 9). Working drawings are available from the author.

Acknowledgments

The contributions of Messrs. A. A. Raffler and S. Szick, Science Workshop, Carleton University, are greatly appreciated in the fabrication of this device. I wish to thank the National Research Council of Canada for generous financial support.

1. J. W. ApSimon, W. G. Craig, P. V. Demarco, D. W. Mathieson, L. Saunders, and W. B. Whalley. Tetrahedron, **23**, 2339 (1967).
2. J. W. ApSimon, W. G. Craig, P. V. Demarco, D. W. Mathieson, L. Saunders, and W. B. Whalley. Tetrahedron, **23**, 2359 (1967).
3. J. W. ApSimon, W. G. Craig, P. V. Demarco, D. W. Mathieson, and W. B. Whalley. Tetrahedron, **23**, 2375 (1967).
4. J. W. ApSimon, W. G. Craig, P. V. Demarco, D. W. Mathieson, A. K. G. Nasser, L. Saunders, and W. B. Whalley. Chem. Commun. 754 (1966).
5. A. Dreiding. Helv. Chim. Acta, **42**, 1339 (1959).
6. J. W. ApSimon, P. V. Demarco, and A. Raffler. Chem. Ind. London, 1792 (1966).
7. C. E. Johnson and F. A. Bovey. J. Chem. Phys. **29**, 1012 (1958).
8. D. H. Williams and D. A. Wilson. J. Chem. Soc. (B), 144 (1966).
9. J. Ronayne and D. H. Williams. J. Chem. Soc. (B), 540 (1967).

The measurement of angles and distances in molecular models. III.[1] A general device

J. W. ApSimon, W. G. Craig, A. Demayo, and A. A. Raffler[2]

Department of Chemistry and Science Workshop, Carleton University, Ottawa, Canada

Received October 19, 1967

A measuring device which can be attached to any bond of Dreiding molecular models for the estimation of angles and distances is described.

Canadian Journal of Chemistry, 46, 809 (1968)

As a continuation of our studies on the effect of anisotropic groups on long range shielding in the nuclear magnetic resonance spectra of diterpenes and steroids (1–4), we have developed measuring devices for use with Dreiding molecular models[1] (5). We now wish to report a unit which, contrary to our previous units[1] (5) which were only of use with specific functional groups, can be used for any bond in these models.

This device is shown in plates I and II and consists of two basic interlocking units. The first piece is locked onto the bond of the Dreiding model at the required position. Location is easy if the model unit being used is first scribed for easy placement of the measuring device. The locking unit is an eccentric cam operated by rotation of the knurled knobs seen in the plates. The stationary unit of the device is calibrated in 5° intervals.

The second unit is the rotatable portion of the model and it locks into the first unit. It can be locked on the bond in the same manner and can be rotated around the longitudinal axis of the bond. A scribe mark on this piece gives a reading of the angle of rotation, though a zero point has to be chosen as the vertical plane through the bond under investigation. Attached to this portion of the model is another scale for measurement of the angle of rotation of the locating

[1]For Part II, see J. W. ApSimon. Can. J. Chem. This issue.

[2]Science Workshop, Carleton University.

Can. J. Chem. Downloaded from www.nrcresearchpress.com by 210.87.254.6 on 09/05/12
For personal use only.

earlier idea (6) to the benzene ring. The protractor and distance measuring device has the same basic design as described before (6) except that three locating arms form part of the base plate of the unit. These arms are arranged so that the unit is automatically centered in the benzene ring on tightening set screws at the ends. The center of the benzene ring then corresponds to the pivot point of the measuring arm. Plate I illustrates the complete device both separately and installed in a model of a ring-C aromatic diterpene. The location of a distant methyl group is then a simple matter; the angles and distance required (6) are readily obtained.

This device can be used readily in the application of Johnson and Bovey's (7) approach to the shielding effects of aromatic systems, and could possibly be of use in the study of solvent effects in nuclear magnetic resonance spectra (8, 9). Working drawings are available from the author.

Acknowledgments

The contributions of Messrs. A. A. Raffler and S. Szick, Science Workshop, Carleton University, are greatly appreciated in the fabrication of this device. I wish to thank the National Research Council of Canada for generous financial support.

1. J. W. ApSimon, W. G. Craig, P. V. Demarco, D. W. Mathieson, L. Saunders, and W. B. Whalley. Tetrahedron, **23**, 2339 (1967).
2. J. W. ApSimon, W. G. Craig, P. V. Demarco, D. W. Mathieson, L. Saunders, and W. B. Whalley. Tetrahedron, **23**, 2359 (1967).
3. J. W. ApSimon, W. G. Craig, P. V. Demarco, D. W. Mathieson, and W. B. Whalley. Tetrahedron, **23**, 2375 (1967).
4. J. W. ApSimon, W. G. Craig, P. V. Demarco, D. W. Mathieson, A. K. G. Nasser, L. Saunders, and W. B. Whalley. Chem. Commun. 754 (1966).
5. A. Dreiding. Helv. Chim. Acta, **42**, 1339 (1959).
6. J. W. ApSimon, P. V. Demarco, and A. Raffler. Chem. Ind. London, 1792 (1966).
7. C. E. Johnson and F. A. Bovey. J. Chem. Phys. **29**, 1012 (1958).
8. D. H. Williams and D. A. Wilson. J. Chem. Soc. (B), 144 (1966).
9. J. Ronayne and D. H. Williams. J. Chem. Soc. (B), 540 (1967).

The measurement of angles and distances in molecular models. III.[1] A general device

J. W. ApSimon, W. G. Craig, A. Demayo, and A. A. Raffler[2]

Department of Chemistry and Science Workshop, Carleton University, Ottawa, Canada

Received October 19, 1967

A measuring device which can be attached to any bond of Dreiding molecular models for the estimation of angles and distances is described.

Canadian Journal of Chemistry, 46, 809 (1968)

As a continuation of our studies on the effect of anisotropic groups on long range shielding in the nuclear magnetic resonance spectra of diterpenes and steroids (1–4), we have developed measuring devices for use with Dreiding molecular models[1] (5). We now wish to report a unit which, contrary to our previous units[1] (5) which were only of use with specific functional groups, can be used for any bond in these models.

This device is shown in plates I and II and consists of two basic interlocking units. The first piece is locked onto the bond of the Dreiding model at the required position. Location is easy if the model unit being used is first scribed for easy placement of the measuring device. The locking unit is an eccentric cam operated by rotation of the knurled knobs seen in the plates. The stationary unit of the device is calibrated in 5° intervals.

The second unit is the rotatable portion of the model and it locks into the first unit. It can be locked on the bond in the same manner and can be rotated around the longitudinal axis of the bond. A scribe mark on this piece gives a reading of the angle of rotation, though a zero point has to be chosen as the vertical plane through the bond under investigation. Attached to this portion of the model is another scale for measurement of the angle of rotation of the locating

[1]For Part II, see J. W. ApSimon. Can. J. Chem. This issue.

[2]Science Workshop, Carleton University.

Can. J. Chem. Downloaded from www.nrcresearchpress.com by 210.87.254.40 on 09/05/12
For personal use only.

pointer; this is locked by a screw and the pointer can be extended to the distant group under consideration.

To date, this device has two disadvantages: firstly, its size makes manipulation an acquired art and the reading of the graduated scales is best performed with the aid of a watchmaker's lens; second, and probably more serious, the center of rotation of the pointer is not on the axis of the bond to which the device is attached (see plates). In our cases this is immaterial since the distant group is still located unequivocally from the bond under study, but, should the actual distances be required, it is simply a matter of solid geometry to convert the observed readings to those desired.[3]

Besides being of use in anisotropy studies, this unit could have use in the assessment of dihedral angles (6) by visually lining up the pointer with the bonds in question and measuring the angle of rotation. Working drawings are available from the first named author and we hope to report improvements in design in the future.

[3]A computer program performing this operation is available from the first named author.

Acknowledgments

We thank the National Research Council of Canada for generous support of this work and Mr. Steven Szick for his craftsmanship in the fabrication of these devices.

1. J. W. ApSimon, W. G. Craig, P. V. Demarco, D. W. Mathieson, L. Saunders, and W. B. Whalley. Tetrahedron, **23**, 2339 (1967).
2. J. W. ApSimon, W. G. Craig, P. V. Demarco, D. W. Mathieson, L. Saunders, and W. B. Whalley. Tetrahedron, **23**, 2359 (1967).
3. J. W. ApSimon, W. G. Craig, P. V. Demarco, D. W. Mathieson, and W. B. Whalley. Tetrahedron, **23**, 2375 (1967).
4. J. W. ApSimon, W. G. Craig, P. V. Demarco, D. W. Mathieson, A. K. G. Nasser, L. Saunders, and W. B. Whalley. Chem. Commun. 754 (1966).
5. J. W. ApSimon, P. V. Demarco, and A. Raffler. Chem. Ind. London, 1792 (1966).
6. M. Karplus. J. Am. Chem. Soc. **85**, 2870 (1963).

Nuclear magnetic resonance spectra of 2-pyrazolines

Wallace S. Brey, Jr. and Carmen M. Valencia
Department of Chemistry, University of Florida, Gainesville, Florida, 32601

Received July 17, 1967

The nuclear magnetic resonance spectral parameters for a series of 3-carbomethoxy-2-pyrazolines are presented and discussed. Substitution of a phenyl group at position-5 has a large effect on the relative chemical shift of the two protons at position-4, although a carbomethoxy group at position-5 has little effect. The *cis* and *trans* vicinal coupling constants in compounds with two protons in position-4 are nearly equal and differ from the values found when there is a substituent in position-4. The presence of three groups in positions-4 and -5 appears to hold the ring in a rigid conformation. The line width for the hydrogen attached to nitrogen depends upon the number of phenyl groups in position-5.

Canadian Journal of Chemistry, 46, 810 (1968)

Several previous studies have demonstrated the relationships of structure and configuration of 2-pyrazolines (1–3). In this investigation, we have obtained additional spectral information about a number of 2-pyrazolines containing a carbomethoxy group in position-3, together with various other substituents in positions-4 and -5. These materials were synthesized by Jones, Sanderfer, and Baarda (4).

The pyrazolines were dissolved in $CDCl_3$ to make nearly saturated solutions. Tetramethylsilane was used as internal reference. Spectra were obtained on a Varian DP-60 spectrometer, and peak positions were measured from audio side bands of which the frequency was determined by a frequency counter. The results are shown in Tables I and II. The ring hydrogen spectrum of compound **1** was of the A_2B type, and those of compounds **2** and **4** were analyzed as ABX patterns. Limited data were reported earlier for compounds **6** (2) and **7** (1).

The *cis* configuration of compound **6** is confirmed by the coupling constant between the protons on C-4 and C-5, which is 13.4 c.p.s., well into the range of 10–14 c.p.s. found by Hassner and Michelson (2) for the *cis* constant. In the

Can. J. Chem. Downloaded from www.nrcresearchpress.com by 210.87.254.40 on 09/05/12
For personal use only.

pointer; this is locked by a screw and the pointer can be extended to the distant group under consideration.

To date, this device has two disadvantages: firstly, its size makes manipulation an acquired art and the reading of the graduated scales is best performed with the aid of a watchmaker's lens; second, and probably more serious, the center of rotation of the pointer is not on the axis of the bond to which the device is attached (see plates). In our cases this is immaterial since the distant group is still located unequivocally from the bond under study, but, should the actual distances be required, it is simply a matter of solid geometry to convert the observed readings to those desired.[3]

Besides being of use in anisotropy studies, this unit could have use in the assessment of dihedral angles (6) by visually lining up the pointer with the bonds in question and measuring the angle of rotation. Working drawings are available from the first named author and we hope to report improvements in design in the future.

[3]A computer program performing this operation is available from the first named author.

Acknowledgments

We thank the National Research Council of Canada for generous support of this work and Mr. Steven Szick for his craftsmanship in the fabrication of these devices.

1. J. W. ApSimon, W. G. Craig, P. V. Demarco, D. W. Mathieson, L. Saunders, and W. B. Whalley. Tetrahedron, **23**, 2339 (1967).
2. J. W. ApSimon, W. G. Craig, P. V. Demarco, D. W. Mathieson, L. Saunders, and W. B. Whalley. Tetrahedron, **23**, 2359 (1967).
3. J. W. ApSimon, W. G. Craig, P. V. Demarco, D. W. Mathieson, and W. B. Whalley. Tetrahedron, **23**, 2375 (1967).
4. J. W. ApSimon, W. G. Craig, P. V. Demarco, D. W. Mathieson, A. K. G. Nasser, L. Saunders, and W. B. Whalley. Chem. Commun. 754 (1966).
5. J. W. ApSimon, P. V. Demarco, and A. Raffler. Chem. Ind. London, 1792 (1966).
6. M. Karplus. J. Am. Chem. Soc. **85**, 2870 (1963).

Nuclear magnetic resonance spectra of 2-pyrazolines

Wallace S. Brey, Jr. and Carmen M. Valencia
Department of Chemistry, University of Florida, Gainesville, Florida, 32601

Received July 17, 1967

The nuclear magnetic resonance spectral parameters for a series of 3-carbomethoxy-2-pyrazolines are presented and discussed. Substitution of a phenyl group at position-5 has a large effect on the relative chemical shift of the two protons at position-4, although a carbomethoxy group at position-5 has little effect. The *cis* and *trans* vicinal coupling constants in compounds with two protons in position-4 are nearly equal and differ from the values found when there is a substituent in position-4. The presence of three groups in positions-4 and -5 appears to hold the ring in a rigid conformation. The line width for the hydrogen attached to nitrogen depends upon the number of phenyl groups in position-5.

Canadian Journal of Chemistry, 46, 810 (1968)

Several previous studies have demonstrated the relationships of structure and configuration of 2-pyrazolines (1–3). In this investigation, we have obtained additional spectral information about a number of 2-pyrazolines containing a carbomethoxy group in position-3, together with various other substituents in positions-4 and -5. These materials were synthesized by Jones, Sanderfer, and Baarda (4).

The pyrazolines were dissolved in $CDCl_3$ to make nearly saturated solutions. Tetramethylsilane was used as internal reference. Spectra were obtained on a Varian DP-60 spectrometer, and peak positions were measured from audio side bands of which the frequency was determined by a frequency counter. The results are shown in Tables I and II. The ring hydrogen spectrum of compound **1** was of the A_2B type, and those of compounds **2** and **4** were analyzed as ABX patterns. Limited data were reported earlier for compounds **6** (2) and **7** (1).

The *cis* configuration of compound **6** is confirmed by the coupling constant between the protons on C-4 and C-5, which is 13.4 c.p.s., well into the range of 10–14 c.p.s. found by Hassner and Michelson (2) for the *cis* constant. In the

Can. J. Chem. Downloaded from www.nrcresearchpress.com by 210.87.254.42 on 09/05/12
For personal use only.

TABLE I

Nuclear magnetic resonance shifts of protons in 2-pyrazolines

			Chemical shift in τ units				
	Substituents*		Ring protons			CH_3O group	
Compound	C-4	C-5	NH	C-4	C-5	at C-3	at C-4 or C-5
1	—	CH_3OOC—	4.10	6.75	5.49	6.24	6.19
2	—	CH_3O—C_6H_4—	3.75	6.74 7.17	5.09	6.25	6.22
3 (*trans*)	*p*Cl—C_6H_4—	CH_3OOC—	3.36	5.80	5.24	6.24	6.10
4	—	C_6H_5—	3.31	6.70 7.14	5.05	6.24	—
5 (*trans*)	C_6H_5—	C_6H_5—	3.27	5.77	5.16	6.39	—
6 (*cis*)	CH_3OOC—	C_6H_5—	3.12	5.74	4.69	6.24	6.85
7 (*trans*)	C_6H_5—	CH_3OOC—	3.04	5.77	5.23	6.29	6.21
8	—	2 C_6H_5—	—	6.45	—	6.24	—
9	CH_3OOC—	2 C_6H_5—	—	5.12	—	6.24	6.86

*Each compound has a CH_3OOC— group at position-3.

TABLE II

Magnitude of the coupling constants* in 2-pyrazolines

	Substituents				
Compound	C-4	C-5	J_{trans}	J_{cis}	J_{gem} C-4
3	*p*-ClC_6H_4—	CH_3OOC—	3.9	—	—
7	C_6H_5—	CH_3OOC—	4.0	—	—
5	C_6H_5—	C_6H_5—	6.5	—	—
1	—	CH_3OOC	8.5†	—	—
4	—	C_6H_5—	9.8	11.5	17.1
2	—	*p*-$CH_3OC_6H_4$—	10.5	11.2	16.9
6	CH_3OOC—	C_6H_5—	—	13.4	—

*Coupling constants in c.p.s.
†Average of J_{trans} and J_{cis}.

compounds **3**, **5**, and **7**, which have two protons *trans* to one another in positions-4 and -5, the coupling constants are much smaller, with values of 3.9 to 6.5. In those compounds with three ring protons, the two coupling constants turn out to be quite close to one another, 10.5 and 11.2 for **2**, and 9.8 and 11.5 for **4**, but the pairs of values are still close to the dividing line between expected values of J_{cis} and J_{trans}. For compound **1**, J_{cis} appeared equal to J_{trans}, but this may be the result of a deceptively simple spectrum.

The chemical shifts of the methyl groups in the carbomethoxy substituent groups follow the same trend as found in earlier work (1). Compounds **1**, **3**, and **7**, with the carbomethoxy substituent at position-5, have resonance peaks for the methyl groups at $\tau = 6.10$ to 6.21; in addition, all compounds have peaks at 6.24 to 6.39 for the group at position-3. The two highest shifts, 6.29 and 6.39, occur in molecules having a phenyl group at position-4. Inspection of models shows that the phenyl group is turned out of the plane of the ring so as to shield the methyl group at position-3, and that the extent of out-of-plane rotation is greater when position-5 also contains a phenyl group. For a carbomethoxy group in position-4 with a *cis* phenyl group in position-5, the methyl resonance is at very much higher field, near $\tau = 6.85$. This is again the result of molecular geometry which causes the methyl group to lie before the face of the phenyl group which is here also twisted considerably out of the molecular plane.

The equivalence of the chemical shift of the two protons at position-4 in compound **1** indicates that substitution of a carbomethoxy group at position-5 has no appreciable anisotropic effect on the chemical shift at the neighboring position. On the other hand, substitution of a phenyl group at position-5 does make the C-4 protons

Can. J. Chem. Downloaded from www.nrcresearchpress.com by 210.87.254.42 on 09/05/12
For personal use only.

nonequivalent, by an amount of about 0.4 p.p.m. The magnitude of the geminal coupling constants in **2** and **4** is characteristic for protons α to a double bond in five-membered rings (5).

For the NH group, there is a wide range of line width as well as some variation in chemical shift. In the absence of a phenyl group, the NH absorption is reasonably sharp; when one phenyl group is present at position-5, the NH resonance is somewhat broadened; and for compounds **8** and **9**, with two phenyl groups in this position, the resonance is not visible, presumably because of extensive broadening. Such broadening could be a consequence of modified exchange rate of the proton attached to nitrogen when a phenyl group is present on the adjacent carbon atom, but it seems more reasonable to attribute it to a specific effect of motions of the phenyl group on the relaxation of the nitrogen nucleus which in turn is transmitted to the attached proton.

In compound **6**, the *cis*-disubstituted material, the resonance of the proton attached to C-5 shows an additional doubling of 2.1 c.p.s., evidently due to coupling to the hydrogen attached to nitrogen. Examination of a space-filling model indicates a rigid conformation for this molecule, and the appearance of coupling in the spectrum is apparently the result of the absence of ring inversion.

Acknowledgment

This research was supported by U.S. Public Health Service Grant GM-09343.

1. W. S. Brey, Jr. and W. M. Jones. J. Org. Chem. **26**, 1912 (1961).
2. A. Hassner and M. J. Michelson. J. Org. Chem. **27**, 3974 (1962).
3. J. Elguero and R. Jacquier. Tetrahedron Letters, 1175 (1965).
4. W. M. Jones, P. O. Sanderfer, and D. G. Baarda. J. Org. Chem. **32**, 1367 (1967).
5. R. C. Cookson, T. A. Crabb, J. J. Frankel, and J. Hudec. Tetrahedron, Suppl. No. 7, 355 (1967).

Erratum: Carbonyl-bridged and related compounds. Structural assignments by nuclear magnetic resonance spectroscopy

C. F. H. Allen
Chemistry Department, Rochester Institute of Technology, Rochester, New York

Received November 3, 1967
(Ref.: Can. J. Chem. **45**, 1201 (1967))

Canadian Journal of Chemistry, 46, 812 (1968)

On p. 1201, column 2, lines 16 and 17 read:

$J_{5.4} = 2.6$ c/s.

This should be changed to read:

$J_{6.5} = 2.6$ c/s.

Can. J. Chem. Downloaded from www.nrcresearchpress.com by 210.87.254.42 on 09/05/12
For personal use only.

Can. J. Chem. Downloaded from www.nrcresearchpress.com by 210.87.254.105 on 09/05/12
For personal use only.

Carcinogenicity of lactones. II.[1] *x*-Ray crystal structure analyses of ±3-benzylamino-4-hydroxypentanoic acid lactone hydrochloride and hydrobromide

J. Bryan Jones, Chung Hoe Koo, Ian P. Mellor, S. C. Nyburg, and John M. Young
Lash Miller Chemical Laboratories, Department of Chemistry, University of Toronto, Toronto, Ontario

Received January 31, 1968

X-Ray crystal structure analysis of the hydrochloride of ±3-benzylamino-4-hydroxypentanoic acid lactone shows the methyl and benzylamino groups to be *trans*-oriented.

The hydrobromide is not isomorphous with the hydrochloride and its crystals are optically active owing to spontaneous resolution during crystallization. Refinement of both crystal structures is in progress.

Canadian Journal of Chemistry, **46**, 813 (1968)

In connection with studies designed to ascertain the nature of the cellular nucleophile which undergoes alkylation during the induction of cancer by certain lactones, the reaction of benzylamine with 4-hydroxypent-2-enoic acid lactone (β-angelicalactone, **1**) was carried out for model purposes. As expected, the Michael addition product **2** was obtained in good yield (1).

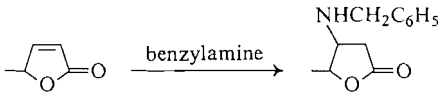

1 **2**

In order to give an indication of the stereochemistry of addition to be expected on alkylation of the cellular nucleophile by carcinogenic lactones such as **1**, it was considered desirable to determine the configuration of **2**. Indirect evidence suggesting a *trans*-orientation of the methyl and benzylamino groups had been presented by Lukes *et al.* (2), but in view of the biological importance of this point, an X-ray analysis of the hydrochloride of **2** has been carried out.

Colorless crystals of the racemate were obtained by recrystallization from methanol–ethanol. System: monoclinic, $a = 9.183(7)$, $b = 11.278(20)$, $c = 12.218(10)$ Å, $\beta = 101.3(1)°$. Space group $P2_1/c$. Density 1.29 g cm^{-3}, calculated as 1.304 for four formula units of $C_{12}H_{16}ClNO_2$ per cell. Phases of 2123 visually estimated independent reflections were assigned by the usual heavy-atom technique using CuKα radiation.

The results (Fig. 1) show unequivocally the *trans*-orientation of the methyl and benzylamino groups in the addition product **2**. The structure analysis is being refined by full-matrix anisotropic least squares procedure and the residual, *R*, stands at present at 0.12. Full details of the structure will appear elsewhere when the refinement is completed.

The observed stereochemistry is in agreement with that predicted from a consideration of the current concepts on the mechanism of the Michael reaction (3) in which perpendicular attack by the nucleophile on the least hindered side of the en-one system is considered to occur under conditions of thermodynamic control. Since none of the diastereomeric lactone **2** with *cis*-orientation of the methyl and benzylamino groups could be detected in the reaction mixture, it appears that the effect of the methyl group is sufficient to ensure that no significant proportion of *cis*-addition product remains in the final equilibrium mixture. In the absence of other orienting factors, the stereochemistry of the corresponding in vivo alkylation reactions should be similarly controlled.

We have also completed the structure analysis of the hydrobromide salt of **2**. System: monoclinic, $a = 6.61(1)$, $b = 10.82(3)$, $c = 9.05(2)$ Å, $\beta = 98.4(3)°$, with $Z = 2$ molecules per cell.

This salt, in which the methyl and benzylamino groups are also *trans*, was of interest

[1]For Part I of this series see ref. 1.

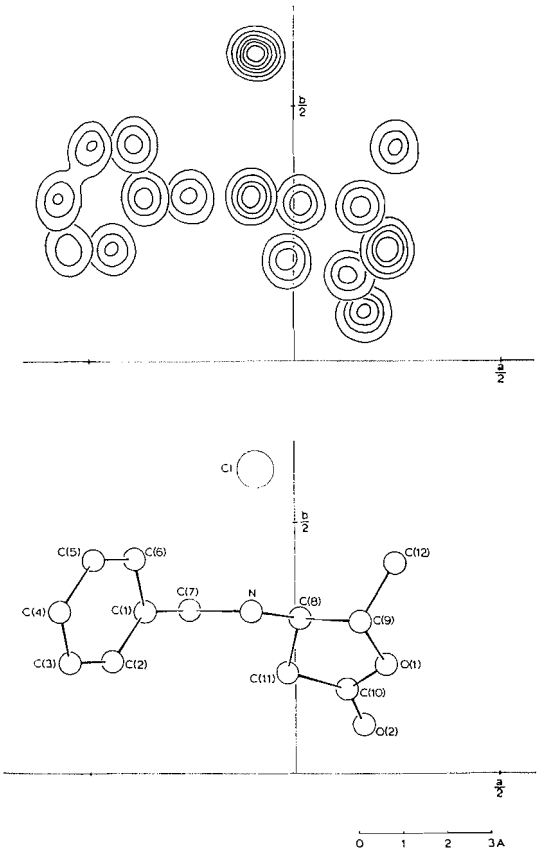

FIG. 1. Final electron density distribution and atomic numbering scheme for the hydrochloride of lactone **2**.

because it is not isomorphous with the chloride and this affords an opportunity to compare the organic moieties in the two compounds.

Our original space group assignment for the hydrobromide was *Pm* but weak $0k0$ reflections with k odd have been confirmed as multiple Renninger reflections. Accordingly, the space group appeared to be $P2_1$ and further refinement confirmed this. This would require the two molecules in any one crystal to be of the same enantiomorph and this, in turn, could only come about by spontaneous resolution on crystallization. Some eight, quite large, crystals were grown from methanol solution and optical rotatory dispersion curves on solutions of each confirmed their individual optical activity; four crystals gave plain positive curves, one crystal gave a plain negative curve, the other three gave too small a rotatory dispersion for a definite assignment. The aminolactone hydrobromide therefore represents yet another case (4) of spontaneous resolution of the positive and negative rotating forms of a racemic modification upon crystallization.

Detailed X-ray analyses of both the hydrochloride and the hydrobromide are being continued.

1. J. B. JONES and J. M. YOUNG. Can. J. Chem. **44**, 1059 (1966).
2. R. LUKES, Z. KOBLICOVA, and K. BLAHA. Coll. Czech. Chem. Commun. **28**, 2183 (1963).
3. E. L. ELIEL, N. L. ALLINGER, S. J. ANGYAL, and G. A. MORRISON. Conformational analysis. Interscience, New York. 1965. pp. 314–317.
4. K. FREUDENBERG. Stereochemie. Franz Deuticke, Leipzig. 1933. pp. 564. E. HAVINGA. Biochem. Biophys. Acta, **13**, 171 (1954).

Can. J. Chem. Downloaded from www.nrcresearchpress.com by 210.87.254.105 on 09/05/12
For personal use only.

Can. J. Chem. Downloaded from www.nrcresearchpress.com by 210.87.254.6 on 09/05/12
For personal use only.

Canadian Journal of Chemistry

Published by THE NATIONAL RESEARCH COUNCIL OF CANADA

VOLUME 46 MARCH 15, 1968 NUMBER 6

New calorimeter for measurement of the enthalpy of mixing of liquids. The enthalpy of mixing of benzene with carbon tetrachloride and of *n*-hexane with cyclohexane[1]

HARRY WATTS, E. C. W. CLARKE, AND D. N. GLEW

Exploratory Research Laboratory, Dow Chemical of Canada, Limited, Sarnia, Ontario

Received September 21, 1967

A high-precision, mixing calorimeter is described for the direct measurement of the enthalpy of liquid mixing under constant pressure conditions. Tests of the calorimeter using the benzene – carbon tetrachloride system at 25 °C show a reaction between mercury and carbon tetrachloride which leads to systematically high values for the heat of mixing. Tests with the *n*-hexane–cyclohexane system at 25 °C give a maximum enthalpy of mixing $\Delta_m h = 222.1_4 \pm 0.2_1$ J/mole at 0.586 cyclohexane mole fraction.

Canadian Journal of Chemistry, **46**, 815 (1968)

Introduction

As part of a study of the mixing properties of volatile nonelectrolytes with water and with deuterium oxide, a high-precision calorimeter has been constructed to measure the enthalpy of mixing of volatile aqueous systems under pressure in the absence of vapor spaces. While existing calorimeter designs were either unsuitable or of insufficient accuracy, general design recommendations for mixing calorimeters (1, 2) were followed, but, in addition, the calorimeter was designed to permit the determination of each experimental parameter to within 0.01% under best conditions. To achieve this, the basic design of Larkin and McGlashan (2) has been modified so that the mixing vessel can be (*a*) filled from a vacuum system, (*b*) weighed on an analytical balance, (*c*) operated under constant pressure, (*d*) stirred in a reproducible manner, and (*e*) operated semi-automatically to reduce the tedium of routine measurement without loss of accuracy.

Older measurements of the enthalpy of mixing of liquids were often subject to gross errors due to vapor spaces, which permitted evaporation or condensation of the mixing liquids, for which the parasitic latent heat changes were of similar magnitude to the mixing enthalpy changes being measured (1). Construction of modern calorimeters without vapor spaces provided high precision liquid-mixing enthalpy measurements (2–4), which may serve as liquid-mixing enthalpy standards for the comparison and assessment of mixing calorimeter performance. McGlashan has given criteria for the selection of suitable liquid-mixing pairs and has advocated use of the benzene – carbon tetrachloride (1) and the *n*-hexane–cyclohexane (5) systems. Tests of our calorimeter with the benzene – carbon tetrachloride system are of interest since they establish a reason for the discordant mixing enthalpy results obtained from recent careful investigations of this system (2, 6–8). Tests with the *n*-hexane–cyclohexane system provide new high-precision measurements for a possible liquid-mixing enthalpy standard.

Experimental

The Mixing Vessel

The mixing vessel shown in Fig. 1 is based on the design of Larkin and McGlashan (2), but includes several modifications. It is made of 347 stainless steel and is highly polished on both the internal and external surfaces. The body of the vessel 1 contains two compartments in which the liquids to be mixed are isolated over mercury with no vapor spaces. The base of the vessel 2, secured by six bolts, carries a slot in which the calibration heater is inserted. During the mixing process the calorimeter is tilted about the horizontal axis R—R to only 60° on either side of the

[1]Contribution No. 155.

Can. J. Chem. Downloaded from www.nrcresearchpress.com by 210.87.254.6 on 09/05/12
For personal use only.

vertical rest position, so that the liquids pass from one compartment to the other without contacting the Teflon gasket between 1 and 2. The calorimeter contains an expansion chamber 3, partly filled with mercury and sealed by a cap 4 to which Nylon pressure tubing 6 is connected. A constant gas pressure is maintained over the mercury through this tube. Mercury can flow between 1 and 3 via tube 14, whose lower end is always under mercury, to compensate for mixing volume changes.

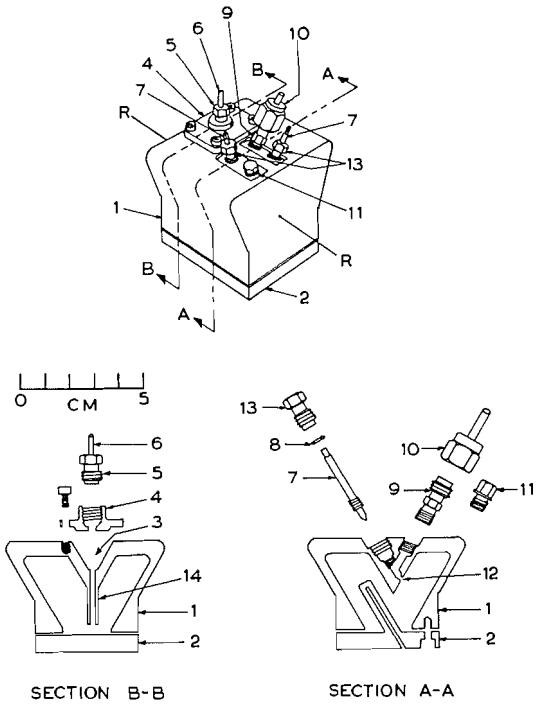

FIG. 1. Isometric and sectional views of mixing vessel: (1) body, (2) base, (3) expansion chamber, (4) chamber cap, (5) tube fitting nut, (6) Nylon pressure tubing, (7) needle valve stem, (8) Teflon O-ring, (9) Swagelok fitting and (10) nut, (11) plug, (12) valve seat, (13) valve packing nut, (14) tube, R—R axis of rotation.

The calorimeter is first evacuated through 6 to less than 10^{-4} Torr; freshly distilled mercury is then run in through 6. The calorimeter is connected to the liquid purification and storage system through coupling 9 and tube 10. Freshly distilled, degassed liquid admitted through the needle valve sealed with Teflon O-ring 8 displaces mercury through 14 into 3. The valve tip 12 is mercury sealed, since it remains under the mercury. The fitting 9 is then removed, the valve cavity filled with mercury, and plug 11 inserted. The valve is thus mercury sealed on the outside to prevent leaks during the mixing process when 12 is no longer covered by mercury on the inside. The amount of each liquid introduced (up to 6 ml) is found by weighing the calorimeter. The calorimeter when full of mercury weighs ~ 999 g; when charged with 5 ml of each liquid it weighs ~ 860 g. The heat capacity of the calorimeter is ~ 400 J/deg.

The Filling System

Figure 2 shows part of the system used to charge the mixing vessel. All storage vessels are pyrex glass and the connecting tubing is 316 stainless steel; Swagelok fittings with Teflon ferrules are used for all metal to glass connections and the control valves are Whitey 0KS2 and 1KS4 needle valves with Kel-F tips. The right hand section is for mercury purification. Mercury, washed successively with dilute aqueous potassium hydroxide, dilute nitric acid, and water, is filtered through a glass sinter 1 into a holding vessel 2 and then into a still 3. It is distilled through a condenser 4 into a receiver 5 and thence run into the calorimeter 6 via 7.

The left hand section beyond tube 16 is duplicated for the second liquid. Purified liquid is passed over an activated alumina column 8 when necessary to remove the last traces of water and the dry liquid is collected in 9. It is subsequently freeze-outgassed five times and vacuum distilled into the glass storage reservoir 10. Liquid is distilled from the reservoir to the graduated filling tube 11, where it is stored over mercury. The calorimeter is connected to 16 and evacuated to the calorimeter valves, and the filling line valve 12 is closed and 13 opened. Air pressure is applied to the two-way stopcock 14 with 15 open to force the liquid around to the calorimeter valve. The calorimeter valve is opened slightly to admit the liquid into the calorimeter. The approximate amount admitted is indicated by the change of the mercury level in

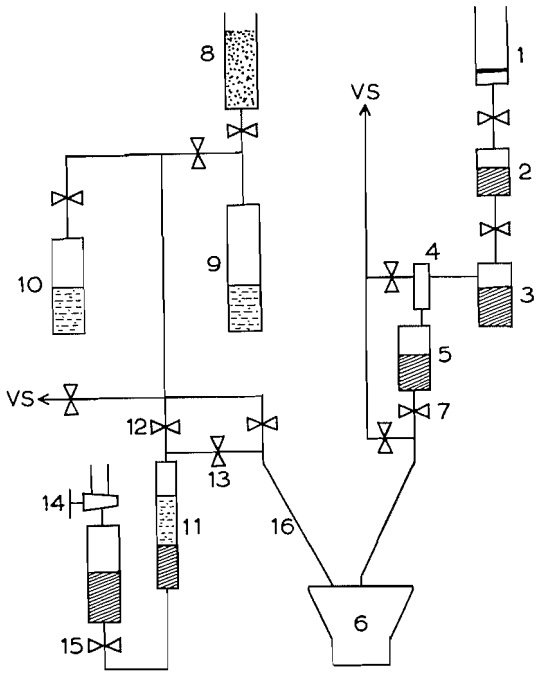

FIG. 2. The filling system: (1) glass-sinter filter, (2) mercury reservoir, (3) mercury still, (4) condenser, (5) mercury receiver, (6) calorimeter mixing vessel, (7) mercury control valve, (8) activated alumina column, (9) liquid receiver, (10) liquid storage, (11) filling tube, (12–15) valves, (16) tube, VS connections to vacuum system.

Can. J. Chem. Downloaded from www.nrcresearchpress.com by 210.87.254.6 on 09/05/12
For personal use only.

11. The residual liquid in tube 16 is condensed back into the reservoir, 16 is evacuated to remove last traces of liquid from the calorimeter valve cavity, and the calorimeter is weighed. The valve cavity is then filled with mercury and plugged.

Temperature Measurement

Temperature changes of the calorimeter are measured by six Veco AX1620 1W5 thermistors, nominal resistance 2000 ohm at 25 °C, mounted one on each face of the calorimeter. These thermistors, connected in a 3 series – 2 parallel array, comprise the 'unknown' arm of a Leeds and Northrup 4232-B high precision Wheatstone bridge, with ratio arms set at 10:1. Power for the bridge is provided by a John Fluke 313A voltage calibrator, so that the voltage (10–14 V) may be selected to allow operation at maximum bridge sensitivity; this voltage remains unchanged throughout an experiment. The off-balance potential is amplified by an Astrodata 121Z nanovoltmeter whose output is fed to a Phillips PR2216U/21 strip chart recorder. All connections in this circuit are made of Inter-8 Weave cable with Co-Netic shielding (Perfection Mica Co.). The cable is laid in soft-iron conduit and the whole calorimeter room is shielded both electrically and magnetically by lining the roof, walls, and floor with galvanized iron sheet. All instrument cases and one point in the bridge circuit are grounded to a copper bus-bar. These extreme precautions are necessary to reduce interference and pickup from nearby electrical equipment. Under most favorable conditions the peak-to-peak noise on the recorder corresponds to a temperature uncertainty of 3×10^{-6} °C.

The temperature of the calorimeter jacket is measured by a calibrated platinum resistance thermometer with a Leeds and Northrup G-2 Mueller bridge. The temperature difference between the calorimeter and the jacket is measured by a single-junction copper–constantan thermocouple. Either the Mueller bridge or the thermocouple is connected to the nanovoltmeter through a Guildline 9145A low-thermal selector switch.

Calibration Circuit

The calibration heater has a resistance of 500 ohm and is made of 0.002″ diam., 188.6 ohm/ft, low temperature coefficient (9) Evanohm wire (Wilbur Driver and Co.) wound on a $\frac{3}{4}'' \times \frac{1}{2}'' \times 0.007''$ alumina wafer (American Lava Corp.) sandwiched between two similar wafers. These thin, dense ceramic alumina wafers promote rapid heat transfer. The high resistance of the heater allows the current leads to be of small diameter (30 B and S gage), reducing heat losses from the calorimeter and eliminating errors from uncertainty in the correct location of the potential leads, which are connected to the current leads at the midpoint between the calorimeter and the calorimeter jacket. Heater power is provided by a Princeton Applied Research TC-100.2BR voltage/current reference source which can supply 0.2 A at up to 100 V. The voltage drop across the heater is measured by a Non-Linear Systems model 9116 digital voltmeter which shows that the heater resistance change is less than 0.02% during the heating period. The heater current and heating time period are not obtained separately; the integrated current through the heater over the whole heating period is obtained from the integrated voltage drop across a standard resistor in series with the heater, measured directly by a Dymec 2401B integrating digital voltmeter to within 0.01%. Switching arrangements allow preselection of calibration energies which are measured to 0.02%.

The Calorimeter Jacket

The filled calorimeter is clamped between Nylon pegs on a fixed bracket inside a 6″ diameter, highly polished, stainless steel cylinder. The electrical connections to the calorimeter pass through the cylinder cover via a Conax seal. The cover is sealed by an O-ring and the cylinder is evacuated to less than 10^{-4} Torr through a flexible stainless steel coupling (Mason–Renshaw Industries). The cylinder is mounted horizontally about its axis, while the calorimeter is mounted within it so that the cylinder axis is coincident with the calorimeter axis R—R shown in Fig. 1; cylinder rotation causes mixing. The cylinder is rotated by a Photocircuits Corp. model 488 printed-armature motor, which can be reversed while running, driving a Tangen Drive (Geneva Motions Corp.) gear system which produces smooth, cyclic displacements of 60° to each side of the upright rest position. A pair of microswitches, actuated by cams on the drive wheel, advance two stepping switches. The first stepping switch actuates a power relay to reverse the motor, return the calorimeter to the rest position, rotate to 60° on the other side, and reverse the motor again. The second stepping switch is preset to count the number of these cycles and, after the preselected number of cycles, actuates a relay cutting the power from the drive motor.

The calorimeter jacket is immersed in a thermostat controlled to within 0.001 °C by a Bayley temperature controller. Short-term temperature fluctuations of the thermostat are attenuated by the $\frac{1}{2}''$ thick stainless steel jacket, so that the jacket inside-surface temperature, controlling heat leaks to the calorimeter, is essentially constant throughout the 60 min period of an experiment.

Procedure for Endothermal Heats of Mixing

The calorimeter, after being filled, is placed in the jacket and the electrical connections are made. The jacket is evacuated and lowered into the thermostat and the whole assembly is left overnight for temperature equilibration. The following morning the thermistor current is switched on and the temperature trace of the calorimeter recorded for 1 h to ensure temperature stability before mixing. The calorimeter shows a slight temperature rise (5×10^{-5} deg min^{-1}) due to heating by the thermistors during this period. Temperature measurements using the thermistors are made in two ways. First, the Wheatstone bridge is nulled at intervals throughout the experiment, using a high detector sensitivity. The recorder chart has a center zero, the bridge resistance is preselected, and the recorder trace shows the passage through the null point. Alternating with these measurements, the bridge is set at a fixed resistance and the bridge off-balance potential is recorded at a sensitivity level such that the complete temperature excursion of the calorimeter is recorded. Figure 3 shows a typical chart for endothermal mixing; some of the null points have been omitted for clarity.

Immediately prior to the mixing, the jacket temperature is measured by the platinum thermometer and the temperature difference between the calorimeter and the jacket is measured by the thermocouple.

At point B in Fig. 3 the heater is switched on to dissipate an amount of energy preset to be nearly equal to that

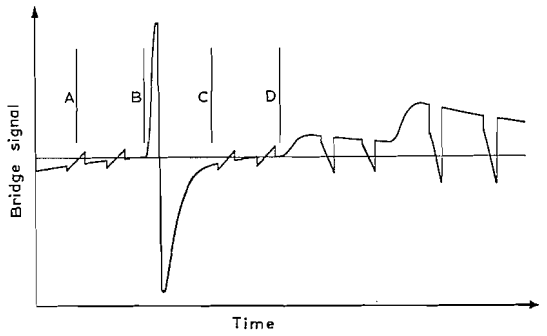

FIG. 3. Typical recorder chart trace of thermistor bridge signal for endothermal mixing. Points A, B, C, and D are spaced at equal time intervals.

expected to be absorbed in the mixing process. The introduction of this compensation energy ensures that the calorimeter temperature is little changed by the mixing. After a short time lag of 1–2 s the calorimeter temperature begins to rise and at the midpoint of the heating period the mixing mechanism is started. As the mixing absorbs heat the temperature falls rapidly and then rises steadily as the remainder of the heat passes from the heater. The calorimeter is tilted 25–50 times to each side of its rest position during 90–180 s. Tests have shown that this is more than adequate for complete mixing, but it is necessary to assist heat exchange between the heater, the mixed liquids, the mercury, and the mixing vessel. Later the mixing mechanism is run for the same number of cycles as in the mixing to determine the thermal effect of stirring (about 1 J), and again with dissipation in the heater of about 1 J. This energy discharge permits the determination of the thermal effect of stirring and of the difference between the compensation heat and the heat of mixing.

The thermistor resistance change during each of these stages is calculated using the Regnault–Pfaundler formula (10)

$$-\Delta R = R_C - R_B + R_A - R_B + (R_C - R_D - R_A + R_B)\left(\frac{\bar{R}_x - \bar{R}_a}{\bar{R}_r - \bar{R}_a}\right).$$

The resistance values R_A, R_B, R_C, R_D are obtained by plotting the high-sensitivity, nulled-bridge resistance readings and selecting the points A, B, C, and D equispaced in time, such that B is immediately prior to the mixing and C is located where the cooling rate first becomes steady after the mixing. The mean resistances $\bar{R}_a$, $\bar{R}_x$, $\bar{R}_r$, during the advance rating, the experimental, and the final rating periods, are obtained by measuring the areas under the sections AB, BC, and CD of the curve obtained at reduced sensitivity, using an Ott planimeter. Since the temperature change of the calorimeter is only a few percent of what it would have been without compensation, the errors from this calculation are insignificant. The resistance changes are converted to temperature changes by Gunn's method (11) and the heats of mixing are evaluated as described by Larkin and McGlashan (2).

Materials

Benzene

Thiophene-free benzene (passes A.C.S. test) was shown by gas chromatography (g.c) to contain toluene, ethyl benzene, and some unspecified aliphatic hydrocarbons. These impurities were removed below limits of detection (10 p.p.m.) by passage through an Autoprep A-100 preparative g.c unit.

Carbon Tetrachloride

Selected material from the production of Dow Chemical of Canada, Limited, was fractionated three times on an efficient column at high reflux ratio. The product, which contained less than 15 p.p.m. chloroform, was passed through a column of Woelm neutral activated alumina which removed the chloroform to better than 2 p.p.m.

n-Hexane and Cyclohexane

Phillips Petroleum Company, Bartlesville, research grade hydrocarbons were dried by passing through a $12'' \times \frac{1}{2}''$ column containing Woelm neutral activated alumina. No further purification was made, as recommended (5). Details of the hydrocarbon purities stated by the manufacturer are: *n-Hexane*, lot no. 1176, purity 99.99 mole % by freezing point determination; the impurity by g.c is methyl cyclopentane. *Cyclohexane*, lot no. 1078, purity 99.99 mole % by freezing point determination, most probable impurity 2,4-dimethylpentane.

Results and Discussion

Benzene – Carbon Tetrachloride

The results obtained at 25 °C for mixing benzene and carbon tetrachloride are given in Table I. Details for each of the approximately equi-molar mixtures are recorded chronologically, showing the temperature, weights of each component, carbon tetrachloride mole fraction, observed energy change, and molar enthalpy of mixing $\Delta_m h$. The series A measurements, numbered in the order obtained, are plotted in Fig. 4 where they are compared with the smoothed results of other workers (2, 6, 7).[2] The measurements of Savini *et al.* (8) are not included in this comparison due to their experimental difficulties with this system. What initially appears to be a scatter in our measurements is revealed as a trend with time when they are considered in the order in which they were obtained. It was observed at the end of a series of measurements that the mercury that had been in contact with carbon tetrachloride in the filling system carried a scum on its surface. The separate A and B

[2]The measurements of Murakami and Fujishiro (19), published since this paper was written, lie between the results of Bennett and Benson and those of Larkin and McGlashan; they were made in a calorimeter containing mercury.

Can. J. Chem. Downloaded from www.nrcresearchpress.com by 210.87.254.6 on 09/05/12
For personal use only.

TABLE I

Enthalpy of mixing of benzene – carbon tetrachloride

Temp. (°C)	Weight (g) CCl_4	Weight (g) C_6H_6	Mole fraction CCl_4	Heat change (J)	$\Delta_m h$ (J/mole)	Series
24.968	6.2205	3.8632	0.44985	10.181	113.2_7	A
25.016	4.5072	2.7626	0.45311	7.392	114.3_0	A
25.017	6.3887	2.6411	0.55125	8.694	115.3_9	A
25.019	5.0265	2.6494	0.49069	7.844	117.8_0	A
24.930	3.6408	1.8993	0.49327	5.544	115.5_4	B
24.983	3.8086	1.8318	0.51358	5.611	116.3_9	B

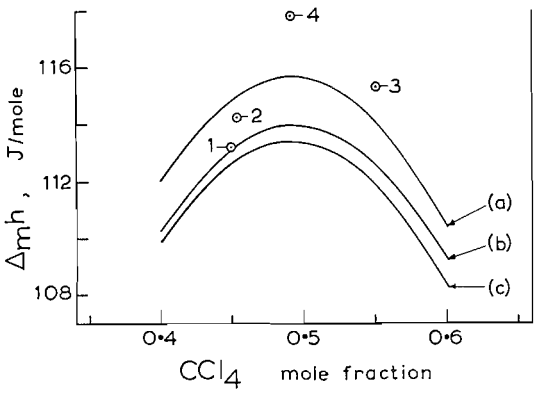

FIG. 4. Enthalpy of mixing of benzene and carbon tetrachloride. Series A results numbered in order of measurement. Smoothed curves are the results of (*a*) Larkin and McGlashan (2), (*b*) Lundberg (6), and (*c*) Bennett and Benson (7).

series of measurements were made, between which the filling system was cleaned and both the mercury and the carbon tetrachloride completely replaced. The deviation of each measurement from the smooth curve of Bennett and Benson (7) is plotted in Fig. 5 against the time of contact of the carbon tetrachloride with mercury in the filling system and in the calorimeter prior to mixing.

Kemball (12) reported that carbon tetrachloride is chemisorbed on mercury and has suggested that a surface reaction occurs. This reaction is possibly that causing the systematic discrepancies observed in our measurements of this system. It is noted (Fig. 4) that the measurements of Larkin and McGlashan (2) are consistently higher than those of Lundberg (6) and those of Bennett and Benson (7); this difference could be due to the amount of reaction occurring between carbon tetrachloride and mercury in the Larkin–McGlashan calorimeter in the time between filling and mixing; this time appears from their paper to be consistently 'overnight'. The large variation within the present measurements cannot arise from the small deviations of the experimental temperatures from 25.000 °C, since the temperature coefficient of $\Delta_m h$ is only about 1.0 J/mole deg for the equimolar system (13). Thus a reaction between mercury and carbon tetrachloride is apparently responsible for the systematically high values obtained for the

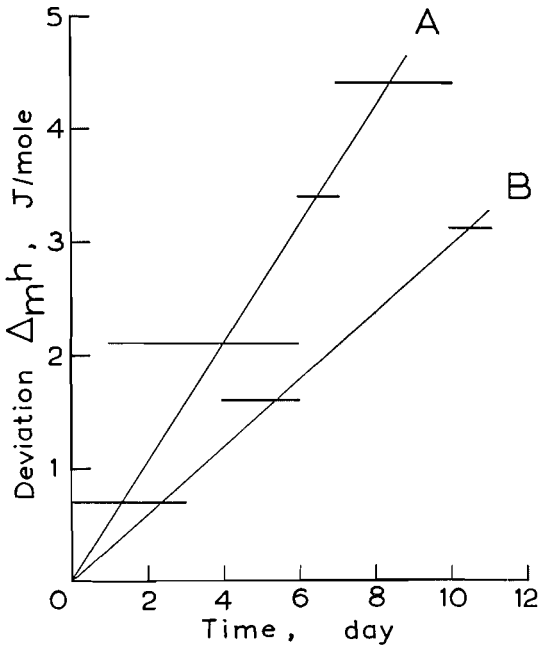

FIG. 5. Deviation of the enthalpy of mixing of benzene and carbon tetrachloride from the value of Bennett and Benson (7) at the same composition, plotted against time of contact of the carbon tetrachloride with mercury. The left hand limit of each line gives the time of contact in the filling system and the length of the line shows the time of contact in the calorimeter for the A and B series.

Can. J. Chem. Downloaded from www.nrcresearchpress.com by 210.87.254.6 on 09/05/12
For personal use only.

TABLE II

Enthalpy of mixing of *n*-hexane–cyclohexane

Temp. (°C)	Weight (g)		*x*, cyclohexane mole fraction	Heat change (J)	$\Delta_m h$ (J/mole)
	Cyclohexane	*n*-Hexane			
25.021	0.7570	3.2297	0.19355	5.409	116.4_0
25.021	1.1770	3.2823	0.26857	7.871	151.1_5
25.006	1.5341	3.3581	0.31870	9.837	171.9_9
25.009	1.9125	3.2201	0.37817	11.449	190.5_2
24.990	2.3086	3.3076	0.41680	13.167	200.0_8
25.015	2.6231	3.2448	0.45288	14.411	209.4_0
25.182	3.0963	3.2364	0.49485	16.136	217.0_4
24.999	3.4677	3.2000	0.52598	17.110	219.4_3
25.024	3.8638	3.2519	0.54886	18.455	220.6_4
25.008	3.8852	2.8730	0.58066	17.686	222.4_4
25.013	4.1158	2.8880	0.59337	18.202	221.8_6
25.001	3.8554	2.6771	0.59590	17.179	223.4_3
25.012	3.8775	2.5709	0.60697	16.837	221.8_1
25.002	3.8670	2.4029	0.62234	16.230	219.8_2
25.128	3.8282	2.2422	0.63613	15.632	218.6_2
25.011	3.8767	2.1168	0.65221	15.180	214.9_4
25.154	3.9513	1.8943	0.68111	14.541	210.9_6
24.993	3.8865	1.5645	0.71781	13.172	204.7_5
25.009	3.8887	1.2984	0.75410	11.599	189.3_0
25.019	3.8565	0.9342	0.80869	9.422	166.2_8
25.026	3.9204	0.6574	0.85928	7.181	132.4_7

enthalpy of mixing of benzene and carbon tetrachloride using mercury-containing mixing calorimeters, so that this system must be considered unsuitable as a standard for mixing calorimeter comparison.

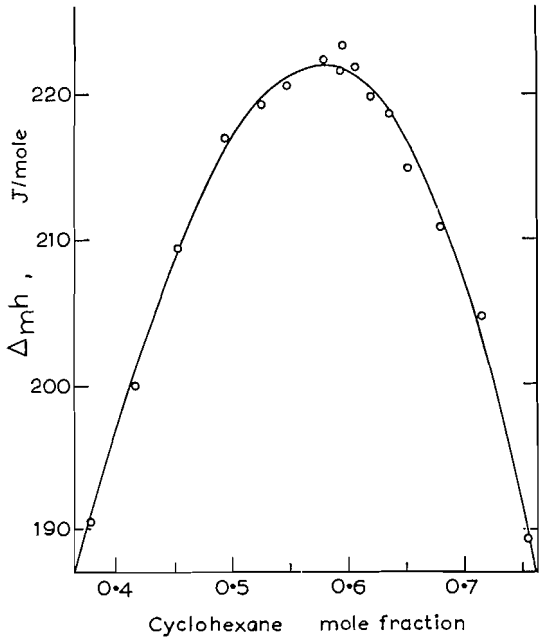

FIG. 6. Enthalpy of mixing *n*-hexane and cyclohexane in the vicinity of the maximum.

n-Hexane–Cyclohexane

In Table II are shown the results for the endothermal enthalpy of mixing *n*-hexane with cyclohexane at temperatures near to 25 °C, calculated using the molecular weights 86.17848 for *n*-hexane, and 84.16254 for cyclohexane. The results in the vicinity of the maximum are plotted in Fig. 6. The mixing temperatures vary slightly due to long-term drifts, but the effect on the $\Delta_m h$ values is so small that these have not been corrected.

The probable error on a typical mixing experiment was estimated to be 0.16% from the known instrumental uncertainties, while the standard error 0.14% is found in the vicinity of the maximum.

The twenty-one $\Delta_m h$ values in Table II were fitted by the method of least squares to give the best-fit equation (16)

$$\Delta_m h = x(1 - x)[867.86 + 258.48(2x - 1) + 101.0(2x - 1)^2],$$

in which x is the cyclohexane mole fraction. The maximum $\Delta_m h$ evaluated from the equation is $222.1_2 \pm 0.3_1$ J/mole at cyclohexane mole fraction 0.5775. The error shown is the standard error for a point calculated from the fitted curve and amounts to 0.14% of the measured value.

At present there are no comparable measure-

Can. J. Chem. Downloaded from www.nrcresearchpress.com by 210.87.254.6 on 09/05/12
For personal use only.

Can. J. Chem. Downloaded from www.nrcresearchpress.com by 210.87.254.6 on 09/05/12
For personal use only.

ments for this system, but it is hoped that other sets may soon become available. Comparison with the earlier measurements of Mathot (14) and of Mathieson and Thynne (15) shows that the precision of the present results is an order of magnitude better than that obtained earlier. To make a proper comparison, both sets of earlier measurements were fitted by the same least squares technique. The values for $\Delta_m h$ and x at the maxima are:

Temp. (°C)	Maximum $\Delta_m h$ (J/mole)	Cyclohexane mole fraction	Observer
20	220.7 ±3.0	0.583	Mathot
20	219.3 ±3.6	0.562	Mathieson and Thynne
25	$222.1_2 \pm 0.3_1$	0.5775	This work

Values of $\Delta_m h$ at both low and high x values are subject to inherently larger errors than those measurements in the vicinity of the maximum for two reasons. First, small weights of one component are used so that weighing errors are enhanced; secondly, the heat being measured is small so that temperature and energy measurement errors are enhanced. For this reason the nine measurements near the maximum, shown in Fig. 6, were fitted by a separate equation and the best fit was obtained for a four-constant equation. The highest point near the maximum in Fig. 6 exhibits a deviation from the best representative curve over three times the standard error. Thus there is a possibility that this is a spurious value. The statistical problem of rejection of outliers has recently received attention (17, 18). The remaining eight data were then refitted, omitting the possibly spurious point, and the best fit was again found with a four-constant equation. The maximum $\Delta_m h$ values found are:

Points fitted	$\Delta_m h$ (J/mole)	x
21 – complete set	$222.1_2 \pm 0.3_1$	0.5775
9 in region of maximum	$222.4_7 \pm 0.3_2$	0.5865
8 near maximum, possible outlier omitted	$222.1_4 \pm 0.2_1$	0.5855

The best fit to the eight points near the maximum, omitting the possibly spurious point, gives a maximum $\Delta_m h$ value which differs insignificantly from that obtained from the fit of all 21 measurements; however, the standard error for the eight-point fit with four degrees of freedom is decreased to 0.1_0%.

Although it is premature to make any final judgment on the suitability of the *n*-hexane–cyclohexane system as an enthalpy of mixing standard, the present indications are that this system will prove to be a suitable standard.

Acknowledgments

This work was supported in part by a grant under the National Research Council of Canada Industrial Research Assistance Programme. We are indebted to C. A. Aitken for his precision work in construction of the mixing vessel and other components, and to J. Almey for many helpful suggestions.

1. M. L. McGlashan. *In* Experimental thermochemistry. Vol. 2. *Edited by* H. A. Skinner. Interscience Publishers, New York. 1962.
2. J. A. Larkin and M. L. McGlashan. J. Chem. Soc. 3425 (1961).
3. I. Brown and W. Fock. Australian J. Chem. **14,** 387 (1961).
4. R. V. Mrazek and H. C. Van Ness. A.I.Ch.E. J. **7,** 190 (1961).
5. M. L. McGlashan. Private communication.
6. G. W. Lundberg. J. Chem. Eng. Data, **9,** 193 (1964).
7. J. E. Bennett and G. C. Benson. Can. J. Chem. **43,** 1912 (1965).
8. C. G. Savini, D. R. Winterhalter, L. H. Kovack, and H. C. Van Ness. J. Chem. Eng. Data, **11,** 40 (1966).
9. G. T. Furukawa, M. L. Reilly, and W. G. Saba. Rev. Sci. Instr. **35,** 113 (1964).
10. W. P. White. The modern calorimeter. Chemical Catalog Company, New York. 1928.
11. S. R. Gunn. Rev. Sci. Instr. **35,** 183 (1964).
12. C. Kemball. Proc. Roy. Soc. London, Ser. A, **201,** 377 (1950).
13. M. L. McGlashan, D. Stubley, and H. Watts. In preparation.
14. V. Mathot. Bull. Soc. Chim. Belg. **59,** 111 (1950).
15. A. R. Mathieson and J. C. J. Thynne. J. Chem. Soc. 3708 (1956).
16. O. Redlich and A. T. Kister. Ind. Eng. Chem. **40,** 345 (1948).
17. F. J. Anscombe. Technometrics, **2,** 123 (1960).
18. F. J. Anscombe and J. W. Tukey. Technometrics, **5,** 141 (1963).
19. S. Murakami and R. Fujishiro. Bull. Chem. Soc. Japan, **40,** 1784 (1967).

Can. J. Chem. Downloaded from www.nrcresearchpress.com by 210.87.254.5 on 09/05/12
For personal use only.

Catalytic decomposition of acetonedicarboxylic acid

D. W. LARSON[1] AND M. W. LISTER
Department of Chemistry, University of Toronto, Toronto, Ontario

Received September 15, 1967

The decomposition of acetonedicarboxylic acid at various pH and in the presence of cobalt, nickel, copper, and zinc perchlorates as catalysts has been investigated. In addition the equilibrium constants for the formation of complexes between the metal ions and the acetonedicarboxylate ion have been measured.

The copper complex appears to differ from the others in being more acidic, and also in its infrared spectrum. The kinetic results have been interpreted in terms of rate constants for the decomposition of each of the complexes, and a qualitative (but not a quantitative) correlation seems to exist between the rate constants and the stability constants of the complexes.

Canadian Journal of Chemistry, **46**, 823 (1968)

The decomposition of acetonedicarboxylic acid to acetoacetic acid and carbon dioxide

$$CO(CH_2COOH)_2 \rightarrow CH_3COCH_2COOH + CO_2$$

was studied by Wiig (1), who determined the rate constants and activation energy for the decomposition, though without considering the extent of ionization of the acid. Krebs (2) examined the effect of various cations as catalysts for the reaction, and a more detailed investigation of this was carried out by Prue (3). He showed, in particular, that the catalytic constants ran parallel to the equilibrium constants for the formation of complexes of the same cations with the malonate ion, which might be expected to behave much like the acetonedicarboxylate ion as a complexing agent. A similar correlation was observed by Gelles, Hay, and Salama (4, 5) for oxaloacetic acid. The object of the present work was to examine the complexing of aqueous acetonedicarboxylic acid directly with various cations, including the effect of pH, and to obtain more information on the kinetics of the decomposition of the acid, its ions, and its metallic complexes.

Experimental

Reagents

Acetonedicarboxylic acid was obtained from Koch Laboratories. Traces of a colored contaminant were removed by activated charcoal before recrystallization of the acid from ethyl acetate. This gave a white powder, m.p. 133–134 °C (Wiig (1) gives 134–135 °C), and an apparent molecular weight by titration with NaOH of 147.0 to 147.7 in different batches (calcd. 146.1). The acid was stored over silica gel, and aqueous solutions were made up as required.

Perchlorate salts (sodium, cobalt, nickel, copper, and zinc) were obtained from the G. F. Smith Co. Solutions of sodium perchlorate were prepared from the anhydrous salt by weight. Stock solutions of the other perchlorates were analyzed by EDTA titration; copper perchlorate was also analyzed iodometrically, and zinc perchlorate by titration with potassium ferrocyanide.

Apparatus

pH Meter

pH measurements were made on a Beckman research pH meter, standardized by potassium acid phthalate at 25 °C. Since most of the solutions examined contained high concentrations of perchlorate ion, the calomel reference electrode was modified to contain saturated sodium chloride solution, instead of the more usual potassium chloride. The latter gave somewhat erratic results, which were attributed to precipitation of potassium perchlorate. In order to convert pH readings to hydrogen ion concentrations, pH measurements were made on solutions of perchloric acid (10^{-2}–10^{-3} *M*) containing sodium perchlorate to ionic strengths of 0.6 and 0.4, as used in the rest of the work. The pH reading was uniformly 0.16 less than $-\log [H^+]$, if the perchloric acid was taken to be completely ionized.

Spectrophotometer

A Beckman DU spectrophotometer was used, modified so that water at 25 °C could be circulated round the cell compartment.

Cell Voltages

These were measured in a glass assembly of conventional design by means of a potentiometer sensitive to 0.01 mV. A sodium perchlorate bridge was used to connect the cell compartments, which always contained a considerable concentration of sodium perchlorate in addition to the cation being studied (e.g. Cu^{2+}) and acetonedicarboxylic acid. The cell was kept at 25.0 °C.

Kinetic Measurements

Reacting solutions were placed in a 500 ml pyrex flask in a thermostat kept at 25.00 ± 0.05 °C. The solution was stirred by a mercury-sealed stirrer, and the flask was connected to a water-jacketed gas burette; air was flushed from the flask and burette with carbon dioxide. The gas evolved (carbon dioxide) was collected over mercury, and gave a measure of the extent of the reaction. The

[1]Present address: Canadian Forces Institute of Aviation Medicine, 1107 Avenue Road, Toronto.

decomposition was also followed by acid–base titration. The technique used was to add enough base to a sample to raise the pH to about 4.5. This largely quenched the reaction. Nitrogen was now bubbled through the sample to remove carbon dioxide, and the titration was then continued to a phenolphthalein end point. When copper or zinc, etc., was present as a catalyst, potassium ferrocyanide was added to precipitate the metal, and the titration was then carried out as described.

Results

Ionization Constants of Acetonedicarboxylic Acid

Although these constants have been measured before (3), they were remeasured under the conditions of the present experiments. pH titrations of acetonedicarboxylic acid with sodium hydroxide were carried out at various temperatures, both solutions containing sodium perchlorate so that the ionic strength was either 0.6 or 0.4. Values of the two ionization constants, K_{a1} and K_{a2}, were calculated from the pH observed when 0.5 and 1.5 moles of sodium hydroxide had been added per mole of acid. The constants are sufficiently close that both stages of ionization have to be taken into account at both pH values. The results are given in Table I. Some confirmation of these values was obtained by following the absorbance at 300 mμ during a similar titration. The curve so obtained followed very closely the one calculated using the dissociation constants in Table I, and the following extinction coefficients: H_2A, 12.1; HA^-, 25.0; A^{-2}, 30.6 M^{-1} cm^{-1}. The values $K_{a1} = 1.8 \times 10^{-3}$ and $K_{a2} = 1.9 \times 10^{-4}$ M^{-1} in ref. 3 are fairly close to the present ones.

H_2A is taken to mean acetonedicarboxylic acid in this and succeeding sections.

TABLE I

Ionization constants of acetonedicarboxylic acid

I	T (°C)	10^3K_{a1}	10^4K_{a2}
0.6	15.6	1.22	1.82
0.6	25.0	0.97	1.52
0.4	15.6	0.99	1.63
0.4	25.0	0.88	1.35

Stability Constants

1. Copper(II)

The formula of the complex in solution, formed by Cu^{2+} and acetonedicarboxylic acid, was found by the method of continuous variation (6) at three pH values, 4.7, 4.2, and 3.6. The absorbance was measured at 400 and 430 mμ, at which wavelengths both Cu^{2+} and acetonedicarboxylic acid absorb very little. The temperature was kept at 25 °C, and the ionic strength at 0.6 by sodium perchlorate. In every case a plot of absorbance against (total copper)/(total copper and acid) gave a sharp symmetrical maximum at 0.5, indicating a 1:1 complex.

The equilibria involved were examined by means of electromotive force (e.m.f.) and absorbance measurements. The e.m.f. measurements were made on cells with two copper electrodes, one dipping into a copper perchlorate solution (roughly 10^{-3} M), and the other into a solution of copper perchlorate and acetonedicarboxylic acid. The pH of the latter solution was adjusted to between 3 and 4.5 by NaOH. Both solutions were at ionic strength 0.6; and 0.6 M sodium perchlorate was used as a bridge between the solutions. The temperature was 25 °C. It was checked, from similar cells with

TABLE II

Data from e.m.f. measurements on the copper acetonedicarboxylate complex

No.	10^3M	10^3a	10^3m	10^2b	10^4h	K_{Cu}	pK_{a3}
1	9.73	16.47	6.14	2.222	3.09	104	3.73
2	13.68	16.00	8.24	2.708	2.18	66	3.36
3	13.68	16.67	8.19	2.708	2.18	90	3.73
4	12.18	10.68	8.94	1.667	2.14	85	3.93
5	9.13	15.29	3.78	2.708	1.44	155	3.88
6	9.32	14.39	4.58	2.553	1.41	102	3.78
7	8.43	16.71	2.44	3.269	0.892	129	3.76
8	5.92	9.08	2.33	1.892	0.66	101	3.80
9	6.08	7.80	2.59	1.667	5.62	132	3.88
10	9.22	11.59	2.83	2.632	5.00	162	3.88
11	10.95	10.17	3.82	2.500	3.71	192	3.96
12	6.00	7.34	2.03	1.781	2.57	50	3.49
					Mean	114	3.76

Can. J. Chem. Downloaded from www.nrcresearchpress.com by 210.87.254.5 on 09/05/12
For personal use only.

Can. J. Chem. Downloaded from www.nrcresearchpress.com by 210.87.254.5 on 09/05/12
For personal use only.

TABLE III

Spectrophotometric data on copper complexes

No.	10^3M	10^3a	D	10^5h	e
1	7.12	7.59	1.105	0.60	190
2	6.89	7.30	1.012	0.74	185
3	10.31	10.47	1.511	1.02	187
4	7.17	7.71	1.024	1.09	188
5	7.34	17.29	1.236	1.18	181
6	7.83	7.16	0.883	1.95	178
7	6.56	24.64	1.011	2.88	170
8	7.34	17.29	1.082	2.88	172
9	7.83	7.69	0.766	3.31	166
10	5.49	17.63	0.714	4.37	158
11	5.54	17.52	0.694	5.13	157
12	9.27	11.27	0.899	5.44	159
13	7.34	17.29	0.838	6.31	154
14	4.86	23.69	0.573	6.76	144
15	5.87	17.24	0.543	10.00	120
16	7.34	17.30	0.617	10.23	129
17	8.82	13.93	0.628	10.70	127
18	7.34	17.30	0.485	13.5	113
19	11.74	14.72	0.678	14.5	120
20	11.74	21.35	0.793	15.1	115
21	11.99	13.03	0.560	18.2	117
22	7.34	29.37	0.454	19.0	95
23	11.74	22.05	0.688	19.5	109
24	11.74	16.11	0.503	20.4	98
25	15.84	28.93	0.615	34.6	86
26	8.39	40.88	0.365	34.6	83
27	15.87	28.37	0.527	38.0	79
28	15.87	28.85	0.503	40.7	86
29	17.27	31.39	0.313	66.0	61
30	13.35	6.58	0.361	66.0	55

two concentrations of copper perchlorate, that the cell voltage was proportional to $\log (m_1/m_2)$, where m_1 and m_2 are the two copper concentrations. These results fitted the line E (mV) = $29.25 \log (m_1/m_2)$, and it was assumed that this equation was obeyed with acetonedicarboxylic acid present. Hence $[Cu^{2+}]$ could be found.

The results are given in Table II. Here M is the total copper concentration, a the total acid, and m the free $[Cu^{2+}]$; b is the concentration of NaOH added, though, of course, this reacts with the acetonedicarboxylic acid; h is the hydrogen ion concentration. Preliminary calculations showed that more hydrogen ion was produced in the solution than could be accounted for if the only effect of the copper was to give the equilibrium

$$Cu^{2+} + A^{-2} \rightleftharpoons CuA \quad (K_{Cu}).$$

It was therefore supposed that CuA might be acidic.

$$CuA + H_2O \rightleftharpoons CuL^- + H_3O^+ \quad (K_{a3}),$$

where L is the new ligand. K_{Cu} and K_{a3} are the equilibrium constants. From the various equilibria and mass balances, it can be calculated that K_{Cu} and K_{a3} are given by the equations

$$mK_{Cu} = \frac{h}{K_{a2}} + 2 - \frac{\left[\frac{h^2}{K_{a1}K_{a2}} + \frac{h}{K_{a2}} + 1\right](h + b + 3m - 3M)}{a + m - M}$$

$$K_{a3} = \frac{h(M - m)\left[\frac{h^2}{K_{a1}K_{a2}} + \frac{h}{K_{a2}} + 1\right]}{mK_{Cu}(a + m - M)} - h.$$

K_{Cu} and K_{a3} were calculated for each solution, with the results also given in Table II. The constants are probably as good as can be expected, since small deviations in voltage or pH alter them considerably. The mean values and average deviations are

$$K_{Cu} = 114\ (\pm\ 33)\ M^{-1}, \text{ and}$$

$$K_{a3} = 1.7\ (\pm\ 0.5) \times 10^{-4}\ M^{-1}.$$

Spectrophotometric studies were made on similar solutions with the results in Table III.

Can. J. Chem. Downloaded from www.nrcresearchpress.com by 210.87.254.5 on 09/05/12
For personal use only.

In this table, D is the absorbance at 400 mμ, at which wavelength only the copper complexes contribute appreciably to the absorbance. These results were interpreted as follows. The same equations that were applied for the e.m.f. data give that

$$[i] \qquad K_{Cu} = \frac{w}{(a - w)(M - w)} \cdot F(h),$$

where

$$F(h) = \frac{K_{a1}K_{a2} + K_{a1}h + h^2}{K_{a1}K_{a2}} \cdot \frac{h}{K_{a3} + h}$$

and w is the total concentration of complexed copper, i.e. [CuA] + [CuL$^-$]. If we define e, the apparent extinction coefficient, as $e = D/w$, then

$$e = \frac{K_{a3}e_2 + he_1}{K_{a3} + h},$$

where e_1 and e_2 are the extinction coefficients of CuA and CuL$^-$ respectively. Substituting in the equation for K_{Cu}, we get

$$[ii] \quad K_{Cu} = \frac{D/e}{(a - D/e)(M - D/e)} \cdot F(h),$$

where $F(h)$ is the function of the hydrogen ion concentration appearing in eq. [i]. Hence if two readings at the same pH are combined, a value of e for that pH can be obtained. This is done with the results shown in Fig. 1. It is evident that e varies with pH. The slope of a plot of e against pH should be greatest at pH = pK_{a3}, and this is seen to be roughly the same value (3.76) deduced from the e.m.f. data. If this value of pK_{a3} and the value of 114 for K_{Cu} are substituted in eq. [ii], values of e at different pH can be calculated. However, these turn out to be consistently rather too low. It was found that if pK_{a3} is taken as 3.86 and K_{Cu} as 110, the values of e so obtained coincide reasonably well with those deduced above. These values are also plotted in Fig. 1. The equation for e above also allows e_1 and e_2 to be calculated. These turn out to be approximately $e_1 = 30$, $e_2 = 205$, and the line in Fig. 1 is calculated from these values of e_1 and e_2, and p$K_{a3} = 3.86$. Taking the average from all measurements, we get the equilibrium constant, K_{Cu}, for $Cu^{2+} + A^{-2} \rightleftharpoons CuA$ to be 112 M^{-1}; CuA is an acid species with p$K_{a3} = 3.81$.

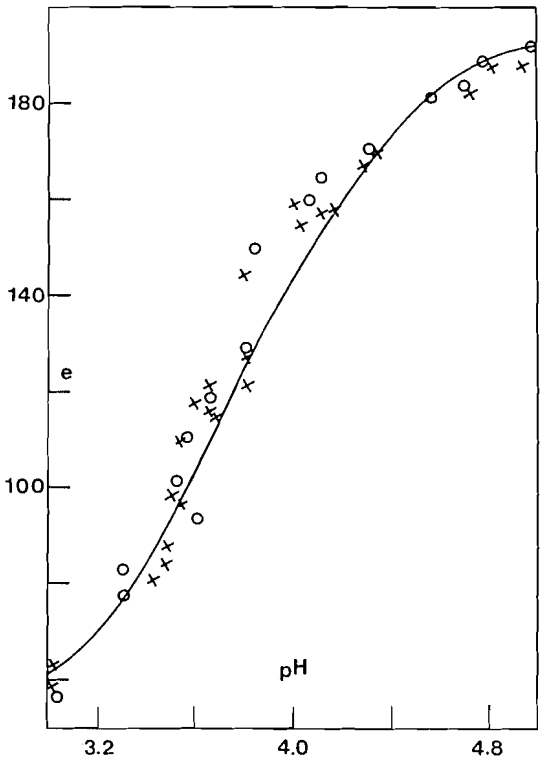

FIG. 1. Apparent absorbance of copper acetonedicarboxylate complexes at various pH: (×) results obtained by combining two measurements at the same pH; (○) results calculated if pK_{a3} is 3.86 and K_{Cu} is 110.

2. Zinc(II)

Since zinc acetonedicarboxylate was found to have no useful absorption spectrum, the complex was investigated by means of an electrochemical cell similar to that used for copper. Somewhat variable results were obtained using zinc rods for electrodes, but zinc amalgam gave satisfactory results, as had been found in earlier work (7–9). An amalgam containing 0.8% zinc by weight was prepared, and stored under nitrogen. The electrodes consisted of a few drops of amalgam in contact with a platinum wire. Their performance was examined when they were in contact with two dilute zinc perchlorate solutions joined by a sodium perchlorate bridge. Both solutions contained sodium perchlorate up to a total ionic strength of 0.60; the cell was maintained at 25.0 °C. The results of this test were as follows.

Log (m_1/m_2)	0.4766	0.3010	0.2038	−0.0967	−0.3966
E (mV)	14.43	9.05	5.73	−2.88	−11.45
Ratio	30.3	30.1	28.1	29.8	29.9

TABLE IV

Data from e.m.f. measurements on the zinc acetonedicarboxylate complex

No.	10^2M	10^2a	10^2m	10^4h	K_{Zn}
1	2.00	5.00	0.98	3.09	96.2
2	2.00	6.00	0.92	3.09	87.8
3	2.00	7.00	0.85	3.09	85.1
4	2.00	8.00	0.78	3.09	84.9
5	1.097	3.00	0.439	0.331	78.4
6	1.097	3.00	0.478	0.692	80.9
7	1.097	3.00	0.531	1.38	88.0
8	1.000	3.00	0.581	2.76	92.9
9	1.097	3.00	0.894	7.94	85.2

The mean ratio of $E/\log(m_1/m_2)$ is 29.6. Here m_1 and m_2 are the concentrations of the zinc solutions, and E is the cell voltage. Results approximately obey an equation

$$E = 29.6 \log (m_1/m_2).$$

The cell ratio is not as constant as could be wished, but the method is evidently capable of giving moderately accurate estimates of concentrations of zinc ions.

To study the zinc acetonedicarboxylate complex, similar cells were made up with known amounts of acetonedicarboxylic acid in one cell compartment. The pH was adjusted with sodium hydroxide or perchloric acid, and was measured. Preliminary results showed that with a high acid to metal ratio, fairly constant equilibrium constants were obtained, if a 1:1 complex was assumed; but at lower ratios deviations occurred which could only be attributed to other species, perhaps M_2A^{2+}. However, no formula for these other species could be established from the data. At high ratios of acid to zinc, a reasonably constant equilibrium constant was obtained for a 1:1 complex, ZnA, as is seen from the data in Table IV. As before, M is the total zinc concentration, a is the total acid, m the free $[Zn^{2+}]$, and h the hydrogen ion concentration. The last column gives the equilibrium constant, K_{Zn}, for

$$Zn^{2+} + A^{2-} \rightleftharpoons ZnA,$$

and its mean value is 86.6 (average deviation 4.1) M^{-1}. It will be seen that K_{Zn} does not vary with pH, at least over the range 2.9 to 4.3. It was also checked, from the amount of sodium hydroxide used in making up the solutions, that the observed pH agreed with a formula ZnA for the complex (as opposed to $ZnAH^+$ or ZnL^-).

3. Cobalt(II)

Cobalt(II) perchlorate has a weak absorption maximum at 510 mμ, which was found to be enhanced, though not shifted, by addition of acetonedicarboxylic acid at pH values around 4. The method of continuous variation (6) was applied to determine the formula of the complex, by plotting $\bar{D}$, the enhancement of the absorbance, against $M/(M + A)$. $\bar{D}$ is defined as

$$\bar{D} = D - e_m \cdot M,$$

where D is the observed absorbance in a solution of total cobalt concentration M, and e_m is the extinction coefficient of Co^{2+}, which was found to be 4.79 at 510 mμ. The results for a pH of 4.35 are plotted in Fig. 2, and show a maximum

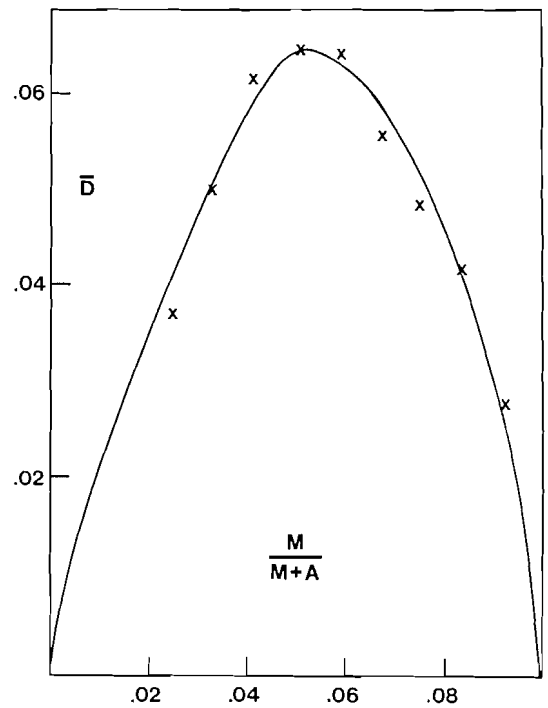

FIG. 2. Continuous variation plot for cobalt acetonedicarboxylate complex.

Can. J. Chem. Downloaded from www.nrcresearchpress.com by 210.87.254.5 on 09/05/12
For personal use only.

TABLE V
Absorbances of cobalt acetonedicarboxylate solutions

No.	10^2M	10^2A	10^5h	D	K_{Co} if $(e_u - e_m)$ is 0.9	1.0	1.1	1.2
1	13.24	4.42	3.09	0.672	252.8	75.5	43.2	29.6
2	11.78	5.88	3.09	0.615	60.1	40.3	30.2	23.8
3	7.36	5.64	7.40	0.386	86.0	58.2	43.2	33.9
4	7.36	5.64	15.5	0.382	78.0	56.6	44.0	35.7
5	7.36	5.64	33.1	0.376	74.7	58.4	47.7	40.1
6	8.83	4.17	7.40	0.451	78.7	52.1	38.2	29.9
7	8.83	4.17	15.5	0.448	72.1	51.9	40.0	32.5
8	8.83	4.17	33.1	0.444	76.9	59.4	48.0	40.1
9	10.30	2.70	7.40	0.513	80.0	49.1	35.1	27.2
10	10.30	2.70	15.5	0.509	55.4	41.3	32.9	27.1
				Mean	91.5	54.3	40.3	32.0
				Av. dev. (%)	34.3	13.5	12.3	14.0

at 0.5, but the curve is unsymmetrical with a bulge towards low values of $M/(M + A)$. Evidently a 1:1 complex predominates, but another complex with more acid is probably also present.

Data on the absorbances at 510 mμ of various mixtures of cobalt perchlorate and acetonedicarboxylic acid at various pH, at 25 °C and an ionic strength of 0.6, are collected in Table V. In all these mixtures cobalt is in excess, and if it is assumed that the only complex is CoA, then the usual equilibrium and mass balance equations give

$$K_{Co} = \frac{(D - e_m \cdot M)(e_u - e_m) \cdot F(h)}{(e_u M - D)[e_u A - D - e_m(M - A)]},$$

where K_{Co} is the equilibrium constant for

$$Co^{2+} + A^{2-} \leftrightharpoons CoA,$$

e_u is the extinction coefficient of CoA, and

$$F(h) = \frac{h^2}{K_{a1}K_{a2}} + \frac{h}{K_{a2}} + 1.$$

This equation contains two unknowns, K_{Co} and e_u, and the method that was adopted was to examine the constancy of the calculated value of K_{Co} for various values of $(e_u - e_m)$. This is done in the last columns of Table V, and it can be seen that there is little to choose between $e_u - e_m = 1.0$ or 1.1. Owing to the small change in absorbance, the value of K_{Co} is necessarily approximate, and the best average value is probably $45 \pm 10\ M^{-1}$.

4. Nickel(II)

The behavior of nickel perchlorate with acetonedicarboxylic acid was similar to that of cobalt perchlorate, and similar absorbance measurements were made at 670 mμ. The method of continuous variation (6) indicated a 1:1 complex, with slight signs of a 1:2 complex at low $M/(M + A)$ ratios. The absorbance values are given in Table VI, and were treated in the same way as those for the cobalt complex. e_m at 670 mμ is 1.85, and Table VI gives values of K_{Ni} calculated for different values of $(e_u - e_m)$. It is seen that the average deviation is least at $(e_u - e_m) = 0.46$, for which the average K_{Ni} is 59.3. Probably one can conclude that K_{Ni} is $60 \pm 5\ M^{-1}$.

With both nickel and cobalt, calculations were made (from the pH, and the amounts of added reagents, including sodium hydroxide) of the degree of protonation of the complex. In both cases, the results supported a formula MA, where M is the metal and H_2A is acetonedicarboxylic acid.

Kinetic Results

1. Acetoacetic Acid

Since the first product of the reaction, acetoacetic acid, also loses carbon dioxide, a brief study was made of this second stage of the reaction, in order to check earlier work. As was already known (10), acetoacetic acid decomposes by a first order, pH dependent reaction. This is interpreted as arising from the simultaneous decomposition of acetoacetic acid and its ion. Pedersen (10) calculated values of 0.99×10^{-3} min^{-1} for the rate constant for the free acid, and 2.06×10^{-5} min^{-1} for the rate constant for the ion, with pK_a of acetoacetic acid equal to 3.30, these values being for 25 °C and an ionic strength

Can. J. Chem. Downloaded from www.nrcresearchpress.com by 210.87.254.5 on 09/05/12
For personal use only.

TABLE VI

Absorbances of nickel acetonedicarboxylate solutions

No.	10^2M	10^2A	10^5h	D	K_{Ni} if $(e_u - e_m)$ is 0.43	0.45	0.46	0.47	0.49
1	10.26	7.34	6.16	0.212	64.7	57.8	50.8	45.6	39.5
2	8.80	8.80	6.16	0.188	94.4	76.4	66.7	63.5	54.0
3	15.94	4.06	3.47	0.311	110.9	70.4	59.3	51.2	40.1
4	15.08	4.92	3.47	0.298	102.2	68.9	59.1	51.6	41.0
5	13.78	6.22	3.47	0.278	90.0	65.7	57.7	51.3	41.8
6	12.92	7.08	3.47	0.265	91.2	68.3	60.5	54.1	44.4
7	8.61	11.39	3.47	0.285	86.8	67.9	61.0	55.3	46.2
				Mean	91.5	67.9	59.3	53.2	43.9
				Av. dev. (%)	10.3	5.2	5.0	7.1	8.5

of 0.51. Table VII gives our results for this reaction, k_2 being the apparent rate constant, defined by the equation: rate $= k_2$[total acetoacetic acid]. It is easily shown that

$$k_2 = \frac{hk_p + K_a k_q}{h + K_a},$$

where k_p and k_q are the rate constants of the acid and its ion respectively. The results in Table VII are for 25 °C and an ionic strength of 0.60, and fit Pedersen's values for k_p and k_q very well if pK_a is taken to be 3.41. The last column gives k_2 calculated from these values. It was also found that 0.0175 M copper perchlorate caused no measurable acceleration of the reaction, although the color indicated that some complex was formed.

TABLE VII

Decomposition of acetoacetic acid at 25 °C

Run	h	10^3k (obs.)	10^3k (calcd.)
1	1.38×10^{-1}	1.00	0.99
2	9.55×10^{-4}	0.717	0.709
3	3.72×10^{-4}	0.478	0.494
4	1.74×10^{-4}	0.321	0.320

2. Acetonedicarboxylic Acid. Uncatalyzed Reaction

This decomposition was also known to be a first order, pH dependent reaction (3); and it was also interpreted in terms of independent reactions of the acid and its ions. The apparent rate constant, k_1, defined as the rate divided by the total concentration of acid, is then given by

$$k_1 = \frac{k_a h^2 + k_b K_{a1} h + k_c K_{a1} K_{a2}}{h^2 + K_{a1} h + K_{a1} K_{a2}},$$

where k_a, k_b, and k_c are the rate constants for H_2A, HA^-, and A^{2-} respectively. In calculating k_1, a correction was made for the decomposition of the acetoacetic acid formed, by means of the values of k_p and k_q obtained above. The fact that the pH changed somewhat during a run as the acid decomposed was also allowed for.

TABLE VIII

Decomposition of acetonedicarboxylic acid

Run	h	10^3k_1 (obs.)	10^3k_1 (calcd.)
1	1.10×10^{-1}	1.26	1.26
2	1.10×10^{-1}	1.26	1.26
3	3.72×10^{-3}	1.64	1.59
4	1.15×10^{-3}	1.86	1.89
5	7.95×10^{-4}	2.02	1.96
6	3.98×10^{-4}	1.91	1.92
7	3.24×10^{-4}	1.81	1.86
8	1.70×10^{-4}	1.51	1.55
9	1.38×10^{-4}	1.39	1.42
10	7.61×10^{-5}	0.97	1.03
11	4.90×10^{-5}	0.70	0.78
12	3.24×10^{-5}	0.56	0.59

The values of k_1 are given in Table VIII. At low pH, K_1 will be approximately equal to K_a, and Table VIII shows that this lower limit of K_1 (and hence K_a) is close to 1.25×10^{-3} min^{-1}. Hence an equation in k_b and k_c could be obtained for each of the other measurements. By subtracting the equation for the highest pH, values of k_b could be obtained: their average was 2.90×10^{-3} min^{-1}, with an average deviation of 0.10×10^{-3}. k_c is evidently small, and is approximately 0.1×10^{-3}. The last column of Table VIII gives values of k_1 calculated from these values of k_a, k_b, and k_c. Prue (3) obtained for 42 °C and an ionic strength of 0.60, as in the present work,

$k_a = 11.0 \times 10^{-3}$, $k_b = 26.5 \times 10^{-3}$, and $k_c = 1.15 \times 10^{-3}$ min^{-1}.

Can. J. Chem. Downloaded from www.nrcresearchpress.com by 210.87.254.5 on 09/05/12
For personal use only.

TABLE IX

Decomposition of acetonedicarboxylic acid catalyzed by copper

Run	10^3M	10^3A	pH	D	10^5 rate	10^2k_{Cu} (min^{-1})
1	8.76	2.35	4.63	0.566	9.64	2.89
2	1.75	3.03	4.53	0.238	6.24	4.33
3	3.50	2.35	4.45	0.370	8.85	3.83
4	5.26	3.19	3.98	0.293	19.5	8.24
5	7.01	6.07	3.84	0.393	35.7	10.03
6	7.01	6.19	3.69	0.404	44.3	10.73
7	7.01	6.07	3.38	0.142	33.3	16.73
8	10.51	7.80	3.23	0.203	52.1	15.23

These results make the activation energy for k_a 23.9 kcal, and k_b 24.3 kcal; the entropy of activation is 0.3 cal/deg for k_a, and 3.3 cal/deg for k_b.

3. Catalysis by Copper(II)

Mixtures were made up containing various amounts of copper perchlorate, acetonedicarboxylic acid, and sodium hydroxide, with sodium perchlorate added to an ionic strength of 0.60. The temperature was 25.0 °C. Readings were taken throughout of the gas evolved, the pH, and the absorbance at 400 mμ. Results are given in Table IX. Initial concentrations of metal and acid are quoted. The rate of gas evolution (converted to g-moles/min l of solution) quoted is for some midpoint in the run where a steady rate was observed; the pH and absorbance readings are interpolated to the same time. The total gas evolution up to this time was also estimated; and, from this and the initial quantity of acetonedicarboxylic acid, the concentrations of acetonedicarboxylic acid and acetoacetic acid at this time were estimated. Allowance was also made for the acid combined in the complex, determined by means of the absorbance and the extinction coefficients obtained earlier.

It was assumed that the total rate was a sum from various first order reactions,

$$\text{rate} = k_1a + k_2b + k_{Cu}u,$$

where a is the total free acetonedicarboxylic acid, whether ionized or not, b the total acetoacetic acid, and u the total copper complex. k_1 and k_2 are the effective rate constants (defined earlier) for the observed pH. k_{Cu} is the rate constant for the complex, and it presumably arises from both CuA and CuL^-. Values of k_{Cu} so calculated are given in Table IX, and it can be seen that k_{Cu} is pH dependent. In this connection, it may be added that three further runs were done at pH 2.48, 2.19, and 0.80. At pH 0.80, the rate was the same as if no copper had been added, and at pH 2.19 it was only about 20% higher. This lack of dependence of rate on the free Cu^{2+} concentration was taken as evidence that the copper catalyzed the reaction by decomposition of the complex, and not by some other mechanism. It will also be seen in Table IX that (with one exception) throughout $M > A$, this being done to avoid possible complications from higher complexes. Returning to the values of k_{Cu}, if we assume that this comes from the decomposition of both CuA and CuL^-, then

$$k_{Cu} = \frac{k_A h + k_L K_{a3}}{h + K_{a3}},$$

where k_A and k_L are the rate constants for CuA and CuL^- respectively, and K_{a3} is the acid ionization constant of CuA. The method of least squares applied to the values of k_{Cu} in Table IX makes $k_A = 0.201$ min^{-1} and $k_L = 0.0056$ min^{-1}, though the value of k_L must be regarded as approximate.

4. Catalysis by Zinc, Cobalt, and Nickel

Since these metals behave similarly, they will be treated together. In each case mixtures of metal perchlorate, acetonedicarboxylic acid, sodium hydroxide, and sodium perchlorate were allowed to decompose at 25 °C. The reaction was followed by titration of the remaining acid. With zinc, the acid was in excess (to avoid Zn_2A^{2+}, etc.), and with cobalt and nickel equal concentrations of metal and acid were used. Rate and pH were extrapolated to zero time. As with copper, it was assumed that the initial rate was the sum of rates for free acetonedicarboxylic acid (and ions) and the metal complex. The con-

Can. J. Chem. Downloaded from www.nrcresearchpress.com by 210.87.254.5 on 09/05/12
For personal use only.

TABLE X

Decomposition of acetonedicarboxylic acid catalyzed by zinc, cobalt, or nickel

Run	Metal	10^2M	10^2A	pH	10^5 rate	10^3k_u
1	Zn	1.71	5.28	4.00	6.49	1.53
2	,,	,,	,,	4.31	4.75	1.48
3	,,	,,	,,	4.47	4.09	1.52
4	,,	,,	,,	4.57	3.72	1.53
1	Co	4.416	4.416	3.76	7.91	2.20
2	,,	,,	,,	3.97	6.57	1.82
3	,,	,,	,,	4.01	6.90	2.10
4	,,	,,	,,	4.19	6.57	2.24
5	,,	,,	,,	4.26	6.41	2.28
1	Ni	5.169	5.169	3.63	11.68	3.12
2	,,	,,	,,	3.79	10.89	2.90
3	,,	,,	,,	3.96	11.58	3.36
4	,,	,,	,,	4.17	10.81	3.23
5	,,	,,	,,	4.44	10.20	3.17

centration of complex was calculated from the equilibrium constants obtained above. The results are given in Table X. The last column gives the values of k_u, the rate constants for the decomposition of the complexes. In no case is any appreciable drift with pH apparent, certainly not as compared with the experimental error. The average values for the rate constants are: $k_{Zn} = 1.52 \times 10^{-3}$ min^{-1}; $k_{Co} = 2.13 \times 10^{-3}$ min^{-1}; and $k_{Ni} = 3.16 \times 10^{-3}$ min^{-1}. The accuracy, of course, depends on the equilibrium constants, as well as the measured rates. However, since the metals are complexed to a considerable extent, the errors from the equilibrium constants are not as bad as might be supposed: for instance a change of K_{Co} from 45 to 40 alters k_{Co} by 4%. Perhaps as an estimate we may write $k_{Zn} = 1.5\ (\pm 0.15) \times 10^{-3}$; $k_{Co} = 2.1\ (\pm 0.2) \times 10^{-3}$; and $k_{Ni} = 3.15\ (\pm 0.3) \times 10^{-3}$ min^{-1}.

Infrared Spectra of Solids

Since copper behaved rather differently from the other metals, an attempt was made to prepare solid metal acetonedicarboxylates and to examine their infrared spectra. The sodium salt (Na_2A) was crystallized from water. Equimolar amounts of the other metal perchlorates and acetonedicarboxylic acid were mixed, the pH was adjusted to about 4 by NaOH, and ethanol was added, when precipitation occurred. The green copper salt was soluble in water, but the others could not be recrystallized, either from water or a variety of organic solvents. The copper salt gave an analysis (for Cu, Na) agreeing with $NaCuL.2H_2O$; the others gave somewhat variable analysis, though the metal content was always high enough to preclude any other ratio of metal to acid than 1:1. While these salts were not obtained pure, the qualitative differences in their spectra (in a Nujol mull) are worth mentioning. The free acid (H_2A) has two strong maxima at 1688 and 1730 cm^{-1}, and the sodium salt (Na_2A) has one at 1587 cm^{-1}. The cobalt, nickel, and zinc salts have strong maxima at 1589 cm^{-1}, and weak maxima at 1700 cm^{-1}. The copper salt has strong maxima at 1574 and 1602 cm^{-1}, a moderate maximum at 1507 cm^{-1}, and weak maximum at 1700 cm^{-1}.

Discussion

The stability and rate constants obtained above are summarized in Table XI, and some comments can be made about them. Firstly the stability constants follow the common pattern of increasing from cobalt to copper and decreasing again for zinc. The rate constants follow the same pattern, but the increase at copper is

TABLE XI

Summary of stability and rate constants (25 °C)

Species	10^3 rate k (min^{-1})	Stability K (M^{-1})	pK_a
H_2A	1.25	—	3.01
HA^-	2.90	—	3.82
A^{2-}	0.1	—	—
CoA	2.1	45	—
NiA	3.15	60	—
CuA	201	112	3.81
CuL^-	5.6	—	—
ZnA	1.5	87	—

Can. J. Chem. Downloaded from www.nrcresearchpress.com by 210.87.254.5 on 09/05/12
For personal use only.

Can. J. Chem. Downloaded from www.nrcresearchpress.com by 210.87.254.5 on 09/05/12
For personal use only.

much more marked, as is the decrease at zinc. However, there seems to be no quantitative correlation between the rate and stability constants given in Table XI.

The formation of the CuL^- species for copper, but not for the other metals, is somewhat surprising. Admittedly the cobalt, nickel, and zinc complexes might behave similarly at higher pH (above 5), so the difference may not be as marked as appears at first. However, the different infrared spectra, as well as the different acid–base behavior, suggests that the neutral copper complex might possibly be **1** and the others of formula **2**. A greater amount of enolization of the copper complex has been noted for the oxaloacetate ion (4, 5), but the difference does not seem to be as great as here.

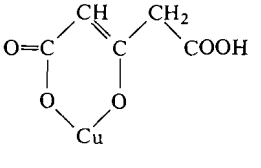

1

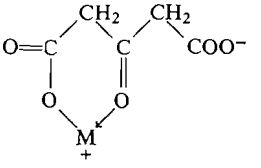

2

It is of interest to note that the CuL^- species is much less reactive than CuA, by roughly the same factor as is A^{2-} compared with HA^-. A tentative explanation is to suggest that in H_2A and HA^- the decarboxylation proceeds through a cyclic electron shift involving the proton (11),

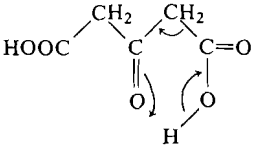

$10^3k = 1.25,$

and that this is easier than the similar reaction with the ion A^{2-}.

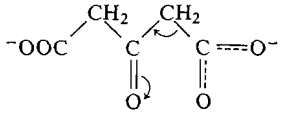

$10^3k = 0.1$

In MA species, where M is Co, Ni, or Zn, the positive charge on the metal assists the electron shift.

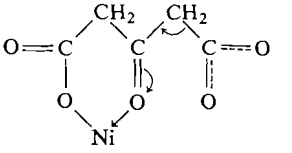

$10^3k = 3.15$

In CuA, a different concerted electron shift is possible,

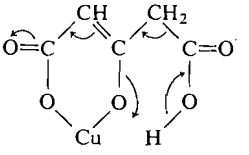

$10^3k = 200,$

which evidently goes more readily; while even in CuL^-, this is still fairly easy, though (as was mentioned above) the drop in rate constant is similar to that between HA^- and A^{2-}.

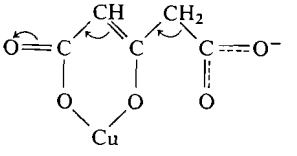

$10^3k = 6$

Acknowledgment

The authors thank the National Research Council of Canada for financial assistance to D. W. L.

1. E. O. Wiig. J. Phys. Chem. **32**, 961 (1928); **34**, 596 (1930).
2. H. A. Krebs. Biochem. J. **36**, 303 (1942).
3. J. E. Prue. J. Chem. Soc. 2331 (1952).
4. E. Gelles and R. W. Hay. J. Chem. Soc. 3673 (1958).
5. E. Gelles and A. Salama. J. Chem. Soc. 3683, 3689 (1958).
6. P. Job. Ann. Chim. Paris, **9**, 113 (1928).
7. R. A. Robinson and R. H. Stokes. Trans. Faraday Soc. **36**, 740 (1940).
8. I. Leden. Z. Physik. Chem. Leipzig, **A188**, 160 (1941).
9. C. J. Nyman, E. W. Murbach, and G. B. Millard. J. Am. Chem. Soc. **77**, 4194 (1955).
10. K. J. Pedersen. J. Am. Chem. Soc. **51**, 2098 (1929).
11. K. J. Pedersen. J. Phys. Chem. **38**, 559 (1934).

Can. J. Chem. Downloaded from www.nrcresearchpress.com by 210.87.254.5 on 09/05/12
For personal use only.

Free radicals by mass spectrometry. XXXVIII. Primary steps in the mercury-photosensitized decompositions of dimethyl sulfide and dimethyldisulfide[1]

A. JONES,[2] S. YAMASHITA,[3] AND F. P. LOSSING
Division of Pure Chemistry, National Research Council of Canada, Ottawa, Canada

Received October 4, 1967

The reaction between mercury ($^3P_1$) atoms and dimethylsulfide at 55 °C has been shown to be exclusively

$$Hg(^3P_1) + CH_3SCH_3 \rightarrow CH_3S + CH_3 + Hg(^1S_0).$$

Two primary modes of dissociation have been established for the corresponding reaction with dimethyldisulfide.

$$Hg(^3P_1) + CH_3SSCH_3 \rightarrow CH_3SS + CH_3 + Hg(^1S_0)$$

$$Hg(^3P_1) + CH_3SSCH_3 \rightarrow 2CH_3S + Hg(^1S_0)$$

The former reaction accounts for $\sim 20\%$ of the primary decomposition at 55 °C. No reaction leading to H-atom removal was found for either compound.

The subsequent reactions of CH_3S and CH_3SS radicals, chiefly combination and disproportionation, have been investigated briefly.

Canadian Journal of Chemistry, **46**, 833 (1968)

Introduction

The mercury-photosensitized decompositions of a large number of hydrocarbons and oxygen- and nitrogen-containing compounds have now been studied and for many the mechanism has been established in some detail (1). Except for some measurements of quenching cross sections, however, no studies have been reported for the $Hg(^3P_1)$-photosensitized decompositions of sulfur-containing compounds.

The production of alkylthiyl radicals in the pyrolysis and direct photolysis of dialkyl sulfides and alkyl disulfides has been reviewed recently (2). The mercury-sensitized photodecompositions of dimethylsulfide and dimethyldisulfide are of interest since they promise to be sources of the methylthiyl (CH_3S) radical, about which our knowledge is rather limited. Interest centers on similarities to, and differences from, the methoxyl radical whose reactions are now well documented.

Experimental

The mercury-photosensitized decompositions were studied using a fast flow system coupled to a mass spectrometer. The apparatus and method of operation have been described previously (3) and it is sufficient here to give only the salient features.

The reactant and mercury vapor at partial pressures of a few microns were carried in a stream of helium at 8 Torr pressure through a tubular reactor which was illuminated by a low pressure mercury lamp of high intensity. In the present experiments the residence time in the reactor at 55 °C was about 1×10^{-3} s. Directly following the illuminated zone, the reaction stream passed over a small orifice leading directly into the ionization chamber of a mass spectrometer. The partial pressures of reactant and product gases in the immediate neighborhood of the orifice can be measured with the mass spectrometer after appropriate determinations of sensitivity coefficients have been made. The reaction conditions resemble those of flash photolysis insomuch as a relatively large concentration of free radicals is generated. Thus reactions between free radicals are favored over radical–substrate reactions.

Dimethylsulfide (B.D.H. Canada Ltd.) and dimethyldisulfide (Eastman Organic Chemicals) were purified by several bulb-to-bulb distillations *in vacuo*. Mass spectra and nuclear magnetic resonance (n.m.r.) analysis were used as tests of purity. The sample of mercury dimethyl-d_6 was prepared by Dr. L. C. Leitch.

Results and Discussion

Decomposition of Dimethylsulfide

Preliminary experiments using low energy ionizing electrons showed an increase at $m/e = 15$ when the reactor was illuminated, indicating the presence of methyl radicals. No increase at $m/e = 47$ (CH_3S) could be detected under the same experimental conditions, suggesting that CH_3S radicals have a lower effective sensitivity in the mass spectrometer than do CH_3 radicals. No increase was found at $m/e = 61$ (CH_3SCH_2).

Analysis at the 50 V mass spectra obtained when the reactor was illuminated showed that the major products of the reaction were dimethyldisulfide, methyl mercaptan, and ethane. Minor

---

[1]NRCC Contribution No. 9864.
[2]NRCC Postdoctorate Fellow 1965–1967.
[3]Visiting Scientist from University of Osaka Prefecture, Japan.

products detected were methane, unreacted methyl radicals, and a trace of carbon disulfide. After the spectra of these products had been subtracted from the composite product spectrum, there remained small peaks at $m/e = 46$ and 45. This residue was shown to be real in a number of experiments concentrating only on this part of the spectrum. The ratio 46/45 was approximately 0.7. This spectrum is attributed to thioformaldehyde, H_2CS (4), the sulfur analog of formaldehyde. Since this compound has not been isolated in monomeric form, no sensitivity coefficient could be obtained and its concentration could not be measured directly. The products expressed in mole % [(number of moles formed per mole of CH_3SCH_3 decomposed) $\times$ 100] are shown in Table I. Since the most abundant products are the dimers of CH_3 and CH_3S radicals, it is evident that the reaction proceeds principally by scission of the carbon–sulfur bond.

TABLE I

Mercury-photosensitized decomposition of CH_3SCH_3 (6.2 microns) in 8 Torr helium (decomposition = 20%)

Product	Mole %	
C_2H_6	40.6	
$CH_3S_2CH_3$	28.8	
CH_3SH	11.8	
CH_4	3.0	
CH_3	7.0	
CS_2	0.76	
H_2CS	Not measured	
C balance	80.6%	87.8%*
S balance	70.2%	85.1%
H balance	82.8%	88.1%

*Balances incorporating CH_2S contribution based on disproportionation mechanism.

[1] $CH_3SCH_3 + Hg(^3P_1) \rightarrow CH_3S + CH_3 + Hg(^1S_0)$

A careful search was made for both hydrogen and the dimer $(CH_3SCH_2)_2$, but neither was present in detectable amounts. A more sensitive search for CH_3SCH_2 radicals was made, using a "titration" of the reaction by a large excess of CH_3 radicals, produced by the simultaneous photodecomposition of $Hg(CH_3)_2$ added to the reaction stream (5). Although a small peak at the parent mass for the $CH_3SCH_2CH_3$ adduct (*m/e* 76) was present, it did not increase with the addition of CH_3 radicals. This is shown in Fig. 1. This peak is also the parent peak of CS_2 which appears to be formed in trace amounts in the reaction. The estimated sensitivity of detection for the CH_3SCH_2 radical by this test is about 2% of the total reaction, and this upper limit may be set for the alternative primary process

[2] $CH_3SCH_3 + Hg(^3P_1) \rightarrow CH_3SCH_2 + H + Hg(^1S_0)$.

A similar titration of the reaction with CD_3 radicals formed from $Hg(CD_3)_2$ gave the results shown in Fig. 2 (curve A). The yield of CH_3SCD_3 increased with increasing CD_3 addition, reaching a limiting yield of 0.62 of the sulfide decomposed (assuming equal sensitivity coefficients for CH_3SCH_3 and CH_3SCD_3). Since the interaction of CH_3S and CD_3 may also lead to disproportionation, this limit represents the minimum fraction of the primary decomposition which gives CH_3S radicals. It can be seen from Fig. 2 (curve B) that the yield of the dimer CH_3SSCH_3 falls correspondingly toward zero as the CH_3S radicals are progressively removed by titration with CD_3 radicals. During this titration experiment it was observed that the fully deuterated sulfide CD_3SCD_3 was produced in small

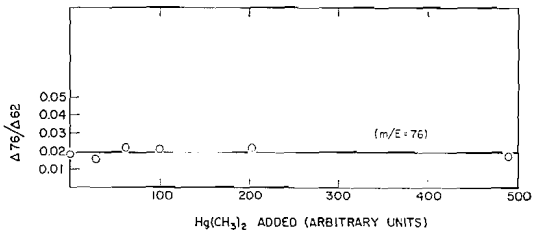

FIG. 1. Effect of adding $Hg(CH_3)_2$ to reaction stream during the decomposition of dimethyl sulfide. Δ76/Δ62 is the ratio of peak heights.

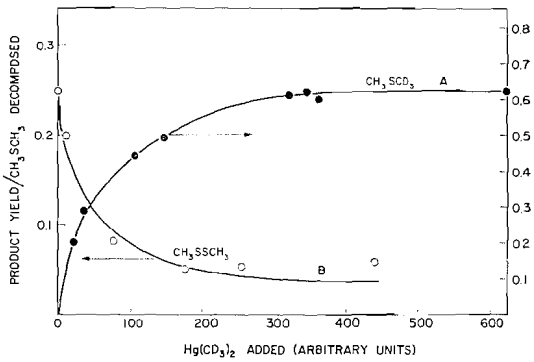

FIG. 2. Curve A. Limiting yield of CH_3SCD_3 formed by addition of $Hg(CD_3)_2$ to reaction stream during the decomposition of dimethyl sulfide. Curve B. Effect of $Hg(CD_3)_2$ addition on the yield of CH_3SSCH_3.

Can. J. Chem. Downloaded from www.nrcresearchpress.com by 210.87.254.5 on 09/05/12
For personal use only.

Can. J. Chem. Downloaded from www.nrcresearchpress.com by 210.87.254.5 on 09/05/12
For personal use only.

amounts, reaching a limiting yield of 0.08. This is thought to result from a secondary photosensitized reaction, according to the sequence:

[3] $CD_3 + CH_3S \rightarrow CH_3SCD_3$

[4] $CH_3SCD_3 + Hg(^3P_1) \rightarrow CH_3 + CD_3S + Hg(^1S_0)$

[5] $CD_3 + CD_3S \rightarrow CD_3SCD_3$.

There is an alternative possibility which must be considered, since it would affect the reliability of the CD_3 titration. The displacement reaction

[6] $CH_3 + CD_3SH \rightarrow CH_3SH + CD_3$

has been reported (6) and the two-step sequence

[7] $CD_3 + CH_3SCH_3 \rightarrow CD_3SCH_3 + CH_3$

[8] $CD_3 + CD_3SCH_3 \rightarrow CD_3SCD_3 + CH_3$

is possible in principle. However, reaction [6] would be $\sim 10^5$ times slower (log $A = 10.73$ mole^{-1} cm^3 s^{-1}, $E = 7.6$ kcal/mole) than the radical combination reactions occurring in the titration. Moreover, the sequence of reactions [7] and [8] would lead to a continuous increase for curve A, Fig. 2, at the higher CD_3 concentrations, rather than the plateau observed.

Effect of Addition of Carbon Monoxide

The effect of carbon monoxide addition on Hg-photosensitized reactions under the conditions employed in this work has been used as a test to show whether a decomposition proceeds through formation of an electronically excited precursor, or by a nonexcited state paraffin-type reaction (3, 7). Two distinct types of behavior are found: a 1.6–2.5-fold increase in the rate of decomposition, attributed to an increased rate of formation of the excited state precursor through the action of a postulated complex HgCO*, or no effect other than a slight decrease in rate attributable to competitive quenching of $Hg(^3P_1)$ by CO. The two types of behavior can in fact be observed for two different primary dissociation processes in the same molecule (7). The effect of the addition of CO to the reaction stream containing CH_3SCH_3 is shown in Fig. 3. According to the interpretation given above, the rate enhancement observed indicates that reaction [1] proceeds by formation of an electronically excited state of CH_3SCH_3, presumably a triplet, which then dissociates by C—S bond rupture.

Decomposition Mechanism

On the basis of the findings given above, the following mechanism can be proposed (where * denotes electronic excitation).

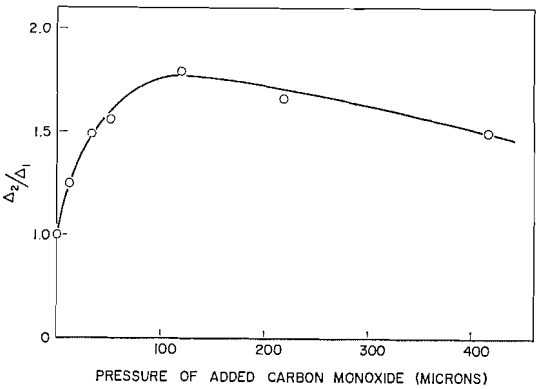

FIG. 3. Effect of added CO on the decomposition of dimethyl sulfide. Δ_2 is the decomposition in the presence and Δ_1 in the absence of added CO.

[9] $CH_3SCH_3 + Hg(^3P_1) \rightarrow CH_3SCH_3^* + Hg(^1S_0)$

[10] $CH_3SCH_3^* \rightarrow CH_3S + CH_3$

[11] $2CH_3S \rightarrow CH_3SSCH_3$

[12] $2CH_3S \rightarrow CH_3SH + H_2CS$

[13] $CH_3 + CH_3S \rightarrow CH_3SCH_3$

[14] $CH_3 + CH_3S \rightarrow CH_4 + H_2CS$

[15] $2CH_3 \rightarrow C_2H_6$

This mechanism leads to the following relationship among the products, where the quantities in brackets are the concentrations measured at the sampling orifice.

$$[16]\quad \tfrac{1}{2}[CH_3S] + [CH_3SH] + [CH_3SSCH_3] = [C_2H_6] + \tfrac{1}{2}[CH_3]$$

Inserting the measured concentrations given in Table I gives $0.47 = 0.51$ for this equality, assuming that $\frac{1}{2}[CH_3S]$ does in fact equal zero, since this radical could not be detected. Assuming, on the other hand that the concentration of undetected CH_3S is equal to that detected for CH_3, the equality becomes exact ($0.51 = 0.51$). The C, S, and H balances for the observed products are given in Table I, in the first column excluding H_2CS, and in the second column including an amount of H_2CS calculated on the basis that $[H_2CS] = [CH_4] + [CH_3SH]$. The good agreement of C, S, and H balances in the latter case supports this assumption. The fate of the missing 15% is not known. The missing component appears to have the same C, S, and H ratio as the dimethylsulfide itself. The

Can. J. Chem. Downloaded from www.nrcresearchpress.com by 210.87.254.5 on 09/05/12
For personal use only.

formation of some polymer was indicated by a progressive deposition of an opaque substance on the reactor walls, which could be removed completely by heating in a stream of air.

The Combination and Disproportionation Reactions of CH_3S

In the above mechanism, the only source of CH_3SH has been taken as reaction [12], and the disproportionation to combination ratio for two CH_3S radicals, k_{12}/k_{11}, would be given by the product ratio $[CH_3SH]/[CH_3SSCH_3]$. The average of several experiments gave this ratio as 0.4 ± 0.1.

The result is in line with previous investigations where disproportionation between two alkylthiyl radicals has been found to occur. Thus Coope and Bryce (8) studied the gas phase pyrolysis of dimethyldisulfide and found 1 mole of methylmercaptan per mole of reacted disulfide, together with a product they believed to be a thioformaldehyde polymer. Later, Rosengren (9) photolyzed a number of alkyl disulfides in a hydrocarbon matrix at 77 °K and recorded spectral changes both at 77° and on warm up. The detection of both products mercaptan and thioaldehyde (or ketone) established the occurrence of disproportionation as the only reaction leading to decomposition.

The results presented here are, however, in disagreement with those obtained by Knight *et al.*, who concluded that the disproportionation reaction for CH_3S radical produced from the direct photolysis of methylmercaptan (10) and dimethyldisulfide (11) was many times slower than the combination. Their conclusion was based on the apparent absence of H_2CS or its trimer among the products and the relatively small amount of CH_3SH produced from dimethyldisulfide photolysis compared with the rate of CH_3S formation. (The authors preferred an abstraction reaction leading to the formation of CH_3SH.) Such a slow disproportionation reaction would be rather surprising in view of its large exothermicity, 42 ± 8 kcal/mole (4), but on the other hand the exothermicity for reaction [11] is even greater. The evidence for $k_{12}/k_{11} = 0.4 \pm 0.1$ obtained from the present work is not unambiguous, owing to the difficulty in making a quantitative analysis for H_2CS, and its concurrent formation from reaction [14]. The magnitude of k_{12}/k_{11} depends, therefore, mainly on the assumption that CH_3SH is formed solely from reaction [12]. There are two alternative sources, abstraction of H atom from the parent sulfide, and from substances adsorbed on the walls of the ion source.

[17] $CH_3S + CH_3SCH_3 \rightarrow CH_3SH + CH_2SCH_3$

[18] $CH_3S + H(wall) \rightarrow CH_3SH$

Reaction [17] as a source for the observed quantity of CH_3SH can be ruled out, since no trace of the expected addition products of the CH_3SCH_2 radical were found. It should be noted that even with a large excess of added CH_3 radical there was no evidence for formation of this radical by the corresponding abstraction reaction

[19] $CH_3 + CH_3SCH_3 \rightarrow CH_4 + CH_2SCH_3$.

Since reaction [19] would be expected to be faster than [17], it is evident that [17] can be neglected. With regard to wall reaction there seems no reason why reaction [18] should be faster than the corresponding reaction of CH_3 radical. In thermal decomposition experiments no difficulty was encountered in obtaining good yields of CH_3S radicals in a similar apparatus (12).

Some conclusions can be drawn about the ratio of disproportionation to combination for $CH_3 + CH_3S$, that is, k_{14}/k_{13}. In the CD_3 titration experiment whose result is shown in Fig. 2, the yield of CH_3SCD_3 was only 0.62, while the results in Table I indicate that at least 85% of the CH_3SCH_3 decomposed to give $CH_3 + CH_3S$ radicals. Assuming that the titration of CH_3S was complete, as suggested by the plateau in curve A, Fig. 2, the combination reaction [3] accounted for 0.62/0.85 of the CH_3S radicals. To this should be added the yield of CD_3SCD_3, 0.08, formed through reactions [3], [4], and [5]. The combination reaction would then account for 0.70/0.85 or 0.82 of the total radical interaction, and the disproportionation reaction

[20] $CD_3 + CH_3S \rightarrow CD_3H + H_2CS$

would account for 0.18. The ratio k_{20}/k_3 then becomes 0.2, with the corresponding ratio for undeuterated species, k_{14}/k_{13}, presumably not greatly different.

Comparison with the $Hg(^3P_1)$-Sensitized Reaction of Dimethyl Ether

Although CH_3OCH_3 and CH_3SCH_3 are analogous species, the modes of reaction with

Can. J. Chem. Downloaded from www.nrcresearchpress.com by 210.87.254.5 on 09/05/12
For personal use only.

$Hg(^3P_1)$ atoms appear to be entirely different. According to the present work CH_3SCH_3 reacts through formation of an electronically excited molecule which dissociates mainly or exclusively by C—S bond scission, without loss of a H atom. The $Hg(^3P_1)$-sensitized reaction of CH_3OCH_3, on the other hand, appears not to involve an electronically excited precursor (7) and proceeds, according to recent work (13), mainly through removal of H atom by $Hg(^3P_1)$ in a reaction apparently similar to that found for paraffins. This difference in the nature of the primary interaction is also illustrated by the large difference in quenching cross sections, 49.3 $Å^2$ for dimethylsulfide and 10 $Å^2$ for dimethyl ether (Procedure II values from ref. 1). The difference presumably results from the greater availability of suitable triplet states in the sulfur compound. The weakness of the C—S bond compared with the C—O bond may also be a factor contributing to the different mode of dissociation.

Decomposition of Dimethyldisulfide

In the decomposition of this compound, an increase in *m/e* 47 was observed with low energy ionizing electrons indicating that CH_3S radicals were formed. Analysis of the product spectra using 50 V electrons, though more complex than for CH_3SCH_3, showed that the products were dimethylsulfide, 2,3,4-trithiopentane (CH_3SSSCH_3), methyl mercaptan, and methane. The peak residues remaining after the spectra of these products had been stripped from the composite spectrum were consistent with the formation of thioformaldehyde, carbon disulfide, and methylhydrodisulfide. These products could not be estimated quantitatively. As mentioned above, thioformaldehyde does not remain in monomeric form, and methylhydrodisulfide appears to be unstable at room temperature (14). The carbon disulfide could not be estimated owing to the possibility of an unknown contribution from the hydrodisulfide. The product yields obtained are given in Table II along with the derived mass balances.

The products found, particularly the trisulfide, indicate that two primary dissociations are occurring; one by the fission of a S—S bond and the other by fission of a C—S bond.

[21] $Hg(^3P_1) + CH_3SSCH_3 \rightarrow 2CH_3S + Hg(^1S_0)$

[22] $Hg(^3P_1) + CH_3SSCH_3 \rightarrow CH_3SS + CH_3 + Hg(^1S_0)$

TABLE II

Mercury-photosensitized decomposition of CH_3SSCH_3 (1.96 microns) in 8 Torr helium (decomposition = 16%)

Product	Mole %
CH_3SCH_3	26.5
CH_3SSSCH_3	25.9
CH_3SH	22.0
C_2H_6	13.4
CH_4	1.9
CH_2S	Not measured
CH_3SSH	Not measured
CS_2	Not measured
Mass balances (CH_2S, CH_3SSH, and CS_2 not included)	
C	77.8%
S	63.2%
H	81.5%

A third possible mode of decomposition is the breaking of a C—H bond.

[23] $Hg(^3P_1) + CH_3SSCH_3 \rightarrow CH_3SSCH_2 + H + Hg(^1S_0)$

A search for hydrogen and the dimer $(CH_3SSCH_2)_2$ was made but neither was present in significant amounts. The absence of CH_3SSCH_2 radical was confirmed in titration experiments using $Hg(CH_3)_2$. No peak at $m/e = 108$, corresponding to the parent peak of the addition compound of CH_3SSCH_2 with CH_3, could be detected. The estimated sensitivity of detection indicates that reaction [23], if it occurs at all, accounts for less than 2% of the primary dissociation.

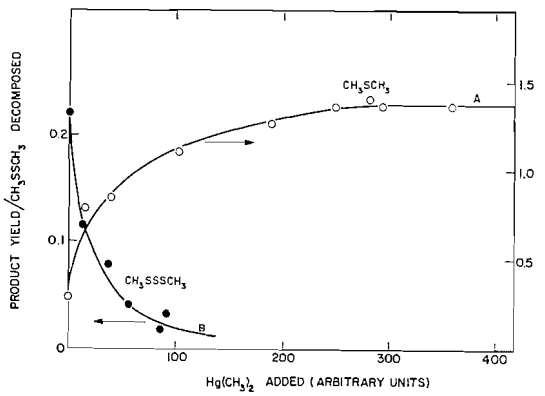

FIG. 4. Curve A. Limiting yield of CH_3SCH_3 formed by addition of $Hg(CH_3)_2$ to the reaction stream during the decomposition of dimethyldisulfide. Curve B. Effect of $Hg(CH_3)_2$ addition on the yield of 2,3,4-trithiopentane.

Can. J. Chem. Downloaded from www.nrcresearchpress.com by 210.87.254.5 on 09/05/12
For personal use only.

Titration experiments using $Hg(CH_3)_2$ and $Hg(CD_3)_2$ gave positive confirmation of the occurrence of the two primary dissociation modes, reactions [21] and [22]. The results of the titration of the CH_3S radical by CH_3 radicals from the addition of $Hg(CH_3)_2$ to the reaction stream are shown in Fig. 4 (curve A). A yield of 1.38 CH_3S radicals per molecule of disulfide decomposed was obtained. Titration with $Hg(CD_3)_2$ showed formation of the fully deuterated dimethyl sulfide (yield .08) explained as before by reactions [3], [4], and [5]. Curve B in Fig. 4 shows the rapid decrease of the 2,3,4-trithiopentane when $Hg(CH_3)_2$ is added to the reaction stream, confirming that the trisulfide arises from the free radical precursors CH_3S and CH_3SS.

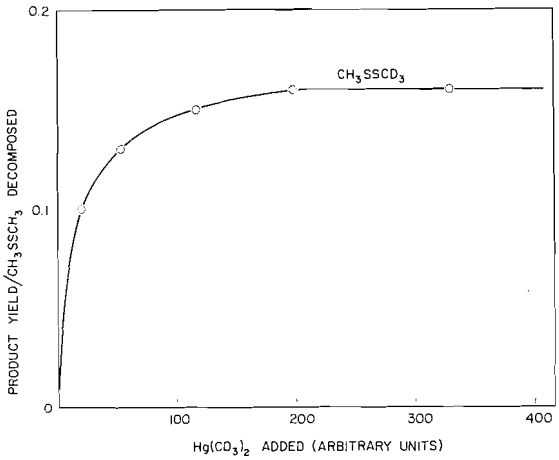

FIG. 5. Limiting yield of CH_3SSCD_3 formed by addition of $Hg(CD_3)_2$ to the reaction stream during the decomposition of dimethyldisulfide.

Titration experiments employing $Hg(CD_3)_2$ demonstrated the presence of methyldithiyl (CH_3SS) radicals in the system by detection of the adduct CH_3SSCD_3. The results are shown in Fig. 5. The height of the plateau indicated a yield of 0.16 CH_3SSCD_3 per substrate molecule decomposed.

Effect of Carbon Monoxide

An effect identical with that found for the dimethylsulfide decomposition was observed with carbon monoxide addition. In a single determination the addition of 200 microns of carbon monoxide to the reaction stream caused the amount of decomposition to increase by a factor of 1.8. It may be concluded that the decomposition, as for that of CH_3SCH_3, proceeds by way of an excited electronic state.

Decomposition Mechanism

The following mechanism, based on the two primary modes of dissociation, is put forward to explain the products observed.

[24] $CH_3SSCH_3 + Hg(^3P_1) \rightarrow CH_3SSCH_3^* + Hg(^1S_0)$

[25] $CH_3SSCH_3^* \rightarrow 2CH_3S$

[26] $CH_3SSCH_3^* \rightarrow CH_3SS + CH_3$

[11] $2CH_3S \rightarrow CH_3SSCH_3$

[12] $2CH_3S \rightarrow CH_3SH + H_2CS$

[27] $CH_3SS + SCH_3 \rightarrow CH_3SSSCH_3$

[28] $CH_3SS + SCH_3 \rightarrow CH_3SSH + H_2CS$

[29] $CH_3SS + CH_3 \rightarrow CH_3SSCH_3$

[13] $CH_3S + CH_3 \rightarrow CH_3SCH_3$

[14] $CH_3S + CH_3 \rightarrow CH_4 + CH_2S$

[15] $2CH_3 \rightarrow C_2H_6$

The titration experiments with $Hg(CD_3)_2$ indicated that decomposition proceeding by C—S split (reaction [26]) accounts for at least 16% of the overall decomposition. The amount of trisulfide formed (see Table II) indicates that this mode accounts for 26% of the decomposition. The difference between these two numbers, though perhaps not much larger than the experimental error, may indicate that combination is more efficient (i.e. less disproportionation) between CH_3SS and SCH_3 than between CH_3SS and CD_3. The usual type of disproportionation reactions between the latter pair does not seem likely;

[30] $CD_3 + CH_3SS \rightarrow CD_3H + (CH_2SS)$,

but a reaction of the type

[31] $CD_3 + CH_3SS \rightarrow CH_3S + CD_3S$

could be possible. In this case titration with CD_3 would produce fully deuterated dimethyl sulfide which could possibly account for some of that observed. Methylhydrosulfide has been assumed to arise by the disproportionation reaction [28]. The alternative possibility that it is formed by abstraction from a substrate molecule is considered unlikely under our conditions in view of the reported unreactive nature of these radicals (see ref. 2). Moreover, no addition products of the CH_2SSCH_3 radical which would be formed in this abstraction reaction were observed.

Acknowledgment

The authors wish to thank Prof. B. G. Gowenlock for access to ref. 2 in advance of publication.

1. R. J. CVETANOVIĆ. Progr. Reaction Kinetics, **2**, 41 (1964).
2. N. J. FRISWELL and B. G. GOWENLOCK. *In* Advances in free radical chemistry. Vol. 2. Logos Press, London. 1967. p. 26.
3. J. B. HOMER and F. P. LOSSING. Can. J. Chem. **44**, 143 (1966).
4. A. JONES and F. P. LOSSING. J. Phys. Chem. **71**, 4111 (1967).
5. J. COLLIN and F. P. LOSSING. Can. J. Chem. **35**, 778 (1957).
6. G. GREIG and J. C. J. THYNNE. Trans. Faraday Soc. **62**, 379 (1966).
7. A. JONES and F. P. LOSSING. Can. J. Chem. **45**, 1685 (1967).
8. J. A. R. COOPE and W. A. BRYCE. Can. J. Chem. **32**, 768 (1954).
9. K. J. ROSENGREN. Acta Chem. Scand. **16**, 1401 (1962).
10. R. P. STEER, B. L. KALRA, and A. R. KNIGHT. J. Phys. Chem. **71**, 783 (1967).
11. P. M. RAO, J. A. COPECK, and A. R. KNIGHT. Can. J. Chem. **45**, 1369 (1967).
12. T. F. PALMER and F. P. LOSSING. J. Am. Chem. Soc. **84**, 4661 (1962).
13. L. F. LOUCKS and K. J. LAIDLER. Can. J. Chem. **45**, 2763 (1967).
14. H. BOHME and G. ZINNER. Ann. **585**, 142 (1954).

Can. J. Chem. Downloaded from www.nrcresearchpress.com by 210.87.254.5 on 09/05/12
For personal use only.

Dielectric studies. Part XVII. Relaxation processes and corresponding enthalpies of activation of some mono-substituted benzenes

J. CROSSLEY
University of Aston in Birmingham, England
AND
S. WALKER
Chemistry Department, Lakehead University, Port Arthur, Ontario

Received August 28, 1967

The dielectric absorption at several microwave frequencies of liquid ethylbenzene, isopropylbenzene, and phenyltrimethylsilane at 15, 37.5, and 50 °C and cyclohexane solutions of *t*-butylbenzene and benzotrichloride at 15, 37.5, 45, and 50 °C has been examined. Benzotrichloride has also been studied in cyclohexane and *p*-xylene solution at 25 °C. Only molecular reorientation can be detected for benzotrichloride, whereas the remainder are all characterized by an absorption that may be analyzed into two relaxation times, one associated with molecular reorientation (τ_1) and a shorter relaxation time (τ_2) which appears to be attributable to an intermolecular process. The enthalpies of activation of the τ_1 process show the expected increase with increasing molecular size, while no temperature dependence is detectable for the shorter relaxation process.

Canadian Journal of Chemistry, 46, 841 (1968)

Can. J. Chem. Downloaded from www.nrcresearchpress.com by 210.87.254.42 on 09/05/12
For personal use only.

Previous work (1, 2) has shown that the mean relaxation times of *o*-xylene, *m*-xylene, toluene, and ethyl-, isopropyl-, and *t*-butyl-benzene were short in comparison with those of rigid molecules of similar shape and size (2, 3). The dielectric absorption of these alkylbenzenes at 25 °C and 1-methyl- and 2-methyl-naphthalene at 50 °C was analyzed in terms of molecular reorientation and also a short relaxation time process. Furthermore, the mean relaxation times of some phenyl-substituted compounds were found to be significantly short (4), indicating a large contribution to the absorption from some short relaxation time process (τ_2). Two explanations have been considered to explain τ_2: (*a*) an intermolecular process, e.g. the decay of some form of charge distortion resulting from molecular collisions, or (*b*) an intramolecular relaxation process involving rotation about the alkyl–aryl bond in which the overlap of the alkyl group orbitals with the π electrons of the ring might vary. This would cause some movement of charge to and fro between the π-electron cloud of the phenyl group and the alkyl group during rotation, and implies oscillation of negative charge. The weight of evidence favored mechanism (*a*). However, it seemed worthwhile examining the dielectric absorption of phenyltrimethylsilane and ethyl-, isopropyl-, and *t*-butylbenzene over a temperature range in order to obtain the enthalpies of activation $\Delta H_0^{\ddagger}$, $\Delta H_1^{\ddagger}$, and $\Delta H_2^{\ddagger}$ associated with the mean relaxation time, τ_1 and τ_2 respectively, and also to determine whether the weight factor of the shorter relaxation process was temperature dependent, the main aim being to gain more information on the characteristics of the τ_2 process.

Experimental Methods

The preparation of phenyltrimethylsilane and the purification of cyclohexane, *p*-xylene, and ethyl-, isopropyl-, and *t*-butyl-benzene have been described elsewhere (1, 4, 5). Benzotrichloride was dried over calcium chloride and fractionally distilled using a 30 theoretical plate spinning band column. A small center fraction was collected and the purity confirmed by gas–liquid chromatography.

The apparatus and techniques employed have been described previously (5, 6). The dielectric constant (ϵ') and loss factor (ϵ'') were determined at 70.00, 35.09, 23.98, 16.20, 9.313, and 6.700 Gc/s. The static dielectric constant (ϵ_0) was measured with a heterodyne beat apparatus at 2 Mc/s.

Experimental Results

The evaluation of the high frequency dielectric constant (ε_∞), distribution coefficient (α), mean relaxation time (τ_0), discrete relaxation times (τ_1 and τ_2), weight factors (C_1 and C_2), and dipole moment (μ) has been described previously (2).

From the relaxation time the free-energy barrier ($\Delta G^{\ddagger}$) separating two equilibrium positions of the relaxing dipole may be evaluated from transition-state theory (7) to be

$$1/\tau = \kappa(kT/h) \exp(-\Delta G^{\ddagger}/RT),$$

Can. J. Chem. Downloaded from www.nrcresearchpress.com by 210.87.254.42 on 09/05/12
For personal use only.

TABLE I

Dielectric constant and loss data for some substituted benzenes in pure liquid and in cyclohexane and *p*-xylene solutions at specified weight fractions (w_2). ε' and ε'' are the measured values while ε'_{calcd} and ε''_{calcd} are the values estimated from the τ_1, τ_2, and C_1 values in Table II

w_2	Frequency (Gc/s)	ε'	ε''	ε'_{calcd}	ε''_{calcd}
	Ethylbenzene at 15 °C				
1.0000	35.09	2.30_0	0.044_7	2.29_6	0.045_8
	23.98	2.30_4	0.057_2	2.31_0	0.055_5
	16.20	2.33_0	0.062_0	2.32_9	0.063_6
	9.313	2.36_1	0.060_7	2.36_2	0.062_1
	6.700	2.38_1	0.060_7	2.38_2	0.062_1
	Ethylbenzene at 37.5 °C				
1.0000	35.09	2.26_2	0.048_9	2.26_1	0.050_0
	23.98	2.28_0	0.059_9	2.27_8	0.057_9
	16.20	2.29_9	0.059_7	2.29_9	0.061_3
	9.313	2.33_2	0.056_8	2.32_9	0.056_0
	6.700	2.34_2	0.048_0	2.34_3	0.048_0
	Ethylbenzene at 50 °C				
1.000	35.09	2.24_6	0.048_7	2.24_1	0.049_2
	23.98	2.26_6	0.059_3	2.25_9	0.057_0
	16.20	2.28_4	0.057_2	2.28_1	0.058_7
	9.313	2.31_4	0.049_9	2.30_9	0.049_3
	6.700	2.31_9	0.042_5	2.32_0	0.040_1
	Isopropylbenzene at 15 °C				
1.0000	35.09	2.26_3	0.035_8	2.26_5	0.036_1
	23.98	2.27_2	0.045_2	2.27_5	0.044_8
	16.20	2.28_8	0.053_2	2.28_8	0.054_3
	9.313	2.32_0	0.067_0	2.31_5	0.065_9
	6.700	2.33_5	0.066_7	2.33_6	0.067_8
	Isopropylbenzene at 37.5 °C				
1.0000	35.09	2.23_2	0.038_8	2.23_4	0.038_7
	23.98	2.24_8	0.049_0	2.24_5	0.049_0
	16.20	2.26_3	0.058_0	2.26_3	0.058_2
	9.313	2.29_6	0.061_6	2.29_5	0.061_1
	Isopropylbenzene at 50 °C				
1.000	35.09	2.21_2	0.041_3	2.21_2	0.041_2
	23.98	2.23_2	0.050_8	2.22_6	0.051_5
	16.20	2.24_8	0.059_4	2.24_6	0.058_5
	9.313	2.27_4	0.056_1	2.27_7	0.056_2
	6.700	2.29_2	0.049_1	2.29_2	0.048_7
	t-Butylbenzene in cyclohexane at 15 °C				
0.6757	35.09	2.17_6	0.017_5	2.17_7	0.017_2
	23.98	2.17_7	0.022_9	2.18_1	0.022_3
	16.20	2.18_7	0.026_4	2.18_8	0.027_6
	9.313	2.20_6	0.034_7	2.20_1	0.034_4
	t-Butylbenzene in cyclohexane at 37.5 °C				
0.6840	35.09	2.14_7	0.019_3	2.14_9	0.019_0
	23.98	2.15_0	0.024_1	2.15_4	0.024_6
	16.20	2.16_9	0.030_0	2.16_3	0.029_9
	9.313	2.17_8	0.033_9	2.17_9	0.033_8
	6.700	2.19_8	0.032_9	2.18_5	0.033_5
	t-Butylbenzene in cyclohexane at 45 °C				
0.6800	35.09	2.13_8	0.020_8	2.13_8	0.020_0
	23.98	2.14_1	0.024_8	2.14_4	0.025_9
	16.20	2.16_0	0.031_6	2.15_3	0.031_2
	9.313	2.17_0	0.033_8	2.17_1	0.033_5
	6.700	2.17_9	0.030_7	2.18_1	0.030_8

TABLE I (*Concluded*)

w_2	Frequency (Gc/s)	ε'	ε''	ε'_{calcd}	ε''_{calcd}
	t-Butylbenzene in cyclohexane at 50 °C				
0.6757	35.09	2.12_6	0.021_6	2.12_5	0.021_5
	23.98	2.13_3	0.025_1	2.13_4	0.025_0
	16.20	2.14_9	0.030_3	2.14_2	0.030_4
	9.313	2.16_3	0.029_7	2.15_8	0.030_9
	6.700	2.16_9	0.030_5	2.16_6	0.027_9
	Phenyltrimethylsilane at 15 °C				
1.0000	35.09	2.32_3	0.012_1	2.33_5	0.012_3
	23.98	2.33_5	0.011_9	2.33_8	0.012_9
	16.20	2.34_4	0.015_0	2.34_1	0.013_5
	9.313	2.35_6	0.014_2	2.34_6	0.015_2
	Phenyltrimethylsilane at 37.5 °C				
1.0000	35.09	2.30_3	0.011_6	2.30_3	0.011_5
	23.98	2.30_5	0.012_7	2.30_7	0.012_3
	16.20	2.30_8	0.011_6	2.31_1	0.012_4
	9.313	2.32_1	0.012_6	2.31_6	0.012_5
	Phenyltrimethylsilane at 50 °C				
1.0000	35.09	2.28_7	0.011_7	2.28_2	0.011_0
	23.98	2.28_7	0.011_7	2.28_5	0.011_8
	16.20	2.28_9	0.010_4	2.28_9	0.011_8
	9.313	2.29_9	0.012_5	2.29_4	0.010_4
	Benzotrichloride in *p*-xylene at 25 °C				
0.07167	70.00	2.28_8	0.024_6		
	34.86	2.29_4	0.033_8		
	23.98	2.30_0	0.048_3		
	16.20	2.31_7	0.064_2		
	9.313	2.34_3	0.079_2		
	Benzotrichloride in cyclohexane at 15 °C				
0.07387	70.00	2.05_2	0.016_5		
	34.86	2.05_9	0.026_8		
	23.98	2.06_5	0.037_9		
	16.20	2.07_6	0.050_6		
	9.313	2.10_7	0.067_9		
	Benzotrichloride in cyclohexane at 25 °C				
0.06200	34.86	2.03_8	0.025_7		
	23.98	2.04_4	0.034_5		
	16.20	2.05_4	0.044_8		
	9.313	2.07_9	0.056_2		
	Benzotrichloride in cyclohexane at 37.5 °C				
0.07315	70.00	2.02_2	0.020_0		
	34.86	2.02_7	0.032_4		
	23.98	2.03_9	0.043_9		
	16.20	2.05_2	0.055_8		
	9.313	2.08_0	0.065_5		
	Benzotrichloride in cyclohexane at 45 °C				
0.07244	35.09	2.01_5	0.033_3		
	23.98	2.02_4	0.044_8		
	16.20	2.04_0	0.055_7		
	9.313	2.07_3	0.063_8		
	6.700	2.09_1	0.061_6		
	Benzotrichloride in cyclohexane at 50 °C				
0.07381	70.00	2.00_3	0.019_8		
	34.86	2.01_1	0.035_4		
	23.98	2.02_5	0.046_7		
	16.20	2.03_5	0.056_0		
	9.313	2.06_7	0.062_7		

where h is Planck's constant, k is the Boltzmann constant, T the absolute temperature, and κ the

TABLE II

Static dielectric constant, high frequency dielectric constant, relaxation times, weight factor, distribution coefficient, and dipole moment data for some substituted benzenes. The relaxation times (in seconds) have been multiplied by 10^{12}

w_2	T (°C)	τ_0	τ_1	τ_2	C_1	α	μ (D)	ε_0	ε_∞
				Ethylbenzene					
1.0000	15	13.7	17.7	5.3	0.7	0.06	0.37	2.424	2.27
1.0000	37.5	10.0	14.4	5.7	0.6	0.06	0.37	2.368	2.23
1.0000	50	8.8	11.6	6.7	0.5	0.02	0.37	2.337	2.21
				Isopropylbenzene					
1.0000	15	19.8	24.6	5.2	0.8	0.08	0.40	2.401	2.24
1.0000	37.5	14.0	15.1	4.0	0.9	0.03	0.39	2.347	2.21
1.0000	50	11.8	13.9	7.8	0.7	0.02	0.40	2.318	2.19
				t-Butylbenzene in cyclohexane					
0.6757	15	24.0	31.7	8.1	0.8	0.12	0.40	2.255	2.16
0.6840	37.5	16.6	20.9	8.1	0.8	0.05	0.39	2.215	2.14
0.6800	45	14.7	16.6	7.5	0.8	0.02	0.39	2.201	2.13
0.6757	50	12.3	17.1	7.0	0.7	0.04	0.38	2.184	2.11
				Phenyltrimethylsilane					
1.0000	15	17.0	38.7	4.0	0.6	0.31	0.25	2.373	2.32
1.0000	37.5	10.3	27.1	3.0	0.5	0.30	0.23	2.331	2.29
1.0000	50	7.3	17.4	5.0	0.4	0.19	0.21	2.302	2.27
				Benzotrichloride in *p*-xylene					
0.07167	25	20.5	20.5	—	1.00	0.00	2.06	2.450	2.06
				Benzotrichloride in cyclohexane					
0.07387	15	25.8				0.05	2.18	2.208	2.05
0.06200	25	23.5				0.05	2.16	2.156	2.03
0.07315	37.5	17.8				0.03	2.18	2.153	2.02
0.07244	45	16.6				0.01	2.15	2.135	2.01
0.07381	50	15.0	15.0	—	1.00	0.00	2.15	2.125	2.00

transmission coefficient normally taken to be 1.

It also follows from transition-state theory that the enthalpy of activation ($\Delta H^{\ddagger}$) may be obtained from the equation

$$\ln \tau T = \Delta H^{\ddagger}/RT + \ln (h/k) - (\Delta S^{\ddagger}/R).$$

The dielectric constant and loss data are presented in Table I. The experimental values ε' and ε'' are compared with those calculated from the Budo equations (8, 9) using the τ_1, τ_2, and C_1 values, given by computer analysis, which are listed in Table II together with the mean relaxation time, weight fraction, dipole moment, static and high frequency dielectric constant, and distribution coefficient.

Discussion

The non-zero distribution coefficient and mean relaxation time of 23.5×10^{-12} s for benzotrichloride in cyclohexane at 25 °C (Table II) is in good agreement with the non-zero distribution coefficient and identical relaxation time reported by Hufnagel and Kilp (10) for this compound in cyclohexane at 20 °C. The non-zero α for benzotrichloride in cyclohexane at 25 °C might suggest a contribution to the dielectric absorption from a τ_2 process of similar origin to that detected for the monoalkylbenzenes (1). However, the dipole moment of benzotrichloride is considerably greater than those of the alkylbenzenes, and for an intramolecular process to be detectable a mesomeric moment appreciably greater than the literature values (11) would be necessary. The mean relaxation time of benzotrichloride in *p*-xylene at 25 °C is a little shorter than in cyclohexane at the same temperature, and the zero distribution coefficients for the *p*-xylene at 25 °C and cyclohexane at 50 °C measurements are against analyzing the dielectric data into contributions from two relaxation times. Thus the measured relaxation time of benzotrichloride may be taken to be a molecular relaxation time value.

For phenyltrimethylsilane and ethyl-, isopropyl-, and *t*-butyl-benzene non-zero distribution coefficients are observed at 15, 37.5, and 50 °C, and their dielectric data may be analyzed in terms of contributions from two relaxation

Can. J. Chem. Downloaded from www.nrcresearchpress.com by 210.87.254.42 on 09/05/12
For personal use only.

Can. J. Chem. Downloaded from www.nrcresearchpress.com by 210.87.254.42 on 09/05/12
For personal use only.

times (Table II) and the analyses fall in line with those for toluene and ethyl-, isopropyl-, and *t*-butyl-benzene at 25 °C (1). The τ_1 values of the alkyl-substituted compounds in Table II are in the sequence of lengthening τ_1 with increasing molecular size and seem reasonable in relation to the molecular relaxation of benzotrichloride, since the van der Waal radii of the chlorine atom and methyl group are 1.8 and 2.0 Å respectively (12).

No systematic variation of C_2 with temperature is discernible for the results in Table II. The τ_2 values of isopropyl- and *t*-butyl-benzene are subject to appreciable errors since C_2 is on the whole fairly small. However, they compare favorably with those obtained by Hassell and Walker (1) at 25 °C. Furthermore, no apparent decrease of these τ_2 values and that for the silicon compound with increasing temperature are apparent, and thus the enthalpy of activation ($\Delta H_2^{\ddagger}$) for the τ_2 process is indistinguishable from zero. Such behavior does not favor intramolecular rotation about the alkyl–aryl bond, since, as models and kinetic data (13) show, the steric hindrance to rotation for *t*-butylbenzene is considerably greater than for toluene. For toluene $\Delta H_2^{\ddagger}$ was found to be 1.3 $\pm$ 1 kcal/mole (1) compared with a potential barrier from gas measurement of 0.5 kcal/mole (14). Unfortunately literature values of barrier heights for the molecules in Table II are not available for comparison.

TABLE III

Enthalpies of activation (kcal/mole) relating to the τ_0 and τ_1 data in Table II for some mono-substituted benzene compounds

Compound	$\Delta H_0^{\ddagger}$	$\Delta H_1^{\ddagger}$
Ethylbenzene	1.8	1.9
Isopropylbenzene	2.4	2.3
t-Butylbenzene	2.5	2.8
Phenyltrimethylsilane	3.1	3.5
Benzotrichloride	2.3	—

The enthalpies of activation obtained from the plots of ln τT against $1/T$ are given in Table III. In the evaluation of the $\Delta H_1^{\ddagger}$ values for the alkylbenzenes the results obtained by Hassell and Walker at 25 °C were incorporated.

In Table III there is close similarity between the $\Delta H_0^{\ddagger}$ and $\Delta H_1^{\ddagger}$ values, and the increase of $\Delta H_1^{\ddagger}$ with increased molecular size (for toluene $\Delta H_1^{\ddagger}$ is 1.1 kcal/mole) is in the expected sequence. Petro and Smyth (15) have measured ethyl- and isopropyl-benzene at three temperatures and reported significant distribution coefficients. They obtained $\Delta H_0^{\ddagger}$ values of 1.9 and 2.5 kcal/mole respectively, which is remarkably good agreement with the values in Table III.

From the work reported in this series the following objections to an intramolecular relaxation process emerge.

(i) The enthalpies of activation for the τ_2 process for toluene and ethyl-, isopropyl-, and *t*-butyl-benzene are indistinguishable from zero.

(ii) The potential barriers to methyl group rotation in *o*- and *m*-xylene in the gas phase are reported to be 2.0 and 0.5 kcal/mole (15) respectively, which are inconsistent with possible analyses for both in terms of a τ_2 value of $\sim 4 \times 10^{-12}$ s.

(iii) The τ_2 value for phenyltrimethylsilane is shorter than that for *t*-butylbenzene although the former contains the larger substituent group and has probably a greater double bond character between the aromatic carbon and the atom of the attached group.

(iv) For an intramolecular relaxation process involving methyl group rotation it is reasonable to suppose that the contribution from such a process would increase with increasing number of substituent groups. However, both toluene and *m*-xylene have similar molecular dipole moments yet the C_2 value for toluene is greater than that for *m*-xylene.

(v) Tetralin is a rigid molecule but shows significant distribution coefficients at 15 and 25 °C.

Thus it seems that the shorter relaxation time may be attributed to an intermolecular process. One possibility is the type visualized by Whiffen (16) for nonpolar molecules, such as benzene, involving a collision-induced dipole and a relaxation time inversely proportional to the frequency of collision.

1. W. F. HASSELL and S. WALKER. Trans. Faraday Soc. **62**, 861 (1966).
2. J. CROSSLEY, W. F. HASSELL, and S. WALKER. J. Chem. Phys. To be published.
3. W. F. HASSELL and S. WALKER. Trans. Faraday Soc. **62**, 2695 (1966).
4. W. F. HASSELL, A. W. P. JARVIE, and S. WALKER. J. Chem. Phys. **46**, 3159 (1967).
5. W. F. HASSELL, M. D. MAGEE, S. W. TUCKER, and S. WALKER. Tetrahedron, **20**, 2137 (1964).
6. D. B. FARMER and S. WALKER. Tetrahedron, **22**, 111 (1965).

7. S. GLASSTONE, K. LAIDLER, and H. EYRING. The theory of rate processes. McGraw-Hill Book Co., Inc., New York. 1941. Chap. 1.
8. A. BUDO. Physik. Z. **39**, 706 (1938).
9. M. D. MAGEE and S. WALKER. Trans. Faraday Soc. **62**, 3093 (1966).
10. F. HUFNAGEL and H. Z. KILP. Naturforsch. **18a**, 769 (1963).
11. J. W. SMITH. Electric dipole moments. Butterworths, London. 1955.
12. L. PAULING. The nature of the chemical bond. Cornell University Press, Ithaca, N.Y. 1945.
13. K. L. NELSON and H. C. BROWN. J. Am. Chem. Soc. **73**, 5605 (1951).
14. M. VOLKENSTEIN. Configurational statistics of polymer chains. Interscience, New York. 1963.
15. A. J. PETRO and C. P. SMYTH. J. Am. Chem. Soc. **79**, 6142 (1957).
16. D. H. WHIFFEN. Trans. Faraday Soc. **46**, 124 (1950).

Can. J. Chem. Downloaded from www.nrcresearchpress.com by 210.87.254.42 on 09/05/12
For personal use only.

Dielectric studies. Part XVIII. Dipole moments and relaxation times of some symmetrically substituted alkylbenzenes

J. CROSSLEY
University of Aston in Birmingham, England
AND
S. WALKER
Chemistry Department, Lakehead University, Port Arthur, Ontario
Received August 28, 1967

The dielectric absorption at four microwave frequencies of pure liquid benzene and *p*-cymene at 25 °C, *p*-xylene and mesitylene at 25, 40, 50, and 60 °C, and solutions of durene and hexamethylbenzene in mesitylene at 60 °C has been examined. All show measurable loss factors and apparent dipole moments of about 0.1 to 0.2 D. These moments are less in magnitude than those associated with the short relaxation time (τ_2) process for the polar monoalkylbenzenes, *o*-xylene and *m*-xylene. Their relaxation times are too short for molecular reorientation and there is a rough correlation between the number of collisions/molecule s and the reciprocal relaxation time.

Canadian Journal of Chemistry, 46, 847 (1968)

Can. J. Chem. Downloaded from www.nrcresearchpress.com by 210.87.254.40 on 09/05/12
For personal use only.

Previous papers in this series (1, 2) have reported a small dielectric loss for *p*-xylene. The results revealed that the frequency maximum in the absorption is greater than 70 Gc/s. This corresponds with a relaxation time less than 2×10^{-12} s which is much shorter than would be anticipated for the molecular reorientation of a molecule of this shape and size, e.g. the molecular relaxation of *p*-chlorotoluene in *p*-xylene at 25 °C is 16×10^{-12} s (3).

Whiffen (4) found that the losses of benzene, carbon tetrachloride, and a few other molecules, having no permanent electric dipole moment, were proportional to the frequency in the range 0.3 to 1.2 cm^{-1}. He suggested that the absorption results from dipole moments induced in molecular collisions where, for example, the C—H bond moment in benzene is the inducing dipole. The induced dipole was regarded as changing direction, not by rotation of the molecule containing it, but because of a new distortion produced at another instant by impact with another neighbor. The plots of loss tangent against frequency suggested Debye behavior and a relaxation time of the order of the time between molecular collisions. Similar results have been reported for nonpolar molecules in both liquid (5) and gaseous (6) states. The gaseous measurements have shown that the absorption is proportional to the square of the gas density and are attributed to temporary dipole moments induced during molecular collisions. DiCarlo and Smyth (7) have measured the dielectric constant and loss at 1.25 and 3.22 cm of several symmetrical molecules. For benzene the dielectric loss at 1.25 cm was about 0.003 at 25 °C, and, in addition, hexamethylbenzene appeared to have a small apparent dipole moment.

The microwave method is well suited to the detection and estimation of small dipole moments, and unlike, for example, the Halverstadt–Kumler approach involves no atomic polarization approximation. It seemed worthwhile determining fairly precise values of apparent dipole moments and relaxation times of some molecules with a center of symmetry, with a view to comparing their magnitude with those obtained for the short relaxation process of the monoalkylbenzenes (8), and also to attempt correlation of the relaxation time for such a process with the number of collisions/molecule s.

Experimental Methods

The apparatus and techniques employed have been described previously (9, 10). The dielectric constant ϵ' and loss factor ϵ'' were determined by the bridge method at frequencies of 70.00, 35.09, 23.98, and 9.313 Gc/s. The static dielectric constant ϵ_0 was measured with a heterodyne beat apparatus at 2 Mc/s.

The compounds were commercially available. Special attention was paid to the purity of the compounds, particularly to the elimination of water. The liquids were treated with sulfuric acid, to remove sulfur compounds, and after preliminary drying with magnesium sulfate, the liquids were allowed to stand over phosphorus pentoxide for 24 h before refluxing and distilling from sodium, using a 30 theoretical plate spinning band column. The

TABLE I

Dielectric loss and apparent dipole moment data for some symmetrically substituted alkylbenzenes. μ_1^1 and μ_2^1 are the apparent dipole moments (in debyes) corresponding to mean relaxation times of 2 and 5×10^{-12} s respectively as calculated from eq. [1]. The loss of the solvent (mesitylene) was subtracted in the case of durene and hexamethylbenzene. The pure liquids were measured at 25 °C and the mesitylene solutions at 60 °C

Solute	w_2	ε_0		Frequency (Gc/s) 70.00	35.09	23.98	9.313
Benzene	1.000	2.278	ε''	0.0059	0.0035	0.0025	0.0003
			μ_1^1	0.10	0.08	0.08	0.05
			μ_2^1	0.11	0.07	0.06	0.03
p-Xylene	1.000	2.263	ε''	0.0063	0.0054	0.0037	0.0022
			μ_1^1	0.12	0.12	0.11	0.11
			μ_2^1	0.13	0.10	0.09	0.09
p-Cymene	1.000	2.244	ε''	0.0071	0.0076	0.0060	0.0047
			μ_1^1	0.15	0.16	0.15	0.17
			μ_2^1	0.16	0.14	0.13	0.15
Mesitylene	1.000	2.275	ε''	0.0074	0.0074	0.0064	0.0034
			μ_1^1	0.14	0.15	0.14	0.14
			μ_2^1	0.15	0.13	0.12	0.12
Durene	0.430	2.239	ε''	0.0039	0.0030	0.0042	0.0034
			μ_1^1	0.17	0.16	0.18	0.22
			μ_2^1	0.18	0.14	0.16	0.20
Hexamethylbenzene	0.126	2.237	ε''	0.0004	0.0000	0.0015	0.0011
			μ_1^1	0.11	—	0.23	0.25
			μ_2^1	0.12	—	0.21	0.23

distillates were stored in amber bottles over sodium wire. Durene and hexamethylbenzene were recrystallized from *p*-xylene and dried in a vacuum oven over phosphorus pentoxide.

Experimental Results

The errors involved in the dielectric constants for low-loss solutions are such that Cole–Cole plots are difficult to formulate, and it is more realistic to examine the absorption in terms of the dielectric losses. The latter are presented in Table I together with the static dielectric constant (ε_0) and dipole moment (μ) data evaluated from the equation

$$[1] \quad \mu = \left(\frac{27kT}{4\pi Nc} \times \frac{\epsilon''}{(\epsilon_0 + 2)^2} \times \frac{1 + \omega^2\tau^2}{\omega\tau}\right)^{1/2},$$

in which k is the Boltzmann constant, T the absolute temperature, N the Avogadro number, ε'' the dielectric loss, ω the angular frequency, and τ the relaxation time.

Some appreciation of the results and an indication of the respective relaxation times are given by the plots of ε'' against log ω (Fig. 1). These plots give some indication of the errors especially for the very low-loss durene and hexamethylbenzene solutions. The broken line curves on these plots were obtained from ε'' values calculated from eq. [1] by substitution of dipole moments and relaxation times giving ε'' values comparable with the experimental values.

Discussion

The dipole moments listed in Table I, calculated from eq. [1], indicate that the values are relatively insensitive to the choice of relaxation time. For benzene the dipole moment values compare favorably with those of 0.06 and 0.02 D calculated from the results of DiCarlo and Smyth (7) at 24.00 and 9.32 Gc/s respectively, using a relaxation time of 5×10^{-12} s.

A comparison of estimates of the frequency of the absorption maximum, in Fig. 1, readily indicates that this frequency decreases with increase in molecular size, and hence, since $\omega\tau = 1$, the observed relaxation time accordingly increases. The different temperature plots for mesitylene and *p*-xylene indicate that the relaxation times are not detectably dependent upon temperature. For benzene the results may be compared with those obtained by Whiffen at 25 °C (4) and DiCarlo and Smyth at 20 °C (7). The plot shows the agreement between the

Can. J. Chem. Downloaded from www.nrcresearchpress.com by 210.87.254.40 on 09/05/12
For personal use only.

Can. J. Chem. Downloaded from www.nrcresearchpress.com by 210.87.254.40 on 09/05/12
For personal use only.

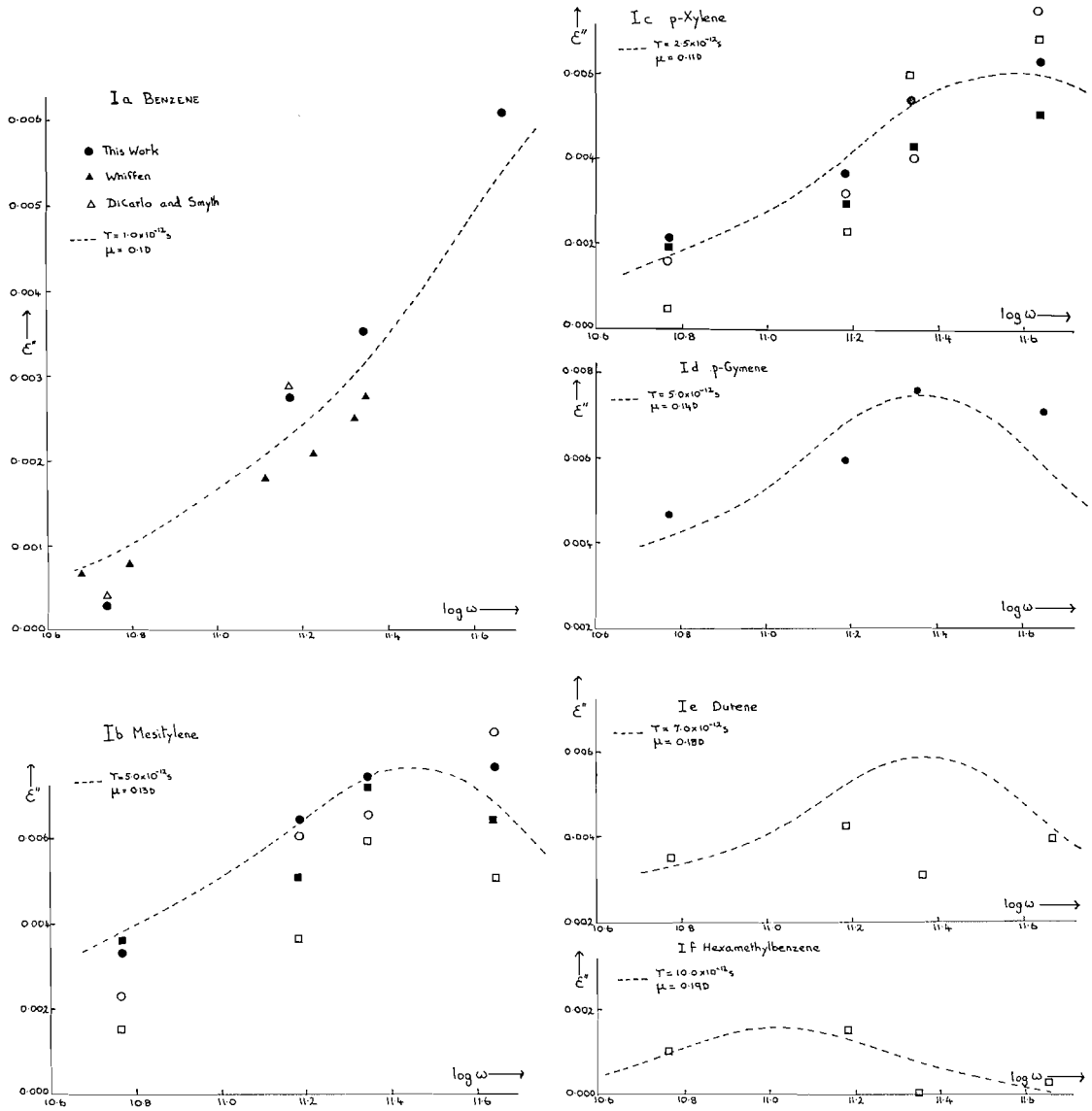

FIG. 1. Plots of ε'' against log ω for benzene and some symmetrically substituted benzenes at (●) 25 °C, (■) 40 °C, (○) 50 °C, and (□) 60 °C. Durene and hexamethylbenzene were measured in mesitylene solution and the loss of the solvent has been subtracted; the remainder were measured as the pure liquid. The broken line indicates a possible loss curve. However, more experimental points would be necessary to establish the true shape.

three sets of results to be remarkably good and supports their validity.

The molecular relaxation times of toluene (8) and bromobenzene in cyclohexane (9) are about 9 and 12 $\times$ 10^{-12} s respectively at 25 °C. Such molecules are of similar shape but of smaller volume than all of the symmetrical alkylbenzenes. In addition, the mean relaxation times of pure liquid *t*-butylbenzene (8) and benzotrichloride in cyclohexane (11) are about 20 and 23 $\times$ 10^{-12} s respectively at 25 °C, compared with a value of approximately 5 $\times$ 10^{-12} s obtained for *p*-cymene, a molecule greater in volume than these mono-substituted compounds. Whiffen and Thompson (12) measured the dielectric absorption of *p*-cymene over a range of temperatures and calculated, using a dipole moment of 0.19 D, relaxation times of 8.0 and

11.0×10^{-12} s at 30 and 10 °C respectively. These values were obtained from measurements at one frequency, and though they are somewhat longer than the value reported in this study, the values are again much shorter than permissible for molecular reorientation.

It is evident that the relaxation times of the symmetrical molecules are not to be attributed to molecular reorientation. Whiffen (4) considered the possibility that the loss tangents are the long wavelength tails of vibrational absorption bands. However, with the exception of benzene, the ε'' against log ω plots show a maximum in the loss either in or close to the microwave region, and the absorption does not detectably increase with temperature for *p*-xylene and mesitylene. Thus, both these features oppose such an assignment.

Satisfactory interpretations of the dielectric absorption of nonpolar liquids (4, 5, 13) and the microwave and far infrared spectrum of compressed gases (6, 14, 15, 18) have been obtained on the basis of electric dipole moments induced during molecular collisions. The number of collisions ($cm^{-3}\ s^{-1}$) between molecules of the same kind is given by (19)

$$[2] \qquad \frac{N^2 d^2}{V^2}\left(\frac{4\pi kT}{m}\right)^{1/2},$$

in which N is the number of molecules in volume V, d the collision diameter, m the mass of a molecule, k the Boltzmann constant, and T the absolute temperature. To gain some insight into collision processes eq. [2], which strictly is applicable to gases, will be applied to our liquid and solution systems.

For a temperature increase 25–60 °C the collision frequency will be increased by a factor $(333/298)^{1/2}$ which is only slightly greater than unity. Similarly, the number of molecules per cc will not be appreciably affected, since the densities of the symmetrical and monoalkylbenzenes show only an approximate 5% decrease over such a temperature range. Thus, a collision process, for which the relaxation time may be governed by the frequency between collisions, would explain the apparent temperature independence shown by the frequency corresponding to the absorption maximum for *p*-xylene and mesitylene. Similarly, the indication that the enthalpy of activation ($\Delta H_2^{\ddagger}$) for the τ_2 process of a number of monoalkylbenzenes was indistinguishable from zero (11) may also be explained.

In order to obtain an estimate of the number of collisions per second experienced by the various alkylbenzenes in question, in the pure liquid state at 25 °C, numerical values have been substituted into eq. [2]. The collision diameter was taken to be 4 Å in every case, since the van der Waals radius of the phenyl group is about 2 Å. The results are compared with the corresponding reciprocal relaxation times in Fig. 2.

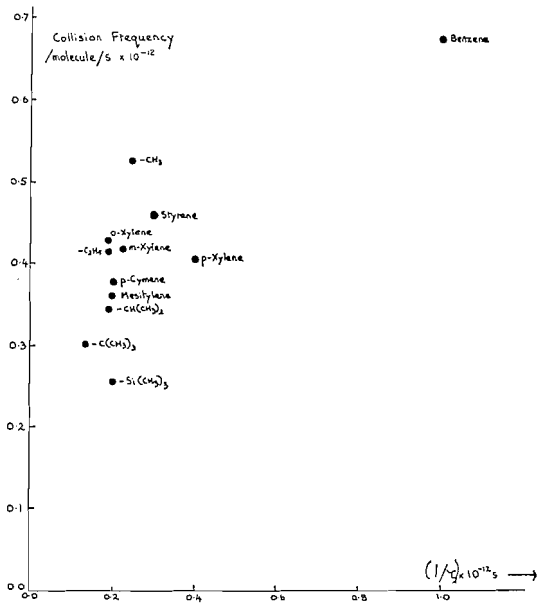

FIG. 2. Plot of number of collisions/molecule s against the reciprocal of relaxation time ($1/\tau_2$) for some alkylbenzenes as the pure liquid at 25 °C. For the low-loss (nonpolar) compounds the τ_2 values are only very rough estimates.

An exact relationship between $1/\tau_2$ and the number of collisions/molecule s is not anticipated because of the inaccuracy of the former and the very approximate estimate of the latter. In addition, it is probable that a favorable orientation of the colliding molecules may be required for a collision to be fruitful. Nevertheless, the plot in Fig. 2 indicates a rough correlation and is in favor of the τ_2 process being dependent on molecular collisions.

The collision frequencies were based on the values for the pure liquid, i.e. the number of molecules per cc; in solution N will decrease and it might be expected that the frequency of

Can. J. Chem. Downloaded from www.nrcresearchpress.com by 210.87.254.40 on 09/05/12
For personal use only.

collision between solute molecules would also decrease. However, the solute molecules will collide with solvent molecules and such collisions could be fruitful, especially so for the durene and hexamethylbenzene which interact with mesitylene.

The τ_2 values for toluene in the pure liquid, carbon tetrachloride, and cyclohexane at 25 °C are 4.3, 3.5, and $\sim 2 \times 10^{-12}$ s respectively (8). The molecular interaction of toluene with itself or of toluene with carbon tetrachloride would be appreciably greater than that of toluene with cyclohexane and this may be a factor in determining the magnitude of τ_2.

For the halobenzenes which have dipole moments about 1.5 D for an induced moment (μ_2) of 0.4 D, and from $C_1/C_2 = \mu_1^2/\mu_2^2$, where μ_1 is the molecular dipole moment, a C_2 value < 0.1 would be predicted. Thus, the zero distribution coefficients observed for these compounds in *p*-xylene solution (2) are not unexpected, since such a small C_2 value would lead to an α tending to zero and this would be even more so for benzotrichloride (in Part XVII) which has a molecular dipole moment of about 2.2 D as opposed to a value of ~ 1.5 D for the monohalobenzenes.

1. J. CROSSLEY, A. HOLT, and S. WALKER. Tetrahedron, **21**, 3141 (1965).
2. W. F. HASSELL and S. WALKER. Trans. Faraday Soc. **62**, 2695 (1966).
3. W. F. HASSELL. Ph.D. Thesis, University of Aston in Birmingham, England. 1966.
4. D. H. WHIFFEN. Trans. Faraday Soc. **46**, 124 (1950).
5. I. R. DAGG and G. E. REESOR. Can. J. Phys. **43**, 1552 (1965).
6. A. A. MARYOTT and G. BIRNBAUM. J. Chem. Phys. **39**, 189 (1961).
7. E. N. DICARLO and C. P. SMYTH. J. Am. Chem. Soc. **84**, 1128 (1962).
8. W. F. HASSELL and S. WALKER. Trans. Faraday Soc. **62**, 861 (1966).
9. W. F. HASSELL, M. D. MAGEE, S. W. TUCKER, and S. WALKER. Tetrahedron, **20**, 2137 (1964).
10. D. B. FARMER and S. WALKER. Tetrahedron, **22**, 111 (1965).
11. J. CROSSLEY and S. WALKER. Can. J. Chem. This issue.
12. D. H. WHIFFEN and H. W. THOMPSON. Trans. Faraday Soc. **42A**, 114 (1946).
13. D. H. WHIFFEN. Proc. Roy. Soc. London, Ser. A, **255**, 78 (1960).
14. J. P. COLPA and J. A. A. KETELAAR. Mol. Phys. **1**, 343 (1958).
15. J. VAN KRANENDONK and Z. J. KISS. Can. J. Phys. **37**, 1187 (1959).
16. H. A. GEBBIE, N. W. B. STONE, and D. H. WILLIAMS. Mol. Phys. **6**, 215 (1963).
17. H. A. GEBBIE and N. W. B. STONE. Proc. Phys. Soc. London, **82**, 543 (1963).
18. G. BIRNBAUM, H. B. LEVINE, and D. A. MCQUARRIE. J. Chem. Phys. **46**, 1557 (1967).
19. H. S. TAYLOR and S. GLASSTONE. A treatise on physical chemistry. Van Nostrand, New York. 1951.

Can. J. Chem. Downloaded from www.nrcresearchpress.com by 210.87.254.40 on 09/05/12
For personal use only.

Ultrasonic study of hydrochloric acid association in N,N-dimethylformamide

SIU C. CHAN[1] AND J. P. VALLEAU
Lash Miller Chemical Laboratory, University of Toronto, Toronto, Ontario

Received September 21, 1967

Ultrasonic absorption and velocity have been measured in anhydrous N,N-dimethylformamide solutions of hydrogen chloride, over the frequency range 13 to 143 mc/s, and the concentration range 0.05 *M* to 3.5 *M*. A large relaxation is observed and ascribed to the association of the acid. The rate constants for this reaction are obtained, and their variations with concentration are discussed. The association rate appears to be entirely diffusion controlled, and the corresponding "reaction distance" is large. This may be related to the very large effect on the sound velocity (and hence on the compressibility) that arises from the introduction of these ions.

Canadian Journal of Chemistry, **46**, 853 (1968)

Can. J. Chem. Downloaded from www.nrcresearchpress.com by 210.87.254.105 on 09/05/12
For personal use only.

Introduction

In the last few years, relaxation techniques have been applied to a large number of proton transfer reactions in aqueous solution (1–4). The reactions of the hydronium ion are generally characterized by extremely large second order rate constants, corresponding to diffusion control of the reactions. An explanation for the remarkable consistency of this result has been sought by postulating a very easy charge transfer through the water molecules adjacent to the solute particles. The charge transfer is thought to occur by a chain mechanism like that of proton conduction in water. This explains the fact that the reactions appear to be entirely diffusion controlled and also that rather long "reaction distances" are deduced for the simplest reactions. Thus H_3O^+ and OH^- appear to react if they come within 8 Å of each other, presumably because charge transfer is very rapid once the ions are separated by only two solvent molecules (1, 4).

Very few corresponding measurements have been done for nonaqueous media (1, 4), and particularly for solvents in which no anomalous proton conduction is expected. This paper describes measurements on solutions of hydrochloric acid in anhydrous N,N-dimethylformamide, using ultrasonic techniques in the range 13 to 143 cm/s.

Experimental

In order to prepare water-free N,N-dimethylformamide (DMF) it is usual to treat the solvent with a drying agent and afterwards to distill it under reduced pressure (5–7). In the present work, the DMF (Fisher certified reagent, water content below 0.05%) was shaken for 12 h with an appropriate "molecular sieve" (Linde Type 4A in (1/16)″ pellets). The liquid was then decanted and distilled under nitrogen in a 10 ft, 50 plate bubble-cap column, the pressure at the head of the column being maintained at about 20 mm of Hg. The specific conductivity of the middle portion of the distillate, which was used for the solutions, was 3.5×10^{-7} ohm^{-1} cm^{-1} at 25 °C.

Anhydrous hydrogen chloride (Matheson, technical grade) was further dried with concentrated sulfuric acid (5), and then bubbled into the purified DMF, which was meanwhile protected from atmospheric moisture with a guard tube. The various solutions were obtained by dilution with purified DMF. These dilutions and other handling of the solutions were carried out under pure nitrogen in a dry box. The concentrations of the individual solutions were measured by greatly diluting aliquots of each with distilled water, then titrating them with standardized sodium hydroxide solution.

The ultrasonic absorption and velocity were measured in a "pulse apparatus" that has been described elsewhere (8). The cell containing the solution was double walled, and the temperature was controlled by circulating fluid from a thermostatted bath. The temperature inside the cell was measured with a copper–constantan thermocouple; the experiments were carried out at (25.2 ± 0.2) °C. In order to prevent atmospheric contamination, especially by water, the cell was fitted with a Teflon top, while the necessary motion of the upper transducer was allowed by installation of a silicone rubber bellows above the Teflon top. This bellows, which was cast in the laboratory, is very limp in order to preclude causing any misalignment of the transducers. The solution was swept with nitrogen presaturated with dry DMF.

It can be seen that precautions were taken to avoid the presence of water in the solutions. In fact, though, small amounts of water, such as that present in the reagent grade DMF, turned out to have little effect on the measured sound absorption.

The amplitude absorption coefficient α of each solution was measured at 13, 39, 65, 91, and 143 mc/s. The possible error in the absorption values is estimated at 3%. The sound velocities are known within about 1%. The frequencies, *f*, were measured with a General Radio type 620A heterodyne frequency meter; the errors in frequency are negligible.

[1]Present address: Department of Chemistry, University of Washington, Seattle, Washington.

Can. J. Chem. Downloaded from www.nrcresearchpress.com by 210.87.254.105 on 09/05/12
For personal use only.

The densities of the solutions were measured at 25.2 °C using a Westphal specific gravity balance. They are known to about 0.2%.

Results

The ultrasonic absorption of pure DMF showed no relaxation in the present frequency range, the value of (α/f^2) being 28×10^{-17} s^2/cm. (The classical sound absorption due to shear viscosity in DMF would amount to 7.2 $\times 10^{-17}$ s^2/cm.) The sound velocity was 1.46 $\times 10^5$ cm/s.

The hydrochloric acid solutions had substantial sound absorption coefficients and showed relaxation in the frequency range studied. At each concentration the results for the absorption coefficients α_i at the five frequencies f_i were fitted to the single relaxation expression

$$[1] \qquad \frac{\alpha_i}{f_i^2} = \frac{A}{1 + (f_i/f_c)^2} + B$$

using weighted least squares. For the weighting factors, w_i, the inverse squares of the experimental values of (α_i/f_i^2) were chosen: this corresponds to the estimated constant percentage uncertainty in the measurements. (This matter of weighting is in no way critical, however. Use of unweighted least squares affects the parameters A, B, and f_c only slightly, and the remaining discussion not at all.) In every case the fit of the results to a single relaxation curve was satisfactory, the experimental points lying within their estimated uncertainty from the fitted curve. At the lowest concentrations the relaxation frequency f_c is below or at the bottom of the frequency range studied, however; there results a larger uncertainty in A and f_c for these cases.

The relaxation frequency f_c, and the parameters A and B, are given in Table I, along with the data on sound velocity c and density ρ. The fifth column of that table, labelled s.d., gives the standard deviation of the experimental points about the fitted curve [1].

$$[2] \quad \text{s.d.} = \sum_{i=1}^{5} w_i \left[\left(\frac{\alpha_i}{f_i^2} \right)_{\text{exp}} - \left(\frac{\alpha_i}{f_i^2} \right)_{\text{fitted}} \right] \Big/ \sum_{i=1}^{5} w_i$$

A and f_c are displayed in Fig. 1.

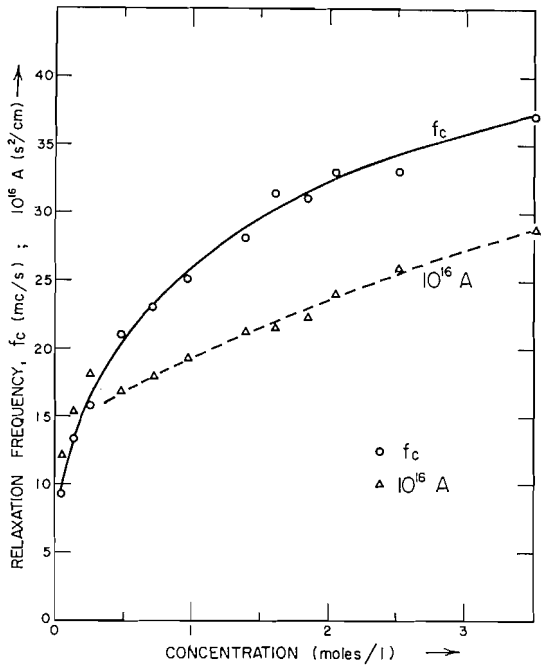

FIG. 1. Relaxation frequency f_c and low frequency absorption A as a function of HCl concentration.

Discussion

One anticipates that the relaxing absorption is due to the acid association reaction

$$[3] \qquad H^+ + Cl^- \rightleftharpoons HCl.$$

If so, A and f_c should vary, in a rough first approximation, as the square root of the HCl concentration. It can be seen in Fig. 1 that this is more or less what has been found. One can certainly eliminate the most obvious alternative absorption mechanisms. Any solvation process, whether involving the ions or the undissociated acid, should yield a relaxation frequency nearly independent of concentration. The same would be true for an internal relaxation of any solvated solute particle. Any process involving the undissociated acid but no ions would have an A value nearly proportional to the concentration, and again a constant relaxation frequency. The experimental results are clearly in accord with the acid association mechanism [3], rather than any of these alternatives, and we shall interpret the results on this basis.

TABLE I

Concentration (moles/l)	$10^{17} \times A$ (s^2/cm)	$10^{17} \times B$ (s^2/cm)	f_c (mc/s)	10^{17} s.d. (s^2/cm)	$10^{-5} c$ (cm/s)	ρ (g/cc)
0.0455	121	27.7	9.3	0.55	1.464	0.945
0.1282	154	27.3	13.3	0.43	1.472	0.947
0.2620	181	28.3	15.8	0.66	1.476	0.950
0.482	168	28.6	21.0	0.52	1.470	0.955
0.710	179	29.2	23.0	0.21	1.482	0.960
0.968	193	29.5	25.1	0.27	1.498	0.966
1.396	212	30.4	28.2	0.40	1.506	0.976
1.610	215	28.8	31.4	0.78	1.517	0.981
1.840	223	31.6	31	0.57	1.509	0.986
2.050	240	28.9	33	1.66	1.513	0.991
2.515	259	33.3	33	2.42	1.532	1.002
3.506	288	39.5	37.2	0.66	1.563	1.024

This reaction [3] may be described by the stoichiometric association quotient Q,

$$[4] \qquad Q = \frac{[HCl]}{[H^+][Cl^-]} = \frac{K}{F},$$

where K is the thermodynamic association constant and F the activity coefficient quotient. F will be given, to a fair approximation, by

$$[5] \qquad F \approx f_\pm^{-2},$$

where $f_\pm$ is the mean ionic activity coefficient of the free ions. For the ultrasonic parameters A and f_c we may then write (9), setting $[HCl] = z$,

$$[6] \quad A = \frac{\pi \rho^2 c (dz/d \ln Q) \delta^2}{RT f_c [1 + (dz/d \ln Q)(\partial \ln F/\partial z)_{T,P}]},$$

$$[7] \quad 2\pi f_c = k_d [1 + Q([H^+] + [Cl^-])] \times [1 + (dz/d \ln Q)(\partial \ln F/\partial z)_{T,P}].$$

In these expressions the derivatives refer to fixed overall composition, and k_d is the rate constant for the dissociation, while δ is the thermodynamic reaction quantity characteristic of ultrasonics, namely

$$[8] \qquad \delta = \Delta V - \left(\frac{\partial V}{\partial T}\right)_p \frac{\Delta H}{C_p},$$

where ΔV and ΔH are the volume and enthalpy of the reaction [3]; C_p and $(\partial V/\partial T)_p$ are the heat capacity and expansion coefficient of the solution.

In order to interpret our results in terms of [6] and [7] we wish the value of Q at each concentration. The only relevant experimental data are on conductivity and at very low concentrations (6). When they are fitted to Ostwald's dilution law (using the least squares method) they yield a limiting equivalent conductivity, Λ^0, of 111 mho cm^2/equiv, and an association constant, Q, of 5.6×10^3 l/mole; the fit is good over the concentration range studied. The ionic strength in these conductivity experiments is near 10^{-4} M, so that this association constant is not far from the thermodynamic constant K. In the case of the ultrasonic experiments, on the other hand, the ionic strengths will be near 10^{-2} M, so that Q may be expected to deviate considerably from K. In order to make some allowance for this, in the following calculations, we have applied an approximation of a type introduced by Güntelberg and used frequently in ion association work (10):

$$[9] \qquad \log f_\pm = -\frac{A I^{1/2}}{1 + 2I^{1/2}},$$

where I is the ionic strength.[2] This approximation represents an improvement over the limiting law of Debye, and corresponds (in DMF solutions) to using an ionic diameter of 4.16 Å in the Debye–Hückel expression for the activity coefficients. The value of A in DMF at 25 °C is 1.60.

Using [9], and repeated approximations for I, values of Q at each concentration may be deduced from the value at low concentrations through [4] and [5]. The resulting values of Q vary by a factor of two over the concentration range studied ultrasonically (cf. Table II). The accuracy of this $f_\pm$ approximation [9] in these

[2]The addition of a small term linear in I improves the fit slightly for aqueous systems. Such a refinement is not possible at present in DMF.

Can. J. Chem. Downloaded from www.nrcresearchpress.com by 210.87.254.105 on 09/05/12
For personal use only.

TABLE II

Concentration (moles/l)	$10^{-3}\,Q$ (l/mole)	I (mole/l)	$\lvert\delta\rvert$ (cc/mole)	$10^{-6}\,k_d$ (s^{-1})	$10^{-9}\,k_a$ (l $mole^{-1}$ s^{-1})	d (Å)	$10^{11}\,\beta$ (cm^2/dyn)
0.0455	3.82	0.00332	19.8	2.41	9.2	12.0	4.94
0.1282	3.41	0.00599	18.8	2.23	7.6	11.6	4.87
0.2620	3.10	0.00903	17.8	1.98	6.1	11.0	4.83
0.482	2.82	0.0129	16.4	2.07	5.8	11.3	4.85
0.710	2.64	0.0162	15.6	1.95	5.2	11.0	4.74
0.968	2.50	0.0195	15.2	1.90	4.8	10.9	4.61
1.396	2.33	0.0243	14.9	1.86	4.3	10.9	4.52
1.610	2.26	0.0265	15.0	1.97	4.5	11.3	4.43
1.840	2.20	0.0287	14.5	1.86	4.1	10.9	4.45
2.050	2.15	0.0307	15.1	1.90	4.1	11.1	4.41
2.515	2.05	0.0348	14.3	1.73	3.5	10.6	4.25
3.506	1.90	0.0427	14.2	1.77	3.4	10.8	4.00

solutions is of course unknown, but it is certain to be a great improvement over assuming ideality; we shall comment below on its importance with respect to our conclusions. Use of [9] also allows us to estimate, in [6] and [7], the "kinetic" correction for the nonideality, $(dz/d \ln Q)(\partial \ln F/\partial z)_{T,P}$, which is small but not negligible (varying from 0.08 to 0.19 for our solutions).

On this basis δ has been extracted from our experimental A values, using [6], and k_d and thus $k_a = k_d Q$ from our experimental relaxation frequencies, using [7]. These parameters are shown in Table II.

It is interesting to examine the magnitude and concentration dependence of the rate constants. The large values of k_a suggest that the association reaction is diffusion controlled, and the following calculations bear this out.

Expressions for the rate constants of diffusion-controlled ionic reactions have been derived by Debye (11) (cf. ref. 1). The result, if one takes into account the "screening", due to the ionic atmosphere, of the type used in the Debye limiting law for activity coefficients, and if the association reaction is truly diffusion controlled,[3] is that

$$[10]\quad 10^{-3}k_a = \frac{4\pi N_0 f_\pm^2 e_0^2 (D_{H^+} + D_{Cl^-})}{\epsilon kT(\exp\,(e_0^2/\epsilon dkT) - 1)},$$

$$[11]\quad k_d \propto D_{H^+} + D_{Cl^-}.$$

[3]See ref. 1, eq. [12]. In that approximation $\exp(b_{IJ}\kappa) = f_\pm^2$, however, which gives our eq. [10]. According to ref. 1 (see pp. 294–296), k_a is independent of concentration. The diffusion coefficients will in fact vary with concentration, however, and that is the point of [11].

In [10], d is the so-called "reaction distance": ions which once diffuse as close to each other as d are supposed certain to react with each other. N_0 is Avogadro's number, e_0 the electronic charge, and ε the dielectric constant, while D_{H^+} and D_{Cl^-} are the self-diffusion coefficients of the ions.

It appears (cf. Table II) that the dissociation rate constant k_d decreases with increasing concentration. Now k_d would be expected to depend on the concentration through the diffusion coefficients (cf. [11]), and one could ask whether this offers an explanation of the observed decrease. (This is a more detailed question than is usually asked of results of the present type and it is therefore asked with some diffidence.) A theory for the concentration dependence of ionic self-diffusion coefficients has been given by Onsager (12, 13); in the language of ionic transport theory, there is no "electrophoretic" effect, but there is a "relaxation" effect given by

$$[12]\quad D_i/D_i^0 = 1 - \gamma I^{1/2},$$

where D_i^0 is the value for infinite dilution. In the present case, for which the transport numbers of the ions are substantially equal (Λ^0_{HCl} is 111 (6), while $\lambda^0_{Cl^-}$ is 55.1 (14)), $\gamma = 0.72$ in DMF at 25 °C. The low concentration limit ($D^0_{H^+} + D^0_{Cl^-}$) is given by $(RT/\mathcal{F}^2)\,\Lambda^0_{HCl}$, where $\mathcal{F}$ is Faraday's constant; one finds $(D^0_{H^+} + D^0_{Cl^-}) = 3.1 \times 10^{-5}$ cm^2/s.

Using these considerations, one can derive from [10], for each concentration, the reaction distance d. This is also given in Table II. There seem to be two things to notice about it. In the first place d is essentially constant around 11 Å,

Can. J. Chem. Downloaded from www.nrcresearchpress.com by 210.87.254.105 on 09/05/12
For personal use only.

Can. J. Chem. Downloaded from www.nrcresearchpress.com by 210.87.254.105 on 09/05/12
For personal use only.

although k_d itself varies substantially. This constancy means that Onsager's theory of the concentration dependence of self-diffusion coefficients does appear to explain the observed trend of k_d with concentration.

The other interesting thing is the large value of the reaction distance (even larger than for the aqueous ions). This is perhaps surprising since one doesn't expect in the present case rapid proton transfer by the "anomalous conduction" mechanism. (It is worth mentioning that these large values for d do not depend on our approximations for $f_\pm$ nor for the concentration dependence of the diffusion coefficients. If we assumed ideal solutions and constant diffusion coefficients we would obtain a slowly varying d, but in the region of 10 Å.) To venture a physical explanation of the large d value, one would have to postulate a substantial region, around one or both of the ions, disturbed in such a way as to allow the rapid passage of the ions.

In this connection it is interesting to examine the adiabatic compressibility of the solutions, which may be calculated from the experimental sound velocities and densities according to

$$[13] \qquad \beta_s \equiv 1/\rho c^2;$$

the values are given in Table II. Compressibility data are often used to obtain "solvation numbers" for ions in solution (15). The argument for doing this is that the h_i solvent molecules, which solvate a molecule of solute i, are effectively withdrawn from the solvent and make no contribution to the compressibility. On that (somewhat questionable) basis we can write, for the present case,

$$[14] \qquad M_{H^+}h_{H^+} + M_{Cl^-}h_{Cl^-} + M_{HCl}h_{HCl} = M_{DMF}(1 - \beta/\beta^0),$$

where M_i and h_i are molality and solvation number of i, while β^0 is the compressibility of the pure solvent. The β data then yield $(h_{H^+} + h_{Cl^-}) \approx 26$, $h_{HCl} \approx 0.4$.

These numbers are rough, since the velocity data is not very precise, but there is no doubt that the ionic "solvation numbers" have a very large value. Now of course one cannot seriously interpret such a large number in terms of the simple solvation model quoted above. What one might infer, however, is that one or both of the ions must be seriously disturbing the structure of a substantial region of the surrounding solvent. This corresponds well with the large "reaction distance" deduced from the rate constants. (A sphere with a radius of 11 Å, the reaction distance, would contain 43 molecules of the solvent.) The solvation number of 0.4 for the undissociated HCl is not surprising in view of the existence of the solid compound HCl:DMF (7, 16).

It is difficult to make very effective use of the values obtained for δ (Table II), because one cannot separate the ΔV and ΔH contributions (cf. [8]). One can estimate a value for ΔH at very low HCl concentrations on the basis of conductivity results (5, 6) at 20 °C and 25 °C; this value is 14.6 kcal per mole. However, ΔH will be concentration dependent;[4] so will $(\partial V/\partial \tau)_p$ and C_p, for which we have only the values appropriate to the pure solvent. It would seem natural to extrapolate our results for δ down to low concentrations to extract a corresponding value of ΔV, but the basis for such an extrapolation is lacking and, besides, there is a large uncertainty in our A values precisely at the lowest concentrations, which are critical in any such extrapolation. It therefore seems that one cannot do better than an order of magnitude estimate of ΔV for the association. If we take the average value of $|\delta|$, 16 cc/mole, and use the low concentration values of ΔH and the other parameters, we find $\Delta V \approx +11$ cc/mole or $+43$ cc/mole, depending on the sign chosen for δ; the former value is more reasonable. An extrapolated value of δ would lead to the lower value of 6 or 7 cc/mole.

Acknowledgments

The authors acknowledge with thanks the support of the National Research Council of Canada. Mr. Chan appreciates a Province of Ontario Graduate Fellowship held in 1965–1966.

1. M. EIGEN, W. KRUSE, G. MAASS, and L. DE MAEYER. Progr. Reaction Kinetics, **2**, 287 (1964).
2. L. DE MAEYER and K. KUSTIN. Ann. Rev. Phys. Chem. **14**, 5 (1963).

[4]The variation in ΔH which may be calculated from the approximation (9) is too small to explain by itself the observed variation in δ.

3. G. G. HAMMES. Ann. Rev. Phys. Chem. **15**, 13 (1964).
4. E. F. CALDIN. Fast reactions in solution. Blackwell Scientific Publications, Oxford. 1964. Chap. 12.
5. L. R. DAWSON, M. GOLBEN, G. R. LEADER, and H. K. ZIMMERMAN, JR. J. Electrochem. Soc. **99**, 28 (1952).
6. P. G. SEARS, R. K. WOLFORD, and L. R. DAWSON. J. Electrochem. Soc **103**, 633 (1956).
7. A. B. THOMAS and E. G. ROCHOW. J. Am. Chem. Soc. **79**, 1843 (1957).
8. J. P. VALLEAU and S. J. TURNER. Can. J. Chem. **42**, 1186 (1964).
9. J. P. VALLEAU. Can. J. Chem. **42**, 1174 (1964).
10. J. N. BUTLER. Ionic equilibrium. Addison-Wesley, Reading, Massachusetts. 1964. p. 436ff.
11. P. DEBYE. Trans. Electrochem. Soc. **82**, 265 (1942).
12. L. ONSAGER. Phys. Rev. **37**, 405 (1931); **38**, 2265 (1931); Ann. N.Y. Acad. Sci. **46**, 241 (1945).
13. R. A. ROBINSON and R. H. STOKES. Electrolyte solutions. 2nd ed. Butterworths, London. 1959. p. 315ff.
14. J. E. PRUE and P. J. SHERRINGTON. Trans. Faraday Soc. **57**, 1795 (1961).
15. S. BARNARTT. Quart. Rev. London, **7**, 84 (1953). See Sect. (1.4).
16. R. C. PAUL, P. S. GURAYA, and R. B. SREENATHAN. Indian J. Chem. **1**, 335 (1963).

Can. J. Chem. Downloaded from www.nrcresearchpress.com by 210.87.254.105 on 09/05/12
For personal use only.

Can. J. Chem. Downloaded from www.nrcresearchpress.com by 210.87.254.42 on 09/05/12
For personal use only.

Pyrochlores. III. X-Ray, neutron, infrared, and dielectric studies of $A_2Sn_2O_7$ stannates[1]

FRANÇOIS BRISSE AND OSVALD KNOP
Department of Chemistry, Dalhousie University, Halifax, Nova Scotia

Received September 13, 1967

A number of compositions $A_2^{3+}Sn_2^{4+}O_7$ and of related mixed phases were prepared and investigated. For the trivalent lanthanons from La to Lu, and for Y, the homogeneous $A_2Sn_2O_7$ phases were of the cubic pyrochlore type (space group *Fd3m*, No. 227). Their lattice parameters gave a very good linear relationship when plotted against the Templeton–Dauben radii of A^{3+}. The applicability of other sets of ionic radii was also tested. The lower limit of the $r(A^{3+}):r(Sn^{4+})$ ratio for cubic pyrochlore stannates is about 1.19 (Ahrens radii), while the upper limit is at least 1.60. Attempts to extend the lower limit by preparing mixed Yb + Sc stannates were only partially successful. $Bi_2Sn_2O_7$ is not a cubic pyrochlore.

The structures of $Y_2Sn_2O_7$ and $Sm_2Sn_2O_7$ were refined from X-ray powder data, and that of $La_2Sn_2O_7$, from neutron powder data. The positional parameter of the majority oxygen atom, $x(O_2)$, has been found to increase with the size of A^{3+}. The distortion of the SnO_6 octahedra in the pyrochlore structure thus decreases with increasing $r(A^{3+})$.

From a systematic study of the infrared spectra of the stannates it appears that it is the size of the Y^{3+} ion rather than its chemistry (as distinct from the Ln^{3+} ions) that determines its place among the 3–4 pyrochlores. No evidence of ferroelectricity was found in Pr, Er, and Lu stannates between room temperature and 4.2 °K.

Canadian Journal of Chemistry, **46**, 859 (1968)

The $A_2^{3+}Sn_2^{4+}O_7$ stannates (A = lanthanons from La to Lu, and Y) form a very complete series of compounds with the cubic pyrochlore structure (Table I). Since La^{3+} is the largest trivalent ion known,[2] the series includes all trivalent ions larger than (and including) Lu^{3+} with the exception of Tl^{3+}, Bi^{3+}, and the 5f-ions. $Bi_2Sn_2O_7$ has been reported, on the evidence of an X-ray powder pattern, to be a distorted pyrochlore (1), but its structure has not been determined. The existence of $Tl_2Sn_2O_7$ has not been investigated, but the 5f-ions are almost certain to form pyrochlore phases.

Two questions arise: What is the smallest trivalent ion still capable of yielding a cubic pyrochlore stannate, and How does the positional parameter $x(O_2)$ of the majority oxygen atom (cf. ref. 2) vary with the size, or the atomic number, of A^{3+}?

The question of the lower size limit may be answered by investigating the stannates of Sc^{3+} and In^{3+}, these ions being nearest in size to Lu^{3+} on the low side. An answer to the second question can only be obtained from a complete determination of the crystal structures of representative members of the stannate series.

To see how $x(O_2)$ varies with the size of A^{3+} it is advantageous to choose trivalent ions at the opposite ends of the series, i.e. La^{3+} and Lu^{3+}. However, the combination La^{3+}–Sn^{4+} in a pyrochlore structure is not too favorable for a structure refinement from X-ray diffraction data. Both atoms are much heavier scatterers than oxygen, and their coherent scattering amplitudes are only 8 units apart at $\theta = 0$. The "difference" reflections, which distinguish the X-ray diffraction pattern of a pyrochlore from that of a defect fluorite, will thus be very weak. In $Lu_2Sn_2O_7$ the difference between f(Lu) and f(Sn) is greater, but Lu scatters even more than La, whereby the sensitivity of the $x(O_2)$ determination is further reduced.

As a compromise it was decided to refine the structure of lanthanum stannate from neutron rather than X-ray data, and to use yttrium and samarium stannates for the X-ray study. The combination of the neutron-scattering amplitudes in $La_2Sn_2O_7$ is quite favorable: b(La) = 0.83, b(Sn) = 0.61, and b(O) = 0.577 (all in 10^{-12} cm, for natural isotopic contents) (3). Y^{3+} is larger than Lu^{3+}, 0.92 Å compared with 0.85 Å (Ahrens radii), but its scattering power for X-rays is 10 units lower than that of Sn^{4+} (at $\theta = 0$) and much lower in absolute value than $f(La^{3+})$. For reliability of a structure refinement yttrium is thus a better choice than any of the lanthanons, but it introduces one uncertainty. While the size of Y^{3+} is close to that of Ho^{3+}, it does not follow that yttrium and

[1]For Part II see ref. 13.
[2]Disregarding Ac^{3+} and possibly Pa^{3+}.

Can. J. Chem. Downloaded from www.nrcresearchpress.com by 210.87.254.42 on 09/05/12
For personal use only.

TABLE I

Preparation and lattice parameters of cubic $A_2Sn_2O_7$ pyrochlores

Composition	$a_0(P)$, Å	Heat treatment*	Reference
$La_2Sn_2O_7$	10.702	1550/1, air-quenched	1
	10.702		4
	10.640†		6
	10.7005 ± 10	1050/48, 1300/48	This work
$Pr_2Sn_2O_7$	10.604		4
	10.6050 ± 10	1350/12, 1400/12	This work
$Nd_2Sn_2O_7$	10.568	1550/1, air-quenched	1
	10.573		4
	10.5695 ± 12	1350/12, 1400/12	This work
$Sm_2Sn_2O_7$	10.507		4
	10.5099 ± 11	1400/18, 1500/24	This work
$Eu_2Sn_2O_7$	10.474		4
	10.4755 ± 7	1000/36, 1100/12, 1400/24	This work
$Gd_2Sn_2O_7$	10.460		4
	10.4600 ± 8	1350/12, 1400/12	This work
$Tb_2Sn_2O_7$	10.428		5
	10.4269 ± 9	1350/12, 1400/12	This work
$Dy_2Sn_2O_7$	10.389		5
	10.4006 ± 6	1350/24, 1400/24, 1500/18	This work
$Ho_2Sn_2O_7$	10.374		5
	10.3756 ± 11	1350/24, 1400/24, 1500/18	This work
$Er_2Sn_2O_7$	10.350		4
	10.3539 ± 9	1000/36, 1100/12, 1400/24	This work
$Tm_2Sn_2O_7$	10.330		5
	10.3291 ± 4	1000/36, 1100/12, 1400/24	This work
$Yb_2Sn_2O_7$	10.304		4
	10.3086 ± 6	1000/36, 1100/12, 1400/24	This work
$Lu_2Sn_2O_7$	10.294		4
	10.2928 ± 13	1000/36, 1100/12, 1400/24	This work
$Y_2Sn_2O_7$	10.371		4
	10.3725 ± 11	1300/3, 1400/32, 1400/48	This work
$(Yb_{0.8}Sc_{0.2})_2Sn_2O_7$	10.2921 ± 21	1400/3 days, 1450/18	This work
$(Yb_{0.6}Sc_{0.4})_2Sn_2O_7$	10.2889 ± 28	1400/3 days, 1450/18; $P + \delta$?	This work
$(Yb_{0.4}Sc_{0.6})_2Sn_2O_7$		1400/3 days, 1450/18; $P + \delta$	This work
$(Yb_{0.2}Sc_{0.8})_2Sn_2O_7$		1400/3 days, 1450/18; P? $+ \delta$	This work
$Sc_2Sn_2O_7$		1000/12, 1400/24, 1400/24; δ	This work
$Sc_4Sn_3O_{12}$		1000/12, 1400/24, 1400/24; δ	This work
$Cr_2Sn_2O_7$		950/12, 1400/6; not P	This work
$In_2Sn_2O_7$		1000/24, 1050/48, 1400/6; not P	This work
$Sb_2Sn_2O_7$		300/24, 500/24, 650/12 (*in vacuo*); no reaction	This work
$Bi_2Sn_2O_7$		950/6, 1000/12, 1000/12; not cubic P	This work
Nd_2SnTiO_7	10.4279 ± 17	1400/48, 1480/2	This work
Ho_2SnTiO_7	10.2368 ± 12	1000/24, 1200/18, 1350/11, 1380/6, 1400/12	This work
$YHoTiSnO_7$	10.2403 ± 8	Same as for Ho_2SnTiO_7	This work
$Y_2(Sn_{0.64}Ti_{0.36})_2O_7$	10.2771 ± 10	950/24, 1200/24, 1450/24	This work
$Y_2(Sn_{0.36}Ti_{0.64})_2O_7$	10.1948 ± 16	950/24, 1200/24, 1450/24	This work
$La_2(Sn_{0.9}Ti_{0.1})_2O_7$	10.6854 ± 11	1350/12, 1400/12	This work
$La_2(Sn_{0.8}Ti_{0.2})_2O_7$	10.6839 ± 20	1350/12, 1400/12; $P + La_2Ti_2O_7$?	This work
$La_2(Sn_{0.7}Ti_{0.3})_2O_7$	10.6845 ± 18	1350/12, 1400/12; $P + La_2Ti_2O_7$?	This work
$(Y_{1-x}Bi_x)_2Sn_2O_7$ (x = 0.2 to 0.8)		950/6, 1000/12, 1100/4, 1100/9; not P	This work
$(Y_{1-x}In_x)_2Sn_2O_7$ (x = 0.2 to 0.8)		950/6, 1000/12, 1300/12; not P	This work

*1550/1 stands for 1550° for 1 h. The firing conditions indicated in refs. 4 and 5 were 1450–1550/5–20.
†The purity of the La_2O_3 used is not clear. The oxide may have contained a substantial amount of Nd and Pr. Firing conditions: 1300–1500° in air, slow cooling in furnace.

holmium, in the pyrochlore structure, are closely similar *chemically*. That is, unless $x(O_2)$ is governed overwhelmingly by the *size* of the trivalent ion, $x(O_2)$ in yttrium stannate need not have a value very similar to that of $x(O_2)$ in holmium stannate. This point will be discussed later.

The fourth stannate structure investigated was that of the mixed phase $Y_2(Sn_{0.36}Ti_{0.64})_2O_7$. This composition is of some interest for the

Can. J. Chem. Downloaded from www.nrcresearchpress.com by 210.87.254.42 on 09/05/12
For personal use only.

application of neutron diffraction to crystal-structure refinement. Assuming that the Sn and Ti atoms are distributed at random over the 16(*d*) sites, the contribution of Sn to the structure factor will be almost completely cancelled by the contribution from Ti, which will be equal in magnitude but of opposite sign.[3] This means that there will be no net diffracted Bragg intensity from atoms in the 16(*d*) sites. The observed intensity will originate only from the contributions from Y and oxygen. One might then expect the isotropic temperature factor B(Sn + Ti) to be eliminated from the refinement, whereby the number of parameters to be refined will decrease by one. This is of consequence, as the number of usable reflections in neutron powder diffraction is invariably small.

As a contribution to the systematic study of cubic pyrochlores it was also decided to redetermine the lattice parameters of the stannates reported earlier (1, 4–6) and to determine the variation of the characteristic infrared frequencies of the stannates with the atomic number of A.

Ferroelectricity in the pyrochlore $Cd_2Nb_2O_7$ and its limited solid solutions with other 2–5 pyrochlores has been known for some time (7–11). No information seems to be available, however, on the existence of ferroelectric transitions in 3–4 pyrochlores. To investigate this matter the permittivities of Pr, Er, and Lu stannates were measured from room temperature down to 4.2 °K.

Experimental

Preparation

The stannates were prepared from SnO_2 (Fisher "Certified" reagent) and freshly calcined lanthanon or yttrium oxides of at least 99.9% purity (Lindsay Chemical Division, American Potash and Chemical Corporation).[4] The TiO_2 and Cr_2O_3 were Fisher "Certified" reagents, Bi_2O_3 and Sb_2O_3 were British Drug Houses reagents, and In_2O_3 of 5N purity was obtained from Koch-Light Laboratories Limited. Spectrographic analysis of the high-purity scandium oxide used in the preparation[5] revealed 0.1% K, 0.02% Na, 0.01% Ca, and (in p.p.m.) 70 Si, 30 Al, 20 Fe, 5 Mg, and 27 Y; no rare-earth impurities were detected.

The oxides were dry-mixed, pressed, and fired in air. The fired disks were cooled with the furnace (for details of preparation see ref. 2). The pressed pellet of Sb_2O_3 + $2SnO_2$ was fired in a recrystallized-alumina crucible which was inside an evacuated and sealed ampoule of transparent silica. The individual firing schedules are noted in Table I. None of the fired disks showed any tendency to swell on exposure to atmospheric air.

X-Ray and Neutron Diffraction

Details of the X-ray and neutron techniques will be found in refs. 2 and 13. CuK radiation filtered with nickel was used throughout ($\lambda\alpha_1$ = 1.540562 Å (14)).

The neutron diffraction patterns were of good quality, but the overlap resulting from the use of a relatively short wavelength, 1.10 Å, was, even with narrow collimation, sufficiently severe to necessitate resorting to Gaussian analysis of the composite peak profiles. Even for resolved reflections it was found of advantage to adjust the peaks to the best Gaussian profiles by least squares.

The raw patterns were reduced to pF_o^2 patterns by correcting for the combined angular and absorption factors. The reduced baseline was then represented by least squares as a polynomial in θ, adjusted to match the baseline of the reduced stannate pattern and subtracted. The reduced peaks were expressed as Gaussian exponentials, $G_i = a_i \exp[-b_i(\theta - \theta_i^0)^2]$, which in turn were expanded into two-term series to fit an iterative least-squares program. The shifts Δa_i and Δb_i were computed from the initial trial values by a full-matrix program written for IBM 1620 (40K). Up to 7 overlapping peaks could be resolved at a time, but the success of the procedure depended to a considerable extent on the choice of the initial trial values. A small empirical correction was added when necessary to position the peaks accurately on the 2θ scale. Integration of the resolved peak areas was simply a matter of evaluating the Gaussian integrals, $a_i(\pi/b_i)^{\frac{1}{2}}$, from the final peak height (a_i) and half-width ($[(\ln 2)/b_i]^{\frac{1}{2}}$) values.

Least-Squares Refinement

The structures were refined from suitably scaled $|F_o|$ that had been extracted from single reflections of the respective diffractometer patterns. The block-diagonal approximation program of ref. 15 was used most of the time. It was supplemented by *ad hoc* programs for computing the correlation matrix and e.s.d.'s of the individual refinement parameters. The weighting scheme employed was W3 of ref. 16.

The X-ray scattering factors for Sm^{3+}, Y^{3+}, and Sn^{4+} (17) and for O^{2-} (18) were corrected for dispersion (real and imaginary parts (19)) and interpolated by a three-function scheme (15). Individual isotropic temperature factors were used throughout. A reduction factor was applied to the shifts in all refinements.

The following abbreviations have been introduced: K, scale factor; n, number of reflections used in a refinement; e.s.d.(w) = e.s.d. × $(\Sigma w)^{\frac{1}{2}}$; $R = \Sigma|\Delta|F||/\Sigma|F_o|$; $D(\Delta I) = \Sigma|\Delta I|/\Sigma I_o$; $D(I) = 1000\Sigma I_c/\Sigma I_o$.

Infrared Spectra

Infrared spectra of the stannates and of comparison compounds were recorded from 4000 to 250 cm^{-1} on a Perkin–Elmer model 521 spectrophotometer using KBr pellets.

Dielectric Measurements

Permittivities of thin ceramic disks were measured, from room temperature down to 4.2 °K and back to room temperature, by Mr. Y. S. Lim in the Department of Physics, Dalhousie University.

[3] b(Ti) = −0.34, b(Y) = 0.80 (in 10^{-12} cm) (3).

[4] For thermogravimetric behavior of the Pr and Tb oxides see ref. 12.

[5] A generous quantity of high-purity scandium oxide was made available to us by Drs. B. I. Pokrovskiĭ and F. M. Spiridonov of the Institute of Inorganic Chemistry, Faculty of Chemistry, Moscow State University.

Can. J. Chem. Downloaded from www.nrcresearchpress.com by 210.87.254.42 on 09/05/12
For personal use only.

The permittivity was measured by a standard balanced-bridge method at a frequency of 1 kc/s and an electric field strength between 15 and 24 V/cm. The disks were electroded by evaporating a thin layer of silver on the disk faces. An indium foil provided connection between the silver coating and copper-disk electrodes.

The permittivity vs. temperature curve for $Cd_2Nb_2O_7$, which was used to check the apparatus, agreed well with that reported by other workers (8, 9). With cadmium niobate the complete cooling–heating cycle took 8 h. Since no ferroelectric transitions were observed in the stannates, individual complete runs could be made in 2 h. The measured values were corrected for porosity of the ceramic specimens (20). The accuracy of both the permittivity and the temperature measurements was estimated to be about 5%.

Results and Discussion

Lattice Parameters and Ionic Radii

All the Ln stannates and $Y_2Sn_2O_7$ were cubic pyrochlores (Table I). Their lattice parameters (at 20 ± 2 °C) agreed very well with those reported by Whinfrey *et al.* (4, 5) and by Roth (1), but the present value of $a_0(La_2Sn_2O_7)$ is about ½% higher than the corresponding value obtained by Padurow and Schusterius (6).

The variation of a_0 with A is represented in Figs. 1–3. A linear relationship was obtained by plotting $a_0(A_2Sn_2O_7)$ (abbreviated in the following to $a_0(P)$) against $a_0(A_2O_3$, *C*-type) (abbreviated to $a_0(C)$). This method of representation does not depend on the choice of an absolute value for the ionic radius of oxygen. In view of this and because of the considerable similarity of the pyrochlore and the *C*-type structures it is not surprising that linearity is so closely satisfied. Using the $a_0(C)$ values of 10.7281 ± 5 Å for Tb_2O_3 (21), 11.140 ± 2 Å for Pr_2O_3 (22), 11.40 Å for La_2O_3 (23), and those of Roth and Schneider (24) for the other oxides, adjusting them to the Cu*K*α value quoted above, and fitting the best straight line by least squares, the regression of $a_0(P)$ on $a_0(C)$ gave $\sigma = 0.0036$ Å, and that of $a_0(C)$ on $a_0(P)$ gave $\sigma = 0.0086$ Å. The very large correlation coefficient of the two regressions, 0.9995, left no doubt about the linearity of the relationship. However, Pr was a conspicuous misfit. When it was omitted the correlation coefficient increased to 0.9998. At the same time the standard deviations decreased by almost one half, indicating a substantial improvement in the fit.

The two sets of a_0 are thus highly consistent, which reflects both the accuracy of the a_0 values and the fact that the A^{3+} ions behave essentially in the same manner in the two oxide structures.

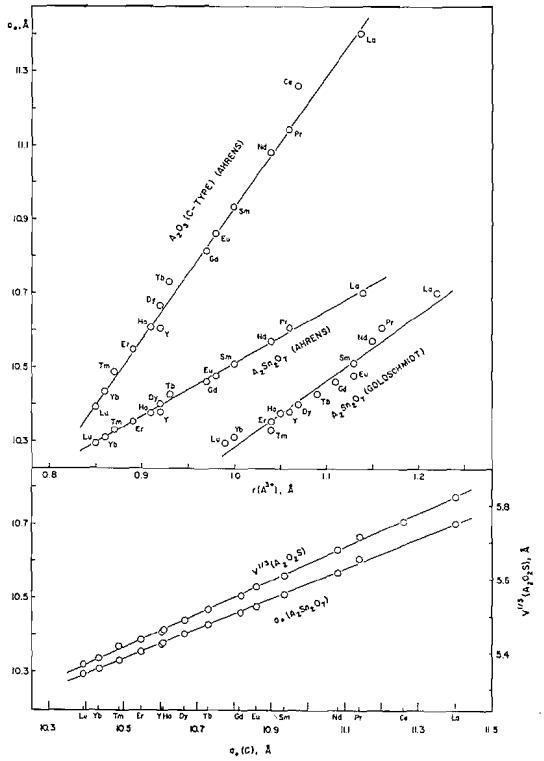

FIG. 1. (*Top*) Dependence of $a_0(A_2Sn_2O_7)$ and $a_0(C)$ on the Ahrens and the Goldschmidt radii of A^{3+}. (*Bottom*) Relationship between $a_0(A_2Sn_2O_7)$ and $a_0(C)$, and between $V^{1/3}(A_2O_2S)$ and $a_0(C)$.

The slope of the $a_0(P)$ vs. $a_0(C)$ line, however, is less than unity, which indicates that $a_0(P)$ increases with $r(A^{3+})$ more slowly than $a_0(C)$.

A plot of $a_0(P)$ against the Ahrens and the Goldschmidt ionic radii gave a far less satisfactory fit. First, as has already been pointed out by Roth and Schneider (24, 25) and elsewhere, it showed that Y^{3+} is misplaced in both sets of radii. Y^{3+} is not similar in size to Dy^{3+}, nor does it appear to fall between Dy^{3+} and Ho^{3+}, as has been stated for the $AFeO_3$ orthoferrites (26); it is somewhat smaller than Ho^{3+}. The present evidence for the position of Y^{3+} in the Ln^{3+} sequence thus fully confirms previous observations on cubic Ln_2O_3 (24, 25), pyrochlore titanates $A_2Ti_2O_7$ (12), oxysulfides A_2O_2S (27), and orthorhombic fluorides AF_3 (28).[6]

[6]When allowance is made in ref. 26 for the stated standard deviation of 0.003 Å, the sequences of the lattice parameters for the orthoferrites can be reconciled with the present observation.

Can. J. Chem. Downloaded from www.nrcresearchpress.com by 210.87.254.42 on 09/05/12
For personal use only.

Secondly, with regard to internal consistency both sets of radii for trivalent lanthanons appear to be in need of revision, but the Goldschmidt more so than the Ahrens radii. In particular, Tb^{3+} is a conspicuous misfit in both the $a_0(P)$ and $a_0(C)$ series (Fig. 1). Roth and Schneider (24) remarked on the failure of Tb_2O_3 to fall in line with the other sesquioxides in their $a_0(C)$ vs. Ahrens radius plot. They suggested that either the Ahrens radius of Tb^{3+} was too small or else not all of the Tb in their Tb_2O_3 was in the trivalent state. Similar misfits have been observed with other Tb compounds, e.g. $Tb_2Sn_2O_7$ (5, and present work), $Tb_2Ti_2O_7$ (12), and Tb_2O_2S (29). Since these compounds were prepared and treated in different ways and have different properties, it is unlikely that they all would have been contaminated with Tb^{4+} to a similar extent. Rather, it is almost certain that the Ahrens value for $r(Tb^{3+})$ is too small.

The set of Ln^{3+} crystal radii proposed by Templeton and Dauben (30)[7] and augmented by Geller's value for $r(Y^{3+})$, 0.893 Å (31), gave a much better linear relationship (Fig. 2). The $a_0(P)$ values can be readily accommodated on the straight lines

$$a_0(P) = 8.6631 + 1.9158r(A^{3+}) \quad \sigma = 0.0032$$

$$r(A^{3+}) = -4.5117 + 0.52157a_0(P) \quad \sigma = 0.0017$$

(correlation coefficient = 0.9996), and similar linear relationships apply to $a_0(C)$, Pr_2O_3 again being an exception (Fig. 2). The $a_0(C)$ vs. $r(A^{3+})$ (Templeton–Dauben) relationship, including $a_0(Ce_2O_3) = 11.26$ Å (32), is expressed by

$$a_0(C) = 6.3876 + 4.7161r(A^{3+}) \quad \sigma = 0.0053$$

$$r(A^{3+}) = -1.3537 + 0.21197a_0(C) \quad \sigma = 0.0011$$

(correlation coefficient = 0.9998; Pr omitted). It is thus almost certain that the value of 11.140 Å for $a_0(Pr_2O_3$, C-type) is too low. The linear relationship of $a_0(P)$ and $r(A^{3+})$ (Templeton–Dauben) may be said merely to reflect the more primary dependence of $a_0(P)$ on $a_0(C)$ of Fig. 1.

The internal consistency of the Templeton–Dauben set is shown in Fig. 2 on another two series of A(III) compounds: the hexagonal A_2O_2S (27) and the orthorhombic AF_3 (28). For these two series the plots of $2V^{1/3}$ vs. $r(A^{3+})$, give very satisfactory smooth lines, although the relationship for AF_3 is not linear and YF_3 does not quite fall on the curve.

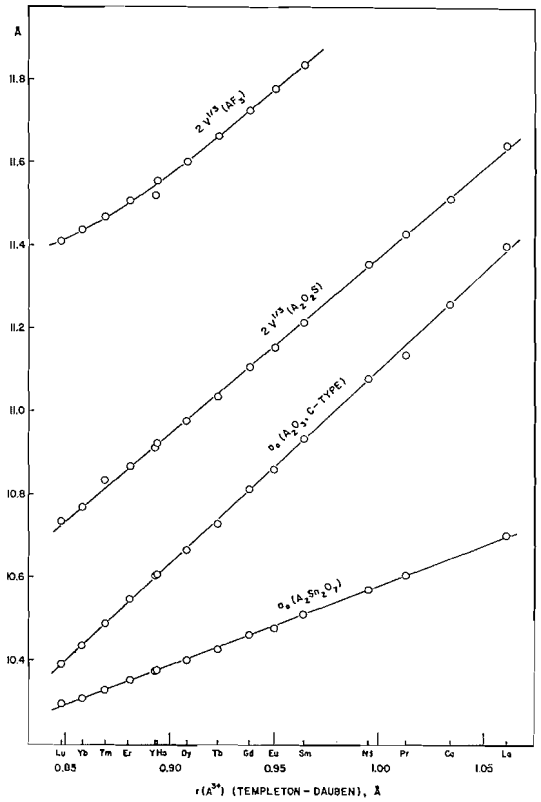

FIG. 2. Variation of $a_0(A_2Sn_2O_7)$, $a_0(C)$, $V^{1/3}(A_2O_2S)$, and $V^{1/3}(AF_3)$ with the Templeton–Dauben radii of A^{3+}.

The set of a_0 values reported for the stannates by Whinfrey *et al.* (4, 5) is also very good. The correlation coefficient, 0.9990, and the standard deviations of the regressions of $a_0(P)$ on $r(A^{3+})$, 0.0026, and of $r(A^{3+})$ on $a_0(P)$, 0.0051, differ only slightly from those quoted for our own values. The Whinfrey set and our set regressed on each other have a very high correlation coefficient, 0.9995, and the two standard deviations are almost identical, 0.0033 Å.

The curve obtained by plotting $a_0(P)$ against the atomic number of the lanthanon displays the familiar cusp at Gd (Fig. 3).

Limits of Existence of the Pyrochlore Structure

The powder pattern of $Sc_2Sn_2O_7$ could be indexed up to $d = 1.119$ Å on a rhombohedral unit cell, $a_{rh} = 7.917$ Å, $\alpha = 72.40°$ ($a_{hex} = 9.353$ Å, $c_{hex} = 17.37$ Å). The reflections at higher angles were too weak and diffuse to permit reliable indexing. This would place the

[7]This set is based primarily on the C-type oxides, so that the radii may be taken as referring nominally to six-coordination.

Can. J. Chem. Downloaded from www.nrcresearchpress.com by 210.87.254.42 on 09/05/12
For personal use only.

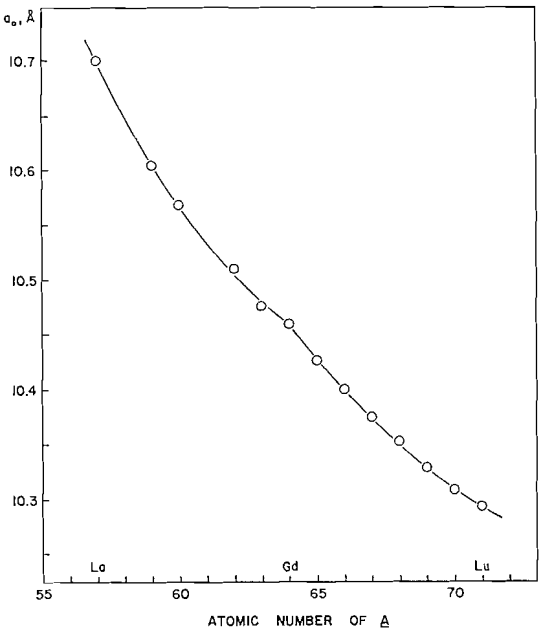

FIG. 3. Variation of $a_0(A_2Sn_2O_7)$ with the atomic number of A.

stannate with the δ phase described by Lefèvre (33) in the system scandia–zirconia, and by other authors in the systems ytterbia–zirconia (34), scandia–titania (35), scandia–hafnia (38), ytterbia–hafnia (38), and lutetia–zirconia (38). These phases may also be related to the rhombohedral phases in the systems U–Y–0 (36, 37), U–Lu–O (37), Tb–O, Pr–O, and Ce–O (33). The clearest demonstration that in A_2O_3–BO_2 systems the (ideal) composition of the δ phase is $A_4B_3O_{12}$ or close to this formula is found in the system scandia–titania (35), where the rhombohedral phase $2Sc_2O_3.3TiO_2$ ($a_{rh} = 7.742 \pm 5$ Å, $\alpha = 71.94 \pm 0.1°$) with a narrow homogeneity range transforms, above $1150 \pm 50°$, to a disordered defect fluorite phase of the same composition. Since the system Sc_2O_3–SnO_2 is presumably sufficiently similar, it was assumed that the composition $Sc_2Sn_2O_7$ corresponded to a mixture of $Sc_4Sn_3O_{12}$ and SnO_2.

However, the strongest lines of the SnO_2 pattern were not visible in the powder photograph of $Sc_2Sn_2O_7$. This is surprising, as a mixture of the assumed composition would contain 20% SnO_2, an amount difficult to overlook. The lattice parameters of $Sc_4Sn_3O_{12}$ were practically the same as those of $\delta(Sc_2Sn_2O_7)$. Assuming that the preparations were reasonably close to the practically attainable state of equilibrium, this would lead to the conclusion that $\delta(Sc_2O_3$–$SnO_2)$ is not limited to the composition $Sc_4Sn_3O_{12}$ but has a homogeneity range extending towards SnO_2, the saturation boundary being somewhere between 60 and 66.6 mole % SnO_2. In this respect the system Sc_2O_3–SnO_2 resembles the systems scandia–zirconia and ytterbia–zirconia, but it differs from the system scandia–titania, although even in the latter the variation, with temperature, of a_0 of the high-temperature disordered fluorite phase corresponding to $\delta(Sc_2O_3$–$TiO_2)$ is small (35).

The lower limit of the pyrochlore stability field for the stannates must thus lie between Sc^{3+} and Lu^{3+}, i.e. between Ahrens radii of 0.81 and 0.85 Å. Since there are no trivalent ions of sizes between Sc^{3+} and Lu^{3+}, a number of mixed compositions $(Sc_{1-x}Yb_x)_2Sn_2O_7$ were prepared, in which the average size of A^{3+} ranged from 0.81 to 0.85 Å ($r(Yb^{3+}) = 0.86$ Å) (Table I). At $x = 0.8$ only lines of the pyrochlore pattern were visible, while at $x = 0.6$ a weak subsidiary pattern appeared. The $a_0(P)$ values in these two compositions were the same, within the stated uncertainty limits. These observations would fix the limit of the pyrochlore phase close to $x = 0.8$, i.e. $r(A^{3+}) = 0.85$ Å (Ahrens). Since this is the ionic radius of Lu^{3+}, it does not appear possible to extend the lower limit in the mixed phases.

Mixed compositions $Y_2(Sn_{1-x}Ti_x)_2O_7$ ($x = 0.36$ and 0.64) and $La_2(Sn_{1-x}Ti_x)_2O_7$ ($x = 0.1$, 0.2, and 0.3) were also prepared and investigated. A plot of a_0 vs. composition for the yttrium compounds (Fig. 4) shows that there is complete solid solubility in the system and the variation of a_0 with x is linear.

Both Ho_2SnTiO_7 and Nd_2SnTiO_7 were pyrochlores. The lattice parameter of the Ho phase was, within the stated uncertainty limits, the same as 10.2377 Å, which is the average of $a_0(Ho_2Sn_2O_7)$ and $a_0(Ho_2Ti_2O_7)$ (12). YHoTi-SnO_7 also was a pyrochlore, but its a_0 was not identical with the average of the individual a_0 of either pair of the pure phases.

Although a continuous solid solution has been said to exist in the system $La_2Sn_2O_7$–$La_2Ti_2O_7$ (6), the only homogeneous composition of the above three was $La_2(Sn_{0.9}Ti_{0.1})_2O_7$ (Table I). Powder photographs of the other two contained

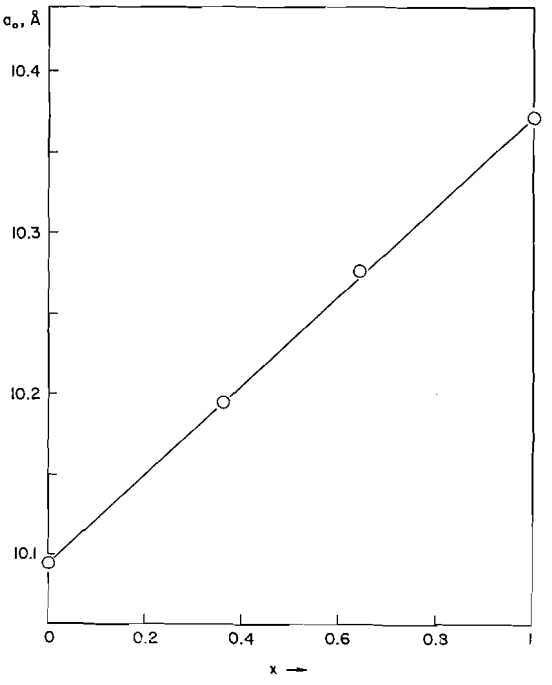

FIG. 4. Relationship between a_0 and composition in the series $Y_2(Sn_{1-x}Ti_x)_2O_7$. For $a_0(Y_2Ti_2O_7)$ see ref. 12.

extra lines, possibly of a foreign phase. Their pyrochlore pattern could be indexed on unit cells that did not significantly differ from a_0 of the homogeneous mixed phase at $x = 0.1$, so that the existence of a limit of substitution of Sn by Ti somewhere near $x = 0.1$ cannot be excluded. The decrease of a_0 on going from $x = 0$ to $x = 0.1$ was only 0.015 ± 2 Å.

These results are difficult to reconcile with the account of Padurow and Schusterius's (6) experiments, not least because these authors are the only ones to report $La_2Ti_2O_7$ to be a cubic pyrochlore (cf. refs. 1 and 12). It is possible that some of the discrepancies can be explained by the higher firing temperatures used by these authors, up to 1550° compared with 1400° in the present work. The powder photograph of their preparation with the approximate formula $(La_{8/12}Nd_{3/12}Pr_{1/12})_2(Sn_{0.375}Ti_{0.625})_2O_7$ ($a = 10.484$ Å) contained a number of extra lines described as v.v.w. (very very weak) that could not be indexed on the pyrochlore cell. This is puzzling, as the presence of a substantial proportion of the smaller Nd^{3+} ion would be expected to favor a homogeneous cubic phase to form, the more readily as $La_2Ti_2O_7$ itself is implied to be a cubic pyrochlore.[8]

As has already been reported by Roth (1), the pattern of $Bi_2Sn_2O_7$ was closely related to the pyrochlore pattern. Both Cr_2O_3 and In_2O_3 reacted with SnO_2, but the products did not give cubic pyrochlore patterns, and the infrared spectra of both and of $Bi_2Sn_2O_7$ were different from the typical spectra of pyrochlore stannates. No reaction was observed between Sb_2O_3 and SnO_2. Attempts to prepare homogeneous cubic pyrochlores of compositions $(Y_{1-x}Bi_x)_2Sn_2O_7$ and $(Y_{1-x}In_x)_2Sn_2O_7$ were not successful (Table I).

Refinement of $Y_2Sn_2O_7$ and $Sm_2Sn_2O_7$ from X-Ray Data

The results of the least-squares refinements are summarized in Table II. Though the convergence was slow, the shifts for both compounds converged to zero. As might be expected, yttrium stannate was the better-behaved structure. The relatively high background of the $Sm_2Sn_2O_7$ diffractometer pattern reduced the reliability of the intensity collection, and the more heavily scattering Sm made the refinement less favorable than for $Y_2Sn_2O_7$. Taking these adverse factors into account, the result, as judged by R and the e.s.d.'s, was reasonably good.

The temperature factors in the $Y_2Sn_2O_7$ refinement were all strongly correlated. This was reflected in the large e.s.d.'s especially of the oxygen atoms: $B(O_2)$ was in fact indeterminate, and $B(O_1)$ was poorly defined and unreasonably high. The situation was worse in samarium stannate. The smallest correlation coefficient was 0.12, while the correlation of B(Sm) and B(Sn) seemed to amount to linear dependence. This time $B(O_1)$ was indeterminate and $B(O_2)$ and B(Sm) were ill-defined.

Although the refinement of samarium stannate cannot be viewed as very satisfactory, it was considered that the appearance of the correlation matrix need not cause alarm (cf. ref. 39). For $2\sigma(x)$ the positional parameter $x(O_2)$ of the Sm

[8]Padurow and Schusterius state that "[natural] pyrochlores have a true cubic symmetry only at elevated temperatures (800–900°). At room temperature all pyrochlore specimens are anisotropic under the microscope; their unit cells are pseudocubic, but the deviation from true cubic cells is always only slight". It is not made clear whether this statement refers to La stannate and the La stannate–titanate as well.

Can. J. Chem. Downloaded from www.nrcresearchpress.com by 210.87.254.42 on 09/05/12
For personal use only.

Can. J. Chem. Downloaded from www.nrcresearchpress.com by 210.87.254.42 on 09/05/12
For personal use only.

TABLE II

Results of the least-squares refinements from X-ray ($Y_2Sn_2O_7$, $Sm_2Sn_2O_7$) and neutron ($La_2Sn_2O_7$) data*

	$Y_2Sn_2O_7$		$Sm_2Sn_2O_7$		$La_2Sn_2O_7$	
	Initial	Final	Initial	Final	Initial	Final
n	17	16	15	15	10	10
After cycle		10		13		11
K	1.000	0.995±1	1.000	0.901±3	1.000	0.978±7
$x(O_2)$	0.4200	0.4120±9	0.4200	0.4167±26	0.4200	0.4216±1
B(A), Å^2	0.15	0.35±17	0.15	0.52±42	0.15	1.20±6
B(Sn), Å^2	0.60	0.41±13	0.60	1.00±59	0.60	1.12±6
$B(O_1)$, Å^2	1.50	3.24±294	1.50	0.53±161	1.50	3.65±10
$B(O_2)$, Å^2	1.50	0.43±57	1.50	2.50±145	1.50	1.07±4
R, %	4.83	0.96	5.09	1.20	3.13	1.92
e.s.d.(w)	10.88	2.23	19.52	3.63	0.315	0.184

*For meaning of symbols see Experimental.

TABLE III

Observed and calculated structure factors for $Y_2Sn_2O_7$ and $Sm_2Sn_2O_7$ (Cu$K\alpha$) and $La_2Sn_2O_7$ (neutrons)

	$Y_2Sn_2O_7$		$Sm_2Sn_2O_7$		$La_2Sn_2O_7$	
hkl	$\|F_o\|$	F_c	$\|F_o\|$	F_c	$100\|F_o\|$	$100F_c$
111	98	101	—	−38	—	67
220		39	—	24	—	163
311	143	−131	—	3	226	−263
222	1167	1160	1423	1416	2253	2268
400	820	818	1064	1082	393	−339
331	—	22	147	158	1250	1270
422	†	−64	—	−49	825	−729
440	1178	1181	1339	1358	4201	4194
531	78	−74	—	55	—	127
620	—	20	—	41	752	702
533*	140	−97	—	12		−448
622	920	918	1085	1096	2166	2176
444	771	774	960	969		679
642	—	6	—	−13	—	−144
800	906	915	1033	1040	3605	3589
733	—	−27	†	−123	1842	−1869
662	764	772	917	900		
840	691	693	832	833		
844	761	749	843	840		
880	638	645	718	716		
10.6.2	601	601	678	668		
12.4.0	583	586	630	636		
10.6.6	533	545	595	591		
12.4.4			562	571		

*Not used in the refinement.
†Intensity not measured.

compound was not significantly different from $x(O_2)$ of $Y_2Sn_2O_7$, but in the context of the results for all three refined stannate structures (see next section) we are inclined to consider the increase of $x(O_2)$ from Y to Sm as real. The inversion of the high-valued thermal parameters $B(O_1)$ and $B(O_2)$ in the two structures is probably a consequence of the strong correlation of all the temperature factors.

Observed and calculated F's are compared in Table III. The $Y_2Sn_2O_7$ refinement gave $D(\Delta I) = 1.45\%$ ($D(I) = 1003$) for reflections used in the refinement, and 2.97% (1034) for all observable reflections (taking I_o of peaks

Can. J. Chem. Downloaded from www.nrcresearchpress.com by 210.87.254.42 on 09/05/12
For personal use only.

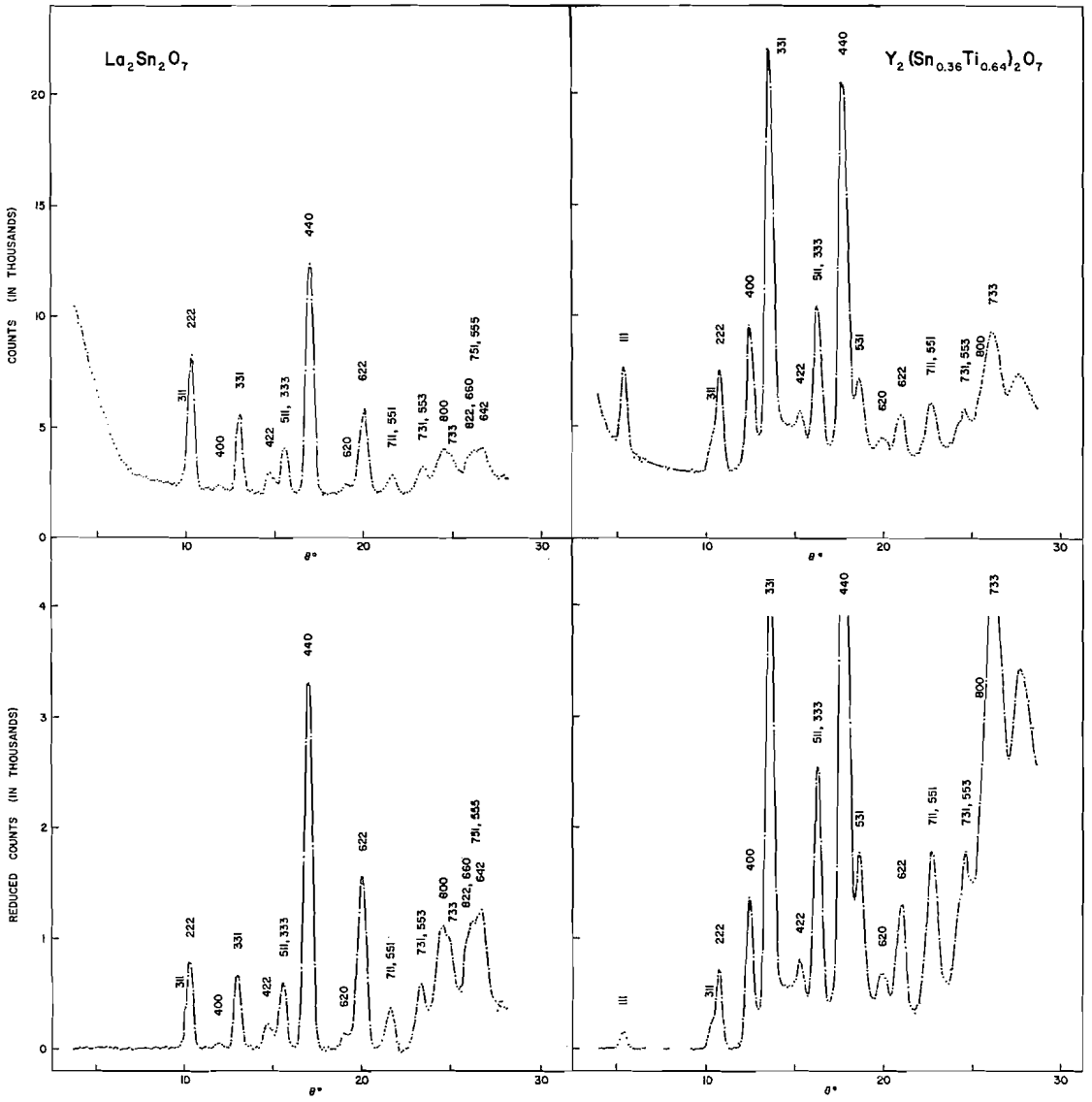

FIG. 5. Raw (*top*) and reduced (*bottom*) neutron diffraction patterns of $La_2Sn_2O_7$ and $Y_2(Sn_{0.36}Ti_{0.64})_2O_7$. The striking difference between the two patterns arises almost entirely from the contribution of the tetravalent atom. The appreciably higher intensity of the Y pattern is caused by the very low absorption in the specimen.

not observed or measured as zero). The corresponding values for the Sm compound were 3.36% (1022) and 3.36% (the second value does not include 10.2.2 + 666, 12.0.0 + 884 and 13.3.1 + 11.7.3 + 977, which were measurable but, as multiple reflections, not counted).

The powder intensity data for both compounds have been submitted to the ASTM file.

Refinement of $La_2Sn_2O_7$ from Neutron Data

The raw and reduced diffraction patterns are shown in Fig. 5. Considering the uncertainties in estimating the baseline and the vagaries of the Gaussian analysis, the 10 single reflections used in the refinement gave surprisingly low e.s.d.'s (Table II) and a good agreement of the structure factors (Table III). While there were only 10 $|F_o|$ for 6 refinement parameters, the large contribution of the oxygen atom to diffraction intensities makes the low e.s.d.'s not unreasonable. The similarity of $D(\Delta I)$ for the 3 classes of reflections indicates that the structure

TABLE IV

Apparent interatomic distances and bond angles in $A_2Sn_2O_7$ pyrochlores*

Distance or angle	Y	Sm	La
	Distances, Å		
Sn—O_2	2.048±8	2.054±22	2.070±4
Sn—O_2	3.956±16	3.965±48	3.991±4
A—$O_1 = a_0\sqrt{3}/8$	2.2457±10	2.2755±10	2.3167±10
A—O_2	2.485±12	2.554±36	2.635±4
$O_2(5)$—$O_2(6)$	2.649±5	2.700±14	2.766±3
$O_2(4)$—$O_2(5)$	3.124±11	3.096±31	3.080±3
$O_1(1)$—$O_2(3)$	2.977±9	3.066±26	3.173±4
$O_1(1)$—$O_2(2)$	3.687±2	3.742±6	3.816±1
O_1—$O_1 = a_0\sqrt{3}/4$	4.4914±18	4.5509±20	4.6334±18
Sn—Sn, A—A, Sn—A $= a_0\sqrt{2}/4$	3.6672±16	3.7158±16	3.7832±14
	Bond angles, °		
$O_2(4)$—Sn(1)—$O_2(5)$	99.4±1.0	97.8±2.4	96.2±0.4
$O_2(5)$—Sn(1)—$O_2(6)$	80.6±1.0	82.2±2.4	83.8±0.4
$O_2(2)$—A(1)—$O_2(3)$	64.4±0.5	63.8±1.3	63.3±0.2
$O_1(1)$—A(1)—$O_2(3)$	77.3±2.2	78.6±5.7	79.4±1.5
$O_1(1)$—A(1)—$O_2(2)$	102.7±2.2	101.4±5.7	100.6±1.5
$O_2(2)$—$O_1(1)$—$O_2(3)$	45.2±0.6	45.4±1.6	45.4±0.3
A(1)—$O_1(1)$—A(2)†	109.47	109.47	109.47

*For atomic positions see Table IV of ref. 2.
†Tetrahedral angle.

determination was on the whole not biased by the selection of peaks for the refinement:

	$D(\Delta I)$	$D(I)$
Reflections used in the refinement	2.66%	1000
Reflections measured	3.60%	1012
All observable reflections up to and including 733	5.02%	1026

$B(O_1)$ was large, though not much more so than $B(O_1)$ in $Y_2Sn_2O_7$, but its e.s.d. was remarkably small. Probably not much emphasis should be placed on the physical significance of the numerical values of these temperature factors.

The temperature factors were again strongly correlated, but generally less so than in the refinements from X-ray data. Of the 15 correlation coefficients 10 were lower than |0.50| and the remaining 5 did not exceed |0.72|.

Refinement of $Y_2(Sn_{0.36}Ti_{0.64})_2O_7$ from Neutron Data

The considerable overlap and the uncertainty in the baseline of an otherwise well-defined pattern (Fig. 5) rendered the Gaussian analysis unreliable. In addition, there was an unusually strong background between 331 and 422 which may have originated in spurious Al(111, 200) and V(110) peaks. Taking these adverse factors into account as best we could 11 $|F_o|$ were extracted and used in a least-squares refinement. Because of the near cancellation of the contributions from Ti and Sn, $B(M^{4+})$ was not included as a parameter of refinement.

After 4 cycles R was reduced from 26.1% to 12.9%, $x(O_2)$ refined from 0.4200 to 0.4183, and $B(Y)$ from 0.15 Å^2 to 1.34 Å^2. However, $B(O_1)$ and $B(O_2)$ kept decreasing from the initial value of 1.50 Å^2 to negative values ($B(O_1)$ strongly negative), and the refinement was discontinued. No improvement resulted on including $B(M^{4+})$ in the refinement. In the circumstances it was not thought profitable to test for the possibility of partial order in the 16(d) sublattice.

Even though the structure could not be successfully refined, it is instructive to compare the pattern of the stannate–titanate with that of $La_2Sn_2O_7$ at the same λ. Since b(La) and b(Y) are similar, the difference in the appearance of the two patterns arises almost entirely from the contribution of Sn in $La_2Sn_2O_7$ and from the difference in $x(O_2)$ of the two pyrochlores.

Interatomic Distances and Bond Angles

The apparent interatomic distances and bond angles (not corrected for thermal motion) are listed in Table IV. The uncertainty limits are based on $2\sigma(x)$ for the refinements from X-ray data, on $4\sigma(x)$ for the refinement from neutron data, and on $4\sigma(a_0)$ for distances independent of $x(O_2)$.

The shortest Sn—O distances in all 3 stannates are practically the same as those reported for six-coordinated Sn(IV) in SnO_2 and $BaSnO_3$ (Table V).

Can. J. Chem. Downloaded from www.nrcresearchpress.com by 210.87.254.42 on 09/05/12
For personal use only.

TABLE V

Metal–oxygen distances in some compounds of La, Sm, Y, and Sn(IV)

Compound	Coordination	Distance, Å	Reference
		La—O distances	
La_2O_3 (*A*-type)	1 O + 3 O + 3 O	2.45±7; 2.37±2; 2.73±2*	43
LaOCl (PbFCl)	4 O (+ 1 Cl + 4 Cl)	2.40	45
LaOBr (PbFCl)	4 O (+ 1 Br + 4 Br)	2.41	45
LaOI (PbFCl)	4 O (+ 1 I + 4 I)	2.42	45
LaOF (rhombohedral)	4 O (+ 4 F)	2.58	46
LaOF (tetragonal)	4 O (+ 4 F)	2.61	46
La_2O_2S	1 O + 3 O (+ 3 S)	2.41; 2.38	47
La_2NiO_4 (K_2MgF_4)	1 O + 4 O + 4 O	2.40±8; 2.62±5; 2.75±1*	48
La_2MoO_6	4 O + 2 O	2.38; 2.33	44
$La_2(SO_4)_3.9H_2O$	6 SO_4 + 6 SO_4	2.60; 2.74	49
	6 H_2O + 3 SO_4	2.74; 2.70	
		Sm—O distances	
Sm_2O_3 (*B*-type)†	1 O + 2 O + 1 O + 2 O + 1 O	2.25; 2.29; 2.49; 2.56; 2.71 (all ±0.06)	50
	1 O + 2 O + 1 O + 2 O + 1 O	2.29; 2.32; 2.38; 2.49; 2.76 (all ±0.06)	
	1 O + 2 O + 1 O + 2 O + 1 O	2.26; 2.28; 2.31; 2.57; 3.12 (all ±0.06)	
SmO (NaCl)	6 O	2.494	51
SmOCl (PbFCl)	4 O(+ 1 Cl + 4 Cl)	2.30	52
		Y—O distances	
Y_2O_3 (*C*-type)	6 O	2.25 (40); 2.250±12 (53); 2.327±40 (3σ)(42)	
	2 O + 2 O + 2 O	2.25; 2.27; 2.34	40
		2.260; 2.354; 2.278 (all ±0.012)	53
		2.228±45; 2.271±42; 2.298±52 (all 3σ)	42
YOOH and YOOD	1 O + 1 O + 2 O + 1 OH + 2 OH	2.24±3; 2.28±2; 2.32±2; 2.38±2; 2.44±2	54
YOF (rhombohedral)	4 O (+ 4 F)	2.44	46
YOF (tetragonal)	4 O (+ 4 F)	2.47	46
$Y(OH)_3$ and $Y(OD)_3$ (UCl_3)	6 O + 3 O	2.403±3; 2.437±3	55
UY_6O_{12}	1 O + 1 O + 2 O + 1 O + 1 O	2.17; 2.28; 2.30; 2.32; 2.40 (all ±0.02)	37
$Y_3Fe_2(FeO_4)_3$ (garnet)	4 O + 4 O	2.368; 2.419	56
YPO_4 (zircon)	4 O + 4 O	2.32; 2.56	57
$Y(EtSO_4)_3.9H_2O$	6 H_2O + 3 H_2O	2.37; 2.55	41
		Sn(IV)—O distances	
SnO_2 (rutile)	4 O + 2 O	2.052±5; 2.056±7	58
$BaSnO_3$ (perovskite)	6 O	2.058	59
$Na_2Sn(OH)_6$	6 OH	1.93	60
$K_2Sn(OH)_6$	6 OH	1.98	60

*Calculated from the authors' unit-cell dimensions and positional parameters.
†It has been suggested that the *B* form is not a polymorph of Sm_2O_3 but a samarium oxide of variable composition (62).

The irregular coordination polyhedra about the La, Sm, or Y atoms (coordination numbers 6, 7, 8, 9, or 12, often with mixed nearest neighbors) make a direct comparison of the metal–oxygen distances in the stannates (coordination 2 + 6) difficult. Even in the sesquioxides there are several M—O distances. The La—O_1 distance is shorter than any listed in Table V, but the Sm—O_1 and Y—O_1 distances are within the range of the M—O distances in the corresponding sesquioxides and other compounds. Interatomic distances longer than Y—O_2 have been reported, but they are not common; the longest Y—O distance in Y_2O_3 does not exceed 2.36 Å. The Sm—O_2 and La—O_2 distances, however, fall within the range quoted for the sesquioxides.

Infrared Spectra

The spectrum of $La_2Sn_2O_7$ consists of a strong, relatively sharp band at 581 cm^{-1} (*A*) and a strong, broader band which has a maximum at ca. 395 cm^{-1}, a sharp shoulder at 327 cm^{-1} (*D*), and an unresolved shoulder in the 470 cm^{-1} region (Fig. 6).

On replacing La with heavier lanthanons *A* and *D* shift to progressively higher wave numbers. The sharpness and intensity of *A* remains, but *D* becomes weaker and eventually (for Yb) degenerates to an unresolved shoulder. The broader band splits up into essentially two component peaks *B* and *C*; the frequency of *C* is almost stationary, while that of *B* progressively increases. The unresolved shoulders and asymmetric peak profiles are evidence of additional

Can. J. Chem. Downloaded from www.nrcresearchpress.com by 210.87.254.42 on 09/05/12
For personal use only.

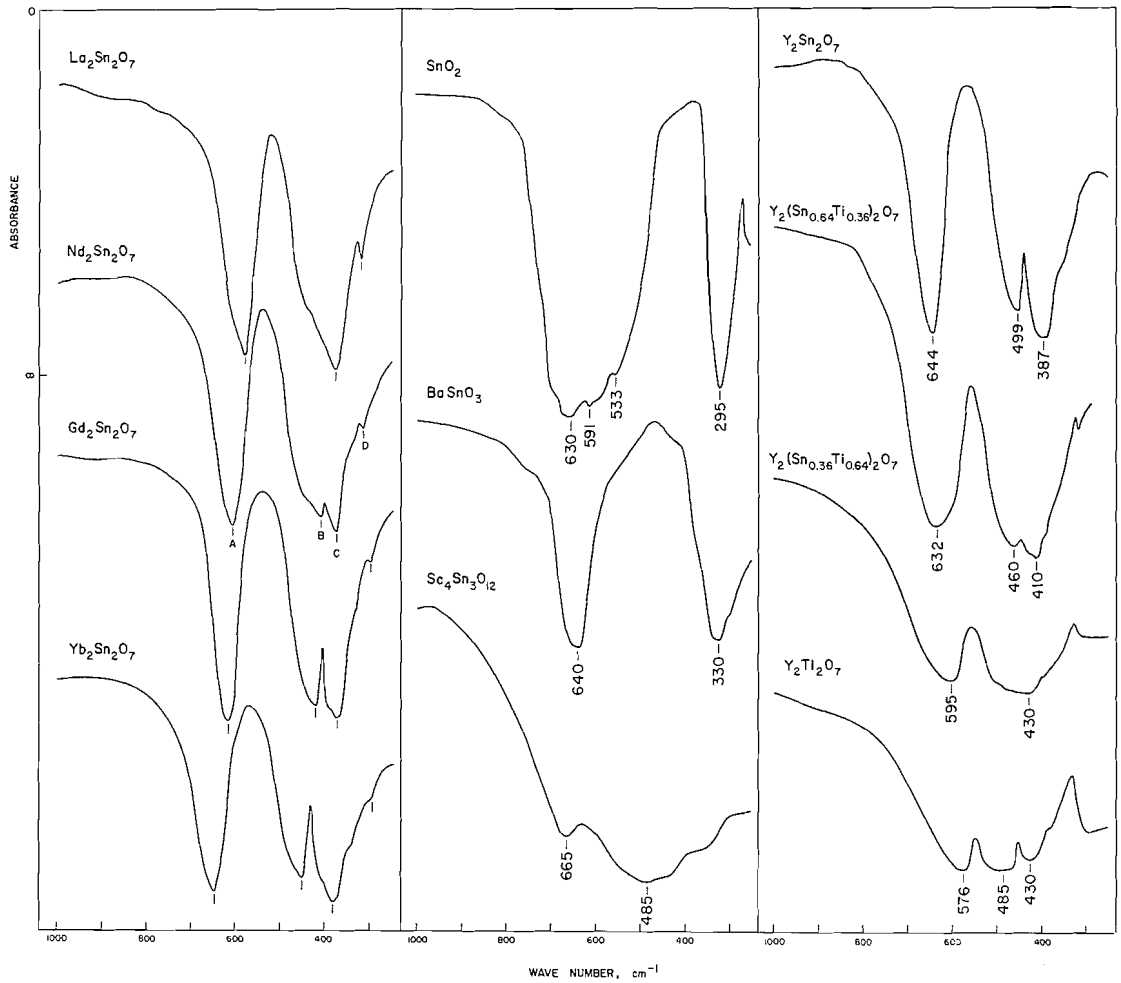

FIG. 6. Infrared transmission spectra of representative pyrochlore stannates and related compounds.

fine structure which, too, depends on the particular lanthanon. A selection of representative spectra is shown in Fig. 6.

When the frequencies of *A*, *B*, and *D* are plotted against Templeton–Dauben's $r(A^{3+})$, the increase of the peak frequencies $\nu(A)$ and $\nu(B)$, and the decrease of $\nu(D)$, with increasing $r(A^{3+})$ are clearly seen (Fig. 7). Although the spread of the points for $\nu(A)$ and $\nu(B)$ is appreciable, the regressions of $\nu(A)$ and $r(A^{3+})$ have a correlation coefficient of -0.983, suggesting that the dependence could not be far from linear. The likelihood of straight-line relationships for $\nu(B)$ and $\nu(D)$ is even more apparent. The slopes of the best straight lines for $\nu(A)$ and $\nu(B)$ are practically identical (Fig. 7).

Similar near-linear relationships, but with slopes of the opposite sign, result when the frequencies are plotted against the atomic numbers or atomic weights of the lanthanons. The frequency $\nu(D)$ decreases with the increasing mass of the lanthanon, as one might perhaps expect, while $\nu(A)$ and $\nu(B)$ increase. However, $\nu(A)$ and $\nu(B)$ of yttrium are very similar to the corresponding frequencies for holmium, thus following ionic size rather than atomic mass. This would suggest that the A and Sn atoms are sufficiently heavy to form a quasistationary inertial framework, while the oxygen atoms move in the potential wells formed by the metal atoms. Since the charge distribution in the well (and hence the vibrational force constant) depends on

Can. J. Chem. Downloaded from www.nrcresearchpress.com by 210.87.254.42 on 09/05/12
For personal use only.

Can. J. Chem. Downloaded from www.nrcresearchpress.com by 210.87.254.42 on 09/05/12
For personal use only.

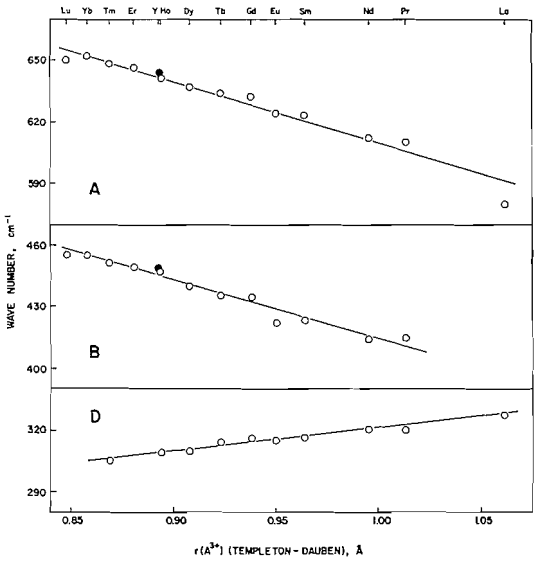

FIG. 7. Variation of the frequencies of the $A_2Sn_2O_7$ absorption maxima *A*, *B*, and *D* with $r(A^{3+})$. Full circles, $Y_2Sn_2O_7$. The straight line for $\nu(A)$ was fitted by least squares.

the effective (equilibrium) interatomic distance which varies with A, the peak frequencies appear to depend on $r(A^{3+})$ rather than on atomic mass; the near-linear dependence of the frequency on the atomic number or atomic weight of the lanthanons is an expression or the change in $r(Ln^{3+})$. Yttrium is thus found with holmium and not outside the frequency range for the lanthanon stannates. An explanation why $\nu(C)$ is stationary, and an assignment of the vibrational modes, would require an analysis beyond the scope of this investigation.

In the series $Y_2Sn_2O_7$–$Y_2Ti_2O_7$ $\nu(A)$ decreased from 644 cm^{-1} in the stannate to 576 cm^{-1} in the titanate. At the same time the band profile of *A* became progressively broader (Fig. 6). The *B* and *C* peaks tended to coalesce at first, but the broad $B + C$ band of $Y_2(Sn_{0.36}Ti_{0.64})_2O_7$ changed into a band with a redistributed fine structure on going over to $Y_2Ti_2O_7$.

Bands similar to the two main bands of the $Ln_2Sn_2O_7$ spectra, *A* and $B + C + D$, are present in the spectra of both SnO_2 (rutile) and $BaSnO_3$ (perovskite) (Fig. 6). Since only lattice modes occur in these structures, these bands no doubt have their origin in similar deformations of the SnO_6 octahedra, which exist in all three structure types, though the networks of the octahedra have unlike connectivities.

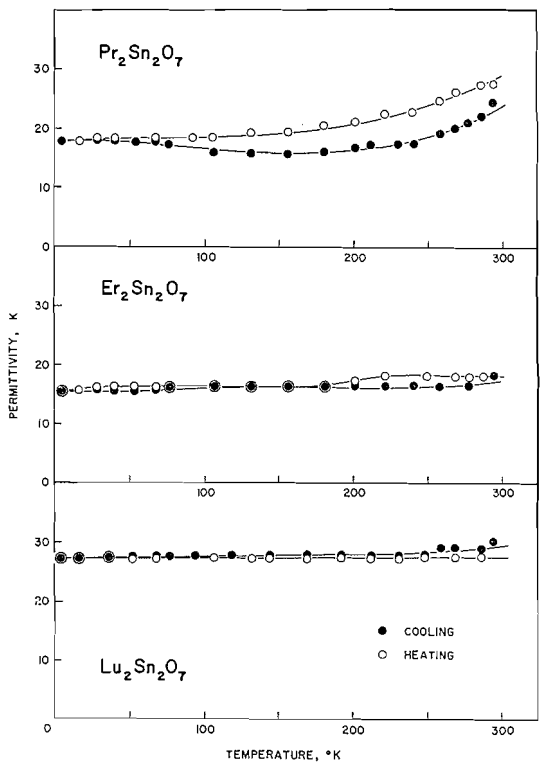

FIG. 8. Dependence of permittivity of three pyrochlore stannates on temperature.

The δ phases $Sc_2Sn_2O_7$ and $Sc_4Sn_3O_{12}$ gave practically identical spectra, but different from those of the cubic stannates. $\nu(A)$ was about 665 cm^{-1}, but instead of an increased separation of the *B* and *C* maxima of the pyrochlore spectra, which might be expected on extrapolating the series to Sc, a broad band with a maximum at 485 cm^{-1} appeared. The separation of *B* and *C* had disappeared, while that of the two main bands, *A* and $B + C$, was very shallow.

Dielectric Measurements

As Fig. 8 shows, there was no indication of ferroelectric behavior in Pr, Er, and Lu stannates. The $Pr_2Sn_2O_7$ disk displayed a considerable thermal hysteresis, probably attributable to dielectric ageing induced by the cooling–heating cycle. The absolute values of the permittivities were undistinguished.

Conclusions

1. As a set of relative ionic (crystal) radii for trivalent lanthanons the Templeton–Dauben set is preferable to the Goldschmidt or the Ahrens

Can. J. Chem. Downloaded from www.nrcresearchpress.com by 210.87.254.42 on 09/05/12
For personal use only.

sets. It is probably the most consistent and complete of all such sets described in the literature. However, it is limited to Ln^{3+} (essentially in six-coordination), and it is not certain how it is related, absolutely, to the radii of cations carrying a different charge, such as those of M^{4+}, which are important in the present context. For this reason it seems practical to retain provisionally the Ahrens radii, in the belief that all the radii of this set are matched, however imperfectly, and thus more likely to give a consistent working picture of the size effect.

In the linear correlation of $a_0(A_2Sn_2O_7)$ and $r(A^{3+})$ (Templeton–Dauben) yttrium appears just below holmium, thus confirming Geller's estimate of its ionic radius.

2. Taking $r(Sn^{4+})$ as 0.71 Å (Pauling, Ahrens) and using the Ahrens radii for A^{3+}, the lower limit of the $r(A^{3+}):r(Sn^{4+})$ ratio for cubic pyrochlores is about 1.19. The upper limit is at least 1.61 (1.49 for the Templeton–Dauben radii). This is the highest ratio yet reported for 3–4 pyrochlores, a possible exception being Pr_2FeSbO_7 (61). The possibility of extending the cubic pyrochlore field towards Ti in the system $La_2Sn_2O_7$–$La_2Ti_2O_7$ was found very limited.

These limits, which are based on ionic size, must be viewed only as *minimum* criteria of existence: Bi^{3+} has a radius ratio of 1.31 but does not form a cubic pyrochlore stannate.

3. Of the three stannate structures refined, $Sm_2Sn_2O_7$ gave the least reliable result. In spite of the large uncertainty limits of $x(O_2)$ in this compound the increase in $x(O_2)$ with the ionic size of A^{3+}, and thus a decrease in the distortion of the SnO_6 octahedra, is evident (Table II).

4. The infrared transmission spectra of the stannates, while exhibiting certain regularities, do not allow of a simple interpretation. They possess, however, a diagnostic value in that they make it possible to distinguish between cubic pyrochlore and other structural arrangements.

The spectrum of $Y_2Sn_2O_7$ is practically identical with that of $Ho_2Sn_2O_7$. This fact, together with the trend in $x(O_2)$ in the series Y, Sm, La stannate, leads to the conclusion that it is the size of Y^{3+} rather than its chemistry (as a 4d-element) that determines its place among 3–4 pyrochlores.

5. No evidence of ferroelectric transitions in Pr, Er, and Lu stannates was found by permittivity measurements between room temperature and 4.2 °K. It is unlikely that ferroelectric properties will be found in other pyrochlore stannates between Pr and Lu.

Acknowledgments

We wish to thank the following individuals and agencies: The staff of the Neutron Physics Branch, Atomic Energy of Canada Limited, for placing at our disposal their neutron diffraction facilities; Mr. H. Nieman for assistance with the neutron diffraction experiments; Dr. F. R. Ahmed for making available to us the least-squares program of ref. 15; Dr. M. Falk for the use of his infrared spectrometer; Mr. Y. S. Lim for carrying out the dielectric measurements; Dr. M. H. Jericho for making possible the low-temperature dielectric study; Drs. B. I. Pokrovskiĭ and F. M. Spiridonov for a gift of high-purity scandium oxide; and the staff of the Dalhousie Computing Centre for their unfailing assistance with machine computation.

This work has been supported in part by a grant in aid of research from the Defence Research Board.

1. R. S. Roth. J. Res. Natl. Bur. Std. **56**, 17 (1956).
2. O. Knop, F. Brisse, L. Castelliz, and Sutarno. Can. J. Chem. **43**, 2812 (1965).
3. G. E. Bacon. Neutron diffraction. 2nd ed. Oxford University Press, Oxford. 1962.
4. C. G. Whinfrey, D. W. Eckart, and A. Tauber. J. Am. Chem. Soc. **82**, 2695 (1960).
5. C. G. Whinfrey and A. Tauber. J. Am. Chem. Soc. **83**, 755 (1961).
6. N. N. Padurow and C. Schusterius. Ber. Deut. Keram. Ges. **31**, 391 (1954).
7. W. R. Cook, Jr. and H. Jaffe. Phys. Rev. **88**, 1426 (1952); **89**, 1297 (1953).
8. G. Shirane and R. Pepinsky. Phys. Rev. **92**, 504 (1953).
9. J. K. Hulm. Phys. Rev. **92**, 504 (1953).
10. F. Jona, G. Shirane, and R. Pepinsky. Phys. Rev. **98**, 903 (1955).
11. V. A. Isupov and O. K. Khomutetskiĭ. Zh. Tekhn. Fiz. **27**, 2704 (1956).
12. O. Knop, F. Brisse, and L. Castelliz. To be published.
13. F. Brisse and O. Knop. Can. J. Chem. **45**, 609 (1967).
14. J. A. Bearden, J. S. Thomsen, A. F. Burr, *et al.* X-ray wavelengths. U.S. Atomic Energy Commission, Div. of Techn. Inform. Extension, Oak Ridge, Tenn. 1964.
15. F. R. Ahmed, E. J. Gabe, G. A. Mair, and M. E. Pippy. A unified set of crystallographic programs for the IBM 1620 computer. September, 1963. Unpublished.
16. Sutarno, O. Knop, and K. I. G. Reid. Can. J. Chem. **45**, 1391 (1967).
17. D. T. Cromer and J. T. Waber. Acta Cryst. **18**, 104 (1965).

18. M. TOKONAMI. Acta Cryst. **19**, 486 (1965).
19. D. T. CROMER. Acta Cryst. **18**, 17 (1965).
20. D. F. RUSHMAN and M. A. STRIVENS. Proc. Phys. Soc. London, **59**, 1011 (1947).
21. N. C. BAENZIGER, H. A. EICK, H. S. SCHULDT, and L. EYRING. J. Am. Chem. Soc. **83**, 2219 (1961).
22. L. EYRING and N. C. BAENZIGER. J. Appl. Phys. **33**, 428 (1962).
23. K. LÖHBERG. Z. Physik. Chem. Leipzig, **B28**, 402 (1935). *Cf. also* F. HUND and U. PEETZ. Z. Anorg. Allgem. Chem. **271**, 6 (1953).
24. R. S. ROTH and S. J. SCHNEIDER. J. Res. Natl. Bur. Std. **64A**, 309 (1960).
25. S. J. SCHNEIDER and R. S. ROTH. J. Am. Ceram. Soc. **43**, 115 (1960).
26. M. EIBSCHÜTZ. Acta Cryst. **19**, 337 (1965).
27. R. W. G. WYCKOFF. Crystal structures. Vol. 2. 2nd ed. Interscience, New York. 1964.
28. A. ZALKIN and D. H. TEMPLETON. J. Am. Chem. Soc. **75**, 2453 (1953).
29. H. A. EICK. J. Am. Chem. Soc. **80**, 43 (1958).
30. D. H. TEMPLETON and C. H. DAUBEN. J. Am. Chem. Soc. **76**, 5237 (1954).
31. S. GELLER. Acta Cryst. **10**, 248 (1957).
32. R. COURTEL and J. LORIERS. Compt. Rend. **230**, 735 (1950).
33. J. LEFÈVRE. Rev. Hautes Temp. Réfractaires, **1**, 229 (1964).
34. M. PEREZ Y JORBA. Ann. Chim. Paris, **7**, 479 (1962).
35. L. N. KOMISSAROVA, B. I. POKROVSKIĬ, and V. V. NECHAEVA. Dokl. Akad. Nauk SSSR, **168**, 1076 (1966).
36. G. A. CHASE. Acta Cryst. **15**, 91 (1962).
37. S. F. BARTRAM. Inorg. Chem. **5**, 749 (1966).
38. F. BRISSE. Ph.D. Thesis, Dalhousie University, Halifax, N.S. 1967.
39. O. KNOP, K. I. G. REID, SUTARNO, and Y. NAKAGAWA. Can. J. Chem. Submitted.
40. A. FERT. Bull. Soc. Franç. Minéral. Crist. **85**, 267 (1962).
41. D. R. FITZWATER and R. E. RUNDLE. Z. Krist. **112**, 362 (1959).
42. O. KNOP and J. M. HARTLEY. To be published.
43. W. C. KOEHLER and E. O. WOLLAN. Acta Cryst. **6**, 741 (1953).
44. L. G. SILLÉN and K. LUNDBORG. Z. Anorg. Allgem. Chem. **252**, 2 (1943).
45. L. G. SILLÉN and A. L. NYLANDER. Svensk Kem. Tidskr. **53**, 367 (1941).
46. W. H. ZACHARIASEN. Acta Cryst. **4**, 231 (1951).
47. W. H. ZACHARIASEN. Acta Cryst. **2**, 60 (1949).
48. A. RABENAU and P. ECKERLIN. Acta Cryst. **11**, 304 (1958).
49. E. B. HUNT, JR., R. E. RUNDLE, and A. J. STOSICK. Acta Cryst. **7**, 106 (1954).
50. D. T. CROMER. J. Phys. Chem. **61**, 753 (1957).
51. H. A. EICK, N. C. BAENZIGER, and L. EYRING. J. Am. Chem. Soc. **78**, 5147 (1956).
52. D. H. TEMPLETON and C. H. DAUBEN. J. Am. Chem. Soc. **75**, 6069 (1953).
53. M. G. PATON and E. N. MASLEN. Acta Cryst. **19**, 307 (1965).
54. A. NØRLUND CHRISTENSEN. Acta Chem. Scand. **19**, 1504 (1965). A. NØRLUND CHRISTENSEN and O. VON HEIDENSTAM. Acta Chem. Scand. **20**, 2658 (1966).
55. A. NØRLUND CHRISTENSEN, R. GRØNBÆK HAZELL, and Å. NILSSON. Acta Chem. Scand. **21**, 481 (1967).
56. A. BATT and B. POST. Acta Cryst. **15**, 1268 (1962).
57. I. R. KRSTANOVIĆ. Acta Cryst. **11**, 896 (1958).
58. W. H. BAUR. Acta Cryst. **9**, 515 (1956).
59. G. WAGNER and H. BINDER. Z. Anorg. Allgem. Chem. **298**, 12 (1959).
60. C. O. BJÖRLING. Arkiv Kemi Mineral. Geol. **15B**, No. 2 (1941).
61. M.-C. MONTMORY and F. BERTAUT. Compt. Rend. **252**, 4171 (1961).
62. V. S. KUTSEV, E. I. SMAGINA, and R. N. MORZHEEDOVA. Russ. J. Inorg. Chem. **8**, 543 (1963).

Can. J. Chem. Downloaded from www.nrcresearchpress.com by 210.87.254.42 on 09/05/12
For personal use only.

Surface oxidation and reduction of platinum electrodes: Coverage, kinetic and hysteresis studies

D. GILROY AND B. E. CONWAY
Department of Chemistry, University of Ottawa, Ottawa, Canada
Received September 20, 1967

Studies on the electrochemical formation and reduction of surface oxide at platinum electrodes have been carried out with particular reference to polarization and hysteresis effects in these processes. Comparisons between the results of galvanostatic and potential sweep techniques have been made for three types of surfaces of platinum electrodes prepared by: (*a*) heating in hydrogen; (*b*) heating in a flame; and (*c*) electrolytically forming platinum black surfaces. The dependence of the quantity of reducible oxide formed under prior steady-state potentiostatic conditions has been related to potential and time of anodic polarization. Polarization effects in the reduction of the surface oxide have been evaluated in terms of the potential dependence of the pseudocapacitance maximum for the oxide reduction process, and a mechanism for the reduction is suggested. The relative slowness of the reduction process is important in regard to the question of the role of oxide in the kinetics of electrocatalytic oxidations at platinum anodes. Hysteresis effects in anodic formation and cathodic reduction of the oxide are discussed in terms of a totally irreversible phase transition involving the ad-layer.

Canadian Journal of Chemistry, 46, 875 (1968)

Can. J. Chem. Downloaded from www.nrcresearchpress.com by 210.87.254.105 on 09/05/12
For personal use only.

Introduction

In recent years, the electrochemistry of oxidized platinum electrodes has received much attention, and a variety of studies on the nature and extent of surface coverage by oxygen species, and on the mechanisms of oxide formation and reduction, have been performed (1–7). Examination of the latter process is of importance in regard to the role of surface oxides in anodic oxidations of organic substances. Such experiments usually involve a change in the electrode surface from one state, defined by a potential and corresponding to a given coverage θ by H- or O-containing species (θ_H or θ_O may be zero), to another, by means of some type of transient. Thus, galvanostatic (1, 3), potential-sweep (4), and potential-step methods (5) have been employed individually or complementarily (2), and in conjunction with ellipsometry (9). Special attention has also been given (6) to the effects of impurities in studies on surface oxidation of platinum, and the initial chemical and electrical condition of the electrode prior to application of the transient must be defined. This factor has often made it difficult to compare various results.

The present paper reports an experimental continuation of our previous studies on transients in relation to the form of capacitance relations for adsorbed, electrochemically generated species at electrodes (8, 9). Results from galvanostatic and potential-sweep methods have been compared and the pseudocapacity–potential relations (8) derived from these transients have been examined with regard to the kinetics and mechanisms of oxide reduction. Particular emphasis has been placed on: (*a*) rate effects in reduction transients (9); (*b*) temperature effects in oxide formation in the range 5–90 °C; (*c*) comparison between smooth and platinum black surfaces; (*d*) oxide film growth over longer times; and (*e*) hysteresis between oxide formation and reduction processes.

The observations at higher temperatures are of importance in relation to the kinetics and mechanism of electrocatalytic oxidations of hydrocarbons at Pt and other noble metals where the surface oxide may behave as a co-reactant or as an inhibitor (10, 11).

Experimental

Cell and Solutions

Experimental measurements were made in an all-glass cell of the type described previously (12), provided with an internally sealed glass coil for circulation of thermostat water; the reference electrode was similarly thermostated.

One molar H_2SO_4 solutions were prepared by dilution of analytical reagent grade acid with triply distilled water, followed by optimum cathodic and anodic pre-electrolysis. Purified nitrogen (12) was bubbled in the working and counter electrode compartments during the experiments.

Electrodes

Three types of electrodes were used: (*a*) platinum wires sealed directly into glass with consequent exposure to the oxygen – natural gas flame; (*b*) platinum black deposited onto platinum wires from a solution of H_2PtCl_6 containing lead acetate; after careful washing, these electrodes were maintained in the cell at 90 °C for several hours to

Can. J. Chem. Downloaded from www.nrcresearchpress.com by 210.87.254.105 on 09/05/12
For personal use only.

sinter the surface (see for example ref. 13) and stabilize its area and properties; (*c*) platinum wires heated in hydrogen at 700 °C for 1 h and then sealed into glass bulbs in a hydrogen atmosphere without contact with the flame.

The glass envelopes of the electrodes were cleaned in chromic acid and soaked in distilled water before use.

Circuits

Conventional circuitry was used to obtain galvanostatic and potential-sweep transients (4); the former were differentiated electronically (14) to give directly the reciprocal electrode capacity dV/dQ, where V is the time-dependent potential in the transient and Q the charge passed at a given time.

Results

Galvanostatic and single potential-sweep transients were obtained after application of the potential–time pretreatment sequences of Fig. 1; the oscilloscope traces were recorded during the periods T. At other times, the electrodes were maintained potentiostatically at 1.5 or 1.2 V to remove oxidizable impurities. Corrections for resistance error effects were made where appropriate.

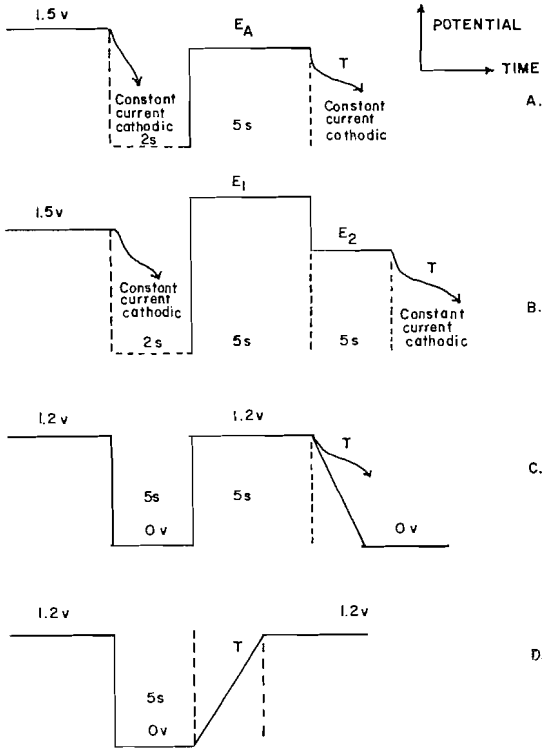

FIG. 1. Potential and time programs in galvanostatic and potentiodynamic reduction of surface oxides at Pt.

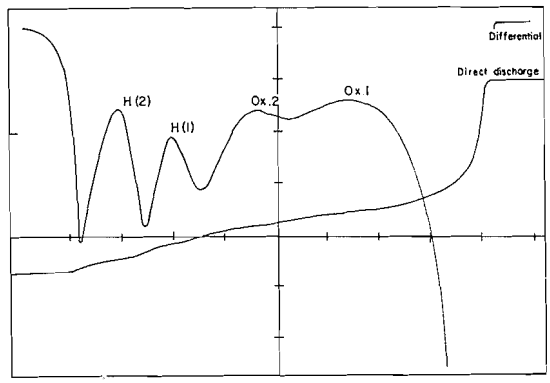

FIG. 2. Galvanostatic and differentiated galvanostatic reduction curves for Pt surface oxide showing two maxima (ox. 1 and ox. 2) in reduction from high anodic potentials (1.6 V E_H). (Based on enlarged projection from 35 mm oscilloscope negative; noise levels < 1 mV.) [35 mA discharge; 2 ms div.$^{-1}$, 0.4 V div.$^{-1}$, vertical].

1. Charge–Potential Relations

Extents of surface oxidation at various given potentials (maintained potentiostatically) were determined from prior anodic steady states by galvanostatic discharge at fairly high current densities using the potential program of Fig. 1A. Transition times for oxide reduction were taken from the beginning of the transients to the maxima in the differential curves (i.e. at the capacity minimum corresponding to the double-layer region) at around 0.4 V, and for hydrogen deposition from the latter region to each of the two differential maxima between 0.3 and 0.0 V. When the initial anodic potential E_A was above 1.6 V, the oxide reduction region became differentiated into two stages[1] easily discernible in the differential galvanostatic curves (Fig. 2). Results for the three different types of electrode at four temperatures are shown in Figs. 3*a*, *b*, *c*. The oxide (Q_O) and hydrogen (Q_H) charges include the double-layer charging contribution but specific corrections for this effect were not made since the ionic double-layer capacity will probably be a function of potential and oxide or H coverage and is thus somewhat indeterminate. A formal correction could be made using the capacity observed at 0.35–0.6 V in the "double-layer" region (e.g. see Fig. 2). It is of interest that the Q_O values for the three types of

[1]A related separation into two regions was observed by Will and Knorr and also Bagotskii and co-workers (4) at high sweep rates in potentiodynamic transients.

Can. J. Chem. Downloaded from www.nrcresearchpress.com by 210.87.254.105 on 09/05/12
For personal use only.

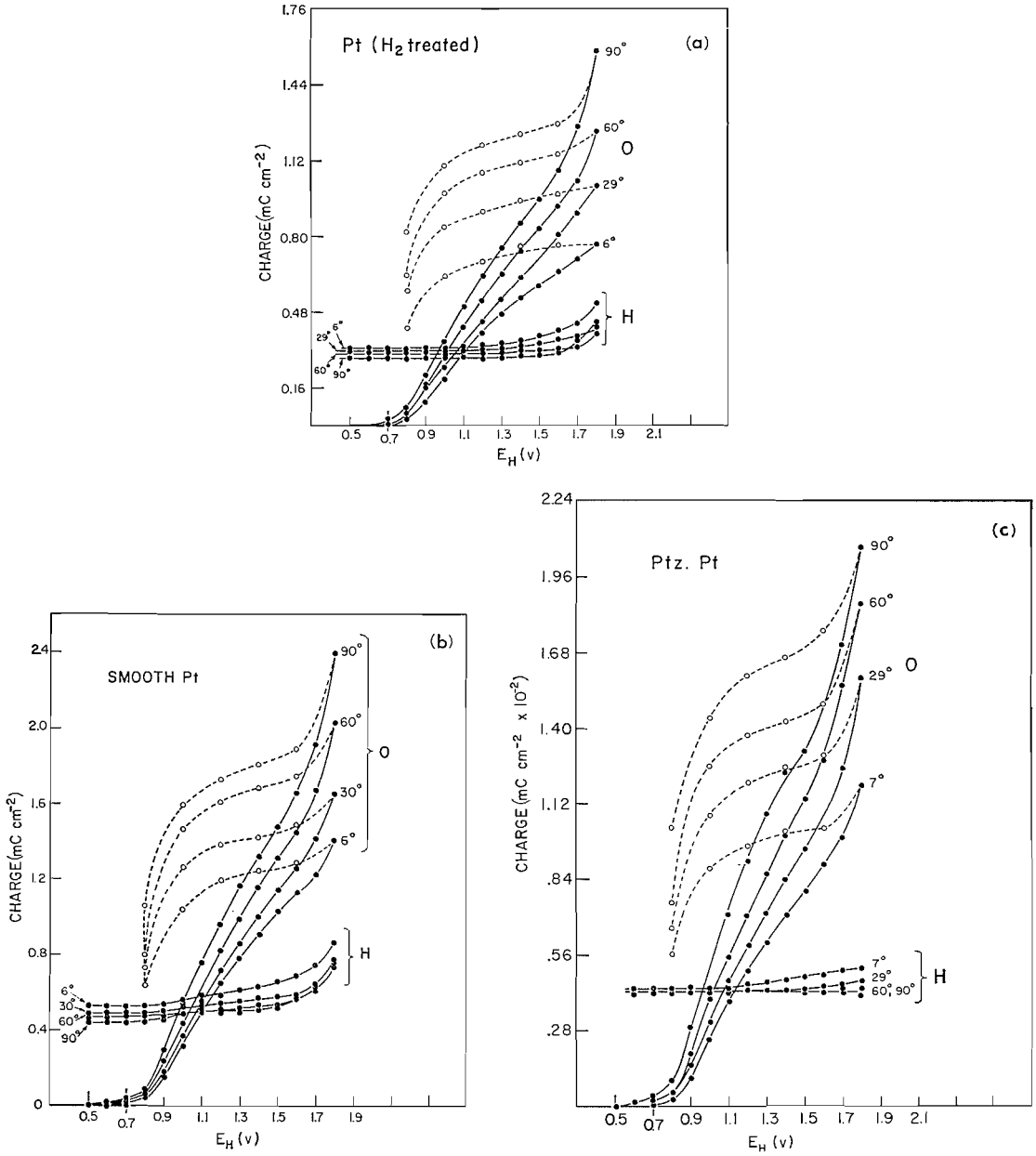

FIG. 3. (*a*) Surface oxide charge and H-atom accommodation at four temperatures for hydrogen-treated smooth Pt. (*b*) As in (*a*) but for flame-treated smooth Pt. (*c*) As in (*a*) but for platinized Pt.

electrode surfaces vary with potential in a closely similar manner, e.g. as indicated by the ratio Q_O/Q_H as a function of potential. Evidently, when platinum is in the "black" condition, no specially characteristic behavior arises at least with regard to the Q_O/Q_H ratio.

Hysteresis effects (15*a*) were examined using program 1B (Fig. 1) in which the electrodes were maintained first at an upper potential E_1 and then at a variable lower one E_2, both for 5 s, before reduction from E_2. The observed charges thus measured have been included in

Can. J. Chem. Downloaded from www.nrcresearchpress.com by 210.87.254.105 on 09/05/12
For personal use only.

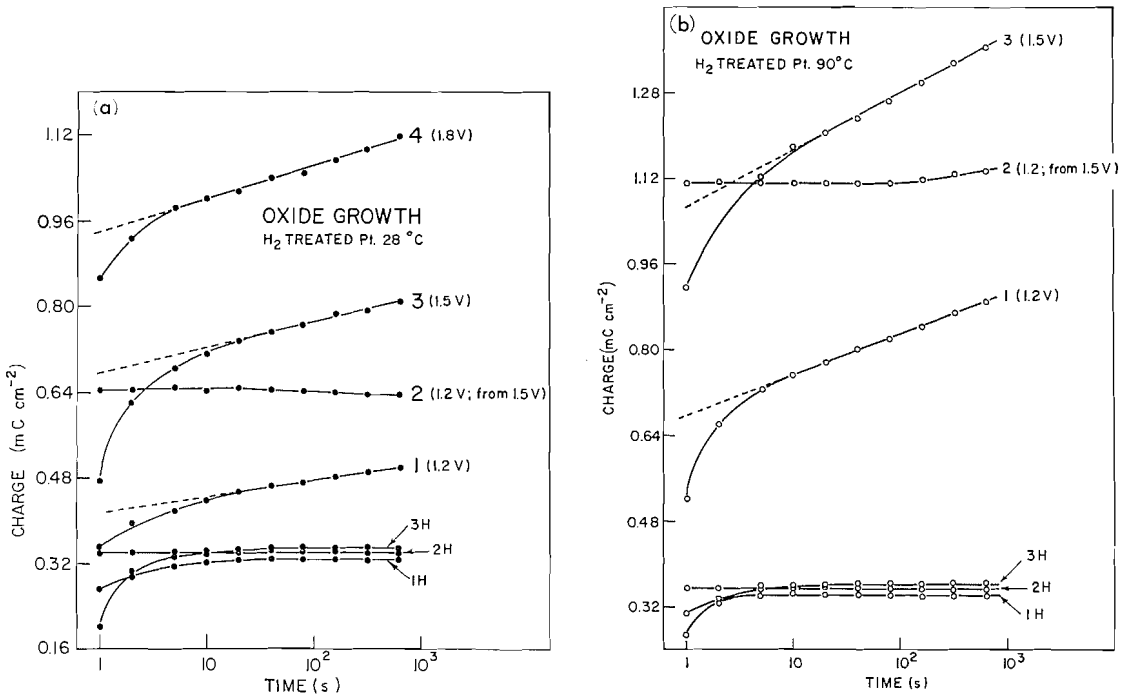

FIG. 4. Oxide growth effects at Pt at 28 °C (*a*) and 90 °C (*b*) in terms of cathodically reducible material in mC cm^{-2}.

Figs. 3 *a–c* as the dotted lines; hysteresis (15*a*) was observed, however, from all potentials in the oxide region and the effects originate in the same way as those found in cyclic voltammetry at Pt: the oxide once formed at a given potential requires a lower potential for its cathodic removal, and the greater is the anodic formation potential, the lower is the potential required for subsequent cathodic reduction (cf. hysteresis in magnetization).[2]

Roughness factors calculated by comparing the quantities Q_H, the charge for hydrogen deposition (from $E_A < 0.7$ V), with a reference value (16) of 0.21 mC cm^{-2} for a plane surface were 1.5 (5) for H_2-treated, 2.5 for flame-treated, and about 180 for platinized Pt.

2. Oxide Growth

Variation of the duration for which the potential was maintained at E_A in program 1A enabled the growth of oxide (in terms of Q_O) to be studied. Up to $E_A = 1.8$ V, the oxide thickened[3] with time, and the length of the reduction wave, or the transition time for reduction, increased logarithmically in time. Typical behavior is shown in Fig. 4. Similar direct logarithmic growth behavior has been found for thin oxide films on Au (17).

Time effects in hysteresis were investigated using the potential program 1B with variation of the time spent at potential E_2. Results for $E_1 = 1.5$ V and $E_2 = 1.2$ V are also shown in Fig. 4. After such a pretreatment program, the oxide apparently does not thicken any further (except after relatively long times) with time at the lower potential; after a "hysteresis" treatment, there is an initial rapid decrease of

[2]The first observations of hysteretic effects in platinum surface oxidation and reduction appear to have been made by Slygin and Frumkin (15*b*) and by Pearson and Butler (15*c*), although no specific attention was given to the origin of the hysteresis behavior.

[3]It is assumed that the effects observed represent a "thickening" with time or an increased penetration of O-species into the surface layer of the metal (cf. the "dermasorption" effect discussed by Schuldiner and Warner (18, and see ref. 6)). It is clear that equivalent effects could arise, however, if there was a progressive increase of valence of the Pt atoms in the surface layer, i.e. an increase of the O:Pt ratio. The first possibility seems the more likely. Oxide film layers up to ca. 10 Å in thickness are deduced in the work on ellipsometry (7), but the present Q_O/Q_H ratios would require a thinner layer, even at 1.8 V.

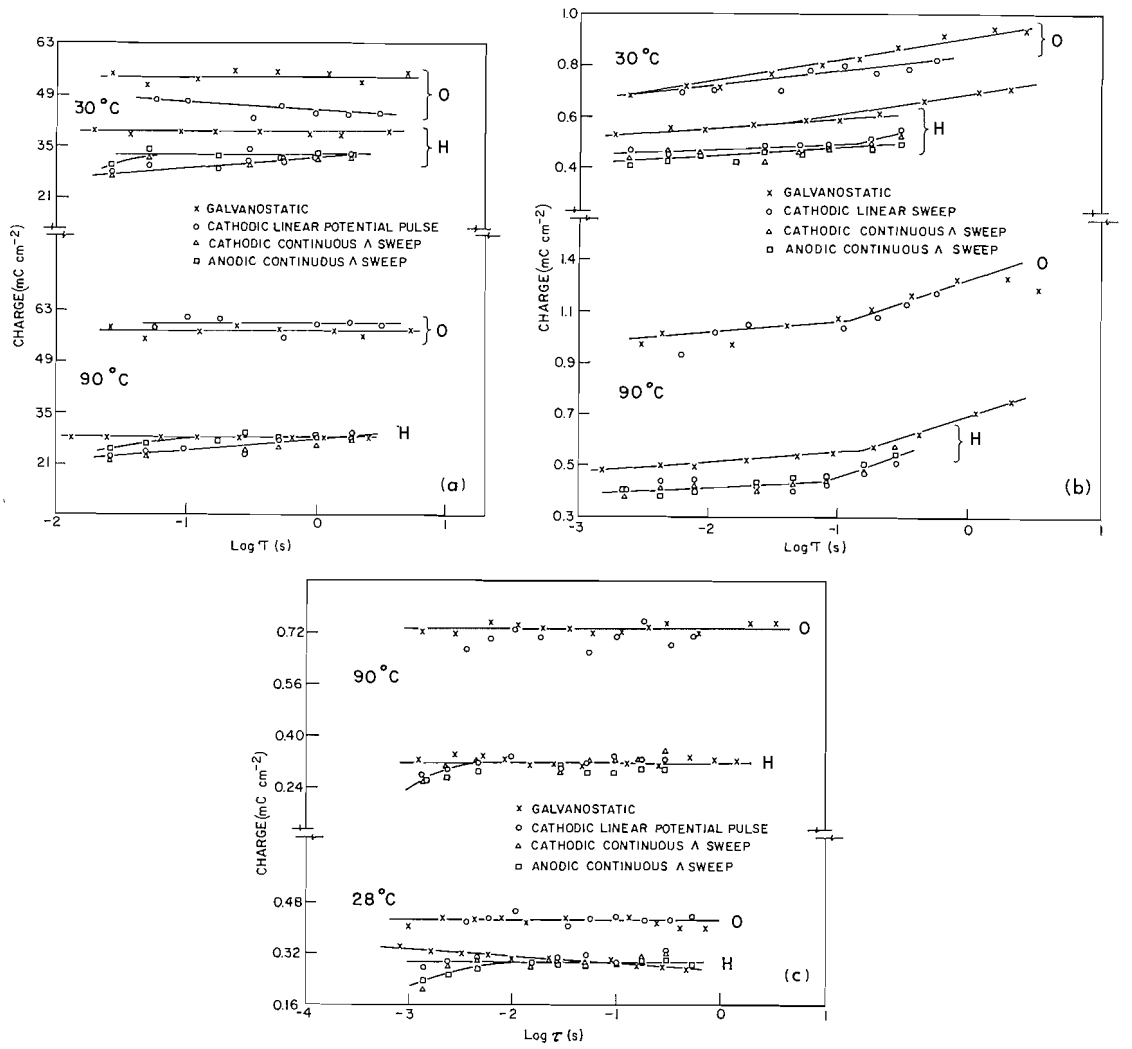

FIG. 5. (*a*) Surface oxide and H charges as a function of transition time in various measurements at platinized Pt at 30 °C and 90 °C. Note: differences between the charges for O and H for the three types of electrodes arise because of the different roughness factors. (*b*) As in (*a*) but for flame-heated smooth Pt. (*c*) As in (*a*) but for hydrogen-treated smooth Pt.

thickness which occurs in a time interval shorter than that studied here, followed by a period in which the quantity of reducible oxide is constant.

3. *Impurity Effects*

Measurement of the total Q_H as a function of time when E_A was kept in the range of potentials for double-layer charging gave indications of slow impurity adsorption, as has also been noted in other work. These effects were minimized by optimum cathodic and anodic pre-electrolysis, and were only significant after extended periods of standing at intermediate potentials, 0.4–0.6 V E_H.

4. *Transition-Time Effects*

The results from galvanostatic and potential-sweep methods were compared by carrying out reductions of the oxide formed at $E_A = 1.2$ V for 5 s using program C (Fig. 1). The appropriate type of transient was introduced over the period T. Again the oxide charge was taken from the beginning of the transient to the capacity

Can. J. Chem. Downloaded from www.nrcresearchpress.com by 210.87.254.105 on 09/05/12
For personal use only.

Can. J. Chem. Downloaded from www.nrcresearchpress.com by 210.87.254.105 on 09/05/12
For personal use only.

minimum around 0.4 V in the potentiodynamic curve. The hydrogen deposition charge was calculated as before for the galvanostatic case, and in the potential-sweep runs by integration over the region from the capacity minimum, at 0.4 V, to 0.00 V. However, the H-charging current was extrapolated linearly to 0.0 V from a potential of about +0.08 V, following a procedure used by Breiter (19) since a Faradaic process becomes significant below this potential. The charges determined as functions of the transition times τ for processes occurring in the "oxygen" and "hydrogen" regions have been plotted in Figs. 5*a*, *b*, and *c* for different modes of preparation of the electrodes and for runs conducted at room temperature and 90 °C. In the single potential-sweep method, the "transition time" was taken as the time required for the potential to traverse the limits of the oxide reduction peak (i.e. from ca. 1.1 to 0.4–0.6 V). Comparison of the results obtained by the galvanostatic and single sweep measurements from prior steady states is considered below in relation to the kinetics of oxide reduction.

5. Repetitive Triangular Potential Sweep

The electrode was subjected to continuous sweeps between 0 and 1.2 V, and the oxygen and hydrogen charges for both anodic and cathodic directions were determined. The hydrogen charges have been included in Figs. 5*a*, *b*, and *c* together with the results from single pulse measurements. Anodic and cathodic oxygen charge balance (cf. refs. 1, 2) between 1.2 V and the potential of the capacity minimum on the cathodic branch was usually better than 90% especially at low sweep speeds. The ratio "total anodic":"total cathodic" charge was usually only somewhat greater than unity [cf. previous conclusions (1)]. Single Λ sweeps are shown in Fig. 6 for various potentials of initiation in the H region and will be discussed later.

6. Anodic Transients

Some anodic galvanostatic transients were recorded and are considered below.

7. Construction of Pseudocapacity–Potential Profiles

The adsorption pseudocapacity C (8, 9) for oxide reduction was calculated from the relation

$$C = i/(\mathrm{d}V/\mathrm{d}t)$$

for the galvanostatic and potential-sweep transients with potential limits of 0.0 V and 1.2 V. Results are presented in Figs. 7 and 8 for various charging currents i and sweep rates $S\,(= \mathrm{d}V/\mathrm{d}t)$. Appreciable kinetic effects in the shapes and positions of the peaks are to be noted and are discussed further below.

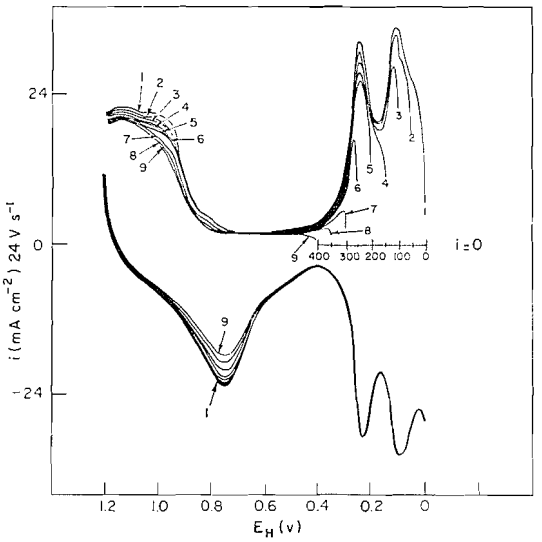

FIG. 6. Repetitive potential-sweep profiles with variation of the lower potential limit (smooth Pt, 28 °C, hydrogen treated).

General Discussion

(1) Estimates of Areas from Oxide and Hydrogen Charges

The "real" electrode areas are of some importance in comparison of results for one electrode and another, and in comparison of results of various workers. The available area of Pt electrodes is usually estimated by charging methods in which the quantity of electrochemically depositable oxygen or hydrogen is determined per unit apparent area. The former technique is not to be recommended since oxides of differing thicknesses and/or formal valences are produced, depending on the anodic potential attained, so that a condition of "full coverage" is difficult to define; also, as suggested here, and elsewhere by Schuldiner and Warner (18, and see ref. 6), oxygen species may diffuse into the bulk metal. Under fairly well-defined conditions, however, hydrogen "charging" of the electrode has been used to estimate areas since in the fully covered state the number of H atoms per unit area is a more definite quantity susceptible to calculation,

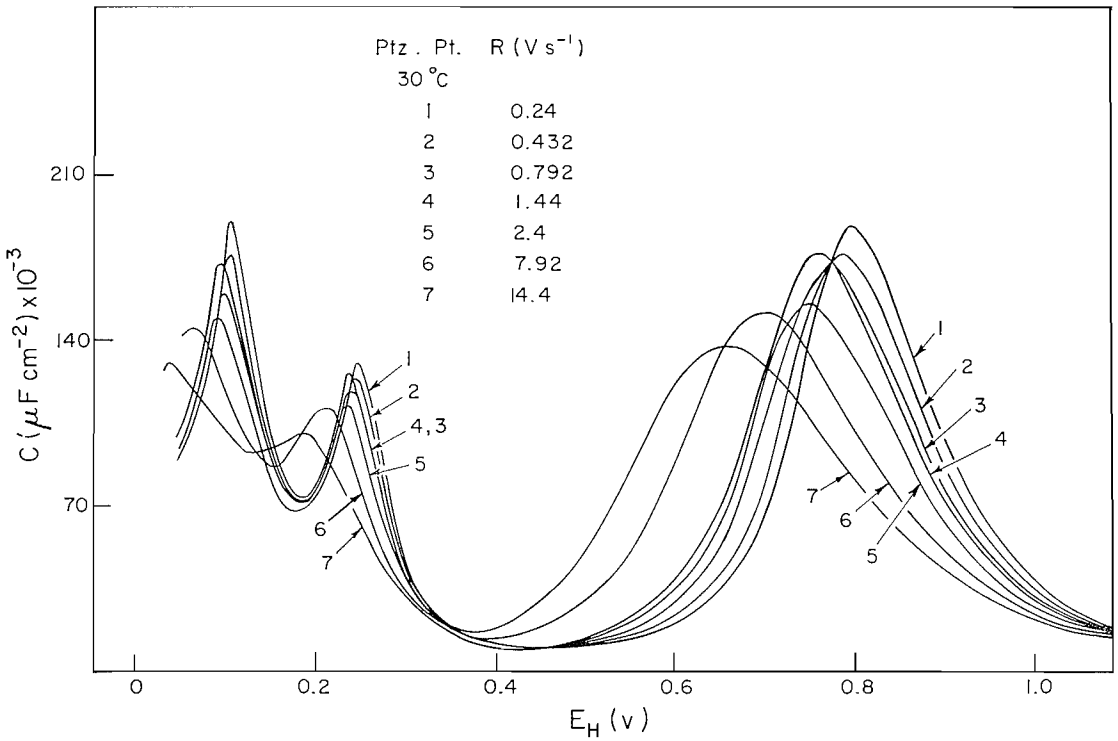

FIG. 7. Pseudocapacitance peaks for surface oxide reduction and H deposition, determined from cathodic single sweep transients (from 1.2 V E_H) at various sweep rates designated here as R.

assuming (20) that there is one H atom for every Pt.[4] Here we have first investigated the reproducibility which can be attained in estimations of various types.

Will and Knorr (4) and French and Kuwana (21) found that it was necessary to clean the surface by formation of a complete layer of surface oxide followed by its removal; H was subsequently deposited in a linear cathodic sweep. At potentials below about 700 mV, the area estimated from the cathodic H accommodation usually decreases with the time the electrode is held before cathodic reduction is commenced, due to adsorption of traces of impurities (cf. refs. 5, 6) or to a deactivation of the surface brought about by the return of displaced Pt atoms to more stable 'original' states (cf. ref. 21). The electrode area should be estimated as soon after the cleaning procedure as possible.

The required potential range and duration of the cleaning pulse must be optimized and may be controlled by the use of a potentiostatic step. After keeping the electrodes at various potentials V in the oxide region (and below) for 5 s, galvanostatic reductions were made at fairly high current densities. Q_O and Q_H were measured from these traces as shown in Figs. 3*a*, *b*, *c*, in which the H charge is seen to follow the oxygen charge to some extent but attains a constant value when measured by a reduction from a series of controlled anodic potentials (cf. refs. 11, 20). The importance of the initial conditions of electrode preparation becomes apparent here. It is evident that the platinized Pt electrodes give the most satisfactory results in that the H charge is constant over a large range of initial potentials, followed, in increasing order of

[4]This is not necessarily the case since H may be also interstitially adsorbed (interstitial H was first considered by Conway and Bockris (32*b*) in regard to the atom–ion mechanism in H_2 evolution) amongst the atoms of the first layer of the metal, as suggested by Conway and Salomon (32*a*) in regard to electrolytic isotope effects (cf. ref. 33; Will also considered interstitial H in the surface). Such a situation seems also to be indicated by the three H desorption peaks found by Will on individual *single crystal* faces of Pt. Diffusion of H into the metal must also be recognized (22) but this complication can be minimized by use of short duration cathodic sweeps and then Q_H is reproducible and constant.

Can. J. Chem. Downloaded from www.nrcresearchpress.com by 210.87.254.105 on 09/05/12
For personal use only.

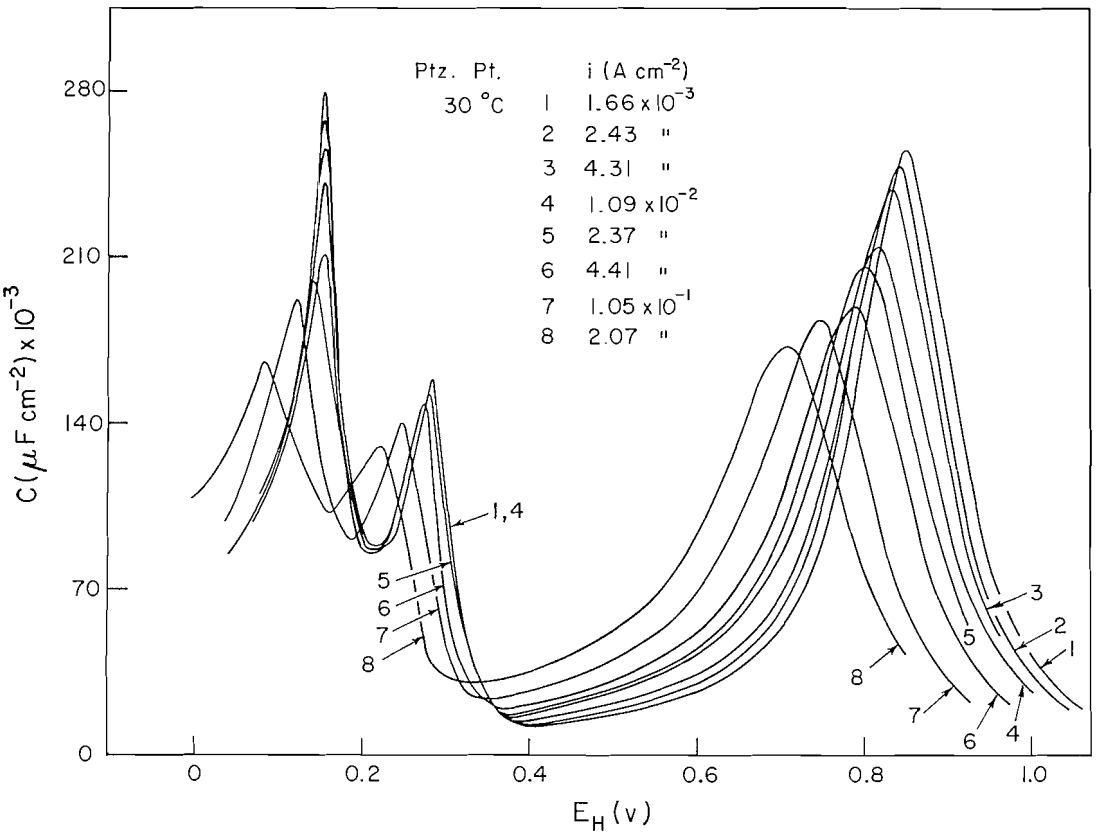

FIG. 8. Pseudocapacitance peaks for surface oxide reduction, H deposition, determined from differentiated cathodic galvanostatic transients (from 1.2 V E_H) at various current densities.

variation of Q_H, by the hydrogen-treated and then the flame-treated surfaces. Evidently, since Q_H becomes constant as V_{anodic} is decreased below ca. 0.7 V, we are really investigating here the resolution of the oxygen and hydrogen waves and the extent to which some oxide is reduced in the H region. Apparently, from this point of view, the flame-treated electrodes are unsatisfactory since it appears that there is always some oxide reduction beyond the usually chosen oxide "end-point" potential. Hydrogen-treated electrodes are quite satisfactory provided that V_{anodic} does not exceed 1300 mV. Although the platinized electrodes give the best results, this may be offset by the fact that (*a*) mechanical instability arises and (*b*) sintering is desirable. In all cases, an increase in temperature gives better resolution of the two regions. The effect of the duration of the cleaning or oxidation pulse may be estimated from the oxide "growth" curves in Fig. 4, from which it may be observed that the cathodic H charge becomes constant when determined from all potentials (in the oxide region) even though the oxide charge itself is observed to increase (cf. ref. 11).

We now examine if there are any significant kinetic differences in the results given by the various methods. Results are shown in Figs. 5*a*, *b*, and *c* for the galvanostatic and linear sweep experiments for various electrode preparations. Oxide was reduced after 5 s formation at 1200 mV. This value of V was chosen because it is below the O_2 evolution potential and yet the surface is probably "fully covered" by oxide; also, for this potential, the oxide is reduced completely on the H_2-treated and platinized electrodes but not on the flame-treated electrode. The difference is apparent in Fig. 5*b* where the H charges for the latter electrode are not constant but depend apparently on current density, being higher in the

Can. J. Chem. Downloaded from www.nrcresearchpress.com by 210.87.254.105 on 09/05/12
For personal use only.

Can. J. Chem. Downloaded from www.nrcresearchpress.com by 210.87.254.105 on 09/05/12
For personal use only.

longer transients. This is possibly also a consequence of the diffusion of oxygen atoms into the metal, to be discussed below. The galvanostatic values of Q_H are significantly higher for the flame-treated electrodes, but with the platinized and H_2-treated electrodes, the two methods give results in good agreement and Q_H is independent of "transition time" except at the highest rates. The Q_H for continuous sweep experiments between 0.0 and 1.2 V are also shown in Figs. 5*a*, *b*, and *c* and correlate well with the data from the single sweep determinations; hence one oxidation sweep only is necessary to clean or activate the electrode reproducibly. The relative accuracy of the galvanostatic and linear sweep methods may be judged by the scatter of the points in the figures. It is evidently easier to obtain reproducible results under galvanostatic conditions. The reasons for this are: (*a*) The end point of the hydrogen wave (around 0 V) is determined more readily on the differentiated galvanostatic trace. In the linear sweep, at potentials near to 0.0 V the passage of a Faradaic current makes an extrapolation necessary (19). The beginning of the hydrogen region and the end of the oxide region is also more easy to distinguish in the galvanostatic method because the differential trace which is proportional to reciprocal capacity in the latter case gives a sharper peak than the current trace (directly proportional to the capacitance) in the sweep method. (*b*) Integration of the linear sweep to obtain the charge is both tedious and sometimes inaccurate. The differential method requires only a calibrated time base and only distances are measured[5] to obtain the charges. For example in Fig. 4, the Q_H for appropriately conditioned electrodes may be reproduced to within 1 or 2%. (*c*) It is more difficult to apply a precisely linear sweep to the system than to apply a constant current, especially at high speeds where the sweep can become noticeably distorted; the resulting *i–V* curves are then difficult to interpret. Also any *iR* effects are *constant* in the galvanostatic method.

After *iR* correction, the values of E_{max} in the H region are independent of current density or sweep rate (up to those rates used in the present work) for all electrodes. We conclude, in agreement with previous work, that H deposition and ionization processes are almost in equilibrium in charging experiments, although there appear to be some slight differences in the values of the peak potentials determined by the two methods depending on electrode preparation [Figs. 11 and 12].

According to kinetic treatments (10, cf. 28) based on considerations of activation polarization, it is expected that dC_{max}/di or $dC_{max}/dS > 0$. Experimentally, the opposite is observed and C_{max} decreases as i or S increases. Since the present and previously published work indicates that the H on the surface is almost at equilibrium, we should expect almost constant C_{max} for various values of i or S. It seems likely that this discrepancy can be explained in terms of diffusion of hydrogen into the metal. Under these circumstances, more charging current is required per cm^2 than would correspond only to production of adsorbed H on the surface itself.[6]

Exploratory calculations based on diffusion theory show that C_{max} would decrease with increasing i but not logarithmically as observed.

Apparently the deposition of H may also activate the process of oxide deposition to a small extent, as illustrated in Fig. 6 where the cathodic end of the sweep has been initiated at various potentials in the H deposition region. There is a decrease[7] of approximately 10% in Q_O as the initiation potential moves from 0 to +400 mV. The cathodic H redeposition regions are identical within the experimental limits of resolution.

2. *Oxidation of the Pt Surface*

(a) Galvanostatic and Potentiodynamic Methods

The surface oxide charges obtained from reductive transients after 5 s at 1.2 V are shown in Figs. 5*a*, *b*, and *c* referred to above. The trends are similar to those observed for the H charges,

[5]In practice, these measurements were made on graph paper by projecting the 35 mm negatives with an enlargement of ca. 6.

[6]Area changes caused by pulsing have been demonstrated by Gilman (38); however, it is doubtful if this is the explanation of the effect discussed here which depends on i or S in single transients, rather than total time of pulse or sweep treatment.

[7]The increased apparent oxide coverage observed after polarization to more cathodic potentials in the H region cannot be accounted for by oxidation of any H that has permeated into the Pt since the reduction of oxide on the returning cathodic sweep also shows a larger peak than that corresponding to less cathodic treatment in the H region.

Can. J. Chem. Downloaded from www.nrcresearchpress.com by 210.87.254.105 on 09/05/12
For personal use only.

i.e. there is more scatter in the results from the sweep method and a dependence of Q on transition time is pronounced only with the flame-treated electrodes. In general, results from the two methods agree quite well, e.g. in the way Q depends on log τ (the transition time) for the flame-treated electrodes. On platinized electrodes, sintering may occur (cf. ref. 13) as is evident from the results shown in Fig. 5*a*, since the area has evidently diminished between the galvanostatic measurements, which were done first, and the sweep measurements. At 30 °C, on these electrodes, the O and H charges in the sweep method decrease and increase, respectively, with log τ. This dependence on τ disappears at 90 °C and the resolution is excellent. In the O region, the H_2-treated electrodes give the best results, insofar as there is least scatter and best agreement between the results from the two methods. Such electrodes are best suited for studies on the O region and platinized ones for the H region.

(b) The Degree and Extent of Surface Oxidation of Pt

While it is difficult to assign valency states to metal atoms in surface phases, the Q–V curves of Figs. 3*a*, *b*, and *c* indicate that a formal mean valency state corresponding to "PtO_2" appears to be eventually reached above 1.8 V in anodic oxidation of Pt. There are, however, no plateaux at any potentials which would correspond to any distinct valency states such as PtOH, PtO, or PtO_2, and time effects (cf. Fig. 4) are usually appreciable. At higher temperatures the observed charges indicate even higher degrees of oxidation, suggesting that more than a surface monolayer is formed since, for monolayer adsorption, it would be expected that oxygen atoms at the surface would take up more space with a consequent lowering of Q_O as temperature was increased. This is indeed observed (19) in the H region where Q_H decreases with T (this is probably a normal effect associated with exothermic adsorption). If the possibility of multilayer formation or "dermasorption" (18, and see ref. 6) is accepted, it obviously becomes difficult to assign a formal valency to the oxide from the Q–V curves alone. Previously we have suggested that the current–potential profiles observed during the oxidation of formate might be explained in terms of various surface oxidation states (24). Nominally the surface layer would be ca. 50% "PtOH" at about 0.9 V, 50% "PtOH" – 50% " PtO" at about 1.5 V, and 100% "PtO" above 1.7 V. These values are, however, lower than would be required for the observed cathodic discharge Q values.

Gilman (5), using a potential-step method, has reported higher values of Q_O at a given V than those in Figs. 3*a*, *b*, *c*, and Laitinen and Enke (1) and Mayell and Langer (23) lower values. However, in the last two cases the electrodes were not maintained at the required potential E_A before estimation but at open circuit so that oxide could have been lost by self-discharge.

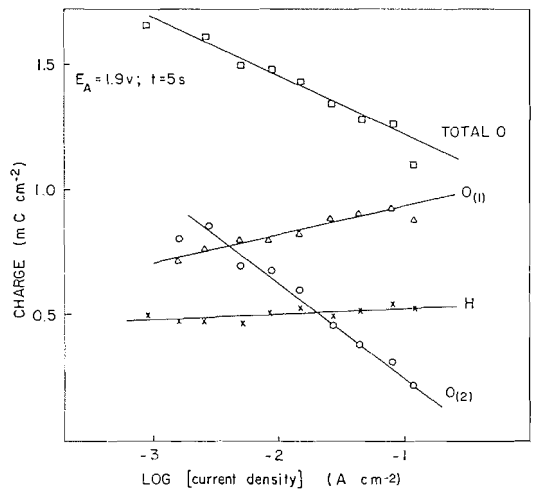

FIG. 9. Oxide and hydrogen charges as a function of cathodic current density at smooth Pt (flame heated). Anodic oxidation at 1.9 V for 5 s; two oxide reduction regions are distinguished.

At high potentials, especially on flamed electrodes, two waves are observed (Fig. 2) in the oxide reduction process, and they become more pronounced as the potential and the cathodic current density are increased. This is perhaps an indication of a second type or phase of oxide. As the reducing current density is decreased the two waves merge into one, evidently because the more anodic wave (termed wave 1) is more irreversible than the lower potential wave (termed wave 2). This is illustrated in Fig. 9, where $E_A = 1.9$ V, which shows the variation of charge for each wave and for the total oxide as a linear function of the logarithm of current density. This seems to preclude the possibility that one wave corresponds to reduction of molecular oxygen from

Can. J. Chem. Downloaded from www.nrcresearchpress.com by 210.87.254.105 on 09/05/12
For personal use only.

solution since in that case a linear dependence of Q on $(i_{cath})^{1/2}$ (with increased charge at decreased current density) would be expected.

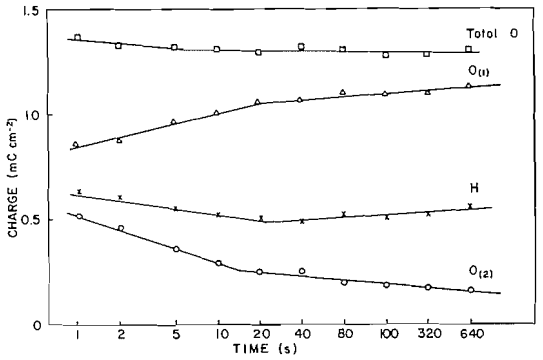

FIG. 10. Time dependence of the two oxide discharge regions (in mC cm^{-2}) and the total oxide and hydrogen charges at smooth flame-heated Pt (transients taken from 1.9 V E_H after the various times indicated on the scale of abscissae).

Wave 2 seems to correspond to the oxide found at lower potentials E_A (i.e. where there is only one oxide wave) since its charge decreases with increasing reduction current density (compare Figs. 5*b* and 9) and it can formally perhaps be designated[8] "PtO". Wave 1 would then represent reduction of a rearranged form of this material which grows with time, at a constant potential, at the expense of the normal type as illustrated in Fig. 10.

(c) Kinetics

(i) Growth Kinetics—At constant potential, the oxide layer grows (Fig. 4), after a short initial period, as a direct (1, 5, 14, 17), rather than an indirect (cf. ref. 26), logarithmic function of time and such behavior for thin films seems rather general. Laitinen and Enke (1) treated the oxidation in terms of a conventional kinetic equation

$$k' \frac{d\theta}{dt} = i = k \exp [V/b]$$

and suggested that k depended exponentially on θ (or Q) (cf. ref. 8). Gilman (5) wrote a similar equation based on the Elovitch adsorption relation with an exp $-r\theta$ term (cf. ref. 8). These treatments seem oversimplified since (*a*) no term was included (e.g. $1 - \theta$) for the activity of free metal sites initially present and (*b*) the back reaction of the charging process has been neglected. If these two factors are included in a modification of the previous treatments, the equation

$$[8] \quad k' \frac{d\theta}{dt} = i = \bar{k}_1(1 - \theta)e^{-r\theta} - \bar{k}_{-1}\theta e^{r\theta}$$

results where $\bar{k}_1$ and $\bar{k}_{-1}$ are electrochemical rate constants containing a constant potential term and a symmetry factor (8) (= 0.5) which is also involved in the r parameter. Integration under Langmuir conditions ($r = 0$) would give

$$[9] \quad \theta = \frac{1}{1 + \bar{K}_1}(1 - \exp -[\bar{k}_1 + \bar{k}_{-1}]t),$$

where $\bar{K}_1 = \bar{k}_1/\bar{k}_{-1}$. This, however, does not lead to the required form in *log t*.

If surface charging only were involved (i.e. if Q_O increased to a limit corresponding to $\theta \to 1$), an asymptotic approach of Q_O to a constant value would be expected as in eq. [9]. The fact that this is not the case indicates either penetration of the oxide oxygen into the metal (cf. ref. 18 and 6) or place exchange (7, 15*a*) between the metal and the oxygen ad-layer to give a "two-dimensional" oxide. We have examined the growth law for Q in terms of diffusion of oxygen atoms [cf. the case for H (22)] into the metal, and Q is found to be proportional to $t^{1/2}$ and not *log t*, as may be expected. We have shown elsewhere (15*a*) that a direct logarithmic law follows for constant *potential* conditions if it is assumed that the potential available across the double layer for the anodic discharge process, leading to oxide formation, decreases with thickness of the film (across which a fraction of the metal-solution potential drop exists) built up at a given time under potentiostatic conditions. For oxide films on Al, a direct log t law can be derived (27) but requires constant *field* conditions.

(ii) Kinetic Effects in Transients for Oxide Reduction—Transient techniques have been used mainly to estimate coverage by ad-species, or, for simple discharge processes, to evaluate charging rates (e.g. ref. 5) or exchange currents; in the case of Pt, kinetic work has been concerned mainly with the anodic oxidation process (5, 35). However, the pseudocapacity–potential profiles

[8]We stress, however, that the representations of the platinum oxide given here and elsewhere in this paper are not intended to refer to any bulk phase species but only to a nominal Pt:O ratio characteristic of the surface oxide produced at a given potential for a certain time.

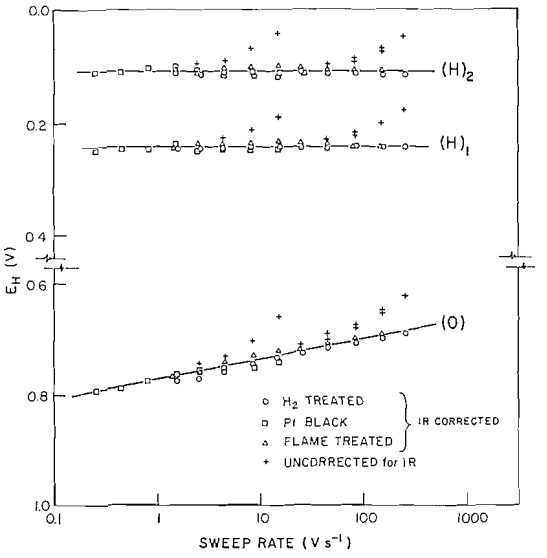

FIG. 11. Potentials of pseudocapacity maxima for cathodic oxide reduction and H deposition as a function of rate of potential sweep.

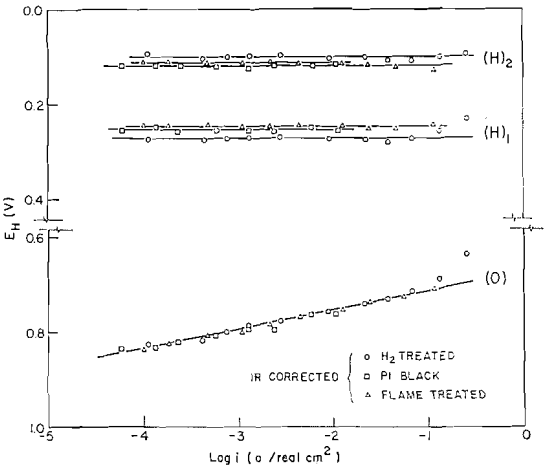

FIG. 12. Potentials of pseudocapacity maxima for cathodic oxide reduction and H deposition as a function of galvanostatic current density.

obtained in reductive transients may also be analyzed theoretically (10, 28). In particular, the variations of the magnitude and position of the pseudocapacitance maximum C_{max} as a function of sweep rate[9] or current density gives information on polarization in the surface charging or discharging reactions (8, 9). Since E_{Cmax} is the potential at which half the oxide originally present remains, the variation of E_{Cmax} with log S or log i provides a measure of polarization at almost constant coverage by oxide species. In general, for surface charging, the values C_{max} and E_{Cmax} are essentially constant for small values of i in the transient, i.e. small displacements from equilibrium but fairly sudden changes will occur at higher values of i. Then, at constant potential, it is easy to show (9) that the calculated capacitance is linear with i at any potential in a galvanostatic transient when an electrochemical Langmuir type of isotherm applies (8).

Figures 7 and 8 show that C_{max} for oxide reduction decreases as i or S increase, and E_{Cmax} (corrected for iR effects) is shifted cathodically (Figs. 11 and 12). Uncorrected values are also shown for the potential sweep case (Fig. 11). For the latter, corrections for area differences between the electrodes are unnecessary since dV/dt is independent of area. However, in the galvanostatic case, the true current densities which depend on roughness factors were obtained on the basis of Q_H values. It is apparent that there is a logarithmic dependence of E_{Cmax} on i or S (and hence transition time τ). The three types of electrode also give results in good agreement. The slopes dE_{Cmax}/d log S are 40 and 38 mV, respectively, over about 4 decades (Figs. 11 and 12). On this basis alone we may conclude that the kinetic characteristics of the oxide reduction are not determined by a simple activation-controlled discharge step[10] considered above, and the process of reduction of surface oxide is evidently markedly displaced from equilibrium in contrast to the behavior in the H region where the iR corrected[11] E_{Cmax} are constant (Figs. 11 and 12). Similarly, plots of C_{max} vs. log i or S are linear and C_{max} *decreases* with increasing i or S. This result is significant since we shall show in a forthcoming paper (29),

[9]The first experimental studies of this kind were made by Will and Knorr (4). Here we have made similar measurements also for the purpose of comparison with the galvanostatic transient results, and for derivation of Tafel slopes.

[10]Conversely, the surface *oxidation* process is associated with a rate-controlling discharge step giving a Tafel slope of ca. $2.3(2RT/F)$ (5).

[11]Since the H deposition and oxidation currents are similar in magnitude to those for reduction of surface oxide, any uncertainties in iR correction could not account for the important qualitative difference between the dependence of E_{Cmax} on i or τ for the H and the oxide processes. In any case, the observed relations in the latter case are *logarithmic* in i or τ, and not linear.

Can. J. Chem. Downloaded from www.nrcresearchpress.com by 210.87.254.105 on 09/05/12
For personal use only.

Can. J. Chem. Downloaded from www.nrcresearchpress.com by 210.87.254.105 on 09/05/12
For personal use only.

developing our previous calculations (8), that the reverse trend is to be expected for most of the possibilities arising in a simple surface charging model. Recently Srinivasan and Gileadi (28) have discussed the effect of sweep rate on the pseudocapacity–potential profile in a development of the work of Conway, Gileadi, and Kozlowska (9); they predict that C_{max} decreases with S to a constant value and that $E_{C_{max}}$ is initially constant and then increases (for an anodic sweep) with log S. This behavior appears at first sight to be contrary to that predicted previously (9) but further theoretical examination of this question in the forthcoming paper (29) shows that two types of cases can arise depending on the range of values of S. A limiting case of infinite capacity arises when $S/\bar{k}_1$ (eq. [8]) is equal to 1.33. Neither of the predictions is, however, in close agreement with the observed trends of C_{max} and $E_{C_{max}}$ considered together.

Two effects are to be considered in the interpretation of the kinetic effects in the transient measurements: (*a*) the linear variation of $E_{C_{max}}$ with log S [first observed by Will and Knorr (4)] or log i and (*b*) the variation of C_{max} with these quantities.

With regard to (*a*), the experimental slope of $E_{C_{max}}$ vs. log S or log i is 40 mV. Gileadi and Srinivasan have shown that for a highly irreversible discharge step, the slope of the $E_{C_{max}}$ vs. log S plot should be the same, approximately, as the steady state Tafel slope for that process. The observed low slope ($<< 2.3(2RT/F)$ and ca. $2.3(\frac{2}{3}RT/F)$ suggests a mechanism more complex than a simple discharge process and could correspond to two steps in oxide reduction with the prior one in quasi-equilibrium, e.g.

[A] $\quad$ "PtO" + H^+ + e $\rightleftarrows$ "PtOH"

[B] $\quad$ PtOH + H^+ + e $\rightarrow$ Pt + H_2O,

with [B] rate determining and concentration of "PtOH" states in the oxide layer potential dependent.[12] Presumably step [A], if quasi-reversible, will be represented by

$$[10] \qquad \frac{\theta_{OH}}{\theta_O} = K_A \exp -VF/RT,$$

since "OH" and "O" sites will occupy more or less similar space on the Pt surface. If $\theta_{O,i}$ is the initial "coverage" prior to reduction,

$$[11] \qquad \frac{\theta_{OH}}{\theta_O} = \frac{\theta_{OH}}{\theta_{O,i} - \theta_{OH}} = \frac{\theta_{OH}/\theta_{O,i}}{1 - \theta_{OH}/\theta_{O,i}} = K_A \exp -VF/RT,$$

so that the relative coverage $\theta_{OH}/\theta_{O,i}$ by "PtOH" species is potential dependent in the usual (8, 25) way. (A surface activity factor exp ($r\theta_{OH}$) might also be included in the general case.) Then reaction [B] will then be associated with a limiting Tafel slope of $2.3(2RT/3F)$, as observed. Rate-controlling reduction through step [A] would presumably give a normal discharge Tafel slope of $2.3(2RT/F)$.

With regard to (*b*), the variation of C_{max}, we are led to the conclusion that, to a limited extent, bulk oxidation has taken place so that at high S or i values, cathodic current is used only to reduce the oxide at the oxide–solution interface. As in the H case, we expect a decrease in C_{max} with i or S. Simply speaking, the longer the time taken during the transient, the more material would be able to diffuse (18, and see ref. 6) and be reduced, so that a larger capacity maximum is observed.[13] It may be noted here that the observed *charge* in reduction is constant because the potential of the electrode is changed between values corresponding to the *same* initial and final states in these experiments. In anodic[14] oxidation, however, the charge would be expected to increase with decreasing log i or log S. This was observed by Gilman (5).

(iii) Hysteresis—It is desirable to examine some of the previous theories of Pt oxidation in the light of the above results which indicate oxidation beyond a monolayer (cf. ref. 7) and,

[12]Nominally, from the observed Q_O values corresponding to the areas under the capacity profiles, the extent of surface oxidation is only a little above (1.3 ×) that corresponding to "PtOH". However, since from whatever potential in the oxide region a reduction transient is taken, the resulting cathodic reduction current profile is almost symmetrical (but smaller with decreasing initial anodic potentials), it is suggested that the surface oxide exists in domains, within which a two-stage reduction involving "PtO" and "PtOH" states can occur. Further discussion of this matter is given in the following section on "Hysteresis".

[13]A similar effect occurs with nickel(III) oxide electrodes; on rapid discharge, the surface layer is preferentially reduced and the potential falls. However, on waiting at open circuit, more oxide can be reduced on further discharge.

[14]The use of anodic galvanostatic transients is unsatisfactory since no well-defined relation between Q and potential (e.g. with respect to time effects) is available and the "end-point" of the transient is arbitrary, being simply the potential at which O_2 evolution occurs at an appreciable rate.

Can. J. Chem. Downloaded from www.nrcresearchpress.com by 210.87.254.105 on 09/05/12
For personal use only.

at high potentials (> 1.6 V), changes in constitution[15] of the oxide (Fig. 2).

Hysteresis effects can originate for several reasons. First, kinetically, if the rate of the desorption process differs from that of the adsorption process, e.g. in the case when slow diffusion effects are operative or when the desorption is endothermic. Secondly, a more fundamental hysteretic effect can arise when the sorbate/sorbent system forms metastable domains (30) which undergo a totally irreversible phase transition to a more stable form before or during desorption. A given coverage is then maintained down to a lower bulk chemical potential of the sorbate in the desorption isotherm, than that required to reach the same coverage in the adsorption isotherm. This is the type of hysteresis involved in the electrochemical oxidation of Pt and the reduction of the resulting surface oxide.

The phenomenon of hysteresis has been associated with the question of charge balance by Laitinen and Enke (1) who, like Böld and Breiter (35), proposed a kinetic explanation. They supposed that if the step I below

$$\mathrm{Pt} \xrightarrow{\mathrm{I}} \mathrm{PtOH} \xrightarrow{\mathrm{II}} \mathrm{PtO}$$

(cf. steps [A] and [B][16] and the steps considered in ref. 35) were slow, then during reduction, the oxide may simply remain in the "PtOH" state. However, this is not a theory which gives a truly irreversible effect, since it would be expected that the PtOH would be reduced given sufficient time, as is indeed indicated by Gilman's charge balance result, and the present work.

The discussion of hysteresis at Pt is complicated by divergences of results regarding the charge balance for anodic oxidation and cathodic reduction; the cathodic charge Q_c has been reported to be about one half (1), or 0.8 (2) of that (Q_A) for anodic oxidation (1, 2). The present results and those of Gilman (5) do not uphold this behavior which may be attributable to impurity adsorption effects (5, 31) since in the work of ref. 1 the electrodes were left on open circuit for appreciable times.

In a cyclic sweep experiment, hysteresis appears at all speeds with no indication of any major change at very slow speeds (cf. ref. 15*a*). In this respect, it seems that the kinetic explanation given by Böld and Breiter of the difference between the anodic-going and the cathodic-going curves, in terms of rate constants, is insufficient to account for the observed type of behavior which is common for a number of metals (15*a*) whether they form "monolayer" oxide films or multiple layers (as e.g. at Ni or Ag, ref. 15*a*) upon anodic oxidation. Also, hysteresis appears at all potentials at which oxide is formed, which would imply [on the above viewpoint, (1)] the conversion of "PtOH" to "PtO" at all potentials; the latter process seems thermodynamically unlikely if a mono-ad-layer is maintained. A completely irreversible transformation from a Pt "OH" or Pt "O" dipolar ad-layer to a two-dimensional oxide (Pt O Pt O . . . in the ad-layer) in domains seems to be the type of explanation required (cf. ref. 30).[17]

The difference in shape of the cathodic oxide reduction profile from that for the anodic oxidation of the platinum surface is a conspicuous feature of all results. The anodic charging curve is in fact almost linear (2, 4, 6, 18) (and the adsorption pseudocapacitance correspondingly almost constant) with potential indicating (as Ohashi *et al.* (2) have implied[18]) a substantial value of r in the coverage term $r\theta$ (cf. ref. 8) in

[15]Studies on the Kolbe reaction to be reported elsewhere (34) indicate inhibition effects at high anodic potentials; this behavior may be associated with changes of constitution of the surface oxide at Pt, since the inhibition effects occur at potentials much higher than those corresponding to inhibition due to the initial formation of surface oxide at ca. 0.8–0.9 V E_H (11, 24).

[16]Thermodynamically, the states written here as "PtOH" and "PtO", in the process of being formed anodically, are not necessarily the same as the similarly written states in the reduction steps [A] and [B], although they have formally the same Pt:O ratio. This may arise because of a two-dimensional transformation of state of the oxide film, of the type referred to in a general way above.

[17]In this connection, it is of interest that low energy electron diffraction studies of O adsorption from the gas phase at metals usually reveals a high degree of order amongst the adsorbate atoms; since the atoms presumably become adsorbed initially at random, a disorder–order transformation of the kind that may also be involved electrochemically must have occurred on the surface. Also, elsewhere (11) we have shown that similar hysteresis occurs with aprotic solvents containing controlled traces of water in quantities which lead only to partial coverage ($\theta_o < 1$) of the electrode by surface oxide. Since the coverage in these experiments is much less than that in water at given anodic potentials, but the hysteresis effects are similar, oxide domains on the surface were suggested.

[18]This is, of course, simply a case such as that considered much earlier by Temkin (36) and applied by Gilman (5) to the case of Pt.

Can. J. Chem. Downloaded from www.nrcresearchpress.com by 210.87.254.105 on 09/05/12
For personal use only.

the exponent $\beta VF - (1 - \beta)r\theta$ relating charging current to potential and coverage. The cathodic reduction profile is, however, much more typical of an ideal redox process (25) and at slow sweep rates is almost perfectly symmetrical. Following our analysis of pseudocapacitance profiles given previously (25), it is easy to show that for a one-electron redox process the observed width of the reduction profile at the half-height (i.e. at $C = 0.5C_{max,\, S\to 0}$) is too large for Langmuir conditions ($r = 0$) to be applicable; in fact, $r/RT \approx 4$ (temperature $T = 300$ °K) accounts for the observed shape of the profile[19] (for a two-electron reduction, the profile would have a higher aspect-ratio and a correspondingly larger value of r would be required). The profile is, however, very symmetrical at low sweep rates ($S < 0.1$ V s^{-1}) so that (37), while the anodic/cathodic profiles are completely irreversible with respect to one another, polarization in the reduction of the surface oxide, *once the latter is formed in the "rearranged" state,* is not an important factor determining the shape. Also nonlinear heterogeneity terms in $r\theta''$ must be insignificant since (25) the reduction profiles are symmetrical. It is for these reasons, amongst others, that we conclude that the different shapes of the anodic-going and cathodic-going curves cannot be explained in conventional kinetic terms alone.

Acknowledgments

Grateful acknowledgment is made to the U.S. Army Engineer Research and Development Labs. for award of Contract No. CP-70 A1-63-4, through the Canadian Commercial Corporation, Ottawa, in support of this work. We also acknowledge the interest taken in this work by Drs. G. R. Freysinger and M. Savitz.

1. H. A. Laitinen and C. G. Enke. J. Electrochem. Soc. **107**, 773 (1960). *See also* S. W. Feldberg, C. G. Enke, and C. E. Bricker. J. Electrochem. Soc. **110**, 826 (1963).
2. K. Ohashi, K. Sasaki, and S. Nagaura. Bull. Chem. Soc. Japan, **39**, 2066 (1966).
3. K. J. Vetter and D. Berndt. Z. Elektrochem. **62**, 378 (1958).
4. F. Will and C. A. Knorr. Z. Elektrochem. **64**, 258, 270 (1960). *See also* V. I. Luk'yanycheva, V. I. Tikhomirova, and V. J. Bagotskii. Elektrokhimiya, **1**, 262 (1965); Dokl. Akad. Nauk SSSR, **159**, 644 (1964).
5. S. Gilman. Electrochim. Acta, **9**, 1025 (1964).
6. S. Schuldiner and T. Warner. J. Electrochem. Soc. **112**, 212 (1965). *See also* L. Formaro and S. Trasatti. Electrochim. Acta, **12**, 1457 (1967).
7. A. K. N. Reddy, M. A. V. Devanathan, and J. O'M. Bockris. J. Electroanal. Chem. **5**, 61 (1963). A. K. N. Reddy, M. A. Genshaw, and J. O'M. Bockris. Abstract No. 41, Electrochemical Society Meeting, Dallas (1967).
8. B. E. Conway and E. Gileadi. Trans. Faraday Soc. **58**, 2493 (1962); Can. J. Chem. **42**, 90 (1964); J. Chem. Phys. **39**, 3420 (1963).
9. B. E. Conway, E. Gileadi, and H. A. Kozlowska. J. Electrochem. Soc. **112**, 341 (1965); J. Electroanal. Chem. **8**, 486 (1964).
10. H. Wroblowa, J. O'M. Bockris, and B. Piersma. J. Electroanal. Chem. **6**, 401 (1963).
11. B. E. Conway, N. Marincic, D. Gilroy, and E. Rudd. J. Electrochem. Soc. **113**, 1144 (1966). J. A. Shropshire. Electrochim. Acta, **12**, 253 (1967).
12. J. J. MacDonald and B. E. Conway. Proc. Roy. Soc. London, Ser. A, **269**, 419 (1962).
13. R. J. Connolley, J. F. Flannery, and B. L. Meyers. J. Electrochem. Soc. **114**, 241 (1967). D. W. McKee. J. Phys. Chem. **67**, 841, 1336 (1963).
14. H. Kozlowska and B. E. Conway. J. Electroanal. Chem. **7**, 109 (1964).
15. (*a*) B. E. Conway and M. Sattar. Proc. Conf. Advisory Group for Aerospace Research and Development, Liège, Belgium, June 1967 (in press, G. Sherman (*Editor*)). (*b*) A. Slygin and A. N. Frumkin. Acta Physicochim. U.R.S.S. **3**, 791 (1935). (*c*) J. Pearson and J. A. V. Butler. Trans. Faraday Soc. **34**, 1163 (1938).
16. S. B. Brummer, J. I. Ford, and M. J. Turner. J. Phys. Chem. **69**, 3424 (1965).
17. A. C. Makrides. Symposium on Electrode Processes, The Electrochemical Society, Cleveland, 1966. p. 371. K. Lehovec and J. D'Amico. J. Electrochem. Soc. **114**, 363 (1967). N. Sato and T. Notoya. J. Electrochem. Soc. **114**, 585 (1967).
18. S. Schuldiner and T. Warner. J. Phys. Chem. **69**, 4048 (1965).
19. M. Breiter. Trans. Faraday Soc. **61**, 749 (1965); *see also* Z. Elektrochem. **64**, 897 (1960).
20. M. Breiter, H. Kammermaier, and C. A. Knorr. Z. Elektrochem. **60**, 37, 119 (1956).
21. W. G. French and T. Kuwana. J. Phys. Chem. **68**, 1279 (1964).
22. D. BenDaniel and F. G. Will. J. Electrochem. Soc. **114**, 909 (1967); cf. **114**, 916 (1967).
23. J. Mayell and J. Langer. J. Electrochem. Soc. **111**, 438 (1964).
24. D. Gilroy and B. E. Conway. J. Phys. Chem. **69**, 1259 (1965).
25. B. E. Conway, E. Gileadi, and M. Dzieciuch. Electrochim. Acta, **8**, 143 (1963).
26. N. F. Mott and H. Cabrera. Trans. Faraday Soc. **36**, 472 (1940); Rept. Progr. Phys. **12**, 163 (1948–49).
27. J. E. Boggio and R. C. Plumb. J. Chem. Phys. **44**, 1081 (1966). *See also* J. R. Anderson and I. M. Ritchie. Proc. Roy. Soc. London, Ser. A, **299**, 354, 371 (1967).
28. S. Srinivasan and E. Gileadi. Electrochim. Acta, **11**, 321 (1966).
29. A. C. Smith, D. Gilroy, and B. E. Conway. In preparation.

[19] In the work of Ohashi *et al.* (2), it was concluded that for the platinum surface oxide reduction process, their λ_c factor, which is related to our r factor, was negligible. The present experimental results do not support this conclusion.

30. D. H. EVERETT and W. I. WHITTON. Proc. Roy. Soc. London, Ser. A, **230**, 91 (1955). D. H. EVERETT and P. NORDON. Proc. Roy. Soc. London, Ser. A, **259**, 341 (1960).
31. S. SCHULDINER and T. WARNER. J. Phys. Chem. **68**, 1223 (1964).
32. (*a*) B. E. CONWAY and M. SALOMON. Ber. Bunsenges. Physik. Chem. **68**, 331 (1964); J. Phys. Chem. **68**, 2009 (1964). (*b*) B. E. CONWAY and J. O'M. BOCKRIS. Can. J. Chem. **35**, 1124 (1957).
33. F. WILL. Extended Abstracts, Electrochemical Society Symposium, Vol. 2, No. 1, 1964; J. Electrochem. Soc. **112**, 451 (1965).
34. B. E. CONWAY and A. K. VIJH. J. Phys. Chem. **71**, 3637, 3655 (1967); Chem. Rev. **67**, 623 (1967).
35. W. BÖLD and M. BREITER. Electrochim. Acta, **5**, 145 (1961).
36. M. I. TEMKIN. Zh. Fiz. Khim. **15**, 296 (1941).
37. E. GILEADI and B. E. CONWAY. J. Chem. Phys. **39**, 3420 (1963).
38. S. GILMAN. J. Electroanal. Chem. **9**, 276 (1965).

Can. J. Chem. Downloaded from www.nrcresearchpress.com by 210.87.254.105 on 09/05/12
For personal use only.

Effects of additives on the e.s.r. of zinc oxide

HISASHI UEDA

Section 6, Government Chemical Industrial Research Institute Tokyo, 2-Mita, Meguroku, Tokyo, Japan

Received May 24, 1967

Solutions of various organic compounds were mixed with zinc oxide powder. The mixtures of these compounds with zinc oxide were prepared by evaporating the solvent. When the zinc oxide with any of the additives is heated at 300 °C, two e.s.r. lines with g factors of 1.960 and 2.004, named I_1 and I_2, were observed. The intensities of I_1 and I_2 come to their equilibrium values after several minutes of heating. The results show that I_1 and I_2 are not from two independently existing species but from the two species R_1 and R_2, whose concentrations are connected with each other by some competitive equilibrium reactions. It was not possible to estimate the two equilibrium constants separately, but their product was estimated to be less than 2.5×10^{-8}. R_1 is concluded to be Zni^+ (interstitial), while R_2 may be Zn^+ or $(ZnO_v)^{-(2v-1)}$, where v is an integer. The compounds which gave strong I_2 were naphthoquinones, naphthols, benzoquinone, hydroquinone, and anthraquinone, while the compounds which gave strong I_1 were benzoin, anthrone, pyrene, and naphthalene.

Canadian Journal of Chemistry, **46**, 891 (1968)

Can. J. Chem. Downloaded from www.nrcresearchpress.com by 210.87.254.5 on 09/05/12
For personal use only.

Introduction

Electron spin resonance (e.s.r.) signals from the paramagnetic species are not strong in an untreated zinc oxide powder if measured at room temperature. However, as shown in Table I, they can be intensified in various ways. Effects of mixed Li_2O and Al_2O_3 were studied by both Kokes (5) and Fujita and Kwan (6). The effect of Al_2O_3 on the intensification of the line with $g = 1.960$ was significant. The effects of adsorbed O_2 (6–8) and Cl_2 (6) were also studied with the specimens pretreated at 500 °C (6, 7) and at 400 °C (8). The present work was undertaken to find the effects of organic additives on the e.s.r. of zinc oxide.

Experimental

The zinc oxide used (Kanto Chemical Co.) was special reagent grade and was prepared by igniting pure zinc. Liquid additives were degassed in vacuum after freezing. These were then distilled. The additive compound was then introduced into evacuated zinc oxide powder in an e.s.r. capillary at the pressure of 20 mm Hg. Solid additives were mostly dissolved in benzene to the concentration of 0.03 g/ml, and 10 ml of the solution thus obtained was poured on 3 g of zinc oxide powder. Evaporation of the solvent in air gave a mixture of the solid additive with zinc oxide. This mixture was evacuated to 5×10^{-2} mm Hg by a vacuum system. The capillary containing zinc oxide and an additive was sealed off from the vacuum system. It was then placed in a heat bath at 300 °C for various lengths of time. Between each heating operation the capillary was cooled to 20 °C to carry out e.s.r. measurements, which were done with a JES–3BX e.s.r. spectrometer with 100 kc/s field modulation. In cases where the additives were insoluble in benzene, ethanol was used as solvent.

Results

Three different e.s.r. lines, with g factors of 1.960, 2.004, and 2.110, were observed in the zinc oxide powder with an additive. The line with $g = 2.110$ was found only with anthracene; the nature of this line is not discussed in the present report. The lines with $g = 1.960$, called I_1, and with $g = 2.004$, I_2, change their intensities during heating; the typical time dependence of the intensities is shown in Fig. 1 and Fig. 2. In Fig. 1 is shown the time dependence of the e.s.r. intensities from the ZnO samples with α-naphthol and α-naphthoquinone, as examples of the many similar curves obtained by various additive compounds. I_2 is observed even before heating is started, while I_1 becomes appreciable after a few minutes of heating. In several minutes the intensities of I_1 and I_2, i.e. I_1 and I_2, come to the equilibrium values. In Fig. 2, I_1 and I_2 from the ZnO to which hydroquinone, quinhydrone, and *p*-benzoquinone are added are shown on the graph with log I_2 as ordinate and log I_1 as abscissa. The point moves along the curve during the heating and the curve ends at the equilibrium point, which is attained in 6 min. In Fig. 3 the e.s.r. spectra I_1 and I_2 are shown. In Fig. 4, the equilibrium points for all the compounds used are plotted on the log I_1 vs. log I_2 plane.

In Fig. 1 it is shown that the concentrations of R_1 and R_2 come to equilibrium after 6 min of heating at 300 °C. From Fig. 2 it is seen that the two species do not exist independently, but are related to each other. If they were independent,

Can. J. Chem. Downloaded from www.nrcresearchpress.com by 210.87.254.5 on 09/05/12
For personal use only.

TABLE I

Paramagnetic species assigned by various authors to the e.s.r. lines from zinc oxide

Authors	Preparation of sample	T_m*	l_1, $g = 1.960$	l_2, $g = 2.004$
Schneider *et al.* (1)	Doped with Zn and Cd	77 °K	Zni^+	
Golubev and Evdokimov (2)	Grinding	20 °C	Less affected by grinding, bulk species	Intensified by grinding, surface species
Geisler and Simmons (3)	Heated to 975 °C	77 °K	Ultraviolet-insensible center	
Baranov *et al.* (4)	Irradiated with 365 mμ light	77 °K	Photodesorption of O from the surface	Chemisorption of atomic O with one unpaired electron
Kokes (5, 9)	Pretreatment at 550 °C, doped with Li, Al, and Ga, some are calcined	24 °C	Conduction electron, bulk species	Adsorbed oxygen radical (9)†
Sancier and Freund (10)	Pretreatment at 550 °C, adsorption of O_2 and CO	20 °C	Decreased with O_2, increased with CO. Ionized donor, mobile electron or oxygen ion vacancy, surface or bulk	Increased with O_2. Various results with CO. O_3^- or O_2^- adsorbed
Ueda, Todo, and Kotera (14)	Adsorption of SO_2, CS_2, and acetonitrile, heated to 300 °C	20 °C	Near surface. Stronger with gamma irradiation	

*Temperature of measurements.
†Showing a part of the spectrum reported in ref. 8.

Can. J. Chem. Downloaded from www.nrcresearchpress.com by 210.87.254.5 on 09/05/12
For personal use only.

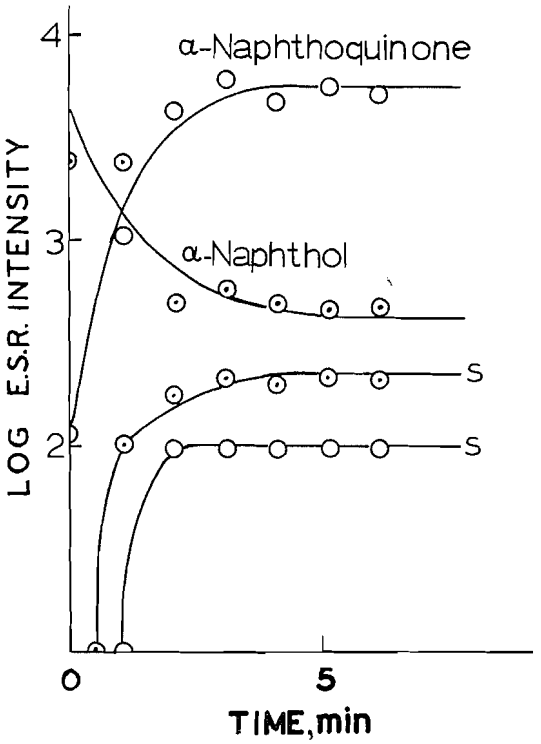

FIG. 1. The e.s.r. intensity of ZnO treated with naphthol and naphthoquinone. The intensity is measured by the height in mm of the first derivative of the absorption curve on recording paper, when the original signal is amplified by 80 dB in current. The curves with the marks s indicate the intensity of I_1, or I_1, while those without it indicate that of I_2, or I_2. The time (min) is the time length during which the specimen is heated at 300 °C.

all the curves, as in Fig. 2, would be (at least in some portion of them) parallel to either the ordinate or the abscissa. Almost all of them are not. In Fig. 4 the equilibrium points for similar compounds, i.e. some aromatic quinones and those compounds which may be formed by hydrogenation of these quinones, lie along the same straight line drawn on a logarithmic plane.

From Fig. 4 it is shown that $\log I_1 + \log I_2 = 5$ is satisfied for aromatic quinones and related compounds. Therefore,

$$[1] \qquad I_1 I_2 = 10^5$$

is a good approximation for the two paramagnetic species in these zinc oxide mixtures. Since $I = 1$ (in mm on recording paper) roughly corresponds to $[R] = 10^{12}$ (spins/ml) and $I = 10^{6.2}$ to $[R] = 7.5 \times 10^{20}$, [1] can be written as

$$[1'] \qquad [R_1][R_2] = 10^{30.7}\ (\text{spins/ml})^2.$$

[1'] suggests that R_1 and R_2 are competing with each other. Experimentally $[R_1]$ does not exceed 10^{16}, while $[R_2]$ can be as high as 10^{20}, or perhaps more. $[R_1][R_2]$, which is constant, is similar to a solubility product constant of a cation and an anion of a difficultly soluble salt in aqueous solution. Therefore, it is quite probable that an overall reaction between R_1 and R_2 leads to stable species S and T.

$$[2] \qquad R_1 + R_2 \rightleftharpoons S + T$$

This overall reaction is greatly enhanced with an additive, e.g. an aromatic quinone. If the unpaired electron observed does not belong mainly to the additive molecules, which will be discussed later, the additive will behave as an electron carrier. Therefore, [2] should be divided into two parts.

$$[3] \qquad S + A^+ \rightleftharpoons R_1 + A;\ K_1$$

$$[4] \qquad T + A \rightleftharpoons R_2 + A^+;\ K_2,$$

where K_1 and K_2 denote the equilibrium constants, S and T denote those species which yield R_1 and R_2 by a charge transfer, and A stands for an additive molecule. From [1'], [3], and [4],

$$K_1 K_2 [S][T] = [R_1][R_2] = 10^{30.7}$$

is obtained.

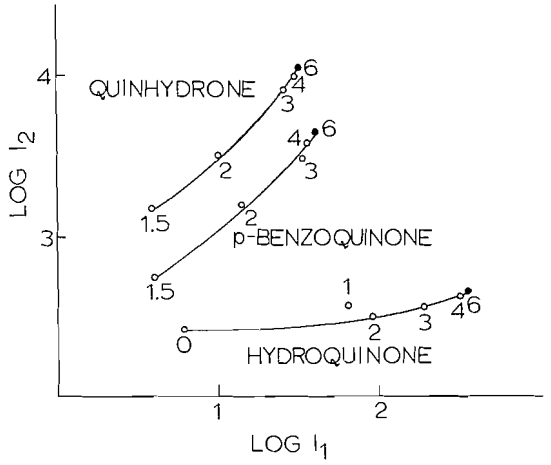

FIG. 2. The e.s.r. intensity of ZnO treated with quinhydrone, *p*-benzoquinone, and hydroquinone. The figure is essentially the same as Fig. 1, but shown on the I_1–I_2 plane. The number under each circle indicates the time length (min) of heating at 300 °C. The black circle indicates the final point observed and shows the equilibrium point.

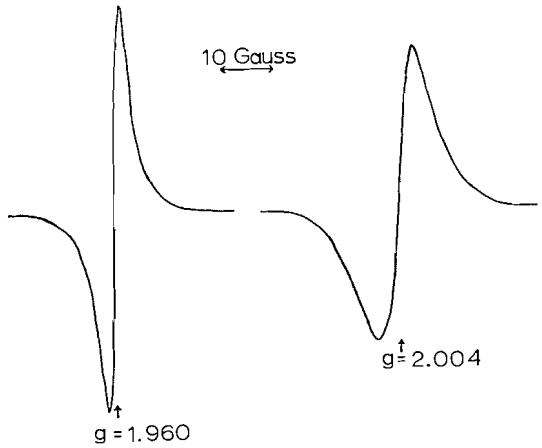

FIG. 3. The shapes of the e.s.r. spectra, l_1 ($g = 1.960$) and l_2 ($g = 2.004$) observed at 20 °C, with 100 kc/s modulation frequency and width of 500 mG. Magnetic field increases from right to left.

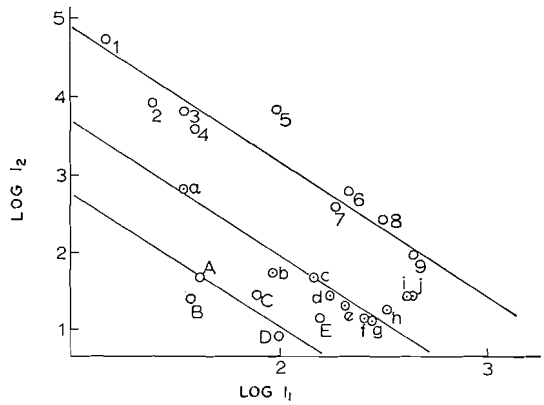

FIG. 4. The e.s.r. intensities of ZnO with various additives and after equilibrium: 1, β-naphthoquinone; 2, quinhydrone; 3, β-naphthol; 4, *p*-benzoquinone; 5, α-naphthoquinone; 6, α-naphthol; 7, hydroquinone; 8, 9,-10-anthraquinone; 9, naphthalene; *a*, resorcinol; *b*, anthracene; *c*, benzophenone; *d*, phenanthrene; *e*, phthalic anhydride; *f*, diphenylamine; *g*, 1,3,5-triphenylimidazole; *h*, benzoine; *i*, pyrene; *j*, anthrone; A, azobenzene; B, triphenylimidazolyl; C, biphenyl; D, acetic anhydride; E, tetramethylphenylenediamine.

Discussion

Various authors have tried to explain the e.s.r. signal from zinc oxide. Their data are summarized in Table I. Experimental conditions varied from author to author. Some took spectra at 77 °K. This was necessary because after prolonged heating of zinc oxide in vacuum and at higher temperatures, e.s.r. measurements are very difficult due to some electrical conductivity caused in zinc oxide. In the present work, however, it was possible to measure all the samples at room temperature. Therefore, the e.s.r. signals observed in some studies at 77 °K with g factors of 1.960 or 2.004 might have been caused by some other species. The g factors of some oxygen-containing radicals depend on temperature. Therefore, direct comparison between the results obtained at 20 °C and 77 °K might not be correct.

The present authors have observed (14) the effect of SO_2 on the e.s.r. of zinc oxide. In that study it was found that oxygen greatly reduces the l_1 signal from SO_2. This fact agrees with the findings of Baranov and Sancier, as shown in Table I.

The purpose of the study of zinc oxide, particularly by means of the e.s.r. method, is to find the location of the unpaired electron formed during the experimental procedures. In the present case the word "location" will mean two things. First, the macroscopic part of the crystal particles, surface or bulk, is meant. Secondly, the atomic orbital or molecular orbitals which are occupied by unpaired electrons are meant. The effect of oxygen on R_1 formed by SO_2 was very fast (14). This may indicate that R_1 is located mainly on or close to the surface. However, one of the main conclusions in the present study is that R_1 and R_2 do not have independent existences. Therefore, it will be more exact to say that either one or both exist on or close to the surface.

The additives which are electrophilic give stronger l_1 while the additives which have tendencies to donate an electron to other molecules give stronger l_2. Therefore it is very probable that an oxidation yields R_1, while a reduction yields R_2. Zni (interstitial) and O^{2-} are to be considered as the species to be oxidized, namely S in [3]. Since the oxidation of O^{2-} by A^+ to form O^- and A is very unlikely, Zni is assumed to be S. In the case of [4], rather rare species such as adsorbed O or O_2 cannot be considered as T, since the e.s.r. intensity of R_2 is very strong; T should be something which is abundant. Therefore Zn^{2+} or Zn^{2+} + (several oxygen anions in crystal lattice) would be suitable for T. The conclusion is, therefore, that Zni, Zn^{2+} or $ZnO^{-2(\nu-1)}$, Zni^+, and Zn^+ or $ZnO^{-(2\nu-1)}$ (where ν denotes some integer) are S, T, R_1, and R_2 respectively.

Can. J. Chem. Downloaded from www.nrcresearchpress.com by 210.87.254.5 on 09/05/12
For personal use only.

Can. J. Chem. Downloaded from www.nrcresearchpress.com by 210.87.254.5 on 09/05/12
For personal use only.

No description has appeared in the literature in which Zn^+ ion in a single crystal matrix was observed by e.s.r. methods. Thus, it is not easy to conclude the existence of Zni^+ and Zn^+ from the present polycrystal e.s.r. data. The only information is the g factor. Since zinc has $3d^{10}4s^2$ configuration, Zn^+ will have $3d^{10}4s^1$ or more likely $3d^94s^2$ configuration. The latter configuration is the same as Cu^{2+} ($3d^9$), which is in a ^2D state. The g factor of the e.s.r. of Cu^{2+} ion is in a wide range (12). If the counter anion is benzoate or tartarate ion, the g factor of a powder specimen is 1.97 (11). This fact, however, does not allow us to say that Zni^+ can have a g factor of 1.960 in the polycrystalline state, because the line widths of the e.s.r. lines from Cu^{2+} ion are enormously large compared with those of the present e.s.r. lines. The different spin densities on the zinc atom between R_1 and R_2 will account for the difference between the g factors of l_1 and l_2.

The conclusion for R_1 in the present discussion does not differ much from those by the other authors. However, the conclusion for R_2 in this work is different. The g factor of the peroxy radicals on ZnO reported by Lunsford and Jayne (8) has three principal values, 2.051, 2.0082, and 2.0020. In the polycrystalline state the main resonance appears around $g = 2.004$. Some authors (9) overlooked the weak resonance at $g = 2.051$. However, the present e.s.r. line, l_2, Fig. 2 right, is clearly different from the e.s.r. line of the peroxy radical. Only the g factor for the main resonance point coincides. The adsorbed oxygen species are, by this reason too, eliminated from the possible species for R_2. R_2 might be Zn^+, but there is no evidence that the unpaired electron is localized in the Zn^+ orbital only. Probably R_2 will be shown to be $(ZnO_v)^{-(2v-1)}$, where v is an integer between 1 and 6 or so.

The possibilities that the unpaired electron, especially for R_2, is not in zinc oxide but in the additive molecule or its fragment can be ruled out for the following reason. If it were, it would be very hard to understand the existence of a paramagnetic organic species so stable and so concentrated at 300 °C. It is also unlikely that the additive decomposes at 300 °C. The fragments thus formed would react with zinc oxide to form, say, OH radical or carbonized fragments. Such species cannot be in equilibrium with Zni^+. Also l_2 can be found in a specimen without any heat treatment and the e.s.r. intensity is reduced by heat treatment if the additive is α-naphthol, as shown in Fig. 1.

The sensitization of the photoconductivity of zinc oxide with phthalic anhydride (13) is also well explained by Zni; Zni forms Zni^+ and e^-, the latter being the charge carrier. In the present study, it is shown that phthalic anhydride intensifies l_1 rather than l_2. These two results agree with each other because l_1 is due to R_1 which is concluded to be Zni^+.

Since (Zn^{2+}) is 2×10^{22} (ions/ml), if 2.5 is used for the apparent density of ZnO powder in the sample tube,

$$K_1K_2(\text{Zni}) = 2.5 \times 10^8 \text{ (spins/ml)}$$

is obtained. Since the upper limit of (Zni^+) is 10^{16}, the available amount of Zni is more than 10^{16}. Therefore,

$$[5] \qquad K_1K_2 \leqslant 2.5 \times 10^{-8}$$

is obtained for aromatic quinones and related compounds at 300 °C.

Since K_1 is for the oxidation of Zni while K_2 is for the reduction of Zn^{2+} (or something including it), it will be true that when K_2 is large, K_1 is small and vice versa. As a result the product K_1K_2 is kept constant for the similar type of additive compounds as shown in [5].

Some authors used a few differently prepared zinc oxide samples. This would not make any appreciable difference in the present study since the magnitude of the e.s.r. intensities is so large in the present samples.

It may be desired to interpret the value $(K_1 \times K_2)$ or K_2 as a function of such quantities as triplet energy level, redox-potential, or half-wave oxidation potential of each compound. Some of them may explain part of the present results, but a complete and consistent understanding of the present results by means of any of these factors has not been possible.

Acknowledgments

The author wishes to thank Norman Shanks who kindly read the manuscript.

1. J. SCHNEIDER and A. RAEUBER. Z. Naturforsch. **16a**, 712 (1961). J. SCHNEIDER and O. SCHIRMER. Z. Naturforsch. **18a**, 20 (1963).
2. V. B. GOLUBEV and B. EVDOKIMOV. Zh. Fiz. Khim. **38**, 477 (1964).

3. C. H. GEISLER and G. L. SIMMONS. Phys. Letters, **11**, 111 (1964).
4. E. V. BARANOV, V. E. KHOLOMOGOROV, and A. N. TERENIN. Dokl. Akad. Nauk SSSR, **146**, 125 (1962).
5. R. J. KOKES. J. Phys. Chem. **66**, 99 (1962).
6. Y. FUJITA and T. KWAN. Private communication.
7. M. SEDAKA and T. KWAN. Bull. Chem. Soc. Japan, **38**, 1414 (1965).
8. J. H. LUNSFORD and J. P. JAYNE. J. Chem. Phys. **44**, 1487 (1966). P. H. KASAI. J. Chem. Phys. **43**, 3322 (1965).
9. R. J. KOKES. *In* 3rd International Congress on Catalysis. *Edited by* W. M. H. Sachtler. North Holland Publ. Co., Amsterdam. 1965. p. 484.
10. K. M. SANCIER and T. FREUND. J. Catalysis, **3**, 293 (1964).
11. F. W. LANCASTER and W. GORDY. J. Chem. Phys. **19**, 1187 (1951); **20**, 740 (1952).
12. G. E. PAKE. Paramagnetic resonance. W. A. Benjamin, Inc., New York. 1962. p. 189.
13. E. INOUE, H. KOKADO, and T. YAMAGUCHI. J. Phys. Chem. **69**, 767 (1965).
14. H. UEDA, N. TODO, and Y. KOTERA. To be published.

Can. J. Chem. Downloaded from www.nrcresearchpress.com by 210.87.254.5 on 09/05/12
For personal use only.

Cinnamaldehydeanil complexes of rhodium(I)

JUNG W. KANG AND P. M. MAITLIS[1]
Department of Chemistry, McMaster University, Hamilton, Ontario
Received November 3, 1967

Cinnamaldehydeanils reacted readily with $[Rh(CO)_2Cl]_2$ under mild conditions to form $Rh(CO)_2ClL$ (**2**), where L is PhCH=CH—CH=NPh or PhCH=CH—CH=NTo (Ph = phenyl, To = *p*-tolyl). Under vigorous conditions $RhCl(CO)L_2$ (**3**) was isolated from this reaction. From the infrared and proton magnetic resonance spectra the ligands, L, appear only to coordinate through the nitrogen atom to the rhodium.

Cinnamaldehyde reacted with $Rh(CO)_2Cl$(*p*-toluidine) to give (**2***b*) in good yield. Heating (**2**) in boiling benzene afforded (**3**) and Rh metal. Triphenylphosphine reacted with (**2**) or (**3**) to form $RhCl(CO)(PPh_3)_2$. The reaction of (**3**) with 1,5-cyclooctadiene gave $(1,5\text{-}C_8H_{12})RhClL$, which was also prepared by reaction of $(1,5\text{-}C_8H_{12}RhCl)_2$ with L.

Some electronegatively substituted acetylenes reacted with (**3**) to yield the stable acetylene complexes $(RC{\equiv}CR)RhClL_2$ (R = CF_3, COOMe).

Canadian Journal of Chemistry, **46**, 897 (1968)

Introduction

Recently Otsuka *et al.* (1) showed that enimines (RCH=CHCH=NR′) reacted with iron carbonyls to give complexes of the type $(RCH{=}CHCH{=}NR')Fe(CO)_3$ where the diene portion was coordinated to the metal. In the course of some investigations on the chemistry of chlorodicarbonylrhodium dimer, (**1**), we became interested in the reactions of enimines and (**1**). This paper describes our results on reactions of (**1**) and cinnamaldehydeanil (PhCH=CHCH=NPh) and cinnamaldehyde *p*-toluidineanil (PhCH=CHCH=NTo).

Results

Chlorodicarbonylrhodium dimer (**1**) reacted readily with cinnamaldehydeanil in ether at 25° to give a 92% yield of the complex (**2***a*). Under more vigorous conditions (benzene–hexane at 80°), the bis-complex (**3***a*) was obtained in 93% yield. The complex (**2***a*) also disproportionated when it was refluxed in benzene at 80° giving rhodium metal and the bis-complex (**3***a*) in 41% yield.

The same reaction also occurred when cinnamaldehyde *p*-toluidineanil was used in place of cinnamaldehydeanil, and the complexes (**2***b*) and (**3***b*) were formed in this way.

Cinnamaldehyde also reacted in benzene at 25° with chlorodicarbonyl(*p*-toluidine)rhodium to give the mono-complex (**2***b*) in nearly quantitative yield.

Triphenylphosphine reacted with the bis-complexes (**3**) in benzene at 80° to give an 83% yield of chlorocarbonylbis(triphenylphosphine)-rhodium (**6**) (2). In contrast, one cinnamaldehydeanil ligand and carbon monoxide were eliminated from (**3***a*) on treatment with 1,5-cyclooctadiene; an 82% yield of chloro(1,5-cyclooctadiene)(cinnamaldehydeanil)rhodium (**4***a*) was isolated. The same compound was obtained by heating chloro(1,5-cyclooctadiene)-rhodium dimer (**5**) (3) with cinnamaldehydeanil. Treatment of the 1,5-cyclooctadiene complexes (**4**) with CO at 1 atm and 25° gave nearly quantitative yields of the mono-complexes (**2**).

On heating the complexes (**3**) with dimethyl acetylenedicarboxylate at 100°, only the carbonyl was substituted, and the dimethyl acetylene-dicarboxylaterhodium complexes (**7**) were obtained. The yields in this reaction were poor and a better method for preparing (**7**) was by treatment of (**3**) with dimethyl acetylenedicarboxylate in tetrahydrofuran in the presence of benzoyl azide. An 87% yield of (**7***a*, R = CH_3OOC) was obtained by this reaction which was also extended to the preparation of the hexafluoro-2-butyne analogue (**8***a*, R = CF_3) in high yield.

On treatment of the acetylene complexes (**7**) and (**8***a*) with carbon monoxide at 1 atm and 25°, the bis-complexes (**3**) were reformed.

Discussion

Otsuka *et al.* (1) have shown that the cinnamaldehydeanil ligand bonds both through the diene and the nitrogen in complexes such as (**9**)

[1]Fellow of the Alfred P. Sloan Foundation and author to whom any correspondence should be addressed.

Can. J. Chem. Downloaded from www.nrcresearchpress.com by 210.87.254.5 on 09/05/12
For personal use only.

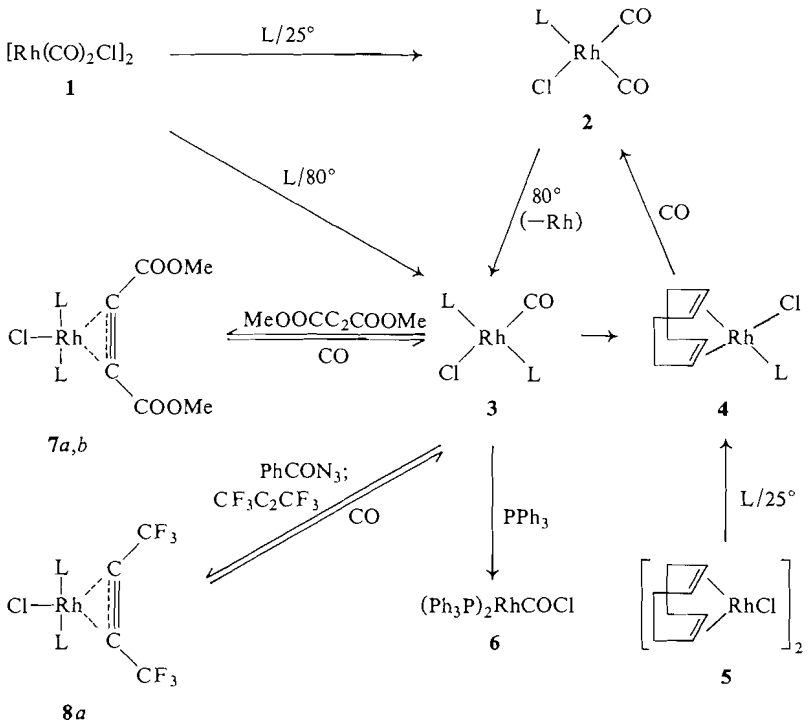

$ToNH_2Rh(CO)_2Cl + PhCH{=}CHCHO \rightarrow$ **2***b*

[*a*, L = PHN=CHCH=CHPh; *b*, L = ToN=CHCH=CHPh; Ph = phenyl, To = *p*-tolyl]

and have suggested the structure to be similar to that of π-butadienetricarbonyliron (**10**) (4). This was shown by the absence of the characteristic

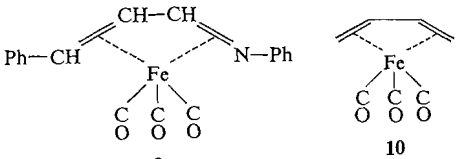

9 **10**

$\nu_{C=C}$ and $\nu_{C=N}$ bands in (**9**) which occurred in the free ligand at 1621 and 1571 cm^{-1}. Instead, bands were found at 1475 and 1429 cm^{-1}, which were assigned to $\nu_{C=C}$ and $\nu_{C=N}$ when co-ordinated to iron. The p.m.r. spectrum of the free ligand, $Ph.CH_a{=}CH_b.CH_c{=}N.Ph$, in CCl_4 solution showed, in addition to phenyl resonances, a quintet at 1.88 and signals at 2.55 and 3.00 τ which were assigned to H_c and H_a or H_b. In the complex (**9**), resonances observed at 2.60 (and 3.30), 4.35, and 6.65 τ were assigned to H_c, H_b, and H_a respectively. Each diene proton therefore suffered a strong up-field shift on complexing to the metal.

The complexes which we have prepared here do not appear to be of this type. In all the complexes of the anil ligands (**2**), (**3**), (**4**), (**7**), and (**8**), bands in the infrared spectra characteristic of the C=C and C=N bonds at ca. 1620 and 1570 cm^{-1} were clearly observed (Table I). The p.m.r. spectra of (**2**) and (**3**), as in the case quoted above, were very difficult to interpret owing to the presence of resonances due to the phenyl protons in the region under discussion. We were, however, able to observe a triplet at 1.82 τ in (**2***a*) and a quintet at 1.32 and two doublets at 1.75 and 1.90 τ in (**3***a*); the latter, following Otsuka *et al.* (1), we ascribe to the diene protons H_c, H_b, and H_a. In neither of these complexes were any resonances to higher field than the phenyl protons (multiplets, 2.1–2.85 τ) observed, as were seen in the complex (**9**).

Both the infrared and p.m.r. spectra of (**2***a*) and (**3***a*) therefore point to a bonding between the ligand and the metal which does not involve the diene function of the ligand; only the nitrogen appears to coordinate with the metal. The spectra of (**2***b*) and (**3***b*) are also consistent with

Can. J. Chem. Downloaded from www.nrcresearchpress.com by 210.87.254.5 on 09/05/12
For personal use only.

TABLE I

Infrared spectra* (cm^{-1})

Compound	ν_{CO}	$\nu_{C=C}$	ν_{CO_2R}	Ligand $\nu_{C=C}$,$\nu_{C=N}$
$C_6H_5CH{=}CH{-}CH{=}N{-}C_6H_5$				1620 (vs) 1570 (vs)
$C_6H_5CH{=}CH{-}CH{=}N{-}C_6H_4CH_3(p)$				1620 (vs) 1575 (vs)
$Rh(CO)_2ClL$ (*2a*)	2075 (vs) 2000 (vs)			1620 (vs) 1565 (vs)
$Rh(CO)_2ClL$ (*2b*)	2080 (vs) 1955 (vs)			1630 (vs) 1580 (vs)
$RhCl(CO)L_2$ (*3a*)	1950 (vs)			1620 (vs) 1570 (vs)
$RhCl(CO)L_2$ (*3b*)	1950 (vs)			1625 (vs) 1575 (vs)
$RhCl(C_8H_{12})L$ (*4a*)				1620 (vs) 1565 (vs)
$RhCl(C_8H_{12})L$ (*4b*)				1625 (vs) 1575 (vs)
$RhClL_2(CH_3O_2CC{\equiv}CCO_2CH_3)$ (*7a*)		1870 (s)	1690 (vs)	1620 (vs) 1575 (vs)
$RhClL_2(CH_3O_2CC{\equiv}CCO_2CH_3)$ (*7b*)		1870 (s)	1685 (vs)	1625 (vs) 1575 (vs)
$RhClL_2(F_3CC{\equiv}CCF_3)$ (*8a*)		1910 (s)		1620 (vs) 1585 (vs)

*All spectra reported are for KBr pellets. Intensities of spectral bands are designated by vs (very strong), s (strong).

this. This is also shown by the stoichiometries of (**2**), (**3**), and (**4**) which clearly point to L functioning as monodentate ligands in square planar rhodium(I) complexes.

The ligand can be arranged about the metal in any one of four different ways

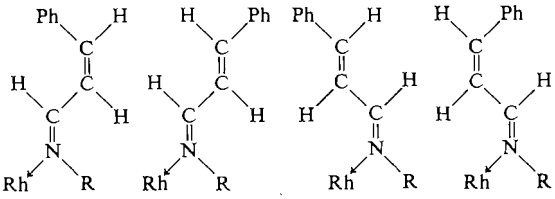

and it is not possible to decide which of these conformations are present in the complexes.

The presence of two terminal metal carbonyl bands in the infrared spectra of complexes (**2**) [Table I] suggests a *cis*-configuration for them.

Lawson and Wilkinson (5) have observed that amines will also cleave the chlorine bridges in (**1**); however, mono-adducts $Rh(CO)_2ClNR_3$ were the usual products and they did not find any cases where one carbonyl was substituted by an amine. Even bipyridyl acted as a monodentate ligand towards (**1**).

In contrast to this behavior the enimine ligands, L, will also, under more vigorous conditions, replace one CO to form the bis-complexes (**3**). The ν_{CO}'s for the bis-complexes (**3**) at 1950 cm^{-1} are close to that reported for $(Ph_3P)_2RhCOCl$ (**6**) (1970 cm^{-1}) (6) and suggest that back-bonding from the metal to anti-bonding orbitals of the enimine ligand must occur to only a slightly smaller extent to that which occurs in the triphenylphosphine complex (**6**). It appears, therefore, that in their properties towards Rh(I) the anil ligands lie somewhere between amines which form only mono-complexes and phosphines which form only bis-complexes such as (**6**) (7). The complexes (**3**) appear more labile than the analogous phosphine complexes; thus one anil and the CO group are replaced by 1,5-cyclooctadiene, while both anils are replaced by triphenylphosphine. In the 1,5-cyclooctadiene complex (**4**), however, it is the diene rather than the anil which is replaced by carbon monoxide.

The reactions of the complexes (**3**) with acetylenes bearing strongly electron-withdrawing groups such as $COOCH_3$ and CF_3 are interesting. When (*3a*) was heated with dimethyl acetylenedicarboxylate, the CO group was replaced by the acetylene to give a low yield of the acetylene complex (*7a*, R = $COOCH_3$). A much better method of preparing this complex was by reaction of the acetylene with (*3a*) in the presence of benzoyl azide. In the iridium series, Collman and Kang (8) showed that the complex $(Ph_3P)_2$-Ir(CO)Cl on treatment with acid azides gives the

Can. J. Chem. Downloaded from www.nrcresearchpress.com by 210.87.254.5 on 09/05/12
For personal use only.

nitrogen complex $(Ph_3P)_2Ir(N_2)Cl$ which reacted readily with acetylenes (ac) to give the complexes $(Ph_3P)_2Ir(ac)Cl$ by substitution of molecular nitrogen. We have not as yet been able to prepare the analogous rhodium nitrogen complex (**11**), but it can be assumed to be an intermediate in this reaction.

$$L_2Rh(CO)Cl \xrightarrow{PhCON_3} [L_2Rh(N_2)Cl] \xrightarrow{RC\equiv CR} (7) \text{ or } (8a)$$
$$[R = COOCH_3, CF_3]$$
11

Using this reaction we were also able to prepare the hexafluoro-2-butyne complex (**8***a*, R = CF_3) in high yield.

The acetylene complexes showed the presence of a modified $\nu_{C\equiv C}$ at 1910 cm^{-1} (**8***a*) and 1870 cm^{-1} (**7***a*). This lowering of $\nu_{C\equiv C}$ from that found in the free acetylenes, 2300 cm^{-1} for $CF_3C\equiv CCF_3$ (9) for example, is a characteristic of metal–acetylene complexes (10) and has been used as a measure of the strength of the metal–acetylene bonding. By comparison with other metal–hexafluoro-2-butyne complexes (10), the bonding in (**8***a*) must be considered rather weak therefore, though the $\Delta\nu_{C\equiv C}$ [$\nu_{C\equiv C}$(free acetylene) — $\nu_{C\equiv C}$(complexed acetylene)] observed of nearly 400 cm^{-1} points to quite a marked decrease in the C≡C bond order in (**8***a*). It is of interest to note that $\nu_{C\equiv C}$ in (**8***a*) is quite close to that observed in $(Ph_3P)_2RhCl(CF_3C_2CF_3)$ (1917 cm^{-1}) (**2**) and this again suggests that electronically the cinnamaldehydeanil ligand has a similar effect to triphenylphosphine in these complexes. Furthermore, Mays and Wilkinson (11) noted that the acetylene in $(Ph_3P)_2RhCl(CF_3C_2CF_3)$ was easily displaced by CO; both our acetylene complexes (**7***a*) and (**8***a*) underwent similar reactions under very mild conditions.

These complexes are obviously of interest in connection with the catalytic properties of many d^8 complexes, particularly of Rh(I). This aspect is currently under investigation.

Experimental

Chlorodicarbonylrhodium dimer (12), chlorodicarbonyl(*p*-toluidine)rhodium (5), cinnamaldehydeanil (13), and cinnamaldehyde-*p*-toluidineanil (14) were prepared by known procedures.

All melting points were determined on a capillary melting point apparatus (Thomas Hoover) and are uncorrected. Infrared spectra were measured on a Beckman model IR-5 spectrophotometer, p.m.r. spectra were measured in $CDCl_3$ solution on a Varian A 60 spectrometer (using tetramethylsilane as internal reference), and ^{19}F n.m.r. spectra were measured on a Varian DP 60 spectrometer using trifluorotoluene as internal standard. Molecular weights were determined in chloroform on a Mechrolab osmometer.

Chlorodicarbonyl(cinnamaldehydeanil)rhodium (2a)

To a solution of 300 mg (0.77 mmole) of chlorodicarbonylrhodium dimer in 5 ml of ether was added a solution of 350 mg (1.70 mmoles) of cinnamaldehydeanil in 5 ml of ether. The pale-yellow solution was stirred at 25° for 10 min under nitrogen and then the solvent was removed under vacuum to give pale-yellow crystals. Recrystallization of the product from ether–hexane afforded 290 mg (92%) of chlorodicarbonyl(cinnamaldehydeanil)rhodium (**2***a*) as yellow crystals, m.p. 120–121° (decomp.).

Anal. Calcd. for $C_{17}H_{13}ClNO_2Rh$: C, 50.81; H, 3.24; Cl, 8.83; N, 3.47; mol. wt., 401. Found: C, 50.93; H, 3.21; Cl, 8.62; N, 3.64; mol. wt., 384.

Chlorodicarbonyl(cinnamaldehyde-p-toluidineanil)rhodium (2b)

The yellow crystalline complex (**2***b*) was prepared in the manner described for (**2***a*) above, yield 305 mg (95%), m.p. 123–125° (decomp.).

Anal. Calcd. for $C_{18}H_{15}ClNO_2Rh$: C, 51.99; H, 3.61; Cl, 8.54; N, 3.35; O, 7.86; Rh, 24.79. Found: C, 51.84; H, 3.66; Cl, 8.39; N, 3.37; O, 7.86; Rh, 24.61.

Chlorocarbonylbis(cinnamaldehydeanil)rhodium (3a)

To a solution of 500 mg (1.29 mmoles) of chlorodicarbonylrhodium dimer in 20 ml of hexane was added a solution of 1.2 g (5.8 mmoles) cinnamaldehydeanil in 10 ml of benzene. The solution was refluxed under nitrogen for 15 h then allowed to cool; the salmon-pink crystals which formed were collected on a filter and washed with hexane and ether to yield 700 mg (93%) of the pure complex (**4***a*), m.p. 172–174° (decomp.).

Anal. Calcd. for $C_{31}H_{26}ClN_2ORh$: C, 63.02; H, 4.48; Cl, 5.97; N, 4.82; mol. wt., 581. Found: C, 64.08; H, 4.48; Cl, 6.10; N, 4.82; mol. wt., 555.

Chlorocarbonylbis(cinnamaldehyde p-toluidineanil)-rhodium (3b)

The salmon-pink crystalline complex was prepared in the same manner as for (**3***a*) above; yield 720 mg (92%), m.p. 177–179° (decomp.).

Anal. Calcd. for $C_{33}H_{30}ClN_2ORh$: C, 65.08; H, 4.93; mol. wt., 609. Found: C, 65.57; H, 5.07; mol. wt., 579.

Reaction of Chlorodicarbonyl(p-toluidine)rhodium with Cinnamaldehyde to Give (2b)

To a solution of 100 mg (0.33 mmole) of chlorodicarbonyl(*p*-toluidine)rhodium in 5 ml of benzene was added a solution of 100 mg (0.75 mmole) of cinnamaldehyde in 2 ml of benzene. The pale-yellow solution was stirred at 25° for 30 min under nitrogen, then the solvent was removed under vacuum to leave a pale-yellow oily residue. Recrystallization of the crude product from ether–hexane afforded 95 mg (71%) of pure (**2***b*) as yellow crystals, m.p. 123–125° (decomp.). The infrared spectrum of this complex was identical with that of an authentic sample.

Can. J. Chem. Downloaded from www.nrcresearchpress.com by 210.87.254.5 on 09/05/12
For personal use only.

Can. J. Chem. Downloaded from www.nrcresearchpress.com by 210.87.254.5 on 09/05/12
For personal use only.

Reaction of Chlorocarbonylbis(cinnamaldehydeanil)-rhodium (3a) with Triphenylphosphine

A mixture of 100 mg (0.17 mmole) of (**3***a*) and 500 mg (1.9 mmoles) of triphenylphosphine in 20 ml of benzene was stirred at 80° for 1 h. The yellow solution was then evaporated under vacuum, and the residue washed with ether. Recrystallization of the product from benzene–methanol afforded 98 mg (83%) of $(Ph_3P)_2Rh(CO)Cl$ (**6**) as yellow crystals, m.p. 195–198° (decomp.). The infrared spectrum of this complex was identical with that of an authentic sample.

Chloro(cinnamaldehydeanil)(1,5-cyclooctadiene)rhodium (4a)

A suspension of 200 mg of chlorocarbonylbis(cinnamaldehydeanil)rhodium (**3***a*) in 5 ml of benzene was refluxed with 1 ml of 1,5-cyclooctadiene under nitrogen for 5 h. The orange solution was cooled, and the solvent evaporated to dryness under vacuum. Recrystallization of the crude product from benzene–hexane afforded 135 mg (74%) of the complex (**4***a*) as orange-yellow crystals, m.p. 146–150° (decomp.), containing benzene of crystallization.

Anal. Calcd. for $C_{23}H_{25}ClNRh.\frac{1}{2}C_6H_6$: C, 63.36; H, 5.73; Cl, 7.19; N, 2.84. Found: C, 63.88; H, 6.00; Cl, 6.90; N, 2.94.

*Reaction of Chloro(1,5-cyclooctadiene)rhodium Dimer (**5**) with Cinnamaldehydeanil to Give (4a)*

The mixture of 100 mg (0.2 mmole) of chloro(1,5-cyclooctadiene)rhodium dimer and 207 mg (1.0 mmole) of cinnamaldehydeanil in 10 ml of benzene was stirred at 25° for 1 h. The orange solution was then evaporated to dryness under vacuum, and the residue washed with ether. Recrystallization of this crude product from benzene–hexane afforded 80 mg (87%) of the complex (**4***a*) as orange-yellow crystals, m.p. 146–150° (decomp.). The infrared spectrum of this complex was identical with that of an authentic sample (**4***a*).

Reaction of Chloro(cinnamaldehydeanil)(1,5-cyclooctadiene)rhodium (4a) with CO

Carbon monoxide was bubbled into a suspension of 100 mg of the complex (**4***a*) in 10 ml of hexane for 1 h. The pale-yellow solution was then allowed to crystallize at −20° under CO to give 86 mg (95%) of (**2***a*). The infrared spectrum of (**2***a*) was identical with that of an authentic sample.

Chlorobis(cinnamaldehydeanil)(dimethyl acetylenedicarboxylate)rhodium (7a)

Method A

A suspension of 500 mg of the complex (**3***a*) in 3 ml of dimethyl acetylenedicarboxylate was heated at 100° with magnetic stirring under nitrogen for 5 h. The reaction mixture was cooled and the orange-yellow product collected on a filter, washed with ether, and dried in air. Recrystallization of the crude product from tetrahydrofuran–hexane afforded 235 mg (31%) of (**7***a*) as orange-yellow crystals, m.p. 165–167° (decomp.).

Anal. Calcd. for $C_{36}H_{32}ClN_2O_4Rh$: C, 62.20; H, 4.60; Cl, 5.11; N, 4.03; mol. wt., 695. Found: C, 62.07; H, 4.77; Cl, 5.04; N, 4.02; mol. wt., 686.

The p.m.r. spectrum showed, in addition to resonances due to the anil ligand, a singlet at 6.75 τ due to the methyl protons of complexed dimethyl acetylenedicarboxylate.

Method B

To a suspension of 500 mg (0.86 mmole) of the complex (**3***a*) and 500 mg (3.5 mmoles) of dimethyl acetylenedicarboxylate in 20 ml of tetrahydrofuran was added a solution of 200 mg (1.46 mmoles) of benzoyl azide in 5 ml of tetrahydrofuran at −10°. The reaction mixture was stirred at this temperature under nitrogen for 30 min, then the yellow solution was heated at 50° for 1 h. The solvent was removed under vacuum and the yellow oily residue was washed with ether to give an orange-yellow solid.

Recrystallization of this solid from tetrahydrofuran–hexane afforded 520 mg (87%) of pure (**7***a*), as orange-yellow crystals, m.p. 165–167° (decomp.). The infrared and p.m.r. spectra of this complex were identical with that of a sample as prepared above.

Chlorobis(cinnamaldehyde p-toluidineanil)(dimethyl acetylenedicarboxylate)rhodium (7b)

The orange-yellow crystalline complex was prepared in the manner outlined above (method B); yield 510 mg (88%), m.p. 176–179° (decomp.).

Anal. Calcd. for $C_{38}H_{36}ClN_2O_4Rh$: C, 63.11; H, 4.99; mol. wt., 723. Found: C, 63.26; H, 5.17; mol. wt., 700.

The p.m.r. spectrum showed, in addition to phenyl and olefinic proton resonances, a singlet at 6.62 τ due to the methyl protons of the ester and a singlet at 7.50 τ due to the *p*-tolyl methyl protons with relative intensities 1:1.

Chlorobis(cinnamaldehydeanil)(hexafluoro-2-butyne)-rhodium (8a)

The reaction was conducted in a 50 ml three-necked flask fitted with a dry-ice reflux condenser and a nitrogen inlet. The flask was charged with 500 mg (0.86 mmole) of (**3***a*), 200 mg (3.5 mmoles) of benzoyl azide, and 20 ml of tetrahydrofuran. The solution was stirred at −78° in a dry ice – acetone bath under nitrogen. Hexafluoro-2-butyne (5 ml) was condensed out into a cold trap and was then allowed to pass slowly through the reaction mixture in a stream of nitrogen. The reaction mixture was then warmed to 50° and was held at this temperature for 3 h, after which it was cooled and the solvent removed under vacuum. The yellow residue was washed with ether and extracted with tetrahydrofuran. The extracts were filtered and concentrated; on addition of excess hexane, the yellow product crystallized. Recrystallization of the crude product from tetrahydrofuran–hexane afforded 530 mg (85%) of pure product (**8***a*) as yellow crystals, m.p. 180–182° (decomp.).

Anal. Calcd. for $C_{34}H_{26}F_6ClN_2Rh$: C, 57.10; H, 3.64; F, 15.96; mol. wt., 715. Found: C, 57.26; H, 3.70; F, 16.15; mol. wt., 703.

The ^{19}F n.m.r. spectrum showed a singlet at −10.1 p.p.m. due to the coordinated hexafluoro-2-butyne.

Acknowledgments

We thank the National Research Council of Canada for financial support, Johnson, Matthey and Mallory for the loan of rhodium trichloride, and Columbian Carbon Co., for a gift of 1,5-cyclooctadiene.

1. S. OTSUKA, T. YASHIDA, and A. NAKAMURA. Inorg. Chem. **6**, 20 (1967).
2. L. VALLARINO. J. Chem. Soc. 2473 (1957).
3. J. CHATT and L. M. VENANZI. J. Chem. Soc. 4735 (1957).
4. R. PETTIT and G. F. EMERSON. Advan. Organometal. Chem. **1**, 4 (1964).
5. D. N. LAWSON and G. WILKINSON. J. Chem. Soc. 1900 (1965).
6. T. A. MANUEL. Advan. Organometal. Chem. **3**, 243 (1966).
7. M. C. BAIRD, J. T. MAGUE, J. A. OSBORN, and G. WILKINSON. J. Chem. Soc. (A), 1347 (1967).
8. J. P. COLLMAN and J. W. KANG. J. Am. Chem. Soc. **89**, 844 (1967).
9. F. A. MILLER and R. P. BAUMANN. J. Chem. Phys. **22**, 1544 (1954).
10. E. O. GREAVES and P. M. MAITLIS. J. Organometal. Chem. **6**, 104 (1966).
11. M. J. MAYS and G. WILKINSON. J. Chem. Soc. 6629 (1965).
12. J. A. MCCLEVERTY and G. WILKINSON. Inorg. Syn. **8**, 211 (1966).
13. O. DOEBNER and W. MILLER. Chem. Ber. **16**, 1664 (1883).
14. C. K. TINKLER. J. Chem. Soc. **103**, 894 (1913).

Can. J. Chem. Downloaded from www.nrcresearchpress.com by 210.87.254.5 on 09/05/12
For personal use only.

Crystal structure of $CdZn_2(PO_4)_2$ and $Cd_2Zn(PO_4)_2$

C. CALVO AND J. S. STEPHENS
Department of Chemistry, McMaster University, Hamilton, Ontario
Received August 14, 1967

The crystal structures of two solid solution phases found to occur in the $Zn_3(PO_4)_2$–$Cd_3(PO_4)_2$ system, one with composition near to $CdZn_2(PO_4)_2$ and the other near to $Cd_2Zn(PO_4)_2$, have been determined. Although these compounds are closely related structurally, there is a miscibility gap between the two phases and an apparent phase transition in only one of these. The compounds, named Bss and Css respectively, have lattice parameters $a = 9.032(4)$ Å, $b = 11.417(5)$ Å, $c = 5.952(6)$ Å, $\beta = 98.8(2)$, and $Z = 4$ for the former compound, and $a = 9.056(8)$ Å, $b = 11.86(1)$ Å, $c = 6.190(9)$ Å, $\beta = 100.1(2)$ and $Z = 4$ for the latter. Both compounds are monoclinic and crystallize with the space group $P2_1/c$ with closely related, but not identical, structures to that of the mineral graftonite. The anions are slightly irregular PO_4^{3-} tetrahedra with average P—O bond distances of 1.538 Å and 1.545 Å for those in Bss and 1.55 Å and 1.56 Å for those in Css. The cations are found to be coordinated to 7, 4, and 5 oxygen atoms for the 3 independent sites per unit cell. In Css the second cation site has a fifth oxygen atom at 2.57 Å in comparison with a length of over 2.9 Å for this same interatomic distance in Bss. The cations appear to be ordered with Cd^{++} preferentially in site 1 in Bss and Zn^{++} preferentially in site 2 in Css.

Canadian Journal of Chemistry, 46, 903 (1968)

Can. J. Chem. Downloaded from www.nrcresearchpress.com by 210.87.254.40 on 09/05/12
For personal use only.

Introduction

Smith and Power (1), by studying changes in the cathodoluminescent emission of Mn^{++} doped mixes of $Zn_3(PO_4)_2$ and $Cd_3(PO_4)_2$, concluded that the system contained six distinct phases. Recent studies by Katnack and Hummel (2) and Brown and Hummel (3) have established the fields of stability of the six phases and further the latter authors indicate that a high temperature phase transformation, possibly of the order–disorder type, occurs at the $Cd_3(PO_4)_2$ rich end of the system. The structures of all these phases, except for the possible disordered forms, have now been determined (4–7) and the results for those having compositions near $CdZn_2(PO_4)_2$ and $Cd_2Zn(PO_4)_2$ will be presented here.

The stability ranges together with the crystallographic character of the various phases in this system present a curious set of observations. $\alpha Zn_3(PO_4)_2$, the low temperature form stable below 942° (2), shows a marked intolerance for the addition of even a modest amount of any other divalent metal ion orthophosphate. The maximum solubility of $M_3(PO_4)_2$, with M = Cd (3), Mg (8), or Mn (9), seems to be about 1 mole %. For temperatures below about 900 °C, a new phase appears upon the addition of increasing amounts of $M_3(PO_4)_2$. The range of stability of this phase, commonly called γ, depends upon the discrete chemical nature of the cation M. For $M = Cd^{++}$ the γ phase is stable between 2 and 8 mole % (3), for $M = Mn^{++}$ the stable range is between 5 and 25 mole % (9), and with $M = Mg^{++}$ it extends from 5 mole % to pure $Mg_3(PO_4)_2$ (8).

The stable form of $Zn_3(PO_4)_2$ between 942 °C and the melting temperature (1060 °C) (2), called the β phase, is found to extend up to 10 to 20 mole % of $Cd_3(PO_4)_2$, depending upon the equilibration temperature (3). A third phase, called "B" solid solution, stable for Cd compositions of roughly 20 to 40 mole %, melts congruently at about 1030 °C and at a composition corresponding almost exactly to that of $CdZn_2(PO_4)_2$. For $Cd_3(PO_4)_2$ content between 55 and 85 mole %, another phase, called "C" solid solution, yields a Debye–Scherrer pattern similar to that of "B"ss. This phase is found to melt incongruently. The sixth phase, that of $Cd_3(PO_4)_2$, shows limited solubility for $Zn_3(PO_4)_2$. This structure is closely related, although not identical, to that of $\beta Zn_3(PO_4)_2$ (7). A miscibility gap exists between each of the phases of mixed composition in this diagram.

We present here the structures of the "B" and "C" solid solution phases. For convenience, these compounds will be called $CdZn_2(PO_4)_2$ and $Cd_2Zn(PO_4)_2$, although in each case the structure studied differed by a few mole % from these nominal compositions. The results for both structures are presented in order to speculate on the nature of the differential thermal analysis anomaly reported by Brown and Hummel (3). In this consideration the structure

TABLE I

Crystal data for $CdZn_2(PO_4)_2$ and $Cd_2Zn(PO_4)_2$

	$CdZn_2(PO_4)_2$	$Cd_2Zn(PO_4)_2$
a (Å)	9.032(4)	9.056(8)
b (Å)	11.417(5)	11.86(1)
c (Å)	5.952(6)	6.190(9)
β	98.8(2)	100.1(2)
Vol. (Å)^3	606.	655.
Z	4	4
Systematic absences	$h0l$ with l odd $0k0$ with k odd	$h0l$ with l odd $0k0$ with k odd
Space group	$P2_1/c$	$P2_1/c$
Linear absorption coefficient (cm^{-1})	121	95

of the mineral graftonite (10), closely related to those presented here, will be contrasted in some detail with those found for "B" and "C" solid solutions.

Experimental Method

(A) $CdZn_2(PO_4)_2$

A sample having composition $(Cd_xZn_{1-x})_3(PO_4)_2$ with $x = 0.2$ was prepared by reacting suitable proportions of $Zn_3(PO_4)_2$, $CdCO_3$, and H_3PO_4 in the form of an aqueous slurry. The mixture was dried, thoroughly ground, and heated to about 600 °C in a covered silica crucible. The sample was then fused in a Vycor tube at a temperature slightly above 1000 °C and slowly cooled to about 950 °C, followed by a quench down to room temperature. The sample showed two types of crystalline morphologies. The first corresponding to the "B" solid solution was needle like in shape and grew out of the second which were flat plates. These appeared to be a $Zn_3(PO_4)_2$–$Cd_3(PO_4)_2$ solid solution having the $\beta Zn_3(PO_4)_2$ structure, since their morphologies appeared similar.[1] Since the original mix corresponded to the eutectic composition as reported by Brown and Hummel (3) the appearance of both phases is not surprising.

A crystal of $CdZn_2(PO_4)_2$ having a diameter of 0.05 mm and a length of 0.5 mm was mounted parallel to the long axis (c) and used to obtain all the crystal data reported here for this compound. Accurate parameters were obtained for a^* and b^* axes from an $hk0$ Weissenberg photograph upon which Al_2O_3 powder lines ($a = 4.75903(3)$ Å, $c = 12.9908(2)$ Å (11)) had been superimposed. The β angle was measured directly from an $h0l$ precession photograph and c^* axis was determined accurately by using the b^* axis previously obtained. The values obtained for these parameters are shown in Table I. The systematic extinctions leading to the selection of $P2_1/c$ as the space group are also given. The density was not determined since it would require that the $\beta(Zn,Cd)_3(PO_4)_2$ crystals be mechanically separated from those of $CdZn_2(PO_4)_2$. If we assume $Z = 4$, however, a value for the volume per molecule in satisfactory agreement with that determined for α (4), β (5), and γ (6) $Zn_3(PO_4)_2$ is obtained.

Intensity measurements were taken with MoKα radiation and since the linear absorption coefficient is 121 cm^{-1} and μR is 0.4, one would expect negligible absorption corrections for the intensities determined within any layer line of data taken perpendicular to the c axis. Since the layer lines were scaled independently, absorption corrections were not necessary. Integrated precession photographs were taken of the {010} and {100} zones and the intensities estimated with a Leeds and Northrup microdensitometer model G-1. The intensities of the reflections in the planes hkn with $n = 0, 1, \ldots 5$ were measured with a scintillation counter using an ω scan and the equi-inclination Weissenberg geometry. These intensities were corrected for dead time and background errors and all the data were subjected to Lorentz and polarization corrections.

A trial structure for the cation positions only was obtained from an interpretation of the real part of the generalized Patterson projections using the hkn data for successive values of n. The positions found were consistent with the $P(U,W)$ and $P(V,W)$ Patterson projections.

[1]This has since been confirmed.

Can. J. Chem. Downloaded from www.nrcresearchpress.com by 210.87.254.40 on 09/05/12
For personal use only.

Can. J. Chem. Downloaded from www.nrcresearchpress.com by 210.87.254.40 on 09/05/12
For personal use only.

A least square refinement on the cationic atomic coordinates and overall temperature factor yielded an

$$R_2\left(= \left[\frac{\sum w[|F_o|^2 - |F_c|^2]}{\sum w|F_o|^2} \right]^{1/2} \right)$$

value of 0.42. The phosphorus atoms were found by the geometric constraint that they lie at least 3.0 Å from each other and from the cations. Only two positions satisfied this criterion and the phosphorus atoms were placed in these positions. These positions were confirmed by calculation of the structure factors although one phosphorus was found to have a suspiciously high temperature factor at this stage. Trial oxygen atom positions were determined by the criterion that they should lie coplanar with the two cations and the phosphorus atom to which it is ligated. This criterion appears to be a feature common to all the pyrophosphates (12) and orthophosphates (5) with cations having radii less than 1 Å investigated to date. Further, the anion, PO_4^{3-}, is commonly found to be nearly regular tetrahedron with a PO bond length near 1.54 Å. Only the radial constraint suggested by the regular tetrahedron was initially explicitly imposed upon the trial structure. Six of the oxygen atoms were found to be located sufficiently close to their proper positions so that they could be refined to their final coordinates. The remaining oxygen atoms were found by imposing the requirement for tetrahedral symmetry about the phosphorus atoms.

A full matrix least square program, prepared by J. S. S., was used to determine the final atomic parameters, both positional and thermal. Atomic scattering factors for Cd^{++}, Zn^{++}, P, and O^- were obtained from the International Tables, Vol. III (13).

The composition of the crystal was determined by allowing the amounts of Cd^{++} and Zn^{++} in each cation site to vary. This calculation resulted in site 1 having a mole fraction of Zn of 0.35 while site 2 had 1.07 and site 3 had 0.94 as their mole fractions of Zn. Although the estimated standard deviations (e.s.d.'s) for these were only 0.05, these latter two values were set to 1.00, since a greater value has no direct physical significance. The occupation number for site 1 was then allowed to vary in subsequent least squares refinement and predicted that the composition should be 79 mole % Zn rather than 75 mole % as determined from the phase diagram, provided that the crystals grew at the eutectic temperature. Since the intergrown crystals (Bss and β) implied that they grew under supersaturated conditions with some finite supercooling, a higher Zn^{++} composition for Bss than that predicted by the equilibrium diagram is not unexpected. Unfortunately, the experimental errors in both this and the phase studies may exceed the compositional difference implied by this analysis.

The final cycles of refinement were performed with the composition of site 2 and 3 taken to be pure Zn^{++}. Weights, ω, were chosen by the criterion suggested by Cruickshank *et al.* (14) where the average value of $\omega|\Delta F|^2$ is made constant independent of the magnitude of F_o. In the case at hand,

$$\omega^{-1} = 4.0 + 0.35|F_o|.$$

Those reflections whose calculated value was less than the minimum observable value, F_o(min.), in their region in reciprocal space were left out of the refinement, and for the remainder of the set of unobserved reflections ΔF was determined from $kF_o(\text{min.}) - F_c$, where k was set at 0.85. The final atomic parameters are listed in Table II and the observed and calculated structure factors are compared in Table III. Of a total of 1999 possible reflections, 1111 were observed, and of these 20 reflections of medium intensity gave unusually high discrepancies and therefore were eliminated from the refinement. The final values of

$$R_1\left(= \frac{\sum||F_o| - |F_c||}{\sum|F_o|} \right)$$

and R_2 for all the reflections are 0.074 and 0.089 respectively.

(B) $Cd_2Zn(PO_4)_2$

Crystals containing on the average about 70 mole % Cd were prepared in a manner entirely analogous to that used for $CdZn_2(PO_4)_2$. Unit cell parameters, shown in Table I, were obtained from photographs calibrated by reflections from $CdZn_2(PO_4)_2$. Intensities of the reflections indexed as $0kl$, hnl with $n = 0$, 1, and 2 and $hk0$ and $hk1$ were estimated by visual comparison. The latter two sets were taken with the Weissenberg camera using MoKα radiation,

Can. J. Chem. Downloaded from www.nrcresearchpress.com by 210.87.254.40 on 09/05/12
For personal use only.

TABLE II

Atomic parameters in $CdZn_2(PO_4)_2$, $Cd_2Zn(PO_4)_2$, and graftonite respectively (estimated standard deviations are enclosed in parentheses)

Atom*	x	y	z	B (Å^2)
M(1)	0.9445(2)	0.3787(1)	0.3321(3)	
	0.9461(2)	0.3769(1)	0.3325(5)	0.24(3)
	0.9472(4)	0.3792(3)	0.3355(10)	1.00(7)
M(2)	0.6960(3)	0.0560(2)	0.3243(3)	
	0.7104(3)	0.0686(3)	0.3293(7)	0.76(5)
	0.7144(4)	0.0790(3)	0.3255(9)	1.44(7)
M(3)	0.3694(2)	0.1942(1)	0.1234(3)	
	0.3581(2)	0.1833(2)	0.1250(5)	0.65(4)
	0.3619(3)	0.1915(2)	0.1295(7)	0.58(6)
P(1)	0.1049(4)	0.1363(3)	0.3970(7)	
	0.0907(7)	0.1345(5)	0.4013(13)	−0.21(7)
	0.0959(5)	0.1338(4)	0.3956(13)	0.22(7)
O(1)	0.0844(10)	0.0658(9)	0.1760(21)	
	0.0806(24)	0.0670(18)	0.1840(58)	1.17(37)
	0.0826(16)	0.0702(11)	0.1787(39)	0.98(26)
O(3)	0.9617(14)	0.2033(11)	0.4301(24)	
	0.9463(19)	0.1918(15)	0.4218(45)	0.32(26)
	0.9390(16)	0.1915(12)	0.4237(38)	1.02(26)
O(5)	0.2354(11)	0.2231(10)	0.3777(21)	
	0.2037(20)	0.2287(17)	0.3721(49)	0.92(33)
	0.2165(11)	0.2299(13)	0.3889(35)	1.32(28)
O(7)	0.1441(13)	0.0598(10)	0.6063(21)	
	0.1432(21)	0.0600(15)	0.6173(47)	0.58(29)
	0.1451(14)	0.0586(11)	0.5961(34)	0.47(23)
P(2)	0.6074(4)	0.4089(3)	0.3059(7)	
	0.6051(7)	0.4056(5)	0.2985(17)	0.11(9)
	0.6011(5)	0.4109(4)	0.3024(12)	0.21(8)
O(2)	0.4776(12)	0.3244(10)	0.3199(19)	
	0.4798(24)	0.3141(19)	0.3276(55)	1.33(39)
	0.4705(17)	0.3258(12)	0.3241(37)	1.10(26)
O(4)	0.6957(11)	0.3722(10)	0.1128(20)	
	0.6946(20)	0.3698(16)	0.1216(47)	0.72(30)
	0.6888(15)	0.3728(11)	0.1235(35)	0.63(23)
O(6)	0.7230(11)	0.0969(9)	0.0206(18)	
	0.7195(18)	0.0966(15)	0.0123(44)	0.31(27)
	0.7242(18)	0.0905(13)	0.0070(39)	1.32(28)
O(8)	0.4590(11)	0.0353(8)	0.2353(21)	
	0.4708(20)	0.0264(17)	0.2470(50)	0.96(35)
	0.4643(15)	0.0368(12)	0.2623(33)	0.72(23)

Anisotropic thermal parameters for $CdZn_2(PO_4)_2$ (Å^2)$\times 10^4$

	U_{11}†	U_{22}	U_{33}	U_{12}	U_{13}	U_{23}
M(1)	139(7)	100(6)	267(16)	8(5)	−28(5)	−59(5)
M(2)	445(14)	383(13)	52(16)	221(11)	53(9)	26(8)
M(3)	95(8)	86(7)	9(15)	16(6)	4(6)	−8(6)
P(1)	46(14)	98(14)	44(22)	−13(10)	28(12)	−17(11)
O(1)	34(39)	92(42)	168(66)	26(29)	12(35)	−46(35)
O(3)	156(60)	269(62)	211(80)	75(44)	147(49)	−9(46)
O(5)	56(42)	202(50)	134(73)	−81(35)	55(38)	−14(42)
O(7)	175(51)	185(51)	146(72)	−51(41)	27(42)	68(42)
P(2)	33(14)	66(13)	46(24)	9(10)	25(11)	2(11)
O(2)	93(46)	207(52)	35(60)	44(35)	16(38)	57(39)
O(4)	55(40)	167(45)	123(64)	−26(35)	74(34)	18(39)
O(6)	61(37)	170(47)	9(61)	−5(32)	16(34)	7(36)
O(8)	82(41)	74(42)	164(69)	14(31)	17(37)	−63(35)

*In the text O(n') is generated from O(n) by the glide plane operation and O($\bar{n}$) and O($\bar{n}'$) represent inversions. Unit cell translations are not separately designated.

†These values were obtained from $\beta_{ij} = 2\pi^2 b_i b_j U_{ij}$ where β_{ij}'s appear as a temperature effect through $\exp[-(\beta_{11}h^2 + 2\beta_{12}hk \ldots)]$ in the structure factor expression and b_i are the reciprocal lattice vectors.

Can. J. Chem. Downloaded from www.nrcresearchpress.com by 210.87.254.40 on 09/05/12
For personal use only.

whereas the rest were taken as precession photographs using AgKα for the {100} zone and MoKα radiation for the remaining data.

The crystal used for the *hk*0 and *hk*1 data had a length of 0.4 mm along the *c* axis and 0.14 mm and 0.20 mm in the plane perpendicular to this axis. The linear absorption coefficient is $\mu = 95$ cm^{-1} and therefore for a μR value of 1.1 the neglect of absorption corrections would lead to errors of 20% in the intensities for the range of data taken. Therefore absorption corrections were applied based upon a cylindrical approximation for the crystal's shape. The remaining data were taken from a crystal of dimensions 0.08 mm × 0.05 mm × 0.14 mm, with the latter value along the *c* axis, and therefore absorption correction could be ignored.

Trial parameters were taken from the final positional parameters obtained for $CdZn_2(PO_4)_2$ with the cations assumed randomly mixed. Individual isotropic temperature factors were used throughout the refinement. After the structure had been partially refined ($R_1 \simeq 0.3$) the multiplicity of the cations were varied. This indicated the Cd^{++} again accumulated in site 1, which shows the highest coordination number, and that site 2 was virtually entirely Zn^{++}. Therefore, the scattering curve subsequently used for site 2 was composed of $0.9f_{Zn}$ and $0.1f_{Cd}$.

The structure was refined to an R_1 value of 0.15 with each reflection equally weighted. The final refinement was then carried through using weights whose reciprocal was expanded in a power series in F_o. The coefficients were determined so as to minimize the average of $\omega\Delta F$ and the function obtained was

$$\omega^{-1} = 2.0 + 0.2F_o + 0.01F_o^2.$$

Unobserved reflections whose calculated value was less than F_o(min.) were given zero weight in the refinement. The final parameters obtained are shown in Table II where they are compared with those of $CdZn_2(PO_4)_2$ and the final structure factors are to be found in Table IV.[2] The value of R_1 is 0.104 and R_2 is 0.129 including all the data. 986 reflections were used of which 663 had observable intensities.

[2]Table IV has been placed in The Depository of Unpublished Data. Photocopies may be obtained, upon request, from: Depository of Unpublished Data, National Science Library, National Research Council of Canada, Ottawa, Canada.

Description of the Structures

(A) $CdZn_2(PO_4)_2$

Both phosphorus atoms are tetrahedrally coordinated to oxygen atoms which lie, on the average, 1.538 Å and 1.545 Å displaced from P(1) and P(2) respectively. The individual P(1)—O bond distances range from 1.520 Å to 1.560 Å, whereas for P(2) the range extends from 1.523 Å to 1.572 Å. Since the estimated standard error on a bond length is about 0.0102 Å, these extremes differ by about twice the sum of their standard errors. Every oxygen atom is ligated to two cations and a phosphorus atom; therefore there is no reason to expect significant deviation from the average P—O bond distance. These values together with the pertinent bond angles are found in Table V where they are compared with those found for $Cd_2Zn(PO_4)_2$ and the mineral graftonite.

The cations are found to lie in polyhedra having three different coordination numbers. Site 1, which contains substantially all the Cd, is coordinated to seven oxygen atoms while site 2 shows fourfold coordination and site 3 shows trigonal bipyramidal coordination. The cation oxygen bond distances range from 2.09 Å to 2.60 Å around site 1 with an average of 2.36 Å. Site 2 has M—O bond distances ranging from 1.90 Å to 2.14 Å with an average of 2.00 Å. Since the bond angles about this cation range from 93° to 140°, deviations from tetrahedral symmetry are substantial. In the mineral graftonite, with nearly the same structure, this site has fivefold coordination in the form of an irregular square pyramid as a result of O(3) bonding to M(2). The O—M(2)—O angles here anticipate this distortion with O(6)—M(2)—O(4) at 140° in contrast with the ideal value of 109°. This angle is 159° in the mineral. For cation site 3 the axial oxygen atoms lie at an average cation oxygen atom separation of 2.145 Å, whereas the equitorial oxygen atoms have average bond lengths of 2.03 Å.

These cation polyhedra are bonded through sharing oxygen atoms to form the framework of the structure. M(3)—O_5 forms infinite chains running parallel to the *c* axis by edge sharing with neighboring *c* glided trigonal bipyramids. The shared edges are all non-equitorial involving O(2), O(2′), O(5), and O(5′). The fifth oxygen atom, O(8), is shared with M(2). This portion of the structure is shown in Fig. 1. Sheets involving

TABLE III

$CdZn_2(PO_4)_2$ observed and calculated structure factors ($\times$ 10) (Unobserved reflections are marked with an asterisk (*), and unreliable reflections with the symbol (ϕ))

H	K		FOBS	FCALC
H	K			L=0
0	4		1869	-1764
0	6		631	-527
0	8		312	-291
0	10		509	413
0	12		977	-1041
0	14	*	302	-92
0	16		649	644
0	18	*	362	-195
1	3		2011	1939
1	4		1446	-1378
1	5		340	364
1	6		362	-306
1	7		865	-730
1	8		1554	1534
1	9	*	226	292
1	10		344	-343
1	11	*	256	-124
1	12		609	-633
1	13	*	287	83
1	14	*	303	204
1	15	*	318	-73
1	16		424	461
1	17	*	348	-222
2	0		555	555
2	1		726	559
2	2		391	-356
2	3		1462	-1549
2	4		883	-899
2	5		1078	-1080
2	6		520	466
2	7		200	249
2	8		863	844
2	9		355	-323
2	10		268	279
2	11		1011	982
2	12		395	-396
2	13	*	290	-18
2	14	*	305	-197
2	15		480	-510
2	16	*	336	222
2	17		206	266
2	18	*	364	8
3	0		1947	2043
3	1		167	-162
3	2		155	-90
3	3	*	159	-34
3	4		548	-560
3	5		607	-581
3	6		253	-245
3	7		1304	-1303
3	8		278	-280
3	9		371	374
3	10		492	519
3	11		480	502
3	12		483	-489
3	13	*	295	211
3	14	*	310	-146
3	15	*	325	-104
3	16		333	342
3	17	*	354	-191
4	0		712	-700
4	1		1278	1253
4	2		314	270
4	3		1289	1325
4	4		144	146
4	5	*	196	43
4	6		300	-278
4	7		305	-303
4	8		489	495
4	9		612	562
4	10		325	-363
4	11		514	520
4	12	*	287	66
4	13		404	-377
4	14	*	316	-82
4	15		619	-563
4	16	*	345	-133
5	0		856	-884
5	1		1323	1273
5	2		859	-873
5	3		497	471
5	4		574	567
5	5		807	-849
5	6	*	221	96
5	7		483	-470
5	8		338	-263
5	9		263	-215
5	10		828	829
5	11		751	718
5	12		346	319
5	13	*	309	-344
5	14	*	323	-174
5	15		465	-493
5	16	*	351	-269
5	17		343	416
5	18	*	376	-165
6	0		695	-573
6	1	*	205	90
6	2	*	208	7
6	3		888	847
6	4		855	802
6	5		651	-682
6	6		464	390
6	7		997	-952
6	8		681	-637
6	9		682	771
6	10		193	-163
6	11	*	293	267
7	0		912	-858
7	1		923	959
7	2		741	738
7	3	*	232	207
7	4		428	374
7	5		277	-383
7	6		296	-413
7	7	*	261	5
7	8	*	271	-222
7	9		386	393
7	10		486	-455
7	11		346	420
7	12		380	446
7	13		698	-691
7	14	*	342	165
7	15		396	-368
7	16	*	366	-362
8	0	*	243	-163
8	1		896	978
8	2		734	-695
8	3	ϕ	465	641
8	4		453	490
8	5	*	261	-144
8	6		203	244
8	7	*	277	-239
8	8		666	-649
8	9	*	296	-135
8	10		495	457
8	11	*	318	148
8	12		445	413
8	13	*	341	-79
9	0		831	-937
9	1		601	-563
9	2	*	266	6
9	3	*	269	-34
9	4		586	686
9	5	*	279	-156
9	6		308	369
9	7		440	-421
9	8	*	302	-78
9	9	*	311	288
9	10		592	-598
9	11	*	332	-160
10	0	*	283	-145
10	1	*	284	168
10	2	*	285	258
10	3		335	-416
10	4	*	292	20
10	5	*	298	107
10	6	*	304	-201
10	7		710	697
10	8	*	319	-224
10	9		305	-266
10	10	*	336	-229
11	0	*	128	-75
11	1	*	303	-252
11	2	*	305	-209
11	3	*	308	91
11	4	*	311	263
11	5		532	511
11	6	*	322	273
12	0		588	-668
12	1		531	-500
12	2	*	325	147
12	3		624	-537
12	4	*	330	229
13	0	*	342	260
H	K			L=1
0	1		228	173
0	2		265	332
0	3		851	-774
0	4	*	106	49
0	5	*	116	-63
0	6		2171	-2278
0	7	*	135	-86
0	8		370	-408
0	9		486	480
0	10		595	570
0	11		602	630
0	12		317	293
0	13		527	-523
0	14		180	137
0	15	*	308	9
1	2		897	869
1	3		1865	1912
1	4		435	418
1	5		1116	-968
1	6		926	-910
1	7	*	191	121
1	8	*	206	-47
1	9		484	-496
1	10		1024	1002
1	11		463	-488
1	12	*	264	160
1	13	*	279	205
1	14		524	-470
1	15	*	309	-249
2	1	ϕ	290	175
2	2		2436	2545
2	3		267	-274
2	4		235	-229
2	5		514	535
2	6		265	-214
2	7		718	-668
2	8	*	211	-86
2	9	*	225	26
2	10		497	573
2	11		601	583
2	12	*	268	120
2	13	*	282	-118
2	14		911	-919
2	15	*	312	-80
3	1		1515	-1514
3	2		579	501
3	3	*	158	31
3	4		980	873
3	5		884	874
3	6		2295	-2364
3	7	*	205	23
3	8	*	218	70
3	9	*	232	-4
3	10		1013	1051
3	11		273	277
3	12	*	273	-212
3	13		219	183
3	14	*	302	4
4	1		250	-148
4	2		538	563
4	3		1476	1523
4	4		1137	-1150
4	5	*	194	-118
4	6		788	-843
4	7	*	216	-202
4	8	*	228	218
4	9		736	-703
4	10		532	553
4	11		218	-151
4	12		284	339
4	13		490	513
4	14		590	-573
4	15	ϕ	322	-426
5	1		191	-223
5	2		943	1032
5	3		445	-461
5	4		710	786
5	5		921	879
5	6	*	218	-71
5	7		492	-574
5	8	*	239	-185
5	9		500	-514
5	10	*	263	108
5	11		556	572
5	12	*	289	26
6	1		1327	-1371
6	2		319	-297
6	3		443	481
6	4		422	451
6	5		624	697
6	6		412	-366
6	7		456	487
6	8	*	252	123
6	9		262	-274
6	10	*	275	50
6	11	*	287	-151
6	12	ϕ	299	-390
6	13		531	470
6	14	*	324	211
7	1	*	223	-221
7	2		460	-501
7	3		364	354
7	4		625	-633
7	5	*	241	255
7	6		613	629
7	7		427	-409
7	8	*	266	-146
7	9		393	-324
7	10		396	-350
7	11	*	298	237
7	12	*	310	299
7	13		500	524
7	14	*	334	-64
8	1	*	242	40
8	2		412	-440
8	3	*	247	81
8	4		850	824
8	5		848	785
8	6		640	583
8	7		532	-607
8	8	*	281	21
8	9		506	-525
8	10		635	-632
8	11	*	311	143
9	1		659	-591
9	2		946	-891
9	3		412	484
9	4	*	270	182
9	5	*	275	-82
9	6		489	531
9	7	*	289	90
10	1	*	280	47
10	2		369	-308
10	3	*	284	190
10	4		535	-472
10	5	*	293	232
10	6		607	722
10	7		468	-467
10	8	*	313	-153
10	9	*	321	-77
10	10		464	-459
10	11	*	338	253
11	1	*	299	70
11	2	ϕ	592	-763
11	3	*	303	-51
12	1	*	318	86
H	K			L=-1
1	3		688	-813
1	4		290	257
1	5		866	-850
1	6		746	-729
1	7		794	756
1	8		161	-222
1	9		1030	968
1	10		336	-337
1	11	*	248	-97
1	12		436	-419
1	13		403	-336
1	14		926	939
1	15	*	308	39
2	2	*	120	80
2	3	*	134	107
2	4		813	-733
2	5		1367	-1273
2	6		400	422
2	7		786	760
2	8		423	373
2	9		119	102
2	10	*	237	85
2	11		1097	-1118
2	12	*	266	46
2	13	*	281	-170
2	14		298	-301
2	15	*	310	213
3	1		2212	2147
3	2		630	557
3	3		1256	-1235
3	4		487	494
3	5		1000	-901
3	6		341	375
3	7	*	201	-75
3	8		369	378
3	9		644	598
3	10		203	-217
3	11	*	256	48
3	12		243	-239
3	13		691	-684
3	14		304	-273
3	15		450	476
3	16	*	328	-7
4	1		234	204
4	2	*	160	-167
4	3		882	-878
4	4		1006	874
4	5		1405	-1354
4	6		998	-923
4	7		1535	1567
4	8		355	-295
4	9		674	681
4	10		286	267
4	11		534	-570
4	12	*	277	-55
4	13	*	291	-207
4	14		412	386
4	15	*	319	227
5	1		1103	1214
5	2		374	268
5	3	*	185	-71
5	4		1540	-1570
5	5		746	-797
5	6		265	-252
5	7		505	498
5	8		309	-246
5	9	*	246	270
5	10		446	504
5	11		797	-757
5	12		614	632
5	13		329	-351
5	14		510	-495
5	15	*	326	213
6	1		688	730
6	2		331	390
6	3		843	-903
6	4		899	935
6	5	*	217	79
6	6		651	-675
6	7		375	-375
6	8	*	246	-72
6	9	*	257	147
6	10		422	414
6	11	*	281	205
7	1		836	-854
7	2	*	216	173
7	3		479	497
7	4		335	349
7	5		446	-384
7	6		620	-612
7	7		698	720
7	8	*	260	-65
7	9		350	321
7	10	*	281	294
8	1	*	233	-68
8	2		701	694
8	3	*	238	-154
8	4		612	-592
8	5	*	250	233
8	6		540	-498
8	7	ϕ	355	-226
8	8		389	-285
8	9	*	284	34
8	10	*	294	365
8	11		487	521
8	12		439	466
8	13	*	328	-166
8	14		403	-459
8	15	*	351	-148
9	1		370	-383
9	2		630	671
9	3		540	496
9	4		862	815
9	5		681	613
9	6		695	-769
9	7		400	-412
9	8	*	289	9
9	9		418	-392
9	10		516	557
9	11	*	318	110
10	1		726	-659
10	2	ϕ	302	447
10	3		414	482
10	4	*	280	-151
10	5	*	284	118
10	6	*	291	-125
10	7	*	298	-139
10	8		220	159
10	9	*	314	-163
11	1	*	290	23
11	2	ϕ	378	544
11	3	*	294	-42
11	4	*	298	59
11	5		363	427
11	6		394	-345
11	7		489	-441
11	8	*	322	-61
12	1	*	309	-281
12	2	*	311	23
12	3		373	314
12	4	*	317	214
12	5	*	321	317
12	6		421	-463
12	7	*	331	-1
12	8	*	338	157
12	9		489	-502
12	10	*	352	154
13	1	*	328	-93
13	2	*	329	-15
13	3	*	331	197
13	4	*	334	-232
13	5	*	338	-59
13	6		442	438
13	7	*	348	-154
14	1	*	346	51
14	2	*	347	-226
15	1	*	362	-99
15	2		446	-486
15	3	*	365	168
16	1	*	376	48
H	K			L=2
0	0		1475	-1490
0	1		831	756
0	2		854	-825
0	3		1512	1455
0	4		392	401
0	5		237	-193
0	6		368	327
0	7		1149	-1071
0	8	*	198	21
0	9		876	933
0	10	*	165	140
0	11	*	170	83
0	12	*	173	206
0	13		245	-239
1	0		1493	-1229
1	2		340	-305
1	3		558	-586
1	4		472	454
1	5		1413	-1399
1	6		336	273
1	7		451	-434
1	8		440	408
1	9		238	228
1	10		386	-325
1	11		995	933
1	12		476	461
1	13		235	-267
1	14	*	295	115
1	15		365	-351
1	16		579	-597
1	17		362	310
1	18	*	340	-62
2	0	*	279	191
2	1		590	586
2	2		614	-526
2	3		407	407
2	4		1101	1089
2	5		605	-532
2	6		383	331
2	7		408	-391
2	8		1364	-1367
2	9	*	220	-196
2	10	*	233	81
2	11		301	323
2	12	*	261	181
2	13	*	275	145
2	14	*	289	234
2	15	*	303	-92
2	16	*	317	-130
2	17	*	330	46
2	18		418	-435
2	19	*	353	-7
2	20		468	437
2	21	*	369	-0
3	0		1915	-1944
3	1		695	-688
3	2	*	150	106
3	3		688	688
3	4		717	737
3	5		1204	1227
3	6		467	466
3	7		314	311
3	8	*	214	-220
3	9		322	286
3	10		608	-632
3	11		558	-463
3	12		546	540
3	13	*	280	-134
4	0		1348	-1315
4	1		619	529
4	2	*	168	-134
4	3		931	-1036
4	4		362	308
4	5		345	277
4	6	*	202	-49
4	7		527	578
4	8	*	224	-85
4	9		1175	-1133
4	10	*	248	188
4	11	*	261	80
4	12		666	647
4	13	*	287	130
5	0	*	183	185
5	1		641	-661
5	2		358	-299
5	3	*	192	-183
5	4		1224	1190
5	5		605	597
5	6		481	415
5	7	*	225	-59
5	8		1295	-1270
5	9		279	-261
5	10	*	258	-122
5	11		305	-273
5	12	*	262	68
5	13		496	517
5	14	*	308	35
5	15		390	370
5	16	*	332	5
6	0		1327	-1197
6	1		904	-881
6	2		739	740
6	3		635	-585
6	4		688	649
6	5		754	756
6	6		490	-561
6	7		877	809
6	8	*	248	-247
6	9	*	258	-176
6	10		570	-551
6	11		574	-575
6	12		448	495
6	13	*	304	-17
6	14	*	316	208
6	15	*	328	111
6	16		350	-283
6	17	*	350	-141
7	0	*	220	-93
7	1	*	220	57
7	2		284	-263
7	3		603	-527
7	4	*	231	-10
7	5		377	386
7	6	*	245	12
7	7		740	722
7	8		292	-290
7	9		752	-810
7	10		538	468
7	11	*	292	-224
7	12		306	310
7	13	*	314	234
7	14	*	326	-95
7	15		311	298
7	16	*	347	-35
8	0	*	238	-108
8	1		747	-753
8	2	*	241	89
8	3		388	-453
8	4	*	248	199
8	5	*	254	-22
8	6	*	260	185
8	7	*	268	-148
8	8	*	276	-59
8	9	*	285	228
8	10	*	295	-95
8	11		476	-402
8	12	*	315	-270
8	13	*	325	167
8	14	*	335	-102
8	15		502	478
8	16	*	354	183
9	0	*	257	130
9	1	*	257	32
9	2		401	385
9	3	ϕ	309	-431
9	4		327	-378
9	5		229	171
9	6		324	-418
9	7		606	590
9	8		336	302
9	9	*	300	12
10	0		567	680
10	1	*	275	15
10	2		417	-333
10	3	*	280	-52
10	4		365	-360
10	5	*	288	125
10	6	*	293	193
10	7	*	300	215
10	8		342	288
10	9	*	314	-250
10	10	*	322	202
10	11	*	331	-242
10	12		483	-445
10	13	*	347	29
11	0		445	402
11	1		488	-472
11	2	*	295	56
11	3	*	298	-144
11	4		668	-652
11	5	*	305	-151
11	6	*	310	52
11	7	*	316	-17
11	8		545	621
11	9		348	389
11	10	*	336	-98
12	0		601	509
12	1		300	265
12	2		380	313
12	3	*	316	-47
12	4		518	-541
12	5	*	322	22
12	6	*	327	-180
12	7	*	332	81
12	8		389	425
12	9	*	343	-229
13	0		316	376
13	1	*	330	-54
13	2		393	-338
13	3	*	333	0
14	0	*	345	148
14	1	*	345	-185
14	2	*	346	168
14	3	*	348	14
14	4	*	350	-293
14	5	*	352	-18
14	6	*	355	-188
14	7	*	358	-147
14	8		420	433
14	9	*	365	208
H	K			L=-2
1	0		1910	1880
1	3		505	-453
1	4		494	589
1	5		967	952
1	6		284	-234
1	7		443	384
1	8		1450	-1493
1	9		300	-346
1	10		312	265
1	11		861	-877
1	12	*	255	76
1	13		545	573
1	14	*	284	-196
1	15		485	482

Can. J. Chem. Downloaded from www.nrcresearchpress.com by 210.87.254.40 on 09/05/12
For personal use only.

TABLE III (*Concluded*)

			FOBS	FCALC
1	16	•	313	-29
1	17		374	-393
1	18	•	339	-172
2	0		1463	-1446
2	3		180	-219
2	4	•	143	90
2	5		1810	1849
2	6		466	-393
2	7		784	844
2	8		473	452
2	9		732	-703
2	10		418	-454
2	11		764	-830
2	12	•	257	98
2	13	•	272	187
2	14	•	286	85
2	15		482	430
2	16	•	314	31
2	17	•	328	-259
2	18		402	453
2	19	•	352	-248
3	0		1302	1184
3	1	•	124	-50
3	2		930	-942
3	3		1548	-1668
3	4		189	-174
3	5	•	167	-104
3	6	•	180	80
3	7		1131	1164
3	8	•	207	51
3	9		499	-483
3	10		905	913
3	11	•	247	-160
3	12		277	-244
3	13	•	275	57
3	14		764	-294
3	15	•	303	115
4	0		1391	1406
4	1		1331	-1358
4	2	Ø	131	235
4	3	•	159	37
4	4		365	-350
4	5		272	-208
4	6		507	-539
4	7		791	-743
4	8	•	215	-49
4	9		237	252
4	10	Ø	522	310
4	11		433	-443
4	12		306	-254
4	13		403	414
4	14	•	294	-201
4	15		566	567
4	16		269	209
4	17	•	334	-278
5	0		219	161
5	1		584	575
5	2		634	610
5	3	•	176	-1
5	4		647	-635
5	5		269	307
5	6		225	-203
5	7		957	985
5	8		816	761
5	9	•	237	-118
5	10		486	-478
5	11	•	261	-8
5	12		451	-465
5	13	•	287	-176
5	14	•	301	13
5	15	•	314	-94
5	16		354	349
5	17	•	339	70
6	0		1633	1608
6	1		362	318
6	2		802	-826
6	3	•	193	-147
6	4		1206	-1205
6	5		228	-197
6	6		176	248
6	7	•	226	-57
6	8		469	520
6	9	•	247	36
6	10		877	870
6	11	•	271	-19
6	12		454	-500
6	13	•	295	-309
6	14	•	308	-119
6	15	•	321	4
6	16		377	397
6	17	•	344	163
7	0		699	738
7	1	•	203	33
7	2		188	186
7	3		391	323
7	4		608	-662
7	5		396	-398
7	6	•	230	-32
7	7		759	-698
7	8		806	876
7	9	Ø	326	454
7	10		333	-310
7	11	•	281	143
7	12		581	-603
7	13	•	305	174
8	0		933	1076
8	1		534	497
8	2		203	216
8	3	•	228	-186
8	4		456	-572
8	5	•	239	-201
8	6	•	246	-188
8	7		298	246
8	8		436	403
8	9	•	272	-128
8	10		286	-263
8	11		433	508
8	12		457	-400
8	13	•	315	-221
8	14	•	326	113

			FOBS	FCALC
8	15		465	-418
8	16	•	347	211
9	0		607	708
9	1	•	240	183
9	2		466	-438
9	3		569	660
9	4		505	-564
9	5	•	255	18
9	6	•	262	167
9	7		305	-372
9	8	•	277	195
9	9	•	286	-22
9	10		405	387
9	11	•	305	131
10	0		555	-612
10	1	•	258	7
10	2		243	207
10	3	•	263	-44
10	4	•	267	-0
10	5		378	-316
10	6	•	278	198
10	7		554	-526
10	8		390	461
10	9	•	301	168
10	10		382	-342
10	11		376	358
10	12	•	328	-93
11	0	•	404	106
11	1	Ø	791	567
11	2	•	278	-9
11	3	•	281	-96
11	4	•	285	137
11	5	•	289	-114
11	6		227	-255
11	7	•	301	94
11	8		310	-294
11	9	•	315	-125
11	10	•	323	293
11	11		440	494
11	12	•	339	149
11	13	•	348	-72
11	14	•	355	-8
11	15		351	-349
11	16	•	367	-150
12	0		320	-284
12	1	•	295	56
12	2		285	-225
12	3		630	656
12	4		377	400
12	5	•	307	98
12	6	•	312	162
12	7	Ø	307	-493
12	8	•	323	-256
13	0		853	-902
13	1	•	313	230
13	2	•	315	146
13	3	•	317	40
13	4	•	320	326
13	5		374	-279
13	6	•	328	-88
13	7	•	333	30
13	8	•	338	57
13	9	•	344	154
13	10	•	349	-162
13	11	•	355	145
13	12		268	288
13	13	•	365	-309
H	K			L=3
0	1		347	-346
0	2		679	-723
0	3		1421	1450
0	4		1164	1126
0	5	•	144	95
0	6	•	149	-71
0	7		333	-309
0	8		374	379
0	9		757	-791
0	10	•	207	33
0	11		378	-406
0	12	•	211	-188
0	13		614	638
0	14	•	295	160
0	15	•	310	-185
0	16		329	-341
0	17	•	338	-152
1	1		698	-784
1	2		524	427
1	3		606	551
1	4		193	132
1	5		505	493
1	6		1240	1329
1	7		529	-491
1	8		305	-220
1	9		476	-462
1	10		867	-843
1	11		771	705
1	12		349	303
1	13		498	488
1	14	•	297	-212
1	15		404	-390
1	16	•	326	-3
1	17		432	-435
1	18	•	352	-85
2	1		1436	-1383
2	2		1332	-1437
2	3		97	107
2	4		491	426
2	5		1484	1440
2	6	•	189	41
2	7		362	-353
2	8		280	-248
2	9		416	-371
2	10		415	-422
2	11		436	460
2	12	•	273	-15
2	13	•	287	-9
2	14		868	821
2	15	•	315	122

			FOBS	FCALC
2	16	•	329	-62
2	17	•	342	-222
2	18		324	-288
2	19	•	364	49
3	1	•	156	113
3	2		1371	-1367
3	3		1300	1286
3	4		617	-564
3	5	•	189	-168
3	6		527	525
3	7		335	-360
3	8		403	410
3	9		630	-608
3	10		193	-275
3	11		266	-221
3	12		284	-255
3	13		419	438
3	14		295	282
3	15		368	-383
3	16	•	333	14
4	1	•	176	-29
4	2		295	293
4	3		238	-234
4	4		238	238
4	5		291	267
4	6		1135	1130
4	7		745	-732
4	8	•	236	-21
4	9	•	248	70
4	10		672	-715
4	11		479	492
4	12	•	286	-11
4	13	•	300	82
4	14	•	313	91
4	15	•	326	73
4	16		314	313
4	17	•	351	-136
5	1		470	-462
5	2		946	-972
5	3		296	-308
5	4		433	387
5	5		491	523
5	6	•	227	-137
5	7		355	372
5	8		362	363
5	9	•	259	109
5	10		437	-435
5	11	•	283	-62
5	12		412	-495
5	13	•	308	-231
5	14		680	603
5	15	•	333	123
6	1		539	542
6	2		523	-599
6	3	•	222	125
6	4		636	-686
6	5		929	-968
6	6		417	447
6	7		328	386
6	8	•	261	204
6	9	•	272	153
6	10		249	-181
6	11		474	-398
6	12	•	306	-83
6	13	•	318	100
6	14	•	330	79
6	15	•	341	59
6	16		323	321
6	17	•	362	132
7	1		849	937
7	2	•	236	234
7	3		823	-851
7	4	•	245	35
7	5	•	251	48
7	6		626	568
7	7	•	267	-41
7	8	•	275	131
7	9	•	285	155
7	10		297	-270
7	11		278	-219
7	12	•	317	-112
7	13		562	-501
7	14	•	339	112
7	15		480	513
7	16	•	359	103
8	1	•	253	263
8	2	Ø	417	-711
8	3		519	-496
8	4	•	263	255
8	5		612	-582
8	6	•	275	-132
8	7		540	531
8	8	•	291	178
8	9		558	501
8	10	•	309	-30
8	11		269	-341
8	12		361	-373
8	13	•	339	-44
9	1		681	593
9	2	•	274	97
9	3		300	-309
9	4		471	-462
9	5		614	-546
9	6	•	292	224
9	7		298	393
9	8	•	306	-173
9	9		349	375
9	10	•	323	-191
9	11		290	-356
9	12		483	481
9	13	•	350	-248
10	1		359	325
10	2	•	293	-200
10	3		482	-510
10	4	•	299	75
10	5	•	303	100
10	6	•	309	-165
10	7	•	315	133
10	8	•	322	37
10	9	•	329	126

			FOBS	FCALC
10	10	•	337	187
10	11	•	345	-133
10	12	•	353	-9
10	13		555	-483
10	14	•	367	-53
11	1	•	310	56
11	2	•	311	68
11	3	•	313	46
11	4	•	317	74
11	5		528	-561
11	6	•	326	-70
11	7	•	331	162
11	8	•	337	32
11	9		420	371
11	10	•	350	208
12	1	•	328	-29
12	2		469	507
12	3	•	331	-131
12	4	•	334	-117
12	5	•	338	140
12	6	•	342	-146
12	7	•	347	11
12	8		398	-385
12	9	•	357	217
13	1	•	345	-81
13	2	•	346	179
13	3	•	348	-8
13	4	•	350	163
13	5	•	353	173
13	6		361	-387
13	7	•	360	-104
13	8	•	364	237
13	9	•	368	26
13	10	•	372	353
13	11	Ø	362	39
13	12	•	377	-108
14	1	•	360	-40
14	2		503	452
14	3	•	362	268
H	K			L=-3
1	4		445	436
1	5		1429	1384
1	6		664	656
1	7		506	-482
1	8		568	558
1	9		344	-335
1	10	•	215	-8
1	11		525	512
1	12		322	-336
1	13	•	256	78
1	14		208	-238
1	15	•	283	92
1	16	•	296	88
1	17		426	-445
1	18	•	320	0
2	3		751	725
2	4		367	299
2	5	•	149	-27
2	6		322	-315
2	7		732	667
2	8	•	190	-118
2	9	•	204	9
2	10		494	-438
2	11	•	230	92
2	12		252	-244
2	13		601	609
2	14		627	635
2	15		367	-359
2	16	•	297	123
2	17		338	-378
2	18	•	321	-181
3	2		1025	-957
3	3		330	386
3	4		1291	-1210
3	5		139	196
3	6		1702	1658
3	7	•	182	38
3	8	•	195	8
3	9		590	-600
3	10		626	-641
3	11	•	234	-153
3	12		319	287
3	13	•	260	122
4	1		963	846
4	2		799	-769
4	3		225	-209
4	4		1114	1114
4	5	•	167	-46
4	6		1103	1114
4	7		716	-670
4	8	•	202	50
4	9	•	214	-15
4	10		676	-689
4	11		364	358
4	12		511	-490
4	13	•	265	-110
4	14		424	499
4	15	•	290	67
5	1		1006	-1056
5	2		503	-577
5	3		390	426
5	4		519	453
5	5		344	-288
5	6		755	762
5	7		523	540
5	8		227	-215
5	9	•	223	140
5	10		779	-786
5	11	•	246	-168
5	12	•	258	-53
5	13		355	339
5	14		603	523
5	15	•	295	-256
5	16	•	307	39
5	17	•	318	308
5	18		298	-282
5	19	•	336	115
6	1		509	530

			FOBS	FCALC
6	2		1197	-1301
6	3	•	180	195
6	4		1070	-1092
6	5	•	194	49
6	6		749	793
6	7		350	-389
6	8	•	222	156
6	9	•	232	-12
6	10		529	-462
6	11	•	255	62
6	12		286	249
6	13		369	-395
6	14	•	290	39
7	1		765	812
7	2		427	-432
7	3	•	196	-180
7	4		708	717
7	5		583	-696
7	6	•	216	-7
7	7		203	-263
7	8		218	172
7	9	•	243	50
7	10	•	254	-183
7	11	•	264	239
7	12		287	-257
7	14		546	551
7	15	•	309	90
8	1		312	-295
8	2		183	243
8	3		198	220
8	4		237	-213
8	5		621	-558
8	6		151	167
8	7		645	607
8	8	•	246	-45
8	9		434	367
8	10	•	265	66
8	11		293	-348
8	12	•	285	-59
9	1		492	458
9	2	•	226	-26
9	3		749	-743
9	4		551	-541
9	5	•	239	32
9	6		309	-288
9	7	•	252	-26
9	8	•	260	101
9	9		389	432
9	10	•	277	96
9	11	•	287	160
9	12	•	296	70
9	13		377	-415
9	14	•	315	-14
10	1		469	434
10	2	•	243	14
10	3	•	246	-126
10	4		615	558
10	5		475	-491
10	6		462	-547
10	7		512	484
10	8	•	274	191
10	9	•	282	166
10	10	•	290	295
10	11		563	-516
10	12	•	307	-117
11	1	•	259	212
11	2		411	481
11	3		347	-333
11	4		303	-325
11	5		477	-502
11	6	•	276	-8
11	7		555	486
11	8	•	288	62
11	9		316	273
11	10	•	303	96
11	11	•	310	-174
11	12	•	318	79
11	13	•	325	-71
11	14		470	-485
11	15	•	338	136
12	1		319	285
12	2	•	277	246
12	3		480	-455
12	4	•	283	327
12	5	•	287	81
12	6		423	-372
12	7	•	297	97
12	8	•	302	-245
12	9	•	309	144
12	10	•	315	176
12	11	•	322	64
12	12	•	328	81
12	13		301	-286
12	14	•	339	114
13	1	•	293	-94
13	2	•	294	-86
13	3	•	296	110
13	4	•	299	59
13	5	•	302	-47
13	6	•	306	-196
13	7	•	311	305
13	8	•	316	-41
13	9	•	321	-32
13	10	•	327	118
13	11		414	-402
13	12	•	336	24
14	1	•	309	155
14	2	•	310	170
15	1	•	323	-199
15	2	•	324	184
15	3	•	325	90
15	4	•	327	332
15	5	•	329	265
15	6		442	-382
15	7	•	335	-117
16	1	•	335	-305
16	2	•	336	-20
16	3		355	317
16	4	•	338	-55
17	1	•	343	68

			FOBS	FCALC
17	2		210	236
17	3	•	344	1
H	K			L=4
0	0		1909	-1802
0	1		834	-854
0	2		673	640
0	3		1337	-1319
0	4		521	433
0	5	•	192	-148
0	6		212	-223
0	7		359	349
0	8		232	198
0	9	•	169	14
0	10		265	-282
0	11	•	206	-217
0	12		536	552
0	13	•	293	24
0	14	•	308	-72
0	15		286	291
0	16		472	-518
0	17	•	350	-5
1	0		1039	1022
1	1		690	704
1	2	•	131	105
1	3		476	-459
1	4	•	160	109
1	5		359	364
1	6		205	-158
1	7		707	691
1	8		746	-737
1	9		892	-867
1	10	•	251	138
1	11	•	266	-217
1	12	•	281	-21
1	13	•	296	165
1	14	•	310	32
1	15		323	348
1	16	•	339	144
2	0	•	143	-66
2	1		638	-698
2	2		345	-393
2	3		589	537
2	4	•	174	-24
2	5		955	962
2	6		368	383
2	7		231	302
2	8		288	295
2	9		458	466
2	10	•	257	-206
2	11		827	-853
2	12		301	-288
2	13	•	300	-238
2	14	•	315	161
2	15		325	379
2	16	•	342	246
3	0		162	-124
3	1	•	168	-83
3	2		263	298
3	3		894	-975
3	4		736	-786
3	5		287	-299
3	6		303	-323
3	7		591	640
3	8		886	929
3	9		507	-442
3	10	•	265	-162
3	11		258	-250
3	12	•	292	41
4	0		1783	1903
4	1		330	-305
4	2	•	193	56
4	3		400	-396
4	4		612	-636
4	5		236	225
4	6		274	219
4	7		270	268
4	8	•	249	-116
4	9		276	-259
4	10	•	274	-47
4	11	•	287	-63
4	12		767	-687
4	13	•	314	265
4	14	•	327	-5
4	15		290	318
4	16		650	607
4	17	•	363	-87
5	0		562	580
5	1		614	-543
5	2		416	406
5	3	•	218	-76
5	4		913	-916
5	5		390	387
5	6		261	-264
5	7		208	134
5	8		785	751
5	9		303	296
5	10		242	-294
5	11		401	-413
5	12		376	-346
5	13	•	323	-63
6	0		287	274
6	1		315	354
6	2	•	232	-143
6	3		364	-315
6	4		710	-673
6	5	•	249	16
6	6	•	257	-50
6	7	•	266	137
6	8		720	748
6	9		522	-502
6	10	•	298	191
6	11		266	277
6	12	•	321	-161
7	0		722	669
7	1		405	-441
7	2	•	252	-203
7	3		238	-246
7	4	•	260	-90

Can. J. Chem. Downloaded from www.nrcresearchpress.com by 210.87.254.40 on 09/05/12
For personal use only.

Can. J. Chem. Downloaded from www.nrcresearchpress.com by 210.87.254.40 on 09/05/12
For personal use only.

TABLE V

Bond distances and angles in $CdZn_2(PO_4)_2$ and $Cd_2Zn(PO_4)_2$ compared with graftonite (e.s.d.'s on the bond lengths are enclosed in parentheses)

	Bond distance (Å)				Bond angle (°)		
	$CdZn_2(PO_4)_2$	$Cd_2Zn(PO_4)_2$	Graftonite		$CdZn_2(PO_4)_2$	$Cd_2Zn(PO_4)_2$	Graftonite
M(1)—O(3)	2.09(1)	2.26(2)	2.25(2)	O(3)—M(1)—O(3′)*	84.1	86.4	86.8
O(1)	2.15(1)	2.27(2)	2.23(1)	—O(1)	144.0	149.9	151.2
O(1)	2.32(1)	2.39(2)	2.36(1)	—O(1′)	111.2	106.2	106.2
O(4)	2.42(1)	2.42(2)	2.47(1)	—O(7)	57.2	57.9	56.7
O(6)	2.45(1)	2.52(2)	2.43(2)	—O(4)	71.0	68.5	66.0
O(7′)	2.51(1)	2.52(2)	2.58(1)	—O(6)	129.1	126.5	124.3
O(3′)	2.60(1)	2.67(2)	2.68(1)	O(3′)—M(1)—O(1)	91.6	94.0	92.8
				—O(1′)	164.5	166.1	164.2
				—O(7)	113.0	116.5	117.5
				—O(4)	98.3	93.4	92.3
				—O(6)	90.7	88.8	88.3
				O(1)—M(1)—O(1′)	78.2	78.3	80.2
				—O(7)	93.3	95.9	99.0
				—O(4)	144.9	141.3	142.7
				—O(6)	86.4	83.6	84.4
				O(1′)—M(1)—O(7)	78.7	76.2	77.8
				—O(4)	85.4	85.8	85.1
				—O(6)	78.0	78.9	77.0
				O(7)—M(1)—O(4)	113.8	114.3	111.1
				—O(6)	156.3	154.6	153.5
				O(4)—M(1)—O(6)	59.7	58.7	58.8
M(2)—O(8)	2.14(1)	2.20(2)	2.26(2)	O(8)—M(2)—O(7)	131.0	117.5	115.6
—O(7)	1.96(1)	2.01(2)	2.04(1)	—O(6)	93.5	91.1	88.0
—O(6)	1.92(1)	2.01(2)	2.01(2)	—O(4)	97.5	94.0	92.1
—O(4′)	1.90(1)	1.98(1)	1.99(1)	O(7)—M(2)—O(6)	99.7	98.5	100.0
—O(3)	2.92(1)	2.57(2)	2.39(2)	—O(4)	101.8	106.3	98.6
				O(6)—M(2)—O(4)	139.7	148.8	159.5
				O(3)—M(2)—O(8)	151.2	158.4	159.4
				—O(7)	77.7	84.1	84.6
				—O(6)	81.0	87.1	93.3
				—O(4)	70.8	77.1	79.6

Can. J. Chem. Downloaded from www.nrcresearchpress.com by 210.87.254.40 on 09/05/12
For personal use only.

TABLE V (*Concluded*)

	Bond distance (Å)				Bond angle (°)		
	$CdZn_2(PO_4)_2$	$Cd_2Zn(PO_4)_2$	Graftonite		$CdZn_2(PO_4)_2$	$Cd_2Zn(PO_4)_2$	Graftonite
M(3)—O(5)	2.10(1)	2.31(2)	2.28(1)	O(5)—M(3)—O(2)	170.6	162.8	168.0
—O(2′)	2.19(1)	2.31(2)	2.27(1)	O(5′)	95.7	88.7	94.0
—O(5′)	1.99(1)	2.17(2)	2.04(1)	O(8)	98.5	105.6	102.0
—O(8)	2.06(1)	2.19(2)	2.08(2)	O(2′)	75.6	75.9	73.2
—O(2)	2.05(1)	2.16(2)	2.11(2)	O(2)—M(3)—O(5′)	74.8	75.9	74.0
				—O(8)	88.7	91.6	88.5
				—O(2′)	108.9	100.7	109.1
				O(5′)—M(3)—O(8)	145.3	149.0	145.3
				—O(2′)	104.9	105.7	106.0
				O(8)—M(3)—O(2′)	109.2	104.4	108.1
P(1)—O(1)	1.529(12)	1.554(34)	1.529(23)	O(1)—P(1)—O(3)	112.3	112.8	110.6
—O(3)	1.541(14)	1.499(18)	1.584(15)	—O(5)	105.3	102.2	106.3
—O(5)	1.558(11)	1.547(20)	1.553(14)	—O(7)	112.5	113.0	115.0
—O(7)	1.518(12)	1.604(26)	1.531(19)	O(3)—P(1)—O(5)	110.6	106.7	109.2
				—O(7)	106.1	108.3	107.1
				O(5)—P(1)—O(7)	110.1	113.0	108.6
P(2)—O(2′)	1.530(12)	1.603(23)	1.548(15)	O(2′)—P(2)—O(4′)	110.7	111.5	110.8
—O(4′)	1.553(13)	1.532(28)	1.524(21)	O —O(6)	111.1	106.0	111.6
—O(6)	1.523(10)	1.531(24)	1.549(21)	—O(8)	108.3	109.7	109.6
—O(8)	1.572(12)	1.593(20)	1.576(15)	O(4)′—P(2)—O(6)	104.2	104.5	103.1
				—O(8)	111.1	112.9	111.7
				O(6)—P(2)—O(8)	111.5	112.0	109.9

*Error in angles are of the order of 0.5° for $CdZn_2(PO_4)_2$ and about twice this number of the remaining compounds.

Can. J. Chem. Downloaded from www.nrcresearchpress.com by 210.87.254.40 on 09/05/12
For personal use only.

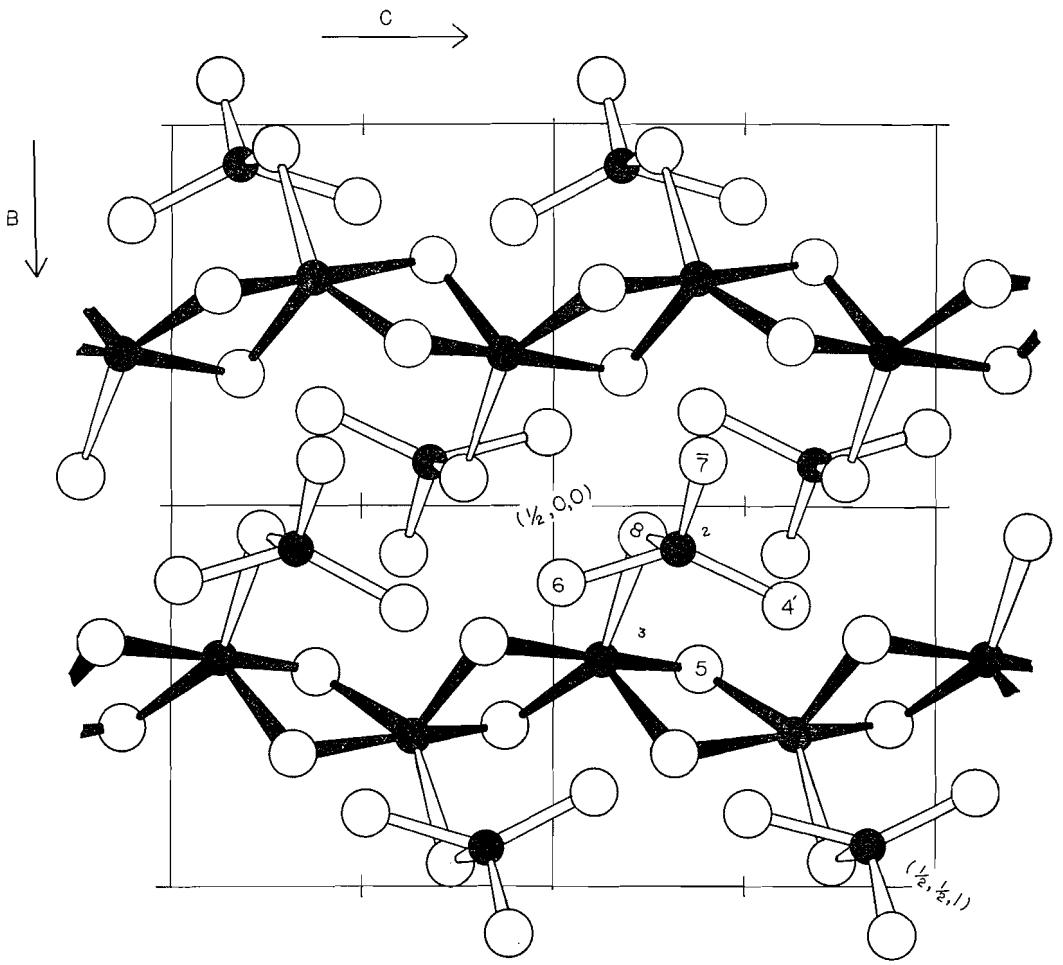

FIG. 1. A portion of the structure of $CdZn_2(PO_4)_2$ is shown in projection onto the *bc* plane. The chains formed by the edge-shared trigonal bipyramids are shown as filled bonds. The cations are filled circles and the oxygen atoms are open circles.

the oxygen polyhedra about site 1 extend in the *bc* plane. These sheets are composed of edge-shared pairs of M(1)—O_7 groups disposed in a face-centered arrangement. The shared edge, O(1) and O($\bar{1}$), arise from centrosymmetrically related polyhedra each of which share corner oxygen atoms, O(3) and O(3′), with the pair of dimeric (M(1)—O_7)$_2$ groups related by the glide plane operations $x, \frac{1}{2} - y, \frac{1}{2} + z$ and $x, -\frac{1}{2} - y, \frac{1}{2} + z$. The three remaining oxygen atoms of cation 2 bridge across the pair of M(1) polyhedra, sharing O(6) with one member and O($\bar{7}$) with the other, and O(4) with the (M(1)—O_7)$_2$ group translated by one unit cell length along the *c* axis. This bonding can be seen in Fig. 2. Thus the tetrahedral cation groups knit together the infinite sheets involving cations of type 1 with the infinite chains involving site 2. The phosphorus tetrahedra, shown in outline in Fig. 2, lie between these chains and sheets.

(B) $Cd_2Zn(PO_4)_2$

Again both PO_4^{3-} tetrahedra are irregular with oxygen atoms lying at an average of 1.55 Å and 1.56 Å from P(1) and P(2) respectively. Since the e.s.d.'s are of the order of 0.02 Å in this compound, no significance can be attached to the difference in the values found here in comparison to those in $CdZn_2(PO_4)_2$. The larger value for e.s.d.'s in "C"ss compared to "B"ss

Can. J. Chem. Downloaded from www.nrcresearchpress.com by 210.87.254.40 on 09/05/12
For personal use only.

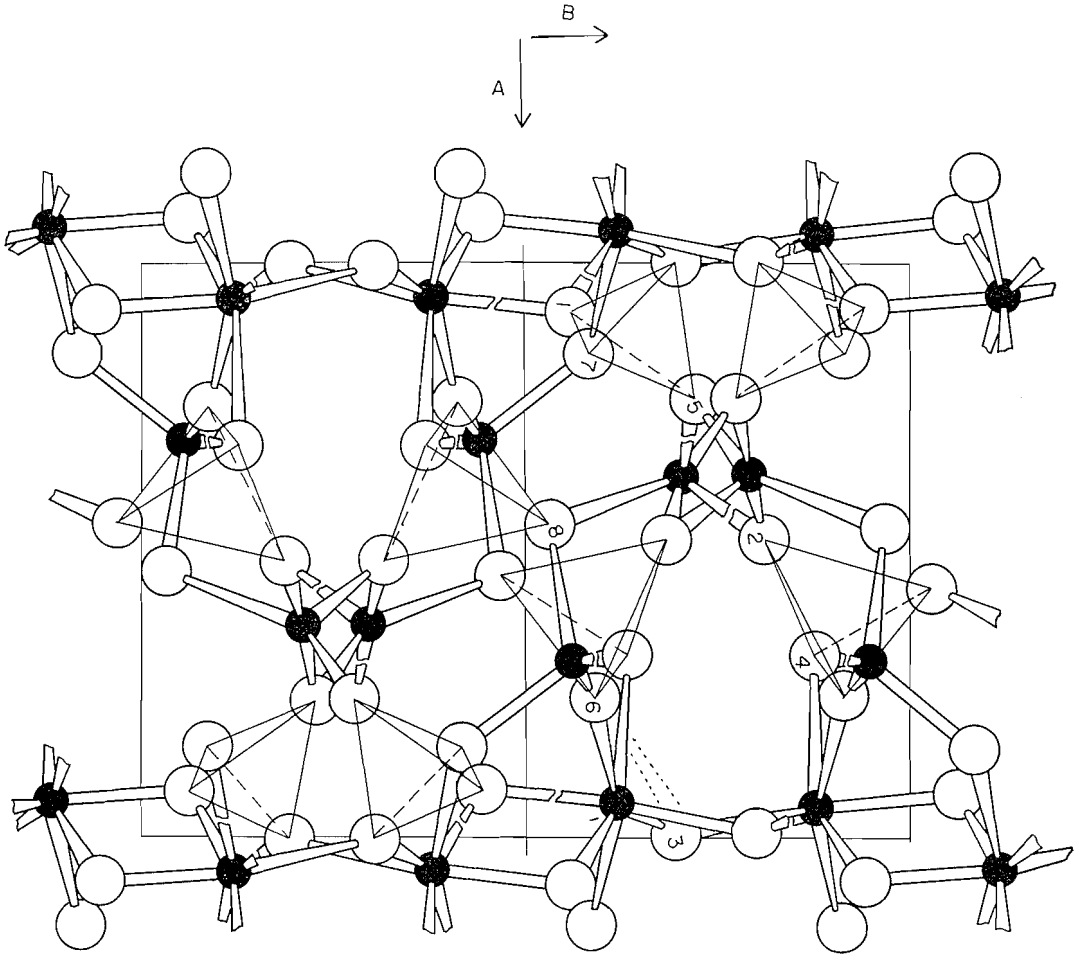

FIG. 2. The structure of $CdZn_2(PO_4)_2$ is shown in projection onto the *ab* plane. The cations are shown as filled circles and the oxygen atoms as open circles. The outlines of the PO_4^{3-} tetrahedra are shown although not the phosphorus atom positions. The bond formed by oxygen atom 3 to cation site 2 in $Cd_2Zn(PO_4)_2$ is shown dotted.

results from the larger relative electron density contributed by the cations and the inherently less accurate visual method of estimating intensities.

Cation 1 is again found in a site showing sevenfold coordination. Five of the oxygen atoms lie roughly in a plane perpendicular to the O(1′)—M—O(3′) axis and lie very approximately in a pentagonal arrangement. The axial cations oxygen bonds, that is those to $O(\bar{1})$ and O(3′), are shorter than the equatorial bonds. These bonds of 2.27 Å and 2.26 Å respectively in Css are also the shorter ones in Bss (2.09 Å and 2.16 Å respectively) and graftonite (2.23 Å and 2.25 Å respectively). The angles show considerable deviations from regularity and, in particular, the angle between O(1′) and O(3′) at M(1) is 166° rather than the ideal 180°.

In Css the cations at site 3 still show trigonal bipyramidal coordination with axial cation–oxygen bond lengths of 2.30 Å and 2.31 Å involving O(2′) and O(5) respectively. The average equatorial M—O bond length is 2.18 Å. For all three structures, the average axial MO bond length exceeds by over 0.1 Å the average equatorial one. This site, which is predominantly occupied by Cd^{2+} has an average metal–oxygen atom bond distance of 2.23 Å as compared with 2.08 Å in Bss where it is occupied entirely by Zn^{2+}. This can be taken as further evidence for the larger cation in this site.

Can. J. Chem. Downloaded from www.nrcresearchpress.com by 210.87.254.40 on 09/05/12
For personal use only.

The major structural difference between $CdZn_2(PO_4)_2$ and $Cd_2Zn(PO_4)_2$ involves site 2. In the latter compound this site has taken on the appearance of an irregular square pyramid involving a fifth oxygen atom, O(3′), lying 2.57 Å from the cation. In $CdZn_2(PO_4)_2$ this oxygen atom is over 2.9 Å away from the cation in site 2. In the mineral graftonite, it lies at 2.39 Å from M(2). The apical oxygen atom, O(7), yields a cation–oxygen atom bond length of 2.01 Å in "C"ss. In comparison with "B"ss, this oxygen atom has moved closer to O(8), as indicated by the decrease from 130° to 117° in the angle between these oxygen atoms subtended at M(2). The only other major angular change is that of O(6)—M—O(4) which is 140° in Bss, 149° in Css, and 160° in the mineral. The average cation oxygen bond length of the four cation oxygen atom bonds common to Bss is 2.05 Å as compared with 1.99 Å in Bss. This change may be a manifestation of the weakening of the shorter bonds due to the presence of the nearly bonded O(3). In Fig. 2, this long bond is shown as a dotted bond length. The atoms in these structures are found to vary significantly from isomorphic positions. P(2) deviates by less than 0.06 Å between the three structures whereas P(1) deviates in $Cd_2Zn(PO_4)_2$ by 0.14 Å from its position in $CdZn_2(PO_4)_2$. In the mineral, the coordinates of P(2) are intermediate. O(3), O(2), O(5) and O(8) show shifts of 0.21 Å, 0.13 Å, and 0.19 Å respectively and these exceeded by a factor of 3 or more the shifts of any of the remaining oxygen atoms. This is expected since the latter three oxygen atoms are bonded to cation 3 which is occupied by Cd^{2+} in "C"ss and Zn^{2+} in "B"ss whereas O(3) forms an additional bond to cation 2. Both M(2) and M(3) show significant shifts whose magnitudes are 0.19 Å and 0.08 Å respectively. In the former case, the motion is primarily in the $a + b$ direction and nearly vectorially opposite to that of O(3). Therefore, the reduced M(2)—O(3) bond distance arises nearly equally from motion of the two bonding atoms.

Discussion

The congruent melting temperatures near the composition represented by $CdZn_2(PO_4)_2$ attest to the stability of this compound. That is, there is probably a minimum in the free energy – composition diagram near the stated composition. By the same token, the lack of a congruent melting compound with composition at $Cd_2Zn(PO_4)_2$ would suggest that there is no particular stability attributable to this composition relative to neighboring points along the composition axis. The stability of Bss might be attributable to the preferred solubility of Cd^{2+} in site 1 and the energy gained by filling such a site and its loss when Cd^{2+} is placed in either of the remaining sites. However, on the surface, it would appear that similar argument would lead to a stable compound at $Cd_2Zn(PO_4)_2$, since here the cations were also found ordered and would also result in a congruent melting point. It appears possible, nevertheless, that the phase transition reported by Hummel and Brown involved a disordering of the cations, probably involving sites 2 and 3 only, above the transition temperature and, therefore, no distinctive minimum in free energy at the proposed compound composition would be expected. At lower temperatures, below the transition point, one might expect a distinct minimum here and this should be reflected in a distinct curvature to the boundary line separating the region containing Bss and Css from the region of Css. Such does not appear to be the case, although the techniques used by Hummel and Brown would not be particularly sensitive to such a behavior.

The existence of a miscibility gap denotes a binodal free energy composition curve with a maximum at some composition around a mole fraction $Cd_3(PO_4)_2$ of 0.5. The fact that the structures of the two phases are so nearly identical helps to hide the reason for the intolerance of Bss to Cd^{2+} for concentrations beyond where site 1 is saturated. In order to occupy either other site Cd^{2+} must distort its environment and perhaps the approach of O(3) to site M(2) results from the distortion so imposed when cation site 3 takes on Cd^{2+}. Since this site is not bound to O(3) directly, the effect must be carried by a rigid displacement of the $P(1)O_4^{3-}$ tetrahedron. That is, with a nearly isotropic displacement of the oxygen atom environment about cation site 3, the tetrahedron containing O(5) will be displaced such as to leave the O(1)—O(7) vector nearly invariant but pushing O(3) towards cation site 2. This is consistent with the displacements discussed above. Thus with those sites containing Cd^{2+} distorting and those with Zn^{2+} resisting the distortion, the free energy

Can. J. Chem. Downloaded from www.nrcresearchpress.com by 210.87.254.40 on 09/05/12
For personal use only.

will increase with increasing composition beyond that of $CdZn_2(PO_4)_2$ until enough Cd^{2+} is added to effect a cooperative distortion to a structure like that of $Cd_2Zn(PO_4)_2$.

The nature of the phase transition reported by Brown and Hummel (3) for $Cd_2Zn(PO_4)_2$ does not have an unambiguous interpretation. It is difficult to conceive of it as a transition of the second kind as treated by Landau and Lifshitz (15) since the structure does not seem to support any continuous change that will result in a phase with higher crystallographic symmetry. This is, of course, under the assumption that the high symmetry phase is the stable form at high temperature. The remaining possibilities are a disordering of the cations or the displacement of O(3) so that at high temperatures, the coordination of cation site 2 is fourfold. This latter possibility seems unlikely in light of the miscibility gap and the fact that it would yield very modest intensity changes which probably would not be seen in a normal X-ray powder pattern. Thus such a change is probably not responsible for the small intensity changes reported by Brown and Hummel (3). Parenthetically in $Cd_3(PO_4)_2$ for which the $l \neq$ O mod 3 reflections are weak (7) a transition resulting in a high symmetry phase is readily conceivable.

One of the most perplexing problems is, accepting the wide variation of structure types corresponding to the composition $M_3(XO_4)_2$, why do these compounds choose the graftonite structure? This structure appears to be a particularly tolerant one since it is composed of sheets of M(1) type cations and chains of M(3) cations bonded somewhat loosely by PO_4 tetrahedron and M(2)—O_n polyhedra. Cation site 1 seems to require a large ion to maintain the pentagonal bipyramidal arrangement of oxygen ligands. With an oxygen atom of radius of 1.4 Å the cation cavity has a radius of 0.93 Å in the plane of the regular pentagon. Therefore, with cations of radii smaller than this in site 1 the structure would be expected to lose stability. In the case of Mn^{2+} with radii of 0.80 Å and Fe^{2+} with radii of 0.75 Å the cations would be expected to be loosely bonded unless the structure is considerably further distorted from the pentagonal bipyramidal arrangement found in these structures. Since $Mn_3(PO_4)_2$ (7) and $Fe_3(PO_4)_2$ (10) adopt these structures it would be of interest to obtain an accurate crystal structure resolution to check this point. On the other hand, for the compound $CaZn_2(PO_4)_2$, the Ca^{2+} ion is probably too large to form the graftonite structure. This seems to be in line with the recent results of Kreidler and Hummel (16) for the $Ca_3(PO_4)_2$–$Zn_3(PO_4)_2$ system.

Acknowledgments

This research has been supported by a grant from the National Research Council of Canada and J. S. Stephens wishes to thank the Ontario Government for providing a fellowship.

1. A. L. Smith and A. D. Power. J. Electrochem. Soc. **101**, 244 (1954).
2. F. L. Katnack and F. A. Hummel. J. Electrochem. Soc. **105**, 125 (1958).
3. J. J. Brown and F. A. Hummel. J. Electrochem. Soc. **110**, 1218 (1963).
4. C. Calvo. Can. J. Chem. **43**, 436 (1965).
5. J. S. Stephens and C. Calvo. Can. J. Chem. **45**, 2303 (1967).
6. C. Calvo. Phys. Chem. Solids, **24**, 141 (1963).
7. J. S. Stephens. Ph.D. Thesis, McMaster University, Hamilton, Ont. 1967.
8. J. F. Sarver, F. L. Katnack, and F. A. Hummel. J. Electrochem. Soc. **106**, 960 (1959).
9. F. A. Hummel and F. L. Katnack. J. Electrochem. Soc. **105**, 528 (1958).
10. C. Calvo. Am. Mineralogist. In press.
11. A. S. Cooper. Acta Cryst. **15**, 578 (1962).
12. B. E. Robertson. Ph.D. Thesis, McMaster University, Hamilton, Ont. 1967.
13. International Tables for X-Ray Crystallography. Vol. III. Kynock Press, Birmingham. 1962.
14. D. W. J. Cruickshank, D. E. Pilling, A. Bujosa, F. M. Louell, and M. R. Truter. *In* Computing methods and the phase problem in X-ray crystal analysis. *Edited by* R. Pepinsky, J. B. Robertson, and J. C. Speakman. Pergamon Press, New York. 1961.
15. L. D. Landau and E. M. Lifshitz. Statistical physics. Addison-Wesley Publishing Company, Inc., Reading, Massachusetts. 1960. p. 439.
16. E. R. Kreidler and F. A. Hummel. Inorg. Chem. **6**, 524 (1967).

Crystal structure of $Cu_3(AsO_4)_2$

SANDRA J. POULSEN[1] AND C. CALVO
Department of Physics, McMaster University, Hamilton, Ontario

Received September 26, 1967

$Cu_3(AsO_4)_2$ forms a monoclinic crystal with lattice parameters $a = 6.327(5)$ Å, $b = 8.642(5)$ Å, $c = 11.313(5)$ Å, $\beta = 92.04(4)°$, and $Z = 4$. The space group is $P2_1/c$. The two orthoarsenate anions in the unit cell have average AsO bond lengths of 1.68 Å and 1.70 Å with mean deviations of 0.02 Å and 0.01 Å respectively. The three cations are fivefold coordinated to oxygen atoms with mean cation oxygen atom bond lengths of 2.005 Å, 2.053 Å, and 2.017 Å for the three independent cations. The range of bond distances extends from 1.892 Å to 2.362 Å. Only one additional cation oxygen distance of less than 3 Å occurs and this lies at 2.76 Å. The cation polyhedra form sheets parallel to the *ab* plane by corner and edge sharing of common oxygen atoms. Adjacent sheets are bonded through the long Cu—O bond distance cited above and by the AsO_4^{3-} anions. Each of the arsenic atoms shares three oxygen atoms with one sheet and one with the adjacent one.

Canadian Journal of Chemistry, 46, 917 (1968)

Can. J. Chem. Downloaded from www.nrcresearchpress.com by 210.87.254.40 on 09/05/12
For personal use only.

Introduction

The crystal structure of $Cu_3(AsO_4)_2$ has been investigated in order to determine if it is related to those previously reported for compounds of the $M_3(XO_4)_2$ type, where the XO_4^{n-} form a tetrahedral group. It would be expected that a modest number of such structure types should be stable. The fact that some arsenates and phosphates are isostructural (1) would support this assumption and suggest that isostructures with the analogous phosphate series should be found among the compounds of this type. This isomorphism has commonly been assumed in the past (2, 3) although it fails for $Cu_3PO_4(OH)_3$–$Cu_3AsO_4(OH)_3$ pair (4) among others.

A further motive for this study is the desire to characterize the geometry of the near neighbor environment of pentavalent As. A limited number of such structures with only oxygen atoms as near neighbors to the As have been determined. These include the anhydrous orthoarsenates, Ag_3AsO_4 (5), the mineral stranskiite ($CuZn_2(AsO_4)_2$) (6), and KH_2AsO_4 (5). The average As—O bond lengths are 1.75 Å, 1.75 Å, and 1.74 Å respectively. The structure of Mg pyroarsenates has been determined by Lukasewicz (7), and recently further refined (8). The average terminal As—O bond length is 1.66 Å whereas the internal or As—O(—As) is 1.68 Å. A number of alkali metal meta-arsenate structures have been reported and all of these have psuedotetrahedral arrangements of oxygen atoms about the arsenic. In $NaAsO_3$ (9), the As—O and As—O(—As) bond lengths are 1.68 Å and 1.77 Å respectively. A number of divalent metal meta-arsenates, however, have been assigned structures that would have sixfold coordinated As^V (10). If this be true, then As^V differs from P^V since the phosphorus invariably is found in tetrahedral environments in the presence of oxygen atoms.

Among the small metal ion $M_3(XO_4)_2$ compounds the lattice parameters found for $Cu_3(AsO_4)_2$, although not the symmetry, would suggest that its structure should be similar to that of either $Mg_3(VO_4)_2$ (11), the mineral graftonite, a solid solution represented as $(Fe,Mn,Ca)_3(PO_4)_2$ (12), or the mineral xanthiosite, $Ni_3(AsO_4)_2$ (13). The lattice parameters of these compounds are compared in Table I. It turns out, however, that the structure of $Cu_3(AsO_4)_2$ is unique among compounds with the same stoichiometry and having tetrahedrally coordinated anions, although it has some features in common with $\beta Zn_3(PO_4)_2$ (14).

Experimental Methods

Crystals of $Cu_3(AsO_4)_2$ were obtained by slowly cooling a melt formed from the precipitate recovered from the reaction of Na_2HAsO_4 and $CuCl_2$ in an aqueous solution. The crystals had either needle-like or plate-like morphologies and several were selected for crystallographic study. The crystals have monoclinic symmetry with the space group $P2_1/c$. The density of 4.8 g/cm^3 was determined with a pycnometer and the sample analyzed for the weight % of Cu. The amount was found to be 40.3 ± 0.5 weight % compared with the theoretical value of 40.7 % calculated for $Cu_3(AsO_4)_2$.

Accurate unit cell parameters were determined from films calibrated with reflections from a TiO_2 crystal

[1]Present address: I.B.M. Corporation, Hamilton, Ontario.

TABLE I

Lattice parameters of a number of $M_3(XO_4)_2$ compounds

	a	b	c	β	Space group
$Cu_3(AsO_4)_2$	6.327	8.642	11.313	92.0	$P2_1/c$
$Mg_3(VO_4)_2$[a]	8.24	11.43	6.05		*Abam*
Graftonite[b]					
$(Fe,Mn,Ca)_3(PO_4)_2$	8.87	11.57	6.17	99°12′	$P2_1/c$
Xanthiosite[c]					
$Ni_3(AsO_4)_2$	10.174	9.548	5.766	92°58.5′	$P2_1/c$

[a]Ref. 11.
[b]Ref. 12.
[c]Ref. 13.

(a = 4.59291(5) Å and c = 2.9591(3) Å (15)) and powder lines of Al_2O_3 (a = 4.75903(3) Å and c = 12.9908(2) Å (16)). The Al_2O_3 lines were superimposed on a zeroth level Weissenberg photograph containing reflections of the $0kl$ type. The pattern was superimposed at the center and the two ends of the film by allowing the exposure to pass through the Weissenberg screen and moving the camera between exposures. The a axis length was determined from a comparison of the layer line spacing of TiO_2 with $Cu_3(AsO_4)_2$ on a film containing patterns from both crystals. The β angle was determined from a direct measurement on a precession photograph of the {010} zone. The crystal parameters are in Table II.

Integrated intensity photographs were obtained for the {010} and {001} zones using MoKα radiation and a precession camera. These data were measured with a Joyce–Lobell microdensitometer. Initially, these data had been measured visually from non-integrated photographs, converted to unitary structure factors, and used to determine the trial structure. Data of the type nkl with n = 0, 1, and 2 were recorded with a manual scintillation counter attached on a Supper Weissenberg camera. These latter data were taken with CuKα radiation and the values measured and corrected, where necessary, for dead time and background errors. All the data were subjected to Lorentz and polarization corrections and adjusted for the effect of absorption. The two crystals used measured 0.16 × 0.08 × 0.08 mm^3 and 0.24 × 0.08 × 0.04 mm^3. The former was used to obtain the data with MoKα radiation with the long axis parallel to c, while the second was used to obtain the remaining data and had the a axis parallel to the long dimension.

Trial structures were obtained from electron density maps prepared with structure factors whose signs were determined by the method of De Vries (17). Reflections with unitary structure factors greater than about 0.2 were used to calculate the probability that the Zachariasen relationship (18)

$$S(\mathrm{H})S(\mathrm{H}')S(\mathrm{H}+\mathrm{H}') = +$$

among the signs S(H)'s of the structure factors $|F(\mathrm{H})|$'s was valid. The numbers of reflections used were 40 out of 102 from the {100} zone, 40 out of 85 from the {010} zone, and 31 out of 112 from the {001} zone. In the latter case 23 signs could be determined in terms of two sign symbols and the two free choices allowed in determining the origin. The four projected electron densities generated from the possible sign choices based on these symbols were calculated. Three of these had atoms on the glide planes but only one had a peak high enough to correspond to the superposition of two atoms expected in this projection. Further, the Patterson functions for the {100} and {010} zones were not consistent with atoms on the glide plane. An R value calculated after 1 cycle of least square refinement using the atomic positions determined from the fourth electron density was 0.31 and, therefore, it was considered to have the greatest likelihood of being correct.

A similar procedure would have determined, at best, only 8 out of the 40 signs originally chosen from the {010} zone in terms of one sign symbol. This was not promising enough, especially with the long projection axis to warrant further pursuit at this stage. For the {100} zone 15 signs could be determined in terms of three sign symbols but only 4 more in terms of an additional sign symbol. Again two free choices were made with the view in mind that this origin might not be the same as the one selected above. In this case, only one sign symbol was chosen and that solution leading to all signs positive was set aside. The signs chosen turned out to lead to the correct structure and the electron densities determined at the initial stages are shown in Fig. 1*a* and *b*. The final positions for the Cu and As ions are superimposed on these diagrams. One sign, that of (008), was determined from Harker–Kasper inequalities (19). It is of interest to note that, although 17 out of the initial 89 Zachariasen relations were wrong, only one sign had been improperly assigned at this stage. The three components x, y, and z of the atomic displacements of Cu and As were determined by combining the results obtained in the two projections and the magnitudes of the peak heights were employed to distinguish between Cu^{2+} and As^{5+}.

TABLE II

Crystal data of $Cu_3(AsO_4)_2$

a = 6.327(5) Å
b = 8.642(5) Å
c = 11.313(5) Å
β = 92.04(4)°
Z = 4
Extinctions for $h0l$, l odd and for $0k0$, k odd
Space group $P2_1/c$
ρ meas. = 4.83 g/cm^3
ρ calcd. = 5.04 g/cm^3
Linear absorption coefficient: μ_{Mo} = 220 cm^{-1}, μ_{Cu} = 260 cm^{-1}

Can. J. Chem. Downloaded from www.nrcresearchpress.com by 210.87.254.40 on 09/05/12
For personal use only.

Can. J. Chem. Downloaded from www.nrcresearchpress.com by 210.87.254.40 on 09/05/12
For personal use only.

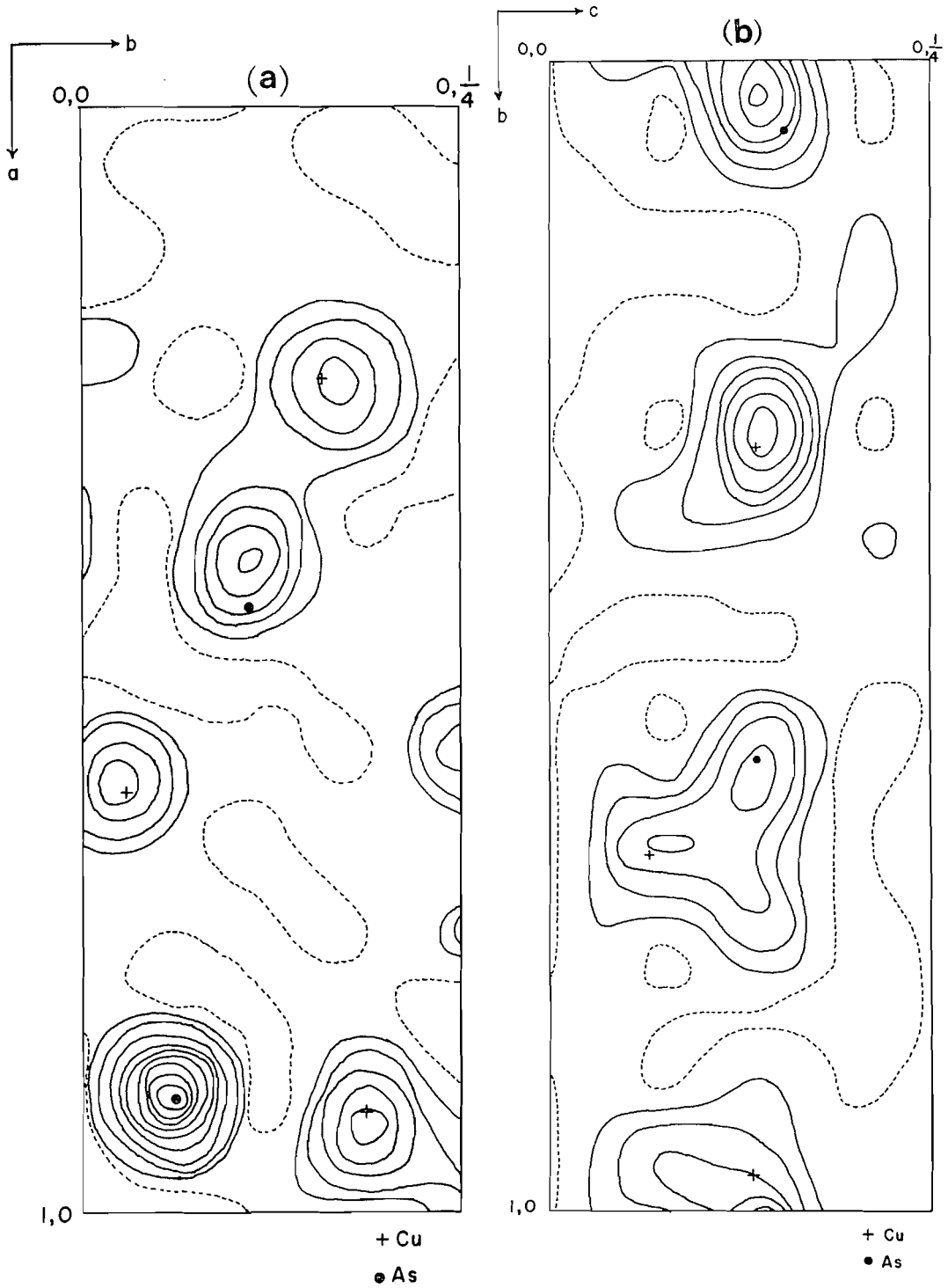

FIG. 1. (*a*) The final atomic positions for Cu and As are shown superimposed on the $\rho(x,y)$ electron density obtained by the use of the sign correlation procedure. (*b*) The final atomic positions for Cu and As are shown superimposed on the $\rho(y,z)$ electron density obtained by the use of the sign correlation procedure.

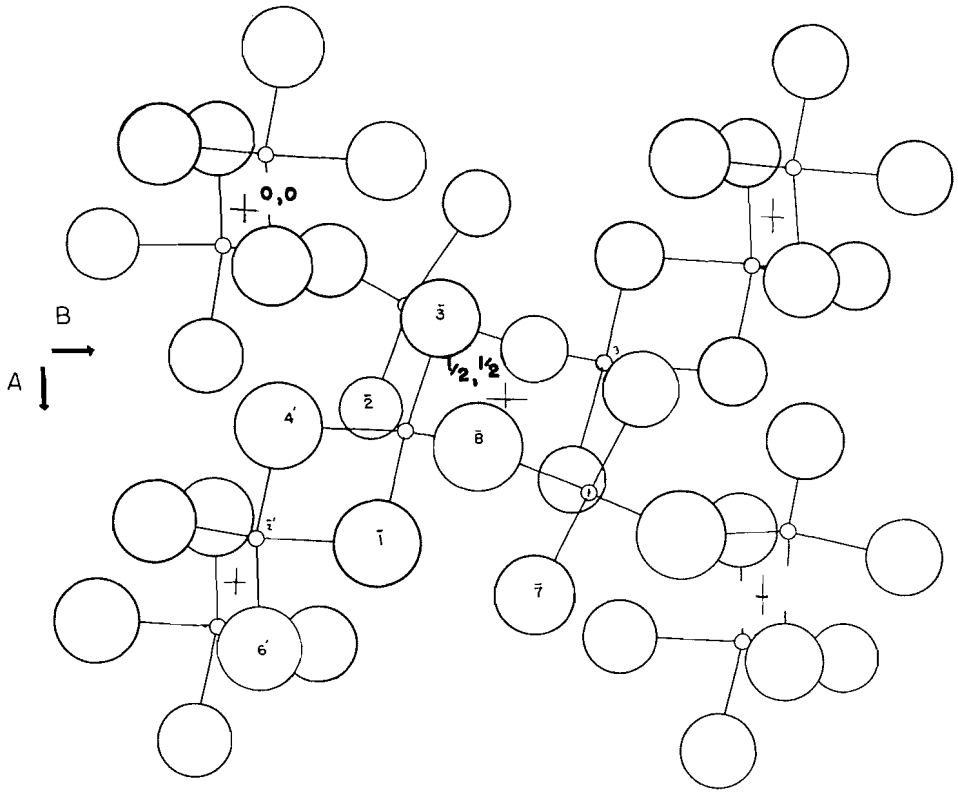

FIG. 2. The bonding between the cation polyhedra is shown in projection onto the $z = 0$ plane. The large spheres represent oxygen atoms while the smaller ones represent the Cu ions.

The oxygen atoms were found by applying the constraint that they should lie at 1.7 Å and be tetrahedrally distributed about the As atoms. Peaks in the difference synthesis satisfying this requirement were assigned to oxygen atoms. Six of the eight oxygen atoms were readily found in this manner but it turned out that the other two, O(5) and O(8), had been interchanged with respect to the appropriate As atoms. Atomic form factors were taken from the International Tables, Vol. III (20). A least squares refinement routine written by J. S. Stephens was employed and yielded an overall R value of 0.20 at this point. Individual isotropic temperature factors were used. Weights were chosen in the manner of Hughes (21). Once the proper positions of the O(5) and O(8) were found the R value dropped to 0.11. Unobserved reflections whose calculated structure factors were less than the minimum observable value in that region of reciprocal space were given zero weight and otherwise taken to be 0.9 of this minimum. Since only a limited amount of data were taken up the a axis, it was felt that a refinement with anisotropic thermal parameters might yield misleading results and therefore were not used. The final structure is shown in projection on the $z = 0$ plane in Fig. 2 and $x = 0$ plane in Fig. 3. The final atomic parameters leading to a

$$R\ (= \frac{\Sigma \| F_o | - | F_c \|}{\Sigma | F_o |}) \text{ of } 0.09$$

$$\text{and } R_2\ (= [\ \frac{\Sigma \omega \| F_o |^2 - | F_c |^2 |}{\Sigma \omega | F_o |^2}\ ]^{1/2}) \text{ of } 0.11$$

for all the data are in Table III. The final combined data for all the layer lines is shown in Table IV. Here the data taken with MoKα radiation have been adjusted for anomalous dispersion to be expected if it had been taken with CuKα radiation, and the final cycles of refinement carried through with the combined data. The values of the atomic coordinates that would allow one to recover the original data are to be found in Table III. Note that, in general, the atomic positions do not differ significantly from the final values reported in Table III, but that the temperature factors do. The larger estimated standard deviations (e.s.d.'s) on the x coordinates of the atoms reflects the limited data taken up the a axis.

The bond distances around the As ions and the Cu ions are shown in Table V. Also included are the bond angles in the various groups. No correction for thermal motion has been applied to these bond lengths. In Table VI, the sum of the bond angles about each of the oxygen atoms is shown. The concept that these are to be near 360° has been a useful one in resolving this structure, although the deviations are quite significant.

Description of Structure

The orthoarsenate ions in this structure form irregular tetrahedra with average AsO bond

Can. J. Chem. Downloaded from www.nrcresearchpress.com by 210.87.254.40 on 09/05/12
For personal use only.

Can. J. Chem. Downloaded from www.nrcresearchpress.com by 210.87.254.40 on 09/05/12
For personal use only.

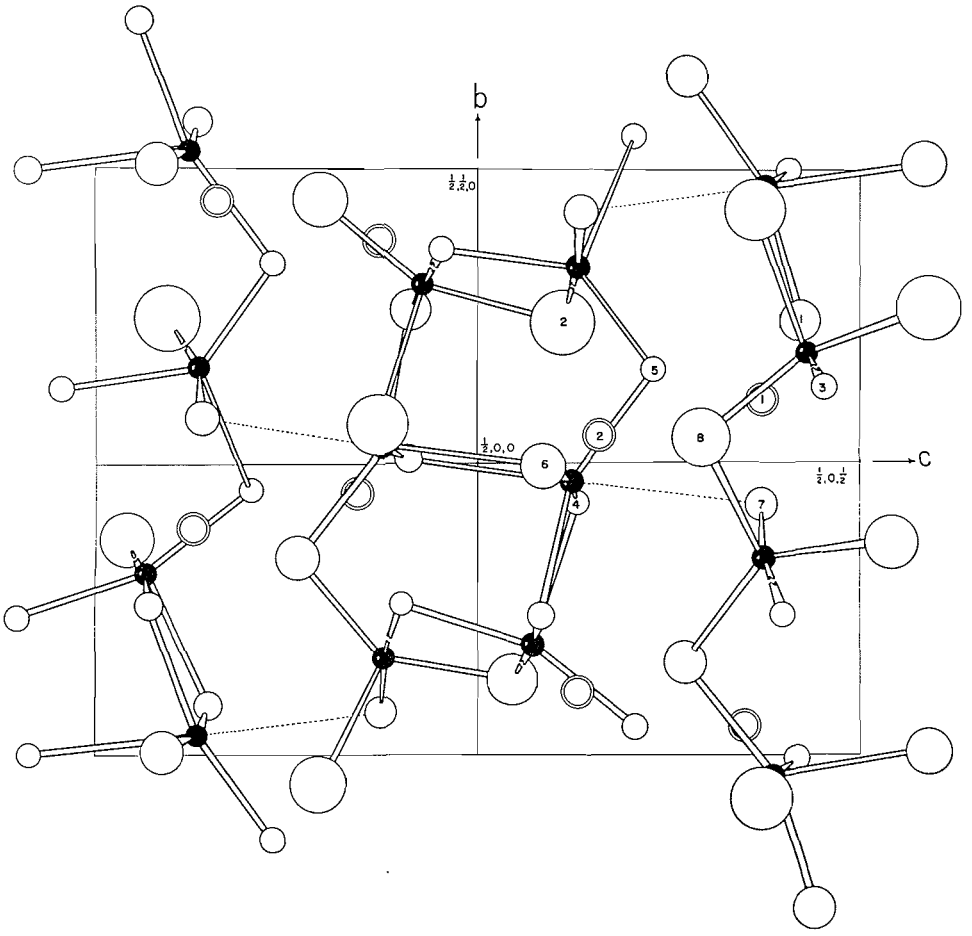

FIG. 3. The structure of $Cu_3(AsO_4)_2$ is shown projected down the *a* axis. The Cu ions are represented by filled circles, the As ions by doubled circles, and the oxygen atoms by large spheres. The long Cu(1)—O(7) bond is shown dotted.

lengths of 1.68 Å for As(1) and 1.70 Å for As(2). These bond lengths range from 1.65 Å to 1.71 Å in the former group and from 1.69 Å to 1.70 Å in the latter group. Since the estimated standard deviation for the As(1)—O(7) bond length is 0.016 Å we can see that at 1.647 Å this bond length deviates by about 3 standard deviations from the average As—O bond length. The range in the O—As—O angle about As(1) is 103° to 117° with an average of 109.6° and a mean deviation of 3.2° and about As(2) is from 105° to 114° with an average of 109.4° and a mean deviation of 2.7°. These values also indicate that the environment of As(1) is the least regular of the two. The more important bond distances and angles are to be found in Table V. Each oxygen atom is bonded to one As atom and two cations, although this requires that one long bond (Cu(2)—O(7)) of 2.76 Å be included.

The environments of the three copper ions differ considerably. Cu(1) has a trigonal bipyramidal environment with O(3), O(5), and O(8) nearly coplanar with Cu(1) while O(2) and O(7) are the axial oxygen atoms of this group. The axial oxygen atoms lie at an average distance of 1.93 Å from the Cu^{2+} whereas the equatorial oxygen atoms lie at 2.05 Å away on the average.

Cu(2) has a tetragonal bipyramidal environment with the cation displaced slightly from the near plane formed by O(1), O(5), O(4), and $O(\bar{6})$ which lie at an average of 1.98 Å from the cation. The first pair of oxygen atoms lie at 2.04 ± 0.01 Å while the latter two lie at 1.905 ± 0.015 Å. The axial oxygen atom O(6) lies at 2.36 Å while

TABLE III

Atomic parameters for $Cu_3(AsO_4)_2$ (e.s.d.'s are enclosed in parentheses). Values in brackets correspond to the parameters used to calculate dispersion corrections so that all the data could be combined

	x	*y*	*z*	β
Cu(1)	0.2415(8)	0.1642(4)	0.6323(3)	1.01(8)
	[0.2414]	[0.1637]	[0.6329]	[0.66]
Cu(2)	0.6161(9)	0.0311(4)	0.8777(4)	1.24(8)
	[0.6176]	[0.0307]	[0.8766]	[0.81]
Cu(3)	0.9082(8)	0.1900(4)	0.4316(3)	1.01(8)
	[0.9074]	[0.1902]	[0.4320]	[0.71]
As(1)	0.4143(6)	0.1134(3)	0.3679(2)	0.76(6)
	[0.4154]	[0.1134]	[0.3677]	[0.49]
As(2)	0.8960(6)	0.0602(3)	0.1507(2)	0.76(6)
	[0.8964]	[0.0618]	[0.1507]	[0.35]
O(1)	0.6062(34)	0.2381(20)	0.4188(14)	0.82(28)
	[0.6038]	[0.2331]	[0.4163]	[0.41]
O(2)	−0.0324(36)	0.2406(21)	0.1063(14)	0.85(28)
	[−0.0370]	[0.2478]	[0.1116]	[0.96]
O(3)	0.2082(39)	0.1309(21)	0.4568(15)	1.24(32)
	[0.2053]	[0.1333]	[0.4556]	[0.33]
O(4)	0.0853(41)	−0.0731(20)	0.1210(16)	1.35(35)
	[0.0894]	[−0.0676]	[0.1232]	[0.62]
O(5)	0.3379(38)	0.1541(19)	0.2284(15)	0.87(29)
	[0.3467]	[0.1561]	[0.2229]	[0.95]
O(6)	0.6701(44)	−0.0046(24)	0.0836(17)	1.50(34)
	[0.6645]	[−0.0078]	[0.0867]	[1.86]
O(7)	0.4809(38)	−0.0705(17)	0.3600(14)	0.78(28)
	[0.4747]	[−0.0705]	[0.3608]	[0.96]
O(8)	−0.1313(42)	0.0528(20)	0.2986(17)	1.28(32)
	[−0.1376]	[0.0413]	[0.2986]	[1.31]

the sixth oxygen atom, O(7), is found at 2.75 Å from the cation.

The third cation shows a highly irregular five-fold coordinated environment roughly disposed as in a trigonal bipyramid. The axial oxygen atoms O(1) and O(3) lie at 1.96 Å and 1.98 Å respectively away from Cu(3) whereas the equatorial oxygen atoms, O(2), O(4), and O(8), show an average cation oxygen bond distance of 2.05 Å. Here one of the equatorial bond angles, O(2)—Cu(3)—O(8), at 159° deviates considerably from the ideal value of 120°.

The cation polyhedra form sheets extended in the *ab* plane through corner and edge sharing. Adjacent sheets are bonded by the arsenate ions which share three oxygen atoms with one sheet and one with the adjacent sheet. In addition, these sheets are bonded through the long Cu(2)—O(7) bond. The structure of these sheets is unique among the $M_3(XO_4)_2$ compounds investigated to date. Cations of type (2) share a non-equatorial edge, consisting of a pair of oxygen atoms, across a center of symmetry. These groups then corner share two oxygen atoms with each of a pair of edge-sharing Cu polyhedra formed from Cu(1) and Cu(3). These pairs alternate forming chains parallel to the *a* direction as shown in Fig. 2. Sheets are formed through corner sharing of oxygen atoms between centrosymmetrically related Cu(1)—Cu(3) polyhedral pairs.

These sheets bear some resemblance to those in $\beta Zn_3(PO_4)_2$ (14), as illustrated in Fig. 1 of that paper. Both structures have rings formed by pairs of edge-shared trigonal bipyramids which corner share oxygen atoms across a center of symmetry. These in turn are bonded, in $\beta Zn_3(PO_4)_2$, through corner sharing between cations 1 and 2, but in contrast with $Cu_3(AsO_4)_2$, no bonding exists between cations 1 and 3 in the same sheet.

The structure of clinoclase, $Cu_3AsO_4(OH)_3$, has a number of features similar to those of $Cu_3(AsO_4)_2$. In the mineral each cation has a tetragonal bipyramidal environment of oxygen atoms which edge share in pairs to form "dimers". As in $Cu_3(AsO_4)_2$ one of these dimers (type I) corresponds to an edge-shared pair across a center of symmetry. Whereas the longest bond of the five is at 2.36 Å in $Cu_3(AsO_4)_2$ the longest one

Can. J. Chem. Downloaded from www.nrcresearchpress.com by 210.87.254.40 on 09/05/12
For personal use only.

Can. J. Chem. Downloaded from www.nrcresearchpress.com by 210.87.254.40 on 09/05/12
For personal use only.

lies at 2.51 Å in clinoclase. The remaining cations in the mineral each have one additional long bond, lying at 2.84 Å and 2.99 Å. The type II dimers are connected by corner sharing to form chains extended along the c^* axis of the mineral much as the edge-shared pair of trigonal bipyramids in $Cu_3(AsO_4)_2$ form chains extended along the a axis. However, in $Cu_3(AsO_4)_2$ both types of dimers participate in the chain. In the mineral four adjacent chains are bonded by corner sharing with one type I dimer whereas in $Cu_3(AsO_4)_2$ the dimers connecting chains are themselves interconnected. In clinoclase only two of the oxygen atoms about As^V are shared strongly with more than one cation while the hydrogen atoms have been assigned to the non-arsenate oxygen atoms. A difference in length among the As—O bonds has been attributed (Ghosh *et al.* (4)) to the fact that the shorter bonds are of higher bond order since they are less strongly bonded to a second cation. A similar phenomenon seems to occur in $Cu_3(AsO_4)_2$ where O(7), bonded strongly to only Cu(1), has an AsO bond length of 1.65 Å whereas the remaining AsO bonds all lie between 1.67 Å and 1.71 Å.

The structure of euchroite, $Cu_2(AsO_4)(OH)\cdot 3H_2O$, has recently been refined by Finney (22). Remarkably he finds the AsO bond distances about AsO_4^{3-} range from 1.615(12) Å to 1.773 (12) Å. The shortest of these is involved in three hydrogen bonds but unbonded to the cations, while the longest is bonded to two cations and participates in only one hydrogen bond. The other oxygen atoms of the tetrahedra are apparently not involved in these bonds. These results do not appear easily reconcilable with those obtained for $Cu_3(AsO_4)_2$.

Crystals of stranskiite are triclinic with space group $P\bar{1}$. The refinement reported by Plieth and Sänger (6) yielded an average As—O bond distance of 1.75 Å. Their data have been further refined (23) using individual isotropic temperature factors with weights, ω, chosen so that $\omega||F_o| - |F_c||$. The average AsO value obtained was 1.68 Å with individual AsO bond distances of 1.70(2) Å, 1.67(1) Å, 1.63(1) Å, and 1.72(2) Å. The shortest of these distances is to that cation which is bonded to only one cation. The Cu ions lie on a center symmetry planar with four equatorial oxygen atoms lying at an average of 1.96 Å away. The next nearest oxygen atoms are two pairs of long axial oxygen atoms at about 3.2 Å away. The Zn ions show fivefold coordination with average Zn—O bond distances of 2.08 Å. These Zn ion polyhedra edge share across a center of symmetry and these in turn corner share with Cu^{2+}. Each of the equatorial oxygen atoms is shared with a separate ZnO polyhedra forming sheets running parallel to the $a + b,c$ plane. Adjacent sheets are bonded by AsO_4^{3-} groups which share two oxygen atoms with each of its neighboring sheets. In this respect stranskiite differs from the sheet structure in $Cu_3(AsO_4)_2$.

In $Mg_3(VO_4)_2$ (11) the cations have obtained fully octahedral environments and this at the expense of a coordination number of four for two of the oxygen atoms. This structure consists of chains of edge-shared octahedra running parallel to the c axis and in this sense resembles the chains of trigonal bipyramids in graftonite. In alternate octahedral holes formed by oxygen atoms from adjacent chains one finds an additional cation. Sheets of these chains lie on the a, $b+c$ plane and are separated by tetrahedrally coordinated V^{5+} which share three oxygen atoms with one sheet and one with the adjacent one.

Whereas phosphate systems seem to show a regularity between P—O and P—O(—P) in terms of valence bond order – bond length as the degree of condensation of the basic XO_4^{n-} tetrahedra increases, such does not appear to be the case for the arsenates. The average As—O bond lengths of 1.70 Å and 1.68[5] Å found for clinoclase and $Cu_3(AsO_4)_2$ respectively differ substantially from the values of 1.75 Å and 1.74 Å reported for Ag_3AsO_4 and KH_2AsO_4 respectively. Stranskiite now shows an average of 1.68 Å. The bond lengths in $Mg_2As_2O_7$, although qualitatively in agreement with chemical bonding considerations in that the terminal bond lengths are shorter (1.66 Å) than the inner AsO bond length (1.68 Å), average to 1.67 Å. This average which should correspond to bond length in an isolated AsO_4^{3-} is lower than the expected value. In this case corrections to the bond lengths arising from the thermal motion of the atoms, particularly for the central oxygen atom, will raise the average AsO bond length to a value near that found in $Cu_3(AsO_4)_2$. The metarsenates should show an even greater discrepancy between the chain AsO bond lengths and the peripheral ones that are found for the

Can. J. Chem. Downloaded from www.nrcresearchpress.com by 210.87.254.40 on 09/05/12
For personal use only.

TABLE IV

Observed and calculated structure factors of $Cu_3(AsO_4)_2$ ($\times$ 10). Reflections marked * were unobserved

K	L	|FØBS|	FCAL	K	L	|FØBS|	FCAL	K	L	|FØBS|	FCAL	K	L	|FØBS|	FCAL
		H = 0		7	2	438	-502	2	2	*107	95	5	11	457	420
				7	3	712	732	2	3	1633	-1626	6	-1	1180	1108
0	2	182	205	7	4	601	651	2	4	719	777	6	-2	1435	1393
0	4	3432	-4038	7	5	*121	86	2	5	971	-1008	6	-3	621	633
0	6	*145	-34	7	6	656	708	2	6	683	682	6	-4	*168	-126
0	8	1475	1477	7	7	930	-979	2	7	986	1021	6	-5	798	-758
0	10	1065	-1048	7	8	580	-629	2	8	165	136	6	-6	911	-949
0	12	879	-777	7	9	169	99	2	9	537	538	6	-7	*144	92
0	14	971	883	7	10	473	-486	2	10	561	-510	6	-8	*141	121
1	2	475	434	8	0	551	-559	2	11	254	-241	6	-9	583	646
1	3	559	-533	8	1	546	624	2	12	311	-229	6	-10	175	369
1	4	1270	1342	8	2	* 88	98	3	-1	372	381	6	0	*156	-80
1	5	207	-216	8	3	734	827	3	-2	563	549	6	1	1491	-1480
1	6	616	631	8	4	160	191	3	-3	1329	1366	6	2	798	-736
1	7	388	382	8	5	597	-629	3	-4	573	-552	6	3	1293	-1269
1	8	332	-342	8	6	213	-242	3	-5	*137	-96	6	4	369	366
1	9	* 95	2	8	7	465	-491	3	-6	266	-279	6	5	853	840
1	10	433	-405	8	8	280	280	3	-7	957	-1007	6	6	434	406
1	11	229	188	8	9	338	398	3	-8	857	830	6	7	610	627
1	12	* 89	-92	9	1	283	-325	3	-9	539	-521	6	8	561	-563
1	13	401	255	9	2	215	222	3	-10	237	190	6	9	474	-468
2	0	803	814	9	3	511	542	3	-11	287	248	6	10	515	-444
2	1	1119	-957	9	4	247	-277	3	-12	573	-486	6	11	161	119
2	2	843	-797	9	5	* 71	62	3	-13	240	197	7	-1	*168	29
2	3	394	-328	9	6	364	-390	3	0	*103	77	7	-2	246	-270
2	4	1052	-1033	9	7	458	-556	3	1	269	-258	7	-3	549	549
2	5	326	-345	10	0	312	-306	3	2	1601	-1535	7	-4	716	-698
2	6	968	1000	10	1	* 97	-55	3	3	426	-409	7	-5	*198	78
2	7	528	-460	10	2	269	308	3	4	* 74	12	7	-6	*196	-58
2	8	836	840					3	5	676	693	7	-7	268	-244
2	9	161	-150	K	L		H = 1	3	6	1221	1271	7	-8	230	228
2	10	209	-216					3	7	292	-139	7	0	629	608
2	11	624	575	0	-2	1186	1131	3	8	595	-512	7	1	630	-595
2	12	252	-269	0	-4	893	874	3	9	876	-797	7	2	501	461
2	13	342	300	0	-6	*187	-157	3	10	392	-344	7	3	476	477
3	1	2663	2680	0	-8	1762	-1888	3	11	*143	-29	7	4	*126	22
3	2	355	337	0	-10	*167	-33	3	12	411	613	7	5	*126	43
3	3	1349	-1311	0	-12	703	730	4	-1	1336	1255	7	6	124	127
3	4	* 74	70	0	-14	169	-214	4	-2	*124	64	7	7	584	-647
3	5	1686	-1664	0	2	566	-539	4	-3	610	-566	7	8	214	-161
3	6	599	-635	0	4	267	311	4	-4	196	-173	7	9	*135	-36
3	7	877	897	0	6	165	171	4	-5	1279	-1359	7	10	230	-192
3	8	440	-450	0	8	399	-458	4	-6	*159	79	8	-1	740	746
3	9	* 76	-37	0	10	580	-538	4	-7	*168	57	8	-2	399	-361
3	10	988	911	0	12	526	566	4	-8	375	468	8	-3	*174	98
3	11	841	-757	0	14	565	465	4	-9	321	313	8	-4	342	349
3	12	559	518	1	-2	941	1029	4	-10	*159	-34	8	-5	725	-714
4	0	434	-463	1	-3	875	-1013	4	-11	*146	-79	8	0	1249	-1217
4	1	411	-399	1	-4	212	-231	4	-12	179	-196	8	1	*168	-12
4	2	335	313	1	-5	*119	107	4	0	406	404	8	2	333	314
4	3	614	607	1	-6	1333	-1510	4	1	* 85	-44	8	3	629	-629
4	4	349	263	1	-7	710	777	4	2	670	-599	8	4	1118	1058
4	5	1531	1543	1	-8	461	-511	4	3	109	90	8	5	*154	85
4	6	588	-546	1	-9	*150	-90	4	4	524	-488	8	6	*146	-109
4	7	330	-375	1	-10	725	696	4	5	835	800	8	7	501	498
4	8	583	-589	1	-11	*107	42	4	6	448	402	8	8	294	-276
4	9	881	-857	1	-12	625	558	4	7	*175	-62	9	-1	754	753
4	10	615	532	1	-13	291	275	4	8	299	238	9	-2	507	479
4	11	* 86	107	1	0	344	-354	4	9	931	-833	9	-3	367	364
4	12	579	481	1	1	569	469	4	10	257	-378	9	-4	290	290
5	1	* 83	40	1	2	256	-226	4	11	*163	-90	9	-5	812	-883
5	2	* 85	-55	1	3	1049	-1066	4	12	328	-228	9	-6	175	-166
5	3	498	-513	1	4	786	854	5	-1	1826	-1738	9	0	220	-215
5	4	* 93	84	1	5	190	-150	5	-2	432	439	9	1	454	-430
5	5	*196	-195	1	6	712	699	5	-3	*149	94	9	2	635	-629
5	6	*145	-112	1	7	1684	1669	5	-4	1184	-1104	9	3	372	-362
5	7	617	683	1	8	1165	-1124	5	-5	678	663	9	4	441	-429
5	8	718	-740	1	9	455	-469	5	-6	251	200	9	5	442	428
5	9	631	618	1	10	330	-377	5	-7	251	-289	9	6	230	235
5	10	464	421	1	11	1149	-997	5	-8	947	935	10	-1	225	-211
5	11	307	-302	1	12	538	434	5	-9	*144	-62	10	-2	*155	48
5	12	426	387	2	-1	1472	1406	5	-10	451	-521	10	-3	*104	-66
6	0	*141	110	2	-2	1408	-1440	5	-11	451	578	10	-4	421	440
6	1	170	180	2	-3	943	-978	5	-12	437	-599	10	0	307	-295
6	2	300	303	2	-4	258	301	5	0	1957	1980	10	1	365	359
6	3	257	234	2	-5	370	-412	5	1	878	-833	10	2	374	376
6	4	233	244	2	-6	688	748	5	2	1145	-1097	10	3	318	320
6	5	491	-495	2	-7	1862	2031	5	3	1567	1540	10	4	291	309
6	6	573	-565	2	-8	403	-423	5	4	1369	-1338	11	0	*166	-31
6	7	663	-661	2	-9	*214	-129	5	5	874	841				
6	8	182	-152	2	-10	*154	73	5	6	582	594	K	L		H = 2
6	9	571	597	2	-11	1367	-1243	5	7	516	-552				
6	10	126	118	2	-12	823	756	5	8	601	663	0	-2	*168	71
6	11	785	708	2	0	748	-754	5	9	*174	53	0	-4	237	202
7	1	288	-330	2	1	1095	986	5	10	395	-247	0	-6	410	414

TABLE IV (*Concluded*)

Observed and calculated structure factors of $Cu_3(AsO_4)_2$ ($\times$ 10). Reflections marked * were unobserved

K	L	|FOBS|	FCAL	K	L	|FOBS|	FCAL	K	L	|FOBS|	FCAL	K	L	|FOBS|	FCAL
0	-8	468	-495	4	-1	*220	71	8	-5	* 81	-81				
0	-10	280	-274	4	-2	1335	-1140	8	-6	698	-674	K	L		H = 5
0	-12	*201	74	4	-3	800	-684	8	-7	* 70	17				
0	-14	304	-336	4	-4	*136	92	8	-8	1030	876	0	-2	*113	48
0	0	487	483	4	-5	206	79	8	0	* 87	-45	0	-4	185	-260
0	2	143	143	4	-6	1209	1070	8	1	* 87	-125	0	-6	*168	-104
0	4	1352	-1287	4	-7	319	250	8	2	510	-560	0	-8	981	987
0	6	469	-510	4	-8	223	-177	8	3	*121	-102	0	-10	*121	140
0	8	345	415	4	-9	1173	-964	8	4	450	461	0	-12	913	-769
0	10	90	96	4	-10	740	-572	8	5	292	353	0	0	*121	-62
0	12	115	150	4	0	304	309	8	6	602	754	0	2	*171	72
0	14	674	599	4	1	1109	966	8	7	*120	70	0	4	460	-528
1	-2	1083	-981	4	2	1407	1304	8	8	242	-264	0	6	*225	-78
1	-3	1106	-1077	4	3	644	580	9	-1	*147	-101	0	8	607	623
1	-4	632	-595	4	4	*127	-80	9	-2	252	-240	0	10	501	547
1	-5	1666	1552	4	5	192	-206	9	-3	464	488	0	12	489	-497
1	-6	507	446	4	6	1086	-1218	9	-4	617	611	1	0	356	-407
1	-7	659	597	4	7	259	-253	9	-5	264	260	2	0	* 96	-80
1	-8	*148	-5	4	8	*187	167	9	-6	308	319	3	0	489	-502
1	-9	1277	-1004	4	9	702	-764	9	0	642	-659	4	0	355	-326
1	-10	893	-718	4	10	535	574	9	1	545	-637	5	0	197	178
1	-11	*127	8	5	-1	349	292	9	2	194	-238	6	0	*166	90
1	-12	290	260	5	-2	724	670	9	3	483	490	7	0	259	-157
1	0	1283	1504	5	-3	855	-773	9	4	172	165	8	0	1036	1091
1	1	2154	2135	5	-4	242	-208	10	-1	349	-374	9	0	228	-170
1	2	790	812	5	-5	1121	-956	10	-2	728	816	10	0	150	157
1	3	627	742	5	-6	*185	28	10	0	243	232				
1	4	478	-548	5	-7	512	585	10	1	248	-264	K	L		H = 6
1	5	1198	-1430	5	-8	*190	-16	10	2	654	-778				
1	6	513	-593	5	-9	1009	771	11	0	*201	-79	0	-2	466	523
1	7	*139	-32	5	-10	*181	18					0	-4	1105	1039
1	8	*150	83	5	-11	314	-248	K	L		H = 3	0	-6	974	-926
1	9	987	931	5	0	*128	-97					0	-8	207	-239
1	10	*148	-124	5	1	119	-99	0	-2	900	-856	0	-10	904	791
1	11	139	-170	5	2	1347	-1264	0	-4	1447	1454	0	0	1645	-1677
2	-1	293	200	5	3	325	-331	0	-6	1013	1030	0	2	771	-766
2	-2	1567	-1394	5	4	297	308	0	-8	824	-938	0	4	1748	1616
2	-3	844	785	5	5	596	603	0	-10	324	-432	0	6	440	399
2	-4	509	-481	5	6	1148	1329	0	-12	531	496	0	8	735	-796
2	-5	174	-172	5	7	539	635	0	-14	179	-195	0	10	306	318
2	-6	1202	1145	5	8	357	-404	0	0	*126	32	1	0	307	-300
2	-7	198	-167	5	9	163	-174	0	2	987	1003	2	0	*148	33
2	-8	*150	15	5	10	472	-606	0	4	1681	-1569	3	0	440	-423
2	-9	303	176	6	-1	*119	-70	0	6	1982	-2163	4	0	523	521
2	-10	389	-354	6	-2	465	423	0	8	1245	1406	5	0	189	121
2	-11	169	107	6	-3	707	-661	0	10	1281	1203	6	0	*254	31
2	-12	254	163	6	-4	1202	1081	0	12	560	-534	7	0	*190	-113
2	-13	260	-88	6	-5	485	436	1	0	1402	1647	8	0	325	252
2	0	359	332	6	-6	*202	-6	2	0	* 89	-40				
2	1	1236	-1282	6	-7	1203	1120	3	0	135	152	K	L		H = 7
2	2	585	597	6	-8	427	-446	4	0	522	517				
2	3	673	-715	6	-9	439	-362	5	0	922	898	0	-2	498	-448
2	4	435	-461	6	-10	450	-363	6	0	318	281	0	-4	614	-641
2	5	1259	1454	6	0	977	-987	7	0	1542	1645	0	-6	144	176
2	6	*158	-31	6	1	*112	115	8	0	465	488	0	-8	612	644
2	7	369	473	6	2	*114	-113	9	0	*193	-128	0	0	227	-245
2	8	951	1048	6	3	617	-670	10	0	*228	69	0	2	138	93
2	9	676	-736	6	4	510	533	11	0	720	-634	0	4	577	561
2	10	208	-218	6	5	307	-384					0	6	163	199
2	11	223	181	6	6	429	-407	K	L		H = 4	0	8	262	-296
2	12	649	-643	6	7	518	648					1	0	*173	-81
3	-1	241	-184	6	8	647	-732	0	-2	403	405	2	0	*163	70
3	-2	839	-730	6	9	*103	104	0	-4	1336	1228	3	0	276	-227
3	-3	651	561	6	10	594	716	0	-6	119	162	4	0	320	-240
3	-4	870	-804	7	-1	483	448	0	-8	150	-119	5	0	882	-720
3	-5	1026	919	7	-2	* 90	-80	0	-10	489	516	6	0	358	-299
3	-6	1257	1169	7	-3	250	240	0	-12	197	-281	7	0	608	-503
3	-7	454	-452	7	-4	491	466	0	-14	837	-693				
3	-8	740	666	7	-5	259	-223	0	0	1685	-1698	K	L		H = 8
3	-9	560	-458	7	-6	272	-219	0	2	290	-290				
3	-10	1016	-812	7	-7	403	399	0	4	323	414	0	-2	235	-299
3	-11	172	-134	7	-8	891	-807	0	6	*182	-66	0	-4	597	-650
3	-12	250	-203	7	0	150	-158	0	8	*127	-0	0	-6	249	256
3	0	1130	1133	7	1	141	-138	0	10	114	73	0	0	431	437
3	1	320	-255	7	2	367	362	0	12	155	175	1	0	355	-317
3	2	595	-491	7	3	119	-172	1	0	1017	1120	2	0	232	191
3	3	*130	-72	7	4	825	871	2	0	1010	-1096	3	0	561	-512
3	4	863	-874	7	5	* 83	49	3	0	582	626	4	0	218	190
3	5	528	-589	7	6	143	-183	4	0	428	-396				
3	6	340	366	7	7	220	-328	5	0	180	-152				
3	7	256	-306	7	8	852	-978	6	0	495	471				
3	8	266	280	8	-1	* 87	64	7	0	210	-174				
3	9	118	153	8	-2	348	329	8	0	290	277				
3	10	172	-184	8	-3	*122	73	9	0	203	-234				
3	11	337	400	8	-4	871	-825	10	0	*174	-25				

Can. J. Chem. Downloaded from www.nrcresearchpress.com by 210.87.254.40 on 09/05/12
For personal use only.

TABLE V

Bond distances and angles in $Cu_3(AsO_4)_2$

Cu(1)—O(2′)	1.931(22) Å	O(2′)—Cu(1)—O(3)	81.3(8)°	O(3)—Cu(1)—O(5̄′)	132.1(7)°
—O(3′)	2.010(17)	—O(5̄′)	90.2(9)	—O(7̄)	92.7(8)
—O(5̄′)	1.993(18)	—O(7̄)	173.8(7)	—O(8̄)	102.1(8)
—O(7̄)	1.933(23)	—O(8̄)	97.2(9)	O(5′)—Cu(1)—O(7̄)	93.6(8)
—O(8)	2.157(9)	O(7̄)—Cu(1)—O(8)	85.7(9)	—O(8)	125.7(7)
Cu(2)—O(1′)	2.050(18) Å	O(1′)—Cu(2)—O(4̄)	81.5(8)°	O(4̄)—Cu(2)—O(5̄)	89.5(9)°
—O(4̄)	1.923(26)	—O(5)	155.3(7)	—O(6̄)	84.8(9)
—O(5)	2.028(17)	—O(6̄)	84.7(7)	—O(6̄)	165.7(8)
—O(6̄)	2.362(20)	—O(6̄)	91.6(9)	—O(7)	99.7(7)
—O(6̄)	1.892(28)	—O(7̄)	95.4(6)	O(5̄)—Cu(2)—O(6)	117.5(7)
—O(7)	2.758(17)	O(6)—Cu(2)—O(6̄)	82.1(9)	—O(6̄)	101.6(9)
		—O(7̄)	175.5(9)	—O(7)	63.4(6)
		O(6̄)—Cu(2)—O(7)	93.4(8)		
Cu(3)—O(1)	1.956(22) Å	O(1)—Cu(3)—O(2′)	98.7(8)°	O(2′)—Cu(3)—O(3̄)	78.4(8)°
—O(2′)	2.087(16)	—O(3̄)	175.1(8)	—O(4′)	89.1(7)
—O(3̄)	1.976(24)	—O(4′)	78.7(9)	—O(8)	158.7(8)
—O(4′)	2.133(18)	—O(8)	88.5(9)	O(3)—Cu(3)—O(4′)	105.1(9)
—O(8)	1.925(19)	O(4̄′)—Cu(3)—O(8)	112.1(7)	—O(8)	92.9(9)
As(1)—O(1)	1.708(19) Å	O(1)—As(1)—O(3)	107.4(9)°	O(3)—As(1)—O(5)	109.9(10)°
—O(3)	1.682(22)	—O(5)	111.3(9)	—O(7)	108.9(10)
—O(5)	1.671(18)	—O(7)	116.5(10)	O(5)—As(1)—O(7)	102.6(8)
—O(7)	1.647(16)				
As(2)—O(2)	1.704(19) Å	O(2)—As(2)—O(4)	111.4(10)°	O(4)—As(2)—O(6)	106.1(11)°
—O(4)	1.704(22)	—O(6)	113.6(10)	—O(8)	105.5(10)
—O(6)	1.690(26)	—O(8)	111.4(10)	O(6)—As(2)—O(8)	108.5(11)
—O(8)	1.689(20)				

TABLE VI

Interatomic angles about oxygen atoms

	Angle (°)	Sum (°)
Cu(2)—O(1)—Cu(3)	101	
Cu(2)—O(1)—As(1)	124	
As(1)—O(1)—Cu(3)	125	350
Cu(1)—O(2)—Cu(3)	99	
Cu(1)—O(2)—As(2)	126	
As(2)—O(2)—Cu(3)	120	345
Cu(1)—O(3)—Cu(3)	100	
Cu(1)—O(3)—As(1)	123	
As(1)—O(3)—Cu(3)	134	357
Cu(2)—O(4)—Cu(3)	99	
Cu(2)—O(4)—As(2)	125	
As(2)—O(4)—Cu(3)	136	360
Cu(1)—O(5)—Cu(2)	110	
Cu(1)—O(5)—As(1)	139	
As(1)—O(5)—Cu(2)	111	360
Cu(2)—O(6)—Cu(2)	98	
Cu(2)—O(6)—As(2)	119	
As(2)—O(6)—Cu(2)	138	355
Cu(1)—O(7)—Cu(2)	105	
Cu(1)—O(7)—As(1)	130	
As(1)—O(7)—Cu(2)	83	318
Cu(1)—O(8)—Cu(3)	106	
Cu(1)—O(8)—As(2)	116	
As(2)—O(8)—Cu(3)	137	359

pyroarsenates. In $NaAsO_3$ these values are 1.77 Å and 1.68 Å respectively, leading to a value of 1.72 Å for the mean AsO bond length. The deviation from the expected here is in the direction opposite to that for the pyroarsenate, if $Cu_3(AsO_4)_2$ is used as the standard for a bond order of 1.5 and if a linear relationship holds between bond order and bond distance. Although the environment might play a greater role here than in the phosphate system, since the electrons involved in the bonding would be less localized, the effect seems to be unusually large.

Acknowledgments

This research has been supported by a grant from the National Research Council of Canada and an Ontario Government Fellowship to S. J. P.

1. A. Durif. Acta Cryst. **12**, 420 (1959).
2. G. R. Fonda. J. Electrochem. Soc. **103**, 400 (1956).
3. F. A. Cotton and G. Wilkinson. Advanced inorganic chemistry. 2nd ed. Interscience Publishers, New York. 1966. p. 517.
4. S. Ghosh, M. Fehlman, and M. Sundaralingam. Acta Cryst. **18**, 777 (1965).
5. L. Helmholtz and D. Levine. J. Am. Chem. Soc. **64**, 354 (1942).
6. K. Plieth and G. Sänger. Z. Krist. **124**, 91 (1967).

Can. J. Chem. Downloaded from www.nrcresearchpress.com by 210.87.254.40 on 09/05/12
For personal use only.

7. K. LUKASEWICZ. Bull. Acad. Polon. Sci. Ser. Sci. Chim. **14**, 725 (1966).
8. C. CALVO and K. NEELAKANTAN. To be published.
9. F. LIEBAU. Acta Cryst. **9**, 811 (1956).
10. J. B. TAYLOR and R. D. HEYDING. Can. J. Chem. **36**, 597 (1958).
11. A. DURIF. Anal. Chem. **31**, 1741 (1959).
12. C. CALVO. Am. Mineralogist. To be published.
13. R. J. DAVIS, M. H. HEY, and A. W. G. KINGSBURY. Mineral. Mag. **35**, 73 (1965).
14. J. S. STEPHENS and C. CALVO. Can. J. Chem. **45**, 2303 (1967).
15. D. J. CROMER and K. HERRINGTON. J. Am. Chem. Soc. **77**, 4708 (1955).
16. A. S. COOPER. Acta Cryst. **15**, 578 (1962).
17. A. DE VRIES. Acta Cryst. **18**, 473 (1965).
18. W. H. ZACHARIASEN. Acta Cryst. **5**, 68 (1952).
19. D. HARKER and J. S. KASPER. J. Chem. Phys. **15**, 70 (1948).
20. International Tables for Crystallography. Vol. III. Kynoch Press, Birmingham. 1962.
21. E. W. HUGHES. J. Am. Chem. Soc. **63**, 1737 (1941).
22. J. J. FINNEY. Acta Cryst. **21**, 437 (1966).
23. C. CALVO and K. Y. LEUNG. Z. Krist. To be published.

Can. J. Chem. Downloaded from www.nrcresearchpress.com by 210.87.254.40 on 09/05/12
For personal use only.

Beryllium and scandium electrode potentials in fused LiCl–KCl eutectic

JAMES A. PLAMBECK
Department of Chemistry, University of Alberta, Edmonton, Alberta
Received October 18, 1967

Electrode potentials of the Be(II)–Be(0) and Sc(III)–Sc(0) systems were measured in dilute solutions of the ionic species in fused LiCl–KCl eutectic at 450 °C. Standard molar electrode potentials of these couples of -2.039 ± 0.013 V and -2.553 ± 0.015 V against a standard molar platinum reference were calculated. It was shown by voltammetric and chronopotentiometric methods that the equilibrium Be(II) + Be(0) $\rightleftarrows$ 2Be(I) suggested by previous authors was not significant in this medium.

Canadian Journal of Chemistry, 46, 929 (1968)

Can. J. Chem. Downloaded from www.nrcresearchpress.com by 210.87.254.40 on 09/05/12
For personal use only.

Introduction

A recent review (1) included an extensive electromotive force series in anhydrous, molten LiCl–KCl at 450°; accurate values of standard potentials of beryllium and scandium couples were not available for inclusion. This paper reports the determination of the Be(II)–Be(0) and Sc(III)–Sc(0) standard potentials in this solvent.

The electrodeposition of beryllium metal from fused chlorides and other media has been extensively studied and the literature reviewed (2). Beryllium metal has been anodically oxidized into, and cathodically plated from, fused LiCl–KCl eutectic as well as other molten chloride mixtures. The electrochemical reaction involved appears to be Be(0), metal $\rightleftarrows$ Be(II), solution + $2e^-$, where Be(II) represents divalent beryllium (probably existing as a chloride–complex ion). A series of papers by Smirnov and coworkers (3–6) have considered the equilibrium Be(II) + Be(0) $\rightleftarrows$ 2Be(I) in fused equimolar NaCl–KCl (3, 4) and other fused salts (5, 6). From their data in LiCl–KCl mixtures at approximately the temperature used in this study (5) it appears that the equilibrium would be far to the left (K = about 10^{-4}) and that comparatively little Be(I) should be produced on anodization of a beryllium wire under the conditions of this study.

Metallic scandium was first prepared (7) by electrolysis of a melt of LiCl–KCl–$ScCl_3$ with a molten zinc cathode; subsequent distillation of the zinc left 94–98% pure scandium metal. The conductance of molten $ScCl_3$ has also been studied (8), and spectrophotometric measurements on tripositive scandium have been made in fused salt media (9). No attempt appears to have been made to determine electromotive force (e.m.f.) values for scandium couples in fused salt media.

Experimental

Apparatus

Potentials were measured with a type K-3 potentiometer (Leeds and Northrup Co., Philadelphia, Pa.). Voltammetric measurements were made with a model FS polarograph (modified to use model XV motors) and metal ions were generated coulometrically using a model IV current source (both E. H. Sargent and Co., Chicago, Ill.). Chronopotentiometric measurements employed a model 6824A power supply/amplifier (Hewlett-Packard, Palo Alto, Calif.), in a constant-current configuration, controlled by appropriate mercury-wetted relay switching circuitry; measurements were recorded on a Hewlett–Packard model 175A oscilloscope equipped with 1750B and 1781B plug-in units and a model 196B camera using ASA 3000 Polaroid film.

The electrolytic cell and glassware preparation procedure used has been described previously (10). The outer glass envelope was contained within a 3″ diameter vertical tube furnace equipped with a model 3120-SCR-477 temperature controller (Marshall Products Co., Columbus, Ohio). Temperatures were measured using a calibrated chromel–alumel thermocouple and the K-3 potentiometer. The thermocouple e.m.f. was measured immediately before and after each measurement of the cell potential, and the mean of these taken as the thermocouple reading appropriate to the cell potential.

Solvent

The solvent used was specially purified LiCl–KCl eutectic (Anderson Physics Labs., Inc., Champaign, Ill.); the method of purification used has been described (11).

Electrodes

Beryllium (A. D. Mackay, New York, N.Y.) and scandium (Johnson, Matthey and Mallory Ltd., Toronto, Ont.) wire, approximately 18 gauge was used as supplied. Surface impurities and oxides were removed by polishing with emery cloth, wiping with damp cotton, and drying with acetone; the wires were used immediately after drying. These wires were connected to platinum leads within the hot zone of the furnace (but above the melt level) to eliminate thermoelectric potential effects.

Counter electrodes used in coulometric generation were either 1/8″ diameter carbon rods (grade U-1 spectroscopic graphite electrodes, United Carbon Products, Inc., Bay City, Mich.) or platinum flags. Both were dried at 150° before use. Each electrode was kept in a separate isolation compartment during a run as described below.

Can. J. Chem. Downloaded from www.nrcresearchpress.com by 210.87.254.40 on 09/05/12
For personal use only.

Procedure

The procedure used was similar to that described previously for rhodium (10). The cell was maintained under a slight positive pressure of dry nitrogen, using a sulfuric acid bubbler, to prevent contamination by atmospheric oxygen and water vapor. Wires or flags used in coulometric generation were rotated, using glass feed-through tubes, to mix the solution within the compartment. Potentials stable to ± 1 mV were obtained within 10 min after such agitation. The chloride content of the isolation compartments was determined by Mohr titration after dissolution in water, and the volume of each compartment calculated as described previously (12). The concentration of metal ion was calculated from the coulombs passed and the compartment volume.

The potentials reported in this paper are with reference to the Pt(II) (1.0 *M*), LiCl–KCl/Pt standard molar platinum electrode (s.m.p.e.) of Laitinen and Liu (12) calculated using the compartment volume as obtained above and conform to the IUPAC "Stockholm" sign convention. Potentials measured against silver reference electrodes were converted to the s.m.p.e. reference using the literature (12) value for the Ag(I)/Ag couple. Least-squares calculations were carried out on the University of Alberta IBM System/360 computer.

Results and Discussion

Beryllium(II)–Beryllium(0) Couple

A total of 47 concentration–potential data points were taken at 450 $\pm$ 1 °C in five separate experiments using the procedure described above; the number of points per experiment varied between 8 and 12. The results for a typical experiment are shown in Fig. 1. The experimental least-square value for the slope of this line was 0.0723 $\pm$ 0.0017 V per log unit as compared with the theoretical Nernst slope of 0.0717 V per log unit for a two-electron process at this temperature. The standard potential (molarity scale) of the Be(II)–Be(0) couple determined in this experiment was −2.023 V, standard deviation 0.002 V, with respect to the s.m.p.e.

Linear Nernst plots were obtained over a range of 0.2 to 0.006 *M* Be(II); at lower concentrations, stable potentials could not be obtained. All of these solutions were colorless. The mean value of *n* was 1.9 $\pm$ 0.2, as determined coulometrically from weight loss of the wire. The standard molarity-scale potential of the Be(II)–Be(0) couple calculated using data from all experiments was −2.039 V, standard deviation 0.013 V, with respect to the s.m.p.e. This corresponds to values of −2.039 and −2.039 V with the same standard deviation on the molality and mole fraction scales respectively (1). Yang and Hudson (13), using the same eutectic and a cell

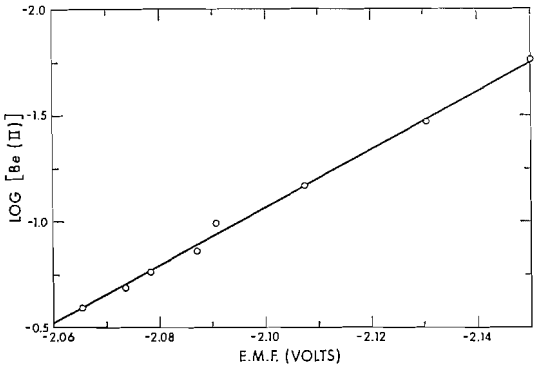

FIG. 1. Electromotive force (vs. s.m.p.e.) as a function of the molar concentration of Be(II) produced by anodization.

similar to the one used in this work, reported the standard mole-fraction-scale potential of the Be(II)–Be(0) couple as −1.997 V at 450 °C with respect to a standard chlorine electrode; this is equivalent to a standard molarity-scale potential of −1.781 V with respect to the s.m.p.e. This value is in poor agreement with the results of the present study, but inasmuch as the lowest temperature at which measurements were made by Yang and Hudson (13) was 488 °C, and these workers used more concentrated solutions (up to 15 mole % $BeCl_2$) for which the behavior was admittedly non-Henrian, it is felt that the results of the present study are to be preferred.

For a fixed concentration of Be(II), plots of measured potential vs. temperature were linear over the range 400–490 °C. Potential readings taken while the temperature was slowly increasing were in good agreement with those taken while it was decreasing. The duration of a single heating and cooling cycle was several hours. The temperature coefficient of potential increased from −0.5 mV/°C for the most dilute Be(II) solutions to −0.6 mV/°C for the most concentrated.

In view of possible complications involving this couple due to the equilibrium between beryllium and its mono- and di-valent ions studied by Smirnov (5), efforts were made to establish the existence of Be(I) in this solvent despite the contraindication of the potentiometric data. Voltammetric scans of melts into which beryllium had been anodized were made in the presence and absence of massive beryllium. In all cases a single wave was observed at $E_{1/2} = -1.9 \pm 0.1$ V prior to lithium deposition. Chronopotentio-

Can. J. Chem. Downloaded from www.nrcresearchpress.com by 210.87.254.40 on 09/05/12
For personal use only.

metric measurements showed only a single diffusion-controlled transition at $E_{\tau/4} = -1.8 \pm 0.1$ V at potentials less negative than lithium deposition. On the basis of these measurements and the potentiometric data it is concluded that univalent beryllium does not exist in significant concentration in fused LiCl–KCl eutectic at 450 °C.

Scandium(III)–Scandium(0) Couple

A total of 49 concentration–potential data points were taken at 450 ± 1 °C in four separate experiments using the procedure described above, with 11 to 14 points per experiment. The results for a typical experiment are shown in Fig. 2. The experimental least-squares value for the slope of this line was 0.0514 V, standard deviation 0.004 V, per log unit as compared with the theoretical Nernst slope of 0.0478 V per log unit for a three-electron process at this temperature. The standard potential (molarity scale) of the Sc(III)–Sc(0) couple determined in this experiment was −2.549 V, standard deviation 0.004 V.

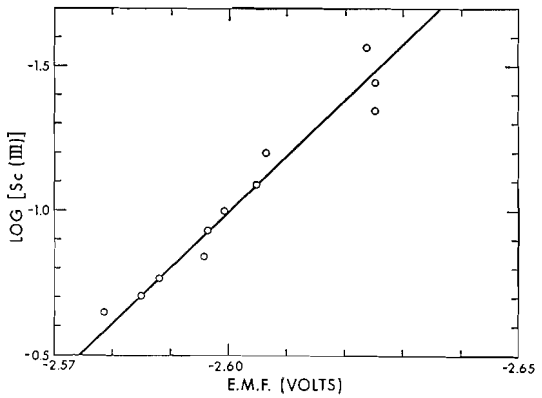

FIG. 2. Electromotive force (vs. s.m.p.e.) as a function of the molar concentration of Sc(III) produced by anodization.

Linear Nernst plots were obtained over a range of 0.02 to 0.23 *M* Sc(III); at lower concentrations, as in the case of beryllium, stable potentials could not be obtained. All scandium solutions were colorless. The mean value of *n* was 3.7 ± 0.8, as determined coulometrically by weight loss. The greater error in the case of scandium is due to a more extensive surface oxidation of the scandium wire not exposed to the melt as compared with beryllium. The standard molarity-scale potential of the Sc(III)–Sc(0) couple, using data from all four runs, was −2.553 V, standard deviation 0.015 V. This corresponds to values of −2.558 and −2.588 V, with the same standard deviation, on the molality and mole fraction scales respectively (1).

Voltammetric and chronopotentiometric curves showed only single waves whose $E_{1/2}$ and $E_{\tau/4}$ values were close to the standard potential of the Sc(III)–Sc(0) couple, indicating that only trivalent scandium was present in solution. No attempt was made to determine the temperature coefficient of the scandium electrode.

Acknowledgments

The author is indebted to W. M. Hope for assistance with part of the experimental work. This work was supported by an Operating Grant from the National Research Council of Canada.

1. J. A. PLAMBECK. J. Chem. Eng. Data, **12**, 77 (1967).
2. I. A. MENZIES, D. L. HILL, and L. W. OWEN. J. Less-Common Metals, **1**, 321 (1959).
3. M. V. SMIRNOV and N. YA. CHUKREEV. Russ. J. Inorg. Chem. English Transl. **4**, 1168 (1959).
4. M. V. SMIRNOV and N. YA. CHUKREEV. Proc. Acad. Sci. USSR, Phys. Chem. Sect. English Transl. **127**, 707 (1959).
5. M. V. SMIRNOV and N. YA. CHUKREEV. Russ. J. Inorg. Chem. English Transl. **6**, 699 (1961).
6. M. V. SMIRNOV, V. E. KOMAROV, and N. YA. CHUKREEV. Russ. J. Inorg. Chem. English Transl. **10**, 1089 (1965).
7. W. FISCHER, K. BRUNGER, and H. GREINEISEN. Z. Anorg. Allgem. Chem. **231**, 54 (1937).
8. W. BILTZ and W. KLEMM. Z. Anorg. Allgem. Chem. **131**, 22 (1923).
9. G. HARRINGTON and B. R. SUNDHEIM. Ann. N.Y. Acad. Sci. **79**, 950 (1960).
10. H. A. LAITINEN and J. A. PLAMBECK. J. Am. Chem. Soc. **87**, 1202 (1965).
11. H. A. LAITINEN, W. S. FERGUSON, and R. A. OSTERYOUNG. J. Electrochem. Soc. **104**, 516 (1957).
12. H. A. LAITINEN and C. H. LIU. J. Am. Chem. Soc. **80**, 1015 (1958).
13. L. YANG and R. G. HUDSON. Trans. AIME, **215**, 589 (1959).

Can. J. Chem. Downloaded from www.nrcresearchpress.com by 210.87.254.42 on 09/05/12
For personal use only.

An accurate determination of the crystal structure of triclinic potassium dichromate, $K_2Cr_2O_7$

J. K. BRANDON[1] AND I. D. BROWN
Department of Physics, McMaster University, Hamilton, Ontario

Received October 12, 1967

The crystal structure of triclinic potassium dichromate has been determined by single crystal X-ray diffraction. The cell constants are $a = 13.367$, $b = 7.376$, $c = 7.445$ Å, $\alpha = 90.75°$, $\beta = 96.21°$, $\gamma = 97.96°$ with four $K_2Cr_2O_7$ units per cell. Refinement of 2600 reflections in both the space groups $P1$ and $P\bar{1}$ leads to the same structure. This is in agreement with the results of anomalous dispersion measurements, confirming that $P\bar{1}$ is the correct space group. The final agreement index, R, is 0.054. The two crystallographically independent dichromate ions are similar, deviating only slightly from C_{2v} symmetry. The Cr—O (terminal) distance is 1.63 Å, the Cr—O (bridging) distance is 1.79 Å and all angles at the chromium atoms are tetrahedral except for one of the O(bridging)—Cr—O(terminal) angles in each ion which is 106°. The angles at the bridging oxygen atoms are 124° and 128°. The geometry of the anion is compared with that found in a number of similar groups.

Canadian Journal of Chemistry, 46, 933 (1968)

Introduction

In 1833 Mitscherlich (1) reported that a phase transition occurs at about 250 °C in potassium dichromate, $K_2Cr_2O_7$. Since that time there has been a succession of papers dealing with the polymorphism and crystallography of potassium dichromate but only recently has the crystal structure of its room temperature phase been reported by Kuz'min, Ilyukhin, and Belov (2). We have independently determined the crystal structure of this phase, and since our results are somewhat more accurate and give a better picture of the detail of the structure, we present them here.

One of the points frequently discussed in earlier papers is whether the correct space group of the room temperature form of potassium dichromate is $P1$ or $P\bar{1}$. Klement and Schwab (3) have reviewed the work up to 1959. More recently, papers have been published by Rao (4), Podisko (5), and Parvov and Shubnikov (6). We give below our reasons for favoring the space group $P\bar{1}$ which was also used by Kuz'min *et al.* (2).

Experimental

Crystals of triclinic potassium dichromate were grown by slowly evaporating a saturated solution of technical grade $K_2Cr_2O_7$ in distilled water at room temperature. The characteristic habit of the clear-orange crystals is shown in

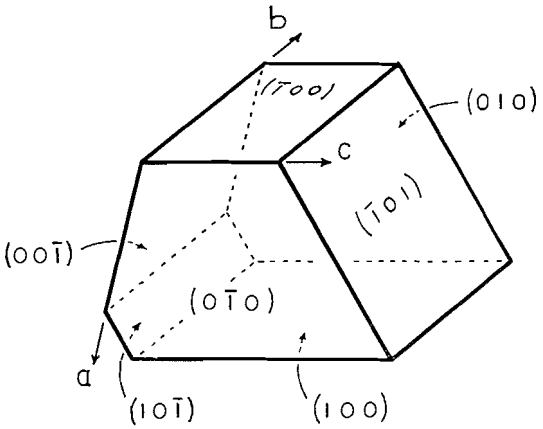

FIG. 1. Habit of triclinic $K_2Cr_2O_7$ crystals.

TABLE I

Crystal data for triclinic $K_2Cr_2O_7$

Formula weight	294.20
System	Triclinic
Space group	$P\bar{1}$
Cell constants	
a	13.367±0.011 Å
b	7.376±0.005 Å
c	7.445±0.006 Å
α	90.75±0.05°
β	96.21±0.07°
γ	97.96±0.05°
Unit cell volume	722.3 Å^3
Density	
Measured	2.66±0.05 gm cm^{-3}
Calculated	2.704 gm cm^{-3}
Number of formula units per unit cell	4
X-ray absorption coefficient (MoK_α)	42.4 cm^{-1}

[1]Present address: Crystallographic Laboratory, Cavendish Laboratory, Free School Lane, Cambridge, England.

TABLE II

Coordinates and temperature factors ($\times 10^5$) of the atoms in triclinic $K_2Cr_2O_7$. The coordinates in parentheses are those reported by Kuz'min *et al.* (2) transformed to the same unit cell. The standard errors are those indicated by the least squares refinement

	Coordinates			Temperature factor components ($\times 10^5$)					
Atom	x	y	z	β_{11}	β_{22}	β_{33}	β_{12}	β_{13}	β_{23}
K1	.15845	.16251	.91463	286	916	879	99	−17	−28
	(.159)	(.160)	(.916)						
K2	−.13591	.19591	.65275	302	1364	1111	90	32	393
	(−.136)	(.198)	(.656)						
K3	.64056	.60346	.66946	253	1376	1124	71	87	−244
	(.639)	(.604)	(.668)						
K4	.34939	.75019	.76701	309	1274	931	221	35	−125
	(.348)	(.749)	(.768)						
σ(K)	.00008	.00012	.00018	5	14	22	7	14	16
Cr1	.11332	.31682	.42610	198	738	667	30	15	−54
	(.113)	(.318)	(.426)						
Cr2	−.08334	.31361	.15240	206	654	668	87	17	22
	(−.083)	(.312)	(.154)						
Cr3	.60718	.09201	.76914	198	723	753	103	52	68
	(.608)	(.092)	(.768)						
Cr4	.41379	.29304	.80714	195	696	725	89	76	73
	(.414)	(.293)	(.808)						
σ(Cr)	.00005	.00007	.00011	3	8	13	4	8	9
OB1	.0228	.4295	.2948	288	735	1093	42	−55	104
	(.024)	(.433)	(.303)						
O11	.1997	.4763	.5166	276	1049	1375	18	−45	−215
	(.199)	(.453)	(.517)						
O12	.1636	.1861	.2948	354	1263	1043	208	128	−333
	(.168)	(.199)	(.295)						
O13	.0605	.1941	.5766	347	1585	1241	65	95	629
	(.064)	(.194)	(.584)						
O21	−.1489	.4584	.0627	448	1214	1737	289	−115	130
	(−.145)	(.463)	(.067)						
O22	−.1517	.1752	.2754	326	1026	1149	−1	198	136
	(−.150)	(.176)	(.279)						
O23	−.0431	.1926	−.0018	305	1619	1027	121	18	−398
	(−.043)	(.187)	(−.005)						
OB3	.5275	.2095	.8919	319	1539	918	363	36	51
	(.522)	(.210)	(.893)						
O31	.7014	.0535	.9120	349	1717	1265	373	−83	146
	(.696)	(.050)	(.905)						
O32	.6487	.2201	.6103	468	1255	1242	70	114	331
	(.651)	(.209)	(.613)						
O33	.5449	−.0982	.6835	397	993	1731	14	41	−75
	(.546)	(−.083)	(.673)						
O41	.3603	.3660	.9728	420	1442	1177	213	269	88
	(.365)	(.364)	(.975)						
O42	.3366	.1370	.6926	368	1182	1496	−29	36	−259
	(.340)	(.142)	(.701)						
O43	.4427	.4606	.6726	313	1085	1358	75	173	371
	(.443)	(.470)	(.675)						
σ(O)	.0003	.0004	.0006	18	50	90	25	50	55

Fig. 1. The choice of axes in Fig. 1 corresponds to those of the actual crystal used in this analysis. Our cell convention has been chosen to allow easy comparison with related structures such as $(NH_4)_2Cr_2O_7$ (7), $K_2S_2O_7$ (8), and β-$Ca_2P_2O_7$ (9).

Accurate cell parameters were measured from precession photographs taken with Zr-filtered Mo-radiation. These films were calibrated with rutile ($a = 4.59373$ and $c = 2.95812$ Å (10)). The crystal data are given in Table I.

The crystal selected for intensity measurements approximated a cylinder (the cylinder axis was [010]) with a mean diameter of 0.25 mm

Can. J. Chem. Downloaded from www.nrcresearchpress.com by 210.87.254.42 on 09/05/12
For personal use only.

Can. J. Chem. Downloaded from www.nrcresearchpress.com by 210.87.254.42 on 09/05/12
For personal use only.

TABLE III

Observed (F_o) and calculated (F_c) *hk*0 and 0*kl* structure amplitudes in units of 1/10 electron per unit cell with the estimated relative standard errors (σ) of the former. The symbols following F_o have the following meaning: -, unobserved reflection; *, unreliable F_o measurement which was given zero weight during refinement; ×, reflection believed to show extinction effects

H	K	L	FØ	FC	σ
0	0	0	0*	5640	***
18	0	0	105*	-102	***
17	0	0	119*	108	***
16	0	0	268	-252	20
15	0	0	36	34	15
14	0	0	130	127	16
13	0	0	32	-26	16
12	0	0	111	110	13
11	0	0	36-	6	18
10	0	0	184	-184	13
9	0	0	65	-60	11
8	0	0	255	257	15
7	0	0	66	27	12
6	0	0	163	160	11
5	0	0	138*	116	***
4	0	0	1226*	-2193	***
3	0	0	45*	-30	***
2	0	0	366*	413	***
1	0	0	9*	-22	***
18	-1	0	120*	116	***
17	-1	0	127	-128	15
16	-1	0	405	-393	23
15	-1	0	40-	33	20
14	-1	0	266	-265	20
13	-1	0	368	375	27
12	-1	0	198	200	14
11	-1	0	262	-274	26
10	-1	0	306	304	26
9	-1	0	554	-593	32
8	-1	0	288	297	21
7	-1	0	274	280	20
6	-1	0	30	35	8
5	-1	0	26	30	7
4	-1	0	561	-579	68
3	-1	0	23*	-24	***
2	-1	0	203*	-237	***
1	-1	0	249*	-209	***
0	-1	0	67*	-90	***
-1	-1	0	318*	-328	***
-2	-1	0	111	-95	11
-3	-1	0	141	-147	13
-4	-1	0	576	606	96
-5	-1	0	26-	-8	13
-6	-1	0	248	266	15
-7	-1	0	309	323	17
-8	-1	0	298	-304	17
-9	-1	0	253	-267	15
-10	-1	0	283	-291	17
-11	-1	0	251	-262	29
-12	-1	0	216	-224	13
-13	-1	0	178	179	13
-14	-1	0	79	-80	7
-15	-1	0	220	223	12
-16	-1	0	285	288	16
-17	-1	0	36-	-2	18
-18	-1	0	164*	180	***
18	-2	0	27*	2	***
17	-2	0	211	-206	12
16	-2	0	308	308	16
15	-2	0	100	98	12
14	-2	0	126	126	8
13	-2	0	303	295	20
12	-2	0	395	-394	22
11	-2	0	428	-439	36
10	-2	0	144	-135	10
9	-2	0	390	-406	28
8	-2	0	298	-301	15
7	-2	0	641	672	41
6	-2	0	186	-175	18
5	-2	0	722	754	96
4	-2	0	959X	1044	172
3	-2	0	492	-489	50
2	-2	0	619	625	74
1	-2	0	929X	-1026	176
0	-2	0	1030*	-1320	***
-1	-2	0	176	165	9
-2	-2	0	959X	-1107	178
-3	-2	0	723	775	76
-4	-2	0	719	760	89
-5	-2	0	118	119	8
-6	-2	0	317	329	18
-7	-2	0	464	-493	26
-8	-2	0	102	108	18
-9	-2	0	157	149	12
-10	-2	0	409	419	38
-11	-2	0	530	555	31
-12	-2	0	161	-167	11
-13	-2	0	59	62	9
-14	-2	0	339	-339	17
-15	-2	0	131	-132	20
-16	-2	0	38-	22	19
-17	-2	0	117*	-117	***
18	-3	0	101*	-99	***
17	-3	0	303	295	18
16	-3	0	40-	-16	20

H	K	L	FØ	FC	σ
15	-3	0	116	120	9
14	-3	0	44	48	12
13	-3	0	507	-501	36
12	-3	0	536	537	32
11	-3	0	91	-93	6
10	-3	0	499	506	30
9	-3	0	923	979	106
8	-3	0	674	-689	64
7	-3	0	245	241	20
6	-3	0	819	-841	94
5	-3	0	635	-671	59
4	-3	0	267	256	15
3	-3	0	617	621	59
2	-3	0	198	194	12
1	-3	0	101	97	5
0	-3	0	291	-297	23
-1	-3	0	433	-435	37
-2	-3	0	339	331	25
-3	-3	0	493	516	36
-4	-3	0	567	-600	56
-5	-3	0	86	-94	6
-6	-3	0	809	-879	89
-7	-3	0	737	-793	79
-8	-3	0	651	682	77
-9	-3	0	184	-178	24
-10	-3	0	558	577	42
-11	-3	0	423	423	26
-12	-3	0	215	-224	12
-13	-3	0	40-	31	20
-14	-3	0	114	-117	14
-15	-3	0	230	-234	25
-16	-3	0	46*	28	***
18	-4	0	76*	-80	***
17	-4	0	125*	129	***
16	-4	0	264	-250	23
15	-4	0	40-	-20	20
14	-4	0	327	-312	18
13	-4	0	298	-303	26
12	-4	0	160*	137	***
11	-4	0	59	72	8
10	-4	0	560	571	41
9	-4	0	477	483	33
8	-4	0	157*	-146	***
7	-4	0	164	-165	9
6	-4	0	595	-603	49
5	-4	0	222	-218	32
4	-4	0	131*	-103	***
3	-4	0	61	56	8
2	-4	0	147	139	8
1	-4	0	57	-63	6
0	-4	0	125	-118	10
-1	-4	0	81	83	4
-2	-4	0	128	-119	7
-3	-4	0	189	-180	12
-4	-4	0	455	474	32
-5	-4	0	35-	46	17
-6	-4	0	420	423	30
-7	-4	0	205	211	13
-8	-4	0	229	-227	13
-9	-4	0	38-	-41	19
-10	-4	0	458	-458	33
-11	-4	0	215	-212	17
-12	-4	0	39-	-4	20
-13	-4	0	78*	-81	***
-14	-4	0	389	398	39
-15	-4	0	126	129	14
-16	-4	0	124*	175	***
17	-5	0	137*	147	***
16	-5	0	215	208	20
15	-5	0	148	-141	15
14	-5	0	253	253	15
13	-5	0	40-	16	20
12	-5	0	222	-216	12
11	-5	0	127	120	8
10	-5	0	607	-620	48
9	-5	0	367	-367	26
8	-5	0	167	162	9
7	-5	0	102	-109	13
6	-5	0	848	892	100
5	-5	0	530	529	37
4	-5	0	177	177	12
3	-5	0	36	-20	11
2	-5	0	139	-135	13
1	-5	0	189	-182	11
0	-5	0	321	-336	23
-1	-5	0	576	583	58
-2	-5	0	370	-378	29
-3	-5	0	65	64	13
-4	-5	0	322	310	19
-5	-5	0	505	-514	36
-6	-5	0	643	671	62
-7	-5	0	38-	-22	19
-8	-5	0	48	58	10
-9	-5	0	108	115	9
-10	-5	0	516	-528	35

H	K	L	FØ	FC	σ
-11	-5	0	39-	-16	20
-12	-5	0	105	-113	12
-13	-5	0	37-	14	18
-14	-5	0	146*	154	***
16	-6	0	115*	120	***
15	-6	0	60	-66	10
14	-6	0	269	263	16
13	-6	0	39-	39	20
12	-6	0	151*	122	***
11	-6	0	154	-145	10
10	-6	0	389	-380	26
9	-6	0	48	42	10
8	-6	0	323	-311	18
7	-6	0	186*	148	***
6	-6	0	257	240	22
5	-6	0	468	-462	30
4	-6	0	175	174	9
3	-6	0	719	-721	71
2	-6	0	35	27	13
1	-6	0	505	486	32
0	-6	0	164	161	15
-1	-6	0	764	799	80
-2	-6	0	56	-70	9
-3	-6	0	391	-385	22
-4	-6	0	337	-356	19
-5	-6	0	304	-300	16
-6	-6	0	295	-282	15
-7	-6	0	188	167	24
-8	-6	0	47	46	11
-9	-6	0	53	52	10
-10	-6	0	303	302	19
-11	-6	0	41	41	11
-12	-6	0	120*	106	***
-13	-6	0	52*	35	***
15	-7	0	218*	-222	***
14	-7	0	92*	-81	***
13	-7	0	37-	43	18
12	-7	0	292	287	18
11	-7	0	95	85	13
10	-7	0	175	168	18
9	-7	0	39*	46	***
8	-7	0	39-	24	20
7	-7	0	39-	17	20
6	-7	0	74*	-46	***
5	-7	0	97	-97	10
4	-7	0	274	-270	15
3	-7	0	44	46	12
2	-7	0	76	-71	13
1	-7	0	215	198	13
0	-7	0	88	83	7
-1	-7	0	90*	-66	***
-2	-7	0	180	173	17
-3	-7	0	90	-99	9
-4	-7	0	160	156	11
-5	-7	0	131	127	15
-6	-7	0	93	-86	9
-7	-7	0	194	184	18
-8	-7	0	204	-199	12
-9	-7	0	70	68	10
-10	-7	0	84	-81	10
-11	-7	0	110*	-122	***
13	-8	0	40*	27	***
12	-8	0	215	-215	21
11	-8	0	63	64	7
10	-8	0	215	-210	12
9	-8	0	76	74	19
8	-8	0	277	252	18
7	-8	0	349	-338	19
6	-8	0	388	387	32
5	-8	0	39-	-6	20
4	-8	0	39-	52	20
3	-8	0	509	506	35
2	-8	0	363	-359	20
1	-8	0	87	-89	12
0	-8	0	403	-390	38
-1	-8	0	536	-534	47
-2	-8	0	39-	19	19
-3	-8	0	38-	0	19
-4	-8	0	271	266	14
-5	-8	0	278	275	17
-6	-8	0	79	75	9
-7	-8	0	48	-52	9
-8	-8	0	187	-182	16
-9	-8	0	28*	-10	***
11	-9	0	88*	89	***
10	-9	0	78*	-76	***
9	-9	0	57*	43	***
8	-9	0	90*	71	***
7	-9	0	117	-121	13
6	-9	0	76*	-63	***
5	-9	0	90*	-94	***
4	-9	0	33	29	14
3	-9	0	49	49	9
2	-9	0	160	174	10
1	-9	0	88	93	7

H	K	L	FØ	FC	σ
0	-9	0	38-	11	19
-1	-9	0	84*	39	***
-2	-9	0	36-	20	18
-3	-9	0	35-	-1	17
-4	-9	0	33-	-3	17
-5	-9	0	124*	-120	***
-6	-9	0	131*	-136	***
7	-10	0	57*	-63	***
6	-10	0	267*	-278	***
5	-10	0	22*	-5	***
4	-10	0	136*	-130	***
3	-10	0	24*	-17	***
2	-10	0	134*	134	***
1	-10	0	54*	-59	***
0	-10	0	244*	223	***
-1	-10	0	20*	-11	***
-2	-10	0	91*	101	***
0	0	-10	27*	-22	***
0	0	-9	194	214	12
0	0	-8	164	-173	8
0	0	-7	91	-82	10
0	0	-6	63	-45	9
0	0	-5	115	110	7
0	0	-4	75	-85	13
0	0	-3	219	209	12
0	0	-2	907	-905	165
0	0	-1	34*	23	***
0	-1	-10	98*	-98	***
0	-1	-9	43-	-34	22
0	-1	-8	156	-166	10
0	-1	-7	185	-190	13
0	-1	-6	77	78	7
0	-1	-5	78	-78	5
0	-1	-4	325	341	18
0	-1	-3	313	321	19
0	-1	-2	24-	9	12
0	-1	-1	344*	338	***
0	-1	0	86*	-90	***
0	-1	1	263*	283	***
0	-1	2	596	-628	62
0	-1	3	267	-246	25
0	-1	4	45	-36	8
0	-1	5	36-	15	18
0	-1	6	721	-758	71
0	-1	7	161	-173	11
0	-1	8	472	469	24
0	-1	9	171	176	17
0	-1	10	147*	142	***
0	-2	-10	115*	131	***
0	-2	-9	40	-39	15
0	-2	-8	66	-55	10
0	-2	-7	225	-230	16
0	-2	-6	40	-39	13
0	-2	-5	418	-410	22
0	-2	-4	264	265	21
0	-2	-3	792	841	81
0	-2	-2	218	215	22
0	-2	-1	831X	927	136
0	-2	0	1023X	-1320	181
0	-2	1	940X	-1095	187
0	-2	2	369	356	21
0	-2	3	205	-202	11
0	-2	4	254	255	30
0	-2	5	435	-439	31
0	-2	6	105	101	6
0	-2	7	38	28	16
0	-2	8	183	187	12
0	-2	9	43-	-23	22
0	-2	10	108*	-120	***
0	-3	-9	99	96	6
0	-3	-8	143	-144	7
0	-3	-7	43	-13	14
0	-3	-6	141	139	7
0	-3	-5	879	931	86
0	-3	-4	451	-448	33
0	-3	-3	889X	-959	88
0	-3	-2	333	339	19
0	-3	-1	178	164	16
0	-3	0	312*	-297	***
0	-3	1	63	8	5
0	-3	2	416	-399	21
0	-3	3	409	-404	24
0	-3	4	136	156	10
0	-3	5	64	49	12
0	-3	6	140	121	16
0	-3	7	526	524	33
0	-3	8	127	-120	10
0	-3	9	181	-193	9
0	-3	10	113*	-156	***
0	-4	-9	82*	-75	***
0	-4	-8	65*	-60	***
0	-4	-7	43-	5	22
0	-4	-6	240	225	15
0	-4	-5	388	383	20
0	-4	-4	181*	161	***

H	K	L	FØ	FC	σ
0	-4	-3	1065	-1149	175
0	-4	-2	265	270	16
0	-4	-1	45	-41	9
0	-4	0	127	-118	13
0	-4	1	35-	-21	18
0	-4	2	249	-219	26
0	-4	3	597	577	45
0	-4	4	96	-100	10
0	-4	5	82	-87	9
0	-4	6	209	-207	13
0	-4	7	61	-70	10
0	-4	8	137	135	21
0	-4	9	39-	2	20
0	-5	-8	170	183	9
0	-5	-7	43-	3	21
0	-5	-6	43-	2	22
0	-5	-5	511	-496	35
0	-5	-4	387	-385	20
0	-5	-3	786	781	68
0	-5	-2	107	100	10
0	-5	-1	47	-32	15
0	-5	0	342	-336	17
0	-5	1	137	-144	14
0	-5	2	405	381	21
0	-5	3	700	690	63
0	-5	4	108	101	7
0	-5	5	232	-226	12
0	-5	6	145	134	8
0	-5	7	132	-133	9
0	-5	8	41-	-14	21
0	-5	9	38*	22	***
0	-6	-8	46*	27	***
0	-6	-7	128	128	13
0	-6	-6	113*	-77	***
0	-6	-5	83	-82	7
0	-6	-4	294	-300	27
0	-6	-3	282	282	18
0	-6	-2	383	372	20
0	-6	-1	43	-29	13
0	-6	0	160	161	17
0	-6	1	98	72	9
0	-6	2	464	473	24
0	-6	3	521	-520	56
0	-6	4	334	-343	18
0	-6	5	35*	-23	***
0	-6	6	145	149	8
0	-6	7	267	272	15
0	-6	8	226	-229	16
0	-7	-7	72*	62	***
0	-7	-6	134	138	14
0	-7	-5	77	-82	8
0	-7	-4	188	194	13
0	-7	-3	194	-186	22
0	-7	-2	137	-143	10
0	-7	-1	85	80	11
0	-7	0	93	83	10
0	-7	1	119	117	6
0	-7	2	43-	16	21
0	-7	3	140	-138	13
0	-7	4	320	-327	19
0	-7	5	108	96	8
0	-7	6	41-	-29	21
0	-7	7	37-	-4	18
0	-8	-6	23*	-14	***
0	-8	-5	65	-63	9
0	-8	-4	120	122	6
0	-8	-3	251	251	13
0	-8	-2	151	158	8
0	-8	-1	68	-62	13
0	-8	0	407	-390	27
0	-8	1	66	67	11
0	-8	2	190	-191	19
0	-8	3	42-	-30	21
0	-8	4	219	228	21
0	-8	5	52	-48	10
0	-8	6	33*	-32	***
0	-9	-4	55*	57	***
0	-9	-3	172	168	9
0	-9	-2	74*	-62	***
0	-9	-1	136	-133	7
0	-9	0	69*	11	***
0	-9	1	50	-39	11
0	-9	2	47	50	11
0	-9	3	197	-195	15
0	-9	4	53	-58	8
0	-9	5	114*	121	***
0	-10	-2	133*	-179	***
0	-10	-1	189*	-204	***
0	-10	0	226*	223	***
0	-10	1	98*	103	***
0	-10	2	52*	-61	***

and a length of 0.46 mm. An integrating precession camera with Zr-filtered Mo-radiation was used to photograph layers with $h = 0$, 1, and 2, and $l = 0$, 1, 2, and 3. The intensities were measured using a recording photomicrodensitometer, and a standard error was estimated for each reflection for use in weighting the data during the least squares refinement. Unobserved intensities were assigned the local minimum observable value. The intensity data consisted of 2604 measured reflections of which 324 were unobserved. During the final stages of refinement 25 low angle reflections suspected of showing extinction effects were given zero weight.

The intensity data and their estimated standard errors were then corrected for Lorentz and polarization effects. Absorption corrections were not considered necessary.

The structure was solved using Patterson function and electron density projections down [001] and [100]. A trial three dimensional structure was formulated in space group $P1$ with

TABLE IV

Interatomic distances (in Å) and angles (in degrees) in triclinic potassium dichromate. Figures in parentheses denote standard errors in the last digits quoted as indicated by the least squares refinement. The true standard errors are probably 5 or 10 times as large. Symmetry transformations from the atom coordinates given in Table II are designated as follows: a = [100], b = [010], c = [001], d = [0$\bar{1}$1], e = [101], f = [$\bar{1}\bar{1}$0], $\bar{a}$ = [$\bar{1}$00], $\bar{b}$ = [0$\bar{1}$0]. The prime denotes inversion in the center of symmetry at either (0, 1/2, 1/2) or (1/2, 1/2, 1/2)

Dichromate ions

Distances	Uncorrected	Thermally corrected	Distances	Uncorrected	Thermally corrected
Cr1—Cr2	3.144(2)	3.144	Cr3—Cr4	3.189(2)	3.189
Cr1—OB1	1.776(3)	1.781	Cr3—OB3	1.780(3)	1.788
Cr2—OB1	1.784(3)	1.790	Cr4—OB3	1.775(3)	1.784
	Mean corrected Cr—O (bridge) = 1.786				
Cr1—O11	1.614(3)	1.624	Cr3—O31	1.618(4)	1.633
O12	1.622(3)	1.634	O32	1.620(4)	1.634
O13	1.610(4)	1.626	O33	1.614(3)	1.629
Cr2—O21	1.583(3)	1.602	Cr4—O41	1.613(4)	1.627
O22	1.632(3)	1.642	O42	1.604(3)	1.619
O23	1.625(3)	1.638	O43	1.633(3)	1.643
	Mean corrected Cr—O (terminal) = 1.629				
OB1—O11	2.71		OB3—O31	2.72	
O12	2.77		O32	2.78	
O13	2.79		O33	2.78	
O21	2.75		O41	2.77	
O22	2.77		O42	2.79	
O23	2.78		O43	2.76	
O11—O12	2.64		O31—O32	2.65	
O13	2.67		O33	2.66	
O12—O13	2.64		O32—O33	2.65	
O21—O22	2.64		O41—O42	2.63	
O23	2.64		O43	2.66	
O22—O23	2.64		O42—O43	2.62	
O12—O23	3.35		O32—O43	3.54	
O13—O22	3.41		O33—O42	3.49	
Angles			Angles		
Cr1—OB1—Cr2		124.0(1)	Cr3—OB3—Cr4		127.6(2)
OB1—Cr1—O11		106.1(1)	OB3—Cr3—O31		106.6(2)
O12		109.4(1)	O32		109.7(1)
O13		110.8(1)	O33		110.1(1)
O11—Cr1—O12		109.5(1)	O31—Cr3—O32		109.8(2)
O13		111.7(1)	O33		110.6(1)
O12—Cr1—O13		109.2(2)	O32—Cr3—O33		110.1(1)
OB1—Cr2—O21		109.6(1)	OB3—Cr4—O41		109.7(1)
O22		108.5(1)	O42		111.2(2)
O23		109.5(1)	O43		108.4(1)
O21—Cr2—O22		110.2(1)	O41—Cr4—O42		109.7(2)
O23		110.6(1)	O43		109.9(2)
O22—Cr2—O23		108.4(1)	O42—Cr4—O43		107.9(1)

K—O distances

K1—O11	3.82	K2—O21c	3.63	K3—O31b	3.70	K4—O41	3.25
O12c	2.83	O22	2.80	O32	2.88	O42b	2.94
O13	2.74	O23c	2.73	O33b	2.70	O43	2.74
O23c	2.87	O13	2.75	O43	2.71	O33b	2.83
O21′	2.82	O11′	2.93	O41′c	2.67	O31′c	2.97
O22′$\bar{b}$	2.83	O12′$\bar{b}$	2.83	O42′	3.34	O32′	2.82
O23′$\bar{b}$	2.97	O13′$\bar{b}$	3.64	O43′	2.68	O33′	*
OB1c	*	OB1	3.86	OB3	3.59	OB3b	3.90
OB1′	*	OB1′	2.96	OB3′c	*	OB3′c	2.86
O41	2.89	O31$\bar{a}$	3.14	O11′a	2.79	O21′	3.29
O42	3.07	O32$\bar{a}$	2.89	O12′a	2.84	O22′	2.76
O31′d	2.84	O41′c	*	O21e	*	O11	3.09

Can. J. Chem. Downloaded from www.nrcresearchpress.com by 210.87.254.42 on 09/05/12
For personal use only.

TABLE IV (*Concluded*)

O—O distances less than 3.20 Å between dichromate ions	
O11—O32′	3.04
O11—O22′	3.16
O12—O31′*b*	3.19
O22—O42′*f*	3.17
O43—O43′	3.15

*These distances are greater than 4 Å.

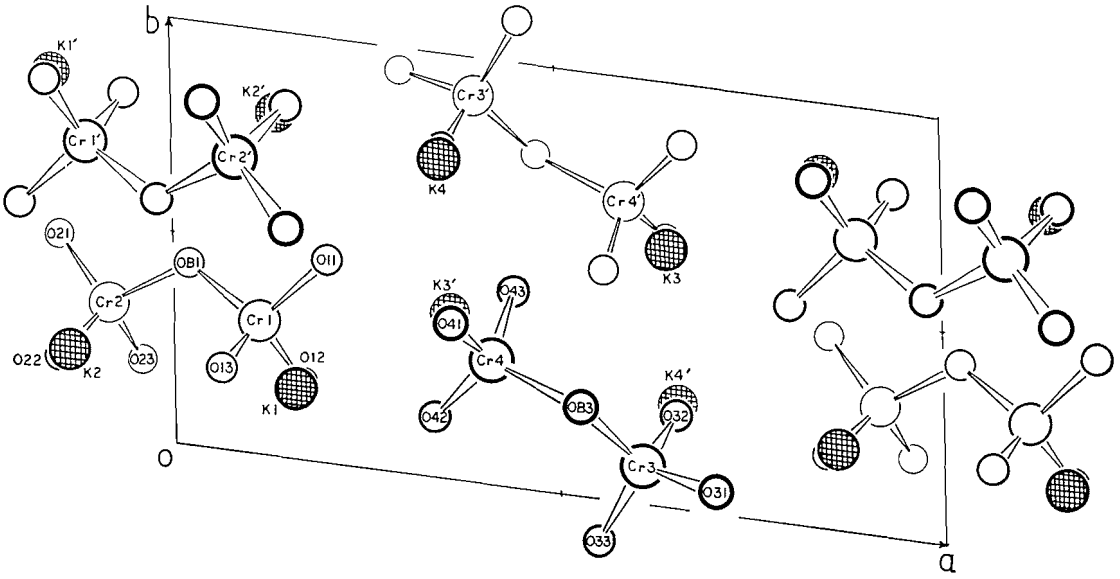

FIG. 2. The structure of triclinic $K_2Cr_2O_7$ projected down [001].

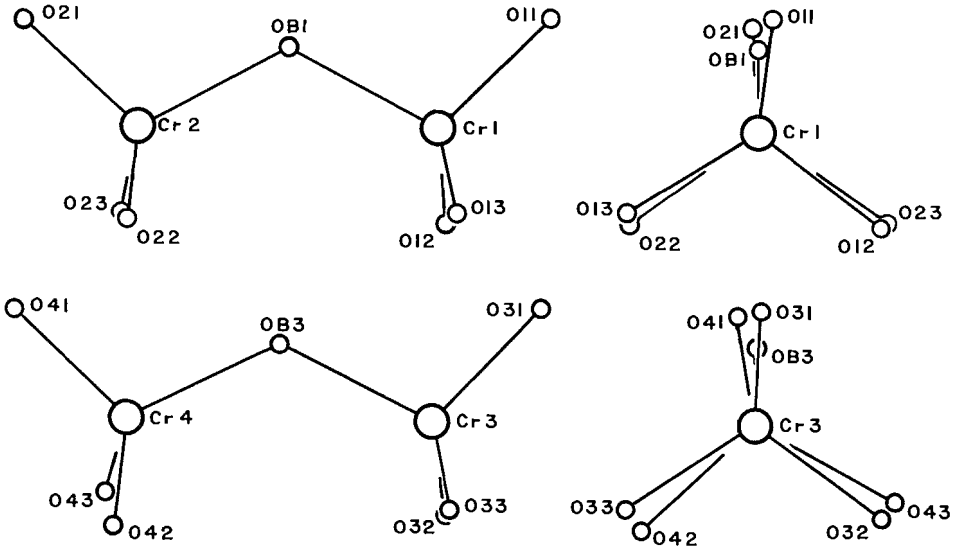

FIG. 3. Side and end views of the two independent $Cr_2O_7^{2-}$ ions in triclinic $K_2Cr_2O_7$.

Can. J. Chem. Downloaded from www.nrcresearchpress.com by 210.87.254.42 on 09/05/12
For personal use only.

Can. J. Chem. Downloaded from www.nrcresearchpress.com by 210.87.254.42 on 09/05/12
For personal use only.

TABLE V

Interatomic distances in various X_2O_7 groups. The naming of the atoms is shown in Fig. 4. The distances (in Å) are generally ± 0.01 Å and the angles (in degrees) are generally $\pm 1°$. Where two figures are given, significantly different values occur within the same crystal. Where the values do not differ significantly, they have been averaged. The angle of eclipse is the angle through which one CrO_4 tetrahedron must be turned to bring the group into an eclipsed configuration

Ion	Angle of eclipse	X—OB—X	X—OB	X—O1	X—O2	OB—X—O1	OB—X—O2	O1—X—O2	O2—X—O2	OB—O1	OB—O2	O1—O2	O2—O2
$Cr_2O_7^{2-}$ ($K_2Cr_2O_7$) (present work)	5, 10	124, 128	1.78	1.61	1.62	110, 106	110	110	109	2.76, 2.72	2.78	2.65	2.64
$P_2O_7^{4-}$ (β-$Ca_2P_2O_7$) (9)	11, 17	131, 138	1.62	1.50	1.53	104	107	113	112	2.45	2.53	2.53	2.53
$P_2O_7^{4-}$ ($Na_4P_2O_7 \cdot 10H_2O$) (16)	23	134	1.61	1.50	1.52	102	106	114	111	2.42	2.53	2.52	2.50
$S_2O_7^{2-}$ ($K_2S_2O_7$) (8)	7	124	1.65	1.43	1.44	101	106	115	113	2.40	2.46	2.40	2.40
Cl_2O_7 (17)	15	119	1.71	1.41	1.41	98	105	115	115	2.36	2.48	2.37	2.37

Can. J. Chem. Downloaded from www.nrcresearchpress.com by 210.87.254.42 on 09/05/12
For personal use only.

44 independent atoms per unit cell. This trial structure possessed approximate centers of symmetry but further refinement was performed without imposing any such constraints.

A full matrix least squares calculation was used to refine the atomic coordinates and isotropic temperature factors of all atoms together with separate scale constants for each of the seven layers of data. Weights for each reflection were set equal to one over the standard error in the observed structure factor (F_o), except for those unobserved reflections for which the calculated structure factor (F_c) was less than the smallest observable F_o. In these cases the weight was set equal to zero. The best weighted agreement index,

$$R \equiv [\sum w^2(|F_o| - |F_c|)^2/\sum w^2|F_o|^2]^{1/2},$$

obtained in the space group $P1$ with individual isotropic temperature factors was 0.075. Since this structure still possessed an approximate center of symmetry a refinement was also performed in the space group $P\bar{1}$ with individual isotropic temperature factors giving an agreement index of 0.096.

Hamilton's statistical tests (11) applied to these agreement indices indicated a less than 0.5% probability of $P\bar{1}$ being the correct space group. However, the $P1$ model was unsatisfactory in that it did not differ in any chemically meaningful way from the $P\bar{1}$ model, and, consequently, an attempt was made to look for anomalous dispersion effects. Structure factor calculations with the $P1$ model indicated that there were several pairs of reflections hkl and $\bar{h}\bar{k}\bar{l}$ whose intensities should be markedly different when photographed with Cu-radiation if the space group really were non-centrosymmetric. A Weissenberg $h0l$ photograph taken with CuK_α radiation failed to show these differences thus indicating that the $P1$ model was wrong. Further examination of the two models showed that during the refinement of the $P1$ model, the extra degrees of freedom were being used to compensate for anisotropic temperature effects. When the $P\bar{1}$ model was refined with anisotropic temperature factors the agreement index dropped to 0.054. It was not possible to refine the $P1$ model with anisotropic temperature factors because of the large correlations between the positional and temperature variables and so it was not possible to use statistical tests to compare the two models at this stage. However, the absence of an observable anomalous dispersion effect, the low value of the agreement index, and the satisfactory molecular geometry of the $P\bar{1}$ model all indicate that any deviations from the $P\bar{1}$ symmetry must be very small.

The atomic coordinates and anisotropic temperature factors are given in Table II for the best anisotropic $P\bar{1}$ model. For comparison, the coordinates of Kuz'min *et al.* (2) are also given. These have been converted to our cell convention by the transformation

$$x = (1/2) - y'; y = (1/2) - z'; z = 1 - x',$$

where x', y', and z' are the coordinates given in their paper. With these coordinates they obtained an agreement index of 0.16.

Table III gives some of the observed structure amplitudes (F_o) and their estimated standard errors (σ) together with the structure factors (F_c) calculated from our parameters in Table II. The complete set of refined structure factor data is given in ref. 12. The atomic scattering factors used were those for K^+, Cr^{3+}, and O^- given in International Tables (13).

Discussion

The present determination of the structure of $K_2Cr_2O_7$ agrees with that of Kuz'min *et al.* (2) but, because of its greater accuracy, it reveals more clearly the configuration of the $Cr_2O_7^{2-}$ ion. This ion consists of two nearly tetrahedral CrO_4 groups joined through a shared oxygen atom. The ion is almost in the eclipsed configuration and is close to having the symmetry C_{2v}. The anisotropic temperature factors of the chromium and oxygen atoms indicate that the $Cr_2O_7^{2-}$ ion undergoes a librational motion with a root mean square amplitude of about 6° around an axis passing through the two chromium atoms.

Interatomic distances and angles calculated for $K_2Cr_2O_7$ from our data are given in Table IV. The bond distances within the $Cr_2O_7^{2-}$ ion are given both before and after corrections have been made for thermal motion (14). Figure 2 shows the structure projected down [001].

Figure 3 shows side and end views of the two crystallographically distinct $Cr_2O_7^{2-}$ ions. When viewed along the Cr—Cr directions, the ions show twists of about 5° and 10° away from an exactly eclipsed configuration, reducing the

Can. J. Chem. Downloaded from www.nrcresearchpress.com by 210.87.254.42 on 09/05/12
For personal use only.

ideal symmetry from C_{2v} to C_2. In addition, one, but only one, of the angles subtended at the chromium atoms in each ion (OB1—Cr1—O11 and OB3—Cr3—O31) is significantly different from 109.5° thus reducing the symmetry further from C_2 to C_1. The Cr—O—Cr bridging angles in the two ions are significantly different with values of 124.0° and 127.6°. In both dichromate ions the two bridging Cr—O distances are equal within experimental error (mean 1.79 ± 0.01 Å) as are the terminal Cr—O distances (mean 1.63 ± 0.01 Å).

It is of interest to compare the geometry of the $Cr_2O_7^{2-}$ ions with those found for similar groups in ionic crystals or in the gas phase. There is, unfortunately, no other determination of the structure of the dichromate ion of comparable accuracy, although three dichromate structures have been reported (2, 7, 15). Accurate structures have been reported for the pyrophosphate ions in β-$Ca_2P_2O_7$ (9) and $Na_4P_2O_7 \cdot 10H_2O$ (16). Like $K_2Cr_2O_7$, β-$Ca_2P_2O_7$ has two non-equivalent anions in the unit cell. The structure of potassium pyrosulfate, in which the $S_2O_7^{2-}$ ion has a crystallographic C_2 symmetry, has also been determined by X-ray diffraction (8) while the structure of Cl_2O_7 has been determined in the gas phase by electron diffraction (17).

In every case, it is found that the immediate environment of both X atoms in the X_2O_7 group has the symmetry C_s, so that two of the four X—O bonds are equivalent within the limits of experimental accuracy. Table V gives, for the various X_2O_7 groups, interatomic distances and angles averaged over all the corresponding values within the crystal.

From this table it can be seen that the groups

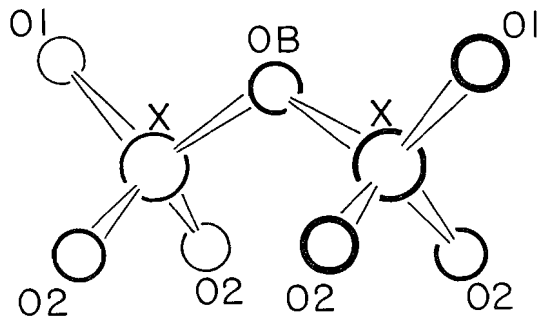

FIG. 4. Idealized view of an X_2O_7 group showing the atom names used in Table V.

are all close to being eclipsed and have X—OB—X angles of about 120 to 130°. These angles vary from group to group even within the same crystal and appear to be sensitive to the crystalline environment. The large deviation from the eclipsed configuration in $Na_4P_2O_7 \cdot 10H_2O$ can be attributed to the hydrogen bonds present. As would be expected, the distance from the central atom (X) to the bridging oxygen atom is always longer than the distances from the central atom to the terminal oxygen atoms. Also, the angles subtended at X by the terminal oxygen atoms (O1—X—O2, O2—X—O2, see Fig. 4 for an explanation of nomenclature) are larger than the angles subtended by the bridging oxygen atoms (OB—X—O1, OB—X—O2) in all groups except $Cr_2O_7^{2-}$. The reason for this can be understood if one realizes that the sum of the van der Waals radii for two oxygen atoms is 2.80 Å. In the smaller ions the oxygen atoms bonded to the same central atom are separated by distances much less than the sum of the van der Waals radii and are under considerable pressure. An additional pressure arises from the coulombic repulsions between the ionic charges which reside on these atoms. Both pressures can be relieved by increasing the angles between the bonds to the terminal oxygen atoms until all the O—O distances are about the same. Examination of the O—O distances in Table V shows that this occurs for all the groups except $Cr_2O_7^{2-}$. In this case, the O—O distances are long enough that no distortion is necessary.

Another common feature in these groups is the small size of the angle OB—X—O1 compared with OB—X—O2. This has been attributed to mutual repulsions between atoms in opposite halves of the X_2O_7 group (17). Like the previous effect, this repulsion is largest when the group is smallest. In an ion the size of $Cr_2O_7^{2-}$ this effect should be absent. In fact, in each of the two crystallographically independent $Cr_2O_7^{2-}$ ions in $K_2Cr_2O_7$ one, but only one, of the OB—X—O1 angles is smaller than the tetrahedral angle. Since any intraionic repulsions should affect both halves of the ion equally, this distortion must be due to the influence of neighboring ions in $K_2Cr_2O_7$. Both $Cr_2O_7^{2-}$ ions are in similar environments. Further work on some of the other phases of the alkali metal dichromates is in progress in this laboratory.

Acknowledgments

We wish to acknowledge the support of a research operating grant from the National Research Council of Canada and one of us (J. K. Brandon) wishes to thank the National Research Council of Canada for a Scholarship.

1. E. MITSCHERLICH. Ann. Physik, **28**, 116 (1833).
2. E. A. KUZ'MIN, V. V. ILYUKHIN, and N. V. BELOV. Dokl. Akad. Nauk SSSR, **173**, 1078 (1967).
3. U. KLEMENT and G. SCHWAB. Z. Krist. **114**, 170 (1960).
4. G. S. RAO. J. Indian Inst. Sci. Sect. A, **41**, 47 (1959).
5. V. S. PODISKO. Tr. Inst. Kristallogr. Akad. Nauk SSSR, **9**, 327 (1954).
6. V. F. PARVOV and A. V. SHUBNIKOV. Kristallografiya, **9**, 435 (1964). (Translation in Soviet Phys.-Cryst. **9**, 361 (1964).)
7. A. BYSTROM and K. WILHELMI. Acta Chem. Scand. **5**, 1003 (1951).
8. H. LYNTON and M. R. TRUTER. J. Chem. Soc. 5112 (1960).
9. N. C. WEBB. Acta Cryst. **21**, 942 (1966).
10. M. E. STRAUMANIS, T. EJIMA, and W. J. JAMES. Acta Cryst. **14**, 493 (1961).
11. W. C. HAMILTON. Acta Cryst. **18**, 502 (1965).
12. J. K. BRANDON. Ph.D. Thesis, McMaster University, Hamilton, Ont. 1967. Table 5-4.
13. INTERNATIONAL TABLES FOR X-RAY CRYSTALLOGRAPHY. Vol. III. Kynoch Press, Birmingham. 1962. Tables 3.3.1A, 3.3.2B.
14. W. R. BUSING and H. A. LEVY. Acta Cryst. **17**, 142 (1964).
15. L. A. ZHUKOVA and Z. G. PINSKER. Kristallografiya, **9**, 44 (1964). (Translation in Soviet Phys.-Cryst. **9**, 31 (1964).)
16. W. S. MCDONALD and D. W. J. CRUICKSHANK. Acta Cryst. **22**, 43 (1967).
17. B. BEAGLEY. Trans. Faraday Soc. **61**, 1821 (1965).

Can. J. Chem. Downloaded from www.nrcresearchpress.com by 210.87.254.42 on 09/05/12
For personal use only.

Interactions in aqueous alkali metal nitrate solutions[1]

D. E. IRISH AND A. R. DAVIS[2]
Department of Chemistry, University of Waterloo, Waterloo, Ontario
Received September 26, 1967

Raman (R) and infrared (I) spectra of aqueous alkali metal nitrate solutions have been recorded at 25 °C for a wide range of concentrations. In dilute solution the nitrate ion is perturbed by solvent water; the effects attributed to cations are nonspecific. The solvated nitrate ion generates the following spectrum: 1404 cm^{-1} (I, R), 1348 cm^{-1} (I, R), 1049 cm^{-1} (R), 825 cm^{-1} (I), 719 cm^{-1} (I, R). In more concentrated solutions band positions, intensities, and especially half-widths show a marked concentration and cation dependence. Changes in band half-width with concentration have been related to hydrated radii of the cations and are discussed in terms of interaction of solvated ions. For solutions of lithium and sodium nitrate more concentrated than 7 *M* a splitting of the $\nu_4(E')$ mode of nitrate ion into components at 720 and 740 cm^{-1} has been detected. Contact between ions is believed to account for the spectral changes observed for these high concentrations although water is shown to still markedly influence the interaction.

Canadian Journal of Chemistry, 46, 943 (1968)

Interactions between ions in concentrated aqueous solutions of strong electrolytes, such as the alkali metal nitrates, which are responsible for apparent deviations of observed properties from properties predicted from theories which assume complete dissociation are often described in terms of "ion-pairs". Methods for the evaluation of the dissociation constant of the ion-pair have been summarized in two recent monographs (1, 2). For the alkali metal nitrates the values of these constants increase as the hydrated radius of the cation decreases (2). Prue has noted that factors outside the scope of the simple electrostatic model must be important and suggests consideration of the molecular nature of the solvent (3). The nature of these ion-pairs and their dependence on the solvent is not well understood. The characterization of the solvent by its bulk properties and the neglect of solvent structure seriously limit the classical theories (4). Ion–solvent interactions are not readily accommodated by the "sphere in continuum" model (4, 5).

The vibrational spectrum frequently presents sufficient information to enable one to distinguish between species in solution (6), and Raman spectroscopy in particular has been used with success in the study of the dissociation of strong acids (7) and of complex ions (8). In addition to the number of modes of vibration, their activity and polarization properties, which together characterize a species, variations in vibrational frequency and the width of spectral lines provide information about environmental influences.

Results of a detailed study of vibrational spectra of aqueous nitrate solutions of lithium, sodium, potassium, and cesium are described below. The Raman spectra of these systems have been described before. The fact that the intensity of the $\nu_1(A_1')$ nitrate line (ca. 1050 cm^{-1}) in the Raman spectra of alkali metal nitrates is proportional to concentration was considered to be sufficient proof of complete dissociation (6). More recently small deviations from linearity have been interpreted in terms of the influence of hydrated cations on the nitrate ion (9).

Other bands in the Raman spectrum have received less attention. Several authors have reported the splitting of the $\nu_3(E')$ band centered at about 1387 cm^{-1} into two other bands for certain solution compositions of certain alkali metal nitrates (10–12) although this has gone unrecorded in at least one compilation of spectral lines (13). The removal of the degeneracy has been attributed to a lowering of the symmetry of the nitrate ion produced by an anisotropic ionic atmosphere (11, and references therein) or by solvent-separated ion-pairs (12). This region of both Raman and infrared spectra is described in detail below.

Aqueous solutions containing polyvalent

[1]Presented in part at the Symposium on the Structures of Ice, Water and Aqueous Solutions, 18th Annual Mid-American Symposium on Spectroscopy, Chicago, Illinois, May 15–18, 1967.

[2]Holder of Ontario Graduate Fellowships, 1965–1967. Present address: Department of Chemistry, Cornell University, Ithaca, New York, 14850.

Can. J. Chem. Downloaded from www.nrcresearchpress.com by 210.87.254.105 on 09/05/12
For personal use only.

Can. J. Chem. Downloaded from www.nrcresearchpress.com by 210.87.254.105 on 09/05/12
For personal use only.

cations may also exhibit splitting of the $\nu_4(E')$ mode (ca. 719 cm^{-1}) (10, 11, 13, 14). The additional line at ca. 740 cm^{-1} is particularly cation sensitive and variations in intensity with composition (Job plots) have been used to characterize the metal-nitrate species (14–16). This line has not hitherto been reported for aqueous solutions of alkali metal nitrates.

The above bands, except for $\nu_1(A_1')$, are also infrared allowed. In addition the infrared spectrum contains a strong sharp band at ca. 825 cm^{-1}, the $\nu_2(A_2'')$. In previous papers (14, 15) we have noted the presence of $\nu_1(A_1')$ in the infrared spectrum and suggested that the ratio of the intensity of the forbidden $\nu_1(A_1')$ mode to the intensity of the allowed $\nu_2(A_2'')$ mode (assuming D_{3h} symmetry for the nitrate ion) provides an empirical criterion to distinguish between nitrates which are covalently bound to metal ions and nitrates which are experiencing ionic interactions. Infrared spectra have now been obtained for many alkali metal nitrate solutions to extend the previous study and complement the Raman data.

Experimental

Aqueous solutions were prepared from weighed quantities of dried portions of the commercial salt and deionized water ($LiNO_3$, Fisher certified reagent; $NaNO_3$, KNO_3, B.D.H. Analar reagent; $CsNO_3$, K and K Laboratories, 99.9% pure). Concentrated solutions of known concentration were diluted by standard volumetric techniques. The solutions were filtered through a Whatman No. 1 filter paper and were clear and colorless.

Raman spectra excited by the 4358 Å line of mercury were recorded on a Cary 81 Raman spectrophotometer. The sample was contained in a cell equipped with a water jacket for temperature control. A Haake constant temperature circulator was used to maintain the temperature at 25 ± 0.02 °C. Undesirable mercury lines were excluded from the spectrum by the ethyl-violet, *o*-nitrotoluene solution supplied by Applied Physics Corp. A slit width of 10 cm^{-1} was used.

Intensities are reported relative to the intensity of the 458 cm^{-1} band of carbon tetrachloride. This spectral line was recorded before and after each measurement of a nitrate solution. Areas were measured with a polar planimeter. The relative integrated intensity was obtained by dividing the area of the particular nitrate band by the average area of the two bracketing CCl_4 bands. The ratio was corrected for differences in instrument sensitivity and sample cells.

Infrared spectra were recorded on a Beckman IR-9 spectrophotometer operated at three times the "standard" slit program provided by the manufacturers. Samples were contained in thermostatted cells supplied by the Research and Industrial Instrument Company; these were equipped with silver chloride windows. The necessary short pathlength was obtained by use of a 0.025 mm Teflon spacer. No reference cell was placed in the reference compartment; some attenuation with a Beckman beam attenuator was necessary.

A hybrid analogue-digital computer routine, described elsewhere (16), was used to resolve band envelopes. The frequency–intensity data are read from spectral charts and punched onto IBM cards. These generate the experimental curve which is displayed on the screen of a storage oscilloscope. A synthetic curve, a sum of invoked component bands each described by a Lorentz–Gaussian product function, is generated. The mean, variance, and area of each component are adjusted until the sum curve and experimental curve superimpose. A difference curve provides a measure of the goodness of fit.

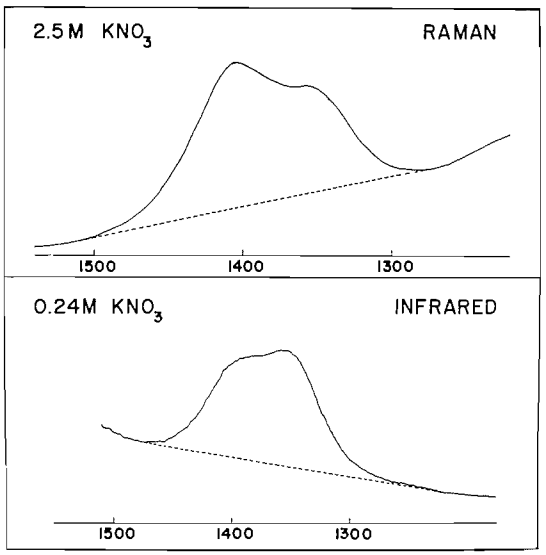

FIG. 1. The Raman spectrum of 2.5 *M* KNO_3 and the infrared spectrum of 0.24 *M* KNO_3 in the region 1100–1500 cm^{-1}.

Results and Discussion

1100–1500 cm^{-1} Region

Two distinct bands are observed in the infrared spectra of dilute aqueous solutions (0.12 to 0.50 *M*) and in the Raman spectra of more concentrated solutions (up to 10 *M* in the case of lithium nitrate) (Fig. 1). The band profiles were resolved by the hybrid analogue-digital computer routine and band frequencies, widths at half-height, and relative integrated intensities obtained.

The infrared-active bands occur at 1349 cm^{-1} and 1397 cm^{-1}; the band positions are independent of concentration for the dilute solutions.

Can. J. Chem. Downloaded from www.nrcresearchpress.com by 210.87.254.105 on 09/05/12
For personal use only.

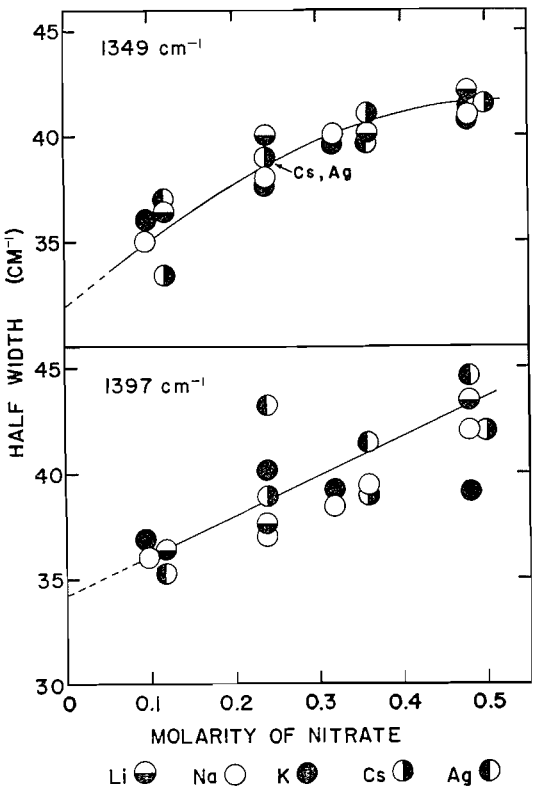

FIG. 2. The variation of half-width of the 1349 and 1397 cm^{-1} infrared bands with the stoichiometric concentration of alkali metal nitrate and silver nitrate.

The band at 1349 cm^{-1} is more intense than the band at 1397 cm^{-1} and the integrated absorbance is directly proportional to concentration for both the total band contour and the individual component bands. The band half-widths exhibit a monatonic increase with increase of concentration, independent of cation (Fig. 2). The variation for silver nitrate is similar to that of the alkali metal nitrates (Fig. 2). The large absorbtivity in this region of the infrared spectrum prevented study of more concentrated solutions.

For more concentrated solutions to the limit of solubility Raman spectra were studied. Again two bands are observed but above 1 *M* the band frequencies are markedly concentration dependent (Fig. 3). (The symbols ν_1 and ν_4 in Fig. 3 conform to the numbering scheme if NO_3^- is considered to have C_{2v} symmetry). Frequencies for solutions of sodium, potassium, and cesium nitrates increase together with increasing concentration whereas the frequencies for lithium nitrate solutions exhibit a different dependence on concentration. The plot of the separation of the two bands versus concentration (lower graph of Fig. 3) suggests that the splitting is 56 cm^{-1} at infinite dilution. The infrared data suggest a splitting of 48 cm^{-1}. These values can be compared with a value of 63 cm^{-1} for aqueous solutions of calcium nitrate (14). Although in the present study detailed information was not obtained for solutions of ammonium nitrate because of the interference of a weak band at 1410 cm^{-1} from NH_4^+, a similar separation of bands was observed.

As the concentration rises above 1 *M* the separation of the component bands increases markedly for lithium nitrate solutions. The value of 71 cm^{-1} at 10 *M* is approaching the value of 83 cm^{-1} observed for aqueous calcium nitrate solutions of the same nitrate concentration (14). Ionic interactions are known to be strong in the

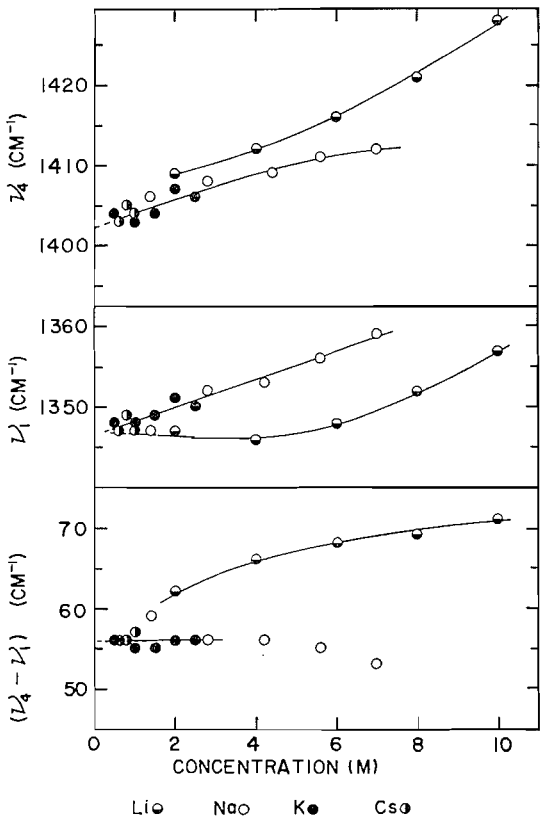

FIG. 3. The variation of band position for the ca. 1350 and 1410 cm^{-1} Raman bands with the stoichiometric alkali metal nitrate concentration.

Can. J. Chem. Downloaded from www.nrcresearchpress.com by 210.87.254.105 on 09/05/12
For personal use only.

calcium system and evidence for similar interaction in concentrated lithium nitrate solutions is presented here.

The Raman band at ca. 1410 cm^{-1} is more intense than the band at ca. 1350 cm^{-1} (the reverse of the infrared bands) and the relative integrated intensity is directly proportional to concentration for both the total band contour and the individual component bands, for all salts to the limit of concentration except lithium. Here a negative deviation from linearity above 8 *M* was observed for the total contour and the 1410 cm^{-1} component, probably due to strong interaction between cation and anion. The intensity ratio $I_{1410}/(I_{1350} + I_{1410})$ is 0.63, independent of the cation. The ratio for calcium nitrate is 0.61 (14).

The half-width of the ca. 1350 cm^{-1} Raman band increases with concentration, independent of cation (Fig. 4). Similarly the half-width of the ca. 1410 cm^{-1} Raman band increases with concentration, independent of cation up to 1.5 *M*. Above this concentration the half-widths exhibit an interesting specific ion effect. The widths become independent of concentration and vary in the sequence Li > Na > K ≃ Cs. The independence of half-width and concentration may arise at a concentration where all water molecules are bound, or at a concentration where ionic interaction with this mode of vibration is maximum.

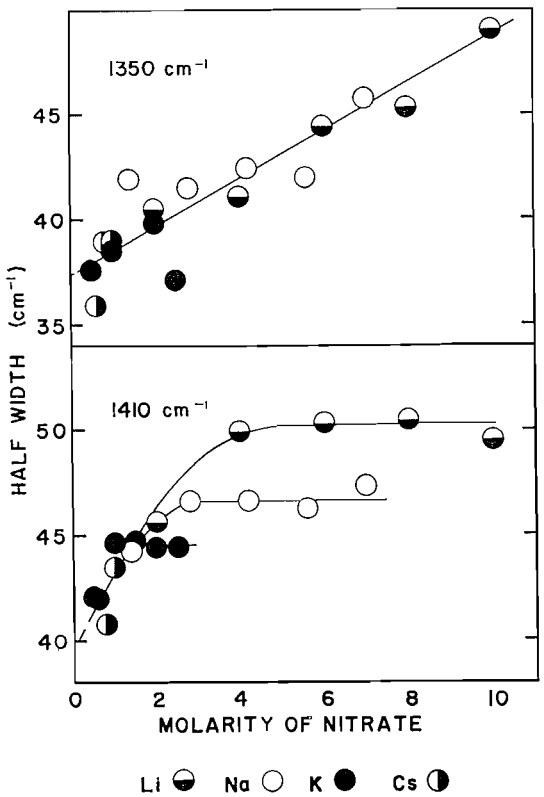

FIG. 4. The variation of half-width for the ca. 1350 and 1410 cm^{-1} Raman bands with the stoichiometric alkali metal nitrate concentration.

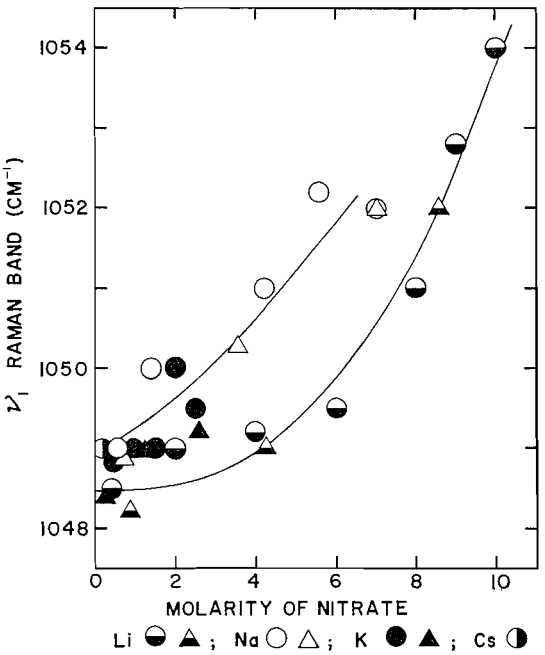

FIG. 5. The variation of band position of the ca. 1050 cm^{-1} Raman band with the stoichiometric concentration of alkali metal nitrate: (○) this work, (△) Vollmar (9).

It appears from the above data that the degeneracy of the $\nu_3(E')$ mode of nitrate is removed by interaction with the solvent water. Variation in the cation-induced polarity of the surrounding solvation sheath causes broadening of the bands but has little effect on the intensity. Above about 1.5 *M* specific ion interaction becomes significant. These conclusions will be substantiated and further developed from the data presented below.

800–1100 cm^{-1} Region

The frequency of the ca. 1050 cm^{-1} Raman band is also markedly concentration dependent (Fig. 5). The observations are in good agreement

Can. J. Chem. Downloaded from www.nrcresearchpress.com by 210.87.254.105 on 09/05/12
For personal use only.

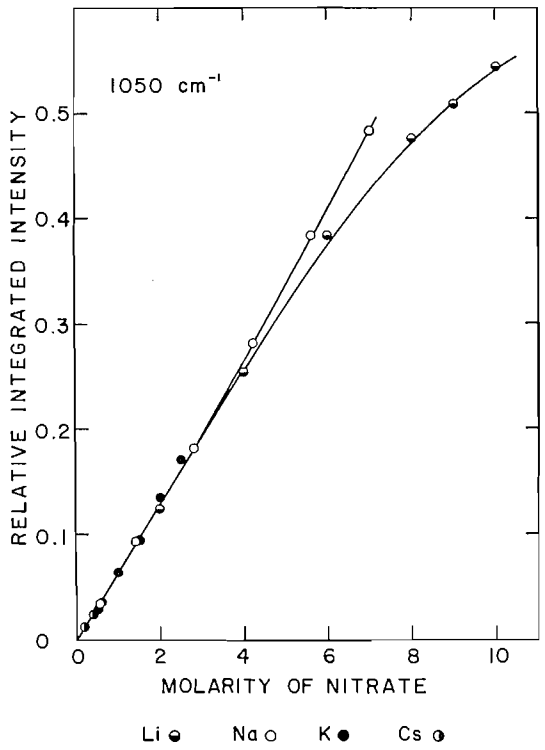

FIG. 6. The variation of relative integrated intensity for the ca. 1050 cm^{-1} Raman band with the stoichiometric concentration of alkali metal nitrate.

with those obtained by Vollmar (9) on a significantly different instrument. In dilute solution the value 1049 $\pm$ 0.5 cm^{-1} is indicated for this vibration. At higher concentrations the value for aqueous $NaNO_3$ is a little larger than that for K, Cs, or Li respectively. Above 7.0 *M* the value for aqueous $LiNO_3$ increases very rapidly with concentration. This is only one of several pronounced spectral changes that occur for solutions of lithium nitrate above approximately 7.0 *M*.

The half-width of the ca. 1050 cm^{-1} band increases with concentration for solutions of lithium nitrate (14.8 to 18.1 cm^{-1}; 0.4 to 10.0 *M*) and to a lesser extent for solutions of sodium nitrate (15.0 to 15.8 cm^{-1}; 0.56 to 7.00 *M*). Below 1.5 *M* the half-widths probably do not differ significantly with differences in cation but above 1.5 *M* they decrease in the order Li > Na > K $\simeq$ Cs, similar to the trend observed for the ca. 1410 cm^{-1} band. Vollmar (9) has noted that the increase in half-width is proportional to an increase in the hydrated radii of cations (17) for a series which included +2 and +3 charge type as well as +1.

A large hydrated radius is indicative of increased polarity of water molecules in the hydration sphere of the cation. Since only a small number of water molecules can be interspersed between ions in concentrated solutions, increase in polarity of the water molecules in the nitrate environment apparently results in increased half-width of the symmetric stretch (cf. ref. 9).

The relative integrated intensity of the ca. 1050 cm^{-1} band is directly proportional to concentration and is independent of the cation up to about 6 *M* (Fig. 6). Above 6 *M* lithium nitrate exhibits a negative deviation from linearity and sodium nitrate a positive deviation. These deviations are similar in sign but not magnitude to those reported by Vollmar (9).

A portion of the infrared spectrum of saturated sodium nitrate in D_2O is shown in Fig. 7. The 1100–1700 cm^{-1} region has been omitted because the absorbance is too large to be recorded. D_2O was used in place of H_2O because the base line is more nearly horizontal at lower wavenumbers. The forbidden $\nu_1(A_1')$ mode at 1049 cm^{-1} is evident; the ratio A_{1049}/A_{825} is 0.34. The band position is somewhat lower for saturated solutions of potassium and cesium nitrates (1046 and 1044 cm^{-1} respectively) but the absorbance ratio is very nearly the same as that for $NaNO_3$. The ratio is 1.0 for a saturated solution of $LiNO_3$. In all cases the intensity ratio rapidly drops to zero with dilution. A value of 1.45 has been reported for the ratio for $Ca(NO_3)_2$ solutions (14) and values of from 2.6 to 7.7 for Ce(IV)–NO_3^-–H_2O systems (15). The values are similarly high for solutions containing Cu^{2+} and Hg^{2+} (16). The low values for

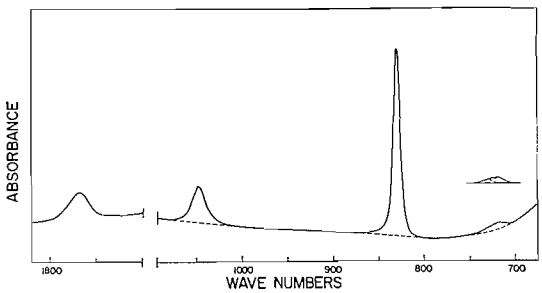

FIG. 7. Portion of the infrared spectrum of saturated sodium nitrate in D_2O.

Can. J. Chem. Downloaded from www.nrcresearchpress.com by 210.87.254.105 on 09/05/12
For personal use only.

the alkali metals are consistent with ionic perturbation of the nitrate ion and contrast with the higher values (greater than 2) which are consistent with covalent bond formation.

The activity of the 1050 cm^{-1} band in the infrared reveals that a dipole moment change is associated with the N—O stretch in the concentrated solution. Scatchard and Prentiss (18, 19) rejected the assumption of an induced dipole as a rationale for the values obtained for mean activity coefficients of alkali metal nitrates in much more dilute solutions. In concentrated solutions at least the value of the dipole moment must be appreciable.

The band at 1768 cm^{-1} in Fig. 7 is assigned to the combination $\nu_1(A_1')$ 1049 cm^{-1} + $\nu_4(E')$ 719 cm^{-1}.

600–800 cm^{-1} Region

The inherently weak 719 cm^{-1} $\nu_4(E')$ deformation mode was studied in detail for lithium nitrate and less thoroughly for sodium nitrate. Below ca. 7.0 *M* $LiNO_3$ a symmetric band at 719 cm^{-1} and a broad, weak band at ca. 689 cm^{-1} are observed. Above 7.0 *M* in the case of lithium nitrate and for saturated solutions of sodium nitrate a high frequency shoulder is observed. The shoulder results from a band at 740 cm^{-1} which can be resolved by the computer routine. The results of the computer analysis are illustrated in Fig. 8 for three samples.

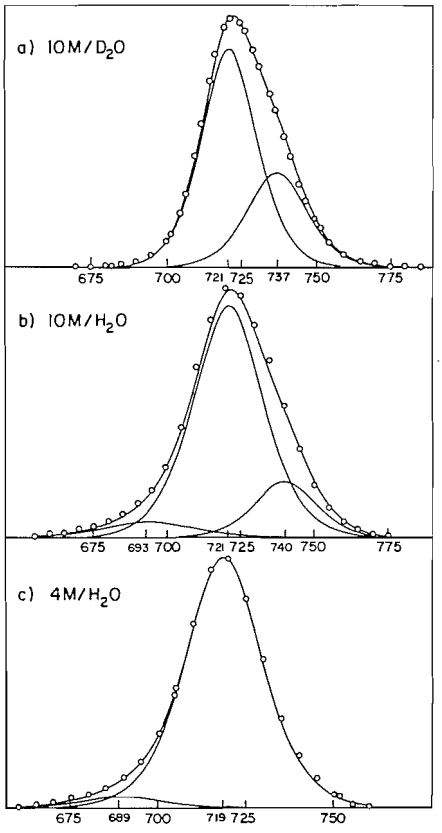

FIG. 8. The analyzed Raman contour from 675 to 775 cm^{-1} of aqueous $LiNO_3$: (*a*) 10.0 *M* in D_2O, (*b*) 10.0 *M* in H_2O, (*c*) 4.0 *M* in H_2O.

The open circles in Fig. 8 are intensity–wavenumber points read from the spectra. The solid lines define the Lorentz–Gaussian product functions which have been introduced to fit the data and also the sum of these functions. The band at 740 cm^{-1} is clearly present for the 10 *M* sample (Fig. 8*b*) but not for the 4 *M* sample (Fig. 8*c*). This band is also present in the infrared spectrum. It can be discerned in Fig. 7. For 10.0 *M* $LiNO_3$ the 740 cm^{-1} infrared band is more intense than the 719 cm^{-1} band. This suggests that an appreciable dipole moment change accompanies the vibration probably induced by a cation in close proximity to nitrate ion.

The total relative integrated intensity of the band envelope is directly proportional to concentration (Fig. 9). The 720 cm^{-1} band intensity exhibits negative deviations from linearity above 7.0 *M* and the 740 cm^{-1} band becomes prominent (Fig. 9).

The band at 689 cm^{-1} is not to be confused with the broad water librational modes in this region. These are known to shift to lower frequencies when solute is added to water (20). The 689 cm^{-1} band has been detected in all aqueous nitrate solutions including those containing polyvalent cations. Its constancy precludes assignment to cation solvation (21). It is absent from the spectrum for the D_2O solution (Fig. 8*a*). We suggest that it is probably due to a nitrate ion – water libration.

General Interpretation

For convenience the results are discussed in terms of four approximate concentration ranges but sharp changes at the limits are not implied. An analogy can be made between these ranges and the "states" proposed by Eigen and Tamm (22) and Atkinson and Kor (23) to account for observed ultrasonic relaxation data. In dilute

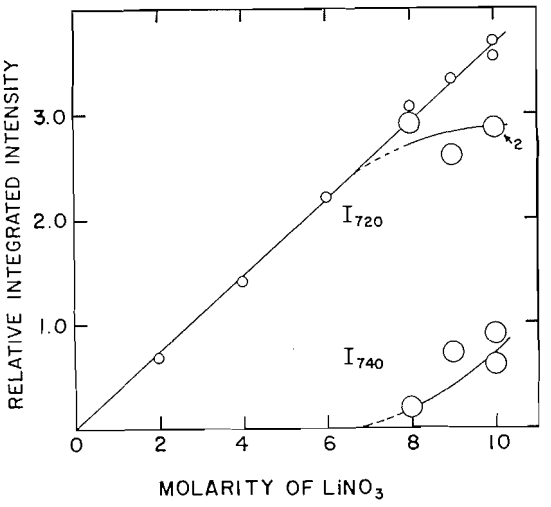

FIG. 9. The variation of relative integrated intensity for the ca. 720 and 740 cm^{-1} Raman bands with the stoichiometric concentration of $LiNO_3$: (o) total relative integrated intensity, (○) relative integrated intensity for resolved components.

solution the system consists of completely solvated ions.

$$M^+(aq) + NO_3^-(aq)$$

In relaxation experiments the ions in this state diffuse together with a rate predicted by the Debye theory and thus the state can be adequately described using conventional solution parameters (solvent dielectric constant, solvent viscosity, ionic charge, and ionic strength) and the "sphere-in-continuum" model (4).

The above description is considered to apply to alkali metal nitrate solutions of concentration less than 1.5 *M*. The vibrational spectrum of the nitrate ion in this concentration range is perturbed primarily by the solvent. The solvated nitrate ion generates the following spectrum: 1404 (I, R), 1348 (I, R), 1049 (R), 825 (I), 719 (I, R). The 56 cm^{-1} split of $\nu_3(E')$ is a measure of the strength of the nitrate ion – water interaction. The observation of the 689 cm^{-1} band, attributed to anion–water libration, is further indication that the nitrate ion possesses a well-defined solvation sphere.

Support for this interpretation comes from three other studies. Strongly bound primary water of solvation has recently been advanced to account for adsorption data for the nitrate ion on a mercury electrode (24). Shifts and intensity changes of the absorption maximum of the 3000 Å ultraviolet band of nitrate ion with change of solvent have been explained in terms of hydrogen bonding between solvent and nitrate ion (25). It has been suggested that the O—H valence stretch of water (ca. 3444 cm^{-1}) will be influenced by anion solvation whereas cation solvation should affect primarily the bending mode (26). It was reported that ions such as F^- and OH^- which are positively hydrated decrease the median frequency of the stretching mode, while strongly structure-breaking ions such as Br^-, I^-, and ClO_4^- increase the frequency of the stretching mode (26). We have observed that the stretching mode is increased 10 cm^{-1} for 2.0 *M* solutions of $LiNO_3$ and KNO_3. This shift must be attributed to the anion and thus provides additional evidence for nitrate–water interactions.

Even in these dilute solutions the nitrate ion is experiencing the field of the cations, as shown by the increase of band half-widths with concentration, but it is essentially a nonspecific effect, i.e. independent of the identity of the +1 cation as required by the Debye–Hückel theory.

Data for concentrated aqueous solutions of $LiNO_3$ can be compared with those for the molten salt. Raman bands at 1439, 1358, 1067, and 726 cm^{-1} have been interpreted in terms of a contact ion pair in the melt with C_{2v} or C_s symmetry (27). The increasing separation of components of $\nu_3(E')$ with increasing concentration has already been noted for aqueous solutions of $LiNO_3$ (see Fig. 3). The frequency separation, $\Delta\nu$, is proportional to the cube root of the molarity, including the value of 81 cm^{-1} for the molten salt (see Fig. 10). $M^{1/3}$ is proportional to a reciprocal distance and this interesting relationship suggests that the perturbation of the nitrate ion arises from coulombic interaction. High values of $\nu_1(A_1')$ (see Fig. 5) are consistent with this interpretation. The slight splitting of the $\nu_4(E')$ mode was probably not observed for the molten salt because of the limitation of photographic detection. This splitting becomes apparent at a concentration of ca. 7 *M* (Fig. 9) where there are only 6 moles of water for every mole of salt. It is reasonable to assume that at concentrations above 7 *M* the nitrate ion occupies a position in the first coordination sphere of lithium ion. However, even for this cation–anion contact, water solvation is important; the splitting of $\nu_3(E')$ is not as great in 10 *M*

Can. J. Chem. Downloaded from www.nrcresearchpress.com by 210.87.254.105 on 09/05/12
For personal use only.

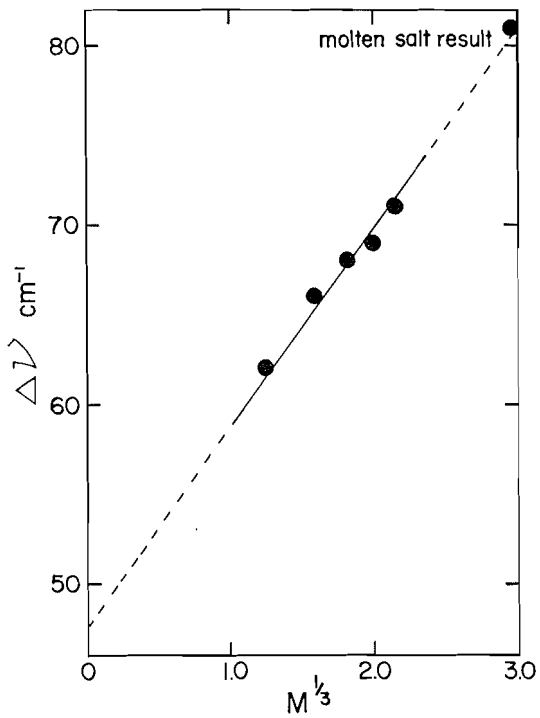

FIG. 10. The frequency split of the $\nu_3(E')$ Raman mode versus cube root of concentration of $LiNO_3$.

aqueous solution as it is for the molten salt. It now seems clear that the presence of a band at about 740 cm^{-1} implies direct metal-nitrate interaction and this has implications for studies of polyvalent nitrates (14, 28).

For the most concentrated solutions (ca. 7 *M*) of $NaNO_3$ there is also evidence of cation–anion contact, viz. the 740 cm^{-1} band observed in the infrared spectrum. Surprisingly, however, the separation of the components of $\nu_3(E')$ decreases slightly as the concentration increases and no splitting is reported for the molten salt (27). The explanation may lie in the symmetry of the ion atmosphere surrounding the nitrate ion. Because of the small size and large charge density of the lithium ion a single Li^+ may contact NO_3^- and at the same time repel other lithium ions, resulting in an anisotropic ion atmosphere. Because of the larger size of the sodium ion the cation repulsion may be of sufficiently smaller magnitude that the ionic environment is isotropic. Thus the splitting of $\nu_3(E')$ observed in aqueous solution for Na^+, K^+, and Cs^+ is essentially all caused by water.

In the concentration range 1.5 to 7 *M* solvent-separated ion-pair interactions are believed to be important. The specific cation effects on the half-width of the ca. 1410 cm^{-1} Raman line correlate with differences in the hydrated radii and hence hydration energy of the cations. The similarity in hydrated radii (17) of K^+, Cs^+, and NO_3^- suggests a similar affinity of each for water; thus each can retain its primary solvation sphere in the presence of the others (e.g. (K^+W) $(W\ NO_3^-)$ where W implies the solvation sphere).

The solvation energies and hence hydrated radii (17) of Na^+ and Li^+ are greater than those of NO_3^-. At sufficiently high concentrations these cations can be expected to perturb and order the peripheral hydration sphere of NO_3^-. The kinetic entity can then be considered to be $(Li^+\ W\ W)(NO_3^-)$.

Thus the solvated potassium ion has its maximum influence on the half-width of the ca. 1410 cm^{-1} Raman band at a concentration of about 1.5 *M* (half-width 44.5 cm^{-1}) and the solubility limit is reached before the nitrate ion is desolvated. The solvated sodium ion has its maximum influence at about 2.5 *M* (half-width 46.5 cm^{-1}) and the solvated lithium ion exerts its maximum influence at about 4.0 *M* (half-width 50.5 cm^{-1}) (see Fig. 4). For concentrations greater than 4.0 *M* ($[H_2O]$:$[LiNO_3] < 12$) ion-pairs of the type $M^+W\ NO_3^-$ are probably important. Prue has suggested that in the absence of specific factors large anions will be unable to displace water from the inner coordination sphere of small cations (3).

Finally it might be noted that this interpretation favors a quasi-lattice-like structure for the concentrated aqueous solution (11, 29, 30). It does not appear to be possible spectroscopically to detect kinetic entities which can be described by an equilibrium expression. Rather, the array of ions and water molecules is being forced by the removal of water into states which pass from completely solvated ions to solvated ions with interacting solvation spheres to ions with shared water of solvation to states involving cation–anion contact, with water still markedly influencing the interaction (cf. refs. 4, 22, 23).

Acknowledgments

This work was supported by grants from the National Research Council of Canada and by

Can. J. Chem. Downloaded from www.nrcresearchpress.com by 210.87.254.105 on 09/05/12
For personal use only.

the Government of Ontario in the form of an Ontario Graduate Fellowship to one of us (A. R. D.). This support, the technical assistance of Mr. G. Hill of the Chemistry Department glass shop, and the assistance of Mr. A. Weerheim and Mr. D. Wallace of the Computer Science Division of the University of Waterloo are gratefully acknowledged.

1. C. W. DAVIES. Ion association. Butterworths and Co., Ltd., London. 1962.
2. C. B. MONK. Electrolytic dissociation. Academic Press Inc., New York. 1961.
3. J. E. PRUE. Ionic equilibria. Pergamon Press Ltd., Oxford. 1966. p. 98.
4. G. ATKINSON and S. PETRUCCI. J. Phys. Chem. **70**, 3122 (1966).
5. J. B. HYNE. J. Am. Chem. Soc. **85**, 304 (1963).
6. O. REDLICH. Chem. Rev. **39**, 333 (1946).
7. T. F. YOUNG, L. F. MARANVILLE, and H. M. SMITH. *In* The structure of electrolytic solutions. *Edited by* W. J. Hamer. John Wiley and Sons, New York. 1959. Chap. 4.
8. D. E. IRISH. *In* Raman spectroscopy, theory and practice. *Edited by* H. A. Szymanski. Plenum Press, New York. 1967. Chap. 7.
9. P. M. VOLLMAR. J. Chem. Phys. **39**, 2236 (1963).
10. I. I. FRIEDMAN. M.Sc. Thesis, State College of Washington, Pullman, Washington. 1944. Referred to in ref. 6.
11. J. P. MATHIEU and M. LOUNSBURY. Discussions Faraday Soc. **9**, 196 (1950).
12. H. LEE and J. K. WILMSHURST. Australian J. Chem. **17**, 943 (1964).
13. R. E. HESTER and R. A. PLANE. Inorg. Chem. **3**, 769 (1964).
14. D. E. IRISH and G. E. WALRAFEN. J. Chem. Phys. **46**, 378 (1967).
15. J. T. MILLER and D. E. IRISH. Can. J. Chem. **45**, 147 (1967).
16. A. R. DAVIS and D. E. IRISH. To be published.
17. E. R. NIGHTINGALE, JR. J. Phys. Chem. **63**, 1381 (1959).
18. H. S. HARNED and B. B. OWEN. The physical chemistry of electrolytic solutions. 3rd ed. Reinhold Publishing Corp., New York. 1958. p. 527.
19. G. SCATCHARD and S. S. PRENTISS. J. Am. Chem. Soc. **56**, 807 (1934).
20. D. A. DRAEGERT. Presented at 18th annual mid-American symposium on spectroscopy. Chicago. May 15–18, 1967.
21. I. NAKAGAWA and T. SHIMANOUCHI. Spectrochim. Acta, **20**, 429 (1964).
22. M. EIGEN and K. TAMM. Z. Elektrochem. **66**, 93, 107 (1962).
23. G. ATKINSON and S. K. KOR. J. Phys. Chem. **69**, 128 (1965).
24. R. PAYNE. J. Phys. Chem. **69**, 4113 (1965).
25. S. J. STRICKLER. Ph.D. Thesis, Florida State University, Tallahassee, Florida. 1961.
26. E. R. NIGHTINGALE, JR. *In* Chemical physics of ionic solutions. *Edited by* B. E. Conway and R. G. Barradas. John Wiley and Sons, New York. 1964. p. 87.
27. S. C. WAIT, JR., A. T. WARD, and G. J. JANZ. J. Chem. Phys. **45**, 133 (1966).
28. R. E. HESTER and K. KRISHNAN. J. Chem. Phys. **46**, 3405 (1967).
29. H. BLOOM and J. O'M. BOCKRIS. *In* Fused salts. *Edited by* B. R. Sundheim. McGraw-Hill Book Co., New York. 1964. p. 5.
30. M. BLANDER. *In* Molten salt chemistry. *Edited by* M. Blander. John Wiley and Sons, New York. 1964. p. 150.

Can. J. Chem. Downloaded from www.nrcresearchpress.com by 210.87.254.105 on 09/05/12
For personal use only.

A view of bond formation in terms of molecular charge distributions

R. F. W. BADER AND A. K. CHANDRA
Department of Chemistry, McMaster University, Hamilton, Ontario

Received June 26, 1967

The process of bond formation as a function of internuclear separation for H_2 and Li_2 is interpreted in terms of the changes in the charge distributions and the forces which they exert on the nuclei. The charge distributions are calculated from extended Hartree–Fock wave functions which reduce to the Hartree–Fock atomic functions for infinite nuclear separation. The results for H_2 indicate that at separations greater than 5 a.u. the net attractive force exerted on the approaching nuclei arises from a simultaneous inwards polarization of the atomic charge distributions. For separations less than 5 a.u. the nuclei are bound by the force exerted by the delocalized component of the charge distribution. The density distributions and forces for He_2 over a range of internuclear separations are compared with those for H_2 to contrast the formation of stable and unstable molecular species in terms of their respective charge distributions.

The final section of the paper examines in detail the changes in the Hartree–Fock molecular charge distribution which arise from the inclusion of electron correlation in the wave function. The maximum error in the Hartree–Fock charge distribution for H_2 is found to be in the region between the nuclei, where it overestimates the charge density by approximately 1%. The errors in the Hartree–Fock charge distribution for Li_2 are found to be of the same order of magnitude as the uncertainty in the calculated density distribution itself.

Canadian Journal of Chemistry, **46**, 953 (1968)

Can. J. Chem. Downloaded from www.nrcresearchpress.com by 210.87.254.40 on 09/05/12
For personal use only.

I. Introduction

In previous publications (1–3) we have interpreted chemical binding in terms of the molecular charge distribution and the forces acting on the nuclei. The interpretation is based on a comparison of the molecular charge distribution and the nature of the forces which it exerts on the nuclei at the equilibrium internuclear separation with the charge densities and their associated forces for the separated atoms. In the present work we employ the same methods in an analysis of the process of bond formation by determining the changes in the atomic charge distribution over a range of internuclear distances.

Wahl and Das (4, 5) have recently obtained extended Hartree–Fock wave functions as a function of the internuclear separation for H_2 and Li_2. These wave functions consist of the Hartree–Fock function modified by the inclusion of the more important valence configurations in a configuration interaction treatment. This method, termed that of the "*Optimized Valence Configurations*" (o.v.c.) was developed specifically to study the process of bond formation with reference to the Hartree–Fock description of the atoms at infinite nuclear separation (4). The added configurations result in a molecular wave function which reduces to the Hartree–Fock atomic functions at large internuclear separations and in addition accounts partially for the increase in correlation energy of the valence electrons when the molecule is formed from the separated atoms. While the configuration mixing is restricted to the valence shell, the inner shells in Li_2 were reoptimized to allow for the changed electronic environment provided by the valence electrons. The results of this method for H_2 and Li_2 give potential energy curves which closely parallel the experimental curves over a large range of internuclear distances.

We have included in this study a similar analysis of the molecular charge distribution as a function of internuclear separation for He_2 using Hartree–Fock wave functions. Since He_2 dissociates into two closed shell atoms, configuration mixing is not required to insure proper behavior of the wave function for extended values of the internuclear distance. The results for H_2 and He_2 provide an interesting contrast of the charge redistributions which accompany the formation of bound and repulsive molecular states.

In the final section of this paper we consider specifically the effect of electron correlation on the Hartree–Fock molecular charge distribution.

Density maps of the total charge distribution are not particularly useful in a discussion of molecular binding. The perturbations of the density distribution caused by the formation of a chemical bond are generally small compared with the total density distribution and hence they

Can. J. Chem. Downloaded from www.nrcresearchpress.com by 210.87.254.40 on 09/05/12
For personal use only.

are effectively masked in total charge density maps. The changes in the original atomic density distributions may be isolated and studied directly by means of a density difference distribution. Such a distribution is constructed by subtracting the superimposed densities of the component (undistorted) *atoms* separated by a distance R from the molecular charge density evaluated at the same value of R.[1] This type of density difference distribution, presented in the form of a contour map for a plane through the molecule and designated by $\Delta\rho(\varepsilon,\eta)$, *provides a detailed picture of the net reorganization of the charge density of the separated atoms accompanying the formation of a molecule.* The density distribution which results from the overlap of the undistorted atomic densities does not place sufficient charge density in the "binding region", (the region between the nuclei) to balance the forces of nuclear repulsion (1). The regions of charge increase in the density difference maps are, therefore, the regions to which charge is transferred *relative to the separated atoms* to obtain a state of electrostatic equilibrium and hence a stable chemical bond. In addition, the location of the principal charge increase in the $\Delta\rho(\varepsilon,\eta)$ maps, whether it is symmetrically placed and shared equally by both nuclei, or whether it is localized in the region of a single nucleus, may be used to characterize the binding as ionic or covalent (2). The principal features of the $\Delta\rho(\varepsilon,\eta)$ maps also reflect differences between bonds which are principally of s or p type. For these reasons the density difference maps are referred to as "bond density maps".

In general, the total force acting on the A nucleus in the molecule AB for any internuclear separation R is given by

$$[1] \qquad \mathfrak{F}_A(R) = \frac{Z_A}{R^2}[Z_B - F_A^e],$$

where F_A^e is the electronic contribution to the force multiplied by R^2,

$$[2] \quad F_A^e = R^2 \int \phi^* \left(\sum_i \frac{\cos\theta_{Ai}}{r_{Ai}^2} \right) \times \phi \, d\vec{\tau}_1 \ldots d\vec{\tau}_N$$

or

$$[3] \qquad F_A^e = R^2 \int \rho(\vec{r}) \frac{\cos\theta_A}{r_A^2} d\vec{\tau}$$

[1]The atomic densities used in the construction of the $\Delta\rho(\varepsilon,\eta)$ maps for Li and He were calculated from the Hartree–Fock atomic functions of Clementi, Roothaan, and Yoshimine (6).

where $\rho(\vec{r})$ is the electron density distribution. The definition of the quantity F_A^e is necessary for the interpretative scheme which relates the change in the nature of both the forces and the density distribution as a function of R to the same reference standard, that of the separated atoms. For the separated atoms the total density distribution may be expressed as a sum of two atomic densities.

$$\rho = \rho_A + \rho_B$$

Since an unperturbed atomic density is centrosymmetric, ρ_A will not contribute to the force on nucleus A. Furthermore at this limit of large R, $r_A \to R$, $\cos\theta_A \to 1$ and thus the contribution of the density on atom B to the force on the A nucleus in terms of F_A^e is

$$[4] \quad F_A^e(R \to \infty) = R^2 \int \rho_B \frac{\cos\theta_A}{r_A^2} d\vec{\tau} = \int \rho_B \, d\vec{\tau} = N_B,$$

where N_B is the number of electrons on the B atom. Thus for a molecule which dissociates into neutral atoms, $Z_B = N_B$ (and $Z_A = N_A$) and the resultant force on both nuclei by eq. [1] is zero. One may interpret the vanishing of the force at large values of R as resulting from each electron on B screening one of the nuclear charges on B from nucleus A. The quantity F_A^e has the dimensions of charge and is numerically equal to the number of point charges which when placed at the B nucleus exerts the same field at the A nucleus as does the actual molecular charge distribution. In the limiting case of the separated atoms, F_A^e reduces to the number of electrons on the B atom as only the density on B exerts a field at A when $R \to \infty$. For values of $R < \infty$, however, the value of F_A^e may be greater than or less than Z_B corresponding respectively to a net force of attraction and the formation of a stable molecule or to a net force of repulsion and the formation of an unstable molecule. A measure of the binding ability of the total molecular charge distribution *relative* to the separated atoms as the reference standard is given by a comparison of the value of $F_A^e(R)$ with N_B, its limiting value for $R = \infty$. This compares the charge equivalent (in terms of a number of charges on B) of the electric field exerted by the electrons in the molecule with the charge equivalent of the field exerted by the

Can. J. Chem. Downloaded from www.nrcresearchpress.com by 210.87.254.40 on 09/05/12
For personal use only.

original atomic distributions. In the formation of a stable molecule, a value of $R\,(=R_e)$ is reached at which point F_A^e is again equal to Z_B, and electrostatic equilibrium is again attained. Thus $F_A^e = Z_B$ at both $R = \infty$ and $R = R_e$. It is one of the purposes of this work to determine the origin of the net attractive force for $\infty > R > R_e$ in terms of the properties of the density distribution as a function of R. Furthermore, the reattainment of a zero force at R_e does not result from a perfect screening of the nuclear charge on B by the density situated solely on B as it does for the separated atom case. The manner in which the molecular charge distribution is disposed so as to balance the forces of nuclear repulsion at R_e is another feature of the density distribution to be investigated.

For interpretative purposes, the charge density of the system, for $R < \infty$, may be expressed as

$$\rho = \rho_A + \rho_B + \rho_D,$$

where ρ_D represents that component of the density distribution which is delocalized over the molecule as a result of the molecular formation. The wave functions employed here are constructed from STO's centered on A and B and thus operationally ρ_A and ρ_B are equated to the atomic populations on A and B and ρ_D to overlap population. For values of $R < \infty$, all three components of the total density distribution contribute to the force on nucleus A and F_A^e may be correspondingly expressed in terms of the three separate contributions

$$[5] \qquad F_A^e = F_A^{(AA)} + F_A^{(BB)} + F_A^{(AB)}.$$

$F_A^{(BB)}$ ($\equiv$ screening force) is the contribution to the force on nucleus A from the atomic charge density ρ_B centered on nucleus B. The screening force is a measure of the electronic shielding of nucleus B from nucleus A by the electrons situated on B. $F_A^{(AA)}$ ($\equiv$ atomic force) denotes the contribution to the partial force on nucleus A from the atomic charge population ρ_A on A. The contribution is zero unless the atomic density remaining on A in the molecule is polarized. $F_A^{(AB)}$ ($\equiv$ overlap force) is the corresponding contribution from the overlap or delocalized charge density, ρ_D.

In the standard reference state the sole contribution to F_A^e is from the screening force, i.e. $F_A^e(\infty) = F_A^{(BB)} = N_B$. In the formation of a stable molecule, $F_A^{(BB)}$ for $R < \infty$ is generally less than N_B, resulting in partially unshielded nuclei and a force of repulsion. The net attractive force is thus exerted by either the delocalized charge density or by polarized atomic densities or both. It is the origin of the net attractive force as a function of R (or repulsive force for an unstable species) in terms of the contributions from ρ_A, ρ_B, and ρ_D which is the primary aim of this investigation.

II. The Formation of the H_2 Molecule

The total force $F_A(R)$ exerted on one of the nuclei in H_2 as calculated from the o.v.c. wave function of Das and Wahl is plotted versus R in Fig. 1. Also shown is an experimental force curve obtained from a Hulbert–Hirschfelder potential function. The most serious discrepancy between the two curves occurs for large values of the internuclear distance, the same discrepancy noted in a comparison of the theoretical and experimental potential curves. The claim by Das and Wahl that their method provides a fruitful means of calculating meaningful potential curves for molecules is borne out for H_2. The comparison of the theoretical and experimental force curves, the derivatives of the potential curves, is a more stringent test of the theoretically derived potential function than is a comparison of the potential functions themselves.

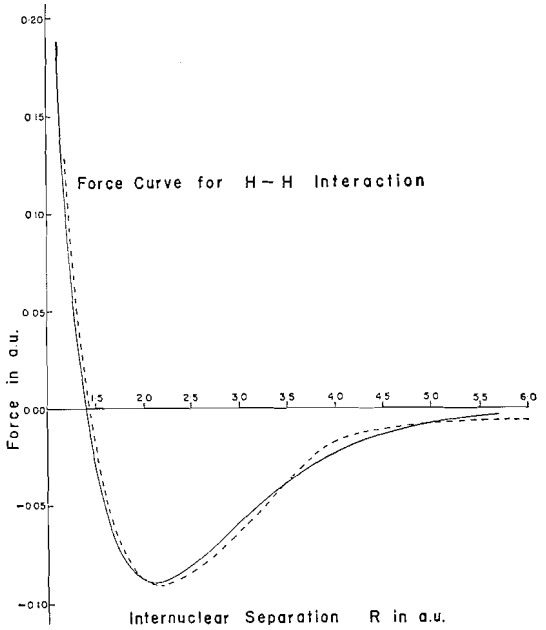

FIG. 1. The experimental (solid line) and theoretical force curves for the H_2 molecule (1 a.u. of force $= e^2/a_0^2 = 8.2378 \times 10^{-3}$ dyn).

Can. J. Chem. Downloaded from www.nrcresearchpress.com by 210.87.254.40 on 09/05/12
For personal use only.

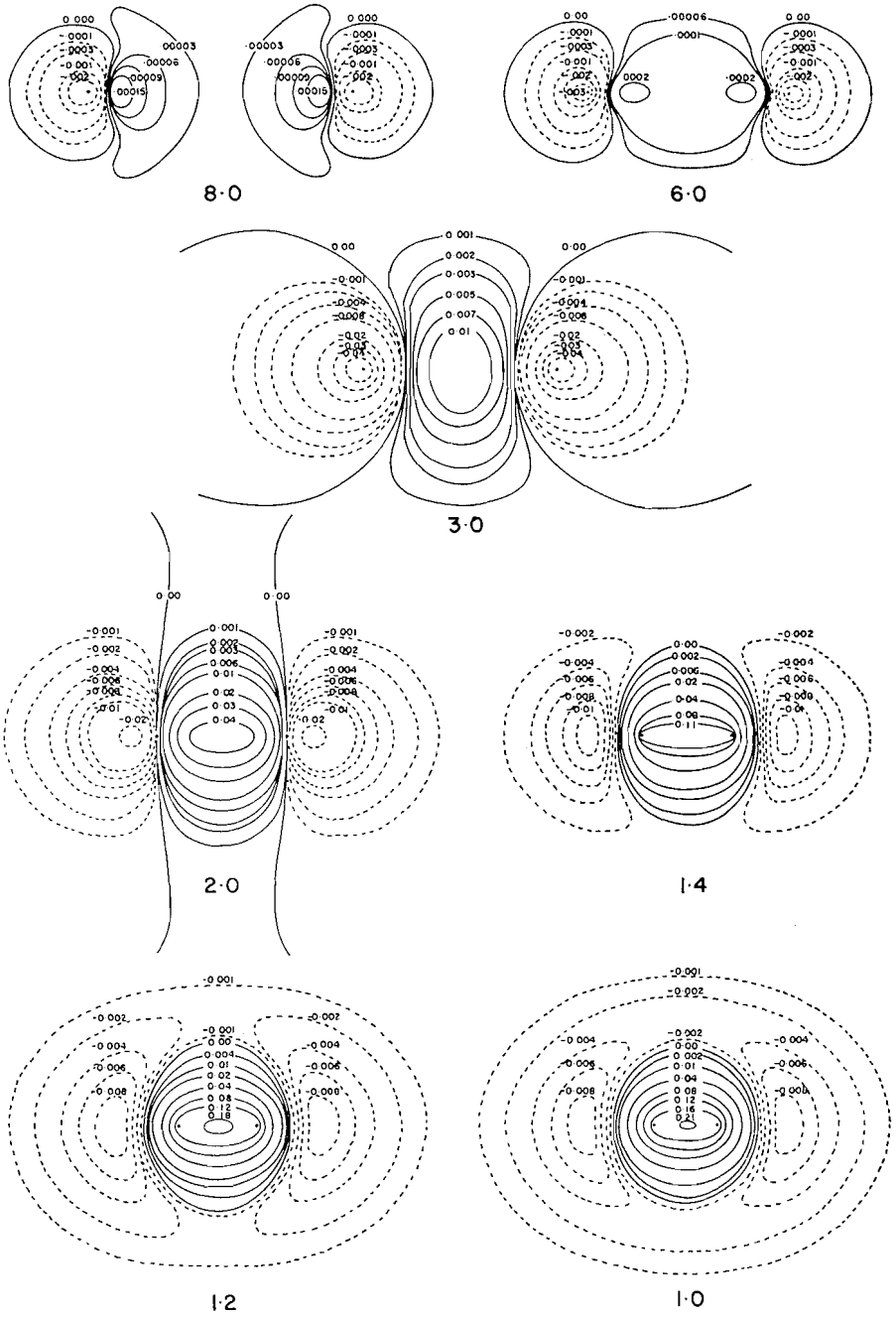

FIG. 2. Density difference contour maps $\Delta\rho(\varepsilon,\eta)$ for H_2 in a.u. at the indicated internuclear distances. The maps at $R = 8.0$ and 6.0 a.u. are drawn to 1/2 scale relative to the others. Note the behavior as a function of R of the zero contours which separate the spatial regions in which the charge density is decreased from those where it is increased relative to the original atomic densities.

Can. J. Chem. Downloaded from www.nrcresearchpress.com by 210.87.254.40 on 09/05/12
For personal use only.

The changing nature of the density distribution which results in the above force curve is illustrated in the density difference maps for H_2 in Fig. 2 and in the profiles of the density difference along the internuclear axis in Fig. 3. The $\Delta\rho(\varepsilon,\eta)$ map for 8 a.u. indicates that the system is best described as two inwardly polarized atoms, there being no evidence of a delocalized component in the charge distribution. The variations with R of the three contributions to the electronic force equivalent, and F_A^e itself, are shown in Fig. 4. The value of F_A^e at 8 a.u. indicates that the distortions of the atomic densities shown in the $\Delta\rho(\varepsilon,\eta)$ map for this internuclear separation exerts a force on either nucleus equivalent to placing 1.33 negative charges on the other nucleus, and hence a *net* attractive force of $-0.33/R^2$. The values of the contributions to F_A^e indicate, as does the $\Delta\rho(\varepsilon,\eta)$ map, that the attractive force operative at large R has its origin in the inwards polarization of the density on each nucleus, i.e. an atomic force, $F_A^{(AA)}$. The contribution from the delocalized component of the density $F_A^{(AB)}$ is zero and the screening contribution is unity, the limiting value for infinite internuclear separation. Thus the charge density on each atom screens its nuclear charge from the other and exactly cancels the nuclear force of repulsion. The *net* attractive force exerted on each nucleus is a result of the inwards polarization of its own atomic density. The attractive forces operative between atoms at this and larger distances are the so-called London dispersion forces. The origin of these forces, as first pointed out by Feynman (7), lies in the *simultaneous* inward polarization of both atomic densities which is induced by their mutual interaction. The long range attractive forces could be aptly described as a "bootstrap effect" as each nucleus is pulled by its own charge density. That the same explanation of the dispersion forces does indeed hold for larger separations has been demonstrated by Eliason and Hirschfelder (8), who have used the Hellmann–Feynman theorem in conjunction with a second-order perturbation function to calculate the force which varies as R^{-7} for the long range interaction of two hydrogen atoms.

At a separation of 6 a.u. the density increase is common to both atoms. The force contributions shown in Fig. 4 indicate that the

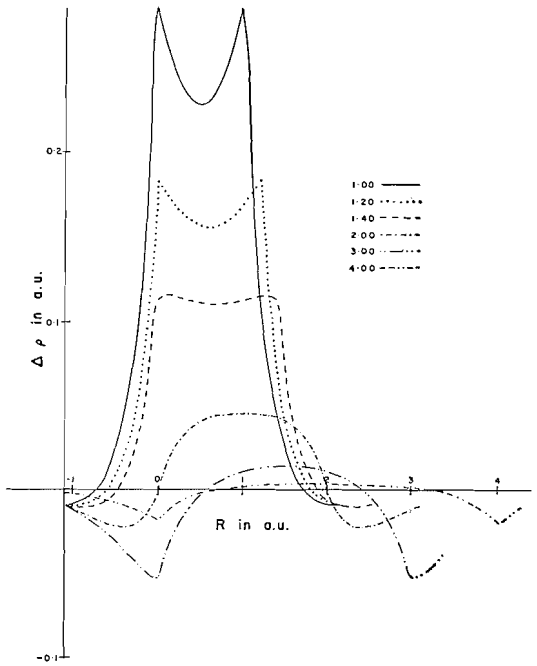

FIG. 3. Profiles of the $\Delta\rho(\varepsilon,\eta)$ maps along the internuclear axis for H_2 as a function of internuclear separation. One nucleus is fixed at the origin and the other is placed at the distances indicated in the figure legend.

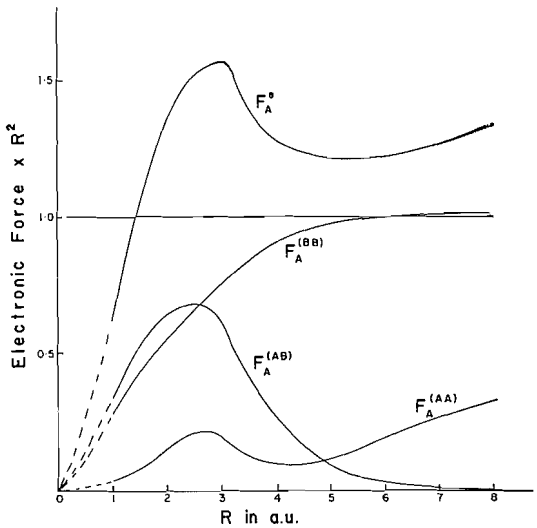

FIG. 4. The variation with R of the charge equivalents of the electronic force and its atomic, overlap, and screening components. The horizontal line at a value of $1(=Z_H)$ is the charge equivalent of the nuclear force of repulsion. The point of intersection of this line and the F_A^e curve represents the equilibrium state of the molecule.

Can. J. Chem. Downloaded from www.nrcresearchpress.com by 210.87.254.40 on 09/05/12
For personal use only.

density increase for $R = 6$ a.u. arises principally from the polarization of the atomic densities rather than from a significant delocalization of the charge density into the internuclear region. However, $F_A^{(AA)}$ is decreasing and $F_A^{(AB)}$ rapidly increasing in this range of internuclear separations. At approximately 5 a.u. the forces exerted by these two contributions are equal and *for distances less than 5 a.u. the delocalized component of the charge density provides the major contribution to the net force which binds the nuclei.* The screening contribution to the force decreases rapidly for separations less than 5 a.u. This is a result of two effects; the transfer of charge to the internuclear region in the formation of the delocalized or overlap component to the charge density and the penetration by each nucleus of the charge density around the other. The decrease in the screening contribution from the limiting separated atom value of unity results in a net force of repulsion acting on the partially unshielded nuclei. This force of repulsion is more than compensated for by the attractive force exerted on the nuclei by the delocalized charge density for values of R in the range $5 > R > R_e$.

Figures 2 and 3 illustrate that at separations down to 2 a.u. the delocalized density is concentrated between the nuclei. At distances less than 2 a.u., an increasing fraction of the delocalized charge density is accumulated on the nonbonded side of the nuclei. This build up of charge in the antibinding region accounts for the sharp decrease in the value of $F_A^{(AB)}$ for distances less than 2 a.u. even though, as is evident from Fig. 3, the amount of density which is delocalized continues to increase. In the united atom limit the density increase at the position of the stationary nucleus in Fig. 3 increases to 2.96 a.u. ($\Delta\rho(0) = \rho_{He}(0) - 2\rho_H(0)$). At this limit, the density increase is symmetrically placed with respect to the united atom nucleus and the electronic force reduces to zero.

The binding in the hydrogen molecule by the molecular charge density at the equilibrium separation of 1.40 a.u. fits the definition of covalent binding proposed earlier (2) in the study of the first-row homonuclear diatomic molecules. The nuclei are descreened at R_e, $F_A^{(BB)} < 1 = Z$ and the resulting force of nuclear repulsion $(Z - F_A^{(BB)})/R_e^2$ is balanced primarily by the force exerted by the delocalized density increase which is shared equally by both nuclei. There are, however, significant differences between the disposition of the bond densities for H_2 and the first-row homonuclear diatomics (2). The $\Delta\rho(\varepsilon,\eta)$ maps for the latter molecules, particularly from $B_2 \rightarrow F_2$, are characterized by separate increases in the charge density in both the antibinding and the binding regions. The charge density is removed from torus-like regions perpendicular to the bond axis and centered at the position of the nuclei. This pattern for the bond density is characteristic of bonds which, in an orbital description, involve the 2p orbitals. A similar pattern for the $\Delta\rho(\varepsilon,\eta)$ maps is found in the region of the A nuclei in the first-row diatomic hydride molecules AH (3). The Li_2 molecule is intermediate in character. It is similar to H_2 in that the charge removal is primarily from the antibinding regions (see Fig. 9) but there is a slight increase in the regions behind the nuclei. The proton in H_2 and in the first-row diatomic hydrides is the only nucleus which does not exhibit a decrease in the charge density at the position of the nucleus in the $\Delta\rho(\varepsilon,\eta)$ maps for stable molecules. It appears that when 2p orbitals are heavily involved in the binding, which they are not in H_2, the density increase in the $p\sigma$ component along the bond axis is at the expense of the $p\pi$ component of the charge density perpendicular to the bond and also of the s density at the position of the nucleus.

The deformation and the delocalization of the original atomic charge densities is very considerable in the formation of molecular hydrogen. The amount of charge density in the internuclear region represents a 70% increase over that obtained from the overlap of the atomic densities. Politzer (9), in an analysis of the charge distribution of the hydrogen molecule, has stated that "the view of the hydrogen molecule as being made up of two atoms slightly polarized toward each other is a reasonable one." This view does not coincide with the facts, either in terms of the density distribution or the forces which it exerts on the nuclei. At R_e the magnitude of the force exerted by the polarization of the atomic densities is less than one-seventh that exerted by the delocalized component of the charge density. Politzer's description does apply at internuclear distances greater than 5 a.u. where both the density and the force analysis

Can. J. Chem. Downloaded from www.nrcresearchpress.com by 210.87.254.40 on 09/05/12
For personal use only.

indicate that the binding is indeed a result of slight polarizations as previously discussed.

III. The Molecular Charge Density and Forces in He_2

Figure 5 presents a series of $\Delta\rho(\varepsilon,\eta)$ maps for He_2 at a number of internuclear distances from 3.0 to 1.5 a.u. calculated from the wave functions of Gilbert and Wahl (10). Figure 6 shows the corresponding $\Delta\rho$ profiles along the internuclear axis. The diagrams are the approximate opposites of the $\Delta\rho(\varepsilon,\eta)$ maps for the hydrogen molecule, particularly for values of $R > 2$ a.u. In the helium molecule the density increase occurs in the immediate vicinity of each nucleus and in the antibinding regions behind each nucleus. This increase occurs at the expense of a density decrease in the binding region between the nuclei. When it is recalled that the $\Delta\rho(\varepsilon,\eta)$ maps are obtained by subtracting from the molecular $\rho(\varepsilon,\eta)$ map a density distribution which itself does not place sufficient charge density between the nuclei to balance the forces of nuclear repulsion, it is clear that the He_2 molecule will be an unstable one. The $\Delta\rho(\varepsilon,\eta)$ maps indicate that the molecular charge distribution places *less* charge density in the binding region than does the standard distribution. It has been previously shown (11) that the antibinding character of the molecular charge distribution for He_2 can be interpreted as a direct consequence of the operation of the Pauli exclusion principle. A $\Delta\rho(\varepsilon,\eta)$ map for He_2 for a molecular density distribution derived from the simple overlap of helium atomic densities and corrected *only* to satisfy the requirements of the Pauli exclusion principle (11), is almost identical to the Hartree–Fock result shown in Fig. 5. The $\Delta\rho(\varepsilon,\eta)$ profile diagrams for H_2 and He_2 provide the most striking contrast of the difference between the charge redistribution which result in the formation of a stable and an unstable molecule.

Figure 7 shows the variation in the total force on the nuclei with R. The theoretically determined force is compared with the recent results of Amdur and Jordan (12). The contributions of the atomic, screening, and delocalized density components to the resultant repulsive force found in He_2 are shown diagramatically in Fig. 8. At infinite internuclear separation the total electronic force is equivalent to the field exerted by two electronic charges, the limiting value of the screening contribution. In the range of R values from 3.0 to 1.5 a.u. the total charge equivalent of the force exerted by the molecular charge distribution is less than the value of two required to balance the force of nuclear repulsion. The resulting net force of repulsion does not have its origin in a descreening of the nuclei by a decrease in the atomic populations. Rather, and unlike the case of H_2, the screening of the helium nuclei by their atomic density distributions increases from the limiting value of two as the value of R is decreased. Thus a symmetrical component of the increase in the charge density at the nuclei noted in the $\Delta\rho(\varepsilon,\eta)$ maps for He_2 is caused by an increase in, or contraction of, the atomic densities and not by a transfer of the delocalized charge density to the immediate region of the nuclei as is the case in H_2. The symmetrical nature of the atomic charge components to the total density is shown by the essentially zero atomic force contribution. The unsymmetrical nature of the charge increase noted in the $\Delta\rho(\varepsilon,\eta)$ maps is caused by a migration of the delocalized component of the density to the *antibinding region* on the nonbonded side of each nucleus. The fact that the charge equivalent of the force exerted by the delocalized density component $F_A^{(AB)}$ is negative in sign implies that this charge density exerts a force which pulls the nuclei away from one another. At 1.5 a.u. the force of repulsion exerted by the delocalized component of the density is equivalent to increasing the *nuclear* charge by $+1.25$ units. This is a sizeable effect and clearly shows the dominating influence of the Pauli exclusion principle on the direction of the migration of the charge density when two closed shell atoms interact.

The total electronic force operative in He_2 may be broken down into its orbital components. Thus

$$F_{He}^{e} = f_{1\sigma_g} + f_{1\sigma_u},$$

where the quantity f_i is the previously defined (2) partial force; the force exerted on the nuclei by the density in the ith molecular orbital multiplied by R^2. Since one electron correlates with each nucleus at infinite separation for a doubly occupied homonuclear diatomic molecular orbital, the limiting value of each f_i is clearly unity. This value corresponds to the screening

Can. J. Chem. Downloaded from www.nrcresearchpress.com by 210.87.254.40 on 09/05/12
For personal use only.

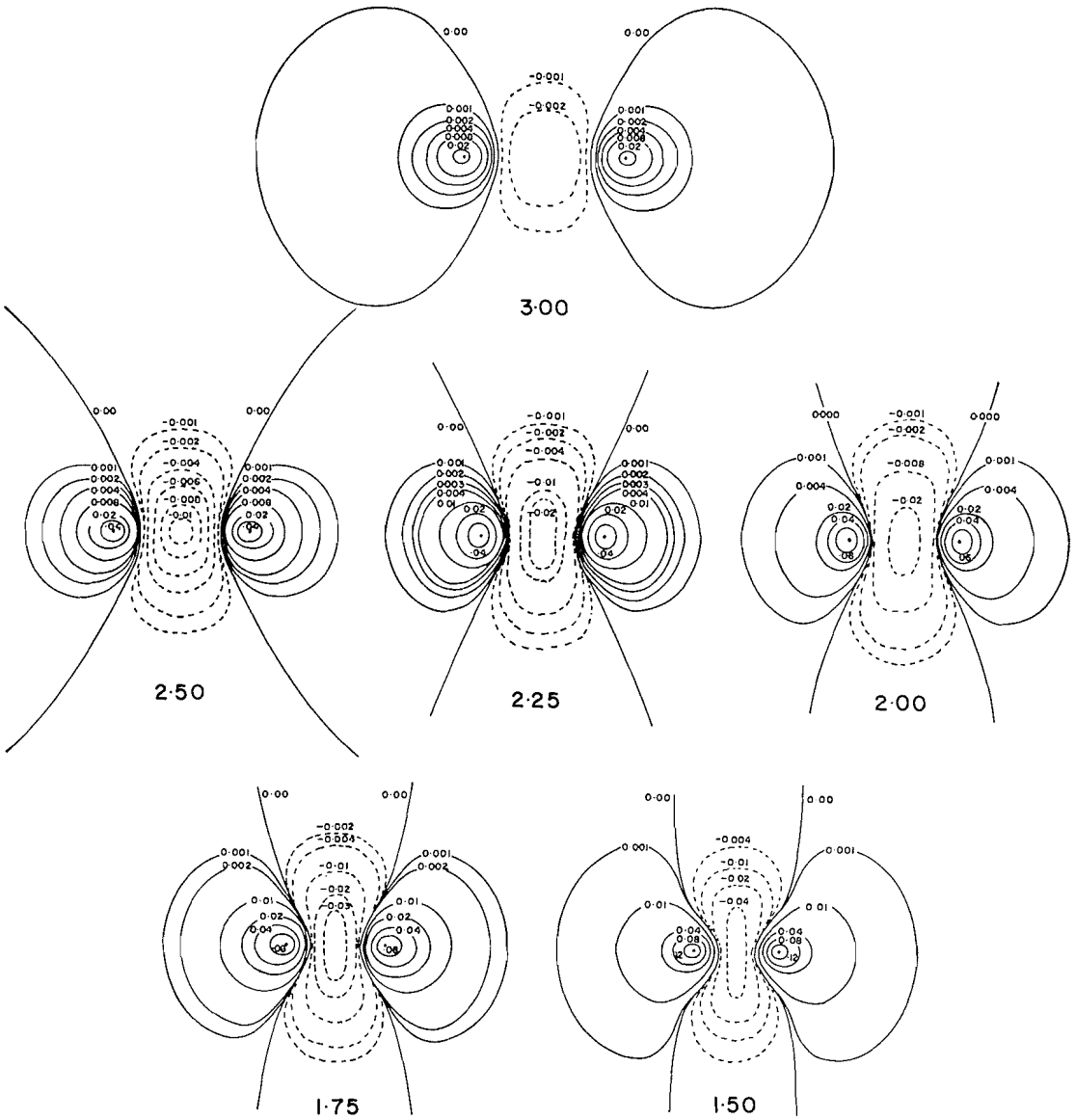

FIG. 5. Density difference contour maps, $\Delta\rho(\varepsilon,\eta)$ for He_2 all drawn to the same scale.

of one nuclear charge on B from A by the single electron from the ith molecular orbital which correlates with atom B. The properties of the $1\sigma_g$ orbital density in helium are similar to those found for the hydrogen molecule for which $F_H^e = f_{1\sigma_g}$. The nuclei are significantly descreened, an effect which increases as R is decreased, there is a small positive atomic force, and the delocalized density exerts an attractive force on the nuclei. This latter contribution is actually larger in the case of helium than in hydrogen for the $1\sigma_g$ density. The $1\sigma_g$ charge density of helium is in fact more binding than is the corresponding charge density in hydrogen as $f_{1\sigma_g}(He) > f_{1\sigma_g}(H)$ over the range of R values considered here. The value of $f_{1\sigma_g}$ for helium attains a maximum value of 1.79 at 1.9 a.u. compared with a maximum value of 1.57 at 3.0 a.u. for hydrogen. Thus out of the two electronic charges in the $1\sigma_g$ density of

Can. J. Chem. Downloaded from www.nrcresearchpress.com by 210.87.254.40 on 09/05/12
For personal use only.

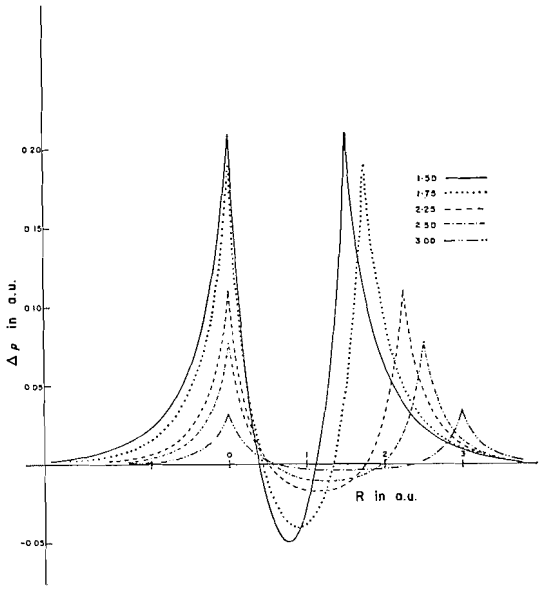

FIG. 6. Profiles of $\Delta\rho(\varepsilon,\eta)$ along the internuclear axis for He_2.

helium, 1.79 of these are effective in binding the nuclei. Since the value of $f_{1\sigma_g}$ exceeds the separated atom value of unity required to just balance the nuclear force of repulsion, the $1\sigma_g$ charge density is classified as *binding*. The $1\sigma_u$ charge density in helium is *antibinding* since the value of $f_{1\sigma_u}$ is less than unity. It is the antibinding character of this orbital charge density which dominates the final forces and form of the density distribution for helium. The screening of the nuclei is increased above the limiting value of unity as R is decreased but the increase in attractive force thus obtained is more than offset by the antibinding force exerted on the nuclei by the delocalized charge components. The very sizeable extent to which the $1\sigma_u$ charge density is transferred to the antibinding regions behind each nucleus is illustrated by the magnitude of the charge equivalent of the force exerted by the $1\sigma_u$ overlap density component, $f^{(AB)}_{1\sigma_u}$. The value of $f^{(AB)}_{1\sigma_u}$ at 1.5 a.u. is -2.1, which implies that the $1\sigma_u$ overlap density pulls the nuclei *away* from one another with a force which is greater than the force of repulsion obtained from the interaction of two bare helium nuclei separated at the same value of R. The $1\sigma_u$ charge density, in addition, exerts a small negative atomic force term which effectively cancels the small positive atomic

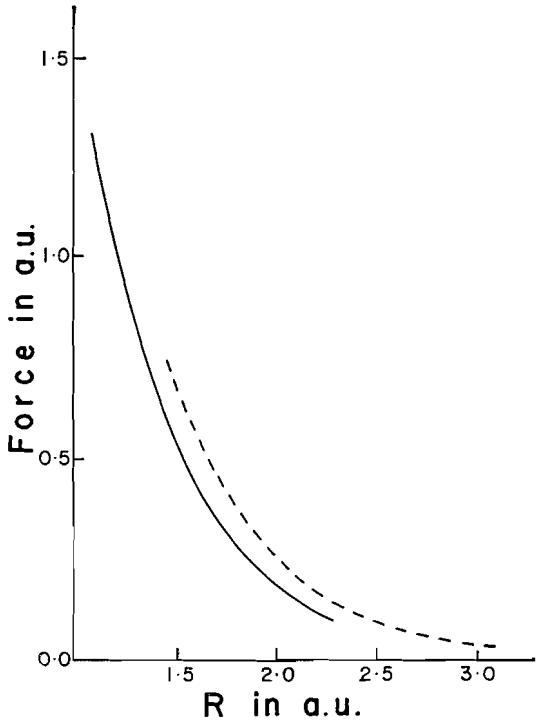

FIG. 7. The theoretical and experimental (12) force curves for He_2.

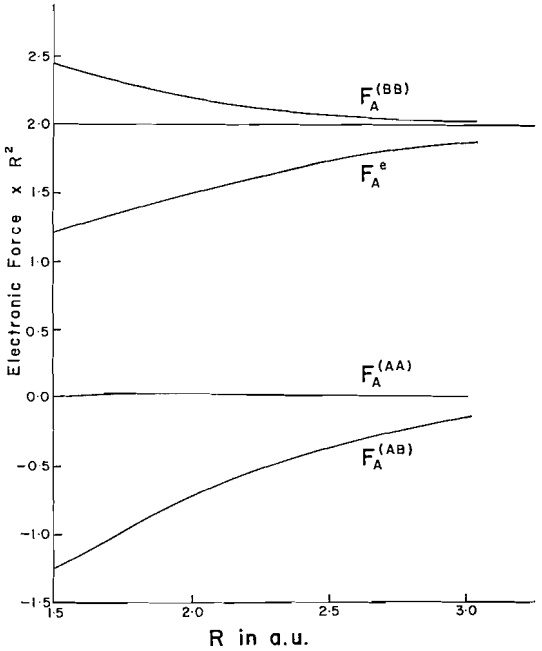

FIG. 8. The charge equivalent of the electronic force and its components for He_2 as a function of internuclear separation. The charge equivalent of the nuclear force of repulsion has a value of $2(=Z_{He})$.

force contribution from the $1\sigma_g$ density. The value of $f_{1\sigma u}$ while less than unity, and, therefore, antibinding, is less than zero (thereby exerting a force drawing the nuclei away from one another) only for values of R less than 2.5 a.u.

IV. The Formation of the Li_2 Molecule[2]

The $\Delta\rho(\varepsilon,\eta)$ map for Li_2 at $R = 5.07$ a.u. (close to the value of $R_e = 5.05$ a.u.) is shown in Fig. 9. The equilibrium charge distributions and the forces which it exerts on the nuclei have been discussed previously (2). The principal features are a diffuse charge increase in the internuclear region and at the nuclei and a removal of charge from the antibinding regions. The density in the immediate vicinity of each nucleus is polarized into the nonbonded region. The nature of the forces exerted on the nuclei by the molecular charge distribution during the *formation* of the molecule is similar to those found for hydrogen with the exception of a negative atomic force arising from the polarizations of the inner shell densities. The screening contribution to the force at 8.0 a.u., 2.8, is slightly less than the limiting value of 3 and decreases continuously to a value of 2.5 at 4.0 a.u. The delocalized charge density is accumulated primarily in the binding region and exerts a binding force on the nuclei which reaches a maximum charge equivalent of 1.00 at 6.0 a.u. The atomic force contribution is, however, negative, a result of the back-polarizations of the core densities which are evident in the $\Delta\rho(\varepsilon,\eta)$ map, Fig. 9. The charge equivalent of the atomic force is a maximum in the region of 5.5 a.u. where it has a value of approximately -0.5. It is slightly less than this at larger and shorter internuclear separations.

The only effect which bond formation has on the inner shell orbitals of the Li atoms is to back-polarize them. The density in the inner orbitals screens two of the charges on each nucleus even at distances as small as 4.0 a.u. and makes no contribution to the delocalized force component. The decrease in the screening contribution from its limiting value of three and the formation of a delocalized density component is confined entirely to a rearrangement of the charge density in the valence shell. The atomic force contribution of the valence density is an attractive one, as it is for H_2. Thus the valence density in Li_2 behaves in a similar fashion to that for H_2. The negative atomic forces which arise from the inner shell polarizations are approximately twice as large in absolute magnitude as those found for the valence density and thus dominate the total density distribution and the forces which it exerts on the nuclei.

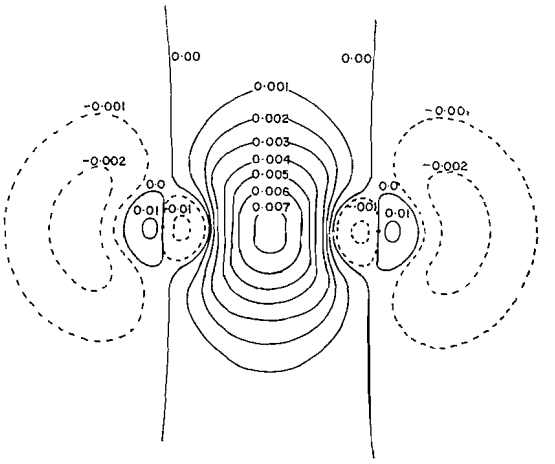

FIG. 9. Density difference map $\Delta\rho(\varepsilon,\eta)$ for Li_2 at $R = 5.07$ a.u.

V. The Effect of Electron Correlation on the Hartree–Fock Charge Density

Aside from the correlation between electrons of like spin introduced by the antisymmetrization requirements of the Pauli principle, a Hartree–Fock wave function, because of its orbital product form, excludes all correlation between electrons of opposite spin. The Hartree–Fock wave function will tend to keep electrons of unlike spin too close together on the average. Thus in terms of the two-electron probability distribution, the correlated wave function is found to yield slightly larger results for the expectation values of operators of the form $\langle(q_i - q_j)^2\rangle$, where q_i and q_j are electronic

[2]The study of Li_2 is not as extensive as that presented for H_2 because of errors in the wave function for Li_2 reported by Das (5). There are three tabulations of this function available; (i) Lab. Mol. Struct. and Spectra Technical Report, p.181 (1966), (ii) Thesis, C. Das, University of Chicago, and (iii) ref. 5. All three copies differ in the values given for the basis orbital vector coefficients, especially for the $2\sigma_u$ and $1\sigma_u$ orbitals. There are still some obvious errors in the latest copy given in ref. 5, and apparently some that are not obvious since the results for a calculation of the forces do not vary smoothly with R. We are reasonably certain of the results we present for R_e and of the qualitative features of the forces as a function of R.

Can. J. Chem. Downloaded from www.nrcresearchpress.com by 210.87.254.40 on 09/05/12
For personal use only.

Can. J. Chem. Downloaded from www.nrcresearchpress.com by 210.87.254.40 on 09/05/12
For personal use only.

coordinates for a pair of electrons. For example, Lyon and Hirschfelder (13) have determined the expectation values of the operators $\langle(\varepsilon_i - \varepsilon_j)^2\rangle$, $\langle(\eta_i - \eta_j)^2\rangle$, $\langle\cos(\phi_i - \phi_j)\rangle$ and $\langle(z_{ai} - z_{aj})^2\rangle$ (where ε,η and ϕ are the confocal elliptic coordinates) for both the Hartree–Fock functions and the Wahl and Das (4,5) extended Hartree–Fock functions for H_2, Li_2, and F_2. The error in these two-electron properties defined by Lyon and Hirschfelder to be

$$\Delta(i,j) = |\langle i,j\rangle_{HF} - \langle i,j\rangle_{EHF}|/\langle i,j\rangle_{EHF}$$

was found to be in the range of 0.1 to 0.2 for H_2 and 0.003 to 0.02 for Li_2.

It is our purpose to investigate what effects the introduction of correlation into the motion of pairs of electrons has on the form of the one-electron probability distribution. Because of Brillouin's theorem, the errors in the uncorrelated Hartree–Fock one-electron density and its dependent properties should be of the second order only (14). Lyon and Hirschfelder (13) found the error functions Δ to have values ranging from 0.00003 to 0.007 in the cases of H_2 and Li_2 for certain one-electron properties, e.g. $\langle 1/r_{ai}\rangle$, $\langle r_{ai}^2\rangle$, $\langle z_{ai}^2\rangle$, and $\langle 3z_{ai}^2 - r_{ai}^2\rangle$. While these errors are very small, they represent averages over the complete density distribution and do not give any information regarding local differences between the Hartree–Fock and extended Hartree–Fock charge densities in particular regions of space.

Figure 10 presents contour maps of $\Delta\rho_e(\varepsilon,\eta)$, the difference between the extended and self-consistent field Hartree–Fock density distributions

$$\Delta\rho_e(\vec{r}) = \rho_{EHF}(\vec{r}) - \rho_{HF}(\vec{r})$$

for both H_2 and Li_2 at their equilibrium internuclear separations. In H_2, the Hartree–Fock density distribution *overestimates* the amount of charge density in the central bonding region and underestimates that present in the regions of the nuclei. An error function for the density may be defined analogously to Δ as $\Delta\rho_e(\vec{r})/\rho_{EHF}(\vec{r})$. This density error function has the average value of 0.003 in the regions of largest positive values of $\Delta\rho_e(\vec{r})$ around the nuclei. The value of the error function in the region of negative $\Delta\rho_e(\vec{r})$ in the central bonding region is approximately -0.01. The value of $\Delta\rho_e(\varepsilon,\eta)$ for Li_2 is everywhere negligible as it is the same order

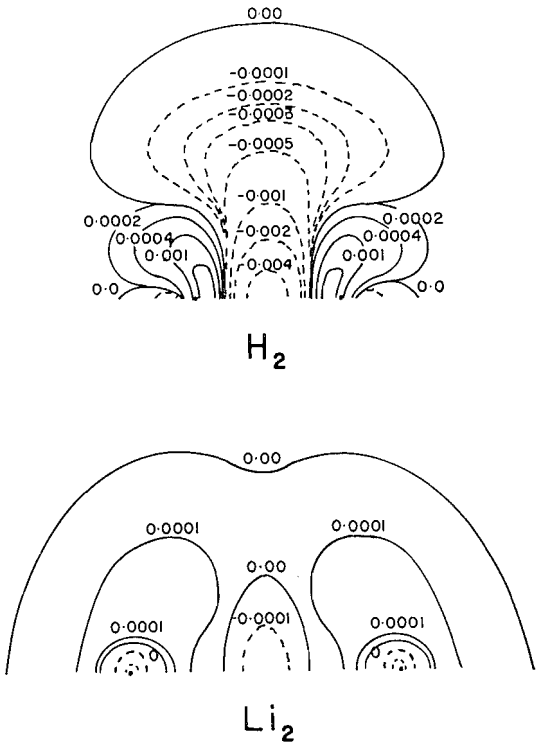

FIG. 10. Density difference maps of $\Delta\rho_e(\varepsilon,\eta)$, the difference between the extended Hartree–Fock and Hartree–Fock density distributions for H_2 at $R = 1.40$ a.u. and Li_2 at $R = 5.07$ a.u.

of magnitude as the accuracy of the density distributions themselves. Kern and Karplus (15) have stated that the percentage error in the one-electron density should be of the same order of magnitude as the percentage error in the total electronic energy. The value of Δ for the energy is 0.02 in the case of H_2 and 0.002 in the case of Li_2.

Figure 10 is, of course, also a plot of the error introduced when the Hartree–Fock molecular charge density is used in the construction of the density difference or bond density maps $\Delta\rho(\varepsilon,\eta)$. It is clear from a comparison of the $\Delta\rho(\varepsilon,\eta)$ in Fig. 2 with $\Delta\rho_e(\vec{r})$ for H_2, that no noticeable error will be introduced by the use of a Hartree–Fock density distribution in the construction of the $\Delta\rho(\varepsilon,\eta)$ map. The value of $\Delta\rho_e(\vec{r})$ is always smaller than $\Delta\rho(\varepsilon,\eta)$ by a factor of 10 or more. Comparison of the corresponding figures for Li_2 illustrates that the use of the Hartree–Fock density distribution for Li_2 in the construction of the $\Delta\rho(\varepsilon,\eta)$ map would entail no

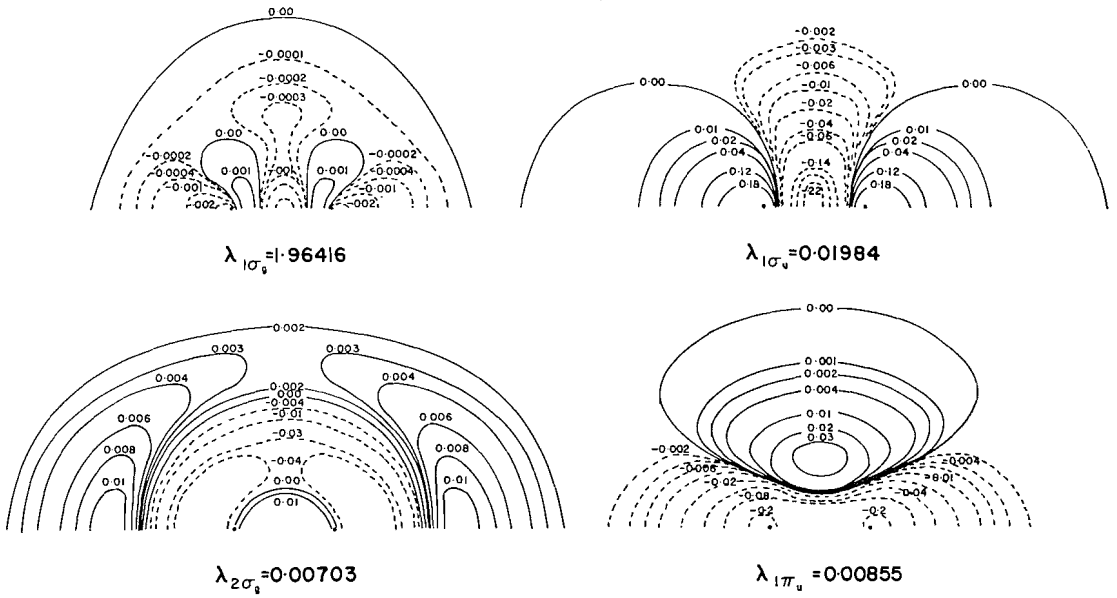

FIG. 11. Density difference maps of $\Delta\rho_c(\varepsilon,\eta)$, the single configuration density minus the Hartree–Fock density for H_2 at $R = 1.40$ a.u. The maps for the $1\sigma_u^2$, $2\sigma_g^2$, and $1\pi_u^2$ configurations illustrate the separate effects of the three principal types of electron correlation on the molecular charge density; left–right, in–out, and angular. Multiplication of the contours in each diagram by the occupation number λ, followed by their addition, yields the $\Delta\rho_c(\varepsilon,\eta)$ map for H_2 in Fig. 11.

detectable error. This is indeed the case as can be verified by comparing the $\Delta\rho(\varepsilon,\eta)$ for Li_2 in this paper with Fig. 3 of ref. 2 which gives a $\Delta\rho(\varepsilon,\eta)$ plot for Li_2 constructed from the Hartree–Fock density distribution. The two maps are superimposable.

The density distribution obtained from an extended Hartree–Fock wave function is best discussed in terms of the *natural orbitals* (13), since the orbitals of both the Hartree–Fock and extended Hartree–Fock functions are the natural orbitals in both approximations. Thus

$$\rho(\vec{r}) = \sum_i \lambda_i \eta_i^* \eta_i,$$

where the η_i are the natural orbitals and the λ_i their occupation numbers. In the case of the hydrogen molecule, each of the orbitals employed in the doubly excited configurations is one of the natural orbitals in the extended Hartree–Fock approximation. The square of the mixing coefficients of the configurations in the total wave function, the $A_{k\lambda}$ of Das and Wahl (4), when doubled to account for the presence of two electrons, are the orbital occupation numbers λ_i. The λ_i are in effect the total electronic charge contributed by each of the natural orbitals in the extended Hartree–Fock description of the electronic ground state of the hydrogen molecule ($\sum_i \lambda_i = N$, the total electronic charge of the molecule).

Figure 11 shows contour plots of the density difference $\rho_c(\vec{r})$, where

$$\Delta\rho_c(\vec{r}) = \rho_i(\vec{r}) - \rho_{HF}(\vec{r}),$$

where $\rho_i(r)$ is the charge density distribution obtained from double occupation of the ith natural orbital η_i. These contour maps show directly the effect of the electron correlation introduced by each added configuration on the Hartree–Fock molecular charge distribution for the hydrogen molecule at R_e. The value of λ_i is shown for each configuration. The configurations $1\pi_g^2$ and $3\sigma_g^2$ have been omitted since their contributions are extremely small, their λ_i values being 0.00033 and 0.00020 respectively. Davidson and Jones (16) have shown that the four configurations illustrated in Fig. 11 account for approximately 90% of the correlation energy in the hydrogen molecule. All of the contours in the $\Delta\rho_c(\vec{r})$ map for the $1\sigma_g^2$ configuration, the dominant term in the natural orbital expansion, are small in value. This indicates that the first

Can. J. Chem. Downloaded from www.nrcresearchpress.com by 210.87.254.40 on 09/05/12
For personal use only.

Can. J. Chem. Downloaded from www.nrcresearchpress.com by 210.87.254.40 on 09/05/12
For personal use only.

natural orbital of the extended Hartree–Fock function is almost identical with the Hartree–Fock natural orbital. Indeed Davidson and Jones (16), in applying the natural orbital expansion to the exact wave function of Kolos and Roothaan (17), found the first natural orbital to have an overlap of 0.999982 with the Hartree–Fock orbital.

Davidson and Jones point out that the three added configurations $1\sigma_u^2$, $1\pi_u^2$, and $2\sigma_g^2$ introduce the three major types of electron correlation (left–right, angular, and in–out respectively). These appelations are simply reflections of the nodal characteristics of the orbitals and the results are clearly evident in Fig. 11. The $1\sigma_u$ orbital possesses a nodal plane midway between the nuclei and its purpose is to keep the electrons at opposite ends of the molecule. Its effect on the one-electron density is to remove charge density from the binding region and to concentrate it in the antibinding regions. It is the correlation introduced by this configuration which is responsible for the negative values of $\Delta\rho_e(\vec{r})$ in the internuclear region of Fig. 10. The inclusion of the $1\pi_u^2$ configuration increases the probability of finding the two electrons on opposite sides of the molecular axis. The net effect of the π^+ and π^- functions on the charge distribution is to decrease the amount of charge density along the internuclear axis and concentrate it in a broad torus-like ring around the axis centered at its midpoint. The nodal property of the $2\sigma_g$ orbital has the effect of keeping one electron in close to the nuclei, and the other further out, in regions removed from the nuclei. Its effect on the Hartree–Fock charge density is to concentrate the density in these same regions. The positive and negative values of $\Delta\rho_e(\vec{r})$ introduced by the $1\pi_u^2$ and $2\sigma_g^2$ configurations nullify the negative and positive values of $\Delta\rho_e(\vec{r})$ from the $1\sigma_u^2$ configuration in the same regions. Indeed, Davidson and Jones (16) stress that the $1\sigma_u^2$, $1\pi_u^2$, and $2\sigma_g^2$ configurations should be considered together for two reasons; they all have λ_i values of the same order of magnitude and they represent correlation in the three orthogonal directions at each point in space. The $\Delta\rho_e(\vec{r})$ maps bear this out in a striking fashion. The regions of charge increase and decrease caused by the introduction of the $1\sigma_u^2$ configuration are approximately the same regions in which the $1\pi_u^2$ and $2\sigma_g^2$ configurations have just the reverse effect upon the Hartree–Fock charge density. The very small net changes in the Hartree–Fock density distribution are the result of a near cancellation of the changes introduced by the three types of correlation. The omission of any one of the three configurations would clearly seriously impair the ability of the resulting wave function to properly describe the small changes in the density distribution caused by electron correlation.

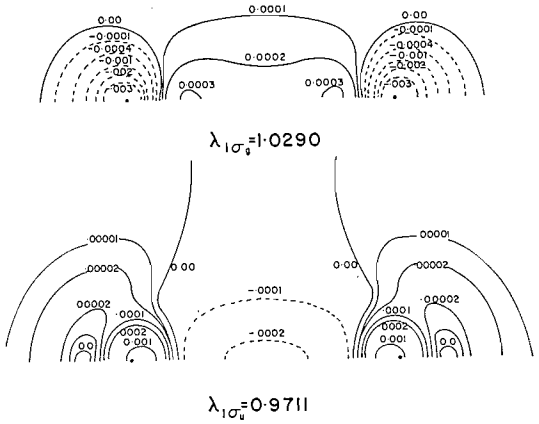

FIG. 12. Density difference maps of the $1\sigma_g^2$ and $1\sigma_u^2$ configuration densities minus the atomic density distributions for H_2 at $R = 8.0$ a.u.

As the internuclear separation is increased the left–right correlation becomes increasingly important, while the other forms become increasingly less important. At 8.0 a.u. the contributions of the $1\sigma_g^2$ and $1\sigma_u^2$ configurations to the total density are close to their limiting values of unity. Figure 12 shows contour maps of the densities derived from the two configurations minus the density of two hydrogen atoms separated at 8.0 a.u. (There is, of course, no single configuration Hartree–Fock density for 8.0 a.u. to use in the construction of a $\Delta\rho_e(\vec{r})$ map.) The contours in these two maps, when multiplied by their λ_i values and added together, produce the $\Delta\rho(\varepsilon,\eta)$ map for 8.0 a.u. shown in Fig. 2. The zero contours of both maps cross the molecular axis in the internuclear region at almost identical places and hence the regions of charge decrease from one configuration tend to cancel the regions of charge increase in the other. The result is the exceedingly small inwardly directed polarization of both atomic densities evident in Fig. 2 for

$R = 8.0$ a.u. One can thus ascribe the origin of the dispersion forces, which result from these polarizations, to a left–right correlation of the electronic motions induced by the mutual interaction of the atoms.

The difference between the atomic, overlap, and screening contributions to the electronic force expressed in terms of their charge equivalents as calculated from the Hartree–Fock and extended Hartree–Fock charge distributions are very small. The results for H_2 and Li_2 indicate that no serious error is entailed when Hartree–Fock molecular charge distributions are employed in an interpretation of molecular binding in terms of the $\Delta\rho(\varepsilon,\eta)$ maps and the forces exerted on the nuclei.

Acknowledgments

We are grateful to Dr. A. C. Wahl, Dr. G. Das, and Dr. T. Gilbert for copies of wave functions in advance of their publication. We also wish to thank Mr. P. Curry for the drawing and assembling of the many diagrams.

1. R. F. W. Bader and W. H. Henneker. J. Am. Chem. Soc. **87**, 3063 (1965).
2. R. F. W. Bader, W. H. Henneker, and P. E. Cade. J. Chem. Phys. **46**, 3341 (1967).
3. R. F. W. Bader, I. T. Keaveny, and P. E. Cade. J. Chem. Phys. **47**, 3381 (1967).
4. G. Das and A. C. Wahl. J. Chem. Phys. **44**, 87 (1966).
5. G. Das. J. Chem. Phys. **46**, 1568 (1967).
6. E. Clementi, C. C. J. Roothaan, and M. Yoshimine. Phys. Rev. **127**, 1618 (1962).
7. R. Feynman. Phys. Rev. **56**, 340 (1939).
8. M. A. Eliason and J. O. Hirschfelder. Univ. Wisconsin Theoretical Chem. Inst. Rept. No. 205 (1966).
9. P. Politzer. J. Phys. Chem. **70**, 1174 (1966).
10. T. L. Gilbert and A. C. Wahl. Unpublished results.
11. R. F. W. Bader and H. J. T. Preston. Can. J. Chem. **44**, 1131 (1966).
12. I. Amdur and J. E. Jordan. J. Chem. Phys. **46**, 165 (1967).
13. W. D. Lyon and J. O. Hirschfelder. J. Chem. Phys. **46**, 1788 (1967).
14. L. Brillouin. Actualités Sci. Ind. Nos. 71, 159, 160 (1933–1934).
15. C. W. Kern and M. Karplus. J. Chem. Phys. **40**, 1374 (1964).
16. E. R. Davidson and L. L. Jones. J. Chem. Phys. **37**, 2966 (1962).
17. W. Kolos and C. C. J. Roothaan. Rev. Mod. Phys. **32**, 219 (1960).

Can. J. Chem. Downloaded from www.nrcresearchpress.com by 210.87.254.40 on 09/05/12
For personal use only.

Can. J. Chem. Downloaded from www.nrcresearchpress.com by 210.87.254.6 on 09/05/12
For personal use only.

Le volume libre dans les liquides[1]

GERMAIN GODBOUT[2] ET YVON SICOTTE
Laboratoire de Chimie Physique, Département de Chimie, Université de Montréal, Montréal, Québec

Reçu le 27 septembre 1967

Le coefficient maximum d'encombrement pour des ellipsoïdes de révolution disposés de façon chaotique est très voisin de celui qu'on obtient pour des sphères, c'est-à-dire 0.64. Le coefficient d'encombrement équivalent pour les liquides à leur point triple est en bon accord avec cette valeur, non seulement pour les liquides à molécules sphériques mais également pour les liquides à molécules non sphériques, indiquant qu'un ensemble d'ellipsoïdes de révolution peut constituer un modèle intéressant pour décrire certaines propriétés de l'état liquide.

Canadian Journal of Chemistry, 46, 967 (1968)

Introduction

De nombreuses propriétés des liquides semblent dépendre, à des degrés divers, de l'importance relative du volume occupé par les molécules elles-mêmes et du volume libre ou interstitiel. La constante diélectrique ou l'indice de réfraction (1, 2), la viscosité (3), la compressibilité (4), ne sont que quelques unes des propriétés où on a tenté d'expliciter cet effet. Au premier chef, le volume molaire semble être la propriété la plus simple à cet égard. Il suffit en effet d'écrire

$$[1] \qquad \phi\bar{V} = N_A v_m,$$

où φ est la fraction de volume occupée par les molécules elles-mêmes, ce que nous appellerons le coefficient d'encombrement; $\bar{V}$ est le volume molaire, N_A le nombre d'Avogadro et v_m le volume d'une molécule.

Malheureusement on se heurte déjà ici à une première difficulté. Il n'est pas possible de définir de façon univoque le volume d'une molécule et il faudra passer par l'intermédiaire de modèles où on représentera la molécule à l'aide des solides réguliers les plus simples, sphères ou ellipsoïdes par exemple. Dans le cas de molécules disposées en réseau, on peut, au volume minimum, relier très simplement le volume total au volume des sphères par lesquelles on voudrait représenter les molécules. Entre autres, pour un réseau hexagonal compact de sphères, on obtient comme coefficient d'encombrement

$$[2] \qquad \phi_{max} = \sqrt{2}\pi/6 = 0.7405.$$

Le réseau cubique à face centrée, où le nombre de voisins immédiats est le même, c'est-à-dire 12, donne le même résultat. Ces deux réseaux sont les plus denses, ce que nous avons symbolisé en indiquant que cette valeur de coefficient d'encombrement est la valeur maximum pour des sphères.

On peut donc, à partir des éqs. [1] et [2] définir le volume v_m de la sphère équivalent à la molécule. Expérimentalement on évalue ce volume à l'aide des volumes molaires cristallins, extrapolés au zéro degré absolu, $\bar{V}_0$. Pour les substances cristallisant dans l'un ou l'autre des systèmes mentionnés, on a donc

$$[3] \qquad 0.74\bar{V}_0 = N_A v_m.$$

Si on admet ensuite, en première approximation, que ce volume est une caractéristique de la molécule considérée, indépendante des conditions, on pourra calculer le coefficient d'encombrement dans les autres conditions, à l'aide de l'éq. [1].

Par ailleurs, dans tout autre cas que le réseau, le calcul théorique du coefficient d'encombrement ne peut se faire que par l'intermédiaire des fonctions de corrélation moléculaire et non seulement des fonctions de corrélation binaire, que l'on sait utiliser, mais également de toute la série des fonctions d'ordre supérieur, où les difficultés deviennent très grandes (5). Evidemment le réseau est un cas spécial où ces fonctions sont entièrement définies et particulièrement simples. On doit donc, pour le moment, se contenter de mesures sur modèles macroscopiques, pour les cas où on peut ainsi reproduire des situations définies ayant une signification physique précise.

On peut se demander par exemple quelle serait la valeur maximum que peut prendre le coefficient d'encombrement pour des sphères

[1]Les résultats utilisés dans le présent travail sont tirés de la thèse de Ph.D. en Chimie de Germain Godbout, Université de Montréal (1966).

[2]Présentement au Centre de Recherches sur les Macromolécules, Strasbourg, France.

Can. J. Chem. Downloaded from www.nrcresearchpress.com by 210.87.254.6 on 09/05/12
For personal use only.

disposées non pas selon un réseau mais de façon chaotique. Plusieurs chercheurs se sont intéressés à ce problème et les résultats obtenus montrent une cohérence remarquable, comme on peut le voir au Tableau I, dans la colonne ϕ_{max}.

TABLEAU I

Coefficients d'encombrement chaotique pour des sphères

Billes utilisées (diamètre en cm)	φ_{max}	φ_{min}	Réf.
Plomb (0.378)	0.641		(6)
Acier (0.635)		0.57	(7)
Verre (0.05)	0.638	0.587	(8)
Acier (0.318)	0.637	0.601	(9)
Nylon (0.287)	0.641	0.596	(10)

On a suggéré qu'un tel ensemble de sphères, distribuées de façon chaotique et occupant un volume minimum, pouvait servir de modèle pour l'état liquide au point triple. Effectivement on retrouve pour les gaz rares liquides à leur point triple une valeur de coefficient d'encombrement très voisine de 0.64 (11, 12). Le but du présent travail était de vérifier si on pouvait étendre ce genre de modèle aux liquides à molécules non sphériques.

Les chercheurs qui ont mesuré le coefficient d'encombrement chaotique pour des sphères ont trouvé que ce coefficient peut varier entre deux valeurs limites bien définies suivant la méthode d'empilement utilisée. Par exemple si on verse des billes dans un contenant rigide et qu'on en frappe délicatement la paroi, le volume occupé diminue graduellement pour atteindre une valeur minimum, correspondant au coefficient maximum d'encombrement chaotique. Par contre, si on renverse alors le contenant et qu'on le ramène ensuite à sa position originale en le faisant tourner lentement sur lui-même, les billes occupent un volume plus grand qu'auparavant, correspondant au coefficient minimum d'encombrement chaotique qui soit stable. Cette valeur minimum apparait également au Tableau I. Ces deux valeurs de coefficient correspondent à des situations bien définies et sont faciles à reproduire; par contre la signification physique que l'on peut attribuer à la valeur inférieure du coefficient, dans le cadre d'un modèle de l'état liquide, est moins immédiate que celle que l'on peut attribuer à la valeur supérieure, comme le font remarquer Bernal et Mason (11).

Si on veut étendre ce modèle aux molécules non sphériques, la suggestion la plus simple qui vient à l'esprit consiste à remplacer les sphères par des ellipsoïdes de révolution qui peuvent représenter convenablement certaines molécules et qui, d'une façon générale, seront du moins plus près de la réalité que les sphères pour ces molécules, tout en demeurant un modèle assez simple. On peut facilement montrer que pour des ellipsoïdes de révolution, le coefficient maximum d'encombrement est, comme pour les sphères, de 0.74, ce qui correspond à un réseau hexagonal compact où les axes identiques des ellipsoïdes sont parallèles. Il s'agissait donc dans notre cas de mesurer le coefficient maximum d'encombrement pour des ellipsoïdes disposés de façon chaotique.

Partie expérimentale

Comme ellipsoïdes, nous avons utilisé des comprimés pharmaceutiques A.B.S. & C. de la maison Rexall, qui sont des ellipsoïdes de révolution applatis presque parfaits et très uniformes. Le petit axe est de 0.371 ± 0.005 cm et le grand est de 0.633 ± 0.003 cm. Ces comprimés à surface dure et polie n'ont pas tendance à adhérer les uns aux autres et résistent bien aux chocs. Dans le but de comparer notre méthode à celles des autres chercheurs, nous avons effectué parallèlement la même mesure sur des billes de verre de 0.500 ± 0.003 cm de diamètre.

Dans ce genre de mesures, comme le fait remarquer Scott (9), il faut corriger les résultats des erreurs introduites par les effets de paroi. Un premier effet provient de ce que la paroi peut amener la formation d'arrangements réguliers, peut amorcer une "cristallisation" à partir de la surface, ce qu'on peut éviter en utilisant des récipients à parois irrégulières (9). D'autre part, la présence de la paroi perturbe les lois de corrélation et crée une zone superficielle dont la densité n'est pas nécessairement celle qu'on a au sein du volume. Pour corriger ce dernier effet, il faut extrapoler les résultats à volume infini. Dans le cas de récipients cylindriques, Scott (9) obtient une relation linéaire entre le coefficient d'encombrement à volume fini et l'inverse de la hauteur, pour un diamètre donné. Il obtient également une relation linéaire entre le coefficient d'encombrement à hauteur infinie et l'inverse du diamètre du cylindre. Cette double extrapolation donne le coefficient d'encombrement à volume infini.

Comme récipients de mesure, nous avons utilisé trois cylindres fabriqués à partir de tube Pyrex, de 3.75, 5.45 et 7.55 cm de diamètre intérieur respectivement. Sur la surface de chacun de ces cylindres, nous avons soufflé vers l'intérieur des demi-sphères de 6 à 10 mm de diamètre, réparties irrégulièrement sur toute la surface et ayant une distance de séparation moyenne de 15 mm. Une extrémité du tube a été bouchée à la paraffine, donnant ainsi un fond plat. Nous avons gradué les cylindres par gravimétrie: la relation entre le volume et la hauteur était linéaire dans les trois cas et correspondait à des diamètres intérieurs effectifs de 3.45, 5.05 et 7.25 cm.

Can. J. Chem. Downloaded from www.nrcresearchpress.com by 210.87.254.6 on 09/05/12
For personal use only.

Dans chacun de ces cylindres, nous avons déterminé le coefficient d'encombrement pour plusieurs hauteurs de remplissage. Le nombre d'ellipsoïdes ou de billes utilisés dans chaque cas a été déterminé par pesée.

Résultats et discussion

Les résultats que nous avons obtenus dans le cas des billes sont entièrement équivalents aux résultats des autres chercheurs et ne font que les confirmer. L'extrapolation à hauteur infinie pour chaque cylindre présente une légère pente négative et l'extrapolation à diamètre infini des données précédentes donne, également avec une pente négative, une valeur de 0.643 comme coefficient d'encombrement maximum, en excellent accord avec les résultats rapportés au Tableau I. La pente négative dans les deux extrapolations traduit le fait que le coefficient d'encombrement près de la surface est plus faible qu'au sein du volume et indique bien qu'il n'y a pas de cristallisation près de la surface.

Le phénomène de cristallisation locale peut par ailleurs se produire indépendamment de la surface comme Scott l'a montré (12) et donner une valeur de coefficient supérieure à 0.64. Scott obtient jusqu'à 0.66. Il s'agit en fait de création d'ordre à courte distance, qu'une agitation convenable élimine facilement. Dans le cas d'ellipsoïdes, on peut prévoir que le phénomène se compliquera de l'apparition de corrélations en orientation; et effectivement nous avons obtenu quelques résultats aberrants, correspondant vraisemblablement à l'apparition de ces corrélations en orientation. Le problème étant beaucoup moins simple que dans le cas des sphères, nous n'avons pas poussé plus loin dans cette direction. Pour éviter ce phénomène, nous avons effectué le remplissage de façon à ce que les ellipsoïdes frappent la paroi sous un angle assez grand et avec une énergie cinétique suffisante pour donner une distribution vraisemblablement chaotique des orientations. Cette utilisation de l'irrégularité de la paroi donne des résultats assez reproductibles et l'énergie cinétique qu'on doit conférer aux ellipsoïdes n'est pas critique. Il faut noter cependant que les résultats obtenus pour les ellipsoïdes sont nettement moins reproductibles que ceux obtenus pour les billes.

La Fig. 1 représente les données de coefficient maximum d'encombrement en fonction de l'inverse de la hauteur de remplissage pour chacun des trois cylindres. Les pentes sont légèrement

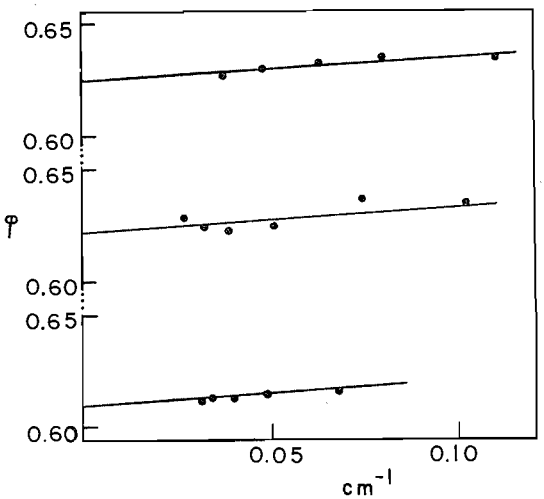

FIG. 1. Variation du coefficient maximum d'encombrement chaotique pour des ellipsoïdes en fonction de l'inverse de la hauteur de remplissage pour les trois cylindres utilisés: de haut en bas, 7.25, 5.05 et 3.45 cm de diamètre effectif.

positives, indiquant qu'au voisinage du fond plat du récipient, le coefficient d'encombrement est plus grand qu'au sein du volume, contrairement aux résultats obtenus pour les sphères. Il s'agit évidemment de corrélations en orientation au voisinage du fond: les ellipsoïdes s'y disposent avec leurs grands axes préférentiellement parallèles au fond. Nous avons déjà fait allusion à des résultats aberrants de coefficients d'encombrement; également il faut souligner que nous avons obtenu des pentes aberrantes, pentes beaucoup plus positives, mais extrapolant à la même valeur de coefficient d'encombrement à hauteur infinie. Les corrélations en orientation près du fond du cylindre devaient vraisemblablement être plus importantes dans ces cas. Comme cet effet disparait de toute façon à hauteur infinie, seule la pente est affectée.

La Fig. 2 représente les coefficients d'encombrement à hauteur infinie en fonction de l'inverse du diamètre effectif des cylindres. La pente est négative et correspond à un coefficient d'encombrement plus faible au voisinage de la paroi irrégulière qu'au sein du volume, contrairement à ce qui se produit au voisinage d'une surface régulière. Les irrégularités à la paroi semblent donc empêcher les corrélations en orientation de se produire.

Nous obtenons donc comme coefficient maximum d'encombrement chaotique à volume

infini pour ces ellipsoïdes une valeur de 0.64, c'est-à-dire identique aux erreurs d'expérience près à celui des sphères. Il aurait évidemment été intéressant de reprendre ces mesures en utilisant des ellipsoïdes de différentes excentricités. Malheureusement, si on peut facilement se procurer des billes bien usinées, de grosseur uniforme, à surface assez dure et assez polie pour se prêter à ce genre de mesures, il est beaucoup plus difficile de trouver des ellipsoïdes possédant les mêmes qualités. Ceci explique que nous n'ayons pu effectuer que les deux mesures que nous venons de décrire. Notons en passant qu'on obtient pour ces ellipsoïdes une valeur de coefficient minimum d'encombrement chaotique de 0.60, qui est aussi en bon accord avec les valeurs rapportées pour les sphères au Tableau I. En première approximation, nous pouvons donc retenir l'hypothèse la plus simple que suggèrent ces résultats: à savoir que le coefficient d'encombrement est indépendant de l'excentricité de l'ellipsoïde et par conséquent est égal à celui des sphères.

Dans cette hypothèse, il est intéressant de vérifier si on retrouve physiquement une valeur de coefficient d'encombrement de 0.64 au point triple pour les liquides à molécules non sphériques, comme c'est le cas pour les gaz rares. On ne dispose malheureusement pas, pour les liquides usuels, de données assez étendues de densités cristallines à basse température pour pouvoir faire ce calcul. Par contre, se basant sur le fait que l'éq. [3] correspond au volume minimum, on estime souvent le volume v_m à l'aide de cette équation, en utilisant comme $\bar{V}_0$ le volume molaire liquide extrapolé au zéro degré absolu. Cette extrapolation se fait généralement en utilisant l'équation de Sugden (13),

$$[4] \qquad \frac{1}{\bar{V}} - \frac{1}{\bar{V}_g} = \frac{1}{\bar{V}_0}\left(1 - \frac{T}{T_c}\right)^{0.3},$$

où $\bar{V}_g$ est le volume molaire de la vapeur saturée à la température T. Aux températures assez éloignées de la température critique T_c, le second terme de gauche est évidemment négligeable devant le premier. La valeur de l'exposant, 0.3, ne coïncide pas avec les prédictions théoriques (14), mais il faut dire que ces dernières concernent surtout le voisinage du point critique. Par ailleurs comme cette relation permet de paramétrer les résultats expérimentaux de façon excellente sur de très larges intervalles de température, elle a été beaucoup utilisée.

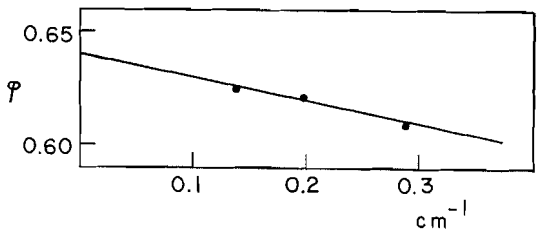

FIG. 2. Variation du coefficient maximum d'encombrement chaotique à hauteur infinie pour des ellipsoïdes en fonction de l'inverse du diamètre effectif des cylindres.

C'est ainsi que Jacobson (4) a tiré les valeurs de $\bar{V}_0$ des données de volume molaire et de température critique pour un grand nombre de liquides. A l'aide des éqs. [1] et [3], nous en avons tiré le coefficient d'encombrement de quelques liquides usuels au point triple ou au point de fusion normal: les deux coefficients sont très voisins pour ces substances. Le Tableau II montre les résultats obtenus.

TABLEAU II

Coefficients d'encombrement équivalents de quelques liquides au point triple ou au point de fusion normal

Acétate d'éthyle	0.66
Acétone	0.66
Benzène	0.61
Bromobenzène	0.65
Chlorobenzène	0.66
Ether éthylique	0.67
Heptane	0.66
Nitrobenzène	0.63
Sulfure de carbone	0.68
Tétrachlorure de carbone	0.62

Il est utile de rappeler ici encore une fois que, en utilisant l'éq. [3], on obtient non pas le volume vrai des molécules, qui physiquement n'a d'ailleurs aucun sens, mais, comme nous l'avons vu, le volume des ellipsoïdes de révolution à axes identiques parallèles, disposés en réseau hexagonal, par lesquels on veut représenter les molécules au volume minimum. La sphère peut évidemment être considérée comme un cas particulier d'ellipsoïde. La grandeur de ce volume est définie de façon univoque par l'éq. [3], peu importe la géométrie de la molécule, mais, selon ce dernier facteur, le volume en question pourra être plus ou moins commode à utiliser. En effet le coefficient d'encombrement qu'on pourra en déduire pour le liquide sous

Can. J. Chem. Downloaded from www.nrcresearchpress.com by 210.87.254.6 on 09/05/12
For personal use only.

Can. J. Chem. Downloaded from www.nrcresearchpress.com by 210.87.254.6 on 09/05/12
For personal use only.

d'autres conditions que le volume minimum, au point triple par exemple, ne coïncidera avec le coefficient d'encombrement calculé pour des ellipsoïdes dans ces conditions que si les molécules peuvent être adéquatement représentées par des ellipsoïdes. Pour cette raison, nous appellerons coefficient d'encombrement équivalent la valeur ainsi obtenue pour les liquides réels.

Par ailleurs la description du point triple en terme de coefficient maximum d'encombrement chaotique, qui semble bien être valable pour les sphères et que nous tentons présentement d'étendre aux molécules non sphériques, fait évidemment abstraction, même dans le cas d'ellipsoïdes parfaits, des corrélations en orientation qui existent au point triple et qui vraisemblablement vont influencer la valeur du coefficient d'encombrement.

Ces deux raisons, ajoutées à l'incertitude sur $\overline{V}_0$ qui est obtenu par extrapolation à l'aide d'une relation empirique, font que le coefficient d'encombrement équivalent calculé de cette façon pour le point triple est entaché d'erreurs dont il est très difficile d'évaluer ne serait-ce que l'ordre de grandeur. Les résultats obtenus justifient cependant la démarche que nous venons de faire. En effet les coefficients d'encombrement équivalents calculés se situent dans une marge étonnamment étroite autour de 0.64 et les causes d'écart signalées ne semblent avoir qu'une importance assez faible.

Conclusion

Il semble donc très probable que le coefficient maximum d'encombrement pour des ellipsoïdes de révolution disposés de façon chaotique soit indépendant de l'excentricité de l'ellipsoïde et qu'il soit par conséquent égal à celui qu'on a pour des sphères.

Il semble également que l'état liquide au point triple soit caractérisé, en première approximation, par un coefficient d'encombrement équivalent très voisin de celui correspondant au modèle décrit plus haut: un ensemble d'ellipsoïdes de révolution disposés de façon chaotique et occupant un volume minimum.

Pour obtenir une description plus rigoureuse de l'état liquide au point triple, il faudrait sinon utiliser une représentation géométrique de la molécule qui soit plus exacte que l'ellipsoïde de révolution, ce qui rendrait malheureusement le modèle pratiquement inutilisable, du moins tenir compte des corrélations en orientation, ce qui est conciliable, du moins formellement, avec le modèle simple utilisé ici.

Remerciements

Nous tenons à exprimer nos remerciements à monsieur G. L. Kitchen ainsi qu'à la maison Rexall, pour nous avoir gracieusement fourni un lot de 10,000 comprimés pharmaceutiques qui nous ont servi d'ellipsoïdes de révolution.

Nous remercions également le Conseil National de Recherches du Canada pour l'octroi d'une subvention de recherche (Y. S.) et de bourses (G. G.).

1. C. J. F. Böttcher. Theory of electric polarisation. Elsevier Press, Inc., New York. 1952.
2. Y. Sicotte. J. Chim. Phys. **63**, 403 (1966).
3. P. B. Macedo et T. A. Litovitz. J. Chem. Phys. **42**, 245 (1965).
4. B. Jacobson. Acta Chem. Scand. **6**, 1485 (1952).
5. H. S. Green. The structure of liquids. Springer-Verlag, Berlin. 1960.
6. W. O. Smith, P. D. Foote et P. F. Busang. Phys. Rev. **34**, 1271 (1929).
7. R. L. Brown et P. G. W. Hawksley. Nature, **157**, 585 (1946).
8. H. Kohn et H. W. Gonell. Staub, **23**, 420 (1950).
9. G. D. Scott. Nature, **188**, 908 (1960).
10. R. Rutgers. Nature, **193**, 465 (1962).
11. J. D. Bernal et J. Mason. Nature, **188**, 910 (1960).
12. G. D. Scott, A. M. Charlesworth et M. K. Mak. J. Chem. Phys. **40**, 611 (1964).
13. S. Sugden. J. Chem. Soc. **2**, 1780 (1927).
14. M. E. Fisher. J. Math. Phys. **5**, 944 (1964)

Can. J. Chem. Downloaded from www.nrcresearchpress.com by 210.87.254.5 on 09/05/12
For personal use only.

Some aspects of *cis–trans*-isomerization mechanisms

M. C. LIN[1] AND K. J. LAIDLER
Department of Chemistry, University of Ottawa, Ottawa, Canada

Received September 6, 1967

It is shown that there is a linear relationship between the activation energy for a thermal *cis–trans* isomerization and the heat of hydrogenation of the C=C bond. There is also a linear relationship between the entropy of activation and the heat of activation, there being a partial compensation effect. It is pointed out that the activation energy for these processes is very close to the π-bond energy of the C=C bond. The significance of these relationships is discussed in terms of the reaction mechanisms.

Canadian Journal of Chemistry, 46, 973 (1968)

Two alternative mechanisms were proposed by Magee, Shand, and Eyring (1) for thermal *cis–trans* isomerizations in the gas phase. Figure 1 is an energy diagram for the singlet and triplet states of an ethylenic compound, and it was suggested that one mechanism of isomerization involves a crossing at point *a* to the triplet state, followed by a crossing at *b* to the singlet state:

$$[I] \qquad AB(^1A) \xrightarrow{\kappa_1} AB^{\ddagger}(^3B) \xrightarrow{\kappa_2} BA(^1A).$$

If the transmission coefficients for the two crossings are κ_1 and κ_2 the overall transmission coefficient is

$$[1] \qquad \kappa = \frac{\kappa_1\kappa_2}{\kappa_1 + \kappa_2}.$$

Alternatively, the system can remain throughout in the singlet state and cross a barrier corresponding to an angle of twist of approximately $\pi/2$:

$$[II] \qquad AB(^1A) \rightarrow AB^{\ddagger}(^1A) \rightarrow BA(^1A).$$

In this case the transmission coefficient will be close to unity.

Early work did indicate very low transmission coefficients for certain *cis–trans* isomerizations, particularly those of dimethyl maleate (2), dimethyl citraconate (3), and butene-2 (4), and it was concluded that these reactions occur by the triplet mechanism. However, as discussed in a review by Cundall (5), the latest evidence (6–8) indicates "normal" frequency factors for these reactions. Table I lists the Arrhenius parameters for a number of reactions for which the evidence seems reliable. It appears from the magnitudes of the frequency factors that all of these reactions occur by mechanism [II].

[1]Present address: Dept. of Chemistry, Cornell University, Ithaca, N.Y.

Recently Terao, Hirokami, Sato, and Cvetanović (15) have estimated that the potential-energy difference between the twisted singlet and twisted triplet states is about 18 kcal/mole. This leads to a value of about 45 kcal/mole for the triplet barriers, a value that is much higher than the

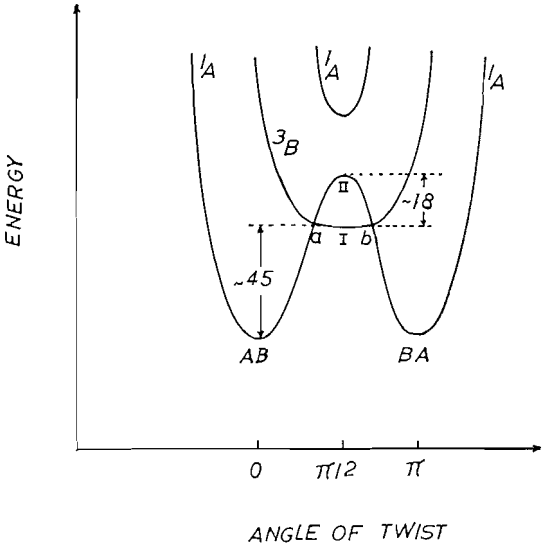

FIG. 1. Schematic potential-energy diagram for a *cis–trans* isomerization.

25 kcal/mole estimated by Magee *et al.* (1). These values allow us to estimate an upper limit for the transmission coefficient corresponding to the hypothetical mechanism [I], whose rate must be less than that by mechanism [II]. Thus for the *cis*-butene-2 isomerization at 723 °K, the rate constant is 8.9×10^{-6} s^{-1}, and Rabinovitch and Michel (6) have estimated a frequency factor of $\sim 10^{14}$ s^{-1}. The same value can be assumed for the hypothetical triplet reaction, and with an activation energy of 45

TABLE I

Summary of Arrhenius parameters and the rate constants at 723 °K for thermal *cis–trans* isomerization of various substituted ethylenes

	Reactants	A (s^{-1})	E (kcal/mole)	k_{723} (s^{-1})	Reference
[*a*]	*cis*-$CH_3CH{=}CHCH_3$	6.1×10^{13}	62.8	6.3×10^{-6}	6
		1.0×10^{14}	62.4	1.4×10^{-5}	7
		3.5×10^{14}	65.0	7.8×10^{-6}	8
[*b*]	*trans*-CHD=CHD	$\sim10^{13}$	65.0	2.2×10^{-7}	9
[*c*]	*cis*-CHCl=CHCl	5.7×10^{12}	56.0	6.7×10^{-5}	10
[*d*]	*trans*-CHCl=CHCl	4.8×10^{12}	55.3	9.0×10^{-5}	10
[*e*]	*cis*-$CH_3CH{=}CHCOOCH_3$	1.6×10^{13}	57.8 ± 1.5	5.4×10^{-5}	11
[*f*]	*cis*-$CH_3CH{=}CHCN$	1.0×10^{11}	51.3 ± 3.7	3.1×10^{-5}	12
[*g*]	*cis*-$C_6H_5CH{=}CHC_6H_5$	6×10^{12}	42.8	0.69	3
[*h*]	*cis*-$C_6H_5CH{=}CHCN$	4×10^{11}	46.0	5.0×10^{-3}	13
[*i*]	*cis*-$C_6H_5CH{=}CHCOOCH_3$	3.5×10^{11}	41.6	9.3×10^{-3}	14

kcal leads to an upper limit of 4×10^{-6} for κ. If κ_1 and κ_2 are equal, their value must be $< 8 \times 10^{-6}$. Upper limits which are much lower are obtained if one uses the value of 25 kcal for the activation energy of the triplet mechanism. The nonoccurrence of triplet mechanisms, as indicated by the "normal" frequency factors and the absence of nonlinear Arrhenius behavior, thus leads us to much lower transmission coefficients for the singlet–triplet transition than had previously been estimated. Theoretical estimates of this quantity are still unreliable.

The discussion of the remainder of this paper is concerned with the variations in energies and entropies of activation and is based on the assumption that the reactions occur by mechanism [II].

Correlation between Energy of Activation and Heat of Hydrogenation

It is reasonable to seek a relationship between the energy of activation and the strength of the C=C bond or some related quantity. A convenient and accessible related quantity is the heat of hydrogenation. Experimental values are available for ethylene and butene-2, while the values for the remaining compounds were calculated using Benson's tables (16) for heats of formation; this procedure is probably reliable to ±1 kcal/mole.

The plot of activation energy against heat of hydrogenation shown in Fig. 2 indicates a reasonably good correlation, and this is confirmed by a statistical test (cf. 17). The correlation coefficient is 0.86, and "Student's t" is 5.1, indicating significance at well below the 0.1% level. If the older results of Kistiakowsky and co-workers (reactions [*g*], [*h*], and [*i*]) are excluded the correlation coefficient is 0.77; "Student's t" is 2.9, indicating significance at the 2% level.

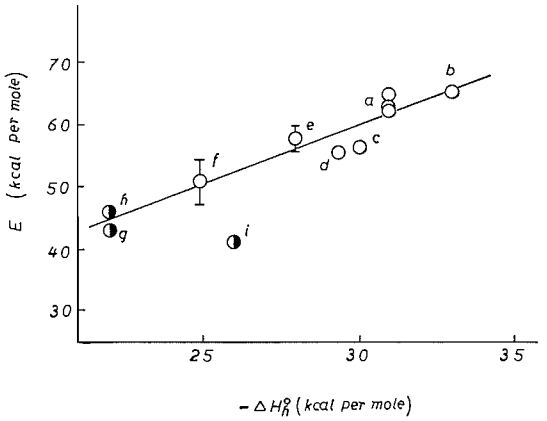

FIG. 2. Plot of E against $-\Delta H_h^\circ$. Half-filled circles are the earlier results of Kistiakowsky and Smith (refs. 3, 13, 14). The letters indicate the reactions referred to in Table I.

The variations with substituents can be explained in a qualitative way in terms of inductive and resonance effects. The activation energies and C=C bond strengths are highest with the deuterated ethylene, the addition of a phenyl group bringing about a reduction. This is attributed to a decrease in the double-bond character, due to resonance of the type

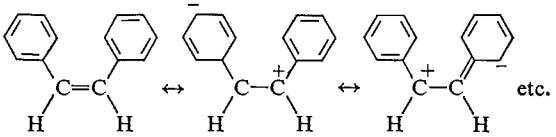

Can. J. Chem. Downloaded from www.nrcresearchpress.com by 210.87.254.5 on 09/05/12
For personal use only.

Can. J. Chem. Downloaded from www.nrcresearchpress.com by 210.87.254.5 on 09/05/12
For personal use only.

Similarly, lowering of the bond strength in methyl crotonate is attributed to resonance such as

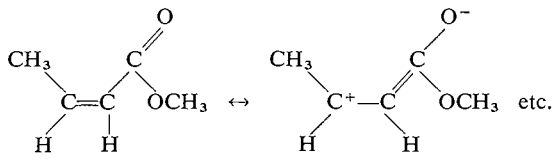

Effects of this kind are indicated by corresponding variations in bond lengths (18).

Correlation between Heat and Entropy of Activation

Figure 3 shows a plot of $\Delta H^{\ddagger}$ against $T\Delta S^{\ddagger}$ for the reactions listed in Table I. The values are calculated using the following relationships:

[2] $$\Delta H^{\ddagger} = E - RT$$

[3] $$\Delta S^{\ddagger} = R \ln Ah/l^{\ddagger}kTe.$$

A and E are the high-pressure values of the frequency factor and activation energy, k and h are the Boltzmann and Planck constants respectively, and $l^{\ddagger}$ is the statistical factor (19); its value is 2 since the isomerization can occur by a twisting about the double bond in either direction. There is seen to be a fairly good correlation, with only two of the 12 points lying at all far from the line. The correlation coefficient for all points is 0.80 and "Student's t" is 4.0, indicating a high degree of significance at well below the 1% level; if reactions [g], [h], and [i] are omitted the correlation coefficient is 0.85 and "Student's t" is 3.9, also corresponding to a high degree of significance at well below the 1% level.

The slope of the plot in Fig. 3 is about 1.6; a slope of unity indicates complete compensation, while one greater than unity indicates only partial compensation. It can be confirmed from the figures in Table I that the lowest rates tend to correspond to the highest activation energies; however, the trend in rates is not as strong as if the $\Delta S^{\ddagger}$ values were constant. The relationship

[4] $$\Delta H^{\ddagger} = 1.6T\Delta S^{\ddagger} + \text{const.}$$

is equivalent to

[5] $$1.6\Delta G^{\ddagger} = 0.6\Delta H^{\ddagger} + \text{const.}$$

or

[6] $$\Delta G^{\ddagger} = 0.38\Delta H^{\ddagger} + \text{const.}$$

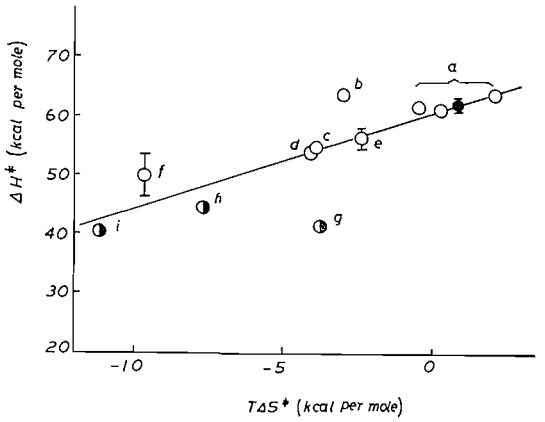

FIG. 3. Plot of $\Delta H^{\ddagger}$ against $T\Delta S^{\ddagger}$. $\ddagger$ was evaluated from $k = 1.3 \times 10^{14} \exp[(-63400 \pm 1000)/RT]$ s^{-1}, obtained by averaging the results of three studies (6, 7, 8); half-filled circles are the earlier results of Kistiakowsky and Smith (refs. 3, 13, 14). The letters indicate the reactions referred to in Table I.

Relationship with π-Bond Energies

Sometimes, as in the case of the C=C bond, a double bond can be envisaged as being formed from a saturated compound by the breaking of two bonds of the same type (e.g. two C—H bonds). In such a case a π-bond energy may be defined (20) as the difference between the bond dissociation energies for the successive breaking of these two bonds. The π-bond energy in ethylene, for example, can be defined as the difference between the C—H bond dissociation energies of H—CH_2CH_3 and H—CH_2CH_2—:

[7] $$Q_{\pi}(C_2H_4) = D(\text{H—}CH_2CH_3) - D(\text{H—}CH_2CH_2\text{—}).$$

The significance of this definition is that D(H—CH_2CH_2—) is abnormally low because a π-bond has been formed at the same time the C—H bond is broken, and that the extent of its lowness is the strength of the π-bond. One may imagine the C—H bond in the C_2H_5 radical to be broken in such a way that the π-bond is not formed, which means that the C_2H_4 produced is in an excited state. On a simple view the energy $D(C_2H_4^*\text{—H})$ required to create this excited $C_2H_4^*$ from C_2H_5 will be the same as that required to break the C—H bond in ethane; thus we may write alternatively

[8] $$Q_{\pi}(C_2H_4) = D(\text{H—}C_2H_4^*) - D(\text{H—}C_2H_4\text{—}).$$

Can. J. Chem. Downloaded from www.nrcresearchpress.com by 210.87.254.5 on 09/05/12
For personal use only.

TABLE II

Thermochemical values used in the calculation of π-bond energies. (All values are in kcal/mole, referred to 0 °K.)

Process ($RMH \rightarrow R\cdot + MH\cdot$)	$\Delta H_f^0(R\cdot)$	$\Delta H_f(MH)$	$D(R—MH)$ ($= D(R—M^*)$)	Process ($RM\cdot \rightarrow R\cdot + M$)	$\Delta H_f^0(RM\cdot)$	$D(R—M)$	Q_π
$C_2H_6 \rightarrow H + C_2H_5$	51.6	30.0	98.1	$C_2H_5 \rightarrow H + C_2H_4$ (21)	30.0	36.2	61.9 (C_2H_4)
$C_3H_8 \rightarrow CH_3 + C_2H_5$	34.2	30.0	83.7	n-$C_3H_7 \rightarrow CH_3 + C_2H_4$ (22)	27.4[a]	21.3	62.4 (C_2H_4)
n-$C_4H_{10} \rightarrow C_2H_5 + C_2H_5$	30.0	30.0	83.7	n-$C_4H_9 \rightarrow C_2H_5 + C_2H_4$ (23)	22.7	21.8	61.9 (C_2H_4)
n-$C_4H_{10} \rightarrow CH_3 + C_3H_7$	34.2	27.4	85.3	s-$C_4H_9 \rightarrow CH_3 + C_3H_6$ (24)	17.8[a]	24.9	60.4 (C_3H_6)

[a]These values are lower than those reported previously (22, 24), by 1.0 and 1.4 kcal/mole; use has now been made of the most recent values of 7.9 and 7.4 kcal/mole (25) instead of 8.9 and 8.8 kcal/mole (26, 27) for the activation energies for the addition of CH_3 to ethylene and propylene respectively.

Can. J. Chem. Downloaded from www.nrcresearchpress.com by 210.87.254.5 on 09/05/12
For personal use only.

In general

[9] $$Q_\pi(\mathrm{M}) = D(\mathrm{R—M^*}) - D(\mathrm{R—M}).$$

These relationships are represented in the energy diagram in Fig. 4.

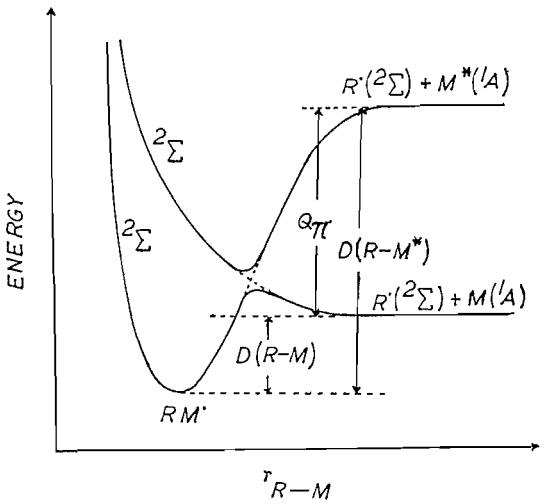

FIG. 4. Schematic energy diagram for the decomposition of an alkyl radical, $RM \rightarrow R^{\cdot} + M$, where M is an olefin.

A slightly different way of looking at the π-bond energy is to regard it as the difference between the energy required to abstract a radical R from a molecule and from a corresponding radical. Thus in terms of butane dissociation energies the π-bond energy of ethylene can be expressed as

[10] $$Q_\pi(\mathrm{C_2H_4}) = D(\mathrm{C_2H_5—CH_2CH_3}) - D(\mathrm{C_2H_5—CH_2CH_2—}).$$

Reliable values for heats of dissociation of C—H bonds in small radicals have recently become available (21–24) from studies of the kinetics of dissociation of the radicals. Table II gives such values together with other information required for the estimation of π-bond energies, which are given in the last column of the table. Heats of formation of radicals were obtained from Rossini (28). There is remarkably good agreement between the four π-bond energies obtained, the average being 61.7 ± 1.0 kcal/mole.

The state of the M* species formed when the energy D(M*—R) is added to the radical M—R, with the breaking of the M—R bond, is presumably the twisted singlet state. In the C_2H_4 case, this is the amount of energy that breaks a C—H bond and converts an sp^3 carbon into an sp^2:

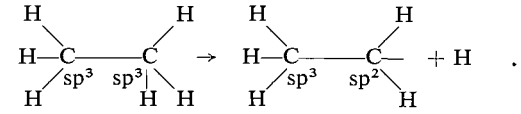

Addition of the same amount of energy will produce a C_2H_4 species in which both carbon atoms are sp^2-hybridized and in which there is no π-bonding:

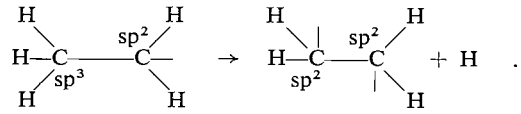

This species, with no π-bonding, can be identified with the twisted state in which there is a minimum of overlapping of the p orbitals which extend at right angles to the planes. In view of this the close relationship between π-bond energies and the activation energies for *cis–trans* isomerizations is easy to understand. It will be interesting to see whether there is a good correlation for the entire series of reactions, but data are as yet not available.

General Discussion

It is now of interest to consider the significance of the above relationships in terms of the mechanisms of these isomerizations. A very simple view is that the partition function for the activated state differs from that for the initial state solely in the absence of the contribution $1/(1 - \exp(-h\nu_0/kT))$ corresponding to the torsional oscillation, all other partition functions remaining the same. If this were the case the rate expression would be simply

[11] $$k = l^* \frac{kT}{h}(1 - \exp(-h\nu_0/kT)) \exp(-E_0/kT).$$

Two considerations, however, show that this concept is too simple:

(1) Insertion of known values for the torsional frequencies does not lead to a reliable prediction of the entropies of activation. The agreement is not bad for some of the reactions of higher entropies of activation (e.g. reaction [*a*], [*b*], and [*e*]), but for reactions with lower ΔS^* values

(e.g. reactions [*f*], [*h*], and [*i*]) the calculated $\Delta S^{\ddagger}$ values are much higher than the experimental ones. Evidently an additional factor is leading to an increased rigidity in the activated complexes for these reactions.

(2) A related argument is based on the experimental $\Delta S^{\ddagger} - \Delta H^{\ddagger}$ correlation. If eq. [11] were valid it would be possible to calculate ν_0 values from the observed $\Delta S^{\ddagger}$ values, and then to interpret the $\Delta H^{\ddagger}$ values on their basis. When this is attempted, however, the ν_0 values are found to vary over an unrealistically wide range (this is essentially point (1) above). Furthermore the energies of activation estimated from these ν_0 values vary over a much greater range than do the experimental values. This was found to be the case when either of two procedures was used:

(*a*) The potential-energy variation with θ was interpreted as the intersection of two purely harmonic curves.

(*b*) The variation was assumed to be given by a cosine function, as employed by Herzberg (29).

In either case the ν_0 values required to interpret the variation in $\Delta S^{\ddagger}$ led to $\Delta H^{\ddagger}$ values covering a much greater range than the range of ~ 20 kcal shown by the values in Table I. Reactions [*a*], [*b*], and [*e*] could be accommodated by treatments of this kind, but the remaining reactions (particularly [*h*] and [*i*]) showed very marked deviations.

In view of this situation it is necessary to suppose that the activation energies, and the corresponding π-bond energies, are related not only to the torsional frequencies but to a considerable extent to interactions between the side groups and the electrons which become unpaired when the bond has become twisted through 90°. Such interactions will reduce the energy required to twist the bond, and also the π-bond energy, and will also lead to an increased rigidity of the activated complex and to a corresponding reduction in its entropy.

1. J. L. MAGEE, W. SHAND, and H. EYRING. J. Am. Chem. Soc. **63**, 677 (1941).
2. G. B. KISTIAKOWSKY and M. Z. NELLES. Z. Physik. Chem. Leipzig, Bodenstein-Festband, 369 (1931).
3. G. B. KISTIAKOWSKY and W. R. SMITH. J. Am. Chem. Soc. **56**, 638 (1934).
4. G. B. KISTIAKOWSKY and W. R. SMITH. J. Am. Chem. Soc. **58**, 766 (1936).
5. R. B. CUNDALL. Progr. Reaction Kinetics, **2**, 165 (1964).
6. B. S. RABINOVITCH and K. W. MICHEL. J. Am. Chem. Soc. **81**, 5065 (1959).
7. R. B. CUNDALL and T. F. PALMER. Trans. Faraday Soc. **57**, 1936 (1961).
8. A. LIFTSHITZ, S. H. BAUER, and E. L. RESLER. J. Chem. Phys. **38**, 2056 (1963).
9. J. E. DOUGLAS, B. S. RABINOVITCH, and F. S. LOONEY. J. Chem. Phys. **23**, 315 (1955).
10. L. D. HAWTON and G. P. SEMELUK. Can. J. Chem. **44**, 2143 (1966).
11. J. N. BUTLER and G. J. SMALL. Can. J. Chem. **41**, 2492 (1963).
12. J. N. BUTLER and R. D. MCALPINE. Can. J. Chem. **41**, 2487 (1963).
13. G. B. KISTIAKOWSKY and W. R. SMITH. J. Am. Chem. Soc. **58**, 2428 (1936).
14. G. B. KISTIAKOWSKY and W. R. SMITH. J. Am. Chem. Soc. **57**, 269 (1935).
15. T. TERAO, S. HIROKAMI, S. SATO, and R. J. CVETANOVIĆ. Can. J. Chem. **44**, 2173 (1966).
16. S. W. BENSON. The foundations of chemical kinetics. McGraw-Hill Book Co., New York. 1960.
17. M. J. MORONEY. Facts from figures. Penguin Books, London. 1957.
18. G. W. WHELAND. Resonance in organic chemistry. John Wiley and Sons, Inc., New York. 1955.
19. D. M. BISHOP and K. J. LAIDLER. J. Chem. Phys. **42**, 1688 (1965).
20. N. N. SEMENOV. Some problems of chemical kinetics and reactivity. Vol. 1. Pergamon Press, London. 1959. p. 59.
21. L. F. LOUCKS and K. J. LAIDLER. Can. J. Chem. **45**, 2795 (1967).
22. M. C. LIN and K. J. LAIDLER. Can. J. Chem. **44**, 2927 (1966).
23. W. E. MORGANROTH and J. G. CALVERT. J. Am. Chem. Soc. **88**, 5387 (1966).
24. M. C. LIN and K. J. LAIDLER. Can. J. Chem. **45**, 1315 (1967).
25. R. J. CVETANOVIĆ and R. S. IRWIN. J. Chem. Phys. **46**, 1694 (1967).
26. R. K. BRINTON. J. Chem. Phys. **29**, 781 (1958).
27. M. MIYOSHI and R. K. BRINTON. J. Chem. Phys. **36**, 3019 (1962).
28. F. D. ROSSINI *et al.* Selected values of physical and thermodynamic properties of hydrocarbons and related compounds. American Petroleum Institute, Pittsburgh. 1953.
29. G. HERZBERG. Infrared and Raman spectra. D. Van Nostrand, New York. 1945. p. 226.

Can. J. Chem. Downloaded from www.nrcresearchpress.com by 210.87.254.5 on 09/05/12
For personal use only.

Can. J. Chem. Downloaded from www.nrcresearchpress.com by 210.87.254.5 on 09/05/12
For personal use only.

Effets ioniques spécifiques sur le taux de formation du ClO_2 par la réaction chlorure–chlorate

F. Lenzi[1] et W. H. Rapson

Department of Chemical Engineering and Applied Chemistry, University of Toronto, Toronto, Ontario

Reçu le 27 décembre 1966

On a observé que des sels ajoutés à la réaction $ClO_3^- + 2H^+ + Cl^- \rightarrow ClO_2 + \frac{1}{2}Cl_2 + H_2O$ en milieux 2.3 *M* et 5.0 *M* H_2SO_4 entraînent des accroissements du taux de la réaction. Ces accroissements de taux, qui sont spécifiques à la nature des ions ajoutés, peuvent être reliés aux nombres d'hydratation de ces ions. La réaction est de douzième ordre par rapport à la concentration stoechiométrique du H_2SO_4 du milieu; ce fait peut s'expliquer par l'hydratation ionique en appliquant les idées de Bascombe et Bell. La réaction chlorure–chlorate peut être considérée comme "amplificateur chimique" pour l'observation des effets d'hydratation.

Rate enhancing specific ion effects have been detected in 2.3 *M* and 5.0 *M* H_2SO_4 for the reaction $ClO_3^- + 2H^+ + Cl^- \rightarrow ClO_2 + \frac{1}{2}Cl_2 + H_2O$. These effects can be related to the hydration numbers of the added ions. This suggests a Bascombe and Bell type of interpretation for the overall twelfth power rate dependence of the above reaction on the sulfuric acid concentration in the reaction medium; the chloride–chlorate reaction acts as a "chemical amplifier" for hydration effects.

Canadian Journal of Chemistry, **46**, 979 (1968)

Introduction

Lors d'une étude cinétique de la formation du bioxyde de chlore par la réaction

[1] $2H^+ + ClO_3^- + Cl^- \rightarrow ClO_2 + \frac{1}{2}Cl_2 + H_2O$

en milieu 2–2.5 *M* H_2SO_4, on a observé (1) des variations surprenantes de l'ordre de réaction par rapport au chlorate avec les changements de concentration du chlorate de sodium. En répétant ces expériences à force ionique constante il a été remarqué que le nitrate de potassium accroit le taux de la réaction [1], alors que le nitrate de sodium a un effet encore bien supérieur.

Par la suite les expériences ont été répétées pour déterminer les taux de la réaction [1] à 5.00 *M* et 2.32 *M* H_2SO_4 en présence des perchlorates de sodium ou de potassium, et des nitrates de lithium, ou de sodium ou de potassium.

Méthodes expérimentales

La réaction [1] a été suivie par spectrophotomètre Beckman DB à 360 mμ. La capacité molaire d'absorption du bioxyde de chlore à 360 mμ est de 115 × 10; cette valeur ne démontre que peu de variation avec l'acidité du milieu et reste inchangée en présence de chlorure, de chlorate ou de chlore (3); les autres espèces chimiques qu'on sait être présentes absorbent peu à cette longueur d'onde (1, 3). La température ambiante fut maintenue à 25.0 ± 0.5 °C, et celle du compartiment à cellules le fut à 25 ± 0.1 °C. Les essais furent effectués en mélangeant deux solutions appropriées dans une cellule spectrophotométrique de 1 cm pour donner les concentration initiales voulues des réactifs. Une des solutions contenait le chlorure de sodium pendant que l'autre contenait le chlorate de sodium et tout autre sel ajouté. Les deux solutions étaient à la même molarité en acide sulfurique. (On fit exception pour le nitrate de potassium en milieu 5.00 *M* H_2SO_4 qui fut dissous dans les deux solutions à cause de sa plus faible solubilité.) Toutes les solutions de chlorate furent préalablement balayées par un courant d'azote pendant 1 h. Les concentrations initiales des réactifs étaient 0.098 *M* $NaClO_3$, 0.0250 *M* NaCl et 5.00 *M* H_2SO_4 pour une série d'expériences, et de 1.20 *M* $NaClO_3$, 0.300 *M* NaCl et 2.32 *M* H_2SO_4 pour l'autre série. La réaction fut observée jusqu'à ce que l'absorption atteigne une valeur de 1.0 ou 1.5; en conséquence on peut considérer que les concentrations des réactifs demeuraient pratiquement constantes. Pour éviter toute confusion les données absorption vs. temps (sans sels ajoutés) pour ces deux séries d'essais seront appelées "données de base".

La cellule-échantillon fut rincée avec une des deux solutions, égouttée et pesée, puis remplie de la même solution au moyen d'une seringue étalonnée munie d'une pointe en teflon (le teflon étant inséré dans la seringue d'une telle façon que la solution n'était en contact qu'avec du verre ou du teflon). Pour chaque essai le volume de solution était ajusté à 1.65 ml. La réaction fut déclenchée en introduisant 1.65 ml de l'autre solution dans la cellule au moyen d'une seringue semblable; ceci demandait 3 s. La cellule fut immédiatement bouchée, agitée énergiquement et placée dans le compartiment à cellules du spectrophotomètre, celui-ci ainsi que l'enregistreuse ayant été préalablement étalonnés avec une solution de chlorate de sodium. Le commencement du tracé d'absorption vs. temps était obtenu en moins de 10 s après le début de la réaction. L'étalonnage du spectrophotomètre et de l'enregistreuse fut contrôlé à la fin de chaque essai en remplissant de nouveau la cellule-échantillon avec une solution de chlorate de sodium. Des essais à blanc furent effectués avec le sel ajouté dissous dans la solution de chlorate de sodium; exception faite des sels d'ammonium, il n'y eut

[1]Département de Génie Chimique, École Polytechnique, Montréal, Québec.

pas d'évolution décelable de bioxyde de chlore dans l'espace de 2 h (les essais eux-mêmes prenaient moins que 15 min).

Chaque expérience comprenait quatre essais: pour deux d'entre eux la solution de chlorate était ajoutée à celle de chlorure; pour les deux autres c'était le chlorure qui était ajouté au chlorate. Aucune différence significative n'a pu être décelée entre les deux paires d'essais. L'écart maximum de pente initiale du tracé absorption–temps pour une série d'essais quelconque en milieu 5.00 M H_2SO_4 était de $\pm 6\%$ de la moyenne, et l'écart moyen de $\pm 3\%$. En milieu 2.32 M H_2SO_4 la reproductibilité des pentes initiales (c.à.d. quand A = absorption = 0) était beaucoup moins bonne, mais les pentes mesurées à des absorptions de 0.2, 0.7 et 1.2 donnaient une meilleure précision: pour une absorption de 0.2 l'écart maximum pour une série quelconque était $\pm 9\%$ et l'écart moyen de $\pm 6\%$.

Le nitrate de sodium et le perchlorate de sodium employés étaient de qualité 'Analar' (B.D.H.), tandis que le nitrate de potassium et le perchlorate de sodium étaient de qualité 'Laboratory' (B.D.H.). Les nitrates de lithium et d'ammonium, et le perchlorate d'ammonium étaient de qualité 'Certified' (Fisher). Le contaminant d'intérêt principal était l'ion chlorure qui pouvait être présent jusqu'à un maximum de 0.15% dans le perchlorate de sodium. Le balayage à l'azote avait pour effet d'éliminer le chlorure par l'entremise de la réaction [1]. Il est à noter que cette réaction n'entraînait qu'une diminution de concentration du chlorate négligeable.

Résultats

Ceux-ci sont représentés aux Figs. 1 et 2.

Dans les deux cas, l'ordonnée est le log du rapport des pentes initiales; c.à.d. le log du rapport de la pente initiale du tracé absorption–temps obtenu avec sel ajouté, à la pente initiale obtenue à partir des données de base. La Fig. 1 s'applique en milieu 5 M H_2SO_4 pour lequel les rapports des pentes initiales ont pû être obtenus directement des tracés absorption–temps. La Fig. 2 correspond au milieu 2.32 M H_2SO_4; cependant dans ce cas les pentes initiales des tracés absorption–temps ne pouvaient être obtenus avec précision, en particulier pour les données de base, parce que la pente décroit trop rapidement à cette acidité, probablement à cause de l'effet inhibiteur du chlore qui est alors augmenté (1, 2). Cet effet, démontré par la Fig. 3, introduit ainsi une incertitude relativement grande dans la détermination de la pente initiale. Pour surmonter cette difficulté, les rapports des pentes aux absorptions de 0.2, 0.7 et 1.2 ont été déterminés et ensuite extrapolés jusquà $A = 0$.

La Fig. 4 représente l'effet de l'addition du $LiNO_3$ sur la réaction [1] en 2.32 M H_2SO_4.

On remarque que les rapports des pentes

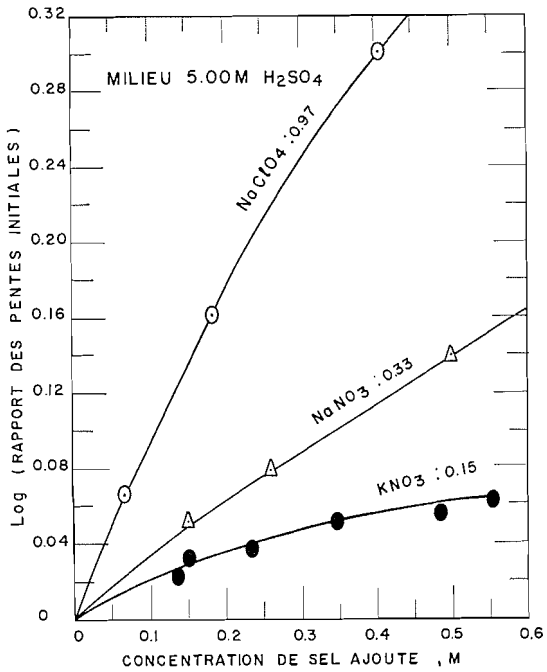

FIG. 1. Effets ioniques spécifiques du $NaClO_4$, $NaNO_3$, KNO_3 sur le taux de réaction de 0.098 M $NaClO_3$ et 0.025 M NaCl en milieu 5.00 M H_2SO_4 à 25.0 ± 0.1 °C. Ordonnée = log (pente initiale du tracé absorption–temps avec sel ajouté/pente initiale des données de base). Le chiffre qui suit la formule du sel ajouté est la pente initiale de la courbe représentée, en $(mole/l)^{-1}$.

augmentent peu ou pas avec l'absorption jusqu'à une concentration de sel ajouté d'environ 0.2 M; l'augmentation devenant plus importante à des concentrations de sel ajouté supérieures. Par exemple pour 0.090 M en $LiNO_3$ le rapport des pentes (= pente du tracé absorption–temps avec $LiNO_3$/pente obtenue d'après les données de base) était de 1.19 pour $A = 0.2$, de 1.19 pour $A = 0.7$ et de 1.20 pour $A = 1.2$, tandis que pour 0.39 M en $LiNO_3$ des rapports de 1.79 pour $A = 0.2$, de 1.95 pour $A = 0.7$ et de 2.08 pour $A = 1.2$ ont été obtenus. Cette augmentation du rapport est assimilable à l'amoindrissement de l'effet inhibiteur du chlore avec augmentation de l'acidité, car, comme il sera démontré ci-dessous, l'addition d'un sel peut être équivalent à une augmentation effective de l'acidité.

Des essais furent aussi effectués en milieu 2.32 M H_2SO_4 avec le perchlorate ou le nitrate d'ammonium; cependant une réaction était

Can. J. Chem. Downloaded from www.nrcresearchpress.com by 210.87.254.5 on 09/05/12
For personal use only.

Can. J. Chem. Downloaded from www.nrcresearchpress.com by 210.87.254.5 on 09/05/12
For personal use only.

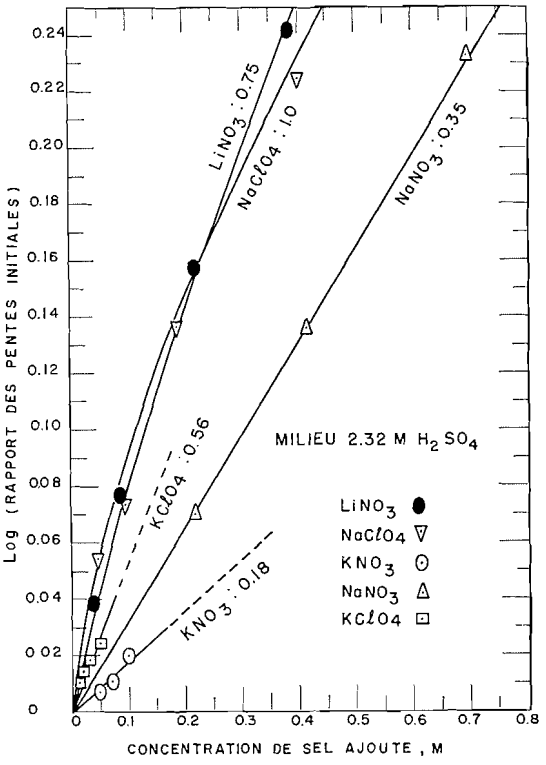

Fig. 2. Effets ioniques spécifiques du $NaClO_4$, $KClO_4$, KNO_3, $NaNO_3$ et $LiNO_3$ sur le taux de réaction de 1.20 M $NaClO_3$ et 0.300 M NaCl en milieu 2.32 M H_2SO_4 à 25.0 ± 0.1 °C. Ordonnée = log (pente initiale du tracé absorption–temps avec sel ajouté/pente initiale des données de base), obtenue à $A = 0$ par extrapolation des rapports de pentes à $A = 0.2$, 0.7 et 1.2. Le chiffre qui suit la formule du sel ajouté est la pente initiale de la courbe représentée, en $(mole/l)^{-1}$.

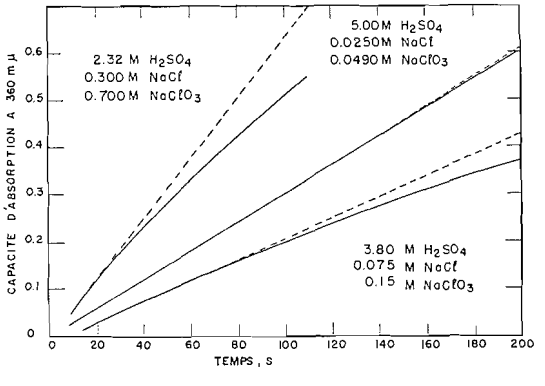

Fig. 3. Différences de l'effet inhibiteur du chlore à diverses acidités pour la réaction [1]. Les pentes initiales des tracés sont représentées en pointillé.

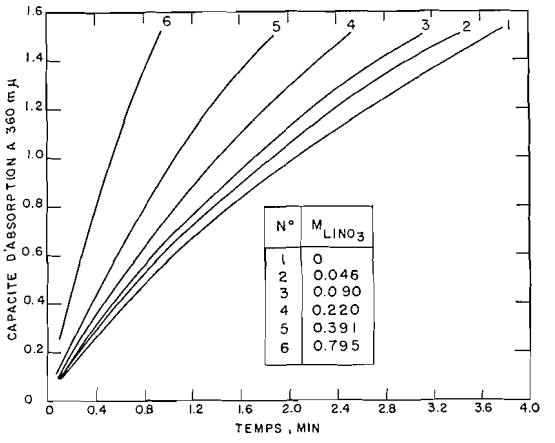

Fig. 4. Effet de l'addition du $LiNO_3$ sur la réaction [1] à 25 °C: 2.32 M H_2SO_4, 0.300 M NaCl, 1.200 M $NaClO_3$.

observée dans l'essai à blanc spectrophotométrique (en absence de chlorure) comprenant le sel d'ammonium et le chlorate de sodium. Les résultats démontraient toutefois un accroissement du taux de la réaction [1] plus grand que dans le cas du sel de sodium correspondant, et même plus grand que celui du lithium pour le cas du nitrate. Ceci est probablement dû à une réaction entre l'ion ammonium et le chlore, ce qui diminuerait l'effet inhibiteur de ce dernier sur le taux de la réaction [1].

Interprétation

Pour éliminer les différences d'association ionique, seules les pentes initiales des courbes représentées aux Figs. 1 et 2 sont comparées. De ces valeurs on tire les rapports

$$\left(\frac{NaClO_4}{KClO_4}\right) = 1.8; \quad 2.32\ M\ H_2SO_4 \qquad \left(\frac{KClO_4}{KNO_3}\right) = 3.1; \quad 2.32\ M\ H_2SO_4$$

$$\left(\frac{NaNO_3}{KNO_3}\right) = 2.2; \quad 5.00\ M\ H_2SO_4 \qquad \left(\frac{NaClO_4}{NaNO_3}\right) = 2.9; \quad 2.32\ M\ H_2SO_4$$

$$\left(\frac{NaNO_3}{KNO_3}\right) = 2.0; \quad 2.32\ M\ H_2SO_4 \qquad \left(\frac{NaClO_4}{NaNO_3}\right) = 2.9 \quad 5.00\ M\ H_2SO_4$$

Malgré l'incertitude assez grande des rapports des pentes initiales des courbes, en particulier dans le cas des sels de potassium, les rapports ci-haut démontrent une certaine spécificité

TABLEAU I

Comparaison des rapports des pentes initiales en 2.32 M H_2SO_4 avec les nombres d'hydratation

		H^+	Li^+	Na^+	K^+	ClO_4^-	NO_3^-
(*a*)	Rapports des pentes expérimentales		0.75	0.35	0.18		
(*b*)	Nombres d'hydratation des chlorures: Robinson and Stokes (4)	8.0	7.1	3.5	1.9		
(*c*)	Nombres d'hydratation des chlorures: Monk (5)	7.3	6.5	3.5	1.9		
(*d*)	Nombres d'hydratation ionique: Glueckauf (6)	3.9	3.4	2.0	0.6	0.3	0
(*e*)	Nombres d'hydratation ionique: Glueckauf and Kitt (7)	3.9	3.3	1.5	0.6		
(*f*)	Nombres d'hydratation ionique: Monk (8)	3.9	4.25	2.9	1.2	0.15	0
	b:*a*		9.5	10	11		
	c:*a*		8.7	10	11		
	d:*a*		4.5	5.7	3.4		
	e:*a*		4.4	4.3	3.4		
	f:*a*		5.7	8.3	6.8		

ionique sur l'accroissement de taux de la réaction [1]; l'effet du sodium est à peu près deux fois plus grand que celui du potassium, et celui du perchlorate est à peu près trois fois celui du nitrate. Ces résultats peuvent être comparés aux nombres d'hydratation du Tableau I. En posant les valeurs respectives de 0.3 et 0.15 de Glueckauf et de Monk pour le nombre d'hydratation du ClO_4^-, le rapport expérimental ClO_4^-: NO_3^- de 3:1 donne 0.1 et 0.05 respectivement pour le nombre d'hydratation de l'ion nitrate. Ces valeurs sont consistantes avec la valeur de zéro donnée par Glueckauf ainsi que par Monk.

Les effets du $LiNO_3$, $NaNO_3$ et KNO_3 en milieu 2.32 M H_2SO_4 peuvent être comparés avec les nombres d'hydratation de Robinson et Stokes (4), Glueckauf (6, 7) et Monk (5, 8). Le Tableau I démontre que les résultats sont sensiblement en accord avec les rapports des nombres d'hydratation de Robinson et Stokes (4) pour les chlorures correspondants, ou encore avec ceux calculés par Monk (5). Il y a aussi accord approximatif avec les rapports des nombres d'hydratation ionique obtenus par Glueckauf (6, 7) ainsi qu'avec ceux calculés par Monk (8).

Les Figs. 5 et 6 représentent les courbes de Van't Hoff pour la réaction [1]. Celles-ci donnent un ordre moyen de 12 par rapport à la concentration stoechiométrique du H_2SO_4 dans l'intervalle 2–6 M. Les données de Young et Blatz (9) indiquent que d'une façon approximative $[H^+] = 1.3\,[H_2SO_4]$ dans l'intervalle 2–6 M H_2SO_4, d'où la réaction [1] peut être considérée comme étant d'ordre 12 par rapport au

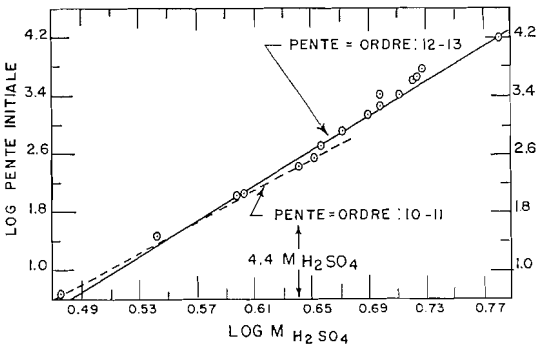

FIG. 5. L'effet du H_2SO_4 sur le taux initial de formation du ClO_2 pour la réaction [1]: 0.100 M $NaClO_3$, 0.0050 M NaCl.

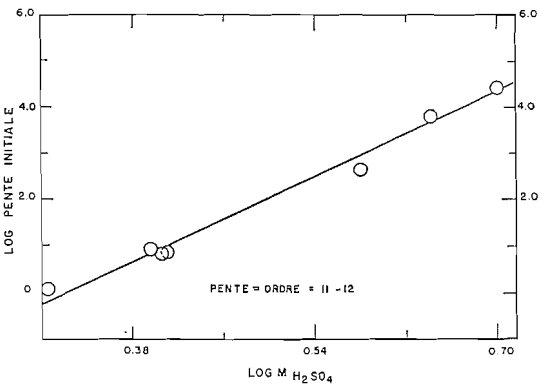

FIG. 6. L'effet du H_2SO_4 sur le taux initial de formation du ClO_2 pour la réaction [1]. 0.500 M $NaClO_3$, 0.0750 M NaCl.

Can. J. Chem. Downloaded from www.nrcresearchpress.com by 210.87.254.5 on 09/05/12
For personal use only.

Can. J. Chem. Downloaded from www.nrcresearchpress.com by 210.87.254.5 on 09/05/12
For personal use only.

H^+. D'autre part il a été démontré à partir des mêmes données (2) que le taux de la réaction [1] est d'ordre 4–5 par rapport à l'activité molale de l'acide sulfurique. L'acidité du milieu exerce donc une influence considérable sur le taux de la réaction [1].

Le parallèle établi entre l'influence des ions ajoutés et les nombres d'hydratation suggère que l'accroissement du taux de la réaction par les sels ajoutés est dû à leur pouvoir d'abstraction d'eau. Leur présence diminuerait la concentration d'eau "libre" (c.à.d. d'eau non rattachée aux ions), augmentant ainsi l'acidité effective.

Cette conclusion est étayée par l'observation que les tracés absorption–temps en milieu 2.32 *M* H_2SO_4 en présence des sels de sodium, lithium et ammonium présentent une diminution de pente qui est beaucoup plus petite que celle obtenue avec peu ou pas d'addition de sel, ou encore addition de sel de potassium; or, il a aussi été observé (Fig. 3) que la diminution de pente décroit avec augmentation d'acidité. (La disparition des réactifs eux-mêmes est trop petite pour entraîner des changements de pente significatifs durant le temps d'observation de la réaction.)

Discussion

On peut tenter de placer la conclusion qualitative ci-haut sur une base plus quantitative. On peut supposer qu'une augmentation de la concentration d'acide sulfurique entraîne les deux effets suivants.

(*a*) Une augmentation de la concentration des protons ou des protons hydratés (effet stoechiométrique H^+).

(*b*) Une diminution de l'activité de l'eau, elle-même entraînée par l'hydratation des protons (effet activité d'eau).

Si on parvient à démontrer que l'effet (*b*) est au moins aussi grand que l'effet (*a*) sur la réaction [1], on expliquerait pourquoi l'addition d'un ion tel que Li^+ (qui a un nombre d'hydratation semblable à celui de H^+) entraîne un effet d'accroissement sensible du taux de la réaction [1], alors même que l'effet (*a*) est absent.

Une augmentation de concentration du H_2SO_4 de 2 *M* à 6 *M* correspond à une augmentation de la concentration des protons par un facteur de trois (9); mais l'augmentation d'acidité effective est beaucoup plus grande, telle que démontrée par les données qui mènent au concept de la fonction d'acidité (10), l'activité des solutions d'acide sulfurique déterminée par mesure de tensions de vapeur (11), ou encore par l'ordre de 12 dont il est question ici. Ces fortes augmentations d'acidité effective peuvent être expliquées d'une façon phénoménologique en employant des fonctions d'acidité ou des coefficients d'activité. Bascombe et Bell (12) ont cependant donné une interprétation plus détaillée du comportement des solutions des acides forts (jusqu'à 8 molale) en fonction de la tétrahydratation du proton. Leur interprétation est supportée par les conclusions indépendantes d'Ackerman (14), de Wyatt (15), de Glueckauf (6, 7) ainsi que par une spéculation (13) sur la pentahydratation globale de l'acide sulfurique.

Il y a probablement plus de quatre molécules d'eau associées à chaque proton; Ackerman (14) fait la distinction entre une couche d'hydratation intérieure et une couche secondaire, et Wyatt (17) remarque que le nombre d'hydratation du proton de quatre n'est qu'une moyenne.

Des échelles d'hydratation très différentes ont été obtenues (16), et le choix de l'une d'elles en particulier, comme celle de Glueckauf ou encore celle de Monk peut être critiqué. Ces dernières échelles donnent des nombres d'hydratation d'à peu près zéro pour des anions tels que Cl^- et NO_3^-, ce qui est aussi discutable. Cependant il y a souvent bon accord entre les rapports de nombres d'hydratation provenant d'échelles différentes: en outre des échelles telles que celle de Glueckauf ou celle de Monk ont l'avantage de se conformer a un nombre d'hydratation protonique de quatre; ce dernier peut être considéré tout simplement comme un paramètre d'hydratation relatif (aux autres ions).

Cinétique de la réaction chlorure–chlorate

La cinétique de la réaction [1] a été déterminée (2) en milieu 2–6 *M* H_2SO_4. Il fut observé que Na^+ exerce une influence marquée sur le taux de la réaction, contrairement à l'ion nitrate. Ainsi l'ordre par rapport au chlorate a donc pu être déterminé en maintenant la concentration de Na^+ constante par l'addition de quantités appropriées de $NaNO_3$ à des concentrations initiales de $NaClO_3$ variées (2). Le mécanisme proposé lorsque le rapport chlorate:chlorure est appréciable est le suivant.

$$[2] \quad 3H^+ + 2Cl^- + ClO_3^- \underset{k_2'}{\overset{k_2}{\rightleftharpoons}} Cl_2 + HClO_2 + H_2O$$

Can. J. Chem. Downloaded from www.nrcresearchpress.com by 210.87.254.5 on 09/05/12
For personal use only.

[3] $$HClO_2 + H^+ + ClO_3^- \underset{k_3}{\rightarrow} 2ClO_2 + H_2O,$$

d'où découle l'équation de taux [4] si l'on tient compte du terme pour l'eau contrairement à ce qui a été fait dans réf. 2

$$[4]\quad \frac{d[ClO_2]}{dt} = \frac{2k_2k_3[H^+]^4[ClO_3^-]^2[Cl^-]^2}{k_2'[Cl_2][H_2O] + k_3[H^+][ClO_3^-]}.$$

A "haute" acidité (6 M H_2SO_4) l'ordre par rapport au chlorate se rapproche de l'unité (1, 2) et l'effet inhibiteur du chlore est plutôt faible (Fig. 3); à "basse" acidité (2 M H_2SO_4) l'ordre par rapport au chlorate se rapproche de 2 et l'effet inhibiteur du chlore est relativement accentué (Fig. 3). A haute acidité $[H_2O]$ est petit (11) relativement a sa valeur à basse acidité tandis que le contraire est le cas pour $[H^+]$. On peut donc supposer qu'en milieu 6 M H_2SO_4 $k_2'[Cl_2][H_2O] < k_3[H^+][ClO_3^-]$, d'où

$$[5]\quad \frac{d[ClO_2]}{dt} \simeq 2k_2[H^+]^3[Cl^-]^2[ClO_3^-]$$

et qu'en milieu 2 M H_2SO_4 $k_2'[Cl_2][H_2O] > k_3[H^+][ClO_3^-]$, d'où

$$[6]\quad \frac{d[ClO_2]}{dt} \simeq \frac{2k_2k_3}{k_2'}[H^+]^4[Cl^-]^2[ClO_3^-]^2 \times [Cl_2]^{-1}[H_2O]^{-1}.$$

Ces équations de taux expliqueraient les observations expérimentales quant à l'influence des concentrations de chlorate, de chlorure et de chlore sur le taux de la réaction [1].

Effet de l'acidité

Considérons maintenant l'effet de l'acidité sur la réaction [1]. Soit l'équilibre entre le proton tétrahydraté et H^+,

$$H^+.4H_2O \rightleftharpoons H^+ + 4H_2O,$$

dont la constante d'équilibre

$$K = \frac{[H^+][H_2O]^4}{[H^+.4H_2O]},\ \text{d'où}\ H^+ = \frac{K[H^+.4H_2O]}{[H_2O]^4}.$$

En substituant cette dernière expression dans l'équation de taux [4] il vient

$$[7]\quad \frac{d[ClO_2]}{dt} = \frac{2k_2k_3K^4[Cl^-]^2[ClO_3^-]^2}{k_2'[Cl_2][H_2O]^{17} + k_3K[H^+.4H_2O][ClO_3^-][H_2O]^{12}}.$$

La validité de l'équation de taux [7] peut être vérifiée assez facilement entre 2 et 4.4 M H_2SO_4, car l'ordre de la réaction [1] par rapport au chlorate est encore relativement grand (1.5 à 4.4 M H_2SO_4 (3). On peut donc encore négliger en première approximation l'effet du chlorate dans le dénominateur de l'éq. [7]. Comparant les taux de formation du bioxyde de chlore à 4.39 M H_2SO_4 et 2.02 M H_2SO_4,

$$\frac{\left(\frac{d[ClO_2]}{dt}\right)_{4.39\ M\ H_2SO_4}}{\left(\frac{d[ClO_2]}{dt}\right)_{2.02\ M\ H_2SO_4}} = \left(\frac{[H^+.4H_2O]_{4.39\ M}}{[H^+.4H_2O]_{2.02\ M}}\right)^4 \left(\frac{[H_2O]_{2.02\ M}}{[H_2O]_{4.39\ M}}\right)^{17}$$

$$= \left(\frac{4.39}{2.02}\right)^4 \times \left(\frac{0.905}{0.651}\right)^{17}$$

$$= 22.4 \times 230 = 5150,$$

démontrant que l'effet activité d'eau est au moins comparable à l'effet stoechiométrique H^+.

Il s'ensuit que l'ordre par rapport à la concentration stoechiométrique du H_2SO_4 entre 2.02 M et 4.39 est égal à log 5150/log (4.39/2.02) = 11 ce qui correspond sensiblement à l'ordre expérimental trouvé pour la région d'acidité en question (voir Figs. 5 et 6). (Des données cinétiques en acidité moindre que 3 M n'ont pas été obtenues pour les concentrations chlorate–chlorure de la Fig. 5.)

La bonne concordance est peut être un peu fortuite, compte tenu des approximations utilisées; cependant si l'on prend des nombres d'hydratation protonique de 3 ou de 5 au lieu de la valeur de 4 préconisée par Bascombe et Bell, le calcul ci-haut donne des ordres de 9 et 13 respectivement pour l'ordre par rapport au H_2SO_4 stoechiométrique dans l'intervalle 2–4.4 M.

Les idées de Bascombe et Bell peuvent donc servir à expliquer l'ordre expérimental élevé par rapport au H_2SO_4 stoechiométrique; ces idées nous mènent aussi à considérer un effet d'activité d'eau qui est au moins comparable à l'effet stoechiométrique H^+, expliquant pourquoi la présence d'un ion comme Li^+ exerce autant d'influence sur le taux de la réaction. Ces concepts permettent une explication plus détaillée qu'antérieurement de la variation de l'effet inhibiteur du chlore avec l'acidité: ceci découle d'une considération du dénominateur de l'éq. [7].

La réaction [1] peut donc être considérée

FOR ERRATA SEE
... 19.... p....

Can. J. Chem. Downloaded from www.nrcresearchpress.com by 210.87.254.5 on 09/05/12
For personal use only.

Page 984, colonne droite, ligne 10: lire 22.3
$271 = 6032$ au lieu de $22.4 \times 230 = 5150$.

Page 984, colonne droite, ligne 15: lire 60
au lieu de 5150.

Page 984, colonne gauche, éq. [7]: lire

$$\frac{2k_2k_3K^4[Cl^-]^2[ClO_3^-]^2[H^+.4H_2O]^4}{k_2'[Cl_2][H_2O]^{17} + k_3K[H^+.4H_2O][ClO_3^-][H_2O]}$$

au lieu de

$$\frac{2k_2k_3K^4[Cl^-]^2[ClO_3^-]^2}{k_2'[Cl_2][H_2O]^{17} + k_3K[H^+.4H_2O][ClO_3^-][H_2O]}$$

Can. J. Chem. Downloaded from www.nrcresearchpress.com by 210.87.254.5 on 09/05/12
For personal use only.

comme un amplificateur chimique pour l'observation des effets d'hydratation en raison de l'exposant élevé de l'activité de l'eau dans l'équation de taux.

Conclusion

1. Les effets d'accroissement de taux de la réaction [1] peuvent être rattachés aux nombres d'hydratation ionique des sels ajoutés; ceci indiquerait que l'addition d'ions bien hydratés aux solutions aqueuses de haute acidité aurait pour effet d'augmenter davantage leur acidité en réduisant l'activité de l'eau: une telle interprétation permet de justifier l'ordre très élévé de la réaction [1] par rapport à la concentration stoechiométrique du H_2SO_4.

2. Pour l'étude cinétique des réactions en milieu de haute acidité, il n'est pas suffisant de maintenir la force ionique 'générale' constante; il faut plutôt maintenir constante la force ionique spécifique (c'est ce qui a dû être fait (2) pour établir l'ordre de la réaction [1]).

3. Du point de vue technologique, l'addition d'un sel relativement très soluble comme le perchlorate de lithium augmenterait considérablement le taux de production du bioxyde de chlore dans le procédé technique "R-2" (18–20), même à acidité relativement basse.

Remerciements

Nous tenons à remercier les professeurs M. W. Lister de l'Université de Toronto et G. Lefebvre de l'Ecole Polytechnique pour leurs conseils; l'un de nous (F. L.) remercie la Faculté de Génie et de Sciences Appliquées de l'Université de Toronto pour l'octroi d'une bourse de recherche.

1. F. Lenzi et W. H. Rapson. Pulp Paper Mag. Can. **63**, (9), T-442 (1962).
2. C. C. Hong, F. Lenzi et W. H. Rapson. Can. J. Chem. Eng. **45**, 349 (1967).
3. F. Lenzi. Ph.D. Thesis, Department of Chemical Engineering and Applied Chemistry, University of Toronto, Toronto, Ontario. 1965.
4. R. A. Robinson et R. H. Stokes. Electrolyte solutions. Butterworths, London. 1955. p. 247.
5. C. B. Monk. Electrolytic dissociation. Academic Press, New York. 1961. p. 87.
6. E. Glueckauf. Trans. Faraday Soc. **51**, 1235 (1955).
7. E. Glueckauf et G. P. Kitt. Proc. Roy. Soc. London, Ser. A, **228**, 322 (1955).
8. C. B. Monk. Electrolytic dissociation. Academic Press, New York. 1961. p. 271.
9. T. F. Young et L. A. Blatz. Chem. Rev. **44**, 93 (1949).
10. M. A. Paul et F. A. Long. Chem. Rev. **57**, 1 (1957).
11. S. Shankman et A. R. Gordon. J. Am. Chem. Soc. **61**, 2370 (1939).
12. K. N. Bascombe et R. P. Bell. Discussions Faraday Soc. **24**, 158 (1957).
13. F. Lenzi. M.A.Sc. Thesis, Department of Chemical Engineering and Applied Chemistry, University of Toronto, Toronto, Ontario. 1956. p. A6.
14. T. Ackerman. Discussions Faraday Soc. **24**, 180 (1957).
15. P. A. H. Wyatt. Discussions Faraday Soc. **24**, 162 (1957).
16. O. Y. Samoilov. Discussions Faraday Soc. **24**, 141 (1957).
17. P. A. H. Wyatt. Discussions Faraday Soc. **24**, 235 (1957).
18. H. de V. Partridge et W. H. Rapson. Tappi, **44**, (10), 698 (1961).
19. W. H. Rapson. Tappi, **41**, (4), 181 (1958).
20. W. H. Rapson. Can. J. Chem. Eng. **36**, 262 (1958).

Can. J. Chem. Downloaded from www.nrcresearchpress.com by 210.87.254.5 on 09/05/12
For personal use only.

Coordination of silicon tetrafluoride with alicyclic ethers and dimethyl ether

J. P. GUERTIN AND M. ONYSZCHUK
Department of Chemistry, McGill University, Montreal, Quebec
Received October 2, 1967

Tensimetric titrations at −78° of silicon tetrafluoride with ethylene oxide, trimethylene oxide, tetrahydrofuran, tetrahydropyran, and dimethyl ether prove the formation of only 1:2 complexes, $SiF_4 \cdot 2$(ether). All are unstable at 25° and either dissociate completely, as do $SiF_4 \cdot 2(CH_2)_4O$, $SiF_4 \cdot 2(CH_2)_5O$, and $SiF_4 \cdot 2(CH_3)_2O$, or decompose into SiF_4 and a polymethylene oxide polymer, as do $SiF_4 \cdot 2(CH_2)_2O$ and $SiF_4 \cdot 2(CH_2)_3O$. Silicon tetrafluoride does not coordinate with 1,4-dioxane in the range −94 to 25° and less than 1 atm pressure. Condensed phase heats of dissociation of $SiF_4 \cdot 2$(ether) complexes follow the order $(CH_2)_3O > (CH_2)_4O > (CH_2)_5O \geq (CH_2)_2O > (CH_3)_2O$, which suggests that this is the relative order of basicities towards SiF_4.

Canadian Journal of Chemistry, 46, 987 (1968)

Can. J. Chem. Downloaded from www.nrcresearchpress.com by 210.87.254.40 on 09/05/12
For personal use only.

Introduction

Few coordination compounds of silicon tetrafluoride and oxygen electron-pair donor molecules have been prepared and characterized. Muetterties (1) has described $SiF_4 \cdot 2(CH_3)_2SO$, $SiF_4 \cdot 2(CH_3)_2NCHO$, and $SiF_4 \cdot xCH_3COCH_2COCH_3$ (where x is indefinite). More recently, Isslieb and Reinhold (2) have reported $SiF_4 \cdot 2(C_6H_5)_3PO$, $SiF_4 \cdot 2(C_6H_{11})_3PO$, $SiF_4 \cdot 2(CH_3)_2NO$, and $SiF_4 \cdot 2C_5H_5NO$. These 1:2 complexes illustrate the marked tendency of silicon to exhibit a coordination number of six, which is especially evident in complexes of silicon tetrafluoride with nitrogen electron-pair donors (1). Although alcohols form 1:4 complexes, $SiF_4 \cdot 4$ROH in which R is CH_3, C_2H_5, i-C_3H_7, and i-C_5H_{11} (3, 4), these probably do not involve eight-coordinate silicon. In a recent detailed study of $SiF_4 \cdot 4CH_3OH$, we concluded that this complex contains tetracovalent rather than hexacovalent silicon and strong hydrogen bonds between methanol and each of the fluorine atoms (5).

The only previous report of an interaction between silicon tetrafluoride and an ether is that by Schmeisser and Elischer (6), who found that ethylene oxide forms a 1:2 complex which decomposes at 10–15° to give 1,4-dioxane. Surprisingly, 1,4-dioxane does not coordinate with silicon tetrafluoride (6), neither do phenyl ethyl ether and isopropyl phenyl ether (3). As part of our continuing interest in the coordination compounds of silicon tetrafluoride, we have studied its interaction with aliphatic cyclic ethers, 1,4-dioxane, and dimethyl ether. Our object has been to determine the conditions of temperature and pressure required for coordination, the stoichiometry of the complexes, and the variation in stability with ring size of the cyclic ethers.

Experimental

Reagents

Commercial samples of ethylene oxide, trimethylene oxide, dimethyl ether, and silicon tetrafluoride were purified by vacuum distillation at low temperatures. Tetrahydrofuran, tetrahydropyran, and 1,4-dioxane were refluxed over freshly cut sodium for 1 h and then fractionally distilled until their boiling points agreed with literature values. The purities of all gaseous compounds were checked by measurements of their vapor pressures, molecular weights, and infrared spectra.

Apparatus

Volatile materials were manipulated in a conventional glass high-vacuum apparatus which had stopcocks lubricated with Kel-F grease and ground-glass joints equipped with Viton rubber O-rings.

Infrared spectra in the range 4000–650 cm^{-1} were recorded on Perkin-Elmer model 21 or Infracord spectrophotometers. Dissociation pressures were measured with a standard tensimeter (7), the temperature of which was kept constant to ±0.2° at any chosen temperature in the range −94 to +14°. Pressures were measured to ±0.1 mm with a cathetometer.

Results

Preparation of $SiF_4 \cdot 2(CH_2)_2O$

In a typical experiment, SiF_4 (8.12 mmoles) was condensed in a vacuum over $(CH_2)_2O$ (6.07 mmoles) and the temperature of the mixture was increased *slowly* from −195 to −78°. After the mixture had been kept at −78° for 30 min, the excess of SiF_4 (5.06 mmoles) was removed by distillation at −129°, and a white solid remained. These results proved that SiF_4 and $(CH_2)_2O$ had combined in a mole ratio of 1:1.99, corresponding to the formula $SiF_4 \cdot 2(CH_2)_2O$. This compound and all other 1:2 SiF_4–ether complexes are formulated as molecular addition compounds

Can. J. Chem. Downloaded from www.nrcresearchpress.com by 210.87.254.40 on 09/05/12
For personal use only.

on the basis of their physical properties described later.

The infrared spectrum of the gas phase at 25° in equilibrium with the solid complex at −65° consisted of bands due to SiF_4 superimposed on those of $(CH_2)_2O$. The molecular weight of this gaseous mixture was 87.2, which compares favorably with 85.1, calculated on the assumption that complete dissociation had occurred and that the liberated SiF_4 was completely in the gas phase while $(CH_2)_2O$ exerted its equilibrium vapor pressure of 10.0 mm at −65°. It was not possible to correct for any lowering of the vapor pressure of $(CH_2)_2O$ by dissolved complex; such a correction would raise the calculated value and thus bring it into closer agreement with the experimental one.

When the temperature of the 1:2 complex was raised to 25°, all of the remaining SiF_4 (3.04 mmoles) was recovered and a colorless, nonvolatile, and viscous liquid resulted, free from ethylene oxide and 1,4-dioxane, the most likely contaminants. The infrared spectrum of the viscous liquid resembled that of 1,4-dioxane except that absorption bands were broader, especially the band in the 1125–1045 cm^{-1} range which is characteristic of the C—O—C stretching vibration. A similar broad band has been observed in the spectra of polyethyleneglycol polymers and in ethylene oxide – acrylonitrile copolymers (8). The broadening of the C—O—C stretching band and the physical properties of the nonvolatile product strongly suggest that it is an ethylene oxide polymer.

It was not possible to obtain pure $SiF_4 \cdot 2(CH_2)_2O$ by a direct synthesis using excess $(CH_2)_2O$ initially. Unconsumed $(CH_2)_2O$ could not be distilled from the mixture of $(CH_2)_2O$ and $SiF_4 \cdot 2(CH_2)_2O$ because the complex has an appreciable dissociation pressure at the temperature at which $(CH_2)_2O$ can be distilled. Therefore, the complex was first prepared at −78° by condensing excess SiF_4 (8.12 mmoles) with $(CH_2)_2O$ (6.07 mmoles); additional $(CH_2)_2O$ (8.32 mmoles) was added, and then the temperature of the mixture was raised to 25° for 1 h. The following fractions were obtained by distillation of the product mixture at temperatures in the range −78 to 25°: (i) a mixture of SiF_4 and $(CH_2)_2O$ which could not be separated by distillation (12.9 mmoles; found: molecular weight (M), 65.0; calcd. for an ideal 1:2 mole mixture of SiF_4 and $(CH_2)_2O$: 64.0); (ii) 1,4-dioxane (1.50 mmoles; found: M, 86.0; calcd.: 88.1); (iii) a small amount of a dark violet, nonvolatile, polymeric material. Thus, there had been a 21% conversion of $(CH_2)_2O$ into 1,4-dioxane and a 9% yield of polymer.

Preliminary experiments indicated that −78° was a suitable temperature for the tensimetric titration of SiF_4 with $(CH_2)_2O$. At this temperature the complex is not greatly dissociated and any excess SiF_4 (b.p. −94.8°) should be entirely in the gas phase. Measured amounts of $(CH_2)_2O$ were added in successive small quantities (~3 mmoles at a time) to a fixed quantity of SiF_4 (12.2 mmoles). After each addition the mixture was warmed quickly to −78° and then kept at this temperature for 15 min, after which time the pressure became constant. A plot of total pressure against mmoles of $(CH_2)_2O$ present shows that the pressure decreased linearly and approached the vapor pressure of pure ethylene oxide (~5 mm at −78°) at a mole ratio $(CH_2)_2O/SiF_4$ equal to 2.03, corresponding to the complex $SiF_4 \cdot 2(CH_2)_2O$.

In the tensimetric titration of $(CH_2)_2O$ under the conditions used in the previously described reverse titration, the pressure remained close to 5 mm (the vapor pressure of $(CH_2)_2O$ at −78°) until the mole ratio $(CH_2)_2O/SiF_4$ decreased to about 2, after which the pressure increased rapidly as more SiF_4 was added. Extrapolation of the final linear portion of this plot to 5 mm pressure gave a mole ratio of 2.00, confirming the formation of the 1:2 complex, $SiF_4 \cdot 2(CH_2)_2O$.

Preparation of $SiF_4 \cdot 2(CH_2)_3O$

Under experimental conditions identical with those used in the preparation of $SiF_4 \cdot 2(CH_2)_2O$, SiF_4 (11.9 mmoles) and $(CH_2)_3O$ (3.86 mmoles) combined in a 1:2.05 mole ratio as evident from the amount of uncombined SiF_4 (10.0 mmoles). Infrared and molecular weight measurements showed that the gas phase at 25° in equilibrium with the solid at 0° consisted of only SiF_4 and $(CH_2)_3O$. (Found: M, 75.0. Calcd.: M, 73.4, assuming complete dissociation of the complex in the gas phase and that the liberated SiF_4 and $(CH_2)_3O$ are completely gaseous. The vapor pressure of $(CH_2)_3O$ of 125 mm at 0° was not established due to the large volume of the reaction vessel.)

Can. J. Chem. Downloaded from www.nrcresearchpress.com by 210.87.254.40 on 09/05/12
For personal use only.

A tensimetric titration of SiF_4 with $(CH_2)_3O$ (added in small portions) showed a combining ratio $(CH_2)_3O/SiF_4 = 2.24$. The discrepancy from the expected 2.00 is probably due to some polymerization of $(CH_2)_3O$. During the titration, the temperature of the mixture had to be raised at a rate of 1° per min to minimize polymerization. When the tensimetric titration was done in reverse, i.e. by addition of successive small portions of SiF_4 to a fixed amount of $(CH_2)_3O$, combining ratios of $(CH_2)_3O$ to SiF_4 were always abnormally high, usually greater than 4:1. This shows clearly that in the SiF_4–$(CH_2)_3O$ system polymerization is enhanced when more $(CH_2)_3O$ is present than is necessary to produce the 1:2 complex. When $(CH_2)_3O$ (8.00 mmoles) was added to previously prepared $SiF_4 \cdot 2(CH_2)_3O$ (1.88 mmoles) and the temperature of the mixture was increased to 25° for 12 h, the products were SiF_4 (1.8 mmoles) and a colorless, viscous, nonvolatile polymer. Thus, SiF_4 had simply catalyzed the polymerization of $(CH_2)_3O$.

An infrared spectrum of the crystalline $SiF_4 \cdot 2(CH_2)_3O$ was taken at −195° using a low-temperature infrared cell. A sample of the complex was sublimed in a vacuum at 3° onto an NaCl plate cooled to −195°. It was difficult to obtain a good spectrum because, in spite of repeated attempts, the thickness of the crystalline film was not uniform and much of the infrared beam was scattered by the microcrystalline deposit. Nevertheless, it was possible to identify the following absorption bands: CH_2 stretching at 2955, 2935, and 2870 cm^{-1}; CH_2 deformation at 1500, 1450, and 1375 cm^{-1}; C—O stretching at 1113 cm^{-1}; Si—F octahedral stretching at 720 cm^{-1}. The intensity of the last band decreased by about 75% when the sample was removed, confirming that the band was due mainly to an absorption by the sample. The remaining absorption was undoubtedly due to SiF_6^{2-} formed by an interaction of $SiF_4 \cdot 2(CH_2)_3O$ with the NaCl surface. A similar reaction occurs between gaseous SiF_4 and NaCl plates (9).

Preparation of $SiF_4 \cdot 2(CH_2)_4O$

Slow cooling of a mixture of SiF_4 (4.94 mmoles) and $(CH_2)_4O$ (4.01 mmoles) from 25 to −78° resulted in excess SiF_4 (2.84 mmoles) and a white solid which contained SiF_4 and $(CH_2)_4O$ in a mole ratio of 1:1.91, corresponding to the complex $SiF_4 \cdot 2(CH_2)_4O$. In several other experiments combining ratios in the range 1:1.91 to 1:2.13 were also obtained.

On raising the temperature of the complex from −78 to 25°, complete dissociation into SiF_4 and $(CH_2)_4O$ occurred, as shown by infrared and molecular weight measurements on the gas phase in equilibrium with the liquid at 25°. (Found: M, 93.9. Calcd.: M, 98.0, assuming complete dissociation of the complex in the gas phase and establishment of the vapor pressure of $(CH_2)_4O$ (125 mm) at 25°.) The absence of polymerization was evident from an infrared spectrum of the liquid phase which showed only the presence of $(CH_2)_4O$.

A tensimetric titration in which $(CH_2)_4O$ was added in successive small portions to SiF_4 (9.43 mmoles) confirmed the formation of only a 1:2 complex, as did the reverse titration of $(CH_2)_4O$ (20.10 mmoles) by successive additions of SiF_4.

Preparation of $SiF_4 \cdot 2(CH_2)_5O$

No visible reaction occurred when SiF_4 (9.03 mmoles) and $(CH_2)_5O$ (2.21 mmoles) were mixed and kept at 25° for 30 min. However, the amount of unreacted SiF_4 (8.00 mmoles) recovered by distillation at −129° indicated that an interaction in a mole ratio of 1:2.14 had occurred at this temperature, producing a white solid corresponding to the complex $SiF_4 \cdot 2(CH_2)_5O$. The large discrepancy between measured and theoretical ratios is undoubtedly due to the fact that the complex is formed only below −54.3°, as evident from subsequent dissociation pressure measurements. At this temperature $(CH_2)_5O$ (m.p. −49°) is a solid so that the complex probably forms slowly at a gas–solid interface.

Infrared and molecular weight measurements on the gas in equilibrium with the liquid at 25° confirmed that the complex was completely dissociated in the gas phase at 25°. (Found: M, 95.0. Calcd.: M, 97.5, assuming complete dissociation of the complex in the gas phase and a vapor pressure of $(CH_2)_5O$ of 70 mm at 25°.) An infrared spectrum of the liquid phase at 25° showed only the presence of $(CH_2)_5O$.

Erratic pressure–composition plots were obtained in tensimetric titrations of SiF_4 with $(CH_2)_5O$ at −95°. Pressure readings were always higher than expected on the assumption that a 1:2 complex, $SiF_4 \cdot 2(CH_2)_5O$, had formed, and the change in slope of the plots was too gradual to show the combining ratio with any degree of

TABLE I

Temperature–pressure data for the SiF_4–1,4-dioxane system

Temperature (°C)	SiF_4 partial pressure (mm)	1,4-Dioxane partial pressure[a] (mm)	Observed total pressure (mm)	Calculated total pressure[b] (mm)
−94	100.0	0	101.5	100.0
−78	102.0	0	104.5	102.0
−45	104.9	0.1	106.0	105.0
−23	105.8	2.1	108.0	107.9
0	106.5	8.5	115.0	115.0
25	107.1	30.9	137.1	138.0

[a]The equilibrium vapor pressures of 1,4-dioxane at the temperature quoted.
[b]Using Dalton's law of partial pressures.

accuracy. These difficulties are attributed, as before, to the occurrence of a slow gas–solid surface reaction between SiF_4 and $(CH_2)_4O$ at temperatures below −49°, the melting point of $(CH_2)_4O$, above which the complex has a high dissociation pressure.

Preparation of $SiF_4 \cdot 2(CH_3)_2O$

A mixture of SiF_4 (3.83 moles) and $(CH_3)_2O$ (3.09 mmoles), prepared at 25° and cooled slowly to −129°, gave unreacted SiF_4 (2.29 mmoles) and a white solid in which the combining ratio of SiF_4 to $(CH_3)_2O$ was 1:2.01, corresponding to the formula $SiF_4 \cdot 2(CH_3)_2O$. This complex dissociated completely into SiF_4 and $(CH_3)_2O$ at 25°, as shown by infrared and molecular weight measurements on the gaseous mixture at this temperature. (Found: M, 65.4. Calcd.: M, 65.4 for a 1:2 mole mixture of SiF_4 to $(CH_3)_2O$.) The formation of only a 1:2 complex at −78° was also confirmed by tensimetric titrations.

Attempted Reaction of SiF_4 with 1,4-Dioxane

Silicon tetrafluoride (1.96 mmoles) and 1,4-dioxane (10.80 mmoles) were condensed together and pressures were measured in the range −94 to 25° and compared with the total pressure calculated assuming no interaction and ideal gaseous behavior according to Dalton's law of partial pressures. The results (Table I) prove that no interaction had occurred in the range −94 to 25°. An infrared spectrum of the gas phase in equilibrium with the liquid at 25° showed absorption bands of SiF_4 superimposed on those of 1,4-dioxane, while a spectrum of the liquid phase contained absorption bands only of 1,4-dioxane, proving that no SiF_4 was dissolved.

Heats of Dissociation

Solid $SiF_4 \cdot 2$(ether) complexes were prepared at low temperatures as previously described and their temperatures were increased slowly until a pressure of about 0.5 mm was observed; thereafter pressure measurements were made at intervals of about 5 to 10°. To be certain that an equilibrium existed at each temperature, a sample of the gas above the solid complex was pumped off and a constant pressure was allowed to reestablish. True equilibrium at a given temperature existed if the pressure before and after the pumping off procedure were identical. Pressure–temperature measurements were made until the complex decomposed irreversibly, as evident by an abnormally large pressure increase and failure to observe identical pressures before and after the pumping off procedure. Equilibrium pressures, approached from above as well as from below a given temperature, were identical in the temperature ranges given in Table II.

The heats of dissociation summarized in Table II were calculated from the slopes of the linear log p_{mm} against T^{-1} plots using the integrated form of the Clausius–Clapeyron equation. Slopes were determined by the method of least squares and error limits are expressed in terms of standard deviations.

Discussion

Preparation of $SiF_4 \cdot 2$(ether) Complexes

The results show that SiF_4 reacts with alicyclic ethers and $(CH_3)_2O$ to form white, solid 1:2 complexes which are stable at −78°. These complexes are not sufficiently stable to be obtained by simply bubbling SiF_4 through solutions of ethers at 25°, as had been attempted unsuccessfully by Muetterties (1), although he was able to prepare SiF_4–oxygen donor complexes such as $SiF_4 \cdot 2(CH_3)_2SO$, $SiF_4 \cdot 2(CH_3)_2NCHO$, and $SiF_4 \cdot x CH_3COCH_2COCH_3$ (where x is uncertain) using this technique. In the preparation

Can. J. Chem. Downloaded from www.nrcresearchpress.com by 210.87.254.40 on 09/05/12
For personal use only.

TABLE II

Heats of dissociation of $SiF_4 \cdot 2(ether)$ complexes

Complex	Temperature–pressure data (°C, mm)	Heat of dissociation ΔH_1^0 (kcal mole^{-1})
$SiF_4 \cdot 2(CH_2)_2O$	−93.2, 0.4; −82.3, 2.1; −77.2, 4.5; −71.8, 10.0; −68.3, 14.3	10.7±0.2
$SiF_4 \cdot 2(CH_2)_3O$	−23.0, 1.2; −17.7, 2.0; −16.2, 2.5; −12.0, 3.5; −11.0, 4.3; −7.3, 5.6; −6.8, 6.2; −3.5, 8.4; 0.3, 12.4; 2.0, 14.0; 5.2, 18.3; 8.1, 23.9; 11.7, 32.7; 13.6, 38.7	13.6±0.1
$SiF_4 \cdot 2(CH_2)_4O$	−69.0, 0.20; −58.9, 0.84; −51.7, 1.90; −45.0, 4.28; −37.7, 9.16; −30.8, 20.2	11.7±0.1
$SiF_4 \cdot 2(CH_2)_5O$	−83.0, 0.44; −76.1, 1.13; −68.7, 3.69; −63.0, 7.40; −58.9, 11.6; −54.3, 17.4	10.9±0.3
$SiF_4 \cdot 2(CH_3)_2O$	−94.0, 0.77; −86.3, 2.25; −85.9, 2.30; −80.9, 4.90; −77.2, 6.81; −76.3, 8.00; −71.7, 13.5; −64.7, 31.8; −60.6, 41.9; −56.6, 57.9	9.0±0.1

of $SiF_4 \cdot 2(CH_2)_2O$ and $SiF_4 \cdot 2(CH_2)_3O$ it was necessary to warm a SiF_4–ether mixture, containing a small excess of SiF_4, *slowly* from −195° (thus providing a good "heat sink" for the heat of reaction) to a temperature at which reaction would just occur and then prevent any further increase in temperature in order to minimize polymerization of the ethers. The excess of SiF_4 was removed at a temperature at which the dissociation pressure of the complex is negligible. For the preparation of the other $SiF_4 \cdot 2(ether)$ complexes, the ether molecules of which do not readily polymerize, it was best to cool the SiF_4–ether mixture containing a small excess of SiF_4 *slowly* from 25° to a temperature sufficiently low to stabilize the complex, and then remove the excess of SiF_4 by distillation at this temperature. It is not possible to obtain pure $SiF_4 \cdot 2(ether)$ complexes by a direct synthesis using an excess of ether initially, because the complexes dissociate at temperatures below which the excess ether can be distilled.

General Properties of $SiF_4 \cdot 2(ether)$ Complexes

All of the $SiF_4 \cdot 2(ether)$ complexes prepared are white solids stable at low temperatures. They did not appear to have a stable liquid state and were completely dissociated in the gas phase at 25°. Only $SiF_4 \cdot 2(CH_2)_3O$ could be sublimed into colorless crystals which were stable only below 13.6°. By contrast, ether complexes of GeF_4 (10) and BF_3 (11) are more stable than those of SiF_4. Thus, $GeF_4 \cdot 2(ether)$ complexes, in which the ether is $(CH_3)_2O$, $(CH_2)_4O$, and $(CH_2)_5O$, are stable solids at 25°, although $GeF_4 \cdot 2(CH_2)_2O$ decomposes above −78° (10). Complexes of BF_3 with $(CH_3)_2O$, $(CH_2)_4O$, and $(CH_2)_5O$ are stable liquids at 25°, and $BF_3 \cdot (CH_3)_2O$ and $BF_3 \cdot (CH_2)_4O$ boil without decomposition (11). Although SiF_4 did not react with 1,4-dioxane even at −94°, GeF_4 forms a 1:1 complex which sublimes at 125°, and BF_3 forms 1:1 and 2:1 complexes both of which are stable at 25°, the former being a white solid and the latter a colorless liquid.

Complexes of $(CH_2)_2O$ with SiF_4, GeF_4, and BF_3 are all similar in their thermal decomposition into 1,4-dioxane and a nonvolatile polymer. These complexes also react with an excess of $(CH_2)_2O$ to produce 1,4-dioxane and a polymer, indicating that they catalyze the dimerization and polymerization of $(CH_2)_2O$. The mechanism of these reactions is probably similar to that proposed for the BCl_3–$(CH_2)_2O$ system (12). In the thermal decomposition of $SiF_4 \cdot 2(CH_2)_3O$, SiF_4 was liberated quantitatively and a nonvolatile, colorless polymer remained. However, $SiF_4 \cdot 2(CH_2)_4O$ and $SiF_4 \cdot 2(CH_2)_5O$ dissociated into their component parts without polymerization of the ethers.

The ease of sublimation and dissociation of the $SiF_4 \cdot 2(ether)$ complexes, as well as the presence of an Si—F octahedral stretching vibration band in the infrared spectrum of $SiF_4 \cdot 2(CH_2)_3O$ at −195°, strongly suggests that the complexes are octahedral molecular adducts in the solid state, although the possibility that they are ionic cannot be ruled out. The spectrum of $SiF_4 \cdot 2(CH_2)_3O$ was not sufficiently resolved to indicate whether ether molecules were in either *cis* or

Can. J. Chem. Downloaded from www.nrcresearchpress.com by 210.87.254.40 on 09/05/12
For personal use only.

TABLE III

Comparisons of heats of dissociation

Dissociation process	Heat of dissociation (kcal mole^{-1})	Ref.
$SiF_4{\cdot}2py_{(s)} = SiF_{4(g)} + 2py_{(l)}$	33.1	16
$SiF_4{\cdot}2iq_{(s)} = SiF_{4(g)} + 2iq_{(hexane\ soln)}$	31.9	16
$SiF_4{\cdot}2NH_{3(s)} = SiF_{4(g)} + 2NH_{3(g)}$	54.6	17
$BF_3{\cdot}(CH_3)_2O_{(s)} = BF_{3(g)} + (CH_3)_2O_{(g)}$	13.3	18
$BF_3{\cdot}(CH_2)_4O_{(s)} = BF_{3(g)} + (CH_2)_4O_{(g)}$	13.4	18

trans octahedral positions. This uncertainty can be resolved only by a detailed X-ray crystallographic study.

Heats of Dissociation of $SiF_4{\cdot}2$(ether) Complexes

In the determination of the measured heats of dissociation, ΔH_1^0, reported in Table II, it was assumed that the complexes were completely dissociated in the gas phase. In the temperature range that dissociation pressures were measured, the dynamic equilibrium was considered to be $SiF_4{\cdot}2(ether)_{(s)} \overset{K_p}{\rightleftarrows} SiF_{4(g)} + 2(ether)_{(l)}$, except for $SiF_4{\cdot}2(CH_2)_5O$ where the $(CH_2)_5O$ was a solid in the temperature range over which pressures were measured. To calculate the equilibrium constant, K_p, it was necessary to assume that the complex was involatile and that the vapor pressure of the liquid ether was negligible by comparison with the pressure of SiF_4. This assumption is justified because even $(CH_3)_2O$, the most volatile ether used, has a vapor pressure about 100 times less than that of SiF_4 in the range -94 to $-56°$. Similar assumptions were made in the calculation of thermodynamic data of BF_3–ether complexes (11). Thus, the dissociation pressure of the complex is due entirely to SiF_4, which gives simply $K_p = p$(atm), and the Clapeyron equation, $\Delta H^0 = -(2.303R\ \Delta\log p)/\Delta T^{-1}$, was used to calculate ΔH^0, since the plot of log p against T^{-1} is equivalent to log K_p against T^{-1}.

The measured heats of dissociation, ΔH_1^0, are related to the true gas phase heats of dissociation, ΔH_2^0, by the following cycle:

$$\begin{array}{ccc} SiF_4{\cdot}2(ether)_{(s)} & \overset{\Delta H_1^0}{\rightleftarrows} & SiF_{4(g)} + 2(ether)_{(l\ or\ s)} \\ \Updownarrow \Delta H_4^0 & & \Updownarrow \Delta H_3^0 \\ SiF_4{\cdot}2(ether)_{(g)} & \overset{\Delta H_2^0}{\rightleftarrows} & SiF_{4(g)} + 2(ether)_{(g)}, \end{array}$$

in which ΔH_4^0 is the heat of sublimation of the complex and ΔH_3^0 is the heat of sublimation or vaporization of the ether. Therefore, $\Delta H_2^0 = \Delta H_1^0 - \Delta H_4^0 + \Delta H_3^0$, so that the measured heats of dissociation must be corrected in order to obtain the true heats of dissociation. Even though values of ΔH_4^0 are not known, they are probably similar in as closely related a series of compounds as $SiF_4{\cdot}2$(alicyclic ether). The heats of vaporization, ΔH_3^0, are reported (13) only for $(CH_2)_2O$ and $(CH_3)_2O$; they are 6.10 and 5.14 kcal mole^{-1} respectively. In the absence of complete data for ΔH_3^0 and ΔH_4^0, it is not justifiable to attach much significance to the absolute values of the measured heats of dissociation. Nevertheless, we believe the trend $(CH_2)_3O > (CH_2)_4O > (CH_2)_5O \geqslant (CH_2)_2O > (CH_3)_2O$ is real and reflects the relative order of basicities towards SiF_4. Exactly the same order has been inferred by others who used a variety of experimental methods (14, and references cited therein). Previous attempts to rationalize this order are examined critically in a separate article in which a new explanation based on electronegativity theory is proposed (15).

Complexes of SiF_4 with nitrogen electron-pair donors have much higher, and BF_3·ether complexes only slightly lower, heats of dissociation than $SiF_4{\cdot}2$(ether) complexes, as evident from the data in Table III. Thus, Si—O coordinate bond energies appear to be less than half those of Si—N and B—O coordinate bonds.

Acknowledgment

We are grateful to the Defence Research Board of Canada for financial assistance (grant number 9530-20, project D46-95-30-20).

1. E. L. Muetterties. J. Am. Chem. Soc. **82**, 1082 (1960).
2. V. K. Isslieb and H. Reinhold. Z. Anorg. Allgem. Chem. **314**, 113 (1962).

Can. J. Chem. Downloaded from www.nrcresearchpress.com by 210.87.254.40 on 09/05/12
For personal use only.

3. J. A. GIERUT, F. J. SOWA, and J. A. NIEWLAND. J. Am. Chem. Soc. **58**, 786 (1936).
4. A. V. TOPCHIEV and N. F. BOGOMOLOVA. Dokl. Akad. Nauk SSSR, **88**, 487 (1953).
5. J. P. GUERTIN and M. ONYSZCHUK. Can. J. Chem. **41**, 1477 (1963).
6. M. SCHMEISSER and S. ELISCHER. Z. Naturforsch. **7b**, 583 (1952).
7. R. T. SANDERSON. Vacuum manipulation of volatile compounds. John Wiley and Sons, Inc., New York. 1958.
8. J. FURNKAWA, T. SAIGUSA, and N. MISE. Makromol. Chem. **38**, 244 (1960).
9. W. R. HESLOP, J. A. A. KETELAAR, and A. BUCHLER. Spectrochim. Acta, **16**, 513 (1960).
10. R. C. AGGARWAL, J. P. GUERTIN, and M. ONYSZCHUK. *In* Proceedings of the VIIIth international conference on co-ordination chemistry. *Edited by* V. Gutmann. Springer-Verlag, Vienna. 1964. p. 198.
11. N. N. GREENWOOD and R. L. MARTIN. Quart. Rev. London, **8**, 1 (1954).
12. J. D. EDWARDS, W. GERRARD, and M. F. LAPPERT. J. Chem. Soc. 348 (1957).
13. Selected values of chemical thermodynamic properties. Circular 500. National Bureau of Standards. U.S. Government Printing Office, Washington, D.C. 1952. p. 599.
14. SISTER M. BRANDON, O.P., M. TAMRES, S. SEARLES, JR. J. Am. Chem. Soc. **82**, 2129, 2134 (1960).
15. J. P. GUERTIN, M. ONYSZCHUK, and M. A. WHITEHEAD. In preparation.
16. J. M. MILLER and M. ONYSZCHUK. J. Chem. Soc. A, 1132 (1967).
17. D. B. MILLER and H. H. SISLER. J. Am. Chem. Soc. **77**, 4998 (1955); **78**, 6412 (1956).
18. H. C. BROWN and R. M. ADAMS. J. Am. Chem. Soc. **64**, 2557 (1942).

Can. J. Chem. Downloaded from www.nrcresearchpress.com by 210.87.254.40 on 09/05/12
For personal use only.

Isomerization of dideuteroethylene photosensitized by $Cd(^3P_1)$

SHIGERU TSUNASHIMA, SHUN-ICHI HIROKAMI, AND SHIN SATO
Department of Applied Physics, Tokyo Institute of Technology, Ookayama, Meguro-ku, Tokyo, Japan
Received August 23, 1967

An investigation of the $Cd(^3P_1)$-photosensitized isomerization of dideuteroethylene has been made over the temperature range 275–350 °C. Principal primary products in the reaction of *trans*-1,2-dideuteroethylene are *cis*-1,2- and *asym*-1,1-dideuteroethylenes. Minor products are ethane, acetylene, and *n*-butane, in amounts which are about three orders of magnitude smaller than those of the isomers.

Decomposition of ethylene into hydrogen and acetylene, which is the principal mode of reaction in the case of $Hg(^3P_1)$, was scarcely observed for the $Cd(^3P_1)$-photosensitized reaction.

The two-excited-states mechanism previously proposed (1, 2) has been applied to explain hydrogen atom scrambling and *cis–trans* isomerization. It has been found necessary to modify the above mechanism to explain the results.

Canadian Journal of Chemistry, 46, 995 (1968)

Can. J. Chem. Downloaded from www.nrcresearchpress.com by 210.87.254.5 on 09/05/12
For personal use only.

Introduction

In the period 1940–1942, LeRoy and Steacie investigated $Cd(^3P_1)$-photosensitized decomposition of ethylene (3–5) and found that the ethylene molecule underwent very little decomposition, but strongly quenched excited cadmium atoms, while in the $Hg(^3P_1)$-photosensitized reaction, ethylene decomposed into hydrogen and acetylene (6).

Recently, the reactions of ethylene and partially deuterated ethylene photosensitized by mercury (7–9), benzene (1), and benzene derivatives (2) have been studied in detail. Hydrogen atom scrambling and *cis–trans* isomerization were explained in terms of the two-excited-states mechanism. Differences in the rate constants for the isomerization reaction of ethylene excited by various photosensitizers were ascribed to differences in the amounts of energy transferred from the photosensitizers. A triplet–triplet energy transfer has been assumed in the case of the photosensitizations by benzene and benzene derivatives. The energy of the $Cd(^3P_1)$ atom is 87.7 kcal, which is nearly equal to the energy of benzene triplet (84.4 kcal). Photosensitization by $Cd(^3P_1)$ may then give rise to reactions similar to those sensitized by benzene. With this prospect in mind, a study of the $Cd(^3P_1)$-photosensitized reactions was undertaken over the temperature range 275–350 °C.

Experimental

Materials

Trans- and *cis*-dideuteroethylenes were synthesized by the method previously reported (10) and *asym*-dideuteroethylene was kindly supplied by Professor Tanaka (Tokyo Institute of Technology). *Cis*-2-butene was purchased from Takachiho-Shoji Co. Gas-chromatographic analysis showed no impurity except for 0.13% *trans*-2-butene. Six 9's cadmium metal was purchased from Soekawa Chemical Co. Ltd.

Apparatus

Two cadmium resonance lamps with argon (2 mm) as a buffer gas were used. The two lamps had different light intensities (A and B). They were heated in a furnace which was kept at 275 °C within ±2 °C by an electric controller. The 2288 Å resonance line was entirely filtered out by UV-29 Toshiba Denki glass filters. The reaction vessel was a 5 cm diameter cylindrical quartz tube (166 ml). The vessel was heated in another furnace, the temperature of which was kept constant to within ±1 °C. The intensity of the cadmium resonance line at 3261 Å was estimated by using the $Cd(^3P_1)$-photosensitized *cis–trans* isomerization of *cis*-2-butene as an actinometer (11). When a value of 0.5 was used for the quantum yield of the isomerization of *cis*-2-butene, the intensity was estimated to be 0.72 μeinstein/min for the lamp A, and 0.32 μeinstein/min for the lamp B at 275 °C.

Analysis

Reaction products were analyzed with a Perkin–Elmer 125 double beam grating infrared spectrophotometer (2) and by gas chromatography using a silica gel column and a flame ionization detector.

Results

Figure 1 shows the time dependence of the mole fractions of *trans*-, *cis*-, and *asym*-dideuteroethylenes at 275 °C, where *trans*-dideuteroethylene (3 mm) was used as a starting compound.

To check for possible interference from mercury-photosensitized reactions, 3 mm of *trans*-ethylene were irradiated by the lamp B for 3 h at room temperature without cadmium vapor in the cell. No detectable *cis–trans* isomerization or decomposition was observed.

Table I summarizes the results of the time dependence. A 1:1:1 ratio of *trans*-:*cis*-:*asym*-dideuteroethylene was obtained after prolonged

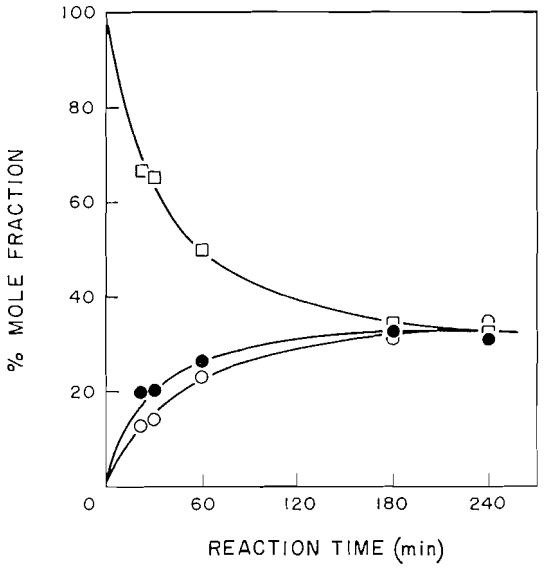

FIG. 1. Time dependence of the $Cd(^3P_1)$-photosensitized isomerization of *trans*-dideuteroethylene at 275 °C: (○) *asym*-dideuteroethylene; (●) *cis*-dideuteroethylene; (□) *trans*-dideuteroethylene.

TABLE I

Time dependence of $Cd(^3P_1)$-photosensitized isomerization of dideuteroethylene at 275 °C

Irradiation time (min)	$C_2H_2D_2$ *Cis* (%)	*Asym* (%)	*Trans* (%)	Lamp
	Trans-$C_2H_2D_2$ (3 mm)			
20	20.2	13.3	66.5	A
30	20.2	14.4	65.4	A
60	26.7	23.3	50.0	A
180	32.3	33.4	34.3	A
241	32.2	35.0	32.8	A
	Asym-$C_2H_2D_2$ (3 mm)			
60	6.1	87.9	6.0	B
300	25.7	49.3	25.0	B
660	32.4	34.1	33.5	B
	Cis-$C_2H_2D_2$ (3 mm)			
660	32.9	32.9	34.2	B

irradiations (6–11 h) at 275 °C of any of the three isomers. These results coincide with those obtained by benzene and benzotrifluoride photosensitizations (1, 2). *Asym*-dideuteroethylene yielded equal amounts of *trans*- and *cis*-dideuteroethylene in each run.

Minor products of $Cd(^3P_1)$ photosensitization at 275 °C were ethane, acetylene, and *n*-butane, which were detected by gas chromatography.

TABLE II

Pressure dependence of $Cd(^3P_1)$-photosensitized isomerization of *trans*-dideuteroethylene at 275, 300, 325, and 350 °C

Ethylene pressure (mm)	$C_2H_2D_2$ *Cis* (%)	*Asym* (%)	*Trans* (%)	Irradiation time (min)
	275 °C Lamp A			
2.0	17.5	12.1	70.4	11
3.0	20.2	13.3	66.5	20
3.95	19.6	13.8	66.6	25
4.95	24.0	20.0	56.0	50
5.0	14.4	8.1	77.5	20
7.05	16.7	9.1	74.2	30
7.65	17.4	9.5	73.1	30
9.6	13.4	4.8	81.8	25
9.9	13.3	5.5	81.2	40
15.2	17.6	7.7	74.7	60
20.0	14.6	5.7	79.7	60
25.2	13.8	4.7	81.5	90
30.0	17.2	6.4	76.4	104
30.1	13.4	4.0	82.6	120
39.9	19.1	5.0	75.9	160
	300 °C Lamp B			
2.9	11.7	8.0	80.3	15
5.1	14.1	7.8	78.1	25
11.1	13.9	6.1	80.0	50
19.6	17.4	7.5	75.1	100
28.4	18.0	6.2	75.8	150
43.6	20.5	6.0	73.5	200
	325 °C Lamp B			
2.9	18.2	12.7	69.1	10
3.3	11.4	7.6	80.9	10
5.15	13.6	7.3	79.1	15
12.5	17.0	8.8	74.2	42
18.6	17.4	7.8	74.8	61
28.4	20.7	9.2	70.1	110
39.4	18.7	5.7	75.6	121
	350 °C Lamp B			
3.0	11.9	8.2	79.9	6
4.8	14.6	7.8	77.6	10
5.9	12.8	6.3	80.9	10
9.8	14.6	7.9	77.5	20
19.6	16.5	6.8	76.7	40
29.3	16.3	6.7	77.0	60
40.3	16.8	5.6	77.6	80

Quantum yields of ethane, acetylene, and *n*-butane were approximately 0.9×10^{-3}, 1.3×10^{-3}, and 1.5×10^{-3}, respectively. Small peaks of C_2H_2 and C_2HD were detected with the infrared spectrometer. Even after prolonged irradiation (6–11 h), noncondensable gas at liquid nitrogen temperature could not be detected. The quantum yield of decomposition was extremely small compared with those of the formation of isomers. No isotopic ethylene, C_2H_3D, and C_2HD_3 could be detected in the infrared spectrum. Table II shows the pressure dependence of isomerization at each temperature.

Can. J. Chem. Downloaded from www.nrcresearchpress.com by 210.87.254.5 on 09/05/12
For personal use only.

Can. J. Chem. Downloaded from www.nrcresearchpress.com by 210.87.254.5 on 09/05/12
For personal use only.

Discussion

Since practically no decomposition has been observed in $Cd(^3P_1)$ photosensitization, the experimental results can be analyzed using the procedure proposed in the previous papers (1, 2).

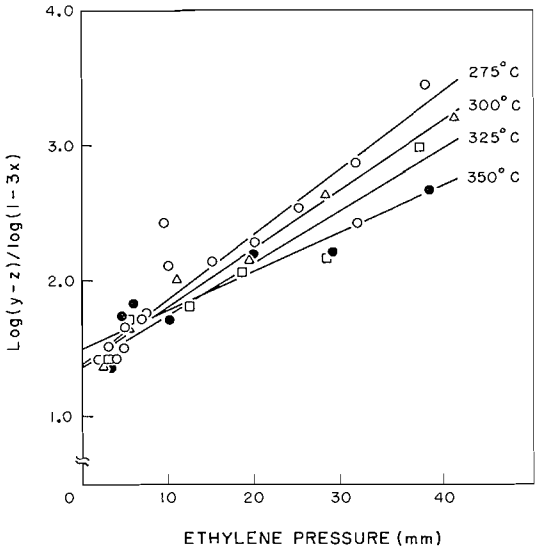

FIG. 2. Pressure dependence of the $Cd(^3P_1)$-photosensitized H-atom scrambling and *cis–trans* isomerization of *trans*-dideuteroethylene: (○) 275 °C; (△) 300 °C; (□) 325 °C; (●) 350 °C.

Figure 2 shows the plots of log $(y - z)$/log $(1 - 3x)$ as a function of the pressure of ethylene at each temperature, 275, 300, 325, and 350 °C, where x, y, and z stand for the fractions of *asym*-, *trans*-, and *cis*-isomers, respectively. At each temperature, an approximately linear relationship was obtained. The slopes and intercepts at each temperature were obtained by the method of least squares. Taking, as before, 4.95 Å for the collision diameter of ethylene, rate constants of the isomerization reaction of excited ethylene (k_2) have been calculated. Table III shows the slopes, intercepts, and k_2 at each temperature.

In the previous papers (1, 2), we have shown that the ratio of two values of k_2 can be calculated on the basis of the classical theory of Kassel. The ratio of k_2 obtained by $Cd(^3P_1)$ photosensitization to that for benzene photosensitization can be readily estimated by using the values 87.7 kcal for the $Cd(^3P_1)$ atom and 84.4 kcal for the lowest triplet ($^3B_{1u}$) benzene

TABLE III

Slopes (k_3/k_2), intercepts, and k_2

Temperature (°C)	$k_3/k_2 \times 10^2$ (mm^{-1})	Intercept	$k_2 \times 10^{-8}$ (s^{-1})
275	4.84±0.55	1.39±0.10	2.47±0.30
300	4.26±0.35	1.41±0.08	2.74±0.25
325	3.85±0.47	1.34±0.10	2.97±0.39
350	2.92±0.47	1.50±0.10	3.84±0.61

molecule. With these values, the calculated ρ $(= (k_2)_{Cd}/(k_2)_{benzene})$ is 2.25. Using a value of k_2 for benzene photosensitization of 8.2×10^7 s^{-1} (2), the value of k_2 for $Cd(^3P_1)$ photosensitization is calculated to be 1.85×10^8 s^{-1}, which is 1.4–2.1 times less than the values obtained in these experiments. The difference must be ascribed to the higher temperature at which $Cd(^3P_1)$ photosensitization has been carried out. The temperature dependence of k_2 may be accounted for in terms of a simple correction in the equation of unimolecular reaction. Corrected vibrational energy of excitation E* at T °K may be expressed as follows,

$$[1] \quad \epsilon(T\,^\circ\mathrm{K}) = \epsilon_{Cd} + \{H_v(T\,^\circ\mathrm{K}) - H_v(293\,^\circ\mathrm{K})\}$$

where $H_v(T\,^\circ\mathrm{K})$ and $H_v(293\,^\circ\mathrm{K})$ represent the heat capacity of vibration of *trans*-1,2-dideuteroethylene at the indicated temperatures. The quantity ϵ_{Cd} is the excess vibrational energy of the ethylene molecule photosensitized by $Cd(^3P_1)$ atom at room temperature (293 °K). The heat capacity of molecular vibration, $H_v(T\,^\circ\mathrm{K})$, is calculated by using the spectroscopic data of *trans*-1,2-dideuteroethylene.[1]

Using eq. [1] and the experimental value of k_2 at each temperature, the values of k_2 at 20 °C are estimated. The average value of k_2 estimated at 20 °C is $(2.0 \pm 0.2) \times 10^8$ s^{-1}, which is in satisfactory agreement with 1.85×10^8 s^{-1} estimated above. However, the real temperature dependence of k_2 may be much more complex.

All intercepts shown in Table III are larger than unity. If the two-excited-states mechanism is strictly applicable, the intercepts should

[1]To calculate the heat capacity of vibration, the following frequency assignments (cm^{-1}) were used; 3065, 3035, 2276, 2271, 1567; 1300, 1282, 1001, 988, 864, 727, 660 (12). Obtained values for H_v(kcal) (at T °K) are as follows: 0.23(293), 1.88(548), 2.12(573), 2.37(598), and 2.63(623).

always be equal to unity. The discrepancy ranges over 0.3 to 0.5, which seems to be greater than the experimental error. A possible explanation for this is that the excited ethylene molecule initially formed may be stabilized without collisional deactivation through a different excited state, possibly a highly vibrationally excited ground state, which undergoes only *cis–trans* isomerization.

We propose the process [2′], which competes with the formation of E**.

[2] $E^* \longrightarrow E^{**}$

[2′] $E^* \searrow E^{\mp}$

$E^{\mp} \rightarrow 1/2$ *trans* $+ 1/2$ *cis*,

where $E^{\mp}$ represents another state which stabilizes into ethylene without collision. Then, eq. [6] in the previous paper (2) is modified into the following form.

$$[3] \quad \log (y - z)/\log (1 - 3x) = 1 + k_2'/k_2 + k_3[M]/k_2$$

The intercept of eq. [3] becomes larger than unity.

LeRoy and Steacie measured the pressure decrease (quantum yield = 0.02) in the Cd-photosensitized decomposition of ethylene and observed small amounts of acetylene as a product (3, 5). They proposed the following mechanism as a primary process.

$$[4] \quad C_2H_4 + Cd^* \rightarrow C_2H_3 + H + Cd$$

We have observed small amounts of ethane, acetylene, and *n*-butane after prolonged irradiation. These products may be explained by the mechanism [4].

The decomposition of ethylene into hydrogen and acetylene was not observed in benzene and Cd photosensitizations. The rate constants of decomposition of excited ethylene can be calculated by using the Kassel equation, which was first applied by Hampson and McNesby (13) to the decomposition of excited ethylene in a number of related systems including the $Hg(^3P_1)$-photosensitized reaction. In a similar manner, we calculated the rates of decomposition of ethylene excited by the $Cd(^3P_1)$ atom and the triplet state of benzene and found that the rates were at least one order of magnitude smaller than that of Hg photosensitization. This explains why the decomposition of ethylene into acetylene and hydrogen is not observed in both Cd and benzene photosensitizations.

Acknowledgments

The authors are indebted to Dr. S. Maeda for the infrared analysis. They also wish to express their thanks to Dr. K. F. Preston (National Research Council of Canada) for assistance in correcting the manuscript.

1. T. Terao, S. Hirokami, S. Sato, and R. J. Cvetanović. Can. J. Chem. **44**, 2173 (1966).
2. S. Hirokami and S. Sato. Can. J. Chem. **45**, 3181 (1967).
3. E. W. R. Steacie and R. Potvin. Can. J. Res. **B18**, 47 (1940).
4. E. W. R. Steacie. Ann. N.Y. Acad. Sci. **41**, 187 (1941).
5. D. J. LeRoy and E. W. R. Steacie. J. Chem. Phys. **10**, 683 (1942).
6. R. J. Cvetanović. *In* Progress in reaction kinetics. Vol. 2. *Edited by* G. Porter. Pergamon, London. 1965. p. 40.
7. A. B. Callear and R. J. Cvetanović. J. Chem. Phys. **24**, 873 (1956).
8. D. W. Setser, D. W. Placzek, R. J. Cvetanović, and B. S. Rabinovitch. Can. J. Chem. **40**, 2179 (1962).
9. D. W. Setser, B. S. Rabinovitch, and D. W. Placzek. J. Am. Chem. Soc. **85**, 862 (1963).
10. B. S. Rabinovitch and F. S. Looney. J. Am. Chem. Soc. **75**, 2652 (1953).
11. S. Tsunashima and S. Sato. To be published.
12. B. L. Crawford, Jr., J. E. Lancaster, and R. G. Inskeep. J. Chem. Phys. **21**, 678 (1953).
13. R. F. Hampson, Jr. and J. R. McNesby. J. Chem. Phys. **43**, 3592 (1965).

Can. J. Chem. Downloaded from www.nrcresearchpress.com by 210.87.254.5 on 09/05/12
For personal use only.

Reactions of thiyl radicals. III. Photochemical equilibrium in the photolysis of liquid disulfide mixtures[1]

K. SAYAMOL AND A. R. KNIGHT

Department of Chemistry and Chemical Engineering, University of Saskatchewan, Saskatoon, Saskatchewan

Received October 30, 1967

The photolysis of mixtures of liquid methyl disulfide and ethyl disulfide at room temperature at wavelengths greater than 2300 Å has been investigated. The sole detectable product is methyl ethyl disulfide which reaches a photostationary state concentration after relatively short irradiation periods. For various initial mixtures, the concentration of the three disulfides in the photostationary state can be correlated in terms of an equilibrium constant, $K = [RSSR']/[RSSR]^{1/2}[R'SSR']^{1/2}$, whose value is 2.05 ± 0.04. The quantum yield of unsymmetrical disulfide formation in the initial stages of the reaction is 330 for an absorbed intensity of 4.70×10^{-2} μeinstein/min when the incident radiation is confined to $\lambda = 2600 \pm 50$ Å. The exceptionally high efficiency of the overall process is ascribed to the chain-propagating step

$$R'S + RSSR \rightarrow R'SSR + RS$$

which likely proceeds through attack of the thiyl radical on the S—S disulfide linkage.

Canadian Journal of Chemistry, 46, 999 (1968)

Introduction

There have been several reports in the literature (1–3) that the liquid phase photolysis of mixtures of disulfides, or disulfides and mercaptans, gives rise to unsymmetrical disulfide formation, but in general no detailed kinetic investigations have been made. Haraldson *et al.* (4) studied the photolysis of alkyl disulfides in 1 *M* cyclohexane solution and found a value for an equilibrium constant, $K' = [RSSR']^2/[RSSR][R'SSR']$, of 5.0. It was noted, however, that the approach to photochemical equilibrium was quite slow and that equilibrium could not be attained with some systems. The reaction was found to be more efficient using non-photochemical methods.

In Part II of this series (5) it was shown that in the gas phase methyl disulfide photolyzes with S—S bond scission. The main fate of the CH_3S radicals produced at substrate pressures between 2 and 25 Torr is recombination to reform the substrate.

Preliminary investigations[2] carried out in this laboratory indicated that in the liquid phase there was virtually no detectable decomposition of pure methyl disulfide, indicating that if the same primary process obtained as in the gas phase, recombination is essentially the sole fate of CH_3S. The reported observation of mixed disulfide formation on co-photolysis of two disulfides is therefore likely due to the same kind of combination reaction involving two different RS radicals.

Experimental

All experiments were carried out at room temperature with samples which were thoroughly degassed by alternate freeze–pump cycles utilizing a simple high vacuum system. Except for the actinometric measurements, the reaction cell was a quartz tube, 10 mm o.d., that contained 8 ml of liquid. The portion of the tube above the liquid level was shielded to prevent any gas phase reaction. The light source was a Hanovia No. 608A-36 100 watt medium pressure mercury lamp mounted in an air-cooled housing with Vycor 7910 window to eliminate wavelengths less than 2300 Å. The lamp tube, $2\frac{3}{4}$ in. in length, was mounted with axis parallel to that of the reaction cell. Methyl disulfide and ethyl disulfide (Eastman) were carefully purified by fractional distillation before use.

At the end of the reaction the reaction mixture was analyzed by thermal conductivity or flame ionization gas chromatography using tricresyl phosphate columns. For each experiment at least two liquid aliquots were analyzed.

In the actinometric runs the reaction cell was a 23 mm square quartz tube containing 20 ml of sample. The cell was enclosed in a light-tight housing with a 1 in. square Baird-Atomic interference filter. The filter has a band pass centered at 2600 Å, with about 15% transmission at λ_{max}, and did not transmit other wavelengths absorbed by the substrates.

Potassium ferrioxalate in aqueous sulfuric acid solution was used as the actinometer (6), and the absorbed light intensity was determined to be 4.70×10^{-2} μeinstein/min.

---

[1]Presented in part to the 50th Chemical Institute of Canada Conference, Toronto, June 1967. From the thesis to be submitted by K. Sayamol in partial fulfilment of the requirements for the M.Sc. degree, University of Saskatchewan, Saskatoon. The research for this paper was supported by the Defence Research Board of Canada, grant number 1675-07.

[2]The authors express their appreciation to Mrs. D. D. Carlson who carried out these experiments.

Can. J. Chem. Downloaded from www.nrcresearchpress.com by 210.87.254.5 on 09/05/12
For personal use only.

Can. J. Chem. Downloaded from www.nrcresearchpress.com by 210.87.254.5 on 09/05/12
For personal use only.

The formation of methyl ethyl disulfide was confirmed via separation of the reaction mixture by fractional distillation at low pressures and mass spectrometric analysis of the "mixed disulfide" fraction.

Gas chromatographic (g.c.) analysis of the reaction mixture showed that no detectable quantities of mercaptans or other products are formed, even in runs as long as 20 h. For ethyl mercaptan, for example, the detection limits were such that this product could be present only to a maximum of 0.05% of the amount of mixed disulfide formed in a given run.

Birch *et al.* (2) found that distillation of disulfide mixtures must be carried out at relatively low temperatures and that the column must be shielded from light, if significant thermal or near ultraviolet photochemical reaction is to be avoided. In the present work it was found that the maximum mole percent of $CH_3S_2C_2H_5$, normal b.p. = 131–133 °C, which can be recovered by distillation "in the dark", but at atmospheric pressure, was 62.3%, indicating the importance of the thermal reaction. Thus the reaction mixture was distilled in the dark at a reduced pressure of 60 Torr where the boiling point of methyl ethyl disulfide is 59.5 °C.

There is also apparently a small amount of disproportionation in the injection block or column of the g.c. units, which amounted to 0.0044 mole % at 70 °C for an equimolar mixture of methyl and ethyl disulfides. This thermal blank is negligible compared with the extensive amount of photodecomposition in irradiations with the full lamp spectrum ($\lambda > 2300$ Å), but must be considered in the quantum yield determinations where the amount of decomposition is quite small because of the low light intensity.

Results

Preliminary investigations showed that in agreement with previous reports photolysis of mixtures of neat methyl disulfide and ethyl disulfide yields the unsymmetrical cross product. In addition, it was apparent that the rate of production of this compound is exceptionally large for a photochemical process. The rate decreases with increasing exposure time and becomes constant after some 60 to 80 min of irradiation. Further irradiation did not alter the proportion of the three disulfides present.

Figure 1 shows the variation in mole fraction of methyl ethyl disulfide for various starting $CH_3S_2CH_3$–$C_2H_5S_2C_2H_5$ mixtures, as a function of exposure time. In each case the percent unsymmetrical disulfide reaches a constant value and undergoes no further change for up to 20 h of irradiation. For any particular exposure time the same results are obtained regardless of whether the irradiation is continuous or interrupted for analysis at earlier stages in the reaction.

Evidence that the photochemical equilibrium

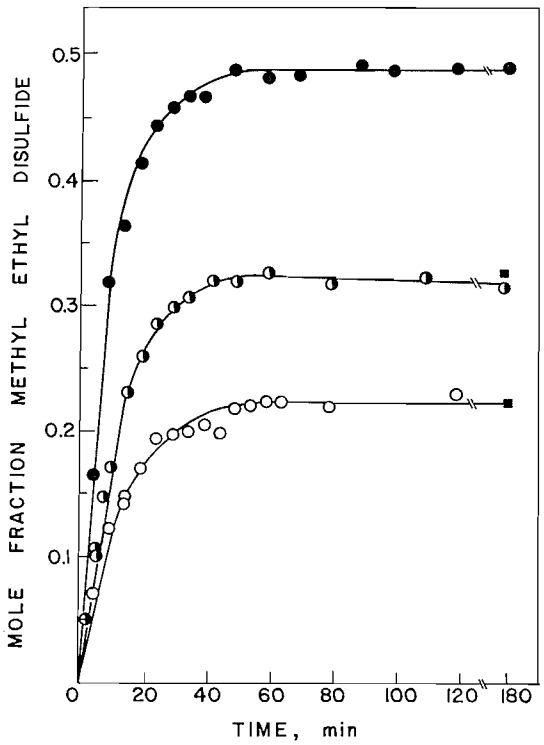

FIG. 1. Variation in mole fraction of methyl ethyl disulfide as a function of exposure time for mixtures of methyl disulfide and ethyl disulfide in which the mole fraction of $CH_3S_2CH_3$ was 0.206, ◑; 0.582, ●; and 0.875, ○. Filled squares indicate exposure times of 20 h.

state can be approached from the opposite direction is presented in Fig. 2, which shows that variation in mole fraction of methyl ethyl disulfide as a function of exposure time beginning with a mixture of all three disulfides, 91.0% $CH_3S_2C_2H_5$, 6.4% $C_2H_5S_2C_2H_5$, and 2.6% $CH_3S_2CH_3$. The mole fraction of the mixed disulfide decreases as the reaction proceeds and again attains a constant value. There is some indication that the mole fraction of $CH_3S_2C_2H_5$ may decline after long exposures, but the change is hardly outside the limits of experimental error.

Since it was apparent from these experiments that a definite equilibrium state is attained in the system, a series of reactions was carried out in which various initial mixtures of the two symmetrical disulfides were photolyzed for 120 min, well into the equilibrium region, and the mole fraction of the disulfides present determined. The data are summarized in Table I which gives the mole fraction of mixed disulfide at equilib-

Can. J. Chem. Downloaded from www.nrcresearchpress.com by 210.87.254.5 on 09/05/12
For personal use only.

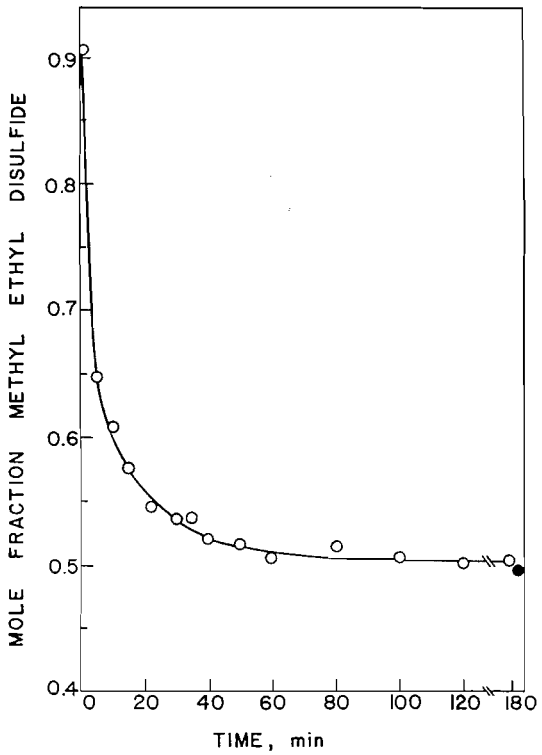

FIG. 2. Variation in mole fraction of methyl ethyl disulfide as a function of exposure time. The initial reaction mixture consisted of 91.0% $CH_3S_2C_2H_5$, 2.6% $CH_3S_2CH_3$, and 6.4% $C_2H_5S_2C_2H_5$. The filled circle indicates the mole fraction after 20 h of exposure.

rium and the value of an equilibrium constant, K, defined as

$$[1] \quad K = [CH_3S_2C_2H_5]/[CH_3S_2CH_3]^{1/2} \times [C_2H_5S_2C_2H_5]^{1/2}$$

and which conveniently correlates the data. The choice of this particular function will be dealt with below. The table also includes two experiments in which the starting mixture contained more than the equilibrium concentration of mixed disulfide. The value of K as defined by eq. [1] remained constant throughout at 2.05 ± 0.04.

The measurement of the quantum yield was carried out using a mixture of methyl disulfide and ethyl disulfide in which $X_{CH_3S_2CH_3} = 0.498$. Since under the conditions of these experiments the amount of reaction in a given time is relatively small because of the small transmittance of the interference filter, a simultaneous blank run was carried out with an identical mixture of disulfides which was kept at room temperature and analyzed for mixed disulfide at the same time as each of the photolysis runs. The amount of exchange in the blank runs remained essentially constant with time, indicating that the reaction likely occurs during g.c. analysis. The amount of mixed disulfide formed in the photolyzed samples was corrected for the contribution from the thermal reaction. A plot of μmoles of mixed disulfide formed vs. time of exposure is linear over the range investigated (mole fraction $CH_3S_2C_2H_5$ up to 0.0328), and the mean rate is 15.5 μmoles/min. With $I_a = 4.70 \times 10^{-2}$ μeinstein/min, this rate indicates a value of 330 for the quantum yield of mixed disulfide formation, $\Phi_{CH_3S_2C_2H_5}$.

TABLE I

Methyl ethyl disulfide formation in the photolysis of liquid disulfide mixtures[a]

$X^b_{CH_3S_2CH_3}$	$X^c_{CH_3S_2C_2H_5}$	K^d
0.122	0.206	2.09
0.206	0.327	2.02
0.258	0.371	2.02
0.316	0.437	2.08
0.410	0.488	2.09
0.582	0.499	2.07
0.735	0.401	2.09
0.808	0.331	2.09
0.848	0.268	2.09
0.875	0.220	2.08
0.934	0.125	2.04
[e]	0.497	2.04
[f]	0.499	2.01

[a]Exposure time = 120 min.
[b]Mole fraction of methyl disulfide present in initial mixture of methyl and ethyl disulfides.
[c]At equilibrium.
[d]Equilibrium constant as defined in text.
[e]Starting mixture = 63.4% $CH_3S_2C_2H_5$, 20.6% $C_2H_5S_2C_2H_5$, and 16.0% $CH_3S_2CH_3$.
[f]From equilibrium region in Fig. 2.

Discussion

Both methyl and ethyl disulfides have almost identical ultraviolet absorption spectra (7), $\lambda_{max} \approx 2500$ Å, and assuming equal efficiencies in the primary process, their rate of photochemical decomposition should be practically the same. By analogy with the gas phase photolysis (5), the primary process is most likely

$$[2] \quad RSSR + h\nu \rightarrow 2RS.$$

Since no detectable decomposition occurs on photolysis of either disulfide alone as pure liquid,

Can. J. Chem. Downloaded from www.nrcresearchpress.com by 210.87.254.5 on 09/05/12
For personal use only.

the only significant fate of RS radicals under these conditions must be the combination

$$[3] \qquad 2RS \rightarrow RSSR.$$

The exothermicity of this equation, equal to D(S—S), 67 kcal/mole for $R = CH_3$ and 69 kcal/mole for $R = C_2H_5$ (8), will result in an excited disulfide molecule but this should be very rapidly deactivated in the condensed phase.

When two different disulfides are co-photolyzed, reaction [3] will give rise to the cross product (in the present system, $CH_3S_2C_2H_5$). As the concentration of this product increases in the system it will begin to compete effectively for absorption of the incident radiation, and its photolysis will become an important source of both methyl and ethyl thiyl radicals.

Since these species can recombine to yield any of the three disulfides, all species will attain a photostationary state after some characteristic exposure time. In the absence of reactions leading to decomposition, the mechanism consists of the three reversible processes

$$[4] \qquad CH_3S_2CH_3 \overset{h\nu}{\rightleftarrows} 2CH_3S$$

$$[5] \qquad C_2H_5S_2C_2H_5 \overset{h\nu}{\rightleftarrows} 2C_2H_5S$$

$$[6] \qquad CH_3S_2C_2H_5 \overset{h\nu}{\rightleftarrows} CH_3S + C_2H_5S,$$

and the overall process can be represented as the equilibrium

$$[7] \qquad \tfrac{1}{2}CH_3S_2CH_3 + \tfrac{1}{2}C_2H_5S_2C_2H_5 \rightleftarrows CH_3S_2C_2H_5$$

to which the equilibrium constant as defined by eq. [1] is applicable. Since there should be the same photolysis rate for all three species, the system amounts simply to a random mixing of CH_3S and C_2H_5S radicals, and therefore a K value of 2 would be expected. Thus the observation that $K = 2.05 \pm 0.04$ indicates that the suggested mechanism is an adequate representation of the system. To compare this value with that obtained by Haraldson *et al.* (4), we note that $K' = K^2$, and thus the data obtained in this investigation yield $K' = 4.2 \pm 0.2$, as compared with 5.0 ± 0.2 (4).

A highly significant feature of this system, however, is the large value of the quantum yield, $\Phi = 330$, which requires that the process be characterized by a chain mechanism. Whatever process may be invoked must be consistent with the important restriction that no detectable decomposition occurs. Thus any process which requires conversion of thiyl radicals to products other than disulfides can be ruled out. The most likely process is an attack of a thiyl radical on the S—S disulfide linkage leading to radical exchange and reformation of a disulfide molecule. For the attack of CH_3S on ethyl disulfide, or C_2H_5S on methyl disulfide, the process can be written as

$$[8] \quad R'S + RSSR \rightleftarrows \left[\begin{array}{c} R\text{—}S \ldots S\text{—}R \\ \cdot\ \cdot\ \cdot \\ S \\ | \\ R \end{array}\right] \rightarrow RSSR' + RS.$$

The suggested form of the cyclic intermediate is speculative, but if the stoichiometry of the process is appropriate then the reactant species must pass through this or some similar trithiyl assembly.

A reaction of this type has been suggested previously (2) on the basis of qualitative evidence for extensive photodecomposition in disulfide systems. The value of the quantum yield obtained from the present work indicates that reaction [8], or some similar process which has the same net effect, must be by far the predominant source of mixed disulfide, and thus the contribution from simple recombination of CH_3S and C_2H_5S radicals is relatively minor. Assuming perfect efficiency in the primary process, each absorbed quantum will yield two thiyl radicals each of which can undergo reaction [8] to form mixed disulfide molecules. Thus the chain length will be $\Phi/2$ or 165. In addition, each thiyl radical can participate in the analogous process with its parent disulfide, but there is no direct method of determining the extent of this reaction. Under the conditions of quantum yield measurements, the concentration of methyl ethyl disulfide itself is negligible and since essentially equal amounts of methyl disulfide and ethyl disulfide are present each thiyl radical, RS, undergoes the same number of exchange reactions with R′SSR′, i.e. 165, as with its parent disulfide, RSSR. At the intensity used in the actinometric measurements, each thiyl radical therefore participates in the exchange reaction about 330 times before recombining with another RS species.

Reaction [8] also represents an alternative to the simple recombination of RS and R′S in reaction [2], and therefore this latter process is

in effect a chain-terminating step. The chain length will thus depend on the photostationary state concentration of thiyl radicals in the system, and since this will vary with incident intensity, the quantum yield will likely be intensity dependent.

Further studies are underway to investigate the effect of intensity and also to measure quantum yields for a variety of other disulfide mixtures. Since the exchange process might be expected to require the proximate approach of the thiyl radical to the S—S bond, this may impose steric restrictions on the efficiency of the reaction, which would be manifested by different quantum yield values for various disulfides at the same incident intensity.

1. M. KLEINMAN. U.S. Patent No. 2 474 849; Chem. Abstr. **44**, 653 (1950).
2. S. F. BIRCH, T. V. CULLUM, and R. A. DEAN. J. Inst. Petrol. **39**, 206 (1953).
3. J. E. EAGER and W. E. SAVIGE. Photochem. Photobiol. **2**, 25 (1963).
4. L. HARALDSON, G. I. OLANFER, S. SUNNER, and E. VARDE. Acta Chem. Scand. **14**, 1509 (1960).
5. P. M. RAO, J. A. COPECK, and A. R. KNIGHT. Can. J. Chem. **45**, 1369 (1967).
6. J. G. CALVERT and J. N. PITTS, JR. Photochemistry. Wiley, New York. 1966. p. 783.
7. J. G. CALVERT and J. N. PITTS, JR. Photochemistry. Wiley, New York. 1966. p. 490.
8. H. MACKLE. Tetrahedron, **19**, 1159 (1963).

Can. J. Chem. Downloaded from www.nrcresearchpress.com by 210.87.254.5 on 09/05/12
For personal use only.

Can. J. Chem. Downloaded from www.nrcresearchpress.com by 210.87.254.40 on 09/05/12
For personal use only.

Homogeneous rate of recombination of hydrogen atoms

F. S. LARKIN[1]
Department of Physical Chemistry, Lensfield Road, Cambridge, (Cambridgeshire), England

Received June 8, 1967

The rate of decay of hydrogen atoms has been measured in a conventional type of discharge-flow system at temperatures between 190–350 °K. The recombination fitted the equation

$$-\mathrm{d[H]/d}t = k_s[\mathrm{H}] + \sum_{\mathrm{M(M}\neq\mathrm{H)}} k_{2,\mathrm{M}}[\mathrm{H}]^2[\mathrm{M}],$$

where k_s is the first order surface rate constant. No three-body recombination for M = H was observed at the low levels of dissociation (2–5%) employed. When the flow gases contained traces of water vapor and (or) oxygen as impurities, the homogeneous rate constants ($k_{2,\mathrm{M}}$) had a small positive activation energy which was due to the influence of a surface reaction between hydrogen atoms and the impurities. In the absence of impurities, true homogeneous rate constants were obtained. A value of $k_{2,\mathrm{Ar}} = 4.6 \pm 0.5 \times 10^{15}$ cm^6 mole^{-2} s^{-1} was found at 291 °K. The temperature variation was approximately $T^{-1/2}$ over the range 190–350 °K.

Canadian Journal of Chemistry, 46, 1005 (1968)

Introduction

Most of the work on the rate of recombination of hydrogen atoms was carried out between 1929–1940. Since then, very little work has been done on this subject. The early investigators (1–9) reported a wide range of values for the homogeneous rate constants at room temperature, and opinions about the kinetics of recombination varied considerably. Experiments were conducted in two ways, viz. by continually pumping hydrogen along a cylindrical tube (dynamical flow method) or by following the course of the recombination in a closed reaction vessel (static method). Most investigators found difficulty in obtaining reproducible results because of rapid wall recombination. Attempts were made to poison surfaces, either by adding 2–3% water vapor to the system (10), or by coating the surface with a suitable material such as syrupy phosphoric acid (11). It is important to note that the influence of these poisons on the kinetics of recombination was not investigated. This is surprising since it was known that passing water vapor through an electric discharge generates active species such as O and OH (12, 13). This problem is discussed in the present work.

Recently, hydrogen atom recombination has been studied at elevated temperatures (1000–5000 °K) in shock tubes and hydrogen–air flames. In the former method, Patch (14) measured atomic profiles by ultraviolet (u.v.) spectroscopy and Rink (15) and Kistiakowsky and Gardiner (16) used an X-ray densitometer. None of these workers was able to measure the temperature coefficient of the rate constants, but arbitrarily assumed a T^{-1} dependence. Sutton (17), however, has reported a T^{-1} dependence for the third bodies H_2 and Ar, using an interferometer and drum camera technique. Comparison of the constants obtained in shock tubes with room temperature values indicates an overall temperature dependence of approximately T^{-1}, in agreement with Sutton's results. In the flame studies (18–20), the rate constants fit between the room temperature and shock tube results on the basis of a T^{-1} temperature dependence if the assumption is made that H_2O is less than an order of magnitude more efficient than H_2 as third body (see, for example, Dixon-Lewis, Sutton, and Williams (18)).

In the present work, the rate of recombination of hydrogen atoms has been reinvestigated in a flow system between 190–350 °K.

Experimental

Experimental rate constants were measured in a conventional type of flow system. Figure 1 shows the essential parts of the apparatus which consisted of a discharge tube, reaction tube, and isothermal calorimeter. Gases were pumped through the reaction tube and a large stopcock and trap by a single stage Edward's vacuum pump which had a maximum pumping capacity of 420 l/min. A 10 l bulb was placed between the trap and pump to smooth the flow pattern and pressure fluctuations. Hydrogen atoms were produced by passing molecular hydrogen, either pure or admixed with an inert gas carrier, through a 100 watt 17 mc/s radiofrequency discharge. Gases were admitted

[1]Present address: Department of Physical Chemistry, McGill University, Montreal, P.Q.

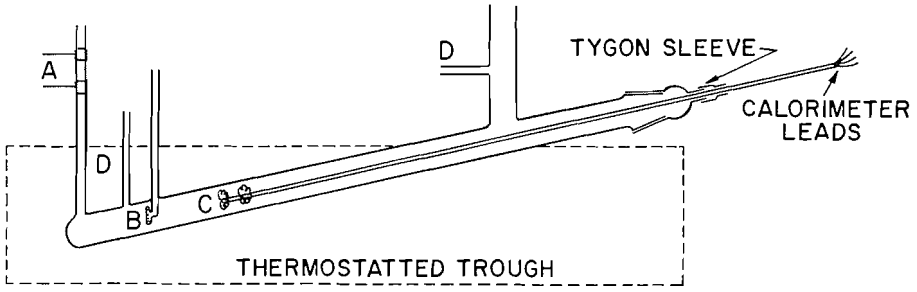

FIG. 1. Diagram of the atomic flow system.

from calibrated flowmeters into the discharge which was established in an 8 mm i.d. quartz tube between two aluminium foil electrodes (A). The products of the discharge flowed into a pyrex glass reaction tube, of 2.5 cm i.d. and 100 cm long, at the upstream end of which was a multiple hole inlet jet (B) for the introduction of reactants with rapid mixing. The whole reaction tube was inclined so that it could be immersed in a well-lagged copper trough. This contained water for experiments at or above room temperature; acetone was used below room temperature. Hydrogen atom concentrations were measured by means of a sliding isothermal calorimeter (C) which was inserted into the reaction tube at the downstream end. A Tygon sleeve provided the vacuum seal for the glass tube carrying the leads to the head of the calorimeter. Two calorimeters were used, each consisting of approximately 50 cm of 34 S.W.G. 13% Rh/Pt wire, wound into a spiral. Each spiral was connected to a separate Wheatstone bridge and they were mounted in tandem about 2–3 cm apart so that the downstream calorimeter could be used to determine the recombination efficiency of the first spiral, which was always greater than 80%. Experiments were generally conducted at total pressures between 2 and 7 mm Hg and at flow velocities between 250 and 1000 cm/s. The total pressure in the system was measured at each end (D) of the reaction tube by silicone oil manometers. Hydrogen atom concentrations of up to 5% could be obtained.

Cylinder gases were used throughout the flow experiments. Commercial grade "high purity" hydrogen, argon, "mineral" helium, and oxygen were obtained from the British Oxygen Company. Deuterium of more than 99.9% purity was obtained from the "20th Century Electronics Company". In early experiments, hydrogen was passed through a "Deoxo" unit at a pressure of 10 p.s.i. to remove oxygen. Argon and helium were dried at atmospheric pressure in glass-wool traps at −80 and −196 °C respectively. The principal impurity in the inert gases was oxygen (less than 0.01%) which was not removed at first. In later experiments, however, flow gases of much higher purity were required. Hydrogen was deoxygenated as before, but in addition passed through glass-wool and molecular sieve traps (B.D.H. grade 4A) at −196 °C and atmospheric pressure. Argon was dried at atmospheric pressure in a P_2O_5 trap and then passed directly into a silica gel trap at −80 °C to remove oxygen impurities. Further purification of the flow gases was effected by passing the hydrogen, or hydrogen-inert gas mixtures, through a "Deoxo" unit and liquid N_2 trap just before entering the discharge. This procedure reduced impurities in the flow stream to a level of approximately 1 p.p.m.

Results and Discussion

In initial experiments, molecular hydrogen was dissociated in unpoisoned reaction tubes, and in this case it was always necessary to have some water vapor in the hydrogen stream to obtain sufficient dissociation (3–5%). The water vapor content was reduced to a suitably low level (about 0.05%) by passing the hydrogen through a trap at −80 °C just before entering the discharge on the low pressure side of the flow-controlling needle valve. Atomic concentrations were measured over distances of up to 50 cm along the tube at intervals from 2–7 cm. Table I shows some typical values of [H] versus x, where x is the distance from the discharge. The rate of recombination should be given by the equation

$$[1] \quad -\mathrm{d[H]}/\mathrm{d}t = k_s[\mathrm{H}] + \sum_{\mathrm{M}(\mathrm{M}\neq\mathrm{H})} k_{2,\mathrm{M}}[\mathrm{H}]^2[\mathrm{M}] + k_{3,\mathrm{H}}[\mathrm{H}]^3,$$

since the recombination on the surface (k_s) is first order (21, 22) and the second two terms represent the recombination by the homogeneous reaction $\mathrm{H} + \mathrm{H} + \mathrm{M} = \mathrm{H}_2 + \mathrm{M}$, where M is the third body. Plots of $[\mathrm{H}]^{-1}$ versus x were smooth curves which were nearly linear when the atomic flow rates, flow-stream velocities, and total pressures were within the range 3–15 μmoles/s, 250–1000 cm/s, and 2–7 mm Hg respectively. Under these conditions, the effects of pressure drop, axial diffusion, and heat gradients were negligible (see Appendix). Experimental measurements were made only when the recombination was predominantly homogeneous. The condition $k_{2,\mathrm{M}}[\mathrm{H}][\mathrm{M}] > \gamma\bar{c}/2r$ (writing k_s

Can. J. Chem. Downloaded from www.nrcresearchpress.com by 210.87.254.40 on 09/05/12
For personal use only.

$= \gamma \bar{c}/2r$, where γ is a surface recombination constant, r is the tube radius, and $\bar{c}$ is the mean atomic velocity (23)) is easily satisfied within the above experimental conditions for $k_{2,M} \sim 10^{16}$ cm^6 mole^{-2} s^{-1} (9), $\gamma \sim 10^{-5}$ (21), and over the temperature range 190–350 °K. In some cases, after many runs, the reaction tube became abnormally catalytic so that surface reactions dominated the recombination, and plots of $[H]^{-1}$ versus x became sharp curves. When this happened, the tube was replaced by a new one which had been carefully washed with distilled water.

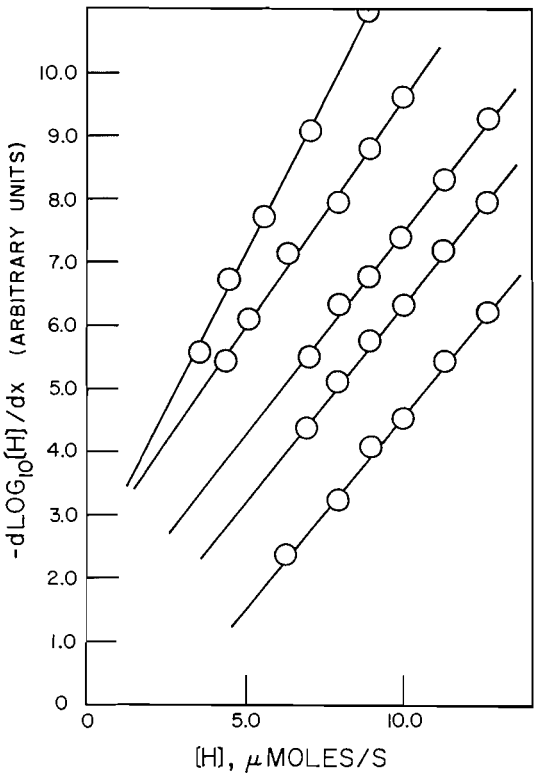

FIG. 2. Plots of $-\mathrm{d}\log_{10}[H]/\mathrm{d}x$ versus [H] for dissociated hydrogen. $-\mathrm{d}\log_{10}[H]/\mathrm{d}x$ (where x is the distance along the reaction tube and is proportional to t) is given in arbitrary units, each of which is equal to 2×10^{-3} cm^{-1}.

Values of $-\mathrm{d}(\ln[H])/\mathrm{d}t$ for various values of [H] were found by measuring gradients of a plot of ln [H] versus t (or x). Plots of $-\mathrm{d}(\ln[H])/\mathrm{d}t$ versus [H] were linear, showing that the last term in eq. [1] is negligible and therefore no significant third order recombination takes place at these low atomic concentrations (2–5% dissociation). Figure 2 shows some of these plots from which $k_{2,M}$ and γ can be readily determined, since eq. [1] becomes

$$[2] \quad -\mathrm{d}(\ln[H])/\mathrm{d}t = \gamma\bar{c}/2r + k_{2,M}[H][M].$$

TABLE I

A typical atomic flow profile for dissociated hydrogen. x is the distance along the reaction tube from the discharge. The data are taken from run 3 of Table II

H (μmoles/s)	x (cm)
13.20	6.2
11.90	9.1
10.93	11.2
9.93	13.3
9.00	15.7
8.01	18.7
7.26	21.6
6.55	24.6
5.88	28.8
4.95	33.5
4.18	39.9
3.08	47.0

During the course of this work, some 30 experimental runs were made at temperatures between 190–350 °K, and 10 reaction tubes were discarded. Table II shows the results of some typical runs. The values of k_{2,H_2} were reproducible at a given temperature and did not vary with pressure. They are thus truly independent of the first order surface reaction. Values of γ vary considerably from run to run, and these results are therefore similar to those of Smallwood (1) and Poole (24), who found that surfaces poisoned with water vapor did not have a reproducible catalytic activity.

In all further experiments, the reaction and discharge tubes were poisoned with "Dri-film" (a mixture of dimethyl-dichlorosilane and trimethyl-chlorosilane (25)). This poison forms a very hard inert surface coating of low vapor pressure and does not have the disadvantages of phosphoric acid coatings which may have reactions with metals or absorb water vapor, etc. In the poisoned system, argon (90%)/hydrogen mixtures could be dissociated to the extent of 3–5% even when the water vapor in the stream was well below 0.05%, or excluded altogether. Addition of water vapor increased the amount of dissociation, but by less than before. It was not necessary to renew reaction tubes during

Can. J. Chem. Downloaded from www.nrcresearchpress.com by 210.87.254.40 on 09/05/12
For personal use only.

TABLE II

Values of k_{2,H_2} and γ. The hydrogen contained traces of water vapor as impurity (about 0.05%)

Run No.	Temp. (°K)	Total flow rate (μmoles/s)	Pressure (mm Hg)	$k_{2,H_2} \times 10^{-16}$ (cm^6 mole^{-2} s^{-1})	$\gamma \times 10^5$
1	289	280	2.93	1.1±0.1	<0.2
2	287	882	5.94	1.3±0.1	<0.2
3	288	562	5.08	1.2±0.1	4.4±0.7
4	289	695	4.16	1.2±0.1	3.1±0.3
5	323	695	5.10	1.7±0.1	0.9±0.4
6	323	723	4.88	1.6±0.1	<0.2
7	273	680	4.75	1.4±0.3	1.1±0.3
8	273	685	4.25	1.3±0.1	<0.2
9	210	577	3.94	0.7±0.1	<0.2
10	215	537	5.60	0.6±0.1	3.5±0.1
11	213	725	6.24	0.7±0.2	6.3±0.2
12	190	756	3.25	0.6±0.1	4.3±0.4

TABLE III

Values of $k_{2,Ar}$ and γ. The argon/hydrogen mixtures contained traces of oxygen as impurity (less than 0.01%)

Run No.	Temp. (°K)	Total flow rate (μmoles/s)	Pressure (mm Hg)	$k_{2,Ar} \times 10^{-16}$ (cm^6 mole^{-2} s^{-1})	$\gamma \times 10^5$
1	290	533	4.57	0.81±0.08	4.3±0.5
2	280	406	4.50	0.81±0.08	0.1?
3	335	540	4.51	1.48±0.15	5.7±0.6
4	335	540	4.21	1.33±0.15	5.1±0.6
5	211	548	4.16	0.42±0.05	4.0±0.5
6	290	530	4.83	0.50±0.07	—
7	211	548	4.16	0.36±0.05	—

these experiments since the catalytic activity was always approximately constant. Table III shows the rate constants obtained for argon/hydrogen mixtures over the same temperature range as before. In runs 6 and 7, the hydrogen was replaced by deuterium. Unfortunately, measurements had to be made in haste because of a limited supply of deuterium, and rate constants could be only approximately estimated from plots of $[D]^{-1}$ versus t. The values of γ were much more reproducible and they agree well with those of Smith (21) and Wood and Wise (22) over this temperature range.

The corresponding results obtained with helium (90%)/hydrogen mixtures dried at liquid N_2 temperature are given in Table IV. Runs 7 and 8 were made with deuterium instead of hydrogen, and rate constants were estimated only approximately from $[D]^{-1}$ versus t plots, as before.

The average room temperature values of the homogeneous rate constants and their temperature variation for the three bodies are given in Table V. The activation energies were determined from simple $\ln k_{2,M}$ versus T^{-1} plots. The present value of k_{2,H_2} at room temperature is almost identical with the value obtained by Steiner (9) in a flow tube of the same diameter. The accompanying positive temperature coefficient raises some difficulties, however. If recombination is considered in terms of the "rigid sphere" model of kinetic theory (26), and H_2^* is the first collision "complex" formed (27), the effective collision diameter of the hydrogen atom would have to be more than 6 Å to account for the observed collision frequencies of $\sim 10^{17}$ cm^6 mole^{-2} s^{-1}. The spectroscopic data on H_2 (28) shows that H_2^* becomes thermally unstable (at room temperature) at atomic separations of more than 4 Å. It is doubtful whether another model for recombination could account for the high collision frequencies. The most reasonable explanation of the present results is that the homogeneous recombination was influenced by some

Can. J. Chem. Downloaded from www.nrcresearchpress.com by 210.87.254.40 on 09/05/12
For personal use only.

TABLE IV

Values of $k_{2,He}$ and γ. The helium/hydrogen mixtures contained traces of oxygen as impurity (less than 0.01%)

Run No.	Temp. (°K)	Total flow rate (μmoles/s)	Pressure (mm Hg)	$k_{2,He} \times 10^{-16}$ (cm^6 $mole^{-2}$ s^{-1})	$\gamma \times 10^5$
1	292	533	5.73	0.46±0.05	2.9±0.4
2	343	532	5.90	0.79±0.08	3.7±0.5
3	196	512	4.70	0.34±0.04	3.0±0.4
4	291	601	6.66	0.49±0.06	2.3±0.2
5	291	608	6.95	0.47±0.06	2.3±0.2
6	292	576	7.02	0.45±0.06	2.8±0.5
7	293	526	5.02	0.44±0.1	—
8	196	518	4.73	0.37±0.1	—

unknown surface reaction (not the first order reaction), since the observed positive activation energy is similar to reported binding energies (29) of physically adsorbed species at room temperatures. This was the conclusion reached by Amdur and Robinson (30), who obtained similar results. The explanation may also partly account for the large errors found in the temperature coefficients of $k_{2,M}$ since a plot of $\ln k_{2,M}$ versus T^{-1} would not necessarily be linear in this case. The question of surface reactions requires further discussion.

TABLE V

Values of $k_{2,M}$ for three third bodies at 293 °K. The activation energies and temperature coefficients are given for temperatures between 190–350 °K

M	$k_{2,M} \times 10^{-16}$* (cm^6 $mole^{-2}$ s^{-1})	Activation energy (kcal/mole)
H_2	1.20±0.1	1.1±0.3
Ar	0.81±0.08	1.2±0.3
He	0.47±0.07	0.9±0.3

*Alternatively the results can be expressed as:
$k_{2,H_2} = 10^{10\pm2} \times T^{2.3\pm0.5}$ cm^6 $mole^{-2}$ s^{-1}.
$k_{2,Ar} = 10^{10\pm2} \times T^{2.4\pm0.5}$ cm^6 $mole^{-2}$ s^{-1}.
$k_{2,He} = 10^{11\pm2} \times T^{1.8\pm0.5}$ cm^6 $mole^{-2}$ s^{-1}.

Surface Reactions

The possibility of additional surface reactions besides the normal first order wall recombination of hydrogen atoms, when hydrogen containing traces of water vapor or oxygen is discharged, was not considered by earlier workers in this field. However, the early experiments of Geib and Harteck (31, 32), and Rodebush and coworkers (33, 34), show that when oxygen is added to a stream of hydrogen atoms or water vapor is dissociated in the discharge, other complex surface reactions occur which produce mainly H_2 and O_2 at room temperature and H_2O_2 at liquid N_2 temperatures. Foner and Hudson (35) have reported OH radicals coming from the surface in the H–O_2 system at room temperature. There is some evidence (36, 37) for the formation of higher oxides of hydrogen (H_2O_3 or H_2O_4) at liquid N_2 temperatures. During experiments with the present flow system, a faint but distinct glow could be seen on the walls of the reaction tube when hydrogen was discharged. The glow disappeared when all water vapor and oxygen impurities were removed from the flow gases. If oxygen was added before or after the discharge, the glow was considerably enhanced, thus suggesting that oxygen promotes surface reactions with hydrogen atoms. The role of impurities in the gas stream was investigated by adding water vapor and oxygen before and after the discharge, and observing the effect on the hydrogen atom profiles in the reaction tube.

In these new experiments, atomic hydrogen concentrations were normally measured with the isothermal calorimeter, but when atomic oxygen concentrations also became significant, the concentrations were determined photometrically by measuring the intensities of the chemiluminescent HNO and NO_2 (air–afterglow) emissions. The emission intensities were recorded on a "Scalamp" galvanometer from the output side of an E.M.I. type 9558-B photomultiplier cell equipped with infrared (Wratten 88A) and green (Wratten 61) transmission filters. The NO concentrations were kept constant and the readings through the 61 and 88A filters were converted so that they were directly proportional to [O] and [H] respectively. This procedure has been described in detail by Clyne and Thrush (38).

Addition of water vapor (maximum amount was 10% of the total flow) through the inlet jet

Can. J. Chem. Downloaded from www.nrcresearchpress.com by 210.87.254.40 on 09/05/12
For personal use only.

TABLE VI

Values of $k_{2,Ar}$ after addition of O_2 or H_2O before the discharge

Temp. (°K)	Flow rate of *Ar/H_2 (μmoles/s)	Flow rate of O_2 (μmoles/s)	Flow rate of H_2O (μmoles/s)	Pressure (mm Hg)	$k_{2,Ar} \times 10^{-16}$ (cm^6 $mole^{-2}$ s^{-1})	O_2 in flow stream (μmoles/s)
290	406	0	14.1	4.50	0.82±0.08	1.06
290	406	0	9.6	4.50	0.81±0.08	0.81
290	406	0	0	4.50	0.80±0.08	0
290	409	4.6	0	4.58	0.80±0.08	2.64
290	409	1.7(5)	0	4.58	0.80±0.08	0.66

*Approximately 90% Ar in mixture.

had no effect on the hydrogen atom profiles. The only observable effect was to reduce the catalytic activity of the calorimeter spirals and reaction tube walls, by surface poisoning. Addition of oxygen through the inlet jet accelerated the hydrogen atom recombination by the first order reaction (39)

[3] $$H + O_2 + M = HO_2 + M.$$

By adding known amounts of O_2 (about 1%) to the products of a discharge through hydrogen in an argon carrier, and by keeping hydrogen atom concentrations below about 0.7%, the recombination became predominantly first order so that the rate constant for reaction [3] could be measured. The results of this work and a comparison with the chemiluminescent measurements of Clyne and Thrush have been published previously (40). When oxygen or water vapor was added before the discharge the recombination was also accelerated by a first order reaction, which was presumably reaction [3]. In addition to the reactions in the discharge which might convert water to molecular oxygen, OH radicals formed in the discharge yield oxygen by the rapid reactions (41)

[4] $$OH + OH = H_2O + O$$

and

[5] $$O + OH = H + O_2.$$

The second order homogeneous rate constants $k_{2,Ar}$ were unaffected, however. This is shown in Table VI where the values of $k_{2,Ar}$ were obtained by plotting $-d(\ln [H])/dt$ versus [H], as in previous experiments. Since the rate constant for reaction [3] was measured, it was possible to estimate the concentration of O_2 in the flow stream from the observed first order acceleration.

Table VII shows the galvanometer current readings from the photomultiplier cell when water vapor was added before and after the discharge. Nitric oxide was added through the inle jet and emission intensities were measured 30 cm further downstream. The readings through the 88A and 61 filter are proportional to [H] and [O] respectively. The galvanometer current readings are expressed in arbitrary units, each of which is equal to 0.048 μA. The concentrations of hydrogen atoms were between 1–2% of the total flow. The oxygen atom concentrations were very small since the emission intensity due to them is approximately 500 times stronger than the corresponding intensity for hydrogen atoms (42). All current measurements were made in a completely darkened room in which even the background infrared emission was negligible. The dark currents are thus a good measure of the intensity of the surface emission. It can be seen that the surface emission was considerably enhanced when water vapor was added before the discharge, but remained approximately unaltered when it was added downstream (decreases a little, probably due to surface poisoning). In general, there was an enhancement of the surface emission whenever oxygen was present in the flow stream, indicating a surface

TABLE VII

Emission intensities through the 88A and 61 Wratten filters for addition of water vapor before and after the discharge. The experimental conditions were: Argon flow 373 μmoles/s, H_2 flow 31 μmoles/s, total pressure (without H_2O) 4.04 mm Hg, temperature 293 °K. The asterisk denotes H_2O addition before the discharge

Wratten filter	H_2O (μmoles/s)	Dark current	Final current
88A	0.0	0.1	206
88A	9.2*	5.3	179
61	0.0	11.3	243
61	9.2*	21.0	108
88A	0.0	0.1	206
88A	14.1	0.1	199
61	0.0	11.3	243
61	14.1	9.1	139

Can. J. Chem. Downloaded from www.nrcresearchpress.com by 210.87.254.40 on 09/05/12
For personal use only.

Can. J. Chem. Downloaded from www.nrcresearchpress.com by 210.87.254.40 on 09/05/12
For personal use only.

TABLE VIII

Typical atomic flow profiles and values of $k_{2,Ar}$, k_{2,H_2}, and γ obtained in Ar/H_2 mixtures containing less than 1 p.p.m. H_2O and O_2 impurities

Run 1		Run 2	
[H] (μmoles/s)	x (cm)	[H] (μmoles/s)	x (cm)
7.88	21.9	7.58	13.2
6.82	28.0	6.49	18.9
5.97	33.5	5.69	24.4
5.17	40.1	4.81	32.5
4.32	49.1	3.90	42.3
3.60	58.1	2.96	57.7

Run No.	Temp. (°K)	Total flow rate (μmoles/s)	Pressure (mm Hg)	$k_{2,Ar} \times 10^{-15}$ (cm^6 $mole^{-2}$ s^{-1})	$\gamma \times 10^5$
1	291	488	5.16	4.5±0.8	3.4±0.8
2	292	524	5.38	4.7±0.8	4.0±0.8
3	213	529	4.54	5.7±0.8	2.7±0.8
4	349	516	5.20	4.1±0.8	5.3±0.8

Run No.	Temp. (°K)	Total flow rate (μmoles/s)	Pressure (mm Hg)	$k_{2,H_2} \times 10^{-15}$ (cm^6 $mole^{-2}$ s^{-1})	$\gamma \times 10^5$
5	291	708	6.35	6.8±1.5	2.6±0.8

reaction between hydrogen atoms and oxygen (or their reaction products).

Further recombination experiments were conducted with very pure flow gases in which water vapor and oxygen impurities were reduced to approximately 1 p.p.m. Under these conditions, dissociation became very difficult. Hydrogen could not be dissociated to any measurable extent (a problem that other workers have reported (43, 44)). Argon/hydrogen mixtures could be dissociated to the extent of 2–3% if the discharge was kept cool by air jets. The extent of dissociation and surface recombination became very dependent on the nature and temperature of the surface under these conditions. Plots of $-d(\ln [H])/dt$ versus [H] were good straight lines (see Fig. 3) and fitted eq. [2]. Table VIII shows typical atomic concentration profiles obtained under these new conditions, together with the values of $k_{2,Ar}$ and γ calculated from several runs. In runs 1–4, the hydrogen content of the mixture was between 4–6%. In run 5, the content was more than 90%, so that a value of k_{2,H_2} could be estimated. $k_{2,Ar}$ was taken as 4.6×10^{15} cm^6 $mole^{-2}$ s^{-1} for this calculation.

The rate constants ($k_{2,M}$) found here are significantly lower than those obtained in flow streams containing traces of water vapor or oxygen impurities. Moreover, $k_{2,Ar}$ has a temperature coefficient of approximately $T^{-1/2}$

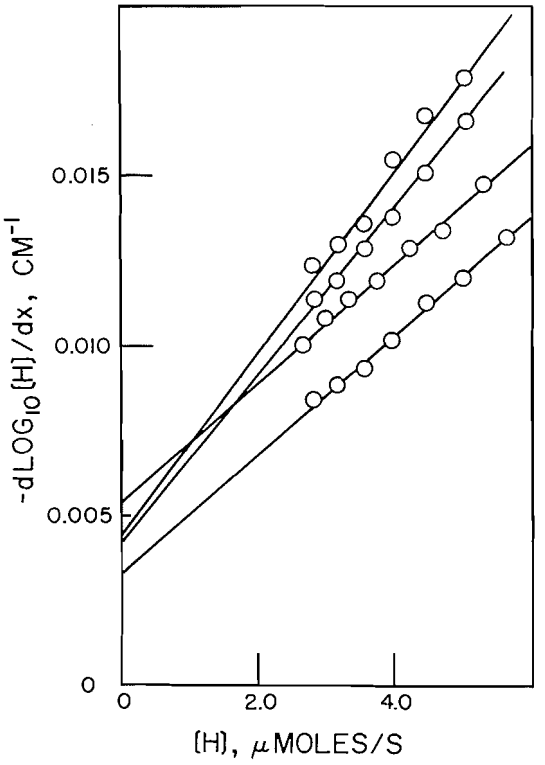

FIG. 3. Typical plots of $-d \log_{10} [H]/dx$ versus [H] for the recombination of hydrogen atoms in an argon carrier (x is the distance along the reaction tube and is proportional to t). The flow gases contained less than 1 p.p.m. O_2 and H_2O impurities.

Can. J. Chem. Downloaded from www.nrcresearchpress.com by 210.87.254.40 on 09/05/12
For personal use only.

TABLE IX

Comparison of present rate constants with those from shock tube and flame studies

Method	Temp. (°K)	M	$k_{2,M} \times 10^{-15}$ (cm^6 $mole^{-2}$ s^{-1})	Ref.
Flow system	213	Ar	5.7±0.8	Present work
"	291	Ar	4.6±0.8	"
"	291	H_2	6.8±1.5	"
"	349	Ar	4.1±0.8	"
Hydrogen–air flames	1273	N_2, H_2, etc	5.0	18
"	1500	"	4.0	19
"	1650	"	6.0	20
Shock tube	3500	Ar	0.86	15
"	"	"	0.42	14
"	"	"	0.34	17
"	"	H_2	4.2	14
"	"	"	1.7(2)	15
"	"	"	1.4(4)	17

compared with the $T^{2.4}$ coefficient found previously. Clearly, the positive temperature coefficient and the high values of $k_{2,Ar}$ obtained in flow streams containing impurities are the result of surface reactions, and the present values of $k_{2,M}$ are the true rate constants. Figure 4 shows a plot of $\log_{10} k_{2,Ar}$ versus $\log_{10} T$ and compares the new rate constants with the shock tube data (14, 15, 17). The general agreement is good, although the overall temperature dependence of $k_{2,Ar}$ seems to be closer to the T^{-1} form used by the shock tube workers in the interpretation of their data than the $T^{-1/2}$ dependence observed in the present experiments. The present values of $k_{2,Ar}$ were obtained by measuring gradients of plots of $\log_{10}$ [H] versus x and the limits of error given in Table VIII were found from the slopes that could be drawn through plots of $-\mathrm{d} \log_{10}$ [H]/dx versus [H] (see Fig. 3). The rather large error limits associated with $k_{2,Ar}$ will strictly allow the temperature dependence to lie anywhere between T^0–T^{-1}, and the $T^{-1/2}$ dependence given here is only an approximate value. It should be noted that only in Sutton's experiments (17) was a T^{-1} dependence of $k_{2,Ar}$ observed.

The values of $k_{2,Ar}$ were not changed within the accuracy of the experiments, when up to 10% water vapor was added after the discharge. These observations were confirmed by measurements of HNO emission. It was concluded that k_{2,H_2O} is not greater than 5×10^{16} cm^6 $mole^{-2}$ s^{-1} at 293 °K. Table IX compares the present results and the shock tube data with the flame studies (18–20), assuming that all the abundant species in hydrogen–air flames give similar values of $k_{2,M}$. This assumption seems reasonable in view of the value of k_{2,H_2O} found here and because the only extensive data on temperature coefficients of a recombination reaction (iodine atoms) for a wide range of third bodies (45, 46) show that the rate constants for different third bodies become more similar as the temperature is raised. It is also interesting to note that the values of γ in Table VIII are in good agreement with Smith's data (21) for water vapor poisoned surfaces over the same temperature range.

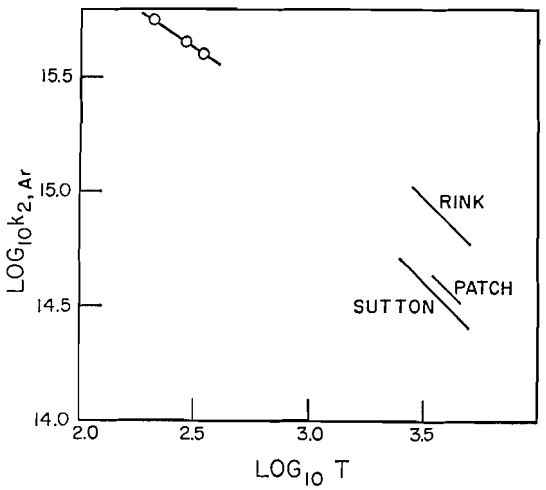

FIG. 4. Plot of $\log_{10} k_{2,Ar}$ versus $\log_{10} T$. Comparison of present room temperature data with shock tube data (see Rink (15), Patch (14), and Sutton (17)).

Can. J. Chem. Downloaded from www.nrcresearchpress.com by 210.87.254.40 on 09/05/12
For personal use only.

The Recombination of Deuterium Atoms

Attempts were made to measure the rate of recombination of deuterium atoms by dissociating Ar (90%)/D_2 mixtures and comparing the atomic decay profiles with those for hydrogen atoms under identical conditions. These profiles were also compared with those for argon/hydrogen mixtures which contained traces of oxygen impurities (less than 0.01%). The experiments were made in a new flow tube of slightly larger internal diameter (2.8 cm). Figure 5 shows some plots of $-\bar{v}\Delta \ln [H]$ versus $[M]\int [H]\, dx$ (rewriting $-\bar{v}d \ln [H]/dx = k_s + k_{2,M}[H][M]$ as $-\bar{v}\Delta \ln [H] = \int k_s dx + k_{2,M}[M]\int [H]dx$, where $\bar{v}$ is the mean linear flow velocity). The plots were curved in pure flow streams, but were linear in those containing impurities. The sensitivity of the experiments was poor, owing to the large proportion of surface recombination. The decrease in the rate constant with increasing pressure in pure flow streams indicates that some of the surface recombination is second order (k_s*). $k_{2,M}$ was obtained by plotting $[M]^{-1}$ versus $k_s^*/[M] + k_{2,M}$ after obtaining the values of the second term from plots of $-\bar{v}d \ln [H]/dx$ versus [H]. A value of $k_{2,Ar} = 4.5 \pm 0.5 \times 10^{15}$ cm^6 mole^{-2} s^{-1} (290 °K) was obtained for hydrogen atoms, in excellent agreement with the previous values. No accurate value of $k_{2,Ar}$ for deuterium atoms could be calculated because of the poor sensitivity of the results. However, comparison with the data for hydrogen atoms shows that the rate constant is smaller and probably lies between 1–4 $\times 10^{15}$ cm^6 mole^{-2} s^{-1} (293 °K). In the flow stream containing impurities, the value of $k_{2,Ar}$ for hydrogen atoms increased to 6.8 $\pm$ 0.5 $\times 10^{15}$ cm^6 mole^{-2} s^{-1} (293 °K).

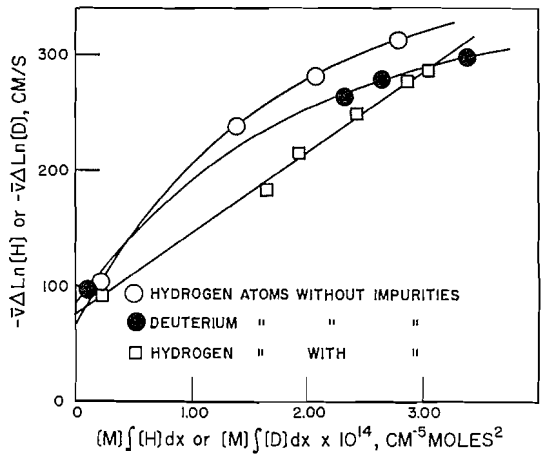

FIG. 5. Plot of $-\bar{v}\Delta \ln [H]$ (and $-\bar{v}\Delta \ln [D]$) versus $[M]\int [H]dx$ (and $[M]\int [D]dx$).

It is not clear why there is some second order surface recombination in these experiments which was not observed previously. A likely explanation is that the surface of the tube was incompletely poisoned, as indicated by the high level of surface recombination, and some impurities were adsorbed on the active surface. Therefore, this is probably a direct observation of the second order surface recombination which falsifies the homogeneous rate constants.

Appendix

The exact mathematical description of the flow method of following fast recombination reactions is extremely complicated when the effects of surface reactions, radial and axial diffusion, and viscous flow are taken into account. Recently, Kaufman (23) has summarized the limiting conditions whereby the effects of diffusion and viscous flow can be neglected for a system undergoing first order homogeneous recombination. This treatment can be readily adapted for the case of second order recombination and allowances can be made for the disturbances arising from the introduction of the isothermal calorimeter.

(a) Pressure Drop

The most serious pressure drop in the present work occurred with Ar/H_2 mixtures. Assuming Poiseuille flow for a pressure of 3 mm Hg and a path length of 40 cm, the drop exceeds 1% for flows faster than about 875 cm/s. The introduction of the isothermal calorimeter caused an increased pressure drop (47), and for a cylindrical calorimeter of 0.8 cm diameter, the flow velocity must be reduced below 405 cm/s for a pressure drop of less than 1%. The pressure drop arising from the recombination of atoms along the tube is less than 1% for 2–3% dissociation.

(b) Diffusion

In the absence of radial convection and radial diffusion effects, the condition for negligible axial diffusion for a homogeneous reaction of order n is $Dk_n[H]^{n-1}/\bar{v}^2 \ll 1$ (where D is the coefficient of diffusion, k_n the nth order rate constant, and $\bar{v}$ the mean linear flow velocity). The

worst cases of axial diffusion in the present experiments arose with pure hydrogen at low linear velocities. For $\bar{v} = 500$ cm/s, a total pressure of 5 mm Hg, and 1.5–2.5% dissociation, the error in the measured rate constant for hydrogen atoms is between 1 and 2% (taking $k_2 = 10^{16}$ cm^6 mole^{-2} s^{-1} and $D = 2.0$ cm^2/s at 1 atm). Axial diffusion becomes increased when the isothermal calorimeter is introduced into the reaction tube. The rapid removal of atoms on the calorimeter surfaces may cause a large perturbation in the atomic flow profile and falsify the measured rate constants. Rate constants of second order or above are validly determined by calorimetry if the condition for negligible axial diffusion is satisfied.

(c) Radial Concentration Gradients

Radial concentration gradients are only negligible when diffusion is sufficiently rapid to destroy the gradients caused by viscous flow and surface recombination. Kaufman's (23) approximate formula for radial concentration gradients modified for second order recombination shows that the worst cases of gradients in the present work occurred with high atomic concentrations (2–3% dissociation) in argon carriers ($D \simeq 1.0$ cm^2/s at 1 atm) and at high pressures (5 mm Hg). In these cases, the concentration variations were between 1–2%, but in most experiments they were below 1/2%.

(d) Heat Gradients

For small heat gradients, the effects of radial convection and heat radiation can be neglected. A calculation based on Fourier conduction shows that in experiments with Ar/H_2 mixtures at total pressures of 5 mm Hg and with 1.5–2.5% dissociation, the maximum temperature difference in a cross section of the reaction tube was from 10–15 °C (taking the conductivity coefficient as 3.9×10^{-5} cal cm^{-1} s^{-1} deg^{-1} at 273 °K and $k_2 = 10^{16}$ cm^6 mole^{-2} s^{-1}). In hydrogen and helium carriers, the temperature differences were only about 1/10 of this.

(e) Total Experimental Errors

The reliability of the experimental values of the rate constants was assessed by estimating the total systematic and random errors. The random errors were estimated by the method outlined by Benson (48). The systematic errors were estimated by calculations such as those outlined in (*a*), (*b*), (*c*), and (*d*). Under a typical set of experimental conditions, the total error in the rate constant measurements was found to be approximately 20%.

Acknowledgments

The author is indebted to Dr. B. A. Thrush and Dr. M. A. A. Clyne for helpful discussions. The research was supported by a studentship and later a fellowship from the Science Research Council, London (England).

1. H. M. Smallwood. J. Am. Chem. Soc. **51**, 1985 (1929).
2. H. M. Smallwood. J. Am. Chem. Soc. **56**, 1542 (1934).
3. H. Senftlenben and O. Reichemeier. Ann. Physik, **6**, 105 (1930).
4. W. Steiner and F. W. Wicke. Z. Physik. Chem. Leipzig, Bodenstein-Festband, 817 (1931).
5. I. Amdur and A. L. Robinson. J. Am. Chem. Soc. **55**, 1395 (1933).
6. L. Farkas and H. Sachsse. Z. Physik. Chem. Leipzig, **B27**, 111 (1934).
7. I. Amdur. J. Am. Chem. Soc. **57**, 856 (1935).
8. I. Amdur. J. Am. Chem. Soc. **60**, 2347 (1938).
9. W. Steiner. Trans. Faraday Soc. **31**, 623 (1935).
10. R. W. Wood. Proc. Roy. Soc. London, Ser. A, **97**, 455 (1920).
11. H. Von Wartenberg and G. Schultze. Z. Physik. Chem. Leipzig, **B2**, 1 (1929).
12. W. H. Rodebush and M. H. Wahl. J. Chem. Phys. **1**, 696 (1933).
13. A. A. Frost and O. Oldenberg. J. Chem. Phys. **4**, 642, 781 (1936).
14. R. W. Patch. J. Chem. Phys. **36**, 1919 (1962).
15. J. P. Rink. J. Chem. Phys. **36**, 262 (1962).
16. G. P. Kistiakowsky and W. G. Gardiner, Jr. J. Chem. Phys. **35**, 1765 (1961).
17. E. A. Sutton. J. Chem. Phys. **36**, 2923 (1962).
18. G. Dixon-Lewis, M. M. Sutton, and A. Williams. Discussions Faraday Soc. **33**, 205 (1962).
19. W. E. Kaskan. Combust. Flame, **2**, 229 (1958).
20. E. M. Bulewicz and T. M. Sugden. Trans. Faraday Soc. **54**, 1855 (1958).
21. W. V. Smith. J. Chem. Phys. **11**, 110 (1943).
22. B. J. Wood and H. Wise. J. Phys. Chem. **66**, 1049 (1962).
23. F. Kaufman. Progr. Reaction Kinetics, **1**, 1 (1961).
24. H. G. Poole. Proc. Roy. Soc. London, Ser. A, **163**, 404 (1937).
25. J. P. Wittke and R. H. Dicke. Phys. Rev. **103**, 620 (1956).
26. S. W. Benson. The foundations of chemical kinetics. McGraw-Hill Book Co., New York. 1960. p. 156.
27. M. Eusuf and K. J. Laidler. Trans. Faraday Soc. **59**, 2750 (1963).
28. G. Herzberg. Molecular spectra and molecular structure. Vol. 1. D. Van Nostrand Co., New York. 1951. Appendix.
29. K. E. Shuler and K. J. Laidler. J. Chem. Phys. **17**, 1212 (1949).
30. I. Amdur and A. L. Robinson. J. Am. Chem. Soc. **55**, 2615 (1933).
31. K. H. Geib and P. Harteck. Chem. Ber. **B65**, 1551 (1932).

Can. J. Chem. Downloaded from www.nrcresearchpress.com by 210.87.254.40 on 09/05/12
For personal use only.

32. K. H. GEIB and P. HARTECK. Z. Physik. Chem. Leipzig, **A170**, 1 (1934).
33. W. H. RODEBUSH, C. W. J. WENDE, and R. W. CAMPBELL. J. Am. Chem. Soc. **59**, 1924 (1937).
34. W. H. RODEBUSH and M. H. WAHL. J. Chem. Phys. **1**, 696 (1933).
35. S. N. FONER and R. L. HUDSON. J. Chem. Phys. **23**, 1974 (1955).
36. N. I. KOBOZEV, I. I. SKOROKHODOV, L. I. NEKRASOV, and E. I. MAKAROVA. Zh. Fiz. Khim. **31**, 1843 (1957).
37. J. A. WOJTOWICZ, F. MARTINEZ, and J. A. ZASLOWSKY. J. Phys. Chem. **67**, 849 (1963).
38. M. A. A. CLYNE and B. A. THRUSH. Proc. Roy. Soc. London, Ser. A, **275**, 544 (1963).
39. M. A. A. CLYNE and B. A. THRUSH. Proc. Roy. Soc. London, Ser. A, **275**, 559 (1963).
40. F. S. LARKIN and B. A. THRUSH. Discussions Faraday Soc. **37**, 112 (1964).
41. F. KAUFMAN and F. P. DEL GRECO. 9th Symp. Combustion, Cornell Univ., Ithaca, N.Y., 1962, p. 659 (1963).
42. M. A. A. CLYNE. Private communication. 1964.
43. T. M. SHAW. J. Chem. Phys. **31**, 1142 (1959).
44. F. C. COFFIN. J. Chem. Phys. **30**, 593 (1959).
45. D. BUNKER and N. DAVIDSON. J. Am. Chem. Soc. **80**, 5085, 5090 (1958).
46. G. PORTER and J. A. SMITH. Proc. Roy. Soc. London, Ser. A, **261**, 28 (1961).
47. D. H. ATHERTON. Trans. ASME, **48**, 145 (1926).
48. S. W. BENSON. The foundations of chemical kinetics. McGraw-Hill Book Co., New York. 1960. p. 87.

Can. J. Chem. Downloaded from www.nrcresearchpress.com by 210.87.254.40 on 09/05/12
For personal use only.

Can. J. Chem. Downloaded from www.nrcresearchpress.com by 210.87.254.6 on 09/05/12
For personal use only.

Absolute rate constants for hydrocarbon oxidation. VIII. The reactions of cumylperoxy radicals[1]

J. A. HOWARD, K. U. INGOLD, AND M. SYMONDS[2]
Division of Applied Chemistry, National Research Council of Canada, Ottawa, Canada

Received October 27, 1967

Absolute rate constants have been measured for the reactions of cumylperoxy radicals with a number of hydrocarbons. The cumylperoxy radicals were produced from cumene hydroperoxide. Sufficient hydroperoxide was present to ensure that only cumylperoxy radicals were involved in the rate-determining propagation reaction.

Primary and secondary deuterium isotope effects have been measured for propagation and termination in the oxidation of cumene. The rate of hydrogen atom abstraction from ring-substituted cumenes by cumylperoxy radicals can be correlated by the Hammett equation using σ^+ substituent constants, $\rho = -0.29$. Primary and secondary peroxy radicals are about 3–5 times more reactive in hydrogen abstraction than tertiary peroxy radicals.

Canadian Journal of Chemistry, **46**, 1017 (1968)

Introduction

The low temperature liquid phase oxidation of cumene can be represented by the following reaction scheme[3] (1–6).

[1] Initiator $\xrightarrow{R_i}$ production of COO·

[2] $\mathrm{COO\cdot + CH \xrightarrow{k_p^{CC}} COOH + C\cdot \xrightarrow{O_2} COO\cdot}$

[6] $\mathrm{COO\cdot + COO\cdot \rightleftarrows}$

$$\mathrm{[COOOOC]_{cage}} \begin{cases} \xrightarrow{\text{direct}} \text{non-radical products} \\ \xrightarrow{\text{indirect}} 2\mathrm{CO\cdot} + \mathrm{O_2} \end{cases}$$

[10] $\mathrm{CO\cdot \xrightarrow{O_2} C_6H_5COCH_3 + CH_3OO\cdot}$

[11] $\mathrm{COO\cdot + CH_3OO\cdot \rightarrow}$ non-radical products

[12] $\mathrm{CO\cdot + CH \xrightarrow{O_2} COH + COO\cdot}$

[13] $\mathrm{CH_3OO\cdot + CH \xrightarrow{O_2} CH_3OOH + COO\cdot}$

CH represents cumene, CO· and COO· the corresponding alkoxy and peroxy radicals, and COOH the hydroperoxide. The overall rate of oxidation is given by

$$[\mathrm{I}] \qquad \frac{-\mathrm{d}[\mathrm{O_2}]}{\mathrm{d}t} = \frac{k_p^{CC}[\mathrm{CH}]R_i^{1/2}}{(2k_t^{CC})^{1/2}},$$

where $2k_t^{CC}$ is a composite rate constant which includes a contribution from reaction [11] as well as from the direct termination in reaction [6]. The value of $2k_t^{CC}$ depends on the experimental conditions since they can affect the fraction of CO· radicals, formed in reaction [$6_{(indirect)}$], which enter into termination via reactions [10] and [11] (4). At 30° $k_p^{CC}/(2k_t^{CC})^{1/2} = 1.5 \times 10^{-3}\ M^{-1/2}\ s^{-1/2}$, $k_p^{CC} = 0.18\ M^{-1}\ s^{-1}$, and $2k_t^{CC} = 1.5 \times 10^4\ M^{-1}\ s^{-1}$ (7).[4] The termination rate constant is an average of values obtained at chain lengths (ν) from 25–50 with 7.17 M cumene.

The addition of cumene hydroperoxide or *t*-butylhydroperoxide to cumene increases the rate of oxidation (3–6). The acceleration is due to the removal of methylperoxy and cumyloxy radicals from the system by the transfer reactions

[9] $\mathrm{CH_3OO\cdot + COOH \xrightarrow{k_{trans}} CH_3OOH + COO\cdot}$

[9′] $\mathrm{CO\cdot + COOH \longrightarrow COH + COO\cdot}$.

Sufficient cumene hydroperoxide (> 0.5 M at 30°) completely suppresses reaction [11] and all termination occurs by the direct process of reaction [6], i.e.

$$[\mathrm{II}] \qquad \frac{-\mathrm{d}[\mathrm{O_2}]}{\mathrm{d}t} = \frac{k_p^{CC}[\mathrm{CH}]R_i^{1/2}}{(2k_{t(direct)}^{CC})^{1/2}}.$$

Under these conditions the rotating sector

[1]NRCC No. 9913.
[2]NRCC Summer Student, 1967.
[3]The reactions and rate constants are numbered in the same way as in ref. 5.

[4]Hendry (6) gives $k_t^{CC} = 1 \times 10^4\ M^{-1}\ s^{-1}$ at 35° which corresponds to $2k_t^{CC} = 1.65 \times 10^4\ M^{-1}\ s^{-1}$ at 30°.

method gives $k_p^{CC} = 0.21\ M^{-1}\ s^{-1}$ and $2k_{t(direct)}^{CC} = 1.1 \times 10^4\ M^{-1}\ s^{-1}$ at 30° (5). However, a more reliable value for $2k_{t(direct)}^{CC} = 6.0 \times 10^3\ M^{-1}\ s^{-1}$ is obtained by substituting $k_p^{CC} = 0.18\ M^{-1}\ s^{-1}$ into the limiting value[5] of $k_p^{CC}/(2k_{t(direct)}^{CC})^{1/2}$ at high COOH concentrations.

In the preceding paper in this series (5) it was shown that cumene hydroperoxide could be used as a chain transfer agent in other oxidizable hydrocarbons. The normal chain-propagating ROO· radical is replaced by a COO· radical,

$$ROO\cdot + COOH \xrightarrow{k_{trans}} ROOH + COO\cdot,$$

and the overall rate of oxidation (at sufficiently high [COOH]) is given by

$$[III] \qquad \frac{-d[O_2]}{dt} = \frac{k_p^{CR}[RH]R_i^{1/2}}{(2k_{t(direct)}^{CC})^{1/2}},$$

where k_p^{CR} is the rate constant for the propagation process

$$COO\cdot + RH \xrightarrow{k_p^{CR}} COOH + R\cdot \quad .$$

In the present paper we have utilized this hydroperoxide addition technique to investigate deuterium isotope effects and ring substitution effects on the oxidation of cumene. Values for the cross propagation constants (k_p^{CR}) for the attack (both abstraction and addition) of cumylperoxy radicals on a number of hydrocarbons have also been measured.

Experimental

The experimental technique has been described in the previous papers in this series (5, and references cited therein).

Cumene-α-d_1, cumene-α-d_1-β-d_6, and cumene-β-d_6 were obtained from Merck, Sharpe and Dohme. The chemical and isotopic purity were checked by vapor phase chromatography (v.p.c.) and mass spectrometry (at low electron energies), respectively. Cumene-α-d_1-β-d_6 and cumene-β-d_6 were 99.5–100% pure by v.p.c. and cumene-α-d_1 was 97.5% pure. The deutero-cumenes gave the following isotopic analysis, α-d_1, $d_0 = 2\%$, $d_1 = 98\%$; α-d_1-β-d_6, $d_6 = 7\%$, $d_7 = 92\%$, $d_8 = 0.9\%$; β-d_6, $d_5 = 5\%$, $d_6 = 94\%$, $d_7 = 0.9\%$. For the purpose of the calculations described below the cumenes were assumed to be 100% deuterated in the named positions.

m- and *p*-methoxycumenes were prepared from the corresponding isopropylphenols (8). *p*-Nitrocumene was prepared by the method of Brown and Bonner (9). *m*-Nitrocumene (99% pure, $n_D^{24} = 1.5277$) was isolated from the *o*- and *p*-isomers by preparative vapor phase chromatography (Varian Aerograph, 25′ × 3/4″ column packed with 2% SE-30 on 45/60 acid-washed chromosorb W). *p*-Carbomethoxycumene was prepared from isopropylbenzoic acid (10). *m*-Bromocumene (11) and *p*-chlorocumene (cf. ref. 12) were prepared from *p*-nitrocumene. *p*-Cyanocumene was prepared by the dehydration of *p*-isopropylbenzaldehyde oxime with acetic anhydride.

Commercial cumene hydroperoxide was purified by successive conversions to its sodium salt until it produced no further increase in the rate of oxidation of cumene (4, 5). *t*-Butylhydroperoxide was dried and recrystallized in bulk at 0 °C. All the rate constants were measured at 30°. The measured rates were corrected for gas evolution and absorption in the non-propagating reactions. The oxidations were initiated either thermally using AIBN or photochemically using azo-bis-cyclohexylnitrile (ACHN). In all cases the rate of initiation R_i was measured by the induction period method (13) using 4-methoxy-2,6-di-*t*-butylphenol.

Results and Discussion

Deuterium Isotope Effects

(i) Deutero-cumenes

Previous workers have reported propagation and termination kinetic isotope effects using cumenes of rather low deuterium content. Russell (14) calculated the true primary isotope effect for hydrogen abstraction, $(k_p^{CC})/(k_p^{CC})_{\alpha D}$, to be 5.5 at 60° using cumene-α-*d* containing 58.4% deuterium. Boozer *et al.* (15) compared cumene with two samples of β-deutero-cumene containing 1.4 and 3.0 atoms of deuterium per molecule. The secondary isotope effect for propagation was measured by adding *p*-nitrophenol or 2,4-dichlorophenol to inhibit the normal termination process. Values of $(k_p^{CC})/(k_p^{CC})_{1.4\text{–}3.0\beta D}$ in the range 1.05–1.27 were obtained at 65°. For the uninhibited oxidations the overall rate exhibited a negative secondary isotope effect[6] ~0.91–0.85, which implied that the normal termination process has a significant positive secondary isotope effect. Our own work confirms the existence, but not the magnitude, of the isotope effects.

The rates and rate constants for the oxidation of cumene and the three deutero-cumenes are summarized in Table I. The two α-deutero-cumenes oxidized too slowly for their absolute rate constants to be measured directly. The small differences in the rate constants for cumene and

[5]From the azo-bis-isobutyronitrile (AIBN) thermally initiated reaction at 30°.

[6]Our own results indicate a positive isotope effect; see Table I.

Can. J. Chem. Downloaded from www.nrcresearchpress.com by 210.87.254.6 on 09/05/12
For personal use only.

TABLE I

Oxidation of deutero-cumenes at 30 °C (rate constants given in units of M^{-1} s^{-1})

Peroxy radical	ROO·			COO·[a]	BOO·[b]
Substrate	$\frac{k_p}{(2k_t)^{1/2}} \times 10^4$	k_p^{RR}	$2k_t \times 10^{-4}$	k_p^{CR}	k_p^{BR}
Cumene	15.0	0.18	1.5	0.18	0.22
Cumene-α-d_1	—	—	—	0.02	0.011
Cumene-α-d_1-β-d_6	0.70	—	—	0.013	—
Cumene-β-d_6	14.0[c]	0.15[c]	1.2[c]	0.11	0.19

[a]Cumene hydroperoxide (COOH), 0.5 *M*.
[b]*t*-Butylhydroperoxide (BOOH), 2.2 *M*.
[c]At $R_i = 3.0 \times 10^{-8}$ *M* s^{-1}, $\nu = 55$, $k_p = 0.13$, and $2k_t = 8.0 \times 10^3$. At $R_i = 7.3 \times 10^{-8}$ *M* s^{-1}, $\nu = 35$, $k_p = 0.18$, and $2k_t = 16.0 \times 10^3$.

cumene-β-d_6 determined with the rotating sector are within the limits of error of this technique.

Considerably more informative results were obtained from the AIBN thermally initiated oxidations of the deutero-cumenes in the presence of excess COOH ($2k_{t(direct)}^{CC} = 6.0 \times 10^3$ M^{-1} s^{-1}) and *t*-butyl hydroperoxide, BOOH ($2k_{t(direct)}^{BB} = 1.3 \times 10^3$ M^{-1} s^{-1}) (16). The COOH increased the rate of oxidation (i.e. $k_p/(2k_t)^{1/2}$) of cumene by 60% but had no effect on the rate of oxidation of cumene-β-d_6 and cumene-α-d_1-β-d_6. This suggests that reaction [11] is relatively unimportant for these two deutero-cumenes under our experimental conditions. Two factors are probably operating to produce this secondary deuterium isotope effect on termination. Firstly, CD_3· will probably be eliminated from the cumyloxy-d_6 radical more slowly than CH_3· from the normal cumyloxy radical.[7] Secondly, there is now considerable evidence that the termination of secondary peroxy radicals involves a significant kinetic isotope effect if the α-H is replaced by deuterium ($k_H/k_D \sim 1.8$–3.0 (14, 18, 19)). By analogy, it seems likely that reaction [11] will be slower for CD_3OO· radicals than for CH_3OO· radicals. We feel that the combination of these two factors can account for the reduction in the termination constant from 1.5×10^4 M^{-1} s^{-1} for cumene to about 6×10^3 M^{-1} s^{-1} for the β-d_6- and α-d_1-β-d_6-cumenes. Abstraction of the β-hydrogen in the termination process, as originally suggested by Boozer *et al.* (15), does not seem to be required by our experimental results (cf. Traylor and Russell (3)).

The cumylperoxy and *t*-butylperoxy propagation constants listed in Table I give primary α-deuterium isotope effects, $(k_p^{CC})/(k_p^{CC})_{\alpha D}$, of 8.0 (α-$d_1$ with COO·), 20 (α-d_1 with BOO·), 8.5 (α-d_1-β-d_6 versus β-d_6 with COO·), and 20 (from the oxidation rates for the last-named pair). The average isotope effect of 14 ± 5 is considerably higher than the value of 5.5 calculated by Russell (14) but it does not seem unreasonable in view of the fairly large activation energy of this reaction (~11 kcal/mole[8]).

The average secondary isotope effect on propagation, $(k_p^{CC})/(k_p^{CC})_{\beta D_6} \approx 1.5$, i.e. $= 1.06 \pm 0.03$ per deuterium. This value is larger than the values reported for the homolytic decomposition of azo-compounds and per-esters (~1.02 per deuterium (23–25)) but is smaller than the values found for S_Ni solvolytic reactions of *t*-butylchloride (~1.10 per deuterium (26–28)).

(ii) Per-deutero-tetralin

The oxidations of tetralin and per-deutero-tetralin were studied in the presence of BOOH. The rate of the thermally initiated (7.6×10^{-3} *M* AIBN) oxidation of tetralin was constant over a range of BOOH concentrations from 0.7–2.2 *M* and the chain is therefore propagated and terminated by BOO· radicals under these conditions. The rate constants are: $k_p^{BR}/(2k_t^{BB})^{1/2} = 43.2 \times 10^{-3}$ $M^{-1/2}$ $s^{-1/2}$ and $(k_p^{BR}/(2k_t^{BB})^{1/2})_D = 2.7 \times 10^{-3}$ $M^{-1/2}$ $s^{-1/2}$, i.e. $k_p^{BR} = 1.5_5$ M^{-1} s^{-1}, $(k_p^{BR})_D = 0.097$ M^{-1} s^{-1} and $(k_p)_H/(k_p)_D = 16$. This isotope effect is a combination of the primary α effect for hydrogen abstraction and secondary α and β effects. It is more reliable than

[7]The radical-chain decomposition of $C_6H_5C(CH_3)(CD_3)OCl$ in cyclohexane–CCl_4 mixtures yields CH_3Cl and CD_3Cl in a ratio of 1.4–1.6 from −9 to 75 °C (17).

[8]$E_p - \frac{1}{2}E_t = 6.3$ (20) and 6.7 (21) kcal/mole and $E_t \approx 9$ kcal/mole (6, 22).

Can. J. Chem. Downloaded from www.nrcresearchpress.com by 210.87.254.6 on 09/05/12
For personal use only.

TABLE II

Rate constants (M^{-1} s^{-1} at 30°) for the oxidation of ring-substituted cumenes

Substituent	[RH] (M)	$R_i \times 10^7$ (M s^{-1})	ν	$\frac{k_p}{(2k_t)^{1/2}} \times 10^3$	k_p	$2k_t \times 10^{-4}$
p-CH_3O-	6.4	1.05	39	2.0	0.40	4.0
None	7.17	1.7	25	1.5	0.19	1.8
None	7.17	0.54	50	1.6	0.16	1.0
m-CH_3O-	6.4	0.34	20	0.60	0.17	8.0
	6.4	0.14	30	0.54	0.11	4.0
p-CH_3-O-C-	5.7	0.96	15	0.83	0.13	2.5
O	5.7	0.31	31	0.97	0.18	3.5

our previous estimate (~57) which was based on the oxidation of the neat hydrocarbons (19).

The Oxidation of Ring-Substituted Cumenes

Russell (29) and later Russell and Williamson (8) measured the rates of oxidation of a number of substituted cumenes. The rates were correlated by the Hammett equation using σ^+ substituent constants, $\rho^+ = -0.41$ (8). The results of co-oxidation studies indicated that the termination constants were the same for cumene and the substituted cumenes. The variation in the rate with substituent was therefore assigned to a variation in the propagation rate constants. Since the co-oxidation procedure is not very sensitive to variations in $2k_t$ (19) we have measured the absolute rate constants for the oxidation of three substituted cumenes, *m*- and *p*-methoxycumene and *p*-carbomethoxycumene. The results together with the results for cumene are given in Table II. The higher termination constants for the substituted cumenes may be due to solvent effects of the substituents on the rate of the direct and/or indirect termination process, since the substituents change the nature of the medium. It is also possible that some primary peroxy radicals are formed from the methoxy or carbomethoxy groups and that these contribute to the higher termination constants (cf. 8, 29).

The rate constants for hydrogen abstraction from 10 substituted cumenes by cumylperoxy radicals are given in Table III. The cumenes were oxidized as 1–2 M solutions in chlorobenzene containing $\geqslant 0.5$ M cumene hydroperoxide. The rate constants can be roughly correlated by the Hammett equation

$$\log_{10}(k_p^{CR}/k_p^{CC}) = (-0.29 \pm 0.04)\sigma^+$$

$$\log_{10}(k_p^{CR}/k_p^{CC}) = (-0.35 \pm 0.07)\sigma.$$

The better correlation with σ^+ implies that there is some separation of charge in the transition state and the ρ value is in good agreement with previous data (8, 29). However, it is rather surprising that k_p^{CR} is nearly constant for electron-attracting substituents with σ^+ values $\geqslant 0.405$.

TABLE III

Rate constants (M^{-1} s^{-1} at 30°) for hydrogen atom abstraction from substituted cumenes by cumylperoxy radicals[a]

Substituent	σ^+	k_p^{CR}
p-Methoxy	−0.778	0.33_5
p-Methyl	−0.311	0.22_5[b]
p-Isopropyl	−0.280	0.24[c]
Hydrogen	0	0.18
m-Methoxy	0.047	0.18
p-Chloro	0.114	0.15_5
m-Bromo	0.405	0.12
p-Carbomethoxy	0.489	0.13
p-Cyano	0.659	0.13_5
m-Nitro	0.674	0.12
p-Nitro	0.790	0.12_5

[a]0.115 M [AIBN], 1–2 M [RH] in chlorobenzene, $R_i = 1.4 \times 10^{-8}$ M s^{-1}, ν = 30–80, [COOH] $\geqslant 0.5$ M.
[b]Corrected for attack on the *p*-methyl group.
[c]Statistically corrected.

It is interesting to note that k_p^{CR} for *p*-methylcumene (*p*-cymene) is greater than the value found for cumene. In contrast, neat *p*-cymene oxidizes more slowly than neat cumene (20, 29) because the methyl substituent gives primary peroxy radicals which have a high termination rate constant.

It is evident from the propagation rate constants in Tables II and III that ring-substituted cumylperoxy radicals are very similar in reactivity to the unsubstituted cumylperoxy radical.

The Reaction of Cumylperoxy Radicals with Hydrocarbons

Measurement of the absolute rate constants for hydrocarbon oxidation have indicated that

Can. J. Chem. Downloaded from www.nrcresearchpress.com by 210.87.254.6 on 09/05/12
For personal use only.

TABLE IV

Rate constants (M^{-1} s^{-1} at 30°) for hydrocarbon oxidation

Propagating radical	ROO· (7)		COO·		
Substrate	$k_p^{RR}/(2k_t^{RR})^{1/2}$ $\times 10^3$	k_p^{RR}	$k_p^{CR}/(2k_{t(direct)}^{CC})^{1/2}$ $\times 10^3$	k_p^{CR}	k_p^{RR}/k_p^{CR}
Toluene[a]	0.014	0.24	0.44	0.034	7.0
Octene-1[a]	0.062	1.0	3.5	0.27	3.7
Bibenzyl[a]	0.13	0.56	2.65	0.20	2.8
Ethylbenzene[a]	0.21	1.3	2.7	0.21	6.2
Diphenylmethane[a]	0.38	2.0[b]	6.5	0.50	4.0
5-Decyne	0.74	2.8	9.05	0.60	4.7
Tetralin[a]	2.3	6.4	21.3	1.65	4.0
Indan[a]	1.7	4.8	22.0	1.7	2.8
9,10-Dihydroanthracene	58.5	175	900	70	2.5
sec-Amylbenzene	0.11	0.07	0.44	0.07	1.0
Cumene	1.5	0.18	2.0	0.18	1.0
2,3-Dimethylbutene-2	3.2	1.7	26.5	1.7	1.0
2,5-Dimethylhexene-3	5.4	2.4	33	2.1	1.1
Styrene	6.3[c]	41	27.5	2.1	19
β-Methylstyrene	9.0[c]	51	54.5	4.2	12
α-Methylstyrene	13	10	51	3.9	2.6

[a]Termination constant measured by rotating sector (see text).
[b]Value obtained by the use of diphenylmethyl hydroperoxide (15). The directly measured propagation constant (4.8 M^{-1} s^{-1} (19)) and termination constant ($2k_t^{RR}$ = 1.6 × 10^8 M^{-1} s^{-1} (19)) should be revised to 2.0 and 2.7 × 10^7 M^{-1} s^{-1} respectively. The high values of k_p^{RR}/k_p^{CR} for toluene and ethylbenzene also suggest that the directly measured propagation and termination constants should be revised downwards.
[c]Previously reported values (ref. 7, Table III) are too large by $\sqrt{2}$.

tetralylperoxy radicals are about four times as reactive as cumylperoxy radicals in hydrogen atom abstraction from aralkanes (5). We have suggested that primary and secondary peroxy radicals are generally more reactive in abstraction than tertiary peroxy radicals (5, 30, 31). This suggestion can be checked by comparing our previously determined (7) oxidation rates and absolute propagation rate constants (k_p^{RR}) with the rates and rate constants (k_p^{CR}) obtained in the presence of >0.5 M cumene hydroperoxide. The results for 15 hydrocarbons are given in Table IV. The k_p^{CR} rate constants were determined both from thermal and photochemical initiated oxidations. For those hydrocarbons marked with an [a] in Table IV the value of $2k_{t(direct)}^{CC}$ was checked by a rotating sector measurement. Agreement with the value found in cumene–COOH mixtures was always satisfactory.

The results in Table IV show that primary and secondary peroxy radicals are generally about 3–5 times more reactive in abstraction than cumylperoxy radicals. However, the tertiary peroxy radicals from 2,3-dimethylbutene-2 and *trans*-2,5-dimethylhexene-3 have a similar reactivity to cumylperoxy radicals.

Chain propagation for the styrenes corresponds to the addition of a peroxy radical to the double bond. The k_p^{RR}/k_p^{CR} ratios for the styrenes giving secondary (styrene and β-methylstyrene) and tertiary (α-methylstyrene) peroxy radicals are about 3–5 times larger than might be expected. The results of rotating sector measurements on these styrenes seem quite reasonable in themselves (32, 33). On the other hand, there is no obvious reason why the polyperoxy radicals should be more reactive in addition than monomeric peroxy radicals (cf. ref. 34). The present results raise the distinct possibility that the directly measured propagation (k_p^{RR}) and termination ($2k_t^{RR}$) rate constants for these styrenes may be too large by a factor of about four because of some unappreciated feature of their copolymerization reactions with oxygen.

1. H. S. BLANCHARD. J. Am. Chem. Soc. **81**, 4548 (1959).
2. P. D. BARTLETT and T. G. TRAYLOR. J. Am. Chem. Soc. **85**, 2407 (1963).
3. T. G. TRAYLOR and C. A. RUSSELL. J. Am. Chem. Soc. **87**, 3698 (1965).
4. J. R. THOMAS. J. Am. Chem. Soc. **89**, 4872 (1967).
5. J. A. HOWARD and K. U. INGOLD. Intern. Oxidation Symp. San Francisco, Preprints, **1**, 3 (1967).
6. D. G. HENDRY. J. Am. Chem. Soc. **89**, 5433 (1967).
7. J. A. HOWARD and K. U. INGOLD. Can. J. Chem. **45**, 793 (1967).

Can. J. Chem. Downloaded from www.nrcresearchpress.com by 210.87.254.6 on 09/05/12
For personal use only.

8. G. A. RUSSELL and R. C. WILLIAMSON, JR. J. Am. Chem. Soc. **86**, 2357 (1964).
9. H. C. BROWN and W. H. BONNER. J. Am. Chem. Soc. **76**, 605 (1954).
10. L. BERT. Bull. Soc. Chim. France, **37**, 1397 (1925).
11. E. C. STERLING and M. T. BOGERT. J. Org. Chem. **4**, 20 (1939).
12. A. I. VOGEL. A textbook of practical organic chemistry. Longmans, Green and Co., London. 1948. p. 576.
13. C. E. BOOZER, G. S. HAMMOND, C. E. HAMILTON, and J. N. SEN. J. Am. Chem. Soc. **77**, 3233 (1955).
14. G. A. RUSSELL. J. Am. Chem. Soc. **79**, 3871 (1957).
15. C. E. BOOZER, B. W. PONDER, J. C. TRISLER, and C. E. WRIGHTMAN. J. Am. Chem. Soc. **78**, 1506 (1956).
16. J. A. HOWARD and K. U. INGOLD. Unpublished result.
17. A. A. ZAVITSAS and S. SELTZER. J. Am. Chem. Soc. **86**, 3836 (1964).
18. J. A. HOWARD and K. U. INGOLD. Can. J. Chem. **43**, 2737 (1965).
19. J. A. HOWARD and K. U. INGOLD. Can. J. Chem. **44**, 1119 (1966).
20. J. A. HOWARD and J. C. ROBB. Trans. Faraday Soc. **59**, 1590 (1963).
21. H. W. MELVILLE and S. RICHARDS. J. Chem. Soc. 944 (1954).
22. J. R. THOMAS and K. U. INGOLD. Intern. Oxidation Symp. San Francisco, Preprints, **1**, 517 (1967).
23. S. SELTZER and E. J. HAMILTON, JR. J. Am. Chem. Soc. **88**, 3775 (1966).
24. T. KOENIG and W. BREWER. Tetrahedron Letters, 2773 (1965).
25. T. KOENIG and R. WOLF. J. Am. Chem. Soc. **89**, 2948 (1967).
26. V. J. SHINER, JR., B. L. MURR, and G. HEINEMANN. J. Am. Chem. Soc. **85**, 2413 (1963).
27. G. FRISONE and E. R. THORNTON. J. Am. Chem. Soc. **86**, 1900 (1964).
28. L. HAKKA, A. QUEEN, and R. E. ROBERTSON. J. Am. Chem. Soc. **87**, 161 (1965).
29. G. A. RUSSELL. J. Am. Chem. Soc. **78**, 1047 (1956).
30. B. S. MIDDLETON and K. U. INGOLD. Can. J. Chem. **45**, 191 (1967).
31. K. U. INGOLD. Lecture presented at the Intern. Symp. on Free Radicals in Solution, University of Michigan, Ann Arbor, Aug. 21–24, 1966.
32. J. A. HOWARD and K. U. INGOLD. Can. J. Chem. **43**, 2729 (1965).
33. J. A. HOWARD and K. U. INGOLD. Can. J. Chem. **44**, 1113 (1966).
34. F. R. MAYO, M. G. SYZ, T. MILL, and J. K. CASLEMAN. Intern. Oxidation Symp. San Francisco, Preprints, **1**, 777 (1967).

Can. J. Chem. Downloaded from www.nrcresearchpress.com by 210.87.254.6 on 09/05/12
For personal use only.

Can. J. Chem. Downloaded from www.nrcresearchpress.com by 210.87.254.6 on 09/05/12
For personal use only.

Pyrolysis of HNCO vapor[1]

R. A. BACK AND J. CHILDS
Division of Pure Chemistry, National Research Council of Canada, Ottawa, Canada

Received November 2, 1967

The pyrolysis of HNCO vapor has been studied briefly at pressures from 5 to 20 Torr and temperatures from 550 to 700 °C. Products observed were CO, N_2, H_2, CO_2, HCN, and C_2N_2; the elemental balance suggests that NH_3 and NH_2CN may also have been products. The pyrolysis is complicated by surface effects, polymerization, and secondary reactions, and is not amenable to quantitative kinetic studies.

Canadian Journal of Chemistry, **46**, 1023 (1968)

The photolysis of HNCO (isocyanic acid) vapor has been studied in some detail in this laboratory (1–6). The pyrolysis, of obvious interest for comparison, has apparently not been examined. The present paper describes a brief study of the pyrolysis.

Experimental

Isocyanic acid was prepared by the reaction of phosphoric acid with saturated aqueous KNCO solution (4). The vapor was pyrolyzed in cylindrical vessels, 3 cm in diameter, 10 cm long, and about 80 cc in volume, made from quartz tubing taken from stock and used with no special treatment of the surface. Two series of experiments were made. In the first, the vapor was pyrolyzed in a vessel permanently mounted within a furnace and attached by capillary tubing through a mercury cutoff to the vacuum line. In the second series of experiments, HNCO at a known pressure was sealed in a well-baked quartz vessel, fitted with a break-seal. The vessel was placed in a hot furnace for the desired reaction time, then removed, attached to the vacuum line via the break-seal, and analyzed.

Products were fractionated at −196 °C, measured in a gas burette, and analyzed by gas chromatography, using a molecular sieve column for the noncondensable fraction and a dinonyl phthalate column for the condensable products (1, 4). The quantitative estimation of HNCO was difficult because of irregular loss by polymerization and decomposition on metal surfaces and columns, but with a glass inlet system and glass columns, fair reproducibility was achieved.

Results and Discussion

The pyrolysis was studied at temperatures from 550 to 700 °C and pressures from 5 to 20 Torr. The reaction was very slow at 500 °C, and almost too fast to study conveniently (complete in 10 min) at 700 °C. Products observed were CO, N_2, H_2, HCN, and CO_2. Figure 1 shows products of the pyrolysis vs. time in the fixed vessel at 600 °C with an initial HNCO pressure of 5 Torr. The shapes of these curves, and the product ratios, are approximately typical of all the experiments in the fixed vessel.

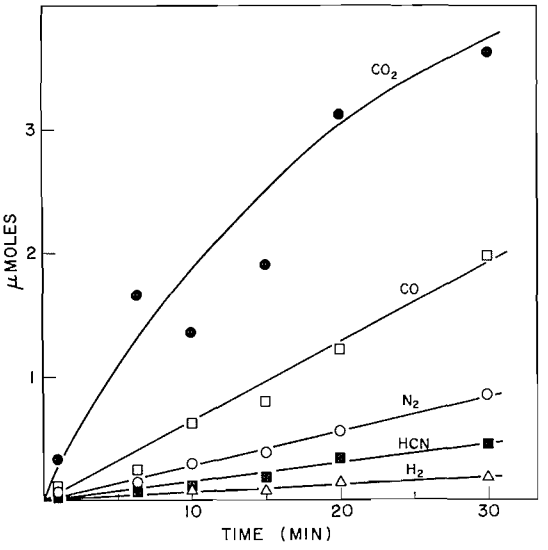

FIG. 1. Products from the pyrolysis of HNCO vapor at 600 °C and 5 Torr.

The loss of HNCO was greater than could be accounted for by the observed products, and it seems probable that trimerization or polymerization in the cold tubing leading to the reaction vessel (in which a white deposit was formed) was responsible. The elemental balance of the products suggests that NH_3 and NH_2CN may also

[1]NRCC No. 9919.

Can. J. Chem. Downloaded from www.nrcresearchpress.com by 210.87.254.6 on 09/05/12
For personal use only.

have been formed in the pyrolysis, the former in conjunction with CO, N_2, and H_2, as in the photolysis, and the latter accompanied by CO_2. Both ammonia and cyanamide are thermally unstable at the temperatures employed, but would, however, be expected to form nonvolatile deposits (ammonia as NH_4NCO) in the cold tubing leading from the reaction vessel, together with trimers and polymers of HNCO. Their analysis in such mixtures presents serious difficulties and was not attempted.

The somewhat variable loss of HNCO by polymerization, and the probable loss of NH_3 and NH_2CN by condensation, made quantitative treatment of the pyrolysis kinetics almost impossible. The experiments in the sealed vessels, in which the entire vessel was at the pyrolysis temperature so that NH_3, HNCO, and NH_2CN would remain in the gas phase, were undertaken to circumvent this problem, and showed some notable differences. The nitrogen yield was markedly higher, somewhat larger than that of CO. The rate of formation of HCN was much higher, and increased sharply with increasing time of reaction, and small amounts of C_2N_2 were observed. These changes are compatible with the occurrence of decomposition and secondary reactions of NH_3 and NH_2CN in the hot vessel. The results were badly scattered, however, and secondary reactions obviously set in very early. Reproducibility with both fixed and sealed pyrolysis vessels was poor, probably because of irreproducible surface conditions. Packing the vessel with quartz tubes increased the rate sharply, and the reaction order, based on initial product yields at several HNCO pressures, was zero order above about 10 Torr. The activation energy, similarly based, was low (~ 25 kcal/mole), and the HNCO loss plotted against time showed at low temperatures a levelling out characteristic of surface poisoning by a product. All these features point to a surface reaction; they were more pronounced at 550° than at 600°, and less so at 700°.

The present results indicate that the pyrolysis mechanism is complex, and is complicated by secondary reactions of products and surface effects. The similarity of the relative yields of CO, N_2, and H_2 suggests that free radical reactions similar to those occurring in the photolysis may account for these products, but further speculation about the mechanism is unjustified. The pyrolysis of HNCO vapor does not seem to be easily amenable to quantitative kinetic investigation, and further studies are not planned in this laboratory at the present time.

1. J. Y. P. Mui and R. A. Back. Can. J. Chem. **41**, 826 (1963).
2. R. A. Back. J. Chem. Phys. **40**, 3493 (1964).
3. J. L. Brash and R. A. Back. Can. J. Chem. **43**, 1778 (1965).
4. W. D. Woolley and R. A. Back. Can. J. Chem. **46**, 295 (1968).
5. R. A. Back and R. Ketcheson. Can. J. Chem. **46**, 531 (1968).
6. N. J. Friswell and R. A. Back. Can. J. Chem. **46**, 527 (1968).

Dielectric relaxation and orientational ordering of water molecules in hexamethylenetetramine hexahydrate[1]

D. W. Davidson
Division of Applied Chemistry, National Research Council of Canada, Ottawa, Canada

Received September 19, 1967

To account for the dielectric properties of hexamethylenetetramine hydrate, which include a static dielectric constant half that of ice, some modification is necessary of the partial orientational ordering of the water molecules proposed by Mak. It is suggested that water hydrogen atoms occupy fixed positions only in the hydrogen bonds with nitrogen.

Canadian Journal of Chemistry, 46, 1024 (1968)

The crystal structure of hexamethylenetetramine (HMT) hexahydrate at −20° has recently been described by Mak and Jeffrey (1, 2). The amine molecules occupy cavities in a hydrogen-bonded framework of water molecules, each cavity being surrounded by eight hexagonal rings of water molecules (Fig. 1). Three nitrogen atoms of the amine are near enough to water oxygen

[1]Issued as NRCC No. 9894.

Can. J. Chem. Downloaded from www.nrcresearchpress.com by 210.87.254.105 on 09/05/12
For personal use only.

have been formed in the pyrolysis, the former in conjunction with CO, N_2, and H_2, as in the photolysis, and the latter accompanied by CO_2. Both ammonia and cyanamide are thermally unstable at the temperatures employed, but would, however, be expected to form nonvolatile deposits (ammonia as NH_4NCO) in the cold tubing leading from the reaction vessel, together with trimers and polymers of HNCO. Their analysis in such mixtures presents serious difficulties and was not attempted.

The somewhat variable loss of HNCO by polymerization, and the probable loss of NH_3 and NH_2CN by condensation, made quantitative treatment of the pyrolysis kinetics almost impossible. The experiments in the sealed vessels, in which the entire vessel was at the pyrolysis temperature so that NH_3, HNCO, and NH_2CN would remain in the gas phase, were undertaken to circumvent this problem, and showed some notable differences. The nitrogen yield was markedly higher, somewhat larger than that of CO. The rate of formation of HCN was much higher, and increased sharply with increasing time of reaction, and small amounts of C_2N_2 were observed. These changes are compatible with the occurrence of decomposition and secondary reactions of NH_3 and NH_2CN in the hot vessel. The results were badly scattered, however, and secondary reactions obviously set in very early. Reproducibility with both fixed and sealed pyrolysis vessels was poor, probably because of irreproducible surface conditions. Packing the vessel with quartz tubes increased the rate sharply, and the reaction order, based on initial product yields at several HNCO pressures, was zero order above about 10 Torr. The activation energy, similarly based, was low (~ 25 kcal/mole), and the HNCO loss plotted against time showed at low temperatures a levelling out characteristic of surface poisoning by a product. All these features point to a surface reaction; they were more pronounced at 550° than at 600°, and less so at 700°.

The present results indicate that the pyrolysis mechanism is complex, and is complicated by secondary reactions of products and surface effects. The similarity of the relative yields of CO, N_2, and H_2 suggests that free radical reactions similar to those occurring in the photolysis may account for these products, but further speculation about the mechanism is unjustified. The pyrolysis of HNCO vapor does not seem to be easily amenable to quantitative kinetic investigation, and further studies are not planned in this laboratory at the present time.

1. J. Y. P. Mui and R. A. Back. Can. J. Chem. **41**, 826 (1963).
2. R. A. Back. J. Chem. Phys. **40**, 3493 (1964).
3. J. L. Brash and R. A. Back. Can. J. Chem. **43**, 1778 (1965).
4. W. D. Woolley and R. A. Back. Can. J. Chem. **46**, 295 (1968).
5. R. A. Back and R. Ketcheson. Can. J. Chem. **46**, 531 (1968).
6. N. J. Friswell and R. A. Back. Can. J. Chem. **46**, 527 (1968).

Dielectric relaxation and orientational ordering of water molecules in hexamethylenetetramine hexahydrate[1]

D. W. Davidson
Division of Applied Chemistry, National Research Council of Canada, Ottawa, Canada

Received September 19, 1967

To account for the dielectric properties of hexamethylenetetramine hydrate, which include a static dielectric constant half that of ice, some modification is necessary of the partial orientational ordering of the water molecules proposed by Mak. It is suggested that water hydrogen atoms occupy fixed positions only in the hydrogen bonds with nitrogen.

Canadian Journal of Chemistry, 46, 1024 (1968)

The crystal structure of hexamethylenetetramine (HMT) hexahydrate at −20° has recently been described by Mak and Jeffrey (1, 2). The amine molecules occupy cavities in a hydrogen-bonded framework of water molecules, each cavity being surrounded by eight hexagonal rings of water molecules (Fig. 1). Three nitrogen atoms of the amine are near enough to water oxygen

[1]Issued as NRCC No. 9894.

Can. J. Chem. Downloaded from www.nrcresearchpress.com by 210.87.254.105 on 09/05/12
For personal use only.

atoms O(2) to form hydrogen bonds. Water molecules O(2) are also hydrogen bonded to three water molecules of the second kind O(1), each of which is only three coordinated. For complete hydrogen bonding, water molecule O(2) must be oriented with one OH group close to the O(2)--N line and O(1) must provide H atoms to two of its three hydrogen bonds O(1)--O(2). With no further restrictions, three orientations of each water molecule are possible. If all allowed orientations are equally likely, the entropy of disorder of N water molecules may be shown to be approximately $(kN/6) \ln (65/27) = 0.29$ cal deg^{-1} mole^{-1}, a value considerably smaller than the maximum orientational entropy $kN \ln (3/2) = 0.81$ cal deg^{-1} mole^{-1} of the disordered ices (3).

In the X-ray work (2) hydrogen atoms were located in the Fourier synthesis patterns not only in the O(2)—H - - N bonds but also on O(1) in the O(1)—H - - O(2) bonds between hexagonal rings. No hydrogen atoms were located within the rings. It was concluded (2) that the proton positions are ordered except within the rings where the possible sites are statistically occupied by half-hydrogen atoms. This degree of disorder results in only two fully hydrogen-bonded ring configurations, those in which all the OH groups point clockwise or counterclockwise around the ring. Since the rings are independent of one another, the entropy of disorder is $(kN/6) \ln 2 = 0.23$ cal deg^{-1} mole^{-1}. This model is inconsistent with the dielectric properties of hexamethylenetetramine hydrate, as outlined below.

The dielectric dispersion locus of Fig. 2 is typical of the water–HMT system at low temperatures. Three samples of different composition and amine purity were studied. All showed a characteristic region of large dielectric absorption, together with a smaller region of absorption at higher frequencies whose amplitude was greatly dependent on the water content of the sample. Only a trace of the second absorption is apparent in the sample of Fig. 2, which was crystallized at 5° from a saturated solution and dried at 0° in a Büchner flask under suction and on a vacuum line for an hour at < 2 mm pressure.

The high-frequency absorption region must be ascribed to ice in which the relaxation has been shifted toward higher frequencies by the presence of impurities, to which the relaxation rate of ice is known to be particularly sensitive (4). The main absorption region arises from reorientation of the water molecules in the hydrate lattice. It is still observable at temperatures above the eutectic at −9° despite serious overlap by ionic conductance after the ice has melted.

There are only 0.58 as many water molecules per cm^3 in HMT hydrate as in ice. The static dielectric constant is more than half as large as that of ice, which is 114 at −57° (5). Reorientation of a water molecule is therefore associated with reorientation of the neighboring water molecules to maintain as great a local correlation between the directions of water dipoles as in ice. The relaxation rate (Fig. 3) is similar to that of ice at high temperatures but is less dependent on temperature. The Arrhenius energy is 9.3 kcal mole^{-1} vs. 13.25 kcal mole^{-1} for ice (5). The maximum value of the dielectric absorption falls with decreasing temperature. This is not, however, at least to −100°, accompanied by a decrease in the amplitude of the dispersion as measured by the static dielectric constant. Rather, a pronounced broadening of the absorption occurs, with the value of the Cole–Cole width parameter α increasing from 0.07 at −38° to 0.23 at −84°.

These results are consistent with threefold orientational disorder at each water-molecule site, as outlined in the first paragraph, but not with the more ordered structure. Twofold disorder within the hexagonal rings would lead to a negligible polarization at an extremely slow rate, since orientational defects would be confined to individual rings. The most likely mechanism of relaxation involves formation of L defects (hydrogen bonds which lack hydrogen atoms) by occasional rotation around the three-coordinated O(1) sites to interchange the non-hydrogen-bonded lone pair and a hydrogen atom in a normal hydrogen bond. L defects can then diffuse through the three-connected water network leaving reoriented fully hydrogen-bonded water molecules in their wake. The magnitude of the activation energy bears a reasonable relationship to that of ice. Thus the formation of one defect requires the breaking of only one hydrogen bond compared with the two which are broken to form a pair of defects in ice (6). Defect diffusion is easier in the hydrate than in ice because of the greater distortion of the O--O--O angles from tetrahedral values. Moreover, at the O(1) sites only one hydrogen bond need be broken in the

Can. J. Chem. Downloaded from www.nrcresearchpress.com by 210.87.254.105 on 09/05/12
For personal use only.

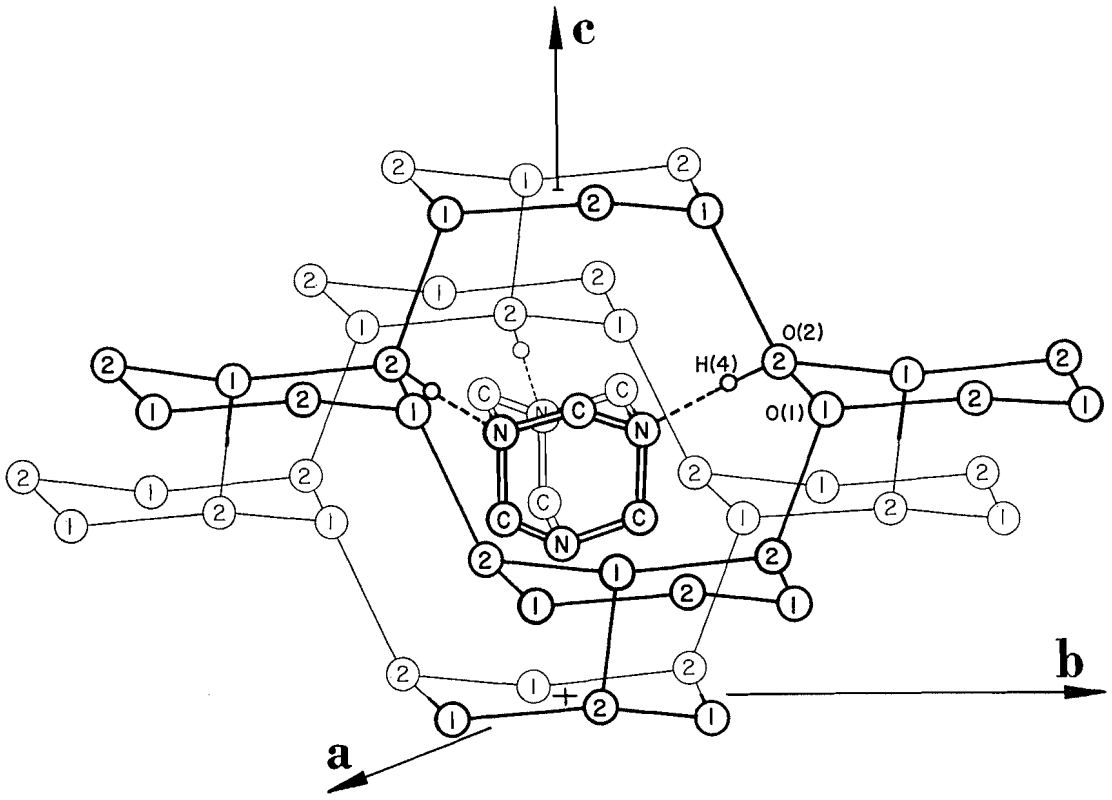

FIG. 1. The structure of hexamethylenetetramine hexahydrate (1, 2). Hydrogen atoms are shown only in the hydrogen bonds to nitrogen.

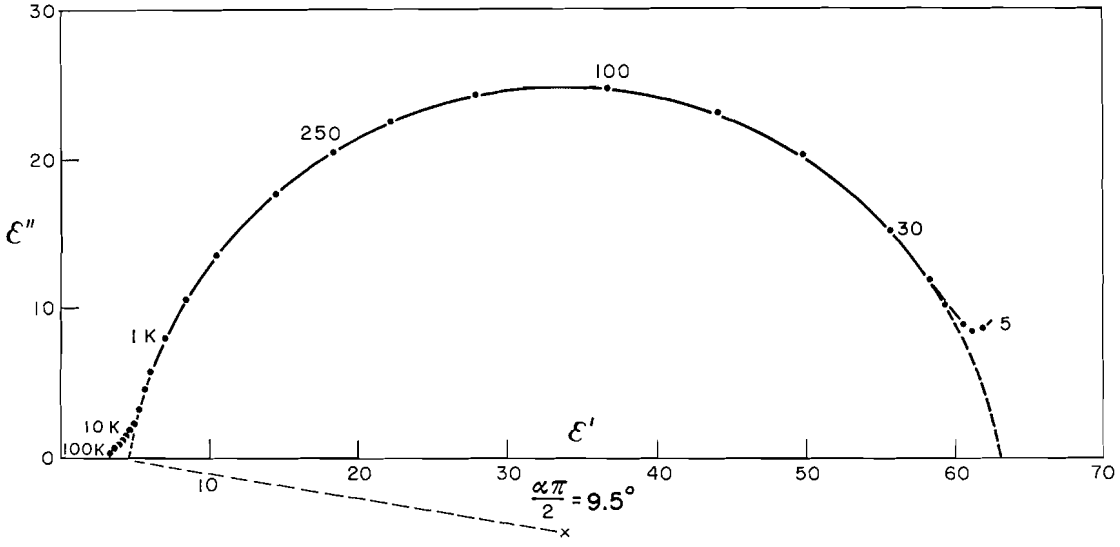

FIG. 2. Complex permittivity locus of HMT. $5.8H_2O$ at −53.3°. Frequencies are in Hz.

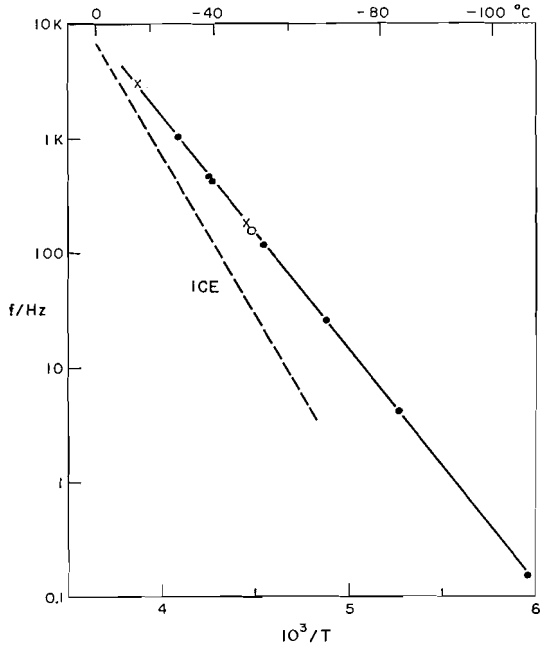

FIG. 3. Dependence of frequency of maximum dielectric absorption of HMT hydrate on temperature. Sample compositions: (●) 5.8, (×) 9, (○) 10 moles of water per mole of HMT. The ice line is from ref. 5.

diffusion step, in contrast to the two required at the O(2) sites and in ice.

The breadth of the absorption curves reflects the presence of some variation in the stability of the different configurations of water molecules. Consideration of first-neighbor interactions only shows orientations of two different stabilities at each of the water-molecule sites. The pronounced broadening at low temperatures suggests that the energy differences between different orientations are temperature dependent. It is possible for this trend to result in long-range ordering at temperatures too low for the relaxation to be followed by dielectric measurements.

Relaxation of the water in HMT hydrate is much less sensitive than that in ice to the presence of impurities, probably because of their reduced ability to enter the lattice interstitially. N.m.r. line narrowing at high temperatures in ice, apparently mainly a result of interstitial diffusion of water molecules, is not so pronounced in hexamethylenetetramine hydrate (7).

Finally, the X-ray results are made fully consistent with the structure adopted to explain the dielectric behavior if the hydrogen atom "seen" at O(1) in the bond between rings is replaced by, on average, two thirds of a hydrogen atom.

I am indebted to Dr. T. C. W. Mak for helpful correspondence.

1. G. A. JEFFREY and T. C. W. MAK. Science, **149,** 178 (1965).
2. T. C. W. MAK. J. Chem. Phys. **43,** 2799 (1965).
3. L. PAULING. Nature of the chemical bond. Cornell University Press, Ithaca. 1948. E. WHALLEY and D. W. DAVIDSON. J. Chem. Phys. **43,** 2148 (1965).
4. H. GRÄNICHER. Physik Kondensierten Materie, **1,** 1 (1963).
5. R. P. AUTY and R. H. COLE. J. Chem. Phys. **20,** 1309 (1952).
6. N. BJERRUM. Kgl. Danske Videnskab. Selskab Mat. Fys. Medd. **27,** 3 (1951).
7. S. K. GARG. Unpublished work.

Preferential solvation of a polar solute by the polar group(s) in the solvents[1]

K. K. DEB[2]
Robert Robinson Laboratories, Oxford Street, Liverpool-7, England

Received September 5, 1967

The rotationally averaged values of the H—H coupling constants in various polar solvents corresponding to a wide range of overall dielectric constant are reported for 1,1,2-trichloroethane. Except for very few solvents, a smooth linear relationship between the observed H—H coupling constants and x ($= (\varepsilon - 1)/(2\varepsilon + 1)$) of the solvents is demonstrated and the data are interpreted as evidence for preferential solvation of 1,1,2-trichloroethane by the polar group(s) in the solvents.

Canadian Journal of Chemistry, 46, 1027 (1968)

[1]This investigation was supported financially by the Science Research Council of Britain.
[2]Present address: The Chemistry Department, The University of South Florida, Tampa, Florida 33620.

Can. J. Chem. Downloaded from www.nrcresearchpress.com by 210.87.254.105 on 09/05/12
For personal use only.

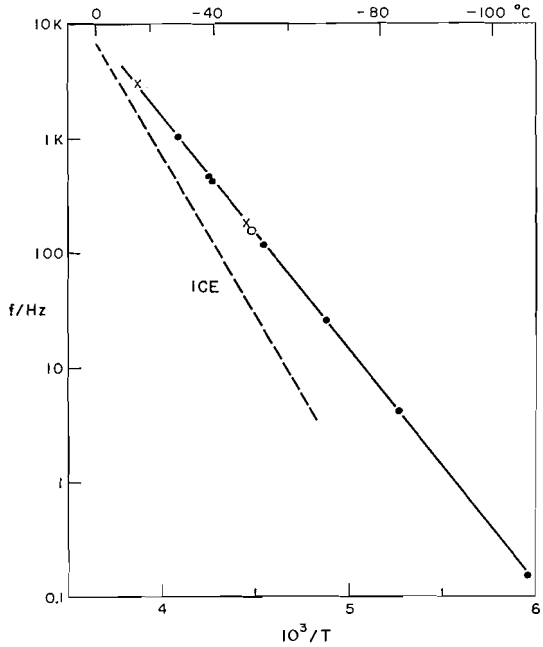

FIG. 3. Dependence of frequency of maximum dielectric absorption of HMT hydrate on temperature. Sample compositions: (●) 5.8, (×) 9, (○) 10 moles of water per mole of HMT. The ice line is from ref. 5.

diffusion step, in contrast to the two required at the O(2) sites and in ice.

The breadth of the absorption curves reflects the presence of some variation in the stability of the different configurations of water molecules. Consideration of first-neighbor interactions only shows orientations of two different stabilities at each of the water-molecule sites. The pronounced broadening at low temperatures suggests that the energy differences between different orientations are temperature dependent. It is possible for this trend to result in long-range ordering at temperatures too low for the relaxation to be followed by dielectric measurements.

Relaxation of the water in HMT hydrate is much less sensitive than that in ice to the presence of impurities, probably because of their reduced ability to enter the lattice interstitially. N.m.r. line narrowing at high temperatures in ice, apparently mainly a result of interstitial diffusion of water molecules, is not so pronounced in hexamethylenetetramine hydrate (7).

Finally, the X-ray results are made fully consistent with the structure adopted to explain the dielectric behavior if the hydrogen atom "seen" at O(1) in the bond between rings is replaced by, on average, two thirds of a hydrogen atom.

I am indebted to Dr. T. C. W. Mak for helpful correspondence.

1. G. A. JEFFREY and T. C. W. MAK. Science, **149,** 178 (1965).
2. T. C. W. MAK. J. Chem. Phys. **43,** 2799 (1965).
3. L. PAULING. Nature of the chemical bond. Cornell University Press, Ithaca. 1948. E. WHALLEY and D. W. DAVIDSON. J. Chem. Phys. **43,** 2148 (1965).
4. H. GRÄNICHER. Physik Kondensierten Materie, **1,** 1 (1963).
5. R. P. AUTY and R. H. COLE. J. Chem. Phys. **20,** 1309 (1952).
6. N. BJERRUM. Kgl. Danske Videnskab. Selskab Mat. Fys. Medd. **27,** 3 (1951).
7. S. K. GARG. Unpublished work.

Preferential solvation of a polar solute by the polar group(s) in the solvents[1]

K. K. DEB[2]
Robert Robinson Laboratories, Oxford Street, Liverpool-7, England

Received September 5, 1967

The rotationally averaged values of the H—H coupling constants in various polar solvents corresponding to a wide range of overall dielectric constant are reported for 1,1,2-trichloroethane. Except for very few solvents, a smooth linear relationship between the observed H—H coupling constants and x ($= (\varepsilon - 1)/(2\varepsilon + 1)$) of the solvents is demonstrated and the data are interpreted as evidence for preferential solvation of 1,1,2-trichloroethane by the polar group(s) in the solvents.

Canadian Journal of Chemistry, 46, 1027 (1968)

[1]This investigation was supported financially by the Science Research Council of Britain.
[2]Present address: The Chemistry Department, The University of South Florida, Tampa, Florida 33620.

Can. J. Chem. Downloaded from www.nrcresearchpress.com by 210.87.254.105 on 09/05/12
For personal use only.

Can. J. Chem. Downloaded from www.nrcresearchpress.com by 210.87.254.105 on 09/05/12
For personal use only.

Recently a classical theory of the solvent dependence of n.m.r. spectrum of rotational isomers has been developed (1). The theory directly evaluates the energy difference (ΔE) between the different rotamers in a medium as a function of the dielectric constant of the medium by the equation

$$[1] \quad \Delta E^{s} = \Delta E^{v} - \frac{kx}{(1 - lx)} + \frac{3hx}{(5 - x)},$$

where $x = (\varepsilon - 1)/(2\varepsilon + 1)$ and $l = 2(n_D{}^2 - 1)/(n_D{}^2 + 2)$, n_D being the refractive index of the solute. k and h are given by $(\mu_g{}^2 - \mu_t{}^2)/a^3$ and $(q_t{}^2 - q_g{}^2)/a^5$, where $\mu_{g,t}$ and $q_{g,t}$ are the dipolar and quadrupolar moments of the *trans* (t) and gauche (g) isomers respectively and 'a' is the molecular radius. It may be noted that the underlying principles giving eq. [1] specifically exclude any chemical bonding between solute and solvent molecules and, in addition, the solvent has been regarded as a medium of uniform dielectric constant. The second assumption is not valid when the effective dielectric constant at the solute molecule is not the same as in the bulk medium. Such a situation usually occurs with a polar solute in the solvents which contain strongly polar groups plus a large hydrocarbon segment. In such solvents the preferential solvation of the polar solute by the polar group(s) in the solvents would be expected to occur and eq. [1] will fail to describe the existing dependence of the relative energies of the different rotamers on the dielectric properties of the solvents. The present investigation is, therefore, undertaken to represent a brief report of experimental evidence for the preferential solvation of a polar solute by a large number of polar solvents corresponding to a wide range of overall dielectric constant. The molecule of 1,1,2-trichloroethane has been chosen for the present investigation because of the simplicity in its n.m.r. spectrum (A_2B system).

The n.m.r. spectra of 1,1,2-trichloroethane in various polar solvents were recorded on a Varian HA-100 spectrometer at the probe temperature of 30 °C and, in all cases, 8–10 spectra were averaged to determine the value of the H—H coupling constants. Solutions of strength 5% by volume were usually used and, in some cases, solutions of varying concentrations were examined but no substantial dilution changes (2) were noticed in the values of the observed H—H couplings. The dielectric constants of some of the solvents have been measured using the capacitance bridge method at the audio frequency region. Table I lists the values of the observed H—H couplings of 1,1,2-trichloroethane in the various solvents which also includes the values of x ($= (\varepsilon - 1)/(2\varepsilon + 1)$) for the solvents adjusted to 30 °C. The plots of the observed H—H couplings versus x exhibit a smoothly linear relation as depicted in Fig. 1*b*, although there seems to be no real prior reason for expecting this to be the case. The best fit curve for observed H—H couplings versus x for 1,1,2-trichloroethane in various suitable solvents has recently been computed (3) using the classical theory (1) (see Fig. 1*a*). It is evident that the observed data for H—H couplings in the solutions of the present series of solvents appear to

TABLE I

The observed H—H coupling constants for 1,1,2-trichloroethane in various polar solvents[a]

Solvent	x	Observed H—H coupling (Hz)	Deviation (Hz)
Ethyl carbonate[b]	0.274	5.89	±0.02
Methyl carbonate[b]	0.293	5.82	±0.02
n-Butyl stearate	0.292	5.98	±0.02
Amyl valerate[b]	0.339	5.88	Nil
Ethyl isovalerate[b]	0.343	5.83	±0.02
Isoamyl acetate	0.354	5.80	±0.02
Cyclohexyl acetate[b]	0.361	5.78	±0.04
Ethyl *n*-butyrate[b]	0.363	5.78	±0.01
Ethyl sebacate	0.364	5.79	±0.02
Isopropyl acetate[b]	0.366	5.74	±0.01
Isobutyl acetate[b]	0.367	5.82	±0.04
Ethyl propionate	0.374	5.78	±0.03
Amyl formate[b]	0.380	5.81	±0.02
Ethyl crotonate[b]	0.384	5.76	±0.04
Ethyl acetate	0.384	5.74	±0.03
Ethyl formate	0.389	5.73	±0.01
Methyl acetate	0.394	5.75	±0.03
Diethyl succinate	0.395	5.69	±0.01
Dimethyl succinate[b]	0.400	5.67	±0.03
Diethyl malonate[b]	0.411	5.61	±0.01
Methyl formate[b]	0.412	5.70	±0.04
2-Octanone	0.428	5.61	±0.03
Sextone B[b]	0.440	5.54	±0.02
4-Methyl-2-pentanone	0.442	5.61	±0.02
Cyclopentanone[b]	0.445	5.52	±0.02
Ethyl acetoacetate[b]	0.454	5.55	Nil
3-Pentanone	0.455	5.56	±0.02
Hexane-2,5-dione[b]	0.456	5.46	±0.01
Cyclohexanone	0.460	5.51	±0.04
Methyl acetoacetate[b]	0.462	5.51	±0.01
Acetylacetone[b]	0.471	5.72	±0.02

[a]All spectra were recorded at 5% by volume solutions in the solvents.
[b]The dielectric constants of these solvents have been measured in the present investigation, otherwise the reported data have been used.

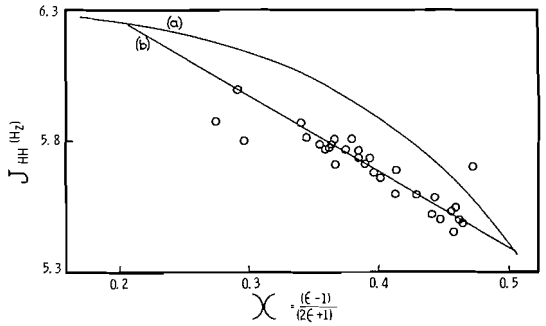

FIG. 1. Plots of the observed H—H coupling constants for 1,1,2-trichloroethane versus x of the various solvents: (*a*) ideal curved line (as shown in ref. 3), (*b*) observed linear relation.

be low, which indicates that the dielectric constant around the solute is now higher than the bulk dielectric constants of the solvents. Such results cannot, however, be attributed to the formation of any chemical complexes or to the changes in the relative energies of the different isomers. On the other hand the results are due to the expected preferential solvation of 1,1,2-trichloroethane in the polar solvents. The electric field of the solute molecule increases due to the preferential solvation and, therefore, the dielectric constant around the solute molecule increases from the bulk dielectric constants of the solvents. The deviations in the values of the observed couplings from the theoretical curve (3) would directly determine the nature and extent of such preferential solvation. It is pertinent to note that in certain solvents such as ethyl or methyl carbonates and acetylacetone apparently abnormal values of H—H couplings are observed and such discrepancies may be attributed to the change in the composition of the conformers due to the specific solvent–solute interactions not involved in the classical theory (1).

Acknowledgment

The author wishes to thank Dr. R. J. Abraham of the Robert Robinson Laboratories for many helpful discussions.

1. R. J. ABRAHAM, K. G. R. PATCHLER, and L. CAVALLI. Mol. Phys. **11**, 471 (1966).
2. K. K. DEB and R. J. ABRAHAM. J. Mol. Spectry. **23**, 393 (1967).
3. R. J. ABRAHAM and M. A. COOPER. J. Chem. Soc. (B), 202 (1967).

Electron spin resonance studies of radiation damage. Part I. An alternating linewidth effect for the $(CH_3)_2\dot{C}OH$ radical in gamma-irradiated acetone at low temperatures

F. P. SARGENT[1]

Department of Chemistry and Chemical Engineering, University of Saskatchewan, Saskatoon, Saskatchewan

Received September 5, 1967

The e.s.r. spectrum of the $(CH_3)_2\dot{C}OH$ radical showed a drastic temperature dependence of linewidth in the range −196 to −100 °C, this being particularly pronounced for the $M_I = \pm 2$ lines. Possible mechanisms are discussed in terms of restricted rotation of the methyl groups and of the OH groups.

Canadian Journal of Chemistry, 46, 1029 (1968)

Examples of alternating linewidth effects in the e.s.r. spectra of paramagnetic species in solution are now quite common and well understood (1). These effects arise from the modulation of the isotropic electron–nuclear hyperfine interaction and quite simple models seem to be satisfactory. The effect is very pronounced for such species as the durosemiquinone cation (2) and the 1,4-dinitrodurene anion (3).

We wish to report an example of an alternating linewidth effect in the solid state which considerably modifies the appearance of the e.s.r. spectrum as the temperature is varied. Samples of aqueous acetone gamma irradiated at −196 °C and examined at −100 °C (i.e. after luminescence (4)) gave spectra similar to that in Fig. 1*a*. These were interpreted in terms of the presence of two species and assigned to the $(CH_3)_2\dot{C}OH$ and $\cdot CH_2COCH_3$ radicals. The first order coupling constants and g values are

[1]NRCC Postdoctorate Fellow 1965–1967.

Can. J. Chem. Downloaded from www.nrcresearchpress.com by 210.87.254.105 on 09/05/12
For personal use only.

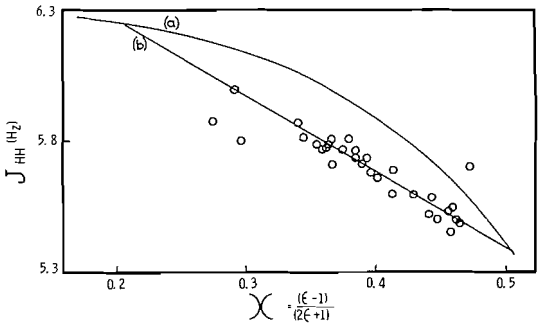

FIG. 1. Plots of the observed H—H coupling constants for 1,1,2-trichloroethane versus x of the various solvents: (*a*) ideal curved line (as shown in ref. 3), (*b*) observed linear relation.

be low, which indicates that the dielectric constant around the solute is now higher than the bulk dielectric constants of the solvents. Such results cannot, however, be attributed to the formation of any chemical complexes or to the changes in the relative energies of the different isomers. On the other hand the results are due to the expected preferential solvation of 1,1,2-trichloroethane in the polar solvents. The electric field of the solute molecule increases due to the preferential solvation and, therefore, the dielectric constant around the solute molecule increases from the bulk dielectric constants of the solvents. The deviations in the values of the observed couplings from the theoretical curve (3) would directly determine the nature and extent of such preferential solvation. It is pertinent to note that in certain solvents such as ethyl or methyl carbonates and acetylacetone apparently abnormal values of H—H couplings are observed and such discrepancies may be attributed to the change in the composition of the conformers due to the specific solvent–solute interactions not involved in the classical theory (1).

Acknowledgment

The author wishes to thank Dr. R. J. Abraham of the Robert Robinson Laboratories for many helpful discussions.

1. R. J. ABRAHAM, K. G. R. PATCHLER, and L. CAVALLI. Mol. Phys. **11**, 471 (1966).
2. K. K. DEB and R. J. ABRAHAM. J. Mol. Spectry. **23**, 393 (1967).
3. R. J. ABRAHAM and M. A. COOPER. J. Chem. Soc. (B), 202 (1967).

Electron spin resonance studies of radiation damage. Part I. An alternating linewidth effect for the $(CH_3)_2\dot{C}OH$ radical in gamma-irradiated acetone at low temperatures

F. P. SARGENT[1]

Department of Chemistry and Chemical Engineering, University of Saskatchewan, Saskatoon, Saskatchewan

Received September 5, 1967

The e.s.r. spectrum of the $(CH_3)_2\dot{C}OH$ radical showed a drastic temperature dependence of linewidth in the range −196 to −100 °C, this being particularly pronounced for the $M_I = \pm 2$ lines. Possible mechanisms are discussed in terms of restricted rotation of the methyl groups and of the OH groups.

Canadian Journal of Chemistry, 46, 1029 (1968)

Examples of alternating linewidth effects in the e.s.r. spectra of paramagnetic species in solution are now quite common and well understood (1). These effects arise from the modulation of the isotropic electron–nuclear hyperfine interaction and quite simple models seem to be satisfactory. The effect is very pronounced for such species as the durosemiquinone cation (2) and the 1,4-dinitrodurene anion (3).

We wish to report an example of an alternating linewidth effect in the solid state which considerably modifies the appearance of the e.s.r. spectrum as the temperature is varied. Samples of aqueous acetone gamma irradiated at −196 °C and examined at −100 °C (i.e. after luminescence (4)) gave spectra similar to that in Fig. 1*a*. These were interpreted in terms of the presence of two species and assigned to the $(CH_3)_2\dot{C}OH$ and $\cdot CH_2COCH_3$ radicals. The first order coupling constants and g values are

[1]NRCC Postdoctorate Fellow 1965–1967.

Can. J. Chem. Downloaded from www.nrcresearchpress.com by 210.87.254.40 on 09/05/12
For personal use only.

TABLE I

The first order g values and hyperfine coupling constants for the $\cdot CH_2COCH_3$ and $(CH_3)_2\dot{C}OH$ radicals

Radical	g value		Coupling constant	
	This work	Zeldes and Livingston*	This work	Zeldes and Livingston*
$\cdot CH_2COCH_3$	2.004	2.0044	20.2 ± 0.3	20.3 to 19.7
$(CH_3)_2\dot{C}OH$	2.003	2.0031	19.1 ± 0.4	19.48 to 19.96

*Zeldes and Livingston, solution e.s.r., see ref. 5. The value of $a_{II} = 20.3$ G for the $\cdot CH_2COCH_3$ radical is that reported by Dixon, Norman, and Buley (8) and quoted by Zeldes and Livingston.

given in Table I together with the recently reported solution values (5). Since the agreement between the solid and solution values is good we assume our assignment to be correct.

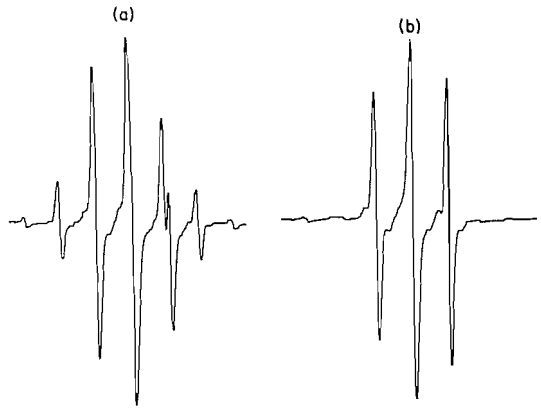

FIG. 1.

When the samples were cooled to -196 °C the spectra became quite different (see Fig. 1*b*). This effect was quite reversible and could be repeated many times without any loss of signal. Examination of this temperature dependence in detail showed a very drastic temperature dependence of the linewidths for the $(CH_3)_2\dot{C}OH$ lines. This was very marked for the $M_I = \pm 2$ lines; however, the $M_I = \pm 3$, i.e. the outermost lines, were not appreciably affected. At -196 °C the $M_I \pm 2$ lines became so broad that they were almost undetectable. We believe that this is the first example of an alternating linewidth effect in the solid state[2] and interpret it in terms of a differential modulation of the relative magnitudes of the methyl proton hyperfine interactions.

[2]Linewidth variations due to slow rotation of one methyl group are well known, see ref. 6.

Since the lines were symmetrical and the spectra of a generally "clean appearance" the g and A anisotropy effects characteristic of some polycrystalline spectra are assumed absent. The out of phase correlation of the methyl proton interactions may arise in two ways. These are spin density modulation via the OH group flipping and modulation via restricted or slow rotation of the methyl groups, both of which lead to a time dependent difference in splittings for the methyl protons.

Spin Density Modulation

If the $(CH_3)_2\dot{C}OH$ radical is planar the OH group will have two possible coplanar configurations. When the OH group is rapidly exchanging between these configurations, i.e. flipping, the time-averaged spectrum will be one of two apparently equivalent methyl groups. If the OH group were locked into a planar configuration, interaction with two non-equivalent methyl groups would be observed provided both groups continue to rotate. However, at intermediate rates of exchange, i.e. flipping, this modulation would lead to an alternating linewidth effect in an analogous manner to that for the durosemiquinone. This would not affect the widths of the $M_I = \pm 3$ lines but all the others would be broadened to varying degrees. In the limit of extreme broadening the spectrum would apparently consist of only four lines of relative intensities 1:9:9:1 instead of the usual seven lines with 1:6:15:20:15:6:1.

Restricted Rotation of the Methyl Groups

Restricted rotation of the methyl groups may lead to an apparent alternating linewidth effect. This has been treated theoretically by Freed and Fraenkel (7) and in the limit of extreme broadening only the $M_I = \pm 3$ and 0 lines would be

Can. J. Chem. Downloaded from www.nrcresearchpress.com by 210.87.254.40 on 09/05/12
For personal use only.

observed. If the two methyl groups are interlocked so that they are rotating in opposite directions the relative intensities of the three sharp lines would be 1:8:1; however, if the two methyl rotations are slow but not correlated in any way, then the relative intensities would be 1:2:1.

Conclusions

Since either mechanism leads to an apparent alternating linewidth effect, it is difficult to decide which effect predominates. The choice is made even more difficult in that methyl groups are known to execute restricted or slow rotation in some radicals at low temperature (6), but spin density modulation via OH group flipping satisfactorily accounts for the linewidth variations observed in radicals where the methyl groups rotate freely (2). It seems quite probable that both mechanisms contribute to the variations observed for the $(CH_3)_2\dot{C}OH$ radical, but because of the complications due to the presence of the $\cdot CH_2COCH_3$ radical it is quite impossible to determine which predominates from our spectra. If the $(CH_3)_2\dot{C}OH$ could be produced in a similar lattice without the complications of a secondary species it should be possible to investigate these effects more fully.

Acknowledgments

The financial support of the National Research Council of Canada is gratefully acknowledged.

1. G. K. Fraenkel. J. Phys. Chem. **71**, 139 (1967).
2. J. R. Bolton and A. Carrington. Mol. Phys. **5**, 161 (1962).
3. J. H. Freed and G. K. Fraenkel. J. Chem. Phys. **37**, 1156 (1962).
4. T. Shida and W. H. Hamill. J. Am. Chem. Soc. **88**, 3683 (1966).
5. H. Zeldes and R. Livingston. J. Chem. Phys. **45**, 1946 (1966).
6. A. Horsfield, J. R. Morton, and D. H. Whiffen. Mol. Phys. **5**, 115 (1962). *See also* I. Miyagawa and K. Itoh. J. Chem. Phys. **36**, 2157 (1962).
7. J. H. Freed and G. K. Fraenkel. J. Am. Chem. Soc. **86**, 3477 (1964).
8. W. T. Dixon, R. O. C. Norman, and A. L. Buley. J. Chem. Soc. 3625 (1964).

Quenching of hexafluoroacetone phosphorescence by mercury[1]

N. C. Lang[2] and K. O. Kutschke
Division of Pure Chemistry, National Research Council of Canada, Ottawa, Canada

Received November 2, 1967

The ratio of the relative yield for fluorescence to that for phosphorescence of hexafluoroacetone excited at 3130 Å was measured; the ratio was a linear function of mercury concentration. This observation confirms that the deactivation of the triplet state proceeds by a reaction which is first order in [Hg]. A quenching constant was obtained which is in excellent agreement with that based on lifetime measurements under mercury-free and mercury-saturated conditions.

Canadian Journal of Chemistry, **46**, 1031 (1968)

It has been reported recently (1, 2) that mercury vapor is an efficient deactivator of the triplet state of hexafluoroacetone. The evidence accumulated to support the identification of mercury as the deactivating agent involved a comparison of experimental quantities measured under mercury-free and mercury-saturated conditions. The quantities involved were the quantum yield of decomposition extrapolated to infinite ketone concentration (2), the lifetime of the triplet state (1, 2), and the ratio of the intensity of the phosphorescence to that of the fluorescence (2). It is reasonable to seek additional confirmation of this identification from measurements made at several intermediate concentrations of mercury.

The present note reports measurements of the ratio Q^f/Q^p as a function of mercury concentration. Q is proportional to the quantum yield of the emission indicated by the superscript although, because of the difference between the spectra of the two emissions (3, 4) and the variation of the sensitivity of the photomultiplier with wavelength, the constant of proportionality is not the same for the two emissions. The overall mechanism advanced for the primary process in this photolysis (4, 5) requires that

$$Q^f/Q^p = K(1 + k_{10}\tau_p[\mathrm{Hg}]).$$

[1]NRCC No. 9928.
[2]Student Summer Assistant, 1967.

Can. J. Chem. Downloaded from www.nrcresearchpress.com by 210.87.254.40 on 09/05/12
For personal use only.

observed. If the two methyl groups are interlocked so that they are rotating in opposite directions the relative intensities of the three sharp lines would be 1:8:1; however, if the two methyl rotations are slow but not correlated in any way, then the relative intensities would be 1:2:1.

Conclusions

Since either mechanism leads to an apparent alternating linewidth effect, it is difficult to decide which effect predominates. The choice is made even more difficult in that methyl groups are known to execute restricted or slow rotation in some radicals at low temperature (6), but spin density modulation via OH group flipping satisfactorily accounts for the linewidth variations observed in radicals where the methyl groups rotate freely (2). It seems quite probable that both mechanisms contribute to the variations observed for the $(CH_3)_2\dot{C}OH$ radical, but because of the complications due to the presence of the $\cdot CH_2COCH_3$ radical it is quite impossible to determine which predominates from our spectra. If the $(CH_3)_2\dot{C}OH$ could be produced in a similar lattice without the complications of a secondary species it should be possible to investigate these effects more fully.

Acknowledgments

The financial support of the National Research Council of Canada is gratefully acknowledged.

1. G. K. Fraenkel. J. Phys. Chem. **71**, 139 (1967).
2. J. R. Bolton and A. Carrington. Mol. Phys. **5**, 161 (1962).
3. J. H. Freed and G. K. Fraenkel. J. Chem. Phys. **37**, 1156 (1962).
4. T. Shida and W. H. Hamill. J. Am. Chem. Soc. **88**, 3683 (1966).
5. H. Zeldes and R. Livingston. J. Chem. Phys. **45**, 1946 (1966).
6. A. Horsfield, J. R. Morton, and D. H. Whiffen. Mol. Phys. **5**, 115 (1962). *See also* I. Miyagawa and K. Itoh. J. Chem. Phys. **36**, 2157 (1962).
7. J. H. Freed and G. K. Fraenkel. J. Am. Chem. Soc. **86**, 3477 (1964).
8. W. T. Dixon, R. O. C. Norman, and A. L. Buley. J. Chem. Soc. 3625 (1964).

Quenching of hexafluoroacetone phosphorescence by mercury[1]

N. C. Lang[2] and K. O. Kutschke
Division of Pure Chemistry, National Research Council of Canada, Ottawa, Canada

Received November 2, 1967

The ratio of the relative yield for fluorescence to that for phosphorescence of hexafluoroacetone excited at 3130 Å was measured; the ratio was a linear function of mercury concentration. This observation confirms that the deactivation of the triplet state proceeds by a reaction which is first order in [Hg]. A quenching constant was obtained which is in excellent agreement with that based on lifetime measurements under mercury-free and mercury-saturated conditions.

Canadian Journal of Chemistry, **46**, 1031 (1968)

It has been reported recently (1, 2) that mercury vapor is an efficient deactivator of the triplet state of hexafluoroacetone. The evidence accumulated to support the identification of mercury as the deactivating agent involved a comparison of experimental quantities measured under mercury-free and mercury-saturated conditions. The quantities involved were the quantum yield of decomposition extrapolated to infinite ketone concentration (2), the lifetime of the triplet state (1, 2), and the ratio of the intensity of the phosphorescence to that of the fluorescence (2). It is reasonable to seek additional confirmation of this identification from measurements made at several intermediate concentrations of mercury.

The present note reports measurements of the ratio Q^f/Q^p as a function of mercury concentration. Q is proportional to the quantum yield of the emission indicated by the superscript although, because of the difference between the spectra of the two emissions (3, 4) and the variation of the sensitivity of the photomultiplier with wavelength, the constant of proportionality is not the same for the two emissions. The overall mechanism advanced for the primary process in this photolysis (4, 5) requires that

$$Q^f/Q^p = K(1 + k_{10}\tau_p[\mathrm{Hg}]).$$

[1]NRCC No. 9928.
[2]Student Summer Assistant, 1967.

Can. J. Chem. Downloaded from www.nrcresearchpress.com by 210.87.254.42 on 09/05/12
For personal use only.

Can. J. Chem. Downloaded from www.nrcresearchpress.com by 210.87.254.42 on 09/05/12
For personal use only.

τ_p is the lifetime of the triplet state in the absence of mercury vapor, 3.4 ms at room temperature (2), and k_{10} is the second order constant of the quenching reaction; a discussion of the detailed mechanism of that reaction is given elsewhere (2). K is independent of [Hg] and is constant for constant ketone concentration if the reaction temperature and exciting wavelength also are constant.

Experiments were done in an apparatus similar to that described earlier (5); excitation was by the filter-isolated 3130 Å line of the mercury arc; all experiments were done with the reaction cell at room temperature. Q for the total emission was measured, after which ~ 10 Torr of air was added and Q^f measured directly as that of the emission not quenched by oxygen; Q^p was taken as $Q^{total} - Q^f$.

The reaction system was composed of the T-shaped cell and a U-tube containing a drop of mercury, both in series with an all-glass piston pump, and a Pyrex spiral gauge used as a null instrument against a mercury manometer. These components were isolated by stopcocks from a conventional storage and pumping system containing mercury. Well-outgassed ketone (2, 4), from Allied Chemical Co. cylinders, was admitted to the reaction system through traps held at -78 °C until a pressure of 22 Torr was attained. These traps also prevented access of mercury vapor to the reaction system during pumping procedures. After condensation of the ketone in the U-tube at -196 °C, the cell, the piston pump, and the connecting tubing were heated with "heat guns" for extended periods (on some occasions for several days) in order to distill all the mercury from the walls of the apparatus to the U-trap. The U-trap was warmed slowly to -78 °C and a measurement of Q^{total} was made after circulation of the ketone vapor through the apparatus to ensure equilibration with the trap of any mercury in the ketone vapor. The constancy of this measurement from one experiment to the next was taken as an indication that the equilibrium mercury vapor pressure had been attained. After warming the U-trap to some desired temperature and allowing for equilibration of the mercury by operation of the pump, a measurement of Q^{total} was taken; this procedure was repeated at successively higher trap temperatures. Q^f was measured, with the trap at room temperature, in the presence of ~ 20 Torr of dry air. Because the vapor pressure of the ketone at -78 °C is greater than 25 Torr and because the U-tube volume was small compared with the total volume of the reaction system, no change in ketone pressure could be observed when the U-tube was warmed above -78 °C.

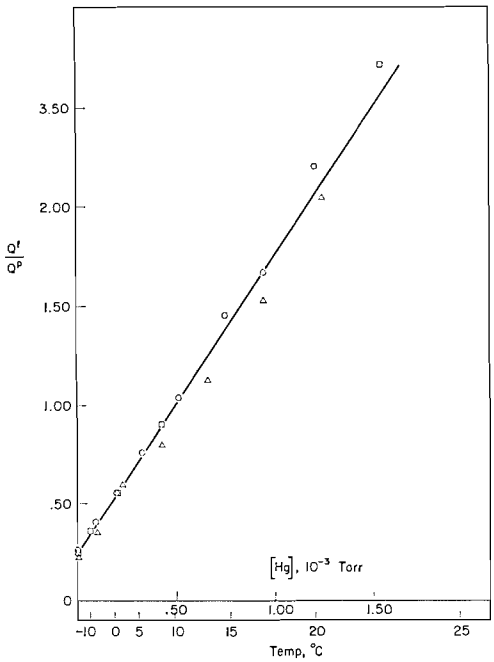

FIG. 1. Effect of [Hg] on Q^f/Q^p. The different symbols represent three different series of experiments.

Figure 1 shows the results of three series of such experiments. The value of Q^f/Q^p measured with the U-tube at -78 °C is 0.25, as shown by the intercept of the plot; this is slightly larger than the value 0.22 found under mercury-free conditions in another apparatus (4). However, the photomultiplier used in that study (EMI 6256S) had a greater sensitivity to the phosphorescence relative to that for the fluorescence than had the photomultiplier (1P21) used here; this experimental difference alone is sufficient to explain the discrepancy observed.

From the ratio of slope/intercept a value $k_{10}\tau_p = 11.2 \times 10^7$ $(\text{mole/l})^{-1}$ is obtained whence $k_{10} = 3.3 \times 10^{10}$ $(\text{mole/l})^{-1}$ s^{-1} when the value of τ_p cited above is used. This evaluation is quite independent of the $k_{10} = 3.1 \times 10^{10}$ $(\text{mole/l})^{-1}$ s^{-1} obtained from a consideration of the triplet lifetime measured under mercury-free

and mercury-saturated conditions (2). This excellent agreement of the two independently determined values of k_{10}, along with the linearity of the data shown in Fig. 1, provides strong support for the postulated kinetics of the overall reaction of mercury with the triplet ketone.

An earlier attempt[3] had been made to obtain data similar to those shown in Fig. 1. For those experiments the reaction system was isolated by Hoke type 413 metal valves. It now is thought that those experiments failed to yield reproducible data because of the difficulty in achieving equilibrium between mercury held in the U-tube and that absorbed on the various metal surfaces of the valves.

[3]By Miss Penny Estabrooks in 1966 during the tenure of a student summer assistantship.

Acknowledgments

The authors are indebted to Dr. A. Gandini and Dr. D. A. Whytock for much useful discussion.

1. A. GANDINI and K. O. KUTSCHKE. Can. J. Chem. **44**, 1720 (1966).
2. A. GANDINI, D. A. WHYTOCK, and K. O. KUTSCHKE. Presented at the International Conference on Photochemistry, Munich, Germany, September 5–10, 1967. Ber. Bunsenges. Physik. Chem. To be published.
3. P. G. BOWERS and G. B. PORTER. J. Phys. Chem. **68**, 2982 (1964).
4. A. GANDINI, D. A. WHYTOCK, and K. O. KUTSCHKE. To be published.
5. R. K. BOYD, G. B. CARTER, and K. O. KUTSCHKE. Can. J. Chem. **46**, 175 (1968).

Application of temperature-programmed desorption to surfaces with physically adsorbed species

H. P. SCHREIBER AND A. G. MACKINNON[1]

Canadian Industries Limited, Central Research Laboratory, McMasterville, Quebec

Received September 21, 1967

Temperature-programmed desorption has been applied to physisorbed aliphatic alcohols and acids on a rutile pigment surface. Reproducible desorption chromatograms for a series of alcohol adsorbates indicate that the same sites are involved in adsorbing the series and that the adsorbate orientation from the surface deviates progressively from normal as the chain length increases. The data also infer a reduction in the activation energy of desorption with increasing chain length. Acid adsorbates also generate reproducible chromatograms, those for formic and acetic acid showing characteristic peaks near 300 °C. The reason for the very high stability of these adsorbates has not yet been resolved.

Canadian Journal of Chemistry, 46, 1033 (1968)

The temperature-programmed desorption (t.p.d.) method has been successfully applied by Amenomiya and co-workers (1–3) for the study of site energy distributions in catalytic surfaces. The method involves gradually desorbing chemisorbed species from active surfaces (e.g. alumina) being heated at a linear rate, sweeping the desorbed material by an inert gas stream into a thermoanalytic cell, giving rise to a desorption chromatogram, and (optionally) trapping and analyzing the desorbed materials. The site energy distribution, relative to physically adsorbed molecules, is of analogous importance in the characterization of adsorbing surfaces. Experimental approaches toward this information generally involve relatively lengthy calorimetric measurements or laborious adsorption isotherm determinations. The application of t.p.d. could therefore offer attractive savings of time and equipment. The present work was undertaken with this in mind, recognizing, however, that because interaction energies in cases of physical (reversible) adsorption run much lower than those in chemisorption, the usefulness of t.p.d. would be restricted to systems with relatively high energies of adsorption. This note presents qualitative confirmation of the applicability of t.p.d. to the characterization of surfaces relative to the physical adsorption of selected probe molecules.

[1]Summer Research Assistant, 1966.

Experimental

The t.p.d. apparatus used in this work was constructed after that of Amenomiya and Cvetanović (1). The substrate to be studied, in this case a 2 g sample of pigment grade TiO_2, having a B.E.T. surface area of

Can. J. Chem. Downloaded from www.nrcresearchpress.com by 210.87.254.42 on 09/05/12
For personal use only.

and mercury-saturated conditions (2). This excellent agreement of the two independently determined values of k_{10}, along with the linearity of the data shown in Fig. 1, provides strong support for the postulated kinetics of the overall reaction of mercury with the triplet ketone.

An earlier attempt[3] had been made to obtain data similar to those shown in Fig. 1. For those experiments the reaction system was isolated by Hoke type 413 metal valves. It now is thought that those experiments failed to yield reproducible data because of the difficulty in achieving equilibrium between mercury held in the U-tube and that absorbed on the various metal surfaces of the valves.

[3]By Miss Penny Estabrooks in 1966 during the tenure of a student summer assistantship.

Acknowledgments

The authors are indebted to Dr. A. Gandini and Dr. D. A. Whytock for much useful discussion.

1. A. GANDINI and K. O. KUTSCHKE. Can. J. Chem. **44**, 1720 (1966).
2. A. GANDINI, D. A. WHYTOCK, and K. O. KUTSCHKE. Presented at the International Conference on Photochemistry, Munich, Germany, September 5–10, 1967. Ber. Bunsenges. Physik. Chem. To be published.
3. P. G. BOWERS and G. B. PORTER. J. Phys. Chem. **68**, 2982 (1964).
4. A. GANDINI, D. A. WHYTOCK, and K. O. KUTSCHKE. To be published.
5. R. K. BOYD, G. B. CARTER, and K. O. KUTSCHKE. Can. J. Chem. **46**, 175 (1968).

Application of temperature-programmed desorption to surfaces with physically adsorbed species

H. P. SCHREIBER AND A. G. MACKINNON[1]

Canadian Industries Limited, Central Research Laboratory, McMasterville, Quebec

Received September 21, 1967

Temperature-programmed desorption has been applied to physisorbed aliphatic alcohols and acids on a rutile pigment surface. Reproducible desorption chromatograms for a series of alcohol adsorbates indicate that the same sites are involved in adsorbing the series and that the adsorbate orientation from the surface deviates progressively from normal as the chain length increases. The data also infer a reduction in the activation energy of desorption with increasing chain length. Acid adsorbates also generate reproducible chromatograms, those for formic and acetic acid showing characteristic peaks near 300 °C. The reason for the very high stability of these adsorbates has not yet been resolved.

Canadian Journal of Chemistry, 46, 1033 (1968)

The temperature-programmed desorption (t.p.d.) method has been successfully applied by Amenomiya and co-workers (1–3) for the study of site energy distributions in catalytic surfaces. The method involves gradually desorbing chemisorbed species from active surfaces (e.g. alumina) being heated at a linear rate, sweeping the desorbed material by an inert gas stream into a thermoanalytic cell, giving rise to a desorption chromatogram, and (optionally) trapping and analyzing the desorbed materials. The site energy distribution, relative to physically adsorbed molecules, is of analogous importance in the characterization of adsorbing surfaces. Experimental approaches toward this information generally involve relatively lengthy calorimetric measurements or laborious adsorption isotherm determinations. The application of t.p.d. could therefore offer attractive savings of time and equipment. The present work was undertaken with this in mind, recognizing, however, that because interaction energies in cases of physical (reversible) adsorption run much lower than those in chemisorption, the usefulness of t.p.d. would be restricted to systems with relatively high energies of adsorption. This note presents qualitative confirmation of the applicability of t.p.d. to the characterization of surfaces relative to the physical adsorption of selected probe molecules.

[1]Summer Research Assistant, 1966.

Experimental

The t.p.d. apparatus used in this work was constructed after that of Amenomiya and Cvetanović (1). The substrate to be studied, in this case a 2 g sample of pigment grade TiO_2, having a B.E.T. surface area of

Can. J. Chem. Downloaded from www.nrcresearchpress.com by 210.87.254.6 on 09/05/12
For personal use only.

Can. J. Chem. Downloaded from www.nrcresearchpress.com by 210.87.254.6 on 09/05/12
For personal use only.

8.7 m^2/g, was placed in a sample cell which could be immersed in coolant or placed within an air furnace. A conventional B.E.T. gas adsorption apparatus, which is part of the experimental arrangement, was used to condition the surface.

In this case the conditioning was designed to lead to a "reproducible" surface in terms of heats of immersion of the TiO_2 in reagent grade xylene. Evacuation for 24 h at 200 °C produced such a surface ($-\Delta H_i = 45$ erg cm^{-2}, using the recently described isothermal calorimeter of Schreiber and Waldman (4)), and this treatment preceded scanning by successive t.p.d. runs up to about 380 °C. The conditioned surface was then covered by adsorbates admitted and metered by conventional vapor adsorption methods. The adsorbates studied included a series of carboxylic acids and alcohols, in addition to water, a common surface contaminant in polar metal oxides. In all cases the surface was saturated by establishing over the surface a partial adsorbate vapor pressure near unity ($p/p_0 \gtrsim 0.95$).

In t.p.d. experiments, helium gas carrier was metered into the system at a constant flow rate of 11.0 ml/min. The inert carrier was first dried by passing through a bed of desiccant ("Dri Rite") then through a liquid N_2 trap. The stream was then split, one portion passing through capillary flow resistors directly to the reference arm of a Gow-Mac AEL 9677 thermal conductivity cell, the other through the sample bed into the detector arm of the conductivity cell, which formed part of a bridge circuit connected to a strip chart recorder. Buffer volumes (3 l) on either side of the conductivity cell helped overcome the effects of minor gas flow fluctuations. A large signal was generated during the initial sweep at room temperature as the excess, loosely adsorbed vapors were swept out of the sample cell by the carrier gas. This decayed in 10–15 min, establishing a steady "base-line". The cell temperature was now increased linearly, the air furnace involved being controlled by a simple circuit programmer. In all of the work reported, a heating rate of 12.5 °C/min was maintained. Gradual desorption generated a peak in the desorption chromatogram, the base-line being reestablished as the surface was depleted. As already noted, the t.p.d. cycle was stopped below 400 °C to avoid thermal damage to the adsorbing surface. A check of the surface area, following completion of the t.p.d. series being reported, gave a value of 8.2 m^2/g, in satisfactory agreement with the initial value reported above.

Results

Three successive desorption chromatograms, obtained from the evacuated TiO_2 sample, are reproduced in Fig. 1, along with one for the surface saturated with water vapor. The evacuated surface obviously releases no appreciable amounts of adsorbate below 300 °C, whereupon a gradual depletion of strongly bonded adsorbate takes place. This high temperature portion of the chromatogram is accentuated following water adsorption, suggesting that the residual adsorbate is strongly adsorbed water. This agrees with reported studies of TiO_2/water interaction (5), which show that full desorption of water from such surfaces does not occur below 400 °C. Since our desorption cycles did not attain this temperature, for reasons already stated, the results discussed below characterize a TiO_2 surface with a small residue of adsorbed water.

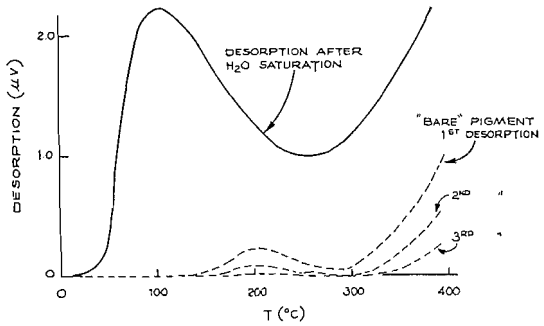

FIG. 1. Successive desorption traces from original TiO_2 surface. T.p.d. trace from TiO_2 following H_2O saturation.

Alcohol Adsorbates

In all t.p.d. experiments reported here, it is assumed that the desorption cycle is begun from constant (near monolayer) surface coverage. The desorption chromatograms for four monofunctional alcohols and ethylene glycol are shown in Fig. 2. The traces are characteristically similar to those obtained by Amenomiya and co-workers (1–3) and display a response peak identified as a temperature maximum, T_M. The T_M value shifts upward as the normal boiling points of the alcohol adsorbates increase. The major glycol peak coincides with the ethanol value, but a secondary peak is evident at about 225 °C. The presence of adjacent —OH anchor groups in the glycol apparently results in strong, neighbor-site adsorption of this adsorbate on roughly one half of the available surface (estimated from the areas under the two desorption peaks). Lateral interaction between OH groups probably enhances the stability of this adsorbate configuration.

The similarity in shape of the aliphatic alcohol desorption traces indicates that the same assembly of surface sites is involved in adsorbing the alcohol series. The strength of the adsorption bonding is suggested by the fact that a substantial proportion of the signal is generated at temperatures above the normal

TABLE I

Chromatogram areas and suggested orientation angles of alkyl chains

Adsorbate	Trace area (in.^{2})	Corrected trace area	Normalized area	Orientational angle (°)
Methanol	1.02	1.020	1.000	90
Ethanol	0.65	0.711	0.697	73
1-Pentanol	0.29	0.391	0.383	64
1-Octanol	0.22	0.357	0.350	62

boiling points of the alcohols; this is increasingly so for shorter chain lengths in the series.

In the case of methanol, desorption is still occurring at temperatures above 325 °C, suggesting that other than purely physical forces may be involved in this adsorbate/adsorbent system. The present data, however, are insufficient to further elaborate on this point.

It is qualitatively evident from Fig. 2 and explicitly shown in Table I, that the areas under the reproducible desorption chromatograms (evaluated by planimeter measurements) decrease sharply as the chain length of the adsorbate increases. In part this is due to the decrease in thermal conductivity of the adsorbates, an effect which can be taken in account using substance specific correction factors for thermal conductivity cells, with He as carrier gas, as given by Kaiser (6). The correction factors, relative to a methanol value of 1.000, are 1.095, 1.342, and 1.624 for ethanol, pentanol, and octanol respectively, and these were applied to calculate the corrected trace areas in Table I. The large residual area decrement is rather surprising if the usual assumption is made that the adsorbates are vertically oriented from the adsorbing surface, to which they are linked via the —OH group (7). This would presumably result in the same packing density of adsorbate, regardless of the chain length, and the corrected area under the desorption trace should be approximately constant. One way of accounting for the results obtained is to assume that alcohols, other than methanol, are not vertically oriented to the surface, and that proportionately greater steric barriers to adsorption are set up as the average orientational angle decreases from 90°. A normalization of the corrected areas under the chromatograms to that of the (assumedly) vertically oriented methanol[2] then provides a means of calculating the apparent angle of orientation, since this datum should be proportional to the average area swept out by the moving alkyl chain above the —OH anchor, and should therefore be proportional to $(\cos \Theta)^2$, where Θ is the angle generated by the mobile chain. The average orientational angle of the adsorbed molecule (relative to the adsorbing surface) then is $(90 - \Theta/2)°$. Calculated values of this angle are entered in Table I.

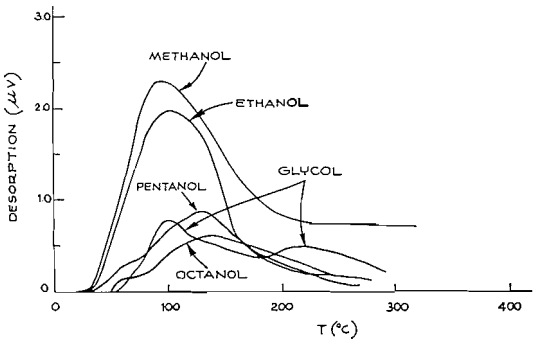

FIG. 2. T.p.d. chromatograms for TiO_2/alcohol systems.

Mathematical analyses of desorption chromatograms for various desorption processes have been given by Redhead (8) and Amenomiya and co-workers (1–3). These are not specifically applicable to the present case of physical adsorption, but within limits of the considerable approximations involved some evidence may be derived from them to show a dependence of the adsorption energy on the alkyl chain length in the alcohol series. The simplest analytical expression pertains to linear heating rates, homogeneous surfaces, and sufficiently high gas flow rates to prevent readsorption. Then it can be shown that

$$[1] \quad 2 \log T_M - \log \beta = \frac{E_d}{2.303RT_M} + \log\left(\frac{E_d}{AR}\right),$$

[2]The area under the methanol peak was defined by joining points at the first lift from the base-line and return to a steady line near 215 °C.

Can. J. Chem. Downloaded from www.nrcresearchpress.com by 210.87.254.6 on 09/05/12
For personal use only.

where β is the heating rate, E_d is the desorption activation energy, R is the gas constant, and A is a desorption rate constant. When β is constant, some plausible value may be chosen for A allowing numerical evaluation of the E_d vs. T_M relationship.[3] Applied to the present case, the calculation cannot provide a meaningful estimate of the absolute E_d value, but shows that the E_d values decrease with increasing alkyl chain length in the relationship

$$[2] \quad (E_d)_{C1} = (E_d)_{C2} + 0.3 \text{ kcal mol}^{-1} = (E_d)_{C5} + 0.9 \text{ kcal mol}^{-1} = (E_d)_{C8} + 1.6 \text{ kcal mol}^{-1}.$$

More complete experimental work would be needed to further confirm and interpret this suggested variation in the activation energy.

Acid Adsorbates

An interesting set of desorption traces was generated for four fatty acid adsorbates, as shown in Fig. 3. Once again a major decrease in the total area under the chromatogram is evident with increasing chain length, the areas being in the ratio 1.00:0.380:0.174:0.132 for formic, acetic, propionic, and isobutyric acid respectively. Conceivably, steric hindrance effects may be even more pronounced than in the case of alcohol adsorbates, but the large apparent effect is obviously related to the unusual character of the formic and acetic acid desorption traces. It is only possible to speculate about the very pronounced T_M values near 290 °C for these acid adsorbates; like all of the chromatograms presented, these are quite reproducible and unmistakably restricted to the initial pair of acid homologues. One possibility is that because of steric hindrance effects exerted by the longer alkyl chains, only these acids can interact with some high energy sites of this complex surface. Ionic bonding is a further possibility, salt formation in the TiO_2 surface being a relatively plausible occurrence. The existence of ionic bonding in TiO_2 surfaces has been previously documented by infrared studies (9). Finally, it is possible that these acids are capable of occupying several neighboring sites simultaneously, with —OH, C=O, or α-hydrogens as laterally interacting anchor groups. The existence of such stable configurations is of inherent interest, and may warrant further investigation.

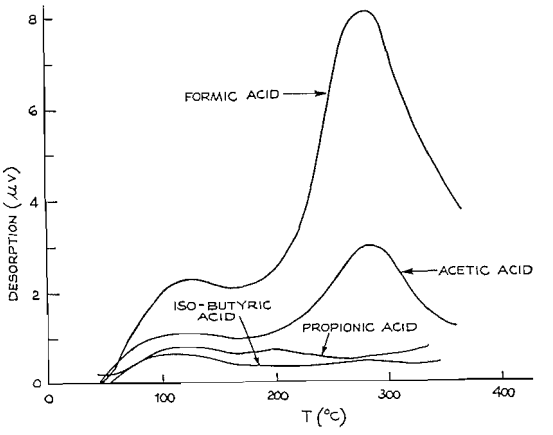

FIG. 3. T.p.d. chromatograms for TiO_2/carboxylic acid systems.

[3]The authors are grateful to a referee for pointing out this approach.

1. Y. AMENOMIYA and R. J. CVETANOVIĆ. J. Phys. Chem. **67**, 144 (1963).
2. Y. AMENOMIYA, J. H. B. CHENIER, and R. J. CVETANOVIĆ. J. Phys. Chem. **68**, 52 (1964).
3. Y. AMENOMIYA, J. H. B. CHENIER, and R. J. CVETANOVIĆ. Proc. Third Int. Congress on Catalysis, Amsterdam, **2**, 1135 (1965).
4. H. P. SCHREIBER and M. H. WALDMAN. J. Polymer Sci. A-2, **5**, 555 (1967).
5. R. E. DAY and G. D. PARFITT. Trans. Faraday Soc. **63**, 708 (1967).
6. R. KAISER. Gas phase chromatography. Vol. III. Butterworths & Co., London. 1963. Chap. 8.
7. P. T. DAWSON, G. T. RICH, and D. A. HAYDON. J. Phys. Chem. **68**, 3550 (1964).
8. P. A. REDHEAD. Trans. Faraday Soc. **57**, 641 (1961).
9. I. T. SMITH. Nature, **201**, 67 (1964).

Can. J. Chem. Downloaded from www.nrcresearchpress.com by 210.87.254.6 on 09/05/12
For personal use only.

Erratum: Comparative formation constants for complexes of copper, nickel, and silver with some substituted pyridines

M. S. SUN AND D. G. BREWER
Department of Chemistry, University of New Brunswick, Fredericton, New Brunswick
Received November 24, 1967

(Ref.: Can. J. Chem. **45**, 2729 (1967))

Canadian Journal of Chemistry, **46**, 1037 (1968)

On page 2735, line 15 of column 1 should read ± 0.03 log units instead of ± 0.3 log units.

Can. J. Chem. Downloaded from www.nrcresearchpress.com by 210.87.254.40 on 09/05/12
For personal use only.

Can. J. Chem. Downloaded from www.nrcresearchpress.com by 210.87.254.40 on 09/05/12
For personal use only.

1,2-Alkylidene and 1,2-ortholactone derivatives of 3,4,6-tri-*O*-acetyl-α-D-glucose

R. U. LEMIEUX AND D. H. DETERT
Department of Chemistry, University of Alberta, Edmonton, Alberta

Received February 5, 1968

Reaction of 3,4,6-tri-*O*-acetyl-1,2-*O*-(1′-*exo*-ethoxyethylidene)-α-D-glucopyranose with ketones in the presence of toluenesulfonic acid provides 3,4,6-tri-*O*-acetyl-1,2-*O*-alkylidene-α-D-glucoses. With butyrolactone the interchange yielded the 1,2-ortholactone.

Canadian Journal of Chemistry, 46, 1039 (1968)

In view of the recent publication by Rees, Tatchell, and Wells (1) on the preparation of 1,2-*O*-alkylidene-α-D-glucopyranoses from tetra-*O*-acetyl-α-D-glucopyranosyl bromide and cadmium dialkyls, we wish to report the results of our own investigations concerning a general method for the preparation of these 1,2-ketals.

p-Toluenesulfonic acid hydrate was dissolved in *N*,*N*-dimethylformamide and an excess of methyl orthoformate was added. The volatile components were then removed by distillation *in vacuo* and the solution was concentrated to an about 2.5 *M* solution of the acid. In a typical experiment, 0.3 ml of this solution was added to 3.5 ml of a 10% solution of dimethoxypropane in dry acetone. Tri-*O*-acetyl-1,2-*O*-(1′-*exo*-ethoxyethylidene)-α-D-glucopyranose (**1**) (2) (750 mg) was added and the solution was left for 20 h at room temperature. The nuclear magnetic resonance (n.m.r.) spectrum of the crude reaction product showed a near quantitative yield of tri-*O*-acetyl-1,2-*O*-isopropylidene-α-D-glucopyranose. After two recrystallizations from ethanol the compound melted at 86.5–88°, $[\alpha]_D$ +26° (*c*, 1 in chloroform). Literature (1), m.p. 87–88°, $[\alpha]_D^{20}$ +30.5° (chloroform). Under similar conditions, tri-*O*-acetyl-1,2-*O*-cyclopentylidene-α-D-glucopyranose (m.p. 113.5–115°, $[\alpha]_D^{25}$ +34.5° (*c*, 1 in chloroform)), tri-*O*-acetyl-1,2-*O*-cyclohexylidene-α-D-glucopyranose (m.p. 68–69°, $[\alpha]_D^{25}$ +33° (*c*, 1 in chloroform)), and a mixture of the diastereoisomeric tri-*O*-acetyl-1,2-*O*-benzylidene-α-D-glucopyranoses were prepared. Strictly anhydrous conditions were necessary (3) and were insured by the addition of about 10% trimethyl orthoformate to dried aldehyde or ketone containing the *p*-toluenesulfonic acid prior to the addition of the 1,2-orthoacetate (**1**).

The n.m.r. spectra for the 1,2-ketals showed $J_{1,2} = 5$, $J_{2,3} = 3$, $J_{3,4} = 3$, and $J_{4,5} = 9$ Hz, values very similar to those reported for acetylated alkyl 1,2-orthoacetate (2) and 1,2-*O*-alkylidene (1, 4) derivatives of D-glucopyranose. These data indicate a distorted, flattened chair conformation (2) as recently found for compounds of this type by X-ray crystallographic analysis (5) rather than the skew-boat suggested by Coxon and Hall (4).

The major isomer formed (about 75%) on reaction of **1** with benzaldehyde had n.m.r. parameters very similar to those presented above. The methine proton of the benzylidene group gave its signal at τ 4.13 in close agreement with the chemical shift, τ 4.10, for the similar proton of 2-phenyldioxolane. The minor component, which has this signal at τ 3.55, has the n.m.r. parameters for the isomer previously reported (1, 6). This isomer is considered to have the phenyl group in the *endo* position since $J_{2,3}$ and $J_{3,4} = 4.5$ Hz and these larger values seem best interpreted as arising from the interaction of the phenyl group with the pyranose ring, as previously discussed by Lemieux and Morgan (2) in connection with the n.m.r. parameters of tri-*O*-acetyl-α-D-glucopyranose 1,2-(methyl orthopivalate).

When 4-butyrolactone was employed as the carbonyl compound, an about equimolar mixture of the *exo* (**2**) ($[\alpha]_D^{25}$ +42° (chloroform)) and *endo* (**3**) (m.p. 116–117°, $[\alpha]_D^{25}$ +85° (chloroform)) isomers of tri-*O*-acetyl-1,2-*O*-(2′-oxacyclopentylidene)-α-D-glucopyranose was obtained which could be separated by chromatography (silicic acid; 0.3% 2,6-lutidine + 3% methanol in benzene). The n.m.r. parameters of the pyranose-ring protons of the *exo*-isomer were virtually identical with those of the acetylated *exo*-alkyl 1,2-orthoacetates of glucose (2). A significant downfield shift of 0.4 p.p.m. was

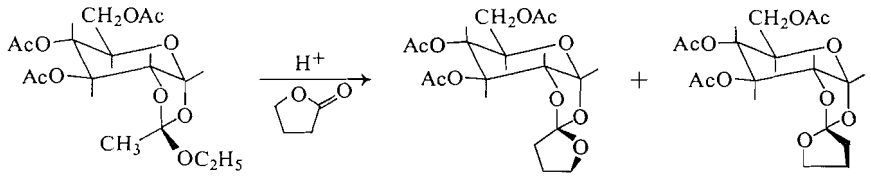

1 2 3

observed for H-3 of the *endo*-isomer and is believed to arise from its close proximity to the oxygen atom of the oxacyclopentylidene ring (7). The values of $J_{2,3} = 4.7$ and $J_{3,4} = 7.0$ Hz were considerably greater than the corresponding values (both 3 Hz) for the *exo*-isomer.

Compounds **2** and **3** were also synthesized from 3,4,6-tri-*O*-acetyl-α-D-glucopyranosyl chloride by way of tri-*O*-acetyl-2-*O*-(4′-hydroxybutyryl)-α-D-glucopyranosyl chloride which was converted to the orthoesters by treatment with tetraethylammonium chloride in 2,6-lutidine (2). These compounds are of interest as reagents for the preparation of D-glucopyranosides (8).

1. R. G. Rees, A. R. Tatchell, and R. D. Wells. J. Chem. Soc. C, 1768 (1967).
2. R. U. Lemieux and A. R. Morgan. Can. J. Chem. **43**, 2199 (1965).
3. R. U. Lemieux and J. D. T. Cipera. Can. J. Chem. **34**, 906 (1956).
4. B. Coxon and L. D. Hall. Tetrahedron, **20**, 1685 (1964).
5. J. Trotter and J. K. Fawcett. Acta Cryst. **21**, 366 (1966).
6. H. B. Wood, H. W. Diehl, and H. G. Fletcher, Jr. J. Am. Chem. Soc. **79**, 1986 (1957).
7. R. U. Lemieux and J. D. Stevens. Can. J. Chem. **43**, 2059 (1965).
8. R. U. Lemieux and A. R. Morgan. IUPAC Symposium, The Chemistry of Natural Products, Kyoto, Japan, April 12–18, 1964. Abstract of Papers, p. 151.

A stereoselective synthesis of α-D-glucopyranosides

R. U. Lemieux, R. Suemitsu,[1] and S. W. Gunner[2]
Department of Chemistry, University of Alberta, Edmonton, Alberta

Received February 5, 1968

Deoximation of 3,4,6-tri-*O*-acetyl-2-oximino-α-D-*arabino*-hexopyranosides to the corresponding 2-ulosides followed by borohydride reduction affords the α-D-glucopyranosides in excellent yields.

Canadian Journal of Chemistry, 46, 1040 (1968)

A main objective of our research in recent years has been the development of a stereoselective synthesis of α-D-glucopyranosides which proceeds in good overall yield based either on the glycosylating agent or the alcohol. This has now been accomplished by deoximation of the readily available 3,4,6-tri-*O*-acetyl-2-oximino-α-D-*arabino*-hexopyranosides (**1**) (1) and borohydride reduction of the resulting ketoglycoside (**2**) followed by deacetylation.

The deoximation has been accomplished under a variety of conditions including oxidation with nitrous acid or lead tetraacetate and transoximations with aldehydes and ketones under acid conditions. To date, the latter conditions appear most reliable and that employing levulinic acid in aqueous hydrochloric acid (2) was used in all the following transformations. Some deacetylation occurs both during the deoximation and in the borohydride reduction and, consequently, no attempt was made to isolate pure compounds after either of these reactions. Instead, the product was acetylated after removal of the boric acid and isolated as the tetraacetate.

In a typical experiment, isopropyl tri-*O*-acetyl-2-oximino-α-D-*arabino*-hexopyranoside (500 mg) which had been obtained in 89% yield using dimeric tri-*O*-acetyl-2-deoxy-2-nitroso-α-D-glucopyranosyl chloride and 1.2 mole equivalent of isopropyl alcohol (1), was treated with 10 ml of levulinic acid containing 1.5 ml of *N* hydrochloric acid at room temperature for 3 h. Extraction with chloroform followed by appropriate washes

[1]University of Alberta Postdoctorate Fellow, 1966–67.
[2]See ref. 1.

Can. J. Chem. Downloaded from www.nrcresearchpress.com by 210.87.254.40 on 09/05/12
For personal use only.

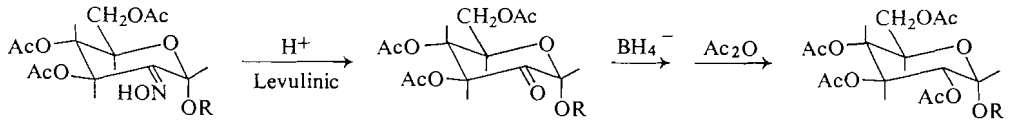

1 2 3

and solvent removal provided a 90% yield of an oil, $[\alpha]_D^{25}$ +80° (chloroform), which exhibited a singlet at τ 5.06 which was assigned to the anomeric proton of **2**. The substance was dissolved in 10 ml of tetrahydropyran and a solution of 120 mg of sodium borohydride in 2 ml of water was added at 0°. The solution was left at room temperature for 1 h and then made acid with excess acetic acid prior to removal of the boric acid with methanol in the usual manner. The residue was acetylated with acetic anhydride at 100°. Gas chromatographic examination of the crude product revealed only a trace (<5%) of component with the retention time of isopropyl tetra-*O*-acetyl-α-D-mannopyranoside. The product crystallized readily and on recrystallization gave an 80% yield of pure isopropyl tetra-*O*-acetyl-α-D-glucopyranoside. The n.m.r. spectrum of this compound shows a doublet for H_1 at τ 4.84 (spacing, 4.0 Hz), a quartet for H_2 at τ 5.24 (spacings, 4.0 and 10 Hz), and a triplet for H_3 at τ 4.54 (spacings, 10 Hz). When borodeuteride was used in the reduction, the spectrum of the product showed a singlet instead of the doublet, the quartet was not present, and the triplet was now a doublet with a spacing of 10 Hz. The signal for H_4 was now clearly apparent as a rough triplet (virtual long-range coupling of H_5 with the H_6's) centered at τ 4.97 with large spacings of about 10 Hz. It was, therefore, clear that indeed the reduction was restricted to the 2-position.

In similar conversions, the phenyl and α-naphthyl tetra-*O*-acetyl-α-D-glucopyranosides were obtained in 70% and 40% yields, respectively. Thus, the procedure shows promise as a general approach for the synthesis of α-D-glucopyranosides and is under further examination.

Acknowledgments

The authors are indebted to the National Research Council of Canada and the Corn Industries Research Foundation for financial assistance.

1. R. U. LEMIEUX, T. L. NAGABHUSHAN, and S. W. GUNNER. Can. J. Chem. **46**, 405 (1968).
2. C. H. DEPUY and B. W. PONDER. J. Am. Chem. Soc. **81**, 4629 (1959).

The photocycloaddition of nitrobenzene to alkenes[1]

J. L. CHARLTON AND P. DE MAYO
Department of Chemistry, University of Western Ontario, London, Ontario

Received February 22, 1968

The photochemical cycloaddition of nitrobenzene to cyclohexene at −70 °C gives an unstable crystalline adduct, an analogue of a molozonide, which has been characterized. Similar results have been obtained with norbornene, hex-1-ene, and 1-methylcyclohexene.

Canadian Journal of Chemistry, 46, 1041 (1968)

In 1956 Büchi and Ayer (1) reported that the irradiation of nitrobenzene in 2-methyl-2-butene gave a complex mixture of products in poor yield. From the structures of those substances identified it could be understood that, in part at least, the ethylenic bond had been oxidatively cleaved. These authors suggested that a derivative of the unknown 1,3,2-dioxazolidine[2] might

[1]Photochemical Synthesis. 21. Preceding paper: P. de Mayo, J.-P. Pete, and M. Tchir, J. Am. Chem. Soc. **89**, 5712 (1967).

[2]1,3,2-Dioxazolidines have been suggested, from time to time, as intermediates in various reactions (refs. 4, 5, 6; see also refs. 7, 8) with varying degrees of credibility.

Can. J. Chem. Downloaded from www.nrcresearchpress.com by 210.87.254.40 on 09/05/12
For personal use only.

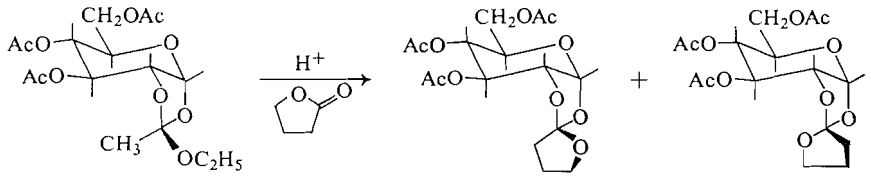

1 2 3

observed for H-3 of the *endo*-isomer and is believed to arise from its close proximity to the oxygen atom of the oxacyclopentylidene ring (7). The values of $J_{2,3} = 4.7$ and $J_{3,4} = 7.0$ Hz were considerably greater than the corresponding values (both 3 Hz) for the *exo*-isomer.

Compounds **2** and **3** were also synthesized from 3,4,6-tri-*O*-acetyl-α-D-glucopyranosyl chloride by way of tri-*O*-acetyl-2-*O*-(4′-hydroxybutyryl)-α-D-glucopyranosyl chloride which was converted to the orthoesters by treatment with tetraethylammonium chloride in 2,6-lutidine (2). These compounds are of interest as reagents for the preparation of D-glucopyranosides (8).

1. R. G. Rees, A. R. Tatchell, and R. D. Wells. J. Chem. Soc. C, 1768 (1967).
2. R. U. Lemieux and A. R. Morgan. Can. J. Chem. **43**, 2199 (1965).
3. R. U. Lemieux and J. D. T. Cipera. Can. J. Chem. **34**, 906 (1956).
4. B. Coxon and L. D. Hall. Tetrahedron, **20**, 1685 (1964).
5. J. Trotter and J. K. Fawcett. Acta Cryst. **21**, 366 (1966).
6. H. B. Wood, H. W. Diehl, and H. G. Fletcher, Jr. J. Am. Chem. Soc. **79**, 1986 (1957).
7. R. U. Lemieux and J. D. Stevens. Can. J. Chem. **43**, 2059 (1965).
8. R. U. Lemieux and A. R. Morgan. IUPAC Symposium, The Chemistry of Natural Products, Kyoto, Japan, April 12–18, 1964. Abstract of Papers, p. 151.

A stereoselective synthesis of α-D-glucopyranosides

R. U. Lemieux, R. Suemitsu,[1] and S. W. Gunner[2]
Department of Chemistry, University of Alberta, Edmonton, Alberta

Received February 5, 1968

Deoximation of 3,4,6-tri-*O*-acetyl-2-oximino-α-D-*arabino*-hexopyranosides to the corresponding 2-ulosides followed by borohydride reduction affords the α-D-glucopyranosides in excellent yields.

Canadian Journal of Chemistry, 46, 1040 (1968)

A main objective of our research in recent years has been the development of a stereoselective synthesis of α-D-glucopyranosides which proceeds in good overall yield based either on the glycosylating agent or the alcohol. This has now been accomplished by deoximation of the readily available 3,4,6-tri-*O*-acetyl-2-oximino-α-D-*arabino*-hexopyranosides (**1**) (1) and borohydride reduction of the resulting ketoglycoside (**2**) followed by deacetylation.

The deoximation has been accomplished under a variety of conditions including oxidation with nitrous acid or lead tetraacetate and transoximations with aldehydes and ketones under acid conditions. To date, the latter conditions appear most reliable and that employing levulinic acid in aqueous hydrochloric acid (2) was used in all the following transformations. Some deacetylation occurs both during the deoximation and in the borohydride reduction and, consequently, no attempt was made to isolate pure compounds after either of these reactions. Instead, the product was acetylated after removal of the boric acid and isolated as the tetraacetate.

In a typical experiment, isopropyl tri-*O*-acetyl-2-oximino-α-D-*arabino*-hexopyranoside (500 mg) which had been obtained in 89% yield using dimeric tri-*O*-acetyl-2-deoxy-2-nitroso-α-D-glucopyranosyl chloride and 1.2 mole equivalent of isopropyl alcohol (1), was treated with 10 ml of levulinic acid containing 1.5 ml of *N* hydrochloric acid at room temperature for 3 h. Extraction with chloroform followed by appropriate washes

[1]University of Alberta Postdoctorate Fellow, 1966–67.
[2]See ref. 1.

Can. J. Chem. Downloaded from www.nrcresearchpress.com by 210.87.254.40 on 09/05/12
For personal use only.

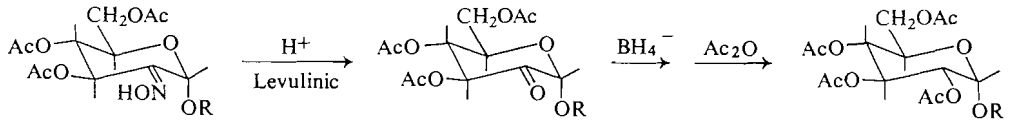

1 2 3

and solvent removal provided a 90% yield of an oil, $[\alpha]_D^{25}$ +80° (chloroform), which exhibited a singlet at τ 5.06 which was assigned to the anomeric proton of **2**. The substance was dissolved in 10 ml of tetrahydropyran and a solution of 120 mg of sodium borohydride in 2 ml of water was added at 0°. The solution was left at room temperature for 1 h and then made acid with excess acetic acid prior to removal of the boric acid with methanol in the usual manner. The residue was acetylated with acetic anhydride at 100°. Gas chromatographic examination of the crude product revealed only a trace (<5%) of component with the retention time of isopropyl tetra-*O*-acetyl-α-D-mannopyranoside. The product crystallized readily and on recrystallization gave an 80% yield of pure isopropyl tetra-*O*-acetyl-α-D-glucopyranoside. The n.m.r. spectrum of this compound shows a doublet for H_1 at τ 4.84 (spacing, 4.0 Hz), a quartet for H_2 at τ 5.24 (spacings, 4.0 and 10 Hz), and a triplet for H_3 at τ 4.54 (spacings, 10 Hz). When borodeuteride was used in the reduction, the spectrum of the product showed a singlet instead of the doublet, the quartet was not present, and the triplet was now a doublet with a spacing of 10 Hz. The signal for H_4 was now clearly apparent as a rough triplet (virtual long-range coupling of H_5 with the H_6's) centered at τ 4.97 with large spacings of about 10 Hz. It was, therefore, clear that indeed the reduction was restricted to the 2-position.

In similar conversions, the phenyl and α-naphthyl tetra-*O*-acetyl-α-D-glucopyranosides were obtained in 70% and 40% yields, respectively. Thus, the procedure shows promise as a general approach for the synthesis of α-D-glucopyranosides and is under further examination.

Acknowledgments

The authors are indebted to the National Research Council of Canada and the Corn Industries Research Foundation for financial assistance.

1. R. U. LEMIEUX, T. L. NAGABHUSHAN, and S. W. GUNNER. Can. J. Chem. **46**, 405 (1968).
2. C. H. DEPUY and B. W. PONDER. J. Am. Chem. Soc. **81**, 4629 (1959).

The photocycloaddition of nitrobenzene to alkenes[1]

J. L. CHARLTON AND P. DE MAYO
Department of Chemistry, University of Western Ontario, London, Ontario

Received February 22, 1968

The photochemical cycloaddition of nitrobenzene to cyclohexene at −70 °C gives an unstable crystalline adduct, an analogue of a molozonide, which has been characterized. Similar results have been obtained with norbornene, hex-1-ene, and 1-methylcyclohexene.

Canadian Journal of Chemistry, 46, 1041 (1968)

In 1956 Büchi and Ayer (1) reported that the irradiation of nitrobenzene in 2-methyl-2-butene gave a complex mixture of products in poor yield. From the structures of those substances identified it could be understood that, in part at least, the ethylenic bond had been oxidatively cleaved. These authors suggested that a derivative of the unknown 1,3,2-dioxazolidine[2] might

[1]Photochemical Synthesis. 21. Preceding paper: P. de Mayo, J.-P. Pete, and M. Tchir, J. Am. Chem. Soc. **89**, 5712 (1967).

[2]1,3,2-Dioxazolidines have been suggested, from time to time, as intermediates in various reactions (refs. 4, 5, 6; see also refs. 7, 8) with varying degrees of credibility.

Can. J. Chem. Downloaded from www.nrcresearchpress.com by 210.87.254.40 on 09/05/12
For personal use only.

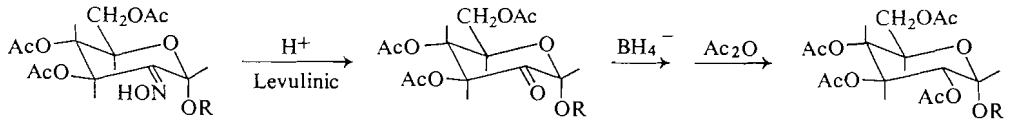

1 2 3

and solvent removal provided a 90% yield of an oil, $[\alpha]_D^{25}$ +80° (chloroform), which exhibited a singlet at τ 5.06 which was assigned to the anomeric proton of **2**. The substance was dissolved in 10 ml of tetrahydropyran and a solution of 120 mg of sodium borohydride in 2 ml of water was added at 0°. The solution was left at room temperature for 1 h and then made acid with excess acetic acid prior to removal of the boric acid with methanol in the usual manner. The residue was acetylated with acetic anhydride at 100°. Gas chromatographic examination of the crude product revealed only a trace (<5%) of component with the retention time of isopropyl tetra-*O*-acetyl-α-D-mannopyranoside. The product crystallized readily and on recrystallization gave an 80% yield of pure isopropyl tetra-*O*-acetyl-α-D-glucopyranoside. The n.m.r. spectrum of this compound shows a doublet for H_1 at τ 4.84 (spacing, 4.0 Hz), a quartet for H_2 at τ 5.24 (spacings, 4.0 and 10 Hz), and a triplet for H_3 at τ 4.54 (spacings, 10 Hz). When borodeuteride was used in the reduction, the spectrum of the product showed a singlet instead of the doublet, the quartet was not present, and the triplet was now a doublet with a spacing of 10 Hz. The signal for H_4 was now clearly apparent as a rough triplet (virtual long-range coupling of H_5 with the H_6's) centered at τ 4.97 with large spacings of about 10 Hz. It was, therefore, clear that indeed the reduction was restricted to the 2-position.

In similar conversions, the phenyl and α-naphthyl tetra-*O*-acetyl-α-D-glucopyranosides were obtained in 70% and 40% yields, respectively. Thus, the procedure shows promise as a general approach for the synthesis of α-D-glucopyranosides and is under further examination.

Acknowledgments

The authors are indebted to the National Research Council of Canada and the Corn Industries Research Foundation for financial assistance.

1. R. U. LEMIEUX, T. L. NAGABHUSHAN, and S. W. GUNNER. Can. J. Chem. **46**, 405 (1968).
2. C. H. DEPUY and B. W. PONDER. J. Am. Chem. Soc. **81**, 4629 (1959).

The photocycloaddition of nitrobenzene to alkenes[1]

J. L. CHARLTON AND P. DE MAYO
Department of Chemistry, University of Western Ontario, London, Ontario

Received February 22, 1968

The photochemical cycloaddition of nitrobenzene to cyclohexene at −70 °C gives an unstable crystalline adduct, an analogue of a molozonide, which has been characterized. Similar results have been obtained with norbornene, hex-1-ene, and 1-methylcyclohexene.

Canadian Journal of Chemistry, 46, 1041 (1968)

In 1956 Büchi and Ayer (1) reported that the irradiation of nitrobenzene in 2-methyl-2-butene gave a complex mixture of products in poor yield. From the structures of those substances identified it could be understood that, in part at least, the ethylenic bond had been oxidatively cleaved. These authors suggested that a derivative of the unknown 1,3,2-dioxazolidine[2] might

[1]Photochemical Synthesis. 21. Preceding paper: P. de Mayo, J.-P. Pete, and M. Tchir, J. Am. Chem. Soc. **89**, 5712 (1967).

[2]1,3,2-Dioxazolidines have been suggested, from time to time, as intermediates in various reactions (refs. 4, 5, 6; see also refs. 7, 8) with varying degrees of credibility.

Can. J. Chem. Downloaded from www.nrcresearchpress.com by 210.87.254.6 on 09/05/12
For personal use only.

Can. J. Chem. Downloaded from www.nrcresearchpress.com by 210.87.254.6 on 09/05/12
For personal use only.

have been an intermediate. Other reaction pathways could be conceived, however, and we have investigated the matter further. Our preliminary results, summarized below, lead us to acknowledge the mechanistic insight of these authors and to report briefly on the properties of these new species.

Whilst irradiation of nitrobenzene at room temperature gave a complex mixture of products, irradiation of nitrobenzene (0.25 g) in cyclohexene (25 cc) at −70 °C until the disappearance of the nitro compound (g.l.c.) gave, on evaporation of the excess solvent at −20 °C, a crystalline solid which could be recrystallized at −80 °C from ethyl acetate. It decomposed over a few minutes at room temperature.

TABLE I

Hydrocarbon	Product	Yield (%) of diol	Yield (%) of aniline
Cyclohexene	*Cis*-cyclohexanediol	51[a]	53
		93[b]	86
Norbornene	*Exo*-norbornanediol	48[a]	47
Hex-1-ene	Hexane-1,2-diol	38[a]	51
1-Methyl-cyclohexene	1-Methylcyclohexane-1,2-diol	33[a]	21

[a]Yields based on hydrogenation of the crude irradiation product and estimated by g.l.c. on 2.5% FFAP on Chromosorb P. No attempt to maximize yields was made.
[b]Yields based on recrystallized adduct.

The infrared spectrum ($CHCl_3$, −20 °C) showed the absence of carbonyl absorption, and bands near 970 cm^{-1} to be attributed to the —O—N— fragment (2, 3). The n.m.r. spectrum (−25 °C, $CDCl_3$) showed benzenoid absorption at 7.38 p.p.m. and, aside from protons on saturated carbon, absorption at 4.38 p.p.m. for two protons attached to carbon bearing oxygen. On allowing the solution to warm, these signals decreased with the concomitant appearance of aldehyde signals at 9.53 p.p.m. These properties are consonant with having the structure **1**.

This was confirmed by catalytic hydrogenation of the crystalline material over pre-reduced platinum catalyst in ethyl acetate at −20 °C.

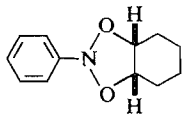

1

Cis-cyclohexanediol (containing <5% *trans* isomer) was obtained in ca. 90% yield, together with an equivalent yield of aniline. The same products could be isolated after hydrogenation of the crude irradiation product (see Table I), but in lower yield. The result of the use of other alkenes is shown in the same table.

The substance **1** is the first member of a class of cyclic derivatives of trivalent nitrogen containing two N—O bonds[3]: the mode of chemical decomposition suggests that the analogy with the molozonides is not purely formal.

Acknowledgments

The financial assistance of the National Research Council of Canada and an NRCC Fellowship to J. L. Charlton are gratefully acknowledged.

1. G. Büchi and D. E. Ayer. J. Am. Chem. Soc. **78**, 689 (1956).
2. V. A. Tartakovskii, I. E. Chlenov, S. S. Smagin, and S. S. Novikov. Izv. Akad. Nauk SSSR Ser. Khim. 583 (1964).
3. M. Davies and N. A. Spiers. J. Chem. Soc. 3971 (1959).
4. J. S. Splitter and M. Calvin. J. Org. Chem. **20**, 1086 (1955).
5. D. L. Hammick and G. Sixsmith. J. Chem. Soc. 580 (1935).
6. I. Ostromisslensky. J. Prakt. Chem. **192**(84), 495 (1911).
7. E. C. Taylor, B. Furth, and M. Pfau. J. Am. Chem. Soc. **87**, 1400 (1965).
8. M. L. Scheinbaum. J. Org. Chem. **29**, 2200 (1964).

[3]The synthesis of substances of type **2**, the first trivalent nitrogen derivatives with two N—O bonds in any system, has been very recently reported (2).

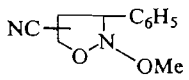

2

Can. J. Chem. Downloaded from www.nrcresearchpress.com by 210.87.254.5 on 09/05/12
For personal use only.

Canadian Journal of Chemistry

Published by THE NATIONAL RESEARCH COUNCIL OF CANADA

VOLUME 46 APRIL 1, 1968 NUMBER 7

Chemistry of episulfides. II.[1] The reactivities of propylene sulfide and propylene oxide towards acetic acid

NEIL S. ISAACS[2] AND K. NEELAKANTAN[3]

University of Reading, Whiteknights Park, Reading, England

Received November 8, 1967

The rates and products of solvolysis of propylene oxide and propylene sulfide in acetic acid have been determined. The results show that terminal attack is preferred, although not exclusively, and that the sulfide is the less reactive by a factor of 50–60. This difference is accounted for mainly in the preexponential factor. Solvent isotope effects are also observed.

Canadian Journal of Chemistry, 46, 1043 (1968)

Pursuing our studies of the reactivities of three-membered heterocycles we now report a comparison of the rates of ring-opening of propylene sulfide **1***a* and propylene oxide **1***b* under acidic conditions (1). Acid catalysis is well established in many reactions of epoxides (2) but has not been examined with the sulfur analogues. It was not found possible to use aqueous solutions of strong acids, however, on account of the extensive polymerization which occurred. The reagent chosen therefore was glacial acetic acid which gave products that could be characterized in good yield both with the epoxide and with the episulfide. As previously, the unsymmetrically substituted rings were chosen in order to be able to study the orientation of ring-opening. Reaction rates have been measured at several temperatures and isotope effects in the presence of acetic acid-*d* noted.

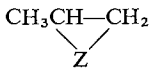

1*a* Z = S
b Z = O

Products of the Reactions

Propylene Oxide and Acetic Acid

Propylene oxide was allowed to react completely with 10 to 20 times its weight of pure acetic acid at temperatures between 30 and 100 °C. After removal of the bulk of the acetic acid by careful fractionation at reduced pressure the resulting solution was analyzed by gas–liquid chromatography (g.l.c.). Two products were apparent; the first, in order of elution, was in major yield and was shown to be 1-acetoxypropan-2-ol **2***a*; the second, minor, constituent was 2-acetoxy-1-propanol, **3***a*.

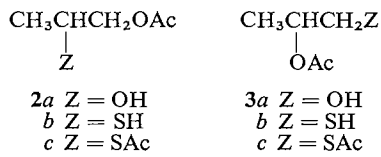

2*a* Z = OH
b Z = SH
c Z = SAc

3*a* Z = OH
b Z = SH
c Z = SAc

The identification of these products was made on the basis of the following evidence. The two compounds gave identical traces with the two monoacetates of propan-1,2-diol (made by incomplete acetylation with acetyl chloride)[4] on two gas chromatographic columns, polypropylene glycol at 120° and 'Antarox' at 140°, conditions under which each compound, the glycol and the diacetate were completely separated. The major component was separated from the minor by preparative gas–liquid chromatography. Its mass spectrum confirmed the molecular weight

[1]For Part I of this series, see N. S. Isaacs, Can. J. Chem. **44**, 395 (1966).

[2]To whom enquiries concerning this work should be made.

[3]Present address: Department of Chemistry, University of Toronto, Ontario.

[4]These are formed in the ratio of 70:30 in order of elution. From previous knowledge of the relative rates of acylation of primary and secondary alcohols (9) it would be expected that the major component would be the primary ester, **2***a*, in agreement with our conclusion.

TABLE I

Ratios of 1-acetoxypropan-2-ol, **2**, and 2-acetoxypropan-1-ol, **3**, formed in various reactions

System	Temperature °C	%**2*** ('normal product')	%**3*** (abnormal product)
		Z = O	
Propylene oxide and acetic acid	30	70	30
Propylene oxide and acetic acid	60	69	31
Propylene oxide and acetic acid	100	67	33
Propan-1,3-diol and 1 mole acetyl chloride		78	22
Propylene oxide and acetic acid/ sodium acetate		80	20
		Z = S	
Propylene sulfide and acetic acid	100	55	45
Propylene sulfide and acetic acid and pyridine		90	10
Propylene sulfide and acetyl chloride		67	33

*Reproducibility = ±5%.

of 118 and gave as base peak a fragment of m/e = 74. This could be interpreted as the extrusion of CO_2, or, more probably since this is not characteristic of esters, to loss of CH_3C—OH which is more consistent with the structure **2***a* than with **3***a*. The second most prominent peak was at m/e = 100, corresponding to a loss of H_2O. The major product was shown to have the same retention time on the above columns and the same infrared spectrum as an authentic sample of 1-acetoxypropan-2-ol prepared by the action of sodium acetate on 1-chloropropan-2-ol, the structure which had been separately established by Stewart and VanderWerf (3). As expected, this compound contained ca. 10% of 2-acetoxypropan-1-ol which was indistinguishable by g.l.c. from the minor product of the reaction. The major product also increased at the expense of the minor on addition of sodium acetate to the reaction mixture, an observation which is consistent with the recognized greater tendency towards terminal attack under basic conditions. The ratios of products were examined at different temperatures, the results being shown in Table I.

Other products observed on the gas chromatogram were a small amount of 1,2-diacetoxypropane (by comparison with an authentic specimen) probably formed by esterification of a primary product and, when propylene oxide was in fairly high concentration, two high boiling components, probably **4** and **5**. These did not appear to be formed to any significant extent under conditions used for the kinetic measurements.

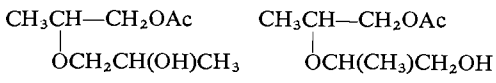

4 **5**

Propylene Sulfide and Acetic Acid

Propylene sulfide was allowed to react with a ten-fold excess of acetic acid at 100° after which the acetic acid was removed by careful distillation under reduced pressure. The products were acetylated by reaction with excess acetyl chloride after which they were subjected to gas chromatography. Two peaks corresponding to 2-acetoxypropyl thiolacetate, **3***c*, and 2-acetoxy-*iso*propyl thiolacetate, **2***c*, were observed and identified by comparison with the retention times on two columns (polypropylene glycol and 'Antarox' both at 150°) of authentic specimens of each compound. The products of the reaction of propylene sulfide and acetic acid are thus 2-acetoxy-propane-1-thiol, **3***b*, and 1-acetoxypropan-2-thiol, **2***b*, in the ratio given in Table I (based on peak areas). This is supported by the infrared spectra of the primary products which show one carbonyl absorption at 1725 cm^{-1} while the acetylated products show an additional band at 1680 cm^{-1} due to the S-acetyl group. In addition to these compounds, the product contained a significant proportion of two higher molecular weight species, separable on the gas chromatograph ('Antarox' at 180°) and probably of structures **6** and **7** by analogy with the product from cyclohexene sulfide and acetic acid (4). The proportion of dimeric product was reduced by carrying out the reaction at greater dilution in

Can. J. Chem. Downloaded from www.nrcresearchpress.com by 210.87.254.5 on 09/05/12
For personal use only.

TABLE II

Measured rate constants

System	T °C	10^5k*	10^5k_N†	10^5k_A‡	k_H/k_D
Propylene oxide and acetic acid	51.80	3.19	2.23	0.96	
Propylene oxide and acetic acid	70.00	14.7	10.29	4.41	
Propylene oxide and acetic acid	90.00	66.3	46.4	19.9	
Propylene oxide and acetic acid-*d*	51.80	1.65			1.93
Propylene oxide and acetic acid-*d*	70.00	9.96			1.48
Propylene oxide and acetic acid-*d*	90.00	43.7			1.52
Propylene sulfide and acetic acid	70.20	0.232	0.127	0.105	
Propylene sulfide and acetic acid	82.00	0.622	0.342	0.280	
Propylene sulfide and acetic acid	92.00	1.06	0.583	0.477	
Propylene sulfide and acetic acid-*d*	90.00	0.627			1.6

*Average for two runs, s^{-1}.
†ie. for attack at C-1 (Normal attack).
‡ie. for attack at C-2 (Abnormal attack).

acetic acid but even at the concentrations employed in the kinetic measurements it probably accounted for one third of the total product.

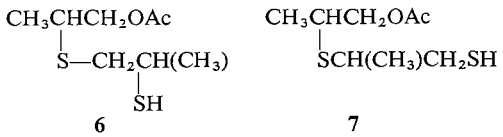

6 7

Experimental

2-Acetoxypropyl thiolacetate, 3*c*, was prepared by the treatment of propylene sulfide with acetyl chloride to give 2-chloropropyl thiolacetate followed by heating with potassium acetate to give 3*c*, b.p. 75° at 10 mm. The structure of this compound has been established by Davies and Savige (5) by hydrolysis to the known 1-mercapto-2-propanol. Gas chromatographic analysis of this product ('Antarox', 120°) showed however a significant proportion of another product inseparable from 2*c*, indicating that ring-opening of propylene sulfide by acetyl chloride gives attack at the 1- and 2-carbons in the ratio of 2:1.

2-Acetoxy*iso*propyl thiolacetate, 2*c*, was prepared by the action of acetic anhydride and pyridine on propylene sulfide, b.p. 100° at 10 mm. Previous workers (5) have shown that the product of this reaction on hydrolysis gives the known 2-mercapto-1-propanol. Gas chromatographic analysis of the product ('Antarox', 120°) shows the presence of approximately 10% of the isomer, 3*c*.

Kinetic measurements were carried out in a water thermostat held to ±0.05° with initial epoxide and episulfide concentrations 0.02–0.05 *M* and analyses conducted by the gas chromatographic technique described previously (1) using a 6 ft silicone column. Propylene oxide was then separated at 75° using as reference a small quantity of cyclopentane added to the reaction mixture and propylene sulfide at 80° using cyclohexane as reference. Peak areas were estimated planimetrically and appeared to be reproducible to ±2 %. First-order rate constants, enthalpies and entropies of activation were calculated using an I.B.M. 1620 computer and least-squares program.

Results

Measured rate constants, dissected where appropriate into separate rates for attack at the primary and secondary carbons ('normal' and 'abnormal' attack, respectively), are shown in Table II. Activation parameters are given in Table III.

Discussion

The rate constants clearly establish that the episulfide is considerably less reactive than the epoxide towards ring-opening in the presence of an acidic reagent, just as it is less reactive towards a base. The difference in rates for the acidic reaction (an average factor of 70 over the temperature range studied) is more pronounced than that for the reaction with aniline (a factor of 2–4). At the same time, the solvent isotope effect, k_H/k_D for both reactions is of the same order of magnitude (ca. 1.5). This indicates that both reactions proceed via the protonated heterocyclic ring **8**, **9**, the isotope effect here being a result of the solvent properties as discussed previously (6).

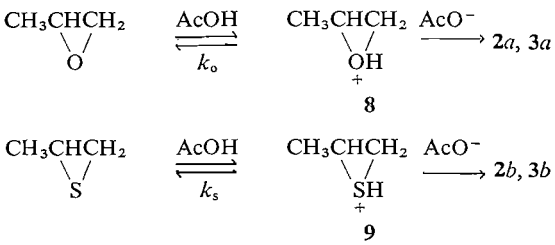

It has recently been shown that in one case at least, a sulfide is more basic than the corresponding ether (7). While it is not reliable to extrapolate too closely the effects of structure

Can. J. Chem. Downloaded from www.nrcresearchpress.com by 210.87.254.5 on 09/05/12
For personal use only.

TABLE III

Activation* parameters for the reactions

System	$\Delta H^{\neq}$ k cal mole^{-1}	$\Delta S^{\neq}$ cal deg^{-1} mole^{-1}
Propylene oxide and acetic acid	18.5±0.9	−24.3±1.5
Propylene sulfide and acetic acid	15.7±1.4	−40.6±4.5

*Average for attack at 1- and 2-carbons.

between two different types of base (8) it is assumed that this gross difference applies also to the three-membered rings although by analogy with ethyleneimine, the actual basicities would be expected to be lower than those of their open-chain analogues. Thus, if it can be assumed that $k_o \gg k_s$, the difference in reactivity results from the greater stability of **9** compared to **8** towards nucleophilic attack. The relative reactivities of propylene sulfide and oxide and of their conjugate acids are in the same order.

The difference in reactivity furthermore appears to originate in the entropy term (Table III) which probably represents a shift in emphasis of the bond-breaking and bond-making processes. Thus the ring-opening of **8** would proceed more or less spontaneously with a good deal of 'S_N1' character while **9** by virtue of its greater stability would require greater concomitant bond-making and more 'S_N2' character involving loss of translational freedom of the reagent in the transition state.

The ratio of attack at the terminal position to attack at C-2 is considerably lower in both cases (approximately 2:1) than was found for reaction under basic conditions. This is commonly experienced in ring-opening reactions of epoxides (2) and is ascribed to the partial carbonium ion character assumed by the secondary rather than the primary carbon atom of the ring although primary attack is favored sterically. It is not, however, apparent why this tendency should be more marked in the case of the episulfide than with the epoxide.

Acknowledgments

We thank the National Research Council of Canada and the University of Victoria for financial support of this work, and Professor J. L. Holmes for mass spectrometric analyses.

1. N. S. Isaacs. Can. J. Chem. **44,** 395 (1966).
2. R. E. Parker and N. S. Isaacs. Chem. Rev. **59,** 737 (1959).
3. C. A. Stewart and C. A. VanderWerf. J. Am. Chem. Soc. **76,** 1259 (1954).
4. C. C. J. Culvenor, W. Davies, and N. S. Heath. J. Chem. Soc. 282 (1949). E. E. Van Tamelen. J. Am. Chem. Soc. **73,** 3444 (1951).
5. W. Davies and W. E. Savige. J. Chem. Soc. 317 (1950).
6. N. S. Isaacs. Tetrahedron Letters, 4549, 4553 (1965).
7. N. S. Isaacs and J. Burns. Tetrahedron Letters, 0000 (1967).
8. E. M. Arnett and C. Y. Wu. J. Am. Chem. Soc. **82,** 4999 (1960).
9. J. Mitchell, W. Hawkins, and D. M. Smith. J. Am. Chem. Soc. **66,** 782 (1944).

Can. J. Chem. Downloaded from www.nrcresearchpress.com by 210.87.254.5 on 09/05/12
For personal use only.

On the selectivity of acylation of unprotected diamino acids

JEAN LECLERC AND LEO BENOITON
Department of Biochemistry, Faculty of Medicine, University of Ottawa, Ottawa, Canada
Received October 18, 1967

p-Nitrophenyl acetate and other esters except formates, will acylate the unprotected diamino acids homolysine, lysine, and ornithine, exclusively at the ω-amino group at pH 11. At lower alkaline pH's, the reaction is preferential but not selective. The reaction with diaminobutyric acid and diaminopropionic acid is not selective at any alkaline pH. ε-*N*-Acetyllysine can be prepared directly by the action of excess phenyl acetate on lysine at pH 11.

Canadian Journal of Chemistry, 46, 1047 (1968)

Can. J. Chem. Downloaded from www.nrcresearchpress.com by 210.87.254.6 on 09/05/12
For personal use only.

We have recently described the synthesis of several ω-*N*-acetyl-α,ω-diamino acid derivatives (1). These were prepared by the action of a *p*-nitrophenyl ester on the copper salt of the amino acid. The copper was used as is done routinely in order to prevent acylation of the α-amino group (2). There exists in the literature, however, a claim to the effect that in making such compounds, selective acylation can be effected successfully even in the absence of copper (3). ω-*N*-Formyllysine and ω-*N*-formylornithine were prepared in this manner (3); moreover, there are other examples of syntheses where ε-*N*-substituted lysine derivatives were prepared without first having protected the α-amino group. These include the synthesis of carbobenzoxy- (4) and trifluoroacetyllysine (5), biocytin (6), peptides of lysine (7) and ornithine (8), and benzylidenelysine (9).

In some cases, evidence for the identity and purity of the products is presented, but only the purified products have been scrutinized. In other cases, e.g. ref. 3, no evidence at all is given. In the case of the carbobenzoxy derivative (4), the α isomer is much more soluble than the ε isomer (9), consequently the two are readily separable. In general, the question of whether the actual acylation reaction was selective remains open. In this paper are described results of a study carried out with the objective of establishing definitely whether or not the acylation of diamino acids is selective for the ω-position, and if so, under what conditions. Because its acylation presents a distinct problem, diaminopropionic acid is discussed separately.

Synthetic standards of the possible isomers in each case were prepared by unequivocal methods as described below and characterized on an amino acid analyzer. The chromatographic data appear in Table I. Acylations were carried out in aqueous solution firstly under the conditions of Okawa and Hase (3) and subsequently all at a constant pH. Reaction mixtures were placed on the amino acid analyzer column and analyzed by comparison with the standards.

The results of the acylation of diamino acids by excess *p*-nitrophenyl ester in the absence of

TABLE I
Chromatographic data from the amino acid analyzer*

Compound	Time (min)	Constant†
α-*N*-Formylornithine	146.0	7.8
α-*N*-Formyllysine	171.8	4.2
α-*N*-Acetyldiaminopropionic acid	70.5	§
α-*N*-Acetyldiaminobutyric acid	112.0	18.0
α-*N*-Acetylornithine	140.6	6.4
α-*N*-Acetyllysine	171.0	4.6
α-*N*-Benzoyllysine	126.8‡	5.7
α-*N*-Propionyllysine	82.0‡	—
α-*N*-Carbobenzoxydiaminopropionic acid	213.0	16.3
δ-*N*-Formylornithine	65.6	20.4
ε-*N*-Formyllysine	99.8	15.8
β-*N*-Acetyldiaminopropionic acid	46.0	18.9
γ-*N*-Acetyldiaminobutyric acid	57.0	18.1
δ-*N*-Acetylornithine	56.0	17.6
ε-*N*-Acetyllysine	77.4	12.1
ε-*N*-Benzoyllysine	70.5‡	22.5
ε-*N*-Chloroacetyllysine	38.0‡	6.9
ε-*N*-Propionyllysine	31.0‡	27.3
β-*N*-Carbobenzoxydiaminopropionic acid	187.0	19.5
ζ-*N*-Acetylhomolysine‖	34.5‡	22.1
Aspartic acid	44.6	20.2
Glycine	89.0	20.6

*Beckman model 120B, 50 cm spherical resin column, eluted with 0.1 *N* sodium citrate, pH 3.28, followed by pH 4.25 buffer at time 85.
†Constant = peak height × width/μmole.
‡pH 4.25 buffer at time 0.
§Constant assumed to be the same as for the β isomer.
‖See ref. 29 for details of synthesis.

Can. J. Chem. Downloaded from www.nrcresearchpress.com by 210.87.254.6 on 09/05/12
For personal use only.

base, i.e., acylation of the amino acid monohydrochloride neutralized with one equivalent of sodium hydroxide (3), appear in Table II. It is seen that in all cases, when formyl and acetyl *p*-nitrophenyl ester were used, both the α and ω derivatives were formed. The products appeared in a ratio of roughly 5 to 1 in favor of the ω derivative, but higher in the case of the acetylation of lysine. The reaction is therefore definitely not selective under these conditions.

TABLE II

Acylation of diaminoacids in absence of base*

Amino acid	Nitrophenyl ester	Derivative formed (relative %) α	ω
Lysine	formate	18	82
	acetate	6	94
Ornithine	formate	17	83
	acetate	13	87
Diaminobutyric acid	acetate	14	86
Diaminopropionic acid	acetate	10	90

*Method of Okawa and Hase (3).

Preparative runs were then worked up as described by Okawa and Hase, and the ω-*N*-formylornithine and ω-*N*-formyllysine were passed on the analyzer. Both compounds were in fact free of α isomer. The conclusion is that the α isomer is more soluble and is lost during the crystallization.

The effect of pH on the selectivity was then studied with lysine, using one equivalent of acylating agent. The results appear in Table III. It was found that, in the pH range of 10.6 to 11.7, only the ω-substituted derivative was formed. Moreover, the amount of starting material remaining was negligible indicating that the reaction was complete. At pH's near neutrality, where more α derivative was formed than at higher pH's, the reaction was far from complete and both the α and ω derivatives were formed. At pH 11, therefore, the acylation of lysine by *p*-nitrophenyl acetate is selective for the ω-position.

Having shown that the acylation of lysine is selective at pH 11, we proceeded to verify if the same was obtained for the other diamino acids. The results in Table IV show that the acylation of homolysine and ornithine is also selective, but the selectivity is lost for the diamino acids of shorter chain length. The results also indicate

TABLE III

Effect of pH on the selectivity of acylation of lysine by *p*-nitrophenyl acetate

pH	Derivative formed (relative %) α	ω	Residual amino acid %
6.2	11	89	72
7.2	13	87	43
7.5	14	86	—
8.0	8	92	—
10.6	0	100	4
11.7	0	100	—

that a one-fold excess of acylating agent is sufficient to force the reaction to completion. But they do not give any information as to whether the reaction proceeds a step further, to the formation of the disubstituted derivative. Calculations indicated that this was not the case. This was confirmed by another experiment. A sample of ε-*N*-acetyllysine was stirred at pH 11.0 in the presence of a four-fold excess of phenyl acetate for 12 h. There was absolutely no change in the ninhydrin color yield of the solution, indicating that ε-*N*-acetyllysine is completely resistant to acylation under these conditions.

TABLE IV

Acylation of diaminoacids by *p*-nitrophenyl acetate at pH 11

Amino acid	Moles of ester	Derivative formed (relative %) α	ω	Residual amino acid %
Homolysine	1	0	100	2.5
Lysine	1	0	100	4
	2	0	100	0
Ornithine	1	0	100	12
Diaminobutyric acid	2	1.2	98.8	0.2
Diaminopropionic acid	1	12	88	38

So far, we have dealt with the acylation of diamino acids by *p*-nitrophenyl acetate. We have also studied the nature of the products formed by other esters as well as by other acylating agents. The results, in Table V, show that at pH 11, the acylation of lysine was selective only if the acylating agent was an ester. Using *p*-nitrophenyl acetate, chloroacetate, or propionate, no α derivative was formed at all, and practically no unreacted amino acid remained in the reaction

Can. J. Chem. Downloaded from www.nrcresearchpress.com by 210.87.254.6 on 09/05/12
For personal use only.

mixture when a one-fold excess of reagent was employed. Using phenyl acetate or propionate, the same results were obtained, even though a larger excess of reagent was required to force the reaction to completion. A different result was obtained when acetic anhydride or benzoyl chloride was used as acylating agent. In both cases, both the α and ω derivatives were formed. In the presence of excess reagent, both were completely converted to the disubstituted derivative, as was expected from other work (10, 11). The selectivity therefore is restricted to acylating agents which are esters.

TABLE V

Acylation of lysine at pH 11

Reagent	Moles of reagent	Derivative formed (relative %) α	ω	Residual amino acid %
p-Nitrophenyl acetate	1	0	100	4
	2	0	100	0
p-Nitrophenyl chloroacetate	5	0	100	<1
p-Nitrophenyl propionate	2	0	100	0
Phenyl acetate	1	0	100	48
	5	0	100	2
Phenyl propionate	5	0	100	18
Acetic anhydride	1	38	62	—
	5	0	0	0
Benzoyl chloride	1	18.8	81.2	41.8
	5	0	0	0

The results obtained with esters of formic acid, however, proved to be different from those obtained with other ester reagents. As seen in Table VI, in the formylation of lysine at pH 11 by either *p*-nitrophenyl formate or ethyl formate, there was always some α derivative formed. In the presence of excess reagent which was required to increase the yield of product, the relative percent of α isomer also increased. The apparent low reactivity[1] of formic acid esters explains the low yields (28%) which we obtained in the synthesis of δ-*N*-formyl-L-ornithine by our method as well as by the method of Okawa and Hase (3).

The selectivity of the acylation of lysine at pH 11 has permitted us to simplify the synthesis of

[1]The reviewer has suggested that the apparent low reactivity of formate esters with amino groups is probably due to the competitive hydrolysis of the reagent by base. Thus, formate esters are actually more reactive (and less specific) than acetate esters.

TABLE VI

Formylation of lysine at pH 11

Reagent	Moles of reagent	Derivative formed (relative %) α	ω	Residual amino acid %
p-Nitrophenyl formate	1	<1	>99	79.6
	2	10	90	53.5
Ethyl formate	1	<1	>99	62
	5	2.5	97.5	18.4
	10	3	97	16.8

ε-*N*-acetyl-L-lysine (1). The latter was prepared in 76% yield by stirring a mixture of lysine with an excess of phenyl acetate for 45 min while keeping the pH at 11 with a pH-stat charged with 2 *N* sodium hydroxide. After the reaction the product was desalted using Dowex 50. Precipitation at the isoelectric point without desalting led to too substantial a loss of material. This method obviates the use of copper, the complete removal of which is often tedious. Phenyl acetate is also preferable in some ways as the acylating agent.

Likely mechanisms which have been postulated for the aminolysis of esters assume a nucleophilic attack by the amine on the carbonyl group of the ester (12, 13). In the present case, for acylation to have occurred exclusively at the ω-position, the nucleophile required would have been the $NH_2(CH_2)_nNH_3^+COO^-$ ion. But this ion does not exist at any pH because the p*K* of the α-amino group is always lower than that of the ω-amino group. Moreover, at high pH's, both amino groups are unprotonated so there is no basis for discriminatory acylation that might depend on the relative concentrations of the protonated and unprotonated forms of the amino groups. However, Bruice *et al.* (14) have noted that the rate constants for the amination of esters depend on the basicity of the nucleophile. Therefore, it would be expected that aminolysis of the ester by the ω-amino group would have been favored. This is what we have observed in all cases. When an acid chloride or anhydride is the acylating agent, the attacking nucleophile is believed to be an acylium ion, $R{=}\overset{+}{C}{=}O$ (15), which because of its high reactivity, attacks any nucleophile without discrimination.

With regard to the preparation of its monosubstituted derivatives, diaminopropionic acid is

Can. J. Chem. Downloaded from www.nrcresearchpress.com by 210.87.254.6 on 09/05/12
For personal use only.

quite different from the other diamino acids. This is due to the unique nature of its copper salt. For the general case, in alkaline solution copper binds to the α-amino group permitting and resulting in reaction exclusively at the ω-amino group (2). But for diaminopropionic acid under these conditions the acylation not only is not selective but it fails completely. This is due to the fact that both the α- and β-amino groups are so close together that they are both bound by the copper (16). The β-amino group is, however, not bound at pH 4 (16). Workers have taken advantage of this to prepare the β-oxalyl (17) and β-ureido (18) derivatives. But in many instances, direct acylation in the absence of copper has been the only recourse. Kjaer (19) has observed that in strongly alkaline solution, the β-position of diaminopropionic acid is preferentially acylated. Other results corroborate this. The β-tosyl (20) and β-chloroacetyl (21) derivatives have been prepared by direct acylation, but the reactions also produced substantial amounts of disubstituted derivatives.

As can be seen in Table IV, the acetylation of diaminopropionic acid with *p*-nitrophenyl acetate at pH 11 has been shown not to be selective. Though it was certainly preferential for the β-position, a substantial amount of α isomer was formed, and much unreacted amino acid remained. Under the same conditions at pH's 7 and 8, only about 10% of the amino acid had reacted, and the relative amounts of α isomer had increased.

With respect to the monoacylation of diaminopropionic acid, Kjaer (19) had suggested that since the pK values of the amino groups are 6.8 and 9.6, at neutral pH, one should be able to expect preferential acylation of the α-amino group since it is uncharged and the β-amino group is charged at this pH. The results cited above indicate that this is not so. Moreover, the authors themselves have shown exactly the opposite, namely that carbobenzoxylation of diaminopropionic acid in a phosphate buffer at pH 7 is highly selective for the β-position (18). They have succeeded in preparing β-carbobenzoxydiaminopropionic acid in 77% yield by this procedure. We have studied the selectivity of the acylation of a dilute solution of diaminopropionic acid with carbobenzoxy chloride in excess sodium bicarbonate and at pH's 7 and 8 using the pH-stat. In all cases, both β and α isomers were formed, in a ratio of about 2 to 1. In more concentrated solutions as described (18), at pH 7, the β-carbobenzoxy derivative precipitates out of solution during the reaction and is, in fact, pure after one recrystallization. However, in all our attempts, there was always some α-isomer present in the filtered reaction mixture. On some occasions, some disubstituted derivative was also formed. We have failed to obtain yields as high as those reported (18). Our conclusion is that acylation of diaminopropionic acid is preferential but not selective at any pH.

Experimental

Materials

Except as otherwise indicated, all ω-*N*-acyl derivatives used as standards were prepared by the action of the corresponding *p*-nitrophenyl ester on the copper salt of the amino acid as has been described for the acetyl derivatives (1). The *p*-nitrophenyl esters were prepared in 70% yield from the acid chloride and sodium *p*-nitrophenylate as described for the chloroacetyl ester (22), except for *p*-nitrophenyl formate (3). ε-*N*-Formyl-L-lysine was purchased from Sigma Chemical Co., St. Louis. ε-*N*-Benzoyl-L-lysine was made as reported (23).

α-*N*-Acetyl-L-lysine (24), α-*N*-acetyl-L-ornithine (24), α-*N*-acetyl-L-diaminobutyric acid (24), α-*N*-benzoyl-L-lysine (25), and α-*N*-formyl-L-lysine (26) were obtained from the corresponding carbobenzoxy derivative followed by hydrogenation. α-*N*-Formyl-L-ornithine was prepared as for the lysine derivative (26), except that contaminating ornithine was removed with Amberlite IRC-50; yield, 59%.

Anal. Calcd. for $C_6H_{12}N_2O_3$: N, 17.5. Found: N, 17.6.

α-*N*-Carbobenzoxy-DL-diaminopropionic acid was prepared from L-cystine as described (27), and acetylated in the presence of *N* NaOH with acetic anhydride. After acidification, the solution was concentrated, the product extracted into ethyl acetate, the solvent evaporated, and the residue hydrogenated over Pd/C to give β-*N*-acetyl-DL-diaminopropionic acid from water–ethanol; yield, 60%.

Anal. Calcd. for $C_5H_{10}N_2O_3$: C, 41.1; H, 6.9; N, 19.2. Found: C, 41.2; H, 7.1; N, 19.2.

β-*N*-Carbobenzoxy-DL-diaminopropionic acid was prepared by the action of phosphorus pentachloride on the dicarbobenzoxy derivative (28).

Acylation Experiments

A solution of diamino acid (1.0 mmole) in 10 ml of water was brought to the required pH with a pH-stat charged with 2 *N* NaOH. Acylating agent was added, and the mixture was magnetically stirred 5 h while the pH was being kept constant. The reaction was usually complete after 3/4 h. When a large excess of reagent was used (Tables V and VI), the reaction was left for 12 h. The solution was then transferred and completed to 100 ml. One ml aliquots were diluted to 5 ml with 0.20 *N* sodium citrate, pH 2.2, and samples were assayed for the appropriate products with a Beckman Amino Acid Analyzer, model 120B.

ε-*N-Acetyl*-L-*lysine*

A mixture of lysine monohydrochloride (1.83 g; 0.01 mole) and phenyl acetate (6.4 ml; 0.05 mole) was stirred for 1 h at pH 11.0 (pH-stat). The solution was removed from the pH-stat and then stirred for an additional hour in the presence of 80 ml of Dowex 50 (H^+ form). The resin was filtered off, washed several times with water, and stirred in 3 *N* NH_4OH for 1/4 h. The resin was removed by filtration, the filtrate evaporated to dryness, and the residue crystallized twice from water–ethanol; yield, 1.37 g (76%).

Anal. Calcd. for $C_8H_{16}N_2O_3$: N, 14.9. Found: N, 14.9.

Acknowledgments

Financial support of this work by the Medical Research Council of Canada and the Department of Education of the Province of Quebec (a scholarship to J. L.) is gratefully acknowledged. We thank Mr. J. H. Seely of this department for the homolysine.

1. L. Benoiton and J. Leclerc. Can. J. Chem. **43**, 991 (1965).
2. J. C. Kurtz. J. Biol. Chem. **122**, 477 (1938).
3. R. Okawa and S. Hase. Bull. Chem. Soc. Japan, **36**, 759 (1963).
4. H. Zahn and H. R. Falkenburg. Ann. **636**, 117 (1960).
5. E. E. Schallenberg and M. Calvin. J. Am. Chem. Soc. 77, 2779 (1955).
6. J. Weijlard, C. Purdie, and M. Tishler. J. Am. Chem. Soc. **76**, 2505 (1954).
7. M. C. Khosla, H. G. Garg, and N. Anand. J. Sci. Ind. Res. India, **21B**, 318 (1962).
8. G. Losse, H. Jeschkeit, and H. Zaschre. Ann. **676**, 232 (1964).
9. B. Bezas and L. Zervas. J. Am. Chem. Soc. **83**, 719 (1961).
10. A. C. Kurtz. Biochem. J. **50**, 690 (1952).
11. S. C. Fu, K. R. Rao, S. M. Birnbaum, and J. P. Greenstein. J. Biol. Chem. **199**, 207 (1952).
12. F. Chattaway. J. Am. Chem. Soc. **59**, 1568 (1937).
13. M. Gordon, J. G. Miller, and A. R. Day. J. Am. Chem. Soc. **70**, 1946 (1948); **71**, 1245 (1949).
14. C. T. Bruice, A. Donzel, R. W. Huffman, and A. R. Butler. J. Am. Chem. Soc. **89**, 2106 (1967).
15. E. S. Gould. Mechanism and structure in organic chemistry. Holt, Rinehart and Winston, New York. 1959. p. 325.
16. A. Albert. Biochem. J. **50**, 690 (1952).
17. S. L. Rao, P. R. Adiga, and P. S. Sarna. Biochemistry, **3**, 342 (1964).
18. A. Kjaer and P. O. Larsen. Acta Chem. Scand. **13**, 1565 (1959).
19. A. Kjaer. Acta Chem. Scand. **3**, 1087 (1949).
20. K. Poduška, J. Rudinger, and F. Šorm. Collection Czech. Chem. Commun. **20**, 1174 (1955).
21. Y. Miyanoki. J. Biochem. Tokyo, **13**, 389 (1931).
22. L. Benoiton. J. Chem. Soc. 763 (1961).
23. A. C. Kurtz. J. Biol. Chem. **140**, 705 (1941).
24. A. Neuberger and F. Sanger. Biochem. J. **37**, 515 (1943).
25. W. F. Ross and L. S. Green. J. Biol. Chem. **137**, 105 (1941).
26. D. E. Wolf, J. Valiant, R. L. Peck, and K. Folkers. J. Am. Chem. Soc. **74**, 2002 (1952).
27. L. Benoiton. Can. J. Chem. To be published.
28. F. Schneider. Ann. **529**, 1 (1937).
29. J. H. Seely and L. Benoiton. Can. J. Biochem. To be published.

Can. J. Chem. Downloaded from www.nrcresearchpress.com by 210.87.254.6 on 09/05/12
For personal use only.

Deuterated amino acids. IV. The synthesis of L-phenyl-d_5-alanine-2,3,3-d_3[1,2]

A. T. BLOMQUIST and R. J. CEDERGREN[3]
Department of Chemistry, Cornell University, Ithaca, New York, 14850
Received November 10, 1967

The synthesis of L-phenyl-d_5-alanine-2,3,3-d_3 is described. The synthetic route involved the enzymatic deacylation of acetylphenyl-d_5-alanine-2,3,3-d_3, which was obtained by catalytic reduction (deuteriumation) of the hydrolyzed 2-methyl oxazolone derivative of benzaldehyde-d_6. The ultraviolet, infrared, and optical rotatory dispersion spectra of L-phenylalanine-d_8 are reported along with some corresponding data on the deuterated intermediates.

Canadian Journal of Chemistry, **46**, 1053 (1968)

Can. J. Chem. Downloaded from www.nrcresearchpress.com by 210.87.254.6 on 09/05/12
For personal use only.

With the general objective of providing highly deuterated amino acids as possible tools for use in the study of a variety of chemical and biological systems, as outlined briefly in a recent article (1), a useful synthesis for the title compound is reported. The synthesis of L-phenyl-d_5-alanine-2,3,3-d_3 is accomplished as outlined in the reaction sequence given below. With reference to this sequence, the formation of benzaldehyde-d_6 requires the addition of sodium chloride to the reaction mixture as a catalyst to guarantee reproducible yields.[4]

The catalytic reduction of the acid **3** in dioxane – ethyl acetate using 10% palladium on carbon as the catalyst is satisfactory but with the solvent–catalyst system of acetic anhydride, deuterium oxide, and platinum oxide (3), substantial reduction of the benzene ring occurs, giving *N*-acetylcyclohexyl-d_{11}-alanine-2,3,3-d_3 (**12**).

Because the activity of the renal acylase varies (4) it is useful to carry out the deacylation reaction simultaneously on separate solutions of the acid **4** and its protio analogue. Since the phenyl protons of the amino acid are distinguishable from the phenyl protons of the *N*-acetyl amino acid in the nuclear magnetic resonance spectrum, the enzymatic deacylation is followed by integration of the two phenyl peaks, and the necessary reaction time is easily determined.

The deuterated L-phenylalanine (**5**) is obtained in 18% yield overall from benzene-d_6.

The ultraviolet and optical rotatory dispersion data for the amino acid **5** are given in the Experimental section. It is to be noted that in the ultraviolet spectrum of **5** all maxima of the deuterated compound are at a lower wavelength than the corresponding maxima of the protio analogue. The higher energy needed to excite the deuterated compound results from the lowered zero point energy associated with deuterium substitution.

Condensation of the aldehyde **1** with *N*-acetylglycine, with 2-mercaptothiazole-5-one, and with hippuric acid affords as products the oxazolone **2**, 2-thio-4-benzylidene-d_6-thiazolone (**9**), and 2-phenyl-4-benzylidene-d_6-oxazolone (**8**) which contain, respectively, 96.4%, 93.9%, and 99.8% deuterium. The reduction of the oxazolone **8** and the thiazolone **9** with deuteriodic acid[5] and red phosphorus gave DL-phenyl-d_5-alanine-d_3 (**7**) in 66% and 51% yields. The product (**7**) from these reactions indicated considerable exchange (81.5%) had occurred rendering these alternate schemes unacceptable.

The observed amount of isotopic dilution of the three condensation products **2** (3.5%), **9** (6%), and **8** (0%) can be rationalized on the basis of tautomerism. Exchange with the solvent of the benzylidene positions of **2** and **9** occurs *via* their respective tautomers, 2-methylene-4-benzyl-Δ^3-oxazolone (**11**) (5, 6)[6] and 2-thio-4-

[1]Part III: A. T. Blomquist, B. F. Hiscock, and D. N. Harpp, J. Org. Chem., **31**, 4121 (1966).
[2]This study was supported in part by the National Science Foundation under grant G-18902.
[3]Present address: Département de biochimie, Université de Montréal, Montréal, Québec.
[4]Certain salts have been shown (2) to catalyze Friedel–Crafts reaction.
[5]Prepared from phosphorus triiodide and deuterium oxide.
[6]An analogous isomerization of certain 2-vinyl-4-benzyloxazolones to 2-ethyl-4-benzylideneoxazolones is described (6). The vinyl oxazolones were prepared by dehydration of acryloyl α-amino acids.

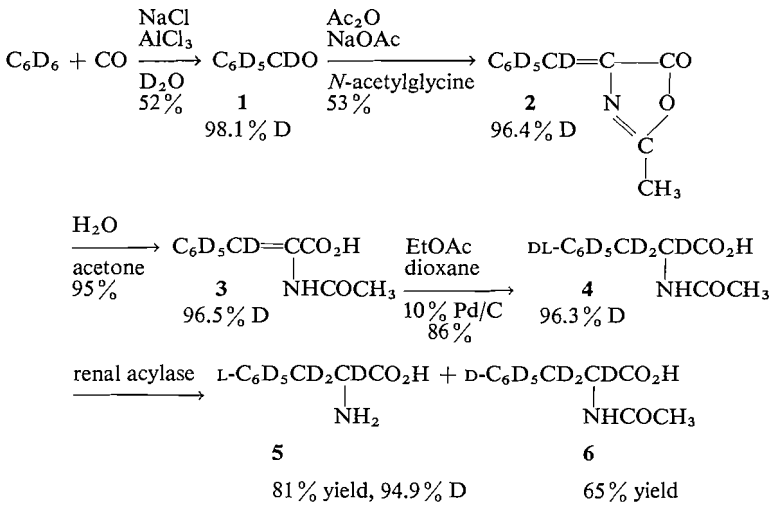

benzyl-Δ^3-thiazolone (**10**); no tautomer is possible for the azlactone **8**.

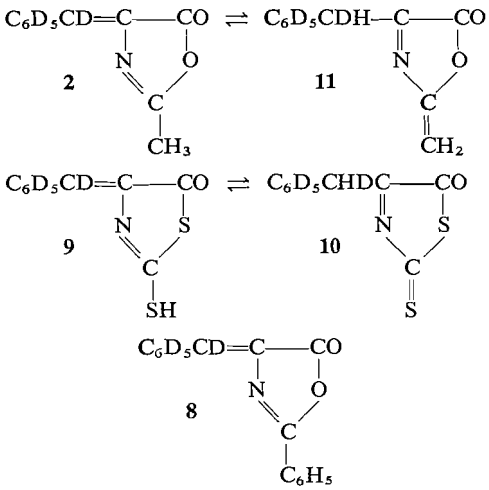

Analysis by mass spectrometry shows the thiazolone **9** to be a mixture of -d_5 (38.9%) and -d_6 (61.1%)[7] species, an indication that exchange occurs at only one position on the molecule. Exchange at the ring positions would give rise to additional species containing only 2, 3, and 4 deuteriums; these were not detected.

Experimental

Materials

Benzene-d_6 was purchased from Ciba Chemical Company, Summit, New Jersey. Phosphorus triiodide was supplied by K and K Fine Chemicals, Jamaica, New York, and renal acylase was obtained from Mann Assayed Biochemicals, New York, New York.

Equipment

The following machines were used in the course of this research: model A-60 Varian nuclear magnetic resonance spectrometer, Cary 14 recording spectrophotometer, Cary 60 spectropolarimeter, Consolidated Engineering model 21-103A mass spectrometer, and a Perkin–Elmer Infracord. A controlled atmosphere box was used throughout this research whenever a possibility of exchange with water vapor in the atmosphere arose. The box was kept dry by maintaining a positive pressure of dry nitrogen in the box, and by placing an evaporation dish containing 1:1 Celite : phosphorus pentoxide in the box. Dry nitrogen referred to in this Experimental section was dried by passing through columns of 1:1 Celite : phosphorus pentoxide.

Analyses

Deuterium analyses were carried out by J. Nemeth, Urbana, Illinois, the B. F. Goodrich Co., Brecksville, Ohio, and by one of the authors (R. J. C.). Microanalyses were performed at Scandinavian Microanalytical Laboratories, Herlev, Denmark, and Galbraith Laboratories, Inc., Knoxville, Tennessee.

Benzaldehyde-d_6 (1)

To a stirred metal autoclave was added 63.8 g (0.760 mole) of benzene-d_6, 112 g of aluminium chloride, 20 g of sodium chloride, and 1.0 ml of deuterium oxide (a modification of the procedure described in ref. 7) under an atmosphere of dry nitrogen. This mixture, pressured with carbon monoxide to 1000 p.s.i., was stirred for 3 h at room temperature; the carbon monoxide was then vented. Deuterium oxide (200 ml) and ether (200 ml) were added slowly and simultaneously to the opened bomb; stirring was continued until evolution of gas ceased. Distillation of the washed and dried ether layer gave 44.1 g (52%) of the aldehyde **1**: b.p. 68° (15 mm), 179° (760 mm); n_D^{25} 1.5414; d_4^{25} 1.1026; λ_{max} (neat) 4.43, 4.79, 6.01 μ.

[7]Deuterium analysis was carried out by the B. F. Goodrich Co., Brecksville, Ohio.

Can. J. Chem. Downloaded from www.nrcresearchpress.com by 210.87.254.6 on 09/05/12
For personal use only.

Can. J. Chem. Downloaded from www.nrcresearchpress.com by 210.87.254.6 on 09/05/12
For personal use only.

Anal. Calcd. for C_7D_6O: C, 74.95; H, 5.94;[8] D, 100 atom %. Found: C, 75.11, 74.96; H, 6.00, 6.07; D, 98.1 atom %.

2-Methyl-4-benzylidene-d_6-oxazolone (2)

Following the procedure of Herbst and Shemin (3), 39.3 g (0.350 mole) of the aldehyde **1**, 44.7 g (0.38 mole) of *N*-acetylglycine, 22.4 g of sodium acetate, and 105 ml of acetic anhydride afforded 35.8 g (53%) of the recrystallized azlactone **2**, m.p. 149–151°.

Anal. Calcd. for $C_{11}H_3D_6NO_2$: C, 68.37; H, 5.00; D, 66.7 atom %. Found: C, 68.43; H, 5.13; D, 64.2 atom % (96.4%).

3-Phenyl-d_5-2-acetamidopropenoic-3-d Acid (3)

Using the reported procedure (3) 38.0 g (0.197 mole) of the azlactone **2** was refluxed in 400 ml of acetone and 150 ml of water for 5 h. After crystallization from water there was obtained 40.1 g (95%) of the acid **3**: m.p. 189–190°; λ_{max} (KBr) 2.85, 3.05, 4.00, 4.40, 5.95, and 6.10 μ.

Anal. Calcd. for $C_{11}H_5D_6NO_3$: C, 62.54; H, 5.53; D, 54.5 atom %. Found: C, 62.74; H, 5.70; D, 52.6 atom % (96.5%).

DL-*N-Acetylphenyl-d_5-alanine-2,3,3-d_3 (4)*

A solution of 9.31 g (0.0437 mole) of the acid **3** in 75 ml of ethyl acetate and 200 ml of dioxane was added to a pressure bottle that contained 1.3 g of 10% palladium on carbon. The bottle was placed in a Parr apparatus and connected directly to an inverted tank of deuterium gas.[9] (The initial deuterium gas pressure was 40 p.s.i.) After 1 h at room temperature, the theoretical amount of deuterium was absorbed. The catalyst was filtered, solvent removed under reduced pressure, and the residual oil crystallized from water to give 8.11 g (86%) of the acetyl derivative **4**: m.p. 147–149°; λ_{max} (KBr) 3.00, 3.50, 4.40, and 5.85 μ.

Anal. Calcd. for $C_{11}H_5D_8NO_3$: C, 61.38; H, 6.50; D, 61.6 atom %. Found: C, 61.19; H, 6.66; D, 59.2 atom % (96.3%).

Reduction of the Acid 3

Following a modification of the reported procedure (3), 34.9 g (0.164 mole) of the acid **3** in 196 ml of acetic anhydride and 42 ml of deuterium oxide was reduced in a Parr apparatus, using 0.83 g of platinum oxide, and a deuterium gas pressure maintained at 40 p.s.i. for 3 h. Filtration followed by evaporation of the filtrate gave 30.6 g of a mixture that comprised 70% compound **4** and 30% *N*-acetylcyclohexyl-d_{11}-alanine-2,3,3-d_3 (**12**).[10]

The mixture, after two recrystallizations from 400 ml of water, gave 7.1 g of the compound **12**: m.p. 172–173°; λ_{max} (KBr) 3.00, 3.50, 4.60, 4.75, and 5.90 μ.

Anal. Calcd. for $C_{11}H_5D_{14}NO_3$: C, 58.09; H, 9.04; D, 73.6 atom %. Found: C, 58.10; H, 8.80; D, 72.5 atom % (98.5%).

2-Phenyl-4-benzylidene-d_6-oxazolone (8)

Using a modification of Buck and Ide's procedure (8), 12.9 g (0.115 mole) of **1**, 20.7 g (0.115 mole) of hippuric acid, 8.4 g of sodium acetate, and 37 ml of acetic anhydride were heated on a steam bath for 2 h. Ethanol (48 ml) was then added, the solvents evaporated, and the solid residue extracted with hot benzene. Concentration of the benzene solution to small volume gave 15.7 g (54%) of the azlactone **8**: m.p. 161–163°; λ_{max} (KBr) 4.42, 5.54, and 6.05 μ.

Anal. Calcd. for $C_{16}H_5D_6NO_2$: C, 75.27; H, 4.57; D, 54.5 atom %. Found: C, 75.14; H, 4.61; D, 54.4 atom % (99.8%).

2-Thio-4-benzylidene-d_6-thiazolone (9)

According to the procedure of Billimoria and Cook (9) from 56.4 g (0.503 mole) of the aldehyde **1** and 56 g (0.421 mole) of 2-mercaptothiazole-5-one,[11] in 500 ml of acetic acid there is obtained 93.1 g (82% based on **1**) of the product **9**, m.p. 208–210°.

Anal. Calcd. for $C_{10}HD_6NOS_2$: C, 53.00; H, 3.38; D, 85.6 atom %. Found: C, 52.85; H, 3.43; D, 80.3 atom % (93.6%), 80.6 atom % (94.2%).

L-*Phenyl-d_5-alanine-2,3,3-d_3 (5) and* D-*N-Acetylphenyl-d_5-alanine-2,3,3-d_3 (6)*

In accordance with the method of Greenstein and Winitz (11), renal acylase (0.245 g) was added to a solution of 6.15 g (0.0286 mole) of the DL-acetyl derivative **4** in 100 ml of water that had been neutralized to pH 7.1 with lithium hydroxide. After standing at 37° for 1 day, 10 drops of acetic acid were added, the mixture heated to 60° and filtered with the aid of charcoal. After addition of 20 ml of ethanol, the filtrate was evaporated to 5 ml. This gave 1.61 g of the L-amino acid **5**. An additional 0.21 g of **5** was obtained by the addition of ethanol to the above ethanol–water filtrate after it had been concentrated to small volume by evaporation.

Acidification to pH 1 of the final aqueous ethanol filtrate gave, after filtration, 2.00 g (65%) of the D-*N*-acetyl derivative **6**: m.p. 167–179°; $[\alpha]_D^{25}$ −36° (*c*, 1, MeOH); λ_{max} (KBr) 3.00, 3.50, 4.42, and 5.95 μ.

The following procedure afforded an additional 0.20 g of the product **5**. The filtrate from the separation of **6** was adjusted to pH 5 and 0.30 g of cupric acetate added. The filtered copper salt was added to 10 ml of water, through which hydrogen sulfide gas was bubbled. The solution of the acid **5** was filtered, concentrated to small volume, and worked up with ethanol as reported above. The total yield of the amino acid **5** was 2.02 g (81%): m.p. 260–262° (decomp.); $[\alpha]_D^{25}$ −34° (*c*, 1, H_2O); λ_{max} (KBr) 3.35, 3.40, 6.15, and 6.50 μ. Ultraviolet

[8]The calculated value for % H on all compounds containing deuterium is that figure which would be obtained in a routine analysis which assumes all water of combustion to be H_2O. The following formula was used, % H = [1.008 A (18.02 + 2.016 B)]/18.02 C × 100 where A equals the total number of H and D atoms in the molecular formula, B is the theoretical atom fraction of D, and C equals the formula weight, including the mass of deuterium.

[9]The ballast tank of the Parr apparatus is not used so as to prevent contamination of the deuterium gas by adsorbed hydrogen.

[10]Ratio determined by the ultraviolet absorption at 258 mμ.

[11]Obtained in 36% yield from ethyl chloroacetate using the procedure described in ref. 10.

absorption spectrum, ε's in parentheses:[12a] λ_{max} (H_2O) 241.8 (77.2), 246.4 (114.2), 251.2 (161.0), 256.8 (189), 262.5 (143.5), and 265.6 mμ (92.6). Molecular rotation (at 25°; *c*, 1; 1 *N* HCl):[12b] [φ] 589, −13.3°; [φ] 470, −18.0°; [φ] 360, 0°; [φ] 275, +313°; [φ] 255, +837°; [φ] 240, +6050°.

Anal. Calcd. for $C_9H_3D_8NO_2$: C, 62.40; H, 6.88; D, 72.7 atom %. Found: C, 62.18; H, 6.99; D, 68.9 atom % (94.9%).

A pilot experiment was used to monitor the above reaction indirectly. An appropriate amount of the protio acetylphenylalanine with renal acylase was reacted in an nuclear magnetic resonance tube. The reaction was followed by the increase in the n.m.r. signal at τ 2.70 due to the phenyl protons of L-phenylalanine and the decrease of the signal at τ 2.80 due to the phenyl protons of acetylphenylalanine. Integration of the peaks gave the percentage of reaction.

Racemization of the Acetyl Derivative **6**

The labile protons were exchanged by stirring 2.00 g of the derivative **6** in 50 ml of deuterium oxide at room temperature. The heavy water was evaporated, 50 ml of acetic anhydride added, and the resulting solution refluxed for 3 h. After this time the solvents were removed *in vacuo* and 15 ml of deuterium oxide added; the evaporation procedure was repeated twice. Finally, the oil was crystallized from 20 ml of water to give 1.27 g (64%) of the racemized derivative **4**; m.p. 142–145°.

Anal. Calcd. for $C_{11}H_5D_8NO_3$: D, 61.6 atom %. Found: D, 65.3 atom % (106%).

[12]The following data were obtained for protiophenylalanine. (*a*) λ_{max} (H_2O), ε's in parentheses: 242.2 (70.6); 247.1 (106); 251.9 (153.2); 257.5 (189); 263.5 (147.5); and 266.8 mμ (82.5). (*b*) [φ] 589, −14.0°; [φ] 470, −18.6°; [φ] 360, 0°; [φ] 275, +312°; [φ] 255, +824°; [φ] 240, +6350°.

1. A. T. Blomquist, R. J. Cedergren, B. F. Hiscock, S. L. Tripp, and D. N. Harpp. Proc. Natl. Acad. Sci. U.S. **55**, 453 (1966).
2. R. T. Arnold and J. Sprung. J. Am. Chem. Soc. **60**, 1699 (1938).
3. R. M. Herbst and D. Shemin. *In* Organic syntheses. Coll. Vol. II. *Edited by* A. H. Blatt. John Wiley and Sons, Inc., New York. 1943. pp. 1 and 491.
4. S. M. Birnbaum, L. Levintow, R. B. Kingsley, and J. P. Greenstein. J. Biol. Chem. **194**, 455 (1952).
5. M. Bergmann and F. Stern. Ann. **448**, 20 (1926).
6. Y. Iwakura, F. Toda, and Y. Torii. Tetrahedron Letters, 4427 (1966).
7. J. H. Holloway and N. W. Krase. Ind. Eng. Chem. **25**, 497 (1933).
8. J. S. Buck and W. S. Ide. *In* Organic syntheses. Coll. Vol. II. *Edited by* A. H. Blatt. John Wiley and Sons, Inc., New York. 1943, p. 55.
9. J. D. Billimoria and A. H. Cook. J. Chem. Soc. 2323 (1949).
10. D. O. Holland. Brit. Patent No. 689, 243 (1953).
11. J. P. Greenstein and M. Winitz. Chemistry of the amino acids. Vol. III. John Wiley and Sons, Inc., New York. 1961. pp. 1831 and 2173.

Can. J. Chem. Downloaded from www.nrcresearchpress.com by 210.87.254.6 on 09/05/12
For personal use only.

Can. J. Chem. Downloaded from www.nrcresearchpress.com by 210.87.254.40 on 09/05/12
For personal use only.

The reaction of 1,2,3-thiadiazoles with base. I. A new route to 1-alkynyl thioethers

R. RAAP AND R. G. MICETICH
R & L Molecular Research, Ltd., 8045 Argyll Road, Edmonton, Alberta

Received October 30, 1967

The reaction between 1,2,3-thiadiazoles, unsubstituted in the 5-position, and a strong base such as an organolithium compound, sodamide, sodium methylsulfinyl carbanion, or potassium *t*-butoxide results in cleavage of the thiadiazole ring system with evolution of nitrogen and formation of alkalimetal alkynethiolate. Subsequent addition of an alkyl or acyl halide to the reaction mixture produces 1-alkynyl thioethers. 4-(5-Phenyl-1,2,3-thiadiazolyl)lithium, obtained from 5-phenyl-1,2,3-thiadiazole and methyl- or phenyllithium, reacts with methyl iodide to give 4-methyl-5-phenyl-1,2,3-thiadiazole.

Canadian Journal of Chemistry, 46, 1057 (1968)

Simple aromatic heterocyclic compounds such as furan (1), thiophene (2), thiazole (3), and isothiazole (4) can all be metallated by treatment with *n*-butyllithium. It was hoped that this behavior would also extend to 1,2,3-thiadiazoles, since this would present a means of introducing substituents in the 4-position and in the 5-position. An investigation into the reaction between 1,2,3-thiadiazoles and *n*-butyllithium was therefore undertaken, a study which led to the discovery of an interesting cleavage reaction of the thiadiazole ring.

1,2,3-Thiadiazoles can be prepared by cycloaddition of diazoalkanes to isothiocyanates (5–8) or thioneesters (9), or from the reaction between α-diazocarbonyl compounds and hydrogen sulfide (10). Synthetically the most convenient method would appear to be the one discovered by Hurd and Mori (11) involving the reaction between thionyl chloride and acylhydrazones containing an α-methylene group. This method was indeed found to be quite versatile and useful. Table I lists the various 1,2,3-thiadiazoles prepared for the present study by this method. Particularly gratifying was the smooth reaction of the carbethoxyhydrazone of ethyl acetoacetate with thionyl chloride to give a 75% yield of ethyl 4-methyl-1,2,3-thiadiazole-5-carboxylate. The free acid could be decarboxylated quantitatively to the previously unknown 4-methyl-1,2,3-thiadiazole, a colorless liquid with an odor reminiscent of pyridine. Ethyl 1,2,3-thiadiazole-5-carboxylate could similarly be prepared from ethyl *N*-carbethoxyhydrazinoformyl acetate, however in much lower yield. The acid in turn was decarboxylated to give 1,2,3-thiadiazole. Wolff (10) prepared this compound by decarboxylation of 1,2,3-thiadiazole-4-carboxylic acid.

When *n*-butyllithium in *n*-hexane was added to an anhydrous tetrahydrofuran solution of 4-phenyl-1,2,3-thiadiazole at −65°, a gas was liberated and a yellow solid precipitated from the intensely colored solution. After the addition of methyl iodide to the reaction mixture a colorless liquid, b.p. 91–93° (1.0 mm), could be isolated. The infrared spectrum contained a sharp band at 2170 cm^{-1}. The nuclear magnetic resonance (n.m.r.) spectrum (CCl_4) consisted of a three-proton singlet at τ 7.63 and a five-proton multiplet centered at τ 2.7. Upon hydrolysis phenylacetic acid was obtained. The elemental analysis agreed with the formula C_9H_8S. The product must hence be 1-methylthio-2-phenylethyne,[1] the formation of which can be rationalized by a cleavage of the thiadiazole ring to nitrogen and lithium 2-phenylethynethiolate which is then alkylated by methyl iodide (Scheme 1). On using ethyl iodide instead of methyl iodide, 1-ethylthio-2-phenylethyne, with comparable physical constants as those reported by Brandsma, Wijers, and Jonker (13*a*), was obtained in 91% yield.

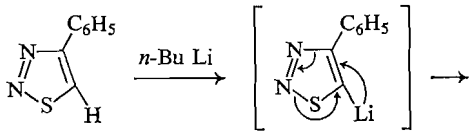

$$N_2 + C_6H_5{-}C{\equiv}C{-}S^{\ominus}\,Li^{\oplus} \xrightarrow{CH_3I} C_6H_5{-}C{\equiv}C{-}SCH_3$$

Scheme 1

[1]Note added in proof: This compound, b.p. 74° (2 mm), has been reported by M. Schmidt and V. Potschka (Naturwissenschaften, **50**, 302 (1963)). We thank Professor J. F. Arens for bringing this paper to our attention.

Can. J. Chem. Downloaded from www.nrcresearchpress.com by 210.87.254.40 on 09/05/12
For personal use only.

TABLE I

1,2,3-Thiadiazoles[a]

	Compound R	R′	Carbethoxyhydrazone		Melting point or boiling point			% calculated				% found			
			Melting point, °C	% yield	(mmHg), °C	% yield	Formula	C	H	N	S	C	H	N	S
1[b]	CH_3	$CO_2C_2H_5$	57–60	99	86(0.2)	75	$C_6H_8N_2O_2S$[b]	33.33	2.78	19.45	22.22	33.55	2.86	19.80	21.80
2	H	$CO_2C_2H_5$	—	60	76(1.0)[c]	25	$C_5H_6N_2O_2S$								
3	C_6H_5	H	117–119	95	77–79(*n*-C_6H_{12})[d]	80	$C_8H_6N_2S$								
4	*p*-$OCH_3C_6H_4$	H	131–132	88	92–94(*n*-C_6H_{12} – C_6H_6)	74	$C_9H_8N_2OS$	56.22	4.20	14.57		55.99	4.44	14.60	
5	*p*-ClC_6H_4	H	138–141	90	137–139 (C_6H_6)	79	$C_8H_5ClN_2S$	48.85	2.56			48.96	2.58		
6	2,4-$Cl_2C_6H_3$	H	146–148[e], 101–105[e]	58, 24	109–112(*n*-C_6H_{12} – C_6H_6)	78	$C_8H_4Cl_2N_2S$	41.57	1.74			41.56	1.96		
7	2-thienyl	H	121–122	85	70–71(*n*-C_6H_{12} – C_6H_6)	86	$C_6H_4N_2S_2$	42.84	2.40	16.66	38.12	43.13	2.59	16.61	37.90
8	5-isothiazolyl	H	151–152	87	119–121(EtOAc)	72	$C_5H_3N_3S_2$	35.49	1.79	24.83		35.64	2.14	24.50	
9	3-pyridyl	H	116–118	88	90–92(*n*-C_6H_{12} – C_6H_6)[f]	86	$C_7H_5N_3S$	51.51	3.09	25.74		51.17	3.24	25.85	
10	H	C_6H_5	88–90[g]	93[g]	52–56[h]; 105(0.2)	72	$C_8H_6N_2S$								
11	CH_3	C_6H_5	95–100	100	116–118(1.3)	84	$C_9H_8N_2S$	61.35	4.58	15.90		61.47	4.71	16.30	
12	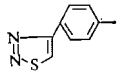	H	236–238 (decomp.)[i]	95[i]	255 (decomp.) (dioxane)	97	$C_{10}H_6N_4S_2$	48.75	2.46	22.75		49.02	2.22	23.03	

[a] 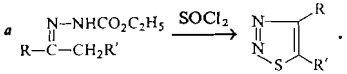

[b]The analyses were performed on the acid, m.p. 173–174° (decomp.), neutralization equivalent 142 (calculated 144).
[c]Reported (12) b.p. 103–105° at 14 mm.
[d]Reported (11) m.p. 77–78°.
[e]Two different isomers were isolated. Both products were converted to 4-(2,4-dichlorophenyl)-1,2,3-thiadiazole upon treatment with thionyl chloride.
[f]HCl salt: m.p. 230–235° (decomp.).
[g]Carbomethoxyhydrazone.
[h]Reported (10) m.p. 53–53.5°.
[i]Dicarbethoxyhydrazone of 1,4-diacetylbenzene.

TABLE II

The effect of base on the yield of 1-methylthio-2-arylethyne*

Base	Solvent	Temperature °C	% yield R = C_6H_5	% yield R = 5-isothiazolyl
n-C_4H_9Li	THF	−65	91	60
CH_3Li	THF	−65	91	90
C_6H_5Li	THF	−65	84	89
$NaNH_2$	NH_3	−60	83	68
$NaCH_2SO—CH_3$	DMSO-THF	−20	88	90
t-C_4H_9OK	t-C_4H_9OH–THF	0	68	77

* 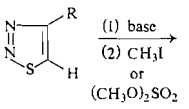

It became immediately evident that the cleavage of 1,2,3-thiadiazoles, unsubstituted in the 5-position, showed great potential as a general synthetic route to 1-alkynyl thioethers[2] and more specifically to those that would not otherwise survive the conditions of the existing routes (13, 14). It was therefore decided to study the scope of the reaction more closely. The result of this investigation is tabulated in Tables II and III. Table II lists the results of a comparative study of the effect on the yields of 1-methylthio-2-phenylethyne and 1-methylthio-2-(5-isothiazolyl)ethyne when various strong bases were employed in the ring opening reaction. Table III summarizes the syntheses of a large number of 1-alkynyl thioethers from 1,2,3-thiadiazoles. The results reported in Tables II and III fully emphasize the general synthetic value of the reaction. A large variety of bases can be employed successfully and especially sodium methylsulfinyl carbanion appears to be a very useful reagent for the preparation of the more sensitive 1-alkynyl thioethers, e.g. 1-methylthio-2-carbomethoxyethyne[3] (Table III, compound 4).

A direct synthetic application of the new cleavage reaction of 1,2,3-thiadiazoles consists of the synthesis of arylacetic acids from arylmethylketones as illustrated in Scheme 2. The overall yields for the preparation of phenylacetic acid, 2-thienylacetic acid and 5-isothiazolylacetic acid by this sequence were 54, 55, and 40% respectively.

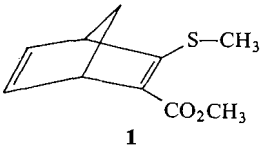

1

4-(1,2,3-Thiadiazolyl)lithium compounds appear to have some degree of stability as was indicated by the behavior of 5-phenyl-1,2,3-thiadiazole towards organolithium compounds. Methyllithium was added to a solution of 5-phenyl-1,2,3-thiadiazole in anhydrous tetrahydrofuran at −65°, followed by the addition of methyl iodide. The expected 4-methyl-5-phenyl-1,2,3-thiadiazole, identical with the material prepared from phenyl-2-propanone by the method of Hurd and Mori (Table I), was isolated in 64% yield. The yield decreased to 34% when phenyllithium was employed whereas the use of n-butyllithium resulted in only trace amounts of the product.

Experimental

All melting points and boiling points are uncorrected. The infrared spectra were recorded on a Perkin–Elmer model 137 "Infracord" spectrophotometer. Nuclear magnetic resonance (n.m.r.) spectra were measured using a Varian Associates model A-60 spectrometer, with tetramethylsilane as a reference. Microanalyses were performed by Dr. G. Weiler and Dr. F. B. Strauss, Microanalytical Laboratory, Oxford, England.

5-Acetylisothiazole

A 1.6 M solution of n-butyllithium in n-hexane (325 ml, 0.53 mole of butyllithium) was added dropwise to a

[2]1-Alkynyl thioethers have been prepared previously by four different methods (13, 14) and their use as synthetic intermediates has been reviewed by Arens (14*a*) in 1960. The mechanistic aspect of the chemistry of 1-alkynyl thioethers is emphasized in a recent review by Drenth (14*b*).

[3]When this compound was heated for 5 h at 95–100° with cyclopentadiene in benzene a 61% yield of a compound, b.p. 95–97° (0.3 mm), was obtained which was assigned the structure of methyl 2-methylthiobicyclo[2,-2,1]hepta-2,5-diene-3-carboxylate (**1**) on the basis of spectral and analytical data.

Can. J. Chem. Downloaded from www.nrcresearchpress.com by 210.87.254.40 on 09/05/12
For personal use only.

Can. J. Chem. Downloaded from www.nrcresearchpress.com by 210.87.254.40 on 09/05/12
For personal use only.

TABLE III

1-Alkynyl thioethers from 1,2,3-thiadiazoles[a]

Compound	RC≡CSR′	X	Base	Melting point or boiling point (mm Hg), °C	% yield	Formula	% calcd. C	H	S	X	% found C	H	S	X
1[b]	$HC{\equiv}CSCH_2C_6H_5$	Cl	*n*-BuLi	73–75 (1.0)	64	C_9H_8S								
2[c]	$CH_3C{\equiv}CSn\text{-}C_4H_9$	Br	*n*-BuLi	74 (16)	60	$C_7H_{12}S$								
3[d]	$HO_2CC{\equiv}CSC_2H_5$	I	*n*-BuLi	—	86	$C_5H_6O_2S$								
4	$CH_3O_2CC{\equiv}CSCH_3$	OSO_3CH_3	$NaCH_2$—SO—CH_3	55–55.5 (1.5)	89	$C_5H_6O_2S$	46.14	4.65	24.64		47.07	4.91	24.50	
5	$C_6H_5C{\equiv}CSCH_3$	I,OSO_3CH_3	*n*-BuLi	91–93 (1.0)	91	C_9H_8S	73.03	5.45	21.66		73.03	5.07	21.45	
6[e]	$C_6H_5C{\equiv}CSC_2H_5$	I	*n*-BuLi	69–70 (0.3)	91	$C_{10}H_{10}S$								
7	$C_6H_5C{\equiv}CSCH_2CO_2C_2H_5$	Br	*n*-BuLi	132–133 (0.3)	80	$C_{12}H_{12}O_2S$	65.45	5.45	14.54		65.86	5.45	14.25	
8[f]	$C_6H_5C{\equiv}CSCH_2CO_2H$	—	—	68–70 (CCl_4)	90	$C_{10}H_8O_2S$	62.48	4.20	16.68		62.47	4.57	17.20	
9	$C_6H_5C{\equiv}CSCO_2CH_3$	Cl	*n*-BuLi	97–98 (0.1)	88	$C_{10}H_8O_2S$	62.48	4.20	16.68		62.70	4.41	17.05	
10	$C_6H_5C{\equiv}CSCO_2C_2H_5$	Cl	*n*-BuLi	102–104 (0.3)	89	$C_{11}H_{10}O_2S$	64.03	4.89	15.54		64.16	5.02	15.49	
11	$C_6H_5C{\equiv}CSCO_2n\text{-}C_3H_7$	Cl	*n*-BuLi	115–116 (0.3)	83	$C_{12}H_{12}O_2S$	65.42	5.49	14.55		65.65	5.89	14.51	
12	$C_6H_5C{\equiv}CSCO_2iso\text{-}C_4H_9$	Cl	*n*-BuLi	114–115 (0.1)	89	$C_{13}H_{14}O_2S$	66.64	6.02			66.82	6.08		
13	$C_6H_5C{\equiv}CSCO\text{-}SCH_3$	Cl	*n*-BuLi	27–28 (*n*-C_6H_{12}); 121–122 (0.2)	81	$C_{10}H_8OS_2$	57.65	3.87	30.79		57.87	3.76	30.80	
14	$C_6H_5C{\equiv}CSCO\text{-}CH_3$	Cl	*n*-BuLi	93–95 (0.5)	58	$C_{10}H_8OS$	68.14	4.58	18.19		68.20	4.66	17.89	
15	$C_6H_5C{\equiv}CSCO\text{-}N(CH_3)_2$	Cl	*n*-BuLi	64–66 (C_6H_6 – *n*-C_6H_{12})	76	$C_{11}H_{11}NOS$	64.35	5.40	15.62	6.82(N)	64.02	5.27	15.22	6.60(N)
16	$C_6H_5C{\equiv}CSCO\text{-}C_6H_5$	Cl	*n*-BuLi	56–57 (*n*-C_6H_{12})	85	$C_{15}H_{10}OS$	75.60	4.23	13.46		75.42	4.68	13.55	
17	$C_6H_5C{\equiv}CSCO\text{-}pClC_6H_4$	Cl	*n*-BuLi	61–62 (*n*-C_6H_{12})	83	$C_{15}H_9ClOS$	66.06	3.33	11.76	13.00(Cl)	65.83	3.55	12.11	12.98(Cl)
18	$p\text{-}OCH_3C_6H_4C{\equiv}CSCO_2C_2H_5$	Cl	*n*-BuLi	49–51 (*n*-C_6H_{12})	76	$C_{12}H_{12}O_3S$	60.98	5.12	13.57		61.21	5.38	13.81	
19	$p\text{-}ClC_6H_4C{\equiv}CSCH_3$	OSO_3CH_3	*n*-BuLi	88–90 (0.4)	73	C_9H_7ClS	59.17	3.86	17.55	19.41(Cl)	58.94	3.83	17.47	19.25(Cl)
20	$p\text{-}ClC_6H_4C{\equiv}CSCO_2C_2H_5$	Cl	*n*-BuLi	30–31; 121–122 (0.1)	80	$C_{11}H_9ClO_2S$	54.88	3.77	13.32		55.02	3.89	13.40	
21	$2,4\text{-}Cl_2C_6H_3C{\equiv}CSCO_2C_2H_5$	Cl	C_6H_5Li	65–67 (*n*-C_6H_{12})	61	$C_{11}H_8Cl_2O_2S$	48.01	2.93	11.65	25.77(Cl)	48.21	3.15	11.91	25.69(Cl)
22	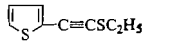	I	*n*-BuLi	72–74 (0.1)	81	$C_8H_8S_2$	57.10	4.79	38.11		56.77	4.47	37.70	
23	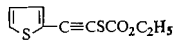	Cl	*n*-BuLi	114–115 (0.5)	80	$C_9H_8O_2S_2$	50.92	3.80	30.21		51.19	3.69	29.81	
24	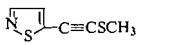	I,OSO_3CH_3	$NaCH_2$—SO—CH_3	68–70 (0.2)	90	$C_6H_5NS_2$	46.43	3.25	41.32		46.32	3.38	41.80	
25	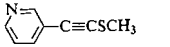	OSO_3CH_3	C_6H_5Li	72–73 (0.2)	65	C_8H_7NS	64.37	4.73	21.49	9.39(N)	64.69	4.90	21.50	9.24(N)
26	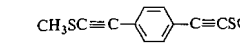	OSO_3CH_3	*n*-BuLi	80–82 (*n*-C_6H_{12})	63	$C_{12}H_{10}S_2$	66.01	4.62	29.38		66.03	4.39	29.65	
27	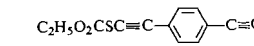	Cl	*n*-BuLi	92–94 (C_6H_6 – *n*-C_6H_{12})	45	$C_{16}H_{14}O_4S_2$	57.47	4.22	19.18		57.75	4.02	19.30	

[a] 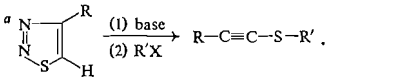

[b] The compound deteriorated rapidly at room temperature and no satisfactory elemental analysis could be obtained. The infrared spectrum, however, contains sharp bands at 3300 and 2040 cm^{-1} while the n.m.r. spectrum ($CDCl_3$) contains singlets at τ 2.75, 6.14, and 7.26 with an integrated area ratio of 5:2:1.

[c] n_D^{26} 1.4880. Reported (14*a*) b.p. 65–67° (12 mm), n_D^{20} 1.4860.

[d] *S*-Benzylthiuronium salt: m.p. 166–167° (decomp.); reported (15) m.p. 165.5–166.5° (decomp.).

[e] n_D^{26} 1.6066. Reported (13) b.p. 132° (14 mm), n_D^{20} 1.6133.

[f] This product was obtained by hydrolysis of the ethyl ester with methanolic NaOH.

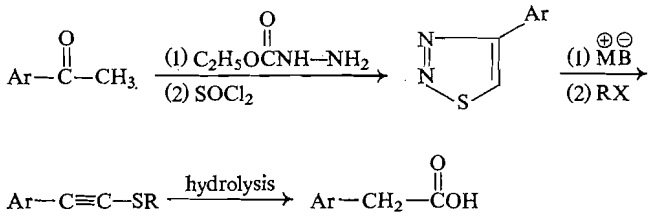

SCHEME 2

stirred solution of isothiazole (42.5 g, 0.50 mole) (16) in 400 ml of anhydrous THF, maintained at approximately −65° (4). The addition was carried out in an N_2 atmosphere. The isothiazolyllithium suspension was slowly siphoned into a vigorously stirred mixture of acetic anhydride (151 g, 1.5 mole) and anhydrous ether (200 ml) cooled in a dry ice – acetone mixture. The reaction mixture was allowed to warm to 0° and then poured into 500 ml of ice-water. The aqueous layer was extracted with two 100 ml portions of ether. The combined organic layers were dried, followed by removal of the solvent. The residue was fractionally distilled to give 35.4 g (56%) of the product, b.p. 62–63° (1.3 mm), m.p. 27°, identical in all respects with a sample of 5-acetylisothiazole prepared by the method of Caton *et al.* (17).

Methyl 1,2,3-Thiadiazole-4-carboxylate

A solution of 1,2,3-thiadiazole-4-carbonyl chloride (460 g, 3.1 mole) (12) in 600 ml of benzene was added dropwise under stirring to 1600 ml of methanol. The temperature of the reaction mixture was allowed to rise to 50°. After the addition was complete the mixture was heated under reflux for 15 min, whereafter the solvent was removed. The product was recrystallized from methanol to give 400 g (90%) of white solid, m.p. 91–93°, reported (12) m.p. 87–88°.

Ethyl 1,2,3-Thiadiazole-5-carboxylate

A solution of the sodium salt of ethyl formylacetate (354 g, 2.6 mole) (18) in 350 ml of water was slowly added to an ice-cooled solution of carbethoxyhydrazine (270 g, 2.6 mole) (19) in 750 ml of 4 *N* hydrochloric acid. After 0.5 h at room temperature the precipitated oil was extracted with ethyl acetate. The carbethoxyhydrazone obtained after drying and removal of the ethyl acetate, solidified upon trituration with *n*-hexane, and amounted to 315 g (60%). The crude ethyl *N*-carbethoxyhydrazinoformylacetate (154 g, 0.76 mole) was carefully added to $SOCl_2$ (220 ml), cooled in ice. When the reaction subdued, the mixture was heated at 80° for 1 h. The excess of $SOCl_2$ was removed and 250 ml of water was added to the residue, followed by extraction with five 100 ml portions of ether. The combined ether extracts were dried and the ether removed. Fractional distillation of the residue yielded 28 g (25%) of crude ester, b.p. 75–82° (3–5 mm), which could be purified further as follows: the ester (170 g) in benzene was added to a column of alumina (500 g) and eluted with 6 l of benzene. Removal of the benzene and distillation of the residue yielded 90 g of colorless oil, sharply boiling at 76° (1.0 mm); reported (12) b.p. 103–105° (14 mm). The n.m.r. spectrum ($CDCl_3$) contained a one proton singlet at τ 0.85, a CH_2 quartet at τ 5.53 and a CH_3 triplet at τ 8.56.

1,2,3-Thiadiazole-5-carboxylic Acid

The ethyl ester (52.7 g, 0.33 mole), cooled in ice, was treated with 112 ml of 3 *N* methanolic NaOH. After 15 min at 0° the methanol was removed and the sodium salt dissolved in 150 ml of water. The solution was acidified and continuously extracted with ether for 24 h. Drying and removal of the ether left the acid (41 g, 96%) as a white solid, m.p. 103° (decomp.), neutralization equivalent 129 (calcd. 130); reported (12) m.p. 104–106° (decomp.).

1,2,3-Thiadiazole

1,2,3-Thiadiazole-5-carboxylic acid (6.5 g, 0.050 mole) was placed in a round bottom flask fitted with a condenser and receiver, the latter cooled in dry ice – acetone and connected to a suction pump. The flask was immersed in an oil bath and heated at 140–150°. Occasional suction was applied to remove the thiadiazole which distilled as a colorless liquid; yield 4.1 g (96%), b.p. 53° (16 mm), m.p. −14°; reported (10) b.p. 83–85° (60 mm). The n.m.r. spectrum (CCl_4) consisted of a complex multiplet at τ 0.92–1.12. The material was also prepared by decarboxylation of 1,2,3-thiadiazole-4-carboxylic acid (11) according to the procedure of Wolff (10). The infrared spectra of the products obtained by the two different methods were superimposable.

Ethyl 4-Methyl-1,2,3-thiadiazole-5-carboxylate

A mixture of ethyl acetoacetate (162.5 g, 1.25 mole), carbethoxyhydrazine (130 g, 1.25 mole), acetic acid (5 ml) and methanol (250 ml) was left at room temperature for 48 h. The mixture was concentrated to dryness and the crude carbethoxyhydrazone (267 g, 99%, m.p. 57–60°) was carefully added, under stirring, to 600 ml of $SOCl_2$ cooled in ice. The reaction mixture was stirred at room temperature for 24 h, whereafter the excess of $SOCl_2$ was removed and the residue distilled *in vacuo* to give 159 g (75%) of a colorless liquid, b.p. 86° (2.0 mm). The infrared spectrum of the neat liquid contained a strong band at 1740 cm^{-1}. The n.m.r. spectrum (CCl_4) consisted of a three proton singlet at τ 7.04, a CH_2 quartet at τ 5.53 and a CH_3 triplet at τ 8.59.

4-Methyl-1,2,3-thiadiazole-5-carboxylic Acid

The ethyl ester (16.7 g, 0.097 mole) was treated with 40 ml of 3 *N* methanolic NaOH and the resultant mixture was left at room temperature for 16 h. The methanol was removed, the sodium salt washed well with ether and dissolved in 100 ml of water. The aqueous solution was cooled and acidified. The product (13.2 g, 94%) was collected by filtration as a white solid and could be recrystallized from ethyl acetate – *n*-hexane, m.p. 173–174° (decomp.). The elemental analyses are reported in Table I.

Can. J. Chem. Downloaded from www.nrcresearchpress.com by 210.87.254.40 on 09/05/12
For personal use only.

Can. J. Chem. Downloaded from www.nrcresearchpress.com by 210.87.254.40 on 09/05/12
For personal use only.

4-Methyl-1,2,3-thiadiazole

This product was obtained in 96% yield by decarboxylation of 4-methyl-1,2,3-thiadiazole-5-carboxylic acid at 185–195° by the same procedure as described for 1,2,3-thiadiazole. The compound distilled at atmospheric pressure (700 mm) at 175–177° with slight decomposition (distillate yellow and odor of H_2S). It distilled at 73–74° at 22 mm pressure as a colorless liquid, n_D^{26} 1.5240, with an odor reminiscent of pyridine. The n.m.r. spectrum ($CDCl_3$) exhibited a one proton signal at τ 1.73 and a three proton signal at τ 7.22.

Anal. Calcd. for $C_3H_4N_2S$: C, 36.00; H, 4.02; N, 27.99; S, 32.04. Found: C, 35.98; H, 3.96; N, 27.61; S, 31.81.

Arylmethylketonecarbethoxyhydrazones

A mixture of arylmethylketone (0.20 mole), carbethoxyhydrazine (0.20 mole), methanol (50–75 ml), and acetic acid (0.5 ml) was heated to the boiling point of the methanol, then left at room temperature overnight. In most instances the product crystallized from the methanolic solution. An additional crop could generally be obtained by the addition of water or ether. The physical constants are given in Table I.

4-Aryl-1,2,3-thiadiazoles

The arylmethylketonecarbethoxyhydrazone (0.10 mole) was added to cold thionyl chloride (50 ml). Upon slight heating a vigorous gas evolution took place. The mixture was heated at approximately 60° for 1 h, whereafter the excess of thionyl chloride was removed. The crude products could be purified by recrystallization after treatment with decolorizing carbon (compounds 3–6), by washing with ether (compound 12), by elution chromatography over alumina using benzene as solvent (compound 7), or by distillation (compounds 10 and 11). Compounds 8 and 9 were obtained as the hydrochlorides from which the free thiadiazoles could be obtained by treatment with ice-water (compound 8) or aqueous sodium carbonate (compound 9). Compound 8 could be further purified by elution chromatography over alumina, using THF as eluant. The physical constants are given in Table I.

1-Alkynyl Thioethers (General Procedures)

(a) With Organolithium Compounds

A 1.6 molar solution of *n*-butyllithium in *n*-hexane (34 ml, 0.055 mole of butyllithium) was added to a stirred suspension of the 1,2,3-thiadiazole (0.050 mole) in 75 ml of anhydrous THF, cooled in dry ice – acetone, at such a rate that the temperature did not exceed −60°. The addition was carried out in an N_2 atmosphere. When the addition was completed the reaction mixture was stirred at −60° for an additional 10 min, whereafter the alkyl halide, dimethyl sulfate, or acyl halide (0.055 mole) was added in one portion. The reaction mixture was allowed to warm to 0° and added to ice-water (75 ml). The organic layer was separated and the aqueous phase extracted with two 50 ml portions of ether. The combined organic layers were dried, whereafter the solvent was removed. The product could be purified by distillation or recrystallization as indicated in Table III. The same procedure was employed with methyllithium (1.66 *M* solution in ether) and phenyllithium (2.1 *M* solution in 3:1 mixture of benzene and ether). The organolithium solutions were obtained from Foote Mineral Company, Exton, Pennsylvania, U.S.A. The physical constants are given in Tables II and III.

(b) With Sodamide

A solution of the 1,2,3-thiadiazole (0.050 mole) in THF was added in 15 min to a stirred suspension of sodamide (prepared from 0.060 g-atom of Na) in approximately 100 ml of liquid ammonia, at −60°. When the addition was completed the reaction mixture was kept at −60° for an additional 2 h, whereafter methyl iodide (14.2 g, 0.10 mole) was added in one portion. The temperature of the mixture was allowed to rise and the ammonia and THF were removed. To the residue was added 100 ml of water and the product was extracted with four 50 ml portions of ether.

(c) With Sodium Methylsulfinyl Carbanion

A solution of sodium methylsulfinyl carbanion was prepared from 0.060 mole of NaH and 30 ml of DMSO by the procedure of Corey and Chaykovsky (20). To this solution was added 50 ml of anhydrous THF, whereafter the mixture was cooled to −20°. A solution of the 1,2,3-thiadiazole in 50 ml of THF was added over 15 min with stirring, while the temperature was maintained at approximately −20°. When the addition was completed the mixture was stirred for an additional 20 min, whereafter the alkyl halide, dimethyl sulfate, or acyl halide (0.060 mole) was added in one portion. Most of the THF was removed, the residue was added to 100 ml of water and the product extracted with three 50 ml portions of ether.

(d) With Potassium t-Butoxide

A solution of 1,2,3-thiadiazole (0.050 mole) in 50 ml of anhydrous THF was added in 15 min to a stirred mixture of potassium *t*-butoxide (from 0.054 g-atom of K), *t*-butyl alcohol (40 ml) and THF (20 ml) at 0°. The reaction mixture was stirred for an additional 15 min whereafter dimethyl sulfate (7.6 g, 0.060 mole) was added in one portion. The reaction mixture was added to 200 ml of ice-water and the product extracted with three 50 ml portions of ether.

Arylacetic Acids from 1-Alkylthio-2-arylethynes

(a) Phenylacetic Acid

A mixture of 1-methylthio-2-phenylethyne (1.0 g), methanol (15 ml) and 3 *N* aqueous H_2SO_4 (15 ml) was heated under reflux for 2 h. Most of the methanol was removed and the oily material extracted with ether. The residue obtained after drying and removal of the ether consisted of a mixture of methyl phenylacetate and methyl phenylthioacetate. This ester mixture was hydrolyzed with 3 *N* methanolic NaOH in the usual manner to give 0.7 g (78%) of phenylacetic acid, m.p. 77–79°. The m.p. was not depressed by the addition of some authentic phenylacetic acid and the infrared spectra were superimposable.

(b) 2-Thienylacetic Acid

A mixture of 1-ethylthio-2-(2-thienyl)ethyne (1.5 g), methanol (20 ml), and 3 *N* aqueous H_2SO_4 (15 ml) was heated under reflux for 4 h. By proceeding in the same manner as above, 1.1 g (88%) of the acid was obtained; m.p. 64–66° (*n*-C_6H_{12} – C_6H_6), reported (22) m.p. 62–63°. The melting point was not depressed by the addition of some authentic 2-thienylacetic acid (21) and the infrared spectra were superimposable.

(c) 5-Isothiazolylacetic Acid

A mixture of 1-methylthio-2-(5-isothiazolyl)ethyne

Can. J. Chem. Downloaded from www.nrcresearchpress.com by 210.87.254.40 on 09/05/12
For personal use only.

(50.0 g), methanol (300 ml), and 50% aqueous H_2SO_4 (60 ml) was heated under reflux for 75 min. Most of the methanol was removed under reduced pressure and the residue added to 600 ml of ice-water. The organic material was extracted with three 150 ml portions of ether. The combined extracts were dried, the ether removed, and the residue distilled *in vacuo* to give 33.0 g (66%) of pale-yellow colored liquid, b.p. 74–86° (0.3–0.5 mm). The infrared spectrum contained, apart from a strong carbonyl band at 1740 cm^{-1}, a weak band at 1690 cm^{-1}, indicating the presence of a small amount of the thioester. The ester mixture (36.5 g, 0.23 mole), dissolved in 50 ml of methanol, was treated with 90 ml of 3 *N* methanolic NaOH. After 2 h at room temperature, the methanol was removed and ether (400 ml) was added to the solid residue. The sodium 5-isothiazolylacetate was removed by filtration, dissolved in 150 ml of water, and acidified with 3 *N* hydrochloric acid (90 ml). After cooling, the white solid was removed by filtration and air-dried; yield 30.0 g (60% overall), m.p. 153–155° (decomp.). The material was the same in every respect as that obtained via an Arndt–Eistert synthesis from isothiazolyl-5-carbonyl chloride (22). The acid could be obtained directly from 1-methylthio-2-(5-isothiazolyl)ethyne in 68% yield when the hydrolysis was carried out in a mixture of 50% aqueous H_2SO_4 and acetic acid (2 h reflux).

Methyl 2-Methylthiobicyclo[2·2·1]hepta-2,5-diene-3-carboxylate

A mixture of 1-methylthio-2-carbomethoxyethyne (10.0 g, 0.077 mole), cyclopentadiene (6.6 g, 0.10 mole) and benzene (30 ml) was heated in an autoclave at 95–100° for 5 h. Removal of the benzene and distillation of the residue *in vacuo* yielded 10.2 g (61%) of a pale-yellow liquid, b.p. 95–97° (0.3 mm). The infrared spectrum of the neat liquid contained a strong carbonyl band at 1680 cm^{-1}. The n.m.r. spectrum (CCl_4) showed a 2-proton AB-type symmetrical multiplet centered at τ 3.29 (H-5,6), other 2-proton multiplets at τ 6.0–6.15 (H-1,4) and τ 7.9–8.05 (H-7), and 3-proton singlets at τ 6.39 (OCH_3) and 7.57 (SCH_3).

Anal. Calcd. for $C_{10}H_{12}O_2S$: C, 61.18; H, 6.17; N, 16.33. Found: C, 60.88; H, 6.21; N, 16.30.

4-Methyl-5-phenyl-1,2,3-thiadiazole

A 1.66 *M* solution of methyllithium in ether (36 ml, 0.060 mole of methyllithium) was added dropwise in 15 min to a stirred solution of 5-phenyl-1,2,3-thiadiazole (8.2 g, 0.050 mole) in 75 ml of anhydrous THF, cooled in dry ice – acetone (N_2 atmosphere). When the addition was completed the mixture was stirred for an additional 15 min whereafter methyl iodide (14.2 g, 0.10 mole) was added in one portion. The mixture was allowed to come to 0° and added to 100 ml of ice-water. The aqueous layer was extracted with two 50 ml portions of ether. The combined organic layers were dried followed by removal of the solvent and distillation of the residue *in vacuo* to give 5.7 g (64%) of product, b.p. 82–83° (0.1 mm). The n.m.r. spectrum (CCl_4) consisted of singlets at τ 2.60 and 7.31 with an integrated area ratio of 5:3 respectively. The material was identical with that prepared from phenyl-2-propanone (Table I).

Acknowledgments

The authors thank Messrs. V. R. Baker, R. A. Fortier, R. R. Thomas, and P. K. Wolfert for their technical assistance and Professor R. U. Lemieux for his interest and advice.

1. V. Ramanathan and R. Levine. J. Org. Chem. **27**, 1216 (1962).
2. V. Ramanathan and R. Levine. J. Org. Chem. **27**, 1667 (1962).
3. J. Beraud and J. Metzger. Bull. Soc. Chim. France, 2072 (1962).
4. M. P. L. Caton, D. H. Jones, R. Slack, and K. R. H. Wooldridge. J. Chem. Soc. 446 (1964).
5. H. Pechmann and A. Nold. Chem. Ber. **29**, 2588 (1896).
6. J. Goerdeler and G. Gnad. Tetrahedron Letters, No. **14**, 795 (1964).
7. D. Martin and W. Mucke. Ann. **682**, 90 (1965).
8. E. Lieber, N. Galvanico, and C. N. R. Rao. J. Org. Chem. **28**, 257 (1963).
9. U. Schmidt, E. Heymann, and K. Kabitzke. Chem. Ber. **96**, 1478 (1963).
10. L. Wolff. Ann. **333**, 1 (1904).
11. C. D. Hurd and R. I. Mori. J. Am. Chem. Soc. **77**, 5359 (1955).
12. D. L. Pain and R. Slack. J. Chem. Soc. 5166 (1965).
13. (*a*) L. Brandsma, H. E. Wijers, and C. Jonker. Rec. Trav. Chim. **83**, 208 (1964). (*b*) H. E. Wijers, P. P. Montijn, L. Brandsma, and J. F. Arens. Rec. Trav. Chim. **84**, 1284 (1965).
14. (*a*) J. F. Arens. *In* Advances in organic chemistry: methods and results. Vol. 2. *Edited by* R. A. Raphael, E. C. Taylor, and H. Wynberg. Interscience Publishers Inc., New York. 1960. p. 117. (*b*) W. Drenth. *In* The chemistry of organic sulfur compounds. Vol. 2. *Edited by* N. Kharash. Pergamon Press, New York. 1966. Chap. 7. (*c*) L. Brandsma, H. J. T. Bos, and J. F. Arens. Chemistry of acetylenic ethers and thioethers. *In* Chapters on the chemistry of acetylenic compounds. *Edited by* H. G. Viehe. Maurits Dekker, New York. In press.
15. J. F. Arens, H. C. Volger, T. Doornbos, J. Bonnema, J. W. Greidanus, and J. H. van der Hende. Rec. Trav. Chim. **75**, 1459 (1956).
16. (*a*) F. Wille, L. Capeller, and A. Steiner. Angew. Chem. Intern. Ed. Engl. **1**, 335 (1962). (*b*) R. Raap. Can. J. Chem. **44**, 1324 (1966).
17. M. P. L. Caton, D. H. Jones, R. Slack, S. Squires, and K. R. H. Wooldridge. J. Med. Chem. **8**, 680 (1965).
18. H. Pechmann. Chem. Ber. **25**, 1040 (1892).
19. O. Diels. Chem. Ber. **47**, 2186 (1914).
20. E. J. Corey and M. Chaykovsky. J. Am. Chem. Soc. **87**, 1345 (1965).
21. J. H. Ford, G. C. Prescott, and D. R. Colingsworth. J. Am. Chem. Soc. **72**, 2109 (1950).
22. R. Raap, R. U. Lemieux, and R. G. Micetich. U.S. Patent No. 3 271 407 (1966); Chem. Abstr. **66**, 2742 (1967).

Can. J. Chem. Downloaded from www.nrcresearchpress.com by 210.87.254.40 on 09/05/12
For personal use only.

Sur la formation de l'*endo* et de l'*exo* acétyl-1 méthyl-6 bicyclo[3·1·0]hexane lors d'une réaction de Friedel–Crafts

NORMAND DUFORT ET JACQUES LAFONTAINE[1]
Département de chimie, Université de Montréal, Montréal, Québec

Reçu le 25 octobre 1967

La condensation du méthyl-1 cyclohexène avec le chlorure d'acétyle en présence de chlorure stannique conduit lors de la deshydrochloruration par une solution alcoolique d'hydroxyde de sodium à la formation de l'acétyl-1 méthyl-2 cyclohexène-2, de l'acétyl-1 méthyl-2 cyclohexène-1 mais en prépondérance à la formation de l'*endo* et de l'*exo* acétyl-1 méthyl-6 bicyclo[3·1·0] hexane.

La formation et la configuration de ces deux composés bicycliques sont confirmées d'une façon certaine par leur synthèse.

Canadian Journal of Chemistry, 46, 1065 (1968)

Dans nos travaux de recherches, il était devenu nécessaire de préparer l'acétyl-1 méthyl-2 cyclohexène-1 comme substance modèle. Nous avons donc utilisé la méthode décrite par Turner et Voitle (1) qui consiste à condenser le chlorure d'acétyle avec le méthyl-1 cyclohexène en présence de chlorure stannique suivie d'une deshydrochloruration par une solution méthanolique d'hydroxyde de sodium.

Au lieu d'obtenir seulement l'acétyl-1 méthyl-2 cyclohexène-2 (**1**) et l'acétyl-1 méthyl-2 cyclohexène-1 (**2**) comme l'indiquait Turner, l'analyse par chromatographie en phase gazeuse a révélé en plus du composé **1** (9%) et du composé **2** (29%) la présence de deux nouveaux composés dans les proportions de 13 et 49%.

La présente publication décrit la séparation et l'identification de ces deux nouveaux composés et rapporte leur synthèse comme preuve de structure.

Chacun de ces composés est obtenu à l'état pur par chromatographie en phase gazeuse préparative. Les composés **1** et **2** sont identifiés comme étant effectivement l'acétyl-1 méthyl-2 cyclohexène-2 (**1**) et l'acétyl-1 méthyl-2 cyclohexène-1 (**2**) par comparaison de leurs constantes physiques et celles de leurs semicarbazones avec les constantes rapportées dans la littérature pour ces composés.

Le composé formé à 13% montre dans l'infrarouge une bande à 1680 cm^{-1} et dans l'ultraviolet un maximum à 213 mμ ($\varepsilon = 3050$). Le spectre de résonance magnétique nucléaire (r.m.n.) présente un doublet à τ 9.04 (3H, $J = 4.0$ c.p.s.) pour le méthyle en β du carbonyle et un singulet à τ 7.89 (3H) pour le méthyle adjacent au carbonyle.

Le composé formé à 49% présente une bande à 1680 cm^{-1} dans l'infrarouge et un maximum à 213 mμ ($\varepsilon = 4530$) dans l'ultraviolet. Le spectre r.m.n. présente un doublet à τ 8.94 (3H, $J = 6.0$ c.p.s.) pour le méthyle en β du carbonyle et un singulet à τ 7.98 (3H) pour le méthyle adjacent au carbonyle.

Ces données spectrales indiquent la présence d'un noyau cyclopropanique conjugué avec un groupe carbonyle (2,3). Le fait que les deux composés résistent à l'ozonolyse confirme l'absence d'une double liaison et la présence d'un anneau cyclopropanique dans leur structure. De plus, par un traitement à l'acide oxalique, ces deux composés s'isomérisent pour donner un mélange des composés **1** et **2** montrant que ces composés sont des isomères.

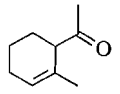

1

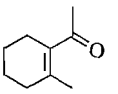

2

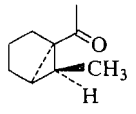

3a

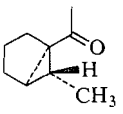

3b

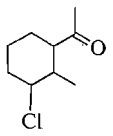

8

[1]Extrait du mémoire présenté par J. Lafontaine en vue de l'obtention du grade de Maître-ès-Sciences, Faculté des Sciences, Université de Montréal, juillet, 1966.

Can. J. Chem. Downloaded from www.nrcresearchpress.com by 210.87.254.40 on 09/05/12
For personal use only.

A l'aide de ces derniers résultats et des données spectrales, on peut conclure que ces deux nouveaux composés sont les deux isomères possibles de l'acétyl-1 méthyl-6 bicyclo[3·1·0]hexane à savoir l'*endo* et l'*exo* **3***a* et **3***b*.

Pour confirmer d'une façon certaine leur structure et pour déterminer leur configuration respective, ces deux composés sont synthétisés de la manière suivante. Le cétal de l'acétyl-1 méthyl-2 cyclohexène-2 (**4**) est obtenu selon la méthode de Rosenkranz *et al.* (4). La réaction suivie par chromatographie sur plaque mince est incomplète. La cétone de départ est éliminée par réduction avec l'hydrure de lithium et d'aluminium suivie d'une chromatographie sur alumine. Le spectre r.m.n. du cétal **4** présente un singulet à τ 8.83 (3H) pour le méthyle en α du groupe cétal, un singulet émergeant d'un massif centré à τ 8.28 (10H) pour le méthyle et les hydrogènes du cycle, un multiplet à τ 6.10 (4H) pour les hydrogènes du groupe cétal et un multiplet à τ 4.35 (1H) pour le proton éthylénique. De plus, le spectre de masse indique un ion moléculaire à *m/e* 182.

L'hydroboration du composé **4** est effectuée selon la méthode proposée par Brown et Subba Rao (5). Or il a été démontré que cette réaction se ferait selon une addition *cis* (6) ce qui signifie que les groupes méthyle et hydroxyle seraient nécessairement *trans* l'un par rapport à l'autre. Comme dans le composé **4**, la double liaison peut en principe être attaquée des deux côtés, il serait possible que les alcools **5***a* et **5***b* se forment.

Après hydrolyse et tosylation, ces deux alcools conduiraient aux cétotosylates correspondants **6***a* et **6***b*. Cependant traités par une base forte, ces cétotosylates s'énoliseraient pour donner un même énolate qui conduirait à la formation du composé **3***b* par une réaction de déplacement anionique intramoléculaire (7). Donc quelque soit le mode d'attaque lors de l'hydroboration, cette méthode constitue une synthèse spécifique du composé **3***b*.

De fait après avoir hydrolysé et tosylé une petite quantité d'alcool obtenu par hydroboration, la détosylation n'a conduit qu'à la formation d'un seul composé: l'*exo* acétyl-1 méthyl-6 bicyclo[3·1·0]hexane (**3***b*). L'analyse par c.p.g. a montré que ce composé était identique au composé obtenu avec un rendement de 13% lors de la réaction de Friedel–Crafts. La configuration d'un des deux composés bicycliques était ainsi déterminée d'une façon certaine.

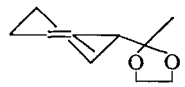

4

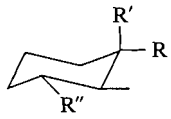

5*a* R = H, R′ = O O, R″ = OH

5*b* R = O O, R′ = H, R″ = OH

6*a* R = H, R′ = $COCH_3$, R″ = OTs

6*b* R = $COCH_3$, R′ = H, R″ = OTs

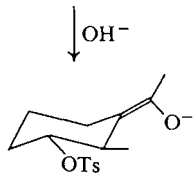

3*b*

Pour déterminer la configuration de l'autre isomère, il a fallu faire la modification suivante qui permet d'obtenir en même temps les deux composés bicycliques. L'alcool obtenu par hydroboration est oxydé par le complexe anhydride chromique – pyridine selon la méthode de Poos *et al.* (8), puis traité par le méthylate de sodium pour donner le composé **7** qui présente une bande cétonique à 1710 cm^{-1} dans l'infrarouge et dans le spectre r.m.n. un singulet à τ 8.79 (3H) pour le méthyle en α du groupe cétal, un doublet à τ 8.91 (3H, J = 7.0 c.p.s.) pour le méthyle du cycle et un singulet à τ 6.18 (4H) pour les hydrogènes du groupe cétal.

La réduction catalytique du composé **7** en présence d'oxyde de platine conduit aux alcools **5***b* et **5***c* qui ne sont pas séparés. Le spectre infrarouge du mélange d'alcools présente des bandes alcools à 985 et 965 cm^{-1} indiquant la présence des deux alcools (9) ce qui sera d'ailleurs confirmé par la formation des deux composés bicycliques **3***a* et **3***b*.

Après hydrolyse du groupe cétal, la tosylation du mélange des deux alcools conduit aux cétotosylates **6***b* et **6***c*.

La détosylation de ce mélange de cétotosylates

Can. J. Chem. Downloaded from www.nrcresearchpress.com by 210.87.254.40 on 09/05/12
For personal use only.

par l'hydroxyde de sodium alcoolique selon la méthode employée par Nelson et Mortimer (7) conduit aux composés bicycliques **3***a* et **3***b*. En effet, l'analyse par c.p.g. sur deux adsorbants différents indique la formation de 36% d'*endo* acétyl-1 méthyl-6 bicyclo[3·1·0]hexane (**3***a*) et de 64% d'*exo* acétyl-1 méthyl-6 bicyclo[3·1·0]-hexane (**3***b*). Ce dernier composé est identifié facilement vu qu'il possède le même temps de rétention sur les deux adsorbants que l'*exo* acétyl-1 méthyl-6 bicyclo[3·1·0]hexane préparé spécifiquement.

Une injection mixte de ces deux composés avec les composés bicycliques formés à 13 et 49% lors de la réaction de Friedel–Crafts montre à l'analyse par c.p.g. que ces composés sont parfaitement identiques. La réaction d'acylation suivie d'une deshydrochloruration par une base forte conduit donc à la formation de 13% d'*exo* acétyl-1 méthyl-6 bicyclo[3·1·0]hexane (**3***b*) et de 49% d'*endo* acétyl-1 méthyl-6 bicyclo[3·1·0] hexane (**3***a*).

Une série de cristallisations a permis d'isoler le cétotosylate **6***b*. Le spectre infrarouge de ce composé présente des bandes à 1710, 1600, 1175 et 1100 cm^{-1} et aucune bande à 3450 cm^{-1}. Le spectre r.m.n. présente un doublet à τ 9.25 (3H, $J = 5.5$ c.p.s.) pour le méthyle du cycle, un singulet à τ 7.90 (3H) pour le méthyle de l'acétyle, un singulet à τ 7.60 (3H) pour le méthyle du toluène et un multiplet à τ 5.85 (1H) pour l'hydrogène attaché au carbone qui porte le groupe tosylate, De plus le spectre de masse indique un ion moléculaire à *m/e* 310. La détosylation de ce produit cristallisé donne un seul composé bicyclique l'*exo* acétyl-1 méthyl-6 bicyclo[3.1.0]-hexane (**3***b*) indiquant que le cétotosylate cristallisé était le composé **6***b*.

Il n'a pas été possible d'obtenir le cétotosylate **6***c* cristallisé. La détosylation des composés recueillis des eaux-mères de cristallisation indique à l'analyse par c.p.g. la formation de 28% du composé **3***b* et de 72% du composé **3***a* comparativement à 64 et 36% avant la cristallisation, ce qui indique un enrichissement de l'isomère **6***c* qui ne voulait pas cristalliser.

Enfin le mélange de composés bicycliques obtenus par synthèse a été séparé par chromatographie en phase gazeuse préparative et le composé **3***b* a été obtenu à l'état pur. Ses constantes physiques et spectrales correspondent parfaitement au composé bicyclique obtenu à 13% lors de la réaction de Friedel–Crafts. Ainsi

7

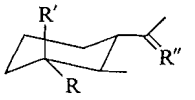

5*b* R = OH, R′ = H, R″ = O O

5*c* R = H, R′ = OH, R″ = O O

6*b* R = OTs, R′ = H, R″ = O

6*c* R = H, R′ = OTs, R″ = O

OH^-

3*a* et **3***b*

la formation et la configuration des composés **3***a* et **3***b* ont été établies d'une façon certaine par cette synthèse.

Toutefois la littérature n'a jamais jusqu'à présent mentionné la formation de tels composés bicycliques lors de ces réactions d'acylation même si beaucoup de travaux ont été faits dans ce domaine (10). C'est pourquoi la formation de tels composés bicycliques nous a incité à examiner davantage cette condensation et nous rapportons brièvement les conclusions tirées de cette étude. Tout essai d'obtenir un composé bicyclique en condensant le chlorure d'acétyle sur le cyclohexène dans les mêmes conditions que pour le méthyl-1 cyclohexène s'est avéré infructueux: on ne décèle que la présence d'acétyl-1 cyclohexène.

La condensation de l'anhydride acétique avec le méthyl-1 cyclohexène faite dans les mêmes conditions qu'avec le chlorure d'acétyle ne donne pas de composé bicyclique mais un mélange de composés **1** et **2** ce qui est d'ailleurs conforme aux travaux de Royals et Hendry (11).

Pour obtenir un rendement optimum en composés bicycliques, il faut une agitation d'au moins 8 h entre le méthyl-1 cyclohexène, le chlorure d'acétyle et le chlorure stannique avant le traitement par une base forte.

Une étude des différents agents deshydrochlorurants a été faite et les résultats sont rapportés dans le Tableau I.

TABLEAU I

Deshydrochloruration des produits d'acylation par différentes bases

Agent deshydrochlorurant	% 3*b*	% **1**	% **2**	% 3*a*
Hydroxyde de sodium	13	9	29	49
Hydrure de sodium	10	5	38	47
t-butoxyde de potassium	14	8	29	49
N,*N*-diméthylaniline	0	35	65	0
Carbonate de sodium	0	75	25	0

De ces deshydrochlorurations, on peut donc déduire que les bases fortes conduisent à peu près à la même quantité de composés cyclopropaniques, tandis que les bases faibles ne conduisent pas à la formation de composés bicycliques.

Ces composés bicycliques **3***a* et **3***b* pourraient s'expliquer par la formation de l'acétyl-1 méthyl-2 chloro-3 cyclohexane (**8**) lors de la condensation du chlorure d'acétyle avec le méthyl-1 cyclohexène. En effet, cette cétone chlorée traitée par une base forte pourrait donner lieu à la formation d'une cétone conjuguée avec un anneau cyclopropanique par une réaction de déplacement anionique intramoléculaire (7).

Il devenait donc intéressant d'essayer d'isoler cette cétone chlorée. Lors d'une condensation et avant la deshydrochloruration, le mélange cétonique indiquait par c.p.g. 39% de cétones éthyléniques et 61% de cétones chlorées. Après deux distillations fractionnées, le chromatogramme de la fraction centrale indiquait trois pics. Le premier pic représentant 2% est identifié comme étant l'acétyl-1 méthyl-2 cyclohexène-1 (**2**). Le second pic représentant 82% et le troisième pic 16% seraient des cétones chlorées. L'analyse centésimale de cette fraction a d'ailleurs donné des résultats très satisfaisants vu la grande fragilité des composés chlorés qui noircissent après quelques heures: elle conduit à la formule $C_9H_{15}OCl$. De plus ces cétones chlorées ayant une bande carbonyle à 1708 cm^{-1} dans l'infrarouge et dans le spectre r.m.n. un doublet à τ 9.10 (3H, $J = 6.4$ c.p.s.) pour le méthyle en β du carbonyle et un multiplet à τ 5.87 (1H) pour l'hydrogène sur le carbone qui porte le chlore pourraient bien être deux isomères de l'acétyl-1 méthyl-2 chloro-3 cyclohexane (**8**). Cependant, il ne fut pas possible de séparer ces cétones à cause de leur instabilité.

Cette présence du chlore en position-γ plutôt qu'en position-β par rapport au groupe acétyle peut s'expliquer par une migration d'hydrure (12).

Ainsi ces composés bicycliques résulteraient de la formation de cétones chlorées en position-γ par rapport au groupe acétyle lors de la condensation de Friedel–Crafts parce que ces cétones traitées par une base forte pourraient donner des composés bicycliques par une réaction de déplacement anionique intramoléculaire.

Partie expérimentale

Les points de fusion ont été déterminés à l'aide d'un appareil de marque "Buchi" et ne sont pas corrigés. Les spectres infrarouges ont été déterminés en solution dans le tétrachlorure de carbone à l'aide d'un spectrophotomètre Beckmann modèle IR-8 à double faisceau.

Les spectres ultraviolets ont été déterminés en solution dans l'éthanol 95% à l'aide d'un appareil "Bausch & Lomb Spectronic 505". Les spectres de résonance magnétique nucléaire ont été déterminés avec un appareil modèle A60, de la compagnie Varian pour des solutions dans le chloroforme deutéré et utilisant le tétraméthylsilane comme référence interne. Les spectres de masse ont été déterminés à l'aide d'un appareil Hitachi – Perkin – Elmer RMU-6D. Les analyses par chromatographie en phase gazeuse ont été effectuées à l'aide d'un appareil F et M modèle 810 en utilisant une colonne de 4m contenant 10% d'hyprose supporté sur du chromosorb P. Les séparations préparatives ont été effectuées à l'aide d'un appareil "Prep/Partitioner" de Fisher modèle 24 en utilisant des colonnes renfermant 10% d'hyprose supporté sur du chromosorb P. Les analyses ont été effectuées par Dr. C. Daesslé "Organic Microanalyses" de Montréal et par "Schwarzkopf Microanalytical Laboratory" de New York.

Condensation du méthyl-1 cyclohexène avec le chlorure d'acétyle

Le méthyl-1 cyclohexène est condensé avec le chlorure d'acétyle en présence de chlorure stannique et le mélange réactionnel est traité par une solution alcoolique d'hydroxyde de sodium selon le procédé décrit par Turner et Voitle (1). L'analyse par chromatographie en phase gazeuse sur une colonne d'hyprose indique la formation de quatre composés qui ont été identifiés comme étant l'*exo* acétyl-1 méthyl-6 bicyclo[3·1·0]hexane (**3***b*) 13%, l'acétyl-1 méthyl-2 cyclohexène-2 (**1**) 9%, l'acétyl-1 méthyl-2 cyclohexène-1 (**2**) 29% et l'*endo* acétyl-1 méthyl-6 bicyclo[3·1·0]hexane (**3***a*) 49%.

Isomérisation du mélange de cétones par l'acide oxalique

Un mélange (50 g) des quatre cétones sont traités par 141 g d'acide oxalique en solution dans l'eau à 105° durant 36 h sous atmosphère d'azote. Les composés organiques sont isolés de la manière habituelle et la chromatographie en phase gazeuse indique la formation de 34% d'acétyl-1 méthyl-2 cyclohexène-2 (**1**) et de 66% d'acétyl-1 méthyl-2 cyclohexène-1 (**2**) qui sont séparés par chromatographie en phase gazeuse préparative. Le composé **1** pur distille à 78–79° à 12 mm (rapporté 83–83.5° à 17 mm (1)); spectre r.m.n.: singulet à τ 8.34 (3H) méthyle

Can. J. Chem. Downloaded from www.nrcresearchpress.com by 210.87.254.40 on 09/05/12
For personal use only.

Can. J. Chem. Downloaded from www.nrcresearchpress.com by 210.87.254.40 on 09/05/12
For personal use only.

sur la double liaison, singulet à τ7.82 (3H) méthyle adjacent au carbonyle, multiplet à τ4.20 (1H) hydrogène sur la double liaison. La semicarbazone cristallisée dans le méthanol fond à 150–151° (rapporté 160–162° (1), 153–155° (13)).

Le composé **2** pur distille à 85–86° à 12 mm (rapporté 89.5–90° à 17 mm (1)); spectre r.m.n.: singulet à τ 8.20 (3H) méthyle sur la double liaison, singulet à τ 7.92 (3H) méthyle adjacent au carbonyle. La semicarbazone cristallisée dans le méthanol fond à 222–223° (rapporté 227–227.5° (1)).

Ozonolyse du mélange de cétones

Le mélange des quatre cétones en solution dans l'éther de pétrole purifié est maintenu à la température du mélange acétone-glace sèche et de l'ozone est barbotté dans la solution jusqu'à ce qu'il y ait un excès d'ozone. La solution est alors décantée; les ozonides jaunâtres restent dans le fond du ballon. Après évaporation de l'éther de pétrole et distillation, la chromatographie en phase gazeuse indique la présence des composés **3***a* et **3***b* seulement. Ces deux composés sont alors séparés par chromatographie en phase gazeuse préparative. L'*exo* acétyl-1 méthyl-6 bicyclo[3·1·0]hexane (**3***b*) pur a un point d'ébullition de 191° à 755 mm; spectre ultraviolet: λ_{max}: 213 mμ, ε 3050; spectre infrarouge: bande carbonyle: 1680 cm^{-1}; spectre r.m.n.: doublet à τ 9.04 (3H, $J = 4.0$ c.p.s.) méthyle en β du carbonyle, singulet à τ 7.89 (3H) méthyle adjacent au carbonyle.

Anal. Calc. pour $C_9H_{14}O$: C, 78.21; H, 10.21. Trouvé: C, 78.38; H, 10.42.

La semicarbazone cristallisée dans le méthanol fond à 213°.

Anal. Calc. pour $C_{10}H_{17}N_3O$: C, 61.51; H, 8.78; N, 21.52; Trouvé: C, 61.70; H, 8.88; N, 21.61.

L'*endo* acétyl-1 méthyl-6 bicyclo[3·1·0]hexane (**3***a*) pur distille à 70–71° à 6 mm; spectre ultraviolet: λ_{max}: 213 mμ, ε 4530; spectre infrarouge: bande carbonyle: 1680 cm^{-1}; spectre r.m.n.: doublet à τ 8.94 (3H, $J = 6.0$ c.p.s.) méthyle en β du carbonyle, singulet à τ 7.98 (3H) méthyle adjacent au carbonyle.

Anal. Calc. pour $C_9H_{14}O$: C, 78.21; H, 10.21. Trouvé: C, 78.20; H, 10.17.

La semicarbazone cristallisée dans le méthanol fond à 206–207°

Anal. Calc. pour $C_{10}H_{17}N_3O$: C, 61.51; H, 8.78; N, 21.52. Trouvé: C, 61.41; H, 9.03; N, 21.43.

Préparation du cétal de l'acétyl-1 méthyl-2 cyclohexène-2

Quarante-cinq gram d'acétyl-1 méthyl-2 cyclohexène-2 (**1**) en solution dans 350 ml de benzène anhydre sont reflués avec 90 ml d'éthylène glycol et 1.5 g d'acide *p*-toluène sulfonique durant 5 h. L'eau formée est éliminée au moyen d'un séparateur d'eau. Après dilution dans l'éther, le mélange est lavé par le carbonate de sodium 10% et l'eau saturée de chlorure de sodium jusqu'à neutralité. Après évaporation des solvants, le résidu est traité par l'hydrure de lithium et d'aluminium de la manière habituelle. Le mélange d'alcool et de cétal est séparé par chromatographie sur alumine. On recueille 22 g du composé **4** qui distille à 227° à 750 mm; spectre infrarouge: bandes à 1115, 1060 et 1040 cm^{-1}, pas de bande à 1705 cm^{-1}; spectre r.m.n.: singulet à τ 8.83 (3H) méthyle en α du groupe cétal, singulet émergeant d'un massif à τ 8.28 (10H) méthyle sur la double liaison et hydrogènes du cycle, multiplet à τ 6.10 (4H) hydrogènes du groupe cétal, multiplet à τ 4.35 (1H) proton éthylénique. Le spectre de masse indique un ion moléculaire à *m/e* 182.

Hydroboration du cétal de l'acétyl-1 méthyl-2 cyclohexène-2

A 20 g du composé **4** et 1.7 g d'hydrure de bore et de sodium en solution dans 65 ml de diglyme sont ajoutés très lentement à 10° et sous atmosphère d'azote, 8.0 g de fluorure de bore fraîchement distillé en solution dans 20 ml de diglyme. Après avoir laissé la réaction se poursuivre durant 1 h, l'excès d'hydrure est détruit par 10 ml d'eau; après l'addition de 20 ml d'hydroxyde de sodium 4*N*, 20 ml de peroxyde d'hydrogène 30% sont ajoutés à une vitesse telle qu'un léger reflux est maintenu. Après extraction et distillation des solvants à pression réduite sous atmosphère d'azote, on obtient 19.5 g d'alcool qui distille à 180° à 12 mm; spectre infrarouge: bandes à 3450, 1115, 1060, 1040 et 985 cm^{-1}; spectre r.m.n.: singulet imbriqué dans un doublet à τ 8.82 (6H) méthyle adjacent au groupe cétal et celui du cycle, singulet à τ 6.31 (1H) hydrogène de l'hydroxyle, singulet à τ 6.10 (4H) hydrogènes du groupe cétal. Le spectre de masse indique un ion moléculaire à *m/e* 200.

Oxydation de l'alcool obtenu par hydroboration

L'alcool (10 g) obtenu par hydroboration en solution dans 100 ml de pyridine anhydre sont ajoutés au complexe anhydride chromique – pyridine formé en ajoutant 24 g d'anhydride chromique à 125 ml de pyridine anhydre. Après une agitation de 20 h à la température de la pièce, le mélange réactionnel est jeté sur de l'eau glacée et extrait par de l'éther. La couche éthérée est lavée par une solution saturée de chlorure de sodium jusqu'à neutralité. Après séchage sur le sulfate de sodium anhydre et évaporation des solvants, le produit est traité par 6 g de méthylate de sodium en solution dans 50 ml de méthanol. Le tout est agité durant 24 h à la température de la pièce. Le précipité est décomposé par l'eau et extrait de la façon habituelle. Après évaporation des solvants et distillation, on recueille 6.5 g du composé **7**; spectre infrarouge: bandes à 1710, 1115, 1060 et 1040 cm^{-1}; spectre r.m.n.: singulet à τ 8.79 (3H) méthyle en α du groupe cétal, doublet à τ 8.91 (3H, $J = 7.0$ c.p.s.) méthyle du cycle, singulet à τ 6.18 (4H) hydrogènes du groupe cétal.

Réduction de la cétone 7

Le cétone **7** (5.5 g) en solution dans 150 ml d'éthanol absolu sont hydrogénés en présence de 2.1 g d'oxyde de platine. Quand l'hydrogénation s'arrête, le catalyseur est éliminé par filtration. Après évaporation du solvant, il reste 4.8 g du mélange d'alcools **5***b* et **5***c*; spectre infrarouge: bandes à 3450, 985 et 965 cm^{-1} indiquant la présence d'alcool équatorial et axial.

Hydrolyse du mélange d'alcools

Un mélange d'alcools **5***b* et **5***c* (4.8 g) en solution dans 100 ml d'éthanol et 14 ml d'acide sulfurique à 10% sont chauffés à reflux durant 2 h et demie et agités à la température de la pièce durant 16 h. Après neutralisation de l'acide par le carbonate de sodium, le tout est extrait de la manière habituelle. Après évaporation des solvants et distillation, on recueille 2.7 g du mélange de cétoalcools correspondants; spectre infrarouge: bandes à 3450, 1710,

Can. J. Chem. Downloaded from www.nrcresearchpress.com by 210.87.254.40 on 09/05/12
For personal use only.

985 et 965 cm^{-1}; (la présence de la bande carbonyle à 1710 cm^{-1} indique l'ouverture du groupe cétal).

Tosylation du mélange de cétoalcools

A 2.7 g du mélange de cétoalcools sont ajoutés 8 g de chlorure de *p*-toluène sulfonyle dans 50 ml de pyridine anhydre. Le mélange laissé à la température de la pièce durant 18 h est ensuite versé sur du HCl 2% refroidi à 0° et le tout est extrait de la façon habituelle. Après évaporation des solvants, le résidu huileux dissous dans l'éther de pétrole cristallise lentement. Après quatre cristallisations, les cristaux sous forme d'aiguilles fondent à 90–91°; spectre infrarouge: bandes à 1710, 1600, 1175 et 1100 cm^{-1}; pas de bande à 3450 cm^{-1}; spectre r.m.n.: doublet à τ 9.25 (3H, $J = 5.5$ c.p.s.) méthyle du cycle, singulet à τ 7.90 (3H) méthyle de l'acétyle, singulet à τ 7.60 (3H) méthyle du toluène, multiplet à τ 5.85 (1H) hydrogène attaché au carbone qui porte le tosylate.

Anal. Calc. pour $C_{16}H_{22}O_4S$: C, 61.93; H, 7.09; S, 10.32. Trouvé: C, 61.82; H, 7.01; S, 10.65.

La détosylation de ces cristaux par une solution alcoolique de NaOH 20% en suivant le procédé décrit ci-dessous ne conduit qu'à la formation du composé **3***b* indiquant que le produit cristallisé était l'isomère **6***b*.

Détosylation du mélange de cétotosylates

A 1.2 g de NaOH dissous dans 6 ml de méthanol sont ajoutés 1.5 g du mélange de cétotosylates non cristallisés **6***b* et **6***c*. Après une agitation de 20 h à la température de la pièce et extraction de la façon habituelle, le mélange de produits obtenus après évaporation de l'éther est analysé par c.p.g.: il y a formation de 64% d'*exo* acétyl-1 méthyl-6 bicyclo[3·1·0]hexane (**3***b*) et 36% d'*endo* acétyl-1 méthyl-6 bicyclo[3·1·0]hexane (**3***a*). Une injection mixte de ces deux composés avec les composés bicycliques formés à 13 et 49% lors de la réaction de Friedel–Crafts montre que ces composés sont parfaitement identiques.

Le composé formé à 64% a été obtenu à l'état pur par chromatographie en phase gazeuse préparative. Les spectres infrarouge, ultraviolet et r.m.n. de ce composé et de celui qui est formé à 13% lors de la réaction de Friedel–Crafts sont parfaitement identiques. De plus à l'analyse par c.p.g. sur une colonne de Polyester de Craig et une colonne d'hyprose, ces deux composés ont le même temps de rétention.

Deshydrochloruration des produits d'acylation par différentes bases

(a) Deshydrochloruration par l'hydrure de sodium

Le mélange de cétones obtenues (6.7 g) lors de l'acylation sont traités par 1 g d'hydrure de sodium selon la méthode décrite par Nelson et Mortimer (7). L'analyse par c.p.g. des produits de deshydrochloruration indique la formation de 10% d'*exo* acétyl-1 méthyl-6 bicyclo-[3·1·0]hexane (**3***b*), 5% d'acétyl-1 méthyl-2 cyclohexène-2 (**1**), 38% d'acétyl-1 méthyl-2 cyclohexène-1 (**2**) et 47% d'*endo* acétyl-1 méthyl-6 bicyclo[3.1.0]hexane (**3***a*).

(b) Deshydrochloruration par le t-butoxyde de potassium

Le mélange de cétones obtenues (6 g) lors de l'acylation en solution dans 150 ml d'alcool *t*-butylique sont traités par une solution formée de 50 ml d'alcool *t*-butylique et de 1.5 g de potassium selon la méthode décrite par Nelson et Mortimer (7). L'analyse par c.p.g. des produits de deshydrochloruration indique la formation de 14% d'*exo* acétyl-1 méthyl-6 bicyclo[3·1·0]hexane (**3***b*), 8% d'acétyl-1 méthyl-2 cyclohexène-2 (**1**), 29% d'acétyl-1 méthyl-2 cyclohexène-1 (**2**) et 49% d'*endo* acétyl-1 méthyl-6 bicyclo[3·1·0]hexane (**3***a*).

(c) Deshydrochloruration par la N,N-diméthylaniline

Les cétones obtenues (6 g) lors de l'acylation sont traités par 5.8 g de *N,N*-diméthylaniline selon la méthode décrite par Royals (11). L'analyse par c.p.g. des produits de deshydrochloruration indique la formation de 35% d'acétyl-1 méthyl-2 cyclohexène-2 (**1**) et de 65% d'acétyl-1 méthyl-2 cyclohexène-1 (**2**).

(d) Deshydrochloruration par le carbonate de sodium

Les cétones obtenues (2 g) lors de l'acylation en solution dans 10 ml de dioxanne purifié et 1 g de Na_2CO_3 sont chauffés sous atmosphère d'azote pendant 2 h et demie. Après dilution par l'éther, la couche organique est lavée par de l'eau jusqu'à neutralité. Après évaporation du solvant, l'analyse par c.p.g. du résidu indique la présence de 75% d'acétyl-1 méthyl-2 cyclohexène-2 (**1**) et de 25% d'acétyl-1 méthyl-2 cyclohexène-1 (**2**).

Isolement d'un mélange de deux cétones chlorées

Un mélange obtenu (12 g) lors de l'acylation et formé de 9% d'acétyl-1 méthyl-2 cyclohexène-1 (**2**) et de 91% de cétones chlorées sont redistillés à travers une colonne Vigreux sous atmosphère d'azote.

La fraction centrale qui distille à 82–83° à 3 mm est analysée par chromatographie en phase gazeuse sur une colonne de glycérol 20% longue d'un mètre cinquante. Le chromatogramme indique la présence de 2% de composé **2** et de 82 et 16% de cétones chlorées qui pourraient être des isomères de l'acétyl-1 méthyl-2 chloro-3 cyclohexane (**8**); spectre infrarouge: bande carbonyle à 1708 cm^{-1}; spectre r.m.n.: doublet à τ 9.10 (3H, $J = 6.4$ c.p.s.) méthyle en β du carbonyle, singulet à τ 7.95 (3H) méthyle adjacent au carbonyle; multiplet à τ 5.87 (1H) hydrogène sur le carbone qui porte le chlore.

Anal. Calc. pour $C_9H_{15}OCl$: C, 61.88; H, 8.65; Cl, 20.29. Trouvé: C, 62.37; H, 8.73; Cl, 20.17.

Remerciements

Les auteurs remercient le Conseil National de Recherches du Canada pour l'aide financière accordée sous forme d'octroi de recherches (A 2030 A14); le service de l'aide aux étudiants de la Province de Québec pour l'aide financière accordée sous forme de bourses d'études (J.L.); le Dr. Pierre Deslongchamps de l'Université de Sherbrooke pour des discussions très utiles.

1. R. B. Turner et D. M. Voitle. J. Am. Chem. Soc. **73**, 1403 (1951).
2. A. B. F. Duncan, W. Gordy, R. N. Jones, F. A. Matsen, C. Sandorfy et W. West. Chemical applications of spectroscopy. Vol. IX. Interscience Publishers Inc., New York. 1956. p. 445.
3. E. M. Kosower. J. Am. Chem. Soc. **80**, 3261 (1958).
4. G. Rosenkranz, J. Pataki et C. Djerassi. J. Org. Chem. **17**, 290 (1952).
5. H. C. Brown et B. C. Subba Rao. J. Am. Chem. Soc. **81**, 6428 (1959).

6. H. C. BROWN et G. ZWEIFEL. J. Am. Chem. Soc. **83**, 2544 (1961).
7. N. A. NELSON et G. A. MORTIMER. J. Org. Chem. **22**, 1146 (1957).
8. G. I. POOS, G. E. ARTH, R. E. BEYLER et L. H. SARETT. J. Am. Chem. Soc. **75**, 422 (1953).
9. E. L. ELIEL. Stereochemistry of carbon compounds. McGraw-Hill Book Company Inc., New York. 1962. p. 217.
10. G. A. OLAH. Friedel–Crafts and related reactions. Vol. III. Part 1. Interscience Publishers Inc., New York. 1964. p. 1033.
11. E. E. ROYALS et C. M. HENDRY. J. Org. Chem. **15**, 1147 (1950).
12. G. A. OLAH. Friedel–Crafts and related reactions Vol. III. Part 1. Interscience Publishers Inc., New York. 1964. p. 1066.
13. N. C. DENO et H. CHAFETZ. J. Am. Chem. Soc. **74**, 3940 (1952).

Can. J. Chem. Downloaded from www.nrcresearchpress.com by 210.87.254.40 on 09/05/12
For personal use only.

Can. J. Chem. Downloaded from www.nrcresearchpress.com by 210.87.254.40 on 09/05/12
For personal use only.

Réduction de cétones conjuguées dans la série acétyl méthyl cyclohexène

NORMAND DUFORT ET EDDY FLAMAND[1]
Département de chimie, Université de Montréal, Montréal, Québec

Reçu le 24 novembre 1967

Quelques cétones conjugées dans la série acétyl méthyl cyclohexène sont préparées et réduites par l'hydrure de lithium et d'aluminium et par l'hydrure de bore et de sodium. Tous les produits de réduction sont également identifiés.

Canadian Journal of Chemistry, 46, 1073 (1968)

Pour nos travaux de recherches, il était important de connaître exactement les résultats de la réduction par l'hydrure de lithium et d'aluminium et par l'hydrure de bore et de sodium de cétones conjuguées de la série acétyl méthyl cyclohexène. Or une revue de la littérature ne permettait pas de tirer des conclusions très précises sur la réduction des cétones de cette série: English et Lamberti (1) rapportaient que la réduction de l'acétyl-1 cyclohexène par l'hydrure de lithium et d'aluminium conduisait uniquement à la formation de l'alcool allylique correspondant alors que Mousseron *et al.* (2) concluaient que la même réduction donnait une prépondérance d'alcool saturé en même temps que l'alcool allylique. D'autre part, Henbest *et al.* (3) rapportaient que la réduction de l'acétyl-1 diméthyl-4,4 cyclohexène par l'hydrure de lithium et d'aluminium conduisait à l'alcool allylique correspondant.

Comme ces résultats ne permettaient pas de déduire des conclusions très nettes, nous avons préparé et réduit les composés suivants: l'acétyl-1 cyclohexène (**1**), l'acétyl-1 méthyl-5 cyclohexène (**2**), l'acétyl-1 méthyl-4 cyclohexène (**3**) et l'acétyl-1 diméthyl-4,4 cyclohexène (**4**) et nous rapportons les résultats de ces réductions.

L'acétyl-1 cyclohexène (**1**) est préparé selon le procédé expérimental décrit par Royals et Hendry (4). L'acétyl-1 méthyl-5 cyclohexène (**2**) est préparé en suivant le procédé rapporté par Mousseron *et al.* (5), mais purifié par chromatographie en phase gazeuse préparative plutôt que par cristallisation fractionnée de sa semicarbazone comme l'avait fait Mousseron.

L'acétyl-1 méthyl-4 cyclohexène (**3**) est préparé selon la méthode de Beumel et Harris (6) en faisant réagir sous atmosphère d'acétylène, la méthyl-4 cyclohexanone avec l'acétylure de lithium complexé avec l'éthylènediamine, suivi d'un traitement par l'acide formique. L'acétyl-1 diméthyl-4,4 cyclohexène (**4**) est également préparé en faisant réagir sous atmosphère d'acétylène, la diméthyl-4,4 cyclohexanone avec l'acétylure de lithium complexé avec l'éthylènediamine, suivi d'un traitement par l'acide formique.

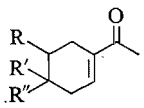

1 R = R′ = R″ = H
2 R = Me, R′ = R″ = H
3 R = R′ = H, R″ = Me
4 R = H, R′ = R″ = Me

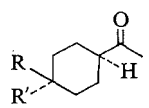

5 R = R′ = H
6 R = R′ = Me
9 R = Me, R′ = H
10 R = H, R′ = Me

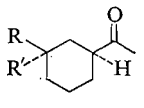

7 R = Me, R′ = H
8 R = H, R′ = Me

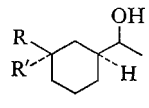

12 R = Me, R′ = H
13 R = H, R′ = Me

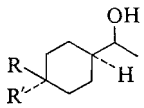

11 R = R′ = H
14 R = Me, R′ = H
15 R = H, R′ = Me
16 R = R′ = Me

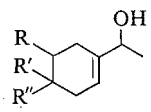

17 R = R′ = R″ = H
18 R = Me, R′ = R″ = H
19 R = R′ = H, R″ = Me
20 R = H, R′ = R″ = Me

Une revue de la littérature révèle que la réduction chimique de cétones conjuguées par l'hydrure de lithium et d'aluminium ou par l'hydrure de bore et de sodium se fait le plus souvent selon un mode d'addition-1,2 pour conduire à l'alcool allylique correspondant (1, 3, 7–12), parfois selon un mode d'addition-1,4 pour donner après hydrolyse la cétone saturée

[1]Extrait du mémoire présenté par E. Flamand en vue de l'obtention du grade de Maître-ès-Sciences, Faculté des Sciences, Université de Montréal, août, 1966.

TABLEAU I

Réduction catalytique des cétones conjuguées

Cétones conjuguées	Catalyseur	Cétones saturées	
Acétyl-1 cyclohexène (**1**)	Pd	Acétylcyclohexane (**5**)	
Acétyl-1 diméthyl-4,4 Cyclohexène (**4**)	Pd	Acétyl-1 diméthyl-4,4 cyclohexane (**6**)	
		Acétyl-1 méthyl-3 cyclohexane	
Acétyl-1 méthyl-5 Cyclohexène (**2**)	Pd/HCl	*cis* (**7**) 52%	*trans* (**8**) 48%
Acétly-1 méthyl-5 cyclohexène (**2**)	Pd/NaOH	88%	12%
		Acétyl-1 méthyl-4 cyclohexane	
Acétyl-1 méthyl-4 Cyclohexène (**3**)	Pd/HCl	*cis* (**9**) 73%	*trans* (**10**) 27%
Acétyl-1 méthyl-4 cyclohexène (**3**)	Pd/NaOH	14%	86%

TABLEAU II

Constantes physiques et pourcentage à l'équilibre des cétones saturées

Cétones saturées	Point d'ébullition, °C	Indice de réfraction à 25°	Pourcentage à l'équilibre
cis Acétyl-1 méthyl-3 cyclohexane (**7**)	191	1.4458	92
trans Acétyl-1 méthyl-3 cyclohexane (**8**)	193	1.4487	8
cis Acétyl-1 méthyl-4 cyclohexane (**9**)	193	1.4490	13
trans Acétyl-1 méthyl-4 cyclohexane (**10**)	190	1.4438	87

correspondante (13–16). Enfin, la littérature mentionne que dans certains cas, une telle réduction peut conduire aux alcools saturés correspondants (2, 9–11, 16–18).

Il devenait donc nécessaire de préparer les cétones saturées correspondantes pour déterminer si la réduction de ces cétones conjuguées par les hydrures complexes donnerait lieu à un mode d'addition-1,4. Les cétones saturées sont préparées par réduction catalytique des cétones conjuguées et les résultats sont rapportés dans le Tableau I. Les cétones saturées *cis* et *trans* acétyl-1 méthyl-3 cyclohexane (**7**) et (**8**) et *cis* et *trans* acétyl-1 méthyl-4 cyclohexane (**9**) et (**10**) sont obtenues à l'état pur par chromatographie en phase gazeuse préparative. Les différentes cétones saturées présentent une bande carbonyle vers 1710 cm^{-1} dans l'infrarouge et aucun proton éthylénique dans le spectre de resonance magnétique nucléaire (r.m.n.) ce qui confirme la formation de ces cétones saturées.

La configuration des isomères *cis* et *trans* de l'acétyl-1 méthyl-3 cyclohexane et de l'acétyl-1 méthyl-4 cyclohexane est déterminée par la mise en équilibre de ces cétones saturées en présence de méthylate de sodium et confirmée par leurs constantes physiques comme l'indique le Tableau II.

Comme cette réduction chimique peut conduire dans certains cas à l'alcool saturé (2, 9–11, 16–18), les différents alcools saturés susceptibles de se former sont préparés à partir des cétones saturées correspondantes par réduction avec l'hydrure de lithium et d'aluminium. Les constantes physiques et l'analyse élémentaire de ces alcools sont rapportées dans le Tableau III. Chacun de ces alcools est obtenu à l'état pur. Les spectres infrarouges de ces composés indiquent la présence d'une bande hydroxyle vers 3340 cm^{-1}, tandis que la bande carbonyle est disparue. De plus, ces différents alcools saturés oxydés par le complexe anhydride chromique –

Can. J. Chem. Downloaded from www.nrcresearchpress.com by 210.87.254.40 on 09/05/12
For personal use only.

TABLEAU III

Constantes physiques et analyse élémentaire des alcools saturés

Alcool saturé	Point d'ébullition, °C	Indice de réfraction à 26°	Trouvé C	Trouvé H	Calculé C	Calculé H
Hydroxy-1 éthyl cyclohexane (**11**)	75–76 à 10 mm	1.4683	—	—	—	—
cis-(Hydroxy-1 éthyl)-1 méthyl-3 cyclohexane (**12**)	203	1.4587	76.22	12.83	76.05	12.67
trans-(Hydroxy-1 éthyl)-1 méthyl-3 cyclohexane (**13**)	205	1.4606	76.01	12.91	76.05	12.67
cis-(Hydroxy-1 éthyl)-1 méthyl-4 cyclohexane (**14**)	207	1.4620	76.17	12.83	76.05	12.67
trans-(Hydroxy-1 éthyl)-1 méthyl-4 cyclohexane (**15**)	204	1.4602	76.12	12.82	76.05	12.67
(Hydroxy-1 éthyl)-1 diméthyl-4,4 cyclohexane (**16**)	210	1.4565	77.20	12.67	76.92	12.82

TABLEAU IV

Constantes physiques et analyse élémentaire des alcools allyliques

Alcool allylique	Point d'ébullition, °C	Indice de réfraction	Trouvé C	Trouvé H	Calculé C	Calculé H
(Hydroxy-1 éthyl)-1 cyclohexène (**17**)	78–80 à 10 mm	1.4834 à 22°	—	—	—	—
(Hydroxy-1 éthyl)-1 méthyl-5 cyclohexène (**18**)	211 à 760 mm	1.4726 à 27°	77.15	11.31	77.03	11.49
(Hydroxy-1 éthyl)-1 méthyl-4 cyclohexène (**19**)	102 à 22 mm	1.4724 à 28°	76.98	11.47	77.03	11.49
(Hydroxy-1 éthyl)-1 diméthyl-4,4 cyclohexène (**20**)	108 à 15 mm	1.4692 à 25°	78.15	11.63	77.92	11.68

pyridine (19) donnent les cétones saturées correspondantes qui sont identifiées par chromatographie en phase gazeuse à l'aide d'échantillons authentiques.

Ayant à notre disposition les cétones et les alcools saturés, les cétones conjuguées sont réduites par l'hydrure de lithium et d'aluminium. L'analyse par c.p.g. des produits de réduction de chaque cétone sur deux adsorbants différents: Hyprose 10% et Polyester de Craig 20% indique la présence d'un seul pic homogène. Les spectres infrarouges montrent la présence d'une bande hydroxyle vers 3380 cm^{-1} et il n'apparaît aucune bande carbonyle. Les spectres r.m.n. présentent un multiplet vers 5.5 p.p.m. pour le proton éthylénique et un singulet vers 4.4 p.p.m. pour le proton de l'hydroxyle; tandis que vers 4.0 p.p.m. apparaît le proton lié au carbone qui porte le groupe hydroxyle. Ces différentes données permettent donc de déduire que la réduction de ces cétones conjuguées conduit uniquement aux alcools allyliques correspondants. Le Tableau IV rapporte les constantes physiques et l'analyse élémentaire de ces alcools.

Pour confirmer leur formation, ces alcools allyliques sont oxydés par le bioxyde de manganèse activé (20). Les produits d'oxydation analysés par c.p.g. indiquent la formation des cétones conjuguées correspondantes qui sont identifiées à l'aide d'échantillons authentiques.

Les cétones conjuguées sont également réduites par l'hydrure de bore et de sodium. L'analyse par c.p.g. des produits de réduction révèle la formation non pas d'un seul mais de deux ou trois composés dépendant de la cétone de départ. De plus, leurs spectres infrarouges ne présentent plus de bande carbonyle mais une bande hydroxyle ce qui permet de déduire la formation d'alcools saturés en plus de l'alcool allylique. Comme les alcools saturés et allyliques

Can. J. Chem. Downloaded from www.nrcresearchpress.com by 210.87.254.40 on 09/05/12
For personal use only.

Can. J. Chem. Downloaded from www.nrcresearchpress.com by 210.87.254.40 on 09/05/12
For personal use only.

provenant de chaque cétone ont des temps de rétention assez différents sur une colonne d'hyprose 10% pour permettre de bien les séparer, il était facile de déterminer le pourcentage de chacun et de les identifier par rehaussement des pics à partir des alcools préparés auparavant. Les résultats de ces réductions sont rapportés dans le Tableau V.

TABLEAU V

Réduction des cétones conjuguées par $NaBH_4$

Cétone conjuguée	Alcool allylique	Alcool saturé
1	**17**: 79%	**11**: 21%
2	**18**: 61%	**12**: 25% et **13**: 14%
3	**19**: 60%	**14**: 16% et **15**: 24%
4	**20**: 80%	**16**: 20%

Les résultats de la réduction de ces cétones conjuguées par l'hydrure de lithium et d'aluminium permettent donc de conclure que cette réduction se ferait uniquement selon un mode d'addition-1,2 pour conduire aux alcools allyliques correspondants.

La réduction de ces mêmes cétones par l'hydrure de bore et de sodium se ferait principalement selon un mode d'addition-1,2 pour donner les alcools allyliques correspondants. Cependant il y aurait un certain pourcentage de réduction selon un mode d'addition-1,4 qui conduirait dans le milieu réactionnel aux cétones saturées qui seraient elles-mêmes réduites selon un mode d'addition-1,2 pour donner les alcools saturés correspondants.

Partie expérimentale

Les points de fusion ont été déterminés à l'aide d'un appareil de marque "Buchi" et ne sont pas corrigés. Les spectres infrarouges ont été déterminés en solution dans le tétrachlorure de carbone à l'aide d'un spectrophotomètre Beckmann modèle IR-8 à double faisceau.

Les spectres ultraviolets ont été déterminés en solution dans l'éthanol 95% à l'aide d'un appareil "Bausch & Lomb Spectronic 505". Les spectres de résonance magnétique nucléaire ont été déterminés avec un appareil modèle A60 de la compagnie Varian pour des solutions dans le chloroforme deutéré et utilisant le tétraméthylsilane comme référence interne. Toutes les analyses par chromatographie en phase gazeuse ont été effectuées à l'aide d'un appareil F et M modèle 810 en utilisant une colonne de 4.5 m contenant 10% d'hyprose supporté sur du chromosorb P. Les séparations préparatives ont été effectuées à l'aide d'un appareil "Prep/Partitioner" de Fisher modèle 24 en utilisant des colonnes renfermant 10% d'hyprose supporté sur du chromosorb P. Les analyses ont été effectuées par Dr. C. Daesslé "Organic Microanalyses" de Montréal et par "Schwarzkopf Microanalytical Laboratory" de New York.

Préparation de l'acétyl-1 cyclohexène

L'acétyl-1 cyclohexène (**1**) est préparé en faisant réagir le cyclohexène avec l'anhydride acétique en présence de chlorure stannique en suivant le procédé décrit par Royals et Hendry (4). L'acétyl-1 cyclohexène distille à 73–75° à 8 mm; n_D^{22}: 1.4890 (rapporté p.e.: 65–69° à 5 mm; n_D^{25}: 1.4883 (4)). La dinitro-2,4 phénylhydrazone cristallisée dans le méthanol fond à 202–203° (rapporté 202° (21)).

Préparation de l'acétyl-1 méthyl-5 cyclohexène

L'acétyl-1 méthyl-5 cyclohexène (**2**) est obtenu en suivant le procédé expérimental décrit par Mousseron *et al.* (5) et le produit est obtenu à l'état pur par c.p.g. préparative. Le composé **2** pur distille à 92° à 10 mm; n_D^{25}: 1.4792 (rapporté 105° à 15 mm; n_D^{25}: 1.5105 (5)). La semicarbazone cristallisée dans le méthanol fond à 210° (rapporté 188° (5)).

Préparation de l'acétyl-1 méthyl-4 cyclohexène

Méthyl-4 cyclohexanone (44.8 g) sont ajoutés lentement sur une période de 15 min à 40.1 g d'acétylure de lithium complexé avec l'éthylènediamine en suspension dans 400 ml de benzène anhydre dans lequel barbotte de l'acétylène. Après une agitation de 4 h à la température de la pièce, 100 ml d'eau sont ajoutés et le tout est chauffé à reflux durant 1 h. Après extraction et évaporation des solvants, la distillation fournit 38 g d'éthynyl-1 méthyl-4 cyclohexanol p.e.: 83° à 16 mm; n_D^{25}: 1.4710 (rapporté 73–75° à 10 mm (22)). L'alcool (30 g) sont alors chauffés à reflux pendant 2 h et demie en présence de 480 ml d'acide formique à 97%. Après neutralisation de l'acide, extraction et évaporation du solvant, la distillation donne 24 g d'acétyl-1 méthyl-4 cyclohexène (**3**) chromatographiquement pur: p.e.: 99–100° à 20 mm; n_D^{27}: 1.4796 (rapporté 86–87° à 11 mm (22)); spectre ultraviolet: ε, 10 250 à 232 mμ. La semicarbazone cristallisée dans le méthanol fond à 213° (rapporté 211° (22)).

Préparation de l'acétyl-1 diméthyl-4,4 cyclohexène

L'acétyl-1 diméthyl-4,4 cyclohexène (**4**) est préparé à partir de la diméthyl-4,4 cyclohexanone en suivant le même procédé expérimental que pour l'acétyl-1 méthyl-4 cyclohexène. L'acétyl-1 diméthyl-4,4 cyclohexène distille à 84° à 7 mm; n_D^{27}: 1.4755 (rapporté p.e.: 102° à 124 mm; n_D^{22}: 1.4795 (3)); spectre ultraviolet: ε, 10 700 à 234 mμ; spectre infrarouge: bande carbonyle à 1670 cm^{-1}. La semicarbazone cristallisée dans le méthanol fond à 220° (rapporté 216–218° (3)).

Réduction catalytique de l'acétyl-1 cyclohexène

L'acétyl-1 cyclohexène (**1**) est hydrogéné en présence de palladium sur charbon 10% en milieu neutre. L'acétyl cyclohexane (**5**) obtenu distille à 74–75° à 22 mm; n_D^{26}: 1.4491 (rapporté 76.2–77° à 25 mm; n_D^{25}: 1.4491 (23)). La dinitro-2,4 phénylhydrazone cristallisée dans le méthanol fond à 137–138° (rapporté 136–136.6° (23)).

Réduction catalytique de l'acétyl-1 diméthyl-4,4 cyclohexène

L'acétyl-1 diméthyl-4,4 cyclohexène (**4**) est hydrogéné en présence de palladium sur charbon 10% en milieu

Can. J. Chem. Downloaded from www.nrcresearchpress.com by 210.87.254.40 on 09/05/12
For personal use only.

neutre. L'acétyl-1 diméthyl-4,4 cyclohexane (**6**) obtenu distille à 211°; n_D^{25}: 1.4469; spectre infrarouge: bande carbonyle à 1705 cm^{-1}.

Anal. Calc. pour $C_{10}H_{18}O$: C, 77.92; H, 11.68. **Trouvé:** C, 77.97; H, 11.86.

La semicarbazone cristallisée dans le méthanol fond à 195°.

Anal. Calc. pour $C_{11}H_{21}N_3O$: C, 62.56; H, 9.95; N, 19.90. Trouvé: C, 62.28; H, 9.89; N, 19.66.

Réduction catalytique de l'acétyl-1 méthyl-5 cyclohexène

L'acétyl-1 méthyl-5 cyclohexène (**2**) est hydrogéné en présence de palladium sur charbon 10% dans l'éthanol 95% acidifié. Après évaporation des solvants, le résidu indique par c.p.g. la formation de 52% de *cis* acétyl-1 méthyl-3 cyclohexane (**7**) et de 48% de *trans* acétyl-1 méthyl-3 cyclohexane (**8**) qui sont séparés par c.p.g. préparative. Le *cis* acétyl-1 méthyl-3 cyclohexane pur distille à 191°; n_D^{25}: 1.4458 (rapporté p.e.: 193°; n_D^{25}: 1.4455 (24)). La semicarbazone cristallisée dans le méthanol fond à 168° (rapporté 160° (24)). Le *trans* acétyl-1 méthyl-3 cyclohexane pur distille à 193°; n_D^{25}: 1.4487 (rapporté 194–195°; n_D^{25}: 1.4469 (24)). La semicarbazone cristallisée dans le méthanol fond à 175° (rapporté 195–196° (24)).

Réduction catalytique de l'acétyl-1 méthyl-4 cyclohexène

L'acétyl-1 méthyl-4 cyclohexène (**3**) est hydrogéné en présence de palladium sur charbon 10% dans l'éthanol 95% acidifié. Après évaporation des solvants, le résidu indique par c.p.g. la formation de 73% de *cis* acétyl-1 méthyl-4 cyclohexane (**9**) et de 27% de *trans* acétyl-1 méthyl-4 cyclohexane (**10**). Ces composés sont séparés par c.p.g. préparative. Le *cis* acétyl-1 méthyl-4 cyclohexane distille à 193°; n_D^{25}: 1.4490.

Anal. Calc. pour $C_9H_{16}O$: C, 77.03; H, 11.49. Trouvé: C, 76.87; H, 11.51.

La semicarbazone cristallisée dans le méthanol fond à 179°.

Anal. Calc. pour $C_{10}H_{19}N_3O$: C, 60.87; H, 9.70; N, 21.29. Trouvé: C, 61.12; H, 9.52; N, 21.37.

Le *trans* acétyl-1 méthyl-4 cyclohexane distille à 190°; n_D^{25}: 1.4438.

Anal. Calc. pour $C_9H_{16}O$: C, 77.03; H, 11.49. Trouvé: C, 77.17; H, 11.38.

La semicarbazone cristallisée dans le méthanol fond à 175°.

Anal. Calc. pour $C_{10}H_{19}N_3O$: C, 60.87; H, 9.70; N, 21.29. Trouvé: C, 61.16; H, 9.59; N, 21.51.

Mise en équilibre d'un mélange de cis et trans acétyl-1 méthyl-3 cyclohexane

A 500 mg d'un mélange formé de 25% de *trans* acétyl-1 méthyl-3 cyclohexane (**8**) et de 75% de *cis* acétyl-1 méthyl-3 cyclohexane (**7**) sont ajoutés 500 mg de méthylate de sodium dissous dans 5 ml de méthanol. Après agitation durant 48 h et décomposition par l'eau, le tout est extrait de la façon habituelle. Après évaporation du solvant, le résidu analysé par c.p.g. indique la présence de 8% de *trans* acétyl-1 méthyl-3 cyclohexane et de 92% de *cis* acétyl-1 méthyl-3 cyclohexane.

Mise en équilibre d'un mélange de cis et trans acétyl-1 méthyl-4 cyclohexane

Un mélange (500 mg) formé de 66% de *cis* acétyl-1 méthyl-4 cyclohexane (**9**) et de 34% de *trans* acétyl-1 méthyl-4 cyclohexane (**10**) sont traités par le méthylate de sodium en suivant le procédé décrit pour la mise en équilibre du mélange de *cis* et *trans* acétyl-1 méthyl-3 cyclohexane. Le résidu analysé par c.p.g. indique la présence de 13% de *cis* acétyl-1 méthyl-4 cyclohexane et de 87% de *trans* acétyl-1 méthyl-4 cyclohexane.

Réduction des cétones saturées par l'hydrure de lithium et d'aluminium

Chaque cétone saturée est réduite selon le procédé suivant: 500 mg de cétone en solution dans 10 ml d'éther sont ajoutés lentement à 200 mg d'hydrure de lithium et d'aluminium en suspension dans 5 ml d'éther. Après un reflux d'une demi-heure, l'excès d'hydrure est détruit en ajoutant de l'eau et le tout est acidifié. Après extraction de la façon habituelle et évaporation du solvant, le résidu est analysé par c.p.g. et distillé. Le Tableau III rapporte les constantes physiques et l'analyse élémentaire des différents alcools saturés.

Oxydation des alcools saturés par le complexe anhydride chromique – pyridine

Chaque alcool est oxydé selon le procédé suivant: 100 mg d'alcool saturé en solution dans 5 ml de pyridine anhydre sont ajoutés au complexe anhydride chromique – pyridine formé en ajoutant lentement 240 mg d'anhydride chromique à 2.5 ml de pyridine anhydre refroidie à 0°. Après une agitation de 24 h à la température de la pièce, le tout est jeté sur de l'eau glacée et extrait de la façon habituelle. Après évaporation du solvant, l'analyse par c.p.g. du résidu indique la présence d'un seul composé qui est identifié comme étant la cétone saturée correspondante à l'aide d'un échantillon authentique.

Réduction des cétones conjuguées par l'hydrure de lithium et d'aluminium

Chaque cétone conjuguée réduite en suivant le procédé expérimental décrit pour la réduction des cétones saturées donne l'alcool allylique correspondant. Le Tableau IV rapporte les constantes physiques et l'analyse élémentaire des différents alcools allyliques.

Oxydation des alcools allyliques par le bioxyde de manganèse activé

Chaque alcool est oxydé selon le procédé suivant: 100 mg d'alcool allylique en solution dans 4 ml d'acétone purifiée sont oxydés par 1.15 g de bioxyde de manganèse en suspension dans 5 ml d'acétone. Après une agitation de 48 h, le tout est filtré sur un gâteau de terre de diatomées. Après évaporation du solvant, l'analyse par c.p.g. du résidu indique la formation d'un seul composé qui est identifié comme étant la cétone conjuguée correspondante à l'aide d'un échantillon authentique.

Réduction des cétones conjuguées par l'hydrure de bore et de sodium

Chaque cétone conjuguée est réduite selon le procédé suivant: 250 mg de cétone en solution dans 4 ml d'isopropanol sont ajoutés à 100 mg d'hydrure de bore et de sodium en solution dans 8 ml d'isopropanol. Après un reflux de 2 h, le borate est décomposé par 10 ml NaOH 10% et le tout est extrait de la façon habituelle. Après distillation des solvants, l'analyse par c.p.g. du résidu indique en plus de l'alcool allylique, la présence d'un ou deux alcools saturés dépendant de la cétone de départ. Le Tableau V rapporte le résultat de ces réductions.

Remerciements

Les auteurs remercient le Conseil National de Recherches du Canada pour l'aide financière accordée sous forme d'octroi de recherches (A 2030); le service de l'aide aux étudiants de la Province de Québec pour l'aide financière accordée sous forme de bourses d'études (E.F.).

1. J. ENGLISH, JR. et V. LAMBERTI. J. Am. Chem. Soc. **74**, 1909 (1952).
2. M. MOUSSERON, R. JACQUIER, M. MOUSSERON-CANET et R. ZAGDOUN. Bull. Soc. Chim. France, 1042 (1952).
3. H. B. HENBEST, B. L. SHAW et G. WOODS. J. Chem. Soc. 1154 (1952).
4. E. E. ROYALS et C. M. HENDRY. J. Org. Chem. **15**, 1147 (1950).
5. M. MOUSSERON, R. RICHAUD et R. GRANGER. Bull. Soc. Chim. France, 222 (1946).
6. O. F. BEUMEL, JR. et R. F. HARRIS. J. Org. Chem. **29**, 1872 (1964).
7. H. B. HENBEST et G. WOODS. J. Chem. Soc. 1150 (1952).
8. O. L. CHAPMAN, H. G. SMITH et R. W. KING. J. Am. Chem. Soc. **85**, 803 (1963).
9. A. C. CURRIE, J. GILLON, G. T. NEWBOLD et F. S. SPRING. J. Chem. Soc. 773 (1960).
10. D. KUPFER. Tetrahedron, **15**, 193 (1961).
11. M. E. CAIN. J. Chem. Soc. 3532 (1964).
12. P. L. SOUTHWICK, N. LATIF, B. M. FITZGERALD et N. M. ZACZEK. J. Org. Chem. **31**, 1 (1966).
13. R. E. LUTZ et J. S. GILLESPIE, JR. J. Am. Chem. Soc. **72**, 2002 (1950).
14. R. E. LUTZ et D. F. HINKLEY. J. Am. Chem. Soc. **72**, 4091 (1950).
15. S. B. KADIN. J. Org. Chem. **31**, 620 (1966).
16. N. W. ATWATER. J. Am. Chem. Soc. **83**, 3071 (1961).
17. J. A. ZDERIC et J. IRIARTE. J. Org. Chem. **27**, 1756 (1962).
18. F. A. HOCHSTEIN et W. G. BROWN. J. Am. Chem. Soc. **70**, 3484 (1948).
19. G. I. POOS, G. E. ARTH, R. E. BEYLER et L. H. SARETT. J. Am. Chem. Soc. **75**, 422 (1953).
20. Houben-Weyl. Methoden der organischen Chemie. Herausgegeben von Eugen Müller. Georg Thieme Verlag. Stuttgart. Band VII. Teil I. 1954. p. 178.
21. E. A. BRAUDE, E. R. H. JONES, F. SONDHEIMER et J. B. TOOGOOD. J. Chem. Soc. 607 (1949).
22. H. RUPE et FR. KUENZY Helv. Chim. Acta, **14**, 701 (1931).
23. R. P. MARIELLA et R. R. RAUBE. J. Am. Chem. Soc. **74**, 518 (1952).
24. M. MOUSSERON, R. GRANGER et J. CLARET. Bull. Soc. Chim. France, 598 (1947).

Can. J. Chem. Downloaded from www.nrcresearchpress.com by 210.87.254.40 on 09/05/12
For personal use only.

Can. J. Chem. Downloaded from www.nrcresearchpress.com by 210.87.254.40 on 09/05/12
For personal use only.

Synthetic studies of hydrazine and guanidine: derivatives of 5-pyrazoles[1,2]

JOSEPH ZAUHAR AND BENOIT F. LADOUCEUR
Department of Chemistry, Collège Militaire Royal de Saint-Jean, Saint-Jean, Québec

Received September 19, 1967

The reactions of several substituted 5-chloropyrazoles with hydrazine hydrate and guanidine, respectively, were investigated in ethanol and dimethyl formamide media. In certain cases, only S_N2 reactions occurred, while in others the 5-hydrazino- and 5-guanidopyrazoles reacted still further to yield related compounds with two pyrazole rings. On the basis of the intermediates and the different condensation products isolated, reaction schemes are proposed for the reactions discussed.

Canadian Journal of Chemistry, 46, 1079 (1968)

Introduction

Studies on the nucleophilic substitution of chlorine in several substituted 5-chloropyrazoles (**1**) by hydroxyl, alkoxyl, and other ions have shown that such reactions were possible whenever electron withdrawing groups were present in the 4-position (1–6). Furthermore, Rojahn and Fegeler (7) claimed that, although 1-phenyl-3-methyl-5-chloropyrazole (**2**) was inert, one or more nitro groups in the benzene nucleus would also labilize the chlorine to a remarkable degree. This conclusion was made as a result of a series of reactions between various nucleophiles and the nitration product of compound **2** (**3**), giving rise to a number of compounds to which the general formula **4** was assigned. Substrate **3**, melting at 181°, was claimed by Michaelis and Behn (8) to be 1(2,4-dinitrophenyl)-3-methyl-5-chloropyrazole. The present investigation elucidates the structure of compound **3** and describes the results of a systematic study of the nucleophilic reactions of substrates (**1**) with hydrazine hydrate and guanidine, respectively, in ethanol and dimethyl formamide media.

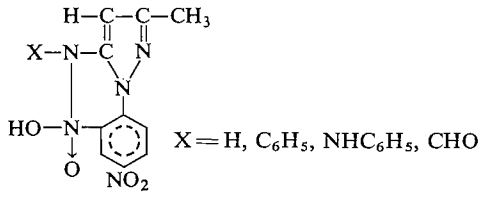

4

[1]Presented in part at the Toronto meeting of the Chemical Institute of Canada, June 1967.

[2]The research for this paper was supported in part by the Defence Research Board of Canada, Grant number 9530-25.

Results and Discussion

The substrates (**1**) required were prepared by chlorinating substituted 5-pyrazolones with phosphorus oxychloride according to a well known method (9–11). Application of the same method to the 2,4-dinitrophenylhydrazone of ethyl acetoacetate (**5**) and that of ethyl benzoylacetate (**6**) over a period of 8 to 10 h yielded, respectively, 1(2,4-dinitrophenyl)-3-methyl-5-chloropyrazole (**9**), m.p. 108–109.5°, and 1(2,4-dinitrophenyl)-3-phenyl-5-chloropyrazole (**10**). The preparation of compound **9** in this way leaves no ambiguity as to its structure. Thus compound **3** must be one of the two remaining possible isomers, 1(2-nitrophenyl)-3-methyl-4-nitro-5-chloropyrazole (**11**) or 1(4-nitrophenyl)-3-methyl-4-nitro-5-chloropyrazole (**12**). The nuclear magnetic resonance (n.m.r.) spectroscopic results shown in Table I indicate that the single nitro group in the 1-phenyl ring lies in the para position. Compound **3** is therefore 1(4-nitrophenyl)-3-methyl-4-nitro-5-chloropyrazole (**12**). This is analogous to the results found by previous investigators (12, 13) who nitrated 1-phenylpyrazole and 2-phenyl-1,2,3,2*H*-triazole by mixed acids and obtained the corresponding 1-*p*-nitro-4-nitro derivatives. Furthermore, the generalized conversion of all 1-phenylpyrazoles to their 1-*p*-nitro-4-nitro compounds via conjugated acids, as predicted by Lynch and Hung (14), well explains why the nitrations in compound **2** were oriented in the 1-para and 4-positions.

Chlorination of **5** and **6** over shorter periods also yielded the corresponding intermediate pyrazolones (**7** and **8**). The complete reaction proceeds as shown in eq. [1] with the hydrazine first undergoing a cyclization by the elimination of ethanol to form the corresponding pyrazolone.

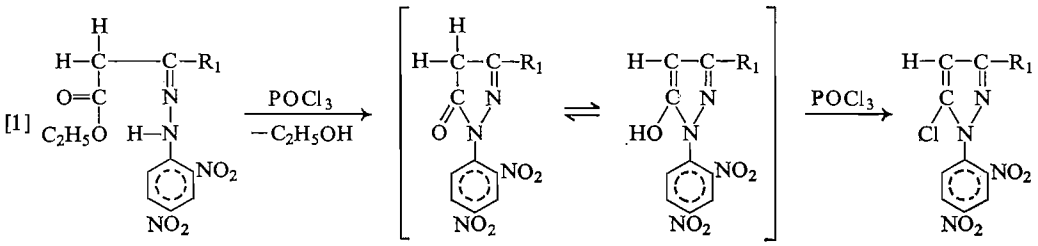

5 $R_1 = CH_3$
6 $R_1 = C_6H_5$

7 $R_1 = CH_3$
8 $R_1 = C_6H_5$

9 $R_1 = CH_3$
10 $R_1 = C_6H_5$

The chlorination of the hydroxypyrazole then proceeds according to the usual manner. It is surprising that the phosphorus oxychloride attack on the carbonyl group occurs only after cyclization of the hydrazone.

In the present work, the nucleophilic substitution reactions of substituted 5-chloropyrazoles (**14–19**) and hydrazine hydrate (**13**) are outlined in Scheme I. With 3-methyl-4-nitro-5-chloropyrazole (**14**) and **13** in ethanol, intermediate **25**, m.p. 128–129°, was isolated. When tested for the chloride ion, this intermediate gave a negative test. This excludes the possibility of the hydrochloride salt being formed. Compound **25** decomposed to **26** whose $R_f = 0.46$ when a dioxane–ethanol (1:2 vol) eluent was used. In addition, a compound with the same elemental analysis and an $R_f = 0.60$ in the same solvent mixture was isolated which is most probably the corresponding dimer. From **13** and **15** in ethanol, compound **21** only was obtained. The nucleophilicity of the end amino group in the latter compound is too weak to react with a second molecule of the chloropyrazole. The hydrazino group shows characteristic bands at 3350, 3240, and 3140 cm^{-1} which is in reasonable agreement with results obtained for methylhydrazine (15). From the reaction of 1-phenyl-3-methyl-4-benzazo-5-chloropyrazole (**16**) and **13** in dimethyl formamide, two products were isoisolated, 5,5′-bis(1-phenyl-3-methyl-4-benzazo-5-amino)-pyrazole (**27**) and 5,5′bis(1-phenyl-3-methyl-4-benzazo)-pyrazole (**29**). Thin-layer chromatography has shown beyond any doubt that **29** arises from the decomposition of **27** and not from the parent substrate. When 1(2-nitrophenyl)-3-phenyl-4-benzazo-5-chloropyrazole (**18**) and **13** were reacted together in the presence of dimethyl formamide in the molar ratio of 1:4, only 1(2-nitrophenyl)-3-phenyl-4-benzazo-5-hydrazinopyrazole (**23**) was obtained (ν_{NH_2} (Nujol) 3340 and 3380 cm^{-1}). Thin-layer chromatographic study of this reaction using benzene as an eluent indicates that **23** ($R_f = 0.18$) was gradually formed from a compound suspected to be 1(2-nitrophenyl)-3-phenyl-4-benzazo-5-chloro-5-hydrazino-2-pyrazoline ($R_f = 0.31$). By heating substrate **19** with **13** in a mixture of

TABLE I

Nuclear magnetic resonance spectra of 1-phenyl-3-methyl-5-chloropyrazole and its dinitro derivatives in acetone-d_6

Compound	Group	Multiplicity*	Chemical shift†
1-phenyl-3-methyl-5-chloropyrazole (**2**)	3-CH_3	s	2.1
	4-H	s	6.25
	5 ϕ H	m	7.44
1-(2,4-dinitrophenyl)-3-methyl-5-chloropyrazole (**9**)	3-CH_3	s	2.12
	4-H	s	6.33
	3-H‡	d, $J = 2$	8.71
	5-H‡	q, $J = 9.2$	8.59
	6-H‡	d, $J = 9$	7.89
1-(4-nitrophenyl)-3-methyl-4-nitro-5-chloropyrazole (**12**)	3-CH_3	s	2.54
	4 ϕ H	q, symmetric	8.15

*s = singlet, d = doublet, q = quadruplet, m = multiplet, J in c.p.s.
†Chemical shift in p.p.m.
‡Hydrogen in 1-phenyl ring.

Can. J. Chem. Downloaded from www.nrcresearchpress.com by 210.87.254.40 on 09/05/12
For personal use only.

Can. J. Chem. Downloaded from www.nrcresearchpress.com by 210.87.254.40 on 09/05/12
For personal use only.

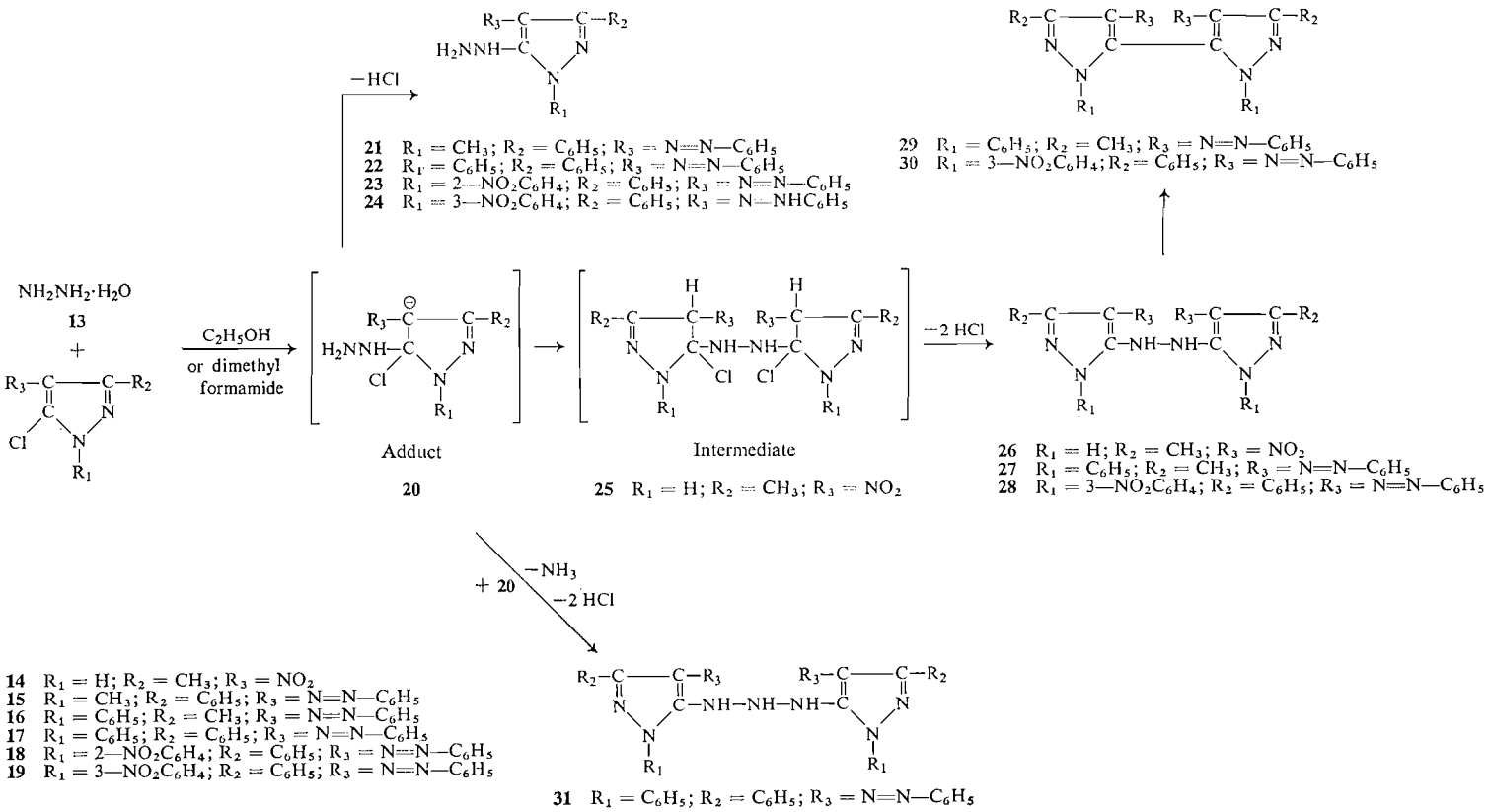

Scheme I

Can. J. Chem. Downloaded from www.nrcresearchpress.com by 210.87.254.40 on 09/05/12
For personal use only.

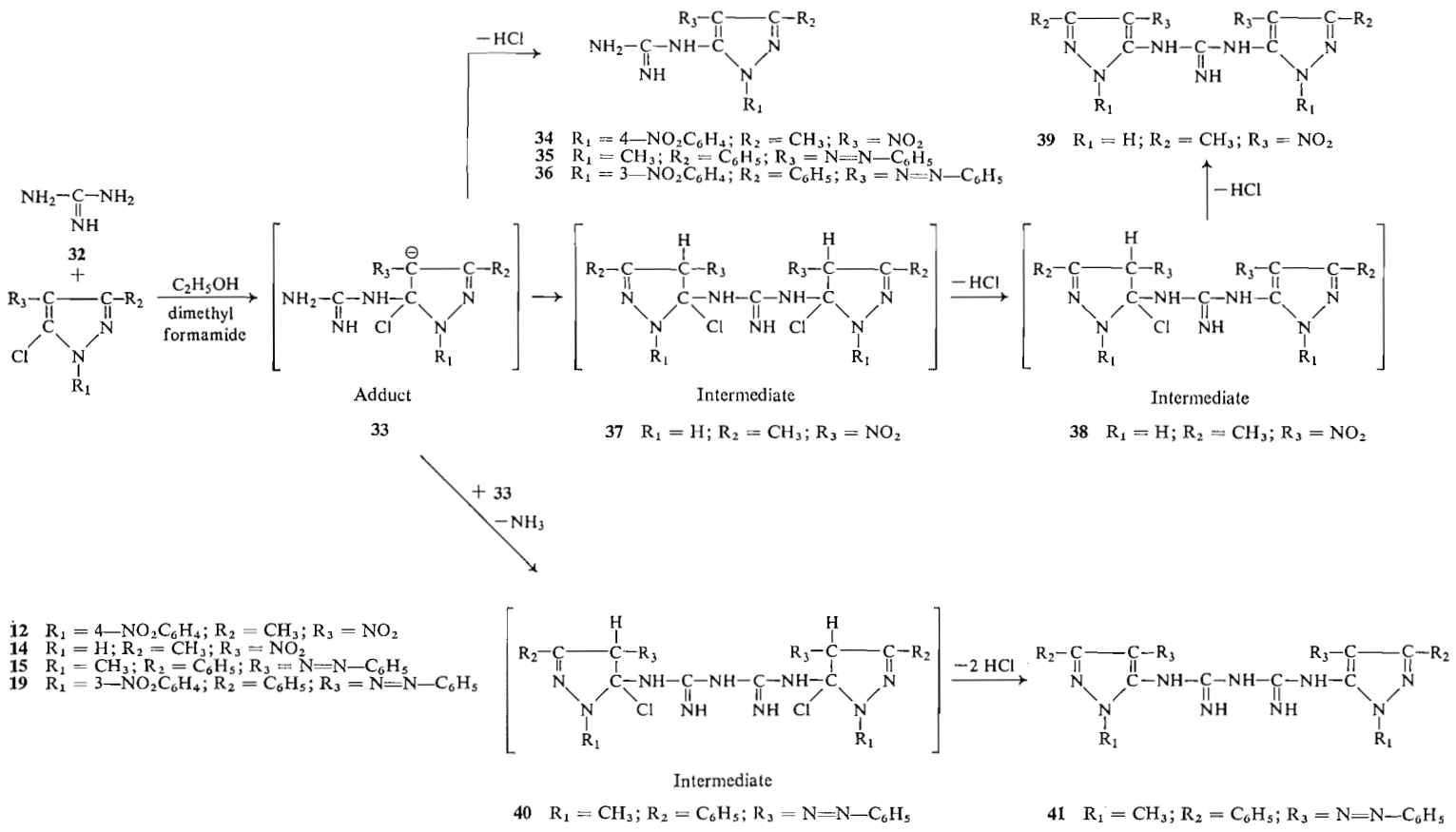

Scheme II

Can. J. Chem. Downloaded from www.nrcresearchpress.com by 210.87.254.40 on 09/05/12
For personal use only.

ethanol and dimethyl formamide, 5,5′-bis(1-(3-nitrophenyl)-3-phenyl-4-benzazo-5-amino)-pyrazole (**28**) is formed and partly decomposed to yield 5,5′-bis(1-(3-nitrophenyl)-3-phenyl-4-benzazo)-pyrazole (**30**). Here again, thin-layer chromatography adequately demonstrates that as the concentration of compound **28** increases and the temperature lies between 75 and 90°, the reaction takes a different course. Adduct **20** then preferably leads to the corresponding 5-hydrazinopyrazole (**24**). On the other hand, the action of **13** on substrate **17** gave rise to both 1,3-diphenyl-4-benzazo-5-hydrazinopyrazole (**22**) and *N*,*N*′-bis(1,3-diphenyl-4-benzazo-5-aminopyrazolyl)-amine (**31**). Chromatographic study of this reaction on thin-layer silica gel plates revealed that both compounds are formed simultaneously from the chloropyrazole. Therefore, direct competition between the simple dehydrohalogenation of adduct **20** and self-condensation of the same adduct through the elimination of ammonia followed by dehydrohalogenation must have occurred in this case.

Both 1(2,4-dinitrophenyl)-3-methyl- (**9**) and 1(2,4-dinitrophenyl)-3-phenyl-5-chloropyrazole (**10**) when heated with hydrazine hydrate (**13**) yielded the degradation product 2,4-dinitrophenylhydrazine. Similar nucleophilic displacements of the pyrazole ring by a hydroxyl or methoxyl group, induced by powerful attracting nitro groups in the ortho and para positions, have been previously reported (16). The former substrate (**9**) also gave a compound whose empirical formula corresponds to $C_6H_8O_3N_6$ and which according to its infrared and n.m.r. spectra could possibly be 2-nitro-4-aminoazoxyphenylhydrazine.

The methochloride salt of 1-methyl-3-phenyl-5-chloropyrazole and **13** in ethanol at room temperature yielded the corresponding 5-hydrazinopyrazole methochloride in two hydrated forms. The 1-phenyl-3-methyl isomer and **13** under the same conditions followed the same reaction path.

3-Phenyl-4-benzazo-5-chloropyrazole did not react with hydrazine hydrate in either ethanol or dimethyl formamide medium. 1-Phenyl-3-methyl-5-chloropyrazole with either an ortho or a para nitro substituent on the phenyl ring behaved likewise. 1(4-Nitrophenyl)-3-methyl-4-nitro-5-chloropyrazole (**12**) with **13** gave a brown polymeric substance whose melting point was above 300° and was not investigated further.

The nucleophilic substitution reactions of several substituted 5-chloropyrazoles (**12**, **14**, **15**, and **19**) with guanidine (**32**) are outlined in Scheme II. The reaction between **14** and **32** in ethanol proceeded slowly at 25° and two important intermediates were isolated, *N*,*N*′-bis-(3-methyl-4-nitro-5-chloro-2-pyrazolin-5-yl-guanidine (**37**) and *N*-(3-methyl-4-nitro-5-pyrazolyl)-*N*′-(3-methyl-4-nitro-5-chloro-2-pyrazolin-5-yl)-guanidine (**38**). Both products tested negatively for ionic chlorine thus excluding the possibility of the formation of the hydrochloride salt. Compound **38** was obtained by the partial dehydrohalogenation of **37** and subsequent dehydrohalogenation of **38** lead to *N*,*N*′-bis-(3-methyl-4-nitro-5-pyrazolyl)-guanidine (**39**).

Substrate **15** and guanidine (**32**) in ethanol did not lead to the corresponding 5-guanidopyrazole or any related compound. Instead **15** reverted back to the parent pyrazolone, 1-methyl-3-phenyl-4-benzazo-2-pyrazolin-5-one. However, in a mixture of ethanol and dimethyl formamide, both **35** and **41** were obtained. Thin-layer chromatographic study of this reaction indicates that both compounds are formed simultaneously from the chloropyrazole. It appears therefore that direct competition between the simple dehydrohalogenation of **33** and self-condensation of **33** through the elimination of ammonia followed by dehydrohalogenation must have occurred. The concentration of compound **41** does not increase at the expense of **35**.

1(3-Nitrophenyl)-3-phenyl-4-benzazo-5-chloropyrazole (**19**) and **32** in dimethyl formamide and ethanol yielded only 1(3-nitrophenyl)-3-phenyl-4-benzazo-5-guanidopyrazole (**36**). In addition to a broad band at 3340 cm^{-1}, attributed to the ν(C═N) of the guanidine group, a ν(N—H) band appears at 3430 cm^{-1}. The end amino group of the guanido group is not reactive enough to proceed to further nucleophilic attack of the substrate. **32** and **12** in ethanolic medium both at room and higher temperatures yielded the corresponding 5-guanidopyrazole **34** exclusively. An absorption band at 3490 cm^{-1} can be assigned to ν(N—H) of the imino group of the guanidine. This band is not present in the infrared spectrum of the nitration product, which nitration according to Wright (17) occurs on the nitrogen doubly bonded to the carbon of the guanidine. The infrared spectrum of compound **34** shows a broad band at 3190 cm^{-1}

which lends support to the chelated structure **42**. No evidence in support of the cyclic structure of the type proposed by Michaelis and Behn (8) (**4**) could be obtained from the infrared spectra.

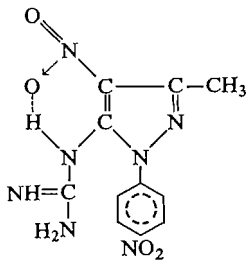

42

3-Phenyl-4-benzazo-5-chloropyrazole was stable towards guanidine in both media previously mentioned. This stability persisted even when a 2-nitrophenyl group was introduced in the 1-position. Similarly, 1-phenyl-3-methyl-5-chloropyrazole with either an ortho or a para nitro substituent in the 1-phenyl ring was equally inert. The methochlorides of 1-phenyl-3-methyl-5-chloropyrazole and its corresponding 1-methyl-3-phenyl isomer behaved likewise. On the other hand, 1(2,4-dinitrophenyl)-3-methyl-5-chloropyrazole (**9**) and 1(2,4-dinitrophenyl)-3-phenyl-5-chloropyrazole (**10**) degraded to 2,4-dinitrophenylguanidine. Crocker and Hall (16) reported a similar cleavage when 1(2,4-dinitrophenyl)-pyrazole was treated with either hot concentrated aqueous–methanolic sodium hydroxyde or boiling methanolic sodium methoxide. The degradation product identified was 2,4-dinitroanisole. It can be concluded therefore, that the electron density on carbon-1 of the phenyl ring is greatly diminished by the presence of the nitro groups, but this effect is not transmitted to carbon-5 of the pyrazole ring. Nucleophilic substitution of **13** and **32** as a result, occurs instead on carbon-1 of the phenyl ring. The two resonating forms of the adduct involved in the reactions with substituted-4-nitro-5-chloro pyrazoles can be represented by **43**, while **44** shows the two probable resonating forms of the adduct involved in the case of the substituted 4-benzazo-5-chloropyrazoles.

The successful isolation of the three intermediates previously described (**25**, **37**, and **38**) indicates that the simplest substitution reactions where 5-hydrazino- and 5-guanidopyrazoles only were obtained, are of the S_N2 type. However, this has not been substantiated by any kinetic studies.

Experimental

All melting points were taken in capillary tubes and were uncorrected. The carbon, hydrogen, nitrogen, and chlorine analyses were made by Micro-Tech Laboratories Inc., Skokie, Illinois. The infrared spectra were determined in Nujol and KBr on a Beckman apparatus, model IR–10, and the nuclear magnetic resonance spectra on a Varian apparatus, model A-60, with tetramethylsilane as an internal standard.

For the thin-layer chromatographic studies Eastman Chromagram sheets, type K301R2, coated with silica gel were used. The 20 cm × 20 cm sheets were cut into 2 cm × 9 cm strips and then activated in a vertical position in an oven at 110°–120°. The best chromatographic separation was obtained when volumes ranging from 1 to 1.5 μl of the reaction mixture were placed on a chromatogram at a point 3/4 in. from one end and then dried. The development was performed in a 125 ml wide mouth glass stoppered bottle containing eluent to a depth of 1 cm measured near the wall of the container.

Ethyl Benzoylacetate 2-Nitrophenylhydrazone

2-Nitrophenylhydrazine (35.5 g, 0.232 mole) was added to ethylbenzoyl acetate (67.0 g, 0.349 mole) and the resulting mixture was then heated while stirring at 95° for a period of 3 h. Upon cooling the reaction flask, a solid cake formed. The product after trituration and recrystallization in 99% ethanol yielded ethylbenzoylacetate 2-nitrophenylhydrazone as yellow needles, m.p. 104–105° (54.2 g, 71.4%), ν_{max} (Nujol) 3310 (NH), 1740 (C=O), 1615 (C=N), 1575 (phenyl), 1530, 1350 (NO_2), 1270 br, 1145 (C—O—C), 760, 735, 685 cm^{-1} (phenyl).

Anal. Calcd. for $C_{17}H_{17}O_4N_3$ (mol. wt, 327.3): C, 62.37; H, 5.23; N, 12.84. Found (mol. wt., Rast method, 311): C, 63.12; H, 5.24; N, 12.92.

1(2-Nitrophenyl)-3-phenyl-2-pyrazolin-5-one

Ethyl benzoylacetate 2-nitrophenylhydrazone (53.0 g, 0.162 mole) was dissolved in glacial acetic acid (400 ml) and the solution was refluxed for 4 h during which time it changed from deep to light red. The resulting solution was then concentrated under reduced pressure until a yellow product separated which was then filtered and washed with ether to remove the unreacted ethylbenzoylacetate 2-nitrophenylhydrazone. The crude product crystallized from ethanol (95%) in cream colored needles, m.p. 164–465° (38.0 g, 83.4%), ν_{max} (Nujol) 1730 (C=O), 1605 (C=N), 1590 (phenyl), 1530, 1350 (NO_2), 775, 750, 740, 695 cm^{-1} (phenyl).

Anal. Calcd. for $C_{15}H_{11}O_3N_3$: C, 64.05; H, 3.94; N, 14.94. Found: C, 64.12; H, 4.12; N, 15.00.

Preparation of 1,3-Disubstituted 4-Benzazo-2-pyrazolin-5-ones

1,3-Disubstituted 2-pyrazolin-5-one (0.10 mole) was dissolved in a minimum amount of dioxane to which a freshly prepared solution of benzenediazonium sulfate (0.11 mole) was added slowly portionwise between 10–20°.

Can. J. Chem. Downloaded from www.nrcresearchpress.com by 210.87.254.40 on 09/05/12
For personal use only.

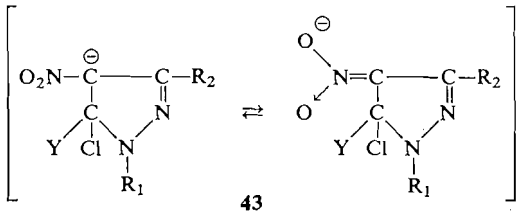

43

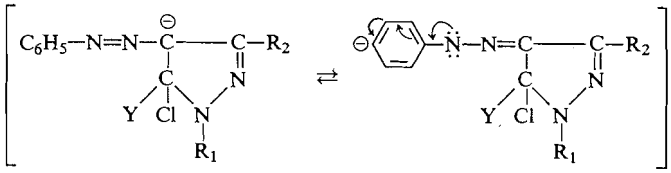

44

$Y = NHNH_2$, $NH-\underset{\underset{NH}{\|}}{C}-NH_2$

An orange-colored solution was produced which gradually gave an orange to brick red precipitate. After the addition of benzenediazonium sulfate was complete, the mixture was further stirred at the above temperature for 45 min, then filtered and finally washed with a large amount of water and dried. The crude product was purified by recrystallization.

1(2-Nitrophenyl)-3-phenyl-4-benzazo-2-pyrazolin-5-one

This compound crystallized from benzene–dioxane in orange needles, m.p. 144–145° (76%), ν_{max} (Nujol) 1660 (C=O), 1600 (C=N), 1565 (phenyl), 1530, 1355 (NO_2), 780, 750, 690 cm^{-1} (phenyl).

Anal. Calcd. for $C_{21}H_{15}O_3N_5$: C, 65.45; H, 3.92; N, 18.17. Found: C, 65.72; H, 4.12; N, 17.48, 17.85.

Two distinct spots on a Chromagram thin-layer silica gel chromatogram were obtained when benzene was used as an eluent, ($R_f = 0.68$ and $R_f = 0.53$).

1(3-Nitrophenyl)-3-methyl-4-benzazo-2-pyrazolin-5-one

Obtained as yellow-orange needles from dioxane, m.p. 200–201° (74%), ν_{max} (KBr) 1660 (C=O), 1590 (phenyl), 1540 (NO_2), 1450 (phenyl), 1340 (NO_2), 880, 760, 730, 710 cm^{-1} (phenyl).

Anal. Calcd. for $C_{16}H_{13}O_3N_5$: C, 59.44; H, 4.05; N, 21.66. Found: C, 59.42; H, 4.20; N, 21.86.

1(4-Nitrophenyl)-3-phenyl-4-benzazo-2-pyrazolin-5-one

This compound was obtained as yellow-orange needles from dioxane, m.p. 241–242° (90%), ν_{max} (KBr) 1660 (C=O), 1590 (phenyl), 1540 (NO_2), 1505 (phenyl), 1360 (NO_2), 850, 785, 760, 745, 705, 695 cm^{-1} (phenyl).

Anal. Calcd. for $C_{21}H_{15}O_3N_5$: C, 65.45; H, 3.92; N, 18.17. Found: C, 65.52; H, 4.04; N, 17.80.

Reactions of Substituted 2,4-Dinitrophenylhydrazones with Phosphorus Oxychloride

Each of the following substituted 2,4-dinitrophenylhydrazones was heated with phosphorus oxychloride in a sealed tube according to the molar ratio, temperature, and time interval indicated below. The reaction tube was cooled, opened, and the contents which were partly viscous and partly gummy were poured over an ice-water mixture. When the ice melted, both a gum which settled to the bottom and a crystalline product were obtained. The crystalline product was separated from the gum by decantation and after filtration was recrystallized from 99% ethanol. The gummy product after standing in water for a few hours and upon trituration yielded an amorphous yellow solid. This solid was purified by crystallization in ethanol after treating the hot solution with activated charcoal.

Ethyl acetoacetate/$POCl_3$ (1.5/1 mole), 130–135°, 5 h gave 43% 1(2,4-dinitrophenyl)-3-methyl-2-pyrazolin-5-one (**7**) as yellow needles, m.p. 145–146°. This compound is identical with the known substance prepared by Khromov-Borisov (18), m.p. and mixture m.p. 144–145°. Also 37% 1(2,4-dinitrophenyl)-3-methyl-5-chloropyrazole (**9**) as colorless rods from ethanol (99%), m.p. 108–109.5°, ν_{max} (Nujol) 1615 (C=N), 1545 (phenyl), 1530 (NO_2), 1500 (phenyl), 1345 (NO_2), 900, 850, 835 cm^{-1} (phenyl).

Anal. Calcd. for $C_{10}H_7O_4N_4Cl$ (mol. wt., 282.6): C, 42.49; H, 2.50; N, 19.83; Cl, 12.54. Found (mol. wt., Rast method, 281): C, 42.55; H, 2.48; N, 19.86; Cl, 12.41.

Ethyl benzoylacetate/$POCl_3$ (2/1 mole), 120–130°, 4 h gave 33% 1(2,4-dinitrophenyl)-3-phenyl-2-pyrazolin-5-one (**8**), m.p. 162–163°. The compound is identical with the compound prepared by Khromov-Borisov (18), m.p. 160–161° and mixture m.p. 161–162°. Also 32% 1(2,4-dinitrophenyl)-3-phenyl-5-chloropyrazole (**10**) as yellow needles from 99% ethanol, m.p. 134–135°, ν_{max} (Nujol) 3120 (OH), 1610 (C=N), 1545 (phenyl), 1525 (NO_2), 1500 (phenyl), 1365, 1340 (NO_2), 895, 830, 810 cm^{-1} (phenyl).

Anal. Calcd. for $C_{15}H_9O_4N_4Cl \cdot \frac{1}{4}C_2H_5OH$: C, 52.26; H, 2.97; N, 15.73; Cl, 9.95. Found: C, 52.87; H, 2.92; N, 15.58; Cl, 9.75.

When the above chlorinations were carried on for an

Can. J. Chem. Downloaded from www.nrcresearchpress.com by 210.87.254.40 on 09/05/12
For personal use only.

Can. J. Chem. Downloaded from www.nrcresearchpress.com by 210.87.254.40 on 09/05/12
For personal use only.

TABLE II

Substituted 5-chloropyrazoles and hydrazine hydrate

Substrate	Reaction solvent	Mole ratio of substrate to hydrazine hydrate	Reaction temperature	Reaction time*	Intermediates and products	Yield† (%)	Melting point (°C)	R_f‡
14	ethanol	1:1.2	25°	1	5,5′-bis(3-methyl-4-nitro-5-amino-5-chloro)-2-pyrazoline (**25**)	28† (*b*)	128–129°	0.10‡ (*g*)
					+			
				2¼	5,5′-bis(3-methyl-4-nitro-5-amino)-pyrazole (**26**)	17† (*c*)	224–225°	0.46‡ (*g*)
					+			
					dimer of (**26**)	10† (*a*)	283–284°	0.60‡ (*g*)
15	ethanol	1:1.2	75–80°	16	1-methyl-3-phenyl-4-benzazo-5-hydrazinopyrazole (**21**)	33† (*a*)	162–163°	0.27‡ (*f*)
16	dimethyl formamide	1:1.5	47–78°	1¼	5,5′bis(1-phenyl-3-methyl-4-benzazo-5-amino)-pyrazole (**27**)	51† (*d*)	264–265°	0.90‡ (*f*)
					+			
			78–132°	26	5,5′-bis(1-phenyl-3-methyl-4-benzazo)-pyrazole (**29**)	23† (*a*)	126–127°	0.72‡ (*f*)
17	ethanol	1:1.1	75–80°	16	1,3-diphenyl-4-benzazo-5-hydrazino-pyrazole (**22**)	21† (*a*)	141–142°	0.35‡ (*e*)
					+			
					N,N′-bis(1,3-diphenyl-4-benzazo-5-aminopyrazolyl)-amine (**31**)	66† (*a*)	139–140°	0.52‡ (*e*)
18	dimethyl formamide	1:4.0	22–95°	1	1(2-nitrophenyl)-3-phenyl-4-benzazo-5-hydrazinopyrazole (**23**)	51† (*c*)	176–178°	0.18‡ (*e*)
19	ethanol – dimethyl formamide	1:1.1	34–75°	5	*N,N′*-bis(1-(3-nitrophenyl)-3-phenyl-4-benzazo-5-amino)-pyrazole (**28**)	20† (*b*)	181–182°	0.40‡ (*e*)
					+			
			34–75°	5	5,5′-bis(1-(3-nitrophenyl)-3-phenyl-4-benzazo)-pyrazole (**30**)	41† (*c*)	159–160°	0.75‡ (*e*)
					+			
			75–90°	6½	1(3-nitrophenyl)-3-phenyl-4-benzazo-5-hydrazinopyrazole (**24**)	18† (*b*)	188–189°	0.50‡ (*e*)

*In hours.
†Recrystallization solvent: ethanol (*a*), benzene (*b*), dioxane–ethanol (*c*), benzene–ethanol (*d*).
‡Eluent: benzene (*e*), chloroform (*f*), ethanol–chloroform 1:5 vol (*g*).

Can. J. Chem. Downloaded from www.nrcresearchpress.com by 210.87.254.40 on 09/05/12
For personal use only.

extended period, between 8 to 10 h, only the corresponding 5-chloropyrazoles (**9** and **10**) were obtained.

1(2-Nitrophenyl)-3-phenyl-4-benzazo-5-chloropyrazole

1(2-Nitrophenyl)-3-phenyl-4-benzazo-5-chloropyrazole was prepared by the method of Michaelis *et al.* (9–11). Treating a hot ethanolic solution of the crude product with activated charcoal and then cooling the resulting filtrate yielded yellow needlelike crystals, m.p. 131–132° (57%), $R_f = 0.83$ using ethanol – carbon tetrachloride (1:5 vol) as eluent, ν_{max} (Nujol) 1610 (C═N), 1530 (NO_2), 1585, 1500 (phenyl), 1340 (NO_2), 780, 770, 750 cm^{-1} (phenyl).

Anal. Calcd. for $C_{21}H_{14}O_2N_5$: C, 62.46; H, 3.49; N, 17.34; Cl, 8.78. Found: C, 62.78; H, 3.48; N, 17.60; Cl, 9.02.

Reactions of Substituted 5-Chloropyrazoles and Hydrazine Hydrate

Each of the substituted 5-chloropyrazoles listed in Table II were respectively dissolved in an appropriate solvent. Hydrazine hydrate was then added in the molar ratio given in the table. The resulting mixture was then stirred and the reaction followed by means of thin-layer chromatography while a temperature increase of 5° every 20 min up to the desired maximum was imposed. Whenever the formation of an intermediate or product was detected at its maximum concentration, a representative sample of the solution was withdrawn from the reaction flask, and the solvent evaporated under vacuum at 0° until the intermediates or products separated from the solution. The compounds were then separated by fractional crystallization and finally recrystallized from an appropriate solvent. The main course of the reaction was carried on until judged to be complete whereupon, the reaction mixture was then concentrated under vacuum until separation of the final product was accomplished. The product after filtration was then recrystallized from an appropriate solvent. In the event of a precipitate being formed during the course of the reaction, the reaction mixture was filtered immediately and the product purified by recrystallization. The reaction was then repeated without removing the precipitate and carried on according to the procedure described above. The intermediates and compounds isolated are listed in Table II while their elemental analyses and principal infrared absorption bands are given in Table III.

1(2,4-Dinitrophenyl)-3-methyl-5-chloropyrazole and Hydrazine Hydrate

The substrate 1(2,4-dinitrophenyl)-3-methyl-5-chloropyrazole (0.01 mole) heated with hydrazine hydrate (0.011 mole) in ethanol at 79° for 6 h yielded two degradation products: 54% 2,4-dinitrophenylhydrazine, m.p. and mixture m.p. with identical sample 197–198° (lit. m.p. 198°), $R_f = 0.52$ using ethanol – carbon tetrachloride (1:5 vol) as eluent.

Anal. Calcd. for $C_6H_6O_4N_4$: C, 36.37; H, 3.05; N, 28.28. Found: C, 36.54; H, 3.00; N, 27.95.

Also, 12% of a compound with empirical formula $C_6H_8O_3N_6$, possibly 2-nitro-4-aminoazoxyphenylhydrazine, m.p. 204–205°, $R_f = 0.03$ using ethanol – carbon tetrachloride (1:5 vol) as eluent, ν_{max} (Nujol) 3315, 3240 (NH), 1615 (phenyl), 1530 (NO_2), 1445 (phenyl), 1335 (NO_2), 1290 (N—N→O), 875, 830, 800 cm^{-1} (phenyl). Nuclear magnetic resonance (DMSO + TMS): 6.86 (5H, broadened singlet, O←N═N—NH_2, NH—NH_2), 7.86 (2H, doublet, 5-H, 6-H) and δ 8.49 (1H, quadruplet, 3-H).

Anal. Calcd. for $C_6H_8O_3N_6$: C, 33.96; H, 3.80; N, 39.61. Found: C, 33.86; H, 3.63; N, 39.80.

1(2,4-Dinitrophenyl)-3-phenyl-5-chloropyrazole and Hydrazine Hydrate

1(2,4-Dinitrophenyl)-3-phenyl-5-chloropyrazole (0.01 mole) and hydrazine hydrate (0.011 mole) in ethanol heated at 79° for 6 h gave 45% 2,4-dinitrophenylhydrazine, m.p. and mixture m.p. 197–198°, $R_f = 0.52$ using ethanol – carbon tetrachloride (1:5 vol) as eluent.

Anal. Calcd. for $C_6H_6O_4N_4$: C, 36.37; H, 3.05; N, 28.28. Found: C, 36.74; H, 3.22; N, 27.75.

Reaction of 1,3-Disubstituted 5-Chloropyrazole Methochlorides with Hydrazine Hydrate

Hydrazine hydrate (4.3 g, 0.085 mole) was slowly added to a solution of each of the methochloride salts (14.5 g, 0.057 mole) in ethanol (100 ml). The resulting yellow solution was then heated for 12 h between 70–75° and then left to cool overnight. A small amount of 1,3-disubstituted 5-chloropyrazole hydrochloride which crystallized from the solution was removed by filtration and the solvent was then stripped from the filtrate under reduced pressure. The 1,3-disubstituted 5-hydrazinopyrazole methochloride then remained as a viscous residue.

1-Methyl-3-phenyl-5-hydrazinopyrazole Methochloride

This compound was obtained as a pale-violet solid by treating the above residue with benzene (250 ml) followed by vigorous stirring. Recrystallization from chloroform gave white needles, m.p. 94–95° (6.4 g, 40%). A positive test was obtained for ionic chlorine. ν_{max} (Nujol) 3400, 3320 (NH), 3160 br (OH), 1675 (NH_2), 1610 (C═N), 1595, 765, 700 cm^{-1} (phenyl).

Anal. Calcd. for $C_{11}H_{15}N_4Cl \cdot 1.5\ H_2O$: C, 49.72; H, 6.83; N, 21.08; Cl, 13.34. Found: C, 50.03; H, 7.16; N, 20.69; Cl, 13.66.

The compound was also isolated as a hydrate with 1/2 molecule of water of crystallization, m.p. 138–139°.

Anal. Calcd. for $C_{11}H_{15}N_4Cl \cdot 0.5\ H_2O$: C, 53.33; H, 6.51; N, 22.62. Found: C, 53.24; H, 6.49; N, 22.05.

1-Phenyl-3-methyl-5-hydrazinopyrazole Methochloride

Treatment of the above residue with an ethanol–ether mixture gave a cream-colored precipitate. The compound was recrystallized from an ethanol–ether mixture as white clustered rods. A positive test for ionic chlorine was obtained, m.p. 209–210° (6.6 g, 41%), ν_{max} (Nujol) 3260, 3140, 1640 (NH), 1560, 1535, 735, 695 cm^{-1} (phenyl).

Anal. Calcd. for $C_{11}H_{15}N_4Cl$: C, 55.35; H, 6.33; N, 23.47; Cl, 14.85. Found: C, 55.13; H, 6.42; N, 23.91; Cl, 14.88.

Reactions of Substituted 5-Chloropyrazoles and Guanidine

The substituted 5-chloropyrazoles listed in Table IV were respectively dissolved in an appropriate solvent to which an ethanolic solution of guanidine was added according to the molar ratio given in Table IV. The mixture was then stirred and the reaction followed by means of thin-layer chromatography, while a temperature increase of 5° every 20 min was maintained until the desired temperature was reached. At the maximum concentration of the intermediate or product formed, a

Can. J. Chem. Downloaded from www.nrcresearchpress.com by 210.87.254.40 on 09/05/12
For personal use only.

TABLE III

Chemical analysis and infrared absorption data

Compound	Formula	Calculated (%)			Found (%)			ν_{max}(Nujol)*
		C	H	N	C	H	N	
21	$C_{16}H_{16}N_6$	65.74	5.52	28.75	65.53	5.50	28.63	3450 (NH), 3240 (NH), 1640 (NH), 1525, 1450 (phenyl), 1360 (C—N) arom., 770, 760, 720, 685 (phenyl).
22	$C_{21}H_{18}N_6$	71.17	5.19	23.71	71.16	5.15	23.27	3380, 3290 (NH), 1595 (C=N), 1585, 1490, 1450, 765, 750, 710, 685 (phenyl).
23	$C_{21}H_{17}O_2N_7 \cdot \frac{1}{2}C_2H_5OH$	62.55	4.77	23.21	63.56	4.60	23.38	3390, 3340 (NH), 1630 (NH), 1545 (NO_2), 1500, 780, 750, 685 (phenyl).
24	$C_{21}H_{17}O_2N_7$	63.15	4.29	24.55	63.46	4.29	24.55	3380, 3290 (NH), 1610 (C=N), 1585 (phenyl), 1520 (NO_2), 1480, 1450 (phenyl), 1340 (NO_2), 860, 795, 725, 710, 690 (phenyl).
25	$C_8H_{12}O_4N_8Cl_2$†	27.06	3.41	31.55	26.69	3.57	31.87	3360, 3300 (NH), 1605 (C=N), 1510, 1340, 825 (NO_2).
26	$C_8H_{10}O_4N_8$	34.05	3.57	39.70	34.62	3.83	39.14	3360, 3310 (NH), 1600 (C=N), 1555, 1345, 825 (NO_2).
Dimer of **26**	$C_{16}H_{20}O_8N_{16}$	34.05	3.57	39.70	34.30	3.88	39.37	3370, 3310, 1645 (NH), 1585 (C=N), 1515, 1325 (NO_2), 1165 (CH_3).
27	$C_{32}H_{28}N_{10}$	69.55	5.11	25.46	70.32	4.93	25.60	No NH, 1595 (C=N), 1585, 1495, 740, 675 (phenyl).
28	$C_{42}H_{30}O_4N_{12} \cdot 1.5\,H_2O$	63.55	4.19	21.17	63.66	4.21	21.16	3350 (NH), 1530 (NO_2), 1450 (phenyl), 1345 (NO_2), 885, 795 (phenyl).
29	$C_{32}H_{26}N_8$	73.54	5.01	21.45	73.02	5.44	21.50	No NH, 1595 (C=N—), 1500, 1450 (phenyl), 1190 (CH_3), 750, 680 (phenyl).
30	$C_{42}H_{28}O_4N_{10}$	68.47	3.83	19.01	68.17	4.10	18.95	No NH, 1530 (NO_2), 1450 (phenyl), 1345 (NO_2), 890, 815, 770, 705 (phenyl).
31	$C_{42}H_{33}N_{11}$	72.92	4.81	22.27	72.88	5.50	21.61	3375 (NH), 1600 (C=N), 1580, 1525, 760, 725, 690 (phenyl).

*The infrared spectra of compounds **21**, **22**, **24**, **27**, **29**, and **31** were taken in KBr disks and are reported in cm^{-1} for the most characteristic bands (group assignments in parentheses.)
†Calculated for Cl: 19.96. Found: 19.33. Negative test obtained for Cl^-.

Can. J. Chem. Downloaded from www.nrcresearchpress.com by 210.87.254.40 on 09/05/12
For personal use only.

TABLE IV

Substituted 5-chloropyrazoles and guanidine

Substrate	Reaction solvent	Mole ratio of substrate to guanidine	Reaction temperature	Reaction time	Intermediates and products	Yield* %	Melting point (°C)	R_f†
14	ethanol	1:1.1	25°	15 min	*N,N'*-bis(3-methyl-4-nitro-5-chloro-2-pyrazolin-5-yl)-guanidine (**37**)	32* (*b*)	195–196°	—
					+			
					N-(3-methyl-4-nitro-5-pyrazolyl)-*N'*-(3-methyl-4-nitro-5-chloro-2-pyrazolin-5-yl)-guanidine (**38**)	61* (*b*)	184–185°	—
					+			
			75°	7 h	dimer of *N,N'*-bis(3-methyl-4-nitro-5-pyrazolyl)-guanidine	71* (*a*)	> 300°	—
15	ethanol – dimethyl formamide	1:1.7	40–70°	7 h	1-methyl-3-phenyl-4-benzazo-5-guanidopyrazole (**35**)	12* (*c*)	194–195°	0.37† (*d*)
					+			
			55–70°	7 h	*N,N'*-bis(1-methyl-3-phenyl-4-benzazo-5-guanylpyrazolyl)-amine (**41**)	11* (*c*)	214–216°	0.12† (*d*)
19	ethanol – dimethyl formamide	1:2.3	25–70°	6 h	1(3-nitrophenyl)-3-phenyl-4-benzazo-5-guanidopyrazole (**36**)	69* (*b*)	203–204°	0.67† (*e*)
12	ethanol	1:1.4	70°	4 h	1(4-nitrophenyl)-3-methyl-4-nitro-5-guanidopyrazole (**34**)	50* (*b*)	249–250°	0.75 (*f*)

*Recrystallization solvent: (*a*) 95% ethanol, (*b*) water, (*c*) ethanol–benzene.
†Eluent: (*d*) benzene, (*e*) ethanol – carbon tetrachloride 1:5 vol, (*f*) ethanol–chloroform 1:5 vol.

Can. J. Chem. Downloaded from www.nrcresearchpress.com by 210.87.254.40 on 09/05/12
For personal use only.

TABLE V

Chemical analysis and infrared absorption data

Compound	Formula	Calculated (%)			Found (%)			ν_{max}(Nujol)*
		C	H	N	C	H	N	
34	$C_{11}H_{11}O_4N_7$	43.28	3.63	32.12	43.68	3.67	31.73	3470, 3370 (NH), 1655 (C═N of guanidine), 1570 (phenyl), 1550 (NO_2), 1510 (phenyl), 1330 (NO_2), 845, 820 (phenyl).
35	$C_{17}H_{17}N_7 \cdot 2.5\ H_2O$	56.03	6.09	26.91	55.60	5.95	27.23	3430, 3300 (NH), 1655 (C═N of guanidine), 1580, 1500, 770, 685 (phenyl).
36	$C_{22}H_{18}O_2N_8$	61.96	4.25	26.28	61.87	4.49	26.02	3460, 3330 (NH), 1645 (C═N of guanidine), 1570 (phenyl), 1525, 1340 (NO_2), 790, 770, 730, 685 (phenyl).
37	$C_9H_{13}O_4N_9Cl_2$†	28.29	3.43	32.99	28.59	3.33	33.30	3450, 3380 (NH), 1670 (C═N of guanidine), 1500, 1345, 825 (NO_2), 760 (C—Cl).
38	$C_9H_{12}O_4N_9Cl$‡	31.27	3.50	36.46	31.55	3.61	36.25	3480, 3460, 3360 (NH), 1660 (C═N of guanidine), 1500, 1360, 820 (NO_2), 760 (C—Cl).
Dimer of **39**	$C_{18}H_{22}O_8N_{18}$	34.95	3.59	40.76	34.14§	3.99§	40.85	3400, 3330 (NH), 1665 (C═N of guanidine), 1540, 1350, 815 (NO_2).
41	$C_{34}H_{31}N_{13} \cdot 2\ H_2O$	62.09	5.36	27.68	62.38	5.48	27.27	3490, 3380, 3310 (NH), 1660 (C═N of guanidine), 1565, 1505, 770, 760, 690 (phenyl).

*Infrared spectra in cm^{-1} for the most characteristic bands (group assignments in parentheses).
†Calculated for Cl: 18.55. Found: 18.70. Negative test for Cl^-.
‡Molecular weight: Calculated: 345.7. Found (Rast method): 348. Positive test obtained for Cl; negative test obtained for Cl^-.
§Could not be purified further.

measured volume of the reaction mixture was withdrawn and the solvent evaporated under reduced pressure at 0–5° until the separation of solids occurred. The intermediates and products formed were then separated by fractional crystallization and recrystallized from an appropriate solvent. The main course of the reaction was carried on to completion, whereupon the reaction mixture was then concentrated under reduced pressure until separation of the final product was accomplished. The product, after filtration, was afterwards recrystallized from an appropriate solvent. Whenever a precipitate formed during the course of the reaction, the latter was separated by filtration and purified in the usual manner. The reaction was then repeated without the removal of the precipitate and carried on according to the method described above. The intermediates and products isolated are given in Table IV while their elemental analyses and principal infrared absorption bands are given in Table V.

1(4-Nitrophenyl)-3-methyl-4-nitro-5-nitroguanidopyrazole

1(4-Nitrophenyl)-3-methyl-4-nitro-5-guanidopyrazole (3.0 g, 0.01 mole) was added portionwise to a mixture of nitric (18.5 g, 0.20 mole, 70%) and sulfuric (51.6 g, 0.52 mole, 98%) acids between 0–5° while stirring vigorously. After all the guanidopyrazole was added, the reaction mixture was further stirred for 45 min at the above temperature and then allowed to rise slowly to 25°. The mixture was then poured over cracked ice and gradually a pale-green precipitate formed. When all the ice melted, the crude product was separated by filtration, washed with water, and dried. 1(4-Nitrophenyl)-3-methyl-4-nitro-5-nitroguanidopyrazole crystallized from ethanol (95%) in clustered rods, m.p. 193–194° (2.8 g, 77%), ν_{max}(Nujol) 3430, 3340 (NH), 3090 (OH), 1685 (NH), 1615 (C=N), 1580 (phenyl), 1530, 1335 (NO_2), 850, 845, 835 cm^{-1} (phenyl).

Anal. Calcd. for $C_{11}H_{10}O_6N_8 \cdot H_2O$: C, 35.87; H, 3.28; N, 30.42. Found: C, 35.99; H, 3.26; N, 30.41.

Acknowledgments

The authors wish to thank Dr. Jean-L. Boivin for his suggestions and the professors of the Department of Chemistry, Collège Militaire Royal de Saint-Jean for their encouragement and stimulating discussions.

1. A. MICHAELIS and H. KLOPSTOCK. Ann. Chem. **354**, 102 (1907).
2. A. MICHAELIS. Ann. Chem. **385**, 1 (1911).
3. C. MUSANTE. Gazz. Chim. Ital. **75**, 109 (1945).
4. A. MICHAELIS and C. A. ROJAHN. Ber. **50**, 737 1917).
5. A. MICHAELIS and F. BENDER. Ber. **36**, 523 (1903).
6. A. MICHAELIS. Ann. Chem. **361**, 251 (1908).
7. C. A. ROJAHN and H. FEGELER. Ber. **63B**, 2510 (1930).
8. A. MICHAELIS and H. BEHN. Ber. **33**, 2595 (1900).
9. A. MICHAELIS and R. PASTERNACK. Ber. **32**, 2398 (1899).
10. A. MICHAELIS and H. DORN. Ann. Chem. **352**, 163 (1907).
11. A. MICHAELIS and W. WILLERT. Ann. Chem. **358**, 171 (1907).
12. I. L. FINAR and R. J. HURLOCK. J. Chem. Soc. 3024 (1957).
13. B. M. LYNCH and T. CHAN. Can. J. Chem. **41**, 274 (1963).
14. B. M. LYNCH and Y. HUNG. Can. J. Chem. **42**, 1605 (1964).
15. D. W. E. AXFORD, G. J. JANZ, and K. E. RUSSELL. J. Chem. Phys. **19**, 704 (1951).
16. H. P. CROCKER and R. H. HALL. J. Chem. Soc. 4489 (1955).
17. G. F. WRIGHT. Can. J. Chem. **30**, 62 (1952).
18. N. V. KHROMOV-BORISOV. Zh. Obshch. Khim. **25** 136 (1955).

Can. J. Chem. Downloaded from www.nrcresearchpress.com by 210.87.254.40 on 09/05/12
For personal use only.

Can. J. Chem. Downloaded from www.nrcresearchpress.com by 210.87.254.105 on 09/05/12
For personal use only.

Concerning the mechanism of the addition of ethanesulfenyl chloride to 3,4-dihydro-2*H*-pyran[1]

M. J. Baldwin and R. K. Brown
Department of Chemistry, University of Alberta, Edmonton, Alberta

Received November 6, 1967

The nuclear magnetic resonance spectrum, at −40°, of the crude mixture obtained by the reaction of ethanesulfenyl chloride with 3,4-dihydro-2*H*-pyran at −40° clearly supports the view that the product is *trans*-2-chloro-3-ethylthiotetrahydropyran. The possibility that there is initial formation of 3-chloro-2-ethylthiotetrahydropyran followed by its rapid rearrangement to 2-chloro-3-ethylthiotetrahydropyran is ruled out because of the stability of 3-chloro-2-ethylthiotetrahydropyran to distillation under vacuum. The latter compound is obtained as a mixture of *cis* and *trans* isomers by the reaction of ethyl mercaptan with 5-chloro-3,4-dihydro-2*H*-pyran in the presence of sulfur dioxide.

Canadian Journal of Chemistry, **46**, 1093 (1968)

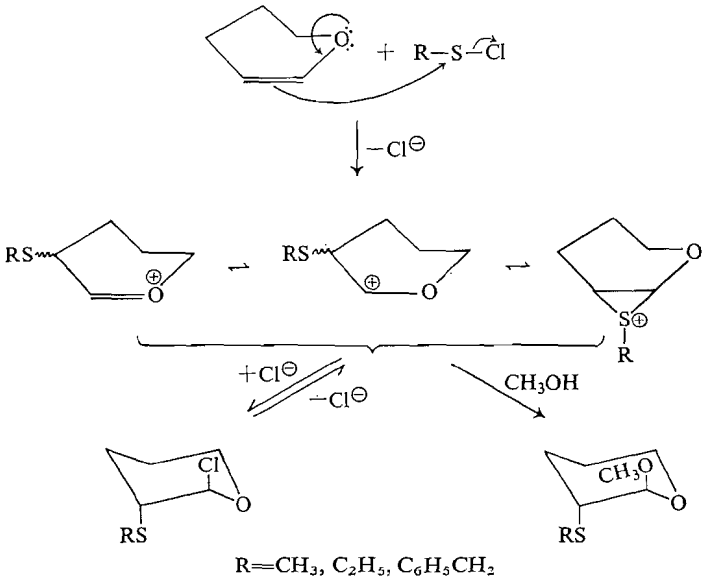

Scheme 1

Introduction

A recent report from this laboratory has described the synthesis of a number of 3-alkylthio-2-methoxytetrahydropyrans by the reaction, at −20°, of alkanesulfenyl halides with 3,4-dihydro-2*H*-pyran (1). Since the reaction first gave, nearly exclusively, the *trans*-3-alkylthio-2-methoxytetrahydropryans which rearranged partly to the *cis* isomers during isolation (thermally) or when exposed to acid catalysts, a mechanism of reaction was proposed as shown in Scheme 1. This involved first a nucleophilic attack of the α,β-unsaturated ether on the alkylsulfenyl halide, to displace the halogen and give an oxocarbonium–episulfonium ion in which the episulfonium contribution is considered to be paramount. Subsequent attack by chloride ion was believed to give, reversibly, 3-alkylthio-2-chlorotetrahydropyran. This α-chloroether decomposed on attempts at its isolation and because of this instability was assigned the *trans* rather than the *cis* configuration since the *trans* arrangement permitted anchimeric assistance by the sulfur atom in enhancing the reactivity of the C—Cl bond.

[1]Taken from the thesis of M. J. Baldwin, to be submitted to the Faculty of Graduate Studies, University of Alberta, Edmonton, Alberta, in partial fulfilment of the requirements for the degree of Doctor of Philosophy.

Can. J. Chem. Downloaded from www.nrcresearchpress.com by 210.87.254.105 on 09/05/12
For personal use only.

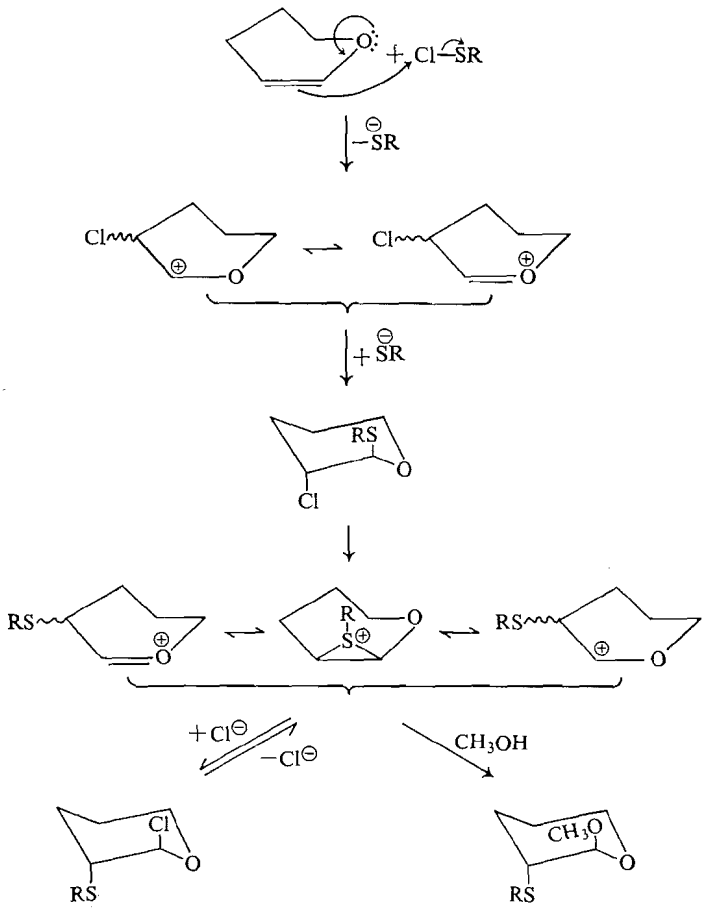

SCHEME 2

Subsequently, in the presence of an alcohol (ROH) the episulfonium ion obtained by loss of the chloride ion then gave, stereoselectively, the *trans*-3-alkylthio-2-alkoxytetrahydropyran. The facile thermal rearrangement to the *cis* isomer agrees with the *trans* configuration, a view also supported by nuclear magnetic resonance (n.m.r.) analysis.

An increasing volume of work in the literature supports the view that, in the absence of radical initiators, the addition of sulfenyl halides to olefins can proceed via an ionic route to give products in which the halogen and alkyl (or aryl) thio groups are *trans*. Kharasch and Havlik (2, 3) showed that the addition of a variety of sulfenyl halides to *cis*- and *trans*-2-butene gave products that were diastereoisomeric racemates. These, upon solvolysis, led to racemic acetates. Enhancement of the rate of acetolysis by sulfur participation was also observed. Kwart and Miller (4) reported that the addition of 2,4-dinitrobenzenesulfenyl chloride to norbornene yields a *trans* product. Their work was confirmed by Cristol *et al.* (5) who showed that addition of *p*-toluenesulfenyl chloride to norbornene, norbornadiene, and 9,10-dihydro-9,10-ethenoanthracene yields *trans* products. They further noted the absence of products which might have arisen by Wagner–Meerwein rearrangement, and attributed this fact to the stabilization of the intermediate carbonium ion species by sulfur participation.

Recently, Mueller and Butler (6) examined the addition of methane- and benzenesulfenyl chlorides to a variety of olefins. The addition of both reagents to acenaphthylene gave stereoselectively the *trans* products. They also reported that addition of these two sulfenyl chlorides to

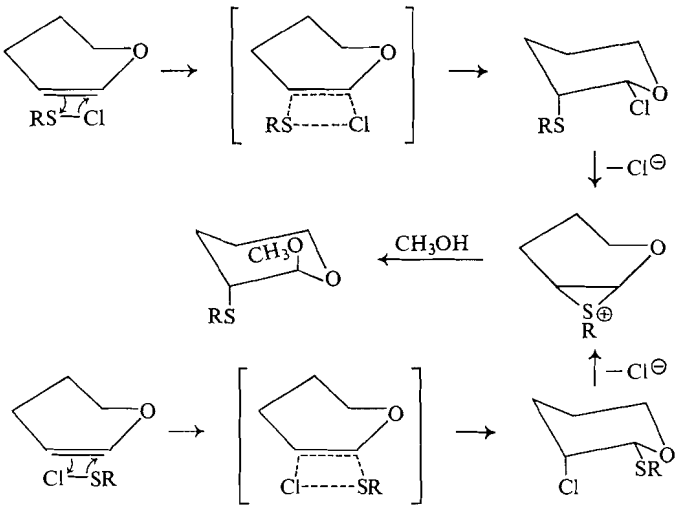

SCHEME 3

propene, 2-methylpropene, 3-methyl-1-butene, and 3,3-dimethyl-1-butene at −20 to −25° gave products which arose from *anti*-Markovnikov addition.[2] Their view was that the pi bond of the olefin first reacted with the sulfur atom of the sulfenyl halide to give, directly, an episulfonium ion which was then attacked by the chloride ion from the direction of least steric hindrance. No evidence was obtained from their reactions of carbonium ion formation. The original *anti*-Markovnikov products then rearranged to "normal" Markovnikov addition products when warmed to ambient temperatures. However, they did find that with an electronically biased substrate such as styrene, only Markovnikov addition was observed. The possibility that in this case also, there had been at first an *anti*-Markovnikov addition followed by a fast rearrangement even at the low reaction temperatures employed, was apparently not explored by these authors (6).

In the light of Mueller and Butler's report (6) a second route to the formation of 3-alkylthio-2-methoxytetrahydropyran must now be considered. This involves initial formation of 2-alkylthio-3-chlorotetrahydropyran, which then rearranges readily, no doubt anchimerically assisted by sulfur participation, either to 3-alkylthio-2-chlorotetrahydropyran or to the episulfonium ion. The latter, or the former by loss of chloride ion, reacts with methyl alcohol to form the isolable 3-alkylthio-2-methoxytetrahydropyran (Scheme 2). As well there exists the possibility, following Mueller and Butler's view, that the episulfonium ion is formed directly and since the pyran is a strongly electronically biased molecule, chloride ion attack would give only *trans*-3-alkylthio-2-chlorotetrahydropyran.

Since the alkylthiochlorotetrahydropyran, proposed as one possible product or an intermediate (Scheme 1) had not been isolated (1), its structure was uncertain. The assumption that it was the *trans*-3-alkylthio-2-chlorotetrahydropyran arose from its apparent instability. The possibility then exists that this intermediate is in fact the *cis* isomer, arising from *cis* addition, probably *via* a four-center reaction (Scheme 3) as has been found for the addition of nitrosyl chloride to glycals (7).

The purpose of the present work was to obtain evidence which would permit a decision concerning the routes of reaction suggested above.

Results and Discussion

The possibility of a free radical addition process was excluded on the basis of Mueller and Butler's (6) observation that the presence of radical inhibitors caused no change in their results or the ease with which the reaction proceeded. As well, we have added methanesulfenyl chloride to 3,4-dihydro-2*H*-pyran in

[2]It is assumed that the chlorine and sulfur atoms in the sulfenyl halide possess a partial negative and partial positive charge respectively.

Can. J. Chem. Downloaded from www.nrcresearchpress.com by 210.87.254.105 on 09/05/12
For personal use only.

Can. J. Chem. Downloaded from www.nrcresearchpress.com by 210.87.254.105 on 09/05/12
For personal use only.

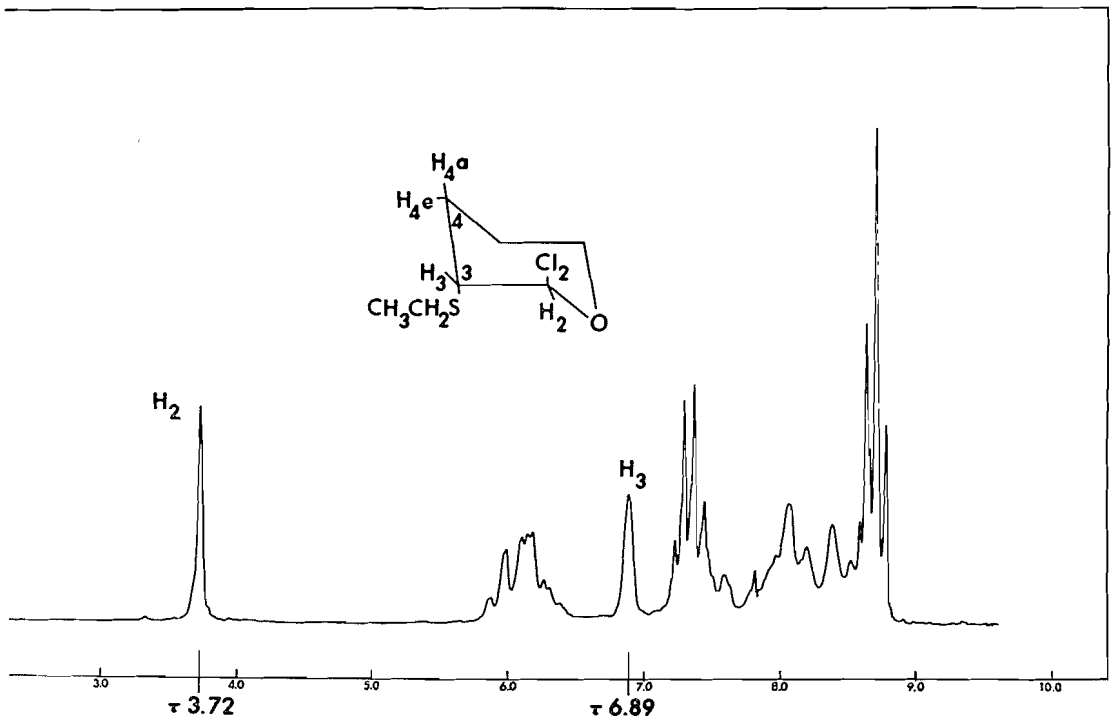

FIG. 1. The 100 Mc.p.s. nuclear magnetic resonance spectrum of 2-chloro-3-ethylthiotetrahydropyran in $CDCl_3$.

the solvent cumene, followed by treatment of the mixture with sodium methoxide in methanol. As before (1) only 3-methylthio-2-methoxymethyltetrahydropyran was obtained in good yield. No products such as dicumyl were found indicative of the intervention of free radicals.

To obtain information concerning the mechanism of this reaction, a slight excess of ethanesulfenyl chloride was added to 3,4-dihydro-2*H*-pyran at −40°. The resulting reaction mixture, kept at −40°, was subjected to n.m.r. analysis (in $CDCl_3$) also at −40°. The 100 Mc.p.s. spectrum (Fig. 1) agrees best with the assignment of the structure of the reaction product as *trans*-2-chloro-3-ethylthiotetrahydropyran in the preferred conformation having the chlorine and ethylthio substituents *trans* diaxial (Scheme 4). The singlet at τ 3.72 (referred to tetramethylsilane) with $w/2 = 4$ c.p.s. was assigned to the anomeric proton (H-2) on the basis of the reported position of the signal for the anomeric proton at τ 3.79 (broad singlet, CCl_4) for 2-chlorotetrahydropyran (8) and at τ 3.97 (broad singlet, $CDCl_3$) for *trans*-2,3-dichlorotetrahydropyran (9). The broad singlet at τ 6.89 ($w/2 = 8$ c.p.s.) in Fig. 1 can be assigned only to H-3. The integration also agrees with these assigments.

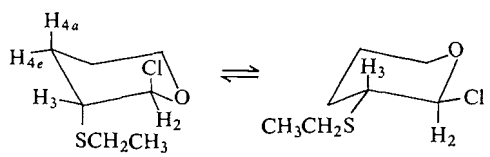

SCHEME 4

The appearance of the signal for H-3 as a broad singlet shows that the couplings with the vicinal protons H-2, H-4*a*, and H-4*e* are all small. This can occur only if H_3 is equatorial since if H-3 were axial its coupling with axial H-4 would be >7 c.p.s. (10), thus resulting in at least a quartet for H-3. The small coupling between H-2 and H-3 is expected whether the anomeric proton H-2 is equatorial or axial. Thus, from this information, no decision can be made concerning the axial or equatorial disposition of the anomeric proton and the chlorine atom attached to the anomeric carbon. However, Anderson and Sepp (8) have found a value of 2.7 kcal/mole in 2-chlorotetrahydropyran for the anomeric effect (11), a figure which indicates that 2-chlorotetrahydropyran is practically completely in that

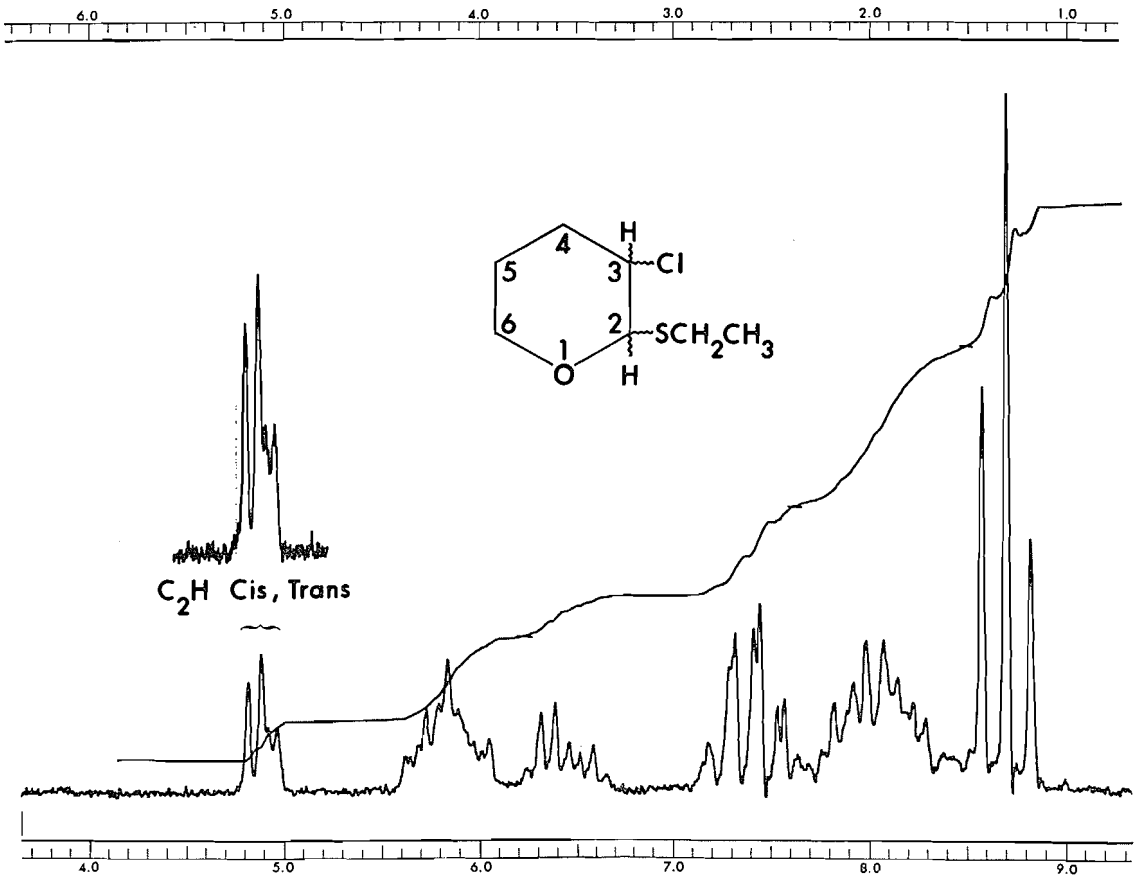

FIG. 2. The 60 Mc.p.s. nuclear magnetic resonance spectrum of 3-chloro-2-ethylthiotetrahydropyran in $CDCl_3$.

conformation wherein the chlorine atom is axial. On this basis one might expect that in either *cis*- or *trans*-2-chloro-3-ethylthiotetrahydropyran the chlorine atom on the anomeric carbon would be in the axial position.

Assuming a value of ~0.4 kcal/mole for the interaction of the ethylthio group with one axial proton in our molecule (ref. 11, p. 44)[3] and accepting the figure of 2.7 kcal/mole for the anomeric effect, 2-chloro-3-ethylthiotetrahydropyran at −40° is biased to the extent of ~2.3 kcal/mole (>99%, using the relation $\Delta G = -RT\ln K$) in the conformation in which the chlorine atom on the anomeric carbon is axial (Scheme 4).

Thus, the evidence above clearly shows that the product obtained from the reaction of ethanesulfenyl chloride with 3,4-dihydro-2*H*-pyran is *trans*-2-chloro-3-ethylthiotetrahydropyran. We do not know whether a fast addition of the ethanesulfenyl chloride occurred first in the reverse manner to form the 3-chloro-2-ethylthiotetrahydropyran, followed by a fast rearrangement, via episulfonium ion formation, but believe that such a process is unlikely under our conditions (−40°). Mueller and Butler (6) found that ambient temperatures were required for similar rearrangement to occur. Indeed, one would expect such ease of C—Cl bond breaking, assisted by sulfur participation, to occur only if the halogen were attached initially to the anomeric carbon, C-2, rather than to C-3, to secure the advantage of stabilization of the positive charge left on the carbon atom vacated by the chloride ion, by participation of the lone pair of electrons on neighboring oxygen.

To test the possible intermediacy of 3-chloro-2-ethylthiotetrahydropyran as postulated in Scheme 2, this compound was synthesized by

[3]Dipolar effects of the ethylthio group are neglected because of lack of available data.

Can. J. Chem. Downloaded from www.nrcresearchpress.com by 210.87.254.105 on 09/05/12
For personal use only.

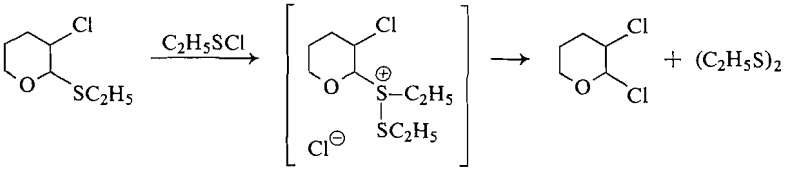

SCHEME 5

the addition of ethanethiol to 5-chloro-3,4-dihydro-2*H*-pyran in the presence of sulfur dioxide catalyst. The 60 Mc.p.s. spectrum (in $CDCl_3$) of this compound is shown in Fig. 2 and agrees with the structural assignment. This spectrum indicates that we have a mixture of *cis* and *trans* isomers since there are two doublets in the anomeric proton region. Gas–liquid chromatography on a column of butanediol succinate on Gas-Chrom P showed only one peak. Ordinary column chromatography was not attempted since our experience with similar compounds has always resulted in failure to separate *cis* and *trans* isomers of the 2,3-disubstituted tetrahydropyrans.

The fact that the above compound could be purified by distillation under vacuum is good evidence that it does not rearrange at −40° to 2-chloro-3-ethylthiotetrahydropyran, certainly as rapidly as is obviously necessary to accommodate Scheme 2.

Treatment of this compound with ethanesulfenyl chloride under conditions similar to those used for the reaction of ethanesulfenyl chloride with 3,4-dihydro-2*H*-pyran gave only a high yield of diethyl disulfide plus 2,3-dichlorotetrahydropyran. There was no evidence of the formation of 2-chloro-3-ethylthiotetrahydropyran either by the n.m.r. spectrum of the reaction mixture or by isolation by fractional distillation.

The above information clearly supports the view that the reaction of ethanesulfenyl chloride with 3,4-dihydro-2*H*-pyran follows the course shown in Scheme 1.

The conversion of 3-chloro-2-ethylthiotetrahydropyran by ethanesulfenyl chloride to 2,3-dichlorotetrahydropyran and diethyl disulfide might occur by a route such as that shown in Scheme 5. Similar reactions of sulfenyl halides with sulfides have been reported by others (12). If this mechanistic pathway (Scheme 5) is correct then it offers support for the assumption that the S—Cl bond of ethanesulfenyl chloride tends to cleave so that the chlorine atom emerges negatively charged.

Experimental

Nuclear magnetic resonance (n.m.r.) spectra were obtained in $CDCl_3$ using Varian Associates HA-100 and A-60 spectrometers operated by Mr. Glen Bigam and Mr. Robert Swindlehurst respectively. Microanalyses were carried out by Mrs. Darlene Mahlow of this Department.

Ethanesulfenyl chloride was prepared according to published directions (13).

3,4-*Dihydropyran* was obtained from the Eastman Kodak Chemical Company.

Addition of 3,4-Dihydro-2H-pyran to Ethanesulfenyl Chloride

A quantity (2.1 g, 0.025 mole) of 3,4-dihydro-2*H*-pyran was added dropwise to a cold (−40°) stirred solution of 2.45 g (0.0254 mole) of ethanesulfenyl chloride in 5 ml of dry $CDCl_3$. The temperature of the reaction mixture was maintained at −40° throughout the addition. The disappearance of the yellow color of the sulfenyl halide provided an indication of the progress of the reaction. When the addition was completed a sample was removed, kept at −40° and immediately subjected to n.m.r. analysis at −40° using the HA-100 spectrometer. The spectrum is shown in Fig. 1 with the two significant signals emphasized.

3-Chloro-2-ethylthiotetrahydropyran

2,3-Dichlorotetrahydropyran was prepared by a modification of the published procedure (14). A solution of anhydrous chlorine (32 g, 0.45 mole) dissolved in 200 ml of dry CCl_4, was cooled to −25°. To this was added dropwise with stirring 37.8 g (0.45 mole) of 3,4-dihydro-2*H*-pyran so that the temperature of the reaction mixture remained at −25°. When the addition was completed the solvent was removed under reduced pressure and the colorless oil then fractionally distilled, b.p., 85° at 21 mm; yield, 64 g (91%); lit. b.p., 79–83° at 18 mm (14).

By distillation of 2,3-dichlorotetrahydropyran at atmospheric pressure according to the method of Riobé (15) an 87% yield of *5-chloro-3,4-dihydro-2H-pyran* was obtained; b.p., 62° at 48 mm; lit. b.p., 139–140° at atmospheric pressure.

3-Chloro-2-ethylthiotetrahydropyran was obtained by a modification of a published procedure (16). A mixture of 3.9 g (0.063 mole) of ethanethiol and 11.8 g (0.1 mole) of 5-chloro-3,4-dihydro-2*H*-pyran was cooled to −20° by means of a dry ice – acetone bath. A slow stream of

Can. J. Chem. Downloaded from www.nrcresearchpress.com by 210.87.254.105 on 09/05/12
For personal use only.

Can. J. Chem. Downloaded from www.nrcresearchpress.com by 210.87.254.105 on 09/05/12
For personal use only.

sulfur dioxide was passed into the solution for 2 min. The mixture was then stirred while it slowly reached room temperature. After standing overnight it was fractionally distilled under reduced pressure giving 8.7 g (77%) of a colorless oil boiling at 63° at 0.15 mm; n_D^{28} 1.5081.

Anal. Calcd. for $C_7H_{13}ClOS$: C, 46.54; H, 7.24; Cl, 19.63. Found: C, 46.70; H, 6.97; Cl, 19.68.

The n.m.r. spectrum is shown in Fig. 2. The signals for the anomeric proton, centered at τ 4.96, indicate the presence of two compounds most likely the *cis* and *trans* isomers whose separation as yet has not been achieved. The spectrum agrees well with the structure assigned.

The Reaction of 3-Chloro-2-ethylthiotetrahydropyran with Ethanesulfenyl Chloride

A solution of 1 g (~0.01 mole) of ethanesulfenyl chloride in 2 ml of dry $CDCl_3$ was cooled to −40° in a dry ice – acetone bath. To the stirred solution was added dropwise 1.8 g (0.01 mole) of 3-chloro-2-ethylthiotetrahydropyran. After the addition, the solution was stirred for 15 min and then freed from solvent by distillation under reduced pressure. The residual oil was fractionally distilled. The following fractions were collected. Fraction I, b.p. 78° at 46 mm (1 g); Fraction II, b.p. 104° at 46 mm (1.3 g). Fractions I and II were found to be identical with diethyl disulfide and 2,3-dichlorotetrahydropyran respectively as shown by comparisons of their boiling points, n.m.r., and infrared spectra with those of authentic samples.

Addition of 3,4-Dihydro-2H-pyran to Methanesulfenyl Chloride in Cumene. Test for Free Radical Intervention

To a cold (−5°) solution of 1.64 g (0.02 mole) of methanesulfenyl chloride (17) in 5 ml of cumene was added dropwise, with cooling, 1.68 g (0.02 mole) of 3,4-dihydro-2*H*-pyran. To the resulting colorless solution was added 1.62 (0.03 mole) of sodium methoxide in 15 ml of methanol. The mixture was stirred ~1 h at room temperature, then the precipitated solid was removed by filtration. The filtrate was freed from methanol under vacuum with a rotary evaporator. The residue was dissolved in ether, washed with water, and dried (Na_2SO_4). The ether was removed by distillation and the oil fractionated under reduced pressure. Cumene (4.2 ml) was collected in a dry ice – acetone trap. Gas–liquid chromatography showed no evidence of any other substance in the cumene. Further distillation of the above oil gave 2.6 g (86%) of 3-methylthio-2-methoxytetrahydropyran; b.p., 46° at 0.2 mm, identical with authentic material (1). A negligible amount of residue remained in the distillation flask.

Acknowledgments

We wish to thank the National Research Council of Canada and the Defence Research Board of Canada for financial support throughout the course of this work. One of us (M. J. B.) is grateful for the award of a Canadian Industries Fellowship (1966–1967).

We also wish to express our appreciation to Mr. Glen Bigam for assistance in the interpretation of the nuclear magnetic resonance spectra.

1. M. J. Baldwin and R. K. Brown. Can. J. Chem. **45**, 1195 (1967).
2. N. Kharasch and A. J. Havlik. J. Am. Chem. Soc. **75**, 3734 (1953).
3. A. J. Havlik and N. Kharasch. J. Am. Chem. Soc. **78**, 1207 (1956).
4. H. Kwart and R. K. Miller. J. Am. Chem. Soc. **78**, 5678 (1956).
5. S. J. Cristol, R. P. Arganbright, G. D. Brindell, and R. M. Heitz. J. Am. Chem. Soc. **79**, 6035 (1957).
6. W. H. Mueller and P. E. Butler. J. Am. Chem. Soc. **88**, 2866 (1966).
7. R. U. Lemieux, G. L. Nagabhushan, and I. K. O'Neill. Tetrahedron Letters, No. 29, 1909 (1964).
8. C. B. Anderson and D. T. Sepp. J. Org. Chem. **32**, 607 (1967).
9. R. U. Lemieux and B. Fraser-Reid. Can. J. Chem. **43**, 1460 (1965).
10. R. U. Lemieux, R. K. Kullnig, H. J. Bernstein, and W. S. Schneider. J. Am. Chem. Soc. **80**, 6090 (1958).
11. E. L. Eliel, N. L. Allinger, S. J. Angyall, and G. A. Morrison. Conformational analysis. Interscience Publishers, New York. 1965. p. 375.
12. C. G. Moore and M. Porter. Tetrahedron, **9**, 58 (1960).
13. H. Brintzinger and M. Langheck. Ber. **86**, 557 (1953).
14. M. Jacobson. J. Am. Chem. Soc. **72**, 1489 (1950).
15. O. Riobé. Bull. Soc. Chim. France, 829 (1951).
16. M. P. Shostakovskii, E. N. Prilezhaeva, and E. S. Shapiro. Izv. Akad. Nauk SSSR, Otd. Khim. Nauk, 357 (1953); Chem. Abstr. **48**, 9311 (1954).
17. H. Brintzinger, K. Pfannstiel, H. Koddebusch, and K.-E. Kling. Ber. **83**, 87 (1950).

Synthesis of anisomycin. Part I. The stereospecific synthesis of *N*-benzoyl-2-(*p*-methoxybenzyl)-3-hydroxy-4-carboxamido pyrrolidine and the absolute configuration of anisomycin

C. M. WONG

Department of Chemistry, University of Manitoba, Winnipeg, Manitoba

Received September 27, 1967

L-Tyrosine was converted stereospecifically to *N*-benzoyl-2-(*p*-methoxybenzyl)-3-hydroxy-4-cyanopyrrolidine (**10**) which had a specific optical rotation $[\alpha]_D^{20}$ +9.7°. Anisomycin was converted also to *N*-benzoyl-2-(*p*-methoxybenzyl)-3-hydroxy-4-cyanopyrrolidine (**16**) which had a specific rotation $[\alpha]_D^{20}$ −11°. The infrared spectra of the synthetic compound and the derivative of anisomycin were superimposable with each other. This result showed that the absolute configuration of the three asymmetric centers in (**10**) of synthetic origin were 2S, 3S, 4S, and those in (**16**) were 2R, 3R, 4R. Thus, anisomycin should have the absolute stereochemistry 2R, 3S, 4S as depicted in the structure (**2**). Hydrolysis of the hydroxy nitriles (**8**) and (**10**) gave an identical amide (**3**) which should have the absolute stereochemistry 2S, 3S, 4R as shown in structure (**3**).

Canadian Journal of Chemistry, 46, 1101 (1968)

Can. J. Chem. Downloaded from www.nrcresearchpress.com by 210.87.254.40 on 09/05/12
For personal use only.

The structure of anisomycin (1) was first proposed in 1965 as shown in (**1**). This structure was revised to (**2**) (2) in 1967 by *x*-ray investigation. However, the *x*-ray study only showed the relative configuration and the absolute configuration of the antibiotic was still unknown. This paper describes the stereospecific synthesis of *N*-benzoyl-2-(*p*-methoxybenzyl)-3-hydroxy-4-carboxamido pyrrolidine[1] (**3**) and the correlation of the synthetic hydroxy nitrile (**10**) with its enantiomer (**16**) obtained from anisomycin.

Results and Discussion

L-Tyrosine was treated with benzoyl chloride in chloroform solution followed by hydrolysis with methanolic sodium carbonate solution to give the acid (**4**). Methylation of the acid (**4**) with methyl iodide in absolute methanol and sodium carbonate solution gave the ester (**5**). Condensation of the ester (**5**) with acrylonitrile in absolute ether solution containing sodium hydride gave an acidic product the infrared spectrum of which showed five-membered ring ketone and cyano group absorptions. All efforts aiming at crystallizing the amorphous acidic product were unsuccessful. It was assumed that this product was a mixture of the ketonitriles (**6**) and (**7**). Sodium borohydride reduction of the acidic ketonitriles in absolute methanol gave a neutral amorphous product. The infrared spectrum showed hydroxy and nitrile bands.

Sodium borohydride reduction of the nitriles (**6**) and (**7**) could give hydroxy nitriles (**8**), (**9**), (**10**), and (**11**). In the reduction of ketonitrile (**6**), the borohydride complex should come mainly from the α side of the pyrrolidine ring to give the hydroxy nitrile (**8**) as the major product. However, two isomeric hydroxy nitriles (**10**) and (**11**) would be expected as a result of the borohydride reduction of the ketonitrile (**7**) with (**10**) being the predominant one. Separation of the reduction product by thin-layer chromatography (t.l.c.) gave two major bands after four developments. The fact that these two fractions were hydroxy nitriles and that they were stereoisomers, could be shown by their extremely similar infrared and mass spectra. One could be easily crystallized while the other remained as an amorphous solid possibly due to the presence of small amounts of other isomers which could not be separated from each other. Hydrolysis of the crystalline and amorphous hydroxy nitriles with concentrated hydrochloric acid led to an identical hydroxy carboxamide (**3**). Of the four possible isomers obtained by sodium borohydride reduction of (**6**) and (**7**), only (**8**) and (**10**) could be the major product and only these two isomers could be converted to the same hydroxy carboxamide (**3**). The crystalline synthetic hydroxy nitrile (**10**) was successfully correlated with its enantiomer (**16**) obtained from anisomycin as described below. This correlation would indicate that the crystalline hydroxy nitrile must have structure (**10**) and the amorphous hydroxy nitrile must have structure (**8**). The conversion of hydroxy nitrile (**8**) to the hydroxy carboxamide (**3**) can be interpreted as going through structure (**12**).

[1]Asymmetric carbons of all compounds are given in absolute configuration.

Can. J. Chem. Downloaded from www.nrcresearchpress.com by 210.87.254.40 on 09/05/12
For personal use only.

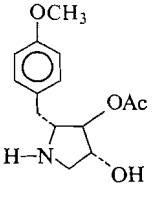

1

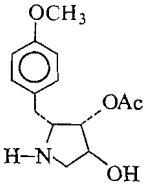

2

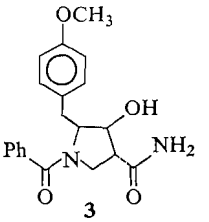

3

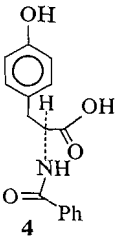

4

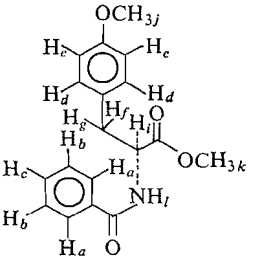

5

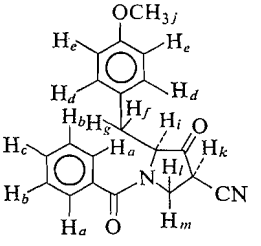

6

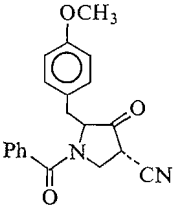

7

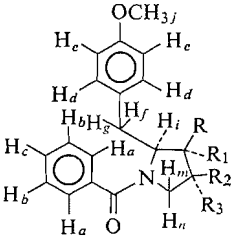

8 R = OH, R_1 = H, R_2 = CN, R_3 = H
9 R = H, R_1 = OH, R_2 = CN, R_3 = H
10 R = OH_k, R_1 = H_p, R_2 = H_1, R_3 = CN
11 R = H, R_1 = OH, R_2 = H, R_3 = CN

Thus, anisomycin was converted into the epoxide[2] (**13**) (1) by treatment with phosphorous pentachloride followed by basic hydrolysis. Opening of the epoxide (**13**) with sodium cyanide should give two basic hydroxy nitriles (**14**) and (**15**). However, this mixture of hydroxy nitriles could not be resolved even after t.l.c. separation and fractional recrystallization. This product was then converted into the corresponding benzoyl derivatives which could be separated into two fractions by t.l.c. Both fractions showed hydroxy nitrile and phenyl carboxamide absorptions in their infrared spectra. One fraction could be easily crystallized while the other remained as an amorphous solid. The crystalline fraction had an infrared spectrum superimposable with that of the hydroxy nitrile (**10**) and an opposite optical rotation. Thus, the crystalline fraction could be represented by the structure (**16**) and the amorphous fraction could be assigned the structure (**17**). Since the hydroxy nitrile (**10**) was prepared from L-tyrosine, the absolute configuration should be 2S, 3S, 4S and the absolute configuration of anisomycin should be 2R, 3S, 4S as

[2]According to the structure proposed by *x*-ray investigation, the chloro compound reported in reference (1) must have structure (*i*). Basic hydrolysis should give the epoxide (**13**). Epoxides (*ii*) and (*iii*) were prepared as intermediates in the successful synthesis of (*dl*)-deacetyl anisomycin. The *N*-acetyl derivative of (**13**) had identical infrared spectrum with that of (*iii*). The synthesis will be reported in a later communication.

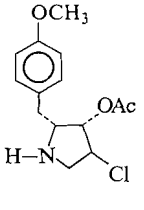

i

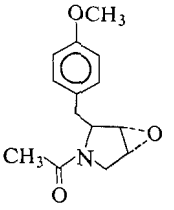

ii

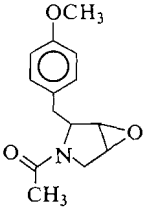

iii

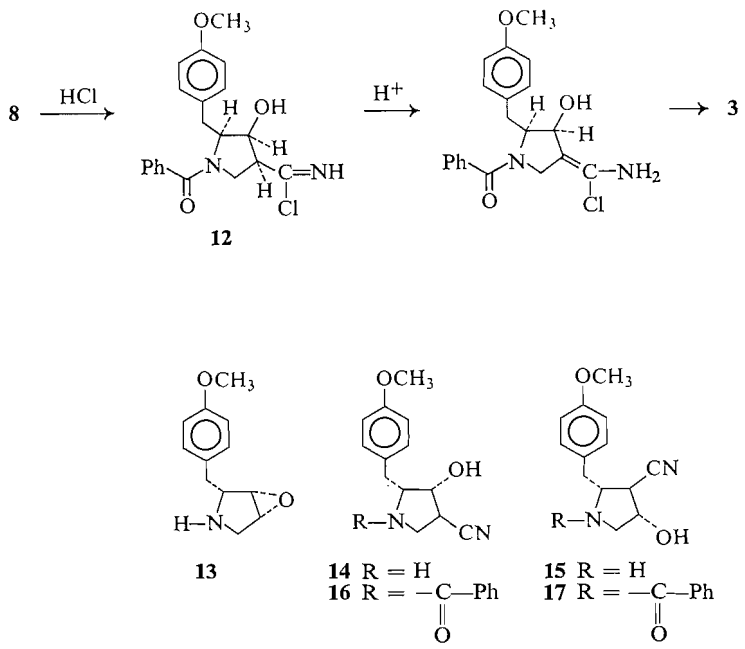

shown in (2). The hydroxy carboxamide (**3**) should have the absolute configuration 2S, 3S, 4R.

Experimental

All infrared spectra were measured on a Perkin-Elmer model 137 spectrophotometer using methylene chloride as solvent. Melting points were measured on a Fisher-Johns apparatus and are uncorrected. Nuclear magnetic resonance (n.m.r.) spectra were measured on a Varian DA 60 or Varian A 56/60 A model. Deuteriochloroform was used as solvent and tetramethylsilane as internal standard. Mass spectra were measured on a Hitachi - Perkin-Elmer RMU-6D mass spectrometer. Microanalyses were performed by Dr. C. Daesslé of Montreal.

Preparation of the Ester (5)

L-Tyrosine (10 g) in a solution of chloroform (100 ml), benzoyl chloride (34 g), and pyridine (8 g) was heated in a 70 °C oil bath under anhydrous condition, for 15 h. The chloroform solution was evaporated under reduced pressure to give a heavy oil. Aqueous methanolic sodium carbonate solution (150 ml, 10%) was added to the oily residue. The solution was stirred at room temperature for 2 h. After acidification with concentrated hydrochloric acid, the solution was extracted with chloroform (5 × 100 ml) and dried over magnesium sulfate. The chloroform solution was then concentrated under reduced pressure. The residue was washed with ether (200 ml). The insoluble material was separated and dried under reduced pressure. The ether washing that contained only benzoic acid was discarded. Methyl iodide (35 ml) was added to the residue together with absolute methanol (100 ml) and sodium carbonate (5 g). After stirring for 24 h at room temperature, the solution was evaporated under reduced pressure to a slurry. The slurry was diluted with water and the aqueous solution was exhaustively extracted by chloroform. The extract, dried over magnesium sulfate, was evaporated to dryness giving a yellow oily residue. Chromatography of the residue on neutral alumina gave the crystalline ester (**5**) (6.5 g) which was recrystallized from ether, m.p. 88–89 °C; infrared absorption: 3400, 2900, 1750, 1670, 1615, 1585, 1515, 1035, 840 cm^{-1}; nuclear magnetic resonance (n.m.r.) τ 2.40 p.p.m. (2 H, multiplet, H_a), 2.59 p.p.m. (3 H, multiplet, H_bH_c), 3.16 p.p.m. (4 H, quadruplet, H_dH_e), 3.47 p.p.m. (1 H, broad singlet, H_1), 5.10 p.p.m. (1 H, broad singlet, H_i), 6.32 p.p.m. (6 H, singlet, H_jH_k), 6.92 p.p.m. (2 H, doublet H_fH_g).

Anal. Calcd. for $C_{18}H_{19}O_4N_1$: C, 69.01; H, 6.07; N, 4.44. Found: C, 67.94; H, 6.26; N, 4.74.

Condensation of the Ester (5) with Acrylonitrile

To a solution of dry ether (200 ml) and ester (**5**) (3.0 g) was added sodium hydride (1.5 g) in mineral oil suspension. The solution was refluxed under anhydrous conditions with stirring, for ½ h. Dry acrylonitrile (4 ml) was injected into the solution which was refluxed for 48 h with vigorous stirring. The excess sodium hydride was decomposed by dropping methanol into the reaction mixture cooled in an ice bath. The solution was then extracted with water (50 ml). The aqueous solution was washed with chloroform (2 × 30 ml). Combining the ether and chloroform solutions gave starting material (620 mg) after chromatography on neutral alumina. The aqueous solution was strongly acidified with concentrated hydrochloric acid. Exhaustive extraction of the cloudy acidic solution with chloroform gave a light-yellow foam (2.3 g) after routine work-up. Chromatography on silica gave white amorphous solid (1.8 g); infrared absorption: 2900, 2275, 2240, 1175, 1650, 1620, 1580,

Can. J. Chem. Downloaded from www.nrcresearchpress.com by 210.87.254.40 on 09/05/12
For personal use only.

1515, 1380, 1110, 1035 cm^{-1}; n.m.r.: 2.61 p.p.m. (5 H, singlet, $H_aH_bH_c$), 3.10 p.p.m. (4 H, quadruplet, H_dH_e), 5.16 p.p.m. (1 H, broad singlet, H_k), 6.10 p.p.m. (1 H, broad singlet, H_l), 6.25 p.p.m. (3 H, singlet, H_j), 6.35–6.75 p.p.m. (4 H, multiplet, $H_fH_gH_iH_m$).

Anal. Calcd. for $C_{20}H_{18}O_3N_2$: C, 71.85; H, 5.39; N, 8.38. Found: C, 72.27; H, 5.02; N, 7.81.

Sodium Borohydride Reduction of the Ketonitriles (6) and (7)

The amorphous mixture of ketonitriles (**6**) and (**7**) (2.2 g) were dissolved in absolute methanol (100 ml). To the solution was added sodium borohydride pellers (8 g) in a period of 3 h. After stirring the solution at room temperature for 12 h, the solution was concentrated to a slurry under reduced pressure. The slurry was diluted with water and extracted with chloroform. Dried over magnesium sulfate and evaporated to dryness, the extract gave an amorphous solid (1.8 g) which was then separated into two components by thin-layer chromatography (t.l.c.) on neutral alumina. The less polar component[3] (**10**) (470 mg) was recrystallized from methanol and ether, m.p., 156–158 °C; infrared absorption: 3590, 2900, 2260, 1640, 1625, 1575, 1505, 1490, 1180, 1100, 1040 cm^{-1}; mass spectrum: *m/e* 336, 215, 163, 121, 105, 85, 83, 78, 77; n.m.r.: τ 2.55 p.p.m. (5 H, singlet $H_aH_bH_c$), 3.00 p.p.m. (4 H, quadruplet, H_dH_e), 5.72 (3 H, unresolved multiplet, $H_iH_nH_m$), 6.0–6.2 p.p.m. (2 H, H_kH_p), 6.26 (3 H, singlet H_j), 6.56–6.71 (3 H, $H_fH_gH_l$), $[\alpha]_D^{20}$ +9.7°($CHCl_3$.)

Anal. Calcd. for $C_{20}H_{20}O_3N_2$: C, 71.43; H, 5.96; N, 8.33. Found: C, 71.69; H, 6.18; N, 8.20.

Hydrolysis of the Hydroxy Nitrile (10)

To the hydroxy nitrile (**10**) (230 mg) was added concentrated hydrochloric acid (3 ml). The solution was stirred at room temperature for 3 h. Water (15 ml) was added and white precipitate appeared. The solution was extracted exhaustively with chloroform and the chloroform solution was dried over magnesium sulfate. Evaporation of the chloroform solution to dryness gave the crystalline amide (**3**) (168 mg) which was recrystallized from methanol and ether, m.p. 175–176 °C; infrared absorption: 3600, 3500, 3410, 2910, 1685, 1640, 1615, 1510, 1470, 1180, 1100, 1040 cm^{-1}; mass spectrum: *m/e* 354, 233, 121, 105, 77.

Anal. Calcd. for $C_{20}H_{22}O_4N_2$: C, 67.80; H, 6.22; N, 7.91. Found: C, 68.00; H, 6.19; N, 7.81.

[3]The amorphous fraction, possibly the hydroxy nitrile (**8**), showed extremely similar infrared and mass spectra with those of the hydroxy nitrile (**10**). It was not further characterized due to the difficulty of bringing it into a crystalline form.

Hydroxy Nitrile (14) from the Epoxide (13)

Epoxide (**13**) (608 mg), prepared according to the procedure described in reference (1), was refluxed with sodium cyanide (4 g) in a solution of *t*-butanol (40 ml) and water (10 ml) for 60 h under nitrogen atmosphere. The *t*-butanol solution was concentrated under reduced pressure and then diluted with water. Exhaustive extraction with chloroform gave, after routine work-up, a yellow oil (580 mg). Chromatography of the oily residue on neutral alumina recovered the epoxide (**13**) (3000 mg) and hydroxy nitrile[4] (**14**) (210 mg). Recrystallization from methanol and ether gave white crystals (170 mg), m.p. 120–124 °C; infrared absorption: 3600, 2900, 2260, 1620, 1510, 1175, 1130, 1040 cm^{-1}.

The hydroxy nitrile (**14**) (170 mg) was then dissolved in dry chloroform (10 ml). To the chloroform solution was added benzoyl chloride (300 mg) and pyridine (5 drops). After stirring for ½ h, the chloroform solution was concentrated to an oily residue. Separation of the residue by t.l.c. on silica plates gave the hydroxy nitrile (**16**) (72 mg) which was purified by recrystallization from ether and methanol, m.p. 156–158 °C, $[\alpha]_D^{20}$ −11°($CHCl_3$). The infrared spectrum was superimposable with that of the synthetic hydroxy nitrile (**10**).

Anal. Calcd. for $C_{20}H_{20}O_3N_2$: C, 71.43; H, 5.96; N, 8.33. Found: C, 71.55; H, 5.97; N, 8.42.

Acknowledgments

The financial support from the National Research Council of Canada and the supply of anisomycin from Dr. Kenneth Butler of Charles Pfizer & Co., Inc. are highly appreciated.

1. J. J. Beereboom, K. Butler, F. C. Pennington, and I. A. Solomons. J. Org. Chem. **30**, 2334 (1965).
2. J. P. Schaefer and P. J. Wheatley. Chem. Commun. **12**, 578 (1967).

[4]The relatively large melting point range would suggest that this compound was possibly contaminated with the isomeric hydroxy nitrile (**15**) which could not be separated from (**14**). The benzoylation product was separated by thin-layer chromatography on silica into two neutral hydroxy nitriles. One was the crystalline hydroxy nitrile (**16**) as shown by comparing the infrared spectrum, optical rotation with those of (**10**). The other hydroxy nitrile could be the hydroxy nitrile (**17**).

Can. J. Chem. Downloaded from www.nrcresearchpress.com by 210.87.254.40 on 09/05/12
For personal use only.

Can. J. Chem. Downloaded from www.nrcresearchpress.com by 210.87.254.40 on 09/05/12
For personal use only.

Diastereoisomeric 2-aryl-6-methyl-3,4 (1,2-piperido)-oxazines[1]

G. A. COOKE AND G. FODOR
Department of Chemistry, Laval University, Quebec 10, Quebec

Received November 2, 1967

The alkaloid sedridine (**1**) is formed stereospecifically by catalytic hydrogenation of optically active α-picolyl methyl carbinol (**2**). The levorotatory **1** gave on action of *p*-nitro benzaldehyde two μ-aryl oxazines, one crystalline and levorotatory, the other oily and dextrorotatory. This is the first example where both epimers of a μ-aryl oxazine could be detected. The configurations and the conformations of these isomers (**10** and **11**) and those of sedridine have been discussed in terms of their nuclear magnetic resonance spectra, with particular reference to spin-decoupling evidence.

Canadian Journal of Chemistry, 46, 1105 (1968)

We have previously reported (1) the synthesis of alkaloid ε-coniceine (**3**). We now wish to discuss in detail one of the intermediates obtained in this series, the enantiomer of the naturally occurring alkaloid (+)sedridine (**1**). The synthesis (2) of **1**, the correlation of the configuration of the piperidine carbon (3) with L(−)pipecolic acid, and the assignment of threo relative configuration have also been made (3).

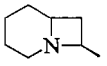

3

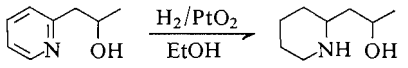

2 1

The reaction sequence used to provide (1) ε-coniceine (**3**) involved the preparation of a pipecolylmethylcarbinol of the same gross structure as sedridine (**1**) by hydrogenation of the corresponding picolylmethyl carbinol (**2**), already carrying one asymmetric center (1). It was quickly observed that reduction of partially resolved **2** proceeded with a considerable degree of asymmetric induction (1). For example, the carbinol (**2**), α_D^{20} −15 to 20° gave the corresponding hexahydro compound (**1**), α_D^{20} −20 to −23° (75%). Improvements in the resolution technique have provided optically pure **2**, α_D^{20} −42°. The reduction of this base with Adams catalyst in ethanol gave a quantitative yield of (−)sedridine (**1**) (m.p. 82–84, α_D^{20} −27.9°). Thus one is dealing, not with a stereoselective reaction, as might have been predicted, but with a stereospecific one. This is rather surprising in view of the apparent absence of compelling reasons for conformational rigidity and in view of the obvious steric-orienting groups in **2**. Closer examination offers an explanation for this specificity.

Infrared dilution studies reveal that the *optically* active carbinol **2** is completely intramolecularly hydrogen bonded. The band at 3340 cm^{-1} is unchanged in $CHCl_3$ and CCl_4 (10^{-2} *M* and 10^{-3} *M* concentration) so there is no evidence for a free hydroxyl. The quasi-bicyclic hydrogen-bonded structure shown in Fig. 1 has the methyl group projecting above the plane of the molecule. Since the reduction of picolyl methyl carbinols leads specifically to (+)sedridine or (−)sedridine, depending on which antimer is used, this indicates the following points: (*a*) the hydrogen bridge must help the molecule to be essentially conformationally immobile; (*b*) the projecting methyl group must be sufficiently bulky to direct the reaction completely; (*c*) the mechanism of the reduction is probably unique.

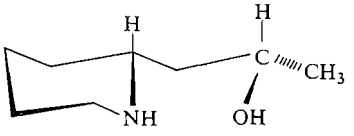

4

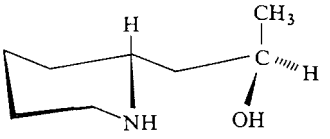

5

[1]This paper forms part of a lecture given by one of us (G.A.C.) at the 50th Canadian Chemical Conference in Toronto, Ontario on June 7, 1967.

Can. J. Chem. Downloaded from www.nrcresearchpress.com by 210.87.254.40 on 09/05/12
For personal use only.

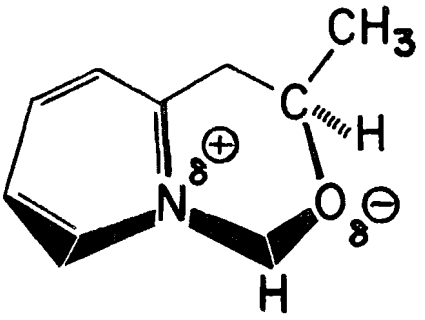

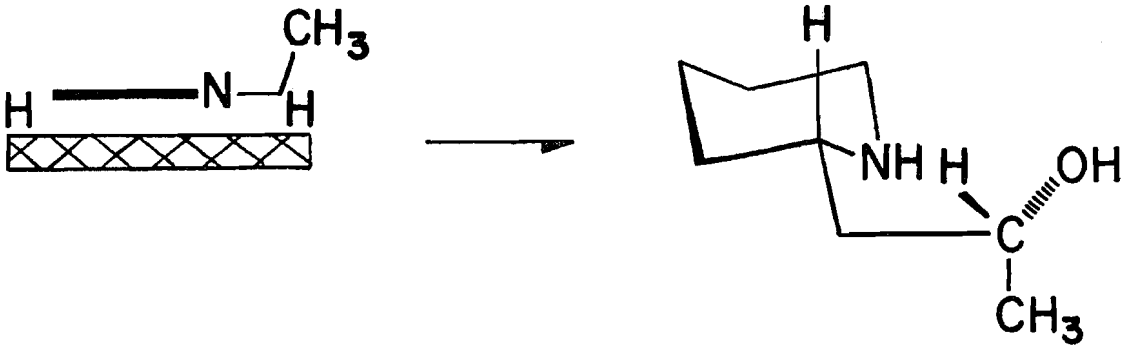

FIG. 1. Possible conformation of **2** during catalytic hydrogenation.

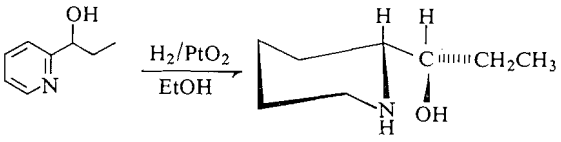

6 7

The generally-accepted mechanism of catalytic reduction at low pressures involves the transfer of activated hydrogen from the catalyst surface to the adsorbed substrate molecule. In this particular case the transfer will take place at the side of the molecule remote from the methyl group, as shown (Fig. 1). Using **2** of indicated absolute configuration, this then allows us to predict the relative configuration of the sedridine produced. It will be erythroid (*S*,*R* in Cahn – Ingold – Prelog terms). The ring asymmetric carbon in (+)sedridine (3) is *S* and therefore *R* for (−)sedridine. The form in Fig. 1 is thus (+)sedridine and so the dextrorotatory carbinol **2** should be *R*. The visualization of the following reactions is, however, easier with the mirror images of those already given, so (−)sedridine will be depicted as **4** in this paper. An analogous reaction (4) i.e. the catalytic hydrogenation of optically active 2-pyridylethylcarbinol (**6**) under conditions identical to those used for the sedridine-forming reaction gave by asymmetric induction conhydrine (**7**) as the major product. This base is known to be erythro, the relative configuration having been established chemically by Sicher and Tichy (5). Taking these facts together the relative configuration **4** (*R*,*S*) is assigned to (−)sedridine. Conversely allosedridine must be **5**.

Beyerman *et al.* (3), however, have already assigned the threo configuration **5** to (±)sedri-

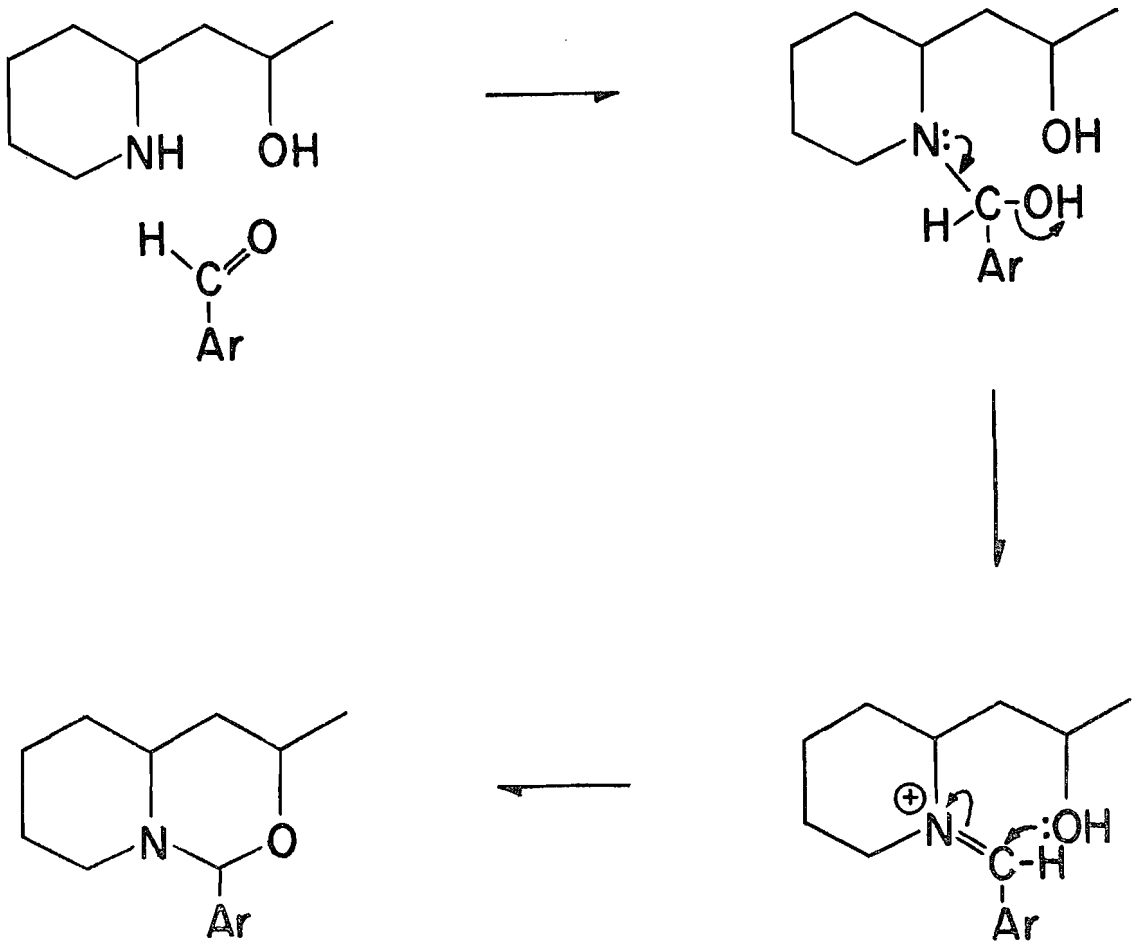

FIG. 2. Mechanism of oxazine ring closure.

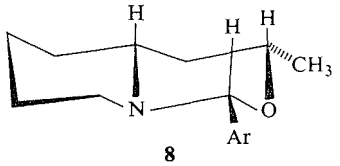

8

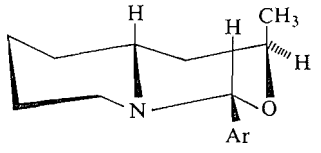

9

dine. This is based on a nuclear magnetic resonance (n.m.r.) analysis of a pair of *p*-substituted phenyloxazines, the *p*-bromophenyl derivatives prepared from racemic sedridine and its diastereoisomer, (±)allosedridine. By careful reasoning it was shown that if **8** and **9** are the aryloxazines produced from the diastereoisomeric pair, then the one derived from sedridine has an equatorial hydrogen on the methyl-bearing carbon. Thus Beyerman's sedridine is threoid (**5**). Yet the course of reduction presented above indicates that sedridine may indeed have erythroid (**4**) relative configuration.

This question will be examined in detail. According to the generally-accepted mechanism (Fig. 2) for the cyclization (6–8) of 1,2-amino alcohols to oxazines, the nitrogen expels the benzylic hydroxyl to give an iminium ion. The assumption that the cyclization does not involve any carbinol carbon–oxygen fission resulting in racemization is absolutely basic to both the position of the Dutch authors and the arguments

Can. J. Chem. Downloaded from www.nrcresearchpress.com by 210.87.254.40 on 09/05/12
For personal use only.

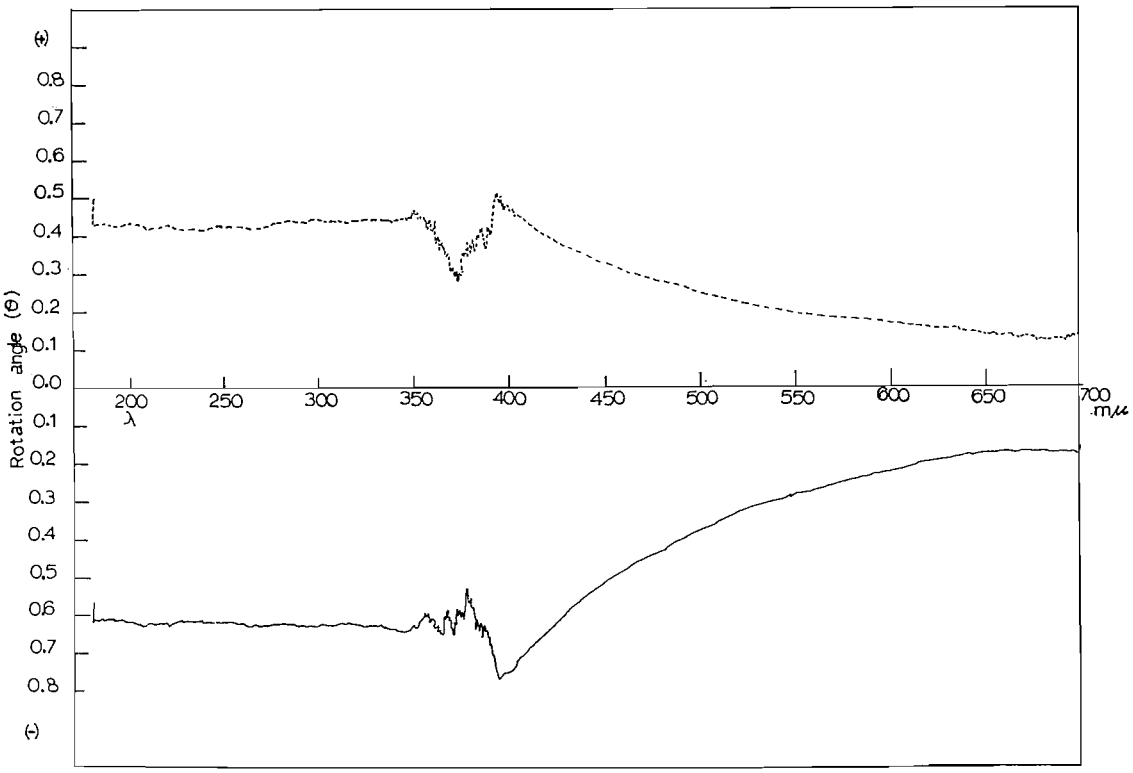

FIG. 3. Optical rotatory dispersion curves. Full line, levorotatory oxazine; dotted line, dextrorotatory oxazine; solvent, dimethyl formamide; angle, 0.5.

to be presented here. Also basic to their position is that (*i*) due to thermodynamic control only one aryloxazine from each diastereoisomer can be formed, with aryl in equatorial position and (*ii*) this has to be the *trans* decalin derivative. In case of (±)sedridine and (±)allosedridine the formation of two different aryloxazines was indeed observed (3) one from each diastereoisomer. The derivative prepared from sedridine displayed an equatorial hydrogen. We must challenge the assumption that these products necessarily are *trans*-chair oxazines.

We consider first the cyclization of the erythro derivative. Depending on whether the cyclization occurs at either the α or β side of the iminium linkage, products **10***a* and **11***a* epimeric at C-2 result. The prediction is thus for the formation of a mixture. Similar arguments pertain to the threo form. One cannot therefore assume either explicitly or implicitly that only the thermodynamically more stable product will be formed in each case.

This argument is now verified by allowing optically pure (−)sedridine to react with *p*-nitrobenzaldehyde. The reaction gave two 2-*p*-nitrophenyl-6-methylpiperidooxazines in approximately equal amounts; one as a crystalline solid (m.p. 128–130°, α_D^{20} −48°), the other as an oil (b.p. 154°, 24μ; α_D^{20} +38°).

The optical rotatory dispersion (o.r.d.) curves (Fig. 3) are nearly mirror images as expected in such examples of diastereoisomerism. The isomers have identical ultraviolet and mass spectra; their infrared spectra also are very similar. Separation by classical methods was successful due to very different solubilities. Further attempts to purify the oily isomer by either thin-layer chromatography (t.l.c.) or gas–liquid chromatography (g.l.c.) led to decomposition. Neither reacts with methyl iodide which indicates that both are weakly basic. This is due to the strong inductive effect by the nitroaryl group and by the hetero oxygen atom.

The n.m.r. spectra of these diastereoisomers (Fig. 4) have been compared carefully, using the same criteria as were used in the analysis of the corresponding pair of *p*-bromophenyl oxazines from (±)sedridine and (±)allosedridine (3).

The most significant signal, that of the proton

Can. J. Chem. Downloaded from www.nrcresearchpress.com by 210.87.254.40 on 09/05/12
For personal use only.

Can. J. Chem. Downloaded from www.nrcresearchpress.com by 210.87.254.40 on 09/05/12
For personal use only.

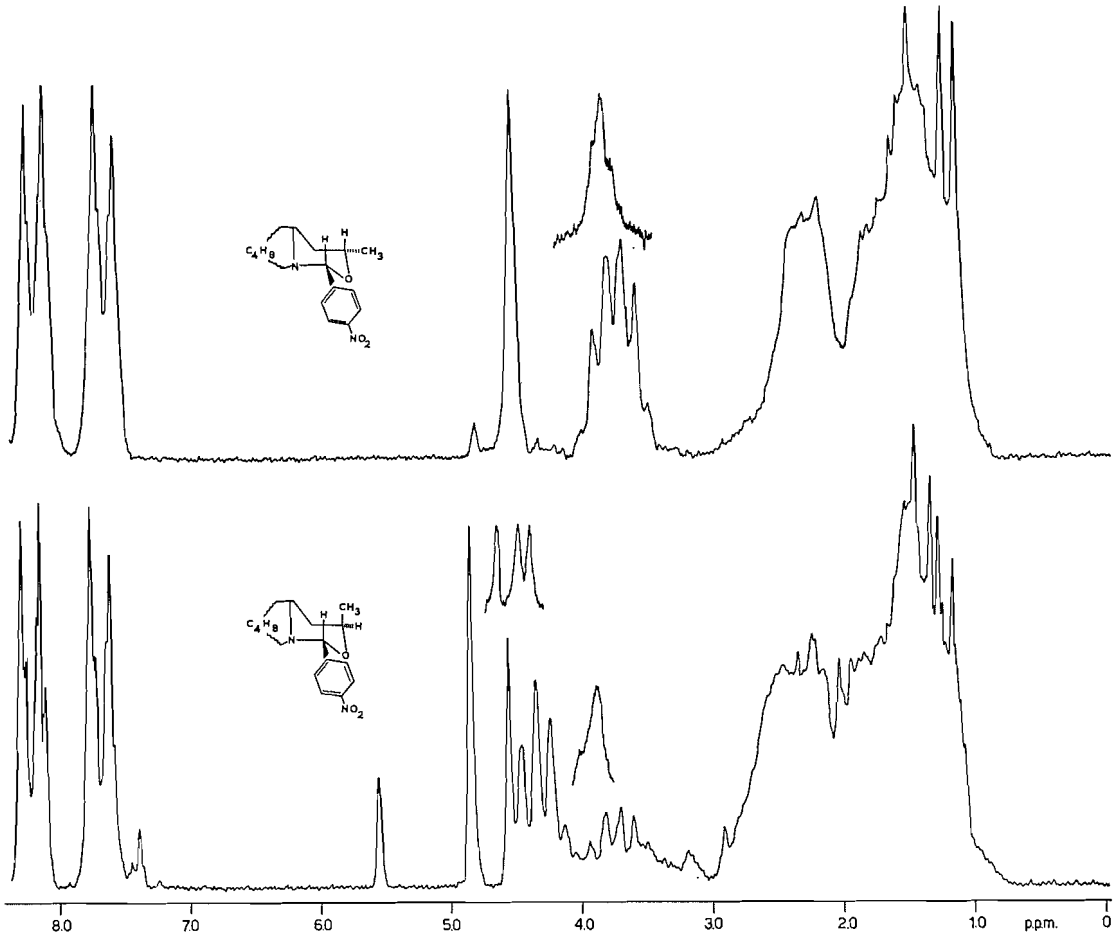

FIG. 4. Nuclear magnetic resonance spectra of the crystalline (−)oxazine (above) and oily (+)oxazine (below); in chloroform-d_3. Double irradiation with spin decoupler model V-6058 A.

on the methyl-bearing carbon (C-6), appears as a quartet centered at δ 4.3 (baseline width 34 c.p.s.) in the dextrorotatory (oily) aryloxazine, while it forms a multiplet around δ 3.65 (baseline 38 c.p.s.) in the case of the levorotatory (crystalline) diastereoisomer. The methyl signal is a doublet in both cases; δ 1.4 in the spectrum of the oily isomer and δ 1.3 in the spectrum of the crystalline isomer. The C-2 proton is strongly deshielded as expected, (δ 4.8 and 4.6, respectively) indicating different chemical environments. Hence the C-6 proton should be equatorial (9) in the oily (+)form and axial for the crystalline (−)isomer and, by inference, the C-6 *methyl is axial in the oily isomer and equatorial in the crystalline form.*

Double irradiation of the C-6 proton with a frequency of +240 c.p.s. causes collapse of the methyl signal in both cases. Irradiation of the methyl group signal simplifies the pattern of the C-6 signal to a broadened doublet in the case of the oily isomer. The signal of the crystalline, (−)form remains still very complex. When the CH_3/H-6 coupling is absent due to double irradiation studies, this proton can only couple with the C-5 methylene. The doublet obtained hereby in the (+)form is a clear indication of an eq/ax coupling while the multiplet obtained with the (−)form results from the simultaneous presence of ax/ax and ax/eq couplings (10, 11). This additional n.m.r. evidence is in harmony with an axial methyl for the oily form and an equatorial methyl for the crystalline isomer. Beyerman *et al.* (3), however, described the crystalline (±)bromophenyloxazine from (±)sedridine as having an axial methyl.

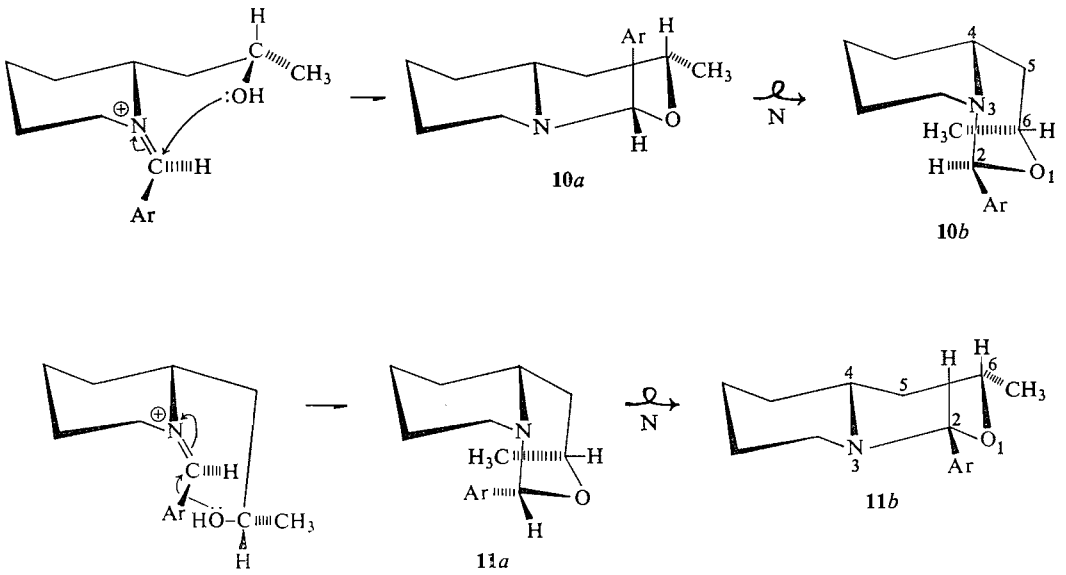

Ours cannot be methyl epimers, since inversion at the carbinol carbon during cyclization of the Schiff base is impossible. The existence of these two stereoisomers from one and the same optically pure (—)sedridine could be explained *a priori* as being a case of epimerism e.g. **10***a* and **11***b*, at the newly formed asymmetric center C-2. This would necessitate, however, identical positions of the C-6 methyl in both forms, which has been disproven by the n.m.r. spectra. The only possibility remaining is that the C-2 epimer with the equatorial aryl group is stable while the axial isomer undergoes stereomutation on nitrogen leading to a different ring junction, i.e. from a *trans*-azaoxadecalin to a *cis*-fused isomer. Inversely by assuming (*i*) an erythro configuration for sedridine and (*ii*) either a β- or an α-attack of the carbinol oxygen on the iminium salt, **10***a* and **11***a* should be formed, which would then rearrange into the more stable *cis* decalin **10***b* and the *trans* decalin **11***b*, respectively. These are different not only at C-2 but also at the nitrogen. In Cahn – Ingold – Prelog terms this means 2*S*:3*R*:4*R*:6*S* for the former and 2*R*:3*S*:4*R*:6*S* for the latter. Assuming the diastereoisomeric threo configuration for sedridine this would only mean the change of 6*S* to 6*R* in both cases with the *trans* decalin having an axial methyl group and the *cis* decalin having an equatorial methyl group. Without chemical evidence of the C-6 configuration, our n.m.r. study merely allows us to assign tentatively **11***b* to the crystalline and **10***b* to the oily isomers. However, the *trans* decalin derivative, **11***b*, with all substituents equatorial, is expected to be higher-melting than the *cis* decalin **10***b* with an axial methyl group.

Unfortunately, we have not succeeded yet in preparing adequate amounts of optically active *allo*sedridine in order to check whether the cyclization gives rise to two diastereoisomers or just one.

The existence of two diastereoisomers (one with an axial and the other with an equatorial 2-*p*-nitrophenyl 6-methylpiperidooxazine instead of only one as reported formerly) invalidates any assignment of a threo configuration for sedridine (3) which is based exclusively on n.m.r. analysis, for equal justification may be provided for an erythro configuration. An explanation is also lacking for the fact that the crystalline *racemic p*-bromophenyloxazine has an axial methyl while the same group is equatorial in the crystalline *optically active p*-nitrophenyloxazine.

Chemical correlation of the carbinol carbon, in either natural sedridine itself or in the intermediate **2**, with a hydroxy compound of known absolute configuration seems therefore indispensable. This work was commenced a year ago by D. Butruille of our Laboratory and is in progress.

Irrespective of our genuine interest in the absolute configuration of the alkaloid sedridine,

Can. J. Chem. Downloaded from www.nrcresearchpress.com by 210.87.254.40 on 09/05/12
For personal use only.

Can. J. Chem. Downloaded from www.nrcresearchpress.com by 210.87.254.40 on 09/05/12
For personal use only.

importance was attached to the fact that a Goodson–Christopher cyclization has produced two μ-diastereoisomers for the first time. The less stable one, carrying an axial aryl group, became stabilized only by basic conformational change, made possible by the configurational flexibility of the tricovalent nitrogen. Diffraction studies using *x*-rays will be started with the (−)*p*-chlorophenyloxazine from (−)sedridine and the configurations of the aryloxazines, assigned by hydrogenation and n.m.r. studies, hopefully will be determined.

Experimental

*(−)Sedridine, 1-(2-Piperidyl)-propan-2-ol (**1**)*

(−)2-Picolylmethyl carbinol **2** (20 g, 0.146 mole), α_D^{20} −39.6° (*c*, 2 in methanol) was dissolved in 95% ethanol (200 ml), then hydrogenated in the presence of Adams platinum oxide (1.8 g) catalyst in a Parr bomb, under 60 p.s.i. for 140 h. The content of unchanged pyridine derivative was determined at intervals by measuring the ultraviolet extinction of an aliquot at 261 mμ.

After shaking for 96 h, 32% of **2** was not reduced; within 140 h, hydrogenation became complete. The solution was then filtered from the catalyst and evaporated to give a white solid **1** (20.1 g), m.p. 55–60°. This has been sublimed (50°, 1 mm) to yield white crystals (19.5 g), m.p. 82–84°; α_D^{20} −27.9° (*c*, 1 in ethanol). Beyerman and Maat recorded (2) m.p. 82° and α_D^{20} +28° for natural (+)sedridine.

2-p-Nitrophenyl-6-methyl-3,4(1,2-piperido)-oxazines

*Levorotatory Oxazine (**11b**)*

(−)Sedridine **1**, (1.0 g, 0.007 mole) was dissolved in chlorobenzene (20 ml) and *p*-nitrobenzaldehyde (1.06 g, 0.0073 mole) was added. The whole was refluxed under a Dean–Stark separator for 24 h with formation of about 0.05 ml water. The solvent was removed in a vacuum and the residue triturated with ether to give brownish colored crystals (0.65 g). Concentration of the filtrate produced a second crop (0.250 g): 46.6% yield, m.p. 123–125°, α_D^{20} −44.65° (*c*, 2 in dimethyl formamide). Recrystallization from petroleum ether (37–54°) of the two crops gave a nearly colorless material, m.p. 128–130° α_D^{20} −48°, (*c*, 1.16 in dimethyl formamide). Optical rotatory dispersion measurement gave α_{590}^{20} −42° and α_{394}^{20} −140.5°, (*c*, 2.745 in dimethyl formamide, angle 0.5).

Anal. Calcd. for $C_{15}H_{20}O_3N_2$: C, 65.19; H, 7.30; N, 10.14. Found: C, 65.11; H, 7.25; N, 10.17.

The mass spectrum showed M + 276.34 (calculated, 276.3392); M − 1 275; *m/e* 261 (loss of methyl); *m/e* 154 as a main peak (M minus nitrophenyl); *m/e* 172 (*p*-nitrophenyl); *m/e* 68 (methylethynyl ketone?). The infrared spectrum showed no free hydroxyl and no NH group, with some indication of Bohlmann bands between 2500–2800 cm^{-1}. The n.m.r. data including those on spin decoupling are indicated in Fig. 4, curve 1.

*Dextrorotatory Oxazine (**10b**)*

The petroleum ether solution gave on evaporation a yellowish oil (0.88 g) which showed no tendency to crystallize after being distilled *in vacuo* (b.p. 154°, 29 μ) and kept in the refrigerator for weeks, alone or in petroleum ether. The infrared and ultraviolet spectra are not too distinct from the crystalline levorotatory stereoisomer, either. The n.m.r. indicates a basically similar spectrum except for the position and the pattern of the C-6 and C-2 protons (Fig. 4, curve 2). There is no more than 10% contamination of the (−)form in the oil, according to n.m.r. and vapor-phase chromatography (v.p.c.) (10% silicon rubber). Purification by t.l.c. on silica was not successful having led to decomposition. Equally important is the α_D^{20} +35.1° (*c*, 1.41; in dimethyl formamide) and α_D^{20} + 38.4° (*c*, 0.612) in another experiment. Optical rotatory dispersion measurement gave α_D^{20} +37.4° and α_D^{20} +111.5° (*c*, 2.4 in dimethyl formamide).

Anal. Found: C, 65.35; H, 6.96; N, 10.53.

The mass spectrum showed an identical pattern with that of the levorotatory oxazine (M +276.34). Nuclear magnetic resonance spectra were taken on Varian A-60, masss pectra with Varian M-66 apparatus, infrared spectra on the Beckman IR-4, optical rotatory dispersion and ultraviolet spectra on the JASCO model ORD/UV-5; g.l.c. on the F & M, model 770 automatic preparative gas chromatograph.

Acknowledgments

Microanalyses have been done by Mrs. I. Beetz (Germany). This project is being supported by the National Research Council of Canada under grant No. A-2839.

1. G. Fodor and G. A. Cooke. Tetrahedron Suppl. **8**, Part I, 113 (1966).
2. H. C. Beyerman and L. Maat. Rec. Trav. Chim. **82**, 1033 (1963).
3. H. C. Beyerman, L. Maat, A. van Veen, A. Zweistra, and W. von Philipsborn. Rec. Trav. Chim. **84**, 1367 (1965).
4. G. Fodor and E. Bauerschmidt. Unpublished results.
5. J. Sicher and M. Tichy. Collection Czech. Chem. Commun. **23**, 2081 (1958).
6. L. H. Goodson and H. Christopher. J. Am. Chem. Soc. **72**, 358 (1950).
7. G. Hardegger and H. Ott. Helv. Chim. Acta, **36**, 1186 (1953).
8. G. Fodor, J. Stefanovski, and B. Kurtev. Chem. Ber. **98**, 705 (1965).
9. J. A. Pople, W. G. Schneider, and H. J. Bernstein. High resolution nuclear magnetic resonance. McGraw-Hill, New York. 1959. Chap. 14. p. 389.
10. J. W. Emsley, J. Feeney, and L. H. Sutcliffe. High resolution nuclear magnetic resonance spectroscopy. Vol. 1. Pergamon, Oxford. 1965. Chap. 9.7. pp. 575–581, 704.
11. R. A. Wohl. Chimia Aarau, **18**, 219 (1964).

Can. J. Chem. Downloaded from www.nrcresearchpress.com by 210.87.254.105 on 09/05/12
For personal use only.

Cationic cyclization of bicyclic diterpenes[1]

O. E. EDWARDS AND R. S. ROSICH[2]
Division of Pure Chemistry, National Research Council of Canada, Ottawa, Canada

Received October 11, 1967

Manool and agathadiol cyclize in formic acid to the 13-epimeric pimara-8,15-dienes and 14α-hydroxyhibane derivatives. The mechanistic and biosynthetic implications of these results are discussed in relation to other work involving cations in tetracyclic diterpenes. The nuclear magnetic resonance spectra of relevant tricyclic and tetracyclic diterpenes are documented.

Canadian Journal of Chemistry, 46, 1113 (1968)

On general chemical considerations a very attractive biosynthetic route from geranylinalool to the tricarbocyclic and tetracarbocyclic diterpenes involves the bicyclic skeleton of type **1** as an intermediate (1). A logical possibility for further cyclization to pimaradienes (e.g. the resin acids) is ionization of the C—O bond of the allylic alcohol system, perhaps with pyrophosphate as the leaving group, to give ions of the type **2**. Electron flow as indicated would then

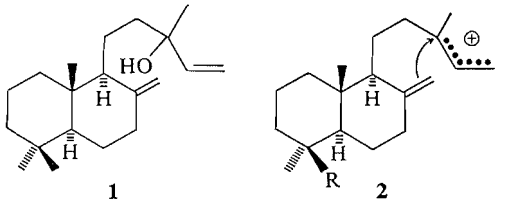

lead to cation **3**. Subsequent elimination of a proton could give the pimaradiene skeleton **4**. Alternatively, cation **3** could give rise to the tetracarbocyclic cation **5** (related to *enantio*-beyerane (hibane) (2) or isohibane (3)) by capture of the electrons of the vinyl group (4).[3]

Further rearrangement of this cation through the nonclassical ions **6** and **6***a* (4) could give the tetracarbocyclic kaurane, phyllocladane, and atisane skeletons. Elimination of a proton from **6** would give the pentacarbocyclic trachylobane (5) skeleton.

Until the present study no clear demonstration of these cyclizations has been reported.[4] However extensive studies of what has become known as the π-route to fused and bridged carbocyclic systems have recently been made (7).

Agathadiol (**7**) and manool (**1**) seemed excellent substrates for an *in vitro* study of the above cyclizations. Furthermore, the axial hydroxymethyl group at C-4 of agathadiol could prove valuable for subsequent building of the hetero ring of the diterpenoid alkaloids if tetracarbocyclic products were obtained. The cation **2** could be formed by solvolysis of an ester such as *p*-nitrobenzoate. However, the excellent model studies of Johnson and co-workers (8, see also ref. 7*b*) in cyclizations of allylic alcohols (e.g. **8** → **9**) suggested the use of formic acid on the allylic alcohols themselves.

In fact, a solution of agathadiol in 98–100% formic acid after 10 min at room temperature was converted almost completely to a mixture of products. This mixture was treated with lithium aluminium hydride to convert formates to alcohols, acetylated under mild conditions, and separated into three fractions (*a*, *b*, and *c*) by chromatography over alumina.

---

[1]NRCC No. 9970. Presented in part at the 150th Meeting, American Chemical Society, Atlantic City, September 1965.

[2]NRCC Post Doctorate Fellow 1964–1966.

[3]Wenkert (4*a*) suggested that pimara-8(14),15-dienes were discrete intermediates but no cyclizations of these have been achieved in the laboratory. A direct cyclization of cation **3** is a more attractive possibility.

[4]Bory and Asselineau (6) showed that manool was converted in H_2SO_4 – HOAc to a hydrocarbon mixture from which a very small yield of a tricyclic diene was characterized. Mme. Bory has informed us (letter dated November 24, 1965) that this hydrocarbon has been identified as sandaracopimara-8,15-diene (**10***c*).

Can. J. Chem. Downloaded from www.nrcresearchpress.com by 210.87.254.105 on 09/05/12
For personal use only.

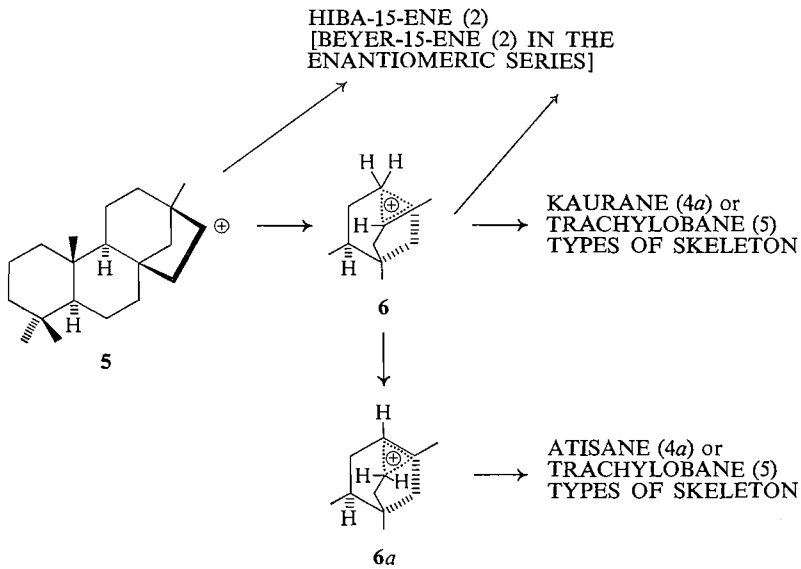

5 6 6a

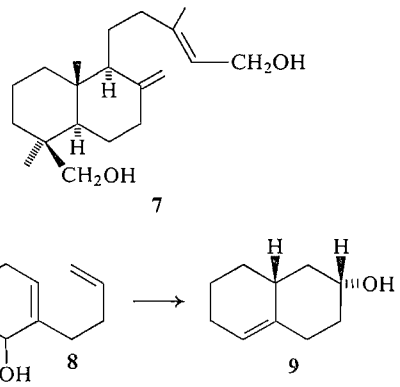

7 8 9

Similarly, a solution of manool[5] in 98—100% formic acid had completely reacted after 20 min. The reaction mixture was treated with lithium aluminium hydride and then directly separated into 3 fractions (*a*, *b*, and *c*) by chromatography.

Tricyclic Products

Fraction *a* of the products from agathadiol was separated into two components by chromatography over silver nitrate impregnated silica gel using the "dry column" technique (9). Their infrared and nuclear magnetic resonance (n.m.r.) spectra were consistent with structures **10***a* and **11***a*. Their mass spectra (parent ion *m/e* 330)

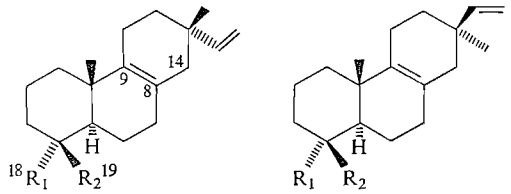

10 **11**

10 *a* $R_1 = CH_3$; $R_2 = CH_2OAc$
b $R_1 = COOCH_3$; $R_2 = CH_3$
c $R_1 = R_2 = CH_3$

11 *a* $R_1 = CH_3$; $R_2 = CH_2OAc$
b $R_1 = COOCH_3$; $R_2 = CH_3$
c $R_1 = R_2 = CH_3$

were identical to each other and similar in their fragmentation pattern to that recorded[6] for methyl isopimara-8,15-diene-18-oate (**10***b*)[7] (methyl sandaracopimarate). The configurations at

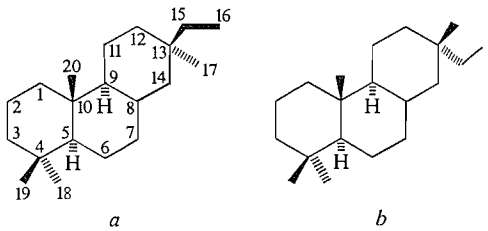

a *b*

[5]A sample of manool was obtained from Koch-Light Laboratories. After careful chromatography the product had m.p. 48–51° and the infrared and nuclear magnetic resonance spectra indicated that it was essentially pure. (Most important, this showed the absence of any of the reaction products that are to be described.)

It is of interest to note that the crude manool, which Mr. D. J. Abbot of Koch-Light Laboratories has kindly informed us came from solvent extraction of the heartwood of Dacrydium biforme, contained a small amount (ca. 2–3%) of a hydrocarbon which appeared to be 13α-pimara-7,15-diene (isopimaradiene).

[6]The mass spectra of the 8,15-dienes are more complicated than those of the 8(14),15-dienes (10).

[7]We are using the names pimarane and isopimarane (formerly sandaracopimarane) for the parent hydrocarbons *a* and *b* respectively.

Can. J. Chem. Downloaded from www.nrcresearchpress.com by 210.87.254.105 on 09/05/12
For personal use only.

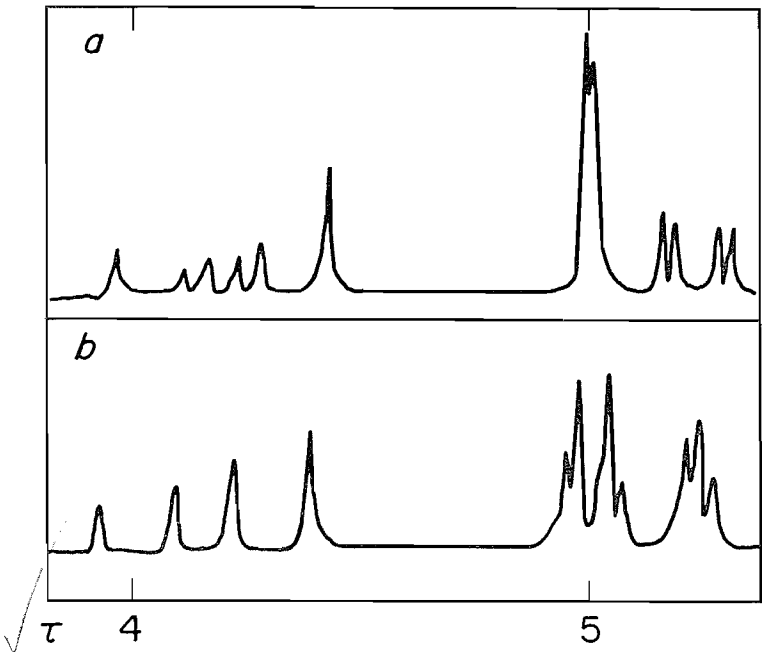

FIG. 1. Vinyl proton absorption patterns: (*a*) isopimara-8,15-diene and its 18- or 19- derivatives, and pimara-8(14),15-diene and its 18- derivatives; (*b*) pimara-8,15-diene and its 18- or 19- derivatives, and isopimara-8(14),15-diene and its 18- derivatives.

C-13 were tentatively assigned by comparison of the vinyl proton signals in their n.m.r. spectra with those of isopimara-8,15-diene and pimara-8,15-diene derivatives (**10***b* and **10***c*, and **11***b*, **11***c* respectively), (see Fig. 1). It is intriguing that moving the double bond from the 8(14) to 8(9) positions or inverting the configuration at C-13 interchanges the vinyl hydrogen patterns.

Confirmation of the structures followed from conversion to known hydrocarbons (11) by reductive cleavage of the ester, oxidation to the aldehydes, conversion to the semicarbazones, and finally Wolff–Kishner reduction. Compound **10***a* gave isopimaradiene (**10***c*) while **11***a* gave pimara-8,15-diene (**11***c*), identified by comparison with authentic specimens.

Fraction *a* of the manool products had an n.m.r. spectrum consistent with an approximately equal mixture of pimara-8,15-diene and its 13-epimer. However, the mixture could not be separated by either thin-layer chromatography (t.l.c.) or column chromatography as used above. Gas–liquid chromatography (g.l.c.) showed the presence of nearly equal amounts of two components with the expected relative retention times (11).

Since approach to the α face of the exocyclic double bond is sterically much more favorable than to the β face, the transition states for the cyclization of cations of type **2** probably resemble **12***a* and **12***b* respectively. The formation of equal amounts of the 13-epimeric dienes must then reflect similar steric requirements of the methyl and vinyl groups in the transition states.

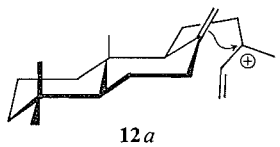

12*a*

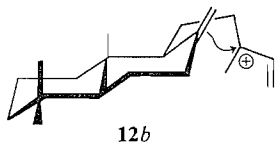

12*b*

The known resin acids of the pimaric family all have their nuclear double bonds in the 7(8) or 8(14) position in contrast to the 8(9) double bond produced in the above experiments.[8] Hence if the *in vivo* cyclizations follow a comparable course to the above cyclization, the enzyme

[8]It was demonstrated that the 7(8) and 8(14) double bonds did not migrate to the 8(9)-position in formic acid under the reaction conditions.

surface must present a unique basic site aiding removal of a 7- or 14-proton.

Tetracyclic Products

Fraction *b* from the agathadiol cyclization products was converted to the alcohol using lithium aluminium hydride. Chromatography on alumina then enabled isolation of a crystalline product (ca. 5% yield) analyzing for $C_{20}H_{34}O_2$ (mol. wt. by mass spectrum 306). This gave no color with tetranitromethane and had only weak end absorption in the ultraviolet (ε at 210 mμ = 80). Its n.m.r. spectrum showed no vinylic proton signals but showed resonance for 3 quaternary methyl groups, a $—CH_2OH$ group on a quaternary carbon, and a *HC*—OH group as a sharp singlet. Hence the compound appeared to be tetracyclic and to have a hibane (**13**) or isohibane (**14**) skeleton.

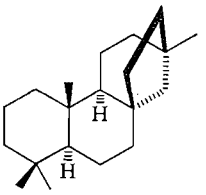

13

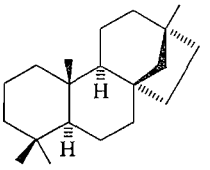

14

The diol was oxidized to the keto-aldehyde which showed the expected infrared and n.m.r. spectra (see Table II). Reduction of the keto-aldehyde under vigorous Wolff–Kishner conditions gave hibane, identified by comparison with an authentic sample (2b).[9] Thus the cyclization product must have structure **15***a* (14-hydroxyl configuration undefined).

Fraction *b* from the cyclization of manool was a combination of eluates whose n.m.r., m.p., and t.l.c. indicated the presence of a single monohydroxy compound **15***b*. Only 40% acetylation of this alcohol was achieved when it was treated with acetic anhydride in pyridine at room temperature for 17 h; but treatment with acetic anhydride in acetic acid containing a trace of *p*-toluenesulfonic acid resulted in complete acetylation. Its mesylate was prepared by treatment with methanesulfonyl chloride in pyridine.

The n.m.r. spectra of these three compounds (alcohol, acetate, and mesylate) each showed signals for four quaternary methyl groups and a single unsplit ($w_{1/2}$ 3 c.p.s.) H—C—O— proton, but gave no indication of unsaturation.

Oxidation of the alcohol **15***b* gave the ketone **16** which was then reduced under Wolff–Kishner conditions to give a hydrocarbon identical with a sample of hibane (**13**).[9] Since the oxygenated carbon atom appeared to be attached to fully substituted carbon atoms (unsplit C*H*OH signal) the alcohol arising in the cyclization reaction must be a 14-hydroxyhibane. In addition, the circular dichroism curve[10] for the ketone **16** showed a negative Cotton effect, in agreement with the proposed formula.

It appeared that we had obtained only one hydroxy isomer since it was considered unlikely that the physical data, especially the n.m.r. spectra, would be the same for both epimers of the alcohol, its acetate, and its mesylate respectively.

An attempt was made to prepare the epimeric alcohol **15***c* by reduction of the ketone. However, reaction with lithium aluminium hydride, lithium tri-*t*-butoxy aluminohydride, or lithium in ethylamine each converted it to an apparently single component identical (t.l.c., n.m.r., m.p., mixture melting point, and *x*-ray powder patterns) with each other and with the cyclization product itself. Furthermore, the acetate of the lithium tri-*t*-butoxy aluminohydride reduction product was identical with the acetate of the original alcohol.

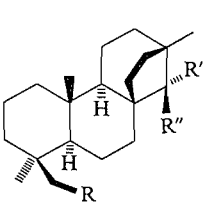

15 *a* R = R′ = OH R″ = H
b R = R″ = H R′ = OH
c R = R′ = H R″ = OH

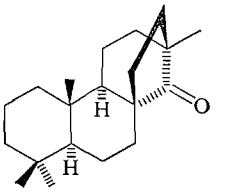

16

Attempts to displace the mesylate of **15***b* with sodium formate in dimethyl formamide or sodium azide in dimethyl formamide, at temperatures up to 125° for up to 2.5 days, were unsuccessful. There was no reaction when the mesylate of **15***b* was heated for 3 days in refluxing aqueous acetone containing sodium acetate. On the other hand, heating overnight in refluxing formic acid

[9]A sample was kindly supplied by Dr. Y. Kitahara.

[10]Obtained through the kind cooperation of Professor R. C. Cookson.

Can. J. Chem. Downloaded from www.nrcresearchpress.com by 210.87.254.105 on 09/05/12
For personal use only.

Can. J. Chem. Downloaded from www.nrcresearchpress.com by 210.87.254.105 on 09/05/12
For personal use only.

containing sodium formate converted the mesylate in part to the formate of the starting alcohol.

The fact that all the chemical reductions of the 14-ketone yield the same alcohol indicates that this arises from "product development control" (12). Consequently, this alcohol is the least hindered of the two 14-epimers. Similarly the S_N1 solvolyses of the mesylate should have given rise to the least hindered formate (most favored approach of formate ion). Molecular models (Dreiding, Fieser) suggest that the 14α-epimer is the least hindered of the two, hence we assign this configuration to the 14-hydroxyhibanes. This assignment is also consistent with mechanistic considerations (see below). We conclude that agathadiol gave 14α,19-dihydroxyhibane (**15***a*) and manool gave 14α-hydroxyhibane (**15***b*).

Careful examination of fractions *c* of the cyclization products of manool or agathadiol, and the polar fractions of the hydrolyzate of fraction *b* from agathadiol failed to reveal any recognizable products. The materials were complex mixtures which appeared to consist largely of products of hydration of the double bonds and of rearrangement of the C-4 substituents in agathadiol. No evidence was obtained for the formation of the triene alcohol communol (**17**) (13) or its isomer **18** (14).

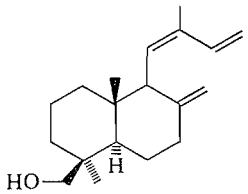

17

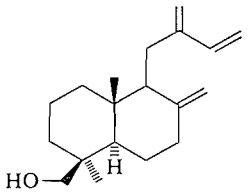

18

Discussion

Examination of molecular models leads us to the conclusion that the observed hibane derivatives are the most likely tetracyclic products to form by cationic cyclization. The preferred conformation for cyclization of the pimaric cation is illustrated in A.

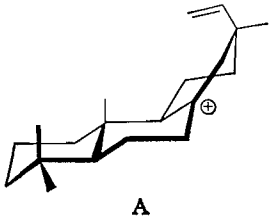

A

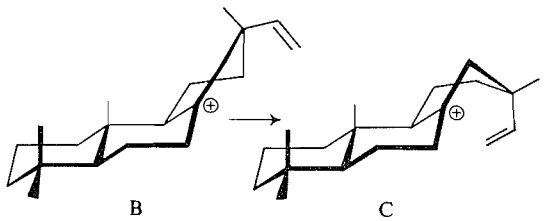

B C

In contrast, the isopimaric cation B, which would lead to the isohibane series (**14**), cannot cyclize until it has adopted the boat conformation C.

As the transition state, for cyclization of A, develops toward tetracyclic cation, the lowest electron density on C-16 is on its *exo* side (see D).

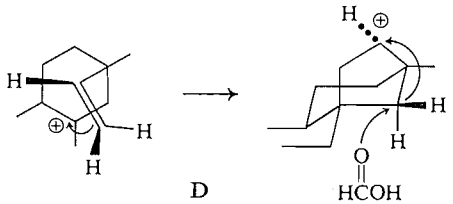

D

This suggests that the developing secondary cation, in this medium of low nucleophilicity (formic acid) is stabilized by bridging[11] from C-14. Formic acid would then complete the process by attack on the opposite face of C-14, leading to the prediction that the secondary hydroxyls in **15***a* and **15***b* have the configuration illustrated. As indicated earlier, this is in accord with other evidence.

While transannular hydride migrations in consort with solvolyses etc. in bridged and medium ring systems are well established (15) a precise analogue of this migration in a bicyclo[3·2·1] system has apparently not been observed previously. However, the above route to the tetracyclic product gives an elegant explanation of the predominant hibane geometry (rather than iso-hibane) that was observed.

Two alternate routes to 14-oxygenated hibane follow. Pimara-8(14),15-dienes are not appreciably transformed into the Δ^8 isomers under our reaction conditions. Therefore, since nearly equal amounts of 13-epimers are formed and no isopimara-8(14),15-diene was found, the amount of the 13β isomers available for cyclization must

[11]For comparable 2 → 6 hydride shifts in norbornyl compounds, there is evidence that a protonated cyclopropane is an intermediate (15*a*), i.e. carbon–carbon participation provides the initial charge delocalization.

Can. J. Chem. Downloaded from www.nrcresearchpress.com by 210.87.254.105 on 09/05/12
For personal use only.

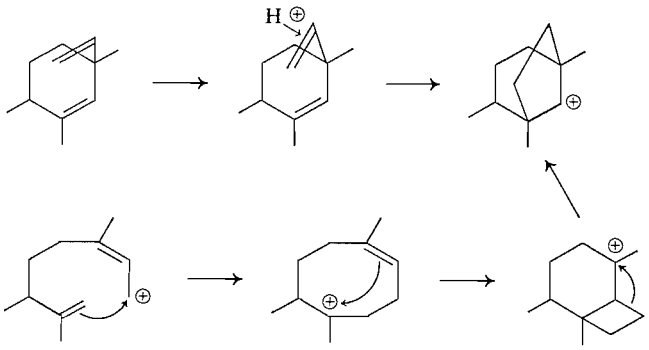

have been small. Hence if route (*a*) were operative it would have to be very efficient. Experiment showed however that the 8(14),15-dienes did not give detectable amounts of 14-oxygenated hibanes under our cyclization conditions, hence (*a*) can be eliminated from consideration.

Route (*b*) is implausible because: (1) The allylic cation will have most of its charge density on the tertiary carbon. (2) Cationic cyclization to an eight membered ring is improbable unless under enzyme control. (3) Cyclization of the cyclooctenyl cation to the 6,4 system should, because of steric interactions with the 10-methyl group, give predominantly the isohibane skeleton contrary to what is observed.

It is of interest to compare the proposed fate of the cation on C-16 with that of cations formed on that carbon by alternative processes. McCrindle and colleagues (16) described the hydrogen chloride catalyzed conversion of beyer-15-ene (**19**) in aprotic solvents to a mixture of (—)kaur-15-ene **20**, (—)kaur-16-ene (isokaurene), and atis-16-ene. Sobti and Sukh Dev (17) found that solvolysis of 16β-tosyloxybeyer-

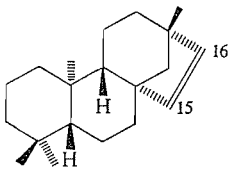

19

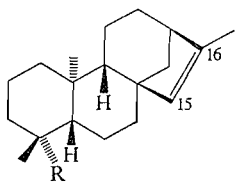

20

ane (**21**) gave (—)kaur-15-ene, (—)isokaurene and kauran-16α-ol. Ghisalberti and Jefferies (18) studied the solvolysis of the related tosylate **22** obtaining the substituted kaurene and isokaurene. Kapadi and Sukh Dev (19*a*) treated 15β, 16β-epoxybeyerane (**23**) with boron trifluoride

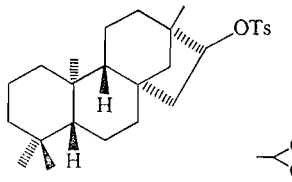

21

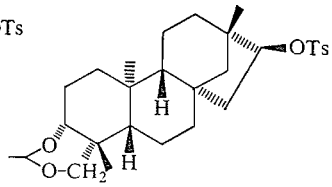

22

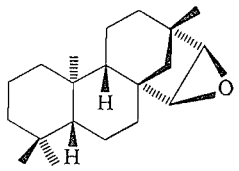

23

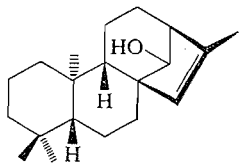

24

etherate. The product was a mixture of 14-hydroxykaur-15-ene (**24**) and the corresponding 16-ene. Similar observations have been made by Hanson (19*b*) and Kitahara and colleagues (19*c*).

In each of these cases the major electron deficiency developed initially on the *endo* size of C-16, in contrast to the situation in our cyclization studies. This was ideal for participation of the 12,13 C—C bond leading to ions of type **25** from which the kaurane cation **26** arose.

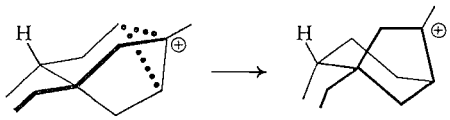

25 26

At present then, the 14 → 16 hydride shift mechanism seems the most plausible route to the 14-oxygenated hibanes but further work is needed to test the hypothesis.

A most interesting related study is that of Ourisson and co-workers (20) on the acid-

TABLE I

Methyl group absorptions in τ units

	—CH_3	Hydrocarbon	19-OH	19-OAC	19-oxo	19R*
Isopimara-8,15-diene	4	9.12, 9.15	9.02	9.04	8.98	8.95
	10	9.04	9.06	9.04	9.16	9.18
	13	9.04	9.04	9.04	9.03	9.04
Pimara-8,15-diene	4	9.12, 9.15	9.01	9.03	8.97	8.97
	10	9.04	9.07	9.03	9.16	9.18
	13	9.07	9.07	9.07	9.08	9.08
	—CH_3	Hydrocarbon	18-OH	R′†	18-oxo	18-R*
Isopimara-8(14),15-diene	4	9.13, 9.14	9.20	8.81		8.90
	10	9.20	9.16	9.17		9.15
	13	8.96	8.96	8.97		8.97
Pimara-8(14),15-diene	4	9.13, 9.15	9.20	8.81	8.92	8.90
	10	9.27	9.22	9.21	9.21	9.20
	13	9.02	9.01	9.01	9.01	9.01

*R = semicarbazone.
†R′ = equatorial 4-methoxycarbonyl.

catalyzed reactions of trachylobane (**27**). However these seem readily accounted for as reactions of edge-protonated cyclopropanes.

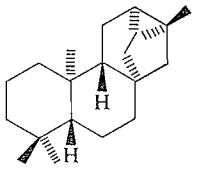

27

Table I summarizes the methyl group absorptions in the n.m.r. spectra of the pimaradienes encountered in this work. Some of the figures for the 8(14),15-dienes (e.g. **4**) have been reported by Wenkert *et al.* (21), but there appears to be an error in the assignments of the signals of pimara-8(14),15-diene. On the basis of Wenkert's assignments, inversion at C-13 to isopimara-8(14),15-diene results in a large shift of one of the C-4 methyl groups. No other such large shift is apparent in derivatives of these hydrocarbons or in the series of 8,15-dienes described in this paper.

The structures of the acetoxy pimaradienes **10***a* and **10***b* described earlier were also supported by other features of their n.m.r. spectra. The center of the pair of doublets arising from the 19-protons in the acetates **10***a* and **10***b* falls at τ 5.85 and 5.86 (*J*, 11 c.p.s.) respectively; in the derived alcohols at τ 6.37 and 6.36 (*J*, 11 c.p.s.); and in the derived aldehydes at τ 0.21 and 0.24 (*J*, 1.2 c.p.s.). These figures are in close agreement with the corresponding absorptions for analogous axial C-4 oxygenated compounds and quite different from the corresponding equatorial C-4 oxygenated derivatives (including those derived from isopimara-8(14),15-diene and pimara-8(14),15-diene-18-oic acids (2*a*, 21, 22).

In the 8(14),15-dienes epimerization at C-13 causes a shift of 0.04–0.06 p.p.m. in the 13-methyl group signal while a similar shift of 0.03–0.05 p.p.m. is observed in the 8,15-dienes. On the other hand, epimerization at C-13 in the 8(14),15-dienes causes a shift of 0.04–0.07 p.p.m. of the 10-methyl group signal whereas in the 8,15-dienes essentially no change in this absorption occurs. The shift to lower field of the 10-methyl signal when the 8(14)-olefin is isomerized to 8(9) is similar to that observed in the steroids (23) and bicyclic diterpenes (24).

Table II summarizes the data for methyl group absorptions relevant to the 14-substituted hibane product.

Insertion of the 14α-hydroxyl group into hibane (*enantio*-beyerane) or its 19-hydroxy derivative has very little effect on the protons attached to C-17 and C-20. A similar behavior is shown by 16β-hydroxybeyerane. The deshielding effect by the 14-ketone group on the protons on C-17 and C-20 would be expected for the structure assigned. In contrast, a 14-ketone in the kaurane series results in a shielding effect, of approximately 0.14 p.p.m., on the 20-protons (19*a*) and a similar effect would be expected for a 14-oxoisohibane structure.

Can. J. Chem. Downloaded from www.nrcresearchpress.com by 210.87.254.105 on 09/05/12
For personal use only.

TABLE II

Methyl group absorptions in τ units

	C-18,C-19	C-20	C-17
16α-(—)-Kaurane	9.15, 9.19	8.99	9.09
Isohibane	9.13, 9.18	9.00	8.99
Beyerane (*enantio* hibane)	9.15, 9.19	9.06	9.06
14α-Hydroxyhibane	9.15, 9.19	9.08	9.08
19-Hydroxybeyerane (calcd)*	9.05	9.08	9.06
14α-19-Dihydroxyhibane	9.05	9.08	9.08
16β-Hydroxybeyerane†	9.14, 9.18	9.06	9.09
14-Oxohibane	9.14, 9.18	8.96	9.01
19-Oxobeyerane (calcd)*	9.01	9.21	9.06
14,19-Dioxohibane	9.00	9.11	8.99
14α-Acetoxyhibane	9.15, 9.19	9.15	9.06
14α-Mesyloxyhibane	9.14, 9.20	9.06	8.98

*Calculated from the known effect of insertion of these substituents into the beyerane skeleton (2*a*, 22). Additivity of these effects is observed when (*i*) there are no conformation differences between the singly- and multisubstituted molecules, and (*ii*) no dipolar or hydrogen bonding interactions occur between these substituents (2*a*, 22, see also ref. 25).

†Unpublished observations in this laboratory.

The 14β-proton absorbs at τ 7.07, 5.55, and 5.89 in the alcohol **15***b*, its acetate, and its mesylate respectively with a $w_{1/2}$ of 3 c.p.s. in each case.

Experimental

Infrared spectra were of Nujol mulls unless otherwise specified and nuclear magnetic resonance (n.m.r.) spectra were determined for deuteriochloroform solutions with tetramethylsilane as internal reference. Optical rotations are of solutions in absolute alcohol unless otherwise noted. Woelm neutral alumina was used for chromatography.

Agathadiol as Substrate

Cyclization of Agathadiol in Formic Acid

Finely powdered agathadiol (2.57 g), prepared by reduction of methyl agathate by lithium aluminium hydride, was dissolved in 98–100% formic acid (200 ml). After 10 min at room temperature (ca. 25°) the solution was poured into a slurry of ice and water containing potassium hydroxide (330 g), extracted with ether, washed with saturated sodium bicarbonate solution, dried, and the volume of the solution reduced to approximately 100 ml. After addition of lithium aluminium hydride, the solution was refluxed for 15 min. The excess reagent was destroyed with a saturated solution of sodium sulfate, the solution dried and then evaporated, leaving a pale-yellow gum (2.49 g).[12] The gum was then acetylated during 2 days in acetic anhydride – pyridine at room temperature. The resulting pale-yellow oily acetate was dissolved in hexane and chromatographed over 50 g of activity III alumina. Elution with hexane (400 ml) gave fraction *a* (1.84 g); hexane–benzene (4:1, 600 ml.) eluted fraction *b* (0.65 g); and finally ether eluted fraction *c* (0.43 g), as colorless oils.

[12]Preliminary experiments had shown that the crude cyclization product was at least partially formylated.

Tricyclic Products

The infrared spectrum of fraction *a* showed the absence of any hydroxylic material. The fraction (900 mg) was chromatographed using the "dry column" technique (9) over 300 g of silica gel impregnated with 75 g of silver nitrate. Hexane–ether (3:1) was used as eluent and 15 ml fractions were collected. The composition of the eluate was determined using vapor-phase chromatography (v.p.c.).[13] Fractions 1–16, 57 mg of oils containing at least 6 components; fractions 17–22, 240 mg of crystals mainly component 1; fractions 23–25, 96 mg of oily mixture of 1 and 2; fractions 26–44, 200 mg of crystals, mainly component 2; fractions 45–155, 105 mg of oils rich in component 2. The balance of fraction *a* combined with fractions 23–25 from the above chromatogram was separated in the same way. The total isolated yields were then 510 mg of component 1 and 440 mg of component 2. However, the total yields estimated using the v.p.c. of the mixed fractions was approximately 600 mg of each component.

19-Acetoxy-isopimara-8,15-diene—Crude component 1 from above chromatogram was recrystallized from aqueous methanol and then sublimed at 115° and 0.02 mm; m.p. 57.5–58.5°; $[\alpha]_D$ +90° (*c*, 0.9). ν_{max}: 1742 cm^{-1} (ester); 3075, 1638, and 906 cm^{-1} (vinyl group). The position of the last band is in agreement for the data of Ireland and Schiess (11*a*) for similar isopimaradienes. The n.m.r. data (see the appropriate section of the discussion) was in agreement with the structural proposals.

Anal. Calcd. for $C_{22}H_{34}O_2$(mol. wt., 330.49): C, 79.95; H, 10.4. Found (mol. wt., mass spectrum, 330): C, 79.8; H, 10.2.

19-Hydroxy-isopimara-8,15-diene—The acetate (445 mg) was treated with excess lithium aluminium hydride during 1 h at room temperature. Working up in the usual

[13]Vapor-phase chromatography was at 200° with a flow rate of 100 ml/min, over a 1 m 15% diethylene glycol succinate on chromosorb W column, in a Perkin–Elmer model 154C gas chromatograph.

Can. J. Chem. Downloaded from www.nrcresearchpress.com by 210.87.254.105 on 09/05/12
For personal use only.

Can. J. Chem. Downloaded from www.nrcresearchpress.com by 210.87.254.105 on 09/05/12
For personal use only.

way, followed by filtration through 12 g of activity III alumina in hexane–benzene (1:1) gave the alcohol as a colorless solid (335 mg). After recrystallization from aqueous-methanol and sublimation at 125° and 0.02 mm this had m.p. 107–108.5°; $[\alpha]_D$ +101° (*c*, 0.18). ν_{max}: 3240 cm^{-1} (hydroxyl) and 3070, 1637, 1001 and 909 cm^{-1} (vinyl group). The n.m.r. data showed the presence of an axial hydroxymethyl group, three quaternary methyl groups, and the vinyl group (see also the appropriate section of the discussion).

Anal. Calcd. for $C_{20}H_{32}O$: C, 83.3; H, 11.2. Found: C, 82.4, 82.5; H, 11.0, 11.1.

19-Oxo-isopimara-8,15-diene and its semicarbazone—The alcohol (145 mg) was dissolved in acetone (10 ml), the solution cooled in ice, and then titrated with Jones' reagent (26). The mixture was poured into water and worked up with ether in the usual way to give the crystalline aldehyde (130 mg), $\nu_{max}(CCl_4)$: 1720 cm^{-1} (aldehyde) and 915 and 1002 cm^{-1} (vinyl group). The n.m.r. spectrum included a peak at τ 0.21 (axial aldehyde proton) as a partially resolved doublet, with *J*, ca. 1.2 c.p.s.

The semicarbazone was prepared in pyridine (10 ml). using a solution of semicarbazide acetate (from 300 mg of semicarbazide hydrochloride and 300 mg of sodium acetate which were dissolved in 0.5 ml of water and 9.5 ml of ethanol) during 2 days at room temperature (27). The mixture was worked up with ether in the usual manner to give 145 mg of the crystalline semicarbazone which was recrystallized first from hexane – ethyl acetate and then from aqueous methanol to give sheaves of colorless needles, m.p. 215°. The n.m.r. spectrum included a maximum at τ 2.97 (—CH=N).

Anal. Calcd. for $C_{21}H_{33}N_3O$: C, 73.4; H, 9.7; N, 12.2. Found: C, 73.6; H, 9.75; N, 12.1.

Isopimara-8,15-diene—The semicarbazone (120 mg) and 5 g of KOH in diethylene glycol (17 ml) were refluxed for 3 h at 200–205° under a nitrogen atmosphere. The mixture was poured into water and worked up with hexane to give 92 mg of a pale-yellow oil which was then chromatographed on 5 g of activity II alumina in 35 ml of hexane to yield 76 mg of a colorless solid. This material gave a single peak on gas chromatography which had the same retention time as an authentic sample (prepared as described by Ireland and co-workers (11)). After recrystallization from methanol and sublimation at 80° and 0.02 mm the material showed m.p. 51–52.5°, $[\alpha]_D$ +119° (*c*, 0.92) undepressed on admixture with an authentic sample.

Anal. Calcd. for $C_{20}H_{32}$ (mol. wt., 272.46): C, 88.2; H, 11.8. Found (mol. wt., 272, mass spectrum): C, 88.4; H, 11.7.

Identity was also established by the infrared (liquid film) (ν_{max} 3078, 1638, 907 cm^{-1}) and n.m.r. spectra and *x*-ray powder patterns.

19-Acetoxypimara-8,15-diene—Crude compound 2 from the above chromatogram was recrystallized from aqueous methanol; m.p. 66–68°, $[\alpha]_D$ +67° (*c*, 0.17). It had ν_{max}: 1745 cm^{-1} (ester); 3080, 1636, and 908 cm^{-1} (vinyl group). The n.m.r. data was in agreement with the structural proposals (see Fig. 1 and Table I).

Anal. Calcd. for $C_{22}H_{34}O_2$ (mol. wt., 330.49): C, 79.95; H, 10.4. Found (mol. wt., 330, mass spectrum): C, 79.7; H, 10.4.

The same sequence was used to prepare the hydrocarbon as for component 1.

19-Hydroxypimara-8,15-diene—After recrystallization from aqueous-methanol this had m.p. 95–97°; $[\alpha]_D$ +78° (*c*, 0.92); ν_{max}, 3369 cm^{-1} (hydroxyl) and vinyl absorption at 3075 and 906 cm^{-1}.

Anal. Calcd. for $C_{20}H_{32}O$: C, 83.3; H, 11.2. Found: C, 83.4; H, 11.0.

Semicarbazone of 19-oxopimara-8,15-diene—The aldehyde was obtained as an oil, $\nu_{max}(CCl_4)$, 1720 cm^{-1} (aldehyde) and 910 and 998 cm^{-1} (vinyl group); while the n.m.r. spectrum included a peak at τ 0.24 (axial aldehyde proton). This signal was a poorly resolved doublet with *J*, ca. 1.2 c.p.s.

The semicarbazone was obtained as plates from aqueous-methanol and had m.p. 192°. The n.m.r. spectrum included a maximum at τ 2.85 (—CH=N—).

Anal. Calcd. for $C_{21}H_{33}N_3O$: C, 73.4; H, 9.7; N, 12.2. Found: C, 73.25; H, 9.5; N, 12.1.

Pimara-8,15-diene—The diene was obtained as a colorless oil which was distilled at 85° and 0.02 mm. Identity with an authentic sample (prepared as described in 11) was established by infrared (liquid film) (ν_{max} 3075, 910 cm^{-1}), n.m.r., and mass spectra and gas chromatography.

Anal. Calcd. for $C_{20}H_{32}$ (mol. wt., 272.46): C, 88.2; H, 11.8. Found (mol. wt., 272, mass spectrum): C, 88.1.; H, 11.7.

Tetracyclic Product

Hiban-14α,19-diol—Fraction *b* from the cyclization sequence showed no hydroxyl or vinyl absorption in its infrared spectrum.

Fraction *b* (600 mg) was dissolved in ether and treated with excess lithium aluminium hydride and after the usual work-up a glass (470 mg) was obtained which was dissolved in hexane–benzene (2:1) and chromatographed on activity IV alumina. Benzene–ether (19:1) eluted a crystalline material (147 mg)[14] which after recrystallization from hexane–acetone had m.p. 204° $[\alpha]_D$−10° (*c*, 0.18). There was only end absorption in the ultraviolet (ε = 80 at 210 mμ in 95% ethanol solution) and no color was obtained with tetranitromethane. The n.m.r. spectrum ($CDCl_3$ and pyridine solutions) showed the presence of three quaternary methyl groups, a —C—C*H*$_2$OH (quartet centered at τ 6.40) and a *H*—C—OH group (singlet at τ 7.09) but no olefinic protons.

Anal. Calcd. for $C_{20}H_{34}O_2$ (mol. wt., 306.47): C, 78.4; H, 11.2. Found (mol. wt., 306, mass spectrum): C, 78.2; H, 11.0.

Hibane—Hiban-14α,19-diol (90 mg) was dissolved in acetone (10 ml) and titrated with the Jones reagent (26), the mixture poured into water, and extracted with ether to give the crystalline 14,19-dioxohibane (80 mg), ν_{max} (CCl_4) (measured on a Perkin–Elmer model 21 spectrometer), 2740 and 1737 cm^{-1} (aldehyde) and 1725 cm^{-1} (ketone). The n.m.r. spectrum showed the presence of three quaternary methyl groups, and an axial aldehyde

[14]From subsequent work in the manool series it became known that acetylation of the 14α-hydroxyl is only approximately 70% complete under the conditions used in the work-up of the product from cyclization of agathadiol. Hence the "true" yield of this diol may be nearer 200 mg (i.e., 7–8%).

Can. J. Chem. Downloaded from www.nrcresearchpress.com by 210.87.254.105 on 09/05/12
For personal use only.

group (τ 0.22, poorly resolved doublet with J, ca. 1.2 c.p.s.).

The keto-aldehyde (70 mg) was refluxed with diethylene glycol (8 ml) and 95% hydrazine (1 ml) for 1½ h under a nitrogen atmosphere. The solution was cooled and pieces of sodium (1 g) added slowly followed by a further 5 ml of diethylene glycol and the mixture refluxed at 220° for 3.5 h, then poured into water and extracted with hexane. A pale-yellow oil (43 mg) was obtained which was chromatographed over activity II alumina in hexane yielding a colorless oil (31 mg) which crystallized on seeding with authentic hibane.[9]

After recrystallization from methanol this had m.p. 39–41.5°, raised to 39–42.5° on admixture with authentic material (m.p. 41–43°). Identity was also established by infrared (measured on a Perkin–Elmer model 21 spectrometer), n.m.r., and mass spectra, and by x-ray powder patterns.

Manool as Substrate

Cyclization of Manool in Formic Acid

Finely powdered manool[15] (6.40 g) was shaken with 98–100% formic acid (100 ml; ca. 0.2 M) for 20 min at room temperature (ca. 25°). All of the solid dissolved within 5 min while an oil began to separate. The mixture was poured onto ice and water containing sodium hydroxide (146 g) and extracted with ether. The residue (6.21 g) was a pale-yellow oil whose n.m.r. spectrum showed the presence of at least some formate group. The ultraviolet spectrum (cyclohexane) had a shoulder near 230 mμ, ε 320 (biformene had λ_{max} 228 mμ $\varepsilon = 15\,300$ (28)). The residue was redissolved in ether and treated with excess lithium aluminium hydride at room temperature for 30 min. Extraction in the usual manner gave a pale-yellow oil (5.98 g) which was dissolved in hexane and chromatographed on 100 g of activity III alumina. Hexane eluted a colorless oil ((4.29 g) fraction *a*) while hexane–benzene (9:1) eluted several crystalline fractions whose melting points and thin-layer chromatograms indicated a single component (fraction *b*; 675 mg).

Tricyclic Product

Isopimara-8,15-diene and pimara-8,15-diene—The n.m.r. spectrum of fraction *a* was that expected of an approximately equal mixture of the two hydrocarbons. The mixture, however, could not be separated. Gas–liquid chromatography on a 6 ft column of 15% diethylene glycol succinate on chromosorb W at 125 °C and flow rate of 20 ml/min (using an F and M model 700 with flame ionization detector) showed the presence of isopimar-8,15-diene and pimara-8,15-diene in the ratio 55:45 (±5%). These were identified by their relative retention times (11) and peak enhancement with authentic materials.

Tetracyclic Products

Hiban-14α-ol—A sample of fraction *b* was recrystallized from aqueous methanol and sublimed at 125° and 0.1 mm; m.p. 114–115°, $[\alpha]_D$ −6° (*c*, 0.91). ν_{max}($CHCl_3$) 3620 cm^{-1} (OH). The n.m.r. spectrum included a singlet at τ 7.58 (H—C—OH).

[15]This had m.p. 48–51° and its infrared and n.m.r. spectra showed it to be free of any of the reaction products to be described below. We thank Professor G. Buchi for a reference sample of crystalline manool.

Anal. Calcd. for $C_{20}H_{34}O$: C, 82.7; H, 11.8. Found: C, 82.55; H, 11.6.

Hiban-14-one—Hiban-14α-ol (209 mg) was dissolved in acetone (20 ml) and titrated with Jones' reagent (26). The mixture was poured into water and extracted with ether to give a pale-yellow solid (202 mg) which was dissolved in hexane and chromatographed on 5 g of activity III alumina to give a colorless solid (140 mg). After recrystallization from aqueous methanol and sublimation at 115° and 0.1 mm it had m.p., 107–108°, ν_{max} 1733 cm^{-1}, $[\alpha]_D$ +11° (*c*, 0.15).

Anal. Calcd. for $C_{20}H_{32}O$: C, 83.3; H, 11.2. Found: C, 83.25; H, 11.1.

Circular dichroism[10] λ_{max} 297 mμ (ΔE − 1.8).

Hibane—Sodium (400 mg) was dissolved in diethylene glycol (15 ml) under a nitrogen atmosphere. Ninety-five percent hydrazine (2.0 ml) and hiban-14-one (85 mg) were added, the mixture refluxed at 180° for 2 h, the temperature then raised to 217° by distillation, and reflux continued for 2 h. The mixture and the distillate were then poured into water and extracted with hexane to give a colorless oil (75 mg). The oil was chromatographed on activity III alumina in hexane (20 ml) to give a colorless oil (73 mg) which crystallized from methanol; m.p. 41.5–43.5°, undepressed on admixture with a recrystallized authentic sample, m.p. 41.5–43.5°. Identity was also established by infrared (liquid film) and n.m.r. spectra and x-ray powder patterns.

Hiban-14α-yl acetate—Hiban-14α-ol (93 mg) was treated with acetic anhydride (2.0 ml) and pyridine (4.5 ml) for 17 h at room temperature (ca. 25°). Working up in the usual way gave a partly solid residue whose n.m.r. spectrum showed only about 40% acetylation. The residue was treated with acetic anhydride (1.5 ml), acetic acid (3 ml) and *p*-toluenesulfonic acid (100 mg) at room temperature overnight. Extraction with ether yielded the acetate (95 mg). This was chromatographed on 5 g of activity III alumina with hexane (70 ml) to give 94 mg of material which after recrystallization from aqueous methanol and sublimation at 105° and 0.1 mm had m.p. 85–86°, ν_{max} 1742 cm^{-1}. The n.m.r. spectrum included a singlet at τ 5.48 (H—C—OAc).

Anal. Calcd. for $C_{22}H_{36}O_2$: C, 79.5; H, 10.9. Found: C, 79.6; H, 11.1.

Hiban-14α-yl mesylate—Hiban-14α-ol (240 mg) was dissolved in pyridine (20 ml) cooled in ice, methanesulfonyl chloride (1.0 g) added, and the mixture left overnight at room temperature. The excess mesyl chloride was destroyed with ice, the mixture poured onto ice-hydrochloric acid, and then extracted with ether to give a solid residue (315 mg). After chromatography on activity I alumina it crystallized from hexane as needles with m.p. 135° ν_{max}($CHCl_3$): 1175 cm^{-1} (—SO_2—O—). The n.m.r. spectrum included a singlet at τ 5.88 (H—C—OMs).

Anal. Calcd. for $C_{21}H_{36}O_3S$: C, 68.8; H, 9.35; S, 8.7. Found: C, 68.7; H, 9.2; S, 8.7.

Reductions of Hiban-14-one

(1) Lithium tri-t-butyoxyaluminohydride—The ketone (99 mg) was treated with excess reductant in tetrahydrofuran for 2 h at room temperature. After the work-up there was obtained 100 mg of a solid whose n.m.r. spectrum was identical to the cyclization product. The residue was chromatographed on 7 g of activity III alumina with hexane (20 ml fractions)—the m.p. and t.l.c. of the frac-

Can. J. Chem. Downloaded from www.nrcresearchpress.com by 210.87.254.105 on 09/05/12
For personal use only.

tions showed that there was only one alcohol produced which after recrystallization from aqueous methanol had m.p. 114–115° undepressed on admixture with the cyclization product. The *x*-ray powder pattern was also identical with that of the cyclization product.

A sample of the reduction product (52 mg) was acetylated with acetic acid (2 ml), acetic anhydride (1 ml) and *p*-toluenesulfonic acid (10 mg). After working up with ether, chromatography on 5 g of activity II alumina in hexane, recrystallization from aqueous methanol, and sublimation at 105° and 0.1 mm, the acetate had m.p. 83.5–85° raised to 84.5–86° on admixture with authentic material. The *x*-ray powder pattern was also identical with that of the acetylated cyclization product.

(2) Lithium aluminium hydride—Hiban-14-one (93 mg) was reduced with excess reductant in refluxing ether during 40 min. The product was examined as in (1) above and was also found to be a single compound identical to the cyclization product. The acetate was not prepared.

(3) Lithium in ethylamine reduction—Hiban-14-one (97 mg) was reduced with lithium in ethylamine using ethanol as the proton source. The product was examined as in (1) and (2) above and was also found to be a single compound identical to the cyclization product. The acetate was not prepared.

Reactions of Hiban-14α-yl Mesylate

(1) Sodium formate in dimethyl formamide—Sixty-two mg of the mesylate in dimethyl formamide (10 ml) were heated with sodium formate (190 mg) at 125° for 2.5 days. The n.m.r. spectrum of the product indicated no apparent reaction.

(2) Sodium azide in dimethyl formamide—The mesylate (104 mg) in dimethyl formamide (12 ml) was heated with sodium azide (200 mg) at 125° for 16 h. The infrared spectrum of the product showed only a trace of absorption at 2100 cm^{-1} (—N_3).

(3) Sodium acetate in aqueous acetone—The mesylate (63 mg), sodium acetate (180 mg), acetone (10 ml), and water (0.5 ml) were refluxed for 3 days. The n.m.r. spectrum of the product showed no apparent reaction.

(4) Sodium formate in formic acid—A solution of the mesylate (98 mg) and sodium formate (27 mg) in formic acid (10 ml) were refluxed for 23 h. Extraction with ether gave a pale-yellow oil (73 mg) whose n.m.r. spectrum showed that it was entirely in the form of a formate (singlets at τ 5.5 and 1.73). This product was treated with excess lithium aluminium hydride in ether at room temperature during 10 min. The colorless solid (72 mg) obtained had an n.m.r. spectrum very similar to the original cyclization product. The product was chromatographed on 7 g of activity III alumina, eluting with hexane (20 ml fractions). The t.l.c. of the fractions showed that only one alcohol (35 mg) was produced. Only 58 mg of material was eluted from the column of which 15 mg had a high R_f on t.l.c. and was presumably an olefinic product while a further 8 mg gave several spots of lower R_f than the mono alcohol. After recrystallization of the product from aqueous methanol it had an n.m.r. spectrum and an *x*-ray powder pattern identical to those of the original alcohol.

Action of Formic Acid on Isopimara-8(14),15-dien-19-oic Acid

To a solution of 66 mg of the acid in 1 ml of chloroform was added 10 ml of 98% formic acid. After 20 min at room temperature the mixture was diluted with 20 ml of water and the resin acids extracted into methylene chloride. After two washes with 20 ml of water to remove formic acid, the methylene chloride solution was dried and distilled. The residue crystallized spontaneously and its n.m.r. spectrum was indistinguishable from that of starting material. The specific rotation however showed a small positive shift (+8°) showing that a slow change was taking place.

Action of Formic Acid on Methyl Pimara-8(14),15-dien-18-oate

The methyl pimarate (116 mg) dissolved within 1 min in 10 ml of 100% formic acid. After 30 min at room temperature the solution was diluted with 25 ml of water and the product extracted into methylene chloride. The organic layer was washed with water, then sodium carbonate solution, dried, and distilled, yielding 117 mg of pale-yellow gum. The n.m.r. spectrum of the gum was nearly identical to that of starting material although the total vinyl hydrogen count had dropped by 30% relative to the OCH_3 signal. No C*H*O—CO— or *H*COO signals were present in the spectrum.

Action of Formic Acid on Pimara-8(14),15-diene

The diene (42 mg) was stirred mechanically with 5 ml of 100% formic acid at room temperature for 75 min. Solution was not complete, some oil drops (formic acid dissolved in diene?) being evident. This simulates closely the conditions during manool cyclization. The reaction mixture was diluted with 20 ml of water, the product extracted into methylene chloride, and the methylene chloride solution washed with sodium carbonate solution. The 44 mg of gum recovered from the solvent had an n.m.r. spectrum very similar to that of starting materials, except for a 20% reduction in intensity of the vinyl proton signals. A weak broad *H*COO— band was present near τ 8.1 but no C*H*O—CO signal was detectable. After hydrolysis with potassium hydroxide in methanol, no C*H*OH signal could be detected in the n.m.r. spectrum.

Acknowledgments

We thank Mr. A. Knoll for valuable technical assistance, Mr. R. Lauzon for high-resolution infrared spectra, and Mr. H. Seguin for microanalyses.

1. L. Ruzicka. Proc. Chem. Soc. 341 (1959). L. Ruzicka. Pure Appl. Chem. **6**, 493 (1963).
2. (*a*) P. R. Jefferies, R. S. Rosich, and D. E. White. Tetrahedron Letters, 1793 (1963). (*b*) Y. Kitahara and A. Yoshikoski. Bull. Chem. Soc. Japan, **38**, 735 (1965).
3. E. Wenkert, P. W. Jeffs, and J. R. Mahajan. J. Am. Chem. Soc. **86**, 2218 (1964).
4. (*a*) E. Wenkert. Chem. Ind. London, 282 (1955). (*b*) W. B. Whalley. Tetrahedron, **18**, 43 (1962).
5. G. Hugel, L. Lods, J. M. Mellor, D. W. Theobald, and G. Ourisson. Bull. Soc. Chim. France, 2882, 2888 (1965).
6. S. Bory and C. Asselineau. Bull. Soc. Chim. France, 1355 (1961).
7. (*a*) P. D. Bartlett, W. S. Trahanovsky, D. A. Bolon, and G. H. Schmid. J. Am. Chem. Soc. **87**, 1314 (1965), and preceding papers of this series (*b*) W. S. Johnson N. P. Jensen, and J. Hooz. J. Am. Chem. Soc. **88**, 3859 (1966); W. S. Johnson and

R. B. KINNEL. J. Am. Chem. Soc. **88**, 3861 (1966); W. S. JOHNSON, P. J. NEUSTAEDTER, and K. K. SCHMIEGEL. J. Am. Chem. Soc. **87**, 5148 (1965), and preceding papers in this series.
8. W. S. JOHNSON, W. H. LUNN, and K. FITZI. J. Am. Chem. Soc. **86**, 1972 (1964).
9. B. LOEV and K. M. SNADER. Chem. Ind. London, 15 (1965).
10. H. H. BRUUN, R. RYHAGE, and E. STENHAGEN. Acta Chem. Scand. **12**, 789 (1958). H. H. BRUUN and S. GASLAND. Acta Acad. Aboensis, Math. Phys. **22**, 24 (1960).
11. (*a*) R. E. IRELAND and P. W. SCHIESS. J. Org. Chem. **28**, 6 (1963). (*b*) R. F. CHURCH and R. E. IRELAND. J. Org. Chem. **28**, 17 (1963).
12. W. G. DAUBEN, G. J. FONKEN, and D. S. NOYCE. J. Am. Chem. Soc. **78**, 2579 (1956).
13. V. P. ARYA, C. ENZELL, H. ERDTMAN, and T. KUBOTA. Acta Chem. Scand. **15**, 225 (1961).
14. C. ENZELL. Acta Chem. Scand. **15**, 1301 (1961).
15. (*a*) A. COLTER, E. C. FRIEDRICH, N. J. HOLNESS, and S. WINSTEIN. J. Am. Chem. Soc. **87**, 379 (1965). (*b*) A. STREITWIESER, JR. Solvolytic displacement reactions. McGraw-Hill, New York. 1962. pp. 141–144. (*c*) C. DANN SARGENT. Quart. Rev. London, **20**, 310–316 (1966). (*d*) A. C. COPE, M. M. MARTIN, and M. A. MCKERNEY. Quart. Rev. London, **20**, 119 (1966).
16. R. A. APPLETON, A. J. MCALEES, A. MCCORMICK, R. C. MCCRINDLE, and R. D. H. MURRAY. J. Chem. Soc. C, 2319 (1966).
17. R. R. SOBTI and SUKH DEV. Tetrahedron Letters, 3939 (1966).
18. E. L. GHISALBERTI and P. R. JEFFERIES. Australian J. Chem. **19**, 1759 (1966).
19. (*a*) A. H. KAPADI and SUKH DEV. Tetrahedron Letters, 1255 (1965). (*b*) J. R. HANSON. Tetrahedron **23**, 793 (1967). (*c*) A. YOSHIKOSHI, M. KITADANI, and Y. KITAHARA. Tetrahedron, **23**, 1175 (1967).
20. G. HUGEL, L. LODS, J. M. MELLOR, and G. OURISSON. Bull. Soc. Chim. France, 2894 (1965).
21. E. WENKERT, A. AFONSO, P. BEAK, R. W. J. CARNEY, P. W. JEFFS, and J. D. MCCHESNEY. J. Org. Chem. **30**, 713 (1965).
22. C. A. HENRICK and P. R. JEFFERIES. Australian J. Chem. **17**, 915 (1964). R. S. ROSICH. Ph.D. Thesis, University of Western Australia, Perth. 1966.
23. R. F. ZÜRCHER. Helv. Chim. Acta, **46**, 2054 (1963). A. I. COHEN and S. ROCK, JR. Steroids, 243 (1964).
24. C. A. HENRICK, P. R. JEFFERIES, and R. S. ROSICH. Tetrahedron Letters, 3475 (1964).
25. R. F. ZÜRCHER. Helv. Chim. Acta, **44**, 1380 (1961).
26. R. G. CURTIS, I. HEILBRON, E. R. H. JONES, and G. F. WOODS. J. Chem. Soc. 457 (1953).
27. R. C. CAMBIE and L. N. MANDER. Tetrahedron, **18**, 465 (1962).
28. R. M. CARMAN and P. K. GRANT. J. Chem. Soc. 2187 (1961).

Can. J. Chem. Downloaded from www.nrcresearchpress.com by 210.87.254.105 on 09/05/12
For personal use only.

Can. J. Chem. Downloaded from www.nrcresearchpress.com by 210.87.254.105 on 09/05/12
For personal use only.

Silicon-containing condensation polymers

SHMUEL MIGDAL, DAVID GERTNER, AND ALBERT ZILKHA
Department of Organic Chemistry, The Hebrew University, Jerusalem, Israel

Received November 7, 1967

Condensation polymers were prepared starting from difunctional silicon-containing carboxylic acids or diols. Dimethyl bis(*p*-carboxymethylphenyl)silane was condensed with various diols to yield polyesters and with various diamines and diisocyanates to yield polyamides. Dimethyl bis(*p*-carboxymethylphenyl)-silane and dimethyl bis(*p*-hydroxymethylphenyl)silane were condensed with dicarboxylic acids to yield polyesters, with diisocyanates to yield polyurethanes, and with ethyl chloroformate to yield a polycarbonate. Some of the properties of the polymers were compared with those of the corresponding polymers prepared from dimethyl bis(*p*-carboxyphenyl)silane.

Canadian Journal of Chemistry, 46, 1125 (1968)

Condensation polymers obtained by the reaction of difunctional monomers such as diacids with diols to yield polyesters, or diacids with diamines to yield polyamides have various important uses. It was interesting to incorporate a metal, such as silicon, into such condensation polymers. Some silicon-containing condensation polymers based on dimethyl bis(*p*-carboxyphenyl)silane were reported (1).

We have recently synthesized (2) dimethyl bis(*p*-carboxymethylphenyl)silane (**1**) and dimethyl bis(*p*-β-hydroxyethylphenyl)silane (**3**) and now report the synthesis of dimethyl bis(*p*-hydroxymethylphenyl)silane (**2**).

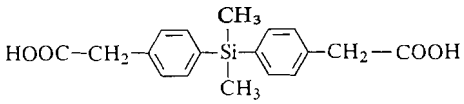

1

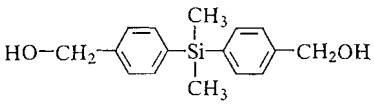

2

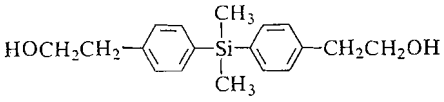

3

These are suitable bifunctional monomers containing silicon which were utilized for the synthesis of polyesters, polyamides, polyurethanes, and a polycarbonate containing silicon in their backbone.

Some of the properties of the polymers were determined and compared with those of the corresponding polymers prepared from dimethyl bis(*p*-carboxyphenyl)silane (**4**).

Equivalent amounts of various diols and **1** were heated to give polyesters (Table I). The reaction mixture was heated initially under atmospheric pressure and then *in vacuo*. The polyesters obtained were low-melting or viscous. They were soluble in acetone, benzene, and *m*-cresol. Their molecular weights were not high and had a low specific viscosity. Diols having a rigid backbone such as 1,4-cyclohexane dimethanol and 2-butyne-1,4-diol gave solid low-melting polymers, ethylene glycol gave a still lower melting product, while its higher homologues gave viscous products. Comparison of these polyesters with the corresponding ones prepared from **4**, shows that the latter had a melting point higher by about 100°.

Silicon-containing polyesters prepared by reaction of **2** with aromatic diacids were solid, with aliphatic diacids such as adipic acid were viscous, while with the silicon-containing diacids **4** and **1** they were solid, the former having the higher melting point (Table I). The polyester obtained by reaction between **3** and **4** was viscous.

Silicon-containing polyamides were obtained by heating the silicon-containing diacids either with diamines (or heating the preformed diammonium salt) or with diisocyanates. Initially the heating is conducted under atmospheric pressure and then *in vacuo*. The polyamide obtained from 1,6-hexane diamine and **1** had a melting point lower by about 90° than the corresponding polyamide obtained from **4**. More rigid diamines gave higher melting polymers. The polyamides were insoluble in ordinary organic solvents, such as chloroform, acetone, and alcohol, but were

Can. J. Chem. Downloaded from www.nrcresearchpress.com by 210.87.254.105 on 09/05/12
For personal use only.

TABLE I

Silicon-containing polyesters*

Diacid	Diol	Melting point °C	% yield	COOH value, mg NaOH/g Polymer	OH value, mg NaOH/g Polymer	— Mn	n	Carbon (%) Calculated†	Carbon (%) Found	Hydrogen (%) Calculated†	Hydrogen (%) Found
1	1,2-Ethane	27	92	12.3	11.7	3330	9.4	67.42	67.42	6.24	6.33
1	1,6-Hexane	—‡	100	16.2	21.9	2100	5.1	69.62	70.18	7.35	7.08
1	Digol	—‡	65	40.4	40.9	980	2.5	65.67	64.53	6.72	6.70
1	1,2-Propane	26	—	44.8	—	—	—	66.84	66.15	6.63	6.71
4	1,4-Cyclohexane Dimethanol	130	64	12.8	13.3	3070	7.5	70.15	69.36	6.89	6.70
4	1,2-Ethane	134§	—	—	—	—	—	—	—	—	—
Adipic	**2**	—‡	82	33.1	34.9	1180	3.1	68.04	68.51	6.87	6.63
Terephthalic	**2**	50	50	40.4	39.4	1010	2.5	70.07	69.65	5.59	5.50
4	**2**	66‖	70	22.5	26.1	1650¶	3.1	70.84	71.68	6.03	6.30
1	**2**	40**	93	10.3	15.4	3160††	5.5	71.96	72.72	6.41	6.40
4	**3**	—‡	86	35.1	35.6	1130	2.1	71.17	71.14	6.46	6.36

*Equivalent amounts of diacid and diol were heated as described before.
†The elementary analyses were calculated for the various n values.
‡Viscous.
§Reported in ref. 1, intrinsic viscosity in m-cresol 0.64 dl/g.
‖Intrinsic viscosity in m-cresol, 0.06 dl/g.
¶Molecular weight as determined by vapor pressure osmometer, 2200.
**Intrinsic viscosity in m-cresol, 0.17 dl/g.
††Molecular weight as determined by vapor pressure osmometer, 2820.

Can. J. Chem. Downloaded from www.nrcresearchpress.com by 210.87.254.105 on 09/05/12
For personal use only.

soluble in formic acid, acetic acid, and in *m*-cresol.

Polyurethanes were prepared by heating **3** at 200–240° with 2,4-toluylene diisocyanate or with 1,6-hexane diisocyanate. The corresponding polymers obtained from **2** had the higher melting points. The polymers obtained from the aromatic diisocyanate had the higher melting point (see Table II).

A polycarbonate was prepared by reacting **2** with ethyl chloroformate in the presence of pyridine to give the dimixed carbonate ester which on heating *in vacuo* in the presence of titanium tetrabutoxide (3) gave the polymer, which was low-melting.

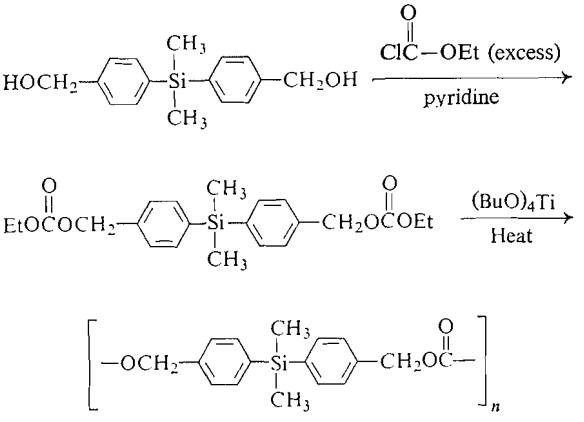

The results show that introduction of an additional methylene group either in the diacid or in the diol lowers the melting point of the condensation polymers.

Experimental

Materials

Compounds **1**, **3**, and **4** were prepared and purified as previously described (1–3). Compound **2** was prepared as follows.

Dimethyl Bis(p-hydroxymethylphenyl)silane (2)

To a suspension of lithium aluminium hydride (3.8 g, 0.1 mole) in dry tetrahydrofuran (200 ml), dimethyl bis(*p*-carboxyphenyl)silane (**1**) (11 g, 0.037 mole) in dry tetrahydrofuran (200 ml), was added dropwise, so that there was a gentle reflux. The reaction mixture was heated under reflux for a further 2 h and cooled in an ice-bath. Crushed ice was added cautiously to destroy excess lithium aluminium hydride, the solvent was evaporated *in vacuo*, and 5% sulfuric acid was added. The mixture was extracted with ether, and the extract was washed with sodium carbonate (10%) followed by water and dried over sodium sulfate. The ether was distilled off *in vacuo*, the residue was left in the cold under petroleum ether, and **2** (7.2 g, 71%) crystallized out and was collected; m.p. 52°.

Anal. Calcd. for $C_{16}H_{20}O_2Si$: C, 70.59; H, 7.35. Found: C, 70.92; H, 7.32.

Number-average Molecular Weights

The carboxyl end groups in the polyesters were determined by direct titration of the polymer in water–acetone solution using phenol–phthalein as indicator.

The hydroxyl end groups were determined by using pyridine – acetic anhydride acetylation reagent (4). Number-average molecular weights were determined from the hydroxyl and carboxyl end groups (5).

The carboxyl and amine end groups in polyamides were determined by anhydrous titration (6, 7). The former by suspending the polyamide in dry dioxane, and titrating with potassium methoxide in benzene–methanol using thymol blue as indicator, and the latter by titrating with perchloric acid in acetic acid, using crystal violet as indicator.

Typical examples of the polycondensations are given below, the rest being summarized in the Tables.

Polyester from Dimethyl Bis(p-carboxymethylphenyl)-silane (1) and 1,4-Cyclohexane Dimethanol

Compound (**1**) (1.08 g, 3.3 mmole) was heated in a glass tube with redistilled 1,4-cyclohexane dimethanol (0.475 g, 3.3 mmole) under argon at atmospheric pressure at 190° for 8 h. The reaction mixture was then heated *in vacuo* (2mm pressure) at 190° for 36 h. The yellowish polyester solidified on cooling, yield 1.33 g (92%), m.p. 45–48°. It had a carboxyl value of 92.3 mg NaOH/g polymer and a hydroxyl value of 62.0 mg NaOH/g polymer, which leads to a molecular weight of 5000 ($n = 11.5$). It is soluble in acetone and benzene and films can be cast from these solvents.

Anal. Calcd. for $(C_{26}H_{32}O_4Si)_n$: C, 71.31; H, 7.35. Found: C, 71.69; H, 7.45.

Salt from (1) and 1,6-Hexanediamine

To a solution of (**1**) (0.5 g, 1.52 mmole) in absolute ethanol (3 ml) and dry ether (10 ml), a solution of 1,6-hexanediamine (0.182 g, 1.57 mmole) in absolute ethanol (3 ml) and dry ether (2 ml) was added. The salt precipitated immediately and the mixture was boiled and cooled, yield 0.62 g (92%), m.p. 185–187°.

Anal. Calcd. for $C_{24}H_{36}O_4N_2Si$: N, 6.31. Found: N, 6.20.

Polyamide from (1) and 1,6-Hexanediamine

The above 1,6-hexanediammonium salt (1.2 g, 2.7 mmole) was heated for 2 h under argon at 190° at atmospheric pressure, and then for 6 h *in vacuo* (2 mm). The polyamide solidified on cooling, yield 0.97 g (89%), m.p. 100°, (polyamide of **4** and 1,6-hexanediamine, m.p. 190°). The carboxyl and amine end groups were determined by anhydrous titration with sodium methoxide and perchloric acid respectively. The polymer contained 0.20 mmole amine groups/g and 0.23 mmole carboxyl groups/g. This gives a number-average molecular weight of 4650 ($n = 11$) for the polymer.

Anal. Calcd. for $(C_{24}H_{32}O_2N_2Si)_n$: C, 70.24; H, 7.86; N, 6.21. Found: C, 69.93; H, 7.75; N, 6.47.

Polyamide from (1) and Ethylenediamine

Equivalent amounts of **1** and redistilled ethylene diamine were heated at 190° as before. The polyamide was obtained in 87% yield, m.p. 140–142°. The polymer was

Can. J. Chem. Downloaded from www.nrcresearchpress.com by 210.87.254.105 on 09/05/12
For personal use only.

TABLE II

Silicon-containing polyurethanes*

Diol	Diisocyanate	Melting point °C	% yield	Formula	Carbon (%)		Hydrogen (%)		Nitrogen (%)	
					Calculated	Found	Calculated	Found	Calculated	Found
2	1,6-Hexane	56	79	$(C_{24}H_{32}N_2O_4Si)_n$	65.3	64.04	7.27	7.18	6.36	6.20
3	2,4-Toluylene	85	99	$(C_{27}H_{30}N_2O_4Si)_n$	68.4	67.30	6.33	6.56	5.92	5.80
3	1,6-Hexane	30	91	$(C_{26}H_{36}N_2O_4Si)_n$	66.66	66.38	7.69	7.77	5.98	5.73

*Equivalent amounts of the diol and diisocyanate were heated as described before.

purified by extraction with boiling ethanol. It contained 6.24 mmole amine end groups/g and 0.30 mmole carboxyl groups/g. This gives a molecular weight of 3700 ($n = 11$) for the polymer.

Anal. Calcd. for $(C_{20}H_{24}O_2Si)_n$: C, 67.87; H, 6.84; N, 7.20. Found: C, 68.18; H, 7.08; N, 6.9.

Polyamide from (1) and 2,4-Toluylene Diisocyanate

Compound (**1**) (1 g, 3.05 mmole) and redistilled 2,4-toluylene diisocyanate (0.531 g, 3.05 mmole) were mixed and heated for 1 h at 190°, and for 3 h at 240°. Polyamide (1.2 g, 95%) was obtained, m.p. 175–180°. It was extracted with boiling ethanol.

Anal. Calcd. for $(C_{25}H_{26}O_2N_2Si)_n$: C, 72.5; H, 6.23; N, 6.77. Found: C, 69.76; H, 6.41; N, 6.73.

Polyurethane from Dimethyl Bis(p-hydroxymethylphenyl)-silane (2) and 2,4-Toluylene Diisocyanate

2,4-Toluylene diisocyanate (0.322 g, 1.85 mmole) and **2** (0.502 g, 1.84 mmole), were heated under argon so that the temperature reached 240° after 30 min. The heating was continued for 3 h. The polymer solidified on cooling and was washed with ethanol, yield 0.74 g (90%).

Anal. Calcd. for $(C_{25}H_{26}N_2O_4Si)_n$: C, 67.26; H, 5.83; N, 6.28. Found: C, 67.02; H, 5.64; N, 6.70.

Polycarbonate from 2

To a solution of **2** (1 g, 3.68 mmole) in pyridine (10 ml), redistilled ethyl chloroformate (1.02 g, 9.45 mmole) was added, and the mixture was stirred in the cold for 2.5 h. Ice (8 g) was added to destroy excess ethyl chloroformate, the mixture was left overnight and extracted with ether. The ether layer was washed by dilute hydrochloric acid (7%) followed by water, dried over magnesium sulfate, and distilled *in vacuo*. The dimixed carbonate ester was extracted with petroleum ether, and the petroleum ether evaporated. To the oily ester, a drop of titanium tetrabutoxide was added, and was heated slowly to 240° for 4 h. The polycarbonate solidified and was washed thoroughly with petroleum ether, ethanol, ether, and then dried; yield 0.38 g (35%), m.p. 47–52°.

Anal. Calcd. for $(C_{17}H_{18}O_3Si)_n$: C, 68.46; H, 6.11. Found: C, 68.30; H, 6.14.

Dimethyl Ester of Dimethyl Bis(p-carboxymethylphenyl)-silane

This ester which is a useful intermediate in the preparation of condensation polymers of (**1**) was prepared as follows: compound (**1**) (2 g, 6.1 mmole) was added to absolute methanol (10 ml), a drop of concentrated sulfuric acid was added and the reaction mixture was refluxed for 6 h. The methanol was driven off *in vacuo*, water was added, and the ester was extracted with ether. The extract was washed with bicarbonate solution, followed by water and dried over magnesium sulfate. The oily ester (1.56 g, 72%) was recovered on evaporation of the ether.

Anal. Calcd. for $C_{20}H_{24}O_4Si$: C, 67.41; H, 6.74. Found: C, 67.08; H, 6.44.

1. S. B. SPECK. J. Org. Chem. **18**, 1689 (1953).
2. A. ROTMAN, D. GERTNER, and A. ZILKHA. Can. J. Chem. **45**, 1957 (1967).
3. H. SCHNELL. Chemistry and physics of polycarbonates. Interscience Publishers, New York, N.Y. 1964. p. 24.
4. B. A. FEIT, D. RAUCHER, and A. ZILKHA. J. Appl. Polymer Sci. **9**, 2379 (1965).
5. W. R. SORENSON and T. W. CAMPBELL. Preparative methods of polymer chemistry. Interscience Publishers, New York, N.Y. 1961. p. 134.
6. A. PATCHORNIK and S. ERLICH-ROGOZINSKI. Anal. Chem. **31**, 985 (1959).
7. M. SELA and A. BERGER. J. Am. Chem. Soc. 77, 1893 (1955).

Can. J. Chem. Downloaded from www.nrcresearchpress.com by 210.87.254.105 on 09/05/12
For personal use only.

Nucleosides. XLIX. Nuclear magnetic resonance studies of 2′-and 3′-halogeno nucleosides. The conformations of 2′-deoxy-2′-fluorouridine and 3′-deoxy-3′-fluoro-β-D-arabinofuranosyluracil

ROBERT J. CUSHLEY,[1] JOHN F. CODINGTON,[2] AND JACK J. FOX

Division of Biological Chemistry, Sloan-Kettering Institute for Cancer Research, Sloan-Kettering Division of Cornell University Medical College, New York 21, New York

Received October 17, 1967

Nuclear magnetic resonance data for a series of 2′-halogeno and 3′-halogeno pyrimidine nucleosides are presented. Using a combination of proton–proton and proton–fluorine couplings vs. dihedral angle values 2′-deoxy-2′-fluorouridine is proposed to have an envelope conformation with C–3′ *endo*, and 1-(3-deoxy-3-fluoro-β-D-arabinofuranosyl)uracil proposed to have a twist conformation with O-ring *endo* and C–1′ *exo*. Correlations between substituent electronegativity and both vicinal coupling constants and internal chemical shifts are discussed.

Syntheses of several new 2′-halogeno and 3′-halogeno nucleosides are described.

Canadian Journal of Chemistry, 46, 1131 (1968)

Can. J. Chem. Downloaded from www.nrcresearchpress.com by 210.87.254.6 on 09/05/12
For personal use only.

Previous reports from this laboratory described the synthesis and structure of several 2′-halogeno-2′-deoxyuridines, (**1**(F,Cl,Br)) (1), and two diacetates (**2**(F,Cl)) (2). The 2′-fluoro compound (**1**(F)) was degraded to a 2-fluoro sugar which was shown to be 2-deoxy-2-fluoro-D-ribose. Its tribenzoate was shown to be 1,3,4-tri-*O*-benzoyl-2-deoxy-2-fluoro-β-D-ribose by chemical studies (3) and nuclear magnetic resonance (n.m.r.) spectroscopy (4).

A complete series of halogeno compounds would provide an extremely interesting group of compounds in which to study, by n.m.r. spectroscopy, the effect of halogeno substituents on the 5-membered furanose ring. Therefore, 2′-deoxy-2′-iodo-uridine (**1**), the diacetates of the 2′-bromo, 2′-iodo, and 2′-deoxy nucleosides (**2**), and the 3′-halogeno nucleosides, **3**(F, Cl, I),were prepared. The complete series studied is listed in Fig. 1.

This report deals with the effect of substituents on chemical shifts of certain protons and the effect of halogens on the conformation of the furanose ring as reflected by the various coupling constants.

In the ideal situation, of course, to study the effects of halogen atoms on coupling constants it is necessary to deal with compounds in a single conformation. At the present time, too, the precise conformation of a furanose ring cannot be determined by proton–proton coupling constants with certainty (5, 6). The various properties, *as well as* bond angles (7), contributing to the coupling constant in the carbohydrate series have been summarized recently (4).

Recent work by Williamson *et al.* (8) and Hall and Manville (9) on the Karplus-type relationship of vicinal proton–fluorine coupling constants and proton–fluorine dihedral angles provided us with the unique opportunity of checking the conformation of the 2′-fluoro nucleoside **1**(F) and 3′-fluoro nucleoside **3**(F), proposed on the basis of the proton–proton couplings, by the vicinal proton–fluorine couplings. Unfortunately the spectrum of the fluoro diacetate **2**(F) was not sufficiently resolved in the solvents used to permit complete analysis of its conformation to be made.

The n.m.r. spectrum of 2′-deoxy-2′-fluoro-β-D-ribofuranosyluracil in DMSO-d_6 – D_2O and D_2O is depicted in Fig. 2. The assignments of H-1′ (δ 5.91), H-2′ (δ 5.02), and H-3′ (δ 4.15) are consistent with the vicinal and geminal H–F couplings found: 17.7, 55, and 19.5 Hz respectively (10). The large proton–fluorine coupling constants allow ready assignments of the protons and also allow a determination of the magnitude of $J_{H\text{-}3',H\text{-}4'}$ to be made by first order analysis of the low-field lines of the H-3′ octet. In D_2O, the n.m.r. spectrum of the region H-3′, H-4′, H-5′, H-5′ becomes clearer (insert, Fig. 2). The splittings $J_{H\text{-}3',H\text{-}4'} = 8.0$ Hz and $J_{H\text{-}2',H\text{-}3'} = 4.6$ Hz

[1]Present address: Section of Physical Sciences, Yale University School of Medicine, New Haven, Connecticut.

[2]Present address: Laboratory for Carbohydrate Research, Departments of Biological Chemistry and Medicine, Harvard Medical School and Massachusetts General Hospital, Boston, Massachusetts.

Can. J. Chem. Downloaded from www.nrcresearchpress.com by 210.87.254.6 on 09/05/12
For personal use only.

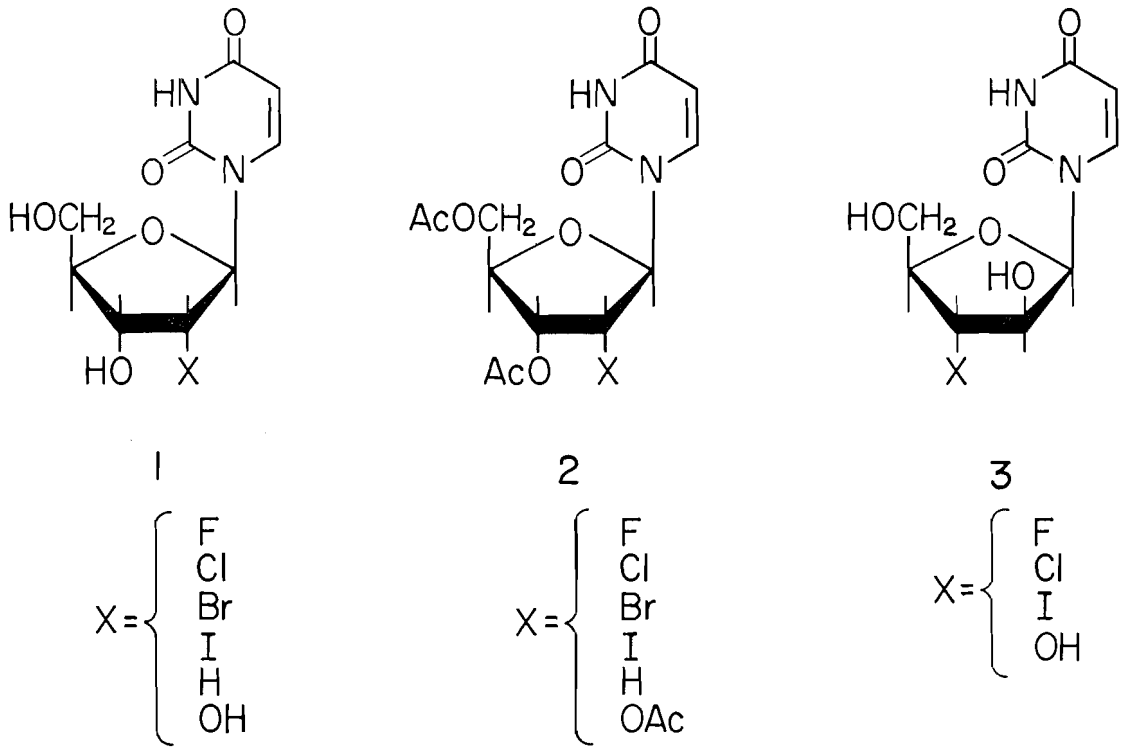

FIG. 1. The series of halogeno compounds studied.

are slightly larger than those determined in DMSO-d_6 – D_2O. Since the chemical shifts are also greater the splittings are more first order. Although all other coupling constants remained unchanged in D_2O, $J_{H\text{-}1',F}$ increased slightly to 18.6 Hz from that shown in the figure.

The n.m.r. spectrum of 3′,5′-di-*O*-acetyl-2′-deoxy-2′-fluoro-β-D-ribofuranosyluracil, **2**(F), could not be analyzed completely since part of the H-2′ signal was buried beneath H-3′, and H-4′ was buried beneath the H-5′ signals. First order analysis along with frequency-sweep double resonance did give, in DMSO-d_6 – D_2O, $J_{H\text{-}1',H\text{-}2'} = 2.0$ Hz, $J_{H\text{-}2',H\text{-}3'} \sim 6.0$ Hz, and $J_{H\text{-}5,H\text{-}6} = 8.0$ Hz. Also ^{19}F spectroscopy (94.1 MHz and frequency-sweep lock mode) gave a multiplet at 144 ± 1 p.p.m. from external CCl_3F, $J_{H\text{-}1',F} = 21.0$ Hz, $J_{H\text{-}2',F} = 52.0$ Hz, and $J_{H\text{-}3',F} = 18.0$ Hz which substantiated the H–F coupling constant values found in the proton spectrum. The values are close to those found for the unacetylated compound **1**(F) but $J_{H\text{-}2',H\text{-}3'}$ has increased from 4.3 Hz for **1**(F) (Fig. 2) to ~6.0 Hz. The increase in $J_{H\text{-}2',H\text{-}3'}$ reflects a decrease in the (3′)C—O, C—F dihedral angle of a few degrees. The large gauche interaction of (3′)-C—OAc, (4′)C—CH_2OAc would be expected to play a greater role in determining the conformation than would the C—F, (3′)C—OAc interaction. Such contributions should be reflected in the lower (3′)C—O,C—F dihedral angle. The (3′)C—OAc, (4′)C—CH_2OAc dihedral angle would thus increase leading to a decreased $J_{H\text{-}3',H\text{-}4'}$ which, unfortunately, we were unable to discern.

Using the data of Williamson *et al.* (8) a rough curve of $J_{H,F}$ vs. dihedral angle (Θ) was constructed using *average* values. A similar rough curve was constructed from the data of Hall and Manville (9). The H,F coupling constants can be expected to be affected by the same factors which influence the H,H coupling constants (7*b*). For instance Williamson *et al.* have shown that for compounds where the dihedral angle, Θ, equals 0° $J^{vic}_{H,F}$ varies from 10.5–30.8 Hz (8) although some distortion of the angle from 0° probably accounts for part of the disparity (8).

The dihedral angles between vicinal nuclei

Can. J. Chem. Downloaded from www.nrcresearchpress.com by 210.87.254.6 on 09/05/12
For personal use only.

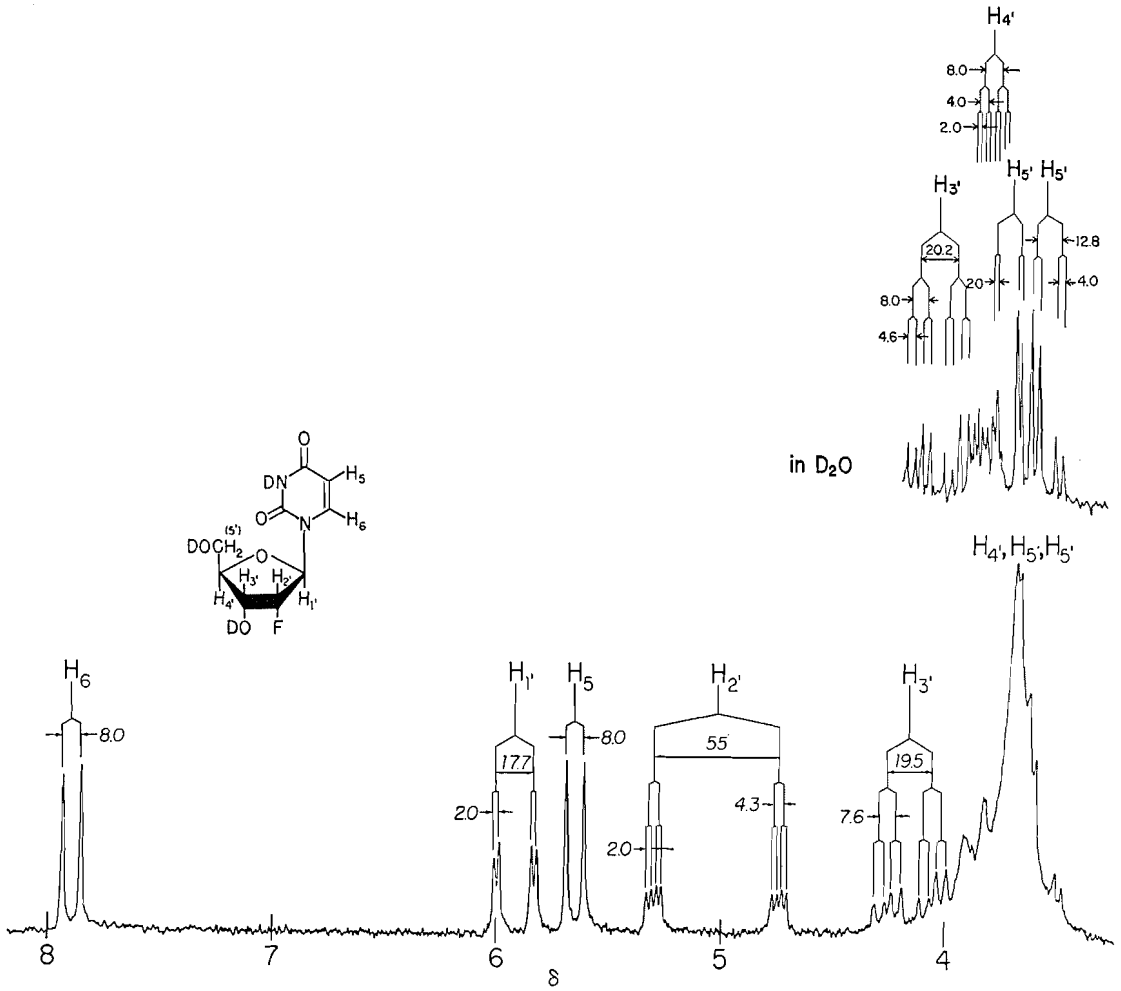

FIG. 2. Proton magnetic resonance spectrum (100 MHz) of 2′-deoxy-2′-fluorouridine, **1**(F), in DMSO-d_6 – D_2O solution with tetramethylsilane as internal standard.

calculated from coupling constants for **1**(F) are given in Table I. The data strongly suggest that in D_2O solution the furanose ring adopts an envelope conformation with C-3′ *endo* as defined by Jardetzky (13). The H,F coupling constants give remarkable agreement with the H,H coupling constants and no other conformation, neither envelope (analogous to C_s symmetry in cyclopentane) nor twist (C_2 symmetry in cyclopentane), agrees nearly as well with the data given in Table I. The conformation presented in Table I is also the one in which the non-bonded interactions are minimal. The conformation does not resemble any previously proposed for 2′-deoxyribofuranosyl nucleosides from n.m.r. data (14–16) or *x*-ray data (17) but is the same as that found by *x*-ray data for cytidine (18), a ribofuranosyl nucleoside, and by n.m.r. data for certain ribofuranosyl pyrimidines (13). Hence it appears that polar effects of the C–F bond rather than steric considerations are mainly responsible for the adoption of the C-3′ *endo* conformation in **1**(F). The C—F,C_1′—N dihedral angle is approximately 149° (*trans*) and the C_3′—O, C—F dihedral angle is 46° (*cis*).

The n.m.r. spectrum of 3′-deoxy-3′-fluoro-β-D-arabinofuranosyluracil, **3**(F), is depicted in Fig. 3. In order to get the best spectrum, it was necessary to use acetone-d_6 – D_2O as solvent.

Frequency sweep decoupling from the center

Can. J. Chem. Downloaded from www.nrcresearchpress.com by 210.87.254.6 on 09/05/12
For personal use only.

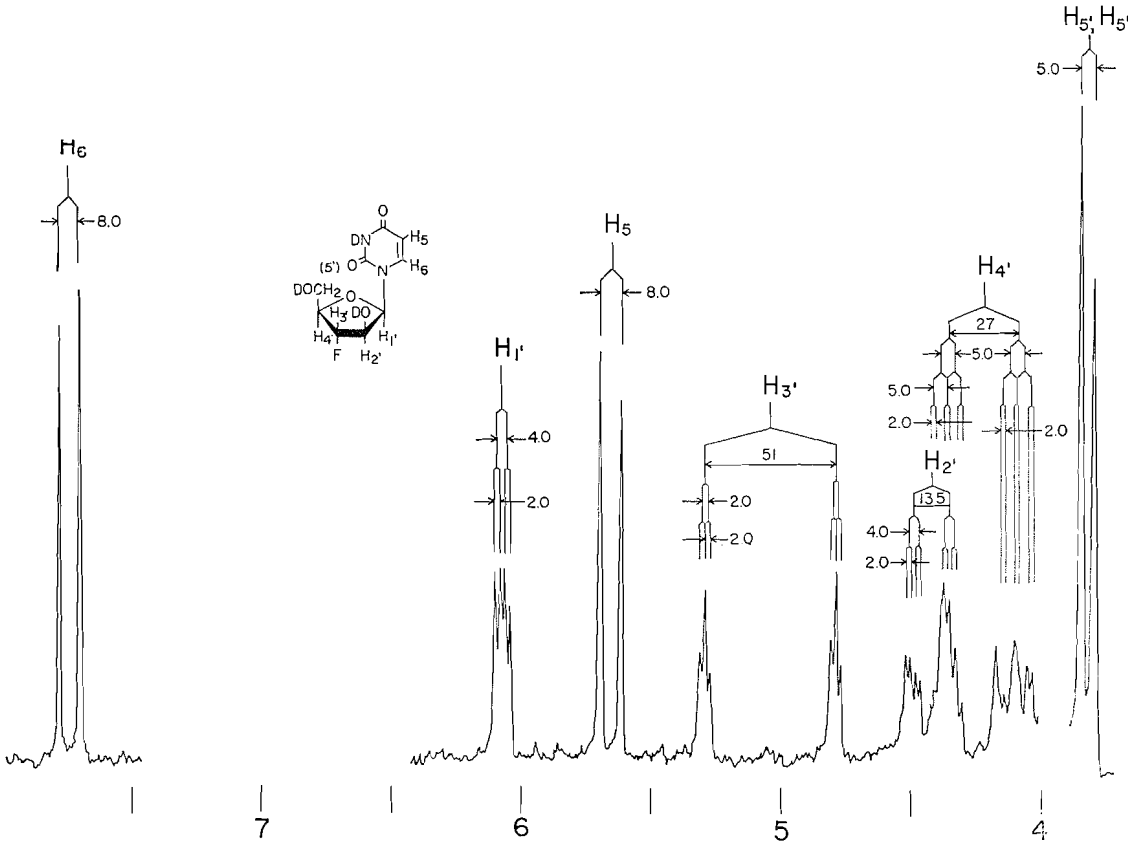

FIG. 3. Proton magnetic resonance spectrum (100 MHz) of 1-(3-deoxy-3-fluoro-β-D-arabinofuranosyl)uracil, 3(F), in acetone-d_6 – D_2O with tetramethylsilane as internal standard.

TABLE I

Conformation of 2′-deoxy-2′-fluorouridine (**1**(F))* from coupling constant data

	Coupling constant (Hz)	Dihedral angle (degrees) Theory†	Calculated
H-1′, H-2′	2.0	91	100‡–119§
H-2′, H-3′	4.6	46	41§– 54‡
H-3′, H-4′	8.0	166	144‡–159§
H-1′, F	18.6	29	7 – 20‖
H-3′, F	20.2	166	158 –160‖

*This compound,

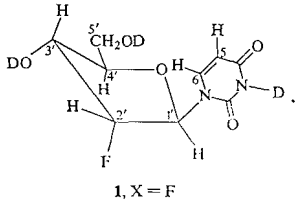

1, X = F

†Based on perfect cyclopentane geometry (11) for an envelope conformation for **1**(F).
‡Value after Lemieux *et al.* (12).
§Value after Karplus (7).
‖Lower value after Williamson *et al.* (8); upper value after Hall and Manville (9).

of the anomeric quartet at δ 6.07 gave a quartet centered δ 4.38, $J_{H\text{-}2',H\text{-}3'} = 2$ Hz, $J_{H\text{-}2',F} = 13.5$ Hz. As well, the two triplets due to H-3′ in the figure sharpened showing a very small H-1′, H-3′ coupling. Furthermore the 12 lines assigned to H-4′ (δ 4.22) were clearly visible. A triple irradiation experiment of both halves of the H-3′ resonance signal was only moderately successful. However, the H-1′ quartet was perturbed, the H-2′ signal showed a rough quartet with $J_{H\text{-}1',H\text{-}2'} \sim 4$ Hz and $J_{H\text{-}2',F} \sim 13.5$ Hz, and the peaks assigned to the H-4′ signal gave a rough doublet of triplets $J_{H\text{-}4',F} \sim 27$ Hz and $J_{H\text{-}4',H\text{-}5'} \sim 5$ Hz. The two C-5′ protons gave a pseudo-doublet ($J = 5.0$ Hz) centered at δ = 3.81 in contrast to the octet seen for the C-5′ protons of **1**(F) (Fig. 2). Such pseudo-doublets for the C-5′ protons have been found for a host of furanosyl pyrimidine nucleosides (19). The assignments of H-2′, H-3′, and H-4′ are consistent with the vicinal and geminal H,F couplings found: 13.5,

Can. J. Chem. Downloaded from www.nrcresearchpress.com by 210.87.254.6 on 09/05/12
For personal use only.

51, and 27 Hz respectively (10). Also, a long-range H,F coupling of 2.0 Hz is found between the anomeric proton, H-1′, and the C-3′ fluorine. It should be noted that from the method of synthesis of **3**(F) (*trans* opening of 1-(2,3-epoxy-β-D-lyxofuranosyl)uracil by HF) the 2′- or 3′-fluoro nucleosides are possible. The n.m.r. data listed above firmly establish the structure of **3**(F) as 1-(3-deoxy-3-fluoro-β-D-arabinofuranosyl)-uracil.

Dihedral angles for **3**(F), calculated from the coupling constant data, are given in Table II. As seen from Table II, the data best fit a twist conformation with the ring oxygen *endo* and C-1′ *exo* based on perfect cyclopentane geometry (11). The fit from the H-F coupling data is not quite as good as that found for compound **1**(F) (Table I) but is by far the best fit of the ten possible conformations based on C_S or C_2 cyclopentane geometry. The conformation depicted is, again, the one which would have been predicted on conformational grounds. Furthermore, decreasing the angle of pucker of O-ring slightly and/or increasing the angle of pucker of C-1′ slightly (placing the aglycon in a more "equatorial" orientation) alters all dihedral angles sufficiently to obtain a better fit with the calculated angles.[3] Increasing the pucker of C-1′ slightly also brings H-1′ and F closer together and could account for the long-range coupling observed. Their positions would approach the *syn*-axial orientation of cyclohexane compounds—an orientation which has been shown to be necessary for long-range H,F coupling in saturated ring systems (21). It should be noted that the discrepancy is in the H,F coupling which might be expected. An envelope conformation with C-1′ *endo* would give an H-4′,F dihedral angle of 0° (calcd. 0°) and an H-2′,F dihedral angle of 29° (calcd. 24–39°) but the H-2′, H-3′ dihedral angle of 149° would be > 30° from that calculated (calcd. 100–119°) and the aglycon and C-4′ hydroxymethyl groups would be *syn*-axially opposed.

[3]The distortion gives an increased C-1′, C-2′ dihedral angle which approaches in magnitude the value proposed by Jardetzky (20) for furanosyl nucleosides. Jardetzky proposed a twist conformation in which the two atoms out of plane (the *endo* and *exo* atoms) have their groups in a staggered ethane configuration (Θ = 60°). This value differs from that proposed by Pitzer and Donath (11) for cyclopentane (Θ = 48°) and would probably occur in compounds bearing "equatorial" substituents at the *endo* and *exo* atoms. Since O-ring is the *endo* atom in **3**(F) the amount of puckering is probably not as great.

TABLE II

Conformation of 3′-deoxy-3′-fluoro-β-D-arabinofuranosyluracil (**3**(F))* from coupling constant data

	Coupling constant (Hz)	Dihedral angle (degrees) Theory†	Calculated
H-1′, H-2′	4.0	39	45§ –59‡
H-2′, H-3′	2.0	105	100‡–119§
H-3′, H-4′	2.0	105	100‡–119§
H-2′, F	13.5	15	24 – 39‖
H-4′, F	27	15	0‖

*This compound,

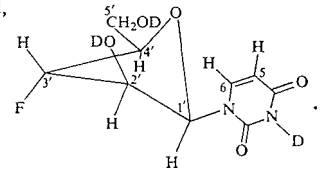

3, X = F

†Based on perfect cyclopentane geometry (11) for a half-chair conformation for 3(F).
‡Value after Lemieux *et al.* (12).
§Value after Karplus (7).
‖Lower value after Williamson *et al.* (8); upper value after Hall and Manville (9).

It should further be noted that application of the vicinal H-F coupling constant vs. dihedral angle correlation, a linear correlation, proposed by White (22) for a series of chlorinated 2,2-difluoropropanes does not apply to the furanose ring systems.

The n.m.r. data for the compounds listed in Fig. 1 are given in Table III. In the case of the 2′-halo compounds (**1**) the halogen atom to a large extent determines the conformation of the compound. Comparison of **1**(F) with **1**(H), whose $J_{H\text{-}1',H\text{-}2'} = 6.9$ Hz, shows that the conformation of 2′-fluoro-2′-deoxyuridine is substantially different from 2′-deoxyuridine. In Table III we see that the $J_{H\text{-}1',H\text{-}2'}$ values vary from 2.0 Hz for **1**(F) to 7.0 Hz for **1**(I). Such a large discrepancy cannot be accounted for solely by an electronegativity effect of the halogen upon the vicinal H,H coupling constant (23–25) and must be due additionally to a gradual change in the conformation of the furanose ring as the substituent varies from fluorine to iodine. Laszlo and Schleyer have found that the effect of electronegativity of substituents on vicinal coupling constants accounts for only a maximum change of 20% in the coupling constant (25).

The $J_{H\text{-}1',H\text{-}2'}$ values for the 2′-halogeno nucleosides are found to increase with the increasing size of 2′-substituent. The calculated dihedral angle between H-1′ and H-2′ increases from

Can. J. Chem. Downloaded from www.nrcresearchpress.com by 210.87.254.6 on 09/05/12
For personal use only.

TABLE III

Nuclear magnetic resonance data for 2′- and 3′-halogeno and related nucleosides

	Compound **1*** in D_2O†						Compound **2*** in DMSO-d_6‡						Compound **3*** in DMSO-d_6‡			
	F	Cl	Br	I	H	OH	F§	Cl	Br	I	H	OAc	F	Cl	I	OH
$\delta_{H\text{-}1'}$	6.23	6.18	6.28	6.47	6.31	5.94	5.85	6.04	6.20	6.35	6.16	6.08	6.07	6.17	6.22	6.04
$\delta_{H\text{-}2'}$	5.46	4.77‖	4.68‖	4.68‖	2.43	4.47‖	5.44‖	5.00‖	5.02	5.03‖	2.40	5.72‖	4.38	4.46‖	4.72‖	~4.0
$\delta_{H\text{-}5}$	6.09	5.97	5.96	6.06	5.93	5.93	5.71	5.76	5.80	5.90	5.70	5.88	5.61	5.61	5.64	5.69
$\delta_{H\text{-}6}$	7.99	7.95	7.94	8.04	7.90	7.91	7.67	7.66	7.74	7.81	7.63	7.93	7.62	7.71	7.87	7.67
$J_{H\text{-}1',H\text{-}2'}$	2.0	4.8	5.6	7.0	6.9	4.0	2.0	6.3	7.0	8.2	7.0	4.1	4.0	5.4	6.0	4.0
$J_{H\text{-}2',H\text{-}3'}$	4.6	—	—	—	~5	—	6.0	6.0	~5.8	—	—	—	2.0	~4.8‖,§	—	~4.0
$J_{H\text{-}5,H\text{-}6}$	8.0	8.2	8.1	8.2	8.3	8.2	8.0	8.1	8.0	8.0	8.0	8.1	8.0	8.0	8.0	8.0
$\delta_{H\text{-}3'}$	4.15	—	—	—	—	—	5.30	5.33	~5.23	—	~5.19	—	5.05	~4.12	~4.14	~4.0

*Compounds 1, 2, and 3 have the structures

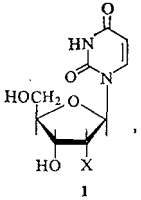
1

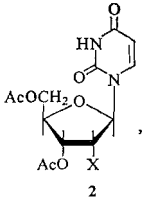
2

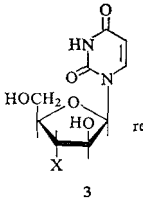
3

respectively.

†Chemical shifts (δ) are in p.p.m. from sodium 2,2-dimethyl-2-silapentane-5-sulfonate as internal standard. Coupling constants are in Hz.
‡Tetramethylsilane as internal standard.
§Small drop of D_2O added to solution.
‖Determined by field sweep decoupling from the H-1′ signal.

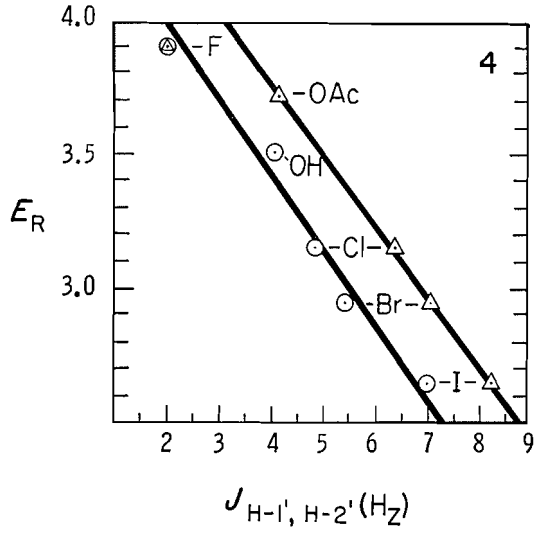

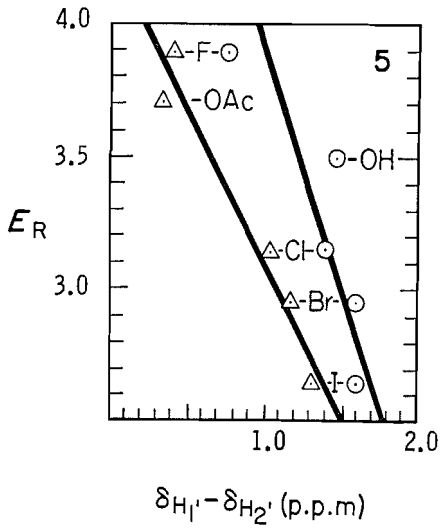

FIG. 4. Plot of electronegativity (E_R) versus coupling constants $J_{H-1',H-2'}$. Notation ⊙ refers to compounds **1** and △ refers to compounds **2**.

FIG. 5. Plot of electronegativity (E_R) versus internal chemical shift $\delta_{H-1'} - \delta_{H-2'}$. Notation ⊙ refers to compounds **1** and △ refers to compounds **2**.

approximately 119° to approximately 151° (Karplus) for the series **1**(F) to **1**(I), thus paralleling the size of the substituent.[4]

Figure 4 lists a correlation between $J_{H-1',H-2'}$ and the Huggins' electronegativity value E_R (26) for both the series of 2′-substituted ribofuranosyluracils (**1**) and their 3′,5′-di-*O*-acetyl derivatives (**2**). The E_R value for OAc is taken from Laszlo and Schleyer (25). In spite of the fact that conformational changes occur in the furanose moiety there is a good correlation between $J_{H-1',H-2'}$ and E_R in both series, and they are in the expected order. This suggests that the effect of electronegativity and dihedral angles are additive in flexible ring systems of the same series and that other effects contributing to the magnitude of vicinal coupling constants (7*b*) are small.

It has been established (27) that not only does J_{vic} vary as E_R but also varies as the orientation of the electronegative substituent. The correlation between J_{vic} and E_R presented here could include a correlation between J_{vic} and the orientation of the electronegative substituent over the vicinal dihedral angle range observed with compounds **1** and **2**.

For the series of 3-substituted arabinofuranosyluracils (**3**) there is also a rough correlation between $J_{H-2',H-3'}$ and E_R. However the series is not complete and some of the coupling constants recorded in Table II are only approximate. Yet with compounds **3**(F), **3**(OH), and **3**(Cl) the vicinal H-2′,H-3′ coupling constant follows the electronegativity of the 3′-substituent. It will be seen that for the 3′-halo nucleosides **3**, the $J_{H-1',H-2'}$ values vary only from 4.0 to 6.0 Hz in contrast with the much greater range encountered in compounds **1** and **2**.

For the compound series **1**, **2** and **3** listed in Table III, the chemical shift data are of interest.

In Fig. 5 are listed the internal chemical shift data H-1′ – H-2′ vs. Huggins' electronegativity values. In all cases the chemical shifts involved were determined by first order analysis or double resonance techniques. Again there is a correlation between internal chemical shift and electronegativity. The fit is seen to be very good for the correlation between internal chemical shift and electronegativity for compounds containing substituents of low electronegativity but, as the electronegativity of the substituent increases, there is a greater deviation from a straight line relationship. For instance the points for **1**(OH and F) and **2**(OAc and F) are farther from their respective plots than those for the other substituents. These results can best be explained on

[4]The actual increase in the C-1′, C-2′ dihedral angle is not 32° since, of course, part of the increase in the magnitude of the coupling constant for the series **1**(F) to **1**(I) is accounted for by the decreasing electronegativity of the substituent (23).

Can. J. Chem. Downloaded from www.nrcresearchpress.com by 210.87.254.6 on 09/05/12
For personal use only.

Can. J. Chem. Downloaded from www.nrcresearchpress.com by 210.87.254.6 on 09/05/12
For personal use only.

the basis of an angular dependence of the internal chemical shifts $\delta_{H\text{-}1'} - \delta_{H\text{-}2'}$ on the dihedral angle between H-1′ and H-2′. As stated above there is a significant change in this dihedral angle in both series of compounds **1** and **2**. Since the shieldings of the two protons can be expected to be most affected by an inductive and an anisotropic effect of the substituent X, it stands to reason that the anisotropic effect (which is angularly dependent) should vary as the orientation of the substituent is varied. In the earlier work by Williamson (23) and Laszlo and Schleyer (25) concerning the effects of electronegativity of substituents on internal chemical shifts in rigid norbornene derivatives, it was suggested that there might be an angular dependence of the substituent electronegativity effects on the internal chemical shifts. However, only two angles were studied, 0° and 120°, and the electronegativity values used were those of Cavanaugh and Dailey (28). Such electronegativity values, which were derived from chemical shift data, probably reflect some magnetic anisotropy contributions (23). On the other hand, our work on the more flexible furanose ring (Fig. 5) uses true electronegativity values and hence does not include a term for variations due to different orientations of the electronegative substituent X.

In the case of the **3**′-substituted *arabino* compounds, **3**, in Table III, there is also a correlation between the internal chemical shifts $\delta_{H\text{-}2'} - \delta_{H\text{-}3'}$ and the Huggins' electronegativity values, E_R. As with that previously described for $J_{H\text{-}2'\text{-}H\text{-}3'}$ vs. E_R, above, the fit is not as good as that found for the series **1** and **2** and is not included in Fig. 5. The poorer fit in this case may again be accounted for simply by the fact that some of the H-3′ signals for the compounds **3** are only approximate.

Synthetic Studies

The reaction of 1-(2,3-epoxy-β-D-lyxofuranosyl)uracil (29) with anhydrous HF in dioxane gave 1-(3-deoxy-3-fluoro-β-D-arabinofuranosyl)-uracil, **3**(F), in crystalline form. The reaction did not proceed readily and after 41 h at 116° starting material was still present in the reaction mixture. The reluctance of 2,3-epoxides of sugars to react with this reagent was consistent with the experience of Taylor *et al.* (30). Under less strenuous conditions, HF in dioxane had been found to give 2′-deoxy-2′-fluoro pyrimidine nucleosides in good yield from the appropriate 2,2′-anhydro derivatives (1). The fluoro nucleoside **3**(F) was separated from other products of the reaction by partition chromatography on Celite (31). Six other crystalline nucleoside derivatives were isolated from the reaction mixture. Although two of these contained approximately one atom of fluorine per molecule, neither was the expected 2′-deoxy-2′-fluoro-β-D-xylofuranosyluracil, as shown by their n.m.r. spectra, and these were not investigated further.

Other 3′-deoxy-3′-halogeno nucleosides of the *arabino* configuration (**3**,(Cl, I)) were prepared by the action of the halogen acid in aqueous medium. The chloro derivative was obtained as two isomorphs. The melting point of one of these agreed with that reported by Naito *et al.* (32).

The 2′-halogeno-2′-deoxy nucleosides **1**(F,Cl, Br) were prepared by the action of the appropriate hydrogen halide on 2,2′-anhydro-1-(β-D-arabinofuranosyl)uracil, as previously described (1). The only halogeno analogue not previously reported, the 2′-iodo nucleoside, was prepared in similar fashion. Unfortunately, the yield was low, and the material was obtained only in an amorphous state. Isolation of **1**(I) was complicated by the presence of additional products in the reaction mixture and chromatographic methods were required.

Experimental

Nuclear magnetic resonance spectra were determined on Varian spectrometers, HA-100 and A-60 (equipped with spin decoupler, Varian, model V-6058A). Melting points were by the capillary method and are corrected. Microanalyses were carried out by Spang Microanalytical Laboratory, Ann Arbor, Michigan.

1-(3,5-Di-O-acetyl-2-deoxy-β-D-erythro-pentofuranosyl)-uracil, 2(H)

A mixture of acetic anhydride (1.1 g, 1.07 mmole) and 1-(2-deoxy-β-D-*erythro*-pentofuranosyl)uracil (2′-deoxyuridine, **1**(H), 0.50 g, 2.2 mmoles) in pyridine (15 ml) was maintained at 25° for 17 h. Unreacted acetic anhydride was decomposed with ethanol, and the solvent removed *in vacuo*. Purification was effected by chromatography, column 1.9 × 27 cm, alumina (Bio-Rad, AG 7). Elution with chloroform–ethanol (1:1) gave (330–400 ml fraction of effluent) a colorless solid, 0.30 g (44%), m.p. 103–107°. Crystallization from ethanol gave colorless needles, m.p. 107–110°, $[\alpha]_D^{25}$ +23° (0.6, chloroform).

Anal. Calcd. for $C_{13}H_{16}N_2O_7$: C, 49.98; H, 5.17; N, 8.97. Found: C, 50.04; H, 5.23; N, 9.04.

1-(3-Deoxy-3-fluoro-β-D-arabinofuranosyl)uracil, 3(F)

A mixture of 1-(2,3-epoxy-β-D-lyxofuranosyl)uracil (2.26 g, 1.0 mmole) and liquid hydrogen fluoride (25 ml)

Can. J. Chem. Downloaded from www.nrcresearchpress.com by 210.87.254.6 on 09/05/12
For personal use only.

in dioxane (300 ml) was heated at 116° for 41 h. Water (60 ml) was added to the cooled solution, which was then neutralized with solid calcium carbonate. After filtration of solids and removal of solvent *in vacuo*, the residue was fractionated by chromatography (Celite, 3.8 × 65 cm) as previously described (31). In addition to **3**(F) several as yet unidentified crystalline products, two containing fluorine, were isolated. The 950–1100 ml fraction gave colorless needles from ethanol, 74 mg (3%), m.p. 179.5–180.5°, $[\alpha]_D^{25}$ +118° (0.2, ethanol).

Anal. Calcd for $C_9H_{11}FN_2O_5$: F, 7.72; N, 11.38. Found: F, 7.96; N, 11.46.

Reaction of 3(F) with Base

A sample of **3**(F) in NaOH (0.05 *N*) was heated at 85–95° for 75 min. Neutralization with solid calcium carbonate and treatment with Dowex 50 (H^+ form) gave, after filtration and removal of water *in vacuo*, a colorless solid. Crystallization from ethanol gave large prisms, m.p. 125–129°, which were identical (identical infrared spectrum and no depression of the m.p. of a mixture) with an authentic sample of 1-(2,3-epoxy-β-D-lyxofuranosyl)uracil (29).[5]

1-(3-Chloro-3-deoxy-β-D-arabinofuranosyl)uracil, 3(Cl)

A solution of 1-(2,3-epoxy-β-D-lyxofuranosyl)uracil (0.05 g, 2.1 mmoles) and hydrochloric acid (3 ml, 3 *N*) in dioxane (5 ml) was heated at 60° for 90 min. Co-distillation with benzene was repeated several times *in vacuo*. From ethanol colorless needles, 0.30 g, m.p. 161–166°, were obtained. Recrystallization from ethanol gave needles, m.p. 163–165°, $[\alpha]_D^{25}$ +90° (0.3, ethanol). Naito *et al.* (32) reported m.p. 159–160°, $[\alpha]_D$ + 91.1° (methanol). An isomorph, 88 mg, m.p. 174–178°, was obtained from the mother liquor. Recrystallization from ethanol gave colorless prisms, m.p. 178–179°, $[\alpha]_D^{25}$ +90.9°. Total yield 0.39 g (67%).

Anal. Calcd. for $C_9H_{11}ClN_2O_5$: Cl, 13.52; N, 10.67. Found: Cl, 13.68; N, 10.77.

1-(3-Deoxy-3-iodo-β-D-arabinofuranosyl)uracil, 3(I)

A solution of 1-(2,3-epoxy-β-D-lyxofuranosyl)uracil (2.0 g, 8.9 mmoles) and freshly prepared hydroiodic acid (5.0 ml, 3.5 *N*) in water (10 ml) was allowed to stand at 25° for 30 min. After removal of water *in vacuo* the residue was triturated with chloroform, and a yellow solid (2.10 g) collected. Crystallization from ethanol gave colorless crystals, 1.70 g, (54%), m.p. 204–205°.

Anal. Calcd. for $C_9H_{11}IN_2O_5$: C, 30.54; H, 3.13; I, 35.85; N, 7.92. Found: C, 30.44; H, 3.43; I, 35.84; N, 7.94.

3′,5′-Di-O-acetyl-2′-bromo-2′-deoxyuridine, 2(Br)

A solution of 2′-bromo-2′-deoxyuridine (**1**(Br), 0.5 g, 1.6 mmole) and acetic anhydride (1.0 g, 10 mmoles) in pyridine (5.0 ml) was allowed to stand at 25° for 17 h. A small piece of ice was added, and the mixture taken to dryness *in vacuo*. The residue was triturated with water, and the water decanted. A dry chloroform solution was placed on a silica gel column (1.9 × 28 cm), and the column washed with chloroform (360 ml). Elution with chloroform–acetone (1:1) gave the product as a pale-yellow amorphous gum in the 50–110 ml fraction of effluent $[\alpha]_D^{25}$ + 8.9° (0.4, ethanol).

Anal. Calcd. for $C_{13}H_{15}BrN_2O_7$: C, 39.92; H, 3.87; Br, 20.43; N, 7.16. Found: C, 39.88; H, 3.81; Br, 20.45; N, 7.09.

2′-Deoxy-2′-iodouridine, 1 (I)

A mixture of 2,2′-anhydro-1-β-D-arabinofuranosyluracil (0.5 g) and dioxane (100 ml) was heated at reflux to effect solution. To the cooled suspension was added a freshly prepared solution of HI in dioxane (20 ml). The mixture was heated at 60–70° for 30 min. The supernatant was decanted and heated at 50–60° for about 15 min. To the undissolved residue was added a solution of hydrogen iodide in dioxane (20 ml) and dioxane (100 ml). After 30 min at 70–100° all solid had entered solution. After heating an additional 15 min the cooled solution was combined with the initial supernatant. To the amber-colored solution was added sodium thiosulfate (7 g in 35 ml water), which removed all color from the solution. This was taken to dryness *in vacuo*, leaving a yellow solid. Passage of the material through a column of silica gel (1.2 × 19.5 cm), using methanol–chloroform (1:1) as eluant, removed the unused acid. Purification was achieved by separation on paper (Whatman 3MM), using 1-butanol – water (86:14) as developing solvent. The product was eluted with ethanol from the band at R_f 0.57–0.85. It was obtained as a nearly colorless hygroscopic amorphous solid, m.p. 80–100°, $[\alpha]_D^{25}$ +22° (0.2, water).

Anal. Calcd. for $C_9H_{11}IN_2O_5$: I, 35.84. Found: I, 35.50, 35.59.

3′,5′-Di-O-acetyl-2′-deoxy-2′-iodouridine, 2(I)

A solution of **1**(I) (80–100 mg) in pyridine (3 ml) was treated with acetic anhydride (0.23 ml). The solution was stirred at 23–25° for 17 h. Ethanol (0.2 ml) was added, and the mixture taken to dryness *in vacuo* with a bath temperature below 26°. The light-yellow residue was triturated twice with water (2–5°) for periods of about 60 min. The supernatants were decanted, the residue dissolved in chloroform, and the solution dried over sodium sulfate. After removal of solvent the yellow gum was dissolved in ether (10 ml) and precipitated as colorless solid by the addition of petroleum ether (b.p. 30–60°). The supernatant was decanted, and the residue dried *in vacuo*. The yield of colorless amorphous solid, m.p. 65–100°, was 30–40 mg.

Anal. Calcd. for $C_{13}H_{15}IN_2O_7$: I, 28.96. Found: I, 29.10, 28.94.

[5]Isomorphic with the sample previously reported, m.p. 139.5–140.5°. Either isomorph adopted the other crystalline form when seeded in a concentrated solution in ethanol and allowed to crystallize.

Acknowledgments

We deeply appreciate the excellent work of Marvin Olsen of this laboratory in determining the 60 MHz spectra and of Ross K. Pitcher of Hoffmann-LaRoche, Inc., Nutley, New Jersey, who has kindly supplied us with the ^{19}F and 100 MHz spectra.

1. J. F. CODINGTON, I. L. DOERR, and J. J. FOX. J. Org. Chem. **29**, 558 (1964); **29**, 564 (1964).

2. I. L. DOERR and J. J. FOX. J. Org. Chem. **32**, 1462 (1967).
3. J. F. CODINGTON, I. L. DOERR, and J. J. FOX. Carbohydrate Res. **1**, 455 (1966).
4. R. J. CUSHLEY, J. F. CODINGTON, and J. J. FOX. Carbohydrate Res. **5**, 31 (1967).
5. R. U. LEMIEUX and D. R. LINEBACK. Ann. Rev. Biochem. **32**, 156 (1963).
6. L. D. HALL. *In* Advances in carbohydrate chemistry. Vol. 19. *Edited by* M. L. Wolfrom. Academic Press, Inc., New York. 1964. p. 51.
7. (*a*) M. KARPLUS. J. Chem. Phys. **30**, 11 (1959). (*b*) M. KARPLUS. J. Am. Chem. Soc. **85**, 2870 (1963).
8. K. L. WILLIAMSON, Y. F. LI, F. H. HALL, and S. SWAGER. J. Am. Chem. Soc. **88**, 5680 (1966).
9. L. D. HALL and J. F. MANVILLE. Abstracts 153rd Meeting of the American Chemical Society, Miami Beach, Florida, April 1967. p. C29.
10. J. JONAS, A. ALLERHAND, and H. S. GUTOWSKY. J. Chem. Phys. **42**, 3396 (1965). L. D. HALL and J. F. MANVILLE. Chem. Ind. London, 991 (1965).
11. K. S. PITZER and W. E. DONATH. J. Am. Chem. Soc. **81**, 3213 (1959).
12. R. U. LEMIEUX, J. D. STEVENS, and R. R. FRASER. Can. J. Chem. **40**, 1955 (1962).
13. C. D. JARDETZKY. J. Am. Chem. Soc. **82**, 229 (1960).
14. C. D. JARDETZKY. Federation Proc. Abstracts, **20**, 355A (1961).
15. R. U. LEMIEUX. Can. J. Chem. **39**, 116 (1961).
16. C. D. JARDETZKY. J. Am. Chem. Soc. **83**, 2919 (1961).
17. D. R. HARRIS and W. M. MACINTYRE. Biophys. J. **4**, 203 (1964).
18. S. FURBERG. Acta Cryst. **3**, 325 (1950).
19. R. J. CUSHLEY. Unpublished results.
20. C. D. JARDETZKY. J. Am. Chem. Soc. **84**, 62 (1962).
21. S. L. SPASSOV, D. L. GRIFFITH, E. S. GLAZER, K. NAGARAJAN, and J. D. ROBERTS. J. Am. Chem. Soc. **89**, 88 (1967). A. D. CROSS. J. Am. Chem. Soc. **86**, 4011 (1964).
22. H. F. WHITE. Anal. Chem. **37**, 403 (1965).
23. K. L. WILLIAMSON. J. Am. Chem. Soc. **85**, 516 (1963).
24. R. J. ABRAHAM and K. G. R. PACHLER. Mol. Phys. **7**, 165 (1963).
25. P. LASZLO and P. v. R. SCHLEYER. J. Am. Chem. Soc. **85**, 2709 (1963).
26. M. L. HUGGINS. J. Am. Chem. Soc. **75**, 4123 (1953).
27. D. H. WILLIAMS and N. S. BHACCA. J. Am. Chem. Soc. **86**, 2742 (1964). H. BOOTH. Tetrahedron Letters, 411 (1965).
28. J. R. CAVANAUGH and B. P. DAILEY. J. Chem. Phys. **34**, 1099 (1961).
29. J. F. CODINGTON, R. FECHER, and J. J. FOX. J. Org. Chem. **27**, 163 (1962).
30. N. F. TAYLOR, R. F. CHILDS, and R. V. BRUNT. Chem. Ind. London, 928 (1964).
31. J. J. FOX, J. F. CODINGTON, N. C. YUNG, L. KAPLAN, and J. O. LAMPEN. J. Am. Chem. Soc. **80**, 5155 (1958).
32. T. NAITO, M. HIRATA, Y. NAKAI, T. KOBAYASHI, and M. KANAO. Chem. Pharm. Bull. Tokyo, **13**, 1258 (1965).

Can. J. Chem. Downloaded from www.nrcresearchpress.com by 210.87.254.6 on 09/05/12
For personal use only.

Nitrations of acetanilides by reagents of NO_2X type[1]

BRIAN M. LYNCH,[2] CATHERINE M. CHEN,[3] AND YUK-YUNG WIGFIELD[4]
Organic Chemistry Laboratory, Saint Francis Xavier University, Antigonish, Nova Scotia
Received October 17, 1967

The distribution of products in the nitration of a series of eight substituted acetanilides has been studied using differing nitrating agents.

With mixed nitric and sulfuric acids, attack *para* to the acetamido group is favored, while with acetyl nitrate or nitronium tetrafluoroborate, predominant *ortho* substitution occurs. It is suggested that *ortho* substitution results from S_N2 displacement by a pair of substituent electrons (on nitrogen or carbonyl oxygen) on the species NO_2X (X = BF_4 or OAc), leading to formation of the most readily accessible σ complex, while the *para* substitution favored in mixed acids results from substitution in the conjugate acid of acetanilide.

Nitroacetanilides follow an unusual path with acetyl nitrate, yielding the corresponding dinitrobenzene in addition to the expected dinitroacetanilides.

Nuclear magnetic resonance spectroscopy efficiently demonstrates the structures of the reaction products, and reveals the preferred intramolecularly hydrogen-bonded conformation of *ortho*-nitroacetanilides.

Canadian Journal of Chemistry, 46, 1141 (1968)

Introduction

Much discussion has centered around aromatic nitrations by preformed nitronium salts as compared with more conventional reagents, since apparent changes in substrate selectivity occur without any great variation in positional selectivity (1–3). A recent report by Ridd (4) indicates that the unusually low substrate selectivities noted for the nitronium-salt nitrations probably reflect diffusion-controlled reaction rates. On the other hand, there are several examples where positional selectivity is highly sensitive to the nature of the substituting agent; little information is available regarding substrate selectivities in these reactions. Thus, nitration of biphenyl by nitric acid – acetic anhydride, by nitrogen pentoxide in acetonitrile, or by nitronium tetrafluoroborate in sulfolane, gives ortho:para ratios exceeding 1, while nitric acid – sulfuric acid gives a ratio of ca. 0.6 (5, 6). Nitration of anisole by nitric acid – acetic anhydride or by nitronium tetrafluoroborate in sulfolane gives ortho:para ratios close to 2, while with nitric acid – sulfuric acid, the ratio is 0.5 (7, 8).

These results have been rationalized by Taylor (6), who proposes direct interaction of *p*- or π-electrons of the aromatic substrate, effecting a nucleophilic displacement on the species NO_2X (which may be an ion-pair), and leading to predominant ortho substitution. This direct interaction is superimposed upon a normal pattern produced by free nitronium ions in the reaction medium.

A specific interaction appropriate to protonated acetyl nitrate (coordination of its electron-deficient carbonyl carbon to the lone pair of the substituent) is not acceptable in view of the similar positional selectivities shown by protonated acetyl nitrate (which is the active species in nitric acid – acetic anhydride mixtures, cf. Bordwell and Garbisch (9)) and nitronium tetrafluoroborate; a postulate of linear coordination between free nitronium ion and substituent lone-pair electrons (7) is also unacceptable, since all sources of nitronium ion should then behave similarly (6).

Acetanilide also exhibits reagent-dependent orientation in nitration; nitric and sulfuric acids yield paranitroacetanilide as major product, while with nitric acid – acetic anhydride, ortho-nitration is favored (10). If Taylor's rationalization is correct, nitration of acetanilides by preformed nitronium salts should yield substituted ortho-nitroacetanilides as the predominant products. This paper reports, *inter alia*, a test of Taylor's proposal for reagent-dependent orientation in nitrations.

We have examined the distribution of products

[1]This investigation was supported by the Petroleum Research Fund (Grant 794-B5) and by the National Research Council of Canada (Grant A-964). Presented in part at the 47th Conference of the Chemical Institute of Canada, Kingston, Ontario, June, 1964.

[2]Enquiries should be addressed to this author.

[3]Graduate Research Assistant, 1966–1967. Present address: State University of New York, Binghamton, New York, U.S.A.

[4]Graduate Research Assistant, 1962–1964. Present Address: University of British Columbia, Vancouver, British Columbia.

Can. J. Chem. Downloaded from www.nrcresearchpress.com by 210.87.254.5 on 09/05/12
For personal use only.

obtained in the nitrations of a series of eight substituted acetanilides, using three different nitrating systems: nitric acid – sulfuric acid, nitric acid – acetic anhydride, and nitronium tetrafluoroborate in acetonitrile. Some competitive nitrations of toluene and acetanilide were also examined.

Experimental

General

Microanalyses were carried out by the Schwarzkopf Microanalytical Laboratory, Woodside, New York. Melting points were measured on a Fisher–Johns apparatus or on a Kofler "Heizbank", and are corrected. Infrared spectra were recorded on a Beckman IR-8 spectrophotometer; samples were examined as suspensions in potassium chloride disks. Proton magnetic resonance spectra were recorded with Varian A-60A or HA-100 spectrometers. Signals are expressed in parts per million from tetramethylsilane, present as an internal reference. Gas–liquid chromatographic analyses were made on an Aerograph A-90P3 instrument with a thermal conductivity detector. Helium was used as the carrier gas, and the analytical column used was 6 ft × 1/4 in 5% silicone SE-30 partitioning phase supported on 60–80 mesh chromosorb P coated with dimethyldichlorosilane. All nitronium-salt nitrations were carried out in a dry box in an atmosphere of purified dry nitrogen.

Starting Materials

The acetanilides were prepared by standard methods from commercial samples of the corresponding anilines. Their melting points were identical with literature values and their nuclear magnetic resonance (n.m.r.) spectra indicated no contamination by isomeric compounds. Nitronium tetrafluoroborate was supplied by K. and K. Laboratories, Plainview, New York.

General Procedures for Nitrations

(a) By Nitric Acid – Acetic Anhydride

A solution of nitric acid (*d*, 1.52, 6 ml) in acetic anhydride (15 ml), prepared at 15–20°, was cooled to −5° and added to a saturated solution of the substituted acetanilide (10 g) in acetic anhydride at 0°, over 15 min. The solution was kept at 0° for 1 h and was poured onto ice. The resulting mixture was extracted with benzene and washed free of acid, and subjected to adsorption chromatography on basic alumina (benzene as eluent), followed by crystallization from ethanol; alternatively, the washed benzene extract was concentrated and injected directly into the inlet port of the gas–liquid chromatograph (column temperature 170–190°); the proportions of the isomeric products were determined by comparison of peak areas and relative retention times with those of authentic samples. Identities were further checked by gas–liquid chromatography of the nitroanilines obtained by hydrolysis of the crude mixture of nitroacetanilides. The results are summarized in Table I.

(b) In Nitric Acid – Sulfuric Acid

The substituted acetanilide (5.0 g) was dissolved in sulfuric acid (*d*, 1.84, 10 ml) and was cooled to 0°, and a mixture of nitric acid (*d*, 1.42, 10 ml) and sulfuric acid (*d*, 1.84, 13 ml) was added at 0°; the mixture was kept at 0° for 1 h and poured into water. The resulting mixture was extracted with benzene and washed free of acid, and the extract was evaporated and the residue was crystallized from ethanol, or the benzene extract was concentrated and injected for gas–liquid chromatographic analysis as above. The results are summarized in Table II.

TABLE I

Nitration of acetanilides by nitric acid – acetic anhydride

Substituent in acetanilide	5-Substituted 2-Nitroacetanilide		Ortho:para ratio†
	Yield (%)*	Melting point °C	
Nil	72	93(93)‡	4.2
3-Br	57	138(139)	8.5
3-Cl	62	118(120)	9.0
3-F	77	90§	9.1
3-I	63	158‖	5.0
3-OMe	56¶	125(125)	4.0
3-Me	58	87(87)	4.5

*Of crystallized product.
†Determined by gas–liquid chromatography.
‡Literature melting points are given in parentheses.
§Anal. Calcd. for $C_8H_7FN_2O_3$: C, 48.89; H, 3.56; N, 14.14. Found: C, 48.88; H, 3.81; N, 13.88.
‖Anal. Calcd. for $C_8H_7IN_2O_3$: C, 31.40; H, 2.15; N, 8.95. Found: C, 31.05; H, 2.38; N, 8.78.
¶In addition to the 5-methoxy-2-nitroacetanilide, 11% of 3-methoxy-4-nitroacetanilide, m.p. 164° (lit. 165°) was obtained.

(c) With Nitronium Tetrafluoroborate

The acetanilide (1 g) was dissolved in acetonitrile (10 ml) and the solution was cooled to −30°. Finely powdered nitronium tetrafluoroborate (1 g) was added slowly at such a rate that the temperature did not rise above −10°. After 30 min, the reaction mixture was poured into cold water, and the precipitated nitroacetanilides were collected, washed, and dried. Yields were virtually quantitative (greater than 90%) for the nitrations of acetanilide, 3-fluoroacetanilide, 3-chloroacetanilide, and 3-iodoacetanilide, and the ortho:para ratios (established, as above, by gas–liquid chromatography) exceeded 10.

Atypical Nitrations

Nitroacetanilides

Nitroacetanilides were unaffected by nitric acid – acetic anhydride at 0°. Reaction at 50–55° using the general conditions specified above yielded 2,5-dinitroacetanilide (4.5 g), m.p. 122° (lit. m.p. 121°) and 1,3-dinitrobenzene (0.5 g), m.p. 88° (lit. m.p. 90°) (infrared and n.m.r. spectra identical with an authentic sample) from 3-nitroacetanilide. In similar reactions with 2- and 4-nitroacetanilides, adsorption chromatography (basic alumina, with benzene as eluent) gave small amounts (0.2 g) of the corresponding dinitrobenzenes as the most rapidly eluted materials. The 1,2-dinitrobenzene was identical in m.p. (118°), infrared and n.m.r. spectra with an authentic sample, while the 1,4-dinitrobenzene had m.p. 172° (lit. 172°) and its n.m.r. spectrum in deuteriochloroform showed a single peak at 8.60 p.p.m.

N-Methylacetanilide

Four grams of material was nitrated at 25° for 12 h using the general conditions of part (*a*) above. Chromatog-

Can. J. Chem. Downloaded from www.nrcresearchpress.com by 210.87.254.5 on 09/05/12
For personal use only.

TABLE II

Nitrations of acetanilides in sulfuric acid

Substituent in acetanilide	Major product	Yield (%)*	Melting point °C	Ortho:para ratio†
Nil	4-nitroacetanilide	75	216(216)‡	0.05
3-Cl	3-chloro-4-nitroacetanilide	60	141(145)	0.04
3-F	3-fluoro-4-nitroacetanilide	52	174§	0.04
3-OMe‖	3-methoxynitroacetanilide	50	164(165)	0.05
3-Br¶	3-bromo-4-nitroacetanilide	40	145**	0.08
3-Br	4,6-dinitro-3-bromoacetanilide	60	166††	—
3-Me	4,6-dinitro-3-methylacetanilide	50	103(103)	—

*Recrystallized product.
†By gas–liquid chromatography.
‡Literature melting points are in parentheses.
§Anal. Found: C, 48.70; H, 3.50.
‖Reaction period: 12 min at 0°.
¶Reaction period: 5 min at 0°.
**Anal. Calcd. for $C_8H_7BrN_2O_3$: N, 10.73. Found: 11.02.
††Anal. Calcd. for $C_8H_6BrN_3O_5$: N, 13.82. Found: 13.55.

TABLE III

Competitive nitration experiments

Reagent	Substrate A	Ortho:para ratio of products	Substrate B	Ortho:para ratio of products	Relative yields of nitration products ($NO_2 \cdot A/NO_2B$)
$HNO_3 - Ac_2O$	acetanilide	4.5 ± 0.5	toluene	1.32 ± 0.10	0.22 ± 0.05
NO_2BF_4 in MeCN	acetanilide	3.5 ± 0.5	toluene	1.30 ± 0.10	1.70 ± 0.10
$HNO_3 - H_2SO_4$	acetanilide	< 0.05	*p*-nitrotoluene	—	0.22 ± 0.03

raphy on alumina (benzene as eluent) yielded 4-nitro-*N*-methylacetanilide (2.8 g), m.p. 150° (lit. m.p. 152–153°) after crystallization from methanol. No ortho-isomer could be detected.

Competitive Nitrations

Equimolar mixtures of the substrates indicated in Table III were nitrated competitively using the conditions outlined above in the general procedures for nitrations, except that the amount of nitric acid or nitronium salt was decreased to 0.10 mole per mole of combined substrates, and the nitronium salt was dissolved in acetonitrile before addition to the substrates (also in acetonitrile). A reaction temperature of 0° was used. The crude nitroacetanilides and nitrotoluenes were collected together with unreacted substrates, after separation from unreacted toluene by chromatography on alumina, and were dissolved in acetic acid-d_4: the composition of the mixtures was established by integration of the n.m.r. signals from the methyl protons of the acetamido and the methyl groups. The relevant chemical shifts (in Hz from tetramethylsilane) were: 2-nitroacetanilide, 136.0; 4-nitroacetanilide, 133.0; 2-nitrotoluene, 152.0; 4-nitrotoluene, 145.0; 2,4-dinitrotoluene, 160.0. Analysis of control mixtures of known composition showed that this method was accurate to $\pm 3\%$. The ortho:para ratios obtained in the nitrations of single compounds were also checked by the n.m.r. integration method, and the results are assembled in Table III.

Attempted Synthesis of N-Nitroacetanilide

N-Nitrosoacetanilide, m.p. 50° (10.0 g), in chloroform (30 ml) was added to a mixture of 30% hydrogen peroxide (6.8 g) and trifluoroacetic anhydride (6.8 g), and the mixture was stirred vigorously for 12 h. The mixture was extracted with sodium bicarbonate, and the residue was dried and chromatographed on alumina using chloroform as eluent. Acetanilide (3.5 g, 47%), m.p. 113° (identical (m.p., mixture m.p., infrared spectra) with an authentic sample) was obtained from the eluted solution on evaporation.

Discussion

Structures of Nitration Products

In most cases, the structures of the major nitration products of the acetanilides obtained using the various reagents were evident from the correspondence of their melting points, and the melting points of the nitroanilines obtained by hydrolysis, with literature values; nuclear magnetic resonance spectra (see section (*d*) below) gave further supporting evidence. The new 5-halogeno-2-nitroacetanilides (the fluoro- and iodo-compounds) were further identified by the fact that their infrared spectra showed the following strong bands in common with those

Can. J. Chem. Downloaded from www.nrcresearchpress.com by 210.87.254.5 on 09/05/12
For personal use only.

Can. J. Chem. Downloaded from www.nrcresearchpress.com by 210.87.254.5 on 09/05/12
For personal use only.

of the known bromo and chloro compounds: 3350 cm^{-1} (ν_{NH}), 1695 cm^{-1} (ν C=O), 1493 and 1333 cm^{-1} (asymmetric and symmetric N—O vibrations), and 865, 845, 820, and 748 cm^{-1} (δ_{C-H}, out-of-plane); this resemblance in major spectral features is to be expected since the heavy halogen atoms have little effect on the vibrations in the rest of the molecule.

However, there is some uncertainty regarding the nature of the nitration products of 3-methoxyacetanilide. Reverdin and Widmer (11) found that nitration by 70% nitric acid at 65° gave two methoxynitroacetanilides, of melting points 125° and 165°, in 65% overall yield, which were hydrolyzed to the corresponding anilines, m.p. 129° and 169°; these were assigned as the 5-methoxy-2-nitro- and 3-methoxy-4-nitro compounds. More recently, Dyall and Pausacker (12) assigned the methoxynitroacetanilide of m.p. 125° as 3-methoxy-4-nitroacetanilide, and describe 3-methoxy-4-nitroaniline as having m.p. 131°. After hydrolysis of their nitration mixture, they obtained a compound, m.p. 157°, which was assigned as 3-methoxy-2,4-dinitroaniline on the basis of a strong infrared absorption band at 830 cm^{-1}, supposedly characteristic of 1,2,3,4-tetrasubstitution. However, Bellamy (13) warns that absorption in this region is "a feature of aromatic nitro compounds, which should not be forgotten when attempts are made to recognize ring-substitution arrangements by the δ—CH frequencies in this region".

We find that the methoxynitroacetanilide of m.p. 125° (obtained as the major product from acetyl nitrate nitration of 3-methoxyacetanilide at 0°) is 5-methoxy-2-nitroacetanilide; the corresponding amine has m.p. 131°. 3-Methoxy-4-nitroacetanilide, m.p. 164°, is also obtained, and yields the corresponding amine, m.p. 169°, on hydrolysis. Definite chemical proof of structure for 5-methoxy-2-nitroaniline is provided by its conversion to 5-methoxybenzofuroxan, m.p. 116°, by oxidation with iodosobenzene diacetate in benzene (cf. Pausacker and Scroggie (14)).

The infrared spectrum of the 3-methoxy-4-nitroaniline showed all the absorption bands quoted for "3-methoxy-2,4-dinitroaniline", and this product should therefore be withdrawn from the literature.

Positional and Substrate Selectivities

The general trend of the results is in agreement with expectations based on Taylor's proposal of S_N2 displacement on a species NO_2X; the 3-substituted acetanilides give predominant ortho substitution with acetyl nitrate and with nitronium tetrafluoroborate, while with mixed nitric and sulfuric acids, where *free* nitronium ions are present, predominant para substitution is observed.

The question remains whether the reaction of an acetanilide with a nitrating agent of NO_2X type occurs as in Scheme 1, path (*a*) (where the electron pair on oxygen is the effective nucleophile) or as in path (*b*) (where the electron pair on carbonyl oxygen is the nucleophile (cf. Norman and Radda (15)).

If path (*a*) is accepted, then there is some evidence that the π-complex represented as an intermediate stage between the reagents Ph·NHAc and NO_2X and the σ-complex for ortho-nitration should not be depicted as the conjugate acid of the hypothetical *N*-nitroacetanilide, since attempts to synthesize *N*-nitroacetanilide by peroxy-acid oxidation of *N*-nitrosoacetanilide (cf. Emmons and Ferris (16)) led to fragmentation to acetanilide in good yield, with no detectable ring-nitration. However, as a referee points out, the conditions for the fragmentation and the normal nitration reactions are not comparable.

If path (*b*) is accepted, then we must postulate that the *O*-nitrated intermediate does not form in highly acid media, since the oxygen atom will be protonated (for evidence of the predominant *O*-protonation of amides, see Gillespie and Birchall (17)). However, the protonated acetamido group will continue to exert a +R effect at the para position, thus accounting for the observed paraorientation.

The small changes in positional selectivity with temperature and with the nature of the nitrating reagent NO_2X are in the expected directions, although scarcely outside experimental reproducibility. Thus, Taylor (5, 6) noted that the ortho:para ratio in the nitration of biphenyl decreases with increasing temperature, in agreement with the differences noted for the nitronium tetrafluoroborate nitrations at −10 and 0°, while at 0°, acetyl nitrate appears to give a slightly greater positional selectivity than nitronium tetrafluoroborate (Table III), possibly reflecting the greater ease of displacement in the ion-pair.

The relative reactivities of toluene and acet-

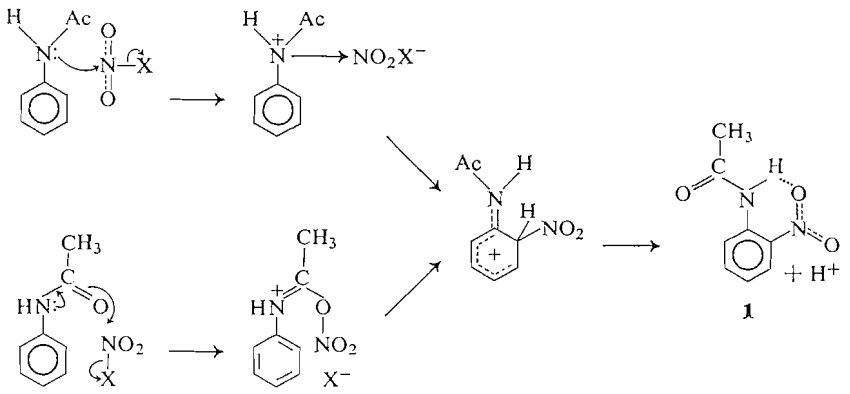

SCHEME 1

anilide towards the nitrating agents would be of interest, and some experiments were carried out seeking this information. The significance of the results with nitronium tetrafluoroborate is questionable, since the reactions are very rapid (Ciaccio and Marcus (18)) found that the rate constant for nitration of *nitrobenzene* by nitronium tetrafluoroborate in acetonitrile at 24° was 0.11 l mole^{-1} min^{-1}), and kinetic control is not certain. However, acetanilide is apparently more reactive than toluene towards nitration by nitronium tetrafluoroborate, and with acetyl nitrate, where kinetic competition was probably observed, toluene is somewhat more reactive. When toluene and acetanilide were allowed to compete for small amounts of nitric acid in sulfuric acid, the toluene was dinitrated to a considerable extent, implying that toluene is far more reactive than the conjugate acid of acetanilide; in confirmation, a competitive experiment with *p*-nitrotoluene and acetanilide using mixed nitrating acids indicated that these compounds were of the same order of reactivity. Once again, however, kinetic competition is not assured under the conditions used.

The results probably allow order-of-magnitude assignments of total reactivity as compared with benzene, as follows: toluene, 25 (1–4); acetanilide/NO_2BF_4, 50; acetanilide/$AcONO_2$, 5; *p*-nitrotoluene, 10^{-7}; conjugate acid of acetanilide, 10^{-8}.

Formation of Dinitrobenzenes from Nitroacetanilides

The formation of small proportions of the corresponding dinitrobenzenes on treatment of the three nitroacetanilides with acetyl nitrate at 50–55° may be explained by postulating that the acetamido group is *N*-nitrosated by nitrosonium ion (perhaps generated by dissociation of N_2O_4 into NO^+ and NO_3^- (19)), then rearranging to the diazoacetate, in turn giving the corresponding diazonium ion, which then undergoes nucleophilic displacement by nitrite ion. This sequence is admittedly speculative, but resembles that suggested previously for the replacement of the acetamido group by bromine using hydrobromic acid – nitric acid (19).

Nuclear Magnetic Resonance Spectra of Nitroacetanilides and Nitroanilines

The spectra of the various nitroacetanilides and nitroanilines obtained from the preparative selective nitrations were sufficiently characteristic for direct assignment of structure. In most cases, the spectra were analyzed as ABX systems (20), and the individual proton chemical shifts were extracted (100 MHz spectra were recorded for compounds where the ABX approximation was not valid at 60 MHz). The shifts are listed in Table IV.

It is to be expected that the acetamido group will exhibit anisotropic deshielding effects at the ortho positions (cf. Carter (21)), but will exert a net shielding effect at meta and para positions; Carter finds that the chemical shifts for the ring protons in acetanilide are shifted from the value for benzene (7.33 p.p.m.) as follows: (+ designates downfield, — upfield shift) ortho-, +0.16; meta-, —0.08; para-, —0.28. Accepting qualitative effects in this order, and using the parameters already available for many other substituents (22, 23), then the ring proton chemical shifts listed in Table IV are consistent in every case with the assigned structures. Further, we have shown (24) that the

Can. J. Chem. Downloaded from www.nrcresearchpress.com by 210.87.254.5 on 09/05/12
For personal use only.

Can. J. Chem. Downloaded from www.nrcresearchpress.com by 210.87.254.5 on 09/05/12
For personal use only.

TABLE IV

Chemical shifts for substituted nitroanilines and nitroacetanilides

Solvent	Ring substituents or ring proton signals at position*						Other signals
	1	2	3	4	5	6	
$CDCl_3$	NHAc	NO_2	8.03(−0.17)	7.60(−0.17)	Br	9.00(+1.23)	Acetyl, 2.27
Me_2CO-d_6	NHAc	NO_2	8.15(−0.05)	7.80(+0.03)	Br	8.85(+1.08)	Acetyl, 2.37
$CDCl_3$	NHAc	NO_2	8.63(−0.52)	NO_2	Br	9.37(+1.40)	Acetyl, 2.33
$CDCl_3$	NHAc	NO_2	8.10(−0.16)	7.07(−0.49)	Cl	8.82(+1.26)	Acetyl, 2.25
DMSO	NH_2	NO_2	7.98(−0.28)	6.63(−0.93)	Cl	7.08(−0.48)	Amino, 7.67
$CDCl_3$	NHAc	NO_2	8.30(+0.04)	6.87(−0.36)	F	8.67(+1.44)	Acetyl, 2.33
$CDCl_3$	NHAc	NO_2	7.92(−0.11)	7.50(−0.44)	I	9.23(+1.29)	Acetyl, 2.27
$CDCl_3$	NHAc	NO_2	8.03(−0.19)	6.50(−0.61)	OMe	8.28(+1.17)	Acetyl, 2.20
DMSO	NH_2	NO_2	7.92(−0.30)	6.22(−0.89)	OMe	6.45(−0.66)	Amino, 7.43
DMSO	NH_2	NO_2	7.90(−0.25)	6.21(−1.16)	Me	6.40(−0.97)	Amino, 7.40
DMSO	NH_2	NO_2	8.73(−0.37)	NO_2	Me	6.90(−0.68)	Amino, ca. 8.00
DMSO	NH_2	6.70(−0.86)	Cl	NO_2	7.78(−0.48)	6.55(−0.87)	
Me_2CO-d_6	NHAc	8.13(+0.57)	Cl	NO_2	8.07(−0.19)	7.67(+0.25)	Acetyl, 2.17
DMSO	NH_2	6.55(−0.68)	F	NO_2	7.83(−0.43)	6.47(−0.85)	Amino, 6.95
Me_2CO-d_6	NHAc	8.32(+0.55)	Br	NO_2	8.05(−0.15)	7.80(+0.29)	Acetyl, 2.17
$CDCl_3$	NHAc	7.78(+0.67)	OMe	NO_2	7.88(−0.36)	6.78(+0.40)	Acetyl, 2.20
DMSO	NH_2	6.33(−1.04)	Me	NO_2	7.85(−0.30)	6.40(−0.90)	Amino, 6.39

*Quantities in parentheses are substituent shifts assigned to the 1-substituent.

Can. J. Chem. Downloaded from www.nrcresearchpress.com by 210.87.254.5 on 09/05/12
For personal use only.

amino proton chemical shifts of substituted anilines in dimethyl sulfoxide are dependent upon the nature and orientation of substituents; here again the observed shifts are consistent with the assigned structures.

It is possible to isolate the effects of the amino or acetamido groups on the various ring proton resonances by assuming that the effects of all other substituents are additive, so that the difference between the observed signal positions and that for benzene (7.33 p.p.m.) arises from the constant specific effects of the other substituents, together with the effect of the amino or acetamido group. The residual shift when the other substituents are taken into account is then assignable to the amino or acetamido group, and the quantities in parentheses in Table IV are these residual shifts.

The shielding effects of the amino group for the 2-nitroanilines in dimethyl sulfoxide are 0.25–0.37 p.p.m. for the 3-proton, 0.89–1.16 p.p.m. for the 4-proton, and 0.48–0.97 p.p.m. for the 6-proton; for the 4-nitroanilines, the effects at the 2- and 6-protons range from 0.68 to 1.04 p.p.m., and at the 5-proton, from 0.30–0.48 p.p.m. For a series of substituted anilines in deuteriochloroform,[5] the mean shifts assignable to the amino group were: 2-proton, 0.82; 3-proton, 0.20; 4-proton, 0.72; 5-proton, 0.27; 6-proton, 0.67 p.p.m., so that the amino group effects in dimethyl sulfoxide are quite consistent with those noted for deuteriochloroform solutions.

The acetamido group in the 2-nitroacetanilides shields the 4-proton by 0.17–0.61 p.p.m., and the 3-proton by a smaller amount (ranging from a deshielding of 0.04 p.p.m. to shielding of 0.19 p.p.m.; the abnormal shielding noted for 5-bromo-2,4-dinitroacetanilide is ascribed to twisting of the 4-nitro group out of the ring plane under the influence of the adjacent bromine). The 6-proton is drastically deshielded (1.17–1.44 p.p.m.), and it is suggested that this effect reflects the existence of a strong intramolecular hydrogen bond between nitro oxygen and acetamido hydrogen, so that the acetamido group is constrained into a conformation with the carbonyl group *cis* to, and coplanar with, the benzene ring, as in structure **1**. The 6-proton in the substituted 2-nitroacetanilides is thus in the deshielding zone of the acetamido carbonyl group. The ortho-deshielding effects are much greater in the planar 2-nitroacetanilides of Table IV than in the non-planar (21, 25) parent acetanilide, and these large shifts are regarded as presumptive evidence for strong intramolecular hydrogen-bonding. Independently, Rae, Sternhell, and their co-workers[5] have reached similar conclusions; the n.m.r. method provides unequivocal indications of the presence of such bonds in suitable 2-substituted acetanilides (contrast the extensive infrared spectroscopic study by Dyall and Kemp (26), where no unique test for intramolecular hydrogen bonding could be established).

It is considered likely that part of the driving force for the ortho-nitrations depicted in Scheme 1 paths (*a*) and (*b*) is this strong hydrogen-bonding interaction between nitro group and acetamido hydrogen; in support of this contention, in the acetyl nitrate nitration of *N*-methylacetanilide, where the hydrogen-bonding interaction is eliminated, 4-nitro-*N*-methylacetanilide is the major reaction product.

Acknowledgments

We thank the donors of the Petroleum Research Fund, administered by the American Chemical Society, for a grant in aid of undergraduate research, and the National Research Council of Canada for continued generous support through operating and major equipment grants.

We are pleased to acknowledge valuable discussions with Dr. I. D. Rae (Monash University), and the courtesy of Mr. R. G. Pitcher (Varian Associates Applications Laboratory, Pittsburgh) in recording 100 MHz nuclear magnetic resonance spectra.

1. G. A. OLAH, S. J. KUHN, and S. H. FLOOD. J. Am. Chem. Soc. **83**, 4571 (1961).
2. W. S. TOLGYESI. Can. J. Chem. **43**, 343 (1965).
3. G. A. OLAH and N. A. OVERCHUK. Can. J. Chem. **43**, 3279 (1965).
4. J. H. RIDD. Studies in chemical structure and reactivity. Methuen, London. 1966. p. 152.
5. R. TAYLOR. J. Chem. Soc. B, 727 (1966).
6. R. TAYLOR. Tetrahedron Letters, 6093 (1966).
7. P. KOVACIC and J. J. HILLER. J. Org. Chem. **30**, 2871 (1965).
8. P. H. GRIFFITHS, W. A. WALKEY, and H. B. WATSON. J. Chem. Soc. 631 (1934).
9. F. G. BORDWELL and E. W. GARBISCH. J. Am. Chem. Soc. **82**, 3588 (1960).
10. F. ARNALL and T. LEWIS. J. Soc. Chem. Ind. London, **48**, 159T (1929).
11. F. REVERDIN and K. WIDMER. Ber. **46**, 4066 (1913).

[5] I. D. Rae. Personal communication.

12. L. K. DYALL and K. H. PAUSACKER. Australian J. Chem. **11**, 491 (1958).
13. L. J. BELLAMY. The infrared spectra of complex molecules. 2nd ed. Methuen, London. 1958. p. 304.
14. K. H. PAUSACKER and J. G. SCROGGIE. Australian J. Chem. **11**, 485 (1958).
15. R. O. C. NORMAN and G. K. RADDA. J. Chem. Soc. 3030 (1961).
16. W. D. EMMONS and A. F. FERRIS. J. Am. Chem. Soc. **76**, 3468 (1954).
17. R. J. GILLESPIE and T. BIRCHALL. Can. J. Chem. **41**, 148 (1963).
18. L. L. CIACCIO and R. A. MARCUS. J. Am. Chem. Soc. **84**, 1838 (1962).
19. W. F. BEECH and N. LEGG. J. Chem. Soc. 961 (1950). F. BELL and K. R. BUCK. J. Chem. Soc. 4601 (1965).
20. J. W. EMSLEY, J. FEENEY, and L. H. SUTCLIFFE. High resolution nuclear magnetic resonance spectroscopy. Vol. I. Pergamon Press, London. 1965. p. 357.
21. R. E. CARTER. Acta Chem. Scand. **21**, 75 (1967).
22. H. SPIESECKE and W. G. SCHNEIDER. J. Chem. Phys. **35**, 731 (1961).
23. P. DIEHL. Helv. Chim. Acta, **44**, 829 (1961).
24. B. M. LYNCH, B. C. MACDONALD, and J. G. K. WEBB. Tetrahedron, **24**, 3595 (1968).
25. M. J. ARONEY, R. J. W. LEFEVRE, and A. N. SINGH. J. Chem. Soc. B, 1183 (1966).
26. L. K. DYALL and J. E. KEMP. Spectrochim. Acta, **22**, 483 (1966).

Can. J. Chem. Downloaded from www.nrcresearchpress.com by 210.87.254.5 on 09/05/12
For personal use only.

Can. J. Chem. Downloaded from www.nrcresearchpress.com by 210.87.254.42 on 09/05/12
For personal use only.

Chemistry of diarylazoalkanes. I. Synthesis of *p,p'*-disubstituted azocumenes and their decomposition products[1,2]

J. Reid Shelton,[3] Joseph F. Gormish, Chih Kuo Liang, Patricia Lyons Samuel,[4] and Peter Kovacic

Department of Chemistry, Case Western Reserve University, Cleveland, Ohio 44106

and

Leroy W. Haynes[5]

Department of Chemistry, College of Wooster, Wooster, Ohio 44691

Received October 24, 1967

p,p'-Disubstituted azocumenes were prepared from the requisite *p*-substituted cumylamines, p-$XC_6H_4C(CH_3)_2NH_2$, X = CH_3, CH_3CH_2, $(CH_3)_2CH$, $(CH_3)_3C$, or Br, by treatment with iodine pentafluoride. The major products from thermal decomposition were dicumyls, along with minor amounts of cumenes and α-methylstyrenes. Syntheses of the corresponding authentic materials are described.

Canadian Journal of Chemistry, 46, 1149 (1968)

The availability in this laboratory of a convenient, new method (1–3) for synthesis of *p*-substituted cumylamines (α,α-dimethylbenzylamines) suggested the use of these compounds as starting materials for preparation of the corresponding *p,p'*-disubstituted azocumenes (**1**) *via* oxidative coupling (4, 5). In keeping with our general interest in the behavior of radical species,

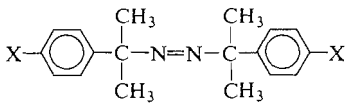

1

X = H, CH_3, CH_3CH_2, $(CH_3)_2CH$, $(CH_3)_3C$, Br

the azo derivatives were desired as precursors for the generation of cumyl-type radicals (for a recent paper in the series, see ref. 6). This note deals with the synthesis and characterization of the azocumenes and their decomposition products.

A description is provided elsewhere of the requisite amines which were obtained by side-chain amination of cumenes with trichloramine–aluminium chloride–*t*-butyl bromide (2, 3). Conversion to the *p,p'*-disubstituted azocumenes was accomplished by adaptation of the directions of Nelsen and Bartlett (5) for the preparation of azocumene (**1**, X = H) from cumylamine and iodine pentafluoride. The decomposition points, extinction coefficients at 367 mμ, elemental analyses, and yields for the five new azo compounds are listed in Table I. The decomposition temperature is dependent upon the rate of heating. Since only one run was carried out in each case, the yields, which refer to analytically pure material, undoubtedly could be improved. A study of the effect of the *para* substituents in the azocumenes on rate of decomposition, activation energy, and product distribution is presented in another report (7).

Nelsen and Bartlett (5) established that the major (94–95%) product from the thermal decomposition of azocumene was dicumyl (**2**, X = H), with the minor ones, cumene (**3**, X = H), and α-methylstyrene (**4**, X = H), resulting from disproportionation of cumyl radicals. Thermal degradation of the substituted analogues in solution gave similar results, >77% (usually >90%) coupling, accompanied by the

[1]This investigation was supported in part by the National Science Foundation under an Academic Year Extension Grant, GY-2170, to L. W. H.

[2]Taken in part from the M.S. Thesis of Chih Kuo Liang, Case Institute of Technology, 1967.

[3]Correspondence should be addressed to this author.

[4]National Science Foundation Undergraduate Research Participant, Case Institute of Technology, summer, 1966.

[5]National Science Foundation College Teacher Research Participant, Case Institute of Technology, summer 1966.

TABLE I

p,p'-Disubstituted azocumenes

p,p'-X,X-Azocumene X =	Melting point (decomp.) °C	$\varepsilon_{367\ m\mu}$	% yield	Formula	Calcd. (%) C	Calcd. (%) H	Calcd. (%) N	Found (%) C	Found (%) H	Found (%) N
H	88.8–90*	47.3†	21	—	—	—	—	—	—	—
Methyl	92–95	49.5	10	$C_{20}H_{26}N_2$	81.63	8.84	9.52	81.54	8.80	9.60
Ethyl	36.5–38	52.4	17	$C_{22}H_{30}N_2$	81.95	9.62	8.69	81.79	9.23	8.82
Isopropyl	55–57.2	51.7	8	$C_{24}H_{34}N_2$	82.23	9.78	7.99	82.18	9.81	7.88
t-Butyl	93.5–97.5	54.2‡	9§	$C_{26}H_{38}N_2$	82.48	10.12	7.40	82.22	10.26	—
Bromo	109.6–110	66.5	22	$C_{18}H_{20}N_2Br_2$	50.96‖	4.75	6.61	50.87‖	4.70	6.60

*Literature (5) m.p. 86.9–88.7°.
†Literature (5) ϵ 44.
‡For material decomposing at 89.5–95°.
§Plus a second crop, m.p. 89.5–95° (decomp.) (7% yield).
‖Br: Calculated, 37.68. Found, 37.84.

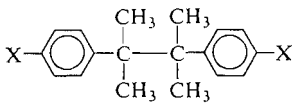

2

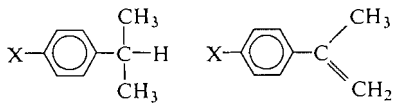

3 4

disproportionation side reaction (7). Authentic samples of the expected products were either purchased or synthesized for use in identification of products by gas–liquid partition chromatography analysis. Only two of the compounds are treated in detail (*p,p'*-dibromo- and *p,p'*-diethyldicumyl) since the others are found in the prior literature.

Experimental[6]

p,p'-Disubstituted Azocumenes

The procedure of Nelsen and Bartlett (5) was used with the indicated modifications. Since iodine pentafluoride decomposes in water (8), the methylene chloride solvent and pyridine were distilled from calcium hydride. Also, the reaction flask was baked overnight in an oven at 200° before use. For the sake of convenience, at the completion of reaction and after water had been added, sufficient ether was introduced to ensure that the organic phase would comprise the upper layer during subsequent work-up. Although methylene chloride or ether was used in the earlier studies (5) as the recrystallization solvent, we found that hot pentane dissolved the azo compounds leaving a brown, insoluble material which could be removed by filtration. If this procedure did not work efficiently, washing the crude solid with small amounts of methanol dissolved the dark impurity leaving the azo compound as a tan powder which could then be recrystallized from pentane or methylene chloride (Table I). Decomposition points were determined in a capillary tube with a heating rate of 1–2°/min.

Decomposition Products from the Azocumenes

p-Substituted Cumenes

p-Cumene was obtained from Eastman Organic Chemicals Department.

p-Ethylcumene—Treatment of cumene with acetyl chloride and aluminium chloride gave *p*-isopropylacetophenone (9) which was converted to *p*-ethylcumene by the Huang-Minlon modification of the Wolff–Kishner reduction (10*a*). The product, b.p. 194–196° (742 mm), lit. (10*b*) b.p. 193° (744 mm), was essentially free of the other isomers according to infrared and gas–liquid partition chromatography (g.l.p.c.) analyses. Attempts to prepare the compound by direct alkylation (10*b*) gave a mixture of isomers not easily separable by distillation.

p-Isopropylcumene was obtained from the Aldrich Chemical Company.

p-t-Butylcumene—Cumene was alkylated with *t*-butyl alcohol in 85% sulfuric acid (11). After work-up, the product was distilled through a column packed with glass helices, b.p. 219–224° (748 mm), lit. (11) b.p. 220° (746 mm). Infrared and g.l.p.c. analyses indicated good purity.

p-Bromocumene was obtained from Columbia Organic Chemicals Company.

p-Substituted α-Methylstyrenes

4-Methyl-α-methylstyrene—This compound, prepared by dehydration of *p*-tolyldimethylcarbinol with potassium hydrosulfate (12*a*), was obtained in 43% yield after redistillation at atmospheric pressure from sodium, b.p. 185–186.5°, n_D^{27} 1.5316, lit. (12*a*) b.p. 187°, lit. (12*b*) n_D^{20} 1.5350.

4-Ethyl-α-methylstyrene—The desired material resulted when the distillation of 4-ethylphenyldimethylcarbinol (13), prepared from acetone and the Grignard reagent of

[6]Decomposition points (uncorrected) were determined with a Thomas-Hoover or Mel-Temp capillary tube apparatus. Elemental analyses were performed by Galbraith Laboratories, Knoxville, Tennessee. The ultraviolet spectra were obtained with a Cary recording spectrophotometer model 14.

Can. J. Chem. Downloaded from www.nrcresearchpress.com by 210.87.254.42 on 09/05/12
For personal use only.

Can. J. Chem. Downloaded from www.nrcresearchpress.com by 210.87.254.42 on 09/05/12
For personal use only.

p-bromoethylbenzene, was attempted. The olefin was purified by distillation from sodium (43% yield based on *p*-bromoethylbenzene), b.p. 84–87° (13 mm), n_D^{25} 1.5285, lit. (14) b.p. 60–61° (6 mm), n_D^{20} 1.531.

4-Isopropyl-α-methylstyrene was obtained from Aldrich Chemical Company.

4-t-Butyl-α-methylstyrene—A mixture of saturated aqueous oxalic acid (50 ml) and 4-*t*-butylphenyldimethylcarbinol (15) (9.63 g, 0.05 mole) was refluxed for 21 h. The organic layer was separated and washed with water, 2% sodium hydroxide, and then water until the washings were neutral. A small amount of ether was added initially to aid the separations. After removal of solvent from the dried solution, the olefin was distilled, 5.6 g, b.p. 102–105° (11 mm), n_D^{28} 1.5192–1.5194. An additional 1.2 g of product was obtained by extracting the combined aqueous phases. The combined fractions were stored over sodium and redistilled to give 5.45 g (60% yield) of the desired material, b.p. 92–94° (8 mm), n_D^{27} 1.5194–1.5200, lit. (14) b.p. 98° (5 mm), n_D^{20} 1.523.

4-Bromo-α-methylstyrene—The procedure involved dehydration of 4-bromophenyldimethylcarbinol (17) with aqueous oxalic acid as described in the preceding section, 48% yield, b.p. 109–116° (12 mm), n_D^{23} 1.5818–1.5822, lit. (18) b.p. 108–110° (11 mm), n_D^{12} 1.5835, lit. (19) b.p. 58–60° (1.8 mm), n_D^{20} 1.5778, lit. (20) b.p. 114.5–117.5° (24 mm), n_D^{20} 1.5834.

p,p′-Disubstituted Dicumyls

p,p′-Dimethyldicumyl—This compound was synthesized in 3% yield according to the method of Farmer and Moore (21), m.p. 154.5–158°, lit. (22) m.p. 157°.

p,p′-Diethyldicumyl—The preparation was first attempted by the method described for *p,p′*-dibromodicumyl. The product, which showed three peaks in g.l.p.c. analysis, was presumed to include coupled side products resulting from abstraction of hydrogen from methylene of the ethyl group.

An alternative pathway was therefore employed. In a flask fitted with a reflux condenser and magnetic stirring bar were placed 20 ml of benzene and 0.5 mmole of *p,p′*-diethylazocumene. The flask was purged with nitrogen and immersed in an oil bath at 85° for 3 days. After removal of most of the solvent by distillation, a brown solid comprised the residue after evaporation for 2 days in air. A solution of this material in absolute ether on evaporation for 5 days in air to remove the disproportionation products gave a light-brown solid (0.095 g, 0.33 mmole), m.p. 73.5–75.2°. The nuclear magnetic resonance spectrum (Varian A60) in carbon tetrachloride with tetramethylsilane internal standard showed the methyl singlet superimposed on the methyl triplet at δ 1.28, the methylene quartet centered at δ 2.59, and the aromatic region centered at δ 6.92. These groups of peaks were in the ratio, 18:4:8, in agreement with that expected for *p,p′*-diethyldicumyl.

Anal. Calcd. for $C_{22}H_{30}$: C, 89.79; H, 10.21. Found: C, 89.53; H, 10.31.

The g.l.p.c. retention time was the same as that for the last of the three peaks obtained from injection of the products from the photolysis reaction.

p,p′-Diisopropyldicumyl—A literature pathway (21) provided the hydrocarbon in 3% yield, m.p. 134–135.5°, lit. (23) m.p. 134–135°.

p,p′-Di-t-butyldicumyl—Use of a prior technique (21) gave a 7% yield of product, m.p. 221–225°, lit. (15) m.p. 225°.

p,p′-Dibromodicumyl—This compound was prepared by a photolytic method developed in this laboratory (16). The apparatus consisted of an outer pyrex reaction vessel equipped with thermometer, nitrogen inlet, condenser, and an inner pyrex insert containing a GE H100-A 4/T mercury lamp. The outer glass jacket of the lamp was removed to allow insertion into the apparatus. Since di-*t*-butyl peroxide shows a broad, regularly increasing absorption from 2200–3400 Å (24), the wavelengths emitted by the lamp which are effective for peroxide decomposition were 3022, 3131, and 3341 Å.

The photolysis apparatus was charged with 0.16 mole of peroxide, 0.64 mole of *p*-bromocumene, and 150 ml of benzene. After a 2 h purge with nitrogen, the mixture was then photolyzed for 25 h at the reflux temperature. Heat for reflux was supplied by the lamp itself, and the desired reflux rate was maintained by passing a stream of air over the light source. Following removal of solvent by rotary evaporation, three recrystallizations of the brown, solid residue from absolute alcohol gave a colorless product, m.p. 174–175.2° (10% yield).

Anal. Calcd. for $C_{18}H_{20}Br_2$: C, 54.79; H, 5.07; Br, 40.13. Found: C, 54.32; H, 4.98; Br, 40.10.

Acknowledgment

We are grateful to Dr. C. W. Uzelmeier for helpful discussions.

1. P. Kovacic and R. J. Hopper. Tetrahedron, **23**, 3965 (1967).
2. P. Kovacic and R. J. Hopper. Tetrahedron, **23**, 3977 (1967).
3. P. Kovacic, J. F. Gormish, R. J. Hopper, and J. W. Knapczyk. Unpublished work.
4. T. E. Stevens. J. Org. Chem. **26**, 2531 (1961).
5. S. F. Nelsen and P. D. Bartlett. J. Am. Chem. Soc. **88**, 137 (1966).
6. J. R. Shelton and C. W. Uzelmeier. J. Am. Chem. Soc. **88**, 5222 (1966).
7. J. R. Shelton, C. K. Liang, and P. Kovacic. J. Am. Chem. Soc. **90**, 354 (1968).
8. Technical Bulletin TA-8532-3. General Chemical Division, Allied Chemical Corp. p. 32.
9. C. F. H. Allen. Organic syntheses. Coll. Vol. II. *Edited by* A. H. Blatt. John Wiley and Sons, Inc., New York. 1963. p. 3.
10. (*a*) Huang-Minlon. J. Am. Chem. Soc. **68**, 2487 (1946). (*b*) C. E. Welsh and G. F. Hennion. J. Am. Chem. Soc. **63**, 2603 (1941).
11. G. F. Hennion, A. J. Driesch, and P. L. Dee. J. Org. Chem. **17**, 1102 (1952).
12. (*a*) W. H. Perkin, Jr. and S. S. Pickles. J. Chem. Soc. **87**, 639 (1905). (*b*) V. N. Ipatieff, H. Pines, and R. C. Olberg. J. Am. Chem. Soc. **70**, 2123 (1948).
13. H. C. Brown, J. D. Brady, M. Grayson, and W. H. Bonner. J. Am. Chem. Soc. **79**, 1897 (1957).
14. H. K. F. Hermans, A. G. Knaeps, and C. A. M. Van der Eycken. Ind. Chim. Belge, **24**, 1467 (1959); Chem. Abstr. **54**, 7592 (1960).

15. M. WALTHER. J. Pharm. Chim. **27**, 476 (1938); Chem. Abstr. **32**, 6237 (1938).
16. C. W. UZELMEIER. Ph.D. Thesis. Case Institute of Technology, Cleveland, Ohio. 1967.
17. H. C. BROWN, Y. OKAMOTO, and G. HAM. J. Am. Chem. Soc. **79**, 1906 (1957).
18. K. ZIEGLER and P. TIEMANN. Ber. **55**, 3406 (1922).
19. E. BERGMANN and A. WEIZMANN. Trans. Faraday Soc. **32**, 1327 (1936).
20. D. SEYMOUR and K. B. WOLFSTIRN. J. Am. Chem. Soc. **70**, 1177 (1948).
21. E. H. FARMER and C. G. MOORE. J. Chem. Soc. 131 (1951).
22. E. BOEDTKER and R. KERLOR. Compt. Rend. **188**, 1681 (1929).
23. Y. ODAIRA and S. TSUTSUMI. Technol. Rept. Osaka Univ. **8**, No. 307, 199 (1958); Chem. Abstr. **53**, 12230 (1959).

Can. J. Chem. Downloaded from www.nrcresearchpress.com by 210.87.254.42 on 09/05/12
For personal use only.

The alkaline decomposition of *o*-phthalaldehyde di-*p*-toluenesulfonylhydrazone

CLIFFORD C. LEZNOFF[1,2]
University Chemical Laboratory, Cambridge, England

Received November 16, 1967

The Bamford–Stevens reaction of *o*-phthalaldehyde di-*p*-toluenesulfonylhydrazone gives *N*-(3,4-dihydrophthalazinyl)*p*-tolylsulfone. The product is synthesized by an independent method.

Canadian Journal of Chemistry, 46, 1152 (1968)

The alkaline decomposition of tosylhydrazones[3] of aldehydes and ketones has been extensively used for the synthesis of olefins (1) and some novel cyclic compounds (2).

The Bamford–Stevens reaction of benzaldehyde tosylhydrazone (1*a*, 1*c*) under aprotic conditions (3) yields an aryl carbene which dimerizes to *trans*-stilbene in high yield. Very little is known about the alkaline decomposition of ditosylhydrazones (1*a*) under aprotic conditions. The ditosylhydrazone of *o*-phthalaldehyde (**1**) could yield a dicarbenoid (4) species (**2**) and hence benzocyclobutadiene (**3**) (5) or some interesting unsaturated macrocyclic compounds.

o-Phthalaldehyde ditosylhydrazone (**1**) was prepared by mixing *o*-phthalaldehyde and *p*-toluenesulfonylhydrazine in a 1:2 ratio in ethanol. The use of acetic acid as solvent (6) gave a colored solution. Heating a solution of **1** in dimethyl formamide at 120°, or in diethyl Carbitol at 160°, with either sodium methoxide or sodium hydride gave *N*-(3,4-dihydrophthalazinyl) *p*-tolylsulfone (**4**) in 5–30% yield, as the only new substance isolated.[4] No products derived from benzocyclobutadiene (**3**) (5) could be detected in the reaction product. Cava and Stein (7) have obtained a similar product by the reaction of phthalaldehydic acid tosylhydrazone with excess acetyl chloride in methanol.

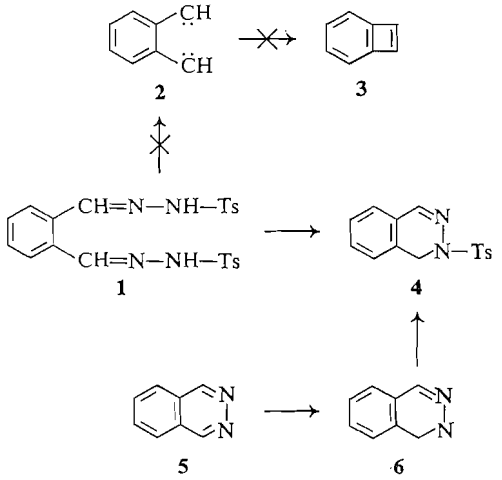

The product **4** was also synthesized by the method of Lemal and Fry (8). Phthalazine (**5**) was reduced with lithium aluminium hydride to 3,4-dihydrophthalazine (**6**), and the crude product was treated directly with *p*-toluenesulfonyl chloride in freshly distilled sulfolane and triethylamine.

Dornow and Bartsch (1*b*) have reported the formation of sulfones from diazoalkanes and aldehyde tosylhydrazones and hence the conversion of **1** to **4** is not surprising. A likely precursor of **4** may involve a monocarbene resulting from loss of one tosylhydrazone group

[1]NRCC overseas Postdoctorate Fellow, 1965–1967.
[2]Present address: Department of Chemistry, York University, Toronto 12, Ontario.
[3]Tosyl = Ts = *p*-toluenesulfonyl.
[4]Ditolyldisulfide and sodium *p*-tolylsulfinate were also formed as side products (see refs. 1*c*, 9).

15. M. WALTHER. J. Pharm. Chim. **27**, 476 (1938); Chem. Abstr. **32**, 6237 (1938).
16. C. W. UZELMEIER. Ph.D. Thesis. Case Institute of Technology, Cleveland, Ohio. 1967.
17. H. C. BROWN, Y. OKAMOTO, and G. HAM. J. Am. Chem. Soc. **79**, 1906 (1957).
18. K. ZIEGLER and P. TIEMANN. Ber. **55**, 3406 (1922).
19. E. BERGMANN and A. WEIZMANN. Trans. Faraday Soc. **32**, 1327 (1936).
20. D. SEYMOUR and K. B. WOLFSTIRN. J. Am. Chem. Soc. **70**, 1177 (1948).
21. E. H. FARMER and C. G. MOORE. J. Chem. Soc. 131 (1951).
22. E. BOEDTKER and R. KERLOR. Compt. Rend. **188**, 1681 (1929).
23. Y. ODAIRA and S. TSUTSUMI. Technol. Rept. Osaka Univ. **8**, No. 307, 199 (1958); Chem. Abstr. **53**, 12230 (1959).

Can. J. Chem. Downloaded from www.nrcresearchpress.com by 210.87.254.40 on 09/05/12
For personal use only.

The alkaline decomposition of *o*-phthalaldehyde di-*p*-toluenesulfonylhydrazone

CLIFFORD C. LEZNOFF[1,2]
University Chemical Laboratory, Cambridge, England

Received November 16, 1967

The Bamford–Stevens reaction of *o*-phthalaldehyde di-*p*-toluenesulfonylhydrazone gives *N*-(3,4-dihydrophthalazinyl)*p*-tolylsulfone. The product is synthesized by an independent method.

Canadian Journal of Chemistry, 46, 1152 (1968)

The alkaline decomposition of tosylhydrazones[3] of aldehydes and ketones has been extensively used for the synthesis of olefins (1) and some novel cyclic compounds (2).

The Bamford–Stevens reaction of benzaldehyde tosylhydrazone (1*a*, 1*c*) under aprotic conditions (3) yields an aryl carbene which dimerizes to *trans*-stilbene in high yield. Very little is known about the alkaline decomposition of ditosylhydrazones (1*a*) under aprotic conditions. The ditosylhydrazone of *o*-phthalaldehyde (**1**) could yield a dicarbenoid (4) species (**2**) and hence benzocyclobutadiene (**3**) (5) or some interesting unsaturated macrocyclic compounds.

o-Phthalaldehyde ditosylhydrazone (**1**) was prepared by mixing *o*-phthalaldehyde and *p*-toluenesulfonylhydrazine in a 1:2 ratio in ethanol. The use of acetic acid as solvent (6) gave a colored solution. Heating a solution of **1** in dimethyl formamide at 120°, or in diethyl Carbitol at 160°, with either sodium methoxide or sodium hydride gave *N*-(3,4-dihydrophthalazinyl) *p*-tolylsulfone (**4**) in 5–30% yield, as the only new substance isolated.[4] No products derived from benzocyclobutadiene (**3**) (5) could be detected in the reaction product. Cava and Stein (7) have obtained a similar product by the reaction of phthalaldehydic acid tosylhydrazone with excess acetyl chloride in methanol.

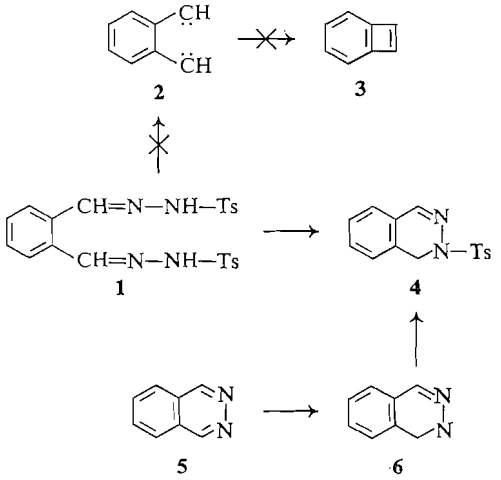

The product **4** was also synthesized by the method of Lemal and Fry (8). Phthalazine (**5**) was reduced with lithium aluminium hydride to 3,4-dihydrophthalazine (**6**), and the crude product was treated directly with *p*-toluenesulfonyl chloride in freshly distilled sulfolane and triethylamine.

Dornow and Bartsch (1*b*) have reported the formation of sulfones from diazoalkanes and aldehyde tosylhydrazones and hence the conversion of **1** to **4** is not surprising. A likely precursor of **4** may involve a monocarbene resulting from loss of one tosylhydrazone group

[1]NRCC overseas Postdoctorate Fellow, 1965–1967.
[2]Present address: Department of Chemistry, York University, Toronto 12, Ontario.
[3]Tosyl = Ts = *p*-toluenesulfonyl.
[4]Ditolyldisulfide and sodium *p*-tolylsulfinate were also formed as side products (see refs. 1*c*, 9).

Can. J. Chem. Downloaded from www.nrcresearchpress.com by 210.87.254.40 on 09/05/12
For personal use only.

from **1** with subsequent carbene insertion to the N–H bond of the remaining tosylhydrazone. The intervention of a protonated diazo compound even under "aprotic" conditions (8, 9) cannot be excluded.

Experimental

Melting points were taken on a Kofler microscope hot-stage and are corrected. Infrared spectra were obtained as KBr discs on a Unicam SP-200 spectrophotometer. Infrared values (ν) are given in cm^{-1}. Nuclear magnetic resonance (n.m.r.) spectra were recorded on a Varian Associates HA-100 spectrometer with tetramethyl silane as an internal standard and deuteriochloroform as solvent. Ultraviolet spectra were obtained in ethanol on a Cary model 14 spectrophotometer. The mass spectra were taken on an A.E.I. MS9 double-focussing mass spectrometer. Woelm alumina (activity II–III) was used for column chromatography.

*o-Phthalaldehyde Ditosylhydrazone (**1**)*

To 2.3 g of *p*-toluenesulfonylhydrazone in 10 ml of warm absolute ethanol was added 0.8 g of *o*-phthalaldehyde in 3 ml of absolute ethanol. The solution was heated to reflux for a few minutes and allowed to stand at room temperature for 3 h. The solid was filtered to give 2.7 g (96%) of **1**, m.p. 151–152° (decomp.). The mass spectrum did not give a parent ion (the unusual splitting pattern of tosylhydrazones is well known (10); n.m.r. (τ), 7.58 s (six protons, Ar—CH), 1.8–3.0 m (complex multiplet which includes aromatic H, CH=N, and NH protons); ν 3300; 3100 (NH), 1640 (C=N), 1595, 1560 (aromatic), 1335, 1165 (SO_2); λ_{max} 225 mμ (ε 28 800), 290 (8650).

Anal. Calcd. for $C_{22}H_{22}N_4O_4S_2$: C, 56.17; H, 4.71; N, 11.91. Found: C, 56.30; H, 5.32; N, 11.81.

*Alkaline Decomposition of o-Phthalaldehyde Ditosylhydrazone (**1**)*

A solution of **1** (2.35 g, 5 mmoles) in 20 ml of dimethyl formamide was added to 0.24 g (10 mmoles) of sodium hydride[5] in 5 ml of dimethyl formamide at 5°. After being stirred for 1 h, the solution was immersed in an oil bath at 120°. After 5 min at this temperature, nitrogen evolution had ceased. The reaction mixture was filtered, the filtrate was extracted into ether, and washed six times with water. The semi-crystalline residue was chromatographed to give 300 mg (21%) of a crystalline compound m.p. 169–171° in the 1:1 pentane : ether fractions. Recrystallization from ether–pentane gave product **4**, m.p. 171–173°. The mass spectrum gave a parent ion at *m/e* 286, as well as large peaks at *m/e* 285, 155, and 130, which would be consistent with structure **4**; n.m.r. (τ) 7.56 s (Ar—CH), 5.54 s (CH_2—N), 2.0–3.0 (eight aromatic protons); ν 3450 br (NH), 1600 (aromatic), 1370, 1180 s (SO_2); λ_{max} 222 mμ (ε 22 100), 290 (9030).

Anal. Calcd. for $C_{15}H_{14}N_2O_2S$: C, 62.93; H, 4.93; N, 9.79. Found: C, 62.80; H, 5.32; N, 9.97.

In a similar reaction in which only one equivalent of sodium hydride was used, the product **4** was obtained in 14% yield. When the reaction was carried out in dry diethyl Carbitol at 160° with two equivalents of sodium methoxide, only a 6% yield of **4** was obtained. All the reactions were carefully examined by thin-layer chromatography for hydrocarbon components, but none could be detected.

*Alternative Synthesis of N-(3,4-Dihydrophthalazinyl)p-tolylsulfone (**4**)*

To a stirred slurry of lithium aluminium hydride (0.38 g, 10 mmoles) in 10 ml of ether under nitrogen, was added dropwise a solution of 1.3 g (10 mmoles) of phthalazine (**5**) in 20 ml of tetrahydrofuran. The mixture was then refluxed for 8 h. Water (1 ml) was added and the mixture was filtered through a filter cel – magnesium sulfate pad. The solvent was removed under reduced pressure. Thin-layer chromatography and elution of the product with ether showed mainly one spot (R_f, 0.8; phthalazine R_f, 0.05). One half of the product (**6**) was dissolved in 17.5 ml of freshly distilled sulfolane, and 0.8 ml (5 mmoles) of triethylamine and 950 mg (5 mmoles) of *p*-toluenesulfonylchloride were added. The solution was heated at 140–150° for 1.5 h, cooled, and then extracted with ether. The resulting oil on chromatography in the 1:1 pentane–ether fractions gave 100 mg of **4**, m.p. 172–174°, undepressed upon admixture with the product obtained above; mass spectrum was identical to that obtained previously.

Anal. Calcd. for $C_{15}H_{14}N_2O_2S$: C, 62.93; H, 4.93; N, 9.79. Found: C, 62.70; H, 4.93; N, 10.20.

[5]The sodium hydride was freed from mineral oil by washing with dry pentane.

Acknowledgment

The author wishes to express his thanks to Professor F. Sondheimer for advice and interest in this work.

1. (*a*) W. R. Bamford and T. S. Stevens. J. Chem. Soc. 4735 (1952). (*b*) A. Dornow and W. Bartsch. Ann. **602**, 23 (1957). (*c*) H. Nozaki, R. Noyori, and K. Sisido. Tetrahedron, **20**, 1125 (1964).
2. G. L. Closs, L. E. Closs, and W. A. Böll. J. Am. Chem. Soc. **85**, 3796 (1963). G. L. Closs and R. B. Larrabee. Tetrahedron Letters, 287 (1965). M. Schwarz, A. Besold, and E. R. Nelson. J. Org. Chem. **30**, 2425 (1965). A. C. Udding, J. Strating, H. Wynberg, and J. L. M. A. Schlatmann. Chem. Commun. 657 (1966).
3. J. W. Powell and M. C. Whiting. Tetrahedron, **7**, 305 (1959). L. Friedman and H. Shechter. J. Am. Chem. Soc. **81**, 5512 (1959). L. Friedman and H. Shechter. J. Am. Chem. Soc. **82**, 1002 (1960).
4. W. Kirmse. *In* Carbene chemistry. *Edited by* A. T. Bloomquist. Academic Press, Inc., New York. 1964. Chap. 10.
5. M. P. Cava and D. R. Napier. J. Am. Chem. Soc. **79**, 1701 (1957). M. Avram, D. Dinu, and C. D. Nenitzescu. Chem. Ind. London, 257 (1959). M. P. Cava and M. J. Mitchell. *In* Cyclobutadiene and related compounds. *Edited by* A. T. Bloomquist. Academic Press, Inc., New York. 1967. Chap. 6.
6. D. G. Farnum. J. Org. Chem. **28**, 870 (1963).
7. M. P. Cava and R. P. Stein. J. Org. Chem. **31**, 1866 (1966).
8. D. M. Lemal and A. J. Fry. J. Org. Chem. **29**, 1673 (1964).
9. J. W. Wilt, C. A. Schneider, H. F. Dabek, Jr., J. F. Kraemer, and W. J. Wagner. J. Org. Chem. **31**, 1543 (1966).
10. A. Bhati, R. A. W. Johnstone, and B. J. Millard. J. Chem. Soc. 358 (1966).

Dimerization of Isoprene

SHOJI WATANABE, KYOICHI SUGA, KEIZO KAMMA, AND IMAKO TORII
Department of Applied Chemistry, Faculty of Engineering, Chiba University, Yayoicho, Chiba, Japan

Received August 3, 1967

The effect of solvents and various amines on the dimerization of isoprene with alkali-metal naphthalene, and the preparation of a new terpenic carboxylic acid, 4,8-dimethyl-3,7-nonadienic acid, by carboxylation of isoprene are described. Tetrahydrofuran, and the 50/50 (v/v) mixture of tetrahydrofuran and dimethyl sulfoxide each gave 40% of isoprene dimer. Sodium naphthalene in tetrahydrofuran solution containing a small amount of *t*-butylamine is active for the reductive dimerization of isoprene.

Canadian Journal of Chemistry, **46**, 1154 (1968)

Can. J. Chem. Downloaded from www.nrcresearchpress.com by 210.87.254.5 on 09/05/12
For personal use only.

Some dimers of isoprene (**1**) have been produced with transition metal complexes (1–2). Recently, we have reported that lithium naphthalene dimerizes conjugated cyclodienes (3), and that it dimerizes **1** to give linear isoprene dimer **2**, a mixture of 2,6-dimethyl-2,6-octadiene and 2,7-dimethyl-2,6-octadiene (4). This paper describes the effect of solvents and various amines on the dimerization of **1** with alkali-metal naphthalene, and the preparation of a new terpenic carboxylic acid by carboxylation of **1**.

The effect of solvents on the behavior of organometallic compounds recently has received considerable attention. When various solvents were mixed with the tetrahydrofuran solution of lithium naphthalene, the solvent effect for the dimerization of **1** was studied, and the typical results are shown in Table I. From these results, tetrahydrofuran and the 50/50 (v/v) mixture of tetrahydrofuran and dimethylsulfoxide each gave equally high yields of **2**.

In the previous paper (4) the authors reported that the lithium naphthalene is active for dimerization of **1**, but sodium naphthalene is not active. The authors have found that the sodium naphthalene in tetrahydrofuran solution containing a small amount of Lewis base, such as *t*-butyl amine or pyridine, is active for the reductive dimerization of **1**, similar to lithium naphthalene in tetrahydrofuran solution. The effect of *t*-butylamine and other Lewis bases on the yields of **2** have also been examined; the results are shown in Table II. From these results, it can be said that the use of 0.1 mole of *t*-butylamine per mole of **1** results in the highest yield of **2** with sodium naphthalene in tetrahydrofuran.

The carboxylation of **1** with carbon dioxide under similar conditions gave a mixture of various carboxylic acids which contained 1% of C_6-monobasic acid (**3**), 28% of C_{11}-monobasic acid (**4**), and 23% of C_{12}-dibasic acid (**5**). The methyl esters of these carboxylic acids were catalytically hydrogenated over palladium on charcoal to give the corresponding saturated methyl esters. Methyl isocaproate from **3** and tetrahydrohomogeranic acid methyl ester from **4** were confirmed by the comparison of the authentic samples. The structure of **4** was determined as 4,8-dimethyl-3,7-nonadienic acid, a new terpenic acid, by spectral evidence as shown in the Experimental section. Compound **5** was a mixture of various isomers the structures of which were not determined since their complete separation had not been successful. The effects

TABLE I

Dimerization of isoprene* by alkali-metal naphthalene

Solvent	Alkali-metal	Yield of dimer (%)
Tetrahydrofuran	Li	40
Diethyleneglycol dimethylether	Li	30
Dimethoxymethane	Li	10
Dioxane	Li	0
Dimethyl formamide	Li	0
Tetrahydrofuran (100 ml), Dimethylsulfoxide (100 ml)	Li	40
Tetrahydrofuran (100 ml), Benzene (100 ml)	Li	12
Tetrahydrofuran (100 ml), Ether (100 ml)	Li	19
Tetrahydrofuran (100 ml), Toluene (100 ml)	Li	6
Tetrahydrofuran (100 ml), *n*-Hexane (100 ml)	Li	4
Tetrahydrofuran (100 ml) Cyclohexane (100 ml)	Li	4
Tetrahydrofuran (100 ml), 1,3-Dioxane (100 ml)	Li	10
Tetrahydrofuran (100 ml), Isopropylether (100 ml)	Li	8
Tetrahydrofuran	Na	5
Tetrahydrofuran (100 ml), Dimethyl sulfoxide (100 ml)	Na	6

*0.1 mole of **1** was used.

TABLE II

Effect of various Lewis bases in tetrahydrofuran*

Alkali-metal	Lewis amines	Molar ratio of Lewis base/isoprene	Yield of dimer (%)
Li	*t*-Butylamine	0.1	40
Na	*t*-Butylamine	1.0	20
Na	*t*-Butylamine	0.5	20
Na	*t*-Butylamine	0.2	30
Na	*t*-Butylamine	0.1	35
Na	*t*-Butylamine	0.05	30
Na	Dibutylamine	0.1	20
Na	Triethylamine	0.1	25
Na	Pyridine	0.1	10
Na	Triphenylphosphine	0.1	20
Na	*p*-Phenylenediamine	0.1	20

*Reaction conditions: tetrahydrofuran (100 ml), alkali-metal (0.1 mole), naphthalene (0.03 mole), and **1** (0.1 mole) were used. Reaction temperature, 30 °C; reaction time, 5 h. The yields of **2** were measured by gas–liquid chromatographic analysis. Column: polyphenylether (20%) on chromosorb W, 3.5 m; temperature 90 °C; carrier gas, helium 40 ml/min.

of reaction temperature on the carboxylation of **1** have also been examined; the results are shown in Table III. From these results, it can be said that the reaction at room temperature affords more C_{11}-monobasic carboxylic acid, but that the reaction at lower temperature gives more C_{12}-dibasic acid.

TABLE III

The effect of temperature on carboxylation of isoprene

Temperature (°C)	Monobasic acid yield (%)	Dibasic acid yield (%)
20	28	17
0	12	18
−20	10	20
−40	7	25
−60	6	38

Experimental

All the experiments were carried out in a dry apparatus under nitrogen and all the reagents were dried over metallic sodium and purified by fractional distillation.

Dimerization of Isoprene (1) with Alkali Naphthalene

The tetrahydrofuran solution of alkali naphthalene was prepared as reported previously (3–4). Lithium naphthalene solutions in solvents other than tetrahydrofuran were prepared similarly. Solutions of lithium naphthalene in solvent mixtures containing tetrahydrofuran were prepared by the addition of the variable solvent to a tetrahydrofuran solution of lithium naphthalene.

A typical procedure using a Lewis base is as follows. To 40 g (0.312 mole) of naphthalene and 150 ml of tetrahydrofuran, 4.5 g (0.65 mole) of lithium cuts were added and the mixture was then agitated at room temperature for 3 h. After addition of 4.7 g (0.065 mole) of *t*-butylamine to the contents, 40 g (0.59 mole) of **1** were added and the mixture was stirred for 3 h more at 30 °C. The reaction mixture was decomposed with methanol and the insoluble matter was dissolved with water. The organic layer was isolated with ether, dried over anhydrous sodium sulfate, and distilled to give 18 g (b.p. 60–110 °C at 40 Torr) of a crude **2**, which was a mixture of 2,6-dimethyl-2,6-octadiene and 2,7-dimethyl-2,6-octadiene. The properties of these hydrocarbons are shown in ref. 4.

Carboxylation of Isoprene (1)

To a mixture of metallic lithium (0.29 mole), naphthalene (20 g) and tetrahydrofuran (100 ml), 20 g (0.29 mole) of **1** was added under an atmosphere of nitrogen during 3 h with stirring. At the conclusion of the reaction, the mixture was poured onto a large excess of crushed Dry Ice (1 000 g) in a beaker. The excess Dry Ice was allowed to evaporate overnight; unchanged lithium in the carboxylated product was then quenched by the cautious addition of 300 cm^3 of water during 0.5 h. Potassium hydroxide (20 g) was then added to the reaction mixture. The nonacidic materials were extracted with isopropyl ether (ether solution *a*) and the remaining solution was made acidic with concentrated hydrochloric acid. The acid was removed completely from the aqueous layer by extraction with isopropyl ether. The ether solution was washed with water, dried over anhydrous sodium sulfate, and the dried ether solution evaporated at reduced pressure to yield 16 g of crude acids. Distillation of these acids gave the following fractions: (*a*) b.p. 60–80 °C at 25 Torr, yield 0.2 g; (*b*) b.p. 117–125 °C at 6 Torr, yield 5.5 g; and (*c*) b.p. 160–180 °C at 5 Torr, yield 4.5 g.

Fraction *a* was esterified with methanol in the usual way to the corresponding methyl ester. It was hydrogenated over palladium on carbon in a methanol solution at 50 °C to give the saturated methyl ester. Isocaproic acid methyl ester was confirmed as the main component by gas–liquid chromatography on a 2 m column of Reoplex 400 (20%) on Celite 545 at a temperature of 120 °C with helium as the carrier gas (40 ml/min). Infrared absorption spectrum of fraction *a* showed a characteristic band of trisubstituted double bond at 810 cm^{-1} and carbonyl group at 1725 cm^{-1}.

Fraction *b* was esterified similarly to the corresponding methyl ester. Distillation of the methylester gave 4,8-dimethyl-3,7-nonadienic acid methylester as the main product; b.p. 90 °C at 4 Torr, n_D^{20} 1.4748, molecular weight 186 (calcd. for $C_{12}H_{20}O_2$, 196), infrared 1745 cm^{-1} (—O—CO—), 1160 cm^{-1} (an ester), 835 cm^{-1} (a trisubstituted double bond), nuclear magnetic resonance (n.m.r.) τ 5.40 (—C*H*=C—), 6.40 (—COOC*H*$_3$), 8.40 (—C=C—C*H*$_3$), saponification value 250 (calcd. for $C_{12}H_{20}O_2$, 288).

Anal. Calcd. for $C_{12}H_{20}O_2$: C, 73.41; H, 10.26. Found: C, 74.04; H, 10.02.

The methyl ester was hydrogenated similarly and absorbed two equivalents of hydrogen to give the corresponding saturated methyl ester. Distillation of the methyl ester gave 4,8-dimethylnonanoic acid methyl ester (homogeranic acid methyl ester) as the main product; b.p. 87 °C at 6 Torr, n_D^{16} 1.4368, n.m.r.: τ 9.15 (C*H*$_3$—), 8.8 (—C*H*$_2$—), 8.6 (—C*H*—), 7.8 (—C*H*$_2$—CO—), 6.4

Can. J. Chem. Downloaded from www.nrcresearchpress.com by 210.87.254.5 on 09/05/12
For personal use only.

(—O—CH_3); infrared 1743, 1170, 1260, and 1370 cm^{-1}. The infrared, n.m.r., and gas–liquid chromatogram agreed with those of its authentic sample.

Fraction *c* was distilled to give a mixture of various dibasic acids but their complete separation was unsuccessful; b.p. 165 °C at 4 Torr, molecular weight 230 (calcd. for $C_{12}H_{18}O_4$; 226). The dimethyl ester was prepared similarly, and had the following properties, b.p. 160–165 °C at 3 Torr, infrared 1745 and 1160 cm^{-1} (carboxylic acid), 785 cm^{-1} (a trisubstituted double bond), saponification value 403 (calcd. for $C_{14}H_{22}O_4$, 444).

Anal. Calcd. for $C_{14}H_{22}O_4$: C, 66.10; H, 8.72. Found: C, 67.10; H, 8.85.

From the ether solution *a*, 2 g of **2** was obtained by fractional distillation.

Infrared Absorption Spectra

These (liquid film) were measured on a Koken IRS spectrophotometer.

Nuclear Magnetic Resonance Spectra

These were determined on a Japan Electron Optics Lab. instrument (60 Mc/s) with carbon tetrachloride solutions and with tetramethylsilane as an internal standard.

Acknowledgment

The authors thank Dr. Sanae Tanaka of Mitsubishi Petrochemical Co., Ltd., for his suggestions and his measurements of the nuclear magnetic resonance spectra.

1. L. I. ZAKHARKIN and G. C. ZHIGAREVA. Izv. Akad. Nauk SSSR, Ser. Khim. (**1**), 168 (1964).
2. A. MISONO, Y. UCHIDA, M. HIDAI, and Y. OHSAWA. Bull. Chem. Soc. Japan, **39**, 2425 (1966).
3. K. SUGA, S. WATANABE, and K. KAMMA. Can. J. Chem. **45**, 933 (1967).
4. K. SUGA and S. WATANABE. Bull. Chem. Soc. Japan, **40**, 1257 (1967).

The synthesis and saponification kinetics of some 4′-substituted 4-phenoxyphenyl acetates

L. A. MATTANO AND J. C. FALK
The Dow Chemical Company, Midland, Michigan

Received September 5, 1967

Phenoxyphenyl acetate and several 4′-substituted derivatives were synthesized and their rates of saponification determined. The nature of the 4′-substituent was correlated with the rate of saponification by means of the Hammett equation.

Canadian Journal of Chemistry, 46, 1156 (1968)

The syntheses and saponification kinetics of esters represent subjects which have been subjected to a great deal of study (1). In the course of these studies both the acyl and alcohol moieties have been extensively varied; however, the syntheses and saponification kinetics of 2′-, 3′-, and 4′-substituted 4-phenoxyphenyl esters (**1**) have been neglected.

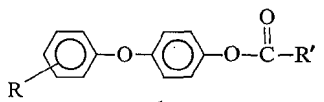

1

Ikawa's synthesis of 4-hydroxy-4′-nitrodiphenyl ether (2), Ungnade's synthesis of 4-carboxy-2′-methyldiphenyl ether (3), and Walker's synthesis of 4-carboxy-4′-hydroxydiphenyl ether (4) suggested that the following route should furnish the desired 4′-substituted 4-phenoxyphenyl acetates.

The substituted 4-phenoxyphenyl acetates synthesized by this route are found in Table I. The acetates were characterized by their ultraviolet and infrared spectra and by elemental analyses.

Precedent exists for assuming that substitution at the 4′-position might affect the rate of saponification of phenoxyphenyl acetates. Since Litvinenko, Tsukerman, Cheshko, and Kolesnikova (5) have shown that the acylation of 4-aminodiphenyl oxide occurs 12 times as fast as the acylation of 4-amino-4′-nitrodiphenyl oxide, similar effects might be expected for the saponification of esters derived from 1-hydroxydiphenyl oxide reported in Table I.

The saponifications were carried out in 25% ethanol/water (v/v), "pH" 10.3, employing phosphate as the buffer species, at 25 °C ±0.01, (ester) = 10^{-4} — 10^{-5} *M*. The course of the reaction was conveniently followed by measur-

Can. J. Chem. Downloaded from www.nrcresearchpress.com by 210.87.254.5 on 09/05/12
For personal use only.

(—O—CH_3); infrared 1743, 1170, 1260, and 1370 cm^{-1}. The infrared, n.m.r., and gas–liquid chromatogram agreed with those of its authentic sample.

Fraction *c* was distilled to give a mixture of various dibasic acids but their complete separation was unsuccessful; b.p. 165 °C at 4 Torr, molecular weight 230 (calcd. for $C_{12}H_{18}O_4$; 226). The dimethyl ester was prepared similarly, and had the following properties, b.p. 160–165 °C at 3 Torr, infrared 1745 and 1160 cm^{-1} (carboxylic acid), 785 cm^{-1} (a trisubstituted double bond), saponification value 403 (calcd. for $C_{14}H_{22}O_4$, 444).

Anal. Calcd. for $C_{14}H_{22}O_4$: C, 66.10; H, 8.72. Found: C, 67.10; H, 8.85.

From the ether solution *a*, 2 g of **2** was obtained by fractional distillation.

Infrared Absorption Spectra

These (liquid film) were measured on a Koken IRS spectrophotometer.

Nuclear Magnetic Resonance Spectra

These were determined on a Japan Electron Optics Lab. instrument (60 Mc/s) with carbon tetrachloride solutions and with tetramethylsilane as an internal standard.

Acknowledgment

The authors thank Dr. Sanae Tanaka of Mitsubishi Petrochemical Co., Ltd., for his suggestions and his measurements of the nuclear magnetic resonance spectra.

1. L. I. ZAKHARKIN and G. C. ZHIGAREVA. Izv. Akad. Nauk SSSR, Ser. Khim. (**1**), 168 (1964).
2. A. MISONO, Y. UCHIDA, M. HIDAI, and Y. OHSAWA. Bull. Chem. Soc. Japan, **39**, 2425 (1966).
3. K. SUGA, S. WATANABE, and K. KAMMA. Can. J. Chem. **45**, 933 (1967).
4. K. SUGA and S. WATANABE. Bull. Chem. Soc. Japan, **40**, 1257 (1967).

The synthesis and saponification kinetics of some 4′-substituted 4-phenoxyphenyl acetates

L. A. MATTANO AND J. C. FALK
The Dow Chemical Company, Midland, Michigan

Received September 5, 1967

Phenoxyphenyl acetate and several 4′-substituted derivatives were synthesized and their rates of saponification determined. The nature of the 4′-substituent was correlated with the rate of saponification by means of the Hammett equation.

Canadian Journal of Chemistry, 46, 1156 (1968)

The syntheses and saponification kinetics of esters represent subjects which have been subjected to a great deal of study (1). In the course of these studies both the acyl and alcohol moieties have been extensively varied; however, the syntheses and saponification kinetics of 2′-, 3′-, and 4′-substituted 4-phenoxyphenyl esters (**1**) have been neglected.

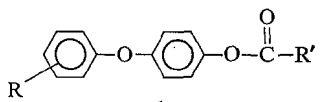

1

Ikawa's synthesis of 4-hydroxy-4′-nitrodiphenyl ether (2), Ungnade's synthesis of 4-carboxy-2′-methyldiphenyl ether (3), and Walker's synthesis of 4-carboxy-4′-hydroxydiphenyl ether (4) suggested that the following route should furnish the desired 4′-substituted 4-phenoxyphenyl acetates.

The substituted 4-phenoxyphenyl acetates synthesized by this route are found in Table I. The acetates were characterized by their ultraviolet and infrared spectra and by elemental analyses.

Precedent exists for assuming that substitution at the 4′-position might affect the rate of saponification of phenoxyphenyl acetates. Since Litvinenko, Tsukerman, Cheshko, and Kolesnikova (5) have shown that the acylation of 4-aminodiphenyl oxide occurs 12 times as fast as the acylation of 4-amino-4′-nitrodiphenyl oxide, similar effects might be expected for the saponification of esters derived from 1-hydroxydiphenyl oxide reported in Table I.

The saponifications were carried out in 25% ethanol/water (v/v), "pH" 10.3, employing phosphate as the buffer species, at 25 °C ±0.01, (ester) = 10^{-4} — 10^{-5} *M*. The course of the reaction was conveniently followed by measur-

Can. J. Chem. Downloaded from www.nrcresearchpress.com by 210.87.254.42 on 09/05/12
For personal use only.

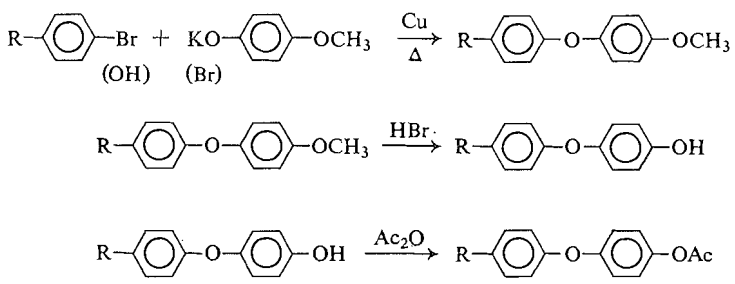

TABLE I

Synthesis of 4′-substituted 4-phenoxyphenyl acetates*

R	R′	R″	Yield %	Melting point (°C)	Boiling point (°C)
—	—	H†	80	—	181 (15 mm)
OCH_3	CH_3	CH_3	49	—	153 (3.2 mm)
Br	OCH_3	Br	14	—	94 (2.2 mm)
OCH_3	NO_2	NO_2	36	62–64	
	OCH_3		9	119–121	
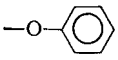	OCH_3	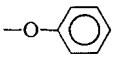	42	69–71	

†Prepared from acetic anhydride and 4-phenoxyphenol.

ing the optical density change of the reaction mixture as a function of time at the wavelength where the product phenolate strongly absorbs (280mμ — 300mμ). First order rate constants were calculated from plots of log (O.D. — $O.D._\infty$) as a function of time by the procedure of Bruice (6) and are tabulated in Table II. Good first order plots were obtained which were reproducible within 2–3%.

TABLE II

Saponification* of 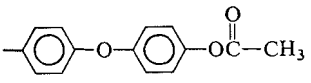

R	$K_1 \times 10^2$ (min^{-1})
H	2.39
CH_3	2.40
Br	4.04
	2.12
NO_2	4.19

*At "pH" 10.3.

The nature of the 4′-substituent may be related to the rate of saponification of the 4′-substituted 4-phenoxyphenyl acetates by use of the Hammett equation (7). A ρ of +0.289, $r = 0.803$, was calculated.

The transmission of electronic effects through the phenoxy bridge may be evaluated by comparison of the ρ obtained in these experiments with the ρ for the saponification of substituted phenyl acetates. Bruice (6) calculated a ρ of +1.15 for the saponification of phenyl acetates in 25% ethanol/water (v/v), "pH" 8.0, at 30°. The shielding effect of the phenoxy bridge is substantial. The ratio ρ/ρ_0 (ρ_0 for substituted phenyl acetates, ρ for 4′-substituted phenoxyphenyl acetates) is 0.25 and agrees with that calculated from transmission coefficients for the transmission of polar effects through oxygen and phenylene links, 0.16 (8).

1. J. Hine. Physical organic chemistry. McGraw-Hill Book Company, Inc., New York. 1962. Chap. 12, and references cited therein.
2. K. Ikawa. Yakugaku Zasshi, **79**, 1493 (1959); Chem. Abstr. **54**, 19022h (1960).

Can. J. Chem. Downloaded from www.nrcresearchpress.com by 210.87.254.42 on 09/05/12
For personal use only.

3. H. E. UNGNADE. J. Am. Chem. Soc. **63**, 2091 (1941).
4. C. R. HARINGTON and R. V. PITT RIVERS. J. Chem. Soc. 1101 (1940). J. WALKER. J. Chem. Soc. 347 (1942).
5. L. M. LITVINENKO, S. V. TSUKERMAN, R. S. CHESHKO, and B. M. KOLESNIKOVA. Zh. Obshch. Khim. **27**, 1663 (1957); Chem. Abstr. **52**, 4546*e* (1958).
6. T. C. BRUICE. J. Am. Chem. Soc. **79**, 1663 (1957).
7. A. A. FROST and R. G. PEARSON. Kinetics and mechanism. John Wiley and Sons, Inc., New York. 1940. p. 186. L. P. HAMMETT. Physical organic chemistry. McGraw-Hill Book Co., Inc., New York. 1940. p. 186 ff.
8. K. BOWDEN. Can. J. Chem. **41**, 2781 (1963).

Can. J. Chem. Downloaded from www.nrcresearchpress.com by 210.87.254.42 on 09/05/12
For personal use only.

Organic and biological spectrochemical studies. XXVII. Electron spin resonance spectra of the pyrene monomer and dimer cation radicals[1]

J. T. COOPER AND W. F. FORBES

Department of Chemistry, University of Waterloo, Waterloo, Ontario and Department of Biochemistry, University of Rochester, Rochester, New York

Received October 12, 1967

The electron spin resonance spectra of pyrene, dissolved in sulfur dioxide – boron trifluoride, are investigated. Two different spectra can be obtained, depending on the experimental conditions, and are ascribed to the monomeric and dimeric hydrocarbon radical cations.

Canadian Journal of Chemistry, 46, 1158 (1968)

Radical dimers of polynuclear hydrocarbons are of some biological interest because they may provide a mechanism whereby metastable free radicals are stabilized. For example, the cation radical dimer of 3,4-benzpyrene has been postulated as a reaction intermediate involved in biological activity (1, 2) and may thus, at least partly, be responsible for the biological activity of that compound. In the course of surveying a number of polynuclear hydrocarbon cation radicals for possible dimer formation, the electron spin resonance (e.s.r.) spectrum of pyrene was investigated in various acid media.

The e.s.r. spectrum of the cation radical of pyrene (**1**) has previously been reported by Lewis and Singer (3); it was obtained by oxidizing the hydrocarbon with antimony pentachloride using methylene dichloride as solvent. However, the spectrum was not well resolved (line-width ca. 150 mG).

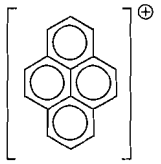

1

For the liquid sulfur dioxide–boron trifluoride system (cf. deBoer and Praat (4)) hydrocarbon and boron trifluoride concentrations of ca. 5×10^{-4} *M* were used. Samples were prepared in liquid nitrogen and allowed to melt in the spectrometer cavity at −50 °C when the spectrum shown in Fig. 1 was obtained.

This spectrum is better resolved (line width ca. 65 mG) and the main lines are well accounted for by a simulated spectrum, assuming the following proton splitting constants: $a_1 = 2.17$ G (four protons; $\rho = 0.098$); $a_3 = 5.39$ G (four protons; $\rho_3 = 0.178$); $a_4 = 1.20$ G (two protons; $\rho_4 = -0.054$) which are in good agreement with the previously reported values (3). The corresponding calculated spin densities, ρ, using the McLachlan molecular orbital – self-consistent field theory (5) are given in parentheses. Generally, for most polynuclear hydrocarbons, which in sulfuric acid afford e.s.r. spectra, the SO_2–BF_3 system appears to give equally well or better resolved spectra.[2] In some cases, for example pyrene and dibenz-(*a*,*c*)triphenylene, a spectrum is obtained in this medium although none can be obtained in sulfuric acid.

Marked changes occur on altering the temperature. The previously blue solution

[1]For part XXVI in this series, see W. F. Forbes and P. D. Sullivan, Can. J. Chem. **46**, 325 (1968).

[2]J. T. Cooper. Unpublished information.

3. H. E. UNGNADE. J. Am. Chem. Soc. **63**, 2091 (1941).
4. C. R. HARINGTON and R. V. PITT RIVERS. J. Chem. Soc. 1101 (1940). J. WALKER. J. Chem. Soc. 347 (1942).
5. L. M. LITVINENKO, S. V. TSUKERMAN, R. S. CHESHKO, and B. M. KOLESNIKOVA. Zh. Obshch. Khim. **27**, 1663 (1957); Chem. Abstr. **52**, 4546*e* (1958).
6. T. C. BRUICE. J. Am. Chem. Soc. **79**, 1663 (1957).
7. A. A. FROST and R. G. PEARSON. Kinetics and mechanism. John Wiley and Sons, Inc., New York. 1940. p. 186. L. P. HAMMETT. Physical organic chemistry. McGraw-Hill Book Co., Inc., New York. 1940. p. 186 ff.
8. K. BOWDEN. Can. J. Chem. **41**, 2781 (1963).

Organic and biological spectrochemical studies. XXVII. Electron spin resonance spectra of the pyrene monomer and dimer cation radicals[1]

J. T. COOPER AND W. F. FORBES

Department of Chemistry, University of Waterloo, Waterloo, Ontario and Department of Biochemistry, University of Rochester, Rochester, New York

Received October 12, 1967

The electron spin resonance spectra of pyrene, dissolved in sulfur dioxide – boron trifluoride, are investigated. Two different spectra can be obtained, depending on the experimental conditions, and are ascribed to the monomeric and dimeric hydrocarbon radical cations.

Canadian Journal of Chemistry, 46, 1158 (1968)

Radical dimers of polynuclear hydrocarbons are of some biological interest because they may provide a mechanism whereby metastable free radicals are stabilized. For example, the cation radical dimer of 3,4-benzpyrene has been postulated as a reaction intermediate involved in biological activity (1, 2) and may thus, at least partly, be responsible for the biological activity of that compound. In the course of surveying a number of polynuclear hydrocarbon cation radicals for possible dimer formation, the electron spin resonance (e.s.r.) spectrum of pyrene was investigated in various acid media.

The e.s.r. spectrum of the cation radical of pyrene (**1**) has previously been reported by Lewis and Singer (3); it was obtained by oxidizing the hydrocarbon with antimony pentachloride using methylene dichloride as solvent. However, the spectrum was not well resolved (line-width ca. 150 mG).

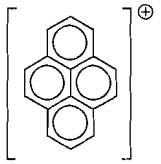

1

For the liquid sulfur dioxide–boron trifluoride system (cf. deBoer and Praat (4)) hydrocarbon and boron trifluoride concentrations of ca. 5×10^{-4} *M* were used. Samples were prepared in liquid nitrogen and allowed to melt in the spectrometer cavity at −50 °C when the spectrum shown in Fig. 1 was obtained.

This spectrum is better resolved (line width ca. 65 mG) and the main lines are well accounted for by a simulated spectrum, assuming the following proton splitting constants: $a_1 = 2.17$ G (four protons; $\rho = 0.098$); $a_3 = 5.39$ G (four protons; $\rho_3 = 0.178$); $a_4 = 1.20$ G (two protons; $\rho_4 = -0.054$) which are in good agreement with the previously reported values (3). The corresponding calculated spin densities, ρ, using the McLachlan molecular orbital – self-consistent field theory (5) are given in parentheses. Generally, for most polynuclear hydrocarbons, which in sulfuric acid afford e.s.r. spectra, the SO_2–BF_3 system appears to give equally well or better resolved spectra.[2] In some cases, for example pyrene and dibenz-(*a*,*c*)triphenylene, a spectrum is obtained in this medium although none can be obtained in sulfuric acid.

Marked changes occur on altering the temperature. The previously blue solution

[1]For part XXVI in this series, see W. F. Forbes and P. D. Sullivan, Can. J. Chem. **46**, 325 (1968).

[2]J. T. Cooper. Unpublished information.

Can. J. Chem. Downloaded from www.nrcresearchpress.com by 210.87.254.6 on 09/05/12
For personal use only.

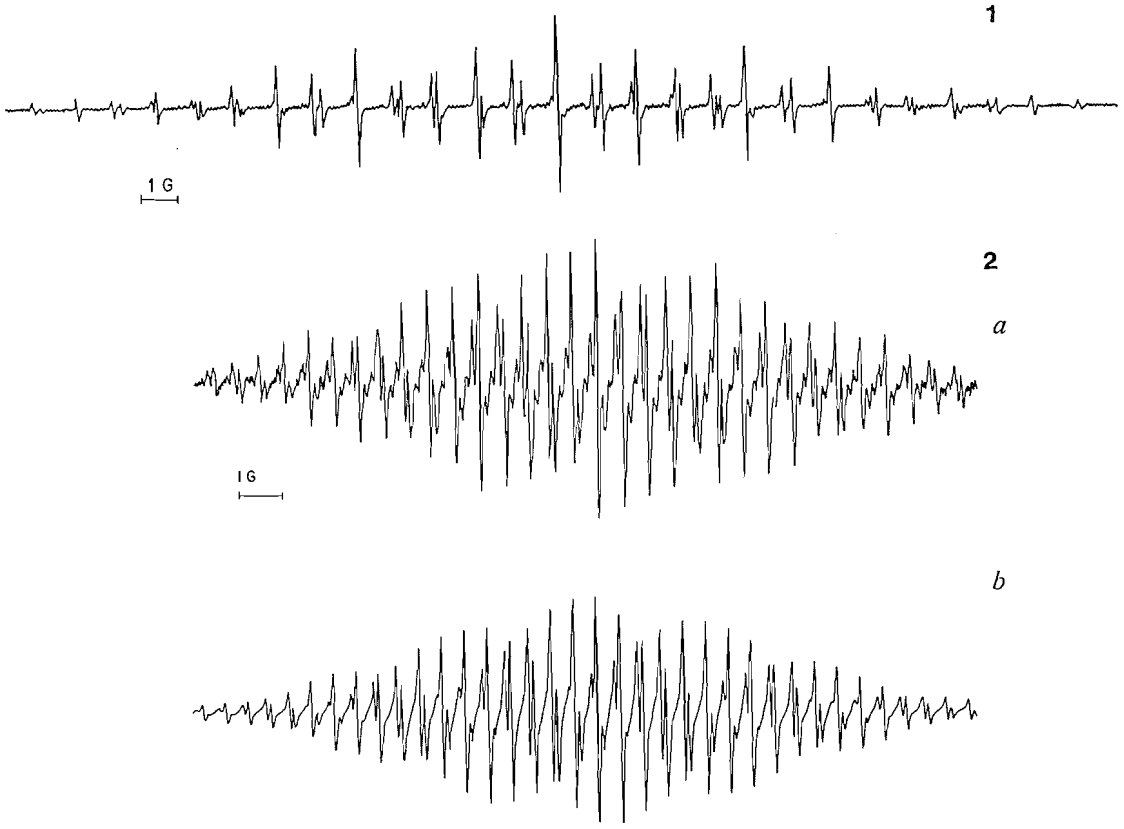

FIG. 1. The e.s.r. spectrum of pyrene in SO_2–BF_3 at −50 °C; the solution was prepared by condensing constituents into a tube cooled in liquid nitrogen.

FIG. 2. (*a*) The e.s.r. spectrum of pyrene, prepared as for Fig. 1, after warming to room temperature and subsequent recooling to −60 °C; (*b*) a computed spectrum using the parameters given in the text.

becomes yellow on warming to 25 °C and the spectrum is considerably changed and broadened. On cooling to −60 °C, the solution turns purple and the line-width decreases to ca. 65 mG (see Fig. 2*a*). This spectrum may be analyzed in terms of: $a_1 = 1.09$ G (eight protons); $a_3 = 2.61$ G (eight protons); $a_4 = 0.56$ G (four protons; see Fig. 2*b*). These values are approximately half those for the cation **1**.

This spectrum is ascribed to the pyrene dimer cation radical, with the unpaired electron density distributed equally over both molecules. Similar dimeric cation radicals have previously been proposed for naphthalene (3), anthracene, and 2,3,6,7-tetramethylnaphthalene (6). Moreover, work in this[2] and other laboratories[3] has shown that dimer radicals are also formed for coronene and possibly other polynuclear hydrocarbons. Dimer formation in solutions of pyrene and other hydrocarbons, involving neutral molecules, has been investigated by fluorescence spectroscopy (8) and the relevant theory discussed (9).

For the pyrene cation radical, dimer formation was inhibited if boron trifluoride was present in about 10-fold excess. Under these conditions, the monomer radical affords well-resolved spectra, even at 50 °C. Conversely, if pyrene is present in excess, the dimer species appeared to be more stable, and was obtained immediately at low temperature.

Pyrene was supplied by the Coal Tar Research Association (Britain) and commercially available sulfur dioxide and boron trifluoride (Matheson) were used. Electron spin resonance

[3]E. deBoer and H. van Willigen. Unpublished information.

Can. J. Chem. Downloaded from www.nrcresearchpress.com by 210.87.254.6 on 09/05/12
For personal use only.

spectra of the vacuum-sealed samples were determined with a Varian E-3 spectrometer. Spectral techniques and computer programs employed were those described previously (7). Splitting constants are believed to be accurate to 0.02 G.

Acknowledgments

This work was supported by the National Cancer Institute of Canada, the Canadian Department of Public Health and Welfare, the National Research Council of Canada, the Defence Research Board of Canada, (Grant No. 1675-04), and by the United States Public Health Service Research Grant RH00392, National Center for Radiological Health.

1. J. ROCHLITZ. Tetrahedron, **23**, 3043 (1967).
2. M. WILK, W. BEZ, and J. ROCHLITZ. Tetrahedron, **22**, 2599 (1966).
3. I. C. LEWIS and L. S. SINGER. J. Chem. Phys. **43** 2712 (1965).
4. E. DEBOER and A. PRAAT. Mol. Phys. **8**, 291 (1964); **7**, 333 (1963).
5. A. D. MCLACHLAN. Mol. Phys. **3**, 233 (1960).
6. O. W. HOWARTH and G. FRAENKEL. J. Am. Chem. Soc. **88**, 4514 (1966).
7. W. F. FORBES and P. D. SULLIVAN. Can. J. Chem. **44**, 1501 (1966).
8. T. FÖRSTER. Pure and Appl. Chem. 7, 73 (1963).
9. J. N. MURRELL and J. TANAKA. Mol. Phys. **7**, 363 (1963).

Can. J. Chem. Downloaded from www.nrcresearchpress.com by 210.87.254.6 on 09/05/12
For personal use only.

4-Substituted 6,7-dimethoxyisoquinolines

ERNEST WENKERT AND R. D. HAUGWITZ
Department of Chemistry, Indiana University, Bloomington, Indiana

Received August 18, 1967

4-Methyl- and 4-ethyl-6,7-dimethoxyisoquinolines have been synthesized by base-induced alkylation of homoveratronitrile, hydrogenation, *N*-formylation of the resultant amines, phosphorus pentoxide-induced cyclization and palladium-catalyzed dehydrogenation. Homoveratronitrile underwent self-condensation to the dimer, 2,4-bis-(3,4-dimethoxyphenyl-)3-aminocrotonitrile, under the influence of potassium *t*-butoxide. 4-Carbomethoxy-6,7-dimethoxyisoquinoline was synthesized by the following sequence of reactions: base-catalyzed condensation of homoveratronitrile with ethyl formate, acid-induced interaction with urethane, pyrolytic cyclization, phosphorus oxychloride treatment, palladium-catalyzed hydrogenolysis, and hydrolysis and esterification of the resultant 4-cyano-6,7-dimethoxyisoquinoline.

Canadian Journal of Chemistry, 46 1160 (1968)

In connection with a problem on alkaloid synthesis we were in need of 4-methyl- (**1***a*), 4-ethyl- (**1***b*), and 4-acetyl- (**1***c*) or 4-carbomethoxy-6,7-dimethoxyisoquinoline (**1***d*). The present communication describes snytheses of three of the four bases.

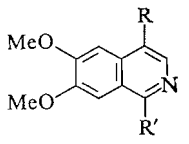

1*a* R = Me, R′ = H
b R = Et, R′ = H
c R = Ac, R′ = H
d R = CO_2Me, R′ = H
e R = CN, R′ = Cl
f R = CN, R′ = H
g R = CO_2Me, R′ = Cl

Exposure of homoveratronitrile (**2***a*) to methyl iodide and potassium *t*-butoxide led to a methylated product (**2***b*) whose hydrogenation in ammoniacal methanol solution over Raney nickel yielded an amine (**3***a*). Treatment of the *N*-formyl derivative (**3***b*) of the latter with phosphorus pentoxide produced a dihydroisoquinoline whose palladium-induced dehydrogenation yielded the desired isoquinoline **1***a*. An identical sequence of reactions except for an initial ethylation of homoveratronitrile generated isoquinoline **1***b*.

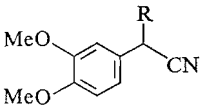

2*a* R = H
b R = Me
c R = Et
d R = Ac
e R = $C(OCH_2)_2Me$
f R = CHO

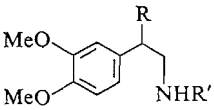

3*a* R = Me, R′ = H
b R = Me, R′ = CHO
c R = Et, R′ = H
d R = Et, R′ = CHO
e R = $C(OCH_2)_2Me$, R′ = H
f R = $C(OCH_2)_2Me$, R′ = CHO

spectra of the vacuum-sealed samples were determined with a Varian E-3 spectrometer. Spectral techniques and computer programs employed were those described previously (7). Splitting constants are believed to be accurate to 0.02 G.

Acknowledgments

This work was supported by the National Cancer Institute of Canada, the Canadian Department of Public Health and Welfare, the National Research Council of Canada, the Defence Research Board of Canada, (Grant No. 1675-04), and by the United States Public Health Service Research Grant RH00392, National Center for Radiological Health.

1. J. ROCHLITZ. Tetrahedron, **23**, 3043 (1967).
2. M. WILK, W. BEZ, and J. ROCHLITZ. Tetrahedron, **22**, 2599 (1966).
3. I. C. LEWIS and L. S. SINGER. J. Chem. Phys. **43** 2712 (1965).
4. E. DEBOER and A. PRAAT. Mol. Phys. **8**, 291 (1964); **7**, 333 (1963).
5. A. D. MCLACHLAN. Mol. Phys. **3**, 233 (1960).
6. O. W. HOWARTH and G. FRAENKEL. J. Am. Chem. Soc. **88**, 4514 (1966).
7. W. F. FORBES and P. D. SULLIVAN. Can. J. Chem. **44**, 1501 (1966).
8. T. FÖRSTER. Pure and Appl. Chem. 7, 73 (1963).
9. J. N. MURRELL and J. TANAKA. Mol. Phys. **7**, 363 (1963).

Can. J. Chem. Downloaded from www.nrcresearchpress.com by 210.87.254.40 on 09/05/12
For personal use only.

4-Substituted 6,7-dimethoxyisoquinolines

ERNEST WENKERT AND R. D. HAUGWITZ
Department of Chemistry, Indiana University, Bloomington, Indiana

Received August 18, 1967

4-Methyl- and 4-ethyl-6,7-dimethoxyisoquinolines have been synthesized by base-induced alkylation of homoveratronitrile, hydrogenation, *N*-formylation of the resultant amines, phosphorus pentoxide-induced cyclization and palladium-catalyzed dehydrogenation. Homoveratronitrile underwent self-condensation to the dimer, 2,4-bis-(3,4-dimethoxyphenyl-)3-aminocrotonitrile, under the influence of potassium *t*-butoxide. 4-Carbomethoxy-6,7-dimethoxyisoquinoline was synthesized by the following sequence of reactions: base-catalyzed condensation of homoveratronitrile with ethyl formate, acid-induced interaction with urethane, pyrolytic cyclization, phosphorus oxychloride treatment, palladium-catalyzed hydrogenolysis, and hydrolysis and esterification of the resultant 4-cyano-6,7-dimethoxyisoquinoline.

Canadian Journal of Chemistry, 46 1160 (1968)

In connection with a problem on alkaloid synthesis we were in need of 4-methyl- (**1***a*), 4-ethyl- (**1***b*), and 4-acetyl- (**1***c*) or 4-carbomethoxy-6,7-dimethoxyisoquinoline (**1***d*). The present communication describes snytheses of three of the four bases.

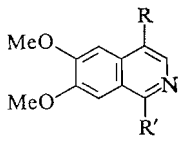

1*a* R = Me, R′ = H
b R = Et, R′ = H
c R = Ac, R′ = H
d R = CO_2Me, R′ = H
e R = CN, R′ = Cl
f R = CN, R′ = H
g R = CO_2Me, R′ = Cl

Exposure of homoveratronitrile (**2***a*) to methyl iodide and potassium *t*-butoxide led to a methylated product (**2***b*) whose hydrogenation in ammoniacal methanol solution over Raney nickel yielded an amine (**3***a*). Treatment of the *N*-formyl derivative (**3***b*) of the latter with phosphorus pentoxide produced a dihydroisoquinoline whose palladium-induced dehydrogenation yielded the desired isoquinoline **1***a*. An identical sequence of reactions except for an initial ethylation of homoveratronitrile generated isoquinoline **1***b*.

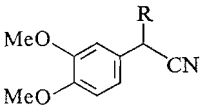

2*a* R = H
b R = Me
c R = Et
d R = Ac
e R = $C(OCH_2)_2Me$
f R = CHO

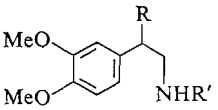

3*a* R = Me, R′ = H
b R = Me, R′ = CHO
c R = Et, R′ = H
d R = Et, R′ = CHO
e R = $C(OCH_2)_2Me$, R′ = H
f R = $C(OCH_2)_2Me$, R′ = CHO

Can. J. Chem. Downloaded from www.nrcresearchpress.com by 210.87.254.40 on 09/05/12
For personal use only.

Base-catalyzed condensation of homoveratronitrile with ethyl acetate yielded the ketone **2***d* (1) whose interaction with ethylene glycol and acid produced the ketal **2***e*. Hydrogenation of the latter yielded an amine (**3***e*) whose treatment with formic acid led to the amide **3***f*. Unfortunately all attempts to convert the formamide into a dihydroisoquinoline failed despite application of a large variety of cyclization procedures. One of these, treatment of **3***f* with phosphorus pentoxide in pyridine (2), yielded the unneeded isocyanide **4** (cf. ref. 3). While a direct approach to the ketone **1***c* thus appeared to be blocked, no alternate route of synthesis was sought in view of the concurrent completion of a synthesis of the equally useful ester **1***d*.

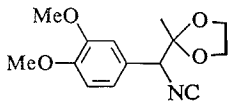

4

Condensation of homoveratronitrile (**2***a*) with ethyl formate, followed by acid-induced interaction of the resultant formyl derivative (**2***f*) with urethane, led to **5** whose pyrolysis in diphenyl ether solution produced the isocarbostyril **6** (cf. ref. 4). Phosphorus oxychloride treatment of the latter gave the chloro compound **1***e* whose palladium-catalyzed hydrogenolysis yielded **1***f*. Hydrolysis and esterification of the cyanide afforded the desired ester **1***d*.

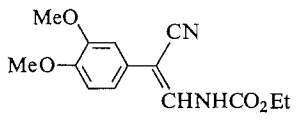

5

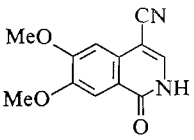

6

Side products of the alkylation of homoveratronitrile (*vide supra*) appeared reminiscent of the product of base-catalyzed dimerization of phenylacetonitrile (5). Self-condensation of homoveratronitrile (**2***a*) under the influence of potassium *t*-butoxide yielded a dimer whose infrared and proton magnetic resonance (p.m.r.) spectral characteristics showed it to possess structure **8***a* and thus to be the tetramethoxy derivative of phenylacetonitrile dimer (**7**). The alkylation side products were shown to be the *N*-alkyl derivatives **8***c* and **8***d* by similar spectral examination.

$C_6H_5CH_2C(NH_2)=C(CN)\ C_6H_5$

7 $[3,4\text{-}(MeO)_2]\,C_6H_3CH_2C(NRR')=C(CN)\text{-}C_6H_3[(OMe)_2\text{-}3,4]$

8*a* R = R′ = H
b R = H, R′ = Ac
c R = Me, R′ = H
d R = Et, R′ = H

Experimental

All melting points were determined on a Reichert microhotstage and are uncorrected. Ultraviolet spectra were obtained on a Cary 14 spectrophotometer. Infrared spectra were determined with a Perkin–Elmer 137B spectrophotometer. Proton magnetic resonance (p.m.r.) spectra of deuteriochloroform solutions containing tetramethylsilane as internal standard were recorded on a Varian Associates A-60 spectrometer. Neutral alumina, activity IV, was used for chromatography.

*4-Methyl-6,7-dimethoxyisoquinoline (**1a**)*

A solution of 3.90 g of potassium, 17.7 g of homoveratronitrile (**2**), and 14.2 g of methyl iodide in 120 ml of *t*-butanol was heated at 100° for 2 h. The solution was concentrated to low volume, acidified with acetic acid, and extracted with chloroform. The extract was evaporated and the residue distilled at 130–140° at 0.05 mm. The liquid product, 11.2 g, consisting of some dimethylated material and **2***b* [μ (neat) C≡N 4.45(w), C=C 6.20(m), 6.25(m); δ C—CH_3 doublet at 1.55 p.p.m. (J = 7.0 c.p.s.), O—CH_3 singlets at 3.81, 3.82 p.p.m.], was reduced without further purification. A mixture of the product and 1.3 g of Raney nickel in 200 ml of methanol saturated with ammonia was hydrogenated in a Paar bomb at 40 p.s.i. for 6 h. The mixture was centrifuged, the supernatant liquid decanted from the catalyst, and the solution evaporated. Distillation of the residue gave 10.5 g of amine composed of some dimethylated product and **3***a* [μ (neat) NH 2.95(w, broad), C=C 6.20(m), 6.25(m); δ C—CH_3 doublet at 1.21 p.p.m. (J = 7.0 c.p.s.), O—CH_3 singlets at 3.79, 3.82 p.p.m.]. A solution of the product in 2.9 g of formic acid was heated at 115° for 3 h. The excess formic acid was removed by distillation. Further distillation at ca. 200° at 0.05 mm yielded 11.3 g of amide encompassing some dimethylated substance and **3***b* [μ (neat) NH 3.07(m), C=O 5.99(s), C=C 6.26(m), 6.34(m); δ C—CH_3 doublet at 1.25 p.p.m. (J = 7.0 c.p.s.), O—CH_3 singlets at 3.79, 3.81 p.p.m.]. A solution of the amide and 30 g of phosphorus pentoxide in 500 ml of toluene was refluxed for 15 min. Another 20 g of phosphorus pentoxide was added and the refluxing continued for 15 min. The solution was decanted from the precipitate and extracted with 10% hydrochloric acid. The precipitate was decomposed with ice-water and the acidic, aqueous solutions combined. They then were washed with chloroform, basified, and extracted with chloroform. The extract was evaporated and the residue distilled under vacuum. This yielded 4.92 g of a mixture of dimethylated dihydroisoquinoline and 3,4-dihydro-**1***a* [μ (neat) C=N 6.14(m), C=C 6.23(m), 6.36(m); δ C—CH_3 doublet at 1.20 p.p.m. (J = 7.0 c.p.s.), O—CH_3 singlets at 3.86, 3.90 p.p.m.]. A mixture of the product and 1.5 g of 10% palladium on charcoal in 200 ml of *p*-cymene was refluxed for 1.5 h. The catalyst was filtered and the filtrate concentrated to 50 ml and extracted with 10% hydrochloric acid. The extract was

Can. J. Chem. Downloaded from www.nrcresearchpress.com by 210.87.254.40 on 09/05/12
For personal use only.

washed with chloroform, made basic with 10% potassium hydroxide, and extracted with chloroform. The extract was evaporated and the residue crystallized from benzene–hexane yielding 1.73 g of **1***a*, m.p. 128°; μ (Nujol) C═C 6.21(m), 6.37(m); δ C—CH_3 singlet at 2.46 p.p.m., two O—CH_3 singlets at 3.97 p.p.m., C_5—H and C_8—H singlets at 6.92, 7.04 p.p.m., C_3—H singlet at 8.17 p.p.m., C_1—H singlet at 8.82 p.p.m.

Anal. Calcd. for $C_{12}H_{13}O_2N$: C, 70.81; H, 6.45; N, 6.89. Found: C, 70.85; H, 6.52; N, 6.92.

*4-Ethyl-6,7-dimethoxyisoquinoline (**1***b*)

The synthesis of **1***b* followed the procedure outlined above for the preparation of **1***a* (except for the use of ethyl iodide in place of methyl iodide in the first reaction). Homoveratronitrile (**2***a*), 1.77 g, was transformed into 0.85 g of its α-ethyl derivative (**2***c*). Hydrogenation of the latter, 8.50 g, gave 6.70 g of amine **3***c*, whose formylation yielded 7.00 g of amide **3***d*. Cyclization of the formamide followed by dehydrogenation of the product (3,4-dihydro-**1***b*), 4.04 g, led to a base whose crystallization from benzene–hexane afforded 1.90 g of **1***b*, m.p. 88°; δ C—CH_3 triplet at 1.36 p.p.m. (J = 7.0 c.p.s.), CH_2 quartet at 2.96 p.p.m. (J = 7.0 c.p.s.), O—CH_3 singlets at 4.01, 4.02 p.p.m., C_5—H and C_8—H singlets at 7.22, 7.27 p.p.m., C_3—H singlet at 8.26 p.p.m., C_1—H singlet at 8.92 p.p.m.; **1***b*·picrate (crystallized from methanol), m.p. 223–225°; μ (Nujol) C═C 6.15(m), 6.20(m), 6.30(m), 6.39(m), 6.50(m).

Anal. Calcd. for $C_{19}H_{18}O_9N_4$: C, 51.12; H, 4.06; N, 12.55. Found: C, 51.64; H, 4.12; N, 12.21.

*α-Acetylhomoveratronitrile Ethyleneketal (**2***e*)

A solution of 23.4 g of homoveratronitrile (**2***a*), 45 ml of ethyl acetate and 9.1 g of sodium in 100 ml of absolute ethanol was refluxed for 2 h. The precipitated salt was filtered, washed with ether, and decomposed in 10% acetic acid. Evaporation of the mixture and crystallization of the residue from methanol yielded 29.0 g of **2***d* (1), m.p. 97–98°; δ C—CH_3 singlet at 2.22 p.p.m., two O—CH_3 singlets at 3.90 p.p.m., benzyl C—H singlet at 4.70 p.p.m.; its enol μ (Nujol) OH 3.22(m, broad), C≡N 4.57(m), C═C 6.18(m), 6.28(w), 6.38(w).

A solution of 10.0 g of **2***d* and 0.3 g of *p*-toluenesulfonic acid in 300 ml of ethylene glycol was distilled slowly at 70–72° at 2.5 mm. After 3 h, 200 ml of ethylene glycol was added and the distillation continued for another 2 h. Chloroform was added to the residual solution, 50–100 ml, and the mixture washed with 10% sodium hydroxide solution. Evaporation of the chloroform solution and crystallization of the residue from methanol yielded 7.9 g of **2***e*, m.p. 85°; μ (Nujol) C≡N 4.45(w), C═C 6.22 (w), 6.28(w); δ C—CH_3 singlet at 1.35 p.p.m., O—CH_3 singlets at 3.88, 3.89 p.p.m., (O—CH_2)$_2$ singlet at 3.96 p.p.m.

Anal. Calcd. for $C_{14}H_{17}O_4N$: C, 63.87; H, 6.51; N, 5.32. Found: C, 63.04; H, 7.86; N, 5.24.

*α-Acetylhomoveratrylamine Ethyleneketal (**3***e*)

A mixture of 4.0 g of **2***e* and 1.0 g of Raney nickel in 200 ml of methanol saturated with ammonia was hydrogenated at room temperature and 40 p.s.i. for 6 h. The mixture was centrifuged and the supernatant liquid decanted and evaporated. The residue was chromatographed on alumina. Distillation of the ethyl acetate and methanol eluates at 200° at 6.5 mm afforded 3.0 g of viscous liquid **3***e*; μ (neat) NH 3.00(w, broad), C═C 6.22(w), 6.28(w); δ NH_2 singlet at 1.08 p.p.m., C—CH_3 singlet at 1.19 p.p.m., O—CH_3 singlets at 3.88, 3.89 p.p.m.

Anal. Calcd. for $C_{14}H_{21}O_4N$: C, 62.90; H, 7.92; N, 5.24. Found: C, 63.04; H, 7.86; N, 5.24.

*N-(α-Acetylhomoveratryl)formamide Ethyleneketal (**3***f*)

A solution of 2.63 g of **3***e* in 0.6 g of 98% formic acid was heated at 120° for 3 h. Distillation of the mixture and collection of a fraction boiling at ca. 200° at 0.3 mm yielded 2.43 g of viscous liquid **3***f*; μ(neat) NH 3.04(m, broad), C═O 6.02(s), C═C 6.22(m), 6.32(m); δ C—CH_3 singlet at 1.17 p.p.m., O—CH_3 singlets at 3.81, 3.82 p.p.m., H—CO doublet at 7.92 p.p.m. (J = 2.0 c.p.s.).

Anal. Calcd. for $C_{15}H_{21}O_5N$: C, 61.00; H, 7.17; N, 4.74. Found: C, 61.26; H, 7.11; N, 4.50.

*Isocyanide **4***

A mixture of 5.0 g of phosphorus pentoxide and 50 g of sand was added in four portions to a boiling solution of 500 mg of **3***f* in 30 ml of pyridine over a period of 6 h. The solution was decanted from the gummy residue which was extracted repeatedly with hot pyridine. The combined pyridine solutions were taken to dryness under vacuum and the residue chromatographed on alumina. Evaporation of the benzene eluates and crystallization of the residual solid from methanol yielded 160 mg of **4**, m.p. 132°; μ (Nujol) C≡N 4.64(s), C═C 6.22(w), 6.30(w); δ C—CH_3 singlet at 1.12 p.p.m., O—CH_3 singlets at 3.88, 3.89 p.p.m., (OCH_2)$_2$ singlet at 3.93 p.p.m.

Anal. Calcd. for $C_{15}H_{19}O_4N$: C, 64.87; H, 6.91; N, 5.05. Found: C, 64.89; H, 6.91; N, 4.93.

*Urethane **5***

A mixture of 8.85 g of homoveratronitrile (**2***a*), 3.80 g of ethyl formate and potassium methoxide, from 1.95 g of potassium, in 40 ml of ether was stirred at room temperature for 5 h. The precipitated salt was filtered, washed with ether, and decomposed in 10% acetic acid solution. The hygroscopic **2***f* enol, 8.00 g, was stored over phosphorus pentoxide. A solution of 26.0 g of **2***f* enol, 11.3 g of ethyl carbamate, and 0.7 ml of concentrated sulfuric acid in 500 ml of toluene was concentrated by slow distillation to a volume of 50 ml. The cooled mixture was filtered and the precipitate washed with benzene. Crystallization of the solid from chloroform–ether yielded 23.9 g of **5**, m.p. 193°; μ (Nujol) NH 3.03(s), C≡N 4.52(m), C═O 5.77(s), C═C 6.10(s), 6.23(w), 6.30(w); δ C—CH_3 triplet at 1.17 p.p.m. (J = 7.0 c.p.s.), two O—CH_3 singlets at 3.92 p.p.m., (O—CH_2) quartet at 4.11 p.p.m. (J = 7.0 c.p.s.).

Anal. Calcd. for $C_{14}H_{16}O_4N_2$: C, 60.48; H, 5.84; N, 10.14. Found: C, 60.64; H, 5.99; N, 10.40.

*4-Cyano-6,7-dimethoxyisocarbostyril (**6**)*

A solution of 11.2 g of **5** in 70 ml of diphenyl ether was refluxed for 50 min. The cooled mixture was filtered and the precipitate washed generously with chloroform. Crystallization of the solid from glacial acetic acid afforded 7.0 g of **6**, m.p. 293–294°; μ (Nujol) NH 3.05(m), C≡N 4.52(m), C═O 6.02(s), C═C 6.07(s), 6.18(m), 6.25(s).

Anal. Calcd. for $C_{12}H_{10}O_3N_2$: C, 62.60; H, 4.38; N, 12.17. Found: C, 62.74; H, 4.50; N, 12.10.

Can. J. Chem. Downloaded from www.nrcresearchpress.com by 210.87.254.40 on 09/05/12
For personal use only.

*1-Chloro-4-cyano-6,7-dimethoxyisoquinoline (**1e**)*

A solution of 11.0 g of **6** in 200 ml of phosphorus oxychloride was refluxed for 2 h and then left standing at room temperature for 12 h. The resultant crystalline precipitate was filtered and washed with hexane yielding 8.75 g of **1e**, m.p. 245°; μ (Nujol) C≡N 4.50(m), C=C 6.24(s), 6.35(w), 6.45(s); δ O—CH_3 singlets at 4.10, 4.12 p.p.m., C_5—H and C_8—H singlets at 7.32, 7.55 p.p.m., C_3—H singlet at 8.44 p.p.m.

Anal. Calcd. for $C_{12}H_9O_2N_2Cl$: C, 57.96; H, 3.57; N, 11.27. Found: C, 58.15; H, 3.86; N, 11.47.

*4-Cyano-6,7-dimethoxyisoquinoline (**1f**)*

A slow stream of hydrogen was passed through a refluxing mixture of 10.0 g of **1e** and 5 g of 10% palladium on charcoal in 500 ml of *p*-cymene for 2.5 h. The hot suspension was filtered through Celite and the filtrate extracted exhaustively with 10% hydrochloric acid solution. The extract was basified with 15% potassium hydroxide solution and the resultant precipitate filtered and dried. Crystallization of the solid from chloroform–methanol yielded 5.2 g of **1f**, m.p. 218–219°; μ (Nujol) C≡N 4.50(m), C=C 6.18(m), 6.35(m); δ O—CH_3 singlets at 4.01, 4.07 p.p.m., C_5—H and C_8—H singlets at 7.18, 7.24 p.p.m., C_3—H and C_1—H singlets at 8.55, 8.99 p.p.m.

Anal. Calcd. for $C_{12}H_{10}O_2N_2$: C, 67.28; H, 4.71; N, 13.08. Found: C, 67.35; H, 4.80; N, 13.10.

*Methyl 1-Chloro-6,7-dimethoxyisoquinoline-4-carboxylate (**1g**)*

A solution of 300 mg of **1e** in 30 ml of methanol and 30 ml of methylene chloride, saturated with hydrogen chloride, was kept at room temperature for 4 days. The mixture was evaporated and the residue treated with 10% sodium carbonate solution and extracted with chloroform. Evaporation of the extract and crystallization of the residue from methanol produced 295 mg of **1g**, m.p. 156–157°; μ (Nujol) C=O 5.83(s), C=C 6.17(m), 6.34(w), 6.40(s).

Anal. Calcd. for $C_{13}H_{12}O_4NCl$: C, 55.42; H, 4.30; N, 4.97. Found: C, 55.30; H, 4.63; N, 4.92.

*Methyl 6,7-Dimethoxyisoquinoline-4-carboxylate (**1d**)*

A mixture of 7.9 g of the nitrile **1f** and 185 ml of concentrated hydrochloric acid was refluxed for 40 h. Removal of water and excess hydrogen chloride by distillation left 8.7 g of **1**·HCl (R = CO_2H, R′ = H), m.p. 230–232°, whose solution in 1.3 l of absolute methanol, saturated with hydrogen chloride, was kept at room temperature for 18 h. The solvent was evaporated and the residue treated with 10% sodium carbonate solution and extracted with chloroform. Evaporation of the extract and crystallization of the residue from hexane–ether led to 6.0 g of the ester **1d**, m.p. 138°; μ (Nujol) C=O 5.82(s), C=C 6.17(m), 6.33(m), 6.61(s).

Anal. Calcd. for $C_{13}H_{13}O_4N$: C, 63.15; H, 5.30; N, 5.67. Found: C, 63.37; H, 5.41; N, 5.80.

Arylacetonitrile Dimers

Phenylacetonitrile, 2.34 g, was treated with a solution of 0.78 g of potassium in 50 ml of *t*-butanol. The solution was evaporated and the residue treated with acetic acid. The mixture was evaporated and the residue extracted with chloroform. The extract was distilled and the fraction boiling at 220–240°at 0.05 mm chromatographed on alumina. The benzene eluate yielded 1.00 g of 2,4-diphenyl-3-aminocrotonitrile (**7**) (5); μ (neat) NH 2.90(s), 3.00(s), 3.10(s), C≡N 4.58(s), C=C 6.10(s), 6.25(s); δ CH_2 singlet at 3.75 p.p.m., NH_2 broad singlet at 4.86 p.p.m. (While aromatic compounds absorb light in the 6.0–6.4μ infrared spectral region, the spectra of neither phenylacetonitrile nor homoveratronitrile (**2a**) revealed the high-intensity enamine band at 6.10μ.)

Homoveratronitrile (**2a**), 1.77 g, was treated with a solution of 0.39 g of potassium in 50 ml of *t*-butanol as above. The distillate solidified. On crystallization from methanol there was obtained 0.90 g of 2,4-bis-(3,4-dimethoxyphenyl-)3-aminocrotonitrile (**8a**), m.p. 133–134°; mass spectroscopy mol. wt. 354; μ (Nujol) NH 2.90(s), 3.00(s), C≡N 4.58(s), C=C 6.10(s); δ four O—CH_3 singlets at 3.81 p.p.m., CH_2 singlet at 3.82 p.p.m., NH_2 broad singlet at 4.82 p.p.m.

Anal. Calcd. for $C_{20}H_{22}O_4N_2$: C, 67.78; H, 6.25; N, 7.90. Found: C, 68.07; H, 6.38; N, 8.07.

A solution of 200 mg of **8a** and 20 mg of *p*-toluenesulfonic acid in 50 ml of acetic anhydride was kept at room temperature for 24 h. It was evaporated and the residue chromatographed on alumina. Benzene elution yielded a solid whose crystallization from ether led to 100 mg of the amide **8b**, m.p. 150°; μ (Nujol) NH 3.03(m), C≡N 4.52(m), C=O 5.89(s), C=C 6.23(s), 6.29(m); δ C—CH_3 singlet at 1.90 p.p.m., four O—CH_3 singlets at 3.83 p.p.m., CH_2 singlet at 3.84 p.p.m.

Anal. Calcd. for $C_{22}H_{24}O_5N_2$: C, 66.65; H, 6.10. Found: C, 67.05; H, 6.10.

Crystallization of the residue of the distillation of **2c** from methanol yielded **8d**, m.p. 170–171°; μ (Nujol) NH 2.98(m), C≡N 4.58(s), C=C 6.21(s), 6.26(s); δ C—CH_3 triplet at 0.93 p.p.m., NCH_2 quartet at 3.11 p.p.m., four O—CH_3, CH_2 and an NH multiplet at 3.8–4.0 p.p.m.

Anal. Calcd. for $C_{22}H_{26}O_4N_2$: C, 69.09; H, 6.85; N, 7.33. Found: C, 68.97; H, 6.99; N, 7.22.

Acknowledgment

The authors are indebted to the Squibb Institute for Medical Research for support of this work.

1. E. Späth and N. Polgar. Monatsh. **51**, 191 (1929).
2. N. Itoh and S. Sugasawa. Tetrahedron, **1**, 45 (1957).
3. W. R. Hertler and E. J. Corey. J. Org. Chem. **23**, 1221 (1958).
4. F. Eiden and B. S. Nagar. Arch. Pharm. **297**, 488 (1964).
5. E. F. J. Atkinson and J. F. Thorpe. J. Chem. Soc. 1906 (1906).

Preparation and structure of dimethyl-α-conidendrin-8-sulfonamide

G. M. BARTON
Department of Forestry and Rural Development, Forest Products Laboratory, Vancouver 8, British Columbia
Received December 1, 1967

The synthesis and structure of a new derivative of α-conidendrin, an extractive from western hemlock (*Tsuga heterophylla* [Raf.] Sarg.), are described. Elemental analyses together with high resolution nuclear magnetic spectroscopy enabled the structure to be designated as 2-naphthoic acid, 1,2,3,4-tetrahydro-3-hydroxymethyl-6,7-dimethoxy-4-(3′,4′-dimethoxyphenyl)-8-sulfonamide γ-lactone.

Canadian Journal of Chemistry, 46, 1164 (1968)

Can. J. Chem. Downloaded from www.nrcresearchpress.com by 210.87.254.42 on 09/05/12
For personal use only.

One of the important challenges of the wood extractive field is the number of pure crystalline compounds potentially available in commercial quantities which are only being used in token amounts at the present time. A good example of one such compound is α-conidendrin, a major phenolic extractive of western hemlock (*Tsuga heterophylla* [Raf.] Sarg.) wood (1) and readily obtainable in commercial amounts from hemlock waste sulfite pulping liquor (2).

In a continuing effort to enhance the usefulness of α-conidendrin, new derivatives have been synthesized. One of these, dimethyl α-conidendrin-8-sulfonamide (2-naphthoic acid, 1,2,3,4-tetrahydro-3-hydroxymethyl-6,7-dimethoxy-4-(3′,4′-dimethoxyphenyl)-8-sulfonamide γ-lactone) has been prepared and submitted for cancer chemotherapy testing.[1] Its structure has been determined as **1**.

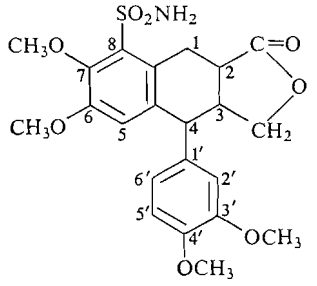

Although it was originally intended to convert a previously prepared derivative of α-conidendrin, namely dimethyl α-conidendrin-8-methyl sulfonate (3), to the sulfonyl chloride intermediate by treatment with phosphorous pentachloride this reaction did not prove to be successful. An alternative procedure was employed with success; this involved the reaction of dimethyl α-conidendrin with monochlorosulfonic acid (4). The sulfonyl chloride intermediate was not isolated, but was reacted immediately with concentrated ammonium hydroxide to give the more easily crystallized sulfonamide. Recrystallization of the resultant sulfonamide from boiling ethanol gave white crystals melting at 291–294 °C. The infrared spectrum of **1** contained strong, broad absorption bands at 1330 and 1150 cm^{-1}; such bands are characteristic of a sulfonamide group.

First order analysis of the nuclear magnetic resonance (n.m.r.) spectra of **1**, together with consideration of the obtained integrals, substantiated the proposed structure and supported the presence of 25 protons. Chemical shifts, decoupling experiments, and comparisons with the spectra of dimethyl α-conidendrin-8-methyl sulfonate (3) resulted in the assignment of most of the protons. The aromatic protons of the pendant ring exhibited remarkably weak coupling and appear as singlets (width at half height 3.0 c.p.s.) probably as a result of the strong electron withdrawing effect of the sulfonamide group. This same electron withdrawing effect also influenced the chemical shift of the four methoxyl groups, and was the basis for the assignment of two of them on carbons C-6 and C-7 to τ 6.32 and 6.24 respectively. The same arguments used in assignment of the methyl sulfonate group (3) to position-8, based on the aromatic proton shifts and steric hindrance, were also applied to the sulfonamide. The structure of the sulfonamide is thus accurately described as **1**.

[1]Dr. H. B. Wood, Jr., Drug Development Branch, Cancer Chemotherapy, National Service Center, Bethesda, Maryland.

Can. J. Chem. Downloaded from www.nrcresearchpress.com by 210.87.254.42 on 09/05/12
For personal use only.

Experimental

Carbon and hydrogen analyses were performed by Mr. P. Broda of the University of British Columbia Chemistry Department. Nitrogen and sulfur analyses were performed by M-H-W Laboratories, Garden City, Michigan. Nuclear magnetic resonance spectra were recorded on a Varian, model HA 100, spectrometer in deuterated dimethyl sulfoxide with tetramethylsilane as an internal standard. Infrared spectra were run in KBr discs on a Baird-Atomic infrared spectrophotometer, model KM-1.

Dimethyl α-Conidendrin-8-sulfonamide

Dimethyl α-conidendrin (5) (2 g) was dissolved in chloroform (50 ml) and the solution cooled to 0 °C. Chlorosulfonic acid (6 ml) was then slowly added to the vigorously stirred, cooled solution. After 20 min the reaction mixture was poured slowly into a beaker of cracked ice. The chloroform layer containing the intermediate sulfonyl chloride was separated from the aqueous phase by means of a separatory funnel and after mixing with an excess of concentrated ammonium hydroxide was allowed to stand overnight at room temperature. The resulting cream-colored precipitate was filtered off and recrystallized from boiling ethanol. Yield of white crystals, m.p. 291–294 °C was 1.0 g (41.5%). Several recrystallizations from ethanol failed to change the melting point.

Anal. Calcd. for $C_{22}H_{25}O_8SN$:C, 57.0; H, 5.4; S, 6.9; N, 3.0. Found: C, 56.5; H, 5.7; S, 7.1; N, 3.3.

Spectra: ν KBr 656 (w), 740(w), 762(w), 775(w), 872 (m, br), 936 (w), 990 (s), 1055 (m), 1096 (m), 1105 (w), 1150 (s, br), 1220 (w), 1260 (m, br), 1330 (s, br), 1380 (w), 1445 (m), 1470 (m), 1512 (s), 1568 (w), 1609 (w), 1755 (s), 2096 (m), 3022 (s) cm^{-1}. Nuclear magnetic resonance $\tau = 2.50$ (2H, amide protons, broad singlet), 2.58 (1H, C5, singlet), 3.26 (1H, aromatic singlet, width at half height 3 c.p.s.), 3.40 (1H, aromatic, singlet, width at half height 3 c.p.s.), 3.78 (1H, aromatic, singlet, width at half height 3 c.p.s.), 5.02 (1H, C-4, doublet, $J = 8$ c.p.s.), 5.84–6.02 (2H, C1, multiplet), 6.24 (3H, C7, singlet), 6.32 (3H, C-6, singlet), 6.40 (3H, C-3[1] or C-4[1], singlet), 6.64 (3H, C-3[1] or C-4[1], singlet), 7.00–7.17 (4H, C-2, C-3 and attached methylene, multiplet).

Acknowledgments

The author thanks Dr. Ross Stewart and Mr. John Manville of the Chemistry Department, University of British Columbia, for their helpful discussions. Technical assistance by Mr. C. R. Daniels of the Wood Chemistry Section, Forest Products Laboratory, is gratefully acknowledged.

The author also wishes to thank Crown Zellerbach, Chemical Products Division, Camas, Washington, for their generous sample of α-conidendrin.

1. F. E. Brauns. J. Org. Chem. **10**, 211 (1945).
2. H. B. Lackey, W. W. Moyer, and W. M. Hearon. Tappi, **32**, 469 (1949).
3. G. M. Barton and J. F. Manville. J. Org. Chem. **30**, 659 (1965).
4. L. F. Fieser. Experiments in organic chemistry. 2nd ed. D. C. Heath and Company. Boston. 1941. p. 262.
5. B. Holmberg. Chem. Ber. **54**, 2389 (1921).

Hydrolytic cleavage of cyclic allylic organoboranes

D. S. Sethi and D. Devaprabhakara
Department of Chemistry, Indian Institute of Technology, Kanpur, India

Received November 7, 1967

It has been shown that cyclic allylic organoborane intermediates obtained from monohydroboration of some 1,2- and 1,3-cyclic dienes with diborane generated *in situ* undergo slow hydrolysis with oxygen-free water to yield monoolefins.

Canadian Journal of Chemistry, 46, 1165 (1968)

It is generally known that organoboranes do not undergo cleavage at carbon–boron bond by water at room temperature (1); however, it has been shown that trisallylborane is unusual in its hydrolysis even at or below room temperature (2). In this connection, we have studied the behavior of certain cyclic allylic organoboranes with oxygen-free water under nitrogen atmosphere to establish the generality of this reaction. We undertook the study with cyclopentadiene, 1,3-cyclohexadiene, 1,3-cyclooctadiene, 1,2-cyclononadiene, and 1,2-cyclodecadiene. Our results with these substrates establish that slow hydrolysis of cyclic allylic organoboranes takes place but not as rapidly as does trisallylborane (2).

Experimental

Carbon and hydrogen analyses were performed by Mr. P. Broda of the University of British Columbia Chemistry Department. Nitrogen and sulfur analyses were performed by M-H-W Laboratories, Garden City, Michigan. Nuclear magnetic resonance spectra were recorded on a Varian, model HA 100, spectrometer in deuterated dimethyl sulfoxide with tetramethylsilane as an internal standard. Infrared spectra were run in KBr discs on a Baird-Atomic infrared spectrophotometer, model KM-1.

Dimethyl α-Conidendrin-8-sulfonamide

Dimethyl α-conidendrin (5) (2 g) was dissolved in chloroform (50 ml) and the solution cooled to 0 °C. Chlorosulfonic acid (6 ml) was then slowly added to the vigorously stirred, cooled solution. After 20 min the reaction mixture was poured slowly into a beaker of cracked ice. The chloroform layer containing the intermediate sulfonyl chloride was separated from the aqueous phase by means of a separatory funnel and after mixing with an excess of concentrated ammonium hydroxide was allowed to stand overnight at room temperature. The resulting cream-colored precipitate was filtered off and recrystallized from boiling ethanol. Yield of white crystals, m.p. 291–294 °C was 1.0 g (41.5%). Several recrystallizations from ethanol failed to change the melting point.

Anal. Calcd. for $C_{22}H_{25}O_8SN$:C, 57.0; H, 5.4; S, 6.9; N, 3.0. Found: C, 56.5; H, 5.7; S, 7.1; N, 3.3.

Spectra: v KBr 656 (w), 740(w), 762(w), 775(w), 872 (m, br), 936 (w), 990 (s), 1055 (m), 1096 (m), 1105 (w), 1150 (s, br), 1220 (w), 1260 (m, br), 1330 (s, br), 1380 (w), 1445 (m), 1470 (m), 1512 (s), 1568 (w), 1609 (w), 1755 (s), 2096 (m), 3022 (s) cm^{-1}. Nuclear magnetic resonance $\tau = 2.50$ (2H, amide protons, broad singlet), 2.58 (1H, C5, singlet), 3.26 (1H, aromatic singlet, width at half height 3 c.p.s.), 3.40 (1H, aromatic, singlet, width at half height 3 c.p.s.), 3.78 (1H, aromatic, singlet, width at half height 3 c.p.s.), 5.02 (1H, C-4, doublet, $J = 8$ c.p.s.), 5.84–6.02 (2H, C1, multiplet), 6.24 (3H, C7, singlet), 6.32 (3H, C-6, singlet), 6.40 (3H, C-3[1] or C-4[1], singlet), 6.64 (3H, C-3[1] or C-4[1], singlet), 7.00–7.17 (4H, C-2, C-3 and attached methylene, multiplet).

Acknowledgments

The author thanks Dr. Ross Stewart and Mr. John Manville of the Chemistry Department, University of British Columbia, for their helpful discussions. Technical assistance by Mr. C. R. Daniels of the Wood Chemistry Section, Forest Products Laboratory, is gratefully acknowledged.

The author also wishes to thank Crown Zellerbach, Chemical Products Division, Camas, Washington, for their generous sample of α-conidendrin.

1. F. E. Brauns. J. Org. Chem. **10**, 211 (1945).
2. H. B. Lackey, W. W. Moyer, and W. M. Hearon. Tappi, **32**, 469 (1949).
3. G. M. Barton and J. F. Manville. J. Org. Chem. **30**, 659 (1965).
4. L. F. Fieser. Experiments in organic chemistry. 2nd ed. D. C. Heath and Company. Boston. 1941. p. 262.
5. B. Holmberg. Chem. Ber. **54**, 2389 (1921).

Hydrolytic cleavage of cyclic allylic organoboranes

D. S. Sethi and D. Devaprabhakara
Department of Chemistry, Indian Institute of Technology, Kanpur, India

Received November 7, 1967

It has been shown that cyclic allylic organoborane intermediates obtained from monohydroboration of some 1,2- and 1,3-cyclic dienes with diborane generated *in situ* undergo slow hydrolysis with oxygen-free water to yield monoolefins.

Canadian Journal of Chemistry, 46, 1165 (1968)

It is generally known that organoboranes do not undergo cleavage at carbon–boron bond by water at room temperature (1); however, it has been shown that trisallylborane is unusual in its hydrolysis even at or below room temperature (2). In this connection, we have studied the behavior of certain cyclic allylic organoboranes with oxygen-free water under nitrogen atmosphere to establish the generality of this reaction. We undertook the study with cyclopentadiene, 1,3-cyclohexadiene, 1,3-cyclooctadiene, 1,2-cyclononadiene, and 1,2-cyclodecadiene. Our results with these substrates establish that slow hydrolysis of cyclic allylic organoboranes takes place but not as rapidly as does trisallylborane (2).

Can. J. Chem. Downloaded from www.nrcresearchpress.com by 210.87.254.6 on 09/05/12
For personal use only.

Can. J. Chem. Downloaded from www.nrcresearchpress.com by 210.87.254.6 on 09/05/12
For personal use only.

Results and Discussion

Monohydroboration was carried out by diborane generated *in situ* (3) by the addition of boron trifluoride etherate to the stirred solution of sodium borohydride and diene in dry diglyme under inert atmosphere of nitrogen at 0 to −5°. The resulting mixture of organoboranes was stirred with a known excess of oxygen-free water at 5 to 10° for 2 h only since the increase of hydrolysis time from 2 to 4 h did not affect the yield of the cyclic monoolefin appreciably. A flash distillation of the resulting product under vacuum gave a mixture of organic and water layers. The organic layer was analyzed by vapor-phase chromatography (v.p.c.) for the residual cyclic diene and the cyclic monoolefin. Under these conditions cyclopentadiene, 1,3-cyclohexadiene, 1,3-cyclooctadiene, 1,2-cyclononadiene, and 1,2-cyclodecadiene gave cyclopentene, cyclohexene, *cis*-cyclooctene, *cis*-cyclononene, and *cis*-cyclodecene respectively. The yield of the cyclic monoolefin was estimated based on the amount of the cyclic diene used in the reaction by v.p.c. technique in each case (4). The results are summarized in Table I.

TABLE I

Percentage yield (by weight) of olefin by vapor-phase chromatography

Diene	Olefin	Yield of olefin
Cyclopentadiene	Cyclopentene	5
1,3-Cyclohexadiene	Cyclohexene	21
1,3-Cyclooctadiene	*cis*-Cyclooctene	35
1,2-Cyclononadiene	*cis*-Cyclononene	18
1,2-Cyclodecadiene	*cis*-Cyclodecene	16

Each cyclic monoolefin was separated by v.p.c. and its identity was established thoroughly by comparison of v.p.c. retention times on carbowax – silver nitrate and ucon columns and infrared spectra using an authentic sample.

The formation of cyclic monoolefins from cyclic dienes may be summarized as follows.

The poor yield of cyclopentene from cyclopentadiene is in agreement with the results of Winstein and co-workers (5) who have observed the predominant formation of 3-cyclopenten-1-ol (94%) in the monohydroboration of cyclopentadiene with diborane. It has been reported by Brown and co-workers (6) that the monohydroboration oxidation of 1,3-cyclohexadiene with diborane gives 34% yield of a mixture of 2-cyclohexen-1-ol (60%) and 3-cyclohexen-1-ol (40%). The lower yield reported may be attributed partly to the competing side reaction of the intermediate allylic organoborane under the hydrolytic experimental conditions. The results with 1,2-cyclononadiene and 1,2-cyclodecadiene further confirm our previous results on monohydroboration oxidation of allenes (7).

We have further confirmed that no other unsaturated organoborane (vinylic or non-allylic) undergoes carbon–boron bond cleavage by water. In support of this we subjected monohydroboration products from 3-hexyne and 1,4-cyclohexadiene to similar study and found no monoolefin formation.

Experimental

All infrared spectra were recorded on a Perkin–Elmer Infrared model 137B with sodium chloride optics. Vapor-phase chromatographic analyses were made with Aerograph model 90P instrument using 6 ft by $\frac{1}{4}$ in. columns. The following liquid phases were employed (percentage by weight on 60/80 mesh chromosorb W): 15% carbowax – silver nitrate and 15% ucon. Cyclic monoolefinic samples were collected by v.p.c. for infrared analysis.

Materials

Diglyme (Ansul Co.) was distilled from lithium aluminium hydride. In order to inhibit peroxidation, 0.01% of sodium borohydride was added. Boron trifluoride ethyl etherate (Eastman) was treated with a small quantity of ethyl ether (to ensure an excess of this component) and distilled under reduced pressure from a few pieces of calcium hydride. Sodium borohydride from Metal Hydrides Inc. (98%) was used without purification.

1,3-Cyclohexadiene (Aldrich), 1,3-cyclooctadiene (Columbia), 1,4-cyclohexadiene (Aldrich), and 3-hexyne (K & K) were used without any purification. Freshly distilled cyclopentadiene from its dimer (Aldrich) was used. 1,2-Cyclononadiene and 1,2-cyclodecadiene were prepared from 9,9-dibromobicyclo[6·1·0]nonane and 10,10-dibromobicyclo[7·1·0]decane according to the procedure of Moore and Ward (8). Their properties corresponded well with those reported.

General Procedure for Monohydroboration and Hydrolysis

In a 250 ml three-necked flask fitted with a condenser, an equilibrating dropping funnel, a thermometer, and an inlet and an outlet (top of the condenser) for nitrogen, was placed pulverized sodium borohydride (2.09 g, 0.055 mole, 10% excess) in dry diglyme (50 ml) and an appropriate cyclic diene or alkyne (0.20 mole). Boron trifluoride etherate (10.28 g, 0.072 mole 10% excess) in diglyme (20 ml) was added dropwise with stirring over a period of 1 h under a slight static pressure of nitrogen while maintaining the temperature of the reaction mixture between 0 to −5°. The stirring was continued for an additional hour at room temperature in order to complete the hydro-

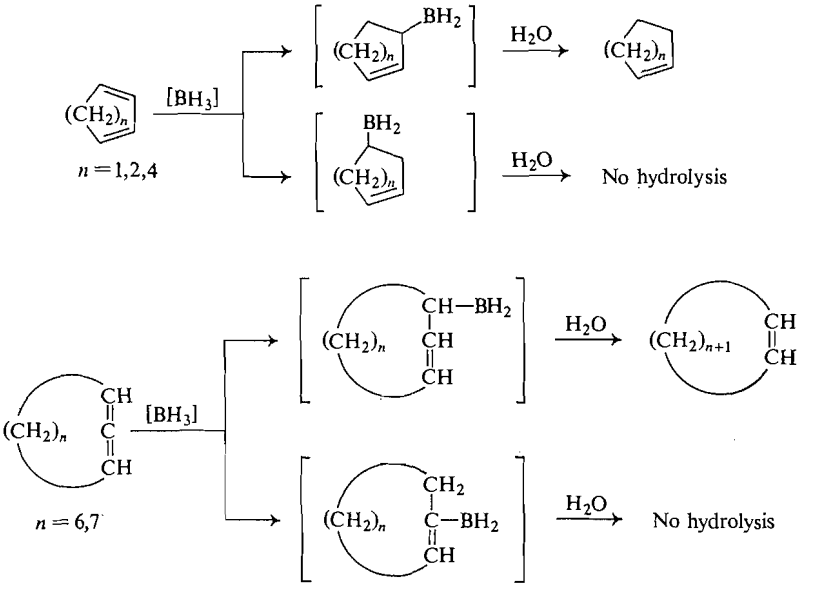

boration. Excess of sodium borohydride was destroyed carefully by dropwise addition of oxygen-free water at 5 to 10° and further 10 ml of oxygen-free water was added and stirred for 2 h.

The resulting mixture was then flash distilled under vacuum to obtain a mixture of water and organic layers. The organic layer was separated, dried, and weighed.

Quantitative measurements of the cyclic monoolefin formed and the unreacted cyclic diene in each case were determined using vapor-phase chromatographic absolute method (4), which involves the direct comparison of a ratio of the areas of the unknown in a mixture with calibration curve obtained from synthetic mixtures containing varying amounts of the components. The yield (percentage by weight) of the cyclic monoolefin was calculated based on the amount of cyclic diene used in the reaction. The identity of each cyclic monoolefin was established by comparison of chromatographic retention times on carbowax – silver nitrate and ucon columns using authentic samples. This was further supported by collecting each cyclic monoolefin by v.p.c. and comparing its infrared spectrum with that of an authentic sample.

Acknowledgment

We thank the Council of Scientific and Industrial Research, New Delhi, India, for financial support of this work.

1. H. C. Brown. Hydroboration. W. A. Benjamin, Inc., New York. 1962.
2. B. M. Mikhailov and F. B. Tutorskaya. Dokl. Akad. Nauk (SSSR), **123**, 479 (1958); Chem. Abstr. **53**, 6990 (1959).
3. H. C. Brown and B. C. Subba Rao. J. Am. Chem. Soc. **81**, 6428 (1959).
4. S. D. Nogare and R. S. Juvet, Jr. Gas-liquid chromatography—theory and practice. Interscience Publishers. New York. 1962. p. 259.
5. E. L. Allred, J. Sonnenberg, and S. Winstein. J. Org. Chem. **25**, 26 (1960).
6. G. Zweifel, K. Nagase, and H. C. Brown. J. Am. Chem. Soc. **84**, 183 (1962).
7. D. Devaprabhakara and P. D. Gardner. J. Am. Chem. Soc. **85**, 1458 (1963).
8. W. R. Moore and H. R. Ward. J. Org. Chem. **27**, 4179 (1962).

Can. J. Chem. Downloaded from www.nrcresearchpress.com by 210.87.254.6 on 09/05/12
For personal use only.

Studies of the chemistry of azole derivatives. IV. New *N*-substituted 2-aminothiazoles

JAG MEGH SINGH
Defence Science Laboratory, Metcalfe House, Delhi, India

Received August 1, 1967

The syntheses of 11 new *N*-substituted 2-aminothiazoles have been accomplished by condensing ω-chloro-3,4-dihydroxy- and ω-chloro-2,3,4-trihydroxyacetophenone with substituted thioureas.

Canadian Journal of Chemistry, **46**, 1168 (1968)

Can. J. Chem. Downloaded from www.nrcresearchpress.com by 210.87.254.105 on 09/05/12
For personal use only.

In a continuation of our earlier investigations (1–3) on azole derivatives we present some details concerning the synthesis of a group of thiazolylamines prepared by condensing ω-chloro-3,4-dihydroxy- and ω-chloro-2,3,4-trihydroxyacetophenone with substituted thioureas.

Interest in the preparation of compounds obtained by this condensation which contain the thiazole nucleus for use as chemotherapeutic agents, has been stimulated by the successful application of several thiazole compounds such as sulfthiazole and promizole in the treatment of various diseases (4). Chelation in medicine has proved very useful and the medical potential of chelating agents was determined when ethylenediaminetetraacetic acid was used to combat lead poisoning; therefore, the possibility of forming metal chelates also prompted us to undertake the synthesis of some thiazoles. Eleven new *N*-substituted 2-aminothiazoles with general structural formula **1**, have been synthesized.

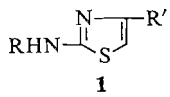

1

Experimental[1]

ω-Chloro-3,4-dihydroxyacetophenone

A mixture of chloroacetic acid (20 g), catechol (20 g), and phosphorous oxychloride (15 g) was dissolved in benzene (80 ml) and heated on a water bath at 60–70° for 24 h. The mixture was cooled, the benzene decanted, water added, and the heavy crystalline precipitate (19 g), ω-chloro-3,4-dihydroxyacetophenone, was collected. The product (yield 58%), was recrystallized from hot water, m.p. 172° (reported (5) m.p. 173°).

ω-Chloro-2,3,4-trihydroxyacetophenone

A mixture of anhydrous pyrogallol (25 g), chloroacetic acid, and phosphorous oxychloride (20 g) was kept at 70° for 6 h. Cold water (150 ml) was then added and the mixture heated until the brown solid dissolved. After clarification with charcoal, the mixture was kept for 24 h at 0° and dark brown needles of ω-chloro-2,3,4-tri-

[1]All melting points are uncorrected.

TABLE I

N-Substituted 2-aminothiazole hydrochlorides

R	Solvent	Formula	Melting point °C	Yield %	Calculated % S	Found % S
		R′ = 3,4-Dihydroxyphenyl-				
Phenyl	Ethanol	$C_{15}H_{13}ClN_2O_2S$	225	40	9.98	9.82
p-Chlorophenyl	50% Ethanol	$C_{15}H_{12}Cl_2N_2O_2S$	240	35	9.01	9.11
p-Tolyl	Methanol	$C_{16}H_{15}ClN_2O_2S$	241	42	9.57	9.59
Allyl	Ethanol	$C_{11}H_{11}ClN_2O_2S$	205	40	11.83	11.65
β-Naphthyl	Ethanol	$C_{19}H_{15}ClN_2O_2S$	233	40	8.68	8.65
		R′ = 2′,3′,4′,-Trihydroxyphenyl-				
Phenyl	Methanol	$C_{15}H_{13}ClN_2O_3S$	220	41	9.50	9.48
p-Chlorophenyl	Benzene	$C_{15}H_{12}Cl_2N_2O_3S$	180	42	8.62	8.59
p-Tolyl	50% Ethanol	$C_{16}H_{15}ClN_2O_3S$	220	45	9.13	9.15
Allyl	Ethanol	$C_{11}H_{11}ClN_2O_3S$	210	40	11.17	10.09
β-Naphthyl	Methanol	$C_{19}H_{15}ClN_2O_3S$	243	41	8.28	8.25
H	Methanol	$C_9H_9ClN_2O_3S$	245	50	12.28	12.25

hydroxyacetophenone separated. These were recrystallized from water; yield 40%, m.p. 166° (reported (6) m.p. 169°). The substituted thioureas were prepared using the method of De Clermont and Wehrlin (7).

N-Substituted 2-Aminothiazoles

A mixture of equimolecular quantities of substituted thioureas and substituted ω-chloroacetophenone in absolute ethanol was refluxed on a water bath for 1 h. The hydrochlorides were separated and recrystallized from appropriate solvents. Data for these products are given in Table I.

Acknowledgment

Thanks are due to Dr. Kartar Singh, Director, Defence Science Laboratory, Delhi, and Dr. H. K. Acharya for their encouragement and for providing facilities to undertake this work.

1. J. M. Singh and S. P. Gupta. J. Indian Chem. Soc. **41**, 867 (1964).
2. J. M. Singh and S. P. Gupta. J. Indian Chem. Soc. **42**, 336 (1965).
3. J. M. Singh and G. R. Chaudhry. J. Indian Chem. Soc. **43**, 272 (1966).
4. L. L. Bombas. J. Am. Chem. Soc. **67**, 671 (1945).
5. T. B. Johnson and E. Gatewood. J. Am. Chem. Soc. **51**, 1817 (1929).
6. J. H. S. Davies and T. Deegan. J. Chem. Soc. 3204 (1950).
7. P. H. De Clermont and E. Wehrlin. J. Chem. Soc. **31**, 70 (1877).

Can. J. Chem. Downloaded from www.nrcresearchpress.com by 210.87.254.105 on 09/05/12
For personal use only.

Can. J. Chem. Downloaded from www.nrcresearchpress.com by 210.87.254.42 on 09/05/12
For personal use only.

Canadian Journal of Chemistry

Published by THE NATIONAL RESEARCH COUNCIL OF CANADA

VOLUME 46 APRIL 15, 1968 NUMBER 8

Phase studies on the iron–selenium system

J. E. DUTRIZAC, M. B. I. JANJUA, AND J. M. TOGURI[1]

Noranda Research Centre, Pointe Claire, Quebec

Received November 20, 1967

The quasi-reduced iron–selenium phase diagram has been determined by a combination of differential thermal analysis, visual polythermal, and liquid sampling techniques. Iron and selenium form two compounds: FeSe with a broad stoichiometry range and $FeSe_2$ with a much narrower composition field. The former compound was found to melt congruently at 1070 °C and 53.5 atomic % selenium, while the latter melted incongruently at 585 °C. Two liquid–liquid regions were observed in this system. One occurred above 790 °C from 73.9 atomic % selenium to about 99.92% selenium with a consolute temperature of 1070 °C at approximately 93 atomic % selenium. The other liquid–liquid region extends upwards from 1520 °C and lies between 3 and 39.5 atomic % selenium.

Canadian Journal of Chemistry, 46, 1171 (1968)

Introduction

Although the iron–selenium system has been extensively studied (1, 2), surprisingly little of the diagram has been actually determined. Troften and Kullerud (3) have shown that $Fe_{1-x}Se$ melts congruently at 1070 ± 5 °C and 53 atomic % selenium. Our data confirm these observations. They also reported that $FeSe_2$ melts incongruently at 585 °C which is consistent with the present work but disagrees with the interpretation of Dudkin and Vaidanich (4) who believed that the 585 °C thermal arrest was caused by a phase change of the marcasite–pyrite type. These latter authors believed that $FeSe_2$ was formed peritectoidally at 790 °C. The only other liquidus datum available for this system is a single point obtained for an iron-saturated melt by Gorokh *et al.* (5). They held an iron–selenium mixture containing an excess of iron at an unspecified temperature between 1300–1400 °C and then cooled and analyzed the resulting mixture of iron and iron selenide. Their single value of 42 weight % selenium is not in close agreement with our data (understandably the data of Gorokh *et al.* indicated additional iron, an observation which is consistent with the problem of trying to separate these two solid phases quantitatively).

Tengner (6) and Fischer (7) have determined the crystal structure of $FeSe_2$. Both workers agree that it is orthorhombic, C18 (marcasite) type. Fischer presented some indirect evidence that $FeSe_2$ exists within fairly narrow composition limits and the present investigation substantiates this view. Work from Japan (8–11) has resolved the crystal structure of FeSe below 400 °C. This compound exists by the creation of iron vacancies and can have compositions lying between Fe_7Se_8 and Fe_3Se_4. At low temperatures there exist two phases: an α (PbO type) and a β (NiAs type) (11). At 350 °C there is a eutectoidal reaction to give a different NiAs structure. Other workers (9, 10) have more recently shown that a low temperature triclinic modification transforms at 240–298 °C to the NiAs structure which subsequently changes to a different hexagonal modification at 320–388 °C. The structure and phase boundaries of "FeSe" have not been determined at elevated temperatures.

In the present work the liquidus of the iron–selenium system has been determined below 1520 °C. The system shows a congruently

[1]Present address: Department of Metallurgy and Materials Science, University of Toronto, Toronto, Ontario.

melting FeSe compound and two liquid–liquid regions at either end of the phase diagram. $FeSe_2$ was found to melt incongruently.

Experimental

Materials Used

Spectrographic grade iron containing at least 99.99% Fe and high-purity selenium shot containing at least 99.99% Se were used.

Preparation of Iron Diselenide

The iron diselenide was prepared by heating stoichiometric amounts of iron wire and selenium in vacuum-sealed Pyrex ampuls at a temperature of 525 °C. The time required for this reaction to go to completion was determined by the disappearance of the reddish selenium vapor in the tube. A typical reaction time using 10 mil iron wire was 6–8 weeks. Once the selenium vapor had vanished, the diselenide was heated for an additional 1–2 weeks to improve the homogeneity of the compound. X-ray diffraction analysis of the product agreed with the published data (6) for this compound.

Preparation of Iron Monoselenide

The iron monoselenide was prepared by heating suitable amounts of iron and selenium in vacuum-sealed silica ampuls at various temperatures. The time required for this reaction was just a few hours even at relatively low temperatures (600 °C). X-ray diffraction patterns obtained for the iron monoselenide prepared by the above method agreed closely with the published data (12).

Experimental Procedure

Differential thermal analysis was used to investigate the entire phase diagram; a Kanthal or silicon carbide furnace was employed depending on the temperature range under consideration. Samples of known composition were vacuum-sealed into small Vycor capsules containing a thermocouple well; for the high temperature regions an alumina sleeve was placed around the capsule to provide added mechanical strength. One junction of a Pt–Pt, 10% Rh thermocouple was placed in the sample well while the other was simply located in the air adjacent to the capsule. The actual temperature of the cell was measured by a calibrated Pt–Pt, 10% Rh thermocouple also placed in the capsule well. The sample was heated to various temperatures, homogenized, and then cooled quickly at approximately 10 °C/min.

The basic method used in this work to determine the liquidus temperatures in the two-liquid region was to observe a sample of known composition as it was slowly heated and to note the temperature at which one phase vanished. The sample was then slowly cooled and the formation of the second phase was likewise observed. The heating and cooling cycle was repeated several times and the liquidus temperature was obtained from the average of the observed values. This method was adopted because insufficient heat is evolved on crossing the liquidus line for detection by conventional methods of thermal analysis. This problem arises because no material is solidifying out of solution and, as a result, no heat of fusion is detected. The only heat effect observed is the small value arising from slight differences in the heats of mixing of the two similar solutions; these small heat effects are usually obscured by normal temperature fluctuations which occur at the elevated temperatures of the experiments.

The measurements were conducted in a non-inductively Kanthal-wound Vycor tube furnace. The sample was observed through a 1 cm × 5 cm slit cut in the furnace refractory bricks on both sides of the clear Vycor tube; in order to reduce temperature gradients, both ends of the slit were blocked off by Pyrex plate windows. With this arrangement, temperature variations in the furnace zone were less than ±5 °C. The temperature of the cell was measured by a calibrated chromel–alumel thermocouple inserted through a small hole in the side of the Vycor tube; the tip of the thermocouple was placed against the outside of the sample cell. The furnace was heated to approximately the liquidus temperature and then a cell containing accurately weighed amounts of high-purity iron wire and selenium pellets, sealed under vacuum in Vycor tubes, was suspended in the hot zone. This cell was homogenized for 24 h and then heated at about 10 °C/h until one of the two liquid phases vanished. The furnace was then cooled at approximately the same rate until the second phase reappeared; the process was repeated a few times to confirm the initial value. The temperatures at which one phase appeared and disappeared agreed to within ±5 °C in all instances.

Since both liquid phases were opaque to visible light at the measuring temperatures, the presence of two phases could not be checked by transmitted radiation. However, there was a significant difference in the reflectivities and emissivities of the two phases, the iron-rich phase reflecting and emitting much more visible light. As a result, the meniscus between the two phases could be detected by the differences in reflectivity and emissivity.

For samples containing between 73.9 and 94.4 atomic % selenium, a straight-wall 13 mm diameter Vycor tube was used to contain the solutions; for mixtures with higher selenium contents, a 4 mm i.d. silica capillary tube was blown onto the bottom of the cell in order to increase the height of the second layer. By adjusting the approximate amounts of each phase present, it was possible to obtain the meniscus of the two liquid phases in the capillary tube. On heating, the meniscus moved downwards and disappeared at the bottom of the capillary; the temperature at which this occurred was then noted. For compositions greater than 99.2 atomic % selenium, there was an insufficient amount of the second layer to allow the visual method to be used. Instead, a vacuum-sealed silica cell was homogenized at a given temperature and then quenched by dropping the capsule into water; after cooling, the selenium in the upper layer was analyzed for iron. To reduce the amount of mixing between the two liquid layers on cooling, the cell consisted of two bulbs connected by about a 1 in. length of fine (4 mm) silica capillary tubing. The amounts of the phases were such that the liquid–liquid interface was in the lower bulb; thus, on cooling, the contents of the upper bulb were prevented from mixing with the denser iron-rich material in the lower bulb. The cells were homogenized at a given temperature for at least 24 h prior to quenching. All the selenium in the upper bulb was used for the determination to eliminate the possibility of segregation on cooling. Some runs were performed by heating the cells to a higher temperature for several

Can. J. Chem. Downloaded from www.nrcresearchpress.com by 210.87.254.42 on 09/05/12
For personal use only.

Can. J. Chem. Downloaded from www.nrcresearchpress.com by 210.87.254.42 on 09/05/12
For personal use only.

hours, cooling to the required temperature, homogenizing, and then quenching. Both methods gave essentially the same results, indicating that the liquid in the upper bulb was in equilibrium with the material in the lower bulb.

Preliminary experiments indicated that the liquidus line of the iron end of the phase diagram increased rapidly with small changes in composition. Consequently, a sampling technique at constant temperature was employed. For these experiments, about 5 g of iron monoselenide was placed in the bottom of a 15 mm silica tube containing a sliding seal. A stiff steel wire threaded into a length of 8 mm diameter iron rod was then placed through the seal. The whole tube containing the iron rod and the iron selenide was evacuated, flushed with nitrogen, and then placed into a hot silicon carbide furnace whose temperature was controlled. The temperature was measured with a Pt–Pt, 10% Rh couple placed in essentially the same position as the reaction tube. When the iron selenide had melted (about 5 min), the iron rod was lowered to the bottom of the tube and then left in contact with the selenide for 2 h at temperatures below 1300 °C and for 1 h at higher temperatures. Initial experiments at the lowest temperature (1016 °C) showed that equilibrium between these phases was achieved in about 10 min; however, additional heating time was given to insure complete homogeneity of the melt. After the desired heating interval, the iron rod was drawn out of the melt by the steel wire passing through the sliding seal. The tube containing the iron-saturated liquid was then quenched and the entire quenched melt was analyzed for iron and selenium in order to eliminate segregation difficulties.

Results and Discussion

The iron–selenium phase diagram as determined in this investigation is shown in Fig. 1. It is important to realize that the pressure over the melts was not 1 atm but rather the equilibrium selenium pressure at a particular temperature–composition. The addition of selenium depresses the melting point of iron to about 1520 °C at 3 atomic % selenium. The monotectic composition is only approximate; it was obtained by heating iron and selenium to a temperature just above 1520 °C, quenching the liquid phases, and then analyzing for selenium in the iron-rich phase. The monotectic temperature appears well established and is accurate to within ±5 °C. Above 1520 °C there is a two-liquid region which was not investigated. At 1490 ± 5 °C, an additional arrest was observed but the cause of this is not known. Between 1490 °C and 960 °C the liquidus, as determined by the liquid saturation experiments, is very steep, especially below about 1300 °C. The shape of the liquidus changed abruptly at 1400 ± 5 °C, the $\gamma \rightarrow \delta$ transformation in iron. The eutectic between iron and iron selenide occurred at 960 ± 5 °C and 44.4 atomic % selenium; these data are in excellent accord with those of Troften and Kullerud (3). FeSe was found to melt congruently at 1070 ± 5 °C and 53.6 atomic % selenium, also in agreement with the data of Troften and Kullerud.

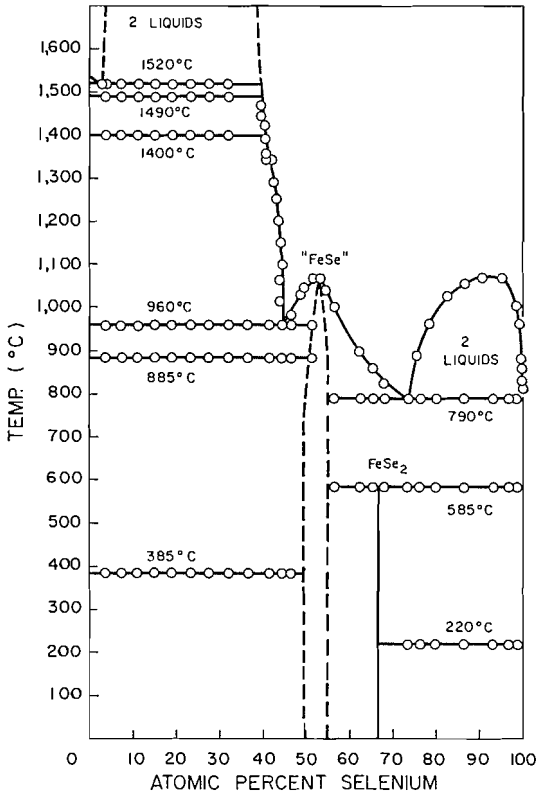

FIG. 1. The quasi-reduced iron–selenium phase diagram.

An arrest at 885 ± 5 °C was observed over the range from pure iron to "FeSe"; the cause of this has not been ascertained. At 385 °C an additional halt was observed; this is believed to be caused by the conversion of one hexagonal modification of FeSe to another (10).

As selenium is added to FeSe, the liquidus drops to the monotectic at 790 ± 5 °C and 73.9 atomic % selenium. A two-liquid region extends upward from 790 °C between 73.9 and 99.98 atomic % selenium; this region has a consolute temperature of 1070 ± 10 °C at approximately 93 atomic % selenium. The liquid–liquid region is quite asymmetrical; it appears to be very

Can. J. Chem. Downloaded from www.nrcresearchpress.com by 210.87.254.42 on 09/05/12
For personal use only.

difficult to dissolve appreciable amounts of iron in selenium under all conditions. As mentioned previously, this region was obtained by a combination of visual and quenching methods. The experimental data obtained by the visual method are given in Table I while the results of the liquid quenching experiments are presented in Table II.

TABLE I

Liquidus temperatures from visual observations

Overall composition (atomic % Se)	Liquidus temperatures (°C)	Mean (°C)
75.7	890, 889	890
78.8	965, 961, 966	964
82.6	1032, 1027, 1033	1031
86.4	1060	1060
90.5	1073, 1073, 1071, 1072	1072
95.1	1070, 1070	1070
98.6	1004, 1005, 1005	1005
99.3	962, 966	964

The temperature arrest at 585 °C, variously reported as the incongruent melting point of $FeSe_2$ (5) or a phase change in $FeSe_2$ (6), has been conclusively identified as the incongruent melting point of $FeSe_2$. This was accomplished by heating both $FeSe_2$ and FeSe (55.7 atomic % Se) in vacuum-sealed ampuls to a temperature slightly above 585 °C (approximately 600 °C), holding at this temperature for 2–3 h, and then quenching. The quenched solids were examined by X-ray diffraction and both patterns were found to be quite similar. In addition, large quantities of selenium were observed to form in the sealed ampul containing $FeSe_2$ at about 585 °C. These results confirm that the arrest at 585 °C is caused by the reaction

$$(1 - x)FeSe_{2(s)} \rightarrow Fe_{1-x}Se_{(s)} + (1 - 2x)Se_{(l)}$$

and not by some crystal change in the iron diselenide. The possibility of confusion exists on this point (6) because the X-ray diffraction pattern obtained by decomposing $FeSe_2$ at 585 °C is different from that published for FeSe which is for the iron-saturated compound. If, however, an iron monoselenide composition is chosen which is nearly selenium saturated (e.g. Fe_3Se_4), then the X-ray pattern is quite similar to that obtained by decomposing $FeSe_2$. It is interesting to note that the $FeSe_2$ diffraction patterns for material prepared at 525 °C are always similar regardless of whether the material was prepared with an excess of selenium or a surplus of iron. This suggests a rather narrow composition range for $FeSe_2$.

TABLE II

Results from liquid quenching experiments

Quenching temp. (°C)	Composition of upper layer (atomic % Fe)	Notes
863	0.25	Previously heated to 918 °C for 15 h, then held at 863 °C for 7 h prior to quenching
855	0.18	Previously heated to 864 °C for 12 h, then held at 855 °C for 4 h prior to quenching
806	0.20	Previously heated to 860 °C for 6 h
812	0.16	—
810	0.17	—
799	0.11	—
799	0.14	—

The arrest at 220 °C is the freezing point of pure selenium; this is in good agreement with the value of 217 °C reported in the literature (13). It is evident from the phase diagram that the solubility of iron in liquid selenium is very low, being only 0.06 weight % (600 p.p.m.) at 790 °C.

Acknowledgment

The authors are grateful to Canadian Copper Refiners Limited for sponsorship of this work.

1. M. HANSEN and K. ANDERKO. Constitution of binary alloys. 2nd ed. McGraw-Hill, New York. 1958.
2. R. P. ELLIOTT. Constitution of binary alloys. 1st suppl. McGraw-Hill, New York. 1965.
3. P. TROFTEN and G. KULLERUD. Carnegie Inst. Washington, Yearbook, **60**, 176 (1961).
4. L. D. DUDKIN and V. I. VAIDANICH. Soviet Phys.–Solid State English Transl. **2**, 1384 (1961).
5. A. V. GOROKH, L. M. KABANOVA, and V. G. DOBOSH. Dokl. Akad. Nauk SSSR, **169**, 639 (1966).
6. S. TENGNER. Z. Anorg. Allgem. Chem. **239**, 126 (1938).
7. G. FISCHER. Can. J. Phys. **36**, 1435 (1958).
8. K. HIRAKAWA. J. Phys. Soc. Japan, **12**, 929 (1957).
9. A. OKAZAKI. J. Phys. Soc. Japan, **16**, 1162 (1961).
10. A. OKAZAKI. J. Phys. Soc. Japan, **14**, 112 (1959).
11. T. HIRONE and S. CHIBA. J. Phys. Soc. Japan, **11**, 666 (1956).
12. A.S.T.M. X-ray Data File 3-0533. American Society for Testing and Materials, Philadelphia, Pa.
13. G. PELLINI and G. VIO. Gazz. Chim. Ital. **36**, 469 (1906).

Velocity of sound in liquid argon at high pressures and temperatures

D. H. BOWMAN, C. C. LIM, AND R. A. AZIZ
Department of Physics, University of Waterloo, Waterloo, Ontario

Received September 5, 1967

Measurements were made of the velocity of sound in liquid argon in the temperature range 86–146 °K and at pressures up to 65 atm. The velocity versus pressure isotherms are steeper and more curved at the higher temperatures. At any one pressure, the velocity is a smoothly decreasing function of temperature. Analysis of the results using existing density data showed that the specific heat ratio, γ, decreases with pressure and increases with temperature in this range. The coefficient in Rao's relation was found to increase with temperature at constant pressure, while that in the relation due to Carnevale and Litovitz exhibited no definite trend with temperature or pressure.

Canadian Journal of Chemistry, 46, 1175 (1968)

Can. J. Chem. Downloaded from www.nrcresearchpress.com by 210.87.254.5 on 09/05/12
For personal use only.

Introduction

Although the pressure dependence of the velocity of sound has been investigated for liquid argon in the temperature region near its normal liquid range (1–3), the interesting region between the normal boiling point and the critical point has not been studied to any great extent. The measurements presented here represent the beginning of such an investigation for the inert gas liquids. The purpose of these measurements is the determination of the temperature and pressure dependence of various thermodynamic quantities of interest and the study, over an extended range, of the relation, proposed by Rao, between the temperature dependence of velocity and the volume expansivity and that proposed by Carnevale and Litovitz between the pressure dependence of velocity and the isothermal compressibility. In addition, the present measurements, together with future measurements on other inert gas liquids, will allow a more thorough investigation of the principle of corresponding states.

Experimental Method

Velocities were measured in the frequency range 1–2 MHz, using a cylindrical barium titanate transducer. The apparatus and method are essentially as described elsewhere (4) but with certain modifications. In order to obtain the high pressures, a pressure cell was connected into the high pressure line to the velocity cell, as shown in Fig. 1. The pressure cell was simply a thick-walled copper chamber of approximately 7 cm^3 capacity, with a "pigtail" attached to the bottom. The pigtail consisted of a copper rod connected to the cell via a thin-walled stainless steel tube. By adjusting the length of the pigtail, hence the amount of thermal decoupling provided by the stainless steel tube, and then cooling the copper rod in liquid nitrogen, it was possible to control the temperature of the pressure cell over a wide range above 77 °K. In addition, the ability to change the position of the pressure cell in the Dewar holding the liquid nitrogen permitted rapid heating or cooling of the cell when desired. The velocity and pressure cells were both tested to 80 atm pressure.

A 1000 p.s.i. Heise gauge was used to measure the pressure. It had been calibrated previously by the manufacturers, using a National Bureau of Standards certified dead-weight tester. After the velocity measurements, we compared it against a Texas Instrument pressure gauge. The accuracy of the Heise gauge was ± 1 p.s.i. (± 0.068 atm).

The argon gas was supplied by Linde and had a rated purity of 99.995%. The purity was possibly improved by the distillation process described in an earlier paper (5).

The temperature of the velocity cell could be controlled by the method described in ref. 4 to better than 0.001 Kelvin degrees. Above 90 °K, the temperature was measured in terms of the "international temperature scale", and below 90 °K in terms of the National Physical Laboratories scale, by means of a platinum resistance thermometer calibrated by the National Physical Laboratories. The accuracy of temperature measurements was limited to ± 0.005 °K by the accuracy of the standard resistor used for comparison.

The procedure for taking measurements was as follows. The pressure cell was cooled to 85 °K, and argon from the low pressure storage vessels was condensed into it until full. The velocity cell was then cooled and controlled at 85 °K, and argon condensed into it until full. The system, consisting of the pressure cell, velocity cell, and Heise gauge, was then shut off from the storage vessels by a high pressure valve, V_1 in Fig. 1, and the valves between the pressure cell, Heise gauge, and velocity cell were opened. The temperature of the velocity cell was then adjusted to a value at which velocity measurements were to be performed, while the pressure cell was heated to room temperature. As a result, the pressure in the system increased to over 65 atm. The pressure cell valve V_2 was then closed, and the pressure cell cooled to liquid nitrogen temperature. Pressures in the velocity cell could then be decreased to those desired for velocity measurements by allowing small amounts of gas back into the cooled pressure cell. Final pressure adjustment was effected by fine metering the gas into the storage vessels using fine-metering valve V_3. A period of about 20 min was allowed in each measurement for pressure equilibrium

TABLE I

Velocity of sound in liquid argon

86.22$_9$ °K		96.99$_8$ °K		108.18$_0$ °K		117.10$_0$ °K		127.05$_0$ °K		136.02$_0$ °K		146.63$_0$ °K	
P (atm)	W (m/s)	P (atm)	W (m/s)	P (atm)	W (m/s)	P (atm)	W (m/s)	P (atm)	W (m/s)	P (atm)	W (m/s)	P (atm)	W (m/s)
6.5$_3$	847.55	4.0$_8$	769.68	13.6$_1$	690.27	13.6$_1$	613.67	23.8$_2$	529.31	26.1$_3$	420.68	42.4$_8$	284.51
14.9$_7$	851.75	13.6$_1$	775.73	23.8$_2$	698.88	23.8$_2$	625.31	34.0$_2$	545.97	28.5$_8$	428.54	44.2$_3$	300.44
23.1$_4$	856.72	23.8$_2$	782.02	34.0$_2$	707.10	34.0$_2$	636.18	44.2$_3$	560.93	34.0$_2$	443.92	46.3$_4$	315.82
34.0$_2$	860.97	34.0$_2$	788.23	44.2$_3$	715.06	44.2$_3$	646.42	54.4$_4$	574.74	44.2$_3$	468.45	48.9$_9$	331.75
44.9$_1$	866.03	44.2$_3$	794.28	54.4$_4$	722.65	54.4$_4$	656.32	64.6$_4$	587.51	54.4$_4$	489.74	52.7$_8$	351.17
54.4$_4$	870.45	54.4$_4$	800.12	64.6$_4$	730.15	64.6$_4$	665.69			64.6$_4$	508.35	54.4$_4$	358.38
65.3$_2$	875.32	64.6$_4$	805.95									58.5$_2$	374.52
												61.2$_4$	384.17
												64.6$_4$	395.19
												64.6$_4$	395.28

to be achieved between velocity cell and pressure gauge. During measurement along any one isotherm, the temperature was held constant to ± 0.001 Kelvin degrees.

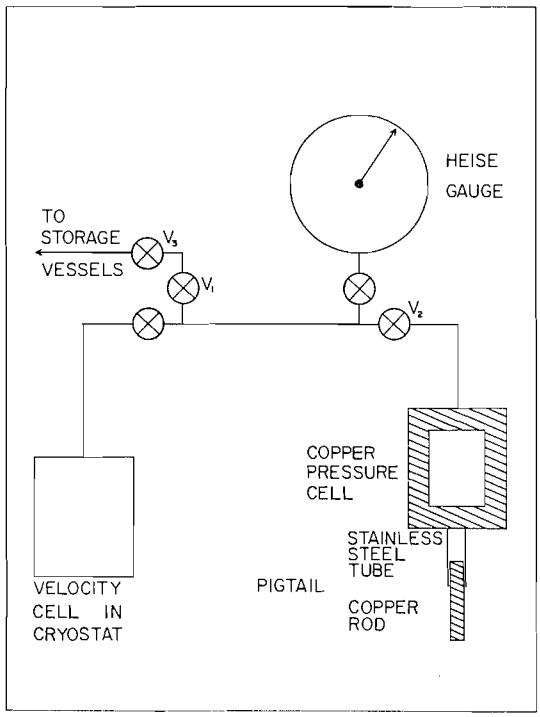

FIG. 1. Schematic diagram of high pressure gas handling system. V_1 and V_2 are shut-off valves, V_3 is a fine-metering valve.

The uncertainty in the pressure measurements was due to the gauge (accuracy ± 0.068 atm) and the unknown hydrostatic pressure head ($+0.04$ atm maximum).

Once the pressure was steady, the velocity could be measured to a precision of better than 0.08% over the entire range of temperature and pressure. The main limitation on accuracy was caused by a slight eccentricity of the transducer, and a consequent relative shift of frequency in the alternate resonance. The accuracy of the velocity data presented is reduced, however, at the highest temperature taken, because of the large change in velocity with pressure. Here, the uncertainty in pressure is equivalent to an error of $\pm 0.15\%$ in the velocity.

Results and Discussion

Forty-seven velocity measurements were made along seven isotherms, at pressures from a small amount above the vapor pressure to 65 atm. One isotherm was at a temperature below the normal boiling point and slightly above the melting temperature at 65 atm. The temperatures of the remaining six isotherms were chosen to be the same as those for which accurate density data were available (6). The resulting velocities, W, are given in Table I, and are shown graphically in Fig. 2, together with values obtained by interpolation from previous results (7) under saturated vapor conditions. At the lower temperatures, W is an almost linear function of pressure P in this pressure range. At higher temperatures, the velocity isotherms are steeper and more curved. The data for each isotherm were fitted to polynomials of successively higher degree by the method of least squares. Polynomials of degree five or less were sufficient to describe the isotherms. The coefficients A_0, A_1, A_2, A_3, A_4, and A_5 of the equation

$$W = A_0 + A_1P + A_2P^2 + A_3P^3 + A_4P^4 + A_5P^5$$

are given for each isotherm in Table II, together with the standard errors of estimate. W and $(\partial W/\partial P)_T$, evaluated at intermediate pressures by the above polynomial, showed smooth variation with pressure, so that the equations were judged suitable for interpolation and evaluation of slopes. They are not necessarily suitable, however, for extrapolation to higher pressures.

Can. J. Chem. Downloaded from www.nrcresearchpress.com by 210.87.254.5 on 09/05/12
For personal use only.

TABLE II

Coefficients in the equation W (m/s) $= A_0 + A_1P + A_2P^2 + A_3P^3 + A_4P^4 + A_5P^5$ (P in atm) and standard error of estimate, σ, for argon

T (°K)	A_0	A_1	$A_2 \times 10^{-3}$	$A_3 \times 10^{-4}$	$A_4 \times 10^{-4}$	$A_5 \times 10^{-4}$	σ
86.22_9	844.26421	0.50693312	−0.48171001				0.016
96.99_8	767.07091	0.64414602	−0.66525705				0.025
108.18_0	678.05865	0.93039365	−2.5981575	0.10359887			0.022
117.10_0	596.87922	1.2955722	−4.7503063	0.18241167			0.031
127.05_0	482.24679	2.2619354	−13.287554	0.53974636			0.027
136.02_0	270.63183	9.3986558	−194.69702	24.056246	−0.11801286		0.026
146.63_0	−12 136.140	1088.9345	−38 631.976	6912.9932	−62.026563	0.22274760	0.106

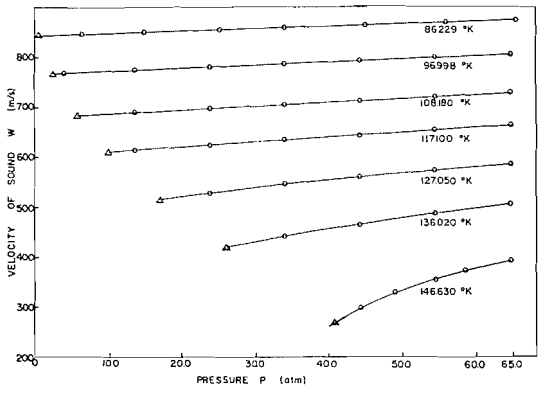

FIG. 2. Liquid argon sound velocity isotherms W (m/s) versus P (atm). (○) Data points from this paper; (△) values interpolated from velocity measurements under saturated vapor pressure (7).

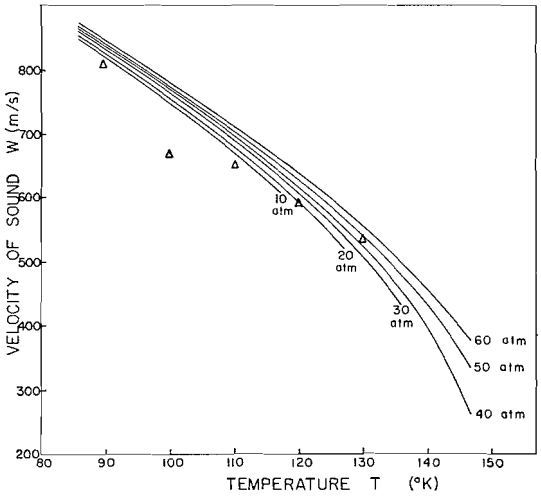

FIG. 3. Liquid argon sound velocity isobars W (m/s) versus T (°K). (△) Values calculated from equation of state by Van Itterbeek *et al.* (6).

Values of W evaluated at 10, 20, 30, 40, 50, and 60 atm pressure are plotted as functions of temperature in Fig. 3. The isobars are nearly linear at low temperatures, becoming steeper and more curved at high temperatures. Polynomials fitted to the isobars, although suitable for interpolation, were judged by the authors to be possibly inaccurate for evaluating slopes.

Dobbs and Finegold (2) have measured the velocity of sound as a function of pressure at 87.2 °K and 90.1 °K. Their results agree to within 0.15% with those found by interpolation of our results. Velocities of sound measured in the temperature range 87–90 °K by Van Itterbeek and Van Dael (3) are higher by about 0.6%. Radovskii (8) has measured the velocity of sound in liquid argon at temperatures above 138 °K and pressures up to 60 atm. The values presented in ref. 8 agree with ours in this region to within the errors of interpolation. It should be noted, however, that at these higher temperatures, the interpolation errors are greater, being possibly as much as 0.4%.

Values of W were calculated by Van Itterbeek *et al.* (6) at various pressures, in the region above 90 °K, using their equation of state and the specific heat values of Eucken and Hauck (9). Those values calculated at 19.3 atm are shown in Fig. 3 for comparison.

Theoretical calculations of W as a function of temperature and pressure have been carried out by David and Hamann (10) using the cell model for a classical Lennard–Jones–Devonshire liquid. Their values (not shown here) are much higher than those presented here. They do show, however, a similar decrease of W with temperature at constant pressure, and an increase in $(\partial W/\partial P)_T$ with temperature.

Derivation of Other Thermodynamic Quantities

It is now possible, using the above velocity data and the density data presented by Van Itterbeek *et al.* (6) and Van Itterbeek and Verbeke

Can. J. Chem. Downloaded from www.nrcresearchpress.com by 210.87.254.5 on 09/05/12
For personal use only.

TABLE III

Adiabatic compressibility χ_S of argon ($atm^{-1} \times 10^{-3}$)

	T(°K)						
P (atm)	86.22_9	96.99_8	108.18_0	117.10_0	127.05_0	136.02_0	146.63_0
1.0	0.101_3						
2.0	0.101_2	(0.129_0)*					
4.0	0.100_9	0.128_5					
6.0	0.100_6	0.127_9	0.173_0				
8.0	0.100_4	0.127_4	0.172_0				
10.0	0.100_1	0.127_0	0.170_9	(0.230_7)			
12.0	0.099_8	0.126_5	0.169_9	0.228_6			
14.0	0.099_5	0.126_0	0.168_9	0.226_5			
16.0	0.099_3	0.125_5	0.168_0	0.224_5			
18.0	0.099_0	0.125_0	0.167_0	0.222_6	0.342_6		
20.0	0.098_7	0.124_6	0.166_1	0.220_6	0.337_2		
25.0	0.098_1	0.123_4	0.163_8	0.216_1	0.324_5	(0.585_1)	
30.0	0.097_4	0.122_3	0.161_6	0.211_7	0.313_1	0.537_8	
35.0	0.096_8	0.121_2	0.159_5	0.207_6	0.302_8	0.500_7	
40.0	0.096_2	0.120_1	0.157_4	0.203_8	0.293_4	0.470_3	(1.85_7)
45.0	0.095_6	0.119_1	0.155_5	0.200_1	0.284_7	0.444_5	1.25_6
50.0	0.095_0	0.118_0	0.153_5	0.196_6	0.276_8	0.422_0	1.01_2
55.0	0.094_4	0.117_0	0.151_7	0.193_2	0.269_4	0.402_1	0.866_3
60.0	0.093_8	0.116_1	0.149_9	0.190_0	0.262_5	0.384_6	0.767_4
65.0	0.093_3	0.115_1	0.148_1	0.186_9	0.256_1	0.369_4	0.693_5

*Values in parentheses are extrapolated.

(11), to derive various thermodynamic quantities of interest.

The adiabatic compressibility, χ_S, was calculated from the relation

$$\chi_S = 1/\rho W^2,$$

where χ_S is in cm^2/dyn, the density ρ is in g/cm^3, and W is in cm/s. The values of χ_S, converted to units of atm^{-1}, are presented in Table III and plotted in Fig. 4. The densities for the first isotherm were obtained from ref. 9. Those for the remaining isotherms were obtained by interpolation, using the method of least squares, of the data of ref. 6. Although the accuracy of the density values had not been quoted, we estimated, from the significant figures retained in the data of ref. 6 and the standard error of estimation of the curves of specific volume V versus pressure P, an accuracy in V or ρ of 0.05%. Thus χ_S is accurate to 0.35% or better. Calculations at intermediate temperatures were avoided because of the greater inaccuracies inherent in the double interpolation which would be required. However, χ_S itself shows a smooth increase with temperature at any one pressure. Our values of χ_S, interpolated at 90.1 °K, agree, to within the accuracy of interpolation, with those of Dobbs and Finegold (2). Any discrepancy between the two sets of results would be due largely to the different density data used.

The specific heat ratio

$$\gamma = C_P/C_V = \chi_T/\chi_S,$$

where the isothermal compressibility

$$\chi_T = \frac{-1}{V}\left(\frac{\partial V}{\partial P}\right)_T,$$

was found by differentiation of the equation for V describing each isotherm. The resulting accuracy of $(\partial V/\partial P)_T$ was estimated as 0.4%. This estimate may be optimistic, however, since we could not judge accurately the errors introduced by the fitted equations. γ values are presented in Table IV. They show an increase in γ with temperature, at constant pressure, and a decrease with pressure at constant temperature. The apparent increase of γ with P in parts of the isotherms at 108.18, 127.05, 136.02, and 146.63 °K probably has no physical meaning, but is just a result of the above-mentioned errors.

The γ values interpolated from our data are slightly higher than those found by Dobbs and Finegold (2) at 90.1 °K and those found by Van Itterbeek *et al.* (1) at 90.3 °K. The difference is again partly a result of the different density data used. At higher temperatures, the agreement between our values and those of Van Itterbeek *et al.* (6) is not good. It is noted here that in the thermodynamic relation used by

Can. J. Chem. Downloaded from www.nrcresearchpress.com by 210.87.254.5 on 09/05/12
For personal use only.

TABLE IV

γ values for argon

	T (°K)						
P (atm)	86.22_9	96.99_8	108.18_0	117.10_0	127.05_0	136.02_0	146.63_0
10.0	2.00	2.45	2.38	(3.00)*			
20.0	2.00	2.37	2.39	2.96	3.04		
30.0	1.99	2.31	2.39	2.91	3.04	3.42	
40.0	1.98	2.26	2.40	2.86	3.02	3.40	(3.11)*
50.0	1.96	2.22	2.40	2.80	2.98	3.32	4.36
60.0	1.95	2.20	2.40	2.75	2.93	3.21	4.40

*Values in parentheses are extrapolated.

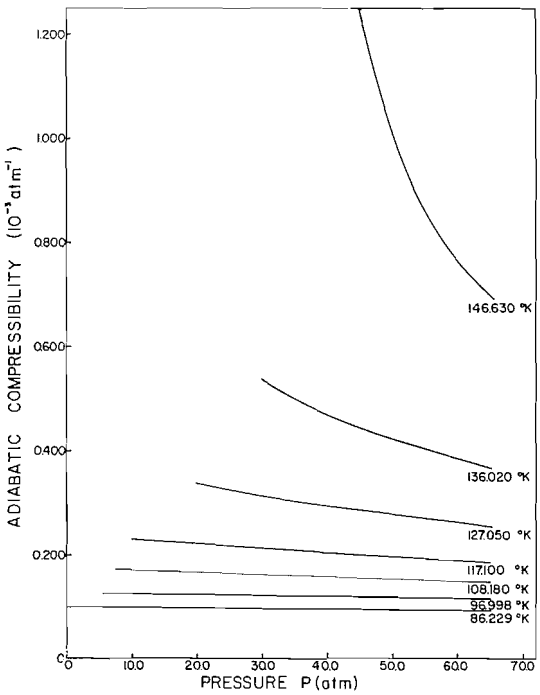

FIG. 4. Adiabatic compressibility, χ_S, of liquid argon, as a function of pressure, for various values of temperature.

Van Itterbeek *et al.*, large errors may be encountered in evaluating $(\partial V/\partial T)_P$ as discussed below.

The molar heat capacity at constant volume, C_V, was calculated from the formulas

$$W = V\left[\frac{T}{MC_V}\left(\frac{\partial P}{\partial T}\right)_V^2 - \frac{1}{M}\left(\frac{\partial P}{\partial V}\right)_T\right]^{1/2}$$

and

$$\left(\frac{\partial P}{\partial T}\right)_V = \frac{-(\partial V/\partial T)_P}{(\partial V/\partial P)_T},$$

where V is the molar volume, and M is the molecular weight.

In calculating C_V, three separate sets of values of V, $(\partial V/\partial P)_T$, and $(\partial V/\partial T)_P$ were used: (*a*) as determined directly from the density data of Van Itterbeek *et al.* (6) and Van Itterbeek and Verbeke (11); (*b*) as tabulated by Van Itterbeek *et al.* (6) at 90, 100, 110, 120, and 130 °K; (*c*) as tabulated by Rowlinson (12) along the liquid–vapor coexistence curve.

The values of C_V so calculated differed by large amounts from each other where they could be compared. The values along the liquid–vapor curve had a large and apparently random variation about smoothed experimental values of C_V tabulated by Rowlinson (12). The variation (greater than 20% in places) was due almost entirely to the uncertainty in $(\partial V/\partial T)_P$ and $(\partial V/\partial P)_T$. For the above reasons, none of the calculated values of C_V are presented here.

Test of Relations between Velocity, Thermal Expansivity, and Isothermal Compressibility

Rao's relationship (13, 14), expressed in the form

$$\frac{1}{W}\left(\frac{\partial W}{\partial T}\right)_P = -K\frac{1}{V}\left(\frac{\partial V}{\partial T}\right)_P,$$

was tested for argon by evaluating K for various temperatures and pressures. Whereas K has been found to be approximately constant and equal to 3 for many organic liquids in their normal liquid ranges, at low pressures, the values of K for argon presented in Table V are in general much less than 3, and show a gradual increase with temperature. The accuracy of our values is uncertain due to the above-mentioned errors in evaluating $(\partial V/\partial T)_P$.

The theoretical predictions of David and Hamann (10) also give K a value much less than 3 for classical Lennard–Jones–Devonshire liquids. They show, contrary to our results, a decrease in K with increasing temperature. Such

Can. J. Chem. Downloaded from www.nrcresearchpress.com by 210.87.254.5 on 09/05/12
For personal use only.

TABLE V

Rao's constant, K, for argon

	T (°K)						
P (atm)	86.22_9	96.99_8	108.18_0	117.10_0	127.05_0	136.02_0	146.63_0
10	1.8	1.9	2.0	(2.1)*			
20	1.7	1.9	1.9	2.0	2.4		
30	1.8	1.8	1.9	2.0	2.2	2.6	
40	1.7	1.8	1.8	1.8	1.9	2.1	(2.8)*
50	1.7	1.8	1.9	2.0	1.9	2.1	2.3
60	1.6	1.8	1.9	2.0	1.9	1.9	1.9

*Values in parentheses are extrapolated.

TABLE VI

Values of coefficient K' in the Carnevale and Litovitz relation for argon

	T (°K)						
P (atm)	86.22_9	96.99_8	108.18_0	117.10_0	127.05_0†	136.02_0	146.63_0
10.0	2.92	2.63	3.16	(2.86)*			
20.0	2.90	2.68	3.04	2.78	3.36†		
30.0	2.88	2.73	2.95	2.72	3.13	3.69	
40.0	2.85_5	2.75	2.88	2.68	2.96	3.20	
50.0	2.83	2.76	2.82_5	2.66	2.85	3.07	3.52
60.0	2.81	2.75	2.80	2.67	2.79	2.94	2.68

*Values in parentheses are extrapolated.
†Values of K' at 127.05_0 °K were suspect, because of lack of data points for this isotherm.

a model (the cell model) of the liquid phase might be expected to be valid only in the high density limit, that is at low temperatures and high pressures. Nozdrev (15) has derived a more complete relation, taking into account the effect of the specific heat ratio, γ, and predicts an increase in K with temperature, in agreement with our findings.

A test of the relation

$$\frac{1}{W}\left(\frac{\partial W}{\partial P}\right)_T = -K'\frac{1}{V}\left(\frac{\partial V}{\partial P}\right)_T$$

due to Carnevale and Litovitz (16) indicates that for argon, over most of the region studied, K' is in the range 2.6–3.4, as shown in Table VI. The possible error in K' is estimated at 1.0% but is possibly greater because of uncertainties in the derivatives, as mentioned earlier. The lack of pressure and temperature dependence of K' could be expected in the light of the theoretical calculations of David and Hamann (10) which predict a constant value of 2.7 for K' over a wide range of temperature and pressure.

Acknowledgment

The authors would like to thank the National Research Council of Canada for their financial support of this investigation.

1. A. Van Itterbeek, W. Grevendonk, W. Van Dael, and G. Forrez. Physica, **25**, 1255 (1959).
2. E. R. Dobbs and L. Finegold. J. Acoust. Soc. Am. **32**, 1215 (1960).
3. A. Van Itterbeek and W. Van Dael. Cryogenics, **1**, 226 (1961).
4. C. C. Lim and R. A. Aziz. Can. J. Phys. **45**, 1275 (1967).
5. R. A. Aziz, C. C. Lim, and D. H. Bowman. Can. J. Chem. **45**, 1037 (1967).
6. A. Van Itterbeek, O. Verbeke, and K. Staes. Physica, **29**, 742 (1963).
7. R. A. Aziz, D. H. Bowman, and C. C. Lim. Can. J. Chem. **45**, 2079 (1967).
8. I. S. Radovskii. Zh. Prikl. Mekhan. i Tekhn. Fiz. **3**, 172 (1964).
9. A. Eucken and F. Hauck. Z. Physik. Chem. Leipzig, **134**, 161 (1928).
10. H. G. David and S. D. Hamann. Australian J. Chem. **14**, 1 (1961).
11. A. Van Itterbeek and O. Verbeke. Physica, **26**, 931 (1960).
12. J. S. Rowlinson. Liquids and liquid mixtures. Butterworth Publications Ltd., London. 1959.
13. M. R. Rao. Indian J. Phys. **14**, 109 (1940).
14. M. R. Rao. J. Chem. Phys. **9**, 682 (1941).
15. V. F. Nozdrev. Application of ultrasonics in molecular physics. Gordon and Breach, New York. 1963.
16. E. H. Carnevale and T. A. Litovitz. J. Acoust. Soc. Am. **27**, 547 (1955).

Can. J. Chem. Downloaded from www.nrcresearchpress.com by 210.87.254.5 on 09/05/12
For personal use only.

Effects of electron scavengers in the radiolysis of water vapor[1]

R. S. Dixon and M. G. Bailey
Atomic Energy of Canada Limited, Whiteshell Nuclear Research Establishment, Pinawa, Manitoba
Received July 31, 1967

Water vapor irradiated with X-rays in the presence of nitrous oxide gives mainly nitrogen and oxygen together with small amounts of hydrogen and, possibly, hydrogen peroxide. The yield of nitrogen, $G(N_2) = 3.0 \pm 0.3$, is constant over a wide range of conditions and $G(O_2) = 1.6 \pm 0.3$ after an induction period. The hydrogen yield is constant at low doses with $G(H_2) = 0.45 \pm 0.1$, but reaches a steady state at higher doses. The nitrogen yield is equated with the yield of scavengeable electrons in water vapor, the value $g(e) = 3.0 \pm 0.3$ being in reasonable agreement with the theoretical value based on $W(H_2O) = 30$ eV. Addition of other electron scavengers to water vapor containing nitrous oxide suppresses the nitrogen yield by competing efficiently for electrons. On the basis of their efficiency in suppressing the nitrogen yield, limiting values for the relative rates of reaction of N_2O, SF_6, CCl_4, and HCl with electrons in water vapor are obtained and comparisons are made with their known electron attachment cross sections in the gas phase.

Canadian Journal of Chemistry, 46, 1181 (1968)

Introduction

Observed radiation decomposition yields of water vapor in the presence of additives are few and there is considerable disagreement amongst the recent data (1–3). The value[2] $g(H) = g(OH) = 11.7$ quoted by Firestone (1) from the β-ray induced exchange of D_2 with H_2O is much higher than the values obtained from water vapor containing organic scavengers where $g(H) = 7$–8 and $g(OH) = 8.5$ (2) and from the H_2O–NH_3–O_2 system where $g(H) = 5.7$ and $g(OH) = 6.5$ (3).

Recent investigations (4, 5) have shown that the hydrogen yield is reduced on addition of nitrous oxide or sulfur hexafluoride to H_2O or D_2O vapor containing organic additives. This reduction is thought to be caused by electron capture by N_2O or SF_6, thus preventing the neutralization reaction

$$e^- + H_3O^+ \rightarrow H + H_2O.$$

The reduction in the hydrogen yield $\Delta G(H_2) \approx 3$ has therefore been equated with the yield of electrons in water vapor.

The importance of the yield and reactions of electrons in the radiation chemistry of water vapor has led us to study irradiated water vapor containing several additives, all of which are known to react with electrons from studies in other systems, and some of which are thought to be specific scavengers for electrons.

[1]Issued as A.E.C.L. No. 3049.
[2]Primary yields are written as $g(x)$ and experimental yields as $G(x)$, molecules per 100 eV.

Experimental

Materials

Water was successively distilled from acid dichromate, from alkaline permanganate, and through a quartz tube at 500 °C in a stream of oxygen. Nitrous oxide, sulfur hexafluoride, and hydrogen chloride (Matheson research grade), carbon tetrachloride and hydrogen peroxide (Fisher certified), and propylene (Phillips research grade) were used without further purification except for several freeze–pump–thaw cycles.

Technique

The irradiation vessels were 450 cc cylindrical quartz cells equipped with a center thermocouple well and a break-seal for analysis. Before filling, the cells were washed with permanganic acid, rinsed with acidified hydrogen peroxide, rinsed several times with triply distilled water, heated in air at 500 °C overnight, cooled, and evacuated to 10^{-6} Torr at room temperature. A weighed amount of water (~0.25 g) was pipetted into a small flask attached to a grease-free preparation line and, after degassing with several freeze–pump–thaw cycles, was distilled into the irradiation vessel immersed in liquid nitrogen. Gases were added by condensing a known volume of gas, at a known temperature and pressure, into the vessel. The vessel and contents were finally evacuated to 10^{-6} Torr at −196 °C before sealing off. The vessel was mounted in a furnace which was kept at 125 ± 2 °C during irradiation. The temperature was controlled by a Honeywell controller/recorder system and was constant to ±1 °C over the whole vessel. The total pressure during irradiation was ~750 Torr. Duplicate irradiations were carried out with X-rays from a 1.5 MeV Van de Graaff accelerator using a water-cooled stainless steel target. After irradiation, the gases not condensable at −196 °C were measured volumetrically and nitrogen, oxygen, and hydrogen were analyzed by gas chromatography using helium (for N_2 and O_2) or argon (for H_2) carrier gas. Hydrogen peroxide was estimated by its oxidation of iodide ion.

Dosimetry

The dose rate of 3.0×10^{17} eV g^{-1} min^{-1} in H_2O (at an electron beam current of 1 mA) was estimated by the nitrous oxide dosimeter irradiated at ambient temperature (~ 25 °C) inside the furnace. A value $G(N_2) = 11.0$ was used (6). The yields of nitrogen from irradiated nitrous oxide at 400 and 700 Torr were linear with dose up to the maximum dose used, 1.4×10^{20} eV g^{-1} (2.8×10^{17} eV ml^{-1} N_2O at s.t.p.), and were independent of pressure within the range used. The relative dose rate was checked periodically with the Fricke dosimeter. The energy absorbed by each additive was calculated by assuming it to be directly proportional to the electron density of the additive.

Results

Water Vapor + N_2O

The yield–dose plots for nitrogen, oxygen, and hydrogen produced from irradiated water vapor containing nitrous oxide are shown in Fig. 1. The slopes of the linear portions give $G(N_2) = 3.0 \pm 0.3$ and $G(O_2) = 1.6 \pm 0.3$, in the latter case after an induction period. The nitrogen yield was independent of dose from 0.15–5.0 $\times 10^{20}$ eV g^{-1}, of dose rate within the range 0.4–3.0 $\times 10^{17}$ eV g^{-1} min^{-1}, and of nitrous oxide concentration between 0.1–10 mole %. The intercept in the nitrogen plot at zero dose is outside experimental error and appears to indicate that $G(N_2) > 3.0$ at low doses. However, this may be due, in part, to air contamination since blank experiments without irradiation always gave small quantities of nitrogen (~ 0.1 μmoles) and oxygen (~ 0.01 μmoles). Thus it is not possible to estimate the magnitude of $G(N_2)$ at doses lower than 10^{19} eV g^{-1} except that it may be greater than the steady state yield of 3.0. As shown in Fig. 1, addition of 1 mole % propylene to water vapor containing 1 mole % nitrous oxide reduced the oxygen yield to zero but did not affect the nitrogen yield.

The yield of hydrogen from water vapor containing 1 mole % nitrous oxide appears to build up to a steady state value of about 0.4–0.5 μmoles cm^{-3} H_2O, though the yields tended to be somewhat erratic. At low doses the hydrogen yield was approximately constant at $G(H_2) = 0.45 \pm 0.1$. Generally nitrogen, oxygen, and hydrogen accounted for all the gaseous products collected. Small quantities of hydrogen peroxide, $G(H_2O_2) \leq 0.15$, were found in some samples. Blank experiments with water vapor containing added hydrogen peroxide (up to 10^{-2} M) but without irradiation showed that greater than 90% of the hydrogen peroxide decomposed, but the oxygen measured from this decomposition was usually less than 10% of that expected.

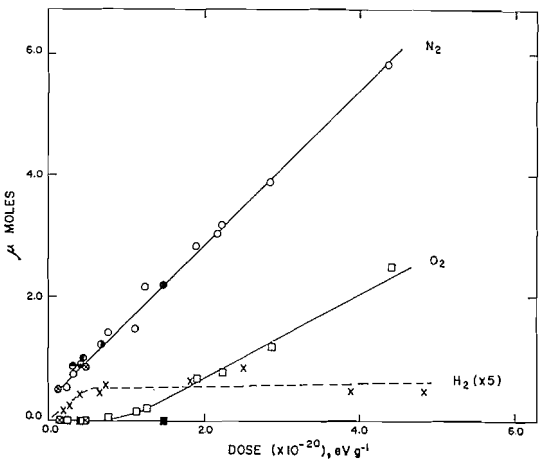

FIG. 1. Product yields from water vapor containing nitrous oxide. Pressure ~ 750 Torr and temp. 125 °C. Dose rate 3×10^{17} eV g^{-1} min^{-1}. N_2 yields: (◓) 0.1 mole % N_2O; (○) 1 mole % N_2O; (◒) 2.2 mole % N_2O; (◐) 5.2 mole % N_2O; (◑) 10 mole % N_2O; (●) 1 mole % N_2O + 1 mole % propylene. O_2 yields: (□) 1 mole % N_2O; (◧) 5.2 mole % N_2O; (■) 1 mole % N_2O + 1 mole % propylene. H_2 yields: (×) 1 mole % N_2O. Dose rate 4×10^{16} eV g^{-1} min^{-1}. N_2 yields: (⊗) 1 mole % N_2O. O_2 yields: (⊠) 1 mole % N_2O.

Water Vapor + N_2O + Additives

Addition of sulfur hexafluoride (0.0016–1.0 mole %) to water vapor containing nitrous oxide (1–10 mole %) caused essentially complete suppression of the nitrogen yield in each case. Small quantities of nitrogen (0.1–0.2 μmoles) were produced in all the samples, which in terms of "yields" amounted to $G(N_2) \sim 0.4$ compared with 3.0 in the absence of sulfur hexafluoride. However, since this "yield" did not change as the N_2O:SF_6 ratio increased from 1:1 to 1250:1 and since the absolute amounts of nitrogen were similar to those produced in blank runs without irradiation, these small quantities of nitrogen are probably due to air contamination. It is concluded that even at a N_2O:SF_6 ratio of 1250:1 the sulfur hexafluoride causes complete suppression of the nitrogen produced by reaction of nitrous oxide with intermediates produced from the water. $G(H_2)$ was ~ 0.4 at doses less than 5 $\times 10^{19}$ eV g^{-1} but decreased at higher doses.

Carbon tetrachloride (0.04–1.2 mole %) had a similar effect in suppressing the nitrogen yield from water vapor containing nitrous oxide (1–6 mole %) at all N_2O:CCl_4 ratios between 1:1 and

110:1. Hydrogen was not measured in these samples.

In water vapor containing nitrous oxide (1 mole %) and hydrogen chloride, $G(N_2)$ decreased from 2.9 to 0.3 as the hydrogen chloride concentration increased from 0.075 to 1 mole %. $G(H_2)$ increased from 0.2 to 3.5 over the same concentration range.

All the above yields were based on the energy absorbed by water only. Corrections for nitrogen and hydrogen produced by direct absorption of energy by nitrous oxide and hydrogen chloride were made using $G(N_2)_{N_2O} = 11.0$ (6) and $G(H_2)_{HCl} = 8.0$ (7). These corrections were made assuming that energy transfer from additive to water does not occur and that addition of sulfur hexafluoride, carbon tetrachloride, or hydrogen chloride does not affect $G(N_2)$ from pure nitrous oxide. It is possible that neither of these assumptions is strictly correct but we estimate that any inaccuracies due to these assumptions will not seriously affect the conclusions arrived at in the present study.

Discussion

Water Vapor + N_2O

The major reactions which produce H and OH in irradiated water vapor are generally assumed to be

$$H_2O \text{—}\wwwarrow H_2O^*, H_2O^+, e^-$$

[1] $$H_2O^+ + H_2O \rightarrow H_3O^+ + OH$$

[2] $$e^- + H_3O^+ \rightarrow H + H_2O$$

[3] $$H_2O^* \rightarrow H + OH \quad .$$

Reaction [1] is extremely fast ($k = 1.26 \times 10^{-9}$ cm^3 $molecule^{-1}$ s^{-1}) (8) thus precluding other reactions of H_2O^+ at the pressure of water vapor used.

The high efficiency of nitrous oxide as an electron scavenger has been postulated in various aqueous solutions (9), organic liquids (10), and gaseous systems (11). Its efficiency in gaseous systems is based on electron impact experiments which have shown it to dissociatively capture electrons close to zero electron energy (12, 13). It therefore seems probable that nitrous oxide is acting as an electron scavenger in water vapor,

[4] $$e^- + N_2O \rightarrow N_2 + O^-,$$

thus preventing the neutralization reaction [2]. If no other reactions produce nitrogen, its yield may therefore be taken as a measure of the yield of scavengeable electrons in water vapor. The value $G(N_2) = 3.0 \pm 0.3 = g(e)$ found over a wide range of dose rate and nitrous oxide concentration is in good agreement with the theoretical value of 3.3 based on the average energy required to form an ion pair in water vapor, $W(H_2O) = 30$ eV (14, 15) and with Baxendale and Gilbert's value (4) of 3.0 ± 0.4 at low nitrous oxide concentration (≤ 0.7 mole %).

Since nitrous oxide concentration has no effect on $G(N_2)$ it appears that the reactions

[5] $$H + N_2O \rightarrow OH + N_2$$

[6] $$OH + N_2O \rightarrow HO_2 + N_2$$

do not compete favorably with other reactions of H and OH. This is confirmed by the lack of effect on the nitrogen yield of propylene, which is known to react rapidly with both H atoms (see for example ref. 16) and OH radicals (17).

Similarly, Fig. 1 clearly shows that the buildup of oxygen does not affect $G(N_2)$, indicating that the quantities of oxygen produced in our experiments are insufficient for electron capture by oxygen to compete with electron capture by nitrous oxide. Also, since $G(N_2)$ is in good agreement with the expected value of $g(e)$ from the W-value in water vapor (14, 15), it appears that the reaction

[7] $$O^- + N_2O \rightarrow N_2 + O_2^-$$

proposed in the propane–nitrous oxide system (11) is not occurring in water vapor under our experimental conditions even at 10 mole % nitrous oxide. The fate of O^- is presumably neutralization,

[8] $$O^- + H_3O^+ \rightarrow OH + H_2O,$$

or reaction with water,

[9] $$O^- + H_2O \rightarrow OH + OH^-,$$

followed by neutralization

[10] $$H_3O^+ + OH^- \rightarrow 2H_2O.$$

Since reaction [8] probably occurs at a rate comparable to the rate of reaction of O^- with the positive ion formed in propane radiolysis (11), where reaction [7] does occur, and since the dose rates are similar in the two studies, the fate of O^- is probably disappearance by reaction [9]. Since the nitrogen yield was unaffected by nitrous oxide concentration up to 10 mole % this indicates k_9

$\geq k_7$, assuming an uncertainty of 10% in $G(N_2)$. For electrons to disappear via [4] in competition with [2] at the dose rate used ($\sim 3 \times 10^{12}$ eV cm^{-3} s^{-1}) and at a minimum concentration of 0.1 mole % nitrous oxide, a steady state treatment of reactions [1], [2], [4], [8], [9], and [10] indicates $k_4/{k_2}^{1/2} \geq 1.5 \times 10^{-10}$, assuming $k_2 = k_8 = k_{10}$ and a 10% uncertainty in $G(N_2)$. Similarly for at least 90% of O^- to disappear via [9] in competition with [8], the steady state treatment shows $k_9/{k_8}^{1/2} \geq 1.5 \times 10^{-13}$. The recombination coefficients k_2 and k_8 are not accurately known but probably lie in the range 10^{-6}–10^{-8} cm^3 $molecule^{-1}$ s^{-1} (18). Hence it follows that $k_4 \geq 1.5 \times 10^{-14}$ cm^3 $molecule^{-1}$ s^{-1} and $k_9 \geq 1.5 \times 10^{-17}$ cm^3 $molecule^{-1}$ s^{-1}, though the true values could be much higher than the minimum values. The former is at least an order of magnitude higher than the specific rate found in propane radiolysis at room temperature (11), assuming the same rates of electron–positive ion recombination in water vapor and propane.

The value of $G(N_2)$ at very low doses is not known but may be greater than 3.0. However, since the small quantities of nitrogen produced in samples containing sulfur hexafluoride, which captures all electrons, were similar to the nitrogen intercept in Fig. 1, then if $G(N_2)$ is greater than 3.0 at low doses, the extra nitrogen probably does not originate from electrons. This is supported by the lack of effect of nitrous oxide concentration on $G(N_2)$ over the whole dose range studied. Thus there seems little doubt that nitrogen is formed by reaction [4] only and that $G(N_2)$ is a measure of the yield of scavengeable electrons in water vapor.

Oxygen is produced with $G(O_2) = 1.6 \pm 0.3$ after a dose of about 5×10^{19} eV g^{-1} and extrapolation of the yield–dose plot for oxygen to zero dose gives a negative intercept of 0.65 μmoles. This suggests that oxygen is either removed by impurities at low doses or is formed by secondary reactions of some product of radiolysis. Our analysis for hydrogen peroxide showed little or no yield, which is in accordance with our observation that hydrogen peroxide is decomposed thermally under our experimental conditions. However, in blank experiments with water vapor containing added hydrogen peroxide (without irradiation) we found less than 10% of the oxygen expected (0.5–1 μmole) from decomposition of the hydrogen peroxide, i.e. oxygen is being removed by some process. Since the extent of this removal is of the same magnitude as the intercept in Fig. 1, we suggest that oxygen is removed during radiolysis either by reaction with impurities or by loss to the walls of the vessel.

Oxygen is probably produced by the following reactions.

[4] $e^- + N_2O \rightarrow N_2 + O^-$

[11] $H_2O_2 \rightarrow OH + OH$

[12] $H + H_2O_2 \rightarrow OH + H_2O$

[13] $OH + H_2 \rightarrow H + H_2O$

[14] $OH + H_2O_2 \rightarrow HO_2 + H_2O$

[15] $OH + OH + M \rightarrow H_2O_2 + M$

[16] $OH + HO_2 \rightarrow H_2O + O_2$

[17] $HO_2 + HO_2 \rightarrow H_2O_2 + O_2$

[18] $H + O_2 + M \rightarrow HO_2 + M.$

Since reaction [4] essentially converts e^- to OH, the presence of nitrous oxide would cause OH to be in excess of H by about 6 G units. Production of oxygen from these "excess" OH radicals would yield $G(O_2) = 1.5$, which is in good agreement with the measured value of $G(O_2) = 1.6 \pm 0.3$. The complete suppression of the oxygen yield found on addition of 1 mole % propylene to water vapor containing 1 mole % nitrous oxide is predicted by the above scheme, since propylene will rapidly react with all the available H and OH radicals (16, 17).

As shown in Fig. 1, hydrogen builds up to a steady state concentration which is presumably limited by the back reaction

[13] $OH + H_2 \rightarrow H + H_2O.$

Although the hydrogen yields are small and somewhat irreproducible, a steady state value of $\sim$0.4–0.5 μmoles cm^{-3} H_2O is reached at a dose of about 5×10^{19} eV g^{-1}, which is similar to the steady state yield found in pure water vapor (3). At doses lower than this, the yield was approximately linear with dose with $G(H_2) = 0.45 \pm 0.1$. This is in reasonable agreement with the molecular hydrogen yield in water vapor found in several independent studies (19–21).

When the steady state concentration of hydrogen is reached the net chemical change will be given by

$$N_2O \rightarrow N_2 + \tfrac{1}{2}O_2$$

assuming that no other products are formed. The

TABLE I

Comparison between the relative rates of reaction of some molecules with electrons in irradiated water vapor and their known electron attachment cross sections in the gas phase[1]

Molecule	Electron energy at 1st maximum (eV)	Relative cross section at: 1st maximum	0.5 eV electron energy	1.0 eV electron energy	Relative integrated cross section over electron energy range: 0–0.5 eV	0–1 eV	Reference	Estimated relative rate of reaction with electrons from present work
SF_6	0.0	150–13000	20–80	0.5	300–3000	40–400	23–26	$\geq 10^4$
CCl_4	0.02	30–65	70	30	330	75	23	$\geq 10^3$
HCl	0.6	1–2	3	0.5	3	2	23	~10
N_2O	~0.6	1	1	1	1	1	12, 13, 22	1
H_2O	6.4	1–2					23	

[1]All values relative to $N_2O = 1$.

results substantiate this since, within the limits of experimental error, the relationship

$$G(N_2) \approx 2G(O_2) = g(e)$$

is seen to hold over the whole range of nitrous oxide concentration.

Water Vapor + N_2O + Additives

Although nitrous oxide captures electrons close to zero electron energy, its capture cross section for such electrons is low (12, 13, 22). The electron capture cross sections of sulfur hexafluoride and carbon tetrachloride are much higher than that of nitrous oxide and their first maxima both occur close to zero electron energy, whereas that of nitrous oxide is at a much higher electron energy (see Table I). Thus the suppression of the nitrogen yield from water vapor – nitrous oxide mixtures is probably due to electron capture by SF_6 and CCl_4,

[19] $$e^- + SF_6 \rightarrow SF_6^-$$

[20] $$e^- + CCl_4 \rightarrow CCl_3 + Cl^-,$$

competing with reaction [4],

[4] $$e^- + N_2O \rightarrow N_2 + O^-,$$

and it appears that even at the lowest SF_6:N_2O and CCl_4:N_2O ratios used, reaction [4] is completely suppressed. Since the lowest SF_6:N_2O and CCl_4:N_2O ratios were 1:1250 and 1:110 respectively, this indicates that the electron capture efficiencies of sulfur hexafluoride and carbon tetrachloride in water vapor are at least 10^4 and 10^3 times greater than that of nitrous oxide. These values are shown in the last column of Table I. The limiting relative rate $k(e^- + SF_6)/k(e^- + N_2O)$ found in the present work is in good agreement with that found by Johnson and Warman in gaseous propane (11).

The effect of hydrogen chloride in irradiated water vapor containing 1 mole % nitrous oxide appears to be somewhat more complex. $G(N_2)$ falls from 2.9, which is approximately the value in the absence of hydrogen chloride, to 0.3 as the HCl:N_2O ratio increases from 0.076:1 to 1:1 (a factor of 13) and $G(H_2)$ increases from 0.2 to 3.5 over the same range. Assuming an uncertainty of about 10% in these G-values, the decrease in $G(N_2)$ with increase in hydrogen chloride concentration is consistent with a simple competition between hydrogen chloride and nitrous oxide for electrons,

[4] $$e^- + N_2O \rightarrow N_2 + O^-$$

[21] $$e^- + HCl \rightarrow H + Cl^-,$$

with $k_{21}/k_4 \sim 10$. However, the hydrogen yields appear to be too low since, although H atoms from reaction [21] will probably react with HCl,

[22] $$H + HCl \rightarrow H_2 + Cl,$$

we would also expect H atoms produced in reaction [3] to react with HCl via reaction [22]. It is possible that secondary products are interfering with the reactions of H atoms but in the absence of a more detailed study, which is outside the scope of this work, we can only deduce that hydrogen chloride probably captures electrons about 10 times more efficiently than nitrous oxide. This is shown in the last column of Table I.

Comparison between the Cross Sections for Electron Attachment and the Relative Rates of Reaction with Electrons in Water Vapor

The probability of electron capture by an additive will be given by an integral of the form

$$N_A \int f(E)\sigma(E)dE,$$

where N_A is the concentration of the additive,

$f(E)$ is the flux of electrons at energy E, and $\sigma(E)$ is the electron capture cross section of the additive at energy E. It is interesting to speculate on the probability of electron capture in irradiated water vapor using available data on electron capture cross sections compared with our values of the relative rates of reaction of electrons with the various additives.

Our experiments show that the majority of electrons are not captured by water even though its concentration is much higher than that of the additive. This is evident from the lack of competition with nitrous oxide for electrons in water vapor containing as little as 0.1 mole % nitrous oxide. The appearance potential of H^- from the reaction

$$[23] \qquad e^- + H_2O \rightarrow H^- + OH$$

is about 5 eV (23) and the capture cross section for H_2O in the 5–7 eV energy range (where the first maximum for H_2O occurs) is higher than those of the additives. Thus the value of $f(E)$ in the 5–7 eV range must be small and the rate of loss of energy for electrons must be reasonably high in this energy range.

Some arbitrary comparisons of the capture cross sections of the molecules studied at low electron energies are shown in Table I. The qualitative correlation between the resonance capture cross sections and our relative reaction rates shows that electrons with energies in the range 0–0.6 eV (the position of the first maximum for N_2O and HCl) are important and $f(E)$ will have significant values in this range. HCl has effectively zero cross section at 0.35 eV (the appearance potential of Cl^-) suggesting that $f(E)$ is significant at values of E greater than this. In general the comparisons show that while the capture cross sections at low electron energies give the correct sequence, SF_6 and CCl_4 capture electrons more efficiently, with respect to N_2O, than the cross sections would suggest. This disparity increases if we compare capture cross sections at energies above 1 eV, but a more quantitative agreement is obtained if we compare integrated cross sections at energies below 0.5 eV, though the available data in this region are sparse.

In general the above observations lead to the conclusion that electron capture occurs at low electron energies, probably less than 0.5 eV, but not necessarily completely at thermal electron energy. However, more information is needed on both electron capture cross sections at low electron energies and the rates of reaction of electrons in irradiated gases before a more detailed comparison may be made.

Acknowledgments

It is a pleasure to acknowledge the critical comments by Drs. P. J. Dyne and A. W. Boyd on earlier forms of the manuscript.

1. R. F. Firestone. J. Am. Chem. Soc. **79**, 5593 (1957).
2. J. H. Baxendale and G. P. Gilbert. Discussions Faraday Soc. **36**, 186 (1963).
3. A. R. Anderson, B. Knight, and J. A. Winter. Trans. Faraday Soc. **62**, 359 (1966).
4. J. H. Baxendale and G. P. Gilbert. Science, **147**, 1571 (1965).
5. G. R. A. Johnson and M. Simic. J. Phys. Chem. **71**, 1118 (1967).
6. J. A. Hearne and R. W. Hummel. Radiation Res. **15**, 254 (1961).
7. R. A. Lee, R. S. Davidow, and D. A. Armstrong. Can. J. Chem. **42**, 1906 (1964).
8. F. W. Lampe, F. H. Field, and J. L. Franklin. J. Am. Chem. Soc. **79**, 6132 (1957).
9. F. S. Dainton and D. B. Peterson. Proc. Roy. Soc. London, Ser. A, **267**, 443 (1962).
10. G. Scholes and M. Simic. Nature, **202**, 895 (1964).
11. G. R. A. Johnson and J. M. Warman. Trans. Faraday Soc. **61**, 1709 (1965).
12. R. K. Curran and R. E. Fox. J. Chem. Phys. **34**, 1590 (1961).
13. G. J. Schultz. J. Chem. Phys. **34**, 1778 (1961).
14. C. Wingate, W. Gross, and G. Failla. Radiation Res. **8**, 411 (1958).
15. J. Booz and H. G. Ebert. Z. Angew. Phys. **13**, 376 (1961).
16. R. J. Cvetanovic. Advan. Photochem. **1**, 115 (1963).
17. E. R. Bell, W. E. Vaughan, and F. F. Rusk. J. Am. Chem. Soc. **79**, 3997 (1957).
18. A. von Engel. Ionized gases. Clarendon Press, Oxford. 1965. p. 155.
19. A. R. Anderson, B. Knight, and J. A. Winter. Nature, **201**, 1026 (1964).
20. J. H. Baxendale and G. P. Gilbert. J. Am. Chem. Soc. **86**, 516 (1964).
21. J. Y. Yang and I. Marcus. J. Am. Chem. Soc. **88**, 1625 (1966).
22. D. Rapp and D. D. Briglia. J. Chem. Phys. **43**, 1480 (1965).
23. I. S. Buchel'nikova. Zh. Eksperim. i Teor. Fiz. **35**, 1119 (1958).
24. W. M. Hickam and R. E. Fox. J. Chem. Phys. **25**, 642 (1956).
25. R. K. Asundi and J. D. Craggs. Proc. Phys. Soc. London, **83**, 611 (1964).
26. B. H. Mahan and C. H. Young. J. Chem. Phys. **44**, 2192 (1966).

Transition from internal to external oxidation in indium–silver alloys[1]

L. D. PETHE, H. B. MATHUR,[2] AND A. B. BISWAS[3]
National Chemical Laboratory, Poona, India

Received January 10, 1967

The kinetics of oxidation of In–Ag alloys of 5, 10, and 15 at. % indium have been studied on a vacuum microbalance. The 15 at. % indium alloy oxidizes externally and the 5 at. % alloy internally. A plot of logarithm of the parabolic oxidation rate, k_p, versus reciprocal of the absolute temperature for 10 at. % indium alloy gives two intersecting straight lines corresponding to the energies of activation of 23 and 39.6 kcal/mole for the oxidation below and above 600 °C respectively. These are comparable to the energies of activation of 23 kcal/mole for the internal oxidation of 5 at. % indium alloy and 40 kcal/mole for the external oxidation of 15 at. % indium alloy. The rate-controlling step in the external oxidation of 15 at. % indium alloy is the diffusion of indium through the alloy. Photomicrographs of the cross sections of the oxidized foils of these alloys confirm the conclusions derived from the kinetic data.

Canadian Journal of Chemistry, **46**, 1187 (1968)

Can. J. Chem. Downloaded from www.nrcresearchpress.com by 210.87.254.6 on 09/05/12
For personal use only.

The high temperature oxidation studies on a series of alloys by Rhines *et al.* (1–3) and Meijering and Druyvesteyn (4) have provided the basis on which the general features of internal oxidation can be adequately explained. When the percentage of the baser metal component in a binary alloy is increased to a certain critical value, the volume of the precipitated oxide of the baser metal becomes so large that its particles condense to form a barrier which inhibits further oxygen diffusion through the alloy matrix, resulting in the transition from internal to external oxidation. Dietrich and Koch (5) found this critical concentration to be 9 atom % indium for In–Ag alloy. Wagner (6) has described the conditions required for this transition mathematically in terms of the diffusion rates of oxygen and the oxide forming baser metal and the molar volumes of the metal and the oxide. Rapp (7) evaluated this theory for the In–Ag system and found his experimental results at 550 °C in agreement with Wagner's theoretical predictions. More recently he has also studied the oxidation of three In–Ag alloys of less than 15 atom % indium, based on the computer-calculated programs for the formation of interruption bands (8). The change in the mechanism of oxidation of indium–silver alloys appears to be solely dependent on the concentration of the less noble metal. However, the kinetics of oxidation have not been studied systematically over a range of temperature in the region of the critical concentration. In this communication, we report the results of such an investigation with the aid of a quartz microbalance.

Experimental Procedure

The quartz microbalance was constructed according to the details described by Bradley (9). As the density of the In–Ag alloy was nearly the same as that of pure silver, the counterpoise weights were prepared from pure silver in order to eliminate corrections due to buoyancy. The sample was suspended in the constant temperature zone of nearly 3.0 cm in the middle of a non-inductively wound resistance furnace.

After suspending the sample the reaction vessel was evacuated to 10^{-5} Torr. Argon was then introduced at the experimental pressure. The furnace, controlled and set at the experimental temperature, was raised over the reaction vessel. The sample was annealed at the experimental temperature for 1 h. Argon was then pumped out and oxygen introduced in its place. The rate of oxidation was then followed by noting the movement of the reference pointer, fixed to the balance beam. As the molecular weights of argon and oxygen are nearly equal, the above procedure enabled us to determine the position of the moving pointer before oxidation started and at the same time avoided corrections due to buoyancy and the thermomolecular effects.

Silver–indium alloys were prepared by melting the spectroscopically pure metals in high purity graphite crucibles, placed inside silica tubes and sealed in a vacuum of 10^{-5} Torr. The metals had the following analysis.

Silver Fe, 0.03%; Si, 0.01%; Mg, 0.003%; Al, 0.003%; and Cu, 0.003%.

Indium Fe, Pb, Sn, Mg, Ag, each 0.003%; Bi and Ni each 0.001%; Si, 0.0003%.

The homogenity of the alloys was tested by the analysis of small fractions of the alloy taken from different portions of the ingot. The ingots were cold rolled to foils of the desired thickness. The foils were abraded successively by 2/0 and 4/0 emery papers under mineral oil, rinsed in low boiling point petroleum ether, and finally suspended in the balance.

---

[1]Communication No. 950 from the National Chemical Laboratory, Poona-8, India.

[2]To whom communications regarding this article should be addressed.

[3]Present address: Indian Institute of Technology, Powai, Bombay-76.

Can. J. Chem. Downloaded from www.nrcresearchpress.com by 210.87.254.6 on 09/05/12
For personal use only.

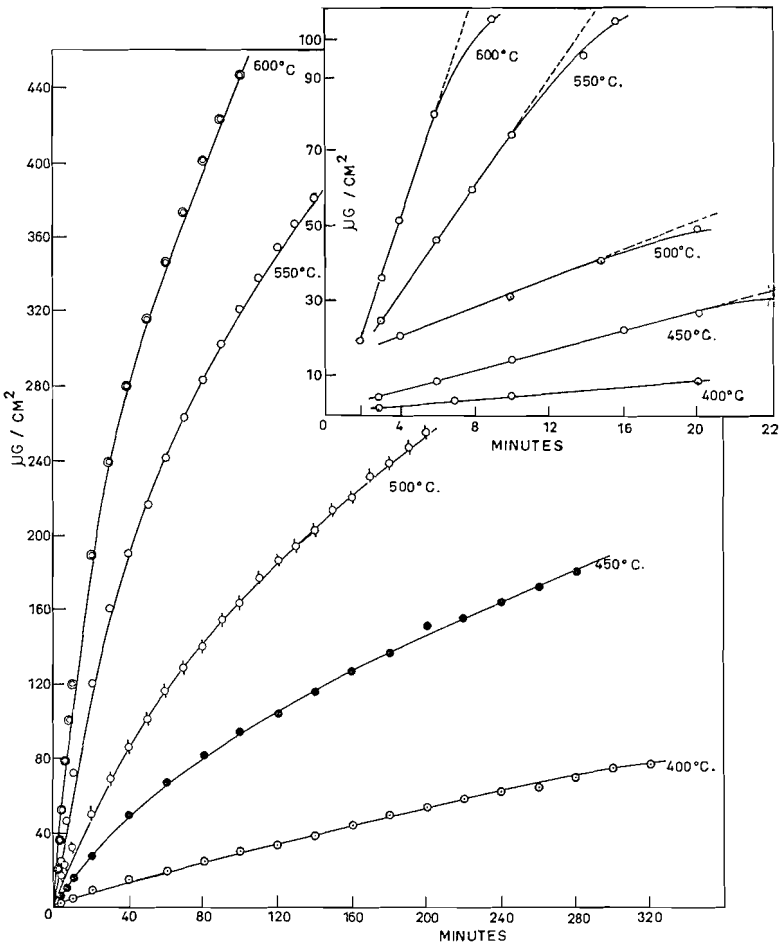

FIG. 1. Kinetics of oxidation of 5/95 In–Ag alloy in 76 Torr oxygen pressure at various temperatures. The initial rate of oxidation of the alloy is shown in the enlarged figure at the top right hand corner.

Spectroscopically pure argon was used and oxygen gas was prepared from analytical reagent grade potassium permanganate.

Results and Discussion

The oxidation studies were undertaken on three alloys of silver containing 5, 10, and 15 atom % indium. The kinetics of oxidation of 5/95 In–Ag alloy in the region 400–600 °C and at 76 Torr oxygen pressure are represented in Fig. 1. The experimental data for all the three alloys have been plotted in Figs. 2–4 as the square of the oxygen uptake versus time.

It may be observed that the rate of oxygen uptake by the alloys decreases sharply with the increase in the indium content. With the exception of a brief initial period, the oxidation of 5 at. % In–Ag alloy in the temperature interval 450–600 °C can be described by means of a parabolic rate law. The rate of oxidation for the first few minutes shows a linear dependence with time as shown in Fig. 1. The interval during which the linear law is obeyed increases with the decrease in temperature. At 400 °C, the oxidation during the entire period of study can be described by a linear rate law. The oxidation kinetics of the 10 at. % In–Ag alloy are also governed by the parabolic rate law, the only exception being the experiment at 675 °C, where the oxidation kinetics deviates from the parabolic rate law after the 80th minute (Fig. 3). For the 15 at. % In–Ag alloy, the parabolic rate law is valid for

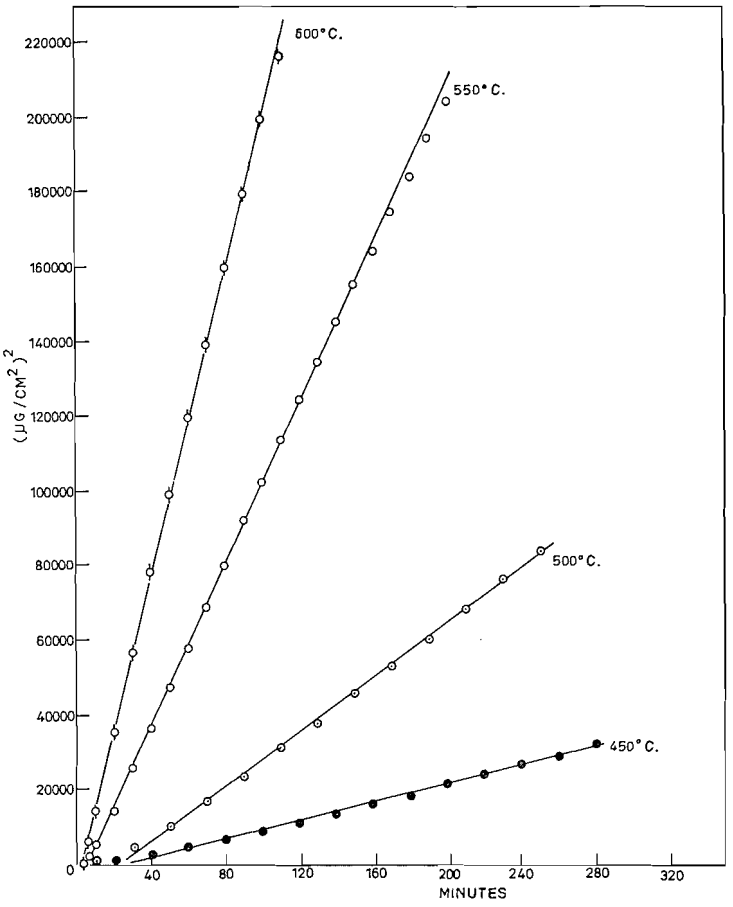

FIG. 2. Parabolic plot of the oxidation of 5/95 In–Ag alloy.

an initial period. With an increase in the period of oxidation, marked departures from the parabolic rate law are observed. The period, over which the parabolic rate law is valid, decreases with an increase in the temperature of oxidation (Fig. 4).

The Arrhenius plots of the parabolic rate constants (Fig. 5) indicate that a single mechanism is responsible for the oxidation of 5 and 15 at. % In–Ag alloys while there are two different processes taking part during the oxidation of 10/90 In–Ag alloy. The change in the mechanism of oxidation takes place at about 600 °C. The obedience of the oxidation kinetics of the 5, 10, 15 at. % In–Ag alloys to the parabolic rate law indicates that the diffusion is the rate-controlling process during their oxidation. The initial linear rate, observed in 5/95 In–Ag alloy, is due to a phase boundary reaction where the dissociation and dissolution of oxygen takes place at the alloy/oxygen interface. Indium atoms act as active sites for the dissociation of the oxygen before it dissolves in the alloy. This gives rise to and maintains the concentration gradient within the alloy which acts as the driving force for the diffusion of oxygen. Once the concentration gradient has been built up, further oxidation is controlled by the diffusion of oxygen through the alloy. The observed linear rate of oxidation at 400 °C indicates that the phase boundary reaction is the rate-controlling step during the entire period of oxidation.

The energies of activation calculated for the oxidation of these alloys from the Arrhenius plots in Fig. 5 are summarized in Table I.

The energy of activation of 23.6 kcal/½mole

Can. J. Chem. Downloaded from www.nrcresearchpress.com by 210.87.254.6 on 09/05/12
For personal use only.

Can. J. Chem. Downloaded from www.nrcresearchpress.com by 210.87.254.6 on 09/05/12
For personal use only.

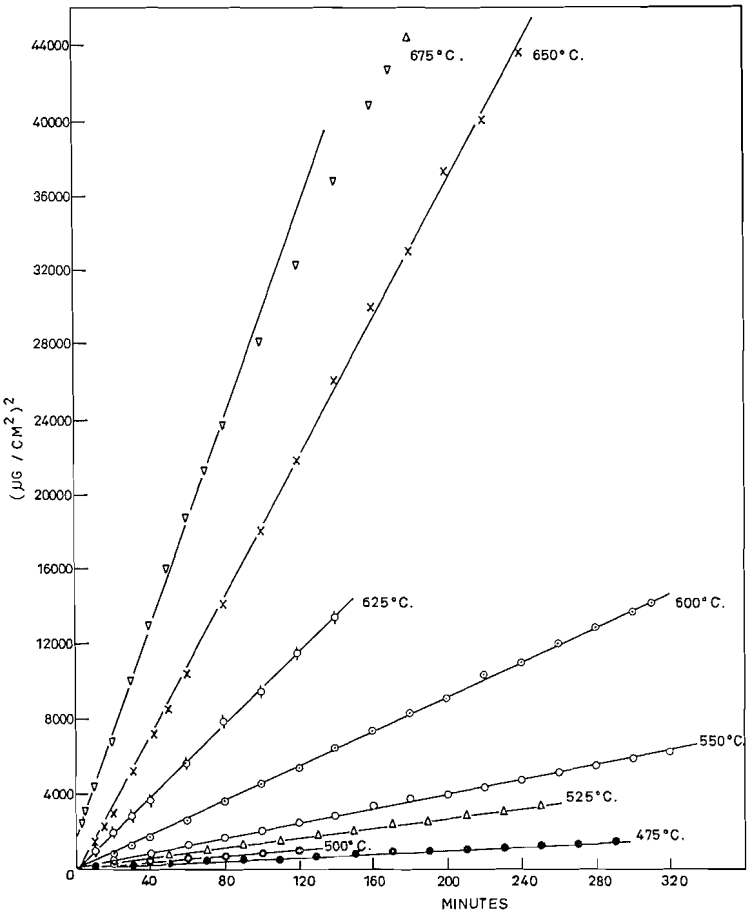

FIG. 3. Parabolic plot of the oxidation of 10/90 In-Ag alloy.

TABLE I

The energies of activation calculated from the slopes of the Arrhenius plots in Fig. 5 for the oxidation of 5, 10, and 15 atom % In-Ag alloys

In-Ag alloy (atom % In)	Activation energy (kcal/mole)
5	23.6
10	23.0, 39.6
15	40.0

observed in the oxidation of 5/95 In-Ag alloy corresponds to internal oxidation. According to Rapp's (7) equation [14], the parabolic constant for internal oxidation is proportional to the product of the oxygen solubility $N_O^{(s)}$ and oxygen diffusivity D_O. Hence,

$$\frac{d[\ln K_p]}{dT} = \frac{d[\ln N_O^{(s)}]}{dT} + \frac{d[\ln D_O]}{dT} = \frac{1}{RT^2}[\Delta H\{\tfrac{1}{2}O_2(g) = O_{(\text{In Ag})}\}] + \frac{\Delta E_{(\text{diff})}}{RT^2}.$$

According to Eichenauer and Muller (10)

$$\Delta H[\tfrac{1}{2}O_2(g) = O_{(\text{In Ag})}] = 11.86 \text{ kcal.}$$
$$\Delta E_{(\text{diff})} = 11.00 \text{ kcal.}$$

Hence,

$$\frac{d \ln K_p}{dT} = \frac{11.86 + 11.00}{RT^2} = \frac{22.86}{RT^2}.$$

The calculated activation energy of 22.86 kcal/$\frac{1}{2}$mole O_2 for the parabolic kinetics is in

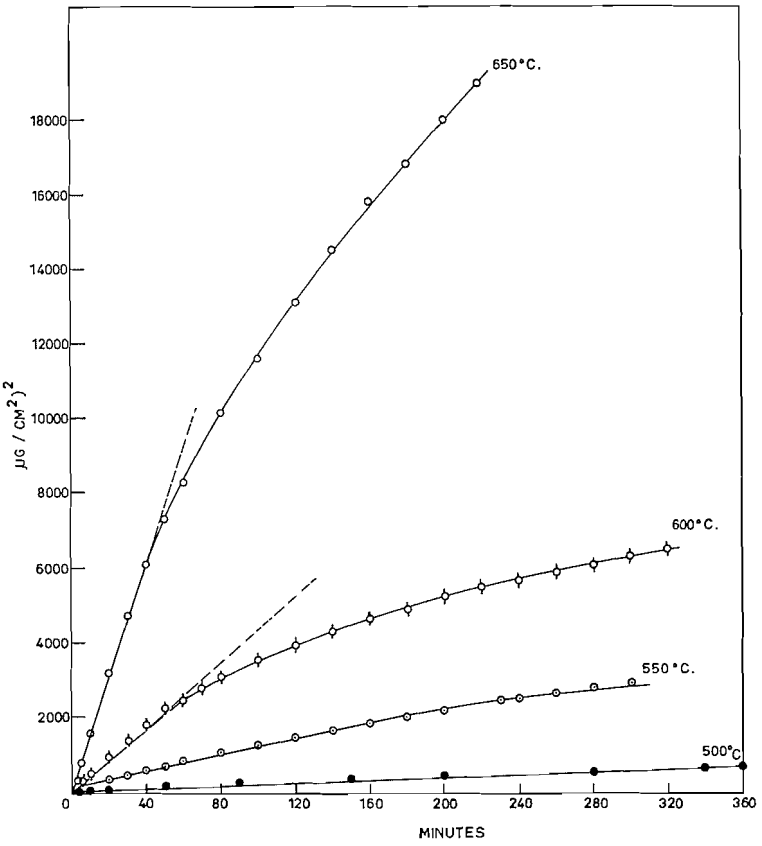

FIG. 4. Parabolic plot of the oxidation of 15/85 In–Ag alloy.

good agreement with the value of 23.6 kcal/mole deduced from the experimental temperature dependence of K_p.

The rate of oxidation of the 15/85 In–Ag alloy has been found to be much lower than that of the 5/95 In–Ag alloy. This is due to the formation of an external oxide layer. The growth of this external scale is controlled by the diffusion of indium ions through it. The oxide was identified as In_2O_3 by electron diffraction.

The energy of activation for the 15/85 In–Ag alloy has been found to be 40.05 kcal/mole and is comparable to the energy of activation of 36.6 kcal/mole reported by Schoen (11) for the diffusion of In through 16.6/93.4 In–Ag alloy. This suggests that the rate-controlling step during the oxidation of 15/85 In–Ag alloy is the diffusion of In through the alloy and not through the oxide as assumed by Rapp (7). An interrupted oxidation of 15/85 In–Ag alloy at 600 °C (described below) supports the above conclusion.

The parabolic law ceases to hold after a certain period of oxidation of the 15/85 In–Ag alloy (Fig. 4). Such a deviation can either be (1) due to the ageing of the oxide layer (12) or (2) due to a decreased diffusion of indium through the oxide on account of the depletion of indium atoms at the alloy/oxide interface. In order to find out which of the two mechanisms is responsible for the deviation, the following experiment was carried out.

A sample of 15/85 In–Ag alloy foil was oxidized at 600 °C and at 76 Torr oxygen pressure for 40 min (the period estimated from the data in Fig. 4), after which the deviation from the parabolic rate law is expected to take place. The oxygen was then replaced by argon at the same pressure. The sample was annealed at the same temperature for 60 min, after which argon was replaced by oxygen and the oxidation reaction continued. The kinetic and the parabolic plots for this experiment (Fig. 6) show that the

Can. J. Chem. Downloaded from www.nrcresearchpress.com by 210.87.254.6 on 09/05/12
For personal use only.

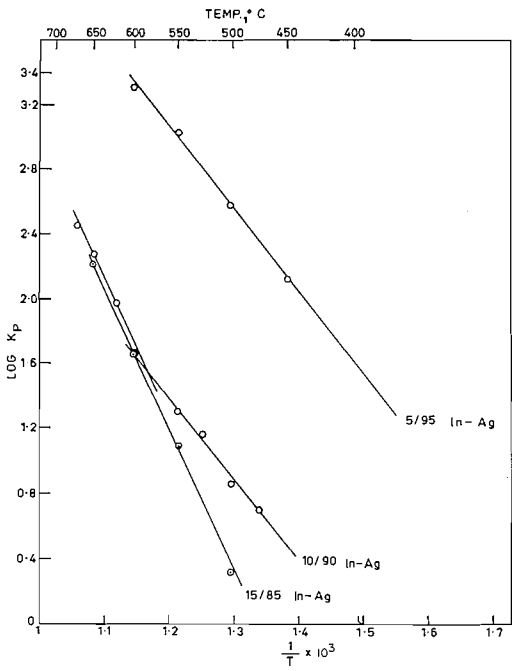

FIG. 5. The variation of logarithm of the parabolic rates of oxidation of 5, 10, and 15 at. % In–Ag alloys as a function of reciprocal of absolute temperature.

interrupted oxidation can still be described by a parabolic rate law in spite of the fact that in a normal conventional run, a deviation from this rate law takes place. This deviation is due to the depletion of the indium atoms at the alloy/oxide interface. In_2O_3 is a *n*-type semiconductor (13) and the growth of In_2O_3 oxide layer may be assumed to take place through the diffusion of interstitial In^{3+} ions through the oxide matrix. If the rate at which the indium atoms are delivered at the alloy/oxide interface is lower than the diffusion rate of indium ions through the oxide, the former step would be rate controlling. If, however, the oxidized sample is annealed in an inert atmosphere, as is done in our interrupted oxidation experiment, the concentration of In in the alloy layer immediately below the alloy/oxide interface would be restored to nearly its original value as a result of the inward diffusion of Ag atoms and the outward diffusion of In atoms during the annealing. This would restore the oxidation kinetics to the parabolic rate law. The oxygen uptake for the first 10 min immediately after the inert gas annealing is higher than the oxygen uptake for the same period immediately preceding the interruption of oxidation as shown in Fig. 6. This observation would immediately rule out the ageing of the oxide film as the cause of the reduction in the oxidation rate of the 15/85 In–Ag alloy at 600 °C (Fig. 4) because ageing of the oxide film would have resulted in a lowering of the oxidation rate. If the oxidation data obtained after the inert gas annealing are plotted according to a parabolic equation by assuming the 100th minute as the zero of the time scale, a parabolic rate constant $k_p = 45$ $\mu g^2/cm^4$ min is obtained. This may be compared with the value of $k_p = 43.5$ $\mu g^2/cm^4$ min during oxidation prior to annealing. Almost equal values of the parabolic rate constants support the conclusions derived earlier.

The energy of activation for the oxidation of 10/90 In–Ag alloy below 600 °C is 23.0 kcal/$\frac{1}{2}$mole and is comparable to the energy of activation of 23.6 kcal/$\frac{1}{2}$mole for the internal oxidation of 5/95 In–Ag alloy (Table I). On the other hand, the energy of activation of 39.6 kcal/mole for the oxidation of this alloy above 600 °C can be attributed to the external oxidation, since it is nearly equal to 40.0 kcal/mole, the activation energy for the external oxidation of 15/85 In–Ag alloy. Hence we conclude that the 10/90 In–Ag alloy oxidizes predominantly internally below 600 °C while it undergoes predominantly external oxidation above 600 °C. In fact, a reduction in the rate of oxidation of 15/85 In–Ag alloy with an increase in the period of oxidation observed at all temperatures (Fig. 4) has also been found in the oxidation rate of 10/90 In–Ag at 675 °C (Fig. 3). This is expected at higher temperatures since the oxide molecules have a higher mobility which facilitates the formation of coarser oxide particles. They obstruct further diffusion of oxygen and hence inhibit internal oxidation. At lower temperatures the oxide molecules are relatively immobile and are dispersed widely as small oxide particles which may not form a barrier to the diffusion of oxygen. This is the cause of the transition from the internal oxidation to the external oxidation of the 10/90 In–Ag alloy at 600 °C. It may be expected that such a transition can also take place in alloys of lower indium contents like the 5/95 In–Ag but only at comparatively higher temperatures.

Photomicrographs of the cross sections of the foils of the three alloys oxidized at 600 °C and 76 Torr oxygen pressure support the above

Can. J. Chem. Downloaded from www.nrcresearchpress.com by 210.87.254.6 on 09/05/12
For personal use only.

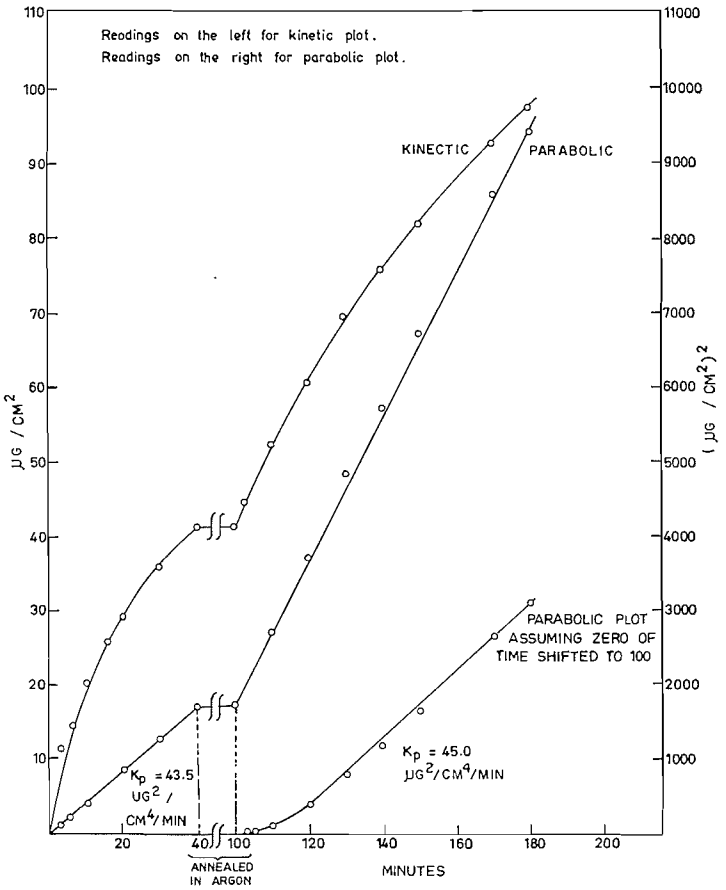

FIG. 6. Oxidation of 15/85 In–Ag alloy at 600 °C and 76 Torr oxygen pressure. The oxidation was interrupted between the 40th and 100th minute by pumping out oxygen from the reaction vessel.

conclusions. Figure 7 shows the two oxidation fronts advancing parallel to the surface of the internally oxidized foil of 5/95 In–Ag alloy. The precipitation of the oxide at the grain boundaries is clearly indicated. Figure 8 shows the cross section of the oxidized 10/90 In–Ag alloy. This alloy oxidizes both internally and externally. Hence, we observe significant precipitation at the grain boundaries, as well as the external oxide scale. The latter is not visible in the photograph due to the uneven rates of dissolution of the alloy and oxide during etching. In contrast to this, Fig. 7 shows no unevenness of the external layer since no external oxide is present. A cross section of the 15/85 In–Ag oxidized foil shown in Fig. 9 indicates that there is no significant precipitation at the grain boundaries and only an external scale is formed, as is evident from the unevenness of the surface.

The process of internal oxidation can be considered to take place in the following three consecutive steps: (*a*) dissociation of oxygen molecules to atoms at the phase boundary, (*b*) dissolution of oxygen atoms in the alloy, and (*c*) diffusion of oxygen atoms in the alloy away from the surface.

If the interface reactions (*a*) and (*b*) are the rate-controlling steps, it is expected that the oxidation would be governed by a linear rate (14). On the other hand, if step (*c*) is rate controlling, we expect the oxidation to be governed by the parabolic rate law. It may be noted that the initial linearity of the oxidation rate for 5/95 In–Ag alloy may be due to the steps (*a*) or (*b*), or both controlling the rate of oxidation. A plot of the logarithm of the linear rate constant versus $1/T$ is a straight line (Fig. 10) and the energy of activation calculated from its slope is

Can. J. Chem. Downloaded from www.nrcresearchpress.com by 210.87.254.6 on 09/05/12
For personal use only.

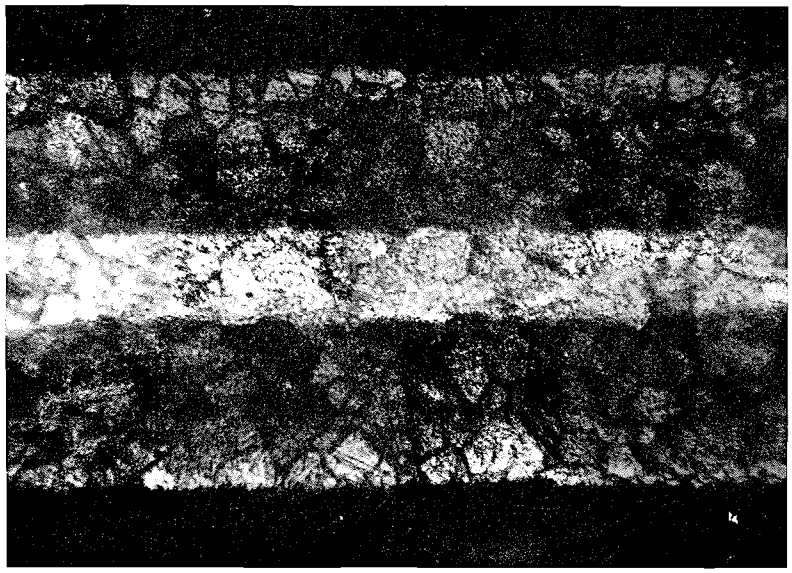

FIG. 7. The cross section of the 5/95 In–Ag alloy foil after oxidation at 600 °C in 76 Torr oxygen pressure for 2 h. The lighter band in the middle is the unoxidized alloy.

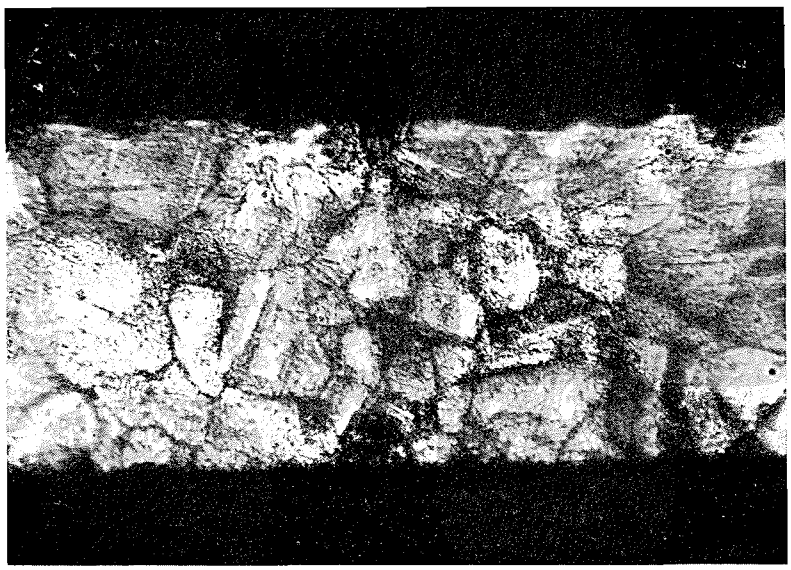

FIG. 8. The cross section of the 10/90 In–Ag alloy after oxidation at 600 °C in 76 Torr oxygen pressure for 4 h.

Can. J. Chem. Downloaded from www.nrcresearchpress.com by 210.87.254.6 on 09/05/12
For personal use only.

FIG. 9. The cross section of 15/85 In–Ag alloy foil after oxidation in 76 Torr oxygen pressure at 600 °C for 4 h. The unevenness of the surface is due to the external oxide layer.

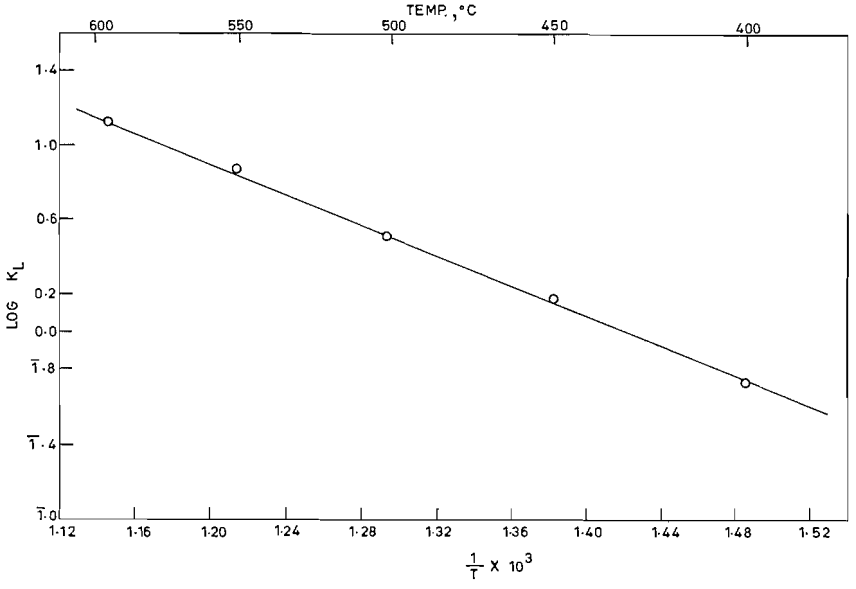

FIG. 10. Variation of the logarithm of linear rate of oxidation of 5/95 In–Ag alloy as a function of the reciprocal of absolute temperature.

Can. J. Chem. Downloaded from www.nrcresearchpress.com by 210.87.254.6 on 09/05/12
For personal use only.

18.5 kcal/½mole O_2. This is very much lower than the energy of activation required for the dissociation of oxygen, viz. 59 kcal/½mole (15), but is of the same order of magnitude as the energy of activation of 11.86 kcal/½mole O_2 found for dissolution of oxygen in pure silver (10). It is therefore suggested that the step (*b*), viz. the dissolution of oxygen atoms at the phase boundary, is the rate-controlling step and responsible for the initial linear oxidation rate of the 5/95 In–Ag alloy. It may, however, be noted that the observed energy of activation of 18.5 kcal/½mole O_2 is for the dissolution of oxygen in the 5/95 In–Ag alloy and hence is likely to be higher than that for pure silver.

1. F. N. RHINES and A. H. GROBE. Trans. Am. Inst. Mining Met. Engrs. **147**, 318 (1942).
2. F. N. RHINES. Trans. Am. Inst. Mining Met. Engrs. **137**, 246 (1940).
3. F. N. RHINES, W. A. JOHNSON, and W. A. ANDERSON. Trans. Am. Inst. Mining Met. Engrs. **147**, 205 (1942).
4. J. L. MEIJERING and M. J. DRUYVESTEYN. Philips Res. Rept. **2**, 81 (1947).
5. I. DIETRICH and L. KOCH. Z. Metallk. **50**, 31 (1959).
6. C. WAGNER. Z. Elektrochem. **63**, 772 (1961).
7. R. A. RAPP. Acta Met. **9**, 730 (1961).
8. R. A. RAPP, D. F. FRANK, and J. V. ARMITAGE. Acta Met. **12**, 508 (1963).
9. R. S. BRADLEY. J. Sci. Instr. **30**, 84 (1953).
10. W. EICHENAUER and G. MULLER. Z. Metallk. **53**, 321 and 700 (1962).
11. A. SCHOEN. Ph.D. Thesis, Physics Department, University of Illinois. 1958.
12. J. L. MEIJERING and M. L. VERHEIJKE. Acta Met. **7**, 331 (1959).
13. O. KUBASCHEWSKI and B. E. HOPKINS. Oxidation of metals and alloys. Butterworth Publications, London. 1962. p. 24.
14. O. KUBASCHEWSKI and B. E. HOPKINS. Oxidation of metals and alloys. Butterworth Publications, London. 1962. p. 110.
15. T. L. COTTRELL. The strength of chemical bonds. Butterworth Scientific Publications, London. 1954.

Can. J. Chem. Downloaded from www.nrcresearchpress.com by 210.87.254.6 on 09/05/12
For personal use only.

Densities and magnetic susceptibilities of thallium amalgams

W. T. FOLEY, REBECCA FAI-YING CHIU, AND JOHN R. DELOREY
Department of Chemistry, St. Francis Xavier University, Antigonish, Nova Scotia

Received October 13, 1967

The densities of solid thallium amalgams were measured pycnometrically at −79.0 °C with the following results in g/ml: 13.946, 13.851, 13.465, 13.379, 13.219, 13.263, 13.267, 13.264, 13.184, 13.180, 13.177, 13.132, 13.063, 13.055 for the concentrations in weight % thallium of 8.72, 11.15, 19.45, 20.40, 21.32, 21.45, 24.58, 29.20, 30.71, 31.29, 32.03, 33.29, 40.54, and 42.99 respectively. The magnetic susceptibilities of the amalgams were measured by the Gouy method over the same concentration range at temperatures from −180 °C to 150 °C. The alloys were diamagnetic and the susceptibilities were compatible with the phase diagram. The densities and the e.m.f. measurements on concentration cells show that the alpha phase at −79 °C extends from 21.35 to 30.7 weight % thallium and at 0 °C the alpha phase extends to 33.75 weight % thallium.

Canadian Journal of Chemistry, 46, 1197 (1968)

Can. J. Chem. Downloaded from www.nrcresearchpress.com by 210.87.254.105 on 09/05/12
For personal use only.

This is a report on the densities of thallium amalgams determined pycnometrically at −79 °C over a concentration range from 0 to 42 weight % thallium. A few densities were determined at 0 °C over the concentration range 29 to 40 weight % thallium. The report also deals with the magnetic susceptibilities of thallium amalgams over a concentration range 0 to 42 weight % thallium and over a temperature range from −180 °C to 150 °C. Taylor (1) has reported that thallium, which has a single unpaired electron, when dissolved in mercury has definite paramagnetism, but not to the extent which one would expect if the thallium atoms were assumed to dissolve in mercury without change. In this work it was found that thallium amalgams are diamagnetic; in the solid state the amalgams are more diamagnetic than mercury, and at 25 °C the liquid amalgams are slightly less diamagnetic than mercury.

Densities of Solid Amalgams

The pycnometer used in the density determinations was a modification of the type proposed by Henglein (2) and it consisted of two Pyrex bulbs joined by capillary tubing which bore engraved calibration marks. The bottom bulb had a volume of 15 ml and the top bulb, which terminated in a standard taper joint, had a volume of 1 ml.

Experimental

The pycnometer was attached to a vacuum line as were also two bulbs, one containing the amalgam and the other containing toluene which had been freed from sulfur-containing compounds by refluxing in the presence of mercuric acetate. The toluene was freed from dissolved oxygen by pumping after it had been cooled to liquid-nitrogen temperature. About 50 g of amalgam were transferred to the pycnometer, which, along with the bulb containing the toluene, was then isolated from the vacuum line. The pycnometer was placed into a Dewar flask containing a mixture of dry ice and acetone and the temperature of this mixture was determined with a platinum resistance thermometer which had been calibrated at the boiling point of oxygen, the freezing point of water, and the melting point of pure zinc. Under oxygen-free conditions, the toluene was added to the pycnometer until the level of the liquid reached the graduation marks on the pycnometer and, after a delay to allow for thermal equilibrium, the volume was recorded. The pycnometer was then transferred to a water bath at 25 °C, the volume of the contents was measured, and finally the weight of the contents was determined. The density of the toluene at 25 °C was also measured. With the use of these data as well as the densities of thallium amalgams at 25 °C (3), the densities of the amalgams at −79.0 °C were calculated. In a similar fashion were determined the densities at 0.0 °C of several amalgams which were solid at 0 °C in the concentration range of interest. The measurement of the density of the 31.29 weight % thallium amalgam was performed after the alloy had been kept at −79 °C for 24 h. Table I contains the results of the measurements at −79.0 °C and at 0.0 °C and the same results are displayed in Fig. 1. The density values are considered to be accurate to ±0.005 g/ml. It was noted that the surface of the solid amalgam at the composition corresponding

FOR ERRATA SEE
..... 19..... P.....

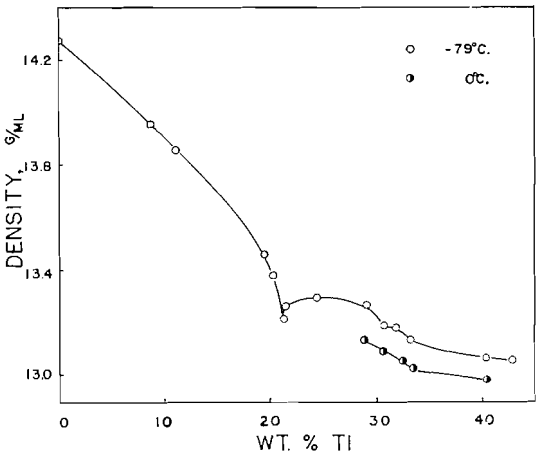

FIG. 1. Densities of solid amalgams at 0 and −79 °C.

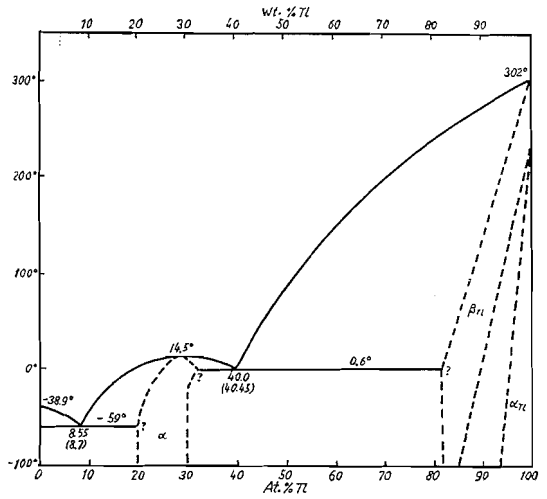

FIG. 2. Mercury–thallium system according to Hansen.

to Tl_2Hg_5 showed to the unaided eye well-defined crystal faces in marked contrast to the surface of the solids whose compositions were slightly different.

The amalgams were prepared and analyzed in a manner already described (4).

TABLE I

Densities of thallium amalgams at −79.0 and 0.0 °C

Wt. % Tl	d^{-79} (g/ml)	Wt. % Tl	d^{-79} (g/ml)	d^{0} (g/ml)
0	14.271	32.03	13.177	
8.72	13.946	33.29	13.132	
11.15	13.851	40.54	13.063	
19.45	13.465	42.99	13.055	
20.40	13.379			
21.32	13.219	28.99		13.131
21.45	13.263	30.87		13.082
24.58	13.267	32.69		13.050
29.20	13.264	33.70		13.020
30.71	13.184	40.54		12.934
31.29	13.180			

Discussion

Figure 1 shows that the density isotherm for −79° is made up of three regions, the first being from 0 to 21.3 weight % thallium, the second between 21.3 and 30.7 weight %, and the third between 30.7 and 43 weight %. A comparison of Fig. 1 with Fig. 2, which shows the phase diagram of the mercury–thallium system according to Hansen (5), enables one to decide that the region between 21.3 and 30.7 weight % thallium belongs to the alpha phase. However, Fig. 1 does not show a maximum at 28.95 weight % thallium, which is the weight % thallium in Tl_2Hg_5. As the thallium content of the alloy increases, there is a steady decrease in density because the density of thallium is about 12% lower than that of mercury. It would be expected that if the densities of the solid were corrected for this steady decrease in value, then the corrected values of the density would reveal the influence of the compound. In Fig. 3 there is plotted against weight % thallium the ratio $(V_1 - V_2)/V_1$, where V_1 is the specific volume of the liquid at 25 °C and V_2 is the specific volume of the solid at −79 °C. This figure clearly reveals a maximum for Tl_2Hg_5.

The density of the 32.03 weight % amalgam at −79 °C does not fall on a smooth plot with the neighboring values. There is no anomaly at this

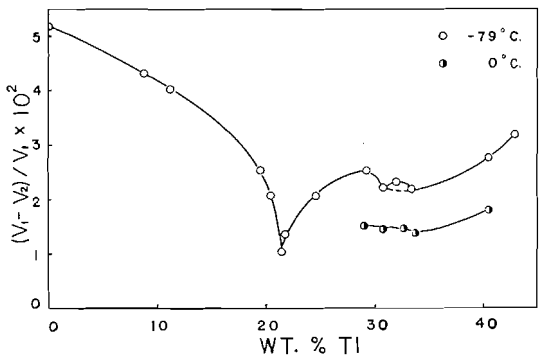

FIG. 3. Relative volume change on solidification.

Can. J. Chem. Downloaded from www.nrcresearchpress.com by 210.87.254.105 on 09/05/12
For personal use only.

Can. J. Chem. Downloaded from www.nrcresearchpress.com by 210.87.254.105 on 09/05/12
For personal use only.

concentration in the plot of the densities measured at 0 °C. In fact, the density curve for 0 °C in Fig. 1 suggests that the alpha phase ends at 33.7 weight % thallium, and also the electromotive force (e.m.f.) measurements described further on in this report substantiate this view. It is believed that the anomalies in the density at 31.29 and at 32.03 weight % thallium at −79 °C are due to the persistence of the alpha phase as a metastable phase. It will later be shown that the magnetic susceptibility data are also anomalous in the same concentration range. In Fig. 3, the dotted line in the graph represents the stable portion of the region and the presumed metastable region is depicted by a solid line in the same concentration range. The concentration cell measurements, described below in this report, indicate that the upper concentration limit of the alpha phase at −79 °C is slightly higher than 30.5 wt. % thallium. On that account, it is considered improbable that the alloy of composition 30.71 wt. % thallium was also metastable.

Magnetic Susceptibility of Thallium Amalgams

Experimental

The magnetic susceptibilities of the samples were determined by the Gouy method and the measurements were made in a nitrogen atmosphere, which has negligible susceptibility. A magnetic shield was incorporated into the design of the apparatus so as to insure that the magnetic field at the outer end of the sample was negligible. The specimen was in the form of a rod of uniform cross section, and the force on the specimen was compared with the force on a sample of mercury of identical dimensions, and at the same field strength. The susceptibility was calculated with the aid of eq. [1].

$$[1] \qquad \chi_a = \chi_s \cdot d_s \cdot F_s / d_a \cdot F_a$$

where χ_a and χ_s are the gram susceptibilities of the alloy and of the mercury, d_a and d_s are the densities, and F_a and F_s are the corrected forces which act on the specimens when the magnetic field is applied.

The magnetic susceptibility measurements were made relative to a solution of nickel chloride as a primary standard and the susceptibility of the nickel chloride was calculated from the equation of Nettleton and Sudgen (6). The nickel chloride solution was prepared from $NiCl_2.6H_2O$ (Fisher Certified), and the nickel content was determined gravimetrically using dimethylglyoxime. Mercury, which was used as a secondary standard, was purified by washing with dilute nitric acid while a stream of air was bubbled through it, and finally the mercury was distilled according to the method of Hulett (7). The feedline of the still-pot was made of capillary tubing and was placed in the gap of a horseshoe magnet which had a field strength of 13 kG. The amalgams were prepared in a manner already described (4).

The magnet used in this study was a Newport 4 in. electromagnet, type A, powered by a type D104 Newport magnet power supply. The balance used to obtain the force on the sample was a Stanton Sm 12 and the cryostat was patterned after the one described by Figgis and Nyholm (8). The Gouy tubes were made from precision-bore glass tubing with an inside diameter of 6 mm. The tubes had flat bottoms and the length of the specimen in the tubes was 12 cm.

The amalgam samples in the loaded Gouy tubes were frozen solid before being introduced into the cryostat and the freezing was performed so that there was little likelihood of the composition varying longitudinally. In general, when an amalgam is frozen the composition of the solid which separates differs from that of the surviving liquid and the differences in density of the two phases could cause stratification. In the Gouy method the force on the sample depends upon the area of the sample, the strength of the magnetic field, and the gradient of the magnetic field. Consequently, a radial variation in the composition would be less objectionable than a vertical variation in composition. The pole pieces of the magnet were adjusted so that the field at the center was uniform over an area as great as the area of the sample. Measurements were made on samples that had been frozen while in the vertical position and measurements also were made on samples that had been frozen in the horizontal position. Results obtained by the former method gave poor agreement with the phase diagram while results obtained by the latter method gave excellent agreement. The procedure for freezing was simple. Attached to the Gouy tube through a standard-taper joint was a capillary tube which was fastened through a right-angled bend to an amalgam reservoir. While the Gouy tube was held horizontally and kept rotating, freezing of

Can. J. Chem. Downloaded from www.nrcresearchpress.com by 210.87.254.105 on 09/05/12
For personal use only.

TABLE II

Mass susceptibilities of solid amalgams in c.g.s. units $\times 10^6$

% Tl	−181 °C	−150 °C	−100 °C	−70 °C	−60 °C	−50 °C	−40 °C	−12 °C	−10 °C	−2 °C	12 °C	14 °C
0	−0.134	−0.117	−0.123	−0.127	−0.141	−0.143	−0.144					
4.04	−0.131	−0.139	−0.139	−0.139	−0.133	−0.133						
8.72	−0.161	−0.160	−0.158	−0.156	−0.157							
22.03	−0.248	−0.239	−0.224	−0.217	−0.214			−0.197				
26.67	−0.217	−0.213	−0.208	−0.204	−0.214				−0.196			
29.12	−0.203	−0.201	−0.199	−0.197	−0.198							−0.197
31.53	−0.201	−0.199	−0.196	−0.196	−0.192						−0.187	
36.00	−0.196	−0.196	−0.195	−0.193	−0.195					−0.186		
42.17	−0.191	−0.189	−0.186	−0.185	−0.184				−0.181			

Can. J. Chem. Downloaded from www.nrcresearchpress.com by 210.87.254.105 on 09/05/12
For personal use only.

the amalgam was initiated by inserting the end of the Gouy tube into a hole drilled in a copper block that was cooled with a mush of dry ice and acetone. As freezing occurred, the tube was slowly pushed further into the block and, when the freezing reached a predetermined level, the excess amalgam was poured off and the Gouy tube was sealed off with a flame. It is not claimed that segregation was entirely prevented but the method seemed to have minimized it considerably. The sample could not be frozen along its entire length at once because such a procedure yielded a solid whose diameter was non-uniform as well as being smaller than the internal diameter of the glass tube.

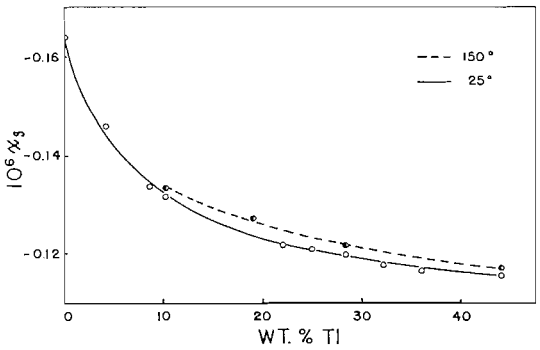

FIG. 4. Isotherms of magnetic susceptibility of liquid thallium amalgams, χ_g, in c.g.s.m. units.

To confirm that the specimens used were free from ferromagnetic impurities, all observations were made at two field strengths.

The results of the susceptibility measurements are given in Table II and Fig. 4. The data of Reuter (9) and of Bates and Baker (10) on the susceptibility of mercury were plotted and a smooth curve was drawn through the points; the result was in quite good agreement with that of this work. The values obtained for the mass susceptibility of mercury in c.g.s. units times 10^6 at 25°, −39°, −100°, and −150 °C by Bates and Baker were −0.167 (−0.165), −0.143 (−0.144), −0.133 (−0.134), and −0.124 (−0.126) respectively. The values obtained in this work are those written in parentheses. The precision of the data is estimated to be 0.6%.

Discussion

A plot of the susceptibility of solid mercury against temperature yields a straight line with a positive slope until the temperature is as low as −152 °C. The absolute value of the susceptibility at −181 °C shows a 6% increase over the value at −152 °C and it does not lie on the straight line: this is in harmony with the work of Bates and Baker. When the data for a concentrated amalgam are plotted against the temperature, the slope is negative. At a composition of 6% thallium by weight, the two opposing tendencies are equal and the susceptibility of the amalgam at this composition is temperature-independent in the solid state.

The relationship between the susceptibility of the solid amalgams and the phase diagram is brought out most clearly by Fig. 5 which shows, as a function of the composition, the values obtained at −70 °C and −150 °C. The straight line relationship obtained for the region between 0 and 22 weight % thallium indicates that, in agreement with the phase diagram, the susceptibility for a given concentration is the sum of (the susceptibility of the mercury times its weight fraction) plus (the susceptibility of the 22% by weight alloy times its weight fraction). Thus at

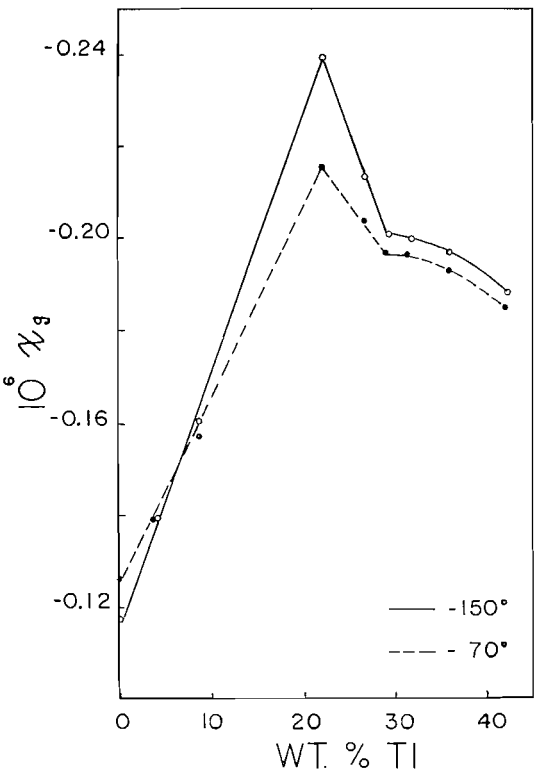

FIG. 5. Isotherms of magnetic susceptibility of solid amalgams, χ_g, in c.g.s.m. units.

Can. J. Chem. Downloaded from www.nrcresearchpress.com by 210.87.254.105 on 09/05/12
For personal use only.

9% thallium by weight, the weight fraction of mercury is 0.59, so that the calculated susceptibility for this concentration at −150 °C is (0.59 × 11.7) + (0.41 × 24.0) = 0.167. Actually, according to the density measurements the alpha phase begins at 21.35 and not 22.03 weight % thallium. It was estimated that the gram susceptibility of the 21.35 weight % alloy would be 0.003 × 10^6 c.g.s. units greater than the value measured for the 22.03% by weight alloy.

The next portion of the susceptibility isotherms shows a straight-line relationship from the beginning of the alpha phase to the composition corresponding to that of Tl_2Hg_5. This doubtless reflects the change in susceptibility as some of the thallium positions in the Tl_2Hg_5 lattice are being replaced by mercury. At the concentration where Tl_2Hg_5 occurs, the slope changes abruptly again until the composition of 30.7 weight % thallium is reached and this composition represents the boundary of the alpha phase at both −150° and −70 °C. One would expect that from the termination of the alpha phase up to 42 weight % thallium there would be a straight-line relationship similar to that which exists between 0 and 21.35 weight % thallium. But the measured values do not lie on a straight line and this may be regarded as evidence to support the view that the 31.53% amalgam contains metastable alpha phase at −150° and −70 °C. By extrapolating the data for 36.00 and 42.17 weight % thallium, one estimates the susceptibility of the 30.70 weight % amalgam at −150 °C and −70 °C to be −0.204 and −0.200 × 10^6 c.g.s. units respectively. Thus, the curve in Fig. 5 is in error at this concentration by only 0.003 × 10^6 c.g.s. units. The anomaly in both the density measurements and in the susceptibility measurements led to a decision to investigate by electrochemical means the equilibria at the thallium-rich boundary of the alpha phase.

Concentration Cell Measurements

Olander (11) studied the phase equilibria in solid thallium amalgams with the aid of a concentration cell over the temperature range −60° to −20 °C. He concluded that the boundary of the alpha phase occurred at 31.5 weight % thallium.

Experimental

An H-type cell was used and the amalgams were introduced in the absence of oxygen. An oxygen-free solution of 1% thallium acetate in 90% alcohol was used as an electrolyte. A two-phase saturated amalgam containing 45% thallium was used in one leg of the H-cell and the amalgam whose composition was within the range of interest in the other leg. Measurements were made with a Leeds and Northrup type K2 potentiometer. Measurements were not made until 12 h had elapsed after the cells had been placed in the constant-temperature bath. The results obtained are shown in Table III.

TABLE III

Voltage of cell (Tl, $Hg)_{two\ phase}$ $TlOCOCH_3$, C_2H_5OH (Tl, $Hg)_\alpha$

	V (mV)	
Wt. % Tl	−79 °C	0 °C
30.5	0.001	11.000
32.0	0.000	2.000
33.3	0.000	0.800
33.5	0.000	0.700
33.7	0.000	0.005

Discussion

If a concentration cell containing the 45 wt. % thallium amalgam at one electrode registers 0 V, this means that the amalgam at the second electrode is in equilibrium with beta-thallium. However, the voltage will not be zero if the second electrode contains the alpha phase. The experimental results suggest that at −79 °C the boundary of the alpha phase has a thallium content between 30.5 and 32.0 wt. % thallium and that at 0 °C the boundary of the alpha phase has a thallium content very slightly greater than 33.7 wt. %. The percent thallium in $TlHg_2$ is 33.75 so that possibly this may be the composition corresponding to the boundary of the alpha phase. It appears that, under the experimental conditions employed in both the density and the magnetic susceptibility measurements, at an amalgam composition close to 31.5% thallium by weight and at a temperature of −79 °C, the alpha phase remained as an unstable phase.

Acknowledgment

Grateful acknowledgment is made by W. T. F. of the grant in aid of research from the National Research Council of Canada.

1. N. W. TAYLOR. J. Am. Chem. Soc. **48**, 854 (1926).
2. F. A. HENGLEIN. Z. Physik. Chem. Leipzig, **115**, 91 (1925).
3. W. T. FOLEY, A. K. BASAK, and J. R. DELOREY. Can. J. Chem. **42**, 2749 (1964).
4. W. T. FOLEY and K. O'SULLIVAN. Can. J. Chem. **45**, 855 (1967).
5. M. HANSEN. Constitution of binary alloys. 2nd ed. McGraw-Hill Book Co., New York. 1958. p. 843.
6. H. NETTLETON and S. SUDGEN. Proc. Roy. Soc. London, Ser. A, **173**, 313 (1939).
7. G. A. HULETT. Phys. Rev. **33**, 307 (1911).
8. B. N. FIGGIS and R. S. NYHOLM. J. Chem. Soc. 331 (1959).
9. K. REUTER. Diplomarbeit, Philipps-Universität, Marburg, West Germany. 1957.
10. L. F. BATES and C. J. W. BAKER. Proc. Phys. Soc. London, **49**, 611 (1938).
11. A. OLANDER. Z. Physik. Chem. Leipzig, A**171**, 425 (1934).

Can. J. Chem. Downloaded from www.nrcresearchpress.com by 210.87.254.105 on 09/05/12
For personal use only.

Can. J. Chem. Downloaded from www.nrcresearchpress.com by 210.87.254.40 on 09/05/12
For personal use only.

Nonempirical s.c.f. calculations on sulfur atom, hydrogen sulfide, and dihydrogen sulfoxide

A. RAUK
Department of Chemistry, Queen's University, Kingston, Ontario

AND

I. G. CSIZMADIA
Lash Miller Chemical Laboratories, Department of Chemistry, University of Toronto, Toronto, Ontario

Received October 11, 1967

This paper reports the first attempt to use Gaussian basis sets in nonempirical self-consistent field (s.c.f.) calculations on sulfur-containing chemical systems. Exponents for Gaussian-type functions (G.t.f.) on S atom are given for the minimal basis set. The optimization procedure is described and the optimized exponents utilized on calculations on S atom, H_2S, and the hypothetical dihydrogen sulfoxide (H_2SO). Calculations by the minimal basis set of G.t.f., using these exponents, gave a value for the HSH angle of H_2S that agrees well with the experimentally determined value. Calculations of H_2SO support a "multiple bond" picture of the S—O bond.

Canadian Journal of Chemistry, 46, 1205 (1968)

Introduction

Ab initio calculations on atoms and small molecules are well established in the chemical literature (1). Accurate results have been obtained using exponential-type functions (e.t.f.) or, as usually referred to, Slater-type orbitals (S.t.o.) as basis functions in the s.c.f. procedure. Satisfactory results have also been obtained using Gaussian-type functions (G.t.f.) or, as sometimes called, Gaussian-type orbitals (G.t.o.), when the basis set size is approximately 2 to 3 times as large as the equivalent basis set of e.t.f. (2). Methane, as a classical example, may be quoted for comparison of the numerical results obtained from e.t.f. and G.t.f. basis sets (3–8). These results are shown in Table I. A compendium of *ab initio* calculations covering the period of 1960–67 which includes results of both e.t.f. and G.t.f. calculations has been prepared (9).

TABLE I

Comparison of *ab initio* m.o.-s.c.f. calculations on methane by G.t.f. and e.t.f. basis sets

Basis	C—H (bohr)	Energy (E)* (hartree)	Reference
9 e.t.f.	2.0000	−39.86	3
9 e.t.f.	2.0000	−40.12568	4
9 e.t.f.	2.0500	−40.12822	4
9 e.t.f.	2.1000	−40.12698	4
27 e.t.f.	2.0665	−40.1804	5
29 G.t.f.	2.0500	−40.0612	6
33 G.t.f.	2.0665	−40.1668	7
52 G.t.f.	2.0530	−40.172	6
52 G.t.f.	2.1200	−40.1983	8

*Hartree–Fock energy = −40.217. Experimental energy = −40.519.

Because it is possible to compute integrals over a basis of G.t.f. about 1000 times faster than over e.t.f., it appears advantageous to use the former, especially when the number of electrons in the problem becomes large. Even with this device it may still be necessary to employ a basis set that is less than adequate for quantitative purposes.

Our primary interest is in the sulfinyl grouping (10). Because even the simplest sulfoxide, H_2SO (**1**), represents a 26-electron problem containing four atoms, it was clear at the outset that a minimal basis set of G.t.f. had to be utilized. Exponents for the S atom were unknown because no S-containing compounds had been previously treated with G.t.f. It was necessary therefore to obtain first an optimal set of exponents for s-type and p-type functions from open shell s.c.f. calculations on S atom in its electronic ground (^3P) state and the exponent for d-type functions from closed shell s.c.f. calculations on H_2S. This paper reports these results. To complete this preliminary study we have also performed closed shell s.c.f. calculations on **1**.

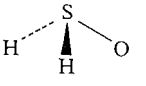

1

The mathematical formalism for the open and closed shell s.c.f. as well as other calculations (dipole moment, population analysis, and electron density contour plots) have been reviewed recently (11) in detail. Consequently only the

Can. J. Chem. Downloaded from www.nrcresearchpress.com by 210.87.254.40 on 09/05/12
For personal use only.

results obtained from computations on S, H_2S, and H_2SO are given in this paper. The computations have been carried out on an IBM 7094-II computer using the Polyatom system (11).

Optimization of spd Exponents (α) of S Atom

The minimal basis set for sulfur consisted of five s-type (5^s) functions, two sets of p-type (2^p) functions, and a set of d-type (1^d) functions. Full optimization of the s-type exponents would have involved five independent nonlinear variables and was not attempted. Rather, the exponents were restricted to a geometric series in the manner described previously (11). This restriction had the advantage of reducing the number of independent variables to two, the "center exponent" and the "ratio of exponents". The effect was not expected to be severe (12) since the exponents for neon (13) and nitrogen (14) were previously optimized for minimal and higher basis sets with the same restriction. The exponents for all of the second row elements had been obtained from neon and nitrogen by a scaling procedure (11, 15) and satisfactory results achieved (16–24). Optimization was performed by varying the s-type exponents systematically until a set was obtained that yielded a minimum energy for the open shell ^3P ground state of sulfur atom.

Since only two p-type exponents were needed, these were varied independently and a paraboloid surface was used to obtain the optimum values. The procedure was iterated for the s- and p-type exponents until three significant figure accuracy was obtained. This involved a triple optimization for the s-type and a double optimization for the p-type G.t.f.

TABLE II

Exponents (α) of G.t.f. for neon and sulfur

Function type	Neon	Sulfur	
		Scaled from neon	Optimized for energy
s	0.922	2.488	0.5581
	4.68	12.63	3.151
	23.8	64.23	17.79
	121.0	326.5	100.44
	613.0	1654.3	567.05
p	0.817	2.272	0.375
	4.80	13.33	6.332
d	—	—	5.42

Minimal basis set calculations on hydrogen sulfide were used to optimize the d-exponent of sulfur (a definition of d-G.t.f. is given in Appendix 1). The results are summarized in the last column of Table II.

In order to have a set of initial orbital exponents for the detailed optimization, the s and p orbital exponents for Ne (9, 11) were scaled according to eqs. [65] and [66] of ref. 11.[1] These values are shown in the third column of Table II. A comparison between the scaled and optimized exponents given side by side in Table I reveals that the scaling procedure from Ne to S, or probably in more general terms, from second to third row elements, is not a successful policy.

TABLE III

Orbital energies of sulfur atom

	Energy (hartree)	Identification	Occupancy
Total	−378.22026	$1s^2 2s^2 2p^6 3s^2 3p^4$	16
	−90.7954	1s	2
	−7.7100	2s	2
	−3.5524	$2p_x$	2
	−3.5524	$2p_y$	2
	−3.5524	$2p_z$	2
s.c.f.–a.o.	0.2100	3s	2
	0.3772	$3p_x$	4/3
	0.3772	$3p_y$	4/3
	0.3772	$3p_z$	4/3
	43.6340	4s	0
	687.5056	5s	0

Results for Sulfur Atom

The atomic orbital energies for sulfur in its ^3P state, using the optimized exponents, are shown in Fig. 1. Numerical values for the orbital energies are given in Table III. Because of the necessity of accommodating 16 electrons in 11 atomic orbitals in an open-shell calculation, only two orbitals are unoccupied, and it is not surprising that some of the occupied orbitals have positive energy. This behavior is characteristic of the inflexibility of the minimal basis set (12). In the atomic calculations, d-type functions were not included because the 3d atomic orbitals are empty in the ground electronic configuration (^3P) of S atom.

[1]It should be noted that eq. [65] of ref. 11 carries a printing error and, in its correct form, both terms must be squared.

Can. J. Chem. Downloaded from www.nrcresearchpress.com by 210.87.254.40 on 09/05/12
For personal use only.

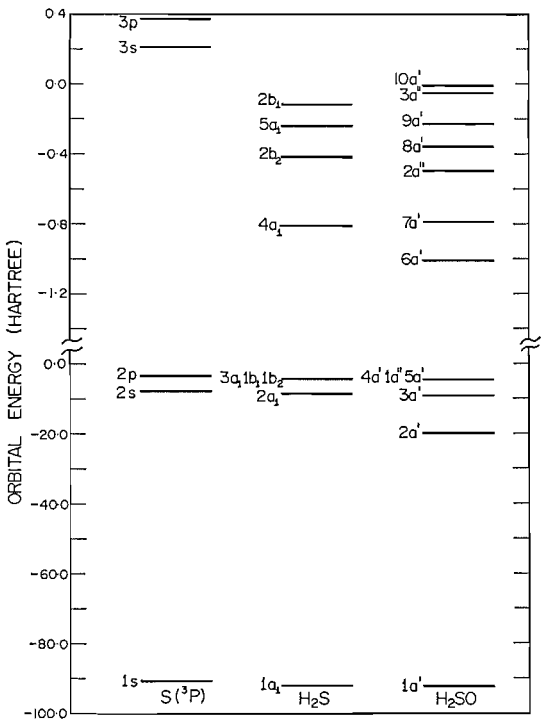

FIG. 1. Orbital energies for sulfur, hydrogen sulfide, and dihydrogen sulfoxide.

Figure 2 shows the radial electron density of sulfur atom as calculated from Hartree–Fock atomic orbitals (25, 26) and from self-consistent field atomic orbitals obtained by expansion in terms of the optimized basis set of G.t.f. The difference between the two radial electron densities is a result of the minimal G.t.f. basis set, but it is evident that the radial electron density distribution has been reproduced reasonably well.

Results for Hydrogen Sulfide

The minimal basis set size for hydrogen sulfide was 19 and consisted of sulfur $5^s\,2^p\,1^d$ and hydrogen 1^s ($\alpha = 0.283$ (15)). The experimentally determined geometry (27) of H_2S was used (HSH = 92.25°; S—H = 2.5228 bohr (1.335 Å)). The molecular orbital energies are listed in Table IV and shown graphically in Fig. 1. Table IV also lists the molecular orbital energies for H_2S without d-G.t.f. on sulfur. It is apparent that the two lowest-lying molecular orbitals benefit most from the inclusion of d-G.t.f. (cf. Appendices).

Figure 3 shows the electron density contour diagrams for the nine occupied orbitals as well as the total electron density contours for H_2S. In every case, the innermost contour represents a density of 1 electron per cubic bohr and the remaining contours decrease by powers of 10.

TABLE IV

Occupied molecular orbitals of H_2S

		Energy (hartree) s,p basis	Energy (hartree) s,p,d basis	Symmetry type
Total*		−379.63700	−381.03894	C_{2v}
	1	−91.8573	−92.0230	$1a_1$
	2	−8.6451	−8.8504	$2a_1$
	3	−4.5198	−4.4283	$3a_1$
	4	−4.5189	−4.4266	$1b_1$
s.c.f.–m.o.	5	−4.5160	−4.4247	$1b_2$
	6	−0.7968	−0.8099	$4a_1$
	7	−0.4223	−0.4173	$2b_1$
	8	−0.2319	−0.2418	$5a_1$
	9	−0.1247	−0.1196	$2b_2$

*The experimental energy of H_2S is estimated (28) to be −400.81 hartree.

The dipole moment of H_2S was calculated to be 1.75 D. The experimental dipole moment (29) is 0.98 D. Details of the electron population analysis are shown in Table V.

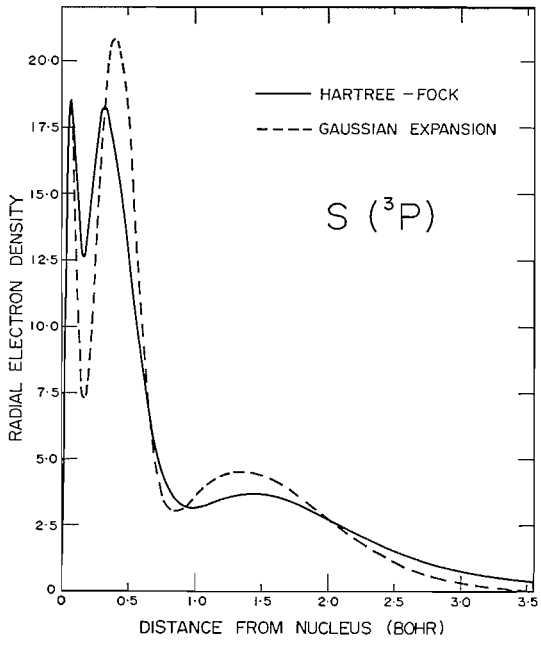

FIG. 2. Radial electron density of sulfur atom.

Can. J. Chem. Downloaded from www.nrcresearchpress.com by 210.87.254.40 on 09/05/12
For personal use only.

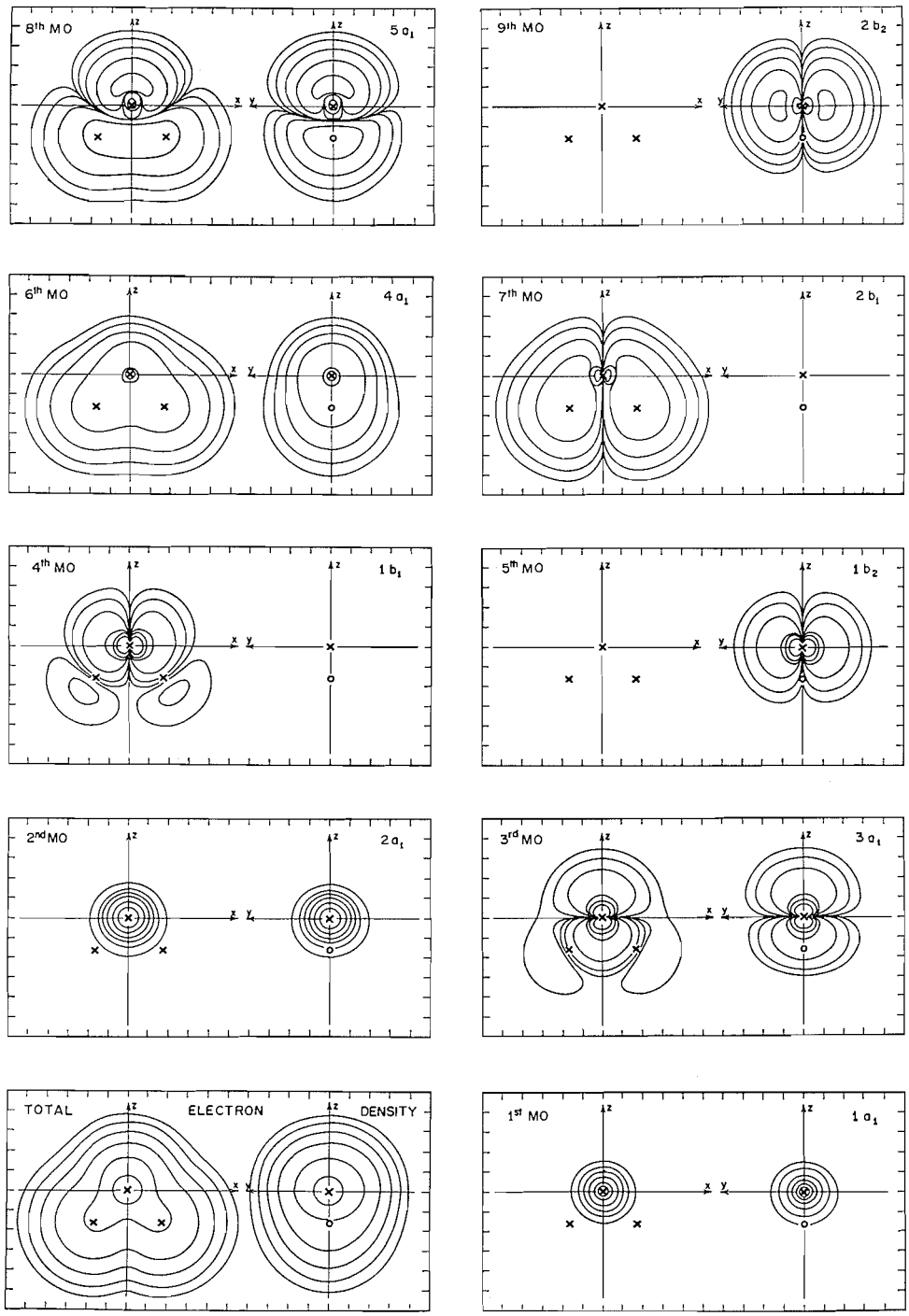

FIG. 3. Electron density contours for hydrogen sulfide.

Can. J. Chem. Downloaded from www.nrcresearchpress.com by 210.87.254.40 on 09/05/12
For personal use only.

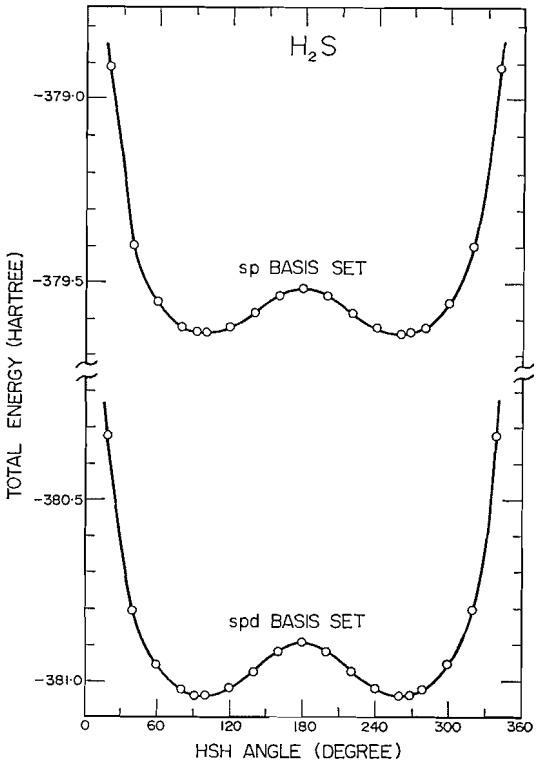

FIG. 4. Variation of total energy of hydrogen sulfide as a function of the HSH angle.

The results of a conformational study in which the HSH angle was varied, keeping the S—H bond length fixed at 2.5228 bohr, are shown in Table VI. The results are graphically presented in Fig. 4. Inclusion of d-type functions leads to a slightly better prediction for the equilibrium HSH angle (98.8°) than does the calculation without d-type functions (99.9°).[2] With d-type functions, the energy barrier in passing through the linear molecule is somewhat higher (0.1475 hartree, 92.3 kcal/mole) than that calculated without the inclusion of d-type functions (0.1212 hartree, 76.0 kcal/mole).[3] There is qualitatively good agreement between the experimentally determined HSH angle and that calculated using the minimal basis set for sulfur.

[2]These values were obtained by fitting parabolas to three points near the minimum.

[3]The inclusion of carbon d-G.t.f. in the basis set of CH_3^- increased the inversion barrier height from 1.16 kcal/mole to 2.94 kcal/mole for a fixed C—H bond length (1.95 bohr) (30).

TABLE V

Electron population analysis of H_2S

Quantity		s,p basis	s,p,d basis
Net charges	Sulfur	0.6462	0.9110
	Hydrogen	−0.3231	−0.4555
Overlap population	S—H bond	0.5276	0.4853

TABLE VI

Variation of HSH angle (θ) of H_2S (H—S bond length = 2.5228 bohr)

θ (deg)	Energy (hartree) sp basis set	spd basis set
180	−379.5183	−380.8930
160	−379.5379	−380.9212
140	−379.5827	−380.9765
120	−379.6223	−381.0208
100	−379.6395	−381.0404
92.25	−379.6370	−381.0390
80	−379.6210	−381.0237
60	−379.5509	−380.9554
40	−379.3981	−380.8043
20	−378.9152	−380.3229

Results for Dihydrogen Sulfoxide (1)

The minimal basis set of G.t.f. for **1** consisted of the same G.t.f. used in the case of H_2S as well as 3^s ($\alpha = 1.20; 9.45; 74.7$) and 1^p ($\alpha = 0.749$) on oxygen. The total basis set size was 25. The geometrical parameters were chosen to be those experimentally determined (27) for dimethyl sulfoxide (HSO = 107°; HSH = 100°; S—O = 2.779 bohr (1.47 Å); S—H = 2.5117 bohr (1.329 Å)[4]).

Table VII gives the energies of the occupied molecular orbitals. The same information is displayed graphically in Fig. 1.

The dipole moment of **1** was calculated to be 2.36 D. The results of the electron population analysis yielding the net charges are given in Table VIII. It is apparent from Table VIII that the S—H bond of **1** is essentially ionic in character. The high net charge on hydrogen and the lower net charge on oxygen reflect the inability of the minimal basis set to represent adequately the electronegativities of the atoms. A similar deviation of the calculated dipole moment vector

[4]The value 1.329 Å is the S—H bond length in mercaptans.

Can. J. Chem. Downloaded from www.nrcresearchpress.com by 210.87.254.40 on 09/05/12
For personal use only.

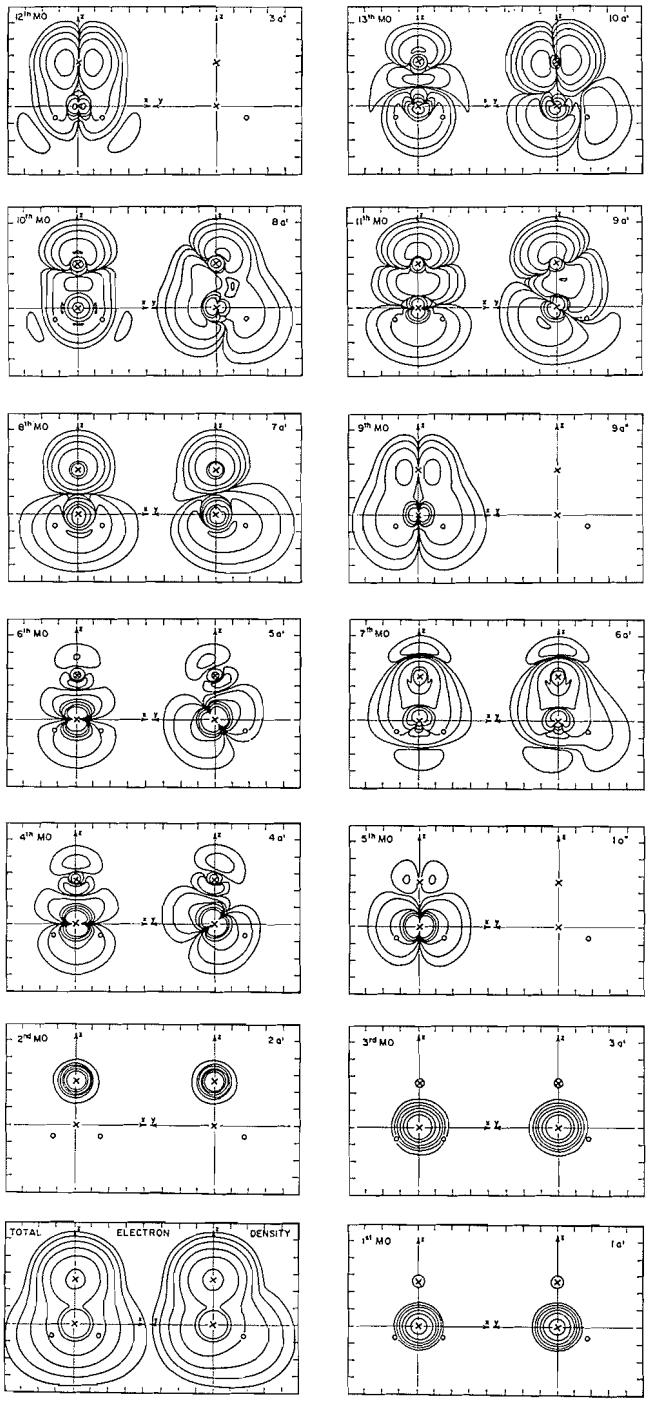

FIG. 5. Electron density contours for dihydrogen sulfoxide.

Can. J. Chem. Downloaded from www.nrcresearchpress.com by 210.87.254.40 on 09/05/12
For personal use only.

TABLE VII

Occupied molecular orbitals for H_2SO (1)

	Energy (hartree)	Symmetry type
Total	−451.11639	C_s
1	−92.2348	$1a'$
2	−19.9258	$2a'$
3	−9.0370	$3a'$
4	−4.6219	$4a'$
5	−4.6211	$1a''$
6	−4.6129	$5a'$
s.c.f.-m.o. 7	−1.0999	$6a'$
8	−0.7893	$7a'$
9	−0.4988	$2a''$
10	−0.3684	$8a'$
11	−0.2309	$9a'$
12	−0.0528	$3a''$
13	−0.0087	$10a'$

from the experimental direction was found previously (24, 31) when a minimal basis set was used. Improvement of the basis set led to proper values of the net charges as well as accurate dipole moments. Significantly, in these examples (24, 31) even the minimal basis set provided an adequate representation of the molecular geometry.

Inspection of the coefficient matrix of **1** revealed that the principal contributions of the d-G.t.f. are to two of the lowest-lying molecular orbitals. These are essentially the sulfur core 1s and 2s orbitals (cf. Appendix 1) and are of no chemical interest. The d-orbitals were found to be unimportant in the higher occupied molecular orbitals. They do become important in the highest antibonding molecular orbitals. The two highest occupied molecular orbitals can be identified as the oxygen lone pairs; the nearest facsimile of the classical lone pair on sulfur is orbital number 10 (Fig. 5).

TABLE VIII

Electron population analysis of H_2SO (1)

Quantity	s,p,d basis	
Net charges	Sulfur	1.1707
	Oxygen	−0.1294
	Hydrogen	−0.5206
Overlap population	S—O bond	0.8600
	S—H bond	0.1509

Orbitals 7, 10, 11, and 12 (Fig. 5) each show some S–O overlap. This is consistent with multiple bonding between sulfur and oxygen (32) as is the relatively high S–O overlap population (Table VIII). Computation (utilizing the optimized exponents presented in this paper) on H—SO—CH_3 and H—SO—$\ddot{C}H_2^{(-)}$ has been communicated recently (33). The full paper describing the above species as well as results on dimethyl sulfoxide and its anion will be published shortly (34).

Acknowledgments

We should like to thank Professor S. Wolfe for many helpful discussions as well as comments and criticism in the course of the research and during the preparation of the manuscript. The continuous financial support of the National Research Council of Canada is gratefully acknowledged. The authors wish to express their appreciation to the Institute of Computer Science of the University of Toronto for making their computer facilities available for this work.

One of us (A. R.) would like to thank Professor D. J. LeRoy for his hospitality in his department at the University of Toronto during the academic year 1966–1967. His (A. R.) thanks are also due to Mr. S. A. Houlden, Mr. M. A. Robb, and Mr. R. E. Kari for valuable advice as well as Miss N. K. Holbrook for technical assistance. A studentship granted to A. R. by the National Research Council of Canada for the period 1966–1967 is gratefully acknowledged.

Appendix 1

Gaussian type functions may be defined in a number of different ways (see for example eqs. [18], [62], and [63] of ref. 11). However, according to Boys' original suggestion (35) unnormalized G.t.f. are defined as

$$\eta = x^{a_1}y^{a_2}z^{a_3}e^{-\alpha r^2}$$

or linear combinations of such functions. Consequently s-, p-, and d-G.t.f. are obtained with the following conditions.

$$\text{s-type:}\quad a_1 + a_2 + a_3 = 0$$

$$\text{p-type:}\quad a_1 + a_2 + a_3 = 1$$

$$\text{d-type:}\quad a_1 + a_2 + a_3 = 2$$

This procedure leads to a single s-type function, three p-type functions, and six d-type functions. The latter can be represented by factors x^2, y^2, z^2, xy, xz, and yz in front of the $e^{-\alpha r^2}$ (Fig. 6).

Can. J. Chem. Downloaded from www.nrcresearchpress.com by 210.87.254.40 on 09/05/12
For personal use only.

Linear combination of those three d-type functions which include the squares of x, y, and z yields a spherically symmetric function since $r^2 = x^2 + y^2 + z^2$:

$$x^2e^{-\alpha r^2} + y^2e^{-\alpha r^2} + z^2e^{-\alpha r^2} = (x^2 + y^2 + z^2)e^{-\alpha r^2} = r^2e^{-\alpha r^2}.$$

Due to its spherical symmetry $r^2e^{-\alpha r^2}$ is also an s-type function (analogous to 3s e.t.f.). This is in agreement with the definition of G.t.f. (p. 197 of ref. 11) which makes them analogous to e.t.f. (eq. [12] of ref. 11):

$$\eta_{e.t.f.} = N_{e.t.f.}r^{n-1}e^{\alpha r}\, S_{l,m}(\vartheta,\varphi)$$

$$\eta_{G.t.f.} = N_{G.t.f.}r^{2(n-1)}e^{-\alpha r^2}\, S_{l,m}(\vartheta,\varphi).$$

Whenever the normalized spherical harmonic $S_{l,m}(\vartheta,\varphi)$ is equal to $\frac{1}{2}\sqrt{\pi}$ (i.e. $l = m = 0$), the function η is, by definition, an s-type function. Consequently the admixture of dx^2-, dy^2-, and dz^2-G.t.f. into the formation of atomic cores is not only not surprising but, in fact, essential. It is worth noting that Krauss in his methane calculations (7) used G.t.f. of the form $r^2e^{-\alpha r^2}$ to represent the carbon atom.

TABLE IX

Orbital energies of sulfide ion with minimal sp and spd basis sets

s.c.f.–a.o.	Degeneracy	Orbital energies (hartree) sp basis	spd basis
1s	1	−89.8255	−89.9717
2s	1	−6.8505	−7.0353
2p	3	−2.7261	−2.7261
3s	1	+0.7607	+0.7387
3p	3	+1.0450	+1.0569
3d	5	—	+10.3191
4s	1	+45.7326	+21.9126
5s	1	+689.6740	+92.2843
6s	1	—	+726.2621

In order to illustrate this point with an example, closed-shell s.c.f. calculations were carried out on the spherically symmetrical sulfide ion (S^{2-}). The orbital energies obtained with the sp and spd basis sets are summarized in Table IX. It is clear that a $5^s + 2^p$ basis set gave five s-type and two sets of p-type self-consistent field atomic orbitals (s.c.f.–a.o.); however, a $5^s + 2^p + 1^d$ basis set gave six s-type, two sets of p-type, and one set of d-type s.c.f.–a.o. It can be seen from the coefficient matrix that the d_{xy}-, d_{xz}-, and d_{yz}-G.t.f. are equivalent to 3d-s.c.f.–a.o.;

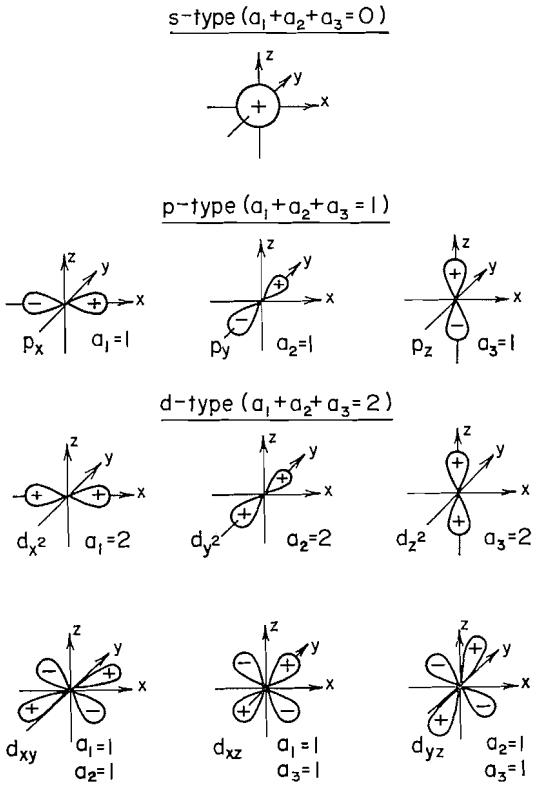

FIG. 6. Pictorial representation of the most frequently used G.t.f. of the type $x^{a_1}y^{a_2}z^{a_3}e^{-\alpha r^2}$.

however, from the d_{x^2}-, d_{y^2}-, and d_{z^2}-G.t.f. one linear combination yields an s-type s.c.f.–a.o. (i.e. $x^2 + y^2 + z^2$), as discussed above, while the remaining two linear combinations give rise to the $3d_{x^2-y^2}$ (i.e. $x^2 - y^2$) and $3d_{3z^2-r^2}$ (i.e. $3z^2 - (x^2 + y^2 + z^2) = 2z^2 - x^2 - y^2$) s.c.f.–a.o.

Appendix 2

It is possible to argue that no conclusion can be made on the basis of this work concerning the importance of d-functions in bonding since the optimized d-exponent was too large, causing the function to possess its maximum value too close to the sulfur nucleus. Setting the first derivative of say d_{z^2} equal to zero, one obtains a relationship between α and Z_{max} (the position where d_{z^2} achieves maximum value):

$$\alpha = \frac{1}{Z^2_{max}} \text{ or } Z_{max} = (1/\alpha)^{1/2}.$$

The optimized α was 5.42 which gave Z_{max} = 0.43 bohr. Remembering that S—H = 2.5228

TABLE X

Characteristics of s.c.f.–m.o. results on H_2S with a basis set of $5^s + 2^p + 2^d$ G.t.f. on the sulfur atom

Occupied s.c.f.–m.o.	Symmetry type	Orbital energy	l.c.a.o. coefficients of d-G.t.f.*					
			x^2	y^2	z^2	xy	xz	yz
1	$1a_1$	−93.3473	−0.005	−0.004	−0.005	—	—	—
			+0.219	+0.219	+0.219	—	—	—
2	$2a_1$	−9.0876	−0.000	−0.001	−0.000	—	—	—
			−0.285	−0.287	−0.285	—	—	—
3†	$1b_1$	−4.6891	—	—	—	—	−0.081	—
			—	—	—	—	−0.001	—
4†	$3a_1$	−4.6880	−0.069	+0.002	−0.065	—	—	—
			−0.001	−0.001	−0.004	—	—	—
5	$1b_2$	−4.6690	—	—	—	—	—	−0.001
			—	—	—	—	—	−0.001
6	$4a_1$	−0.9493	−0.200	−0.162	−0.200	—	—	—
			−0.077	−0.074	−0.077	—	—	—
7	$2b_1$	−0.4554	—	—	—	—	−0.029	—
			—	—	—	—	−0.007	—
8	$5a_1$	−0.3867	+0.243	+0.190	+0.215	—	—	—
			+0.026	+0.030	+0.026	—	—	—
9	$2b_2$	−0.2102	—	—	—	—	—	+0.038
			—	—	—	—	—	+0.001

*The first row of coefficients corresponds to d-G.t.f. of $\alpha = 0.25$ while the second row of coefficients corresponds to d-G.t.f. of $\alpha = 5.42$.
†Note that orbitals $1b_1$ and $3a_1$ are interchanged on the orbital energy scale with respect to the order reported in Table IV. This is not surprising, however, since both $3a_1$ and $1b_1$ m.o. can be looked upon as distorted 2p-a.o. of sulfur.

and S—O = 2.779 bohr it is likely that the maximum electron density of a sulfur-participating bond will be in the neighborhood of 2 bohrs away from the sulfur atom. This distance demands an exponent of 0.25. In order to see whether d-functions are necessary to describe bonding, a calculation was carried out on H_2S at the equilibrium bond angle (92.25°) with a basis set ($5^s + 2^p + 2^d$) consisting of 23 G.t.f. on the sulfur atom. The two sets of d-G.t.f. had exponents of 5.42 and 0.25. The l.c.a.o. coefficients are summarized in Table X.

Because the molecule is not spherically symmetric the x^2-, y^2-, and z^2-G.t.f. do not show identical exponents as they did in sulfide ion (Appendix 1) to form the 1s, 2s, and 3s s.c.f.–a.o. Nevertheless their coefficients in the molecular orbitals of a_1 symmetry type are close enough to each other to justify the conclusion that they participate as a distorted $x^2 + y^2 + z^2$ function (cf. Appendix 1). As might have been expected, d-G.t.f. with the larger exponent contribute to the two lowest symmetric m.o. (i.e. $1a_1$ and $2a_1$) while d-G.t.f. with the smaller exponent contribute to the two highest occupied symmetric m.o. (i.e. $4a_1$ and $5a_1$); however, these contributions are all of the s-type (i.e. $x^2 + y^2 + z^2$). Coefficients of xz and yz d-G.t.f. in the b_1 and b_2 m.o. are still negligible (cf. Table X) implying no appreciable participation of d-orbitals in bonding.

Because the s,p-basis set of the sulfur atom was small ($5^s + 2^p$) it is natural that the d-G.t.f. is overemphasized. A near Hartree–Fock s,p-basis set (say $20^s + 12^p$) would most likely reduce even the present small contribution of xz and yz functions.

1. L. C. Allen and G. M. Karo. Rev. Mod. Phys. **32**, 275 (1960).
2. S. Huzinaga. J. Chem. Phys. **42**, 1293 (1965).
3. J. J. Sinai. J. Chem. Phys. **39**, 1575 (1963).
4. R. M. Pitzer. J. Chem. Phys. **46**, 4871 (1967).
5. B. J. Woznick. J. Chem. Phys. **40**, 2860 (1964).
6. R. Janoschek, G. Diercksen, and H. Preuss. Intern. J. Quantum Chem. **1**, 373 (1967).
7. M. Krauss. J. Chem. Phys. **38**, 564 (1963).
8. C. D. Ritchie and H. F. King. J. Chem. Phys. **47**, 564 (1967).
9. M. Krauss. Compendium of *ab initio* calculations of molecular energies and properties. To be published.[5]
10. A. Rauk, E. Buncel, R. Y. Moir, and S. Wolfe. J. Am. Chem. Soc. **87**, 5498 (1965).
11. I. G. Csizmadia, M. C. Harrison, J. W. Moskowitz, and B. T. Sutcliffe. Theoret. Chim. Acta, **6**, 191 (1966); **7**, 156 (1967).
12. S. S. Seung, M. C. Harrison, and I. G. Csizmadia. Theoret. Chim. Acta, **8**, 281 (1967).

[5]The manuscript has been reproduced at the Ames Laboratory at Iowa State University. The authors would like to thank Dr. Krauss (National Bureau of Standards, Washington, D.C.) for making a copy of the manuscript available.

Can. J. Chem. Downloaded from www.nrcresearchpress.com by 210.87.254.40 on 09/05/12
For personal use only.

13. M. C. HARRISON. J. Chem. Phys. **41**, 495 (1964).
14. C. M. REEVES and M. C. HARRISON. J. Chem. Phys. **39**, 11 (1963).
15. C. M. REEVES. J. Chem. Phys. **39**, 1 (1963).
16. M. C. HARRISON. J. Chem. Phys. **41**, 499 (1964).
17. J. W. MOSKOWITZ and M. C. HARRISON. J. Chem. Phys. **43**, 3550 (1965).
18. L. BURNELL and J. J. KAUFMAN. J. Chem. Phys. **43**, 3540 (1965).
19. I. G. CSIZMADIA. J. Chem. Phys. **44**, 1849 (1966).
20. J. W. MOSKOWITZ and M. C. HARRISON. J. Chem. Phys. **42**, 1726 (1965).
21. J. W. MOSKOWITZ. J. Chem. Phys. **43**, 60 (1965).
22. J. M. SCHULMAN and J. W. MOSKOWITZ. J. Chem. Phys. **43**, 3287 (1965).
23. M. B. ROBIN, R. R. HART, and N. A. KUEBLER. J. Chem. Phys. **44**, 1803 (1966).
24. I. G. CSIZMADIA, M. C. HARRISON, and B. T. SUTCLIFFE. Theoret. Chim. Acta, **6**, 217 (1966).
25. E. CLEMENTI. IBM J. Res. Develop. **9**, 2 (1965).[6]

[6]A supplement entitled "Tables of atomic functions" (a systematic tabulation of atomic Hartree–Fock functions) is available upon request to the Editor of IBM Journal of Research and Development.

26. F. HERMAN and S. SKILLMAN. Atomic structure calculations. Prentice-Hall, New York. 1963. pp. 6–12 to 6–23.
27. H. J. M. BOWEN *et al.* (*Compilers*). Tables of interatomic distances and configuration in molecules and ions. Chem. Soc. London Spec. Publ. No. 11 (1958).
28. R. MOCCIA. J. Chem. Phys. **40**, 2186 (1964).
29. A. L. MCCLELLAN. Tables of experimental dipole moments. W. H. Freeman, San Francisco. 1963.
30. R. E. KARI and I. G. CSIZMADIA. To be published. Presented at the Second Canadian Symposium on Quantum Chemistry, Montreal, June 26–30, 1967.
31. M. A. ROBB and I. G. CSIZMADIA. Theoret. Chim. Acta. In press.
32. P. B. SOLLMAN, R. NAGARAJAN, and R. M. DODSON. Chem. Commun. (11), 550 (1967).
33. S. WOLFE, A. RAUK, and I. G. CSIZMADIA. J. Am. Chem. Soc. **89**, 5710 (1967).
34. S. WOLFE, A. RAUK, and I. G. CSIZMADIA. A quantum mechanical study of proton exchange in sulfoxides with retention and inversion of configuration. In preparation.
35. S. F. BOYS. Proc. Roy. Soc. London, Ser. A, **200**, 542 (1950).

Can. J. Chem. Downloaded from www.nrcresearchpress.com by 210.87.254.40 on 09/05/12
For personal use only.

Studies on the decomposition of tetra-alkylammonium salts in solution. Part I. Phenylbenzylmethylallylammonium iodide[1]

K. T. Leffek and F. H.-C. Tsao
Department of Chemistry, Dalhousie University, Halifax, Nova Scotia

Received July 31, 1967

The loss of optical activity from phenylbenzylmethylallylammonium iodide in chloroform solution has been found to be entirely due to decomposition; racemization as such does not take place. The products are benzyl iodide and allylmethylaniline. A mechanism involving decomposition via a triple ion is deduced from the reaction kinetics. The activation parameters ($\Delta H^{\neq}$ and $\Delta S^{\neq}$) and a secondary deuterium isotope effect are reported.

Canadian Journal of Chemistry, 46, 1215 (1968)

Can. J. Chem. Downloaded from www.nrcresearchpress.com by 210.87.254.105 on 09/05/12
For personal use only.

Introduction

Most standard texts of organic chemistry state that the decomposition of quaternary tetra-alkylammonium salts yields an alkyl halide and tertiary amine, when the dry salt is heated to fairly high temperatures. The reaction

$$R_4N^+X^- \rightarrow R_3N + RX$$

is the reverse of the Menschutkin reaction. Much less well known is the fact that this reaction proceeds for certain salts in solution, particularly in chloroform solution.

About 70 years ago some intensive work was carried out by several groups of workers on the optical activity of tetra-alkylammonium salts which depended for their asymmetry on the central nitrogen atom, to which four different alkyl groups were attached. The first optical resolution of such a compound was made in 1899 by Pope and Peachey (1), who resolved phenylbenzylmethylallylammonium iodide by fractional crystallization of the *d*-10-camphorsulfonate. The dextro iodide was recovered by reaction with potassium iodide. Many other salts were resolved during the following decade, all of which contained the benzyl and phenyl groups (2–7).

The loss of optical activity of the salts in chloroform solution was quantitatively measured and found to take place quite rapidly at room temperature. The results of several investigations established that the iodides decomposed at the same rate as the disappearance of optical activity, at least to within 20% (8, 9). This decomposition went to completion and benzyl iodide was identified as one of the products by its smell. Salts of other halides reached an equilibrium at less than 100% decomposition (10, 11) and one iodide showed similar behavior in ethanol solvent (12).

Nevertheless, a general mechanism of racemization is sometimes given in texts as involving the equilibrium

$$R_4N^+X^- \rightleftharpoons R_3N + RX.$$

The right-hand-side products cannot be optically active so eventually the activity disappears.

As a preliminary to a general investigation of these reverse Menschutkin reactions, it was decided to check the relative rates of decomposition and loss of optical activity.

Results and Discussion

The products of the decomposition of phenylbenzylmethylallylammonium iodide in chloroform solution were found to be only benzyl iodide and methylallylaniline, by vapor phase chromatographic analysis. Authentic samples injected into the column under identical conditions had identical retention times with the two peaks found with the reaction mixture.

The reaction mixtures were found to contain no iodide ion after 3 days at 25 °C, indicating that the decomposition was complete.

Comparison of Rates of Decomposition and Loss of Optical Activity

Wedekind and Paschke (8) and von Halban (9) employed titration methods using standard silver nitrate solution to determine the extent of decomposition. However, the ease with which benzyl iodide hydrolyzes to yield iodide ion

[1]Presented at the 50th Annual Conference of the Chemical Institute of Canada, Toronto, Ontario, June 1967.

Can. J. Chem. Downloaded from www.nrcresearchpress.com by 210.87.254.105 on 09/05/12
For personal use only.

makes a physical method, such as measurement of the conductance of the solution used by Stewart and Weale (13), much more convenient and precise. Good straight line Guggenheim plots (14) were obtained when the conductance values were used, but curves, showing a gradual increase in first order rate constant with time, resulted if these were converted to molar concentrations by means of a calibration curve. All the rate constants quoted refer to the former means of calculation.

The Guggenheim method applied to the loss of optical activity directly gave curved plots. However, when the molar concentrations, as measured by the optical rotation, were converted by means of the conductance–concentration calibration curve to conductance values, straight lines were obtained. The rate constants obtained from the straight line plots for decomposition and loss of optical activity are compared in Table I.

TABLE I

Rate constants for the loss of optical activity and the decomposition of phenylbenzylmethylallylammonium iodide in chloroform solution at 25 °C

No. of runs	Initial conc. (moles/l)	Loss of optical activity 10^5k_1 (s^{-1})	Decomposition 10^5k_1 (s^{-1})
1	0.05	5.51	
1	0.05	5.59	
4	0.05		5.56±0.01

Thus, the loss of optical activity seems to be entirely due to decomposition, confirming the work of Wedekind and Paschke (8) and von Halban (9). The figures in Table I are not directly comparable with those of ref. 8 because the latter have a factor of 2.303 omitted and are averages of rate constants which are actually increasing as the run proceeds. If the different method of calculation is taken into account the present results are consistent with those of Wedekind and Paschke (8).

Mechanism of the Decomposition

Steady first order rate constants are obtained from the equation

$$[1] \qquad k_1 = \frac{2.303}{t}\log_{10}\left(\frac{C_0}{C}\right)$$

in which C_0 and C are the measured conductances at zero time and time t respectively.

For weak electrolytes, the degree of ionization, α, may be equated to Λ/Λ_0, where Λ and Λ_0 are the equivalent conductances at the particular concentration and at infinite dilution. Then eq. [1] becomes a modified first order rate equation

$$[2] \qquad k_1 = \frac{2.303}{t}\log_{10}\left(\frac{\alpha_0}{\alpha_t}\times\frac{a}{(a-x)}\right).$$

The generally low values obtained for the conductances of these solutions makes reasonable the assumption that most of the salt is present as ion-pairs. The degree of ionization is then the fraction of salt which is dissociated into single ions, although at the concentrations used in these experiments, the dissociated species may be a larger aggregate.

The kinetic consequences of several mechanisms of decomposition may be predicted as follows.

An S_N1 decomposition of the ion-pair,

$$R_4N^+I^- \xrightarrow{\text{slow}} R_3N + R^+I^- \xrightarrow{\text{fast}} R_3N + RI,$$

would give

$$\frac{-d[R_4N^+I^-]}{dt} = k_1[R_4N^+I^-].$$

Neglecting activity coefficients, the concentration of $R_4N^+I^-$ is $(1-\alpha)a$, which, if α is small, would be simply equal to the molar concentration a.

An S_N2 mechanism, analogous to that considered by Pocker and Parker (15) for reactions of sulfonium salts in ethanol solution,

$$R_4N^+ + I^- \rightarrow R_3N + RI,$$

would give

$$\frac{-d[R_4N^+I^-]}{dt} = k_2[R_4N^+][I^-] = k_2\alpha^2a^2.$$

For the equilibrium

$$R_4N^+I^- \rightleftharpoons R_4N^+ + I^-$$

$$K = \alpha^2a/(1-\alpha)$$

$$\frac{-d[R_4N^+I^-]}{dt} = k_2(1-\alpha)Ka.$$

Again, if α is small, this would give a rate dependent on the molar concentration of the substrate.

An S_N1 decomposition of the ammonium ion

$$R_4N^+ \xrightarrow{\text{slow}} R_3N + R^+ \xrightarrow[I^-]{\text{fast}} R_3N + RI$$

Can. J. Chem. Downloaded from www.nrcresearchpress.com by 210.87.254.105 on 09/05/12
For personal use only.

yields

$$\frac{-d[R_4N^+]}{dt} = k_1[R_4N^+] = k_1\alpha a.$$

When integrated this yields eq. [2].

However, a free benzyl carbonium ion in chloroform solution is quite unlikely since it is not formed when benzyl halides react in hydroxylic solvents (16, 17), although the benzyl group undoubtedly has some carbonium ion character in the initial state as a result of delocalization of the positive charge. If the salt exists almost entirely in the form of ion-pairs in chloroform solution, it is probable that any small quantity of free ions formed would be almost entirely associated in the form of triple ions, the concentration of which would be nearly equal to αa. The most likely mechanism may be formulated as

$$3R_4N^+I^- \overset{\text{fast}}{\rightleftharpoons} R_4N^+(I^-)_2 + (R_4N^+)_2I^-$$
$$\Big\downarrow \text{slow}$$
$$R_3N + RI + 2R_4N^+I^-,$$

which is probably best described as an ionic internal nucleophilic substitution.

A comparison of the rate constant for decomposition of the iodide with that determined by Stewart and Weale for the bromide (13) shows a difference of a factor of approximately 10 in favor of the iodide, indicating that the anion plays a significant role in the reaction.

The independence of the first order rate constant with respect to the concentration of the reacting ion is verified by the results collected in Table II. It thus appears that the assumption $\alpha = \Lambda/\Lambda_0$ is valid over the concentration range 0.02–0.05 *M*, although this would be expected to break down at low concentrations.

TABLE II

First order rate constants for the decomposition of phenylbenzylmethylallylammonium iodide in chloroform solution at 25 °C

Concentration (moles/l)	10^5k_1 (s^{-1})
0.050	5.52
0.045	5.69
0.040	5.66
0.035	5.63
0.030	5.56
0.025	5.53
0.020	5.55

If the salt exists almost entirely as ion-pairs with a very small concentration of dissociated unsymmetrical ions, the order of the reaction when calculated with respect to the molar concentration of the substrate should be equal to one-half.

In an investigation by Ross *et al.* (18) on the decomposition of benzyldimethylphenylammonium thiocyanate in chloroform solution, using a basic assumption that the mechanism was S_N2, it was concluded that the kinetics fitted a two-thirds order equation and that the salt existed predominantly as triple-ions in solution, although a two-thirds order arising from mixed kinetics was not excluded. On the other hand, Stewart and Weale (13) measured the conductance of benzylphenylmethylallylammonium bromide in chloroform solution and concluded from its magnitude that the salt existed almost entirely as ion-pairs, which seems the more likely state of these salts when dissolved in chloroform.

Although the results of Ross *et al.* (18) fit a two-thirds order equation very well, this is not necessarily a unique analysis. Several runs in the present work were found to fit not only a two-thirds order equation, but also a one-half order equation almost as well. Deviations appear at about 90% reaction. On our analysis, the kinetics would be expected to be one-half order, so long as the degree of ionization, α, was small compared to unity. Thus, towards the end of a run when the concentration of salt has fallen to a low level, α increases so that the concentration of reactive ions becomes less than $[R_4N^+I^-]^{1/2}$, giving rise to deviations in the plot of the square root of the salt concentration versus time. Thus, the fact that the decomposition fits a two-thirds order equation slightly better than a one-half order equation need not be significant.

Another method of determining the kinetic order of a reaction is to plot the logarithm of the initial concentration against the logarithm of the half-life. Nine runs were analyzed to determine their half-lives with respect to molar concentration of the substrate and the graph was plotted. The slope of such a graph is equal to $(n - 1)$, where n is the reaction order. It was found, however, that the fit to a one-half slope was about the same as that to a one-third slope.

Thus the order of the reaction with respect to the molar concentrations cannot be unequivocally determined and therefore it provides only

Can. J. Chem. Downloaded from www.nrcresearchpress.com by 210.87.254.105 on 09/05/12
For personal use only.

secondary evidence for the mechanism of the reaction. Since the kinetic observations of the present investigation definitely preclude an S_N2 mechanism, it is believed that the assumption of a dominant ion-pair state of the salt in chloroform solution with decomposition via a triple ion is a preferable interpretation to that offered by Ross *et al.* (18).

Activation Parameters

The rate constants for the decomposition reaction were measured at 5° intervals between 20 and 45 °C and the results analyzed according to the equation

$$[3]\quad \log_{10}\left(\frac{k}{T}\right) = \log_{10}\left(\frac{k}{h}\right) - \frac{\Delta H^{\ddagger}}{2.303RT} + \frac{\Delta S^{\ddagger}}{2.303R}$$

in which the symbols have their standard transition state theory meanings. Figure 1 shows a graph of $\log_{10}(k/T) + 8$ versus $1000/T$ and also two values reported by Wedekind and Paschke (8). A least squares fit to eq. [3] gives

$$\Delta H^{\ddagger} = 25.91 \pm 0.07 \text{ kcal mole}^{-1}$$

$$\Delta S^{\ddagger} = 8.86 \pm 0.22 \text{ cal mole}^{-1} \text{ deg}^{-1}.$$

The ease with which the reaction takes place at room temperature may be seen to be due to the positive entropy of activation which reduces the effect of the rather large enthalpy of activation. In a reaction such as this decomposition, in which one ion decomposes into two entities, the transition state would be expected to have a greater entropy than the initial state. How much of this positive entropy of activation is the result of the disruption of the initial state solvation shell cannot be ascertained until further studies of other salts and other solvents have been made, but the known sensitivity of the reaction to solvent indicates that solvation plays an important role.

The fact that the activation energy plot shows no curvature over a reasonably large temperature range lends support to the explanation of the kinetics in terms of a single mechanism. If two different ionic species were decomposing simultaneously with different activation energies, deviations from linearity would be expected in Fig. 1.

Secondary Deuterium Isotope Effect

Since the secondary deuterium isotope effects have been measured for some Menschutkin reactions (19, 20), it is of interest to consider this effect in the reverse decomposition. The rate ratios between the normal compound and its methyl-d_3 analogue are shown in Table III. These rate ratios were fitted to eq. [4] by the method of least squares:

$$[4]\quad \log_{10}(k_H/k_D) = \frac{(\Delta H_D^{\ddagger} - \Delta H_H^{\ddagger})}{2.303RT} - \frac{(\Delta S_D^{\ddagger} - \Delta S_H^{\ddagger})}{2.303R}.$$

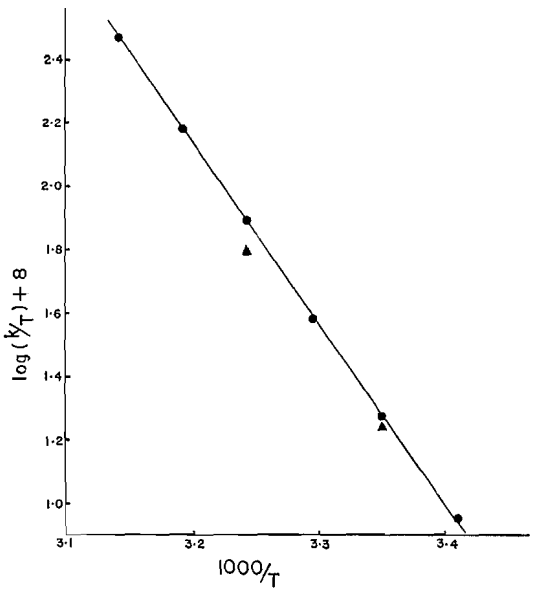

FIG. 1. The temperature dependence of the rate constant of decomposition of phenylbenzylmethylallylammonium iodide in chloroform solution: (●) present work, (▲) Wedekind and Paschke (8).

TABLE III

Secondary deuterium isotope effects for the decomposition of phenylbenzylmethyl-d_3-allylammonium iodide in chloroform solution

Temp. (°C)	$10^5 k_H$ (s^{-1})	$10^5 k_D$ (s^{-1})	k_H/k_D
20.03	2.64_2	2.38_3	1.10_9
25.04	5.51_7	5.06_3	1.09_0
25.06	5.54_6	5.07_2	1.09_3
30.10	11.53	10.67	1.08_1
30.10	11.64	10.74	1.08_4
35.10	23.88	21.96	1.08_7
35.10	23.76	22.03	1.07_9
40.04	47.67	44.3_6	1.07_5
45.09	93.8_9	88.5_1	1.06_1
45.09	92.6_0	85.6_0	1.08_2
45.09	93.3_0	87.7_4	1.06_3

Can. J. Chem. Downloaded from www.nrcresearchpress.com by 210.87.254.105 on 09/05/12
For personal use only.

The enthalpy and entropy differences and their standard deviations were

$$(\Delta H_D^{\ddagger} - \Delta H_H^{\ddagger}) = 226 \pm 43 \text{ cal mole}^{-1}$$

$$(\Delta S_D^{\ddagger} - \Delta S_H^{\ddagger}) = 0.58 \pm 0.14 \text{ cal mole}^{-1} \text{ deg}^{-1}.$$

A detailed discussion of the effect of replacing methyl by deuteromethyl in this reaction should not be attempted without first gaining more information concerning the effects of making more substantial changes in the substrate molecule. This information is currently being gathered (J. T. Burns and K. T. Leffek, unpublished work). However, some discussion is of value. The changes in the two reaction parameters are opposing, with the enthalpy change the major factor. Preliminary results of Burns and Leffek indicate that electron-releasing substituents on the nitrogen atom increase both the enthalpy and entropy of activation for this decomposition. Thus the isotope effect on the enthalpy of activation is in agreement with the greater electron-releasing character, due to an anharmonicity effect, of CD_3 relative to CH_3. In this particular case, therefore, the deuteromethyl group appears to act, qualitatively, in the same manner as any other substituent group. In such cases as this it is tempting to leave the discussion at this physical–organic level as advocated by Halevi (21), but at the same time it should be remembered that a more theoretical analysis, such as that presented by Wolfsberg and Stern (22), is probably necessary to fit all secondary isotope effects into a self-consistent picture.

Experimental

Materials

Phenylbenzylmethylallylammonium Salts

Methylaniline (32 g) and benzyl chloride (38 g) were warmed for 2½ h on a water bath. The hydrochloride which formed was destroyed with concentrated sodium hydroxide solution and the benzylmethylaniline was recovered, dried with anhydrous sodium sulfate, and distilled at reduced pressure. A second distillation gave an almost colorless oil, boiling range 205–210 °C at 60 mm Hg pressure. Yield 53 g (90%).

The benzylmethylaniline (20 g) was shaken with allyl iodide (17 g) and allowed to stand 24 h. The ammonium iodide which formed was separated by filtration, powdered, and crystallized from 50% ethanol, m.p. 140–142 °C. Yield 32 g (93%). Titration of iodide ion indicated a purity of 99.8%.

The iodide and anhydrous silver *d*-10-camphorsulfonate were dissolved, in equimolar proportions, in a solvent consisting of equal parts of acetone and ethyl ether. After repeated recrystallization from boiling acetone, the less soluble *d*-phenylbenzylmethylallylammonium *d*-10-camphorsulfonate was obtained as colorless crystals, m.p. 168–170 °C, $[\alpha]_{5461}^{25}$ 52.3° in H_2O (ref. 1, $[\alpha]_D$ 44.4°). This was reconverted to the iodide by adding an aqueous solution of the salt to aqueous potassium iodide. A white crystalline precipitate formed immediately. This was recrystallized several times from hot 50% ethanol, m.p. 145 °C, $[\alpha]_{5461}^{25}$ 61.1° in 50% acetone–methanol (ref. 1, $[\alpha]_D$ 52.5°).

Phenylbenzylmethyl-d_3-allylammonium Iodide

Methyl-d_3 iodide was prepared by the method of Cotton *et al.* (23). The deuterium content, by mass spectrometric analysis, was 97.5%. This was used to prepare methyl-d_3-aniline by the method of Hepp (24). Acetanilide (15 g) and sodium (4 g) were mixed in xylene (100 ml) and heated at 130 °C for 2–3 h. The material was allowed to cool, then methyl-d_3 iodide (11 g) was added and the reaction maintained by gentle heating. The product was boiled with alcoholic potassium hydroxide (100 ml) for a day, after which the mixture was filtered, the solvent was removed, and the base was neutralized with concentrated hydrochloric acid. Methyl-d_3-aniline was recovered by steam distillation, dried with anhydrous sodium sulfate, and redistilled, b.p. 190–192 °C, yield 30 g (59%). The remainder of the preparation was carried out as described above. The n.m.r. spectrum of the normal salt in chloroform contained a peak at $\tau = 6.3$ due to the *N*-methyl group. The deuterated salt had an identical spectrum except for the absence of this peak.

Chloroform Solvent

Commercial material containing about 1% ethanol

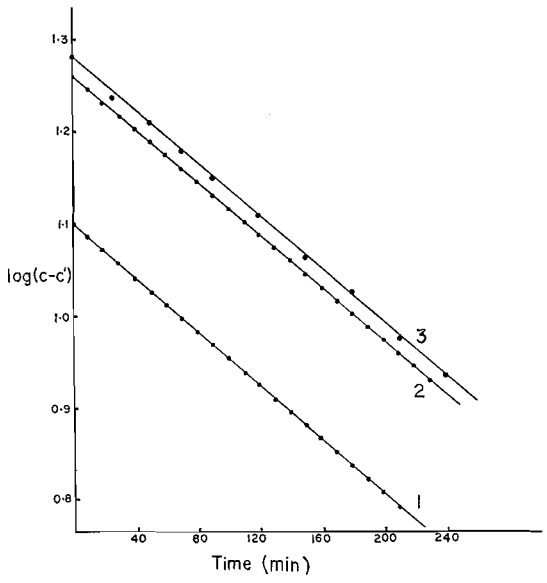

FIG. 2. Guggenheim plots for illustrative kinetic runs for the decomposition of phenylbenzylmethylallylammonium iodide in chloroform solution. 1. Conductimetric, initial conc. 0.040 *M*. 2. Conductimetric, initial conc. 0.050 *M*. 3. Polarimetric, initial conc. 0.050 *M*.

Can. J. Chem. Downloaded from www.nrcresearchpress.com by 210.87.254.105 on 09/05/12
For personal use only.

was purified by extraction with water, dried, and redistilled, b.p. 61 °C. Traces of ethanol were still detectable by v.p.c. analysis.

Kinetic Methods

The rate constants for the decomposition reactions were obtained from conductance measurements carried out with a Wayne-Kerr Universal Bridge type B221. Two runs were carried out simultaneously using cells with shiny platinum electrodes, capacity about 25 ml, cell constants approximately 0.13. The observed conductances (C_l) were used in the place of concentrations in the Guggenheim equation and the first order rate constants were calculated from the slope of the plot of $\log_{10}(C_l - C_l')$ against time (14).

TABLE IV

Decomposition of phenylbenzylmethylallylammonium iodide in chloroform solution at 25.04 ± 0.05 °C

Run 49. Initial conc. substrate = 0.050 *M*

	Conductances (μmho)	
t (min)	At *t* min	At *t* min + 8 h
0	24.43	6.252
10	23.69	6.097
20	22.95	5.950
30	22.25	5.806
40	21.57_5	5.667
50	20.91	5.532
60	20.28	5.402
70	19.68	5.276_5
80	19.07	5.154
90	18.51	5.036
100	17.94_5	4.921_5
110	17.41	4.811
120	16.89	4.705
130	16.40	4.600
140	15.92	4.500
150	15.44	4.406
160	14.99	4.310
170	14.55_5	4.218
180	14.13	4.133
190	13.72	4.047
200	13.32	3.966
210	12.95_5	3.885
220	12.57	3.808
230	12.21_5	3.733

From Guggenheim plot, $k_1 = 5.52 \times 10^{-5}$ s^{-1}

The rate constants for loss of optical activity were derived from measurement of the change of optical activity with time using a 20 mm polarimeter tube in a Bendix-Ericsson automatic polarimeter ETL-NPL type 143A. The rotatory power of each reading was converted to the relative molar concentration and then to the corresponding conductance by means of a calibration curve of molar concentration vs. conductance. The first order rate constant was then calculated again using the Guggenheim method. Figure 2 shows typical Guggenheim plots for three runs, and Table IV contains the conductance values for one of them. The calibration curve was constructed by measuring the conductance of a solution containing appropriate concentrations of substrate and products over a period of time, and extrapolating the conductance, graphically, to the time at which the solution was prepared. Although this is not an ideal method, repeated determinations gave a satisfactory calibration curve (compare line 3 with lines 1 and 2 in Fig. 2).

Acknowledgments

The authors are grateful for financial support by the National Research Council of Canada and by the Research Development Committee of Dalhousie University.

1. W. J. Pope and S. T. Peachey. Trans. Chem. Soc. **75**, 1127 (1899).
2. W. J. Pope and A. W. Harvey. Trans. Chem. Soc. **79**, 828 (1901).
3. H. O. Jones. Trans. Chem. Soc. **85**, 223 (1904).
4. A. W. Harvey. Trans. Chem. Soc. **87**, 1481 (1905).
5. E. Wedekind and E. Frohlich. Ber. **38**, 3933 (1905).
6. E. Wedekind. Ber. **39**, 474 (1906).
7. E. Wedekind. Z. Elektrochem. **12**, 330 (1906).
8. E. Wedekind and F. Paschke. Ber. **41**, 2659 (1908).
9. H. von Halban. Ber. **41**, 2417 (1908).
10. E. G. Williams, M. W. Perrin, and R. O. Gibbon. Proc. Roy. Soc. London, Ser. A, **154**, 684 (1936).
11. W. C. Davies and R. G. Cox. J. Chem. Soc. 614 (1937).
12. J. Syrkin and M. Gubareva. Acta Physicochim. URSS, **8**, 236 (1938).
13. J. M. Stewart and K. E. Weale. J. Chem. Soc. 2849 (1965).
14. E. A. Guggenheim. Phil. Mag. **2**, 538 (1936).
15. Y. Pocker and A. J. Parker. J. Org. Chem. **31**, 1526 (1966).
16. G. Kohnstam. *In* The transition state. Chem. Soc. London Special Publ. No. 16. 1962. p. 179.
17. R. E. Robertson and J. M. W. Scott. J. Chem. Soc. 1596 (1961).
18. S. D. Ross, M. Finkelstein, and R. C. Petersen. J. Am. Chem. Soc. **83**, 4853 (1961).
19. K. T. Leffek and J. W. MacLean. Can. J. Chem. **43**, 40 (1965).
20. H. C. Brown and G. J. McDonald. J. Am. Chem. Soc. **88**, 2514 (1966).
21. E. A. Halevi. Progr. Phys. Org. Chem. **1**, 109 (1963).
22. M. Wolfsberg and M. J. Stern. Pure Appl. Chem. **8**, 325 (1964).
23. F. A. Cotton, J. H. Fassnacht, W. D. Horrocks, Jr., and N. A. Nelson. J. Chem. Soc. 4138 (1959).
24. P. Hepp. Ber. **10**, 327 (1877).

Can. J. Chem. Downloaded from www.nrcresearchpress.com by 210.87.254.105 on 09/05/12
For personal use only.

A simple cell for the electrodeposition of traces of metal on thin metallized plastic films. Applications to the preparation of radioactive sources of Co-60, Ag-110m, Hg-203, Ni-63, and Zn-65[1]

Y. UJIHIRA[2] AND J. C. ROY
Département de Chimie, Université Laval, Québec, Québec

Received September 25, 1967

A simple and rapid electrochemical technique for the preparation of uniform and adherent metal deposits on thin metallized plastic films has been developed. It is based on the use of an electrolytic cell, characterized by the separation of the anode and cathode compartments by a fritted glass disc. Furthermore, electrodeposition is achieved from a solution having a volume of only 0.15 ml. The technique and the conditions used to realize the electrodeposition on thin metallized plastic films is described. The cell has been used to electrodeposit many metals, mostly by spontaneous electrodeposition using a magnesium anode and also by application of an external voltage using a platinum anode. In this paper, we describe the experimental conditions and report the results dealing with the electrodeposition of Co, Ni, Ag, Hg, and Zn. Deposits of less than a microgram to several hundred micrograms per square centimeter were obtained with high yields in 10 to 40 min. The use of the technique for the preparation of radioactive sources of Co-60, Ni-63, Ag-110m, and Hg-203 for absolute rate determinations is reviewed.

Une méthode électrochimique, simple et rapide, a été mise au point pour préparer des dépôts métalliques uniformes et adhérents sur des films plastiques, métallisés, dont l'épaisseur totale est d'environ 50 μg/cm². La méthode repose sur la séparation de la cathode (film métallisé) et de l'anode (bande de magnésium ou fil de platine) par une paroi poreuse et sur l'utilisation d'un très faible volume de solution, soit environ 0.15 ml. La méthode ainsi que les conditions expérimentales pour réaliser l'électrodéposition des métaux sur des films plastiques métallisés sont discutées de façon détaillée. On décrit les conditions expérimentales pour obtenir des dépôts métalliques de Co, Ni, Ag, Hg et Zn par électrolyse interne. Ces dépôts ont des épaisseurs variant de moins d'un microgramme à quelques centaines de microgrammes par centimètre carré et sont obtenus avec des rendements très élevés pour des périodes d'électrolyse de 10 à 40 min. On discute également de l'utilisation de cette méthode électrochimique pour préparer des sources radioactives de Co-60, Ni-63, Ag-110m et Hg-203 pour la mesure absolue de leurs taux de désintégration dans un compteur proportionnel 4π.

Canadian Journal of Chemistry, 46, 1221 (1968)

Introduction

Descriptions in the literature of techniques for the preparation of targets and radioactive sources by electrodeposition on thin metallized plastic films having a total superficial density of the order of 50 μg/cm² are exceedingly sparse. In the exhaustive review made by Yaffe (1) on the preparation of thin films and sources, the only reference bearing on the subject is the work of Blanchard, Kahn, and Birkhoff (2). In fact, it is the only extensive study which has been published on this particular aspect of source preparation. These authors prepared annular sources of eight different radionuclides (Ru-106, Ag-110m, Hg-203, Co-60, In-114, Cr-51, Au-198, and Fe-59) on metallized films of 60 μg/cm² for β-spectrometry. They reported deposition efficiencies above 95% for the spontaneous electrodeposition of these isotopes using a magnesium anode, and of 15 to 95% by the imposition of an external voltage, using a platinum anode; the deposition times varied from 3 to 8 h and the volume of solution was approximately 10 ml. The efficiencies were determined by counting aliquots of the supernatant solution during and after deposition. Although this method of measurement undoubtedly gives the fraction deposited in the course of electrolysis, it does not necessarily give the fraction remaining on the film because dissolution of a metallic deposit after electrodeposition or during washing could lead to significant losses for some metals, as we found and as has been reported by Broyles *et al.* (3) in the case of tin. This point is discussed by Lingane (4) in his book on electroanalytical chemistry, which is an excellent source of information on practical problems associated with electrolysis. Whereas Blanchard *et al.* used an acid solution 0.1 *M* in HCl, Garfinkel and Hutchinson (5) found it necessary to neutralize the solution in order to minimize the dissolution

[1]Paper presented at the Chemical Institute of Canada 50th Conference in Toronto, and reviewed in Chem. Can. **19**, 7, 34 (1967).

[2]Laval University Postdoctorate Fellow. On leave from the University of Tokyo, Japan.

Can. J. Chem. Downloaded from www.nrcresearchpress.com by 210.87.254.105 on 09/05/12
For personal use only.

of the magnesium anode when they attempted to use the procedure of Blanchard *et al.* to electrodeposit Fe-55 on metallized collodion for making sources for 4π-counting. For a similar reason and other reasons to be discussed later, we were not very successful in using their procedure for preparing flat sources of 1 cm^2 for 4π-counting.

Spernol, De Roost, and Lerch (6) have described a cell wherein an external voltage is applied to prepare Co-60 on thin metallized VYNS films (a polyvinylchloride–acetate copolymer) for 4π-counting, but they could not obtain deposition efficiencies higher than 70%.

Parker, De Croës, and Sevier (7) mentioned that some good results have been obtained with a metallized organic substrate used in conjunction with a cell designed to electrodeposit elements on to metal backings. Although no experimental details or data were reported, from the information given in other papers (8, 9), it seems that the organic substrate was Mylar (a polyester compound), the minimum thickness of which was 0.9 mg/cm^2.

This short survey shows that techniques to electrodeposit elements on thin plastic films have not been developed very extensively, although they are useful to prepare targets and sources for alpha and beta spectrometry, and for absolute rate determination of alpha and beta emitters. In particular, they could be very valuable to prepare the kind of sources needed for absolute rate determination of some low energy beta-emitters and in this connection any proposed electrochemical technique, to be appealing to the prospective users, should meet the following requirements: (1) be simple, efficient, and reproducible; (2) give uniform and adherent deposits; (3) require relatively short electrodeposition time and be nearly quantitative.

Since we are particularly interested in this last type of application, we studied different experimental arrangements and a few parameters affecting electrodeposition on thin metallized plastic films. These studies led us to develop an electrolytic cell which fulfills the conditions stated above for preparations of sources of Co-60, Ni-63, Ag-110m, Hg-203, four low energy beta-emitters of special interest in the metrology of radionuclides.

Cells and Electrodes

The cathode was a VYNS film (10) stretched across an aluminium ring, 25 mm inside diameter, 38 mm outside diameter, and 0.6 mm thick, and metallized on one side by vacuum evaporation of gold or of gold – 18% palladium alloy (11, 12). To avoid breakage of the VYNS film during electrodeposition, its superficial density should not be much less than 20 μg/cm^2. VYNS was found to be superior to collodion as a backing. The resistance of the conducting layer between the center of the film and the mount should be less than 60 ohms, otherwise the electrodeposited metal flakes off during or shortly after electrodeposition. With our method of preparation of the films (12), a sufficient conductivity was obtained with a metallic coat of 25 μg/cm^2. Superficial densities of the films were determined gravimetrically; that of the coating was calculated from the equations developed by Holland and Steckelmacher (12, 13) from the total evaporation of a known amount of metal. Thus, as a rule, the total superficial density of the film was about 50 μg/cm^2 except where noted and, for reasons given above, it would be difficult to use much thinner films.

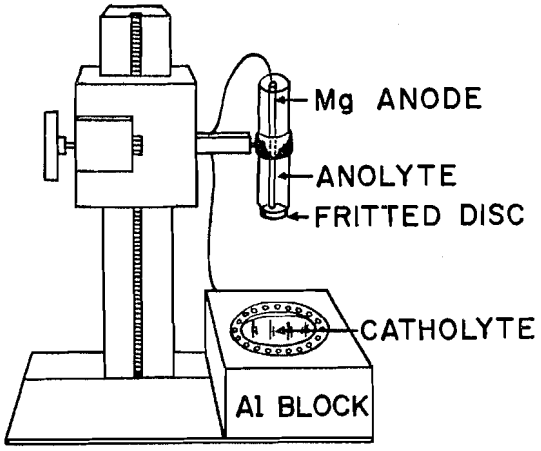

FIG. 1. Apparatus for internal electrolysis.

The cell used in this work is shown in Fig. 1. It is characterized by the separation of the anode and cathode compartments by a fritted glass disc. It has been used to prepare metal deposits of many elements mainly by internal electrolysis (achieved without an external source of electrical energy by simply short-circuiting the two electrodes forming the cell) (4, 14) using a mag-

Can. J. Chem. Downloaded from www.nrcresearchpress.com by 210.87.254.105 on 09/05/12
For personal use only.

nesium anode. A ribbon or a rod of magnesium and the proper anolyte (< 0.1 ml) are placed in the sintered glass tube (medium or fine porosity) of 1 cm in diameter; this constituted one half-cell, the anode. The catholyte (0.1 to 0.15 ml) is placed on the metallized film; this constituted the other half-cell, the cathode. By bringing the fritted disc in contact with the catholyte mixture on the film and making electrical contact between the two electrodes, spontaneous electrodeposition occurs for many elements. The working area of the cathode was ≈ 1 cm^2.

According to our practical experience dealing with the electrodeposition of micro-quantities of metal on thin plastic films from a small volume of solution, the key to a successful operation rests on the separation of the two electrodes by a porous membrane. The use of a fritted disc has been found most convenient to prepare flat sources of 1 cm^2 in area, but it is expected that other types of porous membranes should work equally well. In fact, good results have been obtained with a membrane made of a VYNS film pierced in its center and stretched on a supporting aluminium ring. When we tried to use a platinum or a magnesium anode dipping directly in the mixture in a cell operating with or without an external voltage respectively, we encountered a number of problems such as: the attack of the conducting layer and splashing of the solution by the evolved gases; the rupture of the conducting layer leaving a bare annulus of VYNS around the metal deposit; the formation of a viscous solution of $Mg(OH)_2$ and contamination of the deposit with this hydroxide in internal electrolysis; a poor quality and often porous deposit. The small volume of solution used in the experiments could have been largely responsible for these effects.

Electrodeposition and Methodology

With the cell shown in Fig. 1, the elements studied so far (Fe, Co, Ni, Zn, Cd, Ag, Pt, Au, Hg, Tl, Pb, Bi) have been successfully electrodeposited on thin metallized plastic films. Thallium, however, is readily and completely dissolved by oxidation when exposed to air. Thus, the only way to prepare a source of thallium would be by co-deposition with another metal. All experiments were done at room temperature. The catholyte mixture was prepared by adding, separately on the film, a weighed amount of the radioactive solution, the desired amount of carrier, and the proper electrolyte to have an overall volume of between 0.1 and 0.15 ml as described in Table I. Gravimetric sampling, handling of the solution, and dilution are based on the use of a small polyethylene ampoule called a pycnometer and on techniques already described (15, 16).

In this paper, we shall limit our discussion to the results obtained for the deposition of Co, Ni, Ag, Hg, and Zn by internal electrolysis. We used Co-60, Ni-63, Ag-110m, Hg-203, and Zn-65 as radiotracers to determine the optimum conditions for their electrodeposition. To obtain these, the following approach was found very fruitful:

(1) to use for the catholyte and anolyte the procedure suggested by Schleicher (17) and Schleicher and Schlösser (18) as our first choice for these solutions;

(2) to measure the initial and final pH of the catholyte with narrow range test papers in the preliminary experiments;

(3) to carry out the electrolysis for different periods of time and to observe the course of the current and voltage decay;

(4) to analyze the cathode, the catholyte, the washings, and the anode compartment for the presence of the elements being electrodeposited after each period of electrolysis.

In this last operation, the catholyte was withdrawn with a transfer pipette (19) and kept for analysis, the cathodic deposit was rinsed immediately with 5 to 10 drops of distilled water or methanol, and the washings were withdrawn by decantation and kept for analysis. The excess water was removed with a piece of Kleenex.

The final choice of the catholyte and anolyte was based on the behavior of the system in this series of measurements.

For the gamma-emitting nuclides Co-60, Hg-203, Ag-110m, and Zn-65, analysis of the different fractions was done by gamma spectrometry. The deposition efficiencies (defined as the fraction remaining on the film after washing) were measured by comparing the gamma-emission rates of the electrodeposited metal with that of an evaporated source having the same geometry, except for Hg-203 where the γ-activity on the VYNS film was measured before and after electrodeposition. For nickel, the same operations were done by chemical analysis using a colorimetric method based on the reaction of

Can. J. Chem. Downloaded from www.nrcresearchpress.com by 210.87.254.105 on 09/05/12
For personal use only.

TABLE I

Procedure followed for the preparation of the solutions and experimentally determined optimum conditions for the electrodeposition of Co, Ni, Ag, Zn, and Hg by internal electrolysis

Nuclides	Co-60	Ni-63	Ag-110m	Hg-203	Zn-65
Specific activity and chemical composition of the stock solution	25 μCi/ml 10 μg Co^{++} per ml 0.1 *M* HCl	1.5 mCi/ml 0.024 Ci/g of Ni	25 μCi/ml 300 μg Hg^{++} per ml 0.1 *M* HNO_3	25 μCi/ml 185 μg Hg^{++} per ml 0.1 *M* HNO_3	25 μCi/ml 66 μg Zn^{++} per ml 0.1 *N* H_2SO_4
Preparation of the radioactive solution					
Dilution of stock soln. with:	0.1 *M* HCl	0.1 *N* H_2SO_4	1 *M* NH_4OH	0.1 *N* H_2SO_4	1 *N* H_2SO_4
Dilution factor	7.84	1379.0	3.5	2.75	4.77
Amount of carrier in soln.	1.3 μg/ml	45.3 μg/ml	85.7 μg/ml	67.3 μg/ml	11.1 μg/ml
Preparation of the catholyte: about 10 to 60 mg of the radioactive soln., plus addition of carrier, plus the following electrolyte: Final volume 0.1 to 0.15 ml	≈70 mg conc. NH_4OH	≈70 mg conc. NH_4OH	≈70 mg conc. NH_4OH	1–3 drops H_2O added to radio. soln. ≤0.1 *M* H_2SO_4	50 mg 1 *M* CH_3COONa + ≈30 mg 0.2 *M* NaOH
Anolyte: volume ≈ 0.1 ml except for silver where it is smaller (cf. Discussion)	1 *M* $(NH_4)_2SO_4$	1 *M* $(NH_4)_2SO_4$	0.5 *M* $(NH_4)_2SO_4$	0.2 *M* $MgSO_4$	0.2 *M* $MgCl_2$
Superficial density of cathode					
VYNS (μg/cm²)	24–60	24–60 (cf. Discussion)	24	24	24
Au or alloy (μg/cm²)	25	25	25	25	25
Final pH	Strongly alkaline			7–8	7
Maximum voltage obtained (V)	1.8	1.9	1.8	2.0	1.6
Maximum current obtained (mA)	3.0	2.0	1.0–2.0	0.6–2.0	0.8
Duration of electrolysis (min)	40	20–60	10–40	15–20	30–45
Average yield obtained (%)	85–95	≈98	95–100	20–90 (cf. Discussion)	85–95

Can. J. Chem. Downloaded from www.nrcresearchpress.com by 210.87.254.105 on 09/05/12
For personal use only.

nickel with dithio-oxalate. This method of analysis will be fully described in another paper (20).

The gamma spectrometry was done with a Nuclear Data 128 multi-channel analyzer used in conjunction with a $1\frac{1}{2} \times 1\frac{1}{2}$ in. NaI(Tl) crystal. The variation of the beta-counting rate as a function of the superficial density for Co-60, Hg-203, Ag-110m, and Ni-63 was measured with a 4π gas-flow proportional counter, pill-box type, and the ancillary equipment. Absolutely standardized solutions of Co-60, Hg-203, Ag-110m, obtained from the International Atomic Energy Commission in Vienna, and a stock solution of Ni-63, obtained from Atomic Energy of Canada, were used in these measurements.

The degree of uniformity of the deposits was assessed by autoradiography and photography with 35 mm color film. The autoradiograms were prepared by the techniques outlined by Chase *et al.* (21). Color slides of the electrodeposited film were taken with Kodachrome II, type A, color film (any color film will work) using a 35 mm Zeiss Ikon Contarex camera equipped with a bellows-focusing attachment and mounted on a tripod. This last method is particularly effective for judging the degree of uniformity of a deposit when superficial densities are greater than 10 $\mu g/cm^2$ and it has the advantage that the use of a radiotracer is not required.

Results and Discussion

Table I summarizes the procedure followed for the preparation of solutions and the experimentally determined optimum conditions to carry out the electrodeposition of Co, Ni, Ag, Hg, and Zn. The detailed presentation of important data obtained in these studies is given in Tables II–VI. Scores of sources of each radionuclide have been prepared by following the procedure. The reproducibility was very good for Co, Ni, Ag, and Hg, but only fair for Zn. Deposits of Co, Ni, Ag, Hg, and Zn, having superficial densities of less than 1 $\mu g/cm^2$ to several hundred micrograms per square centimeter, were prepared. The deposits were metallic and very adherent and, when they were observable visually (this requires about 10 $\mu g/cm^2$), they were bright and appeared to be very smooth. Autoradiograms of the sources indicate that the metals were homogeneously deposited on the cathode. The examination of the 35 mm color slides of the sources having superficial density greater than 10 $\mu g/cm^2$ showed that, at times, some deposits were slightly thinner at the center than around the edge. This arose when the catholyte acquired a pronounced convex shape under the pressure exerted by the fritted glass tube and could be corrected by stretching the column of liquid between the two surfaces into a concave form.

From the analysis of the catholyte, washings, and diaphragm, one can infer that nearly complete deposition of microgram quantities of Ni, Ag, Hg, Co, and Zn has been achieved rapidly by internal electrolysis, but dissolution of the cathodic deposit in the catholyte once the electrodes are disconnected and during the washings, probably by air oxidation, could lead to losses, more or less significant, depending on the element. The more noble elements are less prone to be oxidized and, in fact, the losses are limited to less than 1% for Ag and Hg, but they could be large for Co and Zn under certain experimental conditions and could be important for Ni when there are just a few micrograms of Ni^{2+} carrier in solution.

Electrodeposition and Co-deposition of Cobalt

We have found that a strongly ammoniacal solution is the best medium to achieve the electrodeposition of microquantities of cobalt. In a solution less than 5 *M* in NH_4OH, it is very difficult to electrodeposit much more than about 10 μg of cobalt. Above this amount, the precipitation of cobalt hydroxide, which either adhered to the cathode or remained in suspension, prevents the formation of a metallic deposit much thicker than a few $\mu g/cm^2$. For best results, concentrated ammonium hydroxide should be added to the radioactive solution in sufficient amounts to obtain a mixture between 8 and 10 *M* in NH_4OH. The results obtained under these conditions are presented in Table II. Pure and metallic cobalt deposits with yields of 90% can be obtained in 10 to 20 min provided that the dissolution of cobalt can be kept to a minimum when the electrolysis is over. This could usually be achieved by withdrawing the bulk of the catholyte with a transfer pipette and by wiping off the remainder with a piece of Kleenex as soon as possible after the end of the electrolysis. Even then, slight losses occur because there always remains on the film a very adherent layer of liquid into which dissolution takes place. The use

TABLE II

Some of the data on the electrodeposition of cobalt (expt. nos. 1–7) and on the co-deposition of traces of cobalt with nickel (expt. nos. 8–17)

Expt. No.	Molarity of NH_4OH in mixture (M)	Amount of Co^{2+} in soln. (μg)	Amount of Ni^{2+} added (μg)	Duration of electrolysis (min)	Distribution of Co-60 activity		
					Film (%)	Catholyte and washing (%)	Fritted disc (%)
1		0.03	None	28	62	32	5
2		1.0	"	25	84	6	6
3	8–10	8.0	"	25	91	6	3
4		23.3	"	20	92	4	4
5		35.0	"	20	92	4	4
6		53.7	"	25	91	4	5
7		185.0	"	25	94	3	3
8		0.05	8.1	35	80	15	5
9		0.05	15.4	35	86	9	5
10		0.05	31.7	30	86	<1	13
11		0.04	56.2	30	85	5	10
12	5	0.03	88.9	50	93	1	6
13		0.03	152.0	35	96	2	2
14		0.03	294.0	40	93	1	6
15		0.03	459.0	45	91	<1	8
16		0.04	878.0	60	96	<1	3
17		0.04	1312.0	60	96	<1	3

of methanol instead of distilled water for washing the deposit limits the losses to 1–2% during this operation. Even when following this procedure, the losses can sometimes be substantial, especially when the amount of Co^{2+} carrier is very low, as shown in Table II.

Another way to control the dissolution is by co-deposition with another metal which does not exhibit the same tendency. This possibility has been investigated. Zinc and especially nickel have been found efficient in this respect. The data on co-deposition of traces of cobalt with nickel are presented in Table II. The co-deposition of traces of cobalt is best done with nickel in 5–8 M ammoniacal solution and, for best results, it is recommended that no more than 1 μg of Co^{2+} carrier and at least 15 μg of Ni^{2+} be used and that the electrodeposition be carried out for 20–40 min. Thus, this procedure affords another possible method to prepare sources of cobalt when dissolution could be a problem.

Electrodeposition of Mercury

Some of the data obtained in studying the electrodeposition of mercury are presented in Table III. Highest yields are obtained when the electrolysis is not continued over 15 min, when the final pH is between 6 and 8, and when the amount of carrier is less than 20 μg. Above this value, the deposition efficiency drops down fairly regularly to about 20% when the amount of deposited mercury becomes larger. Evidence for a strong adherence of electrodeposited mercury on to the metallized support comes from the observation that no loss of the element occurred over periods of observation of several days. This property renders electrodeposition much more attractive for the preparation of sources for 4π β-counting. In this connection, it might be worthwhile to mention that loss of mercury occurs in sources prepared by various evaporation methods and that sulfide precipitation of mercury seems to have been the only practical method found so far to eliminate this unwanted phenomenon.

Since gold amalgamates readily, the amalgamation of gold on VYNS would be consistent with the results. If this interpretation is correct, the stability of electrodeposited mercury should be linked with the use of gold as a metal coating for VYNS.

Electrodeposition of Nickel and Silver

Nickel and silver give excellent deposits, are easily plated from an ammoniacal solution, and remain on the film with nearly 100% efficiency, as one can see in Tables IV and V. For nickel, one should remark that the superficial densities of some of the VYNS films in Table IV are 36 and

Can. J. Chem. Downloaded from www.nrcresearchpress.com by 210.87.254.105 on 09/05/12
For personal use only.

TABLE III

Data on the electrodeposition of mercury showing (*a*) the effect of the final pH on the deposition for small (expt. nos. 1–4) and large (expt. nos. 5–7) amounts of Hg^{2+} ions and (*b*) the variation of the deposition efficiency with the amount of Hg^{2+} ions initially present in the solution (expt. nos. 8–14). Electrolyte: 1–3 drops of water added to the radioactive solution; the solution was initially about 0.1 *M* in H_2SO_4

Expt. No.	Amount of Hg^{2+} in soln. (μg)	Duration of electrolysis (min)	Final pH	Distribution of Hg-203 activity			
				Film (%)	Catholyte (%)	Washing (%)	Fritted disc (%)
1	2.7	15	7	95	2	<1	3
2	1.5	15	8	89	3	<1	7
3	1.3	15	9	85	—	—	—
4	1.6	20	>10	92	4	<1	4
5	40.8	18	3	54	—	—	—
6	46.9	20	6	57	27	8	9
7	66.5	15	8	52	38	3	7
8	22.3	15	6.5	88	10	<1	2
9	105.3	25	8	45	44	7	5
10	198.0	15	6	46	35	6	10
11	362.0	15	2	28	—	—	—
12	1428.0	15	6	30	51	—	—
13	2617.0	15	6	13	—	—	—
14	3124.0	33	6	23	—	—	—

60 μg/cm^2; thicker films than the usual 24 μg/cm^2 are needed when the amount of deposited nickel becomes greater than about 50 μg. The thinner films tend to break under the strain exerted by a layer of metal greater than 50–70 μg/cm^2. This remark also applies to the co-deposition of Co with Ni. For highest deposition efficiencies, the use of at least 10 μg of Ni^{2+} carrier is recommended.

As can be seen in Table V, a strongly ammoniacal solution is the best medium for carrying out the electrodeposition of silver. It has been found that the current should not be higher than about 1 mA in order to obtain a bright deposit; much above this value, the deposit is black and porous. To control the current at around 1 mA, the volume of the anolyte should be very small, around 0.01–0.02 ml; the technique that we used was to impregnate a piece of filter paper with the anolyte and to place the magnesium anode on it.

Electrodeposition of Zinc

On the basis of different studies on the electrodeposition of zinc (18, 22, 23), a slightly acidic solution of sodium acetate was chosen for the catholyte. Then, we investigated the effect of the pH and other parameters on the behavior of the system. The results, presented in Table VI, show that the pH of the catholyte has a considerable influence on the electrodeposition and that yields of 95% can be obtained in 40–45 min by stopping the electrolysis when the final pH is about 7. To obtain these results, however, the electrolysis has to be done under known and controlled conditions because most of the current generated through the cell is due to the electrolysis of water with the result that the pH of the catholyte increases gradually as the electrodeposition of zinc proceeds. The electrode reactions are discussed in a later section. Briefly, in the case of zinc, the main electrode processes are reactions [1] or [2] where hydroxonium ions are consumed in acidic medium and hydroxyl ions are generated in basic medium. Since zinc is readily soluble in acid, it is not easily deposited at pH lower than about 2, whereas zinc hydroxide precipitates in basic solution. It follows that the best working pH range is between 3 and 7 and that the presence of sodium acetate is required to buffer the solution at these values for a time long enough to allow the electrodeposition of zinc. We found that the best results were obtained by adopting the following conditions:

(*a*) 50 mg of a 1 *M* solution of sodium acetate was added to the radioactive solution on the film;

(*b*) the initial pH of the catholyte was adjusted to about 4; since the radioactive solution was initially 1 *N* in H_2SO_4, this was done by adding

Can. J. Chem. Downloaded from www.nrcresearchpress.com by 210.87.254.105 on 09/05/12
For personal use only.

TABLE IV

Data on the electrodeposition of nickel from an ammoniacal medium about 5 *M* in NH_4OH showing the variation of the deposition efficiency with the amount of Ni^{2+} ions in solution. Note that the thickness of the VYNS film is increased when more than 50 μg/cm² is deposited

Expt. No.	Amount of Ni^{2+} in soln. (μg)	Duration of electrolysis (min)	Thickness of VYNS film (μg/cm²)	Nickel recovered on film (%)
1	3.0	50	24	11
2	4.3	40	24	68
3	16.2	45	24	88
4	21.6	45	24	94
5	33.8	40	24	98
6	52.1	42	24	99
7	84.5	35	36	90
8	167.8	30	36	95
9	213.9	56	60	99
10	395.0	56	60	98
11	510.0	60	60	98

about 30 mg of a 0.2 *M* solution of NaOH to the mixture on the film;

(*c*) the volume of the anolyte and the porosity of the fritted disc were selected in order to obtain a flow of current of 0.8–1.0 mA through the cell;

(*d*) the electrolysis was stopped at pH 7; for the conditions given under (*a*), (*b*), and (*c*) it takes about 40–45 min to raise the pH from 4 to 7.

The reproducibility of the results is not as good as with Co, Ni, Ag, and Hg, first because of the considerable influence of the pH on the electrodeposition and secondly because of a white solid residue which tends sometimes to remain on the film after the catholyte has been removed. This residue can be washed away, but the yields drop to 70–80%. We found, however, that the deposition of a residue rarely occurs when the time of electrodeposition is 30 min or less; thus, shortening the time of electrolysis is a possible way to eliminate this contamination.

Deposition Efficiencies vs. the Duration of Electrolysis

Curves of the deposition efficiencies vs. the duration of the internal electrolysis are shown in Fig. 2 for a given amount of each element initially present in the catholyte. Except for mercury, similar curves were obtained for the different amounts of Co^{2+}, Ni^{2+}, Ag^{+}, and Zn^{2+} carrier used in these studies; Tables II and IV–VI also show this similarity. For mercury, the same behavior was obtained only up to 20 μg carrier, for reasons discussed in the section on the electrodeposition of this element.

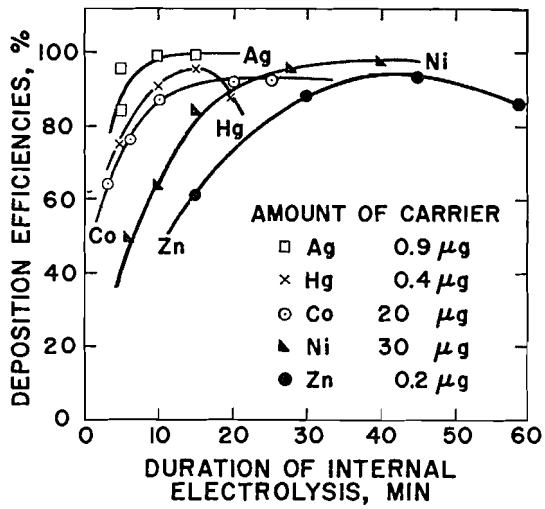

FIG. 2. Curves showing the variation of the electrodeposition yields of Ag, Ni, Co, Hg, and Zn vs. the duration of internal electrolysis.

Electrode Reactions

The nature of the processes taking place in the cell can be interpreted from the analysis of the current decay curves taken with different amounts of carrier, from the observation of reactions taking place at the electrodes, and from the calculation of the quantity of electricity needed to electrodeposit micro-amounts of metal.

Current decay curves obtained in the course of the electrodeposition of Ni are shown in Fig. 3; similar curves have been obtained for Co, Ag, Hg, and Zn. As a rule, the current increases

Can. J. Chem. Downloaded from www.nrcresearchpress.com by 210.87.254.105 on 09/05/12
For personal use only.

TABLE V

Data on the electrodeposition of silver showing (*a*) how the nature of the medium influences the deposition efficiency (expt. nos. 1–7) and (*b*) that in 10 *M* NH_4OH the deposition is nearly quantitative, independent of the amount of Ag^+ ion in solution (expt. nos. 8–14)

Expt. No.	Nature of the medium	Amount of Ag^+ in soln. (μg)	Duration of electrolysis (min)	Silver recovered on film (%)
1	Slightly acidic*	3.6	15	86
2	"	4.0	30	87
3	0.5 *M* NH_4OH	2.7	15	93
4	5 *M* "	2.7	15	94
5	10 *M* "	2.7	25	96
6	10 *M* "	3.4	26	100
7	12 *M* "	2.5	15	98
8		45.2	15	97
9		81.4	15	98
10		113.9	28	99
11	10 *M* NH_4OH	172.5	19	95
12		321.6	37	98
13		438.0	39	98
14		608.0	40	97

*Slightly acidic: 1 drop of 0.02 *M* HNO_3 + 1 drop of 0.03 *M* H_2SO_4 solutions.

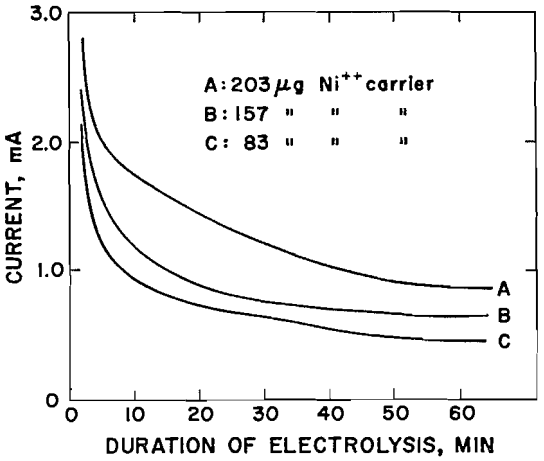

FIG. 3. Current decay curves for different amounts of Ni^{2+} carrier present in the catholyte.

sharply in the first minute or so, due to the diffusion of the anolyte through the fritted disc and the making of a better junction between the two electrode chambers. The curves follow the same trend as long as the amount of metal deposited is no more than a few hundred micrograms. This is an indication that the reaction at the cathode, $M^{n+} \rightarrow M + ne$, contributes only to a small fraction of the total current generated in the cell, a contribution which varies with the amount of metal deposited. Thus, other reactions must take place at the electrodes; in fact, evolution of gas is observed at the cathode and gas bubbles come out of the anolyte when shaken. This can be interpreted by the following electrode reactions taking place in acidic and basic solutions, namely the evolution of hydrogen at the cathode

[1] $2H^+ + 2e \rightarrow H_2$ (acid medium)

[2] $2H_2O + 2e \rightarrow H_2 + 2OH^-$ (basic medium)

and the evolution of oxygen at the anode

[3] $2H_2O \rightarrow O_2 + 4H^+ + 4e$ (acid medium)

[4] $4OH^- \rightarrow O_2 + 2H_2O + 4e$ (basic medium).

Other ions in the solutions could possibly be involved in electrode reactions and, thus, bring their own contribution to the total current, but no experimental verification of this has been made. We have observed, however, that renewing the anolyte in the middle of the electrolysis brings about a sharp increase in the current. This is an indication that the gradual increase of the Mg ions in the anode compartment by dissolution of the magnesium is in large part responsible for the current decay. This interpretation is further supported by the observation already made in the case of silver, where the decrease in current obtained in diminishing the volume of anolyte is due to a slower rate of dissolution of the magnesium anode.

Can. J. Chem. Downloaded from www.nrcresearchpress.com by 210.87.254.105 on 09/05/12
For personal use only.

TABLE VI

Data on the electrodeposition of Zn showing the variation of the deposition efficiency versus the final pH for small (expt. nos. 1–7) and large (expt. nos. 8–12) amounts of Zn^{2+} ions. Electrolyte: 50 mg of a solution 1 *M* in sodium acetate; for adjustment of the initial pH, see the discussion on zinc

Expt. No.	Amount of Zn^{2+} in soln. (μg)	Duration of electrolysis (min)	Final pH	Distribution of Zn-65 activity			
				Film (%)	Catholyte (%)	Washing (%)	Fritted disc (%)
1	0.2	30	3	45	50	3	2
2	0.2	30	6	87	10	3	<1
3	0.2	30	7	97	3	<1	<1
4	0.2	45	7.5	96	3	1	<1
5	0.2	60	8	87	5	3	<5
6	0.2	30	10	82	8	7	3
7	0.1	30	12	40	49	10	<1
8	18	30	2	26	60	14	<1
9	19	30	4	48	35	13	4
10	20	30	4.5	70	20	9	<1
11	20	45	6	85	8	5	2
12	24	60	9	86	5	9	<1
13	180	45	7	95	3	2	<1
14	216	30	5.5	82	13	4	<1

Since the current flowing through the cell is a manifestation of the rate of the electrode reaction, one can calculate the quantity of electricity and the time required to deposit different amounts of metal by placing into Faraday's equation the value of current generated in the cell, which is of the order of 1–3 mA. Assuming that the total current results from the deposition of the metal, complete plating of 100 μg would require about 150 s for Ni and Co and about 75 s for Ag and Hg. Thus, this calculation shows that the deposition of up to 100 μg of metal contributes only a small fraction to the total current and that a much larger amount has to be plated in order to use the current decay curves as an indication of the completeness of the electrodeposition.

Application to Source Preparation for 4π β-counting

In absolute rate determinations of low energy β-emitters by 4π β-counting of solid sources, the chief corrections are those required for absorption of the β in the thin metallized plastic film and in the source. Whereas the first correction can be estimated experimentally or from published curves, the second one is much more difficult to evaluate and is, therefore, the principal uncertainty in 4π-counting. When the activity measurement can be made by coincidence counting or by application of the efficiency tracing technique, the self-absorption correction is eliminated. However, a coincidence apparatus is not a common piece of equipment in most laboratories and the application of the technique to actual measurements is not simple, as has been pointed out by Baerg (24). It remains that in many situations the problem of estimating a self-absorption correction arises.

Self-absorption in sources prepared by various evaporation methods has been studied by Merritt, Taylor, and Campion (25) and the data obtained have been used to set up self-absorption curves for several radionuclides. A rapid variation of self-absorption with source thicknesses was found when the mean superficial density was greater than a certain critical value, whereas below it no simple relationship was found. This behavior is typical of sources prepared by evaporation methods. Because of the lack of homogeneity of such sources, the concept of mean superficial density has little meaning and it follows that this critical value is ill defined. For these reasons, Merritt, Taylor, and Campion warn that curves such as theirs are intended as a guide and are valid for systems prepared under conditions closely similar to theirs.

Distillation techniques developed by Yaffe and co-workers (26, 27) give thin and uniform deposits, but the method is not simple for routine

Can. J. Chem. Downloaded from www.nrcresearchpress.com by 210.87.254.105 on 09/05/12
For personal use only.

Can. J. Chem. Downloaded from www.nrcresearchpress.com by 210.87.254.105 on 09/05/12
For personal use only.

source preparation. Keith and Watt (28) claimed that freeze drying can give uniform sources, but it seems that a great deal of skill is required to achieve this goal. As suggested earlier in this paper, electrodeposition could be used to prepare sources of several radionuclides for 4π β-counting. Besides being simple, efficient, and reproducible, the techniques described here give sources which possess the following attributes, important in 4π β-counting: (1) the sources are uniform; (2) only the metal is deposited; (3) as superficial density can be unambiguously defined, self-absorption corrections and values determined with accuracy could be used with confidence by other workers; (4) the conductivity of the film is not affected since the deposit is metallic.

Electrodeposition, however, has a disadvantage; it cannot be made 100% quantitative because, as discussed before, small losses by dissolution and on the membrane are unavoidable. It is a matter of deciding in each specific case if this disadvantage outweighs the possibility offered by the method of determining self-absorption with a good degree of accuracy. It is timely now to discuss the sources of errors associated with this method in connection with the preparation of sources for 4π β-counting.

The determination of chemical yields by γ-counting or by chemical analysis can easily be made with a precision of $\pm 2\%$ on each individual measurement; this error can be reduced below 1% in preparing several sources in a given series of measurements, as is common practice. The determination of the thickness of the metal deposits and conductive layer can be done with good precision and does not introduce an appreciable error. As the thickness of the VYNS is in the range of 15–40 μg/cm^2, one has to rely on a gravimetric method and the appearance of the film to estimate this quantity; the error could be $\pm 25\%$ in this measurement. Clearly, the development of a routine method for determining VYNS thickness in our working range is needed and we are currently investigating this problem. Ideally, self-absorption corrections as a function of the thickness should be done by the coincidence technique when the method is applicable and we expect to do this in the near future for Co-60, Hg-203, and Ag-110m. As the maximum β-energy of these radionuclides covers a range from 0.31 to 0.086 MeV, the self-absorption data could be used to establish a general curve for self-absorption as a function of the maximum β-energy for various thicknesses.

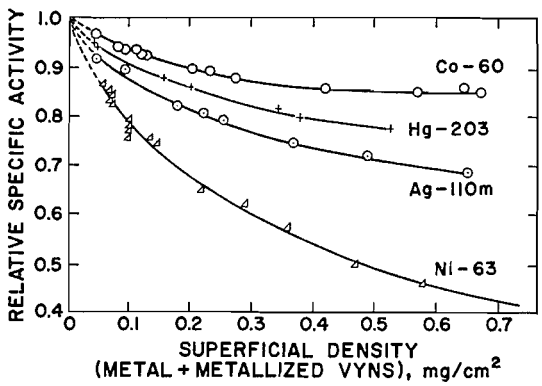

FIG. 4. Plots of the relative specific activity of sources of Co-60, Ni-63, Ag-110m, and Hg-203 vs. the total thickness (metal + metallized VYNS). The relative specific activity is the ratio of the observed disintegration rate per mg of the radioactive solution by the absolute disintegration rate per mg of the same radioactive solution.

For the time being, we have setup self-absorption curves by 4π β-counting electrodeposited sources of different thicknesses and, in Fig. 4, we have plotted relative specific activity vs. the total thickness (metal deposit + metallized VYNS). The self-absorption corrections for the sources of Co-60, Ag-110m, and Hg-203 were calculated by comparing the observed disintegration rates at various thicknesses with those determined by the standardization group at the International Atomic Energy Agency. Since the solution of Ni-63 used in the measurement was not absolutely standardized, we proceeded differently to set up the self-absorption curve. The thinnest nickel deposit used to establish the absorption curve was about 10 μg/cm^2 and the thickness of metallized VYNS was 50 μg/cm^2 for a total thickness of 60 ± 5 μg/cm^2. Then, we assume that the correction determined by Pate and Yaffe (29) for the absorption of the Ni-63 β-rays in metallized VYNS can be applied to the combination described above without introducing a serious error. Consequently, the correction given by Pate and Yaffe for absorption in a source mount of 60 μg/cm^2 was taken as the first point on the curve for Ni-63 in Fig. 4. Because self-absorption should be determined with better accuracy by the

coincidence technique and the thickness of the VYNS by an appropriate method, these curves should only be considered as tentative: they are given to indicate the general trend of self-absorption vs. the thickness for these four radionuclides.

Conclusion

The cell described here has been used for the spontaneous electrodeposition of the metals listed in the section on "Electrodeposition" and also with good results for the electrodeposition of Fe, Co, and Zn by the imposition of an external voltage. It is expected that most metals, which can be electrodeposited from an aqueous solution, could be plated on thin metallized plastic films using this cell; however, the most reactive metals might not have a useful lifetime on the film because of dissolution initiated by air oxidation. The case of thallium, mentioned earlier, is an extreme case of an element which can be easily electrodeposited but which has an ephemeral life when exposed to air.

The cell combines simplicity and versatility. Similar or different electrolyte solutions, aqueous or nonaqueous, can be placed separately in each electrode compartment. This feature should make it easier to perform the electrodeposition of some metals on metallized VYNS. In one experiment, a lithium electrode placed in ethylene glycol in the anode chamber has been used to achieve the spontaneous electrodeposition of Ni from an aqueous solution.

Although the cell has been developed for the preparation of thin and uniform radioactive sources for absolute rate determinations of low energy β-emitters, it is clear that it can be used to prepare solid sources of many other β-emitters and some α-emitters for different applications. The cell offers another technique for the preparation of targets for nuclides which can be electrodeposited, especially when the amount of starting material is low or when the material is a valuable enriched isotope. Finally, this cell should work equally well for the electrodeposition of elements on metal backings and might be an improvement on the devices actually in use.

1. L. YAFFE. Ann. Rev. Nucl. Sci. **12**, 153 (1962).
2. R. L. BLANCHARD, B. KAHN, and R. D. BIRKHOFF. Health Phys. **2**, 246 (1960).
3. C. D. BROYLES, D. A. THOMAS, and S. K. HAYNES. Phys. Rev. **89**, 715 (1953).
4. J. L. LINGANE. Electroanalytical chemistry. 2nd ed. Interscience Publishers, Inc., New York. 1958.
5. S. B. GARFINKEL and J. M. R. HUTCHINSON. Intern. J. Appl. Radiation Isotopes, **13**, 629 (1962).
6. A. SPERNOL, E. DE ROOST, and O. LERCH. Joint Nuclear Research Center Geel Establishment, Belgium. Report Eur. 477.e. 1964.
7. W. PARKER, M. DE CROËS, and K. SEVIER. Nucl. Instr. Methods, 7, 22 (1960).
8. W. PARKER. Methods in the preparation of radioactive material. Boktryckeri Aktiebolag, Göteborg. 1965. pp. 79–88.
9. W. C. PARKER and H. SLÄTIS. *In* Alpha, beta- and gamma-rays spectroscopy. Vol. 1. *Edited by* K. Siegbahn. North-Holland Publ. Co., Amsterdam. 1965. p. 383.
10. B. D. PATE and L. YAFFE. Can. J. Chem. **33**, 15 (1955).
11. C. C. LOWENTHAL and A. M. SMITH. Nucl. Instr. Methods, **30**, 363 (1964).
12. J. C. ROY and J. TURCOTTE. Can. J. Chem. **45**, 1379 (1967).
13. L. HOLLAND and W. STECKELMACHER. Vacuum, **2**, 346 (1952).
14. G. CHARLOT and D. BÉZIER. Méthodes électrochimiques d'analyse. Masson & Cie, Paris. 1954. p. 30.
15. J. S. MERRITT and J. G. V. TAYLOR. Atomic Energy of Canada Ltd., Chalk River. Report CRGP-1256. 1957.
16. J. C. ROY and C. COLAS. Report of Bureau International des Poids et Mesures, Sèvres. 1964.
17. A. SCHLEICHER. Electroanalytische schnellmethoden. Ferdinand Enke Verlag, Stuttgart. 1947.
18. A. SCHLEICHER and O. SCHLÖSSER. Z. Anal. Chem. **130**, 1 (1949).
19. R. W. DODSON, A. C. GRAVES, L. HELMHOLZ, D. L. HUFFORD, R. M. POTTER, and J. G. POVELITES. *In* Miscellaneous physical and chemical techniques of the Los Alamos Project experimental techniques. *Edited by* A. C. Graves and D. K. Froman. McGraw-Hill Book Co., Inc., New York. Natl. Nucl. Energy Ser. Div. V, **3**, 1 (1952).
20. Y. UJIHIRA and J. C. ROY. Can. J. Chem. This issue.
21. G. D. CHASE, S. RITUPER, and J. W. SULCOSKI. Experiments in nuclear science. Burgess Publishing Co., Minneapolis. 1964. p. 62.
22. C. HAENNY and P. MIVELAZ. Helv. Chim. Acta, **31**, 633 (1948).
23. C. J. MALETSKOS and J. W. IRVINE, JR. Nucleonics, **14**, 84 (1956).
24. A. P. BAERG. Metrologia, **2**, 23 (1966).
25. J. S. MERRITT, J. G. V. TAYLOR, and P. J. CAMPION. Can. J. Chem. **37**, 1109 (1959).
26. B. D. PATE and L. YAFFE. Can. J. Chem. **34**, 265 (1956).
27. L. YAFFE and J. B. FISHMAN. *In* Metrology of radionuclides. International Atomic Energy Agency, Vienna. 1960. p. 185.
28. R. L. G. KEITH and D. E. WATT. Nucl. Instr. Methods, **42**, 68 (1966).
29. B. D. PATE and L. YAFFE. Can. J. Chem. **33**, 929 (1955).

Can. J. Chem. Downloaded from www.nrcresearchpress.com by 210.87.254.105 on 09/05/12
For personal use only.

Can. J. Chem. Downloaded from www.nrcresearchpress.com by 210.87.254.105 on 09/05/12
For personal use only.

Spectrophotometric determination of traces of nickel as dithio-oxalate complex

Y. UJIHIRA[1] AND J. C. ROY
Département de Chimie, Université Laval, Québec, Québec

Received September 25, 1967

The reaction between nickel and potassium dithio-oxalate has been developed into a simple, quick, and precise method for the spectrophotometric determination of traces of nickel and has been applied to the analysis of this element in our studies on its electrodeposition on thin metallized plastic films. On making absorption measurements of the colored compound formed by the reaction in various bases and acids at different concentrations, it was found that a dilute sulfuric acid solution is a good medium for preparation of samples and making the measurements. Maximum absorption of the compounds occurs at 500 mμ and obeys the Beer–Lambert law over a suitable range. The effect of various ions on the determination of nickel by the method has been measured along with the absorption curves of the compounds formed by the reaction of potassium dithio-oxalate with cobalt and copper. The relative merits of the method are discussed with reference to other methods of analysis of traces of nickel.

Une méthode spectrophotométrique d'analyse de traces de nickel, basée sur la réaction de cet élément avec le dithio-oxalate de potassium, a été mise au point. Au cours d'essais avec différents acides et bases, il a été trouvé que dans une solution diluée d'acide sulfurique le composé coloré issu de cette réaction se forme rapidement et possède la stabilité requise pour faire des mesures d'absorption. L'absorption est maximale à 500 mμ et obéit à la loi de Beer–Lambert. En plus de mesurer les spectres d'absorption des composés formés par la réaction du dithio-oxalate de nickel avec le cobalt et le cuivre, nous avons déterminé les concentrations tolérables pour plusieurs autres éléments qui contribuent à l'absorption à 500 mμ. Cette méthode a été utilisée avec succès pour l'analyse de nickel dans plus de quarante échantillons, obtenus au cours d'études sur l'électrodéposition de cet élément sur des films plastiques minces. La méthode se caractérise par sa simplicité et présente plusieurs avantages sur celles déjà décrites pour l'analyse de traces de nickel.

Canadian Journal of Chemistry, 46, 1233 (1968)

Introduction

The reaction of nickel with potassium dithio-oxalate, $K_2C_2O_2S_2$, first observed by Jones and Tasker (1) has been used by Fairhall (2) and Yoe and Wirsing (3) for the colorimetric determination of nickel. These investigations indicated that the reagent is extremely sensitive and permits the determination of very small amounts of nickel. The reaction has been further studied in order to establish if it could be developed into a simple, quick, and precise method for the spectrophotometric determination of microgram amounts of nickel in our work on the electrodeposition of the element on thin metallized plastic films (4). Thus, the absorption spectrum of the complex, the application of the Beer–Lambert law, and the effect of various ions and different experimental conditions have been determined. These studies showed that the reaction meets the requirements set above for our specific application and could also be applicable to the analysis of traces of nickel in a wide variety of samples.

[1]Laval University Postdoctorate Fellow. On leave from the University of Tokyo, Japan.

Method and Results

Reagents and Apparatus

The potassium dithio-oxalate was obtained from Eastman Kodak. A 0.05% aqueous solution of potassium dithio-oxalate was freshly prepared, a more concentrated solution tending to form a white turbidity in less than 50 h. The standard nickel solution consisted of 40 μg of Ni^{2+} per ml of a 0.1 *N* H_2SO_4 solution. The absorption measurements were made with a Beckman model DU spectrophotometer.

Reaction of Nickel with Potassium Dithio-oxalate

According to Jones and Tasker (1), the reaction of potassium dithio-oxalate with nickel salts is represented by the following equation.

$$2K_2C_2O_2S_2 + NiX_2 = K_2(C_2O_2S_2)_2Ni + 2KX$$

Our spectrophotometric measurements support this reaction. It follows then that 6.75 μg of $K_2C_2O_2S_2$ will be required to react with 1 μg of nickel. Under our experimental conditions, it has been found that the amount of $K_2C_2O_2S_2$ needed to react with 0–60 μg of nickel should be about 10% higher than the values calculated from

Can. J. Chem. Downloaded from www.nrcresearchpress.com by 210.87.254.105 on 09/05/12
For personal use only.

the above equation. Yoe and Wirsing (3) have made a similar observation and have explained it by a slight decomposition of the reagent. This seems to be the most likely explanation.

Absorbancy of the Complex in Various Media

Absorbancy measurements of the potassium nickelo-dithio-oxalate complex were made in various bases and acids at different concentrations. In solutions where the normality of H_2SO_4 or HNO_3 varies between 1 and 1×10^{-5}, the color development of the complex is not affected by the acidity of the solution. In 0.1 *N* H_2SO_4 solution, the complex reaches its maximum color intensity within 10 s and is stable for at least 90 min, whereas in 1 *N* H_2SO_4 the coloration decreases by about 10% in 30 min, a process which is accelerated at higher concentrations. In 1 *N* HCl or 0.1 *N* NH_4OH, it takes more than 20 min to get the maximum color intensity while in 1 *N* NH_4OH or in 0.1 *N* NaOH no coloration is observed. On the basis of these experiments, a medium approximately 0.1 *N* in H_2SO_4 has been selected to make the spectrophotometric determination of nickel, rather than a more dilute solution, primarily to facilitate the dissolution of the nickel salts in one of the operations required for the preparation of the samples used in studying firstly the absorption characteristics of the complex and secondly the electrodeposition of nickel on metallized thin films.

For the preparation of the first type of sample, the procedure was as follows: (*a*) addition of sufficient standard nickel solution in a 25 ml beaker in order to have from 0–50 μg of Ni^{2+}, evaporation of the solution under an infrared lamp, and dissolution of the residue with 1 ml of 1 *N* H_2SO_4 by swirling the solution; (*b*) dilution with 8 ml of distilled water, making-up of the volume to 10 ml with 1 ml of 0.05% solution of potassium dithio-oxalate, and mixing again by swirling the solution.

When the amount of nickel is in the range of 50–120 μg, the added volume of water and reagent in step (*b*) should be 7 and 2 ml respectively. In using the amount of potassium dithio-oxalate suggested, one avoids the presence of a large excess of reagent which accelerates fading of the coloration of the complex. The additions of the solutions were done with calibrated pipets and the absorbancy measurements were done immediately after the preparation of the mixture using water as blank.

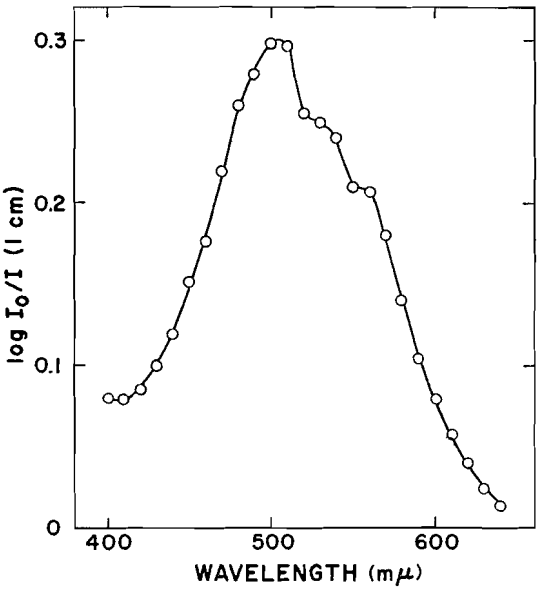

FIG. 1. Absorbancy curve of potassium nickelo-dithio-oxalate compound: 4 μg of Ni per ml of a 0.1 *N* H_2SO_4 solution. Blank: water.

The absorption spectrum of the potassium nickelo-dithio-oxalate complex in 0.1 *N* H_2SO_4 is given in Fig. 1. The absorption maximum is at 500 mμ and this was the wavelength selected to make the spectrophotometric determination of nickel. At this wavelength, the absorbancy is the same, within ±2%, in solutions from 1 to 10^{-5} *N* in sulfuric acid (range of concentrations investigated in these measurements). It follows that within these limits the concentration of sulfuric acid is not critical in the spectrophotometric determination. One should remember, however, that the complex is less stable in 1 *N* H_2SO_4 than in more dilute solution and for this reason a medium about 0.1 *N* in H_2SO_4 was used to make the measurements. We found it more convenient to use water as blank rather than dithio-oxalate solution prepared by the same procedure as the nickel sample. If this practice is followed, it is important to add the same amount of reagent for setting up the calibration curve and for determining the amount of nickel in the unknown because the reagent absorbs light to a slight extent and the absorption follows the Beer–Lambert law at 500 mμ.

Beer–Lambert Law

In Fig. 2 the absorbancy of the complex at 500 mμ is plotted vs. the amount of nickel in

Can. J. Chem. Downloaded from www.nrcresearchpress.com by 210.87.254.105 on 09/05/12
For personal use only.

0.1 N H_2SO_4 solution. The absorption obeys the Beer–Lambert law in the range 0–6 μg of nickel per ml of solution and appears to follow it from 6–12 μg of nickel per ml solution (inasmuch as could be verified with the data obtained). It was difficult to gather precise results in this region because discoloration of the complex goes faster and faster as the amount of nickel increases. The best range for making the measurements is, for absorbancy values between 0.1 to 0.3, that corresponding to 1–4 μg of nickel per ml of solution. The intersection of the calibration curve with the ordinate at 0.011 rather than at 0 is due to the slight absorption of the reagent and to the fact that water was used as blank.

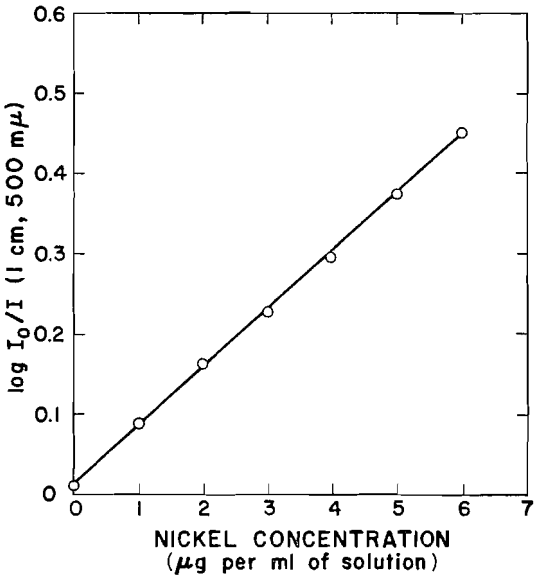

FIG. 2. Calibration curve for determination of nickel by the potassium dithio-oxalate method in a 0.1 N H_2SO_4 solution. Blank: water.

Effect of Various Ions

Jones and Tasker (1) and Yoe and Wirsing (3) have observed that many ions react with potassium dithio-oxalate to form color compounds. We have determined, for many of them, the amount which can be present without interfering with the spectrophotometric analysis of nickel at 500 mμ and have measured the absorption spectra of the compounds formed by the reaction of cobalt and copper with potassium dithio-oxalate (Fig. 3). The concentrations of these two ions must be under 1/20 that of nickel to reduce their contribution to the total absorbancy to about 2% at 500 mμ. One μg per ml of Ag, Au, Hg, Fe(II), or Fe(III) introduces a 5–20% error. The presence of 30 μg/ml of Cr, 300 μg/ml of Cd, 100 μg/ml of La, Ca, or Mn, 300 μg/ml of Mg or Zn does not interfere with the nickel determination and also, in the absence of sulfate ion, 30 μg/ml of Pb and 300 μg/ml of Ba and Sr can be tolerated.

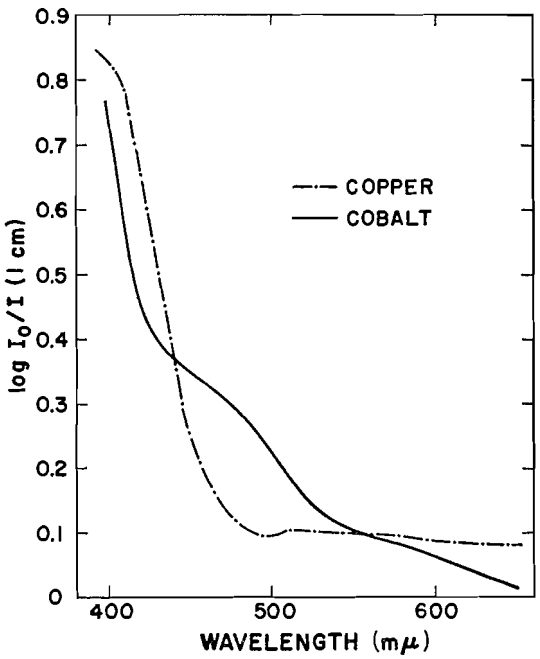

FIG. 3. Absorbancy curves of compounds formed by the reaction of cobalt and copper with potassium dithio-oxalate: 5 μg of either element per ml of a 0.1 N H_2SO_4 solution. Blank: water.

Determination of Nickel Electrodeposited on Thin Films

For this application, the amount of nickel introduced initially into the catholyte is accurately known and varied from 0 to about 500 μg. To begin with, we wished to analyze the distribution of nickel in the catholyte, in the washing, on the membrane, and on the film in order to determine the optimum conditions for its electrodeposition; once these were established, we were mainly interested to know the deposition efficiency and used one of the three following approaches to obtain this quantity: (*a*) direct analysis of nickel on the film and calculation of the chemical yields by taking the ratio nickel on the film/initial amount of nickel; (*b*) analysis of nickel in the combined fractions, catholyte, and washing

Can. J. Chem. Downloaded from www.nrcresearchpress.com by 210.87.254.105 on 09/05/12
For personal use only.

(the amount on the membrane was found to be negligible) and calculation of the yield by difference; (*c*) simultaneous use of modes (*a*) and (*b*) in the same run.

Although the last approach is the best, because it permits cross-checking of the data and estimation of the accuracy of the method, modes (*a*) or (*b*) can be used with confidence and give good results. For this application, method (*b*) was preferred when the amount of nickel in the catholyte and washing was 5–50 μg, otherwise method (*a*) was adopted. By following this rule, the concentration of nickel in the final sample was usually in the best working range for spectrophotometric determination at 500 mμ and, furthermore, a dilution operation could often be eliminated in the procedure. Since the deposition efficiency was of the order of 95%, it meant that in practice method (*b*) was used for sources having superficial densities higher than about 50 μg/cm^2 and method (*a*) for thinner sources.

The general procedure for the preparation of the samples was as follows: (i) if method (*a*) is used, dissolve the nickel deposit with a few drops of conc. HNO_3 under an infrared lamp and evaporate to dryness (gold and palladium remain undissolved on the film); if method (*b*) is used, transfer the catholyte and washings into a 25 ml beaker and evaporate to dryness under an infrared lamp; dissolve the residue in 1 ml of a 1 *N* H_2SO_4 solution; (ii) if the amount of nickel is less than 50 μg, add 8 ml of water, make up the volume to 10 ml with 1 ml of the 0.05% potassium dithio-oxalate solution, mix by swirling, and measure the absorbancy at once; if the amount of nickel is more than 50 μg, transfer the 1 *N* H_2SO_4 solution in a 5, 10, or 20 ml volumetric flask depending on the amount of nickel, add water up to the mark, mix the solution, then pipet at least 2 aliquots of 1 or 2 ml into a 25 ml beaker, make up the solution to 9 ml with water, add 1 ml of the 0.05% solution of potassium dithio-oxalate, mix by swirling, and measure the absorbancy at once.

More than 40 determinations of nickel have been successfully done by following this procedure in our studies on the electrodeposition of nickel. It has been estimated that each of the three operations, setting up the calibration curve, spectrophotometric reading, and preparation of the sample, introduces a ±2% error; since the operations are independent, the errors can be combined quadratically to yield a ±3.5% standard error on each nickel determination. This figure would also represent our estimate of the precision of the method for the analysis of traces of nickel in samples for which its initial concentration is not known.

The sensitivity of the method is good down to 0.5 μg of nickel per ml of solution, but below this limit the precision rapidly decreases.

Conclusion

Yoe and Wirsing have studied the reaction between potassium dithio-oxalate and nickel with reference to its use in colorimetry. In the present investigation, the reaction has been developed into a spectrophotometric method of analysis and thereafter has been used for the routine determination of nickel in different samples resulting from experiments on the electrodeposition of micrograms of this element on thin metallized plastic films. The spectrophotometric determination of nickel as the dithio-oxalate complex has been found to be the most convenient method of analysis for the type of application described in the paper. In fact, it has several advantages over other colorimetric methods (5): color development is obtained in acidic medium and the concentration of the acid is non-critical over a wide range; no extraction by an organic solvent is required to make the absorbancy measurement; the maximum absorption falls at a very convenient wavelength at which to make the measurement; the sensitivity is comparable to the dimethylglyoxime methods; the complex and color are stable for an adequate period of time. The great advantage of the method is its simplicity, the main disadvantage is a poorer selectivity than the other methods. When this requirement is not important, the use of potassium dithio-oxalate becomes very attractive to determine traces of nickel.

1. H. O. Jones and H. S. Tasker. J. Chem. Soc. **95**, 1904 (1909).
2. L. T. Fairhall. J. Ind. Hyg. **8**, 528 (1926).
3. J. H. Yoe and F. H. Wirsing. J. Am. Chem. Soc. **54**, 1866 (1932).
4. Y. Ujihira and J. C. Roy. Can. J. Chem. This issue.
5. E. B. Sandell. Colorimetric determination of traces of metals. 3rd ed. Interscience Publishers, Inc., New York. 1959. p. 665.

Trifluoromethyl-substituted fluorophosphates and fluoroarsenates

S. S. CHAN AND C. J. WILLIS
Department of Chemistry, University of Western Ontario, London, Ontario
Received August 15, 1967

Synthetic routes have been developed to salts containing the anions $[CF_3PF_5]^-$, $[(CF_3)_2PF_4]^-$, $[(CF_3)_3PF_3]^-$, $[(CF_3)_2AsF_4]^-$, and $[(CF_3)_3AsF_3]^-$. These are isolated as stable solids with Cs^+, or sometimes Ag^+, as the cation. Their ^{19}F n.m.r. spectra are discussed, and it is suggested that the bis- and tris-(trifluoromethyl)-substituted fluorophosphates have a *trans* configuration.

Trimethyltrifluoromethyltin, $(CH_3)_3SnCF_3$, forms 1:1 complexes with PF_5, $(CF_3)_2PF_3$, and $(CF_3)_3PF_2$. It is suggested that transfer of a trifluoromethyl group as CF_3^- has occurred here, leading to the formation of trimethyltin derivatives of the trifluoromethyl-substituted fluorophosphates.

Canadian Journal of Chemistry, 46, 1237 (1968)

Can. J. Chem. Downloaded from www.nrcresearchpress.com by 210.87.254.105 on 09/05/12
For personal use only.

Comparatively little is known of substituted halophosphate or haloarsenate anions, i.e. $[R_nPX_{6-n}]^-$ or $[R_nAsX_{6-n}]^-$ where X is a halogen. The ions $[CH_3PF_5]^-$ and $[C_6H_5PF_5]^-$ have been studied, largely using nuclear magnetic resonance (n.m.r.) methods, by Muetterties and Mahler (1) and by Schmutzler and Reddy (2). Other workers have demonstrated by conductance measurements the existence in solution of phenoxy derivatives such as $[(C_6H_5O)_3PBr_3]^-$ (3*a*), $[(C_6H_5O)_2PBr_4]^-$ (3*b*), and $[(C_6H_5O)_2PCl_4]^-$ (3*b*). Several mixed halophosphate ions have also been postulated, again on the basis of conductance measurements (4): these include $[PCl_4F_2]^-$, $[PBr_4F_2]^-$, and $[PCl_5Br]^-$. The chemistry of the hexahaloarsenate ions is even more restricted, and only $[AsF_6]^-$ and $[AsCl_6]^-$ are known.

A number of trifluoromethyl phosphorus(V) halides are well characterized, including the compounds $(CF_3)_3PCl_2$ (5), $(CF_3)_2PCl_3$ (6), CF_3PCl_4 (7), $(CF_3)_3PF_2$, $(CF_3)_2PF_3$, and CF_3PF_4 (8). A similar range of trifluoromethyl arsenic(V) fluorides and chlorides is also known (9).

No reports have appeared on the isolation of trifluoromethyl-substituted halophosphates or haloarsenates as simple metallic salts. Emeléus and Harris (10) suggested the equilibrium

$$2(CF_3)_3PCl_2 \rightleftharpoons [(CF_3)_3PCl]^+ + [(CF_3)_3PCl_3]^-$$

to account for the conductivity of tris(trifluoromethyl)phosphorus dichloride in acetonitrile solution, but did not isolate any compound containing the anion. Reports of related anions include the hydrogen-containing ion $[CF_3PF_4H]^-$ (11) and the antimony derivatives $[(CF_3)_3SbCl_3]^-$ and $[(CF_3)_3SbBr_3]^-$ (12).

Synthetic Routes

In view of the electronegativity of the trifluoromethyl group and the stability of its known compounds with phosphorus and arsenic, it would be expected that derivatives of the type $[(CF_3)_nPF_{6-n}]^-$ and $[(CF_3)_nAsF_{6-n}]^-$ would also be stable, and this we have found to be the case. The most general method of preparation is through the reaction of the appropriate trifluoromethyl phosphorus or arsenic halide with a suspension of cesium fluoride in acetonitrile, when simple addition of a fluoride ion occurs readily to give the above anions, where $n = 1$, 2, or 3 for phosphorus and $n = 2$ or 3 for arsenic.

Another preparative route is through the fluorination of the corresponding salts of the trifluoromethyl oxyacids. The fluorinating agent used was sulfur tetrafluoride, known to be suitable for the replacement of oxygen by fluorine (13), and in this way the silver and cesium salts of the bis(trifluoromethyl)tetrafluorophosphate anion were prepared:

$$Ag[(CF_3)_2PO_2] + 2SF_4 \rightarrow Ag[(CF_3)_2PF_4] + 2SOF_2.$$

However, this method did not appear to be as generally applicable as that mentioned above.

A third possible route to trifluoromethyl-substituted anions is available through the reactions of trimethyltrifluoromethyltin. This compound is known to undergo heterolytic fission of the Sn—CF_3 bond when it reacts with boron trifluoride, giving trimethyltin trifluoromethylfluoroborate (14):

$$(CH_3)_3SnCF_3 + BF_3 \rightarrow [(CH_3)_3Sn]^+[CF_3BF_3]^-.$$

It might be expected, therefore, that reaction with other Lewis acids, such as derivatives of

Can. J. Chem. Downloaded from www.nrcresearchpress.com by 210.87.254.105 on 09/05/12
For personal use only.

P(V) or As(V), would lead to a similar migration of CF_3^- to yield trifluoromethyl-substituted anions, e.g.

$$(CH_3)_3SnCF_3 + PF_5 \rightarrow [(CH_3)_3Sn]^+[CF_3PF_5]^-.$$

In particular, this route alone offers the possibility of putting more than three trifluoromethyl groups on to a phosphorus or arsenic atom, e.g.

$$(CH_3)_3SnCF_3 + (CF_3)_3PF_2 \rightarrow [(CH_3)_3Sn]^+[(CF_3)_4PF_2]^-.$$

This synthetic route did not lead to such clear-cut results as the previous two, but some reactions did occur and the possible structures of the products obtained are discussed below.

The compounds obtained by these three approaches will now be discussed under the headings of phosphorus compounds, arsenic compounds, and trimethyltin derivatives.

Substituted Fluorophosphates

The compounds prepared were the three cesium salts $Cs[(CF_3)_nPF_{6-n}]$, where $n = 1$, 2, or 3, and the silver salt $Ag[(CF_3)_2PF_4]$. The cesium salts were all stable white solids, water-soluble, and recoverable unchanged from aqueous solution. They were also soluble in polar organic solvents. On heating, the solids decomposed above 200° to give fluorocarbons and a residue containing cesium fluorophosphate.

The silver salt was less stable than the cesium salts and decomposed at 120° to give silver fluoride and bis(trifluoromethyl)phosphorus trifluoride. Presumably, the cesium salts do not decompose in a similar way because the various phosphoranes are not stable at the higher decomposition temperatures.

The principal peaks of the infrared spectra of the cesium salts in acetonitrile solution are given in Table I.

Bennett, Emeléus, and Haszeldine (15) observed that the carbon–fluorine stretching modes in a number of trifluoromethylphosphines fell to between 1250 and 1100 cm^{-1}, with a band between 750 and 735 cm^{-1} attributed to a trifluoromethyl deformation mode. In the hexafluorophosphate ion, infrared absorptions are found at 847 and 561 cm^{-1} (16), with a Raman-active absorption at 741 cm^{-1} (17).

The absorption bands present in the trifluoromethylfluorophosphates in the region 1100–1230 cm^{-1} may therefore be assigned to C—F stretching frequencies, while absorptions in the region 620–830 cm^{-1} are mainly associated with P—F bonds. Each spectrum contains at least one absorption in the region associated with C—F deformation frequencies (740–750 cm^{-1}) but these cannot be definitely distinguished from P—F absorptions. The spectrum of the ion $[(CF_3)_2PF_4]^-$ contains fewer absorption peaks in the P—F region, irrespective of the assignment of that at 751 cm^{-1}, suggesting a higher degree of symmetry for this ion than the other two. The infrared spectrum of the silver salt, $Ag[(CF_3)_2PF_4]$, also showed only three bands in the P—F region at 786, 758, and 639 cm^{-1} (Nujol mull). The similarity of these to the frequencies found with the corresponding cesium salt suggests that the ions have the same configuration.

TABLE I

Infrared spectra of cesium trifluoromethylfluorophosphates (acetonitrile solution)

$Cs[CF_3PF_5]$	$Cs[(CF_3)_2PF_4]$	$Cs[(CF_3)_3PF_3]$
1317 (vw)	1307 (w)	1305 (w)
1221 (m)	1230 (s)	1208 (s)
		1175 (m)
1109 (vs)	1119 (vs)	1138 (s)
		1108 (s)
		1056 (vw)
1029 (vw)	1033 (vw)	1028 (vw)
829 (vs)	815 (vs)	810 (m)
804 (s)		
750 (vw)	751 (m)	764 (m)
723 (m)		740 (vw)
657 (m)		706 (m)
636 (w)	635 (s)	620 (s)
549 (m)	578 (w)	

Further information on the structures of the ions was obtained from their n.m.r. spectra, taken in acetonitrile solution. The solubility of the salts in this solvent is limited, leading to an unfavorable signal-to-noise ratio in the ^{19}F resonance spectra and making it impossible to obtain a ^{31}P resonance spectrum.

Since both ^{19}F and ^{31}P have a spin of 1/2, a considerable amount of spin–spin coupling would be expected in the fluorine resonance spectrum, and the fact that this was observed indicates that no interionic exchange of fluorine atoms was occurring. In many cases, however, the resulting multiplets did not appear symmetrical. Muetterties and Mahler (1) also reported distorted spin–spin coupling multiplets in the fluorine n.m.r. spectra of the methylpentafluoro-

Can. J. Chem. Downloaded from www.nrcresearchpress.com by 210.87.254.105 on 09/05/12
For personal use only.

phosphate and phenylpentafluorophosphate anions, attributing this to the fact that the coupling constant between non-equivalent fluorine nuclei is of the same order of magnitude as the difference in their chemical shifts. Pople, Schneider, and Bernstein (ref. 18, p. 96) point out that such distortion is frequently found for interacting non-equivalent nuclei of the same species where the difference in chemical shifts is of the same order of magnitude as the coupling constant.

For the ion $[CF_3PF_5]^-$, only one structure is possible (assuming octahedral coordination about the phosphorus atom): an arrangement of C_{4v} symmetry with a trifluoromethyl group at one vertex. This will lead to three types of fluorine atom in the ion, those in the CF_3 group, four equivalent atoms in an equatorial position (F_e), and one atom *trans* to the CF_3 group in an apical position (F_a).

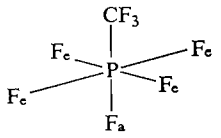

This should produce three resonance signals of relative intensities 3:4:1, with various multiplets produced by spin–spin coupling.

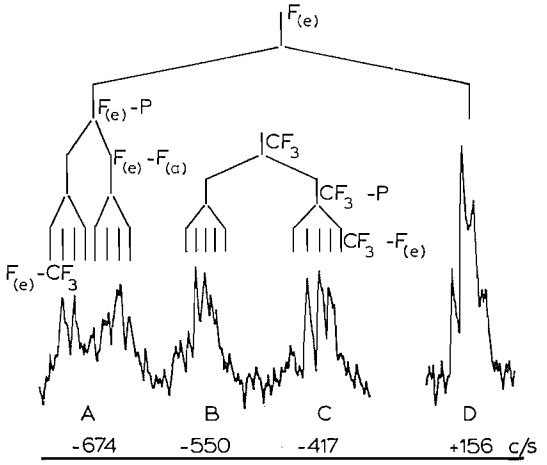

FIG. 1. ^{19}F n.m.r. spectrum of $Cs[CF_3PF_5]$ (acetonitrile solution).

The actual spectrum obtained is shown in Fig. 1, and is quite complex. The coupling pattern shown in the figure, and discussed here, provides a rationalization of the spectrum in terms of the structure of the ion, but this must be regarded with reserve because of the possibility that the spectrum is not first order. It contains groups of absorption peaks centered on −674, −550, −417, and +156 c/s (all chemical shifts are from external trifluoroacetic acid) which are designated as A, B, C, and D respectively. Although peaks A and D are of different appearance, we assign them both to the F_e atoms, the splitting between them (J = 830 c/s) being due to coupling with the phosphorus atom to which they are directly linked. Further splitting, only resolved in peak A, is found in the form of a doublet (J = 52 c/s) due to coupling of the F_e atoms with the F_a atom, and the final splitting into quartets (J = 12 c/s) is assigned to coupling between the F_e atoms and fluorine atoms of the CF_3 group.

The remaining absorption in the spectrum, peaks B and C, is then assigned to the fluorine atoms of the CF_3 group, the primary splitting (J = 133 c/s) being due to coupling with the phosphorus atom. Further splitting into quintets (J = 12 c/s) is then apparent, assigned to coupling with the four F_e atoms. It would be expected that interaction with the single F_a atom would give further splitting into doublets, and on some of the peaks at C a splitting of 4 c/s was observed. The resolution attainable, however, did not permit any definite decision on this point.

Further absorption peaks, associated with the F_a atom, should be present in the spectrum but were not observed. This is presumably due to their lower intensity (only 1/4 that of the F_e peaks) and high degree of multiplicity.

The bis(trifluoromethyl)tetrafluorophosphate anion, $[(CF_3)_2PF_4]^-$, could exist in two octahedral structures, a *trans* arrangement of D_{4h} symmetry (**1**) or a *cis* arrangement of C_{2v} symmetry (**2**).

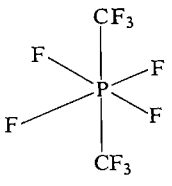

1

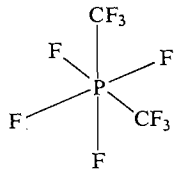

2

Structure **1** contains only two kinds of fluorine atom, the six on the CF_3 groups and

Can. J. Chem. Downloaded from www.nrcresearchpress.com by 210.87.254.105 on 09/05/12
For personal use only.

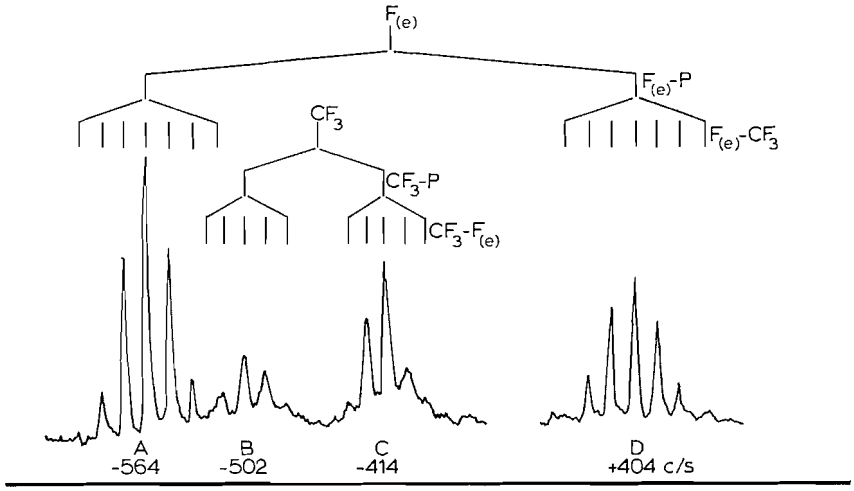

FIG. 2. ^{19}F n.m.r. spectrum of $Cs[(CF_3)_2PF_4]$ (acetonitrile solution).

the remaining four on the phosphorus atom, and it would therefore be expected to give two absorption peaks in an intensity ratio 6:4. Structure **2** contains three types of fluorine atom, since the four attached to the phosphorus atom now form two pairs in different environments, and would therefore give three signals in an intensity ratio 6:2:2.

The ^{19}F n.m.r. spectrum of the ion, Fig. 2, makes it clear that it is present exclusively in the *trans* form, structure **1**.

As in the previous spectrum, absorption peaks are present in four regions, centered on −564, −502, −414, and +404 c/s, which are referred to as A, B, C, and D respectively. The distortion referred to previously is still present, but to a smaller extent.

The peaks at A and D are assigned to the four fluorine atoms directly linked to phosphorus, the splitting between them (968 c/s) being due to coupling with the ^{31}P nucleus. Each peak is split into a septet ($J = 14$ c/s) by coupling with the six equivalent fluorine atoms in the two CF_3 groups.

The remaining absorptions at B and C are associated with the fluorine atoms of the trifluoromethyl groups, the primary splitting ($J = 88$ c/s) being due to coupling with the phosphorus atom and the further splitting into a quintet ($J = 14$ c/s) associated with coupling to the other four fluorine atoms. The relatively simple nature of this n.m.r. spectrum is a consequence of the high symmetry of the ion; it will be recalled that the infrared spectrum of this ion also suggested a symmetrical structure.

The ^{19}F n.m.r. spectrum of the tris(trifluoromethyl)trifluorophosphate ion, $[(CF_3)_3PF_3]^-$, was considerably more complex. Again, two structures are possible, with the three trifluoromethyl groups arranged in either a *trans* configuration of C_{2v} symmetry (**3**) or a *cis* configuration of C_{3v} symmetry (**4**).

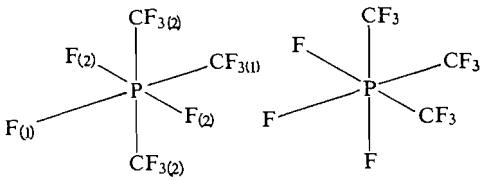

3 **4**

The trifluoromethyl groups in structure **3** are of two types, one is *trans* to a fluorine atom, $CF_{3(1)}$, and two are *trans* to each other, $CF_{3(2)}$. Similarly, there is one fluorine atom on phosphorus, $F_{(1)}$, which is *trans* to a trifluoromethyl group while the other two, $F_{(2)}$, are *trans* to each other. The n.m.r. spectrum should therefore contain four signals in an intensity ratio of 6:3:2:1, each signal being of high multiplicity through spin–spin interactions.

For structure **4**, however, the trifluoromethyl groups are all equivalent, as are the three fluorine atoms on phosphorus, so two signals would be expected in an intensity ratio 9:3.

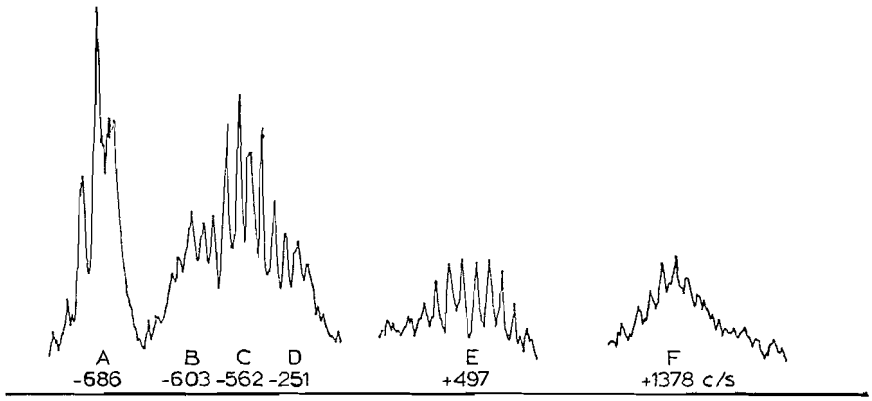

FIG. 3. ^{19}F n.m.r. spectrum of $Cs[(CF_3)_3PF_3]$ (acetonitrile solution).

The observed spectrum is shown in Fig. 3, and its complex appearance indicates that a first order analysis would not be valid. By analogy with the other ions studied, we suggest that the absorption peaks E and F, at higher field, are due to fluorine atoms directly linked to phosphorus, the splitting between them ($J =$ 881 c/s) being caused by coupling with the phosphorus atom. The remaining absorption, in areas A, B, C, and D, is then associated with the fluorine atoms in the trifluoromethyl groups.

Although a complete analysis of this spectrum cannot be made, it is apparent that the *trans* configuration must predominate, its four different types of fluorine atom giving rise to the complex interactions observed. The *cis* configuration, containing only two types of fluorine atom, would be expected to give a recognizable and much simpler spectrum. However, such a spectrum could easily be incorporated within that observed, and we cannot therefore suggest on present evidence that the ion is exclusively present in the *trans* form.

The chemical shifts and coupling constants found in these three ions are summarized in Table II, together with similar data on other ions.

The data obtained in the present work are consistent with those obtained previously. It will be seen that there is a progressive change in the chemical shift of the resonance for the fluorine atoms on the phosphorus as the number of trifluoromethyl groups is increased. For $[PF_6]^-$, the resonance is at -11.6 p.p.m., while for $[(CF_3)_3PF_3]^-$ it has moved up to $+16.6$ p.p.m. In view of the relative electronegativities of the fluorine atom and the trifluoromethyl group, this change will be accompanied by an increase in the electron density around the remaining fluorine atoms, but data accumulated from other sources (ref. 18, p. 172) suggest that it would not be valid to infer a causal relationship between electron density and chemical shift.

Substituted Fluoroarsenates

The cesium salts of the trifluoromethyl-substituted fluoroarsenates were prepared by the same general method as the corresponding phosphorus derivatives: the reaction of cesium fluoride with the appropriate trifluoromethyl arsenic(V) fluoride, e.g.

$$(CF_3)_2AsF_3 + CsF \rightarrow Cs[(CF_3)_2AsF_4].$$

This method was successful for the bis(trifluoromethyl)tetrafluoroarsenate and the tris(trifluoromethyl)trifluoroarsenate, $Cs[(CF_3)_3AsF_3]$, but it could not be applied to the preparation of the mono-substituted ion, $[CF_3AsF_5]^-$, because the parent fluoride, CF_3AsF_4, is not known, and attempts to prepare it were unsuccessful.

The alternative route to these compounds, using sulfur tetrafluoride as a fluorinating agent, was used to prepare silver bis(trifluoromethyl)-tetrafluoroarsenate from the oxygen-containing salt:

$$Ag[(CF_3)_2AsO_2] + 2SF_4 \rightarrow Ag[(CF_3)_2AsF_4] + 2SOF_2.$$

This method, however, did not give the corresponding reaction with the cesium salt, nor could it be used for the preparation of either the cesium or the silver trifluoromethylpentafluoroarsenate.

Can. J. Chem. Downloaded from www.nrcresearchpress.com by 210.87.254.105 on 09/05/12
For personal use only.

TABLE II

Chemical shifts and coupling constants in the ^{19}F n.m.r. spectra of substituted fluorophosphates

Ion	Chemical shifts, p.p.m.			Spin–spin coupling constants, c/s					
	F	CF_3	δ(F—F)†	F_e—P	F_a—P	CF_3—P	F_a—F_e	F—CF_3	Ref.
$[PF_6]^-$	−11.6			710					(19)
$[CF_3PF_5]^-$	−4.4	−8.6		802	N.O.	133	52	12	*
$[(CF_3)_2PF_4]^-$	−1.4	−8.0		968		88		14	*
$[(CF_3)_3PF_3]^-$	+16.6	−11.0 to −10.0		881					*
$[CF_3PF_4H]^-$	−16.1	−11.2		858		156		14.7	(11)
$[CH_3PF_5]^-$			10.3	830	691		39		(1)
$[CH_3PF_5]^-$			11.8	829	680		35		(2*b*)
$[C_6H_5PF_5]^-$			3.7	830	680		41		(1)
$[C_6H_5PF_5]^-$			3.0	820	700		40		(2*c*)

*Data from present work. All spectra recorded at 56.4 Mc/s.
†δ(F—F) represents the difference in chemical shift between F_a and F_e.

The cesium salts were both white solids, soluble in polar organic solvents. They dissolved readily in water, and cesium tris(trifluoromethyl)trifluoroarsenate could be recovered unchanged by freeze-drying. Cesium bis(trifluoromethyl)tetrafluoroarsenate, however, appeared to hydrolyze rapidly and could not be recovered from aqueous solution.

The infrared spectra of the three compounds were consistent with their proposed structures. Emeléus and co-workers (9) reported that the spectra of a number of trifluoromethyl derivatives of arsenic were similar to those of the analogous phosphorus compounds, containing vibrational absorption frequencies of the CF_3 group in the region 1110–1250 cm^{-1} and a deformation band near 735 cm^{-1}. The infrared spectrum of the hexafluoroarsenate ion has been observed by Weidlein and Dehnicke (20) in the compounds $[AsCl_4^+][AsF_6^-]$ and $KAsF_6$. The former showed absorptions in the region 402–389 cm^{-1} with further bands at 706 and 587 cm^{-1}, while the potassium salt showed only a very strong absorption at 700 cm^{-1} and weaker bands in the region 410–389 cm^{-1}.

The principal absorptions in the spectra of the compounds prepared in the present work are shown in Table III.

Strong absorptions of C—F stretching frequencies are present in all spectra, with a deformation mode near 735 cm^{-1} observed in most cases. The expected bands near 400 cm^{-1} associated with As—F bonds only show up in the mulls of the two cesium salts, but the absorptions between 500 and 660 cm^{-1} are presumably also due to As—F vibrations. All the absorption peaks of these compounds were considerably broader than those of the analogous phosphorus compounds.

The ^{19}F n.m.r. spectra of the arsenic compounds were not well resolved and no fine structure could be observed. This effect was to be expected from the known quadrupole moment ($Q = 0.3$) of the ^{75}As nucleus, which causes a broadening of the resonance signals. However, sufficient information was obtained from the n.m.r. spectra to give some evidence for the configuration of the ions.

For the ion $[(CF_3)_2AsF_4]^-$, two configurations are possible, the *trans* and *cis* that were shown as (**1**) and (**2**) for the analogous phosphates. By arguments advanced previously, the *trans* isomer would be expected to show two signals in an intensity ratio of 6:4, while the *cis* isomer would show three absorptions in an intensity ratio of 6:2:2.

The observed spectrum of this ion is shown at (*a*) in Fig. 4. It shows a fairly sharp absorption peak at −13.1 p.p.m. and very broad absorptions centered on −150 and −85 p.p.m. The first of these peaks is presumably associated with the trifluoromethyl groups in the ion and, since no other absorptions were detected, it could be suggested that the two peaks at low field were due to the other four fluorine atoms. Since there are two of them, this would then indicate that the ion is in the *cis* configuration.

This explanation must be regarded with reserve, however, since the two broad peaks are considerably shifted to low field. Muetterties and Phillips (19) have reported that the fluorine

Can. J. Chem. Downloaded from www.nrcresearchpress.com by 210.87.254.105 on 09/05/12
For personal use only.

TABLE III

Infrared spectra of trifluoromethyl fluoroarsenates

$Cs[(CF_3)_2AsF_4]$		$Ag[(CF_3)_2AsF_4]$,	$Cs[(CF_3)_3AsF_3]$	
CH_3CN soln.	Nujol mull	Nujol mull	CH_3CN soln.	Nujol mull
	1268 (w)			1278 (w)
				1265 (w)
		1189 (sh)*		
1150 (vs)	1145 (sh)*	1150 (vs)	1152 (vs)	1144 (s)
1118 (sh)*	1118 (vs)	1125 (sh)*		
	1080 (sh)		1080 (w)	
			1028 (w)	
	756 (m)	744 (w)		
	734 (s)	731 (w)		735 (m)
	723 (w)	721 (w)		727 (m)
		655 (w)		
606 (m)	602 (s)		608 (m)	595 (s)
566 (w)			562 (m)	
				530 (s)
522 (vw)	518 (s)			
	388 (s)			390 (m)

*sh = shoulder.

n.m.r. absorption in the ion $[AsF_6]^-$ is at −18.1 p.p.m., and the evidence available from the other ions studied here suggested that the substitution of a trifluoromethyl group for a fluorine atom should give a shift to high field rather than to low field. In the absence of the further evidence that would have been provided by splitting patterns, these assignments must be tentative only, and the configuration of the ion $[(CF_3)_2AsF_4]^-$ cannot be assigned with certainty.

With the ion $[(CF_3)_3AsF_3]^-$, there are again two possible structures, *cis* and *trans* similar to those shown as (**3**) and (**4**), and these would be expected to give four absorption peaks in a 6:3:2:1 intensity ratio or two peaks in a 9:3 ratio respectively. The observed spectrum is shown at (*b*) in Fig. 4, and contains only two peaks, a strong sharp signal at −14.7 p.p.m. and a much weaker, but reasonably sharp, signal at +24.1 p.p.m. We feel this spectrum gives a clear indication that this ion is present as the *cis* isomer. The stronger peak is associated with the three trifluoromethyl groups, which are all equivalent in the *cis* (but not in the *trans*) isomer. The remaining peak is then due to the three equivalent fluorine atoms on the arsenic atom. The chemical shift of the peak at +24.1 p.p.m. is to a higher field than that of the ion $[AsF_6]^-$ and the peak lies in the region that would be expected by analogy with the trends observed with the phosphorus compounds.

The *trans* configurations observed in the ions $[(CF_3)_2PF_4]^-$ and $[(CF_3)_3PF_3]^-$ are consistent with the steric requirements of the larger trifluoromethyl groups. Since the assignments of *cis* structures in the analogous arsenates rest solely on rather ill-defined n.m.r. spectra, especially for the bis(trifluoromethyl)tetrafluoroarsenate, conclusions on these configurations must be regarded as only tentative until further information is available. However, it may be of significance that the *trans* structures are found with the smaller phosphorus atom at the center of the ion, where steric interactions between trifluoromethyl groups might be of greater effect than in the arsenic compounds.

Trimethyltin Derivatives

The possible reactions of trimethyl(trifluoromethyl)tin with phosphorus(V) fluoride and related compounds were of interest in view of the observation by Clark and O'Brien (21) that trimethyltin hexafluorophosphate appeared to be unstable, decomposing to give trimethyltin fluoride:

$$[(CH_3)_3Sn]^+[PF_6]^- \rightarrow (CH_3)_3SnF + PF_5.$$

It might be expected, therefore, that any similar ionic compound with a trifluoromethyl-substituted fluorophosphate anion would also decompose:

$$(CH_3)_3SnCF_3 + PF_5 \rightarrow [(CH_3)_3Sn]^+[CF_3PF_5]^- \rightarrow (CH_3)_3SnF + CF_3PF_4.$$

By repetition of this process, it might be possible to replace successively further fluorine atoms

Can. J. Chem. Downloaded from www.nrcresearchpress.com by 210.87.254.105 on 09/05/12
For personal use only.

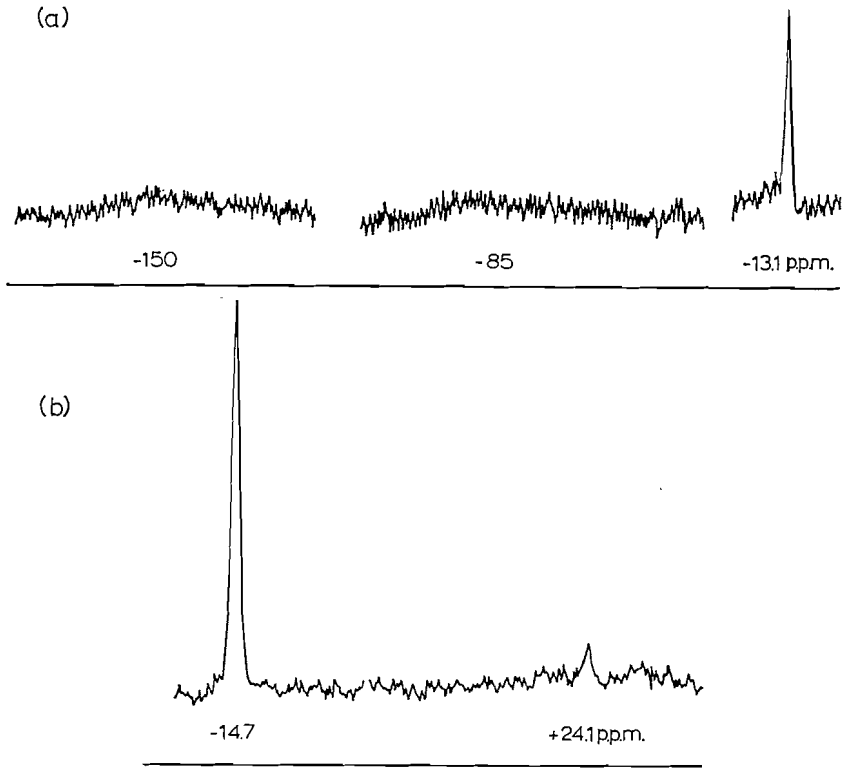

FIG. 4. ^{19}F n.m.r. spectra of (*a*) $Cs[(CF_3)_2AsF_4]$ and (*b*) $Cs[(CF_3)_3AsF_3]$ (acetonitrile solutions).

on the phosphorus atom, up to the fully substituted compound $(CF_3)_5P$. In practice, however, the reaction did not primarily follow this course. When an excess of trimethyl(trifluoromethyl)tin was brought into contact with phosphorus(V) fluoride, an immediate reaction was apparent. Volatile products included small quantities of the compounds CF_3PF_4, $(CF_3)_2PF_3$, and $(CF_3)_3PF_2$, as expected from the above scheme, but a white solid was also produced. Use of equimolar quantities of the reactants favored the production of the solid, and the stoichiometry of its formation showed it to be a 1:1 adduct.

Similar solid 1:1 adducts were also formed between trimethyltrifluoromethyltin and the trifluoromethyl-substituted phosphoranes $(CF_3)_2PF_3$ and $(CF_3)_3PF_2$. The former formed readily from stoichiometric quantities of the reactants, but the latter adduct was only produced in low yield and most of the tin compound was recovered unchanged.

The three adducts were insoluble in common organic solvents and hydrolyzed in contact with water, so it was not possible to carry out ^{19}F n.m.r. studies. Infrared absorptions in the region 500–1300 cm^{-1} are summarized in Table IV.

A comparison of the spectra of the first two adducts with those of the salts $Cs[CF_3PF_5]$ and $Cs[(CF_3)_3PF_3]$, given in Table I, shows that they are generally similar, although the peaks are somewhat broader. We suggest, therefore, that these two adducts of trimethyl(trifluoromethyl)tin may be regarded as the salts $[(CH_3)_3Sn]^+[CF_3PF_5]^-$ and $[(CH_3)_3Sn]^+[(CF_3)_3PF_3]^-$, With the third adduct, that of the phosphorane $(CF_3)_3PF_2$, there is no analogous cesium salt, but the similarity of its spectrum to those of the other two adducts suggests that it also may be regarded as a salt, $[(CH_3)_3Sn]^+[(CF_3)_4PF_2]^-$, in which transfer of a trifluoromethyl group as CF_3^- has occurred. This would constitute the first reported instance of a compound containing four trifluoromethyl groups attached to a phosphorus atom.

Can. J. Chem. Downloaded from www.nrcresearchpress.com by 210.87.254.105 on 09/05/12
For personal use only.

TABLE IV

Infrared spectra of trimethyltin derivatives (Nujol mulls)

$(CH_3)_3SnCF_3.PF_5$	$(CH_3)_3SnCF_3.(CF_3)_2PF_3$	$(CH_3)_3SnCF_3.(CF_3)_3PF_2$
1304 (w)	1300 (sh)	1298 (sh)
	1274 (s)	1278 (s)
1228 (m)	1231 (s)	1216 (s)
1122 (vs)	1126 (s)	1120 (s)
	1078 (sh)	1076 (m)
1023 (s)		
	979 (w)	979 (w)
817 (vs)	844 (s)	810 (sh)
	784 (s)	781 (s)
755 (w)	760 (s)	752 (s)
725 (m)	740 (s)	
	710 (sh)	717 (s)
		676 (vw)
656 (m)		
635 (m)	636 (s)	
594 (w)		
553 (s)		
528 (w)		
513 (m)		

Hydrolysis Reactions

A brief study was made of the hydrolysis of the compounds produced in this work. The usual product of the base hydrolysis of a trifluoromethyl derivative is known to be fluoroform, but this was obtained in surprisingly few instances.

Of the trifluoromethyl-substituted fluorophosphates, the cesium and trimethyltin derivatives gave no volatile product on base hydrolysis. This lends additional support to the proposal that the trifluoromethyl group in the trimethyltrifluoromethyltin adducts has been transferred to the phosphorus atom, since a trifluoromethyl group attached to a tin atom is known to be readily cleaved as fluoroform (22). Surprisingly, the silver salt, $Ag[(CF_3)_2PF_4]$, behaved in a different manner to the corresponding cesium salt and gave 0.98 mole of fluoroform per mole of salt on base hydrolysis.

Under acid hydrolysis conditions, the cesium salts were less stable. The compound $Cs[(CF_3)_2PF_4]$ gave 0.97 mole of silicon tetrafluoride per mole while the compound $Cs[(CF_3)_3PF_3]$ gave 0.87 mole of fluoroform per mole. Cesium trifluoromethylpentafluorophosphate, $Cs[CF_3PF_5]$, still did not give any volatile product, however. No attempt was made to identify any nonvolatile product remaining after hydrolysis.

With the trifluoromethylfluoroarsenates, the hydrolytic stability was lower, and all evolved fluoroform with base. The amounts produced per mole of salt were: $Cs[(CF_3)_2AsF_4]$, 0.98 mole; $Ag[(CF_3)_2AsF_4]$, 1.75 mole; $Cs[(CF_3)_3AsF_3]$, 2.75 mole. The generally lower hydrolytic stability of the trifluoromethylarsenic compounds, as compared with the phosphorus derivatives, is in agreement with previous observations (9), but it will be noted that there is again a difference between the cesium and silver salts of the same anion.

Experimental

General

Conventional vacuum techniques were used throughout for the manipulation of volatile compounds in the absence of air and moisture. All reactants were carefully dried before use. Products were separated by fractional condensation and identified by infrared spectroscopic examination (vapor phase, unless otherwise noted) using Beckman model IR-5 and IR-10 instruments. Reactions were carried out in sealed, previously evacuated Pyrex glass reaction tubes. ^{19}F n.m.r. spectra were determined in acetonitrile solution on a Varian DP-60 instrument at a frequency of 56.4 mc/s using external trifluoroacetic acid as reference. Elemental analyses were performed by Alfred Bernhardt Laboratories, Mulheim, Germany, with the exception of cesium, which was estimated gravimetrically as the tetraphenylborate.

Trifluoromethylphosphines

The phosphines $(CF_3)_3P$, $(CF_3)_2PCl$, and CF_3PCl_2 were prepared by the reaction of trifluoroiodomethane with yellow phosphorus and subsequent chlorination, following the procedure of Bennett, Emeléus, and Haszeldine (5). The various trifluoromethylfluorophosphoranes, which are known to undergo slow decomposition on standing (8), were kept at $-196°$ and their purity was checked by infrared spectroscopic examination immediately before use.

Can. J. Chem. Downloaded from www.nrcresearchpress.com by 210.87.254.105 on 09/05/12
For personal use only.

Can. J. Chem. Downloaded from www.nrcresearchpress.com by 210.87.254.105 on 09/05/12
For personal use only.

Cesium Trifluoromethylpentafluorophosphate

Trifluoromethyldichlorophosphine was converted to trifluoromethylphosphorus tetrachloride by reaction with chlorine (7) and fluorinated to the tetrafluoride using antimony(III) fluoride (8).

Trifluoromethylphosphorus tetrafluoride (0.5 g) was condensed on to an excess of cesium fluoride in acetonitrile (10 ml) and kept at 25° for 15 h. Fractionation showed that all the tetrafluoride had reacted and no volatile product was obtained. The suspension was filtered to remove excess cesium fluoride, then the acetonitrile was removed, leaving a white solid. This was extracted with water, filtered, and freeze-dried to give cesium trifluoromethylpentafluorophosphate.

Anal. Calcd. for CF_8CsP: C, 3.66; F, 46.4; P, 9.45. Found: C, 3.55; F, 46.6; P, 9.62.

Silver Bis(trifluoromethyl)tetrafluorophosphate

Silver bis(trifluoromethyl)phosphinate, $Ag[(CF_3)_2PO_2]$, was prepared from bis(trifluoromethyl)chlorophosphine by the procedure of Emeléus, Haszeldine, and Paul (6). A sample of the silver salt (1.4 g) was allowed to warm up slowly from −196° with an excess of sulfur tetrafluoride (4 g, obtained from the Matheson Co., Joliet, Ill.) and kept at 25° for 1 h. Fractionation showed that the volatile products included a trace of bis(trifluoromethyl)phosphorus trifluoride, together with thionyl fluoride and unreacted sulfur tetrafluoride. The remaining white solid product was silver bis(trifluoromethyl)tetrafluorophosphate.

Anal. Calcd. for $C_2F_{10}AgP$: C, 6.81; F, 53.9. Found: C, 6.68; F, 53.6.

The silver salt decomposed without subliming when heated *in vacuo* to 120°, giving bis(trifluoromethyl)phosphorus trifluoride as the only volatile product.

Cesium Bis(trifluoromethyl)tetrafluorophosphate

Silver bis(trifluoromethyl)phosphinate (1.6 g) was dissolved in water (20 ml) and an equivalent amount of aqueous cesium hydroxide solution added slowly. After keeping for 12 h at 25°, the precipitated silver oxide was removed by filtration and the solution evaporated to give cesium bis(trifluoromethyl)phosphinate, $Cs[(CF_3)_2PO_2]$, which was then fluorinated with sulfur tetrafluoride in the same manner as that described previously for the silver salt to give cesium bis(trifluoromethyl)tetrafluorophosphate.

Anal. Calcd. for $C_2F_{10}CsP$: C, 6.36; F, 50.3; Cs, 35.2. Found: C, 5.82; F, 50.2; Cs, 34.4.

In an alternative route to the same compound, bis(trifluoromethyl)phosphorus trifluoride was prepared by the action of sulfur tetrafluoride on bis(trifluoromethyl)iodophosphine (8). The phosphorane (0.3 g) was then allowed to react with an excess of cesium fluoride suspended in acetonitrile (5 ml) for 15 h at 25°. Fractionation showed no volatile product and filtration, followed by evaporation of solvent, yielded crude cesium bis(trifluoromethyl)tetrafluorophosphate as a yellow solid. The salt was purified by extraction with water, followed by freeze-drying, to give colorless material identical by infrared spectroscopic examination with that produced in the previous reaction.

Cesium Tris(trifluoromethyl)trifluorophosphate

Tris(trifluoromethyl)phosphorus difluoride, $(CF_3)_3PF_2$, was prepared by the reaction of tris(trifluoromethyl)phosphine with sulfur tetrafluoride (8). A sample of the phosphorane (1.5 g) was allowed to react with an excess of cesium fluoride in acetonitrile (10 ml) for 15 h at 25°. Fractionation gave no volatile product, and the solution, which had become brown, was filtered and evaporated *in vacuo* to a thick brown resinous material. On addition of water, the brown impurity appeared to be insoluble, and the clear solution was filtered and evaporated by freeze-drying to give cesium tris(trifluoromethyl)trifluorophosphate as a white solid.

Anal. Calcd. for $C_3F_{12}CsP$: C, 8.42; F, 53.3; Cs, 31.1. Found: C, 8.37; F, 53.6; Cs, 32.6.

Trifluoromethylarsines

The arsines $(CF_3)_3As$, $(CF_3)_2AsI$, and CF_3AsI_2 were prepared by the reaction of trifluoroiodomethane with arsenic following the procedure of Emeléus *et al.* (9).

Cesium Bis(trifluoromethyl)tetrafluoroarsenate

Bis(trifluoromethyl)arsenic trichloride was prepared by the reaction of tris(trifluoromethyl)arsine with chlorine (9). It was converted to the trifluoride by keeping at 25° for 18 h with an excess of dry silver(I) fluoride, the identity of the product being checked by molecular weight measurement (vapor-density, calcd. molecular weight, 270; found: 273). The same compound was also prepared by the fluorination of bis(trifluoromethyl)-iodoarsine with sulfur tetrafluoride.

A sample of bis(trifluoromethyl)arsenic trifluoride (1 g) was condensed into a reaction tube containing excess cesium fluoride suspended in acetonitrile (5 ml). After keeping at 25° for 15 h, no volatile product was found, and filtration of the solution, followed by evaporation of solvent, gave a white solid whose analysis suggested that it was slightly impure cesium bis(trifluoromethyl)tetrafluoroarsenate.

Anal. Calcd. for $C_2F_{10}CsAs$: C, 5.68; F, 45.0. Found: C, 8.07; F, 46.4.

In an attempt to prepare this compound by a different route, bis(trifluoromethyl)arsinic acid was prepared (9) and neutralized with aqueous cesium hydroxide. Freeze-drying gave solid cesium bis(trifluoromethyl)arsinate, $Cs[(CF_3)_2AsO_2]$, which was fluorinated with sulfur tetrafluoride, as described previously, in the hope of preparing cesium bis(trifluoromethyl)tetrafluoroarsenate. Volatile products included thionyl fluoride, indicating that fluorination had occurred, but analysis showed that the solid product had a much lower carbon content than the desired compound, suggesting that trifluoromethyl groups had been cleaved to give some cesium fluoroarsenate.

Silver Bis(trifluoromethyl)tetrafluoroarsenate

Bis(trifluoromethyl)arsinic acid was neutralized with silver oxide to give silver bis(trifluoromethyl)arsinate, $Ag[(CF_3)_2AsO_2]$ (9). The silver salt was then fluorinated with excess sulfur tetrafluoride for 12 h at 25°. Volatile products were only thionyl fluoride and unreacted sulfur tetrafluoride and the solid residue was a white solid which turned grey on exposure to light. The similarity of its infrared spectrum to that of the cesium salt identified it as silver bis(trifluoromethyl)tetrafluoroarsenate. It could be sublimed unchanged *in vacuo* at 140°, but it was insoluble in common organic solvents.

Cesium Tris(trifluoromethyl)trifluoroarsenate

Tris(trifluoromethyl)arsenic dichloride was prepared from tris(trifluoromethyl)arsine and chlorine and con-

Can. J. Chem. Downloaded from www.nrcresearchpress.com by 210.87.254.105 on 09/05/12
For personal use only.

verted to the difluoride using silver fluoride (9). A sample of the difluoride (1 g) was allowed to react with a suspension of cesium fluoride in acetonitrile (5 ml) for 15 h at 25°, after which fractionation gave no volatile products. The solution was filtered and evaporated *in vacuo* to give cesium tris(trifluoromethyl)trifluoroarsenate as a white solid.

Anal. Calcd. for $C_3F_{12}CsAs$: C, 7.63; F, 48.3. Found: C, 7.77; F, 48.5.

The solid readily dissolved in water to give a clear solution from which it could be recovered unchanged (as judged by its infrared spectrum) by freeze-drying.

Attempted Preparation of Cesium Trifluoromethylpentafluoroarsenate

Trifluoromethylarsenic tetrachloride, CF_3AsCl_4, is not known, and attempts to prepare it were not successful. The chlorination of trifluoromethyldichloroarsine with chlorine, a method successfully used for the preparation of other arsenic(V) derivatives, led repeatedly to explosion of the reaction tube. Similar uncontrolled decomposition occurred when trifluoromethyldiiodoarsine was fluorinated with sulfur tetrafluoride. Cesium trifluoromethylarsinate, $Cs_2[CF_3AsO_3]$, was prepared and fluorinated with sulfur tetrafluoride, but extensive decomposition again occurred and the desired product could not be isolated.

Adducts of Trimethyl(trifluoromethyl)tin

(a) With Phosphorus Pentafluoride

Trimethyl(trifluoromethyl)tin was prepared by the irradiation of trifluoroiodomethane with hexamethylditin (22). Phosphorus(V) fluoride was a commercial sample (A. D. Mackay Inc., New York, N.Y.) purified before use by fractional condensation through a trap at −160° to remove phosphorus(V) oxyfluoride.

Phosphorus(V) fluoride (6.61 g, 52.4 mmoles) and trimethyl(trifluoromethyl)tin (1.17 g, 5.02 mmoles) in a sealed tube (20 ml) were kept at 25° for 1 h, by which time a white solid had separated. Unreacted PF_5 (5.82 g, 46.2 mmoles) was recovered, together with traces of the tin compound; no other volatile product was detected. Based on the amount of PF_5 consumed, the ratio of reactants in the solid product, $(CH_3)_3SnCF_3/PF_5$, was 1/1.2.

In a second reaction tube, the reactants were mixed in approximately equimolar proportions. Phosphorus(V) fluoride (2.86 g, 22.7 mmoles) and trimethyl(trifluoromethyl)tin (4.25 g, 18.2 mmoles) were kept together for 1 h. Fractionation of volatile products gave some unreacted PF_5 and tin compound, together with a trace of trifluoromethylphosphorus tetrafluoride. Spectroscopic examination of the solid product showed it to be identical with that produced in the previous reaction.

When a considerable excess of trimethyl(trifluoromethyl)tin (2.46 g, 11.0 mmoles) was kept for 3 h at 25° with phosphorus(V) fluoride (0.204 g, 1.63 mmoles) a small amount of the same solid was produced, but the greater part of the reactants was recovered unchanged. Small amounts of the phosphoranes CF_3PF_4, $(CF_3)_2PF_3$, and $(CF_3)_3PF_2$ were identified spectroscopically, but not quantitatively separated. Attempts to carry out the reaction in carbon tetrachloride solution lead to decomposition giving dark-colored tarry products.

The solid adduct prepared in the above reactions decomposed slowly *in vacuo* at 25°, giving off phosphorus(V) fluoride. On heating, it did not melt or sublime, but started to decompose at 120°, giving PF_5, POF_3, SiF_4 and leaving a brown residue shown by infrared spectroscopic examination to be mainly trimethyltin fluoride. The adduct could not be dissolved without decomposition in water, nor in any common organic solvent.

(b) With Bis(trifluoromethyl)phosphorus Trifluoride

Trimethyl(trifluoromethyl)tin (1.90 g, 8.15 mmoles) and $(CF_3)_2PF_3$ (1.50 g, 6.63 mmoles) were kept in a sealed tube at 25° for 6 h, by which time a grey solid had formed. Fractionation gave unreacted tin compound (0.34 g, 1.46 mmoles) as the only volatile product, indicating that 6.69 mmoles of it remained in the solid adduct for a reacting ratio of 1/1.0. The solid could be sublimed *in vacuo* at 135–140°, but was insoluble in common organic solvents.

(c) With Tris(trifluoromethyl)phosphorus Difluoride

Trimethyl(trifluoromethyl)tin (2.70 g, 11.6 mmoles) and $(CF_3)_3PF_2$ (1.86 g, 6.75 mmoles) were kept at 25° for 6 h, by which time a small amount of white solid had appeared. Fractionation gave unreacted tin compound (2.40 g, 10.4 mmoles) and phosphorane (1.56 g, 5.66 mmoles) as the only volatile products. The stoichiometry of the formation of the solid appeared to be about 1/0.92, but could not be accurately estimated because of the small amount of reaction which had occurred (16%). However, the solid was shown by analysis to be a 1:1 adduct.

Anal. Calcd. for $C_7H_9F_{17}PSn$: C, 16.5; H, 1.77; F, 52.3. Found: C, 16.7; H, 2.50; F, 51.9.

When the reaction temperature was increased to 65° for 2.5 h, the amount of reaction increased to 70%, but the appearance of carbon tetrafluoride, tetrafluoroethylene, and fluoroform in the reaction products indicated that some decomposition was also occurring.

The adduct appeared to be slightly soluble in chloroform and methanol, but the solutions were not sufficiently concentrated for a ^{19}F n.m.r. signal to be detected.

Hydrolysis Studies

The hydrolysis results were obtained by using either 15% aqueous sodium hydroxide or 15% sulfuric acid solution. In either case, a small sample of the compound (ca. 0.2 g) was sealed with the aqueous solution (5 ml) in a small tube (20 ml) and kept at 110–120° for about 12 h. Volatile products were fractionated, weighed, and identified by infrared spectroscopy. No attempt was made to characterize hydrolysis products remaining in solution.

Acknowledgments

The authors gratefully acknowledge financial support for this work from the National Research Council of Canada and the Ontario Department of University Affairs.

1. E. L. Muetterties and W. Mahler. Inorg. Chem. **4**, 119 (1965).
2. (*a*) R. Schmutzler. J. Am. Chem. Soc. 86, 4500 (1964). (*b*) R. Schmutzler. J. Chem. Soc. 5630 (1965). (*c*) R. Schmutzler and G. Reddy. Inorg. Chem. **4**, 191 (1965).
3. (*a*) G. S. Harris and D. S. Payne. J. Chem. Soc. 3038 (1956). (*b*) H. N. Rydon and B. L. Tonge. J. Chem. Soc. 3043 (1956).

4. L. KOLDITZ. *In* Advances in inorganic chemistry and radiochemistry. Vol. 7. *Edited by* H. J. Emeléus and A. G. Sharpe. Academic Press, New York. 1965. p. 1, and references cited therein.
5. F. W. BENNETT, H. J. EMELÉUS, and R. N. HASZELDINE. J. Chem. Soc. 1565 (1953).
6. H. J. EMELÉUS, R. N. HASZELDINE, and R. C. PAUL. J. Chem. Soc. 563 (1955).
7. W. MAHLER and A. B. BURG. J. Am. Chem. Soc. **80**, 6161 (1958).
8. W. MAHLER. Inorg. Chem. **2**, 230 (1963).
9. H. J. EMELÉUS, R. N. HASZELDINE, and E. G. WALASCHEWSKI. J. Chem. Soc. 1552 (1953).
10. H. J. EMELÉUS and G. S. HARRIS. J. Chem. Soc. 1494 (1959).
11. R. G. CAVELL and J. F. NIXON. Proc. Chem. Soc. 229 (1964).
12. H. J. EMELÉUS and J. H. MOSS. Z. Anorg. Allgem. Chem. **282**, 24 (1955).
13. W. C. SMITH. J. Am. Chem. Soc. **82**, 6176 (1960).
14. R. D. CHAMBERS, H. C. CLARK, and C. J. WILLIS. J. Am. Chem. Soc. **82**, 5298 (1960).
15. F. W. BENNETT, H. J. EMELÉUS, and R. N. HASZELDINE. J. Chem. Soc. 3896 (1954).
16. A. DE LATTRE. J. Chem. Phys. **19**, 1610 (1951).
17. L. A. WOODWARD and L. E. ANDERSON. J. Inorg. Nucl. Chem. **3**, 326 (1956).
18. J. A. POPLE, W. G. SCHNEIDER, and H. J. BERNSTEIN. High resolution magnetic resonance. McGraw-Hill, New York. 1959.
19. E. L. MUETTERTIES and W. D. PHILLIPS. J. Am. Chem. Soc. **81**, 1084 (1959).
20. J. WEIDLEIN and K. DEHNICKE. Z. Anorg. Allgem. Chem. **337**, 113 (1965).
21. H. C. CLARK and R. J. O'BRIEN. Inorg. Chem. **2**, 1020 (1963).
22. H. C. CLARK and C. J. WILLIS. J. Am. Chem. Soc. **82**, 1888 (1960). R. D. CHAMBERS, H. C. CLARK, and C. J. WILLIS. Chem. Ind. London, 76 (1960).

Can. J. Chem. Downloaded from www.nrcresearchpress.com by 210.87.254.105 on 09/05/12
For personal use only.

Can. J. Chem. Downloaded from www.nrcresearchpress.com by 210.87.254.6 on 09/05/12
For personal use only.

Measurement of the vapor pressure of methanol–*n*-decanol and ethanol–*n*-decanol mixtures[1]

JASWANT SINGH[2] AND G. C. BENSON
Division of Pure Chemistry, National Research Council of Canada, Ottawa, Canada

Received November 8, 1967

Molar excess Gibbs free energies of mixtures of methanol and ethanol with *n*-decanol were obtained from static vapor pressure measurements over the temperature range 20–50 °C. The molar excess entropies of the system methanol–decanol are predominantly negative at 25 °C; those of ethanol–decanol are positive.

Canadian Journal of Chemistry, 46, 1249 (1968)

I. Introduction

The results of calorimetric and volumetric investigations of a number of binary *n*-alcohol systems have been reported in previous publications from our laboratory (1, 2). In the present paper the study of the thermodynamic properties of these systems is extended by vapor pressure measurements made on methanol–decanol and ethanol–decanol solutions over the temperature range 20–50 °C.

II. Experimental

(a) Description of Apparatus

A schematic diagram of the vapor pressure assembly is given in Fig. 1. Total vapor pressures were measured with a precision quartz gauge (Texas Instruments) which had been calibrated against a mercury manometer; pressure changes of 0.005 mm of mercury could be detected. The quartz spiral of the gauge was thermostated at 60 ± 0.1 °C (i.e. about 10° above the highest temperature at which vapor pressures were determined) and was connected to the vapor pressure cell by a stainless steel capillary tube (1.6 mm i.d.). The temperature of the latter was monitored at several points by iron–constantan thermocouples and was maintained at about 60 °C by a heating jacket.

The vapor pressure cell could be joined through a Hoke bellows valve (type Y441) to a vacuum manifold to which were attached ampuls of the more volatile component of the system under investigation. At the start of a run the cell and a set of ampuls were sealed in position with their charges separated from the vacuum line by fragile glass partitions which could be ruptured later by magnetically activated breakers. The shapes of the cell and an ampul are illustrated in Fig. 2. Prior to loading the cell its internal volume was determined from the weight of water needed to fill it to the seal-off constriction. The water bath surrounding the cell was mounted on a platform which could be raised and lowered by a winch to facilitate connecting the cell to the vacuum line. A Thermotrol controller (Hallikainen Instruments) regulated the temperature of the water bath to ±0.002 °C at temperatures in the range 20–50 °C. The temperature of the bath at the time of each vapor pressure measurement was determined with a Leeds and Northrup platinum resistance thermometer[3] in a Müeller bridge circuit.

The cell and ampuls were filled in separate operations on another vacuum line. In each case the liquid to be loaded was thoroughly degassed by repeated freezing, pumping, and melting as it was distilled back and forth between two traps. Finally an appropriate amount was distilled into the container (cell or ampul) and sealed off. The amount of material was determined from weighings of the empty and sealed off container with corrections applied to allow for changes in buoyancy.

After the cell had been sealed in position, the volume of the line which later would be available to the vapor (i.e. extending from valve K_1 into the pressure gauge) was determined to better than ±0.05 cm³ by expanding dry nitrogen from a known volume attached to the vacuum line and measuring the pressure change. The manifold and line to the gauge were then evacuated for 12 h at 60 °C to remove adsorbed gases; valve K_1 was closed and the cell seal broken.

Vapor pressures of mixtures were measured at 6 temperatures from 20 to 50 °C. Generally the actual temperatures of the measurements were within ±0.1 °C of the "standard set" (20.0, 25.0, 30.0, 35.0, 40.0, and 50.0 °C). Where necessary, values at the rounded temperatures were interpolated by fitting the data with an Antoine form of equation

$$[1] \qquad \log_{10} p(\text{Torr}) = A - \frac{B}{C + t(°\text{C})}.$$

Mixtures were formed by freezing the material in the cell, opening valve K_1, and distilling the contents of one of the ampuls (i.e. the more volatile component) into the cell. Steady pressure readings were usually obtained less than 3 h after each change in composition or alteration of temperature. A stirrer in the cell, coupled magnetically to an external rotor driven by compressed air, was quite effective in decreasing the time needed to achieve equilibrium. Occasionally two runs were carried out at 20 or 25 °C, one at the beginning (after making a new composition) and another following the measurements at 50 °C.

---

[1]Issued as NRCC No. 9937.
[2]NRCC Postdoctorate Fellow 1965–67.
[3]The thermometer was calibrated by the Division of Applied Physics, NRCC, and the R_0 value was checked periodically by measurements at the water triple point.

Can. J. Chem. Downloaded from www.nrcresearchpress.com by 210.87.254.6 on 09/05/12
For personal use only.

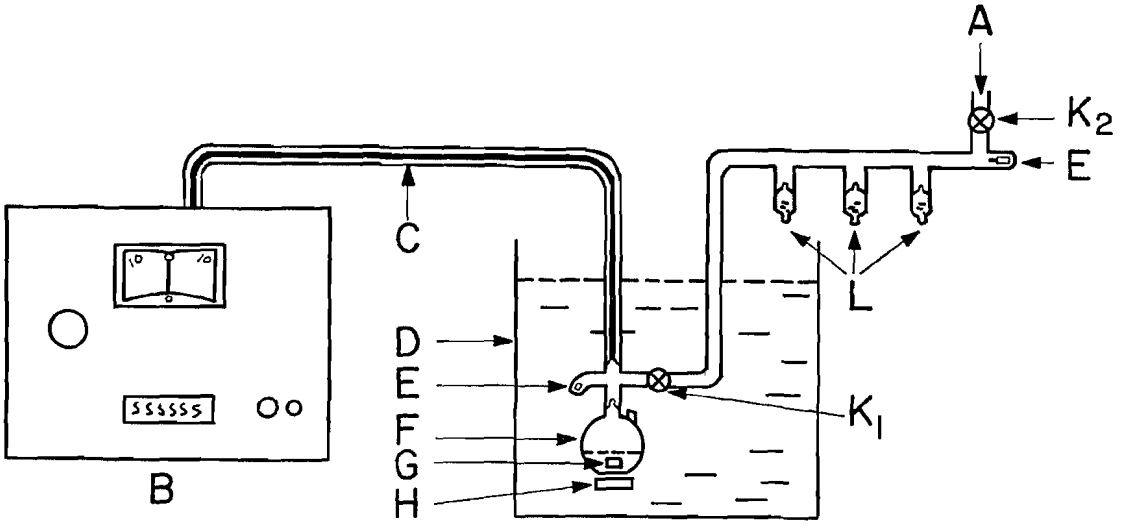

FIG. 1. Vapor pressure assembly. A connection to vacuum line; B quartz spiral pressure gauge; C thermally jacketed stainless steel capillary; D water bath; E breakers for seals; F cell; G magnetic stirrer; H air driven rotor for stirrer; K_1, K_2 metal bellows valves; L ampuls for more volatile component.

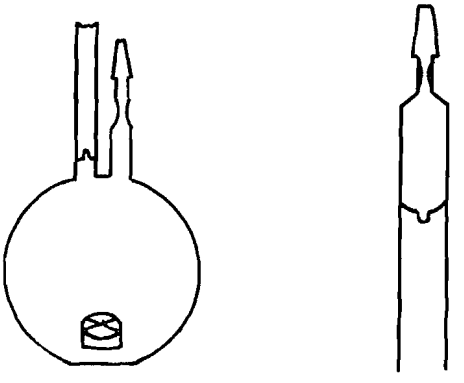

FIG. 2. Cell and ampul prior to attachment to filling line.

The agreement of the results indicated that no degassing had occurred at the higher temperatures.

(b) Composition of Liquid Mixtures

Only the total number of moles of each component (n_1^t, n_2^t) are known directly from weighings of the cell and ampuls. The composition of the liquid phase at any stage in the measurement must be calculated from these by allowing for the material present in the vapor phase. For this purpose, the vapor volume V^g is obtained from

$$[2] \quad V^g = V^{C+L} - (n_1^t - n_1^g)V_1^0 - (n_2^t - n_2^g)V_2^0.$$

This represents the difference between V^{C+L}, the sum of the internal volumes of the cell and line to the gauge (determined as described above), and the volume of the liquid neglecting the volume change which occurs when the pure liquids are mixed. In eq. [2] n_1^g and n_2^g are the moles present in the vapor phase, and V_1^0 and V_2^0 are the molar volumes of the pure liquids.

Values of n_1^g and n_2^g corresponding to each total pressure measurement are estimated by an iterative calculation, in which it is assumed that the partial pressure of the less volatile component (i.e. subscript 2) in the vapor phase in equilibrium with the solution at mole fraction x_1 is given by the Raoult's law expression

$$[3] \quad p_2 = (1 - x_1)p_2^0,$$

where p_2^0 is the vapor pressure of the pure liquid at the temperature of the measurement. This iteration is based on the equation of state

$$[4] \quad V^g = (n_1^g + n_2^g)\left(\frac{RT}{p} + B + Dp^2\right),$$

which has been recommended for the representation of data for pure alcohols (3). In eq. [4], R is the gas constant, and B and D are the second and fourth virial coefficients respectively. Since in the mixtures under investigation, the mole fraction y_2 of decanol in the vapor phase is generally relatively small, we have assumed that

$$[5] \quad B \simeq B_{11}$$

and

$$[6] \quad D \simeq D_{1111},$$

where B_{11} and D_{1111} are the virial coefficients for the pure vapors, and the contributions of all other terms to B and D have been neglected.

(c) Materials

The alcohols used were purified by distillation and (or) chromatographic techniques. In all cases the starting

TABLE I

Vapor pressures of the pure component liquids

Temp. (°C)	Methanol p (Torr)	Methanol δ*	Ethanol p (Torr)	Ethanol δ*	Decanol, p (Torr)
20	97.39	0.09	43.96	−0.10	0.016
25	126.97	0.08	59.10	−0.08	0.026
30	163.91	0.07	78.53	−0.05	0.042
35	209.63	0.04	103.22	−0.02	0.060
40	265.74	−0.03	134.29	0.00	0.089
50	416.59	−0.30	220.88	−0.04	0.210
Antoine coefficients					
A	8.04827		8.09322		
B	1563.49		1586.84		
C	238.012		226.017		
σ	0.018		0.076		

*$\delta = p$ − value from ref. 4.

TABLE II

Molar volumes and virial coefficients of the pure component liquids (Units: V^0 cm^3 mole^{-1}; B cm^3 mole^{-1}; D cm^3 mole^{-1} Torr^{-2}.)

Temp. (°C)	Methanol V_1^0	Methanol B_{11}	Methanol D_{1111}	Ethanol V_1^0	Ethanol B_{11}	Ethanol D_{1111}	Decanol, V_2^0
20	40.505	−1980.	−0.0843	58.366	−3435.	−0.2450	190.644
25	40.730	−1778.	−0.0456	58.682	−2938.	−0.1295	191.428
30	40.955	−1603.	−0.0251	59.004	−2603.	−0.0699	192.207
35	41.184	−1452.	−0.0142	59.331	−2289.	−0.0385	192.980
40	41.421	−1320.	−0.0081	59.666	−2025.	−0.0216	193.748
50	41.927	−1102.	−0.0014	60.363	−1615.	−0.0072	195.278

materials were the best available commercial reagents. Methanol and ethanol were passed through columns of Poropak Q + 5% PEG 20M in a model 775 F & M preparative gas chromatograph, refluxed with magnesium, and stored in flasks on the vacuum line immediately after distillation from the alcoholates. The decanol was purified by passing it through a column of Chromosorb W coated with PEG 1500. Densities measured on samples typical of the materials used in the vapor pressure measurements are: methanol 0.7867_1, ethanol 0.7850_7, and decanol 0.8268_7 g cm^{-3} at 25 °C. Throughout the course of the investigation a number of chromatographic checks were run on all the materials to ensure the detection of any contamination of the samples.

III. Results and Discussion

Vapor pressures of the component liquids at rounded temperatures are summarized in Table I. Coefficients of the Antoine equations used to interpolate in the experimental results for methanol and ethanol are listed at the bottom of the table along with σ, the probable error of the estimate in each case. The deviations of our results for methanol and ethanol from the data tabulated by the American Petroleum Institute (4) are given in columns 3 and 5. Since these show opposite trends, they can not be attributed to a difference of our temperature scale from the "international temperature scale" or to a constant error in experimental technique.

Values of the other properties of the pure component liquids, needed for analysis of the vapor pressure measurements, are collected in Table II. The molar volumes at 25 °C are based on the densities quoted in Section II; coefficients of expansion used in obtaining values at other temperatures were derived from the data of Costello and Bowden (5). Virial coefficients were calculated from formulas given by Kretschmer and Wiebe (3) and involve extrapolation to temperatures 20° lower than considered by those authors.

Results of the vapor pressure measurements on methanol–decanol and ethanol–decanol systems are summarized in Tables III and IV. Included are values of the natural logarithm of the

Can. J. Chem. Downloaded from www.nrcresearchpress.com by 210.87.254.6 on 09/05/12
For personal use only.

TABLE III

Liquid–vapor equilibrium for methanol–decanol mixtures (p in Torr)

x_1	p	y_1	ln γ_1	x_1	p	y_1	ln γ_1	x_1	p	y_1	ln γ_1
	20 °C				25 °C				30 °C		
0.0673	10.55	0.9986	0.4861	0.0671	13.63	0.9982	0.4813	0.0668	17.41	0.9977	0.4759
0.1612	24.53	0.9995	0.4553	0.1608	31.65	0.9993	0.4489	0.1603	40.42	0.9991	0.4425
0.2285	33.63	0.9996	0.4210	0.2280	43.43	0.9995	0.4148	0.2274	55.51	0.9994	0.4088
0.3121	44.07	0.9998	0.3786	0.3116	56.97	0.9997	0.3727	0.3109	72.90	0.9996	0.3671
0.3966	53.68	0.9998	0.3351	0.3961	69.49	0.9998	0.3300	0.3955	89.04	0.9997	0.3251
0.4924	63.51	0.9999	0.2854	0.4921	82.31	0.9998	0.2811	0.4916	105.62	0.9998	0.2770
0.5736	70.86	0.9999	0.2414	0.5733	91.92	0.9999	0.2376	0.5729	118.06	0.9998	0.2339
0.6767	78.85	0.9999	0.1820	0.6765	102.42	0.9999	0.1791	0.6762	131.73	0.9999	0.1763
0.7624	84.40	1.0000	0.1301	0.7623	109.78	0.9999	0.1281	0.7621	141.34	0.9999	0.1261
0.8568	89.59	1.0000	0.0722	0.8568	116.59	1.0000	0.0706	0.8567	150.27	1.0000	0.0693
	35 °C				40 °C				50 °C		
0.0665	22.01	0.9975	0.4707	0.0661	27.54	0.9970	0.4655	0.0652	41.99	0.9953	0.4542
0.1597	51.09	0.9990	0.4365	0.1590	64.00	0.9988	0.4310	0.1571	97.90	0.9982	0.4204
0.2267	70.27	0.9993	0.4033	0.2259	88.15	0.9992	0.3982	0.2238	135.22	0.9988	0.3884
0.3102	92.40	0.9996	0.3621	0.3093	116.10	0.9995	0.3576	0.3070	178.79	0.9992	0.3491
0.3948	113.02	0.9997	0.3206	0.3940	142.17	0.9996	0.3165	0.3918	219.49	0.9994	0.3082
0.4910	134.26	0.9998	0.2730	0.4903	169.14	0.9997	0.2693	0.4885	261.81	0.9996	0.2616
0.5725	150.21	0.9998	0.2304	0.5719	189.44	0.9998	0.2271	0.5705	293.93	0.9997	0.2203
0.6759	167.84	0.9999	0.1735	0.6756	211.96	0.9999	0.1709	0.6747	329.78	0.9998	0.1654
0.7620	180.29	0.9999	0.1241	0.7618	227.95	0.9999	0.1222	0.7612	355.46	0.9999	0.1181
0.8567	191.90	1.0000	0.0682	0.8566	242.94	0.9999	0.0672	0.8564	380.03	0.9999	0.0655

TABLE IV

Liquid–vapor equilibrium for ethanol–decanol mixtures (p in Torr)

x_1	p	y_1	ln γ_1	x_1	p	y_1	ln γ_1	x_1	p	y_1	ln γ_1
	20 °C				25 °C				30 °C		
0.0942	5.35	0.9973	0.2609	0.0941	7.13	0.9967	0.2543	0.0940	9.40	0.9960	0.2481
0.1687	9.33	0.9986	0.2352	0.1686	12.47	0.9983	0.2307	0.1683	16.45	0.9979	0.2260
0.2527	13.66	0.9991	0.2124	0.2525	18.25	0.9989	0.2073	0.2522	24.08	0.9987	0.2025
0.3229	17.09	0.9994	0.1904	0.3227	22.84	0.9992	0.1858	0.3224	30.16	0.9991	0.1814
0.3908	20.30	0.9995	0.1712	0.3902	27.13	0.9994	0.1675	0.3894	35.81	0.9993	0.1639
0.3948	20.49	0.9995	0.1702	0.3946	27.38	0.9994	0.1652	0.3944	36.16	0.9993	0.1607
0.4658	23.66	0.9996	0.1481	0.4656	31.63	0.9996	0.1438	0.4654	41.83	0.9995	0.1401
0.5825	28.60	0.9998	0.1134	0.5823	38.26	0.9997	0.1094	0.5822	50.63	0.9997	0.1061
0.6595	31.68	0.9998	0.0909	0.6594	42.40	0.9998	0.0872	0.6593	56.13	0.9997	0.0842
0.7022	33.18	0.9999	0.0743	0.7020	44.47	0.9998	0.0719	0.7017	58.92	0.9998	0.0700
0.7826	36.12	0.9999	0.0504	0.7824	48.45	0.9999	0.0484	0.7823	64.24	0.9999	0.0468
0.8538	38.60	0.9999	0.0292	0.8537	51.79	0.9999	0.0274	0.8536	68.72	0.9999	0.0263
0.9124	40.61	1.0000	0.0130	0.9124	54.52	1.0000	0.0119	0.9124	72.39	0.9999	0.0113
	35 °C				40 °C				50 °C		
0.0938	12.25	0.9956	0.2426	0.0936	15.80	0.9949	0.2373	0.0930	25.54	0.9925	0.2279
0.1681	21.46	0.9977	0.2212	0.1678	27.69	0.9973	0.2162	0.1669	44.75	0.9961	0.2060
0.2519	31.43	0.9986	0.1979	0.2515	40.61	0.9984	0.1935	0.2505	65.82	0.9976	0.1855
0.3221	39.40	0.9990	0.1772	0.3217	50.94	0.9988	0.1733	0.3206	82.72	0.9983	0.1663
0.3884	46.74	0.9992	0.1604	0.3871	60.36	0.9991	0.1571	0.3839	97.73	0.9987	0.1522
0.3941	47.26	0.9992	0.1567	0.3937	61.14	0.9991	0.1532	0.3927	99.53	0.9987	0.1476
0.4651	54.72	0.9994	0.1367	0.4648	70.87	0.9993	0.1338	0.4639	115.57	0.9990	0.1294
0.5820	66.31	0.9996	0.1035	0.5817	85.99	0.9996	0.1014	0.5811	140.70	0.9994	0.0990
0.6591	73.56	0.9997	0.0819	0.6589	95.44	0.9997	0.0801	0.6584	156.35	0.9995	0.0781
0.7013	77.26	0.9998	0.0685	0.7008	100.29	0.9997	0.0675	0.6995	164.30	0.9996	0.0666
0.7820	84.29	0.9998	0.0458	0.7817	109.51	0.9998	0.0451	0.7810	179.78	0.9997	0.0451
0.8535	90.23	0.9999	0.0256	0.8534	117.30	0.9999	0.0253	0.8530	192.88	0.9998	0.0260
0.9123	95.11	0.9999	0.0110	0.9123	123.71	0.9999	0.0110	0.9122	203.58	0.9999	0.0120

Can. J. Chem. Downloaded from www.nrcresearchpress.com by 210.87.254.6 on 09/05/12
For personal use only.

TABLE V

Coefficients for eqs. [8] and [9]

Temp. (°C)	C_1	C_2	C_3	C_4	$\sigma_{\ln\gamma}$	σ_G (J mole^{-1})
			Methanol–decanol			
20	1835.0	−910.3	661.9	−441.6	0.0054	2.9
25	1839.2	−908.6	664.4	−433.6	0.0052	2.9
30	1842.7	−907.2	665.7	−427.3	0.0052	2.9
35	1846.8	−905.9	666.2	−422.1	0.0051	2.9
40	1851.5	−904.8	665.8	−418.6	0.0051	3.0
50	1857.4	−897.6	658.1	−414.1	0.0053	3.1
			Ethanol–decanol			
20	953.4	−403.0	252.2	−118.7	0.0019	1.0
25	944.9	−390.8	237.5	−118.7	0.0015	0.8
30	937.1	−382.5	228.8	−119.6	0.0013	0.8
35	930.2	−377.3	226.2	−120.3	0.0013	0.7
40	924.0	−375.8	228.4	−121.5	0.0013	0.8
50	915.1	−384.2	245.9	−125.0	0.0018	1.1

activity coefficient of component 1 in the liquid phase, calculated from the formula

$$[7]\quad \ln\gamma_1 = \ln\left(\frac{p_1}{x_1 p_1^0}\right) + \frac{(p - p_1^0)(B_{11} - V_1^0)}{RT} + D_{1111}\frac{(4y_1^3 - 3y_1^4)(p^3 - (p_1^0)^3)}{3RT},$$

which is based on the same equation of state as used in the iterative calculation of the mole fractions x_1 and y_1 for the liquid and vapor phases. Since the corrections for differences in total pressure are negligible, the values obtained from eq. [7] can be used for $\ln\gamma_1$ at atmospheric pressure.

If the molar excess Gibbs free energy G^E is represented by the polynomial

$$[8]\quad G^E = x_1x_2\sum_{r=1}^{n} C_r(x_2 - x_1)^{r-1},$$

it follows that

$$[9]\quad \ln\gamma_1 = \frac{x_2^2}{RT}\sum_{r=1}^{n} C_r(1 - 2rx_1)(x_2 - x_1)^{r-2}.$$

The coefficients C_r were determined by fitting eq. [9] to the experimental results for $\ln\gamma_1$ by the method of least squares. In all cases, use of four constants led to a satisfactory fit, and the resulting values are listed in Table V. Values of $\sigma_{\ln\gamma}$, the probable error of the estimate of $\ln\gamma_1$ calculated with eq. [9], are given in column 6 of the table. The last column contains values of σ_G, the statistical estimate of the root mean square error of G^E, calculated from eq. [8] with the coefficients determined by fitting eq. [9] to the experimental results.

The excess entropy and enthalpy can be derived from the temperature dependence of G^E using the formulas

$$[10]\quad S^E = -\left(\frac{\partial G^E}{\partial T}\right)_p$$

and

$$[11]\quad H^E = G^E + TS^E.$$

For the methanol–decanol system, the values of G^E increase with temperature over most of the concentration range, but the changes are fairly small (i.e. only 8 J mole^{-1} for a 30° change at $x_1 = 0.5$). The value of G^E for the ethanol–decanol system decreases with temperature, but again the changes are relatively small. Thus qualitatively it follows that the excess entropy is predominantly negative in methanol–decanol solutions and positive in ethanol–decanol solutions. By fitting the G^E data for an equimolar solution with a third degree polynomial in the temperature, the temperature derivative at 25° was obtained and values of $H^E = 401$ and 358 J mole^{-1} were calculated for the methanol–decanol and ethanol–decanol systems respectively. These may be compared with the values 397 and 301 J mole^{-1} measured calorimetrically[4]. The agreement is reasonable since the quantitative evaluation of H^E from vapor pressures involves considerable uncertainty (6).

[4]H. D. Pflug, A. E. Pope, and G. C. Benson. Unpublished data.

Can. J. Chem. Downloaded from www.nrcresearchpress.com by 210.87.254.6 on 09/05/12
For personal use only.

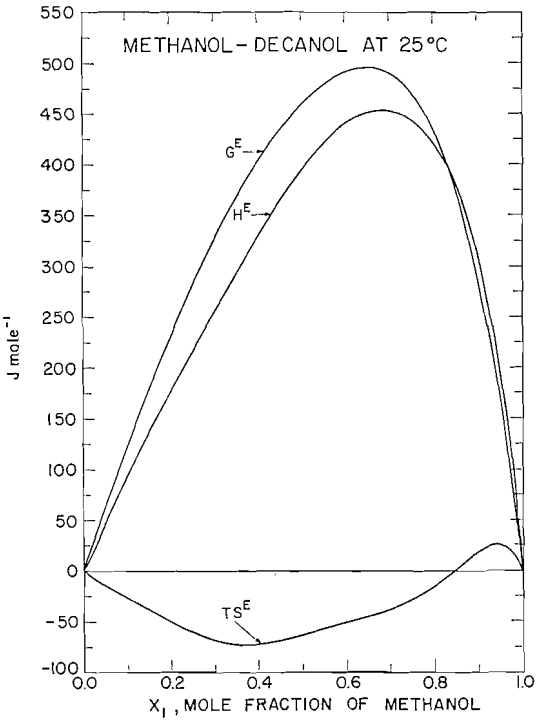

FIG. 3. Excess thermodynamic properties of methanol–decanol mixtures at 25 °C. G^E from vapor pressures; H^E calorimetric results[4]; TS^E calculated from eq. [11].

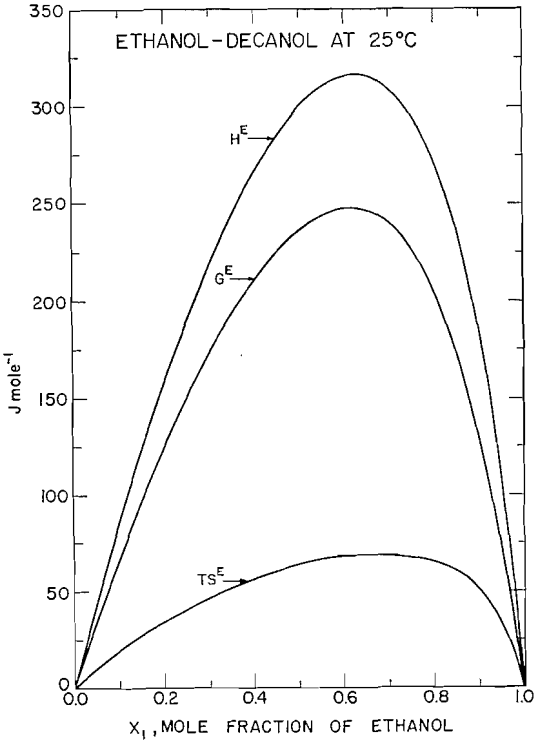

FIG. 4. Excess thermodynamic properties of ethanol–decanol mixtures at 25 °C. G^E from vapor pressures; H^E calorimetric results[4]; TS^E calculated from eq. [11].

It is preferable to use calorimetrically determined values of H^E in eq. [11] to calculate S^E. This has been done in Figs. 3 and 4, where values of G^E obtained from the coefficients in Table V at 25° and of H^E determined calorimetrically[4] have been combined to calculate TS^E. For both systems H^E is positive, probably resulting from a net breaking of hydrogen bonds when solutions are formed. In the case of the ethanol system, there is an accompanying increase in entropy and similar behavior is observed for the more concentrated methanol solutions. However, in the latter system, at mole fractions less than 0.85, the excess entropy is negative, suggesting that the smaller alcohol molecule is able to participate in a more ordered structure of the solution than is possible in the case of ethanol.

Acknowledgments

We are indebted to Dr. D. H. Davies for collaboration in the initial phase of the research. We also wish to thank Mr. C. J. Halpin for carrying out the chromatographic work and for providing invaluable technical assistance throughout the course of the investigation.

1. A. E. POPE, H. D. PFLUG, B. DACRE, and G. C. BENSON. Can. J. Chem. **45**, 2665 (1967).
2. H. D. PFLUG and G. C. BENSON. Can. J. Chem. **46**, 287 (1968).
3. C. B. KRETSCHMER and R. WIEBE. J. Am. Chem. Soc. **76**, 2579 (1954).
4. AMERICAN PETROLEUM INSTITUTE RESEARCH PROJECT 44. Selected values of properties of hydrocarbons and related compounds. Texas A&M University, College Station, Texas. 1953 and later revisions.
5. J. M. COSTELLO and S. T. BOWDEN. Rec. Trav. Chim. **77**, 36 (1958).
6. J. S. ROWLINSON. Liquids and liquid mixtures. Butterworth's Publications Ltd., London. 1959. p. 131.

Can. J. Chem. Downloaded from www.nrcresearchpress.com by 210.87.254.6 on 09/05/12
For personal use only.

Can. J. Chem. Downloaded from www.nrcresearchpress.com by 210.87.254.42 on 09/05/12
For personal use only.

Etard reactions. I. Nature of complexes and their reactions with some oxygen and nitrogen donor molecules

R. C. MAKHIJA[1] AND R. A. STAIRS
Chemistry Department, Trent University, Peterborough, Ontario

Received October 30, 1967

Dilute carbon tetrachloride solutions of chromyl chloride and toluene react to form a product of empirical composition, $C_6H_5CH_3.2CrO_2Cl_2$ (**1**). On refluxing **1** with carbon tetrachloride solutions of pyridine, α-picoline, acetonitrile, dioxan, tetrahydrofuran, and triethylamine, adducts of approximate compositions $C_6H_5CH_3.2CrO_2Cl_2.2D$ (D = donor molecule) are obtained.

Results of magnetic susceptibility, infrared, and preliminary X-ray observations are discussed. Possible structures for **1** and for the ternary adducts are described.

Canadian Journal of Chemistry, 46, 1255 (1968)

Introduction

The reaction of toluene with chromyl chloride yields a product of composition $C_6H_5CH_3.2CrO_2Cl_2$ (**1**), which is not a simple adduct, as the oxidation state of chromium appears to be reduced from VI to IV. Various structures have been suggested for this product (1, 2), but that due to Etard (3) has been most favored (4–7). Etard's structure is

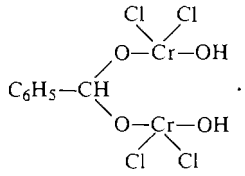

Very little direct work on the structure of **1** has been carried out. Etard's proposal was based on analytical data and the nature of the hydrolysis products. A single magnetic susceptibility measurement by Wheeler (5) appeared to confirm Etard's assignment of oxidation state IV to chromium, but Necsoiu and co-workers (2) reported electron spin resonance (e.s.r.) data which were interpreted as showing only one of the two chromium atoms in this state, the other presumed to be still Cr(VI). E.s.r. measurements on substances not known to be magnetically dilute are difficult to interpret, but so is a magnetic susceptibility measurement at a single temperature.

In order to make molecular weight and conductance measurements, and to facilitate infrared and ultraviolet spectral studies, a solvent for the Etard products was sought. They are decomposed by hydroxylic solvents, and are inert to and insoluble in solvents such as carbon tetrachloride and hydrocarbons. Donor solvents appear to dissolve **1** by reaction,[2] and removal of excess solvent yields new substances of composition $C_6H_5CH_3.2CrO_2Cl_2.2D$. We have prepared and partially characterized, but have not been able to purify, ternary complexes of this sort formed by **1** with pyridine, α-picoline, acetonitrile, triethylamine, dioxan, and tetrahydrofuran. Infrared spectra and some preliminary X-ray data have been obtained. We have also measured the magnetic susceptibility of **1** and of the pyridine complex over a range of temperatures.

Experimental

Chromyl chloride (Allied Chemical) was purified by bubbling dry nitrogen through the liquid to remove traces of hydrogen chloride, and was then distilled through a 30 cm Vigreaux column. The fraction boiling at 114–115 °C was retained. The reagent was protected from light during distillation and storage. Toluene was dried and distilled before use.

The solvents carbon tetrachloride and petroleum ether (b.p. 37–50 °C) were purified by standard methods (8).

Liquid ligands were fractionated, predried off the line over either calcium hydride or phosphoric oxide, and finally distilled under vacuum from a suitable desiccant (sodium for tetrahydrofuran and dioxan, P_2O_5 for acetonitrile). All the purified reagents were stored in a dry box.

Analytical Methods

Chromium was determined as Cr_2O_3. By evaporating the sample nearly to dryness with concentrated nitric acid, a clear green solution was obtained from which hydrous Cr_2O_3 was precipitated with filtered 1:1 ammonia, followed by ignition for several hours at 800 °C. Carbon, hydrogen, and nitrogen were analyzed by Microanalyses, Toronto.

[1]Teaching Postdoctoral Fellow.

[2]R. C. Makhija. Unpublished observations.

Can. J. Chem. Downloaded from www.nrcresearchpress.com by 210.87.254.42 on 09/05/12
For personal use only.

TABLE I

Comparison of infrared spectra and assignments

Etard 1 (cm^{-1})	Etard 1.2CH_3CN (cm^{-1})	Etard 1.2C_5H_5N (cm^{-1})	Etard 1.2$C_5H_4(CH_3)N$ (cm^{-1})	Etard 1.2$(C_2H_5)_3N$ (cm^{-1})	Etard 1.2C_4H_8O (cm^{-1})	Etard 1.2$C_4H_8O_2$ (cm^{-1})	Assignments
3260–3340 sb	3240–3350 sb	—	3350 mb	3300–3400 sb	3140–3360 sb	3300 sb	Associated hydrogen-bonded OH
2900–2960 sb	2900–2960 sb	2960 s 2938 s	2880–2960 sb	2900–2970 sb	2960–2900 sb	2900–2980 sb	C—H stretching
2860 s	2855 s	2860 s	2845 s	2860 s	2855 s	2860 s	Nujol
—	2310 s	—	—	—	—	—	C≡N stretching
—	2295 m	—	—	—	—	—	
1620 s	—	1615 s	1630 s	1617 m	1625 m	1603 s	C=C stretching
1595 s	1595 s	—	—	1595 s	1595 m	1585 s	
1575 s	—	—	—	—	—	—	
—	1530 s	1540 s	1535 m	1535 w	—	1545 s	C=N stretching
—	—	1490 s	1500 ms	—	1485 m	—	
1458 mb	1455 s	1465 sh 1450 s	1455 sb	1465 s	1455 s	1460 s	Nujol
—	1410 m	1418 w	—	1415 m	1418 m	1423 m	Unassigned
1380 m	1375 m	1380 m	1375 m	1380 m 1368 w	1378 s	1380 m	Nujol
1325 m	—	—	1310 m	1320 w	1315 w	1322 m	Fingerprint bands
1290 m	—	—	—	1280 w	—	1300 m	
—	—	—	—	—	—	1260 s	C—N vibrations
1225 m	—	1220 m	1230 m 1210 m	1230 w	1223 m	1225 m	
1170 m	—	1155 m	—	1175 w	1170 m	1175 m	C—H in plane deformation
—	—	—	—	—	—	1115 s	
—	—	1070 m	1065 m	1075 w	1070 w	1080 s	C—O stretching of coordinated dioxan and tetrahydrofuran
—	—	1048 m	1030 s	1040 w	1040 m	1045 s	
1015 m	1015 m	1018 m	—	997 w	1010 m	1015 m	
—	945 m	950 m	945 m	940 w	955 m	955 w	
840 w	860 w	860 m	—	—	865–855 sb	868 s	C—O—C in cyclic ethers
750 m	720 w	—	715 m	722 w	750 w 720 m	755 w	Pyridine vibrations
700 m	—	695 s	—	695 w	680 m	700 w 680 w	
635 m	—	640 m	—	638 w	—	610 m	Unassigned
528 m	510 m	495 mb	545 m	520–560 mb	510–530 mb	535 mb	Cr—O stretching
445 m	450 m	442 m	425 w	410 w	450 w	445 mb	Cr—O stretching
325 mb	340 m	340 mb	330 mb	340 w	320–345 mb	350 w	Cr—Cl stretching
—	—	285 w	290 w	290 w	—	—	Cr—N stretching

NOTE: (i) s = strong, m = medium, w = weak, v = very, sh = shoulder, b = broad, asym = asymmetric, sym = symmetric. (ii) In the region 1420 cm^{-1} to 940 cm^{-1} fingerprint bands appear which are usually combination bands and are difficult to assign. (iii) Nujol absorption interferes between 2920–2710 cm^{-1}, 1470–1410 cm^{-1}, and 1380–1350 cm^{-1}.

Can. J. Chem. Downloaded from www.nrcresearchpress.com by 210.87.254.42 on 09/05/12
For personal use only.

Physical Measurements

Infrared spectra were measured on Nujol mulls using Beckmann IR 10 and Perkin Elmer 621 (grating) spectrophotometers. Magnetic susceptibility measurements were made over the temperature range 96–297 °K on solid samples on a Gouy-type balance. X-ray powder diffraction patterns were taken in 11.46 cm Debye–Scherrer cameras. Copper K_α radiation was used throughout. A nickel screen was used instead of filters. Irradiation was at 20 mA and 32 kV, for 5–15 h.

Reactions

All the reactions were carried out in a dry box flushed with dry nitrogen to avoid hydrolysis of the highly moisture-sensitive materials. Solid products were washed thoroughly with a suitable solvent and dried in vacuum for several hours.

Reaction of Chromyl Chloride with Toluene

A solution of toluene (11.9 g, 129.08 mmoles) in dry carbon tetrachloride (500 ml) was treated dropwise with stirring with a solution of chromyl chloride (4.99 g, 32.27 mmoles) in carbon tetrachloride (150 ml) during 1 h, stirred for 6 h, and allowed to stand at room temperature overnight. The suspension was filtered and the precipitate washed with carbon tetrachloride until washings were colorless, and then dried in vacuum.

Anal. Calcd. for $C_6H_5CH_3.2CrO_2Cl_2$: C, 20.91; H, 2.01; Cr, 25.89. Found: C, 20.89; H, 1.99; Cr, 26.35.

The Etard complex was insoluble in most common organic solvents, e.g. benzene, carbon tetrachloride, chloroform, *n*-hexane, and ether, but was completely soluble in dioxan and tetrahydrofuran. On removal of solvent a residue remained which contained a new complex.

*Reaction of **1** with Pyridine*

Etard complex **1** (2.2834 g, 5.68 mmoles) was refluxed with a dilute solution of pyridine (1.8738 g, 23.72 mmoles) in carbon tetrachloride for 20 h. The product was filtered, washed with solvent, and dried in vacuum. The net gain in weight after the reaction was 0.9046 g, indicating attachment of two molecules of pyridine. The product was a greenish black crystalline solid, insoluble in common organic solvents, and did not melt.

Anal. Calcd. for $2CrO_2Cl_2.C_6H_5CH_3.2Py$: C, 36.43; H, 3.21; N, 5.00; Cr, 18.57. Found: C, 36.08; H, 3.19; N, 7.21; Cr, 17.95.

*Reaction of **1** with Acetonitrile*

1 (0.32 g, 0.79 mmoles) was refluxed with a dilute solution of acetonitrile (0.16 ml, 3.05 mmoles) in carbon tetrachloride for 24 h. The resulting product was filtered, washed, and dried. It was found to be insoluble in common organic solvents, was non-melting, and showed coordination bands in the infrared spectrum. The strong band at 2310 cm^{-1} was due to coordination through nitrogen of the C≡N group.

Anal. Calcd. for $2CrO_2Cl_2.C_6H_5CH_3.2CH_3CN$: C, 27.27; H, 2.89; N, 5.78; Cr, 21.49. Found: C, 26.95; H, 3.04; N, 5.84; Cr, 23.4.

*Reaction of **1** with Dioxan*

1 (2.6271 g, 6.53 mmoles) was dissolved in 35 ml of dry dioxan, giving a dark-brown clear solution. Solvent was removed by vacuum distillation and the resulting solid was dried for 2 days. The net gain in weight was 1.2716 g, indicating attachment of 2.21 molecules of dioxan. The complex was a shining, crystalline, chocolate-colored solid which decomposed in air.

Anal. Calcd. for $2CrO_2Cl_2.C_6H_5CH_3.2$dioxan: C, 31.14; H, 4.15; O, 33.31; Cr, 17.99. Found: C, 28.83; H, 5.83; O, 31.48; Cr, 15.96.

*Reaction of **1** with Tetrahydrofuran*

1 (2.50 g, 6.21 mmoles) was dissolved in 50 ml of dried tetrahydrofuran. An exothermic reaction occurred, giving a dark-brown solution. On removal of the solvent by vacuum distillation, a black residue was left which was dried in vacuum for 48 h. The new reaction product was insoluble in common organic solvents, hygroscopic, and decomposed in moist air. It was very lustrous, and X-ray powder diffraction showed it to be crystalline.

Anal. Calcd. for $2CrO_2Cl_2.C_6H_5CH_3.2C_4H_8O$: C, 32.96; H, 4.4; Cr, 19.04. Found: C, 31.26; H, 4.97; Cr, 19.75.

*Reaction of **1** with Triethylamine*

1 (3.03 g, 7.53 mmoles) was refluxed for 24 h at 50 °C with a 5% solution of triethylamine (4.2 ml, 30 mmoles) in petroleum ether, followed by filtration of the precipitate, washing, and drying in vacuum. The weight of solid remaining after reaction was 5.146 g, showing a net gain in weight of 2.12 g, which implies attachment of 2.8 molecules of base. X-ray examination of the residue showed lines due to triethylamine hydrochloride, and the infrared spectrum shows a band attributed to Cr—N stretching. It appears that complex formation and HCl abstraction have both occurred. It was ash colored and crystalline in appearance, non-melting, and insoluble in common organic solvents.

Anal. Calcd. for $2CrO_2Cl_2.C_6H_5CH_3.2(C_2H_5)N$: C, 37.73; H, 6.38; N, 4.63; Cr, 17.20. Calcd. for $2CrO_2Cl_2.C_6H_5CH_3.3(C_2H_5)_3N$: C, 42.56; H, 7.51; N, 5.95; Cr, 14.74. Found: C, 35.86; H, 7.14; N, 5.31; Cr, 17.58.

*Reaction of **1** with 4-Picoline*

3.35 g of the toluene chromyl chloride complex was refluxed with a 10% solution of 4-picoline (4 ml in 40 ml petroleum ether) for 36 h, followed by filtration, washing, drying, and weighing. The net gain in weight after reaction was 1.6746 g, which was equivalent to 2.15 moles of 4-picoline per mole of Etard complex. The adduct was insoluble, hygroscopic, non-melting, and buff colored.

Anal. Calcd. for $2CrO_2Cl_2.C_6H_5CH_3.2CH_3C_5H_4N$: C, 42.17; H, 3.70; N, 4.68; Cr, 17.39. Found: C, 42.62; H, 4.87; N, 7.27; Cr, 17.09.

Results and Discussion

The infrared spectra of $C_6H_5CH_3.2CrO_2Cl_2$ and $C_6H_5CH_3.2CrO_2Cl_2.2D$ (where D = dioxan, tetrahydrofuran, acetonitrile, pyridine, 4-picoline, or triethylamine) have been recorded and frequency assignments are given in Table I. These were made by comparison with those of chromyl chloride (8) and the donor molecules used (9, 10). Recently Duffin and Tucker (11) reported that **1** was composed of benzaldehyde

TABLE II
Magnetic susceptibility measurements

Etard **1**			Etard $1.2C_5H_5N$			Cr(IV)	
Temperature (°K)	$10^6 \times \chi_g$	Average $\mu_{eff.}$ (B.M.)	Temperature (°K)	$10^6 \times \chi_g$	Average $\mu_{eff.}$ (B.M.)	$\mu_{calcd.}$* (B.M.)	$\mu_{obs.}$† (B.M.)
297	20.315		297	14.658			
273	22.735		278	15.300			
243	25.565		243	17.420			
213	30.039	3.21±0.06	213	19.954	3.28±0.07	2.83	2.8–3.1
174	35.408		164	25.042			
134	44.191		139	28.581			
96	61.612		115	34.650			
			96	40.118			

*Magnetic moment calculated from $\mu = \sqrt{(n(n+2))}$.
†Magnetic moments observed in covalent bond complexes of Cr and other atoms with the same number of unshared electrons.

coordinated to reduced chromyl chloride, on the basis of only one absorption band at 1618 cm^{-1}, which they assign to the carbonyl group with a negative shift on coordination to Cr(IV). Our values for frequencies are similar to those reported by these workers, as shown in Table I.

Further, a broad, strong band at 3300 cm^{-1} was observed which is assigned to hydrogen-bonded OH. We assign our 1620 and their 1618 cm^{-1} band as due to C=C in the ring in toluene. The strong peaks expected for Cr—O asymmetric and symmetric stretching we believe are reduced to medium intensity and shifted to very low frequencies: 528 and 445 cm^{-1}. We can discern only one of the two expected Cr—Cl stretching bands, at 325 cm^{-1}.

The reaction of chromyl chloride with toluene reduces the oxidation state of chromium from VI to IV, while in all other reaction products the oxidation state remains IV, i.e. the reactions of the Etard complex **1** with nitrile, cyclic ethers, pyridine, 4-picoline, and triethylamine do not involve any further reduction. These reaction products are most probably hexa-coordinated through hydroxo- or halogen-bridging.

The infrared spectra of the complexes of **1** with three of the nitrogen bases show bands at 495, 442, 340 cm^{-1} (pyridine), at 545, 425, 330 cm^{-1} (4-picoline), and at 520–560, 410, 340 cm^{-1} (triethylamine), which are tentatively assigned to asymmetric and symmetric Cr—O stretching and Cr—Cl stretching vibrations. The appearance of new bands at 285, 290, and 290 cm^{-1} in these respective complexes are assigned to the Cr—N linkage, indicating the coordination of chromium with the nitrogen of these donor molecules.

The infrared spectrum of $C_6H_5CH_3.2CrO_2Cl_2.2CH_3CN$ shows a strong absorption around 2310 ± 10 cm^{-1} which shows a positive shift of approximately +60 cm^{-1} compared with values obtained in free acetonitrile. This confirms the coordination of the nitrile molecule through nitrogen (12). The far infrared spectrum of this substance shows a single, sharp, medium-intensity band at 340 cm^{-1} which may be ascribed to a Cr—Cl stretching mode.

The infrared spectra of the tetrahydrofuran and dioxan reaction products of **1** are typical of the coordinated ligands in the region 1200–300 cm^{-1}, and in particular the peak associated with the COC antisymmetric stretching mode is split and shows the expected frequency decrease (13, 14). The 1110 cm^{-1} and 1070 cm^{-1} antisymmetric COC absorption peaks in dioxan and

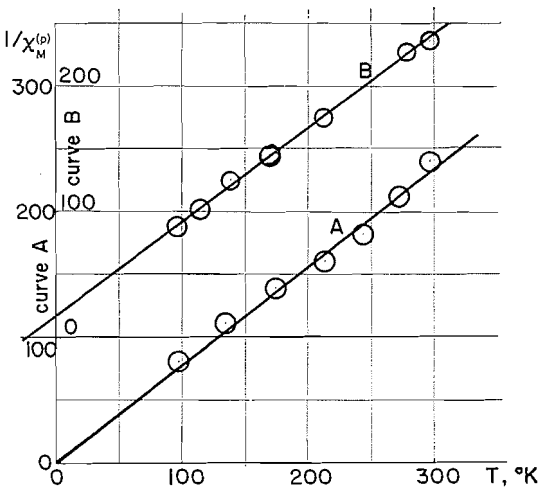

FIG. 1.

Can. J. Chem. Downloaded from www.nrcresearchpress.com by 210.87.254.42 on 09/05/12
For personal use only.

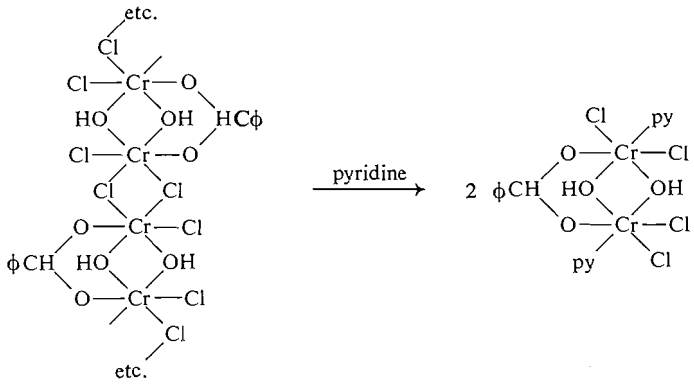

Etard product Ternary complex

FIG. 2.

tetrahydrofuran are reduced to 1080 cm^{-1}, 1045 cm^{-1} and 1040 cm^{-1}, 1010 cm^{-1} respectively in their reaction products. The low infrared frequency assignments shown in Table I may be used to establish the coordination number. Thus for six-coordinated complexes the frequencies for chromium–chlorine stretching modes are expected in the 300–380 cm^{-1} region, although they are higher for five- or four-coordinated complexes (15, 16). The values obtained in our complexes (320–345 cm^{-1} and 350 cm^{-1}) are in accord with six-coordination. We observe an additional peak in the 270–280 cm^{-1} region in the dioxan complex, and in the 275–285 cm^{-1} region in the tetrahydrofuran complex, which we tentatively assign to a stretching mode of the bond between chromium and oxygen of the ligand (dioxan or tetrahydrofuran).

Magnetic Susceptibility

The measured magnetic susceptibilities per gram (χ_g) are recorded in Table II. The reciprocal of the paramagnetic susceptibility per gram-atom of chromium is shown as a function of absolute temperature for the toluene Etard product (**1**) in Fig. 1*a* and for the ternary complex of this with pyridine in Fig. 1*b*. **1** obeys the Curie Law (17, 18), having a Weiss constant zero within experimental error (estimated $\pm 10°$). The ternary complex obeys the Curie–Weiss law, with a Weiss constant about $-30°$. The values of the magnetic moment are for **1**, 3.21 $\pm$ 0.07, and for the pyridine complex, 3.28 $\pm$ 0.07 Bohr magnetons. These are the same within experimental error. The theoretical values for chromium IV are 4.47 for the free Cr^{4+} ion (the ground state presumed to be $^3F_2$), and 2.83 if the orbital contribution is fully quenched. The measured values are sufficiently close to the spin-only value that they may be taken as evidence for chromium IV. Whether the coordination at chromium is essentially tetrahedral, or octahedral, or of lower symmetry cannot be judged from the small excess of the measured over the spin-only moment as there are several different groups attached to the chromium atom. It appears probable, from the observations on the solubility of the Etard complex, that it is polymeric, presumably by the formation of hydroxo or chloro bridges. If this is the case, the coordination number of chromium would be, not 4 as in Etard's structure, but most probably 6.

These magnetic measurements are in agreement with that of Wheeler, and tend to confirm his interpretation (5). It must be concluded that the electron spin resonance result obtained by Necsoiu and co-workers arose because of some peculiarity of the environment of the chromium atoms, such that one half the absorption was so broad as to be unobservable with their apparatus, or in some way suppressed or grossly shifted.

The preliminary X-ray observations clearly show that the toluene Etard complex is most probably amorphous while its reaction products with donor molecules are crystalline. As these substances are complex in structure and of low density, the X-ray powder diffraction patterns were not very satisfactory for indexing, etc. More information on this will be given in a later paper in this series.

Tentative structures for the Etard product and the ternary complexes which are compatible with the above are shown in Fig. 2. Work with models has shown that the proposed linkage by hydroxo

Can. J. Chem. Downloaded from www.nrcresearchpress.com by 210.87.254.42 on 09/05/12
For personal use only.

bridges of two chromiums that are attached to the same carbon (through oxygen) is much less strained than the analogous linkage by chloro bridges. Without the constraining carbon atom, the chloro bridges between chromiums not otherwise linked are not so strained.

Retention of the hydroxo bridges on reaction with pyridine or other bases would explain why the ternary complexes contain one molecule of base only per chromium atom. We cannot find any evidence in the infrared to support any particular arrangement of bridges.

Acknowledgments

The authors wish to acknowledge generous help and advice from Professor A. Westland of Ottawa University, with the magnetic measurements, and from Professor R. D. Heyding of Queen's University at Kingston, with X-rays. The work was made possible by grants from the National Research Council of Canada, Ottawa, and Trent University.

1. W. H. HARTFORD and M. DARRIN. Chem. Rev. **58**, 1 (1958).
2. I. NECSOIU, A. T. BALABAN, I. PASCARU, E. SLIAM, M. ELIAM, and C. D. NENITZESCU. Tetrahedron, **19**, 1133 (1963).
3. A. ETARD. Ann. Chim. Phys. [5], **22**, 218 (1881).
4. F. WESTHEIMER. Chem. Rev. **45**, 419 (1949).
5. O. H. WHEELER. Can. J. Chem. **38**, 2137 (1960).
6. A. BARTECKI. Roczniki Chem. **39**, 167 (1965).
7. K. WIBERG, B. MARSHALL, and G. FOSTER. Tetrahedron Letters, 345 (1962).
8. W. E. HOBBS. J. Chem. Phys. **28**, 1220 (1958).
9. L. J. BELLAMY. The infra-red spectra of complex molecules. 2nd ed. Methuen and Co. Ltd., London. Reprinted 1964.
10. C. N. R. RAO. Chemical applications of infrared spectroscopy. Academic Press Inc., New York. 1963.
11. H. C. DUFFIN and R. B. TUCKER. Chem. Ind. London, 1262 (1966).
12. S. C. JAIN and R. RIVEST. Can. J. Chem. **45**, 139 (1967).
13. G. W. A. FOWLES, P. T. GREENE, and T. E. LESTER. J. Chem. Soc. 2365 (1967).
14. R. J. KERN. J. Inorg. Nucl. Chem. **24**, 1105 (1962).
15. I. R. BEATTIE and T. GILSON. J. Chem. Soc. 6595 (1965).
16. R. J. H. CLARK, R. S. NYHLOM, and D. E. SCARFE. J. Chem. Soc. 1296 (1966).
17. R. S. NYHOLM. Quart. Rev. London, **7**, 377 (1953).
18. P. W. SELWOOD. Magneto chemistry. Interscience Publishers Inc., New York. 1964.

Can. J. Chem. Downloaded from www.nrcresearchpress.com by 210.87.254.42 on 09/05/12
For personal use only.

Can. J. Chem. Downloaded from www.nrcresearchpress.com by 210.87.254.5 on 09/05/12
For personal use only.

Réactions dans le sulfolane. II. Etude électrochimique de systèmes oxydo-réducteurs des halogènes[1]

R. L. Benoit, M. Guay et J. Desbarres[2]
Département de Chimie, Université de Montréal, Montréal, Québec

Reçu le 31 juillet 1967

On a étudié l'oxydation électrochimique des halogénures et la réduction des halogènes dans le sulfolane, un solvant aprotique. La formation d'ions trihalogénures X_3^- stables a été mise en évidence. On a déterminé par potentiométrie les constantes de formation K des ions X_3^- comme étant égales à $10^{7.4}$ (X = I), $10^{6.8}$ (X = Br) et $10^{3.1}$ (X = Cl) en milieu $LiClO_4$ 0.10 *M*. Les valeurs des constantes K ont aussi été déterminées dans le méthanol, un solvant hydroxylique, $10^{4.2}$ (X = I) et $10^{2.3}$ (X = Br) et dans des mélanges des deux solvants (X = I). L'utilisation d'une électrode au ferrocène a permis de montrer approximativement dans quelle mesure les énergies de solvatation des ions X_3^- et X^- varient d'un solvant à l'autre.

The electrochemical oxidation of halides and reduction of halogens have been studied in sulfolane, an aprotic solvent. Stable trihalide ions X_3^- are formed. The formation constants K of these X_3^- ions have been determined by potentiometry as $10^{7.4}$ (X = I), $10^{6.8}$ (X = Br), and $10^{3.1}$ (X = Cl) in a 0.1 *M* $LiClO_4$ medium. The values of the constants K have also been obtained in methanol, a hydroxylic solvent, $10^{4.2}$ (X = I), $10^{2.3}$ (X = Br), and in mixtures of both solvents (X = I). The variations of solvation energies of X_3^- and X^- ions from one solvent to the other were estimated by means of a ferrocene electrode.

Canadian Journal of Chemistry, 46, 1261 (1968)

Dans un précédent mémoire (1) on a exposé les résultats d'une étude électrochimique préliminaire sur la tétraméthylènesulfone (sulfolane), un solvant polaire aprotique. On examine maintenant le comportement électrochimique de systèmes oxydo réducteurs des halogènes, systèmes déjà étudiés dans d'autres solvants. Les constantes de stabilité des ions trihalogénures X_3^- formés ont été déterminées et conduisent à l'ordre $I_3^- > Br_3^- > Cl_3^-$, contrairement aux conclusions d'Iwamoto et coll. (2) pour ce type de solvant. Dans un tout récent article, l'oxydation dans le sulfolane de Br^- en deux étapes et celle de Cl^- en une seule est mentionnée (3).

Résultats

I. Comportement de l'iode

(a) Tracé des courbes intensité–potentiel

Les courbes intensité–potentiel de solutions d'iode et d'iodure sont représentées Fig. 1 (courbes 1 et 2 respectivement, corrigées pour le courant résiduel). Les 4 vagues désignées respectivement par I, II, III, IV apparaissent vers −0.3 à −0.8 V, +0.1 V, +0.8 V et +1.5 V. Le courant de diffusion de la vague I est le double de celui de la vague II. Les valeurs absolues des courants limites de diffusion des vagues I et II sont proportionnelles, et avec le même coefficient, aux concentrations (Fig. 2). Des déterminations coulométriques non rapportées ici, sur les vagues I et II indiquent pour l'oxydation de I^- et la réduction de I_2, des échanges de 0.66 ± 0.06 et 0.33 ± 0.03 électrons équivalents/atome-gramme sur les vagues I et II respectivement. En mélangeant d'autre part des solutions d'iode et iodure, on obtient le spectre de I_3^- avec ses maxima à 292 et 362 mμ (4).

Les vagues I et II correspondent donc respectivement aux réactions suivantes.

[1] $$3I^- \rightleftharpoons I_3^- + 2e$$

[2] $$2I_3^- \rightleftharpoons 3I_2 + 2e$$

On a établi les équations des vagues I et II (5) et comparé les valeurs théoriques des pentes des droites donnant E en fonction de transformées logarithmiques de i et $i^\perp$ (5), aux valeurs expérimentales. Au lieu d'une pente théorique de 29.3 mV par unité de logarithme, on obtient pour les réactions $3I_2 \rightarrow 2I_3^- - 2e$, $2I_3^- \rightarrow 3I_2 + 2e$ et $3I^- \rightarrow I_3^- + 2e$, 30, 32 et 34 mV respectivement. Ces réactions électrochimiques seraient donc "réversibles", toutefois les pentes augmentent lorsque les concentrations dépassent 10^{-3} *M*.

[1]Tiré d'une communication présentée à la Conférence Internationale sur la Chimie des Solvants non-aqueux, tenue à Hamilton du 1 au 3 juin 1967.

[2]En congé du Centre National de la Recherche Scientifique, Paris, France. Présente adresse: Service de Chimie Analytique associé au C.N.R.S., E.S.P.C.I., 10, rue Vauquelin, Paris, France.

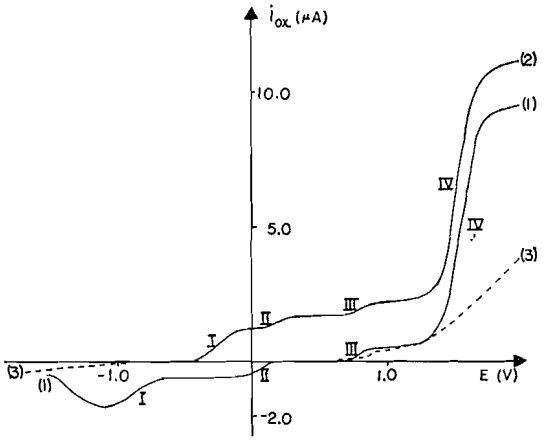

FIG. 1. Courbes intensité-potentiel. (1) I_2 8.5×10^{-4} M; (2) I^- 1.7×10^{-3} M; (3) courant résiduel.

Dans le cas de la réduction de l'iode (vague I), le plateau de diffusion est à peine visible et suivi d'une baisse du courant, un tel phénomène indique généralement des modifications de l'état de surface des électrodes. Popov et Geske (5) ont obtenu des résultats similaires dans l'acétonitrile et suggèrent une interprétation. La non proportionnalité des vagues III et IV avec la concentration (Fig. 2) a été également rencontrée par ces auteurs.

(b) Stabilité de l'ion triiodure dans le sulfolane

Plutôt que de déterminer la constante de formation de I_3^- d'après les différences des potentiels de demi-vague des vagues I et II (2), on a utilisé une méthode potentiométrique (6).

Soit C_{I_2} et C_{I^-} les concentration d'iode et iodure, en moles ou ions-gramme/litre, ajoutées dans une solution,

$$C_{I_2} = [I_2] + [I_3^-] \text{ et } C_{I^-} = [I^-] + [I_3^-].$$

Si en milieu $LiClO_4$ 0.10 M, on prépare deux séries de solutions d'iode iodure telles que

$$C_{I_2} = \tfrac{1}{2}C_{I^-} = C_1 \text{ et } C_{I_2} = 2C_{I^-} = C_2$$

et si l'ion I_3^- est suffisamment stable (sinon des corrections sont effectuées comme dans les cas étudiés plus loin de Cl_3^-, et Br_3^- dans le méthanol) les équations de Nernst appliquées aux réactions [1] et [2] deviennent

$$E_{I_3^-/I^-} = E_{31} = E^1_{31} - 0.0586 \log C_1$$

$$E_{I_2/I_3^-} = E_{23} = E^1_{23} + 0.0293 \log C_2,$$

où E^1_{31} et E^1_{23} sont les potentiels normaux

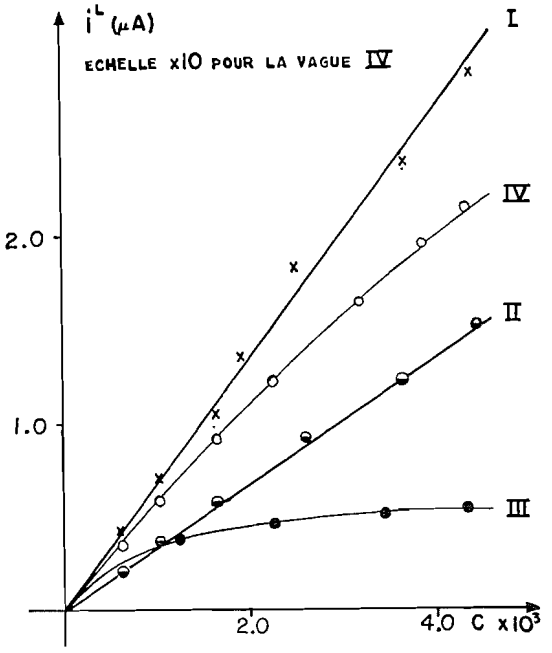

FIG. 2. Relations entre les courants-limites de diffusion et les concentrations. (I) vagues I (I_3^-/I^-), (II) vagues II (I_2/I_3^-), (III) vagues III, (IV) vagues IV (échelle des courants multipliée par 10). Concentrations C exprimées en ion ou atome-gramme/litre.

apparents pour $LiClO_4$ 0.10 M. Les variations de E_{31} et E_{23} en fonction de log C permettent d'obtenir E^1_{31} et E^1_{23} par extrapolation (Fig. 3) $E^1_{31} = -0.570$ V et $E^1_{23} = +0.087$ V. Les pentes des droites expérimentales donnant E en fonction de log C correspondent bien aux pentes théoriques. La constante de formation K de I_3^-, $10^{7.4}$, est ensuite calculée d'après

$$\frac{E^1_{23} - E^1_{31}}{0.088} = \log K.$$

(c) Stabilité de l'ion triiodure dans le méthanol et les mélanges sulfolane méthanol

Les potentiels normaux apparents des systèmes I_3^-/I^- et I_2/I_3^-, E^2_{31} et E^2_{23}, ont été déterminés pour des mélanges sulfolane méthanol par rapport à une électrode au ferrocène dans les mêmes mélanges. On donne Fig. 4 les valeurs de E^2_{31} et E^2_{23} en fonction de la composition du solvant ainsi que celles des constantes K. Les valeurs obtenues dans le méthanol sont $E^2_{31} = -0.131$ V et $E^2_{23} = +0.241$ V, de telle sorte qu'entre le sulfolane et le méthanol on calcule, avec l'électrode au ferrocène comme

Can. J. Chem. Downloaded from www.nrcresearchpress.com by 210.87.254.5 on 09/05/12
For personal use only.

Can. J. Chem. Downloaded from www.nrcresearchpress.com by 210.87.254.5 on 09/05/12
For personal use only.

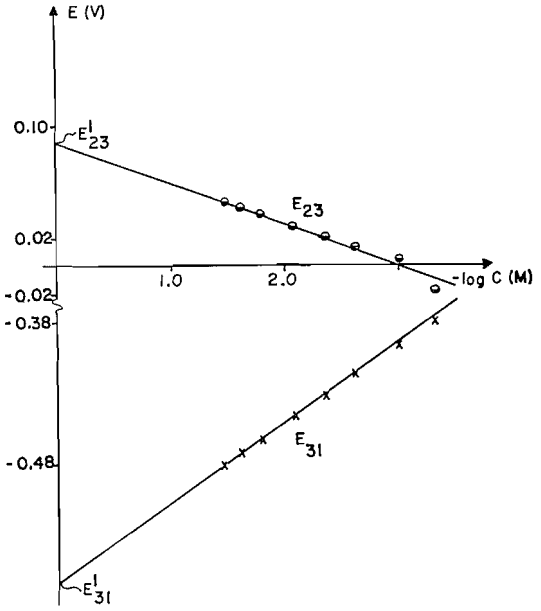

FIG. 3. Variations des potentiels normaux apparents des systèmes I_3^-/I^- (E_{31}) et I_2/I_3^- (E_{23}) en fonction des concentrations C (réf. Ag^+ 10^{-2} M/Ag, $LiClO_4$ 0.10 M).

référence commune, $\Delta E^2_{31} = -0.179$ V et $\Delta E^2_{23} = 0.106$ V. On a aussi déterminé ces ΔE en éliminant l'électrode au ferrocène. On a mesuré la différence de potentiel entre deux solutions, l'une dans le sulfolane l'autre dans le méthanol, de mêmes concentrations en iode et iodure, C_1 dans le premier cas et C_2 dans le

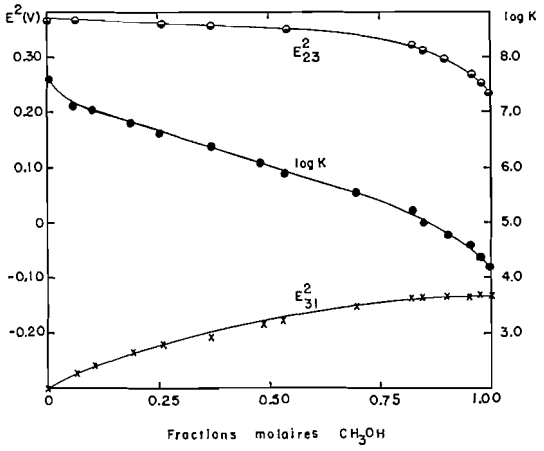

FIG. 4. Variation des potentiels normaux apparents des systèmes I_3^-/I^- (E^2_{31}), I_2/I_3^- (E^2_{23}) (réf. électrode au ferrocène) et de la constante de formation K de I_3^- dans les mélanges sulfolane méthanol.

deuxième. On obtient $\Delta E_{31} = -0.200$ V et $\Delta E_{23} = 0.095$ V c'est-à-dire des différences de seulement 20 à 10 mV avec les valeurs ΔE^2_{31} et ΔE^2_{23}.

II. Comportement des autres halogènes

(1) Brome

Les solutions de brome dans le sulfolane sont peu stables. Les courbes du brome et du bromure ont la même allure que celles de l'iode et de l'iodure (Fig. 5). La hauteur des vagues I et II est aussi proportionnelle à la concentration. La transformée logarithmique de ces deux vagues indique que les réactions sont vraisemblablement rapides en oxydation et lentes en réduction. On a déterminé la constante de formation de Br_3^- par la méthode potentiométrique ($8 \times 10^{-3} \leqslant C_1$ et $C_2 \leqslant 2 \times 10^{-2}$ M), $E^1_{31} = -0.150$ V, $E^1_{23} = 0.450$ V et $\log K_{Br_3^-} = 6.8$. Les valeurs obtenues dans le méthanol en utilisant une électrode au ferrocène sont $E^2_{31} = 0.39$ V, $E^2_{23} = 0.60$ V et $\log K_{Br_3^-} = 2.3$.

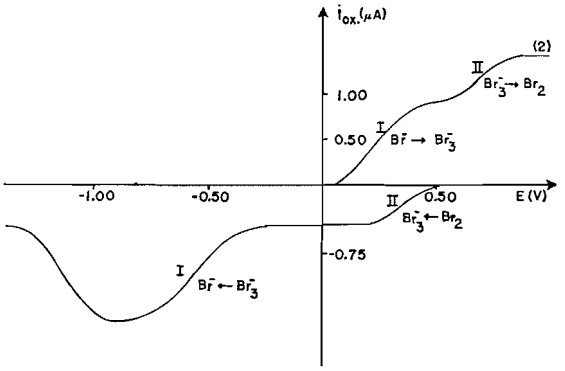

FIG. 5. Courbes intensité-potentiel. (1) Br_2 8.5 $\times$ 10^{-4} M; (2) Br^- 1.7 $\times$ 10^{-3} M.

(2) Chlore

On a seulement tracé la courbe d'oxydation de Cl^-. La vague ne peut s'obtenir que par déduction d'un courant résiduel important. On a obtenu une valeur approximative de la constante de formation de Cl_3^- par potentiométrie, $E^1_{31} = 0.21$ V ($C_1 = 1.23 \times 10^{-3}$ M), $E^1_{23} = 0.48$ V ($C_2 = 2.46 \times 10^{-3}$ M) et $\log K_{Cl_3^-} \sim 3.1$.

(3) Fluor

La courbe d'oxydation d'une solution saturée de LiF se confond avec la courbe du courant résiduel.

TABLEAU I

Constantes d'équilibre

Constante diélectrique	Solvant S	$I_2 + I^- \rightleftarrows I_3^-{}_{(S)}$	$I_2 + S \rightleftarrows I_2.S_{(CCl_4)}$ (12)
43	$(CH_2)_4SO_2$	$10^{7.4}$	0.73
36	CH_3CN	$10^{7.4}$ (6)	0.40
36	CH_3NO_2	$10^{7.7}$ (8)	—
38	$HCON(CH_3)_2$	$10^{6.8}$–$10^{7.3}$ (9, 10)	2.9
49	$(CH_3)_2SO$	$10^{5.4}$ (7)	11.6
33	CH_3OH	$10^{4.2}$	0.47
80	H_2O	$10^{2.9}$ (11)	—

Discussion

Les résultats indiquent la grande stabilité des ions I_3^- et Br_3^- dans le sulfolane. On compare dans le Tableau I les valeurs de la constante de formation de I_3^- dans le sulfolane, 4 autres solvants polaires aprotiques, le méthanol et l'eau. On indique aussi dans ce tableau les valeurs des constantes d'équilibre des réactions donneur–accepteur entre ces solvants et l'iode dans CCl_4 (12). Ces dernières constantes sont peu élevées mais suggèrent, que dans ces solvants aprotiques de constantes diélectriques voisines, les faibles différences de stabilité de I_3^- proviennent en partie des interactions iode–solvants et que les différences des énergies de solvatation de I^- et I_3^- sont voisines. Par contre, la stabilité beaucoup plus faible de I_3^- dans le méthanol, un solvant hydroxylique de constante diélectrique aussi voisine, résulte de solvatations relatives très différentes des ions I^- et I_3^-. Parker (9, 13) attribue ces différences d'énergies de solvatation des anions par les deux groupes de solvants aux liaisons hydrogènes. Les mesures des potentiels des systèmes I_3^-/I^- et I_2/I_3^- par rapport à l'électrode au ferrocène permettent d'évaluer dans quelle mesure le changement de solvatation, du sulfolane au méthanol, affecte I_3^- et I^-. Strehlow (14) a en effet suggéré que le potentiel d'oxydo-réduction du système ion ferricinium/ferrocène pouvait être considéré comme indépendant du solvant. Ce point de vue est confirmé par les faibles valeurs de ΔE mesurées entre des électrodes au ferrocène, dans le sulfolane et le méthanol: 14 ± 3 mV lorsque le pont de $LiClO_4$ 0.10 *M* est une solution dans le méthanol ou le sulfolane. Ces résultats suggèrent que les potentiels de jonction sulfolane–méthanol sont faibles, et que les solvatations relatives de l'ion ferricinium et du ferrocène varient peu du premier solvant au second. Les valeurs voisines des différences de potentiel, des systèmes I_3^-/I^- et I_2/I_3^-, ΔE_{31} et ΔE_{23}, déterminées directement ou par rapport à l'électrode au ferrocène, renforcent ces conclusions. Si le solvant hydroxylique est l'eau au lieu du méthanol, il se peut que l'électrode au ferrocène ne soit pas utilisable comme système de référence, comme en témoignent les conclusions divergentes obtenues avec le couple acétonitrile eau (15, 16). C'est pour cette raison que l'on a choisi ici le méthanol plutôt que l'eau comme solvant hydroxylique.

Les valeurs de $E^2{}_{23}$ et $E^2{}_{31}$ (Fig. 4) dans le sulfolane et le méthanol, respectivement 0.347 V, −0.310 V et 0.241 V, −0.131 V, indiquent que la plus grande stabilité de I_3^- dans le sulfolane est due à la fois à une énergie de solvatation plus forte pour I_3^- et plus faible pour I^-. Un calcul approximatif montre que, si l'on néglige les variations des interactions entre l'iode, et le sulfolane et le méthanol (Tableau I), les contributions des différences d'énergies de solvatation des deux ions à la plus grande stabilité de I_3^- dans le sulfolane sont de 1.9 kcal pour I^- et 2.4 kcal pour I_3^-. Ceci alors que Parker (9) dans le cas du diméthylformamide et du méthanol attribue la variation de stabilité de I_3^- aux différentes énergies de solvatation du seul ion I^-, d'ailleurs en conformité avec sa valeur $\Delta E_{23} \sim 0$ mV. Le diméthylformamide et le sulfolane paraissent ainsi solvater différemment le système I_2/I_3^- puisque l'on a obtenu $\Delta E_{23} = 95$ mV, ceci si l'on néglige les potentiels de jonction (9) dans les deux cas.

Les variations des potentiels $E^2{}_{23}$ et $E^2{}_{31}$ en fonction de la fraction molaire de méthanol (Fig. 4) montrent que de 0 à 0.70 l'énergie de solvatation de I_3^- varie peu alors que celle de

Can. J. Chem. Downloaded from www.nrcresearchpress.com by 210.87.254.5 on 09/05/12
For personal use only.

Can. J. Chem. Downloaded from www.nrcresearchpress.com by 210.87.254.5 on 09/05/12
For personal use only.

I^- augmente, et que de 0.70 à 1.00, les énergies de solvatation de I_3^- et I^- diminuent toutes deux mais cette dernière moins. Les variations de E^2_{23}, E^2_{31} et $E^2_{23} - E^2_{31}$ sont cependant telles, que l'addition de méthanol au sulfolane provoque une diminution continue de la constante de I_3^- (Fig. 4). Ce résultat diffère de ce qui est observé avec une autre paire de solvants aprotique et hydroxylique, le diméthylsulfoxyde et l'eau, où la constante K reste égale à $10^{5.4}$ jusqu'à une fraction molaire de 0.40 d'eau (7). Cette différence paraît dûe aux interactions, fortes entre le diméthylsulfoxyde et l'eau, et faibles entre le sulfolane et le méthanol.

La constante K de Br_3^- dans le sulfolane, $10^{6.8}$ est voisine de celle récemment déterminée dans le nitrométhane $10^{7.2}$ (8) et le diméthylformamide $10^{6.3}$ (9). La stabilité de Br_3^- dans le méthanol est beaucoup plus faible, $10^{2.4}$, et les valeurs de E^2_{23} et E^2_{31} comparées à E^1_{23} et E^1_{21} reflètent les différentes énergies de solvatation des ions Br^- et Br_3^- dans les deux solvants. La faible stabilité de Cl_3^-, $10^{3.1}$, est inattendue (2) mais a aussi été établie dans le nitrométhane (8).

L'ordre de stabilité des ions X_3^- est ainsi $I_3^- > Br_3^- \gg Cl_3^-$, c'est-à-dire l'inverse de celui fréquemment cité (17) et donné par Iwamoto et coll. (2) pour le nitrométhane, l'acétone et l'acétonitrile, trois autres solvants polaires aprotiques. Les conclusions de ces auteurs sont basées sur l'examen des courbes voltampérométriques des halogénures et l'utilisation des $E_{1/2}$. L'unique vague de Cl^- obtenue dans le nitrométhane et l'acétone a été attribuée à l'oxydation de Cl^- en Cl_3^- par comparaison avec les valeurs de $E_{1/2}$ données par Kolthoff et coll. (18) pour les "deux vagues" de Cl^- dans l'acétonitrile. L'absence d'ions Cl_3^- stables dans le nitrométhane a été récemment établie et les calculs des constantes K à partir des $E_{1/2}$ ont été critiqués (8). De plus la présence des deux vagues d'oxydation de Cl^- dans l'acétonitrile n'a pas été confirmée (8). Les arguments avancés pour démontrer la grande stabilité de Cl_3^- ne sont ainsi pas valables. Par ailleures, l'ordre $I_3^- > Br_3^-$ observé dans le sulfolane l'est aussi dans le nitrométhane (8), le diméthylformamide (9). L'ordre de stabilité $I_3^- > Br_3^- > Cl_3^-$ est donc le même dans les solvants polaires aprotiques et l'eau. Si les différences des énergies de solvatation entre les ions X^- et X_3^- dans les solvants polaires aprotiques et l'eau sont considérables, elles diminuent dans l'ordre $I > Br \gg Cl$. Ceci est confirmé par des déterminations potentiométriques en cours dans ce laboratoire, qui indiquent que dans la série I_2X^-, l'ordre de stabilité est aussi $I_2I^- > I_2Br^- > I_2Cl^-$.

Le principe des acides et bases "durs et mous" (19) est ainsi bien applicable (2, 17), l'acide "mou" I_2 formant le complexe le plus stable avec I^-, la base la plus "molle".

La solvatation probablement très faible de F^- dans le sulfolane permettait de penser que l'on aurait pu mettre en évidence l'oxydation électrochimique de F^- en F_2 à un potentiel voisin de celui correspondant à l'oxydation de Cl^- en Cl_2. Les résultats ne permettent pas de conclure vu la faible solubilité de LiF et l'oxydation électrochimique de l'électrolyte support ou du solvant à ces potentiels (courants résiduels importants).

Les effets de solvatation notés pour l'équilibre $X_2 + X^- \rightleftharpoons X_3^-$ sont aussi observés pour des équilibres formellement analogues tels $SO_2 + X^- \rightleftharpoons SO_2X^-$, $AgX\downarrow + X^- \rightleftharpoons AgX_2^-$ et $GeCl_4 + Cl^- \rightleftharpoons GeCl_5^-$, qui sont fortement déplacés vers la droite dans les solvants aprotiques (17, 20, 21).

Partie expérimentale

Réactifs

L'iodure de tétrabutylammonium et le bromure de tétraéthylammonium sont des produits Eastman. Les perchlorates de lithium anhydre et d'argent proviennent de G. F. Smith et le ferrocène (fer dicyclopentadiényl) de Aldrich. Le picrate de ferricinium est préparé suivant le mode opératoire donné par Kolthoff et Thomas (15). Des solutions de perchlorate de ferricinium dans le sulfolane sont aussi obtenues par oxydation in situ du ferrocène par le perchlorate d'argent.

La purification du sulfolane est décrite par ailleurs (1). La teneur en eau du sulfolane utilisé est d'environ 0.1%.

Techniques électrochimiques

Les courbes intensité–potentiel sont tracées à l'aide d'un polarographe Tacussel à trois électrodes. L'électrode indicatrice de platine est une électrode rotative à disque, le diamètre du fil de platine est 1 mm. L'électrode de référence est constituée par un fil d'argent plongeant dans une solution de $AgClO_4$ 10^{-2} M – $LiClO_4$ 0.10 M dans le sulfolane, la réversibilité de cette électrode a été montrée (1). Cette électrode est séparée de la solution par un premier fritté "medium", un compartiment contenant une solution de $LiClO_4$ 0.10 M, et un deuxième fritté. L'électrode auxiliaire est un fil de platine plongeant dans une solution de $LiClO_4$ 0.10 M dans le sulfolane, à l'intérieur d'un compartiment séparé et analogue à celui de l'électrode de référence. La courbe du courant résiduel est donnée Fig. 1.

Déterminations potentiométriques

La détermination potentiométrique des constantes de stabilité des ions trihalogénures X_3^- en milieu $LiClO_4$ 0.10 *M* est faite en utilisant le pH-mètre potentiomètre Radiometer 26. Dans le sulfolane, on mesure les différences de potentiel entre l'électrode de référence à l'argent décrite plus haut et une électrode de platine plongeant dans une solution contenant des mélanges halogène halogénure à des concentrations variables. L'étude de l'influence de l'addition de méthanol sur la stabilité de I_3^- est effectuée en remplaçant l'électrode de référence à l'argent par une électrode au ferrocène, c'est-à-dire un fil de platine plongeant dans une solution de ferrocène picrate de ferricinium aux concentrations 5×10^{-3} *M*; la composition du solvant dans cette demi-cellule est ajustée de la même façon que dans la demi-cellule de mesure. Deux séries de mesures sont faites, soit en ajoutant du méthanol aux solutions dans le sulfolane, soit l'inverse. La jonction entre les deux demi-cellules est assurée par un pont de $LiClO_4$ 0.10 *M* dans le sulfolane ou le méthanol. Pour la détermination de la stabilité de Br_3^- dans le méthanol, on mesure la différence de potentiel entre l'électrode au ferrocène et une électrode de platine plongeant dans une solution de bromure à laquelle on ajoute une solution de Br_2. Afin de réduire la réaction de l'halogène sur le solvant, on utilise dans le cas du brome et du chlore des solutions environ 0.1 *M* dans CCl_4, la faible quantité de CCl_4 ainsi introduite dans les solutions, est sans influence sur la stabilité de X_3^- (6).

Le potentiel de l'électrode au ferrocène dans le sulfolane est de -0.260 V par rapport à l'électrode de référence à l'argent. Toutes les mesures sont faites à 22 ± 2 °C. La précision des valeurs des potentiels normaux apparents est estimée à 10 mV.

Remerciements

Nous remercions le Conseil National de Recherches pour une subvention. Nous sommes reconnaissants à Madame Badoz-Lambling pour l'intérêt qu'elle a porté à ce travail. Nous remercions V. Plichon de sa collaboration initiale, et J. C. Marchon de nous avoir communiqué ses résultats sur le nitrométhane avant leur publication. Le sulfolane a été gracieusement fourni par la Compagnie Shell.

1. R. L. Benoit, P. Pichet et J. Desbarres. Electrochim. Acta. Sous presse.
2. I. V. Nelson et R. T. Iwamoto. J. Electroanal. Chem. 7, 218 (1964).
3. J. B. Headridge, D. Pletcher et M. Callingham. J. Chem. Soc. A, 684 (1967).
4. A. I. Popov et R. F. Swensen. J. Am. Chem. Soc. **77**, 3724 (1955).
5. A. I. Popov et D. H. Geske. J. Am. Chem. Soc. **80**, 1340 (1958).
6. J. Desbarres. Bull. Soc. Chim. France, 502 (1961).
7. F. W. Hiller et J. H. Krueger. Inorg. Chem. **6**, 528 (1967).
8. J. C. Marchon et J. Badoz-Lambling. Bull. Soc. Chim. France, 4660 (1967).
9. A. J. Parker. J. Chem. Soc. A, 220 (1966).
10. C. Sinicki. Bull. Soc. Chim. France, 194 (1966).
11. L. I. Katzin et E. Gebert. J. Am. Chem. Soc. **77**, 5814 (1955).
12. R. S. Drago et K. F. Purcell. *Dans* Non-aqueous solvent systems. *Edité par* T. C. Waddington. Academic Press, Inc., New York. 1965.
13. A. J. Parker. Quart. Rev. London, **16**, 163 (1962).
14. H. Strehlow. *Dans* The chemistry of non-aqueous solvents. *Edité par* J. J. Lagowski. Academic Press, Inc., New York. 1966.
15. I. M. Kolthoff et F. G. Thomas. J. Phys. Chem. **69**, 3049 (1965).
16. J. F. Coetzee et J. J. Campion. J. Am. Chem. Soc. **89**, 253 (1967).
17. R. Alexander, E. C. F. Ko, Y. C. Mac et A. J. Parker. J. Am. Chem. Soc. **89**, 3703 (1967).
18. I. M. Kolthoff et J. F. Coetzee. J. Am. Chem. Soc. **79**, 1852 (1957).
19. R. G. Pearson. J. Am. Chem. Soc. **85**, 3533 (1963).
20. E. J. Woodhouse et T. H. Norris. International Conference on Non-aqueous Solvent Chemistry. McMaster University, Hamilton, Ont. 1967.
21. M. Gauthier. Thèse de M.Sc., Université de Montréal, Montréal, Qué. 1967.

Can. J. Chem. Downloaded from www.nrcresearchpress.com by 210.87.254.5 on 09/05/12
For personal use only.

Radiolysis of cyclohexane in a xenon matrix at 77 °K[1]

J. A. STONE[2]
Research Chemistry Branch, Atomic Energy of Canada Ltd., Chalk River, Ontario
Received September 19, 1967

Low concentrations (less than 7 mole %) of cyclohexane and cyclohexane-d_{12} have been irradiated in xenon matrices at 77 °K. The products are qualitatively the same as those obtained by the radiolysis of the pure hydrocarbon but the yields differ. In particular $G(H_2) = 6.7$ for 6.2 mole % cyclohexane is much higher than that for solid cyclohexane at the same temperature (4.65). (All G values are calculated on energy absorbed in the whole sample.) The G values for products are reduced to limiting values, which are ~ 50–75% of the initial ones, by low concentrations of SF_6. Carbon tetrachloride reduces the yields to a greater extent than does SF_6. Both ionic and nonionic product formation probably occur. Ion chamber dosimetry has been used to determine the energy absorption by xenon which is anomalous due to the presence of low energy, scattered gammas in the cobalt-60 source.

Canadian Journal of Chemistry, 46, 1267 (1968)

Can. J. Chem. Downloaded from www.nrcresearchpress.com by 210.87.254.105 on 09/05/12
For personal use only.

Introduction

Radiolytic yields from a given quantity of a saturated hydrocarbon in a constant gamma ray field are enhanced by the addition of noble gases. This phenomenon has been studied extensively in the gas phase since the initial experiments of Lind and Bardwell (1). Studies in the condensed phase have been more limited (2–4). The enhanced yields have been attributed mainly to charge transfer from the noble gas to the hydrocarbon in the solid and liquid phases and to charge transfer accompanied by energy transfer in the gas phase. In a previous paper (3), the author showed that the radiolysis of cyclohexane in krypton matrices at 77 °K gives products in yields much greater than those expected from the mole fraction of hydrocarbon. Even with a krypton/hydrocarbon molecular ratio of 100/1, $G(H_2) = 1.9$ (this value being calculated according to the energy absorbed in the whole sample). The other major product is cyclohexene. The predominance of unimolecular decomposition was confirmed by the isotopic composition of the hydrogen evolved from mixtures of cyclohexane and cyclohexane-d_{12} irradiated in krypton matrices. The results were interpreted in terms of exothermic charge transfer from krypton to cyclohexane.

In gas phase radiolysis the substitution of one noble gas for another changes the product yields (5, 6). This is interpreted as being due to a change in the differences between the energy levels of hydrocarbon and noble gas. Similar changes in product yields would be expected from the radiolysis of cyclohexane in a xenon matrix as compared with a krypton matrix. This is indeed the case, the overall radiolytic decomposition of cyclohexane being far greater in xenon than in krypton.

An advantage that xenon possesses over krypton as a matrix material is its lower vapor pressure at 77 °K (10^{-3} mm Hg compared with 3 mm Hg), which implies that the matrix will be relatively more stable. The $G(H_2)$ values obtained with xenon–hydrocarbon mixtures show much less scatter than those for the corresponding krypton mixtures. This can be attributed in part to the lower tendency of the hydrocarbon to segregate and in part to the ease of analysis for hydrogen in the xenon system.

Experimental

Materials

Xenon (Matheson Research Grade) was distilled several times from trap to trap. No impurities (< 10 p.p.m.) were detectable by mass spectrometric analysis. Cyclohexane-d_{12} (Merck of Canada Ltd.) and cyclohexane (Fisher Spectranalyzed) were shaken with concentrated sulfuric acid and fractionally distilled. The purified materials when analyzed by gas–liquid chromatography with flame ionization detection showed no peaks due to cyclohexene, benzene, 1-hexene, or *n*-hexane, i.e. impurity concentrations were less than 5×10^{-5} *M*. Sulfur hexafluoride (Matheson 98% minimum purity) and carbon tetrachloride (Fisher Reagent Grade) were used as received.

Sample Preparation

Samples for irradiation were prepared by deposition from the gas phase. The components were well mixed in the gas phase and were then passed slowly into the irradiation vessel which was immersed in liquid nitrogen. The

[1]Issued as A.E.C.L. No. 3048.
[2]Present address: Department of Chemistry, Queen's University, Kingston, Ontario.

TABLE I

Energy absorption for different materials relative to that of carbon

Wall material	Z	Saturation ion current (A $\times 10^8$)	$e^S c/e^S Z$	μ_Z/μ_c
Graphite	6	0.96	1.000	1.00
Aluminium	13	1.05	0.922	1.01
Copper	29	1.37	0.840	1.20
Silver	47	1.75	0.769	1.40
Tantalum	73	2.52	0.719	1.89

method has been described in detail (3). An improvement in the technique was made by the replacement of the manually adjusted variable needle valve by a motor-driven one which was controlled by a servo-mechanism employing a capacitance manometer. A flow rate of 3 ml/min of vapor at s.t.p. was accurately maintained during sample deposition.

Each sample contained 1.28×10^{-2} mole of xenon. The composition of individual samples was determined by the amount of hydrocarbon used. In most of the experiments, except those concerned with the effect of hydrocarbon concentration on product yields, the liquid volume of either c-C_6H_{12} or c-C_6D_{12} used in making up the samples was 0.1 ml (6.2 mole % in each sample). All irradiations were at liquid nitrogen temperatures (77 °K).

Dosimetry

The radiation source was a Gammacell 220 (Atomic Energy of Canada Limited, Commercial Products). The gamma spectrum in such a heavily shielded source contains contributions not only from the cobalt-60 primary gamma rays but also from lower energy scattered Compton gammas. Ferrous sulfate dosimetry can be used to determine the energy absorption in materials containing low Z atoms but is clearly inadequate for high Z atoms such as xenon. Ritz and Attix (7) have shown that the relative amounts of energy absorbed by materials of different Z values may be determined from saturation ion currents in ion chambers whose walls are constructed with these various materials. Their method has been used in the present work to determine the energy absorption in xenon relative to that in graphite.

The geometry of the ion chambers was as described by Ritz and Attix. Ion chambers were constructed of graphite, aluminium, copper, silver, and tantalum with an air volume in each of 1.158 ml. The saturation ion current was measured in each chamber.

If J_Z is the saturation ion current in a chamber with wall material of atomic number Z and J_c is that in a similar chamber with graphite walls then

$$\frac{J_Z}{J_c} = \frac{\mu_Z}{\mu_c} \times \frac{e^S c}{e^S Z},$$

where μ_Z/μ_c is the ratio of the absorption coefficients per electron for material of atomic number Z and carbon in the gamma field and $e^S c/e^S Z$ is the ratio of electron stopping powers. The ratios $e^S c/e^S Z$ were obtained from the tabulated values of Attix, DeLa Vergne, and Ritz (8) and are relatively insensitive to varying incident photon energy whereas μ_Z/μ_c shows a more pronounced variation. The results of the ion chamber measurements are presented in Table I.

By interpolation the ratio of the energy absorption coefficient of xenon ($Z = 54$) to that of carbon is 1.52. The low energy gamma rays will be stopped more effectively by a given thickness of material than will the high energy ones. Ritz and Attix showed that this difficulty could be overcome by using collecting electrodes of different thicknesses but of the same material and obtaining saturation ion currents extrapolated to zero electrode thickness. This would be a second order correction in the present work and so was not attempted. However, the effects of attenuation were minimized by using collecting electrodes of the same thickness, i.e. 0.85 g/cm^2.

From the results of ferrous sulfate dosimetry ($G(Fe^{3+}) = 15.6$) the energy absorption per electron for carbon was calculated to be 3.4×10^{-6} eV/min. This number was used directly to calculate the energy absorption by the hydrocarbon part of a sample. For xenon the weighting factor of 1.52 per electron as determined above was employed.

Product Analysis

After irradiation the samples were brought to room temperature and then frozen again at 77 °K. Noncondensable gases were pumped off through solid nitrogen traps, measured volumetrically, and analyzed mass spectrometrically. The gases determined in this way were H_2, D_2, HD, CH_4, and CD_4, the methanes always being less than 0.5% of the total gas collected. The xenon was allowed to evaporate at 195 °K and the remaining hydrocarbon mixture was diluted with 0.5 ml of c-C_6H_{12}. Liquid products were determined by gas–liquid chromatography, cyclohexene and bicyclohexyl as described previously (9), and n-hexane, n-hexane-d_{14}, 1-hexene, and 1-hexene-d_{12} on a 1/4 in. × 12 ft, 10% squalane column at 50 °C. The latter four products were identified by mass spectral analsis of chromatographic fractions. Deuterated products always had a greater retention time than the corresponding protiated products. This difference was most pronounced for products separated on the columns operated at the lower temperatures. Concentrations of products were determined by peak area on the assumption that deuteration had no effect on the response of the flame ionization detector. All standards used for calibration purposes were protiated ones. The chlorinated products were also determined by gas–liquid chromatography; cyclohexyl chloride and hexachloroethane on a 1/4 in. × 8 ft, 15% Xe-60 column at 120 °C; and chloroform on a 1/4 in. × 8 ft, 10% carbowax 1000 column at 65 °C.

Can. J. Chem. Downloaded from www.nrcresearchpress.com by 210.87.254.105 on 09/05/12
For personal use only.

Can. J. Chem. Downloaded from www.nrcresearchpress.com by 210.87.254.105 on 09/05/12
For personal use only.

Results and Discussion

The radiolysis of both c-C_6H_{12} and c-C_6D_{12} in xenon matrices at 77 °K was studied. More experiments were performed with the c-C_6D_{12}/Xe system since with this system a good check on experimental technique was available. The isotopic composition of the radiolytic hydrogen was the same as that obtained in the radiolysis of c-C_6D_{12} alone, i.e. 95% D_2, 5% HD, and a trace of H_2. If, however, hydrogenated impurities were present, and water was in this category, more HD and H_2 were observed. The mixing flask and irradiation cell were therefore always flamed out under vacuum before use. The rest of the sample preparation apparatus was kept under vacuum at all times.

All G values quoted in this paper are calculated according to the total energy absorbed in the sample, although of course the final products result from the hydrocarbon alone. In all experiments low concentrations (< 7 mole %) of c-C_6H_{12}, c-C_6D_{12}, or mixtures of the two were used. Since the usual analytical technique was used for the quantitative determination of hydrogen, the same absolute amount of hydrogen was required as from a liquid phase radiolysis. This of course means that the % decomposition of the hydrocarbon is high. For example, for 6.2 mole % c-C_6D_{12} in xenon, after a total dose of 5.9 $\times 10^{19}$ eV/g, 1.3% of the hydrocarbon has disappeared (on the rough assumption that $G(-c\text{-}C_6D_{12}) = 2G(D_2)$). For the same dose but the lower c-C_6D_{12} concentration of 0.3 mole %, about 18% of the hydrocarbon has been converted to products. In many of the experiments the % decomposition was high. This was unavoidable with the present analytical techniques. With increasing dose the G values of the major products decreased. The effect of total dose on product yields was determined for samples containing 6.2 mole % of either c-C_6H_{12} or c-C_6D_{12}. A rather long extrapolation is required to obtain initial yields so that the values quoted are subject to considerable error. Much longer extrapolations, with the accompanying increases in the uncertainties of the initial yields, are required at lower hydrocarbon concentrations. The total dose studies were therefore confined to the samples containing high hydrocarbon concentrations.

The radiolytic products are the same as those obtained from the hydrocarbon alone, viz. hydrogen, cyclohexene, bicyclohexyl, and 1-hexene.

Hydrogen

In this discussion the hydrogen yield from c-C_6D_{12} in xenon will be denoted as $G(D_2)$ it being understood that this includes a 5% contribution from HD.

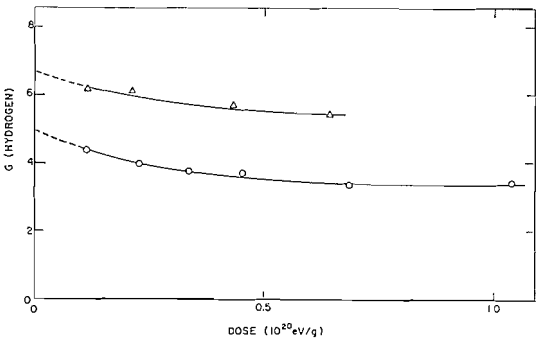

FIG. 1. Hydrogen yields as functions of dose: (△) 6.2 mole % c-C_6H_{12}, (○) 6.2 mole % c-C_6D_{12}.

Figure 1 shows the variations with dose of $G(H_2)$ and $G(D_2)$ from 6.2 mole % of c-C_6H_{12} and c-C_6D_{12} respectively in xenon over the range 1–10 $\times 10^{19}$ eV/g. The yields extrapolated to zero dose are $G(H_2) = 6.7$ and $G(D_2) = 5.0$. These numbers may be compared with the corresponding ones for the radiolysis of the liquid hydrocarbons at 22 °C, $G(H_2) = 5.55$ (10) and $G(D_2) = 4.15$ (11). A better comparison would be with the yields from the pure hydrocarbons in the solid phase at 77 °K when $G(H_2)$ is 4.65 (3), but $G(D_2)$ is not known. Hydrogen is produced with greater efficiency for a given energy absorption when the cyclohexane is dispersed in a xenon matrix than when the pure hydrocarbon is irradiated to the same dose. Although initially most of the energy is absorbed by the xenon, transfer of "reactivity" to the hydrocarbon occurs with high efficiency.

$G(H_2)$ and $G(D_2)$ decrease with increasing dose but this decrease is much more pronounced than that observed in the liquid phase radiolysis of cyclohexane (compare Fig. 1 with Fig. 1 of ref. 10). $G(D_2)$ is always lower than $G(H_2)$ for a given hydrocarbon concentration at the same dose. Figure 1 shows that the yields parallel each other with increasing dose. When mixtures of

TABLE II

The isotopic composition of hydrogen from 3.1 mole % c-C_6H_{12} and 3.1 mole % c-C_6D_{12} in xenon

Dose (10^{19} eV/g)	$G(H_2)$	G(HD)	$G(D_2)$	$G(H_2 + HD + D_2)$
1.3	2.72	1.29	0.49	4.50
4.0	2.12	1.10	0.42	3.64

TABLE III

The isotopic composition of the hydrogen evolved from 50/50 c-C_6H_{12}-c-C_6D_{12} mixtures under various conditions at 77 °K

Sample	% H_2	% HD	% D_2
Xenon matrix	58.1	30.2	11.6
Krypton matrix	66.0	17.0	17.0
Hydrocarbons alone	54.5	32.3	13.2

c-C_6D_{12} and c-C_6H_{12} are irradiated in a xenon matrix the isotope effect is still observable. Two samples each containing 3.1 mole % of c-C_6H_{12} and the same amount of c-C_6D_{12} were irradiated to different total doses. The analysis of the evolved hydrogen gave the results in Table II.

$G(H_2 + HD + D_2)$ is lower than expected when compared with the averaged values of $G(H_2)$ and $G(D_2)$ from 6.2 mole % c-C_6H_{12} and c-C_6D_{12} respectively in xenon. No immediate explanation can be given for this fact especially in view of the large contribution that c-C_6H_{12} makes to the overall hydrogen production. Table III compares the isotopic composition of the hydrogen obtained from mixtures of c-C_6H_{12} and c-C_6D_{12} in the solid phase (3), in a krypton matrix (3) and in a xenon matrix. In each case the total dose is $\sim 4 \times 10^{19}$ eV/g.

The isotopic composition of the hydrogen from the samples containing xenon is almost the same as that for the solid hydrocarbon mixture. In a krypton matrix the % HD is considerably reduced, whereas the % H_2 and % D_2 are greater. This is indicative of a greater relative contribution of unimolecular decomposition to overall product formation in krypton compared with xenon. The liquid product yields confirm this hypothesis. It must, however, be borne in mind that G(hydrogen) in a krypton matrix is about a factor of three less than in a xenon matrix.

At a constant dose of 4.0×10^{19} eV/g $G(H_2)$ and $G(D_2)$ decrease with decreasing hydrocarbon concentration (Fig. 2). However, as noted previously, the % decomposition at the lower hydrocarbon concentration is far greater than at the higher concentrations where, at 4.0×10^{19} eV/g, the yields are ~ 20% lower than the values obtained by extrapolation to zero dose. Figure 2 does not give a true picture. At very low doses all points on the two graphs would be raised, but those at the lower concentrations by a greater amount than those at the higher concentrations. The slopes would therefore be less pronounced. The curves in Fig. 2 certainly do not extrapolate smoothly to the origin. The efficiency of "reactivity" transfer from xenon to cyclohexane is not a sensitive function of cyclohexane concentra-

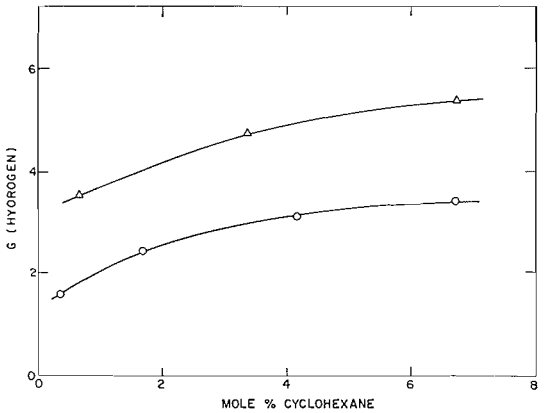

FIG. 2. Hydrogen yields as functions of hydrocarbon concentration: (△) c-C_6H_{12}, (○) c-C_6D_{12}. Dose = 4×10^{19} eV/g.

Can. J. Chem. Downloaded from www.nrcresearchpress.com by 210.87.254.105 on 09/05/12
For personal use only.

TABLE IV

Primary product yields obtained by extrapolation to zero dose (6.2 mole % hydrocarbon)

Product	c-C_6H_{12}/Xe	c-C_6D_{12}/Xe
Hydrogen	6.7	5.0
Cyclohexene	3.0	2.2
Bicyclohexyl	2.3	1.3
1-Hexene	0.5	0.7
Cyclohexylcyclohexene	0.16	0.06

tion over the range studied. A similar conclusion was drawn from the radiolysis of cyclohexane in a krypton matrix (3) where $G(H_2)$ showed little variation over the range 0.2–10 mole % hydrocarbon.

Liquid Products

Cyclohexene and bicyclohexyl are major liquid products and 1-hexene and cyclohexylcyclohexene are minor ones. All were quantitatively determined. Figures 3 and 4 show the variations of the cyclohexene and bicyclohexyl yields with dose for both 6.2 mole % c-C_6H_{12}/Xe and 6.2 mole % c-C_6D_{12}/Xe. The G values, extrapolated to zero dose, for all identified primary products are shown in Table IV.

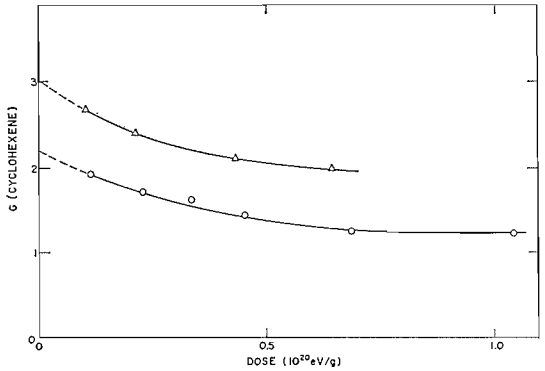

FIG. 3. Cyclohexene yields as functions of dose: (△) 6.2 mole % c-C_6H_{12}, (○) 6.2 mole % c-C_6D_{12}.

A hydrogen balance is not obtained; in each system, products with a hydrogen equivalent of ~1.4 units are missing. However, as emphasized earlier, long extrapolations were required to obtain these yields so that the errors in the tabulated values may be large. There were three small, unidentified peaks near the bicyclohexyl peak in the gas–liquid chromatograms obtained with the XE-60 column. The retention times were

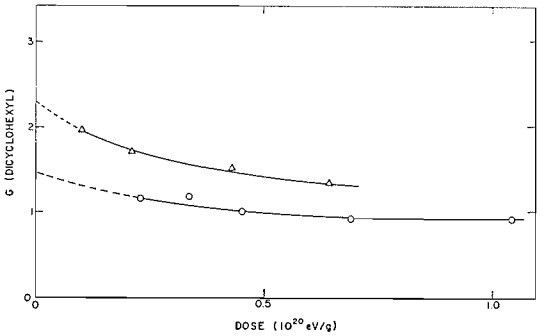

FIG. 4. Bicyclohexyl yields as functions of dose: (△) 6.2 mole % c-C_6H_{12}, (○) 6.2 mole % c-C_6D_{12}.

all less than that for bicyclohexyl and the total peak area was ~25% that of the bicyclohexyl peak. The products responsible for these peaks were probably C_{10} or C_{11} hydrocarbons. They were primary products showing the same variation in yield with dose as did bicyclohexyl. No products were detected ($G < 0.02$) in the C_7–C_9 range. As in the radiolysis of liquid cyclohexane, C—C bond scission leading to fragments of carbon number less than six does not play a major role in product formation. Except for 1-hexene, which makes no contribution to the hydrogen balance, the yields of deuterated liquid products are less than those of the corresponding protiated ones. This is consistent with the H_2 and D_2 yields. The primary yields of bicyclohexyl and cyclohexene from 6.2 mole % c-C_6H_{12}/Xe are comparable with those obtained by the radiolysis of cyclohexane in the liquid phase, as shown in Table V.

The G values for the yields in the krypton matrix have been corrected to allow for the absorption of low energy gamma rays. All G values given in ref. 3 should be decreased by 20%.

1-Hexene has been reported by Ho and Freeman (12) as a primary product ($G = 0.4$) in the

Can. J. Chem. Downloaded from www.nrcresearchpress.com by 210.87.254.105 on 09/05/12
For personal use only.

TABLE V

Yields of bicyclohexyl and cyclohexene under various conditions

Sample	$G(C_6H_{10})$	$G(C_6H_{11})_2$
6.2 Mole % c-C_6H_{12}/Xe (77 °K)	3.0	2.2
4.5 Mole % c-C_6H_{12}/Kr (77 °K) (3)	1.4	0.24
Liquid c-C_6H_{12} (295 °K) (10)	3.27	1.95
Solid c-C_6H_{12} (77 °K) (3)	2.35	1.55

radiolysis of highly purified liquid cyclohexane. This product is formed in both the c-C_6H_{12}/Xe and c-C_6D_{12}/Xe systems but unlike all the other primary products the deuterated species ($G = 0.7$) has a higher yield than the protiated one ($G = 0.5$).

One other liquid product, *n*-hexane, was identified and quantitatively determined. It is a secondary product. In the system 6.2 mole % c-C_6H_{12}/Xe the yield rises to a limiting value of 0.08 G units at 5×10^{19} eV/g. The limiting yield in the corresponding deuterated system is 0.21 G units. Since for both 1-hexene and *n*-hexane the yield of the deuterated species is greater than that of the protiated species it is tempting to designate 1-hexene as the precursor of *n*-hexane. The buildup of *n*-hexane concentration with increasing dose certainly follows the declining yield of 1-hexene but the correlation is not quantitative at the lowest doses. This will be discussed later.

The variations of liquid product yields with hydrocarbon concentration were studied at a constant dose of 4.0×10^{19} eV/g. The yields decreased in the same manner as did those of H_2 and D_2 shown in Fig. 2.

The Effects of the Addition of Sulfur Hexafluoride and Carbon Tetrachloride

The accuracy with which it was possible to measure small gaseous volumes of SF_6 and small liquid volumes of CCl_4 limited the amounts employed to the range 0.03–1.0 mole %. Since in these experiments the concentration of cyclohexane was held constant at 6.2 mole %, the molar concentration of SF_6 or CCl_4 was between 0.5 and 16% that of cyclohexane.

The results obtained upon addition of SF_6 to both the systems c-C_6H_{12}/Xe and c-C_6D_{12}/Xe are most striking. At even the lowest concentration (0.04 mole %) the yields of all primary products are lowered by 25–50%. Increasing the SF_6 concentration fails to cause any further significant decrease. These results, shown in Figs. 5–8, were all obtained at doses of 4.0×10^{19} eV/g. Also marked on the figures are the yields in the absence of SF_6 taken from Table III. For comparison purposes these are not the correct yields to use since the limiting yields, unlike those normally encountered in liquid phase radiolysis (12), are still dose dependent. $G(H_2)$ decreased by ~ 0.4 units for the system 0.5 mole % SF_6/6.2 mole % c-C_6H_{12}/Xe when the dose was increased from 1.3 eV/g to 4.0×10^{19} eV/g. In the absence of SF_6 the decrease is ~ 0.7 units. The yield of the secondary product *n*-hexane was also decreased by SF_6. The limiting yield of *n*-hexane was 0.07 while that of *n*-hexane-d_{14} was 0.13.

The effect of CCl_4 on the c-C_6D_{12}/Xe system is different from that of SF_6. The yields of all products obtained from cyclohexane-d_{12} alone are drastically reduced and, except for that of

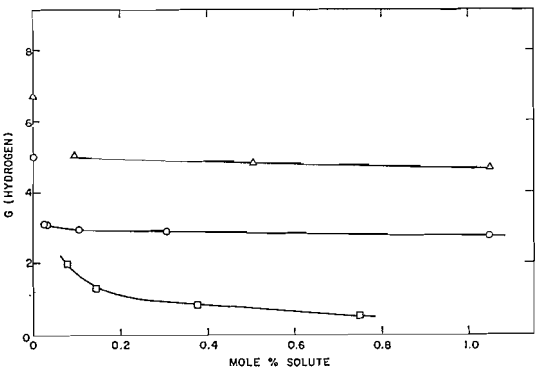

FIG. 5. The effects of SF_6 and CCl_4 on hydrogen yields: (△) 6.2 mole % c-C_6H_{12} + SF_6, (○) 6.2 mole % c-C_6D_{12} + SF_6, (□) 6.2 mole % c-C_6D_{12} + CCl_4. Dose = 4×10^{19} eV/g.

Can. J. Chem. Downloaded from www.nrcresearchpress.com by 210.87.254.105 on 09/05/12
For personal use only.

TABLE VI

Chlorinated product yields in the system 6.2 mole % c-C_6D_{12}/CCl_4/Xe

Mole % CCl_4	$G(CDCl_3)$	$G(C_2Cl_6)$	$G(c\text{-}C_6D_{11}Cl)$	$G(c\text{-}C_6D_{11}CCl_3)$
0.07	0.43	0.30	0.66	0.26
0.14	0.68	0.58	0.95	0.58
0.38	0.90	0.86	1.07	0.66
0.75	1.10	1.22	1.12	0.86

cyclohexene, the yields approach zero at the higher CCl_4 concentration. These results are shown in Figs. 5–7 while in Table VI the yields of chlorinated products for the same experiments are given. At 0.07 mole % CCl_4 G(1-hexene-d_{12}) was 0.13 while G(n-hexane-d_{14}) was 0.1. At higher concentrations the yields of these products were immeasurably small.

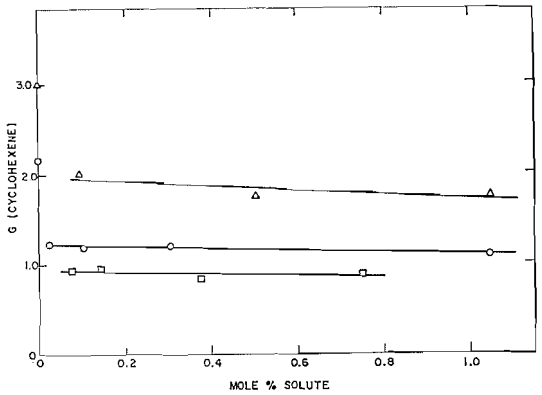

FIG. 6. The effects of SF_6 and CCl_4 on cyclohexene yields: (△) 6.2 mole % c-C_6H_{12} + SF_6, (○) 6.2 mole % c-C_6D_{12} + SF_6, (□) 6.2 mole % c-C_6D_{12} + CCl_4. Dose = 4×10^{19} eV/g.

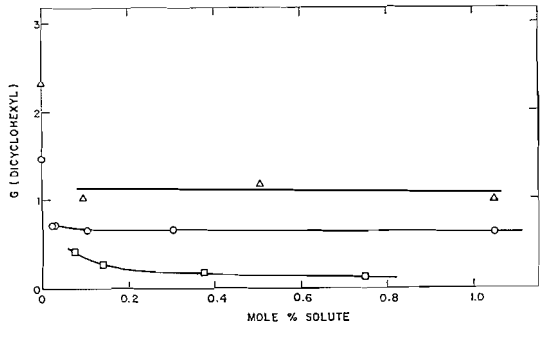

FIG. 7. The effects of SF_6 and CCl_4 on bicyclohexyl yields: (△) 6.2 mole % c-C_6H_{12} + SF_6, (○) 6.2 mole % c-C_6D_{12} + SF_6, (□) 6.2 mole % c-C_6D_{12} + CCl_4. Dose = 4×10^{19} eV/g.

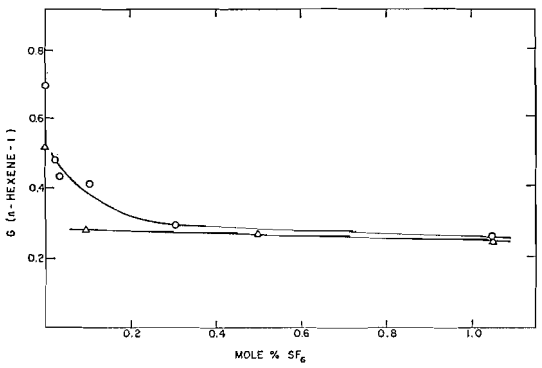

FIG. 8. The effect of SF_6 on n-hexene-1 yields: (△) 6.2 mole % c-C_6H_{12} + SF_6, (○) 6.2 mole % c-C_6D_{12} + SF_6. Dose = 4×10^{19} eV/g.

Mechanism of Product Formation

The results obtained are not those that would be expected from a two-phase system, i.e. the cyclohexane was distributed throughout the xenon rather than being segregated. The structure of the solid could not be ascertained and it may have been that the cyclohexane was present in small molecular clusters rather than single molecules. The results do not show much scatter, which implies that the sample preparation technique was good.

If all the energy absorbed in the xenon were transferred completely to the cyclohexane and if the hydrocarbon decomposed as it does in the pure liquid then the yields from 6.2 mole % c-C_6H_{12}/Xe would be the same as in the liquid. In fact some yields are higher and some are a little lower; $G(H_2)$ is increased by 1.2 units, G(bicyclohexyl) is increased by 0.3 units, and G(cyclohexene) is decreased by 0.3 units. The transfer of "reactivity" from xenon to hydrocarbon must be highly efficient. In a similar type of experiment Davis, Libby, and Kevan (4) reached the same conclusion. They found that the yields and proportions of the isomeric

Can. J. Chem. Downloaded from www.nrcresearchpress.com by 210.87.254.105 on 09/05/12
For personal use only.

Can. J. Chem. Downloaded from www.nrcresearchpress.com by 210.87.254.105 on 09/05/12
For personal use only.

hexenes and dodecanes obtained by the radiolysis of *n*-hexane/xenon solutions remained essentially constant over the concentration range 4.3 to 100 mole % *n*-hexane. They did not measure hydrogen yields or study the effect of total dose.

The results with xenon are very different from those obtained with krypton both in the absolute yields of products and in the relative yields. The product yields in xenon are much greater and the liquid product distribution is more like that in the radiolysis of the liquid hydrocarbon. The very high ratio G(cyclohexene)/G(bicyclohexyl) together with the low % of HD from mixtures of c-C_6D_{12} and c-C_6H_{12} in krypton shows the predominant part played by unimolecular decomposition.

Energy migration in a krypton matrix was ascribed to resonance charge transfer, the subsequent localization of energy at the hydrocarbon site being by exothermic charge transfer. Such processes are equally probable in the present work. Charge transfer from xenon to cyclohexane is exothermic by ~ 2.3 eV. It seems improbable, however, that a $G(H_2)$ value as high as 6.7 is explicable in terms of ionic processes alone since, on the assumption that the W value for xenon in the solid phase is comparable to that in the gas phase, $G(Xe^+)$ is 4.5 (13). Processes other than ionic ones probably contribute to product formation as in the radiolysis of the pure hydrocarbons.

The experiments with added SF_6 and CCl_4 were undertaken in an attempt to distinguish mechanisms of product formation which depend upon ion neutralization by electrons. Both additives capture thermalized electrons with high efficiency (14, 15) but charge transfer between the ground state of Xe^+ and CCl_4 (appearance potential of $CCl_3^+ = 11.65$ eV (16)) is exothermic while charge transfer with SF_6 (appearance potential of $SF_5^+ = 15.85$ eV (16)) is highly endothermic. At room temperature SF_6 is resistant to free radical attack (17) but CCl_4 readily engages in radical chain reactions. Although the present experiments were performed at 77 °K, many of the cyclohexyl radicals formed will be immobilized as in the radiolysis of solid cyclohexane at 77 °K (18). They can be scavenged by CCl_4 when the temperature of the sample is raised. Such a process will not occur with SF_6. The decreases in product yields upon the addition of SF_6 will therefore be ascribed entirely to electron capture. It must, however, be borne in mind that any products whose yields are decreased by SF_6 must be formed subsequent to charge neutralization, i.e. any neutral products formed, for example by dissociative charge transfer, should be unaffected by the addition of SF_6.

With added SF_6 $\Delta G(H_2)$ and $\Delta G(D_2)$ are approximately 1.8 units. The corresponding reductions in G(cyclohexene) + G(bicyclohexyl) are 2.4 for c-C_6H_{12}/Xe and 2.0 for c-C_6D_{12}/Xe. The 1-hexene yields are also reduced and it is to be noted that the difference in yields between 1-hexene and 1-hexene-d_{12} is practically eliminated.

Three conclusions may be drawn from these results:

(1) No products are entirely eliminated by the addition of SF_6, i.e. all products are formed in at least two ways. This is in accord with the mechanism proposed by Dyne for the liquid phase radiolysis of cyclohexane in which the same products are formed by both ionic and nonionic mechanisms (19).

(2) The decrease in hydrogen yield is approximately equal to the sum of the decreases in cyclohexene and bicyclohexyl yields. SF_6 is most probably reacting with a common precursor of all three products. This is presumed to be a thermalized electron.

(3) G(scavengeable electrons), which will be equated to ΔG(hydrogen) + ΔG(1-hexene), is ~ 2.0.

The mechanism by which SF_6 decreases product yields may be formulated

[1] $$Xe^+ + Xe \rightarrow Xe + Xe^+$$

[2] $$Xe^+ + c\text{-}C_6H_{12} \rightarrow Xe + c\text{-}C_6H_{12}{}^+$$

[3] $$c\text{-}C_6H_{12}{}^+ + e \rightarrow c\text{-}C_6H_{12}{}^* \rightarrow \text{products}$$

[4] $$SF_6 + e \rightarrow SF_6{}^-$$

[5] $$SF_6{}^- + c\text{-}C_6H_{12}{}^+ \rightarrow \text{products other than those from [3].}$$

Reaction [1] is the resonance charge transfer process by which the positive charge migrates through the matrix.

In support of such a mechanism a new product was observed in the SF_6/c-C_6D_{12}/Xe system. From its chromatographic retention time this product was judged to be cyclohexyl fluoride. No definite identification was made. The chromatographic peak height increased only

Can. J. Chem. Downloaded from www.nrcresearchpress.com by 210.87.254.105 on 09/05/12
For personal use only.

slightly with increasing SF_6 concentration which would be consistent with $C_6H_{11}F$ production in reaction [5].

CCl_4 should also capture electrons and reduce product yields to the same limiting values as SF_6 does. This has been shown to occur in the gas phase radiolysis of propane when $G(H_2)$ reaches the same limiting value with both additives (20). However, in the c-C_6D_{12}/Xe system, CCl_4 reduces the yields of all products to a greater extent than does an equal concentration of SF_6. The mechanism by which CCl_4 reduces the hydrogen yield below the limiting value obtained with SF_6 raises the bigger problem as to how and when molecular hydrogen is formed in the matrix. Bouldin and Gordy (21) showed by electron spin resonance techniques that D atoms are present when low concentrations of CD_4 are irradiated in xenon at 4 °K. At 77 °K no H-atom signal can be detected when low concentrations of ethane are irradiated in xenon.[3] It must therefore be concluded that the hydrogen is present in the molecular form at 77 °K. About 2% of the hydrogen can be pumped off the solid matrix, the rest is trapped but can be released by melting the sample. Table III shows that radiolysis of c-C_6D_{12}/c-C_6H_{12} mixtures in a xenon matrix yields almost the same isotopic composition of hydrogen as radiolysis of the hydrocarbons alone. The mechanism of hydrogen formation therefore probably involves both molecular elimination and one or more bimolecular processes.

At 77 °K thermalized hydrogen atoms will not abstract Cl from CCl_4 and hot hydrogen atoms should show no preference for reacting with CCl_4 rather than with c-C_6H_{12}. The reduction of hydrogen yields by CCl_4 below the limiting yield obtained with SF_6 must therefore be due to competition between it and c-C_6H_{12} for energy supplied by the matrix. This might take the form of a charge transfer process since Kevan (6) has shown that in the gas phase there is a dependence of product yields on the differences between the recombination energies of noble gas ions and the molecule donating the electron. Kevan's theory would predict that CCl_4, having an ionization potential much closer in value to that of xenon than does c-C_6H_{12}, would be very efficient in donating an electron to Xe^+. However, it was found earlier that CCl_4 is equally effective in reducing product yields in the c-C_6H_{12}/Kr system where its ionization potential is well removed from that of krypton. Some form of nonionic excitation transfer, e.g. from metastable levels of xenon, may also contribute significantly to hydrogen production. CCl_4 must be highly effective in quenching this transfer. This role of CCl_4 in reducing product yields is consistent with the yields of chlorinated products shown in Table VI provided that the process results in the scission of a C—Cl bond.

$$[6] \qquad Xe^* + CCl_4 \rightarrow Xe + \cdot CCl_3 + \cdot Cl$$

$$[7] \qquad \cdot Cl + c\text{-}C_6D_{12} \rightarrow DCl + c\text{-}C_6D_{11}\cdot$$

$$[8] \qquad 2 \cdot CCl_3 \rightarrow C_2Cl_6$$

$$[9] \qquad c\text{-}C_6D_{11}\cdot + \cdot CCl_3 \rightarrow c\text{-}C_6D_{11}CCl_3$$

$$[10] \qquad \rightarrow c\text{-}C_6D_{10} + CDCl_3$$

Pritchard, Pyke, and Trotman-Dickenson (22) found the reaction of chlorine atoms with cyclopentane to be extremely fast ($E_a = 0.58$ kcal mole^{-1}, $A = 2.9 \times 10^{14}$ cc mole^{-1} s^{-1}) so that [7] will occur rapidly even at 77 °K. No attempt was made to detect HCl as a reaction product. Reaction [10] explains why, although the yield of bicyclohexyl is reduced to a very low value with large amounts of CCl_4, the yield of cyclohexene remains high. In fact at 0.75 mole % CCl_4 G(cyclohexene-d_{10}) is 0.9 while $G(D_2)$ is 0.5. These numbers point out the danger of ascribing a cyclohexene yield which is invariant with solute concentration as being due to the unimolecular elimination of hydrogen.

Although the hydrogen, cyclohexene, bicyclohexyl, and 1-hexene yields are reduced by ~70% upon the addition of 0.07 mole % CCl_4 the yields of chlorinated products are not large. However, on increasing the concentration of CCl_4 the yields of chlorinated products increase considerably while there is a much smaller decrease in the yields of products from cyclohexane alone. This lends support to the idea of direct energy transfer from xenon to CCl_4 at the higher CCl_4 concentrations.

Earlier in the paper there was speculation as to whether 1-hexene is the precursor of *n*-hexane. Figure 8 shows that the addition of SF_6 reduces 1-hexene-d_{12} to a greater extent than 1-hexene. At the same time the yield of *n*-hexane-d_{14} is reduced to a greater extent than that of *n*-hexane. This would support the hypothesis.

[3] J. A. Stone and D. R. Smith, unpublished result.

Can. J. Chem. Downloaded from www.nrcresearchpress.com by 210.87.254.105 on 09/05/12
For personal use only.

However, in the presence of 1 mole % SF_6 G(1-hexene-d_{12}) $\approx$ G(1-hexene) but G(n-hexane-d_{14}) is still about twice as great as G(n-hexane). Unless there is a large isotope effect in the production of n-hexane then the designation of 1-hexene as its only precursor becomes doubtful.

The ratio of disproportionation to combination for cyclohexyl radicals is 1.1 in the liquid phase at ambient temperature (23) while from Table V G(cyclohexene)/G(bicyclohexyl) = 1.68 for the liquid phase radiolysis. On the assumption that all the dimer is formed by radical combination then the non-radical yield of cyclohexene is 1.1 G. In solid cyclohexane the ratio is 1.5 and in a xenon matrix it is $\sim$ 1.4. The effect of temperature on the disproportionation–combination ratio of cyclohexyl or any other cyclic radicals is not known. Experiments with smaller alkyl radicals show that disproportionation has a slightly lower activation energy than does combination (24). The present results would suggest that there is little change in the disproportionation–combination ratio with decreasing temperature, if anything the change may be in the opposite direction to that found for other radicals. This of course is still based on the assumption that the dimer is formed only by radical combination. The present results do not provide evidence for or against other methods of dimer formation.

An outstanding feature of the yield curves for primary products (Figs. 1, 3, and 4) is the marked dose dependence. This is much greater that that observed in the liquid phase radiolysis of cyclohexane (10, 12). It is to be noted, however, that the decreases in yields relative to the % decomposition of the hydrocarbon are roughly the same. As an approximation we can equate the number of c-C_6H_{12} molecules decomposing to $G(H_2)$. From Fig. 1 of ref. 10, $G(H_2)$ is reduced by 0.5 units after a dose of 3×10^{20} eV/g. A dose of 2×10^{19} eV/g is required in a xenon matrix containing 6.2 mole % c-C_6H_{12} to effect the same decrease. Since the concentration of cyclohexane in the matrix is about 10% of that in the pure liquid the % decomposition is roughly the same in both cases.

Ho and Freeman (12) found that although the yields of cyclohexene and bicyclohexyl in liquid cyclohexane have decreased to the extent of 30–40% at 3×10^{20} eV/ml the ratio of yields decreases only slightly ($\sim$ 6%). They suggest that this is due to the removal of an unidentified, common precursor. In a xenon matrix containing 6.2 mole % hydrocarbon the ratio shows only a slightly greater variation over the range studied. From the experimental points in Figs. 3 and 4 the ratio changes from 1.36 at the lowest dose to 1.48 at the highest dose for c-C_6H_{12}, while for c-C_6D_{12} the values, over a larger dose range, are 1.45 to 1.30. A common precursor in the xenon matrix might be the cyclohexyl radical. These trapped radicals could act either as traps for electron holes or as H-atom scavengers. However, there seems little likelihood that the former is the case since cyclohexane itself is also an effective trap and is present at a much higher concentration. H-atom scavenging would lead to an increase in the cyclohexene yield relative to that of bicyclohexyl since addition will be accompanied by disproportionation (24). An alternative proposal which would lead to a decrease in the cyclohexene/bicyclohexyl ratio with increasing dose would be the scavenging of hydrogen atoms by cyclohexene. Some cyclohexene is probably formed even at 77 °K particularly at the higher concentrations when the cyclohexane is present in molecular clusters. G(cyclohexene)/G(bicyclohexyl) decreases with increasing dose in the c-C_6D_{12}/Xe system but an increase occurs in the c-C_6H_{12}/Xe system. A decision for or against the involvement of a common precursor cannot be made on the basis of the present results.

Acknowledgments

The author wishes to express his sincere appreciation for the help received from Dr. A. W. Boyd in the dosimetry determinations. He also thanks Dr. Boyd for the many helpful discussions on the substance of this paper. Drs. F. Brown, P. J. Dyne, and N. H. Sagert are thanked for critical comments on the earlier drafts.

1. S. C. Lind and D. C. Bardwell. J. Am. Chem. Soc. **48**, 1575 (1926).
2. P. Ausloos, R. E. Rebbert, and S. C. Lias. J. Chem. Phys. **42**, 540 (1965).
3. J. A. Stone. Can. J. Chem. **43**, 809 (1965).
4. D. R. Davies, W. F. Libby, and L. Kevan. J. Am. Chem. Soc. **87**, 2766 (1965).
5. V. Aquilanti. J. Phys. Chem. **63**, 3434 (1965).
6. L. Kevan. J. Chem. Phys. **44**, 683 (1966).
7. V. H. Ritz and F. H. Attix. Radiation Res. **16**, 401 (1962).

8. F. H. ATTIX, L. DELA VERGNE, and V. H. RITZ. J. Res. Natl. Bur. Std. **60**, 235 (1958).
9. J. A. STONE. Can. J. Chem. **42**, 2872 (1964).
10. P. J. DYNE and J. A. STONE. Can. J. Chem. **39**, 2381 (1961).
11. J. R. NASH and W. H. HAMILL. J. Phys. Chem. **66**, 1097 (1962).
12. S. K. HO and G. R. FREEMAN. J. Phys. Chem. **68**, 2189 (1964).
13. G. G. MEISELS. J. Chem. Phys. **41**, 51 (1964).
14. R. A. LEE and D. A. ARMSTRONG. Nature, **200**, 552 (1964).
15. F. P. GUARINO, M. R. RONAYNE, and W. H. HAMILL. Radiation Res. **17**, 379 (1962).
16. R. E. FOX and R. K. CURRAN. J. Chem. Phys. **34**, 1595 (1961).
17. L. BATT and F. R. CRUICKSHANK. J. Phys. Chem. **70**, 723 (1966).
18. H. SZWARC. J. Chim. Phys. 1067 (1962).
19. P. J. DYNE. Can. J. Chem. **43**, 1080 (1965).
20. G. R. A. JOHNSON and J. M. WARMAN. Trans. Faraday Soc. **61**, 1709 (1965).
21. W. V. BOULDIN and W. GORDY. Phys. Rev. **135**, A806 (1964).
22. H. O. PRITCHARD, J. B. PYKE, and A. F. TROTMAN-DICKENSON. J. Am. Chem. Soc. **77**, 2629 (1955).
23. W. A. CRAMER. J. Phys. Chem. **71**, 1171 (1967).
24. R. KLEIN, M. D. SCHEER, and R. KELLEY. J. Phys. Chem. **68**, 598 (1964).

Can. J. Chem. Downloaded from www.nrcresearchpress.com by 210.87.254.105 on 09/05/12
For personal use only.

Studies on the thermodynamics and conductances of molten salts and their mixtures. Part V. The density, change of volume on fusion, viscosity, and surface tension of sodium chlorate and of its mixtures with sodium nitrate

A. N. CAMPBELL AND E. T. VAN DER KOUWE
Department of Chemistry, University of Manitoba, Winnipeg, Manitoba

Received August 17, 1967

The densities, viscosities, and surface tensions of molten sodium chlorate, and of molten mixtures of sodium chlorate and sodium nitrate, as well as the change of volume on fusion, have been determined.

From the dependence of molar volume on temperature and composition, it appears that the mixing of sodium chlorate and sodium nitrate is a process of dilution rather than of interaction. The viscosity of sodium chlorate is found to be much lower than that of lithium chlorate, a possible indication of greater complexity in the lithium chlorate melt. The activation energy of viscous flow for sodium chlorate is less than that of lithium chlorate. For lithium chlorate – lithium nitrate mixtures, at constant temperature, there is pronounced positive deviation from linearity, when viscosity is plotted against molar composition. For sodium chlorate – sodium nitrate mixtures, the deviation is much less marked though still positive.

The surface tension of sodium chlorate is almost identical with those of lithium and potassium chlorates. The surface heat of sodium chlorate is higher than that of lithium chlorate but it still indicates some degree of covalency. The Guggenheim formula and Sokolov's rule have been applied. In contrast to melts of mixtures of lithium chlorate and lithium nitrate, the sodium salt melts would appear to have simpler constituents and to be more ionic in character.

Canadian Journal of Chemistry, 46, 1279 (1968)

Can. J. Chem. Downloaded from www.nrcresearchpress.com by 210.87.254.6 on 09/05/12
For personal use only.

From previous work on lithium chlorate and lithium chlorate – lithium nitrate melts (1) we concluded that these melts were complex in character. We were unable to say with certainty wherein this complexity consists, except that it seems probable that simple ions are only present to a very limited extent. We did, however, suggest that molten lithium chlorate might consist of clusters of molecules or of molecules and ions, and that the addition of lithium nitrate gave rise to some kind of interaction between the nitrate ion and chlorate lattice, resulting in the formation of complex clusters, with possible bridging of the nitrate ion between two or more clusters. However this may be, the constituents of lithium chlorate melts are complex and of a covalent character. Possibly the melt retains much of its lattice character in the liquid state.

We thought that a similar exhaustive investigation of sodium chlorate and sodium chlorate – sodium nitrate mixtures might yield contrasting information. Because of its higher melting point, it is to be expected that melts containing sodium chlorate would be somewhat more ionic in character. All the measurements made by Campbell *et al.* on $LiClO_3$ and $LiClO_3$–$LiNO_3$ melts (1) have been repeated for the system $NaClO_3$–$NaNO_3$ but, because of the higher temperatures involved, several experimental methods had to be changed. The present communication gives an account of our work on molar volume, volume change on fusion, viscosity, and surface tension.

Previous work on molten sodium chlorate is restricted to an early determination of density (2), a measurement of the heat of fusion (3), and an investigation of the phase diagram of the system $NaClO_3$–$NaNO_3$ (4). An accurate determination of the viscosity of sodium nitrate has been made by Dantuma (5), who used an oscillating sphere. The phase diagram shows an absence of compound formation (in the solid state), but extensive solid solution, both of sodium nitrate in sodium chlorate and of sodium chlorate in sodium nitrate, at the temperature of the eutectic (211 °C). The allotropic transformation of sodium nitrate, occurring at 274.6°, is depressed below 250° by the presence of sodium chlorate in solid solution.

Density determinations were made over the temperature range 240–290°; pure sodium chlorate undergoes incipient decomposition above 290°. Three mixtures of sodium chlorate and sodium nitrate, including the eutectic mixture, were investigated. The changes of molar volume on fusion of pure lithium chlorate, of pure

Can. J. Chem. Downloaded from www.nrcresearchpress.com by 210.87.254.6 on 09/05/12
For personal use only.

sodium chlorate, and of the eutectic mixture of sodium chlorate and sodium nitrate were also determined.

No simple theory relating viscosity to composition of the melt exists. According to Harrap and Heymann (6) the viscosity isotherm exhibits negative deviation from additivity, even if the mixture is ideal in other respects.

The surface tension of molten salt mixtures, apart from its intrinsic interest, gives rise to many other functions of interest in the study of structure. Thus, for example, Guggenheim (7) has derived an expression for the surface tension of an ideal equimolar mixture, involving the surface tensions of the pure components and the average area per molecule in the surface layer. Deviations from the Guggenheim equation have been attributed by many workers (8–10) to thermodynamic nonideality and they have postulated the presence of complex ions where these deviations are large, e.g. in the $CdCl_2$–KCl system (11). Another important relation is the surface heat content per unit area:

$$H^s/a = \gamma - T\frac{d\gamma}{dT}.$$

Since the temperature coefficient of surface tension for molten salts is constant, the surface heat content is independent of temperature and thus provides a fundamental quantity which may be used to compare molten salts and other liquids (12). Bloom *et al.* (9) and Janz and Lorenz (8) have used this parameter as an indication of the molecular character of the melt. When complex formation occurs, it is to be expected that the surface heat will be negative.

Experimental

Sodium chlorate and sodium nitrate were used without further purification, after drying at 130°. Both were Fisher Reagent chemicals; according to the analyses supplied with the reagents, the maximum impurity in the sodium chlorate was 0.005% sodium bromate and that in the sodium nitrate 0.0005% 'heavy metals'. Lithium chlorate was prepared by the method of Campbell and Griffiths (13), using reagent grade barium chlorate and lithium sulfate. The melting point of the preparation was found to be 127.9°, as against 127.6° given by Campbell and Griffiths. The high melting point is sufficient proof of purity.

A mixture of 27.3% lithium nitrate, 18.2% sodium nitrate, and 54.5% potassium nitrate was used as thermostat fluid; it functioned admirably. The double-walled metal thermostat had glass windows on opposite sides. Temperature was controlled with a Princo Magnaset regulator and was constant to ±0.1° over the range 230–290°. Temperature was measured with a copper–constantan thermocouple and a vernier potentiometer capable of measuring to 1 μV.

As fixed points for thermocouple calibration the freezing points of tin (231.9°), bismuth (271.3°), and cadmium (320.9°) were used.

For density determinations of melts, we used the manometric densitometer of Husband (14). It is unnecessary to discuss the theory and operation of this admirable instrument here, since they are given in the original communication. Transfer of material to the densitometer was conducted in a moisture-free atmosphere, in a nitrogen-filled dry box.

Heights of the dibutyl phthalate manometer (cf. Husband (14)) were measured by a cathetometer to ±0.1 mm. The temperature coefficient of density of dibutyl phthalate is about ±0.0001 g ml^{-1} deg^{-1}. Since temperature fluctuations were within 0.1°, this introduces negligible deviations in density. All weighings were made on a precision balance and were correct to better than ±0.0001 g. Hence the overall precision in the density values is ±0.0002 g ml^{-1} or ±0.02%.

For the densities of solid sodium and lithium chlorates, a Weld pycnometer of about 25 ml capacity was used. Silicone oil, in which the salts are completely insoluble, was used as the indifferent liquid. Entrapped air was removed by prolonged evacuation. The drawback to this method, about the only method which can be used for the density of a powder, is the uncertainty as to the complete removal of air. Nevertheless, we estimate the maximum possible error in our determinations of density of solid forms to be not greater than ±0.05%.

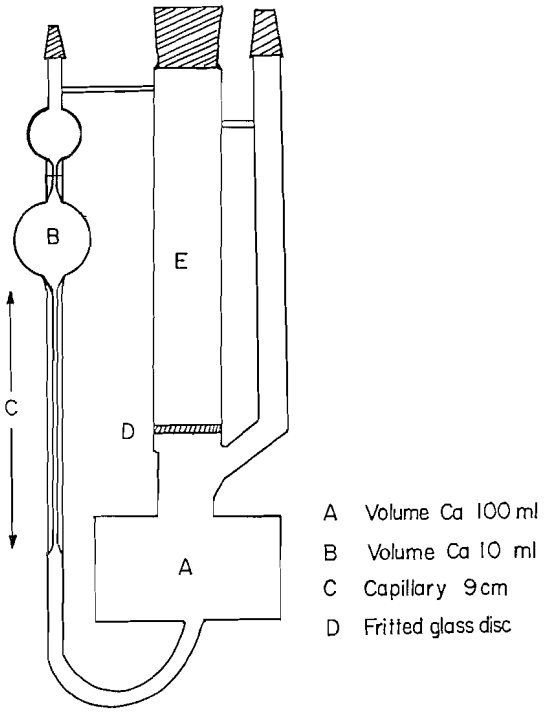

FIG. 1. The viscometer.

TABLE I

Densities, molar volumes, and coefficients of thermal expansion of sodium chlorate and three mixtures of sodium chlorate and sodium nitrate

t (°C)	d (g ml^{-1})	V (ml mole^{-1})
A. Pure sodium chlorate		
263.6	2.101	50.663
266.0	2.099	50.721
267.8	2.097	50.755
270.0	2.095	50.803
272.5	2.093	50.859
275.1	2.091	50.910
277.8	2.088	50.978
281.0	2.086	51.035
285.0	2.082	51.112
Best line $V=45.075+0.021t$		
$\alpha\times10^4=4.66$		
B. Mole fraction sodium nitrate = 0.273		
238.0	2.086	48.212
242.8	2.082	48.288
250.2	2.076	48.462
254.7	2.072	48.556
258.2	2.068	48.636
263.5	2.064	48.735
272.7	2.056	48.932
273.8	2.055	48.958
279.3	2.050	49.058
283.4	2.046	49.152
Best line $V=43.233+0.021t$		
$\alpha\times10^4=4.86$		
C. Mole fraction sodium nitrate = 0.485		
234.6	2.059	46.651
242.8	2.052	46.803
249.8	2.045	46.961
253.6	2.043	47.037
258.6	2.038	47.129
261.4	2.036	47.187
270.0	2.028	47.357
279.2	2.019	47.578
284.3	2.015	47.660
289.2	2.011	47.753
Best line $V=41.851+0.020t$		
$\alpha\times10^4=4.18$		
D. Mole fraction sodium nitrate = 0.611		
250.1	2.025	46.091
253.0	2.022	46.157
255.5	2.020	46.212
260.6	2.015	46.315
262.5	2.014	46.342
266.5	2.010	46.444
270.3	2.007	46.506
280.0	1.999	46.704
284.1	1.995	46.798
286.5	1.993	46.840
Best line $V=40.972+0.021t$		
$\alpha\times10^4=4.21$		

The viscometer used is shown in Fig. 1. It is a modified form of that used by Goodwin and Mailey (15). The important part is the fritted glass disc D. Melts are very liable to contain suspended particles, especially if the melt has been exposed to a high temperature, for instance when sealing an apparatus. The purpose of the disc is to filter out any such particles, which would entirely vitiate a viscosity determination. The large volume (100 ml) of the reservoir A renders the hydrostatic pressure almost independent of the total amount of liquid. The salt was introduced to the upper compartment of E as a powder; after melting, it collected in reservoir A. The melt was sucked into B and allowed to flow back under gravity. Preparation of mixture and transfer to viscometer were carried out in a dry box. The expression for viscosity is

$$\eta = (1 + \alpha\theta)\left(A - \frac{B}{t^2}\right)td,$$

where t = time of flow, d = density, α = thermal coefficient of expansion of Pyrex glass, and θ = °C. A and B are constants characteristic of the viscometer and independent of θ.

The constants A and B were obtained by calibration with water at 6.0 and 25.0°. Flow times were measured to 1 s over a total flow time of about 2000 s. This gives a deviation of $\pm0.05\%$. Densities of molten sodium chlorate and its mixtures were correct to $\pm0.02\%$. This would seem to point to an overall precision of $\pm0.1\%$. Because, however, an additional correction had to be applied to eliminate the effect of change in head of liquid on the time of flow, the overall accuracy is only $\pm1.0\%$. This correction is necessary because of change in cross section of reservoir A and expansion of liquid (15).

The method of determining surface tension has been described previously (16).

Results

A. *Density and Molar Volume*

Table I gives the densities and molar volumes of pure sodium chlorate and of three mixtures with sodium nitrate, at different temperatures, as well as the coefficients of expansion obtained from the equation

$$V = V_0\,(1 + \alpha t).$$

When density and molar volume, respectively, are plotted against temperature, linear graphs are obtained. Calculations of best straight line and standard error were made on a 360 I.B.M. computer. The appropriate straight line equations, in terms of molar volume and temperature, for each mixture, are also given in Table I.

From the graphs of molar volume versus temperature, isotherms were obtained for different temperatures (260 to 290° at 10° intervals).

Can. J. Chem. Downloaded from www.nrcresearchpress.com by 210.87.254.6 on 09/05/12
For personal use only.

Can. J. Chem. Downloaded from www.nrcresearchpress.com by 210.87.254.6 on 09/05/12
For personal use only.

These graphs were linear and satisfy the equation

$$V = A_0 + A_1 n_2,$$

where n_2 is the mole fraction of sodium nitrate, and A_0 and A_1 are constants for a given temperature.

Table II gives the A_0 and A_1 values.

Unlike sodium chlorate, pure solid lithium chlorate exhibits allotropic transition. The transition β-$LiClO_3 \rightleftarrows \alpha$-$LiClO_3$ occurs at 99.1°, α-lithium chlorate being the high temperature form (13).

TABLE II

Values of constants in the equation for the best line $V = A_0 + A_1 n_2$ by the method of least squares

t (°C)	A_0	A_1
260	50.495	−6.799
270	50.703	−6.804
280	50.912	−6.809
290	51.121	−6.814

TABLE III

Densities in the solid state

t (°C)	d (g ml^{-1})	t (°C)	d (g ml^{-1})
A. Sodium chlorate		B. α-Lithium chlorate	
25.0	2.487	102.5	2.309
60.0	2.472	108.0	2.303
84.8	2.461	112.0	2.298
96.1	2.455	114.0	2.295
96.8	2.454	115.6	2.295
121.0	2.445	117.0	2.293
124.5	2.441	119.1	2.290
132.0	2.440	121.0	2.286
138.4	2.436	Best line $V=37.038+0.020t$	
144.8	2.434	C. β-Lithium chlorate	
190.1	2.414	25.0	2.596
208.5	2.405	35.0	2.592
214.0	2.402	81.5	2.576
235.1	2.393	85.5	2.571
248.3	2.388	95.0	2.567
249.4	2.386	110.0	2.563
252.0	2.385	Best line $V=34.692+0.005t$	
Best line $V=42.583+0.008t$		D. Eutectic mixture sodium chlorate – sodium nitrate (57.09 wt % $NaClO_3$)	
		96.3	2.332
		104.5	2.327
		116.4	2.322
		120.0	2.320
		144.5	2.309
		162.6	2.299
		174.3	2.293
		194.8	2.283
		Best line $V=40.332+0.009t$	

The densities of α- and β-$LiClO_3$, of sodium chlorate, and of the eutectic mixture of sodium chlorate and sodium nitrate, at various temperatures, are reproduced in Table III together with the equation for the best straight line.

The molar volume of the solid at the melting point was obtained from the equation for volume as a function of temperature. A similar procedure gave the volume of the liquid at the melting point. From these figures, the change in molar volume on melting was obtained. The equation for the molar volume of liquid lithium chlorate was obtained previously by Campbell and Nagarajan (1). The volume change of the transition was also calculated from the molar volumes of α- and β-lithium chlorate at the transition temperature. The same calculation was made for the eutectic mixture. The results are given in Table IV.

TABLE IV

Volume change on fusion and allotropic transformation

Salt	% increase in volume of low temperature form
α-$LiClO_3$	9.05 (fusion)
β-$LiClO_3 \rightleftarrows \alpha$-$LiClO_3$	10.95 (transition)
$NaClO_3$	11.70 (fusion)
Eutectic $NaClO_3$–$NaNO_3$	9.40 (fusion)

B. Viscosity

The viscosities of pure sodium chlorate and of certain of its mixtures with sodium nitrate are given in Table V. In Fig. 2 log η versus $1/T$ is plotted. All viscosity data were fitted to the equation

$$\eta = \eta_0 \exp \frac{E_\eta}{RT},$$

where E_η is the activation energy of viscous flow. Table V lists the values of η_0 and E_η for the different mixtures.

From the dependence of viscosity on composition, at constant temperature, interpolations at arbitrarily chosen temperatures were made by means of a computer, employing the equation of best fit. The data so obtained were analyzed by the method of least squares and found to fit the equation

$$\eta = B_0 + B_1 n_2 + B_2 n_2^2.$$

TABLE V

Viscosities of pure sodium chlorate and three mixtures of sodium chlorate and sodium nitrate

A. Pure sodium chlorate		Mole fraction sodium nitrate 0.273		0.485		0.611	
t (°C)	η (cP)	t (°C)	η (cP)	t (°C)	η (cP)	t (°C)	η (cP)
261.3	6.95	238.0	8.53	238.0	7.56	249.2	6.11
261.6	6.93	240.0	8.33	241.7	7.24	253.0	5.88
264.2	6.74	245.3	7.77	246.2	6.92	256.2	5.70
264.5	6.70	248.0	7.54	249.5	6.66	256.8	5.67
266.3	6.59	253.0	7.16	253.3	6.38	259.7	5.50
268.5	6.46	256.1	6.91	255.4	6.24	262.0	5.38
272.3	6.19	257.0	6.86	257.3	6.07	268.5	5.06
275.3	5.98	260.3	6.60	258.5	6.14	272.0	4.92
277.3	5.86	263.9	6.37	262.4	5.77	273.5	4.84
280.7	5.71	270.4	5.96	267.8	5.47	276.0	4.77
282.8	5.58	271.2	5.88	272.8	5.22	277.7	4.68
286.0	5.43	275.0	5.66	277.5	5.00	286.2	4.37
		280.3	5.37	282.5	4.79	286.7	4.32
		284.3	5.16			288.3	4.26
		287.5	4.98				
Best fit:							
$\eta = 2.451 \times 10^{-4} \exp(5975/RT)$		$\eta = 2.064 \times 10^{-4} \exp(6093/RT)$		$\eta = 2.428 \times 10^{-4} \exp(5809/RT)$		$\eta = 3.646 \times 10^{-4} \exp(5295/RT)$	

The values of B_0, B_1, and B_2 corresponding to each temperature are given in Table VI.

TABLE VI

Values of B_0, B_1, and B_2 in the equation $\eta = B_0 + B_1 n_2 + B_2 n_2^2$

t (°C)	B_0	B_1	B_2
260.0	0.908	0.149	−0.037
270.0	1.610	−0.068	−0.026
280.0	2.911	−0.563	0.013
290.0	4.466	−1.264	0.082

C. Surface Tension

Table VII reproduces surface tension at different temperatures for pure sodium chlorate and for the three mixtures. The results are expressed analytically in the same table.

The analytical representations of the composition dependence of surface tension, at constant temperature, were obtained from a least squares fit of the experimental values. The results are represented graphically in Fig. 3.

The surface heat of sodium chlorate is constant at 129.6 ergs cm^{-2} over the temperature range 260–290°.

Discussion

In order to establish a comparison between the behavior of the two salts, lithium chlorate and sodium chlorate, suitable temperatures for the comparison must be found. Corresponding temperatures, in the usual sense of the term, cannot be used, since in most cases the critical temperature is unknown. According to Angell

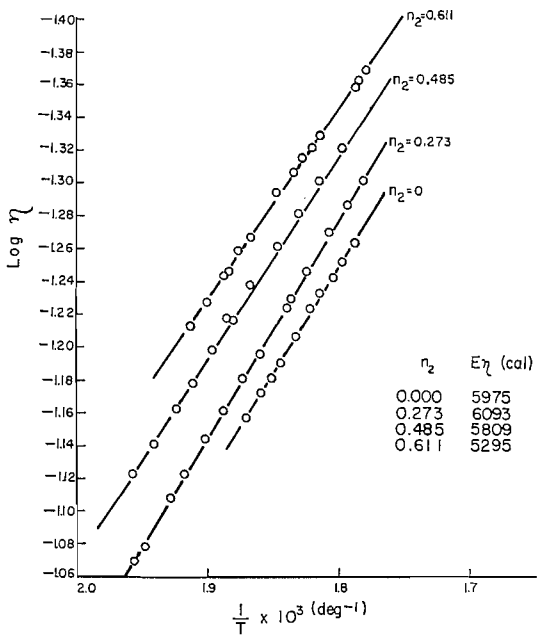

FIG. 2. Plot of log η vs. $1/T$.

Can. J. Chem. Downloaded from www.nrcresearchpress.com by 210.87.254.6 on 09/05/12
For personal use only.

TABLE VII

Surface tensions of pure sodium chlorate and mixtures with sodium nitrate

Pure sodium chlorate		Mole fraction sodium nitrate					
		0.273		0.485		0.611	
t (°C)	Surface tension (dyn cm^{-1})	t (°C)	Surface tension (dyn cm^{-1})	t (°C)	Surface tension (dyn cm^{-1})	t (°C)	Surface tension (dyn cm^{-1})
265.0	90.72	248.5	97.46	224.5	104.13	245.5	105.93
268.5	90.46	253.0	97.33	240.4	103.19	248.0	105.89
275.0	90.00	260.6	96.78	257.5	102.15	260.5	105.10
280.1	89.53	267.8	96.21	264.8	101.58	270.8	104.41
286.5	89.16	275.6	95.75	275.8	100.95	279.5	103.88
290.3	88.85	281.8	95.35	282.8	100.43		
Best line $\gamma=110.28-0.073t$		$\gamma=113.94-0.066t$		$\gamma=118.40-0.063t$		$\gamma=121.19-0.061t$	

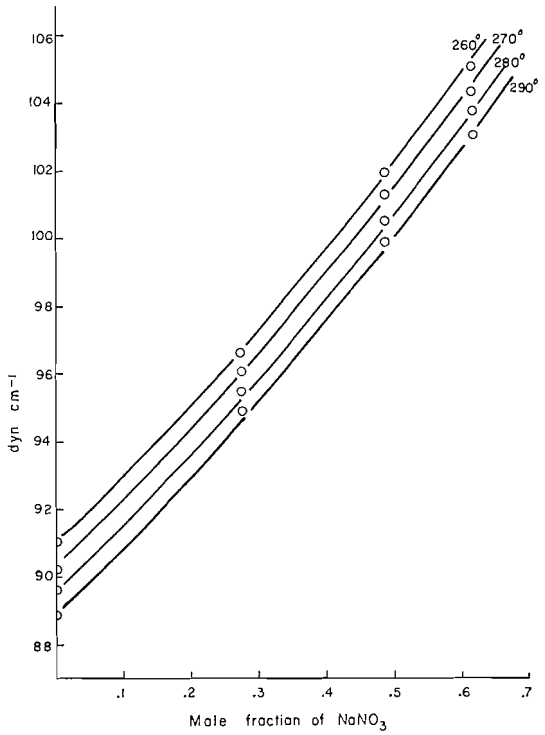

FIG. 3. Surface tension vs. composition.

(17), the ratio of temperature to T_0, where T_0 is the temperature at which the structural entropy is zero, represents a theoretical corresponding temperature. Angell's argument is based upon the nonadherence of liquids at low temperatures (e.g. below their melting points) to the Arrhenius relation. Our liquids, however, obeyed the Arrhenius relation quite well over the small temperature range studied. We contented ourselves with the arbitrary standard laid down by Bloom and Heymann (11), viz. a temperature 10° above the melting point (expressed in °K). On this basis, the following table shows the effect of the three alkali cations, lithium, sodium, and potassium for which data are now available, on three common ion substitutions.

Anion substitution	% change in volume on anion substitution		
	Li	Na	K
ClO_3-Cl	14.95	12.71	13.59
NO_3-Cl	10.41	6.67	4.56
ClO_3-NO_3	4.54	6.04	9.03

While the chlorate–chloride substitution shows approximately the same change in molar volume for all three cations, the chloride–nitrate substitution gives a distinctly larger expansion for the lithium cation than for the other two. On the other hand, the nitrate–chlorate substitution is distinctly smaller for lithium than for the other two cations.

In the sodium chlorate–sodium nitrate system, a linear relation exists between molar volume and molar composition (at constant temperature). This is in sharp contrast to the $LiClO_3$–$LiNO_3$ system, where there is positive deviation from linearity. Boardman *et al.* (18) regard a positive deviation as a sign of complex formation and increasing covalency as the second substance is added. Large deviations have actually been found in systems in which complex formation is known to occur (19).

At 264.5 °C the viscosity of sodium chlorate is 6.6 cP, as compared with 33.0 cP, the viscosity

Can. J. Chem. Downloaded from www.nrcresearchpress.com by 210.87.254.6 on 09/05/12
For personal use only.

Can. J. Chem. Downloaded from www.nrcresearchpress.com by 210.87.254.6 on 09/05/12
For personal use only.

of lithium chlorate at 131.8°. Molten salts in general have viscosities between 1 and 5 cP. The much lower viscosity of sodium chlorate indicates a more ionic character of the melt, although the viscosity is still slightly higher than that of most ionic salts.

The activation energy of viscous flow for sodium chlorate is 5.98 kcal mole^{-1}, as compared with 7.86 kcal mole^{-1} for lithium chlorate. The value for sodium chlorate is comparable with that of most ionic melts, whose activation energies of viscous flow usually lie within the limits 3 to 10 kcal mole^{-1}.

No theoretical treatment exists which connects the viscosity of a molten mixture with composition. The "ideal" isotherm does not appear to be linear because liquid mixtures which behave ideally in other respects (e.g. zero volume change on mixing) still do not show a linear relation for viscosity versus mole fraction. There is a slight positive deviation for the system $NaClO_3$–$NaNO_3$, in comparison with a very pronounced positive deviation for the system $LiClO_3$–$LiNO_3$. Harrap and Heymann (6) reported only negative deviations from additivity for many chloride systems.

The surface tension of sodium chlorate is 91.2 dyn cm^{-1} at the melting point. For simple spherical ions, a marked decrease is observed in surface tension with increasing cation radius, but for the nitrates the surface tension remains almost constant. The same tendency appears with the chlorates, the surface tensions of lithium, sodium, and potassium chlorates at $1.1T$ being 86.2, 87.4, and 81 dyn cm^{-1} respectively. This suggests that the anion determines the surface energy in the Group I chlorates, as with the nitrates.

The surface heat of a molten salt is not temperature dependent and, according to Bloom *et al.* (9), it is a measure of the covalent character of the melt. For some ionic salts the surface heat is high (e.g. NaCl 216.7 ergs cm^{-2}) while for more covalent salts the values are much lower (e.g. $MgCl_2$ 76.7). The surface heat of sodium chlorate is 129.6 ergs cm^{-2} while the value for lithium chlorate is 118. Although the difference is relatively small, it shows that in both salts some covalency is present, sodium chlorate being slightly more ionic in character.

The surface tensions of pure sodium chlorate and its mixtures with sodium nitrate are linearly dependent on temperature. At constant temperature, the surface tension increases with increasing content of sodium nitrate. This is not surprising since the surface tension of sodium nitrate is higher, viz. 120.7 dyn cm^{-1} at the melting point.

TABLE VIII

Sokolov's rule

Temperature (°C)	Molar volume (ml)	Surface tension (dyn/cm) Calcd.	Exp.
260	50.583	—	91.30
270	50.793	90.55	90.57
280	51.003	89.80	89.84
290	51.213	89.07	89.11

Application of the Guggenheim formula for the surface tension of an ideal equimolecular mixture indicates an almost ideal behavior for the sodium chlorate – sodium nitrate mixture. The calculated surface tension is 103.37 dyn cm^{-1} at 260° and the corresponding experimental value 101.5. A similar calculation cannot be made for the lithium chlorate – lithium nitrate mixture because the extrapolations involved would be too drastic: it was not possible, at the temperatures involved, to make a liquid mixture containing more than 0.213 mole fraction lithium nitrate.

Sokolov (20) found the following formula to represent the temperature variation of surface tension, for salts with a complex anion,

$$\gamma_1 = \gamma_2 \frac{V_1}{V_2},$$

where γ_1 and γ_2 are the surface tensions and V_1 and V_2 the molar volumes, at temperatures t_1 and t_2 respectively. This formula applies to pure sodium chlorate, as Table VIII shows.

1. A. N. CAMPBELL and M. K. NAGARAJAN. Can. J. Chem. **42**, 1137 (1964); **42**, 1616 (1964). A. N. CAMPBELL and D. F. WILLIAMS. Can. J. Chem. **42**, 1778 (1964); **42**, 2984 (1964).
2. POINCARRÉ. Ann. Chim. Phys. **6**, 314 (1890).
3. H. M. GOODWIN and T. H. KALMUS. Phys. Rev. **28**, 1 (1909).
4. A. N. CAMPBELL, E. M. KARTZMARK, and M. K. NAGARAJAN. Can. J. Chem. **40**, 1258 (1962).
5. R. S. DANTUMA. Z. Anorg. Allgem. Chem. **175**, 1 (1928).
6. B. S. HARRAP and E. HEYMANN. Trans. Faraday Soc. **51**, 259 (1955).
7. E. A. GUGGENHEIM. Trans. Faraday Soc. **41**, 150 (1945).

8. G. J. JANZ and M. R. LORENZ. Rev. Sci. Instr. **32**, No. 2, 130 (1961).
9. H. BLOOM, F. G. DAVIES, and D. W. JAMES. Trans. Faraday Soc. **56**, 1179 (1960).
10. N. K. BOARDMAN, A. R. PALMER, and E. HEYMANN. Trans. Faraday Soc. **51**, 277 (1955).
11. H. BLOOM and E. HEYMANN. Proc. Roy. Soc. London, Ser. A, **188**, 392 (1946).
12. G. M. BENNETT and A. D. MITCHELL. Z. Physik. Chem. Leipzig, **84**, 475 (1913).
13. A. N. CAMPBELL and J. E. GRIFFITHS. Can. J. Chem. **34**, 1647 (1956).
14. L. J. B. HUSBAND. J. Sci. Instr. **35**, 300 (1958).
15. H. M. GOODWIN and R. D. MAILEY. Phys. Rev. **26**, 44 (1908).
16. A. N. CAMPBELL and D. F. WILLIAMS. Can. J. Chem. **42**, 1778 (1964).
17. C. A. ANGELL. J. Phys. Chem. **70**, 2793 (1966).
18. N. BOARDMAN, E. DORMAN, and E. HEYMANN. J. Phys. Chem. **53**, 375 (1949).
19. H. BLOOM, J. KNAGGS, J. MOLLOY, and D. WELCH. Trans. Faraday Soc. **49**, 1458 (1953).
20. O. K. SOKOLOV. Zh. Neorgan. Khim. **11**, (7), 1703 (1966).

Can. J. Chem. Downloaded from www.nrcresearchpress.com by 210.87.254.6 on 09/05/12
For personal use only.

Studies on the thermodynamics and conductances of molten salts and their mixtures. Part VI. Calorimetric studies of sodium chlorate and its mixtures with sodium nitrate

A. N. CAMPBELL AND E. T. VAN DER KOUWE
Department of Chemistry, University of Manitoba, Winnipeg, Manitoba

Received August 22, 1967

The following properties have been determined by direct experiment for pure sodium chlorate and its mixtures with sodium nitrate: heat capacity (both solid and liquid) and heat of fusion. From these experimental quantities, the following properties have been derived: entropy of fusion, heat of mixing, and free energy and entropy of mixing. The results have been compared with our previous results for the corresponding lithium chlorate – lithium nitrate system. On the whole, the conclusion is justified that the structure of melts containing lithium chlorate is more complex than that of melts involving sodium chlorate.

Canadian Journal of Chemistry, 46, 1287 (1968)

Can. J. Chem. Downloaded from www.nrcresearchpress.com by 210.87.254.105 on 09/05/12
For personal use only.

As the work described here is largely a repeat of previous work on lithium chlorate and lithium chlorate – lithium nitrate mixtures (1), reference should be made to that paper for the theoretical aspect. Calorimetric work on sodium chlorate has been reported by Goodwin and Kalmus (2) but no thermodynamic data are available for sodium chlorate – sodium nitrate mixtures. Goodwin and Kalmus report the heat of fusion of sodium chlorate as 5250 cal $mole^{-1}$ and the molar heat capacity as 32.9 cal $mole^{-1}$ deg^{-1}. Kelley (3) gives values of 5400 and 31.8 respectively.

According to Lumsden (4), the accepted heat of fusion of sodium nitrate is that obtained by Sokolov and Shmidt (5), who found a value of 3600 cal $mole^{-1}$. Goodwin and Kalmus (2) reported a molar heat capacity for liquid sodium nitrate of 36.5 cal $mole^{-1}$ deg^{-1}. As mentioned previously (1) we used a method essentially similar to that of Goodkin, Solomons, and Janz (6) for the determination of heats of fusion.

The most accurate measurements of heats of mixing are due to Kleppa (7–10). Before this method was developed, the heat of mixing was obtained from electromotive force (e.m.f.) measurements or from phase diagrams. In this investigation, a less direct method has been followed, similar to the one used by Gilbert (11) for the system LiF–KF.

Experimental

The apparatus was identical with that used previously (1), except that, instead of the rather cumbersome photoelectric control used for keeping the furnace at constant temperature, we now substituted a copper–constantan thermocouple in conjunction with an electronic relay system. The relay developed an e.m.f. equal to that produced by the thermocouple, at the desired temperature. The details of the arrangement are sufficiently well known. In the region 200–280°, temperature was controlled to $\pm 0.1°$.

The salts were sealed in Vycor tubes and we therefore determined the specific heat of Vycor, using for this purpose a solid Vycor rod. The results are given in Table I.

TABLE I

Specific heat of Vycor glass*

Temperature of furnace (°C)	Specific heat (cal deg^{-1} g^{-1})
210.2	0.1930
239.8	0.1975
257.5	0.2000
265.0	0.2015
306.1	0.2067

*The sample was allowed to cool from furnace to room temperature, so that the figures given are average values.

Results

In order to make a fair comparison between different salts and mixtures, all heats evolved were calculated to the same final temperature, using the equation of Goodkin, Solomons, and Janz (6) where $(t_1 - t_2)$ is the experimental temperature range and t_{sr} the comparison temperature.

$$\Delta H_{corr} = \Delta H_{obs}(t_1 - t_{sr})/(t_1 - t_2)$$

Figure 1 expresses graphically the heat content of sodium chlorate over the range 125.2 to 294.4°, a range which includes the melting point. Analytically expressed, it was found that the heat

TABLE II

Calorimetric data for the sodium chlorate – sodium nitrate system

Mole fraction of sodium nitrate, n_2	Molar heat capacity, C_p (cal deg^{-1} mole^{-1}) Solid	Liquid	Freezing point, T_f (°K)	ΔH_f (cal mole^{-1})	ΔS_f (cal deg^{-1} mole^{-1})
0.000	$10.92+44\times10^{-3}T(\pm0.3)$	32.0±0.2	533.0	5076±19	9.52
0.138	—	32.7±0.2	514.7	4795±22	9.32
0.273	30.9±0.3	33.3±0.2	504.5	4545±23	9.00
0.426	—	34.0±0.2	490.4	4186±22	8.54
0.485	31.2±0.3	34.2±0.2	484.1	4042±18	8.35
0.611	31.5±0.3	34.9±0.2	510.3	4197±20	8.22

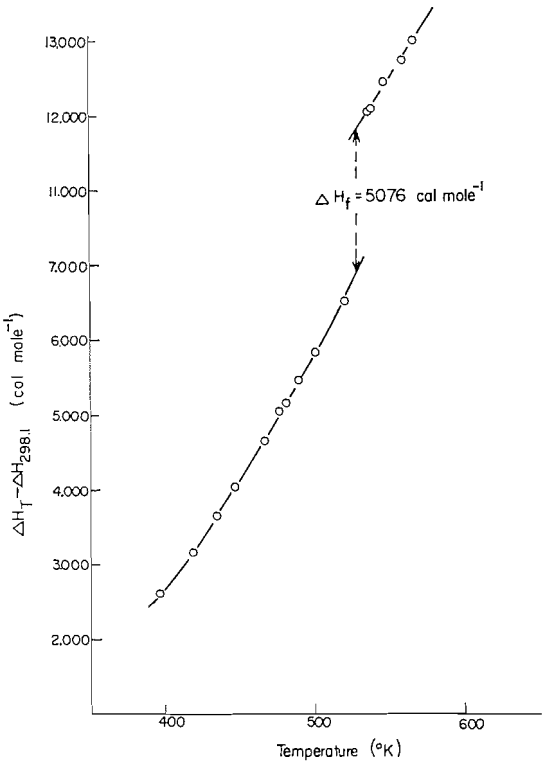

FIG. 1. Heat content data for pure sodium chlorate.

content of the solid form could be represented by the equation

$$\Delta H_T(\text{s}) = 22.0 \times 10^{-3}T^2 + 10.92T - 5266\ (\pm 19)\ \text{cal mole}^{-1}$$

and that of the liquid by

$$\Delta H_T(\text{l}) = 32.05T - 5171\ (\pm 12)\ \text{cal mole}^{-1}.$$

Differentiation of the above equations gives

$$C_p(\text{s}) = 44.0 \times 10^{-3}T + 10.92\ (\pm 0.3)\ \text{cal deg}^{-1}\,\text{mole}^{-1}$$

and $C_p(\text{liq}) = 32.05 \pm 0.2\ \text{cal deg}^{-1}\,\text{mole}^{-1}$.

The molar heat of fusion was obtained from the difference in molar heat contents of the liquid and solid forms at the melting point. The entropy of fusion, $\Delta S_f = \Delta H_f/T_f$, is given in Table II. This table also includes the molar heat capacities of five mixtures of sodium chlorate and sodium nitrate, as well as their heats of fusion and entropies of fusion.

The heat of mixing of sodium chlorate (mole fraction n_1) and sodium nitrate (mole fraction n_2) has been calculated as the difference between the observed and calculated values of heat content at 533 °K, the melting point of pure sodium chlorate.

$$\Delta H^{\text{M}} = \Delta H_{\text{obs}} - \Delta H_{\text{calcd}}$$

The observed heat content was calculated to 533 °K from the formula

$$\Delta H_{\text{obs}} = \Delta H_t(\text{mixture}) + \int_{T_t}^{533} C_p(\text{liq})\,dT,$$

where ΔH_f(mixture) = heat of fusion of the mixture, T_f = freezing point of mixture, and C_p(l) = molar heat capacity of liquid mixture. The calculated heat content was obtained as

$$\Delta H_{\text{calcd}} = n_1\Delta H_t(1) + n_2\Delta H_t(2),$$

where $\Delta H_f(1)$ and $\Delta H_f(2)$ are the molar heats of fusion of pure sodium chlorate and of pure sodium nitrate, at 533°. $\Delta H_f(2)$ was calculated to 533°, using the relation

$$\Delta H_t(2) = \Delta H_t(\text{p}) + \int_{533}^{T_t} \Delta C_p\,dT,$$

where ΔH_f(p) is the heat of fusion of pure sodium

Can. J. Chem. Downloaded from www.nrcresearchpress.com by 210.87.254.105 on 09/05/12
For personal use only.

TABLE III

Heats of mixing in the sodium chlorate – sodium nitrate system at 533 °K

Mole fraction of sodium nitrate, n_2	Heat content calculated (cal mole^{-1})	ΔH_f of sample (cal mole^{-1})	$\int_{T_f}^{533.0} C_p(l)dT$ (cal mole^{-1})	Heat content observed (cal mole^{-1})	ΔH^M (cal mole^{-1})
0.138	4859	4795	599	5394	535
0.273	4766	4545	950	5495	729
0.426	4662	4186	1450	5637	975
0.485	4621	4042	1672	5714	1093
0.611	4532	4197	792	4989	748

nitrate at its melting point and ΔC_p is the difference between the molar heat capacities of solid and liquid sodium nitrate

$$\Delta C_p = C_p^{\,s} - C_p^{\,liq}.$$

Because the system $NaClO_3$–$NaNO_3$ exhibits solid solubility, it is questionable whether the heat of mixing calculation is justified, since a heat of solution in the solid state (unknown) is involved. Except for the pure components and the eutectic mixture, there is no sharp melting temperature: solid and liquid are in equilibrium over a range of temperature. Hence, the heat of fusion does not have its usual significance. An arbitrary correction was applied to the heat of fusion, as follows.

$$\Delta H_{corr} = \Delta H_f - \tfrac{1}{2}(t_1 - t_2)(C_p(s) + C_p(liq)),$$

where ΔH_f is the heat of fusion obtained by subtracting the heat content of the solidus from that of the liquidus, t_2 is the temperature at which the system is completely solid, and t_1 the temperature at which it is completely liquid. In other words, the mean specific heat of solid and liquid forms is used to give the heat effect over the range of temperature in which solid is transforming to liquid. This ΔH_{corr} has been used for the heat of mixing calculations. It has been assumed that the specific heat of sodium nitrate is constant over the temperature range involved. The isothermal heats of mixing are given in Table III. Obviously, they are only approximate.

The activity of sodium chlorate in sodium chlorate – sodium nitrate mixtures was obtained from the equilibrium diagram (12), by means of the equation

$$\ln a = \frac{\Delta H_f}{R}\left(\frac{1}{T} - \frac{1}{T_f}\right) + \frac{\Delta C_p}{R}\left[\ln\frac{T_f}{T} - \left(\frac{T_f - T}{T}\right)\right],$$

where ΔC_p = difference between molar heat capacities of solid and liquid phases. The free energy of mixing then results as $\Delta G^M = RT \ln a$. The entropy of mixing is obtained from $\Delta G^M = \Delta H^M - T\Delta S^M$. The values of free energy, enthalpy, and entropy of mixing are given in Table IV, as well as the ideal entropies of mixing, calculated in the usual way. Figure 2 shows the dependence of ΔG^M, ΔH^M, and $T\Delta S^M$ on n_1.

Discussion

The entropy of fusion of sodium chlorate is puzzling. While the entropies of fusion of the nitrates decrease in the order $LiNO_3 = 12.1$, $NaNO_3 = 6.2$, $KNO_3 = 3.8$, those of the chlorates are irregular, thus $LiClO_3 = 6.1$, $NaClO_3 = 9.5$, $KClO_3 = 7.8$. On the other hand, the molar heats of fusion for the nitrates are $LiNO_3 = 6.39$, $NaNO_3 = 3.60$, $KNO_3 = 2.30$, while the corresponding data for the chlorates are $LiClO_3 = 2.47$, $NaClO_3 = 5.07$, $KClO_3 = 5.0$, that is, the heats of fusion for the chlorates go in the opposite direction to those of the nitrates. If, as we suppose, the lithium chlorate melt has a complicated structure, one might expect the entropy change on fusion of lithium chlorate to be abnormally low: it has, however, a value of 6.1, the normal value for ionized salts. On the other hand, the entropy of fusion of lithium nitrate is exceptionally high. It should be pointed out that, while the heat of fusion of sodium chlorate is an experimental figure, obtained independently by Goodwin and Kalmus (2) and by ourselves, the heat of fusion of potassium chlorate is not an experimental quantity but is derived by calculation, on an assumption which seems to us somewhat doubtful, namely that, in the $KClO_3$–KCl phase diagram, the $KClO_3$ liquidus can be considered ideal, and that therefore the activity is equal to the mole fraction (13). If it should subsequently transpire that this figure for the heat of

Can. J. Chem. Downloaded from www.nrcresearchpress.com by 210.87.254.105 on 09/05/12
For personal use only.

TABLE IV

Free energy, enthalpy, and entropy of mixing in the system sodium chlorate – sodium nitrate, at 533 °K

Mole fraction of sodium nitrate, n_2	ΔG^M (cal mole^{-1})	ΔH^M (cal mole^{-1})	$T\Delta S^M$ (cal mole^{-1})	ΔS^M (cal deg^{-1} mole^{-1})	ΔS^M (ideal) (cal deg^{-1} mole^{-1})
0.138	−179.4	535	714	1.339	0.293
0.273	−289.2	729	1018	1.909	0.632
0.426	−447.6	975	1423	2.669	1.099
0.485	−521.4	1093	1614	3.028	1.171
0.611	−265.3	457	722	1.354	1.384

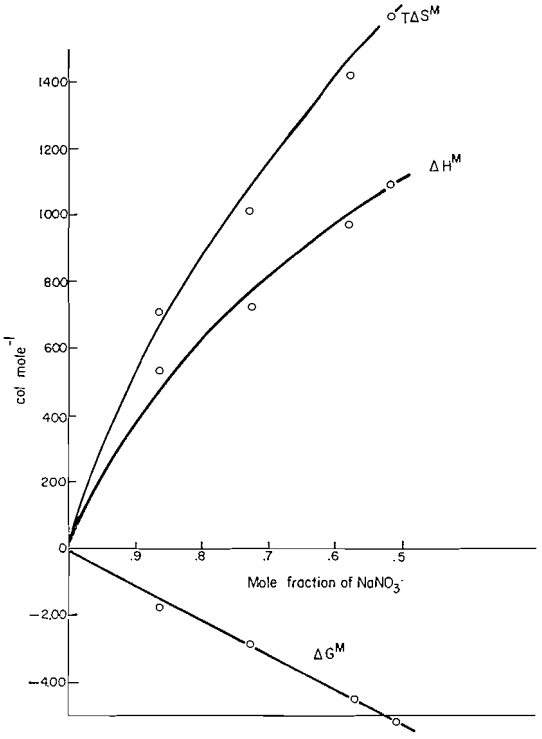

FIG. 2. ΔG^M, ΔH^M, and $T\Delta S^M$ as functions of composition of $NaClO_3$–$NaNO_3$ mixtures.

fusion of potassium chlorate is seriously in error, it might be that the entropy of fusion of potassium chlorate would turn out to be higher than that of sodium chlorate and thus one anomaly, at least, would be removed.

The entropy of fusion of sodium chlorate – sodium nitrate mixtures decreases steadily from 9.52 e.u. for pure sodium chlorate to 8.17 e.u. for the mixture richest in sodium nitrate, viz. 0.611 mole fraction sodium nitrate. There is a very large difference (1778 cal) between the heat of fusion of pure lithium chlorate and the mixture containing 0.25 mole fraction lithium nitrate. This difference is much larger than the corresponding drop in the heat of fusion in the sodium chlorate – sodium nitrate system. The same tendency is reflected in the entropy of fusion, which increases dramatically in the lithium system, while for the sodium system there is only a modest decrease for small additions to the pure sodium chlorate. Although the entropy of fusion of lithium nitrate is very high (12.1 e.u.) the increase in entropy of fusion is much more than that predicted by the mixture rule, e.g. at $n_2 = 0.255$, the additive value should be 7.51 e.u., whereas the observed value is 10.86 e.u. This sharp increase in entropy of fusion on addition of lithium nitrate may arise from some sort of interaction of the nitrate ion with the chlorate lattice, which results in an increased entropy value. The more ideal behavior in the sodium system confirms the view that in this system the process is more that of mixing than of interaction.

The molar heat capacity of sodium chlorate is 32.05 cal deg^{-1} mole^{-1}, as compared with 29.20 for lithium chlorate. The values are similar to those of the nitrates.

The change in molar heat capacity supports the view that addition of lithium nitrate to pure molten lithium chlorate forms a more complex cluster, perhaps by a process of bridging by the nitrate ion. This conclusion is based on the positive deviations of the observed molar heat capacities of lithium chlorate – lithium nitrate mixtures, in both solid and liquid states. The deviation is more pronounced in the liquid state (1). The heat capacity of sodium chlorate – sodium nitrate mixtures shows ideal behavior in the molten state.

The heat of mixing in the molten sodium chlorate – sodium nitrate system at 533 °K (m.p. of sodium chlorate) is positive and increases with addition of sodium nitrate. This agrees with the

Can. J. Chem. Downloaded from www.nrcresearchpress.com by 210.87.254.105 on 09/05/12
For personal use only.

findings of Kleppa and Meschel (14) that in all the anion mixtures studied by them the heat of mixing is positive.

Although the free energy of mixing given in Table IV is only approximate and subject to a number of assumptions, it does give a comparison with the values for the lithium system. The free energy of mixing is calculated from the phase diagram, where the occurrence of solid solubility renders the calculation inaccurate. Admitting a qualitative value, however, the data show that the mixing process is spontaneous, because ΔG^M is negative. The entropy of mixing, derived from the free energy of mixing and therefore equally approximate in character, is much greater for the lithium chlorate – lithium nitrate system than for the corresponding sodium system. The large positive deviations of ΔS^M from ideality suggest that more stable low energy configurations result on the addition of nitrate ion to chlorate ion. This effect is not spectacular in the sodium chlorate – sodium nitrate system. In the sodium system, no such configuration exists possibly because of the higher melting temperature of this system, which seems to destroy the lattice which we presume to exist in molten lithium chlorate.

1. A. N. CAMPBELL and M. K. NAGARAJAN. Can. J. Chem. **42**, 1616 (1964).
2. H. M. GOODWIN and T. H. KALMUS. Phys. Rev. **28**, 1 (1909).
3. K. K. KELLEY. Contributions to the data on theoretical metallurgy. Bulletin 584. U.S. Bureau of Mines, Washington. 1960.
4. J. LUMSDEN. Thermodynamics of molten salt mixtures. Academic Press, New York. 1966. p. 109.
5. V. A. SOKOLOV and N. E. SHMIDT. Izv. Sektora Fiz.-Khim. Analiza Inst. Obshch. Neorgan. Khim. Akad. Nauk SSSR, **26**, 123 (1955).
6. J. GOODKIN, C. SOLOMONS, and G. J. JANZ. Rev. Sci. Instr. **29**, 105 (1958).
7. O. J. KLEPPA. J. Phys. Chem. **67**, 1937 (1960).
8. O. J. KLEPPA and L. S. HERSH. J. Chem. Phys. **34**, 351 (1961).
9. O. J. KLEPPA, R. B. CLARKE, and L. S. HERSH. J. Chem. Phys. **35**, 175 (1961).
10. O. J. KLEPPA and L. S. HERSH. J. Chem. Phys. **36**, 544 (1962).
11. R. A. GILBERT. J. Phys. Chem. **67**, 1143 (1963).
12. A. N. CAMPBELL, E. M. KARTZMARK, and M. K. NAGARAJAN. Can. J. Chem. **40**, 1258 (1962).
13. J. LUMSDEN. Thermodynamics of molten salt mixtures. Academic Press, New York. 1966. p. 136.
14. O. J. KLEPPA and S. V. MESCHEL. J. Phys. Chem. **67**, 668 (1963).

Can. J. Chem. Downloaded from www.nrcresearchpress.com by 210.87.254.105 on 09/05/12
For personal use only.

Studies on the thermodynamics and conductances of molten salts and their mixtures. Part VII. The electrical conductance of sodium chlorate and its mixtures with sodium nitrate

A. N. CAMPBELL AND E. T. VAN DER KOUWE
Department of Chemistry, University of Manitoba, Winnipeg, Manitoba

Received August 28, 1967

The specific and equivalent conductances of molten sodium chlorate and of its mixtures with sodium nitrate have been determined over the temperature range 240–280 °C. The results are treated as temperature functions at constant composition and as composition functions at constant temperature. From these data, the activation energies of conductance have been derived. The results have been compared with various theoretical equations and the conclusion is made that, while melts containing lithium chlorate may be associated or complexed in some way, the sodium chlorate melts show less of such a structure and are more ionic.

Canadian Journal of Chemistry, 46, 1293 (1968)

Can. J. Chem. Downloaded from www.nrcresearchpress.com by 210.87.254.42 on 09/05/12
For personal use only.

The work described here is an exact reproduction, with sodium chlorate and sodium nitrate, of the previous work on lithium chlorate and lithium nitrate (1). The experimental technique is also the same.

Results

The specific conductances of pure molten sodium chlorate, and of its mixtures with sodium nitrate containing 0.273, 0.485, and 0.611 mole fraction sodium nitrate, were determined over the temperature range 240–280 °C. The results are expressed graphically in Fig. 1. Using the density values obtained previously (2), the equivalent conductances of pure sodium chlorate were obtained from the expression

$$\Lambda = M_e \kappa \rho^{-1}.$$

For mixtures, Bloom and Heymann (3) replace M_e, the equivalent weight of the pure salt, by the mean equivalent weight of the mixture, M_m, given by

$$M_m = M_1 n_1 + M_2 n_2,$$

where M_1 and M_2 are the equivalent weights of the two salts and n_1 and n_2 their mole fractions. The equivalent conductances in relation to temperature are represented graphically in Fig. 2. Specific and equivalent conductances are represented analytically by the equations of Tables I and II.

The analytical representations of the isothermal dependence of specific and equivalent conductance on mole fraction of sodium nitrate were obtained from least squares fits and are given in Table III.

The linear relations between log κ or log λ and $1/T$ are expressed analytically by the equation of Table IV.

Discussion

Plester, Rogers, and Ubbelohde (4) noticed that for most molten salts with considerable dissociation, the quantities determined in this paper lie within the following limits

$$\kappa = 1\text{–}5\ \text{ohm}^{-1}\,\text{cm}^{-1}$$

$$\Lambda = 30\text{–}50\ \text{cm}^2\,\text{ohm}^{-1}\,\text{equiv}^{-1}$$

$$\Delta E_\kappa = 1\text{–}5\ \text{kcal mole}^{-1}.$$

The values of κ and λ for sodium chlorate are higher than those for lithium chlorate but lower

TABLE I

Analytical representation of specific conductance

Mole fraction sodium nitrate	Temperature range (°)	Equation	Standard error
0.000	263.7–283.4	$\kappa = -0.5078 + 0.0031t$	0.005
0.273	246.6–284.7	$\kappa = -0.5738 + 0.0037t$	0.001
0.485	241.0–276.6	$\kappa = -0.5213 + 0.0038t$	0.001
0.611	247.2–281.4	$\kappa = -0.5737 + 0.0041t$	0.003

TABLE II

Analytical representation of equivalent conductance*

Equation	Standard error
$\lambda = -27.8236 + 0.1675t$	0.02
$\lambda = -30.2728 + 0.1892t$	0.04
$\lambda = -26.8541 + 0.1874t$	0.06
$\lambda = -28.9703 + 0.2014t$	0.07

*Mole fractions and temperature ranges as in Table I.

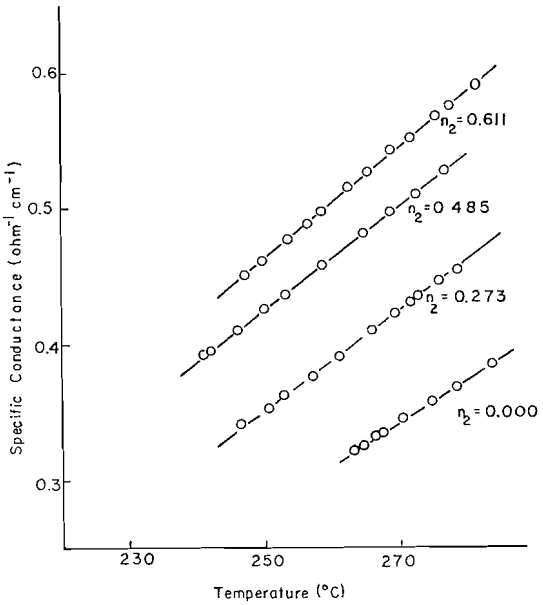

FIG. 1. Specific conductance vs. temperature.

TABLE III

Analytical representation of the change of conductance with mole fraction of sodium nitrate. (The specific conductance obeys the equation $\kappa = A_1 + A_2 n_2 + A_3 n_2^2$ and the equivalent conductance the equation $\lambda = B_1 + B_2 n_2$)

t (°C)	A_1	A_2	A_3	B_1	B_2
260	0.286	0.388	−0.056	15.320	13.310
270	0.313	0.444	−0.125	17.103	13.624
280	0.377	0.284	+0.091	18.886	13.939
290	0.423	0.232	0.164	21.471	11.441

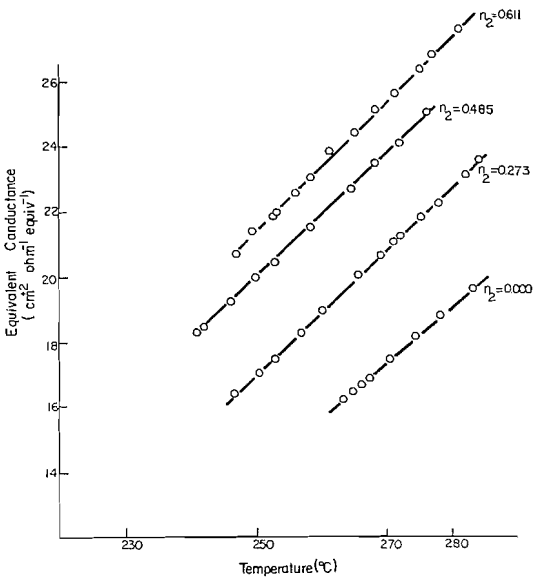

FIG. 2. Equivalent conductance vs. temperature.

TABLE IV

Arrhenius representation of conductance of sodium chlorate – sodium nitrate mixtures

Mole fraction $NaNO_3$	Arrhenius equation, conductance $= A \exp -(\Delta E/RT)$	Activation energy (kcal)
0.000	$\kappa = 45.94 \exp -(5268/RT)$	5.27
	$\lambda = 2910 \exp -(5506/RT)$	5.51
0.273	$\kappa = 53.04 \exp -(5193/RT)$	5.19
	$\lambda = 3253 \exp -(5435/RT)$	5.43
0.485	$\kappa = 37.38 \exp -(4637/RT)$	4.64
	$\lambda = 2160 \exp -(4851/RT)$	4.85
0.611	$\kappa = 37.55 \exp -(4551/RT)$	4.55
	$\lambda = 2114 \exp -(4756/RT)$	4.75

than for most other salts with polyatomic anions which have low melting points.

The ratio of the activation energies of viscosity and conductance usually has a value between 2 and 4 for ionic melts. Such a value is supposed to indicate that the viscous flow in these salts involves a greater configurational change than the flow under influence of an electric field. A lower ratio of the activation energies may indicate association. Both for lithium chlorate and sodium chlorate, the ratio is practically unity; the same value, unity, is frequently observed for nitrates.

Quoting a previous paper by Campbell and Williams (1): "A method of calculating the degree of dissociation of molten electrolytes has been put forward by Greenwood and Martin (5), which is indeed little more than the old classical rule of Arrhenius, and involves gross approximations and untenable assumptions such as the validity of the Walden rule. Nevertheless, the method does sometimes appear to give results in rough agreement with accepted values." Using the viscosity data of a previous

Can. J. Chem. Downloaded from www.nrcresearchpress.com by 210.87.254.42 on 09/05/12
For personal use only.

TABLE V

Enthalpies of jump and hole formation

Ion	Crystallographic ionic radius (Å)	Enthalpy of hole formation (kcal mole^{-1})	$\Delta H_h + \Delta H_j$ (kcal mole^{-1})	$\Delta H^+ + RT$ (kcal mole^{-1})
Na^+	0.95	1.42	2.31	6.7
ClO_3^-	2.00	6.31	10.30	
Na^+	0.95	1.88	2.49	8.0
NO_3^-	2.30	11.04	11.05	

In the above table, the various quantities are obtained as follows. Column 3: enthalpy of hole formation = $4\pi r^2\gamma$. Column 4: $\Delta H_h = 4\pi r^2(\gamma - T(d\gamma/dT))$. Column 5: According to Bockris *et al.* (6), the experimental activation energy for equivalcnt conductance ΔH^+_{exp} is related to the enthalpy of hole formation (ΔH_{hole}) and ionic jump (ΔH_{jump}) as follows: $\Delta H^+_{exp} = \Delta H_{jump} + \Delta H_{hole} - RT$. Column 5 is not derived from the other columns in Table V. The fact that the figures in columns 4 and 5 do not agree is significant and is commented on in the text.

paper (2), we have applied Greenwood and Martin's rule to calculate the degree of ionization of sodium chlorate: the figure obtained is 0.81 against a corresponding figure of 0.80 for lithium chlorate. The Group I nitrates also yield a figure of approximately unity. If any trust is to be placed in this calculation, it would indicate that all these salts are completely ionic in their melts.

Referring once again to the work on lithium chlorate (1), we have again applied the equation of Bockris, Crook, Bloom, and Richards (6),

$$\Delta H^+ = \Delta H_{jump} + \Delta H_{hole} - RT,$$

to sodium chlorate, with the results given in Table V.

The value calculated for the activation enthalpy of conduction for the sodium ion in the chlorate, as well as in the nitrate, is much lower than the experimental enthalpy, whereas the calculated activation enthalpies for the anions are both larger than the experimental enthalpy. Duke and Owens (7) have determined the transport numbers of the lithium and sodium ions in lithium nitrate and sodium nitrate to be 0.84 ± 0.06 and 0.71 ± 0.01 respectively: this indicates that the conductance is primarily uni-ionic. It is possible that the conductances of the ions in lithium chlorate, and to a lesser extent those of sodium chlorate, are also uni-ionic. If, however, the simple ions were the conducting species, the experimental activation enthalpies should be closer to those calculated for the lithium and sodium ions. Because of these discrepancies, the radii of the ionic species involved in ionic migration in the lithium and sodium melts cannot be identical with the crystallographic radii of the lithium and sodium ions. They must be larger, despite the fact that the cation is the principal conducting species. This evidence, together with the similarity of the activation enthalpies of conductance and of viscous flow, indicates that in lithium chlorate melts, and to a lesser degree in sodium chlorate melts, the conducting species are probably associated in some manner.

The internal consistency of the results can be checked with the equation of Martin (8).

$$\Delta E_\lambda = \Delta E_\kappa + RT^2\alpha,$$

where α is the coefficient of thermal expansion, obtained by us in a previous communication (2). $\Delta E_\kappa(5.26) + \alpha RT^2(0.26) = 5.52$, compared with the experimental value of ΔE_λ of 5.50 kcal mole^{-1}.

Harrap and Heymann (9) concluded that deviation from additivity in the conductances of mixtures of molten salts increases as the difference between the equivalent conductances of the components of the mixture increases. Most systems show negative deviations from additivity. The equivalent conductance of the system $NaClO_3$–$NaNO_3$ shows negative deviation, e.g. at 270 °C and $n_2 = 0.256$ mole fraction sodium nitrate, $\Lambda = n_1\lambda_1 + n_2\lambda_2 = 26.20$ cm^2 ohm^{-1} equiv^{-1}, while the experimental value is 23.74. The corresponding lithium system also shows negative deviation. The calculations are inexact, however, since the equivalent conductances of the nitrates have been extrapolated to temperatures much below the melting points.

A striking difference between the two systems is to be seen in the temperature effect. In the lithium mixtures, the specific conductance is almost doubled for a 40° rise in temperature, while for the sodium system the increase is much

Can. J. Chem. Downloaded from www.nrcresearchpress.com by 210.87.254.42 on 09/05/12
For personal use only.

less. At comparable temperatures ($1.10T_f$) the specific and equivalent conductances of sodium chlorate are at least twice as great as those of lithium chlorate.

The activation energies for both specific and equivalent conductances show a decrease in the sodium system with nitrate addition, while in the lithium system the activation energy remains essentially constant, at least as far as it was possible to carry the nitrate addition. Campbell and Nagarajan (10) suggested a possible bridging may occur in the lithium chlorate – lithium nitrate mixtures. This would increase the association present in the chlorate melt and hence increase the activation energy of conductance, though the isothermal conductance of such mixtures would change only slightly if the lithium ion is the charge-carrying ion. The regular behavior of sodium chlorate and its mixtures with sodium nitrate provides no evidence for cluster formation, such as may occur in the lithium chlorate melts. Various techniques (e.g. infrared absorption spectra by Wilmshurst (11)) have failed to provide any precise experimental information as to the nature of the presumed association.

1. A. N. CAMPBELL and D. F. WILLIAMS. Can. J. Chem. **42**, 1984 (1964).
2. A. N. CAMPBELL and E. T. VAN DER KOUWE. Can. J. Chem. This issue.
3. H. BLOOM and E. HEYMANN. Proc. Roy. Soc. London, Ser. A, **188**, 392 (1946).
4. D. W. PLESTER, S. E. ROGERS, and A. R. UBBELOHDE. Proc. Roy. Soc. London, Ser. A, **235**, 469 (1956).
5. N. N. GREENWOOD and R. L. MARTIN. J. Chem. Soc. 1427 (1953).
6. J. O'M. BOCKRIS, E. H. CROOK, H. BLOOM, and N. E. RICHARDS. Proc. Roy. Soc. London, Ser. A, **255**, 588 (1960).
7. F. R. DUKE and B. OWENS. J. Electrochem. Soc. **105**, 548 (1958).
8. R. L. MARTIN. J. Chem. Soc. 3246 (1954).
9. B. S. HARRAP and E. HEYMANN. Trans. Faraday Soc. **51**, 259 (1955).
10. A. N. CAMPBELL and M. K. NAGARAJAN. Can. J. Chem. **42**, 1137 (1964).
11. J. K. WILMSHURST. J. Chem. Phys. **39**, 1779 (1963).

Can. J. Chem. Downloaded from www.nrcresearchpress.com by 210.87.254.42 on 09/05/12
For personal use only.

Can. J. Chem. Downloaded from www.nrcresearchpress.com by 210.87.254.5 on 09/05/12
For personal use only.

Surface energy and surface tension[1]

E. A. FLOOD AND G. C. BENSON
Division of Pure Chemistry, National Research Council of Canada, Ottawa, Canada

Received December 6, 1966

Some thermodynamic properties of surface regions are defined. The interdependence of these properties, the effects of particle size, etc. are examined.

Results of computer summations of Lennard–Jones (6–12) interaction energies of atoms at lattice sites of face-centered cubic arrays are presented. "Shells" of lattice sites are described by reduced lattice vectors of constant magnitude. Such shells contain (1), 6, 8, 12, 24, or 48 atoms.

Sublimation energies of atoms in shells of clusters containing from 1 to 1337 atoms are compared with the sublimation energy per atom of an infinite cluster ε_0. Mean sublimation energies of clusters of 13 and 1337 atoms are, respectively, about $0.36\varepsilon_0$ and $0.83\varepsilon_0$.

Specific surface energies of clusters show relatively little variation with particle size; the specific surface energy of a cluster of 13 atoms is about 0.82 of the specific surface energies of clusters containing from $1337 \rightarrow \infty$ atoms.

It is shown that two bulk phases and the interphase between them can grow in extent from suitable sources of mass, etc. while the nature and state of each of the three regions remain constant. Thus the extensive thermodynamic variables of each of the three regions can behave (mathematically) as homogeneous functions of first degree in one another. If the three regions consist of a single common component, under equilibrium conditions the Gibbs potentials per unit mass of the three regions must be the same. Accordingly if the Helmholtz potential of the surface region exceeds that of, say, the condensed bulk phase by A_s, per gram, the displacement mechanical growth potential, the pv potential per gram, must be less than that of the condensed bulk phase by A_s. If the pv potential of the bulk phase is zero, then $A_s + (pv)_s = 0$ and for a flat interface $A_s = \gamma\sigma$ where γ is the surface tension and σ the area per gram of the flat surface region.

The above ideas underlie Gibb's treatment of surface regions. Such treatments cannot be applied, literally, to systems consisting of only a few atoms or molecules. Thus surface tension in the sense of a negative tangential surface stress of relatively large magnitude is a property of systems of very many molecules (bulk systems) in a state of complete thermodynamic equilibrium.

The surface energies of crystals of molecular dimensions are reasonably meaningful and are only a little less than those of laboratory scale crystals. However, the "surface tensions" of such crystals are largely meaningless. The magnitudes of any negative stresses in the surface regions of such minute crystals are probably very much less than those corresponding to the true surface tension of large crystals; further, the surface stresses of these minute crystals are not closely related to excess surface energies, excess surface Helmholtz free energies, etc.

Canadian Journal of Chemistry, 46, 1297 (1968)

I. Introduction

In order to describe, in any detail, the behavior of systems whose properties are materially influenced by the interfacial regions between phases, it is necessary to know a good deal concerning the properties of the interfacial regions themselves. Thus it is highly desirable to determine the distribution of energies, stresses, and the like in surface regions, as well as to determine the dependence of these properties on sizes of holes in condensed systems and upon sizes of drops, crystals, etc.

The dependence of surface energy on particle size has been studied both experimentally and theoretically by a number of investigators. Detailed statistical mechanical descriptions of surface regions, tensor analyses of the surface forces associated with intermolecular fields, distributions of Gibbs dividing surfaces, etc. appear in the scientific literature (1–12).

In general the rather extensive literature dealing with these subjects suggests that specific surface energies decrease somewhat with decreasing particle size. However, the views expressed are by no means in perfect agreement with one another. Even the definitions of the various surface quantities vary considerably. The relation between surface free energy and surface tension depends largely upon whether or not chemical potentials of surface and interior material are equal. Such questions are usually ignored.

In what follows we present some thermodynamic considerations of surface regions, a brief discussion of the Gibbs adsorption equation, some definitions of surface thermodynamic quantities, and the results of computer summations of Lennard–Jones (6–12) interaction potentials for some idealized systems together

[1]NRCC No. 9892.

Can. J. Chem. Downloaded from www.nrcresearchpress.com by 210.87.254.5 on 09/05/12
For personal use only.

with the corresponding surface energies and surface tensions.

Perhaps the main conclusions of this study are:

(1) Surface tension in the sense of a negative tangential surface stress is primarily a property of bulk systems. It is analogous to an osmotic pressure. Surface tension arises from the differences in Helmholtz potentials of surface and bulk regions when the extensive thermodynamic properties of surface and bulk regions are additive and their chemical potentials are equal. It is not primarily dependent on the range of the intermolecular forces.

(2) Specific surface energies of very small clusters of noble gas like atoms are only a little less than those of large clusters.

(3) The "surface tensions" of very small clusters (molecular dimensions) and holes are probably very much less than those of large clusters and holes.

II. Thermodynamic Equations for Surfaces

(1) Basic Notions

In deriving the thermodynamic condition for internal equilibrium of heterogeneous systems it is usually assumed that the energies, entropies, etc. of the various parts of a system are additive. If such a system is divided into small volumes by imaginary planes, each small volume has an energy, entropy, pv potential, etc. of its own, no energy, no entropy, no pv potential being shared between the various small volumes. In such systems the extensive variables behave as homogeneous functions of first degree in one another. It is usually assumed that we can write

$$[1] \qquad dE = TdS - pdv + \mu dm$$

as the condition that a system be in reversible equilibrium with the externally applied "forces", the temperature, T, the hydrostatic pressure, p, and the chemical potential, or "osmotic" forces, μ. Obviously the equation implies that the time average values of S, v, and m are definite quantities capable of practically infinitesimal variations.

If the energy behaves as a homogeneous function of first degree in S, v, and m between certain limits we can integrate eq. [1] between these limits and write for the increments,

$$[2] \qquad E = TS - pv + \mu m,$$

and rearranging,

$$[3] \qquad E - TS + pv = A + pv = G = \mu m,$$

where A is the Helmholtz free energy or Helmholtz potential and G the Gibbs potential of the system between the specified limits. Eq. [3] leads to the familiar equation

$$[4] \qquad d\mu = -S'dT + v'dp$$

where S' and v' are specific quantities.

If the system is supposed divided into n small volumes by imaginary planes, similar equations are supposed applicable to each small volume, and eq. [3] can be written

$$[5] \quad E - TS + pv = \sum^{n} (E_i - TS_i + pv_i)$$
$$= A + pv = \sum^{n} (A_i + pv_i)$$
$$= G = \sum^{n} G_i$$
$$= \mu m = \sum^{n} \mu m_i,$$

i.e. the potentials are additive. Each small volume of eq. [5] is regarded as being in reversible equilibrium with the "external forces" supplied by the material surrounding it.

The conditions for internal equilibrium with respect to any definable variations follow from

$$(dE)_{S,v,m} \geqslant 0, \quad (dA)_{T,v,m} \geqslant 0, \text{ etc.},$$

leading to T, p, and μ uniform [e.g. the potentials being additive we suppose the system divided into two parts and $A = A_1 + A_2$ and $dA = (\partial A_1/\partial v_1)dv_1 + (\partial A_2/\partial v_2)dv_2$, where $dv_1 + dv_2 = 0$; $dA = (-p_1 + p_2)dv_1 \geqslant 0$, where dv_1 is either + or −, therefore $p_1 = p_2$].

The integration of eq. [1] assumes that it is possible for the system to grow in extent from suitable sources of heat, work, and mass, the "intensive" variables T, p, and μ remaining constant during the growth process. While we write eq. [2] to describe the increments of the system concerned as it grows in extent, the process implies corresponding negative increments of the system or systems from which it grows. The net mechanical displacement work done in the process will be $pv - p_0v_0$, i.e. the work done by the system less the work done on the reference system from which it grows. By taking μ_0 for the reference system as zero, the equation describes the net value of δG for the process. This is practically equivalent to assigning various values of E, TS, pv, etc. to the body itself in some particular state.

If the system is subject to a change in position

Can. J. Chem. Downloaded from www.nrcresearchpress.com by 210.87.254.5 on 09/05/12
For personal use only.

in a scalar potential field in place of eq. [1], we must write

$$[6] \qquad dE = TdS - pdv + f_x dx + \mu dm,$$

where f_x is the force function of the field and x a corresponding positional coordinate.

Potentials such as

$$\int_{x_0}^{x}\left(\frac{\partial E}{\partial x}\right)_{S,v,m} dx, \quad \int_{x_0}^{x}\left(\frac{\partial A}{\partial x}\right)_{T,v,m} dx$$

are not properties of the system alone but are shared between the systems and the field (or the system "producing" the field).

We can write, with S, v, and m constant,

$$[7] \qquad E = E^0 + \int_{x_0}^{x} f_x dx,$$

where E^0 is the "intrinsic energy" with respect to a reference state at x_0 and E is the "total energy" at x. Similar equations can be written for A, G, etc. and eq. [4] becomes

$$[8] \qquad d\mu = -S'dT + v'dp + f_x' dx.$$

When $\partial S'/\partial x = \partial f_x'/\partial T = 0$,

the conditions for equilibrium between systems at x and at x_0 are

$$[9] \qquad T(x) - T(x_0) = 0$$

$$\mu(x) - \mu(x_0) = 0 = \int_{x_0}^{x}\left(v\frac{dp}{dx} + f_x\right)dx$$

but not

$$p(x) = p(x_0).$$

Both the total potentials and intrinsic potentials of systems at x and at x_0 can be additive when the field potential of the system at, say, x is independent of the presence or absence of the system at x_0. Under these latter circumstances we can suppose a system at any position x to grow in extent at constant x while its nature and state remain constant. Thus regarding the whole system as made up of "parts" having various values of x, the extensive variables of the whole system or any of its parts can behave as homogeneous functions of first degree in one another between relatively larger finite limits (e.g. a laboratory scale system in a gravitational field).

When, however, the various parts of the system exert mutual field forces upon one another, the field potential is shared between the various parts and the Helmholtz potentials of the parts are not independent of one another and are not additive. The extensive thermodynamic variables of such systems do not behave, in general, as homogeneous functions of first degree in one another, i.e. it will not always be possible for such systems to grow in extent by appreciable factors, while the intensive variables remain constant.

Since we may assume that mutual field forces exist in surface regions the applicability of eqs. [1] to [5], to surface regions may appear of doubtful validity. However, following Gibbs we can get over this difficulty very easily.

(2) Thermodynamics of Surface Layers

Let the wavy dotted line in Fig. 1 represent the "flat" non-uniform interfacial region between a liquid and its vapor.

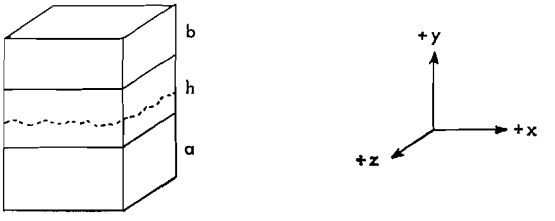

FIG. 1.

We can suppose planes drawn at a and $a + h$ parallel with the apparent position of the interfacial region. The planes are supposed drawn beyond the range of any surface forces so that the whole of the non-uniform region, where mutual field potentials exist, is contained within the two planes. The whole three-part system, the liquid, the non-uniform layer of thickness h, and the vapor, can grow in extent from a suitable reference state, while its nature and state remain constant provided that the growth is parallel with the surface. Since no mutual field forces pass the imaginary planes, the potentials of the three parts are additive. We can suppose the values of a, b, and h known. Accordingly we can consider the variations of the thermodynamic properties of the bulk phases known and we can subtract these variations from the "observed" variations of the whole system and obtain

$$[10] \qquad dE_h = TdS_h - p_T' dv_h + \mu dm_h$$

as a thermodynamic equation for the layer containing the surface region. (p_T' is the mean stress per unit cross-sectional area through the layer between the imaginary planes, i.e. p_T' is a mean principal stress, not a stress per unit area of

Can. J. Chem. Downloaded from www.nrcresearchpress.com by 210.87.254.5 on 09/05/12
For personal use only.

surface in the xz plane but in the yz plane if growth is in the $+x$ direction.)

The terms in eq. [10] refer unambiguously to the layer between the parallel planes containing the surface region. However, the observed values of these terms will depend upon the distance between the parallel planes that we choose to take, as well as upon the exact position of the very thin non-uniform real region of negative stress, i.e. the exact position of the real surface of tension within the parallel planes. Generally the exact position of this real non-uniform surface region will be very difficult if not impossible to determine. Hence the values of the various quantities in eq. [10] as determined by any particular experiment will be largely dependent on experimental details rather than on the thermodynamic properties of the real surface of tension; this will be the case even if the value of h, the distance between the planes, is taken as some standard fixed value. Accordingly it might appear that such thermodynamic equations for surfaces were of very little practical value.

One of the most important aspects of Gibbs treatment is that for multicomponent systems, especially two-component systems, exact equations can be obtained without knowing the position of the surface region. "We are therefore at liberty to choose such a position for the dividing surface as may for any purpose be convenient."

The term $p_T'\mathrm{d}v_h$ in eq. [10] represents the mechanical displacement work of virtual parallel growth of the layer between the imaginary parallel planes. Since the distance, h, between the parallel planes remains constant during growth, we can write $\mathrm{d}v_h = h\mathrm{d}\sigma$, where σ is the surface area. Putting $\gamma = -p_T'h$, γ is a positive tension when p_T' is negative. If the parallel planes had been placed at the limits of the uniform bulk phases so that h were the actual thickness of the non-uniform surface region, then γ would be the actual negative force per unit length (in the z direction for growth in the $+x$ direction) or the tension of the surface region. Accordingly, we shall *define* surface tension for flat surfaces by

$$[11] \qquad \gamma = -p_T h,$$

where h is the actual thickness of the non-uniform interfacial layer.[2]

Putting $p_T\mathrm{d}v_h = -\gamma\mathrm{d}\sigma$ in eq. [10], dropping subscripts, and supposing the system to contain a number of components, we can write

$$[12] \qquad \mathrm{d}E = T\mathrm{d}S + \gamma\mathrm{d}\sigma + \sum\mu_i\mathrm{d}m_i$$

as a fundamental thermodynamic equation for interfaces.

The corresponding increments for parallel growth in extent (cf. eq. [2]) are

$$[13]^2 \qquad E - TS - \gamma\sigma = A - \gamma\sigma = G = \sum\mu_i m_i.$$

The term $\gamma\sigma$ is wholly equivalent to the pv term of bulk systems under hydrostatic states of stress. Evidently the non-uniform interfacial layer can behave thermodynamically very much like a laboratory scale system in equilibrium with externally applied forces.

Equation [13] leads to

$$[14] \qquad \gamma = A/\sigma - \sum\Gamma_i\mu_i$$

and to the so-called Gibbs adsorption equation

$$[15]^3 \qquad (\mathrm{d}\gamma)_T = -\sum\Gamma_i\mathrm{d}\mu_i,$$

where Γ_i is the actual mass or number of moles of the ith component contained in unit area of the non-uniform surface region.

Since the thickness of the non-uniform surface region is not readily determined, and in many cases it will be difficult if not altogether impossible to separate experimentally the non-uniform surface region from the uniform bulk phases, the direct determination of the actual values of Γ_i may present some difficulties. However, there are many cases where it is not necessary to determine the actual values of Γ_i in order to use eq. [15]. There are a large number of other values of the surface "excess" masses, say Γ_i', which will satisfy eq. [15]. These alternative surface excesses depend upon the position chosen for the surface region in the real three-part system with respect to a reference system consisting of the two corresponding bulk phases. Some of these alternative "correct" surface excesses may admit of experimental determination much more readily than the actual values. This is the gist of Gibbs' statement concerning the choice of the position of the dividing surface.

Guggenheim and Adam (13) have given a very complete description of the various conventions that have been found convenient for determining the various permissible values of Γ_i', i.e. sets of

[2]Discussions of h, G for the surface layer, etc. appear in Appendix I.

[3]For a flat surface layer we should write $\Sigma m_i\,\mathrm{d}\mu_i = -S\mathrm{d}T - \sigma\mathrm{d}\gamma$, not $\Sigma m_i\,\mathrm{d}\mu_i = -S\mathrm{d}T + v\mathrm{d}p - \sigma\mathrm{d}\gamma$, since p and γ are not strictly independent variables. Thus $p = P(T,\mu_1,\mu_2\ldots)$ and for the interface between specified phases γ is determined by T,μ_1,μ_2, etc. For n possible phases there will be $n(n-1)/2$ possible flat interphases.

Can. J. Chem. Downloaded from www.nrcresearchpress.com by 210.87.254.5 on 09/05/12
For personal use only.

values of Γ_i' which satisfy $(d\gamma)_T = -\sum\Gamma_i'd\mu_i$. The importance of the difference between the ratios of the concentrations of components in the surface and bulk systems as well as our freedom with respect to the real values of Γ_i may be illustrated by considering a two-component liquid of relatively low vapor pressure. For any given volume of the bulk liquid we can write

$$M_1d\mu_1 + M_2d\mu_2 = vdp,$$

and for an equal volume of the corresponding vapor

$$M_1'd\mu_1 + M_2'd\mu_2 = vdp.$$

Hence after subtraction,

$$(M_1 - M_1')d\mu_1 + (M_2 - M_2')d\mu_2 = 0.$$

If the vapor pressure is low and M_1 and M_2 are at all comparable, $M_1 \gg M_1'$, $M_2 \gg M_2'$. Hence for variable values of μ_1 or μ_2

[16] $$M_1d\mu_1 + M_2d\mu_2 = 0$$

very nearly. (If p and T are constant a two-phase, two-component system is invariant and $d\mu_1 = d\mu_2 = 0$). For the corresponding liquid–vapor interface we can write

[17] $$m_1d\mu_1 + m_2d\mu_2 = -\sigma d\gamma.$$

If $M_2 = bM_1$ and $m_2 = sm_1$, it is easily shown that

$$m_1[b - s]d\mu_2 = \sigma d\gamma$$

or

$$\Gamma_1[b - s]d\mu_2 = d\gamma.$$

While b and $d\mu_2$ may be considered as known (e.g. $d\mu_2/dM_2$ for the bulk systems can be determined, etc.), s and m_1 or Γ_1 may be practically impossible to measure. Any sample of the surface region collected for analysis will certainly contain a large portion of bulk material. However, if we add eqs. [16] and [17] we obtain

$$(m_1 + M_1)d\mu_1 + (m_2 + M_2)d\mu_2 = -\sigma d\gamma.$$

If the quantity of liquid phase that is inadvertently included along with the surface region is $M_1 + M_2$ and if $M_1 + M_2 = x(m_1 + m_2)$ where x is unknown, we can write

$$m_1(x) = m_1 + M_1$$
$$= m_1[1 + x(1 + s)/(1 + b)], \text{ etc.}$$

Putting $m_2(x)/m_1(x) = s(x)$ it is easily shown that

$$m_1(x)[b - s(x)] = m_1[b - s].$$

Hence

$$m_1(x)[b - s(x)] = \sigma d\gamma/d\mu_2$$

or

[18] $$\Gamma_1'(x)[b - s(x)] = d\gamma/d\mu_2.$$

The terms $m_1(x)$ or $\Gamma_1'(x)$ and $s(x)$ are the observed values from the sample collected which consisted of the non-uniform surface region together with an unknown quantity of the bulk liquid phase. When $b < s(x)$ the second component "concentrates" in the surface region or is "adsorbed" by the surface and $d\gamma/d\mu_2$ is negative. When $b > s(x)$ the second component "concentrates" in the liquid phase or is repelled from, or negatively "adsorbed" by, the surface and $d\gamma/d\mu_2$ is positive.

Under the assumed experimental conditions x will be a large number and if b and s are not very different from one another in magnitude $s(x)$ will approach b very closely and $[b - s(x)]$ will approach zero. Hence the "experimentally observed" values of $d\gamma/d\mu_2$ will be subject to large errors. In the case of adsorption of a substance (say, the second component) on the surface of the first component where solution of the second in the first is practically nil, b can be taken as zero, and the relation between $d\gamma/d\mu_2$ and the quantity adsorbed can be calculated in a number of ways. Also experimental measurements of the quantities involved, the various Γ_i' values, are relatively easy. The adsorption of H_2O vapor on Hg was quoted by Gibbs to illustrate the general method. With some reservations the Gibbs adsorption equation can be applied at least as a first approximation to adsorption of gases on solids. However, in these cases we cannot measure the surface stress directly, nor can we distinguish between the surface stress and the stresses of the solid remote from the surface. In the case of solid adsorbents of large internal surface areas we cannot suppose the solid, the surface region, and, say, the gas separated from one another by imaginary planes so that the potentials of the three regions are additive. Hence we cannot give any very definite meaning to the pv or $\gamma\sigma$ potential of the surface layer as distinct from the solid and we cannot apply the Gibbs adsorption equation in any literal sense to these cases although this is often done.

(3) Curved Surfaces

When a surface layer completely envelopes one of the bulk phases or when the layer has an appreciable curvature the situation is somewhat

Can. J. Chem. Downloaded from www.nrcresearchpress.com by 210.87.254.5 on 09/05/12
For personal use only.

more complicated. When surface curvatures are appreciable and there is any real surface tension the tangential surface stresses will have components along the radii of curvature and vice versa, leading to a hydrostatic pressure difference across the surface layer. However, if the surface region can be separated from the bulk phases by imaginary curved surfaces so that the non-uniform surface region is contained wholly within the surface shell, the potentials of the two bulk phases and the surface shell will be additive and the system can be treated in much the same manner as systems with flat surface regions. The formal treatment is straightforward but the measurement of the pv potential of the surface shell as well as the definition of surface tension may present some difficulties. When we attempt to integrate $dE = TdS - p_T dv_s + \mu dm$, as applied to a spherical shell of volume v_s we must suppose the radius and thickness of the shell constant if the "nature and state" are to remain constant during growth. Thus we might write

$$[19] \qquad \delta v_s = (R^3 - R_1{}^3)\delta\omega/3$$

where ω is solid angle, R the outer radius of the shell, R_1 the inner radius, and $R - R_1 = h$, the thickness of the shell. We might also suppose a very large number, n, of shells and write

$$[20] \qquad \delta v_s = 4\pi(R^3 - R_1{}^3)\delta n/3$$

$$\delta v_1 = 4\pi R_1{}^3\delta n/3, \text{ etc.}$$

In any case, if the specific properties of the material in the surface shell of volume, v_s, differ from those of the material in the interior volume v_1 it is necessary that $\delta v/v = \delta v_1/v_1 = \delta v_s/v_s$ if the specific properties of the whole volume, v, are to remain constant during any finite growth. If p is the hydrostatic pressure exerted on the whole volume $v_1 + v_s$ or v, p_1 the hydrostatic pressure of the interior volume v_1, and p_s the effective surface stress of v_s when growth is consistent with constant specific properties, we can write

$$[21] \qquad p_1\delta v_1 + p_s\delta v_s = p\delta v,$$

where $p\delta v$ is the mechanical displacement work of finite growth in volume, mass, etc. of the whole system.

Since $\delta v_1/v_1 = \delta v_s/v_s = \delta v/v$ when the specific properties, "the nature, and state" of the whole system remain constant during growth, we can write

$$[22] \qquad p_1v_1 + p_sv_s = pv.$$

When $\delta v_1 = R_1{}^3\delta\omega/3$, etc. or when $\delta v_1 = 4\pi R_1{}^3\delta n/3$, etc., eq. [22] follows since these relations are consistent with $\delta v_1/v_1 = \delta v_s/v_s$, etc.

If the spherical system consists of a liquid drop (or drops) in equilibrium with its vapor, the thermodynamic properties of the surface layer (or layers) are largely controlled by the dense or liquid-like part of the surface(s). Accordingly it is convenient to compare p_s with the hydrostatic pressure of the normal liquid in the interior, i.e. with p_1. Hence we write

$$[23] \qquad p_s = p_1 + \bar{q}_3,$$

where $p_1 + \bar{q}_3$ represents the average of the surface stresses which yield the correct mechanical displacement work for spherical growth of the surface (the subscript indicates an average over the cube of the radius). Hence substituting this value for p_s in eq. [21] and the appropriate values of δv_1, δv_s, from eq. [19] or [20] we get

$$[24] \qquad p_1 - p = -\bar{q}_3(R^3 - R_1{}^3)/R^3,$$

and putting $R_1 = \eta R$,

$$[25] \qquad p_1 - p = -\bar{q}_3(1 - \eta^3).$$

If, however, we balance forces acting perpendicularly on a plane through the center of the spheres[4] we would have

$$[26] \qquad p_1R_1{}^2 + p_s'(R^2 - R_1{}^2) = pR^2.$$

While we might compare p_s' with p_1 as we did with p_s it seems more convenient to compare p_s' with the external pressure p. Hence we write $p_s' = p + \bar{q}_2$ (the subscript indicates an average over the square of the radius) which leads to

$$[27] \qquad p_1 - p = -\bar{q}_2(1 - \eta^2)/\eta^2$$

and to

$$[28] \qquad \bar{q}_3 = \bar{q}_2(1 + \eta)/(1 + \eta + \eta^2)\eta^2$$

It is worth noting that the p_s' from balancing forces acting perpendicularly on a plane through the center of the sphere is the same as the p_s' for finite cylindrical growth, i.e. for $\delta v_1 = \pi R_1{}^2\delta z$, $\delta v_s = \pi(R^2 - R_1{}^2)\delta z$, etc., where z is a distance along the normal to the area πR^2. Also p_s' is the same as the p_s in the virtual surface stretching

[4]This is analogous to following Maxwell (14) and writing $dp/dR = 2(q - p)/R$ as a condition that the tangential stress forces q and the radial stress forces p balance. In our case, however, the surface forces arise largely from mutual field potentials and although the tangential forces act largely as stress forces, the radial forces are a combination of stress and field forces.

Can. J. Chem. Downloaded from www.nrcresearchpress.com by 210.87.254.5 on 09/05/12
For personal use only.

work at constant thickness, h, where $R = R_1 + h$, i.e. for the virtual process

$$[29] \quad p_1(\partial v_1/\partial R_1)\mathrm{d}R_1 + p_s(\partial v_s/\partial R_1)_h \mathrm{d}R_1 = p(\partial v/\partial R_1)_h \mathrm{d}R_1$$

The spherical growth, cylindrical growth, and virtual stretching are, of course, different processes. In the "stretching" process (eq. [29]) $\mathrm{d}\sigma/\mathrm{d}v = 2\sigma/3v$ whereas for both spherical and cylindrical growth processes $\mathrm{d}\sigma/\mathrm{d}v = \delta\sigma/\delta v$. Again, $\mathrm{d}\sigma/\mathrm{d}v = 2/R$ for both "stretching" and cylindrical growth, while for the spherical growth process $\mathrm{d}\sigma/\mathrm{d}v = 3/R$ (σ is the surface area of v in each case).

The quantities p_s and p_s' are "tangential" stresses, mechanical forces per unit cross sectional area of the surface shell. Surface tension is a force per unit length. When the inner and outer lengths of the perimeters of the surface shell are appreciably different from one another, the question arises as to what length is the most suitable one to correlate with surface tension.

If we think of the surface tension as measuring the net surface stress perpendicular to the radius as in "balancing forces" or in a virtual stretching process then γ will be directly related to p_s' by an equation of the form $\gamma L = -p_s'\pi(R^2 - R_1^2)$, where L is a length. If we write $\pi(R^2 - R_1^2) = \sum L_i\delta h_i = \bar{L}h$ where $\sum\delta h_i = R - R_1 = h$, then $\bar{L} = \pi(R + R_1)$. If p_i is independent of L_i i.e. dependent only on the distance along the radius, then $\sum p_i L_i \delta h_i = \bar{p}\,\bar{L}h = \bar{p}\,\pi(R + R_1)h$ and putting $\bar{p}h = -\gamma$, $\gamma\pi(R + R_1) = -p_s'\pi(R^2 - R_1^2)$. Hence for the spherical shell we shall define γ by

$$[30] \quad \gamma(R + R_1) = -p_s'(R^2 - R_1^2),$$

which is consistent with our definition of γ for flat surfaces. This definition leads to

$$[31] \quad \gamma = -(p + \bar{q}_2)\,R(1 - \eta)$$

and to

$$[32] \quad p_1 - p = \gamma(1 + \eta)/R\eta^2 + p(1 - \eta^2)/\eta^2;$$

when $\eta \to 1$, eq. [32] leads to the familiar relations $p_1 - p = 2\gamma/R$, $(p_1 - p)v = \frac{2}{3}\gamma\sigma$. Note that for a flat surface the pv displacement potential is $-\gamma\sigma$ whereas the pv potential for a spherical surface is only $-\frac{2}{3}\gamma\sigma$. This seemingly paradoxical result is another way of saying that a flat surface of tension will do work amounting to $\frac{1}{3}\gamma\sigma$ on external bodies if allowed to form, reversibly, a spherical surface of the same area and tension. Or as Gibbs puts it "the work [done on the system in forming the spherical mass] consists of two parts of which one is always positive, and is expressed by the product of the superficial tension and the area of the surface of tension, and the other is always negative, and is numerically equal to the product of the difference of pressure by the volume of the interior mass".

The relation between the "pv" potential for a flat and a spherical surface does not depend directly on the definitions of eqs. [23] and [30] but follows from any definition of γ for which $p_1 - p = 2\gamma/R$ together with $p_1v_1 + p_sv_s = pv$, where v_1 and v are concentric spherical volumes of very nearly equal magnitudes.

If a system containing an interface or surface layer were to grow in extent not spherically but in some other way the "pv" potential of the surface layer would be different, e.g. for cylindrical growth the pv potential is $-\gamma\sigma$ as for flat growths. In any system which is not isotropic and where the Helmholtz potentials of the parts are not the same, the Helmholtz potentials, the pv potentials, etc. will depend on how the growth, from suitable sources, is to take place.

The treatment of the surface of a spherical hole in a liquid is much the same as that given above, except that the hydrostatic pressure of the liquid is now the "external" pressure of the system containing the spherical surface.

When the surface region between a solid and its vapor (or any other bulk phase) can be separated by imaginary planes so that the potentials of the three regions are additive, the above relations are equally applicable provided that the intensive variables applicable to the bulk states are limited to T, p, and μ.

In the case of a liquid–vapor interface we can easily measure the surface tension directly by balancing forces. Also, if the system has only a single component, we can reversibly convert bulk liquid to surface system and measure the difference of the pv works concerned. But in the case of a solid there is no very direct way of distinguishing between surface stress and bulk solid stresses, i.e. there is no unambiguous method of measuring surface tension directly.

However, the energy of solid powders can often be measured as a function of surface area, the Helmholtz potential per unit area inferred, and an ideal surface tension of the particles calculated assuming eqs. [3], [13], etc. or equivalent equations.

Can. J. Chem. Downloaded from www.nrcresearchpress.com by 210.87.254.5 on 09/05/12
For personal use only.

(4) Surface Free Energy

"Surface free energy" has been defined as the excess Helmholtz potential of small drops or crystals, compared with equal masses of bulk material, the excess being expressed per unit surface area. For a spherical mass this quantity may be defined by

$$[33] \qquad A^s = AN(\bar{f}\,' - 1)/4\pi R^2,$$

where A is the Helmholtz potential per molecule of bulk material; $A\bar{f}'$ the Helmholtz potential per molecule of the N molecules in the spherical cluster of radius R. Usually $\bar{f}\,' > 1$.

If the entropies of surface and bulk material are the same, or if the temperature is low so that TS is small, A is practically the same as energy so that the "surface free energy" becomes "surface energy". The surface energy can be measured fairly easily.

Writing ε_0 as the sublimation energy, per molecule, of condensed material (i.e. the difference between the Helmholtz potentials of the gas and bulk material) we can write

$$[34] \qquad E^s = \varepsilon_0 N(1 - \bar{f})/4\pi R^2,$$

where $\bar{f} < 1$, and $\varepsilon_0\bar{f}$ is the sublimation energy per molecule of the cluster.[5]

In the case of a "hole" in condensed material, E^s is also given by eq. [34], but N is the number of atoms or molecules removed to form the hole and $N\varepsilon_0\bar{f}$ the sublimation energy of a cluster of N atoms. R is the radius of the "hole" and of the cluster of the N atoms removed.

The relation between A^s and the surface tension as defined by eqs. [30] and [32] is readily obtained, assuming the ideal conditions underlying the derivation of the thermodynamic equation for surfaces eqs. [12], [13], etc.

For spherical drops or clusters we assume $p_1v_1 + p_sv_s = pv$ as before. For equilibrium with respect to diffusive interchange the chemical potential of the surface and interior are equal. Hence, for a one component system we can write

$$[35] \qquad \mu = p_1/\rho_1 + A\bar{f}_1'/m = p_s/\rho_s + A\bar{f}_s'/m,$$

where ρ_1 and ρ_s are the densities of the interior and surface volumes respectively; $A\bar{f}_1'$ and $A\bar{f}_s'$ are the Helmholtz potentials per molecule and m the mass of the molecule. Since p_s is taken as $p_1 + \bar{q}_3$, we get

$$[36] \qquad \bar{q}_3 = 3AN(\bar{f}_1' - \bar{f}')/4\pi R^3(1 - \eta^3) + p_1(\rho_s - \rho_1)/\rho_1,$$

where $\bar{f}' = (N_s\bar{f}_s' + N_1\bar{f}_1')/(N_s + N_1)$ and $N_s + N_1 = N$.

When $\rho_s \to \rho_1$, we get for drops

$$[37] \qquad \gamma = \frac{3\eta^2}{1+\eta}\,\frac{\bar{f}_1 - \bar{f}}{1 - \bar{f}}\,E^s - pR(1 - \eta).$$

For "holes" in a condensed system

$$[38] \qquad \gamma = \frac{3\eta}{1+\eta}\,\frac{N_s\varepsilon_0(\bar{f}_0 - \bar{f}_s)}{4\pi R_1^2} - p\,\frac{R_1(1-\eta)}{\eta},$$

where R_1 is the radius of the hole and $R_1 = \eta R$, where R is the outer radius of the shell. $\varepsilon_0\bar{f}_0$ is the sublimation energy of the material just beyond the outer radius of the shell. If the hole is a hole in a very large bulk system, $\bar{f}_0 = 1$, and we can write

$$[39] \qquad \gamma = \frac{3\eta}{1+\eta}\,E^s - pR_1\,\frac{(1-\eta)}{\eta}.$$

For large drops and large holes $\eta \to 1$ and $\gamma = \frac{3}{2}A^s = \frac{3}{2}E^s$. The displacement work potential, the pv potential, for spherical growth of the shell is $\frac{2}{3}\gamma\sigma = E^s\sigma$.

If we can calculate the values of the sublimation energies of interior and surface atoms as well as the thickness $(R - R_1)$ of the surface region we can calculate E^s and the ideal γ from the above equations. Also if the relative values of the energies change with curvature we can estimate the effect of curvature on surface tension.

In Part III of this paper we shall assume that the difference in sublimation energies or self-potentials of molecules in various regions of face-centered cubic close-packed arrays, as calculated by pair-wise additive summation of the 6–12 Lennard–Jones potentials without relaxation effects, will correspond, approximately, to differences in Helmholtz potentials of such regions in real systems, when the real systems are close-packed Van der Waals' type crystals or dense liquids of very low vapor pressure.

III. Geometry, Surface Energies, and Surface Tensions for Face-Centered Cubic Arrays

The following is an outline of the methods used in calculating the self-potentials or sublima-

[5]The primed and unprimed factors in eqs. [33] and [34] are related by the expression

$$(\bar{f}' - 1)A = \varepsilon_0(1 - \bar{f}).$$

A similar relation holds between $\bar{f}_1'$ and $\bar{f}_1$ used in subsequent equations.

Can. J. Chem. Downloaded from www.nrcresearchpress.com by 210.87.254.5 on 09/05/12
For personal use only.

tion energies of 'noble gas atoms' in various face-centered clusters of atoms.

(i) Geometry of the Face-Centered Cubic Array

Let $\mathbf{i}_1$, $\mathbf{i}_2$, $\mathbf{i}_3$ be unit vectors defining a set of orthogonal Cartesian axes. The sites of a simple cubic lattice with lattice parameter a are located by the vectors

$$[40] \qquad \mathbf{r}_l = a(l_1\mathbf{i}_1 + l_2\mathbf{i}_2 + l_3\mathbf{i}_3),$$

where l_1, l_2, l_3 take integral values, positive, negative, or zero. It is convenient to use a as a unit and to define a reduced lattice vector

$$[41] \qquad \mathbf{L} = l_1\mathbf{i}_1 + l_2\mathbf{i}_2 + l_3\mathbf{i}_3$$

so that $\mathbf{r}_l = a\mathbf{L}$. Hence,

$$[42] \qquad \mathbf{L}\cdot\mathbf{L} = L^2 = l_1^2 + l_2^2 + l_3^2.$$

A face-centered cubic structure can be derived from the simple cubic structure by restricting the positions of the atoms to lattice sites of even parity, i.e. the sum $l_1 + l_2 + l_3$ is an even whole number. The nearest neighbor distance in the face-centered cubic array is $a\sqrt{2}$ where 'a' is the cube edge of the simple cubic lattice from which it is derived.

(ii) Interaction Energies

It is assumed that the condensation energy or self-potential of a cluster of atoms is the sum of the Lennard–Jones (6–12) interaction energies of all pairs of atoms in the cluster. Thus the energy of interaction between a pair of atoms at lattice points i and j separated by the distance r_{ij} can be represented by

$$[43] \qquad u_{ij} = -\alpha r_{ij}^{-6} + \beta r_{ij}^{-12}.$$

The two parameters α and β can be adjusted to fit two experimental values, the heat of sublimation and the lattice spacing of large (infinite) clusters.

The lattice energy per atom of a 'large' cluster (containing N atoms) is

$$[44] \qquad \Phi(a) = \lim_{N\to\infty}\left[\frac{1}{2N}\sum_i \sum_{\substack{j \\ \text{all atoms}}}{}' u_{ij}\right],$$

where the prime indicates omission of terms $i = j$. In the limit $N \to \infty$, $\sum_j' u_{ij}$ is the same for all atoms i, hence

$$[45] \qquad \Phi(a) = \frac{1}{2}\sum_{\substack{l_1+l_2+l_3 \\ \text{even}}}^{\infty}{}' [-\alpha a^{-6}L^{-6} + \beta a^{-12}L^{-12}].$$

Jones and Ingham (15) have tabulated the sums

$$[46] \qquad A_n'' = \sum_{\substack{l_1+l_2+l_3 \\ \text{even}}}^{\infty}{}' L^{-n}$$

and inserting these values

$$[47] \qquad \Phi(a) = \tfrac{1}{2}[-\alpha a^{-6}A_6'' + \beta a^{-12}A_{12}''],$$

where $A_6'' = 1.80674$ and $A_{12}'' = 0.18956$.

If 'a_0' is the equilibrium value of 'a' for the large (infinite) cluster and ε_0 the sublimation energy per atom, then the constants α and β are given by

$$[48] \qquad \alpha = \frac{4\varepsilon_0 a_0^{\,6}}{A_6''}, \qquad \beta = \frac{2\varepsilon_0 a_0^{\,12}}{A_{12}''}$$

The self-potential of an atom in the 'infinite' cluster or crystal is the energy of interaction of one atom in the cluster with all others (i.e. $\sum_j' u_{ij}$ for i fixed) and is equal to $-2\varepsilon_0$.

(iii) Shells of Atoms

The 'primary' atom of shell s will be defined as that atom which occupies the lattice site located by the reduced lattice vector

$$[49] \qquad \mathbf{P}^{(s)} = p_1^{(s)}\mathbf{i}_1 + p_2^{(s)}\mathbf{i}_2 + p_3^{(s)}\mathbf{i}_3,$$

where

$$p_1^{(s)} \geqslant p_2^{(s)} \geqslant p_3^{(s)} \geqslant 0,$$

and

$$p_1^{(s)} + p_2^{(s)} + p_3^{(s)}, \text{ even.}$$

The sites of the other atoms of shell s are located by the vectors

$$[50] \qquad \mathbf{Q}_j^{(s)} = q_{j1}^{(s)}\,\mathbf{i}_1 + q_{j2}^{(s)}\,\mathbf{i}_2 + q_{j3}^{(s)}\,\mathbf{i}_3,$$

where the set of integers

$$(q_{j1}^{(s)},\ q_{j2}^{(s)},\ q_{j3}^{(s)})$$

is derived from $(p_1^{(s)}, p_2^{(s)}, p_3^{(s)})$ by permutation of the $p_1^{(s)}$, $p_2^{(s)}$, $p_3^{(s)}$ or by changes of sign.

The number of atoms in shell s will be indicated by $\nu^{(s)}$ which can have values 1, 6, 8, 12, 24, or 48 depending on the particular set $\mathbf{P}^{(s)}$. Thus for example, if $p_1^{(s)} > p_2^{(s)} > p_3^{(s)} > 0$ then $\nu^{(s)} = 3!\cdot 2^3 = 48$.

The atoms of a shell as defined above are all at the same distance from the origin, i.e. $(\text{distance})^2 = a^2[P^{(s)}]^2$. By convention the shells are numbered consecutively, 0, 1, 2,....., corresponding to the increasing magnitudes of $[P^{(s)}]^2$ starting with the atom at the origin which forms shell 0. It is possible for two shells s and s' to have the same value of $[P^{(s)}]^2$ and in this case s is taken as less than s', when $p_1^{(s)} < p_1^{(s')}$ or if $p_1^{(s)} = p_1^{(s')}$ when $p_2^{(s)} < p_2^{(s')}$.

Can. J. Chem. Downloaded from www.nrcresearchpress.com by 210.87.254.5 on 09/05/12
For personal use only.

TABLE I*

ϕ_k^s

	k									
s	0	1	2	3	4	5	10	20	30	40
0	0.0000000	0.6713164	0.7673669	0.8876495	0.9133525	0.9397931	0.9726812	0.9892426	0.9934387	0.9954249
1	0.9440569	0.3339210	0.4580340	0.7497330	0.8297271	0.8936675	0.9620766	0.9872368	0.9925860	0.9949655
2	0.9839915	0.7357655	0.2730720	0.5409187	0.6080608	0.8404719	0.9468212	0.9844684	0.9915120	0.9944415
3	0.9949882	0.8491387	0.7821770	0.3811226	0.5016384	0.6410883	0.9173493	0.9814996	0.9904060	0.9938424
4	0.9978580	0.9178640	0.8842929	0.6432613	0.3662001	0.5027094	0.8723212	0.9775316	0.9889906	0.9931675
5	0.9988983	0.9669280	0.9088253	0.7693753	0.7011207	0.4317572	0.8083090	0.9702005	0.9868608	0.9923625
10	0.9998103	0.9959670	0.9904298	0.9655269	0.9542911	0.8307548	0.4092896	0.9048724	0.9733028	0.9876051
20	0.9999762	0.9995951	0.9993786	0.9978859	0.9968718	0.9952708	0.9698806	0.4159584	0.8199668	0.9435382
30	0.9999911	0.9998603	0.9997844	0.9993870	0.9990948	0.9985587	0.9928823	0.8602162	0.4043269	0.8043834
40	0.9999957	0.9999369	0.9998980	0.9997429	0.9996580	0.9993530	0.9976178	0.9867161	0.9341365	0.3397991

*Entries lying above or on the diagonal of the table were calculated from eq. [61]; those below the diagonal were obtained from eq. [59].

Can. J. Chem. Downloaded from www.nrcresearchpress.com by 210.87.254.5 on 09/05/12
For personal use only.

Although each shell possesses a center of symmetry, the shells are far from resembling a set of uniform superficial distributions of atoms. The number of atoms in these shells does not increase necessarily as the cluster gets larger and the number of atoms in the 'outermost shell' of a large more or less spherical cluster will be very much less than the effective number of 'surface' atoms. Thus, for example, a cluster comprising shells 0 to 25 contains 603 atoms of which only 48 atoms are in shell 25. However, the 306 atoms of shells 15 to 25 are all within about one nearest neighbor distance of the surface.

(iv) Shell Sums

It is convenient to define shell sums $v_n^{(st)}$ as follows.

$$[51]\quad v_n^{(st)} = \sum_j \left| \boldsymbol{P}^{(s)} - \boldsymbol{Q}_j^{(t)} \right|^{-n}, \; t \neq s$$
$$= \sum_j [(p_1^{(s)} - q_{j1}^{(t)})^2 + (p_2^{(s)} - q_{j2}^{(t)})^2 + (p_3^{(s)} - q_{j3}^{(t)})^2]^{-n/2},$$

where $\sum_j$ indicates a sum over all the $\nu^{(t)}$ atoms of shell t. In the special case $t = s$, we define

$$[52]\quad v_n^{(ss)} = \sum_j{}' \, |\boldsymbol{P}^{(s)} - \boldsymbol{Q}^{(s)}|^{-n},$$

where the prime indicates that the term $|\boldsymbol{P}^{(s)} - \boldsymbol{P}^{(s)}|^{-n}$ must be omitted from the summation.

By considering a very large cluster it can be shown that

$$[53]\quad \sum_t^{\infty}{}_0 \, v_n^{(st)} = A_n''.$$

(v) Energy of Clusters

A cluster of atoms formed by shells 0, 1, 2,.....k will be called a cluster of size $\nu(k)$, where $\nu(k)$ is the number of atoms in the cluster. Evidently

$$[54]\quad \nu(k) = \sum_j^k{}_0 \, \nu^{(s)}.$$

Using eqs. [43], [48], [51], and [52] the total energy of interaction of all of the atoms in the cluster can be expressed as

$$[55]\quad E_k = (-2\varepsilon_0) \sum_s^k{}_0 \nu^{(s)} \Big[\sum_t^{s-1}{}_0 \{ (2/A_6'') \times v_6^{(st)} - (1/A_{12}'') v_{12}^{(st)} \} + \tfrac{1}{2} \{ (2/A_6'') v_6^{(ss)} - (1/A_{12}'') v_{12}^{(ss)} \} \Big].$$

Note that $E_0 = 0$, since by definition $v_n^{(00)}$ vanishes.

The average energy of interaction per atom in the cluster is

$$[56]\quad \bar{E}_k = E_k/\nu(k).$$

For a large cluster it follows that

$$[57]\quad \bar{E}_\infty = \Phi(a_0) = -\varepsilon_0$$

(vi) Distribution of Energies of Shells in Clusters and Near Holes

Suppose we have a hole A in a very large cluster, the hole being formed by removal of atoms in shells 0, 1, 2,..k. The remaining part of the cluster $k + 1$, $k + 2$, . . . ∞ is called B. We wish to calculate the self-potential of an atom at site P in B assuming that the lattice is not distorted. Because of the symmetry we can restrict our consideration to 'primary' atoms in B.

The self-potential of the atom at $\boldsymbol{P}^{(s)}$, when $k + 1 < s < \infty$ and $\nu(k)$ atoms are removed to form the hole, is given by

$$[58]\quad U_k^{(s)} = -\alpha a_0^{-6} \sum_t^{\infty}{}_{k+1} v_6^{(st)} + \beta a_0^{-12} \sum_t^{\infty}{}_{k+1} v_{12}^{(st)}.$$

Defining

$$[59]\quad \phi_k{}^s = 1 - (2/A_6'') \sum_t^k{}_0 v_6^{(st)} + (1/A_{12}'') \sum_t^k{}_0 v_{12}^{(st)}$$

for $s > k$, it can be shown with the aid of eq. [53] that

$$[60]\quad U_k^{(s)} = -2\varepsilon_0 \phi_k{}^s.$$

This same expression can also be used to calculate the self-potential of an atom of shell s in a finite cluster consisting of shells 0, 1, 2,.....k, provided that the definition of $\phi_k{}^s$ for $s \leqslant k$ is taken to be

$$[61]\quad \phi_k{}^s = (2/A_6'') \sum_t^k{}_0 v_6^{(st)} - (1/A_{12}'') \sum_t^k{}_0 v_{12}^{(st)}.$$

Values of $\phi_k{}^s$ were calculated from eqs. [59] and [61] for s and k ranging from 0 to 49. From these results the distribution of energies in the various 'shells' in clusters and in the 'shells' of material surrounding holes can be determined. An abridged set of values of $\phi_k{}^s$ is given in Table I.[6]

[6] A table of the complete set of values calculated for $\phi_k{}^s$ has been placed in the Depository. Photocopies of the deposited material may be obtained upon request to: The Depository of Unpublished Data, National Science Library, National Research Council of Canada, Ottawa, Canada.

Can. J. Chem. Downloaded from www.nrcresearchpress.com by 210.87.254.5 on 09/05/12
For personal use only.

(vii) Radius and Surface Area of Clusters

The apparent radius and surface area of a cluster of a few 'shells' are necessarily rather vague quantities. However, when the number of shells becomes very large the clusters approach spheres having reasonably definite radii and surface areas.

The radius R_k of a cluster comprising shells $0, \ldots k$ (i.e. containing $\nu(k)$ atoms) is defined by the equation

$$[62] \qquad (4/3)\pi R_k^3 = 2a_0^3\nu(k).$$

The corresponding surface area of the cluster is

$$[63] \qquad \sigma_k = 4\pi R_k^2.$$

(viii) Surface Energy and Surface Tension

From Part II it follows that the specific surface energy of a cluster of $\nu(k)$ atoms is the excess of the energy of the cluster over that of the same number of atoms in a large crystal and expressed per unit area of the cluster. Thus in the notation outlined above

$$[64] \qquad E^s = (\bar{E}_k - \bar{E}_\infty)\nu(k)/\sigma_k$$

or

$$[65] \qquad E^s a_0^2/\varepsilon_0 = \frac{[1 - (\bar{E}_k/\bar{E}_\infty)]\nu(k)}{4\pi(R_k/a_0)^2}.$$

By comparison of eqs. [34] and [65] we see that

$$\bar{f} = \bar{E}_k/\bar{E}_\infty.$$

The value of $E^s a_0^2/\varepsilon_0$ for a hole corresponding to $\nu(k)$ missing atoms in an infinite cluster is the same as that for a cluster of $\nu(k)$ atoms.

Calculations of the surface energy from eq. [65] are summarized in Table II for clusters with up to 50 shells. It may be noted that the values of $E^s a_0^2/\varepsilon_0$ fluctuate as increasingly larger clusters are considered, but appear to be approaching a value somewhat larger than 0.2345 estimated (16) for the {110} face of a large undistorted crystal.

We shall write $\gamma_{k_1/k}$ as the apparent surface tension of the surface layer of a cluster formed from shells 0 to k of which shells 0 to k_1 constitute the central core and the remaining $k - k_1$ shells the surface layer. Dropping the negligibly small pressure term in eq. [37], the value of the surface tension is given by

$$[67] \qquad \gamma_{k_1/k}\frac{a_0^2}{\varepsilon_0} = \frac{3\eta^2}{1+\eta}\frac{\bar{f}_1 - \bar{f}}{1 - \bar{f}}E^s\frac{a_0^2}{\varepsilon_0},$$

TABLE II

k	$\nu^{(k)}$	$\nu(k)$	$R_k/a_0\sqrt{2}$	$\bar{f}$	$E^s(a_0^2/\varepsilon_0)$
0	1	1	0.5527	0.0	0.13027
1	12	13	1.2995	0.35987	0.19607
2	6	19	1.4747	0.41591	0.20303
3	24	43	1.9362	0.51807	0.21994
4	12	55	2.1018	0.56277	0.21660
5	24	79	2.3714	0.61376	0.21589
6	8	87	2.4489	0.60944	0.22544
7	48	135	2.8352	0.66605	0.22316
8	6	141	2.8765	0.66556	0.22675
9	12	153	2.9559	0.67190	0.22860
10	24	177	3.1031	0.68704	0.22890
11	24	201	3.2374	0.70992	0.22135
12	24	225	3.3614	0.70851	0.23095
13	24	249	3.4770	0.71726	0.23171
14	48	297	3.6874	0.73857	0.22722
15	24	321	3.7841	0.74301	0.22922
16	48	369	3.9641	0.75798	0.22613
17	12	381	4.0066	0.75917	0.22743
18	24	405	4.0890	0.75578	0.23538
19	24	429	4.1682	0.76350	0.23235
20	24	453	4.2445	0.76688	0.23323
21	6	459	4.2632	0.76562	0.23551
22	48	507	4.4069	0.77609	0.23258
23	24	531	4.4754	0.77792	0.23426
24	24	555	4.5418	0.78386	0.23139
25	48	603	4.6692	0.79076	0.23027
26	24	627	4.7303	0.79240	0.23147
27	48	675	4.8480	0.80165	0.22666
28	8	683	4.8671	0.79930	0.23025
29	48	731	4.9786	0.80128	0.23319
30	12	743	5.0057	0.80140	0.23432
31	24	767	5.0590	0.80141	0.23680
32	24	791	5.1112	0.80440	0.23565
33	24	815	5.1624	0.80532	0.23689
34	24	839	5.2126	0.80628	0.23801
35	48	887	5.3101	0.81067	0.23697
36	48	935	5.4043	0.81795	0.23189
37	24	959	5.4501	0.82058	0.23048
38	48	1007	5.5396	0.82304	0.23105
39	48	1055	5.6262	0.82630	0.23035
40	6	1061	5.6369	0.82547	0.23189
41	24	1085	5.6790	0.82300	0.23693
42	48	1133	5.7616	0.82744	0.23434
43	24	1157	5.8020	0.82741	0.23603
44	24	1181	5.8418	0.82765	0.23732
45	24	1205	5.8811	0.82989	0.23581
46	48	1253	5.9582	0.83274	0.23490
47	12	1265	5.9772	0.83253	0.23594
48	24	1289	6.0147	0.83265	0.23725
49	48	1337	6.0885	0.83490	0.23693

where

$$[68] \qquad \eta = R_{k_1}/R_k$$

and

$$[69] \qquad \bar{f}_1 = (1/\nu(k_1))\sum_{i\,0}^{k_1}\nu^{(i)}\phi_k{}^i.$$

Note that $\varepsilon_0\bar{f}_1$ is the mean energy of sublimation of atoms in the core.

According to the above definitions $\gamma_{0/1}$ is the apparent surface tension of the outer layer (12

Can. J. Chem. Downloaded from www.nrcresearchpress.com by 210.87.254.5 on 09/05/12
For personal use only.

TABLE III

k_1	R_{k_1}/R_{49}	$\phi_{49}{}^{k_1}$,	$\bar{f}_1$	$\gamma_{k_1/49}(a_0{}^2/\varepsilon_0)$
0	0.09077	0.99636	0.99636	0.00525
1	0.21344	0.99604	0.99607	0.02605
2	0.24222	0.99569	0.99595	0.03275
3	0.31801	0.99531	0.99559	0.05308
4	0.34521	0.99486	0.99543	0.06122
5	0.38949	0.99435	0.99510	0.07530
6	0.40222	0.99386	0.99499	0.07952
7	0.46566	0.99318	0.99434	0.10155
8	0.47246	0.99237	0.99426	0.10400
9	0.48550	0.99150	0.99404	0.10871
10	0.50966	0.99152	0.99370	0.11763
11	0.53173	0.99046	0.99332	0.12589
12	0.55210	0.98985	0.99295	0.13363
13	0.57107	0.98844	0.99251	0.14085
14	0.60563	0.98650	0.99154	0.15405
15	0.62152	0.98641	0.99116	0.16026
16	0.65108	0.98218	0.98999	0.17142
17	0.65806	0.97885	0.98964	0.17399
18	0.67160	0.97979	0.98905	0.17907
19	0.68461	0.97482	0.98826	0.18369
20	0.69714	0.97456	0.98753	0.18818
21	0.70021	0.97357	0.98735	0.18926
22	0.72381	0.97056	0.98576	0.19739
23	0.73506	0.96800	0.98496	0.20118
24	0.74597	0.95797	0.98379	0.20430
25	0.76688	0.95055	0.98114	0.20957
26	0.77692	0.94685	0.97983	0.21195
27	0.79626	0.92338	0.97582	0.21414
28	0.79940	0.94247	0.97543	0.21486
29	0.81770	0.92935	0.97240	0.21775
30	0.82215	0.89003	0.97107	0.21747
31	0.83091	0.90689	0.96906	0.21780
32	0.83949	0.83934	0.96513	0.21479
33	0.84789	0.83453	0.96128	0.21168
34	0.85614	0.89597	0.95941	0.21168
35	0.87216	0.83369	0.95261	0.20590
36	0.88762	0.82024	0.94581	0.19930
37	0.89515	0.70412	0.93977	0.19088
38	0.90984	0.63410	0.92519	0.16849
39	0.92407	0.68955	0.91447	0.15204
40	0.92582	0.63882	0.91291	0.14949
41	0.93275	0.67335	0.90762	0.14092
42	0.94631	0.51497	0.89098	0.11108
43	0.95294	0.60405	0.88503	0.10035
44	0.95949	0.65892	0.88043	0.09210
45	0.96594	0.50657	0.87299	0.07782
46	0.97860	0.54707	0.86050	0.05335
47	0.98172	0.40760	0.85621	0.04461
48	0.98789	0.43007	0.84827	0.02826
49	1.00000	0.47585	0.83490	0.00000

atoms) in a cluster of 13 atoms. In this case $\eta = 0.5527/1.2995$, as may be seen from Table II. Thus $\gamma_{0/1} = 0.1852E^s = 0.036\varepsilon_0/a_0{}^2$.

Table III summarizes calculations of some values of $\gamma_{k_1/49}$. These show the effect of varying the core size on the estimation of the surface tension of a cluster containing 1337 atoms.

In the case of 'holes' we write $\gamma_{k_1/k_2/k}$ to indicate the surface tension of the surface layer made up of shells $k_1 + 1$ to k_2 about a hole formed by removing shells 0 to k_1 from a cluster originally containing $k + 1$ shells (the surface layer being compared with the outer shells $k_2 + 1$ to k). Calculation of $\gamma_{k_1/k_2/k}$ is analogous to that of $\gamma_{k_1/k}$ but uses eq. [38] in place of eq. [37]. Some results obtained in this way for holes in a very large cluster are

$$[70] \qquad \gamma_{0/1/\infty} = 0.0783\ \varepsilon_0/a_0{}^2$$

$$\gamma_{40/49/\infty} = 0.1680\ \varepsilon_0/a_0{}^2.$$

All of the clusters or holes considered are small compared with bulk systems, consequently the thickness of the "non-uniform" region is somewhat arbitrary. The values of γ obtained in the above estimates depend on the thickness assumed for the surface region, i.e. the values depend on the choice of R_{k_1}/R_k, etc. The radius of the largest of the clusters considered is only about six atomic diameters. Two reasonably complete surface layers would correspond roughly to $k_1 = 20$ and $k_1 = 30$. Thus perhaps the most meaningful value of γ lies between $\gamma_{20/49}$ and $\gamma_{30/49}$ or about $0.2\varepsilon_0/a_0{}^2$. Of course in much larger clusters where the thickness of the non-uniform region is quite distinct from the interior, the value of η is close to unity and the ambiguity in the values of γ disappears, i.e. $\gamma = (3/2)E^s \approx 0.36\ \varepsilon_0/a_0{}^2$. In general the calculations indicate a small decrease of specific surface energy E^s with decreasing particle size and a somewhat greater decrease in surface tension γ.

From the tables rough estimates of "ideal stress distributions" in surface layers can be made. An "ideal stress distribution" is the distribution of hydrostatic stresses consistent with the distribution of sublimation energies assuming that chemical potentials and specific volumes are equal everywhere. While perhaps these ideal stress distributions are not very realistic they should give some notion of the stress distributions in systems of reasonable size where the assumed conditions are approximately valid.

IV. Validity of the Thermodynamic Equation for Surfaces

Many Molecule Systems

The basic assumptions underlying all of the equations of Part II fall into four categories. (i) The basic concepts of thermodynamics (essentially macroscopic) are applicable to the systems concerned. (ii) The only intensive thermodynamic variables that need to be considered are

Can. J. Chem. Downloaded from www.nrcresearchpress.com by 210.87.254.5 on 09/05/12
For personal use only.

the temperatures, the chemical potentials, and the pressures, the pressures being largely hydrostatic. (iii) The energies, entropies, "pv" potentials, Helmholtz potentials, etc. of the whole non-uniform surface layer and those of the corresponding bulk phases are additive. (iv) The surface layer is in complete thermodynamic equilibrium with the bulk phases, i.e. it is in equilibrium with respect to thermal and material interchange (equality of T and μ) as well as being in mechanical equilibrium (equilibrium with respect to change in relative positions of the parts, i.e. with respect to "strain").

As long as we deal with the time average properties of many molecule systems whose variables are definable and whose interactions with external systems are inherently observable (i) should be reasonably valid.

Assumption (ii), however, is not very likely to be valid in cases where "contact potentials", surface electric fields, polarization energies, stress–strain potentials, etc. of appreciable magnitudes are possible.

To provide for a variety of sources of potential we should write eq. [1] in the form

$$[71]\quad dE = TdS - pdv + \sum Y_j dy_j + \sum X_k dx_k + \sum \phi_l dq_l + \sum \mu_i dm_i,$$

where $\sum Y_j dy_j$ represents those "work" terms in addition to TdS, pdv, and $\sum \mu_i dm_i$ which must be involved as a system grows in extent, its nature and state remaining constant. The y's are extensive variables. The terms $\sum X_k dx_k$ are work terms associated with changes in position in scalar potential fields. (The equation implies that it is possible for the system to grow in extent without change in position, i.e. with the x's constant.) The terms $\sum \phi_l dq_l$ are any other work terms not clearly in the other categories, e.g. polarization energies, strain energies, etc. In the event of p, Y_k, etc. being different in different directions it will be necessary that the system grow in extent in some definite manner (e.g. constant shape) in order that the quantities have definite values, i.e. in order that dE be the derivative of a function. If a crystal in a state of homogeneous strain under non-isotropic stresses maintains its crystal form during growth, p would be $\frac{1}{3}(p_1 + p_2 + p_3)$, where p_1, p_2, p_3 are the principal stresses. If the growth takes place in only two directions in a plane, p will be $\frac{1}{2}(p_1 + p_2)$, where p_1 and p_2 are the principal stresses in the plane of growth. Assuming equations of the form of eq. [71] applicable to a system of two bulk phases and the interface between them and that the whole three-part system can grow in extent from suitable sources of heat, mass, etc., we can follow the same procedure as used in deriving eqs. [10] to [15] of Part II and obtain the more general equation for surfaces in the form

$$[72]\quad dG = -SdT - \sigma d\bar{\gamma} - \sum y_j dY_j + \sum \phi_l dq_l + \sum \mu_i dm_i.$$

For Van der Waals type crystals in the absence of external electric and magnetic fields, in the absence of adsorbed ions, etc., the terms $\sum y_j dY_j$ should be negligible, but terms of the type ϕdq may still contribute appreciably to the equilibrium between the surface and bulk material, especially if one of the bulk phases is a solid. Accordingly, we should write the Gibbs "adsorption equation" in the form,

$$[73]\quad d\bar{\gamma} = \sum \Gamma_i d\mu_i - \phi' dq.$$

This equation should be applicable to the surfaces of reasonably large nonionic crystals. Unless the crystals are highly symmetrical it is unlikely that both surface and bulk phase stresses will be equal in all directions. Accordingly terms of the type ϕdq should contribute to the equilibrium between the surface and bulk material of many solids.

The assumptions of category (iii) are certainly valid for a large number of laboratory scale systems, especially those where the surface volume ratio is comparatively small and the condensed bulk phase is liquid. Where the surface volume ratio is large and the condensed phase is a solid, it is very doubtful that one can suppose the surface region separated from the bulk state by imaginary surfaces such that the potentials of the three regions are additive. If the internal surface area of a porous solid were anything like 10^3 m^2/g this assumption could hardly be valid.

The assumption (iv) of complete thermodynamic equilibrium between surface and bulk phases should be valid in laboratory scale systems of reasonable fluidity, i.e. where self-diffusion rates are reasonably high. However, in such systems as activated carbon at room temperatures, the whole system in a steady state will have a uniform temperature and be in mechanical

Can. J. Chem. Downloaded from www.nrcresearchpress.com by 210.87.254.5 on 09/05/12
For personal use only.

equilibrium, i.e. the field and stress forces will balance, but the chemical potential of the carbon (if it has any meaning in this case) will not be the same everywhere.

However, in many molecule systems, at reasonable temperatures, fluctuations associated with diffusion interchange undoubtedly can and do occur. When such fluctuations in number density are very small compared with the number of molecules in the region concerned the fluctuations will not change the thermodynamic properties per molecule of any of the regions concerned. Accordingly the conditions for equilibrium between many molecule systems whose potentials are not additive are probably much the same as those between systems whose potentials are additive. If the materials constituting the "layers" within the interfacial region can be thought of as having temperatures and chemical potentials, under equilibrium conditions there can be no temperature gradients and no chemical potential gradients along any line passing through the interfacial region, i.e. $\partial T/\partial x = 0$, $\partial\mu/\partial x = 0$, along x, a normal through the interface.

Thus we assume that we can write equations for layers within an interface that are analogous to the thermodynamic equations for equilibrium of bulk systems in scalar potential fields, such as

$$[74] \quad \mu(x) - \mu(x_0) = \int_{x_0}^{x}\left(v\frac{dp}{dx} + \phi\frac{dq}{dx} + f_x\right)dx = 0,$$

where $x - x_0$ is any distance along the normal to the flat surface.

In bulk systems under hydrostatic states of stress, the term ϕdq drops out, and putting $p = -X_x = -Y_y = -Z_z$, where X_x, etc. are principal tractions, eq. [74] can be written in the form

$$[75] \quad \frac{\partial Y_y}{\partial y} = \frac{\partial Z_z}{\partial z} = 0,\ Y_z,\ Z_y, \text{ etc.} = 0.$$

This is a special case of the general equation for equilibrium between tractions and "body forces" of elasticity theory as applied to bulk systems, namely,

$$[76] \quad \frac{\partial X_x}{\partial x} + \frac{\partial X_y}{\partial y} + \frac{\partial X_z}{\partial z} - \rho(x)f_x = 0, \text{ etc.}$$

Equation [74] contains the condition for mechanical equilibrium (equilibrium with respect to change of dimensions in any direction) as well as equilibrium with respect to diffusive interchange of material. Thus as applied to a single component bulk fluid of uniform temperature, the conditions for mechanical equilibrium with respect to pressures and body forces become indistinguishable from the conditions for thermodynamic equilibrium. However, if the system were, say, a solid in a gravitational field supported at the bottom by the traction X_x equal in magnitude to mg, the weight of the solid, and no external stresses applied to the surface anywhere else, the condition for mechanical equilibrium would be as given by eq. [76]. This equation would be applicable to a solid of any shape which could be formed by rotation about the x axis or the direction of the body force g. Although the solid would be in mechanical equilibrium it would not, in general, be in equilibrium with respect to diffusive interchange, i.e. $\mu(x) \neq \mu(x_0)$. The system might be far from being in a state of thermodynamic equilibrium.

Thus eq. [76] of elasticity theory does not, in general, include equality of chemical potentials. It applies to every "point" within a body including the points on the surface, and if the surface tractions and body forces are known, they represent boundary conditions which the stress function must satisfy. The equations enable one to calculate the change in form or the strain, the change in distribution of stress within the body, as the boundary conditions are changed, provided that the elastic properties are known. The equations describe the equilibrium between the "external" forces applied to the surfaces of any small volumes and the field or body forces which may act on the interiors (the center of mass) of the small volumes which the whole system is supposed divided into. Although the small volumes are treated as points, the underlying ideas are essentially macroscopic. There is no very direct way of measuring stresses acting on a molecule or atom and it might seem that such macroscopic notions as stress, pv potential, etc. were meaningless as applied to such ultramicroscopic systems. However, there are a good many cases where the thermodynamic states of stress of very minute volumes can be reasonably definite physical quantities which can be defined with respect to a reference state.

In all condensed systems mutual field potentials exist, i.e. relatively large intermolecular

Can. J. Chem. Downloaded from www.nrcresearchpress.com by 210.87.254.5 on 09/05/12
For personal use only.

forces are involved in the equation of state. In systems where the extensive variables are homogeneous functions of first degree in one another, we can suppose the system divided into small volumes by imaginary planes and each small volume has a time average energy TS, pv, μm, etc. of its own. The implication is that no mutual field forces pass these imaginary planes (the surfaces of the small volumes). The gradient of the time average field potentials of the material constituting these volumes is zero everywhere. In the case of uniform mobile fluids there is practically no lower limit to the size of these imaginary volumes. Their time average properties are constant over relatively short time intervals and are the same everywhere. The "radial" distribution becomes uniform at a relatively short distance from any reference point. However, in the case of crystalline solids, where definite long range order exists over relatively long periods of time, the lower limit of the size of the imaginary volumes would be some multiple of the unit cell including crystal vacancies and the like. The "radial" density and field potential distributions may be regarded as periodic, but no net field forces pass the surfaces of the imaginary small volumes. Evidently if the extensive thermodynamic variables of a uniform bulk system are homogeneous functions of first degree in one another, we can assign definite values to the intensive thermodynamic variables of the smallest interior volumes whose time average extensive thermodynamic variables are additive. When the bulk system is under a hydrostatic pressure approaching zero we take the state of stress of the imaginary small volumes as the standard state of zero hydrostatic stress, regardless of the nature of the intermolecular and thermal forces. (Of course the implication is that the field forces are short ranged, i.e. decrease more rapidly with distance than an inverse square law. A large self-gravitating sphere cannot be in a uniform state of stress and the potentials of its parts cannot be additive.)

Consider a perfect face-centered cubic closed-packed array of identical spherical atoms. If the array is large enough and the interatomic forces short ranged and surface forces, external fields, etc. are negligible, the extensive thermodynamic variables of the whole array will be homogeneous functions of first degree in one another. If the external hydrostatic stress is zero, the thermodynamic state of stress of the smallest volumes whose potentials are additive can also be taken as zero. Since every atom in the interior of the array has the same time average properties we take the "volume" of the atom as the smallest additive volume, i.e. the pressure of each interior atom is zero. If the interatomic potentials are pair-wise additive and the forces limited to nearest neighbor (n.n.) interaction only, the interatomic forces acting between the centers of mass of any pair in the assembly are the same everywhere. In the absence of an applied external stress the repulsive and attractive forces just balance and the net force acting on the "surfaces" of the atoms is zero everywhere. The pv potential of the interior atoms being taken as zero, the pv potentials of the surface atoms in the undisturbed lattice must also be taken as zero.

Assuming the attractive forces somewhat longer ranged than the repulsive forces so that work must be done to separate a pair, the work of removal of an atom from the interior leaving a hole in the otherwise undisturbed lattice would be 12 times the work of separating a pair, say $12W$, while the work of removing an atom from the (100) surfaces would be $9W$.

If the holes are closed after removal and the energy of the array is a homogeneous function of first degree in the number of atoms, the energy of removal or the "sublimation energy" of the interior atoms is $6W$, while the sublimation energy of the (100) surface atoms is $4.5W$.

Assuming TS very small and E large, the Helmholtz potentials of surface atoms must be considerably greater than those of the interior. Since the pressure is zero everywhere the pv potentials are zero everywhere. (No potential gradients pass the surfaces of the small volumes.) While there are different energy levels or self-potential plateaux, the potential of each atom (or volume) is a minimum and $d\Omega/dx_e = 0$. Each atom is at the "bottom of a potential energy well". The fact that there are deeper wells nearby has no effect whatever on the pressure and does not contribute to the equilibrium. Hence the Gibbs potentials of surface atoms are greater than those of the interior atoms. The system will be in thermal and mechanical equilibrium but not in equilibrium with respect to diffusive interchange of material.

We now allow a small statistical relaxation of the lattice and suppose that the atoms have

Can. J. Chem. Downloaded from www.nrcresearchpress.com by 210.87.254.5 on 09/05/12
For personal use only.

sufficient thermal motion so that finite displacements from their minimum energy positions can and do occur. If the displacements are of sufficient magnitude diffusive interchange will occur together with small fluctuations in number density of the various regions. The fluctuations in number density will require equality of chemical potentials when equilibrium is established. Thus there would be a tendency for material to diffuse toward regions of lower chemical potential and the development of a pressure difference. The process would resemble very closely the development of an osmotic pressure in a macroscopic system. For the ideal system considered (strong interatomic forces limited to n.n. distance only) a very small increase or decrease in n.n. distance (probable number density) would correspond to the effects that could be produced by relatively large externally applied stresses without changing the energies appreciably.

Since the chemical potential of the whole system will be controlled by the large interior mass (assuming a semi-infinite slab), the introduction of diffusive interchange will tend to make the chemical potentials of the surface atoms the same as those of the interior atoms. The surface being flat the pressure of the interior will tend to remain zero while the surface will develop a large negative stress, not necessarily hydrostatic by any means. But the pv potential of the surface for parallel growth must be consistent with the difference between the Helmholtz potentials of surface and bulk material as in the Gibbs treatment. Hence we conclude that under conditions of complete thermodynamic equilibrium there can be a large positive surface tension associated with the interface of condensed systems when only n.n. interactions occur (a conclusion somewhat at variance with that of Shuttleworth (5)). But without the requirement of equality of chemical potentials n.n. interatomic forces will not, in general, lead to any stresses in regular lattices, as pointed out by Shuttleworth.

If the interatomic attractive forces are longer ranged than the n.n. distance, the repulsive field of an atom between two others must sustain a larger attractive or "compressive" force than the repulsive field of a pair. This situation is somewhat different from that discussed above. If the potentials are pair-wise additive L–J (6–12) potentials when the array is large, the potentials of the interior volume are uniform. The system as a whole can grow in extent, its nature and state remaining constant. If the external pressure perpendicular to the surface of a semi-infinite slab is zero, the states of stress of all the interior atoms is still taken as zero. However, the repulsive fields of atoms near the surface will be sustaining smaller attractive fields than those in the interior and if we suppose those in the interior to be under zero stress, those near the surface should be regarded as in a negative state of stress, if we can apply such macroscopic notions in this case. The negative stress would be associated not with the difference between n.n. self-potentials of surface and interior atoms but rather with the difference in self-potentials in excess of the difference in n.n. potentials. This relatively small difference in "state of stress" will by no means compensate for the difference in Helmholtz potentials of surface and interior atoms. The surface atoms will not be in equilibrium with respect to diffusive interchange. If we now allow the lattice to relax a little, so that diffusive interchange can occur, relatively large pressure differences can develop, i.e. a true positive surface tension will develop as in the illustration above.

Evidently there are two distinct questions. (1) What stresses are necessarily associated with given field forces in regular lattices of constant n.n. distances in order that stress and field forces balance? (2) What modification of the stresses and n.n. distances in the surface region of lattices must exist when diffusive interchange can occur and the equilibrium involves equality of the chemical potentials? It is clear that the introduction of the "osmotic" forces associated with diffusive interchange (equality of the chemical potentials) must influence very materially the stress structure of many systems consisting of a great many molecules held together largely by their own intermolecular forces.

Few Molecule Systems

Clusters of a very few molecules in a close-packed array cannot in general behave as though the potentials of its parts were additive, i.e. it cannot grow in extent while its specific thermodynamic properties remain constant. Thus there can be little or no meaning to writing $dE = TdS - pdv + \mu dm$ as applied to, say, a close-packed cluster of 13 atoms and certainly we cannot apply such an equation to the imaginary "surface" and

Can. J. Chem. Downloaded from www.nrcresearchpress.com by 210.87.254.5 on 09/05/12
For personal use only.

"interior" volumes of such small clusters. Variations of the type $dE = (\partial E_1 / \partial m_1)\, dm_1 + (\partial E_2/\partial m_2)dm_2 = 0$, $dm_1 + dm_2 = 0$ are obviously meaningless or impossible as applied to such "surface" and "interior" volumes. Statistical fluctuations in atom number densities and diffusive interchange between various parts of a system, the other variables remaining constant, is obviously a property assignable only to systems of large numbers of molecules.[7] Thus, in a cluster of a few molecules held together by their own intermolecular forces, if we can speak of the stress structure at all in such cases, it will be determined by the intermolecular forces alone without any requirement of equilibrium with respect to diffusive interchange. If any meaning can be given to the chemical potentials of its parts they will not be uniform. If we were to suppose that a cluster of 13 atoms has a real surface tension in the sense that the outer layer of atoms are under appreciable negative tangential stresses the components of these stresses along the radius would lead to a large compressive stress on the interior atom, i.e. the repulsive field of the interior would have to sustain a larger force than that of a molecule in a large face-centered cubic array in spite of the fact that the latter must sustain the larger attractive force fields. Evidently we cannot regard the "surface regions" of very small particles as having thermodynamic properties of their own. Similarly in the case of very small holes formed by the removal of a few atoms from the interior of a large many molecule condensed system we cannot regard the "surface region" of the hole as a thermodynamic entity distinct from the hole. The hole and the region surrounding it should be regarded as a statistical fluctuation of the thermodynamic state of the whole condensed system.

Practically none of the basic assumptions underlying the equations relating surface tension, γ, and surface Helmholtz potential, A^s or E^s as defined in Part II, can be applicable to very small particles or to very small holes.

Although we cannot apply equations of the type $dE = TdS - pdv + \mu dm$ to the surface regions of very small particles and holes we can apply $dE = TdS + dw$ (where w is work done on the system by external bodies) to the whole system of particles or to a system of holes in a bulk system. Thus if the Helmholtz potential increases as a result of dividing a crystal into smaller crystals or as a result of the formation of holes or vacancies in a bulk system $dE - TdS$ or $(dA)_T$ would be a measure of the work done on the system. Thus for the change in Helmholtz free energy from its value for a bulk system we could write

$$[77] \qquad A = A^s\sigma,$$

taking the Helmholtz potential of the bulk system of negligible surface area as zero, A^s as the Helmholtz potential per unit surface area of the whole system, and σ its surface area measured or calculated in some particular manner whether fictitious or not (cf. eqs. [33], [63], and [64]).

Equation [77] leads to

$$[78] \qquad (dA)_T = \left(A^s + \frac{dA^s}{d\sigma}\right)d\sigma = \gamma_A' d\sigma = dw \ldots$$

This definition of γ_A' is practically the same as that of A^s or E^s as defined by eqs. [33], [34], and [64], and as we have seen is not necessarily closely related to the real surface tension γ. Thus while A^s is sometimes called surface tension it is certainly not necessarily closely related to tangential surface stresses at all. Even in large bulk systems which are in a state of complete internal thermodynamic equilibrium A^s may be dominated by work terms other than surface "pv" terms.

V. Conclusions

The surface energies calculated by the above method must be regarded as rather crude approximations. However, surface energies of noble gas-like crystals based on much more sophisticated treatments (16) do not differ very much from those calculated from pair-wise additive 6–12 potentials. Hence the variation of E^s with particle size as given in the tables should be approximately correct for the systems treated and should give the order of magnitude of the effect of particle and drop size on E^s values of real systems which are reasonably close to the model, i.e. reasonably close-packed systems of spherical molecules whose vapor pressures are very low.

[7]The isothermal condition for equilibrium between a cluster and the gas, $v_c dp_c = v_g dp_g$, where the subscripts refer, respectively, to the cluster and to the gas, is not applicable to a cluster of only a few atoms or molecules (cf. ref. 2).

Can. J. Chem. Downloaded from www.nrcresearchpress.com by 210.87.254.5 on 09/05/12
For personal use only.

Parts II, III, and IV lead to the following conclusions.

1. The Gibbs thermodynamic equations for surfaces are only applicable to the interfacial region between bulk phases which are in complete thermodynamic equilibrium, i.e. uniformity of chemical potentials, etc.

2. As applied to solid surfaces the Gibbs adsorption equation should include shear–strain potentials.

3. The specific surface energies and specific surface Helmholtz potentials (E^s and A^s) of noble gas-like crystals decrease very little with particle size. For laboratory scale systems the decrease is negligible.

4. Surface tension in the sense of a negative tangential surface stress is primarily a property of bulk systems.

5. The surface tension of laboratory scale particles and holes decreases with particle size a little more rapidly than does A^s, but the decrease is probably negligible for systems resembling condensed noble gas-like structures.

6. The surface tension in the sense of a negative tangential surface stress of particles or of holes of molecular dimensions is either meaningless, very small, or negative and is not closely related to A^s, the specific surface free energy.

Appendix I

The thickness h includes all regions where the surface fields are appreciable. Near the critical temperature the surface fields will become small compared with the gravitational field necessary to maintain the flat surface. The thermodynamic properties of systems very near the critical temperature depend on previous history and the "surface thickness" becomes an indefinite and largely meaningless quantity, but well below the critical temperature it should be a reasonably definite quantity.

Hence when reasonably far from any critical regions we assume that under equilibrium conditions a flat non-uniform region of definite thickness, h, can separate two distinct fluid phases. In general h will vary with T, p, μ_1, μ_2, etc., but for both bulk phases p is a function of T, μ_1, $\mu_2 \ldots \mu_i$. The thickness of an interface between specified phases will be determined by T, μ_1, $\mu_2 \ldots \mu_i$.

Consider a small piece of this non-uniform region. The area is σ, the thickness h. The external stresses are p perpendicular to σ and p_T perpendicular to h. Since no mutual fields pass the surfaces "containing this piece", we can write

[A1] $$dE = TdS - pd\sigma dh - p_T h d\sigma + \sum \mu_i dm_i$$

and

[A2] $$\mu_i = (\partial E/\partial m_i)_{S,h,\sigma,m_1,\ldots m_{i-1}}.$$

This system can grow in extent, reversibly, from suitable sources of m_1, m_2, etc. while T, p, p_T, μ_1, etc. remain constant.

If the growth takes place with both h and σ increasing it is equivalent to increasing the quantities of the bulk phases as well as increasing the quantity of the surface region. Although μ_1, μ_2, etc. will be constant the values of E, S, v, etc. depend on the relative proportions of the three regions. It is only when the growth is parallel to σ (i.e. h constant) that the specific properties of the system all remain constant. In a laboratory scale layer of thickness Z, where $Z = a + b + h$, a referring to, say, the gas phase, b the liquid phase, and h to the non-uniform surface, it would be necessary that a and b as well as h remain constant during growth, if the specific properties are to remain constant.

For parallel growth of the three layers a, b, and h constant

[A3] $$dE = TdS - pad\sigma - pbd\sigma - p_T h d\sigma + \sum \mu_i dm_i \ldots$$

and

[A4] $$\mu_i = (\partial E/\partial m_i)_{S,a,b,h,\sigma m_1,\ldots m_{i-1}}.$$

If desired we could write $p_T'(a + b + h) = pa + pb + p_T h$, but p_T' will vary with the relative values of $a + b$ and h, but with T and μ_i's constant, p and p_T and h are constant.

For the surface layer alone

[A5] $$dE_\sigma = TdS_\sigma - p_T h d\sigma + \sum \mu_i dm_i,$$

and

[A6] $$G_\sigma = E_\sigma - TS_\sigma + p_T h\sigma = E_\sigma - TS_\sigma - \gamma\sigma = \sum \mu_i m_i,$$

and

[A7] $$dG_\sigma = -S_\sigma dT + \sigma d(p_T h) + \sum \mu_i dm_i = -S_\sigma dT - \sigma d\gamma + \sum \mu_i dm_i$$

also

[A8] $$\left(\frac{\partial G_\sigma}{\partial m_i}\right)_{T,h,p_T,m_1\cdots m_{i-1}} = \left(\frac{\partial E_\sigma}{\partial m_i}\right)_{S,h,\sigma,m_1\cdots m_{i-1}} = \mu_i.$$

It will be noted that it is $p_T h$ which varies with $T, \mu_1, \mu_2, \ldots$ etc. and although both p_T and h can vary, the displacement work per unit increase in surface depends only on the product $p_T h$, i.e. $dw = p_T h d\sigma = -\gamma d\sigma$.

If we had put $p_T h = ph - \gamma'$, where p is the hydrostatic pressure of the bulk phases, $dw = (ph - \gamma')d\sigma$ and the value of $ph - \gamma'$ will depend on $T, \mu_1, \ldots$ etc. in the same way as $p_T h$. If we put $ph\sigma = pv$ and hence $p_T h\sigma = pv - \gamma'\sigma$, and for the surface layer write

$$G_\sigma = E_\sigma - TS_\sigma + pv - \gamma'\sigma,$$

we might conclude that $G_\sigma = G_\sigma(T, p, \gamma', \mu_1, \text{etc.})$.

From our point of view the surface displacement potential (or the Gibbs free energy) of the surface is best given by

[A9] $$G_\sigma = E_\sigma - TS_\sigma - \gamma\sigma = \sum \mu_i m_i,$$

as found by Gibbs, rather than

[A10] $$G_\sigma = E_\sigma - TS_\sigma + pv - \gamma'\sigma = \sum \mu_i m_i,$$

as found by some authors.

Hence $\gamma = -p_T h$ seems a better definition of surface tension than

[A11] $$\gamma' = -p_T h + ph,$$

as sometimes suggested.

Acknowledgment

We are indebted to Dr. P. I. Freeman for assistance with some of the calculations described in Part III.

1. G. BAKKER. in Handbuch der Experimentalphysik. W. Wien and F. Harms (*Editors*). Vol. 6. Akad. Verlags., Leipzig. 1928. p. 434.
2. J. H. KEENAN. Thermodynamics. John Wiley and Sons, Inc., New York. 1941. p. 441.
3. R. C. TOLMAN. J. Chem. Phys. **17,** 333 (1949).
4. R. SHUTTLEWORTH. Proc. Phys. Soc. London, **A62,** 167 (1949).
5. R. SHUTTLEWORTH. Proc. Phys. Soc. London, **A63,** 444 (1950).
6. G. C. BENSON and R. SHUTTLEWORTH. J. Chem. Phys. **19,** 130 (1951).
7. R. M. BARRER. Trans. Faraday Soc. **50,** 1074 (1954).
8. M. M. NICOLSON. Proc. Roy. Soc. London, Ser. A, **228,** 490 (1955).
9. S. ONO and S. KONDO. Encyclopedia of Physics. S. Flügge (*Editor*). Vol. 10. Springer-Verlag, Berlin. 1960. p. 134.
10. F. P. BUFF. Advan. Chem. Ser. **33,** 340 (1961).
11. A. BELLEMANS. Physica, **29** (5), 548 (1963).
12. K. S. YUN and G. C. BENSON. J. Chem. Phys. **44,** 2548 (1966).
13. E. A. GUGGENHEIM and N. K. ADAM. Proc. Roy. Soc. London, Ser. A, **139,** 218 (1933).
14. W. D. NIVEN (*Editor*). The scientific papers of James Clerk Maxwell. Vol. 1. Cambridge Press. 1890. *Reprinted by* Dover, New York. 1952 p. 52.
15. J. E. JONES and A. E. INGHAM. Proc. Roy. Soc. London, Ser. A, **107,** 636 (1925).
16. G. C. BENSON and T. A. CLAXTON. Phys. Chem. Solids, **25,** 367 (1964).

Can. J. Chem. Downloaded from www.nrcresearchpress.com by 210.87.254.5 on 09/05/12
For personal use only.

$Hg(^3P_1)$ photosensitized reactions of cyclopropane

O. P. STRAUSZ, P. J. KOZAK,[1] G. N. C. WOODALL, A. G. SHERWOOD,[2] AND H. E. GUNNING
Department of Chemistry, University of Alberta, Edmonton, Alberta

Received February 20, 1967

Under static conditions the major reaction product is a polymer. Polymerization is inhibited by free radical scavengers such as NO, O_2, butadiene-1,3, etc. with a simultaneous large increase in propylene yields. The NO inhibited reaction affords propenaldoxime and acrylonitrile as principal products, indicating the presence of allyl radicals, and N_2O which is indicative of H atoms. Polymerization can also be suppressed by rapid flow: it is entirely a secondary process. The products of the flow experiments are: propylene, biallyl, allylcyclopropane, 4-methyl pentene-1, hexene-1, 2,3-dimethyl butane, C_5 and C_9 hydrocarbons, H_2, CH_4, C_3H_8, and traces of bicyclopropyl. Most of the products can be accounted for by the self-scavenging of H atoms by propylene and the ensuing reactions of isopropyl and allyl radicals. The major primary step is the formation of an electronically excited cyclopropane, possibly the ground state triplet of trimethylene with a large excess of vibrational energy. The primary decomposition is retarded by pressure. Φ(decomp.) > 0.38, at 20 Torr, but is less than unity.

Canadian Journal of Chemistry, 46, 1317 (1968)

Can. J. Chem. Downloaded from www.nrcresearchpress.com by 210.87.254.105 on 09/05/12
For personal use only.

Introduction

A critical evaluation of the status of the mercury sensitization of cyclopropane up to 1962 has recently been given in a review article by Cvetanovic (1), and for this reason discussion of earlier developments on the subject will be omitted here. Only the three most recent articles will be briefly described. Setser, Rabinovitch, and Spittler (S.R.S.) (2) have reported an interesting and revealing study on the *trans* → *cis* isomerization of *trans*-dideutero cyclopropane at pressures up to 70 atm. The relative importance of the two basic products *cis*-Δ-d_2 and polymer was found to be pressure dependent and the fractional yield of the *cis* isomer increased rapidly with pressure between 0.01 and 5 atm and appeared to level off above 5 atm. The isomerization was envisaged via an excited triplet state of cyclopropane (triplet trimethylene diradical). The possibility that polymerization occurs via the same excited species or through the intervention of a second primary step giving cyclopropyl + H atom was also considered. In a subsequent study (3), it was also found that oxygen up to 15% had only a slight effect on the isomerization which was taken as additional evidence that monovalent free radicals are not involved in the mechanism.

While this present study was in progress a brief communication (4) appeared in the literature utilizing the ethylene-^{14}C sampling technique for the mercury sensitization of cyclopropane. From the appearance of pentene-1 as the major reaction product it was concluded that either allyl or cyclopropyl + H-atom split is the major mode of decomposition with the subsequent rapid isomerization of the latter to the former. A minimum value of 0.22 was deduced for the quantum yield of cyclopropane disappearance.

Experimental

Static experiments were carried out in a conventional high vacuum apparatus. The flow system consisted of a large reservoir, a commercial oil flow meter, a mercury saturator and stripper, a 16 mm i.d. tubular quartz cell surrounded with a Hanovia helical mercury resonance lamp, manometer, and flow control valves.

From the cell the reaction mixtures were passed through traps at −117 and −196°. The noncondensables were measured in a gas buret and then analyzed by gas chromatography (g.c.) on a 6 ft molecular sieve column. The −117° fraction was then transferred from the trap to the g.c. sample inlet and analyzed on a 20 ft, 5% 1,2,3-tri(2-cyanoethoxy)propane-on-chromosorb column first at 10°, and subsequent to C_6 hydrocarbon elution at 60° to elute C_9's.

The −196° fraction was transferred to a calibrated volume, allowed to warm, mixed thoroughly, and measured, and then a small aliquot was analyzed by g.c. on a 40 ft 5% silicon grease-on-celite column at 0 °C.

Product identifications were performed by comparison of g.c. retention times and mass spectrometric cracking patterns of g.c. separated components with those of standard samples.

The following products were positively identified: H_2, CH_4, propylene, propane, 2,3-dimethyl butane, 4-methyl pentene-1, hexene-1, and biallyl and allyl cyclopropane. From the −117° fraction one peak appeared on the chromatogram corresponding to the retention time of 3-methyl butene-1 and was assumed to be a C_5 olefin. Also

---

[1]Present address: Imperial Oil Research Laboratories, Sarnia, Ontario.

[2]Present address: Dept. of Chemistry, Simon Fraser University, Vancouver, B.C.

Can. J. Chem. Downloaded from www.nrcresearchpress.com by 210.87.254.105 on 09/05/12
For personal use only.

from the fraction, four components, eluted at 60° corresponding to the retention time range of C_9 hydrocarbons, were assumed to be nonenes.

Two very minor products, which appeared as shoulders on the biallyl and allyl cyclopropane peaks, were thought to be isopropyl cyclopropane and bicyclopropyl. Sufficient quantity of the latter was collected from a number of long runs for mass spectrometric analysis. This was quite similar to, but not identical with (possibly because of incomplete separation from allyl cyclopropane), that obtained on a synthetic sample of bicyclopropyl.

Product determination for CH_4, C_3H_8, and the C_6's were obtained from calibrated g.c. peak areas. For propylene the detector response was taken to be identical with that of cyclopropane and for C_5's it was estimated from C_6's.

The products from the nitric oxide inhibited runs were separated by g.c. on a carbowax 600-on-celite column with temperature programming between 30 and 92°. The compound believed to be propenaldoxime always gave two peaks, presumably owing to the *syn* and *anti* forms. Their mass spectra were similar, each giving an intense parent peak at $m/e = 71$. The infrared (i.r.) spectrum agreed with that obtained on a commercial standard and the n.m.r. spectrum clearly indicated the presence of the allyl skeleton. The next important product eluted at 40° from the column. Its i.r. spectrum showed the presence of the allyl group and its mass spectrum was reminiscent of that of alkyl nitrates. It was tentatively identified as allyl nitrate. From static experiments an additional product was also obtained which, from its g.c. retention time and mass spectrum, was identified as acrylonitrile.

Materials

Cyclopropane (Matheson C.P. or Ohio Chemical Anaesthetic grade) was purified by either of the following procedures: (*a*) a series of low temperature distillations utilizing a LeRoy still; (*b*) preparative g.c. or (*c*) bubbling it through 4 × 1 m columns of saturated aqueous solution of alkaline potassium permanganate, with subsequent low temperature distillation.

Nitric oxide (Matheson) was purified by trap-to-trap distillation terminating at −186°.

All other materials used were of the best available grade and were further purified as found necessary.

The lamp intensity was determined with the N_2O–n-C_4H_{10} actinometer and the yield of N_2 was extrapolated to $[n\text{-}C_4H_{10}]/[N_2O] = 0$, where $\Phi(N_2)$ was taken as unity.

Results

Early studies on the mercury photosensitization of cyclopropane (1) have shown that under static conditions the main characteristic of the reaction is a rapid polymerization with quantum efficiencies below unity. In the present investigation it was found that the nature of the polymer changes with the impurities present in the cyclopropane and with the experimental conditions. In the initial stages of the reaction with scrupulously purified cyclopropane there was no measurable pressure decrease or visible polymer formation. This was followed by a period of solid polymer deposition and the final stage of the reaction was characterized by the appearance of a liquid polymer. On the other hand, cyclopropane containing a few hundredths of a percent propylene impurities gave liquid polymer directly. When the reaction was performed in a single pass system at fast flow, polymer formation was almost completely suppressed, indicating that its origin is entirely secondary in character. The yield of volatile products resulting from static experiments was very low; propane, propylene, along with trace quantities of C_2 hydrocarbons, 1,5-hexadiene, hexene-1, and *n*-hexane were formed. The major component, propylene, slowly reached a photostationary state concentration of ca. 0.01 mole % (the same concentration could be attained by starting with cyclopropane containing more than 0.01 mole % added propylene). This, along with the observation that a 10–20-fold increase in the propylene yield resulted by the addition of relatively small quantities of free radical scavengers, such as butadiene-1,3, CO, or NO to the system, suggested that propylene might be one of the major primary products of the decomposition. Nitric oxide was also effective in suppressing polymerization and it afforded two revealing new products, acrylonitrile and propenaldoxime. Both of these can be accounted for by the reaction of nitric oxide with allyl radicals and the isomerization and subsequent dehydration of the initially formed nitroso propene,

$$CH_2{=}CH{-}CH_2 + NO \rightarrow CH_2{=}CH{-}CH_2NO$$
$$\downarrow$$
$$CH_2{=}CHCN + H_2O \leftarrow CH_2{=}CH{-}CH{=}NOH.$$

The correctness of this sequence was tested in auxiliary experiments by the mercury sensitization of butene-1 in the presence of small concentrations of nitric oxide. The major mode of decomposition of butene-1 is a split into methyl and allyl (1), and the most abundant reaction product found was propenaldoxime.

The cyclopropane – nitric oxide system also gave N_2O and H_2O, the reduction products of NO by H atoms (5),

$$H + NO \rightarrow HNO \rightarrow 0.5N_2O + 0.5H_2O.$$

Finally in the static system three experiments were performed with added O_2. Mixtures of 100

TABLE I

Quantum yield values for product formation

Relative flow	$\Phi \times 10^2$						Sum
		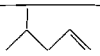	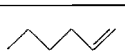	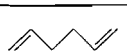	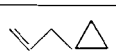		
			$P(\triangle) = 200$ Torr				
28	0.68	0.79	0.77	0.56	0.47	3.24	6.51
60	0.64	1.02	0.84	0.82	0.74	4.29	8.35
100	0.66	1.30	0.94	1.33	0.78	5.56	10.6
200	0.56	1.52	1.00	1.48	1.08	7.42	13.1
250*	0.48	1.41	0.93	1.54	0.92	7.42	12.7
*$\Phi \times 10^2$ $CH_4 = 0.13$; C_3 in C_5's $\simeq 3.2$; in $C_9 \simeq 4.7$; in $C_3H_8 = 0.24$† Φ total in C_3 units $\simeq 0.26$							
			$P(\triangle) = 20$ Torr				
50	0.48	0.39	0.34	0.34	0.38	2.14	4.07
150	0.42	0.64	0.50	0.73	0.86	7.52	10.7
250*	0.58	0.92	0.48	0.99	1.03	12.40	16.4
*$\Phi \times 10^2$ $CH_4 = 0.29$; C_3 in C_5's $\simeq 1.3$; in $C_9 \simeq 4.90$; in $C_3H_8 = 0.29$† Φ total in C_3 units $\simeq 0.25$; Φ total in C_3 units, corrected for incomplete quenching and pressure broadening $\simeq 0.35$							

†Calculated from K_d/K_{com} (isopropyl) = 0.50; lamp intensity = 8.63 μeinsteins/min; exposure time = 3–5 min.

Torr cyclopropane with 5 and 10 Torr O_2 were irradiated. Complete consumption of the oxygen had occurred before 5% of the cyclopropane had reacted. Large quantities of oxidation products, CO, CO_2, and H_2O, were formed, but the yield of the other volatile products was essentially unchanged from the value for pure cyclopropane. In the third experiment the reaction was carried out only to ca. 1% conversion, to ensure that all the oxygen would not be consumed. Under this condition, propane was not observed and the propylene yield increased by a factor of about 2 over the value for pure cyclopropane.

The main conclusion which can be drawn from these static experiments is that propylene, allyl radicals, and H atoms are primary products of the mercury sensitization of cyclopropane.

The reaction was further investigated in the single pass system which had the advantage of eliminating polymer formation and permitting the isolation of the lower molecular weight products resulting directly from the primary fragments of the decomposition, before they had undergone further reactions.

Two series of experiments were performed at 20 and 200 Torr substrate pressures and at various flow rates. The following products were detected: H_2, CH_4, C_3H_8, 2,3-dimethyl butane, 4-methyl pentene-1, 1,5-hexadiene, allyl cyclopropane, an unidentified C_5 which probably was 3-methyl butene-1, four heavier hydrocarbons, probably C_9's, and small amounts of bicyclopropyl together with some other C_9 hydrocarbons. Quantum yield data for the five major C_6 hydrocarbons and propylene are summarized in Table I.

The formation of 2,3-dimethyl butane, 4-methyl pentene-1, hexene-1, and 1,5-hexadiene can be rationalized in terms of the reactions of H atoms, allyl radicals, and propylene, while the allyl cyclopropane seems to indicate the presence of cyclopropyl radicals. However, an alternate route for this latter product may be the secondary mercury-sensitized isomerization of the biallyl product (6). To check this possibility, a few runs (not reported in Table I) were performed at low pressures and low flow rates, under which conditions a large increase resulted in the relative yield of allyl cyclopropane. A similar increase was obtained from a run in which 0.5% of biallyl was added to 12 Torr cyclopropane undergoing mercury sensitization. For this reason the presence of cyclopropyl radicals is subject to doubt. Nevertheless, because the constancy of the allyl cyclopropane to 1,5-hexadiene yield ratios at high flows, and because of the presence of the minor C_6 product which appears to be bicyclopropyl, we are inclined to believe that allyl cyclopropane is not a secondary product in its entirety.

The quantum yield values obtained at 20 Torr cyclopropane pressure have to be corrected for

Can. J. Chem. Downloaded from www.nrcresearchpress.com by 210.87.254.105 on 09/05/12
For personal use only.

Can. J. Chem. Downloaded from www.nrcresearchpress.com by 210.87.254.105 on 09/05/12
For personal use only.

incomplete quenching and for incomplete pressure broadening of the mercury resonance line. Using Holstein's formula for the imprisonment time, $T_i = 0.625\, k_0\, R(\ln k_0 R)^{1/2}\tau$ (7) and a value of 1.1 A^2 for σ^2(cyclopropane) (8), the fractional quenching is 0.91. The collision-broadening cross section of cyclopropane is not known, but should not be greatly different from that of propane. Using the data reported for propane (9), the overall correction factor turns out to be 1.39.

The total quantum yield values derived from the combined product yields, that is the quantum yields for cyclopropane disappearance, were 0.26 and 0.35 at 200 and 20 Torr pressures, respectively, at the highest flow rate used. As seen from the data in the last column of Table I, the Φ values show a rising trend with increasing flow rates and in the low pressure series, at least, this trend would probably continue with further increase in flow. Because of this and because of the possibility that some of the complex products have escaped detection, the measured quantum yields should be regarded as minimum values. The relative yield of propylene, which is produced mainly by a molecular isomerization process, can only be crudely estimated as being 60–70% of the total decomposition products.

The quantum yield for the overall decomposition is relatively low, and although a clear pressure trend appears, it is unlikely that it would attain unity at zero pressure.

The nitric oxide inhibited reaction was also examined in the flow system. A number of runs have been performed with ca. 2% added nitric oxide. The bulk of the fraction condensable at −102° was propenaldoxime (~75%) and a product tentatively identified as allylnitrate (~15%).

Discussion

In considering the primary step of decomposition, two basic alternatives appear: interaction of the excited mercury atoms with the C—H bonds resulting in cyclopropyl radicals and H atoms, or interaction with the carbon skeleton leading to trimethylene formation.

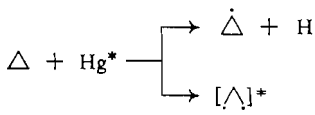

The fact that propylene is the major reaction product makes it immediately clear that [1*b*] is an important mode of decomposition. This is in agreement with the result of S.R.S. (2) on the *trans* → *cis* isomerization of *trans*-Δ-d_2. Step [1*a*] is exothermic by ca. 12 kcal/mole. Thermalized cyclopropyl radicals are relatively stable and readily undergo abstraction reactions (10, 11) or they may recombine to give, at least partly, bicyclopropyl (12). Although they are thermodynamically metastable with respect to allyl (ΔH ~ 30 kcal/mole and a bond dissociation energy for ring cleavage as low as −18 kcal/mole has been estimated (13)), the experimental activation energy for the ring opening reaction

[2] $$\dot{\triangle} \rightarrow \dot{\wedge}$$

is relatively high, 22 kcal/mole (11), rendering step [2] unimportant at room temperature. Therefore the second major primary decomposition product allyl, has to arise via [1*b*]. The propylene product formed from the isomerization of trimethylene

[3] $$[\dot{\wedge}]^* \rightarrow [\wedge]^*$$

may contain excess energy up to 121 kcal/mole and must undergo allylic cleavage quite rapidly. In the mercury sensitization of propylene the lifetime of the excited triplet propylene molecules, having excitation energy of 112 kcal/mole, with respect to decomposition into allyl + H is of the order of 10^{-9} s. The lifetime of chemically activated ground state singlet propylene having an excitation energy of 118 kcal/mole is of the same order of magnitude, 4×10^{-9} s (14). Assuming that stabilization occurs with collision frequency, at 200 Torr pressure 75% of the triplet and 91% of the singlet excited propylene should be stabilized. The experimental value is ~ 63%. Therefore the main source of allyl radicals must be

[4] $$[\wedge]^* \rightarrow \dot{\wedge} + H\ .$$

This conclusion is also supported by the observation that the energy transfer process from excited mercury to cyclopropane does not show the hydrogen deuterium isotope effect ($k_H/k_D \sim 1$), indicating that the primary interaction site is not the C—H bond.

The appearance of methane and C_5 compounds may be explained by methyl split from the excited propylene,

[5] $$[\wedge]^* \rightarrow CH_3 + C_2H_3\ ,$$

Can. J. Chem. Downloaded from www.nrcresearchpress.com by 210.87.254.105 on 09/05/12
For personal use only.

which comprises about 12% of [4] in the mercury sensitization of propylene (15, 16), followed by

[6] 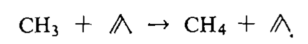

and

[7] $C_2H_3 + C_3 \rightarrow C_5\cdot$

However, the small yield of allyl cyclopropane, about 5% of the total, and the minute quantities of bicyclopropyl detected require the inclusion of step [1*a*] as a minor primary process in the mechanism. Since this reaction, unlike [1*b*], [3], and [4], would provide a pressure independent mode of fragmentation it would probably not represent more than ca. 2% of the total quenching processes.

All of the remaining products can now be easily accounted for on the basis of the self-scavenging of H atoms by propylene,

[8] 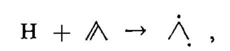

the efficiency of which is explained by the inertness of cyclopropane with respect to H-atom attack (17), and the ensuing radical combination and disproportionation reactions.

[9*a*], [9*b*], [10*a*], [10*b*], [11*a*], [11*b*], [12*a*], [12*b*], [13], [14*a*], [14*b*], [15], [16]

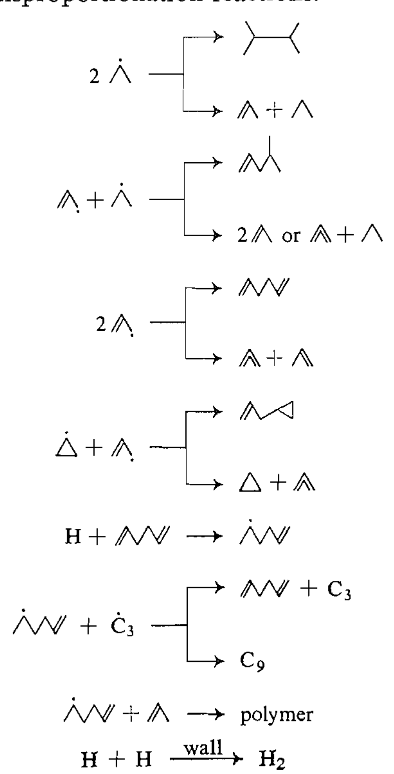

Disproportionation of allyl radicals is generally thought to be unimportant, although a relatively large value of $k_d/k_{com} \simeq 0.16$ has recently been deduced for the reaction of allyl with ethyl (18). If any allene were formed in our system it would not have been detected (the reported total quantum yields are minimal values).

Since polymer formation is inhibited by nitric oxide it is definitely a free radical process for which the responsible species are most likely to be the hexenyl and allyl radicals. The observed phase change of the polymer with the extent of conversion is probably related to the degree of unsaturation in the growing polymer chain; hydrogenation converts the liquid into a solid through crosslinking of the polymeric chains.

Returning now to the primary step, we see that the predominant mode of quenching is the transfer of excitation energy to the carbon skeleton of the ring, promoting a ($\sigma \rightarrow \sigma^*$) type transition, and displaying the well known pseudo olefinic character of the cyclopropane molecule (19).

In the majority of triplet mercury photosensitizations the spin conservation rule is known to be obeyed and we may with reasonable confidence assume that the trimethylene is formed in a triplet state

[17] 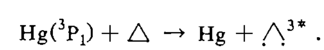

According to recent molecular orbital calculations, the ground state of trimethylene is a triplet (20) and there are a number of low-lying singlets above it (21). For the subsequent reactions the following sequence may be tested,

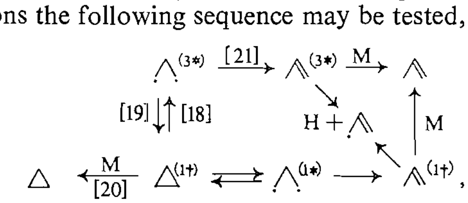

where the number in brackets indicates multiplicity and asterisk and dagger signify electronic and vibrational excitation respectively. At high pressures where ring reopening to give singlet trimethylene is not too significant, it is permissible to neglect the difference in reactivity between singlet and triplet, under which condition steady state approximation gives

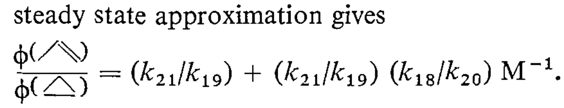

TABLE II

k_{21}/k_{19} values for singlet and triplet trimethylenes

System	Nature of trimethylene	Total energy	Vibrational energy	k_{21}/k_{19}
Hg sensitization of △	Triplet	112	> 58	~0.03
Δ-d_2 thermal decomposition	Singlet	64	—	0.08 (23)
Addition of CH_2 to $C_2H_2D_2$*	Singlet	102	< 48	0.05 (22)
Addition of CH_2 to $C_2H_2D_2$†	Singlet	105	> 51	0.07 (22)

*From photolysis of ketene at 3340 Å.
†From photolysis of ketene at 3200 Å.

Using the data reported by S.R.S. in Table I of ref. 2, and plotting the percentage yield of polymer over twice the percentage yield of *cis*-dideutero cyclopropane [the equivalent term of $\phi(\diagup\!\diagdown)/\phi(\triangle)$] against reciprocal pressure, the six high pressure runs indicate a somewhat scattered straight line relation. Extrapolation of this plot to infinite pressure gives $k_{21}/k_{19} \sim 0.03$, which may be compared to the corresponding values reported in the literature for singlet trimethylenes as listed in Table II.

The linearity of the plot extends to quite low pressures (~0.2 atm) owing to the not too different values of the k_{21}/k_{19} ratios for the singlet and triplet trimethylene species. From the slope, which has a value of $\sim 1.0\ \text{atm}^{-1}$, the value of k_{18} can be calculated if we assume a value for k_{20}. Taking k_{20} equal to the gas kinetic collision rate constant, $\sim 1.2 \times 10^{11}\ M^{-1}\ \text{s}^{-1}$, $k_{18} = 1.5 \times 10^{11}\ \text{s}^{-1}$. This agrees quite well with the value of $1.6 \times 10^{11}\ \text{s}^{-1}$ obtained by Rabinovitch *et al.* (22) from methylene addition to ethylene-d_2 in the 3200 Å photolysis of ketene. The excess energy content in the two systems, 112 and 105 kcal/mole, are also comparable.

The structural isomerization to propylene, step [21], is known to have an activation energy of ca. 1 kcal/mole higher than the ring reclosure step [18] for singlet trimethylene (23). Therefore with increasing amounts of excess vibrational energy in the trimethylene, the ratio k_{21}/k_{19} should increase. The observed low value for triplet trimethylene, in spite of its large excess vibrational energy, indicates that the hydrogen shift in the triplet is not as facile as in the singlet state. This is in agreement with the suggestion of Rabinovitch and co-workers and of Benson (23, 24), that the hydrogen shift in the singlet state is assisted by simultaneous partial double bond formation. If the propylene from triplet trimethylene is formed in its lowest triplet state this assistance is obviously absent, and intersystem crossing to the cyclopropane ground state singlet may become relatively more important. That isomerization to olefins is relatively less important in the triplet than singlet state of trimethylenes is also evidenced by the data of Simons and Rabinovitch (23) on the triplet and singlet methylene addition reactions to *cis*-butene-2; the ratio of the cyclic to the olefin products is decidedly higher for the triplet reactions.

The value of the primary quantum yield of the mercury photosensitization reaction can also be estimated from the combined data of the present study and that of S.R.S. (2). $\phi[1a]$ is found to be ~0.02 and $\phi[1b] \geq 0.37$ and 0.32 at 20 and 200 Torr pressure respectively. This brings up the question of other possible modes of energy dissipation and "primary" processes which might be operative in this system. In view of the fact that no Hg $6(^3P_0)$ atoms participate in the reaction (25), and the intensity of the recently detected band emission (26) around 2600 Å appears to be comparable to that from propane (ϕ(decomposition) ~ 1), no meaningful solution of this problem can be given at present.

Because of its relevance it should be noted that the only other cyclopropyl compound whose mercury-sensitized decomposition has been studied, spiropentane (27), exhibits similar kinetic features as reported here for cyclopropane. The only major primary step is carbon–carbon bond cleavage,

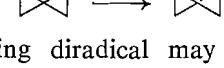

The resulting diradical may undergo unimolecular cleavage to ethylene and allene or may be collisionally stabilized as methylenecyclobutene. The combined yield of the two types of processes is unaltered by pressure and is equal to 0.55, manifesting an inherent quantum inefficiency.

Can. J. Chem. Downloaded from www.nrcresearchpress.com by 210.87.254.105 on 09/05/12
For personal use only.

Acknowledgments

The authors are grateful to the National Research Council of Canada for financial support, to Mr. O. Clement for valuable experimental assistance, and to Professor S. Rabinovitch of the University of Washington, Seattle, for most helpful discussions.

1. R. J. CVETANOVIĆ. *In* Progress in reaction kinetics. Vol. 2. *Edited by* G. Porter. Pergamon Press, London. 1964.
2. D. W. SETSER, B. S. RABINOVITCH, and E. G. SPITTLER. J. Chem. Phys. **35,** 1840 (1961).
3. D. W. SETSER, D. W. PLACZEK, R. J. CVETANOVIĆ, and B. S. RABINOVITCH. Can. J. Chem. **40,** 2179 (1962).
4. R. A. HOLROYD and G. W. KLEIN. J. Phys. Chem. **69,** 2129 (1965).
5. O. P. STRAUSZ and H. E. GUNNING. Trans. Faraday Soc. **60,** 347 (1964).
6. R. SRINIVASAN. J. Am. Chem. Soc. **83,** 4923 (1961).
7. T. HOLSTEIN. Phys. Rev. **83,** 1159 (1951).
8. B. DE B. DARWENT and M. K. PHIBBS. J. Chem. Phys. **22,** 110 (1954).
9. G. R. DE MARÉ, O. P. STRAUSZ, and H. E. GUNNING. Can. J. Chem. **43,** 1329 (1965).
10. P. J. KOZAK. Ph.D. Thesis, University of Alberta, Edmonton, Alberta. 1964.
11. G. GREIG and J. C. J. THYNNE. Trans. Faraday Soc. **62,** 3338 (1966); **63,** 1369, 2196 (1967).
12. Y. ROUSSEAU. Ph.D. Thesis, University of Alberta, Edmonton, Alberta. 1963.
13. H. DAUBEN. Department of Chemistry, University of Washington, Seattle. Private communication.
14. J. W. SIMONS, B. S. RABINOVITCH, and F. H. DOVER. J. Phys. Chem. **70,** 1076 (1966).
15. M. AVRAHAMI and P. KEBARLE. J. Phys. Chem. **67,** 354 (1963).
16. C. A. HELLER and A. S. GORDON. J. Chem. Phys. **42,** 1262 (1965).
17. H. E. GUNNING and E. W. R. STEACIE. J. Chem. Phys. **17,** 351 (1947). R. J. SCOTT and H. E. GUNNING. J. Phys. Chem. **56,** 156 (1952).
18. D. G. L. JAMES and G. E. TROUGHTON. Chem. Commun. 94 (1965).
19. M. Y. LUKINA. Russ. Chem. Rev. English Transl. **31,** 419 (1962).
20. H. E. SIMMONS. Private communication.
21. R. HOFFMANN. Abstracts of the 151st National Meeting of the Am. Chem. Soc., Pittsburgh, Pa., March, 1966. Paper 109K.
22. B. S. RABINOVITCH, E. TSCHUIKOW-ROUX, and E. W. SCHLAG. J. Am. Chem. Soc. **81,** 1081 (1959).
23. E. W. SCHLAG and B. S. RABINOVITCH. J. Am. Chem. Soc. **82,** 5996 (1960). J. W. SIMONS and B. S. RABINOVITCH. J. Phys. Chem. **68,** 1322 (1964). S. W. BENSON. J. Chem. Phys. **34,** 521 (1961). W. B. DEMORE and S. W. BENSON. *In* Advances in photochemistry. Vol. 2. Interscience, New York. 1964.
24. D. W. SETSER and B. S. RABINOVITCH. J. Am. Chem. Soc. **86,** 564 (1964).
25. S. PENZES, A. J. YARWOOD, O. P. STRAUSZ, and H. E. GUNNING. J. Chem. Phys. **43,** 4524 (1965).
26. S. PENZES, O. P. STRAUSZ, and H. E. GUNNING. J. Chem. Phys. **45,** 2322 (1966).
27. G. R. DE MARÉ, L. G. WALKER, O. P. STRAUSZ, and H. E. GUNNING. Can. J. Chem. **44,** 457 (1966).

Can. J. Chem. Downloaded from www.nrcresearchpress.com by 210.87.254.105 on 09/05/12
For personal use only.

Can. J. Chem. Downloaded from www.nrcresearchpress.com by 210.87.254.42 on 09/05/12
For personal use only.

Electrochemical reactions at PbO_2 electrodes. Part III. β-PbO_2 electrodes in acid perchlorate electrolytes at high overpotential

N. A. HAMPSON, P. C. JONES, AND R. F. PHILLIPS
Department of Chemistry, Loughborough University of Technology, Leicestershire, England

Received October 13, 1967

The mechanism of exchange between β-lead dioxide and plumbous ions in solution has been investigated using the galvanostatic technique. Interpretation of the η_D vs. i data is consistent with a change in mechanism from a single two-electron transfer step to two successive single-electron transfer steps as the magnitude of the potential excursion from equilibrium is increased.

Analysis of the slopes obtained from the linear-logarithmic region indicates that the slow step in the reaction is that leading to the formation of a Pb(III) intermediate.

The orders of reaction with respect to the plumbous and hydrogen ions have been obtained from the dependence of the rate of the reaction on the concentration of the electro-reactive species.

A reaction mechanism is suggested on the basis of the kinetic data.

Canadian Journal of Chemistry, 46, 1325 (1968)

Introduction

In Part II (1), galvanostatic measurements at β-PbO_2 electrodes in acid – lead perchlorate electrolytes were described in which the maximum amplitude of the potential excursion undertaken by the electrode was restricted to ±10 mV about the equilibrium potential. There was considerable evidence to show that in this range the exchange reaction involved a simultaneous two-electron transfer. The reaction is more complicated at higher overpotentials, however, and appears to follow two successive single-electron transfer steps. This paper deals with experiments in this higher overpotential region in which the maximum potential excursion is approximately ±300 mV.

Theory

Exchange Current and Rate-Determining Step

The equations for a 2-electron transfer between O and R involving two consecutive electron transfer steps and an intermediate, S, are as follows.

[1*a*] $$O + e = S$$

[1*b*] $$S + e = R$$

Each step has its own characteristic exchange current (i_{0a} and i_{0b}) and cathodic transfer coefficient (α_a and α_b). The exchange currents are defined in terms of concentrations C, and corresponding standard rate constants, k^0, by (2)

[2*a*] $$i_{0a} = Fk_a{}^0 C_O{}^{1-\alpha_a} C_S{}^{\alpha_a}$$

[2*b*] $$i_{0b} = Fk_b{}^0 C_S{}^{1-\alpha_b} C_R{}^{\alpha_b}.$$

By writing for each step a charge-transfer equation (3) for the dependence of the charge-transfer overpotential, η_D, upon current density, i, and then eliminating terms connected with the concentration of the intermediate species, Vetter (4) obtained the equation[1]

[3] $$\frac{i}{2} = \frac{\exp -(\alpha_a + \alpha_b)\frac{F\eta_D}{RT} - \exp(2 - \alpha_a - \alpha_b)\frac{F\eta_D}{RT}}{\frac{1}{i_{0b}}\exp(1-\alpha_a)\frac{F\eta_D}{RT} + \frac{1}{i_{0a}}\exp(-\alpha_b)\frac{F\eta_D}{RT}},$$

where F, R, and T have their usual significance. At high overpotential this equation gives plots of η_D versus $\log_e i$ (Tafel plots) having slopes $-\alpha_a F/RT$ and $(1-\alpha_b)F/RT$ for the cathodic and anodic branches respectively; corresponding intercepts of the rectilinear parts of these plots for $\eta_D = 0$ yield $2i_{0a}$ and $2i_{0b}$. Current–overpotential characteristics corresponding to eq. [3] have been computed by Hurd (5) for a number of i_{0a}/i_{0b} ratios. It was confirmed that the curves passed through the origin ($\eta_D = 0$, $i = 0$) with the slope predicted by eq. [4],

[4] $$-\left(\frac{\partial\eta_D}{\partial i}\right)_{\eta_D=0} = \frac{RT}{4F}\left(\frac{1}{i_{0a}} + \frac{1}{i_{0b}}\right),$$

obtained by differentiating eq. [3] with respect to i and setting $\eta_D = 0$. Vetter and Thiemke (6),

[1]This equation, in common with usage throughout this paper, conforms to I.U.P.A.C. conventions.

Can. J. Chem. Downloaded from www.nrcresearchpress.com by 210.87.254.42 on 09/05/12
For personal use only.

investigating the Tl(III)/Tl(I) reaction, calculated i_{0a} and i_{0b} from intercepts of the cathodic and anodic branches of the Tafel plots and showed that the slope calculated from eq. [4] agreed with that observed at $\eta_D = 0$. This evidence confirmed the view that the Tl(III)/Tl(I) exchange involves two consecutive one-electron transfer stages within the potential range investigated.

For the case of a two-electron transfer involving consecutive single-electron transfer steps in which one step is slow and rate determining, Lovreček (7) in a somewhat more general treatment than Vetter's (4) showed that the slopes of the cathodic and anodic branches of the linear-logarithmic regions are given respectively by

$$[5]^2 \qquad \frac{\partial \log_e i_C}{\partial \eta_D} = \frac{-F}{RT}(n_C^* - 1 + \alpha_i)$$

and

$$[6]^2 \qquad \frac{\partial \log_e i_a}{\partial \eta_D} = \frac{F}{RT}(n_A^* - \alpha_i),$$

where n_C^* (and n_A^*) is the ordinal number of the slowest step in a multistep cathodic (or anodic) reaction, and α_i is α_a or α_b (eqs. [1*a*] and [1*b*]). For the two-step reaction [1], n_C^* may be 1 (or 2) with α_i equal to α_a (or α_b); similarly when n_A^* is 1 (or 2), α_i is α_b (or α_a).

Expressions equivalent to eqs. [5] and [6] can each be obtained from eq. [3] by putting either i_{0a} or i_{0b} respectively equal to infinity. This has the effect of ensuring that the other reaction, for which i_0 is finite, controls the reaction (e.g. considering eqs. [1*a*] and [1*b*] for $i_{0a} = \infty$, i_{0b} is finite and reaction [1*b*] controls). Four $\partial \log_e i/\partial \eta_D$ values (two anodic and two cathodic) are obtained corresponding to $n_A^* = 1$ or 2 and $n_C^* = 1$ or 2 using, in each case, the appropriate value of the transfer coefficient.

The usefulness of Lovreček's treatment lies in the possibility of choosing values of n_A^* and n_C^* consistent with the experimental data and hence identifying the slow step in the multistep process. Lovreček and Marinčić (8) for example applied the method to the Cd(II)/Cd(Hg) exchange.

The Electrochemical Reaction Order

The determination of reaction order by observing the dependence of the rate of the reaction on concentration is well established. It has not, however, been much applied to the study of reactions at electrodes with the exception of Vetter, Gerisher, and their collaborators who have used the method extensively for elucidating electrochemical reactions at mercury and amalgam electrodes (see for example ref. 9). The basis is that, at sufficiently high cathodic overpotentials, the cathodic current flowing at any fixed potential is a function of the concentration of those electro-reactive species directly involved in the cathodic current flow. Conversely, at high anodic overpotentials the reaction rate (measured by i) is a function of the concentration of the reduced species. For comparison of these reaction rates (current densities), potentials must be referred to some standard and in our case the reference potential chosen was that corresponding to arbitrarily selected solutions of fixed composition.

This particular procedure is only possible if either the anodic or cathodic exchange reactions can be suppressed by the application of high overpotentials. In some cases such overpotential measurements are not feasible, but reaction orders may still be deduced, however, from the dependence of the exchange currents on concentration, using relationships of the type given by eq. [2].

Experimental

The experimental apparatus and technique were the same as those detailed in previous parts (1, 10). Galvanostatic polarizations were made corresponding to cathodic and anodic activation overpotentials as high as |300 mV|. A range of electrolytes (constant perchlorate ion concentration 6.85 *M*) of variable $[Pb^{2+}]$ at constant $[H^+]$ and variable $[H^+]$ at constant $[Pb^{2+}]$ were investigated.

Results

Determinations were first made of αZ and i_0 using the iterative method of Farr, Hampson, and Williamson (11). Experimental η_D and i values were introduced into the charge-transfer eq. [3] in the form

$$[7] \quad i = i_0[\exp -\alpha ZF\eta_D/RT - \exp (1-\alpha)ZF\eta_D/RT]$$

(where α is the cathodic transfer coefficient and Z the number of electrons involved in the single step electron-transfer process) and the iterative technique used to determine optimum values of αZ and i_0. This involved minimizing the root-

[2]The present use of the I.U.P.A.C. convention changes the eqs. [5] and [6] from the corresponding ones given in refs. 7 and 8. This has the effect of replacing α by $(1 - \alpha)$. (Care should be taken over signs in reading ref. 8.) Care must be taken in extending equations of types [5] and [6] to more complicated systems (see Wright (16)).

TABLE I

Potential limits of constant αZ. Potential region (about the equilibrium) in which the reaction conforms to a simultaneous two-electron transfer process

Concentration, M	Potential region (± 5 mV)
1. *Lead concentration* at constant $[H^+] = 3.0\ M$, $[ClO_4^-] = 6.85\ M$	
1.47	−28 mV to +12 mV
0.47	−30 mV to +16 mV
0.093	−41 mV to +19 mV
2. H^+ *concentration* at constant $[Pb^{2+}] = 0.1\ M$, $[ClO_4^-] = 6.85\ M$	
3.0	−30 mV to +13 mV
0.48	−32 mV to +15 mV
0.20	−28 mV to +13 mV

mean-square deviation of arbitrarily chosen i_0 values, using an I.C.T. 1905 computer.[3]

Calculations were made over a progressively increasing range of η_D values, each successive increase (with the associated i) being incorporated with the previous η_D vs. i values. For example, 10 sets of η_D vs. i readings at 1 mV intervals were used to cover the range up to 10 mV (point A, Fig. 1). The range of experimental readings was then increased to 15 mV and so on to cover the whole potential range (point B, Fig. 1).

Our results show that in the lower η_D ranges, αZ and i_0 remained constant for both anodic and cathodic polarization, but as the magnitude of η_D was increased in the higher range, these optimum values of αZ and i_0 changed. In Fig. 1 these optimum αZ values are plotted for a particular electrolyte concentration, as a function of the highest value of η_D, ($\eta_{D\,max}$). Table I shows the limits within which αZ is constant. The changes in αZ from the constant value at low anodic and cathodic η_D indicates a change in the charge-transfer process.

Figures 2 and 3 show current–overpotential characteristics presented as log i vs. η_D (Tafel) plots. Figure 2 refers to electrolytes of varying Pb^{2+} and constant H^+ concentration, relative to the reference system 3.0 M H^+, 1.0 M Pb^{2+} (6.85 M ClO_4^- with added $NaClO_4$) at equilibrium. On this scale potentials (represented by E_{3M}) are given by

$$[8]\quad E_{3M} = \eta_D - 0.029 \log_{10} [Pb^{2+}] \text{ at } 25\ ^\circ C.$$

Potentials for the complementary system (varying H^+ and constant Pb^{2+} concentrations) shown in Fig. 3 are relative to the equilibrium potential for the reference system 0.1 M Pb^{2+} and 1.0 M H^+. On this scale, potentials (represented by E'_{1M}) are given by

$$[9]\quad E'_{1M} = \eta_D + 0.118 \log_{10} [H^+] \text{ at } 25\ ^\circ C.$$

The validity of both eqs. [8] and [9] was confirmed for the above systems by potentiometric measurements at equilibrium (i.e. $\eta_D = 0$).

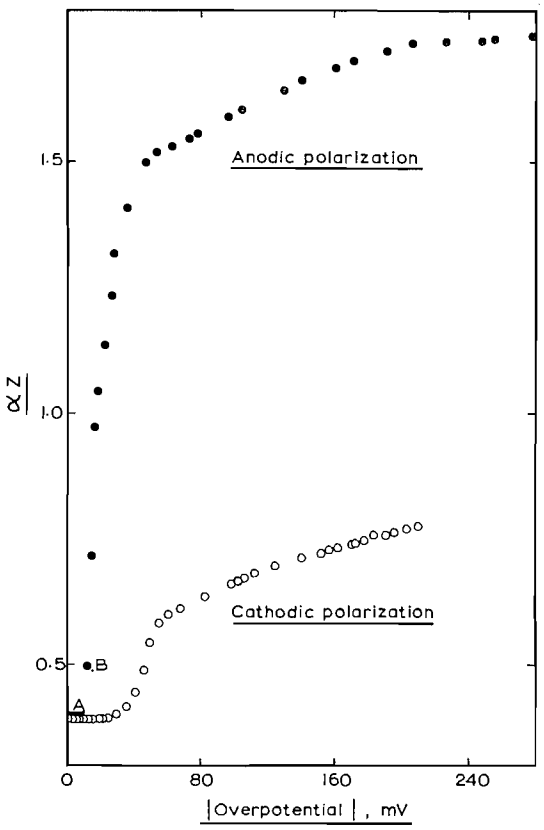

FIG. 1. Variation of transfer coefficient with overpotential β-PbO_2 electrode: electrolyte 0.1 M Pb^{2+} + 0.02 M H^+. Total $[ClO_4^-]$, 6.85 M (with $NaClO_4$); 23 °C.

[3]A program written in Fortran IID is available from the authors.

Can. J. Chem. Downloaded from www.nrcresearchpress.com by 210.87.254.42 on 09/05/12
For personal use only.

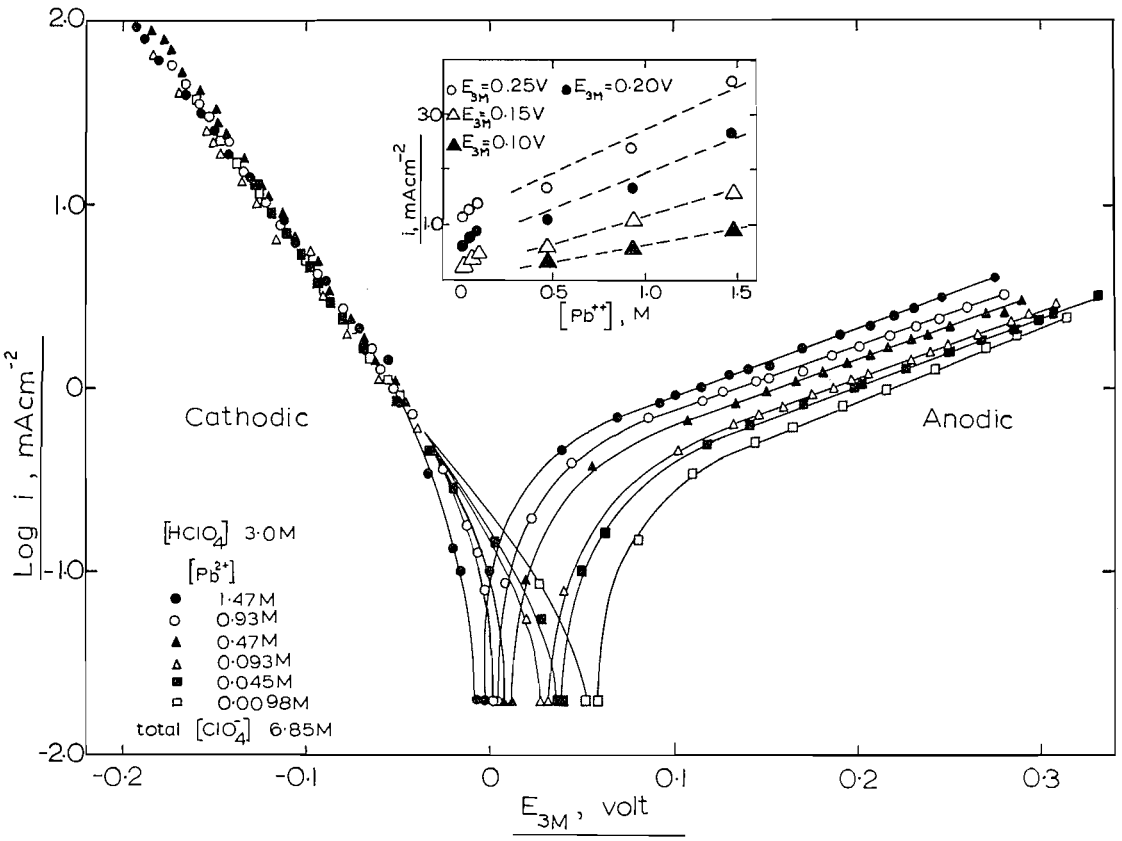

FIG. 2. Anodic and cathodic current density – potential curves for β-PbO_2 at various Pb(II) concentrations in 3.0 *M* $HClO_4$ at 23 °C.

The small diagram in Fig. 2 shows the dependence of anodic current on $[Pb^{2+}]$ at constant potential. Figures 4 and 5 show the dependence of anodic and cathodic currents on $[H^+]$ for polarization within the Tafel region.

The dependence of exchange currents (i_{0a} and i_{0b}) on $[Pb^{2+}]$ is shown in Fig. 6 and on $[H^+]$ in Fig. 7.

Discussion

Process Change

In an earlier paper (1) it was shown that the computed transfer coefficient for the low overpotential region is the same for both anodic and cathodic polarization and that this value agreed with that derived from the dependence of exchange current on lead ion concentration. It was also shown that the exchange currents were identical for both anodic and cathodic polarization for a given electrolyte.

In the present work it has been shown that when the potential excursion from the equilibrium potential is increased sufficiently, a pronounced change is observed in the kinetic parameters, as indicated by significant variations in αZ (Fig. 1, Table I). The constancy of αZ in the lower overpotential regions extends further into the cathodic than into the anodic region. It should be noted that attempts to force η_D vs. i data of the form given by eq. [3] into an expression of the type eq. [7] would result, for small $|\eta_{D\,max}|$, in the computed αZ values being strongly dependent upon $|\eta_{D\,max}|$ with this dependence becoming negligible as $|\eta_{D\,max}|$ increased to high values, results which are at variance with the above observations.

Table II shows the characteristics [i_0 and $(RT/F)\partial \log_e i/\partial \eta_D$] calculated from the linear high overpotential Tafel plots. These results

Can. J. Chem. Downloaded from www.nrcresearchpress.com by 210.87.254.42 on 09/05/12
For personal use only.

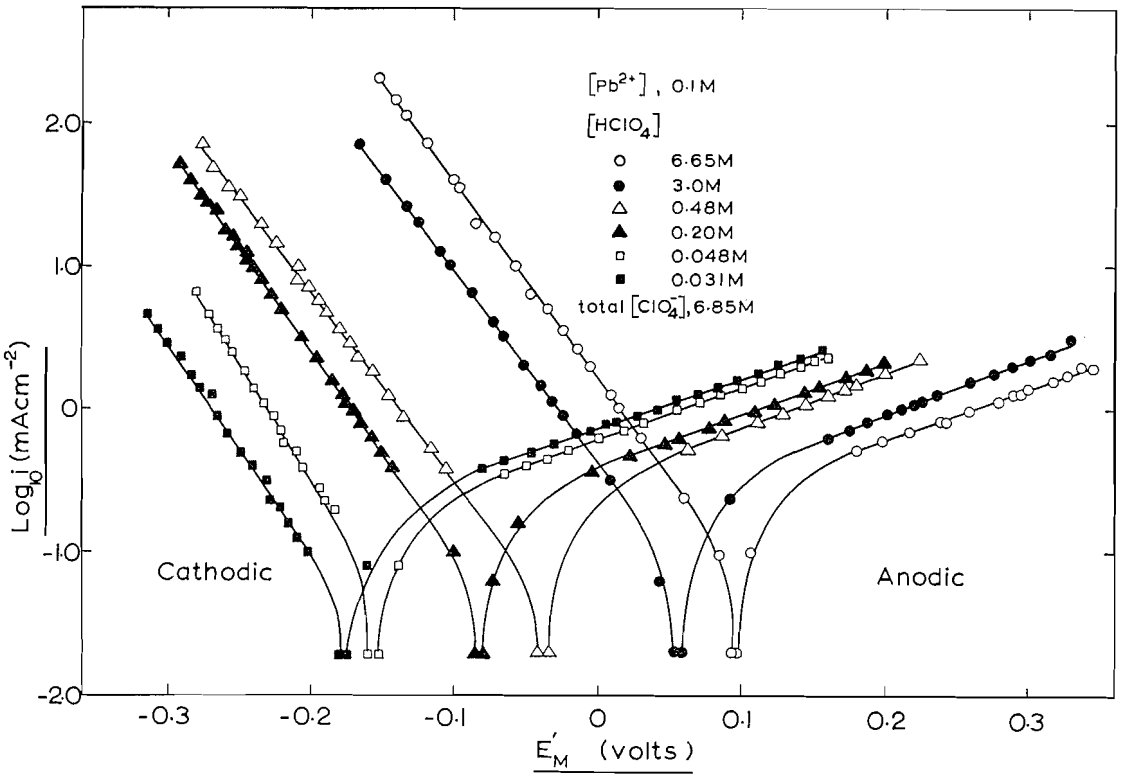

FIG. 3. Anodic and cathodic current density – potential curves for β-PbO_2 at variable H^+ concentration in 0.1 *M* Pb^{2+} at 23 °C.

suggest that in this high overpotential region the reaction involves two consecutive single-electron charge-transfer steps. Thus, (*a*) the sum of the cathodic and anodic coefficients $[-(RT/F)\partial \log_e i_C/\partial\eta_D$ and $(RT/F)\partial \log_e i_A/\partial\eta_D$, respectively] is significantly less than two; (*b*) the anodic and cathodic exchange currents, obtained by extrapolation of Tafel plots to η_D equal zero, are appreciably different; and (*c*) these exchange currents differ from those obtained for the low overpotential region (1). That these consecutive single-electron charge-transfer processes do not, however, occur in the low overpotential region is seen from an analysis of the results in Table III. This follows from a comparison of the experimental charge-transfer resistances (1) (calculated

TABLE II

Characteristics of Tafel plots. β-PbO_2 electrode: total $[ClO_4^-] = 6.85$ *M* (with added $NaClO_4$); 23 °C

Concentration (*M*)		Cathodic coeff., $\frac{-2.303RT}{F}\frac{\partial \log i_C}{\partial\eta_D}$	Anodic coeff., $\frac{2.303RT}{F}\frac{\partial \log i_A}{\partial\eta_D}$	Intercepts at $\eta_D = 0$	
Pb^{2+}	H^+			$2i_{0a}$ (mA cm^{-2})	$2i_{0b}$ (mA cm^{-2})
0.93	3.0	0.84	0.21	0.250	0.331
0.47	3.0	0.88	0.22	0.118	0.285
0.093	3.0	0.82	0.22	0.074	0.257
0.045	3.0	0.90	0.22	0.040	0.250
0.089	0.48	0.84	0.22	0.050	0.220
0.092	0.20	0.86	0.22	0.052	0.200
0.093	0.0032	0.82	0.24	0.042	0.118

Can. J. Chem. Downloaded from www.nrcresearchpress.com by 210.87.254.42 on 09/05/12
For personal use only.

Can. J. Chem. Downloaded from www.nrcresearchpress.com by 210.87.254.42 on 09/05/12
For personal use only.

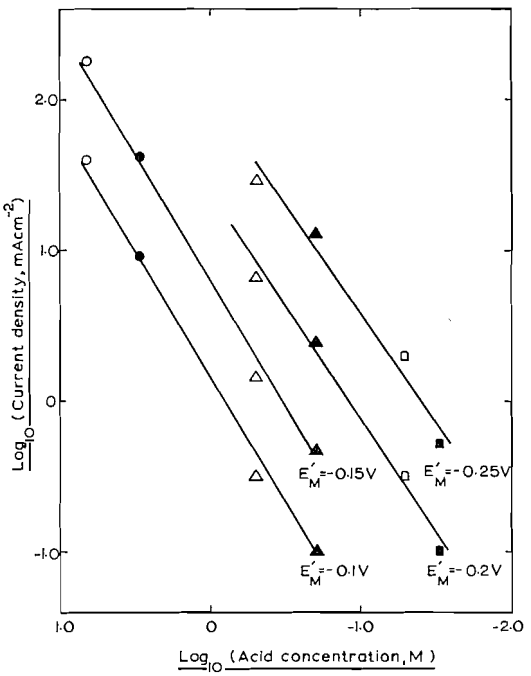

FIG. 4. Dependence of cathodic faradaic current density on H^+ concentration. β-PbO_2 electrode at 23 °C.

for $\eta_D < 10$ mV) with those obtained from the theoretical slope of the appropriate equation [4] for the two-consecutive single-electron transfer steps; the differences in magnitude indicate a change in the reaction mechanism from that applying in the high overpotential region.

TABLE III

Charge-transfer resistances. Comparison of experimental charge-transfer resistances (1) (for $\eta_D < 10$ mV) with those calculated from eq. [4] (for $\eta_D > 50$ mV)

Concentration (*M*)		Charge-transfer resistance (ohm cm²)	
Pb^{2+}	H^+	Experimental (1)	Calculated
0.93	3.0	72	89
0.47	3.0	83	152
0.093	3.0	114	222
0.045	3.0	133	369
0.095	6.65	80	212
0.089	0.48	142	312

Rate-Determining Step

The slopes of Tafel plots for a series of electrolyte compositions are fairly constant (Table II). Interpretation of this data using Lovreček's theory only gives rational values for the charge-transfer coefficients, corresponding to the 1st and 2nd charge-transfer reactions, if n_A^* and n_C^* are each equal to one. Hence, the first charge-transfer step in both the anodic and cathodic directions emerges as the rate-determining step.

On this basis we calculate the charge-transfer coefficients α_a and α_b using eqs. [5] and [6] and the mean Tafel slopes as

[10] $$n_C^* - 1 + \alpha_a = 0.86 \pm 0.1; \quad \alpha_a = 0.86 \pm 0.1$$

[11] $$n_A^* - \alpha_b = 0.24 \pm 0.02; \quad \alpha_b = 0.78 \pm 0.02.$$

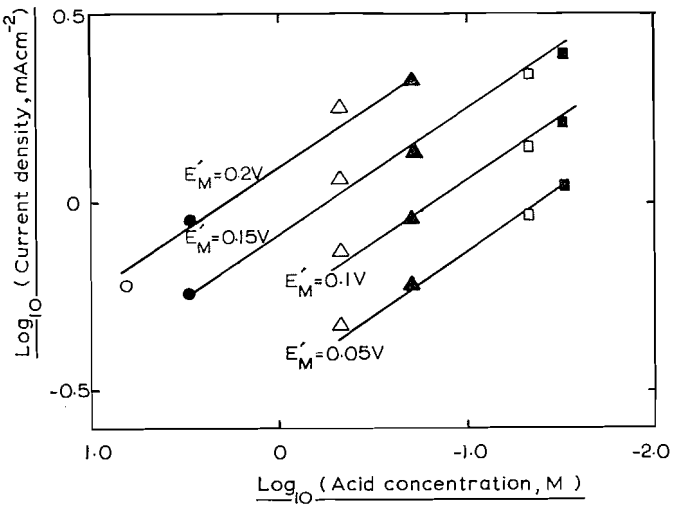

FIG. 5. Dependence of anodic faradaic current density on H^+ concentration. β-PbO_2 electrode at 23 °C.

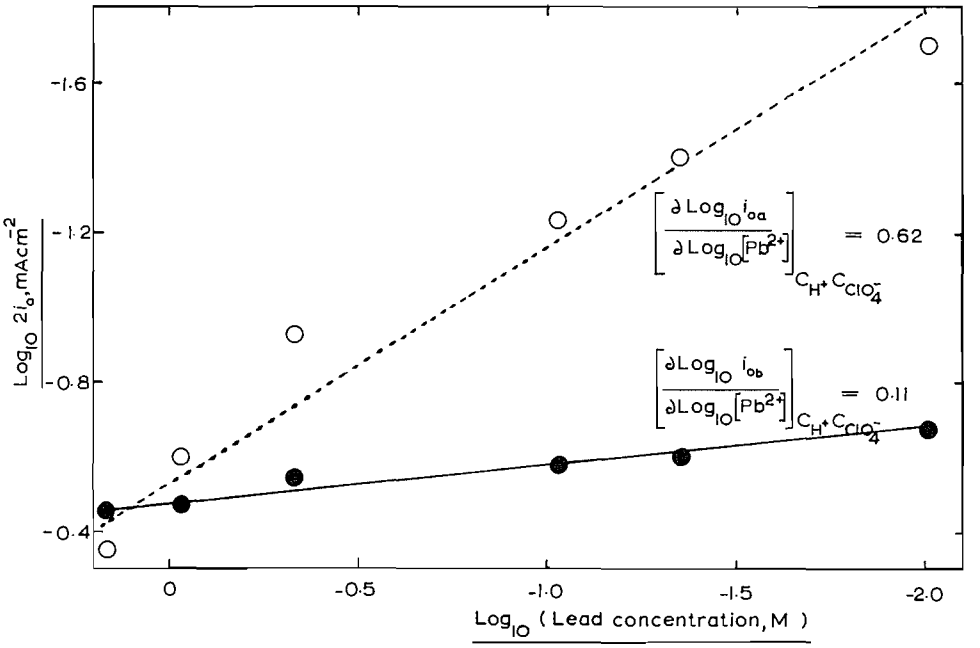

FIG. 6. Variation of exchange current with lead concentration. β-PbO_2 electrode; total [ClO_4^-], 6.85 *M* (with $NaClO_4$); [H^+], 3.0 *M*. 23 °C.

Reaction Order

The dependence of current on [Pb^{2+}] at anodic and cathodic overpotentials is shown in Fig. 2. Referring to the cathodic plot, it will be seen that in the higher overpotential region the experimental results fall on the same straight (Tafel) line. This is to be expected from the fact that the activity of β-PbO_2 is constant.

$$\left(\frac{\partial i_C}{\partial[Pb^{2+}]}\right)_{C_{H^+}, C_{ClO_4^-}, T, E}$$

is therefore zero.

For the anodic side of Fig. 2, a family of parallel linear (Tafel) plots is obtained in the higher overpotential region, and further examination of these plots (inserted plot of Fig. 2) shows that

$$\left(\frac{\partial i_A}{\partial[Pb^{2+}]}\right)_{C_{H^+}, C_{ClO_4^-}, T, E}$$

is constant over a wide concentration range. This suggests that the rate of the reaction is first order with respect to [Pb^{2+}] over this concentration range. However, plots of log i_A vs. log Pb^{2+} at constant potential show a decrease in reaction order in the lower [Pb^{2+}] regions, tending from ~ 1 to ~ 0.3. Various explanations of this low reaction order may be offered. Fleischmann and Liler (12) have observed similar apparently low reaction orders (0.26), in the case of deposition of PbO_2 from acetate solutions, and explained these in terms of the adsorption of Pb^{2+} at the electrode; there is, however, no discernible evidence for Pb^{2+} adsorption in our system (1). Alternatively, self-discharge might occur especially at low [Pb^{2+}]. Since at least one Pb^{2+} ion must, however, be concerned in the electrode reaction, it seems very probable therefore that the reaction is first order with respect to Pb^{2+}.

From the above observations and the following derived information (see Figs. 3, 4, and 5)

$$[12] \quad \left(\frac{\partial \log i_C}{\partial \log C_{H^+}}\right)_{C_{Pb^{2+}}, C_{ClO_4^-}, T, E} = 1.5$$

$$[13] \quad \left(\frac{\partial \log i_A}{\partial \log C_{H^+}}\right)_{C_{Pb^{2+}}, C_{ClO_4^-}, T, E} = -0.4,$$

we may now write for cathodic polarization,

$$[14] \quad i_C = k_C F C_{H^+}^{1.5},$$

and for anodic polarization,

$$[15] \quad i_A = k_A F C_{Pb^{2+}} C_{H^+}^{-0.4},$$

where k_C and k_A are the potential-dependent rate constants.

Can. J. Chem. Downloaded from www.nrcresearchpress.com by 210.87.254.42 on 09/05/12
For personal use only.

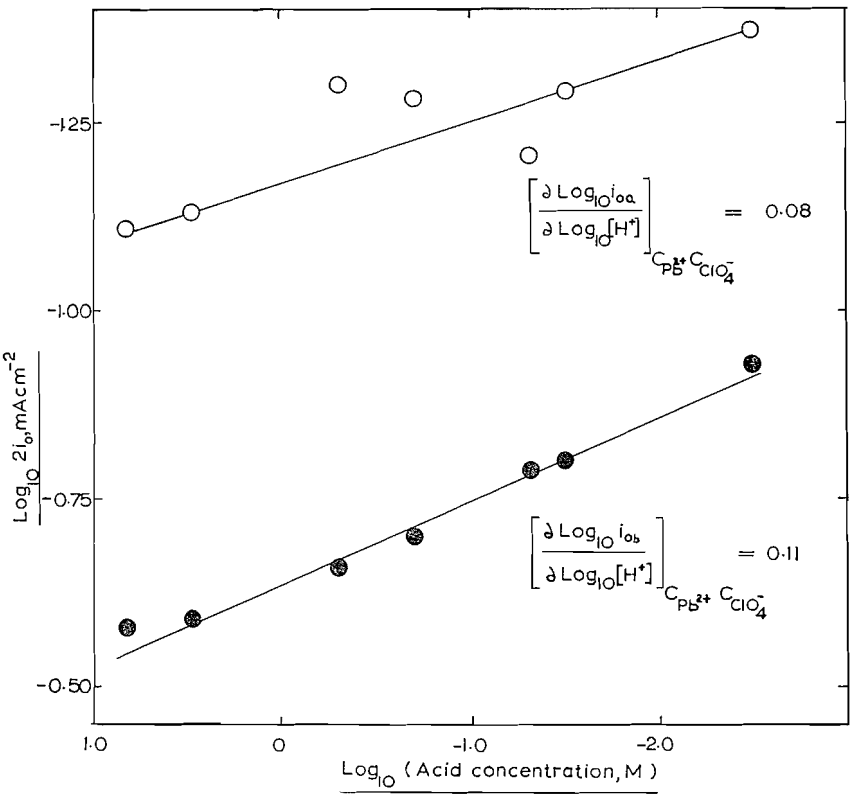

FIG. 7. Variation of exchange current with H^+ concentration. β-PbO_2 electrode; total [ClO_4^-], 6.85 *M* (with $NaClO_4$); [Pb^{2+}], 0.1 *M*. 23 °C.

Mechanism

A possible mechanism (written in the cathodic direction) at high overpotentials is as follows.

[16*a*] $PbO_2 + 2H^+ \rightleftharpoons PbO_2(H^+)_2$ ads.

[16*b*] $PbO_2(H^+)_2$ ads. + e = $[HO.Pb.OH]^+$

[16*c*] $[HO.Pb.OH]^+ + e = Pb(OH)_2$

[16*d*] $Pb(OH)_2 + 2H^+ \rightleftharpoons Pb^{2+} + 2H_2O$

The existence of free Pb^{4+} ions in solution is unlikely. Consequently, it seems probable that the overall reaction involves a Pb(IV) species [16*a*] at the surface, either adsorbed or as part of the lattice. Hydrogen ion adsorption at the PbO_2 lattice has been reported by Rüetschi and Cahan (13) and by Hampson *et al.* (1). The proposed species $PbO_2(H^+)_{2\ ads.}$ may be compared with $Pb(OH)_2^{2+}$, postulated by Fleischmann and Liler (12) as an intermediate in the electrodeposition of PbO_2 from acetate solutions. In the present discussion the $PbO_2(H^+)_{2\ ads.}$ intermediate is considered to arise as a surface species formed as the product of adsorption of H^+ by lattice O atoms on the surface. Such an adsorption would be expected to further weaken the bonds between surface lead atoms and the underlying fully coordinated oxygen atoms of the PbO_2.

The slow stage of the overall reaction is that involving the first electron transfer. This is the stage eq. [16*b*] in which we suggest formation of a Pb(III) hydroxy intermediate, $[HO.Pb.OH]^+$. It may be noted that Varypaev and Fedot'ev (14) similarly considered Pb(III) formation to be the slow step in the electrodeposition of PbO_2 from $Pb(NO_3)_2$ solution; schemes based on a Pb^{3+} ion, however, are more open to objection than those based on a transitory single-charged intermediate.

Our results show that addition of the second electron eq. [16*c*] is fast, leading we suggest to the formation of $Pb(OH)_2$, in line with the view

Can. J. Chem. Downloaded from www.nrcresearchpress.com by 210.87.254.42 on 09/05/12
For personal use only.

Can. J. Chem. Downloaded from www.nrcresearchpress.com by 210.87.254.42 on 09/05/12
For personal use only.

that $Pb(OH)_2$, being a neutral molecule, might be expected to transfer across the double layer more readily than would a charged ion, such as Pb^{2+} (15).

When the process is carried out anodically, the above reactions occur in the reverse order and the slow stage is now eq. [16*c*], again leading to the formation (we suggest) of the same [HO.Pb.OH]$^+$.

For the cathodic reaction (rate control by eq. [16*b*]) we have, at sufficiently high overpotential,

$$[17a] \qquad i_C = k_C F C_{PbO_2(H^+)_2}.$$

From the equilibrium [16*a*], and taking the activity of β-PbO_2 as constant, it then follows, in the absence of adsorption of H^+ ions, that

$$[17b] \qquad i_C = k_C' F (C_{H^+})^2,$$

where k_C' is the appropriate rate constant. The effect of such H^+ ion adsorption would be to reduce the exponent of the C_{H+} term; our observations of an exponent of 1.5 is thus evidence for H^+ adsorption.

For the anodic reaction (rate control [16*c*]) the corresponding equation at sufficiently high overpotential is

$$[18] \qquad i_A = k_A F C_{Pb(OH)_2}.$$

Since, from the equilibrium [16*d*],

$$[19] \qquad K_S = [Pb(OH)_2][H^+]^2/[Pb^{2+}],$$

(where K_S is the equilibrium constant), it then follows that

$$[20] \qquad i_A = k_A' F C_{Pb^{2+}} C_{H^+}^{-2},$$

(where k_A' is the rate constant). In this case H^+ adsorption would increase the value of the C_{H+} exponent, eq. [20]. Our observed value, −0.4, indicates therefore the presence of such adsorption, in further support of the similar conclusions from our cathodic experiments and previous observations (1, 13). There seems no reason to suggest, however, that the same amount of adsorption occurs for both anodic and cathodic processes. Adsorption is likely to be potential dependent, and therefore different for anodic and cathodic polarization.

Apparent Exchange Current

The calculation of exchange current by extrapolation of linear-logarithmic η_D vs. i data to $\eta_D = 0$ assumes that no mechanistic change occurs in the region over which the extrapolation is made. Since such a change does occur, i_0 values calculated this way can only be interpreted hypothetically (for high η_D reaction). These apparent exchange currents, however, depend on the concentration of the electro-reactive species, and we can write from eqs. [16*b*], [16*c*], and [16*d*], in terms of eqs. [2*a*] and [2*b*] for a single-electron cathodic transfer,

$$[21] \qquad i_{0a} = k_a'^0 C_{PbO_2(H^+)_2}^{1-\alpha_a} C_{Pb(III)}^{\alpha_a}.$$

From the equilibrium [16*a*]

$$[22] \qquad K = [PbO_2(H^+)_2]/[H^+]^2,$$

it follows that

$$[23] \qquad i_{0a} = k_a''^0 C_{Pb(III)}^{\alpha_a} C_{H^+}^{2(1-\alpha_a)}.$$

Similarly for the anodic reaction

$$[24] \qquad i_{0b} = k_b'^0 C_{Pb(III)}^{(1-\alpha_b)} C_{Pb(OH)_2}^{\alpha_b},$$

which with eq. [19] gives

$$[25] \qquad i_{0b} = k_b''^0 C_{Pb(III)}^{(1-\alpha_b)} C_{Pb^{2+}}^{\alpha_b} C_{H^+}^{-2\alpha_b},$$

where $k_a'^0, k_a''^0, k_b'^0$, and $k_b''^0$ are rate constants.

Both eqs. [23] and [25] contain a term involving the intermediate Pb(III) species. Since the concentration of this latter is unlikely to be independent of potential (because of its ionic nature), the apparent exchange may only be discussed semiqualitatively.

From eq. [23] are obtained the following two equations for the cathodic reaction.

$$[26]^4 \qquad \left(\frac{\partial \log i_{0a}}{\partial \log C_{Pb^{2+}}}\right) = \alpha_a \left(\frac{\partial \log C_{Pb(III)}}{\partial \log C_{Pb^{2+}}}\right)$$

$$[27]^4 \qquad \left(\frac{\partial \log i_{0a}}{\partial \log C_{H+}}\right) = 2(1-\alpha_a) + \alpha_a \left(\frac{\partial \log C_{Pb(III)}}{\partial \log C_{H+}}\right)$$

Reference to Fig. 6 shows that the l.h.s. of eq. [26] has the numerical value ~0.6, and combining this value with the previously determined value of 0.86 for α_a (eq. [10]), we obtain

$$[28]^4 \qquad \left(\frac{\partial \log C_{Pb(III)}}{\partial \log C_{Pb^{2+}}}\right) = 0.7.$$

Similarly (from Fig. 7) the l.h.s. of eq. [27] has the value ~0.08, leading to

$$[29]^4 \qquad \left(\frac{\partial \log C_{Pb(III)}}{\partial \log C_{H+}}\right) = -0.2.$$

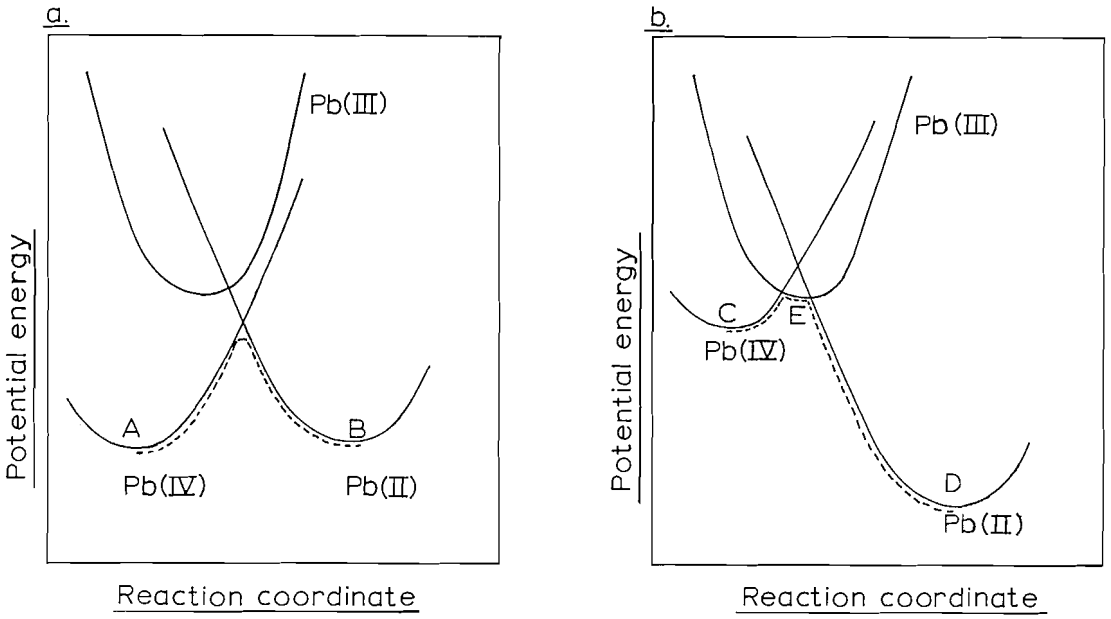

FIG. 8. Potential energy diagram.

In the same way, eq. [25] gives the following two equations for the anodic reaction.

$$[30]^4 \quad \left(\frac{\partial \log i_{0b}}{\partial \log C_{Pb^{2+}}}\right) = \alpha_b + (1 - \alpha_b)\left(\frac{\partial \log C_{Pb(III)}}{\partial \log C_{Pb^{2+}}}\right)$$

$$[31]^4 \quad \left(\frac{\partial \log i_{0b}}{\partial \log C_{H^+}}\right) = -2\alpha_b + (1 - \alpha_b)\left(\frac{\partial \log C_{Pb(III)}}{\partial \log C_{H^+}}\right)$$

The corresponding numerical values for the l.h.s., from Figs. 6 and 7, are 0.11 and 0.11 and these combined with the previously determined α_b value of 0.78 (eq. [11]) give

$$[32]^4 \quad \left(\frac{\partial \log C_{Pb(III)}}{\partial \log C_{Pb^{2+}}}\right) = -3.0$$

$$[33]^4 \quad \left(\frac{\partial \log C_{Pb(III)}}{\partial \log C_{H^+}}\right) = 7.6$$

The two cathodic results (eqs. [28] and [29]) could be interpreted as indicating an increase in the effective concentration of the Pb(III) intermediate with decrease in $[H^+]$ or increase in $[Pb^{2+}]$. These latter changes would, in effect, alter the electrode potential to more negative values and so (as illustrated above) favor the participation of the Pb(III) in the overall reaction. Similarly, in the anodic process (eqs. [32] and [33]), increasing the $[H^+]$ or decreasing the $[Pb^{2+}]$ will raise the electrode potential and again favor the Pb(III) participation. This is in line with the results of the $|\eta_D|$ vs. αZ correlation, Fig. 2. Thus at high positive and at high negative potentials the reaction becomes consecutive electron transfer involving an intermediate.

The above evidence for two consecutive single-electron stages at high overpotential must, however, be considered in conjunction with the earlier evidence (and ref. 1) for a single two-electron stage at low overpotential. Figures 8*a* and 8*b* relate to the lower overpotential and high overpotential conditions respectively. In Fig. 8*a* the reaction path (dotted line) does not cross the energy curve for the Pb(III); there is no transitory intermediate and the two-electron reaction occurs in one step. In 8*b*, however, the cathodic polarization raises curve A to curve C; in this case, the Pb(III) energy curve is intersected so producing a "stable" region (E in Fig. 8*b*) of

[4]In eqs. [26]–[33] the appropriate intensity factors are maintained constant, e.g. in eq. [26], $[H^+]$, $[ClO_4^-]$, T are constant.

Can. J. Chem. Downloaded from www.nrcresearchpress.com by 210.87.254.42 on 09/05/12
For personal use only.

existence of this intermediate in the overall path from C to D, with the result that the overall charge-transfer process now occurs in two consecutive single-electron transfer steps.

Acknowledgment

One of us (PCJ) thanks the Loughborough University of Technology for a grant.

1. N. A. HAMPSON, P. C. JONES, and R. F. PHILLIPS. Can. J. Chem. **45**, 2045 (1967).
2. P. DELAHAY. Double layer and electrode kinetics. Interscience, New York. 1965. Chap. 7. p. 164.
3. W. ERDY-GRUZ and M. VOLMER. Z. Physik. Chem. Leipzig, **150A**, 203 (1930).
4. K. J. VETTER. Z. Naturforsch. **7a**, 328 (1952).
5. R. M. HURD. J. Electrochem. Soc. **109**, 327 (1962).
6. K. J. VETTER and G. THIEMKE. Z. Elektrochem. **64**, 805 (1960).
7. B. LOVREČEK. J. Phys. Chem. **63**, 1795 (1959).
8. B. LOVREČEK and N. MARINČIĆ. Electrochim. Acta, **11**, 237 (1966).
9. K. J. VETTER. *In* Transactions of the symposium on electrode processes, Philadelphia, Pa., 1959. *Edited by* E. Yeager. J. Wiley and Sons, New York. 1961. p. 47.
10. N. A. HAMPSON, P. C. JONES, and R. F. PHILLIPS. Can. J. Chem. **45**, 2039 (1967).
11. J. P. G. FARR, N. A. HAMPSON, and M. E. WILLIAMSON. J. Electroanal. Chem. **13**, 462 (1967).
12. M. FLEISCHMANN and M. LILER. Trans. Faraday Soc. **54**, 1370 (1958).
13. P. RÜETSCHI and B. D. CAHAN. J. Electrochem. Soc. **104**, 406 (1957).
14. V. N. VARYPAEV and N. P. FEDOT'EV. Tr. Leningr. Tekhnol. Inst. im. Lensoveta, **46**, 103 (1958).
15. H. GERISCHER. Anal. Chem. **31**, 33 (1959).
16. G. A. WRIGHT. J. Electrochem. Soc. **114**, 1263 (1967).

Can. J. Chem. Downloaded from www.nrcresearchpress.com by 210.87.254.42 on 09/05/12
For personal use only.

Can. J. Chem. Downloaded from www.nrcresearchpress.com by 210.87.254.42 on 09/05/12
For personal use only.

Cyclic voltammetry of diphenylpicrylhydrazyl in tetrahydrofuran

B. Lionel Funt[1] and Derek G. Gray
Department of Chemistry, University of Manitoba, Winnipeg, Manitoba

Received October 2, 1967

Cyclic voltammetry has revealed four reversible single electron transfer processes in the oxidation and reduction of diphenylpicrylhydrazyl (DPPH) in tetrahydrofuran (THF). These are associated with a cation, a free radical, a monoanion, a dianion radical, and a trianion of DPPH.

THF is a good solvent for cyclic voltammetry as evidenced by the stability of the products generated at the electrodes. It is also one of the few excellent solvents for anionic polymerization and is therefore a remarkably suitable medium for studies of electropolymerization phenomena.

Canadian Journal of Chemistry, 46, 1337 (1968)

Tetrahydrofuran is an excellent solvent for electrolytically initiated anionic polymerization as well as for conventional anionic polymerization (1–3). This led us to an investigation of the suitability of this solvent for an electrochemical study of the initiating process for polymer formation. As a model electroactive compound for organic solvent systems, Solon and Bard (4) suggested the use of diphenylpicrylhydrazyl (DPPH), as they found that this free radical undergoes a reversible one-electron reduction to form a stable anion and a one-electron oxidation to form a stable cation in acetonitrile, methanol, ethanol, acetone, and dimethylsulfoxide.

DPPH is a compound of profound interest in polymer chemistry and has been widely employed as an inhibitor and free radical trap. An elucidation of its redox behavior appeared of intrinsic merit.

Experimental

Tetrahydrofuran (Fisher Certified) was dried over calcium hydride, fractionated, and stored over calcium hydride on the vacuum line. Tetrabutylammonium perchlorate (Southwestern Analytical, polarographic grade) was carefully dried by heating and evacuation. Diphenylpicrylhydrazyl (Eastman) was used as supplied.

High vacuum conditions were used for all solvent transfers and electrolytic measurements. The glass electrolytic cell contained a planar working electrode made from the cross section of a 1/16 in. diameter platinum wire sealed in glass. Because of the risk of contamination from conventional electrodes a silver wire sheathed in a glass capillary was used as a reference electrode. The counter electrode was a 1 in. diameter platinum disc. The complete cell was thermostatted at 25 °C. A Wenking 61RH potentiostat was used, coupled with a Hewlett Packard 3300A function generator and 7030A XY recorder. Background currents were negligible and over the complete range 0.6 V to −3.1 V were less than 0.3 μA.

Results

Figure 1 shows a cyclic voltammogram covering the potential range available in the solvent. In addition to the expected formation of a stable cation (A) and anion (B) at the left (anodic) side of the voltammogram, two further single electron transfers (C), (D) occur at more cathodic potentials. It has been shown (5) that in aprotic solvents, aromatic nitro-compounds undergo reversible one-electron reductions to give stable radical ions. At more negative potentials, dianions, unstable in a dimethyl formamide medium, were formed. The voltammetric evidence here suggests that DPPH undergoes a similar reduction of a nitro-substituent. The four electron transfer processes indicated in Fig. 1 may be written:

Process A	B	C	D
$DPPH^{+} \underset{-e}{\overset{+e}{\rightleftarrows}} DPPH\cdot$	$DPPH\cdot \underset{-e}{\overset{+e}{\rightleftarrows}} DPPH^{-}$	$DPPH^{-} \underset{-e}{\overset{+e}{\rightleftarrows}} DPPH^{--}$	$DPPH^{--} \underset{-e}{\overset{+e}{\rightleftarrows}} DPPH^{---}$

The species represented as ions will presumably exist as ion aggregates with tetra-alkyl ammonium counter ions in this solvent.

Each of the electron transfer steps may be examined individually by cyclic voltammetry. For example, Fig. 2 indicates the effect obtained by varying the scan rate for process B. The theoretically predicted linear relationship between the peak current and the half-power of the scan rate was found (6, 7).

Figure 2 also indicates that the values for peak

[1]Present address: Department of Chemistry, Simon Fraser University, Vancouver, B.C.

TABLE I

Values obtained for all four electron processes

	Process[a]			
	A	B	C	D
Peak potential[b] (V)				
E_{pa} (anodic)	+0.500	−0.122	−1.714	−2.030
E_{pc} (cathodic)	+0.436	−0.183	−1.788	−2.110
$E_{pa}-E_{pc}=DE_p$	0.064	0.066	0.074	0.080
Peak current[c] (μA)				
i_{pa} (anodic)	1.8	1.9	1.6	1.8
i_{pc} (cathodic)	2.2[d]	1.9	1.8	1.6[d]

[a]See Results. Data for 1.0 m*M* DPPH in 0.10 *M* THF–NBu_4ClO_4.
[b]The peak potentials, extrapolated to zero current, are measured versus a silver wire electrode, and hence only the relative values are significant.
[c]Measured from estimated extension of voltammogram for the preceding peak (13). Scan rate, 0.1 V/s.
[d]Approximate values, due to interference from neighboring peak.

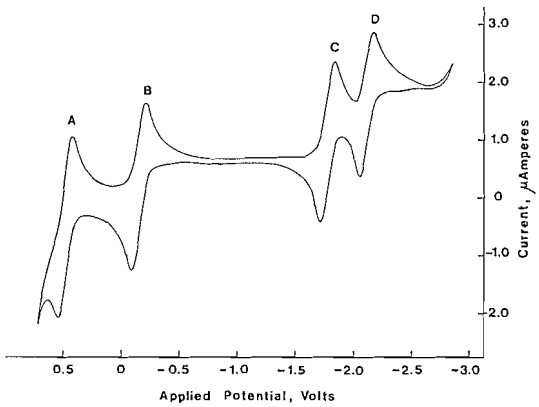

FIG. 1. Cyclic voltammogram of DPPH (1.0 m*M*) in 0.10 *M* NBu_4ClO_4 –THF. Scan rate 0.07 V/s.

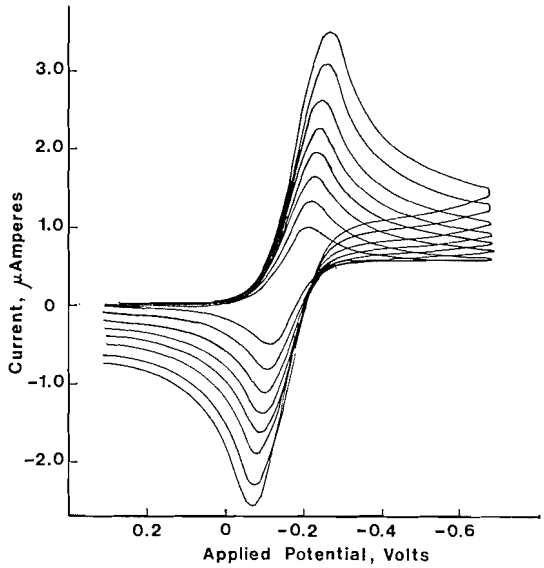

FIG. 2. Effect of variation of scan rate on process B, DPPH $\rightleftharpoons$ DPPH. Scan rates: 0.02, 0.04, 0.07, 0.10, 0.14, 0.20, 0.30, 0.40 V/s.

potentials move linearly with increasing peak currents. The cathodic peaks become more cathodic and the anodic peaks become more anodic as the scan rate is increased. Consequently the peak potentials were determined by extrapolating, for a range of scan rates, the line through the peak maxima to zero current. The values thus obtained for all four electron processes, together with the corresponding anodic and cathodic peak currents, are presented in Table I. From the similarity of all the peak currents, and the nature of the substrate, it appears that each of the four electron transfer steps involves a single electron process. Furthermore, it should be noted that the cathodic and anodic peaks are of similar heights, thus chemical reactions of any of the species subsequent to electron transfer are unimportant in the scan time.

Experimentally, it was found that variation of the scan rate resulted in displacement of all eight peaks along the potential axis, in an anodic direction for anodic peaks and in a cathodic direction for cathodic peaks. The peak potential displacements for every process were linear with peak current, and in all cases corresponded to a shift of 22 ± 2 mV/μA peak height. When the supporting electrolyte concentration was reduced from 0.101 *M* to 0.034 *M* this shift increased to 74 ± 6 mV per μA peak current. We thus conclude that the potential drift with changing scan

Can. J. Chem. Downloaded from www.nrcresearchpress.com by 210.87.254.42 on 09/05/12
For personal use only.

Can. J. Chem. Downloaded from www.nrcresearchpress.com by 210.87.254.42 on 09/05/12
For personal use only.

rate is due to uncompensated ohmic resistance between the reference and working electrodes (8, 9) resulting from the low solution conductance (2.3×10^{-4} ohm^{-1} cm^{-1} for 0.1 M NBu_4ClO_4–THF).

A further criterion for the reversibility of the process B is available. Several voltammograms were obtained at different scan rates, and log i was plotted against E for the lower portion of the cathodic sweep, and $[\log (i_p - i)^{1/2}]/i$ vs. E for almost the complete cathodic sweep (10), where i = current for a corrected potential E and i_p = peak current. In all cases, straight lines of gradient 1/66 mV resulted. This is in good agreement and within experimental error of the value expected for a reversible reaction.

Thus there is every indication that a potential drift is due to uncompensated resistance, and that for the low scan rates employed, all the electron transfer reactions are reversible.

Discussion

THF is a suitable solvent for electrochemical studies in the cathodic range (11, 12) and a preferred solvent for anionic polymerization. Its use in the current work, in a vacuum tight apparatus, parallels closely the conditions employed in the polymerization of living anionic systems. It is expected that further studies by cyclic voltammetry in this solvent will provide valuable insights into the fundamental processes occurring during the initiation and propagation of living anions in polymerization.

The simple silver wire reference electrode proved adequate for cyclic voltammetric measurements involving low current drain for short time intervals. The reliability of reference electrodes in this nonaqueous system and the reproducibility of the results obtained was a source of satisfaction in this work, and an indication that such techniques could be employed further in other studies of electropolymerization.

One of the main findings of this investigation was the proof of the existence of a stable cation and a stable anion of DPPH in THF and that each of these ions was formed by a reversible one-electron transfer. The peaks A and B in Fig. 1 reflect these one-electron transfer steps and each has been investigated as indicated in Fig. 2. A striking feature of Fig. 1 is the cyclic voltammetric evidence for the formation by two consecutive single electron transfers of a dianion radical and trianion of DPPH. The authors are unaware of any other sequence of four electron transfer reactions in nonaqueous systems that show the remarkable reversibility found in this work. It appears that five separate stable oxidation states of DPPH may be produced electrolytically in THF and that each of the processes is reversible and can be studied systematically and quantitatively.

Nicholson (8) showed that potential drift with variation in scan rate is probably due to: 1. Subsequent chemical reaction. 2. Irreversibility of the electron transfer process. 3. Uncompensated ohmic resistance between the working and reference electrodes. The symmetry of the anodic and cathodic peaks eliminates the first possibility. The logarithmic current–potential plots and the peak separation indicate the reversibility of the transfer processes. Thus there is every indication that the potential drift arises from the uncompensated resistance.

In future work it may be desirable to perform more detailed studies of electron transfer processes at higher scan rates. Under these circumstances it would be necessary to employ special circuitry to counteract the large uncompensated resistances which are inevitable in organic systems. However, the present data indicate that electron transfer processes in DPPH are reversible at low scan rates and that it is possible to calculate the value of the resistance and to take it into account in the electron transfer processes in the system at low scan rates.

This study was prompted by our primary interest in electropolymerization. One of the encouraging findings is that THF is a good solvent for studies employing cyclic voltammetry inasmuch as the resultant products of the electrodes were found to be stable. THF is one of the few solvents suitable for "living" anionic polymerization, and has been employed extensively in many investigations. Thus it is obvious that THF is a remarkably suitable medium for studies of anionic electropolymerization. It is expected that electrochemical evidence obtained by techniques similar to those described here will elucidate the mechanisms in electrochemically initiated polymerizations.

Acknowledgments

The authors thank the National Research Council of Canada for a grant, and Chemcell for

the award of a fellowship (D. G.). The financial assistance of the Dow Chemical Company of Canada is gratefully acknowledged.

1. B. L. FUNT. Macromol. Rev. **1**, 35 (1966).
2. B. L. FUNT, D. RICHARDSON, and S. N. BHADANI. J. Polymer Sci. Pt. A, **4**, 2871 (1966).
3. B. L. FUNT and D. G. GRAY. J. Macromol. Chem. **1**, 625 (1966).
4. E. SOLON and A. J. BARD. J. Am. Chem. Soc. **86**, 1926 (1964).
5. W. KEMULA and R. SIODA. Bull. Acad. Polon. Sci. Ser. Sci. Chim. **11**, 394 (1963).
6. P. DELAHAYE. New instrumental methods in electrochemistry. Interscience, New York. 1954.
7. R. S. NICHOLSON and I. SHAIN. Anal. Chem. **36**, 706 (1964).
8. R. S. NICHOLSON. Anal. Chem. **37**, 1351 (1965).
9. R. S. NICHOLSON. Anal. Chem. **37**, 667 (1965).
10. W. H. REINMUTH. Anal. Chem. **33**, 1793 (1961).
11. J. BADOZ-LAMBLING and M. SATO. Acta Chim. Acad. Sci. Hung. **32**, 191 (1962).
12. J. PERICHON and R. BUVET. Electrochim. Acta, **9**, 587 (1964).
13. D. S. POLCYN and I. SHAIN. Anal. Chem. **38**, 370 (1966).

Can. J. Chem. Downloaded from www.nrcresearchpress.com by 210.87.254.42 on 09/05/12
For personal use only.

Can. J. Chem. Downloaded from www.nrcresearchpress.com by 210.87.254.40 on 09/05/12
For personal use only.

Kinetics of neopentyl chloride pyrolysis. I. The molecular decomposition

J. S. SHAPIRO[1] AND E. S. SWINBOURNE[2]
Division of Pure Chemistry, National Research Council of Canada, Ottawa, Canada

Received July 10, 1967

A detailed investigation of the thermal decomposition of neopentyl chloride over the temperature range of 410–496 °C established that the pyrolysis occurs via two concurrent processes: (i) a unimolecular decomposition accompanied by a Wagner–Meerwein rearrangement giving methylbutenes and hydrogen chloride and (ii) a radical-chain decomposition to methane, isobutene, methyl chloride, 1-chloro-2-methylpropene, 3-chloro-2-methylpropene, 1,1-dimethylcyclopropane, and hydrogen chloride. The molecular reaction accounts for 30–40% of the overall decomposition. The Arrhenius equation for the molecular process is given by $k_1(s^{-1}) = 10^{13.26\pm0.36}e^{-60\,000\pm1640/RT}$. The nature of the transition state for the decomposition is discussed in terms of the unique molecular structure of neopentyl chloride.

Canadian Journal of Chemistry, 46, 1341 (1968)

Introduction

The most recent concept of the transition state for the gas-phase molecular elimination of hydrogen halides from halogenated hydrocarbons is best described as a halide carbonium ion-pair **1** (1), or as **2** (2) in which the positive charge is distributed between the α-carbon atoms and the β-hydrogen atoms rather than an earlier model described by **3** (3).

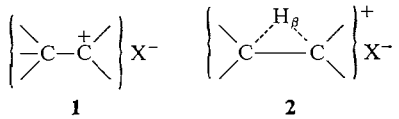

1 **2**

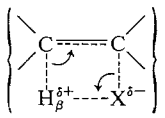

3

In structure **3** hydrogen atoms in the positions β to the halogen atoms are considered to participate in the rate-determining step (the polarization of the C—X bond), whereas in structures **1** and **2** the slow process is regarded as the critical elongation of the carbon—halogen bond resulting from redistribution of intramolecular energy with little assistance from the β-hydrogen atoms, followed by ion-pair formation.

The pyrolysis of neopentyl chloride offers a novel opportunity to test the hypothesis that the β-hydrogen atom has little effect on the rate of hydrogen halide elimination, since the molecule lacks β-hydrogen atoms. Because of the well-established analogies between gas-phase decompositions of alkyl halides and the reactions of these compounds in polar solvents (1, 4) and because solvolytic reactions of neopentyl compounds frequently lead to rearranged products, the kinetic study of this pyrolysis is of outstanding interest.

Maccoll and Swinbourne (5) reporting on the pyrolysis of neopentyl chloride in a preliminary study discussed the process in terms of four concurrent reactions of which the predominant process is the loss of hydrogen chloride, accompanied by a Wagner–Meerwein rearrangement of the carbon skeleton and leading to the formation of methylbutenes. Other products were thought to arise from different modes of C—C bond rupture and were compared with neopentane pyrolysis. Anderson and Benson (6) offered an alternative theory to account for the experimental results by considering the overall reaction as a radical-chain process, with 1,1-dimethylcyclopropane as the major precursor to the methylbutenes. The presence of hydrogen chloride at 444 °C was considered to be unfavorable for the isolation of the initially formed C_5 species which was believed to isomerize rapidly (5, 6). In view of recent work (7) concerned with the catalytic activity of allyl bromide carbons towards olefin isomerization, particularly in systems containing hydrogen halides (8), reinvestigation of neopentyl chloride pyrolysis in greater detail and in vessels coated with one of the decomposition products of the chloride is considered justified.

---

[1]Postdoctorate Fellow, Division of Pure Chemistry, 1965–1967.

[2]School of Chemistry, University of New South Wales, Kensington, N.S.W., Australia.

Can. J. Chem. Downloaded from www.nrcresearchpress.com by 210.87.254.40 on 09/05/12
For personal use only.

Experimental

I. Materials

Neopentyl chloride was prepared by the gas-phase chlorination of neopentane (5). Of the compounds, found as reaction products, which were required for thermal stability studies and for calibration purposes, 1,1-dimethylcyclopropane was prepared from 1,3-dibromo-2,2-dimethylpropane (9), 2-methylbut-1-ene and 2-methylbut-2-ene were purchased from Philip's Petroleum Company, 1- and 3-chloro-2-methylpropenes were purchased from Dr. Theodor Schuchardt (Munchen), and hydrogen chloride, 3-methylbut-1-ene, C_1–C_5 hydrocarbons, and C_2–C_3 olefins were purchased from Matheson Company in research grade gas cylinders. Commercial synthetic ammonia and hydrogen were used directly from cylinders. The purity of the organic compounds was checked by gas chromatography.

II. Procedure and Analysis of Products

Most of the decompositions were carried out in a Pyrex glass vessel (400 ml, $S/V = 0.8\ cm^{-1}$) housed in a heated aluminium alloy block thermostat. A packed vessel (244 ml, $S/V = 5.5\ cm^{-1}$) was also used to test for surface effects. The apparatus and experimental methods have already been described (10). The vessels were coated with the pyrolysis products of 3-chloro-2-methylpropene at 450 °C and "seasoned" with runs of neopentyl chloride. This treatment eliminated the fast starts observed with freshly coated vessels and resulted with a value for the rate of decomposition slightly lower than observed previously (5). Overnight treatment of the vessel with propylene at 450 °C reduced the rate to a lower, reasonably constant value, on prolonged pyrolysis at high temperatures. Between runs the vessel was left in contact with the decomposition products of neopentyl chloride. At the completion of a kinetic run ammonia gas was distilled into the vessel in a slight excess of the calculated hydrogen chloride pressure, after which the entire contents of the vessel were distilled into a tapped vessel (~ 1 l.) at −196 °C. The sampling vessel was allowed to warm up then made up to atmospheric pressure with dry nitrogen gas. Ammonia addition prior to sampling is necessary to avoid the facile combination of hydrogen chloride with the olefinic products. Separate control experiments have shown that the presence of ammonia has little effect on the reaction rate and on the distribution of products. Hydrogen chloride determinations were carried out on separate kinetic runs, the reaction products being trapped in a 200 ml bulb containing 50 ml of 1:1 ethanol/water mixture at −196 °C. The bulb was warmed to 80 °C, then allowed to cool overnight (this treatment results in complete hydrolysis of tertiary and secondary chlorides with negligible hydrolysis of the primary chlorides). The contents of the bulb were then titrated with alkali. The organic products were analyzed by gas chromatography in a laboratory-made unit with a flame-ionization detector. Hydrogen was determined separately with a thermal-conductivity chromatograph. Reproducible analyses were obtained with samples injected by means of a gas-tight syringe. Four columns were used:

1. 20% w/w squalane with 1% w/w Tween 20 on Celite (100–120 mesh, acid washed, dry sil treated), 4′ long; useful for separation of methane, methyl chloride, isobutene, the three isomeric methylbutenes, 1-chloro-2-methylpropene, and neopentyl chloride.

2. 5% w/w Dow Corning high vacuum silicone grease, 5% w/w silicone oil F96 (General Electric) 0.3% w/w Atpet 800 and 0.1% w/w Alketerge T on Celite (100–120 mesh, dry oil treated), 12′ long. This column was mainly used to separate 3-methylbut-1-ene from 1,1-dimethylcyclopropane but was also effective in separating other hydrocarbons from olefins of the same number of carbon atoms.

3. 20% w/w ββ′-oxydipropronitrile with 1% w/w Tween 20 on Celite (100–120 mesh, acid washed, dry sil treated) 4′ long; used to separate the isomeric chloro-2-methylpropenes, also gives partial separation of *t*-pentyl and neopentyl chlorides.

4. Molecular Sieve 5A column, prepared by coating finely powdered Molecular Sieve 5A on Celite (100–200 mesh), followed by conditioning with oxygen-free nitrogen at 250 °C (11). Separation of methane and hydrogen is complete on this column.

Besides products already reported in neopentyl chloride pyrolysis (5), 1,1-dimethylcyclopropane and 3-chloro-2-methylpropene were found among the reaction products, the latter in small amounts. The identity of the product believed to be 1,1-dimethylcyclopropane was confirmed by comparison of its retention time on three chromatographic columns (1–3) with those of a synthetic sample, and by means of n.m.r. spectroscopy. Minor products included hydrogen, ethane, propane, ethylene, and propylene, together with traces of neopentane. Together, these amount to less than 1% of the reaction products in the early stages of the decomposition. Variation of total pressure with time and of reaction products with total pressure are illustrated in Figs. 1–3. Similar plots were obtained at other temperatures.

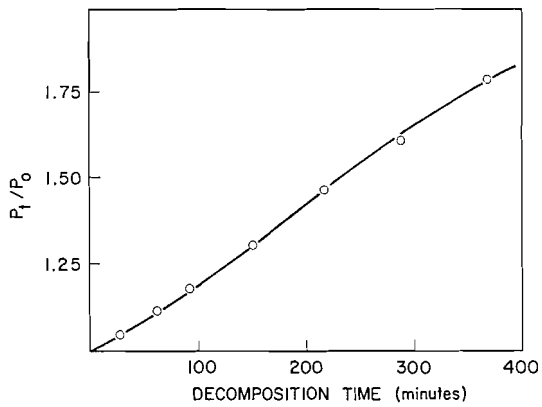

FIG. 1. Variation of total pressure with time of decomposition of neopentyl chloride at 444 °C. P_0 and P represent the initial pressure of neopentyl chloride and total pressure after decomposition time, respectively. Each point represents a mean of 5–10 runs. $P_0 \sim 200$ mm.

III. The Stoichiometry of the Reaction

In terms of the observed reaction products and of separate control experiments on the thermal stability of these, the stoichiometry of the overall reaction can be

represented as follows:

$$\rightarrow HCl + C_5H_{10} \text{ (2-methylbut-1-ene and 2-methylbut-2-ene)} \quad [I]$$

$$\rightarrow HCl + C_5H_{10} \text{ (1,1-dimethylcyclopropane)} \quad [II]$$

$$(CH_3)_3C(CH_2Cl) \rightarrow CH_3Cl + \textit{iso}\text{-}C_4H_8 \quad [III]$$

$$\rightarrow CH_4 + 1\text{-}C_4H_7Cl \text{ (1-chloro-2-methylpropene)} \quad [IV]$$

$$\rightarrow CH_4 + 3\text{-}C_4H_7Cl \text{ (3-chloro-2-methylpropene)} \quad [V]$$

These are followed by two important secondary reactions:

$$\text{1,1-dimethylcyclopropane} \xrightarrow{HCl} \text{2-methylbut-2-ene} + \text{3-methylbut-1-ene} \quad [VI]$$

$$\text{2-methylbut-1-ene} \quad [VII]$$

$$(CH_3)(CH_2Cl)C{=}CH_2 \xrightarrow{HCl} \text{polymer} + HCl\ (+ \text{ traces of } CH_4, \textit{iso}\text{-}C_4H_8) \quad [VIII]$$

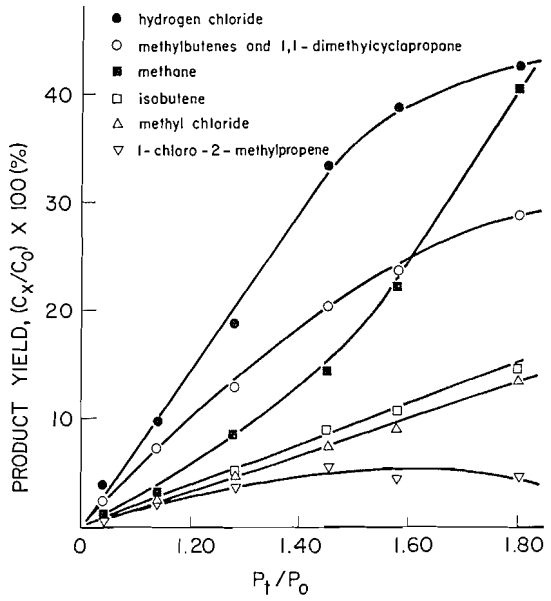

FIG. 2. Product yield at different stages of decomposition of neopentyl chloride at 444 °C (% moles of product per 100 initial moles of neopentyl chloride). P_0 and P_t represent the initial pressure of neopentyl chloride and total pressure after decomposition time, t, respectively. C_X and C_0 represent the concentration of product X and the initial concentration of neopentyl chloride, respectively. Each point represents a mean of 2–3 runs. $P_0 \sim 200$ mm.

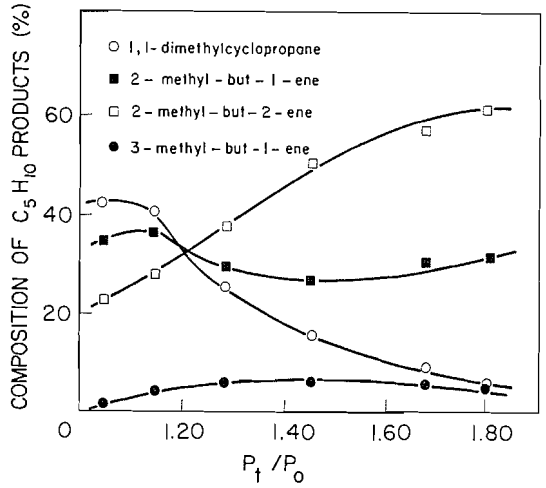

FIG. 3. Composition of C_5H_{10} products at different stages of decomposition of neopentyl chloride at 444 °C. P_0 and P_t represent the initial pressure of neopentyl chloride and total pressure after decomposition time, t, respectively. Each point represents a mean of 2–3 runs. $P_0 \sim 200$ mm.

It was deduced from the mass balance that reactions [IV] and [V] were almost equal in rate; however, only small amounts of 3-chloro-2-methylpropene were detected among the products owing to its rapid decomposition under the experimental conditions. The initial composition of C_5H_{10} products at 444° is (Fig. 3) 44% 1,1-dimethylcyclopropane, 36% 2-methylbut-1-ene, and 20% 2-methylbut-2-ene. It appears likely that 3-methylbut-1-ene is not formed directly from neopentyl chloride but is produced by isomerization of the other C_5H_{10} products. Separate studies on 2-methylbut-2-ene and 2-methylbut-1-ene in the presence of hydrogen chloride showed that 3-methylbut-1-ene does not come readily from these; however, it is formed from 1,1-dimethylcyclopropane (12). Since, under the reaction conditions, the rate of disappearance of 3-methylbut-1-ene can be considered negligibly small[3] in the early stages of neopentyl chloride decomposition (to $P_t/P_0 \sim 1.25$), the amount of 3-methylbut-1-ene present in the reaction mixture provides a key to the amount of 1,1-dimethylcyclopropane which has isomerized, thus allowing separate estimates to be made of reactions [I] and [II] over these stages of neopentyl chloride decomposition. Reactions [VI] and [VII] complicated these estimates to some extent, but the following procedure was found

[3]A separate study at 444 °C showed that in the presence of an equal pressure of hydrogen chloride 3-methylbut-1-ene isomerizes slowly to 2-methylbut-1-ene. It also decomposes slowly to methane and isobutene.

Can. J. Chem. Downloaded from www.nrcresearchpress.com by 210.87.254.40 on 09/05/12
For personal use only.

Can. J. Chem. Downloaded from www.nrcresearchpress.com by 210.87.254.40 on 09/05/12
For personal use only.

TABLE I

Variation of product yield of organic products with added substances

	Product yield (%)*			
Time (min)	60	60	50	60
P_0 (mm)	212	201	159	212
Added substance	—	Isobutene	Propylene†	Hydrogen chloride
$P_{\text{added sub.}}$ (mm)	—	102	144	100
Neopentyl chloride decomposed (%)	11	3	4	25
Product				
Methane	2.45	0.50	0.48	5.04
Methyl	1.42	0.11	—	3.99
Isobutene	1.88	—	0.31	4.03
1,1-Dimethylcyclopropane‡	1.94(2.66)	0.40	0.28	2.84
3-Methylbut-1-ene‡	0.24(0.00)	0.02	0.02	0.32
2-Methylbut-1-ene‡	1.90(1.66)	1.66	1.92	2.32
2-Methylbut-2-ene‡	1.24(1.00)	0.87	0.90	3.64
1-Chloro-2-methylpropene	1.58	0.27	0.32	5.66

*% moles of product per100 initial moles of neopentyl chloride.
†Pyrolysis after prolonged use of vessel.
‡Figures in brackets give the amounts of methylbutenes after allowance is made for contribution from 1,1-dimethylcyclopropane isomerization.

fruitful: Flowers and Frey (12) have shown that 1,1-dimethylcyclopropane isomerizes homogeneously to 3-methylbut-1-ene and 2-methylbut-2-ene in a 1:1 ratio. The results were reproduced in the present apparatus. A separate study at 444 °C of the hydrogen chloride catalyzed isomerization of 1,1-dimethylcyclopropane established 2-methylbut-1-ene as the only major product, after allowance was made for the homogeneous isomerization. Since the rate of the catalyzed isomerization to 2-methylbut-1-ene was found to be close to 1/2 the rate of the homogeneous isomerization to 3-methylbut-1-ene and 2-methylbut-2-ene, the concentration of isomerized 1,1-dimethylcyclopropane is given by:

$$-\Delta(\text{1,1-dimethylcyclopropane}) \sim 3(\text{3-methylbut-1-ene}).$$

After allowing for the isomerization, subtraction of the total 1,1-dimethylcyclopropane from the sum of C_5H_{10} products produced in the overall reaction leaves the sum of the methylbutenes produced by reaction [I] alone.

In Table I are given the amounts of the major reaction products of the pyrolysis of neopentyl chloride at 444° carried out in the presence of added substances. The marked inhibiting effect of propylene and isobutene and the catalytic effect of hydrogen chloride upon the formation of methane, methyl chloride, isobutene, 1-chloro-2-methylpropene, and 1,1-dimethylcyclopropane indicate that reactions [II]–[V] are radical processes. The effects of these additions upon the formation of 2-methylbut-1-ene and 2-methylbut-2-ene are much smaller; these apparent effects are further diminished when allowance is made for isomerization of 1,1-dimethylcyclopropane. This behavior is consistent with reaction [I] being molecular.

TABLE II

Effect of S/V ratio on formation of products at 444 °C

	Product yield (%)*					
	$S/V = 0.8\ \text{cm}^{-1}$ (*a*)			$S/V = 5.5\ \text{cm}^{-1}$ (*b*)		
Time (min)	10	30	60	10	30	60
P_0 (mm)	190	196	193	199	190	194
Neopentyl chloride decomposed (%)	2	5	11	2	6	26
Product						
Methane	0.35	1.03	3.50	0.17	0.80	2.83
Methyl chloride	0.14	0.48	1.45	0.09	0.49	1.51
Isobutene	0.26	0.73	1.99	0.17	0.73	2.33
1,1-Dimethylcyclopropane	0.18	0.87	1.86	0.15	0.68	1.48
3-Methylbut-1-ene	0.03	0.04	0.18	0.01	0.05	0.25
2-Methylbut-1-ene	0.38	0.66	2.31	0.58	2.44	6.24
2-Methylbut-2-ene	0.29	0.69	1.93	0.35	1.93	8.72
1-Chloro-2-methylpropene	0.31	0.85	1.32	0.12	0.56	1.46

*% mole of product for 100 initial moles of neopentyl chloride.
(*a*) Results from runs in vessel after ~ 30 kinetic runs.
(*b*) Results from runs in vessel after ~ 10 kinetic runs.

TABLE III

Effect of hydrogen chloride on formation of products in vessels of different S/V ratio

	Product yield (%)*					
	$S/V = 0.8\ cm^{-1}$ (*a*)			$S/V = 5.5\ cm^{-1}$ (*b*)		
P_0 (mm)	212	202	208	212	201	206
P_{HCl}/P_0	0.00	0.09	0.24	0.47	0.00	0.24
Product						
Methane	2.45	2.81	3.71	5.04	0.57	3.38
Methyl chloride	1.42	2.25	3.33	3.99	0.34	2.47
Isobutene	1.88	2.49	3.48	4.03	0.42	2.61
1,1-Dimethylcyclopropane	1.94	2.77	3.10	2.84	0.40	2.78
3-Methylbut-1-ene	0.24	0.28	0.28	0.32	0.03	0.05
2-Methylbut-1-ene	1.90	1.83	2.16	2.32	2.42	2.49
2-Methylbut-2-ene	1.24	2.75	2.69	3.64	1.47	1.98
1-Chloro-2-methylpropene	1.58	2.76	3.70	5.66	0.32	2.29

*% moles of product per 100 initial moles of neopentyl chloride.
(*a*) Pyrolysis of neopentyl chloride at 444 °C for 60 min after ~ 90 kinetic runs.
(*b*) Pyrolysis of neopentyl chloride at 444 °C for 20 min after ~ 30 kinetic runs.

TABLE IV

Effect of hydrogen bromide on formation of products in the packed vessel (*a*, *b*)

	Product yield (%)*		
P_0	201	204	203
P_{HBr}/P_0	0	1.5×10^{-4} (*c*)	0.25
Product			
Methane	0.57	23.8	36.6
Methyl chloride	0.34	7.4	10.2
Isobutene	0.42	11.7	27.4
1,1-Dimethylcyclopropane	0.40	4.7	0.8
3-Methylbut-1-ene	0.03	0.7	0.8
2-Methylbut-1-ene	2.42	5.4	5.0
2-Methylbut-2-ene	1.47	9.2	13.1
1-Chloro-2-methylpropene	0.32	6.6	4.2

*moles of product per 100 initial moles of neopentyl chloride.
(*a*) $S/V = 5.5\ cm^{-1}$.
(*b*) Pyrolysis of neopentyl chloride at 444 °C for 20 min after 30 kinetic runs.
(*c*) 100 mm of HBr were introduced into the evacuated vessel, then pumped out after 10 min until the pressure dropped to 3×10^{-1} mm.

Runs in the packed vessel showed that a sevenfold increase in S/V ratio resulted in only a slight change in the rates of formation of products in the early stages (~ 5%) of neopentyl chloride decomposition (see Table II). This is consistent with the pyrolysis being homogeneous in both vessels at least over this range of decomposition. Beyond this point, the formation of products was significantly more rapid in the packed vessel than in the unpacked vessel, particularly in respect of the formation of methylbutenes. This marked autocatalytic behavior in the packed vessel appeared to be associated with the hydrogen chloride acting in combination with the increased surface area: the catalytic activity of added hydrogen chloride was much more marked in the packed than in the unpacked vessel, and such additions in the packed vessel caused a marked increase in the rate of formation of 1,1-dimethylcyclopropane (see Table III). Two runs carried out in the packed vessel in the presence of hydrogen bromide showed it to be an even more effective catalyst than hydrogen chloride (see Table IV) as may be expected from the observations of Failes and Stimson (29) concerning the catalytic activity of these two substances.

Examination of Figs. 1 and 2 shows that, in contrast to the behavior in the packed vessel, decomposition of neopentyl chloride in the unpacked vessel proceeded smoothly with no sudden acceleration in the rate, and it is probable that decomposition in this vessel was essentially homogeneous well beyond the 5% decomposition point.[4]

[4]There was indirect evidence that the surface/HCl effect was also operating to a lesser extent in the unpacked vessel. Thus, the overall rate of decomposition of neopentyl chloride was slightly less in vessels which had been in use over a prolonged period and there was also a slightly different product distribution in these vessels. These changes, however, did not relate to reaction [I] (see Table V, also Table III, Part II). It is possible that the surface may act as a secondary generating source of chlorine atoms via the reaction

$$S + HCl \rightarrow SH + Cl.$$

Can. J. Chem. Downloaded from www.nrcresearchpress.com by 210.87.254.40 on 09/05/12
For personal use only.

The extent of reaction [I] which is believed to be molecular can be expressed as a function of the overall decomposition in the unpacked vessel. It is represented here by θ which is given by:

$$\theta = \frac{(\Sigma C_5H_{10})_{[I]} + (HCl)_{[I]}}{[\Sigma(\text{reaction products})_{[I]-[VIII]}]}$$

$$= \frac{2[\Sigma(C_5H_{10})_{[I]-[III]} - (1,1\text{-dimethylcyclopropane}) + 3(3\text{-methylbut-1-ene})]}{[\Sigma(\text{reaction products})_{[I]-[VIII]}]},$$

since $(\Sigma C_5H_{10})_{[I]} = (HCl)_{[I]}$.

Evaluation of θ in this manner applies only to the early stages of neopentyl chloride decomposition (to $P_t/P_0 < 1.25$), since at greater extents of reaction the rate of disappearance of 3-methylbut-1-ene becomes significant. Under normal experimental conditions values of θ were in the range 0.35 ± 0.05 regardless of pyrolysis temperature and of the initial pressure of the reactant.

Direct gas chromatographic analysis of undecomposed neopentyl chloride was not readily reproducible (owing presumably to adsorption of the vapor by the silicone stopcock grease) and it was found more accurate to deduce this quantity from a mass balance based upon the amounts of products formed. For example, from reactions [I]–[VIII] it is evident that

$$-\Delta(C_5H_{11}Cl) = (HCl) + (CH_3Cl) + (1\text{-}C_4H_7Cl).^5$$

In cases where hydrogen chloride determinations were not carried out, empirical relationships such as the following were found applicable:

$$(HCl) = (\text{methylbutenes}) + (1,1\text{-dimethylcyclopropane}) + (1\text{-}C_4H_7Cl).^5$$

The concentrations of reactant decomposed by the molecular and radical-chain processes are then given by $-\Delta(C_5H_{11}Cl)\theta$ and $-\Delta(C_5H_{11}Cl)(1-\theta)$, respectively, and the concentrations of unreacted chloride, and hence given by:

$$C_{MOL} = C_0 - \Delta(C_5H_{11}Cl)\theta$$

$$C_{RAD} = C_0 - \Delta(C_5H_{11}Cl)(1-\theta).$$

The remainder of this paper deals with the molecular mode of decomposition, while the radical-chain pyrolysis will be closely examined in the following paper.

Results

Table V shows the rate coefficient (k_1) for the unimolecular decomposition of neopentyl chloride, estimated from C_0, C_{MOL} and from the first order law

$$k_1 = (2.303/t)\log(C_0/C_{MOL}),$$

applicable for early stages of decomposition. No significant variation of k_1 with initial pressure is evident. Insensitivity of k_1 to propylene, isobutene, ammonia, and hydrogen chloride is illustrated in Table VI. Variation of k_1 (39 values) with temperature is shown as an Arrhenius plot in Fig. 4. The line, determined by least squares procedure, and the 90% confidence limits (assuming that all errors reside in log k_1 and none in T) are given by $\log k_1 = 13.26 \pm 0.36 - (60\,000 \pm 1640/2.303\,RT)$.

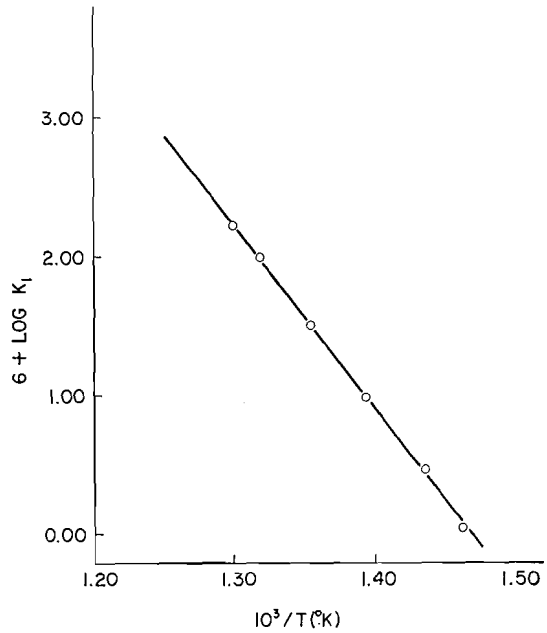

FIG. 4. Arrhenius plot for the molecular decomposition of neopentyl chloride. The points correspond to mean rate coefficients. The line drawn through the points was determined by the least squares method.

Discussion

The present experimental results confirm the findings of the previous experiment (5) that the decomposition of neopentyl chloride occurs via two parallel pathways: (i) molecular elimination of hydrogen chloride and formation of methylbutenes and (ii) a radical-chain process.

[5] 1-C_4H_7Cl and 3-C_4H_7Cl formed in equal amounts.

Can. J. Chem. Downloaded from www.nrcresearchpress.com by 210.87.254.40 on 09/05/12
For personal use only.

TABLE V

Lack of dependence of k_1 on initial pressure (444 °C)

P_0 (mm)	312	250	212	214*	215*	93	65	26
$10^6 k_1$ (s^{-1})	8.8	8.2	8.4	8.8	7.5	9.8	8.5	10.1

*For runs carried out after prolonged use of vessel at high temperatures.

TABLE VI

Decompositions in the presence of added substances at 444 °C

P_0 (mm)	206	201	265	171	111	53	202	212	130
Additive	Isobutene	Isobutene	Propene	Propene	Propene	Propene	HCl*	HCl*	NH_3
P_{add} (mm)	42	102	59	150	207	243	18	100	101
$10^6 k_1$ (s^{-1})	7.4	7.4	9.3	8.5	10.8	9.6	9.3	13.2	10.3

*Correction was applied for the decomposition of 3-methylbut-1-ene.

The molecular nature of (i) is established by the pressure independence of k_1, by the insensitivity of k_1 to olefinic inhibitors and to hydrogen chloride, and by a value of $\sim 10^{13}$ s^{-1} for the Arrhenius pre-exponential factor of the reaction. The effect of surface on the molecular elimination was found to be small, confirming the homogeneous nature of the process.

It is evident from Table VII that the Arrhenius expression for the molecular decomposition of neopentyl chloride is in line with those observed for the other primary chlorides. The normal value for the activation energy supports the view that the decomposition proceeds through reaction pathway with an energy barrier of comparable height to those of the other chlorides, hence takes place via a common mechanism. No additional energy is necessarily required for the isomerization of the neopentyl ion to the *t*-pentyl ion as thermochemical calculations (18) indicate that this transformation is exothermic by 31 kcal/mole.

Comparison of relative rates of solvolysis in polar solvents and gas-phase pyrolyses of neopentyl and ethyl derivatives is instructive in view of previously stressed analogies (1–4). The relative rates of solvolysis of ethyl and neopentyl bromide and *p*-toluene sulfonate in formic acid are compared with pyrolysis rates for unimolecular elimination of hydrogen chloride in the gas phase in Table VIII.

In the case of the solvolyses (S_N1 processes

TABLE VII

Arrhenius parameters for the decomposition of primary alkyl chlorides

Alkyl chloride	Temperature range (°C)	log A (s^{-1})	E (kcal $mole^{-1}$)	Ref.
Ethyl	400–490	14.60	60.8	13
	420–500	13.63	56.8	14
n-Propyl	420–478	13.45	55.5	15
n-Butyl	430–470	14.00	57.0	15
Isobutyl	417–474	14.02	56.9	16
n-Pentyl	396–456	14.60	58.3	17
Neopentyl	410–496	13.26	60.0	This study

TABLE VIII

Relative rates of primary alkyl compounds

Reaction	Ethyl	Neopentyl	Reference
RBr, HCOOH, 95 °C	1.0	0.6	19
ROTS*, HCOOH, 75 °C	1.0	1.0	20
RCl, gas phase, 444 °C	1.0	0.08	13, and present study

*OTS represent *p*-toluene sulfonate group.

Can. J. Chem. Downloaded from www.nrcresearchpress.com by 210.87.254.40 on 09/05/12
For personal use only.

Can. J. Chem. Downloaded from www.nrcresearchpress.com by 210.87.254.40 on 09/05/12
For personal use only.

leading to rearranged products) the migrating methyl group does not appear to assist C—X heterolysis since similar rates are observed for both ethyl and neopentyl compounds. This observation has been interpreted (21, 22) as an indication that the rate of methyl migration in the initially formed carbonium ion is faster than the rate of reaction with the surrounding solvent. In the gas phase a different situation exists since the pyrolysis rate of ethyl chloride is about 12 times faster than that of neopentyl chloride. The role of a β-hydrogen atom in unimolecular gas-phase dehydrohalogenation reactions has been considered to be the same as that of the polar solvent in S_N1 and E1 reactions of halides (3). The decrease in rate of pyrolysis in a molecule lacking β-hydrogen atoms leads to the conclusion that β-hydrogen atoms do play an important part in the rate-determining process of charge separation between the α-carbon atom and the chlorine atom to which it is bonded. In the case of neopentyl chloride the critical elongation of the carbon–chlorine bond is probably assisted by one of the γ-hydrogen atoms, the interaction being less effective than in a molecule possessing β-hydrogen atoms.

With the molecular nature of the reaction established, it is worthwhile to speculate on the nature of the transition state. Maccoll and Swinbourne have considered (5) an ion-pair transition state **4** with five possible modes for its decomposition depending upon the manner of hydrogen chloride elimination and on which of the hydrogen atoms is eliminated. From Fig. 3, it is evident that the two major C_5H_{10} products produced initially are 1,1-dimethylcyclopropane and 2-methylbut-1-ene. Since the rate of isomerization of the former to the latter in the early stages of the neopentyl chloride decomposition cannot account for the bulk of the 2-methylbut-1-ene, this must be formed by a molecular reaction. This conclusion is consistent with structure **5**, in which a γ-hydrogen atom is attacked by the departing chloride ion.

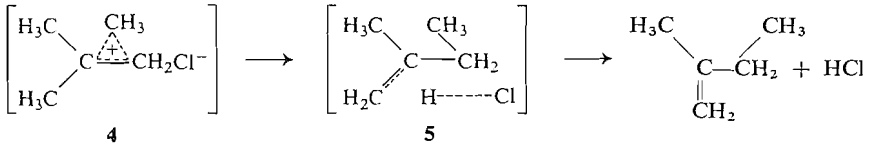

4 **5**

Similarly, although 2-methylbut-2-ene is formed in smaller amounts, the quantities present in the early stages of neopentyl chloride decomposition suggest that some 2-methylbut-2-ene is independently produced from neopentyl chloride via a unimolecular mechanism[6] probably involving transition state **6**, proposed by Maccoll and Swinbourne (5).

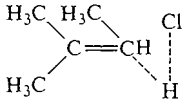

6

The gas-phase pyrolysis of neopentyl chloride thus leads to the formation of a methylbutene mixture containing a larger proportion of 2-methylbut-1-ene than expected from thermodynamic data (23) and from the equilibrium composition observed after prolonged pyrolysis (see Fig. 3). It appears that methylbutenes with abnormal proportions of methylbutenes are not uncommon in other reactions of neopentyl compounds in which skeletal rearrangement is observed in solution (24), in the gas-phase (25), and on alumina (26). In each of these cases a carbonium ion not having a *t*-pentyl structure was proposed as a precursor to the methylbutenes. This situation applies to the present case where the most likely carbonium ion intermediate is represented by a methyl-bridged structure **4**. A similar transition state was proposed for liquid-phase reactions of neopentyl compounds (27).

The most likely factor accounting for difference between the composition of methylbutenes produced from neopentyl chloride in the present and the preliminary study (5) is the nature of the pyrolytic carbon which was found to be less active than allyl bromide carbon in promoting isomerization of olefins in the presence of hydrogen chloride (8).

[6]In a recent communication (28) it was stated that 2-methylbut-2-ene might possibly be formed from neopentyl chloride via a free-radical intermediate; however the more recent analysis of results, as discussed in this paper, supports a unimolecular mechanism for its formation.

Acknowledgments

We thank Professor V. R. Stimson for helpful discussions and Mr. M. K. Withers for valuable advice on the gas chromatographic analysis. One of us (J. S. S.) is indebted to C.S.I.R.O. for the award of a Postgraduate Senior Studentship.

1. A. MACCOLL. Theoretical organic chemistry. Kekulé Symposium. Butterworth, London. 1958.
2. A. MACCOLL. Advan. Phys. Org. Chem. **3**, 91 (1965).
3. A. MACCOLL and P. J. THOMAS. Nature, **176**, 392 (1955).
4. A. MACCOLL. The transition state. Chem. Soc. London Spec. Publ. No. 16. 1962. pp. 159–173.
5. A. MACCOLL and E. S. SWINBOURNE. J. Chem. Soc. 149 (1964).
6. K. H. ANDERSON and S. W. BENSON. J. Chem. Phys. **39**, 1673 (1963).
7. M. R. BRIDGE and J. L. HOLMES. J. Chem. Soc. B, 713 (1966).
8. K. A. HOLBROOK and J. J. ROONEY. J. Chem. Soc. 247 (1965).
9. C. E. BOORD, R. A. CRAIG, J. M. DERFER, K. E. CREENLEE, and R. W. SHORTRIDGE. J. Am. Chem. Soc. **70**, 946 (1948).
10. E. S. SWINBOURNE. Australian J. Chem. **11**, 314 (1958).
11. C. E. BOORD and G. KYRYACOS. Anal. Chem. **29**, 787 (1957).
12. M. C. FLOWERS and H. M. FREY. J. Chem. Soc. 3953 (1959).
13. D. H. R. BARTON and K. E. HOWLETT. J. Chem. Soc. 155 (1949).
14. N. CAPON and R. A. ROSS. Trans. Faraday Soc. **62**, 1560 (1966).
15. D. H. R. BARTON and K. E. HOWLETT. J. Chem. Soc. 2033 (1949).
16. K. E. HOWLETT. J. Chem. Soc. 4487 (1952).
17. R. C. S. GRANT and E. S. SWINBOURNE. J. Chem. Soc. 4423 (1965).
18. R. TAUBERT and F. P. LOSSING. J. Am. Chem. Soc. **84**, 1523 (1962).
19. I. DOSTROVSKY, E. D. HUGHES, and C. K. INGOLD. J. Chem. Soc. 173 (1946).
20. H. J. MARSHALL and S. WEINSTEIN. J. Am. Chem. Soc. **74**, 1120 (1952).
21. A. STREITWIESER, JR. Solvolytic displacement reactions. McGraw-Hill, New York. 1962.
22. Y. POCKER. *In* Molecular rearrangements. Vol. 1. *Edited by* P. De Mayo. Interscience, New York. 1963.
23. F. D. ROSSINI *et al.* Selected values of physical and thermodynamic properties of hydrocarbons and related compounds. Carnegie Press, Pittsburgh. 1953.
24. M. S. SILVER. J. Am. Chem. Soc. **83**, 3482 (1961).
25. W. C. HERNDON and E. S. LEWIS. J. Am. Chem. Soc. **83**, 5230 (1961).
26. C. W. PILLAI and H. PINES. J. Am. Chem. Soc. **83**, 3274 (1961).
27. G. J. KARABATOS, S. MEYERSON, and C. E. ORZECH. J. Am. Chem. Soc. **86**, 1994 (1964).
28. J. S. SHAPIRO and E. S. SWINBOURNE. Chem. Commun. 465 (1967).
29. R. L. FAILES and V. R. STIMSON. Australian J. Chem. **17**, 851 (1964).

Can. J. Chem. Downloaded from www.nrcresearchpress.com by 210.87.254.40 on 09/05/12
For personal use only.

Kinetics of neopentyl chloride pyrolysis. II. The radical-chain decomposition

J. S. SHAPIRO[1] AND E. S. SWINBOURNE[2]

Division of Pure Chemistry, National Research Council of Canada, Ottawa, Canada

Received July 10, 1967

The radical-chain thermal decomposition of neopentyl chloride was studied in the temperature range of 410–496 °C and over the pressure range of 22 to 340 mm. A small surface effect was noted after prolonged conditioning of the vessel and in a vessel of high surface/volume ratio. The reaction is of three-halves order and the rate coefficient is expressible by $k_{3/2}$ ($l^{1/2}$ mole$^{-1/2}$ s^{-1}) $= 10^{13.55\pm0.67} \times e^{-56300\pm2100/RT}$. The experimental facts are shown to be consistent with a mechanism involving chlorine atoms as the principal propagating radicals, with a first-order initiation step and a termination step involving the combination of methyl and chloromethyl radicals. The relative concentrations of the various radicals, calculated from known and estimated kinetic parameters, have been shown to be dependent on the hydrogen chloride produced from the concurrent unimolecular decomposition of neopentyl chloride reported in Part I. 1,1-Dimethylcyclopropane, found as a reaction product, is believed to be formed directly from neopentyl chloride by a radical-chain mechanism.

Canadian Journal of Chemistry, 46, 1351 (1968)

Can. J. Chem. Downloaded from www.nrcresearchpress.com by 210.87.254.6 on 09/05/12
For personal use only.

Introduction

It has been proposed by Barton and Onyon (1) that, apart from a molecular mechanism, alkyl halides may decompose by themselves thermally via a radical-chain mechanism. It was proposed that alkyl chlorides decompose via reaction schemes of this type only if two conditions are fulfilled: (i) the molecule has a hydrogen atom in the position β to the chlorine atom so that μ-radicals (2) capable of decomposition are produced and (ii) the olefinic products of such reactions are inefficient inhibitors (otherwise chlorine atoms will be removed rapidly from the system).

The radical-chain decomposition of neopentyl chloride presents an interesting case of an alkyl chloride lacking β-hydrogen atoms, and which on decomposition yields products such as methylbutenes which should be highly efficient radical scavengers (28).

1,1-Dimethylcyclopropane has been observed as a product of the pyrolysis of neopentyl chloride. Maccoll and Swinbourne (22) have proposed that this compound could be formed from neopentyl chloride via a unimolecular mechanism involving an ion-pair type transition state, while Anderson and Benson (10) have proposed its formation via a free-radical intermediate. Other reactions involving neopentyl compounds have resulted in the formation of 1,1-dimethylcyclopropane. These include the reaction between neopentyl chloride and sodium (3, 4), and between neopentyl chloride and phenyl sodium (5), both of which are believed to proceed via a carbene intermediate with elimination of a hydrogen atom in the position α with respect to the carbon atom to which the chlorine is attached. Other examples are the pyrolysis of neopentyl chloroformate (8) and the thermal dehydration of neopentyl alcohol on alumina (9), for each of which a mechanism has been proposed with a transition state involving charge separation.

The present study is expected to permit selection of the most likely process leading to the formation of 1,1-dimethylcyclopropane in neopentyl chloride pyrolysis.

Experimental

Preparation of materials, description of apparatus, procedure and analysis of products have been described in Part I.

Results

I. Reaction Mechanism

In Figs. 1–3 (Part I) the variation of total pressure with pyrolysis time and of yields of reaction products with total pressure were illustrated for the pyrolysis at 444 °C. In Figs. 1–3, shown below, the corresponding plots are given for the propylene-inhibited pyrolysis. These results together with others shown in Table I (Part I) indicate that the major products of the radical-chain decomposition are: methane,

[1]Postdoctorate Fellow, Division of Pure Chemistry, 1965–1967.

[2]School of Chemistry, University of New South Wales, Kensington, N.S.W., Australia.

TABLE I

Analysis of minor products of neopentyl chloride pyrolysis at 444 °C. Initial pressure of neopentyl chloride ~ 200 mm

	Product yield* (%)				
Pyrolysis time (min)	20	40	80	160	320
Hydrogen	—	—	—	0.016	2.20
Ethane	0.0006	0.004	0.015	0.047	0.38
Ethylene	0.004	0.015	0.028	0.074	0.36
Propane	0.0000	0.000	0.007	0.02	0.16
Propylene	0.0007	0.002	0.003	0.09	0.40
3-Chloro-2-methylpropene	0.01	0.17	0.30	0.70	0.60
Isobutene	0.30	0.64	1.46	3.36	7.65

*moles of product formed/100 initial moles of neopentyl chloride.

isobutene, methyl chloride, 1-chloro-2-methylpropene, 1,1-dimethylcyclopropane, and hydrogen chloride. 3-Chloro-2-methylpropene, an expected major product, was found only in small quantities presumably because of its thermal instability at the temperature range studied. A separate study of its pyrolysis, alone and in the presence of an equal pressure of hydrogen chloride, revealed that it decomposes more rapidly than neopentyl chloride to a polymer, hydrogen chloride, and small amounts of methane and isobutene.

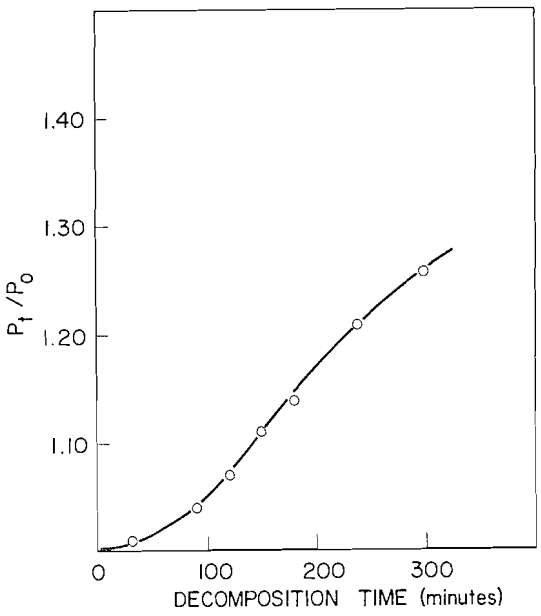

FIG. 1. Variation of total pressure with time of decomposition of neopentyl chloride at 444 °C in the presence of added propylene. Initial molar ratio of neopentyl chloride to propylene = 1:1. P_0 and P_t represent the initial pressure of neopentyl chloride and total pressure after decomposition time, t, respectively. $P_0 \sim 150$ mm.

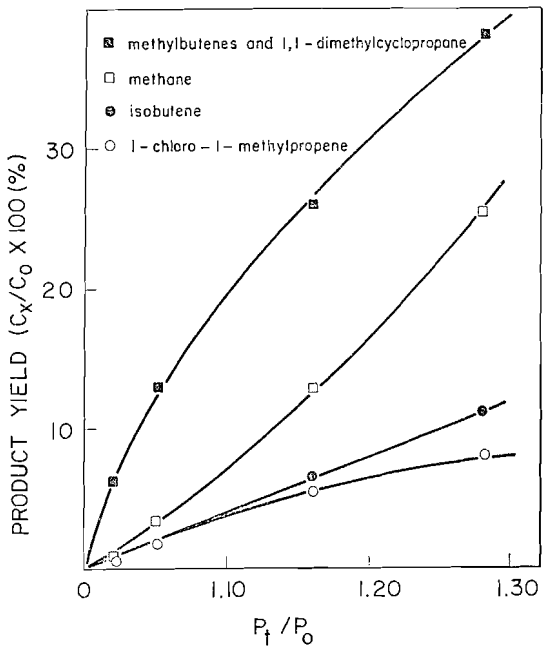

FIG. 2. Product yield at different stages of decomposition of neopentyl chloride at 444 °C in the presence of added propylene (% moles of product per 100 initial moles of neopentyl chloride). Initial molar ratio of neopentyl chloride to propylene = 1:1. P_0 and P_t represent the initial pressure of neopentyl chloride and total pressure after decomposition time, t, respectively. C_X and C_0 represent the concentration of product X and HCl initial concentration of neopentyl chloride, respectively. $P_0 \sim 150$ mm.

In Table I are listed the yields of the minor reaction products at various stages of decomposition. Isobutene is included in the table for comparison. Since the yields of the minor products are very small and tend to increase rapidly with extent of reaction these products are probably formed by secondary decomposition of the major pyrolysis products.

Can. J. Chem. Downloaded from www.nrcresearchpress.com by 210.87.254.6 on 09/05/12
For personal use only.

Can. J. Chem. Downloaded from www.nrcresearchpress.com by 210.87.254.6 on 09/05/12
For personal use only.

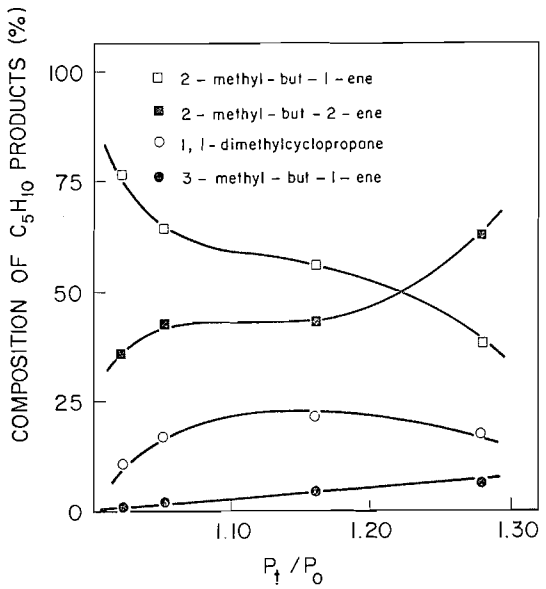

FIG. 3. Composition of C_5H_{10} products at different stages of decomposition of neopentyl chloride at 444 °C in the presence of added propylene. Initial molar ratio of neopentyl chloride to propylene = 1:1. P_0 and P_t represent the initial pressure of neopentyl chloride and total pressure after decomposition time, t, respectively. $P_0 \sim 150$ mm.

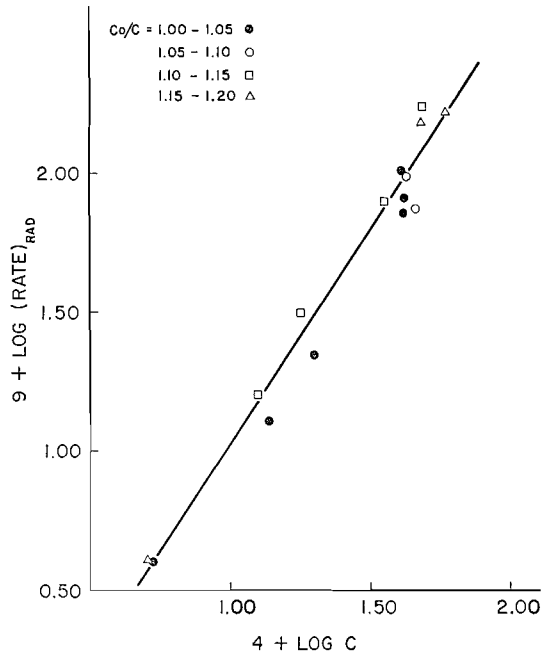

FIG. 4. Double logarithmic plot for the determination of reaction order for the radical-chain decomposition of neopentyl chloride at 444 °C. C represents the concentration of neopentyl chloride. C and $(rate)_{RAD}$ are given in mole l^{-1} and mole l^{-1} s^{-1} respectively.

II. Reaction Order

The procedure for resolving the overall rate of decomposition of neopentyl chloride into molecular and radical-chain components is outlined in Part I. The rate of the radical reaction is given by $d(C_0 - C_{RAD})/dt$ or $(C_0 - C_{RAD})/t$ for small amounts of decomposition, where C_0 and C_{RAD} represent the initial concentration, and concentration of undecomposed neopentyl chloride after reaction time, t. From the results at the early stages of the decomposition a plot of log $(rate)_{RAD}$ versus log C is shown in Fig. 4. The slope of the line of best fit corresponds to a reaction order of 1.5. Similar logarithmic plots for the formation of methane, methyl chloride, isobutene, 1-chloro-2-methylpropene, and 1,1-dimethylcyclopropane also gave an order of 1.5 in each case. In contrast, the reaction order for the formation of the methylbutenes (2-methylbut-1-ene and 2-methylbut-2-ene) estimated with a similar plot is 1.

III. Kinetic Results

The rate coefficient for these radical chain decompositions $(k_{3/2})$ was calculated from the expression:

$$k_{3/2} = 2(C_0^{1/2} - C_{RAD}^{1/2})/tC_0^{1/2}C_{RAD}^{1/2}.$$

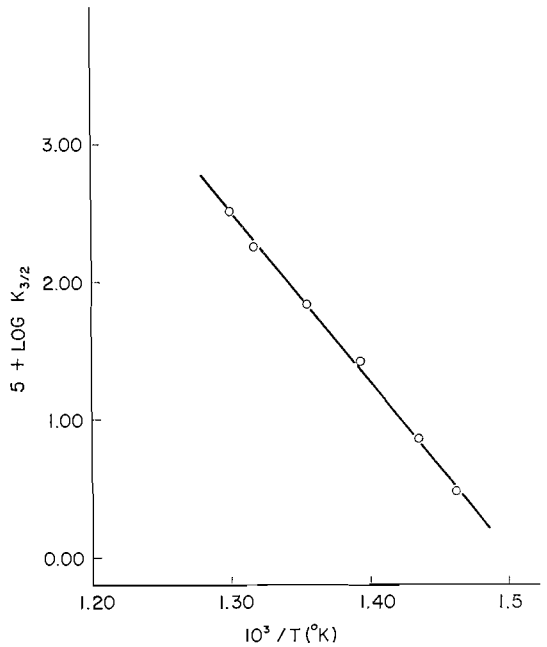

FIG. 5. Arrhenius plot for the radical-chain decomposition of neopentyl chloride. The points correspond to mean rate coefficients. The line drawn through the points was determined by the least squares method.

TABLE II

Effect of added substances on isobutene/methyl chloride and isobutene/1-chloro-2-methylpropene ratios. Pyrolysis of neopentyl chloride (~ 200 mm) at 444 °C for 60 min

Added substance	Isobutene/methyl chloride	Isobutene/1-chloro-2-methylpropene
None	1.33*	1.18*
2-Methylbut-2-ene	2.21(34), 5.34(98)	1.25(34), 0.91(98)
Hydrogen chloride	1.11(18), 1.04(50), 1.01(100)	1.01(18), 1.05(50), 0.80(100)

*Average of 3 kinetic runs. Figures in parentheses give the pressures (mm) of added substances.

TABLE III

Typical decompositions at 444 °C

P_0 (mm)	190	196	179	194	214†	213†	215†	198†
C_0/C^*	1.02	1.05	1.11	1.24	1.02	1.05	1.11	1.27
$10^4\, k_{3/2}(l^{1/2}\ \text{mole}^{-1/2}\text{s}^{-1})$	2.36	2.85	3.06	2.42	0.71	1.51	1.91	2.56

*C_0 and C represent the measured or estimated values of initial concentration and concentration remaining after pyrolysis, of neopentyl chloride, respectively.
†Runs after prolonged use of vessel at high temperatures.

The temperature dependence of the rate coefficient is shown in Fig. 5 for 31 runs in the range 410–496 °C. The Arrhenius expression, determined by the method of least squares together with the 90% confidence limits (assuming all the error resides in log $k_{3/2}$ and none in $1/T$) is given by $k_{3/2}(l^{1/2}\ \text{mole}^{-1/2}\ \text{s}^{-1}) = 10^{13.55\pm0.64}e^{-56300\pm2100/RT}$.

IV. Effect of Added Substances

The effect of added propylene, isobutene, and hydrogen chloride on the rate of formation of products is demonstrated in Table I (Part I). Both olefins reduce the rates of formation of organic products other than methylbutenes by factors of 5–10 while hydrogen chloride enhances these rates by factors of 2–3. Rough estimates of the reaction order with respect to added isobutene and hydrogen chloride are minus 1 and plus 1/2 respectively.

Addition of olefins and of gas-phase catalysis affects the rate of formation of certain products more than others. This observation particularly applies to isobutene and methyl chloride which are expected to be formed in a stoichiometric ratio via the same elementary reaction (see reaction scheme, Part I). For example, olefins reduce the rate of formation of methyl chloride more than the rate of formation of isobutene. In Table II are given the isobutene/methyl chloride ratios together with the isobutene/1-chloro-2-methylpropene ratios observed during the pyrolysis, alone and in the presence of 2-methylbut-2-ene[3] and hydrogen chloride.

V. Effect of Surface Conditioning

Prolonged use of the vessel ($S/V = 0.8\ \text{cm}^{-1}$) at high temperatures was found to have a significant effect on the rate of radical-chain decomposition as shown in Table III. Inspection of Table III points to the existence of an induction period in runs carried out at 444 °C after prolonged use of a vessel at high temperatures. No definite induction period was found during the earlier experiments, though it was noted that induction periods are produced if the vessel was treated with propylene overnight at 444 °C. Hence the vessel was left in contact with the decomposition products of neopentyl chloride between kinetic runs.

Discussion

Reaction scheme 1, although speculative, accounts for most of the experimental observations reported here on the decomposition of neopentyl chloride.

The following notation is used in the discussion given below: $(CH_3)_2C(CH_2Cl)$ and $(CH_3)_3C(\dot{C}HCl)$ are both represented by R_2. CH_3 and

[3]2-Methylbut-2-ene was used instead of isobutene since gas chromatographic analysis for methyl chloride in the presence of a large excess of isobutene is unsatisfactory. This olefin was found to have an inhibiting effect of the same order of magnitude as isobutene.

Can. J. Chem. Downloaded from www.nrcresearchpress.com by 210.87.254.6 on 09/05/12
For personal use only.

[1] $(CH_3)_3C(CH_2Cl) \rightarrow \begin{matrix} CH_3CH_2(CH_3)C{=}CH_2 \\ (CH_3)_2C{=}CH(CH_3) \end{matrix} + HCl$ (molecular decomposition)

[2] $(CH_3)_3C(CH_2Cl) \xrightarrow{a} (CH_3)_2\dot{C}(CH_2Cl) + \dot{C}H_3((CH_3)_2\dot{C}(CH_2Cl) \rightarrow (CH_3)_2C{=}CH_2 + Cl)$

$(CH_3)_3C(CH_2Cl) \xrightarrow{b} (CH_3)_3\dot{C} + \dot{C}H_2Cl$

[3] $\dot{C}H_3$ or $\dot{C}H_2Cl + HCl \rightleftharpoons CH_4$ or $CH_3Cl + \dot{C}l$

[4] $(CH_3)_3C(CH_2Cl) + \begin{matrix} +\dot{C}H_3 \xrightarrow{a} CH_4 \\ \dot{C}H_2Cl \xrightarrow{b} CH_3Cl + (CH_3)_2\dot{C}(CH_2Cl) \text{ or } (CH_3)C(\dot{C}HCl) \\ +\dot{C}l \xrightarrow{c} HCl \end{matrix}$

[5] $(CH_3)_2\dot{C}(CH_2Cl) \begin{matrix} \xrightarrow{a} \dot{C}H_3 + (\dot{C}H_3)(CH_2Cl)C{=}CH_2 \\ \xrightarrow{b} \dot{C}H_2Cl + (CH_3)_2C{=}CH_2 \\ \xrightarrow{c} \dot{C}l + (CH_3)_2\langle \end{matrix}$

$(CH_3)_3C(\dot{C}HCl) \xrightarrow{d} \dot{C}H_3 + (CH_3)_2C{=}CHCl$

[6] olefin $+ \begin{matrix} \dot{C}H_3 \\ \dot{C}H_2Cl \\ \dot{C}l \end{matrix} \begin{matrix} \xrightarrow{a} CH_4 \\ \xrightarrow{b} CH_3Cl + \\ \xrightarrow{c} HCl \end{matrix} \left\{ \begin{matrix} \text{olefinic radical} \\ \text{abstraction} \end{matrix} \right\}$ or $\left\{ \begin{matrix} \text{large olefinic radical} \\ \text{addition} \end{matrix} \right\}$

[7] $\dot{C}H_3 + \dot{C}H_3$ or $\dot{C}H_2Cl \rightarrow C_2H_6$ or C_2H_5Cl ($C_2H_5Cl \rightarrow C_2H_4 + HCl$)

[8] $\dot{C}H_3$ or $\dot{C}H_2Cl + (CH_3)_2\dot{C}(CH_2Cl)$ or $(CH_3)_3C(CHCl) \rightarrow$ termination products

[9] $(CH_3)_2\dot{C}(CH_2Cl) + (CH_3)_2\dot{C}(CH_2Cl)$ or $(CH_3)_3C(\dot{C}HCl) \rightarrow$ termination products

[10] $\dot{C}l + (CH_3)_2\dot{C}(CH_2Cl)$ or $(CH_3)_3C(\dot{C}HCl) \rightarrow$ termination products

[11] 2 olefinic radicals $\rightarrow$ termination products

REACTION SCHEME 1.

CH_2Cl are both represented by R_1 and all olefinic radicals are represented by R^1. RCl, R_1H, and R^1H designate neopentyl chloride, methane, or methyl chloride, and any of the olefinic products formed during the pyrolysis, respectively. No formal distinction is made here between the two types of R_1 and R_2 radicals, and between the different types of R^1.

Can. J. Chem. Downloaded from www.nrcresearchpress.com by 210.87.254.6 on 09/05/12
For personal use only.

TABLE IV

Kinetic parameters for elementary reactions

Reaction	Log k_{444}°	Log A	E	References or remarks
[1]	−5.0	13.26	60.0	See Part I
[2]	−7.7	16.1	78.0	(23)
[3]	7.5	9.0	5.0	(15)
[−3]	9.5	10.7	3.9	(15)
[4*a*]	5.5	8.3	10.2	(24)
[4*b*]	5.5	8.3	10.2	Assumed that $k_{4a}=k_{4b}$
[4*c*]	10.0	10.5	1.5	Assumed the same A and E as for C_2H_5Cl (15)
[5]	4.7	13.2	28*	Assumed from related reactions (13, 15)
[6*a*]	6.2	8.0	6.0	Assumed the same as for methyl addition to propylene (26)
[6*b*]	6.2	8.0	6.0	Assumed that $k_{6a}=k_{6b}$
[6*c*]	11.0	11.3	1±1	Assumed from related reactions (14)
[7]	10.4	10.4	0	(15)
[8]	10.4	10.4	0	Assumed that $k_7=k_8$
[9]	11.0	11.0	0	Assumed
[10]	11.3	11.3	0	(15)
[11]	7.4	7.4	0	(25)

k, A, and E refer to the Arrhenius equation $k = Ae^{-E/RT}$. k and A are given in s^{-1} or in $l\,mole^{-1}\,s^{-1}$ and E in kcal/mole.
*Activation energies for reactions [5*a*]–[5*d*] were estimated from bond dissociation energies and standard heats of formation (18, 27). Benson's additivity rules (12) were used where data was not otherwise available.

In Table IV are listed the Arrhenius parameters of the elementary reactions together with rate coefficients at 444 °C. No distinction is made between initiation steps [2*a*] and [2*b*], although from a statistical viewpoint and from the consideration of the two carbon–carbon bonds which are of comparable strength, reaction [2*a*] is more likely to predominate. In order to simplify the solution of the kinetic equations, a single (average) set of values for the Arrhenius parameters has been chosen to account for reactions [5(*a*–*d*)]. These parameters are not known with any certainty, but the analytical results suggest that the relative rates of these reactions are approximately equal over the temperature range studied.

On the assumption of long radical chains, the steady state expressions are given by:

$$[a]\quad \mathrm{d(Cl)}/\mathrm{d}t = k_3(\mathrm{R_1})(\mathrm{HCl}) + k_{5c}(\mathrm{R_2}) - k_{4c}(\mathrm{Cl})(\mathrm{RCl}) - k_{6c}(\mathrm{Cl})(\mathrm{RH^1}) - k_{-3}(\mathrm{Cl})(\mathrm{R_1H}) = 0$$

$$[b]\quad \mathrm{d(R_1)}/\mathrm{d}t = (k_{5a} + k_{5b} + k_{5d})(\mathrm{R_2}) - k_3(\mathrm{R_1})(\mathrm{HCl}) + k_{-3}(\mathrm{Cl})(\mathrm{R_1H}) - (k_{4a} + k_{4b})(\mathrm{R_1})(\mathrm{RCl}) - (k_{6b} + k_{6c})(\mathrm{R_1})(\mathrm{RH^1}) = 0$$

$$[c]\quad \mathrm{d(R_2)}/\mathrm{d}t = [(k_{4a} + k_{4b})(\mathrm{R_1}) + k_{4c}(\mathrm{Cl})](\mathrm{RCl}) - (k_{5a} + k_{5b} + k_{5c} + k_{5d})(\mathrm{R_2}) = 0$$

$$[d]\quad \mathrm{d(R^1)}/\mathrm{d}t = [(k_{6a} + k_{6b})(\mathrm{R_1}) + k_{6c}(\mathrm{Cl})](\mathrm{R^1H}) - k_{11}(\mathrm{R^1})^2 = 0.$$

From expressions [*a*] and [*c*], on neglecting small terms,

$$\frac{(\mathrm{Cl})}{(\mathrm{R_1})} = \frac{4k_3(\mathrm{HCl})}{3k_{4c}(\mathrm{RCl})\phi} \quad \text{and}$$

$$\frac{(\mathrm{R_1})}{\mathrm{R_2})} = \frac{k_{5c}\phi}{k_3(\mathrm{HCl})},$$

where $$\phi = 1 + \frac{4k_{6b}(\mathrm{RH^1})}{3k_{4c}(\mathrm{RCl})}.$$

Substitution of numerical values for the rate coefficients at 444 °C, listed in Table IV, and taking (RCl) = 50×10^{-4} mole l^{-1} (equivalent to 220 mm) lead to the following relative ratios of radical concentrations:

1% reaction:	(Cl)/(R_1) = 8×10^{-5};	(R_1)/(R_2) = 57
5% reaction:	3×10^{-4}	16
10% reaction:	4×10^{-4}	12
20% reaction:	6×10^{-4}	9

The calculated ratios indicate that R_1 radicals are in the greatest concentration in the early stages of the decomposition, hence reaction [7] is the most important termination step. From the steady state assumption it follows that $k_2(\mathrm{RCl}) = k_7(\mathrm{R_1})^2$ or $(\mathrm{R_1}) = (k_2/k_7)^{1/2}(\mathrm{RCl})^{1/2}$ on substitution for (R_1) in the ratio (Cl)/(R_1),

Can. J. Chem. Downloaded from www.nrcresearchpress.com by 210.87.254.6 on 09/05/12
For personal use only.

$$(Cl) = \frac{4k_3}{3k_{4c}}\left(\frac{k_2}{k_7}\right)^{1/2}\frac{(HCl)}{\phi(RCl)^{1/2}}.$$

The rate of disappearance of neopentyl chloride by the radical-chain reaction is then given by the expression:

$$\left[\frac{-d(RCl)}{dt}\right]_{RAD} = k_{4c}(Cl)(RCl) = \frac{4k_3}{3\phi}\left(\frac{k_2}{k_7}\right)^{1/2}(HCl)(RCl)^{1/2}.$$

From the analysis of reaction products, the concentration of hydrogen chloride, (HCl), is related to the extent of the overall decomposition, in the early stages, by the expression: (HCl) = 0.37 [(RCl_0) − (RCl)], where (RCl_0) and (RCl) represent the initial concentration and concentration remaining after pyrolysis, of neopentyl chloride, respectively. The rate expression for neopentyl chloride radical-chain decomposition can then be expressed entirely in terms of (RCl) thus:

$$[A]\quad \left[\frac{-d(RCl)}{dt}\right]_{RAD} = \frac{4k_3}{3\phi}\frac{k_2^{1/2}}{k_7}0.37\left[\frac{(RCl_0)}{(RCl)} - 1\right](RCl)^{3/2} = k_{3/2}^{1}(RCl)^{3/2}.$$

This mechanism predicts a reaction order of 1.5 with respect to neopentyl chloride. The rate coefficient is expected to be constant for decompositions carried out to the same extent of reaction but to change with the progress of the reaction, the change in rate coefficient being dependent on the ratio $[(RCl_0)/(RCl) - 1]/\phi$. The experimental finding shown in Fig. 4 is in agreement with the predicted mechanism. From Fig. 4 it is seen that points corresponding to runs of approximately the same extent of decomposition lie along a straight line with a slope of 1.5. From values of rate coefficients at 444 °C listed in Table IV and from analysis of products the calculated values of $k_{3/2}^{1}$ for $(RCl_0)/(RCl) =$ 1.05, 1.10, and 1.20 at 444 °C are 6.6×10^{-4}, 9.4×10^{-4}, and 12.0×10^{-4} $l^{1/2}$ $mole^{-1/2}$ s^{-1}, respectively. Observed values of $k_{3/2}$ at 444 °C showed a tendency to increase with extent of reaction but because of poor reproducibility these values were scattered about a mean of 2.7×10^{-4} $l^{1/2}$ $mole^{-1/2}$ s^{-1}. Other cases may arise (11): (i) when $(R_1) \sim (R_2)$; (ii) when $(R_2) > (R_1)$; and (iii) when $(R^1H) \geqslant (RCl)$.

(i) This case corresponds to decompositions in the presence of added hydrogen chloride ($(HCl)/(RCl) \leqslant 1$). For $(HCl)/(RCl) \sim 0.25$ $(R_1)/(R_2) \sim 1.2$ and 1.8 at 1% and 10% decomposition respectively, and for $(HCl)/(RCl) \sim 1$, $(R_1)/(R_2) \sim 0.6$ and 0.9 at 1% and 10% reaction respectively. Under these circumstances the predicted major termination step is [8] and the rate of disappearance of neopentyl chloride via the radical mechanism is given by the expression:

$$[B]\quad \left[\frac{-d(RCl)}{dt}\right]_{RAD} = \frac{4}{3\phi^{1/2}}\left(\frac{k_2k_3k_{5c}}{k_8}\right)^{1/2}(HCl)^{1/2}(RCl)^{1/2} = \frac{4(0.37)^{1/2}}{3\phi^{1/2}}\left(\frac{k_2k_3k_{5c}}{k_8}\right)^{1/2}\left[\frac{(RCl_0)}{(RCl)} - 1\right](RCl) = k^{1}(RCl).$$

(ii) In the presence of a large excess of hydrogen chloride $(HCl)/(RCl) \geqslant 1$ or in the presence of hydrogen bromide, $(R_2) \gg (R_1)$ and the most important termination step is [9]. The rate of disappearance of neopentyl chloride is then given by expression [C] which is independent of the concentrations of added hydrogen halides.

$$[C]\quad \left[\frac{-d(RCl)}{dt}\right]_{RAD} = \frac{4}{3}k_{5c}\left(\frac{k_2}{k_8}\right)^{1/2}(RCl)^{1/2}$$

(iii) For the olefin-inhibited pyrolysis and for the decomposition at extents greater than 25% contributions of processes [6*a*], [6*b*], [6*c*] become important, particularly that of [6*c*]. Under such conditions olefins compete with neopentyl chloride for propagating radicals, of which chlorine atoms are the most reactive since the ratio $6_{6c}/k_{4c}$ is estimated to be ~ 10. This ratio plays a predominant part in the expression for the rate of disappearance of neopentyl

Can. J. Chem. Downloaded from www.nrcresearchpress.com by 210.87.254.6 on 09/05/12
For personal use only.

Can. J. Chem. Downloaded from www.nrcresearchpress.com by 210.87.254.6 on 09/05/12
For personal use only.

chloride by processes corresponding to eqs. [A] and [B]. Reaction [6*c*] represents a general type of process involving chlorine atoms in addition/abstraction reactions with olefins containing primary as well as secondary and tertiary hydrogen atoms (e.g. isobutene, 2-methylbut-1-ene, and 3-methylbut-1-ene, respectively). Since a rather larger pre-exponential factor is predicted for abstraction of secondary and tertiary hydrogen atoms by chlorine atoms than in the case of primary hydrogen atoms (14), the ratio $k_{6c}/k_{4c} \sim 10$ is probably of a reasonable order of magnitude.

Thus under the above stated conditions reaction [11] becomes the most important termination step. From [*d*] and from the steady state expression $k_2(\mathrm{RCl}) = k_{11}(\mathrm{R}^1)^2$, on neglecting unimportant terms,

$$[\mathrm{D}] \qquad \left[\frac{-\mathrm{d}(\mathrm{RCl})}{\mathrm{d}t}\right]_{\mathrm{RAD}} = \frac{k_2}{k_{6c}}\frac{(\mathrm{RCl})^2}{(\mathrm{R^1H})}.$$

Though detailed measurements were not made of the initial rates of pyrolysis in the presence of either hydrogen chloride or olefins, the rough estimates of reaction order with respect to these substances (see previously) are in agreement with rate expressions [B] and [D]. In the presence of added hydrogen bromide, even at very low concentrations, $(\mathrm{R}_2) \gg (\mathrm{R}_1)$ since the analogous reaction to [3] involving hydrogen bromide (16) occurs at least 10 times faster than reaction [3] at 444 °C. Appropriate substitution in expression [C] gives a rate for the radical reaction which is about 6 times greater than the predicted value for the "normal" pyrolysis at 444 °C given by [A]. The observed rates of formation of products from the radical reaction were increased by factors of 20–40 in the presence of hydrogen bromide (see Part I).

In Table II it was shown that the isobutene/methyl chloride ratio increases in the presence of added 2-methylbut-2-ene and decreases in the presence of added hydrogen chloride, the change in this ratio depending on the amount of added substance. A possible explanation for this is that the radical chains in neopentyl chloride pyrolysis are short and a substantial contribution of isobutene comes from the decomposition of the chloro tertiary butyl radicals ($(\mathrm{CH_3})_2\dot{\mathrm{C}}(\mathrm{CH_2Cl})$) produced in the initiation reaction [2*a*]. This would lead to large isobutene/methyl chloride concentration ratios for decomposition in the presence of olefins and to smaller ratios for decompositions in the presence of added hydrogen chloride because of long radical chains in the latter case. This is in agreement with the observed results for isobutene/methyl chloride ratios shown in Table II, but is inconsistent with observations on the isobutene/1-chloro-2-methylpropene ratio which remains almost unchanged in the presence of added substances. Since in the normal pyrolysis isobutene and 1-chloro-2-methylpropene are formed at approximately the same rate, a corresponding increase in the isobutene/1-chloro-2-methylpropene ratio can be expected if the excess isobutene is indeed formed from the decomposition of chloro tertiary butyl radicals. Since this is not the case, the remaining possibility is that no significant amounts are produced in this way, instead some chloromethyl radicals (as well as methyl radicals) are lost from the system via reactions [6*a*], [6*b*], and 8. Isobutene concentration was therefore used instead of that of methyl chloride to monitor reaction [5*b*].

Addition of ammonia gas prior to sampling for analysis or organic products (see Part I) has little effect on the rate of radical reaction. The expected rate of hydrogen atom abstraction from ammonia by methyl (17) and chloromethyl radicals is of the same order of magnitude as the rate of abstraction from neopentane. Some chlorine atoms are probably removed from the system by ammonia but rather slowly since $D(\mathrm{H—NH_2}) \sim D(\mathrm{H—Cl})$ (27).

The outstanding difference between the present study and the earlier work (22) lies in the nature of the carbonaceous material coating the inner walls of the vessel. In the study by Maccoll and Swinbourne (22) 1,1-dimethylcyclopropane isomerized very rapidly to methylbutenes and the methylbutenes isomerized to give an equilibrium mixture. This process obscured the extent of the radical-chain process. Pyrolytic carbon from allyl bromide decomposition was shown by Bridge and Holmes (19) only to promote the isomerization of butenes but not to affect the rate of *n*-butyl bromide pyrolysis at 370–420 °C (20), contrary to the proposal by Laidler and Wojciechowski (21). With the pyrolytic carbon used in the present study (from 3-chloro-2-methylpropene and propene treatment) there are indications that while the surface is less efficient in promoting the isomerization of the

Can. J. Chem. Downloaded from www.nrcresearchpress.com by 210.87.254.6 on 09/05/12
For personal use only.

methylbutenes than is allyl bromide carbon, a heterogeneous process leading to the formation of 2-methylbut-1-ene and hydrogen chloride occurs on the surface in a vessel of high S/V ratio (see Part I). Interaction of this heterogeneous reaction with the radical-chain decomposition could take place through the hydrogen chloride produced by the former process, via reaction [3]. However, the interplay between the surface and the radical-chain decomposition is likely a more complex process than can be accounted for by the heterogeneous reaction alone since the rate of formation of products representative of the radical-chain process increases more in the vessel of high S/V ratio in the presence of hydrogen chloride (see Part I). Traces of ammonium chloride, found in the analysis of the pyrolytic carbon vessel with S/V ratio $= 0.8\ cm^{-1}$ at the conclusion of the experiment, may be partly responsible for the heterogeneous process.

This work establishes that 1,1-dimethylcyclopropane is formed during the pyrolysis of neopentyl chloride via a largely homogeneous radical-chain reaction rather than via a quasi-heterolytic process (22) or via a carbene intermediate (6, 7). Although the exact mechanism leading to its formation from chloro-neopentyl chloride radicals is not confirmed unequivocally, of the two possible transition states shown below, **1** is more probable since it involves least scrambling of atoms in the transition state.

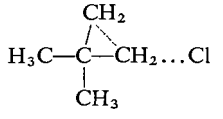

1

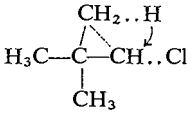

2

While Anderson and Benson's proposal (10) that 1,1-dimethylcyclopropane is a radical-chain decomposition product of neopentyl chloride is verified here, their hypothesis that the methylbutenes are formed exclusively via the cyclopropane is disproved. Formation of the methylbutenes by methyl radical addition to the chloro-2-methylpropenes and to isobutene, also suggested by these authors, was found to be negligible from studies on the pyrolysis of neopentyl chloride in the presence of 1-chloro-2-methylpropene.

Acknowledgments

The authors thank Professor S. V. Stimson for helpful discussion. One of us (J. S. S.) gratefully acknowledges a C.S.I.R.O. Postgraduate Senior Studentship.

1. D. H. R. Barton and P. F. Onyon. Trans. Faraday Soc. **45**, 726 (1949).
2. P. Goldfinger, M. Letort, and M. Niclause. Contribution à l'étude de la structure moléculaire. Vol. Commem. Victor Henri. Desoer, Liège. 1948. p. 283.
3. H. L. Bernstein, A. H. Popkin, F. C. Whitmore, and J. P. Wilkins. J. Am. Chem. Soc. **63**, 124 (1941).
4. J. R. Pfister, A. H. Popkin, and F. C. Whitmore. J. Am. Chem. Soc. **61**, 1616 (1939).
5. F. C. Whitmore and H. D. Zock. J. Am. Chem. Soc. **64**, 1783 (1942).
6. J. G. Berger and L. Friedman. J. Am. Chem. Soc. **83**, 500 (1961).
7. A. P. Krapcho and P. S. Skell. J. Am. Chem. Soc. **83**, 754 (1961).
8. W. C. Herndon and E. S. Lewis. J. Am. Chem. Soc. **83**, 5230 (1961).
9. C. N. Pillai and H. Pines. J. Am. Chem. Soc. **83**, 3274 (1961).
10. K. H. Anderson and S. W. Benson. J. Chem. Phys. **39**, 1673 (1963).
11. R. L. Failes and V. R. Stimson. Australian J. Chem. **17**, 851 (1964).
12. S. W. Benson and J. H. Buss. J. Chem. Phys. **29**, 546 (1958).
13. J. A. Kerr and A. F. Trotman-Dickenson. *In* Progress in reaction kinetics. Vol. 1. *Edited by* G. Porter. Pergamon, London. 1961.
14. G. C. Fettis and J. H. Knox. *In* Progress in reaction kinetics. Vol. 2. *Edited by* G. Porter. Pergamon, London. 1967.
15. G. Chiltz, P. Goldfinger, G. Huybrechts, G. Martens, and G. Verbeke. Chem. Rev. **63**, 355 (1963).
16. B. H. Eckstein, H. A. Scheraga, and E. R. Van Artsdalen. J. Chem. Phys. **22**, 28 (1954).
17. P. Gray and J. C. J. Thynne. Trans. Faraday Soc. **60**, 1047 (1964).
18. F. D. Rossini *et al.* Selected values of physical and thermodynamic properties of hydrocarbons and related compounds. Carnegie Press, Pittsburgh. 1953.
19. J. L. Holmes. Private communication.
20. M. R. Bridge and J. H. Holmes. J. Chem. Soc. B, 713 (1966).
21. K. J. Laidler and B. W. Wojciechowski. Trans. Faraday Soc. **59**, 369 (1963).
22. A. Maccoll and E. S. Swinbourne. J. Chem. Soc. 148 (1964).
23. Wing Tsang. J. Chem. Phys. **44**, 4283 (1966).
24. A. F. Trotman-Dickenson. Free radicals. Methuen, London. 1959. p. 65.
25. R. J. Akers and J. J. Throssell. Chem. Commun. 432 (1966).
26. L. E. Mandelcorn and E. W. R. Steacie. Can. J. Chem. **32**, 79 (1954).
27. J. A. Kerr. Chem. Rev. **66**, 465 (1966).
28. M. N. Kale and A. Maccoll. J. Chem. Soc. 5033 (1957).

Mercury-sensitized photolysis of perfluorocyclobutene and 1,3-perfluorobutadiene

WAYNE STUCKEY AND JULIAN HEICKLEN[1]
Aerospace Corporation, El Segundo, California

Received September 13, 1967

The mercury-sensitized photolyses of cyclo-C_4F_6 and 1,3-C_4F_6 were examined in the vapor phase. In the *c*-C_4F_6 system, the major product was 1,3-C_4F_6; in the 1,3-C_4F_6 system, *c*-C_4F_6. In both cases, an excited molecule is formed which can pass to a common intermediate structure. The intermediate reverts to 1,3-C_4F_6 about 86% of the time and to *c*-C_4F_6 about 14% of the time. The efficiencies of quenching the excited mercury atom, relative to N_2O, are 0.71 and 1.38 for *c*-C_4F_6 and 1,3-C_4F_6 respectively.

Canadian Journal of Chemistry, 46, 1361 (1968)

Can. J. Chem. Downloaded from www.nrcresearchpress.com by 210.87.254.5 on 09/05/12
For personal use only.

I. Introduction

In the study of the mercury-sensitized photolysis of C_4F_8-2, *cis–trans* isomerization occurred. Thus, the formation of an excited-molecule intermediate was indicated (1). Except for the *cis–trans* isomerization, no other chemical change occurred at temperatures up to 370°.

Perfluorocyclobutene and 1,3-perfluorobutadiene are isomers with the same carbon–fluorine bonding. Therefore, interconversion of the two compounds does not require the difficult step of fluorine-atom migration. It has been shown by Schlag and Peatman (2) that the isomerization can be induced thermally at temperatures above 192° by a homogeneous unimolecular reaction with no side complications. They deduced both rate constants in the temperature range 192 to 266°. The purpose of the present paper is to elucidate the isomerization induced by mercury sensitization.

II. Experimental

The fluorocarbons used in this study were obtained from the Peninsular ChemResearch Co., Inc. Each was degassed at −196° prior to use; gas chromatographic analysis, employing a column at 0° packed with Union Carbide Perfluorolube FS-5 on firebrick, showed about 0.3 and 0.7% of an impurity with a retention time similar to C_2F_6, respectively, for *c*-C_4F_6 and 1,3-C_4F_6. Nitrous oxide was from the Matheson Co. and also was degassed at −196° before use.

The experimental procedure is the standard one used in our laboratory, originally described by Saunders and Heicklen (3). Irradiation was from a Hanovia, flat, spiral, low-pressure mercury arc. The incident light passed through a Corning 9-54 glass (to remove radiation below 2200 Å) and, for some runs, through screens (to reduce the intensity) before entering one arm of the X-shaped cell through a quartz window. The other arm of the cell was situated in the sample path of a Beckman IR-5 spectrometer. The cell was encased in a wire-wound aluminium block so that elevated temperatures could be obtained, if desired.

For runs in which the C_4 perfluoroolefin was sensitized, the growth of its isomer was monitored by *in situ* infrared spectroscopy. The 7.10 and 7.52 μ bands of *c*-C_4F_6 and 1,3-C_4F_6 were used, respectively.

When mixtures of N_2O and the C_4 perfluoroolefin were sensitized, the N_2 produced was measured after exposure was terminated. The reaction mixture was expanded through a trap at −196°, and the pressure of the non-condensable gas was measured in a McLeod gauge.

We determined the absolute intensity of the lamp by monitoring CF_2O production in the mercury-sensitized photolysis of 500 Torr of N_2O in the presence of 20 Torr of C_2F_4. Under these conditions, $\Phi(CF_2O)$ was equal to 1.0 (4).

III. Results

The absorption at 2537 Å of *c*-C_4F_6 and 1,3-C_4F_6 was measured on a Cary model 15 spectrometer. Perfluorocyclobutene was essentially transparent, but 38 Torr of 1,3-C_4F_6 had an optical density of 0.066 in a 10 cm cell. Thus, with *c*-C_4F_6 the primary process is entirely mercury sensitization. However, with 1,3-C_4F_6, a small amount of direct absorption of the radiation will occur, too.

The mercury sensitization of perfluorocyclobutene yielded 1,3-C_4F_6 almost exclusively. With 20 Torr of *c*-C_4F_6, gas chromatographic analysis showed 97.9% 1,3-C_4F_6, and two unidentified products of 0.7 and 1.4%. By infrared analysis, the only product detected was 1,3-C_4F_6 under all conditions.

The irradiation of about 20 Torr of 1,3-C_4F_6 produced 91.8% *c*-C_4F_6, 1.5% C_3F_6, 2.2% of a compound with the retention time of C_2F_6, and 0.7, 0.9, and 2.9% of three unidentified products, as obtained by gas chromatographic analysis. Only *c*-C_4F_6 could be detected by infrared analysis.

In both cases, the failure to detect the minor products by infrared analysis was due to the

[1]Present address: Department of Chemistry, Pennsylvania State University, University Park, Pa. 16802.

Can. J. Chem. Downloaded from www.nrcresearchpress.com by 210.87.254.5 on 09/05/12
For personal use only.

insensitivity of this technique and not to peculiarities in the system. However, this deficiency prohibited us from monitoring their quantum yields in all the runs.

With c-C_4F_6, the minor products are so small that they could hardly have any influence on the conclusions. With 1,3-C_4F_6, the minor products may come from the direct absorption of the radiation by 1,3-C_4F_6, and thus would be a side issue to the purpose of this manuscript. In any event, the sum of their quantum yields is only 0.01. It was felt that a separate study of the direct photolysis at 1,3-C_4F_6 would be more fruitful in unraveling their mechanism of formation, and they are not discussed further in this paper.

At room temperature and low pressures, some runs were done to extended conversions starting with each isomer. Both isomers were monitored and, to within 10%, the sum of their pressures was constant; thus, there was no extensive loss of material by polymerization.

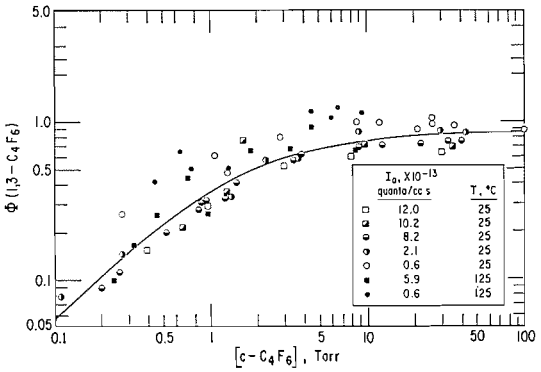

FIG. 1. Log–log plot of $\Phi(1,3\text{-}C_4F_6)$ vs. $[c\text{-}C_4F_6]$ in the mercury-sensitized photolysis of c-C_4F_6.

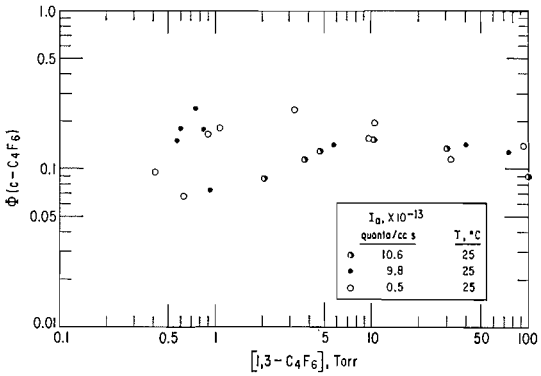

FIG. 2. Log–log plot of $\Phi(c\text{-}C_4F_6)$ vs. $[1,3\text{-}C_4F_6]$ in the mercury-sensitized photolysis of 1,3-C_4F_6.

The initial quantum yields of product formation as a function of pressure of the starting material are shown in Figs. 1 and 2. The data exhibit considerable scatter, but definite conclusions can be made: First, a 20-fold change in intensity has little, if any, effect in either system. Second, in the c-C_4F_6 system, the results are essentially the same at 25 and 125 °C. However, the points at the lower intensity at 125° are above the other points. We feel that this is an artifact caused by the difficulty in the actinometer runs under these conditions. It was found that when N_2O–C_2F_4 mixtures were exposed under these conditions, the CF_2O produced slowly disappeared after exposure. Thus, the absorbed intensity measurements may have been somewhat low. As a result, the values for $\Phi(1,3\text{-}C_4F_6)$ would be too high. Measurements at 125° were not made with 1,3-C_4F_6 as a starting gas because polymerization was extensive. As a third conclusion, in the 1,3-C_4F_6 system, $\Phi(c\text{-}C_4F_6)$ is 0.14 ± 0.02 independent of 1,3-C_4F_6 pressure between 4 and 100 Torr. Measurements were made to pressures as low as 0.4 Torr. However, in order that the back reaction be minimized, the amount of c-C_4F_6 produced was extremely small, and the scatter of the data increased markedly as can be seen in Fig. 2. Nevertheless, $\Phi(c\text{-}C_4F_6)$ is not measurably affected. Fourth, in the c-C_4F_6 system, $\Phi(1,3\text{-}C_4F_6)$ is about 0.86 at high pressures (definitely less than 1.0) but drops measurably as the c-C_4F_6 pressure is lowered.

To obtain the relative quenching cross section of the C_4 compounds for the excited mercury atom, we irradiated mixtures of N_2O and the perfluoroolefin. Small amounts of C_2H_6 also were present to scavenge the oxygen atoms produced from N_2O decomposition. The quantum yields of N_2 obtained in these runs are listed in Table I. They increase toward 1 as the ratio of N_2O pressure to perfluoroolefin pressure is enhanced.

IV. Discussion

The primary photolytic act is mainly the absorption of radiation by Hg vapor.

[a] $\quad Hg + h\nu(2537\ Å) \rightarrow Hg^*$

The excited mercury atom Hg* is scavenged by the perfluoroolefin

[b] $\quad Hg^* + B \rightarrow Hg + B^*$

[c] $\quad Hg^* + C \rightarrow Hg + C^*,$

TABLE I

Mercury-sensitized photolysis of N_2O–perfluoroolefin mixtures at 25°, $I_a \sim 10^{14}$ quanta/cc s

$[N_2O]$, Torr	$[C_4F_6]$, Torr	$\Phi(N_2)$
	c-C_4F_6	
7.6	84	0.122
17.1	95	0.20
49.4	98	0.41
109	103	0.59
	1,3-C_4F_6	
40	72	0.30
50.3	85	0.32
61.7	175	0.192
66.5	96	0.37
115	100	0.41
241	100	0.59

where B and C are 1,3-C_4F_6 and *c*-C_4F_6 respectively, and the superscript * denotes an electronically excited state (presumably a triplet).

Since the excited molecules isomerize reversibly, there must be a common intermediate form (designated I). The invariance of $\Phi(c\text{-}C_4F_6)$ in the 1,3-C_4F_6 system with conditions suggests that all B* molecules convert to I.

[*d*] $$B^* (+ M) \rightarrow I (+ M)$$

However, in the *c*-C_4F_6 system, $\Phi(1,3\text{-}C_4F_6)$ falls as the pressure is reduced below 10 Torr. The falloff at low pressures suggests that either the light absorbed is reduced (because of the pressure-broadening effect on absorption) or that all the Hg* is not quenched by C. In the latter case reaction [*c*] would be in competition with

[*e*] $$Hg^* \rightarrow Hg + h\nu .$$

To check this possibility, we studied the mercury-sensitized photolysis of N_2O in the presence of small amounts of C_2H_6 (to scavenge the oxygen atoms produced). The rate of N_2 production at 0.1 Torr of N_2O was 0.25 that at the high-pressure limit. Thus, reaction [*e*] must be important. Since it will be shown that *c*-C_4F_6 is only 0.71 times as efficient as N_2O in quenching Hg*, $\Phi(1,3\text{-}C_4F_6)$ should be reduced by a factor of 5.6 at 0.1 Torr of *c*-C_4F_6. The data in Fig. 1 show a reduction of about a factor of 15. There is considerable scatter in the data, especially at the low pressures, and it is possible that these two numbers are within experimental error of each other.

If the difference between 5.6 and 15 is real, then the additional falloff could be explained in two ways. The first possibility is that the 1,3-C_4F_6 product was formed with excess energy and either decomposed or polymerized before stabilization at low pressures, thus resulting in a low yield. The second possibility is that there was a competition for C*

[*f*] $$C^* \rightarrow C$$

[*g*] $$C^* + C \rightarrow I + C .$$

The intermediate then converts to one of the stable isomeric configurations

[*h*] $$I \rightarrow B$$

[*i*] $$I \rightarrow C .$$

The mechanism predicts that in the *c*-C_4F_6 system

$$[1] \quad \Phi(1,3\text{-}C_4F_6) = \left(\frac{k_c[C]}{k_e + k_c[C]}\right)\left(\frac{k_h}{k_h + k_i}\right) \times \left(\frac{k_g[C]}{k_f + k_g[C]}\right),$$

where [ ] indicates concentration, whereas in the 1,3-C_4F_6 system

$$[2] \quad \Phi(c\text{-}C_4F_6) = \left(\frac{k_b[B]}{k_e + k_b[B]}\right)\left(\frac{k_i}{k_h + k_i}\right).$$

The equations predict that at sufficiently high pressures, the quantum yields are independent of pressure or absorbed intensity with $\Phi(1,3\text{-}C_4F_6) = k_h/[k_h + k_i]$ and $\Phi(c\text{-}C_4F_6) = k_i/[k_h + k_i]$. Consistent values of 0.86 and 0.14 are obtained for the respective rate constant ratios. As the pressure is reduced, the expressions predict that the quantum yields will drop. This occurs in the *c*-C_4F_6 system, but not in the 1,3-C_4F_6 system. However, the lowest pressure for which data could be obtained in the 1,3-C_4F_6 system was 0.4 Torr. It will be shown that 1,3-C_4F_6 is 1.38 times as efficient as N_2O in scavenging Hg*, so that k_e/k_b is 0.22 Torr in this system. Thus, even at 0.4 Torr, $\Phi(c\text{-}C_4F_6)$ should have dropped to only 0.093; at 0.7 Torr, to 0.11. The uncertainty in the data at these pressures is so large that the effect was masked.

To obtain the relative quenching efficiencies for reactions [*b*] and [*c*], we irradiated mixtures of N_2O and the perfluoroolefin. With N_2O the reaction is

Can. J. Chem. Downloaded from www.nrcresearchpress.com by 210.87.254.5 on 09/05/12
For personal use only.

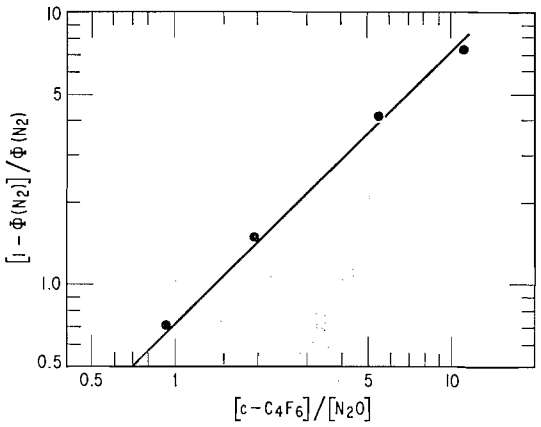

FIG. 3. Log–log plot of $[1 - \Phi(N_2)]/\Phi(N_2)$ vs. $[c\text{-}C_4F_6]/[N_2O]$ in the mercury-sensitized photolysis of $c\text{-}C_4F_6$–N_2O mixtures.

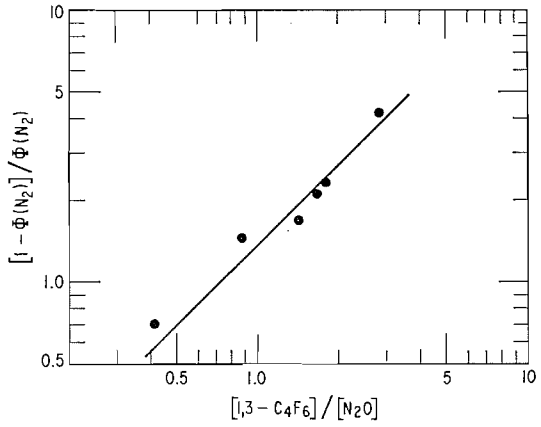

FIG. 4. Log–log plot of $[1 - \Phi(N_2)]/\Phi(N_2)$ vs. $[1,3\text{-}C_4F_6]/[N_2O]$ in the mercury-sensitized photolysis of $1,3\text{-}C_4F_6$–N_2O mixtures.

[j] $Hg^* + N_2O \rightarrow Hg + N_2 + O$.

$\Phi(N_2)$ should obey the equation

$$[3] \qquad \frac{1 - \Phi(N_2)}{\Phi(N_2)} = \frac{k_c[C]}{k_j[N_2O]}$$

or

$$[4] \qquad \frac{1 - \Phi(N_2)}{\Phi(N_2)} = \frac{k_b[B]}{k_j[N_2O]}.$$

Figures 3 and 4 are the appropriate plots. The log–log graphs are linear with slopes of 1. The intercepts yield values of 0.71 ± 0.03 and 1.38 ± 0.18, respectively, for k_c/k_j and k_b/k_j.

The rate constant information obtained in this study is summarized in Table II.

TABLE II

Summary of rate constant information

Ratio	Value	Source
$k_h/[k_h+k_i]$	0.86	Eq. 1, Fig. 1
$k_i/[k_h+k_i]$	0.14	Eq. 2, Fig. 2
k_c/k_j	0.71	Eq. 3, Fig. 3
k_b/k_j	1.38	Eq. 4, Fig. 4

Acknowledgments

The authors wish to thank Mrs. Barbara Peer for assistance with the manuscript. Financial assistance through Air Force Contract No. 04-(695)-1001 is gratefully acknowledged.

1. D. SAUNDERS and J. HEICKLEN. J. Phys. Chem. **69**, 3205 (1965).
2. E. W. SCHLAG and W. B. PEATMAN. J. Am. Chem. Soc. **86**, 1676 (1964).
3. D. SAUNDERS and J. HEICKLEN. J. Am. Chem. Soc. **87**, 2088 (1965).
4. D. SAUNDERS and J. HEICKLEN. J. Phys. Chem. **70**, 1950 (1966).

Can. J. Chem. Downloaded from www.nrcresearchpress.com by 210.87.254.5 on 09/05/12
For personal use only.

Photometric analysis of trace amounts of hydrazine with *p*-dimethylaminobenzaldehyde. Chemical equilibria. Part II[1]

DONALD S. GAMBLE
Analytical Chemistry Research Service, Research Branch, Canada Agriculture, Ottawa, Canada

Received November 7, 1967

Additional chemical equilibrium data are presented for aqueous solutions into which have been put *p*-dimethylaminobenzaldehyde, HCl, and hydrazine sulfate. The photometric measurement of the thermodynamic equilibrium constant for *p*-dimethylaminobenzaldehyde protonation agrees to within experimental error with the value from solubility experiments. The average of the two is $\mathcal{K}_1 = 44.$ (molal)$^{-1}$ ± 2%.

Some analytical chemical applications are discussed.

Canadian Journal of Chemistry, 46, 1365 (1968)

Can. J. Chem. Downloaded from www.nrcresearchpress.com by 210.87.254.105 on 09/05/12
For personal use only.

Introduction

p-Dimethylaminobenzaldehyde reacts with hydrazine in aqueous strong acid solution to give a colored compound. The photometric method of analysis based on this reaction was pioneered by Pesez and Petit (1), and has been improved several times since (2–4). Gamble and Hoffman have described the main features of the chemical equilibria in this system, and have measured some of the constants and activity coefficient ratios (5). The purpose of this work is to provide further quantitative data for these equilibria, so that this method of analysis may be more readily improved or adapted to various needs.

The first experimental step is to measure the acid dependence of the *p*-dimethylaminobenzaldehyde protonation equilibrium. The ultraviolet–visible spectrum for the aldehyde in aqueous strong acid solution shows absorbance peaks at 350 mμ and 240 mμ. Among the evidence for protonation reaction is the fact that strong acid depresses the 350 mμ peak while enhancing that at 240 mμ (6). This suggested the idea of photometric measurements of the protonation equilibrium. The protonated and unprotonated forms of the aldehyde have similar absorbances at $\lambda = 240$ mμ, so that the total absorbance is not a very sensitive function of the extent of reaction. The 350 mμ peak, however, is excellent for measuring this equilibrium. Because the aldehyde concentrations used are three to four orders of magnitude lower than those of the acid, it is most practical to measure absorbance at $\lambda = 350$ mμ as a function of total aldehyde concentration, with acid concentration being the parameter of the family of curves.

The second step consists of making photometric measurements on the color-forming reaction itself. These experiments are very similar to some of those already reported (5), and consist of absorbance measurements at $\lambda = 455$ mμ for solutions into which have been put strong acid, hydrazine sulfate, and *p*-dimethylaminobenzaldehyde.

These two sets of measurements are used for estimating the mass action quotient for the color-forming reaction between the aldehyde and hydrazine. HCl was chosen as the strong acid most useful for this study.

Experimental

(a) Chemicals

Hydrazine sulfate, formula weight 130.130; Fisher Certified Reagent, assay 99.3%, American Chemical Society standard. The reagent was dried to constant weight over P_2O_5 at room temperature.

p-Dimethylaminobenzaldehyde, formula weight 149.195; Analar Analytical Reagent, melting point 73.0–75.0 °C. Maximum ash, 0.05%. The reagent was dried to constant weight over P_2O_5 at room temperature.

Hydrochloric acid, 37–38%, Baker Analysed Reagent, American Chemical Society grade. Maximum total impurity, 0.008%.

(b) Equipment

Beckman DU spectrophotometer, with thermostatted cell compartment.

Constant temperature bath, 25.000 ± 0.005°.

A matched pair of quartz sample cells, 1.00 cm path length.

The calibrations of the spectrophotometer and its sample cells have been described elsewhere (5).

(c) Method for p-Dimethylaminobenzaldehyde Protonation Equilibrium

Standard HCl solutions were prepared with concentrations from 0.025 *m* to 1.0 *m*, and used for making stock

[1]Contribution No. 96, Analytical Chemistry Research Service.

TABLE I

Absorbance at 350 mμ as a function of *p*-dimethylaminobenzaldehyde molality, with HCl molality as the parameter. Least squares results for the family of straight lines. 25.00 °C

c_3, HCl molality	$(\partial A_1/\partial c_1)_{c_3} \times 10^{-5}$	c_1 range $\times 10^5$	Number of measurements	$\sigma \times 10^5$, stand. deviation of straight line
0.02525	0.137	1.0 to 3.9	7	0.0035
0.05053	0.0886	1.0 to 9.1	9	0.0058
0.1014	0.0507	2.6 to 18	9	0.0046
0.1997	0.0270	1.9 to 18	9	0.0016
0.3010	0.0176	2.4 to 18	9	0.0016
0.3990	0.0118	2.1 to 18	9	0.0029
0.5034	0.00896	2.0 to 18	9	0.0010
0.5971	0.00784	1.9 to 18	8	0.0078
0.7150	0.00548	2.0 to 19	6	0.0046
0.8186	0.00453	2.5 to 21	9	0.038
0.9416	0.00370	2.4 to 22	9	0.0025
1.034	0.00318	2.4 to 22	9	0.0021

solutions of the reagent. These were 0.01 *m* aldehyde in aqueous HCl.

0.1 to 0.9 g aliquots of the stock solution and enough of the corresponding HCl standard solutions were weighed into flasks, to give 50 g of total solution. One hour of equilibration at 25.000 °C gave reproducible absorbance readings, which were taken at $\lambda = 350$ mμ. The corresponding HCl solutions served as blanks.

(d) Method for the Color-Forming Reaction

Standard HCl solutions were prepared with concentrations from 0.4842 *m* to 0.7322 *m*; 0.1 *m* and 0.02 *m* aldehyde solutions in aqueous HCl were made from these. 2 g to 6 g aliquots of 0.1 *m* aldehyde, or 11 g to 12.5 g aliquots of 0.02 *m* aldehyde, were weighed into flasks. 4.9×10^{-5} *m* hydrazine sulfate in aqueous HCl was also made with the same HCl standard solutions. 12 g to 12.5 g aliquots of hydrazine sulfate stock solution were weighed into each flask to give 25 g total solution. After 30 min of equilibration at 25.000 °C, the absorbance was read at $\lambda = 455$ mμ. The blanks lacked only the hydrazine sulfate.

Results and Calculations

Symbols

m_1 = *p*-dimethylaminobenzaldehyde molality.

$m_2 = H^+$ molality.

m_3 = protonated aldehyde molality.

$m_4 = m_{10} + m_{11}$.

m_5 = benzaldazine molality.

m_6 = benzaldazine quinoidal cation molality.

$m_{10} = N_2H_4$ molality.

$m_{11} = N_2H_5^+$ molality.

a_i = molal activity of ion or molecule *i*.

γ_i = molal activity coefficient of ion or molecule *i*.

$\mathcal{K}_j$ = thermodynamic equilibrium constant.

K_j = mass action quotient corresponding to $\mathcal{K}_j$.

A_1 = total absorbance at $\lambda = 350$ mμ, of aldehyde in aqueous HCl.

A_2 = absorbance at 455 mμ, of the benzaldazine quinoidal cation.

l = light path (cm) in the sample.

ε_1 = molar extinction coefficient at $\lambda = 350$ mμ, of unprotonated aldehyde in aqueous HCl.

ε_3 = molar extinction coefficient at $\lambda = 350$ mμ, of protonated aldehyde in aqueous HCl.

ε_2 = molar extinction coefficient at $\lambda = 455$ mμ, of the benzaldazine quinoidal cation.

W = (kg of H_2O)/(liter of solution).

The p-Dimethylaminobenzaldehyde Protonation Equilibrium

The absorbance at $\lambda = 350$ mμ was measured as a function of *p*-dimethylaminobenzaldehyde molality, with total HCl molality being the parameter. The temperature was constant at 25.000 ± 0.005 °C during equilibration. The method of least squares showed the data to be linear, with zero intercepts. The slopes, $(\partial A_1/\partial c_1)_{c_3}$, and other information for the resulting family of straight lines are given in Table I.

The total absorbance in this system is given by

$$[1] \qquad A_1 = lW(\varepsilon_1 m_1 + \varepsilon_3 m_3).$$

The material balance relations for total aldehyde and total acid are given by eqs. [2] and [3].

$$[2] \qquad c_1 = m_1 + m_3$$

$$[3] \qquad c_3 = m_2 + m_3.$$

Substituting [2] into [1] gives

$$[4] \qquad (A_1/lW) = (\varepsilon_1 - \varepsilon_3)m_1 + \varepsilon_3 c_1.$$

The protonation equilibrium is described by eq. [5];

$$[5] \qquad K_1 = m_3/m_1 m_2.$$

Can. J. Chem. Downloaded from www.nrcresearchpress.com by 210.87.254.105 on 09/05/12
For personal use only.

Can. J. Chem. Downloaded from www.nrcresearchpress.com by 210.87.254.105 on 09/05/12
For personal use only.

Since $m_3 < c_1$, then when $c_1 \ll c_3$, as with the present work, [3] reduces to

$$c_3 \approx m_2.$$

Substituting this and [2] into the mass action expression [5] gives

$$[6] \qquad m_1 = c_1/(K_1c_3 + 1).$$

Absorbance as a function of total acid and total aldehyde is found by combining [4] and [6];

$$[7] \quad (A_1/lW) = \left[\frac{(\varepsilon_1 - \varepsilon_3)}{(K_1c_3 + 1)} + \varepsilon_3\right] c_1.$$

Assuming that $W = W(c_3)$ is independent of c_1, the slope of [7] is

$$[8] \quad (1/lW)(\partial A_1/\partial c_1)_{c_3} = \frac{(\varepsilon_1 - \varepsilon_3)}{(K_1c_3 + 1)} + \varepsilon_3.$$

$$\text{Since } \lim_{c_3 \to 0}\left[\frac{1}{lW}(\partial A_1/\partial c_1)_{c_3}\right] = \varepsilon_1,$$

a simple extrapolation of $(1/lW)(\partial A_1/\partial c_1)_{c_3}$ vs. c_3 might be expected to yield the molar extinction coefficient of the unprotonated aldehyde.[2] In practice, however, eq. [8] approaches the $c_3 = 0$ limit asymptotically, so that the intercept is unobtainable. A more tractable relationship is found by multiplying both sides of eq. [8] by $(K_1{}^*c_3 + 1)$, where $K_1{}^*$ is some arbitrary value for K_1;

$$[9] \quad \frac{1}{lW}(\partial A_1/\partial c_1)_{c_3}(K_1{}^*c_3 + 1) = \left(\frac{K_1{}^*c_3 + 1}{K_1c_3 + 1}\right)(\varepsilon_1 - \varepsilon_3) + (K_1{}^*c_3 + 1)\varepsilon_3.$$

Equation [9] has the same intercept as does [8], but if $K_1{}^*$ is of the same order of magnitude as K_1, then it will approach the $c_3 = 0$ limit much less steeply, and in a more nearly linear fashion. The intercept thus becomes accessible. The accurate calculation of ε_1 requires, however, that the properties of [9] near the $c_3 = 0$ limit be examined in detail. For $c_3 < 0.025\ m$, $K_1 \approx \mathscr{K}_1$. If the term $(K_1{}^*c_3 + 1)\varepsilon_3$ is not too big, then three conditions are possible in this region:

(*a*) $K_1{}^* \equiv \mathscr{K}_1$. Then $(K_1{}^*c_3 + 1)/(K_1c_3 + 1)$ approaches unity, and the plot of $(1/lW)(\partial A_1/\partial c_1)_{c_3}(K_1{}^*c_3 + 1)$ vs. c_3 becomes nearly horizontal for $c_3 < 0.025\ m$. The intercept will give an accurate value of ε_1.

(*b*) $K_1{}^* < \mathscr{K}_1$. Since $K_1 \geqslant \mathscr{K}_1$, then as c_3 approaches zero, $(K_1{}^*c_3 + 1)(K_1c_3 + 1)$ rises ever more steeply toward unity. The quantity $(1/lW)(\partial A_1/\partial c_1)c_3(K_1{}^*c_3 + 1)$ then rises correspondingly steeply toward the true intercept. Consequently the shape of the curve cannot be determined between $c_3 = 0$ and the first experimental point. As a result, the apparent intercepts give ε_1 values that are too low.

(*c*) $K_1{}^* > \mathscr{K}_1$. As c_3 decreases toward zero, there will be a point at which $K_1{}^* \equiv K_1$, so that the curve of $(1/lW)(\partial A_1/\partial c_1)_{c_3}(K_1{}^*c_3 + 1)$ vs. c_3 has zero slope. Then as c_3 further approaches zero, the curve will drop ever more steeply to the true intercept. As before, this yields the wrong intercept, leading this time to ε_1 values that are too high. Figure 1 illustrates this behavior. In Fig. 2, the apparent intercept is accordingly plotted as a function of $K_1{}^*$, for the determination of ε_1. It is evident that, as expected, the apparent intercept becomes constant at ε_1 as $K_1{}^*$ approaches $\mathscr{K}_1$ from either direction. ε_1 is readable from this graph to more significant figures than are justified by the photometric accuracy. The result is

$$\varepsilon_1 = 0.293 \times 10^5 \text{ (mole} \times \text{cm}^{-1}) \pm 0.6\%.$$

By using this answer and assuming, on the strength of Fig. 2, that $K_1 \approx 45$ at $c_3 = 0.05053\ m$ (see Table I), it was found from eq. [8] that ε_3 is zero to within the errors of measurement. With these values of the molar extinction coefficients,

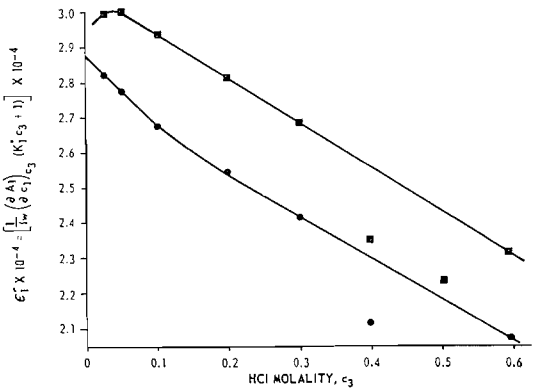

FIG. 1. The effect of $K_1{}^*$ on the calculation of ε_1. ●, $K_1{}^* = 42$; ■, $K_1{}^* = 47$. $\lambda = 350$ mμ. See eq. [9].

[2]Dr. R. C. Turner has correctly pointed out that in [8], the approximation $m_2 \approx c_3$ becomes invalid as c_3 approaches zero. Because c_1 is of the order of $10^{-5}\ m$ in the lower c_3 region, however, the term affected, K_1c_3, becomes negligible compared with unity before the approximation breaks down. Hence the numerical value of ε_1 is not affected within the number of significant figures experimentally justified.

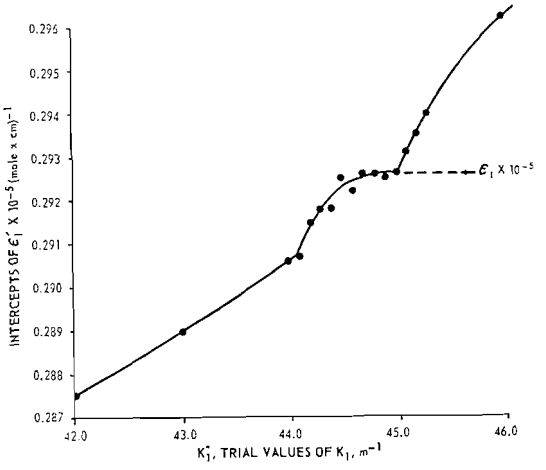

FIG. 2. The calculation of ε_1 from the intercepts of ε_1'. See Fig. 1 and eq. [9].

eq. [8] was used for calculating K_1', the preliminary values of K_1 and $\mathscr{K}_1$ shown in Fig. 3. This gives

$$\mathscr{K}_1 = 45.\ (\text{molal})^{-1} \pm 2\%,$$

which agrees to within the experimental errors with the value of 43. $(\text{molal})^{-1} \pm 2.4\%$ from solubility measurements (6). The value finally adopted therefore is the average,

$$\mathscr{K}_1 = 44.\ (\text{molal})^{-1} \pm 2\%.$$

By definition, $\mathscr{K}_1 = K_1(\gamma_3/\gamma_1\gamma_2)$.
The values of $(\gamma_3/\gamma_1\gamma_2)$ in Table II were accordingly calculated from eq. [10].

$$[10] \qquad (\gamma_3/\gamma_1\gamma_2) = (45./K_1').$$

The finally adopted values of K_1 are consequently given by Table II and eq. [11].

$$[11] \quad K_1 = 44.(\gamma_1\gamma_2/\gamma_3)\ (\text{molal})^{-1} \pm 2\%.$$

The error in K_1 is found to be only $\pm 2\%$, because of the cancellation in eq. [11] of errors from a common source.

Finally, the results of the solubility work (6, 7), in the form of eq. [12] and the published values of $(\gamma_3/\gamma_2)_s$ and m_{2s} permitted the calculation of the molal activity coefficient of unprotonated aldehyde, γ_1.

$$[12] \quad \text{Log}\,(\gamma_3/\gamma_2) = \log\,(\gamma_3/\gamma_2)_s - 0.60(m_2 - m_{2s}).$$

The substitution $m_2 \approx c_3$ was again used here.

TABLE II

Activity coefficient data for *p*-dimethylaminobenzaldehyde in aqueous HCl. $0 \leqslant c_1 \leqslant 22 \times 10^{-5}$ *m*

c_3, total HCl, *m*	$(\gamma_3/\gamma_1\gamma_2)$ (± 4%)	(γ_3/γ_2); from solubility experiments (± 4%)	γ_1 (± 8%)
0.02525	0.99	0.99	1.0
0.05053	0.99	0.99	1.0
0.1014	0.96	0.94	0.98
0.1997	0.91	0.83	0.91
0.3010	0.85	0.73	0.85
0.3990	0.79	0.64	0.81
0.5034	0.72	0.56	0.76
0.5971	0.68	0.49	0.73
0.7150	0.62	0.42	0.67
0.8186	0.58	0.36	0.62
0.9416	0.54	0.31	0.57
1.034	0.53	0.28	0.52

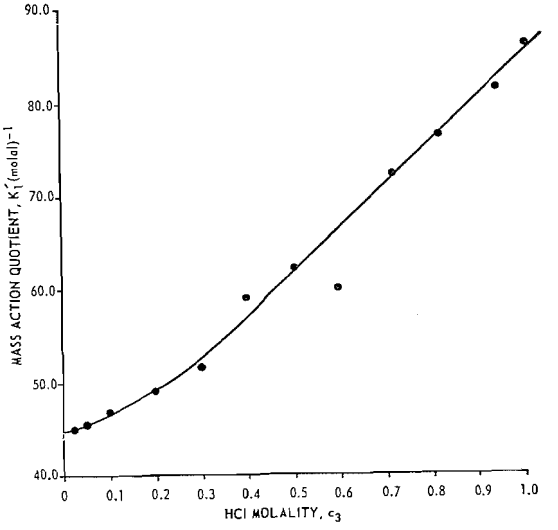

FIG. 3. *p*-Dimethylaminobenzaldehyde protonation equilibrium. Preliminary values, K_1', of the mass action quotient. Experimental error = ±2%.

The Color Formation Equilibrium

Table III gives the measurements, in the form of absorbance at $\lambda = 455$ mμ, of quinoidal cation concentrations in aqueous HCl solutions into which have been put aldehyde and hydrazine sulfate. From the work of Gamble and Hoffman, the quinoidal cation molality is given by eq. [13].

$$[13] \qquad m_6 = A_2/(0.566 \times 10^5 lW).$$

The material balance equations for total aldehyde and total acid for these solutions are

$$[14] \qquad c_1 = m_1 + m_3 + 2m_6$$

$$[15] \qquad c_3 = m_2 + m_3 + m_6.$$

Can. J. Chem. Downloaded from www.nrcresearchpress.com by 210.87.254.105 on 09/05/12
For personal use only.

TABLE III

Color formation equilibrium; measurements error in A is $\pm 0.5\%$

c_1, total DAB, m	c_2, total hydrazine, $m \times 10^5$	A_2, absorbance at 455 mμ	c_3, total HCl, m
0.008178	2.305	0.421	
0.01179	2.356	0.594	
0.01456	2.444	0.800	0.4842
0.01577	2.288	0.727	
0.01848	2.317	0.880	
0.01992	2.263	0.879	
0.009030	2.369	0.429	
0.01005	2.310	0.483	
0.01219	2.452	0.596	0.5866
0.01361	2.431	0.661	
0.01571	2.468	0.718	
0.01796	2.412	0.789	
0.01983	2.430	0.859	
0.009803	2.431	0.542	
0.01008	2.416	0.577	
0.01254	2.425	0.713	
0.01474	2.422	0.718	
0.01480	2.430	0.770	0.6328
0.01508	2.428	0.819	
0.01738	2.435	0.859	
0.01782	2.423I	0.900	
0.01968	2.430	0.920	
0.01971	2.422	0.935	
0.01018	2.437	0.469	
0.01095	2.455	0.525	
0.01296	2.444	0.665	
0.01489	2.413	0.686	
0.01689	2.449	0.780	0.7322
0.01888	2.439	0.833	
0.01984	2.438	0.843	
0.02180	2.429	0.918	
0.02385	2.420	0.965	
0.02474	2.467	0.980	

Using these to eliminate m_2 and m_3 from eq. [5] gives eq. [16], from which m_1 is calculated.

$$[16] \quad 44.(\gamma_1\gamma_2/\gamma_3) = \frac{(c_1 - 2m_6) - m_1}{(c_3 - c_1 + m_6)m_1 + {m_1}^2}.$$

In general,

$$(\gamma_3/\gamma_1\gamma_2) = f(c_3,c_1).$$

Table II gives, essentially,

$$(\gamma_3/\gamma_1\gamma_2) = f(c_3,0).$$

Applying these data from Table II to the color formation experiments for which $c_1 \neq 0$ therefore raises the problem of correcting them accordingly. Since eqs. [12], [2], and [3] permit this correction for (γ_3/γ_2), the problem reduces to a consideration of γ_1. The dependence of γ_1 on c_1 is quite unknown. The following observations are, however, relevant.

(*a*) The total effect of c_1 on (γ_3/γ_2) is minor compared with the variation of (γ_3/γ_2) with c_3, being generally somewhat less than the outside limit of 2%.

(*b*) γ_1 is less strongly dependent on c_3 than is (γ_3/γ_2).

(*c*) The effects of c_3 on γ_1 and on (γ_3/γ_2) partly cancel.

(*d*) Generally, the effects of electrolyte composition are secondary relative to the effects of total electrolyte concentration.

As a guess then, it is assumed that the effect of c_1 on γ_1 is small, and may even partly cancel the effect of c_1 on (γ_3/γ_2). For the subsequent calculations, the effect of c_1 on $(\gamma_3/\gamma_2\gamma_1)$ has been neglected. This approximation is unlikely to introduce an error as great as 2% into the calculation of m_1.

The color-forming reaction between *p*-dimethylaminobenzaldehyde and hydrazine is described by eq. [17].

Can. J. Chem. Downloaded from www.nrcresearchpress.com by 210.87.254.105 on 09/05/12
For personal use only.

Can. J. Chem. Downloaded from www.nrcresearchpress.com by 210.87.254.105 on 09/05/12
For personal use only.

[17] $$2DAB + N_2H_5^+ \overset{K_2}{\rightleftharpoons} AZH^+ + 2H_2O$$

$$K_2 = m_6/m_1^2 m_4.$$

The product AZH^+ is the benzaldazine quinoidal cation that absorbs light at $\lambda = 455$ mμ (5). The material balance equation for total hydrazine is

[18] $$c_2 = m_4 + m_6.$$

K_2 values calculated from eqs. [16], [17], and [18] are shown in Fig. 4.

Discussion

The three mass action quotients chosen for giving a full description of the equilibria in this system (5) are K_1, K_2 (see eqs. [5] and [17]), and $K_3 = (m_5 m_2/m_6)$. Of these, K_3 was earlier shown to be not applicable to solutions with acid concentration in the range used. K_1 and its corresponding equilibrium constant have now been very adequately measured. It is unlikely that K_2 can be evaluated at present to better than ±15%. One reason for this is that it contains a squared factor. The results can nevertheless be usefully applied.

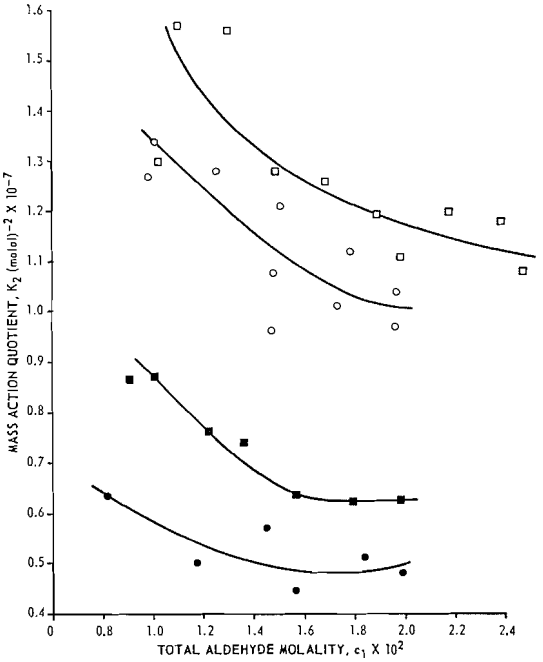

FIG. 4. Color-forming reaction equilibrium. ●, 0.4842 *m* HCl; ■, 0.5866 *m* HCl; ○, 0.6328 *m* HCl; □, 0.7322 *m* HCl. Experimental error = ±15%.

If the HCl concentration and an upper limit for hydrazine concentration are given, then the *p*-dimethylaminobenzaldehyde concentration required for complete conversion of the hydrazine to the colored quinoidal cation can be estimated. This is done by using γ_1 with the $(\gamma_3/\gamma_1\gamma_2)$ values in Table II, and K_2 values interpolated from Fig. 4. Assuming that these K_2 values have an error of ±20%, then the estimate of the required total reagent concentration, c_1, will be good to about ±10%. Since the calculation cannot be done for complete conversion ($m_4 = 0$), it is carried out by setting $m_6 \approx c_2$, and $m_4 \approx 2\%$ of c_2. In this way it is possible to avoid both the incompleteness of color formation on one hand, and an unreasonable excess of reagent on the other. Conversely, if absorbance, total acid concentration, and total aldehyde concentration are known, a calculation can indicate whether or not unreacted hydrazine is likely to exist.

The previously published (K_2/γ_1^2) data of Gamble and Hoffman are in rough agreement with the present results, and may serve as a guide to the analytical chemist. The K_2 values calculated from them, however, could be in error by as much as 36%, leading to c_1 estimates in error by 20%.

The existing methods of hydrazine analysis based on the reaction with *p*-dimethylaminobenzaldehyde typically employ 0.6 *M* to 1 *M* H_2SO_4 in the sample solutions. Apart from the fact that at least some acid is required to produce the quinoidal cation, acid concentrations as great as this are generally used to avoid reagent solubility problems. With *p*-dimethylaminobenzaldehyde solubility measurements and other equilibrium data now at hand, it becomes possible to explore improvements in the method of analysis. For example, the aqueous HCl solubility curve makes it possible to prepare a solution for which

$c_3 = 0.2\ m$ HCl
$c_2 = 1.14 \times 10^{-5}\ m$ hydrazine
$c_1 = 0.04\ m$ aldehyde.

The hydrazine will be fully converted to the quinoidal cation and have, in a 1 cm sample cell, an absorbance of about 0.65 at $\lambda = 455$ mμ. The advantages to be gained from improved procedure are:

1. Complete conversion of the hydrazine to

the colored product absorbing at 455 mμ ensures maximum reproducibility. (This has been done before, but with more difficulty.)

2. The use of smaller reagent concentrations, which is permitted by the smaller acid concentrations, makes the blanks less absorbing. Random error in the preparation of blanks will therefore contribute less experimental error to the absorbance reading.

3. The use of smaller reagent concentrations, by making the blanks less absorbing, opens the way to increased sensitivity of the method through increased path lengths (3 to 5 cm).

4. When the hydrazine is known to be fully converted to the colored product, then its concentration can be calculated from the molar extinction coefficient ($\varepsilon_2 = 0.566 \times 10^5$ (mole cm)$^{-1}$). Thus the analysis does not depend solely on standards, which therefore become independent checks.

The estimated error in γ_1 in Table II is $\pm 8\%$. Because γ_1 approaches unity at low HCl concentrations, despite the fact that it was calculated with ($\gamma_3/\gamma_1\gamma_2$) values and ($\gamma_3/\gamma_2$) values from independent experiments, it is suspected that the data may be better than this.

Acknowledgments

The work at the bench was done mainly by Mr. D. Hindle, with help from Mr. K. Wilson. The author thanks Dr. R. C. Turner for reading and commenting on the manuscript.

1. M. Pesez and A. Petit. Bull. Soc. Chim. France, 122 (1947).
2. G. W. Watt and J. D. Chrisp. Anal. Chem. **24**, 2006 (1952).
3. P. R. Wood. Anal. Chem. **25**, 1879 (1953).
4. I. Hoffman. J. Assoc. Offic. Agr. Chemists, **44**, 723 (1961).
5. D. S. Gamble and I. Hoffman. Can. J. Chem. **45**, 2813 (1967).
6. D. S. Gamble. Can. J. Chem. **45**, 2805 (1967).
7. H. S. Harned and B. B. Owen. The physical chemistry of electrolytic solutions. 3rd ed. A.C.S. Monograph Series, Reinhold Publishing Corp., New York. 1950. pp. 602–613.

Can. J. Chem. Downloaded from www.nrcresearchpress.com by 210.87.254.105 on 09/05/12
For personal use only.

Chemisorption sites on porous silica glass and on mixed-oxide catalysts

N. W. CANT[1] AND L. H. LITTLE

Department of Physical Chemistry, University of Western Australia, Nedlands, Western Australia

Received October 2, 1967

It has been shown previously that two types of adsorption sites exist on the surface of porous silica glass (Corning code no. 7930) for the adsorption of polar molecules, such as ammonia. One site is the surface hydroxyl group which forms a hydrogen bond to the adsorbate molecule. The second type of site is provided by traces of foreign oxides on the glass surface.

In the present study, the infrared spectrum of ammonia adsorbed on the silica glass has been compared with that of ammonia adsorbed on samples prepared by adding B_2O_3, ZrO_2, and Al_2O_3 to a pure silica powder. This comparison suggests that surface boron atoms (a Lewis acid) are the adsorption sites for ammonia on the porous silica glass. An additional type of site (a Bronsted acid or a different type of Lewis acid site, such as aluminium atoms) may exist in small concentrations on the glass and be responsible for isomerization and polymerization reactions with olefins.

Canadian Journal of Chemistry, 46, 1373 (1968)

Can. J. Chem. Downloaded from www.nrcresearchpress.com by 210.87.254.6 on 09/05/12
For personal use only.

Introduction

In recent years the nature of the acidic sites present on the surface of silica–alumina cracking catalysts has been the subject of many studies. The infrared measurements of Parry (1) and Basila, Kantner, and Rhee (2) have demonstrated the existence of both Lewis (electron acceptor) and Bronsted (proton donor) acid sites on silica–alumina.

The corresponding surface properties of porous silica glass (Corning code no. 7930) have been much less studied. Little, Klauser, and Amberg (3) first showed that the glass could isomerize and polymerize certain hydrocarbons and associated this ability with the small quantities of other oxides such as Al_2O_3, ZrO_2, and B_2O_3, which are present in the glass. Chapman and Hair (4) found that when some of the surface hydroxyl groups were replaced by fluorine atoms the ability of the glass to crack cumene was greatly enhanced. This was attributed to the electronegative fluorine atoms which increased the acidity of the neighboring hydroxyl groups, i.e. the catalytic sites were Bronsted acids. The explanation was supported by the ineffectiveness of a fully fluorinated glass (containing no surface hydroxyl groups) to crack cumene. Chapman and Hair failed to detect radical cations which may be formed by the abstraction of electrons from anthracene molecules adsorbed on Lewis acid centers on the glass surface.

Folman and Yates (5) studied the adsorption of ammonia on porous glass and interpreted data on length changes and infrared spectra to indicate two adsorption sites; one was definitely shown to be a surface hydroxyl group, the other was thought to be a surface silicon or oxygen atom, although ammonia adsorbed on the latter site was not distinguished spectroscopically. Using thinner samples of glass, Cant and Little (6) were able to make this distinction, finding that ammonia adsorbed on a surface hydroxyl group gave bands at 3400 cm^{-1} and 3320 cm^{-1}, which were removed on room temperature evacuation. Ammonia adsorbed on the second site produced bands at 3365 cm^{-1} and 3280 cm^{-1} and was not greatly affected by evacuation at 150 °C. Because of the similarity of the 3365 cm^{-1} and 3280 cm^{-1} bands to those in the spectrum of the Lewis acid–base complex $F_3B{:}NH_3$ the second site was interpreted as a Lewis acid site, possibly a surface boron atom. This assignment was supported by investigations which showed that pure silica only possessed adsorption sites of the first type (7, 8).

The aim of this study has been to determine which, if any, of the other oxides present in porous silica glass is responsible for the chemisorption of ammonia. Since this work was completed Low, Ramasubramanian, and Subba Rao (9) have reported further studies to define the adsorption sites on porous glass.

Experimental

The technique in this study has been to add small quantities of other oxides to a silica powder whose adsorption properties for ammonia are known. By comparing the spectrum of ammonia adsorbed on porous glass with the spectrum of ammonia adsorbed on these

[1]Present address: Mellon Institute, Pittsburgh, Penn., U.S.A.

Can. J. Chem. Downloaded from www.nrcresearchpress.com by 210.87.254.6 on 09/05/12
For personal use only.

modified silicas, the nature of the chemisorption site on porous glass could then be assigned with more confidence.

The silica powder employed was Degussa Aerosil. Its adsorption properties for ammonia were identical with those of Cab-O-Sil silica used previously (8). Its surface area was approximately 180 m^2/g determined by the B.E.T. method using nitrogen. Small quantities of B_2O_3, ZrO_2, and Al_2O_3 were incorporated in the aerosil by making a slurry of aerosil with a solution of boric acid, zirconium nitrate, and aluminium nitrate, respectively. Laboratory grade materials were used in each case and the concentration was such that the resulting adsorbents had an oxide concentration of about 3%. The slurries were dried for 2 h at 120 °C and calcined at 400 °C for 10 h. The surface areas of these impregnated silicas were unchanged from that of the original aerosil. It is known that silica–alumina catalysts made in this way are active in cumene cracking (10).

In order to obtain the infrared spectra, the adsorbents were ground to a fine powder and compressed into thin self-supporting discs under a pressure of 10 tons/sq. in. The thickness was chosen such that after 450 °C evacuation, the optical density of the hydroxyl band at 3750 cm^{-1} was in the range 0.6–0.9. Discs of silica impregnated with zirconia, as described above, had only limited transmission and samples with higher transmission were prepared by soaking a compressed disc of aerosil in the zirconium nitrate solutions and then drying and calcining as before. Mathieson anhydrous (99.99% pure) ammonia gas was used without further treatment.

The spectrometer used was an all-grating Perkin Elmer model 521, and most spectra were recorded with computed spectral slit widths between 6.0 and 1.2 cm^{-1} for the frequency range 4000–700 cm^{-1}. The instrument was calibrated as required against atmospheric water vapor or ammonia gas present in the cell. The frequencies quoted are limited in accuracy to about 5 cm^{-1} by the difficulty of assigning frequencies to comparatively broad bands. Many of the spectra were recorded using the linear absorbance attachment available on the instrument, to facilitate comparison of band intensities.

The cell was similar to the windlass type described by Little, Klauser, and Amberg (3). It was carefully aligned in the infrared beam and all manipulations were carried out without changing the alignment. It was possible to wind the sample from the infrared beam to the furnace section and back again without significant changes in the spectrum. Another cell with identical path length and connected to the same gas line was arranged in the reference beam to ensure compensation for absorption by ammonia gas.

The following procedure was employed. The compressed disc was evacuated in the furnace section at 450 °C to an ultimate vacuum of less than 10^{-4} mm. It was then wound down into the infrared beam and the spectrum recorded from 4000 cm^{-1} to about 1300 cm^{-1}, at which frequency the sample absorbed all radiation. A known pressure (usually about 5 cm) of ammonia gas was then admitted to both sample and reference cells and the spectrum recorded after standing for 1 h. No changes were observed on further standing. Gas phase ammonia was then removed by room temperature evacuation and another spectrum recorded. The temperature of evacuation was gradually raised and spectra recorded after each further period of evacuation.

Results

Table I summarizes some of the available data for the NH vibrations of ammonium salts and ammine complexes. The former are characterized by strong absorption near 1450 cm^{-1}, the latter by two bands, one near 1600 cm^{-1} and the other below 1400 cm^{-1}, arising in each case from NH deformation vibrations. The low frequency band for ammonia coordinated to the surface occurs below 1350 cm^{-1} (15) and in the present study could not be observed due to strong absorption by the adsorbent. The vibration occurs at even lower frequency for ammonia hydrogen bonded to surface hydroxyl groups (16). However, it is possible to distinguish ammonia chemisorbed in the coordinated form (to a Lewis acid site) from that in the protonated form (produced by Bronsted acid sites) by the infrared absorption bands near 1600 and 1450 cm^{-1}.

The frequencies of the corresponding NH stretching bands do not enable such positive identification to be made. Symmetry considerations show that the infrared spectrum of NH_4^+ should produce a single absorption (due to ν_3) in this region and the 3332 cm^{-1} band of NH_4BF_4 is assigned to this vibration. Stronger perturbations in other crystalline salts, such as ammonium chloride, displace this frequency to lower values and produce additional bands due to overtone, combination, and the normally infrared-forbidden ν_1 vibration (12). There are two infrared-active NH stretching fundamentals of ammine complexes, the frequencies of which are sensitive to the environment.

In the absence of strong surface perturbations, ammonia chemisorbed as ammonium ion on Bronsted acid sites should produce a single absorption band near 3300 cm^{-1}. Ammonia coordinated to Lewis acid sites should produce two bands in this region separated by 50–100 cm^{-1}.

When the experiments detailed previously were performed with aerosil containing 3% B_2O_3, the spectra of Fig. 1 were obtained. The spectrum of the evacuated adsorbent differs in two respects from that of pure silica. Firstly, a sharp band appears at 3707 cm^{-1} in addition to the one at 3747 cm^{-1} which is found for the pure silica. This is assigned to a hydroxyl group on a boron atom. A similar band was observed by Kozirovski and Folman (17) in the spectrum of some of their samples of porous glass, and more recently by Low and Ramasubramanian (18) for

TABLE I

Some of the available data for NH vibrations of ammonium salts and ammine complexes

Assignment	Absorption frequencies			Reference
	v (NH)	δ_{asym}(NH)	δ_{sym}(NH)	
NH_3 gas	3444, 3337	1627	932, 968	(11)
NH_3 physically adsorbed on hydroxyl groups	3400, 3320	1630		(7, 8)
NH_4Cl	3138	1403		(12)
NH_4BF_4	3332	1433		(12)
$F_3B{:}NH_3$	3340, 3285	1596	1440, 1420	(13)
$Co(NH_3)_6Cl_3$	3070 (broad)	1603	1325	(14)
$Co(NH_3)(ClO_4)_3$	3320, 3240	1630	1352	(14)

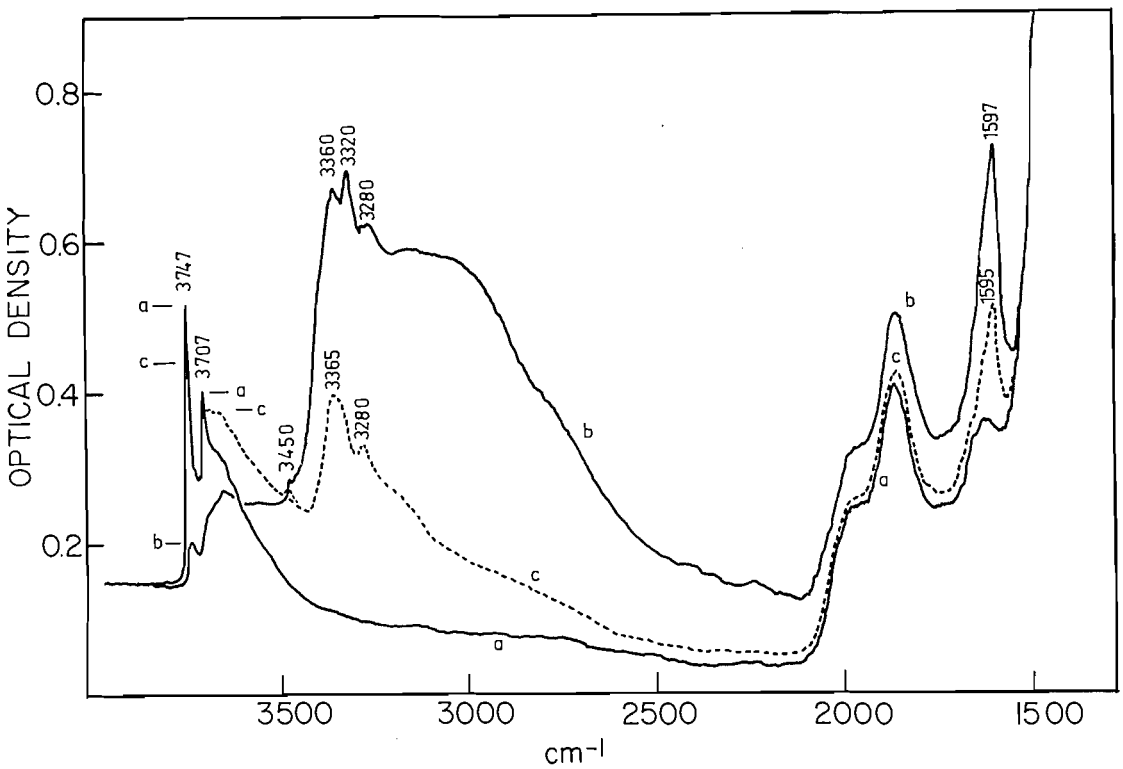

FIG. 1. (*a*) Infrared spectrum of boric oxide – silica mixture evacuated at 450 °C, (*b*) after addition of 5 cm of ammonia, (*c*) after evacuation at 20 °C.

boric oxide – silica mixtures. Secondly, as found with 0.1 mm porous silica glass, the sample absorbs completely below 1450 cm^{-1} compared with 1330 cm^{-1} for pure silica. This is probably due to a vibration of B_2O_3, and Hanst, Early, and Klemperer (19) have observed a broad band at 1400 cm^{-1} in the spectrum of B_2O_3 vapor at 1200 °C.

Spectrum (*b*) of Fig. 1 shows that in the presence of gas phase ammonia there is adsorption onto free hydroxyl groups (both Si—OH and B—OH) similar to that observed with the Si—OH groups of pure aerosil (8). Room temperature evacuation removed this physically adsorbed ammonia but did not affect a chemisorbed species which absorbs at 3365 cm^{-1}, 3280 cm^{-1}, and 1595 cm^{-1} (spectrum (*c*), Fig. 1). As the temperature of evacuation was raised the intensity of the three bands was reduced in the same ratio, suggesting that only one adsorbed

Can. J. Chem. Downloaded from www.nrcresearchpress.com by 210.87.254.6 on 09/05/12
For personal use only.

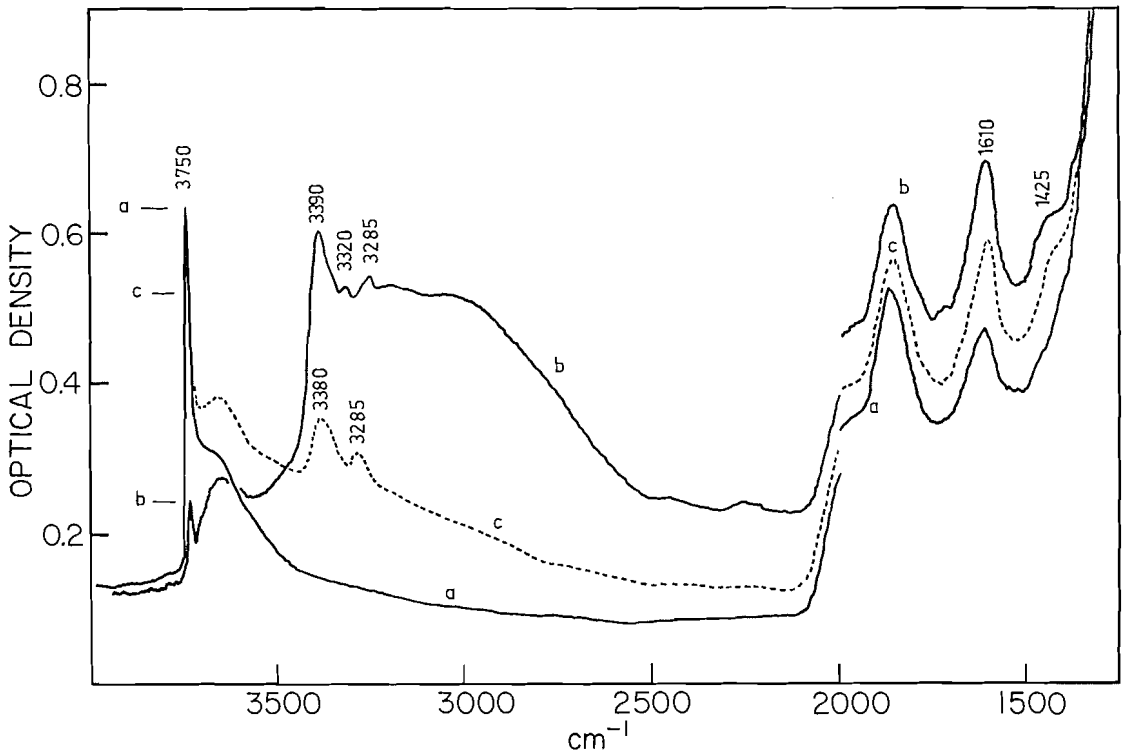

FIG. 2. (*a*) Infrared spectrum of zirconia–silica mixture evacuated at 450 °C, (*b*) after addition of 5 cm of ammonia, (*c*) after evacuation at 20 °C.

species was present. This species was not removed by evacuation until the temperature was raised to 200 °C. The appearance of the intense band at 1595 cm^{-1} confirms that the major chemisorbed species is NH_3, probably coordinated to a surface boron atom, i.e. a Lewis acid site. An additional band arising from the ν_2 vibration would be expected between 1400 and 1300 cm^{-1} but this cannot be checked since the adsorbent is opaque in this region. Ammonia adsorbed as ammonium ions on Bronsted acid sites could not be distinguished from coordinated ammonia by spectra in the 3300 cm^{-1} region if the two forms were desorbed at similar rates during evacuation. However, ammonium ions are unlikely to be present in large quantities in view of the similarity between the spectrum of the chemisorbed species and that of $F_3B{:}NH_3$.

An additional weak band appeared at 3450 cm^{-1} in the spectrum of ammonia adsorbed on boric oxide – silica. This band has been assigned (9, 20) to a secondary amine group such as

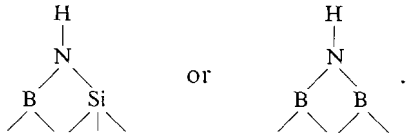

No evidence of bands due to primary amine groups $\equiv B{-}NH_2$ or $\equiv Si{-}NH_2$ was found.

Figure 2 shows the corresponding spectra for ammonia adsorbed on aerosil impregnated with zirconia. The spectrum of the evacuated disc prior to the adsorption of ammonia is identical with that of pure aerosil. In the presence of ammonia gas, physical adsorption by hydrogen bonding to surface hydroxyl groups is apparent. Chemisorbed species are also present which absorb at 3380 cm^{-1}, 3285 cm^{-1}, 1610 cm^{-1}, and 1425 cm^{-1}. Evacuation at increasing temperatures reduced the intensity of all bands until the ammonia was completely removed at 200 °C. A small quantity of ammonium ion is thought to be responsible for the 1425 cm^{-1} band, while

Can. J. Chem. Downloaded from www.nrcresearchpress.com by 210.87.254.6 on 09/05/12
For personal use only.

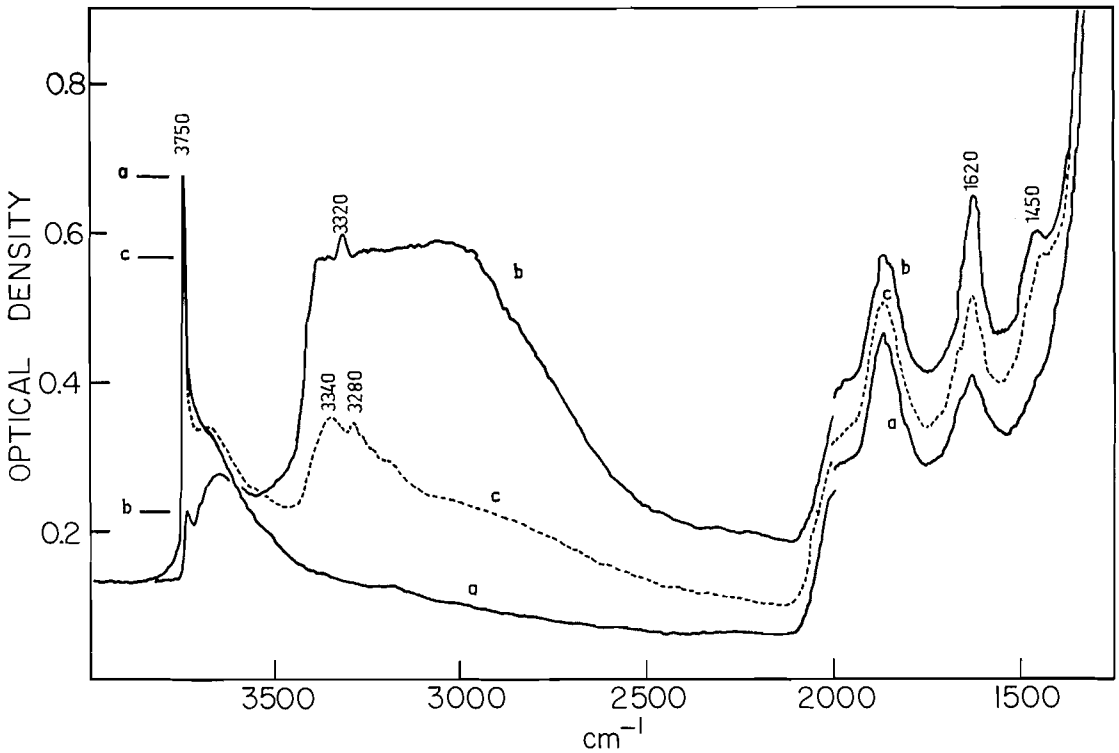

FIG. 3. (*a*) Infrared spectrum of alumina–silica mixture evacuated at 450 °C, (*b*) after addition of 5 cm of ammonia, (*c*) after evacuation at 20 °C.

ammonia coordinately bonded to surface zirconium atoms produced the other bands. The presence of proton donor sites on the silica–zirconia is supported by its catalytic activity in olefin isomerization (21).

When ammonia was adsorbed on aerosil impregnated with alumina the spectra of Fig. 3 were obtained. The frequencies of the bands at 3340 cm^{-1}, 3280 cm^{-1}, 1620 cm^{-1}, and 1450 cm^{-1} are similar to those reported for ammonia adsorbed on a silica–alumina cracking catalyst (22). Lewis and Bronsted sites thus exist on the impregnated silica–alumina sample similar to those reported for the cracking catalyst.

Discussion

Because of the method of preparation it is expected that the surface of porous glass will be of variable composition. After the acid leaching process it is considered that few boron or aluminium atoms will exist on the surface (23). However, if the glass is heated above 500 °C (and this is usually done during most spectroscopic studies) it is known that boron atoms diffuse through the glass and form "whiskers" of B_2O_3 on the surface (23). Presumably, other impurity atoms may do the same.

The quantity of other oxides in porous glass has been found to vary. The specifications of porous silica glass (Corning code no. 7930) show a B_2O_3 content of 3%, an Al_2O_3 content of 0.3%, and trace amounts only of ZrO_2 and other oxides (23). Chapman and Hair (4) quote the following figures for their samples: B_2O_3, 3% and trace amounts of Al_2O_3 and As_2O_3. Our samples (6) were too small to analyze for Al_2O_3 or ZrO_2 but were found to contain about 3% B_2O_3. In contrast, Little, Klauser, and Amberg (3) from spectrochemical analysis report: B_2O_3, 2.1% and approximately 0.4% each of Al_2O_3 and ZrO_2. They also showed that leaching with acid for 6 h subsequent to the initial preparation did not affect the B_2O_3 content although it approximately halved both the Al_2O_3 and ZrO_2 contents. Acid-leached glass showed less ability

Can. J. Chem. Downloaded from www.nrcresearchpress.com by 210.87.254.6 on 09/05/12
For personal use only.

Can. J. Chem. Downloaded from www.nrcresearchpress.com by 210.87.254.6 on 09/05/12
For personal use only.

to polymerize and isomerize hydrocarbons. For this reason Little, Klauser, and Amberg considered that Al_2O_3 and ZrO_2 were responsible for the hydrocarbon reactions rather than B_2O_3. Of course, the analysis figures refer to the bulk porous glass. The acid leaching process may have significantly reduced the surface boron content without causing a measurable change in its bulk content.

In the region of NH stretching vibrations the infrared spectrum of ammonia chemisorbed on aerosil impregnated with boria (Fig. 1) is very similar to the spectrum of chemisorbed ammonia on porous glass that we have presented previously (6). The frequencies of the bands of the adsorbed species are identical in the two cases and the intensity ratio between the two bands are similar. The same dependence on the temperature of desorption is also apparent. For these reasons we consider that surface boron atoms (Lewis acid sites) are responsible for the chemisorption of ammonia on porous glass. We have been able to detect only one chemisorbed NH_3 species on silica–boria and on the porous silica glass, in addition to the small quantity of secondary amine responsible for the band at 3450 cm^{-1}.

Previously, we (6) had not been able to detect a band due to the asymmetric bending vibration of adsorbed ammonia on porous glass. From the band intensities observed in the present study, it can be shown that the intensity of this band would be too weak to detect for ammonia adsorbed on the thin glass samples previously employed.

Infrared spectroscopic investigations of the adsorption of ammonia have revealed the presence of Bronsted acid sites on silica–alumina and to a lesser extent on silica–zirconia. The latter catalyst, moreover, shows less activity than silica–alumina in the isomerization and polymerization of butenes (21).

Recent spectroscopic studies (21) with boric oxide – silica systems have shown that surface boron atoms are not catalytically active sites for the olefin reactions reported previously with silica glass (3). However, it is possible that Bronsted acid sites or other Lewis acid sites such as aluminium atoms exist on porous silica glass and are responsible for hydrocarbon reactions that have been observed (3). The number of these catalytically active sites may be small in relation to the total number of acid sites and the ammonia chemisorbed to them would be indistinguishable by infrared spectroscopy.

Acknowledgment

Financial assistance from the Australian Research Grants Committee is gratefully acknowledged.

1. E. P. PARRY. J. Catalysis, **2**, 371 (1963).
2. M. R. BASILA, T. R. KANTNER, and K. H. RHEE. J. Phys. Chem. **68**, 3197 (1964).
3. L. H. LITTLE, H. E. KLAUSER, and C. H. AMBERG. Can. J. Chem. **39**, 42 (1961).
4. I. D. CHAPMAN and M. L. HAIR. J. Catalysis, **2**, 145 (1963).
5. (*a*) M. FOLMAN and D. J. C. YATES. Proc. Roy. Soc. London, Ser. A, **246**, 32 (1958). (*b*) M. FOLMAN and D. J. C. YATES. J. Phys. Chem. **63**, 183 (1959).
6. N. W. CANT and L. H. LITTLE. Can. J. Chem. **42**, 802 (1964).
7. I. D. CHAPMAN and M. L. HAIR. Trans. Faraday Soc. **61**, 1507 (1965).
8. N. W. CANT and L. H. LITTLE. Can. J. Chem. **43**, 1252 (1965).
9. M. J. D. LOW, N. RAMASUBRAMANIAN, and V. V. SUBBA RAO. J. Phys. Chem. **71**, 1726 (1967).
10. W. B. HORTON and R. W. MAATMAN. J. Catalysis, **3**, 113 (1964).
11. W. S. BENEDICT and E. K. PLYLER. Can. J. Phys. **35**, 1235 (1957).
12. T. C. WADDINGTON. J. Chem. Soc. 4340 (1958).
13. J. GOUBEAU and H. MITSCHELEN. Z. Physik. Chem. Frankfurt, **14**, 61 (1958).
14. K. NAKAMOTO. Infrared spectra of inorganic and co-ordination compounds. John Wiley and Sons, Inc., New York. 1963. p. 143.
15. M. VAN TONGELEN. J. Catalysis, **5**, 535 (1966).
16. N. W. CANT and L. H. LITTLE. Can. J. Chem. **45**, 3055 (1967).
17. Y. KOZIROVSKI and M. FOLMAN. Trans. Faraday Soc. **60**, 1532 (1964).
18. M. J. D. LOW and N. RAMASUBRAMANIAN. J. Phys. Chem. **70**, 2740 (1966).
19. P. L. HANST, V. H. EARLY, and W. KLEMPERER. J. Chem. Phys. **42**, 1097 (1965).
20. N. W. CANT and L. H. LITTLE. Unpublished data.
21. G. A. BLOMFIELD and L. H. LITTLE. Unpublished data.
22. N. W. CANT and L. H. LITTLE. Nature, **211**, 69 (1966).
23. T. H. ELMER, I. D. CHAPMAN, and M. E. NORDBERG. J. Phys. Chem. **67**, 2219 (1963).

Can. J. Chem. Downloaded from www.nrcresearchpress.com by 210.87.254.6 on 09/05/12
For personal use only.

Colorimetric determination of molybdenum with 5,7-dibromo-8-hydroxyquinoline

I. I. M. Elbeih and M. A. Abou-Elnaga
Department of Chemistry, Faculty of Science, University of Cairo, Giza, Egypt

Received November 3, 1967

A new method for the colorimetric determination of molybdenum(VI) uses 5,7-dibromo-8-hydroxyquinoline as coloring reagent. Molybdenum(VI) is separated from other elements by paper chromatography using a butanol – nitric acid – acetylacetone solvent mixture.

Canadian Journal of Chemistry, 46, 1379 (1968)

Introduction

Several methods have been described (1) for the colorimetric determination of minute amounts of molybdenum in complex materials. These methods depend on the separation of molybdenum from other elements by precipitation, extraction, and ion-exchange methods. The present work describes a new method for the colorimetric determination of molybdenum(VI), using 5,7-dibromo-8-hydroxyquinoline which forms a canary-yellow color with molybdenum-(VI). This method depends on the separation of molybdenum(VI) from interfering ions by descending paper chromatography using a new solvent mixture which consists of *n*-butanol, 1.5 *N* nitric acid, and acetylacetone (50:50:1). The method proved to be simple, sensitive, and accurate.

Experimental

Apparatus and Reagents

Instrument

Absorbance measurements were made with a Unicam spectrophotometer model SP.500 using 1.00 cm cells.

Reagent Solution

0.2 g of 5,7-dibromo-8-hydroxyquinoline was dissolved in 500 ml ethanol, left for 2 h, and then filtered if necessary.

Standard Molybdenum Solutions

A stock solution was prepared by dissolving 0.9200 g of A.R. ammonium molybdate in 500 ml of 0.1 *N* nitric acid. From this stock solution (which is 0.1%) other standard solutions were prepared to contain 20, 40, 60, 80, 100, 120, 140, and 150 μg molybdenum per ml.

Buffer Solution pH = 1.09

50 ml *N* sodium acetate + 70 ml *N* hydrochloric acid were diluted to 250 ml with distilled water.

Absorption and Calibration Curves

Blank Reagent Solution

To 4.5 ml of buffer solution (pH = 1.09), 12 ml ethanol, and 5.5 ml of the reagent solution, ethanol was added to the mark in a 25 ml volumetric flask.

Standard Molybdenum Reagent Solutions

To the standard molybdenum solution in 0.1 *N* nitric acid, 4.5 ml buffer solution (pH = 1.09), 12 ml of ethanol, and 5.5 ml of the reagent solution, ethanol is added to the mark in a 25 ml volumetric flask.

The absorption curve of the standard molybdenum reagent solution is shown in Fig. 1. It is clear from this

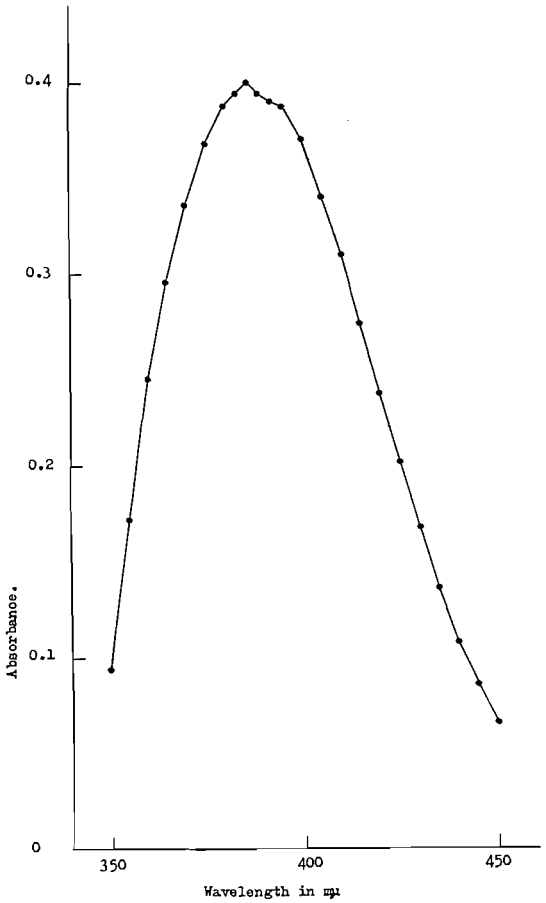

FIG. 1. Absorption curve for Mo^{6+}, maximum absorption at 386 mμ.

curve that the maximum absorption for the molybdenum reagent solution is at 386 mμ, the spectrophotometer being set on the blank reagent solution as reference.

A calibration curve was prepared using the standard molybdenum reagent solutions and setting the spectrophotometer on the blank reagent solution as reference. It was clear from this curve that Beer's law is obeyed over the concentration range 20–150 μg of molybdenum per 25 ml of solution.

Effect of pH

The optimum pH value was found to be 1.09 (sodium acetate and HCl). At higher pH values the color of the solution fades quickly.

Stability of the Reaction

At pH = 1.09 the color of the molybdenum complex (bright canary-yellow) was found to be stable for at least 1 h. However, it was found that readings should not be taken before 10 min from mixing the reagents thoroughly, as the absorption of the colored solution reaches a maximum after a period of 10 min. The absorbance for 100 μg of molybdenum was found to be 0.272 after 10 min from mixing the reagents, and the same value was again obtained for the same solution after a period of 1 h.

Effect of Solvents

Water causes precipitation of 5,7-dibromo-8-hydroxyquinoline. The molybdenum complex is unstable in acetone; the best medium should contain about 80% ethanol.

Sensitivity of Reaction

The reaction was found to be sensitive to a concentration of 2 μg of molybdenum per 25 ml of solution. The optical density reading obtained for this solution was 0.003.

Effect of Diverse Ions

Tests were made for the presence of several ions in the standard molybdenum reagent solution. A solution containing 100 μg of molybdenum per 25 ml of solution was used for these tests. Table I shows the tolerance to other ions.

TABLE I

Tolerance to other ions

Ion	Concentration below which no interference occurs (μg)
Ag^{+}	A precipitate due to HCl in buffer solution
Pb^{2+}	A precipitate due to HCl in buffer solution
Cu^{2+}	A precipitate appears
Hg^{2+}	85
Bi^{3+}	5
Cd^{2+}	35
Co^{2+}	40
Ni^{2+}	35
Zn^{2+}	50
Mn^{2+}	100
Al^{3+}	100
Cr^{3+}	30
Fe^{3+}	3
Sn^{2+}	2
Mg^{2+}	85
Ca^{2+}	75
Sr^{2+}	90
Ba^{2+}	100
K^{+}	150
Th^{4+}	40
U^{6+}	30
Ti^{4+}	1
V^{5+}	5
Be^{2+}	30
Na^{+}	Present in buffer solution
Cl^{-}	Present in buffer solution
F^{-}	100
Br^{-}	100
I^{-}	100
SO_4^{2-}	100
SO_3^{2-}	135
CO_3^{2-}	150

The Chromatographic Separation of Molybdenum

A new solvent for the chromatographic separation of molybdenum(VI) was prepared: 50 ml of *n*-butanol are shaken in a separatory funnel with 1 ml acetylacetone, then 50 ml of 1.5 *N* nitric acid are added. The mixture is shaken thoroughly and left for complete separation of the two phases. Then a conventional unit for descending paper chromatography is employed; the lower layer is placed on the bottom of the tank and the upper layer is put in the trough and left for a few hours to assure equilibration. The tank is kept in an insulated cupboard which keeps the inside temperature constant during the experiment. Filter paper sheets (for chromatography) are cut out into strips 18 × 52 cm and the trough height is adjusted to permit the strips to be hung on both sides of the trough. Four loaded and four blank zones are used for each determination. Each of the sheets is pencilled into a zone chromatogram, as shown in Fig. 2, to provide a central zone and two locating strips. Ten drops (each exactly 0.01 ml) of the sample solution are placed with a microsyringe along the starting line of the middle area of each strip to be loaded, and two drops on the locating strips (on the small crosses). The drops are allowed to dry, the top edge of each paper is placed in the trough and the tank closed. The papers are allowed to develop until the solvent front travels about 30 cm from the starting line. The development time for this solvent mixture is about 18 h. The sheets are then removed from the tank and dried in a stream of hot air. The locating strips are cut from each sheet and sprayed with the general sprays (2) to locate the cation spots. The locating strips are first sprayed with the kojic acid – oxine mixture (1 g kojic acid and 5 g oxine in 1 l of 60% ethyl alcohol), dried, and observed under ultraviolet illumination. They are again sprayed with ammoniacal hydrogen sulfide water, dried, and observed in daylight.

It was found that this solvent mixture gives concentric spots with most cations except Al^{3+} which gives a faint forward shadow, V^{5+} which gives an elongated spot, and Hg^{+}, Hg^{2+} which give faint backward tailings. Mo^{6+} moves as a concentric spot with the acid front. The position of the molybdenum spot is marked on the locating strips with a pencil. These strips are placed against their respective sheets and the position of the molybdenum zone is marked with a pencil. Four loaded and four blank zones are cut out and collected in two glass containers. The R_F values of several cations in the butanol – acetylacetone – nitric acid solvent mixture are given in Table II.

Can. J. Chem. Downloaded from www.nrcresearchpress.com by 210.87.254.6 on 09/05/12
For personal use only.

Can. J. Chem. Downloaded from www.nrcresearchpress.com by 210.87.254.6 on 09/05/12
For personal use only.

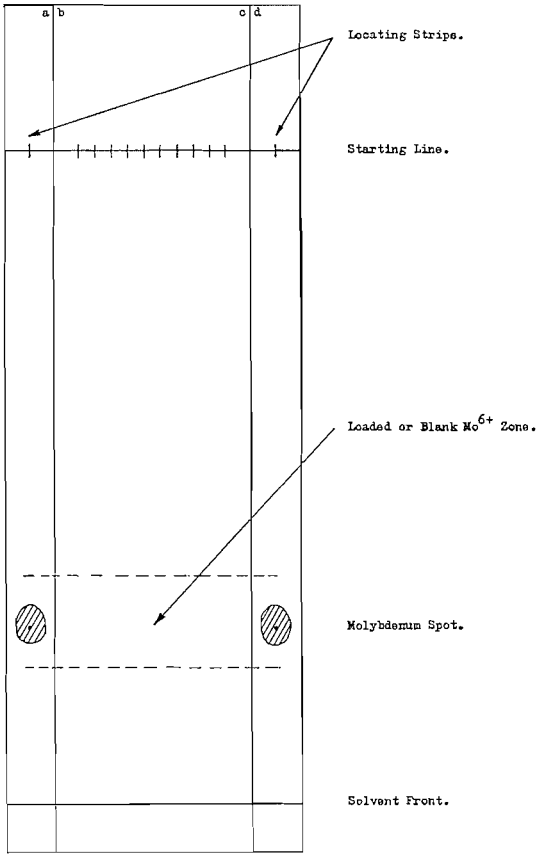

FIG. 2. Zone chromatogram for estimation of molybdenum(VI).

TABLE II

R_F values of cations with butanol – acetylacetone – nitric acid solvent mixture

Cation	R_F	Cation	R_F	Cation	R_F
Sb^{3+}	0.00	Ni^{2+}	0.09	Li^{+}	0.21
Sn^{4+}	0.00	Tl^{+}	0.09	V^{5+}	0.22
Ba^{2+}	0.03	Cr^{3+}	0.10	Be^{2+}	0.30
Sr^{2+}	0.04	Co^{2+}	0.10	Ti^{4+}	0.30
Th^{4+}	0.04	Zn^{2+}	0.10	U^{6+}	0.30
Ce^{3+}	0.05	Cd^{2+}	0.11	Fe^{3+}	0.40
Ca^{2+}	0.06	Al^{3+}	0.11	As^{3+}	0.50
K^{+}	0.07	Mn^{2+}	0.11	Mo^{6+}	0.73
Pb^{2+}	0.08	Ag^{+}	0.12	Hg^{+}	0.74
Na^{+}	0.08	Cu^{2+}	0.12	Hg^{2+}	0.76
Mg^{2+}	0.09	Bi^{3+}	0.19	Sn^{2+}	0.77

It is clear from Table II that only mercury and stannous ions interfere in the chromatographic separation of molybdenum.

Extraction and Determination of Molybdenum Zones

(1) One blank zone is shredded, placed in a clean silica crucible, and ignited at 600 °C for ½ h in a muffle furnace.

(2) When the crucible is cool, 2.5 ml of concentrated hydrochloric acid are added to the greyish-brown residue, and the mixture is boiled gently for a few seconds on a hot plate. About 8 ml of distilled water are added and the solution is boiled for ½ min.

(3) The acid solution is transferred to a 50 ml beaker and the crucible is washed three times with 10, 10, and 5 ml of boiling water. The washings are transferred to the beaker.

(4) The solution is boiled gently on a hot plate, using a small clean glass rod to regulate the boiling, until the total volume is reduced to about 4 ml.

(5) The solution is made alkaline with 40% sodium hydroxide solution (about 30 drops), then it is made just acid with 75% nitric acid (about 15 drops), and the sides of the beaker are rinsed with 2 ml ethanol.

(6) The solution is filtered through a sintered glass funnel No. 3 into a 25 ml volumetric flask and the beaker washed thoroughly twice with 3 ml ethanol.

(7) To the filtered solution, 4.5 ml buffer solution (pH = 1.09) and 5.5 ml of 5,7-dibromo-8-hydroxyquinoline solution are added.

(8) The solution is made up to the mark with ethanol and shaken well.

(9) The extraction is repeated with the other blank zones. The solution obtained is used as a blank reagent solution.

(10) One loaded molybdenum zone is shredded, ignited, and extracted in the same manner as the blank zone. The extraction is repeated with the other loaded zones. The solution obtained is used as an unknown molybdenum reagent solution. (In fact parallel experiments of four blank and four loaded zones are carried out at the same time.)

(11) The absorbance of the unknown molybdenum reagent solution is determined at a wavelength of 386 mμ after 10 min using the blank reagent solution as reference.

(12) By referring to the calibration curve, the amount of molybdenum in the unknown is estimated.

Results

The satisfactory nature of the above procedure was established using drops taken from standard ammonium molybdate solutions. These drops were chromatographed, extracted, and estimated as given above; typical results are shown in Table III.

TABLE III

Typical results of ammonium molybdate solutions

	μg of molybdenum		
Expt.	Taken	Found	Error
1	55	55	0
2	75	75	0
3	100	99	−1
4	120	119	−1
5	150	149	−1

The application of the above technique was also investigated with a number of cationic mixtures, examples of which are given in Table IV.

TABLE IV

Typical results of molybdenum mixtures

Mixture	μg of molybdenum		
	Taken	Found	Error
Mo^{6+}, Hg^{2+}, Be^{2+}	100	100	0
Mo^{6+}, Fe^{3+}, Ca^{2+}	100	99	−1
Mo^{6+}, V^{5+}, Cd^{2+}	100	100	0
Mo^{6+}, Sn^{2+}, Sn^{4+}	100	101	+1

The cations other than Mo^{6+} are each present in amounts of 30–40 μg.

Discussion

Although the technique described above is fairly simple, there are still certain points to be considered in order to obtain the best results.

(1) Molybdenum is completely separated chromatographically from most cations and especially from V^{5+} and Fe^{3+}, which interfere seriously with the coloring reagent.

(2) The volume of molybdenum chloride must not be reduced by evaporation to less than 4 ml, otherwise volatilization of molybdenum chloride takes place and low absorption values of molybdenum are obtained on the calibration curve.

(3) Increase of acidity with nitric acid, when neutralizing the sodium hydroxide solution, gives low absorption readings.

1. E. B. SANDELL. Colorimetric determination of traces of metals. 3rd ed. Interscience Publishers, Inc., New York. 1959.
2. I. I. M. ELBEIH and M. A. ABOU-ELNAGA. Anal. Chim. Acta, **17**, 397 (1957).

Can. J. Chem. Downloaded from www.nrcresearchpress.com by 210.87.254.6 on 09/05/12
For personal use only.

Can. J. Chem. Downloaded from www.nrcresearchpress.com by 210.87.254.5 on 09/05/12
For personal use only.

Chélates du fer (III) avec des anions dicarboxylates

M. Deneux, R. Meilleur et R. L. Benoit
Département de Chimie, Université de Montréal, Montréal, Québec

Reçu le 14 juillet 1967

La formation de complexes entre le fer(III) et les anions oxalate, malonate, succinate, glutarate et acétate a été étudiée par potentiométrie et spectrophotométrie à 25 °C, force ionique 0.52 ± 0.02, $[H^+]$ ≃ 0.5 et 0.1 *M*. Les constantes d'acidité des acides dicarboxyliques et les constantes de formation des monochélates du fer(III) ont été déterminées. L'ordre de stabilité est le suivant: oxalate ≃ malonate > succinate ≃ glutarate.

Complex formation between iron(III) and oxalate, malonate, succinate, glutarate, and acetate ions has been studied by potentiometric and spectrophotometric methods at 25 °C, ionic strength 0.52 ± 0.02, and ≃ 0.5 and 0.1 *M* H^+ concentrations. The acidity constants of the dicarboxylic acids and the formation constants of the monochelates of iron(III) have been determined. The stability order is as follows: oxalate ≃ malonate > succinate ≃ glutarate.

Canadian Journal of Chemistry, 46, 1383 (1968)

Introduction

Parmi les facteurs affectant la stabilité des chélates en solution, la dimension du cycle formé par le métal et les atomes du ligand joue un rôle important. Les résultats expérimentaux obtenus avec des ions métalliques M^{2+} indiquent un maximum de stabilité des cycles comportant cinq chaïnons, ou six s'il y a des effets de résonance. C'est ainsi que les anions dicarboxylates $[O_2C—(CH_2)_n—CO_2]^{2-}$ forment avec les ions M^{2+} des premiers éléments de transition, des complexes dont la stabilité varie dans l'ordre oxalate > malonate ≫ succinate ≃ glutarate (1–3). Les rares données concernant les complexes des ions M^{3+} semblent confirmer des variations similaires (4). Cependant, lors de travaux sur les complexes oxalates et malonates du germanium(IV), des expériences préliminaires ont révélé que les complexes de l'ion ferrique Fe^{3+} avec les anions oxalate et malonate avaient des stabilités voisines. Une étude plus complète des complexes de Fe^{3+} avec les quatre premiers anions dicarboxylates, $0 \leqslant n \leqslant 3$, a donc été effectuée afin de préciser l'ordre des stabilités. Durant ces travaux, deux articles ont paru (5, 6) sur les complexes monooxalates du fer(III), où des conclusions contraires sont tirées quant à l'existence d'un complexe protoné $FeHC_2O_4^{2+}$.

Partie expérimentale

A. Réactifs

Les solutions de fer(II) et de fer(III) destinées à l'étude potentiométrique sont préparées par dissolution, en présence de fil de platine, de fer électrolytique dans l'acide perchlorique "Baker and Adamson", qualité "reagent", convenablement dilué. On ajoute ensuite de l'eau oxygénée de manière à oxyder partiellement ou totalement le fer(II). On dose ce dernier par le cérium(IV). La concentration en ions H^+ est vérifiée (7).

La pureté des ligands utilisés: acides oxalique et malonique (Matheson Coleman and Bell), acide succinique (Fisher Scientific Company), acide glutarique (Eastman Organic Chemicals) déterminée par dosage potentiométrique varie entre 99.1 et 100.1% à 0.7% près. Le produit $LiClO_4,3H_2O$ est de "G. F. Smith".

B. Appareillage

Les mesures potentiométriques sont effectuées avec un potentiomètre Leeds and Northrup, auquel est adjoint un galvanomètre de zéro. Les densités optiques sont déterminées à l'aide d'un spectrophotomètre Zeiss PMQII muni de cuves de quartz de 10.0 mm. Le pH est mesuré avec un appareil Radiometer 22. Les mesures sont faites à 25.0 ± 0.1 °C et à force ionique 0.52 ± 0.02 ($LiClO_4$).

C. Méthodes

a. Potentiométrie

La formation de complexes entre les ions Fe^{3+} et les ligands oxalate et malonate est étudiée par potentiométrie. On détermine les variations de potentiel d'électrode d'une solution de fer(III) et de fer(II) $2\text{–}6 \times 10^{-3}$ *M* dans $HClO_4$ 0.50 *M* ou 0.10 *M* lors de l'addition du ligand. On utilise deux demi-cellules de 100 ml recouvertes extérieurement d'un film plastique noir (8). La jonction est assurée par un tube en U rempli d'une solution $HClO_4$ 0.50 *M* ou $HClO_4$ 0.10 *M* + $LiClO_4$ 0.40 *M*. Une atmosphère d'azote est maintenue au-dessus des solutions. Une électrode de platine plonge dans chaque demi-cellule. La composition de la demi-cellule de référence reste inchangée, tandis que l'on ajoute dans la demi-cellule de mesure une solution de ligand $3 \times 10^{-2} - 8 \times 10^{-1}$ *M* sensiblement de mêmes acidité et force ionique, ainsi qu'une solution de fer(III) et de fer(II) de manière à maintenir constantes les concentrations totales de ces derniers ions. Des valeurs du potentiel stables à ±0.5 mV sont obtenues en moins de 2 min et la reproductibilité est de l'ordre du mV.

Can. J. Chem. Downloaded from www.nrcresearchpress.com by 210.87.254.5 on 09/05/12
For personal use only.

Les potentiels pris par les électrodes sont respectivement:

$$[1]\quad E_{réf} = E_0 + \frac{RT}{F}\,\mathrm{Log}\,\frac{[Fe^{3+}]_{réf}}{[Fe^{2+}]_{réf}} = E_0 + \frac{RT}{F}\,\mathrm{Log}\,\frac{C_M}{\left(1+\frac{K_H}{[H^+]}\right)C_{Fe^{2+}}}$$

et

$$[2]\quad E_{mes} = E_0 + \frac{RT}{F}\,\mathrm{Log}\,\frac{[Fe^{3+}]}{[Fe^{2+}]},$$

où C_M représente la concentration totale constante de Fe(III) ($C_M = 4.7 \times 10^{-3}$ et 2.35×10^{-3} M respectivement en milieu $[H^+] \simeq 0.5$ et 0.1 M), $C_{Fe^{2+}}$ la concentration totale constante de Fe(II) ($C_{Fe^{2+}} = 5.8 \times 10^{-3}$ et 2.9×10^{-3} M respectivement en milieu $[H^+] \simeq 0.5$ et 0.1 M), K_H la constante d'hydrolyse des ions ferriques, $K_H = [FeOH^{2+}][H^+]/[Fe^{3+}]$, $[Fe^{3+}]$ et $[Fe^{2+}]$ les concentrations de Fe(III) et Fe(II) libres.

On mesure:

$$[3]\quad \Delta E = E_{mes} - E_{réf} = \frac{RT}{F}\,\mathrm{Log}\left[\frac{[Fe^{3+}]\left(1+\frac{K_H}{[H^+]}\right)C_{Fe^{2+}}}{[Fe^{2+}]\,C_M}\right] = \frac{RT}{F}\,\mathrm{Log}\left[\alpha_0\left(1+\frac{K_H}{[H^+]}\right)\frac{C_{Fe^{2+}}}{[Fe^{2+}]}\right]$$

en fonction de C_L, la concentration totale du ligand.

Les différents bilans-matières dans la cellule de mesure:

$$[4]\quad C_L = [H_2L] + [HL^-] + [L^{2-}] + [FeL^+] + 2[FeL_2^-] + 3[FeL_3^{3-}] + [FeL]$$

$$[5]\quad C_M = [Fe^{3+}] + [FeOH^{2+}] + [FeL^+] + [FeL_2^-] + [FeL_3^{2-}]$$

$$[6]\quad C_{Fe^{2+}} = [Fe^{2+}] + [FeL]$$

nous conduisent à l'expression finale en fonction des constantes de formation β_n des différents complexes de Fe(III), FeL_n

$$\beta_n = \frac{[FeL_n]}{[Fe^{3+}][L^{2-}]},$$

de la constante K_H et de la constante de formation β_1' du complexe avec Fe(II)

$$\beta_1' = \frac{[FeL]}{[Fe^{2+}][L^{2-}]}$$

$$[7]\quad C_L = [L]\left(1+\frac{[H^+]}{K_2}+\frac{[H^+]^2}{K_1K_2}\right) + \frac{C_M(\beta_1[L] + 2\beta_2[L]^2 + 3\beta_3[L]^3)}{1+\frac{K_H}{[H^+]}+\beta_1[L]+\beta_2[L]^2+\beta_3[L]^3} + \frac{C_{Fe^{2+}}\beta_1'[L]}{1+\beta_1'[L]}.$$

L'hydrolyse de Fe(III) et la formation de complexes avec Fe(II) apparaissant à titre correctif, les valeurs des constantes K_H et β_1' ne nécessitent pas une grande précision. Nous avons utilisé: $K_H = 1.8 \times 10^{-3}$ (9–11) et $\beta_1' = 4 \times 10^4$ (8).

Dans une première approximation, en négligeant la faible variation de $[H^+]$ due à la formation de complexes, l'hydrolyse de Fe(III) et la formation de complexes avec Fe(II), on calcule α_0 à l'aide de l'éq. [3] simplifiée $\Delta E = (RT/F)\,\mathrm{Log}\,\alpha_0$. A partir de la relation entre α_0 et C_L, on atteint par approximations successives, en posant

$$\bar{n} = \frac{-\mathrm{d}\,\log\alpha_0}{\mathrm{d}\,\log[\sum H_2L]} \text{ et } C_L = [\sum H_2L] + \bar{n}C_M,$$

la correspondance entre α_0 et $[\Sigma H_2L]$, $[\Sigma H_2L]$ étant la concentration en ligand libre:

$$[\sum H_2L] = [H_2L] + [HL^-] + [L^{2-}].$$

A l'aide de fonctions telles que

$$[8]\quad \frac{1-\alpha_0}{\alpha_0[\sum H_2L]} \simeq \beta_1^* + \beta_2^*[\sum H_2L]$$

$$[9]\quad \frac{1-\alpha_0}{\alpha_0[\sum H_2L]^2} \simeq \beta_2^* + \beta_3^*[\sum H_2L],$$

on détermine graphiquement les valeurs approchées des constantes de stabilité apparentes

$$\beta_n^* = [FeL_n]/([Fe^{3+}][\sum H_2L]^n)$$

valables à l'acidité considérée.

Compte tenu de

$$[10]\quad \beta_n = \beta_n^*\left(1+\frac{[H^+]}{K_2}+\frac{[H^+]^2}{K_1K_2}\right)^n,$$

nous calculons les valeurs approchées des constantes β_n.

On porte alors ces valeurs approchées dans l'éq. [7], on calcule [L] par approximations, puis

$$[11]\quad \alpha_0 = \frac{1}{1+\frac{K_H}{[H^+]}+\beta_1[L]+\beta_2[L]^2+\beta_3[L]^3}$$

et ΔE (à l'aide de l'éq. [3]). L'on ajuste ensuite les différentes valeurs de β_n de manière à faire coïncider à ± 1 mV les ΔE calculés et expérimentaux. Ces dernières valeurs nous permettent de calculer les concentrations des différentes espèces en solution et ainsi d'atteindre une meilleure valeur de $[H^+]$. On ajuste à nouveau les β_n jusqu'à obtention d'une bonne concordance à ± 1 mV entre les ΔE calculés et expérimentaux.

b. Spectrophotométrie

La méthode potentiométrique précédente n'a pu être appliquée aux cas des acides succinique et glutarique, les différences de potentiel observées étant trop faibles à $[H^+] = 0.1$ M. Dans la méthode spectrophotométrique utilisée, on mesure l'augmentation d'absorption de solutions ferriques causée par l'addition du ligand, à force ionique 0.51, $[H^+] = 0.101 \pm 0.001$ M, $C_M = 2$–3×10^{-3} M et C_L variable.

Les spectres des complexes FeL présentent un maximum d'absorption assez étalé dans la région 280–320 mμ par rapport au fer(III) pris comme référence. Dans

cette zone de longueur d'onde, l'absorption correspondant à H_2L, HL^- et L^{2-} est négligeable. On a:

$$[12] \qquad A_{réf} = \epsilon_{Fe} C_M,$$

où ε_{Fe} est le coefficient d'extinction effectif du fer(III). Dans les conditions expérimentales choisies, $[FeL_2^-]$ est négligeable: la proportion maximale $[FeL_2^-]/[FeL^+]$ calculée en posant $\beta_2 \leqslant 10^{12}$ ne dépasse pas 0.9%, 0.3% et 0.4% pour les ligands malonate, succinate et glutarate.

Nous avons:

$$[13] \quad A_{mes} = \epsilon_{Fe}[Fe^{3+}] + \epsilon[FeL] = (\epsilon - \epsilon_{Fe})[FeL] + \epsilon_{Fe} C_M$$

où ε est le coefficient d'extinction du complexe FeL.

On mesure:

$$[14] \quad A_{mes} - A_{réf} = \Delta A = (\epsilon - \epsilon_{Fe})[FeL] = \Delta\epsilon[FeL]$$

En tenant compte de la constante β_1^*, on arrive à l'expression:

$$[15] \qquad \frac{\Delta A}{C_L - [FeL]} = \Delta\epsilon\beta_1^* C_M - \beta_1^* \Delta A.$$

[FeL] étant négligeable devant C_L, ($[FeL^+]/C_L \leqslant 0.018$) on obtient:

$$[16] \qquad \frac{\Delta A}{C_L} = \Delta\epsilon\beta_1^* C_M - \beta_1^* \Delta A$$

C_M restant constante et C_L étant la variable, la pente de la droite $\Delta A/C_L = f(\Delta A)$ est égale à β_1^*.

c. Constantes d'acidité des ligands

Les constantes d'acidité des acides dicarboxyliques et de l'acide acétique sont déterminées par analyse des courbes de titrage potentiométrique de solutions d'acides environ $2 \times 10^{-2} M$ par de la soude 0.5 *M*. Des solutions d'acide perchlorique de concentration connue et de force ionique 0.50 servent à la standardisation du pH-mètre. La linéarité de réponse de l'électrode de verre a été vérifiée dans l'intervalle $1.70 < -\log [H^+] < 3.30$.

Les constantes K_1 et K_2 ont été déterminées par approximations successives à l'aide des fonctions

$$[17] \qquad pH = pK_1 + \log \frac{C_B + [H^+]}{K_2(2C_L - C_B - [H^+])[H^+]^{-1} + C_L - C_B - [H^+]}$$

$$[18] \qquad pH = pK_2 + \log \frac{[H^+](C_B + [H^+])K_1^{-1} + C_B[H^+] - C_L}{2C_L - C_B - [H^+]}$$

où C_B représente la concentration de NaOH ajoutée.

L'équation [17] n'étant pas applicable à l'acide oxalique, le pH bas des solutions conduisant à des erreurs de calcul importantes, le pK_1 de ce ligand a été donné par la pente de la droite d'équation:

$$[19] \quad [H^+](C_B + [H^+]) = K_1[K_2(2C_L - C_B - [H^+])[H^+]^{-1} + C_L - C_B - [H^+]]$$

et a été confirmé par étude spectrophotométrique à $\lambda = 215$ mμ, avec $C_L = 1.7 \times 10^{-3}$ *M* et $[H^+]$ variant de 0.1 à 0.5 *M*.

Résultats et discussion

Dans le Tableau I, les constantes d'acidité des acides dicarboxyliques et acétique obtenues en milieu $LiClO_4$ 0.5 *M* sont comparées aux valeurs déterminées en milieu KCl 0.2 *M* (16). Par rapport à ces dernières, nos valeurs de pK_1 et pK_2 sont respectivement inférieures de 0.15 et 0.20 environ: ces écarts résultent vraisemblablement des milieux différents.

La méthode potentiométrique d'étude des complexes a conduit à des différences de potentiel ΔE allant jusqu'à 190 et 270 mV pour des concentrations maximales en acide oxalique 6.7×10^{-2} et 2.9×10^{-2} *M* en milieu $[H^+] = 0.495 \pm 0.005$ *M* et $[H^+] = 0.105 \pm 0.003$ *M* respectivement, mais seulement de 13 et 70 mV pour l'acide malonique (concentration maximale: 0.18 *M* dans les deux cas) aux acidités voisines. On a porté sur la Fig. 1 les points expérimentaux donnant ΔE en fonction de C_L, ainsi que les points calculés. On note un bon accord. La Fig. 2 représente les variations de la fonction [16] pour les différents ligands considérés. On a regroupé dans les Tableaux II et III les valeurs des constantes β_1^* et β_n obtenues par potentiométrie et spectrophotométrie respectivement.

On note la concordance de notre valeur de β_1^*, constante apparente en milieu $[H^+] = 0.50$ *M*, avec celle de Bauer et Smith (5). Cette dernière a été déterminée par spectrophotométrie en utilisant des solutions de fer(III) 10 fois moins concentrées que les nôtres. On peut ainsi conclure à l'absence de complexes polynucléaires dans ces milieux. La valeur de Moorhead et Sutin (6), en milieu $[H^+] = 0.50$ *M*, $[NaClO_4] = 0.50$ *M*, est aussi voisine.

Nos valeurs de β_1 ne dépendent que peu de l'acidité. Celles de Bauer et Smith varient plus et ces auteurs ont expliqué ces variations en postulant l'existence d'un complexe protoné $FeHC_2O_4^{2+}$, dont ils ont calculé la constante de formation:

$$\log \beta_1'' = \log \frac{[FeHC_2O_4^{2+}]}{[Fe^{3+}][HC_2O_4^-]} = 4.35.$$

Can. J. Chem. Downloaded from www.nrcresearchpress.com by 210.87.254.5 on 09/05/12
For personal use only.

Can. J. Chem. Downloaded from www.nrcresearchpress.com by 210.87.254.5 on 09/05/12
For personal use only.

TABLEAU I

Constantes d'acidité des ligands

Ligand	pK_1	pK_2	pK_1 (16)	pK_2 (16)
Acide oxalique	1.00±0.05	3.50±0.03	1.14	3.85
Acide malonique	2.53±0.03	5.01±0.03	2.69	5.24
Acide succinique	3.92±0.03	5.05±0.03	4.07	5.28
Acide glutarique	4.09±0.03	4.84±0.03	4.21	5.06
Acide acétique	4.48±0.03		4.67	

TABLEAU II

Constantes de stabilité β_n et β_n* déterminées par potentiométrie

Ligand	$[H^+]$ (M)	log β_1	log β_2	log β_3	log β_1*
Oxalate	0.495±0.005	7.56	13.63	—	—
Oxalate	0.105±0.003	7.49	13.64	18.49	—
Oxalate[a]	0.5				3.58
	0.1				4.67
Malonate	≃0.50	7.47			0.54
Malonate	≃0.10	7.45			1.89

[a]Calculée à l'aide de l'éq. [10].

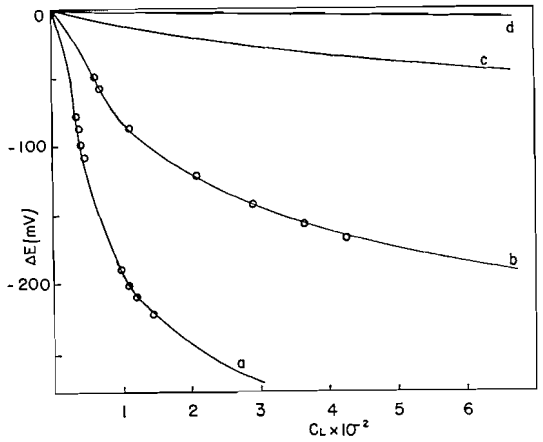

FIG. 1. Variations de ΔE en fonction de la concentration totale en ligand. Les courbes expérimentales sont représentées en trait plein (les points marqués ont été calculés). (*a*) Oxalate, $[H^+] = 0.103 \pm 0.003$ M, $C_M = 2.35 \times 10^{-3}$ M, $C_{Fe^{2+}} = 2.9 \times 10^{-3}$ M; (*b*) oxalate, $[H^+] = 0.495 \pm 0.005$ M, $C_M = 4.7 \times 10^{-3}$ M, $C_{Fe^{2+}} = 5.8 \times 10^{-3}$ M; (*c*) malonate, $[H^+] = 0.10$ M, $C_M = 2.35 \times 10^{-3}$ M, $C_{Fe^{2+}} = 2.9 \times 10^{-3}$ M; (*d*) malonate, $[H^+] = 0.50$ M, $C_M = 4.7 \times 10^{-3}$ M, $C_{Fe^{2+}} = 5.8 \times 10^{-3}$ M.

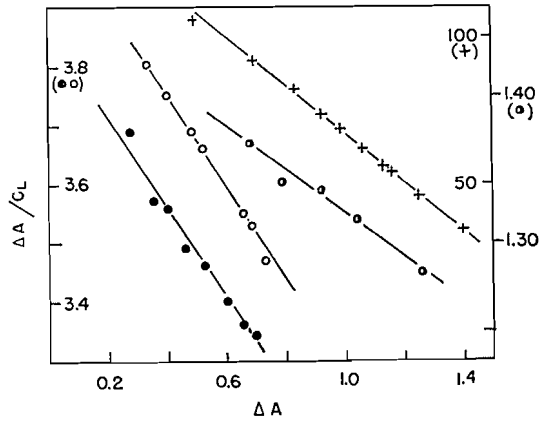

FIG. 2. Détermination spectrophotométrique des β_1* pour les différents systèmes ferriques (en milieu $[H^+] = 0.100$ M). (+) = malonate, $C_L = 0.466$–4.163×10^{-2} M, $C_M = 10^{-3}$ M, $\lambda = 310$ mμ; (○) = succinate, $C_L = 0.859$–2.11×10^{-1} M, $C_M = 2 \times 10^{-3}$ M, $\lambda = 300$ mμ; (●) = glutarate, $C_L = 0.745$–2.086×10^{-1} M, $C_M = 2 \times 10^{-3}$ M, $\lambda = 300$ mμ; (◑) = acétate, $C_L = 0.493$–0.985 M, $C_M = 2 \times 10^{-3}$ M, $\lambda = 295$ mμ.

Compte tenu de la formation de ce complexe, ils trouvent log β_1 égal à 7.39. Si nous admettions leur hypothèse, on calculerait:

$$\log \beta_1 = 7.48 \text{ et } \log \beta_1'' = 3.60.$$

Moorhead et Sutin obtiennent pour β_1 des valeurs indépendantes de l'acidité entre $[H^+] = 0.50$ M et $[H^+] = 1.00$ M à force ionique 1.0,

TABLEAU III

Constantes de stabilité β_1* et β_1 déterminées par spectrophotométrie

Ligand	$[H^+]$ (M)	log β_1*	log β_1
Acide malonique	0.101	1.91±0.01	7.46
Acide succinique	0.100	−0.10±0.01	6.88
Acide glutarique	0.100	−0.15±0.02	6.78
Acide acétique	0.100	−0.85±0.05	2.63

TABLEAU IV

Constantes de formation du complexe monooxalate du fer(III) et constantes d'acidité de l'acide oxalique

$\log \beta_1$*	$\log \beta_1$	pK_1	pK_2	Milieu	Référence
3.54	7.86			$[HClO_4]=0.50\ M$	(5)
4.06	7.65			$[HClO_4]=0.20\ M$, $[NaClO_4]=0.30\ M$	
		1.20 ± 0.01		$[NaClO_4]\simeq0.45\ M$, $[HClO_4]\simeq0.05\ M$	
			3.66 ± 0.02	$[NaClO_4]\simeq0.5\ M$	
3.48	7.57			$[HClO_4]=0.50\ M$, $[NaClO_4]=0.50\ M$	(6)
2.95	7.61			$[HClO_4]=1.00\ M$	
		1.08 ± 0.01		$[NaClO_4]\simeq0.91\ M$, $[HClO_4]\simeq0.09\ M$	
			3.55 ± 0.01	$[NaClO_4]\simeq1.0\ M$	
3.58	7.56			$[HClO_4]=0.495\pm0.005\ M$	Présent travail
4.67	7.49			$[HClO_4]=0.105\pm0.003\ M$, $[LiClO_4]=0.4\ M$	
		1.00 ± 0.05		$[H^+]=4\times10^{-3}$–$0.5\ M$, $\mu=0.50(LiClO_4)$	
			3.50 ± 0.03	$[LiClO_4]=0.50\ M$, $\mu=0.52(LiClO_4)$	

ainsi qu'à force ionique 3.0 entre $[H^+] = 0.50$ M et $[H^+] = 3.00$ M. Ces auteurs rejettent donc l'existence du complexe protoné. Il faut toutefois noter que tous ces résultats admettent implicitement, et ceci est discutable, que les coefficients d'activité des différents ions restent constants lorsque le milieu passe de $[HClO_4] \simeq 0.1\ M + [NaClO_4] \simeq 0.4$–$2.9\ M$ (ou $[HClO_4] \simeq 0.1\ M + [LiClO_4] \simeq 0.4\ M$) à $[HClO_4] = 0.5$–$3\ M$ (voir Tableau IV), et ainsi, que K_1 est indépendant du milieu. Il semble que l'existence de tels complexes protonés "labiles", déjà difficile à établir aux faibles acidités utilisées pour caractériser les complexes oxalates du Cu^{2+} (12, 13), l'est d'autant plus, aux fortes acidités employées dans le cas des complexes oxalates du fer(III). Nous adoptons $\log \beta_1 = 7.53 \pm 0.1$.

Cette valeur est nettement plus faible que celles déterminées aux faibles acidités, en tenant compte de l'hydrolyse des ions Fe^{3+}: 8.15–9.4 (4).

Les valeurs de β_1 du complexe malonate obtenues par potentiométrie et spectrophotométrie sont voisines, $\log \beta_1 = 7.46$. Les constantes β_1 des complexes succinate et glutarate n'ont été déterminées qu'à $[H^+] = 0.10\ M$ et sont respectivement $\log \beta_1 = 6.88$ et 6.78. La valeur donnée pour le succinate dans la littérature est $\log \beta_1 = 7.49$ (4).

La stabilité nettement plus faible du complexe acétate, $\log \beta_1 = 2.63$, semblerait indiquer que les complexes des anions dicarboxylates sont des chélates, la substitution de CH_3— par ^-COO—$(CH_2)_n$— ne devant que peu modifier la stabilité. De même, au complexe monodenté $FeC_2O_4H^+$ devrait correspondre $\log \beta_1'' < 2.6$ vu le remplacement de CH_3— par HOOC—. La valeur calculée par Bauer et Smith ($\log \beta_1'' = 4.35$), semblerait donc, si elle était confirmée, devoir être attribuée à un complexe bidenté.

L'ordre de stabilité des complexes du fer(III) est ainsi: oxalate $\simeq$ malonate $>$ succinate $\simeq$ glutarate. On retrouve la séquence suivie généralement par la plupart des complexes des métaux bivalents, à ceci près que l'on enregistre pour Fe(III) des variations faibles ($\Delta \log \beta_1 \simeq 0.6$) entre les complexes malonates et succinates, alors que la décroissance est rapide de l'oxalate au glutarate pour les éléments de transition bivalents. Bien que l'on explique souvent la diminution de stabilité avec une augmentation des dimensions du cycle formé comme étant un effet d'entropie, des mesures récentes de ΔH et ΔS ont montré que le problème était plus complexe, les effets de l'enthalpie et de l'entropie sur β_1 pouvant être opposés (3). Si l'on compare les résultats obtenus pour Fe(III) avec ceux déjà connus pour La(III) (1) et

Can. J. Chem. Downloaded from www.nrcresearchpress.com by 210.87.254.5 on 09/05/12
For personal use only.

Cr(III) (14), la nature du métal paraît jouer un rôle important dans la détermination de l'ordre de stabilité des complexes dicarboxylates des métaux trivalents. Les résultats impliquent ainsi des limitations aux corrélations entre, d'une part la stabilité des complexes d'un métal et d'autre part la basicité des ligands ou la stabilité des complexes d'un autre métal (15).

Remerciements

Nous remercions le Conseil National de Recherches du Canada pour une subvention et le Conseil des Arts du Canada pour une bourse (M. D.).

1. J. M. PEACOCK et J. C. JAMES. J. Chem. Soc. 2233 (1951).
2. M. YASUDA, K. YAMASAKI et H. OHTAKI. Bull. Chem. Soc. Japan, **33**, 1067 (1960).
3. A. MCAULEY, G. H. NANCOLLAS et K. TORRANCE. Inorg. Chem. **6**, 136 (1967).
4. L. G. SILLÈN et A. E. MARTELL. Stability constants of metal ion complexes. Spec. Publ. No. 17. The Chemical Society, London. 1964.
5. R. F. BAUER et W. MACF. SMITH. Can. J. Chem. **43**, 2755 (1965).
6. E. G. MOORHEAD et N. SUTIN. Inorg. Chem. **5**, 1866 (1966).
7. W. C. SCHUMB, M. S. SHERRIL et S. B. SWEETSER. J. Am. Chem. Soc. **59**, 2360 (1937).
8. M. B. SCHIGOL. Russ. J. Inorg. Chem. English Transl. **6**, 171 (1961).
9. A. S. WILSON et H. TAUBE. J. Am. Chem. Soc. **74**, 3509 (1952).
10. C. BROSSET. Svensk. Kem. Tidskr. **53**, 434 (1941).
11. W. C. BRAY et A. V. HERSHEY. J. Am. Chem. Soc. **56**, 1889 (1934).
12. L. CIAVATTA et M. VILLAFIORITA. Gazz. Chim. Ital. **95**, 1247 (1965).
13. A. MCAULEY et G. H. NANCOLLAS. Trans. Faraday Soc. **56**, 1165 (1960).
14. H. MURO et R. TSUCHIYA. Bull. Chem. Soc. Japan, **39**, 1589 (1966).
15. H. FREISER, Q. FERNANDO et G. E. CHENEY. J. Phys. Chem. **63**, 250 (1959).
16. R. K. CANNAN et A. KIBRICK. J. Am. Chem. Soc. **60**, 2314 (1938).

Can. J. Chem. Downloaded from www.nrcresearchpress.com by 210.87.254.5 on 09/05/12
For personal use only.

Can. J. Chem. Downloaded from www.nrcresearchpress.com by 210.87.254.42 on 09/05/12
For personal use only.

Nuclear spin–spin coupling constants; equilibrium and kinetic studies for fluoroberyllate complexes in solution

J. FEENEY
Varian Associates, Walton-on-Thames, England

AND

R. HAQUE, L. W. REEVES, AND C. P. YUE
Department of Chemistry, University of British Columbia, Vancouver, British Columbia

Received June 7, 1967

^{19}F nuclear magnetic resonance signals of aqueous solutions containing beryllium and fluoride ions have been used to study the equilibrium and kinetic processes occurring. Detailed studies of line widths, intensities, chemical shifts, and coupling constants have been made. This leads to an equilibrium constant determination $K_c = 8.0 \pm 2.0 \times 10^{-2}$ mole kg^{-1} for the dissociation reaction

$$BeF_4^{2-} \underset{k_{-1}}{\overset{k_1}{\rightleftharpoons}} BeF_3^- + F^-.$$

The line width studies show that in addition to the above reaction there is fluoride ion exchange involving all three species. Rate constants at 33 °C are: $k_1 = 23.8$ (s^{-1}), $k_{-1} = 3 \times 10^2$ mole^{-1} s^{-1}, $k_2 = 4.3 \times 10^2$ mole^{-1} s^{-1} (for F^- ion exchange with BeF_4^{2-}), $k_3 = 4.5 \times 10^2$ mole^{-1} s^{-1} (for F^- ion exchange with BeF_3^-), $k_4 = 4.5 \times 10^2$ mole^{-1} s^{-1} (for F^- ion exchange between BeF_3^{2-} and BeF_4^-). These values are determined within a factor of three. The equilibrium constant K_c is independent of temperature in the range 2 to 50 °C. An entropy of reaction ~ -5 e.u. is indicated.

Studies of BeF_2 solutions show that at least two fluoroberyllate complexes are present and these are assigned as monomeric BeF_2 and $(BeF_2)_n$. Values of coupling constants and line widths in the absence of exchange processes strongly suggest the structures $BeF_3(H_2O)^-$ and $BeF_2(2H_2O)$ for the tri- and di-fluoride species.

The reduced coupling constants j_{X-F} in the isoelectronic series BeF_4^{2-}, BF_4^-, CF_4, and NF_4^+ correlate with atomic number in the same manner as the series TeF_6, SbF_6^-, and SnF_6^{2-}. A change in sign of the coupling constant j_{X-F} is suggested between NF_4^+, CF_4, BF_4^- as a group and BeF_4^{2-}. The variation of coupling constants j and $|\Psi^2_{ns}(0)|$ with atomic number is presented for a wide range of elements. The question of the origin of the sign of the coupling in relation to the atomic number dependence is related to a recent theory of Pople and Santry (16).

Canadian Journal of Chemistry, 46, 1389 (1968)

Introduction

The study of beryllium fluoride complexes of the type $BeF_n^{(2-n)-}$ by nuclear magnetic resonance (n.m.r.) has not been extensive. In the solid state, studies of $(NH_4)_2BeF_4$ have been made by Leane and Richards (1) and Blinc and Levstek (2).

Gutowsky and Hoffmann (3) reported spectra of aqueous BeF_2 solutions as part of an early survey of the chemical shifts of fluoride molecules. Recently Francis and Lawrenson (4) made a qualitative study of the ^{19}F spectra of ammonium tetrafluoroberyllate solutions. They resolved a quadruplet signal of chemical shift +85.5 from trifluoroacetic acid (TFA). The components of the quadruplet were broad ($\sim$ 24 c.p.s.) and the reported coupling constant J_{Be-F} was 33.7 c.p.s. No other resonances were reported.

We have been able in this work to detect several other resonances in these solutions and to compute the equilibrium constant for the reaction

$$BeF_4^{2-} \rightleftharpoons BeF_3^- + F^-$$

as well as study the kinetics of fluoride exchange. The measurement of the coupling constant J_{BeF} in BeF_4^{2-} affords an opportunity to consider coupling constants in the isoelectronic series BeF_4^{2-}, BF_4^-, CF_4, and NF_4^+ in the context of the atomic number dependence and to further extend the relationship between the '*s*' contact interaction and coupling constants from more recent measurements (17, 18).

Experimental

Ammonium tetrafluoroborate and beryllium fluoride were supplied by K. and K. Laboratories and used without further purification. Ammonium fluoride was an analytical grade reagent supplied by B.D.H. Laboratories Ltd. Solutions were made by weighing both the water and the salt.

TABLE I*

Chemical shift and line width of the peak associated with BeF_4^{2-} and other fluoroberyllate complexes when Be^{2+} ion is added to a solution containing F^- ion

Concentration of beryllium nitrate (mole l)	Chemical shift of the new peak (p.p.m.)	Line width (c.p.s.)	Remark
0.1	84.8	27.2†	Quartet
0.2	85.0	30.5	,,
0.3	85.1	37.0	,,
0.4	84.4	142.0‡	Quartet collapses into a broad peak
0.5	85.0	170.0	,,
0.6	86.7	210.0	,,
0.8	89.4	252.0	,,
1.0	89.9	260.0	,,

*Concentration of NH_4F is 5.0 M; coupling constant $J_{^9Be-^{19}F} \sim 32$–34 c.p.s.; the chemical shift of $F^- \sim 36.8$ p.p.m.
†Line width of one component of the resolved quartet.
‡Line width of the peak due to the collapse of quartet.

^{19}F spectra were observed using Varian HR 60 and HR 94.1 spectrometers. ^9Be resonances were obtained in 15 mm sample tubes at 7.75 Mc/s with a Varian variable frequency n.m.r. spectrometer. The field modulation frequency was 200 c.p.s. and the audio phase detector was adjusted so as to observe only first side bands in absorption mode. The external standard was TFA for ^{19}F chemical shifts and a saturated solution of $Be(NO_3)_2$ for the ^9Be chemical shifts. Intensities were measured by repeated tracings onto good bond paper and then weighing the cutouts. The nucleus ^9Be has spin 3/2.

Results

(a) Addition of Be^{2+} to Ammonium Fluoride Solutions

A 5.0 *m* solution of ammonium fluoride was treated with beryllium nitrate solutions in varying amounts. The ratio $[F^-]/[Be^{2+}]$ was varied between 50 and 5. The resulting solutions had two fluorine magnetic resonance signals, one with chemical shift +36.8 p.p.m. and the second +85 p.p.m. from an external TFA reference. The signal at +36.8 p.p.m. is assigned to the F^- ion and the second signal to the species BeF_4^{2-}. The latter high field peak varied considerably in character, depending on the ratio $[F^-]/[Be^{2+}]$. At high values of $[F^-]/[Be^{2+}]$ it was resolved as a quadruplet with the components considerably broadened. The coupling constant J_{Be-F} was always between 32 and 34 cycles and the apparent value obtained depended on the line width of the components, which in turn depend upon an exchange process involving the F^- ion. The major fluoride ion complex present in these solutions is always assigned as BeF_4^{2-} on the basis of further studies of ammonium tetrafluoroborate solutions. Table I gives a summary of the data obtained for ammonium fluoride/beryllium nitrate solutions. When $[F^-]/[Be^{2+}] < 14$ the quadruplet structure collapses to a single broad resonance.

(b) Studies of Ammonium Tetrafluoroberyllate Solutions

A complete study of the concentration dependence of ^{19}F chemical shifts, line widths, and signal intensities was made at 33 °C and selected solutions were studied over the temperature range +2 °C to 50 °C. At ambient temperature, 33 °C, the number and complexity of the ^{19}F magnetic resonance peaks depend markedly on concentration of ammonium tetrafluoroberyllate in water.

In concentrated solutions > 0.6 *m* there are two broad signals which can be assigned to the F^- ion and BeF_4^{2-} ions on the basis of their chemical shifts. As the salt is diluted, however, a third fluorine resonance is resolved on the high field side of the BeF_4^{2-} ion peak; it is of considerably lower intensity and appears initially as a broad peak $\sim$ 100 c.p.s. in width. As the ammonium tetrafluoroberyllate is diluted further the new peak develops a quadruplet structure at ~ 0.3 *m*. As further dilution is made the quadruplet structure on both high field peaks, $\delta = +85$ p.p.m. and $\delta = +88.5$ p.p.m., becomes sharper as the exchange process causing line broadening becomes slower. The area of the new peak with $\delta = +88.5$ p.p.m. is always three times that of the F^- ion signal in the same solution, so it is assigned to the BeF_3^- ion. The exact nature of

Can. J. Chem. Downloaded from www.nrcresearchpress.com by 210.87.254.42 on 09/05/12
For personal use only.

TABLE II

Chemical shifts and intensities of ^{19}F nuclear magnetic resonance signals in $(NH_4)_2BeF_4$ solutions at various concentrations. I_4/I_3 = intensity of BeF_4^{2-} ion resonance/intensity of BeF_3^- ion resonance

Molality $(NH_4)_2BeF_4$	$\frac{\text{Intensity } BeF_4^{2-}}{\text{Intensity } BeF_3} = \frac{I_4}{I_3}$	Chemical shifts (p.p.m.)*		
		BeF_4^{2-}	BeF_3^-	F^-
0.0476	0.608	86.2	88.6	—
0.1001	0.681	86.2	87.5	40.3
0.1206	1.068	86.0	88.5	—
0.1840	1.350	85.8	88.4	39.6
0.2610	1.390	85.7	88.5	38.6
0.554	1.793	85.4	88.3	—
1.308	3.280	†	†	30.0

*External TFA reference.
†BeF_4^{2-} and BeF_3^- resonances become a single peak due to a rapid exchange process.

the BeF_3^- ion is not directly available but the line widths of the ^{19}F resonance in dilute solutions at 2 °C (~ 7.0 Hz) probably indicate a symmetrical structure since spin–spin relaxation through interruption of scalar coupling to a ^9Be nucleus of spin 3/2 cannot be appreciable. This is consistent with a structure $[BeF_3(H_2O)]^-$ where 1 water molecule replaces a fluoride ion. The chemical shift data for these resonances are summarized in Table II. The F^- ion resonance position is somewhat concentration dependent.

The addition of excess F^- ion to these solutions causes a decrease in line width of both quadruplet signals to a minimum value of 10 Hz half width at 33 °C in the limit of large excess of F^- ion. The chemical shifts of signals assigned to BeF_4^{2-} and BeF_3^- ions do not change. Addition of Be^{2+} ion in the form of the nitrate salt results in considerable broadening of the BeF_4^{2-} and BeF_3^- peaks and leads to collapse of the two signals into one broad peak which moves to high field on adding excess Be^{2+} ion.

In Fig. 1 selected spectra in the region of the BeF_4^{2-} and BeF_3^- resonance peaks are indicated at several temperatures and concentrations for an ^{19}F Larmor frequency of 94.1 MHz. The relative intensities and chemical shift data are recorded in Table II for various concentrations of ammonium tetrafluoroberyllate at ambient temperature 33 °C. Table III lists similar data and the computed equilibrium constants to be discussed later for the variable temperature experiments. Line widths for the quadruplet components and the F^- ion signal were also measured in the solutions at ambient temperature and were used to derive the kinetic parameters, for the exchange processes taking place in these solutions.

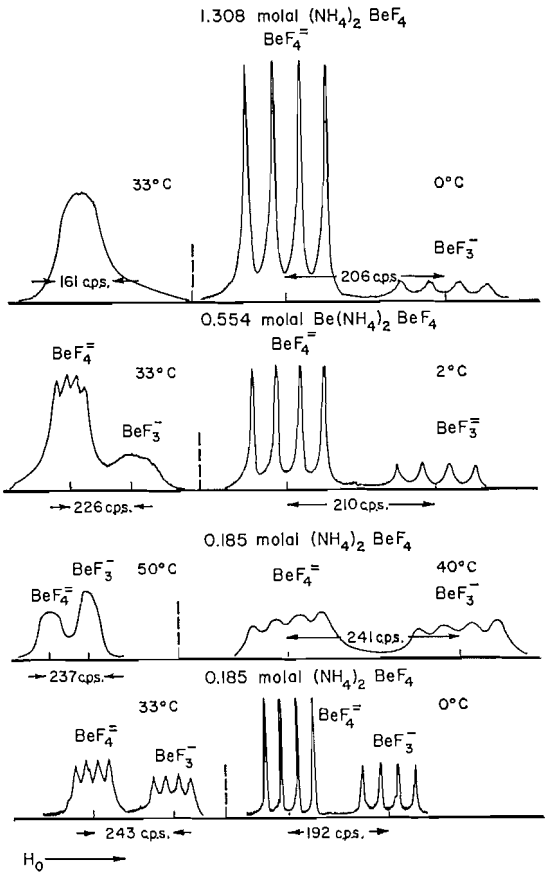

FIG. 1. ^{19}F n.m.r. spectra of ammonium tetrafluoroberyllate solutions at selected temperatures and concentrations.

Can. J. Chem. Downloaded from www.nrcresearchpress.com by 210.87.254.42 on 09/05/12
For personal use only.

TABLE III

Collected data on equilibrium constants from intensity measurements for the reaction $BeF_4^{2-} \rightleftharpoons BeF_3^- + F^-$ at a series of temperatures and concentrations

Concentration $(NH_4)_2BeF_4$ (moles/1000 g)	Temperature (°C)	$R = I_4/I_3$	Equilibrium constant, $K_c \times 10^2$ (moles kg^{-1})
0.185	0	1.43	8.32
0.185	10	1.31	9.50
0.185	20	1.52	7.5
0.185	25	1.23	10.35
0.185	33	1.39	9.02, 8.7
0.185	40	1.31	9.40
0.185	50	1.14	11.6
0.544	2	3.53	6.5
1.308	0	6.94	4.04
0.048	33	0.608	7.06
0.121	33	1.07	8.30
0.261	33	1.79	8.28
0.554	33	3.28	6.5

(c) Studies of BeF_2 Solutions

A single fluorine nuclear magnetic resonance signal was observed in concentrated solutions of beryllium difluoride at room temperature. Typical signals are illustrated in Fig. 2 for 1.81 *m*, 0.362 *m*, and 0.181 *m* solutions. At the lower concentrations two signals appear in the spectrum; the high field one has a quadruplet structure. The chemical shifts are +90 p.p.m. and +92.4 TFA, while the single broad resonance in concentrated solutions is centered around +91.7 p.p.m., indicating that rapid interconversion is occurring between the two species which are resolved separately in dilute solutions. It should be noted that the high field quadruplet is approximately twice as intense as the broad resonance in dilute solutions. Details of the coupling constant measurement and chemical shift measurements are listed in Table IV from 0.181 *m* to 1.810 *m* BeF_2. No fluoride ion resonance was observed in any of the beryllium difluoride solutions. At least two beryllium fluoride complexes are present and these do not appear to be dissociative to give fluoride ion.

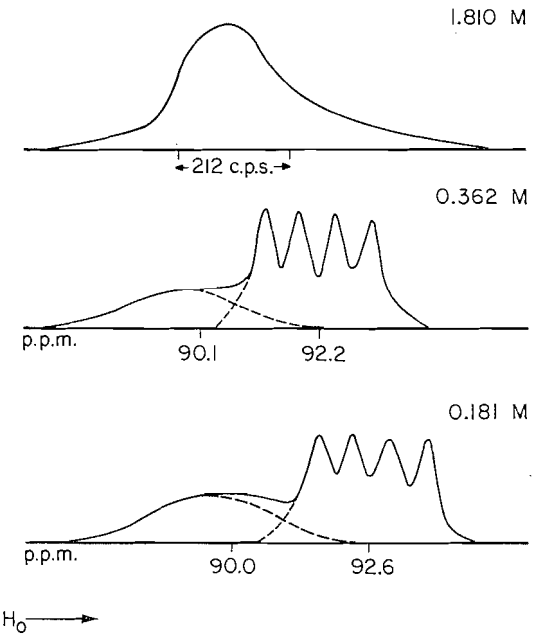

FIG. 2. ^{19}F n.m.r. spectra of beryllium difluoride solutions at three concentrations.

(d) Studies of the ^9Be Nuclear Resonance

It is expected that changes in ^9Be chemical shifts are quite small (5) and this was our experience in several solutions of beryllium complex ions measured. The intrinsic line width on the spectrometer used was 15 to 20 Hz because of field inhomogeneity. The only noticeable effect of adding Be^{2+} ions to solutions containing the fluoride ion was some line broadening and chemical shift changes near the limits of experimental error ± 8 Hz ($\sim \pm 1$ p.p.m.). An attempt was made to investigate the well-known polymeric substances (6) produced when beryllium carbonate is dissolved in solutions of beryllium salts or bases such as sodium hydroxide are added to aqueous solutions of the nitrate. The solutions become viscous in the limit of high Be^{2+} concentrations. Some line

Can. J. Chem. Downloaded from www.nrcresearchpress.com by 210.87.254.42 on 09/05/12
For personal use only.

TABLE IV

Chemical shifts and coupling constant of species present in aqueous BeF_2 solutions. A* refers to the single broad peak and B* refers to the quadruplet. The coupling constant is noted in column 4

Concentration of BeF_2 (moles/l)	Chemical shifts (p.p.m.) A*	Chemical shifts (p.p.m.) B*	Coupling constant (c.p.s.)
0.181	90.0	92.6	40.0
0.362	90.1	92.2	39.9
0.724	90.0	92.2	39.8
1.086	90.0	92.2	39.0
1.448	92.0		—
1.810	91.9		—

broadening of the ^9Be n.m.r. signal occurred and there was a chemical shift change to low field of approximately 1.6 p.p.m. from saturated beryllium nitrate in the limit of incipient gelatinous precipitation. It is evident that a spectrometer of higher resolution and stability is required for a complete study of the ^9Be nuclear magnetic resonance in these systems.

Discussion

Equilibrium Studies

The species present in ammonium tetrafluoroberyllate solutions are quite clearly associated with the equilibrium

[1] $$BeF_4^{2-} \rightleftharpoons BeF_3^- + F^-,$$

which probably represents the exchange of a fluoride ion for a water molecule

[2] $$BeF_4^{2-} \rightleftharpoons [BeF_3(H_2O)]^- + F^-.$$

The limiting line widths at low temperature (2 °C) and low concentrations (2.4 Hz for BeF_4^{2-} and 7.0 Hz for BeF_3^-) indicate that even in the BeF_3^- ion the actual structure is close to tetrahedral about the beryllium (7).

The intensity measurements lead to an evaluation of K_c at various temperatures,

[3] $$K_c = \frac{[BeF_3^-][F^-]}{[BeF_4^{2-}]}$$

[4] $$K_e = \frac{c\alpha^2}{1-\alpha} \cdot \frac{\gamma_{BeF_3^-}\gamma_{F^-}}{\gamma_{BeF_4^{2-}}} = K_c K_\gamma,$$

where c = molality of the BeF_4^{2-} ion, α = degree of dissociation of the BeF_4^{2-} ion, and $\gamma_{BeF_4^{2-}}$, $\gamma_{BeF_3^-}$, and γ_{F^-} are activity coefficients for the respective ions.

If I_4 and I_3 represent areas of the ^{19}F nuclear magnetic resonance signals for BeF_4^{2-} and BeF_3^- ions respectively then K_c can be written

[5] $$K_c = 16c/3(4R + 3R^2)^{-1} \text{ moles kg}^{-1},$$

where $R = (I_4/I_3)$. The values of K_c obtained by this method are listed in Table III for the solutions investigated. It is clear that K_c is reasonably independent of concentration at the ambient temperature 33 °C; the mean value is assigned as $8.0 \pm 2 \times 10^{-2}$ mole kg^{-1}. K_γ is not determined but appears to be independent of concentration. There is no sensible temperature dependence of K_c so that ΔH for reaction [1] appears to be close to zero. Using $\Delta G^0 = 1.5$ kcal from the equilibrium constant and $\Delta H^0 = 0$ then $\Delta S^0 \cong -5$ e.u. The only other determination of K_c, from optical density studies, gave a value 1×10^{-2} mole l^{-1} at room temperature (8).

The equilibria in BeF_2 solutions are more difficult to assign. No doubt in all these solutions a very low concentration of species such as BeF^+ occurs but these would not be detected and the predominant equilibrium seems to be a non-dissociative type. It is reasonable to suggest

[5] $$n BeF_2 \rightleftharpoons (BeF_2)_n,$$

where n is unknown and the beryllium is located in an unsymmetrical environment in the polymer leading to rapid relaxation of the ^9Be nuclear spin and loss of the quadruplet structure. Signal overlap is serious enough to preclude intensity measurements of sufficient precision to investigate the equilibrium thoroughly. There is also a rapid exchange in concentrated solutions which complicates an analysis of the equilibrium. The species $BeF_2(H_2O)_2$ has been reported (5) and is consistent with the resolution of a quadruplet, in

Can. J. Chem. Downloaded from www.nrcresearchpress.com by 210.87.254.42 on 09/05/12
For personal use only.

Can. J. Chem. Downloaded from www.nrcresearchpress.com by 210.87.254.42 on 09/05/12
For personal use only.

a fairly symmetric electric field gradient for an approximately tetrahedral shape.

Connick and Poulson (9) observed separate resonances for AlF^{2+} and AlF_2^+ in mixed solutions of sodium fluoride and aluminium nitrate, but the much larger quadrupole moment of ^{27}Al and possibly unsymmetric environment precluded measurement of a scalar coupling.

Chemical Shifts and Coupling Constants

In order of decreasing fluoride ion content the chemical shifts and coupling constants J_{BeF} are: BeF_4^{2-} $\delta = +86 \pm 0.5$ from TFA, $J = 33 \pm 1$ Hz; BeF_3^- $\delta = +88.5 \pm 1$ p.p.m., $J = 36 \pm 0.5$ Hz; BeF_2 (monomeric) $\delta = +92.2 \pm 0.5$, $J = 39.6 \pm 0.5$ Hz; $(BeF_2)_n$ $\delta = 90 \pm 1$ p.p.m., no coupling resolved. The increase in the absolute magnitude of the coupling constants is approximately proportional to the chemical shift changes.

It is interesting to consider the coupling constants to the central atom in BeF_4^{2-}, BF_4^-, CF_4, and NF_4^+ as an isoelectronic series.

The reduced coupling constants taken as $j_{XF} = J_{XF}/\gamma_X\gamma_F$ (where j_{X-F} is in Hz, γ_X and γ_F are nuclear moments in nuclear magneton units divided by the spin I in units of $\hbar$) for fluorides of the first period elements are: NF_4^+ 110.35; NF_3 75.45; ONF_3 63.90; CF_4 38.8; BF_3 1.11; BF_4^- 0.12; BeF_4^{2-} 8.00; BeF_3^- 8.73; BeF_2 9.60; and HF 17.752 (10–15). These reduced couplings j_{AB} are related to those defined by Pople and Santry (16), K_{AB}, given in units of cm^{-3} by the following conversion formula.

$$[6] \qquad K_{AB} = \frac{h}{\mu_N^2} j_{AB},$$

where $j_{AB} = J_{AB}/\gamma_A\gamma_B$ as defined above. $h =$ Plank's constant and μ_N is the nuclear magneton in ergs G^{-1}. The factor $h/\mu_N^2 = 2.598 \times 10^{20}$ $erg^{-1}\,G^{-2}$ s. The gyromagnetic ratio of all nuclei are positive except for ^9Be where K_{AB} and j_{AB} will differ in sign from J_{AB}.

The correlation of j_{X-Y} in a series of compounds of related symmetry with atomic number is now well established for Y = H and X = a central atom in a molecule or ion (17, 18), and some correlation is also noted for Y = F (19, 20). The linear relation $|j|^{1/2} = AZ_X + B$ where A and B are empirical constants is widely applicable.

We have indicated (17) that the origin of this empirical law lies in the magnitude of the '*s*' electron contact interaction which is always positive because it is the square of the state function at the nucleus. Since, however, it would be unlikely that j could change sign in a series of compounds which fit the linear relation fairly well, we have taken this to indicate all such couplings j have the same sign. There has as yet been no experimental determination of relative signs which contradicts this statement.

Before proceeding further with a discussion of the fluorine compounds it is profitable to illustrate how well the couplings to protons follow the magnitude of the '*s*' electron contact interaction as a function of atomic number. Since the earlier publications (17, 18) more experimental determination of spin–spin coupling constants have been made and it is also possible to obtain fairly reliable estimates of the contact interaction since such data has been important in the measurement of the isotropic contributions to hyperfine interactions in e.p.r. spectra. In Fig. 3(*a*) the dependence of the contact interaction $|\Psi^2_{ns}(0)|^{1/2}$, where n is the valence shell of the atom, is given as a function of atomic number for a wide variety of elements. Curve (1) refers to the alkali metal atoms, curve (2) to the group IV elements, and curve (3) to the group VI elements. After the first 10 elements the contact interaction is close to a linear dependence on the atomic number of the atom.

Some remarks are necessary regarding the source and precision of the data. Fermi-contact interactions can be determined from hyperfine structure separations in atoms which have simple spectroscopic states (21) or by using an empirical formula due to Goudsmit (22) based on pseudo-hydrogen-like behavior of more complex atoms. In some cases refined Hartree–Fock wave functions are available from computer calculations and these give a good estimation of the amplitude of the state function at the nucleus (23, 24). A further source of data is to be found in the book by Kopfermann (25).

Several corrections should be applied in order to get precise estimates of the contact energy. These include relativistic corrections which are more serious with heavy atoms, the finite size of the nucleus, and spin polarization of inner '*s*' shells (23, 26). Some of the data in Fig. 3(*a*) is corrected and some relies on the point nucleus model with no corrections. The refinements even

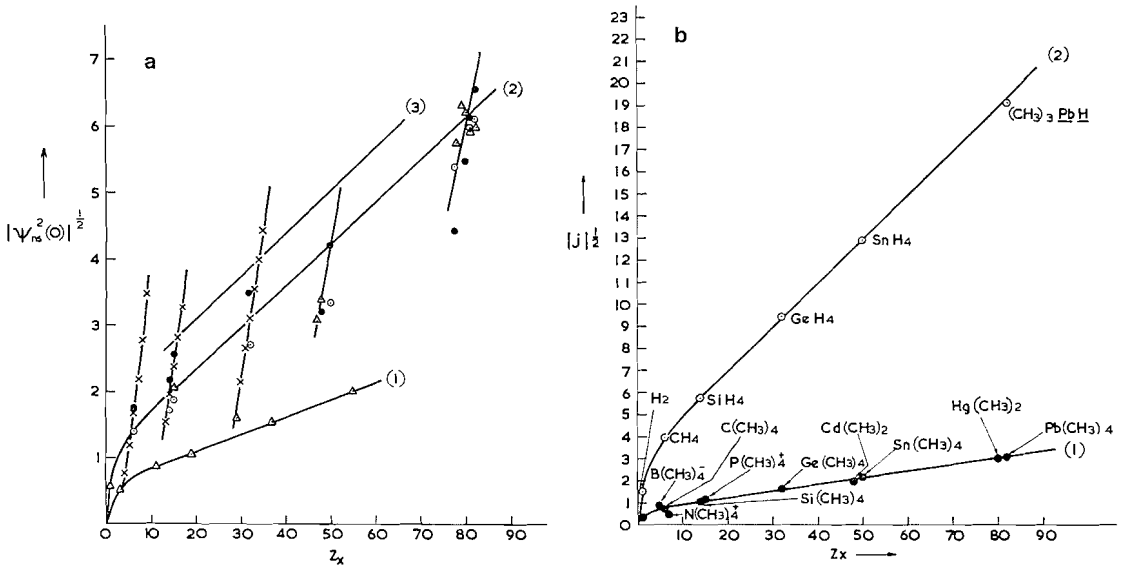

FIG. 3. (*a*) Values $|\Psi^2_{ns}(0)|^{1/2}$ for atoms plotted versus atomic number Z_X of the atoms. The designation of points relates to the method of calculating $|\Psi^2_{ns}(0)|$: (×) self-consistent field calculation (23); △ hyperfine structure separations; (●) Hartree–Fock wave function (24); (⊙) Goudsmit method (22). (*b*) Reduced coupling constants $|j_{X-H}|^{1/2}$ and $|j_{X-C-H}|^{1/2}$ plotted as a function of atomic number Z_X. Note that changes of hybridization at 'X' have been accounted for in H_2, $Cd(CH_3)_2$, and $Hg(CH_3)_2$.

with heavy atoms is not significant enough to affect the overall correlation represented in Fig. 3(*a*). The units of $\Psi^2_{ns}(0)$ are atomic and may be converted to cm^{-3} by multiplying by a factor $a_0{}^3$ in cm^3.

Remarkable agreement with this Z_X dependence is shown in the plot of $|j|^{1/2}$ versus Z_X (Fig. 3(*b*)) for couplings in the symmetrical tetrahedral species XH_4 and $X(CH_3)_4$. Some of this data has been presented before but more comprehensive values of $|j|$ are now available (17–19). The vertical scales in Figs. 3(*a*) and 3(*b*) for $|\Psi^2_{ns}(0)|^{1/2}$ and $|j|^{1/2}$ have been arranged so that for the group IV elements C, Si, Ge, Sn, and Pb the two curves designated (2) in both Figs. 3(*a*) and 3(*b*) are actually coincident. There was too much data available to combine the two dependences in one graph. Curve (1) in Fig. 3(*b*) refers to the indirect couplings j_{X-C-H}. Both $|j|^{1/2}$ and $|\Psi^2_{ns}(0)|^{1/2}$ give a nonlinear dependence up to element 10, neon, where the lack of shielding by d shells produces a deviation from the equations $|j|^{1/2} = AZ_X + B$ and $|\Psi^2_{ns}(0)|^{1/2} = aZ_X + b$ where A, B and a, b are empirical constants. The parallelograms bounded by curves (2) and (3) for groups IV and VI in Fig. 3(*a*) are completed by the variation of $|\Psi^2_{ns}(0)|^{1/2}$ across a period of the periodic table. This produces a much larger variation in $\Psi^2_{ns}(0)$. The lines from left to right with the much steeper slope correspond to the 2nd period Li to fluorine, 3rd period Na to Cl, 4th period K to Br, and 5th period Rb to I. The data is much more fragmentary for the heavy element elements. The transition period elements where the '*s*' contact interaction has not been evaluated must have low values of $|\Psi^2_{ns}(0)|$, though the apparent linearity of $|\Psi^2_{ns}(0)|^{1/2}$ versus Z_X cannot continue to give a zero value at any finite Z_X. The general appearance of Fig. 3(*a*) is:

(a) vindication of the parallelogram rule for couplings presented earlier (19);

(b) excellent demonstration that the value of j is dominated by 'Fermi' contact interaction terms; and

(c) an explanation of the very low values of j in compounds where fluorine is directly bonded to a transition metal such as WF_6 (11), MoF_6 (12), and NbF_6^- (28).

The obvious problem of taking the square root of a number which may have a negative sign for j can be circumvented by the fact that $\Psi^2_{ns}(0)$ is always positive and the sign contribution to j arises from another term.

Can. J. Chem. Downloaded from www.nrcresearchpress.com by 210.87.254.42 on 09/05/12
For personal use only.

Can. J. Chem. Downloaded from www.nrcresearchpress.com by 210.87.254.42 on 09/05/12
For personal use only.

Pople and Santry (16) express the contract contribution to 'K', a reduced coupling constant, as

$$[7]\quad K_{AB}=\left(\frac{64\pi^2}{9}\right)\beta^2(S_A|\delta(r_A)|S_A)\times(S_B|\delta(r_B)|S_B)\pi_{s_As_B}$$

where

$$[8]\quad \pi_{\mu\nu}=4\sum_{i}^{occ}\sum_{j}^{unocc}(\epsilon_i-\epsilon_j)^{-1}C_{i\mu}C_{i\nu}C_{j\mu}C_{j\nu}.$$

$(\varepsilon_i-\varepsilon_j)$ are the energy differences between the highest occupied molecular orbital and the excited triplet states j which are unoccupied.

$C_{i\mu}$, C_{iv}, etc. are coefficients of the atomic orbital 's' wave functions used in the linear combination atomic orbital approximation. Pople and Santry (16) point out that the sign of K resides in the term $\pi_{\mu\nu}$. The matrix elements

$$[9]\quad (S_A|\delta(r_A)|S_A)(S_B|\delta(r_B)|S_B)=|\Psi_{ns_A}(0)|^2|\Psi_{ns_B}(0)|^2$$

are always real and positive. The dependence of j or K on Z_X relates only to the absolute magnitudes as we point out (17). In the average energy approximation when $\Sigma_i\Sigma_j(\varepsilon_i-\varepsilon_j)$ is replaced by an average energy, the sign information is also lost. Pople and Santry (16) further show that for directly bonded atoms where the s electrons on one atom are tightly bound, i.e. the energy of an s electron is well below that of the p electron function with which it is mixed and the s electron on the other atom, then the value of j may become *negative*. They predict that such a factor does produce a negative j in CF_4 and HF and indeed the C—F coupling in CF_4 has been shown to be opposite in sign to C—H which is positive (29, 30).

We may write the coupling constant K in the following form.

$$[10]\quad K_{AB}=j_{AB}\cdot\frac{h}{\mu_N^2}=a\pi_{s_As_B}|\Psi^2{}_{ns_A}(0)||\Psi^2{}_{ns_B}(0)|$$

a is a numerical constant and $\pi_{s_As_B}$ is of uncertain sign. Combining all numerical constants and adding the empirical law for the dependence of $|j|$ and $|\Psi^2{}_{ns}(0)|$ on Z_X,

$$[11]\quad |j_{AB}|^{1/2}=b(\pm1)^{1/2}[\pi_{s_As_B}|\Psi^2{}_{ns_A}(0)||\Psi^2{}_{ns_B}(0)|]^{1/2}=(\pm1)^{1/2}[AZ_X\pm B].$$

The vertical scale of $|j|^{1/2}$ is a real axis in Fig. 3(*b*) for $|j_{X-H}|$, curve (2), and an imaginary axis for the $|j_{X-C-H}|$, curve (1). It is always a real axis for $|\Psi^2{}_{ns}(0)|^{1/2}$.

The question arises in some cases when the empirical constant B is negative that $|j|^{1/2}$ becomes zero at some finite Z_X. When $AZ_X < B$ a change in sign of the term $[AZ_X + B]$ occurs. We must interpret this as merely a discontinuity in the periodic dependence of $|\Psi^2{}_{ns}(0)|^{1/2}$ as indicated in Fig. 3(*a*), for each period of the periodic table.

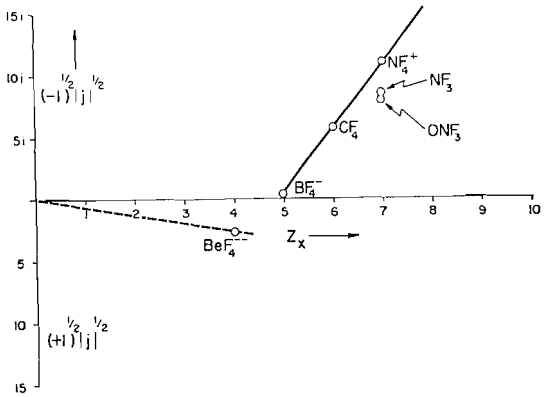

FIG. 4. Reduced coupling constants $|j_{X-F}|^{1/2}$ in simple fluorides of the second period.

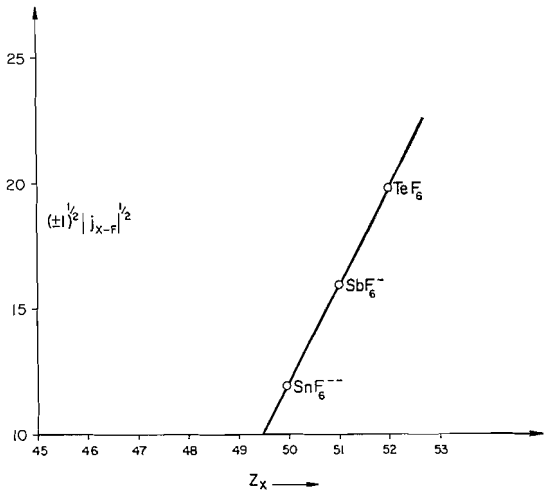

FIG. 5. Reduced coupling constants $|j_{X-F}|^{1/2}$ in the isoelectronic series TeF_6, SbF_6^-, and SnF_6^{2-} as a function of atomic number.

The isoelectronic series NF_4^+, CF_4, BF_4^-, and BeF_4^{2-} are an example of a negative B and

Can. J. Chem. Downloaded from www.nrcresearchpress.com by 210.87.254.42 on 09/05/12
For personal use only.

almost zero coupling at boron. In Fig. 4 the empirical law

$$[12] \quad |j_{X-F}|^{1/2} = (\pm 1)^{1/2}[5.37\, Z_X - 26.6]$$

for BF_4^- (13, 14), CF_4 (31), and NF_4^+ (10) is illustrated. It is evident that there is a change in sign of the coupling in going from BF_4^- to BeF_4^{2-}. We suggest in agreement with Pople (16) that j is negative in BF_4^-, CF_4, and NF_4^+ but positive[1] in BeF_4^{2-}. In order to represent this discontinuity in some manner in Fig. 4, the positive ordinate is labelled $(-1)^{1/2}j^{1/2}$ while the negative ordinate is labelled $(+1)^{1/2}j^{1/2}$. Further coupling constants j for simple fluorides of the second period elements are also plotted in Fig. 4. They appear at sensible positions with respect to the symmetric tetrahedral species. As a further illustration of the applicability of this particular type of Z_X dependence the recently available series TeF_6, SbF_6^-, and SnF_6^{2-} (11, 31) are also plotted in Fig. 5. Here the sign of j is uncertain but the linear dependence is quite clear.

Kinetic Studies on $(NH_4)_2BeF_4$ Solutions

The line widths of the ^{19}F n.m.r. lines in ammonium tetrafluoroberyllate solutions vary with concentration as demonstrated in Fig. 1. Qualitatively an increase in concentration of $(NH_4)_2BeF_4$ at ambient temperature 33 °C results in an increase in line width for all three species present in solution F^-, BeF_3^-, and BeF_4^{2-}. The fact that the line width of the BeF_4^{2-} ion resonance is a function of concentration indicates that a fluoride ion exchange process occurs in addition to simple dissociation and re-association. The line widths of all signals have been measured and in the case of the BeF_4^{2-} and BeF_3^- resonances a mean of four measurements involving each component of the quadruplet is obtained. The mechanism of the kinetic processes measured corresponds to the following scheme.

$$[13] \quad BeF_4^{2-} \underset{k_{-1}}{\overset{k_1}{\rightleftarrows}} BeF_3^- + F^-$$

$$[14] \quad BeF_4^{2-} + F^{*-} \xrightarrow{k_2} BeF_3F^{*2-} + F^-$$

$$[15] \quad BeF_3^- + F^{*-} \xrightarrow{k_3} BeF_2F^{*-} + F^-$$

$$[16] \quad BeF_4^{2-} + BeF_2F^{*-} \xrightarrow{k_4} BeF_3F^{*2-} + BeF_3^-$$

[1]The actual sign of J will be negative because γ_{Be} is negative.

An analysis of this reaction scheme can be made according to standard methods (32). Let the sites BeF_4^{2-}, BeF_3^-, and F^- be denoted as A, B, and C respectively. The mean lifetime of a fluorine nucleus in these sites can be written (32)

$$[17] \quad \tau_A^{-1} = \frac{1}{[BeF_4^{2-}]}\frac{d[BeF_4^{2-}]}{dt}$$

$$[18] \quad \tau_B^{-1} = \frac{1}{[BeF_3^-]}\frac{d[BeF_3^-]}{dt}$$

$$[19] \quad \tau_C^{-1} = \frac{1}{[F^-]}\frac{d[F^-]}{dt}.$$

The full line width at half height $\Delta\nu_{1/2}$ in Hz is related to the mean lifetime τ_i on site 'i' by the simple equation

$$[20] \quad \tau_i^{-1} = \pi\Delta\nu_{1/2} - \frac{1}{T^*_2},$$

where $1/T^*_2$ is the contribution to line width from all other sources than the exchange processes. The kinetic scheme represented by eqs. [13] to [16] leads to the following expressions for τ_A, τ_B, and τ_C.

$$[21] \quad \tau_A^{-1} = k_1 + k_2[F^-] + k_4[BeF_3^-] = k_1 + (k_2 + k_4)K_c(3/4)R$$

$$[22] \quad \tau_B^{-1} = (k_{-1} + k_3)K_c(3/4)R + k_4K_c(9/16)R^2$$

$$[23] \quad \tau_C^{-1} = (k_{-1} + k_3)(3/4)K_cR + k_2K_c(9/16)R^2,$$

where $K_c = 8.0 \pm 0.9 \times 10^{-2}$ mole kg^{-1} at 33 °C determined earlier and $R = (I_4/I_3)$ as in eq. [5]. By plotting τ_A^{-1} versus R, k_1 and $(k_2 + k_4)$ were determined from the slope of the lines and the intercepts when $R = 0$. By fitting the values of τ_B^{-1} and τ_C^{-1} to equations of the form quadratic in R (eqs. [22] and [23]) all rate constants could be separately determined.

It is known that line widths are not a very accurate method of determining rate constants (33), however, the linearity of experimental points in eq. [21] is quite satisfactory and the quadratic behavior of points in eqs. [21], [22] is also quite good. We estimate that the rate constants determined and listed below should

be regarded as satisfactory within a factor of three.

$$k_1 \cong 23.8\ s^{-1}$$
$$k_{-1} \cong 3 \times 10^2\ mole^{-1}\ s^{-1}$$
$$k_2 \cong 4.3 \times 10^2\ mole^{-1}\ s^{-1}$$
$$k_3 \cong 8 \times 10^2\ mole^{-1}\ s^{-1}$$
$$k_4 \cong 4.5 \times 10^2\ mole^{-1}\ s^{-1}$$

It is interesting that the slowest process is the dissociation or water replacement involving the tetrahedral arrangement BeF_4^{2-} but that fluoride ion exchange as in [14] or [16] is still quite fast. The values of T_{2A}^*, T_{2B}^*, and T_{2C}^* are 0.8 s, 0.8 s, and 0.1 s respectively. These are reasonable values and allow some additional consistency in the kinetic analysis. They correspond to relaxation times plus inhomogeneity broadening effects in the absence of the exchange processes considered. The values 0.8 s indicate the field inhomogeneity estimated at $\sim$ 0.5 Hz. The fluoride ion ^{19}F relaxation time is considerably shorter and this is consistent with our own unpublished observations that the fluoride ion takes part in other exchange processes not involving the fluoroberyllate ions. These processes are at present under study.

Acknowledgment

The support of this research by the National Research Council of Canada is gratefully acknowledged.

1. J. B. Leane and R. E. Richards. Spectrochim. Acta, **10**, 154 (1957).
2. R. Blinc and I. Levstek. Phys. Chem. Solids, **12**, 295 (1960).
3. H. S. Gutowsky and C. J. Hoffmann. J. Chem. Phys. **19**, 1259 (1951).
4. P. F. Francis and I. J. Lawrenson. J. Inorg. Nucl. Chem. **26**, 1462 (1964).
5. H. S. Gutowsky and C. S. Juan. J. Chem. Phys. **40**, 1714 (1964).
6. D. A. Everest. The chemistry of beryllium. Elsevier Publishing Co., 1964.
7. J. A. Pople. Mol. Phys. **1**, 168 (1958).
8. K. E. Kleiner. Soviet research in fluorine chemistry. Part II. Consultants Bureau Inc., New York. 1959. p. 85.
9. R. E. Connick and R. E. Poulson. J. Am. Chem. Soc. **79**, 5153 (1957); J. Phys. Chem. **63**, 568 (1959).
10. K. O. Christe, J. P. Guertin, A. E. Parlath, and W. Sawodny. Inorg. Chem. **6**, 533 (1967).
11. E. L. Muetterties. J. Am. Chem. Soc. **81**, 1084 (1959).
12. N. Bartlett, J. Passmore, and E. J. Wells. Chem. Commun. 213 (1966).
13. K. Kuhlmann and D. M. Grant. J. Phys. Chem. **68**, 3208 (1964).
14. R. Haque and L. W. Reeves. J. Phys. Chem. **70**, 2753 (1966).
15. C. McLean. Discussions Faraday Soc. No. 34, 200 (1962).
16. J. A. Pople and D. P. Santry. Mol. Phys. **8**, 1 (1964).
17. L. W. Reeves and E. J. Wells. Can. J. Chem. **41**, 2698 (1963).
18. L. W. Reeves. J. Chem. Phys. **40**, 2128 (1964).
19. L. W. Reeves. J. Chem. Phys. **40**, 2423 (1964).
20. P. T. Inglefield and L. W. Reeves. J. Chem. Phys. **40**, 2425 (1964).
21. E. Fermi. Z. Physik, **60**, 320 (1930).
22. S. Goudsmit. Phys. Rev. **43**, 636 (1933).
23. D. M. Whiffen. J. Chem. Phys. 1589 (1964).
24. G. W. Smith. J. Chem. Phys. **42**, 435 (1965).
25. H. Kopfermann. Nuclear moments. *Translated by* E. E. Schneider. 2nd ed. Academic Press, New York. 1957.
26. N. F. Ramsey. Nuclear moments. Wiley Publ. Co., New York. 1953.
27. G. W. Smith. General Motors Research Publication G.M.R. 444 Warren, Michigan.
28. K. J. Packer and E. L. Muetterties. J. Am. Chem. Soc. **85**, 3035 (1963).
29. G. V. D. Tiers. J. Phys. Chem. **67**, 1373 (1963).
30. N. Muller and D. T. Carr. J. Phys. Chem. **67**, 112 (1963).
31. P. A. W. Dean and D. F. Evans. Proc. Chem. Soc. 407 (1964).
32. A. Loewenstein and T. M. Connor. Ber. Bunsenges. Physik. Chem. **67**, 280 (1963).
33. L. W. Reeves. Advan. Phys. Org. Chem. **3**, 187 (1965).

Can. J. Chem. Downloaded from www.nrcresearchpress.com by 210.87.254.42 on 09/05/12
For personal use only.

Can. J. Chem. Downloaded from www.nrcresearchpress.com by 210.87.254.40 on 09/05/12
For personal use only.

Chemical shifts for compounds of the group IV elements silicon[1] and tin[2]

B. K. HUNTER AND L. W. REEVES
Chemistry Department, University of British Columbia, Vancouver, British Columbia

Received August 2, 1967

Chemical shifts for ^{29}Si in seven series of molecules of the type X_nSiY_{4-n} have been measured where Y is an alkyl group and X varies widely in electronegativity. A considerable amount of proton and fluorine chemical shift data has been obtained for the same compounds and in one series $(CH_3)_nSiCl_{4-n}$ the ^{13}C chemical shifts in the methyl groups have been measured.

The gross features of the ^{29}Si chemical shifts are understood by considering the series $(Alkyl)_3SiX$ with the electronegativity of X widely varied. The hybridization at silicon is approximately conserved in these series and the theoretically anticipated linear dependence on electronegativity of X is demonstrated. The ligands X = O, N, and F are exceptional and these ^{29}Si chemical shifts have a high field shift. This additional shielding has been associated with $(p \rightarrow d)\pi$ bonding. The approximate nature of present chemical shift theories is not likely to provide a measure of the order of $(p \rightarrow d)\pi$ bonding.

The ^{29}Si chemical shifts in the series X_nSiY_{4-n} are discussed and also indicate a net shielding effect with $(p \rightarrow d)\pi$ bonding. A comparison is always made with corresponding ^{13}C chemical shifts. A long range proton–proton coupling in molecules Me_3SnX and Me_2SnX_2, *H*—C—Si—C—*H*, is observed when and only when X = O, (N?), F.

^{119}Sn chemical shifts in a series of alkyltin compounds have been measured. The same dependence on the electronegativity of X in the series $(Alkyl)_3SnX$ is noted, but the variation of X is much more limited. Some shielding due to $(p \rightarrow d)\pi$ bonding in the series $(n\text{-Butyl})_nSnCl_{4-n}$ is suggested. The tin chemical shift has been measured as a function of concentration and solvent for simple methyltin bromides and chlorides. In donor solvents, it has been possible to obtain equilibrium constants for complex formation from tin dilution chemical shifts. The nature of the bonding in complexes suggested previously is consistent with the variations in the coupling constant $|J_{Sn-C-H}|$ with concentration. The distinction between ionization and complex formation with the solvent for $(CH_3)_2SnCl_2$ can be made on the basis of the concentration dependence of $|J_{Sn-C-H}|$.

The spin–lattice relaxation time T_1 for ^{13}C and ^{29}Si in natural abundance in several pure degassed compounds has been measured. These are not in the case of ^{13}C (as has been suggested) of the order several minutes, but are always less than 50 s and in one case as low as 3–4 s. Both ^{29}Si and ^{13}C T_1 values follow what might be expected on the basis of a dipole–dipole mechanism from the closest protons. The short value of 35 s in CS_2 is probably a result of spin–rotation interaction in the liquid state.

Canadian Journal of Chemistry, 46, 1399 (1968)

Introduction

Although ^{13}C chemical shifts in organic compounds are becoming available at an increasing rate (1, 2), so far only two papers have appeared in which ^{29}Si and ^{119}Sn have been studied (3, 4). In both cases the investigators have lacked a systematic set of compounds, but the work on ^{119}Sn carried out by Lauterbur and Burke with tin compounds was a comprehensive investigation which included solvent effects and predicted a considerable use for tin magnetic resonance in following the nature of tin compounds in solution. Reeves and co-workers recently measured the spin–spin coupling constant for ^{117}Sn—^{119}Sn in hexamethylditin from a study of the ^{119}Sn spectrum (5).

Clearly, there is a need for further data, particularly of a systematic nature, regarding the chemical shifts of Si and Sn in organometallic compounds. It is the aim of this study to fill some of this gap, especially with respect to ^{29}Si chemical shifts which have not yet been studied systematically.

Experimental

(a) N.M.R. Measurements

Proton magnetic resonance measurements were made on a Varian HA100 or a Varian A60 spectrometer. With silicon compounds, because of the possibility of near overlap with the tetramethylsilane (TMS) signal, a small amount of benzene was used to provide a lock signal and to serve as an internal reference peak. Subsequently, all proton chemical shift data was referenced to 1% TMS with low field shifts reported with a negative sign in parts per million. The tin compounds were usually measured on a Varian A60 with a 1% TMS internal reference signal included. With suitable care, the chemical shifts of protons are given to ± 0.01 p.p.m. and coupling constants to ± 0.05 Hz.

Fluorine n.m.r. spectra were obtained from either Varian HR 60 or HR 100 spectrometers tuned to 56.4 MHz or 94.1 MHz respectively. Monofluorotrichloromethane (FTCM) was added in small amount ($\sim 2\%$ by volume) to each solution and served as an internal standard for fluorine chemical shift measurements. Spin

[1]Presented at the 8th E.N.C. meeting, Pittsburgh, Pa. March (1967).

[2]Presented at the 7th E.N.C. meeting, Pittsburgh, Pa. February (1966).

Can. J. Chem. Downloaded from www.nrcresearchpress.com by 210.87.254.40 on 09/05/12
For personal use only.

coupling constants to fluorine have a mean square deviation ± 0.1 Hz, while fluorine chemical shifts are given to ± 0.01 p.p.m.

^{29}Si nuclear magnetic resonance spectra (n.m.r.) were obtained from a spectrometer assembled largely from parts manufactured by Varian Associates. The magnetic field strength was 9.41 kG, and the detecting frequency 7.95 MHz. Field sweep was provided by a V3507 slow sweep unit and signals were recorded on a Varian G10 recorder. The V4311 radiofrequency (r.f.) transmitter and receiver unit was driven by highly regulated power supplies which allow increased stability over those available in a Varian spectrometer. The B+ voltage was supplied from a Lambda Electronics Corporation model 32 power supply and the 12 V d.c. filament source was a Lectronic Research Associates Inc. model T.R. 32–34 0.01% regulated power supply. The silicon signals were all recorded with rapid passage dispersion mode ($\sim$ 1 G/min sweep rates) at high r.f. power levels. Relaxation time measurements (T_1) for ^{13}C and ^{29}Si were measured as will be described in the Results section of this paper. The samples were neat liquids in 10 mm o.d. thin wall tubes and immersed in some reference liquid in standard 15 mm o.d. test tubes. The external standard was tetramethoxysilane in almost all cases. Sweep rate calibrations were achieved by using a sample of trimethylsilane. The doublet structure with spacing 184 Hz was measured from the proton spectrum and this corresponds to 23 p.p.m. in the silicon spectrum. The sweep standard was observed with increasing and decreasing magnetic field and the doublet recorded. The external reference and unknown sample were then recorded at exactly the same sweep rates four times in each direction and finally replaced by the sweep standard to assure no drift in sweep rates.

The ^{119}Sn nuclear magnetic resonance signal was observed with a modified Varian V4310C r.f. unit at 22.3822 MHz in a field 14.1 kG. In this case the signals are somewhat stronger and display through a Varian V3521 base line stabilizer was possible. This latter instrument employs an audio modulation frequency of 1996 Hz in our case, and in most experiments an absorption-made signal was presented. The modulation frequency provides a calibration for spectra. Heteronuclear double resonance at high power levels at the proton resonance frequency using an NMR Specialties S.D. 60 decoupler causes collapse of the scalar coupling to protons and simplifies the measurement of tin chemical shifts. In many cases, the ^{119}Sn signal is badly split due to coupling to many non-equivalent protons in the molecule.

(b) Sample Preparation

Organosilicon compounds were purchased from several sources (N.M.R. Specialties Co.; Peninsular Chem-Research Corp.; Aldrich Chemical Co.). Several samples were kindly donated by the Dow Corning Corporation. The purchased and donated samples were used without further purification.

Several samples were prepared by standard techniques (6) as listed below. Standard vacuum techniques were used where necessary. Samples were usually purified by distillation and purities checked by n.m.r. spectra run on a Varian A-60.

The silanes $(C_6H_5)_2SiH_2$, $(C_6H_5)SiH_3$, SiH_4, Me_3SiH, Me_2SiH_2, and $MeSiH_3$ were prepared by reduction of the corresponding chlorides with $LiAlH_4$ under a dry nitrogen environment.

The methyl and phenyl fluorides were prepared from the chlorides using various fluorinating agents as shown below. Silicon tetrafluoride (SiF_4) was prepared from the reaction of Na_2SiF_6 and H_2SO_4 on a silica gel (7). The phenylmethylsilanes were prepared from phenyllithium and the corresponding methylchlorosilanes. Triphenylsilane was prepared from phenylmagnesium bromide and trichlorosilane.

Preparation of fluorosilanes

Compound	Fluorinating agent
Me_3SiF	AgF/Et_2O
Me_2SiF_2	PbF_2/reflux
$MeSiF_3$	HF/Et_2O (low yield)
ϕ_2SiF_2	HF/Et_2O

The organotin compounds were obtained from Peninsular Chemical Company or graciously supplied by M and T chemical company as research samples through the agency of Dr. Considine. In most cases, the purity of the supplied material was adequately assured from the proton magnetic resonance spectrum, but in a few cases distillation of the materials was made to provide a pure sample.

Results

Silicon Compounds

(a) Accuracy of Silicon-29 Chemical Shift Data

The error in the ^{29}Si shift measurements is estimated to be ± 1 p.p.m. This estimate is based on two facts. First, the standard deviation on a series of seven measurements of the chemical shift in a $(MeO)_4Si$/TMS sample was found to be 0.4 p.p.m. Second, many samples give ^{29}Si spectra which are split into multiplets by direct ^{29}Si—H coupling. The coupling constants may be measured from the ^{29}Si spectrum and compared with the value obtained from the ^{1}H spectrum. The values from ^{29}Si spectra consistently agree to ± 5 Hz with those obtained from ^{1}H spectrum. For example, $J_{^{29}Si-H}$ in ϕ_2SiMeH was found from the ^{29}Si spectrum to be 190–200 Hz and from the ^{1}H spectrum to be 196 Hz. In some cases, for example the methylchlorosilanes, the ^{29}Si spectrum cannot be observed except under very fast sweep and higher than normal power conditions. The errors are consequently somewhat larger, about ± 5 p.p.m. Also, some signals, particularly tetravinylsilane, are considerably broadened by spin coupling and the error is increased to ± 3 p.p.m.

While the random error in the ^{29}Si measurements is ± 1 p.p.m., there is a systematic error in the measurements which has not been taken into account. Since an external standard is being

Can. J. Chem. Downloaded from www.nrcresearchpress.com by 210.87.254.40 on 09/05/12
For personal use only.

used, a correction should be made for differences in bulk susceptibility of the various samples (8). This correction may be applied using the following equation.

$$\delta_{\text{sphere}} = \delta_{\text{obs}} + \frac{2\pi}{3}(\chi_{v,\text{ref}} - \chi_{v,\text{sample}}),$$

where δ_{sphere} = spherical or true chemical shift, δ_{obs} = observed chemical shift, $\chi_{v,\text{ref}}$ = volume susceptibility of reference, and $\chi_{v,\text{sample}}$ = volume susceptibility of sample. The bulk susceptibility correction will be less than 1 p.p.m. and can probably be ignored. As a check, the chemical shift between Me_3SiH and $(MeO)_4Si$ was measured from internal and external standards. For the internal standard the shift is 62.6 p.p.m. and for the external standard it is 61.5 p.p.m. It is questionable whether or not this difference is significant. In any case, the small error introduced by failure to apply a bulk susceptibility correction is bound to be preferable to the possibility of larger errors introduced by solvent effects.

(b) N.M.R. Studies of Silicon Compounds

The main object has been to collect as complete data as is possible on a series of organosilicon derivatives of related structure. Seven series of the type SiX_nY_{4-n} have been measured where the ligands X and Y are varied among the following: —OMe, —H, —OEt, —OAc, —Cl, —ϕ, —F, and —Me. An incomplete set of data on the vinyl ligand is also available as well as other miscellaneous silicon chemical shifts which do not fall into regular series. The data is compounded into a series of tables which have adequate legends. In Appendix I, all previously reported silicon chemical shifts are also listed in order to serve as a reference point (2, 3). Whenever there was overlap with this previous data and disagreement in values occurred, our measurements were repeated several times in order to ensure that our reported values were correct. An example of a typical silicon-29 spectrum with calibrated sweep is shown in Fig. 1. In 1A, trimethylsilane with tetramethoxysilane as an external sample was recorded in one sweep. The doublet with 184 Hz, splitting for trimethylsilane is clearly seen. In the lower spectrum 1B at the same sweep rate and in the same field direction, the trimethylsilane is replaced by TMS and the chemical shift of 79.5 p.p.m. is recorded. The average chemical shift reported in the tables is

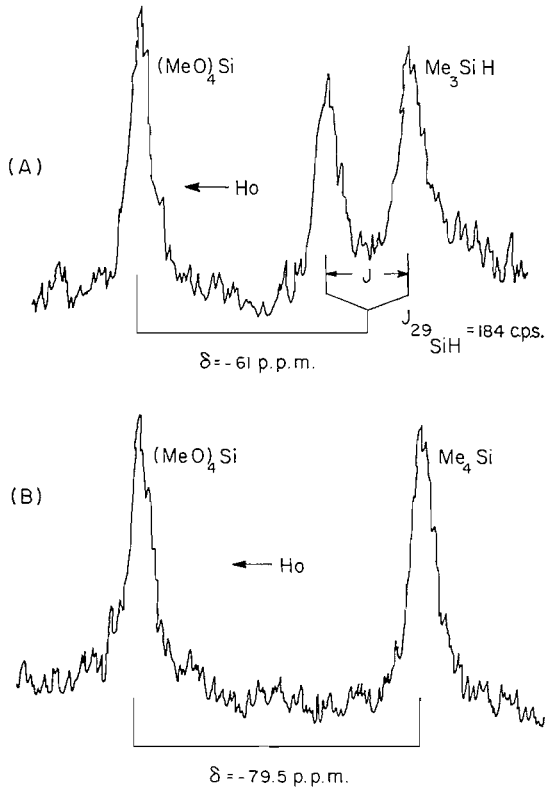

FIG. 1. ^{29}Si magnetic resonance spectra in rapid passage dispersion mode. The upper spectrum is used to calibrate the sweep. The sample is tetramethoxylane with trimethylsilane as an external sweep standard. The lower spectrum shows the −79.5 p.p.m. chemical shift change between $(CH_3)_4Si$ and $(CH_3O)_4Si$ at the same sweep rate.

obtained, of course, from several such sweeps in both increasing and decreasing field direction.

The general features of the data in Tables I to VII inclusive can be summarized as follows. When an oxygen ligand replaces methyl groups on silicon, there is a shift to low field for the first alkoxy group, and for the further addition of alkoxy groups a shift change to high field is observed. This behavior is very similar to that reported by Lauterbur (2) for the methoxy series. There are small differences of up to 10 p.p.m. in the range of chemical shifts for methoxy, ethoxy, and acetoxy groups. The dominant effect, therefore, must be the exchange of carbon for oxygen in the bonding to silicon. Changes in proton chemical shifts of the methyl groups directly bonded to silicon are small and much less characteristic of the ligands on silicon. The value of $|J_{^{13}C-H}|$ in the silicon methyl increases

TABLE I

N.m.r. data for $Me_xSi(OMe)_{4-x}$

	Si[a] (p.p.m.)	Me[b] (p.p.m.)	OMe[b] (p.p.m.)	$J_{^{29}SiCH}$ (c.p.s.)	$J_{^{29}SiOCH}$ (c.p.s.)	$J_{^{13}CH}$[c] (c.p.s.)
Me_4Si	−79.5	−0.0	—	6.62	—	118.1
Me_3SiOMe	−96.5	−0.21	−3.49	6.65	4.13	118.0
$Me_2Si(OMe)_2$	−77	−0.19	−3.55	7.2	3.90	118.5
$MeSi(OMe)_3$	−38	−0.12	−3.58	8.35	3.82	119.1
$Si(OMe)_4$	0	—	−3.60	—	3.55	—

[a]Silicon-29 chemical shift in p.p.m. from $(MeO)_4Si$.
[b]^1H chemical shift in p.p.m. from TMS.
[c]$J_{^{13}CH}$ is for a methyl group directly attached to silicon.

with oxygen substitution at silicon, but the effect is much more pronounced with the acetoxy group. The coupling constant $|J_{Si-C-H}|$ is also enhanced as oxygen ligands are added. While the ^{13}C satellites of TMS are single sharp lines, in the case of Me_3SiX and Me_2SiX_2, where X = O, F, fine structure is resolved. In the Me_3SiX compounds, the side bands have a septet structure, while for Me_2SiX_2 compounds, a quadruplet is resolved. For the oxygen and fluorine ligands which are probably bound to silicon by partial $(p \rightarrow d)\pi$ bonds there is a long range proton coupling between equivalent methyl protons, $J_{H-C-Si-C-H}$. The splitting is always $J = 0.35 \pm 0.1$ Hz. We shall consider this feature in the Discussion section.

Tin Compounds

(a) Chemical Shifts

These series of compounds available were not particularly systematic, though some major trends in the effects of substituents can be seen. The chemical shifts measured are listed as miscellaneous tin chemical shifts in Table IX. If the tin compounds are solids, the chemical shifts correspond to measurements in saturated chloroform solutions. The internal or external reference peak is always the ^{119}Sn shift in tetramethyltin. The chemical shift range encountered corresponds to ~250 p.p.m., which is considerably less than the total range of chemical shifts for tin compounds (2, 4, 8). The present list is restricted to alkyltin compounds, and does not include the tetra- and di-valent halides which have large chemical shifts to high field (8). Tin chemical shifts often exhibit a concentration dependence in polar solvents (4), and this was the object of a quantitative study. In the list of tin chemical shifts, solvent conditions are specified where a study was made.

(b) Solvent Dilution Studies

Solvent studies were made on trimethyltin bromide and chloride. The ^{119}Sn resonance position could be located with good precision (±1.0 p.p.m.) to dilutions of approximately 10 mole % in the solvents investigated. These results are plotted for the polar solvents acetone and acetonitrile in Fig. 2. The open circle points are tin chemical shifts relative to the chemical shift equal to zero for tetramethyltin. The right hand scales correspond to this chemical shift in p.p.m. Trimethyltin bromide is a liquid, but trimethyltin chloride is a solid with maximum solubility ~ 40 mole % in acetone and acetonitrile.

Dilution of the two trimethyltin halides in

TABLE II

N.m.r. data for $Me_xSi(OEt)_{4-x}$

	Si[a] (p.p.m.)	Me[b] (p.p.m.)	$J_{^{29}SiCH}$ (c.p.s.)	$J_{^{13}CH}$ (c.p.s.)
Me_4Si	−79.5	0.0	6.62	118.1
Me_3SiOEt	−93	−0.23	6.67	118.0
$Me_2Si(OEt)_2$	−72	−0.20	7.08	118.2
$MeSi(OEt)_3$	−34	−0.16	8.35	119.2
$Si(OEt)_4$	+4	—	—	—

[a]Silicon-29 chemical shift in p.p.m. from $(MeO)_4Si$.
[b]^1H chemical shift in p.p.m. from TMS.

Can. J. Chem. Downloaded from www.nrcresearchpress.com by 210.87.254.40 on 09/05/12
For personal use only.

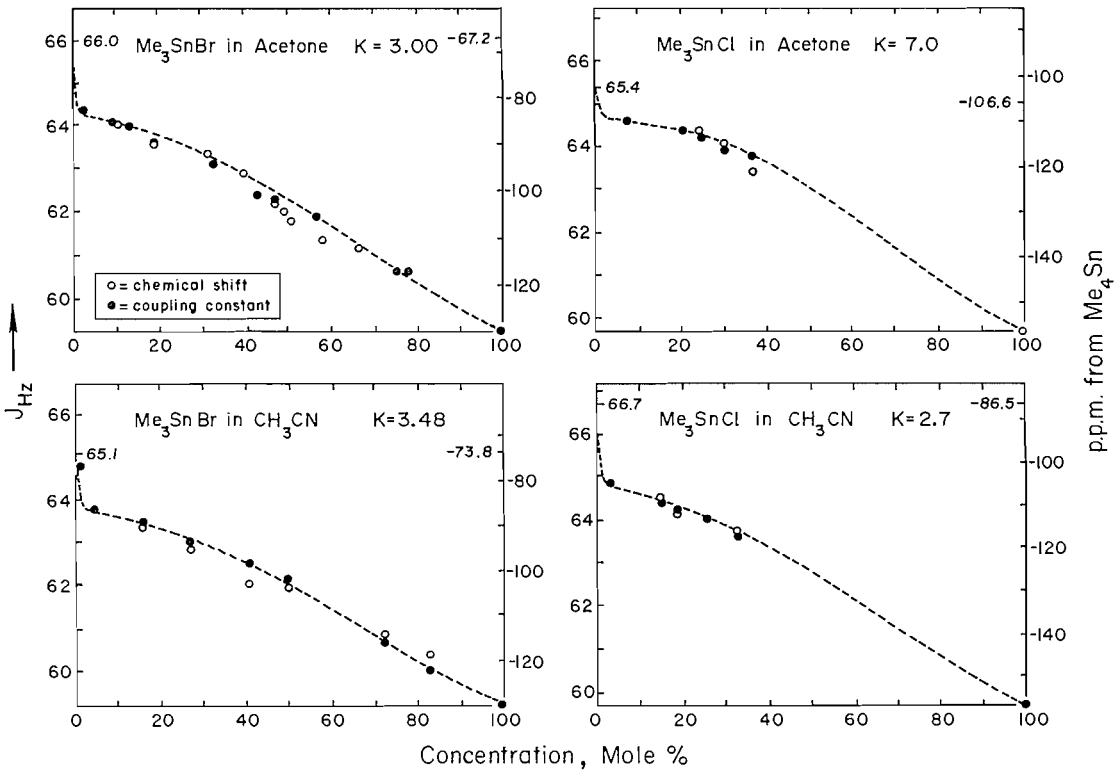

FIG. 2. Concentration dependence of ^{119}Sn chemical shifts and spin-spin couplings J_{Sn-C-H} for trimethyltin halides in donor solvents.

nonpolar solvents, such as chloroform, benzene, and carbon tetrachloride, does not change the chemical shifts of ^{119}Sn more than 5 p.p.m. from the pure compound value. The extrapolated infinite dilution chemical shifts for trimethyltin bromide are +5, 0, and −5 p.p.m. for carbon tetrachloride, benzene, and chloroform respectively. The corresponding figures for trimethyltin chloride are the same within experimental error. The relatively large extrapolation and small observed change leave an uncertainty of approximately ±2 p.p.m. in these figures. The lack of large changes in chemical shift with dilution in these solvents is indicative that no complexing occurs between the tin compound and the solvent and, furthermore, no self-association occurs in the trimethyltin halides. On the other hand, it is clear that some complexing between the trimethyltin halides and acetone and acetonitrile does occur. Further studies on dioxane solutions of trimethyltin bromide were made. These, too, indicated a large change in chemical shift (~ 45

TABLE III

N.m.r. data for $Me_xSi(OAc)_{4-x}$

	Si[a] (p.p.m.)	Me[b] (p.p.m.)	$J_{^{29}SiCH}$ (c.p.s.)	$J_{^{13}CH}$ (c.p.s.)
Me_4Si	−79.5	0	6.62	118.1
Me_3SiOAc	−103	−0.36	7.10	119.5
$Me_2Si(OAc)_2$	−85	−0.53	7.77	121.3
$MeSi(OAc)_3$	−35	−0.67	9.5	123.4
$Si(OAc)_4$	−5	—	—	—

[a]Silicon-29 chemical shift in p.p.m. from $(MeO)_4Si$.
[b]^1H chemical shift in p.p.m. from TMS.

Can. J. Chem. Downloaded from www.nrcresearchpress.com by 210.87.254.40 on 09/05/12
For personal use only.

TABLE IV

N.m.r. data for Me_xSiCl_{4-x}

	Si[a] (p.p.m.)	C[b] (p.p.m.)	Me[c] (p.p.m.)	$J_{^{29}SiCH}$ (c.p.s.)	$J_{^{13}CH}$ (c.p.s.)
Me_4Si	−79.5	190	0	6.62	118.1
Me_3SiCl	−115	176	−0.39	7.00	120.77
Me_2SiCl_2	−120	190	−0.45	7.61	123.6
$MeSiCl_3$	−96	210	−1.05	9.07	125.5
$SiCl_4$	−63	—	—	—	—

[a]^{29}Si chemical shift in p.p.m. from $(MeO)_4Si$.
[b]^{13}C chemical shift in p.p.m. from CS_2.
[c]^{1}H shift in p.p.m. from TMS.

TABLE V

N.m.r. data for $Me_xSi(C_6H_5)_{4-x}$

	Si[a] (p.p.m.)	Me[b] (p.p.m.)	$J_{^{29}SiCH}$ (c.p.s.)	$J_{^{13}CH}$ (c.p.s.)
Me_4Si	−79.5	0	6.62	118.1
$Me_3Si\phi$	−75	−0.26	6.60	119.0
$Me_2Si\phi_2$	−72	−0.52	6.60	120.5
$MeSi\phi_3$	−67	−0.74	6.64	[c]
$Si\phi_4$	[c]	—	—	—

[a]^{29}Si chemical shift relative to $(MeO)_4Si$.
[b]^{1}H chemical shift relative to Me_4Si.
[c]Too insoluble to be measured.

p.p.m. to high field at infinite dilution) consistent with molecular complexing between dioxane and trimethyltin bromide.

These studies were complemented by a similar study of the changes in chemical shift of the protons with dilution in the same solvents. As expected, the only appreciable change in the proton chemical shift occurred in benzene solutions. The changes in chemical shift of the protons of trimethyltin bromide between the pure compound and infinite dilution are −0.033 p.p.m. in $CHCl_3$, −0.066 p.p.m. in acetone, −0.1 p.p.m. in CH_3CN, −0.13 p.p.m. in dioxane, and −0.47 p.p.m. in benzene. These shifts are characteristic only of the well-known changes in chemical shift that occur with non-polar solvents (such as cyclohexane) in benzene due to its large molecular diamagnetic anisotropy (8). The proton magnetic environment must be considered virtually insensitive to the complex formation, which is known to involve donation into d orbitals on the central tin atom. These observations are a complete vindication of the promise held out by Burke and Lauterbur (4) regarding the utility of tin magnetic resonance for the study of solution complexes of tin.

While it is not expected that proton chemical shifts should be sensitive to complexing at the tin

TABLE VI

N.m.r. data for Me_xSiF_{4-x}

	Si[a] (p.p.m.)	Me[b] (p.p.m.)	F[c] (p.p.m.)	$J_{^{29}SiF}$ (c.p.s.)	$J_{^{29}SiCH}$ (c.p.s.)	$J_{^{13}CH}$ (c.p.s.)	J_{HCSiF} (c.p.s.)
Me_4Si	−79.5	0	—	—	6.62	118.1	—
Me_3SiF	−110	−0.19	158	276	7.40	120.0	7.23
Me_2SiF_2	−84	−28	130		7.60		6.25
$MeSiF_3$	[d]	+0.2	133	278	8.8		4.14
SiF_4	[d]	—	161.8	178	—	—	—

[a]^{29}Si chemical shift relative to $(MeO)_4Si$.
[b]^{1}H chemical shift from TMS.
[c]^{19}F chemical shift from $CFCl_3$.
[d]Too volatile to be measured.

Can. J. Chem. Downloaded from www.nrcresearchpress.com by 210.87.254.40 on 09/05/12
For personal use only.

Can. J. Chem. Downloaded from www.nrcresearchpress.com by 210.87.254.40 on 09/05/12
For personal use only.

TABLE VII

N.m.r. data for Me_xSiH_{4-x}

	Si[a] (p.p.m.)	Me[b] (p.p.m.)	H[c] (p.p.m.)	J_{SiH} (c.p.s.)	$J_{^{29}SiCH}$ (c.p.s.)	$J_{^{13}CH}$ (c.p.s.)	J_{HCSiH} (c.p.s.)
Me_4Si	−79.5	0	—	—	6.62	118.1	—
Me_3SiH	−61	−0.20	−4.20	183.8	7.20	119.35	3.76
Me_2SiH_2	−38	−0.26	−4.03	188.5	7.5	120.8	4.15
$MeSiH_3$	[c]	−0.27	−3.71	194.6	7.9	123.6	4.67
SiH_4	[c]	—	[c]	202.5	—	—	—

[a] ^{29}Si chemical shift from $(MeO)_4Si$.
[b] ^{1}H chemical shift from TMS.
[c] Too volatile to be measured.

TABLE VIII

Miscellaneous ^{29}Si chemical shifts

Compound	Chemical shift[a] (p.p.m.)
$ViSi(OEt)_3$[b]	−15.5
$C_6H_5SiH_3$	−18
$C_6H_5Si(OEt)_3$	−19
$(MeO)_6Si_2$	−27
$(C_6H_5)_2SiH_2$	−45
$(C_6H_5)Si(OEt)_2$	−45
$(C_6H_5)_2{}^2SiF_2$	−49
Vi_4Si	−57
Me_6Si_2	−59
$Me(C_6H_5)_2SiH$	−60
$[(MeO)_2MeSi]_2$	−72
Et_2SiF_2	−80
$ClCh_2SiMe_3$	−81.5
$(Me_3Si)_2O$	−83.5
$Me_3SiO\phi t$-Bu	−92

[a] Relative to $(MeO)_4Si$.
[b] Vi ≡ vinyl.

atom, the indirect spin–spin coupling from ^{119}Sn to the methyl protons is very sensitive to dilution in the same manner as the ^{119}Sn chemical shifts. Any change in coordination at the tin atom will result in variations in the use of the '*s*' electron state function for any particular bond to the tin. This must be reflected in changes in coupling constant through the Fermi contact interaction $|\Psi_{5s}(0)|^2$. A complementary study of $J_{^{119}Sn-C-H}$ in the same solvents for the trimethyltin halides has been made.

These studies are summarized with the chemical shift data in Fig. 2. The solid circles on each graph show changes in coupling constant J_{Sn-C-H} referred to the left hand scales as indicated. The sensitivity of the proton resonance signal allows the detection and measurement of peaks to a limit of about 1 mole % for the ^{119}Sn side bands. The points for chemical shift and coupling constant are plotted so that the scale on the left and right of each graph corresponds to the same linear distance for changes in these parameters in going from pure compound to infinite dilution.

Dimethyltin dichloride has limited solubility in most solvents (less than 40 mole%). A dilution study from a saturated solution was made for the variation of $|J_{Sn-C-H}|$ in the following solvents: acetonitrile, acetone, methanol, 50/50 mole % acetone–water, and water. The first three solvents were carefully dried over vacuum-baked anhydrous calcium sulfate. The results of this study are shown in Fig. 3. In nonpolar solvents such as chloroform, benzene, and carbon tetrachloride the variation in $|J_{Sn-C-H}|$ from the pure compound in very dilute solutions was less than ±3 Hz.

The dilution studies of $|J_{Sn-C-H}|$ shown in Fig. 3 are of two types. In water and water/acetone, the value of the coupling constant

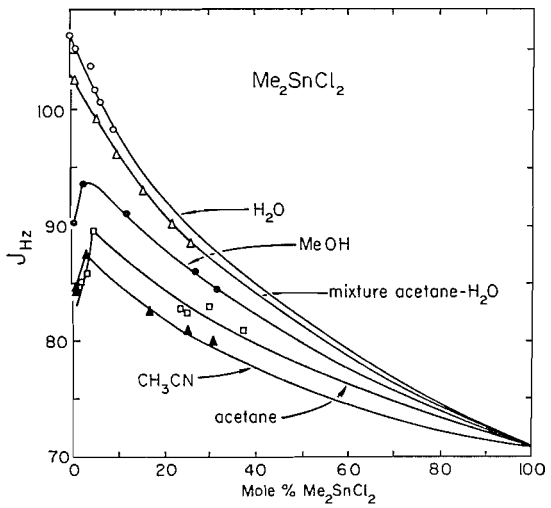

FIG. 3. Concentration dependence of the spin–spin couplings J_{Sn-C-H} for dimethyltin dichloride in various solvents.

TABLE IX

^{119}Sn chemical shifts

Compound	Solvent	(p.p.m.) tetramethyltin $\delta = 0$
$(CH_2{=}CH)_4Sn$	None	+165.1
$(CH_3)SnCl_3$	Acetone[a]	+103.6 to +151.2
$(CH_3)SnCl_3$	Water[a]	+474 to +481
Triphenyltin -2 ethylhexoate	$CHCl_3$	+115.3
Triphenyltin -cyclohexyl	Pure $CHCl_3$	+113.7 +125
$(CH_3)_3Sn{-}Sn(CH_3)_3$	None	+109.0
Diphenyltin -dicyclohexyl	$CHCl_3$	+106.5
Phenyltin -tricyclohexyl	$CHCl_3$	+102.5
Diphenyltin bis-thiobenzoate	$CHCl_3$	+101.2
Triphenyltin SS dimethylthiocarbonate	$CHCl_3$	+94.5
$(CH_2{=}CH)_2Sn(n\text{-Butyl})_2$	None	+86.4
Bis-triphenyltin oxide	$CHCl_3$	+80.6
$(n\text{-Butyl})_6Sn_2$	None	+79.5
$(CH_3)_2Sn(CH{=}CH_2)_2$	None	+79.4
Diphenyltin -dibutyl	None	+65.9
$(CH_3)_2Sn\phi_2$	None	+59.8
bis(triphenyltin sulfide)	None	+48.7
Triphenyltin chloride	None	+46.0
Tetraisopropyltin	None	+43.9
Phenyltintributyl	None	+41.7
$(CH_2{=}CH)_2SnCl_2$	None	+40.9
$(CH_3)_3Sn(CH{=}CH_2)$	None	+35.4
$(CH_3)_3Sn$phenyl	None	+30.3
$(n\text{-Propyl})_4Sn$	None	+16.8
$(CH_3CH_2)_4Sn$	None	+6.7
$(CH_3)_3Sn(CH_2CH_2CH_3)$	None	+2.9
$(CH_3)_3Sn$ cyclohexyl	None	+1.7
$(CH_3)_4Sn$	None	0.0
$(CH_3)_2Sn(n\text{-Butyl})_2$	None	−0.4
$(CH_3)_3Sn(CH_2CH_3)$	None	−5.9
$(CH_3)_3Sn$(Isopropyl)	None	−9.9
$(CH_3)_3Sn(t\text{-Butyl})$	None	−17.5
Diphenyltin sulfide	$CHCl_3$	−19.5
Tris(Trimethyltin -orthophosphate	None	−24.9
Trimethyltin chloride – pyridine complex	CH_3CH	−20.2
	$CHCl_3$	−25.4
$(CH_3)_3SnOH$	MeOH	−51.8
$(CH_3)_3SnMn(CO)_5$	Cyclohexane	−66.3
$(CH_3)_2SnBr_2$	$CHCl_3$	−74.3
$(CH_3)_2SnS$	CS_2	−125.6
$(CH_3)_3SnBr$	None	−130.7
$(CH_3)_3SnBr$ – aniline complex	$CHCl_3$	−149.9
$(CH_3)_3SnCl$	Cyclohexane[a]	−155.7 to −158.6
$(CH_3CH_2)_3SnCl$	None	−155.9

[a]Range of chemical shift noted; dependent on concentration.

always increases with dilution, but in the polar organic solvents between 5 and 8 mole % tin chloride the coupling constant decreases sharply in absolute magnitude to a lower value at infinite dilution. The estimates of the infinite dilution coupling constants are: 107 Hz in water, 103 Hz in water/acetone, 90 Hz in methanol, and 84 Hz in acetonitrile and acetone. The coupling constants and chemical shifts in the pure supercooled halides are estimated from the linear dependence

Can. J. Chem. Downloaded from www.nrcresearchpress.com by 210.87.254.40 on 09/05/12
For personal use only.

Can. J. Chem. Downloaded from www.nrcresearchpress.com by 210.87.254.40 on 09/05/12
For personal use only.

of these parameters on the relative mole concentration of halogen in their mixtures. Rapid halogen exchange is occurring in these solutions.

TABLE X

Tin chemical shifts in trimethyltin halides as a function of concentration in various solvents

Compound	Solvent	Mole %	In p.p.m. from pure compound
$(CH_3)_3SnCl$	H_2O	14.0	+102.0
,,	,,	9.9	+120.5
,,	,,	7.2	+121.4
,,	,,	5.2	+124.4
,,	,,	2.8	+125.0
,,	,,	0	+128.6*
,,	MeOH	21.8	+107.4
,,	,,	18.9	+111.5
,,	,,	14.2	+114 8
,,	,,	10.1	+117.9
,,	,,	0	+124.4*
,,	Acetone–H_2O	27.6	+109 4
,,	,,	22.8	+118.2
,,	,,	15.9	+125.7
,,	,,	10.6	+134.0
$(CH_3)_3SnBr$	H_2O	4.7	+90.5
,,	,,	3.9	+93.0
,,	,,	3.2	+96.8
,,	Acetone–H_2O	34.0	+77.4
,,	,,	24.0	+82.4
,,	,,	14.2	+102.3
,,	,,	9.7	+107.5

*Extrapolated values.

In Table X, the tin chemical shifts related to the pure compound are given for trimethyltin bromide and chloride for various accessible dilutions in water and 50/50 mole % acetone/water mixtures. In the case of trimethyltin chloride, the data also include solutions in methanol.

Relaxation Times T_1 for Some Silicon and Carbon Compounds

The measurement of spin–lattice relaxation times for ^{13}C usually observed in 1.1% natural abundance of spin 1/2 and ^{29}Si in 4.7% natural abundance, spin 1/2 in liquid samples of their compounds has received no attention in the published literature, although for ^{13}C they are often alluded to as long or worse, quoted as several minutes without measurement. In view of the increasing interest in observing ^{13}C by the direct field/frequency lock techniques and accumulated scans of absorption mode spectra, we felt it worthwhile to measure a few values of T_1 in typical pure compounds of these elements.

The method used is based on the adiabatic rapid passage method. The conditions $dH_0/dt \ll |\gamma H_1^2|$ and τ, the time spent in resonance, $\cong H_1/(dH_0/dt) \ll T_1$, T_2 were satisfied in all measurements (9). The procedure consisted of increasing power levels on the V4311 r.f. unit to 20 db below 0.5 W, the full output, then sweeping rapidly at $\sim$ 1 G/min through the ^{13}C or ^{29}Si signal in natural abundance in the purified vacuum-degassed liquids. Probe balance proved to be the limiting factor on the amount of power that could be produced at the sample. The single adiabatic passage inverts the magnetization to the negative z direction, taking positive z as the H_0 field direction. Subsequently, recovery at a relaxation rate $1/T_1$ occurs back to the positive z direction. The signal strength at constant gains in the adiabatic passage is proportional to the magnetization $M(t)$ at any time, since it is the act of precession of a macroscopic vector of length $M(t)$ through the xy plane perpendicular to H_0 which induces a proportional signal in the receiver coil (9). If the sample is left in the magnetic field H_0 for a period at least $10T_1$, then the first adiabatic passage gives a signal proportional to $M(0)$. A second adiabatic passage a time 't' later performs a precession of the magnetization remaining in the negative z direction back into the positive z direction. The signal height is proportional to $-M(t)$. The signal width under adiabatic conditions is proportional to the H_1 field which remains constant for all traverses of the resonance. By varying the interval 't', the signal heights can be measured and T_1 determined from the first order recovery law

$$[1] \qquad \ln\left(1 + \frac{I_t}{I_0}\right) = \ln 2 - \frac{t}{T_1}.$$

I and I_0 are heights of the signal at times t and $t = 0$.

The plots of $\ln (1 + I/I_0)$ versus t give a straight line of slope $1/T_1$ and intercept $\ln 2$. These experimental results are shown for the ^{13}C resonances in pure benzene, acetone carbonyl carbon, and CS_2 at 7.95 MHz and 7.45 kG, and for the ^{29}Si resonances in tetramethoxysilane, tetramethylsilane, and hexamethyldisiloxane at 7.95 MHz and 9.41 kG (Fig. 4). Table XI contains the list of T_1 values. After this work was completed, Drs. Paul Lauterbur and Ray Ettinger made us aware that they had obtained similar measurements on enriched compounds some years ago (10). There is only one compound

TABLE XI

Compound	Nucleus	T_1 (s)	Reference
Benzene	^{13}C	14	*a*
Acetone carbonyl	^{13}C	19	*a*
CS_2	^{13}C	35	*a,b,c*
$*^{13}CO_2$ in H_2O	^{13}C	35	*b*
$*^{13}CO_2$ in D_2O	^{13}C	45	*b*
$*^{13}CO_2$ in CS_2	^{13}C	24	*b*
*OCS	^{13}C	20	*b*
$*H^{13}CO_3^-$	^{13}C	9	*b*
$*NH_2{}^{13}COONH_4$	^{13}C	5	*b*
$*(C_2H_5O)_2{}^{13}CO$	^{13}C	51	*b*
$*(CH_3O)_2{}^{13}CO$	^{13}C	49	*b*
$*(C_2H_5O)_4{}^{13}C$	^{13}C	47	*b*
$*^{13}CH_3I$	^{13}C	~3.5	*c*
$(CH_3O)_4Si$	^{29}Si	73	*a*
$(CH_3)_4Si$	^{29}Si	16	*a*
$[(CH_3)_3Si]_2O$	^{29}Si	40	*a*

*Enriched to 55% ^{13}C in the appropriate position.
(*a*) Present work.
(*b*) Ettinger and Lauterbur. Private communication.
(*c*) Ettinger and Johnson. Private communication.

which is common to both sets of measurements, CS_2, and the agreement is excellent. Subsequent to our measurements, Ettinger and Johnson (11) rechecked the value of 35 s for $^{13}CS_2$ and in an enriched sample of Me_3I found T_1 to be 3–4 s. As far as is known, the results in Table II are the only known values of T_1 for ^{13}C and ^{29}Si in liquids.

Discussion

Silicon Chemical Shifts

Chemical shift theories for isotropic liquids have followed the formulation of Ramsey (12, 13), who treated the electron–nucleus interaction in the complete Hamiltonian to second order perturbation. Notable exceptions to this include a variation method calculation of O'Reilly (14).

More recent attempts to use the Ramsey method in more approximate forms, usually with an average excitation energy approximation, have met with some success in explaining the gross features of the chemical shift behavior of heavier nuclei (15–20). The paramagnetic contribution in the Ramsey formulation (12, 13) is considered only for the atom containing the nucleus in question (except in Cornwell's paper (19)). The σ and π systems used in bonding and the ionicity of these bonds are a requirement in computing the matrix elements for the perturbation calculation. Bond orders must be known. If the p and d content of all bonding orbitals remains an invariant factor in a series of molecules, the assumptions lead to the general result that chemical shift is a linear function of p and d

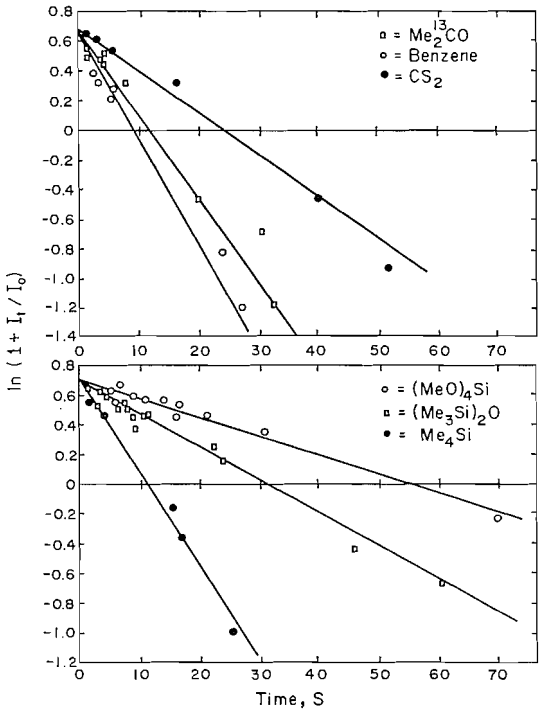

FIG. 4. Results for T_1 measurements for ^{13}C and ^{29}Si signals in six compounds. I/I_0 represents the ratio of the peak intensities at arbitrary times t and $t = 0$; ln $(1 + I/I_0)$ is plotted versus t.

orbital occupancy, which is often empirically represented by differences in electronegativity. At present, the theory of Saika and Slichter (15) with respect to p orbital occupancy in the F—X bond remains less than satisfactory. Numerous exceptions are found among experimentally measured fluorine chemical shifts (21).

In the compounds of silicon, the participation of (p → d) bonding from a suitable ligand has been a subject of some controversy (22–26). Bond shortening in Si—N, Si—O, and Si—F can be characterized using the criteria of Shomaker and Stevenson (27) and the unusual bond angles of silylamines and silyl ethers are well known (26). It is to be hoped that the chemical shifts, which are also crudely dependent on electronegativity differences, can, when taken in consideration with carbon, point out the peculiarity of certain silicon–X bonds. Previous studies of proton chemical shifts in silicon compounds cannot be expected to show bonding changes at silicon so well.

Gutowsky and Juan (34) have an approximate

Can. J. Chem. Downloaded from www.nrcresearchpress.com by 210.87.254.40 on 09/05/12
For personal use only.

Can. J. Chem. Downloaded from www.nrcresearchpress.com by 210.87.254.40 on 09/05/12
For personal use only.

expression for the chemical shift based on either valence bond or linear combination atomic orbital – molecular orbital calculations. They consider only the second order paramagnetic term on the bonding orbitals of the atom in question and an equation may be written.

$$[2] \quad \sigma^2 = -\left(\frac{2e^2\hbar^2}{3\Delta m^2c^2}\right)\left(\left\langle\frac{1}{r_p^3}\right\rangle P_u + \left\langle\frac{1}{r_d^3}\right\rangle D_u\right)$$

Δ is a mean ground state to triplet state excitation energy and e, h, m, and c are constants. $\langle 1/r_p^3\rangle$ and $\langle 1/r_d^3\rangle$ are mean inverse cubes for distances electrons to nucleus and P_u and D_u may be called the 'electron unbalance' for valence p and d orbitals respectively.

P_u and D_u are dependent on coordination number, hybridization of atomic orbitals in bonding, and ionicity of bonds. In order to extract the dependence on ionicity, one assumes that Δ, $\langle 1/r_p^3\rangle$, and $\langle 1/r_d^3\rangle$ can be approximately constant in a series of compounds and, further, that one can arrange a series such that the coordination number and hybridization do not change. For silicon compounds, it is convenient to choose the series $(CH_3)_3Si$—X where X varies in electronegativity as widely as possible. In order to avoid any dependence on an n.m.r. scale of electronegativities, the ^{29}Si chemical shifts of $(CH_3)_3Si$—X compounds have been plotted against the Pauling electronegativity (28) difference between silicon and X in Fig. 5. The lower half of the figure is devoted to ^{29}Si chemical shifts in $(CH_3)_3SiX$ compounds and the upper half to previously published data on ^{13}C chemical shifts in CH_3X compounds (2). Features which distinguish ^{13}C chemical shift dependence on electronegativity have been discussed (1, 2). The odd feature in the experimental data is the high field shifts for CH_3I, CH_3Br, and CH_3Cl, which stand out as exceptions to the gross linear dependence on electronegativity. The shifts for the three odd methyl halides depend within themselves linearly on electronegativity, but the line through them is well displaced from zero chemical shift change for the C—C bond, which is arbitrarily set at zero for zero electronegativity difference. This aspect of ^{13}C chemical shift behavior has received some attention (29, 30). Both diamagnetic anisotropy and intramolecular dispersion forces have been suggested as contributing a shielding effect for these halides.

The silicon chemical shift data in the lower

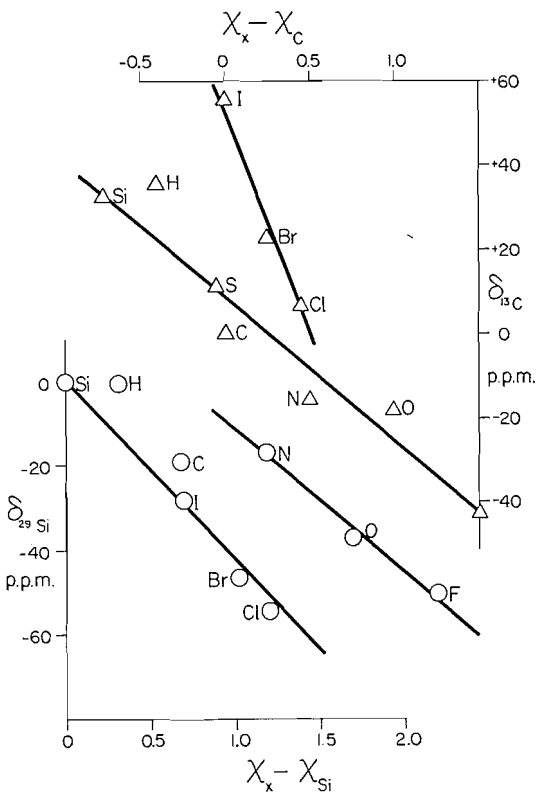

FIG. 5. ^{29}Si chemical shifts in $(CH_3)_3SiX$ and ^{13}C chemical shifts in CH_3X compounds plotted against the electronegativity differences $(\chi_X - \chi_{Si})$ and $(\chi_X - \chi_C)$. The ^{13}C chemical shifts are given in the figure at the upper right.

half of Fig. 5 show marked contrasts to the ^{13}C data. In this case a regular linear trend is seen for the elements Si, C, I, Br, and Cl, with the expected zero relative shift with Si = X in $(CH_3)_3Si$—$Si(CH_3)_3$ being on the line. With X = N, O, and F, an additional shielding effect becomes operative. The shift with X = H seems in both ^{13}C and ^{29}Si shifts to be a little displaced to high field from what might be expected for the electronegativity of hydrogen. Bonds to hydrogen are known to be exceptional even with regard to bond length, e.g. Si—H bonds are longer than calculated from electronegativities and covalent radii (27). Gutowsky and Larmann (31) computed chemical shifts for tervalent phosphorous compounds where no appreciable $(p \rightarrow d)\pi$ back donation of charge occurs. In tetravalent phosphorous compounds, calculations have been extended to include arbitrary

Can. J. Chem. Downloaded from www.nrcresearchpress.com by 210.87.254.40 on 09/05/12
For personal use only.

$(p \rightarrow d)\pi$ donation (32). In this paper, the use of an experimental shielding in conjunction with a crude theoretical estimate of a σ bond contribution to the chemical shift to determine the quantitative amount of $(p \rightarrow d)\pi$ bonding must be subject to large uncertainties. The more qualitative dependence on electronegativity for silicon chemical shifts is, however, established here and the role of $(p \rightarrow d)\pi$ bonds in shielding the silicon is similar to the behavior of tetrahedral phosphorous derivatives.

The tables of silicon chemical shifts 1–8 for the series $SiX_{4-n}Y_n$ do show the 'sagging' behavior characteristic of phosphorous compounds as the value of n is changed (32). The empirical rule of Letcher and Van Wazer, who find that deviations from linearity of changes in chemical shift with 'n' are constant for ^{31}P chemical shifts do not apply to silicon chemical shifts. The compounds $M(CH_3)_n(OR)_{4-n}$ give opposite trends for the M chemical shift. If M = carbon, the addition of —OR groups is strongly deshielding, while for M = silicon the effect is strongly shielding after the first (OR) group. Similar behavior is also noted for nitrogen and fluorine ligands. On the assumption that appreciable $(p \rightarrow d)\pi$ bonding causes a shielding effect, whereas the increasing polarity of the sp^3 hybrid orbitals causes deshielding (one assumes as a first approximation orthogonality of the sp^3–σ orbitals and $(p \rightarrow d)\pi$ bonds), it follows that the net shielding effect of the π bonds is greater and results in a net high field shift after the first (OR), —F, or $—N(Me)_2$ group.

An interesting observation is the behavior of the chloromethylsilanes, which have a chemical shift at lowest field for Me_2SiCl_2. Jaffé (25) has tabulations which enable crude estimates of $(p \rightarrow d)\pi$ overlap to be made for Si—O, Si—F, and Si—Cl bonds. The overlap integrals are 0.2, 0.2, and 0.15 respectively. For the larger halogens overlap will be even smaller because of the large mean radius of the valence shell. The $(p \rightarrow d)\pi$ donation will be less effective for chlorine and the $(p \rightarrow d)\pi$ bond order smaller. This is in agreement with the regular behavior of the trimethylsilyl chloride in Fig. 5 and lack of a strong shielding effect in the series $Me_{4-n}SiCl_n$ as n is increased (see Table IV).

The overlap between silicon d orbitals and molecular π electrons in the vinyl and phenyl groups will be smaller because of the larger size of the silicon d orbitals compared with the $2p$–π carbon orbitals. An electronegativity effect is almost entirely absent in series such as $(Vinyl)_{4-n}Si(CH_3)_n$ and $(Phenyl)_{4-n}Si(CH_3)_n$, since all bonds are Si—C at silicon. In both cases, there is a linear shielding effect as the number of vinyl and phenyl groups is increased. The shielding effect is 4 p.p.m. per phenyl group and 5.6 p.p.m. per vinyl group. In series $(Alkyl \text{ or } Aryl)_4SiH_{4-n}$, the hydrogen leads to increased shielding as n increases, but this effect is small and difficult to interpret. Chemical shifts in the molecules $MeSiH_3$ and SiH_4 proved too difficult to measure because of volatility and explosion hazards in preparation.

Spin-Couplings in Silicon Compounds

A new feature of spin-coupling constants in silicon compounds is the appearance of a long range interaction *H*—C—Si—C—*H* when the silicon is bound to oxygen or fluorine. There are similar long range couplings known, for instance the 0.4 Hz coupling in acetone *H*—C—C—C—*H* and in mercury dimethyl *H*—C—Hg—C—*H* (33). The fact that this coupling constant in silicon compounds can be observed only when a $(p \rightarrow d)\pi$ donor such as fluorine and oxygen is bonded to silicon suggests that the use of silicon d orbitals to transmit coupling via the electronic system is facilitated by partial occupancy. Otherwise, silicon proton, carbon, and silicon fluorine couplings are quite regular in behavior and they have been discussed at length by other workers (34).

Recently, the small long range couplings in dimethyl sulfide *H*—C—S—C—*H* (35), disilyl sulfide *H*—Si—S—Si—*H* (36), and germyl methyl sulfide *H*—Ge—S—C—*H* (37) have been reported. The availability of low lying unoccupied or partly occupied p or d orbitals appears to be a prerequisite for such couplings.

Tin Chemical Shifts

The chemical shift range encountered in tin compounds is much larger than silicon or carbon because of the increased magnitude of $\langle 1/r^3 \rangle$ for valence p and d electrons in eq. [2] as indicated by spin–orbit interactions (20). The values of $\langle a_0^3/r^3 \rangle_{np}$ in atomic units for carbon silicon and tin are 1.7, 2.5, and 8.0 (38) approximately. It has been suggested (20) that the contracted chemical shift range encountered in silicon compounds is the result of a shielding effect due to $(p \rightarrow d)\pi$ bonds with the ligands oxygen and

Can. J. Chem. Downloaded from www.nrcresearchpress.com by 210.87.254.40 on 09/05/12
For personal use only.

fluorine. The results here support this suggestion. These ligands would otherwise give strong low field chemical shifts for the bonded silicon. $(p \rightarrow d)\pi$ bonding in tin compounds should occur with larger ligands, such as chlorine and bromine, where overlap is more favorable, but the $(p \rightarrow d)\pi$ bonding order is expected to be lower than in silicon compounds because the σ bonding will not be as ionic with these more electropositive ligands (23). A chemical shift range of 1900 p.p.m. in tin compounds compared with 316 p.p.m. in carbon reflects the same order of change in $\langle 1/r^3 \rangle_{np}$. The chemical shifts measured in this work are only a small fraction of this range, ~ 500 p.p.m., and consist mainly of alkyltin (X) compounds or tin ions in aqueous media.

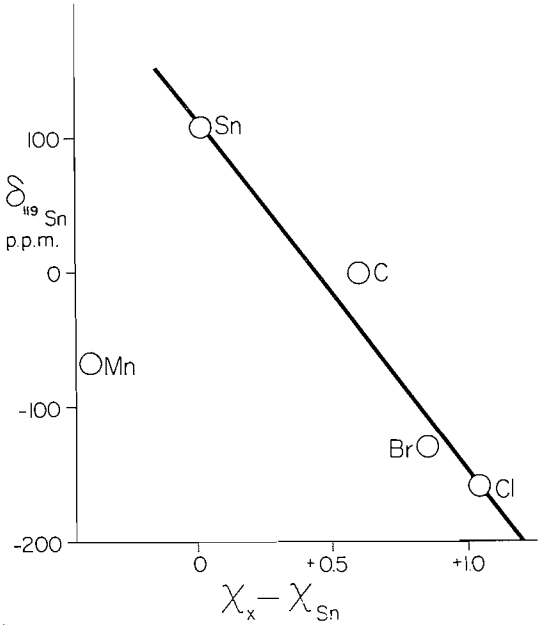

FIG. 6. ^{119}Sn chemical shifts in $(Alkyl)_3SnX$ compounds as a function of $(\chi_X - \chi_{Sn})$.

There are several similarities between silicon and tin chemical shifts with respect to molecular structure. The *n*-butyltin chlorides give the same 'sagging' dependence on the number of chlorine atoms that is reported earlier in this paper for silicon bonded to oxygen and fluorine. The first chlorine atom produces a deshielding effect, but all subsequent chlorine atoms to $SnCl_4$ are shielding. The figures for these results are a combination of the data of Lauterbur (4) and our present work. The shifts are: $(n\text{-Bu})_4Sn$ +12 p.p.m. (4); $(n\text{-Bu})_3SnCl$ −143 p.p.m. (4), −139 p.p.m. (present work); $(n\text{-Bu})_2SnCl_2$ −71 p.p.m. in acetone solution (4), −56 p.p.m. (present work); $(n\text{-Bu})SnCl_3$ +3 p.p.m. (4); $SnCl_4$ +150 p.p.m. (4, present work).

The results for vinyltin compounds are similar to the silicon vinyls. Apart from $Sn(C_2H_3)_3CH_3$, which was not available, the increase in tin shielding per vinyl group is constant at 40 p.p.m. per vinyl added. This shielding effect is almost an order of magnitude larger than for silicon vinyl derivatives and reflects the increased overall sensitivity of tin chemical shifts to molecular structure.

The general form of the dependence of tin chemical shifts on Pauling electronegativity difference in $(Alkyl)_3SnX$ compounds follows the same form as those for silicon in the lower half of Fig. 4. The number of chemical shifts available is disappointingly small and limited by the formation of solid polymeric substances with the very electronegative elements. A gross linear dependence can be noted for the elements —Sn, —C, —Br, and —Cl. The availability[3] of $(CH_3)_3SnMn(Co)_5$ enabled us to get a ^{119}Sn chemical shift of −66.3 p.p.m. It is plotted as a $(CH_3)_3Sn$—X compound in Fig. 5. The chemical shift is quite irregular. The much larger slope of the chemical shift versus electronegativity in tin compounds is again a manifestation of the use of (5p) valence electrons for bonding rather than (3p) in silicon. The hybridization of bonding orbitals will be approximately the same.

The Changes in ^{119}Sn Chemical Shifts with Solvent and Concentration

It is known that nonaqueous donor molecules complex with tetrahedral tin compounds to form penta- and hexa-coordinated tin complexes (39–41). Some equilibrium constants have been measured from infrared intensity data (42). Burke and Lauterbur (4) concluded that these tin complexes are formed with large accompanying changes in tin chemical shifts. No quantitative study has followed these earlier observations.

The dissolution of trimethyltin chloride and bromide in donor organic solvents such as acetone, acetonitrile, and dioxane proceeds to a 1:1 complex formation.

[3]We thank Professor H. C. Clark for providing this sample.

Can. J. Chem. Downloaded from www.nrcresearchpress.com by 210.87.254.40 on 09/05/12
For personal use only.

We can write

$$(CH_3)_3SnX + :D \rightleftharpoons (CH_3)_3SnX{:}D \text{ 1:1 complex.}$$

If we assume there is 1 mole of halide plus donor and C moles of halide and αC moles of complex are formed at equilibrium, then the equilibrium constant in mole fraction units for the above reaction is given by

$$[3] \qquad K = \frac{\alpha(1 - C\alpha)}{(1 - \alpha)(1 - C - C\alpha)}.$$

The tin chemical shift observed is the time weighted average of the complexed and free forms. If the chemical shifts are referenced to zero for pure trimethyltin halide then

$$[4] \qquad \delta_0 = \alpha\delta_c.$$

δ_0 = observed tin chemical shift in a solution of arbitrary concentration, δ_c = chemical shift in the complex, and K is given by

$$[5] \qquad K = \frac{\delta_0(\delta_c - C\delta_0)}{\delta_c^2(1 - C) + C\delta_0^2 - \delta_0\delta_c}.$$

A simple computer program was devised to choose trial values of K and δ_c and compute the dilution chemical shift curves shown in Fig. 2. The dotted curve on each graph is the computed dilution chemical shift dependence in each case for the values of K recorded on the top right hand side of each plot, and for an infinite dilution chemical shift δ_c recorded on the right. The figures are: Me_3SnBr in acetone $\delta_c = -67.2$ p.p.m. with respect to tetramethyltin, $K = 3.00$; Me_3SnBr in CH_3CH $\delta_c = -73.8$, $K = 3.48$; Me_3SnCl in acetone $\delta_c = -106.6$, $K = -106.6$; Me_3SnCl in CH_3CN $\delta_c = -86.5$, $K = 2.7$.

As noted earlier, the spin-coupling constant J_{Sn-C-H} is modulated in the same way by the same exchange process. By assuming that the coupling constant J_{Sn-C-H} in the complex takes arbitrary values and knowing the coupling constant in the pure halide, then the dotted curve obtained from best computed results also represents the variation of coupling constant with dilution. The infinite dilution values of coupling constants in the complexed form are: Me_3SnBr:acetone $J_c = 66.0$ Hz; Me_3SnBr:acetonitrile $J_c = 65.1$ Hz; Me_3SnCl:acetonitrile $J_c = 66.7$ Hz.

The dimethyltin dihalides are known to be better acceptors and with the same donor molecules complexing takes place in two steps (43).

$$(CH_3)_2SnCl_2 + :D \rightleftharpoons [(CH_3)_2SnCl_2{:}D]$$

$$(CH_3)_2SnCl_2{:}D + :D \rightleftharpoons [(CH_3)_2SnCl_2{:}2D]$$

In aqueous or mixed aqueous/organic solvents, both the trimethyltin halides and dimethyltin dihalides ionize. In the case of the dihalides, ionization proceeds in two steps to give in dilute solutions the dimethyl stannic ion (44). For dimethyltin dichloride, the equilibrium constants are known (44).

$$(CH_3)_2SnCl_2 \underset{}{\overset{K_1}{\rightleftharpoons}} (CH_3)_2SnCl^+ + Cl^-$$

$$(CH_3)_2SnCl^+ \underset{K_2}{\rightleftharpoons} (CH_3)_2Sn^{2+} + Cl^-$$

$K_1 = 3.48$ moles l^{-1} in water and $K_2 = 0.417$ moles l^{-1} in water.

The study of dimethyltin dichloride in various solvents is summarized in Fig. 3. In methanol, acetone, and acetonitrile the values of J_{Sn-C-H} can be interpreted in terms of the formation of a penta-coordinated tin complex in concentrated solutions followed in dilute solution by the predominant formation of a hexa-coordinated tin complex with two donor molecules. The value of $J_{^{13}C-H}$ in the methyl group changes by less than 1–2 Hz in all solutions and this locates the center of the complexing reaction as being at the tin atom. The approximate proportionality between J_{Sn-C-H} and the s electron character used in bonding at the tin to the carbon has been established (45). It appears, therefore, that the 's' character used in bonding increases in going from $(CH_3)_2SnCl_2$ to $[(CH_3)_2SnCl_2{:}D]$ and decreases in proceeding to $[(CH_3)_2SnCl_2{:}2D]$. If the bonding changes at tin can be approximately described as $(sp^3) \rightarrow (sp^2)dp \rightarrow (dsp^2)(dp)$, then the Sn—C bond at the tin has 1/4, 1/3, and 1/4 's' electron character respectively. This accounts, at least qualitatively, for the shape of the observed dilution curves. There is support for this bonding scheme in the known bond lengths. The donor molecules occur as axial ligands with longer bonds (41). Extrapolated values of J_{Sn-C-H} from the concentrated regions of the solution are 90 to 96 Hz, depending on the solvent, compared with 71 Hz in the pure dihalide. The approximate ratio of 4/3 is satisfactory. The infinite dilution values of the coupling are less certain because the extrapolation is difficult to make in view of the rapid decrease of J and decreasing signal to noise.

Ionization in water and acetone/water mixtures is accompanied by an increasing value of J

Can. J. Chem. Downloaded from www.nrcresearchpress.com by 210.87.254.40 on 09/05/12
For personal use only.

to infinite dilution values 107 Hz and 103 Hz respectively. The linear $(CH_3)_2Sn^{2+}$ ion has a tin–proton coupling constant which is sensitive to solvation, therefore. Addition of excess sodium chloride to the water solutions does not change the coupling, hence water/acetone competition in the solvation process must occur.

Tin chemical shifts in aqueous media are given at a series of dilutions for $(CH_3)_3SnCl$ and $(CH_3)_3SnBr$ in Table X. The latter compound does not dissolve an appreciable amount of water, but is solubilized by addition of acetone. A considerable high field displacement of chemical shifts occurs with ionization. The infinite dilution chemical shift of $(CH_3)_3SnCl$ is sensitive to the solvent mixture, indicating some role played by the second solvent component in the solvation process.

Acknowledgments

The support of the National Research Council of Canada is gratefully acknowledged. We are also indebted to Mrs. Cyr for making some tin chemical shift measurements.

Appendix

Si^{29} chemical shifts (2, 3)

Compound	Chemical shift (p.p.m.)
$[(CH_3)_3SiO]_4Si$	81.5
$SiBr_4$	68
Sodium silicate solution	64
$(C_2H_5O)_4Si$	59.5
$[(CH_3)_3SiO]_3SiCH_3$	42.5
$C_6H_5SiH_3$	39
$(C_2H_5O)_3SiH$	21.5
$C_6H_5(CH_3)SiH_2$	14.8
$(CH_3SiHO)_5$	13.1
$(CH_3SiHO)_4$	12
$(C_6H_5)_2SiH_2$	11.8
$[(CH_3)_2SiO]_x$	0
$[(CH_3)_2SiO]_4$	−2.2
$[C_2H_5(CH_3)SiO]_4$	−2.3
$C_6H_5(CH_3)_2SiH$	−4.5
$SiCl_4$	−6
$[(CH_3)_2SiO]_2O$ (C_6H_6 solution)	−12.1
$[(CH_3)_3SiCH{=}CH_2]$	−15.1
$[(CH_3)_2SiH]_2O$	−17.2
$(CH_3)_3SiC_6H_5$	−17.8
$(C_6H_5)_2CH_3SiOC_2H_5$	−18.2
$[(CH_3)_2SiNH]_3$	−18.7

Si^{29} chemical shifts (2, 3)

Compound	Chemical shift (p.p.m.)
$[(CH_3)_3Si]_2NH$	−19.8
$(CH_3)_3SiCH_2OH$	−21.8
$(CH_3)_4Si$	−22.0
$[(CH_3)_3Si]_2CH_2$	−22.5
$(CH_3)_3SiCH_2NH_2$	−23.2
$(CH_3)_3SiCH_2C_6H_5$	−23.4
$(CH_3)_3Si(CH_2)_3CH_3$	−23.8
$(CH_3)_3SiCH_2Cl$	−25.5
$(CH_3)_3SiCH_2NCS$	−28.2
$[(CH_3)_3Si]_2O$	−28.7
$(CH_3)_3SiOC_2H_5$	−29.4
$[(CH_3)_3SiO]_3SiCH_3$	−29.4
CH_3SiCl_3	−30
$[(CH_3)_3SiO]_4Si$	−30.4
$(CH_3)_3SiI$	−30.6
$(CH_3)_2Si(CH_2Si)CHCl_2$	−31.2
$[(CH_3)_3SiO]_3PO$	−35
$(CH_3)_3SiBr$	−48.4
$(CH_3)_3SiCl$	−51
$(CH_3)_3SiF$	−53.1
$(CH_3)_2SiCl_2$	−54
$(CH_3)_3SiOSO_3H$	−57.6

1. J. B. STOTHERS. Quart. Rev. London, **19**, 144 (1965).
2. P. C. LAUTERBUR. *In* Determination of organic structures by physical methods. *Edited by* F. C. Nachod and W. D. Phillips. Vol. 2. Academic Press, New York and London. 1962. Chap. 4.
3. G. R. HOLZMAN, P. C. LAUTERBUR, J. H. ANDERSON, and W. KOTH. J. Chem. Phys. **25**, 172 (1956).
4. J. J. BURKE and P. C. LAUTERBUR. J. Am. Chem. Soc. **83**, 326 (1961).
5. H. C. CLARK, J. T. KWON, L. W. REEVES, and E. J. WELLS. Can. J. Chem. **42**, 941 (1964).
6. C. EABORN. Organosilicon compounds. Butterworths, London. 1960.
7. C. EABORN. J. Chem. Soc. 2840 (1952).
8. J. A. POPLE, W. G. SCHNEIDER, and H. J. BERNSTEIN. High resolution nuclear magnetic resonance. McGraw-Hill Book Co., 1959.
9. A. ABRAGAM. Principles of nuclear magnetism. Oxford University Press. 1961. pp. 65–66.
10. R. ETTINGER. Ph.D. Thesis, State University of New York, Stony Brook, N.Y. 1962.
11. R. ETTINGER and L. JOHNSON. Private communication.
12. N. F. RAMSEY. Phys. Rev. **78**, 699 (1950).
13. N. F. RAMSEY. Phys. Rev. **78**, 540 (1950).
14. D. E. O'REILLY. J. Chem. Phys. **36**, 855 (1962).
15. A. SAIKA and C. P. SLICHTER. J. Chem. Phys. **22**, 26 (1954).
16. J. S. GRIFFITH and L. E. ORGEL. Trans. Faraday Soc. **53**, 601 (1957).
17. M. KARPLUS and T. P. DAS. J. Chem. Phys. **34**, 1683 (1961).
18. C. W. KERN and W. M. LIPSCOMB. J. Chem. Phys. **37**, 260 (1963).
19. C. D. CORNWELL. J. Chem. Phys. **44**, 874 (1966).

20. C. J. JAMESON and H. S. GUTOWSKY. J. Chem. Phys. **40**, 1714 (1964); **40**, 2285 (1964).
21. J. FEENEY, N. EMSLEY, and L. H. SUTTCLIFFE. High resolution nuclear magnetic resonance. Vol. 2. Pergamon Press, 1966.
22. D. W. J. CRUICKSHANK. J. Chem. Soc. 5486 (1964).
23. C. P. CRAIG, A. MACCOLL, R. S. NYHOLM, L. E. ORGEL, and L. E. SUTTON. J. Chem. Soc. 332 (1954).
24. F. G. A. STONE and D. SEYFERTH. J. Inorg. Nucl. Chem. **1**, 112 (1955).
25. H. H. JAFFÉ. J. Phys. Chem. **58**, 185 (1954).
26. E. A. V. EBSWORTH. Volatile silicon compounds. Pergamon Press, New York. 1963.
27. V. SCHOMAKER and D. P. STEVENSON. J. Am. Chem. Soc. **63**, 37 (1961).
28. L. PAULING. The nature of the chemical bond. Cornell University Press, Ithaca, N.Y. 1939.
29. H. SPIESECKE and W. G. SCHNEIDER. J. Chem. Phys. **35**, 722 (1961).
30. T. SCHAEFFER, W. F. REYNOLDS, and Y. YONEMOTO. Can. J. Chem. **41**, 2969 (1963).
31. H. S. GUTOWSKY and J. LARMANN. J. Am. Chem. Soc. **87**, 3815 (1965).
32. J. H. LETCHER and J. R. VAN WAZER. J. Chem. Phys. **44**, 815 (1966); **45**, 2916 (1966).
33. K. A. MCLAUGHLAN, D. H. WHIFFEN, and L. W. REEVES. Mol. Phys. **10**, 131 (1966).
34. H. S. GUTOWSKY and C. S. JUAN. J. Chem. Phys. **37**, 2198 (1962).
35. E. A. V. EBSWORTH and J. J. TURNER. J. Chem. Phys. **36**, 2628 (1962).
36. N. VAN MEURS. Spectrochim. Acta, **19**, 1695 (1963).
37. T. J. WANG and C. H. VAN DYKE. Chem. Commun. 612 (1967).
38. R. G. BARNES and W. V. SMITH. Phys. Rev. **93**, 95 (1954).
39. C. A. KRAUS and W. N. GREEN. J. Am. Chem. Soc. **45**, 3078 (1923).
40. R. HULME. J. Chem. Soc. 1524 (1963).
41. A. B. THOMAS and E. G. ROCHOW. J. Inorg. Nucl. Chem. **4**, 205 (1957).
42. N. A. MATWICOFF and R. S. DRAGO. Inorg. Chem. **3**, 337 (1964).
43. I. R. BEATTIE. Quart. Rev. London, **17**, 382 (1963).
44. T. N. FARRAR, M. M. MCGRADY, and R. S. TOBIAS. J. Am. Chem. Soc. **87**, 5019 (1965).
45. J. R. HOLMES and H. D. KAESZ. J. Am. Chem. Soc. **83**, 3903 (1961).

Can. J. Chem. Downloaded from www.nrcresearchpress.com by 210.87.254.40 on 09/05/12
For personal use only.

Can. J. Chem. Downloaded from www.nrcresearchpress.com by 210.87.254.40 on 09/05/12
For personal use only.

Chemistry of phosphorus pentaselenide. I. Its reaction with alcohols

MOHAN V. KUDCHADKER, RALPH A. ZINGARO, AND KURT J. IRGOLIC
Department of Chemistry, Texas A&M University, College Station, Texas

Received September 26, 1967

The reaction of phosphorus pentaselenide with a number of alcohols has been studied. The predicted products, the dialkyldiselenophosphoric acids, were unstable. Derivatives were isolated as the potassium salts or as the chromium(III) complexes. When the salts of the acids were not isolated from the reaction mixture, different derivatives having bridged selenium atoms, viz. $(RO)_4P_2Se_4$ and $(RO)_4P_2Se_5$, were isolated. The properties of these compounds as measured using infrared, ultraviolet, n.m.r. spectroscopic and differential thermal analytical methods are reported.

Canadian Journal of Chemistry, 46, 1415 (1968)

Introduction

Phosphorus pentasulfide is widely used as the starting material for the preparation of a large number of organosulfur compounds. Its selenium analogue, P_2Se_5, may be useful for the synthesis of phosphorus bearing organoselenium compounds, but it has been investigated to a very limited extent. This paper describes the reaction of P_2Se_5 with alcohols.

The existence of P_2Se_5 was suggested by Berzelius (1) as early as 1834, but its preparation was reported for the first time by Carius and Bogen (2) in 1862. They obtained it in the form of a dark red-brown mass by the fusion of stoichiometric amounts of red phosphorus and selenium in an atmosphere of CO_2. This preparation was confirmed by other workers (3).

Rathke (4) in 1869 reported that the P_2Se_5 obtained in the above fashion was purified by recrystallization from CCl_4 at 200°. Behrens and Haschka (5) reported that it could be purified by sublimation in high vacuum at 300–350°. We were unable to reproduce these findings.

There are few reports in the literature concerning the reactions of P_2Se_5 with organic compounds. The reaction between P_2Se_5 and ethanol (2) has been reported to proceed as follows.

$$P_2Se_5 + 5C_2H_5OH = H_2Se + H_2O + C_2H_5OP(O) \times (SeC_2H_5)_2 + C_2H_5OP(O)(SeC_2H_5)(SeH)$$

The products isolated from this reaction in the present study differ from these. Rathke (4) studied the reaction of P_2Se_5 with CCl_4, and he reported the formation of CSe_2 as a major product. This was recently confirmed by Yarovenko and co-workers (6). Rathke (4) also reported on the reaction of P_2Se_5 with KOH and $ROSO_3K$. He obtained R_2Se and R_2Se_2 as the principal products. Pall (7) observed the formation of selenophene in the reaction of acetylacetone with P_2Se_5. Jensen and co-workers (8) converted ureas to the corresponding selenourea derivatives with P_2Se_5.

In 1961 Behrens and Haschka (5) studied the reaction of P_2Se_5 with liquid ammonia. Depending upon the temperature used, various products could be isolated as indicated by the following scheme.

$$P_2Se_5 + NH_3 \xrightarrow{20°} [NH_4]_2[PSe_3NH_2]$$

Filter; cool the filtrate −70°

$$[NH_4]_3[PSe_4] + [NH_4]_2[PSe_2(NH_2)NH]$$

$$[NH_4]_2[PSe_3NH_2] \xrightarrow[-33°]{NH_3} [NH_4]_3[PSe_3NH]$$

$$[NH_4]_2[PSe_3NH_2] \xrightarrow[20°]{-NH_3} [NH_4][PSe_3NH_3]$$

$$[NH_4]_2[PSe_2(NH_2)NH] \xrightarrow[20°,\ vacuo]{-NH_3} [NH_4][PSe_2(NH_2)_2]$$

Stolle and Gutmann (9) converted dibenzyl- and diacetyl-hydrazides to the corresponding selenodiazoles with P_2Se_5. Van den Hende and Klingsberg (10) used P_2Se_5 to affect the following conversion.

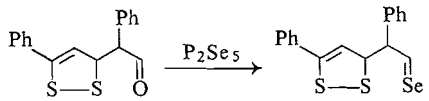

To the best of our knowledge these examples describe the known reactions of P_2Se_5 with organic substrates.

Can. J. Chem. Downloaded from www.nrcresearchpress.com by 210.87.254.40 on 09/05/12
For personal use only.

TABLE I

Analytical data for the products isolated from P_2Se_5–alcohol reactions

Compound		C (%)	H (%)	P (%)	Molecular weight	Melting point (°C)	Color	Recrystallization solvent	Approximate yield (%)
a. $(C_2H_5O)_2P(Se)SeK$	Calcd.	15.10	3.17			132–136	Colorless	95% ligroin	60
	Found	14.70	3.13					+5% EtOH	60
b. *n*-$(C_3H_7O)_2P(Se)SeK$*	Calcd.	20.81	4.08			92–95	Colorless	95% ligroin	
	Found	20.94	4.17					+5% EtOH	55–60
c. $(C_4H_9O)_2P(Se)SeK$	Calcd.	25.67	4.86			92–93	Colorless	95% ligroin	
	Found	25.64	4.99					+5% EtOH	50
d. $(C_6H_{11}O)_2P(Se)SeK$	Calcd.	33.80	5.21			202–208	Colorless	80% ligroin	
	Found	33.99	5.39			(decomp.)		+20% EtOH	60
e. $(C_5H_{11}O)_2P(Se)SeK \cdot H_2O$	Calcd.	28.57	5.77			132–133	Colorless	ligroin	35
	Found	28.43	5.52						
f. $[Se_2P(OC_2H_5)_2]_3Cr$	Calcd.	16.21	3.41	10.45		160	Olive green	EtOH	45
	Found	15.99	3.64	10.45					
g. *n*-$[Se_2P(OC_3H_7)_2]_3Cr$*	Calcd.	22.21	4.36	9.55					
	Found	22.16	4.20	9.44					
h. *i*-$(C_3H_7O)_4P_2Se_4$†	Calcd.	23.47	4.60	10.09	614 (chloroform)	83	Dark green	EtOH	35–40
	Found	23.65	4.67	9.86	610 (chloroform)	102–102.5	Orange-red	Benzene	75
i. $(C_6H_{11}O)_4P_2Se_4$	Calcd.	37.22	5.74	8.00	774 (chloroform)	115–116	Orange-red	Benzene	70
	Found	36.98	5.71	8.00	772 (chloroform)				
j. $(C_2H_5O)_4P_2Se_5$	Calcd.	15.08	3.17	10.05	637 (benzene)	84	Golden yellow	Cyclohexane	70
	Found	15.00	3.30	10.20	612 (benzene)				
				61.97‡					
				62.10§					

n-Propyl derivative. †Isopropyl derivative. ‡Se (%) Calcd. §Se (%) Found.

Can. J. Chem. Downloaded from www.nrcresearchpress.com by 210.87.254.40 on 09/05/12
For personal use only.

Experimental

Reagents

The various alcohols were purchased from the Aldrich Chemical Company. They were dried over calcium oxide for a period of 6 h and then distilled. Red amorphous phosphorus was purchased from the Fisher Chemical Company. Grey selenium was supplied by the Canadian Copper Refiners, Ltd.

Cyclohexane, *n*-heptane, and toluene were purchased from the Aldrich Chemical Company. These were dried over phosphorus pentoxide and distilled before use. Spectral grade CCl_4, CS_2, and cyclohexane were purchased from the Curtin Chemical Company.

Spectra

All infrared spectra were recorded on the Beckman model IR-12 as KBr pellets or as solutions. The ultraviolet spectra were recorded on the Cary model 14-R. The n.m.r. spectra were recorded on the Varian model A-60. The potassium salts were run as solutions in D_2O, the tetraselenides in CCl_4, and the pentaselenide in CS_2. Whenever it was possible to do so, tetramethylsilane was used as the internal reference standard. Methylene chloride was used as the external standard for the D_2O solutions.

Phosphorus Pentaselenide

Red phosphorus was first washed with anhydrous ether and then dried *in vacuo*. Stoichiometric amounts of the dry phosphorus and finely powdered grey selenium were mixed intimately by rolling for 12 h in a ball-mill. The mixture was introduced into a heavy-walled glass container which was evacuated and then filled with nitrogen. The neck of the container was sealed and placed in a furnace where it was heated at 450 °C for 12 h. The container was removed from the furnace and allowed to cool overnight before it was broken.[1]

P_2Se_5 was obtained as a glassy black-purple solid. It was powdered in a ball-mill, preferably under a dry, inert atmosphere and then stored in a desiccator over P_2O_5. The finely powdered solid was examined on a G.E. X-ray diffractometer. Both rapidly and slowly quenched samples were examined, but no scattering patterns were observed. P_2Se_5 appears to be an amorphous solid. Analysis of a typical sample gave the values P 13.47% and Se 84.37%, which compares with the calculated values of 13.56% for P and 86.44% for Se. No success was achieved in the preparation of samples of this material which were sufficiently thin to allow for measurement of its infrared absorption. It was either totally insoluble or decomposed, in the usual organic solvents. P_2Se_5 hydrolyzes in air with the evolution of large amounts of gaseous H_2Se.

The P_2Se_5 prepared according to the method of Muthmann and Clever (3) was far less reactive than that described in this report. A definite loss of reactivity was observed on aging and this was probably due to hydrolysis of the sample when the container was opened to the atmosphere at various times during storage.

Preparation of Bis(O,O'-diethyldiselenophosphato)-selenium(II)

In a three-necked flask equipped with a mechanical stirrer, reflux condenser, and a separatory funnel a suspension of freshly ground P_2Se_5 (14 g, 0.034 mole) in 75 ml of cyclohexane was taken to reflux under an atmosphere of nitrogen. Then, 4.61 g of absolute ethanol (0.1 mole) was added dropwise until the evolution of H_2Se ceased, ~3.5 h. Any H_2Se was swept out by the nitrogen and trapped in sodium hydroxide. The suspension was filtered and to the bright orange-yellow filtrate was added 50 ml of low-boiling ligroin.[2] The solvent was stripped in a film type evaporator at reduced pressure until bright-yellow needles began to separate. The saturated solution was stored under nitrogen and cooled for 24 h. The bright-yellow crystals were separated by filtration and rapidly removed to a nitrogen-filled desiccator. The yields varied from 60–75%, based upon the reaction of 4 moles of alcohol with excess P_2Se_5.

As obtained the compound is analytically pure. It decomposes in air, depositing selenium, and invariably undergoes decomposition upon recrystallization. It can be recrystallized from cyclohexane and is readily soluble in CS_2 or CCl_4. The CS_2 solutions remain clear and stable for several hours. The pertinent analytical data are given in Table I.

Preparation of Bis(O,O'-dialkyldiselenophosphates)

Isopropyl or cyclohexyl alcohol was added to a boiling suspension of P_2Se_5 in *n*-heptane in the same molar ratio and under conditions identical with those described in the immediately preceding section. The filtrate, having a bright red-orange color was reduced in volume under reduced pressure until the formation of red-orange crystals was observed. The saturated solutions were cooled under nitrogen and yielded large, well-formed crystals whose stoichiometry corresponded to the formulation $(RO)_4P_2Se_4$. The yields averaged 75% and the pertinent analytical data are given in Table I.

These compounds were kept in air for indefinite periods without any apparent decomposition. They were readily soluble in CCl_4, CS_2, or benzene and were easily recrystallized from absolute ethanol.

Preparation of Tris(O,O'-dialkyldiselenophosphato)-chromium(III)

The filtrate obtained following the reaction of either ethanol or *n*-propanol with P_2Se_5 was treated with a slight excess of $CrCl_3 \cdot 6H_2O$ in ethanol. The volume of ethanol is just sufficient to dissolve the chromium salt. For each 6 moles of the alcohol used in the reaction, 1 mole of the chromium salt was added. For example, to the filtrate obtained from the reaction of 40 g of P_2Se_5 (~0.088 mole) with 25 ml (0.33 mole) of *n*-propanol in 100 ml of cyclohexane was added 18 g (0.067 mole) of $CrCl_3 \cdot 6H_2O$ in the minimum volume of ethanol required

[1] *Caution*: On several occasions the container exploded quite violently upon fracture of the glass neck. To avoid such potentially dangerous explosions it is recommended that the glass tube be enclosed in a screw-capped iron pipe. The narrow neck of the glass container is permitted to emerge through a hole drilled into one of these caps. The glass can then be broken by breaking the emergent neck. Should the container explode, the glass fragments will be contained within the pipe.

[2] The addition of ligroin was found to inhibit the deposition of selenium as a decomposition product.

Can. J. Chem. Downloaded from www.nrcresearchpress.com by 210.87.254.40 on 09/05/12
For personal use only.

to effect its dissolution. The mixture was refluxed for 30 min on a steam bath and filtered. Following overnight storage in a refrigerator, large, shiny, dark-green, almost black crystals of tris(O,O′-*n*-propyldiselenophosphato)-chromium(III) are deposited. The compounds were recrystallized from ethanol. The pertinent analytical data for the ethyl and *n*-propyl derivatives are given in Table I.

Preparation of the Potassium Salts of O,O′-dialkyldiselenophosphoric Acids

The preparation of potassium O,O′-di-*n*-butyldiselenophosphate will be described. This procedure is generally applicable for the preparation of the potassium salts.

Under an atmosphere of nitrogen, 14.82 g (0.20 mole) of *n*-butanol was added, with stirring, to a boiling suspension of finely divided P_2Se_5 (25 g, 0.055 mole) in 100 ml of *n*-heptane. The evolution of H_2Se ceased after 4 h. The solution was filtered. To the clear filtrate was added a solution containing 5.6 g of KOH (0.1 mole) in 25 ml of absolute ethanol. The combined solutions were stirred for 1 h. The solution was evaporated under reduced pressure until a precipitate began to separate. The saturated solution was stored under dry nitrogen and refrigerated for 12 h. The colorless crystals were separated by filtration under an atmosphere of dry nitrogen. The crystals were dried *in vacuo* (~0.1 mm) at a temperature of 35–45°.

The alcoholic KOH must be added to the reaction mixture immediately following the period of reflux. The potassium salts were all exceedingly hygroscopic and in the case of the *n*-amyl derivative continuous pumping for a period of 72 h at a temperature of 65° was necessary to obtain a solid of constant stoichiometry which was obtained as the monohydrate.

Potassium ethoxide was used successfully in place of KOH for the preparation of the potassium salts. The pertinent data for the five potassium salts which were characterized are given in Table I.

Results and Discussion

Physical Properties of Phosphorus Pentaselenide

The dark, almost black color of this compound, the absence of any crystalline structure, its glass-like appearance, and its tendency to fracture suggest that it possesses a band-type structure. One of the obvious ways to determine whether a solid possesses such a structure is to examine the widths of its spectral absorption bands. Although such experiments were attempted with thin slices of P_2Se_5, it began to decompose immediately upon contact with atmospheric moisture, as evidenced by the rapid evolution of H_2Se and the surface deposition of selenium. This behavior obviated the acquisition of any meaningful results. Although it has been reported that P_2Se_5 is red in color, this color is probably due to separation of red selenium as a result of decomposition of the sample or to incomplete fusion of the elements. The freshly fused material, unexposed to air, did not possess any red color.

The claim of Rathke (4) that P_2Se_5 could be recrystallized from carbon tetrachloride appears to be very doubtful. Attempts to reproduce his results by heating P_2Se_5 in CCl_4 in sealed tubes always resulted in decomposition of the compound. This claim may be further discounted in view of the fact that P_2Se_5 has been found to react with this solvent with the formation of carbon diselenide (6). Although it was found that P_2Se_5 did not undergo sublimation under the conditions used in this study, the possibility does exist that at sufficiently low pressure it may undergo such a transition.

Two important observations were made during the course of the preparation of P_2Se_5. They are: (*a*) the compound prepared by quenching the sealed tube from 450° to room temperature was found to possess a higher reactivity (towards alcohols) than the compound obtained on slow cooling and (*b*) aging rendered the material less reactive, the probable reason being that it undergoes hydrolysis on exposure to atmospheric moisture through handling.

It is very important that both the red phosphorus and selenium be thoroughly dried before fusion in the sealed tube.

Reaction of Phosphorus Pentaselenide with Alcohols

Although none of the O,O′-dialkyldiselenophosphates were isolated as free acids, their formation during the course of the reaction with phosphorus pentaselenide is inferred from the isolation of the potassium salts of O,O′-dialkyldiselenophosphates. The primary reaction of P_2Se_5 with alcohols is, therefore, represented by the equation

$$4ROH + P_2Se_5 = 2(RO)_2P(Se)SeH + H_2Se.$$

In all of the reactions, the ratio of the number of moles of the alcohol to that of the P_2Se_5 used was close to 4:1. The formation of $(RO)_2P(Se)SeH$ must be the primary reaction because (1) it was found necessary to add an ethanolic KOH solution *immediately* in order to get the salts, (2) the potassium salts were obtainable in every case, and (3) the potassium salts could not be prepared from either the bis(O,O′-dialkyldiselenophosphates) or bis(O,O′-diethyldiselenophosphato)selenium(II).

Can. J. Chem. Downloaded from www.nrcresearchpress.com by 210.87.254.40 on 09/05/12
For personal use only.

The potassium O,O′-dialkyldiselenophosphates were rather unstable and turned red upon storage. These salts were best preserved in sealed tubes under an atmosphere of nitrogen.

The preparation of the tris(O,O′-dialkyldiselenophosphato)chromium(III) complexes is similar to the preparation of their sulfur analogs (11). The formation of these chromium complexes may be represented by the equations

$$4ROH + P_2Se_5 = 2(RO)_2P(Se)SeH + H_2Se$$

$$3(RO)_2P(Se)SeH + CrCl_3\cdot 6H_2O = Cr[Se_2P(OR)_2]_3 + 3HCl + 6H_2O.$$

The chromium complexes were quite stable and did not require any special precautions for their storage. Jorgensen (12) prepared inner complexes of O,O′-diethyldiselenophosphate in low yields by the use of a fused mixture of 0.2 g-atom yellow phosphorus and 0.3 g-atom selenium powder. The yield of the tris(O,O′-diethyldiselenophosphato)chromium(III) was greatly improved when phosphorus pentaselenide was used as a reagent.

The formation of bis(O,O′-dialkyldiselenophosphate) and that of bis(O,O′-diethyldiselenophosphato)selenium(II) was rather unique and unexpected. The mechanism of their formation is not clear and requires further study. However, the first step almost certainly involves the formation of the O,O′-dialkyldiselenophosphoric acid. The bis(O,O′-dialkyldiselenophosphate) and bis(O,O′-diethyldiselenophosphato)selenium(II) could then form by the atmospheric oxidation of the P-bonded selenium.

$$2(RO)_2P(Se)SeH \xrightarrow{[O]} (RO)_4P_2Se_4 + H_2O$$

$$2(C_2H_5O)_2P(Se)SeH \xrightarrow[Se]{[O]} (C_2H_5O)_4P_2Se_5 + H_2O$$

There is always elemental selenium present in reaction mixtures of this type due to decomposition of the P_2Se_5 or of the O,O′-dialkyldiselenophosphoric acid itself. The H_2Se evolved during the course of the reactions could easily become a source of elemental selenium. There is a possibility that the O,O′-dialkyldiselenophosphoric acids could react with P_2Se_5 in the absence of air to yield the bis(O,O′-dialkyldiselenophosphate) and the bis(O,O′-diethyldiselenophosphato)selenium(II) along with the formation of a lower phosphorus selenide and elemental selenium.

$$2(RO)_2P(Se)SeH + 2P_2Se_5 = (RO)_4P_2Se_4 + P_4Se_3 + H_2Se + 6Se$$

$$2(RO)_2P(Se)SeH + 2P_2Se_5 = (RO)_4P_2Se_5 + P_4Se_3 + H_2Se + 5Se$$

There is a marked difference in the stabilities of the two types of compounds. Although the two bis(O,O′-dialkyldiselenophosphates) are quite stable, the bis(O,O′-diethyldiselenophosphato)selenium(II) was found to decompose rapidly. The colors of the two compounds also differ. Both of the tetraselenides are orange-red in color, while the pentaselenide is golden yellow. These differences will be discussed more quantitatively in the section dealing with their electronic spectra.

The possibility that the compounds with stoichiometry $(RO)_4P_2Se_4$ may be dimers of the O,O′-dialkyldiselenophosphoric acid, $[(RO)_2P(Se)SeH]_2$, was excluded because (1) no acid hydrogen could be detected upon titration with a standard base, (2) no absorption bands were observed in the region 2260–2350 cm^{-1}, which is the range assigned to absorption due to Se—H vibrational frequency (13–15), and (3) n.m.r. spectra in CCl_4 solutions failed to show the presence of any acidic protons.

By analogy with compounds having the formula (26), $R_2P(Se)—Se_n—P(Se)R_2$, structure (**1**) is assigned to the compounds with stoichiometry $(RO)_4P_2Se_4$ and $(RO)_4P_2Se_5$.

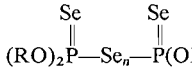

(1)

($n = 2$ for $(RO)_4P_2Se_4$; $n = 3$ for $(RO)_4P_2Se_5$)

The final structural assignments will be possible only after making a complete X-ray crystallographic study. Such a study has been initiated and preliminary data (16) for bis(O,O′-dicyclohexyldiselenophosphate) showed that the crystals are monoclinic with $a = 12.01_9$ Å, $b = 14.59_8$ Å, $c = 9.80_1$ Å, $\beta = 65.58°$, space group $P2_1/c$.

Proton N.M.R. Spectra

Lalezari and Sharghi (17) have recently investigated the proton shift of the SeH group in selenomercaptans and selenols. They reported a chemical shift 7.20–8.75 τ in a series of nine selenols. However, no mention of the size of the coupling constants is made in this paper, nor

TABLE II

^{1}H n.m.r. data for O,O′-dialkyldiselenophosphate derivatives

Compound	^{1}H chemical shift (τ scale)			$J_{CH_2CH_3}$		J_{P-CH_2}
$(CH_3CH_2O)_4P_2Se_5$	CH_3 8.62	CH_2 5.88		7.2		10.5
$(CH_3-\underset{\displaystyle CH_3}{\underset{\vert}{C}}H-O)_4P_2Se_4$	CH_3 8.62	$-\underset{\vert}{C}-H$ 5.2		J_{CH-CH_3} 6.5		J_{P-CH_2} ~0
$(CH_3CH_2O)_2P(Se)SeK$	8.85	6.09		$J_{CH_2CH_3}$ 7.2		J_{P-CH_2} 9.5
$(\overset{\gamma}{C}H_3\overset{\beta}{C}H_2\overset{\alpha}{C}H_2O)_2P(Se)SeK$	9.08	β CH_2 8.38	γ CH_2 6.06	$J_{CH_2CH_3}$ 7.2	$J_{P-\overset{\alpha}{C}H_2}$ 9.1	$J_{CH_2CH_2}$ 6.2
$(C_6H_{11}O)_4P_2Se_4$	C_6H_{10} 8.45	α-H 5.43		—		
$(C_6H_{11}O)_2P(Se)SeK$	C_6H_{10} 8.55	α-H 5.68				

was any integration of the peak areas carried out. These results cannot be considered conclusive at the present time. An examination of the ^{1}H n.m.r. spectra of bis(O,O′-diethyldiselenophosphato)selenium(II), bis(O,O′-diisopropyldiselenophosphate), and bis(O,O′-dicyclohexyldiselenophosphate) did not show any absorption in the region 7.20–8.75 τ, the region assigned to the Se—H proton by Lalezari and Sharghi.

The ^{1}H resonance spectra of phosphorus-containing compounds are rather complicated due to the possible long range coupling to ^{31}P which has a spin of 1/2. In the present study coupling by ^{31}P to the nearest methylene group was observed in the case of compounds having an ethyl or *n*-propyl group. The methine proton in the isopropyl group did not show any splitting due to ^{31}P. In the case of the cyclohexyl group, the poorly resolved 10-proton multiplet appeared as a broad band centered at ~ 8.45–8.55 τ. Coupling to the phosphorus could not be observed for lack of resolution. The eleventh proton, attached to the oxygen-bonded carbon, appeared as a small broad band around 5.68 τ. In all cases, when ^{31}P coupling was observed it was only to those protons attached to the α-carbon atom.

Ideally, the methylene protons of an ethyl group adjacent to a phosphorus atom should show an eight line spectrum. Coupling of the methylene protons to a single phosphorus nucleus will yield a doublet. Each of the two components of the doublet will then couple to the methyl protons to yield a set of two quartets, or a total of eight lines. The intensity of these lines will be in the ratio 1:3:1:3:3:1:3:1.

The ^{1}H spectrum of bis(O,O′-diethyldiselenophosphato)selenium(II) in CS_2 ideally illustrates the points made in the discussion immediately preceding. The methylene protons yield a well-defined eight line spectrum (Fig. 1), while the methyl protons, even under high resolution,

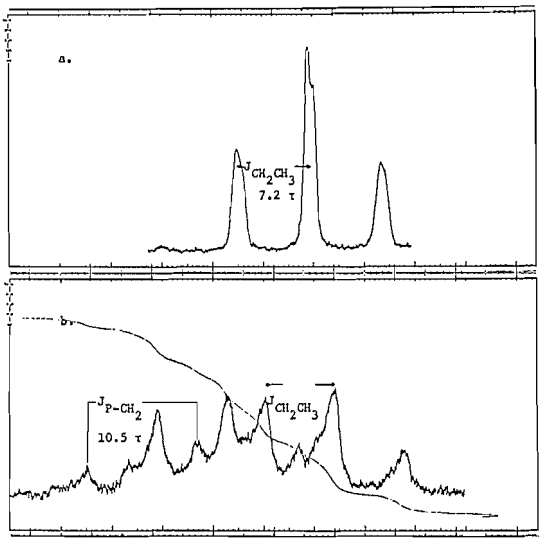

FIG. 1. Nuclear magnetic resonance spectrum of $(C_2H_5O)_4P_2Se_5$ in CS_2, 50 c.p.s. sweep: (*a*) methyl triplet; (*b*) methylene octet.

Can. J. Chem. Downloaded from www.nrcresearchpress.com by 210.87.254.40 on 09/05/12
For personal use only.

Can. J. Chem. Downloaded from www.nrcresearchpress.com by 210.87.254.40 on 09/05/12
For personal use only.

show the normal triplet without any splitting arising out of coupling to the phosphorus nucleus.

Table II summarizes the ^{1}H n.m.r. shifts and related coupling constants observed for the compounds prepared in this study. In the case of potassium O,O′-diethyldiselenophosphate the n.m.r. signal from the methylene protons was also observed as an octet. The n.m.r. spectrum of potassium O,O′-di-*n*-propyldiselenophosphate also showed coupling of the α-methylene protons to ^{31}P. In this case, a well-defined sextet was observed in what would otherwise be a triplet. In this molecule the protons of the β-methylene group and the terminal methyl group yielded the normal spectrum with no coupling to ^{31}P.

Overlapping of the multiplet components to yield a spectrum having fewer lines than the number expected has been observed (18). In the case of triethylphosphate, for example, the methylene protons appear as a quintet, 4.11 τ, and this is only one of a number of examples of such partial overlap reported in the literature (19) for similar compounds.

The absence of ^{31}P coupling to the methine proton in the case of the isopropyl derivative could possibly be due to shielding by the two attached methyl groups. The absence of such coupling has also been reported in triisopropylphosphate (19) and other isopropyl derivatives.

Harris *et al.* (20) studied the proton resonance spectra of a number of esters of pyrophosphoric and hypophosphoric acids and their sulfur analogs. All of the observations made in the present study, viz. ^{31}P coupling to the α-carbon only and the values of the chemical shifts and the coupling constants, are consistent with their work.

Infrared Spectra

Chittenden and Thomas (21) have observed two bands which they ascribe to ν(P=Se) in compounds of the type $(RO)_3PSe$, $(RO)_2RPSe$, and (RO)(HO)(R)PSe. To the higher frequency band they assign the number I, and to the lower frequency band the number II. Because, in the compounds which are the subject of this study, two bands were observed in the region of ν(P=Se), this notation is used. However, it should be pointed out that in a series of phosphine selenides, R_3PSe, ν(P=Se) was observed as a singlet (22).

In Table III the compounds which were studied in this investigation have been classified into one of three groups.

TABLE III

Observed frequencies for ν(P—Se) in various O,O′-dialkylselenophosphates and derivatives

Compound	P—Se stretching frequencies (cm^{-1}) I*	II*
Group A		
$(C_2H_5O)_2P(Se)SeK$	584	520
$(n\text{-}C_3H_7O)_2P(Se)SeK$	610	500
$(n\text{-}C_4H_9O)_2P(Se)SeK$	589	525
$(n\text{-}C_5H_{11}O)_2P(Se)SeK\cdot H_2O$	580	520
$(C_6H_{11}O)_2P(Se)SeK$	582	530
Group B		
$(i\text{-}C_3H_7O)_4P_2Se_4$	529	469
$(C_6H_{11}O)_4P_2Se_4$	512	477
$(C_2H_5O)_4P_2Se_5$	531	449
Group C		
$[(C_2H_5O)_2P(Se)Se]_3Cr(III)$	488	454
$[(n\text{-}C_3H_7O)_2P(Se)Se]_3Cr(III)$	500	460

*Chittenden and Thomas (21) notation.

The potassium salts exhibit an intense absorption which is observed over the rather narrow range 580–610 cm^{-1}. These values fall within the range assigned by several other workers (21–24). A second band, of lower intensity, which is tentatively assigned as band II falls within the range 500–530 cm^{-1}. In these molecules the two P—Se linkages may be expected to be equivalent, i.e. the structure may be described by the resonance form $(RO)_2P\begin{matrix}\diagup\!\!\!\diagup Se\\ \diagdown\!\!\!\diagdown Se\end{matrix}\ominus$. The two vibrations may arise from a number of well-known causes, but it would be highly speculative to specify a cause in such complicated molecules without additional experimental information.

The tetraselenides and the pentaselenide, which make up Group B, exhibit absorption due to P—Se stretching at frequencies lower than those of Group A. A strong, higher frequency band is observed in the range 512–531 cm^{-1} while band II, of medium intensity, falls within the limits 449–477 cm^{-1}. Structure (**1**), which has been assigned to these compounds, is consistent with the infrared data. The selenium atoms

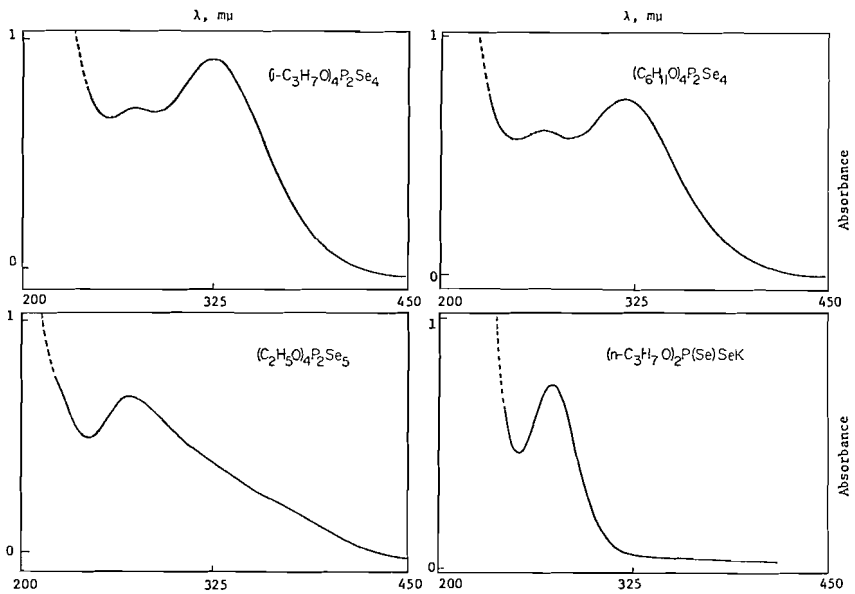

FIG. 2. Ultraviolet spectra of various dialkyldiselenophosphate derivatives in absolute ethanol.

attached to each of the phosphorus atoms in such a structure are non-equivalent and the higher frequency band presumably arises from the P—Se link having the higher bond order.

Group C is made up of the chromium(III) complexes. Values observed for the two P—Se frequencies are the lowest among the compounds studied. It should be noted that the two P—Se vibrations reported in Table III for these compounds are almost equal in their intensities. That these bands can be assigned with confidence to ν(P—Se) was corroborated by comparison of these spectra with those of the thio-analogues, i.e. $[(RO)_2P(S)S]_3Cr(III)$. The latter were prepared and they were found to be completely transparent in the region of ν(P—Se).

The absence of any absorption due to (Se—H) in any of the compounds has been mentioned earlier.

Electronic Spectra

The electronic spectrum of tris(O,O′-diethyldiselenophosphato)chromium(III), prepared in this study, exhibited absorption maxima at 727 mμ, 565 mμ, and 309 mμ (ε 430, 340, 14 000 respectively). These results are in excellent agreement with those reported by Jorgensen (12), who assigned them to the following transitions in the respective order

$$^4\Gamma_2 \rightarrow {}^4\Gamma_5,\ {}^4\Gamma_2 \rightarrow a^4\Gamma_4 \text{ and } \pi \rightarrow \gamma_3$$

The compounds bis(O,O′-diethyldiselenophosphato)selenium(II), bis(O,O′-diisopropyldiselenophosphate), and bis(O,O′-dicyclohexyldiselenophosphate) exhibited absorption maxima as recorded in Table IV.

TABLE IV

Absorption spectra of bis(O,O′-dialkyldiselenophosphates) and bis(O,O′-diethyldiselenophosphato)-selenium(II)

Compound	λ_{max} (mμ)	ε
$(C_2H_5O)_4P_2Se_5$	271	14 500
$(i\text{-}C_3H_7O)_4P_2Se_4$	(*a*) 324	9 800
	(*b*) 273	7 600
$(C_6H_{11}O)_4P_2Se_4$	(*a*) 318	9 500
	(*b*) 265	7 700

The compounds listed in Table IV, as can be seen in Fig. 2, show strong absorption in the ultraviolet region. These bands possess a long wavelength tail which extends well into the visible region. This long wavelength tail is undoubtedly responsible for the orange or yellow color of these compounds. Fredga (25) observed that among acids having the general formula, $HOOC—CH_2—Se—(CH_2)_n—Se—CH_2—COOH$, those with $n \neq 0$ were colorless, whereas, the acid with $n = 0$ was yellow. In the course of the synthesis of diethyldiselenophosphinic acid and its derivatives, Kuchen and Knop

Can. J. Chem. Downloaded from www.nrcresearchpress.com by 210.87.254.40 on 09/05/12
For personal use only.

Can. J. Chem. Downloaded from www.nrcresearchpress.com by 210.87.254.40 on 09/05/12
For personal use only.

(26) isolated compounds with the general formula $(C_2H_5)_2$—P(Se)—Se_n—P(Se)$(C_2H_5)_2$. They observed that the compound with $n = 1$ was colorless, whereas that with $n = 3$ was orange-red. Finally, Bergson and co-workers (27) cite a number of examples involving compounds having a Se—Se linkage, all of which are yellow to orange-red in color. It seems reasonable to conclude that the diselenide group constitutes a special chromophoric system. In the current study all of the potassium salts, which do not possess a Se—Se linkage, were observed to be colorless. The tetraselenides and the pentaselenide (structure **1**), on the other hand, are colored orange-red and yellow respectively. This further suggests the presence of a Se—Se bond in these compounds.

A simplified molecular orbital diagram has been constructed for dialkyldisulfides and diselenides (27), which utilizes only the σ-electron pair between the S or Se atoms and the two pairs of π-electrons on these atoms. In the compounds presently under consideration, however, such a simplification cannot be justified because of the presence of a large number of dissimilar atoms having higher energy levels. Jorgensen (12) has constructed a molecular orbital diagram for a central transition metal ion octahedrally surrounded by three $ROPSe_2^-$ groups. In his treatment, the lowest energy levels are the σ_{SeP} ones. Hence, the electrons from these levels are not expected to be easily excited. The intermediate levels are in the order σ_{SeM} and π_{+SeSe}(bonding) while the highest ligand levels below the metal d levels are the π_{-SeSe}(antibonding).

If the assumption is made that the σ_{SeP} levels in the tetra- and penta-selenides lie below the π_{SeSe} levels, as suggested by Jorgensen for the metal complex, then the molecular orbital diagram of Bergson and co-workers (27) may describe, in a very simple way, the transitions that are observed in these molecules. That is, they are transitions which arise from energy levels derived from the Se—Se bridge. However, the possibility that transitions among π_{PSe} levels may be involved cannot be ruled out. Unfortunately, such levels were not discussed in the Jorgensen treatment.

It is to be noted that the two bis(O,O′-dialkyldiselenophosphates) have almost identical spectra with respect to both the location of the maxima and their intensities. This suggests an equivalent structure with respect to the arrangements of the phosphorus and selenium atoms, as is to be expected.

The potassium salts prepared in this study also absorbed in the ultraviolet region. The two salts whose spectra were measured, the ethyl and *n*-propyl derivatives, possessed a single maximum at 273 mμ (ε 1200) and 262 mμ (ε 3200) respectively. These bands were much less intense than those observed for the penta- and tetra-selenides and did not extend into near ultraviolet or visible region (Fig. 2), and they are colorless.

Differential Thermal Analysis

The data obtained from the differential thermal analysis (d.t.a.) curves observed for the various compounds prepared in this study are recorded in Table V.

TABLE V

Differential thermal analysis data for O,O′-dialkyldiselenophosphate derivatives

Compound	Change at °C			
	Exothermic		Endothermic	
P_2Se_5	137	vw		
	148	vw		
	157	vw		
	161	vw		
	165	s		
	247	vw		
	370	s		
$(C_2H_5O)_4P_2Se_5$	105	s	75	s
	108	s		
	120	sh		
$(i\text{-}C_3H_7O)_4P_2Se_4$	138	s	108	s
	140	s	135	s
	142	sh		
	148	sh		
	157	sh		
$(C_6H_{11}O)_4P_2Se_4$	110	s	94	s
$Cr[Se_2P(OC_2H_5)_2]_3$	152	s	215	vw
	175	s		
$Cr[Se_2P(OC_3H_7)_2]_3$	172	s	82	s
			216	w
$Cr[S_2P(OC_2H_5)_3]$	211	s	154	s

ABBREVIATIONS: s = sharp, w = weak, vw = very weak, sh = shoulder, b = broad.

A few comments regarding some of the changes observed can be made. Tetraphosphorus triselenide melts at 245–246°. Sharp exothermic peaks were observed at ~239° and ~250°, indicating a possible spontaneous decomposition at a temperature near the observed m.p. of the material. Phosphorus pentaselenide showed a

well-defined exothermic peak at ~370°, indicating a decomposition of the compound at about this temperature.

The d.t.a. curve for bis(O,O′-diethyldiselenophosphato)selenium(II) showed a sharp endothermic peak at ~75°. The observed m.p. of the compound was 84°.

Bis(O,O′-diisopropyldiselenophosphate) was characterized by a sharp endothermic peak at 108°, the observed melting point of the same compound was 102–102.5°. Bis(O,O′-dicyclohexyldiselenophosphate) showed a sharp exothermic peak at 110°; its observed m.p. was 115–116°. This suggests a decomposition near the melting point. Tris(O,O′-diethyldiselenophosphato)chromium(III) showed a sharp exothermic peak at 152° while its observed m.p. was 160°. This also suggests a decomposition near the melting point. Further, a weak endothermic peak was observed at ~215°. The melting point of grey selenium is 217°. Hence, the endothermic peak at 215° may result from the formation of elemental selenium and subsequent decomposition.

Tris(O,O′-di-*n*-propyldiselenophosphato)-chromium(III) had a m.p. of 83°. The d.t.a. curves for the compound were characterized by a sharp endothermic peak at 82°. As in the previous case, a weak endothermic peak at 216° suggested the formation of elemental selenium. A m.p. of 160° has been recorded for tris(O,O′-di-*n*-propyldithiophosphato)chromium(III). Its d.t.a. curve had an exothermic maximum at 154°.

It should be noted that the temperatures on the recorder were not calibrated.

Acknowledgments

The authors wish to acknowledge the financial support furnished by the Selenium–Tellurium Development Association, Inc., the U.S. Atomic Energy Commission under contract No. AT-(40-1)-2733, and the Robert A. Welch Foundation, Houston, Texas. We appreciate the assistance of Dr. B. M. Benjamin, Oak Ridge National Laboratory, for running the n.m.r. spectra of some of our samples at a time when our instrument was not operative.

1. J. J. BERZELIUS. *In* Gmelins Handbuch der anorganischen Chemie. Sys. no. 9–12. Verlag Chemie, Weinheim/Bergstr. 1942. p. 244.
2. L. CARIUS and W. BOGEN. Ann. **124**, 57 (1862).
3. W. MUTHMANN and A. CLEVER. Z. Anorg. Chem. **13**, 191 (1897).
4. B. RATHKE. Ann. **152**, 200 (1869).
5. H. BEHRENS and G. HASCHKA. Ber. **94**, 1191 (1961).
6. N. N. YAROVENKO, G. B. GAZIYEVA, V. N. SHEMANINA, and N. A. FEDOROVA. Zh. Obshch. Khim. **29**, 940 (1959).
7. C. PALL. Ber. **18**, 2255 (1885).
8. K. A. JENSEN, G. SELBERT, and B. KAGI. Acta Chem. Scand. **20**, 281 (1965).
9. R. STOLLE and L. GUTMANN. J. Prakt. Chem. **69**, 509 (1934).
10. J. H. VAN DEN HENDE and E. KLINGSBERG. J. Am. Chem. Soc. **88**, 5045 (1966).
11. D. E. COLDBERY, W. C. FERNELIUS, and M. SHAMMA. Inorganic syntheses. Vol. VI. McGraw-Hill Book Company, Inc., New York. 1960. pp. 142–143.
12. C. K. JORGENSEN. Mol. Phys. **5**, 485 (1962).
13. N. SHARGHI and I. LALEZARI. Spectrochim. Acta, **20**, 237 (1964).
14. A. B. HARVEY and M. K. WILSON. J. Chem. Phys. **45**, 678 (1966).
15. D. M. CAMERON, W. C. SEARS, and H. H. NIELSEN. J. Chem. Phys. **7**, 994 (1939).
16. R. F. COPELAND. Private communication.
17. I. LALEZARI and N. SHARGHI. Spectrochim. Acta, **23**, 1948 (1966).
18. N. S. BHACCA, L. F. JOHNSON, and J. N. SHOOLERY (*Compilers*). High resolution n.m.r. spectra catalog. Vol. 2. Analytical and Instrument Division, Varian Associates, Pasadena, California. 1962. Spectrum no. 482.
19. Catalog of nuclear magnetic resonance spectral data. Manufacturing Chemists' Association Research Project, Chemical Thermodynamic Properties Center, Texas A&M University, College Station, Texas. Loose-leaf data sheets, extant, 1967. Serial Nos. 3–55.
20. R. K. HARRIS, A. R. KATRITZKY, S. MUSIEROWICZ, and B. TERNAI. J. Chem. Soc. (A), 37 (1967).
21. R. A. CHITTENDEN and L. C. THOMAS. Spectrochim. Acta, **20**, 1679 (1964).
22. R. A. ZINGARO. Inorg. Chem. **2**, 192 (1963).
23. L. C. THOMAS and R. A. CHITTENDEN. Chem. Ind. London, 1913 (1961).
24. E. GRYSZKIEWICZ-TROCHIMOWSKI, J. QUINCHON, O. GRYSZKIEWICZ-TROCHIMOWSKI, and M. LESECH. Bull. Soc. Chim. France, 739 (1961).
25. A. FREDGA. Svensk Kem. Tidskr. **48**, 91 (1936).
26. W. KUCHEN and B. KNOP. Angew. Chem. 77, 259 (1965).
27. G. BERGSON, G. CLAESON, and L. SCHOTTE. Acta Chem. Scand. **16**, 1159 (1962).

Can. J. Chem. Downloaded from www.nrcresearchpress.com by 210.87.254.40 on 09/05/12
For personal use only.

Chemistry of phosphorus pentaselenide. II. Its reaction with amines

ROBERT G. MELTON AND RALPH A. ZINGARO
Department of Chemistry, Texas A&M University, College Station, Texas

Received September 26, 1967

The reaction of phosphorus pentaselenide with amines may yield, as products, selenophosphoric triamides, $(RNH)_3PSe$; alkylammonium diselenophosphoric diamides, $(RNH)_2P(Se)Se^-RNH_3^+$; or alkylammonium monoacidbis(diselenophosphoric diamides), $\{[(RNH)_2P(Se)Se]_2H\}^-RNH_3^+$, where R is an alkyl group. The preparation of potassium diselenophosphoric diamides, $(RNH)_2P(Se)Se^-K^+$, is also described.

Canadian Journal of Chemistry, 46, 1425 (1968)

Can. J. Chem. Downloaded from www.nrcresearchpress.com by 210.87.254.6 on 09/05/12
For personal use only.

This paper describes the reaction of phosphorus pentaselenide with primary amines. The reactions of phosphorus pentaselenide which were previously reported have been reviewed in the first paper of this series (1). In this part, selenophosphoric triamides, $(RNH)_3PSe$ (**1**); alkylammonium diselenophosphoric diamides, $(RNH)_2P(Se)Se^-RNH_3^+$ (**2**); potassium diselenophosphoric diamides, $(RNH)_2P(Se)Se^-K^+$ (**3**); and alkylammonium monoacidbis(diselenophosphoric diamides), $\{[(RNH)_2P(Se)Se]_2H\}^-RNH_3^+$ (**4**), where R is an alkyl group, have been prepared by the reactions of P_2Se_5 with primary amines.

The nature of the reaction of phosphorus pentasulfide with primary amines has been known for several years (2) and the subject has been reviewed by Cowley (3). The reaction of P_2Se_5 with primary amines has not been the subject of previous investigations.

Experimental

Reagents

All amines were purchased from the Baker Chemical Company and were stored over sodium hydroxide. They were distilled just prior to use. Red phosphorus powder was purchased from Mallinckrodt Chemical Company. It was washed several times with anhydrous ethyl ether and dried *in vacuo* over phosphorus pentoxide before use. Selenium powder was supplied by the Canadian Copper Refiners Ltd. Heptane (96–100°) and ligroin (66–75°) was purchased from Eastman Organic Chemicals Company. Ethanol (absolute) was purchased from the U.S. Industrial Chemical Company.

Phosphorus Pentaselenide

Phosphorus pentaselenide was prepared according to the procedure described by Kudchadker *et al.* (1). Stoichiometric amounts of dry red phosphorus powder were intimately mixed with selenium powder. The mixture was sealed in a glass container under an atmosphere of nitrogen and was then heated to 450° for 12 h. After cooling to room temperature, the glass container was broken and the glassy, grayish black P_2Se_5 was removed and ground into a fine powder in a ball-mill before use.

N,N',N''-Tris(cyclohexyl)selenophosphoric Triamide

This compound was prepared by the dropwise addition of a stoichiometric amount (0.9 mole) of cyclohexylamine to a suspension of powdered P_2Se_5 (0.1 mole) in 200 ml of heptane at 50°, with stirring, under an atmosphere of nitrogen, over a period of 2 h. After the reaction mixture was stirred for an additional 3 h, the solid cyclohexylammonium hydrogen selenide which precipitated was separated, along with other solids, from the reaction mixture. The filtrate, which contained a suspension of colloidal selenium, was allowed to remain in a stoppered flask until the red selenium converted to the stable gray form which settled rapidly. Finally, the filtrate was refiltered and the product $(C_6H_{11}NH)_3PSe$ was recovered from the second filtrate by evaporation of the heptane solvent in a film-type evaporator at reduced pressure. Purification was accomplished by first washing the solid product with ligroin. It was redissolved in the minimum volume of a *cool* heptane–ethanol mixture. The solvents were slowly removed by evaporation at reduced pressure until the crystalline product separated. The latter was removed, dried *in vacuo*, and stored in evacuated, sealed glass tubes.

Alkylammonium Diselenophosphoric Diamides

Compounds of the type $(RNH)_2P(Se)Se^-RNH_3^+$ were prepared by the addition of a stoichiometric amount of the amine (0.7 mole) to a suspension of powdered P_2Se_5 (0.1 mole) in heptane. The reaction conditions and methods of recovery and purification were the same as those just described for the preparation of N,N',N''-tris(cyclohexyl)selenophosphoric triamide. It must be emphasized that the solution containing the compound should not be evaporated to dryness. Continued pumping on the solvent-free crystals will cause the loss of a mole of amine and conversion to the acid salt.

Potassium N,N'-Bis(butyl)diamidodiselenophosphate

Potassium N,N'-bis(butyl)diamidodiselenophosphate, $(C_4H_9NH)_2P(Se)Se^-K^+$, was prepared by the reaction of butylammonium N,N'-bis(butyl)diamidodiselenophosphate (0.01 mole) with a stoichiometric amount of alcoholic potassium hydroxide (0.01 mole) in ethanol under an atmosphere of nitrogen. After refluxing the reaction mixture for 2 h, the solution was filtered and evaporated to dryness at reduced pressure (0.1 mm).

TABLE I

Data for selenophosphoric amides*

Compound		Calcd. (%)	Found (%)	Melting point (°C)	Yield (%)	ν(P=Se) (cm^{-1})
N,N′,N″-Tris(cyclohexyl)selenophosphoric triamide	C	53.46	53.35	168–169	10	599
	H	8.97	8.91			
	P	7.66	7.62			
	Se	19.52	19.28			
Hexylammonium N,N′-bis(hexyl)diamidodiselenophosphate	C	43.99	43.87	88–89 (decomp.)	4	543
	H	9.02	9.12			
	P	6.30	6.42			
	Se	32.13	32.05			
Butylammonium N,N′-bis(butyl) diamidodiselenophosphate	C	35.38	35.61	117–120 (decomp.)	6	540
	H	7.93	8.02			
	N	10.31	10.42			
	P	7.60	7.80			
	Se	38.77	39.01			
Isobutylammonium N,N′-bis(isobutyl)-diamidodiselenophosphate	C	35.38	35.15	164–166 (decomp.)	7	552
	H	7.93	8.06			
	P	7.60	7.33			
	Se	38.77	38.50			
sec-Butylammonium N,N′-bis(*sec*-butyl)-diamidodiselenophosphate	C	35.38	35.49	132–134 (decomp.)	11	547
	H	7.93	8.00			
	P	7.60	7.57			
	Se	38.77	38.52			
Isobutylammonium monoacidbis[N,N′-bis(isobutyl)diamidodiselenophosphate]	C	32.39	32.30	86	11	580
	H	7.20	7.34			
	N	9.45	9.26			
	P	8.35	8.54			
	Se	42.60	43.04			
sec-Butylammonium monoacidbis[N,N′-bis(*sec*-butyl)diamidodiselenophosphate]	C	32.39	32.08	95–96	8	566
	H	7.20	7.25			
	P	8.35	8.18			
	Se	42.60	42.10			
Potassium N,N′-bis(butyl)diamidodiselenophosphate	C	25.82	25.64	Above 300°	Quantitative based on onium salt	545
	H	5.37	5.50			
	Se	42.44	42.25			

*Analyses were performed by the Galbraith Laboratories, Knoxville, Tennessee, and by the Schwarzkopf Laboratories, Woodside, New York.

The resulting solid was purified by dissolution in the minimum volume of a heptane–ethanol mixture at room temperature followed by filtration and evaporation under reduced pressure until crystals of the solid separated.

Isobutylammonium Monoacidbis[N,N′-bis(isobutyl)-diamidodiselenophosphate]

$\{[(C_4H_9NH)_2P(Se)Se]_2H\}^-C_4H_9NH_3^+$ was prepared by the evaporation, at reduced pressure (0.1 mm), of a heptane–ethanol solution (1:1 by volume) of isobutylammonium N,N′-bis(isobutyl)diamidodiselenophosphate. Following the complete removal of the solvent, pumping was continued on the crystals until they acquired a constant weight. Free amine was collected in the cold trap of the vacuum pump. Purification of the resulting solid product was accomplished in the manner described for the compounds prepared in the preceding sections. The same procedure was used for the preparation of *sec*-butylammonium monoacidbis[N,N′-bis(*sec*-butyl)diamidodiselenophosphate].

Spectra

The infrared spectra of all of the compounds were recorded on a Beckman IR 12 double beam spectrophotometer. The KBr pellet technique was used. Samples were scanned between 200 and 4000 cm^{-1}. Nuclear magnetic reasonance (n.m.r.) spectra were run on a Varian A-60 n.m.r. spectrometer.

Results and Discussion

The eight selenophosphoric amides which were prepared in this study are listed in Table I along with other pertinent physical data. All of the selenophosphoric amides were found to be

Can. J. Chem. Downloaded from www.nrcresearchpress.com by 210.87.254.6 on 09/05/12
For personal use only.

Can. J. Chem. Downloaded from www.nrcresearchpress.com by 210.87.254.6 on 09/05/12
For personal use only.

unstable in air. This was especially true of the alkylammonium salts of the diselenophosphoric diamides (**2**). For this reason, all reactions and recovery and recrystallization of the products were carried out in a dry, nitrogen atmosphere. The reported yields are not the highest attainable. No systematic study was made for the purpose of maximizing the yields.

In contrast with the analogous reactions of P_2S_5 with primary amines in which large amounts of H_2S are evolved, viz.

$$12RNH_2 + P_4S_{10} \rightarrow 4(RNH)_3PS + 6H_2S$$

$$8RNH_2 + P_4S_{10} \rightarrow 4(RNH)_2P(S)SH + 2H_2S,$$

H_2Se and $(RNH)_2P(Se)SeH$ were never isolated as the free acids, but only as the alkylammonium salts, $RNH_3^+HSe^-$ and $(RNH)_2P(Se)\text{-}Se^-RNH_3^+$. Both H_2Se and the selenophosphoric acids are expected to be stronger acids than the corresponding thio-derivatives. Thus, they readily form salts with the excess amine present in the reaction mixture. The formation of the products that were isolated is described by the following reactions.

$$9RNH_2 + P_2Se_5 \rightarrow 2(RNH)_3PSe + 3RNH_3^+HSe^-$$

$$7RNH_2 + P_2Se_5 \rightarrow 2(RNH)_2P(Se)Se^-RNH_3^+ + RNH_3^+HSe^-$$

$$(RNH)_2P(Se)Se^-RNH_3^+ + KOH \xrightarrow{EtOH} (RNH)_2P(Se)Se^-K^+ + RNH_2 + H_2O$$

$$2(RNH)_2P(Se)Se^-RNH_3^+ \xrightarrow{vacuum} \{[(RNH)_2P(Se)Se]_2H\}^-RNH_3^+ + RNH_2$$

In comparison with the reaction of P_2Se_5 with alcohols in which compounds containing bridged Se_2 and Se_3 bonds were formed (1), the reactions of P_2Se_5 with primary amines proceeded in the manner expected. This was probably due to the fact that the free acids that were formed were rapidly converted to the stable alkylammonium salts. This precluded any secondary reactions involving the unstable, free acids.

Except for the reaction of cyclohexylamine, triamides were not isolated at atmospheric pressure. Since Buck and co-workers (2) reported that dithiophosphoric diamides were intermediates in the formation of thiophosphoric triamides, the conversion of selenophosphoric diamides to the triamides may be possible if the reactions are carried out under pressure. It is probable that the failure to isolate ethyl or *n*-propyl derivatives was due to the loss of these volatile amines under the conditions under which these reactions were carried out. These derivatives could probably be prepared under reaction conditions which would involve the use of high pressures.

Infrared and N.M.R. Spectra

The assignment of the P═Se vibration was based on previous work which established the location of the fundamental P═Se vibration (4–6) and was corroborated in the case of the selenophosphoric triamide by a comparison of the series of molecules $(C_6H_{11}NH)_3P{=}O$ (7), $C_6H_{11}NH)_3P{=}S$, and $(C_6H_{11}NH)_3P{=}Se$. The fundamental P═Se vibrational band of all selenophosphoric amides occurs as a singlet in the predicted region. The frequencies observed for ν(P—Se) are listed in Table I.

Nuclear magnetic resonance spectra did not distinguish between the protons on the corresponding ammonium, $(RNH)_2P(Se)Se^-RNH_3^+$, and ammonium monoacid salts, $\{[(RNH)_2P(Se)\text{-}Se]_2H\}^-RNH_3^+$. The protons on the ammonium cation and any acid proton, if present, appeared as a rather broad peak at 5.99 τ with respect to tetramethylsilane. When treated with D_2O, this peak disappeared very rapidly showing that any acid proton was in rapid exchange with the protons attached to the N-onium atom. No resonance peaks were observed at 8.75 τ which Lalezari and Sharghi (8) have recently reported as the region for the Se—H proton in selenols. The infrared spectra of the alkylammonium and alkylammonium monoacid salts were essentially identical.

A hydrogen bond between two selenium atoms, Se—H···Se may possibly exist in anions of the type (**4**) prepared in this study. This is very unlikely, however, because of the relatively large size and low electronegativity of selenium. It is more likely that the proton is associated, probably through hydrogen bonding, to the smaller, electronegative nitrogen atoms attached to the phosphorus.

X-ray Data

Preliminary X-ray crystallographic data on a single crystal of isobutylammonium monoacid-bis[N,N′-bis(isobutyl)diamidodiselenophosphate] indicates a triclinic space group and a molecular weight of $(730 \pm 10)/p$, where p is an integer (the actual molecular weight is 741.45).

It was found that $a = 11.24$ Å, $b = 19.96$ Å, $c = 15.88$ Å, $\gamma = 93.0°$, $\alpha = 93.5°$, and $\beta = 93.5°$.[1] Inasmuch as the assumed molecular weight is that of the acid salt and because the molecular weight of any other reasonable species is totally inconsistent with these data, the assumption of a structure involving an acid anion seems very reasonable. The final results of this X-ray study should prove to be most interesting.

Acknowledgments

We express our appreciation for financial assistance to The Robert A. Welch Foundation of Houston, Texas, and to the U.S. Atomic Energy Commission for support under Contract No. AT-(40-1)-2733. We wish to thank Dr. Edward A. Meyers and Dr. Nancy Smith for furnishing us with their crystallographic data. Also we thank the Selenium–Tellurium Developement Association, Inc., for the gift of selenium and the Stauffer Chemical Company for a sample of thiophosphoryl trichloride.

[1]E. A. Meyers, Texas A&M University. Unpublished results.

1. M. V. KUDCHADKER, R. A. ZINGARO, and K. J. IRGOLIC. Can. J. Chem. This issue.
2. A. C. BUCK, J. D. BARTLESON, and H. P. LANKELMA. J. Am. Chem. Soc. **70**, 744 (1948).
3. A. H. COWLEY. J. Chem. Educ. **41**, 530 (1964).
4. L. C. THOMAS and R. A. CHITTENDEN. Technical Paper 784. Chemical Defense Experimental Establishment, Great Britain. July 28, 1961.
5. V. V. TURKEVICH and I. F. VIBLII. Zh. Prikl. Spectroskopii, Akad. Nauk Belorussk. SSR, **4**, 77 (1966).
6. R. A. ZINGARO. Inorg. Chem. **2**, 192 (1963).
7. L. F. AUDRIETH and A. D. F. TOY. J. Am. Chem. Soc. **64**, 1553 (1942).
8. I. LALEZARI and N. SHARGHI. Spectrochim. Acta, **23A**, 1948 (1967).

Can. J. Chem. Downloaded from www.nrcresearchpress.com by 210.87.254.6 on 09/05/12
For personal use only.

Vacuum ultraviolet chemiluminescence from the reactions of active nitrogen with I_2, IBr, ICl, and ICN

L. F. PHILLIPS
Chemistry Department, University of Canterbury, Christchurch, New Zealand

Received August 10, 1967

Numerous emission lines from excited I, Br, and Cl atoms have been observed between 1261 and 2062 Å. For the flames with I_2, IBr, and ICl it is possible to assign excitation mechanisms on the basis of the dependence of emission intensity on either [N] or $[N]^2$. In the case of dependence on [N] the emission is the result of energy transfer from an excited nitrogen molecule, which is produced by reaction of N with NI, has an energy of 185 ± 3.5 kcal/mole, and is identified with the predicted $^3\Delta_u$ species. The dissociation energy of NI is found to lie between 35.6 and 40 ± 3.5 kcal/mole. It is proposed that excited nitrogen molecules can be produced as well as removed very rapidly by processes of the type

$$N(^4S) + N_2(^3\Delta_u) \rightarrow N_2(^1\Sigma_g^+, v \gg 0) + N(^4S)$$

$$N(^4S) + N_2(^1\Sigma_g^+, v \gg 0) \rightarrow N_2(^3\Sigma_u^+) + N(^4S).$$

Canadian Journal of Chemistry, 46, 1429 (1968)

Can. J. Chem. Downloaded from www.nrcresearchpress.com by 210.87.254.5 on 09/05/12
For personal use only.

Introduction

Previous studies (1–6) of chemiluminescence arising from reactions of active nitrogen with halogens were concerned mainly with the processes leading to emission by excited halogen molecules, although the ready excitation of atomic iodine lines at 2062 and 1876 Å has also been known for a long time (2).

In the present work the observations of flame spectra have been extended into the vacuum ultraviolet (u.v.), as far as the lithium fluoride cutoff at 1024 Å. The unexpected outcome of these studies is that a rich emission spectrum has been found, with many strong atomic lines between 1500 and 1900 Å, and with weaker lines as far down as 1261 Å. Practically all of the emission is due to excited iodine atoms, though chlorine and bromine lines have also been observed.

In order to obtain some information about the excitation mechanisms of these lines their intensities were measured as a function of the nitrogen atom concentration in the reaction tube. For ICN the results of such measurements have no ready interpretation at present, but from the results for I_2, IBr, and ICl it has been possible to deduce a reaction scheme which provides a unified interpretation of (i) the vacuum u.v. emission from I_2, IBr, and ICl flames; (ii) the banded visible and u.v. emission from these flames; (iii) the visible and u.v. line emission from flames of active nitrogen with metal halides (7) and carbonyls (8).

The main novel feature of this scheme is the important role which it assigns to nitrogen molecules in the $^3\Delta_u$ state. Energy transfer from $^3\Delta_u$ molecules was earlier postulated by Kenty (9) to account for excitation processes in weak electrical discharges through nitrogen. The present results provide support for his conclusions as to the energy and radiative lifetime of this species. The $A.^3\Sigma_u^+$ state of N_2, which has been observed at low concentrations in the N–I_2 flame (10), and which was previously believed to be responsible for exciting the banded emission from this flame, is now considered to be present largely as a consequence of collisional deactivation of the $^3\Delta_u$ state by atomic nitrogen.

For emission features which require more excitation energy than is available from the $^3\Delta_u$ state a different excitation mechanism, one involving $^5\Sigma_g^+$ nitrogen molecules, is postulated. Such a mechanism was previously proposed for the flames with metal halides, and is probably also applicable to the flames with metal carbonyls.

Experimental

Active nitrogen from a microwave discharge at ca. 3 Torr entered a 25 mm o.d. pyrex reaction tube, where it was mixed with I_2, IBr, ICl, or ICN carried in a stream of nitrogen from a simple saturator. The saturator flow was adjusted to produce an intense visible reaction flame in the 5 cm length of tube between the halogen inlet and the pumping lead. The flame normally extended a further 30 cm to the cold-trap protecting the pump. A countercurrent of nitrogen prevented any solid reaction products (either CN polymer, or I_2O_5 resulting from the presence of a trace of O_2 in the prepurified nitrogen) from reaching a Harshaw lithium fluoride window situated at the far end of the reaction tube, 15 cm from the halogen inlet jet. ICN was prepared[1] by the method of Goy, Shaw, and

[1]I am grateful to Mr. Q. J. F. Grady for preparing this sample of ICN.

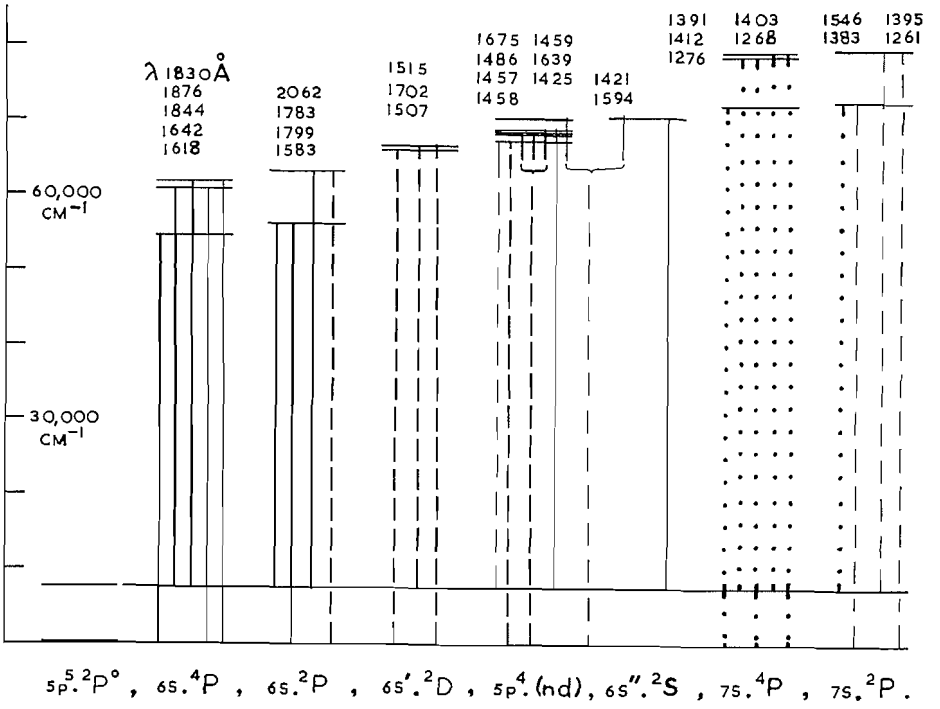

FIG. 1*a*. Transitions from the observed excited states of atomic iodine. Heavy unbroken lines indicate strong emission, thin unbroken lines moderately strong, heavy broken lines weak, thin broken lines very weak, and dotted lines very very weak or unobserved emission. The following groups of lines were not able to be resolved because of the need to use wide slits: 1457.5, 1458.0, and 1458.8 Å; 1383.2, 1390.8, 1392.5, and 1395.0 Å; 1261.3 and 1267.6 Å.

Pritchard (11); other materials were as previously described (6). The spectrometer was a McPherson model 218, with a 2400 lines/mm grating, sodium salicylate screen, and EMI type 9514 SA photomultiplier. Entrance and exit slit widths were varied from 10 μ, for the strongest lines, to 400 μ for lines below 1400 Å. The nitrogen afterglow intensity halfway along the 5 cm length of reaction tube was monitored with an RCA type 1P21 photomultiplier in combination with a Spectrolab P-type interference filter of 15 Å half-width at 6250 Å. Nitrogen atom concentrations were varied, when necessary, by varying the power supplied to the discharge.

Results

(*i*) *The Observed Transitions*

The observed emission lines of atomic iodine are shown in Fig. 1*a* (energy levels from Moore (12)). The same lines were present in each of the four flames, but with noticeably lower intensity in the flames of ICl and ICN. Essentially all the predicted transitions to the lowest (^{2}P) term of iodine (I) were observed for the terms 6s.^{4}P, 6s.^{2}P, 6s'.^{2}D, 5p^4.nd, 6s''.^{2}S, and 7s.^{2}P. There is some uncertainty about the transitions from

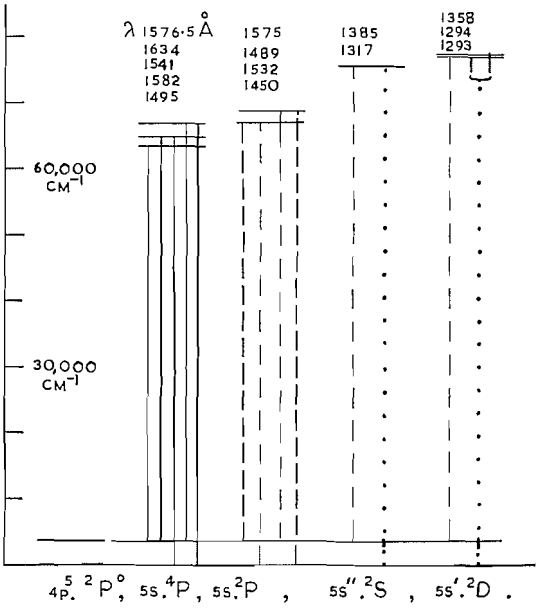

FIG. 1*b*. Transitions from observed excited states of atomic bromine. Strengths indicated as in Fig. 1*a*.

Can. J. Chem. Downloaded from www.nrcresearchpress.com by 210.87.254.5 on 09/05/12
For personal use only.

Can. J. Chem. Downloaded from www.nrcresearchpress.com by 210.87.254.5 on 09/05/12
For personal use only.

$7s.^4P$; of the two lines which would not be confused with transitions from $7s.^2P$, that at 1276 Å was classified as very very weak, and that at 1403 Å was not observed at all. These lines are expected to be relatively weak because of the change of spin that is involved in going to the ground state. The most energetic transition observed, that at 1261 Å, required an excitation energy of 226.6 kcal/mole.

In the IBr flame lines of Br (I) were observed below 1650 Å, with intensity comparable to that of iodine lines in the same region. The observed transitions are shown in Fig. 1*b*. Corresponding Cl (I) lines lie below 1400 Å, where the necessity of using wide slits made identification a problem. However, there was a definite feature at 1360 Å which could be attributed to the transitions from $4s.^2P_{1\frac{1}{2}}$ and $4s.^2P_{\frac{1}{2}}$ to $3p^5.^2P_{\frac{1}{2}}$. A less definite feature near 1340 Å probably represented the transitions from these same excited levels to $3p^5.^2P_{1\frac{1}{2}}$. No transitions could be observed from $4s.^4P$ levels, presumably because spin conservation is a powerful constraint in the case of atomic chlorine. No short-wavelength emission from CN radicals was observed, neither in the ICN flame, nor in a separate experiment with cyanogen.

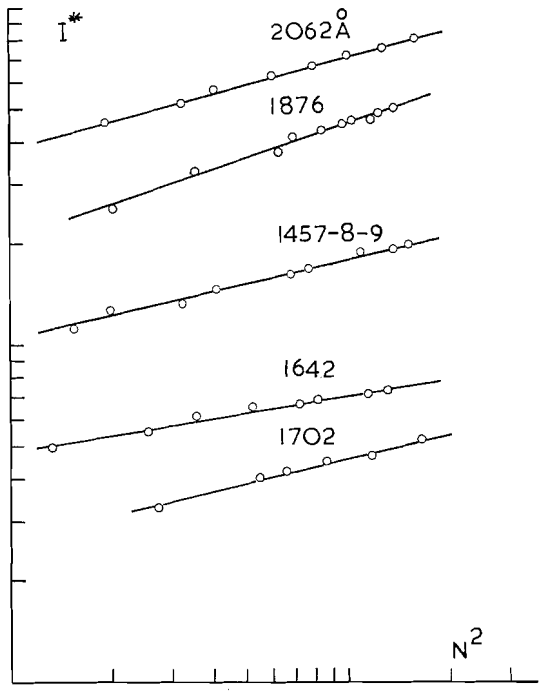

FIG. 2. ICN flame: representative graphs of log intensity for various iodine lines versus log intensity at 6250 Å (nitrogen afterglow region). Results obtained by measuring intensities simultaneously as the discharge power was varied.

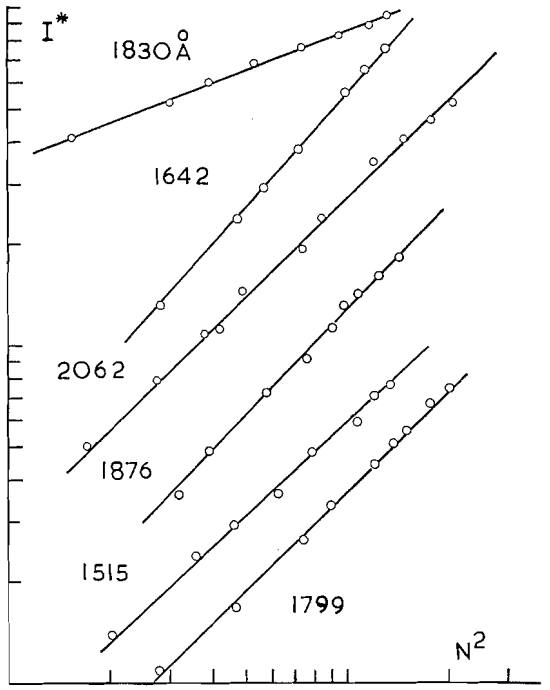

FIG. 3. ICl flame: representative graphs of log intensity of atomic iodine lines versus log intensity of the nitrogen afterglow.

(ii) Dependence of Intensity on Nitrogen Atom Concentration

The data here consist of simultaneous values of intensity for the nitrogen afterglow, proportional to $[N]^2$ (13), and for the individual atomic lines. Typical results are plotted logarithmically in Figs. 2, 3, 4, and 5.

In the case of ICN the lines show only a slow variation with nitrogen atom concentration (approximately $[N]^{1/2}$). With I_2 and IBr the lines arising from $6s.^2P$ and $6s.^4P$ levels of atomic iodine vary as [N], while those arising from higher levels (this includes all bromine lines) vary as $[N]^2$. In the case of ICl the lines all vary as $[N]^2$, with the exception of the line at 1830 Å which varies as [N]. It is noteworthy that the banded emission from these flames varied as [N] in the case of I_2 and IBr, and as $[N]^2$ in the case of ICl (6).

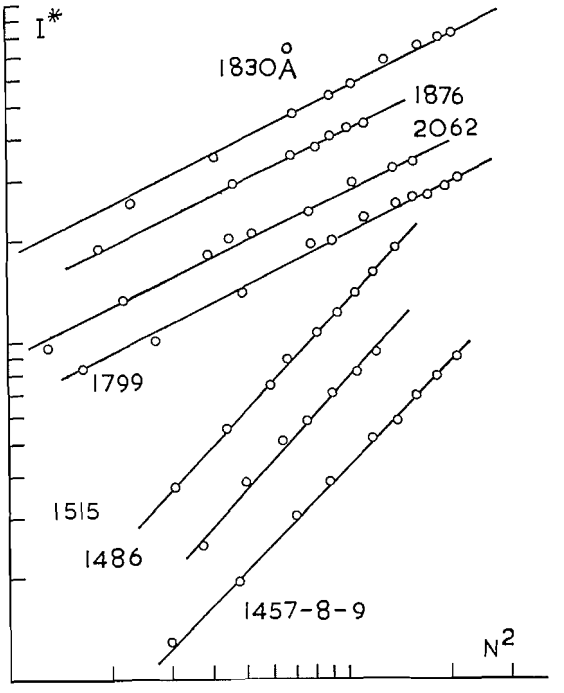

FIG. 4. I_2 flame: as in Fig. 3.

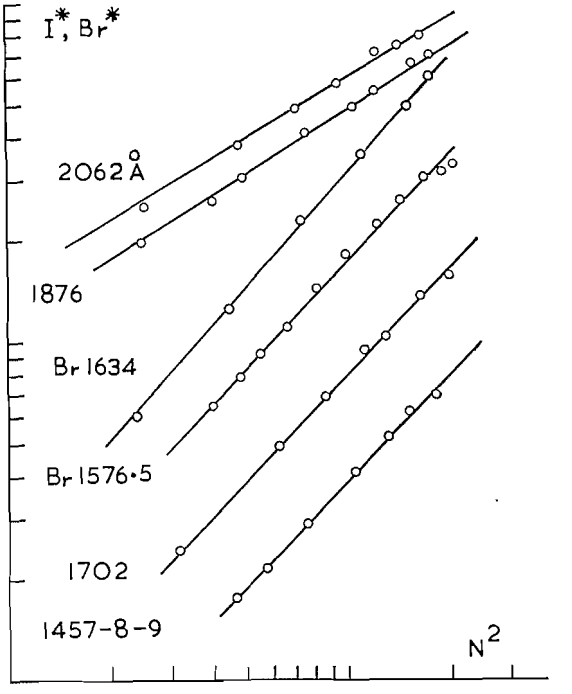

FIG. 5. IBr flame: representative graphs of log intensity versus log afterglow intensity for atomic iodine and bromine lines.

Discussion

Two basic mechanisms which have been proposed to account for luminescence excited by active nitrogen are as follows:

(i) the termolecular mechanism (as proposed for metal halides)

$$[1] \qquad N + N + M \rightarrow N_2^* + M$$

$$[2] \qquad N_2^* + M \rightarrow N_2 + M$$

$$[3] \qquad N_2^* + I \rightarrow N_2 + I^*;$$

(ii) the bimolecular mechanism (as proposed for I_2 and IBr)

$$[4] \qquad N + IX \rightarrow NI + X$$

$$[5] \qquad N + NI \rightarrow N_2^{**} + I$$

$$[6] \qquad N_2^{**} + I \rightarrow N_2 + I^*$$

$$[7] \qquad N_2^{**} + M \rightarrow N_2 + M.$$

In each instance the intensity of luminescence is proportional to the concentration of excited nitrogen molecules, so that for (i) we have, in the steady state,

$$[8] \qquad \text{intensity} \propto \frac{k_1[N]^2[M]}{k_2[M] + k_3[I]}$$

$$[9] \qquad \sim k_1[N]^2/k_2,$$

and for (ii)

$$[10] \qquad \text{intensity} \propto \frac{k_4[N][IX]}{k_6[I] + k_7[M]}$$

$$[11] \qquad \sim k_4[N][IX]/k_7[M],$$

where "M" includes the species IX.

The first mechanism can account for excitation processes requiring up to 225 kcal/mole (or slightly more with a contribution from kT), assuming the N_2^* species to begin its career in the $^5\Sigma_g^+$ state. The second mechanism, on the other hand, is limited by the energy of N_2^{**}, which in turn is limited to 225.1 kcal/mole minus the dissociation energy of NI.

The results for the ICN flame do not fit either of these simple mechanisms, and the attempt to explain the behavior of this rather complex system is therefore postponed, at least until the results of a current study of the banded emission at longer wavelengths become available.

In the I_2 and IBr flames the lower energy lines, like the banded emission between 1900 and 6000

Can. J. Chem. Downloaded from www.nrcresearchpress.com by 210.87.254.5 on 09/05/12
For personal use only.

Can. J. Chem. Downloaded from www.nrcresearchpress.com by 210.87.254.5 on 09/05/12
For personal use only.

Å, vary as [N], and it is therefore reasonable to attribute them to mechanism (ii). When this mechanism fails, because of insufficient energy in the species N_2**, it is to be expected that the intrinsically less efficient termolecular mechanism will take over, to account for the emission down to 1261 Å. In accord with this hypothesis, all of the higher energy lines which are sufficiently intense to measure as a function of [N] have been found to vary as $[N]^2$. The changeover from one mechanism to the other occurs between the $6s.^2P_{\frac{1}{2}}$ level of iodine, at 63 186.76 cm^{-1} and the $5s.^4P_{2\frac{1}{2}}$ level of bromine, at 63 429.82 cm^{-1}. Thus the energy of N_2** appears to be 63 310 $\pm$ 120 cm^{-1}, or 180.9 $\pm$ 0.3 kcal/mole. However, this can be criticized on the grounds that no excitation of Br by N_2** has been observed, and the process could be inefficient near its upper energy limit. Hence it seems preferable to set the upper limit at the $6s'.^2D_{2\frac{1}{2}}$ level of iodine (66 020.64 cm^{-1}), and to state the energy of N_2** as 185 $\pm$ 3.5 kcal/mole. This should be compared with Kenty's result (9) that the energy of the $^3\Delta_u$ state of N_2 lies between 182 and 190 kcal/mole. As was pointed out previously (5), both NCl and NBr are too stable to form $N_2(^3\Delta_u)$ by reaction with N. If the excited species were merely vibrationally excited, electronic ground-state N_2, rather than a definite, metastable, electronically excited molecule, there would be no reason for the marked difference found between iodine and other halogens in their reactions with atomic nitrogen.

For ICl we consider first the lines other than that at 1830 Å. Since they vary as $[N]^2$ we conclude that the termolecular mechanism (i) applies, and must also apply to the banded emission, which shows the same variation. It follows that the reaction

[12] $$N + ICl \rightarrow NCl + I$$

occurs to the exclusion of

[13] $$N + ICl \rightarrow NI + Cl.$$

This is reasonable, since the production in reaction [5] of N_2** having 185 $\pm$ 3.5 kcal/mole implies that D^0_{NI} is less than 40 $\pm$ 3.5 kcal/mole. Thus reaction [13] is endothermic to the extent of at least 9.8 $\pm$ 3.5 kcal/mole (14), and is expected to be slow. Since reaction [4], with X = I, is quite rapid at room temperature and has almost no temperature coefficient, the value of D^0_{NI} must also be greater than 35.6 kcal/mole. If we believe, in addition, that reaction [4] occurs as written with X = Br, then the lower limit for D^0_{NI} is raised to 41.9 kcal/mole. However, this is doubtful because the results obtained with IBr can also be explained in terms of the reactions of an equilibrium proportion of I_2, IBr vapor being about 8% decomposed to I_2 and Br_2 at equilibrium, at room temperature. It thus seems a better deduction that the reaction of N with IBr is entirely according to

[14] $$N + IBr \rightarrow NBr + I.$$

The apparent high efficiency of reaction [4] in producing $N_2(^3\Delta_u)$ suggests that this reaction is nearly thermoneutral, i.e. that the dissociation energy of NI is in fact close to 40 $\pm$ 3.5 kcal/mole.

In an attempt to explain the [N] dependence of the 1830 Å line, which has the lowest excitation energy of the lines observed, we consider the reaction

[15] $$N + NCl \rightarrow N_2 + Cl.$$

The dissociation energy of NCl is estimated to be about 62 kcal/mole (14), so that the nitrogen molecule resulting from reaction [15] could possess up to 163 kcal/mole of excess energy, probably in vibrational form. The rather close correspondence of the energy available with that required to excite the 1830 Å line raises the possibility that energy transfer could be very efficient. The number of such excited molecules needed to account for the 1830 Å emission could thus be insufficient to affect the kinetics of emission at other wavelengths, particularly in the banded region.

One other discrepancy remains in connection with the ICl flame. In the previous work (6) the decay of the banded emission with time was found to be similar to the decay of [N], whereas the intensity measured at a fixed point in the flame was proportional to $[N]^2$. The most likely explanation of this is that the dependence of intensity on $[N]^2$ was found relatively early in the flame, but by the time the banded emission had begun to decay the system was effectively an N–I_2 flame, as a consequence of wall recombination of iodine atoms formed in reaction [12], and the decay followed the usual N–I_2 kinetics.

Several authors (15, 16) have proposed that electronically excited molecules are able to be

quenched very efficiently by reaction with ground state atoms, for example:

[16] $N_2(A.^3\Sigma_u^+) + N(^4S) \rightarrow N(^4S) + N_2(X.^1\Sigma_g^+, v \gg 0)$.

Rate constants quoted for this sort of process are typically 2×10^{-10} cm^3 molecule^{-1} s^{-1}, i.e. not appreciably less than the rate constant for binary collisions. Considerations of microscopic reversibility make it difficult to see why the reverse reactions should not be equally efficient, i.e. why a highly vibrationally excited, electronic ground-state molecule should not cross into a higher electronic state as a result of an atom interchange reaction. Thus in a system containing electronically excited molecules and ground-state atoms one would expect to find a cascade deactivation process, in which appreciable populations would be produced in intermediate electronic levels. For the present reaction systems the processes involved would include

[17] $N_2(^3\Delta_u) + N(^4S) \rightarrow N(^4S) + N_2(^1\Sigma_g^+, v_1)$

[18] $N_2(^1\Sigma_g^+, v_1) + M \rightarrow N_2(^1\Sigma_g^+, v_2) + M$

[19] $N_2(^1\Sigma_g^+, v_2) + N(^4S) \rightarrow N(^4S) + N_2(^3\Sigma_u^+)$

[20] $N_2(^3\Sigma_u^+) + N(^4S) \rightarrow N(^4S) + N_2(^1\Sigma_g^+, v_2)$

and so on, with probably also the one-step process

[21] $N_2(^3\Delta_u) + N(^4S) \rightarrow N(^4S) + N_2(^3\Sigma_u^+, v_3)$.

Evidence in support of this scheme is provided by our previous observation (10) of small concentrations of $A.^3\Sigma_u^+$ nitrogen molecules in the N–I_2 flame. At the time the A state was believed to be mainly responsible for excitation occurring in the N–I_2 flame; the present results appear to provide a much more satisfactory explanation.

NOTE ADDED IN PROOF: In a current publication Kenty (17) discards his previous estimate of the energy of the $^3\Delta_u$ state in favor of a value of about 170 kcal/mole. This does not affect the identification of N_2** as $^3\Delta_u$ provided this species can transfer both electronic and vibrational excitation energy to atomic iodine. The next higher metastable state of N_2, $a'.^1\Sigma_u^-$ at 194 kcal/mole, has too much energy for production by reactions [4] and [5]. A consecutive excitation mechanism involving $I(^2P_{\frac{1}{2}})$ would lead to dependence of intensity on $[N]^2$, and is also ruled out.

Acknowledgments

This work was supported by The New Zealand Universities Research Committee and by Grant AF-AFOSR-1265-67 from the United States Air Force Office of Scientific Research. I am grateful to Mr. G. J. Smith for making preliminary observations below 2000 Å.

1. R. J. STRUTT and A. FOWLER. Proc. Roy. Soc. London, Ser. A, **86**, 105 (1911).
2. L. H. EASSON and R. W. ARMOUR. Proc. Roy. Soc. Edinburgh, **48**, 1 (1928). A. ELLIOTT. Proc. Roy. Soc. London, Ser. A, **174**, 273 (1940).
3. E. R. V. MILTON, H. B. DUNFORD, and A. E. DOUGLAS. J. Chem. Phys. **35**, 1202 (1961).
4. C. G. FREEMAN and L. F. PHILLIPS. J. Phys. Chem. **68**, 362 (1964).
5. K. S. RAXWORTHY and L. F. PHILLIPS. Can. J. Chem. **42**, 2928 (1964).
6. M. R. GRIGOR and L. F. PHILLIPS. 11th Symposium (International) on Combustion. The Combustion Institute, Pittsburgh. 1967. p. 751.
7. L. F. PHILLIPS. Can. J. Chem. **41**, 732, 2060 (1963).
8. W. R. BRENNAN and G. B. KISTIAKOWSKY. J. Chem. Phys. **44**, 2695 (1966).
9. C. KENTY. J. Chem. Phys. **35**, 2267 (1961).
10. D. I. WALTON, M. J. MCEWAN, and L. F. PHILLIPS. Can. J. Chem. **43**, 3095 (1965).
11. C. A. GOY, D. H. SHAW, and H. O. PRITCHARD. J. Phys. Chem. **69**, 1504 (1965).
12. C. E. MOORE. Natl. Bur. Std. U.S. Circ. 467, Vol. I (1949); Vol. II (1952); Vol. III (1958).
13. J. BERKOWITZ, W. A. CHUPKA, and G. B. KISTIAKOWSKY. J. Chem. Phys. **25**, 457 (1956).
14. V. I. VEDENEYEV, L. V. GURVICH, V. N. KONDRATIEV, V. A. MEDVEDEV, and YE. L. FRANKEVICH. Bond energies, ionization potentials and electron affinities. Edward Arnold, London. 1966. (Russian ed. Acad. Sci. U.S.S.R., Moscow. 1962).
15. D. R. BATES. J. Atmospheric Terrest. Phys. **6**, 171 (1955).
16. R. A. YOUNG. Can. J. Chem. **44**, 1171 (1966). K. L. WRAY. J. Chem. Phys. **44**, 623 (1966).
17. C. KENTY. J. Chem. Phys. **47**, 2545 (1967).

Can. J. Chem. Downloaded from www.nrcresearchpress.com by 210.87.254.5 on 09/05/12
For personal use only.

Carbon-13 kinetic isotope effects. III.[1] Temperature dependence of k_{12}/k_{13} for 1-bromo-1-phenylethane alcoholysis

JAN BRON AND J. B. STOTHERS
Department of Chemistry, University of Western Ontario, London, Ontario

Received November 2, 1967

The temperature dependence of k_{12}/k_{13} for methanolysis and ethanolysis at the α-carbon of 1-bromo-1-phenylethane has been determined over the ranges 25° and 45° respectively. It is found that the kinetic isotope effect *increases* with increasing temperature for these systems. This result offers support for earlier interpretations on the ^{13}C fractionations measured previously and the data are considered in terms of the original Bigeleisen equation. The results indicate that primary kinetic ^{13}C isotope effects may be useful for distinguishing between bimolecular and unimolecular substitution mechanisms.

Canadian Journal of Chemistry, 46, 1435 (1968)

Can. J. Chem. Downloaded from www.nrcresearchpress.com by 210.87.254.5 on 09/05/12
For personal use only.

Introduction

Some time ago a study of the kinetic isotope effect at the α-carbon of 1-bromo-1-phenylethane in alcoholysis was described (1). From the results of this work, it seemed reasonable to suggest that there is appreciable bond strengthening between the α-carbon and the phenyl ring in the transition state of the rate-determining step. Recently, other evidence has been presented by Kresge, Lichtin, Rao, and Weston (2) to support this view. The latter authors have shown that the Ar—C^+ bonds in the triphenylcarbonium ion must be considerably strengthened relative to those for the uncharged species. One of the weaknesses of the previous work in the 1-bromo-1-phenylethane system (1) is the fact that k_{12}/k_{13} was measured at a single temperature in each of the solvents methanol and ethanol. A knowledge of the temperature dependence of these ^{13}C fractionations could shed further light on the origins of these kinetic isotope effects and provide data for comparisons with the variation of k_{12}/k_{13} in bimolecular substitution processes (3).

In this paper the results of measurements of k_{12}/k_{13} for methanolysis at 0 °C and ethanolysis at 0 and 25 °C are presented. Thus, with the earlier data (1), the variations of k_{12}/k_{13} over a range of 25° and 45° are known for methanolysis and ethanolysis respectively. The experimental results are considered in terms of the Bigeleisen equation (4).

Experimental

The general techniques employed have been described in detail previously (1). Some modifications were introduced in the present work to improve the reliability of our measurements. The purity of the product samples was checked by gas chromatography to insure that the samples were free of starting material and styrene. All distillations were carried out on a Nester-Faust spinning, platinum band column. An isotope-ratio, 15 in. Nier-type mass spectrometer was used for the isotopic abundance measurements of the carbon dioxide samples. The signal for the mass 45 peak was compared with the signal for the 44 and 46 masses. These ratios were corrected for ^{17}O and ^{18}O contributions and the isotope effects calculated in the usual fashion (1). Measurements of the reaction kinetics were done for each of the systems by acid–base titration of the hydrogen bromide formed. Each reaction was followed to at least one half-life.

Results

The rate constants found for methanolysis at 0° and ethanolysis at 0° and 25° are listed in Table I together with the data reported by Fainberg and Winstein (5). The agreement between these two sets of data is favorable and any differences would not affect the calculated kinetic isotope effects significantly.

TABLE I
Kinetic results of alcoholyses of 1-bromo-1-phenylethane

Solvent	Temp. (°C)	$k_1 \times 10^6$ (s^{-1}) Found	Lit.*
Methanol	0	1.84	1.7
Ethanol	0	0.194	0.199
	25	6.70	6.28

*Reference 5.

The results for the kinetic isotope effect determinations for methanolysis and ethanolysis are collected in Tables II and III respectively. For each system a sufficient quantity of 1-bromo-1-phenylethane was prepared and purified for the

[1]Part II, ref. 3*d*.

TABLE II

^{13}C kinetic isotope effects in the methanolysis of 1-bromo-1-phenylethane

Temp. (°C)	Expt. No.	Extent of reaction (%)	k_{12}/k_{13}	$(k_{12}/k_{13} - 1)100$
0	1	4.8	1.0032	0.32
	2	4.8	1.0055	0.55
	3	4.7	1.0064	0.64
	4	4.7	1.0045	0.45
	5	4.7	1.0046	0.46
	6	4.8	1.0055	0.55
		Mean values	1.0050 ± 0.0010*	0.50 ± 0.10*
25		Mean values†	1.0065 ± 0.0007*	0.65 ± 0.07*

*Standard deviations.
†Reference 1.

entire series of runs. A small sample was degraded to carbon dioxide via benzoic acid in our usual manner (1) and this served as the standard for comparisons of the $^{12}C/^{13}C$ ratios measured for the products from each individual run. The extent of reaction is indicated for each experiment in the tables. The rate constant ratios (k_{12}/k_{13}) and "percent isotope effects", $(k_{12}/k_{13} - 1) \times 100$, are listed in the last two columns. For comparisons and discussion, the earlier results (1) of isotope effect measurements in these systems are included in the tables.

Discussion

An isotopic rate constant ratio such as k_{12}/k_{13} in the present systems can be viewed as the product of two factors: the so-called temperature independent factor, t.i.f., and the temperature dependent factor, t.d.f. Thus we have

$$[1] \qquad k_{12}/k_{13} = (\text{t.i.f.})(\text{t.d.f.}).$$

The t.i.f. can be evaluated from the masses of the molecular fragments formed by rupture of the bond undergoing change, as discussed previously (1) the C—Br or C—O bond in the present instance. Experimental support for the choice of this fragment model, originally suggested by Bigeleisen and Wolfsberg (4), has been presented for these reactions (1). The second term, t.d.f., represents the contribution to the isotope effect of isotopic frequency shifts in the vibrational modes available to the reactants and activated complexes. According to an equation due to Bigeleisen (4), the t.d.f. can be written,

$$[2] \quad \text{t.d.f.} = [1 + \sum_{i}^{3n-6} G(u_i)\Delta u_i - \sum_{i}^{3n^{\ddagger}-7} G(u_i{\ddagger})\Delta u_i{\ddagger}],$$

where $u_i = h\nu_i/kT$ and

$$G(u_i) = \frac{1}{2} - \frac{1}{u_i} + \frac{1}{e^{u_i} - 1}$$

[values for the latter function are readily available in the tables of Bigeleisen and Mayer (6)].

As noted previously (1), it seems reasonable to assume that alcoholysis of the 1-phenylethyl halides proceeds by a S_N1-type mechanism in which a cationic intermediate is involved and there is reason to suggest that much of the substitution occurs through an intimate ion-pair (7). Thus there are two transition state models which can be envisaged as the source of the kinetic isotope effect; both of which must be closely related to the intimate ion-pair. Since both were considered in detail earlier (1), it is sufficient to note that the magnitude of t.i.f. contribution is in the range 1.0011–1.0021 according to the molecular fragment model for the two transition states. From eq. [1] it follows that the t.d.f. must be 1.005 or less depending on which of the observed results is considered.

From eq. [2] it is seen that the contributions to t.d.f of the initial state are opposite in sign to those of the transition state. Furthermore, there is ample reason (3*c*, 4) to expect that the temperature dependence will be inverse since the t.d.f. approaches unity as the high temperature

Can. J. Chem. Downloaded from www.nrcresearchpress.com by 210.87.254.5 on 09/05/12
For personal use only.

TABLE III

^{13}C kinetic isotope effects in the ethanolysis of 1-bromo-1-phenylethane

Temp. (°C)	Expt. No.	Extent of reaction (%)	k_{12}/k_{13}	$(k_{12}/k_{13}-1)100$
0	1	5.2	1.0014	0.14
	2	5.6	1.0014	0.14
	3	4.5	1.0030	0.30
	4	4.8	1.0020	0.20
	5	6.5	1.0010	0.10
		Mean values	1.0018±0.0007*	0.18±0.07*
25	1	4.7	1.0032	0.32
	2	4.6	1.0054	0.54
	3	4.4	1.0056	0.56
	4	4.5	1.0038	0.38
	5	4.5	1.0041	0.41
		Mean values	1.0044±0.0009*	0.44±0.09*
45		Mean values†	1.0064±0.0007*	0.64±0.07*

*Standard deviations.
†Reference 1.

limit. In a number of nucleophilic bimolecular substitutions, k_{12}/k_{13} for the carbon at the site of displacement has been shown to decrease with increasing temperature (3*c*, 3*e*) as expected. In the present systems, however, the opposite behavior is found such that the ^{13}C isotope effect increases with increasing temperature. Qualitatively this can be explained in terms of eq. [2] by a difference in the temperature dependencies of the initial and transition state terms.

The fact that the observed k_{12}/k_{13} ratios are relatively small is consistent with the conclusion that the contributions of the transition state are comparable to those of the initial state and the observed temperature dependencies substantiate this conclusion. Presumably the strengthening of the Ar—C_α bond in the cation is sufficient to offset the effect of the loss of the C—Br vibrational modes. This view had been expressed earlier on the basis of our original results (1) and, more recently, indirect support was presented from a study of the equilibrium isotope effect for the dissociation of trityl alcohol in concentrated sulfuric acid (2).

There has been evidence presented to show that valid calculations of isotope effects can be obtained from a consideration of grossly abbreviated models of larger systems (2, 8). For the present case the major contribution to the isotopic fractionation at the α-carbon can be expected to arise from vibrational changes of the bonds with which this atom is directly involved. These are the C—H, C—Me, C—Ph, and C—Br bonds of the initial state and the C—H, C—Me, and C—Ph bonds in the transition state, which we can assume to resemble those of the cation. The vibrational energy differences for a tertiary C—H bond in a process involving the hybridization change $sp^3 \rightarrow sp^2$ have been discussed by Streitwieser *et al.* (9) for which an aldehyde or olefin was suggested as a suitable model for estimating the frequencies associated with the trigonal case. Choosing the olefin as a model for the present case we can consider the stretching mode changing from $\sim 2900 \rightarrow \sim 3020\ cm^{-1}$, while one of the bending modes is little affected ($\sim 1350\ cm^{-1}$) and one is lowered substantially $\sim 1350 \rightarrow \sim 800\ cm^{-1}$. In addition, the C—C stretching modes in the initial state can be assigned nominal values of $1210\ cm^{-1}$ on the basis of other estimates (2). In the transition state, it is reasonable to suppose that both the C—Me and C—Ph bonds will be somewhat "tightened" due to resonance and hyperconjugative interactions. Presumably the effect of the phenyl ring will be the greater and, as a first approximation, we assign to it a frequency of $1450\ cm^{-1}$. For the C—Me we have chosen $1350\ cm^{-1}$. It is difficult to estimate frequencies for the bending modes of these C—C bonds in either state but we have chosen 400 and $600\ cm^{-1}$ for the initial and transition states, respectively. Finally, the contribution of the C—Br bond ($550\ cm^{-1}$) must be included in the initial state term.

Can. J. Chem. Downloaded from www.nrcresearchpress.com by 210.87.254.5 on 09/05/12
For personal use only.

TABLE IV

Contributions to t.d.f. for solvolysis of 1-bromo-1-phenylethane

State	Bond	ν_i	$\Delta\nu_i$	273° u_i	273° $G(u_i)\Delta u_i$	318° u_i	318° $G(u_i)\Delta u_i$
Initial	C—Br	550	19	2.899	0.0214	2.489	0.0162
	C—H	2900	9	15.286	0.0206	13.123	0.0173
		1350	4	7.116	0.0076	6.109	0.0061
	C—C	1210	23	6.378	0.0418	5.475	0.0335
		400	8	2.108	0.0069	1.810	0.0052
Transition	C—H	3020	9	15.919	0.0207	13.666	0.0174
		800	2	4.217	0.0029	3.610	0.0023
	C—C^+	1450	28	7.643	0.0546	6.562	0.0442
		1350	26	7.116	0.0494	6.109	0.0398
		600	12	3.163	0.0144	2.715	0.0110

Using these frequencies, with the simple diatomic model to calculate the effect of the mass change, $^{12}C \rightarrow {}^{13}C$, on these, one can evaluate t.d.f. from eq. [2]. The results are set out in Table IV for each of two temperatures, 273 and 318 °K. Vibrational modes which are not altered during reaction, such as the in-plane bending mode for the tertiary C—H bond, need not be included since these cancel. Using these data the $\sum G(u_i)\Delta u_i$ terms can be evaluated for the initial and transition states. Including two of each of the C—C contributions $\sum G(u_i)\Delta u_i$ is 0.1470 (273°) and 0.1170 (318°) while $\sum G(u_i\ddagger)\Delta u_i\ddagger$ is 0.1564 (273°) and 0.1257 (318°). Thus, t.d.f. is 0.9906 (273°) and 0.9913 (318°), which when combined with the t.i.f. contributions mentioned above yield kinetic isotope effects in the range, 0.9920–0.9934. Specific values are listed in Table V. We conclude, therefore, that, although the estimates are crude, bond strengthening in the transition state can offset the loss of the C—Br mode in the initial state sufficiently to account for the relatively small kinetic isotope effects observed.

TABLE V

Carbon-13 isotope effects in ethanolysis of 1-bromo-1-phenylethane

Temp. (°C)	t.i.f.*	t.d.f.†	k_{12}/k_{13} Calcd.	k_{12}/k_{13} Obsd.
0	1.0021	0.9906	0.9927	1.0018
	1.0014	0.9906	0.9920	
45	1.0021	0.9913	0.9934	
	1.0014	0.9913	0.9927	1.0064

*"Temperature independent factor", values from ref. 1.
†"Temperature dependent factor", see text.

Although the above estimates lead to an inverse isotope effect (i.e. $k_{12}/k_{13} < 1.0$), it is important to note that the choice of bending frequencies for the C—C bonds can be the decisive factor. If the true values for these are less than those given in Table IV for the transition state terms, $G(u_i)\ddagger\Delta u_i\ddagger$ is reduced correspondingly and the calculated isotope effect increases. It seems reasonable, however, that the frequencies of the bending modes for the C—C^+ bonds will be higher than those for normal C—C bonds. Since accurate estimates are difficult, more precise predictions of the t.d.f. values are not possible. These problems, however, do not affect the important conclusion regarding the small observed isotope effect.

The "abnormal" temperature dependency found for these 1-bromo-1-phenylethane alcoholyses is interesting but difficult to interpret in a unique way. Perhaps the isotopic shifts of the vibrational frequencies are different for cationic species than those for stable molecules. It has been noted by Kresge *et al.* (2) that some of the infrared assignments for the triphenylcarbonium ion suggest smaller isotopic shifts. If this is the case, the temperature dependence of the $G(u_i\ddagger)\Delta u_i\ddagger$ terms will be significantly different from that of the $G(u_i)\Delta u_i$ terms and this could produce the observed variation of k_{12}/k_{13} with temperature.

Another possibility which merits mention in the present case is one of those discussed by Yankwich and Buddenbaum (10) in their recent critical discussion of the temperature dependence of kinetic carbon isotope effects. For solvolyses proceeding through an intimate ion-pair in

Can. J. Chem. Downloaded from www.nrcresearchpress.com by 210.87.254.5 on 09/05/12
For personal use only.

equilibrium with an organic halide, eq. [1] may be rewritten as

$$[3] \quad k_{12}/k_{13} = (\text{t.i.f.})(\text{t.d.f.})_{kin}(\text{t.d.f.})_{equil}$$

in which $(\text{t.d.f.})_{kin}$ arises from the activation step leading to the products and $(\text{t.d.f.})_{equil}$ represents isotopic fractionation for an equilibrium preceding the rate-determining step. The temperature dependencies of these two temperature dependent factors may well be different and this difference may account for the observed results.

Yankwich and Buddenbaum (10) have delineated the difficulties associated with interpretations of kinetic isotope effect results obtained "over the modest temperature ranges covered by most studies of solution reactions". Nevertheless, it is tempting to suggest that the temperature dependence of the primary carbon isotope effect may serve as a useful distinction between the limiting S_N1 and typical S_N2 mechanisms for nucleophilic displacement, since the latter are found to behave "normally", i.e. $k/k' \approx f(1/T)$, in several instances (3*c*, 3*e*, 10, 11). The extremely tentative nature of this proposal cannot be overemphasized and, unfortunately, it would appear to be difficult to confirm or disprove.

Acknowledgment

We are grateful to the National Research Council of Canada for research funds to support this study.

1. J. B. Stothers and A. N. Bourns. Can. J. Chem. **38**, 923 (1960).
2. A. J. Kresge, N. N. Lichtin, K. N. Rao, and R. E. Weston. J. Am. Chem. Soc. **87**, 437 (1965).
3. (*a*) M. L. Bender and D. F. Hoeg. J. Am. Chem. Soc. **79**, 5649 (1958). (*b*) M. L. Bender and G. J. Buist. J. Am. Chem. Soc. **80**, 4304 (1958). (*c*) K. R. Lynn and P. E. Yankwich. J. Am. Chem. Soc. **83**, 790, 3220 (1961). (*d*) J. B. Stothers and A. N. Bourns. Can. J. Chem. **40**, 2007 (1962). (*e*) J. Bron and J. B. Stothers. Unpublished observations.
4. J. Bigeleisen and M. Wolfsberg. Advan. Chem. Phys. **1**, 15 (1958).
5. A. H. Fainberg and S. Winstein. J. Am. Chem. Soc. **79**, 1602 (1957).
6. J. Bigeleisen and M. G. Mayer. J. Chem. Phys. **15**, 261 (1947).
7. E. Grunwald, A. Heller, and F. S. Klein. J. Chem. Soc. 2604 (1957).
8. M. Wolfsberg and M. J. Stern. Pure Appl. Chem. **8**, 225 (1964).
9. A. Streitwieser, R. H. Jagow, R. C. Fahey, and S. Suzuki. J. Am. Chem. Soc. **80**, 2326 (1958).
10. P. E. Yankwich and W. E. Buddenbaum. J. Phys. Chem. **71**, 1185 (1967).
11. A. J. McNamara and J. B. Stothers. Unpublished data.

Can. J. Chem. Downloaded from www.nrcresearchpress.com by 210.87.254.5 on 09/05/12
For personal use only.

Can. J. Chem. Downloaded from www.nrcresearchpress.com by 210.87.254.105 on 09/05/12
For personal use only.

NOTES

Adsorption and coprecipitation of silver on hydrous ferric oxide

WILLY DYCK
Geological Survey of Canada, Ottawa, Canada

Received August 23, 1967

With silver-110m as a tracer, detailed investigations were carried out on the adsorption of silver on freshly prepared hydrous ferric oxide in the pH region 4–8, and silver equilibrium concentration range 10^{-4}–10^{2} p.p.m. The results fit Freundlich adsorption isotherms, and may be explained in terms of hydrogen–silver ion exchange. They also show that adsorption is essentially complete in less than 5 min and is strongly dependent on pH and the manner in which the precipitate was prepared, but is independent of temperature in the 0–50 °C range, of moderate concentrations of sodium nitrate ($\sim$ 10 g/l), and of trace concentrations of sodium chloride ($\lesssim 1.5 \times 10^{-3}$ g/l) during test periods ranging from 1 to 3 days.

Tests also showed that under equilibrium conditions and similar chemical environments the amounts of silver coprecipitated or adsorbed were identical.

Canadian Journal of Chemistry, 46, 1441 (1968)

Introduction

The hydrous oxides of iron and manganese that occur in nature have been found to contain considerable quantities of trace elements such as Ag, Co, Ni, etc. (1–4). It is generally accepted that adsorption plays a dominant role in concentrating trace elements in these oxides.

The nature of hydrous oxides of iron has been studied extensively by Weiser (5, 6). The adsorption of silver on ferric oxide gels has been studied by a number of Russian scientists (7–10). The silver concentration range investigated by these workers is indicated by the dotted rectangle in Fig. 1A. In general, their results show that adsorption of silver is strongly influenced by the presence of anions which form insoluble silver salts; the less soluble the salt, the greater the adsorption.

This report deals with a detailed investigation of the adsorption and coprecipitation of silver on freshly prepared hydrous ferric oxides in the silver concentration range and pH range normally encountered in natural waters.

Experimental

Procedures

The experimental results were obtained by batch type experiments in which the silver ion concentration or the pH was varied and the amount of hydrous ferric oxide was kept constant throughout at 2.53×10^{-3} mole Fe^{3+} equivalent.

The adsorption tests were carried out by precipitating the iron with base (NaOH, NH_4OH, or urea), washing the precipitate, and then adding the desired amount of silver at the predetermined pH. The amount of silver adsorbed was determined by measuring the change in the activity of the solution. After equilibrium was established, the activity of the washed precipitate was also measured. The coprecipitation tests were carried out by precipitating the iron with base from mixtures of iron and silver solutions. For example, the values shown in Fig. 1 were obtained as follows: 100 ml of 1410 p.p.m. Fe^{3+} solution was titrated with dilute NaOH with vigorous stirring. The resulting precipitate was washed 3 times with 60 ml hot 1% $NaNO_3$ adjusted to the pH at which the experiment was to be carried out. The $NaNO_3$ was used to prevent the hydrolysis of the precipitate at low pHs. The precipitate was then mixed with pH-adjusted $AgNO_3$ solution containing 2 g $NaNO_3$ and sufficient water to make a total volume of 200 ml. The resulting mixture was stirred intermittently. All pH adjustments were made with NaOH or HNO_3. The Ag^+ concentration changes were measured periodically by centrifuging a 30 ml aliquot and measuring the counting rate of two 5 ml aliquots of the clear solution. These aliquots were then returned to the mixture. These measurements are referred to as 'solution measurements'.

After 1–3 days, the precipitates were washed in a 1% $NaNO_3$ solution at the pH of the experiment until the counting rate of the precipitate approached a constant value (8 to 10 washes). This washing resulted in10–20% loss of precipitate, hence all washed precipitates were dissolved after silver analysis and the iron content was determined colorimetrically. These silver and iron measurements are referred to as 'washed precipitate measurements'.

The values shown in Fig. 2 were obtained by the same general procedure except that the precipitates were prepared by boiling the iron solution with urea as described by Willard and Tang (11).

Solutions

Pure solutions containing silver were prepared by accurate dilution of a 0.02 *N* $AgNO_3$ stock solution. To minimize adsorption on walls of storage bottles, the pH

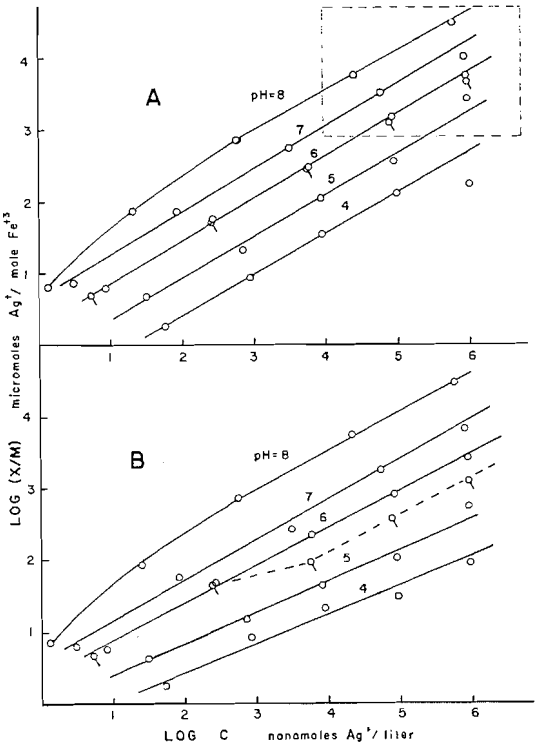

FIG. 1. Room temperature (~ 25 °C) adsorption isotherms of silver and hydrous ferric oxide prepared with sodium hydroxide: A, solution measurements; B, washed precipitate measurements. (For details of tests see experimental section.) Points with tail were obtained without $NaNO_3$.

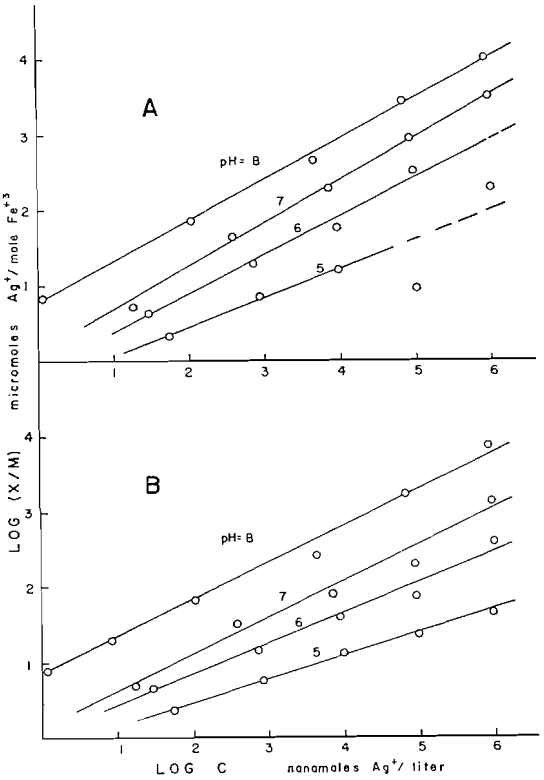

FIG. 2. Room temperature (~ 25 °C) adsorption isotherms of silver and hydrous ferric oxide prepared with urea: A, solution measurements; B, washed precipitate measurements. (For details of tests see experimental section.)

of the diluted solutions was kept below 2. A convenient quantity, approximately 20 μCi of silver-110m, was added to 1 l of solution to measure subsequent silver concentration changes. The secondary stock solutions contained 216, 21.6, 2.16, 0.216, and 0.022 p.p.m. Ag^+.

Reagent grade $Fe(NO_3)_3.9H_2O$ was dissolved in water and kept at pH 1 with HNO_3 to prevent the formation of colloidal iron. The stock solution was standardized gravimetrically and colorimetrically. Aliquots of this stock solution were then diluted to give 1410 p.p.m. Fe^{3+} secondary stock solution.

Instruments

All pH measurements were made with a model 22 Radiometer pH meter. To avoid chloride contamination of experimental solutions the KCl in the calomel–salt bridge was replaced by KNO_3. Silver concentration changes were measured with a Harshaw 3″ well type NaI (Tl) crystal and a single-channel pulse-height analyzer Victoreen model 851A. The instrument was set to record the 0.656 MeV gamma ray of silver-110m.

Errors

Because a large silver concentration range was covered, cross contamination was found to be one of the most troublesome factors. To achieve an average reproducibility of ±5%, as was eventually attained in this study, several experiments had to be carried out with a set of laboratory ware conditioned to a particular silver concentration. Counting errors and volume measurement errors were easily kept below ±1% in most cases. By adding sufficient tracer to the solutions, the 10 000 counts required to give an error of ±1% (95% confidence limit) were easily accumulated in all but a few cases where adsorption exceeded 98%. At low silver concentrations, extraneous loss of silver was minimized by using large volumes of solution in all-glass apparatus.

Results and Discussion

As is evident from Figs. 1 and 2, the adsorption of Ag^+ by freshly prepared hydrous ferric oxides from very dilute solutions can be represented by the well-known Freundlich adsorption equation

$$X/M = kC^{1/n},$$

where X/M = ratio of the amounts of silver and iron in the precipitate at the equilibrium silver

Can. J. Chem. Downloaded from www.nrcresearchpress.com by 210.87.254.105 on 09/05/12
For personal use only.

concentration C. It is also evident that the hydrogen ion concentration greatly influences the amount of silver adsorbed. From the constant spacing of the isotherms, one can readily infer that a plot of pH vs. log C at constant X/M also gives straight lines. A pH vs. log C relationship, as well as one form of the Freundlich adsorption isotherm, can be deduced from the expression for the equilibrium constant of the ion exchange reaction

$$Ag^+ + \overline{H} = H^+ + \overline{Ag},$$

where the barred quantities refer to the respective ions in the solid phase. Although $\overline{H}$ cannot be measured directly, it is proportional to the amount of hydrous oxide M, hence the ratio $\overline{Ag}/\overline{H}$ is proportional to X/M. Thus a linear relationship is obtained if any one quantity on the right side of the equation

$$\log K = \log H^+ - \log Ag^+ + \log (\overline{Ag}/\overline{H})$$

is kept constant. Here K is the equilibrium constant of the above reaction.

Part A of Figs. 1 and 2 represents solution measurements and part B washed precipitate measurements (for details of procedures see Experimental section). Extensive washing did not change X/M appreciably at the lower concentration range even though 10–20% of the silver and iron were lost during washing. At the high equilibrium concentrations but low pH, relatively more silver was washed out than iron, i.e. X/M decreased somewhat. This silver–iron correspondence suggests that the adsorption forces which bind silver to hydrous iron oxide are nearly as strong as those binding the hydrated iron oxide molecules to each other. Yet silver ferrites $(AgFeO_2)_3$ are known to form only under extreme conditions, such as boiling in NaOH (12).

X/M values obtained from measurements with precipitates prepared with urea (Fig. 2) are generally about 2–4 times lower than those from NaOH precipitations. Since the amount of iron was kept constant in all experiments, it follows that about 2–4 times less silver is adsorbed by these precipitates. This could be due to the fact that the precipitates prepared with urea were approximately 1.5 times denser than those from NaOH, indicating closer packing of the oxide. Ammonia, it was found, does not appreciably affect adsorption of silver below pH = 6. The values represented by tailed points in Fig. 1 (adsorption isotherm pH = 6) were obtained without $NaNO_3$ and show that the electrolyte does not interfere with the adsorption of silver. The lower X/M values of this isotherm in Fig. 1B coincide with excessive loss ($\sim 30\%$) of precipitate during washing. Apparently much of the iron went into a colloidal state and carried with it relatively larger amounts of silver.

A comparison study showed that adsorption and coprecipitation values were the same within the limits of experimental error, indicating a rather open structure for the hydrous oxide. Below pH 6 the values obtained with precipitates prepared with NH_4OH were only slightly lower than those obtained with precipitates prepared with NaOH. Above pH 6 appreciable complexing of silver was noted when NH_4OH was present.

The effect of temperature on adsorption was found to be negligible in the temperature range 2–50 °C.

Because ions forming insoluble silver salts can influence the adsorption of Ag^+ appreciably, chloride tests were carried out to determine what role Cl ions would play in the adsorption tests described here. These tests showed that only after increasing the Cl^- concentration by a factor of 10 from that added initially with the various salts (as calculated from impurity labels on reagent bottles) is an increase in the adsorption of Ag^+ observed.

Igneous rocks have an average Ag:Fe ratio of 1:500 000; the lowest Ag:Fe ratio in the experimental mixtures described above is 1:70 000. Even at this ratio essentially all of the silver was adsorbed by the hydrous ferric oxide. Assuming indiscriminate leaching for the two elements and no Ag^+ complexing, subsequent precipitation of iron will carry with it essentially all of the silver. Hence natural waters near the neutral point cannot be expected to carry Ag^+ in solution in easily detectable quantities whenever there is evidence of iron oxide formation. Limonite, on the other hand, can be expected to contain silver if the ion was present in the solution from which the limonite precipitated.

1. R. W. Boyle. Bull. Geol. Surv. Can. No. 111 (1965).
2. R. W. Boyle, W. M. Tupper, J. Lynch, G. Friedrich, M. Ziauddin, M. Shafiqullah, M. Carter, and K. Bygrave. Geol. Surv. Can. Paper 65-42 (1966).

Can. J. Chem. Downloaded from www.nrcresearchpress.com by 210.87.254.105 on 09/05/12
For personal use only.

3. P. LJUNGGREN. Geol. Foren. Stockholm Forh. **77**, 33 (1955).
4. E. BONATTI and O. JOENSUN. Science, **154**, 643 (1966).
5. H. B. WEISER. Inorganic colloid chemistry. Vol. II. The hydrous oxides and hydroxides. John Wiley and Sons, Inc., New York. 1935.
6. H. B. WEISER. Colloid chemistry. 2nd ed. John Wiley and Sons, Inc., New York. 1950.
7. V. A. KARGIN, P. S. VASILEV, and O. I. DMITRIENKO. Zh. Fiz. Khim. **14**, 1628 (1940).
8. T. N. CHERNIKOVA and E. N. GAPON. Kolloidn, Zh. **11**, 120 (1949).
9. O. I. DMITRIENKO, V. A. KARGIN, and A. A. RYABININA. Kolloidn. Zh. **13**, 3 (1951).
10. O. I. DMITRIENKO and A. A. RYABININA. Kolloidn. Zh. **15**, 29 (1953).
11. H. H. WILLARD and N. K. TANG. J. Am. Chem. Soc. **59**, 1190 (1937).
12. A. KRAUSE and K. PILAWSKI. Z. Anorg. Chem. **197**, 301 (1931).

Can. J. Chem. Downloaded from www.nrcresearchpress.com by 210.87.254.105 on 09/05/12
For personal use only.

Circular dichroism of the tetracyanonickelate(II) ion

ROLAND A. HAINES AND ANTHONY A. SMITH
Department of Chemistry, University of Western Ontario, London, Ontario

Received October 20, 1967

When $[Ni(CN)_4]^{2-}$ is dissolved in optically active 1,2-propanediol, two circular dichroism bands are observed which can be attributed to electronic transitions in the complex. Based on previous molecular orbital calculations, the relative energy levels of the d orbitals have been determined as $d_{xz}, d_{yz} < d_{xy} < d_{z^2} < d_{x^2-y^2}$.

Canadian Journal of Chemistry, 46, 1444 (1968)

In the last few years there has been considerable interest in the electronic structures of square planar metal complexes. Much of this interest has been due to the fact that the relative energies of the d orbitals in square planar complexes are not known with certainty, even in compounds of D_{4h} symmetry. Information regarding the ordering of the energy levels of the d orbitals often may be obtained by examining the absorption spectra of the complexes. However, for many of the square planar complexes it has been difficult to observe the bands due to d–d transitions because of very strong overlapping with the charge transfer bands. This is particularly found to be the case when π-bonding ligands such as CN^- are present and as a consequence the d–d absorption bands usually occur only as shoulders in the region of the low energy charge transfer band or are completely hidden.

Gray and other workers (1–4) have studied various square planar complexes with cyanide ions and have attempted to determine energy levels from the observed transitions. However, in most cases the peaks due to the d–d transitions were well hidden. We wish to report a study of the $[Ni(CN)_4]^{2-}$ ion which gives further insight into the relative ordering of the energy levels of the molecular orbitals in this type of compound.

The study was suggested by a recent paper (5) in which circular dichroism (c.d.) was reported for the $[PtCl_4]^{2-}$ ion in optically active 2,3-butanediol. In the region of one of the d–d transitions, a c.d. band was observed and this was attributed to the concentration of the dissymmetric influences of the solvent to the tetragonal ($+z$ and $-z$) positions of the ion.

We have examined the $[Ni(CN)_4]^{2-}$ complex in a similar optically active solvent (*d*-1,2-propanediol) and have found evidence for two c.d. bands. The observed spectra are shown in Fig. 1. The bands are quite reproducible for a given set of conditions and remain relatively unchanged over a period of 1 to 2 weeks. Due to very strong absorption by both the solvent and solute, the c.d. maximum for the high energy band could not be obtained. However, it is unquestionable that a second negative c.d. peak does occur and some rounding of the curve at approximately 272 mμ is indicated.

For $[PtCl_4]^{2-}$, the observed c.d. was attributed to the ${}^1A_{1g} \rightarrow {}^1A_{2g}$ transition (5). This assignment would correspond to an arrangement of the d-orbitals which is different from that given by Gray and Ballhausen (1). Recently new molecular orbital calculations have been made (6) and the ordering of energy levels in $[PtCl_4]^{2-}$ is now given as $d_{z^2} < d_{xz}, d_{yz} < d_{xy} < d_{x^2-y^2}$. The results of the c.d. study for $[PtCl_4]^{2-}$ are consistent with this new arrangement.

The $[Ni(CN)_4]^{2-}$ complex has D_{4h} symmetry

3. P. LJUNGGREN. Geol. Foren. Stockholm Forh. **77**, 33 (1955).
4. E. BONATTI and O. JOENSUN. Science, **154**, 643 (1966).
5. H. B. WEISER. Inorganic colloid chemistry. Vol. II. The hydrous oxides and hydroxides. John Wiley and Sons, Inc., New York. 1935.
6. H. B. WEISER. Colloid chemistry. 2nd ed. John Wiley and Sons, Inc., New York. 1950.
7. V. A. KARGIN, P. S. VASILEV, and O. I. DMITRIENKO. Zh. Fiz. Khim. **14**, 1628 (1940).
8. T. N. CHERNIKOVA and E. N. GAPON. Kolloidn, Zh. **11**, 120 (1949).
9. O. I. DMITRIENKO, V. A. KARGIN, and A. A. RYABININA. Kolloidn. Zh. **13**, 3 (1951).
10. O. I. DMITRIENKO and A. A. RYABININA. Kolloidn. Zh. **15**, 29 (1953).
11. H. H. WILLARD and N. K. TANG. J. Am. Chem. Soc. **59**, 1190 (1937).
12. A. KRAUSE and K. PILAWSKI. Z. Anorg. Chem. **197**, 301 (1931).

Circular dichroism of the tetracyanonickelate(II) ion

ROLAND A. HAINES AND ANTHONY A. SMITH
Department of Chemistry, University of Western Ontario, London, Ontario

Received October 20, 1967

When $[Ni(CN)_4]^{2-}$ is dissolved in optically active 1,2-propanediol, two circular dichroism bands are observed which can be attributed to electronic transitions in the complex. Based on previous molecular orbital calculations, the relative energy levels of the d orbitals have been determined as $d_{xz}, d_{yz} < d_{xy} < d_{z^2} < d_{x^2-y^2}$.

Canadian Journal of Chemistry, 46, 1444 (1968)

In the last few years there has been considerable interest in the electronic structures of square planar metal complexes. Much of this interest has been due to the fact that the relative energies of the d orbitals in square planar complexes are not known with certainty, even in compounds of D_{4h} symmetry. Information regarding the ordering of the energy levels of the d orbitals often may be obtained by examining the absorption spectra of the complexes. However, for many of the square planar complexes it has been difficult to observe the bands due to d–d transitions because of very strong overlapping with the charge transfer bands. This is particularly found to be the case when π-bonding ligands such as CN^- are present and as a consequence the d–d absorption bands usually occur only as shoulders in the region of the low energy charge transfer band or are completely hidden.

Gray and other workers (1–4) have studied various square planar complexes with cyanide ions and have attempted to determine energy levels from the observed transitions. However, in most cases the peaks due to the d–d transitions were well hidden. We wish to report a study of the $[Ni(CN)_4]^{2-}$ ion which gives further insight into the relative ordering of the energy levels of the molecular orbitals in this type of compound.

The study was suggested by a recent paper (5) in which circular dichroism (c.d.) was reported for the $[PtCl_4]^{2-}$ ion in optically active 2,3-butanediol. In the region of one of the d–d transitions, a c.d. band was observed and this was attributed to the concentration of the dissymmetric influences of the solvent to the tetragonal ($+z$ and $-z$) positions of the ion.

We have examined the $[Ni(CN)_4]^{2-}$ complex in a similar optically active solvent (*d*-1,2-propanediol) and have found evidence for two c.d. bands. The observed spectra are shown in Fig. 1. The bands are quite reproducible for a given set of conditions and remain relatively unchanged over a period of 1 to 2 weeks. Due to very strong absorption by both the solvent and solute, the c.d. maximum for the high energy band could not be obtained. However, it is unquestionable that a second negative c.d. peak does occur and some rounding of the curve at approximately 272 mμ is indicated.

For $[PtCl_4]^{2-}$, the observed c.d. was attributed to the ${}^1A_{1g} \rightarrow {}^1A_{2g}$ transition (5). This assignment would correspond to an arrangement of the d-orbitals which is different from that given by Gray and Ballhausen (1). Recently new molecular orbital calculations have been made (6) and the ordering of energy levels in $[PtCl_4]^{2-}$ is now given as $d_{z^2} < d_{xz}, d_{yz} < d_{xy} < d_{x^2-y^2}$. The results of the c.d. study for $[PtCl_4]^{2-}$ are consistent with this new arrangement.

The $[Ni(CN)_4]^{2-}$ complex has D_{4h} symmetry

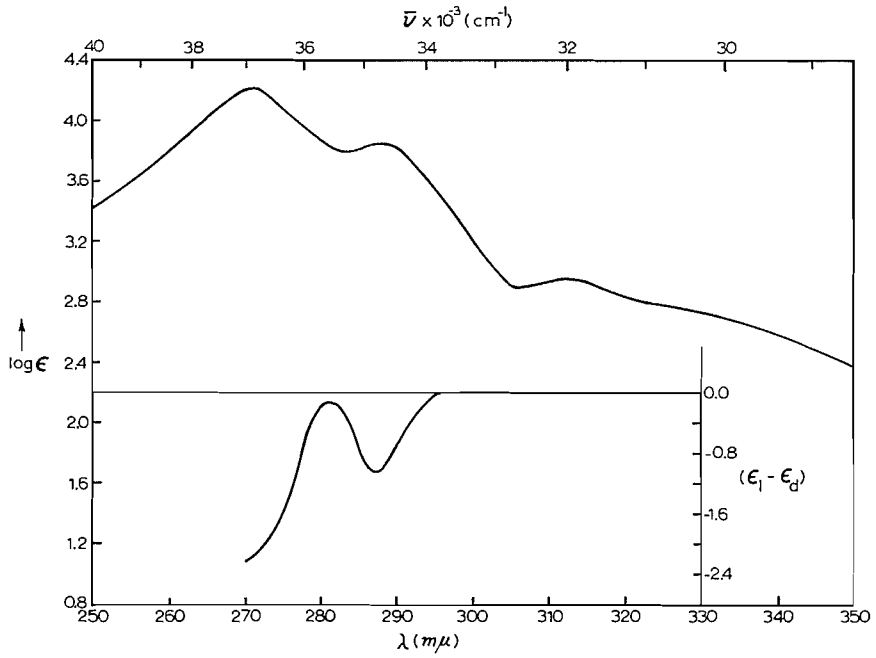

FIG. 1. Absorption spectrum and circular dichroism of $[Ni(CN)_4]^{2-}$ in *d*-1,2-propanediol.

and hence should be optically inactive. The fact that circular dichroism is observed must be due to dissymmetry caused by the presence of the optically active solvent. In dissymmetric complexes strong circular dichroism is observed for those absorption bands which are magnetic dipole allowed (7). In a given point group this requirement is met when the direct product of the symmetries of the electronic wave functions belongs to a representation containing a rotation. For $[Ni(CN)_4]^{2-}$ only two transitions meet this requirement, namely $^1A_{1g} \rightarrow {}^1A_{2g}$ and $^1A_{1g} \rightarrow {}^1E_g$. These correspond to the orbital transitions $d_{xy} \rightarrow d_{x^2-y^2}$ and d_{xz}, $d_{yz} \rightarrow d_{x^2-y^2}$. Charge transfer bands involve transitions between the d levels and low energy π-antibonding levels. If Gray's assignment of the molecular orbital energy levels is correct, the lowest-lying antibonding orbital is a_{2u}. The lowest energy charge transfer bands arise from transitions from the various d orbitals to this level and circular dichroism should not be observed for these bands. Thus the c.d. which is observed should be due to the two d–d transitions given above. Certain charge transfer bands could exhibit c.d. but these are of higher energy; the a_{2u} orbital would be expected to be of lower energy since it is stabilized by overlap with the $4p_z$ orbital (1).

The three observed absorption bands at 31 950, 34 720, and 36 900 cm^{-1} in propanediol are charge transfer bands as predicted previously (1). The shoulder at 30 500 cm^{-1} is a d–d transition and since no c.d. is observed for this band, it must be $^1A_{1g} \rightarrow {}^1B_{1g}$, corresponding to an electron transfer from d_{z^2} to $d_{x^2-y^2}$. Since no c.d. is observed at lower energies, the two magnetic dipole allowed d–d bands must be hidden under the intense charge transfer bands. The positions of the two observed c.d. bands (34 840 cm^{-1} and $\sim$ 37 000 cm^{-1}) compare favorably with estimates made by Gray and Ballhausen (1) for the d–d transitions. The high energy band should be the $^1A_{1g} \rightarrow {}^1E_g$ transition since this corresponds to transitions involving the d_{xz} and d_{yz} orbitals which should be of lowest energy and the most energy would be required for this case. The other c.d. band must therefore be $^1A_{1g} \rightarrow {}^1A_{2g}$ and corresponds to a transition from the d_{xy} orbital. The c.d. spectra thus supports the ordering of d-orbital energy levels as d_{xz}, $d_{yz} < d_{xy} < d_{z^2} \ll d_{x^2-y^2}$. Gray's recent work (6) has pointed out that for $[Ni(CN)_4]^{2-}$ the d_{z^2} orbital would be expected to be of higher energy than d_{xz} and d_{yz} and not in the reverse order as was found for $[PtCl_4]^{2-}$. Our c.d. results are consistent with his views and those of other workers (4).

The conclusions made in this work have been based on the assumption that Gray's antibonding levels are correct. Other interpretations are possible only with much rearrangement of the antibonding orbitals and the present ordering is quite feasible on the basis of currently available data. The ordering of the d-orbitals given for $[Ni(CN)_4]^{2-}$ may not necessarily be valid for $[Pd(CN)_4]^{2-}$ and $[Pt(CN)_4]^{2-}$ since the crystal field strength of ligands coordinated to second and third row transition metals is usually greater than that observed for transition metals of the first row. As a result, the levels of d_{z^2} and d_{xy} may reverse to yield the arrangement given by Gray and Ballhausen (1). These other complexes absorb at much higher energies and have large extinction coefficients so that the technique which we have used is not readily applicable.

Experimental

Potassium tetracyanonickelate(II) monohydrate was prepared by the method of Fernelius and Burbage (8). The orange-red crystals were dried at 100 °C under vacuum to yield the yellow anhydrous compound. Optically active *d*-1,2-propanediol was obtained from the Aldrich Chemical Co., Milwaukee, Wisconsin.

Solutions containing the complex in *d*-1,2-propanediol were prepared by weighing both solvent and solute into a weighing bottle; the density of the solvent was then used to calculate concentrations. Solutions used for c.d. measurements were approximately 4×10^{-3} *M*. Circular dichroism spectra were recorded on a Durrum-Jasco ORD-UV-5 spectropolarimeter and absorption spectra were obtained using a Beckman DK-1 spectrophotometer.

Acknowledgment

We are grateful to the National Research Council of Canada for financial support of this work.

1. H. B. GRAY and C. J. BALLHAUSEN. J. Am. Chem. Soc. **85**, 260 (1963).
2. H. B. GRAY. *In* Transition metal chemistry. Vol. 1. *Edited by* R. L. Carlin. Marcel Dekker, Inc., New York, N.Y. 1965. p. 239.
3. J. R. PERUMAREDDI, A. D. LIEHR, and A. W. ADAMSON. J. Am. Chem. Soc. **85**, 249 (1963).
4. C. J. BALLHAUSEN, N. BJERRUM, R. DINGLE, K. ERIKS, and C. R. HARE. Inorg. Chem. **4**, 514 (1965).
5. B. BOSNICH. J. Am. Chem. Soc. **88**, 2606 (1966).
6. H. BASCH and H. B. GRAY. Inorg. Chem. **6**, 365 (1967).
7. W. MOFFITT. J. Chem. Phys. **25**, 1189 (1956).
8. W. C. FERNELIUS and J. J. BURBAGE. Inorg. Syn. **2**, 227 (1946).

Refinement of the crystal structure of scandium oxide

OSVALD KNOP AND JEAN M. HARTLEY
Department of Chemistry, Dalhousie University, Halifax, Nova Scotia

Received August 30, 1967

The crystal structure of Sc_2O_3 (*C*-type; $a_0 = 9.8459 \pm 15$ Å at 20 ± 2 °C) was refined from X-ray powder diffractometer data. Isotropic individual temperature factors were used in full-matrix *F* (19 reflections) and F^2 (41 reflections) programs. The positional parameters were determined as $u(Sc) = -0.0355 \pm 1$, $x(O) = 0.3933 \pm 3$, $y(O) = 0.1513 \pm 3$, and $z(O) = 0.3835 \pm 3$. The merits and limitations of refining from careful powder diffractometer data are briefly discussed.

Canadian Journal of Chemistry, 46, 1446 (1968)

The crystal structure of Sc_2O_3 is of the *C*-type (space group $Ia3$–T_h^7), with 8 Sc_1 in 8(*b*) ($\frac{111}{444}$ etc.), 24 Sc_2 in 24(*d*) ($u0\frac{1}{4}$ etc.), and 48 O in 48(*e*) (*xyz* etc.) (1). The structure has been refined by least squares, first from 19 $|F_o|$ extracted from accurate powder diffractometer intensities of single well-resolved reflections (for details see ref. 2), and then from 41 $\sum_i F_o^2$. The latter set contained 17 single ($i = 1$), 21 double ($i = 2$), and 3 triple ($i = 3$) reflections. Only those multiple reflections were utilized in which both or all three component F_o^2's had the same multiplicity, e.g. 420 + 240 or 611 + 532 + 352. The peaks were step-scanned at 0.01° θ intervals wherever this appeared desirable. Individual isotropic temperature factors were employed. Both parts of the dispersion correction (3) were applied to the scattering factors of Sc^{3+} (4) and O^{2-} (5). Three least-squares programs were used: a block-diagonal approximation *F*-program of ref. 6 written for IBM 1620 (40K), and *ad hoc* full-matrix *F* and

The conclusions made in this work have been based on the assumption that Gray's antibonding levels are correct. Other interpretations are possible only with much rearrangement of the antibonding orbitals and the present ordering is quite feasible on the basis of currently available data. The ordering of the d-orbitals given for $[Ni(CN)_4]^{2-}$ may not necessarily be valid for $[Pd(CN)_4]^{2-}$ and $[Pt(CN)_4]^{2-}$ since the crystal field strength of ligands coordinated to second and third row transition metals is usually greater than that observed for transition metals of the first row. As a result, the levels of d_{z^2} and d_{xy} may reverse to yield the arrangement given by Gray and Ballhausen (1). These other complexes absorb at much higher energies and have large extinction coefficients so that the technique which we have used is not readily applicable.

Experimental

Potassium tetracyanonickelate(II) monohydrate was prepared by the method of Fernelius and Burbage (8). The orange-red crystals were dried at 100 °C under vacuum to yield the yellow anhydrous compound. Optically active *d*-1,2-propanediol was obtained from the Aldrich Chemical Co., Milwaukee, Wisconsin.

Solutions containing the complex in *d*-1,2-propanediol were prepared by weighing both solvent and solute into a weighing bottle; the density of the solvent was then used to calculate concentrations. Solutions used for c.d. measurements were approximately 4×10^{-3} *M*. Circular dichroism spectra were recorded on a Durrum-Jasco ORD-UV-5 spectropolarimeter and absorption spectra were obtained using a Beckman DK-1 spectrophotometer.

Acknowledgment

We are grateful to the National Research Council of Canada for financial support of this work.

1. H. B. GRAY and C. J. BALLHAUSEN. J. Am. Chem. Soc. **85**, 260 (1963).
2. H. B. GRAY. *In* Transition metal chemistry. Vol. 1. *Edited by* R. L. Carlin. Marcel Dekker, Inc., New York, N.Y. 1965. p. 239.
3. J. R. PERUMAREDDI, A. D. LIEHR, and A. W. ADAMSON. J. Am. Chem. Soc. **85**, 249 (1963).
4. C. J. BALLHAUSEN, N. BJERRUM, R. DINGLE, K. ERIKS, and C. R. HARE. Inorg. Chem. **4**, 514 (1965).
5. B. BOSNICH. J. Am. Chem. Soc. **88**, 2606 (1966).
6. H. BASCH and H. B. GRAY. Inorg. Chem. **6**, 365 (1967).
7. W. MOFFITT. J. Chem. Phys. **25**, 1189 (1956).
8. W. C. FERNELIUS and J. J. BURBAGE. Inorg. Syn. **2**, 227 (1946).

Refinement of the crystal structure of scandium oxide

OSVALD KNOP AND JEAN M. HARTLEY
Department of Chemistry, Dalhousie University, Halifax, Nova Scotia

Received August 30, 1967

The crystal structure of Sc_2O_3 (*C*-type; $a_0 = 9.8459 \pm 15$ Å at 20 ± 2 °C) was refined from X-ray powder diffractometer data. Isotropic individual temperature factors were used in full-matrix *F* (19 reflections) and F^2 (41 reflections) programs. The positional parameters were determined as $u(Sc) = -0.0355 \pm 1$, $x(O) = 0.3933 \pm 3$, $y(O) = 0.1513 \pm 3$, and $z(O) = 0.3835 \pm 3$. The merits and limitations of refining from careful powder diffractometer data are briefly discussed.

Canadian Journal of Chemistry, 46, 1446 (1968)

The crystal structure of Sc_2O_3 is of the *C*-type (space group $Ia3$–T_h^7), with 8 Sc_1 in 8(*b*) ($\frac{111}{444}$ etc.), 24 Sc_2 in 24(*d*) ($u0\frac{1}{4}$ etc.), and 48 O in 48(*e*) (*xyz* etc.) (1). The structure has been refined by least squares, first from 19 $|F_o|$ extracted from accurate powder diffractometer intensities of single well-resolved reflections (for details see ref. 2), and then from 41 $\sum_i F_o^2$. The latter set contained 17 single ($i = 1$), 21 double ($i = 2$), and 3 triple ($i = 3$) reflections. Only those multiple reflections were utilized in which both or all three component F_o^2's had the same multiplicity, e.g. 420 + 240 or 611 + 532 + 352. The peaks were step-scanned at 0.01° θ intervals wherever this appeared desirable. Individual isotropic temperature factors were employed. Both parts of the dispersion correction (3) were applied to the scattering factors of Sc^{3+} (4) and O^{2-} (5). Three least-squares programs were used: a block-diagonal approximation *F*-program of ref. 6 written for IBM 1620 (40K), and *ad hoc* full-matrix *F* and

Can. J. Chem. Downloaded from www.nrcresearchpress.com by 210.87.254.105 on 09/05/12
For personal use only.

TABLE I

Results of the least-squares refinements

	Initial values	Block-diagonal approximation	Full-matrix F-refinement	Full-matrix F^2-refinement	Ref. 9
Number of $\|F_o\|$ or ΣF_o^2, n		19	19	41	172
After cycles		12	3	3	
Scale factor, K	1.000	1.168±1	1.170±1	1.168±1	
u	−0.030	−0.0350±3	−0.0346±3	−0.0355±1	−0.0351±2
x	0.375	0.3921±7	0.3929±7	0.3933±3	0.3928±7
y	0.150	0.1528±6	0.1521±6	0.1513±3	0.1528±7
z	0.375	0.3842±6	0.3838±6	0.3835±3	0.3802±7
$B(Sc_1)$, Å^2	0.40	0.78±7	0.95±7	0.79±2	Not stated
$B(Sc_2)$, Å^2	0.40	0.88±5	0.88±5	0.82±2	Not stated
$B(O)$, Å^2	1.00	0.99±9	1.02±9	1.21±4	Negative
R_1, %*	34.1	2.01	1.42		7†
R_2, %*				1.63	
$[\Sigma w(\Delta\|F\|)^2/(n-m)\Sigma w]^{1/2}$	16.0	0.73	0.82		
$[\Sigma w(\Delta F^2)^2/(n-m)\Sigma w]^{1/2}$				134.7‡	

* $R_1 = \Sigma||F_o| - |F_c||/\Sigma|F_o|$; $R_2 = \Sigma|F_o^2 - F_c^2|/\Sigma F_o^2$.
†It is not made clear in ref. 9 to which stage of refinement this R value refers.
‡157.3 for initial trial values.

F^2 programs written for IBM 1800. The weighting scheme was W3 of ref. 7.

The intensity of each reflection was measured at least three times. The reproducibility varied with the integrated intensity as follows (intensities normalized to I_c (222)):

Intensity range	Number of reflections	Standard deviation, %	
		Range	Average
10–100	4	0.3–1.7	1.0
5–10	5	0.6–3.6	2.0
2–5	12	1–4.4	2.2
<2	16	1–14.8	7.2

Reflections 220, 752 + 572, and 965 + 695, which were not observed in the diffractometer pattern, were entered at $I_o = 0$. Reflection 664 was observed but its intensity was too low, relative to the background, to be measured with any accuracy. $I_o(664)$ was therefore estimated by comparison with $I_o(833) = 0.5$. The only eligible reflection not included in the refinement was 200.

The high-purity scandium oxide was kindly donated by Drs. B. I. Pokrovskiĭ and F. M. Spiridonov of the Institute of Inorganic Chemistry, Faculty of Chemistry, Moscow State University. Spectrographic analysis revealed the following impurities: 0.1% K, 0.02% Na, 0.01% Ca, and (in p.p.m.) 70 Si, 30 Al, 20 Fe, 5 Mg, and 27 Y. No rare-earth impurities were detected.

The powder patterns of the original material taken with Ni-filtered CuK radiation were weak and not very sharp. To improve the crystallinity two pressed disks of the oxide were heated to 1100 °C for 12 h followed by firing at 1400 °C for 2 h. One of them was then kept at 1600 °C for 2 h and subsequently fired at 1700 °C for 18 h in argon. Only the disk fired at 1700 °C sintered with appreciable shrinkage. Since there did not appear to be further improvement in the definition of the powder lines on firing to 1700 °C, the less sintered 1400 °C material was used in the X-ray study. The lattice parameter, $a_0 = 9.8459 \pm 15$ Å (at 20 ± 2 °C), agreed well with that reported in ref. 8, 9.845 Å (at 25 °C), but not with the recent value of 9.810 ± 2 Å (9).[1]

The initial F-refinement was carried out with the block-diagonal approximation program starting with reasonable estimates of the parameter values (Table I). After 12 cycles the unweighted R reached 2.01%, with all the shifts well within the corresponding e.s.d.'s and converging absolutely. When the final parameter values were used as the initial trial values in the full-matrix F-program, very small changes in the parameters resulted after 3 cycles.

The correlation matrix contained 3 terms whose absolute values were greater than |0.5|, viz. $B(Sc_1) - u$ (0.65), $B(O) - y$ (−0.53) and

[1]This value appears to have been reported by mistake. It has been corrected to 9.844 ± 2 Å (cf. Z. Krist. In press).

Can. J. Chem. Downloaded from www.nrcresearchpress.com by 210.87.254.105 on 09/05/12
For personal use only.

TABLE II

Observed and calculated structure factors

hkl	$10\|F_o\|$	BDA* $10\ F_c$	FMF* $10\ F_c$	FMF²* $10(\Sigma\|F_o\|^2)^{1/2}$	FMF²* $10(\Sigma F_c^2)^{1/2}$
211	764	799	792	764	809
220	0	−101	−105	0	99
222	4653	−4634	−4635	4652	4629
321, 231				325	346
400	1802	1805	1805	1801	1811
411	632	627	640	632	678
420, 240				585	641
332	1374	−1381	−1375	1373	1375
422	453	460	440	453	464
431, 341				1321	1293
521, 251				947	920
440	4674	4713	4718	4672	4693
433	686	−718	−721	686	745
611, 532, 352				1208	1229
620, 260				830	878
541, 451				1218	1227
622	2578	−2619	−2621	2577	2613
631, 361				1442	1486
444	1428	1439	1438	1427	1435
543, 453				743	767
640, 460				1003	938
642, 462				805	798
800	2715	2749	2745	2714	2732
653, 563				942	931
662	1700	−1690	−1688	1700	1667
752, 572				0	137
840, 480†	1091	1112	1113	1091	1116
833	600	−619	−619	600	620
842, 482				775	800
664	300‡	428	397	300‡	413
844	1650	1611	1611	1650	1589
10.1.1, 772				695	659
943, 493				743	764
10.3.3, 961, 691				1117	1052
10.4.2, 4.10.2				1249	1199
800	1025	1026	1022	1025	1005
10.4.4, 882				885	779
10 6.2, 6.10.2†	718	−704	−695	718	693
965, 695				0	407
12.2.0, 2.12.0				1342	1313
12.2.2, 10.6.4, 6.10.4				1102	1052

*BDA, block-diagonal approximation; FMF, full-matrix *F*-program; FMF², full-matrix F^2-program.
†$I(hkl) = I(khl)$.
‡Estimate for the local conditions of background and peak-to-background ratio.

$B(Sc_2) - u$ (0.66), but the low e.s.d.'s suggested that the correlations, if actually present, could not have interfered significantly with the refinement and that the numerical accuracy of the matrix inversion was adequate (cf. ref. 10).

The initial trial values in the F^2-program were again those obtained in the block-diagonal approximation refinement. The results after 3 cycles (Table I) were all within, or very close to, 2σ of the final parameter values produced by the full-matrix *F*-refinement, but the e.s.d.'s were appreciably lower. The correlation coefficients $B(Sc_2) - u$, $B(O) - y$, and $B(Sc_2) - y$ were 0.86, −0.66, and 0.52 respectively. The absolute values of all the others were below |0.5|, and 14 of them below |0.1|. The agreement of the observed and calculated structure factors was satisfactory for all the refinements (Table II).

The intensity agreement indices $D(\Delta I)$ and $D(I)$ (cf. ref. 7) show that the selection of $|F_o|$ and $\sum_i F_o^2$ for the refinements was reasonably balanced, so that the results may be considered as representative for the complete set of intensities.

Can. J. Chem. Downloaded from www.nrcresearchpress.com by 210.87.254.105 on 09/05/12
For personal use only.

TABLE III

Sc—O distances in Sc_2O_3 and other scandium compounds

Compound	Coordination	Distance, Å	Reference
Sc_2O_3	(Sc_1 -) 6 O	2.12 ± 0.036 (3σ)	9
	(Sc_2 -) 2 O + 2 O + 2 O	2.08; 2.09; 2.16 (all ± 0.039, 3σ)	
	(Sc_1 -) 6 O	2.159 ± 0.016	This work*
	(Sc_2 -) 2 O + 2 O + 2 O	2.071 ± 0.018; 2.107 ± 0.018; 2.146 ± 0.017	
$ScVO_4$ (zircon)	4 O + 4 O	2.07; 2.38	11
ScOF (monoclinic ZrO_2)	4 O + 3 F	2.08; 2.08; 2.10; 2.14 (all ± 0.02)	12
α-ScOOH (diaspore)	2 O + 1 O + 2 OH + 1 OH	2.06 ± 0.03; 1.97 ± 0.04; 2.29 ± 0.03; 2.18 ± 0.04	13
γ-ScOOH (boehmite)	2 O + 2 O + 2 O	2.06; 2.08; 2.17	14
$Sc(OH)_3$	6 OH	2.0_8 ± 0.05	15
$CaSc_2O_4$ ($CaFe_2O_4$)	2 O + 2 O + 1 O + 1 O	2.07; 2.15; 2.18; 2.22 (all ± 0.05)	16
	1 O + 1 O + 2 O + 2 O	2.04; 2.12; 2.16; 2.17 (all ± 0.05)	
$Sc_2(WO_4)_3$	6 O	2.020 ± 0.016; 2.026 ± 0.015; 2.051 ± 0.013; 2.053 ± 0.015; 2.103 ± 0.016; 2.124 ± 0.010	17

*Based on the final parameter values (± 3σ) from the full-matrix F^2-refinement. Not corrected for thermal motion.

	$D(\Delta I)$	$D(I)$
Reflections used in the *F*-refinement (19)	2.64%	1010
Reflections used in the F^2-refinement (41)	3.60%	1005
All reflections measured (65)	4.81%	986
Reflections observable within the CuKα sphere up to and including 11.6.1 + 6.11.1 + 10.7.3 + 7.10.3 (69)	5.01%	988

Refinements from $\sum_t F_o^2$ work best when all the component F_c^2's in a sum change in the same direction for a given set of parameter shifts, i.e. when they all simultaneously increase or all decrease. When the changes are in opposing directions, there might occur, in the extreme case, a complete compensation, so that the net change in the $\sum_t F_c^2$ would be zero and the particular sum term would not contribute to the refinement. For Sc_2O_3 the changes are in opposing directions in a few of the sums, but usually the absolute values of the individual component F_c^2's in a sum and their rates of change are combined in such a way that refinement does take place, albeit with reduced efficacy. The result of the F^2-refinement is thus to be preferred to that of the full-matrix *F*-refinement, but as noted above the differences in the parameters obtained are small.

The present values of the refined parameters are not very different from those obtained recently by Geller *et al.* (9) using a single crystal and photographic methods (Table I). There is an almost complete agreement in *u*, *x*, and *y*, but the difference in *z* is outside the stated 3σ limits, and all our temperature factors are reasonable. By contrast, Geller *et al.* reported that their *B*(O) was negative, and "the standard deviations of the thermal parameters indicated that the values were not very meaningful". However, the elements of their correlation matrix were all less than 0.15.

The Sc_1—O and Sc_2—O distances (both for irregular six-coordination) are compared with Sc—O distances in other scandium compounds in Table III. Geller's Sc—O values all fall within our 3σ uncertainty intervals of the individual distances. The unweighted average of the four different values for the Sc—O distances (present work), 2.121 Å, agrees with Norrestam's unspecified average of 2.122 Å quoted in ref. 12.

The present results may be regarded as demonstrating the usefulness and reliability of refinement of simple structures from accurate powder diffractometer data. They also confirm the view that the presence of even relatively large linear correlation coefficients need not prejudice the accuracy and reliability of a least-squares refinement.

The advantages of refining from powder data are the elimination of approximate absorption corrections and of empirical correlation factors which are required to bring (photographic)

Can. J. Chem. Downloaded from www.nrcresearchpress.com by 210.87.254.105 on 09/05/12
For personal use only.

single-crystal data to the same scale, and minimization of extinction and double reflection as well as of problems arising from local imperfections and inhomogeneities, which in a small single crystal might seriously affect the observed intensities. On the other hand, the powder data are usually insufficient for a full anisotropic refinement; they do not permit evaluation of the anisotropy of the local background which may be associated with a reflection; and specimen preparation must be designed and executed so as to counteract possible tendency to preferred orientation of the powder and aging of the pressed disk or grease mount. Extraction of very weak reflections from the background may also present problems. However, where single crystals are not obtainable, there is no choice of method, and then it is reassuring to know that careful powder diffractometry, where applicable, is capable of yielding results which are comparable with those from single-crystal data.

Acknowledgments

Financial support of this investigation by the National Research Council of Canada and a grant to J. M. H. from the Atlantic Provinces Inter-University Committee on the Sciences are hereby acknowledged.

1. L. PAULING and M. D. SHAPELL. Z. Krist. **75**, 128 (1930).
2. O. KNOP, F. BRISSE, L. CASTELLIZ, and SUTARNO. Can. J. Chem. **43**, 2812 (1965).
3. D. T. CROMER. Acta Cryst. **18**, 17 (1965).
4. International tables for x-ray crystallography. Vol. III. Kynoch Press, Birmingham. 1962.
5. M. TOKONAMI. Acta Cryst. **19**, 486 (1965).
6. F. R. AHMED, E. J. GABE, G. A. MAIR, and M. E. PIPPY. A unified set of crystallographic programs for the IBM 1620 computer. September 1963. Unpublished.
7. SUTARNO, O. KNOP, and K. I. G. REID. Can. J. Chem. **45**, 1391 (1967).
8. H. E. SWANSON, R. K. FUYAT, and G. M. UGRINIC. Natl. Bur. Std. U.S. Circ. 539, **3**, 27 (1954).
9. S. GELLER, P. ROMO, and J. P. REMEIKA. Z. Krist. **124**, 136 (1967).
10. W. C. HAMILTON. Statistics in physical science. The Ronald Press Company, New York. 1964. pp. 201–202. C. SCHERINGER. Acta Cryst. **19**, 504 (1965).
11. W. O. MILLIGAN and L. W. VERNON. J. Phys. Chem. **56**, 145 (1952).
12. B. HOLMBERG. Acta Chem. Scand. **20**, 1082 (1966).
13. A. NØRLUND CHRISTENSEN and S. J. JENSEN. Acta Chem. Scand. **21**, 121 (1967).
14. W. O. MILLIGAN and J. L. MCATEE. J. Phys. Chem. **60**, 273 (1956).
15. K. SCHUBERT and A. SEITZ. Z. Anorg. Allgem. Chem. **256**, 226 (1948).
16. H. MÜLLER-BUSCHBAUM and H. G. SCHNERING. Z. Anorg. Allgem. Chem. **336**, 295 (1965).
17. S. C. ABRAHAMS and J. L. BERNSTEIN. J. Chem. Phys. **45**, 2745 (1966).

Can. J. Chem. Downloaded from www.nrcresearchpress.com by 210.87.254.105 on 09/05/12
For personal use only.

Infrared emission from the $N–I_2$ reaction flame

L. F. PHILLIPS

Chemistry Department, University of Canterbury, Christchurch, New Zealand[1]

Received September 20, 1967

The flame spectrum between 1 and 3 μ consists mainly of nitrogen first positive bands, plus the atomic iodine line at 1.315 μ. The intensity of the emission bands increases markedly when iodine is added.

Canadian Journal of Chemistry, **46**, 1450 (1968)

The emission spectrum of the active nitrogen–iodine flame has previously been observed to consist mainly of bands and continua of molecular iodine in the visible and near ultraviolet (1), together with numerous atomic iodine lines below 2100 Å (2). In the present work these observations have been extended into the infrared as far as 3 microns.

The spectrometer was an evacuated model 84-111 Jarrell-Ash half-metre Ebert monochromator, used with 3 mm slits and a 295 grooves/mm grating blazed at 2.1 μ. Window materials were Linde sapphire or calcium fluoride. For most of the experiments radiation below 1.1 μ was removed with a Spectrolab anti-reflection coated silicon blank. The detector was a Unicam SP50 Golay detector with KBr window, contained in a Pfund condensing unit. A 12 c.p.s. light chopper, tuned lock-in amplifier, and phase-sensitive

[1]Present address: Inorganic Materials Research Division, Lawrence Radiation Laboratory, University of California, Berkeley, California.

single-crystal data to the same scale, and minimization of extinction and double reflection as well as of problems arising from local imperfections and inhomogeneities, which in a small single crystal might seriously affect the observed intensities. On the other hand, the powder data are usually insufficient for a full anisotropic refinement; they do not permit evaluation of the anisotropy of the local background which may be associated with a reflection; and specimen preparation must be designed and executed so as to counteract possible tendency to preferred orientation of the powder and aging of the pressed disk or grease mount. Extraction of very weak reflections from the background may also present problems. However, where single crystals are not obtainable, there is no choice of method, and then it is reassuring to know that careful powder diffractometry, where applicable, is capable of yielding results which are comparable with those from single-crystal data.

Acknowledgments

Financial support of this investigation by the National Research Council of Canada and a grant to J. M. H. from the Atlantic Provinces Inter-University Committee on the Sciences are hereby acknowledged.

1. L. PAULING and M. D. SHAPELL. Z. Krist. **75**, 128 (1930).
2. O. KNOP, F. BRISSE, L. CASTELLIZ, and SUTARNO. Can. J. Chem. **43**, 2812 (1965).
3. D. T. CROMER. Acta Cryst. **18**, 17 (1965).
4. International tables for x-ray crystallography. Vol. III. Kynoch Press, Birmingham. 1962.
5. M. TOKONAMI. Acta Cryst. **19**, 486 (1965).
6. F. R. AHMED, E. J. GABE, G. A. MAIR, and M. E. PIPPY. A unified set of crystallographic programs for the IBM 1620 computer. September 1963. Unpublished.
7. SUTARNO, O. KNOP, and K. I. G. REID. Can. J. Chem. **45**, 1391 (1967).
8. H. E. SWANSON, R. K. FUYAT, and G. M. UGRINIC. Natl. Bur. Std. U.S. Circ. 539, **3**, 27 (1954).
9. S. GELLER, P. ROMO, and J. P. REMEIKA. Z. Krist. **124**, 136 (1967).
10. W. C. HAMILTON. Statistics in physical science. The Ronald Press Company, New York. 1964. pp. 201–202. C. SCHERINGER. Acta Cryst. **19**, 504 (1965).
11. W. O. MILLIGAN and L. W. VERNON. J. Phys. Chem. **56**, 145 (1952).
12. B. HOLMBERG. Acta Chem. Scand. **20**, 1082 (1966).
13. A. NØRLUND CHRISTENSEN and S. J. JENSEN. Acta Chem. Scand. **21**, 121 (1967).
14. W. O. MILLIGAN and J. L. MCATEE. J. Phys. Chem. **60**, 273 (1956).
15. K. SCHUBERT and A. SEITZ. Z. Anorg. Allgem. Chem. **256**, 226 (1948).
16. H. MÜLLER-BUSCHBAUM and H. G. SCHNERING. Z. Anorg. Allgem. Chem. **336**, 295 (1965).
17. S. C. ABRAHAMS and J. L. BERNSTEIN. J. Chem. Phys. **45**, 2745 (1966).

Can. J. Chem. Downloaded from www.nrcresearchpress.com by 210.87.254.5 on 09/05/12
For personal use only.

Infrared emission from the $N–I_2$ reaction flame

L. F. PHILLIPS
Chemistry Department, University of Canterbury, Christchurch, New Zealand[1]

Received September 20, 1967

The flame spectrum between 1 and 3 μ consists mainly of nitrogen first positive bands, plus the atomic iodine line at 1.315 μ. The intensity of the emission bands increases markedly when iodine is added.

Canadian Journal of Chemistry, **46**, 1450 (1968)

The emission spectrum of the active nitrogen–iodine flame has previously been observed to consist mainly of bands and continua of molecular iodine in the visible and near ultraviolet (1), together with numerous atomic iodine lines below 2100 Å (2). In the present work these observations have been extended into the infrared as far as 3 microns.

The spectrometer was an evacuated model 84-111 Jarrell-Ash half-metre Ebert monochromator, used with 3 mm slits and a 295 grooves/mm grating blazed at 2.1 μ. Window materials were Linde sapphire or calcium fluoride. For most of the experiments radiation below 1.1 μ was removed with a Spectrolab anti-reflection coated silicon blank. The detector was a Unicam SP50 Golay detector with KBr window, contained in a Pfund condensing unit. A 12 c.p.s. light chopper, tuned lock-in amplifier, and phase-sensitive

[1]Present address: Inorganic Materials Research Division, Lawrence Radiation Laboratory, University of California, Berkeley, California.

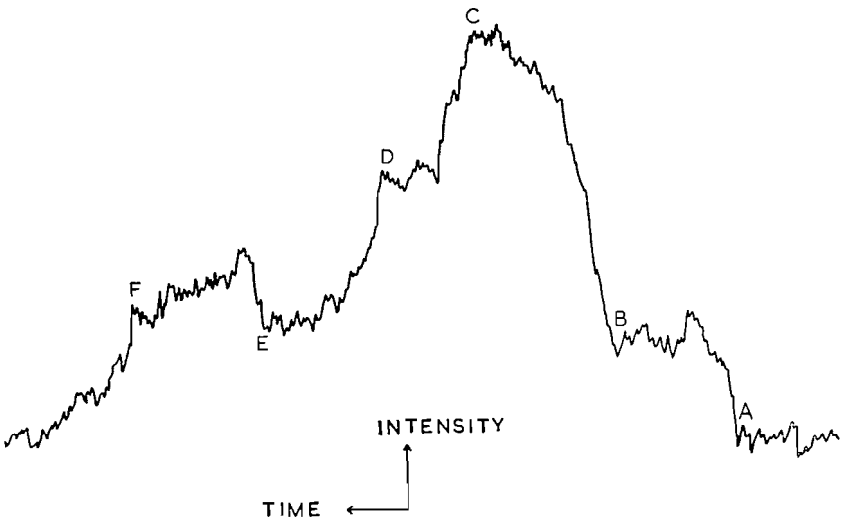

FIG. 1. Enhancement of the (0,1) first positive emission by addition of iodine to discharged nitrogen. Intensity of emission in arbitrary units versus time. At A the discharge is turned on, at B a trace of iodine (ca. 10^{-4} Torr) is added, at C and D successively larger amounts of iodine are added (to ca. 10^{-2} Torr), at E the iodine is removed, and at F the discharge is turned off. Duration of experiment ca. 7 min.

detector were used. The total light path through air (mainly in the condensing unit) was about 15 cm.

Matheson prepurified nitrogen was dried at −180 °C, pumped through a microwave discharge at ca. 3 Torr, and allowed to react with analytical reagent grade iodine, carried in a stream of the same nitrogen, in a 40 cm × 25 mm o.d. Pyrex tube having a sapphire window at the end furthest from the iodine inlet. The discharge was separated from the reaction tube by 30 cm of 15 mm o.d. tubing having two right-angle bends in different planes before a final T-join to the reaction tube. There was a tendency for the energetic "pink afterglow" to occur in this T-join; to avoid complications from this source the microwave power level was always reduced well below the point at which a more energetic region could be seen. Addition of iodine caused the color of the gas stream to change first from yellow to almost white, then to blue as more iodine was added. Most of the observations were made under conditions where the visible emission from the reaction tube was blue except for a short region near the iodine inlet. Typical partial pressures of atomic nitrogen (prior to reaction) and iodine were 2×10^{-2} and 2×10^{-3} Torr, respectively.

The strongest emission features between 1.1 and 3 μ were the atomic iodine line at 1.315 μ and the (0,1) band of the N_2 first positive system at 1.238 μ. Other features were essentially the same as the bands found by Hepner and Herman (3) in the emission from energetic discharges through helium–nitrogen mixtures, but the resolution and signal-to-noise ratio were much poorer in the present study because of the relatively low light intensity. Thus the observed emission mostly belonged to the first positive system. It was notable that the emission increased greatly in intensity when a trace of iodine was added to the discharged nitrogen. Typical behavior is shown for the (0,1) first positive band in Fig. 1. A subsequent investigation in the visible region, using narrow slits, a grating blazed at 5000 Å, and a 1P21 photomultiplier (with Corning filters for order separation), showed that in fact all first positive bands, up to at least $v' = 12$, increased in intensity when a trace of iodine was added. The maximum enhancement, and the amount of additional iodine required to bring about a net decrease in intensity, were least at high v', but the decrease was quite gradual; no effect was observed which could be attributed to energy resonance in a process such as (2, 4, 5)

$$[1] \qquad N_2^* + N(^4S) \rightarrow N(^4S) + N_2(^3\Pi_g, v'),$$

where N_2^* is an excited species produced by reaction of N with NI (2). The simplest interpretation of these observations is that I_2, or I, is a particularly efficient third body for promoting recombination of nitrogen atoms into the $^5\Sigma_g^+$ state.

Can. J. Chem. Downloaded from www.nrcresearchpress.com by 210.87.254.5 on 09/05/12
For personal use only.

Acknowledgments

This work was supported by the New Zealand Universities Research Committee and by Grant AF-AFOSR-1265-67 from the United States Air Force Office of Scientific Research.

1. A. ELLIOTT. Proc. Roy. Soc. London, Ser. A, **174**, 272 (1940).
2. L. F. PHILLIPS. Can. J. Chem. This issue.
3. G. HEPNER and L. HERMAN. Ann. Geophys. **13**, 242 (1957).
4. K. L. WRAY. J. Chem. Phys. **44**, 623 (1966).
5. R. A. YOUNG. Can. J. Chem. **44**, 1171 (1966).

Can. J. Chem. Downloaded from www.nrcresearchpress.com by 210.87.254.5 on 09/05/12
For personal use only.

Can. J. Chem. Downloaded from www.nrcresearchpress.com by 210.87.254.5 on 09/05/12
For personal use only.

Correlation of specific rotation with conformation. A new approach to the study of conformational equilibria

R. U. LEMIEUX AND A. A. PAVIA[1]
Department of Chemistry, University of Alberta, Edmonton, Alberta

Received March 14, 1968

The marked changes in optical rotation which occur on dissolving the methyl 2-deoxy-α-L-and 3-deoxy-β-L-*erythro*-pentopyranosides in a variety of solvents including chloroform, acetone, acetonitrile, pyridine, dimethylsulfoxide, and water were found by nuclear magnetic resonance to result almost exclusively from changes in conformational equilibria. The changes in rotation are in agreement with those expected from Brewster's rules.

Canadian Journal of Chemistry, 46, 1453 (1968)

The profound influence of solvent on the conformational properties of methyl 2-deoxy-α-D-*erythro*-pentopyranoside (1) prompted a further examination of this and related phenomena.

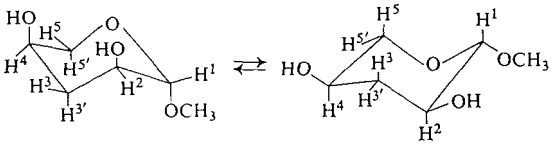

1*a* **1***b*

Methyl 3-deoxy-β-L-*erythro*-pentopyranoside (**1**) was prepared by reaction of methyl 4-*O*-acetyl-2,3-anhydro-β-L-ribopyranoside (2) with sodium iodide in acid acetone (3) followed by hydrogenolysis of the resulting methyl 4-*O*-acetyl-3-deoxy-3-iodo-β-L-xylopyranoside using palladium on carbon as catalyst. The deacetylated product was converted to the di-*O*-*p*-nitrobenzoate of **1**, m.p. 123.5–124.5°, $[\alpha]_D$ +51.2° (*c*, 1.3 in chloroform) for purification. Saponification followed by vacuum distillation afforded analytically pure **1** as a colorless oil.

The nuclear magnetic resonance (n.m.r.) spectrum of **1** in deuterium oxide required the compound to exist largely in the 1C conformation (**1***b*) since $J_{1,2} = 6.0$, $J_{2,3} \simeq J_{3,4} \simeq 8.9$, $J_{2,3'} \simeq J_{3',4} = 4.5$, and $J_{3',5'} = 1.9$ Hz. In this conformation, the compound is expected (4) to possess a specific rotation of +100°. A specific rotation of +95° was observed. When deuteriochloroform was used as solvent, $J_{1,2}$ decreased to 2.2 Hz and it was clearly evident that H_3 and $H_{3'}$ were weakly (<3 Hz) coupled with both H_2 and H_4. Similarly H_4 was weakly coupled with both H_5 and $H_{5'}$. It was therefore apparent that the compound now existed largely in the Cl conformation (**1***a*). Indeed, for the compound in this conformation a specific rotation of +137° is expected and the value observed was +142°. It was possible to show that the relative chemical shifts observed for the various ring protons were in good agreement with those expected based on the empirical rules proposed by Lemieux and Stevens (5).

The above data infer that the change in rotation was to a good approximation the result of the change in conformational equilibria which occurred on changing the solvent. It could be expected, therefore, that in such situations studies of change in conformation with change in environment could be examined by simple polarimetry. To test this hypothesis, the rotations and n.m.r. spectra of compound **1** were measured in a variety of solvents. The results presented in Fig. 1 show that a linear relationship was obtained between the coupling constant of H_1 with H_2 ($J_{1,2}$ as displayed by the spacing of the doublet for H_1) with the specific rotation. The value for $J_{1,2}$ is considered to be a measure of the relative populations of the conformations **1***a* and **1***b* for **1**.

Preliminary studies with the α and β anomers for methyl 2-deoxy-L-*erythro*-pentopyranoside

[1]University of Alberta Postdoctorate Fellow, 1967–1968.

Can. J. Chem. Downloaded from www.nrcresearchpress.com by 210.87.254.5 on 09/05/12
For personal use only.

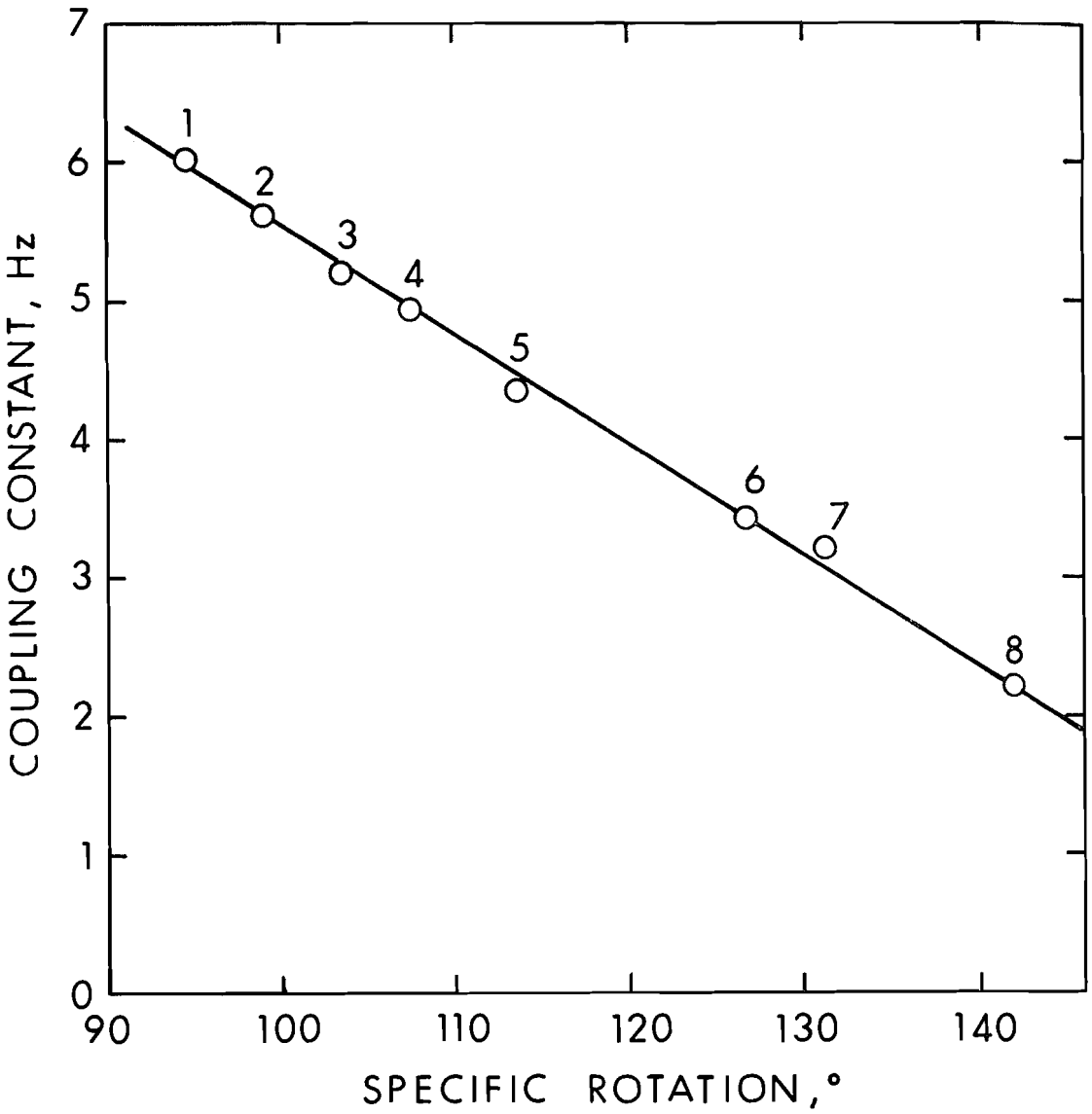

FIG. 1. Relationship between specific rotation ($[\alpha]_D^{25}$) and the coupling constant at 35° for H^1 and H^2 of methyl 3-deoxy-β-L-*erythro*-pentopyranoside (**1**) with change in solvent at concentrations (g/100 ml) of 9 ± 1 (except for acetonitrile and pyridine, 7 ± 1): 1, D_2O; 2, $(CD_3)_2SO$; 3, 6.4 g $(CD_3)_2SO$/g $CDCl_3$; 4, 2.57 g D_2O/g $(CD_3)_2CO$; 5, C_5D_5N; 6, CD_3CN; 7, $(CD_3)_2CO$; 8, $CDCl_3$.

(**2** and **3**, respectively) confirmed these conclusions. The earlier observations (1) for compound **2** were confirmed. In deuterium oxide, the coupling constants $J_{1,2}$ and $J_{1,2'}$ were 7.2 and 3.3 Hz, respectively, values which require a high concentration of conformation **2***a*. Indeed, in this conformation, the compound is expected (4) to have a specific rotation of 0°, and a specific rotation of −50° was observed. On changing the solvent to deuteriochloroform, the values of $J_{1,2}$ and $J_{1,2'}$ became near equal at 3 Hz and the specific rotation changed to −169°. A specific rotation of − 169° is expected (4) for the compoundin conformation **2***b*. The β-anomer **3** showed $J_{1,2} \simeq J_{1,2'} \simeq 2.9$ Hz both in water and deuteriochloroform. In accord with this observation the

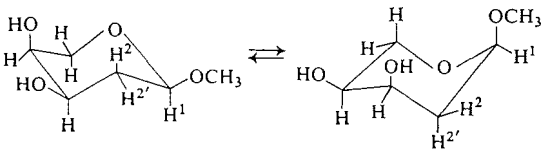

2a 2b

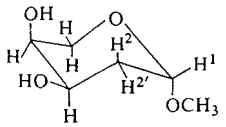

3

specific rotation appeared virtually independent of solvent. This is apparent from the specific rotations of +197°, +201°, and +192° observed in water, chloroform, and dimethylsulfoxide, respectively. Brewster's rules would predict a specific rotation of +209° for the compound in the C1 conformation shown. The presence of the C1 conformation (**2***b*) to an extent of about 25% for compound **2** in water is not eliminated by the n.m.r. parameters and may account for the observed rotation. For compounds **2** and **3**, the specific rotations were measured at much lower concentrations (about 1%) than were the n.m.r. spectra (about 10%).

We are therefore led to the important conclusion that the changes in rotation, noted for the changes in solvent, can be primarily related to the change in conformation of the compound. That is, solvent molecules in the solvent shell made contributions which were relatively small as compared to the measured rotation. It is evident, therefore, that in such cases, studies of the changes in rotation of compounds which occur on changing solvent can provide an important tool for the study of conformational equilibria and thereby of solvation phenomena. A consideration of the data in Fig. 1 obviously shows that the conformational changes are the result of specific solvation of the substrate. Through a net gain of electron density, the change in the electronic state of the oxygen atoms involved in the hydrogen bonds with solvent appears to have an important influence on the conformational equilibrium. This will be discussed in a forthcoming communication, which will deal with a variety of derivatives of compounds **1** and **2**.

Acknowledgment

The research was supported by the National Research Council of Canada Grant T-172 to R.U.L.

1. R. U. LEMIEUX and S. LEVINE. Can. J. Chem. **42**, 1473 (1964).
2. S. MUKHERJEE and A. R. TODD. J. Chem. Soc. 969 (1947).
3. R. U. LEMIEUX, E. FRAGA, and K. A. WATANABE. Can. J. Chem. **46**, 61 (1968).
4. J. H. BREWSTER. J. Am. Chem. Soc. **81**, 5483 (1959).
5. R. U. LEMIEUX and J. D. STEVENS. Can. J. Chem. **43**, 2059 (1965).

Stable complexes of bromine with some phthalazines[1]

A. HIRSCH[2] AND D. ORPHANOS
Canadian Technical Tape, Ltd., Montreal, Quebec

Received March 12, 1968

Bromine complexes of phthalazine and several phthalazine derivatives have been prepared. The yields are quantitative and the compounds exhibit good stability. The complexes may be utilized as sources of bromine in bromination reactions.

Canadian Journal of Chemistry, 46, 1455 (1968)

When a solution of phthalazine in carbon tetrachloride was treated with 1 molar equivalent of bromine, a solid separated. Isolation of the reaction product and drying in high vacuum gave a yellow-colored crystalline powder, m.p. 122–123°. The yield obtained was exactly the sum of the quantities of the two reactants used, a fact which reasonably suggested that the elemental composition was $C_8H_6Br_2N_2$ (**1**). Additional support for this molecular formulation

[1]We gratefully acknowledge the support of the National Research Council of Canada.

[2]Present address: Standard Packing Corporation, Clifton, New Jersey.

Can. J. Chem. Downloaded from www.nrcresearchpress.com by 210.87.254.5 on 09/05/12
For personal use only.

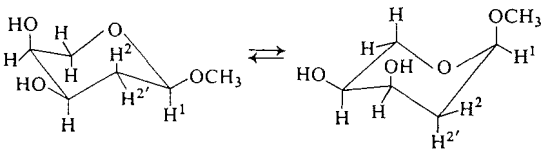

2a 2b

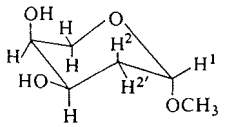

3

specific rotation appeared virtually independent of solvent. This is apparent from the specific rotations of +197°, +201°, and +192° observed in water, chloroform, and dimethylsulfoxide, respectively. Brewster's rules would predict a specific rotation of +209° for the compound in the C1 conformation shown. The presence of the C1 conformation (**2***b*) to an extent of about 25% for compound **2** in water is not eliminated by the n.m.r. parameters and may account for the observed rotation. For compounds **2** and **3**, the specific rotations were measured at much lower concentrations (about 1%) than were the n.m.r. spectra (about 10%).

We are therefore led to the important conclusion that the changes in rotation, noted for the changes in solvent, can be primarily related to the change in conformation of the compound. That is, solvent molecules in the solvent shell made contributions which were relatively small as compared to the measured rotation. It is evident, therefore, that in such cases, studies of the changes in rotation of compounds which occur on changing solvent can provide an important tool for the study of conformational equilibria and thereby of solvation phenomena. A consideration of the data in Fig. 1 obviously shows that the conformational changes are the result of specific solvation of the substrate. Through a net gain of electron density, the change in the electronic state of the oxygen atoms involved in the hydrogen bonds with solvent appears to have an important influence on the conformational equilibrium. This will be discussed in a forthcoming communication, which will deal with a variety of derivatives of compounds **1** and **2**.

Acknowledgment

The research was supported by the National Research Council of Canada Grant T-172 to R.U.L.

1. R. U. LEMIEUX and S. LEVINE. Can. J. Chem. **42**, 1473 (1964).
2. S. MUKHERJEE and A. R. TODD. J. Chem. Soc. 969 (1947).
3. R. U. LEMIEUX, E. FRAGA, and K. A. WATANABE. Can. J. Chem. **46**, 61 (1968).
4. J. H. BREWSTER. J. Am. Chem. Soc. **81**, 5483 (1959).
5. R. U. LEMIEUX and J. D. STEVENS. Can. J. Chem. **43**, 2059 (1965).

Stable complexes of bromine with some phthalazines[1]

A. HIRSCH[2] AND D. ORPHANOS
Canadian Technical Tape, Ltd., Montreal, Quebec

Received March 12, 1968

Bromine complexes of phthalazine and several phthalazine derivatives have been prepared. The yields are quantitative and the compounds exhibit good stability. The complexes may be utilized as sources of bromine in bromination reactions.

Canadian Journal of Chemistry, 46, 1455 (1968)

When a solution of phthalazine in carbon tetrachloride was treated with 1 molar equivalent of bromine, a solid separated. Isolation of the reaction product and drying in high vacuum gave a yellow-colored crystalline powder, m.p. 122–123°. The yield obtained was exactly the sum of the quantities of the two reactants used, a fact which reasonably suggested that the elemental composition was $C_8H_6Br_2N_2$ (**1**). Additional support for this molecular formulation

[1]We gratefully acknowledge the support of the National Research Council of Canada.

[2]Present address: Standard Packing Corporation, Clifton, New Jersey.

Can. J. Chem. Downloaded from www.nrcresearchpress.com by 210.87.254.42 on 09/05/12
For personal use only.

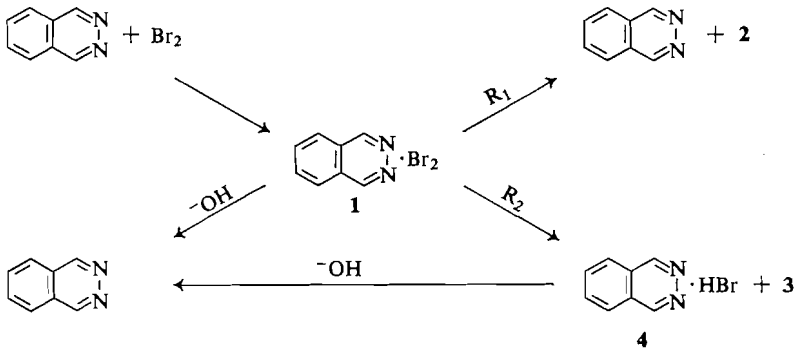

(R_1 = cyclohexene; R_2 = acetone)

REACTION SCHEME 1.

was obtained by bromine analysis. Thus, the product obtained was quite stable and after 6 months of storage showed no indication of change in its melting point and infrared spectrum. Its tetrahydrofuran solution was bright yellow and, upon addition of compounds reactive towards bromine, the color was discharged. The chemical changes depicted in Reaction Scheme 1 can only be compatible with the formulation **1**.

2 and **3** are bromocompounds arising from R_1 and R_2 respectively. In no case was an attempt made to isolate and identify **2** and **3**. Furthermore, it was found that 1-phenylphthalazine, 1,4-dichlorophthalazine, and 1,4-dibromophthalazine, available in our laboratory, can also combine with bromine to form stable complexes of the type **1**. The yields obtained were quantitative and in agreement with the complexing of the phthalazine compound with 1 molar equivalent of bromine. These new compounds reported in the experimental part showed sharp melting points and characteristic colors.

Experimental[3]

Bromine and Phthalazine Complex (1)

To a solution of phthalazine (1.3 g) in carbon tetrachloride (80 ml) at room temperature and under vigorous stirring, a solution of bromine (1.6 g) in carbon tetrachloride (20 ml) was added in 2–3 min. The resulting mixture was stirred for 30 additional min. The yellow precipitate was collected, washed with carbon tetrachloride, and dried in high vacuum. A yellow crystalline powder was obtained melting at 122–123° to a red liquid; yield quantitative. This product upon heating at about 100° for several hours acquires a violet color without any change in its melting point and infrared spectrum. Bromine analysis showed the value 55.51%, which was compatible with the theoretical calculated 55.12%.

[3]Melting points are uncorrected. Analyses were carried out by Dr. C. Daessle, Montreal, Quebec.

Chemical properties of **1**: (*a*) The yellow-colored tetrahydrofuran solution of **1** was decolorized upon addition of an excess of cyclohexene. From the resulting colorless solution pure phthalazine could properly be isolated. The recovery of phthalazine was quantitative. (*b*) Addition of **1** into acetone resulted in a yellow-colored solution. This solution on standing overnight or refluxing for 1 min was decolorized while a white crystalline material separated. It melted at 254–255° with foaming and by mixed melting point and infrared spectrum was identified as phthalazine hydrobromide **4**. (*c*) Treatment of **1** with an aqueous solution of NH_3 or NaOH results in the quantitative recovery of phthalazine.

Phthalazine Hydrobromide (4)

This derivative has not been described previously, and for identification purposes its preparation was requested. Phthalazine (0.65 g) was dissolved under stirring in 2 ml of a 48% aqueous solution of hydrobromic acid. The resulting clear solution, upon addition of 50 ml of acetone, separated a white crystalline solid, m.p. 254–255° with foaming; yield 1.02 g.

Anal. Calcd. for $C_8H_7BrN_2$: Br, 37.85. Found: Br, 38.26.

1-Phenylphthalazine-Bromine Complex

This complex was prepared by a procedure similar to that applied for **1**. It was obtained as a red-colored powder melting at 105°; yield quantitative.

1,4-Dibromophthalazine-Bromine Complex

1,4-Dibromophthalazine (0.01 mole) was dissolved in chloroform (15 ml). The volume of the resulting solution was increased to 100 ml by adding carbon tetrachloride (85 ml). Then, under vigorous stirring, bromine (1.6 g; 0.51 ml; 0.01 mole) in carbon tetrachloride (10 ml) was added dropwise. The orange-colored solution was stirred for 20 additional min and upon removal of the solvent afforded an orange-colored powder melting at 195°; yield quantitative.

1,4-Dichlorophthalazine-Bromine Complex

It was prepared by the procedure given above for the 1,4-dibromophthalazine–bromine complex. The product was obtained as a yellow-colored powder melting at 155°; yield quantitative.

Can. J. Chem. Downloaded from www.nrcresearchpress.com by 210.87.254.42 on 09/05/12
For personal use only.

The mechanism of isomerization of cyclopropanes

ROBERT J. CRAWFORD AND THOMAS R. LYNCH
Department of Chemistry, University of Alberta, Edmonton, Alberta

Received March 21, 1968

The racemization rate of *trans*-(−)-1,2-diphenylcyclopropane has been observed to be greater than that of *trans–cis* isomerization, in support of a trimethylene intermediate.

Canadian Journal of Chemistry, 46, 1457 (1968)

Can. J. Chem. Downloaded from www.nrcresearchpress.com by 210.87.254.42 on 09/05/12
For personal use only.

The isomerization of 1,2-disubstituted cyclopropanes may proceed through an "expanded ring" (1) or trimethylene species **1** (2) or via the concerted twist mechanism of Smith (3). The latter is attractive in that it follows the principle of least motion; ref. 4 gives an excellent review of this concept. The trimethylene species has the geometry **1** and if it plays a role[1] in the isomerization of **2** to **3** then (−)-**2** will be racemized on reaching **1**. Thus by the Smith mechanism the racemization rate constant (k_{rac}) will be equal to the rate constant for *trans* to *cis* isomerization (k_{tc}).

We have undertaken a study of the rate of geometrical isomerization and the rate of racemization of *trans*-(−)-1,2-diphenylcyclopropane (5). This compound was selected on the basis of its large rotation, the lack of any competing olefin formation, and the convenient temperature of isomerization (6). Table I gives the rate constants observed for the measurements carried out in 1-butanol 0.2 *M* in *trans*-1,2-diphenylcyclopropane.

The value k_{tc} was obtained from the observed rate of approach to equilibrium from the *trans* isomer (7). The values k_{tc} and k_{ct} are in good agreement with those previously reported by others (6).

That the racemization of **2** is faster than its conversion to **3** is consistent with a mechanism suggesting the trimethylene species as an intermediate and cannot be explained by the Smith mechanism alone.

Acknowledgment

The authors wish to express their thanks to

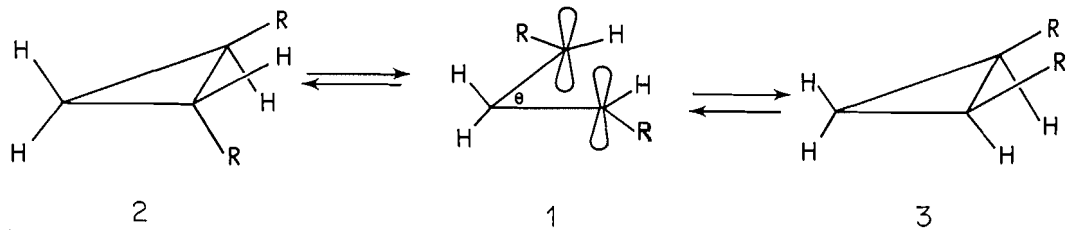

2 1 3

TABLE I

Rate constants for the isomerization and racemization of (−)1,2-diphenylcyclopropane

Temperature	k_{rac} (10^6 s^{-1})	$k_{tc} + k_{ct}$ (10^5 s^{-1})	K^c	k_{rac}/k_{tc}
204.5±0.2	6.80±0.06[a]	6.10±0.18[b]	11.8	1.42±0.03
220.7±0.3	25.6 ±1.3	20.1 ±1.0	10.7	1.49±0.05
229.0±0.5	49.1 ±2.6	36.5 ±2.1	10.3	1.52±0.03

[a]Errors are standard deviations.
[b]Racemization and geometrical isomerization rates were measured for each sample, thus minimizing the errors from temperature deviations and the errors in the ratios of the last column.
[c]Equilibrium values obtained starting from pure *cis* and pure *trans*.

[1]The symmetry state of the trimethylene species **1** is dependent upon the angle θ in **1** and thus both con- and dis-rotatory ring closure from **1** are possible (2*b*).

the National Research Council of Canada for a grant.

1. B. S. RABINOVITCH, E. W. SCHLAG, and K. B. WIBERG. J. Chem. Phys. **28**, 504 (1958).
2. (*a*) R. J. CRAWFORD and A. MISHRA. J. Am. Chem. Soc. **88**, 3963 (1966). (*b*) R. HOFFMANN. Abstracts of the 151st National Meeting of the American Chemical Society, Pittsburgh, Pa. March 1966. Paper 109K. (*c*). R. J. CVETANOVIC, H. E. AVEY, and R. S. IRWIN. J. Chem. Phys. **46**, 1993 (1967).
3. F. T. SMITH. J. Chem. Phys. **29**, 235 (1958).
4. J. HINE. J. Org. Chem. **31**, 1236 (1966).
5. I. TÖMÖSKÖZI. Chem. and Ind. London, 689 (1965).
6. (*a*) C. H. DE PUY and L. B. RODEWALD. Tetrahedron Letters, 2951 (1964). (*b*) C. D. DEBOER. Ph.D. Thesis, California Institute of Technology. 1966.
7. K. J. LAIDLER. Chemical kinetics. McGraw-Hill Book Co., Inc., New York. 1950. p. 19.

Can. J. Chem. Downloaded from www.nrcresearchpress.com by 210.87.254.42 on 09/05/12
For personal use only.

Can. J. Chem. Downloaded from www.nrcresearchpress.com by 210.87.254.5 on 09/05/12
For personal use only.

Canadian Journal of Chemistry

Published by THE NATIONAL RESEARCH COUNCIL OF CANADA

VOLUME 46 MAY 1, 1968 NUMBER 9

Steroids and steroidases. VI.[1] On the C-17 specificity of the Δ^5-3-ketoisomerase of *Pseudomonas testosteroni* and evidence for substrate micelle formation

J. BRYAN JONES AND DONALD C. WIGFIELD

Lash Miller Chemical Laboratories, Department of Chemistry, University of Toronto, Toronto 5, Ontario

Received November 27, 1967

Studies on the acid-, base-, and enzyme-catalyzed isomerizations of several variously C-17 substituted Δ^5-3-ketosteroids have indicated micellar aggregation of relatively non polar substrates in the dilute aqueous methanol assay solvent to be an important consideration when evaluating specificity data. Further evidence that the isomerase is sensitive to the presence of 17α-substituents in its substrates has been obtained and the probability that tyrosine is the acid catalytic group at the active center is discussed.

Canadian Journal of Chemistry, 46, 1459 (1968)

Introduction

The literature reports concerning the C-17 specificity of the Δ^5-3-ketoisomerase of *Pseudomonas testosteroni* (1–3), and, in particular, that cholest-5-en-3-one (**1***d*) is not a substrate of the enzyme (1), prompted us to investigate systematically the behavior of a series of variously C-17 substituted Δ^5-3-ketosteroids towards acid-, base-, and enzyme-catalyzed isomerizations to the corresponding αβ-unsaturated ketones.

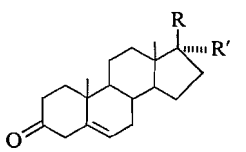

1

1*a*, R,R′ = O
b, R = OH, R′ = H
c, R = H, R′ = H
d, R = C_8H_{17}, R′ = H
e, R = OH, R′ = CH_3
f, R = OH, R′ = C≡CH
g, R = H, R′ = OH

All the substrates reported to undergo significant enzyme-catalyzed isomerization have one striking feature in common, *viz.* a polar, oxygen containing, functional group at or near the C-17 position, whereas the only Δ^5-3-ketosteroid with a negligible enzymic isomerization rate, cholest-5-en-3-one (**1***d*), possessed a nonpolar C_8H_{17} C-17 substituent. In an attempt to ascertain the reasons for this marked specificity difference, systematic studies on the series of Δ^5-3-ketones **1***a–d*, with groups of graded polarity at C-17, were carried out.

Experimental

Preparation of Δ^5-3-Ketosteroids[2]

(a) By Oxidation (5)

Androst-5-ene-3,17-dione (**1***a*), androst-5-en-3-one (**1***c*), and cholest-5-en-3-one (**1***d*) were prepared by dimethyl sulfoxide – dicyclohexylcarbodiimide oxidation of the corresponding 3β-alcohols as described previously (4).

(b) By Deconjugation (6)

17α-Hydroxyandrost-5-en-3-one (1g)—A solution of 17α-hydroxyandrost-4-en-3-one (400 mg) and potassium *t*-butoxide (1.5 g) in *t*-butyl alcohol (10 ml) was stirred under nitrogen for 90 min at 20°, and the reaction was then quenched by the rapid addition of 10% aqueous acetic acid. Excess aqueous sodium bicarbonate (40 ml, saturated solution) was added and the mixture was extracted with ether (4 × 20 ml). The combined ether extracts were washed with water (3 × 10 ml), dried ($MgSO_4$) and rotary evaporated at room temperature. The residue was washed with cold *n*-hexane (10 ml) to remove *t*-butyl alcohol and the precipitate was then

[1]For Part V of this series, see J. B. Jones and D. C. Wigfield. J. Am. Chem. Soc. **89**, 5294 (1967).

[2]Full details of the purification and analytical procedures used to obtain pure Δ^5-3-ketosteroids are given in an earlier communication (4).

recrystallized from acetone to give 17α-hydroxyandrost-5-en-3-one as plates (260 mg) m.p. 175–180°, ν_{max} ($CHCl_3$) 3584 (OH), and 1715 cm^{-1} (C=O).

Anal. Calcd. for $C_{19}H_{28}O_2$ (288.4): C, 79.12; H, 9.79. Found: C, 79.28; H, 9.81.

The following compounds were also obtained by the above procedure:

17β-Hydroxyandrost-5-en-3-one (1b)—From 17β-hydroxyandrost-4-en-3-one (400 mg), plates (320 mg, from acetone) m.p. 162–164° (lit. (7) m.p. 160–168°), ν_{max} ($CHCl_3$) 3690 (OH) and 1712 cm^{-1} (C=O).

17β-Hydroxy-17α-methylandrost-5-en-3-one (1e)—From 17β-hydroxy-17α-methylandrost-4-en-3-one (400 mg), prisms (325 mg, from acetone) m.p. 168–172° (lit. (8) m.p. 156–157°), ν_{max} ($CHCl_3$) 1712 cm^{-1} (C=O).

17β-Hydroxy-17α-ethynylandrost-5-en-3-one (1f)—From 17β-hydroxy-17α-ethynylandrost-4-en-3-one (400 mg), prisms (260 mg, from acetone) m.p. 238–240°, ν_{max} ($CHCl_3$) 3584 (OH), 3311 (≡C—H), and 1715 cm^{-1} (C=O); nuclear magnetic resonance (n.m.r.), δ 0.91 and 1.20 (3H singlets, C_{18}-CH_3 and C_{19}-CH_3), 2.54 (1H, singlet, ≡C—H), and 5.3 p.p.m. (1H, multiplet, C_6-H).

Anal. Calcd. for $C_{21}H_{28}O_2$ (312.4): C, 80.73; H, 9.03. Found: C, 80.84; H, 9.00.

Androst-5-ene-3,17-dione (1a)—From androst-4-ene-3,17-dione (400 mg), plates (250 mg, from methanol) m.p. 153–154° (lit. (4) m.p. 150–155°). (Since **1a** is very soluble in *n*-hexane, the crude product was not washed prior to recrystallization.)

General Isomerization Kinetics Procedures (1–3)

All isomerizations were performed in 3 ml, 1.0 cm light path, quartz cuvettes using a Beckmann D.U. spectrophotometer fitted with a thermostatted (25°) cell compartment. The wavelength selector was set to the wavelength of maximum absorption of the Δ^4-3-ketones produced from **1***a–g*. The isomerizations were then followed by observing the rate of increase of absorbance (in optical density units) as a function of time. For the faster reactions, the absorbance value was preset and the time noted on a split hand stopwatch as the bridge circuit came into balance. Using this technique,[3] readings could be taken every 8 s. The absorbance of the reaction mixture at infinite time (at least six half-lives) was also determined. The data were then analyzed by the now standard procedure (1–3).

For the acid- and base-catalyzed reactions, methanolic stock solutions containing 0.5 mg/ml of steroid were used. These solutions were always freshly prepared immediately prior to each run. For the substrates **1***a–d*, these stock solutions provided a concentration of ~0.03 μ mole per ml in the final reaction mixture. (This steroid concentration minimized the solubility difficulties encountered and provided convenient optical density values for following the kinetic runs.) For the isomerizations of all the new Δ^5-3-ketosteroids, and for those incompletely documented in the literature, the formation of the corresponding Δ^4-3-ketone was verified by its isolation.

For all the kinetic runs, the absorbance values were obtained using a reference cell containing all components except the steroid substrate. Also all data were corrected for the uncatalyzed rate of substrate isomerization by evaluating reaction mixtures in which the catalyst solution was replaced by an equivalent volume of CO_2-free water. In addition, for the enzyme-catalyzed processes, owing to the anomalous behavior of **1***d*, it was necessary to do blank reactions in which 1% aqueous bovine serum albumin (present in all enzyme solutions used) replaced the isomerase solution. The larger of the two uncatalyzed rates was then used in calculating the net enzymic rate of isomerization. All runs were carried out at least twice, and the reproducibility was $\leq \pm 3\%$.

Buffer Solutions

Tris-(hydroxymethyl)-aminomethane – hydrochloric acid (Tris – HCl), carbonate – bicarbonate, potassium chloride – hydrochloric acid (KCl – HCl) were prepared as described by Gomori (9); borate – hydroxide – carbonate buffer was the Fisher certified reagent.

Acid-catalyzed Isomerizations

The kinetic data were obtained with 3 ml reaction mixtures of the following composition.

3.3% Aqueous Methanol

Aqueous hydrochloric acid pH 1.00[4] (2.90 ml), methanol (0.05 ml), steroid stock solution (0.05 ml).

27% Aqueous Methanol

KCl–HCl buffer solution[5] of 0.15 *M* and pH 1.10 (2.20 ml), methanol (0.75 ml), steroid stock solution (0.05 ml).

75% Aqueous Methanol

KCl–HCl buffer solution (2.95 ml of a solution prepared from methanol (64.5 ml) and aqueous 0.15 *M* KCl–HCl pH 1.16 (24.0 ml)), steroid stock solution (0.05 ml).

The results obtained for the substrates evaluated, **1***a–d*, are summarized in Table I.

Base-catalyzed Isomerizations

Isomerization of a methanol solution of androst-5-ene-3,17-dione (**1***a*) with 0.2 *M* carbonate – bicarbonate buffer, pH 8.5–9.0, or with aqueous sodium hydroxide pH 8.5–9.0 gave products shown by thin-layer chromatographic analysis to contain at least four components.[6]

When 0.05 *M* Tris–HCl buffers, pH 8.5–9.0, or aqueous sodium hydroxide pH > 10.0, were used, clean isomerizations were obtained from which a quantitative yield of pure androst-4-ene-3,17-dione could be isolated. The kinetic data were obtained with 3 ml reaction mixtures of the following composition.

[3]We are grateful to Dr. P. Talalay for introducing us to this method.

[4]In all cases, the pH values quoted refer to those of the parent aqueous buffer. The pH values of the various water–methanol mixtures were not determined.

[5]For acid-catalyzed isomerizations carried out in aqueous solutions containing >5% methanol it became necessary to use KCl–HCl buffers as the catalysts since reproducible results could no longer be obtained with HCl alone.

[6]Subsequently, the formation of such mixtures was found to be less serious than indicated by the initial thin-layer chromatography analyses since 95–99% of the expected product, androst-4-ene-3,17-dione, was formed in each case (10).

449183

Can. J. Chem. Downloaded from www.nrcresearchpress.com by 210.87.254.5 on 09/05/12
For personal use only.

TABLE I

Acid- and base-catalyzed isomerizations of Δ^5-3-ketosteroids*

	1*a*		1*b*		1*c*		1*d*	
Solvent (pH)†	Reaction order‡	Rate constant§	Reaction order	Rate constant	Reaction order	Rate constant	Reaction order	Rate constant
3.3% MeOH (1.00)	1	9.08	1	10.5	Multiple‖	—	Multiple‖	—
27% MeOH (1.10)	1	5.29	1	5.88	1	5.23	‖Multiple	—
75% MeOH (1.16)	1	1.20	1	1.44	1	1.55	1	1.53
1.6% MeOH (8.82)	1	0.46	1	0.47	Multiple‖	—	Multiple‖	—
27% MeOH (8.54)	1	0.29	1	0.28	1	0.49	‖Multiple	—
75% MeOH (10.0)	1	65.9	1	47.5	1	47.6	1	46.1

*All measurements taken at 25 °C with a steroid concentration of 0.008 mg (~0.03 μmole)/ml.
†pH refers to that of the aqueous solution prior to addition of methanol.
‡With respect to steroid concentration.
§All rate constants in $min^{-1} \times 10^2$.
‖Reaction proceeds more rapidly than for 1*a* or 1*b*.

TABLE II

Enzyme-catalyzed isomerizations of Δ^5-3-ketosteroids*

	Relative rate†						
Solvent	1*a*	1*b*	1*c*	1*d*	1*e*	1*f*	1*g*
1.6% MeOH	100‡	102‡	~0§	~0§	40	33	30
27% MeOH	100‡	249‡	579‡	~0§	—‖	—‖	—‖

*All measurements taken at 25 °C with a steroid concentration of 0.055 μmole/ml.
†Relative to androst-5-ene-3,17-dione (1*a*) = 100, under each set of conditions. All rates corrected for the uncatalyzed reaction and for the effect of added protein.
‡Immeasurably fast when enzyme concentration was increased 10-fold.
§Unaffected by up to 100-fold increases in enzyme concentration.
‖Not determined.

1.6% Aqueous Methanol

0.05 *M* Tris–HCl buffer pH 8.82 (2.95 ml), steroid stock solution (0.05 ml).

27% Aqueous Methanol

0.05 *M* Tris–HCl buffer pH 8.54 (2.20 ml), methanol (0.75 ml), steroid stock solution (0.05 ml).

75% Aqueous Methanol

Buffer solution (2.95 ml of a solution prepared from methanol (64.5 ml) and 0.05 *M* aqueous borate – hydroxide – carbonate pH 10.0 (24.0 ml)), steroid stock solution (0.05 ml).

The results obtained for the steroids evaluated, 1*a–d*, are summarized in Table I.

Enzyme-catalyzed Isomerizations

Preparation of Solutions of the Δ^5-3-Ketoisomerase

Pseudomonas testosteroni was cultivated and the cells converted to an acetone powder as described by Talalay *et al.* (1). To extract the enzyme, acetone powder (100 mg) was ground (pestle and mortar) with alumina (100 mg) in ice-cold 0.03 *M* phosphate buffer pH 7.0 (5 ml) containing 1% bovine serum albumin until a homogeneous mixture was obtained. The mixture was then centrifuged (6000 *g*) at 2° for 10 min and the supernatant was stored at 0°. When required, dilutions of this enzyme supernatant solution were made with 0.03 *M* phosphate buffer pH 7.0 containing 1% bovine serum albumin.

Kinetic data were obtained using the assay method developed by Talalay and his co-workers (1). Typical reaction mixtures had the following composition.

1.6% Aqueous Methanol

Aqueous potassium phosphate buffer (100 μ moles) pH 7.0 (2.90 ml), 0.175 μ mole steroid (in 0.05 ml methanol), 0.05 ml of the 1000 times diluted enzyme solution.

5% Aqueous Methanol

As for 1.6% aqueous methanol except that the 3 ml reaction volume contained a total of 0.15 ml methanol.

27% Aqueous Methanol

As above except that the reaction volume contained 0.80 ml methanol, and 0.05 ml of 10 times diluted isomerase solution was used.

The results obtained, and the range of conditions applied in obtaining the relative substrate activities of 1*a–g*, are given in Table II.

Results and Discussion

For comparison purposes model isomerizations employing acid catalysis were first undertaken. Enzymic catalyses of βγ-unsaturated ketones are routinely carried out in dilute aqueous methanol at 25° (1, 3) and accordingly the initial acid (HCl)-catalyzed isomerizations of 1*a–d* were performed in 3.3% aqueous methanol

Can. J. Chem. Downloaded from www.nrcresearchpress.com by 210.87.254.5 on 09/05/12
For personal use only.

Can. J. Chem. Downloaded from www.nrcresearchpress.com by 210.87.254.5 on 09/05/12
For personal use only.

at the above temperature, under conditions approximating those of the enzymic assay as closely as practicable.[7] The results obtained (Table I) showed that only for the two substrates with an oxygen function at C-17, **1***a* and **1***b*, was a pseudo first order dependence on steroid concentration observed. In contrast, for **1***c* and **1***d*, with H and C_8H_{17} respectively as the 17β-groups, the isomerizations did not obey first order kinetics. Their overall rates were much faster than for **1***a* and **1***b* but the orders of reaction observed were multiple. The orders observed were in the range 2–3 and were found to change as the isomerization proceeded; they also varied from one run to another.

These data, together with the fact that precipitation of **1***c* and **1***d* occurred during some isomerizations, indicated that the influence of the nonpolar nature of the C-17 groups on the solubility of these steroids caused their aggregation into micelles in the aqueous medium employed for the kinetic analyses. If this was so, increasing the steroid solvating ability of the aqueous solvent by raising the methanol concentration should reflect itself in a progressive breakdown of the micellar aggregations. The experimental observations supported this view. As the proportion of methanol was gradually increased, the multiplicity of the acid-catalyzed reaction orders for **1***c* and **1***d* decreased until in 27% aqueous methanol pseudo first order kinetic behavior was observed for the isomerization of androst-5-en-3-one (**1***c*). However, for cholest-5-en-3-one (**1***d*), with the most nonpolar C-17 substituent of the series, the kinetics did not become first order until a methanol concentration of 75% was reached.

The kinetic data cited above were obtained spectrophotometrically by monitoring the change in optical density of the reaction solution at the wavelength of maximum absorption of the αβ-unsaturated ketone product (244–248 mμ). The remote possibility was considered that the abnormalities observed in very dilute aqueous methanol might be due to deviations from the Beer–Lambert law. However, a close reexamination of the final molar extinction coefficients obtained did not reveal any evidence for this, and, in addition, the ultraviolet and optical rotatory dispersion spectra of freshly prepared solutions of **1***a–d* in polar (methanol) and nonpolar (cyclohexane) solvents were in no way unusual.[8]

In view of the acid-catalysis evidence for micelle formation by the more nonpolar substrates, it became of interest to extend the model isomerization studies into the pH range 6–9 where the isomerase itself operates at maximum efficiency (13). In contrast to the well studied isomerizations of Δ^5-3-ketosteroids at low pH (2, 3) few measurements had been made in basic solution presumably owing to the complications arising from multiple product formation (2). That the base-catalyzed reaction was not straightforward (2) was confirmed by the observation that isomerization of androst-5-ene-3,17-dione (**1***a*) in a sodium hydroxide solution of pH 9 afforded a mixture containing at least three components. A similar result was obtained when a carbonate – bicarbonate buffer solution of the same pH was employed.[6] However, when Tris–HCl buffer of pH 8.8 was used the isomerizations of all the Δ^5-3-ketones **1***a–d* proceeded cleanly and accordingly this medium was used for all the base-catalysis kinetic measurements in solutions containing up to 27% methanol. In water containing 75% methanol, the addition of the Tris–HCl buffer effected isomerization only very slowly and it was found necessary to substitute borate – hydroxide – carbonate buffer of pH 10 in order to achieve convenient rates.

The data obtained are summarized in Table I; they follow a similar pattern to those of the acid-catalyzed reactions and thus provide further evidence that substrates **1***c* and **1***d*, with nonpolar substituents at C-17, form micelles in aqueous solution.

A comparison of the rate constants for the acid- and base-catalyzed isomerizations of **1***a–d* in 75% aqueous methanol shows that those for **1***b–d* do not differ by >7 and >3% respectively. This indicates that the rates observed for cholest-5-en-3-one are normal and it seems likely

[7]Most enzymic assays have been carried out in 1.6% aqueous methanol (1, 3) but owing to the frequent solubility difficulties encountered with **1***c* and **1***d* in this solvent, 3.3% aqueous methanol proved a more satisfactory solvent for the acid-catalyzed reactions. For the subsequent base-catalyzed isomerizations, it was possible to use 1.6% aqueous methanol although some data in this medium were invalidated by steroid precipitation during the isomerization.

[8]Caution is required when interpreting the spectra of some βγ-unsaturated ketones possessing remote carbonyl groups unless the compounds and solutions are examined immediately after their preparation (11, 12).

Can. J. Chem. Downloaded from www.nrcresearchpress.com by 210.87.254.5 on 09/05/12
For personal use only.

therefore that all the micelles have been broken down in solutions of this composition.

Surprisingly, the steroid that is anomalous, in 75% aqueous methanol, is the standard enzyme substrate, androst-5-ene-3,17-dione (**1***a*), since its acid- and base-catalyzed isomerization rates are significantly slower and faster respectively than those of the other Δ^5-3-ketones. This constitutes yet another example of the many long range substituent effects which have been observed in steroidal systems (see ref. 14 for some leading references). The influence of the carbonyl group can in this case be satisfactorily rationalized in terms of polar transmission (14, 15) whereby the inductive effect of the carbonyl group would tend to destabilize the positively charged enolic transition state involved in acid catalysis, but would stabilize the negatively charged enolate intermediate of the base-catalyzed reaction.

In view of the preceding kinetic evidence for micelle formation by **1***c* and **1***d* in aqueous solution, the possibility arose that the negligible enzymic isomerization rate reported for cholest-5-en-3-one might be due to such aggregation and that the fully solvated molecule might well be a good substrate. Unfortunately, the fact that a methanol concentration of 75% is necessary to ensure the complete breakdown of cholest-5-en-3-one micelles precluded the substrate evaluation of the monomeric molecule, since, as expected, the enzyme was completely denatured under such conditions.

Nevertheless, a comparison of the relative rates of enzymic isomerization of **1***a–c* (see Table II) provided firm evidence that substrate aggregation into micelles can indeed give rise to an apparent C-17 specificity of the enzyme.

In 1.6% aqueous methanol **1***a* and **1***b*, with =O and β-OH groups respectively at C-17, are both good substrates and the substitution of β-OH for =O has a negligible influence on the rate. For **1***c*, however, with no functional group at C-17, the rate of enzyme-catalyzed isomerization in this solvent was negligibly small, and, in contrast to those of **1***a* and **1***b*, was not increased when higher (up to 100-fold) enzyme concentrations were applied.

The next step, *viz.* increase of the methanol concentration, was approached with some trepidation owing to the increasing denaturation most proteins undergo when the organic solvent concentration of their solutions in water is raised. The activity of the isomerase was assayed as a function of methanol concentration, and, as anticipated, progressive loss of activity was observed. Using androst-5-en-3,17-dione (**1***a*) as the standard substrate it was found that the addition of 3,5, and 10% methanol destroyed 5,17, and 76% respectively of the enzyme's isomerization capacity. In 27% methanol, 99% of the activity was lost; fortunately, this could be counterbalanced by using greater quantities of enzyme and satisfactory rates were obtained in 27% aqueous methanol by increasing the enzyme concentration 100 times. In such solutions the isomerase activity was found to be constant over the period of kinetic measurement (3 min) and 75% of this activity was still present after 1 h.

When **1***c* was assayed in 27% aqueous methanol, in which solution it is present as the fully solvated molecule, it became a better substrate of the enzyme than either **1***a* or **1***b*. This observation establishes beyond all doubt that an oxygen function at or near C-17 is not a requirement for substrate activity.[9]

As expected, for **1***d* negligible enzymic catalysis was observed in 1.6 and 27% aqueous methanol even when the enzyme concentration was increased 100-fold.

It should be stressed that the relative rates for **1***a–d* given in Table II are those due to the *enzyme*-catalyzed process *alone* and do not necessarily reflect the *total* rate of product formation under the assay conditions. It is necessary to make this distinction since for androst-5-en-3-one the uncatalyzed reaction in the assay medium lacking only the enzyme was quite rapid both in 1.6 and 27% aqueous methanol. Even greater caution was required when evaluating the enzyme-catalyzed process for cholest-5-en-3-one since the uncatalyzed rate of isomerization was substantially increased by the addition of the enzyme preparation. However, increases in enzyme concentration of up to 100-fold did not further augment the rate and it was subsequently established that the velocity increase observed on addition of the enzyme was

[9]The results obtained in this unusual, for an enzyme, solvent are considered valid since (*i*) **1***a* and **1***b* remain good substrates in the solvent of higher methanol content; (*ii*) their rates of isomerization in both 1.6 and 27% aqueous methanol, and that of **1***c* in the latter solvent, are proportional to the amount of enzyme added.

Can. J. Chem. Downloaded from www.nrcresearchpress.com by 210.87.254.5 on 09/05/12
For personal use only.

due only to the addition of protein; the addition of 1% aqueous bovine serum albumin alone (with which all the enzyme preparations were diluted prior to use) caused a similar increase in the uncatalyzed isomerization rate of **1***d*. In contrast, for **1***a* and **1***b* the uncatalyzed rates in 1.6 and 27% aqueous methanol were low and were unaffected by the addition of bovine serum albumin. In arriving at each of the net enzymic relative rates summarized in Table II, both the uncatalyzed reaction and the effect of bovine serum albumin were taken into account.

As stated earlier, it was not possible to evaluate the enzymic substrate activity of cholest-5-en-3-one under conditions ensuring its existence as a monomer.[10] From the data of **1***a–c* it seems likely that the observed specificity with respect to **1***d* results from a combination of micelle formation[11] and a true specificity effect of the large C_8H_{17} group. In an attempt to clarify the relative contributions of these two factors further experiments systematically examining the influence of C-17 hydrocarbon substituents are being carried out.

Although the negligible enzymic isomerization of cholest-5-en-3-one is by far the most dramatic feature of the currently available specificity data, smaller, but real, rate differences have been reported for other substrates, particularly for those with 17α-substituents (1, 2). The 17α-specificity of the enzyme was corroborated by comparison of the isomerizations in 1.6% aqueous methanol of 17β-hydroxy-17α-methylandrost-5-en-3-one (**1***e*), 17β-hydroxy-17α-ethynylandrost-5-en-3-one (**1***f*), and 17α-hydroxyandrost-5-en-3-one (**1***g*). As Table II shows, their rates relative to that of androst-5-en-3,17-dione (**1***a*) are very much diminished. The unlikely (since **1***e–g* all contain a C-17 hydroxyl function) possibility that the rate differences might be explained, at least in part, by some substrate micellation, was eliminated by a comparison of the isomerization rates of **1***a*, **1***e*, and **1***f* in 1.6 and 5% aqueous methanol; the rate ratios in both solvents were identical.

Since the 17α-groups of **1***e–g* differ markedly in polarity, the observed specificity presumably reflects an increased steric interaction of this region of the substrate with the active site.

The elegant fluorescence studies carried out by Talalay and his co-workers (13) on isomerase-19-nortestosterone complexes implicate tyrosine at the binding site. Their data suggest this to be a polar interaction involving the C-3 or C-17 region of the steroid but do not enable the two possibilities to be distinguished. The above specificity results, and particularly that monomeric androst-5-en-3-one is an excellent substrate, argue against any significant C-17 tyrosine interaction of this kind. The mechanism of action of the isomerase outlined by Malhotra and Ringold (3) proposes the concurrent participation of an acidic and a basic group in the rate determining enolization step. They suggest that the acidic group protonates (partly or fully) the C-3 carbonyl group and it now seems likely that the phenolic group of a tyrosine at the active site fulfills this role. The activation parameters for the isomerization (18) are consistent with this view and further supporting evidence will be presented shortly.

[10]The isomerase from beef adrenals does not appear to require monomeric substrates (16).

[11]The influence micelle formation may have on enzymic and related processes is attracting increasing attention (17).

Acknowledgments

The generous support of the National Research Council of Canada and the Province of Ontario, Department of University Affairs, and the award (to D. C. W.) of a Commonwealth Scholarship, are gratefully acknowledged.

1. F. S. Kawahara, S.-F. Wang, and P. Talalay. J. Biol. Chem. **237**, 1500 (1962).
2. W. R. Nes, E. Loeser, R. Kirdani, and J. Marsh. Tetrahedron, **19**, 299 (1963).
3. S. K. Malhotra and H. J. Ringold. J. Am. Chem. Soc. **87**, 3228 (1965).
4. J. B. Jones and D. C. Wigfield. Can. J. Chem. **44**, 2517 (1966).
5. K. E. Pfitzner and J. G. Moffatt. J. Am. Chem. Soc. **85**, 3027 (1965); **87**, 5670 (1965).
6. H. J. Ringold and S. K. Malhotra. Tetrahedron Letters, 669 (1962).
7. R. E. Schaub and M. J. Weiss. Chem. Ind. London, 2003 (1961).
8. J. Iriate, C. Djerassi, and H. J. Ringold. J. Am. Chem. Soc. **81**, 436 (1959).
9. G. Gomori. *In* Methods in enzymology. Vol. 1. Academic Press Inc., New York, New York. 1955. pp. 138–144.
10. J. B. Jones and V. Vlasinich. Unpublished results.
11. R. E. Ballard, S. F. Mason, and G. W. Vane. Trans. Faraday Soc. **59**, 775 (1963).
12. R. Grinter, S. F. Mason, and G. W. Vane. Trans. Faraday Soc. **60**, 285 (1964).
13. S.-F. Wang, F. S. Kawahara, and P. Talalay. J. Biol. Chem. **238**, 576 (1963).

14. E. L. ELIEL, N. L. ALLINGER, S. J. ANGYAL, and G. A. MORRISON. Conformational analysis. Interscience Publishers, Inc., New York, New York. 1965. pp. 345–350.
15. H. B. HENBEST. Proc. Chem. Soc. 159 (1963).
16. H. WERBIN, W. EWALD, and I. L. CHAIKOFF. Biochim. Biophys. Acta, **107**, 596 (1965).
17. J. R. KNOWLES and C. A. PARSONS. Chem. Commun. 755 (1967), and references therein.
18. J. B. JONES and D. C. WIGFIELD. J. Am. Chem. Soc. **89**, 5294 (1967).

Can. J. Chem. Downloaded from www.nrcresearchpress.com by 210.87.254.5 on 09/05/12
For personal use only.

Can. J. Chem. Downloaded from www.nrcresearchpress.com by 210.87.254.40 on 09/05/12
For personal use only.

Studies in terpenoids. IV.[1] Synthetic studies in juvabiones and analogues. Conversion of *ar*-(+)-turmerone to *ar*-(+)-juvabione[2]

K. Subrahmania Ayyar[3] and G. S. Krishna Rao
Department of Organic Chemistry, Indian Institute of Science, Bangalore 12, India

Received July 31, 1967

Synthetic work leading to the preparation of todomatuic acids[4] (**2***a*), juvabiones (**2***b*), and *ar*-(±)-juvabione (**8***d*) and the successful conversion of *ar*-(+)-turmerone (**9**) to *ar*-(+)-juvabione (**3***b*) is presented. The synthetic compounds **2***b* and **3***b* exhibit juvenile hormone activity.

Canadian Journal of Chemistry, 46, 1467 (1968)

By hydrolysis of the oil derived from *Abies sachalinensis* Mast., Tuchihashi and Hanzawa (1) isolated todomatuic acid and its structure, deduced by Momose (2), was confirmed by Nakazaki and Isoe (3) who also assigned its absolute configuration (**1***a*). Very recently highly active sesquiterpenoid juvenile hormones called juvabione (4, 5) and dehydrojuvabione (5, 6) were isolated from the wood of the balsam fir, *Abies balsamea* L., the former identified as the methyl ester (**1***b*) of todomatuic acid.

This paper[2,5] describes the synthetic work[6] leading to the preparation of todomatuic acids[4] (**2***a*), juvabiones (**2***b*), and *ar*-(±)-juvabione (**8***d*), the successful conversion of *ar*-(+)-turmerone (**9**) to *ar*-(+)-juvabione (**3***b*), and the chemical correlations of the various compounds.

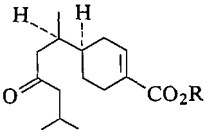

1 *a*, R = H
b, R = Me

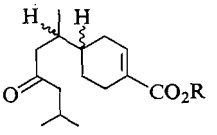

2 *a*, R = H
b, R = Me

p-Methoxystyrylisobutyl ketone (7) on conjugate addition (8) with CH_3MgI furnished the

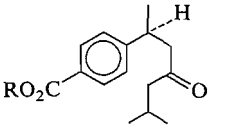

3 *a*, R = H
b, R = Me

1,4-addition product **4***a*.[7] Birch reduction of the anisyl alcohol **4***b* and hydrolysis of the resulting dihydroanisole gave the unconjugated keto alcohol **5***a*. Its acetate **5***b* was hydrogenated to **6***a* which was then converted to the cyanohydrin acetate **6***b* by an exchange reaction (10). The dehydration of **6***b* furnished the acetoxy unsaturated nitrile **7***a* as a major product[8] which on alkaline hydrolysis gave the hydroxy unsaturated acid **7***b*. Oxidation (Jones' reagent) of **7***b* gave the keto acids **2***a*,[9] m.p. 65–66° (lit. (6) m.p. 66–67°) when regenerated from its *S*-benzylthiuronium salt, m.p. 162°. It gave an infrared spectrum (CCl_4) almost superimposable with that of the natural todomatuic acid (**1***a*).[10] Several attempts to separate the two racemates of the methyl ester **2***b* by thin-layer chromatography (t.l.c.), including $AgNO_3$–SiO_2 (11), gas–liquid chromatography (g.l.c.),[11] and inverted dry column chromatography (12) were unsuccessful.

[1]For Part III in this series, see L. R. Subramanian and G. S. Krishna Rao, Tetrahedron, **23**, 4167 (1967).

[2]For a preliminary account of this work, see K. Subrahmania Ayyar and G. S. Krishna Rao, Tetrahedron Letters, 4677 (1967).

[3]Present address: Forest Research Laboratory, Bangalore 3, India.

[4]The suffix *s* indicates diastereomixture.

[5]For a recent report on the synthesis of (±)-juvabione from Japan, see K. Mori and M. Matsui. Tetrahedron Letters, 2515 (1967).

[6]Part of this work was presented and published as an abstract at the "Symposium on Recent Advances in the Chemistry of Terpenoids", National Chemical Laboratory, Poona, India, in June 1965.

[7]For an alternate synthesis of **4***a* in support of its structure, see K. Subrahmania Ayyar, Ph.D. Thesis. Indian Institute of Science, Bangalore, India. 1967.

[8]The structure of the minor product was established (9) to be a deacetoxy diene nitrile (**7***a*, with OAc substituted by a double bond).

[9]The synthesis of todomatuic acids[4] (**2***a*) was also achieved by the route: **5***a* → **6***c* → **6***d* → **6***e* → **7***c*. Though **7***c* furnished **2***a* on acid hydrolysis, its hydrolysis by alkali gave a solid nonketonic diene acid. Its structure and the related transformations will be published separately.

[10]We thank Dr. S. Isoe for the authentic samples.

[11]We thank Dr. Sukh Dev for the gas–liquid chromatography of **2***b* and its nuclear magnetic resonance spectrum.

Can. J. Chem. Downloaded from www.nrcresearchpress.com by 210.87.254.40 on 09/05/12
For personal use only.

Gas–liquid chromatography gave a single peak on two different columns. Besides showing on t.l.c. identical R_f value as juvabione **1***b*, **2***b* exhibited juvenile hormone activity[12] against *Pyrrhocoris apterus* L. and *Dysdercus intermedius* at 10 μg per one bug dosage. The natural and synthetic juvabione*s* exhibited surprisingly almost identical infrared spectra.[12]

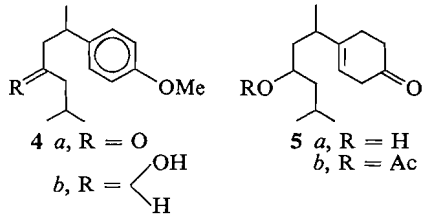

4 *a*, R = O
b, R = OH, H

5 *a*, R = H
b, R = Ac

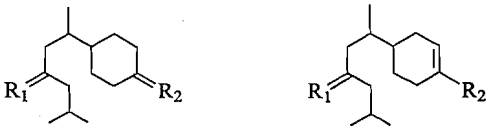

6 *a*, R_1 = OAc, H; R_2 = O
b, R_1 = OAc, H; R_2 = OH, CN
c, R_1 = OH, H; R_2 = O
d, R_1 = OH, H; R_2 = OH, CN
e, R_1 = O; R_2 = OH, CN

7 *a*, R_1 = OAc, H; R_2 = CN
b, R_1 = OH, H; R_2 = CO_2H
c, R_1 = O; R_2 = CN

The synthetic todomatuic acid*s* (**2***a*) gave desoxo- and the anilide (m.p. 125°) of *trans*-dihydrodesoxotodomatuic acids (3) which gave superimposable infrared spectra (in CCl_4) with the corresponding samples derived from the natural acid **1***a*.[10]

The synthesis of *ar*-todomatuic acid arose from a consideration that the occurrence in nature, in different sources or often in the same source, of perhydroterpenoids and the corresponding aromatized compounds is quite widespread (13).

Conjugate addition of CH_3MgI to the styrylisobutyl ketone (14) furnished 2-phenyl-6-methylheptan-4-one (**8***a*). Chloromethylation of **8***a* gave the chloromethyl ketone **8***b* which was converted by standard procedures to the keto acid **8***d* and *ar*-(±)-juvabione **8***e* *via* the aldehyde **8***c*. Dehydrogenation of the keto acid*s* **2***a* to give the *ar*-keto acid **8***d* provided mutually confirmatory support to both the structures.

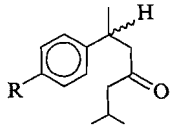

8 *a*, R = H
b, R = CH_2Cl
c, R = CHO
d, R = CO_2H
e, R = CO_2Me

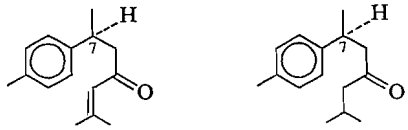

9 **10**

Alternatively *ar*-(+)-turmerone (**9**) of known absolute configuration (15) at C-7 appeared to be an attractive starting material for the preparation of optically active *ar*-todomatuic acid (**3***a*) and *ar*-juvabione (**3***b*).

Aromatization of the sesquiterpene ketone fraction from *Curcuma longa* L. consisting chiefly of turmerone and *ar*-turmerone by the hydrogen transfer technique of Kindler and Luhrs (16) gave *ar*-(+)-turmerone (**9**).[13] On oxidation (17, 18) by a modified procedure (CrO_3 – AcOH – H_2O), *ar*-(+)-dihydroturmerone (**10**) gave *ar*-todomatuic acid (**3***a*) contaminated with terephthalic acid. Purification of the esterified material by chromatography gave *ar*-(+)-juvabione (**3***b*). The *ar*-analogue (+)-**3***b* also exhibited juvenile hormone properties[12] like the keto esters **1***b* and **2***b*.

In Table I are summarized the optical rotations of some of the related compounds under study. It is interesting to note that while the *ar*-compounds with *S*-chirality at C-7 (type A) exhibit dextro rotation, the *trans*-dihydrodesoxotodomatuic acid with R chirality at C-7 (type B) also exhibits dextrorotation. Since compounds of type C will be levorotatory (antipodal to A), it follows that aromatization of B would lead to reversal in the sign of rotation.

[12]We thank Prof. F. Sorm for the t.l.c. and infrared comparison of **1***b* and **2***b*, and comparative hormonal evaluation of **1***b*, **2***b*, and **3***b*.

[13]We thank Dr. A. S. Rao for the infrared spectrum of authentic *ar*-turmerone (15).

TABLE I

Serial No.	Compound	Chirality at C–7	Rotation
1	Todomatuic acid (**1***a*)	*R*(5)	$[\alpha]_D^{25}$ +87° (4) M_D +233° (3)
2	Desoxo-todomatuic acid	*R*(5)	M_D +224° (3)
3	*trans*-Dihydro-desoxo-todomatuic acid	*R*(5)	M_D +34° (3)
4	Juvabione (**1***b*)	*R*(6)	$[\alpha]_D^{20}$ +79.5° (5)
5	Turmerone fraction	*S*(17)	$[\alpha]_D$ −7 to −27° (15); −32.6° *
6	Turmerone		$[\alpha]_D^{25}$ −61.7° (19)
7	*ar*-Turmerone (**9**)	*S*(17)	$[\alpha]_D$ +68° (15); +60 to +69° *
8	*ar*-Juvabione (**3***b*)	*S*	$[\alpha]_D^{27}$ +22.93° *

*Present work.

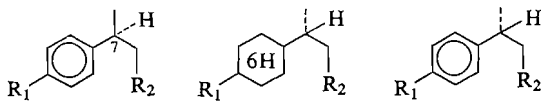

A, (+)- B, (+)- C, (−)-

It may therefore be predicted that the naturally occurring dextrorotatory todomatuic acid, juvabione, and dehydrojuvabione will furnish the corresponding levorotatory compounds on aromatization of the ring.

Experimental

Bath temperatures (b.t.) are given for short-path distillations. Melting points are not corrected. Infrared spectra were taken on Perkin–Elmer Infracord, model 137. Petroleum ether used had boiling range 40–60°. The organic extracts were washed appropriately and dried (Na_2SO_4) before removal of the solvent. Microanalyses were carried out by Messrs. B. R. Seetharamia, D. P. Bose, and H. S. Thyagarajan of this department.

2-(p-Methoxyphenyl)6-methylheptan-4-one (4a)

To a solution of the Grignard reagent prepared from magnesium (15.8 g) and methyl iodide (50 ml) in dry ether was added at 0° with stirring anhydrous cuprous chloride (3 g). *p*-Methoxystyrylisobutyl ketone (7) (50 g) in dry ether (100 ml) was slowly added to the reaction mixture at 0°. Along with the addition of the ketone more cuprous chloride (3.0 g) was added in small lots. After leaving the reaction mixture overnight, it was refluxed (1h) and decomposed under cooling (ice and salt) by the slow addition of HCl aqueous (1:1) with vigorous stirring. The ether layer was separated, washed with water, saturated aqueous $Na_2S_2O_3$ and again water. Removal of solvent furnished **4***a*, b.p. 131–136° at 1.5 mm (37.5 g), n_D^{23} 1.5025; infrared (neat); 1724 cm^{-1} (saturated $\rangle C{=}O$); λ_{max} (EtOH) 276 mμ (ε757.5).

Anal. Calcd. for $C_{15}H_{22}O_2$: C, 76.9; H, 9.4. Found: C, 77.0; H, 9.3.

2-(p-Methoxyphenyl)6-methylheptan-4-ol (4b)

The ketone **4***a* (20 g) in dry ether (100 ml) was added dropwise with vigorous stirring to a suspension of lithium aluminium hydride (4 g) in dry ether (100 ml). Stirring was continued (1 h) and the reaction mixture was left overnight. The excess lithium aluminium hydride was decomposed with ethyl acetate (50 ml); water (40 ml) and aqueous HCl (1:6, 200 ml) were added and the product was extracted with ether. Removal of solvent furnished the alcohol **4***b*, b.p. 140–141° at 0.5 mm (14 g); n_D^{29} 1.5090; infrared (neat); 3448 cm^{-1} (−OH).

Anal. Calcd. for $C_{15}H_{24}O_2$: C, 76.3; H, 10.2. Found: C, 76.4; H, 10.2.

4-4'(-Hydroxy-6'-methyl-2'-heptyl)cyclohex-3-en-1-one (5a)

To a solution of the alcohol **4***b* (25 g) in absolute ethanol (125 ml), and liquid ammonia (500 ml) sodium (34 g) in small pieces was added in small lots. Each further lot of sodium was added after the disappearance of the blue color. More ammonia (500 ml) was collected to replenish the ammonia lost by evaporation and the addition of sodium completed (6 h). Evaporation of ammonia followed by the usual work-up gave the corresponding dihydroanisole (27 g) which did not show aromatic absorption in the ultraviolet; infrared (neat); 3509 (−OH); 1706, 1672, 1217 cm^{-1} (enol ether) (20). It was immediately used in the next reaction.

To the above crude enol ether (27 g) in acetone (194 ml) and methanol (106 ml), oxalic acid (5 g in 120 ml water) was added and the reaction mixture was stirred vigorously (1.5 h). It was poured into water (1 l) and extracted with petroleum ether. The solvent was removed at room temperature under reduced pressure to furnish **5***a* (24 g). An analytical sample was prepared by chromatography (SiO_2). The keto alcohol **5***a*, eluted with 1:1 benzene–ether had b.t. 120–140° at 1 mm, n_D^{23} 1.4740; infrared (neat); 3571 (—OH), 1724 (saturated $\rangle C{=}O$) and, 800 cm^{-1} ($\rangle C{=}CH{-}$). No absorption for α,β-unsaturated ketone was noticed in the ultraviolet even after equilibration with alkali.

Anal. Calcd. for $C_{14}H_{24}O_2$: C, 75.0; H, 10.7. Found: C, 74.9; H, 10.7.

The above keto alcohol **5***a* (5 g), acetic anhydride (8.3 ml) and pyridine (0.7 ml) were mixed together and left overnight. It was then poured into water (100 ml) and extracted with petroleum ether. Removal of the solvent furnished the *acetate* **5***b* (6.2 g) which was used as such for the next reaction. An analytical sample prepared by short-path distillation had b.t. 100–120° at 1 mm, n_D^{24} 1.4725; infrared (neat); 1727 and 1236 cm^{-1} (acetate).

Anal. Calcd. for $C_{16}H_{26}O_3$: C, 72.2; H, 9.8. Found: C, 72.2; H, 9.7.

4-(4'-Acetoxy-6'-methyl-2'-heptyl)cyclohexan-1-one (6a)

The compound **5***b* (6.2 g) was hydrogenated in acetic acid (25 ml) with Adams catalyst (150 mg) at room temperature and pressure till slightly more than one mole of H_2 was adsorbed (6 h). The catalyst was removed by filtration and the product **6***a* (5.8 g) was worked up. An analytical sample prepared by short-path distillation had b.t. 135–140° at 1 mm, n_D^{25} 1.4630; infrared (neat); 1724 and 1236 cm^{-1} (acetate).

Can. J. Chem. Downloaded from www.nrcresearchpress.com by 210.87.254.40 on 09/05/12
For personal use only.

Can. J. Chem. Downloaded from www.nrcresearchpress.com by 210.87.254.40 on 09/05/12
For personal use only.

Anal. Calcd. for $C_{16}H_{28}O_3$: C, 71.6; H, 10.5. Found: C, 71.8; H, 10.8.

4-(4'-Acetoxy-6'-methyl-2'-heptyl)cyclohexan-1-one Cyanohydrin (6b)

The keto acetate **6a** (5.8 g), acetone cyanohydrin (18 ml), and 10% aqueous NaOH (1 ml) were mixed together and left overnight. The reaction mixture was poured with stirring into ice-water slurry (1 kg) containing acetic acid (4 ml). Extraction with ether and removal of the solvent furnished the acetoxy cyanohydrin (**6b**) which was used directly for dehydration. Infrared (neat); 3571 (—OH), 2273 (saturated —C≡N), 1730, and 1238 cm^{-1} (acetate).

4-(4'-Acetoxy-6'-methyl-2'-heptyl)cyclohex-1-ene-1-nitrile (7a)

To the acetoxy cyanohydrin **6b** (6 g) in dry pyridine (27 ml), $POCl_3$ (9 ml) was added under cooling (ice). The reaction mixture was heated on a steam bath (15 min). It was cooled and poured into crushed ice with vigorous stirring. Extraction with petroleum ether followed by washing with aqueous HCl (1:1), 10% aqueous $NaHCO_3$ and then with water and removal of solvent gave a residue (5.2 g) which was chromatographed (SiO_2–I). Benzene eluted the deacetoxynitrile[8] and other by-products (1.7 g), while ether eluted the required acetoxy unsaturated nitrile, **7a** (3.3 g) which had b.t. 115–125° at 1 mm (2 g), n_D^{25} 1.4795; infrared (neat); 2242 (conjugated —C≡N), 1730 and 1238 (acetate), and 1645 cm^{-1} (conjugated C=C) and no absorption maxima in the region 220 to 330 mμ (21).

Anal. Calcd. for $C_{17}H_{27}NO_2$: C, 73.6; H, 9.8; N, 5.1. Found: C, 73.4; H, 9.5; N, 5.1.

4-(4'-Hydroxy-6'-methyl-2'-heptyl)cyclohex-1-ene-1-carboxylic Acid (7b)

The acetoxy nitrile **7a** (1.6 g) was refluxed (20 h) with ethanolic KOH (5.6 g KOH in 28 ml of distilled alcohol) and worked up to give the hydroxy unsaturated acid **7b** (1.45 g) which was directly used in the subsequent step. An analytical sample of **7b** was obtained on short-path distillation (150–170° at 1 mm) as a low-melting solid. Infrared (CCl_4); 2985, 2667, and 1689 (—COOH) and 1645 cm^{-1} (conjugated C=C). The infrared of the Ag salt showed a strong peak at 3404 nm^{-1} (—OH).

Anal. Calcd. for $C_{15}H_{26}O_3$: C, 70.9; H, 10.2. Found: C, 70.4; H, 9.8.

The *S-benzylthiuronium* salt had m.p. 134–136°.

Anal. Calcd. for $C_{23}H_{36}O_3N_2S$: N, 6.7. Found: N, 6.5.

4-(4'-Keto-6'-methyl-2'-heptyl)cyclohex-1-ene-1-carboxylic Acid: Todomatuic Acids[4] *(2a)*

To a solution of the hydroxy acid **7b** (1 g) in acetone (20 ml), Jones' reagent (22) (8 ml) was added dropwise with stirring (magnetic) and cooling (ice). After the addition was over, it was left for 15 min and poured into water (200 ml), extracted with ether, and the acidic product (0.9 g) worked up. An analytical sample of **2a** prepared by short-path distillation had b.t. 150–160° at 1 mm; infrared (CCl_4); 3636–3077 (broad, O=C—*OH*), 1712, 1695 (acid and ketone carbonyl), and 1647 cm^{-1} (conjugated C=C).

Anal. Calcd. for $C_{15}H_{24}O_3$: C, 71.4; H, 9.5. Found: C, 71.6; H, 9.6.

The *S-benzylthiuronium* salt had m.p. 162°.

Anal. Calcd. for $C_{23}H_{34}N_2O_3S$: N, 6.7. Found: N, 6.8.

The keto acid regenerated from the *S*-benzylthiuronium salt by the usual procedure was obtained as a white solid, m.p. 65–66°. It had an infrared spectrum (CCl_4) almost superimposable with todomatuic acid *(1a)*.[10]

The *methyl esters* **2b** *(juvabiones*[4]*)*, prepared by refluxing (6 h) the solution of the keto acid **2a** (0.3 g) in dry acetone (10 ml) with dimethyl sulfate (0.22 g) and anhydrous K_2CO_3 (0.22 g) followed by the usual work-up had b.t. 115–120° at 1 mm, n_D^{27} 1.4815; infrared (neat); 1721 (shoulder, unsaturated ester), 1715 (ketone), and 1647 cm^{-1} (conjugated C=C). Nuclear magnetic resonance,[11] δ (solvent CCl_4, reference TMS) 0.86 (d, J = 6 Hz) and 0.88 (d, J = 6 Hz) 9H, 3.67 (—COO*CH*$_3$), 6.87 (*H*—C=C—CO_2CH_3).

Anal. Calcd. for $C_{16}H_{26}O_3$: C, 72.2; H, 9.8. Found: C, 71.8; H, 9.9.

The keto acid **2a** was subjected to Wolff–Kishner reduction (3). An analytical sample of the corresponding *desoxotodomatuic acid* had b.t. 155–160° at 1 mm (0.4 g), n_D^{26} 1.4850. The infrared spectrum (in CCl_4) was superimposable with that of the authentic sample.[10]

Anal. Calcd. for $C_{15}H_{26}O_2$: C, 75.6; H, 10.9. Found: C, 75.4; H, 10.7.

Hydrogenation of the above desoxoacid (0.35 g) in acetic acid (25 ml) at room temperature and pressure over Adams catalyst (0.1 g) till there was no more absorption of H_2 gave the crude *dihydrodesoxotodomatuic acid*. An analytical sample had b.t. 155–160° at 1 mm (0.25 g), n_D^{30} 1.4730; infrared (neat); 2976, 2615, and 1712 cm^{-1} (—COOH).

Anal. Calcd. for $C_{15}H_{28}O_2$: C, 75.0; H, 11.7. Found: C, 75.0; H, 11.9.

The *methyl ester* of the above dihydrodesoxo acid (0.25 g) was prepared by esterification with diazomethane generated from nitrosomethylurea (0.85 g) and 40% aqueous KOH (2.5 ml). An analytical sample (0.1 g) had b.t. 115–120° at 1 mm, n_D^{20} 1.4555; infrared (neat); 1742 cm^{-1} (ester).

Anal. Calcd. for $C_{16}H_{30}O_2$: C, 75.6; H, 11.8. Found: C, 75.7; H, 11.8.

trans (±)-Dihydrodesoxotodomatuic Acid

The above methyl ester (0.6 g) was equilibrated with NaOEt (5) and hydrolyzed to the *trans* acid. An analytical sample had b.t. 150–155° at 1 mm (0.52 g), n_D^{30} 1.4635; infrared (neat); 2976, 2695, and 1712 cm^{-1} (—COOH).

Anal. Calcd. for $C_{15}H_{28}O_2$: C, 75.0; H, 11.7. Found: C, 74.6; H, 11.4.

The *anilide* of *trans*-(±)-dihydrodesoxotodomatuic acid prepared in the usual manner by treatment of the acid with thionyl chloride, followed by aniline had m.p. 125° (dilute MeOH) [Lit. (3) m.p. 106° for the anilide of optically active acid], with its infrared spectra in CCl_4 and in $CHCl_3$ completely identical with the authentic sample.[10]

Anal. Calcd. for $C_{21}H_{33}NO$: N, 4.4. Found: N, 4.5.

2-Phenyl-6-methylheptan-4-one (8a)

To a solution of the Grignard reagent prepared from magnesium (11 g) and methyl iodide (35 ml) in dry ether,

Can. J. Chem. Downloaded from www.nrcresearchpress.com by 210.87.254.40 on 09/05/12
For personal use only.

was added at 0° with stirring, anhydrous Cu_2Cl_2 (3 g). Styrylisobutyl ketone (14) (35 g) in dry ether (100 ml) was slowly added to the reaction mixture at 0°. Along with the addition of the ketone more anhydrous Cu_2Cl_2 (3 g) was added in small lots. After leaving the reaction mixture overnight, it was refluxed (1 h) and decomposed under cooling (ice-salt) by the slow addition of aqueous HCl (1:1) with vigorous stirring. The residue (34 g) from the ethereal extract was fractionated and the fraction b.p. 109–114° at 1/mm (22.8 g) had n_D^{27} 1.5040; infrared (neat); 1712 cm^{-1} saturated $\rangle C{=}O$).

Anal. Calcd. for $C_{14}H_{20}O$: C, 82.4; H, 9.8. Found: C, 82.6; H, 9.8.

4-(4'-Keto-6'-methyl-2'-heptyl)benzaldehyde (8c)

To the ketone **8***a* (5 g) taken in a suspension of anhydrous $AlCl_3$ (2.3 g) in nitrobenzene (10 ml), chloromethyl methyl ether (7 g) (23) was added dropwise with stirring at room temperature (5 min). Stirring was continued at room temperature (30 min) and then at 50° (3 h). After leaving overnight, the reaction mixture was poured into crushed ice with stirring and extracted with ether. From the ethereal extract which contained both the chloromethyl derivative *(8b)* and nitrobenzene, some nitrobenzene (9 ml) was distilled off at b.t. 100° at 1 mm. The crude product thus obtained was used for the Sommelet reaction.

To the crude chloromethyl compound **8***b* (5 g) in aqueous HOAc (1:1, 25 ml), hexamethylenetetramine (24) (6.2 g) was added. The reaction mixture was refluxed (30 min). Aqueous HCl (1:1, 20 ml) was added and the refluxing continued (10 min). The reaction mixture was cooled, poured into water, and extracted with ether. The crude residue from the ethereal extract containing the aldehyde **8***c* was used as such for the next reaction. An analytical sample of the aldehyde **8***c* obtained by purification *via* the Girard T complex had b.t. 120–125° at 1 mm; infrared (neat); 2817 ($O{=}\overset{|}{C}{-}H$) and 1709 cm^{-1} (ketone and aldehyde $\rangle C{=}O$).

Anal. Calcd. for $C_{15}H_{20}O_2$: C, 77.6; H, 8.6. Found: C, 77.4; H, 8.8.

ar-(±)-Todomatuic Acid (8d)

(a) By Oxidation of 8c

To the crude aldehyde **8***c* (5 g) taken in ethanol (65 ml) and aqueous $AgNO_3$ (3.1 g in 32.5 ml water), aqueous NaOH (3.1 g in 31 ml water) (25) was added dropwise with vigorous stirring (30 min). After stirring for 3 h, the reaction mixture was filtered and the alcohol distilled off under reduced pressure. The residue was diluted with water (250 ml) and extracted with ether to remove all neutral matter. The clear alkaline aqueous portion was acidified with aqueous HCl (1:1) and the liberated acid extracted with ether. The residue (1.6 g) from the extract on short-path distillation, b.t. 180–185° at 1 mm, gave an analytical sample (1.23 g) of **8***d*. It solidified to a low-melting yellow solid. Infrared (CCl_4); 3676–3021 (broad, $O{=}\overset{|}{C}{-}O{-}H$), 1715 (sh) and 1695 (carboxyl and ketone $\rangle C{=}O$) and 1613 cm^{-1} (aromatic C=C).

Anal. Calcd. for $C_{15}H_{20}O_3$: C, 72.6; H, 8.1. Found: C, 72.7; H, 7.9.

The methyl ester, *ar-(±)-juvabione* (**8***e*) prepared by esterifying the above acid (1.23 g) with diazomethane generated from nitrosomethylurea (4 g) and 40% aqueous KOH (12 ml), had b.t. 134–135° at 1 mm; infrared, *(vide infra)*.

Anal. Calcd. for $C_{16}H_{22}O_3$: C, 73.3; H, 8.4. Found: C, 73.3; H, 8.3.

(b) By Dehydrogenation of Synthetic Todomatuic Acids[4] *(2a)*

The keto acid (0.1 g) and sulfur (70 mg) were heated (1 h) at 240–260°. The reaction mixture was cooled to room temperature and was then repeatedly digested with thiophene free dry benzene and filtered. The filtrate was refluxed (2 h) with freshly precipitated copper (1 g). The solid was filtered off and the benzene was removed from the filtrate. The residue (50 mg) was esterified with diazomethane generated from nitrosomethylurea (200 mg) and 40% aqueous KOH (0.6 ml). The crude ester obtained was purified by preparative thin-layer chromatography. The infrared spectrum *(vide infra)* of the pure ester (20 mg) was superimposable in all respects with that of methyl *ar-(±)*-todomatuate (**8***e*), as prepared above.

ar-Turmerone (9)

The oil (161 g) of *Curcuma longa* L., supplied by Techno Chemical Industries, Calicut, India, was fractionated and the sesquiterpene ketone fraction (31 g) distilling at 115° at 1 mm was collected, α_D^{26} −32.6°, n_D^{26} 1.5050; infrared (neat); 1695 (unsaturated $\rangle C{=}O$), 1626 (conjugated C=C), and 1515 cm^{-1} (ar C=C). *ar*-Turmerone in the ketone fraction was spectrophotometrically estimated to be ca. 65%.[14]

A mixture of the ketone fraction (13.2 g), xylene (100 ml), cinnamic acid (27 g), and 10% palladium on carbon (1 g) was refluxed (2 h). After cooling to room temperature, the reaction mixture was filtered, and the filtrate diluted with ether. The residue (13 g) from the ethereal extract on fractionation gave *ar*-turmerone **9** (9 g) which had b.p. 146° at 8 mm; α_D^{26}—69° (homogeneous by t.l.c.) and an infrared spectrum superimposable with that of the authentic sample.[13]

ar-Dihydroturmerone (10)

ar-Turmerone (**9**) (2.2 g) was hydrogenated at room temperature and pressure over 5% palladium on carbon (0.5 g) in ethanol (25 ml) till there was no more absorption of hydrogen. The catalyst was filtered and the alcohol distilled off from the filtrate. The residue (2.2 g) was fractionated to furnish *ar*-dihydroturmerone (**10**) b.p. 115° at 1 mm (1.6 g) which had n_D^{22} 1.4890, α_D^{27} +37.4°; infrared (neat); 1712 cm^{-1} (saturated $\rangle C{=}O$).

Anal. Calcd. for $C_{15}H_{22}O$: C, 82.5; H, 10.2. Found: C, 82.4; H, 10.3.

ar-(+)-Juvabione (Methyl ar-(+)-Todomatuate) (3b)

ar-(+)-Dihydroturmerone (**10**) (6 g) was added to a solution of CrO_3 (24 g) in AcOH (320 ml) containing

[14]The estimation was carried out, on the suggestion of one of the referees, in a separate experiment on a different batch of the fraction.

water (37 ml). The reaction mixture was left aside for 24 h. Methanol (100 ml) was added to destroy excess CrO_3 and the acetic acid and methanol were distilled off under reduced pressure. The residue was diluted with water (500 ml) and extracted with petroleum ether. The acid (0.9 g) reextracted from the organic phase was dissolved in absolute methanol (25 ml). Potassium hydroxide (0.3 g) and methyl iodide (5 ml) were added and the reaction mixture was refluxed (6 h). Methanol was distilled off and the residue was extracted with ether after dilution with water. The residue (0.9 g) from the ethereal extract was chromatographed (SiO_2). The methyl ester (0.4 g) after one more chromatography followed by purification by preparative t.l.c. and short-path distillation gave an analytical sample of *ar*-(+)-juvabione[12] (**3***b*) which had b.t. 125–130° at 1 mm, n_D^{27} 1.4960; and $[\alpha]_D^{27}$ +22.93° ($CHCl_3$ concentration 17.88); infrared ($CHCl_3$); 1710 (ester $\rangle C{=}O$), and 1288 cm^{-1} ($O{=}\underset{|}{C}{-}O{-}Me$). The infrared spectrum, displaying several sharp bands, was completely superimposable with the spectra of the methyl esters prepared from (*a*) *ar*-(±)-todomatuic acid (**8***d*) and (*b*) synthetic todomatuic acids (**2***a*) (*vide supra*).

Anal. Calcd. for $C_{16}H_{22}O_3$: C, 73.3; H, 8.4. Found: C, 73.1; H, 8.6).

Acknowledgments

We are grateful to Prof. D. K. Banerjee of this department for his encouragement and his interest in this work. One of us (K. S. A.) thanks the authorities of the Indian Institute of Science for the award of a scholarship.

1. R. Tuchihashi and T. Hanzawa. J. Chem. Soc. Japan, **61**, 1041 (1940); Chem. Abstr. **37**, 258 (1943).
2. T. Momose. J. Pharm. Soc. Japan, **61**, 288 (1941); Chem. Abstr. **44**, 9383 (1950).
3. M. Nakazaki and S. Isoe. Bull. Chem. Soc. Japan, **36**, 1198 (1963).
4. W. S. Bowers, H. M. Fales, M. J. Thompson, and E. C. Uebel. Science, **154**, 1020 (1966).
5. V. Cerny, L. Dolejs, L. Labler, F. Sorm, and K. Slama. Tetrahedron Letters, 1053 (1967).
6. K. Mori and M. Matsui. Tetrahedron Letters, 4853 (1967).
7. J. C. Bardhan and D. N. Mukherji. J. Chem. Soc. 4629 (1956).
8. H. O. House, W. L. Respess, and G. M. Whitesides. J. Org. Chem. **31**, 3128 (1966).
9. K. Subrahmania Ayyar. Ph.D. Thesis. Indian Institute of Science, Bangalore, India. 1967.
10. H. J. Ringold. J. Am. Chem. Soc. **82**, 961 (1960).
11. A. S. Gupta and Sukh Dev. J. Chromatog. **12**, 189 (1963).
12. V. K. Bhalla, U. R. Nayak, and Sukh Dev. J. Chromatog. **26**, 54 (1967).
13. W. Sandermann. *In* Comparative biochemistry. *Edited by* M. Florkin and H. S. Mason. Vol. III. Academic Press, Inc., New York. 1962; Chaps. 10 and 11. H. Erdtman and T. Norin. *In* Chemistry of organic natural products. *Edited by* L. Zechmeister. Vol. 24. Springer-Verlag, Wien. 1966; Sukh Dev. J. Sci. Ind. Res. India, **25**, 494 (1966).
14. R. P. Mariella and R. R. Raube. J. Am. Chem. Soc. **74**, 521 (1952).
15. V. K. Honwad and A. S. Rao. Tetrahedron, **20**, 2921 (1964).
16. K. Kindler and K. Luhrs. Ann. **685**, 36 (1965); Chem. Ber. **99**, 227 (1966).
17. C. Enzell and H. Erdtman. Tetrahedron, **4**, 361 (1958).
18. K. B. Wiberg. *In* Oxidations in organic chemistry. *Edited by* K. B. Wiberg. Part A. Academic Press, Inc., New York. 1965.
19. H. Mima. Yakugaku Zasshi, **79**, 644 (1959); Chem. Abstr. **53**, 16471*e* (1959).
20. L. J. Chinn and H. L. Dryden, Jr. J. Org. Chem. **26**, 3904 (1961).
21. E. A. Braude and O. H. Wheeler. J. Chem. Soc. 320, 325 (1955).
22. P. J. Neustaedter. *In* Steroid reactions. *Edited by* C. Djerassi. Holden-Day, San Francisco. 1963. p. 116.
23. R. C. Fuson and C. H. McKeever. *In* Organic reactions. *Edited by* R. Adams. Vol. I. John Wiley and Sons, Inc., New York. 1942.
24. S. J. Angyal. *In* Organic reactions. *Edited by* R. Adams. Vol. VIII. John Wiley and Sons, Inc., New York. 1954.
25. K. J. Clark, G. I. Fray, R. H. Jaeger, and R. Robinson. Tetrahedron, **6**, 217 (1959).

Can. J. Chem. Downloaded from www.nrcresearchpress.com by 210.87.254.40 on 09/05/12
For personal use only.

Can. J. Chem. Downloaded from www.nrcresearchpress.com by 210.87.254.6 on 09/05/12
For personal use only.

The photolysis of benzil in cyclohexane solution[1]

DAVID L. BUNBURY AND CHIOU TONG WANG[2]
St. Francis Xavier University, Antigonish, Nova Scotia

Received October 13, 1967

Benzil has been irradiated in cyclohexane solution. The principal products are: benzoic acid; benzaldehyde; phenyl cyclohexyl ketone; benzoin; benzoin benzoate; a compound tentatively identified as desyl benzoyloxydesyl ether; another compound not yet identified; and approximately one-third of the reacted benzil that was not accounted for. A small amount of unsaturation is also found. As long as there is enough benzil present (presumably to absorb all of the light) the benzil disappearance is linear with time. All products appear at the shortest times checked and so cannot be secondary products. If one neglects the benzoic acid approximately 19% of the benzoyl groups that react do so in the form of benzoyl radicals. No evidence for phenyl radical formation was found. The upper limit for the quantum yield of benzil disappearance at 366 mμ is 0.25. The benzoic acid does not arise directly during the photolysis but only when the solution is exposed to oxygen during the work-up. Preliminary experiments in cumene solution have shown that the amount of benzil lost for the same length of irradiation increases by a factor of about 1.5. In 2-propanol solution the increase is by a factor of 2.5. When 2-propanol is the solvent, a new product appears which is most probably the dimer of the ketyl radical which is formed when an excited benzil abstracts a hydrogen atom. This product is very unstable.

Canadian Journal of Chemistry, 46, 1473 (1968)

Introduction

The photoreduction of benzophenone and other phenyl ketones to the corresponding pinacols is a well studied reaction (1–4). Aliphatic 1,2-diketones such as 5,6-decanedione give 2-hydroxycyclobutanones on photolysis with remarkable yields, practically 100% of all ketone reacting (5). On the other hand biacetyl, which is unable to form a cyclic intermediate for hydrogen abstraction from itself, undergoes a radical split into two acetyl radicals on photolysis in mineral oil, heptane, and perfluorooctane (6). In ethanol solution biacetyl undergoes photoreduction to the 3,4-dimethyl-3,4-dihydroxyhexane-2,5-dione in analogy to the formation of benzpinacol in 2-propanol (7).

Benzil was irradiated in cyclohexane solution in an effort to see which path or combination of the two is followed. Cyclohexane was chosen as the initial solvent as its hydrogens are moderately easy to abstract, but there would still be a chance for the split into radicals to occur. In retrospect it would have been better to have started at one of the extremes.

Experimental

Materials

Benzil was Matheson, Coleman, and Bell reagent grade which was twice recrystallized from methanol. Cyclohexane (Fisher certified reagent) was freshly distilled. Silica gel used in column chromatography was 100–200 mesh Fisher certified grade and washed with ethyl ether before use. The silica gel used in thin-layer chromatography (t.l.c.) was silica G according to Stahl from E. Merck and was pretreated in the following way. It was allowed to stand overnight with methanol, filtered, and rinsed with methanol. The washed adsorbent was dried in an oven at 120–130 °C for 6 h. All other solvents used were distilled before use.

Apparatus

All melting points were taken on a Fisher–Johns melting point apparatus and are uncorrected. Infrared (i.r.) spectra were determined on a Beckman IR 8 double-beam instrument. Nuclear magnetic resonance (n.m.r.) spectra were determined on a Varian A-60A instrument. Analyses and molecular weights were by Schwarzkopf Microanalytical Laboratory, 56-19 37th Avenue, Woodside, New York 11377. Gas–liquid chromatography (g.l.c.) was performed on a Burrell model K-1 with thermal conductivity detector. The column was 250 cm long, ¼ in. in diameter, and was filled with 20% Dow Corning high-vacuum silicone grease on 80–100 mesh Chromosorb W. Standard solutions were run alternately with the irradiated solution for each peak of interest. Three Raymaster Uviarc high-pressure mercury lamps 420-U1 (George W. Gates and Co., Franklin Square, Long Island, N.Y.) were used in all but the actinometry run.

Irradiation

Two types of irradiation were carried out. In the first type, the reaction vessel was a Vycor cylinder and had a volume of 50 ml. Benzil (0.530 g) was placed in this cell which was then attached to a high-vacuum line by a ground joint and evacuated. Cyclohexane (35 ml) was put into another container and after degassing by conventional freeze–pump–thaw cycles was distilled onto the benzil. The reaction cell was then sealed off from the line, allowed to warm up to room temperature, and the benzil was dissolved by shaking. After all the benzil had

[1]Presented at the Annual Meeting of the Atlantic Section of the Chemical Institute of Canada on August 25 and 26, 1966. Taken in part from the M.Sc. thesis of Chiou Tong Wang.

[2]Present address: University of North Dakota, Grand Forks, North Dakota.

Can. J. Chem. Downloaded from www.nrcresearchpress.com by 210.87.254.6 on 09/05/12
For personal use only.

dissolved, the cell was placed in a Vycor cylinder of about twice the diameter of the cell and water (20–30 °C) circulated through this cylinder during irradiation. The bath with cell was surrounded by the three mercury lamps. The arrangement of reflectors was such that most of the light was reflected back and forth until it was absorbed. Irradiation was for 2 h.

In the second type, 34.5 g of benzil was dissolved in 2.3 l of cyclohexane (the concentrations used in both types are close to saturation). The resulting solution was poured into a 3-l three-necked round-bottom Pyrex flask fitted with reflux condenser and nitrogen sparger connections. Before irradiation the solution was flushed for 30 min with nitrogen (99.997% purity, Matheson Co., Whitby, Ontario). The flask was then surrounded with the same three ultraviolet lamps. The progress of reaction during irradiation was followed by withdrawing small portions for g.l.c. and t.l.c.

Thin-layer Chromatography

The plates were coated with a slurry of Silica Gel G (25 g in 50 ml of distilled water) to 0.25 mm thickness and allowed to stand overnight prior to use. Where available, standards were run as well as the irradiated solution. The developing solvent was petroleum ether (30–60°): ethyl ether (4:1). Visualization was both by ultraviolet light and by iodine.

Column Chromatography

The reaction mixtures of 10 sealed-tube runs were combined and added to 30 g of silica gel (100–200 mesh) with continuous shaking. The cyclohexane was removed by a rotary evaporator, the dried product ground in a mortar with *n*-hexane, and the slurry then slowly added to the *n*-hexane layer on top of 300 g of silica gel in a previously packed column. The column was eluted with 6 l of hexane – ethyl ether which varied in concentration from 0 to 70% ethyl ether (v/v), then 2.5 l each of acetone and ethyl alcohol. Each fraction was examined by either t.l.c. or g.l.c. The first compound eluted was phenylcyclohexyl ketone, the second benzil, and the third benzoic acid, which was purified using sodium hydrogen carbonate. The materials eluted by acetone and ethyl alcohol could not be identified.

In nitrogen-flushed photolyses the cyclohexane was removed under reduced pressure and the residue divided into four equal parts each of which was treated in the following way. The irradiated mixture was adsorbed on silica gel then placed on top of a silica gel column. The column was eluted with 10 l of ethyl ether – hexane, which varied in concentration from 0 to 50% ethyl ether (v/v). Five per cent ether brought out phenylcyclohexyl ketone and 15% brought out the unreacted benzil. The fractions eluted by 25% ether were combined, concentrated, and extracted with sodium hydrogen carbonate. The sodium hydrogen carbonate extract was acidified and the liberated benzoic acid extracted, recovered, and weighed. The material remaining after removal of the benzoic acid was subjected to further column chromatography and yielded four compounds. The material eluted from the first column by 50% ether could not be separated any further and was brownish in color. The i.r. and n.m.r. spectra showed the presence of aliphatic hydrogen atoms, presumably in cyclohexyl residues. There was also some material which could not be removed from the column.

Isolation Identification and Estimation of Products

Benzaldehyde

In both types of irradiation the solution was injected into the gas chromatograph and a peak obtained with the same retention time as authentic benzaldehyde. The solvent was distilled under reduced pressure and checked again on the gas chromatograph. The peak belonged to the distillate. The presence of benzaldehyde in the distillate was confirmed by precipitating its 2,4-dinitrophenylhydrazone, observed m.p. 237 °, lit. 237 °. Quantitative measurement of benzaldehyde was made by comparing its area on the gas chromatograph with that of a standard solution.

Phenylcyclohexyl Ketone

In sealed-tube photolyses this compound was identified by trapping its peak from the gas chromatograph and comparing its infrared spectrum with that of an authentic sample prepared by standard procedures. Quantitative measurement was made by comparing the peak area in the irradiated solution with that of a standard solution. In nitrogen-flushed irradiations, the isolated material was also weighed.

Unreacted Benzil

Its peak from the gas chromatograph was trapped and identified by its i.r. spectrum. The area was compared with that of standard solutions. The recovered material was weighed.

Unsaturation

The irradiated solution of some sealed-tube photolyses was distilled under reduced pressure or at atmospheric pressure using chlorobenzene as a chaser. The distillate was treated according to the method of Hardwick (8) (addition of glacial acetic acid, bromine, then KI, followed by thiosulfate titration). The unsaturation was assumed to indicate cyclohexene.

Benzoic Acid

After its recovery from the bicarbonate extracts benzoic acid was identified by its melting point and i.r. spectrum. It was measured by weighing.

The following products were isolated only from nitrogen-flushed irradiations following rechromatography and after removal of the benzoic acid (although t.l.c. showed their presence in sealed-tube experiments).

Benzoin Benzoate

The first fraction eluted gave a substance which after recrystallization had a m.p. of 128 °C, lit. 125 °C. The mixture melting point with benzoin benzoate showed no depression and the i.r. and n.m.r. spectra were identical with an authentic sample prepared by refluxing benzoyl chloride and benzoin in *sym*-collidine. Interestingly, no ester was formed when pyridine was used as the solvent. The substance was weighed.

Benzoin

The third substance eluted has a m.p. of 134 °C on recrystallization, lit. 137°. A mixture melting point with benzoin showed no depression and its i.r. spectrum was identical with that of an authentic sample (Matheson, Coleman, and Bell). It was weighed.

An earlier attempt in the sealed-tube runs to separate this material on an alumina column led to the formation of benzil. Authentic benzoin gave the same reaction. A similar reaction is known to occur at 150 °C (9).

Can. J. Chem. Downloaded from www.nrcresearchpress.com by 210.87.254.6 on 09/05/12
For personal use only.

Desyl Benzoyloxydesyl Ether (4)

This was the second substance eluted and after recrystallization had a melting point of 218–219 °C. It was weighed.

Anal. Calcd. for $C_{35}H_{26}O_5$ (formula weight, 526.5): C, 79.83; H, 4.98. Found (mol. wt., 558, isothermal distillation): C, 80.19; H, 4.80.

The carbonyl absorption in the infrared is a doublet, 1712 and 1680 cm^{-1}. Between 1600 and 1430 cm^{-1} there are four other peaks whose position and relative intensities were more or less the same as in 11 other benzoyl compounds. In five other benzoyl compounds either the third or fourth peak is missing. The presence of the two bands at about 1600 and 1582 cm^{-1} in all benzoyl compounds examined by Rasmussen *et al.* has already been pointed out (10). The correspondence of these four bands with those of benzoin and benzoin benzoate is particularly marked. The n.m.r. spectrum consists only of unresolved aromatic absorption. The low solubility of the compound did not allow a decision to be made on the presence or absence of the lone aliphatic hydrogen atom.

On hydrolysis, this compound would be expected to yield benzoin, benzil, and benzoic acid. When refluxed for 4 h with KOH in ethanol no reaction occurred. When refluxed with 6 *N* HCl in ethanol for 3 h no reaction occurred. However, a ketal should be very sensitive to acid hydrolysis. A small amount was refluxed overnight with 10% KOH in ethylene glycol, water added, and the mixture extracted with methylene chloride. The methylene chloride was evaporated in a mortar and an infrared spectrum taken of the residue. It appeared to be hydrobenzoin. Both benzoin and benzil when refluxed with 10% KOH in ethylene glycol (b.p. 197 °C) for 24 h yielded hydrobenzoin. It is known that when a primary alcohol is heated with sodium hydroxide or potassium hydroxide the sodium or potassium salt of the corresponding fatty acid is formed with the evolution of hydrogen (11). Acidification of the water layer, extraction with methylene chloride, followed by evaporation gave a material that showed the presence of benzoic acid.

We also obtained 0.5 g of a substance that came out initially with the benzoin. The benzoin was removed by extraction with hot methanol and colored substances were removed by recrystallization. After recrystallization from a large volume of methyl ethyl ketone the m.p. was 227–228 °C. There was no evidence for aliphatic hydrogens in either the n.m.r. or i.r. spectra. The carbonyl peak in the i.r. is a doublet at about 1718 and 1662 cm^{-1}. The four peaks mentioned before as being characteristic of the benzoyl group are all present. The elementary analysis of the compound was found to be: C, 75.99; H, 5.26, the best fit for which is $C_{16}H_{13}O_3$. We would like to think that the compound is 1,2,3,4-tetraphenyl-1,4-butanedione-2,3-diol dibenzoate but that would give an analysis of: C, 80.0; H, 4.80. The reported molecular weight is 300 by the Rast method, but, since the compound decomposes on melting, this is almost surely wrong. The insolubility of the compounds prevents use of the isothermal distillation method and also prevents a good n.m.r. spectrum from being obtained.

Results and Discussion

From a comparison of runs B-3, B-4, and B-5 in Table I it will be seen that the disappearance of benzil is approximately linear with time and that the production of benzaldehyde and phenylcyclohexyl ketone also increases with time. Because of variations in the quality of the cooling water and in the voltage to the lamps, reproducibility was difficult to obtain. Runs 1–10 in Table I exhibit this clearly. From a comparison of runs B-9, B-10, B-11, and B-12, it is seen that neither concentration nor total amount of benzil present had any effect on the actual number of moles destroyed as long as the percent destroyed did not reach the very high value of run B-8. The course of a nitrogen-flushed photolysis, followed by withdrawing small amounts for gas–liquid chromatography, showed that the benzil disappearance and the production of phenylcyclohexyl ketone and benzaldehyde were linear with time. Table II shows a complete analysis of a nitrogen-flushed photolysis and a comparison with the sum of runs 1–10 of the sealed-tube photolysis. A complete analysis of run 11 was not possible since at the time all of the products were not known. In sealed-tube photolysis it was impossible to analyze for benzoin and higher molecular weight products by gas–liquid chromatography as they would either decompose or not come off at all. Since the percent benzaldehyde and phenylcyclohexyl ketone produced in the two types is the same within experimental error it is assumed that the same mechanism is operative in each case. Since the Pyrex cell and flask give the same result as the Vycor cell, light of wavelength below 280 mμ is not necessary. The photochemically reactive state of benzil is presumably the lowest energy triplet as in most other carbonyl compounds. Calvert and Pitts (12) record that the quantum yield for intersystem crossing ($s_1 \rightarrow t_1$) for benzil is 0.92.

Although a complete material balance has not been obtained, 68% of the benzoyl groups lost have been accounted for. Four products require a split of the benzil into benzoyl radicals: benzaldehyde, phenylcyclohexyl ketone, benzoin benzoate (**2**), and desyl benzoyloxydesyl ether (**4**). Equations [1–13] can account for their formation.

Equation [6] leading to the addition of benzaldehyde to cyclohexene is a well-known type of reaction (13). In support of eqs. [8], [9], and [10], benzaldehyde is known to add photochemically to phenanthraquinone though by a

TABLE I

Reaction variables and products for the photolysis of benzil in cyclohexane

Run no.	Time (min)	Solvent	Volume (ml)	Sample		Benzil destroyed		C_6H_5CHO (mmoles)	Unsaturation (mmoles)	Cyclohexylphenyl ketone (mmoles)
				Benzil (mmoles)	Conc. (mmoles/l)	(mmoles)	(%)			
B-3	140	Cyclohexane	35	3.09	88.3	1.23	39.8	0.076	0.025	0.064
B-4	62	Cyclohexane	35	2.95	84.3	0.66	22.4	0.059	0.014	0.054
B-5	30	Cyclohexane	35	3.04	86.0	0.22	7.2	0.021	0.000	0.039
B-6*	95	Cyclohexane	35	2.86	81.6	1.03	36.0	0.066	0.020	0.078
B-7	62	Hexane	5	0.25	50.0	—	—	—	—	—
B-8†	30	Cyclohexane	5	0.09	18.3	0.08	83.5	0.014	—	0.010
B-9	30.5	Cyclohexane	35	0.64	18.3	0.39	60.4	0.025	0.010	0.023
B-10	30	Cyclohexane	35	2.82	80.6	0.42	14.9	0.000	0.006	0.032
B-11	30	Cyclohexane	25	1.74	80.6	0.44	25.1	0.025	0.021	0.031
B-12	30	Cyclohexane	25	0.80	31.9	0.37	46.2	0.030	0.004	0.030
B-13	30	Cumene	20	2.21	110.8	0.74	33.4	trace	—‡	—
B-14	30	Cumene	20	2.21	110.6	0.60	27.2	trace	—	—
B-16	85	2-Propanol	35	4.58	131.0	3.01	65.8	—	—	—
1	120	Cyclohexane	35	2.52	72.0	1.01	40.1	0.122	—	0.127
2	120	Cyclohexane	35	2.55	72.9	0.91	35.7	0.094	—	0.117
3	120	Cyclohexane	35	2.57	73.5	0.83	32.2	0.094	—	0.106
4	120	Cyclohexane	35	2.59	74.0	1.19	46.0	0.169	—	0.127
5	120	Cyclohexane	35	2.58	73.8	1.06	41.2	0.085	0.022	0.074
6	120	Cyclohexane	35	2.54	72.5	0.94	37.1	0.142	0.026	0.101
7	120	Cyclohexane	35	2.56	73.1	0.94	36.7	0.122	—	0.122
8	120	Cyclohexane	35	2.54	72.5	1.13	44.5	0.178	—	0.133
9	120	Cyclohexane	35	2.44	69.7	0.99	40.6	0.170	—	0.059
10	120	Cyclohexane	35	2.56	73.1	1.12	43.8	0.076	—	0.079

*A Pyrex cell was used.
†The original cell broke at the end of this run.
‡Not measured.

TABLE II

Comparison of sealed-tube and nitrogen-flushed photolysis

	Sealed-tube		Nitrogen-flushed		Nitrogen-flushed	
	Sum of runs 1–10	% Benzoyl groups lost	Run 11	% Benzoyl groups lost	Run 12	% Benzoyl groups lost
Time (h)	2		24		24	
Cyclohexane (ml)	350		2300		2300	
Benzil starting (mmoles)	25.4		164.0		164.0	
Benzil disappeared (mmoles)	10.1		65.5		60.8	
Benzaldehyde (mmoles)	1.25	6.2	8.2	6.25	7.91	6.5
Phenylcyclohexyl ketone (mmoles)	0.96	4.8	7.2	5.5	6.96	5.7
Cyclohexene (calculated on two runs) (mmoles)	0.24				1.45*	
Benzoic acid (mmoles)	6.3	31.1			23.75	19.5
Benzoin benzoate (mmoles)					6.32	15.6
Desyl benzoyloxydesyl ether (mmoles)					1.71	7.1
Benzoin (mmoles)					5.65	9.3
Compound with 3 or 6 benzoyl groups						3.9

*Calculated.

Can. J. Chem. Downloaded from www.nrcresearchpress.com by 210.87.254.6 on 09/05/12
For personal use only.

Can. J. Chem. Downloaded from www.nrcresearchpress.com by 210.87.254.6 on 09/05/12
For personal use only.

[1] $C_6H_5COCOC_6H_5 \longrightarrow [C_6H_5COCOC_6H_5]^*$

[2] $[C_6H_5COCOC_6H_5]^* \longrightarrow 2C_6H_5CO\cdot$

[3] $C_6H_5CO\cdot + C_6H_{12} \longrightarrow C_6H_5CHO + C_6H_{11}\cdot$

[4] $C_6H_5CO\cdot + C_6H_{11}\cdot \longrightarrow C_6H_5COC_6H_{11}$

[5] $2C_6H_{11}\cdot \longrightarrow C_6H_{10} + C_6H_{12}$

[6] $C_6H_5CO\cdot + C_6H_{10} \longrightarrow$ 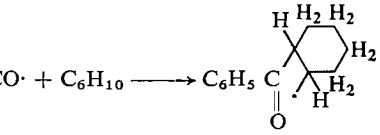

[7] 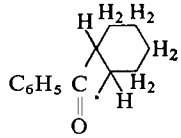 $+ C_6H_5CHO \longrightarrow C_6H_5COC_6H_{11} + C_6H_5CO\cdot$

[8] $C_6H_5CO\cdot + C_6H_5COCOC_6H_5 \longrightarrow$ 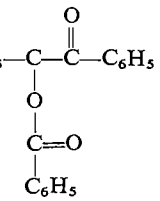

1

[9] 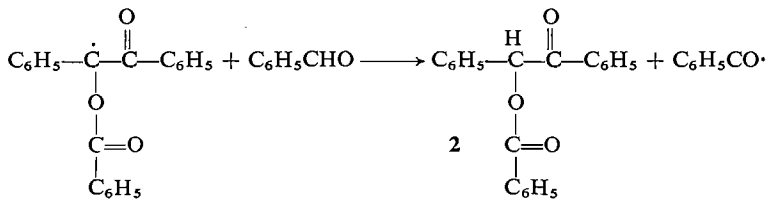

1 **2**

[10] $\mathbf{1} + C_6H_{12} \rightarrow \mathbf{2} + C_6H_{11}\cdot$

[11] 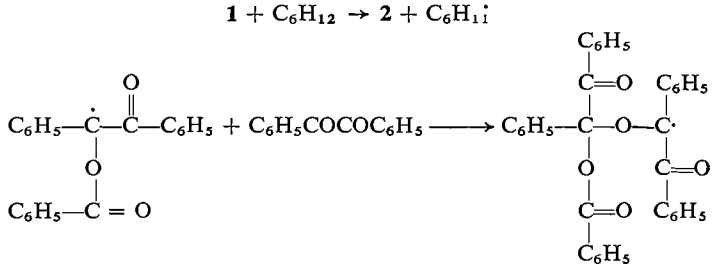

3

[12] $\mathbf{3} + C_6H_5CHO \longrightarrow$ 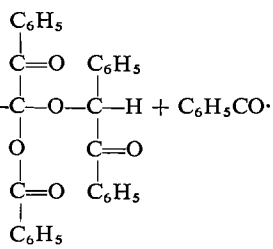

4

[13] $\mathbf{3} + C_6H_{12} \longrightarrow \mathbf{4} + C_6H_{11}\cdot$

Can. J. Chem. Downloaded from www.nrcresearchpress.com by 210.87.254.6 on 09/05/12
For personal use only.

slightly different mechanism. In that case, after the addition of the benzoyl radical to the oxygen of the quinone, it is an oxygen radical rather than a carbon radical that removes the hydrogen atom in eq. [13] (14). In support of eqs. [8] and [11], benzil is known to be an efficient radical trap (15). All nonaromatic hydrogens must originate from the cyclohexane so there should be an equivalent number of cyclohexyl residues (one cyclohexene equivalent to two residues). The sum of benzaldehyde, benzoin benzoate, desyl benzoyloxydesyl ether, and twice the benzoin in run 12 is 27.2 mmoles. The sum of phenyl cyclohexyl ketone and twice the cyclohexene is 9.86 mmoles. A search was made for bicyclohexyl but none was found, in contrast to the photoreaction of benzophenone in cyclohexane (16). The missing cyclohexyl residues must be in the remaining unidentified material which did show evidence of aliphatic hydrogens. Pitts and others (17) found that cyclohexene strongly inhibits the formation of benzpinacol in irradiated olefin – alcohol – benzophenone systems and thought that this might be due to reaction of the ketyl radical with the cyclohexene: no adducts could be isolated however.

The benzoin is thought to arise from an excited benzil which abstracts a hydrogen from the solvent or from benzaldehyde and forms the ketyl radical (5). The ketyl radical then dis-

[14] $[C_6H_5COCOC_6H_5]^* + C_6H_{12} \longrightarrow$

$$C_6H_5\overset{OH}{\overset{|}{C}}\cdot\!\!-\!\!\overset{O}{\overset{\|}{C}}\!\!-C_6H_5 + C_6H_{11}\cdot$$

[15] $2C_6H_5\dot{C}OHCOC_6H_5 \longrightarrow$

$$C_6H_5COCOC_6H_5 + C_6H_5CHOHCOC_6H_5$$

proportionates. That the ketyl radical is formed is not in doubt as Beckett, Osborne, and Porter (18) report its spectrum in flash-photolyzed, degassed ethanol solutions and triplet benzophenone will abstract hydrogen from hexane as well as alcohols though with a lower quantum yield (3). No product which could be assigned to coupling of the ketyl radicals of benzil could be found. In support of this observation, Porter and others (18) suggest that the ketyl radicals from benzil, unlike those from benzophenone, acetophenone, and benzaldehyde, disproportionate owing to a steric effect, as one of the products that they find in the flash photolysis of benzil in ethanol is benzoin. Also, in studying the thermal decomposition of 1,1,2,2-tetraphenylethanol in the presence of benzil, Metzger (19) finds benzoin among his products and suggests that it arises from the disproportionation of the same ketyl radical. He does not report any of the coupling product. However, later work here has shown that when benzil is irradiated in degassed isopropyl alcohol a precipitate that has a hydroxyl band in the infrared and a benzoyl group, and which is not benzoin appears. This product is very unstable thermally and in solution in the presence of oxygen it forms benzil. We believe that this is the dimer of the ketyl radical; however, further work concerning elucidation of its structure is being done.[3]

The product which is most difficult to explain and which appears in such large amounts is the benzoic acid. In the sealed-tube experiments particularly, only a very small trace of oxygen can be present during the irradiation. Therefore, some product must be formed which reacts quickly with oxygen to form benzoic acid after the irradiation is over and during the work-up. In an attempt to check this a sealed-tube photolysis was performed in which 0.26 g of benzil was decomposed. Immediately on opening the cell, the contents were poured into sodium bicarbonate through which CO_2 had been bubbled for about 15 min. On shaking, separation, acidification, extraction, and evaporation of the solvent, 0.02 g of benzoic acid was recovered. If the same proportion of benzoic acid as in run 12 had been produced 0.06 g should have been obtained. Stevens and Dubois (20) have observed that the major product of aerated solutions of biacetyl in hexane, when exposed to sunlight, is acetic acid. A possible reaction path they suggest is one involving reaction of the ketyl radical of biacetyl with oxygen. If some product in the benzil case is in equilibrium with the ketyl radical from benzil, this could lead to benzoic acid when exposed to air. During the photolysis of benzophenone in alcohols Pitts and others (17) have observed the formation of a reactive intermediate which is quickly destroyed by oxygen. This intermediate was formed in deaerated solutions and at high light intensities.

[3] *Note added in proof*—This work (not yet published) has confirmed the suggested structure and shown that the appearance of the precipitate is temperature, concentration, and solvent dependent.

Can. J. Chem. Downloaded from www.nrcresearchpress.com by 210.87.254.6 on 09/05/12
For personal use only.

Our intensities were at least as strong. They also refer to earlier work by J. Boeseken who irradiated terephthalophenone in cyclohexanol and observed a visibly colored "photosubstance" which was destroyed on shaking with oxygen. In this work the precursor of benzoic acid might be the analogous intermediate.

Rust, Seubold, and Vaughn (21) found that heating benzaldehyde with *t*-butyl peroxide led to the formation of dihydrobenzoin dibenzoate in high yield by a mechanism involving the attack of a benzoyl radical on the oxygen of another benzaldehyde molecule followed by coupling of the resulting radicals. We have attempted to check on the reaction of benzoyl radicals with benzil by adding benzil to the mixture of benzaldehyde and *t*-butyl peroxide. The products obtained were of relatively high molecular weight and did not correspond to any of our photolytic products nor were they the dibenzoate.

An attempt to determine the quantum yield of the reaction failed when the lamp broke after 2 h, and only an upper limit of 0.25 for benzil disappearance at 366 mμ could be calculated. The quantum yield for the disappearance of benzophenone in hexane is about 0.5 (3). It is not known what fraction of the benzil initially splits into radicals but a relatively high proportion of these can be expected to recombine and thus lower the quantum yield. This is supported by the fact that MacKay, Marx, and Waters (22) found 29 moles of benzil produced per 100 moles of azodibenzoyl decomposed photochemically in benzene, and in their case the initial benzoyl radicals would have been separated by a molecule of nitrogen. As would be expected, the amount of benzil destroyed in the same time increases in cumene solution and in isopropyl alcohol solution when runs B-10, B-13, and B-14, and B-10 and B-16 are compared. In cumene solution there was no increase in the amount of benzaldehyde produced so the increased disappearance must have been due to more hydrogen abstraction by excited benzil and/or reaction of the benzoyl radicals with benzil. That the benzoyl radical is a poor hydrogen abstractor is shown by the fact that MacKay and others (22) found only a trace of benzaldehyde when azodibenzoyl was photolyzed in cumene solution. All products appear at the earliest times and so presumably do not arise by secondary photolysis. In run B-1 a special search was made for benzene to check the possibility of phenyl radicals being formed but none was found.

If one neglects the benzoic acid whose mode of formation is unknown, one finds that approximately 19% of the benzoyl groups of the benzil that react, do so as benzoyl radicals.

Acknowledgments

The authors would like to thank the National Research Council of Canada for generous support and Dr. Brian M. Lynch for nuclear magnetic resonance spectra and many helpful discussions.

1. W. M. Moore, G. S. Hammond, and R. P. Foss. J. Am. Chem. Soc. **83**, 2789 (1961).
2. G. S. Hammond, W. P. Baker, and W. B. Moore. J. Am. Chem. Soc. **83**, 2795 (1961).
3. A. Beckett and G. Porter. Trans. Faraday Soc. **59**, 2038 (1963).
4. A. Beckett, A. D. Osborne, and G. Porter. Trans. Faraday Soc. **60**, 873 (1964).
5. W. H. Urry and D. J. Trecker. J. Am. Chem. Soc. **84**, 118 (1962).
6. S. A. Greenberg and L. S. Foster. J. Am. Chem. Soc. **83**, 4339 (1961).
7. W. D. Cohen. Chem. Weekblad, **13**, 590 (1916).
8. T. J. Hardwick. J. Phys. Chem. **64**, 1623 (1960).
9. Y. Halpern, M. Michman, and S. Patai. J. Chem. Soc. B, 149 (1966).
10. R. S. Rasmussen, D. D. Tunnicliff, and R. Brattain. J. Am. Chem. Soc. **71**, 1068 (1949).
11. E. Reid, H. Worthington, and A. W. Larcher. J. Am. Chem. Soc. **61**, 99 (1939).
12. J. G. Calvert and J. N. Pitts. Photochemistry. John Wiley & Sons, New York. 1966. p. 309
13. W. A. Pryor. Free radicals. McGraw-Hill Book Co., New York. 1966. p. 219.
14. R. F. Moore and W. A. Waters. J. Chem. Soc. 238 (1953).
15. H. C. McBay and S. M. McBay. Papers presented at the 135th Meeting, American Chemical Society, Division of Paint, Plastics and Printing Ink, Chemistry. Boston, 1959. Vol. 19, No. 1.
16. C. Walling and M. J. Gibian. J. Am. Chem. Soc. **86**, 3902 (1964).
17. J. N. Pitts, Jr., R. L. Letsinger, R. P. Taylor, J. M. Patterson, G. Recktenwald, and R. B. Martin. J. Am. Chem. Soc. **81**, 1068 (1959).
18. A. Beckett, A. D. Osborne, and G. Porter. Trans. Faraday Soc. **60**, 873 (1964).
19. S. H. Metzger. Ph.D. Thesis, University of Illinois, Urbana, Ill. 1962. p. 73.
20. B. Stevens and J. T. Dubois. J. Chem. Soc. 2813 (1962).
21. F. F. Rust, F. H. Seubold, and W. E. Vaughn. J. Am. Chem. Soc. **70**, 3258 (1948).
22. D. MacKay, U. F. Marx, and W. A. Waters. J. Chem. Soc. 4793 (1964).

Can. J. Chem. Downloaded from www.nrcresearchpress.com by 210.87.254.40 on 09/05/12
For personal use only.

Models for the assignment of the chemical shifts for protons on the epoxide ring of 2,3-anhydroglycopyranosides[1]

F. SWEET AND R. K. BROWN
Department of Chemistry, University of Alberta, Edmonton, Alberta

Received December 1, 1967

The signal assignments for the protons of the epoxide ring in several 3,4-epoxy-2-alkoxytetrahydropyrans have been made by spin decoupling. Because of the close resemblance of these tetrahydropyrans to 2,3-anhydroglycopyranosides, these results have been used to make chemical shift assignments for the H-2 and H-3 protons of the latter compounds. For the compounds examined, the H-2 proton signal occurs at higher field compared to the position of the H-3 proton signal.

Canadian Journal of Chemistry, 46, 1481 (1968)

In a recent paper (1), nuclear magnetic resonance (n.m.r.) data of a number of glycopyranosides, each of which contained a 2,3-epoxy, 2,3-episulfide, or 2,3-epimine function (Scheme 1) were reported. A relationship was found between the H-1,H-2 coupling constant (as shown in the signal for the anomeric proton) and the *cis* or *trans* orientation of the anomeric

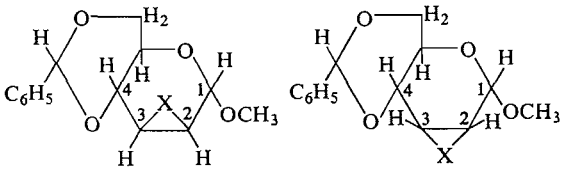

1 **2**

X = O, S, NH, NAc

SCHEME 1

alkoxy group and the C-2,C-3 epi function. In all cases presented, when these two groups were *trans*, the H-1,H-2 coupling was very small ($J_{1,2} \sim$ O), whereas when they were in the *cis* arrangement, the H-1,H-2 coupling was 2.5 to 4.5 Hz. This useful information has permitted an assignment of the signals for the C-3 methylene protons in indene oxide and has simplified the analysis of the n.m.r. spectra of a variety of cyclopentene oxides (1).

Since it was found that $J_{1,2} \sim J_{3,4} \sim 0$ for **1** (X = O), no assignment of the signal position of H-2 and H-3 (1) could be made on this basis. However, by a comparison of the n.m.r. spectra of **2** (X = O) and **1** (X = O) an assignment was apparently possible (1) although the rationale for this is obscure to us. The signals for the H-3 and H-2 protons of **1** (X = O) were reported to be at τ 7.25 and τ 6.93 respectively. Assignments of the H-2 and H-3 signal positions of the analogues of **1** (Scheme 1) were then made by analogy (1).

During the course of work in this laboratory, we have prepared a number of 2,3-epoxytetrahydropyrans[2] (Scheme 2) as possible intermediates for the preparation of carbohydrate models. These now prove to be well-suited to the study of the n.m.r. spectra of the 2,3-anhydropyranosides.

In these compounds (**3**–**5**) the signals for the protons on C-4 are well upfield and are separated from those of the protons on the remaining carbon atoms. This simplifies the assignment of

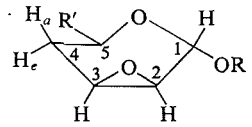

3*a* R = CH_3; R′ = H
4 R = *t*-C_4H_9; R′ = H
5 R = CH_3; R′ = CH_2-OCH_3

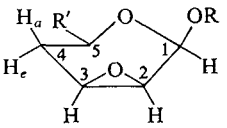

3*b* R = CH_3; R′ = H

SCHEME 2

[1]Taken from the thesis of F. Sweet to be submitted to the Faculty of Graduate Studies, University of Alberta, Edmonton, Alberta, as part of the requirements for the degree of Doctor of Philosophy.

[2]The numbering system used here is not that recommended for the tetrahydropyran series, but is that which is applied to the pyranosides wherein the anomeric carbon is designated as position-1.

signals and the problem of their separation, contrary to the situation prevailing in the 2,3-anhydropyranosides which possess an oxygen atom attached to each carbon atom. Moreover, it is highly unlikely that $J_{1,2} \sim J_{3,4a} \sim J_{3,4e} \sim 0$, a condition which would make the assignment of the signals for H-2 and H-3 more difficult as in the case of **1** (1). A further advantage of our models is the elimination of the possibility that virtual coupling (2, 3) might affect the magnitude of the spacing from which $J_{2,3}$ is measured.

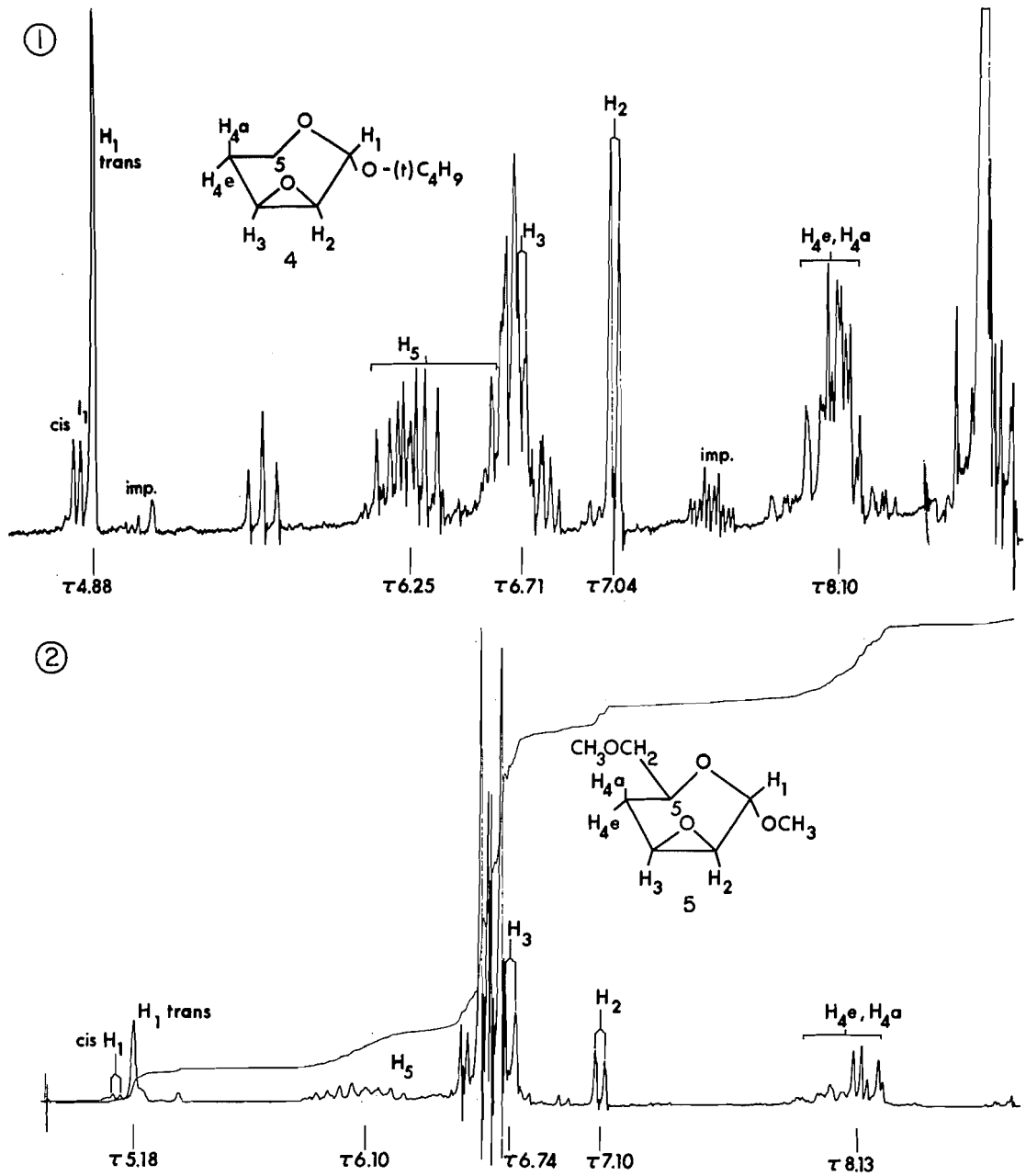

FIG. 1. The 100 MHz nuclear magnetic resonance spectrum of **4** (*trans* and some *cis*) in $CDCl_3$ as solvent (imp. = impurity).

FIG. 2. The 100 MHz nuclear magnetic resonance spectrum of **5** (*trans* and some *cis*) in $CDCl_3$ as solvent.

Can. J. Chem. Downloaded from www.nrcresearchpress.com by 210.87.254.40 on 09/05/12
For personal use only.

TABLE I

Observed chemical shifts (in τ units) and first order coupling constants*

Compound†	τ H-1	$J_{1,2}$	τ H-2	τ H-3	$J_{2,3}$
3*a* 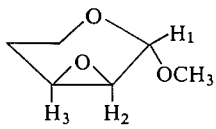	5.22	0	7.04	6.71	4.0
3*b* 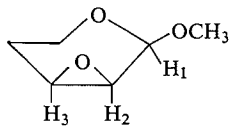	5.15	2.5	6.72	~6.58	4.0
4 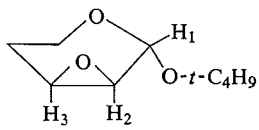	4.88	0	7.13	6.74	4.0
5 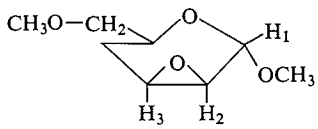	5.18	0	7.10	6.74	4.0
6 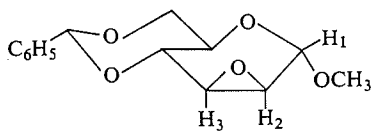	5.14	0	6.88	6.56	3.8

*In Hz.
†The solvent for these compounds was $CDCl_3$.

The n.m.r. spectra of compounds **3–5** are shown in Figs. 1–4 and the significant τ and *J* values are listed in Table I. For compounds **3***a*, **4**, and **5**, wherein H-1 and H-2 are *trans*, two characteristic signals are observed. The anomeric proton appears as a singlet ($J_{1,2} \sim 0$) in the region τ 4.88–5.22. A doublet ($J = 4.0$)[3] is observed at τ 7.06–7.13. These results are similar to those reported (1). Decoupling experiments clearly show the latter doublet to be due to H-2, not H-3.

When the nucleus with the doublet at ~τ 7.1 was irradiated, the complex pattern at ~τ 6.7 simplified to a quartet but no change was observed in the region τ 7.9–8.2 (H-4*a* and H-4*e*). Irradiation at τ 6.7 caused the doublet at τ 7.1 to collapse to a singlet and the development of a simpler pattern at τ 7.9–8.2. Irradiation at τ 8.13 gave no change in the doublet at τ 7.10 but collapse occurred in the signals at ~τ 6.7. This information shows that the signal for H-2 is that at τ 7.1 ($J_{2,3} = 4.0$) while that for H-3 is at a somewhat lower field (see Table I).

The close similarity of these model compounds to the 2,3-anhydropyranosides clearly indicates that the reported signal assignments for H-2 and H-3 (1) should be reversed. Further support for this is found in the n.m.r. spectrum (Fig. 5) of methyl 4,6-*O*-benzylidene-2,3-anhydro-α-D-mannopyranoside, **6**. Significant signal assignments of **6** are shown in Table I and in Fig. 5.

[3]The practically constant value of 4.0 Hz for $J_{2,3}$ in compounds **3***a*, **4**, and **5** should be compared to the range of $J_{2,3}$ of 3.8–4.5 Hz found for analogous pyranosides (1). The effect of virtual coupling on the observed coupling constant may be responsible for this reported (1) variation.

Can. J. Chem. Downloaded from www.nrcresearchpress.com by 210.87.254.40 on 09/05/12
For personal use only.

Can. J. Chem. Downloaded from www.nrcresearchpress.com by 210.87.254.40 on 09/05/12
For personal use only.

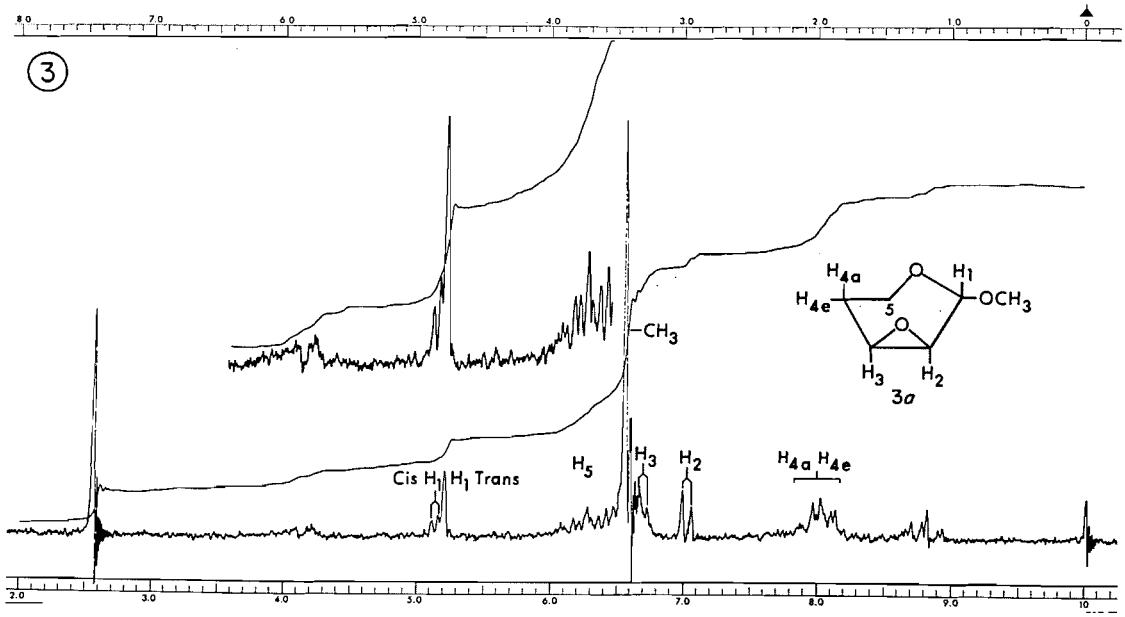

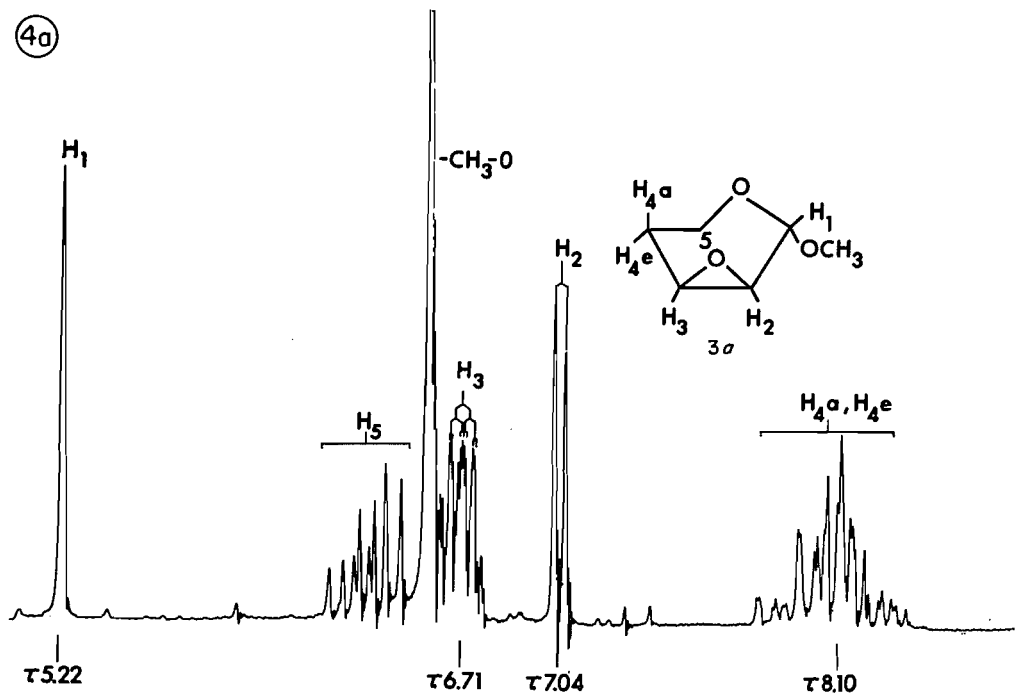

FIG. 3. The 60 MHz nuclear magnetic resonance spectrum of a *cis*, *trans* mixture of 3*a* in $CDCl_3$ as solvent.
FIG. 4*a*. The 100 MHz nuclear magnetic resonance spectrum of 3*a* in $CDCl_3$ as solvent.

Can. J. Chem. Downloaded from www.nrcresearchpress.com by 210.87.254.40 on 09/05/12
For personal use only.

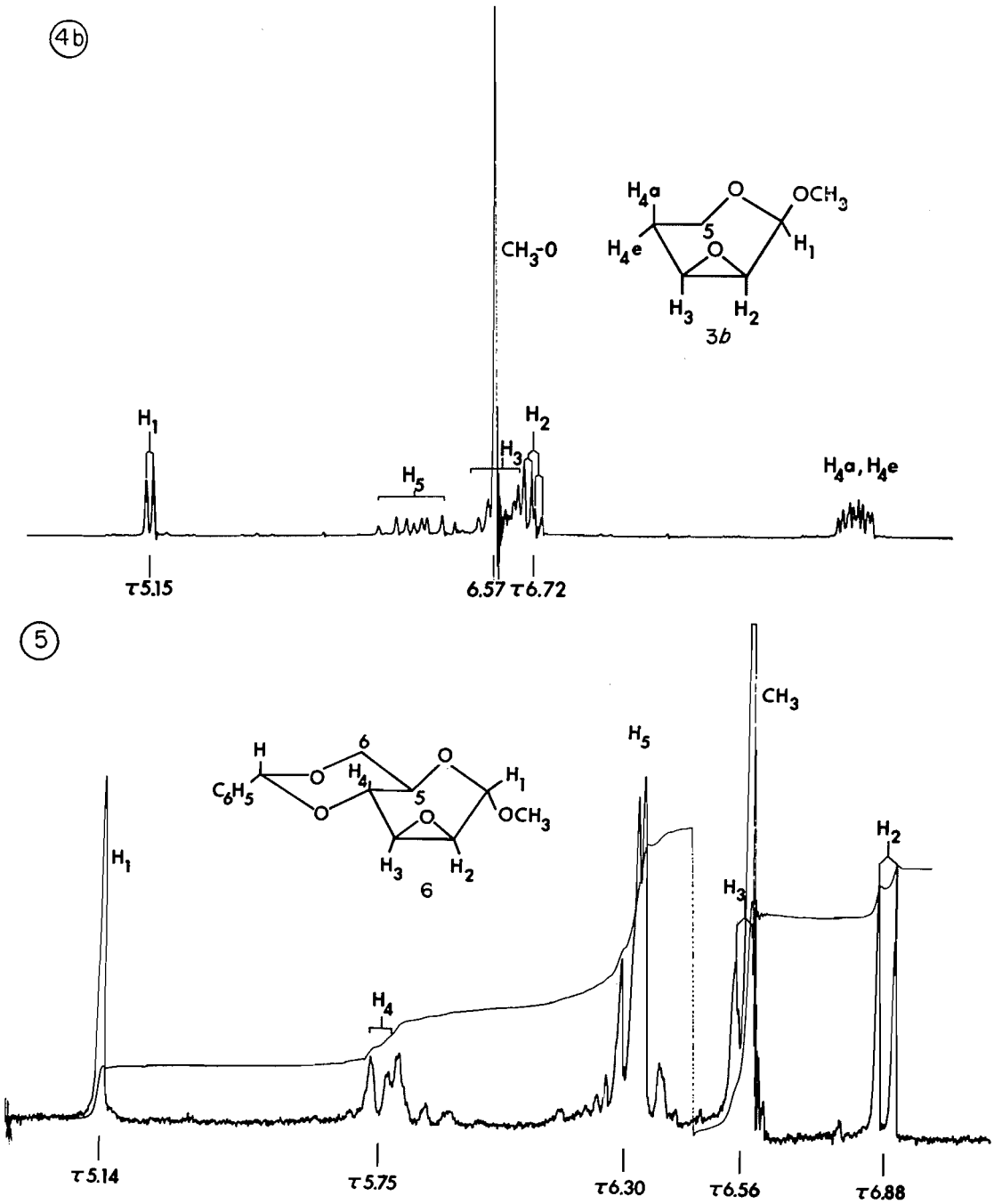

FIG. 4*b*. The 100 MHz nuclear magnetic resonance spectrum of 3*b* in $CDCl_3$ as solvent.
FIG. 5. The 100 MHz nuclear magnetic resonance spectrum of **6** in $CDCl_3$ as solvent.

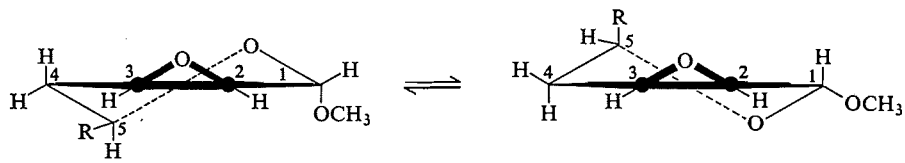

Irradiation at τ 6.56 (H-3) caused the doublet at τ 6.88 (H-2) to collapse to a singlet as well as a sharpening of the signals at ~τ 5.75 (H-4). Irradiation at ~τ 5.75 (H-4) caused a sharpening of the signal at τ 6.56 (H-3) and a marked collapse of the multiplet at τ 6.30 (H-5) but no change in the doublet at τ 6.88 (H-2).

The conformational implications of the information in Table I are interesting. The benzylidene group provides methyl 4,6-*O*-benzylidene-2,3-anhydro-α-D-mannopyranoside with a greater degree of rigidity than is found in the epoxytetrahydropyrans **3** and **4**. The methoxymethyl group of **5** would no doubt result in the existence of **5** largely in the conformer in which the methoxymethyl group is equatorial. Models show that **3** and **4** possess considerable conformational freedom between the two extremes shown below. Such mobility is associated with rotation about the C-1,C-2 and C-3,C-4 bonds with consequent change in the dihedral angle, coupling constant, and signal position (chemical shift) of the protons concerned. No doubt the values observed are time–averaged. Yet in all cases, for **3***a* and *b*, **4**, and **5**, the couplings are $J_{1,2} \sim 0$ and $J_{2,3} = 4.0$ indicating a marked similarity of their conformational equilibria. It is interesting to compare $J_{2,3} = 3.8$ Hz in methyl 4,6-*O*-benzylidene-2,3-anhydro-α-D-mannopyranoside, **6**.

Experimental

The nuclear magnetic resonance spectra were obtained with Varian A60 and HR100 spectrometers operated by Mr. Robert Swindlehurst and Mr. Glen Bigam respectively. The HR100 spectrometer was operated at the normal probe temperature of 35 °C. Tetramethylsilane was the internal reference and the solvent was $CDCl_3$ in all cases. Spin decoupling was performed using Johnson's procedure (4).

The following compounds were prepared by literature methods: *cis*- and *trans*-3,4-epoxy-2-methoxytetrahydropyran (**3***b* and **3***a*) (5), *trans*-2-*t*-butoxy-3,4-epoxytetrahydropyran (5), methyl 2,3-anhydro-4-deoxy-6-*O*-methyl-α-DL-*lyxo*-hexopyranoside,[4] and methyl 4,6-*O*-benzylidene-2,3-anhydro-α-D-mannopyranoside (6).

Acknowledgment

The authors are grateful to the National Research Council of Canada for financial assistance throughout the course of this work.

1. D. H. Buss, L. Hough, L. D. Hall, and J. F. Manville. Tetrahedron, **21**, 69 (1965).
2. J. I. Musher and E. J. Corey. Tetrahedron, **18**, 791 (1962).
3. R. U. Lemieux and J. D. Stevens. Can. J. Chem. **44**, 249 (1966).
4. L. F. Johnson. Varian Associates Technical Bulletin No. 87-100-082 (1962).
5. F. Sweet and R. K. Brown. Can. J. Chem. **46**, 707 (1968).
6. G. J. Robertson and C. F. Griffith. J. Chem. Soc. 1193 (1935).

[4]F. Sweet and R. K. Brown. To be published.

Can. J. Chem. Downloaded from www.nrcresearchpress.com by 210.87.254.40 on 09/05/12
For personal use only.

Can. J. Chem. Downloaded from www.nrcresearchpress.com by 210.87.254.42 on 09/05/12
For personal use only.

Mass spectra of alkylquinolines

P. M. Draper and D. B. MacLean
Department of Chemistry, McMaster University, Hamilton, Ontario

Received September 1, 1967

A study has been made of the fragmentation upon electron impact of monomethylquinolines, dimethylquinolines, monoethylquinolines, and monopropylquinolines. Deuterium labelled analogues of some of the alkylquinolines have been prepared and their fragmentation studied to gain insight into the mechanism of fragmentation. The fragmentation of the alkylquinolines is closely analogous to that of alkylbenzenes. Rearrangement of the molecular ion appears to precede the fragmentation process in many of the compounds studied. The fragmentation of 2- and 8-ethyl- and *n*-propylquinolines are influenced by the proximity of their alkyl side chains to the nitrogen atom.

Canadian Journal of Chemistry, **46**, 1487 (1968)

Sample *et al.* (1) have recently reported a study of the mass spectral fragmentation of alkylquinolines and isoquinolines. We have also carried out a study of alkylquinolines with the object of using mass spectrometry in the identification of degradation products from alkaloid studies, and we report here the results of our investigation.

Until the recent work, the spectra of only a few alkylquinolines had been discussed (2–5). However, the spectra of other alkylated aromatic compounds including alkylpyridines (6–8), alkylindoles (9), and alkylbenzenes (10, 11) have been discussed in some detail. Our results show that the fragmentation patterns observed for alkylpyridines and alkylbenzenes can be applied in many cases to the alkylquinolines.

Sample *et al.* (1) observed that the major fragmentation of monomethylquinolines proceeds through the sequence $M \rightarrow M{-}H \rightarrow M - (H + HCN)$. Since they found that the $M - (H + HCN)/M{-}H$ ratio was constant for the 2-, 3-, and 4-isomers, they concluded that the loss of HCN must proceed from a common intermediate, which they postulated to be the azatropylium ion **2** as shown in Scheme 1.

They noted that ion **2** might form either by rearrangement of the benzyl ion **1** or direct from the molecular ion but they were unable to differentiate between the routes since they had no deuterated methylquinolines available.

In the case of methylquinolines substituted in the benzene ring they found that the ratio $M - (H + HCN)/M{-}H$ was constant for the four isomers but much lower than that observed for the compounds substituted in the pyridine ring. They postulated two routes to these ions as shown in Scheme 2.

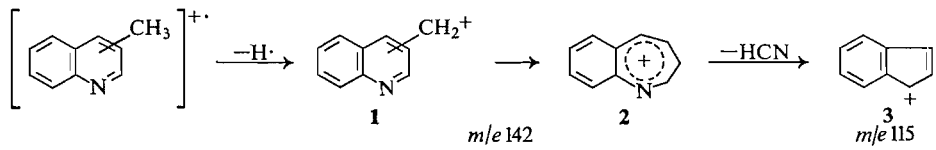

SCHEME 1

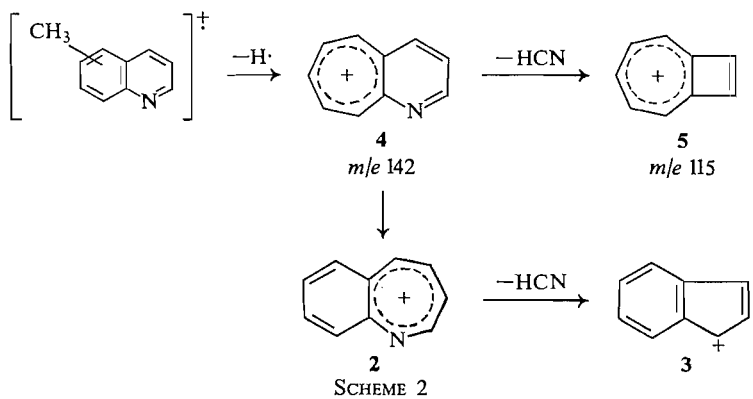

SCHEME 2

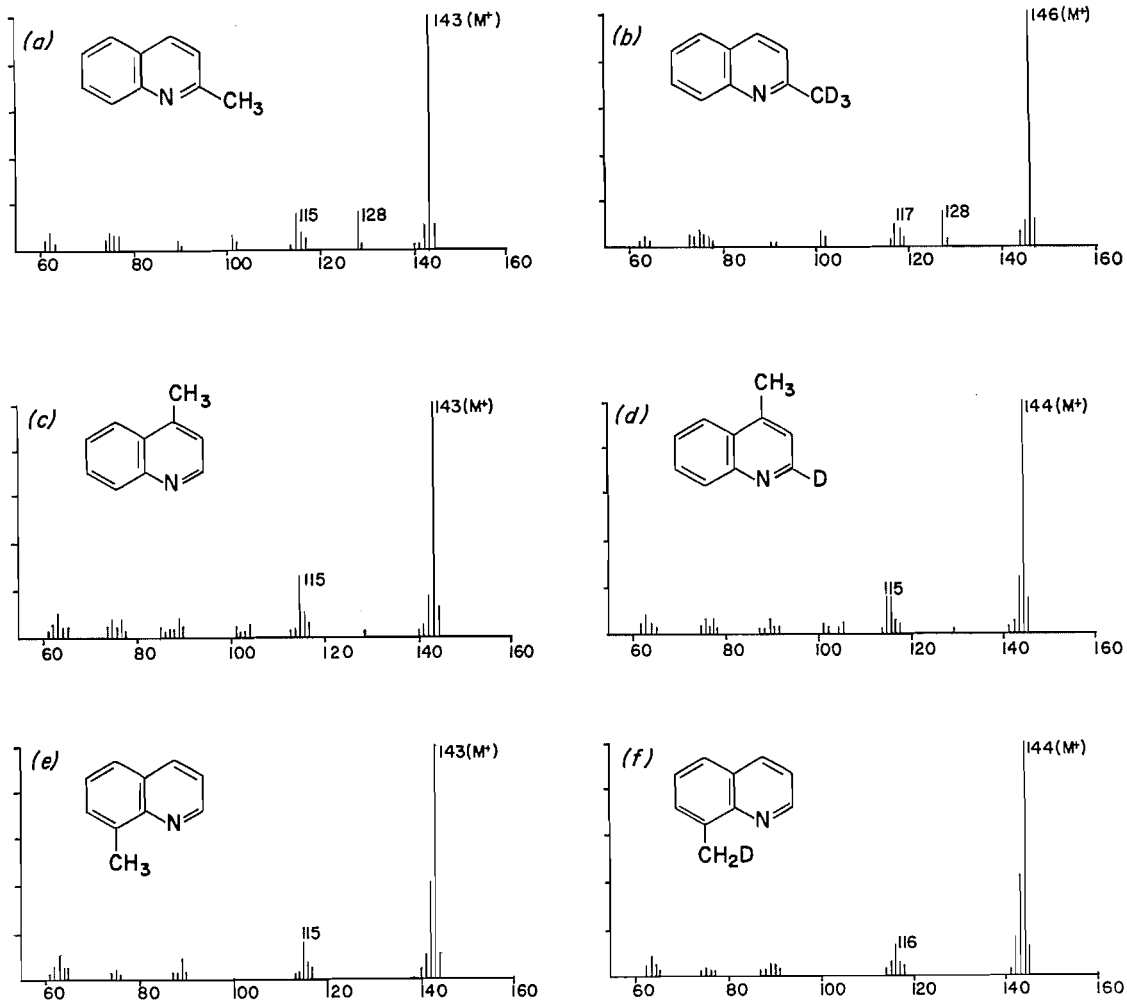

FIG. 1. Mass spectra of (*a*) 2-methylquinoline, (*b*) 2-methylquinoline-α-d_3, (*c*) 4-methylquinoline, (*d*) 4-methylquinoline-2-d_1, (*e*) 8-methylquinoline, and (*f*) 8-methylquinoline-α-d_1.

We also examined the seven monomethylquinolines obtaining results similar to those reported. In addition, we have examined the spectra of three labelled compounds, 2-methylquinoline-α-d_3, 4-methylquinoline-2-d_1, and 8-methylquinoline-α-d_1. The spectra of the three labelled compounds and their corresponding unlabelled analogues are shown in Fig. 1.

Among the monomethylquinolines the 2-methyl compound is characterized by the presence of an M — 15 ion (about 16% of the molecular ion in intensity). This feature allows 2-methylquinoline to be differentiated from other members of the series. In the deuterated analogue (Fig. 1*b*) this peak is observed at M — 18 showing that the loss of methyl proceeds without randomization of hydrogen. 2-Methylquinoline has prominent peaks at M — 1 and M — 28. In the α-d_3 analogue the peak corresponding to M — 1 in the unlabelled compound appears at M — 1 and M — 2. The relative intensities of M — 1 and M — 2 are not compatible with a benzyl ion or with a simple expansion of the pyridine ring of the quinoline system to a benzazatropylium ion. The ratio is more in accord with a random loss of H and D from the whole system. The peak appearing at M — 28 (*m/e* 115) is distributed over three masses in the labelled compound appearing

Can. J. Chem. Downloaded from www.nrcresearchpress.com by 210.87.254.42 on 09/05/12
For personal use only.

TABLE I

Mass spectra of dimethylquinolines

	M+	M−1	M−15	M−28	M−42	M−(CH$_3$ + HCN) / M−CH$_3$
2,3	100	22	12	6	25	2.1
2,4	100	14	8	5	14	1.8
2,6	100	33	9	3	10	1.1
2,7	100	26	12	4	12	1.0
2,8	100	28	10	4	10	1.0
3,4	100	38	40	10	17	0.42
3,5	100	34	22	6	8	0.36
3,6	100	34	20	6	8	0.40
3,7	100	34	20	8	10	0.50
3,8	100	30	16	4	6	0.38
4,6	100	31	16	4	6	0.38
4,8	100	30	28	6	10	0.36
5,6	100	34	86	6	8	0.09
5,7	100	40	47	5	6	0.12
5,8	100	52	34	3	4	0.12
6,7	100	38	45	5	6	0.13
6,8	100	32	34	4	4	0.12
7,8	100	54	30	10	4	0.13

at *m/e* 116, *m/e* 117, and *m/e* 118 indicating retention of all three deuterium atoms in the ion of *m/e* 118. In this region of the spectrum the undeuterated compound also shows peaks of low intensity at M − 27, emanating either from direct loss of HCN from the molecular ion or from loss of acetylene from M − H, and at M − 26 possibly through loss of C_2H_2 from the molecular ion. Calculation of the ratio of loss of HCN to DCN in the deuterated compound is impractical without a knowledge of the C and N composition of the ions in this region.

The spectrum of 4-methylquinoline-2-d_1 and its unlabelled analogue are shown in Fig. 1*d* and Fig. 1*c*, respectively. In the spectrum of 4-methylquinoline-2-d_1 it is not clear that loss of H is a random process since there is only a very small contribution to the ion of M-2 in the deuterated analogue, relative to the undeuterated sample. However, the loss of DCN from the system is not specific for the ion appearing at *m/e* 115 in the undeuterated compound and is now found at both *m/e* 115 and 116.

In Fig. 1*e* and Fig. 1*f* the spectra of 8-methylquinoline and its α-d_1 analogue are recorded. The M − 1 peak found in the undeuterated sample is now distributed over M − 1 and M − 2 in the deuterated sample. The ratio of M − 1 to M − 2 (7:1) is such that randomization of all nine hydrogens appears to occur although the possibility that it involves only the benzenoid ring hydrogens and the methyl hydrogens is not rigorously excluded. The peak appearing at *m/e* 115 in the undeuterated compound is now distributed over *m/e* 115 and 116 in the deuterated analogue with the latter making the larger contribution. Again the interpretation is rendered difficult by the presence of peaks at *m/e* 116 and 117 in the spectrum of the unlabelled sample.

The labelling experiments, therefore, suggest a rearrangement of the molecular ion prior to loss of hydrogen. Randomization of the nine hydrogens of the system appears to occur but the labelling experiments are not extensive enough at this stage of our study to propose a structure for the intermediate species. The azatropylium ion **2** is, however, a convenient representation of the M − 1 ion bearing in mind that randomization of H has occurred in its formation.

The dimethylquinolines which we have examined are recorded in Table I. The intensities of the major fragment ions are listed as well as the M − (CH$_3$ + HCN)/M—CH$_3$ ratio. Sample *et al.* recorded only the spectra of 2,3- and 2,4-dimethylquinoline. They discussed the formation of ions, M − 1, M − 28, and M − 42 in the two systems but failed to remark upon the peak at M − 15 which is present in the two compounds and which is prominent in all of the other isomers. They imply that the M − 42 ion is formed from M − 1 through loss of CH_3CN. Our results indicate that although this scheme may apply to 2,3- and 2,4-dimethylquinoline it cannot be generally applied to dimethylquinolines.

Can. J. Chem. Downloaded from www.nrcresearchpress.com by 210.87.254.42 on 09/05/12
For personal use only.

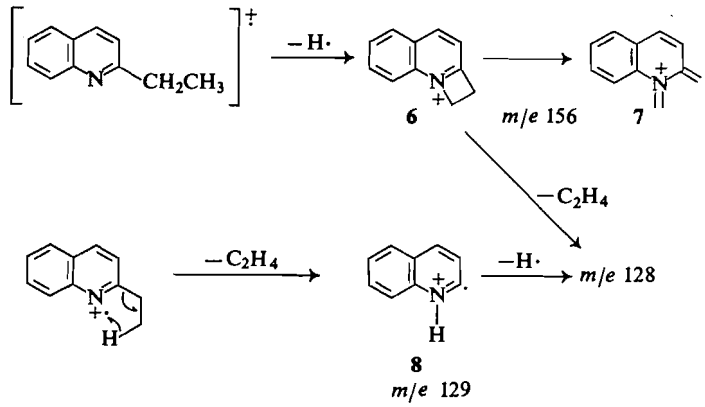

SCHEME 3

We believe that the major pathway to the M − 42 ion proceeds through the sequence M → M—CH_3 → M − (CH_3 + HCN). This sequence is supported by the presence of metastable peaks corresponding to the two transformations in all the isomers which we have examined. Moreover, the loss of acetonitrile from M—H in a single step in any but the 2-substituted dimethylquinolines would require extensive rearrangement.

A second but less general route to the M − 42 ion, namely M → M—CH_3CN → M − (CH_3CN + H), has been detected in all our 2-substituted dimethylquinolines.[1] In their spectra there is a metastable peak at 86.0 corresponding to the transformation M → M—CH_3CN and we find that the peak at M − 41 is more intense than expected of an isotope peak of M − 42.

The fact that all the dimethylquinolines show both M − 1 and M − 15 ions is reminiscent of the behavior of the xylenes (10). The loss of methyl is in accord with fragmentation of a ring-expanded molecular ion since the monomethylquinolines (2-methyl excepted) show little tendency to lose methyl. Further fragmentation of the M − 1 and M − 15 ions seems to proceed through loss of HCN in all cases.

Examination of the M − (CH_3 + HCN)/M—CH_3 ratios in Table I shows that the dimethylquinolines can be divided roughly into three groups in order of decreasing ratios, namely (*i*) 2-substituted dimethylquinolines, (*ii*) 3,4-dimethylquinoline and dimethylquinolines with a methyl group in each ring but excluding those in (*i*), and (*iii*) dimethylquinolines which have both methyl groups in the benzene ring. The order parallels that observed with the monomethylquinolines where the M − 1 ion formed from methylquinolines with a substituent in the pyridine ring shows a much greater tendency to eliminate HCN than the M − 1 ion formed from methylquinolines with the substituent in the benzene ring. The higher ratios in the case of 2,6-, 2,7-, and 2,8-dimethylquinoline relative to other dimethylquinolines with a methyl group in each ring may be a consequence of a significant contribution to the M − 42 ion by the alternative pathways discussed previously. The very high values observed for the 2,3- and 2,4-isomers may also be caused by the same factors coupled with a generally lower tendency of these two compounds, relative to other isomers, to undergo rearrangement and lose a methyl group.

There is still no satisfactory explanation why the M − 15 ions from the three groups of dimethylquinolines show such different tendencies to lose HCN. Similarly there is no satisfactory explanation for the difference observed between the two groups of monomethylquinolines. Labelling studies on the dimethylquinolines and further studies with the monomethyl compounds may help to resolve these problems.

Of the ethylquinolines, only 2- and 7-ethylquinoline were examined previously (1). It was noted that loss of H and CH_3 are the important fragmentations of the ethylquinolines and that the relative importance of these processes varies with the position of the substituent. The origin of

[1]Loss of CH_3CN from a molecular ion has recently been reported in two related systems. See W. H. Paudler and T. J. Kress, J. Org. Chem. **32**, 2616 (1967) and T. J. Batterham, A. C. K. Triffett, and J. A. Wunderlich, J. Chem. Soc. (B), (9), 892 (1967).

Can. J. Chem. Downloaded from www.nrcresearchpress.com by 210.87.254.42 on 09/05/12
For personal use only.

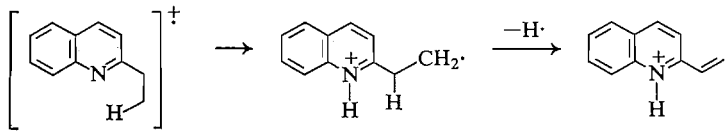

9 10
m/e 156

SCHEME 4

the M — 1, M — 28, and M — 29 ions found in the spectrum of 2-ethylquinoline was discussed and a mechanism proposed for their formation (Scheme 3). It was pointed out that the M — 29 ion may form by loss of hydrogen from **8** or by loss of C_2H_4 from **6** but a metastable peak corresponding to the pathway M — 1 → M — 29 was observed.

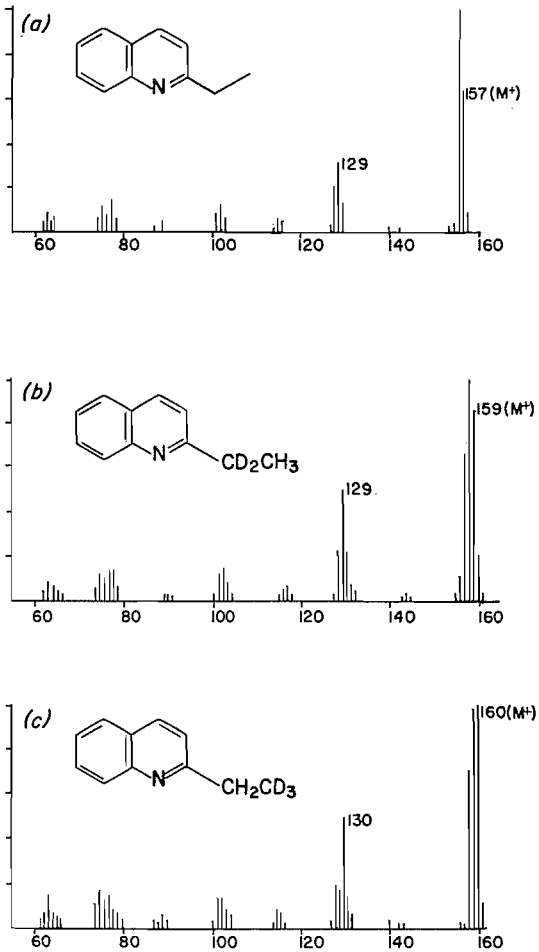

FIG. 2. Mass spectra of (*a*) 2-ethylquinoline, (*b*) 2-ethylquinoline-α-d_2, and (*c*) 2-ethylquinoline-β-d_3.

We examined the spectra of five ethylquinolines and three deuterated ethylquinolines and found features in their fragmentation which escaped the earlier workers. The spectra of 2-ethylquinoline, 2-ethylquinoline-α-d_2, and 2-ethylquinoline-β-d_3 are recorded in Fig. 2*a*, *b*, and *c*, respectively. The spectra reveal that hydrogen is lost from both the α- and β-carbons in the formation of the M — 1 ion. Calculations based on the spectra of the deuterated compounds show that approximately 40% of the hydrogen lost originates in the methyl group and 40% in the methylene group. The remainder may be the result of a random loss from the nucleus or there may be an isotope effect favoring the loss of H. Examination of the spectrum of the α-β-d_5 compound would be required to determine if H were lost from the nucleus. Scheme 3 provides a satisfactory representation of hydrogen loss from the β-carbon. To account for hydrogen loss from the α-position we propose a second independent mechanism in which the molecular ion rearranges with β-H transfer to nitrogen, ion **9**, followed by elimination of α-hydrogen yielding ion **10** (Scheme 4).

Ring expansion followed by loss of H is an alternative mechanism for loss of the α-hydrogen. We favor the mechanism of Scheme 4, however, because there is not an appreciable peak at M — 15 expected from a ring expanded molecular ion (as observed in the spectra of 3-, 4-, and 6-ethylquinoline). Moreover, a higher retention of deuterium in the spectrum of 2-ethylquinoline-α-d_2 would be expected if ring expansion had occurred.

Our labelling experiments show that ion **8** is derived from **9** through loss of ethylene. In both the α-d_2 and β-d_3 compound the M — 28 peak observed in the undeuterated sample is shifted to M — 30. The M — 29 ion in the unlabelled compound may form by loss of C_2H_4 from ion **6**, by loss of H from M — 28 (ion **8**) or by α-elimination of the ethyl group (by analogy with loss of

Can. J. Chem. Downloaded from www.nrcresearchpress.com by 210.87.254.42 on 09/05/12
For personal use only.

Can. J. Chem. Downloaded from www.nrcresearchpress.com by 210.87.254.42 on 09/05/12
For personal use only.

methyl from 2-methylquinoline). Any one of these mechanisms is compatible with the spectra of ethylquinoline and ethylquinoline-α-d_2. For the β-d_3 analogue, however, peaks are present at both M — 31 and M — 32. The M — 32 ion is expected for α-cleavage or for loss of $CD_2{=}CH_2$ from ion **6**. The M — 31 peak suggests a major contribution from the pathway in which hydrogen is lost in a random fashion from ion **8**.

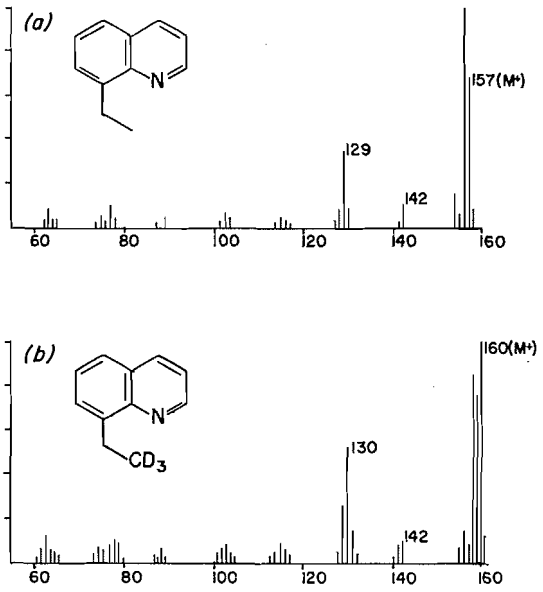

FIG. 3. Mass spectra of (*a*) 8-ethylquinoline and (*b*) 8-ethylquinoline-β-d_3.

The spectra of 8-ethylquinoline and 8-ethylquinoline-β-d_3 are shown in Fig. 3*a* and Fig. 3*b* respectively. The spectrum of 8-ethylquinoline resembles that of 2-ethylquinoline but may be differentiated from it by virtue of a much stronger M — 15 ion. The situation resembles that of the methoxyquinolines where the 2- and 8-isomers showed a fragmentation distinctly different from the other isomers (12). The major fragment ions are observed at M — 1 and M — 28. The labelling experiments show that loss of H from the CH_3 group accounts for approximately 55% of the M — 1 ion, which may be formulated as ion **15**. The remainder, by analogy with the 2-isomer, may be derived from the α-carbon through the sequence **11** → **12** → **14**, or by ring expansion followed by loss of hydrogen. The M — 28 ion, **13**, seems to be derived from the rearranged molecular ion **12** through loss of ethylene since there is a metastable peak corresponding to the transition 157 → 129 and since the M — 28 peak in the undeuterated compound is shifted almost quantitatively to M — 30 in the deuterated compound. These fragmentations are outlined in Scheme 5.

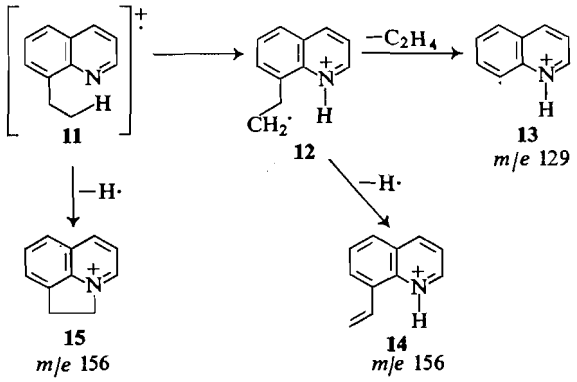

SCHEME 5

The loss of methyl yielding the ion M — 15 is specific since the peak is quantitatively shifted to M — 18 in the β-d_3 analogue. An anomaly in the spectrum of the deuterated compound for which we offer no explanation is the relatively intense peak at M — 31.

The behavior of 8-ethylquinoline on electron impact is different from the 6-isomer, Fig. 4*a*, which we have examined, and the 7-isomer, examined earlier (1). In the latter compounds the loss of 15 mu accounts for the major fragment ion in the spectrum while loss of H and ethylene are relatively less important processes. The 6- and 7-ethylquinolines thus resemble the behavior of ethylbenzene (10) and from our studies on the dimethylquinolines it seems likely that ring expansion occurs prior to the elimination of the methyl group. The 3- and 4-ethylquinolines, Fig. 4*b* and Fig. 4*c*, respectively, exhibit a pattern similar to that of the 6- and 7-isomers in that the M — 15 ion is the most intense fragment ion in the spectrum. They may be differentiated from the 6- and 7-isomers, however, by virtue of a much more intense M — 42 ion. Thus, the elimination of HCN from the M—15 ion is a much more favorable process when the ethyl group is in the 3- and 4-position than when it is in the 6- or 7-position. This behavior is in accord with the behavior of the methylquinolines and the dimethylquinolines. The

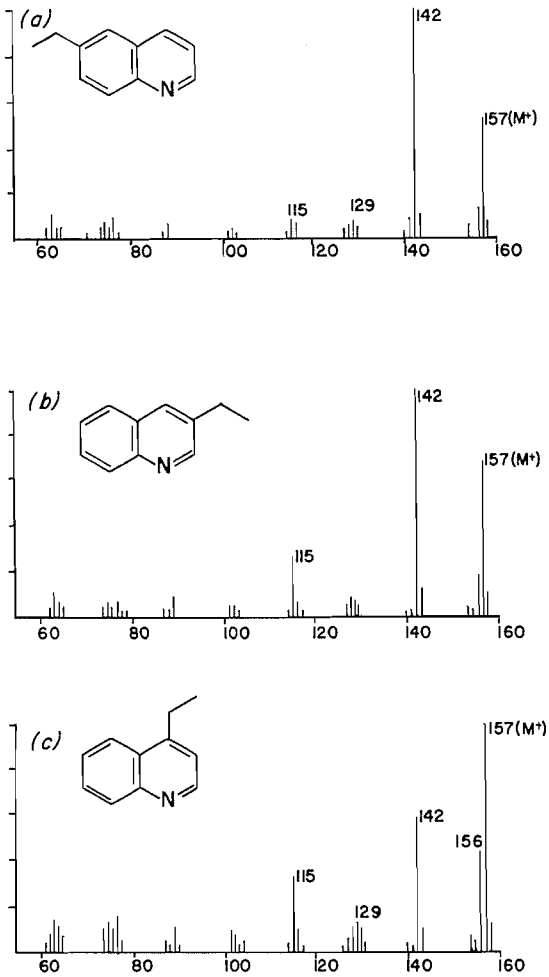

FIG. 4. Mass spectra of (*a*) 6-ethylquinoline, (*b*) 3-ethylquinoline, and (*c*) 4-ethylquinoline.

more intense M − 1 ion in the 4-isomer relative to that observed in the 3-, 6-, or 7-isomers may be a consequence of radical stabilization by cyclization to the 5-position as suggested (1) for other 4-substituted alkylquinolines. We have not, however, carried out labelling experiments to test this hypothesis.

In Table II the metastable peaks observed in the spectra of the ethylquinolines are recorded. They support the mechanisms which we have proposed for the fragmentation of these compounds.

In summary, it appears that 2- and 8-ethylquinoline may be easily differentiated from one another and from the other isomers by mass spectrometry. The remaining isomers fragment

TABLE II

Metastable ions observed in spectra of ethylquinolines

Transformation	Calculated	Observed in the spectra of
M → M−1	155.0	2-, 3-, 4-, 6-, 8-
M → M−2		2-α-d_2, 2-β-d_3, 8-β-d_3
M → M−15	128.4	3-, 4-, 6-
M → M−28	106.0	8-
M → M−30	105.6	2-β-d_3
M−1 → M−29	105.0	2-, 8-
M−2 → M−32	103.6	2-β-d_3
M−15 → M−42	93.1	3-, 4-, 6-, 8-
M−29 → M−56	79.7	2-, 8-

in a similar manner but show sufficient differences from one another in their spectra that mass spectrometry alone should be an adequate method for their identification.

β-Cleavage accompanied by hydrogen transfer (Scheme 6) has been shown to dominate the fragmentation of the 2-*n*-propyl, 2-*n*-butyl, and 2-isobutylquinolines (1) and to play a role in the fragmentation of 6-, 7-, and 8-*n*-propylquinolines.

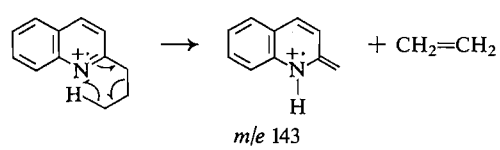

SCHEME 6

In this study we examined the spectra of 2-, 3-, 4-, 6-, and 8-*n*-propylquinolines, 2-*n*-propylquinoline-γ-d_3, and 8-*n*-propylquinoline-γ-d_3. Our results and our interpretation of the fragmentation of 2- and 6-*n*-propylquinolines are in agreement with those already reported and need not be discussed.

β-Cleavage is the most important fragmentation pathway of 3-*n*-propylquinoline (Fig. 5*a*), and again loss of HCN from the *m/e* 142 ion is favored in propylquinolines substituted in the pyridine ring over those substituted in the benzene ring. β-Cleavage with hydrogen rearrangement is negligible in 3-*n*-propylquinoline.

The spectrum of 4-*n*-propylquinoline as shown in Fig. 5*b*, is dominated by peaks originating from β-cleavage with hydrogen rearrangement (ion **16**) and by simple β-cleavage. The latter results in the base peak in the spectrum of 4-*n*-propylquinoline. Peaks at M − 15, ion **17**, and M − 17, ion **18**, may be due to stabilization of the

Can. J. Chem. Downloaded from www.nrcresearchpress.com by 210.87.254.42 on 09/05/12
For personal use only.

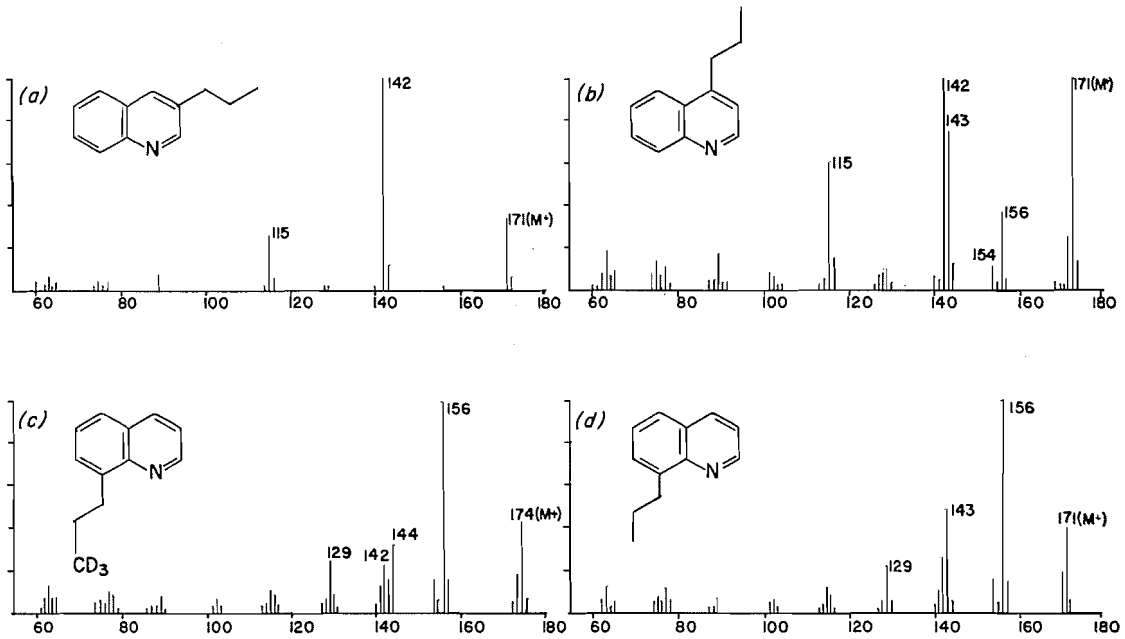

FIG. 5. Mass spectra of (*a*) 3-*n*-propylquinoline, (*b*) 4-*n*-propylquinoline, (*c*) 8-*n*-propylquinoline-γ-d_3, and (*d*) 8-*n*-propylquinoline.

resulting fragments by cyclization to the 5-position as shown in Scheme 7, but we have not carried out labelling experiments to substantiate this hypothesis. This scheme is analogous to that proposed in the fragmentation of 4-isobutylquinoline (1).

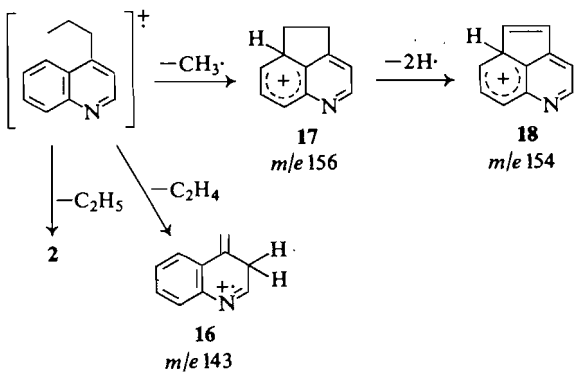

SCHEME 7

Our spectrum of 8-*n*-propylquinoline, as shown in Fig. 5*d*, is similar to that recorded earlier but we have been able to clarify the fragmentation through examination of the γ-d_3 analogue, Fig. 5*c*. The base peak in the spectrum of the undeuterated compound arises from loss of CH_3 from the molecular ion. The peak is shifted to M − 18 in the γ-d_3 isomer showing that the terminal methyl is lost, and that the resulting fragment is probably stabilized by the nitrogen as suggested earlier (1). Our labelling experiments show that only about 20–25% of the hydrogen loss originates from the terminal carbon in formation of the M − 1 ion. Likely alternatives are loss of α- and β-hydrogens (as in 2- and 8-ethylquinolines) resulting in fragments **19** and **20**, respectively, as shown in Scheme 8.

The peak at *m/e* 143 is partially shifted (some scrambling) to *m/e* 144 in the labelled compound indicating transfer of a terminal hydrogen to nitrogen and loss of ethylene. The peak at *m/e* 142 in the unlabelled compound remains at *m/e* 142 in the labelled analogue and is probably caused by a simple β-cleavage. The peak at *m/e* 129 may originate from transfer of a β-hydrogen to nitrogen followed by loss of propylene, by analogy with the rearrangement involving expulsion of ethylene observed in the spectra of 2- and 8-ethylquinolines.

The transformations which we have discussed for the *n*-propylquinolines are supported by the presence of metastable peaks in their spectra. These are recorded in Table III.

Can. J. Chem. Downloaded from www.nrcresearchpress.com by 210.87.254.42 on 09/05/12
For personal use only.

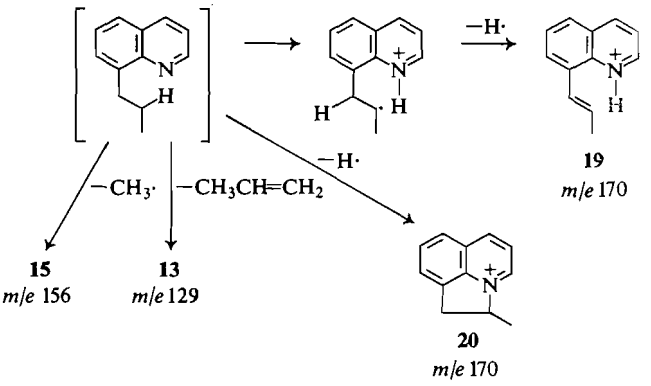

SCHEME 8

TABLE III

Metastable ions observed in spectra of propylquinolines

Transformation	Calculated	Observed in the spectra of
M → M−1	169.0	4-, 8-*n*-propyl
M → M−15	142.3	2-isopropyl
M → M−28	119.6	2-, 4-*n*-propyl, 2-isopropyl
M → M−29	117.9	3-, 4-, 6-*n*-propyl
M−15 → M−43	105.0	2-isopropyl
M−29 → M−56	93.1	2-, 3-, 4-, 6-, 8-*n*-propyl

Finally we have determined the spectra of 2-isopropylquinoline, 2-isopropylquinoline-β-d_3, and 2-isopropylquinoline-β-d_6 (Fig. 6*a*, *b*, and *c*, respectively). The spectra of 2-isopropylquinoline and 2-*n*-propylquinoline are readily differentiated by the relative intensities of peaks at M^+, M − 15, and M − 28. The spectrum of 2-isopropylquinoline-β-d_3 (Fig. 6*b*) shows that the M − 15 peak arises from loss of methyl and that CD_3 is lost more readily than CH_3.

Loss of 28 mu is a minor process in the fragmentation of 2-isopropylquinoline and the fragmentation mechanism is unknown. The spectrum of the β-d_6 isomer indicates a loss of C_2HD_3, while the spectrum of the β-d_3 isomer suggests a randomization of the 6 terminal hydrogens in the loss of the two-carbon unit. Results of our labelling experiments show that the origin of peaks at M − 1, M − 42, and M − 43 can be accounted for by mechanisms similar to those proposed for peaks at M − 1, M − 28, and M − 29 respectively in 2-ethylquinoline (Scheme 3).

In conclusion mass spectrometry appears to be a useful tool for determining the position and extent of substitution of the quinoline nucleus. In the monomethyl series those substituted in the benzene ring can be differentiated from those substituted in the pyridine ring, while in the dimethylquinoline series an unknown can be placed in one of three groups according to the M − (CH_3 + HCN)/M—CH_3 ratio. As the length of the alkyl chain increases the position of

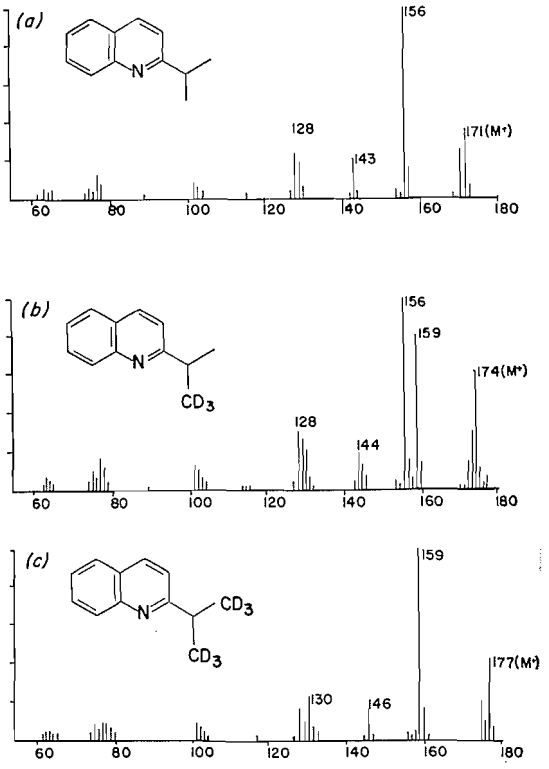

FIG. 6. Mass spectra of (*a*) 2-isopropylquinoline, (*b*) 2-isopropylquinoline-β-d_3, and (*c*) 2-isopropylquinoline-β-d_6.

Can. J. Chem. Downloaded from www.nrcresearchpress.com by 210.87.254.42 on 09/05/12
For personal use only.

substitution can be determined with greater certainty although the 6- and 7-isomers (and probably the 5- also) show similar spectra.

Experimental

Apparatus, Methods and Materials

Mass spectra were determined on a Hitachi Perkin–Elmer RMU-6A mass spectrometer at an ionizing potential of 80 eV and an ionizing current of 50 μA. Samples were introduced through an all-glass inlet system maintained at 200 °C. Spectra are plotted in terms of relative abundance, with the most intense peak (base peak) taken as 100%. Only peaks equal to or greater than 2% of the base peak are recorded.

All samples for mass spectrometry were purified by gas–liquid chromatography (g.l.c.) on a 6 ft column of 20% apiezon M on Celite. The column temperature was maintained at 180 to 220 °C depending on the volatility of the material.

CD_3I (99 atom% D) and CD_3CH_2Br (98 atom% D) were obtained from Merck, Sharp and Dohme of Canada Ltd.

The 4-, 6-, 7-, and 8-methylquinolines and 4,6-dimethylquinoline were obtained commercially.

5-Methylquinoline and 2,7-, 2,8-, 3,5-, 3,6-, 3,7-, 3,8-, 4,8-, and 5,6-dimethylquinolines were obtained from Dr. W. A. Ayer of the University of Alberta.

Nuclear magnetic resonance (n.m.r.) spectra were determined in $CDCl_3$ solution on a Varian A-60 spectrometer. Chemical shifts are expressed in parts per million (δ) from tetramethylsilane used as an internal standard.

Preparation of Alkylquinolines

Many of the alkylquinolines used in this study were prepared by procedures already described in the literature. Table IV lists the quinolines which we have prepared by previously described methods and provides the pertinent references to their preparation. In some cases picrates were prepared. The melting points of the picrates which we recorded are given, with the values quoted in the literature given in brackets.

2-Methylquinoline-α-d_3

The labelled 2-methylquinoline was prepared from *N*-ethoxyquinolinium iodide and CD_3MgI by the method of Červinka *et al.* (23). The composition of the deuterated sample determined by low voltage mass spectrometry was $d_0 = 0.5\%$, $d_1 = 1\%$, $d_2 = 4\%$, and $d_3 = 94.5\%$. An n.m.r. singlet at δ 2.78 (3H) in the undeuterated compound was absent in the labelled compound.

4-Methylquinoline-2-d

To a stirred suspension of 100 mg $LiAlD_4$ in anhydrous tetrahydrofuran was added 215 mg lepidine in tetrahydrofuran. The reaction was heated under reflux for 24 h and excess $LiAlD_4$ destroyed with water. This process was repeated twice and the product isolated and purified by chromatography over alumina for n.m.r. analysis. The composition of the deuterated sample, determined by low voltage mass spectrometry was $d_0 = 8\%$, $d_1 = 90\%$, and $d_2 = 2\%$. The n.m.r. spectrum of the undeuterated compound showed a pair of doublets at 7.36 (1H) and δ 9.04 (1H), ($J = 4.5$ c.p.s.) assigned to the protons at C-3 and C-2 respectively, while the labelled compound showed a singlet at δ 7.39.

TABLE IV

Preparation of alkylquinolines

Alkylquinoline	Melting point picrate (°C)		Reference
2-methyl	193.5–195.5	(195)	13
3-methyl	187–190	(190)	14
2,3-dimethyl	229–232	(235)	15
2,4-dimethyl	194–196	(196)	16
2,6-dimethyl	189–190	(191)	13*
3,4-dimethyl	219–221	(221)	14
2-ethyl	151–153	(148)	17
2-ethyl-β-d_3	— —	—	17†‡
2-*n*-propyl	163–164.5	(159)	17
2-*n*-propyl-γ-d_3	— —	—	17§‖
4-ethyl	191–192	(200)	18
4-*n*-propyl	204–207	(205, 207)	18
6-ethyl	205–206	(205–206)	19
6-*n*-propyl	173.5–174.5	(171–172)	19¶
8-ethyl**	146–149	(146)	20
8-*n*-propyl	138–140	(142)	19††
5,7-dimethyl	243–245	(249)	14‡‡
5,8-dimethyl	180–182	(186)	14‡‡
6,7-dimethyl	273–275	(278)	14‡‡
6,8-dimethyl	223–225	(230)	14‡‡
7,8-dimethyl	196–198	(198)	14‡‡

*The procedure described for the preparation of 2-methylquinoline was used except that *p*-toluidine was substituted for aniline.
†CD_3I was used instead of CH_3I.
‡Low voltage measurements showed the composition of the deuterated sample to be $d_2 = 3\%$; $d_3 = 97\%$.
§CD_3CH_2I was used instead of CH_3CH_2I.
‖Low voltage measurements showed the composition of the deuterated sample to be $d_1 = 2\%$; $d_2 = 5\%$; $d_3 = 93\%$.
¶*p*-Propylaniline was prepared by the method of Long and Schofield (21).
**Nitrate.
††*o*-Propylaniline was prepared by the method of W. P. Neumann (22).
‡‡These quinolines were prepared by J. K. Tandan of this laboratory.

8-Methylquinoline-α-d_1

A solution of 300 mg 8-bromomethylquinoline (24) in 1.5 ml CH_3CO_2D (25) was added dropwise to a stirred mixture of 130 mg zinc metal (granular), 0.8 ml D_2O, and 1.0 ml CH_3CO_2D. The reaction mixture was stirred overnight at room temperature and then refluxed for 1h. The reaction was cooled, water added, and the mixture basified with NH_3 and extracted with ether. The composition of the product determined by low voltage mass spectrometry was $d_0 = 5.5\%$ and $d_1 = 94.5\%$.

2-Ethylquinoline-α-d_2

2-Ethylquinoline (1.5 mmoles) in anhydrous ether was added to 1.4 ml of a 1.6 *N* hexane solution of *n*-butyllithium. One equivalent of D_2O was added with stirring after the reaction mixture had been heated for 0.75 h under nitrogen.

This process was repeated an additional five times. The reaction mixture was poured into D_2O, acidified, and washed with ether. The acid layer was then basified and extracted with ether. The ether layer was dried over

Can. J. Chem. Downloaded from www.nrcresearchpress.com by 210.87.254.42 on 09/05/12
For personal use only.

Can. J. Chem. Downloaded from www.nrcresearchpress.com by 210.87.254.42 on 09/05/12
For personal use only.

Na_2SO_4 and the ether evaporated. The product was purified by chromatography over alumina (g.l.c. caused back exchange). The composition determined by low voltage mass spectrometry was $d_0 = 2.7\%$, $d_1 = 15.2\%$, $d_2 = 69.0\%$, $d_3 = 11.7\%$, and $d_4 = 1.4\%$.

3-Ethylquinoline and 3-n-Propylquinoline

Ethyl ethylmalonanilate (26) (2.5 g) was heated under reflux with 12.5 g phosphorus oxychloride for 10 h. The mixture was cooled, poured on crushed ice, basified and extracted with ether. The resulting 2,4-dichloro-3-ethylquinoline was converted to 3-ethylquinoline by heating with 15 g of tin metal and 55 ml hydrochloric acid for 1 h. The yield of 3-ethylquinoline was 0.46 g (27% based on the ethyl ethylmalonanilate); picrate m.p. 197–198.5 °C (lit. 199 °C (27)).

3-*n*-Propylquinoline was prepared in a similar manner from ethyl *n*-propylmalonanilate. The yield was 12.5% based on ethyl *n*-propylmalonanilate; picrate m.p. 168–169 °C (lit. 174–175 °C (28)).

8-Ethylquinoline-β-d-3 and 8-n-Propylquinoline-γ-d_3

An ether solution of 8-bromomethylquinoline (24) (0.015 mole) was added dropwise to an ether solution of CD_3MgI (0.03 mole). The reaction mixture was heated with stirring for about 45 min. The excess Grignard reagent was destroyed and the crude reaction product isolated by conventional procedures. 8-Ethylquinoline-β-d_3 was separated from the crude product by g.l.c. The composition determined by low voltage mass spectrometry was $d_1 = 0.5\%$, $d_2 = 2\%$, and $d_3 = 97.5\%$.

8-*n*-Propylquinoline-γ-d_3 was prepared in a similar manner; CD_3CH_2Br was substituted for CD_3I in the preparation of the Grignard solution. The composition determined by low voltage mass spectrometry was $d_2 = 5\%$ and $d_3 = 95\%$. Yields were low in both preparations.

2-Isopropylquinoline

Quinaldine was treated with an equivalent of *n*-butyllithium followed by an equivalent of methyl iodide (17). A second equivalent of *n*-butyllithium and methyl iodide was then added to the reaction. The reaction was quenched by pouring into water and the work-up was similar to that described for 2-ethylquinoline-α-d_2. The picrate melted at 154–155 °C (lit. 155–157 °C (29)). The n.m.r. spectrum had a doublet at δ 1.43 and a septet at δ 3.39 ($J = 7.2$ c.p.s.).

2-Isopropylquinoline-β-d_3

The procedure used was that described above except that CD_3I was substituted for the second equivalent of CH_3I. The composition of the product determined by low voltage mass spectrometry was $d_0 = 1.5\%$, $d_1 = 1\%$, $d_2 = 2.5\%$, $d_3 = 80\%$, $d_4 = 3.5\%$, $d_5 = 2.5\%$, and $d_6 = 9\%$.

2-Isopropylquinoline-β-d_6

The procedure used was that described above except that CD_3I was substituted for CH_3I. The composition of the product determined by low voltage mass spectrometry was $d_3 = 1\%$, $d_4 = 1\%$, $d_5 = 2.5\%$, $d_6 = 91\%$, $d_7 = 1\%$, and $d_8 = 3.5\%$.

Acknowledgments

We thank Dr. W. A. Ayer for providing samples of many of the dimethylquinolines used in this study. The award of a bursary and studentships by the National Research Council of Canada to P. M. Draper is gratefully acknowledged. This work was supported through a grant from the National Research Council of Canada.

1. S. D. Sample, D. A. Lightner, O. Buchardt, and C. Djerassi. J. Org. Chem. **32**, 997 (1967).
2. R. W. Sauer, F. W. Melpolder, and R. A. Brown. Ind. Eng. Chem. **44**, 2606 (1952).
3. C. LaLau. Anal. Chim. Acta, **22**, 239 (1960).
4. H. Budzikiewicz, C. Djerassi, and D. H. Williams. Interpretation of mass spectra of organic compounds. Holden-Day, Inc., San Francisco. 1964. p. 257.
5. W. A. Ayer, T. E. Habgood, V. Deulofeu, and H. R. Juliani. Tetrahedron, **21**, 2169 (1965).
6. K. Biemann. Mass spectrometry: organic chemical applications. McGraw-Hill Book Co., Inc., New York. 1962. pp. 130, 134–135, 152.
7. R. A. Khmel'nitskii, P. B. Terent'ev, A. A. Polyakova, and A. N. Kost. Dokl. Akad. Nauk SSSR, **167**, 1066 (1966); Chem. Abstr. **65**, 5980 (1966).
8. G. Spiteller. Massenspectrometrische Strukturanalyse organischer Verbindungen. Verlag Chemie, Weinheim. 1966. p. 172.
9. J. H. Beynon and A. E. Williams. Appl. Spectry. **13**, 101 (1959); **14**, 27 (1960).
10. H. M. Grubb and S. Meyerson. *In* Mass spectrometry of organic ions. *Edited by* F. W. McLafferty. Academic Press Inc., New York. 1963. Chap. 10.
11. F. Meyer and A. G. Harrison. J. Am. Chem. Soc. **86**, 4757 (1964).
12. D. M. Clugston and D. B. MacLean. Can. J. Chem. **44**, 781 (1966).
13. W. H. Mills, J. E. G. Harris, and H. Lambourne. J. Chem. Soc. **119**, 1294 (1921).
14. R. H. F. Manske, L. Marion, and F. Leger. Can. J. Res. **B20**, 133 (1942).
15. S. G. P. Plant and R. J. Rosser. J. Chem. Soc. 1864 (1929).
16. A. Combes. Compt. Rend. **106**, 142 (1888).
17. K. Ziegler and H. Zeiser. Ann. **485**, 174 (1931).
18. A. E. Tchitchibabine. Bull. Soc. Chim. France, [5], **3**, 1607 (1936).
19. R. Long and K. Schofield. J. Chem. Soc. 2350 (1953).
20. R. A. Glenn and J. R. Bailey. J. Am. Chem. Soc. **63**, 639 (1941).
21. R. Long and K. Schofield. J. Chem. Soc. 2066 (1953).
22. W P. Neumann. Ann. **618**, 90 (1958).
23. O. Červinka, A. Fabryova, and L. Matouchova. Collection Czech. Chem. Commun. **28**, 535 (1963).
24. B. Prijs, R. Gall, R. Hinderling, and H. Erlenmeyer. Helv. Chim. Acta, **37**, 90 (1954).
25. M. J. S. Dewar and R. C. Fahey. J. Am. Chem. Soc. **85**, 2245 (1963).
26. F. D. Chattaway and J. M. D. Olmsted. J. Chem. Soc. **97**, 938 (1910).
27. W. P. Utermohlen. J. Org. Chem. **8**, 544 (1943).
28. R. W. Brown and G. Dougherty. J. Am. Chem. Soc. **69**, 2232 (1947).
29. W. Koenigs. Ber. **32**, 223 (1899).

Can. J. Chem. Downloaded from www.nrcresearchpress.com by 210.87.254.42 on 09/05/12
For personal use only.

Mass spectra of tetrahydroquinolines

P. M. DRAPER AND D. B. MACLEAN
Department of Chemistry, McMaster University, Hamilton, Ontario

Received September 25, 1967

The mass spectra of 1,2,3,4-tetrahydroquinoline and 5,6,7,8-tetrahydroquinoline have been recorded. The spectra of the 1-d_1, 2,2-d_2, 3,3-d_2, and 4,4-d_2 analogues of 1,2,3,4-tetrahydroquinoline, and the spectra of the 5-d_1, 6,6-d_2, and 8,8-d_2 analogues of 5,6,7,8-tetrahydroquinoline have aided in the interpretation of the fragmentation mechanisms. The spectra of both isomers are characterized by fragment ions at M − 1, M − 15, and M − 16 while the 5,6,7,8-isomer has an additional peak at M − 28. The spectra of 2-, 3-, 4-, and 6-methyl-1,2,3,4-tetrahydroquinolines have also been examined. Substitution of a hydrogen by a methyl group in the 2- and 4-positions results in an intense M − 15 peak, and substitution in the 3-position results in a peak at M − 29. The main features of these spectra can be predicted from the proposed fragmentation pathways of the parent tetrahydroquinoline.

Canadian Journal of Chemistry, **46**, 1499 (1968)

In a recent paper we reported on the mass spectrometric fragmentation of alkylquinolines with the object of using mass spectrometry for identification of degradation products in alkaloid studies (1). We have also studied the mass spectra of some tetrahydroquinolines for the same reason, and we report here the results of our study.

Although the spectra of tetrahydroquinolines have not been reported, the spectra of many other saturated heterocycles including piperidine (2–4), the piperidine alkaloids (5), and oxygen heterocycles (6, 7) have been studied in detail. In addition, the spectra of tetrahydronaphthalenes (8, 9) and tetrahydroisoquinoline (10) have been reported. It might be expected that the spectra of 1,2,3,4-tetrahydroquinolines would show fragmentation pathways similar to the piperidines, and that the spectrum of 5,6,7,8-tetrahydroquinoline would be similar to that of tetrahydronaphthalene. Our results show that similarities as well as differences exist.

The mass spectra of 1,2,3,4-tetrahydroquinoline and its 1-d_1, 2,2-d_2, 3,3-d_2, and 4,4-d_2 analogues are shown in Fig. 1. The base peak in the spectrum of the unlabelled compound results from loss of hydrogen from the molecular ion. Our labelling experiments show that about 70% of the hydrogen lost originates from C-2 giving ion **1** (Scheme 1). Loss of an α hydrogen is expected by analogy with the spectra of piperidine and pyrrolidine (2). The remainder of the hydrogen appears to be lost from the rest of the molecule in a random fashion. Ring expansion

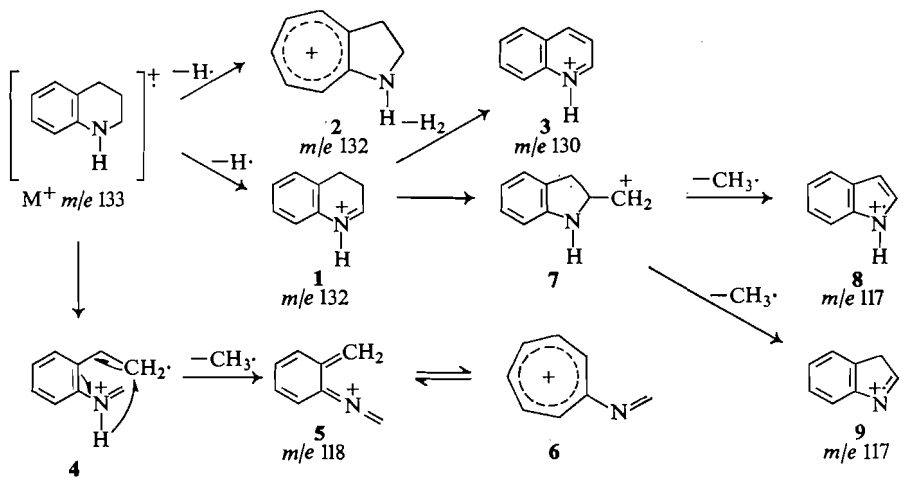

SCHEME 1

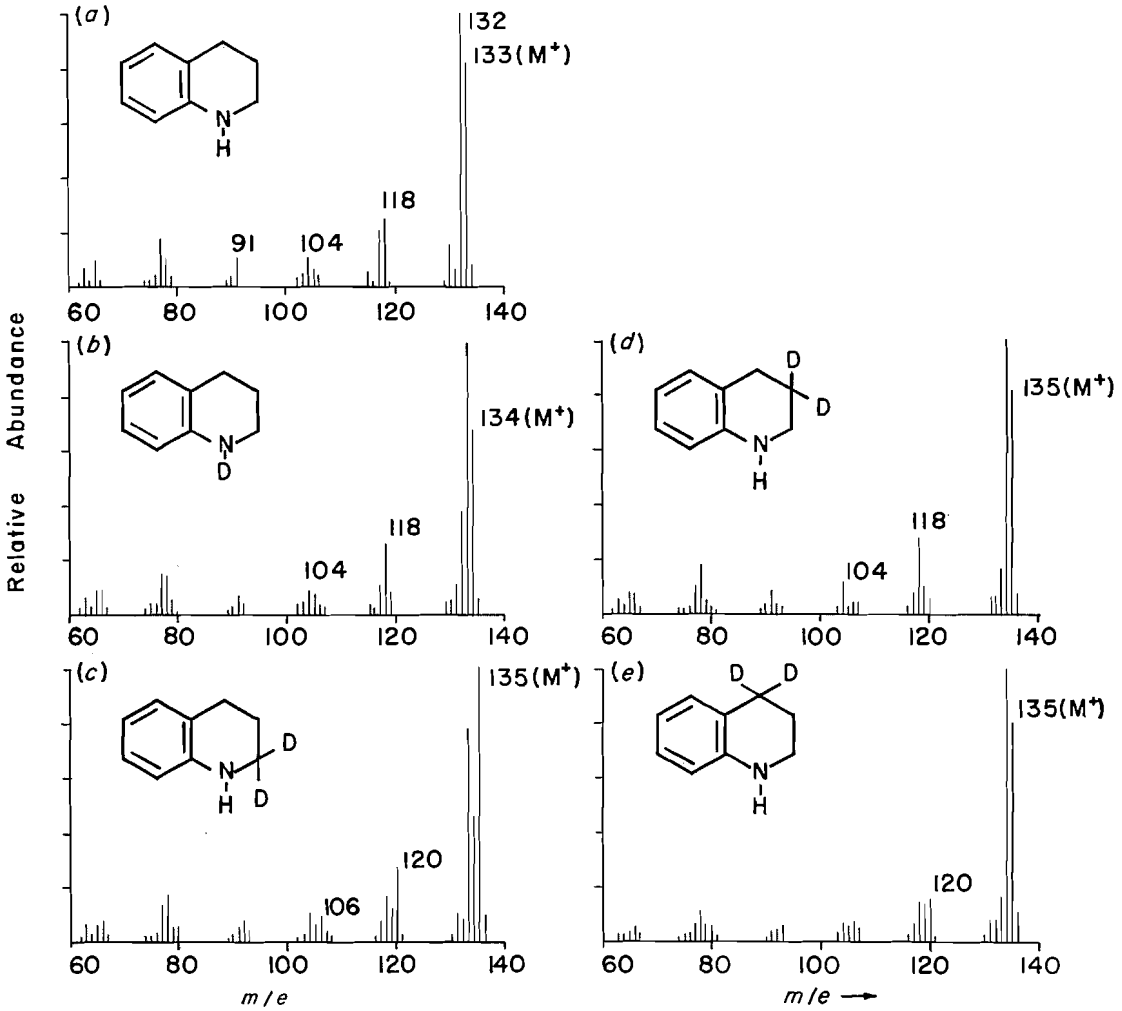

FIG. 1. Mass spectra of (*a*) 1,2,3,4-tetrahydroquinoline, (*b*) 1,2,3,4-tetrahydroquinoline-1-d_1, (*c*) 1,2,3,4-tetrahydroquinoline-2,2-d_2, (*d*) 1,2,3,4-tetrahydroquinoline-3,3-d_2, and (*e*) 1,2,3,4-tetrahydroquinoline-4,4-d_2.

involving C-4 with random loss of hydrogen to give tropylium ion **2** by analogy with the spectrum of toluene (11) is a possible route. The peak at M — 3 presumably arises from aromatization of ion **1** resulting in ion **3**.

Peaks at M — 15 (*m/e* 118) and M — 16 are the only other peaks of appreciable intensity in the spectrum of 1,2,3,4-tetrahydroquinoline. The peak at M — 15 is partially shifted (about 70%) to M — 16 in the spectrum of the 1-d_1 analogue and to M — 16 and M — 17 in the 3,3-d_2 analogue. These results indicate that the major portion of the M — 15 peak arises from loss of C-3 and its hydrogens as well as the hydrogen atom on the nitrogen. The proposed fragmentation mechanism is illustrated in Scheme 1 ($M^+ \rightarrow$ **4** $\rightarrow$ **5** or **6**).

A similar mechanism supported by labelling experiments has been proposed to account for the M — 15 peak found in the spectrum of piperidine (2). C-3 and its associated hydrogens are lost in both compounds; in piperidine the third hydrogen is transferred from C-6 while in tetrahydroquinoline the third hydrogen is transferred from nitrogen.

The M — 16 peak found in the spectrum of 1,2,3,4-tetrahydroquinoline can arise by two pathways, namely, by loss of H from M — 15 or by loss of CH_3 from M — 1. The latter pathway is supported by the presence of a metastable

Can. J. Chem. Downloaded from www.nrcresearchpress.com by 210.87.254.42 on 09/05/12
For personal use only.

Can. J. Chem. Downloaded from www.nrcresearchpress.com by 210.87.254.42 on 09/05/12
For personal use only.

peak at 103.9 (calculated, 103.7) and probably represents the major route. Examination of the spectra of the labelled compounds has helped to elucidate its mode of formation but its origin is not straightforward. From the spectra of the labelled compounds it is observed that the M — 16 peak is not appreciably shifted in the 2,2-d_2 analogue, that it is partially shifted (ca. 40%) to M — 17 in the 1-d_1 compound, to M — 17 and M — 18 in the 3,3-d_2 compound and to M — 17 in the 4,4-d_2 compound. The 3,3-d_2 compound appears to show the greatest shift suggesting that C-3 is lost accompanied by three hydrogens from among the 1-, 3-, and 4-positions. A possible mechanism involving in the first step ring contraction of ion **1** to ion **7** is shown in Scheme 1. Hydrogen transfer from nitrogen or C-4 followed by loss of a methyl radical would yield ions **8** or **9**. The driving force for this rearrangement may lie in the formation of the stable indole system.

Other peaks in the spectrum of 1,2,3,4-tetrahydroquinoline are of low intensity and their formation difficult to interpret even though the labelled analogues are available. The peak at *m/e* 91 may be derived from ion **5** or **6** through loss of HCN since a metastable peak is present corresponding to the transformation *m/e* 118 → *m/e* 91. The series of peaks centered at *m/e* 104 probably arise through successive losses of HCN and one or more hydrogens from M — 1 and M — 3. Thus, metastable peaks are present for the transformation *m/e* 132 → 105 and *m/e* 130 → 103. The spectrum of 1,2,3,4-tetrahydroquinoline is easily differentiated from its 5,6,7,8-isomer (Fig. 3*a*) and the isomeric 1,2,3,4-tetrahydroisoquinoline (10) thus allowing mass spectrometry to be used in its identification.

The spectra of four monomethyltetrahydroquinolines are recorded in Fig. 2. The spectra show that a methyl group on the hydroaromatic ring is more readily lost than a methyl group on the aromatic ring.

The spectra of 2- and 4-methyl-1,2,3,4-tetrahydroquinolines are similar in that they both show weak M — 1 peaks and a base peak at M — 15. The M — 15 fragment from the 2-methyl isomer may be represented by ion **1** which then loses two hydrogens or CH_3 (Scheme 1) to give peaks at M — 17, ion **3**, and M — 30, ion **8**, respectively. The formation of the latter is supported by the presence of a metastable peak at *m/e* 103.9 (calculated, 103.7). The M — 15 ion in the spectrum of the 4-methyl isomer may be stabilized by ring expansion to ion **2** and this ion in turn may lose hydrogen to give a peak at M — 17.

The M — 30 ion in the 4-methyl compound apparently arises from M — 15 through loss of a CH_3 radical since a corresponding metastable peak is present at *m/e* 103.9 (calculated, 103.7). Since the M — 15 to M — 30 ratio is similar for the 2- and 4-isomers it appears that the M — 15 ion derived from the two isomers may have a common structure. Loss of methyl from C-4 followed by hydrogen rearrangement could lead to ion **1** for which a mechanism for loss of 15 mu has already been proposed.

The spectrum of 3-methyl-1,2,3,4-tetrahydroquinoline (Fig. 2*b*) shows an intense M — 1 peak, a less intense M — 15 peak and an intense M — 29 peak relative to its 2- and 4-isomers. The M — 1, M — 29 and M — 30 peaks can form in a manner analogous to the M — 1, M — 15, and M — 16 peaks of the parent compound as shown in Scheme 1. However, the presence of a metastable peak corresponding to the transformation *m/e* 132 → *m/e* 117 indicates that, in part at least, the M — 30 ion forms from M — 15 through loss of a methyl group. We propose that the M — 15 ion formed by loss of the 3-methyl group may rearrange to ion **1** by H transfer before expulsion of the second methyl group in a manner similar to the M — 15 ion derived from the 4-isomer. The M — 15 ion may also lose two hydrogens to give the peak observed at M — 17 which is represented as ion **3** in Scheme 1.

All three compounds show peaks at M — 1, M — 16, and M — 17. In the case of the 3-methyl compound there are metastable peaks corresponding to the transformations M — 1 → M — 16 and M — 16 to M — 17. The 2- and 4-methyl compounds show a metastable for the latter but not the former transformation. Thus there is a pathway to the M — 17 ion for all three compounds other than that described previously.

The spectrum of 6-methyl-1,2,3,4-tetrahydroquinoline (Fig. 2*d*) is similar to that of tetrahydroquinoline since the substitution is not in the saturated ring and accordingly has little effect on the fragmentation. A difference from the parent compound is the presence of a peak at M — 17 in the spectrum of the 6-methyl compound which is caused by loss of hydrogen from the M — 16 species. A ring expanded ion **12** is

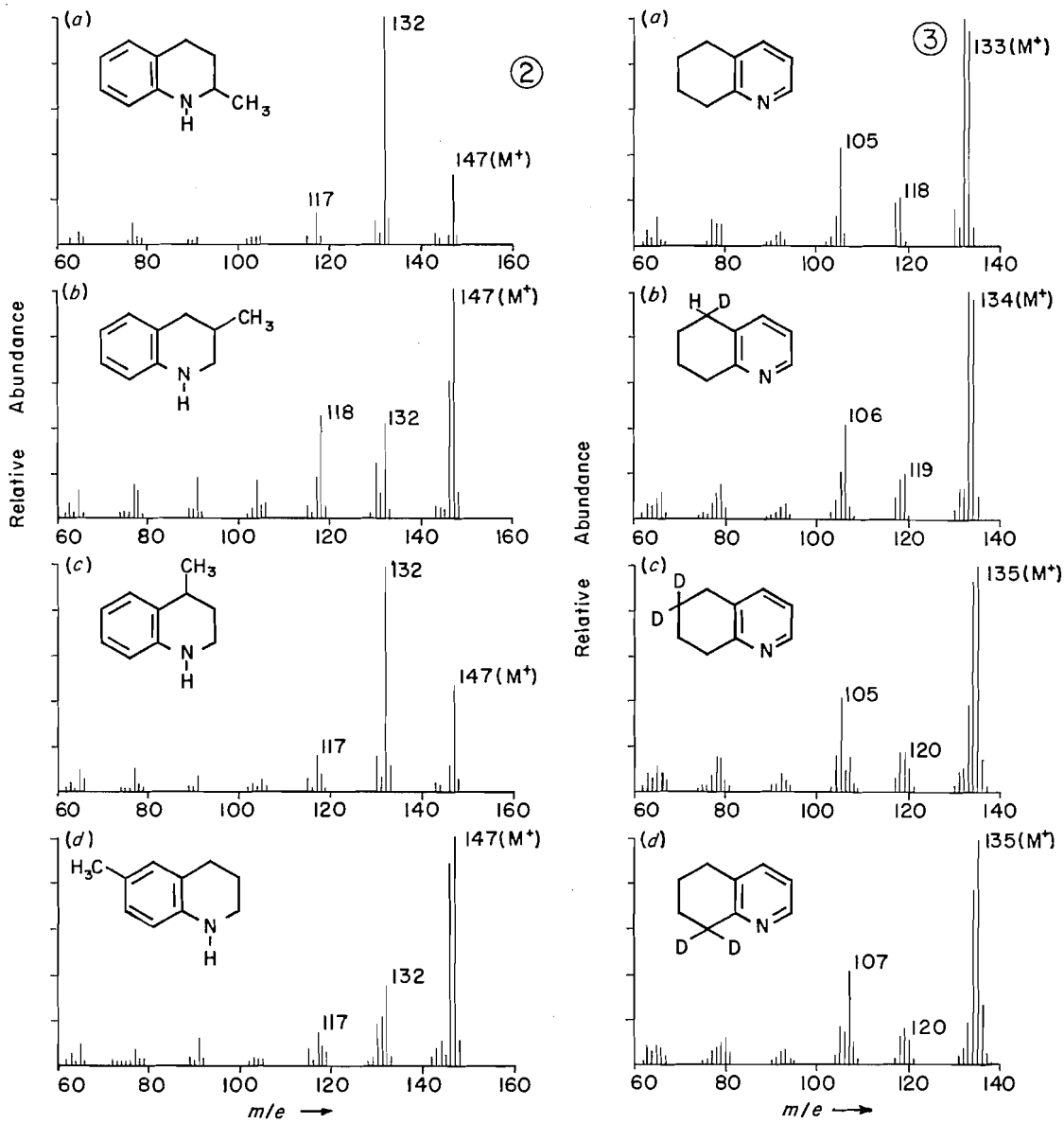

FIG. 2. Mass spectra of (*a*) 2-methyl-1,2,3,4,-tetrahydroquinoline, (*b*) 3-methyl-1,2,3,4-tetrahydroquinoline, (*c*) 4-methyl-1,2,3,4-tetrahydroquinoline, and (*d*) 6-methyl-1,2,3,4-tetrahydroquinoline.

FIG. 3. Mass spectra of (*a*) 5,6,7,8-tetrahydroquinoline, (*b*) 5,6,7,8-tetrahydroquinoline-5-d_1, (*c*) 5,6,7,8-tetrahydroquinoline-6,6-d_2, and (*d*) 5,6,7,8-tetrahydroquinoline-8,8-d_2.

probably formed through the sequence, $M^+ \rightarrow$ **10** $\rightarrow$ **11** $\rightarrow$ **12** (Scheme 2).

The mass spectra of 5,6,7,8-tetrahydroquinoline and its 5-d_1, 6,6-d_2, and 8,8-d_2 derivatives are shown in Fig. 3*a–d* respectively. The spectrum of 5,6,7,8-tetrahydroquinoline may be differentiated from that of the 1,2,3,4-isomer by virtue of the intense peak at M − 28 (*m/e* 105) in the former isomer.

The base peak in the spectrum of 5,6,7,8-tetrahydroquinoline corresponds to loss of hydrogen from the molecular ion. The labelling experiments indicate that the hydrogen loss is not specific. A significant contribution from C-6 is observed (Fig. 3*c*) and a similar contribution from C-7 might be expected. A large proportion of the hydrogen lost may originate from the pyridine ring possibly by ring expansion with

Can. J. Chem. Downloaded from www.nrcresearchpress.com by 210.87.254.42 on 09/05/12
For personal use only.

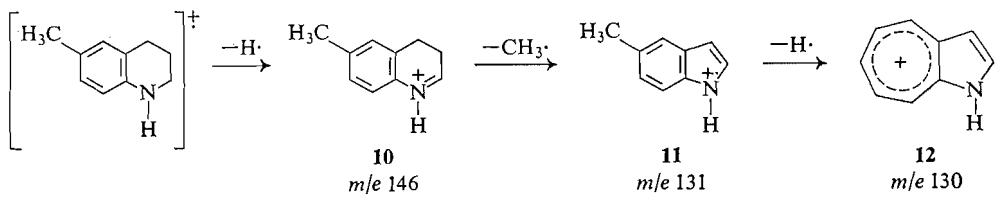

SCHEME 2

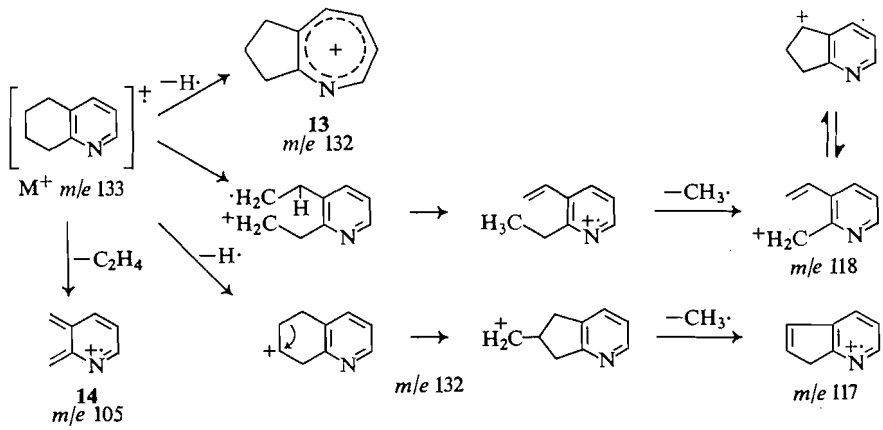

SCHEME 3

random loss of hydrogen to give ion **13**, as shown in Scheme 3.

The labelling experiments do not shed much light on the origin of peaks at M − 15 and M − 16. In all the labelled compounds partial shifts to M − 16 and M − 17 are observed but evaluation is difficult because of the two adjacent peaks. The results indicate that scrambling of hydrogen occurs or that a series of competing reactions may contribute to the M − 15 and M − 16 ions. A tentative mechanism for the formation of ions at M − 15 and M − 16 is outlined in Scheme 3. For formation of the M − 15 ion, a C-6–C-7 bond fission is postulated followed by H transfer and expulsion of a methyl radical. As depicted in Scheme 3, C-7 and its associated hydrogens are lost along with a hydrogen from C-5. It is equally probable that C-6 and its associated hydrogens along with a hydrogen from C-8 would be lost. In the formation of the M − 16 ion, a loss of H from C-7 is followed by ring contraction and elimination of methyl. In this case C-6 and its associated hydrogens are lost along with a hydrogen from C-5 or C-8. By losing hydrogen initially from C-6, C-7 and its associated hydrogens along with a single hydrogen from C-5 or C-8 would be lost. This mechanism accounts for the fact that some deuterium is lost in all the labelled compounds which we have studied, and that deuterium loss is not specific for the M − 15 or M − 16 ions. It is noteworthy that peaks at M − 15 and M − 16 are also found in the spectrum of tetrahydronaphthalene (8, 9) but to our knowledge their origin has not been discussed.

The peak at *m/e* 105 (ion **14**) may be explained by a retro Diels–Alder fragmentation since deuterium is retained in the 5-d_1 and 8,8-d_2 isomers while it is lost in the 6,6-d_2 isomer. A similar loss of ethylene has been observed in the spectrum of tetrahydronaphthalene (8, 9).

Experimental

Apparatus, Methods and Materials

Mass spectra were determined on a Hitachi Perkin–Elmer R.M.U.-6A mass spectrometer at an ionizing potential of 80 eV and an ionizing current of 50 μA. Samples were introduced through an all-glass inlet system maintained at 200 °C. Spectra are plotted in terms of relative abundance, with the most intense peak

Can. J. Chem. Downloaded from www.nrcresearchpress.com by 210.87.254.42 on 09/05/12
For personal use only.

Can. J. Chem. Downloaded from www.nrcresearchpress.com by 210.87.254.42 on 09/05/12
For personal use only.

(base peak) being taken as 100%. Only peaks equal to or greater than 2% of the base peak are recorded.

Nuclear magnetic resonance (n.m.r.) spectra were determined in $CDCl_3$ solution on a Varian A–60 spectrometer. Chemical shifts are expressed in parts per million (δ) from tetramethylsilane used as an internal standard.

All samples were purified by gas–liquid chromatography (g.l.c.) on a 6 ft column of 20% Apiezon M on Celite. The column temperature was maintained at 180 to 220 °C depending on the volatility of the sample.

1,2,3,4-tetrahydroquinoline, 2-methyl-1,2,3,4-tetrahydroquinoline, and 6-methyl-1,2,3,4-tetrahydroquinoline were obtained commercially. CH_3OD (99 atom % D) was obtained from Merck, Sharp and Dohme of Canada Ltd.

1,2,3,4-Tetrahydroquinoline-1-d_1

A sample of tetrahydroquinoline, purified by g.l.c. was treated with 0.3 ml CH_3OD and the CH_3OD evaporated in a vacuum desiccator. The process was repeated three times. A small amount of CH_3OD was pumped through the mass spectrometer to minimize back exchange. The composition of the product determined by low voltage mass spectrometry was: $d_0 = 29\%$ and $d_1 = 71\%$.

1,2,3,4-Tetrahydroquinoline-2,2-d_2

3,4-Dihydrocarbostyril (12) (100 mg) was heated under reflux with 80 mg $LiAlD_4$ in 15 ml anhydrous ether for 2 h. The excess $LiAlD_4$ was destroyed by adding wet ether, then water. The precipitate was removed by filtration and the ether solution dried over Na_2SO_4. The yield of product was 82 mg and its composition determined by low voltage mass spectrometry was: $d_1 = 2\%$ and $d_2 = 98\%$. The n.m.r. spectrum showed a triplet at δ 1.96 (2H) and a triplet at δ 2.84 (2H) ($J = 6.5$ c.p.s.) while the spectrum of the nondeuterated compound showed a multiplet at δ 1.87 (2H), a triplet at δ 2.75 (2H) ($J = 6.5$ c.p.s.), and a triplet at δ 3.25 (2H) ($J = 6.0$ c.p.s.).

1,2,3,4-Tetrahydroquinoline-3,3-d_2

3,4-Dihydrocarbostyril (12) (85 mg) and sodium methoxide (45 mg) were heated under reflux with 1 ml CH_3OD for 3 h. The solvent was evaporated and the process repeated. The residue was extracted with chloroform and the product reduced with lithium aluminium hydride as described above. The composition of the product determined by low voltage mass spectrometry was: $d_1 = 10\%$ and $d_2 = 90\%$. The n.m.r. spectrum showed singlets at δ 2.81 (2H) and δ 3.32 (2H).

1,2,3,4-Tetrahydroquinoline-4,4-d_2

4-Ketotetrahydroquinoline (13) (100 mg) was reduced to 1,2,3,4-tetrahydroquinoline-4,4-d_2 by heating with excess $LiAlD_4$ in ether for 3 h (14). The 1,2,3,4-tetrahydroquinoline-4,4-d_2 was isolated from the crude product (which also contained quinoline and some unreacted starting material) by g.l.c. The composition of the product determined by low voltage mass spectrometry was: $d_1 = 6\%$, $d_2 = 90\%$, and $d_3 = 4\%$. The desired product was formed in insufficient yield for n.m.r. analysis.

3- and 4-Methyl-1,2,3,4-tetrahydroquinolines

The corresponding methylquinoline was reduced by heating it under reflux with excess tin and hydrochloric acid for 48–72 h. The product was isolated by basification and steam distillation of the reaction mixture followed by extraction of the distillate with ether. Yields of both compounds were about 60%.

The picrate of 3-methyltetrahydroquinoline melted at 153–155 °C (*lit.* 155–156 °C (15)) and that of 4-methyltetrahydroquinoline at 134 °C (lit. 157 °C (16) and 138 °C (17)). The *N*-benzoyl derivative of 4-methyltetrahydroquinoline melted at 135–137 °C (lit. 138 °C (17)).

5,6,7,8-Tetrahydroquinoline

5,6,7,8-Tetrahydroquinoline was prepared from 5,6,7,8-tetrahydrocarbostyril (18) by the method of von Braun and Lemke (19). The picrate melted at 155–157 °C (lit. 160–161 °C (19)).

5,6,7,8-Tetrahydroquinoline-5-d_1

5-Aza-1-tetralone was reduced to 5-aza-1-tetralol-1-*d* by the method of Zymalkowski and Rimek (20) except that $NaBD_4$ was substituted for $NaBH_4$, 110 mg of the alcohol was added to excess $LiAlH_4$ (80 mg) in anhydrous tetrahydrofuran and the mixture heated under reflux overnight. The composition of the product determined by low voltage mass spectrometry was: $d_0 = 5\%$, $d_1 = 94\%$, and $d_2 = 1\%$. Reduction of the tetralone with $LiAlD_4$ resulted in large amounts of d_3 and d_4 species (probably by exchange in the pyridine ring) (1).

5,6,7,8-Tetrahydroquinoline-6,6-d_2

5-Aza-1-tetralone (20) (180 mg) was treated with 50 mg CH_3ONa and 1 ml CH_3OD for 1 h at room temperature. The solvent was then evaporated under reduced pressure and the process repeated. The residue was extracted with ether and the ether layer dried over Na_2SO_4. The exchanged tetralone was reduced to 5,6,7,8-tetrahydroquinoline-6,6-d_2 by refluxing it with excess $LiAlH_4$ in tetrahydrofuran for 15 h. The composition of the product determined by low voltage mass spectrometry was: $d_0 = 3\%$, $d_1 = 12\%$, $d_2 = 81\%$, and $d_3 = 4\%$.

5,6,7,8-Tetrahydroquinoline-8,8-d_2

5,6,7,8-Tetrahydroquinoline (20 mg), CH_3ONa, and CH_3OD (1 ml) were sealed in a glass tube and heated in a steam bath for about 3 weeks. The composition of the product determined by low voltage mass spectrometry was: $d_0 = 2\%$, $d_1 = 8.5\%$, $d_2 = 70\%$, $d_3 = 16\%$, and $d_4 = 3.5\%$.

Acknowledgments

This work was supported by a grant from the National Research Council of Canada. The award of a bursary (1964–1965) and studentships (1965–1968), to P. M. Draper by the National Research Council of Canada is gratefully acknowledged.

1. P. M. Draper and D. B. MacLean. Can. J. Chem. This issue.
2. A. M. Duffield, H. Budzikiewicz, D. H. Williams, and C. Djerassi. J. Am. Chem. Soc. **87**, 810 (1965).
3. L. W. Daasch. J. Phys. Chem. **69**, 3196 (1965).
4. H. Budzikiewicz, C. Djerassi, and D. H. Williams. Interpretation of mass spectra of organic compounds. Holden-Day, Inc., San Francisco. 1964. pp. 100–103.

5. M. SPITELLER-FRIEDMANN and G. SPITELLER. Monatsh. **96**, 104 (1965).
6. B. WILLHALM, A. F. THOMAS, and F. GAUTSCHI. Tetrahedron, **20**, 1185 (1964).
7. C. S. BARNES and J. L. OCCOLOWITZ. Australian J. Chem. **17**, 975 (1964).
8. K. BIEMANN. Mass spectrometry: organic chemical applications. McGraw-Hill Book Co., Inc., New York. 1962. p. 105.
9. Z. KECKI and H. WINCEL. Nukleonika, **8**, 117 (1963).
10. M. BALDWIN, A. G. LOUDON, A. MACCOLL, L. J. HAYNES, and K. L. STUART. J. Chem. Soc. C, [2], 154 (1967).
11. H. M. GRUBB and S. MEYERSON. *In* Mass spectrometry of organic ions. *Edited by* F. W. McLafferty. Academic Press Inc., New York, N.Y. 1963. Chap. 10.
12. L. H. BRIGGS and G. C. DE ATH. J. Chem. Soc. 456 (1937).
13. W. S. JOHNSON, E. L. WOROCH, and B. G. BUELL. J. Am. Chem. Soc. **71**, 1901 (1949).
14. W. S. JOHNSON and B. G. BUELL. J. Am. Chem. Soc. **74**, 4517 (1952).
15. M. AVRAMOFF and Y. SPRINZAK. J. Am. Chem. Soc. **78**, 4090 (1956).
16. A. TCHITCHIBABINE and C. BARKOVSKY. Compt. Rend. **212**, 914 (1941).
17. N. V. BRINGI and P. V. DESHMUKH. J. Org. Chem. **27**, 4117 (1962)
18. J. THESING and A. MÜLLER. Ber. **90**, 711 (1957).
19. J. VON BRAUN and G. LEMKE. Ann. **478**, 191 (1930).
20. F. ZYMALKOWSKI and H. RIMEK. Arch. Pharm. **294**, 759 (1961).

Can. J. Chem. Downloaded from www.nrcresearchpress.com by 210.87.254.42 on 09/05/12
For personal use only.

Can. J. Chem. Downloaded from www.nrcresearchpress.com by 210.87.254.105 on 09/05/12
For personal use only.

Enantiomeric 3-hydroxypent-4-enethionamides from thioglucosides of Crambe and Brassica seeds by action of ferrous salts

F. L. AUSTIN, C. A. GENT, AND I. A. WOLFF

Northern Regional Research Laboratory, Northern Utilization Research and Development Division, Agricultural Research Service, United States Department of Agriculture, Peoria, Illinois 61604

Received December 11, 1967

epi-Progoitrin, the major thioglucoside of *Crambe abyssinica* seed, is cleaved by ferrous salts to yield (*S*)-1-cyano-2-hydroxy-3-butene and (*S*)-3-hydroxypent-4-enethionamide. The products are the same whether obtained from the purified thioglucoside or from the seed meal. Identical behavior was observed for seed meal of *Brassica napus*, which gave corresponding derivatives of the opposite configuration. Optical rotatory dispersion and proton magnetic resonance studies suggest the existence of solvent-dependent differences in rotamer composition for the 3-hydroxypent-4-enethionamides.

Canadian Journal of Chemistry, 46, 1507 (1968)

Earlier publications from this laboratory have detailed the chemistry of *epi*-progoitrin, the major thioglucoside in seed meal of *Crambe abyssinica* Hochst ex R. E. Fries and of its enzymic conversion products (1–3). The enzymic reaction may lead to two distinct types of products. One, 5-vinyl-oxazolidinethione or (*R*)-goitrin, is formed by spontaneous cyclization of an intermediate β-hydroxy isothiocyanate (4); the other consists of open-chain nitriles derived from the aglucon of *epi*-progoitrin. Three of this group have been recognized: (*S*)-1-cyano-2-hydroxy-3-butene and a diastereoisomeric pair of episulfides related to this unsaturated nitrile.

Several species of Brassica contain a thioglucoside with a similar structure to that found in Crambe. The two thioglucosides differ only in configuration about the asymmetric carbon atom in the aglucon portion of the molecule (1). The configurations persist without racemization during enzymic conversion, so that two series of enantiomorphic compounds result, depending on the source material (1, 2). A scheme showing these relationships, together with the absolute configurational assignments, was recently given (5).

The occurrence of enantiomers of a compound in related plant families is unusual but not unique for Crambe and Brassica. The situation with respect to the thioglucosides of these species has been discussed by Daxenbichler *et al.* (1) who also cited other substances, mainly terpenes, which occur in nature as enantiomers. Analogous observations were noted for an alkaloid (20) and for the butanol derivative, betuligenol (21).

Although enzymic transformation of the thioglucosides present in members of the *Cruciferae* and in a limited number of other plant families frequently proceeds via the isothiocyanate pathway, the route leading to nitriles may occur almost exclusively or the two types of products can be formed concurrently. Schwimmer (6) noted that the decomposition of sinigrin by myrosinase (thioglucosidase, EC3.2.3.1) in the presence of ascorbate and protein yielded nitrile at pH 3.0 but isothiocyanate at higher pH values. Further studies of this system by Ettlinger *et al.* (7) supported pH dependence of the observed ratio of nitrile to isothiocyanate produced. The results were explained in terms of the nonenzymatic breakdown of a labile intermediate whose rate was determined by pH. The intermediate was identified as the sinigrin aglucon.

These studies provide fairly clear results in the case of isolated thioglucoside plus enzyme systems. However, a more complex situation was demonstrated by VanEtten *et al.* (8) for *Crambe abyssinica* seed meal subjected to the action of endogenous enzymes. Age, storage conditions, and prior heat treatment of the seed, as well as such factors as amounts of water, temperature, and pH during autolysis, affected the relative amounts of (*R*)-goitrin and nitrile products formed. In fact, exclusive production of nitrile components was usual for the majority of recently harvested seed samples. Essentially the same autolysis pattern was noted for *Brassica napus* (a species of commercial rapeseed) as for Crambe.

The explanation for these variations was obscure, and more subtle influences were sought.

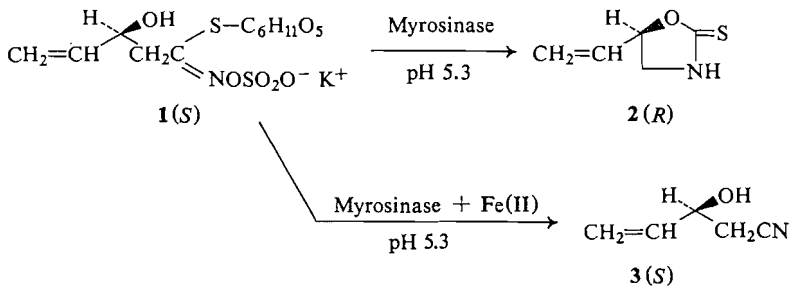

SCHEME 1

Miller (9) noted that potassium silver sinigrate was converted quantitatively to allyl cyanide by iodide in the presence of ferrous ion, whereas other metal salts or iodide alone gave predominantly allyl isothiocyanate. Enzymic conversion of sinigrin also yielded nitrile when ferrous ion was present.

We found that ferrous ion also exerts a directive influence on the enzymic conversion of isolated *epi*-progoitrin (**1**). At pH 5.3 in the absence of iron, the addition of myrosinase produced (*R*)-goitrin (**2**) only, whereas under the same conditions but with low concentrations of ferrous salts, the major product was the unsaturated nitrile (**3**). There was only a trace of **2**. The enzymic reaction also was more rapid with ferrous ion.

Although ferrous salts exerted a profound influence on the course of the enzymic reaction, they also unexpectedly cleaved the thioglucoside without the mediation of an enzyme (10). In this instance the products were **3** and (*S*)-3-hydroxypent-4-enethionamide (**4**). Enzymic reaction [1] is compared with nonenzymic reaction [2] in Scheme 1.

Youngs and Perlin (11) describe the nonenzymic decomposition of sinigrin by ferrous sulfate at 95°. In their work, only allyl cyanide was obtained.

Results and Discussion

The nonenzymic degradation of *epi*-progoitrin (**1**) was slow at room temperature and required a considerable excess (six to eight equivalents) of ferrous salt for best results. Other metal ions, including stannous, cobaltous, nickel, and ferric, as well as hydroquinone, did not degrade **1**. Neither was the pentaacetate of **1** (1) attacked by ferrous salts.

Traces of residual enzyme in the preparation of **1** were considered an unlikely explanation for the reaction on the grounds of the isolation procedure, the differences in products, and the relatively large ferrous ion requirement. This explanation was excluded by boiling an aqueous solution of **1** for 5 min. Ferrous salt was added to the cooled solution and the reaction allowed to proceed at room temperature. Both the ratio of products and yields were the same as from **1** not subjected to heat.

In defatted Crambe meal, the native enzyme(s) of which had been inactivated by heat, thioglucoside degradation by ferrous ion proceeded as observed for isolated **1**. Contact of the meal with a solution of a ferrous salt resulted in the production of both nitrile (**3**) and thionamide (**4**).

Similarly, we found that defatted, enzyme-inactivated seed meal of *Brassica napus* L. (rapeseed), in contact with a solution of a ferrous salt, also produced nitriles and a thionamide. Although significant amounts of thioglucosides other than progoitrin are present in rapeseed (12), only a single thionamide was obtained from this source. It proved to be the enantiomer of the corresponding compound from Crambe meal.

Crambe and rapeseed meals were used as source material for the isolation and investigation of

Can. J. Chem. Downloaded from www.nrcresearchpress.com by 210.87.254.105 on 09/05/12
For personal use only.

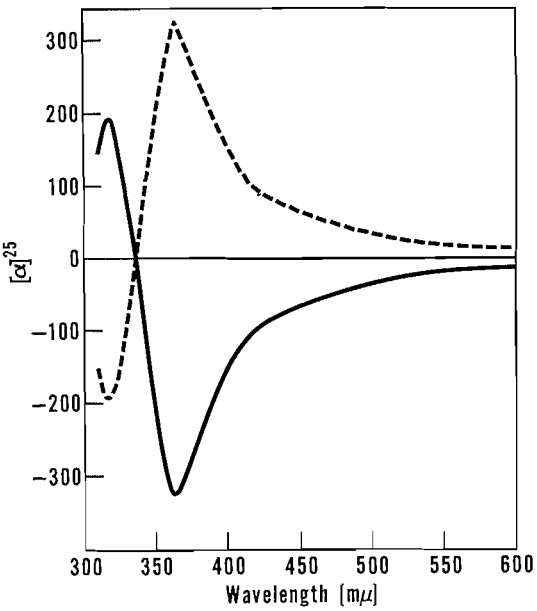

FIG. 1. Optical rotatory dispersion curves in methanol [3-hydroxypent-4-enethionamides: —— (*S*)-enantiomer from *Crambe abyssinica*; - - - - (*R*)-enantiomer from *Brassica napus*.

the two optical isomers of 3-hydroxypent-4-enethionamide. Both compounds had the same melting point but exhibited equal and opposite rotatory dispersion curves (see Fig. 1). The (*S*)-thionamide (**4**) from Crambe exhibited a negative Cotton effect, whereas the configurationally related (*S*)-unsaturated nitrile (**3**) showed a plain positive rotatory dispersion curve (2). A negative Cotton effect was noted as an exception by Burakevich and Djerassi (13) for the (*S*)-*N*-methylthionamide of *O*-acetyllactic acid. They attributed the deviation from the general positive Cotton effect for (*S*)-thionamides to the lack of correlation between bulk and priority in the Cahn–Ingold notation when a hetero atom was involved. The same argument would be valid for the hydroxythionamide from **1**.

Ultraviolet spectra of the thionamides in alcohol were typical of those for thioacetamide and dimethyl thioacetamide (14). A weak band was present at 330 mμ and a strongly absorbing band at 267 mμ, The higher wavelength band undergoes a bathochromic shift of 20 mμ in chloroform solution, whereas the position of the high intensity band is scarcely affected. This behavior has been observed with other thionamides (15) and interpreted as an $n \rightarrow \pi^*$ transition for the longer wavelength band and a $\pi \rightarrow \pi^*$ transition near 267 mμ. The absorption data are summarized in Table I.

TABLE I

Ultraviolet absorption of (*S*)- or (*R*)-3-hydroxypent-4-enethionamide

Solvent	λ_{max} $n \rightarrow \pi^*$ (mμ)	Log ε	λ_{max} $\pi \rightarrow \pi^*$ (mμ)	Log ε
Water	318	1.76	265	4.04
95% Ethanol	330	1.73	267	4.05
Chloroform	350	1.75	269	4.01

Bach and co-workers studied the anomalous rotatory dispersion and circular dichroism curves for *N*-thiobenzoyl and *N*-phenylthioacetyl derivatives of amino acids in solvents of differing polarity (16). Their suggested explanation for unexpected shifts in sign of the Cotton effects implicated solvent-influenced changes in rotamer composition. We made a similar investigation of the rotatory dispersion curves of (*S*)-3-hydroxypent-4-enethionamide in water and chloroform. The position of the extrema varied with solvent as expected from the absorption maxima for the longer wavelength transition (Table I). In addition, the Cotton effect was negative in both solvents, but its amplitude differed more than threefold. These data are summarized in Table II.

TABLE II

Optical rotatory dispersion of (*S*)-3-hydroxypent-4-enethionamide

Solvent	$[\alpha]_D^{25}$	First extremum	Second extremum
Water	−9°	$[\alpha]_{347}$ −278°	$[\alpha]_{305}$ +320°
Chloroform	−96°	$[\alpha]_{383}$ −1102°	$[\alpha]_{335}$ +884°

Burakevich and Djerassi (13) demonstrated considerable conformational mobility in thionamides by measuring the circular dichroism maxima over the temperature range −192° to 168°. Without resort to temperature studies, our observed amplitude differences suggest that polarity of the solvent affects the rotamer population of the 3-hydroxypent-4-enethionamides. This deduction is supported by the nuclear magnetic resonance (n.m.r.) spectra of the compounds. The region of absorption by the

Can. J. Chem. Downloaded from www.nrcresearchpress.com by 210.87.254.105 on 09/05/12
For personal use only.

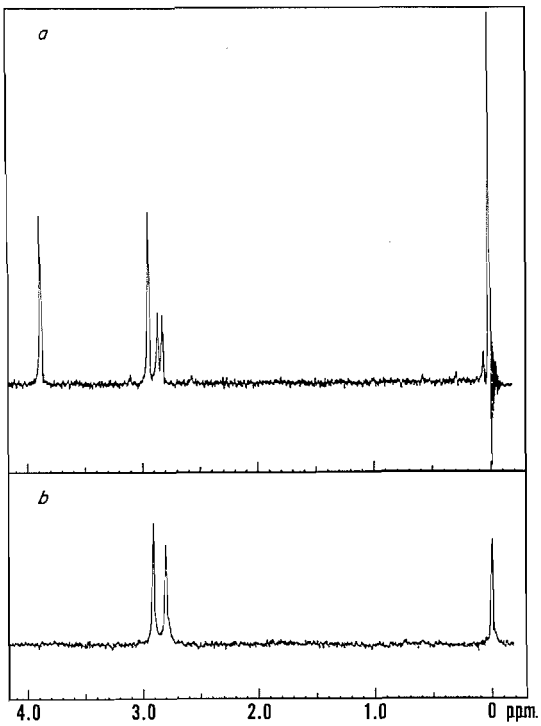

FIG. 2. High field proton magnetic resonance spectra of 3-hydroxypent-4-enethionamides. *a*, in deuteriochloroform; *b*, in deuterium oxide.

methylene protons at δ 2.8 to 3.0 was of interest because it showed an unsymmetrical two proton triplet in deuteriochloroform, which became a two proton doublet in deuterium oxide (see Fig. 2). Most likely, the spectrum observed in deuteriochloroform indicates a small chemical shift difference between two magnetically nonequivalent protons. Jackman and Bowman (17) have discussed such nonequivalent geminal protons and cited several examples of alteration of the chemical shift with change in solvent or concentration. The behavior of 2-butanol on dilution in carbon tetrachloride was interpreted in terms of a change in rotamer population.

Other features of the n.m.r. spectra of the 3-hydroxypent-4-enethionamides were essentially like the published spectrum (2) of (*S*)-1-cyano-2-hydroxy-3-butene in deuteriochloroform. The only differences were a shift in position of the hydroxyl proton from δ 3.8 to 3.9 and the addition of a broad band from δ 7.9 to 8.6 for the two amide protons.

The structure of the thionamides was confirmed chemically by reaction with silver nitrate in aqueous solution. Silver sulfide precipitated, and 1-cyano-2-hydroxy-3-butene was isolated in nearly quantitative yield after ether extraction. Kindler and Finndorf (18) first reported the reaction of either silver or lead salts with thioacetamide to form acetonitrile.

The unsaturated nitrile from (*S*)-3-hydroxypent-4-enethionamide was identical to the (*S*)-1-cyano-2-hydroxy-3-butene derived from **1** in Crambe seed meal on enzymic cleavage (2). Comparison was made of the infrared absorption and of mobility on thin-layer chromatography. The plain positive optical rotatory dispersion curves also were the same. Thus configurational integrity of the asymmetric center was maintained during nonenzymic degradation of **1** and also through the subsequent steps of purification of **4** and its dehydrosulfuration by silver nitrate.

Experimental

Assays for goitrin and unsaturated nitrile were carried out by the procedures of Daxenbichler *et al.* (2). Thionamide was determined with a Beckman[1] DK-2 instrument by measurement of the ultraviolet absorption at 267 mμ in alcohol solution; the extinction value ($\log \varepsilon = 4.05$) was determined from a purified sample. Usually background absorption was negligible. Optical rotatory dispersions were made with a Cary 60 recording spectropolarimeter. Initial sample concentrations were between 0.1 and 0.2% and diluted further if necessary to record the extrema. Proton magnetic resonance spectra were determined with a Varian A-60 instrument.

Isolated *epi*-progoitrin (**1**) (estimated purity 90%) was obtained from defatted Crambe meal by the procedure of Daxenbichler *et al.* (1).

Enzymic Degradation of 1

1 (100 mg, 0.21 mmoles) was dissolved in water (5 ml) and mustard myrosinase (15 mg) added. The pH was maintained at 5.3 by addition of 0.1 *N* sodium hydroxide with an automatic recording titrator (radiometer). After alkali consumption ceased (2 h), the solution was extracted five times with 10-ml portions of ether. The ether solution, dried over sodium sulfate, was evaporated in a stream of nitrogen. The residue was dissolved in chloroform (1 ml) for nitrile assay. Solvent was then replaced with alcohol, the solution appropriately diluted, and the ultraviolet absorption determined (assay for goitrin or thionamide). Results of the assays showed 21.7 mg of (*R*)-goitrin (80% yield) and only a negligible yield of unsaturated nitrile (< 5%).

[1]Mention of firm names or products does not imply endorsement by the United States Department of Agriculture over other firms or similar products not mentioned.

Can. J. Chem. Downloaded from www.nrcresearchpress.com by 210.87.254.105 on 09/05/12
For personal use only.

Can. J. Chem. Downloaded from www.nrcresearchpress.com by 210.87.254.105 on 09/05/12
For personal use only.

This reaction was repeated, except that ferrous ammonium sulfate (20 mg, 0.05 mmoles) was added to the solution of **1** before introduction of the enzyme. In this instance the enzyme reaction was faster than before (20 min for alkali consumption to cease). Assay of the ether-soluble products showed only 0.4 mg of (*R*)-goitrin (1.5% yield) but 12.3 mg of unsaturated nitrile (60% yield).

Nonenzymic Degradation of ***1***

1 (100 mg, 0.21 mmoles) was dissolved in 25 ml of pH 5.3 buffer (acetic acid – sodium acetate) and ferrous ammonium sulfate (600 mg, 1.53 mmoles) was added. The solution was covered with nitrogen and allowed to stand overnight at room temperature. On spectral examination of the reaction mixture at the end of this time period, **1** (λ_{max} = 227 mμ) was no longer detectable, but a peak was present at 265 mμ. The aqueous solution was saturated with salt and extracted five times with 50-ml portions of ether. The extract was dried over sodium sulfate, the solvent removed, and the residue assayed. There were 3.3 mg of unsaturated nitrile (16% yield) and 12.0 mg of the thionamide (43% yield).

These results were typical. Although stoichiometric conversions were not achieved, from 90–100% of the total ether extractable material was represented by nitrile and thionamide. Buffered solutions were not essential, and the reaction proceeded in the same way in distilled water. Ferrous sulfate could be used in place of ferrous ammonium sulfate without affecting the results.

Action of Ferrous Salts on Crambe Meal

Enzyme(s) in defatted Crambe meal were inactivated by the procedure of VanEtten *et al.* (19). For the purpose, Crambe meal (100 g), which assayed 6.7% *epi*-progoitrin, was heated on a steam bath, covered with boiling water (700 ml), and maintained above 90° with stirring for 10 min. Ferrous ammonium sulfate (50 g) was added to the cooled mixture. It was covered with nitrogen and allowed to stand 16 h at room temperature. The reaction mixture was divided into four portions, residual meal solids were removed by centrifugation, and each solid fraction was washed four times with 50-ml portions of water. The combined aqueous extracts and washes were saturated with sodium chloride and extracted with five 600-ml portions of ether. Centrifuging was necessary to break emulsions. The ether extracts were dried over sodium sulfate, partially concentrated, and made to 100 ml. Samples were removed for assay. The average yield of thionamide from 10 runs was 590 mg (29%). The accompanying nitrile amounted to 190 mg (12%).

Separation of ***3*** *and* ***4***

Ether extracts from two Crambe meal reactions were evaporated. The residue (containing 1.05 g of thionamide and 0.41 g of nitrile) was dissolved in chloroform (10 ml) and transferred to a column (40 × 2.5 cm) of aluminium oxide (Camag, chromatographic grade, acidic) prepared by slurrying the adsorbent in chloroform. The column was eluted with chloroform and eluate collected in 200-ml fractions. The initial fraction contained (*R*)-goitrin (0.05 g, 1.2% based on thioglucoside content of the meal). This low level of (*R*)-goitrin was not observed during assay of crude extracts in the presence of larger amounts of thionamide. The second and third fractions contained most of the (*S*)-1-cyano-2-hydroxy-3-butene (0.40 g, 97% recovery). The infrared curve was identical to that of a known sample (2). A composite of nitrile-containing fractions from the aluminium oxide column was evaporated, dissolved in water, and chromatographed on Sephadex G-10 by the method of Daxenbichler *et al.* (3). All the product eluted was in the range corresponding to the unsaturated nitrile and no evidence for the presence of episulfide nitriles was found.

Elution of the aluminium oxide column with additional chloroform (600 ml) was continued to remove final traces of **3**. The eluting solvent was then changed to a mixture of chloroform:methanol (95:5). After an intermediate fraction (100 ml), most of **4** was removed from the column in the two succeeding 200-ml fractions (1.00 g, 95% recovery).

*(S)-3-Hydroxypent-4-enethionamide (****4****)*

The thionamide-containing fractions from the chromatographic column were concentrated to remove solvent. The residue was dissolved in acetone and the solution centrifuged to separate a trace of insoluble matter. After evaporation of the acetone, benzene (5 ml) was added. The product formed on refrigeration was recrystallized from ether–benzene followed by washing with cold ether. Recovery, 0.82 g of colorless crystals, m.p. 56.5–57°; $[\alpha]_D^{25}$ −20° (*c*, 0.16; methanol).

Anal. Calcd. for C_5H_9NOS (mol. wt., 131): C, 45.8; H, 6.9; N, 10.7; S, 24.4. Found (mol. wt., 134): C, 46.2; H, 6.9; N, 10.7; S, 24.0.

(R)-3-Hydroxypent-4-enethionamide

Defatted seed meal of *Brassica napus* L. (200 g) was heated in water to inactivate enzyme(s), the cooled suspension was allowed to stand in the presence of ferrous ammonium sulfate (100 g), and products were isolated by ether extraction as described for Crambe. Assay showed the presence of 390 mg of nitrile and 740 mg of thionamide. The products, separated on aluminium oxide, gave recoveries of 351 mg of nitrile and 550 mg of the (*R*)-3-hydroxypent-4-enethionamide, m.p. 56.5–57°; $[\alpha]_D^{25}$ +21° (*c*, 0.104; methanol).

Anal. Calcd. for C_5H_9NOS: C, 45.8; H, 6.9; N, 10.7; S, 24.4. Found: C, 45.8; H, 6.9; N, 10.6; S, 24.0.

Racemic 3-Hydroxypent-4-enethionamide

Equal amounts (19.5 mg) of (*S*)- and (*R*)-3-hydroxypent-4-enethionamide were dissolved separately in ether (1 ml). The solutions of the enantiomers were combined and half the solvent was evaporated. Benzene (1.5 ml) was added and the colorless racemate recovered, m.p. 87–87.5°.

A melting point for the racemate 30° higher than that of the optical isomers is unusual, but has a counterpart in the 14° difference observed between the enzymic product (**2**) and racemic goitrin (**1**).

Dehydrosulfuration of (S)-3-Hydroxypent-4-enethionamide

(*S*)-3-Hydroxypent-4-enethionamide (100 mg, 0.763 mmoles) in 5 ml of water was added dropwise to a stirred solution of 0.1 *N* silver nitrate (16.5 ml). Stirring was continued for 10 min longer. The black precipitate of silver sulfide was removed by gravity filtration. After

saturation with salt, the filtrate was extracted five times with 50-ml portions of ether. The extract, dried over sodium sulfate and with solvent removed, gave 64 mg (87%) of (*S*)-1-cyano-2-hydroxy-3-butene. The infrared absorption and optical rotatory dispersion curves were indistinguishable from those of the known cyano compound (2) obtained from enzymic hydrolysis of **1**. R_f values were the same in a parallel thin-layer chromatogram (Silica Gel G; developed with ether–hexane, 5:3).

Acknowledgments

We express our appreciation to K. L. Mikolajczak for optical rotatory dispersion curves; to Walter Boyd for proton magnetic resonance spectra; and to Clara McGrew, Bonita Heaton, and L. P. Burgess for analytical results.

1. M. E. DAXENBICHLER, C. H. VANETTEN, and I. A. WOLFF. Biochemistry, **4**, 318 (1965).
2. M. E. DAXENBICHLER, C. H. VANETTEN, and I. A. WOLFF. Biochemistry, **5**, 692 (1966).
3. M. E. DAXENBICHLER, C. H. VANETTEN, and I. A. WOLFF. Chem. Commun. 526 (1966).
4. A. KJAER. Fortschr. Chem. Org. Naturstoffe, **18**, 122 (1960).
5. M. E. DAXENBICHLER, C. H. VANETTEN, W. H. TALLENT, and I. A. WOLFF Can. J. Chem. **45**, 1971 (1967).
6. S. SCHWIMMER. Acta Chem. Scand. **14**, 1439 (1960).
7. M. G. ETTLINGER, G. P. DATEO, JR., B. W. HARRISON, T. J. MABRY, and C. P. THOMPSON. Proc. Natl. Acad. Sci. U.S. **47**, 1875 (1961).
8. C. H. VANETTEN, M. E. DAXENBICHLER, J. E. PETERS, and H. L. TOOKEY. J. Agr. Food Chem. **14**, 426 (1966).
9. H. E. MILLER. Thesis, Rice University, Houston, Texas. 1965. p. 56.
10. F. L. AUSTIN and C. A. GENT. Chem. Commun. 71, 1967.
11. C. G. YOUNGS and A. S. PERLIN. Can. J. Chem. **45**, 1801 (1967).
12. A. KJAER and R. B. JENSEN. Acta Chem. Scand. **10**, 1365 (1956).
13. J. V. BURAKEVICH and C. DJERASSI. J. Am. Chem. Soc. **87**, 51 (1965).
14. M. J. JANSSEN. Rec. Trav. Chim. **79**, 454 (1960).
15. J. SANDSTROM. Acta Chem. Scand. **16**, 1616 (1962).
16. E. BACH and A. KJAER; R. DAHLBOM, T. WALLE, and B. SJOBERG; E. BUNNENBERG, C. DJERASSI, and R. RECORDS. Acta Chem. Scand. **20**, 2781 (1966).
17. L. M. JACKMAN and N. S. BOWMAN. J. Am. Chem. Soc. **88**, 5565 (1966).
18. K. KINDLER and F. FINNDORF. Ber. **54**, 1079 (1921).
19. C. H. VANETTEN, M. E. DAXENBICHLER, J. E. PETERS, and I. A. WOLFF. J. Agr. Food Chem. **13**, 24 (1965).
20. Z. HARII, M. HANAOKA, Y. YAMAWAKI, and Y. TAMURA. Tetrahedron, **23**, 1165 (1967).
21. W. H. TALLENT. J. Org. Chem. **29**, 988 (1964).

Can. J. Chem. Downloaded from www.nrcresearchpress.com by 210.87.254.105 on 09/05/12
For personal use only.

Can. J. Chem. Downloaded from www.nrcresearchpress.com by 210.87.254.42 on 09/05/12
For personal use only.

Studies on chitan (β-(1 → 4)-linked 2-acetamido-2-deoxy-D-glucan) fibers of the diatom *Thalassiosira fluviatilis*, Hustedt. III. The structure of chitan from *x*-ray diffraction and electron microscope observations[1,2]

N. E. DWELTZ[3] AND J. ROSS COLVIN
Division of Biosciences, National Research Council of Canada, Ottawa, Canada

AND

A. G. MCINNES
Atlantic Regional Laboratory, National Research Council of Canada, Halifax, Nova Scotia

Received October 27, 1967

The form and crystal structure of the fibers attached to the diatom *Thalassiosira fluviatilis* were studied by the electron microscope and *x*-ray diffraction.

These fibers, which were shown previously to be pure, highly crystalline β-(1 → 4) linked poly-*N*-acetyl-D-glucosamine (chitan), are strap-like in cross section, 1000–2000 Å in width at their widest point close to the base, from which they taper uniformly to a very small tip at their outer extremity. Three connected filaments or microfibrils form the fiber at its widest point.

The unit cell of chitan is monoclinic with the space group $P2_1$. The parameters of the unit cell are $a = 4.80$, $b = 10.32$, $c = 9.83$ Å, and $\beta = 112°$. The density of the chitan fibers is 1.495 g/cm^3. There is only one polymeric chain per unit cell with a two-fold screw axis and therefore the chains are parallel to each other. A three-dimensional structure is proposed for chitan which is reasonable from stereochemical considerations and which is in good agreement with all observed *x*-ray diffraction data.

Canadian Journal of Chemistry, 46, 1513 (1968)

Introduction

A previous publication (1) described the production and isolation of extracellular fibers attached to the planktonic, euryhaline diatom *Thalassiosira fluviatilis*. The extracellular "mucilage" surrounding each diatom was shown to be due to long, narrow fibers, each composed of a number of microfibrils, which grew from marginal and central pores in the ends of the diatoms. Later evidence (2) showed that these extracellular fibers consisted entirely of pure, highly crystalline poly-*N*-acetyl-D-glucosamine, $(C_8H_{13}O_5N)_n$, linked by β-(1 → 4)-bonds. This polymeric substance was given the name *chitan* to distinguish it from chitin, as it is isolated from other sources. It is not a chemically distinct species but has a radically different *x*-ray diffraction pattern and infrared spectrum (2). The name *chitan* was selected for this polysaccharide to conform with modern nomenclature.

The present paper records the results of a combined *x*-ray diffraction and electron microscope study of these extracellular fibers and proposes a probable structure for the crystalline polysaccharide. The atomic positions and chain configuration were first approximately assumed from known chemical and stereochemical criteria and these were then adjusted by trial and error until the calculated structure factors were in best agreement with the observed structure factors. Thirteen structure factors were studied quantitatively and fifteen were studied qualitatively.

Experimental

Methods for production and isolation of the chitan fibers have been described previously (1).

Electron Microscopy

Washed diatoms and the associated extracellular fibers were suspended in distilled water and drops of a dilute suspension transferred to specimen grids bearing carbon films. The grids were then dried in a desiccator over anhydrous $CaSO_4$ prior to shadowing with Pd:Au (60:40) at 15 °C. Both unshadowed as well as shadowed specimens were examined in a Philips EM 100C electron microscope at 80 kV.

x-Ray Diffraction

Both powder and fiber *x*-ray diffraction photographs of chitan were taken. The finely-powdered chitan, used to obtain the powder diffraction photographs, was prepared as follows: clean, dry mats of fibers (1, 2), frozen in a

---

[1]This investigation was reported in detail to the National Meeting of the American Chemical Society, Cellulose, Wood, and Fiber Chemistry, Chicago, September 11, 1967.

[2]Issued as NRCC No. 9927.

[3]NRCC Postdoctorate Fellow, 1966–1967. Present address: Physics Division, ATIRA, Ahmedabad-9, India.

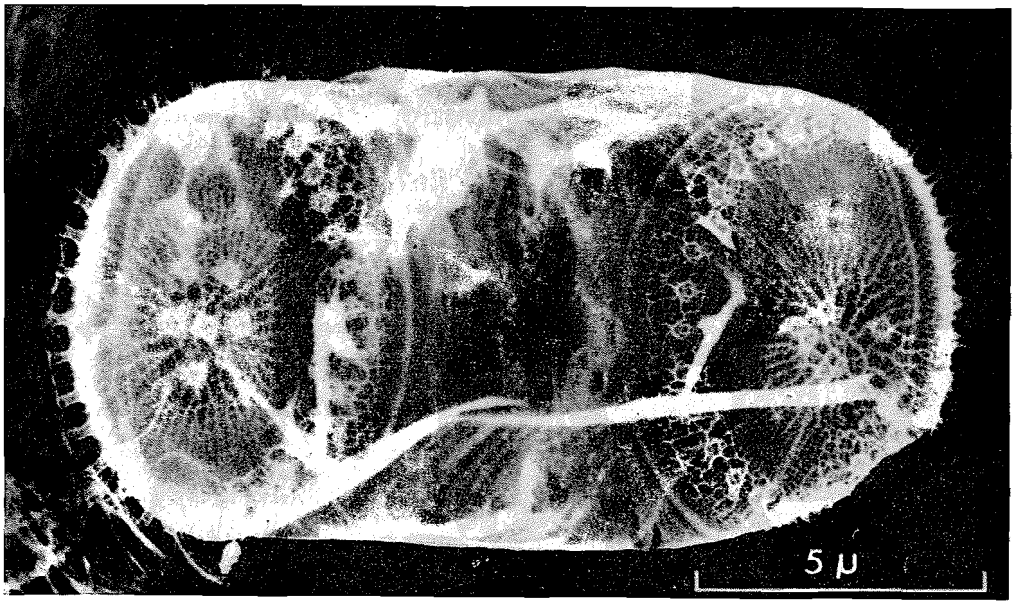

FIG. 1. Electron micrograph of the shell of an unshadowed diatom, *Thalassiosira fluviatilis*, in girdle view.

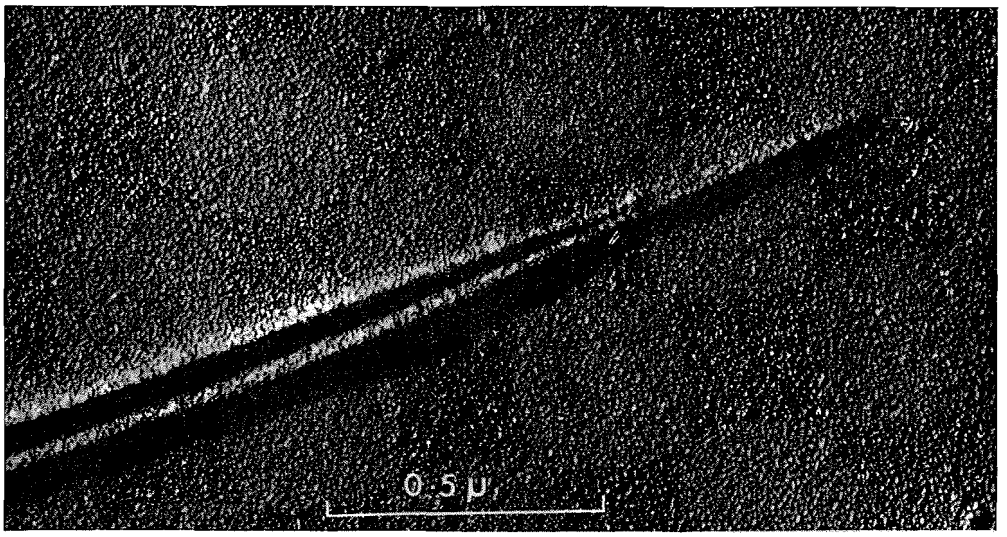

FIG. 2. Photograph of the shadowed basal end of a fiber which was embedded in the diatom prior to examination.

matrix of ice, were ground to a fine powder in an agate mortar. The powder was subsequently lyophilized.

Uniform, highly oriented fiber bundles, 0.1 mm in diameter and about 1 cm in length, were used for fiber *x*-ray diffraction photographs. The bundles were drawn slowly from a viscous slurry of chitan fibers in distilled water, the process being interrupted periodically to allow partial air drying before continuing the extension. Finally, the fiber bundles were air-dried completely.

The powder and oriented fiber *x*-ray diffraction photographs were obtained using a Philips "Norelco" microcamera. Nickel-filtered CuK α *x*-radiation of wavelength 1.542 Å was employed with a specimen to film distance of 15 mm. The collimator diameter was 0.002 in. and the microcamera was kept evacuated during exposure. The diffraction photographs were recorded on flat films.

Results and Discussion

Electron Microscope Studies

Electron micrographs of the shells of single diatoms, as well as single extracellular fibers, were taken. Figure 1 shows an electron micro-

Can. J. Chem. Downloaded from www.nrcresearchpress.com by 210.87.254.42 on 09/05/12
For personal use only.

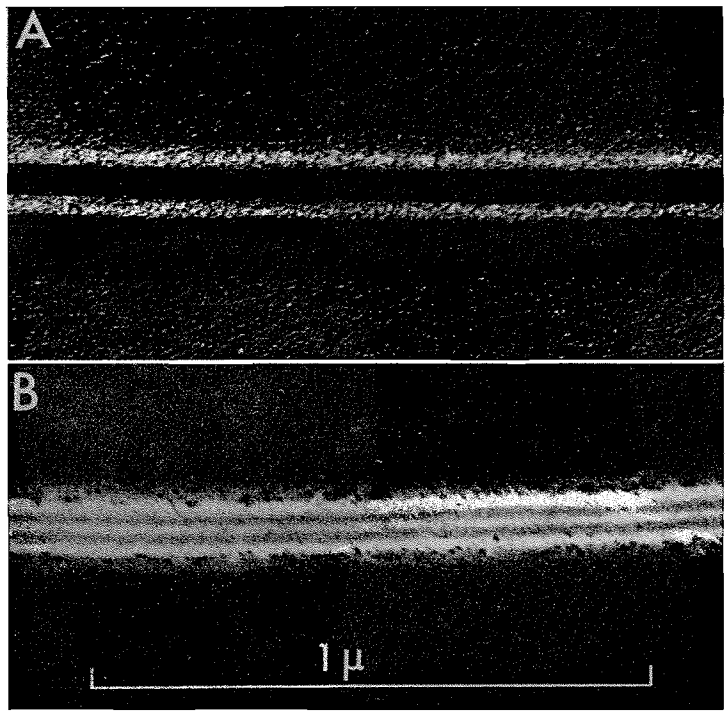

FIG. 3. Photographs of segments of: (A) a shadowed fiber close to the basal end and of; (B) a similar unshadowed segment.

graph of the shell of a single diatom in girdle view. Diatom lengths are in the range 12 to 15 μ. At the periphery of both ends of the cylindrical structure can be seen a circular array of tiny, hollow protrusions or pores. In addition, similar pores can be seen in the center of the circular ends. It is through these pores that the extracellular chitan fibers extend (1). The diatom shell is weakly siliceous with no *N*-acetyl-D-glucosamine present (1) which is further evidence that there is no close connection between the fibers and the wall.

Previous observations showed that the individual fibers have a strap-like form and are 60–80 μ in length with a maximum width of 0.1–0.2 μ (1). Present studies confirmed and extended these conclusions. Figure 2 is a photograph of the basal end of a fiber which was embedded in the diatom prior to examination. It tapers rapidly and resembles the quill tip of a feather. Figure 3A is a photograph of a short segment of a fiber, close to the base and after shadowing and Fig. 3B a photograph of a similar unshadowed segment. Each segment has a maximum width of 0.2 μ and a thickness which is much less (of the order of 0.05 μ). Furthermore, in these segments three parallel filaments are connected to each other laterally by two strips of the same material which are less electron dense. Therefore, two longitudinal grooves are present along both sides of the strap-like fiber close to its base and also in the center. On shadowing, both these grooves fall within the shadow created by the Au–Pd alloy and only the thicker, outer filaments are seen (Fig. 3A). Although it is not practical to illustrate all their length in a single photograph, the fibers also taper slowly and uniformly from a point close to their basal end to their outer extremity. Figure 4 shows the extreme outer tip of a fiber, where it tapers to a point below the resolution of the microscope. Although not shown in Fig. 4, the two longitudinal grooves gradually disappear as the tip of the fiber is approached. In summary, each chitan fiber is like a small strap with two grooves along each side, tapering rapidly towards one end and very slowly towards the other.

Because the fibers taper slowly towards their outer extremities and because they grow in length by extrusion from the cell, new chains of

Can. J. Chem. Downloaded from www.nrcresearchpress.com by 210.87.254.42 on 09/05/12
For personal use only.

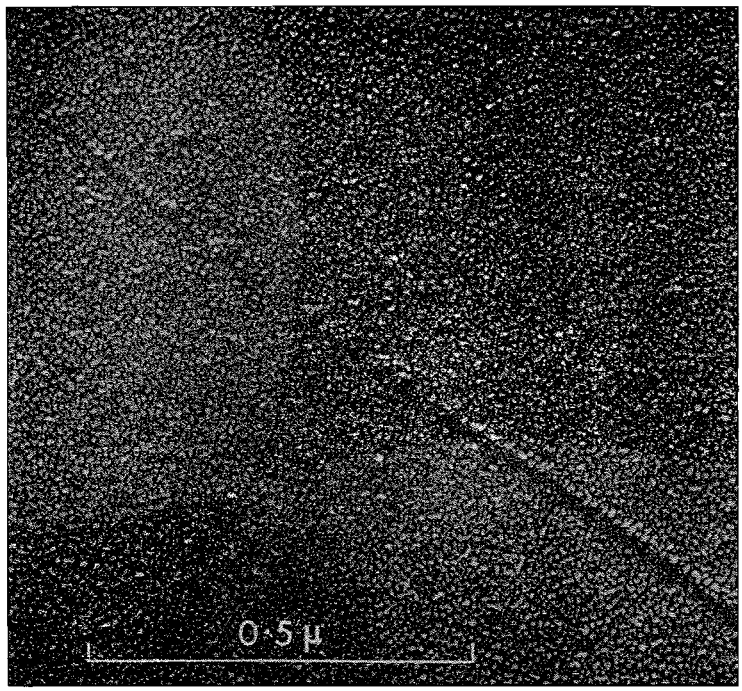

FIG. 4. An electron micrograph of the shadowed, tapering outer tip of a fiber.

poly-*N*-acetylglucosamine must be added to the periphery of the fibers as they extend at the base. However, nothing is yet known about the details of this process.

x-Ray Diffraction Studies

(a) Unit Cell of Chitan

The unit cell was determined from the *x*-ray diffraction pattern of completely randomized, finely powdered chitan, using the general method of Zsoldos (3) for a monoclinic lattice, because it was not possible to index all reflections on the basis of a unit cell of higher order. The *d* and $\sin^2\theta$ values of every observed ring were calculated and the first observed reflection of highest *d* spacing was assumed to be 001. The rest of the reflections were indexed with the aid of a graph in which the values of $(\sin^2\theta - l^2\sin^2\theta_{001})$ were plotted as ordinates and *l* the Miller index, as abscissa. From the indexed diffraction pattern, the unit cell parameters were deduced as $a = 4.80$, $b = 10.32$, $c = 9.83$ Å, and $\beta = 112°$. Fiber diffraction patterns were taken in order to check the unit cell parameters deduced from the powder ring analysis (3), to determine the correct space group of the monoclinic cell and to determine the structure factors of the observed reflections. The parameter $b = 10.32$ Å obtained earlier is in agreement with the fiber repeat distance calculated from the layer line spacings of a well-oriented bundle of chitan fibers (Fig. 5) where the fiber axis is vertical. Furthermore, the highest *d* value is an equatorial reflection and the earlier assumption that it was 001 is justified. All well-resolved reflections may be indexed with the unit cell derived above. Further, on the fiber diagram reproduced in Fig. 5 only the even order reflections were present on the meridian and all the odd order reflections *OkO* with *k* odd were absent. It was therefore concluded that there was a screw axis parallel to the fiber axis. As no further systematic absences were noted, it was concluded that the space group was $P2_1$.

(b) Structure of Chitan

The density of chitan was determined by the flotation method using well oriented bundles of chitan fibers in a mixture of bromoform and benzene. It was found to be 1.495 g/cm^3.

From the volume of the unit cell and the density it was calculated that there are two residues of *N*-acetylglucosamine, $C_8H_{13}O_5N$,

Can. J. Chem. Downloaded from www.nrcresearchpress.com by 210.87.254.42 on 09/05/12
For personal use only.

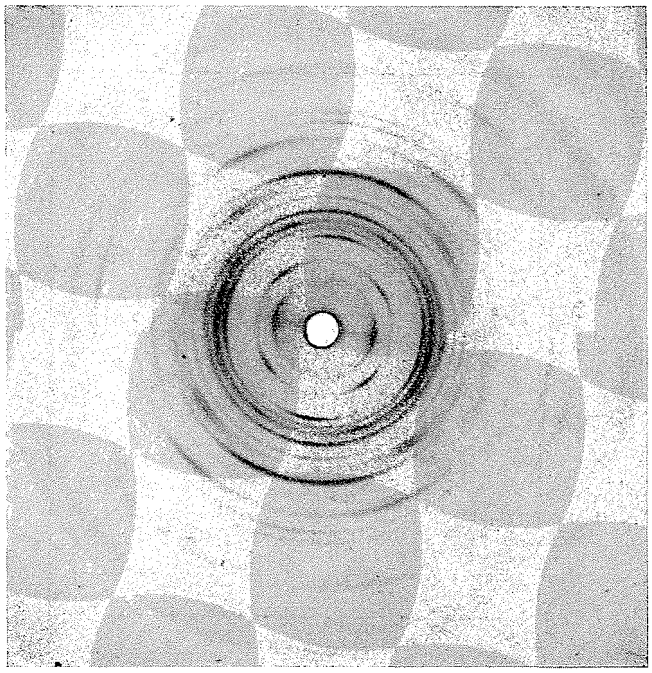

FIG. 5. *x*-Ray diffraction pattern of a bundle of longitudinally oriented chitan fibers recorded on flat film using Nickel-filtered CuK α radiation. Fiber axis vertical. The pattern has been enlarged to correspond to a specimen to film distance D = 4 cm.

per unit cell of chitan. Since chitan is a polymer with a crystallographic chain repeat of 10.32 Å and since the β-(1 → 4) repeat distance of a single *N*-acetyl-D-glucosamine residue from stereochemical criteria is 5.16 Å, there must be two residues in a repeat of 10.32 Å. Therefore, the two residues of *N*-acetylglucosamine in each unit cell must belong to the same chain. Furthermore, since there is a screw axis parallel to the fiber axis demanded by the space group, these two residues are crystallographic counterparts obtainable by a screw operation.

The cross-sectional area of the base of the unit cell (*ac*–plane) allows only one chain of poly-*N*-acetyl-D-glucosamine to pass through each parallelopiped without steric hindrance. Consequently, all the polymer chains in the crystalline part of the structure must run in the same direction and the structure of chitan is parallel crystallographically.

Using the above facts and the finding that the *N*-acetylglucosamine residues were linked by β-(1 → 4) bonds (2), scale model polymer chains were built in crystallographic array so that good lateral hydrogen bonding between neighboring chains was obtained. The coordinates of all carbon, oxygen and nitrogen atoms in one residue of *N*-acetylglucosamine were then determined with due consideration for stereochemical criteria regarding interatomic covalent and hydrogen bonds.

From the atomic coordinates the structure factors were calculated, F_c, for all possible reflections whose $\sin^2\theta$ values were less than 0.13, because no reflections were recorded outside this range. The calculations were made using a computer programmed with the standard expression for structure factors for space group $P2_1$.

Individual atoms within a single molecule were moved, as well as chains rotated as a whole, until good general agreement between calculated and observed structure factors was obtained. This process was carried out entirely by trial and error.

The *x*-ray intensities of all observed reflections from the fiber pattern were determined using a recording microdensitometer and following the method of Langridge *et al.* (4). The variation of optical density was measured for each reflection

Can. J. Chem. Downloaded from www.nrcresearchpress.com by 210.87.254.42 on 09/05/12
For personal use only.

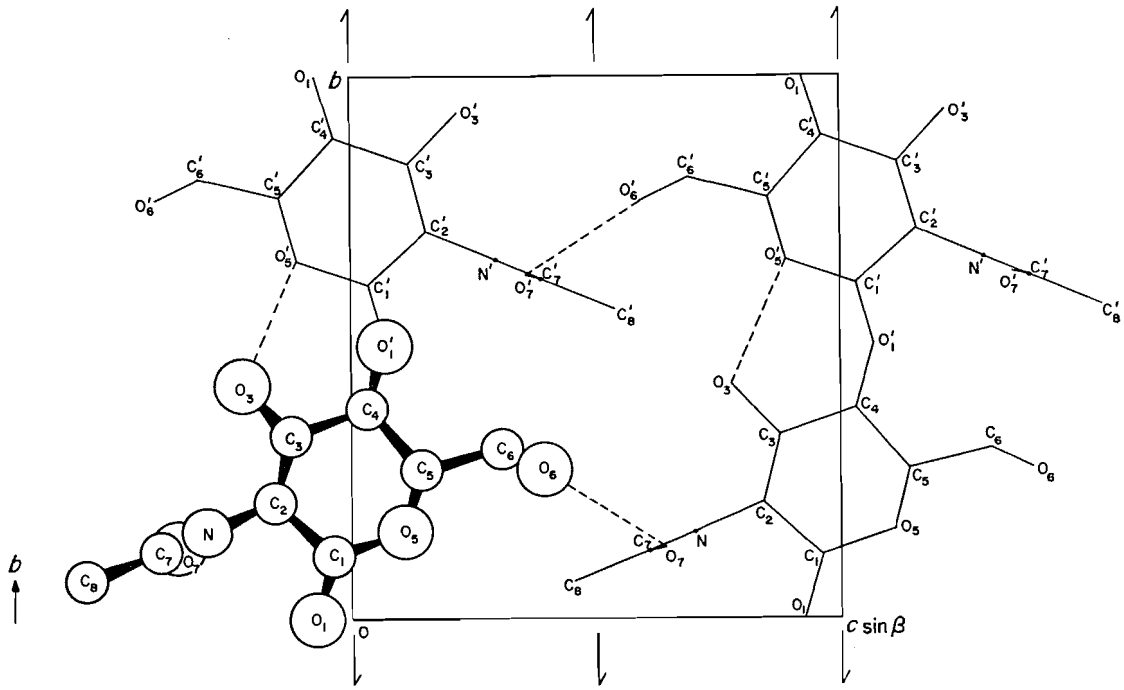

FIG. 6. The *a*-projection of the structure proposed for chitan. The fiber axis is vertical.

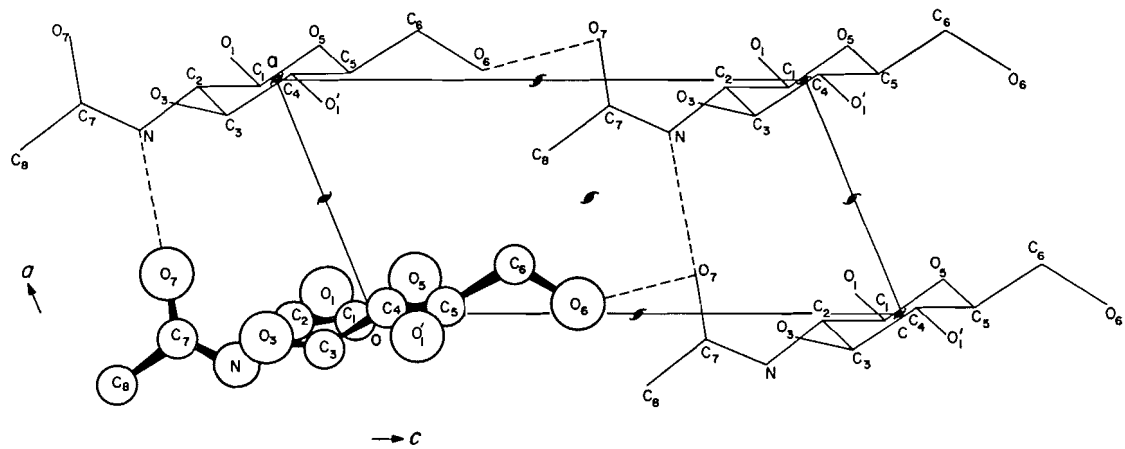

FIG. 7. The *b*-projection (fiber axis projection) of the structure proposed for chitan. For simplicity, only one half of the residues in the unit cell have been included.

in all the four quadrants of the photograph along a radius passing through the center of each spot. In practice, an image of a slit was traversed across each reflection, the length of the slit lying along the arc length. The integrated intensity was then calculated from the observed maximum by the method proposed by Franklin and Gosling (5). The first seven correction factors given by them were employed in these studies. The last, a correction for absorption by the specimen, was ignored. The average integrated intensity from all four quadrants was calculated in each case and the square root taken as the observed structure factor, F_o.

Can. J. Chem. Downloaded from www.nrcresearchpress.com by 210.87.254.42 on 09/05/12
For personal use only.

Can. J. Chem. Downloaded from www.nrcresearchpress.com by 210.87.254.42 on 09/05/12
For personal use only.

In order to scale correctly the F_o to the F_c, and to correct the F_c for the temperature effect, the following procedure was adopted. The value ln F_c/F_o was plotted against $\sin^2\theta/\lambda^2$ for all observed reflections and a straight line graph obtained. The intercept of this line on the ln F_c/F_o axis gave the scale factor and its slope gave the value of B to be used in the standard temperature factor. The value of B was 14 Å^2 which is considered reasonable for a fibrous material.

Figure 6 shows the projection along the a-axis of the final structure proposed for chitan. The atoms of one residue of N-acetylglucosamine are represented by circles and the covalent bonds by continuous lines. Hydrogen bonds are shown by broken lines. Figure 7 shows the projection along the b-axis. Here just one molecule on each of 4 adjacent chains has been projected in order to prevent overlap of atoms in projection.

Figures 6 and 7 show that there are three hydrogen bonds for every residue of N-acetylglucosamine. Of these three, one is an intra-chain $O_3H\ldots O_5$ bond of length 2.68 Å, and two are inter-chain: $O_6H\ldots O_7$ bond of length 2.75 Å and $NH\ldots O_7$ bond of length 2.73 Å. Both inter-chain stabilizing hydrogen bonds are bifurcated as the oxygen atom O_7 takes part in both. The six-membered rings are "chair" shaped and are connected to one another along the chain axis by bridge oxygen atoms in the β-(1 → 4) linkage. The 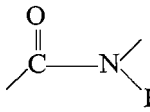 amide group is planar and has the conventional bond distances. There are no short contacts in the proposed structure.

Table I gives the d-values and hkl Miller indices of all observed reflections from the fiber pattern and also shows the agreement between F_c and F_o. In Table I, the F_c values have been corrected for the temperature effect, and the F_o values have been suitably scaled to the F_c. There were a few observed reflections which were too weak to determine their intensities accurately and these have been included in Table I as faint (F) or very faint (V.F.). Where two or more reflections overlapped the F_o of individual reflections could not be recorded, and here again the F_o have been included in Table I in symbolic terms. It is quite clear from Table I that

TABLE I

Calculated and observed structure factors for chitan

hkl	$\sin^2\Theta$ (calculated)	F_c	F_o	$\sin^2\Theta$ (observed)	d (Å) (observed)
001	0.0072	22.81	22	0.007	9.12
10$\bar{1}$	0.0262	61.60	61	0.026	4.76
002	0.0286	3.13			
100	0.0300	88.00	83	0.030	4.45
10$\bar{2}$	0.0367	18.58	19	0.037	4.03
101	0.0481	0.39	V.F.*	0.048	3.52
10$\bar{3}$	0.0615	1.51			
003	0.0644	8.73	V.F.*	0.065	3.02
102	0.0806	5.02			
10$\bar{4}$	0.1006	10.89			
20$\bar{2}$	0.1047	15.46	M	0.105	2.38
20$\bar{1}$	0.1052	28.96			
004	0.1145	15.50			
20$\bar{3}$	0.1185	0.69			
200	0.1200	6.23			
103	0.1273	6.28			
010	0.0056	0			
011	0.0127	15.14	16	0.013	6.80
11$\bar{1}$	0.0318	25.09	26	0.032	4.31
012	0.0342	13.48	14	0.034	4.18
110	0.0356	7.00			
11$\bar{2}$	0.0422	9.18	V.F.*	0.042	3.76
111	0.0537	10.14	V.F.*	0.053	3.35
11$\bar{3}$	0.0670	16.57	W	0.068	2.96
013	0.0700	17.43			
112	0.0862	0.99			
11$\bar{4}$	0.1061	9.09			
21$\bar{2}$	0.1103	12.10	F†	0.110	2.32
21$\bar{1}$	0.1108	7.85			
014	0.1200	16.23	F†	0.120	2.23
21$\bar{3}$	0.1241	6.00			
210	0.1256	12.23			
020	0.0223	32.12	33	0.022	5.16
021	0.0295	16.65	17	0.030	4.45
12$\bar{1}$	0.0485	9.46	8	0.049	3.48
022	0.0509	15.05	16	0.051	3.41
120	0.0523	13.75	V.F.*	0.057	3.23
12$\bar{2}$	0.0590	9.59			
121	0.0705	18.73	V.F.*	0.070	2.91
12$\bar{3}$	0.0838	6.61			
023	0.0867	8.23			
122	0.1029	3.72			
12$\bar{4}$	0.1229	6.95			
22$\bar{2}$	0.1270	7.46			
22$\bar{1}$	0.1275	0.88			
030	0.0502	0			
031	0.0574	30.09	30	0.058	3.20
13$\bar{1}$	0.0764	22.47			
032	0.0788	30.90	36	0.077	2.78
130	0.0802	11.30			
13$\bar{2}$	0.0869	10.05	V.F.*	0.089	2.58
131	0.0984	8.92			
13$\bar{3}$	0.1117	13.60	F†	0.110	2.32
033	0.1146	7.58			
040	0.0893	13.43	F†	0.089	2.58
041	0.0964	9.92	F†	0.097	2.48
14$\bar{1}$	0.1155	8.75			
042	0.1179	8.62			
140	0.1193	4.44			
14$\bar{2}$	0.1259	10.42	F†	0.126	2.17

*V.F. = very faint.
†F = faint.

there is good agreement between F_c and F_o, and that the structure proposed for chitan is probably correct. In this structure determination the contribution by the hydrogen atoms was ignored as the intensity data available are not accurate enough to warrant their inclusion.

TABLE II

Fractional coordinates of one *N*-acetylglucosamine residue (except hydrogens), corrected to 3 places of decimals derived from the final structure for chitan

Atom	*x/a*	*y/b*	*z/c*
C-1	−0.028	0.116	−0.036
C-2	−0.024	0.211	−0.156
C-3	−0.154	0.338	−0.120
C-4	0.028	0.384	0.036
C-5	0.028	0.271	0.142
C-6	0.209	0.307	0.305
C-7	−0.101	0.122	−0.390
C-8	−0.307	0.067	−0.541
N	−0.226	0.159	−0.297
O-1	0.089	0.000	−0.069
O-3	−0.102	0.427	−0.220
O-5	0.153	0.160	0.110
O-6	0.039	0.275	0.393
O-7	0.175	0.130	−0.356

Table II gives the final fractional coordinates of one *N*-acetylglucosamine residue without the hydrogen atoms which resulted in the satisfactory agreement between calculated and observed structure factors. Tables III and IV give the covalent and hydrogen bond distances involved in each residue of *N*-acetylglucosamine. All bond distances are satisfactory.

TABLE III

Intramolecular covalent bond distances in Å derived from the final structure for chitan

Bond	Distance
C_1—C_2	1.54
C_1—O_1	1.41
C_1—O_5	1.44
C_2—C_3	1.55
C_2—N	1.47
C_3—C_4	1.53
C_3—O_3	1.44
C_4—C_5	1.56
C_5—C_6	1.55
C_5—O_5	1.39
C_6—O_6	1.43
C_7—C_8	1.55
C_7—N	1.32
C_7=O_7	1.24
C_4—O_1	1.41

TABLE IV

Intermolecular hydrogen bond distances in Å for the final structure of chitan

Bond	Distance
O_3 (H).....O_5	2.68
O_6 (H).....O_7	2.75
N (H).....O_7	2.73

(c) Modifications of Chitan

An earlier study (2) reported that when chitan was immersed for a short time in hot, aqueous (50%) lithium thiocyanate, it was changed irreversibly into a form with an infrared spectrum and *x*-ray diffraction pattern indistinguishable from those of ordinary crustacean chitin (α-chitin). During the present investigation, this result was confirmed but we wish to stress that this change in the original chitan is accompanied by a marked loss of crystallinity and order in the

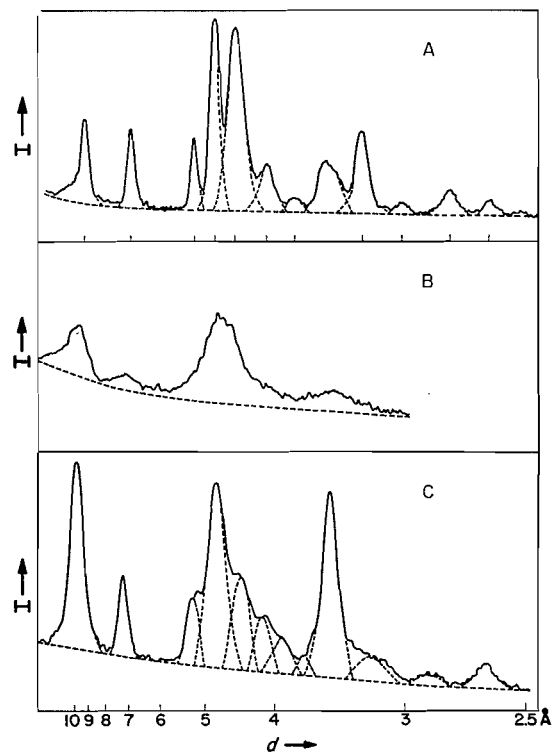

FIG. 8. Radial microdensitometer scans of: (A) *x*-ray powder diagrams of chitan; (B) chitan swollen in hot aqueous lithium thiocyanate (50%) for 15 s, washed, and dried; and (C) crustacean chitin.

Can. J. Chem. Downloaded from www.nrcresearchpress.com by 210.87.254.42 on 09/05/12
For personal use only.

specimen, as reflected both by the infrared spectrum (compare Fig. 3A with Fig. 3B of ref. 2) and *x*-ray diffraction powder patterns. Figure 8 shows uncorrected, radial, microdensitometer scans of the intensity distribution on flat film, powder, *x*-ray diffraction photographs of chitan, chitan swollen in hot aqueous lithium thiocyanate (50%) for 15 s, and crustacean chitin. The differences observed in the sharpness, intensities, and positions of the bands in microdensitometer tracings *a* and *c* add further support to the previous conclusion (2) that the macrostructure of unmodified chitan is markedly different from and much more crystalline than that of crustacean chitin. The lack of detail and broadness of the bands in scan *b* as compared with those in scan *a* clearly reflect a marked loss of order in the modified chitan. A similar comparison of scan *b* with scan *c* indicates that modified chitan has a lower degree of order than crustacean chitin, and consequently it is not possible to conclude unambiguously that modified chitan and crustacean chitin (α-chitin) have identical macrostructures.

Note added in proof—After this paper was submitted for publication, a recent short communication by Blackwell *et al.* (6) came to our notice in which a new unit cell was proposed for chitan based on *d*-spacings from fiber photographs. The parameters of the monoclinic unit cell with space group $P2_1$ were given as $a = 4.85$, $b = 10.38$ (fiber repeat), $c = 9.26$ Å, and $\beta = 97.5°$. This gives rise to essentially the same lattice as the one derived independently by us and proposed in this paper. The two unit cells can be derived from one another by a transformation of axes. The essential difference between the two is that a basal *ac*-plane diagonal in the present unit cell becomes the basal cell edge in the unit cell proposed by Blackwell *et al.* (6). The reason why the present unit cell was retained by us was because it is the one derived by the method proposed by Zsoldos (3) in which the reflection with the highest *d*-spacing is indexed as 001. Thus there is essentially no difference between the unit cell proposed here and the one given by Blackwell *et al.* (6). The space group and parallel chain arrangement are also confirmed independently.

1. J. McLachlan, A. G. McInnes, and M. Falk. Can. J. Botany, **43**, 707 (1965).
2. M. Falk, D. G. Smith, J. McLachlan, and A. G. McInnes. Can. J. Chem. **44**, 2269 (1966).
3. L. Zsoldos. Acta Cryst. **11**, 835 (1958).
4. R. Langridge, H. R. Wilson, C. W. Hooper, M. H. F. Wilkins, and L. D. Hamilton. J. Mol. Biol. **2**, 19 (1960).
5. R. E. Franklin and R. G. Gosling. Acta Cryst. **6**, 678 (1953).
6. J. Blackwell, K. D. Parker, and K. M. Rudall. J. Mol. Biol. **28**, 383 (1967).

Can. J. Chem. Downloaded from www.nrcresearchpress.com by 210.87.254.42 on 09/05/12
For personal use only.

Can. J. Chem. Downloaded from www.nrcresearchpress.com by 210.87.254.40 on 09/05/12
For personal use only.

Fermentation of long-chain compounds by *Torulopsis apicola*. IV. Products from esters and hydrocarbons with 14 and 15 carbon atoms and from methyl palmitoleate[1,2]

A. P. Tulloch and J. F. T. Spencer
National Research Council of Canada, Prairie Regional Laboratory, Saskatoon, Saskatchewan

Received November 22, 1967

Esters and hydrocarbons, containing 14 and 15 carbon atoms, are converted to the hydroxy fatty acid portions of glycosides by *Torulopsis apicola* in yields of 10–20%. When C-15 compounds are fermented, almost half of the hydroxy acids which are produced are 16-hydroxy C-17 acids. The carbon chain of the substrate is first lengthened by two carbon atoms and then hydroxylated. Direct hydroxylation also occurs, to a lesser extent, giving both 14-hydroxy- and 15-hydroxypentadecanoic acids. Similar results are obtained when C-14 compounds are used. Lengthening of the chain followed by hydroxylation gives rise to hydroxy C-16 acids and direct hydroxylation produces 13-hydroxy- and 14-hydroxytetradecanoic acids. Primary and secondary C-14 and C-15 alcohols were also isolated from the products of hydrocarbon fermentation (2.5–5% yield). Methyl palmitoleate is converted to hydroxy fatty acids in yields of 40–70%, the major component of which is 16-hydroxy-*cis*-9-hexadecenoic acid.

Canadian Journal of Chemistry, **46**, 1523 (1968)

Several years ago we reported the discovery of a yeast of the genus *Torulopsis* which produced extracellular glycosides consisting of partly acylated sophorosides of hydroxy fatty acids (1). The yeast, which was formerly thought to be a strain of *Torulopsis magnoliae* (1), has since been examined at the Centraalbureau voor Schimmelcultures in Delft and has been identified as *Torulopsis apicola* (Hajsig). As well as producing glycosides when grown on glucose, the yeast also converted long chain hydrocarbons and fatty acids directly to the hydroxy fatty acid portion of the glycosides (2). When compounds with 16 or more carbon atoms were fermented they were converted to hydroxy fatty acid glycosides in quite high yield, but when compounds with 15 or fewer carbon atoms were used the yield of glycoside was much lower. We have now investigated the composition of the hydroxy fatty acid portion of the glycosides obtained when compounds with 14 and 15 carbon atoms are fermented. In all the fermentations the hydroxy acids consisted of a mixture of acids with the hydroxyl group on the terminal carbon atom, (ω-hydroxylation), and acids with the hydroxyl group on the penultimate carbon atom ((ω−1)-hydroxylation). The relative amounts of these acids varied considerably. Our earlier work with 16–18 carbon compounds (2) suggested that the degree of ω-hydroxylation increased as the length of the substrate molecule decreased. We wished to determine if still higher proportions of ω-hydroxy acids were formed when the shorter chain acids were used, particularly, since one of the possible products, ω-hydroxypentadecanoic acid, is used to prepare the macrocyclic musk "exaltolide".

The products of the fermentation of methyl palmitoleate were also investigated, since it appeared (2) that an ester with one *cis* double bond reacted like a saturated ester with one less carbon atom. It was suggested (2) that this was because the molecules of such a pair of esters were similar in length. Methyl palmitoleate might therefore be expected to react in the same way as methyl pentadecanoate.

Fermentation of 14 and 15 Carbon Compounds

When either esters or hydrocarbons with 14 and 15 carbon atoms were fermented, 10–20% of the substrate was converted to hydroxy fatty acid sophoroside. Sometimes the rest of the added compound was completely metabolized by the yeast, but on other occasions about half could be recovered unchanged.

The compositions of the hydroxy fatty acid portions of the products obtained after the fermentation of methyl pentadecanoate and pentadecane were determined by gas–liquid chromatography (g.l.c.) (3, 4). They are shown in Table I. The mixtures were more complicated than

[1]Issued as NRCC No. 10003.
[2]Presented in part at the 49th Canadian Chemical Conference of the Chemical Institute of Canada, Saskatoon, June 1966.

those obtained from earlier fermentations and the individual components had to be concentrated by column chromatography, distillation, and fractionation of the acetates by urea complex formation, and finally purified by g.l.c., before characterization. The strain of yeast, used to ferment the ester, had been kept in laboratory culture longer than that used to ferment the hydrocarbons and formed hydroxy fatty acids with a greater degree of unsaturation than it had produced when first isolated (1).

TABLE I

Composition of hydroxy acid portion of fermentation products from C-15 compounds

	Compound fermented	
	Methyl pentadecanoate	Pentadecane
Hydroxy acid	Percentage of hydroxy acid	
14 OH 15:0	13	14
15 OH 15:0	14	17
15 OH 16:0	1	1
16 OH 16:0	2	1
16 OH 17:0	13	30
16 OH 17:1	29	13
17 OH 17:0	3	2
17 OH 18:0	6	8
17 OH 18:1	12	9
18 OH 18:0	1	1
18 OH 18:1	2	2
Unidentified components	4	2

Table I shows that hydroxypentadecanoic acids are produced but these form only about 25% of the total. The amounts of ω-hydroxy- and (ω−1)-hydroxypentadecanoic acids are approximately equal, which is similar to the ratio of ω-hydroxy to (ω−1)-hydroxy acid obtained by fermenting methyl palmitate ((2) and Table III). The major components are (ω−1)-hydroxy C-17 acids but ω-hydroxy C-17 acids are very minor components. The remainder consists of hydroxy C-18 acids which, together with 2–3% of hydroxy C-16 acids, are probably produced by the "normal" fermentation of the organism which sometimes continues in the presence of long-chain substrates (2).

The hydroxy acids were shown to be produced by direct hydroxylation of the substrate (2) and this reaction no doubt accounts for the formation of 14-hydroxy and 15-hydroxy C-15 acids. The formation of 16-hydroxyheptadecanoic acid was much more unexpected. However, the carbon chain of pentadecanoic acid is probably lengthened by two carbon atoms and the resulting heptadecanoic acid is then hydroxylated. The relative amounts of (ω−1)-hydroxy and ω-hydroxy C-17 acids are about the same as those found when heptadecanoic acid was fermented (2). The unsaturated 16-hydroxy C-17 acid was isolated and shown to be 16-hydroxy-*cis*-9-heptadecenoic acid. Thus it appears that, when the chain length is too short for good conversion to hydroxy acids, the chain can be elongated to a more suitable length; also a double bond can be introduced at the 9,10-position.

TABLE II

Composition of hydroxy acid portion of fermentation products from C-14 compounds

	Compound fermented		
	Methyl myristate	Tetradecane	None
Hydroxy acid	Percentage of hydroxy acid		
13 OH 14:0	13	7	—
14 OH 14:0	14	9	—
15 OH 16:0	10	18	8
15 OH 16:1	5	1	—
16 OH 16:0	11	18	9
16 OH 16:1	11	5	4
17 OH 18:0	6	15	19
17 OH 18:1	25	20	48
18 OH 18:0	—	1	4
18 OH 18:1	3	2	4
Unidentified components	2	4	4

Table II shows the compositions of the fatty acid portions of the glycosides obtained from C-14 ester and hydrocarbon. The composition of the fatty acids, obtained when the strain used to ferment the methyl ester was grown in the absence of long-chain substrate, is included for comparison. Up to 25% of the acids are produced by direct hydroxylation giving 13-hydroxy and 14-hydroxytetradecanoic acids in about a 1:1 ratio. It is likely that elongation of the chain, giving rise to hydroxy C-16 acids, also occurs since these acids form about 40% of the total compared to about 20% formed without added long-chain compounds. The unsaturated 16-hydroxy C-16 acid was isolated and the double bond shown to be at the 9,10-position.

Can. J. Chem. Downloaded from www.nrcresearchpress.com by 210.87.254.40 on 09/05/12
For personal use only.

Can. J. Chem. Downloaded from www.nrcresearchpress.com by 210.87.254.40 on 09/05/12
For personal use only.

In addition to hydroxy acids, the hydrolyzed fermentation products produced from C-14 and C-15 hydrocarbons contained alcohols. Those from tetradecane were a mixture of 1-tetradecanol and 2-D-tetradecanol, and those from pentadecane were a mixture of 1-pentadecanol and 2-D-pentadecanol. In both cases the ratio of secondary alcohol to primary alcohol was about 4:1. The alcohols are probably formed by hydroxylation and then converted to glycosides without further oxidation to acids. The higher proportion of secondary alcohols compared to the 1:1 ratio of (ω−1)-hydroxy to ω-hydroxy acids suggests that secondary alcohols are less readily converted to hydroxy acids than are primary alcohols. The secondary alcohols are assigned the D-configuration because of their positive rotation (5), but as explained before (1), the rules of nomenclature require that the dextrorotatory (ω−1)-hydroxy acids be named as L-hydroxy acids.

Fermentation of Methyl Palmitoleate

The yields of glycoside obtained from methyl palmitoleate were much better than those from methyl pentadecanoate. One strain of yeast converted about 40% of the substrate to hydroxy acids and another converted about 70%. The composition of the product, which was the same for both strains of yeast, is shown in Table III; the hydroxy esters obtained by fermenting methyl palmitate are shown for comparison. The major components have been produced by direct hydroxylation in both cases, but using the unsaturated substrate, the ratio of ω-hydroxy to (ω−1)-hydroxy acid is about 4:1 and for palmitate it is 1:1. If methyl palmitoleate had been fermented in the same way as methyl pentadecanoate a 1:1 ratio would have been expected. Thus it appears that the theory relating degree of ω-hydroxylation with length of substrate molecule (2) does not hold in this case, though it seems that the presence of a *cis* double bond favors ω-hydroxylation.

16-Hydroxy-*cis*-9-hexadecenoic acid, which had previously been isolated from shellac (6), was obtained from the hydrolyzed fermentation product by column chromatography. By analogy with the fermentation of methyl pentadecanoate, chain extension of the substrate by two carbon atoms might occur, giving *cis*-11-octadecenoic acid which might then be hydroxylated to the corresponding 17-hydroxy acid. The fractions, obtained during the isolation of 16-hydroxy-9-hexadecenoate which contained unsaturated C-18 hydroxy esters and unsaturated 15-hydroxy and 16-hydroxy C-16 esters, were oxidized with the permanganate periodate reagent and the products analyzed by g.l.c. (7). However, since the only dibasic acid produced was azelaic acid, the unsaturated C-18 ester must be 17-hydroxyoleate and cannot be derived from palmitoleate by simple chain extension.

TABLE III

Composition of hydroxy acid portion of fermentation products from C-16 esters

	Compound fermented	
	Methyl palmitoleate	Methyl palmitate
Hydroxy acid	Percentage of hydroxy acid	
15 OH 16:0	4	36
15 OH 16:1	13	1
16 OH 16:0	4	42
16 OH 16:1	55	4
17 OH 18:0	9	5
17 OH 18:1	13	10
18 OH 18:0	trace	trace
18 OH 18:1	2	2

Experimental

Nuclear magnetic resonance (n.m.r.) spectra were measured with a Varian HA-100 spectrometer, using carbon tetrachloride as solvent. Silicic acid (Bio-Sil A from Bio-Rad Laboratories, Richmond, California) was used for column chromatography. Gas–liquid chromatography (g.l.c.) was carried out as described previously (2–4, 7).

Method of Fermentation

The medium used was: glucose (10%), yeast extract (1%), and urea (0.1%). Methyl esters (0.5–1 g portions) were fermented with strain 148-64 in shaken flasks containing medium (50 ml) as described previously (2). Strain 325-66 was used to ferment the hydrocarbons. Medium (3 l) was inoculated with 50 ml of shaken culture and agitated at 385 r.p.m. for 4 days at 24 °C with an air flow of 1 l/min in 5-l fermentors. Portions (35 g) of the hydrocarbons were added on each of the first three days. The extracellular glycosides were extracted with ethyl acetate and the solvent removed, the gum was then taken up in 80% methanol–water, and unreacted substrate extracted by shaking with hexane, the aqueous methanol was removed on a rotatory evaporator.

Products of the Fermentation of C-15 Compounds

Glycoside (4.85 g) was obtained from methyl pentadecanoate (8 g in 8 flasks), and hydrolysis with methanolic

Can. J. Chem. Downloaded from www.nrcresearchpress.com by 210.87.254.40 on 09/05/12
For personal use only.

hydrogen chloride (4%) (1) gave hydroxy ester (1.93 g). Pentadecane (200 g) gave glycoside (51.5 g) and unreacted starting material (100 g) was recovered.

Isolation of C-15 Alcohols

Hydrolysis of the above glycoside from pentadecane gave hydroxy esters and alcohols (21 g). This mixture was saponified with aqueous alkali and the alcohols (3.5 g) extracted with hexane; acidification of the aqueous portion and ether extraction gave the hydroxy acids (15.2 g). The alcohols and their acetates were analyzed by g.l.c. using silicone and polyester columns (3, 4), comparison of the retention times with those of 2- and 1-pentadecanols (and their acetates) indicated that the alcohols consisted of 2-pentadecanol (80%) and 1-pentadecanol (20%).

The mixture of alcohols was acetylated by refluxing with acetic anhydride and the acetate of 1-pentadecanol concentrated to about 60% by urea complex formation, as previously described in the purification of methyl 18-hydroxyoctadecanoate (2). The two acetates were then separated in batches by g.l.c. using a silicone column (2) and the alcohols isolated after deacetylation. 1-Pentadecanol crystallized from hexane and had m.p. 43–43.5 °C, an authentic sample had m.p. 44–45 °C and the mixed m.p. was 44–45 °C. 2-D-Pentadecanol was crystallized from hexane and had m.p. 39–40 °C and $[\alpha]_D^{28}$ +6.2° (*c*, 1.5 in methanol).

Anal. Calcd. for $C_{15}H_{32}O$: C, 78.87; H, 14.12. Found: C, 78.80; H, 13.93.

The location of the hydroxyl group at C-2 was confirmed by the n.m.r. spectrum which showed a methyl doublet at 1.10 p.p.m. for CH_3 adjacent to CHOH (8).

Identification of the Hydroxy Acids

Portions of the hydroxy methyl esters derived from the products of the fermentation of C-15 esters and hydrocarbons were acetylated and analyzed by g.l.c. (ethylene glycol succinate column (4)). Using this column methyl 16-acetoxy 9-heptadecenoate has almost the same emergence time as methyl 16-acetoxy hexadecanoate; therefore, part of the acetylated esters was hydrogenated and reanalyzed and the percentages of the overlapping peaks calculated by difference. Figure 1 shows the curves obtained in the analysis of the esters before and after hydrogenation.

Isolation of Hydroxy C-15 Esters

Acids (15.2 g), from the fermentation of pentadecane, were taken up in acetone (160 ml) and allowed to crystallize at room temperature. After filtration of the saturated acids (4.7 g), the mother liquors, which contained unsaturated acids and an increased proportion of hydroxy C-15 acids, were converted to methyl esters and acetylated. Fractional distillation at 0.2 mm through a short Vigreux column gave a fraction (2.4 g), b.p. 140–145 °C, which contained 14-acetoxypentadecanoate (30%) and 15-acetoxypentadecanoate (25%). This fraction was treated with urea (2 g) in methanol (25 ml) and gave a urea complex (1.4 g) which yielded esters (0.37 g) after decomposition. These esters, which contained 52% of ω-acetate, were separated on the silicone column and gave methyl 15-hydroxypentadecanoate after deacetylation. Crystallization from hexane gave the ester with m.p. and mixed m.p. 47.5–48.5 °C.

The mother liquors from the urea fractionation were distilled to give a concentrate of 14-acetoxy ester which was purified by g.l.c. Deacetylation and crystallization from hexane gave methyl 14-L-hydroxypentadecanoate with m.p. 40–41 °C and $[\alpha]_D^{28}$ +4.5 (*c*, 1.3 in methanol).

Anal. Calcd. for $C_{16}H_{32}O_3$: C, 70.54; H, 11.84. Found: C, 70.75; H, 11.80.

The n.m.r. spectrum confirmed the structure (methyl doublet at 1.10 p.p.m. (8)).

Isolation of Hydroxy C-17 Acids

The saturated hydroxy acids (4.7 g) obtained from the fermentation of pentadecane, above, were converted to methyl esters and acetylated. Methyl 16-acetoxyheptadecanoate, which formed about 60% of the mixture, was isolated by preparative g.l.c. (2). Deacetylation gave methyl 16-hydroxyheptadecanoate which was crystallized from hexane; the m.p. and mixed m.p. with an authentic sample (2) was 50.5–51.5 °C.

The unsaturated hydroxy C-17 ester was isolated from hydroxy esters obtained by fermentation of methyl pentadecanoate since they contained a relatively high percentage of this component. These esters were acetylated and separated on a silver nitrate–silicic acid column (9). Elution with benzene–hexane 1:1 gave saturated esters, and elution with benzene–hexane 4:1 gave unsaturated esters which consisted of a mixture of acetoxy C-17 and C-18 compounds. The mixture was separated by g.l.c. and the C-17 product deacetylated to give methyl 16-hydroxy-9-heptadecenoate. Oxidation with the permanganate periodate reagent gave azelaic acid which was identified by g.l.c. (7). The n.m.r. spectrum showed a methyl doublet at 1.12 p.p.m. (8) and a multiplet at 5.24 p.p.m. for the two protons of a relatively isolated *cis* double bond (10).

Products of the Fermentation of C-14 Compounds

Methyl myristate (0.5 g per flask) was fermented in two flasks giving glycoside (1.4 g); hydroxy esters (0.53 g) were obtained on hydrolysis. Tetradecane (200 g) gave glycoside (65 g) and unreacted hydrocarbon (*c*, 100 g) was recovered.

Isolation of C-14 Alcohols

The above glycoside (65 g) gave a mixture (25 g) of hydroxy esters and alcohols on hydrolysis. Alcohols (3 g) were isolated and separated into 1-tetradecanol (20%) and 2-tetradecanol (80%) by the procedures used with the C-15 alcohols. 1-Tetradecanol was crystallized from hexane and had m.p. and mixed m.p. 38–39 °C. 2-D-Tetradecanol, crystallized in the same way, had m.p. 33.5–34.5 °C and $[\alpha]_D^{28}$ +6.2 (*c*, 1.6 in methanol).

Anal. Calcd. for $C_{14}H_{30}O$: C, 78.43; H, 14.11. Found: C, 78.25; H, 13.88.

The n.m.r. spectrum had a methyl doublet signal at 1.12 p.p.m.

Isolation of C-14 and C-16 Hydroxy Acids

The acids remaining after the separation of alcohols were converted to methyl esters (17 g) and fractionated on a silicic acid column. Elution with hexane–acetone (96:4) gave a fraction (8 g) with C-18 esters as major components and elution with hexane–acetone (92:8) gave

Can. J. Chem. Downloaded from www.nrcresearchpress.com by 210.87.254.40 on 09/05/12
For personal use only.

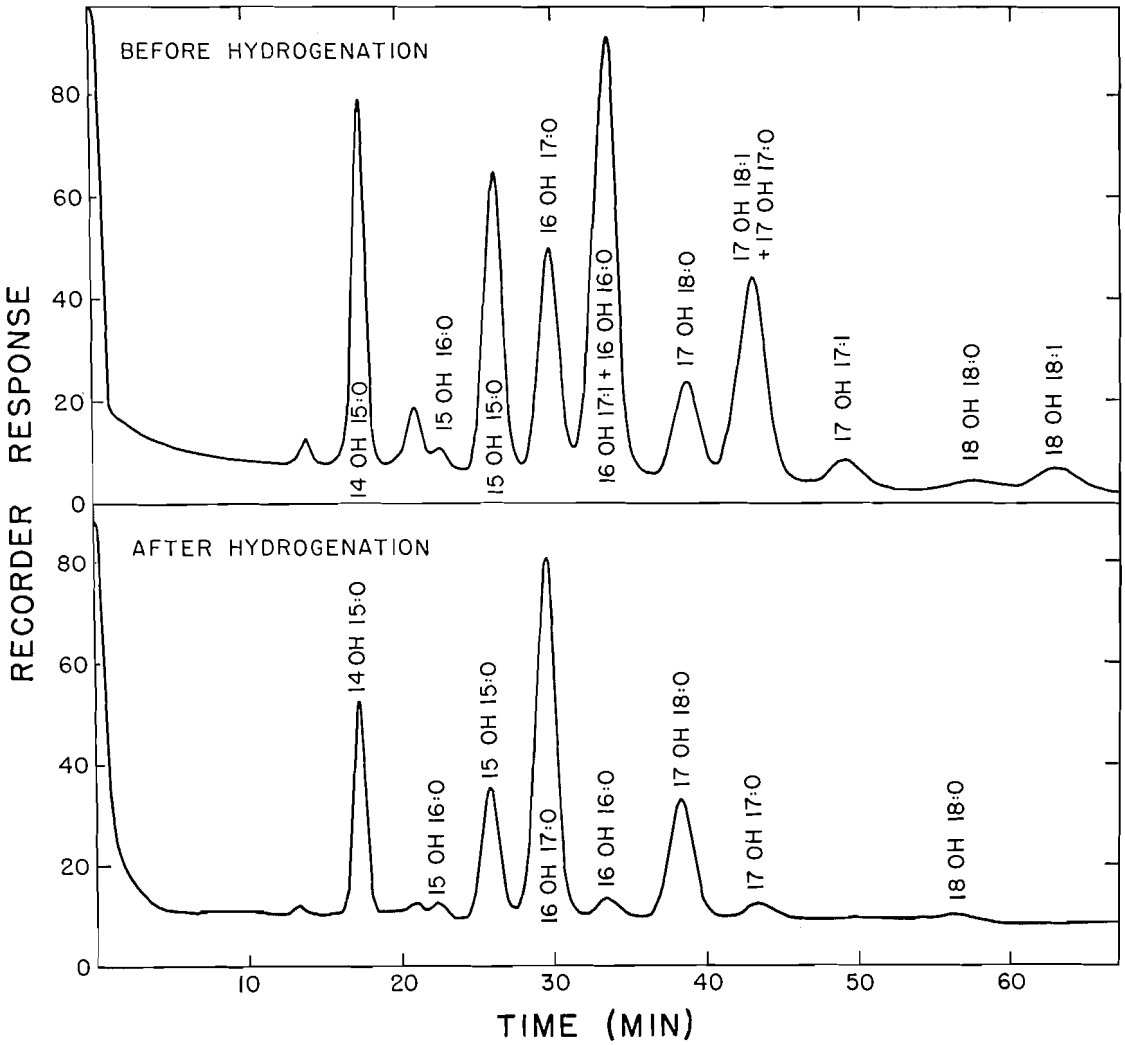

FIG. 1. Gas–liquid chromatographic separation of acetylated hydroxy esters derived from the fermentation of methyl pentadecanoate.

material (4.8 g) composed mainly of C-14 and C-16 esters. This material (4.8 g) was acetylated and chromatographed on a silver nitrate – silicic acid column (250 g) giving saturated esters (2.8 g) (elution with benzene–hexane 1:1) and unsaturated esters (1.8 g) (elution with benzene–ether 95:5).

Isolation of Saturated C-14 and C-16 Hydroxy Esters

The saturated esters were deacetylated and chromatographed on a silicic acid column. Elution with hexane–chloroform (3:1) gave crude methyl 15-hydroxyhexadecanoate which, after rechromatography and crystallization from hexane, had m.p. and mixed m.p. 46.5–47.5 °C (2). A mixture of methyl 16-hydroxypalmitate and methyl 13-hydroxytetradecanoate was eluted next, and finally methyl 14-hydroxytetradecanoate was eluted with hexane–chloroform (1:1). Methyl 14-hydroxytetradecanoate was crystallized from hexane and had m.p. 46–46.5 °C (lit. (11) gives 47°); 14-hydroxytetradecanoic acid was obtained by saponification and had m.p. 90–91 °C (lit. (11) gives 91–91.5 °C). Methyl 16-hydroxyhexadecanoate was isolated by rechromatography and had m.p. and mixed m.p. 56–56.5 °C (2). A fraction containing a relatively high proportion of methyl 13-hydroxytetradecanoate was acetylated and the pure acetoxy ester obtained by preparative g.l.c. Deacetylation and crystallization from hexane gave methyl 13-L-hydroxytetradecanoate with m.p. 41–42 °C and $[\alpha]_D^{28}$ +6.2 (*c*, 1.1 in methanol).

Anal. Calcd. for $C_{15}H_{30}O_3$: C, 69.72; H, 11.70. Found: C, 69.51; H, 11.63.

In the n.m.r. spectrum the terminal CH_3 signal was a

doublet at 1.11 p.p.m. A 13-hydroxytetradecanoic acid has been reported to be present in the bark of white fir (12), but the configuration of the optical center was not determined.

Isolation of Unsaturated Hydroxy C-16 Acid

When the unsaturated acetoxy esters (1.8 g) were deacetylated and chromatographed on silicic acid in chloroform–hexane (1:3) fractions containing methyl 17-hydroxy-9-octadecenoate (0.9 g) and methyl 16-hydroxy-9-hexadecenoate (0.4 g) were obtained. Both yielded azelaic acid on oxidation with the permanganate periodate reagent (7). 16-Hydroxy *cis*-9-hexadecenoic acid was obtained by hydrolysis of the second fraction, after crystallization from acetone the m.p. was 28–28.5 °C. Conversion to the methyl ester and hydrogenation gave methyl 16-hydroxyhexadecanoate with m.p. and mixed m.p. 56–57 °C (2).

Products of the Fermentation of Methyl Palmitoleate

Methyl palmitoleate was isolated from Emery oleic acid (Emersol 233LL) which was previously shown to contain 12% of hexadecenoic acids (4). The acid was converted to methyl esters and the esters of the C-16 acids were separated by distillation through a spinning band column. Fractional crystallization from methanol at −10 to −20 °C removed the less soluble methyl palmitate and also the *trans* ester leaving pure methyl palmitoleate.

Methyl palmitoleate (0.5 g per flask) was fermented in two flasks with strain 148-64 giving glycoside (1.78 g) which gave hydroxy esters (0.76 g) on hydrolysis. Using strain 319-67, ester (4 g) (1 g per flask) gave glycoside (5.8 g) and hydroxy esters (1.50 g).

The hydroxy esters (1.4 g) were chromatographed on silicic acid (50 g) and eluted with hexane–chloroform (3:1). The first fraction (0.23 g) contained hydroxy C-18 esters and the second (0.51 g) consisted of approximately equal amounts of unsaturated 15-hydroxy and 16-hydroxy C-16 and 17-hydroxy C-18 esters. Portions of each of these fractions were oxidized with the permanganate periodate reagent in 60% *t*-butanol (7) and the dicarboxylic acids produced were shown by g.l.c. (7) to consist almost entirely of azelaic acid. The latter fractions from the silicic acid column contained pure methyl 16-hydroxy-*cis*-9-hexadecenoate (0.50 g), which gave 16-hydroxy-*cis*-9-hexadecenoic acid on hydrolysis; the m.p. was 23.5–25.5 °C (Lit. (6) gives 17–19 °C). Part of this acid was esterified with diazomethane and hydrogenated to give methyl 16-hydroxyhexadecanoate m.p. and mixed m.p. 54.5–55.5 °C.

Acknowledgments

The authors wish to thank Mr. L. L. Hoffman and Mr. N. R. Gardner for experimental assistance, Mr. M. Mazurek for nuclear magnetic resonance measurements and Mr. W. C. Haid for microanalyses.

1. P. A. J. Gorin, J. F. T. Spencer, and A. P. Tulloch. Can. J. Chem. **39**, 846 (1961).
2. A. P. Tulloch, J. F. T. Spencer, and P. A. J. Gorin. Can. J. Chem. **40**, 1326 (1962).
3. A. P. Tulloch. J. Am. Oil Chemists' Soc. **41**, 833 (1964).
4. A. P. Tulloch and J. F. T. Spencer. J. Am. Oil Chemists' Soc. **43**, 153 (1966).
5. J. A. Mills and W. Klyne. Progr. Stereochem. **1**, 205 (1954).
6. W. W. Christie, F. D. Gunstone, H. G. Prentice, and S. C. Sen Gupta. J. Chem. Soc. 5833 (1964).
7. A. P. Tulloch and B. M. Craig. J. Am. Oil Chemists' Soc. **41**, 322 (1964).
8. A. P. Tulloch. J. Am. Oil Chemists' Soc. **43**, 670 (1966).
9. B. DeVries. J. Am. Oil Chemists' Soc. **40**, 184 (1963).
10. C. Y. Hopkins. Progr. Chem. Fats Lipids, **8**, Part 2, 213 (1965).
11. P. Chuit and J. Hausser. Helv. Chim. Acta, **12**, 463 (1929).
12. H. L. Hergert and E. F. Kurth. Tappi, **36**, 137 (1953).

Can. J. Chem. Downloaded from www.nrcresearchpress.com by 210.87.254.40 on 09/05/12
For personal use only.

The deamination of 16-acetyl-17-aminoandrosta-5,16-dien-3β-ol[1]

L. Rodríguez-Hahn and J. Romo
Instituto de Química de la Universidad Nacional Autónoma de México, México 20, D.F., México

Received November 20, 1967

The deamination of 16-acetyl-17-aminoandrosta-5,16-dien-3β-ol (**2***a*) with nitrous acid afforded two products. Their structures have been established as **3***a* and **3***b*.

Canadian Journal of Chemistry, 46, 1529 (1968)

Can. J. Chem. Downloaded from www.nrcresearchpress.com by 210.87.254.42 on 09/05/12
For personal use only.

Nitrous acid deamination of several steroidal amines has been reported in the literature (1). It is well known that rearrangements often take place in the course of this reaction. Apparently, there has not been recorded the deamination of a steroidal enamine; for this reason we became interested in the examination of the behavior of such a function upon treatment with nitrous acid.

The 16-acetyl-17-aminoandrosta-5,16-dien-3β-ol (**2***a*) is a stable enamine whose diacetyl derivative (**2***b*) was obtained by a Beckmann rearrangement of the acetoxime of pregna-5,16-dien-3β-ol-20-one acetate (**1**) (2) in acetic anhydride solution using boron trifluoride etherate as catalyst. When the enamine **2***a*, in acetic acid solution, was treated with sodium nitrite, two products were isolated after chromatography. Evidence is presented herewith for assignment of structures **3***a* and **3***b* to these products.

Product **3***a* obtained in small amounts showed m.p. 230–231° and analyzed for $C_{23}H_{34}O_5$. In the infrared (i.r.) spectrum it showed a free hydroxyl band at 3600 cm^{-1} and a carbonyl band at 1735 cm^{-1}. Its nuclear magnetic resonance (n.m.r.) spectrum[2] exhibited two singlets at 0.85 and 1.02, corresponding to the angular methyl groups. A singlet (intensity 6 protons) at 2.15 is assigned to the 16-acetyl group already present in **2***a* and an acetoxy group. At lower field (5.38) is observed only a multiplet corresponding to the 6-vinylic proton; therefore, the acetoxy group must be substituted on a tertiary carbon atom.

Product **3***b*, m.p. 206–208° ($C_{25}H_{36}O_6$) also showed a free hydroxyl i.r. band at 3600 cm^{-1} and a carbonyl band at 1740 cm^{-1}. In the n.m.r. spectrum the singlets ascribed to the angular methyl groups are observed at 0.80 and 1.02. Three singlets at 2.05, 2.08, and 2.15 were assigned to the methyl group of the 16-acetyl side chain and to two acetoxy groups. A proton attached to a carbon atom bearing an acetoxy group which is not coupled with other hydrogen atoms is responsible for a singlet at 5.25. A multiplet at 5.35 corresponds to the 6-vinylic hydrogen.

Chromium trioxide oxidation (3) of **3***b* in acetone solution followed by mild acid treatment afforded the α,β-unsaturated ketone **4** (λ_{max}, 240 mμ; ε, 15 200) which in the i.r. spectrum did not show free hydroxyl bands. It had carbonylic bands at 1675 cm^{-1} (α,β-unsaturated 6-membered ketone) and at 1745 cm^{-1} (acetyl groups).

Acetic anhydride – pyridine acetylation of **3***a* or **3***b* gave the same product (**3***c*) ($C_{27}H_{38}O_7$), m.p. 248–250°, which did not exhibit free hydroxyl i.r. bands. The n.m.r. spectrum of **3***c* indicates the presence of three acetoxy and one acetyl groups. It showed singlets at 2.05 (6 H), at 2.08 (3 H), and at 2.16 (3 H). A broad multiplet found at 4.55 is characteristic of the proton bonded to the 3-carbon atom carrying an acetoxy group. The n.m.r. spectrum of **3***c* also showed the singlet at 5.25 (1 H) attributed to a proton bonded to a carbon bearing an acetoxy group and the multiplet at 5.40 corresponding to the 6-vinylic hydrogen. The newly formed hydroxyl groups are substituted in the 6-membered ring of **3***c* since alkaline hydrogen peroxide oxidation of **3***c* afforded a dicarboxylic acid, characterized as its dimethyl ester – acetate and identified as the diester **5**, prepared following the method described by von Seeman and Grant (4).

Lithium aluminium hydride reduction of the ketone **3***c* gave a mixture of two stereoisomeric tetrols containing three vicinal hydroxyl groups.

---

[1]Contribution No. 259 from the Instituto de Química de la Universidad Nacional Autónoma de México.

[2]The nuclear magnetic resonance spectra were determined by Mr. Eduardo Díaz on a Varian A-60A spectrometer in $CDCl_3$ solution, using tetramethylsilane as internal reference. All chemical shifts are reported in p.p.m. as δ values.

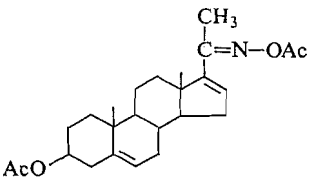

1

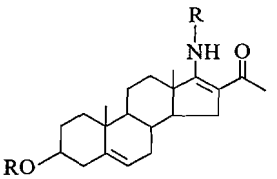

2 *a*, R = H
b, R = Ac

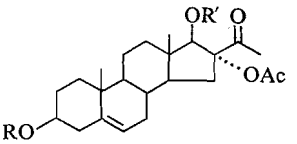

3 *a*, R = R′ = H
b, R = H,R′ = Ac
c, R = R′ = Ac

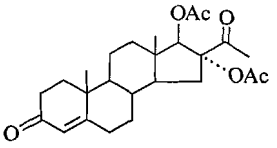

4

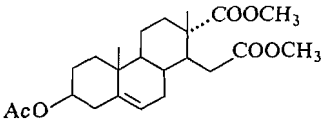

5

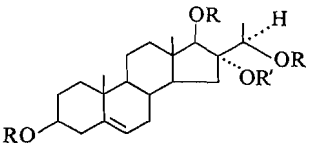

6 *a*, R = R′ = H
b, R = Ac,R′ = H
c, R = R′ = Ac

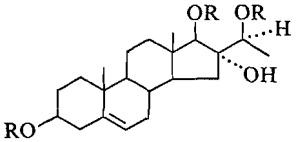

7 *a*, R = H
b, R = Ac

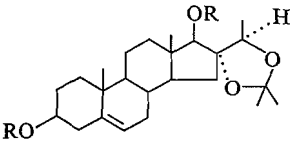

8 *a*, R = H
b, R = Ac

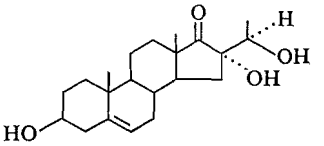

9

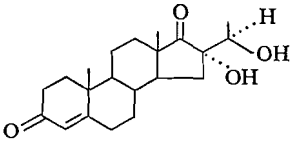

10

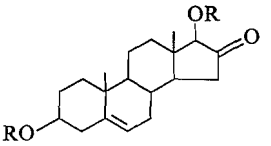

11 *a*, R = H
b, R = Ac

Only one of them (**6***a*) formed an acetonide (**8***a*) when the mixture was treated with acetone in the presence of hydrochloric acid. In this way the tetrol **7***a* could be readily separated from the acetonide (**8***a*). The latter showed a free hydroxyl i.r. band at 3625 cm^{-1} and formed the diacetate **8***b*.

Hydrolysis of the acetonide **8***a* gave the tetrol **6***a*. Acetylation of **6***a* with acetic anhydride–pyridine afforded the triacetate **6***b* which still showed in the i.r. spectrum a free hydroxyl band at 3600 cm^{-1} indicating the presence of a tertiary hydroxyl group. The latter could be acetylated under acid conditions. The resulting tetraacetate exhibited four n.m.r. singlets at 1.96, 2.03, 2.05, and 2.1 assigned to four acetoxy groups. The tetrol **7***a* yielded the triacetate **7***b*.

Sodium borohydride reduction of **3***c* in tetrahydrofuran solution was accompanied by migration of the acetate function from the tertiary 16-hydroxyl group to the newly formed secondary hydroxyl group in the side chain, yielding the triacetate **6***b*.

Chromium trioxide oxidation (3) of the acetonide **8***a* followed by acid treatment afforded a mixture of the ketones **9** and **10**. Both products had free hydroxyl i.r. bands. The i.r. spectrum of **9** had only a carbonylic band at 1750 cm^{-1} corresponding to a 5-membered ketone. Product **10** is a diketone since its i.r. spectrum had bands at 1735 cm^{-1} (cyclopentanone) and at 1660 cm^{-1} (α,β-unsaturated 6-membered ketone) (λ_{max} at 240 mμ; ε, 15 800).

Periodic acid oxidation of the tetrol **6***a* gave acetaldehyde, characterized as its 2,4-dinitrophenylhydrazone. When this reaction was carried out under mild conditions the ketol **11***a* was obtained. The diacetate **11***b* was prepared. Both

Can. J. Chem. Downloaded from www.nrcresearchpress.com by 210.87.254.42 on 09/05/12
For personal use only.

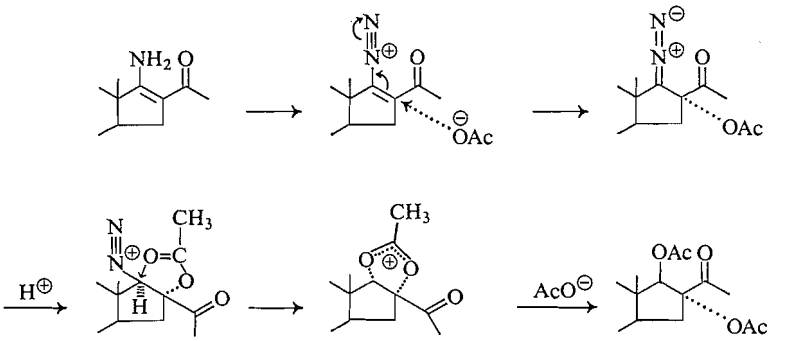

products were identified with authentic samples prepared according to a method previously described (5).

We suggest the following mechanism for the deamination of **2***a*.[3]

Some considerations concerning the stereochemistry of the deamination products **3***a* and **3***b* are pertinent: A β configuration is assigned to the 16-acetyl side chain since the optical rotatory dispersion curve of **3***c* exhibited a strong negative Cotton effect (6) consequently the 16-tertiary acetoxy group possesses an α orientation. The β configuration of the 17-acetoxy group of **3***c* is deduced from that of the ketol **11***a* (7), and is in accordance with the proposed mechanism. Construction of models of the tetrols **6***a* and **7***a* indicates that there is a steric interaction between the 17β-hydroxyl group and the methyl group of the side chain when an (*S*) configuration is assumed at the side chain asymmetric center. Therefore the formation of an acetonide is thermodynamically unfavored. Such steric crowding is not observed in the tetrol having an (*R*) configuration at that asymmetric center and consequently the latter is the tetrol (**6***a*) which forms the acetonide.

Experimental[4]

Nitrous Acid Treatment of 16-Acetyl-17-amino-androsta-3,16-dien-3β-ol (2a)

A solution of sodium nitrite (5 g) in water (25 ml) was added dropwise in 25 min with mechanical stirring to a suspension of the amino derivative **2***a* (4.60 g) in acetic acid (100 ml) at 15°. The mixture was stirred for 0.5 h more, poured in water, and extracted with chloroform. The organic extract was washed with water, dried on anhydrous sodium sulfate, and evaporated to dryness. The residue was chromatographed on alumina (100 g). The crystalline fractions eluted with benzene – ethyl acetate 9:1 were combined and recrystallized from acetone–hexane. This yielded the diacetate **3***b* (650 mg), m.p. 206–208°; $[\alpha]_D$ −135°; i.r. bands at 3600 cm^{-1} (hydroxyl group) and at 1740 cm^{-1} (ketone and acetyl groups).

Anal. Calcd. for $C_{25}H_{36}O_6$: C, 69.42; H, 8.39; O, 22.19. Found: C, 69.20; H, 8.31; O, 22.53.

The crystalline fractions eluted with benzene – ethyl acetate 4:1 were combined and recrystallized from methanol–ether. This yielded the monoacetate **3***a* (50 mg), m.p. 230–231°; $[\alpha]_D$ −80°; i.r. bands at 3600 cm^{-1} (hydroxyl groups) and at 1735 cm^{-1} (ketone and acetyl groups).

Anal. Calcd. for $C_{23}H_{34}O_5$: C, 70.74; H, 8.78; O, 20.48. Found: C, 71.15; H, 8.52; O, 20.81.

The combined mother liquors were acetylated and chromatographed on alumina (80 g). Elution with benzene–hexane 1:1 and benzene gave **3***c* (2 g). The analytical sample showed m.p. 248–250° (needles from acetone–hexane), $[\alpha]_D$ −153°; i.r. bands at 1740 cm^{-1} (ketone and acetyl groups); optical rotatory dispersion (dioxan); $[\alpha]_{550}$ −126°; $[\alpha]_{450}$ −214; $[\alpha]_{330}$ −484; $[\alpha]_{315}$ −494; $[\alpha]_{310}$ −494.

Anal. Calcd. for $C_{27}H_{38}O_7$: C, 68.33; H, 8.07; O, 23.60. Found: C, 68.17; H, 8.08; O, 23.84.

The same product (**3***c*) was obtained when **3***a* and **3***b* were acetylated with acetic anhydride and pyridine.

Chromium Trioxide Oxidation of the Diacetate 3b

A solution of the diacetate **3***b* (300 mg) in acetone (15 ml) was treated with 8 *N* chromium trioxide at 5° until the persistence of an orange color. After 5 min the solution was diluted with water and the precipitate filtered. The crude material was dissolved in methanol (8 ml) treated with a drop of concentrated hydrochloric acid and left at room temperature for 15 min. The solution was diluted then with water and the precipitate filtered and washed with water. The crude product was chromatographed on alumina (5 g). The crystalline fractions eluted with benzene – ethyl acetate 9:1 were combined and recrystallized from ether–hexane. This yielded the ketone **4** (150 mg) m.p. 190–191°; $[\alpha]_D$ −24°; λ_{max},

[3]We are grateful to the referees for valuable suggestions concerning this mechanism.

[4]Melting points are uncorrected. The alumina used in the chromatograms was Alcoa F-20 (washed with ethyl acetate). Analyses by Dr. F. Pascher, Bonn, Germany. Ultraviolet spectra: 95% EtOH solution, Beckmann DK2 spectrophotometer. Infrared spectra: $CHCl_3$ solution, (unless noted otherwise) Perkin–Elmer 21 double beam spectrophotometer. Rotations in chf at 20°. We are grateful to Syntex, S. A., for the determination of the rotations.

Can. J. Chem. Downloaded from www.nrcresearchpress.com by 210.87.254.42 on 09/05/12
For personal use only.

Can. J. Chem. Downloaded from www.nrcresearchpress.com by 210.87.254.42 on 09/05/12
For personal use only.

240 mμ; ε, 15 200; i.r. bands at 1745 cm^{-1} (acetate and acetyl groups), at 1675 cm^{-1} (α,β-unsaturated 6-membered ketone), and at 1620 cm^{-1} (C = C double bond).

Anal. Calcd. for $C_{25}H_{34}O_6$: C, 69.74; H, 7.96; O, 22.30. Found: C, 69.91; H, 7.89; O, 22.35.

Hydrogen Peroxide Oxidation of the Triacetate 3c

A solution of the triacetate **3c** (500 mg) in methanol (25 ml) was treated with 30% hydrogen peroxide (5 ml), potassium hydroxide (1 g) in water (5 ml), and heated under reflux for 1 h. Thirty percent hydrogen peroxide (5 ml) was added and the reflux continued for 1 h more. The solution was concentrated, diluted with water, and extracted with ether. The ethereal extract was discarded. The aqueous solution was acidified with dilute hydrochloric acid and extracted with ether. The ethereal extract was washed with water, dried, and evaporated to dryness. The gummy residue was treated with an ethereal solution of diazomethane (prepared from 2 g of *N*-nitrosomethylurea), left at 4° overnight, treated with a few drops of acetic acid to destroy the excess of diazomethane, and evaporated to dryness. The residue was acetylated with acetic anhydride - pyridine for 1 h on the steam bath. Crystallization from ether–hexane afforded the diester **5** (40 mg) as needles from ether–hexane m.p. 145–147°; $[\alpha]_D$ −87°. This product was identified by the standard methods with an authentic specimen prepared according to a method previously reported (4).

Lithium Aluminium Hydride Reduction of the Triacetate 3c.

A solution of the triacetate **3c** (3 g) in anhydrous tetrahydrofuran (300 ml) was treated with lithium aluminium hydride (3.5 g) and heated under reflux for 4 h. The excess of lithium aluminium hydride was destroyed with ethyl acetate. A saturated aqueous solution of sodium sulfate (10 ml) was added, the mixture filtered, and the solution evaporated to dryness *in vacuo*. The residue (2 g) suspended in acetone (100 ml) was treated with concentrated hydrochloric acid (2.5 ml) and heated under reflux for 1 h. The solution was concentrated to a small volume *in vacuo*, cooled, diluted with ethyl acetate, and washed with a saturated aqueous solution of sodium bicarbonate, dried and evaporated. The oily residue crystallized from acetone. This yielded the tetrol **7a** (200 mg) m.p. 250–255°. The analytical sample showed m.p. 272–273° (prisms from methanol - ethyl acetate); $[\alpha]_D$ −38°; i.r. bands (Nujol) at 3500 and 3200 cm^{-1} (hydroxyl groups).

Anal. Calcd. for $C_{21}H_{34}O_4$: C, 71.96; H, 9.78; O, 18.26. Found: C, 71.72; H, 9.92; O, 18.50.

Acetylation of **7a** with acetic anhydride - pyridine on the steam bath for 1 h yielded the triacetate **7b**, m.p. 209–210°; $[\alpha]_D$ −44°; i.r. bands at 3550 cm^{-1} (hydroxyl group) and at 1740 cm^{-1} (acetyl groups).

Anal. Calcd. for $C_{27}H_{40}O_7$: C, 68.04; H, 8.46; O, 23.50. Found: C, 68.20; H, 8.33; O, 23.79.

The acetone mother liquors were evaporated to dryness and the residue chromatographed on alumina (20 g). Elution with benzene - ethyl acetate 1:1 gave the acetonide **8a** (1.47 g) m.p. 138–142°. The analytical sample showed m.p. 142–144° (needles from acetone–hexane), $[\alpha]_D$ −41°; i.r. band at 3625 cm^{-1} (hydroxyl groups).

Anal. Calcd. for $C_{24}H_{38}O_4$: C, 73.81; H, 9.81; O, 16.38. Found: C, 73.64; H, 10.01; O, 16.58.

Acetylation of the acetonide **8a** with acetic anhydride - pyridine for 1 h on the steam bath, furnished the diacetate **8b**, m.p. 190–193° (needles from acetone–hexane); $[\alpha]_D$ −93°; i.r. band at 1745 cm^{-1} (acetyl group).

Anal. Calcd. for $C_{28}H_{42}O_6$: C, 70.85; H, 8.92; O, 20.23. Found: C, 70.72; H, 8.97; O, 20.17.

Tetrol 6a

The acetonide **8a** (500 mg) in methanol (5 ml) was treated with hydrochloric acid (0.5 ml) and water (1 ml) heated under reflux for 10 min and left 0.5 h at room temperature. The solution was concentrated *in vacuo*, water was added, and the precipitate collected and washed with water. Crystallization from methanol - ethyl acetate yielded prisms (170 mg) m.p. 240–242°; $[\alpha]_D$ −63°; i.r. band (Nujol) at 3300 cm^{-1} (hydroxyl group).

Anal. Calcd. for $C_{21}H_{34}O_4$: C, 71.96; H, 9.78; O, 18.26. Found: C, 71.58; H, 9.86; O, 18.75.

Triacetate of the Tetrol 6a

Acetylation of the tetrol **6a** with acetic anhydride - pyridine for 1 h on the steam bath and crystallization from acetone–hexane afforded prisms m.p. 199–201°; $[\alpha]_D$ −48°; i.r. bands at 3600 cm^{-1} (hydroxyl group) and at 1740 cm^{-1} (acetyl groups).

Anal. Calcd. for $C_{27}H_{40}O_7$: C, 68.04; H, 8.46; O, 23.50. Found: C, 67.82; H, 8.64; O, 23.71.

Tetraacetate of the Tetrol 6a

A solution of the tetrol **6a** (150 mg) in acetic anhydride (5 ml) containing *p*-toluenesulfonic acid (50 mg) was left at room temperature overnight and poured in water. After the hydrolysis of the anhydride the precipitate was extracted with ethyl acetate. The organic extract was washed with aqueous sodium bicarbonate, dried, and evaporated. The gummy residue dissolved in benzene was passed through alumina (2 g). Crystallization from acetone–hexane yielded needles (65 mg) m.p. 132–134°; $[\alpha]_D$ −32°; i.r. band at 1740 cm^{-1} (acetyl groups).

Anal. Calcd. for $C_{29}H_{42}O_8$: C, 67.16; H, 8.16; O, 24.68. Found: C, 67.38; H, 7.94; O, 24.55.

Acetylation of the triacetate **6b** as described above afforded also the tetraacetate **6c**.

Sodium Borohydride Reduction of the Triacetate 3c

A solution of the triacetate **3c** (250 mg) in tetrahydrofuran (15 ml) was treated with sodium borohydride (250 mg) and heated under reflux for 1.5 h. Water was added and the mixture acidified with acetic acid. The precipitate was extracted with ethyl acetate. The organic extract was washed with water, dried, and evaporated. The solid residue was crystallized from ether–hexane. This yielded the triacetate **6b** (100 mg) m.p. 200–201°. This was identified by the standard methods with the triacetate **6b** obtained previously by acetylation of **6a**.

Chromium Trioxide Oxidation of the Acetonide 8a

A solution of the acetonide **8a** (320 mg) in acetone (12 ml) was treated at 5° with 8 *N* chromium trioxide (3) until the persistence of an orange color. It was then proceeded as described in a previous case. Crystallization of the crude product from ether and methanol afforded the ketone **9** (35 mg) m.p. 248–250°; $[\alpha]_D$ 67° (dioxane); i.r. bands (Nujol) at 3300 and 3450 cm^{-1} (hydroxyl group) and at 1750 cm^{-1} (cyclopentanone).

Anal. Calcd. for $C_{21}H_{32}O_4$: C, 72.38; H, 9.26; O, 18.36. Found: C, 72.41; H, 9.44; O, 18.13.

The ethereal mother liquors were evaporated to dryness and the residue, dissolved in benzene was passed through alumina (5 g). Crystallization from acetone–hexane afforded the diketone **10** (50 mg) as prisms m.p. 138–140°; $[\alpha]_D$ 202°; λ_{max}, 240, 303 mμ; ε, 15 800, 600; i.r. bands at 3600 cm^{-1} (hydroxyl groups), at 1735 cm^{-1} (cyclopentanone), at 1660 cm^{-1} (α,β-unsaturated 6-membered ketone), and at 1615 cm^{-1} (C = C double bond).

Anal. Calcd. for $C_{21}H_{30}O_4$: C, 72.80; H, 8.73; O, 18.47. Found: C, 72.60; H, 8.84; O, 18.52.

Periodic Acid Oxidation of the Tetrol 6a

A solution of the tetrol **6***a* (550 mg) in methanol (30 ml) was treated with periodic acid (425 mg) in water (2 ml). The mixture was left at room temperature for 5 h then poured in water and extracted with ethyl acetate. The organic extract was washed with water, dried, and evaporated. Crystallization of the residue from ethyl acetate – hexane afforded the ketol **11***a* (250 mg), m.p. 186–190°. Further crystallizations from ethyl acetate – ether raised the m.p. to 193–195°; i.r. bands (Nujol) at 3450 cm^{-1} (hydroxyl groups) and at 1750 cm^{-1} (cyclopentanone).

Acetylation of the ketol **11***a* with acetic anhydride – pyridine for 1 h on the steam bath gave the diacetate **11***b* m.p. 120–121°; $[\alpha]_D$ −189°; i.r. bands at 1740 and at 1750 cm^{-1} (acetyl groups) and at 1770 cm^{-1} (cyclopentanone).

Anal. Calcd. for $C_{23}H_{32}O_5$: C, 71.10; H, 8.30; O, 20.60. Found: C, 71.05; H, 8.54; O, 20.79.

The ketol **11***a* and its diacetate **11***b* proved to be identical with samples prepared following a procedure previously described (5).

The periodic acid oxidation of **6** (300 mg) was repeated and after 5 h at room temperature the solution was distilled and the distillate collected in a solution of 2,4-dinitrophenylhydrazine hydrochloride in aqueous methanol. The precipitate was collected and washed with water. Crystallization from methanol–chloroform afforded the 2,4-dinitrophenylhydrazone of acetaldehyde m.p. 156–158°. It showed no depression in mixture m.p. with an authentic specimen and the i.r. spectra were identical.

1. R. ANLIKER, O. ROHR, and H. HEUSSER. Helv. Chim. Acta, **39**, 1494 (1956). H. HEUSSER, P. T. HERZI, A. FÜRST, and P. A. PLATTNER. Helv. Chim. Acta, **33**, 1093 (1950). W. G. DAUBEN and P. LANG. Tetrahedron Letters, **11**, 453 (1962). W. L. WENDLER. Rearrangements in steroids. *In* Molecular rearrangements. *Edited by* P. de Mayo. Interscience Publishers, New York. 1964. Part 2. p. 1019.
2. J. ROMO and A. ROMO DE VIVAR. J. Am. Chem. Soc. **81**, 3446 (1959).
3. A. BOWERS, T. G. HALSALL, E. R. H. JONES, and A. J. LEMIN. J. Chem. Soc. 2548 (1953).
4. C. VON SEEMANN and G. A. GRANT. J. Am. Chem. Soc. **72**, 4073 (1950).
5. F. H. STODOLA, E. C. KENDALL, and B. F. MCKENZIE. J. Org. Chem. **6**, 841 (1941).
6. P. CRABBÉ. Tetrahedron, **19**, 51 (1963).
7. N. S. LEEDS, D. K. FUKUSHIMA, and T. F. GALLAGHER. J. Am. Chem. Soc. **76**, 2943 (1954).

Can. J. Chem. Downloaded from www.nrcresearchpress.com by 210.87.254.42 on 09/05/12
For personal use only.

Can. J. Chem. Downloaded from www.nrcresearchpress.com by 210.87.254.5 on 09/05/12
For personal use only.

Franserin and confertin: new pseudoguaianolides isolated from *franseria* and *ambrosia* species[1]

J. Romo, A. Romo de Vivar, A. Vélez, and E. Urbina
Instituto de Química de la Universidad Nacional Autónoma de México, México 20, D.F., México

Received January 12, 1968

Two pseudoguaianolides were isolated from *Franseria ambrosioides* Cav.: damsin of known structure and franserin whose constitution was established as a 10-hydroxytetrahydroambrosin (**2**). From *Ambrosia confertiflora* DC. were isolated the known desacetylconfertiflorin (**12**) and confertin, a new lactone found also as constituent of *Ambrosia tenuifolia* Harv et Gray. It was identified as the ketolactone **9** previously prepared from cumanin (**11**).

Canadian Journal of Chemistry, 46, 1535 (1968)

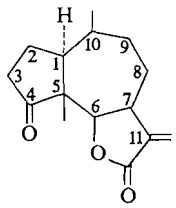

1

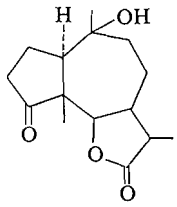

2

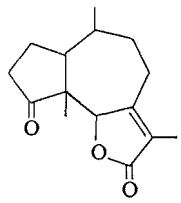

3

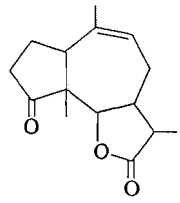

4

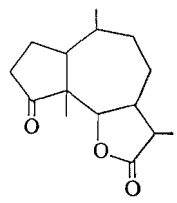

5

Franseria ambrosioides Cav. is a Compositae widely distributed in the northwestern part of Mexico. In the less polar fractions of the chromatogram of the ethanol extract of the plant we have isolated a crystalline product ($C_{15}H_{20}O_3$) m.p. 111°, identified as damsin (**1**) (1) by its spectral features. Furthermore, isomerization of its double bond to endocyclic conjugation under hydrogenation conditions gave dihydroisoambrosin (**3**) (2). Treatment of our product with toluenethiol in the presence of piperidine followed by desulfurization with Raney nickel of the intermediary adduct yielded the C-11 epimer of tetrahydroambrosin (**5**) (2). It had infrared (i.r.) bands at 1770 cm^{-1} (γ-lactone) and at 1740 cm^{-1} (cyclopentanone). The tetrahydro derivative **5** showed in the nuclear magnetic resonance (n.m.r.) spectrum[2] a doublet ($J = 8$ c.p.s.) at 4.46 corresponding to the C-6 proton. Two doublets ($J = 7$ c.p.s.) at 1.23 and 1.10 were ascribed to two secondary methyl groups. A tertiary group is responsible for a singlet at 1.11 partially superimposed on one of the doublets. When an authentic sample of ambrosin (**6**) was submitted to a similar treatment as described above for damsin (**1**) the tetrahydro derivative **5** was also obtained.

From the more polar fractions of the chromatogram there was isolated a crystalline pseudoguaianolide which we propose to name franserin.

Franserin (**2**) m.p. 225–227° and $[\alpha]_D \pm 0°$ had an analysis of $C_{15}H_{22}O_4$. It contains a cyclopentanone and a five-membered ring lactone as shown by i.r. bands at 1740 and 1775 cm^{-1}. The latter group is not conjugated with an exocyclic methylene group as frequently occurs in this type of lactones since franserin (**2**) did not show end ultraviolet (u.v.) absorption and its n.m.r. spectrum did not exhibit low field signals besides that corresponding to the proton attached to the carbon bearing the lactone closure. This grouping must be oriented to C-6 since the signal appears as a doublet ($J = 8$ c.p.s.) at 4.45.

Franserin (**2**) possesses a tertiary hydroxyl group (i.r. band at 3550 cm^{-1}) (n.m.r. singlet at 1.64 which disappears on equilibration with deuterium oxide). It is not acetylated with acetic anhydride – pyridine nor oxidized with chromium trioxide.

The following evidence indicates that the tertiary hydroxyl group of franserin (**2**) is located at C-10. The n.m.r. spectrum of franserin (**2**)

[1]Contribution No. 260 from the Instituto de Químico de la Universidad Nacional Autónoma de México.

[2]The nuclear magnetic resonance spectra were determined by Mr. Eduardo Díaz on a Varian A-60A spectrometer in $CDCl_3$ solution using tetramethylsilane as internal reference. All chemical shifts are reported in p.p.m. as δ values.

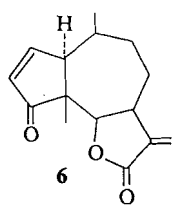
6

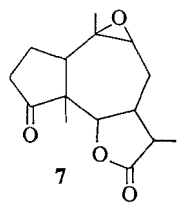
7

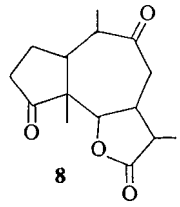
8

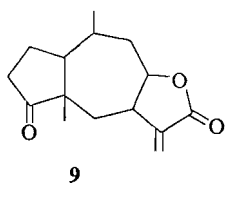
9

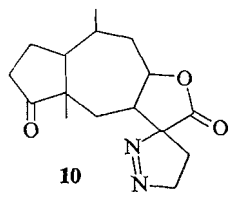
10

showed in the methyl region a singlet at 1.10 and a doublet ($J = 7$ c.p.s.) at 1.25 ascribed to a tertiary and a secondary methyl group, respectively. A singlet at 1.37 corresponds to a methyl group attached to a carbon atom carrying a hydroxyl group. Anhydrofranserin (**4**) prepared by dehydration of a pyridine solution of franserin (**2**) with thionyl chloride exhibited in its n.m.r. spectrum a singlet at 0.95 and a doublet ($J = 7$ c.p.s.) at 1.18 assigned to a tertiary and a secondary methyl group, respectively. A vinylic methyl group is responsible for a triplet ($J = 0.5$ c.p.s.) at 1.79. A multiplet at 5.56 was ascribed to a vinyl proton. A doublet ($J = 6.5$ c.p.s.) at 4.53 corresponds to the C-6 proton. Oxidation of anhydrofranserin (**4**) with *m*-chloroperbenzoic acid gave the epoxide **7**. Its n.m.r. spectrum exhibited a singlet at 1.40 corresponding to the methyl group linked to the carbon bearing the epoxide. A triplet at 3.02 is attributed to the proton at C-9. Treatment of **7** with boron trifluoride etherate afforded the ketone **8**. It showed in the i.r. spectrum three carbonyl bands, at 1775 cm^{-1} (γ-lactone), at 1750 cm^{-1} (cyclopentanone), and at 1720 cm^{-1} (cycloheptanone).

The structure of franserin (**2**) was established when hydrogenation of anhydrofranserin (**4**) afforded a product identified with the tetrahydro derivative **5** obtained as described above from damsin (**1**) and ambrosin (**6**). Therefore, franserin is correctly represented by formula **2** with its asymmetric centers at C-1, C-5, C-6, and C-7 oriented as in ambrosin (**6**).

Chromatography of the ethanol extract of *Ambrosia confertiflora* DC yielded in the less polar fractions a sesquiterpene lactone which we propose to name confertin. It was found also as a constituent of *Ambrosia tenuifolia* Harv et Gray. Confertin m.p. 145–146°, showed in the i.r. spectrum a band at 1740 cm^{-1} corresponding to a five-membered ring ketone. Confertin also contains an exocyclic methylene group conjugated with a γ-lactone as shown by i.r. bands at 1770 and 1665 cm^{-1} by end absorption in the u.v. spectrum (λ_{max} 211 mμ; ε, 10 500) and confirmed by the formation of a pyrazoline (**10**). The structure of confertin was elucidated when it was identified as the ketolactone **9** previously obtained by dehydration of cumanin (**11**) (3).

From the more polar fractions of the chromatogram of the ethanol extract of *A. confertiflora* there was obtained a crystalline product ($C_{15}H_{20}O_4$), m.p. 201–204°, $[\alpha]_D$ +16°. It was identified as desacetylconfertiflorin (**12**) of known structure and stereochemistry (4). Chromium trioxide oxidation of **12** gave another proof of the relative position of the secondary hydroxyl group. It yielded the lactone **13** which contains the double bond conjugated with the lactone carbonyl and with the newly formed ketone (λ_{max} 245 mμ; ε, 9700). It had i.r. bands at 1695 and 1640 cm^{-1} attributed to the α,β-unsaturated cycloheptanone. The n.m.r. spectrum of **13** exhibited a singlet at 0.83, a doublet ($J = 7$ c.p.s.) at 1.04, and a doublet ($J = 2$ c.p.s.) at 2.30 corresponding to a tertiary, a secondary,

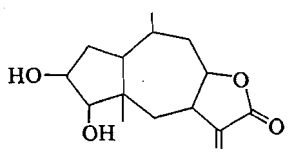
11

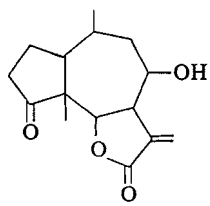
12

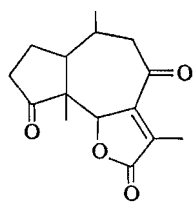
13

Can. J. Chem. Downloaded from www.nrcresearchpress.com by 210.87.254.5 on 09/05/12
For personal use only.

Can. J. Chem. Downloaded from www.nrcresearchpress.com by 210.87.254.5 on 09/05/12
For personal use only.

and a vinylic methyl group, respectively. The signal assigned to the proton at C-6 shows homoallylic coupling and appears as a quadruplet ($J = 2$ c.p.s.) at 5.28.

Experimental[3]

Isolation of the Lactones from Franseria ambrosioides

The plant was collected in September in the neighborhood of Río del Quelite (State of Sinaloa). The dried plant (without roots, 300 g) was extracted twice with ethanol (3 l) for 8 h. The combined ethanol extracts were concentrated to 500 ml and treated with a solution of lead acetate (25 g) in water (500 ml). The mixture was left at room temperature for 1 h, filtered, diluted with water (1 l), and extracted with chloroform. The extract was evaporated to dryness and the gummy residue (12 g) dissolved in benzene–hexane 1:1 was chromatographed on alumina. The crystalline fractions eluted with benzene–hexane 1:1, 2:1, and 3:1 were combined and crystallized from isopropyl ether. This yielded damsin (**1**) (2.43 g), m.p. 109–111°; λ_{max} 213 mμ; ε, 8400; i.r. bands at 1770 cm^{-1} (γ-lactone), at 1750 cm^{-1} (cyclopentanone), and at 1665 cm^{-1} (C=C double bond).

Anal. Calcd. for $C_{15}H_{20}O_3$: C, 72.55; H, 8.12; O, 19.33. Found: C, 72.33; H, 8.21; O, 19.47.

In the nuclear magnetic resonance (n.m.r.) spectrum it showed the following signals: a pair of doublets ($J = 2.5$ c.p.s.) at 6.23 and 5.60 (exocyclic methylene), a doublet ($J = 8$ c.p.s.) (C-6 proton), a singlet at 1.08, and a doublet ($J = 7$ c.p.s.) at 1.11 (secondary and tertiary methyl groups, respectively).

Franserin (**2**) was obtained in the polar fractions eluted with benzene and increasing proportions of ether. Crystallization of **2** from ethyl acetate – ether yielded small needles (140 mg) m.p. 225–227°: $[\alpha]_D \pm 0°$ (dioxan); i.r. bands (KBr) at 3550 cm^{-1} (hydroxyl group), at 1775 cm^{-1} (γ-lactone) and at 1740 cm^{-1} (cyclopentanone).

Anal. Calcd. for $C_{15}H_{22}O_4$: C, 67.64; H, 8.33; O, 24.03. Found: C, 67.98; H, 8.35; O, 23.90.

Dihydroisoambrosin (3)

A solution of damsin (**1**) (400 mg) in ethyl acetate (30 ml) was stirred in an atmosphere of hydrogen in the presence of 5% Pd–C (60 mg); after 2 h the solution was filtered and evaporated to dryness. The residue crystallized from acetone–hexane yielding 290 mg dihydroisoambrosin; m.p. 165° which was identified with an authentic specimen by the standard methods.

11-Epitetrahydroambrosin (5)

A solution of ambrosin (**6**) (400 mg) in benzene (25 ml) was treated with toluenethiol (2 ml) and piperidine (2 ml) and heated under reflux for 6 h. The solution was washed with dilute hydrochloric acid, water, dried on anhydrous sodium sulfate, and evaporated to dryness. The residue dissolved in ethanol (40 ml) was treated with Raney nickel (7 g), heated under reflux for 14 h, filtered, and evaporated to dryness. The residue crystallized from isopropyl ether. This yielded 11-epitetrahydroambrosin (**5**) (120 mg) m.p. 115°; $[\alpha]_D$ +27°; i.r. bands at 1770 cm^{-1} (γ-lactone) and at 1740 cm^{-1} (cyclopentanone).

Anal. Calcd. for $C_{15}H_{22}O_3$: C, 71.97; H, 8.86; O, 19.17. Found: C, 71.99; H, 9.01; O, 19.08.

When this reaction was carried out with damsin (**1**) (400 mg), a dihydroderivative (170 mg) m.p. 115° was obtained. It was identified with 11-epitetrahydroambrosin (**5**) by the standard methods.

Anhydrofranserin (4)

A solution of franserin (**2**) (600 mg) in pyridine (10 ml) was treated at 5° with thionyl chloride (1.5 ml). After 5 min the mixture was poured in ice-water and extracted with ethyl acetate. The organic layer was washed with dilute hydrochloric acid, water, dried on anhydrous sodium sulfate, and evaporated to dryness. The gummy residue dissolved in benzene–hexane 1:1 was chromatographed on alumina. The crystalline fractions eluted with benzene–hexane 1:1 and increasing proportions of benzene were combined and crystallized from ether–hexane. This yielded 270 m.p. 91–94°. Further crystallizations from acetone – isopropyl ether raised the m.p. to 107–108°; $[\alpha]_D$ −5°; i.r. bands at 1770 cm^{-1} (γ-lactone) and at 1740 cm^{-1} (cyclopentanone).

Anal. Calcd. for $C_{15}H_{20}O_3$: C, 72.55; H, 8.12; O, 19.33. Found: C, 72.43; H, 8.04; O, 19.58.

Hydrogenation of Anhydrofranserin (4)

A solution of anhydrofranserin (150 mg) in ethyl acetate (20 ml) was hydrogenated with Adams catalyst (50 mg) until the absorption of hydrogen ceased. The solution was filtered and evaporated to dryness. The residue crystallized from isopropyl ether. This yielded a dihydro derivative (45 mg) m.p. 115–116° which was undepressed on admixture with a sample of 11-epitetrahydroambrosin. The i.r. spectra were superimposable.

Franserin Epoxide (7)

A solution of anhydrofranserin (**4**) (200 mg) in chloroform (10 ml) was treated with *m*-chloroperbenzoic acid (400 mg). The mixture was heated under reflux for 4 h, washed with aqueous sodium bicarbonate solution, dried on anhydrous sodium sulfate, and evaporated to dryness. The residue was chromatographed on alumina. The crystalline fractions eluted with hexane and increasing proportions of benzene were combined and crystallized from chloroform–ether. This yielded the epoxide (**7**) (130 mg) m.p. 145–148°; $[\alpha]_D$ +33°; i.r. bands at 1780 cm^{-1} (γ-lactone) and at 1750 cm^{-1} (cyclopentanone).

Anal. Calcd. for $C_{15}H_{20}O_4$: C, 68.16; H, 7.63; O, 24.21. Found: C, 68.26; H, 7.60; O, 24.24.

Ketofranserin (8)

A solution of the epoxide **7** (100 mg) in benzene at 10° was treated with boron trifluoride etherate (0.5 ml) and the mixture was left overnight at room temperature. It was then washed with aqueous sodium bicarbonate solution, dried, and evaporated. The residue was purified by chromatography on alumina. Crystallization from acetone – isopropyl ether afforded prisms m.p. 141–143°; $[\alpha]_D$ +12°; i.r. bands at 1775 cm^{-1} (γ-lactone), at 1750 cm^{-1} (cyclopentanone) and at 1720 cm^{-1} (cycloheptanone).

[3]Melting points are uncorrected. Infrared spectra and rotations were measured in chloroform, and ultraviolet spectra in 95% ethanol. The alumina used in the chromatograms was Alcoa F-20 (washed with ethyl acetate). The analyses were carried out by Dr. Franz Pascher, Bonn, Germany. We are grateful to Syntex, S.A., for the determination of the rotations.

Anal. Calcd. for $C_{15}H_{20}O_4$: C, 68.16; H, 7.63; O, 24.21. Found: C, 67.74; H, 7.41; O, 24.56.

Isolation of the Lactones from Ambrosia confertiflora DC

The plant was collected in June, 19 km to the north of San Luis Potosí. The dried plant (1100 g) was extracted as described in the previous case.

Chromatography on alumina of the residue afforded confertin (**9**) in the less polar fractions eluted with hexane and increasing proportions of benzene. Crystallization from acetone–hexane yielded needles (565 mg) m.p. 145–146°. Undepressed on admixture with a sample of anhydrocumanin (**9**) (3). The i.r. spectra were superimposable. The polar fractions eluted with benzene and increasing proportions of ethyl acetate afforded desacetylconfertiflorin (**12**). Crystallization from ethyl acetate – ether furnished needles m.p. 201–204°; $[\alpha]_D$ +16° (dioxan); λ_{max} 210 mμ; ε, 8800; i.r. bands at 3620 and 3500 cm^{-1} (hydroxyl group), at 1775 cm^{-1} (γ-lactone), at 1750 cm^{-1} (cyclopentanone), and at 1660 cm^{-1} (C=C double bond).

Anal. Calcd. for $C_{15}H_{20}O_4$: C, 68.16; H, 7.63; O, 24.21. Found: C, 68.33; H, 7.73; O, 24.20.

Mixture m.p. with an authentic sample was undepressed and the i.r. spectra were superimposable.

*Dehydroisodesacetylconfertiflorin (**13**)*

A solution of desacetylconfertiflorin (**12**) (300 mg) in acetone (8 ml) was treated at 5° with Jones reagent until the persistence of an orange color. After 5 min the mixture was diluted with ethyl acetate washed with water, aqueous sodium bicarbonate, dried on anhydrous sodium acetate, and evaporated to dryness. The residue was purified by chromatography on alumina. Crystallization from chloroform – isopropyl ether gave material (60 mg) m.p. 118°; $[\alpha]_D$ −132°; λ_{max} 245 mμ; ε, 9700; i.r. bands at 1765 cm^{-1} with a shoulder at 1750 cm^{-1} (γ-lactone and cyclopentanone), at 1695 cm^{-1} (cycloheptenone), and at 1640 cm^{-1} (C=C double bond).

Anal. Calcd. for $C_{15}H_{18}O_4$: C, 68.68; H, 6.92; O, 24.40. Found: C, 68.49; H, 6.96; O, 24.57.

*Pyrazoline of Confertin (**10**)*

A solution of **9** (300 mg) in methanol (5 ml) was treated with an ethereal solution of diazomethane (prepared with 1 g of *N*-nitrosomethylurea) and left at 4° overnight. The crystalline precipitate was collected and recrystallized from chloroform–ether. This yielded prisms (270 mg) m.p. 137° decomposition; $[\alpha]_D$ +405° (dioxan); λ_{max} 322 mμ; ε, 240; i.r. bands at 1765 cm^{-1} (γ-lactone) and at 1750 cm^{-1} (cyclopentanone).

Anal. Calcd. for $C_{16}H_{22}O_3N_2$: C, 66.18; H, 7.64; O, 16.53; N, 9.65. Found: C, 66.04; H, 7.70; O, 16.59; N, 9.79.

*Isolation of Confertin (**9**) from Ambrosia tenuifolia Harv et Gray*

The dried plant (520 g) collected on the highway México-Laredo (85 km) was extracted with ethanol. It was then processed as in the previous case. From the less polar fractions of the chromatogram there was obtained confertin (**9**) (1.895 g) m.p. 145–146° undepressed on admixture with the lactone **9** isolated from *A. confertiflora* The i.r. spectra were identical.

Acknowledgments

We are grateful to Dr. Tom J. Mabry of the Cell Research Institute and Department of Botany, the University of Texas, Austin, Texas, for a sample of desacetylconfertiflorin.

Franseria ambrosioides was collected by Mr. Hermilo Quero of the Instituto de Biología de la U.N.A.M. under voucher number Q-24 at Herbario Nacional de la U.N.A.M. (MEXU). *Ambrosia confertiflora* was collected by Miss Silvia del Amo of the Instituto de Biología de la U.N.A.M. under voucher number A-10 at Herbario Nacional de la U.N.A.M. (MEXU).

1. H. A. Abu-Shady and T. O. Soine. J. Am. Pharm. Assoc. **42**, 387 (1953).
2. H. A. Abu-Shady and T. O. Soine. J. Am. Pharm. Assoc. **43**, 365 (1964). F. Sorm, M. Suchy, and V. Herout. Collection Czech. Chem. Commun. **24**, 1548 (1959). W. Herz, H. Watanabe, M. Miyazaki, and Y. Kishida. J. Am. Chem. Soc. **84**, 2601 (1962).
3. J. Romo, P. Joseph-Nathan, and G. Siade. Tetrahedron, **22**, 1499 (1966).
4. N. H. Fisher and T. J. Mabry. Tetrahedron, **23**, 2529 (1967).

Can. J. Chem. Downloaded from www.nrcresearchpress.com by 210.87.254.5 on 09/05/12
For personal use only.

Can. J. Chem. Downloaded from www.nrcresearchpress.com by 210.87.254.40 on 09/05/12
For personal use only.

Odoratin: a new pseudoguaianolide isolated from *Hymenoxis odorata* DC.[1]

A. Ortega, A. Romo de Vivar, and J. Romo
Instituto de Química de la Universidad Nacional Autónoma de México, México 20, D. F., México

Received November 20, 1967

The structure of odoratin, a constituent of *Hymenoxis odorata* DC. has been established as a pseudoguaianolide **1***a* with a stereochemistry related to the sesquiterpene lactones isolated in the genus *Helenium*.

Canadian Journal of Chemistry, 46, 1539 (1968)

Hymenoxis odorata DC. is a Compositae occurring commonly in the High Plateau of Mexico. The bitter taste of this plant suggests the presence of sesquiterpene lactones and led us to undertake its chemical examination. Chromatography of its ethanol extract afforded in the polar fractions a substance of formula $C_{15}H_{22}O_4$, m.p. 165–167°, and $[\alpha]_D$ +71° which we propose to name odoratin. In the infrared (i.r.) spectrum odoratin (**1***a*) showed only one carbonyl band at 1760 cm^{-1} ascribed to a γ-lactone very probably conjugated with an exocyclic methylene group since **1***a* exhibited an ultraviolet (u.v.) maximum at 214 mμ (ε, 9900) and a weak i.r. band at 1660 cm^{-1}.

Odoratin (**1***a*) possesses two hydroxyl groups as shown by the bands at 3610 and 3450 cm^{-1} present in the i.r. spectrum of **1***a* which disappear in its diacetate (**1***b*). The latter exhibited i.r. bands at 1765 and 1740 cm^{-1} assigned to the five-membered ring lactone and acetyl groups.

The hydroxyl functions of odoratin (**1***a*) are in a vicinal position since **1***a* gave a positive periodic acid test.

The nuclear magnetic resonance (n.m.r.) spectrum[2] of odoratin (**1***a*) showed a pair of low-field doublets ($J = 2$ c.p.s.) at 5.64 and 6.29 confirming the presence in **1***a* of an exocyclic methylene. The proton attached to the carbon bearing the ethereal oxygen of the lactone is responsible for a multiplet which could be defined as a pair of lateral doublets and a central triplet centered at 4.81, indicating a lactone function oriented at C-8. A multiplet at 4.10 and a doublet at 3.64 are attributed to the protons on the carbon atoms carrying the hydroxyl groups. These signals are displaced downfield in the n.m.r. spectrum of the diacetate **1***b*. A broad signal at 3.23 in the n.m.r. spectrum of **1***a* is ascribed to an allylic proton. A singlet (2 H) at 2.60 which disappears on equilibration with deuterium oxide corresponded to the hydroxyl protons. A doublet ($J = 7$ c.p.s.) at 1.00 and a singlet at 0.85 are assigned to a secondary and a tertiary methyl group, respectively. The n.m.r. spectrum of diacetylodoratin (**1***b*) exhibited two singlets at 2.13 and 2.06 assigned to two acetoxy groups.

Isomerization of the double bond to endocyclic conjugation with the lactone carbonyl group (1) occurred in attempts to hydrogenate odoratin (**1***a*). The resulting derivative **2***a* showed a u.v. maximum at 220 mμ (ε, 15 200). A vinylic methyl group with an apparent homoallylic coupling is responsible for a triplet ($J = 1$ c.p.s.) at 1.81 in the n.m.r. spectrum of diacetylisoodoratin (**2***b*).

Dehydration of odoratin (**1***a*) with potassium bisulfate (2, 3) resulted in the formation of a lactone (**3**) (λ_{max}, 213 mμ; ε, 10 100) containing a five-membered ring ketone as shown by an i.r. band at 1740 cm^{-1}. The n.m.r. spectrum of **3** exhibited the following signals: two low field doublets ($J = 2$ c.p.s.) at 6.24 and 5.65 (exocyclic methylene protons). A multiplet centered at 4.73 (hydrogen attached to the carbon bearing the lactone closure). A doublet ($J = 6.5$ c.p.s.) at 1.10 and a singlet at 0.92 (secondary and tertiary methyl groups respectively).

Baeyer–Villiger oxidation of the ketone **3** afforded a dilactone **4** (1, 2). It had bands at 1765 cm^{-1} (γ-lactone) and at 1730 cm^{-1} (six-membered ring lactone). The n.m.r. spectrum of **4** indicates that the ethereal oxygen of the six-membered lactone is attached to C-5. It exhibited a displaced singlet at 1.39 corresponding to the

[1]Contribution No. 258 from the Instituto de Química de la Universidad Nacional Autónoma de México.

[2]The nuclear magnetic resonance spectra were determined by Mr. E. Díaz on a Varian A-60A spectrometer in $CDCl_3$ solution using tetramethylsilane as internal standard. All chemical shifts are reported in p.p.m. as δ values.

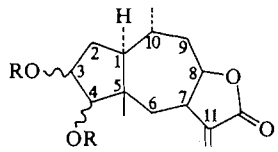

1 *a*, R = H
b, R = Ac

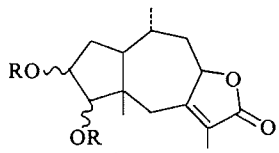

2 *a*, R = H
b, R = Ac

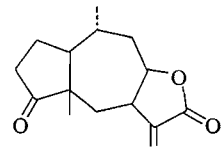

3

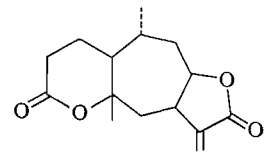

4

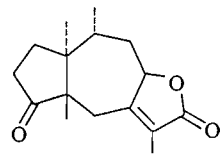

5

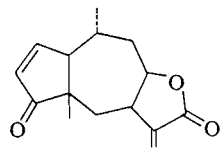

6

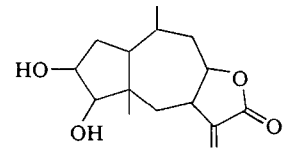

7

angular methyl group; a pair of low field doublets ($J = 2$ c.p.s.) at 6.32 and 5.72 (exocyclic methylene protons); a multiplet centered at 4.86 (C-8 hydrogen); and a doublet at 1.17 (secondary methyl group).

The evidence described above indicates that the keto group of the lactone **3** is attached to C-4. Therefore the hydroxyl groups of odoratin (**1***a*) are bonded to C-3 and C-4.

The double bond of the lactone **3** was isomerized to endocyclic conjugation when **3** was submitted to hydrogenation conditions in the presence of palladium on charcoal catalyst. The resulting lactone (**5**) (λ_{max}, 218 mμ; ε, 9500) showed in its n.m.r. spectrum a triplet ($J = 1$ c.p.s.) at 1.89 ascribed to a vinylic methyl group.

The structure of odoratin (**1***a*) was elucidated when the lactone **5** was identified as desoxydihydroisohelenalin (dihydroisoaromatin) (4–6). Mixture melting points of both products was undepressed and the i.r. spectra were superimposable. Therefore, odoratin possesses structure **1***a* with the asymmetric centers at C-1, C-5, C-8, and C-10 oriented as in aromatin (**6**). Biogenetic considerations render it very probable that odoratin (**1***a*) has the β configuration at C-7 as several lactones of this series (7). The orientation of the hydroxyl groups of odoratin (**1***a*) must be *trans* since an acetonide or a cyclic sulfite could not be obtained. These derivatives are readily prepared in the cumanin series (2, 3).

The gross structures of odoratin (**1***a*) and cumanin (2) (**7**) are identical. They differ in the configuration of the C-10 methyl group, which in odoratin (**1***a*) has an α orientation identical to that of the lactones isolated in the genus *Helenium*. Geigerinin (8, 9), a sesquiterpene lactone which possesses the same gross structure as **1***a* and whose stereochemistry has not been defined, also differs from odoratin (**1***a*).

Experimental[3]

Isolation of Odoratin (1a)

Hymenoxis odorata DC.[4] was collected 20 km to the north of Matehuala (State of San Luis Potosí) on the highway to Saltillo. The dried plant (500 g) was extracted twice with ethanol (4 l) under reflux for 10 h. The ethanol extract was concentrated to 500 ml, treated with a solution of lead acetate (40 g) in water (500 ml), left at room temperature for 2 h, filtered, diluted with water (1 l), and extracted with chloroform. The extract was evaporated to dryness and the residue (20 g) chromatographed on alumina. The more polar fractions eluted with chloroform – 5% ethanol crystallized. They were combined and recrystallized from ethyl acetate. This yielded 3.28 g of **1***a* m.p. 132–134°. Further crystallizations from acetone raised the m.p. to 165–167°; $[\alpha]_D$ +71° (dioxan); λ_{max} 214 mμ; ε, 9900; infrared (i.r.) bands at 3610 and 3450 cm^{-1} (hydroxyl groups), at 1760 cm^{-1} (five-membered ring lactone), and at 1660 cm^{-1} (exocyclic methylene group).

Anal. Calcd. for $C_{15}H_{22}O_4$: C, 67.64; H, 8.33; O, 24.03. Found: C, 67.57; H, 8.29; O, 24.31.

Odoratin Diacetate (1b)

Acetylation of **1***a* with acetic anhydride – pyridine on the steam bath for 1 h afforded the diacetate **1***b* m.p. 132–133° (needles from acetone – isopropyl ether); $[\alpha]_D$ −33°; λ_{max} 213 mμ; ε, 10 000; i.r. bands at 1765 cm^{-1} (γ-lactone), at 1740 cm^{-1} (acetyl groups), and at 1650 cm^{-1} (exocyclic methylene group).

Anal. Calcd. for $C_{19}H_{26}O_6$: C, 65.12; H, 7.48; O, 27.40. Found: C, 65.09; H, 7.49; O, 27.53.

---

[3]Melting points are uncorrected. Analyses were done by Dr. F. Pascher, Bonn, Germany. Infrared spectra and rotations were run in $CHCl_3$; ultraviolet spectra in 95% EtOH. The alumina used in the chromatograms was Alcoa, F-20 (washed with AcOEt).

[4]We are grateful to Mr. H. Quero for the identification of the plant (voucher Q-19 of the Instituto de Biología de la Universidad Nacional Autónoma de México).

Can. J. Chem. Downloaded from www.nrcresearchpress.com by 210.87.254.40 on 09/05/12
For personal use only.

Isoodoratin (2a)

A solution of odoratin (**1***a*) (500 mg) in ethyl acetate (60 ml) was hydrogenated in the presence of 5% Pd–C (70 mg) until the absorption of hydrogen ceased. The solution was filtered and evaporated to dryness. The solid residue crystallized from chloroform–ether. This yielded prisms (310 mg) m.p. 148–150°. Further crystallizations from acetone–ether raised the m.p. to 151–153°; $[\alpha]_D$ −2°; λ_{max} 220 mμ; ε, 15 200; i.r. bands at 3610 and 3450 cm^{-1} (hydroxyl groups), at 1760 cm^{-1} (γ-lactone), and at 1670 cm^{-1} (C=C double bond).

Anal. Calcd. for $C_{15}H_{22}O_4$: C, 67.64; H, 8.33; O, 24.03. Found: C, 67.13; H, 8.77; O, 24.42.

Isoodoratin Diacetate (2b)

Acetylation of **2***a* with acetic anhydride and pyridine on the steam bath for 1 h yielded the diacetate **2***b*, m.p. 215–216° (prismatic needles from acetone–hexane); $[\alpha]_D$ −110°; λ_{max} 218 mμ; ε, 16 500; i.r. bands at 1750 cm^{-1} (broad, γ-lactone and acetyl groups) and at 1675 cm^{-1} (C=C double bond).

Anal. Calcd. for $C_{19}H_{26}O_6$: C, 65.12; H, 7.48; O, 27.40. Found: C, 65.11; H, 7.46; O, 27.60.

Dehydration of Odoratin (1a) with Potassium Bisulfate

An intimate mixture of **1***a* (500 mg) and potassium bisulfate (2.5 g) was heated under high vacuum. The lactone **3** began to sublime at 150°; the mixture was heated at increasing temperature until no more sublimate was produced (240°). The sublimate (180 mg) was chromatographed on alumina. The crystalline fractions were combined and recrystallized from acetone – isopropyl ether. This yielded the lactone **3** m.p. 108–110°; $[\alpha]_D$ +152°; λ_{max} 213 mμ; ε, 10 100; i.r. bands at 1760 cm^{-1} (γ-lactone), at 1740 cm^{-1} (five-membered ring ketone) and at 1660 cm^{-1} (exocyclic methylene group).

Anal. Calcd. for $C_{15}H_{20}O_3$: C, 72.55; H, 8.12; O, 19.33. Found: C, 72.61; H, 8.06; O, 19.26.

Baeyer–Villiger Oxidation of the Lactone 3

A solution of the lactone **3** (300 mg) in chloroform (25 ml) was treated with *m*-chloroperbenzoic acid (550 mg) and *p*-toluenesulfonic acid (200 mg) and heated under reflux for 16 h. The solution was washed with aqueous sodium bicarbonate, dried, and evaporated to dryness. The gummy residue dissolved in benzene–hexane 1:1 was chromatographed on alumina (6 g). The crystalline fractions were combined and recrystallized from acetone – isopropyl ether. This yielded 150 mg of **4** m.p. 142–143°; $[\alpha]_D$ −21°; λ_{max} 212 mμ; ε, 10 000; i.r. bands at 1765 cm^{-1} (γ-lactone), at 1730 cm^{-1} (six-membered ring lactone) and at 1665 cm^{-1} (C=C double bond).

Anal. Calcd. for $C_{15}H_{20}O_4$: C, 68.16; H, 7.63; O, 24.21. Found: C, 67.99; H, 7.67; O, 24.42.

Isolactone 5

A solution of the ketone **3** (200 mg) in ethyl acetate was hydrogenated in the presence of 5% Pd–C (40 mg). When the absorption of hydrogen ceased, the solution was filtered and evaporated to dryness. Crystallization from acetone–hexane afforded the lactone **5** (130 mg), m.p. 146°; λ_{max} 218 mμ; ε, 15 500. Mixture m.p. with dihydroisoaromatin (4, 5) showed no depression. The i.r. spectra were superimposable.

1. W. Herz, A. Romo de Vivar, J. Romo, and N. Viswanathan. J. Am. Chem. Soc. **85**, 19 (1963).
2. J. Romo, P. Joseph-Nathan, and G. Siade. Tetrahedron, **22**, 1499 (1966).
3. J. Romo, P. Joseph-Nathan, A. Romo de Vivar, and C. Alvarez. Tetrahedron, **23**, 529 (1967).
4. W. Herz, P. Jayaraman, and H. Watanabe. J. Am. Chem. Soc. **82**, 2276 (1960).
5. J. Romo, P. Joseph-Nathan, and F. Díaz. Chem. Ind. London, 1839 (1963).
6. J. Romo, P. Joseph-Nathan, and F. Díaz. Tetrahedron, **20**, 79 (1964).
7. J. Romo and A. Romo de Vivar. Fortschr. Chem. Org. Naturstoffe, **25**, 90 (1967).
8. J. P. de Villiers. J. Chem. Soc. 2412 (1959).
9. J. P. de Villiers and K. Pachler. J. Chem. Soc. 4989 (1963).

Can. J. Chem. Downloaded from www.nrcresearchpress.com by 210.87.254.40 on 09/05/12
For personal use only.

Can. J. Chem. Downloaded from www.nrcresearchpress.com by 210.87.254.105 on 09/05/12
For personal use only.

Cis- and *trans*-2,4-dimethoxytetrahydropyran.[1] Models for the study of the anomeric effect

F. SWEET AND R. K. BROWN
Department of Chemistry, University of Alberta, Edmonton, Alberta

Received December 29, 1967

Acid-catalyzed methanolysis of 2-methoxy-5,6-dihydro-2*H*-pyran gave, in good yield, a 4.0:1.0 mixture of *trans*- and *cis*-2,4-dimethoxytetrahydropyran. Mild acid hydrolysis of 2-methoxy-5,6-dihydro-2*H*-pyran followed by acid-catalyzed reaction with methanol gave a *cis–trans* mixture of 4-hydroxy-2-methoxytetrahydropyran in very poor yield.

From the equilibrium mixture of *trans*- and *cis*-2,4-dimethoxytetrahydropyran (4.0:1.0), the magnitude of the anomeric effect of the 2-methoxy group was calculated to be 1.4 kcal/mole.

Canadian Journal of Chemistry, 46, 1543 (1968)

Introduction

As part of a study of the effect of substituents on the ease and direction of C—O bond cleavage in substituted tetrahydropyrans (1), we required the compounds *cis*- and *trans*-4-hydroxy-2-methoxytetrahydropyran and their 4-*O* methylated derivatives. Furthermore, the *cis*- and *trans*-2,4-dimethoxytetrahydropyrans are considered to be more suitable simple carbohydrate analogues useful in studying the anomeric effect than the compounds *cis*- and *trans*-4-methyl-2-methoxytetrahydropyran previously employed for this purpose (2). This paper describes the results of our work on the preparation of these compounds.

Results and Discussion

When 2-methoxy-5,6-dihydro-2*H*-pyran was heated in methanol in the presence of a catalytic amount of *p*-toluenesulfonic acid there was obtained by *fractional distillation* a 92% yield of a mixture of what proved to be *trans*- and *cis*-2,4-dimethoxytetrahydropyran in the ratio 4.0:1.0 respectively. Gas–liquid chromatography (g.l.c.) showed these to be the only significant products of this reaction. Their separation was readily achieved by preparative g.l.c. on a column of 20% butanediol succinate on Gas-Chrom P.

The mixture, as well as the separated components, was analyzed by nuclear magnetic resonance (n.m.r.) spectroscopy (Figs. 1 and 2) and showed for the anomeric proton signals of the major and minor constituents respectively a triplet at τ 5.28 ($J_{2,3'} = J_{2,3} = 2.9$ Hz) and a quartet at τ 5.68 ($J_{2,3'} = 8.3$ Hz, $J_{2,3} = 2.8$ Hz). These coupling values enabled the identification of the major and minor constituents as the *trans* and *cis* isomers respectively and showed that both isomers existed preferentially in the conformer in which the C-4 methoxy group was equatorial (2–4). The pattern of signals observed for the anomeric protons also confirms the position of the methoxy group at C-4 rather than at C-3, since if the latter were the case, the signal for the anomeric proton in both isomers would be a doublet or a broad singlet.

Each of the two separated isomers was allowed to isomerize at room temperature in methanol containing a small amount of *p*-toluenesulfonic acid. Equilibrium was reached within 7 days at room temperature (25 °C) and the equilibrium mixture in each case was found by g.l.c. analysis to be composed of the *trans* and *cis* isomers in the ratio of 4.0:1.0 respectively.

The formation essentially of only the two components, *trans*- and *cis*-2,4-dimethoxytetrahydropyran shows that a highly selective reaction had occurred between methanol and 2-methoxy-5,6-dihydro-2*H*-pyran. It has already been established that both *trans*- and *cis*-3,4-epoxy-2-methoxytetrahydropyran will react with lithium aluminium hydride to give in high yield *only* that product which results from the cleavage of the epoxide C—O bond remote from the anomeric carbon (5). This phenomenon was attributed to the marked destabilizing effect which the two oxygen atoms, attached to the

[1]Taken from the thesis of F. Sweet to be submitted to the Faculty of Graduate Studies as part of the requirements for the degree of Doctor of Philosophy.

Can. J. Chem. Downloaded from www.nrcresearchpress.com by 210.87.254.105 on 09/05/12
For personal use only.

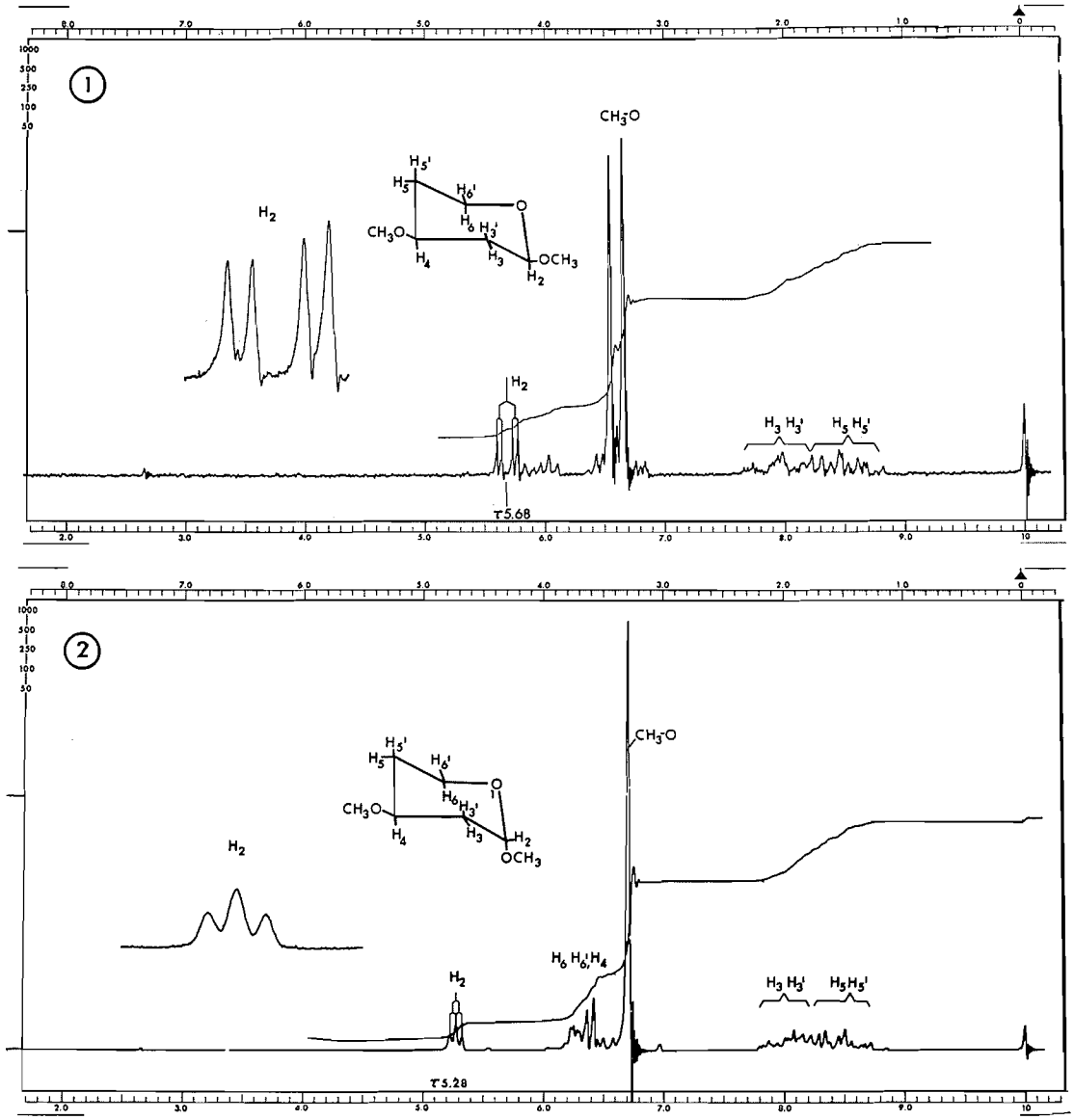

FIG. 1. The 60 MHz nuclear magnetic resonance spectrum of *trans*-2,4-dimethoxytetrahydropyran in solvent $CDCl_3$.

FIG. 2. The 60 MHz nuclear magnetic resonance spectrum of *cis*-2,4-dimethoxytetrahydropyran in solvent $CDCl_3$.

anomeric carbon, had on carbonium ion formation arising from cleavage of the epoxide C—O bond nearest the anomeric center. The results obtained in the present work strongly suggest that a similar polar effect occurs when the double bond is protonated. The more stable protonated state, then, is that in which the carbon of the double bond more remote from the anomeric center becomes positive. This effect is quite powerful since we have not been able to detect, either by g.l.c. or by n.m.r. spectroscopy, any of the 2,3-dimethoxy isomers (4) whose retention times are clearly different from those of the 2,4-dimethoxy compounds. Accordingly a possible route by which the *cis*- and *trans*-2,4-dimethoxytetrahydropyrans are made can be represented as shown in Scheme 1.

Since the reaction was carried out in an acidic

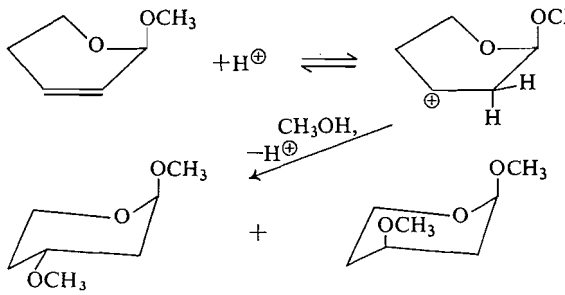

SCHEME 1

medium in which acetals are known to be unstable, a second route to the formation of the 2,4-dimethoxytetrahydropyrans can be devised. This is shown in Scheme 2 and involves a preferred protonation of the oxygen atoms rather than the double bond. Two pathways, *a* and/or *b*, might be followed. In pathway *a*, removal of methyl alcohol would result in an allylic carbonium ion stabilized by participation of the oxygen atom. Attack of methyl alcohol on the C-4 would result in 4-methoxy-2,3-dihydro-4*H*-pyran which should be thermodynamically more stable than 2-methoxy-5,6-dihydro-2*H*-pyran. The 4-methoxy-2,3-dihydro-4*H*-pyran would then react as expected with methanol in the presence of acid to produce the 2,4-dimethoxytetrahydropyran. In pathway *b*, the ring is cleaved first, to yield an allylic carbonium ion which, as in *a*, is stabilized further by oxygen participation. Here also that product should accumulate in which reaction of methanol occurs at the C-4 carbon atom to yield a dimethoxy olefin alcohol which would then readily cyclize to yield the 2,4-dimethoxytetrahydropyran. The possibility exists that the dimethoxy olefin might react with the solvent methanol to form the acetal 3,5,5-trimethoxy-1-pentanol. But it is expected that under acidic conditions this would lose the methoxy group and give the cyclized product, 2,4-dimethoxytetrahydropyran. The instability of such δ-hydroxy acetals in acid media and their tendency to cyclize to the more stable tetrahydropyrans has been shown previously (6).

An unsuccessful attempt was made to determine the relative stability of 2-methoxy-5,6-dihydro-2*H*-pyran and 4-methoxy-2,3-dihydro-4*H*-pyran by heating 2-methoxy-5,6-dihydro-2*H*-pyran in refluxing ether containing some boron trifluoride etherate. Only unchanged material and much polymeric substance was obtained. This formation of polymeric substance is not surprising in view of the reactivity of 3,4-dihydro-2*H*-pyrans (12).

Since methanolysis of 2-methoxy-5,6-dihydro-2*H*-pyran had produced *cis*- and *trans*-2,4-dimethoxytetrahydropyran in good yield, it was thought possible, by hydrolysis followed by treatment with acidic methanol to prepare 4-hydroxy-2-methoxytetrahydropyran. An early report (7) states that attempts to convert 2-methoxy-5,6-dihydro-2*H*-pyran by mild acid hydrolysis to 5-hydroxy-2-pentenal resulted only in a polymeric product unless carried out in the presence of 2,4-dinitrophenylhydrazine. However, steam distillation of the hydrolysis mixture gave a 55% yield of 2,4-pentadienal, a product obtained from the dehydration of 5-hydroxy-2-pentenal (7).

Our attempts to hydrolyze 2-methoxy-5,6-dihydro-2*H*-pyran in 0.1 *N* sulfuric acid at 95–100 °C gave only the dehydration product 2,4-pentadienal (isolated as the 2,4-dinitrophenylhydrazone) along with some polymeric material. Such vigorous conditions were discarded in favor of room temperature hydrolysis of 2-methoxy-5,6-dihydro-2*H*-pyran in the presence of the acidic ion–exchange resin, Amberlite IR 120. When the viscous oil obtained from this reaction was treated with acidic methanol a mixture of 5 products was obtained. Three of these proved to be starting material, and *trans*- and *cis*-2,4-dimethoxytetrahydropyran. The remaining two substances, both of retention time greater than those of the other three constituents, were isolated by g.l.c. as a mixture (2% overall yield) of the isomers *cis*- and *trans*-4-hydroxy-2-methoxytetrahydropyran. These were shown to be different from the isomeric mixture of authentic *cis*- and *trans*-3-hydroxy-2-methoxytetrahydropyran (4) whose retention times were lower than those of the 4-hydroxy-2-methoxytetrahydropyrans. The n.m.r. spectra of the mixture of *cis*- and *trans*-4-hydroxy-2-methoxytetrahydropyrans showed two sets of overlapping multiplets in the anomeric proton region of τ 5.10–5.35, whereas the *cis*- and *trans*-3-hydroxy 2-methoxytetrahydropyrans showed doublets at τ 5.44 and 5.75 for the anomeric protons.

Methylation (8) of the mixture of *cis*- and *trans*-4-hydroxy-2-methoxytetrahydropyran gave a mixture of *cis*- and *trans*-2,4-dimethoxytetrahydropyran identical, both by their n.m.r. spectra and g.l.c. analyses, with those obtained above.

The 4.0:1.0 *trans*:*cis* equilibrium obtained at

Can. J. Chem. Downloaded from www.nrcresearchpress.com by 210.87.254.105 on 09/05/12
For personal use only.

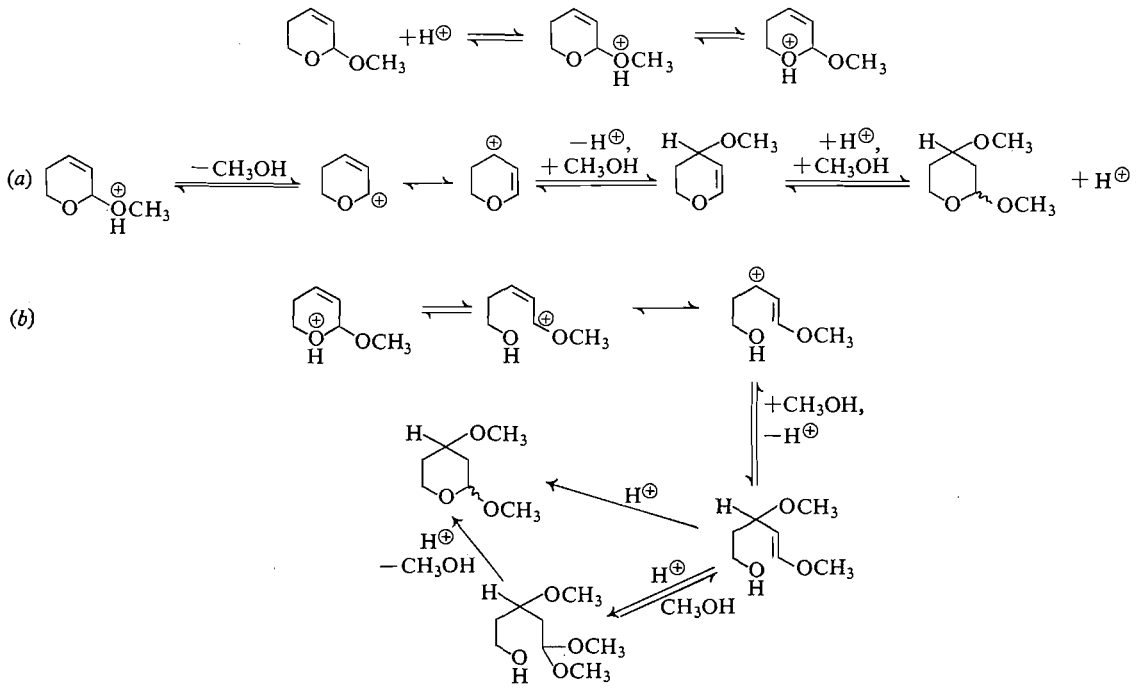

SCHEME 2

25 °C when either *cis*- or *trans*-2,4-dimethoxytetrahydropyran was dissolved in dry methanol containing some *p*-toluenesulfonic acid, shows that the axial C-2 methoxy group is favored over the equatorial C-2 methoxy to the extent of $-\Delta F = 0.82$ kcal/mole (9). The anomeric effect quantitatively is equal to the sum of the free energy difference between the anomers and the *A* value of the C-2 methoxy group (2). Using the *A* value of 0.6 kcal/mole (10) for the methoxy group, Anderson and Sepp (2) have calculated the anomeric effect in 2-methoxy-4-methyltetrahydropyran (in methanol) to be 1.08 kcal/mole. In the present work, using the same value of 0.6 kcal/mole for the *A* value of the methoxy group (cf. 0.7 kcal/mole, ref. 9, p. 44), the anomeric effect in 2,4-dimethoxytetrahydropyran is 1.4 kcal/mole. This difference between our value and that of Anderson and Sepp must be due to the nature of the C-4 substituent. The fact that replacement of the C-4 methyl group by the methoxy substituent *increases* the anomeric effect by ~0.3 kcal/mole supports the view (11) that the anomeric effect is caused by intramolecular dipolar interactions. In Scheme 3 it is quite clear that the electron attracting

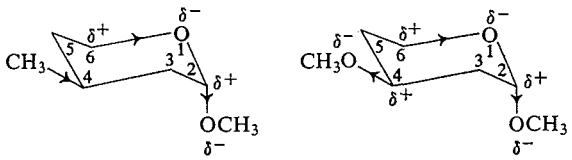

SCHEME 3

methoxy group at C-4 will create a partial positive charge on the C-4 atom, just as the ring oxygen causes a partial positive charge on C-6. These two positive charges will provide greater stabilization of the partial negative charge on the anomeric oxygen atom in the *axial* position than would be the case if the C-4 substituent were the methyl group.

Experimental

Boiling points are uncorrected.

Elemental analyses were done by Mrs. Darlene Mahlow, Department of Chemistry, University of Alberta, Edmonton.

Nuclear magnetic resonance (n.m.r.) spectra were made by Mr. R. Swindlehurst and associates, Department of Chemistry, University of Alberta, Edmonton.

Cis- and Trans-2,4-dimethoxytetrahydropyran

To a stirred solution of 100 mg of *p*-toluenesulfonic

Can. J. Chem. Downloaded from www.nrcresearchpress.com by 210.87.254.105 on 09/05/12
For personal use only.

Can. J. Chem. Downloaded from www.nrcresearchpress.com by 210.87.254.105 on 09/05/12
For personal use only.

acid in 100 ml of anhydrous methanol was added 11.4 g (0.10 mole) of 2-methoxy-5,6-dihydro-2*H*-pyran (7). The mixture warmed spontaneously over the next 5–10 min and was subsequently heated under reflux for 4 h. The cooled solution was neutralized with powdered sodium methoxide and the bulk of the solvent then removed by fractional distillation. The residue, dissolved in 100 ml of ether, was washed with 15 ml of water then dried ($MgSO_4$), filtered, and freed from solvent by fractional distillation. The residual oil, distilled under reduced pressure, gave 13.5 g (92%) of material which by g.l.c. and by n.m.r. was shown to be a mixture of two isomeric components in the ratio 4.0:1.0. The boiling point of the mixture, 109 °C at 100 mm; n_D^{25}, 1.4330.

Anal. Calcd. for $C_7H_{14}O_3$: C, 57.51; H, 9.65. Found: C, 57.44; H, 9.33.

The two isomers were separated by g.l.c. with a model A700 Aerograph Autoprep equipped with a $\frac{1}{4}$ in. (O.D.) × 12 ft stainless steel column packed with 20% butanediol succinate on Gas–Chrom P. Helium was the carrier gas at a flow rate of 110 ml/min. The column temperature was 160 °C and 175 μl quantities were injected manually. Retention times for the major and minor constituents were 190 s and 260 s respectively. Re-injection of these collected fractions showed that they consisted of only one component each and had suffered no decomposition.

The major component (*trans* isomer) had n_D^{25} and 1.4324.

Anal. Calcd. for $C_7H_{14}O_3$: C, 57.51; H, 9.65. Found: C, 57.54; H, 9.47.

The minor component (*cis* isomer) had n_D^{25} and 1.4370. Found: C, 57.06; H, 9.30.

The n.m.r. spectra are shown in Figs. 1 and 2. The *trans* isomer (Fig. 1); H-2 (anomeric) exhibited a triplet centered at τ 5.28, $J_{2,3'} = J_{2,3} = 2.9$ Hz, and referred to tetramethylsilane. The *cis* isomer (Fig. 2); H-2 (anomeric) exhibited a quartet centered at τ 5.68, $J_{2,3'} = 8.3$ Hz, $J_{2,3} = 2.8$ Hz. All couplings are the observed values.

Equilibration of Cis- and Trans-2,4-dimethoxytetrahydropyrans

To separate solutions of 50 mg of each isomer in 5 ml of dry methanol was added 5 mg of *p*-toluenesulfonic acid. The solution was stirred at room temperature (25 °C) for several days. At regular intervals aliquots were removed from each solution and analyzed by g.l.c. using the system described above. Equilibrium was attained within 7 days and in both cases a 4.0:1.0 ratio of *trans* and *cis* isomers was obtained.

Cis- and Trans-4-hydroxy-2-methoxytetrahydropyran

A mixture of 2 g of Amberlite IR 120 (H^+) ion-exchange resin and 10 g (0.087 mole) of 2-methoxy-5,6-dihydro-2*H*-pyran in 100 ml of water was stirred for 3 h at room temperature. The resin was removed by filtration and washed with water (4 × 10 ml). The combined filtrate and washings were freed from water on a rotary evaporator under vacuum at 45 °C. The residue was shaken with 50 ml of dry benzene and the solution freed of solvent in a rotary evaporator under vacuum thus removing the last of the water by azeotropic distillation. The syrupy residue was taken up in 100 ml of dry methyl alcohol and to this was added 10 g of anhydrous $MgSO_4$ and 100 mg of *p*-toluenesulfonic acid. This mixture was stirred at room temperature for 48 h, then neutralized with powdered sodium methoxide and filtered. The filtrate was freed from solvent in a rotary evaporator under vacuum. The oily residue was dissolved in 50 ml of ether, washed with 10 ml of water, and dried ($MgSO_4$). The ether solution was filtered and freed from solvent to give 2.5 g of a crude oil. Gas–liquid chromatographic analysis of this oil was done with the apparatus described above. The column temperature in this case was 180 °C. Five components were obtained. In order of increasing retention time the first three were found, by comparison with authentic samples, to be respectively, 2-methoxy-5,6-dihydro-2*H*-pyran, *trans*- and *cis*-2,4-dimethoxytetrahydropyran. The final two components to emerge were found to be *trans*- and *cis*-4-hydroxy-2-methoxytetrahydropyran. These last two components were collected as a mixture by preparative g.l.c. using the Aerograph as described above. The boiling point (micro) was 56–58 °C at 3 mm, n_D^{25}, 1.4560.

Anal. Calcd. for $C_6H_{12}O_3$: C, 54.53; H, 9.15. Found: C, 54.63; H, 9.24.

Gas–liquid chromatographic analysis of a mixture of the above *cis*- and *trans*-4-hydroxy-2-methoxytetrahydropyrans and *cis*- and *trans*-3-hydroxy-2-methoxytetrahydropyrans (4) showed *four* peaks. The retention times of the first two peaks were identical with those for the *cis*- and *trans*-3-hydroxy-2-methoxytetrahydropyrans (with the *cis* isomer coming out of the column first).

The signals due to the anomeric protons in the n.m.r. spectra (in $CDCl_3$) of the isomeric 3-hydroxy-2-methoxy compounds were found at τ 5.44 (doublet) and τ 5.75, (doublet). The reference was tetramethylsilane. The signals for the anomeric protons of the *cis*- and *trans*-4-hydroxy-2-methoxytetrahydropyran appeared as two sets of overlapping multiplets in the region τ 5.10–5.35.

Methylation of the isomeric mixture of *cis*- and *trans*-4-hydroxy-2-methoxytetrahydropyran was accomplished by the general procedure described previously (8). To 100 mg of the *cis–trans* mixture in 25 ml of dry ether at room temperature was added 3 g of methyl iodide followed by 1 g of sodium hydride. Stirring was continued for 1 h at room temperature. The mixture was filtered under vacuum and the solvent removed from the filtrate. The oily residue (85 mg) was analyzed by g.l.c. No starting material was observed. Only two components were present in the product. These were found to be identical in retention times to the *cis*- and *trans*-2,4-dimethoxytetrahydropyrans prepared above.

Attempted Equilibration of 2-Methoxy-5,6-dihyrdo-2H-pyran

A solution of 2.24 g (0.02 mole) of 2-methoxy-5,6-dihydro-2*H*-pyran in 50 ml of dry ether to which was added 10 drops of freshly distilled boron trifluoride etherate, was heated under reflux for 24 h. The solution was cooled and shaken with 2 g of commercial sodium methoxide in 25 ml of dry ether. The resulting mixture was washed successively with 20 ml of 5% aqueous sodium carbonate, and 20 ml of saturated aqueous sodium chloride. The ether solution was dried (Na_2SO_4), filtered, and freed from solvent by careful fractional distillation. The residual oil was distilled under vacuum to give 1.05 g (47%) of starting material (b.p. 65–66 °C at

65 mm) and a yellow viscous residue (1.1 g) which could not be distilled. The infrared spectrum of the recovered starting material showed no absorption in the region of 1650 cm^{-1} indicative of the presence of an α,β unsaturated ether such as 4-methoxy-1,2-dihydro-4*H*-pyran.

The polymeric substance was analyzed for carbon and hydrogen.

Anal. Calcd. for $(C_6H_{10}O_2)_n$: C, 63.14; H, 8.83. Found (mol. wt., 241, osmometric, acetone as solvent): C, 63.83; H, 8.93.

The molecular weight was indicative of a dimeric species.

Acknowledgment

The authors gratefully acknowledge the financial assistance provided by the National Research Council of Canada.

1. U. E. DINER and R. K. BROWN. Can. J. Chem. **45**, 2547 (1967).
2. C. B. ANDERSON and D. T. SEPP. Chem. Ind. London, 2054 (1964); J. Org. Chem. **32**, 607 (1967).
3. R. U. LEMIEUX, R. K. KULLNIG, H. J. BERNSTEIN, and W. G. SCHNEIDER. J. Am. Chem. Soc. **80**, 6098 (1958).
4. F. SWEET and R. K. BROWN. Can. J. Chem. **44**, 1571 (1966).
5. F. SWEET and R. K. BROWN. Can. J. Chem. **46**, 707 (1968).
6. D. M. LEMAL, P. D. PACHT, and R. B. WOODWARD. Tetrahedron, **18**, 1275 (1962).
7. G. F. WOODS and H. SANDERS. J. Am. Chem. Soc. **68**, 2483 (1946).
8. U. E. DINER, F. SWEET, and R. K. BROWN. Can. J. Chem. **44**, 1591 (1966).
9. E. L. ELIEL, N. L. ALLINGER, S. J. ANGYAL, and G. A. MORRISON. Conformational analysis. Interscience Publishers, New York. 1965. p. 11.
10. E. L. ELIEL and M. H. GIANNI. Tetrahedron Letters, 97 (1962).
11. R. U. LEMIEUX. *In* Molecular rearrangements. *Edited by* P. de Mayo. John Wiley and Sons, Inc., New York. 1964. pp. 738–741.
12. C. P. BROWN and A. R. MATHIESON. J. Chem. Soc. 3608 (1957).

Can. J. Chem. Downloaded from www.nrcresearchpress.com by 210.87.254.105 on 09/05/12
For personal use only.

Conversion of β-chloro-L-alanine to α-carbobenzoxy-DL-diaminopropionic acid

LEO BENOITON
Department of Biochemistry, Faculty of Medicine, University of Ottawa, Ottawa, Canada
Received October 18, 1967

Several *N*-acyl-β-chloroalanine esters have been prepared from the ester which was obtained by chlorination of L-cystine diester. Reaction of benzoyl-β-chloro-L-alanine ethyl ester with potassium phthalimide followed by acid hydrolysis yielded DL-diaminopropionic acid. Reaction of carbobenzoxy-β-chloro-L-alanine ethyl ester with potassium phthalimide followed by saponification and mild acid hydrolysis yielded α-carbobenzoxy-DL-diaminopropionic acid. The racemization took place during the amination step.

Canadian Journal of Chemistry, 46, 1549 (1968)

Can. J. Chem. Downloaded from www.nrcresearchpress.com by 210.87.254.40 on 09/05/12
For personal use only.

Simple routes to derivatives of optically active diaminopropionic acid (DAPr) are lacking because the amino acid itself is not readily available, and because selective reaction at one of the amino groups presents difficulties. This paper describes an attempt at the preparation of mono-*N*-substituted DAPr derivatives from β-chloro-L-alanine.

Present sources for L-DAPr include isolation from seeds of *Mimosa palmeri* (1), enzymatic resolution of the racemate with acylase (2), and Hofmann degradation of acetyl- (3), carbobenzoxy- (4), or tosylasparagine (5). Only the latter directly provides a useful mono-substituted DAPr derivative, α-tosyl-L-DAPr, which is an intermediate in the degradation.

β-*N*-Substituted derivatives of DAPr are not accessible by the route usually used for preparing ω-*N*-substituted diamino acid derivatives. This approach, involving the protection of the α-amino group by cupric ion (6), fails for DAPr because the copper binds both amino groups under the alkaline conditions used (7). At pH 4, the β-amino group is free, but the derivatives so far obtained under these conditions (8, 9) are not useful starting materials for further synthesis. In the absence of copper, in alkaline solution, preferential acylation of the β-amino group does take place (10), having provided β-tosyl- (11), β-chloroacetyl- (12), and β-carbobenzoxy – DAPr (10), but not without concomitant formation of α,β-disubstituted derivative. Reaction in a pH 7.0 buffer has, however, provided β-carbobenzoxy – DAPr in good yield (9).

In 1960, Baganz and Dransch showed that chlorination of disulfides resulted in cleavage, with replacement of the sulfur atoms by chlorine atoms. β-Chloroalanine ester was prepared by bubbling chlorine through a suspension of cystine dimethyl ester dihydrochloride in chloroform (13). This appeared to us as a possible simple route to mono-*N*-substituted DAPr derivatives and eventually mixed peptides, as well as a quick source for β-chloroalanine derivatives, so this was investigated. The series of reactions carried out appears in Scheme 1. At first, cystine methyl ester was used as starting material, but this was abandoned in favor of the ethyl ester which gave derivatives which were easier to crystallize. Both cystine esters were initially prepared by the classical hydrogen chloride method (14), however, because of the limited solubility of the ethyl ester in the reaction medium, the thionyl chloride procedure (15) was adopted. The chlorination was carried out essentially as described in the original paper (13). The yield of β-chloroalanine methyl ester was higher, but the ethyl ester was preferred for subsequent reactions.

Acid hydrolysis of the ester (**2**) provided β-chloro-L-alanine (**3**) in good yield. This compound is usually obtained from serine by the action of PCl_5 on the ester (16). The route described here seems to be more attractive. The carbobenzoxy derivative (**4**) was obtained without difficulty. Synthesis of the latter has since been reported (17).

Five different acylchloroalanine esters (**5**) were prepared. Baganz and Dransch had reported the acetylmethyl ester, obtained with acetic anhydride, as being hydroscopic (18). By using thioacetic acid as acylating agent, both the acetylmethyl and acetylethyl esters have been obtained and adequately characterized, but the other derivatives are simpler to prepare and purify. The benzoylethyl and carbobenzoxyethyl

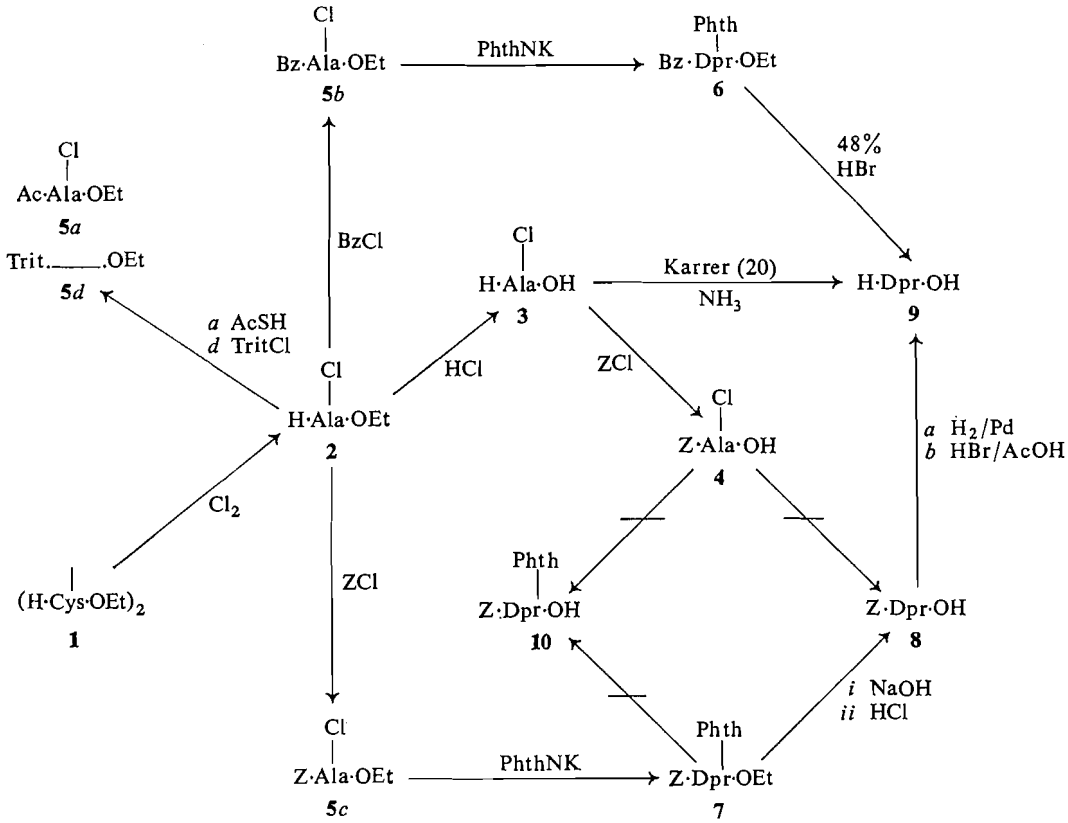

SCHEME 1

Bz = benzoyl
Z = carbobenzoxy
Dpr = diaminopropionic acid

Phth = phthalyl
Trit = trityl

esters both crystallize out during the reaction in yields of over 80%. The trityl ester is also a suitable derivative for further use.

Since the carbobenzoxy group is sometimes labile under alkaline conditions, the next reaction was first explored with the benzoyl derivative. Amination was effected with potassium phthalimide in hot dimethylformamide to give crystalline ethyl α-benzoyl-β-phthalyldiaminopropionate (**6**). Hydrolysis in one step with concentrated hydrobromic acid gave DL-DAPr. Since it is known that DAPr is gradually racemized in hot hydrochloric acid (9), the zero rotation was first believed due to the stringent hydrolytic conditions.

The amination was repeated with the carbobenzoxy ester (**5***c*), but the product (**7**) could not be crystallized. The oil was saponified in a sodium hydroxide – dioxane mixture. This also cleaved one of the phthalimido C—N bonds to leave an *o*-carboxyphenyl substituent which could be removed by mild acid hydrolysis. The carbobenzoxy group survived these conditions. This gave α-carbobenzoxy-DL-DAPr (**8**), a compound not yet reported in the literature. Direct amination of carbobenzoxy-β-chloroalanine with ammonia or potassium phthalimide was also attempted, but without success. Mild acid hydrolysis of the carbobenzoxyphthalyl ester also failed to give the free disubstituted acid (**10**).

The α-carbobenzoxy – DAPr obtained was found to be devoid of optical activity. Samples converted to free DAPr by hydrogen bromide in acetic acid or hydrogenation also gave racemic DAPr. In view of this, the racemization could have taken place only during the amination reaction with potassium phthalimide. Racemization could be accounted for by assuming a base cat-

Can. J. Chem. Downloaded from www.nrcresearchpress.com by 210.87.254.40 on 09/05/12
For personal use only.

Can. J. Chem. Downloaded from www.nrcresearchpress.com by 210.87.254.40 on 09/05/12
For personal use only.

alyzed β-elimination reaction leading to the formation of an acyldehydroalanine ester as the first step in the reaction. Another explanation would invoke participation of the amide carbonyl group in the loss of the β-chlorine atom as postulated for the *O*-desulfoxylation of a serine derivative (19).[1] The latter could account for the fact that only partial racemization was observed by Karrer in the synthesis of DAPr from β-chloro-L-alanine and liquid ammonia (20).

Experimental

Melting points were determined with a Kofler Hot-bench. Optical rotations were determined at 23° with a Rudolph model 62 polarimeter using a 2-dm tube. Compounds were dried at 60° before analysis. Chloroform was redistilled after washing with sulfuric acid and water.

L-Cystine Diethylester Dihydrochloride (1)

Thionyl chloride (51 ml; 0.7 mole) was added (*caution*) to a suspension of L-cystine (24 g; 0.1 mole) in ethanol (600 ml). The mixture was refluxed while being stirred until all the amino acid had dissolved (10 h).[2] Ether (700 ml) was then added, and after cooling, the product (29.2 g) was filtered off. A second crop (6.5 g) was obtained from the mother liquor. This material (95% yield) had m.p. 187°, $[\alpha]_D$ −47.5° (4, water), lit. m.p. 188°, $[\alpha]_D^{20}$ −48° (21), and was used without further purification. It contained about 1% cystine (amino acid analyzer).

β-Chloro-L-alanine Ethyl Ester Hydrochloride (2)

A stream of chlorine was passed into a suspension of ester (**1**) (40 g) in purified chloroform (700 ml) for 1 h at 0° while the mixture was being stirred (13). The solution was clear after ½ h. The flask was stoppered and kept at 0° for 48 h. The mixture was then allowed to warm to 20°, ether (500 ml) was added, and air was bubbled through for 1 h. The precipitate was filtered off and washed four times with ether; yield, 27.5 g (68%).

β-Chloro-L-alanine Methyl Ester Hydrochloride (2a)

This compound was prepared in 87% yield (70% recrystallized) from methanol–ether, m.p. 153° as described above (13) from the appropriate ester (23).

Carbobenzoxy-β-chloro-L-alanine (4)

The ethyl ester (**2**) (5.64 g) was converted to the free β-chloro-L-alanine hydrochloride (**3**) by refluxing 1 h in 2 *N* HCl (60 ml) (13). The mixture was repeatedly evaporated to dryness with the addition of water and finally ethanol, and the residue was crystallized from methanol–ether; yield, 4.0 g (80%), $[\alpha]_D$ −10.8° (3.2, water containing one equivalent of NaOH), corresponding to $[\alpha]_D$ −14.0° (2.5, water) for the free acid, lit. $[\alpha]_D$ −15.0° (9.9, water) (22).

A mixture of this acid (**3**) (4.8 g; 0.03 mole), sodium bicarbonate (10 g; 0.12 mole), and carbobenzoxy chloride (6 ml) was stirred vigorously for 4 h. The mixture was extracted twice with ether and the aqueous layer was acidified to Congo Red. The oil which separated out was extracted into ethyl acetate, the extract was dried, and then evaporated to dryness. The residue was crystallized from carbon tetrachloride (if the mixture forms a gel, trituration results in crystallization after a day or two); yield, 6.4 g (82.8%), m.p. 89°, $[\alpha]_D$ −4.0° (2, dimethylformamide), $[\alpha]_D$ +14.25° (2, methanol), lit. m.p. 88°, $[\alpha]_D^{25}$ +27° (1, methanol) (17).[3]

Anal. Calcd. for $C_{11}H_{12}ClNO_4$ (mol. wt., 257.7): C, 51.3; H, 4.7; N, 5.4. Found: C, 51.2; H, 4.7; N, 5.3.

Acetyl-β-chloro-L-alanine Methyl Ester (5)

To a cooled solution of methyl ester (**2a**) (6.19 g; 0.035 mole) and triethylamine (4.9 ml; 0.035 mole) in chloroform (30 ml) and acetonitrile (30 ml) was added thioacetic acid (5.25 ml; 0.07 mole). After 3 days, air was bubbled through the mixture, the solvent was evaporated, and the residue was taken up in ethyl acetate (100 ml). The mixture was filtered through Celite, the filtrate was washed successively with *N* HCl, water, aqueous $NaHCO_3$, water, and finally dried. The solvent was evaporated and the solid residue was collected with the aid of cold petroleum ether. After thorough drying, the acetylmethyl ester was recrystallized from petroleum ether (b.p. 80–100°); yield, 3.8 g (60%), m.p. 100–102°, $[\alpha]_D$ −12.7° (1, dimethylformamide), soluble in water.

Anal. Calcd. for $C_6H_{10}ClNO_3$ (mol. wt., 179.6): C, 40.1; H, 5.6; N, 7.8. Found: C, 39.8; H, 5.4; N, 7.8.

Acetyl-β-chloro-L-alanine Ethyl Ester (5a)

This derivative was prepared as described for (**5**) from the corresponding ester (**2**); yield, 60%. It can be recrystallized from ether, carbon tetrachloride, or petroleum ether (b.p. 67°), but with considerable loss of material. A sample crystallized twice from ether had m.p. 95°, $[\alpha]_D$ −14.3° (1, dimethylformamide).

Anal. Calcd. for $C_7H_{12}ClNO_3$ (mol. wt., 193.6): C, 43.4; H, 6.25; N, 7.2. Found: C, 43.4; H, 6.3; N, 7.3.

Benzoyl-β-chloro-L-alanine Ethyl Ester (5b)

Benzoyl chloride (6 ml; 0.051 mole) was added dropwise to a stirred aqueous solution of chloroalanine ester (**2**) (9.4 g; 0.05 mole) and sodium bicarbonate (8.4 g; 0.1 mole) at 0°. After 1 h of additional stirring at 25°, the precipitate was collected, dried, and recrystallized from ethanol–water; yield, 11.2 g (88%), m.p. 112°, $[\alpha]_D$ −24.7° (2, dimethylformamide), soluble in ether and tetrahydrofuran.

Anal. Calcd. for $C_{12}H_{14}ClNO_3$ (mol. wt., 255.7): C, 56.35; H, 5.5; N, 5.5. Found: C, 56.5; H, 5.4; N, 5.35.

Carbobenzoxy-β-chloro-L-alanine Ethyl Ester (5c)

A mixture of the chloroalanine ester (**2**) (11.3 g; 0.06 mole), sodium bicarbonate (15.1 g; 0.18 mole), and carbobenzoxy chloride (10 ml) in water was stirred vigorously for 4 h. The precipitate was filtered and recrystallized from ethanol–water; yield, 14.0 g (82%), m.p. 60°, $[\alpha]_D$ −18.8° (2, dimethylformamide), soluble in ether and tetrahydrofuran.

[1]We thank one of the referees for this suggestion.

[2]The product sometimes begins to come out of solution before all the starting material disappears.

[3]We have no explanation for the discrepancy in the rotation values.

Can. J. Chem. Downloaded from www.nrcresearchpress.com by 210.87.254.40 on 09/05/12
For personal use only.

Anal. Calcd. for $C_{11}H_{12}ClNO_4$ (mol. wt., 257.7): C, 51.3; H, 4.7; N, 5.4. Found: C, 51.2; H, 4.7; N, 5.3.

*Trityl-β-chloro-*L*-alanine Ethyl Ester (5d)*

A mixture of chloroalanine ester (**2**) (3.76 g; 0.02 mole), triethylamine (6 ml; 0.044 mole) and triphenylchloromethane (5.6 g; 0.02 mole) in chloroform (30 ml) was left at 25° for 6 h. The solution was washed twice with water, dried, repeatedly evaporated down to dryness with the addition of acetone, and the residue was crystallized twice from methanol; yield, 5.65 g (72%), m.p. 87°, $[\alpha]_D$ +18.0° (2, dimethylformamide).

Anal. Calcd. for $C_{24}H_{24}ClNO_2$ (mol. wt., 393.9): C, 73.2; H, 6.1; N, 3.6. Found: C, 73.0; H, 6.1; N, 3.45.

*Ethyl α-Benzoyl-β-phthalyl-*DL*-diaminopropionate (6)*

A mixture of benzoylchloroalanine ester (**5***b*) (7.67 g; 0.03 mole) and potassium phthalimide (8.33 g; 0.045 mole) in dimethylformamide (40 ml) was stirred at 90° for 3 h. Water (100 ml) and chloroform (100 ml) were added. After shaking, the organic layer was washed with 0.1 *N* NaOH, then with water, dried, and evaporated to small volume. The residue was crystallized from ethanol containing a few drops of water; yield, 8.46 g (77%), m.p. 59°, $[\alpha]_D$ 0.0° ($CHCl_3$ or acetic acid).

Anal. Calcd. for $C_{20}H_{18}N_2O_5$ (mol. wt., 366.4): C, 65.6; H, 4.95; N, 7.65. Found: C, 65.8; H, 4.9; N, 7.6.

*α-Carbobenzoxy-*DL*-diaminopropionic Acid (8)*

A mixture of the carbobenzoxy ester (**5***c*) (4.28 g; 0.15 mole) and potassium phthalimide in dimethylformamide (15 ml) was stirred at 90° for 3 h. Water (100 ml) and chloroform (100 ml) were added, and after shaking, the organic layer was washed with 0.1 *N* NaOH, then with water, dried, and evaporated to an oil. Tetrahydrofuran (15 ml) and *N* NaOH (30 ml) were added, and after 1 h, the tetrahydrofuran was removed under reduced pressure. *N* HCl (60 ml) was added and the mixture was refluxed for 1 h. The cooled solution was extracted twice with ether and then adjusted to pH 6 with *N* NaOH. After cooling for 1 h, the crystals were filtered off, washed thoroughly with water, and dried over P_2O_5; yield, 2.42 g (67.8%). Found: N, 11.95.

The carbobenzoxy – diaminopropionic acid was recrystallized by dissolving in *N* HCl, treating with charcoal, and adding an equal volume of *N* NaOH; yield, 1.69 g (47.5%), $[\alpha]_D$ −0.7° (2, *N* HCl).

Anal. Calcd. for $C_{11}H_{14}N_2O_4$: C, 55.45; H, 5.9; N, 11.8. Found: C, 55.5; H, 5.9; N, 11.7.

DL*-Diaminopropionic Acid Monohydrobromide (9)*

*From Ethyl α-Benzoyl-β-phthalyl-*DL*-diaminopropionate (6)*

The benzoyl derivative (**6**) (3.66 g) was refluxed for 2 h in 48% hydrobromic acid (35 ml). The mixture was cooled, diluted with water (35 ml), filtered, and the filtrate repeatedly evaporated to dryness. The residue was solidified by trituration in ethanol, and the product was crystallized from water–ethanol; yield, 2.93 g (80%), $[\alpha]_D$ +1.0° (2, 5 *N* HCl).

Anal. Calcd. for $C_3H_9BrNO_2$ (mol. wt., 185.0): C, 19.5; H, 4.9; N, 15.1. Found: C, 19.7; H, 5.0; N, 15.0.

*From α-Carbobenzoxy-*DL*-diaminopropionic Acid (8)*

To the carbobenzoxy derivative (**8**) (0.24 g) dissolved in dry acetic acid (5 ml) was added a 35% hydrogen bromide in acetic acid solution (5 ml). After 1 h, several volumes of ether were added and the precipitate was collected and recrystallized from water–ethanol; yield, 0.12 g (62%), $[\alpha]_D$ 0° (1, 6 *N* HCl). Found: C, 19.7; H, 5.0; N, 15.2.

Acknowledgments

The technical assistance of Mrs. H. Williams during part of this work and the financial support of the Medical Research Council are gratefully acknowledged.

1. R. Gmelin, G. Straus, and G. Hasenmaier. Z. Physiol. Chem. **314**, 28 (1959).
2. J. P. Greenstein and M. Winitz. Chemistry of the amino acids. John Wiley & Sons, Inc., New York, N.Y. 1961. p. 2466.
3. P. Karrer and A. Schlosser. Helv. Chim. Acta, **6**, 411 (1923).
4. F. Schneider. Ann. **529**, 1 (1937).
5. J. Rudinger, K. Poduŝka, and M. Zaoral. Collection Czech. Chem. Commun. **25**, 2022 (1960).
6. A. C. Kurtz. J. Biol. Chem. **122**, 477 (1938).
7. A. Albert. Biochem. J. **50**, 690 (1952).
8. S. L. Rao, P R. Adiga, and P. S. Sarna. Biochemistry, **3**, 432 (1964).
9. A. Kjaer and P. O. Larsen. Acta Chem. Scand. **13**, 1565 (1959).
10. A. Kjaer. Acta Chem. Scand. **3**, 1087 (1949).
11. K. Poduŝka, J. Rudinger, and F. Ŝorm. Collection Czech. Chem. Commun. **20**, 1174 (1955).
12. Y. Miyanoki. J. Biochem. Tokyo, **13**, 389 (1931). F. Schneider. Biochem. Z. **291**, 328 (1937).
13. H. Baganz and G. Dransch. Ber. **93** 782 (1960).
14. J. P. Greenstein and M. Winitz. Chemistry of the amino acids. John Wiley & Sons, Inc., New York, N.Y. 1961. p. 925.
15. M. Brenner and W. Huber. Helv. Chim. Acta, **36**, 1109 (1953).
16. E. Fischer and K. Raske. Ber. **40**, 3717 (1907).
17. M. Wilchek, C. Zioudrou, and A. Patchornik. J. Org. Chem. **31**, 2865 (1966).
18. H. Baganz and G. Dransch. Ber. **94**, 2597 (1961).
19. A. M. Gold and D. Fahrney. Biochemistry, **3**, 783 (1964).
20. P. Karrer. Helv. Chim. Acta, **6**, 957 (1923).
21. E. Abderhalden and E. Wybert. Ber. **49**, 2449 (1916).
22. G. B. Brown and V. du Vigneaud. J. Biol. Chem. **140**, 767 (1941).
23. J. T. Edsall. J. Polymer Sci. **12**, 253 (1954).

Can. J. Chem. Downloaded from www.nrcresearchpress.com by 210.87.254.40 on 09/05/12
For personal use only.

Acid-catalyzed rearrangement of hydroperoxides. I. Benzhydryl hydroperoxides[1]

GLENN H. ANDERSON
Exploratory Research Laboratory, Dow Chemical of Canada, Limited, Sarnia, Ontario

AND

JAMES G. SMITH
Department of Chemistry, University of Waterloo, Waterloo, Ontario

Received August 29, 1967

Substituted benzhydryl hydroperoxides have been synthesized and rearranged using sulfuric acid as the catalyst and acetone as the solvent. The products have been analyzed in order to determine the migration aptitudes for the various aryl groups. A linear relationship exists between the log of the migration aptitude and the σ^+ values of the substituents. Ortho substituents deviate from this relationship but the extent of deviation is much smaller than expected. The migration aptitude of hydrogen versus phenyl in the rearrangement of benzhydryl hydroperoxide has been found to vary markedly depending on the solvent. These observations and their bearing upon the mechanism of the rearrangement are discussed.

Canadian Journal of Chemistry, 46, 1553 (1968)

Introduction

Hydroperoxides are well known to undergo rearrangement under acid conditions producing, in the case of benzhydryl hydroperoxide, phenol

$$Ph_2CHOOH \xrightarrow{H^+} PhOH + PhCHO$$

and benzaldehyde (1). Qualitatively, the migration aptitude of substituted phenyl groups has been examined by several investigators (2–5). Such studies (2–4) often relied upon the generation of the hydroperoxide and its rearrangement in the same medium rather than upon the stepwise preparation and isolation of the hydroperoxide followed by a separate rearrangement. However, these studies did establish that electron-donating substituents on the aryl group facilitated its rearrangement while electron-attracting groups inhibited it.

A quantitative comparison of the effects of substituents on aryl migration has been made by van Steveninck and Kooyman (6) for a series of substituted cumene hydroperoxides. A comparison of these results with those derived from competitive migration of two different aryl groups within the same molecule was felt to be of interest.

For this study, several substituted benzhydryl hydroperoxides were examined. These were chosen so as to provide an independent comparison with the two triarylmethyl hydroperoxides which have also been studied (7).

In addition, the complication of olefin formation (3) which might arise from compounds such as 1,1-diarylethyl hydroperoxide, was avoided.

Results

The hydroperoxides were prepared from the corresponding alcohols by the method of Davies *et al.* (8). In the case of benzhydryl hydroperoxide and the methylbenzhydryl hydroperoxides, this procedure proved quite satisfactory. However, the chlorobenzhydrols reacted so slowly that mixtures of the starting alcohol and hydroperoxide arose. These proved difficult to separate.

Extending the reaction time 10-fold, resulted in satisfactory production of hydroperoxide. This variation of the procedure was accompanied by a reduced yield of product due to its slow concomitant rearrangement to phenol and aldehyde. These latter impurities were extracted with dilute alkali from the crude product, the aldehyde having been oxidized to the acid under the reaction conditions.

Table I presents a summary of the hydroperoxides prepared.

Substituted benzhydryl hydroperoxides rearrange to a mixture of two phenols and two benzaldehydes. From an analytical viewpoint, the ideal system for performing the rearrangement of the hydroperoxides would be one in

[1]Contribution No. 153 from the Exploratory Research Laboratory, Dow Chemical of Canada, Limited, Sarnia, Ontario.

TABLE I

Benzhydryl hydroperoxides*

X	Reaction time (h)	Melting point (°C)	Iodometric purity	Analysis: Found C	Found H	Found Cl	Calculated C	Calculated H	Calculated Cl
H	6	49–51.5†	99						
o-CH_3	4	62–63.5	94	78.53	6.53		78.52	6.59	
m-CH_3	3.5	oil	96.5	78.47	6.63				
p-CH_3	1.5	50.5–52	100	78.06	6.30				
o-Cl	63	48–51.5	92	66.66	4.72	15.07	66.53	4.72	15.11
m-Cl	63	38.5–40.5	90	66.72	4.83	15.14			
p-Cl	18	56–58‡	98.5	66.65	4.86	15.09			

*Compounds of structure 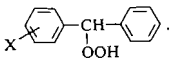 .

†Reported m.p. 50–52° (8).
‡Reported as an oil (9).

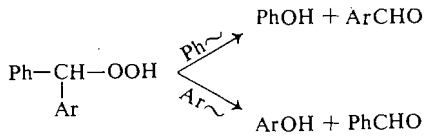

which the final reaction mixture could be injected directly into a gas chromatography unit for analysis after the mineral acid had been neutralized. Acetic acid as a reaction medium, while frequently described in the literature, was found unsatisfactory for our purposes. This solvent tailed badly on the vapor-phase chromatographic (v.p.c.) unit and, while neutralization of the solvent with aqueous sodium bicarbonate was possible, it increased the danger of air oxidation of the aldehydes. Furthermore, trial experiments with *p*-methylbenzhydryl hydroperoxide demonstrated that appreciable amounts of the *p*-cresol formed during the reaction, were esterified to form *p*-cresyl acetate. The final mixture was difficult to analyze with sufficient accuracy.

The use of benzene with a ferric chloride catalyst (10) was also examined and found to produce anomalously low amounts of the phenolic product, possibly due to complexing with the catalyst.

Several solvents were examined as possible replacements for acetic acid. Of those studied, diethyl ether and dioxane slowed the reaction inconveniently (11) and produced a large amount of benzophenone in addition to the normal rearrangement products, phenol and benzaldehyde.

Acetone proved to be a satisfactory solvent; the reaction proceeded rapidly producing high yields of phenol and benzaldehyde and low yields of benzophenone. By using an internal standard it was shown that the rearrangement products, phenol and benzaldehyde, were obtained in 91% and 93% yield respectively while benzophenone was obtained in 3.1% yield. These results compare favorably with those obtained using acetic acid as a solvent.

The rearrangement was carried out at 20 °C under nitrogen with sulfuric acid catalyst. The reaction was monitored using the starch-acidified potassium iodide test for unreacted peroxides. When the reaction was complete, a sample was withdrawn for analysis followed by a second sample approximately 30 min later. After the mineral acid was neutralized by addition of sodium bicarbonate, the samples were analyzed by v.p.c. on a column calibrated with known mixtures. The results reported are an average of the analyses on these two samples. Migration aptitudes were calculated from the areas of the aldehyde peaks only. The phenols tended to tail and overlap in the v.p.c. and the analyses were not reproducible.

The migration aptitudes are tabulated in Table II. Their logarithms are plotted in Fig. 1 against the σ^+ values of Brown and Okamoto (12, 13) for the meta and para substituents and against the Taft σ^* constants (14) for the ortho substituents. A linear relationship is evident with deviations noticeable in the case of the

Can. J. Chem. Downloaded from www.nrcresearchpress.com by 210.87.254.40 on 09/05/12
For personal use only.

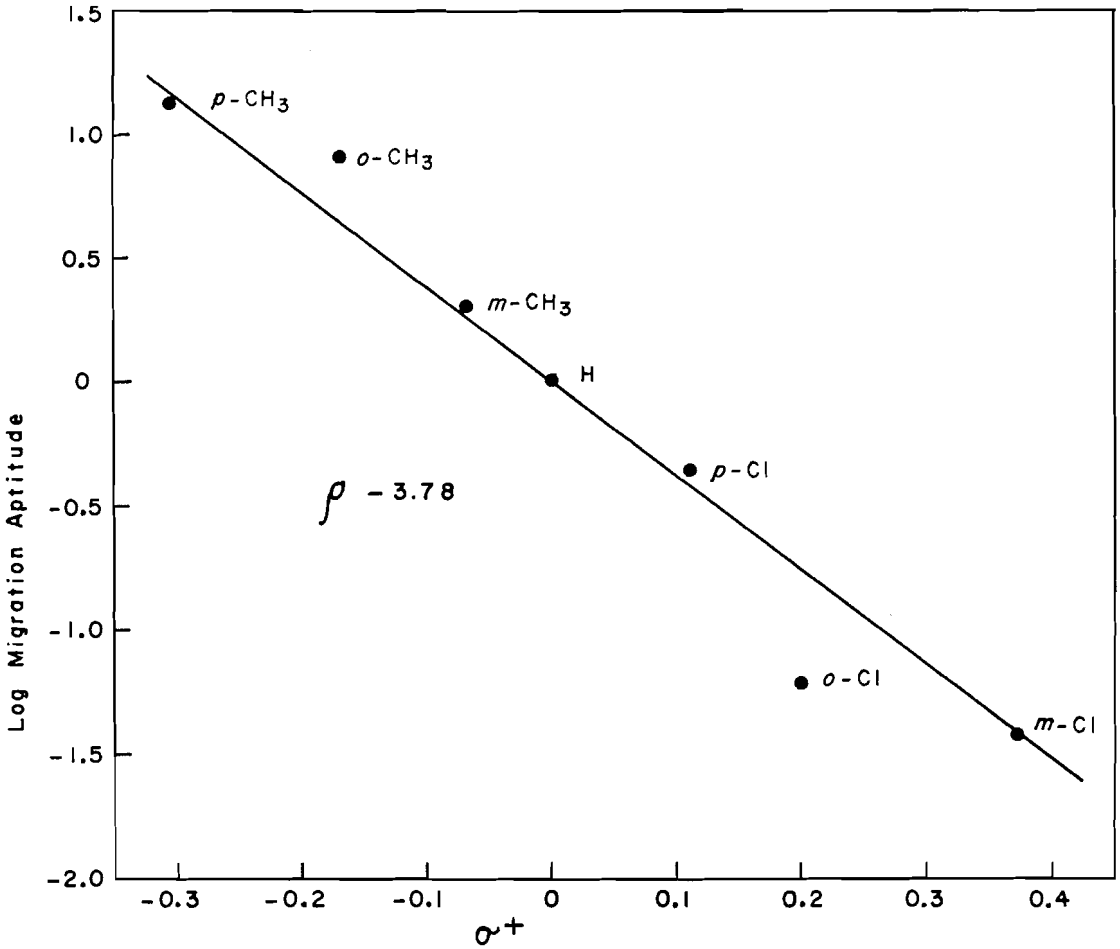

FIG. 1. Migration aptitude in the rearrangement of benzhydryl hydroperoxides.

ortho substituents. Such a linear relationship was not obtained when Hammett σ constants (15) were used.

TABLE II

Migration Aptitudes[a] for PhCH(Ar)OOH

Ar	Ar/Ph	σ^{+}[b]
C_6H_5	1.00	0
o-$CH_3C_6H_4$	6.56	−0.17[c]
m-$CH_3C_6H_4$	2.03	−0.069
p-$CH_3C_6H_4$	13.4	−0.306
o-ClC_6H_4	0.061	+0.20[c]
m-ClC_6H_4	0.037	+0.373
p-ClC_6H_4	0.445	+0.112

[a]In acetone, 20 °C.
[b]From references 12 and 13.
[c]From reference 14.

Discussion

The present results can be compared to those obtained in previous studies. In the rearrangement of substituted cumene hydroperoxides, van Steveninck and Kooyman (6) found a ρ value of −4.57 compared with −3.78 found here. In the case of triarylmethyl hydroperoxides, migration aptitudes (relative to phenyl) of 10.6–12.3 for *p*-tolyl and 0.45 for *p*-chlorophenyl can be calculated from the data reported by Bissing *et al.* (7). The minor differences between the above values and those found in the present study are no doubt due to the different solvent systems and the different temperatures employed.

This study supports the accepted mechanism for the acid-catalyzed rearrangement of hydroperoxides (1). The structure favored in the

Can. J. Chem. Downloaded from www.nrcresearchpress.com by 210.87.254.40 on 09/05/12
For personal use only.

TABLE III

σ^+ Values for ortho substituents

	Experimental		Literature values	
Ortho	Present work	Calcd. from ref. 6	Taft's σ^* (ref. 14)	Ref. 17
CH_3	−0.21	−0.12	−0.17	−0.09, −0.15
Cl	+0.32	+0.42	+0.20	+0.28

transition state (A) is that in which the developing positive charge is most stabilized. Thus an aryl group bearing an electron-donating sub-

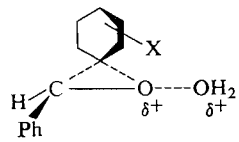

A

stituent migrates in preference to a phenyl group while a phenyl group migrates in preference to an aryl group bearing an electron-attracting substituent.

Perhaps the most interesting observation is the effect of ortho substituents on the migration aptitudes. In pinacol rearrangements, an ortho substituent hinders migration of the group because the steric requirements of the ortho substituent prevent the aryl group from assuming the preferred conformation for migration (16). In the case of hydroperoxides, this argument is less applicable. First, the migration terminus is an oxygen atom bearing only the departing protonated hydroxyl group and this probably offers little in the way of steric interaction. Second, the migration origin bears a proton and a phenyl group and only the latter can be expected to offer any steric interaction.

Thus, it might be expected that the migration of an ortho-substituted group in the hydroperoxide rearrangement would occur in a manner reflecting more closely the nature of the substituent than in the pinacol rearrangement. That this is true can be seen in Table III where σ^+ values are calculated for *o*-methyl and *o*-chloro substituents on the assumption that their migration aptitudes and their σ^+ values are related in the same manner as those of para and meta substituents. The agreement of these values and those calculated in the same manner from the data of van Steveninck and Kooyman (6) with values determined in other ways suggests that the assumption has some merit. Possibly, a study of the acid-catalyzed rearrangement of hydroperoxides with less steric hinderance at the migration origin would provide a means of directly determining ortho σ^+ constants.

The behavior of ortho substituted phenyl groups in the Baeyer–Villiger oxidation is quite different. In fact, Saunders (18) concluded that there is no essential difference between the migration of such groups to an oxygen or to a carbon. For example, the *o*-tolyl group was observed to migrate less than a phenyl group.

The principal difference in the transition state (19) of the Baeyer–Villiger oxidation (B) and that of the hydroperoxide rearrangement is the

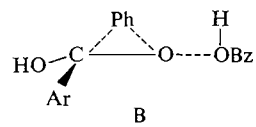

B

presence of a hydroxyl group (instead of hydrogen) on the migration origin. Seemingly, the steric bulk of the hydroxyl group in combination with that of the phenyl group is sufficient to produce the "normal ortho effect".

The formation of benzophenone as a product in the rearrangement of benzyhydryl hydroperoxide can be interpreted as a migration of the benzylic proton in competition with the phenyl groups. On this basis, a striking effect of

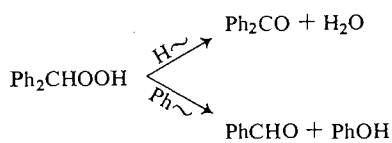

solvent upon the migratory aptitude of hydrogen (relative to phenyl) is apparent, and is summarized in Table IV.

Such a variation has been noted by Collins *et al.* (20–22) when different acids are used in the pinacol rearrangement. In this case, the explanation advanced depended upon the changed steric

Can. J. Chem. Downloaded from www.nrcresearchpress.com by 210.87.254.40 on 09/05/12
For personal use only.

TABLE IV

Solvent effect in the rearrangement of benzhydryl hydroperoxide

Solvent	Migration aptitude	
	H/Ph (Ph CHO)*	H/Ph (Ph OH)†
Acetic acid	0.017	0.016
Acetone	0.067	0.062
Diethyl ether	0.475	0.455

*Based on benzaldehyde and henzophenone mole ratio.
†Based on phenol and benzophenone mole ratio.

requirements of the transition state caused by the acids employed. Whether such an explanation is applicable here or whether the nonpolar solvent, diethyl ether, is suppressing the ionic rearrangement and thus allowing a free radical decomposition of the hydroperoxide to become the predominant reaction mode, can only be determined by further experiment.

Experimental

Melting points were taken on a Gallenkamp melting point apparatus and are uncorrected. Iodometric titrations were performed using the procedure of Kharasch and Burt (4). Elemental analyses were performed by A. B. Gygli, Microanalyses Laboratory, Toronto, Ontario. Gas–liquid chromatographic analyses were done on an F and M model 700 gas chromatograph with dual flame ionization detectors using an 8 ft by 1/4 in. column packed with 15% XF 1150 on Anakrom ABS substrate, operated at 150° with injection port at 275° and detectors at 220°. The system was calibrated with standards using purified samples of the commercially available aldehydes. Purification of the aldehydes was effected by washing the aldehyde with 5% sodium bicarbonate solution, drying, and distilling under vacuum. Three aldehydes were found to be contaminated with substantial amounts of non-aldehydic materials and were purified by preparing their bisulfite adducts, washing the dried adducts with hexane until free of the impurity, regenerating the aldehyde with aqueous sodium carbonate solution, extracting with hexane, and distilling. These aldehydes were *m*-chlorobenzaldehyde, *m*-methylbenzaldehyde, and *o*-methylbenzaldehyde.

The starting alcohols used for the preparation of the hydroperoxides were obtained by the addition of benzylmagnesium chloride to the appropriate substituted benzaldehyde (23).

Preparation of Hydroperoxides

The procedure used is exemplified by *p*-methylbenzhydryl hydroperoxide. The only parameter adjusted was the reaction time.

A solution of 0.20 ± 0.01 g of concentrated sulfuric acid in 15 ml of 90% hydrogen peroxide was prepared and cooled in an ice-water bath. This solution was stirred vigorously with a magnetic stirrer and a solution of 4.07 g of *p*-methylbenzhydrol in 15 ml of diethyl ether added rapidly. The mixture was stirred in the ice bath for 30 min. After this, the ice bath was removed allowing the reaction mixture to warm to room temperature. Stirring was continued for a further 60 min.

At the end of this time, the mixture was diluted with ice and water and the ether phase was separated, washed once with 15 ml water, once with 15 ml 2% sodium hydroxide and ice (separated rapidly while cold), and three times with water. The ether was then dried and removed under vacuum at room temperature. The residue, 4.0 g, crystallized rapidly and titrated as 96% *p*-methylbenzhydryl hydroperoxide.

Recrystallization was effected by dissolving the crude material in 10 ml of benzene at room temperature, stirring, and diluting the solution with 100 ml of hexane. The solution was seeded and cooled to 5°. The material (2.2 g), which slowly separated, titrated as 100% pure, and had m.p. 50.5–52°.

Both *o*-methyl- and *m*-methylbenzhydrol were converted to their hydroperoxides in this manner. *p*-Chloro-, *m*-chloro-, and *o*-chlorobenzhydrol required the longer reaction times shown in Table I. The effect of reaction time on the degree of conversion of the benzhydrol to its hydroperoxide is shown in Fig. 2.

Rearrangement of Hydroperoxides in Acetone

The hydroperoxide (250 mg) was dissolved in 2.0 ml of acetone. The solution was placed in a bath at 20° and treated with 2.0 ml of a freshly prepared solution of 1.0 g concentrated sulfuric acid in 25 ml of acetone. The reacting solution was stirred and periodically, approximately 0.25 ml samples were withdrawn and added to an aqueous solution of potassium iodide acidified with acetic acid, followed by 4 drops of saturated starch solution.

When the reaction gave a negative test for peroxides, a 1 ml sample was withdrawn and added to a large excess of solid sodium bicarbonate. The neutralized solution was stored over the sodium bicarbonate until the analysis was completed.

A second sample was withdrawn 0.5 to 1.0 h later and also analyzed. Each sample was analyzed five times and the resulting values averaged to give the final value.

Rearrangement of Benzhydryl Hydroperoxide

A solution of 150 mg of benzhydryl hydroperoxide in 1.5 ml of diethyl ether and 60 mg of 1,2,4,5-tetrachlorobenzene was treated with 2.0 ml of the same solvent containing 0.080 g of concentrated sulfuric acid. After 15 h the solution gave a negative test for peroxides and a sample was withdrawn, added to solid sodium bicarbonate to neutralize the acid, and analyzed by vapor-phase chromatography as described before but with a column temperature of 165°.

Similar experiments were carried out with acetone as a solvent and with acetic acid. In the last case, the internal standard proved to be insoluble and only a relative analysis could be obtained. Reaction times were 2 h with acetone and 5 h with acetic acid. The results are reported in Table IV.

p-Cresyl Acetate Formation

A solution of 125 mg of *p*-cresol in 2.5 ml of acetic acid was treated with 2.5 ml of acetic acid containing 0.080 g

Can. J. Chem. Downloaded from www.nrcresearchpress.com by 210.87.254.40 on 09/05/12
For personal use only.

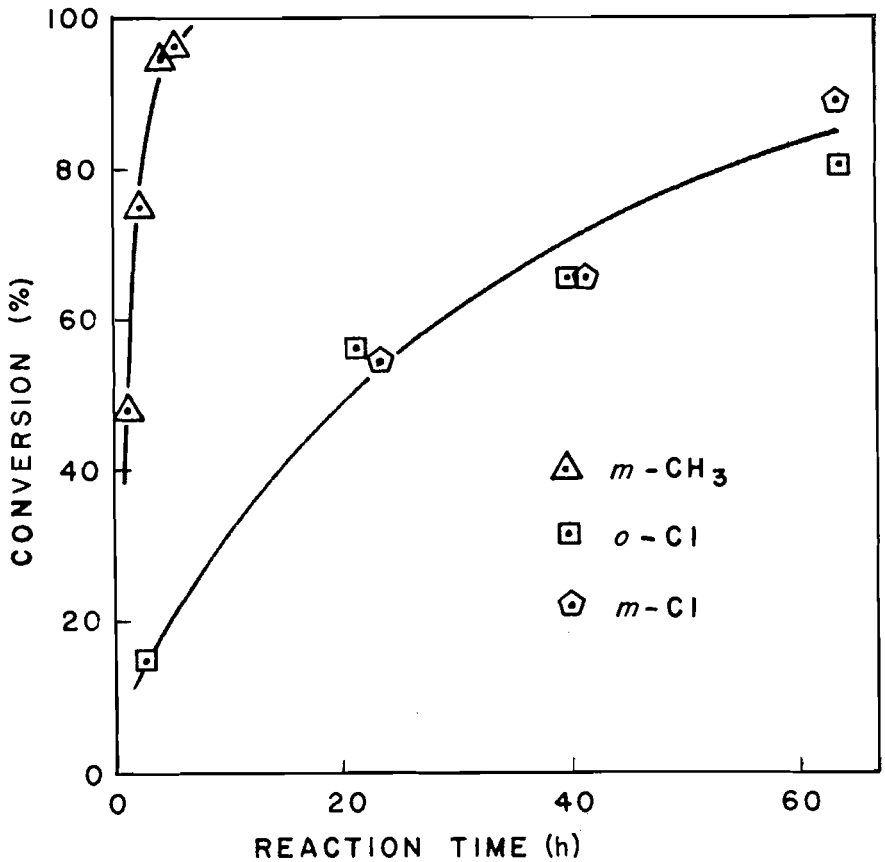

FIG. 2. Preparation of substituted benzyhydryl hydroperoxides.

of concentrated sulfuric acid. After 5 h at 25°, a sample was neutralized with sodium carbonate and analyzed. The product contained 4% (by vapor-phase chromatography area) of *p*-cresyl acetate.

Acknowledgments

We are indebted to Mr. R. E. Mortimer (Dow Chemical of Canda, Limited) for his analyses of the hydroperoxides and to Miss Gudrun Wieczorek for assistance in the early stages of the study. We also wish to express our appreciation to Dr. R. Hiatt (Brock University, St. Catharines, Ontario) for several stimulating discussions.

1. P. A. S. SMITH. *In* Molecular rearrangements. Vol. 1. *Edited by* P. de Mayo. Interscience Publishers, Inc., New York. 1963. p. 573.
2. W. DILTHEY, F. QUINT, and H. DIERICHS. J. Prakt. Chem. **151**, 25 (1938).
3. M. S. KHARASCH, A. FONO, W. NUDENBERG, and A. C. POSHKUS. J. Org. Chem. **15**, 775 (1950).
4. M. S. KHARASCH and J. G. BURT. J. Org. Chem. **16**, 150 (1951).
5. P. D. BARTLETT and J. D. COTMAN, JR. J. Am. Chem. Soc. **72**, 3095 (1950).
6. A. W. DE RUYTER VAN STEVENINCK and E. C. KOOYMAN. Rec. Trav. Chim. **79**, 413 (1960).
7. D. E. BISSING, C. A. MATUSZAK, and W. E. MCEWEN. J. Am. Chem. Soc. **86**, 3824 (1964).
8. A. G. DAVIES, R. V. FOSTER, and A. M. WHITE. J. Chem. Soc. 1541 (1953).
9. A. G. DAVIES and R. FELD. J. Chem. Soc. 4637 (1958).
10. M. S. KHARASCH, A. FONO, and W. NUDENBERG. J. Org. Chem. **15**, 748 (1950).
11. W. PRITZKOW and R. HOFMANN. J. Prakt. Chem. [4] **14**, 131 (1961).
12. H. C. BROWN and Y. OKAMOTO. J. Am. Chem. Soc. **79**, 1913 (1957).
13. Y. OKAMOTO and H. C. BROWN. J. Org. Chem. **22**, 485 (1957).
14. J. HINE. Physical organic chemistry. McGraw-Hill, New York. 1962. p. 98.
15. L. P. HAMMETT. Physical organic chemistry. McGraw-Hill, New York. 1940. p. 184.
16. C. K. INGOLD. Structure and mechanism in organic chemistry. Cornell University Press, Ithaca, N.Y. 1953. p. 478.

Can. J. Chem. Downloaded from www.nrcresearchpress.com by 210.87.254.40 on 09/05/12
For personal use only.

17. I. J. SOLOMON and R. FILLER. J. Am. Chem. Soc. **85**, 3492 (1963).
18. W. H. SAUNDERS, JR. J. Am. Chem. Soc. **77**, 4679 (1955).
19. P. A. S. SMITH. *In* Molecular rearrangements. Vol. **1**. *Edited by* P. de Mayo. Interscience Publishers, Inc., New York. 1963. p. 580.
20. C. J. COLLINS. J. Am. Chem. Soc. **77**, 5517 (1955).
21. B. M. BENJAMIN and C. J. COLLINS. J. Am. Chem. Soc. **78**, 4329 (1956).
22. C. J. COLLINS, W. T. RAINEY, W. B. SMITH, and I. A. KAYE. J. Am. Chem. Soc. **81**, 460 (1959).
23. J. H. LAMNECK, JR. and P. H. WISE. J. Am. Chem. Soc. **76**, 1104 (1954).

Can. J. Chem. Downloaded from www.nrcresearchpress.com by 210.87.254.40 on 09/05/12
For personal use only.

Can. J. Chem. Downloaded from www.nrcresearchpress.com by 210.87.254.105 on 09/05/12
For personal use only.

Acid-catalyzed rearrangement of hydroperoxides. II.

Phenylcycloalkyl hydroperoxides[1]

GLENN H. ANDERSON
Exploratory Research Laboratory, Dow Chemical of Canada, Limited, Sarnia, Ontario

AND

JAMES G. SMITH
Department of Chemistry, University of Waterloo, Waterloo, Ontario

Received October 13, 1967

The acid-catalyzed rearrangement of 1-phenylcycloalkyl hydroperoxides has been investigated using the cyclohexyl, cyclopentyl, and cyclobutyl compounds. Evidence was sought for rearrangement of the cycloalkyl group in competition with migration of the phenyl group during the reaction. Such a rearrangement would result in ring expansion of the cycloalkyl group to give, ultimately, products formed by cycloalkyl ring opening.

No evidence for such a reaction was found in the case of 1-phenylcyclohexyl hydroperoxide; only the expected products, phenol and cyclohexanone, were detected. However, rearrangement of 1-phenylcyclopentyl hydroperoxide gave, besides the expected phenol and cyclopentanone, significant amounts of the ring-opened compound 4-hydroxyvalerophenone as its acetate. A second product, 1-phenylcyclopentene, arose by elimination of hydrogen peroxide from the hydroperoxide.

1-Phenylcyclobutyl hydroperoxide proved to undergo ring expansion with great facility. Only the ring expanded products, 2-phenyl-2-tetrahydrofuryl hydroperoxide and its corresponding peroxide, could be isolated in the treatment of 1-phenylcyclobutanol with hydrogen peroxide using catalytic amounts of mineral acids. However, in the absence of catalysts, 1-phenylcyclobutyl hydroperoxide was formed in detectable amounts and its presence was demonstrated by decomposition with ferrous sulfate to butyrophenone and 1,6-dibenzoylhexane.

It seems reasonable that ring strain is the factor promoting the ring expansion of 1-phenylcyclobutyl hydroperoxide. In the case of 1-phenylcyclopentyl hydroperoxide, it is suggested that the steric interaction of the ortho hydrogens of the phenyl group with the cyclopentyl ring protons has the effect of slowing the migration of the phenyl group sufficiently that alkyl migration can occur to give the observed ring-opened products.

Canadian Journal of Chemistry, **46**, 1561 (1968)

Introduction

The acid-catalyzed rearrangement of aralkyl hydroperoxides is believed to involve the initial protonation of the hydroperoxide followed by dissociation of the protonated species with a concerted migration of the aryl group to the positive oxygen (1). While, in general, aryl groups migrate to the virtual exclusion of alkyl groups (2), it is evident that this is a matter of the relative ease of migration of aryl groups compared to alkyl. The latter are known to migrate when they are not faced with such formidable competitors as aryl groups (3). Indeed, there are examples in which the alkyl group migrates appreciably even in the presence of competing aryl groups (4, 5).

Because it was of interest to examine some of the factors affecting the migration of alkyl groups in hydroperoxides, we have studied the behavior of phenylcycloalkyl hydroperoxides with the expectation that as the cycloalkyl ring size decreased, an increasing tendency for alkyl migration to occur at the expense of phenyl migration would be apparent.

Results

The acid-catalyzed rearrangement of the first member of the series, 1-phenylcyclohexyl hydroperoxide, had been examined in the past and high yields of phenol and cyclohexanone reported (6–10). The rearrangement of this hydroperoxide was reexamined under the conditions selected for the present study, i.e. in acetic acid solution at 25° with sulfuric acid catalyst. A 95% yield of phenol and cyclohexanone was produced as determined by vapor-phase chromatographic (v.p.c.) analysis.

[1]Contribution No. 154 from the Exploratory Research Laboratory, Dow Chemical of Canada, Limited, Sarnia, Ontario.

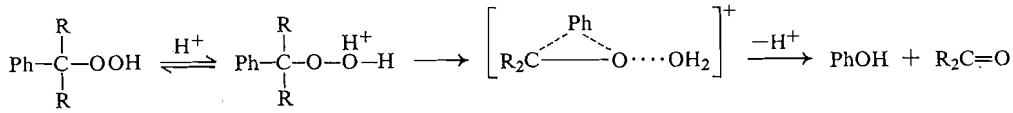

The next member of the series, 1-phenylcyclopentyl hydroperoxide, had also been reported in the literature (11–13). However, its acid-catalyzed rearrangement had been studied (12) largely in terms of its rate of rearrangement relative to that of cumyl hydroperoxide.

The acid-catalyzed rearrangement of 1-phenylcyclopentyl hydroperoxide under the conditions selected for the cyclohexyl analogue produced only a 60–65% yield of phenol and cyclopentanone. In addition, a product was observed by v.p.c. which appeared to be 1-phenylcylopentene. This last product had been reported by van Steveninck and Kooyman (12).

The neutral products from a large scale rearrangement were separated by column chromatography. These products proved to be 1-phenylcyclopentene (11% yield), valerophenone (3% yield), 5-acetoxyvalerophenone (12% yield), and at least one other unidentified compound. Identification of the 1-phenylcyclopentene was made by comparison of its infrared and nuclear magnetic resonance (n.m.r.) spectra to that of an authentic sample. The valerophenone was identified on this basis as well as by its 2,4-dinitrophenylhydrazone derivative.

The structure of 5-acetoxyvalerophenone was established by its analysis, its infrared, and n.m.r. spectra, and by its conversion to 1-phenylpentanediol-1,5 with lithium aluminium hydride.

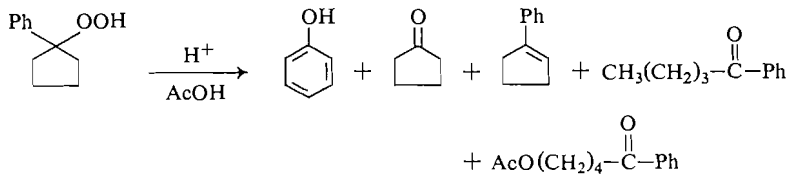

In an attempt to prepare the next homologue, 1-phenylcyclobutyl hydroperoxide, 1-phenylcyclobutanol was treated with 90% hydrogen peroxide and a catalytic amount[2] of sulfuric acid (9). However, the product obtained proved, on examination by thin-layer chromatography (t.l.c.), to consist of four compounds containing active oxygen. Of the four, three liberated iodine rapidly from the acidified potassium iodide detecting spray and were judged to be hydroperoxides. The remaining material liberated iodine slowly and proved to be a peroxide.

It was found that the concentration of this peroxide (**1**) increased on storage of the crude reaction mixture. Isolation was effected by column chromatography and its analysis, molecular weight and peroxide titer, established its molecular formula as $C_{20}H_{22}O_4$.

Even though the infrared spectrum showed the absence of hydroxyl or carbonyl groups, heating the peroxide with strongly acidic 2,4-dinitrophenylhydrazine solution produced the derivative of 4-hydroxybutyrophenone while reduction of the peroxide with lithium aluminium hydride produced 1-phenylbutanediol-1,4.

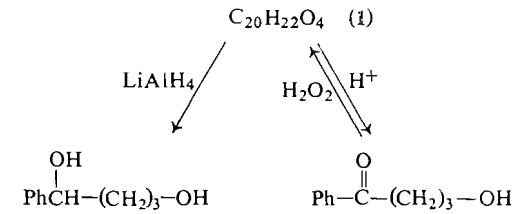

This chemical behavior coupled with the fact that in the n.m.r. spectrum four aliphatic protons were much further downfield than the remaining eight, indicated that the compound had one of the following two structures, **1***a* or **1***b*. Additional confirmation for these structures was obtained when it was found that 4-hydroxybutyrophenone could be converted under certain reaction conditions to a mixture containing

[2]On two occasions, violent explosions occurred completely demolishing the flask and stirring apparatus. Extreme caution should be observed with this reaction and special care should be taken to moderate the initial exothermic reaction with cooling.

Can. J. Chem. Downloaded from www.nrcresearchpress.com by 210.87.254.105 on 09/05/12
For personal use only.

Can. J. Chem. Downloaded from www.nrcresearchpress.com by 210.87.254.105 on 09/05/12
For personal use only.

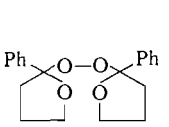

1*a*

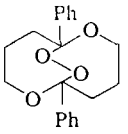

1*b*

the peroxide. These two structures were distinguished by mass spectral analysis. The peroxide (**1**) showed no molecular ion peak, the largest ion-peak observed being at *m/e* of 163 or half the molecular weight. This behavior would be expected from (**1***a*) which should readily cleave at the —O—O— bond. Such a behavior is unlikely in the case of a compound of structure (**1***b*) which would be expected to show ion peaks greater than 163 but less than 326.

While this identified one product from the oxidation of 1-phenylcyclobutanol, it was established by t.l.c. that the major product was a hydroperoxide (**2**) and the peroxide (**1**) was only detected after the oxidation product was aged. On the basis of the similarity of the infrared spectrum of the hydroperoxide (**2**) to that of the peroxide (**1**) (with the obvious exception of the presence of an OH absorption band in the former) and on the basis of the conversion of (**2**) to (**1**) on standing, the structure 2-phenyl-2-tetrahydrofuryl hydroperoxide was assigned to (**2**).

The chemical behavior of hydroperoxide (**2**) substantiated this structure. Reduction of (**2**) with sodium sulfite produced 4-hydroxybutyrophenone while peroxide (**1**) was unaffected by this reducing agent. Furthermore, treatment of 4-hydroxybutyrophenone with 30% hydrogen peroxide generated the hydroperoxide (**2**) and, on aging, peroxide (**1**). Hydroperoxides similar to (**2**) have been reported to form peroxides readily (14, 15).

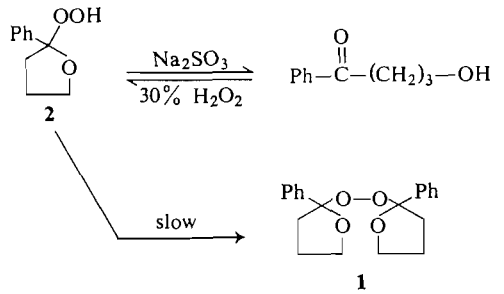

Attention was then turned to the oxidation of 1-phenylcyclobutanol with 90% hydrogen peroxide in the absence of acid. Under these conditions a slow formation of a second hydroperoxide (**3**) was observed, different from 2-phenyl-2-tetrahydrofuryl hydroperoxide (**2**), but identical by t.l.c. to one of the minor hydroperoxides detected in the acid-catalyzed oxidation of 1-phenylcyclobutanol. As the reaction continued, the concentration of this second hydroperoxide increased and 2-phenyl-2-tetrahydrofuryl hydroperoxide (**2**) began to appear as well.

Hydroperoxide (**3**) is believed to be 1-phenylcyclobutyl hydroperoxide which would be the anticipated initial product from the alcohol and hydrogen peroxide. It might be noted here that the oxidation of 4-hydroxybutyrophenone with hydrogen peroxide does not produce this hydroperoxide as a minor product. If hydroperoxide (**3**) were 1-phenylcyclobutyl hydroperoxide, it could not be formed in this manner.

Column chromatography of the oxidation product of 1-phenylcyclobutanol and hydrogen peroxide separated (**3**) from the other hydroperoxides but not from the unconsumed alcohol. Further separation could not be effected. Treatment of this hydroperoxide – alcohol mixture with ferrous sulfate caused radical decomposition of the hydroperoxide with formation of 1,6-dibenzoylhexane and butyrophenone. By analogy with the known behavior of similar hydroperoxides (9, 16) these reaction products provide strong evidence for the presence of 1-phenylcyclobutyl hydroperoxide (**3**) in the original mixture.

Discussion

It is evident that the reaction products observed in the acid-catalyzed rearrangement of phenylcycloalkyl hydroperoxides demonstrate that cycloalkyl groups can rearrange competitively with migration of aryl groups under favorable circumstances. In fact, qualitatively, it may be said that alkyl migration is the major reaction in the 1-phenylcyclobutyl system, it occurs significantly in the 1-phenylcyclopentyl but occurs only slightly if at all in the 1-phenylcyclohexyl analogue.

Two reports in the literature (6, 17) suggest that alkyl migration may occur even in the 1-phenylcyclohexyl system under special reaction conditions. The first of these involved the treatment of the hydroperoxide with chromium trioxide in acetic acid while the second involved treatment with acid-washed clays. However,

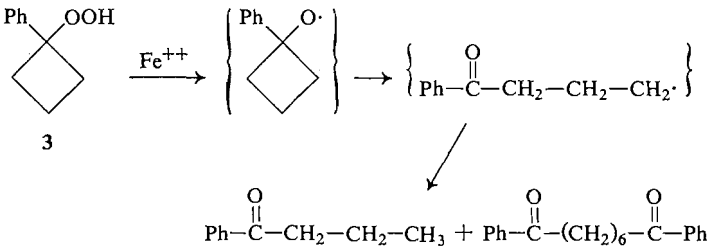

3

under our reaction conditions, such rearrangement products were not observed.

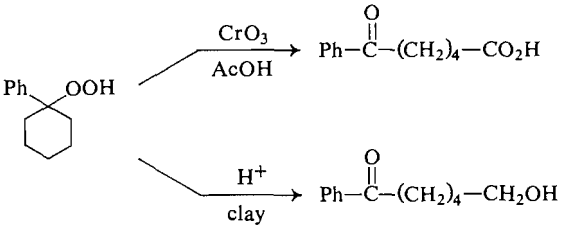

1-Phenycyclopentyl hydroperoxide appeared to undergo acid-catalyzed decomposition by at least three different paths. These are outlined in Scheme 1.

Protonation of the hydroperoxide group can occur in two ways, either on the ether–oxygen to give (**4**) or on the hydroxyl–oxygen to give (**5**). As noted by Smith (18) protonated species such as (**4**) do not lead to rearrangement. Apparently, in this particular case, olefin formation by elimination of hydrogen peroxide is particularly favorable and occurs in competition with the rearrangement reaction. The formation of hydrogen peroxide has been observed by van Steveninck and Kooyman (12). This behavior agrees with the qualitative observation that 1-phenylcyclopentanol dehydrates with ease in the presence of acids.

Two paths are involved in the decomposition of protonated species (5), one involving aryl migration and the other alkyl migration. The former reaction mode produces phenol and cyclopentanone while the latter effects ring enlargement with the eventual production of ring-opened products. Similar ring enlargements with formation of acetoxy ketones have been observed with 1-methylcyclohexyl hydroperoxide (19–21).

The valerophenone detected in the reaction mixture represents a reduction product of the starting hydroperoxide. Its formation is puzzling and may indicate that a small amount of homolytic decomposition is occurring as well.

Ring strain is evidently an important factor in the reaction of 1-phenylcyclobutanol with hydrogen peroxide. The initially formed 1-phenylcyclobutyl hydroperoxide (**3**) rearranged sufficiently fast under the acidic reaction conditions that only low concentrations of (**3**) were detected, the principal product being the rearranged hydroperoxide (**2**). Even in the absence of mineral acid, this tendency for rearrangement was manifested although higher concentrations of the hydroperoxide (**3**) could be obtained.

While ring expansion is understandable in the case of the cyclobutyl compound, it is more difficult to explain in the case of the cyclopentyl analogue. One possibility is that the driving force for the reaction is the reduction of ring proton–proton interactions when the five-membered ring expands to six. If this were true, one would anticipate that the rate of rearrangement of the cyclopentyl compound would be greater than that of the cyclohexyl because of this additional driving force. In actual fact, the cyclopentyl hydroperoxide rearranges less than half as fast as the six-membered ring (12).

However, this rate difference may simply reflect the differing basicities of the hydroxylic oxygen in the 1-phenylcyclohexyl and 1-phenylcyclopentyl hydroperoxides.[3] Such a difference in basicity would be reflected in a different concentration of the respective protonated species such as (**5**) and thus a different reaction velocity in the rate-controlling rearrangement step. If this were true, it would be difficult to select the structural features of the two compounds causing the difference in basicities. Inductive effects in both compounds are similar as are the steric effects in the vicinity of the hydroxyl group. It would seem that the explanation lies elsewhere.

The slower rearrangement of the cyclopentyl compound relative to its cyclohexyl analogue suggests that the rearrangement of the aryl group is inhibited in the former case. An examination

[3]A possibility suggested by a referee.

Can. J. Chem. Downloaded from www.nrcresearchpress.com by 210.87.254.105 on 09/05/12
For personal use only.

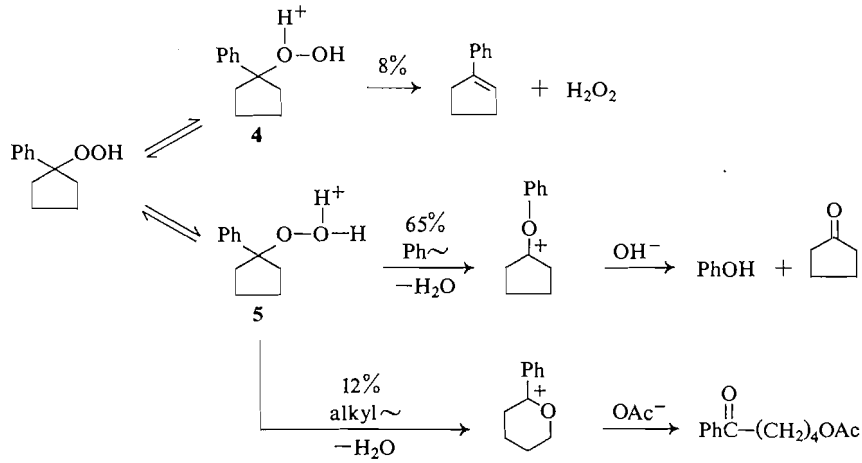

SCHEME 1

of Stuart–Briegleb molecular models demonstrates that when the phenyl group is positioned for maximum interaction of the π-electrons with the positive oxygen (22), the interaction of the ortho-hydrogens and the cycloaliphatic ring hydrogens is greater in the cyclopentyl compound than in the cyclohexyl. It is possible, then, that this steric interaction slows the migration of the aryl group sufficiently that rearrangement of the cyclopentyl group with resultant ring expansion can occur to an appreciable extent.

Experimental

Melting points are uncorrected and were determined in an open capillary with a Gallenkamp melting point apparatus. Infrared spectra were recorded on a Perkin–Elmer 337 grating spectrophotometer using carbon tetrachloride solutions with a reference blank. Nuclear magnetic resonance (n.m.r.) spectra were recorded on a Varian A-60 spectrometer, using deuterated chloroform solutions, with tetramethylsilane as an internal reference. The chemical shifts reported are in parts per million downfield from the tetramethylsilane. Mass spectra were recorded on a Bendix TOF mass spectrometer at room temperature using a direct probe inlet. Vapor-phase chromatography (v.p.c.) analyses were made on an F and M 700 gas chromatograph equipped with a dual flame ionization detector. Eastman type K301R silica gel chromatogram sheets were used for thin-layer chromatography. The method of Kharasch and Burt (2) was used in the iodometric titrations for active oxygen.

1-Phenylcyclohexyl Hydroperoxide

This hydroperoxide was prepared by the method of Hey *et al.* (9) from 1-phenylcyclohexanol (Aldrich Chemical Co., Inc.; m.p. 61–63°). The compound was a white crystalline solid m.p. 59–60 °C and was 99% pure by iodometric titration. Nuclear magnetic resonance: aromatic H's 7.1–7.5 (5.09 H), the aliphatic H's were in a broad band 1.4–2.3 (10.00 H).

Rearrangement of 1-Phenylcyclohexyl Hydroperoxide

1-Phenylcyclohexyl hydroperoxide (100 mg) and 100 mg of *p*-dichlorobenzene (the internal standard) were dissolved in 5 ml of glacial acetic acid and 0.1 ml of concentrated sulfuric acid was added, with stirring, to the solution. After 2 h at room temperature the reaction mixture was dissolved in 20 ml of ether and washed with three 50 ml portions of saturated aqueous sodium bicarbonate solution. The combined bicarbonate wash was extracted five times with 10 ml portions of ether. The combined ether extracts were analyzed by v.p.c. at 165° using an 8 ft by ¼ in. column packed with 15% Ucon 50/HB/2000 on Chromosorb 60–80 mesh. The analyses were made by comparison of the ratio of the peak heights of the products and internal standard to those of mixtures of known composition. The yields were: phenol, 95% and cyclohexanone, 95%.

Preparation of 1-Phenylcyclopentanol

Phenylmagnesium bromide was prepared from 12.0 g (0.50 moles) of magnesium, 52 ml (0.50 moles) of bromobenzene, and 450 ml of diethyl ether. To this, a solution of 45 ml (0.50 moles) of cyclopentanone in 100 mls of ether was added dropwise with stirring and this was followed by ½ h of reflux.

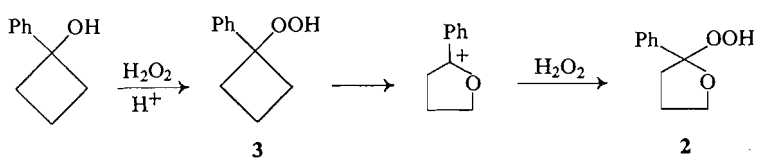

Can. J. Chem. Downloaded from www.nrcresearchpress.com by 210.87.254.105 on 09/05/12
For personal use only.

Can. J. Chem. Downloaded from www.nrcresearchpress.com by 210.87.254.105 on 09/05/12
For personal use only.

After cooling, a solution of 250 mls of 10% aqueous ammonium chloride was added slowly. The gelatinous precipitate which formed was removed by filtration, the organic phase was washed with: 100 ml of water, 100 ml of 2% aqueous sodium carbonate solution, 100 ml of water, dried over anhydrous magnesium sulfate, and evaporated under vacuum. The yellow oily residue of crude 1-phenylcyclopentanol was vacuum distilled in the presence of 0.25 g of sodium carbonate yielding 39.5 g (50% yield) b.p. 99–102° at 2 mm. Nuclear magnetic resonance: aromatic H's 7.0–7.4 (5.00 H), the aliphatic H's had a sharp peak at 1.84 (7.70 H) and the hydroxyl H at 2.29 (1.13 H).

Preparation of 1-Phenylcyclopentyl Hydroperoxide

This hydroperoxide was synthesized by the procedure of Hey *et al.* (9). The product so prepared had an iodometric titration of 94%. Further purification could be effected by the sodium salt method of Kwart and Keen (6) but the recovery was quite low. The purified product had an iodometric tritration of 98% n_D^{20} 1.5452. Nuclear magnetic resonance: aromatic H's 7.0–7.4 (5.00 H), aliphatic H's in a broad band at 1.5–2.4 (7.63 H).

Rearrangement of 1-Phenylcyclopentyl Hydroperoxide

(*a*) *Phenol Determination*

1-Phenylcyclopentyl hydroperoxide (0.395 g) and 0.216 g of *p*-dichlorobenzene (internal standard) were dissolved in 6 ml of glacial acetic acid and 0.1 ml of concentrated sulfuric acid was added while stirring the solution in an ice-water bath. The solution developed a red color and after 2.5 h at room temperature, a negative test for hydroperoxides was obtained (acidified potassium iodide and starch). After 5 h all carbonyl compounds in the mixture were precipitated as 2,4-dinitrophenylhydrazones by the addition of 10 ml of aqueous 2,4-dinitrophenylhydrazine reagent (23) and were removed by filtration. The filtrate was extracted with 10 ml of ether and the organic phase washed with two 50 ml portions of saturated aqueous sodium bicarbonate solution. The combined bicarbonate wash was back extracted with two 20 ml portions of ether. The combined ether extracts were analyzed by v.p.c. at 165° using an 8 ft by $\frac{1}{4}$ in. column packed with 15% Ucon 50/HB/2000 on Chromosorb 60–80 mesh. The analysis was made by comparing the ratio of the peak height for phenol and *p*-dichlorobenzene to those of mixtures of known composition. The yield of phenol was 65%.

(*b*) *Cyclopentanone Determination*

The 2,4-dinitrophenylhydrazone mixture was chromatographed on a column of 80 g of Woelm grade IV neutral alumina using benzene as the eluting solvent. The largest band to appear on the column, cyclopentanone 2,4-dinitrophenylhydrazone, was isolated; 0.336 g, m.p. 140–142°, and mixture melting point with an authentic sample, 141–142°. This represented a yield of 57% of cyclopentanone.

The rearrangement was run at 10–15° with the yields being; phenol 64% and cyclopentanone 57% and at 40° with yields of phenol 65% and cyclopentanone 55%.

(*c*) *Identification of Minor Products*

A solution of 4.0 g of 1-phenylcyclopentyl hydroperoxide (assay 94%) in 50 ml of glacial acetic acid and 3 drops of concentrated sulfuric acid was stirred at room temperature for 5 h. The solution was washed with 400 ml of 10% sodium hydroxide and this alkaline extract was back extracted with two 50 ml portions of ether. The combined ether extract was concentrated by evaporation to 2–3 ml. The ether concentrate was applied to the top of a column of 80 g of Woelm grade IV neutral alumina and eluted in series with 250 ml of *n*-pentane, 250 ml of benzene, and 300 ml of chloroform. Fractions were cut at 100 ml intervals, their composition checked by thin-layer chromatography and like fractions were combined. The following products listed in the order in which they were eluted, were isolated, and identified: 1-phenylcyclopentene (0.345 g, 11% yield), valerophenone (0.113 g, 3% yield), 5-acetoxyvalerophenone (0.606 g, 12% yield), and unknown (0.178 g, —).

Identification

1-Phenylcyclopentene

This compound was identified by comparison of its infrared and n.m.r. spectra to those of an authentic sample. Nuclear magnetic resonance: aromatic H's 6.7–7.2 (5.00 H), the aliphatic H's were in two complex bands at 1.55–2.14 (2.22 H), and 2.18–2.75 (3.94 H) and the vinyl H at 5.75–5.95 (0.92 H).

Preparation of 1-Phenylcyclopentene

1-Phenylcyclopentene was prepared by the acid-catalyzed dehydration of 1-phenylcyclopentanol; b.p. 109° at 14 mm, n_D^{20} 1.5710.

Valerophenone

This compound was identified by comparison of its infrared and n.m.r. spectra to those of an authentic sample (Eastman Organic Chemicals) and by it 2,4-dinitrophenylhydrazone derivative, m.p. 160 – 162°, mixture m.p. 160 – 162°. Nuclear magnetic resonance: aromatic H's are split into two complex bands at 7.15–7.40 (3.04 H) and 7.60–7.85 (1.96 H), aliphatic H's have a broad band at 0.70–1.90 (7.01 H), and a triplet at 2.80 (1.98 H).

5-Acetoxyvalerophenone

This compound, m.p. 45–48°, was identified by: its analysis; its infrared spectrum (ester carbonyl 1735 cm^{-1}, aromatic ketone 1690 cm^{-1} and a C—O—C stretch at 1240 cm^{-1} characteristic of CH_3—CO—OR); and its n.m.r. spectrum. The aromatic protons split into two bands at 7.15–7.40 (3.56 H) and 7.65–7.85 (1.43 H), the aliphatic protons split into two distorted triplets, one at 2.88 (1.77 H) and the other at 3.95 (1.95 H), and also split into a broad band at 1.50–2.10 overlapping the acetoxy methyl singlet at 1.93 (total area 7.12 H).

Anal. Calcd. for $C_{13}H_{16}O_3$: C, 70.90; H, 7.27. Found: C, 70.89; H, 7.16.

$LiAlH_4$ Reduction of 5-Acetoxyvalerophenone

A solution of 0.178 g of 5-acetoxyvalerophenone in 50 ml of diethyl ether was slowly added to a suspension of 0.025 g of $LiAlH_4$ in 20 ml of diethyl ether with stirring and then refluxed for $\frac{1}{2}$ h. Ethyl acetate (10 ml) was added dropwise followed by 15 ml of 10% sulfuric acid. The ether phase was washed with 50 ml of water and evaporated on a steam bath. The yellow oil (0.130 g) of crude reduced product crystallized when 20 ml of *n*-hexane was added. This solid, m.p. 48–52°, had a mixture m.p. of 50–54° with 1-phenyl-1,5-pentanediol. Its infrared spectrum (Fluorolub 3690–1350 cm^{-1} and Nujol mull 1350–610 cm^{-1}) had a broad OH band at 3100–3400

Can. J. Chem. Downloaded from www.nrcresearchpress.com by 210.87.254.105 on 09/05/12
For personal use only.

cm^{-1}, a primary OH stretch at 1050 cm^{-1}, and a secondary OH stretch at 1090 cm^{-1}. This spectrum was identical with that of an authentic sample of 1-phenyl-1,5-pentanediol (m.p. 53–54°) prepared by the $LiAlH_4$ reduction of 4-benzoylbutyric acid (Aldrich Chemical Co., Inc.).

Synthesis of 1-Phenylcyclobutanol

Phenylmagnesium bromide was prepared from 1.72 g (0.071 moles) of magnesium, 11.20 g (0.071 moles) of bromobenzene, and 65 ml of diethyl ether. To this, a solution of 5 g (0.71 moles) of cyclobutanone in 10 ml of diethyl ether was added dropwise with stirring. After refluxing for 0.5 h, the reaction mixture was hydrolyzed with a solution of 50 ml of 10% hydrochloric acid. The organic layer was separated, washed with 100 ml of saturated aqueous sodium bicarbonate solution, 100 ml of water, dried through a bed of anhydrous magnesium sulfate, and evaporated under vacuum. A yellow crystalline residue of crude 1-phenylcyclobutanol (8.8 g) was left m.p. 35–40 °C. On recrystallization from *n*-pentane, pale-yellow rhombic crystals formed, 7.0 g (67% yield) m.p. 41–43 °C.

Its infrared spectrum had a sharp peak at 3580 cm^{-1}, a broad OH at 3200–3500 cm^{-1}, and a tertiary OH stretch at 1135 cm^{-1} whereas its nuclear magnetic resonance had aromatic H's 7.05–7.50 (4.95 H), aliphatic H's in a very broad complex band 1.50–2.60 (6.00 H) and the OH proton at 2.85 (1.01 H).

Acid-catalyzed Oxidation of 1-Phenylcyclobutanol (THIS REACTION SHOULD BE RUN BEHIND A SAFETY BARRIER)

A solution of 2.0 g of 1-phenylcyclobutanol in 10 ml of ether was added dropwise with stirring in an ice-water bath to 10 ml of 90% hydrogen peroxide acidified with 0.01 ml of concentrated sulfuric acid. The mixture was stirred at 0° for 2½ h. At the end of the reaction time, 25 ml of ice-water was added. The organic phase was washed with: 25 ml of cold water, 25 ml of saturated aqueous sodium bicarbonate solution, 25 ml of water, dried through a bed of anhydrous magnesium sulfate, and evaporated under an air stream. A yellow oil remained 1.50 g. Iodometric titration showed a 14% yield of peroxy compound based on the molecular weight of 1-phenylcyclobutyl hydroperoxide.

Identification of the Oxidation Products

A thin-layer chromatogram (t.l.c.) of the residue using 1:1 benzene, chloroform solution as the developing solvent and aqueous potassium iodide solution acidified with acetic acid as the detecting spray revealed three peroxy compounds with the following R_f values: 0.19, 0.32, and 0.51. The 0.32 spot was several times larger in area than the other two. After the crude reaction product stood for several hours, a second t.l.c. showed a fourth peroxy spot with R_f 0.66 characterized by a slow development of color (5–10 min) after spraying with the detecting agent and an additional intense peroxy spot at the origin. After several days standing, subsequent chromatograms of the crude reaction product showed an increase in the relative areas of the spots at R_f 0.66 and the origin and a decrease in the relative area of the spot at R_f 0.32.

Twelve days after the initial oxidation, the residue was chromatographed on 80 g of Woelm grade IV neutral alumina using 1:1 chloroform benzene solution as the eluting solvent. Four fractions of 75 ml each were collected and each was analyzed by t.l.c. The first fraction contained the compound, R_f 0.66, the rest were mixtures.

Fraction one was evaporated under an air stream leaving a white crystalline residue, 0.663 g. The residue was recrystallized from *n*-hexane m.p. 104–107 °C. The infrared spectrum showed no OH peak, no carbonyl peak, but strong C—O—C stretch at 1055 cm^{-1}, and aromatic substitution band at 700 cm^{-1}. Nuclear magnetic resonance: aromatic H's 7.10–7.75 (10.40 H) aliphatic protons in two complex bands 3.60–4.40 H (4.00 H) and 1.50–2.45 (7.70 H). Mass spectrogram: ion peak of highest significance *m/e* 163, no peaks were present greater than 163 and no molecular ion peak appeared at *m/e* 326.

Anal. Calcd. for $C_{20}H_{22}O_4$ (mol. wt., 326): C, 73.6; H, 6.80. Found (mol. wt., 336, osmometer; 320–350, iodometric titration): C, 73.51; H, 6.72.

Preparation of a 2,4-Dinitrophenylhydrazone from Compound R_f 0.66

A sample of the crystalline compound R_f 0.66 was heated with a solution of 2,4-dinitrophenylhydrazine in ethanol strongly acidified with sulfuric acid. A red crystalline derivative formed which was recrystallized from methanol, m.p. 167.5–170°. The mixture melting point with an authentic sample of the 2,4-dinitrophenylhydrazone of 4-hydroxybutyrophenone was 168–170°.

$LiAlH_4$ Reduction of Compound R_f 0.66

A sample (0.10 g) of the crystalline compound R_f 0.66 was reduced by refluxing with 0.08 g of lithium aluminium hydride in 3 ml of ether. After 1 h, 1 ml of ethyl acetate was added followed by 3 ml of concentrated hydrochloric acid. The organic phase was diluted with 10 ml of chloroform, washed with 5 ml of water, 5 ml of saturated aqueous sodium bicarbonate solution, 5 ml of water, dried through a bed of anhydrous magnesium sulfate, and evaporated on a steam bath. A white crystalline residue 0.058 g was left, which after recrystallization from benzene had a m.p. 63–66°. The mixture melting point with an authentic sample of 1-phenyl-1,4-butanediol was 63–66°.

Synthesis of 1-Phenyl-1,4-butanediol

This compound, m.p. 64–66°, was synthesized by the lithium aluminium hydride reduction of 3-benzoylpropionic acid (Aldrich Chemical Co., Inc.)

Treatment of Compound R_f 0.66 with Sodium Sulfite

A suspension of 0.056 g of compound R_f 0.66 (m.p. 97–102.5°) was stirred in 10 ml of aqueous sodium sulfite solution (11.0 g/100 ml water) for 2½ h. The suspension was extracted with 2 ml of ether and the ether extract checked by t.l.c. No change was evident. The ether was stripped off under an air stream leaving 0.038 g of white crystalline residue m.p. 101–104°. The mixture melting point with the starting material was 98–103°.

Identification of Compound R_f 0.32, 2-Phenyl-2-tetrahydrofuryl Hydroperoxide

A solution of 1.0 g of 1-phenylcyclobutanol in 5 ml of ether was added dropwise with stirring in an ice-water

Can. J. Chem. Downloaded from www.nrcresearchpress.com by 210.87.254.105 on 09/05/12
For personal use only.

bath, to 5 ml of 90% hydrogen peroxide acidified with 0.01 ml of concentrated sulfuric acid. The mixture was stirred at 0° for 2½ h. The reaction was terminated with the addition of 15 ml of ice-water. The organic phase was washed with 20 ml of water, 20 ml of saturated aqueous sodium bicarbonate solution, 20 ml of water, dried through a bed of anhydrous magnesium sulfate, and evaporated under an air stream. A yellow oil 0.68 g was left. Thin-layer chromatography showed that the residue was mainly one compound, R_f 0.32, with a small amount of two other peroxy compounds R_f 0.19 and 0.51. Infrared spectrum: almost identical with that of peroxide R_f 0.66 save for a strong OH band 3700–3100 cm^{-1}. Nuclear magnetic resonance: aromatic H's 7.12–7.60, aliphatic H's are in a triplet at 4.09 and a broad peak at 1.65–250.

Preparation of p-Nitrobenzoate Perester of Compound R_f 0.32 (3)

A solution of 0.496 g of the oxidation product in 5 ml of dry pyridine was added to a solution of 0.540 g of *p*-nitrobenzoyl chloride in 15 ml of dry pyridine with stirring in an ice bath. The mixture was kept at 0° for 21 h, then poured into a flask containing 5 ml of concentrated hydrochloric acid and 15 g of cracked ice. A creamy-white precipitate formed and was filtered off. It was suspended in 25 ml of ether in which most of it dissolved. The solution was washed with; 30 ml of 10% hydrochloric acid, 30 ml of 10% sodium hydroxide solution, and dried through a bed of magnesium sulfate. The ether was stripped on a steam bath leaving 0.286 g of yellow oil. This residue was chromatographed on 80 g of Woelm grade IV neutral alumina using 1:1 chloroform benzene solution as the eluting solvent. One 75 ml fraction was collected and evaporated under an air stream leaving a yellow residue 0.242 g. The residue was recrystallized from 1:1 ether, *n*-pentane giving a crystalline compound decomposing above 70°.

Anal. Calcd. for $C_{17}H_{15}NO_6$: C, 62.0; H, 4.56; N, 4.26. Found: C, 64.18; H, 4.54; N, 4.25.

Oxidation of 4-Hydroxybutyrophenone

A solution of 0.13 g of 4-hydroxybutyrophenone in 10 ml of ether was added dropwise with stirring in an ice-water bath to 10 ml of 30% hydrogen peroxide acidified with 0.01 ml of concentrated sulfuric acid. The mixture was stirred for 2½ h. The organic phase was washed with: 15 ml of water, 15 ml of saturated aqueous sodium bicarbonate solution, 15 ml of water, dried through a bed of anhydrous magnesium sulfate, and evaporated under an air stream. A colorless oil 0.10 g was left. Thin-layer chromatography showed one large spot at R_f 0.32. The infrared spectrum of this material showed no carbonyl band indicating substantially complete conversion of the hydroxy ketone to the hydroperoxide and appeared identical to that of 2-phenyl-2-tetrahydrofuryl hydroperoxide prepared by the oxidation of 1-phenylcyclobutanol with hydrogen peroxide in the presence of sulfuric acid.

On standing overnight, the reaction product deposited a few crystals. These were isolated by crystallization from hexane and shown to be (2-phenyl-2-tetrahydrofuryl) peroxide by their melting point, R_f value, and infrared spectrum.

Sodium Sulfite Reduction of Compound R_f 0.32

A solution of 2.03 g of 1-phenylcyclobutanol in 10 ml of ether was stirred at 0 °C with 10 ml of acidified 90% hydrogen peroxide for 1½ h. The organic phase was washed with: 20 ml of water, 20 ml of saturated aqueous sodium bicarbonate solution, 20 ml of water, dried through a bed of anhydrous magnesium sulfate, and evaporated under an air stream leaving 1.96 g of yellow oil. Thin-layer chromatographic analysis showed one large peroxy spot R_f 0.32 and small amounts of three others at R_f 0.19, 0.51, and 0.66.

A 0.10 g sample of the oxidation product was stirred with 10 ml of 10% aqueous sodium sulfite solution for 2½ h. The mixture was extracted with 2 ml of ether and checked by t.l.c. The peroxy spot at R_f 0.32 had disappeared, leaving the faint peroxy spots at R_f 0.19, 0.51, and 0.66. When the chromatogram was exposed to iodine vapor a spot at R_f 0.15 appeared corresponding to that of an authentic sample of 4-hydroxybutyrophenone.

The ether was stripped and a yellowish oil having an infrared spectrum identical with that of 4-hydroxybutyrophenone was left. A 2,4-dinitrophenylhydrazone was prepared from this residue, m.p. 168.5–170° and mixture m.p. 168–170° with the 2,4-dinitrophenylhydrazone from an authentic sample of 4-hydroxybutyrophenone.

Acid-free Oxidation of 1-Phenylcyclobutanol: a Time Study

A solution of 2.0 g 1-phenylcyclobutanol in 10 ml of ether was added to 10 ml of 90% hydrogen peroxide with stirring in an ice-water bath. After stirring 2½ h at 0° a sample of the organic phase was analyzed by t.l.c. using a 1:1 chloroform, benzene developing solution. When sprayed with acidified aqueous potassium iodide solution a faint peroxy compound with R_f 0.51 appeared. A second t.l.c. developed simultaneously with the first and then exposed to iodine vapor revealed spots at R_f 0.35 and R_f 0.51, the former spot corresponding to the starting alcohol. After 6 h the procedure was repeated. Two faint peroxy compounds were detected at R_f 0.51 and 0.32 in addition to the starting material at R_f 0.35. After 24 h the peroxy spots at R_f 0.51 and 0.32 were quite large and they obliterated that of the starting material.

Acid-free Oxidation of 1-Phenylcyclobutanol

A solution of 2.00 g of 1-phenylcyclobutanol in 10 ml of ether was added to 10 ml of 90% hydrogen peroxide with stirring in an ice-water bath. The mixture slowly warmed to room temperature over a 3 h period and was stirred for 15½ h. The reaction was terminated by adding 100 ml of ice-water. The organic phase was washed with two 75 ml portions of water and the aqueous phase was back extracted with 30 ml of ether. The combined ether extracts were dried through a bed of anhydrous magnesium sulfate and the ether was stripped under an air stream. Thin-layer chromatography showed two large peroxy spots at R_f 0.51 and 0.32. The residue was chromatographed on 80 g of Woelm grade IV neutral alumina using benzene as the eluting solvent. One hundred ml of solvent were collected before the first band came through. Ten fractions of 10 ml each and two of 25 ml were collected. Each fraction was analyzed by t.l.c. The first three fractions had only peroxy compound R_f 0.51 and starting alcohol (detected with iodine vapor) in them. The re-

Can. J. Chem. Downloaded from www.nrcresearchpress.com by 210.87.254.105 on 09/05/12
For personal use only.

maining fractions were mixtures of the two peroxy compounds and the starting material.

Ferrous Sulfate Reduction of Compound R_f 0.51

The above fractions containing 1-phenylcyclobutanol and the hydroperoxide R_f 0.51 were combined and evaporated under an air stream leaving 1.157 g of a yellow oil. A saturated aqueous ferrous sulfate solution (75 ml) was added cautiously with stirring to the residue. The mixture turned from green to muddy brown and a white precipitate separated. The solution was extracted with three 20 ml portions of ether. The combined ether extracts were dried through a bed of anhydrous magnesium sulfate and evaporated under an air stream. A sweet smelling semi-crystalline residue was left, 0.863 g. The residue was taken up in 10 ml of hot *n*-hexane and allowed to cool. A crystalline solid precipitated, was removed by filtration, and was recrystallized from *n*-hexane, yield 0.064 g, m.p. 84.5–88.5°. The mixture melting point with an authentic sample of 1,6-dibenzoylhexane of m.p. 87–88.5° was 85–88.5°. The filtrate was evaporated under an air stream leaving 0.710 g of yellow liquid. Thin-layer chromatography using benzene as the developing solvent and iodine vapor as the detecting agent showed three spots with R_f 0.35, 0.45, and 0.61. These corresponded to the R_f values of 1-phenylcyclobutanol, 1,6-dibenzoylhexane, and butyrophenone respectively. The spot corresponding to 1-phenylcyclobutanol was much larger than the other two.

The residue was heated with 10 ml of acidified methanolic 2,4-dinitrophenylhydrazine solution. Nothing precipitated from solution. However, when the solution was checked by t.l.c. two yellow spots appeared with R_f 0.48 and 0.66 (benzene as the eluting solvent). A sample of the butyrophenone 2,4-dinitrophenylhydrazone had an R_f value of 0.66 under these conditions while the bis (2,4-dinitrophenylhydrazone) of 1,6-dibenzoylhexane had an R_f of 0.48.

A sample of the residue was analyzed by v.p.c. on a 4 ft by $\frac{1}{4}$ in. SE-52 silicon rubber column at 140°. One peak appeared, and its retention time was identical with that of *n*-butyrophenone.

Synthesis of 4-Hydroxybutyrophenone (25)

Sodium ethoxide was prepared by reacting 4.5 g (0.196 moles) of sodium, cut into small cubes, with 90 ml of ethanol. When the sodium was consumed, 34 g (0.177 moles) of ethyl benzoylacetate was added slowly with stirring to the solution. After cooling to 5°, 9.0 g (0.204 moles) of ethylene oxide was added with stirring. The temperature was kept at 5° for 2 h, then the solution was allowed to warm to room temperature.

After two days, the yellow-brown gelatinous precipitate was removed by filtration and washed thoroughly with ether leaving a white solid. This was dissolved in 100 ml of water and acidified with glacial acetic acid. The solution turned milky, cleared, and separated into two phases. The organic phase was diluted with 25 ml of ether, washed with 50 ml of saturated aqueous sodium bicarbonate solution and 50 ml of water, dried through a bed of anhydrous magnesium sulfate, and evaporated under vacuum. The residual yellow oil was vacuum distilled. Three fractions were collected, 4.19 g, b.p. 98–103° at 0.4 mm of ethyl benzoylacetate, 1.343 g, b.p. 103–140° at 0.4 mm and 4.04 g 140–145° at 0.4 mm of ethyl 2-benzoyl-4-hydroxybutyrate.

Fraction three was refluxed with 40 ml of 10% potassium hydroxide solution for 3 h. Potassium carbonate (4.0 g) was added and the mixture was extracted with 40 ml of ether. The ether extract was dried through a bed of anhydrous magnesium sulfate and evaporated on a steam bath. The residual amber oil was distilled giving 2.27 g, b.p. 124–129° at 0.6 mm. This fraction was crystallized from *n*-hexane giving 4-hydroxybutyrophenone, m.p. 31–33°. Infrared spectrum: broad OH peak 3300–3700 cm^{-1}, carbonyl peak 1680 cm^{-1}, aromatic substitution peak at 700 cm^{-1}. Nuclear magnetic resonance: aromatic H's split into two complex bands 7.15–7.60 (3.58 H) and 7.80–8.07 (1.91 H), aliphatic H's are in a triplet at 3.70 (1.71 H) and at 3.08 (2.00 H) and a quartet at 1.94 (2.29 H) and hydroxyl proton at 2.51 (1.45 H). The 2,4-dinitrophenylhydrazone was prepared m.p. 168–170°

Anal. Calcd. for $C_{16}H_{16}N_4O_5$; C, 55.7; H, 4.65; N, 16.25: Found: C, 55.84; H, 4; 85; N, 16.02.

Synthesis of 1,6-Dibenzoylhexane

This compound was synthesized by the procedure described for 1,4-dibenzoylbutane (26). The product had a m.p. 82–85° (reported (27) 85–86°) and its bis (2,4-dinitrophenylhydrazone) had a m.p. 243–244°.

Anal. Calcd. for $C_{32}H_{30}N_8O_8$: C, 58.8; H, 4.59; N, 17.15. Found: C, 58.96; H, 4.82; N, 17.14.

Acknowledgment

The authors are indebted to Mr. H. Mak (Dow Chemical of Canada, Limited) for his assistance in recording and interpreting the n.m.r. spectra, to Mr. R. Mortimer (Dow Chemical of Canada, Limited) for the analysis of the peroxides, and to Mrs. Marcia Dilling (The Dow Chemical Company, Midland, Michigan) for the mass spectral analyses. The authors also wish to express their appreciation for several stimulating discussions with Dr. R. Hiatt (Brock University, St. Catharines, Ontario).

1. P. A. S. Smith. *In* Molecular rearrangements. Vol. 1. *Edited by* P. de Mayo. Interscience Publishers, Inc., New York. p. 573.
2. M. S. Kharasch and J. G. Burt. J. Org. Chem. **16**, 150 (1951).
3. E. Hedaya and S. Winstein. J. Am. Chem. Soc. **89**, 1661 (1967).
4. B. Yoemans and D. P. Young. J. Chem. Soc. 2288 (1958).
5. W. Treibs and R. Schollner. Ber. **91**, 2282 (1958).
6. H. Kwart and R. T. Keen. J. Am. Chem. Soc. **81**, 943 (1959).
7. E. B. McCall and D. S. P. Roebuck. Brit. Patent No. 681, 613 (1952) to Monsanto Chemicals, Ltd.
8. G. Caprara and G. Lemetre. Chim. Ind. (Milan) **42**, 974 (1960).

9. D. H. HEY, C. J. M. STIRLING, and G. H. WILLIAMS. J. Chem. Soc. 1054 (1957).
10. S. AKIYOSHI, N. TASHIRO and S. KANAYAMA. Kogyo Kagaku Zasshi **60**, 286 (1957), Chem. Abstr. **53**, 8058*e* (1959).
11. H. KROPF. Ann. **637**, 93 (1960).
12. A. W. DE RUYTER VAN STEVENINCK and E. C. KOOYMAN. Rec. Trav. Chim. **79**, 413 (1960).
13. B. V. EROFEEV, A. I. CHIRKO, and I. I. URBANOVICH. Zhidkofaznoe Okislenie Nepredel'nykh Organ. Soedin., Sb 1961, No. 1, 15; Chem. Abstr. **58**, 427*a* (1963).
14. A. RIECHE and E. SCHMITZ. Ber. **90**, 1082 (1957).
15. A. RIECHE. Angew. Chem. **70**, 251 (1958).
16. E. G. E. HAWKINS and D. P. YOUNG. J. Chem. Soc. 2804 (1950).
17. E. J. VANDENBERG. U. S. Patent No. 2,950,320 (1960) to Hercules Powder Company.
18. P. A. S. SMITH. *In* Molecular rearrangements. Vol. 1. *Edited by* P. de Mayo. Interscience Publishers, Inc., New York. p. 576.
19. F. F. RUST and E. R. BELL. U. S. Patent No. 2,717, 264 (1955) to Shell Development.
20. N. J. LEONARD. U. S. Patent No. 2,594,322 (1952) to Phillips Petroleum Company.
21. W. PRITZKOW and K. A. MULLER. Ber. **89**, 2321 (1956).
22. C. K. INGOLD. Structure and mechanism in organic chemistry. Cornell University Press, Ithaca, New York. 1953 p. 478.
23. R. L. SHRINER, R. C. FUSON, and D. Y. CURTIN. The systematic identification of organic compounds. 5th ed. John Wiley and Sons, Inc. New York. 1965. p. 253.
24. A. BURGER and R. D. BENNETT. J. Med. Pharm. Chem. **11**, 687 (1960); Chem. Abstr. **55**, 11324*i* (1961).
25. G. V. CHELINTZEV and E. D. OSETROVA. Compt. rend. acad. sci. URSS. **2**, 251 (1935), Chem. Abstr. **29**, 6223 (1935).
26. R. C. FUSON and J. T. WALKER. Organic syntheses. Collective Vol. II. John Wiley and Sons, Inc., New York. 1955. p. 169.
27. H. O. HOUSE and J. W. BLAKER. J. Org. Chem. **23**, 334 (1958).

Can. J. Chem. Downloaded from www.nrcresearchpress.com by 210.87.254.105 on 09/05/12
For personal use only.

Can. J. Chem. Downloaded from www.nrcresearchpress.com by 210.87.254.105 on 09/05/12
For personal use only.

Synthesis of benzylidene-flavanones

T. SZÉLL AND M. ZARANDY
Department of Applied Chemistry, University of Szeged, Hungary

Received December 22, 1967

Various procedures for the preparation of benzylidene-flavanones have been examined and von Kostanecki's method was found to give best results. A number of new 6-nitroflavanones are reported.

Canadian Journal of Chemistry, 46, 1571 (1968)

Recent interest in the 6-nitro-3-benzylidene-flavanones as bacteriostatic materials has led us to reinvestigate the methods for their preparation (1–7). Reaction of the flavanone with the appropriate benzaldehyde in ethanol–hydrogen chloride according to von Kostanecki's method (1) was found to give best results. Attempts to develop a one-step synthesis from the acetophenones and benzaldehydes listed in Table I, using basic (5, 6) or acidic (7) catalysts, were generally unsuccessful. This failure is believed to be inherent in the reaction process; the initially-formed chalcone must isomerize to flavanone before condensing with the benzaldehyde, but isomerization is a relatively slow process and occurs under conditions which promote the decomposition of benzylidene-flavanones. In agreement with earlier observation (8), flavanones and benzaldehydes in which the substituents have negative Hammett constants can be successfully condensed in the presence of acids.

Experimental

Attempted Synthesis of 6-Nitro-3-benzylidene-flavanones from 5-Nitro-2-hydroxyacetophenone and the Appropriate Aldehyde

Base-catalyzed condensations (6) were unsuccessful. For the acid-catalyzed condensations, the acetophenone (0.037 g) and 4-methylbenzaldehyde (1 g) were dissolved

TABLE I

Experimental data for benzylidene-flavanones*

Benzaldehyde	Product R_1	R_2	R_3	R_4	Heating times (min)	Yield %	Melting point† (°C)	Formula	% nitrogen Calculated	Found
4-CH_3-	H	H	CH_3	H	10	75	178–179	$C_{23}H_{17}NO_4$	3.8	3.7
4-*i*-C_3H_7	H	H	*i*-C_3H_7	H	5	81	163	$C_{25}H_{21}NO_4$	3.5	3.5
4-OH-	H	H	OH	H	10	33	186–188	$C_{22}H_{15}NO_5$	3.8	3.7
4-OCH_3-	H	H	OCH_3	H	room temperature, 2.5 days	81	153–154	$C_{23}H_{17}NO_5$	3.6	3.7
2-OCH_3-	OCH_3	H	H	H	5	53	168–170	$C_{23}H_{17}NO_5$	3.6	3.7
2-OC_2H_5-	OC_2H_5	H	H	H	8	29	181–182	$C_{24}H_{19}NO_5$	3.5	3.5
4-F-	H	H	F	H	25	86	172–173	$C_{22}H_{14}NO_4F$	3.7	3.8
3-F-	H	F	H	H	15	69	158–159	$C_{22}H_{14}NO_4F$	3.7	3.7
2-F	F	H	H	H	15	51	153	$C_{22}H_{14}NO_4F$	3.7	3.6
2,5-diOCH_3	OCH_3	H	H	OCH_3	room temperature	85	197–198	$C_{24}H_{19}NO_6$	3.4	3.3
3,4-dioxymethylene	H	O-CH_2-O		H	room temperature, 1 day	76	220–222	$C_{23}H_{15}NO_6$	3.5	3.6

*Compounds of structure 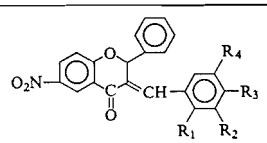 .
†Uncorrected.

in 15 ml of dry ethanol, saturated with HCl at 0 °C, allowed to stand for 30 min, refluxed 25 min, diluted with water, and evaporated to dryness. The residue was crystallized from ethyl acetate – aqueous ethanol, the crystals washed with 2*N* ethanolic sodium hydroxide, then recrystallized from ethanol – ethyl acetate; yield 11%, m.p. 185–187°.

A similar attempt with 3-fluorobenzaldehyde gave only 8.8% yield of benzylidene-flavanone, m.p. 187–189 °C.

Syntheses from 6-Nitroflavanone

6-Nitroflavanone (9) (0.040 g) and the appropriate benzaldehyde (0.5–3 mmole) in 1.5 ml dry ethanol were saturated with hydrogen chloride at 0°. The solutions, often deeply colored, were allowed to stand for some time at room temperature, refluxed briefly, then placed overnight in the refrigerator. The resulting yellow crystals were recrystallized from ethanol – ethyl acetate (1:1). With 4-methoxy-, 2,5-dimethoxy-, and 3,4-dioxymethylene-benzaldehydes, the HCl solutions were not refluxed but were allowed to stand 1–3 days at room temperature.

3-(*p*-Methylbenzylidene)-6-nitro-4′-methylflavanone was prepared from 6-nitro-4′-methylflavanone in a yield of 75% by this procedure; m.p. 185–187°.

Anal. Calcd. for $C_{24}H_{19}NO_4$: N, 3.6. Found: N, 3.7.

The new starting flavanone (m.p. 120–121 °C) was prepared by a method developed for this purpose (9). The remaining products are described in Table I.

Acknowledgments

The generous gift of a number of benzaldehydes from the National Research Council of Canada is gratefully acknowledged. The authors are indebted to Mrs. C. Lakos-Láng and Mrs. G. Bartók-Bozóki of the University of Szeged for microanalyses. The work was supported in part by the Hungarian Ministry of Education.

1. A. KATSCHALOWSKY and ST. VON KOSTANECKI. Chem. Ber. **37**, 3169 (1904).
2. H. RYAN and G. CRUESS-CALLAGHAN. Proc. Roy. Irish Acad. 124 (1929).
3. K. AUWERS and F. ARNDT. Chem. Ber. **42**, 2711 (1909).
4. H. DE DIESBACH and H. KRAMER. Helv. Chim. Acta, **28**, 1399 (1945).
5. M. K. SEIKEL, M. J. LOUNSBURY, and S.-C. WANG. J. Org. Chem. **27**, 2952 (1962).
6. P. R. SHAH and N. M. SHAH. Chem. Ber. **97**, 1453 (1964).
7. T. SZÉLL and R. E. M. UNYI. J. Org. Chem. **28**, 1146 (1963).
8. T. SZÉLL, A. M. EASTHAM, and G. SIPOS. Can. J. Chem. **42**, 2417 (1964).
9. T. SZÉLL. Monatsh. **94**, 992 (1963).

Sur la réduction par les hydrures complexes d'éthers énoliques dérivés de formyl-2 cyclanones. III. Ethers dérivés de la formyl-2 diméthyl-6,6 cyclohexanone

JEAN-CLAUDE RICHER ET JEAN-MARIE HACHEY[1]

Département de chimie, Université de Montréal, Montréal, Québec

Reçu le 27 décembre 1967

La réduction des éthers *O*- et *S*-butylés dérivés de l'hydroxyméthylène-2 diméthyl-6,6 cyclohexanone conduit à l'aldéhyde attendu et au méthylène-2 diméthyl-6,6 cyclohexanol.

The reduction of the *O*- and *S*-butylether derived from the 2-hydroxymethylene-6,6-dimethylcyclohexanone yields, in addition to the expected unsaturated aldehyde, 2-methylene-6,6-dimethylcyclohexanol.

Canadian Journal of Chemistry, **46**, 1572 (1968)

Introduction

Dans le cadre de nos travaux (1, 2) sur les facteurs affectant les réductions 1:2 vs. 1:4 des groupes carbonylés conjugués avec des doubles liaisons, nous avons réexaminé la réduction de l'éther énolique (**1***a*) dérivé de la formyl-2 diméthyl-6,6 cyclohexanone (**2**). Dans le cas similaire de l'éther énolique (**1***b*), Seifert et Schinz (3) n'avaient rapporté que la formation de l'aldéhyde insaturé (**3**) provenant d'une addition initiale 1:2 de l'hydrure sur le groupe carbonyle.

Résultats et discussion

L'éther énolique (**1***a*), préparé à partir de la formyl-2 diméthyl-6,6 cyclohexanone (**2**) d'après

[1]Les résultats rapportés dans ce travail sont tirés du mémoire de maîtrise déposé par Jean-Marie Hachey, Faculté des Sciences, Université de Montréal, mai 1966.

Can. J. Chem. Downloaded from www.nrcresearchpress.com by 210.87.254.105 on 09/05/12
For personal use only.

in 15 ml of dry ethanol, saturated with HCl at 0 °C, allowed to stand for 30 min, refluxed 25 min, diluted with water, and evaporated to dryness. The residue was crystallized from ethyl acetate – aqueous ethanol, the crystals washed with 2*N* ethanolic sodium hydroxide, then recrystallized from ethanol – ethyl acetate; yield 11%, m.p. 185–187°.

A similar attempt with 3-fluorobenzaldehyde gave only 8.8% yield of benzylidene-flavanone, m.p. 187–189 °C.

Syntheses from 6-Nitroflavanone

6-Nitroflavanone (9) (0.040 g) and the appropriate benzaldehyde (0.5–3 mmole) in 1.5 ml dry ethanol were saturated with hydrogen chloride at 0°. The solutions, often deeply colored, were allowed to stand for some time at room temperature, refluxed briefly, then placed overnight in the refrigerator. The resulting yellow crystals were recrystallized from ethanol – ethyl acetate (1:1). With 4-methoxy-, 2,5-dimethoxy-, and 3,4-dioxymethylene-benzaldehydes, the HCl solutions were not refluxed but were allowed to stand 1–3 days at room temperature.

3-(*p*-Methylbenzylidene)-6-nitro-4′-methylflavanone was prepared from 6-nitro-4′-methylflavanone in a yield of 75% by this procedure; m.p. 185–187°.

Anal. Calcd. for $C_{24}H_{19}NO_4$: N, 3.6. Found: N, 3.7.

The new starting flavanone (m.p. 120–121 °C) was prepared by a method developed for this purpose (9). The remaining products are described in Table I.

Acknowledgments

The generous gift of a number of benzaldehydes from the National Research Council of Canada is gratefully acknowledged. The authors are indebted to Mrs. C. Lakos-Láng and Mrs. G. Bartók-Bozóki of the University of Szeged for microanalyses. The work was supported in part by the Hungarian Ministry of Education.

1. A. KATSCHALOWSKY and ST. VON KOSTANECKI. Chem. Ber. **37**, 3169 (1904).
2. H. RYAN and G. CRUESS-CALLAGHAN. Proc. Roy. Irish Acad. 124 (1929).
3. K. AUWERS and F. ARNDT. Chem. Ber. **42**, 2711 (1909).
4. H. DE DIESBACH and H. KRAMER. Helv. Chim. Acta, **28**, 1399 (1945).
5. M. K. SEIKEL, M. J. LOUNSBURY, and S.-C. WANG. J. Org. Chem. **27**, 2952 (1962).
6. P. R. SHAH and N. M. SHAH. Chem. Ber. **97**, 1453 (1964).
7. T. SZÉLL and R. E. M. UNYI. J. Org. Chem. **28**, 1146 (1963).
8. T. SZÉLL, A. M. EASTHAM, and G. SIPOS. Can. J. Chem. **42**, 2417 (1964).
9. T. SZÉLL. Monatsh. **94**, 992 (1963).

Sur la réduction par les hydrures complexes d'éthers énoliques dérivés de formyl-2 cyclanones. III. Ethers dérivés de la formyl-2 diméthyl-6,6 cyclohexanone

JEAN-CLAUDE RICHER ET JEAN-MARIE HACHEY[1]

Département de chimie, Université de Montréal, Montréal, Québec

Reçu le 27 décembre 1967

La réduction des éthers *O*- et *S*-butylés dérivés de l'hydroxyméthylène-2 diméthyl-6,6 cyclohexanone conduit à l'aldéhyde attendu et au méthylène-2 diméthyl-6,6 cyclohexanol.

The reduction of the *O*- and *S*-butylether derived from the 2-hydroxymethylene-6,6-dimethylcyclohexanone yields, in addition to the expected unsaturated aldehyde, 2-methylene-6,6-dimethylcyclohexanol.

Canadian Journal of Chemistry, **46**, 1572 (1968)

Introduction

Dans le cadre de nos travaux (1, 2) sur les facteurs affectant les réductions 1:2 vs. 1:4 des groupes carbonylés conjugués avec des doubles liaisons, nous avons réexaminé la réduction de l'éther énolique (**1***a*) dérivé de la formyl-2 diméthyl-6,6 cyclohexanone (**2**). Dans le cas similaire de l'éther énolique (**1***b*), Seifert et Schinz (3) n'avaient rapporté que la formation de l'aldéhyde insaturé (**3**) provenant d'une addition initiale 1:2 de l'hydrure sur le groupe carbonyle.

Résultats et discussion

L'éther énolique (**1***a*), préparé à partir de la formyl-2 diméthyl-6,6 cyclohexanone (**2**) d'après

[1]Les résultats rapportés dans ce travail sont tirés du mémoire de maîtrise déposé par Jean-Marie Hachey, Faculté des Sciences, Université de Montréal, mai 1966.

Can. J. Chem. Downloaded from www.nrcresearchpress.com by 210.87.254.40 on 09/05/12
For personal use only.

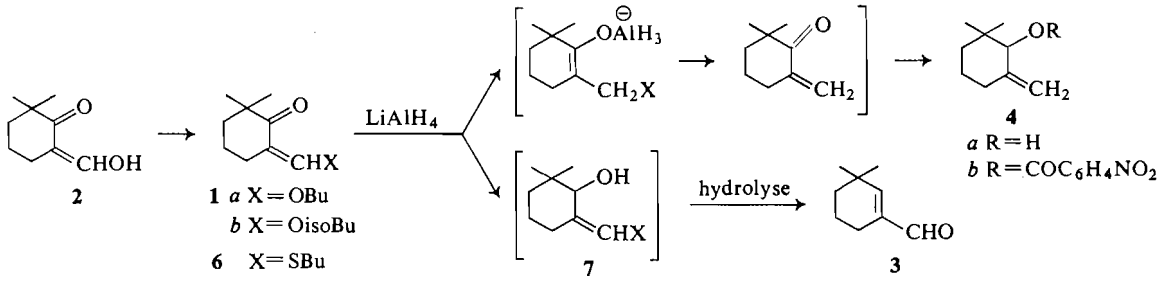

le procédé habituel (4), a été réduit par l'hydrure double de lithium et d'aluminium en suivant les indications de Seifert et Schinz (3). Il a été observé que les produits de la réaction sont formés de 15 à 20% de méthylène-2 diméthyl-6,6 cyclohexanol (**4***a*) et de 80 à 85% de l'aldéhyde attendu (**3**).

L'aldéhyde a été caractérisé par comparaison de ses propriétés physiques et celles de ses dérivés avec les propriétés correspondantes rapportées dans la littérature (3). Quant à l'alcool insaturé **4***a*, sa présence a été mise en évidence d'une part par superposition de pics en c.p.g. avec un échantillon authentique préparé par réduction (5) par $LiAlH_4$ de la formyl-2 diméthyl-6,6 cyclohexanone (**2**). D'autre part, le traitement du mélange brut de la réduction (80% de **3** et 20% de **4***a*) avec de l'acide, transforme l'alcool **4***a* en triméthyl-2,2,6 cyclohexanone (**5**) mise en évidence par superposition de pics en c.p.g. avec un échantillon authentique. Cette transformation, qui a maintenant été observée par plusieurs auteurs (2, 6) a aussi été réalisée sur l'alcool **4***a* pur.

Le thioéther énolique **6**, préparé à partir de l'hydroxyméthylène-2 diméthyl-6,6 cyclohexanone (**2**) et du butanethiol, a pu être désulfurisé en utilisant les indications de Ireland et Marshall (7) pour fournir un échantillon authentique de triméthyl-2,2,6 cyclohexanone (**5**). Le thioéther énolique **6** a aussi été réduit par $LiAlH_4$; la décomposition de l'intermédiaire (**7**) par H_2SO_4 concentré conduit à un mélange réactionnel brut contenant 90 à 95% de l'aldéhyde **3** et 5 à 10% du méthylène-2 diméthyl-6,6 cyclohexanol (**4***a*).

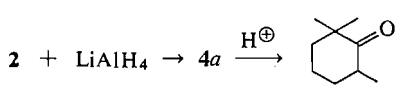

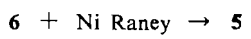

Les résultats obtenus dans le présent travail montrent donc que les additions 1:4 d'hydrures sur des groupements carbonyles conjugués avec des doubles liaisons seraient plus générales que l'on aurait pu le croire d'après les travaux précédents et principalement ceux de Schinz et ses collaborateurs (3, 8). Conformément aux résultats obtenus dans la série du camphre (2) il est noté à nouveau que les quantités d'addition 1:4 d'hydrures sont plus grandes dans le cas des *O*-éthers énoliques (**1***b*) que dans le cas des thioéthers énoliques (**6**).

Partie expérimentale

Les analyses par chromatographie en phase gazeuse (c.p.g.) ont été effectuées à l'aide d'un appareil de la Compagnie F & M, modèle 810, muni d'un détecteur à flamme ionisante sur une colonne spiralée de cuivre de 2.5 m. contenant 10% d'Hyprose sur Chromosorb P 30–60. Température de la colonne, 140 °C, débit du gaz porteurs (He) 60 ml/min.

Butoxyméthylène-2 diméthyl-6,6 cyclohexanone (1a)

Préparé (4) avec un rendement de 85%, ce dérivé présente les caractéristiques suivantes: p.e.: 104 °C/0.4 mm Hg; n_D^{25}: 1.4854; ultraviolet: λ_{max} 275 mμ log ε: 4.21; résonance magnétique nucléaire (r.m.n.) (produit pur): δ 4.00 (t,2H,—O—CH_2—) et δ 7.20(t,1H, vinylique).

Anal. Calc. pour $C_{13}H_{22}O_2$: C, 74.24; H, 10.54. Trouvé: C, 74.17; H, 10.45.

Méthylène-2 diméthyl-6,6 cyclohexanol (4a)

La réduction de 9.1g d'hydroxyméthylène **2** par 2.8 g d'hydrure de lithium et d'aluminium selon les indications de Dreiding et Hartman (5) conduit à 9.0 g de produits bruts qui contiennent d'après la c.p.g. 91% du méthylène alcool désiré (**4***a*). Purifié par distillation fractionnée sous atmosphère d'azote, l'alcool présente les caractéristiques suivantes: p.e.: 135 °C/10 mm Hg; n_D^{24}: 1.4805; infrarouge: bandes à 3420 (OH); 885 (=CH_2); r.m.n.: (solvant, $CDCl_3$), δ 3.67(1H, carbinolique) et δ 4.80(2H, vinyliques).

p-Nitrobenzoate 4b

Préparé à la manière habituelle (9), ce dérivé présente les caractéristiques suivantes: p.f.: 48–49 °C; r.m.n.: (solvant, CCl_4), δ 4.80(m, 2H, vinyliques), 5.20(m, 1H, carbinolique), et 8.10(s, 4H, aromatiques).

Can. J. Chem. Downloaded from www.nrcresearchpress.com by 210.87.254.40 on 09/05/12
For personal use only.

Anal. Calc. pour $C_{16}H_{19}NO_4$: C, 66.42; H, 6.62; N, 4.84. Trouvé: C, 66.07; H, 6.37; N, 4.97.

Remerciements

Les auteurs remercient vivement le Conseil National de Recherches du Canada et la Compagnie Bristol Laboratories pour l'aide financière apportée sous forme de subventions de recherches.

1. J. C. Richer et R. Clarke. Tetrahedron Letters, 935 (1964).
2. J. C. Richer et C. Lamarre. Can. J. Chem. **45**, 1581 (1967).
3. P. Seifert et H. Schinz. Helv. Chim. Acta, **34**, 728 (1951).
4. J. C. Richer et R. Clarke. Can. J. Chem. **42**, 2073 (1964).
5. A. S. Dreiding et J. A. Hartman. J. Am. Chem. Soc. **75**, 939 (1953).
6. A. S. Dreiding et J. A. Hartman. J. Am. Chem. Soc. **78**, 1216 (1956).
7. R. E. Ireland et J. A. Marshall. J. Org. Chem. **27**, 1615 (1962).
8. R. Vondervahl et H. Schinz. Helv. Chim. Acta, **35**, 2368 (1952).
9. R. L. Shriner, R. C. Fuson, et D. Y. Curtin. The systematic identification of organic compounds. John Wiley & Sons, Inc., New York, N. Y. 1962.

Can. J. Chem. Downloaded from www.nrcresearchpress.com by 210.87.254.40 on 09/05/12
For personal use only.

The $AlCl_3$–$LiAlH_4$ reduction of $\Delta^{9(11)}$-12-oxo and $\Delta^{9(11)}$-12-hydroxy steroids

P. Ziegler and J. C. Grivas

Research and Development Laboratories, Canada Packers Limited, Toronto, Ontario

Received December 6, 1967

Desoxycholic acid and 3α,12α-dihydroxypregnane were transformed to the corresponding $\Delta^{9(11)}$-12-oxo compounds. These steroids and their $NaBH_4$ reduction products were then hydrogenolyzed with $AlCl_3$–$LiAlH_4$ to provide $\Delta^{9(11)}$-compounds in good yield.

Canadian Journal of Chemistry, 46, 1574 (1968)

Introduction

Aluminium chloride – lithium aluminium hydride reagents have been used effectively for the elimination of oxygen functions from allylic alcohols and α,β-unsaturated ketones (1–6). Aside from the olefins which are the main reaction products, conjugated dienes and saturated alcohols have been isolated in smaller amounts. In general, these hydrogenolyses have provided the products that are expected to arise from intermediary carbonium ions. For example (6), pulegone yielded 41% of Δ^3-menthene, 35% of $\Delta^{4(8)}$-menthene, 12% of $\Delta^{2,4(8)}$-menthadiene, and 13% of $\Delta^{3,8}$-menthadiene. Hydrogenolysis of Δ^1-cholesten-3-one provided 20% of Δ^1-cholestene and 10% of Δ^2-cholestene (3), but Δ^4-cholesten-3-one gave 85–90% of Δ^4-cholestene (1, 2, 5). It was decided to apply the $AlCl_3$–$LiAlH_4$ reaction to $\Delta^{9(11)}$-12-oxo- and $\Delta^{9(11)}$-12-hydroxy steroids. The latter compounds are readily accessible from some bile acids and sapogenins, and it was hoped that this route would lead to an efficient synthesis of $\Delta^{9(11)}$-steroids which, in turn, can be converted by established methods to 11-oxygenated corticosteroids.

Results and Discussion

Desoxycholic acid was transformed to methyl 3α-acetoxy-12-oxocholanate (**1**) by a known (7–9) sequence of reactions comprising methylation of the carboxyl group, preferential acetylation of the 3α-hydroxy group, and oxidation of the 12α-hydroxy function with chromic acid. Dehydrogenation of the product (**1**) could be effected in excellent yield using selenium dioxide in refluxing acetic acid (10) but the reaction did not proceed well in tertiary butanol (containing traces of pyridine) under conditions that have been reported (11) to provide good yields of $\Delta^{9(11)}$-12-oxo compounds in the sapogenin series. Summarizing the above reactions, it is apparent that methyl 3α-acetoxy-$\Delta^{9(11)}$-12-oxocholenate (**2***a*) or its saponification product (**2***b*) can be obtained in 80–85% yield from desoxycholic acid. Hydrogenolysis of methyl 3α-acetoxy-$\Delta^{9(11)}$-12-oxocholenate (**2***a*) with $AlCl_3$–$LiAlH_4$ reagents in ether provided 60% of 3α,24-dihydroxy-$\Delta^{9(11)}$-cholene (**4**). Better overall results (80–85%) were obtained when 3α-hydroxy-$\Delta^{9(11)}$-12-oxocholenic acid (**2***b*) was first reduced with sodium borohydride to a

Anal. Calc. pour $C_{16}H_{19}NO_4$: C, 66.42; H, 6.62; N, 4.84. Trouvé: C, 66.07; H, 6.37; N, 4.97.

Remerciements

Les auteurs remercient vivement le Conseil National de Recherches du Canada et la Compagnie Bristol Laboratories pour l'aide financière apportée sous forme de subventions de recherches.

1. J. C. Richer et R. Clarke. Tetrahedron Letters, 935 (1964).
2. J. C. Richer et C. Lamarre. Can. J. Chem. **45**, 1581 (1967).
3. P. Seifert et H. Schinz. Helv. Chim. Acta, **34**, 728 (1951).
4. J. C. Richer et R. Clarke. Can. J. Chem. **42**, 2073 (1964).
5. A. S. Dreiding et J. A. Hartman. J. Am. Chem. Soc. **75**, 939 (1953).
6. A. S. Dreiding et J. A. Hartman. J. Am. Chem. Soc. **78**, 1216 (1956).
7. R. E. Ireland et J. A. Marshall. J. Org. Chem. **27**, 1615 (1962).
8. R. Vondervahl et H. Schinz. Helv. Chim. Acta, **35**, 2368 (1952).
9. R. L. Shriner, R. C. Fuson, et D. Y. Curtin. The systematic identification of organic compounds. John Wiley & Sons, Inc., New York, N. Y. 1962.

Can. J. Chem. Downloaded from www.nrcresearchpress.com by 210.87.254.40 on 09/05/12
For personal use only.

The $AlCl_3$–$LiAlH_4$ reduction of $\Delta^{9(11)}$-12-oxo and $\Delta^{9(11)}$-12-hydroxy steroids

P. Ziegler and J. C. Grivas

Research and Development Laboratories, Canada Packers Limited, Toronto, Ontario

Received December 6, 1967

Desoxycholic acid and 3α,12α-dihydroxypregnane were transformed to the corresponding $\Delta^{9(11)}$-12-oxo compounds. These steroids and their $NaBH_4$ reduction products were then hydrogenolyzed with $AlCl_3$–$LiAlH_4$ to provide $\Delta^{9(11)}$-compounds in good yield.

Canadian Journal of Chemistry, 46, 1574 (1968)

Introduction

Aluminium chloride – lithium aluminium hydride reagents have been used effectively for the elimination of oxygen functions from allylic alcohols and α,β-unsaturated ketones (1–6). Aside from the olefins which are the main reaction products, conjugated dienes and saturated alcohols have been isolated in smaller amounts. In general, these hydrogenolyses have provided the products that are expected to arise from intermediary carbonium ions. For example (6), pulegone yielded 41% of Δ^3-menthene, 35% of $\Delta^{4(8)}$-menthene, 12% of $\Delta^{2,4(8)}$-menthadiene, and 13% of $\Delta^{3,8}$-menthadiene. Hydrogenolysis of Δ^1-cholesten-3-one provided 20% of Δ^1-cholestene and 10% of Δ^2-cholestene (3), but Δ^4-cholesten-3-one gave 85–90% of Δ^4-cholestene (1, 2, 5). It was decided to apply the $AlCl_3$–$LiAlH_4$ reaction to $\Delta^{9(11)}$-12-oxo- and $\Delta^{9(11)}$-12-hydroxy steroids. The latter compounds are readily accessible from some bile acids and sapogenins, and it was hoped that this route would lead to an efficient synthesis of $\Delta^{9(11)}$-steroids which, in turn, can be converted by established methods to 11-oxygenated corticosteroids.

Results and Discussion

Desoxycholic acid was transformed to methyl 3α-acetoxy-12-oxocholanate (**1**) by a known (7–9) sequence of reactions comprising methylation of the carboxyl group, preferential acetylation of the 3α-hydroxy group, and oxidation of the 12α-hydroxy function with chromic acid. Dehydrogenation of the product (**1**) could be effected in excellent yield using selenium dioxide in refluxing acetic acid (10) but the reaction did not proceed well in tertiary butanol (containing traces of pyridine) under conditions that have been reported (11) to provide good yields of $\Delta^{9(11)}$-12-oxo compounds in the sapogenin series. Summarizing the above reactions, it is apparent that methyl 3α-acetoxy-$\Delta^{9(11)}$-12-oxocholenate (**2***a*) or its saponification product (**2***b*) can be obtained in 80–85% yield from desoxycholic acid. Hydrogenolysis of methyl 3α-acetoxy-$\Delta^{9(11)}$-12-oxocholenate (**2***a*) with $AlCl_3$–$LiAlH_4$ reagents in ether provided 60% of 3α,24-dihydroxy-$\Delta^{9(11)}$-cholene (**4**). Better overall results (80–85%) were obtained when 3α-hydroxy-$\Delta^{9(11)}$-12-oxocholenic acid (**2***b*) was first reduced with sodium borohydride to a

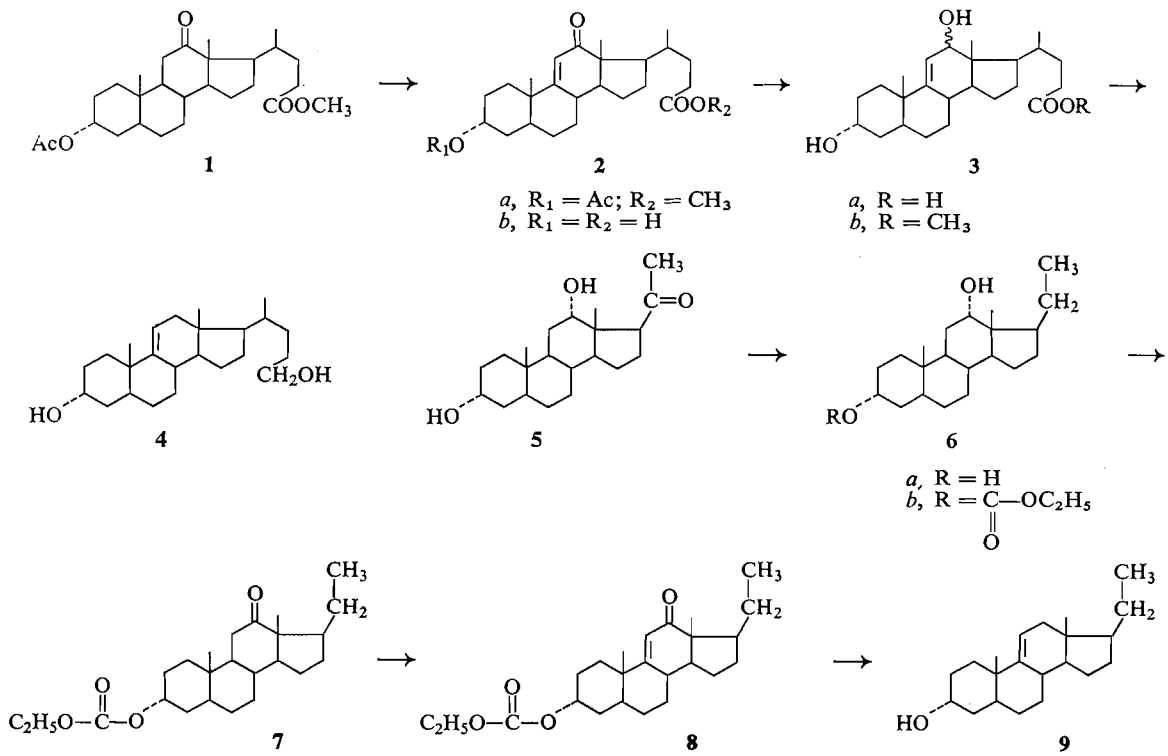

mixture of the 12-epimeric alcohols (**3***a*) which, after methylation with diazomethane, was hydrogenolyzed with $AlCl_3$–$LiAlH_4$. These reactions were carried out in ether and optimum yields were obtained when the molar proportions of steroid:$LiAlH_4$:$AlCl_3$ were 1:5:16.

Hydrogenolysis with $AlCl_3$–$LiAlH_4$ was then applied to $\Delta^{9(11)}$-12-oxopregnenes. The Wolff–Kishner reduction product (**6***a*) of 3α,12α-dihydroxypregnan-20-one (**5**) was esterified preferentially with ethyl chloroformate, and the 3α-monoester (**6***b*) was then oxidized with chromic acid and dehydrogenated with selenium dioxide to afford 3α-ethoxycarbonyloxy-$\Delta^{9(11)}$-12-oxopregnene (**8**). The latter compound was reduced with $NaBH_4$ and the crude reduction product was hydrogenolyzed with $AlCl_3$–$LiAlH_4$, under the same conditions as described earlier, to yield 72% of 3α-hydroxy-$\Delta^{9(11)}$-pregnene (**9**).

Attempts were then made to extend this hydrogenolysis reaction to $\Delta^{9(11)}$-12-oxopregnenes containing an esterified hydroxyl group in the 20α- or 20β-position. Elimination of the 12-oxygen function did not take place in good yield in these cases.

Experimental

Methyl 3α-Acetoxy-$\Delta^{9(11)}$-12-oxocholenate (2a)

Methyl 3α-acetoxy-12-oxocholanate (**1**; 191 g) was dissolved in warm glacial acetic acid (1.8 l), and selenium dioxide (20 g) was added. The mixture was refluxed and stirred for 31 h and, during this time, four additional portions of selenium dioxide (20 g each) were added at regular intervals. The cooled mixture was then filtered, and the dark-orange filtrate was diluted by slow addition of water (5 l). The resulting precipitate was removed by filtration, washed with water, and vacuum-dried to yield 172 g of product, m.p. 142–145 °C. One crystallization from methanol, with charcoaling, provided material with m.p. 146.5–148.5 °C and λ_{max} (ethanol) 240 mμ (ε 11 840). Reported (12), m.p. 145–147 °C and λ_{max} (ethanol) 241 mμ (ε 11 480).

3α,24-Dihydroxy-$\Delta^{9(11)}$-cholene (4)

(a) By Direct $AlCl_3$–$LiAlH_4$ Hydrogenolysis of Methyl 3α-Acetoxy-$\Delta^{9(11)}$-12-oxocholenate (2a)

Methyl 3α-acetoxy-$\Delta^{9(11)}$-12-oxocholenate (**2***a*; 2.35 g) was taken up in ether (80 ml) and the suspension was added within 20 min to a stirred, ice-cold solution of $AlCl_3$–$LiAlH_4$ reagent in ether. The reagent had been prepared by carefully dissolving anhydrous aluminium chloride (8.45 g) in cold, dry ether (50 ml) and adding lithium aluminium hydride (1 g) thereto in several portions. The hydrogenolysis was carried out by refluxing the mixture for 4.5 h. The mixture was then treated cautiously, first with a few ml of water then with dilute

Can. J. Chem. Downloaded from www.nrcresearchpress.com by 210.87.254.40 on 09/05/12
For personal use only.

Can. J. Chem. Downloaded from www.nrcresearchpress.com by 210.87.254.40 on 09/05/12
For personal use only.

sulfuric acid, the ether layer was separated, and the aqueous phase was extracted with methylene chloride. The combined solvent extracts were washed with water, dried over $MgSO_4$, and evaporated to yield 1.94 g of residue. The latter was crystallized from ether to give 1.14 g (60%) of product, m.p. 173–177 °C, and this was shown by thin-layer chromatography (t.l.c.) to be 90% pure. Repeated recrystallization from methylene chloride–ether gave pure 3α,24-dihydroxy-$\Delta^{9(11)}$-cholene (4), m.p. 178–180 °C and $[\alpha]_D^{22}$ +50.6° (*c*, 0.488, dioxane).

Anal. Calcd. for $C_{24}H_{40}O_2$: C, 79.94; H, 11.18; O, 8.88. Found: C, 79.86, 79.94; H, 11.18, 11.11; O, 9.05.

(b) By $NaBH_4$ Reduction of 3α-Hydroxy-$\Delta^{9(11)}$-12-oxocholenic Acid (2b) Followed by $AlCl_3$–$LiAlH_4$ Treatment

The steroid (**2***b*; 36.5 g) was dissolved in a solution of sodium hydroxide (4.2 g) in distilled water (185 ml). Sodium borohydride (8.9 g) was added, the mixture was stirred at 20° for 23 h, and the clear solution was then added dropwise to a stirred solution of concentrated sulfuric acid (10 ml) in water (300 ml). The resulting precipitate was filtered, washed with water, and vacuum-dried at 60° to give 35.4 g of crude 3α,12ξ-dihydroxy-$\Delta^{9(11)}$-cholenic acid (**3***a*), showing negligible absorption at 240 mμ.

This crude acid was methylated with ethereal diazomethane, and a solution of the methyl ester (**3***b*; 4.04 g; 0.01 mole) in ether (80 ml) was added dropwise with stirring to a reagent prepared from aluminium chloride (21.3 g; 0.16 mole) and lithium aluminium hydride (1.9 g; 0.05 mole) in ether (80 ml). The mixture was refluxed for 4 h, and the products were isolated in the manner described previously. Crystallization of the residue (3.59 g) from ether yielded 2.85 g (79%) of 3α,24-dihydroxy-$\Delta^{9(11)}$-cholene (**4**), m.p. 177–179°, identical on t.l.c. and mixture m.p. with an authentic sample.

For further identification this compound was acetylated with acetic anhydride – pyridine, and the residue was crystallized from methanol to provide 3α,24-diacetoxy-$\Delta^{9(11)}$-cholene, m.p. 89–91 °C and $[\alpha]_D^{27}$ +58.7° (*c*, 0.98, dioxane); reported (13), m.p. 87–88 °C and $[\alpha]_D^{25}$ +59° (dioxane).

3α-Ethoxycarbonyloxy-12-oxopregnane (7)

Application of the Huang–Minlon modification (14) of the Wolff–Kishner reduction to 3α,12α-dihydroxypregnan-20-one (**5**) gave, in nearly quantitative yield, 3α,12α-dihydroxypregnane (**6***a*). The latter compound (16 g) was dissolved in pyridine (50 ml), the solution was cooled by ice-water, and ethyl chloroformate (21.5 g) was added dropwise. The mixture was kept at 20° for 2 h, it was then diluted with water, acidified with dilute hydrochloric acid, and the products were extracted with ether. The solvent extract was washed with water, dried, and evaporated to a small volume to yield 11.2 g of material, m.p. 159–172 °C. Recrystallization from ether afforded 5.3 g of **6***b*, m.p. 174–176 °C. Examination of **6***b* by t.l.c. showed the presence of approximately 5% of a less polar contaminant.

A solution of 3α-ethoxycarbonyloxy-12α-hydroxypregnane (**6***b*; 4.1 g) in acetic acid (40 ml) was treated at 20° with a solution of chromic acid (1 g) in water (3 ml), acetic acid (15 ml), and sulfuric acid (0.2 ml). The addition took 20 min and, after stirring the mixture for 3 h, water was added slowly to precipitate the product. Filtration yielded 3.8 g of material, m.p. 90–93 °C. Recrystallization from methanol afforded large, prismatic needles of **7**, m.p. 107–109 °C and $[\alpha]_D^{25}$ +123.5° (*c*, 0.566, chloroform).

Anal. Calcd. for $C_{24}H_{38}O_4$: C, 73.80; H, 9.81. Found: C, 73.97, 74.03; H, 9.90, 9.80.

For further characterization, this ester was saponified with methanolic potassium hydroxide. The product was crystallized from aqueous methanol to yield 3α-hydroxy-12-oxopregnane, m.p. 127–128 °C and $[\alpha]_D^{25}$ +129.9° (*c*, 0.292, chloroform); reported (15) m.p. 129–130 °C.

Anal. Calcd. for $C_{21}H_{34}O_2$: C, 79.19; H, 10.76. Found: C, 79.43; H, 10.97.

3α-Ethoxycarbonyloxy-$\Delta^{9(11)}$-12-oxopregnene (8)

3α-Ethoxycarbonyloxy-12-oxopregnane (**7**; 3 g) was dissolved in glacial acetic acid (50 ml), selenium dioxide (1.5 g) was added, and the mixture was refluxed and stirred for 27 h. An additional 2 g of selenium dioxide was added in two portions during this time. The cooled mixture was filtered, the orange filtrate was diluted with water, and the resulting precipitate was collected, washed, and dried to give 2.63 g of product, m.p. 121–128 °C. Crystallization from methanol, with charcoaling, yielded a pure sample, m.p. 128–130 °C, $[\alpha]_D^{24}$ +122.8° (*c*, 0.235, chloroform), and λ_{max}(ethanol) 240.5 mμ (ε 13 300).

Anal. Calcd. for $C_{24}H_{36}O_4$: C, 74.19; H, 9.34. Found: C, 74.43, 74.33; H, 9.50, 9.48.

A small sample of the ester was saponified with methanolic potassium hydroxide, then isolated by crystallization from hexane–ether to give 3α-hydroxy-$\Delta^{9(11)}$-12-oxopregnene, m.p. 125 °C, $[\alpha]_D^{24}$ +125.3° (*c*, 0.399, chloroform), and λ_{max}(ethanol) 240.5 mμ (ε 12 500).

Anal. Calcd. for $C_{21}H_{32}O_2$: C, 79.70; H, 10.19. Found: C, 79.58, 79.62; H, 10.40, 10.36.

3α-Hydroxy-$\Delta^{9(11)}$-pregnene (9)

A solution of 3α-ethoxycarbonyloxy-$\Delta^{9(11)}$-12-oxopregnene (**8**; 1 g) in tetrahydrofuran (20 ml) was treated with a solution of sodium borohydride (0.3 g) in water (1.5 ml) and the mixture was refluxed for 5 h. After decomposition with very dilute sulfuric acid, the product was extracted with ether, and the solvent extract was washed, dried, and evaporated to give an amorphous residue (0.97 g).

A solution of this residue in ether (30 ml) was added dropwise to a reagent prepared from aluminium chloride (5.5 g) and lithium aluminium hydride (0.49 g) in ether (30 ml). After refluxing for 4 h, the cooled mixture was treated carefully with water followed by dilute sulfuric acid, the products were extracted with ether, and the solvent extract was washed, dried, and evaporated. The residue (750 mg) was crystallized from ether – isooctane to yield 580 mg (75%) of product with double m.p. 121–122° and 128–129° and $[\alpha]_D^{24}$ +45.5° (*c*, 0.364, chloroform).

Anal. Calcd. for $C_{21}H_{34}O$: C, 83.38; H, 11.33. Found: C, 83.41, 83.42; H, 11.32, 11.20.

1. J. BROOME and B. R. BROWN. Chem. Ind. (London), 1307 (1956).
2. O. H. WHEELER and J. L. MATEOS. Chem. Ind. (London), 395 (1957).

3. R. ALBRECHT and CH. TAMM. Helv. Chim. Acta, **40**, 2216 (1957).
4. A. J. BIRCH and M. SLAYTOR. Chem. Ind. (London), 1524 (1956).
5. J. BROOME, B. R. BROWN, A. ROBERTS, and A. M. S. WHITE. J. Chem. Soc. 1406 (1960).
6. J. H. BREWSTER and H. O. BAYER. J. Org. Chem. **29**, 105 (1964).
7. T. REICHSTEIN and M. SORKIN. Helv. Chim. Acta, **25**, 797 (1942).
8. T. F. GALLAGHER and W. P. LONG. J. Biol. Chem. **162**, 521 (1946).
9. B. F. MCKENZIE, W. F. MCGUCKIN, and E. C. KENDALL. J. Biol. Chem. **162**, 555 (1946).
10. E. SCHWENK and E. STAHL. Arch. Biochem. **14**, 125 (1947).
11. A. BOWERS, E. DENOT, M. B. SANCHEZ, F. NEUMAN, and C. DJERASSI. J. Chem. Soc. 1859 (1961).
12. E. SEEBECK and T. REICHSTEIN. Helv. Chim. Acta, **26**, 536 (1943).
13. L. F. FIESER and S. RAJAGOPALAN. J. Am. Chem. Soc. **73**, 118 (1951).
14. HUANG-MINLON. J. Am. Chem. Soc. **71**, 3301 (1949).
15. J. W. HUFFMAN, D. M. ALABRAN, T. W. BETHEA, and A. C. RUGGLES. J. Org. Chem. **29**, 2963 (1964).

Etude de configuration en série bicyclo[2·2·1] hepténique

G. M. BROWN ET P. DUBREUIL
Département de chimie, Université de Sherbrooke, Sherbrooke, Québec

Reçu le 4 décembre 1967

Deux réactions de Diels–Alder ont été étudiées: celle de l'anhydride maléique avec l'acétate de furfuryle et celle du même anhydride avec l'alcool furfurylique. La configuration des composés obtenus a été déterminée à l'aide de la résonance magnétique nucléaire comme étant *exo–cis*.

Canadian Journal of Chemistry, 46, 1577 (1968)

La condensation de l'acétate de furfuryle avec l'anhydride maléique a été faite pour la première fois en 1931 par Diels *et al.* (1). Toutefois aucune preuve de structure n'est donnée par ces chercheures ni par Bitler et Nicholl (2) dont le but est d'utiliser ce composé et ses dérivés comme plastifiants. Il a donc été décidé d'étudier la structure de ce produit d'addition Diels–Alder entre l'acétate de furfuryle et l'anhydride maléique au moyen de la résonance magnétique nucléaire.

Ce dérivé oxa-7 [2·2·1] hepténique **1** présente cinq absorptions sur le spectre de résonance magnétique nucéaire (r.m.n.) (Tableau I). Les absorptions des protons en 5 et 6 correspondent bien aux emplacements des pics d'absorption des mêmes protons du produit de condensation furanne – anhydride maléique (3). Le proton en tête de pont n'est couplé qu'avec le proton en position-5, donc il n'est pas couplé avec le proton en 3; ce qui prouve que les deux protons en 2 et 3 sont *endo*. Cette absence de couplage est bien connue; parmi un nombre considérable de travaux on peut citer quelques références (4–7). Il est facile d'identifier les autres bandes r.m.n. car en comparant le spectre de ce composé à celui du produit de condensation de l'alcool furfurylique et de l'anhydride maléique **2** (réaction connue (8)), il devient évident que la plus grande différence de glissement chimique est celle qui existe entre les bandes d'absorption de τ 5.35 (pour l'acétate) et de τ 6.09 (pour l'alcool). Cette bande d'absorption appartient aux méthylènes en position-1. Par conséquent les bandes à τ 6.49 (pour l'acétate) et à τ 6.64 (pour l'alcool) sont dues aux protons en 2 et 3. Les couplages sont typiques des protons *endo–endo* (9).

Il faut ajouter que certaines difficultés sont apparues lors de l'étude en r.m.n. de l'anhydride **2**. Car s'il est possible de prendre le spectre de cet anhydride à la température de la pièce, il se décompose en solution dans le diméthylsulfoxyde à la température de 60 °C et encore plus rapidement à 85 °C.

Shono et Hachihama, en préparant l'anhydride de l'acide hydroxyméthyl-1 oxa-7 bicyclo-[2·2·1]heptène-5 dicarboxylique-2,3 (**2**, 8), n'en donnèrent pas la configuration, ce produit instable n'étant pas l'objet de leurs recherches. Plus récemment Yuldashev et Tsukervanik (10) firent la condensation de l'alcool furfurylique avec l'anhydride maléique et affirmèrent que l'addition donnait un produit "endoxo". La réduction et du dérivé acétylé **1** et du dérivé hydroxylé **2** démontre que les deux composés possèdent la même configuration, car elle donne un produit unique **3**. Le spectre de ce triol **3** est trés compliqué (Tableau I).

Can. J. Chem. Downloaded from www.nrcresearchpress.com by 210.87.254.40 on 09/05/12
For personal use only.

3. R. ALBRECHT and CH. TAMM. Helv. Chim. Acta, **40**, 2216 (1957).
4. A. J. BIRCH and M. SLAYTOR. Chem. Ind. (London), 1524 (1956).
5. J. BROOME, B. R. BROWN, A. ROBERTS, and A. M. S. WHITE. J. Chem. Soc. 1406 (1960).
6. J. H. BREWSTER and H. O. BAYER. J. Org. Chem. **29**, 105 (1964).
7. T. REICHSTEIN and M. SORKIN. Helv. Chim. Acta, **25**, 797 (1942).
8. T. F. GALLAGHER and W. P. LONG. J. Biol. Chem. **162**, 521 (1946).
9. B. F. MCKENZIE, W. F. MCGUCKIN, and E. C. KENDALL. J. Biol. Chem. **162**, 555 (1946).
10. E. SCHWENK and E. STAHL. Arch. Biochem. **14**, 125 (1947).
11. A. BOWERS, E. DENOT, M. B. SANCHEZ, F. NEUMAN, and C. DJERASSI. J. Chem. Soc. 1859 (1961).
12. E. SEEBECK and T. REICHSTEIN. Helv. Chim. Acta, **26**, 536 (1943).
13. L. F. FIESER and S. RAJAGOPALAN. J. Am. Chem. Soc. **73**, 118 (1951).
14. HUANG-MINLON. J. Am. Chem. Soc. **71**, 3301 (1949).
15. J. W. HUFFMAN, D. M. ALABRAN, T. W. BETHEA, and A. C. RUGGLES. J. Org. Chem. **29**, 2963 (1964).

Etude de configuration en série bicyclo[2·2·1] hepténique

G. M. BROWN ET P. DUBREUIL
Département de chimie, Université de Sherbrooke, Sherbrooke, Québec

Reçu le 4 décembre 1967

Deux réactions de Diels–Alder ont été étudiées: celle de l'anhydride maléique avec l'acétate de furfuryle et celle du même anhydride avec l'alcool furfurylique. La configuration des composés obtenus a été déterminée à l'aide de la résonance magnétique nucléaire comme étant *exo–cis*.

Canadian Journal of Chemistry, 46, 1577 (1968)

La condensation de l'acétate de furfuryle avec l'anhydride maléique a été faite pour la première fois en 1931 par Diels *et al.* (1). Toutefois aucune preuve de structure n'est donnée par ces chercheures ni par Bitler et Nicholl (2) dont le but est d'utiliser ce composé et ses dérivés comme plastifiants. Il a donc été décidé d'étudier la structure de ce produit d'addition Diels–Alder entre l'acétate de furfuryle et l'anhydride maléique au moyen de la résonance magnétique nucléaire.

Ce dérivé oxa-7 [2·2·1] hepténique **1** présente cinq absorptions sur le spectre de résonance magnétique nucéaire (r.m.n.) (Tableau I). Les absorptions des protons en 5 et 6 correspondent bien aux emplacements des pics d'absorption des mêmes protons du produit de condensation furanne – anhydride maléique (3). Le proton en tête de pont n'est couplé qu'avec le proton en position-5, donc il n'est pas couplé avec le proton en 3; ce qui prouve que les deux protons en 2 et 3 sont *endo*. Cette absence de couplage est bien connue; parmi un nombre considérable de travaux on peut citer quelques références (4–7). Il est facile d'identifier les autres bandes r.m.n. car en comparant le spectre de ce composé à celui du produit de condensation de l'alcool furfurylique et de l'anhydride maléique **2** (réaction connue (8)), il devient évident que la plus grande différence de glissement chimique est celle qui existe entre les bandes d'absorption de τ 5.35 (pour l'acétate) et de τ 6.09 (pour l'alcool). Cette bande d'absorption appartient aux méthylènes en position-1. Par conséquent les bandes à τ 6.49 (pour l'acétate) et à τ 6.64 (pour l'alcool) sont dues aux protons en 2 et 3. Les couplages sont typiques des protons *endo–endo* (9).

Il faut ajouter que certaines difficultés sont apparues lors de l'étude en r.m.n. de l'anhydride **2**. Car s'il est possible de prendre le spectre de cet anhydride à la température de la pièce, il se décompose en solution dans le diméthylsulfoxyde à la température de 60 °C et encore plus rapidement à 85 °C.

Shono et Hachihama, en préparant l'anhydride de l'acide hydroxyméthyl-1 oxa-7 bicyclo-[2·2·1]heptène-5 dicarboxylique-2,3 (**2**, 8), n'en donnèrent pas la configuration, ce produit instable n'étant pas l'objet de leurs recherches. Plus récemment Yuldashev et Tsukervanik (10) firent la condensation de l'alcool furfurylique avec l'anhydride maléique et affirmèrent que l'addition donnait un produit "endoxo". La réduction et du dérivé acétylé **1** et du dérivé hydroxylé **2** démontre que les deux composés possèdent la même configuration, car elle donne un produit unique **3**. Le spectre de ce triol **3** est trés compliqué (Tableau I).

Can. J. Chem. Downloaded from www.nrcresearchpress.com by 210.87.254.42 on 09/05/12
For personal use only.

TABLEAU I

Valeurs de glissement chimique (τ) et de constantes de couplage (J, c.p.s.)

Composé	H-5	H-6	H-4	H-2,H-3	CH_2 en 1
1† 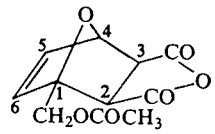	3.30 (q)* $J_{5,6} = 5.8$ $J_{4,5} = 1.6$	3.45 (d) $J_{6,5} = 5.6$	4.64 (d) $J_{4,5} = 1.6$	6.49 (q)* $J = 6.8$	5.35 (q)* $J = 12.5$
2‡ 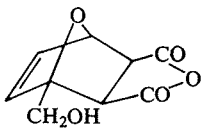	3.47 (s)	3.47 (s)	4.73 (s)	6.64 (q)* $J = 6.0$	6.09 (q)* $J = 12.0$
3§ 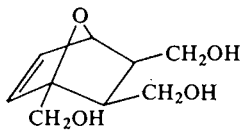	3.47 (s)	3.62 (s)	5.19 (s)	7.97 (q)* $J = 5.0$	6.00 (q)* $J = 12.2$
4† 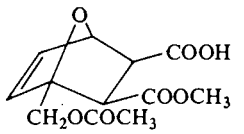	3.38 (q)* $J_{5,6} = 5.8$ $J_{4,5} = 1.6$	3.55 (d) $J_{5,6} = 5.8$	4.67 (d) $J_{4,5} = 1.6$	7.02 (s)	5.44 (q)* $J = 10.8$
5† 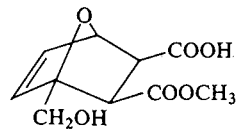	3.54 (s)	3.54 (s)	4.77 (s)	7.10 (s)	6.04 (s)

*q = quadruplet.
†Solvant: CD_3COCD_3.
‡Solvant: CD_3SOCD_3.
§Solvant: D_2O.

La réaction de l'anhydride **1** avec le méthanol donne, même s'il y a beaucoup de décomposition, un diester monoacide **4** dont l'emplacement des bandes d'absorption en spectroscopie r.m.n. dans l'acetone-d_6 est rapporté dans le Tableau I. Le pic du proton acide apparaît à $\tau - 1.81$ dans la pyridine.

Dans ce composé, le groupement acide et le groupement ester pourraient être aussi bien l'un et l'autre en position-2 ou en position-3.

Si la fonction acide de notre produit est en position-2, le départ de l'acétyle en milieu alcalin et puis l'acidification devrait donner lieu à cette lactone dont la formation semble assez facile selon les modèles moléculaires.

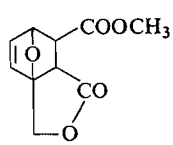

Mais aprés hydrolyse partielle, le produit obtenu ne possède pas de fonction lactone dans l'infrarouge. La possibilité de la formation de la lactone, laquelle s'hydrolyse par la suite, n'est pas exclue mais nous semble peu probable dans ces conditions. Nous favorisons donc la structure **4** pour le monoester.

Dans le Tableau I, il est montré que les composés **4** et **5** possèdent tous les deux la configuration *exo*; fait toujours basé sur l'absence de couplage entre le proton en 4 et le proton en 3.

Partie expérimentale

Les points de fusion ont été déterminés à l'aide de la plaque chauffante Fisher–Johns et ne sont pas corrigés. Les spectres de résonance magnétique nucléaire ont été pris sur l'appareil Varian A-60 à des concentrations variant de 10 à 15%. Les microanalyses ont été effectuées par le laboratoire de microanalyse Schwarzkopf à Woodside, New York.

Can. J. Chem. Downloaded from www.nrcresearchpress.com by 210.87.254.42 on 09/05/12
For personal use only.

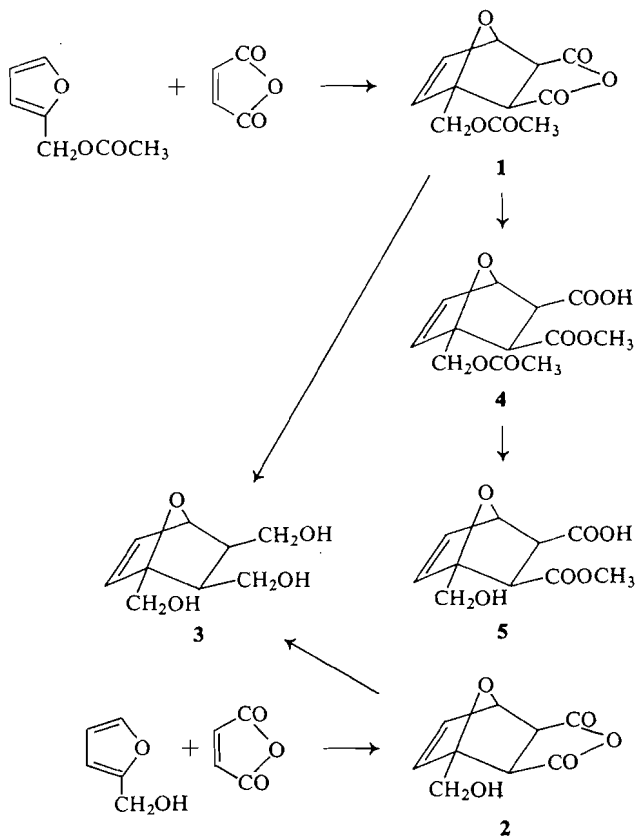

Anhydride de l'acide exo–cis acétoxyméthyl-1 oxa-7 bicyclo [2·2·1]heptène-5 dicarboxylique-2,3 (1)

Ce produit fut préparé par la méthode de Bitler et Nicholl (2), f = 114–115 °C; litt. f = 114 °C (1). Rendement: 75%; infrarouge (CH_2Cl_2) en cm^{-1}: 1859 et 1786 (carbonyles de l'anhydride), 1748 (carbonyle de l'ester).

Anhydride de l'acide exo–cis hydroxyméthyl-1 oxa-7 bicyclo[2·2·1]heptène-5 dicarboxylique-2,3 (2)

Même mode opératoire que pour le composé **1**, f = 88–89° (acétonitrile); litt. f = 82–83 °C (11) et f = 80 °C (10). Rendement: 82%; infrarouge ($CHCl_3$) en cm^{-1}: 1855 et 1779 (carbonyles de l'anhydride).

Exo–cis trihydroxyméthyl-1,2,3 oxa-7 bicyclo[2·2·1]-heptène-5 (3)

(a) Réduction de l'anhydride 1

Une solution de l'anhydride **1** (6.4 g, 0.03 mole) dans 30 ml de tétrahydrofuranne sec fut ajoutée lentement a une suspension de $LiAlH_4$ (4.0 g, 0.10 mole) dans 50 ml de tétrahydrofuranne sec. Le mélange fut agité 4 h à la température de la pièce. L'exces d'hydrure fut détruit par un peu d'eau et la suspension hydrolysée par une solution de tartrate de K et de Na à 20%. La solution tètrahydrofurannique fut séchée sur $MgSO_4$, puis le solvant fut chassé et le produit recristallisé dans le méthanol, f = 151–152 °C. Rendement: 3.0 g, (60%); infrarouge (acétonitrile) en cm^{-1}: 3610 (hydroxyles).

Anal. Calc. pour $C_9H_{14}O_4$: C, 58.05; H, 7.58. Trouvé: C, 57.67; H, 7.54.

(b) Réduction de l'anhydride 2

La réduction de cet anhydride (5.0 g, 0.025 mole) par $LiAlH_4$ (2.5 g, 0.06 mole) dans le tétrahydrofuranne fut faite selon (*a*). 3.0 g (64%) du produit de réduction fondant à 151–152 °C (méthanol) furent obtenus. Le point de fusion mixte des produits des réductions (*a*) et (*b*) n'est pas abaissé.

Acide exo–cis acétoxyméthyl-1 carbométhoxy-2 oxa-7 bicyclo[2·2·1]heptène-5 carboxylique-3 (4)

L'anhydride **1** (21.0 g, 0.09 mole) fut chauffé dans 200 ml de méthanol pendant 7 h, après quoi le méthanol fut chassé sous vide et le résidu mis au froid. Le produit est repris par le chloroforme, f = 121–122 °C, Rendement: 2.4 g, (10%), infrarouge ($CHCl_3$) en cm^{-1}: 1742 (carbonyle d'ester) et 1715 (carbonyle d'acide).

Anal. Calc. pour $C_{12}H_{14}O_7$: C, 53.33; H, 5.22. Trouvé: C, 53.63; H, 5.37.

Acide exo–cis carbométhoxy-2 hydroxyméthyl-1 oxa-7 bicyclo[2·2·1]heptène-5 carboxylique-3 (5)

Le diester monoacide **4** (2.2 g, 0.008 mole) dans 100 ml de méthanol fut ajouté à une solution de K_2CO_3 (13.3 g) dans 120 ml d'eau. Ce mélange fut agité pendant 1h à la température de la pièce. Le méthanol fut chassé, la solution fut acidifiée jusqu'à pH 3 par HCl dilué, puis le volume de la solution fut réduit à 25 ml sous vide. La

Can. J. Chem. Downloaded from www.nrcresearchpress.com by 210.87.254.42 on 09/05/12
For personal use only.

solution aqueuse fut extraite à l'acètate d'éthyle. Cette solution fut séchée sur $MgSO_4$, puis le solvant fut chassé sous vide. 300 mg (16%) d'un produit fondant à 118–120 °C (acétate d'éthyle-éther de pétrole) furent obtenus. Après deux recristallisations dans l'acétate d'éthyle, f = 119.5–120 °C, infrarouge (pastille de KBr) en cm^{-1}: 1742 (carbonyle de l'ester) et 1675 (carbonyle de l'acide).

Anal. Calc. pour $C_{10}H_{12}O_6$: C, 52.63: H, 5.30. Trouvé: C, 52.78; H, 5.59.

Remerciements

Nous remercions Monsieur J. R. Martin de l'Université de Sherbrooke d'avoir bien voulu faire les spectres de résonance magnétique nucléaire.

Nous exprimons également notre gratitude envers le Conseil National de Recherches d'avoir accordé un octroi (G.M.B.) et envers la Ministère de l'Education du Gouvernement du Quèbec pour une bourse (P.D.).

1. O. Diels, K. Alder, H. Nienburg et O. Schmalbeck. Ann. Chem. **490**, 243 (1931).
2. W. P. Bitler et L. Nicholl. U.S. Patent No. 2, 406, 657 (27 août 1946).
3. F. A. L. Anet. Tretrahedron Letters, 1219 (1962).
4. J. Meinwald, Y. C. Meinwald et T. N. Baker. J. Am. Chem. Soc. **85**, 2513 (1963).
5. J. Meinwald et Y. C. Meinwald. J. Am. Chem. Soc. **85**, 2514 (1963).
6. P. Laszlo et P. Schleyer. J. Am. Chem. Soc. **86**, 1171 (1964).
7. L. A. Paquette. J. Org. Chem. **30**, 629 (1965).
8. T. Shono et Y. Hachihama. Kogyo Kagaku Zasshi, **56**, 259 (1953).
9. D. Gagnaire et E. Payo-Subiza. Bull. Soc. Chim. France, 2627 (1963)
10. Kh. Yu. Yuldashev et I. P. Tsukervanik. Uzbeksk. Khim. Zh. **9**, 27 (1965).
11. Y. Hachihama et T. Shono. Technol. Rept. Osaka Univ. **5**, 479 (1955).

Reaction of 3-*O*-*p*-bromophenylsulfonyl-1,2:5,6-di-*O*-isopropylidene-α-D-glucofuranose with dimethylamine[1]

Derek Horton, Jon S. Jewell, and H. S. Prihar
Department of Chemistry, The Ohio State University, Columbus, Ohio 43210

Received February 28, 1967

The *p*-bromobenzenesulfonate (**3**) of 1,2:5,6-di-*O*-isopropylidene-α-D-glucofuranose (**4**) reacts with dimethylamine by aromatic nucleophilic substitution to give the *p*-dimethylaminobenzenesulfonate (**5**) of (**4**), rather than by attack at C-3 of the sugar moiety.

Canadian Journal of Chemistry, 46, 1580 (1968)

As part of a program in this laboratory concerning the synthesis of amino sugars and dimethylamino sugars related to antibiotics (1), it was of interest to study the feasibility of displacements at C-3 by dimethylamine with various sulfonic esters of 1,2:5,6-di-*O*-isopropylidene-α-D-gluco(and D-allo)furanose. The *p*-tolylsulfonyloxy group in 1,2:5,6-di-*O*-isopropylidene-3-*O*-*p*-tolylsulfonyl-α-D-glucofuranose (**1**) (2) is very resistant to displacement by nucleophiles (3–6) with the exception of hydrazine (4–8), although displacements in the D-*allo* analogue of **1** are relatively facile (9). The supposedly better leaving-group characteristics (10) of the 3-substituent in the 3-*p*-nitrobenzenesulfonate analogue (**2**) of **1** did not facilitate displacement at C-3 by ammonia; the reaction gave mostly black tar (6).

The present report records the reaction of dimethylamine with the *p*-bromobenzenesulfonate (**3**) of 1,2:5,6-di-*O*-isopropylidene-α-D-glucofuranose (**4**) for 24 h at 160°; it is observed that the nucleophile attacks **3**, not at C-3, but on the aromatic system, to replace the bromine atom by the dimethylamino group and give 3-*O*-(*p*-dimethylaminophenylsulfonyl)-1,2:5,6-di-*O*-isopropylidene-α-D-glucofuranose (**5**), isolated crystalline in 42% yield. The product was characterized by elemental analysis, by the similarity of the nuclear magnetic resonance (n.m.r.) parameters (Table II) of the sugar moiety of **5**

[1]Supported, in part, by funds from the United States National Institutes of Health, Public Health Service, Department of Health, Education, and Welfare, Bethesda, Maryland under Grant GM-11976-02 (The Ohio State University Research Foundation Project 1820). Funds for the purchase of the nuclear magnetic resonance spectrometer were provided by the National Science Foundation, Washington, D.C.

Can. J. Chem. Downloaded from www.nrcresearchpress.com by 210.87.254.42 on 09/05/12
For personal use only.

solution aqueuse fut extraite à l'acètate d'éthyle. Cette solution fut séchée sur $MgSO_4$, puis le solvant fut chassé sous vide. 300 mg (16%) d'un produit fondant à 118–120 °C (acétate d'éthyle-éther de pétrole) furent obtenus. Après deux recristallisations dans l'acétate d'éthyle, f = 119.5–120 °C, infrarouge (pastille de KBr) en cm^{-1}: 1742 (carbonyle de l'ester) et 1675 (carbonyle de l'acide).

Anal. Calc. pour $C_{10}H_{12}O_6$: C, 52.63: H, 5.30. Trouvé: C, 52.78; H, 5.59.

Remerciements

Nous remercions Monsieur J. R. Martin de l'Université de Sherbrooke d'avoir bien voulu faire les spectres de résonance magnétique nucléaire.

Nous exprimons également notre gratitude envers le Conseil National de Recherches d'avoir accordé un octroi (G.M.B.) et envers la Ministère de l'Education du Gouvernement du Quèbec pour une bourse (P.D.).

1. O. Diels, K. Alder, H. Nienburg et O. Schmalbeck. Ann. Chem. **490**, 243 (1931).
2. W. P. Bitler et L. Nicholl. U.S. Patent No. 2, 406, 657 (27 août 1946).
3. F. A. L. Anet. Tretrahedron Letters, 1219 (1962).
4. J. Meinwald, Y. C. Meinwald et T. N. Baker. J. Am. Chem. Soc. **85**, 2513 (1963).
5. J. Meinwald et Y. C. Meinwald. J. Am. Chem. Soc. **85**, 2514 (1963).
6. P. Laszlo et P. Schleyer. J. Am. Chem. Soc. **86**, 1171 (1964).
7. L. A. Paquette. J. Org. Chem. **30**, 629 (1965).
8. T. Shono et Y. Hachihama. Kogyo Kagaku Zasshi, **56**, 259 (1953).
9. D. Gagnaire et E. Payo-Subiza. Bull. Soc. Chim. France, 2627 (1963)
10. Kh. Yu. Yuldashev et I. P. Tsukervanik. Uzbeksk. Khim. Zh. **9**, 27 (1965).
11. Y. Hachihama et T. Shono. Technol. Rept. Osaka Univ. **5**, 479 (1955).

Reaction of 3-*O*-*p*-bromophenylsulfonyl-1,2:5,6-di-*O*-isopropylidene-α-D-glucofuranose with dimethylamine[1]

Derek Horton, Jon S. Jewell, and H. S. Prihar
Department of Chemistry, The Ohio State University, Columbus, Ohio 43210

Received February 28, 1967

The *p*-bromobenzenesulfonate (**3**) of 1,2:5,6-di-*O*-isopropylidene-α-D-glucofuranose (**4**) reacts with dimethylamine by aromatic nucleophilic substitution to give the *p*-dimethylaminobenzenesulfonate (**5**) of (**4**), rather than by attack at C-3 of the sugar moiety.

Canadian Journal of Chemistry, 46, 1580 (1968)

As part of a program in this laboratory concerning the synthesis of amino sugars and dimethylamino sugars related to antibiotics (1), it was of interest to study the feasibility of displacements at C-3 by dimethylamine with various sulfonic esters of 1,2:5,6-di-*O*-isopropylidene-α-D-gluco(and D-allo)furanose. The *p*-tolylsulfonyloxy group in 1,2:5,6-di-*O*-isopropylidene-3-*O*-*p*-tolylsulfonyl-α-D-glucofuranose (**1**) (2) is very resistant to displacement by nucleophiles (3–6) with the exception of hydrazine (4–8), although displacements in the D-*allo* analogue of **1** are relatively facile (9). The supposedly better leaving-group characteristics (10) of the 3-substituent in the 3-*p*-nitrobenzenesulfonate analogue (**2**) of **1** did not facilitate displacement at C-3 by ammonia; the reaction gave mostly black tar (6).

The present report records the reaction of dimethylamine with the *p*-bromobenzenesulfonate (**3**) of 1,2:5,6-di-*O*-isopropylidene-α-D-glucofuranose (**4**) for 24 h at 160°; it is observed that the nucleophile attacks **3**, not at C-3, but on the aromatic system, to replace the bromine atom by the dimethylamino group and give 3-*O*-(*p*-dimethylaminophenylsulfonyl)-1,2:5,6-di-*O*-isopropylidene-α-D-glucofuranose (**5**), isolated crystalline in 42% yield. The product was characterized by elemental analysis, by the similarity of the nuclear magnetic resonance (n.m.r.) parameters (Table II) of the sugar moiety of **5**

[1]Supported, in part, by funds from the United States National Institutes of Health, Public Health Service, Department of Health, Education, and Welfare, Bethesda, Maryland under Grant GM-11976-02 (The Ohio State University Research Foundation Project 1820). Funds for the purchase of the nuclear magnetic resonance spectrometer were provided by the National Science Foundation, Washington, D.C.

Can. J. Chem. Downloaded from www.nrcresearchpress.com by 210.87.254.5 on 09/05/12
For personal use only.

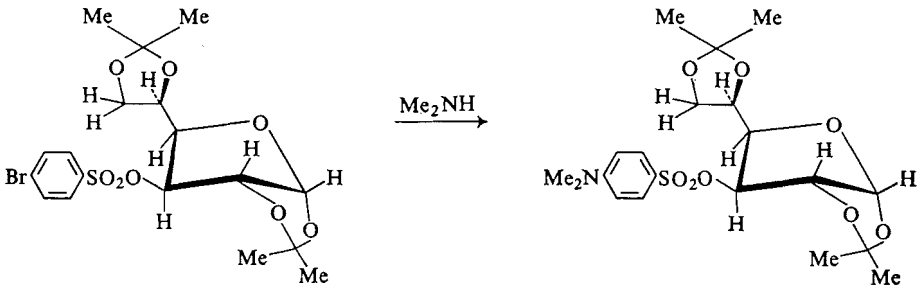

3 5

with those of **1**, **3**, and the 3-*O*-(methylsulfonyl) (**6**) (11) and 3-*O*-(phenylsulfonyl) (**7**) derivatives of (**4**), and by the fact that the aryl protons of **5** gave a 4-proton A_2X_2 system (12) in the n.m.r. spectrum. Details of characterization of the sulfonic esters are given in Table I and in the Experimental section.

At least five possible modes of attack of a nucleophile on **3** can be postulated; abstraction of H-4 (or, conceivably H-2) leading to elimination; rearside attack on C-3 leading to displacement of the sulfonyloxy group; attack on sulfur leading to formation of **4**; or displacement of bromine by aromatic nucleophilic substitution. The fact that the last of these processes was observed as a major pathway in the reaction of **3** with dimethylamine further illustrates the hindrance to rearside (*endo*) attack at C-3 in this bicyclo[3·3·0]system, and indicates that the use of a good leaving group, such as *p*-bromobenzenesulfonate, does not facilitate the displacement at C-3 to a degree suitable for preparative purposes.

Experimental

Melting points were determined with a Hershberg type of apparatus and are uncorrected. Specific rotations were determined in a 2-dm polarimeter tube. Infrared spectra were measured with a Perkin–Elmer model 137 "Infracord" infrared spectrometer. Nuclear magnetic resonance (n.m.r.) spectra were measured at 60 MHz with a Varian A-60 n.m.r. spectrometer. Chemical shifts are given on the τ-scale and all spectra were measured at ~40° with solutions (~10%) in chloroform-*d*, with tetramethylsilane (τ = 10.00) as the internal standard. Spectra were analyzed on a first-order basis, and the *J* values recorded are the measured peak spacings. The width at half-height is denoted by $w_{\frac{1}{2}}$. Microanalyses were determined by W. N. Rond. Thin-layer chromatography was performed with Silica Gel G (E. Merck, Darmstadt, Germany) on plates activated at 110°. The developing solvent was 3:1 chloroform–ether and indication was effected with sulfuric acid.

Preparation of Sulfonic Esters of 1,2:5,6-Di-O-isopropylidene-α-D-glucofuranose

A solution of 1,2:5,6-di-*O*-isopropylidene-α-D-glucofuranose (**4**, 26.0 g, 0.100 mole) in dry pyridine (50 ml) was treated, with cooling, with the appropriate sulfonyl chloride (0.110 mole) and the solution was kept at 25°. Separation of pyridinium chloride was observed (sulfonyl chloride and the time of reaction when pyridinium chloride began to separate is given): methanesulfonyl chloride; 2 min; *p*-nitrobenzenesulfonyl chloride; 10 min; *p*-bromobenzenesulfonyl chloride; 60 min; benzenesulfonyl chloride; 120 min; *p*-toluenesulfonyl chloride; 120 min. The products were isolated after 18, 24, 48, 48, and 48 h, respectively, by adding 20 ml of water with cooling to the reaction mixture. This was followed by a further 350 ml of water 15 min later. Substances **1**, **3**, **6**, and **7** crystallized on trituration and were filtered,

TABLE I

Characterization data for 3-sulfonic esters of 1,2:5,6-di-*O*-isopropylidene-α-D-glucofuranose

Ester	Melting point °C	$[\alpha]_D^{24°}$ (*c*, 1; $CHCl_3$)	R_f	Analytical data C	H	Br	S
p-Bromophenylsulfonyl* (**3**)	149–150	−79.7±0.6	0.95	45.07	4.80	16.97	6.58
Methylsulfonyl† (**6**)	80–82	−49 ±1	0.80				
p-Nitrophenylsulfonyl‡ (**2**)	109–111	−78 ±0.6					
Phenylsulfonyl§ (**7**)	150–152	−78.5±0.9	0.85	54.21	6.39		8.19
p-Tolylsulfonyl‖ (**1**)	122.5–123.5	−71.8±0.6	0.88				

*Calcd. for $C_{18}H_{23}BrO_8S$: C, 45.09; H, 4.84; Br, 16.63; S, 6.70.
†Lit. (11) m.p. 83–84°, $[\alpha]_D$ −50° (chloroform).
‡Lit. (6) m.p. 110°, $[\alpha]_D$ −81.2° (chloroform).
§Calcd. for $C_{18}H_{24}O_8S$: C, 53.98; H, 6.05; S, 8.00.
‖Lit. (2) m.p. 120–121°, $[\alpha]_D$ −81.7° (1,1,2,2-tetrachloroethane).

Can. J. Chem. Downloaded from www.nrcresearchpress.com by 210.87.254.5 on 09/05/12
For personal use only.

TABLE II

Nuclear magnetic resonance spectral data for 3-sulfonic esters of 1,2:5,6-di-*O*-isopropylidene-α-D-glucofuranose

Ester	Chemical shifts (τ)				
	H-1($J_{1,2}$, Hz)	H-2* H-3	H-4, 5, 6, 6′	CMe_2	Aryl
p-Bromophenylsulfonyl (**3**)	4.09 (3.5)	5.13–5.27	5.92–6.19	8.51, 8.69, 8.79, 8.84	2.05–2.42
p-Dimethylaminophenylsulfonyl† (**5**)	4.11 (3.8)	5.16–5.30	5.80–6.18	8.52, 8.69, 8.76, 8.78	2.30, 3.35‡
Methylsulfonyl§ (**6**)	4.07 (3.7)	5.25 5.03‖	5.73–6.11	8.51, 8.59, 8.68, 8.68	
Phenylsulfonyl (**7**)	4.10 (3.7)	5.12–5.26	5.88–6.21	8.52, 8.70, 8.81, 8.87	1.95–2.54
p-Tolylsulfonyl** (**1**)	4.11 (3.5)	~5.21	5.90–6.22	8.54, 8.70, 8.80, 8.84	2.18, 2.65††

*In each example $J_{2,3}$ was ~0 Hz.
†6-Proton singlet (NMe_2) at τ 6.95.
‡Two 2-proton doublets, broadened at base, A_2X_2 system, $J_{A,X}$ = 9 Hz.
§3-Proton singlet ($MeSO_2$) at τ 6.91.
‖Multiplet, $w_{\frac{1}{2}}$ 4 Hz.
Nuclear magnetic resonance data for **1 in acetone solution have been reported in ref. 13.
††Two 2-proton doublets, broadened at base, A_2X_2 system, $J_{A,X}$ = 8 Hz; a 3-proton singlet (Me of Ts) is observed at τ 7.58.

washed well with water, dried, and recrystallized from methanol. Substance **2** did not crystallize directly, and was extracted with 1,2-dichloroethane. The extract was washed at 0° with *N* sulfuric acid, and then with aqueous sodium hydrogen carbonate. The dried (magnesium sulfate) extract was evaporated and the product was crystallized from the minimum volume of boiling methanol. The relative solubilities of the five compounds in methanol was **6** > **2** > **1** > **7** > **3**. The yields of once-recrystallized product were: **1**, 32 g (78%); **2**, 34 g (77%); **3**, 36 g (75%); **6**, 25 g (77%); **7**, 27 g (68%). Additional crops of each compound could be obtained by concentrating the mother liquors and adding water to incipient turbidity. Details of characterization of **1**, **2**, **3**, **6**, and **7** are given in Table I, and Table II gives n.m.r. spectral data for **1**, **3**, **6**, and **7**.

The *p*-nitrobenzenesulfonate **2** was not stable on storage. Even after careful recrystallization it darkened, liquified, and eventually gave a black tar having the odor of acetone, when kept at room temperature for a period of 30 days. The *p*-bromobenzenesulfonate **3** darkened slowly over a period of several months. Carefully recrystallized samples of the methanesulfonate **6**, benzenesulfonate **7**, and *p*-toluenesulfonate **1** appeared stable on prolonged storage, but slow decomposition took place if small proportions of impurities were present.

3-O-(p-Dimethylaminophenylsulfonyl)-1,2:5,6-di-O-isopropylidene-α-D-glucofuranose (5)

A mixture of **3** (5 g) and dimethylamine (10 g) was heated in a steel bomb for 24 h at 160°. The resultant mixture was evaporated, crystallized from propyl alcohol, and recrystallized from chloroform to give **5**, yield 1.94 g (42%), m.p. 132°, $[\alpha]_D^{23}$ −71° (*c*, 0.8, chloroform), R_f 0.78; λ_{max} (KBr) 6.23, 6.62 (aryl C=C), 7.28 (sulfonate, CMe_2), 8.60 μm (sulfonate). The n.m.r. data are given in Table II.

Anal. Calcd for $C_{20}H_{29}NO_8S$: C, 54.16; H, 6.59; N, 3.16; S, 7.23. Found: C, 53.93; H, 6.77; N, 3.03; S, 7.34.

Thin-layer chromatography of the uncrystallized portion of the reaction product revealed the presence of a major component having the mobility of **5**, together with at least four other components. The syrup rapidly decolorized bromine in carbon tetrachloride, suggesting that 3-deoxy-1,2:5,6-di-*O*-isopropylidene-α-D-*erythro*-hex-3-enofuranose (3) was present.

Acknowledgment

The authors thank Dr. J. L. Godman for some of the nuclear magnetic resonance spectral measurements.

1. A. E. El-Ashmawy and D. Horton. Carbohydrate Res. **1**, 164 (1965); **3**, 191 (1967). D. Horton and J. S. Jewell. Carbohydrate Res. **3**, 255 (1967).
2. K. Freudenberg and O. Ivers. Ber. **55**, 929 (1922).
3. K. Freudenberg and F. Brauns. Ber. **55**, 3233 (1922).
4. M. L. Wolfrom, J. Bernsmann, and D. Horton. J. Org. Chem. **27**, 4505 (1962).
5. K. Freudenberg, O. Burkhart, and E. Braun. Ber. **59**, 714 (1926).
6. B. Coxon and L. Hough. J. Chem. Soc. 1643 (1961).
7. R. U. Lemieux and P. Chu. J. Am. Chem. Soc. **80**, 4745 (1958).
8. M. L. Wolfrom, F. Shafizadeh, and R. K. Armstrong. J. Am. Chem. Soc. **80**, 4885 (1958). M. L. Wolfrom, F. Shafizadeh, R. K. Armstrong, and T. M. Shen Han. J. Am. Chem. Soc. **80**, 3716 (1959).
9. K. W. Buck, A. B. Foster, R. Hems, and J. M. Webber. Carbohydrate Res. **3**, 137 (1966).
10. M. S. Morgan and L. H. Cretcher. J. Am. Chem. Soc. **70**, 375 (1948).
11. B. Helferich, H. Dressler, and R. Griebel. J. Prakt. Chem. [2] **153**, 285 (1939).
12. J. A. Pople, W. G. Schneider, and H. J. Bernstein. High-resolution nuclear magnetic resonance. McGraw-Hill Book Co., Inc., New York. 1959.
13. R. J. Abraham, L. D. Hall, L. Hough, and K. A. McLauchlan. J. Chem. Soc. 3699 (1962).

Can. J. Chem. Downloaded from www.nrcresearchpress.com by 210.87.254.5 on 09/05/12
For personal use only.

Thermal and photolytic decomposition reactions of diazo compounds in the bicyclo[4·1·0]heptane series[1,2]

IAN W. J. STILL AND D. T. WANG
Department of Chemistry, University of Toronto, Toronto 5, Ontario

Received December 1, 1967

The photochemical and thermal decomposition reactions of 5-diazo-3-caren-2-one have been studied. Thermal decomposition led to the corresponding azine (93%), while photochemical decomposition in aqueous dioxan led to the azine (7%) and to 3-carene-2,5-dione (9%). Photochemical decomposition in methanol led to a third product $C_{20}H_{24}O_4$ (3%). Experiments on the photochemical decomposition of the isomeric 2-diazo-3-caren-5-one are also described.

Canadian Journal of Chemistry, 46, 1583 (1968)

Can. J. Chem. Downloaded from www.nrcresearchpress.com by 210.87.254.105 on 09/05/12
For personal use only.

The thermal and photolytic decomposition reactions of α-diazoketones have been studied extensively (1–3). In many cases the reaction proceeds by loss of nitrogen followed by Wolff rearrangement of the presumed carbenoid intermediate. We felt that it would be of some interest to investigate a diazoketone in which rearrangement was precluded by the molecular structure and in which the diazo group is γ- to the α,β-unsaturated carbonyl function.

The compound we chose for our initial study was 5-diazo-3-caren-2-one (**1**)[3] which could be prepared in 67% yield from 3-carene-2,5-dione-5-oxime (**2**) (4), using the modification of the Forster (6) reaction with chloramine, as described by Cava *et al.* (5). The diazoketone is a reddish violet solid, m.p. approximately 40° (decomp.), with very intense bands in the infrared at 4.88 and 6.01μ and a maximum in the ultraviolet at 378 mμ (ε 16 000) in methanol, and at 350 mμ (ε 17 000) in *n*-hexane. The nuclear magnetic resonance (n.m.r.) spectrum revealed signals at τ 3.22, 7.95, 8.22, 8.69, and 8.91. Exact integration was not possible since the diazoketone was decomposed by attempts at purification.

When the diazoketone (**1**) was heated at 40° under nitrogen, in the absence of solvent and in the dark, it was converted to a high-melting orange solid in 93% yield. This compound was found to have the molecular formula $C_{20}H_{24}N_2O_2$, on the basis of mass spectral and elemental analysis. The azine structure (**3**) was indicated by its infrared, ultraviolet, and n.m.r. spectra. The particular configuration was assigned on the basis of the n.m.r. signals for the bridgehead protons. Two of these protons appear as a doublet at τ 7.87 ($J = 7$ c.p.s.) and the others as a doublet at τ 7.28 ($J = 7$ c.p.s.). In 3-carene-2,5-dione (**4**) on the other hand, the two bridgehead protons appear as a singlet at τ 7.79, while in 3-carene-2,5-dione-5-oxime (**2**) two doublets ($J = 7$ c.p.s.) were again observed at τ 7.88 and 7.28. Since it has been shown (7) that the oxime function in (**2**) is *syn* to the cyclopropyl group, we have assigned to the azine structure (**3**) in which the N—N bond is *syn* relative to both cyclopropane rings. Chemical support for the gross structure of the azine was obtained by its reaction with excess hydroxylamine hydrochloride, which afforded 3-carene-2,5-dione-2,5-dioxime (**5**) in more than 50% yield. The azine was also obtained when the diazoketone (**1**) was kept at 25° in the absence of light for a few days.

The irradiation of 5-diazo-3-caren-2-one (**1**) in 0.2% solution in 50% aqueous dioxan under nitrogen could readily be followed by watching the disappearance of the diazo band at 4.88μ in the infrared. After 8 h, complete decomposition had occurred, and chromatography on silica gel led to the isolation of the azine (**3**) (7%) and 3-carene-2,5-dione (**4**) (9%). The remaining material consisted largely of polymer, together with small amounts of impure liquid fractions. The carenedione may arise by a mechanism similar to that proposed by Bartlett and Traylor (8) for the conversion of diphenyldiazomethane, in the presence of oxygen, to benzophenone. We have found, however, that the yield of 3-carene-2,5-dione is surprisingly insensitive either to more rigorous removal of oxygen from the system or

[1]Presented in part at the 50th Annual Conference of the Chemical Institute of Canada, Toronto, June 5–7, 1967.

[2]From the M.Sc. thesis of D. T. Wang, University of Toronto, 1967.

[3]Numbering of the carane system used throughout is that used in structure (**1**).

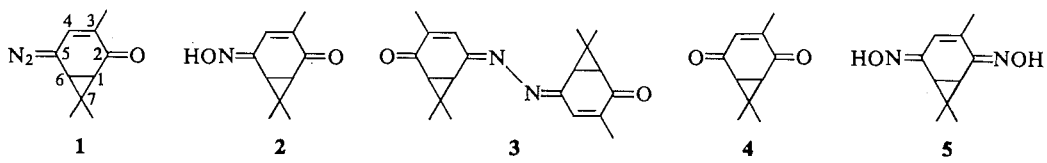

1 2 3 4 5

to attempts to increase the yield by bubbling air through the irradiated solution of the diazoketone, so that a mechanism involving the solvent, or solvent impurities, cannot be excluded at this stage.[4]

When the irradiation of (**1**) was conducted under similar conditions, in methanol as the solvent, three products were isolated. In addition to 3-carene-2,5-dione (12%) and the azine (**3**) (3%), a colorless solid, m.p. 140° (decomp.), was obtained in 3% yield. Nitrogen was not present in this compound, and the elemental analysis indicated the empirical formula $(C_5H_6O)_n$. No molecular ion was observed in the mass spectrum but a peak at *m/e* 296 might arise by (thermal) loss of O_2 from $C_{20}H_{24}O_4$. Some support for this view was obtained by the fact that the unknown solid gave a strong peroxide test when a chloroform solution was shaken with dilute acidified potassium iodide. Two carbonyl bands were observed in the infrared at 5.90 and 6.04μ, which were shifted to slightly longer wavelength when the compound was heated under nitrogen for 10 min at 150°. The amount of material then remaining was too small to permit further characterization.

The isomeric 2-diazo-3-caren-5-one (**8**) was obtained similarly by the reaction of 3-carene-2,5-dione-2-oxime (**7**) with chloramine. The oxime in turn was prepared as shown by a modification of the published procedure of Corey and Burke (4), starting from eucarvone (**6**).

The diazoketone so obtained was slightly con-

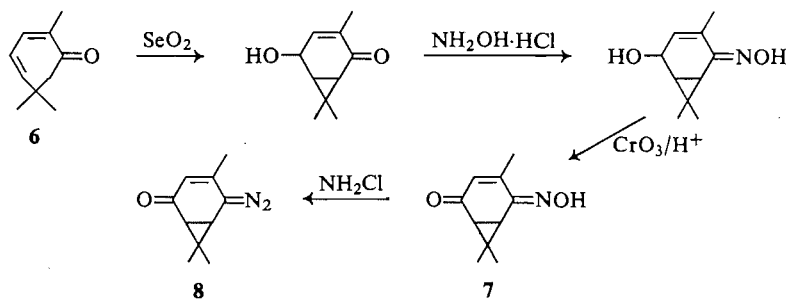

6 8 7

taminated by traces of unreacted oxime (**7**) but possessed the expected bands at 4.80 and 6.05μ. It was felt that the very small amount of oxime present would not significantly affect the decomposition of the diazoketone, and in view of the lability of the diazo grouping, no further attempts were made at purification.

Thermal decomposition was accomplished by heating (**8**) at 55° under nitrogen for 24 h. Polymeric material only was obtained. The greater stability of the diazo function when present at the 2-position (as reflected in the greatly increased time required for complete decomposition) indicates that loss of nitrogen and development of a carbenoid center at the 5-position in the isomeric diazoketone (**1**) may be facilitated by conjugative electron-release from the 3-methyl group. Irradiation of a 0.2% solution of the diazoketone (**8**) in 50% aqueous dioxan for 8 h led to the formation of a dark resinous oil from which small amounts of the starting oxime (**7**) and 3-carene-2,5-dione (**4**) were isolated. No azine could be detected in this reaction. A third product, isolated in extremely low yield, possessed pronounced spectral similarities with the unidentified product from the photolysis of (**1**) in methanol.

[4]We thank one of the referees for this suggestion.

Can. J. Chem. Downloaded from www.nrcresearchpress.com by 210.87.254.105 on 09/05/12
For personal use only.

Can. J. Chem. Downloaded from www.nrcresearchpress.com by 210.87.254.105 on 09/05/12
For personal use only.

To complete our study of diazo compounds in this series, we attempted to convert 3-carene-2,5-dione-2,5-dioxime (**5**) into the bisdiazo compound (**9**), using chloramine. The inherent difficulty involved arises from the fact that the 5-oxime group undergoes conversion to the 5-diazo group more readily than that at the 2-position, while the 5-diazo function so formed undergoes much more rapid thermal decomposition than the 2-diazo group, as we have already observed. Some material was obtained from this reaction with a band at 4.89μ. Infrared examination, however, also revealed the presence of substantial amounts of hydroxylic material (**5** + **10**) and this reaction was not pursued further.

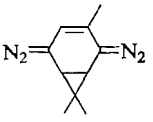

9

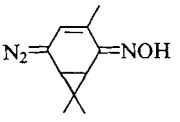

10

In conclusion, oxygenation of a carbenoid precessor, with the formation of the corresponding ketone (9), has been observed in low yield in both cases. Further investigation will be carried out to determine whether attack of ground-state oxygen on triplet carbene species is responsible. Azine formation was observed in virtually quantitative yield in the thermal decomposition of (**1**) and it has been suggested (10) that attack of a diazo group on the singlet carbene may be responsible. Minor products observed during the photolyses of these γ-diazoketones may be cyclic peroxides, but further investigation of these compounds is necessary to substantiate this view. Products corresponding to nucleophilic attack of water or methanol on an electron-deficient (singlet) carbene could not be detected in any of our photolyses, nor were any products corresponding to formal coupling of two carbenoid species obtained.

Experimental

All irradiations were carried out in Pyrex vessels using a 125 W medium-pressure Hanovia mercury lamp.[5] Infrared spectra were recorded on a Perkin–Elmer model 237B grating spectrometer and the ultraviolet spectra on Bausch and Lomb 505 or Unicam SP 800 recording spectrophotometers. Nuclear magnetic resonance spectra were taken on Varian A-60 or HA-100 instruments, with tetramethylsilane as internal standard. Mass spectra were measured using the AE1 MS-902 machine, and the microanalyses were carried out in the laboratory of Mr. A. B. Gygli, Toronto. All melting points are uncorrected.

5-Diazo-3-caren-2-one (1)

A solution of carenedione-5-oxime (**2**) (2.3 g, 0.013 mole) in a mixture of water (100 ml) and 33% sodium hydroxide (3.8 ml, 0.031 mole) was cooled to 0°. Twenty-eight percent ammonium hydroxide (7 ml, 0.55 mole) was added, followed by 12% sodium hypochlorite solution (32 ml, 0.052 mole) added dropwise over a period of 20 min. After the addition of the hypochlorite, the ice bath was slowly warmed up, and stirring was continued for an additional hour. The deep red solid (1.45 g, 67%) was collected by filtration and washed with ice-cold water. The solid melted at 40° (decomp.). The infrared spectrum showed intense bands at 4.88 and 6.01μ, λ_{max}(hexane) 350 mμ (ε 17 000), λ_{max}(MeOH) 378 mμ (ε 16 000).

Thermal Decomposition of 5-Diazo-3-caren-2-one

(*a*) The diazoketone (**1**) (0.2 g, 0.0011 mole) was exposed to air, in the dark, at room temperature for 8 h. The resulting orange solid (0.17 g, 92%) was recrystallized from 95% ethanol, m.p. 189–191°; infrared bands ($CHCl_3$) at 6.05, 6.18, 6.40 μ; λ_{max}(MeOH) 340 mμ (ε 13 400); τ($CDCl_3$) 8.88 (6 H), 8.70 (6 H), 8.05 (6 H), 7.87 (2 H), 7.28 (2 H), and 3.01 (2 H).

Anal. Calcd. for $C_{20}H_{24}N_2O_2$: C, 74.10; H, 7.41; N, 8.62. Found: C, 74.25; H, 7.69; N, 8.60.

(*b*) The diazoketone (**1**) (0.2 g, 0.0011 mole) was heated over boiling methylene chloride for 4 h, and the same orange-colored solid (0.18 g, 93%) was obtained.

Photolysis of 5-Diazo-3-caren-2-one (1)

(*a*) *In 50% Aqueous Dioxan*

A 0.2% solution (100 ml) of 5-diazo-3-caren-2-one in 50% aqueous dioxan was irradiated under nitrogen for 8 h. The orange-colored solution was diluted with water (100 ml) and extracted repeatedly with ether. The organic layer was dried and evaporated to give an oil. Chromatography on silica gel and elution with 5% and 10% ether–benzene mixtures afforded two distinct fractions—one being a pale-yellow crystalline solid, and the other an orange-colored solid. The pale-yellow solid proved to be 3-carene-2,5-dione (**4**) (0.019 g, 9.4%), identical in melting point and infrared spectrum with the material obtained on deoximation of 3-carene-2,5-dione-5-oxime. The orange solid was the azine (**3**) (0.012 g, 6.7%) identical in melting point, mixture melting point, and infrared spectrum with the material obtained on thermal decomposition of (**1**).

(*b*) *In Methanol*

A 1% solution (100 ml) of 5-diazo-3-caren-2-one in methanol was irradiated under nitrogen for 8 h. Chromatography of the crude product on silica gel and elution with 5%, 10%, and 20% ether–benzene mixtures, gave on evaporation 3-carene-2,5-dione (**4**) (0.15 g, 16%), the azine (**3**) (0.03 g, 3%), and a colorless crystalline solid (0.03 g, 3%), respectively.

The colorless solid, after recrystallization from carbon tetrachloride had m.p. 140–144° (decomp.); infrared bands ($CHCl_3$) at 5.90 and 6.04 μ; λ_{max}(MeOH) 227 mμ (ε 27 000) and 287 mμ (ε 15 000); τ($CDCl_3$) 8.87, 8.77,

[5]Engelhard Hanovia Lamps, Bath Road, Slough, England.

8.17, 7.94, 7.41, 5.16, 3.75, and 2.70; mass spectrum *m/e* 296.

Anal. Calcd. for $C_{20}H_{24}O_4$: C, 73.16; H, 7.32. Found: C, 73.88, H, 7.60.

Pyrolysis of Compound $C_{20}H_{24}O_4$

Compound $C_{20}H_{24}O_4$ (0.001 g, 0.000003 mole) was placed in a small test tube, which was heated in an oil bath at 155° under a nitrogen atmosphere. After 10 min, gas evolution ceased and the solid turned into a yellowish oil. Infrared bands were present ($CHCl_3$) at 5.92 and 6.10μ; λ_{max}(MeOH) were at 220 mμ (ε 8500), 294 mμ (ε 7000), and 350 mμ (ε 5500).

Conversion of 3-Carene-2,5-dione-5-azine (3) into 3-Carene-2,5-dione-2,5-dioxime (5)

3-Carene-2,5-dione-5-azine (**3**) (0.1 g, 0.0003 mole) was dissolved in a 1:1 pyridine – absolute alcohol solution (10 ml). Hydroxylamine hydrochloride (0.2 g, 0.004 mole) was added and the mixture was heated on a steam bath for 30 min. After removal of the solvents, the residue was triturated thoroughly with water and a white solid (0.067 g, 57%) m.p. 187–188°, was filtered, washed with water, and dried in air. This material was identical (mixture melting point and infrared spectral comparison) with 3-carene-2,5-dione-2,5-dioxime (**5**) obtained from 3-carene-2,5-dione-5-oxime (**2**) (4), τ (DMSO-d_6) 9.18 (3 H), 8.70 (3 H), 8.05 (3 H), 7.66 (2 H), 3.83 (1 H), −1.48 (1 H), and −1.72 (1 H).

2-Diazo-3-caren-5-one (8)

3-Carene-2,5-dione-2-oxime (**7**) (0.25 g, 0.0014 mole) was dissolved in 33% sodium hydroxide solution (0.4 ml, 0.0032 mole). The solution was diluted with water to 10 ml and cooled to −5° in a dry ice – carbon tetrachloride bath. Ammonium hydroxide (0.8 ml, 0.006 mole) was added, followed by 12% sodium hypochlorite (3.2 ml, 0.0052 mole), added dropwise over a period of 5 min. After completion of the addition of sodium hypochlorite, the mixture was allowed to warm up slowly to room temperature. The alkaline reaction mixture was then extracted with ether and removal of the solvent gave a dark orange-colored oil (0.15 g), infrared bands ($CHCl_3$) at 2.80, 3.06, 4.80, and 6.05μ. No purification was attempted.

Photolysis of 2-Diazo-3-caren-5-one (8)

The crude diazoketone (0.10 g) was dissolved in 50% aqueous dioxan (20 ml). The solution was irradiated under nitrogen, for 8 h. The resulting solution was diluted with water (100 ml) and was extracted with ether (3 times). The combined ether extracts on drying and evaporation yielded an oil. Chromatography on silica gel and elution with 5%, 10%, and 20% ether–benzene mixtures gave 3-carene-2,5-dione (**4**) (0.0025 g), 3-carene-2,5-dione-2-oxime (**7**) (0.0062 g), and a trace of a third, unidentified compound, respectively. The third product showed infrared bands ($CHCl_3$) at 2.78, 3.00, 5.88, and 6.02μ; λ_{max}(MeOH) 220 mμ (ε 6400) and 283 mμ (ε 4600).

Acknowledgment

We wish to thank the National Research Council of Canada for their financial support of this research.

1. W. KIRMSE. Carbene chemistry. Academic Press, New York. 1964.
2. R. O. KAN. Organic photochemistry. McGraw-Hill, New York. 1966.
3. D. C. NECKERS. Mechanistic organic photochemistry. Reinhold, New York. 1967.
4. E. J. COREY and H. J. BURKE. J. Am. Chem. Soc. **78**, 174 (1956).
5. M. P. CAVA, R. L. LITLE, and D. R. NAPIER. J. Am. Chem. Soc. **80**, 2257 (1958).
6. M. O. FORSTER. J. Chem. Soc. 260 (1915).
7. G. L. BUCHANAN, R. A. RAPHAEL, and I. W. J. STILL. J. Chem. Soc. 4372 (1963).
8. P. D. BARTLETT and T. G. TRAYLOR. J. Am. Chem. Soc. **84**, 3408 (1962).
9. E. J. MORICONI and J. J. MURRAY. J. Org. Chem. **29**, 3577 (1964).
10. G. CAUQUIS and G. REVERDY. Tetrahedron Letters, 1493 (1967).

Convenient synthesis of 3-amino-3-deoxy-D-ribose

WALTER SOWA

Department of Organic Chemistry, Ontario Research Foundation, Sheridan Park, Ontario

Received January 5, 1968

3-Amino-3-deoxy-D-ribose and D-ribose were prepared from a derivative of D-xylose. 1,2-*O*-Isopropylidene-5-*O*-triphenylmethyl-α-D-xylofuranose (**2**) was oxidized by dimethyl sulfoxide – acetic anhydride to 1,2-*O*-isopropylidene-5-*O*-triphenylmethyl-α-D-*erythro*-pentofuranos-3-ulose (**3**). The oxime (**4**) of this 3-keto sugar derivative was reduced with lithium aluminium hydride to 3-amino-3-deoxy-1,2-*O*-isopropylidene-5-*O*-triphenylmethyl-α-D-ribofuranose (**5**), isolated as the acetamido derivative (**6**). Hydrolysis yielded 3-amino-3-deoxy-D-ribose hydrochloride. **3** was reduced by sodium borohydride to 1,2-*O*-isopropylidene-5-*O*-triphenylmethyl-α-D-ribofuranose (**7**), which yielded D-ribose on hydrolysis.

Canadian Journal of Chemistry, 46, 1586 (1968)

In recent years many unusual amino and deoxy sugars have been identified as components of a number of antibiotic substances (1). One of these sugars, 3-amino-3-deoxy-D-ribose, is of interest because it occurs in puromycin (2) and in 3′-amino-3′-deoxyadenosine (3). Puromycin, which has been identified as 6-dimethylamino-9-[3-(*p*-methoxy-L-phenyl-alanylamino)-β-D-ribo-

Can. J. Chem. Downloaded from www.nrcresearchpress.com by 210.87.254.105 on 09/05/12
For personal use only.

8.17, 7.94, 7.41, 5.16, 3.75, and 2.70; mass spectrum *m/e* 296.

Anal. Calcd. for $C_{20}H_{24}O_4$: C, 73.16; H, 7.32. Found: C, 73.88, H, 7.60.

Pyrolysis of Compound $C_{20}H_{24}O_4$

Compound $C_{20}H_{24}O_4$ (0.001 g, 0.000003 mole) was placed in a small test tube, which was heated in an oil bath at 155° under a nitrogen atmosphere. After 10 min, gas evolution ceased and the solid turned into a yellowish oil. Infrared bands were present ($CHCl_3$) at 5.92 and 6.10μ; λ_{max}(MeOH) were at 220 mμ (ε 8500), 294 mμ (ε 7000), and 350 mμ (ε 5500).

Conversion of 3-Carene-2,5-dione-5-azine (3) into 3-Carene-2,5-dione-2,5-dioxime (5)

3-Carene-2,5-dione-5-azine (**3**) (0.1 g, 0.0003 mole) was dissolved in a 1:1 pyridine – absolute alcohol solution (10 ml). Hydroxylamine hydrochloride (0.2 g, 0.004 mole) was added and the mixture was heated on a steam bath for 30 min. After removal of the solvents, the residue was triturated thoroughly with water and a white solid (0.067 g, 57%) m.p. 187–188°, was filtered, washed with water, and dried in air. This material was identical (mixture melting point and infrared spectral comparison) with 3-carene-2,5-dione-2,5-dioxime (**5**) obtained from 3-carene-2,5-dione-5-oxime (**2**) (4), τ (DMSO-d_6) 9.18 (3 H), 8.70 (3 H), 8.05 (3 H), 7.66 (2 H), 3.83 (1 H), −1.48 (1 H), and −1.72 (1 H).

2-Diazo-3-caren-5-one (8)

3-Carene-2,5-dione-2-oxime (**7**) (0.25 g, 0.0014 mole) was dissolved in 33% sodium hydroxide solution (0.4 ml, 0.0032 mole). The solution was diluted with water to 10 ml and cooled to −5° in a dry ice – carbon tetrachloride bath. Ammonium hydroxide (0.8 ml, 0.006 mole) was added, followed by 12% sodium hypochlorite (3.2 ml, 0.0052 mole), added dropwise over a period of 5 min. After completion of the addition of sodium hypochlorite, the mixture was allowed to warm up slowly to room temperature. The alkaline reaction mixture was then extracted with ether and removal of the solvent gave a dark orange-colored oil (0.15 g), infrared bands ($CHCl_3$) at 2.80, 3.06, 4.80, and 6.05μ. No purification was attempted.

Photolysis of 2-Diazo-3-caren-5-one (8)

The crude diazoketone (0.10 g) was dissolved in 50% aqueous dioxan (20 ml). The solution was irradiated under nitrogen, for 8 h. The resulting solution was diluted with water (100 ml) and was extracted with ether (3 times). The combined ether extracts on drying and evaporation yielded an oil. Chromatography on silica gel and elution with 5%, 10%, and 20% ether–benzene mixtures gave 3-carene-2,5-dione (**4**) (0.0025 g), 3-carene-2,5-dione-2-oxime (**7**) (0.0062 g), and a trace of a third, unidentified compound, respectively. The third product showed infrared bands ($CHCl_3$) at 2.78, 3.00, 5.88, and 6.02μ; λ_{max}(MeOH) 220 mμ (ε 6400) and 283 mμ (ε 4600).

Acknowledgment

We wish to thank the National Research Council of Canada for their financial support of this research.

1. W. KIRMSE. Carbene chemistry. Academic Press, New York. 1964.
2. R. O. KAN. Organic photochemistry. McGraw-Hill, New York. 1966.
3. D. C. NECKERS. Mechanistic organic photochemistry. Reinhold, New York. 1967.
4. E. J. COREY and H. J. BURKE. J. Am. Chem. Soc. **78**, 174 (1956).
5. M. P. CAVA, R. L. LITLE, and D. R. NAPIER. J. Am. Chem. Soc. **80**, 2257 (1958).
6. M. O. FORSTER. J. Chem. Soc. 260 (1915).
7. G. L. BUCHANAN, R. A. RAPHAEL, and I. W. J. STILL. J. Chem. Soc. 4372 (1963).
8. P. D. BARTLETT and T. G. TRAYLOR. J. Am. Chem. Soc. **84**, 3408 (1962).
9. E. J. MORICONI and J. J. MURRAY. J. Org. Chem. **29**, 3577 (1964).
10. G. CAUQUIS and G. REVERDY. Tetrahedron Letters, 1493 (1967).

Convenient synthesis of 3-amino-3-deoxy-D-ribose

WALTER SOWA

Department of Organic Chemistry, Ontario Research Foundation, Sheridan Park, Ontario

Received January 5, 1968

3-Amino-3-deoxy-D-ribose and D-ribose were prepared from a derivative of D-xylose. 1,2-*O*-Isopropylidene-5-*O*-triphenylmethyl-α-D-xylofuranose (**2**) was oxidized by dimethyl sulfoxide – acetic anhydride to 1,2-*O*-isopropylidene-5-*O*-triphenylmethyl-α-D-*erythro*-pentofuranos-3-ulose (**3**). The oxime (**4**) of this 3-keto sugar derivative was reduced with lithium aluminium hydride to 3-amino-3-deoxy-1,2-*O*-isopropylidene-5-*O*-triphenylmethyl-α-D-ribofuranose (**5**), isolated as the acetamido derivative (**6**). Hydrolysis yielded 3-amino-3-deoxy-D-ribose hydrochloride. **3** was reduced by sodium borohydride to 1,2-*O*-isopropylidene-5-*O*-triphenylmethyl-α-D-ribofuranose (**7**), which yielded D-ribose on hydrolysis.

Canadian Journal of Chemistry, 46, 1586 (1968)

In recent years many unusual amino and deoxy sugars have been identified as components of a number of antibiotic substances (1). One of these sugars, 3-amino-3-deoxy-D-ribose, is of interest because it occurs in puromycin (2) and in 3′-amino-3′-deoxyadenosine (3). Puromycin, which has been identified as 6-dimethylamino-9-[3-(*p*-methoxy-L-phenyl-alanylamino)-β-D-ribo-

Can. J. Chem. Downloaded from www.nrcresearchpress.com by 210.87.254.6 on 09/05/12
For personal use only.

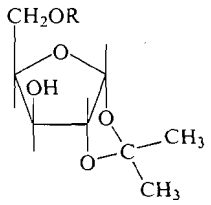

1 R = H
2 R = $C(C_6H_5)_3$

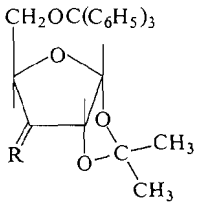

3 R = O
4 R = NOH

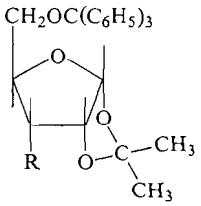

5 R = NH_2
6 R = $NHCOCH_3$
7 R = OH

furanosyl]purine (4), has become an important biochemical tool since its inhibitory effect on protein biosynthesis was demonstrated (5). Both nucleosides exhibit significant antitumor activity (6, 7) and 3-amino-3-deoxy-D-ribose has been described as an intermediate useful for the preparation of compounds antagonistic to vitamins B_2 and B_{12} (8). Numerous synthetic 3′-amino-3′-deoxynucleosides have been reported (9–14).

Several procedures have been published for the synthesis of 3-amino-3-deoxy-D-ribose. The first two are similar in principle. Ammonolysis of 2,3-anhydropentose derivatives yields intermediate 3-acetamido-3-deoxypentose compounds; the required configurational inversion of these is obtained by the attack of the acetamido group on a neighboring *trans*-methylsulfonate (15, 16). Another method (17) depends on the inversion which takes place when the *p*-tolylsulfonoxy group of 1,2;5,6-di-*O*-isopropylidene-3-*O*-*p*-tolylsulfonyl-α-D-glucofuranose undergoes hydrazinolysis. Reduction of the hydrazino compound yields a derivative of 3-amino-3-deoxy-D-allose which is then converted to 3-amino-3-deoxy-D-ribose *via* periodate oxidation and borohydride reduction. A fourth procedure (18) is shorter and more direct than the others. Periodate oxidation of methyl β-D-xylopyranoside followed by treatment of the intermediate dialdehyde with nitromethane and sodium yields the sodium salt of methyl 3-*aci*-nitro-3-deoxy-β-D-ribopyranoside. This is converted to the free nitropentoside with potassium bisulfate and anhydrous sodium sulfate in a ball-mill. Methyl 3-amino-3-deoxy-β-D-ribopyranoside is obtained by hydrogenation of the nitropentoside with platinum catalyst in the presence of hydrochloric acid.

The present communication reports a new and simple method for preparing 3-amino-3-deoxy-D-ribose. 1,2-*O*-Isopropylidene-α-D-xylofuranose (**1**), readily obtained by hydrolysis of 1,2;3,5-di-*O*-isopropylidene-α-D-xylofuranose (19), was treated with triphenylchloromethane to protect the primary alcohol group. Oxidation of the ether (**2**) by dimethyl sulfoxide – acetic anhydride (20) provided the 3-keto derivative (**3**). The oxime (**4**) of **3** was reduced by lithium aluminium hydride to 3-amino-3-deoxy-1,2-*O*-isopropylidene-5-*O*-triphenylmethyl-α-D-ribofuranose (**5**), isolated as the acetamido derivative (**6**). Hydrolysis of **6** afforded 3-amino-3-deoxy-D-ribose as the crystalline hydrochloride in an overall yield of about 45% based on **1**. The yield in the slightly shorter nitromethane procedure (18) is about 17% based on methyl β-D-xylopyranoside.

The 3-keto derivative (**3**) was reduced by sodium borohydride to 1,2-*O*-isopropylidene-5-*O*-triphenylmethyl-α-D-ribofuranose (**7**), thus providing a facile route to D-ribose. A similar conversion of a derivative of D-xylose to one of D-ribose has been reported using chromium trioxide in *t*-butyl alcohol for oxidation and hydrogen over platinum oxide at 60 atm pressure for reduction (21).

Experimental

Solutions were concentrated under reduced pressure using a rotary evaporator and a water bath at a temperature of 50° or less. Thin-layer chromatography utilized Silica Gel G, benzene–methanol (97:3 v/v) and sprays of 50% sulfuric acid or *p*-anisidine hydrochloride reagent (22) followed by heating at 120°. Rates of movement are quoted relative to that of 1,2,3,4,6-penta-*O*-acetyl-β-D-glucopyranose (R_p = 1.0). Melting points were determined on a calibrated Fisher–Johns apparatus. Optical rotations were measured in chloroform solutions at 21–22° unless stated otherwise. Nuclear magnetic resonance spectra were recorded on a Varian A-60 spectrometer using tetramethylsilane as an internal standard; the concentration of the samples was approximately 10% in deuteriochloroform or carbon tetrachloride.

1,2-O-Isopropylidene-5-O-triphenylmethyl-α-D-xylofuranose (2)

1,2-*O*-Isopropylidene-α-D-xylofuranose (**1**) (19) (19.0 g) and triphenylmethyl chloride (30.7 g) were stirred in dry pyridine (100 ml) for 20 h at room temperature. The

Can. J. Chem. Downloaded from www.nrcresearchpress.com by 210.87.254.6 on 09/05/12
For personal use only.

Can. J. Chem. Downloaded from www.nrcresearchpress.com by 210.87.254.6 on 09/05/12
For personal use only.

solution was poured into a mixture of ice and water (700 ml) which was then stirred for 30 min and extracted with ether (3 × 200 ml). The combined ether extracts were washed successively with cold dilute sulfuric acid (2 × 200 ml, 10% v/v), water (1 × 100 ml), saturated sodium bicarbonate solution (2 × 100 ml), and water (2 × 100 ml). The solution was dried over anhydrous sodium sulfate and evaporated to a syrup (41 g). This was crystallized from ether–hexane to obtain the triphenylmethyl ether (**2**) (35.5 g, 82%), m.p. 118–120° and R_p 1.10. After recrystallization it had m.p. 121° and $[\alpha]_D$ +13.3° (*c*, 4.9). The nuclear magnetic resonance spectrum (CCl_4) showed: δ 1.25 and 1.40 (—$C(CH_3)_2$), 2.69 (—OH, multiplet), 3.41 (—CH_2, multiplet), 4.10 (C-3 and C-4 protons, multiplet), 4.33 (C-2 proton, doublet), 5.83 (C-1 proton, doublet), 7.31 (aromatic protons, multiplet).

Anal. Calcd. for $C_{27}H_{28}O_5$:C, 74.97; H, 6.54. Found: C, 75.19; H, 6.63.

1,2-O-Isopropylidene-5-O-triphenylmethyl-α-D-erythro-pentofuranos-3-ulose (3)

Acetic anhydride (4 ml) was added to a solution of **2** (4.2 g) in anhydrous dimethyl sulfoxide (30 ml). After 22 h at room temperature, the reaction mixture was poured into an aqueous solution of sodium bicarbonate (800 ml, 10% w/v). This mixture was stirred for 1 h and then extracted with chloroform (4 × 300 ml). The combined chloroform extracts were washed with water (4 × 400 ml), dried over anhydrous sodium sulfate, and evaporated. The residue was dissolved in ethyl acetate – light petroleum or ether–hexane to crystallize the oxidized product (**3**), R_p 1.21, m.p. 132° and $[\alpha]_D$ +132° (*c*, 4.7). The yields from several preparations varied between 65 and 79%. Nuclear magnetic resonance spectrum (CCl_4): δ 1.41 (—$C(CH_3)_2$), 3.33 (—CH_2, multiplet), 4.27 (C-4 proton, multiplet), 4.36 (C-2 proton, doublet), 6.20 (C-1 proton, doublet), 7.29 (aromatic protons, multiplet).

Anal. Calcd. for $C_{27}H_{26}O_5$: C, 75.32; H, 6.10. Found: C, 75.58; H, 6.26.

1,2-O-Isopropylidene-5-O-triphenylmethyl-α-D-erythro-pentofuranos-3-ulose Oxime (4)

To a solution of hydroxylamine hydrochloride (12.5 g) in water (50 ml) was added an equal volume of sodium hydroxide solution (10% w/v) followed by a solution of **3** (5.0 g) in methanol (100 ml). The mixture was stirred at 65° for 2 h and then allowed to cool to room temperature. The product (**4**) was collected by filtration (5.1 g, 99%). It had R_p 0.90, m.p. 168–169° and $[\alpha]_D$ +154° (*c*, 2.3). Nuclear magnetic resonance spectrum ($CDCl_3$): the oxime was a mixture of *syn* and *anti* forms; except for the anomeric and hydroxyl protons, overlapping signals were obtained for the corresponding protons in each form; δ 1.39 (—$C(CH_3)_2$), 3.42 (—CH_2, broad multiplet), 5.18 (C-2 and C-4 protons, broad multiplet), 6.18, and 6.28 (C-1 proton, doublets), 7.74 and 7.94 (—NOH, singlets), 7.33 (aromatic protons, multiplet).

Anal. Calcd. for $C_{27}H_{27}NO_5$: C, 72.78; H, 6.12; N, 3.16. Found: C, 72.69; H, 6.25; N, 3.13.

Reduction of 1,2-O-Isopropylidene-5-O-triphenylmethyl-α-D-erythro-pentofuranos-3-ulose Oxime

A solution of the oxime (**4**) (1.5 g) in dry ether (40 ml) was added dropwise to a stirred mixture of lithium aluminium hydride (2.0 g) in dry ether (75 ml) at room temperature. The reaction mixture was refluxed with stirring for 7½ h, cooled, and excess hydride was destroyed by slow addition of water. The aqueous layer was separated from the ether layer and extracted with ether (3 × 75 ml). The combined ether solutions were washed with water, dried over anhydrous sodium sulfate, and evaporated to a syrup (1.3 g). Chromatography revealed that the product (**5**), R_p 0.80, was accompanied by a small amount of a second compound, R_p 0.59. The latter was not identified but was probably the epimeric amino sugar having the *xylo* configuration. The crude product (1.3 g) was dissolved in ethanol (25 ml) and treated with acetic anhydride (2 ml). After 30 min stirring, the mixture was poured into a solution of sodium bicarbonate to give 1.2 g (75% based on **4**) of acetamido derivative (**6**), R_p 0.74 and m.p. 180–181°. After recrystallization from ether–hexane, it had m.p. 185° and $[\alpha]_D$ +46.4° (*c*, 4.1). The nuclear magnetic resonance spectrum ($CDCl_3$) showed: δ 1.33 and 1.53 (—$C(CH_3)_2$), 1.90 (—$COCH_3$, singlet), 3.35 (—CH_2, multiplet), 3.79 (C-4 proton, multiplet), 4.25 (C-3 proton, multiplet), 4.59 (C-2 proton, triplet), 5.64 (—NH—, broadened doublet), 5.86 (C-1 proton, doublet), and 7.33 (aromatic protons, multiplet).

Anal. Calcd. for $C_{29}H_{31}NO_5$: C, 73.54; H, 6.61; N, 2.96. Found: C, 73.66; H, 6.63; N, 3.22.

A solution of **6** (1.0 g) in hydrochloric acid (50 ml, 1*N*) was refluxed for 4 h, cooled, filtered, and evaporated. The residue was crystallized from ethanol to yield 3-amino-3-deoxy-D-ribose hydrochloride (0.27 g, 93%) having m.p. 166° (decomp.) and $[\alpha]_D$ −23.0° (*c*, 4.1 in water). Literature values (16) are m.p. 160° (decomp.) and $[\alpha]_D^{24}$ −25.0° (*c*, 2% in water).

1,2-O-Isopropylidene-5-O-triphenylmethyl-α-D-ribofuranose (7)

To a cooled and stirred solution of **3** (1.0 g) in aqueous ethanol (100 ml, 80% v/v) was added a solution of sodium borohydride (1.0 g) in water (25 ml) over a period of 20 min. After the mixture had been stirred for 1 h at room temperature, it was poured into a mixture of ice and water (200 ml). The precipitate was collected by filtration and crystallized from ether–hexane to obtain **7** (0.62 g, 62%), R_p 1.22, m.p. 117° and $[\alpha]_D$ +25.8° (*c*, 4.5). The nuclear magnetic resonance spectrum (CCl_4) showed: δ 1.33 and 1.51 (—$C(CH_3)_2$), 1.97 (—OH, broad multiplet), 3.23 (—CH_2, multiplet), 3.75 (C-3 and C-4 protons, multiplet), 4.45 (C-2 proton, triplet), 5.79 (C-1 proton, doublet), 7.30 (aromatic protons, multiplet).

Anal. Calcd. for $C_{27}H_{28}O_5$: C, 74.97; H, 6.54. Found: C, 75.00; H, 6.48.

A portion of **7** was hydrolyzed with 0.1 *N* sulfuric acid at 100° for 1 h. The cooled hydrolyzate was filtered, neutralized with barium carbonate, and filtered again. The filtrate was chromatographed on Whatman No. 1 paper developed in ethyl acetate – acetic acid – formic acid – water (18:3:1:4 v/v). Ribose was the only sugar detected with the *p*-anisidine hydrochloride spray reagent.

Acknowledgments

The author expresses his appreciation to Dr. F. J. Hopton for helpful discussions concerning

the nuclear magnetic resonance spectra, and to Mrs. Brigitte Licht for technical assistance. The research was made possible by funds received from the Province of Ontario through the Department of Economics and Development.

1. J. D. DUTCHER. Advan. Carbohydrate Chem. **18**, 259 (1963).
2. C. W. WALLER, P. W. FRYTH, B. L. HUTCHINGS, and J. H. WILLIAMS. J. Am. Chem. Soc. **75**, 2025 (1953).
3. N. N. GERBER and H. A. LECHEVALIER. J. Org. Chem. **27**, 1731 (1962).
4. P. W. FRYTH, C. W. WALLER, B. L. HUTCHINGS, and J. H. WILLIAMS. J. Am. Chem. Soc. **80**, 2736 (1958).
5. M. B. YARMOLINSKY and G. L. DE LA HABA. Proc. Natl. Acad. Sci. U.S. **45**, 1721 (1959).
6. W. TROY, S. SMITH, G. PERSONEUS, L. MOSER, E. JAMES, S. J. SPARKS, M. STEVENS, S. HALLIDAY, D. MCKENZIE, and J. J. OLESON. Antibiotics Annual 1953–1954. Medical Encyclopedia, Inc., New York. 1953. pp. 186–190.
7. L. H. PUGH and N. N. GERBER. Cancer Res. **23**, 640 (1963).
8. AMERICAN CYANAMID CO. Brit. Patent No. 762,540 (Nov. 28, 1956); Chem. Abstr. **52**, 11912 (1958).
9. B. R. BAKER, R. E. SCHAUB, and H. M. KISSMAN. J. Am. Chem. Soc. **77**, 5911 (1955).
10. H. M. KISSMAN and M. J. WEISS. J. Am. Chem. Soc. **80**, 2575 (1958).
11. B. R. BAKER, J. P. JOSEPH, and R. E. SCHAUB. U.S. Patent No. 2,852,505 to American Cyanamid Co. (Sept. 16, 1958); Chem. Abstr. **53**, 8175 (1959). L. GOLDMAN and J. W. MARSICO. U.S. Patent No. 2,852,506 to American Cyanamid Co. (Sept. 16, 1958); Chem. Abstr. **53**, 8174 (1959).
12. L. GOLDMAN and J. W. MARSICO. J. Med. Chem. **6**, 413 (1963).
13. N. N. GERBER. J. Med. Chem. **7**, 204 (1964).
14. K. A. WATANABE and J. J. FOX. J. Org. Chem. **31**, 211 (1966).
15. B. R. BAKER and R. E. SCHAUB. J. Org. Chem. **19**, 646 (1954).
16. B. R. BAKER, R. E. SCHAUB, and J. H. WILLIAMS. J. Am. Chem. Soc. **77**, 7 (1955).
17. R. U. LEMIEUX and P. CHU. J. Am. Chem. Soc. **80**, 4745 (1958).
18. H. H. BAER and H. O. L. FISCHER. J. Am. Chem. Soc. **81**, 5184 (1959).
19. B. HELFERICH and M. BURGDORF. Tetrahedron, **3**, 274 (1958).
20. J. D. ALBRIGHT and L. GOLDMAN. J. Am. Chem. Soc. **87**, 4214 (1965).
21. K. ODA and H. WADA. Yakugaku Zasshi, **83**, 890 (1963); Chem. Abstr. **60**, 1825 (1964).
22. L. HOUGH, J. K. N. JONES, and W. H. WADMAN. J. Chem. Soc. 1702 (1950).

Kinetics of hydrolyses of *o*-methylbenzylideneaniline and *o*-hydroxybenzylideneaniline

ALFRED V. WILLI AND JOSÉ F. SIMAN[1]

College of Pharmaceutical Sciences, Columbia University, New York, New York 10023

Received November 23, 1967

Rates of hydrolysis have been measured for *o*-methylbenzylideneaniline, *o*-hydroxybenzylideneaniline, and benzylideneaniline in various buffer solutions in 20% (by volume) aqueous methanol at 29.9 °C. Rate constants for the *o*-CH_3 compound and the unsubstituted Schiff base agree within experimental error which indicates that there is no appreciable rate retarding steric effect. The *o*-OH group decreases the hydrolysis rate at pH = 5.6 – 6.6 by approximately one power of ten. This effect is caused by the hydrogen bond between the OH group and the azomethine N, which renders the Schiff base less accessible to acid-catalyzed hydrolysis.

Canadian Journal of Chemistry, **46**, 1589 (1968)

Introduction

Although the kinetics of hydrolyses of aliphatic and aromatic Schiff bases has been studied extensively (for a recent review see ref. 1 and also refs. 2–5), very little is known about the effects of ortho substituents on the rates. Benzylideneaniline and most of the substituted benzylideneanilines hydrolyze rapidly, even in weakly acidic solutions (pH = 5.6 or lower), with half-lives of a few minutes or even a fraction of a minute (2). On the other hand, *o*-hydroxybenzylideneaniline ("salicylidene aniline") appears to be more stable, for it has been reported that chelate complexes may be prepared by reacting the Schiff base with (weakly acidic!) solutions of heavy metal salts (6). Such a decelerating effect on the rate of hydrolysis may be explained with the aid of two different assumptions: (*a*) the ortho hydroxy group causes steric hindrance of the attack of H_2O or OH^- on the azomethine carbon of the N-protonated Schiff base, or (*b*) a hydrogen bond between the ortho hydroxy group and the azomethine nitrogen

[1]National Science Foundation undergraduate research participant, Summer 1967.

Can. J. Chem. Downloaded from www.nrcresearchpress.com by 210.87.254.6 on 09/05/12
For personal use only.

the nuclear magnetic resonance spectra, and to Mrs. Brigitte Licht for technical assistance. The research was made possible by funds received from the Province of Ontario through the Department of Economics and Development.

1. J. D. DUTCHER. Advan. Carbohydrate Chem. **18**, 259 (1963).
2. C. W. WALLER, P. W. FRYTH, B. L. HUTCHINGS, and J. H. WILLIAMS. J. Am. Chem. Soc. **75**, 2025 (1953).
3. N. N. GERBER and H. A. LECHEVALIER. J. Org. Chem. **27**, 1731 (1962).
4. P. W. FRYTH, C. W. WALLER, B. L. HUTCHINGS, and J. H. WILLIAMS. J. Am. Chem. Soc. **80**, 2736 (1958).
5. M. B. YARMOLINSKY and G. L. DE LA HABA. Proc. Natl. Acad. Sci. U.S. **45**, 1721 (1959).
6. W. TROY, S. SMITH, G. PERSONEUS, L. MOSER, E. JAMES, S. J. SPARKS, M. STEVENS, S. HALLIDAY, D. MCKENZIE, and J. J. OLESON. Antibiotics Annual 1953–1954. Medical Encyclopedia, Inc., New York. 1953. pp. 186–190.
7. L. H. PUGH and N. N. GERBER. Cancer Res. **23**, 640 (1963).
8. AMERICAN CYANAMID CO. Brit. Patent No. 762,540 (Nov. 28, 1956); Chem. Abstr. **52**, 11912 (1958).
9. B. R. BAKER, R. E. SCHAUB, and H. M. KISSMAN. J. Am. Chem. Soc. **77**, 5911 (1955).
10. H. M. KISSMAN and M. J. WEISS. J. Am. Chem. Soc. **80**, 2575 (1958).
11. B. R. BAKER, J. P. JOSEPH, and R. E. SCHAUB. U.S. Patent No. 2,852,505 to American Cyanamid Co. (Sept. 16, 1958); Chem. Abstr. **53**, 8175 (1959). L. GOLDMAN and J. W. MARSICO. U.S. Patent No. 2,852,506 to American Cyanamid Co. (Sept. 16, 1958); Chem. Abstr. **53**, 8174 (1959).
12. L. GOLDMAN and J. W. MARSICO. J. Med. Chem. **6**, 413 (1963).
13. N. N. GERBER. J. Med. Chem. **7**, 204 (1964).
14. K. A. WATANABE and J. J. FOX. J. Org. Chem. **31**, 211 (1966).
15. B. R. BAKER and R. E. SCHAUB. J. Org. Chem. **19**, 646 (1954).
16. B. R. BAKER, R. E. SCHAUB, and J. H. WILLIAMS. J. Am. Chem. Soc. **77**, 7 (1955).
17. R. U. LEMIEUX and P. CHU. J. Am. Chem. Soc. **80**, 4745 (1958).
18. H. H. BAER and H. O. L. FISCHER. J. Am. Chem. Soc. **81**, 5184 (1959).
19. B. HELFERICH and M. BURGDORF. Tetrahedron, **3**, 274 (1958).
20. J. D. ALBRIGHT and L. GOLDMAN. J. Am. Chem. Soc. **87**, 4214 (1965).
21. K. ODA and H. WADA. Yakugaku Zasshi, **83**, 890 (1963); Chem. Abstr. **60**, 1825 (1964).
22. L. HOUGH, J. K. N. JONES, and W. H. WADMAN. J. Chem. Soc. 1702 (1950).

Kinetics of hydrolyses of *o*-methylbenzylideneaniline and *o*-hydroxybenzylideneaniline

ALFRED V. WILLI AND JOSÉ F. SIMAN[1]

College of Pharmaceutical Sciences, Columbia University, New York, New York 10023

Received November 23, 1967

Rates of hydrolysis have been measured for *o*-methylbenzylideneaniline, *o*-hydroxybenzylideneaniline, and benzylideneaniline in various buffer solutions in 20% (by volume) aqueous methanol at 29.9 °C. Rate constants for the *o*-CH_3 compound and the unsubstituted Schiff base agree within experimental error which indicates that there is no appreciable rate retarding steric effect. The *o*-OH group decreases the hydrolysis rate at pH = 5.6 – 6.6 by approximately one power of ten. This effect is caused by the hydrogen bond between the OH group and the azomethine N, which renders the Schiff base less accessible to acid-catalyzed hydrolysis.

Canadian Journal of Chemistry, **46**, 1589 (1968)

Introduction

Although the kinetics of hydrolyses of aliphatic and aromatic Schiff bases has been studied extensively (for a recent review see ref. 1 and also refs. 2–5), very little is known about the effects of ortho substituents on the rates. Benzylideneaniline and most of the substituted benzylideneanilines hydrolyze rapidly, even in weakly acidic solutions (pH = 5.6 or lower), with half-lives of a few minutes or even a fraction of a minute (2). On the other hand, *o*-hydroxybenzylideneaniline ("salicylidene aniline") appears to be more stable, for it has been reported that chelate complexes may be prepared by reacting the Schiff base with (weakly acidic!) solutions of heavy metal salts (6). Such a decelerating effect on the rate of hydrolysis may be explained with the aid of two different assumptions: (*a*) the ortho hydroxy group causes steric hindrance of the attack of H_2O or OH^- on the azomethine carbon of the N-protonated Schiff base, or (*b*) a hydrogen bond between the ortho hydroxy group and the azomethine nitrogen

[1]National Science Foundation undergraduate research participant, Summer 1967.

Can. J. Chem. Downloaded from www.nrcresearchpress.com by 210.87.254.42 on 09/05/12
For personal use only.

Can. J. Chem. Downloaded from www.nrcresearchpress.com by 210.87.254.42 on 09/05/12
For personal use only.

decreases the basicity of the nitrogen and renders the Schiff base less accessible to acid-catalyzed hydrolysis. If the rate decrease is caused by steric hindrance, a similar effect must be expected for any other ortho substituent. If that be the case, a systematic study of ortho effects in Schiff base hydrolysis would supply important information on the rate determining step under various conditions, e.g., pH. In order to distinguish between the two theoretical possibilities mentioned above, we have carried out a kinetic study of the hydrolyses of *o*-methylbenzylideneaniline and *o*-hydroxybenzylideneaniline in comparison to benzylideneaniline.

Experimental

Benzylideneaniline, *o*-methylbenzylideneaniline, and *o*-hydroxybenzylideneaniline were prepared and purified according to known methods (3). Rates of hydrolysis were followed by observing the change of the ultraviolet absorption with time in a Beckman DU spectrophotometer. The temperature of the cell compartment of the instrument was kept constant at +29.9 °C (±0.15) with the aid of thermospacers and a circulation thermostat. (A temperature constancy within ±0.15° is sufficient for these kinetic experiments since the activation energies for the hydrolyses of benzylideneanilines are low (2). The pcH values of the buffer solutions in 20% (by volume) aqueous methanol were measured at 29.9° C in a thermostated cell with a glass electrode Metrohm, type U, and a silver – silver chloride electrode, using a Metrohm pH meter, type E388. The cell was calibrated with a solution of 0.0100 *N* hydrochloric acid and 0.090 *N* KCl in 20% (by volume) aqueous methanol (pcH = 2.000).

Results

Kinetic experiments have been done in 20% (by volume) aqueous methanol at a constant ionic strength of $\mu = 0.100\ N$ at +29.9 °C. Rates are too fast for measurement in 10^{-2} or $10^{-3}\ N$ hydrochloric acid (complete decomposition within 1 min), but they become measurable when the pH is increased above 5.5 or 6.3, respectively. The reaction follows a first order course at least up to 75% decomposition. Pseudo first order rate constants obtained in various buffer solutions are collected in Table I. The estimated precision of the rate constants is within ±3 %. Compositions of the buffer solutions are reported in Table II. According to the results in Table III, the rate constant increases with increasing buffer concentration, even if pH and ionic strength are kept constant.

TABLE I

Rate constants for Schiff base hydrolyses*

Buffer no.	pcH	benzalanil-ine k (s^{-1})	*o*-Methyl benzalanil-ine k (s^{-1})	*o*-Hydroxy-benzalanil-ine k (s^{-1})
A1	5.59	Too fast	Too fast	2.2×10^{-2}
A2	5.89	Too fast	Too fast	1.24×10^{-2}
A3	6.37	4.83×10^{-2}	5.25×10^{-2}	4.79×10^{-3}
A4	6.59	3.26×10^{-2}	3.14×10^{-2}	4.11×10^{-3}
T1	7.38	2.91×10^{-3}	2.86×10^{-3}	2.92×10^{-3}
T2	7.89	1.20×10^{-3}	1.18×10^{-3}	4.75×10^{-3}
T3	8.33	7.15×10^{-4}	7.20×10^{-4}	7.07×10^{-3}
C1	9.85	1.54×10^{-4}	1.96×10^{-4}	9.9×10^{-3}
C2	9.96	1.42×10^{-4}	$2\ 08 \times 10^{-4}$	1.21×10^{-2}
C3	10.27	1.54×10^{-4}	$1\ 80 \times 10^{-4}$	1.48×10^{-2}

*20% (by volume) aqueous methanol at 29.9 °C, $\mu = 0.100\ N$.

Discussion

The data in Table III indicate general acid catalysis for the hydrolyses of *o*-methylbenzylideneaniline and *o*-hydroxybenzylideneaniline, in agreement with previous findings for benzylideneaniline and some parasubstituted benzylideneanilines (2, 3). No attempt has been made in this study to collect enough rate data for extrapolations to zero buffer concentration at each of the pH values. Therefore, it is not possible at present to derive empirical equations for k as a function of $[H_3O^+]$. However, it can be seen that in the pH region of 6.3–8.3 the rate constants for benzylideneaniline and *o*-methylbenzylideneaniline in the same buffer solutions

TABLE II

Buffer solutions employed in kinetic experiments*

No.	Buffer base (M)	Buffer acid (M)	C_{KCl} (M)
	acetate – acetic acid		
A1	0.00952	0.0185	0.0905
A2	0.00952	0.00926	0.0905
A3	0.0143	0.00463	0.0860
A4	0.0238	0.00463	0.0760
	tris(hydroxymethyl)aminomethane – conjugate acid		
T1	0.00476	0.0143	0.0860
T2	0.00952	0.00952	0.0905
T3	0.0286	0.00952	0.0905
	carbonate – bicarbonate		
C1	0.00476	0.0143	0.0715
C2	0.00476	0.00952	0.0810
C3	0.00952	0.00952	0.0715

*Solvent: 20% (by volume) aqueous methanol.

Can. J. Chem. Downloaded from www.nrcresearchpress.com by 210.87.254.42 on 09/05/12
For personal use only.

are identical within experimental error. At pH values above 8.3 *o*-methylbenzylideneaniline is hydrolyzed faster than the unsubstituted compound. On the basis of previous findings for *p*-substituted benzylideneanilines it may be concluded that the electronic substituent effect of the *o*-CH_3 group must be small, presumably due to approximate cancellation of opposing effects in consecutive steps. Consequently, these results indicate that the ortho methyl substituent does not cause any noticable rate retarding steric effect in benzylideneaniline hydrolysis.

Such an effect might possibly occur if two *o*-CH_3 groups are present, provided that attack of nucleoplile on the azomethine carbon is rate limiting. However, it is not completely certain whether this step can be rate limiting in the reaction under study, since in acid-catalyzed esterification and ester hydrolysis steric hindrance is effective already in the presence of one ortho substituent (7). (As far as the conformation of benzylideneaniline is concerned, there is ultraviolet spectroscopic evidence which indicates that the ring bonded to the nitrogen is not in the same plane with the azomethine group. The other aromatic ring, however, appears to be coplanar with the CN double bond (8).

TABLE III

Dependence of the rate constant on the buffer concentration*

Buffer base (M)	Buffer acid (M)	pcH	k (s^{-1})
tris(hydroxymethyl)aminomethane – conjugated acid, *o*-methylbenzalaniline			
0.00952	0.00952	7.89	1.18×10^{-3}
0.0190	0.0190	7.89	1.46×10^{-3}
0.0286	0.0286	7.89	1.91×10^{-3}
acetate – acetic acid, *o*-hydroxybenzalaniline			
0.00952	0.00926	5.89	1.24×10^{-2}
0.0190	0.0185	5.89	1.77×10^{-2}
0.0286	0.0276	5.89	2.01×10^{-2}

*Solvent: 20% (by volume) aqueous methanol, 29.9 °C, $\mu = 0.100N$

o-Hydroxybenzylideneaniline is hydrolyzed about 10 times more slowly than benzylideneaniline at pH 6.6 (Table I), but 10 times as fast at pH = 8.3 and 100 times as fast as benzylideneaniline at pH = 10.0. In weakly acidic solutions, in the presence of metal salts, the hydrolysis of *o*-hydroxybenzylideneaniline cannot compete with the formation and precipitation of the chelate complex. Furthermore, the complex is probably more stable with respect to hydrolysis than the Schiff base itself (9).

As the rate decreasing effect of the *o*-OH group at pH < 7 cannot be caused by steric hindrance, we have to consider the alternative possibility of the explanation based on hydrogen bond formation. In the infrared spectra of *o*-hydroxybenzylideneaniline, formation of an intramolecular hydrogen bond is indicated by a strong shift of the OH stretching frequency to lower wave numbers (10). Consequently, it must be expected that the hydrogen bond decreases the basicity of the nitrogen, in the same manner as the intramolecular hydrogen bond in salicylate ion decreases the basicity of the carboxylate group (11). Experimental data are available on the pK values of the nitrogen in ortho and meta hydroxybenzylidene-2-aminopropane (12), they indicate the presence of such a basicity decreasing hydrogen bond effect in the ortho compound.

A decreased basicity of the nitrogen leads to a decreased rate of the acid-catalyzed pathway of the Schiff base hydrolysis. Conditions are changed in the high pH region because the hydrolysis of *o*-hydroxybenzylideneaniline is also subject to base catalysis: The rate constant as a function of pH goes through a minimum near pH = 7, and then increases with increasing pH (Table I). Base catalysis in the hydrolysis of unsubstituted benzylideneaniline is not noticable below pH = 12 (13).

Base-catalyzed as well as uncatalyzed reactions of *o*-hydroxy Schiff bases (see also Reeves' results for *o*-HOC_6H_4—CH = N—$C_6H_4NMe_3^+$ (4)) probably go through intermediates in which the OH group is deprotonated. Then, the rate decreasing effect of the hydrogen bond would be replaced by a strong accelerating effect of the negative charge.

Acknowledgments

The authors are grateful to the National Science Foundation for financial support of this work through Grant no. GY-2875 of the undergraduate research participation program. They also wish to thank one of the referees for having drawn their attention to references 8 and 12.

1. W. P. Jencks. Progr. Phys. Org. Chem. **2**, 63 (1964).

2. A. V. WILLI and R. E. ROBERTSON. Can. J. Chem. **31**, 361 (1953). A. V. WILLI. Helv. Chim. Acta, **39**, 1193 (1956).
3. E. H. CORDES and W. P. JENCKS. J. Am. Chem. Soc. **84**, 826, 831 (1962); **85**, 2843 (1963). R. K. CHATURVEDI and E. H. CORDES. J. Am. Chem. Soc. **89**, 1230 (1967).
4. R. L. REEVES, J. Am. Chem. Soc. **84**, 3332 (1962). R. L. REEVES and W. F. SMITH. J. Am. Chem. Soc. **85**, 724 (1963). R. L. REEVES. J. Org. Chem. **30**, 3129 (1965).
5. R. B. MARTIN. J. Phys. Chem. **68**, 1369 (1964).
6. T. J. LANE and A. J. KANDATHIL. J. Am. Chem. Soc. **83**, 3782 (1961). K. K. CHATTERJEE, N. FARRIER, and B. E. DOUGLAS. J. Am. Chem. Soc. **85**, 2919 (1963).
7. E. W. TIMM and C. N. HINSHELWOOD. J. Chem. Soc. 862 (1938). R. W. TAFT. *In* Steric effects in organic chemistry. *Edited by* M. S. Newman. John Wiley and Sons, Inc., New York. 1956.
8. W. F. SMITH. Tetrahedron, **19**, 445 (1963). P. BROCKLEHURST. Tetrahedron, **18**, 299 (1962).
9. G. L. EICHHORN and N. D. MARCHAND. J. Am. Chem. Soc. **78**, 2688 (1956).
10. G. M. BADGER and A. G. MORITZ. J. Chem. Soc. 3437 (1958).
11. G. E. K. BRANCH and D. L. YABROFF. J. Am. Chem. Soc. **56**, 2568 (1934).
12. W. BRUYNEEL, J. J. CHARETTE, and E. DE HOFFMANN. J. Am. Chem. Soc. **88**, 3808 (1966).
13. B. KASTENING, L. HOLLECK, and G. A. MELKONIAN. Z. Elektrochem. **60**, 130 (1956).

The preparation of methyl 4-deoxy-3-*O*-methyl-α,β-DL-*threo*-pentopyranoside[1]

F. SWEET and R. K. BROWN
Department of Chemistry, University of Alberta, Edmonton, Alberta

Received January 22, 1967/1968

Methyl 4-deoxy-3-*O*-methyl-α,β-DL-*threo*-pentopyranoside has been prepared by a highly selective reaction of methanol with *cis*-, *trans*-, or *cis–trans*-3,4-epoxy-2-methoxytetrahydropyran in the presence of a catalytic amount of *p*-toluenesulfonic acid. The structure was supported by its conversion, after hydrolysis, to the phenylosazone and, by nitric acid oxidation, to *O*-methyl-DL-tartaric acid.

Canadian Journal of Chemistry, 46, 1592 (1968)

It has been shown recently (1) that 2-alkoxy-5,6-dihydro-2*H*-pyran reacts with *m*-chloroperoxybenzoic acid to give a preponderance of the epoxide in which the 3,4-anhydro ring is *trans* to the 2-alkoxy substituent and that opening of the epoxide ring by $LiAlH_4$ occurs exclusively by breaking the C—O bond remote from the C-2 alkoxy substituent.

We have now employed this approach to prepare a mixture of methyl 4-deoxy-3-*O*-methyl-α- and β-DL-*threo*-pentopyranosides starting with the *cis*-, *trans*-, or *cis–trans*-2-alkoxy-3,4-epoxytetrahydropyran (**1** and **2**).

When **1** and/or **2** were heated in methanol containing some *p*-toluenesulfonic acid as catalyst, a distillable oil was obtained in 76% yield, (Scheme 1) which contained in each case the same mixture of just two substances as shown by gas–liquid chromatography (g.l.c.). That these two substances were isomers was shown by the analysis of the binary mixture which was correct for methyl 4-deoxy-3-*O*-methyl-α (or β)-DL-*threo*-pentopyranoside. The result could be rationalized on the reasonable assumption that the first reaction which occurred was that in which the methanol attacked the protonated epoxide exclusively on that carbon atom remote from the anomeric center. This was then followed by a slower isomerization to produce an equilibrium mixture of the α and β anomers of the DL mixture.

The structures of the products **3** and **4** were proved in the following manner.

The mixture (**3** and **4**) obtained from methanolysis of **1** and **2** was hydrolyzed to give a syrup. Treatment of the syrup with phenylhydrazine gave a solid phenylosazone, which analyzed correctly for the phenylosazone of 4-deoxy-3-*O*-methyl-DL-*threo*-pentose, thus proving the location of the methoxy group at position-4 in the tetrahydropyran ring system. Conversion of the mixture **3** and **4** to the 3,5-dinitrobenzoate gave a solid whose nuclear magnetic resonance (n.m.r.) spectrum showed doublets for the anomeric protons at τ 5.55 ($J_{1',2'} = 7$ Hz) and τ 5.03 ($J_{1,2} = 3.3$ Hz) for the two epimers, and

[1]Taken from the thesis of F. Sweet to be submitted to the Faculty of Graduate Studies, University of Alberta, Edmonton, Alberta, as part of the requirements for the degree of Doctor of Philosophy.

FOR ERRATA SEE
Vol. 46 No. 21 1968 ... P. 3419 ...

Can. J. Chem. Downloaded from www.nrcresearchpress.com by 210.87.254.42 on 09/05/12
For personal use only.

Can. J. Chem. Downloaded from www.nrcresearchpress.com by 210.87.254.5 on 09/05/12
For personal use only.

2. A. V. WILLI and R. E. ROBERTSON. Can. J. Chem. **31**, 361 (1953). A. V. WILLI. Helv. Chim. Acta, **39**, 1193 (1956).
3. E. H. CORDES and W. P. JENCKS. J. Am. Chem. Soc. **84**, 826, 831 (1962); **85**, 2843 (1963). R. K. CHATURVEDI and E. H. CORDES. J. Am. Chem. Soc. **89**, 1230 (1967).
4. R. L. REEVES, J. Am. Chem. Soc. **84**, 3332 (1962). R. L. REEVES and W. F. SMITH. J. Am. Chem. Soc. **85**, 724 (1963). R. L. REEVES. J. Org. Chem. **30**, 3129 (1965).
5. R. B. MARTIN. J. Phys. Chem. **68**, 1369 (1964).
6. T. J. LANE and A. J. KANDATHIL. J. Am. Chem. Soc. **83**, 3782 (1961). K. K. CHATTERJEE, N. FARRIER, and B. E. DOUGLAS. J. Am. Chem. Soc. **85**, 2919 (1963).
7. E. W. TIMM and C. N. HINSHELWOOD. J. Chem. Soc. 862 (1938). R. W. TAFT. *In* Steric effects in organic chemistry. *Edited by* M. S. Newman. John Wiley and Sons, Inc., New York. 1956.
8. W. F. SMITH. Tetrahedron, **19**, 445 (1963). P. BROCKLEHURST. Tetrahedron, **18**, 299 (1962).
9. G. L. EICHHORN and N. D. MARCHAND. J. Am. Chem. Soc. **78**, 2688 (1956).
10. G. M. BADGER and A. G. MORITZ. J. Chem. Soc. 3437 (1958).
11. G. E. K. BRANCH and D. L. YABROFF. J. Am. Chem. Soc. **56**, 2568 (1934).
12. W. BRUYNEEL, J. J. CHARETTE, and E. DE HOFFMANN. J. Am. Chem. Soc. **88**, 3808 (1966).
13. B. KASTENING, L. HOLLECK, and G. A. MELKONIAN. Z. Elektrochem. **60**, 130 (1956).

The preparation of methyl 4-deoxy-3-*O*-methyl-α,β-DL-*threo*-pentopyranoside[1]

F. SWEET and R. K. BROWN
Department of Chemistry, University of Alberta, Edmonton, Alberta

Received January 22, ~~1967~~ 1968

Methyl 4-deoxy-3-*O*-methyl-α,β-DL-*threo*-pentopyranoside has been prepared by a highly selective reaction of methanol with *cis*-, *trans*-, or *cis–trans*-3,4-epoxy-2-methoxytetrahydropyran in the presence of a catalytic amount of *p*-toluenesulfonic acid. The structure was supported by its conversion, after hydrolysis, to the phenylosazone and, by nitric acid oxidation, to *O*-methyl-DL-tartaric acid.

Canadian Journal of Chemistry, 46, 1592 (1968)

It has been shown recently (1) that 2-alkoxy-5,6-dihydro-2*H*-pyran reacts with *m*-chloroperoxybenzoic acid to give a preponderance of the epoxide in which the 3,4-anhydro ring is *trans* to the 2-alkoxy substituent and that opening of the epoxide ring by $LiAlH_4$ occurs exclusively by breaking the C—O bond remote from the C-2 alkoxy substituent.

We have now employed this approach to prepare a mixture of methyl 4-deoxy-3-*O*-methyl-α- and β-DL-*threo*-pentopyranosides starting with the *cis*-, *trans*-, or *cis–trans*-2-alkoxy-3,4-epoxytetrahydropyran (**1** and **2**).

When **1** and/or **2** were heated in methanol containing some *p*-toluenesulfonic acid as catalyst, a distillable oil was obtained in 76% yield, (Scheme 1) which contained in each case the same mixture of just two substances as shown by gas–liquid chromatography (g.l.c.). That these two substances were isomers was shown by the analysis of the binary mixture which was correct for methyl 4-deoxy-3-*O*-methyl-α (or β)-DL-*threo*-pentopyranoside. The result could be rationalized on the reasonable assumption that the first reaction which occurred was that in which the methanol attacked the protonated epoxide exclusively on that carbon atom remote from the anomeric center. This was then followed by a slower isomerization to produce an equilibrium mixture of the α and β anomers of the DL mixture.

The structures of the products **3** and **4** were proved in the following manner.

The mixture (**3** and **4**) obtained from methanolysis of **1** and **2** was hydrolyzed to give a syrup. Treatment of the syrup with phenylhydrazine gave a solid phenylosazone, which analyzed correctly for the phenylosazone of 4-deoxy-3-*O*-methyl-DL-*threo*-pentose, thus proving the location of the methoxy group at position-4 in the tetrahydropyran ring system. Conversion of the mixture **3** and **4** to the 3,5-dinitrobenzoate gave a solid whose nuclear magnetic resonance (n.m.r.) spectrum showed doublets for the anomeric protons at τ 5.55 ($J_{1'2'} = 7$ Hz) and τ 5.03 ($J_{1,2} = 3.3$ Hz) for the two epimers, and

[1]Taken from the thesis of F. Sweet to be submitted to the Faculty of Graduate Studies, University of Alberta, Edmonton, Alberta, as part of the requirements for the degree of Doctor of Philosophy.

FOR ERRATA SEE
Vol. 46 #2 19 68 P. 3419

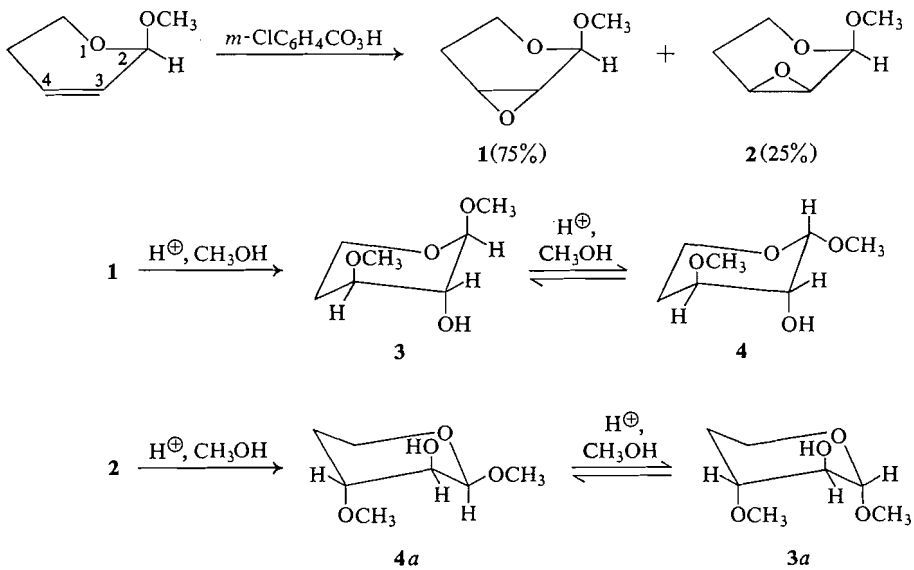

SCHEME 1

quartets centered at τ 4.92 ($J_{2',3'} = 8$ Hz and $J_{1'2'} = 7$ Hz) and τ 4.97 ($J_{2,3} = 8$ Hz and $J_{1,2} = 3.3$ Hz) for the protons H-2, and H-2 on the carbon atom bearing the 3,5-dinitrobenzoyloxy group in the two anomers respectively.[2] Irradiation of the signal position for the anomeric proton H′ at τ 5.55 collapsed the quartet centered at τ 4.92 to a doublet centered at τ 4.92 ($J_{2'3'} = 8$ Hz) thus showing that the two protons concerned must be on adjacent carbon atoms and thus locating the position of the free hydroxyl group on C-2 of the xylopyranoside ring system.

The xylose configuration was established on the basis of the oxidative degradation, with concentrated nitric acid, of the syrup resulting from the hydrolysis of **3** and **4**. There was obtained a solid, melting at 196–202 °C (decomp.). The infrared spectrum of this compound was practically identical with that of authentic *O*-methyl-L-tartaric acid kindly donated by Woo *et al.*[3] (2) who prepared it by nitric acid oxidation of 4,6-dideoxy-3-*O*-methyl-D-glucose (chalcose) and by methylation of authentic L-tartaric acid. The melting point of *O*-methyl-L-tartaric acid was 179–182 °C (1) whereas our material melted at 196–202 °C and is therefore a racemic *compound* rather than a racemic mixture (3, 4).

[2]Here the numbering is that for the xylopyranoside ring system in which the anomeric carbon is number 1.

[3]We are indebted to Dr. Woo and associates of the Parke, Davis and Company, Detroit, Michigan, for their sample of *O*-methyl-L-tartaric acid and a copy of its infrared spectrum.

Experimental

Methyl 1-4-Deoxy-3-O-methyl-α,β-DL-threo-pentopyranoside

A quantity (9.95 g, 0.076 mole) of the 1:3 mixture of *cis*- and *trans*-3,4-epoxy-2-methoxytetrahydropyran was dissolved in 100 ml of anhydrous methanol containing 100 mg of *p*-toluenesulfonic acid. The solution was heated under reflux overnight, then cooled to room temperature and neutralized by the addition of solid sodium methoxide. The methanol was then removed at 45 °C in a rotary evaporator under the vacuum obtained by a water pump. The residue, in 100 ml of methlyene chloride, was washed with 10 ml of saturated aqueous sodium carbonate solution then with 10 ml of water. The combined washings were extracted with 25 ml of methylene chloride. The combined methylene chloride extract and solution were dried (Na_2SO_4), filtered, and then freed from solvent at 45 °C under vacuum in a rotary evaporator. Distillation of the oily residue afforded 9.8 g (76%) of a colorless, viscous oil. The boiling point was 63–66 °C at 0.75 mm; n_D^{23}, 1.4575.

Anal. Calcd. for $C_7H_{14}O_4$: C, 51.84; H, 8.70. Found: C, 51.61; H, 8.43.

The nuclear magnetic resonance (n.m.r.) spectrum in $CDCl_3$ (reference, tetramethylsilane) at 60 MHz using a Varian Associates A60 spectrometer showed two anomeric proton signals at τ 5.79 (doublet, $J_{1,2} \sim 2$ Hz) and at τ 5.92 (doublet, $J_{1',2'} \sim 7$ Hz).

Gas–liquid chromatography (g.l.c.) on a 12 ft, ⅛ in. O.D. column of 20% butanediol succinate on Gas-Chrom

Can. J. Chem. Downloaded from www.nrcresearchpress.com by 210.87.254.5 on 09/05/12
For personal use only.

P 60–80 mesh, with helium as the carrier gas at a flow rate of 40 ml/min, column temperature 180 °C, showed the presence of only two components, clearly resolvable.

The 3,5-dinitrobenzoate, obtained in the usual manner, melted at 131–135 °C (from methanol–water).

Anal. Calcd. for $C_{14}H_{16}O_9N_2$: C, 47.19; H, 4.43; N, 7.86. Found: C, 47.09; H, 4.36; N, 8.13.

The n.m.r. spectrum in $CDCl_3$ (reference tetramethylsilane) (obtained with a Varian Associates HR 100 spectrometer) clearly showed the presence of two isomers. Analysis of the spectrum is described in the discussion section.

*4-Deoxy-3-O-methyl-α,β-*DL*-threo-pentose*

Methyl 4-deoxy-3-*O*-methyl-α,β-DL-*threo*-pentopyranoside (2 g) was placed in 125 ml of water containing 3 g of Amberlite IR 120 (H^+). The mixture was stirred while being heated on a steam bath to 85–90 °C for 20 h. The cooled mixture was filtered (gravity) and the ion–exchange resin washed with 15 ml of water and separated. The combined filtrates were freed from water at 45 °C in a rotary evaporator under reduced pressure and gave 2 g of a colorless syrup. Attempts to crystallize this from a variety of solvents (ethyl acetate, Skellysolve B, methanol, water) failed.

The n.m.r. spectrum in pyridine (reference, tetramethylsilane; A60 spectrometer) showed the presence of two isomers since two anomeric proton signals were obtained — τ 4.45 (doublet, $J_{1,2} \sim 2.0$ Hz) and τ 5.12 (doublet, $J_{1',2'} \sim 7.0$ Hz). No starting material was detected.

*Phenylosazone of 4-Deoxy-3-O-methyl-α,β-*DL*-threo-pentose*

To 0.4 g of 4-deoxy-3-*O*-methyl-α,β-DL-*threo*-pentose was added 0.8 g of phenylhydrazine hydrochloride followed by 1.2 g of crystalline sodium acetate and then 8 ml of water. To the cloudy solution was added 1 ml of saturated aqueous sodium bisulfite to prevent air oxidation of the product. The mixture, frequently shaken, was heated in a beaker of boiling water for 40 min. After 7 min of heating, light-amber colored oil droplets appeared and accumulated. When the solution was cooled, the oil droplets formed an amorphous solid from which the liquid could be decanted. The solid was crystallized from 25 ml of ethanol–water (3:1 by volume) and gave yellow needles. Two further crystallizations from the same solvent mixture gave 350 mg of the pure phenylosazone of 4-deoxy-3-*O*-methyl-α,β-DL-*threo*-pentose. The melting point (with decomposition) was 121 °C.

Anal. Calcd. for $C_{18}H_{22}O_2N_4$: C, 66.23; H, 6.79; N, 17.17. Found: C, 66.44; H, 6.94; N, 17.38.

*Nitric Acid Oxidation of 4-Deoxy-3-O-methyl-*DL*-threo-pentose*

The 4-deoxy-3-*O*-methyl-DL-xylose (1 g) was added to a solution of 4 ml of concentrated nitric acid in 10 ml of water in a porcelain evaporating dish. The mixture was heated on a steam bath, in an efficient hood, until about 2–3 ml of viscous liquid remained. Cooling failed to induce crystallization. The crude material was transferred with 10 ml of water to a flask. The water was removed by a rotary evaporator under vacuum whereupon a colorless solid appeared. This was taken up in 15 ml of hot ethyl acetate, filtered, and stored overnight in a refrigerator. The colorless crystals were separated by filtration under vacuum and again crystallized from 10 ml of ethyl acetate; yield, 550 mg (55%) of pure *O*-methyl-DL-tartaric acid. The melting point (with decomposition) was 196–202 °C. Literature melting point for *O*-methyl-L-tartaric acid was 179–182 °C (2).

Anal. Calcd. for $C_5H_8O_6$: C, 36.59; H, 4.91. Found: C, 36.48; H, 4.80.

The infrared spectrum (KBr pellet) was identical with that supplied by Woo *et al.* (2).

Acknowledgment

The authors are grateful to the National Research Council of Canada for financial support of this work.

1. F. Sweet and R. K. Brown. Can. J. Chem. **46**, 707 (1968).
2. P. W. K. Woo, H. W. Dion, and L. F. Johnson. J Am. Chem. Soc. **84**, 1066 (1962).
3. L. F. Fieser and M. Fieser. Advanced organic chemistry. Reinhold Publishing Company, New York. 1961. p. 84.
4. H. W. Bakhuis-Roozeboom. Ber. **32**, 537 (1899).

Can. J. Chem. Downloaded from www.nrcresearchpress.com by 210.87.254.5 on 09/05/12
For personal use only.

Can. J. Chem. Downloaded from www.nrcresearchpress.com by 210.87.254.40 on 09/05/12
For personal use only.

COMMUNICATIONS

Effect of substituents on the chemical shift of benzylic protons: evidence for a conformational dependence

ROBERT R. FRASER, GURUDATA, CESAR REYES-ZAMORA, AND ROBERT B. SWINGLE
Department of Chemistry, University of Ottawa, Ottawa, Canada

Received March 5, 1968

The benzyl proton shifts in 11 series of *para*-substituted toluenes bearing different α substituents have been determined. In each series, a plot of the benzylic shift against the Hammett σ values of the *para*-substituent is linear. The slope of these plots varies from 0.2 to 0.0 p.p.m./σ. The variation is found to be conformationally dependent, a fact which is not explicable by current theory. A hyperconjugative interaction is proposed to account for these results and for several anomalies in the literature.

Canadian Journal of Chemistry, 46, 1595 (1968)

In the last decade a large number of authors have presented data showing a correlation between the effect of substituents on the chemical shifts (SCS) of protons on a benzene ring, and the Hammett σ values of the substituents (1–3). More recently, correlations between σ values and the SCS of protons in the side chain of aromatics have been reported (4, 5, and references therein). It is usually assumed that the SCS results from the inductive and resonance effects of the substituent, which alter the electron density at the ring carbon atoms. This change is then transmitted through the π electrons to the proton in question. An alternative explanation involving field and mesomeric effects (the F–M correlation) has recently been put forward by Dewar and Takeuchi (6).

We wish to report the determination of the *para*-substituent effect on the benzylic proton shifts, in eleven series of compounds of the formula $X—C_6H_5—CH_2—Z$. For each Z, at least five X substituents were studied whose range of σ values was 0.95 or greater.[1] An example of the Hammett correlation for the benzylic protons of eight tetrahydropyranyl ethers is shown in Fig. 1. This plot is typical of the degree of correlation found in all series. In each series the point for chlorine deviates the most and lies above the best straight line by 1–3 c.p.s.[2] In all series the slope of the best straight line, ρ, is negative. In Fig. 1, ρ has values of 0.16 and 0.15 (p.p.m. per σ) for the two diastereotopic protons of the benzyl group.

The ρ values for the remaining series are listed in Table I. It can be seen that ρ varies widely (0.22–0.00) as the nature of Z is altered. If we accept the premise that any *para*-substituent affects only the π electron distribution of the benzene ring, then the variation in ρ must be due to the variation in Z. The most important properties of Z which change with electronegativity and size and from series to series, are also listed in Table I.

It can be seen that changes in electronegativity of Z bear no relation to changes in ρ. On the other hand there is a reasonably consistent parallel between ρ and the size of Z, the sulfones and toluenes being the only exceptions. This indicates that ρ depends to a large extent on the conformation of the methylene group with respect to the benzene ring.

This conclusion is most strikingly supported by the data for the sulfoxides. When $Z = SOC_6H_5$, the two diastereotopic protons of

[1]All chemical shifts were measured on a Varian DA-60 nuclear magnetic resonance spectrometer using dilute solutions (0.2 *M*) in $CDCl_3$, except in the case of compounds whose methylene protons were magnetically non-equivalent. In these cases 0.3 *M* solutions were used. In each series, 0.1 *M* solutions were also studied and dilution shifts beyond the experimental error of 0.2 c.p.s. could not be detected. Satisfactory elemental analyses were obtained for all new compounds included in this study.

[2]Because of the variable deviation of chlorine, we have not included it when drawing the best straight line for each series. If it were included, the standard errors given in Table I would increase by 30%. We have chosen the standard error of measurement to indicate the accuracy of each correlation, rather than the more commonly used correlation coefficient *r*, since *r* varies with ρ (7).

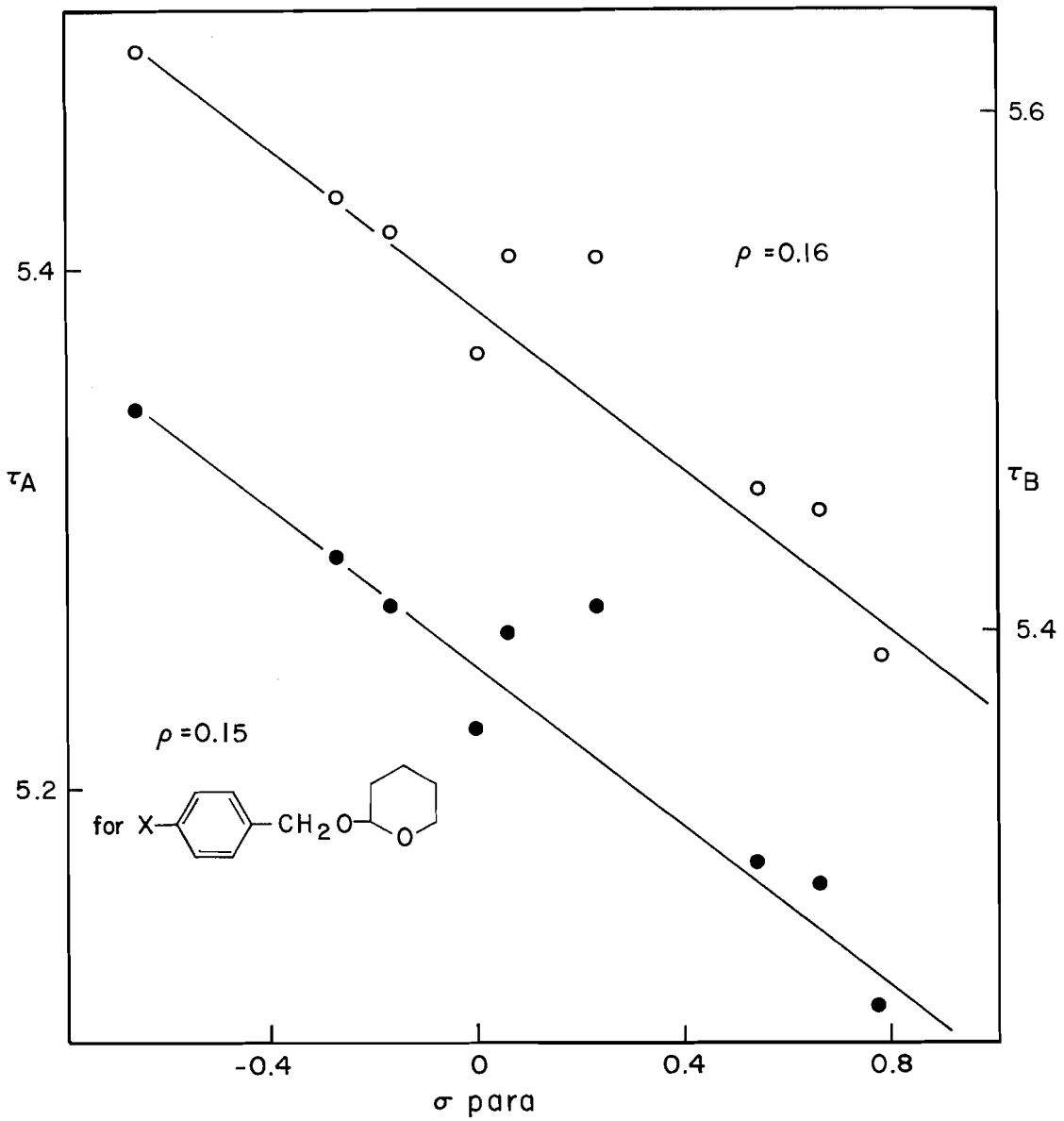

FIG. 1. A Hammett plot of the benzylic proton shifts of nine para-substituted benzyl tetrahydropyranyl ethers.

the methylene group have ρ's of 0.00 and 0.20 in spite of the fact that the electronegativity of Z is the same for each. In the most probable conformation for this sulfoxide depicted as **1**, the bulky phenyl rings are *trans* and the oxygen atom which is larger than the electron pair is located further from the *ortho* proton of the benzene ring. As a result, the diastereotopic protons are placed differently with respect to the plane of the adjacent benzene ring. If the substituent effect is maximal when the C—H bond of a benzylic proton is colinear with the adjacent *p*-orbital, and minimal when at a right angle to it, then the results for this sulfoxide, and for the decrease in ρ with increasing size of Z, would be accounted for.[3] In other words, when Z is small the conformation shown in **2**

[3]It is also possible that H_A, because it is *trans* to the sulfoxide oxygen, has a different ρ than H_B, which is *gauche* to the oxygen. However, this interpretation cannot explain any of the other data in Table I and is therefore less likely.

Can. J. Chem. Downloaded from www.nrcresearchpress.com by 210.87.254.40 on 09/05/12
For personal use only.

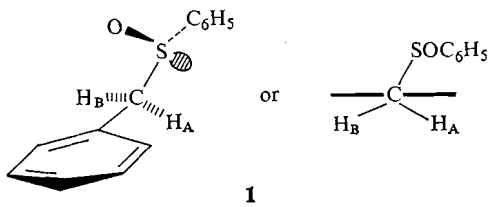

1

2 3

will predominate, and when Z is large the conformation shown in **3** will predominate. Our previous studies of geminal coupling constants in the tetrahydropyranyl ethers and sulfoxides (**9**), which indicated the former to have **2** and the latter to have **3** as their predominant conformations, support this proposal.

TABLE I

Rho values of substituent chemical shift – Hammett plots for X—⟨⟩—CH_2Z

Z	−ρ	Van der Waals radius*	Electronegativity*	Standard error†	N‡
H§	0.20	1.2	2.1	1.0	8
CH_3‖	0.22	2.0	2.5	0.9	7
OH	0.21	1.4	3.5	1.7	6
OCH_3	0.15	1.4	3.5	1.4	6
OTHP	0.16; 0.15	1.4	3.5	1.1	8
Cl	0.11	1.8	3.0	0.8	5
SCH_3	0.10	1.85	2.5	0.8	4
SC_6H_5	0.08	1.85	2.5	1.4	5
$SOCH_3$	0.10; 0.14	1.85	2.5	1.3	5
SOC_6H_5	0.00; 0.20	1.85	2.5	1.9	5
SO_2CH_3	0.16	1.85	2.5	0.9	5
$SO_2C_6H_5$	0.16	1.85	2.5	1.4	5
Br	0.02	1.95	2.0	1.0	5

*Values of the Van der Waals radius and electronegativity of the atom attached to the methylene group are quoted from ref. 18.
†The standard error of estimate (8) is given in units of c.p.s.
‡N represents the number of compounds studied in each series.
§This value was calculated from the data in ref. 4.
‖This value was calculated from the data in ref. 19.

There does not appear to be any explanation for the conformational variation of ρ within the present framework of proton shift theory. Current theory (10, 11) recognizes three main factors which determine the chemical shift of a proton; (*a*) diamagnetic shielding, (*b*) anisotropy, and (*c*) solvent effects. Neither the field nor the inductive mechanism of altering the diamagnetic shielding can account for the conformational dependence of ρ. The effect of a substituent on benzene ring anisotropy is generally assumed to be negligible (12). A proposal has recently been put forward suggesting that all substituents decrease the "ring current" effect by increasing the contributions of the quinonoid form (13). However, using the reported values, we have calculated the substituent effect on anisotropy to be an order of magnitude smaller than that observed in our results and the effect shows no correlation with σ. Since the solvent was $CDCl_3$ in all series, solvent effects are also eliminated. Thus we are forced to conclude that a previously unrecognized factor influences the chemical shift of benzylic protons. Two possibilities which would be conformationally dependent are hyperconjugation or, alternatively, the paramagnetic shielding term of Ramsey's formula (11, p. 159), each of which would be sensitive to a substituent effect.

We wish to emphasize the fact that, regardless of its origin, this new factor merits *careful* attention. It cannot be explained by existing theories, and its magnitude must be anticipated to be considerably greater than the observed perturbation by substituents, through which it was revealed. There are several large anomalous shifts in the literature which can be explained by a hyperconjugative or paramagnetic effect. In α-haloketones, an axial α-proton appears ~1 p.p.m. to lower field than normal (14, 15), in 7,12-dihydropleidenes the pseudoaxial proton appears 1–2 p.p.m. to lower field than the pseudoequatorial proton (16), and in the dibenzhomotropyl methyl ethers of Childs and Winstein (17) a similar discrepancy was observed. Furthermore since this factor influences benzylic shifts (and possibly the shift of any proton α to an sp^2 hybridized atom) their magnitudes must not be used to derive Δχ values. Finally, a greater understanding of this effect could provide an important method of conformational analysis. Further studies to this end are in progress.

Acknowledgments

The authors thank the National Research Council of Canada for financial support of this research.

1. R. R. Fraser. Can. J. Chem. **38**, 2226 (1960).
2. H. Spiesecke and W. G. Schneider. J. Chem. Phys. **35**, 731 (1961).
3. J. W. Emsley, J. Feeney, and L. H. Sutcliffe. High resolution nuclear magnetic resonance spectroscopy.

Can. J. Chem. Downloaded from www.nrcresearchpress.com by 210.87.254.40 on 09/05/12
For personal use only.

Vol. II. The Pergamon Press, Ltd., London. 1966. pp. 749–770.
4. S. H. MARCUS, W. F. REYNOLDS, and S. I. MILLER. J. Org. Chem. **31**, 1872 (1966).
5. T. A. WITTSTRUCK and E. N. TRACHTENBERG. J. Am. Chem. Soc. **89**, 3503 (1967).
6. M. J. S. DEWAR and Y. TAKEUCHI. J. Am. Chem. Soc. **89**, 390 (1967).
7. C. D. RITCHIE and W. F. SAGER. Progr. Phys. Org. Chem. **2**, 323 (1964).
8. A. L. EDWARDS. Statistical methods. Henry Holt and Co., New York. 1967. p. 85.
9. R. R. FRASER, P. HANBURY, and C. REYES-ZAMORA. Can. J. Chem. **45**, 2481 (1967).
10. R. F. ZURCHER. *In* Progress in magnetic resonance. Vol. II. *Edited by* J. W. Emsley, J. Feeney, and L. H. Sutcliffe. The Pergamon Press, Ltd., London. 1967.
11. J. A. POPLE, W. G. SCHNEIDER, and H. J. BERNSTEIN. High-resolution nuclear magnetic resonance. McGraw-Hill Book Co., Inc., New York. 1959. p. 175.
12. T. K. WU and B. P. DAILEY. J. Chem. Phys. **41**, 2796 (1964).
13. H. P. FIGEYS and R. FLAMMANG. Mol. Phys. **12**, 581 (1967).
14. A. NICKON, M. A. CASTLE, R. HARADA, C. E. BERKOFF, and R. O. WILLIAMS. J. Am. Chem. Soc. **85**, 2185 (1963).
15. G. J. KARABATSOS, G. C. SONNICHSEN, N. HSI, and D. J. FENOGLIO. J. Am. Chem. Soc. **89**, 5067 (1967).
16. P. T. LANSBURY, J. F. BIERON, and A. J. LACHER. J. Am. Chem. Soc. **88**, 1482 (1966).
17. R. F. CHILDS and S. WINSTEIN. J. Am. Chem. Soc. **89**, 6348 (1967).
18. L. N. FERGUSON. The modern structural theory of organic chemistry. Prentice-Hall, Inc., New York. 1962.
19. K. L. WILLIAMSON. J. Am. Chem. Soc. **86**, 4021 (1964).

Binuclear copper(I) complexes with bridging bis(diphenylphosphino)acetylene groups

A. J. CARTY AND A. EFRATY
Department of Chemistry, University of Waterloo, Waterloo, Ontario

Received March 20, 1968

The preparations of some novel copper(I) complexes of the ligand bis(diphenylphosphino)acetylene are described.

Canadian Journal of Chemistry, 46, 1598 (1968)

Acetylenic ditertiary phosphines of the type $R_2PC{\equiv}CPR_2$ are potentially interesting ligands in view of the possibility of using the π orbitals of the acetylenic group for coordination in addition to the two phosphorus atoms. Moreover, the linear P—C—C—P skeleton suggests that these compounds may exhibit markedly different coordinating properties from the related tertiary alkylene and tertiary *o*-phenylene diphosphines (1). We have recently prepared a number of complexes of bis(diphenylphosphino)-acetylene **1** which have several novel structural features. Increasing interest in complexes of unsaturated ditertiary phosphines (2) prompts us to report the results of our studies on copper(I) compounds.

Hydrated copper(II) chloride, bromide, and nitrate in ethanolic solution are immediately reduced by **1** with the formation of stable, white, crystalline, diamagnetic compounds insoluble in ethanol but readily recrystallized from dichloromethane. Analyses indicated a composition $(CuX)_2(DPPA)_3$ (X = Cl, Br, NO_3; DPPA = bis(diphenylphosphino)acetylene) in each case. Reaction of potassium thiocyanate with $CuCl_2{\cdot}3H_2O$ in ethanol, followed by addition of **1** yielded, on extraction with dichloromethane, a thiocyanate $(CuSCN)_2(DPPA)_3$. The corresponding iodide complex was prepared by metathetical reaction of the chloride with potassium iodide.

$Ph_2PC{\equiv}CPPh_2$

1

2

We suggest a structure **2** for these compounds in which three diphosphine molecules symmetrically bridge two tetrahedral copper(I) ions. Our main evidence is summarized below.

Osmometric molecular weight measurements in dibromomethane indicate binuclear $(CuX)_2(DPPA)_3$ species in solution. $\nu(C{\equiv}C)$ is infrared inactive in the free ligand but appears in the Raman at 2100 cm^{-1}. Coordination of an

Can. J. Chem. Downloaded from www.nrcresearchpress.com by 210.87.254.40 on 09/05/12
For personal use only.

Vol. II. The Pergamon Press, Ltd., London. 1966. pp. 749–770.
4. S. H. MARCUS, W. F. REYNOLDS, and S. I. MILLER. J. Org. Chem. **31**, 1872 (1966).
5. T. A. WITTSTRUCK and E. N. TRACHTENBERG. J. Am. Chem. Soc. **89**, 3503 (1967).
6. M. J. S. DEWAR and Y. TAKEUCHI. J. Am. Chem. Soc. **89**, 390 (1967).
7. C. D. RITCHIE and W. F. SAGER. Progr. Phys. Org. Chem. **2**, 323 (1964).
8. A. L. EDWARDS. Statistical methods. Henry Holt and Co., New York. 1967. p. 85.
9. R. R. FRASER, P. HANBURY, and C. REYES-ZAMORA. Can. J. Chem. **45**, 2481 (1967).
10. R. F. ZURCHER. *In* Progress in magnetic resonance. Vol. II. *Edited by* J. W. Emsley, J. Feeney, and L. H. Sutcliffe. The Pergamon Press, Ltd., London. 1967.
11. J. A. POPLE, W. G. SCHNEIDER, and H. J. BERNSTEIN. High-resolution nuclear magnetic resonance. McGraw-Hill Book Co., Inc., New York. 1959. p. 175.
12. T. K. WU and B. P. DAILEY. J. Chem. Phys. **41**, 2796 (1964).
13. H. P. FIGEYS and R. FLAMMANG. Mol. Phys. **12**, 581 (1967).
14. A. NICKON, M. A. CASTLE, R. HARADA, C. E. BERKOFF, and R. O. WILLIAMS. J. Am. Chem. Soc. **85**, 2185 (1963).
15. G. J. KARABATSOS, G. C. SONNICHSEN, N. HSI, and D. J. FENOGLIO. J. Am. Chem. Soc. **89**, 5067 (1967).
16. P. T. LANSBURY, J. F. BIERON, and A. J. LACHER. J. Am. Chem. Soc. **88**, 1482 (1966).
17. R. F. CHILDS and S. WINSTEIN. J. Am. Chem. Soc. **89**, 6348 (1967).
18. L. N. FERGUSON. The modern structural theory of organic chemistry. Prentice-Hall, Inc., New York. 1962.
19. K. L. WILLIAMSON. J. Am. Chem. Soc. **86**, 4021 (1964).

Binuclear copper(I) complexes with bridging bis(diphenylphosphino)acetylene groups

A. J. CARTY AND A. EFRATY
Department of Chemistry, University of Waterloo, Waterloo, Ontario

Received March 20, 1968

The preparations of some novel copper(I) complexes of the ligand bis(diphenylphosphino)acetylene are described.

Canadian Journal of Chemistry, 46, 1598 (1968)

Acetylenic ditertiary phosphines of the type $R_2PC{\equiv}CPR_2$ are potentially interesting ligands in view of the possibility of using the π orbitals of the acetylenic group for coordination in addition to the two phosphorus atoms. Moreover, the linear P—C—C—P skeleton suggests that these compounds may exhibit markedly different coordinating properties from the related tertiary alkylene and tertiary *o*-phenylene diphosphines (1). We have recently prepared a number of complexes of bis(diphenylphosphino)-acetylene **1** which have several novel structural features. Increasing interest in complexes of unsaturated ditertiary phosphines (2) prompts us to report the results of our studies on copper(I) compounds.

Hydrated copper(II) chloride, bromide, and nitrate in ethanolic solution are immediately reduced by **1** with the formation of stable, white, crystalline, diamagnetic compounds insoluble in ethanol but readily recrystallized from dichloromethane. Analyses indicated a composition $(CuX)_2(DPPA)_3$ (X = Cl, Br, NO_3; DPPA = bis(diphenylphosphino)acetylene) in each case. Reaction of potassium thiocyanate with $CuCl_2{\cdot}3H_2O$ in ethanol, followed by addition of **1** yielded, on extraction with dichloromethane, a thiocyanate $(CuSCN)_2(DPPA)_3$. The corresponding iodide complex was prepared by metathetical reaction of the chloride with potassium iodide.

$Ph_2PC{\equiv}CPPh_2$

1

2

We suggest a structure **2** for these compounds in which three diphosphine molecules symmetrically bridge two tetrahedral copper(I) ions. Our main evidence is summarized below.

Osmometric molecular weight measurements in dibromomethane indicate binuclear $(CuX)_2(DPPA)_3$ species in solution. $\nu(C{\equiv}C)$ is infrared inactive in the free ligand but appears in the Raman at 2100 cm^{-1}. Coordination of an

Can. J. Chem. Downloaded from www.nrcresearchpress.com by 210.87.254.5 on 09/05/12
For personal use only.

acetylene to a transition metal causes $\nu(C\equiv C)$ to appear weakly in the infrared at a frequency 200–400 cm^{-1} lower than in the free ligand (3). There are no absorptions between 2100 cm^{-1} and 1600 cm^{-1} in the infrared of these complexes suggestive of a lowering of symmetry of the ligand due to coordination of the acetylenic triple bond. Moreover, $\nu(C\equiv C)$ appears at 2120 cm^{-1} in the Raman spectra of methylene dichloride solutions of the complexes, 20 cm^{-1} higher than in the free ligand. We therefore conclude that only the phosphorus atoms are used for coordination. The infrared spectrum of $(CuNO_3)_2(DPPA)_3$ shows two strong bands at 1440 cm^{-1}, 1296 cm^{-1} and a medium band at 1028 cm^{-1} readily assignable to $\nu_4(\nu_a NO_2)$, $\nu_1(\nu_s NO_2)$, and $\nu_2(\nu NO)$ of coordinated nitrate. $(CuSCN)_2(DPPA)_3$ has a single sharp $\nu(C\equiv N)$ absorption at 2060 cm^{-1} and two weak $\nu(C—S)$ bands at 798 cm^{-1} and 805 cm^{-1} characteristic of N-bonded thiocyanate (4). There are no data in the literature on metal–halogen stretching frequencies in copper(I) complexes. However, comparison of the analogous complexes shows that $\nu(Cu—Cl)$ appears as a single strong band at 267 cm^{-1} and $\nu(Cu—Br)$ at 202 cm^{-1}. These values are lower than the frequency ranges for $\nu(Cu—X)$ modes in tetrahedral copper(II) complexes and agree with the single $\nu(Cu—X)$ (A_2'') mode expected for **2** of D_{3h} symmetry (5).

In the many complexes of **1** we have examined, the ligand always appears to be bridging. Reasons for this are readily apparent on examination of the molecular geometry. The bite[1] of the ligand, calculated from recent X-ray data on $P(C\equiv CC_6H_5)_3$ (6) is 4.7 Å. This compares with 3.1 Å for *o*-phenylene bis(diethylphosphine) and is considerably larger than the distance between adjacent positions in tetrahedral copper(II) and copper(I) complexes[2] or between *cis* positions in square planar phosphine complexes of platinum(II) halides (7). The ligand is therefore clearly incapable of chelating in the same way as other diphosphines. An X-ray structure investigation of $(CuNO_3)_2(DPPA)_3$ is now in progress and metal carbonyl complexes of **1** are also being examined.

[1]Distance between the donor atoms.

1. G. Booth. Advan. Inorg. Chem. Radiochem. **6**, 1 (1964).
2. (*a*) W. R. Cullen, P. S. Dhaliwal, and C. J. Stewart. Inorg. Chem. **6**, 2256 (1967). (*b*) H. N. Ramaswamy, H. B. Jonassen, and A. M. Aguiar. Inorg. Chem. Acta, **1**, 141 (1967).
3. J. Chatt, R. G. Guy, and L. A. Duncanson. J. Chem. Soc. 827 (1961).
4. M. E. Farago and J. M. James. Inorg. Chem. **4**, 1706 (1965).
5. D. M. Adams and P. J. Lock. J. Chem. Soc. A, 620 (1967).
6. V. D. Mootz and G. Sasmannshausen. Z. Anorg. Allgem. Chem. **355**, 200 (1967).
7. G. G. Messmer, E. L. Amma, and J. A. Ibers. Inorg. Chem. **6**, 725 (1967).
8. F. G. Mann, D. Purdie, and A. F. Wells. J. Chem. Soc. 1503 (1936).
9. S. J. Lippard and K. M. Melmed. Inorg. Chem. **6**, 2223 (1967).

[2]In the tetrameric copper compound $[CuIAsEt_3]_4$ the distance along a tetrahedral edge is 2.5 Å (8). $Cu(PPh_3)_2BH_4$ is the only copper(I) phosphine complex structurally characterized (9). Although the P—Cu—P bond angle is unusually large (123.26°) the P—P distance is still only 4.0 Å.

Can. J. Chem. Downloaded from www.nrcresearchpress.com by 210.87.254.5 on 09/05/12
For personal use only.

Can. J. Chem. Downloaded from www.nrcresearchpress.com by 210.87.254.42 on 09/05/12
For personal use only.

Canadian Journal of Chemistry

Published by THE NATIONAL RESEARCH COUNCIL OF CANADA

VOLUME 46 MAY 15, 1968 NUMBER 10

Solvent effects on the boron–fluorine coupling constant and on fluorine exchange in the tetrafluoroborate anion

R. J. GILLESPIE, J. S. HARTMAN, AND M. PAREKH

Department of Chemistry, McMaster University, Hamilton, Ontario

Received November 10, 1967

The ^{11}B—^{19}F spin–spin coupling constant in $AgBF_4$ is shown to have an opposite sign in water from that found in a number of organic solvents. Application of the hypothesis of Bell and Danyluk indicates that it has a positive sign in water. Evidence is presented for association, probably in the form of solvent-separated ion pairs, in aqueous $LiBF_4$ and $NaBF_4$ solutions, and for the formation of more tightly bound ion pairs in solvents of lower dielectric constant. In contrast, there apparently is no solute association in $AgBF_4$ solutions in water, DMSO, DMF, or acetonitrile. The pronounced changes observed in the ^{11}B—^{19}F coupling constant support the postulate that its small size is a result of near cancellation of large opposing terms.

The collapse of the ^{10}B—^{11}B isotope shift at high temperatures in the ^{19}F spectra of solutions of $AgBF_4$ in acetonitrile and in acetone provides evidence for exchange of fluorine among boron atoms; a mechanism is proposed for this process.

Canadian Journal of Chemistry, 46, 1601 (1968)

Introduction

The remarkable variation with concentration of the ^{11}B—^{19}F coupling constant of sodium tetrafluoroborate in aqueous solution was first clearly demonstrated by Kuhlmann and Grant (1). These authors found that $J_{^{11}B-^{19}F}$ is dependent not only on the concentration of $NaBF_4$ but also on the presence of other ions in solution. They found that in $NaBF_4$ solutions the value of the coupling constant varies from an extrapolated value of 1.1 Hz at infinite dilution to 4.8 Hz in a saturated solution, and at a given concentration it is increased by the addition of $NaNO_3$ and $LiNO_3$. An equilibrium between free BF_4^- and BF_4^- associated with Na^+ (or Li^+) in an ion pair was postulated to explain the results. Since the coupling constant in ammonium tetrafluoroborate was found to be 1.1 Hz and essentially independent of concentration, it was concluded that the NH_4^+ ion does not form an ion pair with BF_4^-.

Haque and Reeves (2) pointed out that if ion-pair formation occurs in aqueous solutions then the coupling constant should increase in low dielectric constant solvents where ion-pair formation should be more extensive. They found, however, that for $NaBF_4$ in acetone–water and dioxane–water mixtures the coupling constant is slightly decreased and that in dimethyl sulfoxide–water mixtures it decreases from 2.0 to 0.8 Hz over the range 0–65% dimethyl sulfoxide (DMSO). A similar decrease in the coupling constant from 3.5 to 1.3 Hz had been observed in these laboratories by Quail (3) for solutions of $NaBF_4$ in diglyme–water mixtures over the range 0–70% diglyme. In all the solvent mixtures studied by Haque and Reeves the coupling constant increases with increasing $NaBF_4$ concentration as it does in water. They found that the changes in coupling constant that they observed with increasing concentration of $NaBF_4$ were paralleled by changes in the chemical shift. They concluded that their results could not be interpreted in terms of ion-pair formation and they also discussed other evidence against this hypothesis. The X-ray diffraction results of Ryss and Radchenko (4) show that in solutions of $NaBF_4$ (2–9 *M*) in water the Na^+ ion is hexacoordinated by water and therefore there can be no direct contact of Na^+ with BF_4^-. Also the ^{19}F spectrum is a sharp quartet although ^{11}B has a quadrupole moment; the presence of the

Can. J. Chem. Downloaded from www.nrcresearchpress.com by 210.87.254.42 on 09/05/12
For personal use only.

Na^+ ion in an ion pair would be expected to create an appreciable field gradient at the ^{11}B nucleus and hence cause broadening or collapse of the quartet. Further evidence against an intimate ion pair has been provided by a study of the ^7Li resonance in aqueous solutions of $LiBF_4$ in which narrow resonance lines were obtained (5). The absence of broadening due to quadrupole relaxation implies that the environment around the Li^+ ion is symmetrical.

Haque and Reeves postulated that all the observations could be explained by assuming that the observed changes in the coupling constant, J,[1] can be attributed to changes in B—F...H—O hydrogen bonding. They assumed that increased hydrogen bonding lowers the coupling constant. They attributed the concentration dependence of the coupling constant in aqueous $NaBF_4$ solutions to removal of water by hydration of the sodium ion and thus to a decrease in the number of water molecules that are available to hydrogen bond with the BF_4^- ion. The difficulty with this explanation is that even in quite dilute solution there is an appreciable dependence of the coupling constant on concentration, e.g. from 1.1 Hz at infinite dilution to 1.9 Hz at 1 M (1). In a 1 M solution there are over 50 molecules of water per Na^+ ion and it seems unlikely that a single sodium ion could influence 50 molecules of water sufficiently that their ability to hydrogen bond with BF_4^- is appreciably reduced.

Haque and Reeves attributed the marked decrease of the coupling constant with decreasing water concentration in dimethyl sulfoxide–water mixtures to specific solvation of BF_4^- by the conjugate acid of dimethyl sulfoxide which is formed in the following protolysis equilibrium.

$$DMSO + H_2O \rightleftharpoons DMSOH^+ + OH^-$$

The absence of a similar decrease in the coupling constant in dioxane–water and acetone–water mixtures was attributed to the fact that they undergo the above protolysis reaction to a much smaller extent. However, it has been estimated that the ionic concentrations in a 1:1 H_2O–DMSO mixture are only 4×10^{-4} M (6). Thus it seems unlikely that an appreciable fraction of the BF_4^- ions could be solvated in this way.

It appears, therefore, that no entirely satisfactory and consistent explanations have been given for the variation of the coupling constant in the tetrafluoroborate ion with concentration and with added cations in aqueous sodium tetrafluoroborate solutions and with the variation of the solvent composition in organic solvent–water mixtures. The present work provides further information which enables a more comprehensive explanation of all the observations to be given.

In a preliminary report of this work (7) we have shown that J for solutions of $AgBF_4$ changes sign on changing the solvent from water to acetonitrile.

Results

The ^{11}B—^{19}F coupling constant J of silver tetrafluoroborate was investigated by ^{19}F n.m.r. in the solvents water, acetonitrile, dimethyl sulfoxide (DMSO), dimethylformamide (DMF), acetone, diglyme, and pyridine and in some mixtures of these solvents. Some solutions of other tetrafluoroborates were also studied.

In solutions of the silver salt in the pure solvents water, acetonitrile, dimethyl sulfoxide, and dimethylformamide the 1:1:1:1 quartet due to coupling with boron-11 ($I = 3/2$) was observed. In the case of acetonitrile, however, the observed splitting of 0.39 Hz was only just detectable. In acetone, diglyme, and pyridine no splitting was observed although the peak had a width of 1.4–6 Hz. The peak due to fluorine on boron-10, which was shifted 0.050 p.p.m. to lower field, did not have observable multiplet structure in any of the solutions except concentrated solutions in water for which a splitting corresponding to $J_{^{10}B-^{19}F} = 0.4 \pm 0.1$ Hz was observed; this agrees well with the corresponding $J_{^{11}B-^{19}F}$ value of 1.07 ± 0.07 Hz. In most other solutions of the silver salt the expected ^{10}B—^{19}F splittings were below the limit of resolution of the spectrometer which was about 0.35 Hz. The coupling constants obtained in these various solvents are summarized in Table I. We note that in the pure solvents and in the 50:50 mole % CH_3CN–H_2O mixture the coupling constant is essentially independent of concentration. This simplifies the investigation of the effects of changing the solvent.

The mean value of J for $AgBF_4$ in aqueous solution, 1.07 ± 0.07 Hz, appears to be independent of concentration and is the same within experimental error as was obtained by Kuhlmann and Grant for NH_4BF_4 solutions (1). It appears

[1]The coupling constant $J_{^{11}B-^{19}F}$ is hereafter denoted simply by the symbol J.

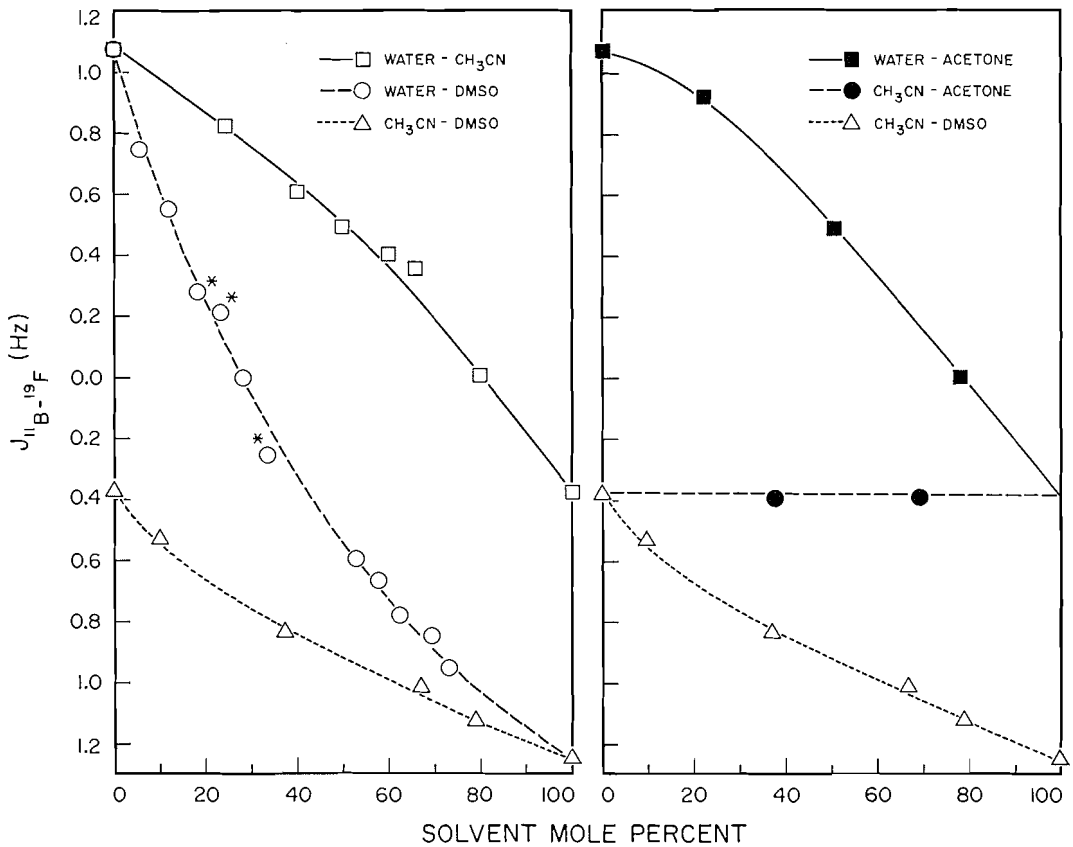

FIG. 1. Variation of $J_{^{11}B-^{19}F}$ with solvent composition in solutions of silver tetrafluoroborate. (*) No splitting was observed in these cases; J was estimated from the width of the single peak.

that in water there is no specific interaction of the BF_4^- ion with either the Ag^+ or NH_4^+ cations. The value of J for $LiBF_4$ solutions in water, however, increases with concentration in a manner similar to that for $NaBF_4$ solutions.

Figure 1 shows the variation of J with solvent composition for solutions of $AgBF_4$ in CH_3CN–H_2O, acetone–H_2O, DMSO–H_2O, CH_3CN–acetone, and CH_3CN–DMSO mixtures. In all the organic solvent–water mixtures the magnitude of J decreases, becomes zero, and then increases again as the percentage of organic solvent increases. Smooth curves are obtained only if it is assumed that the coupling constant decreases from the value observed in water to a value of zero and then changes sign, so that in the pure organic solvents its sign is opposite to that in aqueous solutions. Further evidence that J does indeed change sign in all the water–organic solvent systems studied is provided by the results of measurements on solutions of $AgBF_4$ in CH_3CN–acetone and CH_3CN–DMSO mixtures which clearly indicate that the coupling constant remains of the same sign in these mixtures (Fig. 1).

TABLE I

$J_{^{11}B-^{19}F}$ values for $AgBF_4$ solutions
(temperature 25° unless otherwise specified)

Molality	J (Hz)	Molality	J (Hz)
Water		50 mole % CH_3CN–H_2O	
0.11	1.05	0.08	0.53
0.58	1.13	0.57	0.50
0.58	1.13 (69°)	1.49	0.43
0.58	0.98 (96°)	DMSO	
0.91	1.14	0.48	1.20
2.05	1.19	0.86	1.22
2.35	1.04	1.52	1.35
2.86	1.07	1.80	1.24
CH_3CN		1.80	1.17 (47°)
0.16	0.33 (0°)	1.80	1.24 (69°)
0.16	0.36	1.80	1.28 (91°)
1.16	0.42 (5°)	DMF	
1.16	0.37	1.01	0.96

Can. J. Chem. Downloaded from www.nrcresearchpress.com by 210.87.254.42 on 09/05/12
For personal use only.

Can. J. Chem. Downloaded from www.nrcresearchpress.com by 210.87.254.42 on 09/05/12
For personal use only.

Aqueous solutions of sodium tetrafluoroborate show a small but distinct decrease in J at higher temperatures. A brief investigation showed that one sample with $J = 4.37 \pm 0.1$ Hz at room temperature yielded $J = 3.60 \pm 0.2$ Hz at 98°. A second sample with $J = 2.03 \pm 0.1$ Hz at room temperature yielded $J = 1.7 \pm 0.1$ Hz at 83°. These changes were not due to extensive irreversible reaction since the original room temperature value could be obtained again on cooling; however, a small additional multiplet appeared which apparently arises from BF_3OH^- (1). The shift of J towards the infinite dilution value as the temperature is raised is further evidence supporting Kuhlmann and Grant's postulate of an equilibrium between free and ion-paired BF_4^- in these solutions. Solutions of silver tetrafluoroborate, on the other hand, do not show marked changes in J with temperature. Table I shows that the J values obtained for an aqueous solution of $AgBF_4$ at 69° and 96° are within 0.1 Hz of the average room temperature value of 1.07 Hz. In solutions of $AgBF_4$ in DMSO splittings due to B—F coupling were clearly visible at several temperatures between room temperature and 91°; J remained constant at 1.24 ± 0.1 Hz. The absence of marked changes in J with temperature, such as are observed in solutions of the sodium salt, is a further indication of the lack of any appreciable interactions of BF_4^- with the Ag^+ ion. A brief investigation suggested that the tetramethylammonium salt behaves similarly in aqueous solution. The fact that essentially the same value of J is obtained in aqueous solutions of the ammonium, tetramethylammonium, and silver salts, and that this value is equivalent to the infinite dilution value of aqueous solutions of the sodium and lithium salts, is good evidence that NH_4^+, $N(CH_3)_4^+$, and Ag^+ do not interact appreciably with the BF_4^- ion. On the other hand, aqueous solutions of $LiBF_4$, like those of $NaBF_4$, show a clear dependence of J on concentration (Fig. 2). However, the effect is less than in the sodium salt by a factor of about 2; results previously obtained for the sodium salt are shown in Fig. 2 for comparison. Clearly both Li^+ and Na^+ tend to form ion pairs with BF_4^-.

The very closely spaced quartet structure due to boron–fluorine coupling was difficult to observe at room temperature in solutions of $AgBF_4$ in acetonitrile. Slightly better resolution, with no change in the size of the small splittings, was obtained at rather lower temperatures. Above room temperature the small splittings due to J disappeared completely. At high temperatures the separate peaks arising from F-on-^{10}B and F-on-^{11}B (7) collapsed to yield a single sharp peak, which showed no further change at higher temperatures up to 150°. The temperature range of peak coalescence was 90–100° in the more dilute solutions (0.52 and 0.65 m $AgBF_4$) and 80–90° in the more concentrated solutions studied (3.1 and 3.8 m $AgBF_4$). This collapse of the isotopically shifted peaks at high temperatures is strong evidence for rapid exchange of fluorine among boron atoms at these temperatures. Because of the small relative chemical shift of the F-on-^{10}B and F-on-^{11}B peaks and the broadening due to B—F coupling at lower temperatures the changes in signal shape as the peaks collapsed could not be observed in as much detail as one would wish for the calculation of detailed kinetic data for the process. However, the occurrence of peak coalescence at somewhat lower temperatures in the more concentrated solutions is in accord with an exchange mechanism which is greater than first order in tetrafluoroborate anion.

A solution of $AgBF_4$ (1.51 m) and BF_3 (1.42 m) in acetonitrile gave separate ^{19}F peaks for BF_4^- and for BF_3 (as $CH_3CN.BF_3$), each with an isotope shift, at −17°. A partially collapsed spectrum showing two distinct maxima was obtained at 0° and a single broad peak (width at half-height 8.6 Hz) at room temperature. Higher temperatures caused some reaction, shown by the appearance of new small peaks in the ^{19}F and ^{1}H spectra.

Solutions of $AgBF_4$ in acetone (0.22, 0.74, and 1.29 m) gave broadened ^{19}F spectra in which the F-on-^{11}B peak had a width at half-height of 1.4–2.0 Hz, but with no splittings visible. In the 1.29 m sample, spectra essentially identical with the room temperature spectrum were obtained at 10.5°, −39°, and −56°. In a 1.19 m sample the separate peaks arising from F-on-^{10}B and F-on-^{11}B collapsed at ~70°. Thus rapid fluorine exchange occurs at high temperatures in acetonitrile and acetone, but not in water or DMSO.

Solutions of $AgBF_4$ in diglyme and pyridine gave room temperature ^{19}F spectra consisting of a single broad peak with a width at half-height of 4–6 Hz.

Can. J. Chem. Downloaded from www.nrcresearchpress.com by 210.87.254.42 on 09/05/12
For personal use only.

Discussion

Boron–Fluorine Coupling

Kuhlmann and Grant (1) noted that the $^{11}B—^{19}F$ coupling constant is anomalously small compared with the isoelectronic molecules BeF_4^{2-} and CF_4, which have $^{9}Be—^{19}F$ and $^{13}C—^{19}F$ coupling constants of 33.7 and 259 Hz, respectively (8, 9). Haque and Reeves (2) have expressed these values in terms of the reduced coupling constant j, which corrects for the changes in the magnetogyric ratios γ_X of the nuclei.

$$[1] \qquad \left| j_{X-F} \right| = \left| \frac{J_{X-F}}{\gamma_X \gamma_F} \right|$$

This yields the absolute values of the reduced coupling constants j_{Be-F}, j_{B-F}, and j_{C-F} as 8.16, 0.16, and 34.9 respectively. Further evidence of the anomaly in BF_4^- is provided by the larger B—F coupling constants in the closely related species BF_3OH^- and $CF_3BF_3^-$ which are 12.7 and 39.0 Hz respectively (1, 10).

Pople and Santry, who carried out calculations of nuclear spin–spin coupling constants by molecular orbital theory (11), showed that only the Fermi contact mechanism is important in the case of direct interaction between light nuclei and that the anomalously small size of J in BF_4^- is a result of a close balance between large terms of opposite sign in the atom–atom polarizibility. These conclusions have been supported by additional calculations by Murrell *et al.* (12).

The suggestion that the small values of J in BF_4^- are due to a close balance between large coupling terms of opposite sign is strongly supported by the evidence given in this paper for a change of sign of the coupling constant J between water and organic solvents. Since the absence of a concentration or temperature dependence of J in $AgBF_4$ solutions in different solvents strongly suggests that free BF_4^- is present rather than an associated species, changes as striking as those observed are to be expected only if the contributing terms are large, so that a change of no more than a few percent in one or more of these could change the sign of J.

As an illustration that the magnitude of the observed changes in J in BF_4^- is not unusually large, we may consider the changes in $^{119}Sn—^{19}F$ coupling in tetraethylammonium hexafluorostannate, recently reported by Dean and Evans (13). $J_{^{119}Sn-^{19}F}$ was found to vary from 1557 Hz in water to 1593 Hz in DMSO, and was virtually independent of concentration in the solvents studied. The lack of concentration dependence contrasts with the results obtained from the di-*n*-propylammonium salt, in which a concentration dependence of $J_{^{119}Sn-^{19}F}$ was evident in all of the solvents studied, and for which ion pairing was proposed. The tetraethylammonium salt was postulated to give free SnF_6^{2-} ions in solution, and the differences in $J_{^{119}Sn-^{19}F}$ in the different solvents were postulated to arise from differing degrees of solvation of the ion. The maximum observed changes with solvent of $J_{^{119}Sn-^{19}F}$ and $J_{^{11}B-^{19}F}$ in $(Et_4N)_2SnF_6$ and $AgBF_4$ are 36 Hz and 2.4 Hz respectively, and correspond to changes in reduced coupling constants j (eq. [1]) of 3.29 and 0.26. Thus the change in j is an order of magnitude smaller in BF_4^-, in spite of the fact that the sign changes.

Although a number of studies of solvent dependence of coupling constants have been reported (ref. 1 of ref. 14), the causes of the solvent dependence are not always clear; in many, but not all, cases the effect can be attributed to molecular complex formation or association. It has been postulated (14, 15) that in the absence of such strong interactions variations in solute coupling constants are caused mainly by the electric field of the solvent. Bell and Danyluk (15) proposed that the solvent interaction takes the form of different reaction fields at the different solute atoms, which change the solute electron distribution to some extent and affect the amount of s character in the molecular orbitals, and thus affect the spin–spin coupling. Dean and Evans (13) have applied the arguments of Bell and Danyluk (15), which are based on the molecular orbital treatment of Pople and Santry (11), to the trend of $J_{^{119}Sn-^{19}F}$ in SnF_6^{2-} with solvent polarity and have estimated that the absolute sign of the reduced coupling constant is negative. (Since $\gamma_{^{119}Sn}$ and $\gamma_{^{19}F}$ have opposite signs, $J_{^{119}Sn-^{19}F}$ would then be positive.) A similar estimate can be made from the available data for the BF_4^- ion in solutions of $AgBF_4$. We consider that as the solvent polarity increases as we move from the organic solvents to water, a more positive reaction field, resulting from orientation of solvent dipoles, builds up near the fluorines; this increases the polarity of

Can. J. Chem. Downloaded from www.nrcresearchpress.com by 210.87.254.42 on 09/05/12
For personal use only.

the B—F bonds. Since according to the Pople–Santry treatment the negative contribution to j_{B-F} decreases as the B—F bond polarity increases, j_{B-F} becomes more positive as we move from the organic solvents to water. Thus j_{B-F} should be positive in water and negative in the organic solvents studied; since both ^{11}B and ^{19}F have positive magnetogyric ratios $J_{^{11}B-^{19}F}$ also will be positive in water and negative in the organic solvents.

Haque and Reeves (2) have rejected Kuhlmann and Grant's hypothesis that $NaBF_4$ is associated into ion pairs in aqueous solution, apparently on the assumption that any significant interaction would have to involve an inner-sphere ion pair. Their reasons for discarding an inner-sphere ion pair are convincing; however, a solvent-separated ion pair is not excluded by any of their evidence. It is possible that in a solvent-separated ion pair the symmetry at boron is not decreased sufficiently to collapse the splitting due to boron–fluorine coupling, although the coupling constant is nevertheless affected; this seems reasonable especially since the postulate of opposing coupling terms provides that small interactions can strongly affect the observed small J.

Structure **1** appears possible for the ion pair in aqueous solution; the very small differences in the fluorine environments between it and structure **2** for the free solvated anion could cause

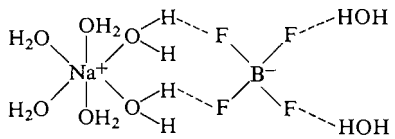

1

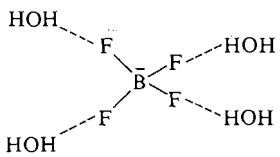

2

changes in J and in the chemical shift. Structure **1** is in accord with a very small electric-field gradient about boron and also with hexacoordination of water molecules about Na^+ as has been demonstrated by Ryss and Radchenko (4). Both structures **1** and **2** are also in reasonable agreement with Ryss and Radchenko's estimate that each fluorine of BF_4^- has 1.1 nearest neighbor water molecules. There would presumably be an equilibrium between **1** and **2** and the equilibrium constant determined by Kuhlmann and Grant would still be valid. The existence of an equilibrium such as that between **1** and **2** is further supported by our observation that J decreases as the temperature is raised, corresponding to a greater degree of dissociation of **1** at higher temperatures.

Further evidence that ion pairs exist in $NaBF_4$ solutions is provided by the increase of J from 1.1 to 4.8 Hz in these solutions as the concentration is raised. We have concluded above that j_{B-F} and J are negative in the organic solvents and become positive in aqueous solution as a result of increasing polarity of the B—F bonds. In an ion pair such as **1** there should be a greater degree of polarity in the B—F bonds than would be found in free aqueous BF_4^-; the coupling constant should thus become more positive. A marked change in this direction is in fact observed. This additional correlation tends to confirm both Bell and Danyluk's hypothesis of reaction field effects on directly bonded coupling constants and Kuhlmann and Grant's postulate of ion pairs in aqueous $NaBF_4$ solutions.

The concentration dependence of J in aqueous solutions of $LiBF_4$ (Fig. 2) provides good evidence that Li^+ also forms an ion pair with BF_4^-, as was previously indicated by Kuhlmann and Grant's study of the effects of adding lithium salts to solutions of $NaBF_4$ (1). However, it is surprising that the increase in J from the infinite dilution value is less by a factor of two at a given concentration for the lithium salt than for the sodium salt. This would appear to suggest that $LiBF_4$ does not form ion pairs as readily as $NaBF_4$; however, this is unlikely in view of the smaller size and greater polarizing power of the Li^+ ion. The difference might arise, instead, from the presence of tetrahedral, rather than octahedral, coordination of water about Li^+, which would affect the nature of the solvent-separated ion pair, and hence the coupling constant. This may be a simple statistical effect in that there are 12 possible ways that a BF_4^- ion can hydrogen bond to two *cis* water molecules of $Na(H_2O)_6^+$ but only 6 possible ways in which it can hydrogen bond to two *cis* water molecules in $Li(H_2O)_4^+$.

The apparent correlation of the coupling constant with the boron–fluorine bond polarity can explain the difficulties encountered by Haque

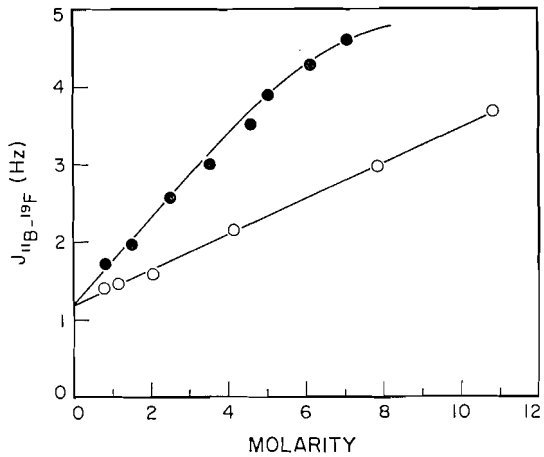

FIG. 2. The concentration dependence of $J_{^{11}B-^{19}F}$ in aqueous solutions of lithium and sodium tetrafluoroborates. Legend: (○) $LiBF_4$ (this work); (●) $NaBF_4$ (ref. 1).

and Reeves in accounting for the results of their studies of variations of J in solutions of $NaBF_4$ in mixed solvents. Ion pairs, which would be expected to be formed to a greater extent and to be held more tightly in solvents of lower dielectric constant, should increase the B—F bond polarity, while the decreased reaction field of the solvent with respect to that of water should decrease it. Thus the choice of the sodium salt for studies of the dependence of J on solvent was unfortunate, as the presence of two opposing effects of unknown relative magnitudes does not allow clear conclusions to be drawn.

The presence of splittings due to B—F coupling in the ^{19}F spectra of $AgBF_4$ solutions, and of n.m.r. evidence for a rapid exchange of fluorine among boron atoms at high temperatures, appears to be related to the dielectric constant of the solvent. Table II indicates this relationship; the data for methylene chloride solutions were obtained by Sharp and co-workers, who studied solutions of triphenylmethyl tetrafluoroborate (16). It is seen that solutions of BF_4^- in solvents of low dielectric constant do not give rise to splittings due to boron–fluorine coupling. This is apparently not due to a coupling constant of zero since the peaks are not sharp, but is probably a result of quadrupole relaxation of boron. Because of the lower dielectric constant and the probable absence of a stable solvation shell about the cation, intimate or inner-sphere ion pairs are probably present in these solvents and there could be a sufficiently large field gradient at boron to collapse the small splittings.

A study by Packer and Muetterties (17) of ^{19}F spectra of solutions of potassium hexafluoroarsenate provides precedent for the postulate that the absence of splittings due to B—F coupling in solutions of the tetrafluoroborate ion in solvents of low dielectric constant is due to quadrupole relaxation. The AsF_6^- ion is similar to the BF_4^- ion in that it is a highly symmetrical species with a central spin-3/2 nucleus, and in aqueous solution it gives rise to a ^{19}F spectrum consisting of a 1:1:1:1 quartet. However, its much larger spin–spin coupling constant ($J_{^{75}As-^{19}F} = 933$ Hz (18)) allows the characteristic ^{19}F signal shapes expected (19) for intermediate rates of quadrupole relaxation of ^{75}As to be distinguished. ^{19}F spectra of $KAsF_6$ in the series of solvents of decreasing dielectric constant, water, acetonitrile, acetone, and glyme, showed increasing amounts of quadrupole relaxation. In these solvents it was possible to obtain the entire range of line shapes for a spin-1/2 nucleus coupled to a spin-3/2 nucleus. A further study by Arnold and Packer (18) using ^{75}As resonance was interpreted as indicating association of AsF_6^- with cations rather than with solvent molecules.

In solutions of $AgBF_4$ the B—F splittings are so small that even relatively slow quadrupole relaxation of boron should be sufficient to prevent resolution of the ^{19}F quartet. In the present study the absence of splitting due to B—F coupling in acetone solutions provides the best evidence for quadrupole relaxation of boron in a solvent of low dielectric constant. Our studies with acetonitrile–acetone solvent mixtures provide evidence that J is not zero in acetone but that a broadening process obscures the splittings. Thus as the mole fraction of acetone is increased, the small splittings become less well resolved and eventually disappear, but as long as they are visible they do not change appreciably in size from those observed in pure acetonitrile. The disappearance of the splittings due to J cannot be due to moderately fast fluorine exchange as the same broadened spectrum was obtained at low temperatures. The effect is not dependent on concentration as essentially identical spectra were obtained over a considerable range of concentrations. The most reasonable explanation is association of the solute; ion pairs are the most likely type of association. In this system, as

Can. J. Chem. Downloaded from www.nrcresearchpress.com by 210.87.254.42 on 09/05/12
For personal use only.

TABLE II

Correlation of ^{19}F spectra of $AgBF_4$ with solvent dielectric constant

Solvent	Dielectric constant at 20°	Splittings due to J observed at room temp.	Evidence for rapid fluorine exchange		Coalescence temperature
			At room temp.	Above room temp.	
Water	80	Yes	No	No	—
DMSO	47	Yes	No	No	—
Acetonitrile	38	Yes	No	Yes	90°
Dimethylformamide	37	Yes	No	—	—
Acetone	21	No	No	Yes	70°
Pyridine	12	No	Uncertain	—	—
Methylene chloride	9	No	Yes*	—	—

*Exchange between BCl_4^- and BF_4^- (as triphenylmethyl salts) is indicated by ^{19}F and ^{11}B n.m.r. (16).

the solvent changes from acetonitrile to acetone, the decreasing ability of the solvent to solvate the ions could cause an increasing proportion of them to exist in the form of intimate ion pairs, with resultant broadening and disappearance of the closely spaced 1:1:1:1 multiplet. Previous work has shown that the degree of solvation of Ag^+ appears to vary with the solvent in the order acetone < acetonitrile < DMSO (20). This could explain why the splittings due to boron–fluorine coupling are observed only in solvents with dielectric constants equal to or greater than that of dimethylformamide; these are the better coordinating solvents, and the formation of intimate ion pairs, *in contrast to solvent-separated ion pairs such as 1*, should be favored by the absence of a stable solvation shell about the cation. Since Ag^+ appears to have especially high complexing ability towards a number of nonaqueous solvents (21) it would not be expected to form an intimate ion pair with BF_4^- in these solvents. In accord with this there appears to be no quadrupole relaxation of the BF_4^- ion in $AgBF_4$ solutions in these solvents since very small splittings down to 0.3 Hz can be observed.

Fluorine Exchange

Rapid exchange of fluorine among boron atoms is proved by the collapse of the ^{10}B—^{11}B isotope shift at high temperatures in solutions of $AgBF_4$ in acetonitrile and acetone. The absence of such rapid exchange in water and in DMSO is demonstrated by the ^{19}F n.m.r. spectra at 90° which clearly show both the isotope shift and the splitting due to J. The results suggest that the exchange process is facilitated by solvents of low dielectric constant (Table II); since solvents of low dielectric constant tend to solvate ions less efficiently, the exchange may be a result of poorer solvation of the anion. The results of Sharp and co-workers (16) on solutions in methylene chloride are included in Table II although these results are not strictly analogous, the observed exchange being between fluorine and chlorine, rather than among fluorines.

Various mechanisms are possible for the fluorine exchange; e.g. a simple reversible dissociation of BF_4^- into F^- and BF_3. In view of the fact that exchange seems to be much faster in acetonitrile solution when BF_3 is added, we suggest a mechanism involving a slight initial dissociation of BF_4^- to yield BF_3, which can then take part in several reversible reactions, including the formation of a fluorine-bridged $B_2F_7^-$ ion [3] which we propose as the principal intermediate in the fluorine exchange.

(i) $BF_4^- \rightleftharpoons BF_3 + F^-$

[3] (ii) $BF_3 + BF_4^- \rightleftharpoons$ 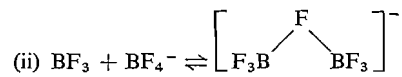

3

(iii) BF_3 + solvent $\rightleftharpoons BF_3$.solvent

Complexing of BF_3 with the solvent as indicated by step (iii) is not directly involved in fluorine exchange but would be expected to occur in donor solvents and would decrease the amount of free BF_3 in solution and affect the exchange rate. Evidence for the existence of the proposed intermediate $B_2F_7^-$ as a stable species in methylene chloride solution has been provided by Brownstein and co-workers (22).

The fluorine scrambling reaction in solutions of $AgBF_4$ and $CH_3CN.BF_3$ in acetonitrile may be analogous to that in solutions of $(n\text{-}C_3H_7)_4N.$-

Can. J. Chem. Downloaded from www.nrcresearchpress.com by 210.87.254.42 on 09/05/12
For personal use only.

Can. J. Chem. Downloaded from www.nrcresearchpress.com by 210.87.254.42 on 09/05/12
For personal use only.

PF_6 and $CH_3CN.PF_5$ in the same solvent, reported by Tebbe and Muetterties (23) on the basis of the collapse of the doublet due to P—F coupling in the ^{19}F spectrum of $CH_3CN.PF_5$ when the hexafluorophosphate salt is added. In the absence of the hexafluorophosphate salt the collapse of the doublet was found to occur only at high temperatures. Tebbe and Muetterties proposed a three-step reaction scheme analogous to [2] for the exchange process. They did not discuss the mechanism of exchange between PF_5 and PF_6^-; we suggest as the intermediate or transition state the fluorine-bridged dimer $P_2F_{11}^-$, analogous to $B_2F_7^-$. Step (ii), probably the chief fluorine scrambling step in both of the analogous schemes involving BF_3/BF_4^- and PF_5/PF_6^-, would be most effective when both the anion and the Lewis acid are present in considerable concentration. This would explain the increase in the rate of fluorine exchange in both systems on adding the second of the two species.

To explain the results of their ^{11}B and ^{19}F n.m.r. studies which showed that rapid halogen exchange occurs between BCl_4^- and BF_4^- in methylene chloride solution, Sharp and coworkers (16) postulated reactions similar to (i) and (ii) of scheme [2], but with the important difference that the presence of BCl_4^- is required. Their work showed that BF_4^- does not exchange halogen with Cl^- in this solvent, and thus it would appear that BF_4^- does not dissociate as in (i). However, they proposed that BCl_4^- does dissociate in a reaction analogous to (i), and that the BCl_3 so formed exchanges halogen with BF_4^-. The mechanism of this halogen exchange reaction is probably analogous to (ii), with the formation of a halogen-bridged ion. An equilibrium of BCl_4^- with BCl_3 and Cl^- in methylene chloride has also been proposed by Thompson and Davis (24) to explain the variation of the ^{11}B chemical shift of the BCl_4^- ion with concentration of chloride ion in this solvent. The apparent inability of BF_4^- to take part in reaction (i) is in keeping with the very poor solvation expected for fluoride ion in methylene chloride; no ionic fluoride is known which is soluble in this solvent (16).

Summary

The tetrafluoroborate ion has proved to be especially amenable to study by high-resolution ^{19}F n.m.r. spectroscopy. The sensitivity of the boron–fluorine coupling constant to small changes in the environment of the ion provides an accurate probe for small differences in solvation and for association. The possibility of quadrupole relaxation of boron provides a further approach to the detection of association. The existence of an isotope shift allows observation of a fluorine scrambling process. The BF_4^- ion is most unusual in that near cancellation of large opposing coupling terms allows small changes in these large terms to have readily observable effects on the spectrum.

Experimental

Hydrated lithium tetrafluoroborate was prepared by dissolving reagent grade lithium hydroxide monohydrate in an equimolar amount of purified grade 48–50% fluoroboric acid. Excess fluoroboric acid was added to this solution and was carefully evaporated at 90–100° to yield crystalline $LiBF_4.3H_2O$. Anhydrous lithium tetrafluoroborate was prepared by carefully drying the trihydrate at 90–100°.

Sodium tetrafluoroborate (Harshaw) and the silver and tetramethylammonium tetrafluoroborates (Alfa Inorganics) were used without further purification. The reagent grade solvents acetone, acetonitrile, DMSO, DMF, and pyridine were dried over molecular sieves before use. Boron trifluoride was purified as described previously (25).

Tetrafluoroborate solutions were prepared directly in precision 5 mm n.m.r. tubes. Addition of the tetrafluoroborate salt was carried out in a dry-box. The mixtures were degassed by passing a slow stream of nitrogen through the liquid for 10 min; this also served to mix the sample and effect complete solution. Passage of nitrogen caused a negligible weight loss in solutions in water, DMSO, DMF, or pyridine, but a significant loss in solutions containing acetone or acetonitrile. The solution containing BF_3 was made up on a high-vacuum system.

^{19}F n.m.r. spectra were obtained at 56.4 MHz on a Varian Associates HR-60 spectrometer equipped with a variable temperature probe.

Acknowledgments

We thank the United States Air Force Office of Scientific Research and the National Research Council of Canada for financial support of this work. We also thank the National Research Council of Canada for the award of a Studentship (to J. S. H.).

1. K. KUHLMANN and D. M. GRANT. J. Phys. Chem. **68**, 3208 (1964).
2. R. HAQUE and L. W. REEVES. J. Phys. Chem. **70**, 2753 (1966).
3. J. W. QUAIL. Ph.D. Thesis, McMaster University, Hamilton, Ontario. 1963.

4. A. I. Ryss and I. V. Radchenko. J. Struct. Chem. USSR, English Transl. **5**, 489 (1964).
5. M. Parekh and N. N. Greenwood. Unpublished results.
6. J. R. Holmes, D. Kivelson, and W. C. Drinkard. J. Am. Chem. Soc. **84**, 4677 (1962).
7. R. J. Gillespie and J. S. Hartman. J. Chem. Phys. **45**, 2712 (1966).
8. P. E. Francis and I. J. Lawrenson. J. Inorg. Nucl. Chem. **26**, 1462 (1964).
9. R. K. Harris. J. Phys. Chem. **66**, 768 (1962).
10. R. D. Chambers, H. C. Clark, L. W. Reeves, and C. J. Willis. Can. J. Chem. **39**, 258 (1961).
11. J. A. Pople and D. P. Santry. Mol. Phys. **8**, 1 (1964).
12. J. N. Murrell, P. E. Stevenson, and G. T. Jones. Mol. Phys. **12**, 265 (1967).
13. P. A. W. Dean and D. F. Evans. J. Chem. Soc. A, 698 (1967).
14. S. L. Smith and A. M. Ihrig. J. Chem. Phys. **46**, 1181 (1967).
15. C. L. Bell and S. S. Danyluk. J. Am. Chem. Soc. **88**, 2344 (1966).
16. R. D. W. Kemmitt, R. S. Milner, and D. W. A. Sharp. J. Chem. Soc. 111 (1963).
17. K. J. Packer and E. L. Muetterties. Proc. Chem. Soc. 147 (1964).
18. M. St. J. Arnold and K. J. Packer. Mol. Phys. **10**, 141 (1966).
19. J. Bacon, R. J. Gillespie, and J. W. Quail. Can. J. Chem. **41**, 3063 (1963).
20. D. C. Luers, R. T. Iwamoto, and J. Kleinberg. Inorg. Chem. **5**, 201 (1966).
21. Stability constants. Chem. Soc. London Spec. Publ. No. 17 (1964).
22. S. Brownstein and J. Paasivirta. Can. J. Chem. **43**, 1645 (1965). P. J. Burchill, S. Brownstein, and A. M. Eastham. Can. J. Chem. **45**, 17 (1967).
23. F. N. Tebbe and E. L. Muetterties. Inorg. Chem. **6**, 129 (1967).
24. R. J. Thompson and J. C. Davis. Inorg. Chem. **4**, 1464 (1965).
25. R. J. Gillespie and J. S. Hartman. Can. J. Chem. **45**, 859 (1967).

Can. J. Chem. Downloaded from www.nrcresearchpress.com by 210.87.254.42 on 09/05/12
For personal use only.

Can. J. Chem. Downloaded from www.nrcresearchpress.com by 210.87.254.40 on 09/05/12
For personal use only.

Behavior of a sulfur vapor electrode in sulfide melts

W. T. THOMPSON AND S. N. FLENGAS
Department of Metallurgy and Materials Science, University of Toronto, Toronto, Ontario
Received December 13, 1967

The reversible potentials for the formation cell

$$(-)\ \mathrm{Ag}\ \left|\begin{matrix}\mathrm{Ag_2S}\\ \mathrm{AgCl}\end{matrix}\right|\ \text{graphite},\ \mathrm{S_{vapor}}\ (+)$$

have been measured for concentrations of silver sulfide in silver chloride up to 12 mole %, in the temperature range 490 to 860 °C. Nernst behavior with respect to the partial pressures of the various sulfur species present in the vapor phase over the electrode is observed in the range 10^{-3} to 1.0 atm. Calculations of partial pressures are based on existing mass spectrometric data. The concentration dependence of the cell voltage follows the Nernst law only in very dilute silver sulfide solutions. The data are used to calculate the thermodynamic properties of silver sulfide in solution with silver chloride.

Canadian Journal of Chemistry, 46, 1611 (1968)

Introduction

In spite of recent developments in the field of sulfide electrochemistry, high temperature formation cells employing gaseous sulfur electrodes have not yet been investigated.

Pure heavy metal sulfides are known to be electronic conductors even in the liquid state. However, recent investigations (1–6) have shown that the solutions of these sulfides in molten metal chlorides are ionic over appreciable concentration and temperature ranges specific to each system. For those solutions a gaseous sulfur electrode may be used in conjunction with a metal electrode to realize the formation of the metal sulfide in solution and, thereby, study its thermodynamic properties.

A liquid sulfur electrode has been developed by Kiukkola and Wagner (7) and used with a solid silver iodide electrolytic membrane to investigate the thermodynamic properties of pure silver sulfide in the temperature range 150 to 425 °C. A similar sulfur electrode used with a sodium electrode and ceramic electrolyte for energy storage purposes has been announced recently (8).

Verduch and Wagner (9) investigated solid double sulfides at temperatures up to 400 °C using a galvanic cell fitted with a solid electrolyte membrane and two sulfur vapor electrodes. The cell arrangement was such that the properties of the sulfur electrode could not be observed as the sulfur pressure did not enter into the expression for the cell potential.

In the present investigation a formation cell employing a sulfur vapor electrode in conjunction with a silver electrode has been developed and used to study the binary solutions of Ag_2S–AgCl in the temperature range 490 to 860 °C. It is shown that the sulfur pressure dependence of the cell voltage at different temperatures follows Nernst behavior consistent with a two electron electrode process per sulfur atom. For this interpretation, it is necessary to calculate the partial pressures of the various molecular forms of sulfur vapor over the electrode using equilibrium constants obtained from mass spectrometric data (10). The concentration dependence of the cell voltage is similarly consistent with the Nernst equation for dilute silver sulfide solutions where Henry's law is expected to be valid. These data also indicate a two electron process.

The technique described herein may be used in the study of other sulfide–chloride systems in their range of ionic behavior. It is only required that the chloride solvent be stable under an applied sulfur pressure.

Experimental

The electrochemical cell

$$(-)\ \mathrm{Ag}\ \left|\begin{matrix}\mathrm{Ag_2S}\\ \mathrm{AgCl}\end{matrix}\right|\ \text{graphite},\ \mathrm{S_{vapor}}\ (+)$$

and the connected apparatus for handling the argon and sulfur vapor mixtures are given in Figs. 1 and 2. The cells were made entirely of glass. The high temperature parts of the apparatus containing the sulfide melts were made from quartz tubing connected to the Pyrex using graded seals. The silver electrodes were 2 to 4 mm diameter pure silver rods dipping into the melt; these were maintained in an argon atmosphere. The inert electrodes for sulfur

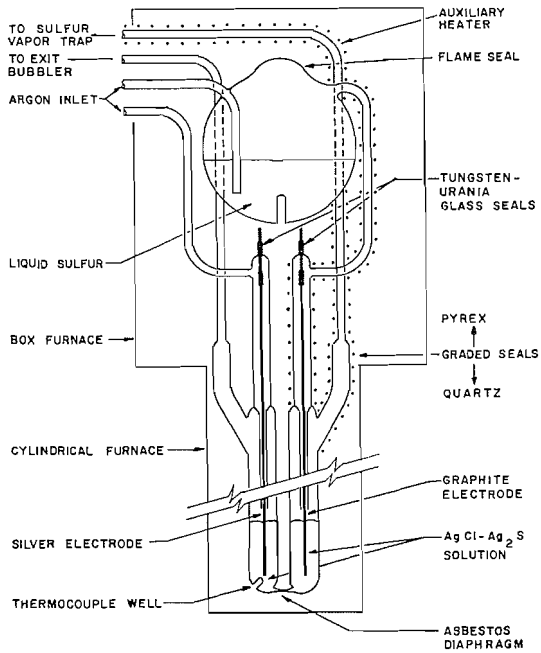

FIG. 1. Experimental cell design.

were 2 mm diameter spectroscopic graphite rods. Prior to use, these were heated in vacuum at 1000 °C for about 24 h to remove volatile matter. To test its reactivity the graphite was heated in a flowing (about 60 ml/min) sulfur–argon mixture at 850 °C. After 2 weeks exposure to a sulfur pressure of 10^{-2} atm, only 0.5 mg of carbon had reacted. This corresponds to less than one part in a thousand of the theoretical weight loss based on the formation of carbon disulfide. Therefore, graphite may be considered as essentially inert with respect to sulfur at temperatures up to 850 °C.

The sulfur pressure was created by bubbling preheated argon through molten sulfur. The molten sulfur was contained in a 1000 ml flask located in a furnace equipped with removable top and front panels, the latter having a double wall glass window.

The lower part of the cell, containing the sulfide solution, was in a second independently temperature-regulated furnace. During the experiments, the temperature of the upper furnace was controlled to ± 1 °C, while the sulfide melt temperature was controlled to ± 2 °C.

The silver chloride was either reagent grade or made by precipitation from an aqueous silver nitrate solution with hydrochloric acid. Silver sulfide was similarly prepared using ammonium sulfide. The prepared compounds were washed with distilled water and alcohol, followed by vacuum drying at 120 °C. The sulfur was laboratory reagent grade. Purification by repeated sublimation was not performed since the impurities in this material consisted chiefly of insoluble matter, and these are known not to affect the sulfur pressure (11). The sulfur was dried "in situ" under vacuum at 90 to 100 °C prior to its use in an experiment.

TABLE I

Experimental e.m.f. measurements

X_{Ag_2S}	E (mV)	T_B (°C)	T_E (°C)
.081	221	147	491
	234	163	488
	255	203	490
	274	253	491
	284	327	489
	281	285	491
	270	234	490
.081	232	183	558
	289	305	556
	298	368	554
	296	329	557
	285	280	557
	271	240	556
	256	206	555
	229	172	556
	199	141	557
.045	225	161	613
	259	202	610
	283	240	610
	311	315	614
	321	353	612
	306	297	610
	296	269	611
	277	232	614
	248	186	610
.081	188	169	701
	194	175	699
	231	215	700
	162	146	699
	286	320	698
	301	359	700
	302	368	700
	265	273	700
	250	243	699
	215	198	699
	174	157	700
.045	219	188	753
	268	255	752
	318	368	752
	302	317	757
	295	301	757
	289	286	756
	264	242	756
.081	161	184	855
	178	194	855
	181	198	856
	219	236	858
	163	187	857
	264	320	860
	165	188	860
	263	302	860
	163	187	858
	280	347	857

During measurements, dry oxygen-free argon was slowly bubbled through the liquid sulfur in the bulb. The sulfur-saturated argon was led to the electrode and over the surface of the sulfide melt. The gas mixture leaving the electrode then passed to a sulfur condenser from which sulfur-free argon was expelled to the atmosphere through a sulfuric acid bubbler. The saturation of the argon with

Can. J. Chem. Downloaded from www.nrcresearchpress.com by 210.87.254.40 on 09/05/12
For personal use only.

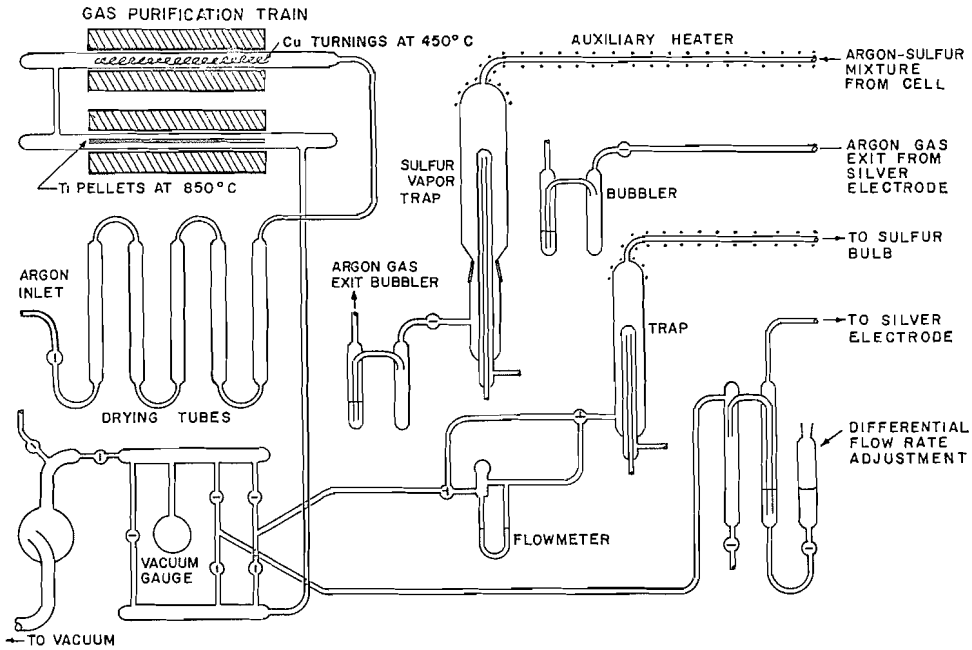

FIG. 2. Apparatus for handling the sulfur–argon gas mixtures and controlling the differential flow rates of argon and total pressures.

sulfur was verified by approximate dew point measurements taken on the tube leading from the bulb. Condensed sulfur could be seen on the tubing when the latter was 4 to 5 °C cooler than the sulfur bath. In order to be certain that the temperature of the liquid sulfur in the bulb would control the sulfur pressure at the electrode, it was necessary to heat all tubing conducting the vapor from the bulb to the condenser. This was accomplished by wrapping the tubing with auxiliary heating elements. It was also required to use hot internal electrode connections. These were made using tungsten leads sealed in urania glass, the electrodes being threaded or silver soldered to the tungsten. The metal exposed to the sulfur vapor rapidly formed a thin sulfide layer which rendered the connections immune to further sulfur attack.

The two electrode compartments contained melts of the same composition but were separated by means of an asbestos diaphragm. This diaphragm was made by collapsing quartz tubing around a small pre-fired strand of asbestos fibers, the continuity of the fibers being preserved (12). The capillaries formed between the interstices of the fibers allowed electrolytic contact but effectively prevented the diffusion of dissolved sulfur to the silver electrode. In experiments conducted with cells in which a simple U-tube, without the asbestos fiber diaphragm, connected the two electrode compartments, dissolved sulfur attacked the silver electrode. This effect could be minimized by operating the cells at a low sulfur pressure and was, for all practical purposes, eliminated by the introduction of the diaphragm described above.

The temperatures were measured using calibrated chromel–alumel thermocouple wires. Thermocouple and cell voltages were measured with a Leeds and Northrup type K-3 potentiometer. The cell e.m.f. was found to be reproducible on increasing and decreasing temperature and pressure cycles, and with the exception of the most dilute solution investigated, the reproducibility was better than 3 mV.

Early experiments showed that the e.m.f. was insensitive to changes in argon flow rate in the range 20 to 100 ml/min. For the experimental measurements included in this paper, the flow rate was 60 to 80 ml/min.

Results

The effect of sulfur pressure on the e.m.f. was investigated by varying the liquid sulfur temperature T_B in the range 140 to 370 °C for electrode temperatures T_E from 490 to 860 °C. These data are shown in Table I at the corresponding sulfide concentration of the solution.

Table II shows the electromotive force measurements as a function of temperature at various silver sulfide concentrations. For these measurements the temperature of the liquid sulfur was low so that the sulfur pressure would be small. The measurements shown in this and the previous table are in chronological order and indicate that the measurements are reproducible on increasing and decreasing electrode temperature

Can. J. Chem. Downloaded from www.nrcresearchpress.com by 210.87.254.40 on 09/05/12
For personal use only.

Can. J. Chem. Downloaded from www.nrcresearchpress.com by 210.87.254.40 on 09/05/12
For personal use only.

TABLE II
Experimental e.m.f. measurements

X_{Ag_2S}	E (mV)	T_B (°C)	T_E (°C)
.011	229	154	821
	244	157	774
	250	155	674
	257	151	573
	265	141	504
	264	142	548
	247	144	624
	237	150	729
	227	154	828
.015	262	176	599
	276	175	505
	269	174	562
	258	176	639
	244	178	738
	236	182	832
	246	186	799
	259	184	681
	269	174	561
	277	168	485
.024	204	165	815
	211	179	850
	236	177	691
	228	170	709
	235	167	656
	234	159	615
	237	147	555
	210	160	759
	224	188	831
	240	171	644
	247	143	480
	234	148	560
	228	156	633
.045	208	171	727
	224	166	629
	236	159	517
	208	175	746
	197	179	824
	193	181	861
	201	176	789
	221	173	676
	226	162	606
	233	164	576
	243	158	500
.081	175	185	827
	171	182	747
	203	176	661
	232	183	558
	221	147	491
	168	171	782
	182	169	718
	199	163	628
	213	147	517
	172	166	748
	164	176	826
	188	169	701
.119	211	173	585
	190	175	676
	166	178	774
	176	177	733
	223	177	549
	231	175	498
	206	182	633

and pressure cycles. At high temperatures equilibrium was reached within 1 h after adjusting the experimental variables; at lower electrode temperatures (below 600 °C) significantly longer periods of time were required to achieve a steady cell voltage.

At the end of each experiment, samples of the melt in each electrode compartment were analyzed for sulfur. It was found that during the 1 to 2 weeks of continuous cell operation the sulfide concentration of the sulfur electrode compartment had increased slightly. This can be attributed to a small amount of chlorine evolution resulting from the displacement reaction

[1] $$2AgCl + \tfrac{1}{2}S_2 \rightarrow Ag_2S + Cl_2.$$

Although the standard free energy for the reaction as written is about +25 kcal in the temperature range of this investigation, chlorine can be evolved since the flowing sulfur–argon mixture prevents the true equilibrium chlorine pressure from being established over the melt. This displacement was minimized by restricting the silver sulfide concentration to no less than 1 mole % and also by operating the cell at low sulfur pressures, whenever possible. The largest relative increase in sulfide concentration was in the most dilute solution where the sulfide concentration increased from 1.00 to 1.12 mole % silver sulfide over a period of a week. For the most concentrated solution containing 11.9 mole % sulfide, no change in sulfide concentration was detected. For calculation purposes the small junction potential which this effect might introduce has been neglected and the concentrations reported in the table are the average of the analyzed values for each compartment.

Discussion

Theoretical Considerations

If sulfur were a simple vapor that could exist only in one molecular form, the sulfur pressure at the electrode would be equal to the vapor pressure of sulfur in equilibrium with the liquid in the bulb. It is known, however, that sulfur in the vapor phase is a complex mixture of various molecular species ranging essentially from S_2 to S_8, the concentration of each being temperature and pressure dependent. For this reason the relative concentrations of the various molecules will be different at the electrode than in the bulb. Assuming that the vapor passes through the

Can. J. Chem. Downloaded from www.nrcresearchpress.com by 210.87.254.40 on 09/05/12
For personal use only.

temperature gradient from bulb to electrode while at all times preserving local equilibrium, it is possible to calculate the composition of the sulfur vapor at the electrode when both bulb and electrode temperatures are known. The assumption of equilibrium is reasonable since, in the pressure range of the investigation, the number of sulfur–sulfur collisions per unit time is expected to be very high, and the time constants for dissociation and association processes are small (13). Therefore, before a sulfur molecule can move an appreciable distance within the temperature gradient, it will enter the equilibrium required by the temperature and total sulfur pressure in the new position.

For calculation purposes, it is convenient to consider the vapor in the sulfur bulb and at the electrode as consisting of $\bar{v}_B$ and $\bar{v}_E$ mean number of sulfur atoms per molecule, respectively. These numbers may be defined by a relationship of the following form,

$$[2] \qquad \bar{v} = \frac{\sum_{v=2}^{8} vP_{S_v}}{\sum_{v=2}^{8} P_{S_v}},$$

where P_{S_v} is the partial pressure of species S_v, and v is an integral number having values between 2 and 8. Therefore, upon passage from temperature T_B to temperature T_E, the sulfur dissociation may be represented by

$$[3] \qquad (S_{\bar{v}_B})_{T_B} \rightarrow \frac{\bar{v}_B}{\bar{v}_E} (S_{\bar{v}_E})_{T_E}.$$

For calculation purposes a volume element V_B containing n_A moles of argon and $n_{S_{\bar{v}_B}}$ moles of species $S_{\bar{v}_B}$ at a total pressure of 1 atm and temperature T_B will be considered. When the temperature is increased to T_E, dissociation will take place and the volume will expand to V_E to accommodate the increased number of molecules at a total pressure of 1 atm, fixed experimentally by the exit bubbler head. At temperature T_E there are $(\bar{v}_B/\bar{v}_E)n_{S_{\bar{v}_B}}$ moles of species $S_{\bar{v}_E}$ and n_A moles of argon if argon diffusion from the volume element under consideration can be ignored.

$$[4] \qquad P_{S_{\bar{v}_E}} = \frac{n_{S_{\bar{v}_E}}}{n_A + n_{S_{\bar{v}_E}}} = \frac{(\bar{v}_B/\bar{v}_E)n_{S_{\bar{v}_B}}}{n_A + (\bar{v}_B/\bar{v}_E)n_{S_{\bar{v}_B}}}$$

Multiplying the numerator and denominator of eq. [4] by RT_B/V_B and substituting

$$[5] \qquad (P_A)_B = 1 - P_{S_{\bar{v}_B}},$$

the sulfur pressure at the electrode is given as:

$$[6] \qquad P_{S_{\bar{v}_E}} = \frac{\bar{v}_B/\bar{v}_E}{1 + (\bar{v}_B/\bar{v}_E - 1)P_{S_{\bar{v}_B}}} \times P_{S_{\bar{v}_B}}.$$

Because it is necessary for the total gas pressure to always equal the exit bubbler pressure (eq. [5]), it follows that there is a decrease in the argon pressure as sulfur dissociates. The argon partial pressure at the electrode is given as:

$$[7] \qquad (P_A)_E = \frac{1}{(P_A)_B + (\bar{v}_B/\bar{v}_E)(1 - (P_A)_B)} \times (P_A)_B.$$

At the low sulfur pressures employed during most of the experimental measurements where $(P_A)_B$, is approaching unity, $(P_A)_E$ is only slightly lower than $(P_A)_B$. Thus, the assumption in the development of eq. [6], namely that there be no argon diffusion, is justified since not only is there little time in the flowing gas stream for diffusion to occur, but also the partial pressure difference is generally small.

The most comprehensive data on sulfur vapor comes from the mass spectrometric studies of Berkowitz and Marquart (10). Their results show in graphical form the equilibrium constants relating the various partial pressures as functions of temperature. These generate the following six independent equations:

$$[8] \qquad 3 \log P_{S_2} - 2 \log P_{S_3} = -6.00 \times 10^3 T^{-1} + 8.50$$

$$[9] \qquad 2 \log P_{S_2} - \log P_{S_4} = -5.73 \times 10^3 T^{-1} + 6.49$$

$$[10] \qquad \log P_{S_5} - \tfrac{5}{8} \log P_{S_8} = -2.87 \times 10^3 T^{-1} + 3.28$$

$$[11] \qquad \log P_{S_6} - \tfrac{3}{4} \log P_{S_8} = -1.22 \times 10^3 T^{-1} + 1.52$$

$$[12] \qquad \log P_{S_7} - \tfrac{7}{8} \log P_{S_8} = -1.16 \times 10^3 T^{-1} + 1.55$$

$$[13] \qquad 4 \log P_{S_2} - \log P_{S_8} = -20.9 \times 10^3 T^{-1} + 23.6.$$

Due to uncertainty in the experimental values for the S_2–S_8 equilibrium constants, the data for this case is taken from calculations based on

Can. J. Chem. Downloaded from www.nrcresearchpress.com by 210.87.254.40 on 09/05/12
For personal use only.

vibrational assignments for the S_8 molecule (14). The calculated line is in fair agreement with the experimental mass spectrometric data.

The equilibrium constant equations can be applied to calculate the partial pressures for all sulfur species when an additional independent relationship among the various partial pressures is available. For vapor in equilibrium with liquid, the vapor pressure equation provides this relationship (15).

$$[14] \quad \text{Log } P_{\text{sulfur}} = \frac{-4830}{T_B} - 5.0 \log T_B + 21.00,$$

where $$P_{\text{sulfur}} = \left(\sum_{v=2}^{8} P_{S_v} \right)_B .$$

Hence, for conditions that exist in the bulb, $\bar{v}_B$ and $P_{S\bar{v}_B}$ can be evaluated and therefore $P_{S\bar{v}_E}$ can be related to $\bar{v}_E$ from eq. [6] for any temperature T_B. This reduced form of eq. [6] together with eqs. [8]–[13] evaluated now at the electrode temperature T_E allows the calculation of the partial pressures of all molecular forms of sulfur vapor over the sulfide melt.

The calculation is illustrated in Fig. 3. Curve (*a*) represents the variation of $\bar{v}_B$ with respect to log $P_{S\bar{v}_B}$. The family of curves (*b*) represents the variation of $\bar{v}_E$ with respect to log $P_{S\bar{v}_E}$, as determined by eq. [6] in which $P_{S\bar{v}_B}$ and $\bar{v}_B$ have values that are determined by T_B. The curves (*c*) represent the variation of $\bar{v}_E$ with respect to log $P_{S\bar{v}_E}$ for various electrode temperatures. It may be seen from the figure that each set of temperatures T_B and T_E defines only one total sulfur pressure at the electrode; this is given by the intersection of the appropriate curves of sets (*b*) and (*c*).

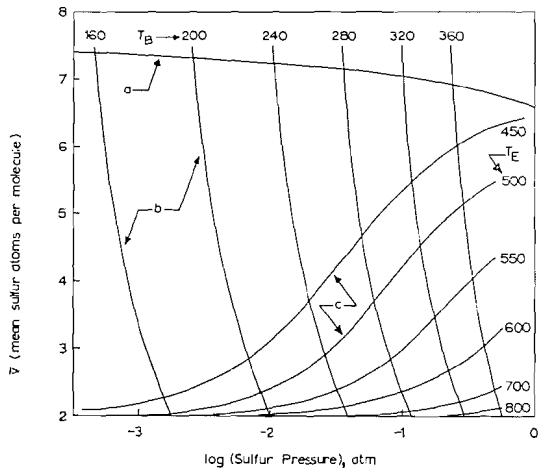

FIG. 3. Sulfur pressures plotted as a function of the number of sulfur atoms per sulfur vapor molecule for the saturated vapor (*a*) and non-saturated vapor (*c*) at various electrode temperatures. Curve (*b*) is the variation of the mean number of sulfur atoms per molecule at the electrode temperature plotted against total sulfur pressure at corresponding sulfur bulb temperatures.

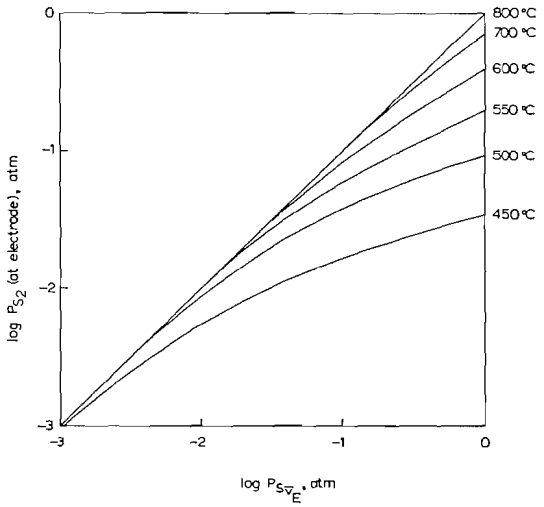

FIG. 4. Variation of the partial pressure of S_2 species at various temperatures and total sulfur pressure at the electrode.

Figure 4 shows the relationship between total sulfur pressure and S_2 pressure for various temperatures of importance to this investigation. The partial pressure of other molecules can now be simply related to the S_2 pressure from the equilibrium constant expressions [8]–[13] and so a complete knowledge of the vapor over the melt, necessary for the proper understanding of electrode behavior, is possible. In the following discussion, the subscript with v will be omitted, it being understood that v applies to the sulfur vapor at the electrode.

For the electrochemical cell

$$(-)\ \text{Ag} \left| \begin{matrix} \text{Ag}_2\text{S} \\ \text{AgCl} \end{matrix} \right| \text{graphite}, S_v\ (+)$$

the primary cell process is the formation of Ag_2S according to the equation

$$[15] \quad 2\text{Ag}_{(\text{solid})} + \frac{1}{v} S_{v(\text{vapor})} \rightarrow \text{Ag}_2\text{S}_{(\text{solution})},$$

Can. J. Chem. Downloaded from www.nrcresearchpress.com by 210.87.254.40 on 09/05/12
For personal use only.

for which the Nernst expression is

$$[16] \qquad E = E^0_{Ag_2S} - \frac{RT}{2F} \ln \frac{a_{Ag_2S}}{P_{S_v}^{1/v}},$$

where E, E^0, and a, represent measured and standard cell potentials and activity, respectively. In eqs. [15] and [16], v can have any integral value from 2 to 8. The standard cell potential will also have different values depending upon the choice of the standard state for the sulfur vapor. However, the value of E for a given set of experimental conditions is uniquely defined and is independent of the value of v since it is expected that all the vapor molecules must be in equilibrium at the electrode. The choice for the value of v is therefore a matter of preference. Since S_2 is the major component of the sulfur vapor in most of the experiments, v will be taken to be 2, thus making the standard state for sulfur pure S_2 vapor at 1 atm pressure.

The overall cell reaction may be realized by considering either formation or concentration cell reactions. In the formation cell the following reactions are considered to occur:

At the silver electrode,

$$[17] \qquad 2Ag \rightarrow 2Ag^+ + 2e^-.$$

At the graphite electrode,

$$[18] \qquad \tfrac{1}{2}(S_2)_{vapor} + 2e^- \rightarrow S^{2-}.$$

Hence, the overall cell process is as in eq. [15].

The cell may also be considered as a sulfur vapor concentration cell. In this case, the reactions are:

At the silver electrode,

$$[19] \qquad S^{2-} \rightarrow \tfrac{1}{2}(S_2)_{vapor} + 2e^-.$$

At the graphite electrode, the reaction is again as in eq. [18]. The overall process is now

$$[20] \qquad \tfrac{1}{2}(S_2)_{\substack{graphite\\electrode}} \rightarrow \tfrac{1}{2}(S_2)_{\substack{silver\\electrode}}.$$

Reaction [20] represents the process of transfer of sulfur from high to low partial pressure for which the cell potential is

$$[21] \qquad E = \frac{RT}{4F} \ln \frac{(P_{S_2})_{\text{sulfur electrode}}}{(P_{S_2})_{\text{silver electrode}}}.$$

Equation [16] and eq. [21] are equivalent only when the partial pressure of sulfur at the silver electrode is the decomposition pressure for dissolved silver sulfide in equilibrium with pure silver. For this condition,

$$[22] \qquad (P_{S_2})_{\text{silver electrode}} = \exp\left(\frac{2\mu_{Ag_2S} - 4\mu^0_{Ag} - \mu^0_{S_2}}{RT}\right),$$

where μ and μ^0 represent chemical potentials in the solution and standard state respectively.

In a cell without a diaphragm separating the two compartments, the sulfur pressure at the silver electrode will not have the equilibrium value given by eq. [22] due to sulfur diffusion through the electrolyte. In this case the cell potential should be described as a mixed potential and does not have a simple thermodynamic interpretation. By introducing a diaphragm into the cell, the silver electrode operates under essentially equilibrium conditions and, hence, the measurements can be used for thermodynamic calculations in accord with eq. [16].

Interpretation of Results

The plot of cell e.m.f. vs. the logarithm of the total sulfur pressure over the melt is shown in curve (*a*) of Fig. 5, the data being taken from Table I. The changing slope of this curve indicates changes in the distribution of the sulfur pressure among the different sulfur molecules. For this reason, the Nernst equation is not directly applicable. Lines (*b*, *c*, *d*) represent the same plot with respect to the partial pressure of S_2, S_4, and S_8, calculated as previously indicated. The relationships are now linear with respect to log P and correspond to an electron change n of 1.93. Considering the accuracy of the voltage measurements and, more particularly, the accuracy of the sulfur vapor data in the pressure calculations, this experimental value for n can be taken to substantiate the two electron electrode process represented in eq. [18]. The corresponding lines for other forms of sulfur, S_3, S_5, S_6, and S_7, also give the expected slopes. These have not been plotted for the sake of brevity. It should be noted that lines (*a*) and (*b*) asymptotically approach each other, indicating that at low sulfur pressure (less than 10^{-3} atm), S_2 is the main sulfur vapor molecule at 490 °C.

The effect of temperature on the pressure dependence of the e.m.f. is shown in Fig. 6. The data for this plot are taken from Table I. In order to plot all the data on the same graph, the lines shown at 612 and 755 °C, respectively, were corrected for the concentration effect and made to correspond to X_{Ag_2S} of 0.081.

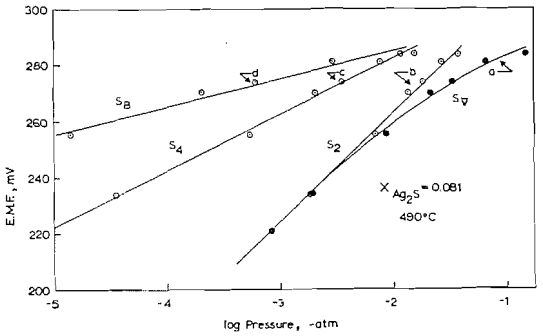

FIG. 5. Variation of cell potential with respect to the logarithm of the partial pressures of S_2, S_4, S_8, and S_v sulfur species.

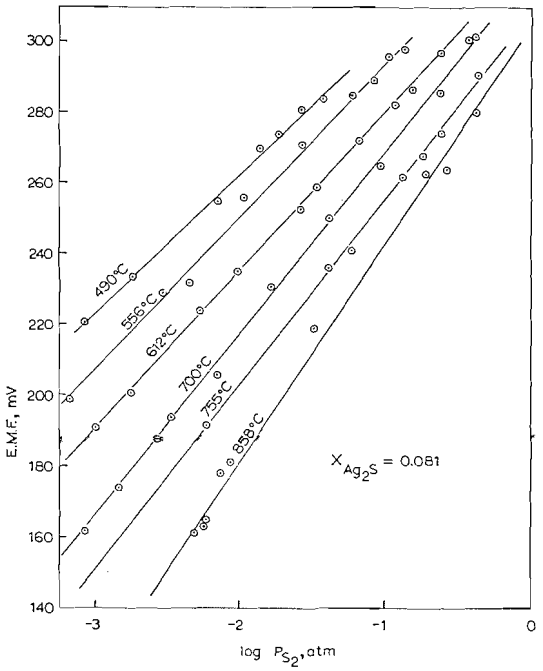

FIG. 6. Cell e.m.f. against log P_{S_2} at various electrode temperatures.

The least squares slopes for all lines in Fig. 6 give a value of n of 1.91 $\pm$ 0.06. This is taken as indicating that the process in eq. [18] occurs over the entire temperature range of importance to this investigation.

The variation of the e.m.f. vs. temperature at fixed sulfide concentration for various calculated total sulfur pressures at the electrode is given in Fig. 7. The temperature dependence is linear in the high temperature – low pressure region where S_2 is essentially the only vapor molecule present. At lower temperature and higher pressure where heavier molecules exist in significant concentrations, the curve again deviates from linearity. The diagonal dotted line indicates the temperature–pressure limits beyond which the electrode can be operated without extensive calculations. For low pressures, where $\bar{v}_E$ equals 2, eq. [6] reduces to

$$[23] \qquad (P_{S_2})_{electrode} = \frac{\bar{v}_B}{2} (P_{S_{\bar{v}}})_{bulb},$$

and so the sulfur pressure over the electrode depends only on the temperature of the liquid sulfur in the bulb.

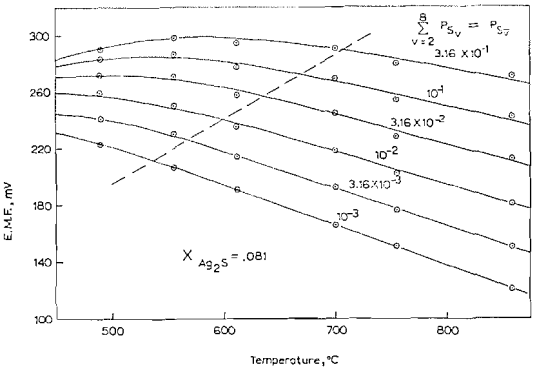

FIG. 7. Effect of total sulfur pressure on the temperature dependence of cell e.m.f. Region to the right of the diagonal dashed line represents a vapor consisting entirely of S_2 species.

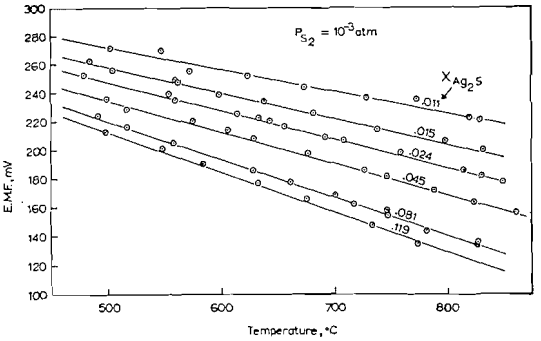

FIG. 8. Effect of temperature on the cell potential at various silver sulfide concentrations.

The concentration dependence of the cell potential as a function of temperature at fixed sulfur pressure is given in Fig. 8. The data are taken from Table II. Most of these measurements were conducted at a pressure level where sulfur at the electrode was essentially S_2, thereby allow-

Can. J. Chem. Downloaded from www.nrcresearchpress.com by 210.87.254.40 on 09/05/12
For personal use only.

ing eq. [23] to be used. For some of the low temperature measurements, however, the extended calculations were required. The equations determined by linear regression are shown in Table III, the e.m.f. being given with respect to a standard sulfur electrode (S_2 at 1 atm). Standard deviations are also included. Measurements at higher concentration than 12 mole % Ag_2S were not taken because the electrolyte is known to no longer conduct completely ionically (2).

TABLE III

Temperature dependence of e.m.f. vs. S_2 electrode at 1 atm

X_{Ag_2S}	e.m.f. (mV) vs. temp. (°K)	Standard deviations (mV)
0.011	$E = 391 - 0.00414T$	3.5
0.015	$E = 396 - 0.0291T$	1.5
0.024	$E = 404 - 0.0522T$	1.2
0.045	$E = 403 - 0.0684T$	1.5
0.081	$E = 422 - 0.113T$	1.5
0.119	$E = 430 - 0.131T$	1.4

The plot of E vs. log X_{Ag_2S} is shown in Fig. 9. The dotted lines indicate the liquidus for this system (1). The solid points are calculated from the free energy measurements of Rosenqvist (16) for solid Ag_2S as interpreted by Richardson and Jeffes (17). The curvature of the plot at higher concentrations is indicative of the change in activity coefficient along an activity isotherm. At the lower concentrations, Henry's law is valid and the slopes of the lines shown are in agreement with the process represented in eq. [18].

From the data available in Table III, the heat and entropy changes for reaction [15] can be obtained for v equal to 2. By subtracting from these properties the heat and entropy of formation of pure Ag_2S, the partial molar enthalpy and entropy of mixing may be determined. These values are plotted as a function of concentration in Fig. 10.

The uncertainty in the heats of formation of dissolved silver sulfide calculated from the standard deviations represent error limits of the order of ± 50 to 100 cal/mole. However, it is possible that other errors that cannot be readily accounted for, such as the uncertainty in the equilibrium constants for the sulfur pressure calculation and the slight change in melt composition during a run, could make the error limits wider. Furthermore, since the heats of formation of pure silver sulfide are not known with confidence, the partial molar properties for the solutions have not been tabulated. The curves in Fig. 10 indicate that the partial molar heats of mixing of silver sulfide decrease with increasing sulfide concentration and the solutions approach nearly athermal behavior at about 20 mole %

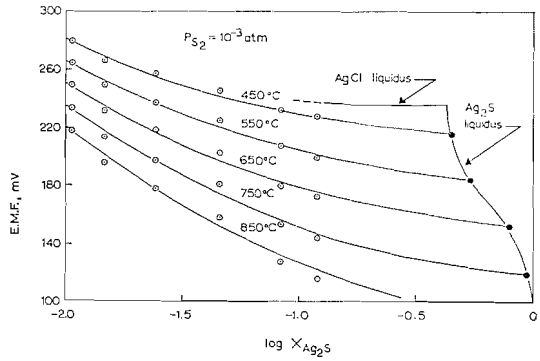

FIG. 9. Variation of cell potential with respect to the logarithm of silver sulfide concentration at constant temperatures. Solid points are on the silver sulfide liquidus and were calculated from existing free energy data.

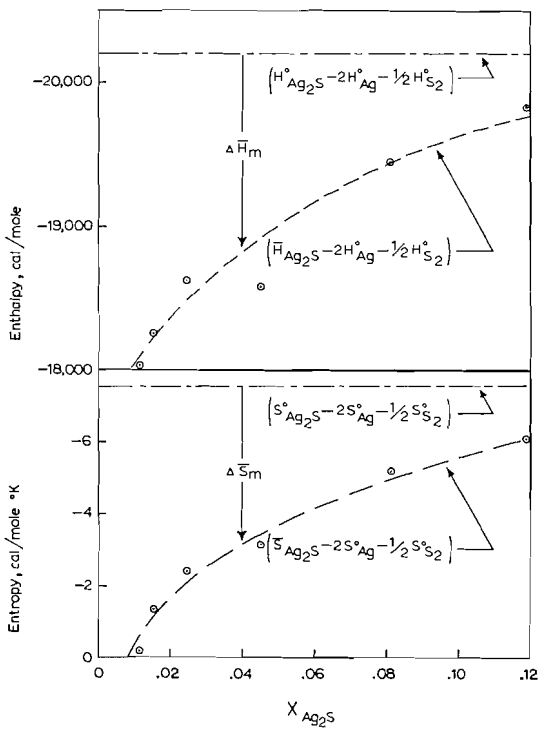

FIG. 10. Enthalpies and entropies of formation of dissolved silver sulfide.

Can. J. Chem. Downloaded from www.nrcresearchpress.com by 210.87.254.40 on 09/05/12
For personal use only.

Can. J. Chem. Downloaded from www.nrcresearchpress.com by 210.87.254.40 on 09/05/12
For personal use only.

sulfide. It appears that the partial molar heats of mixing are all small positive quantities.

The activity isotherm for Ag_2S is given in Fig. 11 at the melting point of Ag_2S. The open circles represent activities calculated from the e.m.f. measurements made in this investigation using Rosenqvist's value for the standard cell potential. The solid line for concentrated sulfide solutions represents cryoscopic activities calculated from the van't Hoff equation, wherein it is assumed that the heat of fusion, ΔH_f, of silver sulfide is temperature independent and has a value of 800 cal/mole (16).

$$[24] \qquad \ln a_{Ag_2S} = \frac{-\Delta H_f}{R}\left(\frac{1}{T_L} - \frac{1}{T_F}\right)$$

Although the activities actually apply only to the liquidus temperature, their use at higher temperatures is justified in constructing Fig. 11, since the temperature dependence of the activity as given by the partial molar heat of mixing is seen from Fig. 10 to be very low for the concentrated sulfide solutions. It is evident that the cryoscopic and electrochemical measurements are in substantial agreement.

The positive deviations from ideality indicated by the activities are consistent with a tendency of the like species in this system to associate in the liquid. The positive heats of mixing indicate a decrease of activity with temperature and the solutions tend towards ideality at the higher temperatures, as expected.

The present results indicate that the previously suspected incongruently melting compound in this system (1) does not exist and that the unusual shape of the silver sulfide liquidus should be attributed to the positive deviations from ideality and to the tendency towards immiscibility. Immiscibility appears to be a general trend, particularly, in reciprocal metal chloride – metal sulfide systems. For example, a large miscibility gap has been found in the system NaCl–Ag_2S and in other metal sulfide – alkali and alkaline earth chloride systems currently under investigation in this laboratory (18, 19).

As mentioned in the introduction, silver chloride solutions rich in silver sulfide conduct electronically over wide temperature and composition ranges (2). From the present results it appears that association of like species is the only structural property of the melt that may be related to its abnormal electrical properties.

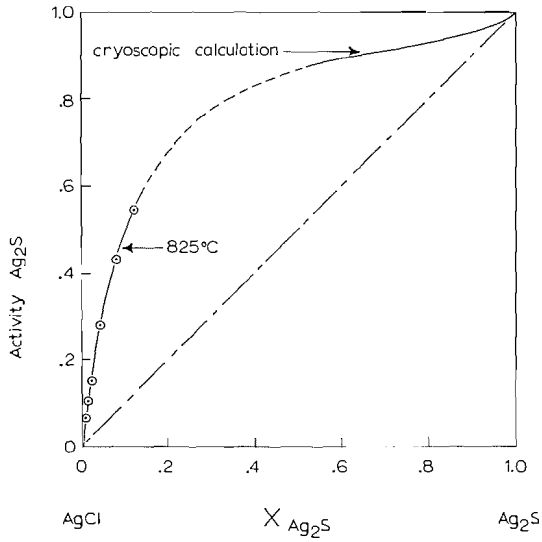

FIG. 11. Activity isotherm for silver sulfide at 825 °C. Points are experimental; the solid line represents activities calculated from the phase diagram.

Acknowledgments

The authors wish to express their gratitude to the National Research Council of Canada for financial support. The authors thank Mr. R. H. Chappell for his assistance in constructing the glass apparatus.

1. M. C. BELL and S. N. FLENGAS. J. Electrochem. Soc. **111**, 569 (1964).
2. M. C. BELL and S. N. FLENGAS. J. Electrochem. Soc. **111**, 575 (1964).
3. M. C. BELL and S. N. FLENGAS. J. Electrochem. Soc. **113**, 27 (1966).
4. M. C. BELL and S. N. FLENGAS. J. Electrochem. Soc. **113**, 31 (1966).
5. A. K. GARBEE. M.A.Sc. Thesis, University of Toronto, Toronto, Ontario. 1966.
6. M. BOURGON, G. DERGE, and G. M. POUND. Trans. AIME, **209**, 1454 (1957).
7. K. KIUKKOLA and C. WAGNER. J. Electrochem. Soc. **104**, 379 (1957).
8. FORD MOTOR CO. Press release, Jan. 1967.
9. A. G. VERDUCH and C. WAGNER. J. Phys. Chem. **61**, 558 (1957).
10. J. BERKOWITZ and J. R. MARQUART. J. Chem. Phys. **39**, 275 (1963).
11. W. A. WEST and A. W. MENZIES. J. Phys. Chem. **33**, 1880 (1929).
12. S. N. FLENGAS and T. R. INGRAHAM. Can. J. Chem. **36**, 780, 1103 (1958).
13. S. PETER. Z. Elektrochem. **57**, 289 (1953).
14. G. B. GUTHRIE, D. W. SCOTT, and G. WADDINGTON. J. Am. Chem. Soc. **76**, 1488 (1954).
15. O. KUBASCHEWSKI and E. EVANS. Metallurgical thermochemistry. Pergamon Press Ltd., London. 1955.
16. T. ROSENQVIST. Trans. AIME, **185**, 451 (1949).
17. F. D. RICHARDSON and J. H. E. JEFFES. J. Iron Steel Inst. London, **171**, 165 (1952).
18. M. C. BELL. Ph.D. Thesis, University of Toronto, Toronto, Ontario. 1964.
19. A. D. PELTON and S. N. FLENGAS. To be published.

Gas–solid exchange reactions: Zinc vapor and polycrystalline zinc selenide

E. A. SECCO AND CHIEN-HUO SU
Chemistry Department, St. Francis Xavier University, Antigonish, Nova Scotia
Received November 28, 1967

The exchange kinetics of zinc vapor with polycrystalline zinc selenide have been studied in a static system in the temperature range 720–800 °C.

The kinetic data are consistent with a diffusion-controlled process from the initial stage, in contrast with existing exchange data on ZnO and ZnS powders. The diffusion equation is given as:

$$D = 10^3 \exp(-79.5 \pm 5 \text{ kcal}/RT) \text{ cm}^2 \text{ s}^{-1}.$$

Canadian Journal of Chemistry, 46, 1621 (1968)

Can. J. Chem. Downloaded from www.nrcresearchpress.com by 210.87.254.40 on 09/05/12
For personal use only.

Introduction

This study is a continuation of a program of research on heterogeneous isotopic exchange reaction involving a metallic vapor and a solid compound. The program is an attempt to understand the kinetics and mechanism of gas–solid interaction. Previous studies reporting on the Zn–ZnO (1) and Zn–ZnS (2) systems have shown the rate to be controlled by two processes, an initial first-order rate followed by a diffusion rate.

The compound ZnSe, while belonging to the family of compounds which includes ZnO and ZnS, possesses a zinc blende cubic structure in contrast to the wurtzite hexagonal structure of ZnO and ZnS previously studied. The exchange study between Zn vapor and solid ZnSe shows that the gas–solid reaction is diffusion controlled over the entire range of the reaction fraction investigated.

Experimental

The polycrystalline ZnSe used in this work was from A. D. MacKay, Inc. 99.9995% purity. The X-ray diffractogram showed a pattern identical with the ZnSe diffraction pattern recorded in A.S.T.M. index No. 5-0522. The surface area of the selenide powder was found to be 0.64 m^2/g by nitrogen adsorption measurements. The particle radius is calculated to be ca. 8.7×10^{-4} cm. The selenide powder was stored in an oven at 150 °C before use.

The exchange runs were carried out in a static system with the use of quartz vessels, and the reaction fraction was determined by the uptake of radio-zinc, as previously described (3).

Results

In Fig. 1 are shown typical log $(1 - \alpha^*)$ versus time plots at different temperatures for constant Zn pressure (0.10 atm) and constant mole fraction of zinc selenide (0.50); α^* is the reaction fraction. The logarithms of the rate constants, k_e, obtained from the slopes of the straight lines in Fig. 1 are plotted against the reciprocal of the absolute temperature in Fig. 4, line *a*, to give a straight line corresponding to an energy of 80.5 ± 3 kcal. The characteristic feature of the common non-zero intercept of Fig. 1, whose value of -0.20 corresponds to 40% reaction, is evident as in previously reported gas–solid exchange studies.

The noticeable absence in Fig. 1 of a straight line for the initial exchange stage as previously observed suggested the probing of the initial stage in greater detail. The results in the form of log $(1 - \alpha^*)$ versus time plots are given in Fig. 2. The absence of the zero intercept persisted while the common non-zero intercept in Fig. 2 now appears at -0.10. The logarithms of the rate constants, k_e', obtained from the slopes of the straight lines in Fig. 2 when plotted against $1/T$ °K in Fig. 4, line *b*, give a linear relation whose slope also corresponds to an energy of 80 ± 5 kcal.

It is obvious that a single process prevails in the zinc vapor – selenide solid exchange reaction with an activation energy of 80 ± 3 kcal. The significance of the lower value for the common non-zero intercept at shorter durations is simply one of tangential origins, thus attesting to the singularity of the exchange rate. With an activation energy of 80 kcal, it is most probable that the exchange process is a diffusion-controlled transport mechanism whose rate is a function of depth. If such is the case, the diffusion process is operative at the outset of the exchange reaction.

The particular solution to the diffusion equation of interest in this type of experiment is that in which a solid specimen is bathed in an atmosphere containing the diffusion species. For the case of the sphere, to which the polycrystalline

Can. J. Chem. Downloaded from www.nrcresearchpress.com by 210.87.254.40 on 09/05/12
For personal use only.

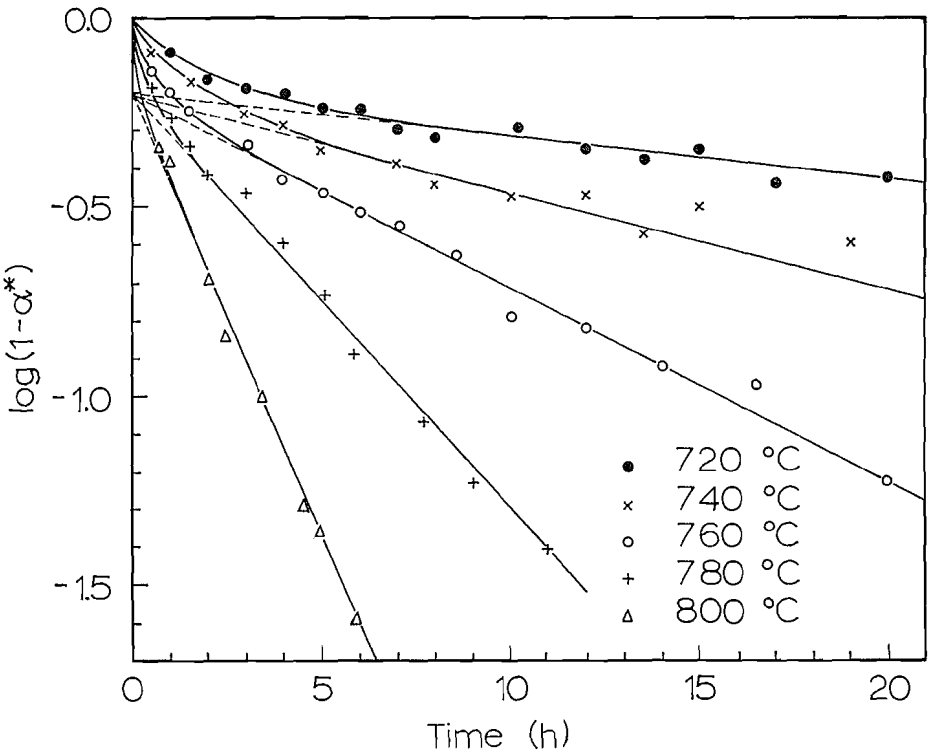

FIG. 1. Plot of log $(1 - \alpha^*)$ versus time at various temperatures.

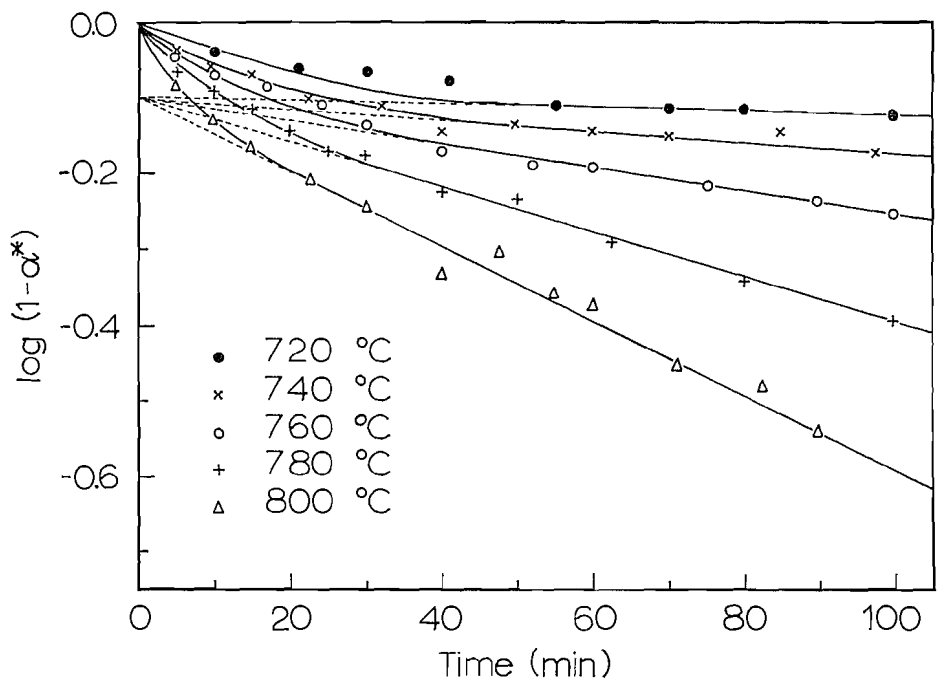

FIG. 2. Plot of log $(1 - \alpha^*)$ versus time at various temperatures for early stage of reaction

Can. J. Chem. Downloaded from www.nrcresearchpress.com by 210.87.254.40 on 09/05/12
For personal use only.

powder is assumed to approximate quite well, the solution to the problem is given by Crank (4) in the form:

$$[1]\quad \frac{M_t}{M_\infty} = 1 - \sum_{n=1}^{\infty} \frac{6\beta(\beta-1)}{9+9\beta+q_n^2\beta^2} e^{-Dq_n^2 t/r^2}.$$

This gives the total amount of M_t of tracer in the solid at time t as a fraction of the amount M_∞ at equilibrium. β is the ratio of the moles of zinc in the vapor to the number of moles of zinc in the solid, n^g/n^s; D is the diffusion coefficient, and r is the radius of the spherical particle. The q_n's are the non-zero positive roots of

$$[2]\quad \tan q_n = \frac{3q_n}{3+\beta q_n}.$$

In order to test the applicability of the diffusion equation and to evaluate the diffusion coefficients, a theoretical plot is made of (M_t/M_∞) against $x^2 = Dt/r^2$ and from this curve a value of x^2 is read from each experimental value of M_t/M_∞. These values of x^2 are plotted against the time t. If the diffusion equation is followed, the resulting graph should be a straight line through the origin, the slope of which is D/r^2. Figure 3 shows such a plot of the nondimensional (Dt/r^2) as a function of time for ^{65}Zn exchange with ZnSe at the different temperatures up to 12 h. The very good fit of the experimental data with the theoretical diffusion expression supports the view that the exchange reaction is governed by a diffusion process at the outset.

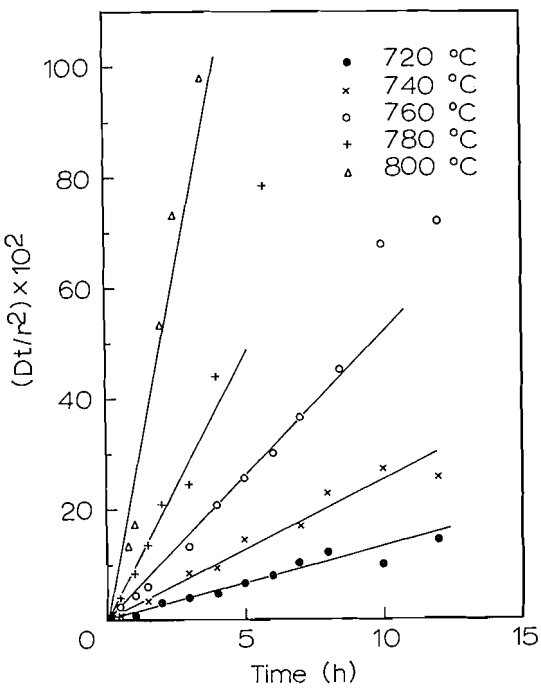

FIG. 3. Plot of nondimensional Dt/r^2 versus time.

The diffusion coefficients at the various temperatures were evaluated as the product of the slope of the straight line in Fig. 3 and the square of the particle radius, r^2. The logarithm of the diffusion coefficients versus $1/T$ °K yields a straight line, Fig. 4, line c, corresponding to an activation energy of 79.5 ± 5 kcal, which is identical with the previously obtained energy values. The diffusion equation is given as $D = 10^3 \exp(-79.5 \pm 5 \text{ kcal}/RT)\ \text{cm}^2\ \text{s}^{-1}$.

Discussion

It is well recognized that in such a simple reaction as gas–solid exchange, i.e.

$$Zn^*_{(g)} + ZnX_{(s)} \rightleftharpoons Zn^*X_{(s)} + Zn_{(g)},$$

where the reactants and products are chemically and structurally identical, thus precluding product–reactant interface effects, in addition to the actual exchange process, there may occur the part-processes of chemisorption of vapor and phase-boundary reaction along with the dissolution and transport of the vapor in the solid to the exchange site, any one of which may be rate determining. However, our exchange studies on ZnO and ZnS systems indicate that, of all the part-processes possible, only two processes have played rate-determining roles, namely (i) first-order rate and (ii) diffusion or transport process. The interpretation of the Zn–ZnSe exchange data in terms of a single diffusion-controlled mechanism is an interesting contrast to the previously reported studies. The obvious question is what factors determine the interplay of these two rate-determining processes?

Let us consider the initial step as an adsorptive one, viz.

$$Zn_{(g)} + site_{(s)} \overset{K}{\rightleftharpoons} (Zn_{ads}.site)_{(s)},$$

and assume the surface exchange reaction to be proportional to the concentration of adsorbed Zn. The total exchange rate, by applying the law of mass action and the Langmuir adsorption isotherm, is given by

$$[3]\quad k = \frac{ak_eKp_{Zn}}{(RT)+Kp_{Zn}},$$

where a = number of occupied adsorption sites, k_e = exchange rate constant, K = equilibrium

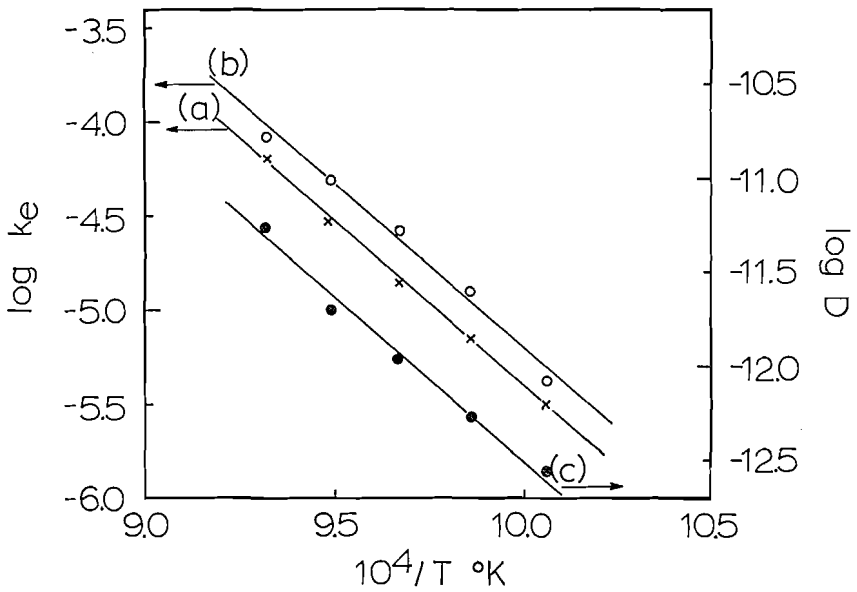

FIG. 4. Plot of log k_e versus $1/T$ °K.

constant for adsoprtion, and p_{Zn} = pressure of zinc vapor.

The exchange studies on Zn–ZnO and Zn–ZnS (5) systems have shown the measured rate constant to be a product of the exchange rate constant and an adsorption constant which is a limiting case of eq. [3], i.e. $Kp_{Zn} \gg RT$, so that $k_1' = ak_e$, a condition corresponding to complete coverage *or* high K value at constant p_{Zn}. In the ZnO and ZnS systems, the exchange reaction followed a first-order rate for the initial 30–50% of the exchange for the inequality condition $D_{Zn} > k$, i.e. the diffusion coefficient of Zn is greater than the composite rate constant. As the reaction progressed beyond 50%, the inequality is reversed, i.e. $k > D_{Zn}$, and the reaction is controlled by a diffusion process. Evidently the latter inequality prevails in the Zn–ZnSe exchange reaction from the outset.

The inequality $D_{Zn} > k$ implies that the solid is relatively permeable and the exchange sites are readily accessible to the vapor, whereas for $D_{Zn} < k$ the reverse is implied. Since the studies on ZnO and ZnS involved hexagonal structures while ZnSe is cubic, this structural aspect merits further study. It would be especially useful to carry out exchange studies between Zn vapor and the cubic form of ZnS.

Acknowledgments

This research work has received generous support from the National Research Council of Canada.

1. E. A. SECCO. *In* Fourth international symposium on reactivity of solids. *Edited by* J. H. deBoer. Elsevier Publishing Co. Inc., Amsterdam. 1960. p. 188.
2. E. A. SECCO. Can. J. Chem. **42**, 1396 (1964).
3. E. A. SECCO and W. J. MOORE. J. Chem. Phys. **26**, 942 (1957).
4. J. CRANK. The mathematics of diffusion. Clarendon Press, Oxford. 1956. pp. 88–90.
5. A. J. MACKINNON, R. R. MARTIN, and E. A. SECCO. Can. J. Chem. **42**, 2334 (1964).

Can. J. Chem. Downloaded from www.nrcresearchpress.com by 210.87.254.40 on 09/05/12
For personal use only.

Can. J. Chem. Downloaded from www.nrcresearchpress.com by 210.87.254.6 on 09/05/12
For personal use only.

Radiolysis of ethyl iodide and carbon tetrachloride mixtures at 77 °K

R. M. LEBLANC,[1] F. C. THYRION,[2] AND J. A. HERMAN
Department de Chimie, Université Laval, Québec, Québec

Received December 7, 1967

The radical yields of $C_2H_5^{\cdot}$ and $CCl_3^{\cdot}$ observed by electron spin resonance of $CCl_4 + C_2H_5I$ mixtures irradiated by γ rays at 77 °K are compared with yields of HCl, I_2, and HI measured after thawing. The dissociative capture of thermalized electrons by CCl_4 is extremely effective and accounts for most of the observed radicals. The difference between yields of HCl and $CCl_3^{\cdot}$ results from charge transfer from $C_2H_5I^+$ to $CCl_3^{\cdot}$. The formation of iodine proceeds both from neutralization processes of Cl^- ions with positive ions formed from C_2H_5I, and from ion–molecule reactions.

On compare les rendements radicalaires observés par la résonance électronique paramagnétique aux rendements en HCl, I_2 et HI observés après réchauffement de mélanges de CCl_4 et de C_2H_5I soumis aux irradiations des rayons γ. La capture d'électrons thermalisés est très efficace dans le cas du CCl_4 et fournit la plus grande partie des radicaux observés. L'écart entre les rendements en HCl et $CCl_3^{\cdot}$ est dû au transfert de charge que subit $C_2H_5I^+$ avec $CCl_3^{\cdot}$. Les réactions de neutralisation de Cl^- avec une entité positive issue de C_2H_5I et les réactions ion–molécule sont à la base de la production d'iode.

Canadian Journal of Chemistry, Volume 46, 1625 (1968)

Introduction

It has been shown that some γ-irradiated halogenated alkanes form anions efficiently by electron capture, as indicated by the corresponding visible and u.v. spectra of the ionic species in organic glasses at −196 °C (1). In the same way, Hamill and his co-workers (1) have established a scale of relative efficiency of electron capture for a whole series of solutes dissolved in suitable solvents; these measurements were based on competitive reaction abilities of solutes for thermalized electrons produced within the medium; however, they were confined to low solute concentrations.

It seems worthwhile to extend such a study over a wider range of concentration in a mixture of two solutes chosen from the Hamill scale. However, at high concentration the technique of measuring the optical spectrum of organic glasses at 77 °K does not give sufficient precision, therefore another experimental approach was preferred: the e.s.r. spectrum of radicals in frozen solutions and the subsequent chemical analysis of reaction products enabled us to establish a reaction scheme in such a system. In addition, irradiation in the solid phase has the advantage of limiting the reactions, especially of formed products, by preventing diffusion of bulky fragments in the solid.

We have chosen ethyl iodide and carbon tetrachloride as components of the mixture, both being known as good scavengers for thermalized electrons. Besides, numerous investigations of the irradiation of ethyl iodide in the pure state and in solutions have been made. Complete agreement on yields and on reaction mechanisms has not yet been fully established, and during this study new values of radiochemical yields were found, which give a better understanding of the observed behavior of γ-irradiated ethyl iodide.

Experimental

Carbon tetrachloride (Baker Company) labeled "Spectroscopic Grade" was distilled on a Todd column with a reflux ratio of 25:1. Ethyl iodide (BDH reagent) was purified on a silica gel and then distilled on a column of 40 theoretical plates. In the next step both reactants were successively vacuum distilled through a mixture of soda lime and magnesium sulfate and from trap to trap at liquid nitrogen temperature, and finally stored in darkened vessels. The purity of the reactants was checked by gas chromatography and only in C_2H_5I did an unidentified impurity remain of concentration less than 0.005%.

The solutions were prepared under vacuum (10^{-5} Torr) by mixing by volume (precisions ±5%) known quantities of the components (total of 5 ml). After admission to the irradiation cell they were frozen rapidly in order to obtain glassy solids. The irradiation cell reserved for chemical analysis was hemispherical in shape with a flat bottom (diameter 5 cm) and equipped with a break-seal. This particular geometry allows the solution to spread into a thin layer (< 2 mm). Once the irradiation was completed the cell was withdrawn from the liquid nitrogen bath, some water was poured over the break-seal, and the latter was broken. In this way the thin solid

[1]Holder of a NRCC Student Fellowship.
[2]Present address: Laboratoire de Chimie-Physique III, Université de Louvain, Belgium.

Can. J. Chem. Downloaded from www.nrcresearchpress.com by 210.87.254.6 on 09/05/12
For personal use only.

layer of organic solution is warmed very quickly by water which is sucked into the cell. In such a way one prevents to a considerable extent the reactions of HCl and HI with radicals during the thawing period, the two acids being immediately extracted by water. In addition a small excess of water still remaining over the broken break-seal prevents any losses of acids by evaporation.

Our purpose being the study of primary reactions only, the chemical analysis was limited to HCl, HI, and I_2 and was performed in the following manner. The aqueous solution collected after successive extractions was washed 2 to 4 times with cyclohexane "Spectroscopic Grade" to remove iodine and all other organic compounds which might be dissolved in the aqueous phase. A part of that aqueous solution was used for determination of hydrogen iodide by spectrophotometry at 226 mμ wavelength. The determination of the total concentration of acids, HCl, and HI, by the method of Bergman and Sanik (2), was performed on the remaining aqueous solution. Following this method, the concentration of the $Fe(SCN)^{2+}$ complex proportional to the concentration of halogen ions was measured spectrophotometrically at $\lambda_{max} = 460$ mμ. The iodine present in the organic phase was extracted with freshly prepared KI 2 *M* solution, and determined by absorption of the I_3^- ion at 350 mμ ($\varepsilon = 2.77 \times 10^4$ l mole^{-1} cm^{-1} (3)).

The e.s.r. study of free radicals formed during irradiation was performed on 0.2 ml samples of the same solutions rapidly frozen at 77 °K in Suprasil tubes. Before sealing, the sample was evacuated for several hours at 10^{-4} Torr. The free radical spectra were obtained with a Varian (model 4500 – 10 A, X-band) e.p.r. spectrometer, which was equipped with variable temperature dual-cavity and cooling system. The spectra were obtained at 77 °K or at a higher temperature, the temperature being maintained within 0.5 °C. The first derivative spectra were obtained with a X–Y recorder. The radical concentration was determined by calibration with diphenylpicrylhydrazyl (DPPH) in biphenyl.

The irradiation cell and the Suprasil tubes were irradiated in a Gammacell 220 irradiator (A.E.C.L.) at a dose of 2.92×10^{19} eV g^{-1}. Yields are reported relative to $G = 15.6$ for the Fricke dosimeter, but corrections have been made for the low energy components in the cylindrical ^{60}Co source, which caused a significant increase in the energy absorbed by the iodine atoms (4).

Results

The results of the spectrophotometric determination of HCl, I_2, and HI as a function of the ethyl iodide fraction are given in Fig. 1 and Table I. We have adopted the electron fraction as being characteristic of the energy absorption by the two constituents of the mixture, but we are aware that no particular reason can be advanced to justify such a procedure (5).

There is a significant difference between our values and those of Arnikar and Willard (3) for the yields of iodine and hydrogen iodide from the radiolysis of pure ethyl iodide in the glassy

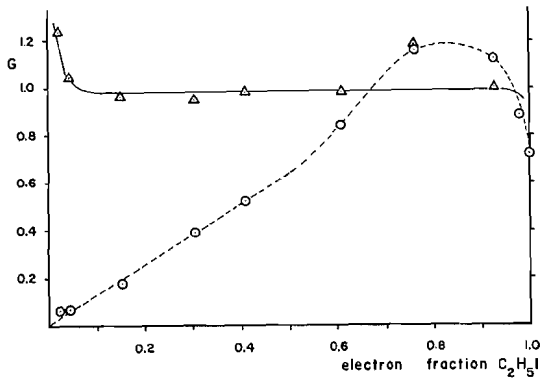

FIG. 1. $G(I_2)$ (○) and G(HCl) (△) of mixtures of C_2H_5I – CCl_4 irradiated at 77 °K.

state at 77 °K. However, the sum of the yields for iodine, G(HI) + $2G(I_2)$, are comparable in both cases. A value of G(HI) in the present study higher than that of Arnikar and Willard (3) or that of Hermann and Harrah (6) can be explained by a better prevention of the reaction between free radicals and HI, which is known to be a very efficient reaction (7). These authors could lose an appreciable amount of HI in such a reaction during the thawing of the solid ethyl iodide. For this reason the experimental method adopted here is justified.

It can be seen that an addition of minute quantities of CCl_4 decreases dramatically the yield of HI (Table I), while the yield of iodine increases slightly (Fig. 1). However, a further addition of CCl_4 to C_2H_5I brings about a linear decrease in the yield of iodine. On the other hand, the yield of HCl is remarkably constant over a wide range of concentration. This result can be compared with that of Van Dusen and Hamill (8) and Urban and Bednar (9) obtained in irradiated mixtures containing CCl_4.

The e.s.r. spectrum of irradiated pure CCl_4 was the same as described by others (10–12), and is attributed to the $CCl_3^{\cdot}$ radical. It consists of one broad asymmetric band (g=2.014) which begins to show structure at 120 °K and finally disappears at 217 °K.

Pure C_2H_5I in the glassy state displays an e.s.r. specturm of 6 lines, whose characteristics are identical with that observed by others (6, 13) and is attributed to the $C_2H_5^{\cdot}$ radical. The g factors being different for $CCl_3^{\cdot}$ and $C_2H_5^{\cdot}$ radicals, their e.s.r. spectra are slightly separated and this allows one to calculate the respective con-

TABLE I
Electron fraction of C_2H_5I

		1.00	0.98	0.93	0.76	0.61	0.41	0.31	0.16
Present work	G(HI)	3.2	2	0.013	0.002	0.003	0.008	0.008	—
	$G(I_2)$	0.72							
Reference 3	G(HI)	1.9							
	$G(I_2)$	1.2							
Reference 6	G(HI)	1.25							
	$G(I_2)$	1.45							

centrations of the radicals in irradiated mixtures. The ratio of concentration of these radicals is influenced only slightly by increasing the temperature. However, the temperature of disappearance of the radicals decreases steadily with increasing C_2H_5I content in the mixtures.

The variation of the free radical concentrations was usually linear with absorbed doses. However, highly concentrated solutions of CCl_4 show a small (several %) decrease from linearity.

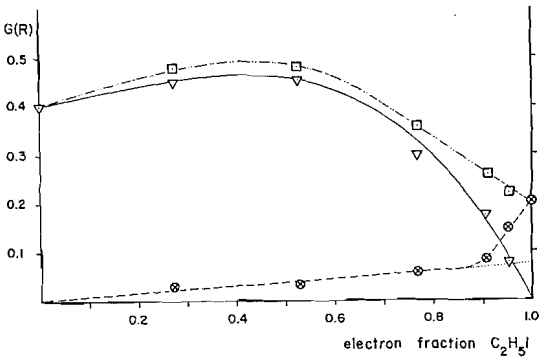

FIG. 2. Radical yields $G(CCl_3^{\cdot})$ (▽) and $G(C_2H_5^{\cdot})$ (⊗), and total radical yield G(R) (□) of mixtures of $C_2H_5I - CCl_4$ irradiated at 77 °K.

The total yield of radicals, G(R), and the yields of each radical species, $G(C_2H_5^{\cdot})$ and $G(CCl_3^{\cdot})$, are given as a function of the electron fraction of ethyl iodide in Fig. 2. If one admits that any deviation from the theoretical yield is represented by a curve, which does not coincide with the straight line of the mixture law (14) (line issued from the origin and passing through the experimental yield of the pure component), then $G(C_2H_5^{\cdot})$ shows a negative deviation, while $G(CCl_3^{\cdot})$ is characterized by a positive deviation relative to the theoretical yields. These deviations can be represented by the following formulas:

$$\bar{g}(C_2H_5^{\cdot}) = G_x(C_2H_5^{\cdot}) - XG^0(C_2H_5^{\cdot})$$

$$\bar{g}(CCl_3^{\cdot}) = G_x(CCl_3^{\cdot}) - (1 - X)G^0(CCl_3^{\cdot}),$$

where X is the electron fraction of C_2H_5I, G_x represent the experimental yields at concentration X and G^0 the yields of radicals in pure components, and $\bar{g}(C_2H_5^{\cdot})$ and $\bar{g}(CCl_3^{\cdot})$ represent losses and gains relative to the mixture law. It can be seen in Fig. 3 that there is no compensation of the gains of the $CCl_3^{\cdot}$ radical yields by the losses of the $C_2H_5^{\cdot}$ yields; the excess total radical yield, $\bar{g}$(R),

$$\bar{g}(R) = G(R) - [(1 - X)G^0(CCl_3^{\cdot}) + XG^0(C_2H_5^{\cdot})],$$

is also represented in Fig. 3. Roginskii *et al.* (11) found a similar relationship for irradiated mixtures of methanol in carbon tetrachloride.

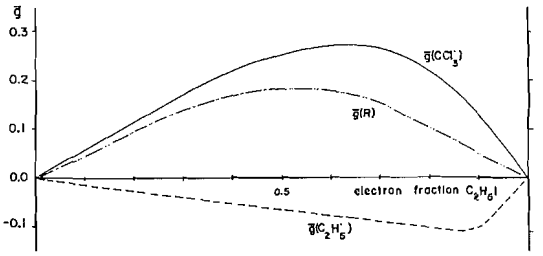

FIG. 3. Deviations of radical yields relative to the mixture law.

Discussion

The analytical procedures for measuring the concentrations of radicals and reaction products are realized in such a manner that any comparison between these measurements must be done very carefully. Indeed, the difficulty of measuring the amplitude and the nature of the reactions taking place during the thawing of the sample is the principal obstacle limiting the validity of

Can. J. Chem. Downloaded from www.nrcresearchpress.com by 210.87.254.6 on 09/05/12
For personal use only.

Can. J. Chem. Downloaded from www.nrcresearchpress.com by 210.87.254.6 on 09/05/12
For personal use only.

any conclusion. However, the radical yields being much less than that of reaction products, it can be assumed that reactions of these radicals during the warming period will modify only slightly the quantities of products formed during irradiation. Moreover, the irradiation doses were chosen to prevent significant accumulation of reaction products within the system, thus reducing the possibility of secondary reactions.

Ions and excited molecules of both components in the mixtures are formed in primary processes, as a result of the absorption of energy in the system:

$$[1] \qquad C_2H_5I \xrightarrow{\gamma} C_2H_5I^+ + e^-$$

$$[1a] \qquad C_2H_5I \xrightarrow{\gamma} C_2H_5I^*$$

$$[2] \qquad CCl_4 \xrightarrow{\gamma} CCl_4^+ + e^-$$

$$[2a] \qquad CCl_4 \xrightarrow{\gamma} CCl_4^*$$

Although there is no evidence from mass spectrometric measurements for the existence of CCl_4^+, its presence in the solid phase at low temperature has been postulated by Hamill *et al.* (15, 16). They tentatively ascribed the 4800 Å absorption band produced in the irradiation at 77 °K of 3-methylpentane (3-MP) containing CCl_4 to CCl_4^+ ions formed by charge transfer from excited 3-MP^+ ions. However, the study of Claridge and co-workers (17) calls in question the assignment of this band to CCl_4^+ ions. More recently, Shida and Hamill (18) observed in γ-irradiated polycrystalline CCl_4 at 77 °K a band centered at 4000 Å, which they attributed to trapped positive holes in the CCl_4 matrix, the calculated yield, G(hole), being around 1.9. They suppose that (positive) holes in carbon tetrachloride may correspond to $(CCl_3\text{—}Cl)^+$ entities having an increased internuclear separation. However, CCl_4^+ is an ion-radical and therefore should be detected by the e.s.r. method. If so, it should be included in the experimental radical yield of pure CCl_4, which in the present case is 0.4 (Fig. 2). The discrepancy between this value and that of Shida and Hamill should not be interpreted as a nonexistence of the CCl_4^+ ion, but rather may point out the efficiency of the recapture process in pure carbon tetrachloride between anions and (positive) holes.

The species formed in processes [1], [1*a*], [2], and [2*a*] will enter into a series of reactions in order to dissipate the accumulated energy. Thermalized electrons can undergo dissociative capture with ethyl iodide and carbon tetrachloride (12, 15, 19, 20) in the following reactions:

$$[3] \qquad C_2H_5I + e^- \rightarrow (C_2H_5I)^- \rightarrow C_2H_5^{\cdot} + I^-$$

$$[4] \qquad CCl_4 + e^- \rightarrow (CCl_4)^- \rightarrow CCl_3^{\cdot} + Cl^-,$$

where parentheses indicate anions which might be long lived. Hamill and his co-workers (8, 21) have shown that the solvolysis of CCl_4^- is greatly promoted in polar media. However, it would be wrong to presume that solvolysis must necessarily separate $CCl_3^{\cdot}$ and Cl^- in the solid phase. On the contrary, Claridge and Willard (12) showed, that in the case of irradiated methyl halides in the solid phase, both $CH_3^{\cdot}$ and X^- fragments are formed in the same solvent envelope.

On the other hand, because of the low concentrations of HI and I_2 compared with that of mixture components, the electron capture processes by these reaction products can be ignored, notwithstanding that the cross section for electron attachment of I_2 is higher than that of CCl_4, and that of HI is higher than that of C_2H_5I (1, 22).

Another possibility for the degradation of the internal energy of the primary species is the charge transfer from ions formed in reactions [1] and [2]. If the ionization potential (i.p.) of CCl_4 is taken as 11.47 eV (23) (it is actually the appearance potential of CCl_3^+), this value being greater than that of C_2H_5I (i.p. = 9.33 eV) (24), reaction [5] is plausible.

$$[5] \qquad CCl_4^+ + C_2H_5I \rightarrow CCl_4 + C_2H_5I^+$$

Even reaction [6],

$$[6] \qquad C_2H_5I^+ + CCl_3^{\cdot} \rightarrow C_2H_5I + CCl_3^+,$$

might take place because the i.p. of $CCl_3^{\cdot}$ is only 8.78 eV (25). However, the low concentrations of reactants in reaction [6] suggest that this reaction may be less important than reaction [5]. On the other hand, the electroluminescence experiments on 3-methylpentane, tretramethylene-*p*-phenylenediamine solutions (26) are interpreted as evidence for trapping of electrons in close proximity to the parent ion. If this also applies to the present system, $C_2H_5I^+$ and $CCl_3^{\cdot}$ (formed in reaction [4]) might not be too far from one another, and assuming a chain of positive charge transfer, reaction [6] can be significant. Since CCl_3^+ ion can not be detected

Can. J. Chem. Downloaded from www.nrcresearchpress.com by 210.87.254.6 on 09/05/12
For personal use only.

by e.s.r., reaction [6] might be tentatively invoked to explain the differences in yields of CCl_3· and HCl.

Charge neutralization processes will play an important role either during irradiation or during the thawing period of the sample. Neutralization of the primary ions, CCl_4^+ and $C_2H_5I^+$, by that fraction of electrons which have not escaped the coulombic attraction of parent ions and return back in less than 10^{-13} s, leads to highly excited neutral species which resemble those formed in reactions [1*a*] and [2*a*]. It is normally assumed that such highly excited neutral molecules will dissociate (in the gas phase) into radical fragments:

[7] $$C_2H_5I^* \rightarrow C_2H_5\cdot + I\cdot.$$

However, Claridge and Willard (12) showed that in 3-methylpentane glasses, direct dissociation of R—X molecules by photon absorption does not occur. The reason for this might be a strong cage effect in the solid phase, as seen by the difference of radiochemical yields in the solid and liquid state (22, 27). If the same behavior applies to the present system, formation of CCl_3· and C_2H_5· radicals in the homolytic dissociation reactions of excited neutral molecules is not important, and the contribution to $G(CCl_3\cdot)$ and $G(C_2H_5\cdot)$ is small. In such a way, we assume that the small, but measurable, radiochemical yield of C_2H_5· radicals in the concentration range less than 0.9 of ethyl iodide (Fig. 2) results from reaction [7] and accounts for a $g_7(C_2H_5\cdot) = 0.07$ in pure C_2H_5I.

Luebbe and Willard (28), who photolyzed pure ethyl iodide at 93 °K, concluded from kinetic results that HI is formed in a homolytic splitting reaction:

[8] $$C_2H_5I^* \rightarrow C_2H_4 + HI.$$

However, Timm (29) did not find any evidence for reaction [8] in the photolysis of ethyl iodide in a hydrocarbon matrix at 77 °K. In the present case, if such reaction occurs, the formation of HI should follow the C_2H_5I content over the whole range of concentrations. It is clear from Table I that such is not the case and for this reason we reject the occurrence of the homolytic dissociation reaction [8].

One of the following ion–molecule reactions should be considered:

[9] $$C_2H_5I^+ + C_2H_5I \rightarrow (C_2H_5I)_2^+$$

[10] $$\rightarrow (C_2H_5)_2I^+ + I\cdot.$$

The conversion of $C_2H_5I^+$ to $(C_2H_5I)_2^+$ or $(C_2H_5)_2I^+$ ions in a solid matrix at 77 °K is attributable to a preexisting neutral dimer, $(C_2H_5I)_2$, caused by permanent dipole pairing. The occurrence of reaction [9] is based on the work of Mittal and Hamill (30), who attributed the absorption band at 7600 Å in the γ-irradiated alkyl iodide to $(RI)_2^+$ ion, whereas Claridge and Willard (31) assigned the same band also to the R_2I^+ ion. The evidence that this absorption band belongs to a cationic species is convincing; likewise, its attribution to a species having RI^+ ion as precursor seems reasonable. However, the assignment of the 7600 Å absorption band to $(RI)_2^+$ only is based on an approximate energetic consideration of the ionization efficiency curve of the $(C_2H_5I)_2^+$ ion in the gas phase and therefore might be not definitive. Mechanistically, reaction [10] is more interesting in the present case, because it can explain the relatively important formation of molecular iodine (Fig. 1), while reaction [9] cannot. Moreover, reaction [10] might explain partly the difference between $G(C_2H_5\cdot)$ and $G(I) = 2G(I_2)$.

The neutralization reactions between positive and negative ions are probably the main processes accounting for decomposition products. Such neutralization processes in the solid phase were recently invoked by Mittal and Hamill (30) in order to explain the slow decay of ionic spectra of alkyl halides in hydrocarbon glasses at 77 °K. In the present system the following reactions must be considered:

[11] $$(C_2H_5)_2I^+ + X^- \rightarrow (C_2H_5)_2I.X$$

[12] $$(C_2H_5I)^+ + X^- \rightarrow (C_2H_5I).X,$$

where X^- stands for Cl^- or I^-. During the warming period, when the matrix is softening, the complexes (RI).X and (R_2I).X enter into a series of reactions which are similar to radical reactions within spurs in the liquid phase. We assume that HCl and HI are formed by the reactions [13*a*] and [13*b*].

[13*a*] $$(C_2H_5)_2I.Cl \rightarrow HCl + C_2H_4 + C_2H_5I$$
$$(C_2H_5I).Cl \rightarrow HCl + I\cdot + C_2H_4$$

[13*b*] $$(C_2H_5)_2I.I \rightarrow HI + C_2H_4 + C_2H_5I$$
$$(C_2H_5I).I \rightarrow HI + I\cdot + C_2H_4$$

Reactions [11] and [12] are of special interest. Since carbon tetrachloride is extremely effective in dissociative electron capture, its addition in

Can. J. Chem. Downloaded from www.nrcresearchpress.com by 210.87.254.6 on 09/05/12
For personal use only.

even small amount will strongly diminish the neutralization processes [11] and [12] with I^-, and therefore could be the reason for the dramatic decrease of G(HI) (Table I), inasmuch as we admit that the formation of HCl prevails over formation of HI in reaction [13*a*].

Radical Yields

The free radicals measured by e.s.r. are mainly formed in reactions [3] and [4]. Wentworth *et al.* (20) showed that reaction [4] seems to be temperature independent, contrary to reaction [3]. Moreover, Hamill *et al.* (1) and Buchel'Nikova (32) showed that carbon tetrachloride is more efficient in electron capture than ethyl iodide. In the present case, a $G(CCl_3\cdot)$ superior to that given by the mixture law supports this view (Fig. 2). Ethyl iodide acts as an efficient electron capturer only when its electron fraction is greater than 0.9; in this range of concentrations the increase of $G(C_2H_5\cdot)$ is proportional to the decrease of $G(CCl_3\cdot)$, as measured from the slopes of the two curves.

Indeed, if $N(X^-)$ is the number per ml of X^- anions formed by dissociative capture (reactions [3] and [4]), the following equality must hold:

$$[14] \qquad \frac{N(Cl^-)}{N(I^-)} = \frac{\sigma_{CCl_4}}{\sigma_{C_2H_5I}} \frac{[CCl_4]}{[C_2H_5I]},$$

where σ stands for dissociative capture cross section. A straightforward steady state kinetic derivation confined only to reactions [1], [3], and [4] gives an expression of the well-known form:

$$[15] \qquad \frac{1}{g(I^-)} = \frac{1}{g^0(I^-)} + \frac{1}{g^0(I^-)} \frac{\sigma_{CCl_4}}{\sigma_{C_2H_5I}} \frac{[CCl_4]}{[C_2H_5I]},$$

where $g(I^-)$ and $g^0(I^-)$ are calculated yields in mixtures and in pure ethyl iodide respectively of iodine ions formed in reaction [3]. This yield is defined by the difference $g(I^-) = G(C_2H_5\cdot)_{tot} - g_7(C_2H_5\cdot)$, which for pure ethyl iodide is equal to $g^0(I^-) = 0.20 - 0.07 = 0.13$ (Fig. 2). A plot of the reciprocal of $g(I^-)$ as a function of the ratio of concentrations $[CCl_4]/[C_2H_5I]$ should give a straight line, from whose slope it should be possible to calculate the ratio of σ's. From the linear portion of such a plot one finds a ratio $\sigma_{CCl_4}/\sigma_{C_2H_5I} = 16$, which compares very favorably with the value of 18 calculated from Lee's coefficients of electron attachment (33).

The shape of the $G(C_2H_5\cdot)$ curve (Fig. 2) indicates that another mechanism must be invoked in order to explain the small, but measurable, yield in the concentration range less than 0.9. The homolytic dissociation of excited C_2H_5I molecules formed in reactions [1*a*] and [7] might be the process responsible for this slow decrease of $G(C_2H_5\cdot)$. On the other hand, at high concentrations of ethyl iodide ($> X = 0.6$) the observed $G(CCl_3\cdot)$ decreases, notwithstanding that one might expect that the yield of $CCl_3\cdot$, being the counterpart of Cl^- by reaction [4], should not differ much from that measured at low and moderate concentrations. Because $G(CCl_3\cdot)$ decreases with increasing C_2H_5I concentration, it might be assumed that this radical has better chances for a charge transfer with increasing concentration of $C_2H_5I^+$ ions (reaction [6]). Finally, the nonvanishing excess total radical yield, $\bar{g}$(R) (Fig. 3), might result from the combined effect of preferential electron capture by CCl_4, the polarity of the medium, and an undetermined contribution of homolytic dissociation of excited CCl_4* into $CCl_3\cdot$ and Cl atom.

Iodine Formation

In the solid matrix at 77 °K there is no evidence for formation of I_2, as inferred from the absence of characteristic band absorption of this molecule. However, the I_2^- was assumed to exist in glassy C_2H_5I (31)[3], and is formed by the reaction

$$[16] \qquad I^- + I \rightarrow I_2^-.$$

This ion might be the precursor for the molecular iodine, if we propose that the neutralization by positive ions does not induce secondary reactions consuming iodine. Even if such would be the case, reaction [16] can only be important for pure and very concentrated ethyl iodide, because the addition of a small amount of CCl_4 will decrease very strongly the concentration of iodine anions. For this reason we prefer reaction [17] for the formation of molecular iodine at moderate and low concentrations of ethyl iodide.

$$[17] \qquad I\cdot + I\cdot \rightarrow I_2$$

Assuming that the molecular iodine formed during the thawing period does not react further, and thus does not change its concentration appreciably, and provided that the iodine pro-

[3]Recently Mittal and Hamill (30) attributed the absorption band of I_2^- (4050 Å) to RI.I neutral complex.

Can. J. Chem. Downloaded from www.nrcresearchpress.com by 210.87.254.6 on 09/05/12
For personal use only.

duction in reactions [3] and [16] is equivalent to $G(C_2H_5^{\cdot})$, the excess of $G(I)$ over $G(C_2H_5^{\cdot})$ must result from the two other reactions [10] and [13]. In the case of pure ethyl iodide, this excess can come only from reactions [10] and [13*b*] and accounts for $g(I) = G(I)_{tot} - G(C_2H_5^{\cdot}) = 1.24$. One can verify these assumptions when looking, for instance, for yields of $I^{\cdot}$ and $C_2H_5^{\cdot}$ radicals at an electron fraction of 0.9 for C_2H_5I. We observe a $G(I) = 2.3$ and a $G(C_2H_5^{\cdot}) = 0.07$; if we add to the latter value the calculated $g(I)_{10,13b}$, then we find that the yield $g(I)_{13a}$ is about unity, and this corresponds well to the observed $G(HCl)$.

The relative importance of the above mechanisms is valid only in the range of high concentrations of C_2H_5I (0.9 to 1.0). With diminishing concentrations of ethyl iodide, the importance of (RI).I complexes decreases, because the concentrations of $(C_2H_5)_2I^+$ and $C_2H_5I^+$ decrease. Nevertheless, even at low concentrations of ethyl iodide, the concentration of the RI^+ ion may be sufficient to produce the main part of the iodide, as shown by Croft and Hanrahan (34) and Forrestal and Hamill (35).

Hydrogen Chloride Yield

Several authors (9, 36) have assumed that formation of HCl in the mixtures of hydrocarbons and carbon tetrachloride results essentially from the attack on CCl_4 by H atoms. Similarly it was proposed (37) that formation of radicals in the solid phase might also originate from homolytic dissociation of H atoms from excited hydrocarbon molecules and a subsequent attack on neighboring molecules by these hydrogen atoms. However, the low yields of hydrogen for irradiated liquid C_2H_5I (38, 39) and, in the present case, the invariance of HCl and HI yields in the solid phase with increasing concentration of ethyl iodide, suggest that the above-mentioned process is not very important. Therefore, the reaction

[18] $$H^{\cdot} + CCl_4 \rightarrow HCl + CCl_3^{\cdot}$$

should have only a limited importance for formation of HCl and $CCl_3^{\cdot}$, in spite of the fact that such a process has been postulated in mixtures of methanol in carbon tetrachloride (9, 11, 40).

We have seen previously that at high C_2H_5I concentrations equal amounts of iodine atoms and HCl are formed in reaction [13*a*], which accounts for the radiochemical yields of about unity for each of these species. We assume that the same reaction [13*a*] is still responsible for yields of HCl at moderate and low concentrations of ethyl iodide. Indeed, examination of Figs. 1 and 2 to the extent of $X = 0.6$ shows some parallelism in the $CCl_3^{\cdot}$ and HCl yields. This observation, coupled to the regular aspect of $G(HCl)$, might be explained by assuming that originally there is a unique Cl^- species. Providing that the concentration of Cl^- remains constant, as a result of the high efficiency of electron capture and of the polarity of the medium, a constant yield of the charge neutralization reactions [11] and [12] will be found, in spite of the decrease of CCl_4 content of the mixture. Finally, the possibility of formation of HCl in reaction [18] cannot be disregarded at high concentrations of CCl_4.

Acknowledgments

The authors wish to thank the National Research Council of Canada for financial support of this work. We are also grateful to the "Counseil des Arts du Canada" for a postdoctoral fellowship to one of us (F. C. T.). Assistance of the solid state research center of this University is also gratefully acknowledged.

1. J. P. Guarino, M. R. Ronayne, and W. H. Hamill. Radiation Res. **17**, 379 (1962).
2. J. G. Bergman and J. Sanik. Anal. Chem. **29**, 241 (1957).
3. H. J. Arnikar and J. E. Willard. Radiation Res. **30**, 204 (1967).
4. W. Bernstein and R. Schuler. Nucleonics, **13**, No. 11, 110 (1955).
5. A. J. Swallow. *In* Energy transfer in radiation process *Edited by* G. O. Phillips. Elsevier, Amsterdam. 1966. p. 121.
6. G. L. Hermann and L. A. Harrah. U.S. At. Energy Comm. Accession No. 33327, Rept. No. AD 634912 (1966).
7. D. L. Bunbury, R. R. Williams Jr., and W. H. Hamill. J. Am. Chem. Soc. **78**, 6228 (1956).
8. W. Van Dusen and W. H. Hamill. J. Am. Chem. Soc. **84**, 3648 (1962).
9. J. Urban and J. Bednar. Collection Czech. Chem. Commun. **31**, 4221 (1966).
10. J. E. Bennet and A. Thomas. Intern. Symp. Free Radicals, 6th, Cambridge, England, 1963.
11. V. A. Roginskii, A. G. Kotov, and S. Ya. Pzhezhetskii. Russ. J. Phys. Chem. English Transl. **39**, 1544 (1965).
12. R. F. C. Claridge and J. E. Willard. J. Am. Chem. Soc. **87**, 4992 (1965).
13. H. W. Fenrick, S. W. Filseth, A. L. Hanson, and J. E. Willard. J. Am. Chem. Soc. **85**, 3731 (1963).
14. M. Burton. Actions chimiques et biologiques des

radiations. *Edited by* M. Haissinsky. 3rd series Masson et Cie, Paris. 1958. p. 15.
15. J. P. GUARINO and W. H. HAMILL. J. Am. Chem. Soc. **86**, 777 (1964).
16. D. W. SKELLY and W. H. HAMILL. J. Phys. Chem. **70**, 1630 (1966).
17. R. F. C. CLARIDGE, R. M. IYER, and J. E. WILLARD. J. Phys. Chem. **71**, 3527 (1967).
18. T. SHIDA and W. H. HAMILL. J. Chem. Phys. **44**, 2369 (1966).
19. D. W. SKELLY, R. G. HAYES, and W. H. HAMILL. J. Chem. Phys. **43**, 2795 (1965).
20. W. E. WENTWORTH, R. S. BECKER, and R. TUNG. J. Phys. Chem. **71**, 1652 (1967).
21. P. S. RAO, J. R. NASH, J. P. GUARINO, M. R. RONAYNE, and W. H. HAMILL. J. Am. Chem. Soc. **84**, 500 (1962).
22. C. CAPELLOS. Radiation chemistry of alkyl halides. Rept. No. AD 632704. U.S. Dept. of Commerce. 1967.
23. K. WATANABE, T. NAKAYAMA, and J. MOTTL. J. Quant. Spectry. Radiative Transfer, **2**, 369 (1962).
24. K. WATANABE. J. Chem. Phys. **26**, 542 (1957).
25. J. B. FARMER, I. H. HENDERSON, F. P. LOSSING, and D. G. H. MARSDEN. J. Chem. Phys. **24**, 348 (1956).
26. G. E. JOHNSON and A. C. ALBRECHT. Abstracts of papers presented at the Intern. Conf. of Photosensitization in Solids, Chicago, Ill., June 1964. (Cited by Claridge and Willard in ref. 12.)
27. I. W. SCHULTE. J. Am. Chem. Soc. **79**, 4643 (1957).
28. R. H. LUEBBE and J. E. WILLARD. J. Am. Chem. Soc. **81**, 761 (1959).
29. D. TIMM. Acta Chem. Scand. **20**, 2219 (1966).
30. J. P. MITTAL and W. H. HAMILL. J. Am. Chem. Soc. **89**, 5749 (1967).
31. R. F. C. CLARIDGE and J. E. WILLARD. J. Am. Chem. Soc. **88**, 2404 (1966); **89**, 510 (1967).
32. N. S. BUCHEL'NIKOVA. Zh. Eksperim. Teor. Fiz. **35**, 1119 (1958).
33. T. G. LEE. J. Phys. Chem. **67**, 360 (1963).
34. T. S. CROFT and R. J. HANRAHAN. J. Phys. Chem. **66**, 2188 (1962).
35. L. J. FORRESTAL and W. H. HAMILL. J. Am. Chem. Soc. **83**, 1535 (1961).
36. W. H. HAMILL. Direct and indirect effects on chemical systems. *In* Comparative effects of radiation. *Edited by* M. Burton, J. S. Kirby-Smith, and J. L. Magee. J. Wiley and Sons, New York. 1960.
37. V. V. VOEVODSKII and YU. N. MOLIN. Radiation Res. **17**, 366 (1962).
38. R. SCHULER and R. PETRY. J. Am. Chem. Soc. **78**, 3954 (1956).
39. R. M. LEBLANC. Unpublished results.
40. V. A. ROGINSKII, A. G. KOTOV, and S. YA. PZHEZHETSKII. Dokl. Akad. Nauk SSSR, **163**, 1433 (1965).

Can. J. Chem. Downloaded from www.nrcresearchpress.com by 210.87.254.6 on 09/05/12
For personal use only.

Can. J. Chem. Downloaded from www.nrcresearchpress.com by 210.87.254.6 on 09/05/12
For personal use only.

Determination of the heat of formation of trimethylindium and calculation of the mean In—CH_3 bond dissociation energy

W. D. CLARK[1] AND S. J. W. PRICE
Department of Chemistry, University of Windsor, Windsor, Ontario

Received November 20, 1967

The enthalpy of reaction of $In(CH_3)_3$,c with a chloroform solution of bromine is -162.5 kcal mole^{-1}. With this value $\Delta H_f^0{}_{298}[In(CH_3)_3,c] = 29.5$ kcal mole^{-1} and $\Delta H_f^0{}_{298}[In(CH_3)_3,g] = 41.1$ kcal mole^{-1}. Combining the latter with $\Delta H_f^0{}_{298}[CH_3,g] = 33.2$ kcal mole^{-1} and $\Delta H_f^0{}_{298}[In,g] = 58.2$ kcal mole^{-1} then gives $E(In—CH_3) = 38.9$ kcal mole^{-1}. From previous kinetic studies $D[(CH_3)_2In—CH_3] + D[In—CH_3] = 87.9$ kcal mole^{-1}. Hence $D[CH_3In—CH_3] = 28.8$ kcal mole^{-1}.

Canadian Journal of Chemistry, 46, 1633 (1968)

Introduction

The pyrolysis of trimethylindium has been studied in a toluene carrier system (1). From the kinetic data the following values were estimated: $D[(CH_3)_2In—CH_3] = 47.2$ kcal mole^{-1}, $D[In—CH_3] = 40.7$ kcal mole^{-1}. The kinetic mechanism proposed assumed that under all conditions used reaction [2] was much faster than reaction [1].

[1] $$In(CH_3)_3 \rightarrow In(CH_3)_2 + CH_3$$

[2] $$In(CH_3)_2 \rightarrow InCH_3 + CH_3$$

The present work was undertaken to determine the mean metal–carbon bond dissociation energy in trimethylindium and hence $D[CH_3In—CH_3]$.

Fowell and Mortimer (2) used the reaction of trimethylgallium with excess iodine to determine the heat of formation of this alkyl. Because of the high strength of the gallium–carbon bond in methylgallium (3) only two methyl radicals were readily displaced. Concentrated iodine solution at an elevated temperature was required to obtain sufficient extent of reaction to allow the heat of formation of the alkyl to be determined. Bromine was chosen over iodine for the present work because a reliable value for $\Delta H_f^0{}_{298}(InBr_3, c)$ was available.

Experimental

Materials

(*a*) Trimethylindium was prepared by refluxing indium metal with dimethylmercury in an atmosphere of dry nitrogen using mercuric chloride as catalyst (4). After 8 days the reaction flask was cooled to 0 °C (vapor pressure of trimethylindium, 0.2 mm) and the unreacted dimethylmercury (vapor pressure, 17 mm) was distilled off. The crude trimethylindium was transferred to the main alkyl storage system where the remaining dimethylmercury was removed by repeated degassing at 0 °C. The final product melted at 89.5 °C and gave vapor pressure measurements consistent with literature values (4). It was stored under its own vapor pressure at −190 °C.

(*b*) Chloroform and bromine were fractionally distilled and then degassed by bulb to bulb distillation. Sufficient bromine was vacuum distilled into chloroform to give approximately 1 *N* solution. The resulting solution was stored under a nitrogen atmosphere.

(*c*) $InBr_3$ was dried in a nitrogen atmosphere using phosphorus pentoxide.

Apparatus and Procedure

The apparatus used was similar to that of Fowell and Mortimer (2). The temperature rise was measured with a Beckman thermometer equipped with a magnifying lens so that the relative temperature could be estimated to within 0.001°. A 0.20 W bare wire chromel immersion heater was used for electrical calibration.

The normality of the bromine solution was checked before each run by addition of excess potassium iodide followed by titration of the liberated iodine with standard sodium thiosulfate. Similar titrations were used to determine the amount of bromine consumed in a run. Titrations before and after blank runs showed that no measurable loss of bromine occurs.

Trimethylindium was distilled under vacuum into a weighed ampul, sealed, and reweighed. The ampul was attached to a rod fitted into the reaction vessel through a ground glass sleeve. To start an experiment, the ampul was crushed against the bottom of the reaction vessel by depressing the rod. Blank runs showed that no measurable heat is generated when an empty evacuated ampul is broken.

Results and Discussion

The results are shown in Table I. All experiments were carried out at approximately 25 °C. Within the experimental scatter the observed heats of reaction are consistent with the percentage of the alkyl undergoing reaction. The data are limited, but inspection of Fig. 1 indicates a pattern of reaction similar to that previously observed by Fowell and Mortimer for the

[1]Recipient of an NRCC Fellowship.

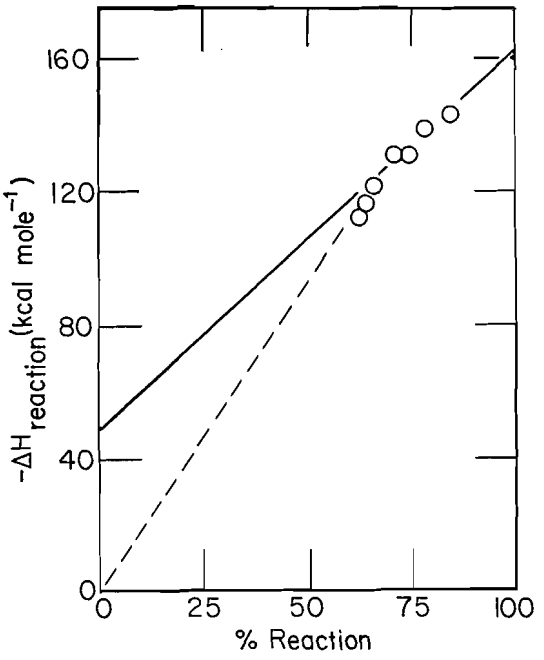

FIG. 1. Variation of the heat of reaction of trimethylindium with bromine in chloroform solution at 25 °C. The percent reaction is based on replacement of all three methyl groups by bromine. Solid line, linear least mean squares line obtained using the points above 66% reaction; broken line, plot obtained if the first two methyl groups are readily replaced by bromine so that a linear relationship holds from 0–66.7% conversion.

TABLE I

Enthalpy of reaction of trimethylindium with bromine in chloroform solution

Sample weight (g)	Normality of Br_2 solution*	Conversion† (%)	ΔH_{rx} (kcal mole^{-1})
0.0897	1.085	84	143
0.1043	0.972	78	139
0.0657	0.053	75	131
0.0907	0.656	71	132
0.1461	0.827	66	121
0.0805	0.658	65	116
0.1422	1.055	63	112

*25.0 ml bromine solution used in each run.
†Based on replacement of all three methyl groups by bromine.

reaction of trimethylgallium with iodine (2), quantitative replacement of two methyl radicals by halogen followed by slow replacement of the third methyl group. The linear least mean squares extrapolation to 100% based on this mechanism gives $\Delta H = 162.5$ kcal mole^{-1} for reaction [3].

[3] $In(CH_3)_3(c) + 3\,Br_2(soln.) \rightarrow InBr_3(soln.) + 3CH_3Br(g)$

No correction has been made for the heat of solution of any CH_3Br which remains in solution. The heat of solution of $InBr_3$,c in chloroform was determined in separate experiments as $\Delta H_{soln} = -1.4 \pm 0.3$ kcal mole^{-1}. The enthalpy of solution of bromine in chloroform is 0.7 kcal mole^{-1} (5). With $\Delta H_f^0{}_{298}(InBr_3,c) = -102.5$ kcal mole^{-1} (6) and $\Delta H_f^0{}_{298}(CH_3Br,g) = -9.0$ kcal mole^{-1} (7), $\Delta H_f^0{}_{298}(In(CH_3)_3,c) = 29.5$ kcal mole^{-1}. Combining this with $\Delta H_{sublimation}(In(CH_3)_3,c) = 11.6$ kcal mole^{-1} (4) gives $\Delta H_f^0{}_{298}(In(CH_3)_3,g) = 41.1$ kcal mole^{-1}. With $\Delta H_f(CH_3) = 33.2$ (5) and $\Delta H_f(In,g) = 58.2$ (6) the mean metal–methyl bond dissociation energy in trimethylindium, $E(In—CH_3)$, is 38.9 kcal mole^{-1}. This gives $D[CH_3In—CH_3] = 28.8$ kcal mole^{-1}, a value consistent with the previously proposed kinetic mechanism for the decomposition of trimethylindium in a toluene carrier system (1).

Acknowledgment

This work has been supported by a grant from the National Research Council of Canada.

1. M. G. JACKO and S. J. W. PRICE. Can. J. Chem. **42**, 1198 (1964).
2. P. A. FOWELL and C. T. MORTIMER. J. Chem. Soc. 3734 (1958).
3. M. G. JACKO and S. J. W. PRICE. Can. J. Chem. **41**, 1560 (1963).
4. L. M. DENNIS, R. W. WORK, E. G. ROCKOW, and E. M. CHARMOT. J. Am. Chem. Soc. **56**, 1047 (1934).
5. Selected values of chemical thermodynamic properties. Natl. Bur. Std. U.S. Tech. Notes, No. 270-1 (1965).
6. Selected values of chemical thermodynamic properties. Natl. Bur. Std. U.S. Tech. Notes, No. 270-2 (1965).
7. P. FOWELL, J. R. LACHER, and J. D. PARK. Trans. Faraday Soc. **61**, 1324 (1965).

Can. J. Chem. Downloaded from www.nrcresearchpress.com by 210.87.254.6 on 09/05/12
For personal use only.

Can. J. Chem. Downloaded from www.nrcresearchpress.com by 210.87.254.105 on 09/05/12
For personal use only.

Theory of the thermoelectric power of ionic crystals

A. R. ALLNATT[1] AND P. W. M. JACOBS
Department of Chemistry, University of Western Ontario, London, Ontario

Received July 31, 1967

A thermodynamic analysis of the interface between a metal and an ionic crystal is performed and a differential equation for the potential difference Φ between the electrode and the crystal is derived. This equation can be used to give a new expression for the heterogeneous contribution to the thermoelectric power of an ionic crystal MX between electrodes M′. Addition of the homogeneous contribution gives the total thermoelectric power θ. A complete *a priori* evaluation of this expression for θ is only possible by making assumptions about the contribution to the potential difference between the surface and bulk of the crystal, $\varphi^S - \varphi^B$, which comes from the relaxation of cations and anions in the surface layers of an ionic crystal. Some information on this point is provided by the marked decrease in θ which occurs at low temperatures. While an analysis of experimental data in terms of the theory provides acceptable values for the ionic heats of transport, there is, as yet, no explanation of the remarkable Λ-point in the thermoelectric power of pure KCl.

Canadian Journal of Chemistry, 46, 1635 (1968)

I. Introduction

It was first pointed out by Frenkel (1) that if the free energies of formation of cation vacancies and anion vacancies are unequal then a potential difference will develop between the surface and the bulk of an ionic crystal. In this and all other treatments of the space-charge problem, the crystal was assumed to be at a uniform temperature. If two opposite faces of a crystal are at different temperatures then the temperature dependence of this space charge will make a contribution to the heterogeneous thermoelectric power. The purpose of this paper is to evaluate this contribution. If the electrodes are perfectly polarized so that no charge crosses the crystal/electrode boundaries this space-charge contribution will in fact constitute the whole of the heterogeneous thermoelectric power. The theory presented is thus in complete contrast to formulations (2–4) in which thermodynamic equilibrium between the crystal and electrode phases is expressed by equating the electrochemical potentials of all species common to the two phases. The ideally polarized electrode we are considering may not exist in practice, but it is necessary to examine this model because the other theories have not been successful when applied to systems of the form M′ | MX | M′ in which the electrodes M′ do not have a cationic or anionic species in common with the salt MX.

Contact between a metal and an ionic crystal has been considered only once previously, in a paper by Grimley and Mott (5). These authors, however, discussed only the silver/silver bromide interface and so neither their results nor their technique are applicable to the present problem. Lehovec (6) has also considered the space-charge problem, obtaining a solution for the potential distribution which is exact for crystals whose thickness is large compared with the Debye length. The most recent attack on the space-charge problem is given in a series of four papers by Kliewer (7–10). Here general solutions for the potential distribution are obtained which are exact, provided $e(\varphi^S - \varphi^B) \ll kT$ and the only form of defect interactions are those in which defects of opposite virtual charge occupy nearest neighbor sites. In neither of these contributions, however, is there a specific discussion of the metal/salt interface.

II. Theory

The interfacial region σ comprises parts of both phases; in particular it includes the actual geometrical interface between phase α (the crystal MX) and the phase β (the metal M′) together with that part of α in which a space charge occurs. Since there is no applied potential difference between β and a second electrode, any space charge will be localized near the surface so that the region of α in σ is small but finite. Temperature and pressure may therefore be assumed to be uniform in σ. Our starting point is

[1]Permanent address: Department of Chemistry, The University, Manchester 13, England.

Can. J. Chem. Downloaded from www.nrcresearchpress.com by 210.87.254.105 on 09/05/12
For personal use only.

the Gibbs–Duhem equation for the interfacial region σ,

$$[1]\quad S\,dT - V\,dP + A\,d\gamma + \sum_{j,\alpha} N_j^{\alpha}\,d\tilde{\mu}_j^{\alpha} = 0.$$

N_j^{α} is the number of species j (ions, vacancies, etc.) in that part of α included in σ; $\tilde{\mu}_j^{\alpha}$ is similarly the electrochemical potential of species j in that part of α which is in σ, and the other symbols have their usual thermodynamic significance. Now

$$[2]\quad d\tilde{\mu}_j^{\alpha} = -s_j^{\alpha}\,dT + v_j^{\alpha}\,dP + [d\mu_j^{\alpha}]_{T,P} + ez_j^{\alpha}\,d\varphi^{\alpha}.$$

Equations [1] and [2] yield

$$[3]\quad A\,d\gamma + \sum_{j,\alpha} N_j^{\alpha}[d\mu_j^{\alpha}]_{T,P} + \sum_{\alpha} q^{\alpha}\,d\varphi^{\alpha} = 0.$$

q^{α} is the total charge in phase α, φ^{α} the potential of α and ez_j^{α} the charge carried by species j in α, e being the charge on the proton. Note that z^{α} is zero for vacancies, which carry no charge.

We consider a crystal MX in which the defects are of the Schottky type, containing a fraction c of divalent impurity ion, M^{2+}. The crystal is in contact with two electrodes M′ which are at different temperatures T, $T + \Delta T$. In phase α the species j are M^+, X^-, impurity ions (subscript i), cation vacancies (subscript +), anion vacancies (subscript −), and complexes[2] (subscript k). In phase β the species are cations M'^{z+} of charge ze and electrons e^-. Since the phase β is in internal equilibrium,

$$[4]\quad N_{M'^{z+}}\,d\tilde{\mu}_{M'^{z+}} + N_{e^-}\,d\tilde{\mu}_{e^-} = \frac{-q^{M'}}{e}\,d\tilde{\mu}_{e^-}.$$

In phase α, equality of the number of cation sites and the number of anion sites requires

$$[5]\quad N_{M^+} + N_+ + N_i + 2N_k = N_{X^-} + N_- = N,$$

where N is the total number of sites on each sublattice. Electroneutrality is not conserved in the separate surface phases but

$$[6]\quad N_{M^+} + 2N_i + 2N_k - N_{X^-} = -N_+ + N_i + N_- = \frac{q^{MX}}{e} = \frac{-q^{M'}}{e}$$

because there are equal but opposite charges on each side of the interface. It is important to note that N_+, N_i are, respectively, the number of *free*, that is uncomplexed, cation vacancies and impurity ions present in phase α. Enumerating the appropriate species j in [3] and utilizing [4] and [6] gives

$$[7]\quad A\,d\gamma + N_k(d\mu_k - 2\,d\mu_{M^+}) + N_{X^-}(d\mu_{M^+} + d\mu_{X^-}) + N_-(d\mu_+ + d\mu_-) - \frac{q^{M'}}{e}(d\mu_{M^+} - d\mu_+) + N_i(d\mu_i + d\mu_+ - 2\,d\mu_{M^+}) + q^{M'}(d\varphi^{M'} - d\varphi^{MX}) = 0,$$

where the subscripts T,P have been omitted to avoid an excessively clumsy notation. Define the surface excess of j in α by

$$[8]\quad \Gamma_j = \frac{(n_j^{\alpha} - n_j^{B})V^{\alpha\sigma}}{A}$$

where A is the area of the interface, n_j is the number of species j per unit volume, $V^{\alpha\sigma}$ is the volume of α in σ, and B denotes the bulk phase of MX, away from the space-charge region. Substituting [8] into [7] and using the Gibbs–Duhem equation for the bulk phase (where there is no space charge) gives

$$[9]\quad e\,d\Phi = -\frac{e\,d\gamma}{\sigma^{M'}} + \frac{e\Gamma_+}{\sigma^{M'}}(d\mu_{M^+} + d\mu_{X^-} - d\mu_+ - d\mu_-) + \frac{e\Gamma_k}{\sigma^{M'}}(2\,d\mu_{M^+} - d\mu_k) + \frac{e\Gamma_i}{\sigma^{M'}}(d\mu_{M^+} - d\mu_{X^-} - d\mu_i + d\mu_-) - d\mu_{X^-} + d\mu_-,$$

where $\Phi = \varphi^{M'} - \varphi^{MX}$ and $\sigma^{M'} = q^{M'}/A$ is the surface charge on the metal.

Since there is equilibrium between the surface space-charge layer and the bulk at the same temperature

$$[10]\quad \tilde{\mu}_{M^+}{}^{\sigma} + \mu_+{}^{B} = \tilde{\mu}_{M^+}{}^{B} + \mu_+{}^{\sigma}.$$

The appropriate chemical potentials for substitution in [10] have been given elsewhere (4). The result of these substitutions is

$$[11]\quad n_+{}^{\sigma}(x) = n_+{}^{B}\ \exp\{e(\varphi^{\sigma}(x) - \varphi^{B})/kT\},$$

where $n_+{}^{\sigma}(x)$ and $\varphi^{\sigma}(x)$ denote respectively the number of cation vacancies per unit volume and the potential at a distance x below the surface in

[2]A complex consists of a divalent cation and a cation vacancy on nearest neighbor sites.

Can. J. Chem. Downloaded from www.nrcresearchpress.com by 210.87.254.105 on 09/05/12
For personal use only.

the surface region σ. The analogous expressions for anion vacancies and impurity ions are

$$[12]\quad n_-^{\sigma}(x) = n_-^{B}\exp\{-e(\varphi^{\sigma}(x) - \varphi^{B})/kT\}$$

$$[13]\quad n_i^{\sigma}(x) = n_i^{B}\exp\{-e(\varphi^{\sigma}(x) - \varphi^{B})/kT\}.$$

There is no gradient of complexes in the space-charge region. In deriving eqs. [11]–[13] we have used approximate formulas for the chemical potentials which are valid when $n_+ \ll n_{M+}$, $n_- \ll n_{X-}$. If we do not make these approximations in μ, the expressions derived are

$$[11^1]\quad \frac{n_+^{\sigma}(x)}{n_+^{B}} = \frac{K(1 - c_i^{\sigma} - 2c_k^{\sigma})}{1 + c_+^{B}(K-1) - c_i^{B} - 2c_k^{B}} \simeq \frac{K}{1 + c_+^{B}K}, \quad \text{when } K \gg 1,$$

$$[12^1]\quad \frac{n_-^{\sigma}(x)}{n_-^{B}} = \frac{K^{-1}}{1 + c_-^{B}(K^{-1} - 1)} \simeq \frac{K^{-1}}{1 + c_-^{B}K^{-1}}, \quad \text{when } K \to 0,$$

and

$$[13^1]\quad \frac{n_i^{\sigma}(x)}{n_i^{B}} = \frac{K^{-1}(1 - c_i^{\sigma} - 2c_k^{\sigma})}{1 + c_+^{B}(K-1) - c_i^{B} - 2c_k^{B}} \simeq \frac{K^{-1}}{1 + c_+^{B}K}, \quad \text{when } K \gg 1.$$

When K is of 0(1), eqs. [11¹], [12¹], and [13¹] reduce respectively to eqs. [11], [12], and [13]. Actually for alkali halides and for other pure crystals of similar Schottky defect concentration, the condition is far less restrictive than $K = 0(1)$ and eqs. [11]–[13] will be valid for $10^{-3} < K < 10^3$ or $|\varphi^{\sigma}(x) - \varphi^{B}| < \sim 450$ mV.

The charge density is

$$[14]\quad \rho(x) = e\{n_-(x) + n_i(x) - n_+(x)\}.$$

Substituting for $\rho(x)$ in Poisson's equation

$$[15]\quad \frac{d^2\varphi(x)}{dx^2} = \frac{-4\pi\rho(x)}{\epsilon}$$

and integrating once gives

$$[16]\quad \left|\frac{d\varphi(x)}{dx}\right| = \left[\frac{8\pi kT}{\epsilon}\sum_j n_j^{B} \times \{\exp[-z_j e\{\varphi(x) - \varphi^{B}\}/kT] - 1\}\right]^{1/2},$$

where z_j is defined to be $+1$ for impurity ions and anion vacancies and -1 for cation vacancies. A second integration [cf. refs. 6 and 7] would give the potential distribution but this is not our immediate concern.

The surface charge per unit area is

$$[17]\quad -\sigma^{MX} = \sigma^{M'} = -\int_0^{\infty}\rho(x)\,dx = \frac{-\epsilon}{4\pi}\left[\frac{d\varphi(x)}{dx}\right]_{x=0},$$

which, on substituting from [16], gives

$$[18]\quad |\sigma^{M'}| = \left\{\frac{\epsilon kT}{2\pi}\sum_j n_j^{B} \times [\exp\{-z_j e(\varphi^{S} - \varphi^{B})/kT\} - 1]\right\}^{1/2},$$

where $\varphi^{S} = \varphi^{\sigma}(x)$ at $x = 0$. Since $n_+^{B} - n_-^{B} = n_i^{B}$,

$$[19]\quad \sigma^{M'} = \left(\frac{2\epsilon kT n_+^{B}}{\pi}\right)^{1/2}\sinh\left\{\frac{e(\varphi^{S} - \varphi^{B})}{2kT}\right\},$$

where we have chosen the + sign because $\varphi^{S} > \varphi^{B}$ when $\sigma^{M'}$ is positive.

The surface excess of species j is

$$[20]\quad \Gamma_j = \int_0^{\infty}(n_j^{\sigma}(x) - n_j^{B})\,dx.$$

Substituting from [11]–[13] in [20] and integrating gives

$$[21]\quad |\Gamma_j| = \left(\frac{\epsilon kT n_j^{B}}{2\pi}\right)^{1/2}\frac{1}{z_j e} \times \{\exp(-z_j e(\varphi^{S} - \varphi^{B})/2kT) - 1\},$$

where the negative sign must be used for Γ_j when j denotes cation vacancies and the positive sign when j denotes impurity ions or anion vacancies. Finally, substituting for $\sigma^{M'}$, Γ_+, and Γ_i in [9] and noting that Γ_k is zero yields

$$[22]\quad e\,d\Phi = -\frac{e\,d\gamma}{\sigma^{M'}} + \frac{e^{y/2}}{e^{y/2}+1}(d\mu_{M^+} + d\mu_{X^-} - d\mu_+ - d\mu_-) - \left(\frac{n_i^{B}}{n_+^{B}}\right)^{1/2}\frac{1}{e^{y/2}+1}(d\mu_{M^+} - d\mu_{X^-} - d\mu_i + d\mu_-) - d\mu_{X^-} + d\mu_-,$$

where y is an abbreviation for $e(\varphi^{S} - \varphi^{B})/kT$.

The chemical potentials are

$$[23]\quad \mu_i = \mu_i^{0} + kT\ln c_i, \quad \mu_+ = g_+ + kT\ln c_+, \quad \mu_- = g_- + kT\ln c_-,$$

Can. J. Chem. Downloaded from www.nrcresearchpress.com by 210.87.254.105 on 09/05/12
For personal use only.

where c_j is the site fraction of j. It is a valid approximation to set c_{M^+} and c_{X^-} equal to unity and so $[d\mu_{M^+}]_T = 0 = [d\mu_{X^-}]_T$. Substituting from the eqs. [23] in [22] and dropping the term in $d\gamma/dT$ (which is difficult to evaluate precisely but is certainly small) gives

$$[24]\quad e\frac{d\Phi}{dT} = \frac{-e^{y/2}}{e^{y/2}+1}\left[\left(\frac{\partial\mu_+}{\partial c_+}\right)_T\frac{dc_+}{dT} + \left(\frac{\partial\mu_-}{\partial c_-}\right)\frac{dc_-}{dT}\right] - \left(\frac{c_1}{c_+}\right)^{1/2} \times \frac{1}{e^{y/2}+1}\left[\left(\frac{\partial\mu_-}{\partial c_-}\right)_T\frac{dc_-}{dT} - \left(\frac{\partial\mu_1}{\partial c_1}\right)_T\frac{dc_1}{dT}\right] + \left(\frac{\partial\mu_-}{\partial c_-}\right)_T\frac{dc_-}{dT} \equiv e\theta_{het},$$

where θ_{het} denotes the heterogeneous contribution to the thermoelectric power. The expression for the homogeneous contribution is (2, 4)

$$[25]\quad e\theta_{hom} = t_+\left(\frac{\partial\mu_+}{\partial c_+}\right)_T\frac{dc_+}{dT} - t_-\left(\frac{\partial\mu_-}{\partial c_-}\right)_T\frac{dc_-}{dT} - t_+\frac{Q_{M^+}}{T} + t_-\frac{Q_{X^-}}{T},$$

where t_j is the transference number of species j and Q_{M^+}, Q_{X^-} are the ionic heats of transport for cations and anions respectively. Adding [24] and [25] gives

$$[26]\quad Te\theta = -Q_{M^+} - t_-(h - Q_{MX}) + h/(e^{y/2}+1) - \left(\frac{c_1}{c_+}\right)^{1/2}\frac{T}{e^{y/2}+1}\left\{\left(\frac{\partial\mu_-}{\partial c_-}\right)_T\frac{dc_-}{dT} - \left(\frac{\partial\mu_1}{\partial c_1}\right)_T\frac{dc_1}{dT}\right\},$$

where we have used the fact that

$$[27]\quad \left(\frac{\partial\mu_+}{\partial c_+}\right)_T\frac{dc_+}{dT} + \left(\frac{\partial\mu_-}{\partial c_-}\right)_T\frac{dc_-}{dT} = \frac{h}{T}.$$

Q_{MX} is the sum of the individual ionic heats of transport, $Q_{M^+} + Q_{X^-}$, and h is the enthalpy change accompanying the formation of a Schottky defect pair. The term in braces in eq. [26] is evaluated with the help of four relations.

$$[28]\quad c_+c_- = K_1 = \exp(-g/kT)$$

$$[29]\quad \frac{c_k}{c_+c_1} = K_2 = \exp(\zeta/kT)$$

$$[30]\quad c_k = c - c_1$$

$$[31]\quad c_- = c_+ - c_1$$

Substitution of the result in [26] gives the final expression for the thermoelectric power

$$[32]\quad Te\theta = -Q_{M^+} - t_-(h - Q_{MX}) + \frac{1}{e^{y/2}+1} \times \left[h - \frac{(c_1c_+)^{1/2}}{2c_+ - c_1(1-p)}\{h(1+p) - 2p\chi\}\right],$$

where p is the degree of association ($= c_k/c$) and $-\chi$ is the enthalpy change accompanying the formation of a complex from an unassociated cation vacancy and a divalent impurity ion.

The high-temperature limiting form of [32] when $c_+ \gg c_i$, $p \to 0$, is

$$[33]\quad Te\theta = -Q_{M^+} - t_-(h - Q_{MX}) + \frac{h}{e^{y/2}+1}.$$

The first two terms on the right-hand side of [33] represent an approximate expression for $Te\theta$ which was developed previously (11); this previous result is clearly only valid when the potential difference $\varphi^S - \varphi^B$ is large in comparison with kT, and so is of rather limited applicability. The new result, eq. [33], should apply to pure crystals at high temperatures, i.e. in the intrinsic region, whenever the conditions $c_+{}^B K \ll 1$, $c_-{}^B K^{-1} \ll 1$ are satisfied.

When $c_i \simeq c_+$, $t_- \to 0$, the limiting form of [32] is

$$[34]\quad Te\theta = -Q_{M^+} - \frac{1}{e^{y/2}+1}\left[\frac{2p\chi}{1+p}\right].$$

This result should apply either to crystals doped with divalent cation impurities or to nominally pure crystals at low temperatures. Again when $\varphi^S - \varphi^B$ is large compared with kT, [34] degenerates to the previous approximate result (11), $Te\theta = -Q_{M^+}$.

Equation [26] may also be used to derive the result for the precipitation region in which the impurity concentration exceeds the solubility

Can. J. Chem. Downloaded from www.nrcresearchpress.com by 210.87.254.105 on 09/05/12
For personal use only.

limit. The excess impurity precipitates as a separate phase taking a corresponding number of cation vacancies from solution. The concentration of impurity ions and cation vacancies in solution is then limited by the relation

$$[35] \qquad c_+c_i = \exp\,(g_p/kT),$$

where g_p is the free energy change on removing an isolated cation vacancy and an isolated impurity ion from solution into the precipitated phase. Combining eqs. [23], [26], and [35] the result for the limit where $t_- \to 0$ and $c_i \simeq c_+$ is

$$[36] \qquad Te\theta = -Q_{M^+} - \frac{h_p}{e^{y/2}+1},$$

where h_p is the enthalpy corresponding to g_p. This equation is valid in the presence of association of unprecipitated defects.

III. Comparison with Experiment

There are a few modern measurements of the thermoelectric power of cells of the type M′ | MX | M′ which cover a reasonable temperature range. These consist of two sets of measurements on KCl (11, 12) and another two on NaCl (13, 14). Platinum electrodes have been used almost exclusively. The most extensive measurements, in terms of temperature range, are those of Jacobs and Maycock (11) on KCl. Some of their data are reproduced in Fig. 1. The most striking features of these results are as follows:

(i) The value of $Te\theta$ decreases at low temperatures. This is characteristic of both the pure and the doped salt although for the latter it occurs at higher temperatures.

(ii) In the data for pure KCl there is a pronounced Λ-point in the region of 820 °K.

(iii) There is remarkably little concentration dependence in θ since the pure KCl crystal contains about 10^{-6} mole fraction of divalent impurities, whereas c was 1.2×10^{-3} for the crystal doped with $SrCl_2$.

(iv) $Te\theta$ for both pure and doped crystals decreases linearly with temperature apart from the features mentioned under (i) and (ii). The temperature slopes are remarkably similar also.

(v) The data for two nominally pure crystals which are illustrated in Fig. 1 do not show quantitative agreement. Run 20 refers to KCl twice recrystallized from distilled water before being grown by the Kyropoulos method from a platinum crucible. Run 2 refers to a KCl crystal grown from A.R. KCl in a silica crucible by the Stockbarger method. Alternating current conductivity measurements show that the Kyropoulos crystal is purer with the larger value of t_- at equivalent temperatures. The differences between the two runs are not necessarily connected with the use of Rh electrodes in run 2 and Pt electrodes in run 20, since additional data obtained with Pt electrodes show differences of the same order.

The theory outlined in II provides a reasonable explanation of some, but not all, of the features observed. The difficulty in making a quantitative test centers on the calculation of $\varphi^S - \varphi^B$. By considering the equilibrium between the atom in the bulk and an atom at a kink site on the surface one has

$$[37] \qquad \tilde{\mu}_{M^+}{}^B = \mu_+{}^B + \tilde{\mu}_{M^+}{}^S,$$

which gives

$$[38] \qquad e(\varphi^S - \varphi^B) = -(g_+ + kT\log n_+{}^B) + (\mu_{M^+}{}^B - \mu_{M^+}{}^S).$$

The first parenthetical term represents the difference in potential for an idealized crystal in which surface properties are neglected and is the result stated by Lehovec (6). The presence of the second term was clearly recognized by Grimley and Mott (5). It may contribute an appreciable potential difference since a relative displacement of the positive and negative ions, in the crystal plane at the interface, over a few tenths of an angstrom is sufficient to set up a potential of ~0.5 V. Unfortunately, accurate estimates of this quantity are not available. We refer to the first and second parenthetical terms in [38] as the space-charge part and the lattice part of $\varphi^S - \varphi^B$ respectively.

The calculation of the first term, although much simpler, is by no means precise at present. Conductivity measurements (15) for KCl yield $h = 2.259$ eV, $s = 0.463 \times 10^{-3}$ eV deg^{-1}. A recent theoretical calculation (16) yields the same value of h and gives $h_+ = 0.956$ eV, $h_- = 1.303$ eV. In the absence of either experimental or theoretical information we take $s_- = 0.31 \times 10^{-3}$ eV deg^{-1} and $s_+ = 0.15 \times 10^{-3}$ eV deg^{-1}.

For the doped crystal, neglecting the small effect of association, the first term in [38] contributes −0.52 V to −0.56 V in the range 600

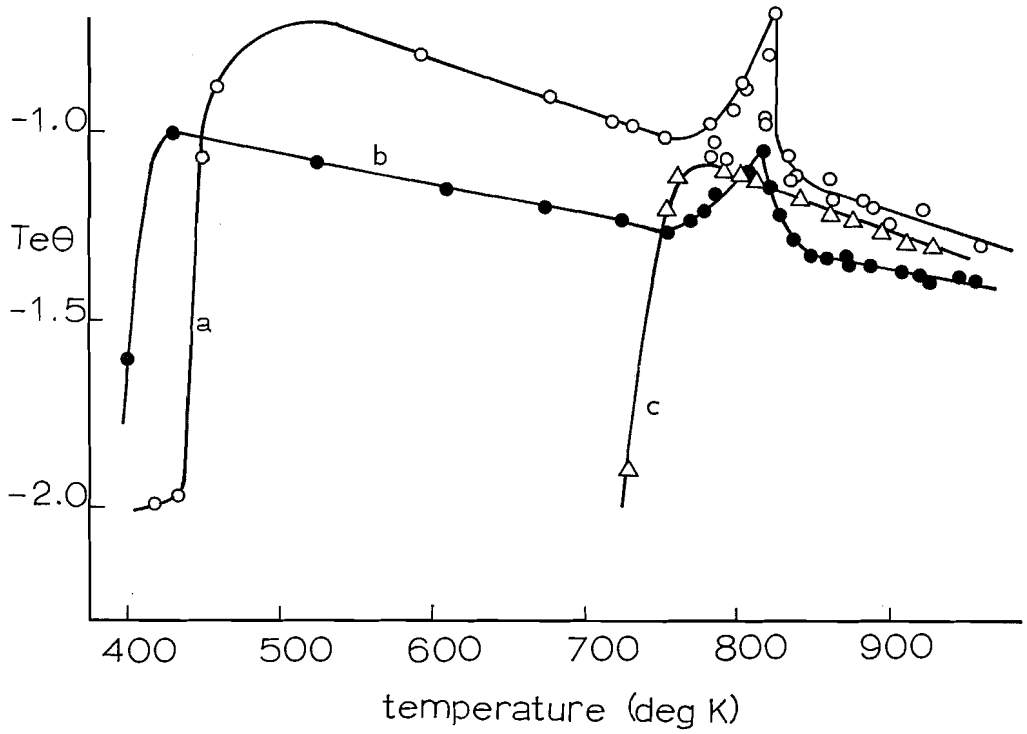

FIG. 1. Thermoelectric power of KCl. (*a*) Run 2, pure KCl between rhodium electrodes. (*b*) Run 20, pure KCl between platinum electrodes. (*c*) Run 11, KCl containing $SrCl_2$ ($c = 1.2 \times 10^{-4}$).

to 900 °K. If the Grimley and Mott estimate of the second term is accepted then $\varphi^S - \varphi^B$ may lie in the range 0 to -1 V depending on the sign of $(\mu_{M^+}{}^B - \mu_{M^+}{}^S)$. In a previous paper the approximate form of [34] without the association term was used for the doped crystal as would be correct for $y \gg 1$. The present estimate suggests that this is not valid but that the correct answer lies between the limiting values

$$[39] \quad Te\theta = -Q_{M^+} - \frac{p\chi}{1+p}, \qquad y = 0 \quad (e^{y/2} = 1)$$

$$[40] \quad Te\theta = -Q_{M^+} - \frac{2p\chi}{1+p}, \qquad y \ll -1 \quad (e^{y/2} = 0).$$

The experimental value of χ is 0.42 eV, so that the association correction is actually quite small. Thus for $y = 0$, Q_{M^+} is 0.97 eV at 800 °K and 1.13 eV at 900 °K, compared with 0.80 eV and 0.97 eV respectively for $y \ll -1$, and 1.14 eV and 1.28 eV respectively for $y \gg 1$.

The decrease of thermoelectric power at low temperatures occurs at approximately the temperature of impurity precipitation as detected by conductance measurements. According to eqs. [34] and [36] the decrease in $Te\theta$ is

$$\frac{1}{e^{y/2}+1}\left(h_p - \frac{2p\chi}{1+p}\right).$$

For $SrCl_2$, $h_p = 1.43$ eV (17) and the decrease in thermoelectric power is therefore $1.08/(e^{y/2} + 1)$ eV and $1.25/(e^{y/2} + 1)$ eV for doped and pure crystals respectively. This analysis is therefore consistent with the experimental results if $e^{y/2} \ll 1$. The experimental values of θ at these temperatures are the least accurate because of isothermal space-charge effects. Precise experimental values of h_p are also difficult to determine. If one tentatively assumes, therefore, that $e^{y/2} + 1 \leqslant 1.1$, and if agreement between theory and experiment is to be attained, then the lattice part of $\varphi^S - \varphi^B$ is $\leqslant 0.2$ V.

We conclude that [34] and [36] correctly predict the large effect of precipitation and lead to reasonable values for the cation heat of transport for KCl, and also (14) for NaCl. These heats of transport are not strongly temperature dependent and are greater than the corresponding activation energies. Since the association

Can. J. Chem. Downloaded from www.nrcresearchpress.com by 210.87.254.105 on 09/05/12
For personal use only.

Can. J. Chem. Downloaded from www.nrcresearchpress.com by 210.87.254.105 on 09/05/12
For personal use only.

effect is rather small the theory predicts that the concentration dependence of θ in doped crystals is very weak, in contrast to previous theories which predict a dependence from a term $-k \log c_i (1 - p)$ (14). Further measurements may therefore distinguish between the two kinds of theories in a relatively simple manner. It would also be valuable to obtain a more accurate comparison of theory and experiment for the precipitation point, and hence obtain a reliable value for the lattice part of $\varphi^S - \varphi^B$.

For the pure crystal, comparison between theory and experiment is more difficult. Such a comparison is extremely sensitive to the values of transport numbers, concerning which uncertainty persists, and to the smallness of the observed differences between θ for pure and doped crystals. Furthermore, there is a still unexplained experimental irreproducibility between runs on different specimens in the intrinsic conductance region in KCl, and to an apparently smaller degree in NaCl. With these factors in mind the results for KCl may be considered. (It should be stated that no explanation for the Λ-point is provided either by the present theory or by previous theories.)

For the pure crystal (with Pt electrodes) one finds from [38] that at 900 °K the first term contributes 0.11 V to $\varphi^S - \varphi^B$ corresponding to a contribution to y of 0.04. In a previous paper the pure crystal results have been used to calculate Q_{X-} from [33] assuming $e^{y/2} + 1 \gg h$ so that the last term may be neglected. Using the tentative value for the lattice part of $\varphi^S - \varphi^B$ obtained above, 0.2 V, and assuming that it is independent of temperature, one finds that the neglected term is approximately 0.27 eV. Using $Q_{M+} = 0.97$ eV, consistent with the estimate of 0.2 V for the lattice part of $\varphi^S - \varphi^B$, the amended value of Q_{X-} is 0.4 eV.

IV. Conclusions

The present theory has been successful in explaining both the low-temperature falloff in $Te\theta$ and the apparent lack of a strong concentration dependence for the thermoelectric power of alkali halides. Neither it nor any other theory yet proposed explains the curious Λ-point found for pure KCl nor the lack in reproducibility in the data for pure alkali halides. The theory gives values for the cation heat of transport which are of a reasonable magnitude, i.e. somewhat greater than the migration activation energy. An approximate value for the anion heat of transport can also be obtained and this is rather less than half the anion migration energy. On the Wirtz (18) picture this would mean that, for the anion jump, rather more energy must be expended in preparing the site to receive the jumping anion. This in turn implies that there is a greater relaxation around an anion vacancy than around a cation vacancy, a conclusion which is supported by the theoretical calculations of Boswarva and Lidiard (16).

1. J. Frenkel. Kinetic theory of liquids. Oxford University Press, London. 1946.
2. R. E. Howard and A. B. Lidiard. Discussions Faraday Soc. **23**, 113 (1957); Phil. Mag. **2**, 1462 (1957).
3. R. W. Christy. J. Chem. Phys. **34**, 1148 (1961).
4. A. R. Allnatt and P. W. M. Jacobs. Proc. Roy. Soc. London, Ser. A, **260**, 350 (1961).
5. T. B. Grimley and N. F. Mott. Discussions Faraday Soc. **1**, 3 (1947).
6. K. Lehovec. J. Chem. Phys. **21**, 1123 (1953).
7. K. L. Kliewer and J. S. Koehler. Phys. Rev. **140**, A1226 (1965).
8. K. L. Kliewer. Phys. Rev. **140**, A1241 (1965).
9. K. L. Kliewer. Phys. Chem. Solids, **27**, 705 (1966).
10. K. L. Kliewer. Phys. Chem. Solids, **27**, 719 (1966).
11. P. W. M. Jacobs and J. N. Maycock. Trans. Met. Soc. AIME, **236**, 165 (1966).
12. A. R. Allnatt and P. W. M. Jacobs. Proc. Roy. Soc. London, Ser. A, **267**, 31 (1962).
13. R. W. Christy, Y. W. Hsueh, and R. C. Mueller. J. Chem. Phys. **38**, 1647 (1963).
14. A. R. Allnatt and A. V. Chadwick. J. Chem. Phys. **47**, 2372 (1967).
15. J. H. Beaumont and P. W. M. Jacobs. J. Chem. Phys. **45**, 1496 (1966).
16. I. M. Boswarva and A. B. Lidiard. At. Energy Res. Estab. Gt. Brit. Rept. TP232 (1966).
17. A. R. Allnatt and P. W. M. Jacobs. Trans. Faraday Soc. **58**, 116 (1962).
18. K. Wirtz. Physik. Z. **44**, 221 (1943).

Can. J. Chem. Downloaded from www.nrcresearchpress.com by 210.87.254.40 on 09/05/12
For personal use only.

Partition coefficient of methyl iodide between vapor and water[1]

R. A. HASTY
Battelle Memorial Institute, Pacific Northwest Laboratory, Richland, Washington

Received September 12, 1967

The Ostwald's partition coefficient for the solubility of methyl iodide in water was determined from 4.85 to 68.5 °C. The partition coefficient measured for 10^{-7} to 10^{-8} *M* solutions was found to be from 20 to 30% lower than for 10^{-2} *M* solutions. A new rapid gas chromatographic technique is described for the determination of partition coefficients in dilute systems.

Canadian Journal of Chemistry, 46, 1643 (1968)

Introduction

The removal of methyl iodide in the p.p.m. concentration range by the action of sprays has been investigated in this laboratory and elsewhere (1, 2). The mass transfer of methyl iodide from the gas phase to the liquid involves the partition coefficient of methyl iodide between the vapor phase and the aqueous phase. The partition coefficient is also known as the Ostwald's absorption coefficient. Estimates (2, 3) and measurements (4) of the partition between vapor and aqueous solution of methyl iodide have been reported. It was felt that a determination of the partition coefficient for the p.p.m. concentration range would be valuable for the calculation of rate of mass transport in our studies and would also extend the knowledge of the behavior of methyl iodide to dilute systems.

Experimental

The partition coefficient, β, expressed in units of (g-moles CH_3I/liter of solution)/(g-moles CH_3I/liter of vapor) can be calculated from the concentration, C^0, of methyl iodide in a known volume, V_T, where no solution is present, and the concentration of methyl iodide in the gas phase, C, when the container of volume, V_T, has a volume of liquid, V_L, present.

The partition coefficient is defined as

$$[1] \qquad \beta = \frac{C_L}{C} = \left(\frac{N_T - N_G}{N_G}\right)\left(\frac{V_G}{V_L}\right),$$

where C_L is the concentration of methyl iodide in the liquid phase. Rearrangement of eq. [1] gives

$$[2] \qquad \beta = \left[\frac{C^0}{C} - 1\right]\left(\frac{V_G}{V_L}\right) + \frac{C^0}{C}.$$

A Research Specialties gas chromatograph, equipped with a Warner Chilcot electron capture detector, was used. A 1/4″ o.d. × 6′ stainless steel column packed with Chromosorb P coated with 20% SE 30 (silicone gum) under isothermal conditions (50 °C) was employed to separate the methyl iodide from the other gases, N_2 and H_2O, in aliquots. The carrier gas and scavenger gas flow rates were adjusted to 30.4 ml/min and 39.3 ml/min, respectively, to give an optimum between sensitivity and linearity of detector response for methyl iodide. The lower detection limit of the system was determined to be 2×10^{-12} g methyl iodide. A linear correlation was obtained for peak height for aliquots which contained up to 6×10^{-10} g methyl iodide.

Jacketed Pyrex vessels were maintained at a specified temperature, ±0.05 °C, by circulation of an ethylene glycol – water mixture from a thermostatted bath through the jacket of the vessel. The vessel was cylindrical with an i.d. of 2.7 cm and a volume of 55.3 ± 0.1 ml. A 6 mm i.d. tube at the top of the vessel was sealed with a rubber serum bottle stopper to permit sampling. Adsorption of methyl iodide by the stopper during the measurement of the partition coefficient was shown to be negligible.

Methyl iodide was obtained from Eastman Organic Chemicals and stored at 4 °C until needed. To obtain a desired concentration of methyl iodide in an experiment, appropriate dilutions were made of saturated methyl iodide – air mixtures (20.0 °C). A reproducibility of dilution was shown to be within ±3.6%. The accuracy of the determination of the methyl iodide concentration was estimated to be ca. 7% at 30 °C.

An initial dilution of approximately 300 was made of the saturated vapor of methyl iodide at 20.0 °C. A subsequent set of dilutions of approximately 10^3 is made into a set of three vessels. One vessel is used as a standard, i.e. without liquid present. The other two vessels with water present have the same total amount of methyl iodide in the system. Aliquots are taken from each of the vessels. The vessels which contain both liquid and gas phases are shaken vigorously after each sampling to ensure that equilibrium is reached. It was observed that one shaking was usually sufficient to obtain equilibrium, as shown by a constant concentration in the gas phase.

Results and Discussion

The measurement of partition coefficient of methyl iodide between vapor and liquid is limited

[1]This paper is based on work performed under United States Atomic Energy Commission Contract AT(45-1)-1830. Permission to publish is gratefully acknowledged.

at the lower temperatures by the freezing point of the solution and at the upper temperature by the hydrolysis of methyl iodide by the solvent. The effect of the hydrolysis (5) was negligible between 60 and 70 °C. An additional limitation was found which lowered the reliability of the partition coefficient at temperatures above 50 °C. Sampling of the gas mixtures at temperatures above ambient with a syringe at ambient temperature is thought to cause partial condensation of water vapor within the syringe.

The effect of concentration of methyl iodide on the partition coefficient was examined from 6.4×10^{-9} M to 1.28×10^{-7} M at 29.90 °C and found to be constant within experimental error. The average of six values for the partition coefficient is 2.75 with a standard deviation of ± 0.15. The maximum deviation from the average is 7.9%. The uncertainty[2] calculated for the partition coefficient is 7.3% ($V_G/V_L = 1.21$, $\beta = 2.75$). From the data of Glew and Moelwyn-Hughes (4), a value of the partition coefficient of 3.95 at 29.90 °C and a vapor concentration of ca. 5×10^{-3} g-mole/liter is calculated. This value decreases by 3% over a concentration range of from 4.046×10^{-2} to 2.085×10^{-2} g-moles/liter in the solution. The decrease in partition coefficient with a decrease in methyl iodide concentration is unlike the behavior of methyl chloride and methyl fluoride (4, 6). The partition coefficient for methyl bromide (4) shows a small increase (ca. 0.5%) over the concentration range 2.4×10^{-1} to 7.3×10^{-2} g-mole/liter.

The values of partition coefficient for methyl iodide between vapor and an aqueous solution determined in this work are shown in Fig. 1. Between 4.8 and 68.5 °C, the partition coefficient can be represented by

$$[3] \qquad \log_{10}(\beta) = -4.82 + \frac{1597}{T},$$

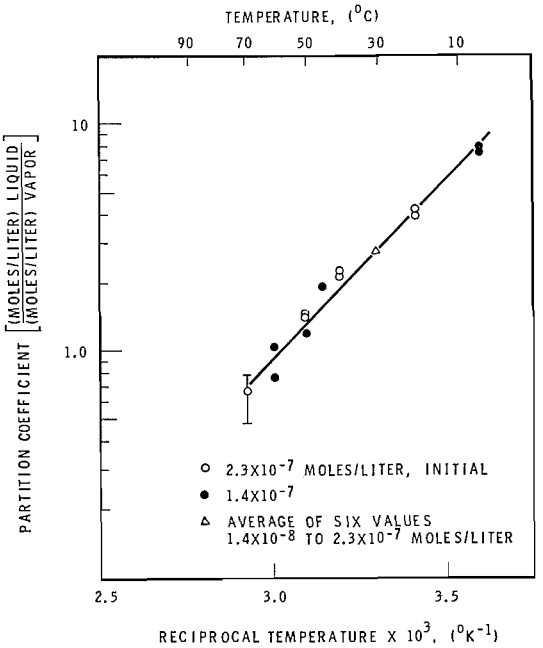

FIG. 1. Partition coefficient of methyl iodide as a function of the reciprocal temperature. ○, 2.3×10^{-7} mole/l, initial; ●, 1.4×10^{-7} mole/l, initial; △, average of six values with concentration between 1.4×10^{-8} to 2.3×10^{-7} mole/l.

where T is the temperature in °K. The partition coefficient as represented by eq. [3] is 22% lower than the value reported by Rex (7) and 32% lower than the value reported by Glew.

[2]The uncertainty of the partition coefficient, $\delta\beta$, can be shown to be

$$\frac{\delta\beta}{\beta} = \left[\frac{\beta + (V_G/V_L)}{\beta}\right]\left[\left(\frac{\sigma_{C^0}}{C^0}\right)^2 + \left(\frac{\sigma_C}{C}\right)^2\right]^{1/2},$$

where σ_{C^0} and σ_C are the uncertainties of C^0 and C. All other terms have the same definitions as in eq. [1].

1. R. A. HASTY. J. Chem. Eng. Data, in press. J. Mishima, L. C. Schwendiman, L. L. Burger, and R. A. Hasty. Proc. Ninth Air Cleaning Conf., U.S. At. Energy Comm. CONF-660904 (1966).
2. R. E. ADAMS, B. A. SOLDANO, and W. T. WARD. Behavior of fission products in gas–liquid systems. Nuclear Safety Program Annual Report, U.S. At. Energy Comm. Rept. ORNL-4071 (March 1967).
3. H. R. DIFFEY, C. H. RUMARY, M. J. S. SMITH, and R. A. STINCHOOMBE. At. Energy Res. Estab. Gt. Brit. Rept. AERE-R-4882 (1965).
4. D. N. GLEW and E. A. MOELWYN-HUGHES. Discussions Faraday Soc. **15**, 150 (1953).
5. E. A. MOELWYN-HUGHES. Proc. Roy. Soc. London, Ser. A, **220**, 386 (1953).
6. E. A. MOELWYN-HUGHES. Proc. Roy. Soc. London, Ser. A, **164**, 295 (1938).
7. A. REX. Z. Physik. Chem. Leipzig, **1**, 355 (1906).

Can. J. Chem. Downloaded from www.nrcresearchpress.com by 210.87.254.40 on 09/05/12
For personal use only.

Can. J. Chem. Downloaded from www.nrcresearchpress.com by 210.87.254.105 on 09/05/12
For personal use only.

Electric moments and conformation of substituted fluoroformates in benzene solutions

E. Bock, D. Iwacha, H. Hutton,[1] and A. Queen
Parker Chemistry Laboratory, University of Manitoba, Winnipeg, Manitoba

Received October 11, 1967

The dipole moments of methyl-, ethyl-, *n*-propyl-, *n*-butyl-, *n*-amyl-, and phenyl-fluoroformate were determined in dilute benzene solutions at 25 °C. The experimental results suggest that the conformation of the fluoro-esters is similar to the conformation of the chloro-esters and differs from the conformation of the normal esters; viz. the ester hydrocarbon group and the fluorine atom are *cis* to each other. Results of fluorine and proton n.m.r. measurements on these molecules support the conclusions based on the dipole moment data if a "through-space" coupling mechanism is assumed for the long range spin–spin coupling J_{H-F}[1-5].

Canadian Journal of Chemistry, 46, 1645 (1968)

Introduction

On the basis of the experimental data on the dipole moments of the first five members of the chloroformate homologous series, determined in this laboratory (1), it was concluded that the most probable conformation of these molecules in benzene solution differed from the now well-established conformation of the normal esters and carboxylic acids, in general, by having the chlorine atom situated *cis* to the hydrocarbon moiety. Although this conclusion is in agreement with the observations of Mizushima and Kubo (2) on the temperature dependence of the vapor phase dipole moments of methyl and ethyl chloroformate, it is nevertheless a surprising result. The only other paper in the literature, concerning the structure of methyl chloroformate, is the paper by O'Gorman, Shand, and Schomaker (3), who determined the electron-scattering spectra of methyl chloroformate. These authors interpreted their results in terms of a structure in which the chlorine atom was *trans* to the methyl group; a structure which, in a sense, is directly opposite to the one proposed earlier in this laboratory. To investigate this matter further, it was decided to determine the dipole moments of a number of fluoroformates. The particular molecules used were selected because the presence of the fluorine atom in them offered the possibility of an independent study of their conformations by fluorine and proton n.m.r. studies.

[1]Department of Chemistry, Brandon University, Brandon, Manitoba.

Experimental

Solvent

Fisher certified reagent benzene was used as solvent. The benzene was dried by repeated shaking with Linde molecular sieve 4A. The purity of the solvent was checked by gas chromatography as well as by determining the usual physical constants, viz. the boiling point, refractive index, and density, and comparing the latter with the appropriate literature values.

Solute

The fluoro-esters were synthesized after the method of Nakanishi, Myers, and Jensen (4), with one slight modification. It was found that the yield of the product was increased and the reaction time decreased considerably if in addition to constant stirring the reaction mixture was simultaneously subjected to gentle refluxing for several hours. The product was distilled from fresh, dry thallous fluoride at reduced pressure and further purified by gas chromatography. Moreover since the most likely chief impurity in the fluoroformates would be the corresponding chloroformate, all solute samples were checked for the presence of chlorine by hydrolyzing the sample and adding aqueous silver nitrate. All samples remained clear, thus confirming the absence of chloride ions. The boiling points and refractive indices of the synthesized molecules are summarized in Table I. The dipole moment apparatus and experimental procedure have been described elsewhere (5). The proton and fluorine n.m.r. spectra were determined on degassed, 5% benzene solutions containing tetramethylsilane (TMS) and $CFCl_3$ as internal references, using a Varian DP-60 spectrometer. The fluorine line positions were determined relative to $CFCl_3$ using the superposition of sidebands technique and the locked frequency sweep technique. When using the latter technique the field was "locked on" to the $CFCl_3$ signal.

Results and Discussion

The experimental data are shown in Table II. The dipole moments derived from these data by the method of Smith (6) are summarized in

TABLE I

Boiling points and refractive indices of prepared fluoroformates

Compound	Boiling point (°C) Exp.	Boiling point (°C) Lit.	n_D^{25} Exp.	n_D^{25} Lit.
Methyl fluoroformate	39	37–40[a] 40[b]		
Ethyl fluoroformate	56	55–57[a] 57[b], 55.6–57[c] 57[d]	1.3292	1.3295[c]
n-Propyl fluoroformate	78	90–102[b]	1.3463	
n-Butyl fluoroformate	94	97–99[b]		
n-Amyl fluoroformate	78–80 at 80 mm		1.3810	
Phenyl fluoroformate	150	153[d]	1.4649	

[a]Reference 19.
[b]Reference 20.
[c]Reference 21.
[d]Reference 22.

Table III. The dipole moments were calculated using the equation

$$[1] \qquad u^2 = \frac{27kT}{4\pi N} \frac{M_2}{d_1(\epsilon_1 + 2)^2} (\alpha - \nu),$$

where k is the Boltzmann constant, T the absolute temperature, N the Avogadro number, M_2 molecular weight of the solute, d_1 and ε_1 the density and dielectric constant of the pure solvent, α the slope of curve $\varepsilon_{12} = \varepsilon_1 + \alpha w_2$, where ε_{12} is the dielectric constant of the solution and w_2 the weight fraction of the solute in solution, and ν the slope of the curve $n_{12}^2 = n_1^2 + \nu w_2$, where n_{12} and n_1 is the refractive index of the solution and solvent respectively. The reliability of the calculational method used was tested by comparing the derived dipole moment for methyl fluoroformate with the value obtained for the same molecule by the use of the Halverstadt–Kumler equation (7) in conjunction with accepted bond refractivities (8). Both methods yielded the same value of 2.61 D. Included in Table III, to facilitate comparison, are the dipole moments of the normal esters and of the chloro-esters. The chemical shifts and coupling constants are given in Table IV.

From Table III, it is apparent that the dipole moments of all fluoro-esters are uniformly higher, by about 0.2 D, than the corresponding chloro-esters. A vector-model, bond-moment calculation based on the structural data for methyl formate as determined by Curl (9) and accepted bond moments (8) (see Fig. 1) was

TABLE II

Weight fraction, w, dielectric constant, ε, refractive index, n, and density d of benzene solutions at 25 °C

$w \times 10^3$	ε	n	d
Methyl fluoroformate ($\alpha = 8.88$ $\nu = -0.60$)			
0.897	2.2810	1.4977	0.8738
2.022	2.2906	1.4975	0.8740
4.529	2.3129	1.4971	0.8744
6.679	2.3317	1.4967	0.8748
Ethyl fluoroformate ($\alpha = 9.15$ $\nu = -0.44$)			
1.093	2.2828	1.4978	0.8738
2.672	2.2973	1.4974	0.8740
3.890	2.3080	1.4972	0.8742
5.407	2.3216	1.4971	0.8743
n-Propyl fluoroformate ($\alpha = 8.20$ $\nu = -0.47$)			
0.844	2.2796	1.4978	0.8731
1.789	2.2873	1.4977	0.8735
4.255	2.3077	1.4972	0.8738
5.495	2.3172	1.4971	0.8744
7.726	2.3355	1.4968	0.8744
n-Butyl fluoroformate ($\alpha = 7.23$ $\nu = -0.48$)			
1.058	2.2804	1.4976	0.8738
1.816	2.2858	1.4975	0.8738
3.862	2.3005	1.4973	0.8739
7.461	2.3260	1.4970	0.8743
n-Amyl fluoroformate ($\alpha = 6.47$ $\nu = -0.49$)			
0.833	2.2775	1.4978	0.8737
2.405	2.2886	1.4975	0.8738
4.098	2.2990	1.4973	0.8740
7.019	2.3169	1.4971	0.8742
Phenyl fluoroformate ($\alpha = 5.14$ $\nu = -0.32$)			
1.196	2.2787	1.4977	0.8740
2.953	2.2876	1.4977	0.8744
4.681	2.2968	1.4977	0.8748
6.227	2.3048	1.4976	0.8752

Can. J. Chem. Downloaded from www.nrcresearchpress.com by 210.87.254.105 on 09/05/12
For personal use only.

Can. J. Chem. Downloaded from www.nrcresearchpress.com by 210.87.254.105 on 09/05/12
For personal use only.

TABLE III

Dipole moments in debye units, D, of normal, chloro-, and fluoro-formate esters derived from dilute benzene solutions

	Formate	Chloroformate	Flouroformate
Methyl	1.75 (16)	2.38 (1)	2.61* ± 0.02
Ethyl	1.96 (17)	2.66 (1)	2.85* ± 0.02
n-Propyl	1.91 (17)	2.70 (1)	2.91* ± 0.02
n-Butyl	2.03 (1)	2.71 (1)	2.92* ± 0.02
n-Amyl	1.92 (gas) (17)	2.71 (1)	2.93* ± 0.02
Phenyl	—	2.39 (1)	2.65* ± 0.02

*Values obtained in this work.

compatible with the conformation in which the fluorine atom was *cis* to the hydrocarbon moiety. This result is in agreement with a similar calculation carried out for the chloro-esters (1). As in ref. 1, the vector model calculations were based on bond moments given by Smith (8), viz. H—C = 0.4 D, C—O = 0.8 D, C=O = 2.4 D, C—F = 1.4 D. It was also assumed that the group moment of CH_3 was equal to the H—C moment and that the direction of the latter was along the CH_3—O bond. From Fig. 1, it is quite apparent that the dipole moment decreases with increase in the angle θ and assumes a minimum value for $\theta = \pi$. Thus, $u = 2.33$ D for $\theta = 0$, and $u = 1.64$ D for $\theta = \pi$. The calculated moment for the *cis* conformation, 2.33 D, is smaller than the experimentally determined value of 2.61 D. This discrepancy may be due to a number of effects, viz. induction effects, mesomeric effects, or other effects. However, in our opinion, no great significance should be read into the observed discrepancy between calculated and experimental dipole moment. It is well known that such calculations give qualitative results only; e.g. on the basis of bond moments one would predict that chloromethane and chloroform molecules should have identical dipole moments. But, in fact, the dipole moment of the chloromethane molecule is 1.87 D and that of the chloroform molecule is 1.01 D (18).

The n.m.r. results support the above conclusions based on dipole moment data but only if a "through-space", coupling mechanism is assumed. The fluorine n.m.r. spectrum of methyl fluoroformate consists of a single line of about 0.8 c/s width at half-height. The slight broadening of the line suggests that some coupling exists between the fluorine nucleus and methyl protons, but the coupling is too small to be resolved by our instrument. The ethyl fluoro-

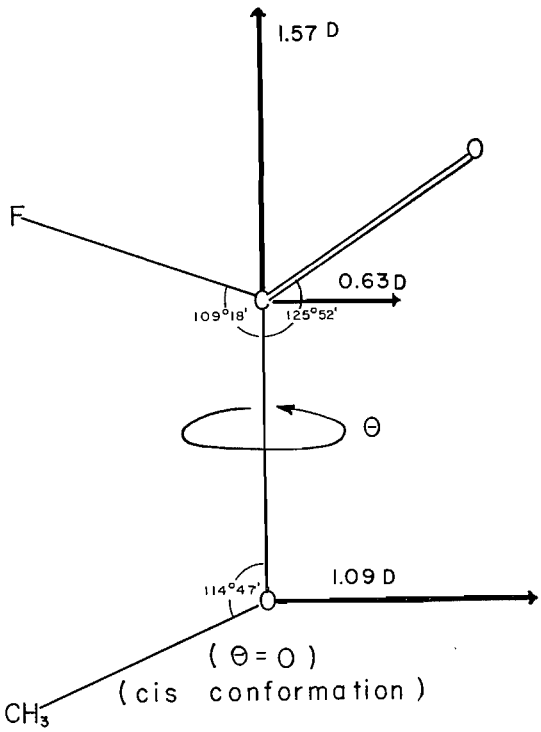

FIG. 1. Vector model for methyl fluoroformate molecule.

formate spectrum consists of a well-developed quartet, indicating quite definitely that the fluorine is coupled to the methyl protons by a long range spin–spin coupling ($J_{H-F}J^{1-5}$). All other higher alkyl fluoroformates exhibit triplet spectra only, indicating that the fluorine is coupled to a methylene group. Proton spectra of *n*-propyl fluoroformate showed definitely that in this molecule the coupling is also $J_{H-F}J^{1-5}$, viz. the fluorine is coupled to the β-methylene group. The proton spectrum of *n*-propyl fluoroformate (from low to high field) consists of a triplet, followed by a multiplet, which seems to consist of seven lines, followed by another triplet. The spectrum is very similar to that of *n*-propyl alcohol with the obvious exception that the hydroxyl proton line is missing and that the number of lines due to the β-methylene protons is increased from four to approximately seven. It is very tempting to explain the observed long range spin–spin coupling ($J_{H-F}{}^{1-5}$) in ethyl and propyl fluoroformate in terms of a "through-space" coupling mechanism. Such a mechanism has been proposed from time to time in the literature (10–15). If such a coupling mechanism

TABLE IV

Fluorine chemical shifts at 56.4 Mc/s and coupling constants

Compound	Solvent	Chemical shift*	Coupling constant J_{H-F}†
Methyl fluoroformate	C_6H_6 (5%)	1064.0±0.2	—
Ethyl fluoroformate	" "	987.2±0.2	1.76±0.10
n-Propyl fluoroformate	" "	1001.7±0.1	1.61±0.04
n-Butyl fluoroformate	" "	989.2±0.1	1.55±0.07
n-Amyl fluoroformate	" "	985.5±0.2	1.54±0.07
Phenyl fluoroformate	" "	927.1±0.1	(Splitting= 0.58±0.07)

*In c/s from internal $CFCl_3$.
†In c/s.

is adopted in the present case, then the distance between the fluorine atom and the methyl or methylene carbon in ethyl fluoroformate or *n*-propyl fluoroformate respectively turns out to be, on the basis of the observed coupling constants, about 2.7 Å (9). But this is just the sort of distance one would expect if indeed the fluorine atom were *cis* to the hydrocarbon moiety, a structure postulated earlier for the chloro- and fluoro-esters on the basis of the dipole moment data. However, the existence of the "through-space" coupling mechanism is by no means unequivocally established. It is quite possible that coupling takes place through the bonds, in which case the n.m.r. results would have no bearing on the dipole moment data. That not all is well with the "through-space" coupling mechanism interpretation is illustrated by the fluorine spectrum of methyl fluoroformate. Instead of the expected quartet of lines the spectrum consists of one slightly broadened line. Yet the distance between the methyl carbon and the fluorine atom is approximately the same as that between the methyl carbon and the fluorine atom in ethyl fluoroformate. The obvious difference between the two molecules is that in the former the fluorine atom and the proton to which it is coupled are separated by four bonds, whereas in the latter molecule these two atoms are separated by five bonds. This observation alone seems to suggest that the coupling may occur through the bonds after all. Further work designed to elucidate the nature of the coupling mechanism is in progress, e.g. effect of temperature, selective deuteration of the various sites in the molecule, and solvent effect on the magnitude of the coupling constants. The fluorine spectrum of phenyl fluoroformate also appears to be far from being straightforward. The spectrum appears to possess some doublet splitting with superimposed fine structure.

Acknowledgments

We thank Mr. R. Schwenk and Mr. J. W. S. Lee for running the n.m.r. spectra. We also thank Dr. T. Schaefer for his help in the interpretation of some n.m.r. spectra. The financial assistance of the National Research Council of Canada is deeply appreciated. We thank one of the referees for several helpful suggestions.

1. E. Bock and D. Iwacha. Can. J. Chem. **45**, 3177 (1967).
2. S. Mizushima and M. Kubo. Bull. Chem. Soc. Japan, **13**, 174 (1938).
3. J. M. O'Gorman, W. Shand, Jr., and V. Schomaker. J. Am. Chem. Soc. **72**, 4222 (1950).
4. S. Nakanishi, T. C. Myers, and E. V. Jensen. J. Am. Chem. Soc. **77**, 3099 (1955).
5. E. Bock and E. F. Dojack. Can. J. Chem. **45**, 1097 (1967).
6. J. W. Smith. Trans. Faraday Soc. **46**, 394 (1950).
7. I. F. Halverstadt and W. D. Kumler. J. Am. Chem. Soc. **64**, 2988 (1942).
8. J. W. Smith. Electric dipole moments. Butterworths Scientific Publications, London. 1955.
9. R. F. Curl, Jr. J. Chem. Phys. **30**, 1529 (1959).
10. P. C. Myhre, J. W. Edmonds, and J. D. Kruger. J. Am. Chem. Soc. **88**, 2459 (1966).
11. L. Petrakis and C. H. Sederholm. J. Chem. Phys. **35**, 1243 (1961).
12. S. Ng and C. H. Sederholm. J. Chem. Phys. **40**, 2090 (1964).
13. A. D. Cross. J. Am. Chem. Soc. **86**, 4011 (1964).
14. K. L. Servis and J. D. Roberts. J. Am. Chem. Soc. **87**, 1339 (1965).
15. F. A. L. Anet, A. J. R. Bourn, P. Carter, and S. Winstein. J. Am. Chem. Soc. **87**, 5429 (1965).
16. E. Bock. Can. J. Chem. **45**, 2761 (1967).
17. A. L. McClellan. Tables of experimental dipole moments. W. H. Freeman & Co., San Francisco and London. 1963.
18. R. D. Nelson, Jr., D. R. Lide, Jr., and A. A. Maryott. Selected values of electric dipole moments for molecules in the gas phase. NSRDS–NBS10. Washington, D.C. 1967.
19. H. Kitano and K. Fukui. Kogyo Kagaku Zasshi, **58**, 603 (1955).
20. G. Olah and I. Kuhn. J. Org. Chem. **21**, 1319 (1956).
21. S. Nakanishi, T. C. Myers, and E. V. Jenzen. J. Am. Chem. Soc. **77**, 3099 (1955).
22. H. J. Emeleus and J. F. Wood. J. Chem. Soc. 2183 (1948).

Can. J. Chem. Downloaded from www.nrcresearchpress.com by 210.87.254.105 on 09/05/12
For personal use only.

Can. J. Chem. Downloaded from www.nrcresearchpress.com by 210.87.254.40 on 09/05/12
For personal use only.

Phosphine-substituted carbonyl halide complexes of chromium and molybdenum

A. D. Allen and P. F. Barrett[1]
Department of Chemistry, University of Toronto, Toronto, Ontario
Received December 1, 1967

A number of phosphine tetracarbonyl halide salts of the Group VI metals have been prepared of the type: *cis*-$[Et_4N][PR_3M(CO)_4X]$ where PR_3 = $(p\text{-}FC_6H_4)_3P$ or $(p\text{-}ClC_6H_4)_3P$, M = Cr or Mo for X = Cl, and M = Mo for X = Br, by the reaction of phosphines with the pentacarbonyl halides $[Et_4N][M(CO)_5X]$. A new method for the preparation of *cis*-$(P\phi_3)_2Mo(CO)_4$ complexes from the phosphine tetracarbonyl halides is described.

Assignments are made for the bands in the carbonyl stretching region of the infrared spectra of these complexes.

Canadian Journal of Chemistry, **46**, 1649 (1968)

Although a number of phosphine-substituted carbonyl halide complexes of manganese have been prepared (1–3), no corresponding complexes of the Group VI transition metals have been reported. Since the pentacarbonyl halide complexes of these metals can be prepared by the reaction of the hexacarbonyls with a tetra-alkylammonium halide (4),

$$R_4NX + M(CO)_6 \rightarrow [R_4N]^+[M(CO)_5X]^- + CO,$$

where X = Cl, Br, or I, and M = Cr, Mo, or W, it was felt that the phosphine tetracarbonyl halide complexes could be prepared in a similar manner by reacting complexes of the type $PR_3M(CO)_5$ with a tetra-alkylammonium halide:

$$R_4NX + PR_3M(CO)_5 \rightarrow [R_4N]^+[PR_3M(CO)_4X]^- + CO.$$

Reactions of this type were carried out in diglyme at 120 °C under nitrogen with complexes containing a variety of substituted triaryl phosphines. Products were isolated in some cases which gave good analyses for the proposed phosphine tetracarbonyl halide complexes. Unfortunately, however, the yields from these reactions were very poor because a considerable amount of decomposition occurred at the high temperatures necessary for the preparations.

An alternative method for the preparation of these compounds was suggested by the method for the preparation of the corresponding manganese compounds (1). The manganese pentacarbonyl halides react with a phosphine at room temperature, a carbonyl group being replaced by a phosphine. The analogous reactions of some of the Group VI metal pentacarbonyl halides with phosphines were found to proceed smoothly at room temperature in diglyme under nitrogen to produce the desired phosphine tetracarbonyl halides:

$$[1] \quad [R_4N][M(CO)_5X] + PR_3 \rightarrow [R_4N][PR_3M(CO)_4X] + CO.$$

Table I lists the complexes of this type that were prepared, with their analytical data. All these complexes were bright orange-yellow in color and were only moderately stable in air.

We could not prepare pure samples of any iodo complexes, or any bromo complexes of chromium by this method. In addition, pure samples of the product could not be obtained with aryl phosphines containing electron-releasing groups, or with triphenylphosphine itself. Although products were obtained in these cases which showed peaks in the carbonyl region of the infrared spectra similar to those observed for the pure complexes in Table I, additional peaks were also evident, indicating the presence of other products.

Angelici and Basolo (2) have found that the reaction of *cis*-$Mn(CO)_4LX$ with L′ (L and L′ represent a variety of tertiary phosphines, arsines, and stibines) results in the replacement of one of the carbonyl groups by L′ to form *cis*-$Mn(CO)_3LL'X$. In an attempt to prepare the corresponding *cis*-tricarbonyl complexes of the Group VI metal halides, we have reacted the *cis*-phosphine tetracarbonyl halides prepared as above with additional phosphine. During the course of these reactions in diglyme a precipitate of the tetra-alkylammonium halide was formed and pale-yellow complexes were isolated from

[1]Present address: Department of Chemistry, Trent University, Peterborough, Ontario.

TABLE I

Complex	% C		% H	
	Calcd.	Obsd.	Calcd.	Obsd.
$[Et_4N][(p\text{-}FC_6H_4)_3PCr(CO)_4Cl]$	55.75	55.31	5.00	5.49
$[Et_4N][(p\text{-}ClC_6H_4)_3PCr(CO)_4Cl]$	51.81	51.09	4.65	5.09
$[Et_4N][(p\text{-}FC_6H_4)_3PMo(CO)_4Cl]$	52.22	51.47	4.68	4.91
$[Et_4N][(p\text{-}ClC_6H_4)_3PMo(CO)_4Cl]$	48.73	48.94	4.37	4.65
$[Et_4N][(p\text{-}FC_6H_4)_3PMo(CO)_4Br]$	49.06	48.92	4.40	4.68
$[Et_4N][(p\text{-}ClC_6H_4)_3PMo(CO)_4Br]$	45.96	45.63	4.12	4.43

TABLE II

Complex	Melting point (°C)	% C		% H	
		Calcd.	Obsd.	Calcd.	Obsd.
$(P\phi_3)_2Mo(CO)_4$	148–150 (decomp.)	65.57	65.58	4.14	4.15
$[(p\text{-}FC_6H_4)_3P]_2Mo(CO)_4$	158–160 (decomp.)	57.15	56.91	2.88	2.76
$[(p\text{-}ClC_6H_4)_3P]_2Mo(CO)_4$	142–145 (decomp.)	51.14	49.88	2.58	2.42

the solution. The molybdenum complexes analyzed quite well for $(PR_3)_2Mo(CO)_4$ (see Table II) and the chromium complexes had infrared spectra and melting points identical with those for the *trans*-$(PR_3)_2Cr(CO)_4$ complexes (5). Thus in the case of the Group VI metal complexes it appears that the halide rather than the carbonyl group is replaced by the phosphine. The reactions can be represented by

[2] $[Et_4N][PR_3M(CO)_4X] + PR_3 \rightarrow (PR_3)_2M(CO)_4 + Et_4NX.$

The possibility of this reaction occurring during the preparation of the phosphine tetracarbonyl halide complexes explains why pure products were obtained in some cases and not in others. The ratio of the two possible products formed, $[Et_4N][PR_3M(CO)_4X]$ and $(PR_3)_2M(CO)_4$, would depend on the relative rates of the two reactions [1] and [2]. Only when reaction [2] is slow compared with [1] could the $[Et_4N][PR_3M(CO)_4X]$ complexes be prepared in a pure state. A kinetic study of these reactions has been carried out and is reported in a later paper.

Attempts to prepare the mixed phosphine complexes, $(PR_3)(PR'_3)M(CO)_4$, by this reaction have been unsuccessful. Compounds have been isolated with infrared spectra similar to those of the $(PR_3)_2M(CO)_4$ complexes, but good analyses for these compounds could not be obtained. From the infrared spectra and the analytical data it could be seen that the reagent phosphine partly replaced the phosphine already present in the complex, in addition to replacing the halide, thus resulting in a mixture of products.

Discussion of Infrared Spectra and Structures

$[Et_4N][PR_3M(CO)_4X]$ Complexes

The infrared spectra of all the $[Et_4N][PR_3M(CO)_4X]$ complexes in the carbonyl stretching region showed four bands: a high frequency peak of medium intensity, a moderately intense low frequency peak, and two moderately intense peaks at intermediate frequencies. The two peaks at intermediate frequencies were often so close together that it was not possible to resolve them. Thus the absolute positions of these two peaks are often in doubt. A typical spectrum is shown in Fig. 1.

Two isomers of the $[PR_3M(CO)_4X]^-$ anions are possible in which the phosphine group is either *cis* or *trans* to the halide. The *trans* configuration would have C_{4v} symmetry and only three carbonyl bands would be predicted. The *cis* configuration with C_{1h} symmetry would be expected to show four bands: a high frequency band of medium intensity and three moderately intense bands at lower frequencies.

The observed spectra of the phosphine tetracarbonyl halide complexes prepared corresponded exactly to that predicted for the *cis* configuration. This structure is also in agreement with that predicted on electronic grounds. The weaker π-bonding ability of the halide compared

Can. J. Chem. Downloaded from www.nrcresearchpress.com by 210.87.254.40 on 09/05/12
For personal use only.

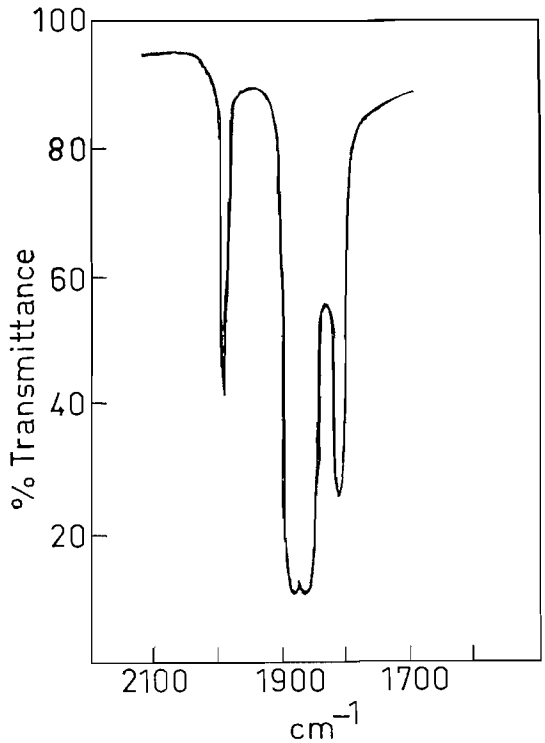

FIG. 1. Infrared spectrum in diglyme of *cis*-$[Et_4N][(p\text{-}FC_6H_4)_2PCr(CO)_4Cl]$ [(0.03 *M*). Cell thickness = 0.1 mm.

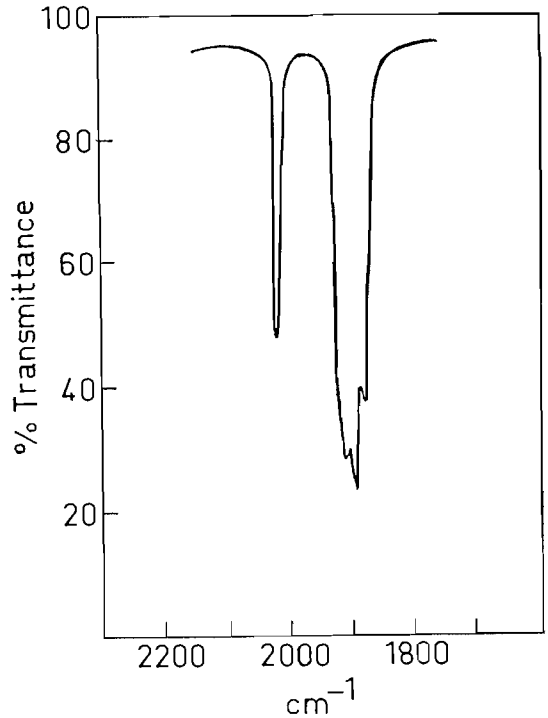

FIG. 2. Infrared spectrum in diglyme of *cis*-$(P\phi_3)_2Mo(CO)_4$ (0.02 *M*). Cell thickness = 0.1 mm.

with carbon monoxide should result in the metal–carbon bond *trans* to the halide being stronger than the other metal–carbon bonds in $[M(CO)_5X]^-$, so that the *cis* carbonyls might be expected to be replaced more easily than the *trans* carbonyl in these complexes.

$(PR_3)_2Mo(CO)_4$ Complexes

The infrared spectra of all the molybdenum compounds $(PR_3)_2Mo(CO)_4$ showed four bands in the carbonyl stretching region: one medium intensity band at the highest frequency and three closely spaced (and sometimes unresolved) intense bands at lower frequencies. Figure 2 shows a typical spectrum in the carbonyl stretching region.

These complexes have been assigned the *cis* configuration since the infrared spectra are consistent with C_{2v} symmetry, which should give four active carbonyl stretching modes. The *trans* configuration having D_{4h} symmetry would show only three bands.

The chromium complexes, $(PR_3)_2Cr(CO)_4$, on the other hand, had infrared spectra identical with those of the *trans*-$(PR_3)_2Cr(CO)_4$ compounds (5). Although the halide replaced by the phosphine is *cis* to the phosphine already present in the starting material, *cis*-$[PR_3Cr(CO)_4X]^-$, the complex rearranges during the course of the reaction so that in the final product the phosphine groups are *trans* to each other. It seems that there is too much steric interaction between two triaryl phosphine groups for the *cis* configuration to be formed in the chromium series.

The reaction of the *cis*-phosphine tetracarbonyl halide complexes of molybdenum with phosphines appears to be a better method to prepare the *cis*-$(PR_3)_2Mo(CO)_4$ complexes than by the direct reaction of the hexacarbonyl with a phosphine. Since the former reaction can be done at room temperature, there appears to be no tendency for isomerism to the *trans* complex to occur. The method of Poilblanc and Bigorgne (6) resulted in the formation of mixtures of the *cis* and *trans* isomers which were difficult to separate.

Can. J. Chem. Downloaded from www.nrcresearchpress.com by 210.87.254.40 on 09/05/12
For personal use only.

Can. J. Chem. Downloaded from www.nrcresearchpress.com by 210.87.254.40 on 09/05/12
For personal use only.

Assignment of Carbonyl Stretching Bands

For the purpose of assigning the carbonyl stretching frequencies observed in the infrared to particular modes of vibration for the complexes *cis*-$(PR_3)_2Mo(CO)_4$ and *cis*-$[Et_4N][PR_3M(CO)_4X]$, only the triphenylphosphine complexes of molybdenum will be discussed in detail. The modes of vibration and the observed bands for solution spectra in diglyme are given below.

Cis-$(P\phi_3)_2Mo(CO)_4$ — C_{2v} *Symmetry*

$A_1^{(a)}$ B_1 $A_1^{(b)}$ B_2

Absorption bands (cm^{-1}): 2022(m), 1917(s), 1903(s), 1882(s).

Cis-$[Et_4N][P\phi_3Mo(CO)_4Br]$ — C_{1h} *Symmetry*

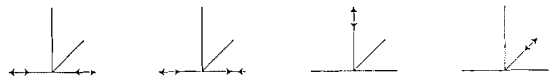

$A'_{(a)}$ A'' $A'_{(b)}$ $A'_{(c)}$

Absorption bands (cm^{-1}): 2005(m), 1890(s), 1875(s), 1818(s)

Trans-$(P\phi_3)_2Mo(CO)_4$ has an intense band at 1896 cm^{-1} in diglyme and this has been assigned to the E_u mode (7). The B_1 mode in *cis*-$(P\phi_3)_2Mo(CO)_4$ is similar to the E_u mode of the *trans* complex, since they involve the asymmetric stretching of two *trans* carbonyl groups. In both cases there are two carbonyl groups and two phosphines *cis* to these carbonyl groups so that the frequencies of these two modes should be almost identical (8). The 1903 cm^{-1} band in the *cis* complex is the closest to the 1896 cm^{-1} band in the *trans* complex and has been assigned to the B_1 mode. This assignment is also supported by the relative intensities of the bands; the B_1 mode should give rise to the most intense band, and the 1903 cm^{-1} is in fact the most intense.

Since in most carbonyl complexes *trans* pairs of carbonyl groups have stronger force constants than carbonyl groups *trans* to substituents (8, 9), the highest frequency band in *cis*-$(P\phi_3)_2Mo(CO)_4$ at 2022 cm^{-1} can be assigned to the $A_1^{(a)}$ mode. Also since symmetrical stretching modes of vibration are at higher frequencies than the corresponding asymmetical modes of vibration (10), the $A_1^{(b)}$ mode and the B_2 mode in *cis*-$(P\phi_3)_2Mo(CO)_4$ can be assigned to the 1917 cm^{-1} peak and the 1882 cm^{-1} peak respectively.

A summary of the assignments of the carbonyl frequencies for the *cis*-$(PR_3)_2Mo(CO)_4$ complexes is given in Table III.

The separation between the $A_1^{(a)}$ mode and the B_1 mode in *cis*-$(P\phi_3)_2Mo(CO)_4$ is 119 cm^{-1} and we would expect the separation between the corresponding $A'_{(a)}$ and A'' modes in *cis*-$[Et_4N][P\phi_3Mo(CO)_4Br]$ to be similar. The $A'_{(a)}$ mode can easily be assigned to the 2005 cm^{-1} band so that the 1890 cm^{-1} band can be assigned to the A'' mode. This assignment is also supported by intensity arguments. The lower π-bonding ability of the bromide compared with the phosphine leads us to assign the lowest frequency peak at 1818 cm^{-1} to the $A'_{(c)}$ mode, leaving the $A'_{(b)}$ mode to be assigned to the band at 1875 cm^{-1}.

A summary of the assignments of the infrared spectra of the *cis*-$[Et_4N][PR_3M(CO)_4X]$ complexes is given in Table IV. The assignments for the chromium complexes were made on the basis of the similarity in the profiles of their spectra to those of the molybdenum complexes.

Experimental

Cis-[Et₄N][PR₃M(CO)₄X] Complexes

A mixture of 0.001 mole of $[Et_4N][M(CO)_5X]$ and 0.0011 mole of PR_3 in 10 ml diglyme was stirred under nitrogen at room temperature for about 1 h. The solution was then filtered under nitrogen and the product was precipitated from solution with low boiling petroleum ether (b.p. 40–60 °C). The solvent was then decanted off and the yellow-orange product washed several times with petroleum ether and dried under vacuum. The $[Et_4N][M(CO)_5X]$ complexes used in this method were prepared by the method of Abel, Butler, and Reid (4).

Cis-(PR₃)₂Mo(CO)₄ Complexes

A mixture of 0.0008 mole of $[Et_4N][Mo(CO)_5Br]$ and 0.0011 mole PR_3 was stirred in 30 ml tetrahydrofuran under nitrogen for about $\frac{1}{2}$ h. A further 0.0011 mole of PR_3 was then added and the mixture was stirred for $1\frac{1}{2}$ h at about 40 °C. The Et_4NBr precipitated during the reaction was filtered off and the solvent was evaporated under reduced pressure. The resulting product was extracted with chloroform and recrystallized from a mixture of chloroform and methanol, giving pale-yellow needle crystals in about 70% yield.

Infrared Spectra

Infrared spectra were recorded with a Perkin–Elmer 521 grating spectrophotometer.

TABLE III

Infrared spectra of *cis*-$(PR_3)_2Mo(CO)_4$ complexes in diglyme (frequencies in cm^{-1})

PR_3	$A_1^{(a)}$ mode	$A_1^{(b)}$ mode	B_1 mode	B_2 mode
$P\phi_3$	2022	1917	1903	1882
$(p\text{-}ClC_6H_4)_3P$	2024	1925	1909	1890
$(p\text{-}FC_6H_4)_3)P$	2024	1923	1907	1890

TABLE IV

Infrared spectra of *cis*-$[Et_4N][(p\text{-}XC_6H_4)_3PM(CO)_4X']$ in diglyme (frequencies in cm^{-1})

M	X	X′	$A'_{(a)}$ mode	A'' mode	$A'_{(b)}$ mode*	$A'_{(c)}$ mode*
Cr	Cl	Cl	1995	1887	1867	1821
Cr	F	Cl	1995	1885	1864	1820
Mo	Cl	Cl	2005	1889	1877	1820
Mo	F	Cl	2004	1886	~1870	1818
Mo	Cl	Br	2005	1890	~1877	1817
Mo	F	Br	2005	~1888	~1877	1819

*The $A'_{(b)}$ mode represents the vibration of the carbonyl group *trans* to the phosphine, and the $A'_{(c)}$ mode represents the vibration of the carbonyl group *trans* to the halide.

Acknowledgment

One of us (P. F. B.) wishes to thank the National Research Council of Canada for scholarships.

1. R. J. Angelici and F. Basolo. J. Am. Chem. Soc. **84**, 2495 (1962).
2. R. J. Agelici and F. Basolo. Inorg. Chem. **2**, 728 (1963).
3. R. J. Angelici, F. Basolo, and A. J. Poë. J. Am. Chem. Soc. **85**, 2215 (1963).
4. E. W. Abel, I. S. Butler, and J. G. Reid. J. Chem. Soc. 2068 (1963).
5. P. F. Barrett. Ph.D. Thesis, University of Toronto, Toronto, Ontario. 1965.
6. R. Poilblanc and M. Bigorgne. Compt. Rend. **250**, 1064 (1960).
7. C. S. Kraihanzel and F. A. Cotton. Inorg. Chem. **2**, 533 (1963).
8. L. E. Orgel. Inorg. Chem. **1**, 25 (1962).
9. M. A. El-Sayed and H. D. Kaesz. J. Mol Spectry. **9**, 310 (1962).
10. M. A. El-Sayed and H. D. Kaesz. Inorg. Chem. **2**, 158 (1963).

Can. J. Chem. Downloaded from www.nrcresearchpress.com by 210.87.254.40 on 09/05/12
For personal use only.

Can. J. Chem. Downloaded from www.nrcresearchpress.com by 210.87.254.40 on 09/05/12
For personal use only.

Kinetics of some substitution reactions of the Group VI metal carbonyl halides

A. D. ALLEN AND P. F. BARRETT[1]
Department of Chemistry, University of Toronto, Toronto, Ontario

Received December 1, 1967

The kinetics in diglyme are reported for the two reactions of $[Et_4N][M(CO)_5X]$ with aryl phosphines to form *cis*-$[Et_4N][PR_3M(CO)_4X]$ and $PR_3M(CO)_5$ where M = Cr, Mo, or W, X = Cl, Br, or I, and PR_3 = $P\phi_3$, $(p\text{-}FC_6H_4)_3P$, or $(p\text{-}ClC_6H_4)_3P$. The reactions of *cis*-$[Et_4N][PR_3M(CO)_4X]$ with excess phosphine to form $(PR_3)_2M(CO)_4$ have also been studied kinetically. Possible mechanisms for these three types of reactions are discussed.

Canadian Journal of Chemistry, 46, 1655 (1968)

Recently we reported the preparation of complexes of the type *cis*-$[Et_4N][PR_3M(CO)_4X]$ by the reaction of $[Et_4N][M(CO)_5X]$ with various tertiary phosphines. The reactions of these complexes with excess phosphine to form $(PR_3)_2M(CO)_4$ were also described (1). Kinetic studies are now reported for the following reactions in the solvent diglyme:

$$[1]\quad [Et_4N]\,[M(CO)_5X] + PR_3 \xrightarrow{k_1} \textit{cis}\text{-}[Et_4N]\,[PR_3M(CO)_4X] + CO$$

$$[2]\quad [Et_4N]\,[M(CO)_5X] + PR_3 \xrightarrow{k_2} PR_3M(CO)_5 + Et_4NX$$

$$[3]\quad \textit{cis}\text{-}[Et_4N]\,[PR_3M(CO)_4X] + PR_3 \xrightarrow{k_3} (PR_3)_2M(CO)_4 + Et_4NX,$$

where $PR_3 = P\phi_3$, $(p\text{-}FC_6H_4)_3P$, or $(p\text{-}ClC_6H_4)_3P$, X = Cl, Br, or I, and M = Cr, Mo, or W.

Experimental

Preparation and Purification of Materials

The complexes $[Et_4N][M(CO)_5X]$ were prepared by the method of Abel, Butler, and Reid (2). Our recently reported methods were used for the preparation of the complexes *cis*-$[Et_4N][PR_3M(CO)_4X]$ (1). Triphenylphosphine was obtained from Eastman Organic Chemicals Ltd. and was used without further purification. $(p\text{-}FC_6H_4)_3P$ and $(p\text{-}ClC_6H_4)_3P$ were prepared by the method of Cook (3). Diglyme was thoroughly dried over sodium and freshly distilled before each run.

Determination of Rates

The rates of reactions [1] and [2] were determined by following the disappearance of the highest frequency carbonyl band of $[Et_4N][M(CO)_5X]$ as it reacted with PR_3 to form *cis*-$[Et_4N][PR_3M(CO)_4X]$ and $PR_3M(CO)_5$. The fact that *cis*-$[Et_4N][PR_3M(CO)_4X]$ reacts further with phosphine to produce $(PR_3)_2M(CO)_4$ is of no consequence since this product is also transparent in the region of the peak followed in the kinetics. To study the rate of reaction [3], the *cis*-$[Et_4N][PR_3M(CO)_4X]$ complexes were isolated and then reacted with excess phosphine and the disappearance of the lowest frequency carbonyl band in these complexes was followed.

To carry out the kinetic runs a weighed amount of the carbonyl complex was added to a flask in a bath whose temperature was maintained to ± 0.1 °C. A slow stream of dry nitrogen was continously passed through the flask. A thermostated solution of known phosphine concentration in diglyme was added to the flask at time zero and the mixture was stirred briefly to dissolve the carbonyl complex. Samples were withdrawn with a syringe and inserted into the infrared cell. During the course of the reaction usually only a 50 cm^{-1} range of the spectrum was scanned in the region of the peak being studied. The base line of the spectrum was obtained from the absorbance of a solution of the phosphine run against the reference solvent diglyme. From the transmittances, linear plots of log (o.d.$_t$ − o.d.$_\infty$) against time were obtained and the first order rate constants were calculated from the slopes of these lines. In these calculations, o.d.$_t$ is the optical density at time t and o.d.$_\infty$ the optical density at $t = \infty$; o.d.$_\infty$ was found to be zero in all cases.

During the course of both reactions [2] and [3] a precipitate of Et_4NX was formed since it is quite insoluble in diglyme. In an attempt to avoid this precipitation, the tetrabutyl-ammonium complex was prepared and used in reaction [3] since the tetrabutyl-ammonium halide formed in the reaction would be more soluble in diglyme. Under these conditions, however, the reaction did not go to completion but reached an equilibrium. The precipitate did not prove to be a problem since it settled to the bottom of the reaction flask and the samples for kinetic studies could be withdrawn from the clear supernatent liquid. Added solid tetraethyl-ammonium halide did not change the rates of the reactions. It was therefore concluded that the precipitate did not have any catalytic effect.

Results

Reactions of the Pentacarbonyl Halides

The pentacarbonyl halides react with phosphines via two paths to produce *cis*-$[PR_3M(CO)_4X]^-$ (path [1]) and $PR_3M(CO)_5$ (path [2]). The formation of $PR_3M(CO)_5$ was discovered to

[1]Present address: Department of Chemistry, Trent University, Peterborough, Ontario.

TABLE I

k_{obs} for reactions of $[Et_4N][Mo(CO)_5X]$ with PR_3 in diglyme ($[Mo(CO)_5X]^- \sim 0.03\ M$)

Temp. (°C)	PR_3	$[PR_3]$ (mole/l)	X	$k_{obs} \times 10^4$ (s^{-1})
19.6	$P\phi_3$	0.35	Br	2.88
19.6	$P\phi_3$	0.40	Br	2.98[a]
19.6	$P\phi_3$	0.45	Br	3.09[a]
19.6	$P\phi_3$	0.50	Br	3.52[a]
19.6	$P\phi_3$	0.55	Br	3.64[a]
19.6	$P\phi_3$	0.60	Br	3.82[a]
29.8	$P\phi_3$	0.40	I	1.85
29.8	$P\phi_3$	0.45	I	2.02
29.8	$P\phi_3$	0.50	I	2.04
29.8	$P\phi_3$	0.55	I	2.11
29.8	$P\phi_3$	0.60	I	2.21
29.8	$(p\text{-}FC_6H_4)_3P$	0.40	I	2.24
29.8	$(p\text{-}FC_6H_4)_3P$	0.50	I	2.54
29.8	$(p\text{-}FC_6H_4)_3P$	0.60	I	2.71
29.8	$(p\text{-}FC_6H_4)_3P$	0.70	I	3.06
29.8	$(p\text{-}ClC_6H_4)_3P$	0.40	I	2.60
29.8	$(p\text{-}ClC_6H_4)_3P$	0.50	I	2.88
29.8	$(p\text{-}ClC_6H_4)_3P$	0.60	I	3.30
29.8	$(p\text{-}ClC_6H_4)_3P$	0.70	I	3.68

[a]Average value of several runs.

take place when the pentacarbonyl halides were reacted with a large excess of phosphine. Under these conditions additional peaks appeared in the infrared identical with those of the $PR_3M(CO)_5$ complexes already reported (1). Hence the halide as well as a carbonyl group in the pentacarbonyl halides can be replaced by phosphines. Experimentally the rate of disapperance of the pentacarbonyl halide was followed so that the observed pseudo first order rate constant was a function of the rate constants for both these reaction paths.

Problems arose in studying reactions [1] and [2] simultaneously when the rates of these two reactions were vastly different or when one of them was quite rapid. If the diffrence in the rates was too great, the faster reaction went nearly to completion before a significant portion of the slower reaction had taken place. Under these conditions it was not possible to obtain a rate constant for the slower reaction. If one of the reactions was quite rapid, the overall rate of the two reactions was too fast to study accurately with the apparatus used.

Table I lists the pseudo first order rate constants for the disappearance of $[Et_4N][Mo(CO)_5X]$ via the two reactions paths [1] and [2].

The reactions of $[Et_4N][Mo(CO)_5Cl]$ with PR_3 and $[Et_4N][Mo(CO)_5Br]$ with $(p\text{-}ClC_6H_4)_3P$ or $(p\text{-}FC_6H_4)_3P$ were too fast to be studied accurately by this method.

Table II lists the pseudo first order rate constants for the disappearance of $[Et_4N][Cr(CO)_5X]$. In the case of $[Et_4N][Cr(CO)_5Cl]$ there was no infrared evidence for the formation of $PR_3Cr(CO)_5$, whereas both *cis*-$[Et_4N][PR_3Cr(CO)_4Br]$ and $PR_3Cr(CO)_5$ were formed in the reactions of $[Et_4N][Cr(CO)_5Br]$ with phosphines. No appreciable reaction occurred with $[Et_4N][Cr(CO)_5I]$ and phosphines after 2 h.

Table III lists the values of the pseudo first order rate constants for the reactions of $[Et_4N][W(CO)_5Cl]$ with triphenylphosphine. A comparision of the infrared spectrum of the products of this reaction with those of the other Group VI metal complexes suggested that both *cis*-$[P\phi_3W(CO)_4Cl]^-$ and $P\phi_3W(CO)_5$ were formed, but there was no evidence for *cis*-$[P\phi_3W(CO)_4Cl]^-$ reacting further to give $(P\phi_3)_2W(CO)_4$. The reactions of $[Et_4N][W(CO)_5Br]$ were too slow to be studied.

Except for the reactions of $[Et_4N][Cr(CO)_5Cl]$ with phosphines, the results in Tables I, II, and III indicate that the rates of reaction of the pentacarbonyl halides are dependent on both the nature and concentration of the incoming ligand. Plots of the pseudo first order rate constants against phosphine concentration gave straight lines with a common non-zero intercept for all the phosphines. This indicates that only one of the reaction paths is dependent on the phosphine concentration and the intercept at

Can. J. Chem. Downloaded from www.nrcresearchpress.com by 210.87.254.40 on 09/05/12
For personal use only.

Can. J. Chem. Downloaded from www.nrcresearchpress.com by 210.87.254.40 on 09/05/12
For personal use only.

TABLE II

k_{obs} for the reactions of $[Et_4N][Cr(CO)_5X]$ with PR_3 in diglyme ($[Cr(CO)_5X]^- \sim 0.03\ M$)

Temp. (°C)	PR_3	$[PR_3]$ (mole/l)	X	$k_{obs} \times 10^4$ (s^{-1})
19.6	$P\phi_3$	0.40	Cl	1.45
19.6	$P\phi_3$	0.50	Cl	1.57
19.6	$P\phi_3$	0.60	Cl	1.56[a]
19.6	$(p\text{-}FC_6H_4)_3P$	0.40	Cl	1.67[a]
19.6	$(p\text{-}FC_6H_4)_3P$	0.50	Cl	1.65
19.6	$(p\text{-}FC_6H_4)_3P$	0.60	Cl	1.64
19.6	$(p\text{-}ClC_6H_4)_3P$	0.30	Cl	1.49
19.6	$(p\text{-}ClC_6H_4)_3P$	0.40	Cl	1.57
19.6	$(p\text{-}ClC_6H_4)_3P$	0.50	Cl	1.57
19.6	$(p\text{-}ClC_6H_4)_3P$	0.60	Cl	1.55
29.8	$P\phi_3$	0.40	Br	1.19[a]
29.8	$P\phi_3$	0.45	Br	1.32
29.8	$P\phi_3$	0.50	Br	1.25
29.8	$P\phi_3$	0.55	Br	1.40
29.8	$P\phi_3$	0.60	Br	1.48
29.8	$P\phi_3$	0.70	Br	1.61
29.8	$(p\text{-}FC_6H_4)_3P$	0.40	Br	1.29
29.8	$(p\text{-}FC_6H_4)_3P$	0.45	Br	1.38
29.8	$(p\text{-}FC_6H_4)_3P$	0.50	Br	1.48
29.8	$(p\text{-}FC_6H_4)_3P$	0.55	Br	1.53
29.8	$(p\text{-}FC_6H_4)_3P$	0.60	Br	1.56
29.8	$(p\text{-}FC_6H_4)_3P$	0.70	Br	1.73
29.8	$(p\text{-}ClC_6H_4)_3P$	0.40	Br	1.38
29.8	$(p\text{-}ClC_6H_4)_3P$	0.45	Br	1.42
29.8	$(p\text{-}ClC_6H_4)_3P$	0.50	Br	1.53
29.8	$(p\text{-}ClC_6H_4)_3P$	0.55	Br	1.59
29.8	$(p\text{-}ClC_6H_4)_3P$	0.60	Br	1.69

[a]Average value of several runs.

TABLE III

k_{obs} for the reactions of $[Et_4N][W(CO)_5Cl]$ with PR_3 in diglyme ($[W(CO)_5Cl]^- \sim 0.03\ M$)

Temp. (°C)	PR_3	$[PR_3]$ (mole/l)	$k_{obs} \times 10^4$ (s^{-1})
29.8	$P\phi_3$	0.40	2.30
29.8	$P\phi_3$	0.50	2.42
29.8	$P\phi_3$	0.60	2.57
29.8	$P\phi_3$	0.65	2.65
29.8	$P\phi_3$	0.70	2.72

zero phosphine concentration gives a value of the rate constant for the phosphine independent path. At $t = \infty$, the products are $PR_3M(CO)_5$ (which does not react further at the temperatures used) and $(PR_3)_2M(CO)_4$. On increasing the concentration of the phosphine, relatively more $PR_3M(CO)_5$ was formed than $(PR_3)_2M(CO)_4$, as indicated by the intensities of the infrared bands of these products. Hence the path to form $PR_3M(CO)_5$ must be the phosphine dependent path.

The observed pseudo first order rate constant, k_{obs}, can thus be expressed as

$$k_{obs} = k_1 + k_2[PR_3],$$

where k_1 is the first order rate constant for reaction [1], and k_2 is the second order rate constant for reaction [2]. Figure 1 shows a plot of the data obtained for the reactions of $[Et_4N][Mo(CO)_5I]$ with phosphines. Table IV summarizes the values of k_1 and k_2 from similar plots for the other reactions studied.

Reactions of the Phosphine Tetracarbonyl Halides

Phosphines react with the *cis*-phosphine tetracarbonyl halides to produce the diphosphine tetracarbonyl (path [3]) by the replacement of the halide. The products formed with the molybdenum complexes have the *cis* configuration, while those with the chromium complexes have the *trans* configuration (1). It is possible that the *cis* complexes of chromium are formed initially but rearrange rapidly because of steric interaction. The tungsten complex, *cis*-$[P\phi_3W(CO)_4Cl]^-$ did not react to form $(P\phi_3)_2W(CO)_4$ under the conditions used.

Table V lists the pseudo first order rate constants obtained by following the disappearance of the lowest frequency carbonyl band of the *cis*-$[Et_4N][PR_3M(CO)_4X]$ complexes during their reaction with excess phosphine.

TABLE IV

Rate constants for the following reactions in diglyme

[1] $[Et_4N][M(CO)_5X] + PR_3 \xrightarrow{k_1} cis\text{-}[Et_4N][PR_3M(CO)_4X] + CO$

[2] $[Et_4N][M(CO)_5X] + PR_3 \xrightarrow{k_2} PR_3M(CO)_5 + Et_4NX$

Temp. (°C)	M	X	PR_3	$k_1 \times 10^4$ (s^{-1})	$k_2 \times 10^4$ (l $mole^{-1}$ s^{-1})
19.6	Mo	Cl	$P\phi_3$	Rapid	—*
19.6	Mo	Br	$P\phi_3$	1.34	4.1
29.8	Mo	I	$(p\text{-}FC_6H_4)_3P$	1.13	2.76
29.8	Mo	I	$(p\text{-}ClC_6H_4)_3P$	1.13	3.59
29.8	Mo	I	$P\phi_3$	1.13	1.81
19.6	Cr	Cl	$(p\text{-}FC_6H_4)_3P$	1.56	Negligible
19.6	Cr	Cl	$(p\text{-}ClC_6H_4)_3P$	1.56	Negligible
19.6	Cr	Cl	$P\phi_3$	1.56	Negligible
29.8	Cr	Br	$(p\text{-}FC_6H_4)_3P$	0.7	1.72
29.8	Cr	Br	$(p\text{-}ClC_6H_4)_3P$	0.7	1.72
29.8	Cr	Br	$P\phi_3$	0.7	1.37
29.8	Cr	I	$P\phi_3$	Slow	Slow
29.8	W	Cl	$P\phi_3$	1.73	1.39

*Since k_1 is so large it was not possible to obtain a value for k_2, although some $P\phi_3Mo(CO)_5$ was detected in the infrared so that the rate of this reaction must be greater than with the Cr—Cl complex.

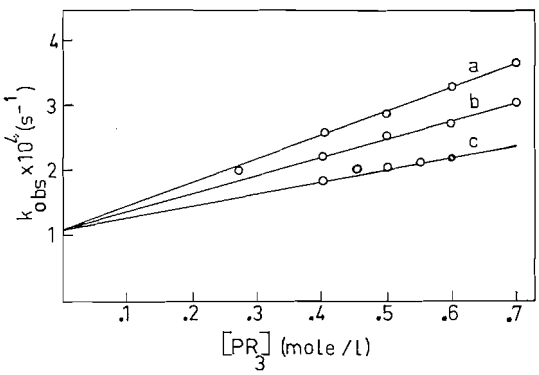

FIG. 1. k_{obs} for the reactions of $[Et_4N]$ $[Mo(CO)_5I]$ with phosphines in diglyme at 29.8 °C. (*a*) $PR_3 = (p\text{-}ClC_6H_4)_3P$, (*b*) $PR_3 = (p\text{-}FC_6H_4)_3P$, (*c*) $PR_3 = P\phi_3$.

Plots of k_{obs} against the concentration of phosphine gave straight lines passing through the origin, indicating that the reactions were first order in both the complex and the phosphine. It was not possible to study some reactions kinetically because of the difficulty in preparing pure starting material from the first step in the following reaction sequence.

$$[M(CO)_5X]^- + PR_3 \rightarrow cis\text{-}[PR_3M(CO)_4X]^- \xrightarrow{PR_3} (PR_3)_2M(CO)_4$$

In a number of cases the second reaction was fast compared with the first so that it was not possible to isolate the intermediate complex *cis*-$[Et_4N][PR_3M(CO)_4X]$. Under these circumstances it was only possible to obtain relative rates for the reactions of the different phosphines by following the appearance of $(PR_3)_2M(CO)_4$ from a mixture of $[M(CO)_5X]^-$ and phosphine. Since the rate of formation of the intermediate is independent of the phosphine used, the relative rates of formation of $(PR_3)_2M(CO)_4$ give a measure of the reactivity of the phosphine in the second step. Under these preparative conditions so low a concentration of phosphine was used that virtually no $PR_3M(CO)_5$ was formed. In all cases the rates of reaction of the complexes with different phosphines decreased in the order: $P\phi_3 > (p\text{-}FC_6H_4)_3P > (p\text{-}ClC_6H_4)_3P$.

Table VI lists the second order rate constants for the reactions of the phosphine tetracarbonyl halides with phosphines, obtained from the slopes of the plots of k_{obs} against $[PR_3]$. Figure 2 shows the plots of the rate data for the reactions of *cis*-$[Et_4N][PR_3M(CO)_4Br]$.

Discussion

Reaction [1]

$$[M(CO)_5X]^- + PR_3 \rightarrow cis\text{-}[PR_3M(CO)_4X]^- + CO$$

The rates of the reaction of the Group VI metal pentacarbonyl halide complexes with phosphines to form the phosphine tetracarbonyl

Can. J. Chem. Downloaded from www.nrcresearchpress.com by 210.87.254.40 on 09/05/12
For personal use only.

Can. J. Chem. Downloaded from www.nrcresearchpress.com by 210.87.254.40 on 09/05/12
For personal use only.

TABLE V

k_{obs} for the reactions of *cis*-$[Et_4N][PR_3M(CO)_4X]$ with PR_3 in diglyme (*cis*-$[PR_3M(CO)_4X]^- \sim 0.02\ M$)

Temp. (°C)	M	X	PR_3	$[PR_3]$ (mole/l)	$k_{obs} \times 10^4$ (s^{-1})
29.8	Mo	Cl	$P\phi_3$	0.60	~1.0
19.6	Mo	Br	$P\phi_3$	0.35	2.98
19.6	Mo	Br	$P\phi_3$	0.40	3.84
19.6	Mo	Br	$P\phi_3$	0.50	4.65
19.6	Mo	Br	$P\phi_3$	0.60	5.34
29.9	Mo	Br	$(p\text{-}FC_6H_4)_3P$	0.40	1.36
29.9	Mo	Br	$(p\text{-}FC_6H_4)_3P$	0.50	1.70
29.9	Mo	Br	$(p\text{-}FC_6H_4)_3P$	0.60	2.04
29.9	Mo	Br	$(p\text{-}ClC_6H_4)_3P$	0.20	0.56
29.9	Mo	Br	$(p\text{-}ClC_6H_4)_3P$	0.40	1.23
29.9	Mo	Br	$(p\text{-}ClC_6H_4)_3P$	0.60	1.92
29.9	Mo	I	$(p\text{-}ClC_6H_4)_3P$	0.40	4.28
29.9	Mo	I	$(p\text{-}ClC_6H_4)_3P$	0.50	5.75
29.9	Mo	I	$(p\text{-}ClC_6H_4)_3P$	0.60	6.60
29.8	Cr	Cl	$(p\text{-}FC_6H_4)_3P$	0.40	1.82
29.8	Cr	Cl	$(p\text{-}FC_6H_4)_3P$	0.40	1.75
29.8	Cr	Cl	$(p\text{-}FC_6H_4)_3P$	0.50	2.13
29.8	Cr	Cl	$(p\text{-}FC_6H_4)_3P$	0.60	2.49
29.8	Cr	Cl	$(p\text{-}FC_6H_4)_3P$	0.70	3.02

TABLE VI

Second order rate constants for the reactions of *cis*-$[Et_4N][PR_3M(CO)_4X]$ with PR_3 in diglyme

Temp. (°C)	M	X	PR_3	$k_3 \times 10^4$ (l $mole^{-1}$ s^{-1})
29.9	Mo	Cl	$P\phi_3$	~1.7
29.9	Mo	Br	$(p\text{-}FC_6H_4)_3P$	3.4
29.9	Mo	Br	$(p\text{-}ClC_6H_4)_3P$	3.0
19.6	Mo	Br	$P\phi_3$	9.2
29.9	Mo	I	$(p\text{-}ClC_6H_4)_3P$	11.1
19.6	Mo	I	$P\phi_3$	Rapid
29.8	Cr	Cl	$(p\text{-}FC_6H_4)_3P$	4.3
29.8	W	Cl	$P\phi_3$	Slow

halides were found to be independent of both the nature and the concentration of the added phosphine. This suggests that the first step in the mechanism of these reactions involves the unimolecular dissocation of a carbonyl group followed by the rapid attack of the phosphine on the five-coordinated intermediate:

$$[M(CO)_5X]^- \xrightarrow[\text{slow}]{-CO} [M(CO)_4X]^- \xrightarrow[\text{fast}]{PR_3} \textit{cis}\text{-}[PR_3M(CO)_4X]^-.$$

This is the mechanism Angelici and Basolo have proposed for the reactions of the manganese pentacarbonyl halides with a variety of ligands (4). It is interesting to note that evidence has been obtained for the presence of $M(CO)_5$ (M = Cr, Mo, and W) in the photochemically induced reactions of the hexacarbonyl (5, 6) so that it is not unreasonable to assume that the five coordinate $[M(CO)_4X]^-$ is an intermediate in the above reaction.

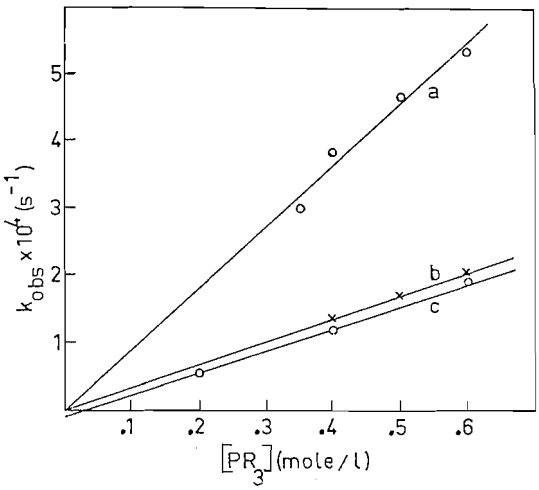

FIG. 2. k_{obs} for the reactions of *cis*-$[Et_4N][PR_3Mo(CO)_4Br]$ with phosphines in diglyme. (*a*) $PR_3 = P\phi_3$ (at 19.6 °C), (*b*) $PR_3 = (p\text{-}FC_6H_4)_3P$ (at 29.9 °C), (*c*) $PR_3 = (p\text{-}ClC_6H_4)_3P$ (at 29.9 °C).

The rates were found to decrease with changes of the halide in the order Cl > Br > I. This can be explained on the basis of the electronegativity or polarizability of the halides, as has been done

Can. J. Chem. Downloaded from www.nrcresearchpress.com by 210.87.254.40 on 09/05/12
For personal use only.

for the corresponding reactions of the manganese pentacarbonyl halides (4).

The molybdenum complexes react more readily than either the chromium complexes or the tungsten complexes and this is presumably due to the variation in the metal–carbon bond strengths between these complexes. Although there are no data for the bond strengths in these complexes, the metal–carbon bond strengths are known for the Group VI metal hexacarbonyls and indicate that the metal–carbon bond is weaker for molybdenum than for chromium or tungsten (7). Our results are then reasonable if the molybdenum–carbon bond is the weakest in the three pentacarbonyl halides.

Reaction [2]

$$[M(CO)_5X]^- + PR_3 \rightarrow PR_3M(CO)_5 + X^-$$

The rates of both reactions involving the replacement of a halide ligand by a phosphine ligand (reactions [2] and [3]) were found to be dependent on both the nature and the concentration of the phosphine. Because second order kinetics were observed, one possible mechanism for these reactions would be an S_N2 displacement mechanism, involving a seven-coordinated intermediate. Another possibility, however, would involve the establishment of an equilibrium between the starting material and an intermediate (which may or may not be solvated) followed by the slow reaction of this intermediate with a phosphine:

$$MX^- \underset{k_b}{\overset{k_f}{\rightleftharpoons}} M^*(\text{solvent}) + X^- \overset{PR_3}{\rightarrow} MPR_3,$$

where $M^* = M(CO)_5$ for reaction [2], $M^* = PR_3M(CO)_4$ for reaction [3].

In this case the rate could also show a second order dependence on the phosphine concentration, but at high concentrations this dependence could disappear if the overall rate reached the rate of the forward reaction k_f. At the concentrations of phosphine used this effect has not been observed, but this of course does not rule out the mechanism.

The rates of reaction [2] decrease with changes in the phosphine in the order: $(p\text{-}ClC_6H_4)_3P > (p\text{-}FC_6H_4)_3P > P\phi_3$. Since the basicity increases in this sequence, one might have expected the order of the rates to be reversed. In this case, however, the important factor must be the ability of the phosphine to accept d orbital electrons from the metal. The greater the tendency for this to occur, the less would be the repulsion between the nonbonding d electrons on the metal and the electron pair on the phosphorous, allowing an easier approach of the metal and the phosphorous in the transition state. Thus the increase in the ability of the phosphines to accept metal d orbital electrons caused by electron-withdrawing substituents, must override the accompanying decrease in the basicity of the phosphines in these reactions. Edwards and Pearson (8) have pointed out that this polarizability factor plays the chief role in cases where the central element has several outer orbital electrons, in particular with transition metals with a full compliment of d electrons.

The results for this reaction indicate that the bromide is replaced more readily than either the chloride or the iodide. Presumably the M—X bond strengths follow a smooth trend on changing the halide from chloride to bromide to iodide and would determine the rates on the basis of an S_N1 mechanism. However, in an S_N2 displacement mechanism, steric factors would be expected to play a large role as well. If the metal–halide bond strengths increase in the order $I < Br < Cl$, the iodide complex would not necessarily react the fastest because of the greater steric difficulty in forming the seven coordinate transition state. Since the bromide complexes react the most rapidly, we regard this as evidence against an S_N1 mechanism, thereby giving weight to an S_N2 mechanism.

The rates of reaction [2] are greater for the tungsten and molybdenum complexes than for the chromium complexes. For an S_N1 mechanism involving the dissociation of the halide we would expect the rates to parallel the order of the M—X bond strengths. Using the infrared data of Bennett and Clark (9) for the M—Cl stretching frequencies in $[M(CO)_5Cl]^-$, crude calculations for the M—Cl force constants were made on the assumption that the M—Cl portion of the molecule approximates a diatomic system. These showed that the M—Cl bond strengths increased in the order $Cr < Mo < W$ and this predicts that the chromium complex should react the fastest. On the basis of an S_N2 mechanism, however, the larger tungsten and molybdenum atoms would be more susceptible to an S_N2 attack, resulting in their complexes reacting faster than those of chromium, as is observed.

Hence all our data are consistent with an S_N2

Can. J. Chem. Downloaded from www.nrcresearchpress.com by 210.87.254.40 on 09/05/12
For personal use only.

mechanism and we are led to propose this mechanism for reaction [2].

Reaction [3]

$$cis\text{-}[PR_3M(CO)_4X]^- + PR_3 \rightarrow (PR_3)_2M(CO)_4 + X^-$$

The rates of the above reactions were found to decrease with changes of the phosphine in the order $P\phi_3 > (p\text{-}FC_6H_4)_3P > (p\text{-}ClC_6H_4)_3P$, which is the reverse order found for the replacement of a halide by a phosphine in the pentacarbonyl halides. It is difficult to predict the order of rates that might be expected on the basis of an S_N2 mechanism because of the phosphine already present in the complex. However, the observed order of rates might be predicted on the basis of an S_N1 mechanism involving the breaking of the metal–halogen bond. The greater the basicity of the phosphine in the complex, the weaker the metal–halogen bond would be and the faster would be the rate. This is supported by the work of Bennett and Clark (9), who have shown that the metal–halogen stretching frequencies in substituted derivatives of $Mn(CO)_5X$ decrease with increasing basicity of the substituents.

The rates of reaction [3] increase with change of the halide in the order Cl < Br < I. Although no information is available on the metal–halide bond strengths in these complexes, molecular models have shown that there is considerable steric interaction between the halide and the phosphine which increases with the size of the halide. Thus the strength of the metal–halogen bond and hence the rates of the reactions can be explained on steric grounds.

Finally the rates of these reactions decrease with changes of the central metal in the order: Cr > Mo > W. If the metal–halogen bond strengths in these complexes can be assumed to follow the same order as that proposed for the $[M(CO)_5X]^-$ complexes (W > Mo > Cr), the rates would be expected to follow the observed order if the breaking of this bond is the important step in the reaction. A steric factor may also be involved since the smaller the central atom, the greater would be the steric repulsion between the halide and the phosphine, allowing the metal–halogen bond to break more easily.

All our results are thus consistent with an S_N1 mechanism in which the breaking of the metal–halogen bond in reaction [3] is the rate-determining step. Although an S_N2 mechanism was proposed for the replacement of the halide in the pentacarbonyl halides, it appears that the presence of the phosphine in the phosphine tetracarbonyl halides makes it sterically impossible to form a seven-coordinated intermediate with another phosphine via an S_N2 mechanism.

Acknowledgment

One of us (P. F. B.) wishes to thank the National Research Council of Canada for scholarships.

1. A. D. Allen and P. F. Barrett. Can. J. Chem. This issue.
2. E. W. Abel, I. S. Butler, and I. G. Reid. J. Chem. Soc. 2068 (1963).
3. C. D. Cook. Ph.D. Thesis, University of Toronto, Toronto, Ontario. 1962.
4. R. J. Angelici and F. Basolo. J. Am. Chem. Soc. **84**, 2495 (1962).
5. G. R. Dobson, M. A. El-Sayed, I. W. Stolz, and R. K. Sheline. Inorg. Chem. **1**, 526 (1962).
6. I. W. Stolz, G. R. Dobson, and R. K. Sheline. J. Am. Chem. Soc. **84**, 3589 (1962).
7. H. G. Schuster-Woldan and F. Basolo. J. Am. Chem. Soc. **88**, 1657 (1966), and references therein.
8. J. O. Edwards and R. G. Pearson. J. Am. Chem. Soc. **84**, 16 (1962).
9. M. A. Bennett and R. J. H. Clark. J. Chem. Soc. 5560 (1964).

Can. J. Chem. Downloaded from www.nrcresearchpress.com by 210.87.254.40 on 09/05/12
For personal use only.

Cumulative yields in the 14-MeV neutron fission of ^{238}U

D. J. GORMAN[1] AND R. H. TOMLINSON
Department of Chemistry, McMaster University, Hamilton, Ontario

Received November 20, 1967

The isotopic abundances of the elements xenon, krypton, and cesium formed in the 14-MeV neutron fission of ^{238}U have been measured mass spectrometrically. The relative yields of some isotopes of krypton, strontium, zirconium, molybdenum, ruthenium, iodine, xenon, barium, cerium, and neodymium were measured using a Ge(Li) detector. The ratios were normalized through isobaric nuclides, and absolute yields were obtained by normalizing the sum of the heavy-mass yields to 100%.

The results indicate that the fine structure persists at this excitation energy. In particular, the peak at $A = 134$ which is so characteristic of thermal fission is still prominent in 14-MeV fission.

Canadian Journal of Chemistry, 46, 1663 (1968)

Introduction

Fine structure in the mass-yield curve has been well established for thermal or pile neutron fission of ^{235}U (1), ^{233}U (2), ^{238}U (3), ^{239}Pu (4), ^{241}Pu (5), and ^{229}Th (6), but no single comparable work exists for fission by neutrons of 14-MeV energy.

All of the yields for 14-MeV fission reported to date have been determined by radiochemical methods. Wahl (7) measured yields of ^{131}I–^{135}I in ^{235}U 14-MeV fission and observed that the fine-structure peak at $A = 134$ present in thermal fission was almost washed out at the higher energy. Ames *et al.* (8), Cuninghame (9), and James *et al.* (10) determined yields for the 14-MeV fission of ^{238}U but were unable to establish the presence of any fine structure, since in none of these works were yields for more than two consecutive masses determined. Broom (11) measured iodine yields in the mass region 131–135 and observed a fine-structure peak at $A = 132$. This was in agreement with the structure observed in spontaneous fission of ^{238}U but not with the work of Wahl (7) on ^{235}U or with the work done in this laboratory on the fast fission of ^{238}U (3).

In the present work the relative yields of xenon, krypton, and cesium isotopes were determined mass spectrometrically. The yields of some isotopes of krypton, strontium, zirconium, molybdenum, ruthenium, iodine, xenon, barium, cerium, and neodymium were determined relative to mass 99 by gamma-ray measurement with a Ge(Li) detector using the method of Gordon *et al.* (12). The xenon and cesium yields were related through their isobars at mass 135; the yields obtained from mass spectrometry and gamma-ray spectrometry were related through the isobars at masses 131, 132, 133, and 135. By combining these two methods it has been possible to obtain yields for all mass numbers between 131 and 147 with the exception of masses 138, 143, 144, 145, and 146. These were obtained by interpolation. Mass yields above 146 and below 131 were extrapolated with the aid of radiochemical data. Absolute yields were obtained by normalizing the sum of the relative yields in the heavy-mass peak to 100%.

Experimental

The principal limitation in this work was the 14-MeV neutron flux available. All irradiations were done with a Texas Nuclear model 9509 neutron generator which produces 14-MeV neutrons by the $^3H(d,n)^4He$ reaction. The neutron flux averaged over a target lifetime of about 5 h was 5×10^7 n cm^2/s. For a 30 h irradiation of 10 g of uranium, the number of atoms of a fission product formed in 6% yield is approximately 10^{19}. For cesium this is just at the limit of detection with the mass spectrometer. Because of the small sample size, contamination by naturally occurring elements was a problem and special precautions had to be taken to eliminate the contamination or to reduce it to a tolerable level.

(a) Mass Spectrometry

The samples used to obtain the krypton and xenon ratios consisted of 10 g of UCl_4 sealed in quartz. The UCl_4 was prepared by allowing uranium metal to react with chlorine in a closed system. The rare gases were released from the UCl_4 by heating it until it sublimed. The analyses were performed in a 10 in. radius, 90° sector, gas-source spectrometer with magnetic scanning. The irradiation data for these samples are given in Table I.

The samples for the determination of cesium consisted of approximately 50 g of UF_6 sealed in quartz. The UF_6

[1]Holder of NRCC Scholarship 1963–66 and B.A. Oil Co. Ltd. Fellowship 1966–67. Present address: Lawrence Radiation Laboratory, University of California, Berkeley, California, U.S.A.

Can. J. Chem. Downloaded from www.nrcresearchpress.com by 210.87.254.40 on 09/05/12
For personal use only.

TABLE I

Irradiation data for samples used to obtain relative yields of krypton and xenon isotopes

Sample	Length of irradiation (h)	t_1* (h)	t_2† (h)
1	23.5	6100‡	160
2	41.0	1920‡	670
3	41.0	2090‡	450
4	9.0	13.17	1.0
5	9.0	118.7	1.76
6	7.0	97.3	6.3

*t_1 = time from end of irradiation to extraction of rare gases.
†t_2 = time from extraction of rare gases to analysis of sample.
‡An average time taken from the midpoint of a series of irradiations over a period of 1 week.

was purchased from Atomergic Chemetals Co. and was purified using the fractional distillation procedure described by Claassen, Weinstock, and Malm (13). After irradiation, the UF_6 was distilled out of the sample tube leaving the nonvolatile fission products behind on the walls. The fission products were dissolved in a small amount of pure dilute HCl, evaporated to one drop, and applied to the filament of the mass spectrometer. The pure HCl was prepared by dissolving HCl gas in water which was purified by passage through a cation exchange column of Dowex 50W-X8. The analyses were performed in a 10 in. radius, 90° sector, solid-source mass spectrometer with magnetic scanning and a 12 stage electron multiplier. The UF_6 samples were irradiated for 6–8 h each day over a period of 1 week, and were allowed to cool for several months before the mass spectra were determined. The irradiation data are given in Table II.

TABLE II

Irradiation data for samples used to obtain relative yields of cesium isotopes

Sample	Length of irradiation (h)	Time from irradiation to analysis* (days)
1	23.5	71
2	21.0	101

*An approximate time taken from the midpoint of the series of irradiations.

(b) Gamma-ray Spectrometry

Three identical samples of natural uranium foil weighing 80 mg each were sealed in 0.5 mm thick polyethylene. These constituted samples A, B, and C. Sample A was irradiated in the thermal column of the McMaster reactor for 5 h at a thermal neutron flux of approximately 10^8 n cm^{-2} s^{-1}. Under these conditions only the ^{235}U in the sample undergoes fission; therefore sample A was used as the ^{235}U standard. Samples B and C were irradiated in a 14-MeV neutron flux of 10^8 n cm^{-2} s^{-1}. Since these samples contain 99.27% ^{238}U, and since the 14-MeV fission cross sections of ^{238}U and ^{235}U are comparable (14), essentially all of the fissions are from ^{238}U, as discussed below.

The detector used was an ORTEC model 8145 lithium-drifted germanium detector with a volume of 2 cm^3. The pulses were amplified with an ORTEC model 118A FET preamplifier and a model 410 linear amplifier. The full width at half-maximum of the 662-keV ^{137}Cs line was about 3.4 keV. Pulses were analyzed and stored in a Nuclear Data 4096 channel pulse height analyzer.

Gross fission-product gamma-ray spectra were obtained for samples A, B, and C at 3, 5, 6, 18, and 24 h after the end of the irradiation, with the samples still sealed in polyethylene. Thereafter spectra were recorded once a day for the first week and every 2 or 3 days for the next 2 weeks.

Because the fission cross section of ^{238}U (1.17 b) (15) is comparable to the (n,2n) cross section (880 mb) (16) at a neutron energy of 14 MeV, ^{237}U was produced in approximately the same yield as the fission products. ^{237}U has a number of gamma rays with energies less than 100 keV and these completely obscured any fission-product gamma rays below this energy, in particular the 91.1-keV gamma ray from ^{147}Nd. Therefore, in order to obtain the yield of ^{147}Nd it was necessary to separate it from the uranium after the irradiation. To accomplish this, another set of samples was prepared. Sample D was used as a standard and it consisted of 2 mg of U_3O_8 enriched to 93.18% in ^{235}U. This was sealed in a quartz capsule and irradiated in the McMaster reactor for 1 h at a flux of approximately 10^8 n cm^{-2} s^{-1}. Samples E and F consisted of 1 g of reagent grade uranyl nitrate sealed in a polyethylene capsule. They were irradiated in a 14-MeV neutron flux of 10^8 n cm^{-2} s^{-1} for 1 h. The uranyl nitrate was purified by adsorbing the uranium on Dowex AGl-X8 anion exchange resin in 9 *M* HCl solution. The rare earths were eluted with 9 *M* HCl and the uranium was eluted with water (17).

TABLE III

Irradiation data for samples used in activity measurement*

Sample	Neutron energy	Type of fission	Length of irradiation (h)
A	Thermal	^{235}U	5
B	14 MeV	^{238}U	5
C	14 MeV	^{238}U	5
D	Thermal	^{235}U	1
E	14 MeV	^{238}U	1
F	14 MeV	^{238}U	1

*In all cases the neutron flux was approximately 10^8 n cm^{-2} s^{-1}.

Approximately 12 h after the irradiation, samples D, E, and F were broken open and dissolved in 9 *M* HCl, and a mixture of rare earths was added as a carrier. The uranium was adsorbed on Dowex AGl-X8 anion exchange resin. Both uranium and rare-earth fractions were evaporated to dryness and spectra were taken of each. In samples D, E, and F, spectra were recorded once a day for 5 days after the irradiation.

The composition of these samples and the irradiation data are summarized in Table III and the prominent gamma rays observed are given in Table IV.

TABLE IV

Prominent gamma rays observed from fission products (reproduced from ref. 12)

Nuclide	Energy of peaks analyzed (keV)	Time analyzed after end of irradiation
4.4-h $^{85}Kr^{m}$	151.1	First day
9.7-h ^{91}Sr – 51-min $^{91}Y^{m}$	555.7	First 2 days
65-d ^{95}Zr – 35-d ^{95}Nb*	724.5, 757.2; 766.2	After 10 days
17-h ^{97}Zr – 73-min ^{97}Nb	743.5; 658.0	First 3 days
67-h ^{99}Mo – 6.0-h $^{99}Tc^{m}$	140.5	First 2 weeks
40-d ^{103}Ru	497.4	After 10 days
8.05-d ^{131}I	364.5	After 5 days
78-h ^{132}Te – 2.3-h ^{132}I	228.2; 667.8, 772.8	First 2 weeks
20.8-h ^{133}I – 5.3-d ^{133}Xe	529.9	First 3 days; after 2 weeks
9.2-h ^{135}Xe	249.7	First 3 days
82-min ^{139}Ba	165.8	First day
12.8-d ^{140}Ba – 40-h ^{140}La	537.4; 487.3	After 5 days
33-d ^{141}Ce†	145.6	After 10 days
33-h ^{143}Ce†	293.3	First 5 days
284-d ^{144}Ce*	133.3	After 1 month
11.1-d ^{147}Nd†	91.1	After 2 weeks
2.35-d ^{230}Np	209.4, 228.2, 277.5 316.2, 334.8	After 2 weeks
6.75-d ^{237}U	207.5	

*Not observed in ^{238}U spectra because of low activity of sample.
†Separated from uranium and measured first 5 days after irradiation.

Results

The isotopic abundances of fission-product krypton measured relative to mass 86 are shown in Table V. The final relative yields have been corrected for the presence of atmospheric krypton and for HBr background in the mass spectrometer.

The relative abundances of the xenon isotopes are given in Table VI. These have been corrected for contamination by atmospheric xenon and for decay and branching in the 133 and 135 mass chains.

[1] ^{133}I (20.8 h) → 0.024 → $^{133}Xe^{m}$ (2.3 d); ^{133}I (20.8 h) → 0.976 → ^{133}Xe (5.27 d) → ^{133}Cs (stable)

[2] ^{135}I (6.70 h) → 0.30 → $^{135}Xe^{m}$ (15.6 m); ^{135}I (6.70 h) → 0.70 → ^{135}Xe (9.20 h) → ^{135}Cs

The relevant equations are

$$[3]\quad N_1 = \frac{R_1}{\lambda_1}[1 - e^{-\lambda_1 T}]e^{-\lambda_1 t}$$

$$[4]\quad N_2 = N_2^{*}\, e^{-\lambda_2 t_2}$$

$$[5]\quad N_3 = N_3^{*}\, e^{-\lambda_3 t_2} + N_2^{*}\frac{\lambda_2}{\lambda_3 - \lambda_2} \times [e^{-\lambda_2 t_2} - e^{-\lambda_3 t_2}],$$

where

$$[6]\quad N_2^{*} = aR_1\left[\frac{(1 - e^{-\lambda_1 T})}{\lambda_2 - \lambda_1} e^{-\lambda_1 t_1} - \frac{\lambda_1(1 - e^{-\lambda_2 T})}{\lambda_2(\lambda_2 - \lambda_1)} e^{-\lambda_2 t_1}\right] + \frac{R_2}{\lambda_2}(1 - e^{-\lambda_2 T})\, e^{-\lambda_2 t_1}$$

and

$$[7]\quad N_3^{*} = aR_1\left[\frac{\lambda_2(1 - e^{-\lambda_1 T})}{(\lambda_2 - \lambda_1)(\lambda_3 - \lambda_1)} e^{-\lambda_1 t_1} - \frac{\lambda_1(1 - e^{-\lambda_2 T})}{(\lambda_2 - \lambda_1)(\lambda_3 - \lambda_2)} e^{-\lambda_2 t_1} + \left(\frac{1}{\lambda_3} + \frac{\lambda_1}{(\lambda_2 - \lambda_1)(\lambda_3 - \lambda_2)} - \frac{\lambda_2}{(\lambda_2 - \lambda_1)(\lambda_3 - \lambda_1)}\right)\right.$$

Can. J. Chem. Downloaded from www.nrcresearchpress.com by 210.87.254.40 on 09/05/12
For personal use only.

Can. J. Chem. Downloaded from www.nrcresearchpress.com by 210.87.254.40 on 09/05/12
For personal use only.

TABLE V

Relative yields of krypton isotopes

Sample	Relative abundance					
	80	82	83	84	85	86
1 Measured ratio	0.0616	0.1407	0.459	1.117	0.119	1.000
Relative yield (*a*)*			0.423	0.738	0.140	1.000
(*b*)			0.423	0.738	0.652	1.000
Standard deviation			0.007	0.020	0.015	
2 Measured ratio	0.0330	0.1502	0.464	1.281	0.103	1.000
Relative yield (*a*)			0.408	0.721	0.132	1.000
(*b*)			0.408	0.721	0.598	1.000
Standard deviation			0.017	0.022	0.014	
3 Measured ratio	0.0274	0.0803	0.449	0.967	0.130	1.000
Relative yield (*a*)			0.425	0.716	0.144	1.000
(*b*)			0.425	0.716	0.640	1.000
Standard deviation			0.006	0.008	0.007	
Average			0.423	0.716	0.635	1.000
Standard deviation			0.004	0.007	0.006	

*(*a*) Ratio corrected assuming that masses 80 and 82 are a mixture of atmospheric krypton and HBr; (*b*) krypton-85 corrected for decay assuming a 10.6-y half-life for Kr-85 and assuming that 22.5% of the 4.4-h isomer decays to the ground state of krypton.

TABLE VI

Relative yields of xenon isotopes

Sample	Relative abundance						
	129	131	132	133	134	135*	136
1 Measured ratio	0.983	1.168	1.482		1.000		0.873
Relative yield (*a*)†		0.622	0.782		1.000		0.888
Standard deviation		0.008	0.012				0.009
2 Measured ratio	0.0237	0.632	0.777		1.000		0.879
Relative yield (*a*)		0.618	0.759		1.000		0.880
Standard deviation		0.003	0.005				0.005
3 Measured ratio	0.332	0.798	0.995		1.000		0.885
Relative yield (*a*)		0.612	0.756		1.000		0.891
Standard deviation		0.006	0.006				0.010
4 Measured ratio	0.0143			0.388	1.000	0.315	0.882
Relative yield (*a*)				0.390	1.000	0.317	0.882
(*b*)†				0.934	1.000	0.906	0.882
Standard deviation				0.001		0.016	0.005
5‡ Measured ratio	0.0521			0.564	1.000		
Relative yield (*a*)				0.574	1.000		
(*b*)				0.987			
Standard deviation				0.009			
6 Measured ratio	0.0254			0.593	1.000		0.886
Relative yield (*a*)				0.592	1.000		0.887
(*b*)				0.948	1.000		0.887
Standard deviation				0.014			0.007
Average		0.618	0.760	0.935	1.000	0.906	0.883
Standard deviation		0.002	0.004	0.001		0.016	0.003

*Assuming independent yield of ^{135}Xe is 3.0 ± 1.5% of the chain.
†(*a*) Ratio corrected assuming that mass 129 is 100% natural xenon; (*b*) ratio corrected for holdup in isomeric state and independent yield of xenon.
‡Sample discarded due to large hydrocarbon contamination.

$$\times (1 - e^{-\lambda_3 T})\, e^{-\lambda_3 t_1}\Big]$$

$$+ bR_1\Big[\frac{(1 - e^{-\lambda_1 T})}{\lambda_3 - \lambda_1} e^{-\lambda_1 t_1}$$

$$- \frac{\lambda_1(1 - e^{-\lambda_3 T})}{\lambda_3(\lambda_3 - \lambda_1)} e^{-\lambda_3 t_1}\Big]$$

$$+ R_2\Big[\frac{(1 - e^{-\lambda_2 T})}{\lambda_3 - \lambda_2} e^{-\lambda_2 t_1}$$

$$- \frac{\lambda_2(1 - e^{-\lambda_3 T})}{\lambda_3(\lambda_3 - \lambda_2)} e^{-\lambda_3 t_1}\Big]$$

$$+ \frac{R_3}{\lambda_3}(1 - e^{-\lambda_3 T})\, e^{-\lambda_3 t_1}.$$

Here, T is the length of the irradiation, t_1 is the time from the end of the irradiation to the separation of the xenon from the iodine precursor, and t_2 is the time from the separation from the iodine to the determination of the ratios. N_1 represents ^{133}I or ^{135}I, N_2 is $^{133}Xe^m$ or $^{135}Xe^m$, and N_3 is ^{133}Xe or ^{135}Xe. R_1 is the rate of production of N_1 during the irradiation; R_2 and R_3 are the rates of production of N_2 and N_3 independently during the irradiation. The constants a and b are the branching ratios for the iodine. For the 133 mass chain $a = 0.024$, $b = 0.976$ and for the 135 chain $a = 0.30$, $b = 0.70$ (18). The independent yields of ^{133}Xe and ^{135}Xe were calculated using the Coryell displacement method (19). The fractional chain yield of ^{133}Xe is less than 0.008% and it was neglected. The fractional chain yield of ^{135}Xe was taken as 3.0 ± 1.5%. The corrected ^{135}Xe yield is not sensitive to the ratio R_2/R_3; it remains within the quoted errors for all values of this ratio from zero to infinity.

In spite of the precautions taken to purify the uranium, the cesium samples were found to contain a large amount of ^{133}Cs contamination, relative to the size of the sample, which was of the order of 10^9–10^{10} atoms of cesium. Because this contamination was 10^3–10^4 times the amount of ^{135}Cs and ^{137}Cs, it was not possible to measure any fission-product ^{133}Cs. Table VII gives the relative abundances of fission-product ^{135}Cs and ^{137}Cs corrected for contamination by natural barium from the ion-source filaments.

TABLE VII

Relative yields of cesium isotopes

Sample		Relative abundance 135	137
1	Measured ratio	1.00	0.860
	Relative yield (*a*)*	1.00	0.860
	(*b*)	1.00	0.863
	Standard deviation		0.116
2	Measured ratio	1.00	0.936
	Relative yield (*a*)	1.00	0.853
	(*b*)	1.00	0.863
	Standard deviation		0.130
Average		1.00	0.863
Standard deviation			0.086

*(*a*) Ratio corrected for natural barium contamination; (*b*) ratio corrected assuming a half-life for Cs-137 of 30.4 y.

The results from gamma-ray spectrometry are summarized in Tables VIII and IX. In each spectrum the peak areas were determined by

TABLE VIII

Results of measurements on gross fission-product spectra*

Mass chain (x)	y_x^{235}/y_{99}^{235}	R	Number of determinations	y_x^{238}/y_{99}^{238}
85 (Kr)	0.215	0.944±0.033	7	0.203±0.007
91 (Y)	0.964	0.691±0.045	6	0.666±0.043
97 (Zr;Nb)	1.005	0.954±0.062	19	0.959±0.062
99 (Tc)	1.000	1.000	—	1.000
103 (Ru)	0.495	1.89±0.24	10	0.936±0.120
131 (I)	0.484	1.46±0.14	16	0.707±0.068
132 (I)	0.723	1.10±0.12	32	0.795±0.087
133 (I)	1.092	1.01±0.08	13	1.10±0.09
135 (Xe)	1.064	1.04±0.06	9	1.11±0.06
139 (Ba)	1.059	0.861±0.041	4	0.912±0.043
140 (Ba,La)	1.031	0.800±0.087	10	0.825±0.090
143 (Ce)	0.942	0.822±0.076	14	0.744±0.072

*Fission yields for the heavy fragments in ^{235}U fission were taken from the work of Farrar and Tomlinson (1) and those for the light fragments from Katcoff (20).

Can. J. Chem. Downloaded from www.nrcresearchpress.com by 210.87.254.40 on 09/05/12
For personal use only.

TABLE IX

Results of activity measurements on separated rare-earth fraction*

Mass chain (x)	y_x^{235}/y_{143}^{235}	R	Number of determinations	y_x^{238}/y_{143}^{238}
141 (Ce)	1.004	1.14±0.04	11	1.14±0.04
143 (Ce)	1.000	1.000	—	1.00
147 (Nd)	0.378	1.26±0.07	5	0.476±0.026

*Fission yields for ^{235}U were taken from Farrar and Tomlinson (1).

summing the channels under the peak and subtracting a background which was estimated by averaging four channels on each side of the peak. The relative yields were determined using the following relation

$$[8] \quad \frac{y_x^{238}}{y_s^{238}} = \left(\frac{y_x^{235}}{y_s^{235}}\right)\left(\frac{h_x^{238}/h_s^{238}}{h_x^{235}/h_s^{235}}\right) = R\left(\frac{y_x^{235}}{y_s^{235}}\right),$$

where y_x^{238} = yield of nuclide x in ^{238}U 14-MeV neutron fission, y_s^{238} = yield of standard nuclide in ^{238}U 14-MeV fission, y_x^{235} = yield of nuclide x in ^{235}U thermal fission, y_s^{235} = yield of standard nuclide in ^{235}U thermal fission, h_x^{238} = measured peak area of nuclide x in spectrum from 14-MeV fission of ^{238}U, h_s^{238} = measured peak area of standard in ^{238}U fission, h_x^{235} = measured peak area of nuclide x in ^{235}U thermal fission, h_s^{235} = measured peak area of standard in ^{235}U fission.

The 140-keV ^{99}Tc peak was chosen as a standard in samples A, B, and C, since it is prominent in the spectrum for the first 2 weeks after the irradiation, during which time most of the measurements were made.

Because of the low activity of the samples it was necessary to correct for the presence of ^{234}Th contamination in samples E and F. ^{234}Th is produced from the α-decay of ^{238}U and it emits a gamma ray of the same energy as ^{147}Nd (91 keV). During the 19 h that elapsed between the purification of the ^{238}U and its final separation from the rare-earth fission products enough thorium was formed to interfere with the determination of the ^{147}Nd, as the ion-exchange procedure used did not separate thorium from the rare earths.

In order to correct this, a sample was prepared of the same weight as samples E and F, using uranyl nitrate in which the uranium and the thorium were in secular equilibrium. The activity of this sample was measured for the same length of time (4 h), with the same geometry as the sample containing the ^{147}Nd, and the number of counts in the peak was determined. The ratio of the thorium activity in the uranium sample soon after separation to the activity at equilibrium is

$$[9] \quad r = e^{-\lambda_1 t} - e^{-\lambda_2 t},$$

where λ_1 and λ_2 are the decay constants for ^{238}U and ^{234}Th respectively. From the measured count rate of the thorium at equilibrium the count rate of the thorium in the rare-earth sample was calculated using eq. [9]. This correction amounted to between 29 and 43% of the measured 91.1-keV peak area, depending on the length of time between the irradiation and the measurement of the peak.

In samples D, E, and F, the ^{99}Tc could not be used as a standard as it remained with the uranium fraction. In these samples, ^{143}Ce was taken as a secondary standard since its yield relative to ^{99}Tc was determined from samples A, B, and C. The relevant data for samples D, E, and F are given in Table IX.

The krypton yields were normalized to the yields obtained by counting through the ^{85}Kr yield which was measured by both methods, the

TABLE X

Relative and absolute yields of the light-mass fragments in 14-MeV fission of ^{238}U

Mass	Relative yield	Absolute yield (%)
83	0.115±0.006	0.748±0.043
84	0.194±0.010	1.26±0.071
85	0.172±0.009	1.12±0.06
86	0.271±0.014	1.76±0.10
91	0.563±0.042	3.66±0.29
97	0.811±0.060	5.27±0.41
99	0.846±0.032	5.50±0.24
103	0.792±0.105	5.15±0.69

Can. J. Chem. Downloaded from www.nrcresearchpress.com by 210.87.254.40 on 09/05/12
For personal use only.

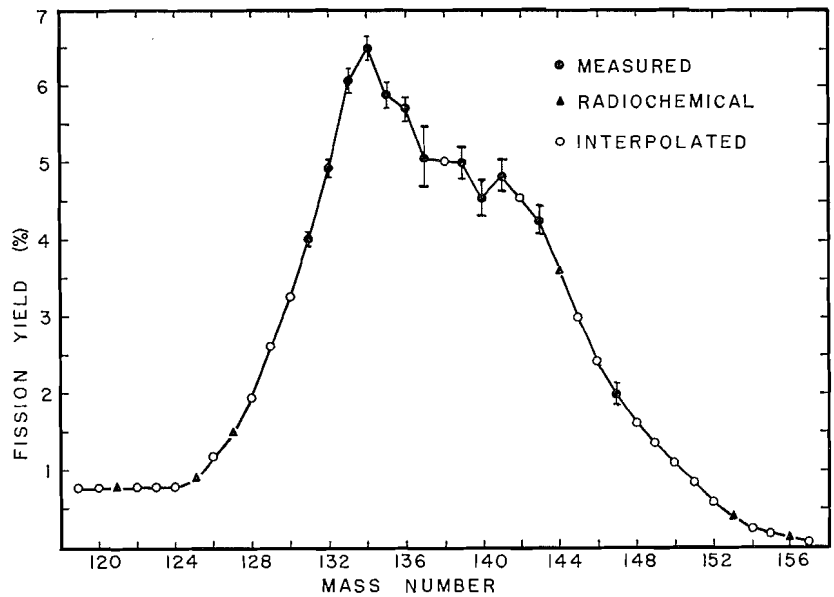

FIG. 1. Mass-yield curve for the heavy fragments in the 14-MeV neutron fission of ^{238}U.

xenon yields through the mass chains 131, 132, 133, and 135 which were measured by both methods. The relative yields thus obtained are shown in Tables X and XI.

In order to obtain absolute yields, the relative yields of the heavy-mass fission products were normalized such that they add up to 100%. In the mass region 131–147 only five relative yields were not experimentally determined, those of masses 138, 142, 144, 145, and 146. These were instead obtained by interpolation. Using the relative abundances of ^{153}Sm and ^{156}Eu determined by Cuninghame (9) and those of ^{121}Sn, ^{125}Sn, ^{127}Sb, and ^{144}Ce of Ames *et al.* (8), all with respect to ^{140}Ba, it was possible to extrapolate the mass-yield curve and obtain relative yields of masses 118–130 and 148–157. The absolute yields of the light fragments were computed using the calculated absolute yield of mass 134. The absolute yields thus obtained along with their standard deviations are given in Tables X and XI. These include a 2.3% normalization error as discussed below. The heavy-mass yields are plotted in Fig. 1 where the error bars indicate the standard deviation of the mean of the measured values.

TABLE XI

Relative and absolute yields of the heavy fragments in 14-MeV fission of ^{238}U

Mass	Relative yield	Absolute yield (%)
119–130*	2.456	15.98
131	0.618±0.002	4.02±0.09
132	0.760±0.004	4.94±0.11
133	0.935±0.001	6.08±0.14
134	1.000	6.50±0.15
135	0.906±0.016	5.89±0.17
136	0.883±0.003	5.74±0.13
137	0.782±0.079	5.08±0.52
138*	0.775	5.04±0.51†
139	0.772±0.047	5.02±0.33
140	0.698±0.081	4.54±0.53
141	0.745±0.058	4.84±0.39
142*	0.700	4.55±0.47†
143	0.655±0.066	4.26±0.44
144*	0.549	3.57±0.37†
145*	0.460	2.99±0.31†
146*	0.370	2.40±0.24†
147	0.312±0.036	2.03±0.24
148–157*	1.010	6.53
Total	15.386	100.00

*Obtained by interpolation and extrapolation.
†Estimated errors.

Discussion

The relative abundances reported in this work have been obtained by both mass-spectrometric and counting methods, both of which have their own different sources of errors.

Errors in the mass-spectrometric yields can arise through statistical and systematic errors in the measurements, and from the corrections for

Can. J. Chem. Downloaded from www.nrcresearchpress.com by 210.87.254.40 on 09/05/12
For personal use only.

Can. J. Chem. Downloaded from www.nrcresearchpress.com by 210.87.254.40 on 09/05/12
For personal use only.

decay and contamination. In general, the statistical errors have been less than 1% as can be seen from the standard deviations quoted for the individual measurements. Systematic errors can arise through mass discrimination in the source and at the electron multiplier in the mass spectrometer. Clarke,[2] using the same machine, has found no isotopic fractionation among the xenon isotopes and less than 1% between mass 82 and 86 among the krypton isotopes. Previous investigations (1–6) in this laboratory have shown no mass discrimination effect among the cesium isotopes. It was thus concluded that the mass discrimination effect was negligible in all cases reported here.

The correction for natural contamination involved in the xenon ratios was small, and the results from the six samples were all consistent within the quoted statistical errors. Only the ^{133}Xe and ^{135}Xe required corrections for decay and so these yields are affected by the values used for the half-lives and branching ratios. The largest uncertainty is the correction for the independent yield of ^{135}Xe and this is responsible for the larger error given for ^{135}Xe. Including the effects of uncertainty in half-lives, branching ratios, and independent yields, the ^{133}Xe and ^{135}Xe yields are believed to be reliable to 2% whereas the other xenon yields are believed to be within 1% of the true value.

The contamination correction for the krypton yields is less certain than that for the xenon yields and so the resulting krypton ratios are considered to be less accurate than the xenon ratios. It is unlikely that the ^{83}Kr and ^{85}Kr are in error by more than 5% but the ^{84}Kr could be in error by as much as 10%.

The statistical uncertainty (10%) in the cesium ratios is so large that effects such as mass discrimination, small errors in contamination corrections, and uncertainty in half-lives will be negligible in comparison.

There are three principal ways in which errors can arise in the yields measured by the counting technique: interference by another gamma ray of the same energy (within 1–2 keV), errors in the reported yields of the ^{235}U standard, and, where a chemical separation was performed, fractionation of different elements.

Interference by another gamma ray in the case of the ^{235}U is unlikely, since Gordon *et al.* (12) have made a study of this by determining the energies and half-lives of all the peaks that were measured here, and our resolution was comparable to that reported by these authors. It is possible that in ^{238}U 14-MeV fission, some nuclide (probably in the valley region) which is formed in higher yield than in ^{235}U might have a gamma ray which would interfere with one of those being measured. However, this should manifest itself in the ratio R (as defined in eq. [8]), changing systematically with time, since it is unlikely that the interfering nuclide would have both the same gamma-ray energy and half-life as those of the one being measured. Since R remained constant within statistical errors, the measured gamma rays seemed free of interference.

The heavy-mass yields in ^{235}U thermal fission were taken from the work of Farrar and Tomlinson (1). In the light-mass region the yields were normalized to the yields of Katcoff (20). In this work these yields were considered to be exact. This is reasonable, since their precision is certainly much better than the precision obtained in counting the low-activity samples obtained in this work.

The ^{147}Nd yield could be in error if, during the removal of the uranium, the neodymium and cerium somehow became partially fractionated. This is unlikely, as the anion exchange procedure used has been extensively studied (17) and the rare earths, with the exception of Ce(IV), are not adsorbed from 9 *M* HCl solution. The presence of Ce(IV) is ruled out, as it is unstable in hot hydrochloric acid solution, being reduced to Ce(III) with the simultaneous liberation of chlorine (21).

In general, the relative yields from masses 131–136 are believed to be accurate to 1%, while the remaining yields in the heavy peak are thought to have an accuracy of 5–10%.

Since natural uranium was used in the irradiations there is the possibility that a thermal-neutron component in the 14-MeV neutron flux might cause fission in the ^{235}U that is present. This can be ruled out as a possible source of error because no ^{239}Np was observed in the 14-MeV fission product spectrum from the ^{238}U. It was calculated that if no ^{239}Np were detected, the thermal flux would have to be less than 10^6 n cm^{-2} s^{-1}. Since ^{235}U comprises only 0.72% of the uranium in the sample, the maximum contri-

[2]W. B. Clarke, private communication.

TABLE XII

Absolute yields of fragments in ^{238}U 14-MeV fission

Mass chain	Absolute total chain yields				
	Ames *et al.* (1958) (8)	Cuninghame (1957) (9)	Broom (1962) (11)	James *et al.* (1964) (10)	This work
83				0.68	0.75
84				1.33	1.26
85					1.12
86					1.76
89	3.0	2.30	2.0		
90			3.4		
91		2.78	2.6		3.66
93				4.11	
97	4.8			5.97	5.27
99	5.7	5.58		6.47	5.50
103					5.15
105	3.4			2.65	
109				1.20	
111	0.87	0.81	0.6	0.98	
112				0.79	
113			0.6	0.87	
115	0.71	0.64		0.64	
121	0.73				
125	0.83				
127	1.43				
129				1.18	
131			2.7	4.60	4.02
132	4.7		4.5		4.94
133			2.6	6.65	6.08
134			4.7		6.50
135			5.0	5.59	5.89
136					5.74
137					5.08
139			4.4	4.92	5.02
140	4.6	4.41	4.3	4.67	4.54
141					4.84
143		3.91		3.51	4.26
144	3.4	2.68			
147		1.99			2.03
153		0.39			
156	0.22	0.13			

bution from ^{235}U fission products is less than 0.5%.

In order to determine absolute yields, the relative yields in the heavy-mass peak were normalized such that they add up to 100%. This procedure necessitated interpolation of the yields at masses 138, 142, 144, 145, and 146, and extrapolation of the curve above mass 147 and below mass 131. To aid in this, radiochemical yields at masses 153, 156 (9), 121, 125, 127, and 144 (8) were taken relative to ^{140}Ba.

Unless there is significant fine structure at masses 138, 142, 144, 145, and 146, it is unlikely that the interpolated yields will be systematically either high or low in comparison with the measured relative yields, and hence they will not contribute significantly to the normalization error.

The total of the measured and interpolated yields relative to ^{134}Xe given in Table XI is 15.386; the total of the extrapolated yields is 3.466. It may therefore be seen that, if the extrapolations had both been either high or low by 10%, the resulting error in the normalization would be only 2.3%. Although the extrapolations may be either high or low by 10%, it is unlikely that both would be high or low. Nevertheless, the 2.3% normalization error has been used.

The values of the fission yields from Tables X and XI are reproduced in Table XII along with the values of Ames *et al.* (8), Cuninghame (9), Broom (11), and James *et al.* (10) for comparison. In assessing these results, we must consider the fact that the relative xenon yields reported here are far superior in precision to any which have

Can. J. Chem. Downloaded from www.nrcresearchpress.com by 210.87.254.40 on 09/05/12
For personal use only.

Can. J. Chem. Downloaded from www.nrcresearchpress.com by 210.87.254.40 on 09/05/12
For personal use only.

been previously reported. Therefore, the reliability of any existing data which does not have approximately the same relative yields for masses 131–136 must be seriously questioned.

Particular attention is drawn to the work of Broom (11) whose iodine yields are in disagreement with this work. This author claimed to have observed a fine structure peak at $A = 132$; however, we find no evidence of this. On the basis of our results, the peak is definitely at mass 134, as predicted by Cuninghame (9).

The only other workers who have measured more than one yield in the region 131–136 are James *et al.* (10) and their relative yields at 131, 133, and 135 are in general agreement with our more accurate ones. The absolute yields quoted by James *et al.* are believed to be somewhat less reliable than those reported here in that, although they used the same method of normalization, their measured yields amounted to only 56% out of 200%, while our measured yields totalled 59% out of 100%.

The agreement between our absolute yields and those of Cuninghame (9) is quite remarkable, considering that his absolute yields were obtained by normalizing the area under the entire mass-yield curve on the basis of only 12 measured yields totalling 29% out of 200%.

It is difficult to compare the work of Ames *et al.* (8) with this work, since very few yields are common to both; however, in the cases where the same yield has been measured, the agreement seems reasonable.

In this work more consecutive heavy-mass yields have been determined than in any previous work, and because of the methods used, the errors are more easily assessed. Although other individual radiochemical yields might prove to be more accurate, the data reported here should certainly give the best overall picture of the general shape of the heavy-fragment mass-yield curve.

The most significant feature of the mass-yield curve for 14-MeV fission as shown in Fig. 1 is the persistence of the fine structure.

The large peak appears at mass 134 as predicted by Cuninghame (9) while the peak at $A = 132$ reported by Broom (11) was not observed.

Acknowledgments

We wish to thank Dr. W. B. Clarke for his help in analyzing the rare gas samples.

The financial support of the National Research Council of Canada and the British American Oil Co. Ltd. is gratefully acknowledged.

1. H. Farrar and R. H. Tomlinson. Nucl. Phys. **34**, 367 (1962).
2. D. R. Bidinosti, D. E. Irish, and R. H. Tomlinson. Can. J. Chem. **39**, 628 (1961).
3. C. K. Mathews. Ph.D. Thesis, McMaster University, Hamilton, Ontario. October 1964.
4. H. R. Fickel and R. H. Tomlinson. Can. J. Phys. **37**, 926 (1959).
5. H. Farrar, W. B. Clarke, H. G. Thode, and R. H. Tomlinson. Can. J. Phys. **42**, 2063 (1964).
6. J. W. Harvey, W. B. Clarke, H. G. Thode, and R. H. Tomlinson. Can. J. Phys. **44**, 1011 (1966).
7. A. C. Wahl. Phys. Rev. **99**, 730 (1955).
8. D. P. Ames, J. P. Balagna, J. W. Barnes, A. A. Comstock, G. A. Cowan, P. B. Elkin, C. P. Ford, J. S. Gilmore, D. C. Hoffman, C. W. Knobelock, E. J. Lang, M. A. Melnick, C. D. Minkkinen, B. D. Pollock, J. E. Sattizahn, C. W. Stanley, and B. Waren. LA-1997 (declassified, 1958).
9. J. G. Cuninghame. J. Inorg. Nucl. Chem. **5**, 1 (1957).
10. R. H. James, C. R. Martin, and D. J. Silvester. Radiochim. Acta, **3** (1/2), 76 (1964).
11. K. M. Broom. Phys. Rev. **126**, 627 (1962).
12. G. E. Gordon, J. W. Harvey, and H. Nakahara. Nucleonics, **24**(12), 62 (1966).
13. H. H. Claassen, B. Weinstock, and J. G. Malm. J. Chem. Phys. **25**, 426 (1956).
14. E. K. Hyde. The nuclear properties of the heavy elements. Vol. III. Fission phenomena. Prentice-Hall, New York. 1964.
15. A. Hemmendinger. Proc. U.N. Intern. Conf. Peaceful Uses At. Energy, 2nd, Geneva, 1958, **15**, p. 344, P/663 (1958).
16. Table of cross sections for fast neutron reactions. 2nd ed. Texas Nuclear Corp., Austin, Texas. January 1964.
17. K. A. Kraus and F. Nelson. Proc. Intern. Conf. Peaceful Uses At. Energy, Geneva, 1955, **7**, p. 113, P/837 (1955).
18. C. M. Lederer, J. M. Hollander, and I. Perlman. Table of isotopes. 6th ed. Wiley, New York. 1967.
19. C. D. Coryell, M. Kaplan, and R. D. Fink. Can. J. Chem. **39**, 646 (1961).
20. S. Katcoff. Nucleonics, **18** (11), 201 (1960).
21. I. M. Kolthoff and E. B. Sandell. Textbook of quantitative inorganic analysis. 3rd ed. Macmillan, New York. 1952. p. 581.

Can. J. Chem. Downloaded from www.nrcresearchpress.com by 210.87.254.42 on 09/05/12
For personal use only.

Dielectric properties of the hydrates of argon and nitrogen[1]

S. R. GOUGH, E. WHALLEY, AND D. W. DAVIDSON
Division of Applied Chemistry, National Research Council of Canada, Ottawa, Canada

Received December 5, 1967

The dielectric relaxation of water in the structure I clathrate hydrates of argon and nitrogen was studied over a range of temperature and pressure. Hydrates were slowly grown at pressures of 1 to 2 kbar in a coaxial cell enclosed in a pressure vessel. The complex permittivity loci resemble circular arcs with static dielectric constants of ~ 56 at 0 °C and high-frequency dielectric constants of 2.85 $\pm$ 0.05. Relaxation near 0 °C is about as slow as in ice I, but activation energies and entropies are much smaller. Formation of Bjerrum defects probably takes place preferentially near the occasional sites at which argon and nitrogen molecules have replaced water molecules in the lattice. The much faster relaxations found previously in the isostructural hydrates of ethers arise from orientational defects induced in the water lattice by the encaged molecules, a small proportion of which may form hydrogen bonds with water. The effect of small gaps in series with samples showing circular-arc dispersion behavior was evaluated.

Canadian Journal of Chemistry, 46, 1673 (1968)

Dielectric relaxation associated with the reorientation of water molecules in ice (1, 2) and its high-pressure modifications (3, 4) has been previously studied. The gas, or clathrate, hydrates (5) are further examples of ices whose lattices consist of hydrogen-bonded four-coordinated water molecules. Stability is conferred upon these hydrates by the presence in the lattice cages of guest molecules, which typically seem to interact only weakly with the water molecules of the host lattice (5, 6).

The earlier dielectric studies of the water relaxation in clathrate hydrates were mainly confined to hydrates of rather large water-soluble ethers and ketones, viz. those of acetone (7); ethylene oxide (8); tetrahydrofuran, 2,5-dihydrofuran, propylene oxide, and trimethylene oxide (9); 1,3-dioxolane (10); dimethyl ether and cyclobutanone (11). In these hydrates the relaxation rates were found to be several orders of magnitude faster than in ice I and the activation energies only about half as great. Although the shapes of the dispersion loci appeared to be characteristic of the lattice structure for the structure II hydrates (9–11), the relaxation rates depended somewhat on the nature of the guest molecules. Except for the structure I hydrate of ethylene oxide (12), the smaller cages of all these hydrates are essentially unoccupied. Moreover, all of these hydrate formers are capable of relatively strong interaction, i.e. of hydrogen bonding, with water molecules. It is known from microwave absorption measurements (6) that in ethylene oxide and tetrahydrofuran hydrates the rotation of the guest molecules is only slightly hindered, but this does not exclude the possibility that a guest molecule may occasionally hydrogen bond to a lattice water molecule. Since these factors may well affect the details of the mechanism of relaxation of the water lattice, it is of considerable interest to examine the relaxation behavior of hydrates of small nonpolar molecules which fill both large and small cages almost quantitatively and which are incapable of hydrogen bonding to the water molecules of the lattice.

The results of a study of the temperature and pressure dependence of the dielectric properties of argon and nitrogen hydrates are reported here. Argon is the smallest molecule known to form a clathrate hydrate. Its hydrate is stable at 0 °C under argon pressures greater than 96 bars (13). Nitrogen hydrate is stable at 0 °C under pressures above 160 bars (13, 14). The decomposition pressures of both hydrates reach 1700 bars at 25 °C.

Experimental Methods

The cell (shown schematically in Fig. 1) consisted of a three-terminal stainless-steel coaxial electrode system mounted in a Teflon cylinder B which was contained by a brass sleeve. The bottom of B was attached to the lower pressure head by the binding post C, which was electrically connected to the outer (high-potential) electrode. The low-potential electrode A was guarded at the bottom. A brass ring D provided shielding between the binding posts C and E in the gas-filled region where their mutual capacitance would otherwise be variable. A small fixed capacitance resulted from interaction within the insulation between binding posts and mounting screws. This

[1]Issued as NRCC No. 9962.

Can. J. Chem. Downloaded from www.nrcresearchpress.com by 210.87.254.42 on 09/05/12
For personal use only.

and the cell constant were measured by calibration with air, cyclohexane, and conductivity water. The electrical connections, seals, and pressure vessel were as previously described (2).

Pressure was generated by a compressed-air-driven oil pump and transmitted to argon or nitrogen by a 3-kbar gas compressor. Pressures were read on a large calibrated 3-kbar Heise gauge. The pressure vessel containing the cell was immersed in an ethanol bath cooled to as low as −100 °C by a three-stage refrigeration unit designed and built by the Plant Engineering Division of NRCC. The bath temperature was regulated by adjustment of the flow rate of refrigerant through the cooling coils and by thermistor-controlled immersion heaters. Temperatures were measured by a calibrated copper–constantan thermocouple F (Fig. 1) inserted into the lower head of the pressure vessel to within 3″ of the center of the sample.

Capacitance and loss between 50 Hz and 500 kHz were measured by the earlier methods (15). For nitrogen hydrate measurements were extended to 0.05 Hz by use of a low-frequency bridge constructed according to a design of Professor R. H. Cole, to whom we are indebted.

The hydrates were grown in situ by subjecting freshly degassed conductivity water to gas pressures much above the hydrate decomposition pressure. Formation of hydrate, which was followed by changes in the dielectric properties of the sample, was very slow, presumably because of a hydrate crust formed at the water–gas interface. Repeated temperature and pressure cycling between about +10 and −40 °C and 1 and 3 kbar increased the formation rate, probably by cracking this crust. Even so, complete conversion to hydrate usually required from 3 to 5 weeks.

The problem of quantitative formation of clathrate hydrates of water-insoluble molecules, even with shaking, has long plagued attempts to define their compositions accurately. (See, for example, ref. 16 for a review of early disagreements in analyses, and ref. 13 for a recent unsuccessful attempt to directly determine the composition of methane hydrate.) For the present hydrates, the conductances measured at frequencies small in comparison with the frequency of maximum dielectric absorption were particularly sensitive to small quantities of water in the sample and served to monitor the disappearance of liquid water. Excess water in a sample of argon hydrate formed at 3 kbar led at low temperatures to a separate absorption region at higher frequencies whose amplitude diminished with conditioning and which was attributed to ice III.

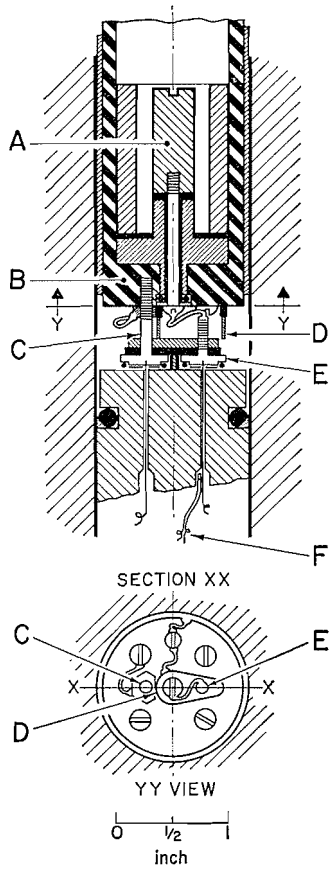

FIG. 1. Schematic of dielectric cell assembly.

Results

The Dispersion Loci

Typical experimental complex dielectric constant plots of argon and nitrogen hydrates are given in Figs. 2 and 3. In all some 50 such curves were obtained. The shapes conform quite closely to depressed circular arcs. The Cole–Cole α parameter increases greatly with decreasing temperature from values of about 0.1 at temperatures above 0 °C to 0.25 (for nitrogen hydrate) at −70 °C. The dispersion loci of nitrogen hydrate are somewhat broader than those of argon hydrate at the same temperature.

As with the hydrates previously studied (7, 9, 10) there are noticeable departures from arcs at low temperatures, especially at high frequencies where ε'' approaches the ε' axis more steeply than the circular arc. Departures of this kind also are observed on the low-frequency side of the absorption region when not obscured by the additional absorption associated with ionic conductance (see Fig. 3, upper locus).

In deriving dielectric parameters from the experimental data, we have taken the Cole–Cole representation (see eq. [1], p. 1676) to be adequate, except for ε_∞, which was obtained by extrapolation to the ε' axis of the high-frequency side of the experimental locus rather than from the best fit of a circular arc to the locus as a whole.

Can. J. Chem. Downloaded from www.nrcresearchpress.com by 210.87.254.42 on 09/05/12
For personal use only.

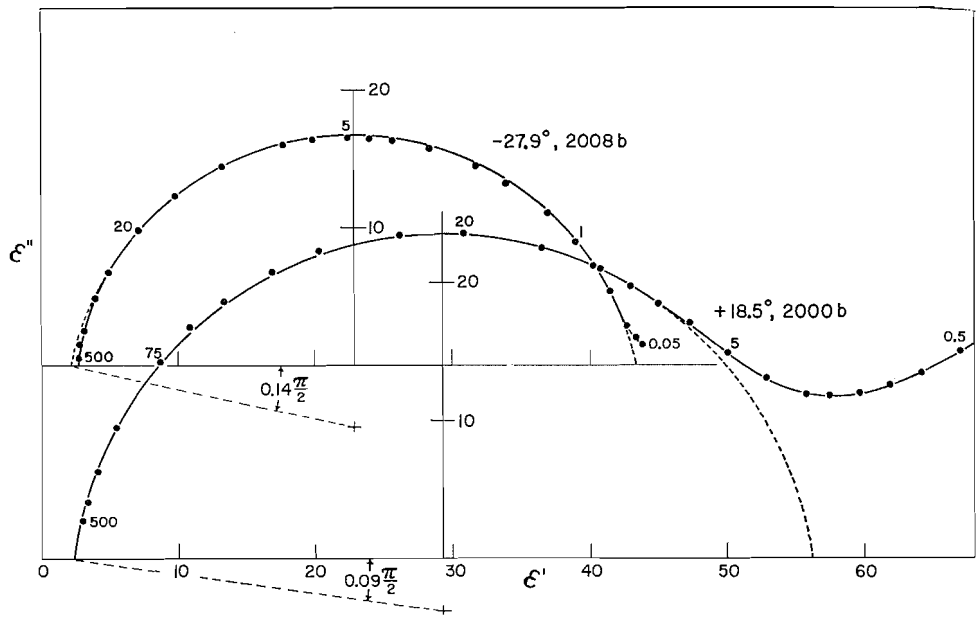

FIG. 2. Complex permittivity loci of argon hydrate. Numbers on loci are frequencies in kHz.

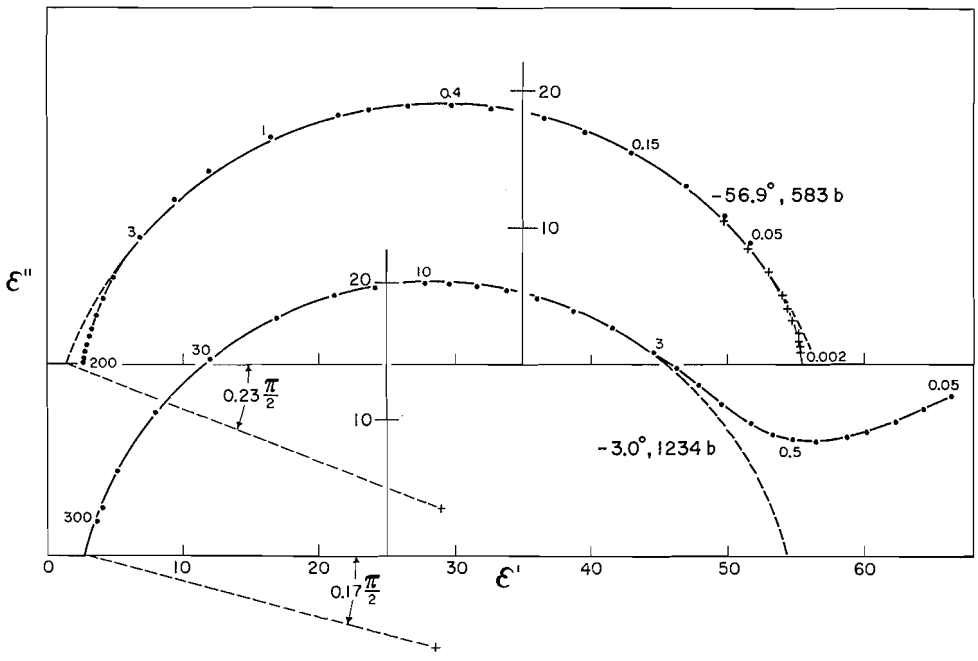

FIG. 3. Complex permittivity loci of nitrogen hydrate. Crosses refer to low-frequency bridge measurements.

TABLE I

Representative dielectric parameters

Sample	t (°C)	P/bar	ε_0(exp)	τ(exp)/μs	α	ε_0 (eq. [9])	τ/μs (eq. [8])	$10^3\,\delta$
				Argon hydrate				
1	18.5	2000	54.3	8.0	.08	53.7	8.0	0
1	18.8	2985	48.3	7.3	.08	54.2	8.3	3
1	9.2	2080	41.6	9.5	.09	55.4	13.0	9
2	3.9	2010	48.7	11.4	.12	56.4	13.5	4
1	−4.5	1990	33.9	11.8	.09	58.0	21.2	18
2	−13.3	2028	45.8	20.4	.12	59.8	27.6	8
2	−22.8	2013	43.4	27.0	.13	61.9	40.6	10
2	−28.1	2000	41.4	31.8	.14	63.2	52.0	13
				Nitrogen hydrate				
3	10.5	1795	~60	8.2	.11	55.0	8.2	0
2	3.0	1233	58	12.6	.14	56.1	12.6	0
1	−9.3	592	55.4	21.7	.17	58.2	23.0	1
1	−21.8	620	52.4	39.8	.20	60.9	48.1	3
2	−35.4	1235	64.6	161	.21	64.5	161	0
1	−45.6	1255	53.7	242	.20	67.2	319	5
3	−50.3	3	57.4	215	.22	67.7	317	3
3	−69.8	1	43.2	730	.26	73.8	1520	10
2	−70.8	808	67.6	1150	.23	74.8	1320	2

Some representative experimental values of static dielectric constant ε_0(exp), α, and relaxation time τ(exp) are given in Table I. Values of ε_∞ lay in the range 2.70 to 2.85.

At relatively high temperatures the measured static dielectric constants (e.g. 54 ± 2 for argon hydrate at 20 °C, 56 ± 2 for nitrogen hydrate at 0 °C) were quite reproducible and, despite the difference of lattice structure, similar to values (e.g. 57 ± 2 at 20 °C) estimated from earlier measurements of structure II hydrates of polar molecules (9, 10) with the dipolar contribution of the guest molecules subtracted. At lower temperatures, however, the apparent values of the static dielectric constant varied considerably from sample to sample and with sample history. They sometimes showed a decrease with decrease of temperature, especially marked for argon hydrate, rather than the increase expected. These effects undoubtedly arose from cracking or shrinkage of the samples away from the electrode surfaces. Such sample contraction affects not only the amplitude of the measured dispersion locus, but also its dependence on frequency. An analysis of contraction effects follows.

The Uniform Gap Model for Cole–Cole Behavior

The complex dielectric constant of the Cole–Cole locus is (17)

$$[1] \qquad \varepsilon^* = \varepsilon_\infty + \Delta\varepsilon[1 + (ix)^\beta]^{-1},$$

where $\Delta\varepsilon$ is $(\varepsilon_0 - \varepsilon_\infty)$, $x = \omega\tau$, τ is the relaxation time corresponding to $1/\omega$ at the frequency of maximum dielectric absorption, and $\beta = 1-\alpha$.

If the effect of sample shrinkage may be represented by a gap of uniform thickness a fraction δ of the interelectrode distance, in series with the sample, the measured complex dielectric constant is

$$[2] \qquad \varepsilon^*(\text{exp}) = k\varepsilon^*[\delta\varepsilon^* + (1 - \delta)k]^{-1},$$

where ε^* is the sample complex dielectric constant and k is the dielectric constant (assumed to have only a real component) of the medium which fills the gap. Substitution of [1] in [2] leads to

$$[3] \qquad \varepsilon^*(\text{exp}) = [k\varepsilon_0 + k\varepsilon_\infty(ix)^\beta] \times [b + a(ix)^\beta]^{-1},$$

in which $a = \delta\varepsilon_\infty + (1 - \delta)k$ and $b = \delta\varepsilon_0 + (1 - \delta)k$. At the low- and high-frequency limits eq. [3] reduces to

$$[4] \qquad \varepsilon_0(\text{exp}) = k\varepsilon_0/b \text{ and } \varepsilon_\infty(\text{exp}) = k\varepsilon_\infty/a.$$

Substitution for ε_0 and ε_∞ in eq. [3] gives

$$[5] \qquad \varepsilon^*(\text{exp}) = \varepsilon_\infty(\text{exp}) + \Delta\varepsilon(\text{exp})[1 + (a/b)(ix)^\beta]^{-1}$$

in which $\Delta\varepsilon(\text{exp}) = \varepsilon_0(\text{exp}) - \varepsilon_\infty(\text{exp})$. Equation [5] has the same form as the Cole–Cole eq. [1] and describes a locus of the same shape. However, $x^\beta = \omega^\beta\tau^\beta$ has been replaced by

Can. J. Chem. Downloaded from www.nrcresearchpress.com by 210.87.254.42 on 09/05/12
For personal use only.

TABLE II

Effect of the gap corrections for nitrogen hydrate

t (°C)	P/bar	ε_0(exp)	τ(exp)/μs	α	ε_0 (eq. [9])	τ/μs (eq. [8])	$10^3\ \delta$
−3.03	1234	54.3	16.8	0.17	57.3	17.9	1.3
−3.24	1888	48.4	15.6	0.17	57.6	19.2	4.7
−3.26	601	52.2	15.9	0.17	57.0	17.7	2.0
−3.32	1233	47.1	14.5	0.17	57.3	18.3	5.1

$(a/b)x^\beta = \omega^\beta(a/b)\tau^\beta$, that is, the apparent relaxation time is now

$$[6] \qquad \tau(\text{exp}) = (a/b)^{1/\beta}\tau.$$

To the extent that the observed dispersion loci are Cole–Cole arcs the adequacy of this model may be tested by the consistency of the values of τ derived from experimental relaxation times by use of eq. [6]. For this purpose the proper values of ε_0 and ε_∞ are required. A knowledge of k is not explicitly required for eq. [6], but is necessary for an estimation of the effective gap thickness

$$[7]^2 \qquad \delta = k\left[\frac{\epsilon_0}{\epsilon_0(\text{exp})} - 1\right](\epsilon_0 - k)^{-1}.$$

If δ and ε_∞ are small, and $\varepsilon_0 \gg \varepsilon_\infty$, little error is introduced by putting $a/b = \varepsilon_0(\text{exp})/\varepsilon_0$, whence

$$[8] \qquad \tau = [\varepsilon_0/\varepsilon_0(\text{exp})]^{1/(1-\alpha)}\tau(\text{exp}).$$

Application of the Gap Model to the Data

For application of eq. [8], ε_0 as a function of temperature and pressure is required. For argon and nitrogen hydrates we take

$$[9] \qquad \varepsilon_0 = (4.0 + 14200/T)(1 + 0.010P),$$

where P is the pressure in kbar. This equation fits the experimental values of ε_0 (± 2) at high temperatures, when the gaps are inappreciable, and allows for variations of ε_0 with temperature and pressure similar to those of the other forms of ice (1–3).

Values of ε_0 from [9] and of τ from [8] are included in Table I, along with the estimates of the relative gap thickness δ from [7]. Values of k were crudely evaluated by extrapolating to lower temperatures the dielectric constants of gaseous argon and nitrogen measured under pressure (18, 19). Values of δ did not exceed 0.015 for nitrogen hydrate and 0.018 for argon hydrate.

The gap correction reduces considerably the variability of the original relaxation time τ(exp). The data in Table II for sample 2 of nitrogen hydrate at −3 °C illustrate this. The relaxation times for the two sets of measurements at 1230 bar are brought into close agreement and the τ's now clearly increase with increasing pressure as they do for other ices (2–4). Figure 4 shows the general improvement in consistency which results.

The series-gap treatment does not reduce the scatter of the relaxation times, particularly between different samples, to the level of uncertainty (ca. 1%) with which τ may be measured in the absence of gaps. Some of the residual scatter suggests overcorrection for the larger gaps. This may arise because the real static dielectric constants are somewhat less than those given by eq. [9] or the gaps are not of uniform thickness. However, certain consistent differences between results for different samples suggest some variation of the relaxation behavior with the conditions of preparation and history of the sample. Thus initial measurements on sample 3 of nitrogen hydrate at a number of temperatures (not shown in Fig. 4) yielded smaller α's and τ's than those previously measured. These anomalies, which do not seem attributable to the presence of ice, disappeared after several days of conditioning.

Discussion

High-Frequency Dielectric Constants

Values of ε_∞ for both argon and nitrogen hydrate (2.85 ± 0.05 at −30 °C after small gap

[2]Strictly, δ is the ratio of gap thickness to electrode separation only for parallel plate electrodes. For cylindrical coaxial electrodes of radii u and v, δ in the above equations is replaced by $\Delta r/[r \ln (v/u)]$, where r is the radial position of a small gap of uniform thickness Δr. In the likely event that contraction occurs by shrinkage away from the outer electrode, δ is replaced, for the actual electrodes used, by $0.78\delta'$, where $\delta' = \Delta r/(v-u)$.

Can. J. Chem. Downloaded from www.nrcresearchpress.com by 210.87.254.42 on 09/05/12
For personal use only.

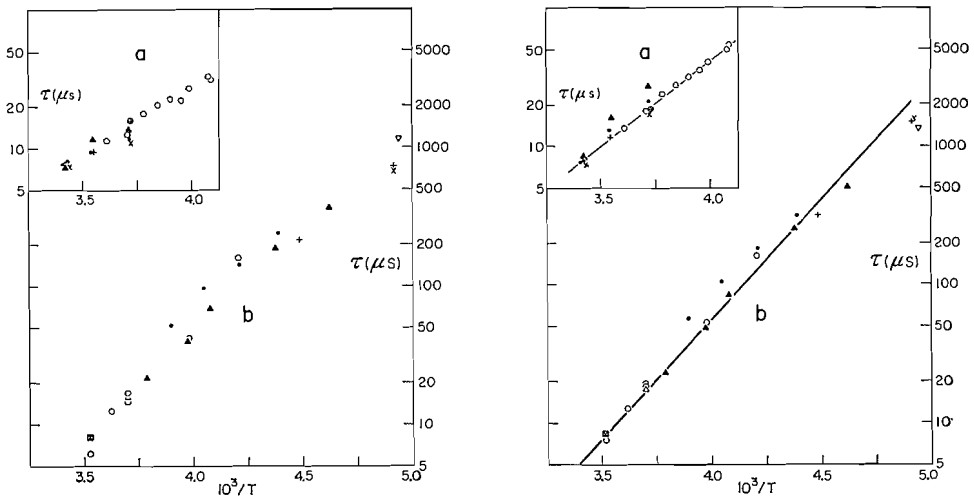

FIG. 4. Experimental (left) and gap-corrected (right) relaxation times at various pressures. (*a*) Argon hydrate. Sample 1: ⊕, 300; +, 800; ×, 1100; ●, 2000; ▲, 3000 bar. Sample 2: ○, 2000 bar. (*b*) Nitrogen hydrate. Sample 1: ▲, 600; ●, 1240 bar. Sample 2: △, 620; ▽, 810; ○, 1240 bar. Sample 3: +, 1; ×, 310;□, 1800 bar.

corrections) are similar to that of ice (3.1), in contrast to the much higher values found for the hydrates of dipolar molecules, to which the reorientation of the guest molecules makes a large contribution (6, 9, 10).

For a solution of argon or nitrogen in the structure I hydrate lattice the Onsager equation may be written (20)

$$[10]\quad \frac{(\epsilon_\infty - 1)(2\epsilon_\infty + 1)}{3\epsilon_\infty} = \frac{4\pi N_0\alpha_0}{1 - f_0\alpha_0} + \frac{4\pi N_1\alpha_1}{1 - f_1\alpha_1},$$

where N is the number density of molecules, α is the molecular polarizability, $f\alpha$ allows for the reaction field, and the subscripts 0 and 1 refer respectively to water and argon or nitrogen. The empty lattice contribution cannot be evaluated in terms of the polarizability of the isolated water molecule since lattice vibrations make important contributions. Instead, we take

$$[11]\quad \frac{4\pi N_0\alpha_0}{1 - f_0\alpha_0} \simeq \left[\frac{(\epsilon_\infty - 1)(2\epsilon_\infty + 1)}{3\epsilon_\infty N_0}\right]_{\text{Ice I}} N_0,$$

in which ϵ_∞ and N_0 in the square brackets refer to ice I. Equation [11] assumes a contribution, per water molecule, of the empty hydrate lattice equal to that of ice and leads to a value of ϵ_∞ of 2.78 for the empty lattice if the unit cell dimension is 12.05 Å. Addition of the contribution of the encaged molecules gives $\epsilon_\infty = 2.90$ for argon hydrate and $\epsilon_\infty = 2.91$ for nitrogen hydrate if all the cages are occupied.

Thus eq. [11] appears to provide a good approximation to the effective polarizability of the water lattice in these hydrates. As in ice, ϵ_∞ is considerably greater than n_D^2 which is ~ 1.72 for both hydrates and ice. It is probable that the lattice vibrations are similar, especially the translational modes which are associated with the optical density maximum in ice at 229.2 cm^{-1} at 100 °K (21). Even after correction for gaps, values of ϵ_∞ for nitrogen hydrate decrease slightly with decrease of temperature, despite the increase of density. This decrease amounts to 0.08 ± 0.04 between −30 and −94 °C and probably arises from a general shift toward higher frequencies of the lattice modes.

Static Dielectric Constants

Since encaged argon and nitrogen molecules contribute only about 0.1 to the dielectric constants, the static dielectric constants are essentially those of the ice-like lattice. Substitution of $\epsilon_0 = 56$ at 0 °C into the Kirkwood equation in the form

$$[12]\quad \epsilon_0 - \epsilon_\infty = 2\pi N_0[(n^2 + 2)/3]^2 g\mu^2/kT,$$

with $n^2 = 1.60$ (from the Lorentz–Lorenz equation and $n^2 = 1.72$ for ice) and $\mu = 1.84$ D,

Can. J. Chem. Downloaded from www.nrcresearchpress.com by 210.87.254.42 on 09/05/12
For personal use only.

TABLE III

Relaxation times and activation parameters for structure I hydrates and ices I and III at 0 °C

	P/bar	τ/μs	E_A (kcal mole^{-1})	$\Delta S^{\neq}$ (cal deg^{-1} mole^{-1})	$\Delta V^{\neq}$ (cm^3 mole^{-1})	Reference
Argon hydrate	2000	16	5.7	−17.5	3	This work
Nitrogen hydrate	1200	15	7.9	− 9.4	2	This work
Ethylene oxide hydrate	1	0.027	6.7	− 1.2		8
Trimethylene oxide hydrate*	1	0.005	5.8	− 1.3		9
Ice I	1	21.5	13.25	+ 9.5	2.9 (−23 °C)	1, 2
Ice III†	3000	0.19	11.6	+13.0	4.5 (−30 °C)	3

*Extrapolated from data below −74 °C.
†Extrapolated from data below −22 °C.

gives a g value of 2.5. This is significantly smaller than the value of 3.3 for ice I, but is comparable to the value of 2.7 found for ice III (3) and for structure II hydrates (9). Clearly again the hydrogen bonding imposes a considerable local correlation between the directions of the dipole moments of water molecules.

Relaxation Times

Reorientation of the water molecules in argon and nitrogen hydrates is remarkably slow in comparison with their reorientation in the clathrate hydrates previously studied. The relaxation times at 0° C (Table III) are larger by several orders of magnitude than those of the isostructural hydrates of ethylene oxide (8) and trimethylene oxide, the latter extrapolated from results at much lower temperatures (9).[3] The structure II hydrates of several ethers and ketones (7, 9–11), have relaxation times of about 0.1 μs at 0 °C.

At relatively high temperatures, argon and nitrogen hydrates relax as slowly as ice I, the slowest of the disordered ices to relax. The relaxation times depend much less on temperature, however, and the activation energies (Table III) are similar to those of other hydrates.

The activation volumes (2 or 3 cm^3 mole^{-1}) are indistinguishable from the activation volume of ice I. Because of small differences between samples, and the small effect of pressure on the relaxation times, activation volumes were derived only from measurements on the same sample. They almost certainly refer to hydrates of constant composition, rather than to hydrates whose compositions attain new equilibrium values in response to a change of pressure.

Shape of the Dispersion Curves

The shapes of the dispersion loci of structure II hydrates and their change with temperature appear to be characteristic of the crystal structure (9–11). This is not the case for the four structure I hydrates for which information is available if the shapes are compared at the same temperatures. Values of α of about 0.1 are found above 0 °C for argon and nitrogen hydrates, at −80 °C for ethylene oxide hydrate, and at −110 °C for trimethylene oxide hydrate, at which temperatures the relaxation times of all these hydrates are similar. However, if the width of the dispersion is entirely dictated by the degree of non-equivalence of water molecule sites and hydrogen bonds in the lattice, identical structures should lead to identical α's at the same temperature. The size of the unit cell is known to vary slightly for different encaged molecules (23, 24). The extent to which the positions of the water molecules vary within the unit cell is unknown, but is likely to be too small to markedly affect the value of α. The relatively broad loci shown by argon and nitrogen hydrates are probably partly due to factors other than non-equivalence of the hydrogen bonds (see next section).

Mechanism of Relaxation

There are several suggestive regularities in the activation parameters for relaxation of the various phases of "ice" listed in Table III of this paper and in Table III of the following paper (25). The Arrhenius activation energies fall into two groups, with values in the ranges 5.7 to 8.7 (average about 7) and 11.0 to 13.3 kcal mole^{-1}, respectively. The group with high

[3]In addition to a hydrate of structure II, trimethylene oxide forms a second hydrate (9) which Calvert's X-ray diffraction studies (22) have now confirmed to be structure I.

Can. J. Chem. Downloaded from www.nrcresearchpress.com by 210.87.254.42 on 09/05/12
For personal use only.

Can. J. Chem. Downloaded from www.nrcresearchpress.com by 210.87.254.42 on 09/05/12
For personal use only.

activation energies is also characterized by relatively high positive entropies of activation, 9 to 13 cal deg^{-1} $mole^{-1}$. The group with low activation energies may be subdivided into the ether and ketone hydrates, with entropies of activation close to zero, and argon and nitrogen hydrates, with large negative activation entropies.

According to the Bjerrum model of relaxation in ice (26), reorientation of water molecules occurs by the diffusion of D and L defects, that is, of O - - - O "bonds" which have either two hydrogen atoms or none near them. In pure ice I these defects are formed by thermal excitation of normal hydrogen bonds N

$$2N \rightleftharpoons D + L,$$

for which an enthalpy and entropy of formation of 15.7 kcal $mole^{-1}$ and −4.2 cal deg^{-1} $mole^{-1}$ may be estimated (27). The activation enthalpy and entropy for the diffusion of the defects are then 4.9 kcal $mole^{-1}$ and 11.6 cal deg^{-1} $mole^{-1}$, where the dielectric Arrhenius energy (Table III) has been converted to an enthalpy of activation at 0 °C.

Ices III, V, VI, and VII have (high) energies and entropies of activation like ice I and appear to relax by essentially the same mechanism (2–4). The hydrogen bonding between the water molecules of the clathrate hydrates of types I and II approaches more closely that in ice I than does the hydrogen bonding in the high-pressure ices. All water molecules are four-coordinated and in the structure I ethylene oxide hydrate at −25 °C (12) for example the average nearest-neighbor O - - - O distance is 2.79 Å and the average departure of the O - - - O - - - O angles from tetrahedral is only 3.7°. It is therefore likely that the clathrate hydrates also relax by diffusion of orientational defects, although the details of the Bjerrum mechanism must be modified to account for the appreciable lowering of the energies and entropies of activation.

The similarity of the activation parameters shown by the ices proper, despite their diverse structures, suggests that the thermodynamic parameters for the formation and diffusion of the defects responsible for relaxation are similar in these phases. We neglect small differences and assume, because of the structural similarities, that the parameters for the *intrinsic* formation and diffusion of the defects are the same in the clathrate hydrates as in ice I.

The fact that the ether and ketone hydrates relax faster than ice suggests that, in addition to intrinsic defects, defects are introduced into the lattice of these clathrate hydrates by interaction of the water with guest molecules. This is further indicated by the existence of differences between the relaxation rates of the isostructural hydrates of different ethers and ketones. The most probable form of this interaction with a guest molecule M produces something resembling an L defect

$$M + N \rightleftharpoons M - - - H—O + L,$$

where N stands for a normal hydrogen bond. The equilibrium constant is

$$K = \frac{c_N}{c_M}\alpha^2,$$

where α is the fraction of normal bonds converted to defects. The ratio c_N/c_M of the concentration of normal bonds to the concentration of guest molecules varies from 11.5 for structure I hydrates with all cages occupied to 34 for structure II hydrates. From the representative Arrhenius energy and entropy of activation of 7 kcal $mole^{-1}$ and 0 cal deg^{-1} $mole^{-1}$ for these hydrates, the energy and entropy of formation of defects are about 3 kcal $mole^{-1}$ and −23 cal deg^{-1} $mole^{-1}$, K is about 2×10^{-8} at −10° C, and α is about 3×10^{-5}. In ice I the fraction α of defect to normal bonds is much less, about 10^{-7} at −10 °C. The energy of defect formation is reasonable: the geometry is less favorable than for hydrogen bonding within the lattice and very roughly half the energy of a hydrogen bond has to be paid. The entropy of formation is also reasonable since a large part of the translational and rotational entropy of the guest is lost when it is tied at one point.

It is not possible to explain the large negative apparent entropies of activation of argon and nitrogen hydrates by such an interaction between the encaged and host molecules as has been suggested above for the ether and ketone hydrates. The most likely explanation is that argon or nitrogen molecules occasionally substitute for water molecules as "impurities" in the lattice during the formation of the hydrate at about 2 kbar gas pressure. The van der Waals radii (1.90 Å for argon and 2.05 Å for nitrogen)

Can. J. Chem. Downloaded from www.nrcresearchpress.com by 210.87.254.42 on 09/05/12
For personal use only.

are somewhat larger than the effective radius of the water molecule (1.40 Å) and some distortion of the local structure would accompany substitution. Each substitution would tend to inject up to 2 D defects into the lattice. Such a mechanism of defect formation would account for the unexpected breadth of the dispersion loci and for its large temperature dependence (last section), as well as for the differences between the activation energies and entropies of the two hydrates. It is consistent with the volumes of activation.

It is instructive to compare the effect of impurities, including air, on the relaxation of ice I. For "slightly impure" ice, $\log \tau$ vs. $1/T$ plots show curvature toward decreasing slopes at low temperatures in both dielectric (11) and spin-lattice (28, 29) relaxation time measurements. In the dielectric case, additional absorption appears at relatively high frequencies to broaden the dispersion loci. Impurities clearly act as sources of orientational defects, the effect of which is not purely local since the whole relaxation spectrum is shifted to higher frequencies. At low enough temperatures defects so originating outnumber those arising intrinsically in ice and the activation energy and entropy become appreciably smaller.

Since argon and nitrogen hydrates have nearly the same relaxation times as ice I at 0 °C, about the same fraction of normal bonds is converted to defects, i.e. about 3×10^{-7}. The impurity-induced defects must be more numerous than the intrinsic defects or the activation energy would be temperature dependent.

This semiquantitative discussion has neglected the differences between the different "ice" structures and between the D and L defects, and is by no means complete. It does, however, serve to explain in a general way the dielectric behavior.

The lattice impurity mechanism suggested for argon and nitrogen hydrates would not be expected to determine the rate of defect formation in the hydrates of much larger molecules which would substitute with more difficulty. Relaxation in SF_6 hydrate is considered in the following paper (25).

Acknowledgments

We are indebted to R. E. Hawkins for help in the construction of the cell and to A. Lavergne for installation and maintenance of the high-pressure equipment.

1. R. P. Auty and R. H. Cole. J. Chem. Phys. **20**, 1309 (1952).
2. R. K. Chan, D. W. Davidson, and E. Whalley. J. Chem. Phys. **43**, 2376 (1965).
3. G. J. Wilson, R. K. Chan, D. W. Davidson, and E. Whalley. J. Chem. Phys. **43**, 2384 (1965).
4. E. Whalley, D. W. Davidson, and J. B. R. Heath. J. Chem. Phys. **45**, 3976 (1966).
5. G. A. Jeffrey and R. K. McMullan. *In* Progress in inorganic chemistry .Vol. 8. *Edited by* F. A. Cotton. Interscience Publishers, New York. 1967.
6. D. W. Davidson, M. M. Davies, and K. Williams. J. Chem. Phys. **40**, 3449 (1964).
7. G. J. Wilson and D. W. Davidson. Can. J. Chem. **41**, 264 (1963).
8. D. W. Davidson and G. J. Wilson. Can. J. Chem. **41**, 1424 (1963).
9. R. E. Hawkins and D. W. Davidson. J. Phys. Chem. **70**, 1889 (1966).
10. A. Venkateswaran, J. R. Easterfield, and D. W. Davidson. Can. J. Chem. **45**, 884 (1967).
11. D. W. Davidson. Unpublished work.
12. R. K. McMullan and G. A. Jeffrey. J. Chem. Phys. **42**, 2725 (1965).
13. D. R. Marshall, S. Saito, and R. Kobayashi. A.I.Ch.E. J. **10**, 202, 723 (1964).
14. A. van Cleeff and G. A. M. Diepen. Rec. Trav. Chim. **79**, 582 (1960); **84**, 1085 (1965).
15. A. D. Potts and D. W. Davidson. J. Phys. Chem. **69**, 996 (1965).
16. W. Schroeder. Ahren's Sammlung Chemischer und Chemisch-technischer Vortrage, **29**, 1 (1926).
17. K. S. Cole and R. H. Cole. J. Chem. Phys. **9**, 341 (1941).
18. A. Michels, C. A. ten Seldam, and S. D. J. Overdijk. Physica, **17**, 781 (1951).
19. A. Michels, A. Jaspers, and P. Sanders. Physica, **1**, 627 (1934).
20. C. J. F. Böttcher. Theory of electric polarization. Elsevier Publishing Co., New York. 1952. p. 318.
21. J. E. Bertie and E. Whalley. J. Chem. Phys. **46**, 1271 (1967).
22. L. D. Calvert. Private communication.
23. M. von Stackelberg and W. Jahns. Z. Elektrochem. **58**, 162 (1954).
24. D. F. Sargent and L. D. Calvert. J. Phys. Chem. **70**, 2689 (1966).
25. Y. A. Majid, S. K. Garg, and D. W. Davidson. Can. J. Chem. This issue.
26. N. Bjerrum. Kgl. Danske Videnskab. Selskab Mat. Fys. Medd. **27**, 3 (1951).
27. H. Gränicher. Physik Kondensierten Materie, **1**, 1 (1963).
28. K. Kume. J. Phys. Soc. Japan, **15**, 1493 (1960).
29. D. E. Barnaal. Ph.D. Dissertation, University of Minnesota, Minneapolis, Minnesota. 1965. University Microfilms 65-7867, Ann Arbor, Mich.

Can. J. Chem. Downloaded from www.nrcresearchpress.com by 210.87.254.6 on 09/05/12
For personal use only.

Dielectric and nuclear magnetic resonance study of the hydrate of sulfur hexafluoride[1]

Y. A. MAJID, S. K. GARG, AND D. W. DAVIDSON
Division of Applied Chemistry, National Research Council of Canada, Ottawa, Canada

Received December 5, 1967

In its dielectric and proton magnetic resonance behavior (except T_1) the clathrate hydrate of SF_6 is similar to ice I. Reorientation of water molecules appears to be little affected by the guest SF_6 molecules and probably depends on the diffusion of rotational Bjerrum defects formed in numbers intrinsic to the lattice structure. The Arrhenius energy and activation entropy for dielectric relaxation are 12.3 ± 0.5 kcal mole^{-1} and 6.8 ± 2.0 cal deg^{-1} mole^{-1}, respectively. The proton rigid-lattice second moment is 32.8 ± 0.5 G^2 at -180 °C. The ^{19}F second moment agrees with the value calculated for rapid isotropic rotation of SF_6 molecules in the large cages only. Diffusion of water molecules in the hydrate is slower than in ice, which suggests that diffusion in ice occurs by migration of interstitial molecules through the channels in ice rather than by migration of lattice vacancies.

Canadian Journal of Chemistry, **46**, 1683 (1968)

A dielectric study (1) of the structure I clathrate hydrates of argon and nitrogen showed that the water molecules undergo reorientation at a much slower rate than in the isostructural hydrates of ethylene oxide and trimethylene oxide. Nevertheless the activation energies for reorientation were considerably less than for ice I (2) and other ices (3). In structure I hydrates the O---O---O angles of the water lattice are distorted from tetrahedral values to a much smaller extent (4), than in ices III (*5a*), V (*5b*), and VI (*5c*), and a smaller hydrogen-bond energy is not to be expected. It was tentatively suggested (1) that, under the high pressure of gas necessary for preparation of their hydrates, argon and nitrogen molecules occasionally replace water molecules in the lattice. Mobile orientational defects of the Bjerrum type may originate at the sites of such substitution and lead to relatively rapid reorientation of the water molecules.

Of the hydrates of the related structure II (6), that of sulfur hexafluoride (7) appears to approach most closely the ideal clathrate (8). SF_6 is too large (van der Waals' diameter 6.1 Å) to readily replace water (2.8 Å) in the lattice. As the result of its octahedral symmetry, SF_6 possesses no dipole, quadrupole, or octupole moment. The relaxation of the water lattice of SF_6 hydrate is therefore expected to be less affected by the encaged molecules than in the structure II hydrates of ethers and ketones previously studied (9–11).

We report here the results of dielectric and wide-line n.m.r. studies of SF_6 hydrate. These two techniques usefully supplement one another. The proton resonance line of the water molecules may be narrowed by diffusion (as appears to be the case for ice I) as well as by the reorientation responsible for the dielectric relaxation. The shape of the ^{19}F resonance line is determined by the motion of the encaged SF_6 molecules to which the dielectric properties are insensitive.

Experimental Methods

Preparation of the Hydrate

SF_6 hydrate is stable under 0.8 atm of SF_6 at 0 °C (12). It was prepared by subjecting conductivity water to pressures of 3 to 4 atm of SF_6 at about 0 °C with occasional cooling to lower temperature to ensure nucleation. Initially, hydrate was formed in a pressure-tight cylindrical dielectric cell under static conditions. The electrical properties always showed these samples to incompletely fill the interelectrode region, despite attempts to improve the filling factor. Samples more satisfactory for dielectric measurement were pressed at low temperatures under 5000 p.s.i. into discs about $\frac{1}{4}$'' thick which were inserted into a pre-cooled cell equipped with a bellows to maintain contact between the parallel-plate electrodes and the sample. Hydrate for pressing was prepared in a small Teflon-lined pressure vessel equipped with a cooling jacket and mounted in a mechanical shaker.

Purity of Hydrate

The early measurements with the cylindrical cell showed that the dielectric behavior of SF_6 hydrate is quite similar to that of ice. This was indicated by the persistence of ice-like properties to temperatures well in excess of 0 °C. The complex permittivity locus at +2 °C shown in the inset of Fig. 1 is typical of the results obtained with the cylindrical cell, in which the absence of significant quantities of ice in the sample was indicated

[1]Issued as NRCC No. 9963.

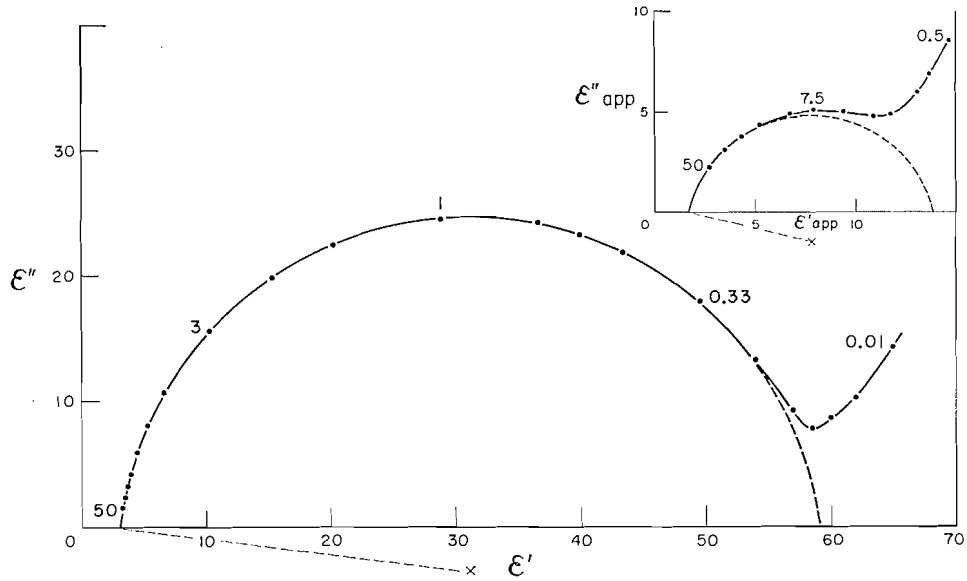

FIG. 1. Complex permittivity locus of SF_6 hydrate at −26.6 °C. Inset: apparent permittivity locus at +2.0 °C. Frequencies are in kHz.

by the absence of discontinuities in dielectric properties as the sample was heated through 0 °C. This method of analysis could not be used with the parallel-plate cell, which was not sealed against loss of SF_6. The SF_6 content was estimated by the loss of weight and the volume of gas evolved when the hydrate decomposed. Some samples prepared in the presence of 1 atm of air discharged more gas than corresponded to $SF_6 \cdot 17H_2O$, which indicated some incorporation of nitrogen and oxygen in the smaller latitce cages. It is believed that all samples consisted of at least 90% hydrate.

Dielectric Measurements

Electrical measurements were made with three-electrode cells by techniques previously described (1, 10, 13).

N.M.R. Measurements

Proton and ^{19}F resonance lines were obtained at 16 MHz with a Varian wide-line n.m.r. spectrometer equipped with Fieldial control of the field of the 12″ electromagnet. The derivative of the absorption mode was observed by means of a Princeton Applied Research JB4 lock-in amplifier and an X–Y recorder. Temperatures in the range between −180 and +2 °C were obtained with a thermocouple-calibrated Varian V-4540 variable temperature accessory; temperature control and measurement were to ±1 °C. Second moments of line width were measured with a curve-reader attached to an EAI analog computer programmed to perform the necessary integrations and were corrected for modulation broadening.

Results

Dielectric Dispersion

The complex permittivity locus shown in Fig. 1 is representative of the loci obtained for SF_6 hydrate in the parallel-plate cell. These loci are quite well described by Cole–Cole arcs, with values of α which vary from about 0.05 at −12 °C to about 0.15 at −65 °C. These width parameters are maximum values. Measurements on samples known to contain appreciable quantities of ice showed additional absorption at relatively high frequencies. Ice present to the extent of a few percent may have contributed some high-frequency absorption even in the best samples, leading to a broadening of the loci, particularly at low temperatures where the two absorption regions are further apart. As is common for slowly relaxing polar solids, the curves are poorly defined at low frequencies where there is overlap from ionic conductance and polarization effects. Values of the high-frequency permittivity ε_∞ lay in the range 2.94 ± 0.06 at temperatures between −30 and −65 °C, in agreement with the value 2.97 calculated by the Onsager equation by the method used for argon and nitrogen hydrates (1). The unit cell dimension was taken as 17.21 Å (7) and the polarizability of SF_6 as 6.46 $Å^3$. Again (1), there was an anomalous decrease of ε_∞ with decreasing temperature. This decrease was of the order of 0.04 between −45 and −65 °C.

At the higher temperatures static dielectric constants are close to, if a few permittivity units less than, the value expected for structure II

Can. J. Chem. Downloaded from www.nrcresearchpress.com by 210.87.254.6 on 09/05/12
For personal use only.

TABLE I
Dielectric data for SF_6 hydrate

T (°C)	ε_0(exp)	ε_∞	τ/μs(exp)	α	ε_0(ass)	τ/μs ("corr")	$\delta \times 10^3$
−11.8	57	3.0	49.3	0.045	57		0
−26.2	59	3.0	175.	0.08	59		0
−40.0	59	3.0	727.	0.12	63	782	1
−55.3	58	2.9	3 280.	0.12	67	3 890	2
−65.4	60	2.9	10 700.	0.16	70	12 800	2

hydrates (10, 11). The difference between the experimental value (58 ± 2) at −15 °C and the value anticipated (64 ± 2) from the earlier work on isostructural hydrates of ethers (10) may arise from incomplete exclusion of voids from the sample during pressing. At −65 °C these values are 61 and 76, respectively, and it is likely that cracks or gaps have developed, as suggested also by the behavior of the relaxation times (next subsection).

Dielectric Relaxation Times

The relaxation times corresponding to the frequencies of maximum absorption for samples of SF_6 hydrate prepared in the absence and presence of air are plotted vs. $1/T$ in Fig. 2. They are similar to those of ice I for which the broken line gives the results of Auty and Cole (2). The effect of the presence of air, and therefore of the incorporation of some nitrogen and oxygen molecules in the smaller cages, is to increase slightly the relaxation times.

The Arrhenius energy is 12.3 kcal mole^{-1} at the higher temperatures. Below −40 °C the apparent activation energy decreases, an effect at least partly caused by cracking of the samples. Application of a correction for the effect of a gap parallel to the electrodes on the relaxation times by the method previously outlined (1) removes some of the curvature of the log τ vs. $1/T$ plot (Fig. 2). Some of the data are given in Table I, together with values of the static dielectric constants ε_0 assumed for calculating the corrections and ratios δ of effective gap thickness to electrode separation.

Proton Resonance Lines

A typical derivative tracing of a proton resonance line is given in Fig. 3. There is a partially resolved doublet structure which is more pronounced at about −50 °C than at lower or higher temperatures. The origin of the doubling, as was first pointed out by Pake (14) for polycrystalline $CaSO_4 \cdot 2H_2O$, is the dominant magnetic interaction between the protons of the same water molecule.

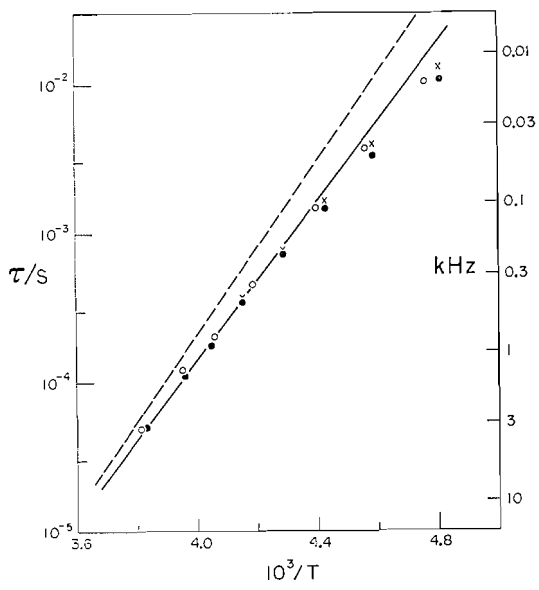

FIG. 2. Dielectric relaxation times of SF_6 hydrate. ● and ○: hydrate prepared in the absence and presence of air, respectively. ×: points ● corrected for series air gaps. The dashed line for ice is from ref. 2.

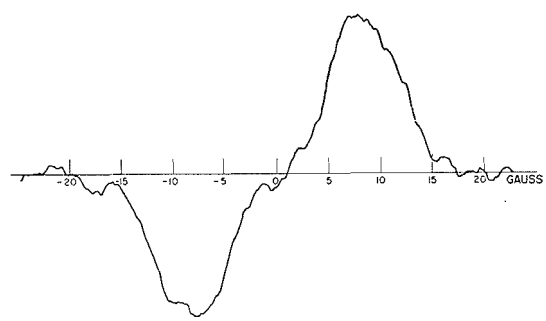

FIG. 3. Derivative curve of ^1H absorption line at −60 °C. Radio frequency field 7 mG, modulation field 1.6 G, sweep rate 1 G/min, time constant 10 s.

Can. J. Chem. Downloaded from www.nrcresearchpress.com by 210.87.254.6 on 09/05/12
For personal use only.

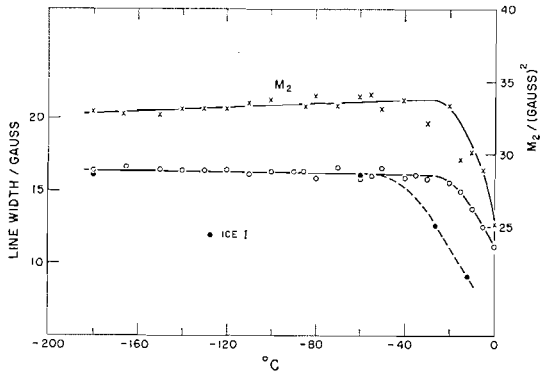

FIG. 4. Temperature dependence of ^1H second moment (upper curve) and ^1H line width. The data for polycrystalline ice are from ref. 15.

The experimental second moment of the proton line (Fig. 4, upper curve) *increases* slightly with increasing temperatures from 32.8 G^2 at −180 °C to 33.8 G^2 at −50 °C. The amount of this increase appears to exceed significantly the experimental error in the relative second moment values: the average difference between the 14 moments measured at temperatures between −180 and −50 °C and the (least-squares) straight line drawn was ±0.27 G^2. The probable uncertainty in the absolute values of the second moment given by the linear relationship between −180 and −50 °C is no more than ±0.5 G^2.

Kume reported (15) the second moment of polycrystalline ice at −180 °C to be 36.7 G^2, with a standard deviation of 1.7 G^2. The accuracy of the measurements on "pure" ice is severely limited by saturation of the radiofrequency (r.f.) signal at low temperatures. Thus Kume found it necessary to reduce the r.f. field to 40 μG in ice at −180 °C. Saturation was not important in SF_6 hydrate for fields as high as 20 mG at temperatures down to −180 °C. This difference is undoubtedly a result of the rapid motion of the encaged molecules.

In the lower two curves of Fig. 4 the temperature dependences of the line widths (between *extrema* of the derivative curves) of SF_6 hydrate and "pure" polycrystalline ice (15) are compared. Over most of the temperature range the line widths are essentially the same. However, the temperature of the onset of narrowing is considerably higher for SF_6 hydrate. The lattice of this hydrate remains "rigid" to much higher temperatures than those of the clathrate hydrates previously studied (16), including the isostructural lattices of the hydrates of tetrahydrofuran, dihydrofuran, and propylene oxide.

A liquid line appeared at 0 °C which corresponded to decomposition of a few percent of the hydrate.

Fluorine Resonance Lines

The ^{19}F resonance lines are narrow and well defined (see Fig. 5A for example) at all temperatures studied. The shapes are almost indistinguishable from Gaussian. With increasing temperature the second moment (Fig. 5B) decreases linearly from 1.20 G^2 at −176 °C to 1.14 G^2 at −60 °C and thereafter somewhat more rapidly to about 0.90 G^2 at 0 °C, where the hydrate decomposes at a noticeable rate. The small ^{19}F second moments at temperatures where the proton second moments are essentially those of the rigid lattice are consistent only with rapid isotropic rotation of encaged SF_6 molecules.

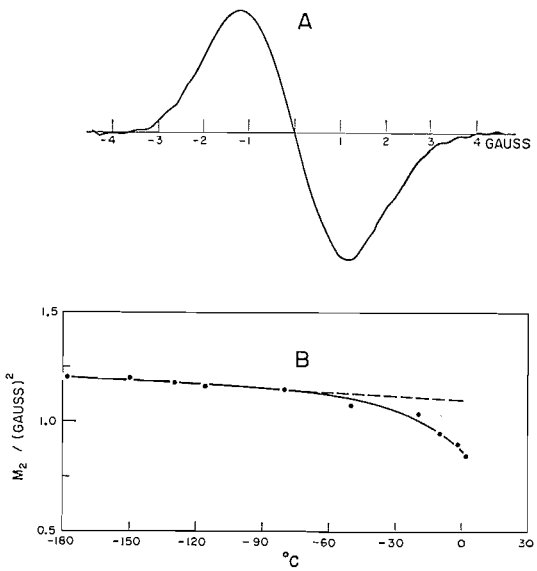

FIG. 5. (A) ^{19}F derivative curve of SF_6 hydrate at −178 °C. Radiofrequency field 9 mG, modulation field 0.17 G, time constant 10 s, sweep rate 1 G/min. (B) Second moments of ^{19}F resonance line in SF_6 hydrate.

Discussion

^{19}F Second Moments

The calculation of the second moment of the ^{19}F resonance line is similar to the one previously

Can. J. Chem. Downloaded from www.nrcresearchpress.com by 210.87.254.6 on 09/05/12
For personal use only.

TABLE II

Contributions to the fluorine second moment in SF_6 hydrate at 0 °C

Interaction	R_j or R_k	Multiplicity	Contribution to M_2
Protons in cage	4.423 Å	42	0.893 G^2
Protons on near ends of radial bonds	5.66	14	0.068
Protons on remote ends of radial bonds	6.40	14	0.033
More distant protons (estimated)			0.10
^{19}F in first neighbor SF_6's	7.45	4×6	0.044
^{19}F in second neighbor SF_6's	12.17	12×6	0.007
	Total second moment		1.15 G^2

made for the proton second moment of tetrahydrofuran deuterate (16). SF_6 molecules are taken to be rotating isotropically around their centers of mass located at the centers of the large structure II cages. The protons are assumed to lie on the O---O bonds of the rigid water lattice 1.01 Å away from an O atom. The Bernal–Fowler rules require that, for the 28 water molecules that constitute the cage, 42 protons lie on the surface of the cage and 14 on bonds extending radially outward. The geometric model differs from the previous one (16) only in the adjustment of distances to fit the unit cell dimensions of SF_6 hydrate, given by von Stackelberg and Jahns (7) as 17.21 Å at 0 °C.

The main contribution to the ^{19}F second moment comes from interactions with the protons. In the polycrystalline case this contribution is 159.1 $\sum_j R_j^{-6}$ G^2, where R_j is the distance of proton j from the cage center in Å. Interaction with the fluorine spins of SF_6 molecules in neighboring cages contributes to the second moment 317.4 $\sum_k R_k^{-6}$ G^2, where R_k is the distance between a cage center and the center of a neighboring cage which contains fluorine nucleus k. The contributions to the second moment are listed on Table II, along with the number of nuclei at distances R_j and R_k.

For comparison with the value of 1.15 G^2 calculated from the lattice parameter at 0 °C the linear portion of Fig. 5B has been extrapolated to 0 °C to give an experimental second moment of 1.10 G^2. The extent of this agreement seems to indicate that there is no appreciable effect on the second moment of the "rattling" vibrations of the SF_6 molecules.

The slope of the linear region of the curve in Fig. 5B may be used to estimate the coefficient of expansion of SF_6 hydrate, if it be assumed that the only effect of temperature change is to change all R_j's and R_k's in proportion to the change in size of the unit cell. A value of $\sim 78 \times 10^{-6}$ deg^{-1} is obtained for the mean linear coefficient between −176 and −60 °C. Sargent and Calvert (17) give an average coefficient of 75×10^{-6} deg^{-1} between −163 and 0 °C from their X-ray studies of six structure II hydrates.

^1H *Second Moments*

The structure of SF_6 hydrate suggests that the proton second moment should be similar to that of ice (see next paragraph). For polycrystalline ice Barnaal and Lowe (18) have calculated a second moment of 30.8 G^2, before vibrational correction, for a model in which the OH distance is 1.01 Å, the O---O distance 2.76 Å, and the angles tetrahedral. For Peterson and Levy's neutron-diffraction model of D_2O ice at −50 °C (19) we calculate a second moment of 31.2 G^2 as an average of 8 proton positions in the unit cell, with a total of 196 nearest protons placed randomly at positions which conform to the Bernal–Fowler rules.

In ice about 57% of the second moment is contributed by the intramolecular proton. The exact geometries of the water molecules in SF_6 hydrate are not known. Mak and McMullan's results (6) for the isostructural tetrahydrofuran – hydrogen sulfide double hydrate show that the O---O---O angles depart on average from tetrahedral by only 3°. The average O---O distance is 2.77 Å, scaled to the smaller unit cell dimension of SF_6 hydrate at 0 °C. Thus the environments of the water molecules in the hydrate are sufficiently similar to those in ice to suggest that the geometry of the water molecules and the intramolecular contribution to the second

Can. J. Chem. Downloaded from www.nrcresearchpress.com by 210.87.254.6 on 09/05/12
For personal use only.

Can. J. Chem. Downloaded from www.nrcresearchpress.com by 210.87.254.6 on 09/05/12
For personal use only.

moment are not appreciably different. The protons of the four nearest-neighbor water molecules contribute one third of the second moment of ice. For SF_6 hydrate this contribution will again be almost identical; although the average O---O distance (at 0 °C) is somewhat longer, there is a slightly larger contribution in the hydrate because all neighbors are in eclipsed configurations with respect to the O---O bonds: in ice three neighbors have staggered configurations. The contribution from more distant protons is about 20% or 0.6 G^2 less in the hydrate since the density of water molecules is about 90% as great as in ice. Finally, interaction with the ^{19}F spins of the SF_6 molecules adds about 0.2 G^2 to the hydrate second moment. Thus, before vibrational corrections, it appears that the second moments of SF_6 hydrate and ice are the same to within less than 1 G^2. The corrections for molecular and lattice vibrations again will be nearly the same in the two cases. Barnaal and Lowe (18) have estimated these corrections to be -1.2 G^2 for polycrystalline ice.

The large moment measured for polycrystalline ice by Kume (36.7 ± 1.7 G^2 at -180 °C) may have been affected by saturation. Barnaal and Lowe (18) obtained the value 32.1 ± 2 G^2 by analysis of the free induction decay shape at -35 °C. The present value of 33.8 ± 0.5 G^2 for SF_6 hydrate at -50 °C, in view of the arguments of the last paragraph, suggests that the proper value for ice is near the upper end of the uncertainty range given by Barnaal and Lowe, i.e. near 34 G^2. It is possible that at -35 °C some diffusional narrowing occurs.

The calculated second moment for the Peterson–Levy model (19), without vibrational correction, is smaller than the experimental one by about 3 G^2. The most probable explanation of the difference is that the effective H—O—H angle is not almost teterahedral but, at -50 °C, some 3 or 4 degrees less. Use of the rather uncertain vibrational corrections of Barnaal and Lowe (18) leads to a further reduction of this angle.

An increase of second moment with increasing temperature is opposite to the usual effect of density and motional changes. However, as Gutowsky *et al.* (20) have pointed out, the line widths of single crystal ice measured at right angles to the *c* axis (a direction in which the line shows no doubling) by Kume and Hoshino (21) show an increase of about 4% between -183 °C and the onset of motional narrowing.

From the coefficient of expansion given in the last section the density of SF_6 hydrate at -180 °C is about 3% greater than at -50 °C which should increase the intermolecular contribution to the second moment by about 0.8 G^2. The observation that in fact M_2 is smaller at -180 °C by 1.0 G^2 than at -50 °C means that it is about 1.8 G^2 less than expected. In a strictly formal way this may be accounted for by an increase in the H—O—H angle by about 2 degrees. The electrostatic interaction between the proton and the oxygen atom to which it is hydrogen bonded has, however, a much larger component in the direction of increasing O—H bond length than in the direction corresponding to increase of the H—O—H angle. An increase in bond length of about 2% is required to account for the full effect. In fact both an opening of the angle and an increase in the bond length probably take place with decrease of temperature. Part of the change in moment with temperature may also be due to change in excitation of lattice vibrations.

Dielectric and N.M.R. Relaxation

The dielectric relaxation times at -30 °C and the activation parameters of a number of structure II hydrates and ices are listed in Table III. Because of some uncertainty in the effects of gaps, the estimated errors in the activation parameters for SF_6 hydrate (± 0.5 kcal mole^{-1} in E_A and ± 2.0 in $\Delta S^{\neq}$) are larger by about a factor of two than for the other substances listed. The parameters for the structure II hydrates of acetone (9), propylene oxide (10), dihydrofuran (10), and trimethylene oxide (10) lie between those shown for dioxolane and cyclobutanone hydrates.

At -30 °C the relaxation time of SF_6 hydrate is longer by two to three orders of magnitude than the relaxation times of the isostructural hydrates of ethers and ketones. SF_6 molecules clearly affect the reorientation of the water molecules much less than these other guest molecules, all of which have appreciable dipole moments and can form hydrogen bonds with water. The activation energy and, to a less extent, the entropy of activation of SF_6 hydrate are similar to those of the ices (Table III). This suggests that in SF_6 hydrate the relaxation be-

TABLE III

Relaxation times and activation parameters for structure II hydrates and ices at −30 °C

	τ (μs)	E_A (kcal mole^{-1})	$\Delta S^{\ddagger}$ (cal deg^{-1} mole^{-1})	Ref.
Sulfur hexafluoride hydrate	270.	12.3	6.8	This work
Tetrahydrofuran hydrate	0.51	7.8	0.8	10
Dioxolane hydrate	2.6	8.7	1.3	11
Cyclobutanone hydrate	0.28	6.5	−3.5	*
Ice I	430.	13.25	9.8	2
Ice III (3 kbar)	2.7	11.6	13.1	3
Ice V (5 kbar)	5.6	11.5	11.3	3
Ice VI (8 kbar)	5.4	11.0	9.2	3

*D. W. Davidson, unpublished work.

havior is approaching that intrinsic to the structure II water lattice.

At 0 °C the dielectric relaxation time of SF_6 hydrate (18 μs) resembles the relaxation times of argon and nitrogen hydrates (16 and 15 μs at 2.0 and 1.2 kbar, respectively (1)), but the activation parameters are much different. The unexpectedly low activation energies and large negative entropies of activation of argon and nitrogen hydrates are not found for SF_6 hydrate. This provides support for the view (1) that Bjerrum defects in the former hydrates originate predominantly, especially at low temperatures, at sites where argon or nitrogen molecules have replaced water molecules in the lattice. Such a mechanism is possible because of the small size of these molecules and the high pressures under which their hydrates were formed (1). In SF_6 hydrate Bjerrum defects probably originate, as they do in pure ice, at normal lattice sites.

Molecular reorientation alone cannot account for the observation that the proton resonance line of SF_6 hydrate narrows at a higher temperature than that of polycrystalline ice (Fig. 2). The faster average dielectric relaxation rate and the presence of a distribution of relaxation times in SF_6 hydrate predict the opposite. This clearly suggests that the main contribution to motional narrowing in ice is the diffusion of water molecules. Onsager and Runnels (22) have indicated that diffusion of free interstitial water molecules is responsible for the low spin-lattice relaxation times of ice. This mechanism of diffusion in ice is consistent with a lower diffusion coefficient in SF_6 hydrate, which lacks the channels present in hexagonal ice. Diffusion by migration of lattice vacancies (23) would almost certainly be faster in the hydrate than in ice.

The motions responsible for proton spin-lattice relaxation in SF_6 hydrate are those of the encaged SF_6 molecules and not, as in pure ice, diffusion and rotation of the water molecules. The value of T_1 measured in ice at 30 MHz has reached 100 s at −38 °C (15) and serious saturation occurs at low temperatures. The absence of saturation in SF_6 hydrate shows T_1 to be less than 1 s at 16 MHz even at −180 °C.

Comparison with the Results of McDowell and Raghunathan

These authors have recently published (24) the results of a study of the ^{19}F resonance line of SF_6 hydrate. Their results are in rough agreement with the present results at temperatures between −123 and −30 °C but show a "sharp motional transition" at −123 °C, below which much higher second moments (~2.0 G^2) were obtained. No evidence of such a transition was found in any of the three samples studied by us. It is difficult to account for a transition of this kind on the basis of the geometries of the SF_6 molecule and the cage which it occupies.

Acknowledgment

The authors are much indebted to Dr. S. Brownstein for helpful discussions.

1. S. R. Gough, E. Whalley, and D. W. Davidson. Can. J. Chem. This issue.
2. R. P. Auty and R. H. Cole. J. Chem. Phys. **20**, 1309 (1952).
3. G. J. Wilson, R. K. Chan, D. W. Davidson, and E. Whalley. J. Chem. Phys. **43**, 2384 (1965).
4. R. K. McMullan and G. A. Jeffrey. J. Chem. Phys. **42**, 2725 (1965).
5. (*a*) W. B. Kamb and S. K. Datta. Nature, **187**, 140 (1960). (*b*) B. Kamb, A. Prakash, and C. Knobler. Acta Cryst. **22**, 706 (1967). (*c*) B. Kamb. Science, **150**, 205 (1965).

Can. J. Chem. Downloaded from www.nrcresearchpress.com by 210.87.254.6 on 09/05/12
For personal use only.

6. M. VON STACKELBERG and H. R. MÜLLER. Z. Elektrochem. **58**, 25 (1954). T. C. W. MAK and R. K. MCMULLAN. J. Chem. Phys. **42**, 2732 (1965).
7. M. VON STACKELBERG and W. JAHNS. Z. Elektrochem. **58**, 163 (1954).
8. H. M. POWELL. J. Chem. Soc. 61 (1948).
9. G. J. WILSON and D. W. DAVIDSON. Can. J. Chem. **41**, 264 (1963).
10. R. E. HAWKINS and D. W. DAVIDSON. J. Phys. Chem. **70**, 1889 (1966).
11. A. VENKATESWARAN, J. R. EASTERFIELD, and D. W. DAVIDSON. Can. J. Chem. **45**, 884 (1967).
12. L. D. SORTLAND and D. B. ROBINSON. Can. J. Chem. Eng. **42**, 38 (1964).
13. A. D. POTTS and D. W. DAVIDSON. J. Phys. Chem. **69**, 996 (1965).
14. G. E. PAKE. J. Chem. Phys. **16**, 327 (1948).
15. K. KUME. J. Phys. Soc. Japan, **15**, 1493 (1960).
16. S. BROWNSTEIN, D. W. DAVIDSON, and D. FIAT. J. Chem. Phys. **46**, 1454 (1967).
17. D. F. SARGENT and L. D. CALVERT. J. Phys. Chem. **70**, 2689 (1966).
18. D. E. BARNAAL and I. J. LOWE. J. Chem. Phys. **46**, 4800 (1967).
19. S. W. PETERSON and H. A. LEVY. Acta Cryst. **10**, 70 (1957).
20. C. K. COOGAN, G. G. BELFORD, and H. S. GUTOWSKY. J. Chem. Phys. **39**, 3061 (1963).
21. K. KUME and R. HOSHINO. J. Phys. Soc. Japan, **16**, 290 (1961).
22. L. ONSAGER and L. K. RUNNELS. Proc. Natl. Acad. Sci. U.S. **50**, 208 (1963).
23. R. O. RAMSEIER. J. Appl. Phys. **38**, 2553 (1967).
24. C. A. MCDOWALL and P. RAGHUNATHAN. Mol. Phys. **13**, 331 (1967).

Can. J. Chem. Downloaded from www.nrcresearchpress.com by 210.87.254.6 on 09/05/12
For personal use only.

Can. J. Chem. Downloaded from www.nrcresearchpress.com by 210.87.254.40 on 09/05/12
For personal use only.

La détermination de la température optimale de précipitation de l'iodate de thorium

R. COLLÉE

Laboratoires de Sciences Nucléaires Appliquées, Institut de Chimie et Métallurgie, Faculté des Sciences Appliquées, Université de Liège, Liège, Belgique

Reçu le 14 juin 1967

Une étude expérimentale a été entreprise au moyen d'un cryostat-ultra-thermostat. Des investigations ont porté d'une part sur des produits purs de thorium et de cérium, isolés ou en mélange et d'autre part sur des solutions de lixiviation de minerais de monazites. Les résultats expérimentaux montrent que le choix de températures de l'ordre de 5 à 10 °C entraîne des erreurs excédentaires appréciables dans les déterminations analytiques. Par ailleurs, l'entraînement intempestif du cérium subit l'influence de la présence du thorium. Au surplus, il ne suffit pas de refroidir simplement les solutions car la température optimale de précipitation est de l'ordre de −2 °C.

Le respect de la température optimale de précipitation permet d'obtenir une plus grande exactitude des résultats analytiques et d'assurer ainsi un meilleur contrôle de bilan des opérations métallurgiques.

Canadian Journal of Chemistry, 46, 1691 (1968)

Introduction

Les méthodes de détermination analytique du thorium dans les minerais et les produits métallurgiques thorifères sont assez nombreuses et leur choix dépend de multiples facteurs tels que la précision désirée, l'importance de la teneur, la nature et l'importance des autres éléments, la rapidité éventuellement exigée, le prix des appareillages nécessaires (1–16). Les procédés les plus courants sont la gravimétrie par l'iodate ou par le thiosulfate (1, 11), la titrimétrie par le molybdate ou l'oxinate, la colorimétrie par l'acide arsénophénylazonaphtol-disulfonique (2–12), la fluorimétrie par l'amino-hydroxyanthraquinone (12), la spectrophotométrie par l'acide diméthyl aminophénylarsinique (2, 4), la fluorescence, la polarographie et l'analyse spectrale (1, 7, 11), la complexométrie (8, 9), l'échange ionique et l'extraction liquide–liquide (13–23).

Une méthode d'analyse particulièrement intéressante est essentiellement basée sur les propriétés complexantes de l'acide éthylène diaminotétraacétique (EDTA, Titriplex) (8–10, 18, 20, 24). Dans certaines conditions, ce réactif complexe les terres rares sans complexer le thorium. Le procédé est simple et rapide et convient particulièrement aux études d'orientation n'exigeant pas une exactitude rigoureuse. La complexation est cependant délicate en présence de certains ions tels que le fer, le zirconium, le bismuth, l'aluminium et l'antimoine.

Nous avons particulièrement étudié la mise au point d'une méthode d'analyse radiochimique basée sur l'irradiation et la spectométrie du rayonnement gamma. Le procédé rend de grands services dans de nombreux cas particuliers, mais postule notamment l'emploi d'un appareillage très coûteux (24–26).

Au cours de plusieurs études relatives aux minerais et aux produits thorifères, nous avons étudié les performances et les conditions d'emploi de toutes ces méthodes d'analyses et l'expérience montre que dans le cas où les teneurs en thorium sont supérieures à 1% et où il est nécessaire d'obtenir des déterminations quantitatives précises permettant le contrôle et le bilan des opérations métallurgiques, la meilleure méthode est encore la gravimétrie par l'iodate. En principe, le thorium est précipité par un excès d'iodate de potassium en milieu nitrique très acide, tandis que les iodates de cérium et des terres rares restent en solution. Les autres impuretés doivent être séparées au préalable, par exemple par un traitement à l'acide oxalique.

Malgré son grand intérêt, l'exposé de la méthode technique opératoire par les auteurs spécialisés comporte de nombreuses imprécisions qui tendent à démontrer que ces auteurs, ayant étudié consciencieusement les opérations, ont constaté dans leurs résultats des variations ne leur permettant pas de donner des indications plus formelles. En particulier, la température de précipitation n'est pas précisée, les auteurs recommandant simplement de "refroidir" ou de "tenir la solution bien froide". Comme certaines anomalies sont apparues dans quelques-uns de

Can. J. Chem. Downloaded from www.nrcresearchpress.com by 210.87.254.40 on 09/05/12
For personal use only.

nos contrôles analytiques, il nous a semblé utile de consacrer quelques expériences à la détermination de la température optimale de précipitation de l'iodate de thorium, en vue de contribuer à une meilleure connaissance de ce métal qui prend une importance toujours plus grande dans l'expansion du génie nucléaire.

Partie expérimentale

L'obtention d'une température réglable et constante se fait au moyen d'un cryostat-ultra-thermostat KT 40 S Colora, modèle 1962, auquel nous avons apporté quelques modifications. Cet appareillage est muni d'un compresseur semi-hermétique refroidi par l'air, du type SWM-Copeland, modèle 411 L-301-1 et d'un moteur PW 7 × 14. L'agent frigorifique est le fréon (R 22). Tous les éléments de commande, de distribution et de service sont réunis sur un élément spécial. Le bain isotherme a un volume de 22 l, une pompe foulante assure la circulation du bain et par conséquent une température uniforme. Celle-ci peut être réglée à des valeurs s'étendant de +40 à −40 °C avec une précision de 0.02 à 0.05 °C.

Comme constituant liquide du bain nous avons employé soit l'eau désionisée pour les températures supérieures ou égale à 5 °C, soit le méthanol techniquement pur pour les températures inférieures à 5 °C.

Comme ce type d'appareil, tel qu'il a été conçu par le fabricant, ne permet pas la réalisation simultanée de plusieurs expériences et comme d'autre part le dispositif de la pompe foulante et du serpentin auxiliaire n'est pas prévu pour assurer une circulation extérieure du liquide au débit souhaitable, nous avons adjoint à l'installation plusieurs bains isothermes réglés par thermostat et mettant à profit le même compresseur frigorifique.

Les expériences relatives à l'étude des composés purs de thorium et de cérium ont été réalisées en partant des produits suivants. Nous avons préféré travailler sur des constituants de plusieurs origines car l'expérience de problèmes analogues nous a montré que des résultats peuvent varier selon l'histoire ou l'hérédité des produits traités.

Nitrate de thorium pour analyse, Merck 12.511-Darmstadt.

Thoriumnitrat reinst. Dr. Th. Schuckardt, Munchen.

Thoriumnitrat chemisch rein. Riedel-CRB.

Nitrate thorium pur.

Thorium sulfate, BDH. British Drug Houses Ltd.

Thorium sulfate. Société des Produits chimiques de Terres rares, Paris.

Nitrate de cérium pour analyse, Merck 150.066 et 150.064.

Ceric sulfate, British Drug Houses Ltd-769.229-620.123.

Cerium IV sufuricum pro analysis-Merck 2274-426.991.

Cerium IV Sulfat für Analyse-Riedel de Haen, 12502. Hannover.

Sulfate cérique pour analyse, Union Chimique Belge.

Iodate de potassium pour analyse, 5051-728.049-Merck Ag Darmstadt.

Lorsque les composés de départ sont des nitrates, ceux-ci sont mis directement en solution aqueuse nitrique et soumis à la méthode à l'iodate. Comme l'analyse des minerais se fait généralement après lixiviation sulfurique, un certain nombre d'expériences ont été effectuées sur des sulfates purs et sur des minerais de monazites.

Résultats

Expériences relatives à des mélanges de cérium et de thorium

Les premières expériences de détermination de la température optimale de précipitation de l'iodate ont été réalisées sur des solutions de nitrates équipondérales en thorium et en cérium. Les températures des expériences ont été de 40, 20, 10, 7, 5, 2, 0, −2, −5, −7 et −10 °C. Les solutions à analyser et les solutions d'iodate sont amenées séparément à la température choisie, ensuite mélangées à cette température et maintenues isothermes pendant 1 h. Les résultats obtenus sont illustrés par le Tableau I.

TABLEAU I

Résultats en thorium et en cérium obtenus expérimentalement par la méthode d'analyse à l'iodate à diverses températures

Température de l'expérience (°C)	Métal (Th) précipité par l'iodate (%)*	Métal (Ce) analysé dans le filtrat après précipitation par l'iodate (%)*
40	83.1	114.2
20	101.7	96.7
15	109.6	93.1
10	111.4	91.9
7	110.9	92.1
5	110.3	89.8
2	104.6	94.8
0	100.9	101.2
−2	99.8	100.5
−5	99.6	100.2
−7	97.9	104.5
−10	95.5	110.7

*Les résultats sont donnés en pourcentage du thorium ou du cérium, contenus dans la solution analysée et déterminés par la pesée des composés purs de départ.

Le précipité final d'iodate est considéré comme un composé de thorium exempt de cérium tandis que le filtrat est réputé contenir le cérium exempt de thorium.

Les résultats expérimentaux montrent notamment que pour des températures de l'ordre de 40 °C, la quantité de thorium précipitée par l'iodate est largement déficitaire et plus de 15% de thorium restent dans la solution et s'ajoutent au cérium du filtrat comme le montre le résultat excédentaire de l'analyse du cérium. Ce phénomène est connu des auteurs spécialisés qui recommandent parfois de "refroidir la solution" ou de

Can. J. Chem. Downloaded from www.nrcresearchpress.com by 210.87.254.40 on 09/05/12
For personal use only.

"tenir la solution bien froide" lors de la précipitation.

Toutefois, ils ne donnent aucune précision relativement à la température optimale et "refroidir la solution" ou "tenir la solution bien froide" se fait le plus souvent en plaçant simplement les ballons contenant les solutions à refroidir dans un bassin à eau courante et la température obtenue de cette manière est généralement de l'ordre de 5 à 15 °C. Or c'est précisément pour ces températures que les erreurs sont les plus importantes dans la détermination du thorium. Ces erreurs peuvent dépasser 10%. Même dans le cas, rare d'ailleurs, où le refroidissement se fait par immersion dans la glace fondante, l'erreur est encore supérieure à 4%. Il est dès lors vraisemblable qu'à ces températures, une partie du cérium est précipité par l'iodate, dans les conditions opératoires classiques, comme semble le confirmer la coloration de ce précipité, qui est nettement jaune au dessus de 2 °C et blanc aux températures inférieures. De surcroît, la quantité de thorium est finalement déterminée par pesée de l'oxyde et le facteur de conversion en métal est plus élevé pour le thorium que pour le cérium. Dès lors la présence d'oxyde de cérium dans le produit réputé être exclusivement de l'oxyde de thorium accentue encore l'erreur par excès des résultats en thorium. De même, dans la détermination du cérium dans l'expérience réalisée à 40 °C, la présence d'oxyde de thorium dans un produit réputé être exclusivement de l'oxyde de cérium, renforce l'erreur par défaut.

Aux températures inférieures à −5 °C, les résultats expérimentaux de détermination du thorium deviennent déficitaires vraisemblablement parce que les conditions physiques de précipitation sont modifiées comme semble le confirmer un changement dans l'aspect du précipité.

Selon les résultats expérimentaux obtenus, la température optimale de précipitation devrait être comprise entre 0 et −5 °C et serait de l'ordre de −2 °C.

Application aux sulfates, aux mélanges non équipondéraux et aux minerais

Dans l'analyse des principaux minerais de thorium, le thorium et le cérium sont le plus souvent lixiviés en milieu sulfurique et d'autre part la teneur en cérium est généralement de loin plus élevée que la teneur en thorium. Aussi avons-nous appliqué l'étude de la température de précipitation par l'iodate à des mélanges de ces deux métaux dans lesquels la teneur en cérium est 5 fois, 10 fois et 20 fois plus importante que celle en thorium, à des solutions sulfatées et à des minerais de monazite à 0.3%–2% et 14% de thorium. Les résultats expérimentaux confirment ceux obtenus ci-dessus. En effet, le choix de températures de 2 à 20 °C pour la précipitation par l'iodate entraîne des erreurs excédentaires relatives de 5 à 20% sur les teneurs en thorium. Toutefois, les quantités de cérium qui accompagnent le thorium dans la précipitation restent faibles et ne sont nullement proportionnelles au thorium. Par ailleurs, les températures optimales de précipitation sont encore de l'ordre de −2 °C.

Précipitation de solutions pures contenant un seul des métaux étudiés

En vue de préciser les rôles respectifs du thorium et du cérium en fonction de la température au cours de la méthode de précipitation par l'iodate, deux séries d'expériences ont été effectuées d'une part sur des solutions pures de thorium exemptes de cérium et d'autre part sur des solutions pures de cérium exemptes de thorium.

Dans le cas des solutions de thorium, les résultats montrent normalement que la précipitation de ce métal par l'iodate, dans les conditions opératoires décrites ci-dessus, est complète pour des températures comprises entre 15 et −5 °C. Dans le cas des solutions de cérium, une faible quantité de cérium est précipitée pour des températures supérieures à 0 °C et notamment entre 5 et 15 °C, mais les quantités précipitées sont inférieures à 5% de celles alimentées dans les solutions analysées et sont donc nettement plus faibles que les écarts constatés dans les résultats ci-dessus relatifs aux analyses des solutions contenant simultanément les deux métaux. Dès lors, l'entraînement du cérium dans les précipités à ces températures ne serait donc pas dû uniquement à la solubilité intrinsèque de l'iodate de cérium mais serait provoqué ou du moins accentué par la présence du thorium.

Par ailleurs, les précipités d'iodate de cérium, obtenus lors de la première précipitation par la solution contenant 15 g de KIO_3, ont une coloration jaune aux températures supérieures à 2 °C

mais nettement blanche aux températures inférieures. Ainsi, le changement de coloration de l'iodate en fonction de la température ne peut être, à lui seul, un critère de la pureté de l'iodate de thorium ou de sa pollution par de l'iodate de cérium.

Conclusion

Selon les renseignements fournis par les ouvrages spécialisés, la précipitation de l'iodate de thorium doit se faire en "solution froide". Toutefois l'imprécision relative à la température peut faire supposer à l'utilisateur, dont ce n'est pas le rôle spécifique d'établir la méthode analytique, que des températures de l'ordre de 5 à 10 °C conviennent parfaitement.

Une étude expérimentale, employant notamment un appareillage ultrathermostat-cryostat nous a permis de constater formellement que le choix de telles températures entraîne des erreurs excédentaires appréciables dans les déterminations analytiques. Les résultats expérimentaux montrent qu'il ne suffit pas de refroidir les solutions mais que la température optimale de précipitation est de l'ordre de −2 °C. Cette valeur a été vérifiée sur des mélanges de composés purs et sur des minerais naturels.

Par ailleurs, l'influence perturbatrice du cérium ne dépend pas uniquement des propriétés intrinsèques de ce métal mais subit l'influence de la présence de thorium.

La détermination de la température optimale permet donc d'obtenir une plus grande exactitude analytique et d'assurer ainsi un meilleur contrôle du bilan des opérations métallurgiques.

1. C. DUVAL. Traité de microanalyse minérale qualitative et quantitative. Tome II. Presses scientifiques internationales, Paris. 1955.
2. M. PINTA. Recherche et dosage des éléments traces. Dunod, Paris. 1962. pp. 161, 529.
3. P. F. THOMASON *et al.* Anal. Chem. **21**, 1239 (1949).
4. C. V. BANKS et C. H. BURD. Anal. Chem. **25**, 416 (1953).
5. D. W. MARGERUM *et al.* Anal. Chem. **25**, 416, 1219 (1953).
6. F. M. GRIMALDI et M. H. FLETCHER. Anal. Chem. **28**, 812 (1956).
7. D. COZZI et S. VIVARELLI. Mineral Ital. 10 (1953).
8. G. SCHARZENBACH. Die komplexometrische Titration. F. Enke Verlag, Stuttgart. 1955.
9. Méthodes d'analyses complexométriques par les titriplex. E. Merck A.G., Darmstadt. 1963.
10. R. MALAT *et al.* Chem. Listy, **48**, 533 (1954).
11. W. R. SCHOELLER et A. R. POWELL. The analysis of minerals and ores in the rare elements. Charles Griffin and Co., Ltd., London, England. 1955. p. 156.
12. G. CHARLOT et R. GAUGUIN. Dosages colorimétriques. Masson, Paris. 1952. p. 224.
13. F. G. ASSELIN *et al.* J. Phys. Chem. **54**, 640 (1950).
14. D. DYRSSEN. Svensk Kem. Tidskr. **65**, 43 (1953).
15. Z. HAGIWARA. Technol. Rept. Tôhoku Univ. **18**, 16 (1953).
16. M. W. LERNER et G. PETRETIC. Anal. Chem. **25**, 227 (1956).
17. D. DYRSSEN. Rec. Trav. Chim. **75**, 753 (1956).
18. R. MACEK et L. MORAVEK. Nature, **178**, 103 (1956).
19. R. BOCK et E. BOCK. Naturwissenschaften, **36**, 344 (1949); Chem. Abstr. **44**, 5749 (1950).
20. R. A. NAGLE et T. K. MURTHY. Current Sci. India, **26**, (1957); Chem. Abstr. **52**, 6052 (1958).
21. D. DYRSSEN et V. DAHLBERG. Acta Chem. Scand. **7**, 1186 (1953).
22. W. E. BROWN et W. RIEMEN. J. Am. Chem. Soc. **74**, 1278 (1952).
23. H. A. GRINIER. Comm. Energie At. France, Rappt. No. 374 (1955).
24. R. COLLÉE, J. GOVAERTS et L. WINAND. Progr. Nucl. Energy, Ser. IX, 289 (1959).
25. R. COLLÉE. Rev. Universelle Mines, **10**, 329 (1965).
26. R. COLLÉE. Génie Chim. **98**, 5, 703 (1967).

Can. J. Chem. Downloaded from www.nrcresearchpress.com by 210.87.254.40 on 09/05/12
For personal use only.

Studies on the surface area of zeolites, as determined by physical adsorption and X-ray crystallography

D. J. C. YATES
Central Basic Research Laboratory, Esso Research and Engineering Company, Linden, New Jersey
Received September 18, 1967

The determination of the surface areas of zeolites is discussed. It is shown that it is incorrect to use the multilayer isotherm method of Brunauer, Emmett, and Teller for solids where only little more than one monolayer can be adsorbed, in cavities little larger than the adsorbed molecules. The areas of such materials can, however, be determined from the beginning of the linear portion of their isotherms (point B). In addition, X-ray spectra can provide an independent method of measuring changes in the surface areas of zeolites.

Canadian Journal of Chemistry, **46**, 1695 (1968)

Can. J. Chem. Downloaded from www.nrcresearchpress.com by 210.87.254.6 on 09/05/12
For personal use only.

Introduction

Although there is now a very considerable volume of work dealing with adsorption on zeolites, there is very little of it that is concerned with the problem of the determination of the surface area of such materials.

In general, although there has been considerable criticism of its theoretical basis (see review in refs. 1*a*, 2, 3*a*), the equation derived by Brunauer, Emmett, and Teller (B.E.T.) (4) has gained wide acceptance as a valid method of determining the surface area of solids. Nevertheless in some instances, it is considered that the B.E.T. equation, at least as regards surface area determination, has its main utility in being a convenient analytical method (1*b*, 2*a*) of locating point B (5), the point on the isotherm where a monolayer is adsorbed.

Most solid surfaces have physical adsorption isotherms of type II in Brunauer's classification (6), and their geometrical structure is such that there is no physical restriction on the number of layers of gas that can be adsorbed. Such multimolecular layers cannot form on zeolites (and some charcoals), as their very small cavities are of similar dimensions to molecules which are adsorbed (7–9). Under such conditions, the isotherms are expected to be of type I in nature. Such isotherms have been reported by many workers using the natural zeolites analcite (9), chabazite (7–9), erionite (10), and mordenite (7, 11), and with the synthetic zeolites faujasite (7, 12–17), mordenite (18), and type A (7, 19). Some values of surface areas have been given in the above work (10, 15, 19) and in reviews (20, 21). There has, however, been no agreement on the best method of area determination, some workers using the B.E.T. method (15, 19, 22, 23), others (10, 19) using the Langmuir equation (2*b*). Barrer has introduced (20, 21) the concept of monolayer equivalent area for zeolites.

Some data on a synthetic faujasite are presented, where the area values obtained with the B.E.T. equation are compared with those obtained by the point B method. It is stressed that the B.E.T. equation should not be used for materials with very small pores, such as zeolites. As zeolites are crystalline, the possibility exists of measuring relative surfaces areas by X-ray crystallography. This has been examined, and it is shown that this method can easily be used to monitor surface area changes in zeolites.

Experimental

Apparatus and Materials

All isotherms were determined volumetrically, using argon at 77 °K. For most of the work, conventional Pyrex glass cells and vacuum systems were used, the pressures being measured with mercury manometers (24). In some cases, however, a quartz Bourdon gauge was used to measure pressures (17).

The X-ray equipment consisted of a Phillips diffractometer, using copper Kα radiation, with a Geiger counter detector. The zeolite samples were exposed to air while their spectra were being measured.

The synthetic faujasite used was an experimental material donated by the Davison Division of W. R. Grace & Co., and had a silica-to-alumina ratio similar to that of zeolite Y of the Linde Co. (25, 26). The structure of this zeolite is similar to that of synthetic zeolite Linde X, which is fairly well known (26–28). The material contained some 15% of a binder, but the nature and surface area of the binder were not given by the manufacturer. The argon, of purity 99.5%, was obtained from the Matheson Co., East Rutherford, New Jersey.

Procedure

In addition to the fresh material, 11 samples were available which had been used, under varying degrees of

severity, for drying gases. All samples were handled identically. For the surface area measurements 1 g was loaded into the Pyrex cells, and evacuation begun. The cell was then heated to 150 °C while pumping. After a good vacuum was reached at this temperature, the temperature was increased to 370 °C. Pumping was then continued until a vacuum of 2×10^{-5} Torr or better was obtained. The cell was then closed, cooled to 77 °K, and argon added. After the isotherm was determined, the argon was evacuated while the sample was warmed to room temperature. The cell was then recooled to 77 °K and helium added to calibrate the cell. After this, the sample was taken out of the cell and weighed. All of the surface area values are given per gram of anhydrous zeolite. The samples were ground in a mortar and pestle for X-ray examination, and that portion which passed through a 300 mesh screen was used. The powder was pressed into a holder using McCreery's procedure as discussed in detail by Klug and Alexander (29).

Results

Surface Area Values

As referred to earlier (1*a*, 1*b*, 2*a*, 3*a*, 4–6), for physical adsorption isotherms, point B corresponds to the adsorption of a monolayer of molecules. If a molecule of known size such as nitrogen or argon is used, the surface area of the solid can be calculated from a knowledge of the number of moles of gas adsorbed, per gram of solid, at point B on the isotherm.

There are two widely accepted methods of determining point B (1*a*, 2). The first is simply to measure the isotherm in sufficient detail so that the shape of the "knee" near point B can be determined accurately. The other method is to use the B.E.T. equation and to determine two or more points on the isotherm in the relative pressure (p/p_0) region between 0.05 and 0.30. As the B.E.T. plot gives a straight line, the slope and intercept of which give the monolayer capacity, a minimum of two isotherm points is needed. In practice, for an accurate determination, it is usual to measure 3 or 4 points on an isotherm.

For molecular sieves, as they contain such small cavities, the isotherm is not type II, and the B.E.T. equation should not be used. The only way, therefore, that the surface areas can be determined is by measuring the isotherm in a fairly detailed fashion. This has been done in this work, and argon isotherms at 77 °K are shown in Figs. 1 and 2. From the first of these isotherms, it was determined that the point B occurred at a pressure of 1.5 cm ($p/p_0 = 0.071$), and this pressure was used to define the point B on subsequent isotherms. This meant that the isotherm

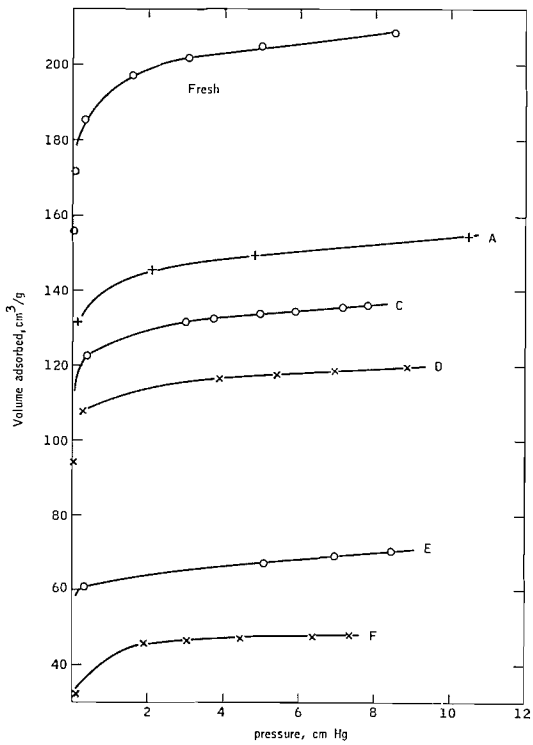

FIG. 1. Argon isotherms at 77 °K on a series of sodium faujasites.

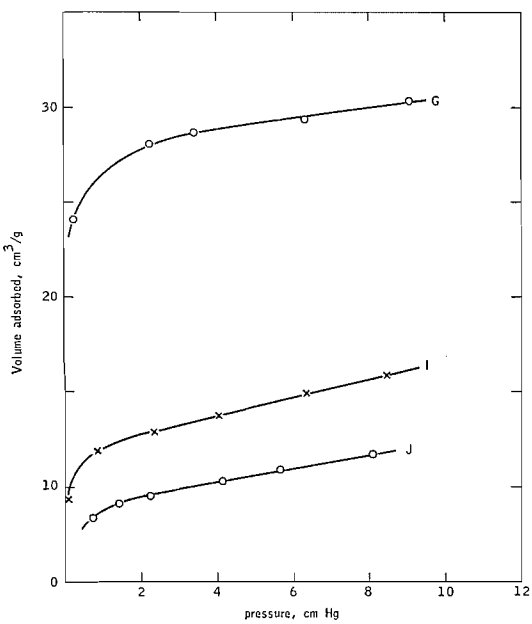

FIG. 2. Argon isotherms at 77 °K on a series of sodium faujasites.

Can. J. Chem. Downloaded from www.nrcresearchpress.com by 210.87.254.6 on 09/05/12
For personal use only.

TABLE I

Surface areas of Na—Y zeolites by two methods

Sample	Monolayer capacity from point B (cm^3/g)	Surface area from point B (m^2/g)	Surface area as % of fresh sample	Surface area using the B.E.T. equation (m^2/g)	Ratio of areas $\frac{\text{B.E.T. equation}}{\text{point B method}}$
Fresh	205.2	805.9	100	675.0	0.84
A	182.3	715.9	88.8	609.1	0.85
B	181.0	710.9	88.2	620.3	0.87
C	154.2	605.7	75.1	517.0	0.85
D	130.2	511.5	63.5	425.4	0.83
E	77.2	303.0	37.6	251.8	0.83
F	48.4	190.0	23.6	168.9	0.89
G	24.7	96.9	12.0	88.5	0.91
H	7.9	31.2	3.9	30.25	0.97
I	7.6	29.7	3.7	26.9	0.91
J	4.1	16.2	2.0	14.6	0.89
K	3.8	15.2	1.9	15.1	0.99

only had to be closely defined in this region, and that the isotherms did not have to be measured at pressures higher than about 10 cm. After the experiment was finished, the sample was taken out of the cell and rapidly weighed before it could adsorb water from the air. Using this dry weight, the surface areas were calculated, and these values are given in Table I. The areas have also been expressed as a percentage of the area of the fresh sieve. The area of the adsorbed argon atoms needed to calculate the surface area from the monolayer capacity has been taken as 14.6 $Å^2$, following Livingston (30).

In order to show the inapplicability of the B.E.T. equation to zeolites, we have also constructed a B.E.T. plot for every isotherm. In most cases, satisfactory B.E.T. plots were obtained, but the areas obtained from them (see Table I) were always found to be considerably lower than those obtained by the point B method, except for the samples of extremely low area (H–K). The latter had obviously lost most of their zeolitic character. As the area of the zeolite increased (i.e. going towards the fresh material), the B.E.T. equation gave areas with lower and lower values relative to the areas obtained from point B. It will be seen that the use of the B.E.T. equation with a normal zeolite would cause an underestimate of the area by about 20%.

Determination of Changes in Crystallinity

The unique characteristic of zeolites as adsorbents is that they are crystalline. Most silicas are amorphous, and some aluminas are partly crystalline, but the very development of the adsorptive property of a zeolite depends on its long-range order, as shown by its regular array of tetrahedrally coordinated cubo-octahedral structural units.

With specific reference to faujasite, a considerable amount of work on its structure and properties has been published (12, 26–28). In particular, its crystal structure has been determined by a three-dimensional Fourier analysis of its X-ray diffraction patterns by Broussard and Shoemaker (27). While their work was on the 13X faujasite, the structure of 13Y faujasite is quite similar (26). It has been found that various batches of synthetic zeolites, of the Na—X type, have variations in crystallinity depending on the variations in their manufacture.[1] These differences are proportional to the peak height at a given diffraction angle. Hence, if the instrumental conditions of the X-ray diffractometer are kept constant, changes in crystallinity can be easily followed with reference to the original zeolite. This has been done with all the samples used here. Their X-ray diffraction spectra have been determined, all under identical instrumental conditions, and the decrease in crystallinity has been determined with reference to the peak heights of the fresh zeolite. The peaks with Miller indices 331, 533, and 555 (see ref. 27) have been used. These have *d*-spacings of 5.70, 3.78, and 2.855 Å, and occur at 2θ values of about 15.5, 23.5, and 31.3. The complete spectra of Na—X over a range of 2θ values from 5 to 55 degrees is given in Fig. 1 of ref. 27. In this work

[1]D. J. C. Yates. Unpublished observations.

Can. J. Chem. Downloaded from www.nrcresearchpress.com by 210.87.254.6 on 09/05/12
For personal use only.

the spectra were also measured over the same range of 2θ values. However, to make the diagram simpler, typical spectra obtained for our samples are shown in Fig. 3 only for 2θ values between 14 and 34 degrees. In all cases the three peak heights were measured and expressed for each of the peaks as a percentage of the peak height of fresh zeolite. The average of these three peaks was then taken and used as the best indication of the overall crystallinity of the sample. The data are given in Table II.

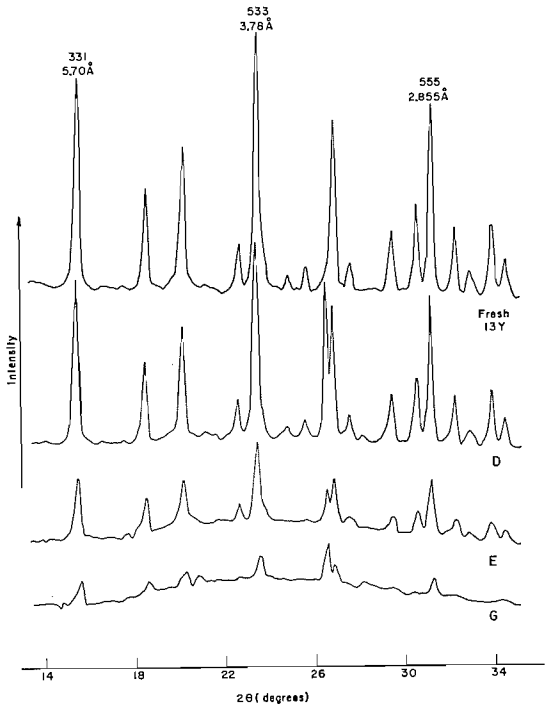

FIG. 3. X-ray diffraction patterns of a series of faujasites of decreasing surface area.

TABLE II

Crystallinity changes in Na—Y zeolites

Sample	Average crystallinity (%)	*d*-spacings 5.7 Å (% of fresh)	3.78 Å (% of fresh)	2.85 Å (% of fresh)
Fresh	100	100	100	100
A	95.7	100	92.2	94.8
B	97.0	98.5	92.5	100
C	80.1	82.5	78.4	79.4
D	76.2	77.5	74.5	76.5
E	32.6	35.0	31.0	31.8
F	30.5	34.2	28.4	28.9
G	10.5	11.6	9.5	—
H	6.8	8.3	6.4	5.6

I, J, and K all have zero crystallinity

Discussion

Adsorption Measurements

It has been known for some considerable time that most zeolites have type I (6) adsorption isotherms (7–9, 11–14, 18, 19), which are characteristic of monolayer adsorption, and capillary condensation is absent (2, 3*a*). The B.E.T. theory, on the other hand, applies to the case of multilayer adsorption (1*a*, 2, 3*a*), most commonly seen as type II isotherms. Under these circumstances, it is not surprising that the application of the B.E.T. equation to type I isotherms yields an incorrect value of v_m, the monolayer capacity. In this work, on a faujasite containing a binder, the B.E.T equation gave v_m values about 20% less than those obtained directly from point B.

Similar discrepancies can be found in the literature. For example, Eberly (15) used the B.E.T. equation to determine the area of Linde NaX faujasite and obtained a value of 760 m^2/g. In some isotherms on NaX using argon at 77 °K, when the point B was at 3.0 cm, we obtained monolayer capacity values of 228 cm^3/g (of dehydrated zeolite) for Lot No. 13961 and 230 cm^3/g for Lot No. 133692-R. These materials have been used in earlier work (17, 31, 32). Assuming an argon area of 14.6 $Å^2$, these capacities correspond to surface areas of 895 and 903 m^2/g. Again the B.E.T. value is too low.

In later work on erionite, Eberly (10) used both the B.E.T. equation and the Langmuir equation and considered the latter more reliable. Here, again, the B.E.T. values were considerably lower than the Langmuir values (10). Similar effects had been observed considerably earlier with A type zeolites by Breck and co-workers (19).

Other values obtained (23) by the B.E.T. method seem low, although a range of values was given (600–800 m^2/g) for zeolites A, X, and Y, with no further details.

For some considerable time it has been recognized that isotherms in zeolites can be represented by the Langmuir equation (7–14, 18, 19, 33, 34). In many cases, this equation has been used to obtain zeolite monolayer capacities, and hence surface areas. However, there are many problems in the use of the Langmuir equation to obtain v_m values (3*b*). For instance, there are numerous isotherms which give excellent straight-line Langmuir plots, but which fail to give consistent v_m values (3*c*). When consideration is given to

Can. J. Chem. Downloaded from www.nrcresearchpress.com by 210.87.254.6 on 09/05/12
For personal use only.

Can. J. Chem. Downloaded from www.nrcresearchpress.com by 210.87.254.6 on 09/05/12
For personal use only.

the assumptions underlying the Langmuir equation, it seems very unlikely that they could apply to adsorption in zeolitic cavities. In fact, it has been stated by Young and Crowell (2*c*): "Charcoal and chabazite are the only adsorbents characterized by type I isotherms and it is certain that adsorption on these two porous solids does not even approximate the severely simple Langmuir picture." With the addition of other zeolites, the above seems a fair summary of the situation.

From the above discussion, it will be seen that the B.E.T. multimolecular isotherm gives, as might be predicted for a type I isotherm, incorrect surface areas for zeolites. The Langmuir equation applies to type I isotherms. It does not necessarily follow, however, that the v_m values derived from the equation will be correct (2*c*, 3*b*, 3*c*). This would seem to eliminate all methods, except that of the recognition of point B as the completion of the monolayer. As the zeolite isotherms are type I with no rise in the amount adsorbed at saturation pressure (p_0), the possibility exists of using this point as a measure of surface area. For example, with the Na—X sample, which had an argon v_m value of 230 cm^3/g (corresponding to a surface area of 903 m^2/g), the amount adsorbed at saturation was 247 cm^3/g.

Very similar values (248 cm^3/g) have been reported by Barrer and Sutherland (12). If this value is taken as equivalent to a monolayer, the area would then be 970 m^2/g.

On balance, the use of the point B, which is very well established with adsorbents with type II isotherms, is considered the most reliable. It is also relatively insensitive to the particular pressure chosen for point B, as shown by the data in Table III for argon at 77 °K on NaX (Lot No. 133692-R). If point B is taken at 3.0 cm, v_m is 230 cm^3/g. However, if it were to be taken anywhere in the pressure region from 1.5 to 5 cm, the v_m value would be within $\pm 2.5\%$ of that at 3 cm. This is very much less than the uncertainty in the area (σ_m) which the argon atom occupies (30) in the monolayer (14.6 $Å^2$). The problems in assigning a unique σ_m value to a given molecule have been discussed recently (2*d*). Even nitrogen (at −195 °C), which has probably been used more than any other adsorbate, has been assigned σ_m values ranging from 15.4 $Å^2$ to 16.2 $Å^2$ (1*c*, 30).

In conclusion, providing that no molecular sieve effects interfere (e.g. neither A nor N_2 are adsorbed (19) on Na—A at −195 °C) it is proposed that the determination of point B on an isotherm of a simple, small, nonpolar molecule such as argon, nitrogen, or oxygen offers the most accurate means of measuring the surface areas of zeolites. Other adsorbents which give type I isotherms with the above gases (for example some kinds of charcoal (35)) should also be treated in the same fashion. Some remarks in a recent paper (36) also draw attention to the difficulties of using the B.E.T. equation for zeolites, and a procedure is suggested which seems similar to that used here, although point B was not determined explicitly.

TABLE III

Argon isotherm at 77 °K on Na—X

Pressure (cm Hg)	Volume adsorbed (cm^3/g)	Corresponding surface area (m^2/g)
1.0	219	860
1.5	224	880
2.0	226.5	889
2.5	228	895
3	230	903
4	232.5	913
5	234	919
10	238	935
15	242	950
21(sat. press.)	247	970

X-Ray Measurements

Although some considerable effort has been put into using low-angle X-ray scattering as a method of measuring surface areas (1*d*), it has not been too successful. The difficulty is that only crystallite sizes are given, rather than total surface area.

This limitation does not apply here, as the unique characteristic of zeolites as adsorbents is that they are entirely crystalline and normal X-ray techniques can be used. Despite this, there has apparently been only one attempt made very recently (36) to use the X-ray spectra of zeolites as a measure of their surface area. The only details given were: "The changes in surface area as determined by N_2 adsorption and in crystallinity as determined by X-ray analysis were always found to be in general agreement."

Before this work was started, there was very little information available in the literature about the usefulness of the X-ray spectra as a measure of the decreasing surface areas of zeolites. It should also be stressed that there are almost no data on, and less understanding of, the reasons

Can. J. Chem. Downloaded from www.nrcresearchpress.com by 210.87.254.6 on 09/05/12
For personal use only.

for the breakdown of zeolites at elevated temperatures. For instance, it is conceivable that the outer portions of the sieve crystals might decompose most readily. If the products of this decomposition were amorphous silica and alumina, it is possible that this amorphous material would block the very small (13 Å) holes in the outside of the crystal. It is then probable that the surface area would drop considerably, as there would be a much restricted access to the interior of the crystals. However, such a process would not readily be detected by X-rays, as the overall crystallinity of the material would be but little affected.

Data given in Tables I and II and Fig. 4 show that the above process only occurs to a small extent under the conditions used here. If the surface area and crystallinity decreased to exactly the same extent, the points would all fall on the 45° line shown in Fig. 4. This line is defined by the fresh zeolite (100% surface area and 100% crystallinity) and the origin, when all surface area and all crystallinity are lost. The points in Fig. 4 lie fairly close to this line, considering the difficulties in measuring the crystallinities. However, there are 6 points below the line (greater loss in area than in crystallinity) and 3 above it, so there is some slight evidence that surface area is lost to a greater degree than is crystallinity.

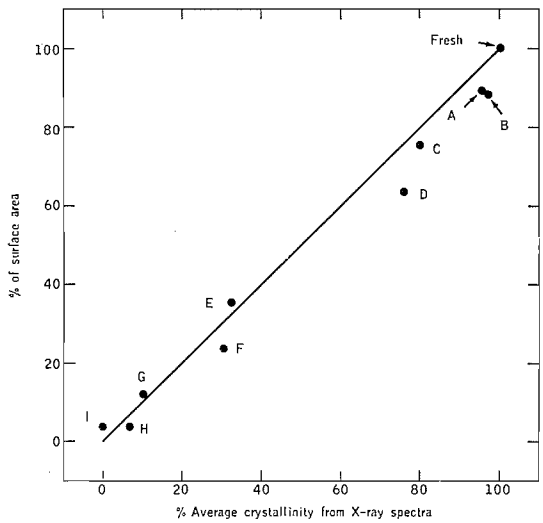

FIG. 4. Relation between average crystallinity and surface area for a series of faujasites.

It is concluded that, under the above conditions, surface area changes in zeolites can be measured equally well by gas adsorption or by X-ray crystallinity measurements. Nevertheless, the gas adsorption method is the most generally applicable, as there are times when the X-ray spectra vary for other reasons than surface area changes. For instance, if it is desired to ascertain whether the zeolite structure has not been damaged as a result of ion exchange, the X-ray spectra cannot readily be employed to do this. The expected changes in surface area per gram of dehydrated zeolite can be calculated, and values close to these have been found (17) for the Ag—X and Li—X. On the other hand, if a series of zeolites with the same structure and cation but varying areas are under study, the X-ray method may be faster than the adsorption method, although the latter method is probably the most accurate.

Absolute Areas

Zeolites are unique among highly dispersed materials, as they are crystalline in nature. If its structure is fully understood, and its dimensions established, a given zeolite can then have an "absolute" surface area, that is, an area defined crystallographically. Such an area will be independent of the errors and uncertainties inherent in area values derived from physical adsorption isotherms.

For the X form of faujasite, many X-ray measurements of its structure have been reported (12, 26–28, 37), and the volumes of its supercages have been calculated and converted into surface area values (38, 39). It is known that gases such as argon and krypton do not enter the sodalite cages (17, 40), so that area values obtained from isotherms of these gases can be directly compared with values calculated from the size of the supercages. For argon, with the point B method, the sample of Na—X used in this work has a surface area of 903 m^2/g. One of the calculations (38) gave a value of 1400 m^2/g for Na—X, which seems rather high. Other calculations (39) gave values between 960 and 1132 m^2/g, depending on the model used. In view of the fact that most samples of zeolites probably contain some amount of noncrystalline material, surface area values calculated from crystallographic data should be higher than values obtained from isotherm measurements. With this proviso, it is felt that the experimental value (903 m^2/g) is in

quite good agreement with the calculated (39) values (960–1132 m^2/g).

As calculations become more precise in the future, it should be possible to use the difference between the experimental and calculated surface areas as a measure of absolute degree of crystallinity of a given sample. At present, no samples of known crystallinity seem to be available, so that X-ray spectra cannot be used to measure the absolute crystallinity of zeolites. The value of 100% average crystallinity was assigned to the fresh NaY zeolite in Table II solely to enable relative comparisons to be made, and should not be taken to imply that this material is entirely crystalline (apart from its binder content, whose nature is unknown).

1. P. H. EMMETT. *In* Catalysis. Vol. 1. Reinhold Publishing Corp., New York, N.Y. 1954. (*a*) p. 31; (*b*) p. 40; (*c*) p. 38; (*d*) p. 63.
2. D. M. YOUNG and A. D. CROWELL. Physical adsorption of gases. Butterworths and Co. Ltd., London. 1962. (*a*) p. 190; (*b*) p. 183; (*c*) p. 109; (*d*) p. 226.
3. S. BRUNAUER, L. E. COPELAND, and D. L. KANTRO. *In* The solid–gas interface. Vol 1. *Edited by* E. A. FLOOD. M. Dekker Inc., New York, N.Y. 1967. (*a*) p. 77; (*b*) p. 80; (*c*) p. 83.
4. S. BRUNAUER, P. H. EMMETT, and E. TELLER. J. Am. Chem. Soc. **60**, 309 (1938).
5. P. H. EMMETT and S. BRUNAUER. J. Am. Chem. Soc. **59**, 1553 (1937).
6. S. BRUNAUER. The adsorption of gases and vapors. Princeton University Press, Princeton, N.J. 1945.
7. W. E. ADDISON and R. M. BARRER. J. Chem. Soc. 757 (1955).
8. P. H. EMMETT and T. W. DEWITT. J. Am. Chem. Soc. **65**, 1253 (1943).
9. R. M. BARRER. Proc. Roy. Soc. London, Ser. A, **167**, 393 (1938).
10. P. E. EBERLY. Am. Mineralogist, **49**, 30 (1964).
11. R. M. BARRER. Trans. Faraday Soc. **40**, 555 (1944).
12. R. M. BARRER and J. W. SUTHERLAND. Proc. Roy. Soc. London, Ser. A, **237**, 439 (1956).
13. R. M. BARRER and W. I. STUART. Proc. Roy. Soc. London, Ser. A, **249**, 464 (1959).
14. R. M. BARRER and P. J. REUCROFT. Proc. Roy. Soc. London, Ser. A, **258**, 431 (1960).
15. P. E. EBERLEY. J. Phys. Chem. **65**, 68 (1961).
16. H. W. HABGOOD. Can. J. Chem. **42**, 2340 (1964).
17. D. J. C. YATES. J. Phys. Chem. **70**, 3693 (1966).
18. R. M. BARRER and D. L. PETERSON. Proc. Roy. Soc. London, Ser. A, **280**, 466 (1964).
19. D. W. BRECK, W. G. EVERSOLE, R. M. MILTON, T. B. REED, and T. L. THOMAS. J. Am. Chem. Soc. **78**, 5963 (1956).
20. R. M. BARRER. 10th Colston Symposium on the structure and properties of porous materials. Butterworths, London. 1958. p. 6.
21. R. M. BARRER. Brit. Chem. Eng. **4**, 267 (1959).
22. P. B. VENUTO, E. L. WU, and J. CATTANACH. Paper presented at Molecular Sieve Symposium, Soc. Chem. Ind., London, April 1967.
23. R. L. MAYS and P. E. PICKERT. Paper presented at Molecular Sieve Symposium, Soc. Chem. Ind., London, April 1967.
24. D. J. C. YATES, W. F. TAYLOR, and J. H. SINFELT. J. Am. Chem. Soc. **86**, 2996 (1964).
25. D. W. BRECK. U.S. Patent No. 3 130 007 (1964).
26. D. W. BRECK. J. Chem. Educ. **41**, 678 (1964).
27. L. BROUSSARD and D. P. SHOEMAKER. J. Am. Chem. Soc. **82**, 1041 (1960).
28. R. M. BARRER. Endeavour, **23**, 122 (1964).
29. H. P. KLUG and L. E. ALEXANDER. X-ray diffraction procedures. J. Wiley and Sons, Inc., New York, N.Y. 1954. p. 300.
30. H. K. LIVINGSTON. J. Colloid Sci. **4**, 447 (1949).
31. J. L. CARTER, P. J. LUCCHESI, and D. J. C. YATES. J. Phys. Chem. **68**, 1385 (1964).
32. D. J. C. YATES. J. Phys. Chem. **69**, 1676 (1965).
33. P. CANNON. J. Phys. Chem. **63**, 160 (1959).
34. P. CANNON and C. P. RUTKOWSKI. J. Phys. Chem. **63**, 1292 (1959).
35. S. BRUNAUER and P. H. EMMETT. J. Am. Chem. Soc. **59**, 2682 (1937).
36. C. V. MCDANIEL and P. K. MAHER. Paper presented at Molecular Sieve Symposium, Soc. Chem. Ind., London, April 1967.
37. R. M. BARRER, F. W. BULTITUDE, and J. W. SUTHERLAND. Trans. Faraday Soc. **53**, 1111 (1957).
38. M. M. DUBININ. Izv. Akad. Nauk SSSR Ser. Khim. 209 (1964).
39. A. V. KISELEV and A. A. LOPATKIN. Kinetika i Kataliz, **4**, 786 (1963).
40. L. V. C. REES and C. J. WILLIAMS. Trans. Faraday Soc. **60**, 1973 (1964).

Can. J. Chem. Downloaded from www.nrcresearchpress.com by 210.87.254.6 on 09/05/12
For personal use only.

Temperature dependence of the electron resonance spectrum of the hydrazine positive ion

H. R. FALLE
Theoretical Chemistry Laboratory, McGill University, Montreal, Quebec
Received November 16, 1967

A temperature study of the hydrazine positive ion, $N_2H_4^+$, showed that the ratio of the nitrogen hyperfine splitting to the proton hyperfine splitting, $|a_N/a_H|$, increased with increasing temperature. The increase in $|a_N/a_H|$ was approximately 3%, while the increase in a_N itself was less than 1% over the 50 °C temperature range. This effect is attributed to torsional vibration about the N—N bond and is assessed on this basis.

Canadian Journal of Chemistry, 46, 1703 (1968)

Can. J. Chem. Downloaded from www.nrcresearchpress.com by 210.87.254.5 on 09/05/12
For personal use only.

Introduction

The temperature dependence of amino proton hyperfine splitting has been reported for the 4-amino-2,6-di-*t*-butyl phenoxy radical (1). This effect was attributed to torsional vibration of the amino group with respect to the plane of the aromatic ring (2). A temperature study of the hydrazine positive radical-ion has shown similar behavior; the ratio $|a_N/a_H|$ was found to increase with increasing temperature. An e.p.r. spectrum of $N_2H_4^+$ is shown in Fig. 1, and the variation of the ratio $|a_N/a_H|$ with temperature is displayed in Fig. 2. As pointed out by Adams and Thomas (3), assessment of the relative intensities of the 25 line spectrum of $N_2H_4^+$ leads to the assignment $a_N > a_H$. Had the proton hyperfine splitting, a_H, been greater than a_N, the intensities of the lines which are circled in Fig. 1 would have been in the ratios 3:8:6 instead of 6:8:3.

Experimental

Using the method of Adams and Thomas (3), $N_2H_4^+$ was generated by the aqueous flow technique using preheated solutions of 0.16 *M* aqueous hydrazine and 0.08 *M* ammonium ceric sulfate in 1 *M* sulfuric acid. A Varian V-4500-10A EPR spectrometer was employed, and to determine the temperature variation of $|a_N/a_H|$, only the three central "groups" of hyperfine lines were recorded (see Fig. 1). The temperature was monitored with a copper–constantan thermocouple inserted into the outlet stream just outside the microwave cavity. Each temperature cited in Fig. 2 is the average, taken to the nearest 0.5 °C, of the temperature measured at the first and third of the three central line-groups recorded. A capillary tube containing dilute peroxylamine disulfonate solution was affixed to, and sufficiently insulated from, the quartz flat-cell to serve as the calibration standard. Interference between the high-field line of the standard and the third line-group $N_2H_4^+$ recorded was negligible. Preliminary determinations of the variation of $|a_N/a_H|$ with temperature using a perylene positive-ion field-scan calibration, that is without the above calibration setup, showed essentially the same slope as reported here. Hence it is inferred that the nitrogen hyperfine coupling in peroxylamine disulfonate is independent of temperature, at least over the temperature range under consideration. The magnetic field-strength was determined using a Varian F-8 fluxmeter coupled with a Schomandl FD-1 frequency meter.

Discussion

The factor $g = 2.00346$ (std. dev. 0.00003), the hyperfine coupling $a_N = 32.5$ Mc/s, and the ratio $|a_N/a_H| = 1.047$ at 25 °C obtained in this study are in agreement with published results (3). A least-squares analysis of the temperature variation of the ratio $|a_N/a_H|$ gave the intercept at 0 °C as 1.027 and the slope as 0.00080 per deg C with a standard error of 0.0025. The mean of the values for the nitrogen hyperfine coupling was found to be $a_N = 32.52$ Mc/s (std. dev. 0.21), whereas the method of least squares gave the intercept at 0 °C as 32.35 Mc/s and the slope as 0.005 Mc/s per deg C with a standard error of 0.20.

Since the data show little justification for assuming any temperature dependence of the nitrogen hyperfine coupling, a_N will be considered to have a constant value of 32.5 Mc/s in the treatment to follow. The increase in the ratio $|a_N/a_H|$ with temperature in $N_2H_4^+$ can be explained using the torsional vibration treatment due to Stone and Carrington (2). The ion $N_2H_4^+$ is iso-electronic with the mono-negative ion of ethylene and hence, the unpaired electron can be assigned to the antibonding orbital

$$\frac{1}{\sqrt{2}}[(2p_z)_{N_1} - (2p_z)_{N_2}],$$

which has a node between the two nitrogen atoms. The atoms in $N_2H_4^+$ are labelled as

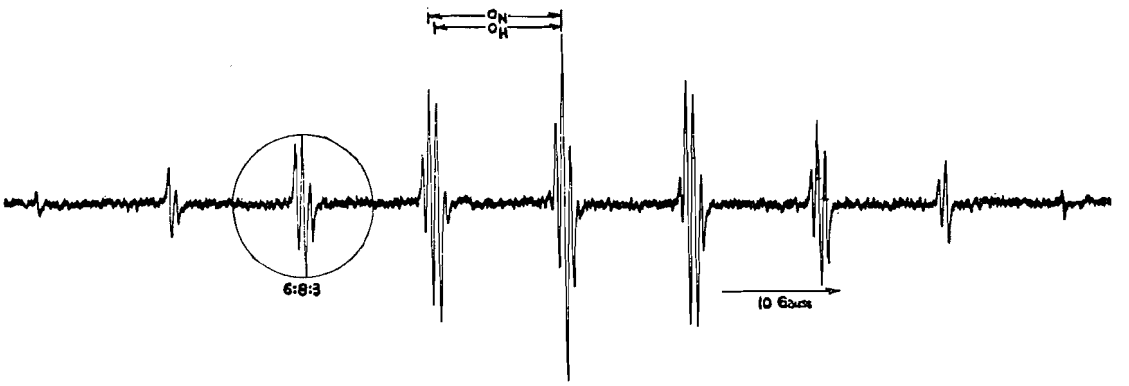

FIG. 1. The first-derivative e.p.r. spectrum of the radical-ion $N_2H_4^+$ in aqueous solution at 35 °C.

shown in the inset in Fig. 2. In the equilibrium position, $\theta = 0°$, the hyperfine coupling a_{N_1} and a_{H_a} $(= a_{H_b})$ are proportional to the unpaired π-electron spin population on nitrogen atom 1. This follows from the usual concepts embodied in the relationships (4)

$$[1] \qquad a_N = Q_N \rho_N^{\pi} \quad (Q_N > 0)$$

and

$$[2] \qquad a_H = Q_H \rho_N^{\pi} \quad (Q_H < 0),$$

where Q is the proportionality constant which relates the hyperfine coupling, a, to the unpaired spin population, ρ^{π}.

When the angle between the planar halves of $N_2H_4^+$ is $\theta > 0°$, overlap can occur between any antisymmetric combination of the bonding σ-orbitals ($\sigma_{N_1H_a}$ and $\sigma_{N_1H_b}$) of the amino group incorporating N_1 and the $2p_z$-orbital of N_2. Overlap can also occur between the orbital $(2p_z)_{N_2}$ and an antisymmetric combination of the antibonding orbitals $\sigma^*_{N_1H_a}$ and $\sigma^*_{N_1H_b}$. Thus, the perturbation imposed on the $2p_z$-orbital of nitrogen atom 2 can be expressed in the form of two equations:

$$[3] \quad (C_\sigma/\sqrt{2})[\sigma_{N_1H_a} - \sigma_{N_1H_b}] + C_N[(2p_z)_{N_2}]\lambda' \sin\theta$$
$$(C^*_\sigma/\sqrt{2})[\sigma^*_{N_1H_a} - \sigma^*_{N_1H_b}] + C_N[(2p_z)_{N_2}]\lambda'' \sin\theta.$$

Similar expressions hold for the pertubation experienced by nitrogen atom 1 due to the σ-orbitals of the N_2 amino group. Hence, the effect of torsional displacement through $\theta°$ would be to introduce positive spin density at the protons, which would bring about an overall decrease in the proton hyperfine coupling, a_H. This treatment can be simplified by assuming that the torsional displacement is small so that the perturbed coefficient, C_N, is approximately equal to the coefficient of the unperturbed $2p_z$-orbital, C_N^0, and that the resonance integral, β_{NN}, remains essentially constant. As a consequence, $Q_N = 65.0$ Mc/s follows from eq. [1], since $\rho_N^{\pi} = |C_N^0|^2 = 0.5$ and the mean value of a_N is 32.5 Mc/s.

The contribution to the proton coupling arising from the perturbations due to the torsional motion will be proportional to $|C_N|^2 \sin^2\theta$ and can be expressed as

$$[4] \qquad Q_t \rho_N^{\pi} \sin^2\theta$$

where $Q_t > 0$. The proton hyperfine couplings at a given angle of displacement will then be

$$[5] \quad a_{H_a} = a_{H_b} = Q_H \rho_{N_1}^{\pi} + Q_t \rho_{N_2}^{\pi} \sin^2\theta$$
$$a_{H_c} = a_{H_d} = Q_H \rho_{N_2}^{\pi} + Q_t \rho_{N_1}^{\pi} \sin^2\theta$$

and since $\rho_{N_1}^{\pi} = \rho_{N_2}^{\pi} = 1/2$, the hyperfine coupling for all protons as a function of θ becomes

$$[6] \qquad a_H(\theta) = \frac{Q_H}{2} + \frac{Q_t}{2} \sin^2\theta.$$

Thus, the formula for the temperature variation of a_H will contain the torsional vibration frequency and the extent of orbital mixing since Q_t contains the parameters λ' and λ''.

Proceeding as previously described (2), $a_H(\theta)$ can be averaged over a given vibrational state by utilizing the relationship

$$[7] \qquad \langle\theta^2\rangle_\nu = \left[(\nu + \tfrac{1}{2})\frac{\Delta E_\nu}{K}\right],$$

where ΔE_ν is the energy of the state with quantum number ν above the ground state, and K is

Can. J. Chem. Downloaded from www.nrcresearchpress.com by 210.87.254.5 on 09/05/12
For personal use only.

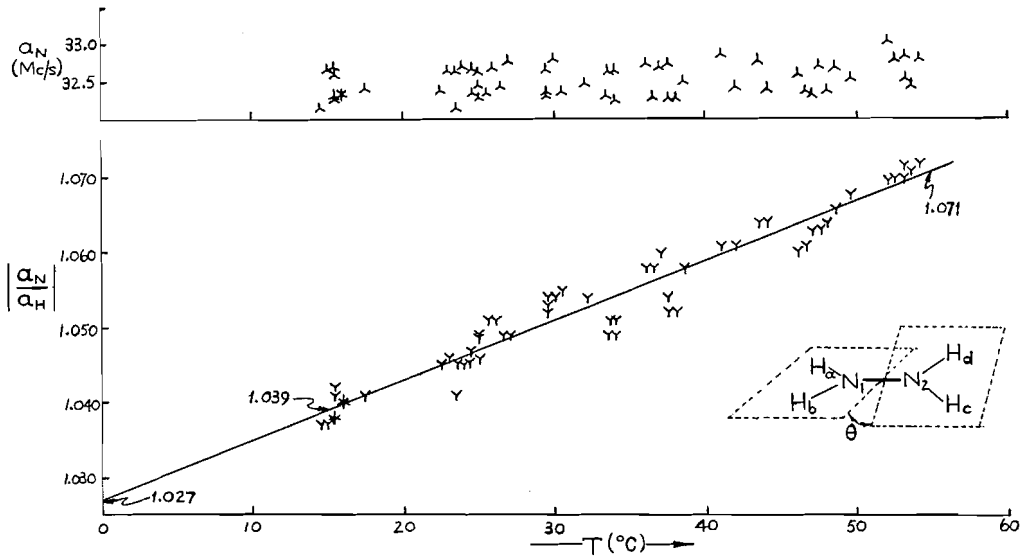

FIG. 2. The nitrogen coupling, a_N, and the temperature variation of the ratio $|a_N/a_H|$ in the radical $N_2H_4^+$.

the vibrational force constant (in energy unit rad^{-2}). This affords the average,

$$[8] \qquad \langle a_H \rangle_\nu = \frac{Q_H}{2} + \frac{Q_t}{2}\left[(\nu + \tfrac{1}{2})\frac{\Delta E_\nu}{K}\right],$$

but because the radical is subject to random tumbling in solution, the time average of the proton hyperfine coupling is assumed to be equivalent to a Boltzmann average over the vibrational states (2). Hence the observed proton hyperfine coupling should be given by

$$[9] \qquad a_H = Z^{-1}\sum_{\nu=0}^{\infty}\langle a_H\rangle_\nu \exp\frac{(-\nu\Delta E_\nu)}{kT},$$

where Z^{-1} is the vibrational partition function. At a given temperature then, the proton hyperfine coupling for $N_2H_4^+$ will be

$$[10] \quad a_H(T) = \frac{Q_H}{2} + \frac{Q_t}{2}\frac{(\Delta E_\nu)}{K}Z^{-1} \times \sum_{\nu=0}^{\infty}(\nu + \tfrac{1}{2})\exp\frac{(-\nu\Delta E_\nu)}{kT},$$

whence

$$[11] \quad 2a_H(T) = Q_H + Q_t\frac{(\Delta E_\nu)}{K} \times \left\{\frac{1}{2} + \left[\exp\frac{(\Delta E_\nu)}{kT} + 1)\right]^{-1}\right\} = Q_H + Q_t\frac{(\Delta E_\nu)}{K} \times \left\{\frac{1}{2}\coth\frac{(\Delta E_\nu)}{kT}\right\}.$$

In C_2H_4, the torsional band lies at 825 cm^{-1}, whereas it is at 580 cm^{-1} for C_2D_4 (5). The value for $N_2H_4^+$ is expected to be lower due to the additional electron in the antibonding π-orbital. The torsional vibration of hydrazine has been assigned to a band centered at 376.7 cm^{-1} in the gas phase (6) and to bands at 404 and 383 cm^{-1} using a N_2 matrix (7), while the torsional vibrations for C_2H_6 and C_2D_6 are at 275 and 200 cm^{-1}, respectively (5). It now remains to choose a reasonable value for the torsional vibration frequency in the planar $N_2H_4^+$ ion and hence to derive an estimate of the magnitudes of Q_H and Q_t. Though rather arbitrarily, the value $\Delta E_\nu = 450$ cm^{-1} is chosen and, using $r_{N-H} = 1.02$ Å (6) and $H\hat{N}H = 120°$ for $N_2H_4^+$, this corresponds to a vibrational force constant, K, of 4730 cm^{-1} rad^{-2}. From Fig. 2, the two points a_H (15 °C) $= -31.30$ Mc/s and a_H (55 °C) $= -30.36$ Mc/s were used in calculating the values of Q_H and Q_t in eq. [11]. The best fit to the temperature variation of the ratio, $|a_N/a_H|$ for 450 cm^{-1}, was obtained with $Q_H = -89.5$ Mc/s and $Q_t = 459$ Mc/s.

The magnitudes of $Q_N = 65.0$ Mc/s and $Q_H = -89.5$ Mc/s are reasonable, being greater than the corresponding values for NH_3^+ (8) but comparable with those for various nitrogen semiquinones (4, 9, 10). The magnitude of $Q_t = 459$ Mc/s is comparable with the frequency dependent $Q_\sigma = 400$ Mc/s derived for the

Can. J. Chem. Downloaded from www.nrcresearchpress.com by 210.87.254.5 on 09/05/12
For personal use only.

2,6-di-*t*-butylphenoxy radical (2). But Q_t is considerably larger than the values of Q_H'', 112 Mc/s (11) and 120 Mc/s (12), derived from experimental β-proton hyperfine couplings using an expression (11):

$$[12] \qquad a_H = Q_H' + Q_H'' \cos^2 \Theta.$$

However, the magnitudes of Q_H and Q_t, particularly the latter, are sensitive to the frequency used for the torsional vibration in $N_2H_4^+$. For example, choosing $\Delta E_v = 400$ cm^{-1} ($K = 3740$ cm^{-1} rad^{-2}) leads to the values $Q_H = -86.3$ and $Q_t = 336$ Mc/s, whereas $\Delta E_v = 500$ cm^{-1} ($K = 5840$ cm^{-1} rad^{-2}) yields $Q_H = -93.2$ and $Q_t = 606$ Mc/s.

It should be mentioned that the invocation of wagging vibrations and the consequent breakdown in orthogonality between the nitrogen $2p_z$-orbital and the N—H σ(bonding) and σ*-(antibonding) orbitals would lead to an increase in a_N (2). Wagging vibrations should also be expected to result in a larger increase in a_H than in a_N and thus a resultant decrease in the ratio $|a_N/a_H|$ (2, 3, 8). However, the probable frequencies for deformation modes in $N_2H_4^+$ should be relatively high (~900 cm^{-1}) (5, 7) and since a_N is independent of temperature, the wagging vibrations are deemed to be unimportant. Deuterium substitution could provide the data necessary to confirm the foregoing torsional vibration hypothesis in the case of $N_2H_4^+$ as well as in the 2,6-di-*t*-butylphenoxy radical.

Acknowledgments

The author wishes to thank the International Order of the Daughters of the Empire (Canada) for an overseas scholarship during 1966–67, when this research was carried out in affiliation with the Department of Theoretical Chemistry, Cambridge, England. Thanks are extended to Dr. A. Carrington, who suggested this problem, and to Dr. A. J. Stone and Dr. M. A. Whitehead for helpful discussions. The author is also indebted to the referees for a number of valuable comments.

1. K. Scheffler and H. B. Stegmann. Tetrahedron Letters, 3035 (1964).
2. A. J. Stone and A. Carrington. Trans. Faraday Soc. **61**, 2593 (1965).
3. J. Q. Adams and J. R. Thomas. J. Chem. Phys. **39**, 1904 (1963).
4. B. L. Barton and G. K. Fraenkel. J. Chem. Phys. **41**, 695 (1964).
5. G. Herzberg. Infrared and Raman spectra. D. Van Nostrand, Princeton, N. J. 1945.
6. A. Yamaguchi, I. Ichishima, T. Shimanouchi, and S.-I. Mizushima. Spectrochim. Acta, **16**, 1471 (1960).
7. E. Catalano, R. H. Sanborn, and J. W. Fraser. J. Chem. Phys. **38**, 2265 (1963).
8. T. Cole. J. Chem. Phys. **35**, 1169 (1961).
9. B. L. Barton and G. K. Fraenkel. J. Chem. Phys. **41**, 1455 (1964).
10. J. R. Bolton, A. Carrington, and J. dos Santos-Veiga. Mol. Phys. **5**, 465 (1962).
11. C. Heller and H. M. McConnell. J. Chem. Phys. **32**, 1535 (1960).
12. D. Pooley and D. H. Whiffen. Mol. Phys. **4**, 81 (1961).

Can. J. Chem. Downloaded from www.nrcresearchpress.com by 210.87.254.5 on 09/05/12
For personal use only.

Can. J. Chem. Downloaded from www.nrcresearchpress.com by 210.87.254.105 on 09/05/12
For personal use only.

Formation et stabilité de complexes hydroxo-ammonio en solution aqueuse. I. Complexes de zinc

A. O. GUBELI ET J. STE-MARIE
Département de Chimie, Université Laval, Québec, Québec

Reçu le 16 août 1966
Approuvé pour publication le 26 septembre 1967

On a développé une nouvelle méthode de calcul pour déterminer les constantes de formation de complexes en équilibre avec un précipité en solution aqueuse. Cette méthode a été appliquée à l'étude des complexes ammonio et hydroxo-ammonio du zinc en présence de son hydroxyde. Les courbes de solubilité en fonction du pH et de $pNH_{3\ tot}$ ont été établies au moyen de l'isotope ^{65}Zn à 25 °C et force ionique unitaire avec $NaClO_4$.

A new method has been developed for the calculation of the formation constants of complexes in equilibrium with a precipitate in aqueous solution. This has been applied to the study of ammonio and ammonio-hydroxo complexes of zinc in the presence of the hydroxide. The curves of solubility vs. pH and $pNH_{3\ tot}$ have been established by means of ^{65}Zn at 25 °C and ionic strength 1.0 with $NaClO_4$.

Canadian Journal of Chemistry, 46, 1707 (1968)

Introduction

Lorsqu'un précipité existe en équilibre avec une solution contenant, outre des ions produits par la dissociation du précipité, des ions ou des molécules qui peuvent servir de ligands, des complexes peuvent non seulement se former à partir des ions métalliques et des ligands en solution mais également entre les ligands et le précipité en équilibre avec la solution. Dans le premier cas on obtient normalement des complexes simples et les méthodes courantes de calcul peuvent être utilisées. Dans le second cas par contre, les complexes formés peuvent être mixtes, c'est-à-dire formés de plus d'une espèce de ligand.

Comme l'étude des complexes mixtes est toute récente et que les méthodes de calcul ne leur sont pas facilement applicables, il fallut mettre au point une méthode particulière à la détermination des constantes de formation de ces complexes mixtes.

Traitement mathématique

Traitement général

Lorsque l'on précipite l'hydroxyde $M(OH)_2$ d'un métal bivalent de coordination n en présence d'ammoniaque, un système d'équilibres simultanés peut s'établir en solution. Ces divers équilibres peuvent être groupés de la manière suivante.

(*a*) Equilibre de dissociation de NH_4^+.

$$[1] \qquad NH_4^+ \rightleftarrows NH_3 + H^+$$

$$k_a = \frac{[NH_3][H^+]}{[NH_4^+]}$$

(*b*) Equilibre de précipitation de $M(OH)_2$.

$$[2] \qquad M^{2+} + 2OH^- \rightleftarrows M(OH)_2$$

$$K_{ps} = [M^{2+}][OH^-]^2$$

(*c*) Equilibres de formation des complexes simples et mixtes.

$$[3] \qquad M^{2+} + xOH^- + yNH_3 \rightleftarrows M(OH)_x(NH_3)_y^{2-x}$$

$$\phi_{xy} = \frac{[M(OH)_x(NH_3)_y^{2-x}]}{[M^{2+}][OH^-]^x[NH_3]^y}$$

Comme la concentration totale de métal en solution est égale à la somme des concentrations de l'ion métallique et de tous les complexes en équilibre, on peut écrire l'équation générale

$$[4] \qquad [M_{tot}] = \sum_{x=0}^{n-y} \sum_{y=0}^{n-x} \phi_{xy}[M^{2+}][OH^-]^x[NH_3]^y.$$

Dans cette équation générale, les concentrations $[M^{2+}]$, $[OH^-]$ et $[NH_3]$ peuvent être exprimées en fonction de $[H^+]$ et de $[NH_{3\ tot}]$ (concentration totale d'ammoniaque en solution). En effet, comme la solution est en équilibre avec l'hydroxyde $M(OH)_2$ précipité:

$$[5] \qquad [M^{2+}] = \frac{K_{ps}}{[OH^-]^2}.$$

De plus, si la concentration des complexes contenant NH_3 est faible comparée à la concentration totale d'ammoniaque en solution, on peut écrire:

$$[6] \qquad [NH_{3\ tot}] = [NH_4^+] + [NH_3]$$

$$= \frac{[NH_3][H^+]}{k_a} + [NH_3]$$

Can. J. Chem. Downloaded from www.nrcresearchpress.com by 210.87.254.105 on 09/05/12
For personal use only.

et

$$[7] \quad [NH_3] = \frac{k_a}{[H^+] + k_a}[NH_{3\,tot}] = F_n(H^+)[NH_{3\,tot}].$$

L'équation [4] devient finalement:

$$[8] \quad [M_{tot}] = \sum_{x=0}^{n-y}\sum_{y=0}^{n-x} \phi_{xy} K_{ps} K_w^{x-2} [H^+]^{2-x} \times [NH_{3\,tot}]^y F_n(H^+)^y.$$

Si $[H^+] \gg k_a$, $F_n(H^+) = k_a/[H^+]$

et l'éq. [8] devient:

$$[9] \quad [M_{tot}] = \sum_{x=0}^{n-y}\sum_{y=0}^{n-4} \phi_{xy} K_{ps} K_w^{x-2} \times k_a^y [NH_{3\,tot}]^y [H^+]^{2-x-y}.$$

Si $k_a \gg [H^+]$, $F_n(H^+) = 1$

et l'éq. [8] devient:

$$[10] \quad [M_{tot}] = \sum_{x=0}^{n-y}\sum_{y=0}^{n-x} \phi_{xy} K_{ps} K_w^{x-2} \times [NH_{3\,tot}]^y [H^+]^{2-x}.$$

Méthode d'identification de complexes en concentration prédominante en solution par l'interprétation de courbes de solubilité d'hydroxydes peu solubles

On sait qu'il existe rarement en solution plus de deux ou trois complexes en équilibre en concentration prédominante. La concentration totale de métal en solution, $[M_{tot}]$, devient donc à toute fin pratique égale à la somme d'un nombre limité de concentrations. Or, on peut étudier de façon expérimentale les variations de $[M_{tot}]$ en fonction du pH et de la concentration totale d'un ligand en solution. Il est de plus possible de calculer, à partir de la loi d'action de masse, les variations de la concentration d'un complexe donné en fonction des mêmes variables.

Si, dans une région donnée de pH et dans un intervalle de concentration de ligand, les variations trouvées expérimentalement pour $[M_{tot}]$ correspondent aux variations prédites pour un complexe donné dans les mêmes conditions d'équilibre, on peut alors conclure que $[M_{tot}]$ correspond à la concentration de ce complexe. Le complexe se trouve donc identifié et sa constante de formation peut être calculée à partir de la valeur de $[M_{tot}]$, de $[H^+]$ et de $[NH_{3\,tot}]$. Si l'on étudie toutes les régions du pH ainsi qu'un intervalle assez étendu de la concentration totale de ligand, on pourra ainsi identifier tous les complexes se formant en concentration appréciable en solution.

On peut dériver les éqs. [9] et [10], après les avoir mises sous forme logarithmique, selon $pNH_{3\,tot}$ et selon le pH; on obtient les équations suivantes.

$$[11] \quad \frac{\partial \log [M_{tot}]}{\partial\, pNH_{3\,tot}} = -y$$

$$[12] \quad \frac{\partial \log [M_{tot}]}{\partial\, pH} = x + y - 2, \quad \text{si } pH < pk_a$$

$$[13] \quad \frac{\partial \log [M_{tot}]}{\partial\, pH} = x - 2, \quad \text{si } pH > pk_a$$

Les complexes prédominants dans les diverses régions de pH et de $pNH_{3\,tot}$ peuvent donc être identifiés à partir des pentes des courbes de solubilité selon le pH et $pNH_{3\,tot}$. A cette fin, on construit un graphique en perspective de log $[M_{tot}]$ en fonction du pH et de $pNH_{3\,tot}$ (Fig. 1). Parallèlement et en partant des équations données ci-dessus, on peut déduire la valeur des pentes caractéristiques de tous les complexes possibles. Ces valeurs sont résumées au Tableau I pour chacune des 15 espèces susceptibles d'être en équilibre avec l'hydroxyde précipité, pour un métal de coordination quatre. On remarque qu'il n'existe pas deux combinaisons semblables.

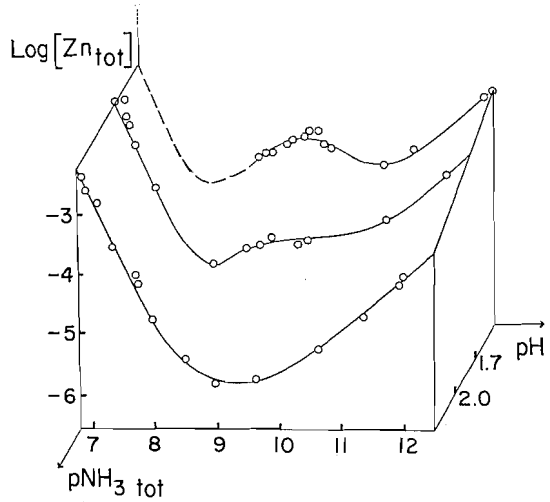

FIG. 1. Graphe tridimensionnel de la solubilité de $Zn(OH)_2$ en fonction du pH et de $pNH_{3\,tot}$.

Méthode expérimentale

Constantes de formation des complexes hydroxo-ammonio de zinc en présence de $Zn(OH)_2$

Les solutions en équilibre avec $Zn(OH)_2$ ont été préparées dans des fioles volumétriques de 50 et 100 ml. Continuellement agitées pendant les premiers jours

TABLEAU I

Pentes caractéristiques de la courbe de solubilité pour des complexes de formule générale $M(OH)_x(NH_3)_y^{2-x}$

x	y	Complexe	$\frac{\partial \log [M_{tot}]}{\partial pH}$ (pH < pk_a)	$\frac{\partial \log [M_{tot}]}{\partial pH}$ (pH > pk_a)	$\frac{\partial \log [M_{tot}]}{\partial pNH_{3\ tot}}$
0	0	M^{2+}	−2	−2	0
1	0	$M(OH)^+$	−1	−1	0
2	0	$M(OH)_2$	0	0	0
3	0	$M(OH)_3^-$	1	1	0
4	0	$M(OH)_4^{2-}$	2	2	0
0	1	$M(NH_3)^{2+}$	−1	−2	−1
0	2	$M(NH_3)_2^{2+}$	0	−2	−2
0	3	$M(NH_3)_3^{2+}$	1	−2	−3
0	4	$M(NH_3)_4^{2+}$	2	−2	−4
1	1	$M(OH)(NH_3)^+$	0	−1	−1
1	2	$M(OH)(NH_3)_2^+$	1	−1	−2
1	3	$M(OH)(NH_3)_3^+$	2	−1	−3
2	1	$M(OH)_2(NH_3)$	1	0	−1
2	2	$M(OH)_2(NH_3)_2$	2	0	−2
3	1	$M(OH)_3(NH_3)^-$	2	1	−1

TABLEAU II

Solubilité de $Zn(OH)_2$ en fonction du pH en présence de NH_3 0.005 *M*

Solution	pH	pZn_{tot}
1	6.80	2.49
2	6.87	2.71
3	7.30	3.58
4	7.69	4.06
5	7.71	4.22
6	7.95	4.79
7	8.48	5.41
8	8.96	5.81
9	9.60	5.75
10	10.63	5.27
11	11.35	4.76
12	11.94	4.23
13	12.00	4.11
14	12.02	4.11

d'équilibre, ces solutions reposèrent ensuite pour que le précipité solide puisse se déposer complètement au fond des récipients. Après 5 ou 6 jours d'équilibre, 4 échantillons de 5 ml furent pris dans chacune des solutions et transférés dans des contenants en matière plastique pour le comptage de la radioactivité. Les pH furent déterminés à l'aide de couples d'électrodes verre–calomel.

Toutes les solutions d'équilibre furent conservées dans des bains à température constante, réglés à 25 °C et leur force ionique fut portée à l'unité avec $NaClO_4$. Aucun tampon ne fut utilisé pour obtenir un pH particulier afin d'éviter toute interaction possible entre le tampon et la solution étudiée. Seuls $HClO_4$ et NaOH furent donc utilisés.

Trois séries de solutions contenant respectivement des concentrations 0.005, 0.02 et 0.04 *M* de NH_3 furent ainsi préparées.

Résultats

Nous avons groupé les résultats expérimentaux aux Tableaux II, III et IV. De plus, ces résultats sont représentés à la Fig. 1 par un graphique en perspective de log Zn_{tot} en fonction du pH et de $pNH_{3\ tot}$.

Les courbes de solubilité montrent en milieu neutre une pente de −2 par rapport au pH et une pente de 0 par rapport à $pNH_{3\ tot}$; l'ion correspondant à ces pentes dans le Tableau I est Zn^{2+}. Commes les courbes se superposent dans cette région à celle de l'hydroxyde seul, publiée précédemment, on a une preuve que le précipité est bien le même pour chacun des cas étudiés, soit $Zn(OH)_2$.

TABLEAU III

Solubilité de $Zn(OH)_2$ en fonction du pH en présence de NH_3 0.02 *M*

Solution	pH	pZn_{tot}
15	6.63	2.14
16	6.80	2.19
17	6.87	2.24
18	6.88	2.31
19	6.92	2.50
20	6.94	2.63
21	7.05	2.95
22	7.07	2.90
23	7.37	3.62
24	8.27	4.89
25	8.83	4.63
26	8.89	4.62
27	9.04	4.59
28	9.25	4.48
29	9.67	4.59
30	9.82	4.53
31	11.12	4.22
32	12.08	3.48

Can. J. Chem. Downloaded from www.nrcresearchpress.com by 210.87.254.105 on 09/05/12
For personal use only.

Can. J. Chem. Downloaded from www.nrcresearchpress.com by 210.87.254.105 on 09/05/12
For personal use only.

TABLEAU IV

Solubilité de $Zn(OH)_2$ en fonction du pH en présence de NH_3 0.04 *M*

Solution	pH	pZn_{tot}
33	8.64	3.74
34	8.76	3.68
35	8.87	3.64
36	9.08	3.55
37	9.20	3.49
38	9.33	3.41
39	9.46	3.36
40	9.60	3.38
41	9.68	3.55
42	9.80	3.61
43	10.64	3.93
44	11.15	3.68
45	12.31	2.84
46	12.47	2.75

Ces courbes présentent, en outre, deux caractéristiques: l'apparition d'un maximum vers pH 9.5 et une pente de 1 en milieu plus alcalin. On remarque aussi que dans la région du maximum, la courbe de solubilité selon $pNH_{3\,tot}$ a une pente de -4 et que cette pente est de -1 en milieu plus alcalin. Or, d'après le Tableau I, on voit que le seul complexe pouvant donner une pente de -4 selon $pNH_{3\,tot}$ à la courbe de solubilité est $Zn(NH_3)_4^{2+}$ et que, en milieu alcalin, des pentes de 1 selon le pH et de -1 selon $pNH_{3\,tot}$ correspondent au complexe $Zn(OH)_3(NH_3)^-$. Ces deux complexes sont en concentration prédominante en solution ammoniacale.

Calcul des constantes d'équilibre

(1) Produit de solubilité de $Zn(OH)_2$

Tous les points expérimentaux situés sur les segments des courbes de solubilité de pente -2, selon le pH, peuvent être introduits directement dans le calcul du produit de solubilité de l'hydroxyde de zinc. En effet, pour tous ces points $[Zn_{tot}]$ est égal à $[Zn^{2+}]$. Comme par définition

$$K_{ps} = [Zn^{2+}][OH^-]^2,$$

on peut écrire

$$[14] \quad K_{ps} = [Zn_{tot}][OH^-]^2 = K_w^2[Zn_{tot}][H^+]^{-2},$$

ou, sous forme logarithmique

$$[15] \quad pK_{ps} = 2pK_w - 2pH + pZn_{tot}$$

où $pK_w = 14.00$ (pour $I = 1.0$ et $t = 25\,^\circ C$).

Des courbes de solubilité obtenues, 15 points expérimentaux peuvent servir au calcul du produit de solubilité de $Zn(OH)_2$ selon l'éq. [15]; on trouve comme valeur moyenne:

$$pK_{ps} = 16.76 \pm 0.03.$$

(2) Constantes de formation des complexes hydroxo–ammonio et ammonio de Zn

Par les pentes des courbes de solubilité, il a été possible d'identifier deux complexes dont la concentration est prépondérante dans deux régions données du pH et de $pNH_{3\,tot}$. Ce sont les complexes $Zn(NH_3)_4^{2+}$ et $Zn(OH)_3(NH_3)^-$ que nous avons mentionnés. Nous avons donc fait le calcul des constantes de formation de ces deux complexes et comme ce calcul pour le premier complexe demandait la connaissance de la constante de dissociation de l'ammoniaque, nous avons préféré trouver cette valeur à partir des courbes de solubilité disponibles plutôt que prendre une valeur donnée en littérature pour une autre force ionique.

(a) Constante de dissociation de l'ammoniaque

Cette constante a été calculée en même temps que la constante de formation de $Zn(NH_3)_4^{2+}$. En effet, dans la région de pH et $pNH_{3\,tot}$ où ce complexe est prédominant, il est possible d'écrire:

$$[16] \quad [Zn(NH_3)_4^{2+}] = [Zn_{tot}] = \phi_{04}[Zn^{2+}][NH_3]^4.$$

Or nous savons d'après l'éq. [7] que

$$[NH_3] = \frac{k_a[NH_{3\,tot}]}{[H^+] + k_a},$$

l'éq. [16] est donc une équation à deux inconnues, k_a et ϕ_{04} que l'on peut écrire de la manière suivante:

$$[17] \quad \left(\frac{[H^+] + k_a}{k_a}\right)^4 = \phi_{04}[NH_{3\,tot}]^4 \frac{[Zn^{2+}]}{[Zn_{tot}]}.$$

Les concentrations $[Zn_{tot}]$, $[NH_{3\,tot}]$ et l'activité $[H^+]$ sont déterminées expérimentalement et, connaissant le pH de la solution et le produit de solubilité de $Zn(OH)_2$, $[Zn^{2+}]$ peut être évaluée. Ainsi chacun des points expérimentaux de la région de pH et $pNH_{3\,tot}$ considérée donne une équation particulière si les valeurs des concentrations sont introduites dans l'équation générale [17]. Par exemple, pour un point *i*, on aura

$$[i] \quad \left(\frac{[H^+]_i + k_a}{k_a}\right)^4 = \phi_{04}[NH_{3\,tot}]_i^4 \frac{[Zn^{2+}]_i}{[Zn_{tot}]_i},$$

TABLEAU V

Valeurs de la constante de dissociation k_a de l'ammoniaque

Points choisis							
i	j	$pZn_i^{2+} - pZn_{tot}$	$pZn_j^{2+} - pZn_{tot}$	pA_{ij}	pH_i	pH_j	pk_a
33	37	2.30	3.67	0.34	8.64	9.20	9.16
33	38	2.30	4.01	0.43	8.64	9.33	9.22
33	39	2.30	4.32	0.51	8.64	9.46	9.24
33	40	2.30	4.58	0.57	8.64	9.60	9.30
33	41	2.30	4.57	0.57	8.64	9.68	9.25
33	42	2.30	4.65	0.59	8.64	9.80	9.24
34	38	2.60	4.01	0.35	8.76	9.33	9.25
34	39	2.60	4.32	0.43	8.76	9.46	9.32
34	40	2.60	4.58	0.50	8.76	9.60	9.37
34	41	2.60	4.57	0.49	8.76	9.68	9.28
34	42	2.60	4.65	0.51	8.76	9.80	9.26
35	38	2.86	4.01	0.29	8.87	9.33	9.33
35	39	2.86	4.32	0.37	8.87	9.46	9.40
35	40	2.86	4.58	0.43	8.87	9.60	9.40
35	41	2.86	4.57	0.43	8.87	9.68	9.33
35	42	2.86	4.65	0.45	8.87	9.80	9.31
36	40	3.37	4.58	0.30	9.08	9.60	9.48
36	41	3.37	4.57	0.30	9.08	9.68	9.38
36	42	3.37	4.65	0.32	9.08	9.80	9.34
37	42	3.67	4.65	0.25	9.20	9.80	9.35
38	42	4.01	4.65	0.16	9.33	9.80	9.20

et pour un point j

$$[j] \quad \left(\frac{[H^+]_j + k_a}{k_a}\right)^4 = \phi_{04}[NH_{3\ tot}]_j^4 \frac{[Zn^{2+}]_j}{[Zn_{tot}]_j}.$$

Si $[NH_{3\ tot}]_i = [NH_{3\ tot}]_j$, on obtient en divisant l'éq. $[j]$ par l'éq. $[i]$:

$$[18] \quad \frac{[Zn_{tot}]_i[Zn^{2+}]_j}{[Zn^{2+}]_i[Zn_{tot}]_j} = A_{ij}^4 = \left(\frac{k_a + [H^+]_j}{k_a + [H^+]_i}\right)^4.$$

Le symbole A_{ij} est introduit pour simplifier l'écriture. L'équation [18] transformée, on aboutit finalement à:

$$[19] \quad k_a = \frac{A_{ij}[H^+]_i - [H^+]_j}{1 - A_{ij}}.$$

Les valeurs obtenues pour la constante de dissociation k_a de l'ammoniaque sont données au Tableau V; elles proviennent de l'éq. [19] en y introduisant les valeurs expérimentales de plusieurs couples de points; les solutions correspondant aux points choisis pour les calculs contenaient toutes la même concentration totale d'ammoniaque.

On trouve comme valeur moyenne de la constante de dissociation de NH_4^+ en H^+ et NH_3: $pk_a = 9.30 \pm 0.02$.

(b) Constante de formation de $Zn(NH_3)_4^{2+}$—Une fois k_a déterminée, la constante de formation de $Zn(NH_3)_4^{2+}$ peut être calculée à partir des mêmes points expérimentaux. En effet, si l'on remplace $[Zn^{2+}]$ dans l'équation modifiée [17] par $K_{ps}K_w^{-2}[H^+]^2$, on obtient

$$[20] \quad \phi_{04} = \frac{K_w^2[Zn_{tot}]([H^+] + k_a)^4}{K_{ps}[H^+]^2k_a^4[NH_{3\ tot}]^4},$$

qui devient sous forme logarithmique:

$$[21] \quad p\phi_{04} = pZn_{tot} - 2pH - 4pNH_{3\ tot} + 4p([H^+] + k_a) - 4pk_a + 2pK_w - pK_{ps}.$$

Les valeurs ainsi obtenues pour les 10 points expérimentaux choisis sont données au Tableau VI; on trouve comme valeur moyenne

$$p\phi_{04} = -10.84 \pm (0.02 + 0.11)$$

(la valeur 0.11 correspond à l'écart moyen fait sur la détermination de k_a et de K_{ps}). Afin de simplifier le tableau, les valeurs calculées pour les concentrations de Zn^{2+} et NH_3 sont données directement; en effet

$$pZn^{2+} = pK_{ps} + 2pH - 2pK_w \text{ et}$$
$$pNH_3 = pNH_{3\ tot} + pk_a - p([H^+] + k_a).$$

(c) Constante de formation de $Zn(OH)_3(NH_3)^-$—Comme on l'a vu la présence du complexe en solution a été déterminée à partir de la courbe de solubilité en milieu fortement alcalin de pentes 1 et -1 selon le pH et $pNH_{3\ tot}$.

Can. J. Chem. Downloaded from www.nrcresearchpress.com by 210.87.254.105 on 09/05/12
For personal use only.

TABLEAU VI

Calcul de la constante de formation de $Zn(NH_3)_4^{2+}$

Solution	pH	pZn_{tot}	pZn^{2+}	$pNH_{3\ tot}$	pNH_3	$4pNH_3$	$-p\phi_{04}$
33	8.64	3.74	6.04	1.41	2.15	8.60	10.90
34	8.76	3.68	6.28	1.41	2.06	8.24	10.84
35	8.87	3.64	6.50	1.41	1.98	7.92	10.78
36	9.08	3.55	6.92	1.41	1.83	7.32	10.69
37	9.20	3.49	7.16	1.41	1.76	7.04	10.79
38	9.33	3.43	7.42	1.41	1.70	6.80	10.81
39	9.46	3.36	7.68	1.42	1.65	6.60	10.92
40	9.60	3.38	7.96	1.41	1.59	6.36	10.94
41	9.68	3.55	8.12	1.41	1.56	6.24	10.81
42	9.80	3.61	8.36	1.41	1.53	6.12	10.87

Réciproquement, tous les points se trouvant sur le segment de courbe de pente 1 peuvent servir au calcul de la constante de formation du complexe mixte $Zn(OH)_3(NH_3)^-$. Pour tous ces points, $[Zn_{tot}] = [Zn(OH)_3(NH_3)^-]$ et l'on peut écrire:

$$[22] \quad \phi_{31} = \frac{[Zn(OH)_3(NH_3)^-]}{[Zn^{2+}][OH^-]^3[NH_3]} = \frac{[Zn_{tot}]}{K_{ps}[OH^-][NH_3]}.$$

Or, pour les points choisis $[H^+]$ est beaucoup plus petite que k_a et dans ce cas, d'après l'éq. [7], $[NH_3]$ devient égale à $[NH_{3\ tot}]$. On a donc

$$[23] \quad \phi_{31} = \frac{[Zn_{tot}]}{K_{ps}[OH^-][NH_{3\,tot}]} = \frac{[Zn_{tot}][H^+]}{K_{ps}K_w[NH_{3\ tot}]},$$

qui sous forme logarithmique devient:

$$[24] \quad p\phi_{31} = pZn_{tot} + pH - pNH_{3\ tot} - pK_{ps} - pK_w.$$

Les valeurs ainsi trouvées pour les sept points choisis en milieu très alcalin sont données au Tableau VII. On obtient comme valeur moyenne:

$$p\phi_{31} = -16.94 \pm (0.01 + 0.03).$$

(d) Constante de formation de $Zn(OH)_2(NH_3)_2$—Pour vérifier si seuls les complexes $Zn(NH_3)_4^{2+}$ et $Zn(OH)_3(NH_3)^-$ sont en équilibre avec Zn^{2+} et le précipité $Zn(OH)_2$, il est possible de calculer ce que l'on devrait théoriquement trouver comme valeur de pZn_{tot} pour les points des courbes de solubilité non utilisés dans le calcul des constantes de formation de ces complexes. Il suffit donc d'additionner les concentrations des ions Zn^{2+}, $Zn(NH_3)_4^{2+}$ et $Zn(OH)_3(NH_3)^-$ calculées à partir des constantes déjà trouvées ainsi que le pH et $pNH_{3\ tot}$ des points choisis. Les valeurs ainsi obtenues sont données au Tableau VIII, à la fois pour pZn_{tot} calculé et trouvé expérimentalement.

On remarque que la différence entre les valeurs expérimentale et calculée de pZn_{tot} est assez grande pour les solutions 7, 8, 9 et 10 si l'on considère uniquement la différence entre les logarithmes (p = —log). Du point de vue absolu cependant, elle correspond à une différence de concentration de 0.000002 *m* en Zn.

Dans le cas des solutions 24, 25, 26, 27, 28 et 29, la différence entre les valeurs expérimentale et calculée s'explique très bien par l'erreur sur les points expérimentaux et la valeur de l'écart moyen des constantes de formation.

TABLEAU VII

Calcul de la constante de formation de $Zn(OH)_3(NH_3)^-$

Solution	pH	pZn_{tot}	$pNH_{3\ tot}$	$pH + pZn_{tot} - pNH_{3\ tot}$	$-p\phi_{31}$
11	11.35	4.76	2.30	13.81	16.95
12	11.94	4.23	2.30	13.87	16.89
13	12.00	4.11	2.30	13.81	16.95
14	12.02	4.11	2.30	13.83	16.93
32	12.08	3.48	1.70	13.86	16.90
45	12.31	2.84	1.41	13.74	17.02
46	12.47	2.75	1.41	13.81	16.95

Can. J. Chem. Downloaded from www.nrcresearchpress.com by 210.87.254.105 on 09/05/12
For personal use only.

TABLEAU VIII

Calcul de la constante de formation de $Zn(OH)_2(NH_3)_2$

Solution	pH	pZn^{2+}	$pZn(NH_3)_4^{2+}$	$pZn(OH)_3(NH_3)^-$	pZn_{tot} (calc.)	pZn_{tot} (exp.)
7	8.48	5.72	7.60	8.52	5.72	5.41
8	8.96	6.68	7.04	7.66	6.49	5.81
9	9.60	7.96	7.04	6.70	6.52	5.75
10	10.63	10.02	8.46	5.51	5.51	5.27
24	8.27	5.30	5.54	8.32	5.10	4.89
25	8.83	6.42	4.78	7.29	4.77	4.63
26	8.89	6.54	4.70	7.18	4.69	4.62
27	9.05	6.86	4.58	6.91	4.57	4.59
28	9.25	7.26	4.54	6.60	4.54	4.48
29	9.67	8.10	4.66	6.00	4.64	4.59
30	9.82	8.40	4.80	5.81	4.76	4.53
31	11.12	11.00	6.96	4.40	4.40	4.22
43	10.64	10.04	4.88	4.60	4.42	3.93
44	11.15	11.06	5.90	4.09	4.08	3.70

Enfin, pour les solutions 30, 31, 43 et 44, la différence entre pZn_{tot} calculé et trouvé expérimentalement est assez grande pour que l'on suppose la présence d'un autre complexe dans cette région de pH et $pNH_{3\ tot}$. D'après les différences remarquées, la concentration de ce complexe augmente légèrement avec le pH mais est proportionnelle au carré de la concentration de NH_3 en solution. Or, le Tableau I montre que le complexe qui correspond à une pente voisine de 0 selon le pH et une pente de -2 selon $pNH_{3\ tot}$ des courbes de solubilité a pour formule $Zn(OH)_2(NH_3)_2$. Bien que nous n'avions que quatre points disponibles pour calculer la constante de formation de ce complexe, il nous a semblé intéressant d'effectuer ce calcul afin de comparer la constante ainsi obtenue avec celle déjà déterminée pour le complexe mixte $Zn(OH)_3(NH_3)^-$. Cette constante ϕ_{22} peut être calculée de la manière suivante

$$[25] \quad \phi_{22} = \frac{[Zn(OH)_2(NH_3)_2]}{[Zn^{2+}][OH^-]^2[NH_3]^2} = \frac{[Zn_{tot}]_{exp} - [Zn_{tot}]_{calc}}{K_{ps}[NH_3]^2},$$

qui, sous forme logarithmique, devient

$$[26] \quad p\phi_{22} = p\Delta Zn_{tot} - 2pNH_3 - pK_{ps},$$

où $p\Delta Zn_{tot} = p([Zn_{tot}]_{exp} - [Zn_{tot}]_{calc})$.

Les valeurs obtenues pour le calcul de la constante de formation du complexe $Zn(OH)_2(NH_3)_2$ sont données au Tableau IX, ainsi que les résultats obtenus à partir de l'éq. [26] pour les quatre solutions concernées. On trouve comme valeur moyenne:

$$p\phi_{22} = -15.53 \pm (0.05 + 0.03).$$

Discussion

Alors que Bjerrum (1) en 1941 et Spike et Parry (2) en 1953 rapportèrent la formation de $Zn(NH_3)^{2+}$, $Zn(NH_3)_2^{2+}$, $Zn(NH_3)_3^{2+}$ et $Zn(NH_3)_4^{2+}$, nous n'avons remarqué que la présence de $Zn(NH_3)_4^{2+}$. De plus, la valeur de $-p\beta_4$ (correspondant à notre $-p\phi_{04}$) obtenue par Bjerrum pour ce complexe est plus faible que celle que nous avons trouvée nous-mêmes (9.48 en comparaison de 10.84). Cette différence serait encore plus grande si la constante de dissociation de 9.61 utilisée par Bjerrum dans

TABLEAU IX

Valeurs de la constante de formation de $Zn(OH)_2(NH_3)_2$

Solution	pH	pNH_3	$2pNH_3$	$pZn(OH)_2(NH_3)_2$ ($p\Delta Zn_{tot}$)	$-p\phi_{22}$
30	9.82	1.81	3.62	4.92	15.46
31	11.12	1.70	3.40	4.69	15.47
43	10.64	1.42	2.84	4.10	15.50
44	11.15	1.42	2.84	3.93	15.67

Can. J. Chem. Downloaded from www.nrcresearchpress.com by 210.87.254.105 on 09/05/12
For personal use only.

ses calculs était substituée à celle de 9.30 trouvée et utilisée dans nos calculs de ϕ_{04}.

Les conditions expérimentales étant différentes, il est évidemment malaisé d'établir une comparaison. En effet, le travail de Bjerrum n'a été effectué qu'en milieu homogène, entre pH 5.8 et 8.3 dans une solution 2 *M* de NH_4NO_3, alors que nos résultats proviennent de solutions en équilibre avec l'hydroxyde de zinc dans une région de pH allant de 6 à 13 et pour des concentrations d'ammoniaque de 0.005 à 0.04 *M*.

Etant donné qu'il nous a été relativement difficile de calculer la valeur des constantes de formation de trois complexes dans un intervalle de 8 unités de pH et de 0.9 unité de $pNH_{3\ tot}$, on peut se demander comment Bjerrum a pu réussir à déterminer quatre constantes dans un intervalle de 2.5 unités de pH sans changer la concentration totale d'ammoniaque et d'ions ammonium en solution. Une remarque semblable a d'ailleurs été faite en 1954 par Wormser (3) qui a montré, en reprenant les calculs de Bjerrum à partir de la courbe expérimentale, que cette courbe de Bjerrum pourrait aussi bien s'expliquer par la présence en solution des seuls complexes $Zn(NH_3)_4^{2+}$ et $Zn(NH_3)_2^{2+}$.

De toute évidence, la théorie de Wormser était fondée puisque nos travaux démontrent la présence du seul complexe $Zn(NH_3)_4^{2+}$ en solution, exception faite des deux complexes mixtes $Zn(NH_3)_2(OH)_2$ et $Zn(NH_3)(OH)_3^-$ que Bjerrum n'aurait pu par sa méthode différencier de $Zn(NH_3)_2^{2+}$ et $Zn(NH_3)^{2+}$; cet auteur n'a d'ailleurs pas tenu compte dans ses travaux de la possibilité de formation de complexes mixtes.

Une étude des complexes hydroxo–ammonio du zinc a été entreprise par Bode (4) en 1962. Mais il introduit dans ses calculs les constantes déjà trouvées par Bjerrum pour la formation de $Zn(NH_3)^{2+}$, $Zn(NH_3)_2^{2+}$, $Zn(NH_3)_3^{2+}$ et $Zn(NH_3)_4^{2+}$. Bode propose toute une série de complexes mixtes, possibles et en "trouve" les constantes de formation en construisant, à l'aide de ses données expérimentales, un système de sept équations où apparaissent sept constantes β inconnues en plus des valeurs de Bjerrum. Des sept valeurs trouvées, deux correspondent respectivement aux complexes $Zn(OH)_2(NH_3)_2$ et $Zn(OH)_3(NH_3)^-$. Comme on pouvait s'y attendre, ces valeurs sont plus faibles que celles que nous avons trouvées; en effet, si l'on tient compte de la formation de complexes qui en réalité n'existent pas, on accorde relativement moins d'importance aux complexes réels et de ce fait les constantes de formation calculées sont trop basses.

Remerciements

Nous désirons remercier la "Canadian Industries Ltd." et le Conseil National de Recherches du Canada pour leur aide financière qui a permis la réalisation de ce travail.

1. J. BJERRUM. Metal amine formation in aqueous solutions. P. Haase and Son, Copenhagen. 1941.
2. C. G. SPIKE et R. W. PARRY. J. Am. Chem. Soc. **75**, 3770 (1953).
3. Y. WORMSER. Bull. Soc. Chim. France, 387 (1954).
4. H. BODE. Z. Anorg. Allgem. Chem. **317**, 3 (1962).

Can. J. Chem. Downloaded from www.nrcresearchpress.com by 210.87.254.105 on 09/05/12
For personal use only.

Can. J. Chem. Downloaded from www.nrcresearchpress.com by 210.87.254.5 on 09/05/12
For personal use only.

Preparation and infrared spectra of alkali and alkaline earth metal chlorosulfates

J. A. CIRUNA AND E. A. ROBINSON
Lash Miller Chemical Laboratories and Erindale College, University of Toronto, Toronto, Ontario

Received December 8, 1967

A new method for the preparation of alkali and alkaline earth metal chlorosulfates is described which involves the precipitation of the salts from saturated solutions in chlorosulfuric acid using thionyl chloride. The infrared spectra of all the chlorosulfates in the region 400–1500 cm^{-1} have been measured and the assignment of the frequencies is discussed.

Canadian Journal of Chemistry, 46, 1715 (1968)

Introduction

Salts of chlorosulfuric acid, although not always recognized as such, have been prepared previously by reacting metal chlorides with sulfur trioxide (1–5). Very recently, $NaSO_3Cl$ has been obtained by the reaction between sodium perchlorate and dimethyl formamide–sulfuryl chloride adduct in acetonitrile solvent (6).

The reaction of metal chlorides and sulfur trioxide gives various products. For example Iler (4) and Hixon and Tinney (5) have described commercial methods that give adducts between the alkali metal chlorides and sulfur trioxide. In the presence of excess SO_3, compounds of the type $NaCl{\cdot}nSO_3$ ($n > 1$) were obtained which lost SO_3 at temperatures above 100 °C to give $NaCl{\cdot}SO_3$, which was found to be relatively stable. Similarly, much earlier, Schultz-Sellack (1) found that when NaCl and KCl, respectively, are exposed to sulfur trioxide for a considerable time, compounds of the type $NaCl{\cdot}4SO_3$ and $KCl{\cdot}8SO_3$ (which are presumably best formulated as $NaS_4O_{12}Cl$ and $KS_8O_{24}Cl$, the salts of chloropolysulfuric acids) are obtained.

In 1960 Waddington and Klanberg (7) showed that reaction of tetramethylammonium chloride and phosphorus pentachloride, respectively, with chlorosulfuric acid gave crystalline compounds which, on the basis of their infrared spectra, were formulated as the chlorosulfates $Me_4N^+{\cdot}SO_3Cl^-$ and $PCl_4^+{\cdot}SO_3Cl^-$, respectively.

In the present work alkali and alkaline earth metal chlorosulfates have been obtained by reacting anhydrous metal chlorides with chlorosulfuric acid,

$$[1] \quad MCl_n + nHSO_3Cl = M(SO_3Cl)_n + nHCl,$$

a method which parallels that of Gillespie and co-workers (8), who have prepared the analogous very pure fluorosulfates by reacting metal chlorides with fluorosulfuric acid.

Vibrational Spectra

Previously, Waddington and Klanberg (7) assigned the infrared spectrum of the chlorosulfate anion in its tetramethylammonium and tetrachlorophosphonium salts by analogy with Sharp's assignment of the spectrum of the fluorosulfate anion in its alkali metal salts (9). More recently, Gillespie and Robinson (10) measured the Raman spectra of solutions of chlorosulfates in dimethylsulfoxide and chlorosulfuric acid, respectively. Very recently, Steger and Ciurea (11) have reported the infrared spectrum of $NaSO_3Cl$ between 300 and 1600 cm^{-1}.

Experimental

Reagents

Chlorosulfuric acid was used directly as obtained from the British Drug Houses Ltd., since attempts to purify it further by simple or fractional distillation gave acid containing appreciable quantities of the anhydride $S_2O_5Cl_2$ (see also ref. 12). Alkali and alkaline earth metal chlorides were commercial samples: barium, calcium, cesium, potassium, and sodium chlorides were B.D.H. Analar reagents; lithium and strontium chlorides were B.D.H. reagent grades; and rubidium chloride was Fisher certified reagent grade. All the salts were carefully dried before use. Thionyl chloride (Fisher) was distilled at atmospheric pressure, and the fraction boiling at 76 °C collected and used.

The handling and transfer of all reagents was carried out in a dry box under an atmosphere of dry nitrogen.

Preparation of Chlorosulfates

In a typical experiment 50 ml of chlorosulfuric acid were transferred under dry nitrogen into a 250 ml flask equipped with a microcondenser. The anhydrous metal chloride was added through the condenser until the solution was saturated at the boiling point of the acid. When the evolution of hydrogen chloride was complete the solution was allowed to cool and thionyl chloride added slowly until the metal chlorosulfate precipitated from solution. The mixture was transferred to the

apparatus shown in Fig. 1 and the salt filtered onto a sintered glass plate and washed several times with thionyl chloride from the reservoir B. The solvent was repeatedly drawn off by opening S_1 and S_2 and applying a vacuum through S_2. After the final washing S_1 and S_4 were closed and remaining thionyl chloride pumped off under reduced pressure into the traps C and D. The dry product was ground to a fine powder and stored in sealed ampuls.

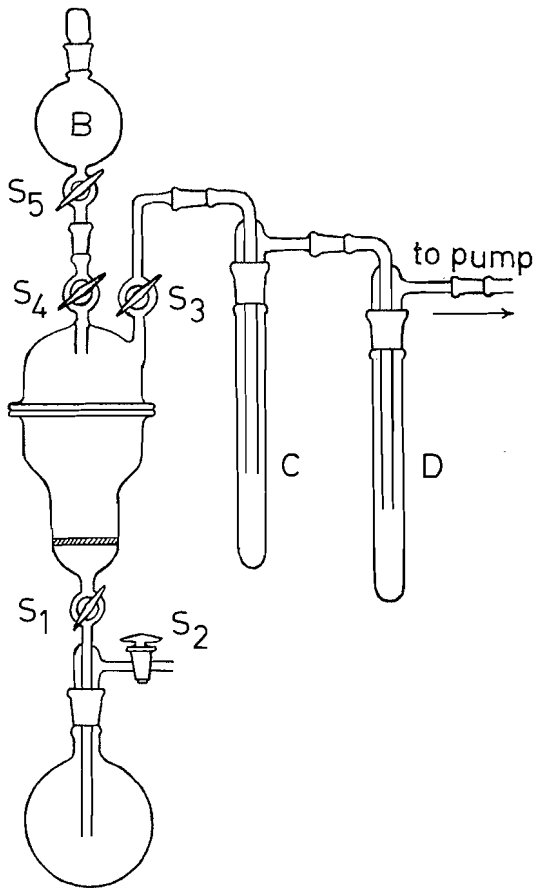

FIG. 1. Apparatus for preparing chlorosulfates.

The metal chlorosulfates were analyzed by hydrolyzing known weights and determining the total acid and chloride content.

[2] $$M(SO_3Cl)_n + 3nH_2O = M^{n+} + nSO_4^{2-} + nCl^- + 2nH_3O^+$$

Typical analyses are shown in Table I.

An alternative method of preparation, which was found to be less successful, was to distill chlorosulfuric acid onto the anhydrous metal chloride, allow the reaction to go to completion, and then distill off the excess acid under reduced pressure. Salts obtained in this way were generally of poor quality compared with those prepared by precipitation, probably due to partial hydrolysis during the distillation procedure, e.g.,

[3] $$2HSO_3Cl = S_2O_5Cl_2 + H_2O$$

[4] $$MSO_3Cl + H_2O = MHSO_4 + HCl$$

TABLE I
Analysis of metal chlorosulfates

	mequiv acid/g		% Cl	
	Found	Theor.	Found	Theor.
$NaSO_3Cl$	14.37	14.44	25.23	25.60
KSO_3Cl	12.87	12.93	22.52	22.93
$Ba(SO_3Cl)_2$	10.72	10.86	19.27	19.25

Spectra

The infrared spectra were obtained on Nujol mulls prepared in an inert atmosphere from finely powdered samples of the salts. The mulls were contained between silver chloride plates and the spectra measured using a Perkin-Elmer 521 grating spectrometer in the range 400–1500 cm^{-1}.

Results and Discussion

The infrared spectra of the alkali and alkaline earth metal chlorosulfates obtained as Nujol mulls in the region 400–1500 cm^{-1} are shown in Table II. Six normal modes of vibration are expected for the chlorosulfate ion (C_{3v} symmetry) all of which should be active in both the infrared and Raman. They are conveniently described (10) as a SO_3 symmetric stretch, ν_1, an asymmetric stretch, ν_4, a SO_3 symmetric bend, ν_3, an asymmetric bend, ν_5, a S—Cl stretch, ν_2, and a S—Cl wag, ν_6.

Waddington and Klanberg (7) assigned the spectra of $Me_4N{\cdot}SO_3Cl$ and $PCl_4{\cdot}SO_3Cl$ by comparison with the spectra of fluorosulfates (9); however, the Raman study of Gillespie and Robinson (10) showed that the band at 540 cm^{-1} assigned by Waddington and Klanberg to the S—Cl stretching mode was in fact the SO_3 symmetric band. The four bands at 533, 555, 600, and 640 cm^{-1}, respectively, observed in the infrared spectrum of $NaSO_3Cl$ by Steger and Ciurea (11), were assigned in terms of removal of the expected degeneracy of the asymmetric bend (533, 555 cm^{-1}) and a Fermi resonance interaction between the symmetric SO_3 bend and a combination band of the S—Cl stretch (392 cm^{-1}) and the S—Cl wag (220 cm^{-1}) (10) to give the 600 and 640 cm^{-1} frequencies.

The present infrared spectra of the metal chlorosulfates, although somewhat complex, are

Can. J. Chem. Downloaded from www.nrcresearchpress.com by 210.87.254.5 on 09/05/12
For personal use only.

Can. J. Chem. Downloaded from www.nrcresearchpress.com by 210.87.254.5 on 09/05/12
For personal use only.

TABLE II

Infrared spectra of chlorosulfates

(*a*)	Li^+	Na^+	K^+	Rb^+	Cs^+	Ca^{2+}	Sr^{2+}	Ba^{2+}	Assignment	
220	[233]	[240]	[244]	[249]	[251]	[229]	[240]	[242]	ν_6 (E)	S—Cl wag
395	[395]	[395]	[376]	[395]	[395]	[417]	[386]	[390]	ν_2 (A)	S—Cl stretch
—	—	—	—	502 vw	505 vw	—	—	—	($2\nu_6$)	
535	539 w	529, 554 vw	535, 551 s	545 m	550 w,sh	545 m	535 w	529 m	ν_3 (A)	Sym. SO_3 deform.
585	585 w,sh	598 m	593 vs	575 vs	570, 592 s	568, 599 w	569 m	566 m	ν_5 (E)	Asym. SO_3 deform.
—	651 s	645 m	620 vs	—	—	637 m	613	603	($\nu_2+\nu_6$)	
—	674 s	—	—	—	—	657 w,sh	639	632	($\nu_1-\nu_2$)	
—	—	—	—	774 m	775 w	770 w	—	—	($\nu_3+\nu_6$)	
—	842 vw	856 w	—	880 vw	856 m	869 w	871 s	849 m	($\nu_6+\nu_5$)	
—	917 w	917 w	—	—	—	—	—	—	($\nu_2+\nu_3$)	
—	—	1017	962 w,sh	970 vw	—	972 vw	975 w	970 m	($\nu_2+\nu_5$)	
1050	1073 vs	1060 s	1047 s	1041 s	1035 s	1077 s	1071 vs	1055 vs	ν_1(A)	Sym. SO_3 stretch
—	—	1080 w	—	1088 vw	1081 w	1100 m	1082 s,sh	1070 m	($2\nu_3$)	
—	—	1163 m,sh	1165 m,sh	—	—	—	—	—	($\nu_3+\nu_5$)	
—	1165 w	1208 s,sh	—	1168 m,sh	1168 m	1162 s	1170 m,sh	1193 vs	($2\nu_5$)	
1195	1240 vs	1245 vs	1250 vs	1270 vs	1245 vs	1242 m,sh	1261 s,sh	1262 vs	ν_4 (E)	Asym. SO_3 stretch
—	1306 vs	1300 m	1291 vs	1290 s,sh	1286 s,sh	1306 m	—	—	($\nu_1+\nu_6$)	

(*a*) Raman spectrum in solution (ref. 10).

satisfactorily explained in terms of overtones and combinations of the fundamental frequencies. The frequencies ν_6 and ν_2, which were estimated from combination frequencies, compare favorably, as do the other fundamentals, with the frequencies in the Raman spectra of chlorosulfate solutions (10). These assignments, however, which hold consistently for the entire series of salts, do not support Steger and Ciurea's postulate of Fermi resonance to explain the peaks in the SO_3 bending region of the spectrum of sodium chlorosulfate.

Apart from ν_6 and ν_2, which were not determined directly, the remaining fundamental frequencies are consistent with the expected C_{3v} symmetry of the chlorosulfate anion. If any appreciable covalent bonding existed between the metal and chlorosulfate the symmetry of MSO_3Cl would, at best, have been reduced to C_s with the appearance of at least nine fundamentals.

However, the steady decrease in the chlorosulfate symmetric stretching frequency, ν_1, with the change in metal cation in the order Li^+ to Cs^+ and Ca^{2+} to Ba^{2+}, is consistent with a decreasing interaction between M^+ and SO_3Cl^- as the polarizing power of the cation decreases. For the large cations where interionic interactions are least likely, the chlorosulfate ion exhibits the lowest S—O symmetric stretching frequency. This behavior is consistent with that postulated to explain differences in the electrical conductivities of the salts in chlorosulfuric acid (12).

Acknowledgments

The National Research Council of Canada is thanked for the award of a scholarship (to J. A. Ciruna) and for generous financial assistance.

1. C. SCHULTZ-SELLACK. J. Chem. Soc. **24**, 193 (1871).
2. O. RUFF. Ber. **34**, 3513 (1901).
3. H. H. SISLER and L. F. ANDRIETH. J. Am. Chem. Soc. **61**, 3392 (1939).
4. R. K. ILER. U.S. Patent No. 2,219,103. 1941.
5. A. W. HIXON and A. H. TINNEY. Ind. Eng. Chem. **33**, 1472 (1964).
6. H. A. LEHMANN, C. RINGLL, and V. KÖLTZSCH. Z. Chem. **5**, 313 (1965).
7. T. C. WADDINGTON and F. KLANBERG. J. Chem. Soc. 2339 (1960).
8. R. J. GILLESPIE, J. BARR, and R. C. THOMPSON. Inorg. Chem. **3**, 1149 (1964).
9. D. W. SHARP. J. Chem. Soc. 3761 (1957).
10. R. J. GILLESPIE and E. A. ROBINSON. Can. J. Chem. **40**, 644 (1962).
11. VON E. STEGER and I. C. CIUREA. Z. Anorg. Allgem. Chem. **350**, 225 (1967).
12. J. CIRUNA and E. A. ROBINSON. Can. J. Chem. This issue.

Can. J. Chem. Downloaded from www.nrcresearchpress.com by 210.87.254.5 on 09/05/12
For personal use only.

Can. J. Chem. Downloaded from www.nrcresearchpress.com by 210.87.254.40 on 09/05/12
For personal use only.

The chlorosulfuric acid solvent system. Part I. Electrical conductivity, transport number, and density measurements on solutions of simple bases

E. A. Robinson and J. A. Ciruna
Lash Miller Chemical Laboratories and Erindale College, University of Toronto, Toronto, Ontario

Received December 8, 1967

Electrical conductivity, transport number, and density measurements on solutions of some simple bases, including alkali metal and alkaline earth metal chlorosulfates, are reported in the chlorosulfuric acid solvent system. The SO_3Cl^- ion was found to have a high mobility compared with, for example, the mobilities of the alkali metal and alkaline earth metal cations, and is believed to conduct by an abnormal Grotthus-type chain mechanism. Alkali metal chlorosulfates appear to behave as fully dissociated electrolytes, whereas alkaline earth metal chlorosulfates are incompletely dissociated. Difficulties encountered in preparing pure chlorosulfuric acid are discussed.

Canadian Journal of Chemistry, 46, 1719 (1968)

Introduction

Although Williamson (1) first synthesized chlorosulfuric acid in 1857 little interest has been shown in its properties as a nonaqueous solvent. However, since sulfuric acid and fluorosulfuric acid are known to be good solvents for a wide variety of inorganic and organic solutes, it is to be expected that chlorosulfuric acid might be equally useful.

Early work by Walden (2) in 1902 established the acid to be a good ionizing solvent and a value of 1.72×10^{-4} ohm^{-1} cm^{-1} was found for its specific conductivity at 25 °C. More recently Paul and co-workers (3) have studied the electrical conductivities of solutions of a few tertiary bases and alkali chlorosulfates; they postulated the following modes of solvent self-dissociation,

[1] $$HSO_3Cl \rightleftharpoons H^+ + SO_3Cl^-$$

[2] $$HSO_3Cl \rightleftharpoons HSO_3^+ + Cl^-,$$

and concluded that the high specific conductivities of solutions of potassium and sodium chlorosulfates in chlorosulfuric acid infer that the acid ionizes according to eq. [1] rather than eq. [2]. Quinoline and α-picoline also gave highly conducting solutions; it was claimed that this could be due to either

[3] $$HSO_3Cl + RN \rightleftharpoons RNH^+ + SO_3Cl^-$$

or

[4] $$HSO_3Cl + RN \rightleftharpoons RNSO_3H^+ + Cl^-.$$

To further confirm the validity of eq. [1] the conductivities of solutions of the Lewis acids $AlCl_3$, $SbCl_3$, $SnCl_4$, $TiCl_4$, and SO_3 were determined; it was found that all these solutes behave essentially as nonelectrolytes. This behavior was interpreted as ruling out eq. [2].

Gillespie and White (4) found that the dielectric constant of chlorosulfuric acid is 60 ± 10 at 14 °C and Palm (5) has determined the Hammett acidity function to be −1.89 units more negative than that of pure sulfuric acid, showing that HSO_3Cl is a stronger acid than H_2SO_4. The latter result was confirmed by Barr, Gillespie, and Robinson (6), who found that chlorosulfuric acid behaves as a very weak acid in 100% H_2SO_4. Waddington and Klanberg (7) found that chlorosulfuric acid behaves also as an acid in liquid hydrogen chloride,

[5] $$HSO_3Cl + HCl \leftrightharpoons H_2Cl^+ + SO_3Cl^-.$$

The greater acidity of chlorosulfuric acid as compared with sulfuric acid, its relatively high dielectric constant, and its potential use as a solvent for inorganic and organic chlorides prompted us to start a systematic investigation of its properties as a nonaqueous solvent. This paper reports the results of some electrical conductivity, transport number, and density measurements on solutions of simple bases.

Experimental

Chlorosulfuric acid (British Drug Houses, reagent grade) was used without further purification. The normal method of purification has been by distillation, but we have found it impossible to obtain pure samples in this manner. Attempts to purify chlorosulfuric acid by distillation at atmospheric (and reduced) pressures gave a product containing increased amounts of pyrosulfuryl chloride (Table I). The $S_2O_5Cl_2$ content was determined by the method of Zararov (12) by extracting the nonpolar anhydride into anhydrous carbon tetrachloride. Ten milliliters of chlorosulfuric acid in 20 ml of 100% H_2SO_4

Can. J. Chem. Downloaded from www.nrcresearchpress.com by 210.87.254.40 on 09/05/12
For personal use only.

was extracted with three 20 ml portions of CCl_4. Aliquots (25 ml) from the combined extractions were then hydrolyzed with 75 ml of water and titrated to give the total acid and chloride content. The original HSO_3Cl/H_2SO_4 sample was extracted with two additional 20 ml portions of CCl_4 to give standards for correcting the HSO_3Cl–H_2SO_4 partition in carbon tetrachloride. The presence of pyrosulfuryl chloride as the impurity in distilled chlorosulfuric acid was verified from its Raman spectrum and by a constant total acid to chloride ratio of 3 to 1 (exp. 3.00 ± 0.02) obtained on hydrolysis.

[6] $$S_2O_5Cl_2 + 3H_2O = 2H_2SO_4 + 2HCl$$

Other possible decomposition products (e.g. SO_2Cl_2, HS_2O_6Cl, $SOCl_2$, HCl, or SO_3) would give acid to chloride ratios different from 3 to 1.

The difficulty in preparing pure chlorosulfuric acid arises because of the ease with which it decomposes thermally,

[7] $$2HSO_3Cl = S_2O_5Cl_2 + H_2O$$

and

[8] $$3HSO_3Cl = S_2O_5Cl_2 + H_2SO_4 + HCl.$$

Decomposition appears to occur under all distillation conditions, and since $S_2O_5Cl_2$ and HSO_3Cl have very similar boiling points, it has proved impossible to separate them effectively (Table I).

TABLE I

Percentages of $S_2O_5Cl_2$ in distilled HSO_3Cl

	Boiling range (°C)	% $S_2O_5Cl_2$
1.	152–153 at 760 mm	13.7
2.	151.5–153 at 760 mm	15.3
3.	151.5–152.5 at 760 mm	16.6
4.	68–69 at 30 mm	22.6
5.	70–71 at 28 mm	9.2
6.	*	0.66
7.	*	0.62

*B.D.H. reagent grade acid.

Fortunately, the $S_2O_5Cl_2$ content of commercial grade chlorosulfuric acid (British Drug Houses) was found to be 0.7% or less. This acid has a rather low specific conductivity (approximately 4×10^{-4} ohm^{-1} cm^{-1}), and reagent grade HSO_3Cl has proved to be a very satisfactory starting material for most of our physical measurements. It certainly appears to be a suitable solvent for the study of the conductimetric behavior of most electrolytes which typically give specific conductivities of the order of 10^{-2} ohm^{-1} cm^{-1}.

Alkali and alkaline earth metal chlorosulfates were prepared from the reaction between an anhydrous metal chloride and chlorosulfuric acid. The details of preparation have been described previously (13). *Sodium chloride*, *potassium chloride*, *cesium chloride*, *ammonium chloride*, *calcium chloride*, and *barium chloride* were B.D.H. Analar reagents; *lithium chloride* and *strontium chloride* were B.D.H. laboratory reagents; *rubidium chloride* was Fisher certified reagent. *Benzoic acid* was recrystallized twice from absolute alcohol and dried at 75 °C. The crystals were fused at 130 °C in a platinum dish and ground to a fine powder (m.p. 122.3 to 123.0 °C); *acetic acid* was prepared by refluxing glacial acetic acid with acetic anhydride for 12 h and fractionating the mixture. The fraction boiling at 118 °C was collected (f.p. 16.56 °C); *p-aminobenzoic acid* was Fisher certified reagent grade; *hydrazine dihydrochloride* was B.D.H. reagent grade; *p-phenylenediamine* was Fisher certified reagent grade.

The conductivity cells were modified versions of those described by Gillespie and co-workers (14). The standard form consisted of two 125 ml Erlenmeyer flasks connected by a supporting glass rod, an electrode chamber, and a 10 mm pyrex tube. A bevelled standard taper on one flask facilitated the addition of solutes to the acid. The electrodes were platinized according to the method of Jones and Bollinger (15). Initially the platinized electrodes were greyed at red heat and then replatinized. The optimum platinizing procedure which gave minimum electrode polarization was to electrolyze the chloroplatinic acid/plumbous acetate solution suggested by Kohlrausch (16) with a direct current of 19.3 mA for 3 min, reversing the current every 30 s. The cell constant was found by using minimum conducting sulfuric acid (14) as a secondary standard. Conductances were measured using a Wayne Kerr B221 universal bridge operating at a set frequency of 1592 c.p.s. with the solution thermostated at 25 ± 0.003 °C.

Conductivity cells were filled under dry nitrogen with chlorosulfuric acid from a delivery burette connected to a reservoir fitted with an efficient drying tube. Solid samples were added from individual ampuls filled in a dry box under an atmosphere of dry nitrogen; liquids were added from bottles equipped with dropping pipettes with standard taper joints.

Density measurements were carried out at 25 °C using Weld specific gravity bottles fitted with ground glass covers and standardized with doubly distilled water. Individual solutions were made up by weight in a dry box under an atmosphere of dry nitrogen.

Transport numbers were measured in a Hittorf cell similar to that used by Gillespie and Wasif (17). After the solution was electrolyzed with a current supplied from a Sargent coulometric source, the contents of the cell compartments were analyzed gravimetrically after hydrolysis for total sulfate content to determine the change in metal ion concentration.

Results and Discussion

Some of the important physical constants of chlorosulfuric acid are summarized in Table II; however, the accuracy of some of the literature values is doubtful since it is not certain that the measurements were performed on pure chlorosulfuric acid.

Electrical Conductivities and Transport Numbers

By analogy with other protonic solvents we assume that chlorosulfuric acid undergoes autoprotolysis.

[9] $$2HSO_3Cl \rightleftharpoons H_2SO_3Cl^+ + SO_3Cl^-$$

Can. J. Chem. Downloaded from www.nrcresearchpress.com by 210.87.254.40 on 09/05/12
For personal use only.

Thus, according to the solvo-system definition, *bases* are defined as substances that increase the concentration of chlorosulfate ion, SO_3Cl^-, and *acids* as substances which increase the concentration of the chlorosulfuric acidium ion, $H_2SO_3Cl^+$. By analogy with the behavior of hydrogen sulfates in sulfuric acid (18), and fluorosulfates in fluorosulfuric acid (19), the alkali and alkaline earth metal chlorosulfates are expected to behave as strong bases of the chlorosulfuric acid solvent system.

TABLE II

Some physical properties of chlorosulfuric acid

		Ref.
Boiling point	62 °C at 2.4 mm	(8)
	78 °C at 21.5 mm	(2)
	152 °C at 760 mm	(8)
Melting point	−80 °C	(8)
Density	1.7410 g/cc	*a*
Viscosity (25 °C)	0.0243 P	(9)
Dielectric constant (14 °C)	60 ± 10	(4)
Molar susceptibility	46.60	(10)
Specific heat	0.282 cal/g	(11)
Hammett acidity value	−12.78	(5)
Specific conductance (25 °C)	1.72×10^{-4} ohm^{-1} cm^{-1}	(2)
	4.0×10^{-4} ohm^{-1} cm^{-1}	*a*

(*a*) Present results.

The results of our conductivity measurements on solutions of metal chlorosulfates in chlorosulfuric acid at 25 °C are given in Table III.

Since chlorosulfuric acid is a stronger acid than sulfuric acid, any organic base that is fully ionized in sulfuric acid is expected to be also fully ionized in chlorosulfuric acid. Thus, acetic and benzoic acids which are strong bases of the sulfuric acid system (20, 21) are expected to be fully protonated in chlorosulfuric acid.

[10] $CH_3COOH + HSO_3Cl = CH_3COOH_2^+ + SO_3Cl^-$

[11] $PhCOOH + HSO_3Cl = PhCOOH_2^+ + SO_3Cl^-$

The proton n.m.r. spectra of acetic and benzoic acid, respectively, in both sulfuric and chlorosulfuric acid were found to be identical.

The results of electrical conductivity measurements on solutions of these solutes are also given in Table III. The specific conductivity curves for the alkali metal chlorosulfates and acetic and benzoic acids are remarkably similar (Fig. 1, which shows that the alkali metal chlorosulfates are indeed fully ionized bases of the chlorosulfuric acid system). Solutions of calcium, strontium, and barium chlorosulfate, on the other hand, have appreciably lower specific conductances which must be attributed to either incomplete ionization or incomplete dissociation due to the formation of ion pairs.

The rather high specific conductances of solutions in chlorosulfuric acid, which are much greater than would be expected if the only contribution to conductance was from a normal diffusion-controlled transport process, suggests that most of the current in the solutions is carried by the chlorosulfate ions which conduct by an abnormal proton transfer mechanism similar to that found for HSO_4^- ions in sulfuric acid (17) and SO_3F^- ions in fluorosulfuric acid (19). This arises from a Grötthus-type chain mechanism in which protons are transferred along chains of solvent molecules. The phenomenon is shown diagramatically for the chlorosulfate ion in Fig. 2.

Abnormal conduction by the SO_3Cl^- ion was verified by transport number measurements on

TABLE III

Interpolated values for the specific conductances of the alkali and alkaline earth metal chlorosulfates in chlorosulfuric acid at 25 °C

	Concentration (equivalents per kilogram of solution)										
	0.02	0.04	0.06	0.08	0.10	0.12	0.14	0.16	0.18	0.20	0.22
$LiSO_3Cl$	0.314	0.573	0.821	1.051	1.266	1.469	1.658	1.832	1.996	—	—
$NaSO_3Cl$	0.313	0.569	0.802	1.023	1.230	1.425	1.610	1.778	1.937	2.086	2.225
KSO_3Cl	0.313	0.572	0.813	1.030	1.248	1.450	1.642	1.817	1.973	2.125	2.267
$Ca(SO_3Cl)_2$	0.266	0.465	0.649	0.807	0.950	1.077	1.198	1.310	1.411	1.501	—
$Sr(SO_3Cl)_2$	0.290	0.518	0.723	0.905	1.070	1.228	1.370	1.502	1.628	1.743	—
$Ba(SO_3Cl)_2$	0.292	0.531	0.751	0.961	1.147	1.320	1.478	1.623	1.760	1.886	—
CH_3COOH	0.314	0.587	0.843	1.091	1.315	1.528	1.729	1.916	2.091	2.260	—
$PhCOOH$	0.314	0.583	0.839	1.070	1.289	1.490	1.675	1.844	2.008	—	—

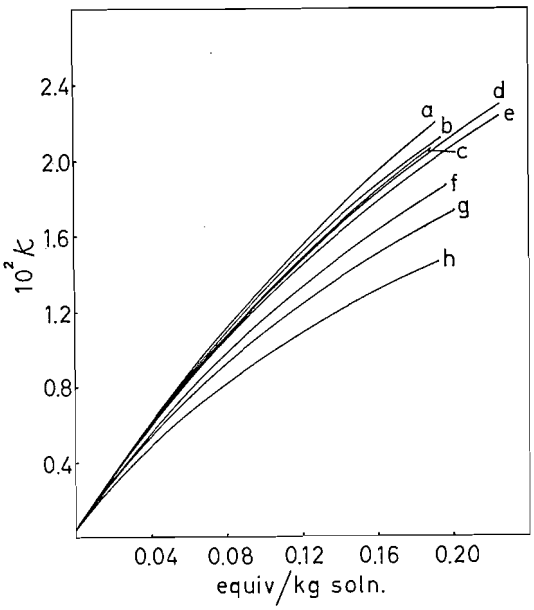

FIG. 1. Specific conductivities of solutions of *a*, acetic acid; *b*, benzoic acid; *c*, lithium chlorosulfate; *d*, potassium chlorosulfate; *e*, sodium chlorosulfate; *f*, barium chlorosulfate; *g*, strontium chlorosulfate; and *h*, calcium chlorosulfate in chlorosulfuric acid.

solutions of sodium and barium chlorosulfate, respectively, in chlorosulfuric acid. The results are given in Table IV. Difficulties in accurately analyzing for low cation concentrations limited the measurements to solutions of relatively high concentration. There appears to be no dependence of the cation transport number on concentration (Fig. 3) and on this basis, the transport numbers of the sodium and barium cations are 0.11 and 0.06, respectively.

TABLE IV

Transport numbers of the sodium and barium cations in chlorosulfuric acid at 25 °C

Soln.[a] conc.	Mequivalents of current	t_c[b]	t_a[c]	t_{av}
		Na^+ cation		
0.0541	1.7000	0.108	0.122	0.115
0.0624	2.0000	0.105	0.108	0.107
0.0779	2.0860	0.114	0.130	0.122
0.0930	2.0600	0.127	0.128	0.128
0.1035	2.2720	0.119	0.114	0.117
0.1204	2.1153	0.087	0.084	0.086
0.1273	2.5401	0.119	0.088	0.104
0.1482	2.1660	0.082	0.116	0.099
		Ba^{2+} cation		
0.0824	2.0000	—	0.061	0.061
0.0838	2.0000	0.042	0.064	0.053
0.0852	2.0000	0.043	0.031	0.037
0.1052	2.0000	0.057	0.059	0.058
0.1112	2.0000	0.059	—	0.059
0.1436	2.0000	0.058	0.038	0.048
0.1652	2.0000	0.062	0.077	0.070

[a] Solution concentration (equivalents per kilogram of solution).
[b] c, cathode.
[c] a, anode.

At low concentrations, below 0.05 mole per kilogram of solution, the specific conductance curves for sodium and barium chlorosulfate are linear, giving equivalent conductances of 79.5 and 72.0 ohm^{-1} cm^2, respectively. Thus the limiting cation mobilities of Na^+ and Ba^{2+} are 9 and 4 ohm^{-1} cm^2, respectively, and the limiting mobility of the chlorosulfate ion is 71 and 68 ohm^{-1} cm^2 for the two electrolytes, respectively; the mobility of the chlorosulfate ion is clearly some 8 to 18 times that of a typical metal cation.

The difficulty in preparing highly pure samples of the alkali and alkaline earth metal chloro-

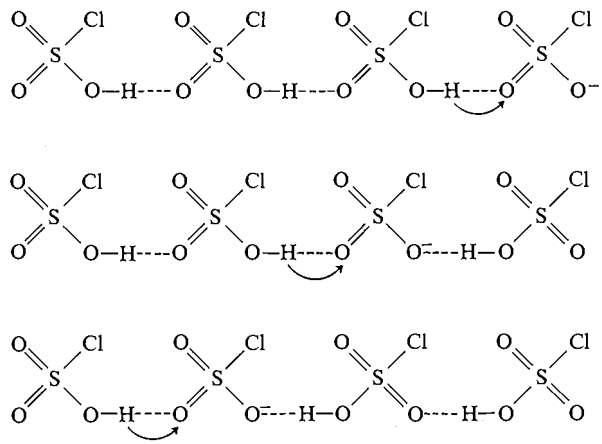

FIG. 2. Abnormal proton conduction by SO_3Cl^- in chlorosulfuric acid.

Can. J. Chem. Downloaded from www.nrcresearchpress.com by 210.87.254.40 on 09/05/12
For personal use only.

Can. J. Chem. Downloaded from www.nrcresearchpress.com by 210.87.254.40 on 09/05/12
For personal use only.

TABLE V

Interpolated values for the specific conductances of the alkali and alkaline earth metal chlorides, hydrazine dihydrochloride, *p*-phenylenediamine, and *p*-aminobenzoic acid in chlorosulfuric acid at 25 °C

	Concentration (equivalents per kilogram of solution)										
	0.02	0.04	0.06	0.08	0.10	0.12	0.14	0.16	0.18	0.20	0.22
LiCl	0.305	0.572	0.820	1.048	1.261	1.468	1.660	1.836	2.002	2.165	—
NaCl	0.305	0.572	0.820	1.048	1.267	1.475	1.670	1.845	2.008	—	—
KCl	0.305	0.572	0.830	1.068	1.288	1.497	1.690	1.872	2.038	2.195	—
RbCl	0.320	0.589	0.845	1.090	1.318	1.530	1.730	1.911	2.086	2.248	2.396
CsCl	0.324	0.595	0.851	1.096	1.325	1.539	1.744	1.937	2.111	2.280	2.441
NH_4Cl	0.320	0.590	0.850	1.098	1.328	1.548	1.752	1.942	2.115	2.284	—
$CaCl_2$	0.249	0.435	0.600	0.751	0.888	1.014	1.128	1.230	1.326	1.415	1.500
$SrCl_2$	0.260	0.468	0.660	0.830	0.993	1.141	1.278	1.401	1.521	—	—
$BaCl_2$	0.275	0.511	0.723	0.920	1.100	1.270	1.433	1.580	1.715	1.839	—
$NH_2NH_2.2HCl$	0.280	0.520	0.749	0.954	1.149	1.334	1.508	1.668	1.815	1.951	—
p-NH_2PhNH_2	0.283	0.528	0.758	0.973	1.180	1.371	1.550	1.715	1.871	2.018	2.157
p-$NH_2PhCOOH$	0.277	0.512	0.726	0.926	1.114	1.285	1.445	1.593	1.733	1.865	—
HCl	0.050	0.063	0.076	0.087	0.097	0.105	0.112	—	—	—	—

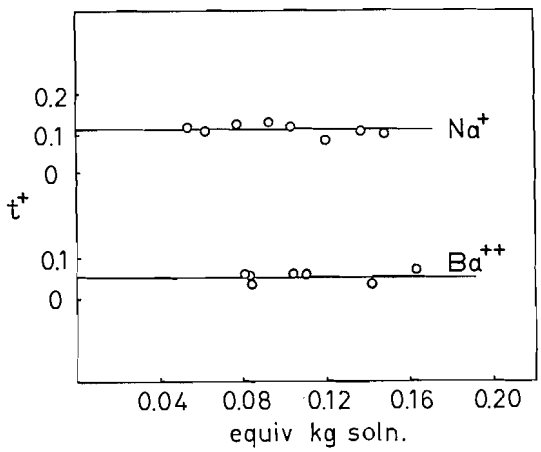

FIG. 3. Sodium and barium ion transport numbers in chlorosulfuric acid.

sulfates led us to investigate the specific conductivities of the anhydrous metal chlorides of Groups IA and IIA in chlorosulfuric acid. The results are given in Table V. The specific conductivity curves for the alkali metal chlorides (Fig. 4) are all very similar and compare favorably with those for solutions of the alkali metal chlorosulfates.

[12] $MCl + HSO_3Cl = M^+ + SO_3Cl^- + HCl$

Quantitatively, the specific conductivity curves of the alkali metal chlorides are all slightly higher than those for the alkali metal chlorosulfates. This is due to the presence of hydrogen chloride in solution which behaves as a very weak base.

[13] $HCl + HSO_3Cl \rightleftharpoons H_2Cl^+ + SO_3Cl^-$

The ionization constant was calculated by comparing concentrations of HCl and KSO_3Cl (reference base) that give the same specific conductivity. To a first approximation, the ratio of these concentrations gives the degree of ionization of the base in chlorosulfuric acid. Hence,

[14] $$K_b = \frac{[H_2Cl^+][SO_3Cl^-]}{[HCl]} = \frac{\alpha^2 w}{1-\alpha} = 3.0 \times 10^{-4} \text{ mole kg}^{-1},$$

where $\alpha = [KSO_3Cl]/[HCl]$ at a given specific conductivity.

In contrast to the similarity of the specific conductivities of the alkali metal chlorides, the chlorides of Group IIA show a greater diversity in their specific conductivities (Fig. 4). In comparison with the specific conductances of *p*-aminobenzoic acid, *p*-phenylenediamine, and hydrazine dihydrochloride, which were used as dibasic standards in a manner similar to the monobases acetic acid and benzoic acid,

[15] *p*-$NH_2PhCOOH + 2HSO_3Cl \rightleftharpoons$ *p*-$NH_3^+PhCOOH_2^+ + 2SO_3Cl^-$

[16] *p*-$NH_2PhNH_2 + 2HSO_3Cl =$ *p*-$NH_3^+PhNH_3^+ + 2SO_3Cl^-$

[17] $NH_2NH_2.2HCl + 2HSO_3Cl = NH_3^+NH_3^+ + 2SO_3Cl^- + 2HCl,$

the conductivities of the alkaline earth metal chlorosulfates are lower, markedly so in the case of the strontium and calcium salts.

The relatively low dielectric constant of chlorosulfuric acid ($\varepsilon = 60$) as compared with sulfuric acid ($\varepsilon = 100$) and fluorosulfuric acid

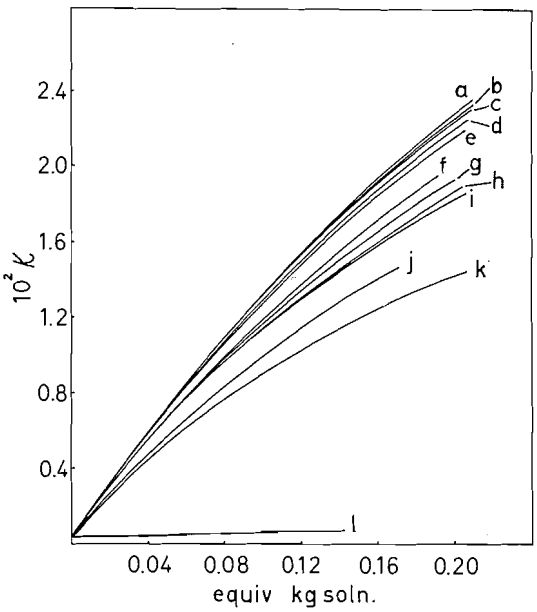

FIG. 4. Specific conductivities of solutions of *a*, ammonium chloride; *b*, cesium chloride; *c*, rubidium chloride; *d*, potassium chloride; *e*, lithium and sodium chloride; *f*, *p*-phenylenediamine; *g*, hydrazine dihydrochloride; *h*, *p*-aminobenzoic acid; *i*, barium chloride; *j*, strontium chloride; *k*, calcium chloride; and *l*, hydrogen chloride in chlorosulfuric acid.

($\varepsilon = 120$) would encourage the formation of ion pairs, especially in the case of divalent cations with small radii. This would effectively reduce the concentration of free chlorosulfate ions in solution and, since the SO_3Cl^- ion carries about 90% of the current, this would lead to a significant decrease in the specific conductivities of the solutions. It seems unreasonable that the low specific conductivities of the strontium and calcium chlorosulfates could be due to incomplete ionization, since chlorosulfuric acid would favor the dissociation of simple salts.

The specific conductivity curve for *p*-aminobenzoic acid falls lower than the curves for hydrazine dihydrochloride and *p*-phenylenediamine, suggesting that protonation on the amino and carboxyl groups may be incomplete. This is consistent with the behavior of these compounds in sulfuric acid, where the intrinsic basicity of an amino group is such that, even for a polyamine, all the amino groups are completely protonated regardless of their position in the molecule. But for an amino acid, the fully protonated amino group decreases the basicity of the carboxyl group in proportion to the decreasing separation of the groups (22).

TABLE VI

Densities of sodium, potassium, and barium chlorosulfate solutions in chlorosulfuric acid

$NaSO_3Cl$		KSO_3Cl		$Ba(SO_3Cl)_2$	
ω	ρ	ω	ρ	ω	ρ
0.0238	1.7426	0.0208	1.7422	0.0157	1.7466
0.0492	1.7443	0.0454	1.7437	0.0407	1.7546
0.0792	1.7455	0.0565	1.7451	0.0583	1.7609
0.1151	1.7488	0.0923	1.7474	0.0798	1.7678
0.1392	1.7499	0.1148	1.7491	0.1163	1.7808
0.1648	1.7518	0.1412	1.7500		
0.1774	1.7519	0.1597	1.7523		
		0.1897	1.7543		

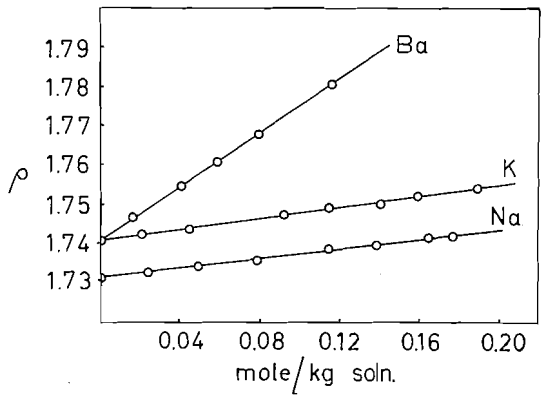

FIG. 5. Densities of solutions of sodium, potassium, and barium chlorosulfate in chlorosulfuric acid. The sodium curve is displaced vertically downward by 0.01 density units.

Densities

The densities of sodium, potassium, and barium chlorosulfate solutions were found to be linear functions of the concentration (Table VI and Fig. 5) and can be expressed in the form

$$[18] \qquad \rho = 1.7410 + A\omega,$$

where the constant A has the following values:

Metal cation	A
Na^+	6.586×10^{-2}
K^+	6.875×10^{-2}
Ba^{2+}	3.400×10^{-1}

The apparent molar volumes, ϕv, of the chlorosulfates can be calculated from the densities of their solutions through the relation

$$[19] \qquad \phi v = M_2/\rho^0 + 10^3(1/\rho - 1/\rho^0)/\omega,$$

where M_2 is the molecular weight of the solute, ρ^0 is the density of the solvent, and ω is the concentration of the solute in moles per kilogram

Can. J. Chem. Downloaded from www.nrcresearchpress.com by 210.87.254.40 on 09/05/12
For personal use only.

Can. J. Chem. Downloaded from www.nrcresearchpress.com by 210.87.254.40 on 09/05/12
For personal use only.

of solution (23). If the apparent molar volume of the chlorosulfate ion is assumed to be the same as that of a chlorosulfuric acid molecule (67 cm^3), the apparent molar volumes of the cations can then be calculated. The negative or zero values that are obtained for ϕv^+ (Table VII) indicate that these ions cause a decrease in the volume of the solution. This is attributed to different degrees of solvation; solvent molecules are tightly bound to the metal cations and occupy less volume than free solvent molecules (23, 24).

TABLE VII

Contraction volumes for the sodium, potassium, and barium cations from apparent molar volumes

	ϕv (cm^3)	ϕv^+ (cm^3)	r_+ (A)	V^+ (cm^3)	$V^+ - \phi v^+$ (cm^3)
Na^+	58	−9	0.95	2.2	11
K^+	67	0	1.33	5.9	6
Ba^{2+}	100	−34	1.35	6.1	40

If the true volume of the cation is known, the contraction that it produces in solution can be calculated by subtracting the apparent molar volume of the cation, ϕv^+, from the observed molar volume, V^+. To a first approximation, the true volumes of the cations can be calculated from values of their crystal radii (25). The contractions calculated in this manner are given in column 6 of Table VII. It is reasonable to assume that the degree of contraction would depend on the strength of the solvent–cation interaction so that the extent of solvation increases in the following order:

$$K^+ < Na^+ < Ba^{2+}.$$

This is also the order that would be expected on the assumption that the extent of solvation increases with the increasing polarizing power of the ion, and is exactly the order of decreasing specific conductivity that was found for the chlorosulfates of Groups IA and IIA. As the degree of solvation increases around a metal cation, there is a reduction in the number of free solvent molecules that can partake in the abnormal proton conduction and this results in a lowering of the specific conductivity as one goes to ions with an increasing polarizing power.

Acknowledgments

The National Research Council of Canada is thanked for generous financial assistance and the award of a scholarship (to J. A. Ciruna).

1. A. W. Williamson. J. Chem. Soc. **10**, 97 (1857).
2. P. Walden. Z. Anorg. Chem. **29**, 371 (1902).
3. R. C. Paul, S. K. Vasisht, K. C. Malhotra, and S. S. Pahil. J. Sci. Ind. Res. India, **21B**, 528 (1962).
4. R. J. Gillespie and R. F. White. Trans. Faraday Soc. **54**, 1846 (1958).
5. V. A. Palm. Proc. Acad. Sci. USSR Chem. Sect. English Transl. **108**, 249 (1956).
6. J. Barr, R. J. Gillespie, and E. A. Robinson. Can. J. Chem. **39**, 1266 (1961).
7. T. C. Waddington and F. Klanberg. J. Chem. Soc. 2332 (1960).
8. C. R. Sanger and Riegel. Proc. Am. Acad. Arts Sci. **47**, 673 (1912).
9. G. P. Luchinski. Z. Physik. Chem. Leipzig, **169**, 269 (1934).
10. A. Clow, H. M. Kirton, and J. M. C. Thompson. Trans. Faraday Soc. **36**, 1018 (1940).
11. J. Ogier. Compt. Rend. **96**, 646 (1883).
12. G. V. Zararov. Zavodsk. Lab. **27**, 1208 (1961).
13. E. A. Robinson and J. A. Ciruna. To be published.
14. R. J. Gillespie, J. V. Oubridge, and C. Solomons. J. Chem. Soc. 1804 (1958).
15. G. Jones and D. B. Bollinger. J. Am. Chem. Soc. **57**, 280 (1935).
16. F. Kohlrausch. Wied. Ann. **60**, 315 (1897).
17. R. J. Gillespie and S. Wasif. J. Chem. Soc. 209 (1953).
18. S. J. Bass, R. H. Flowers, R. J. Gillespie, and E. A. Robinson. J. Chem. Soc. 4315 (1960).
19. J. Barr, R. J. Gillespie, and R. C. Thompson. Inorg. Chem. **8**, 1149 (1964).
20. R. J. Gillespie, E. D. Hughes, and C. K. Ingold. J. Chem. Soc. 2473 (1950).
21. R. J. Gillespie and S. Wasif. J. Chem. Soc. 221 (1953).
22. R. J. Gillespie and E. A. Robinson. Sulphuric acid. *In* Non-aqueous solvent systems. *Edited by* T. C. Waddington. Academic Press, London and New York. 1965. p. 188 ff.
23. R. H. Flowers, R. J. Gillespie, and E. A. Robinson. J. Chem. Soc. 845 (1960).
24. R. J. Gillespie and S. Wasif. J. Chem. Soc. 215 (1953).
25. L. C. Pauling. The nature of the chemical bond. Cornell University Press, Ithaca, N.Y. 1960. p. 514.

Can. J. Chem. Downloaded from www.nrcresearchpress.com by 210.87.254.5 on 09/05/12
For personal use only.

Electrochemistry of zinc, cadmium, and mercury ions in fused $AlCl_3$–NaCl–KCl eutectic[1]

D. A. Hames and James A. Plambeck
Department of Chemistry, University of Alberta, Edmonton, Alberta

Received November 28, 1967

The electrochemistry of the ions of zinc, cadmium, and mercury in the $AlCl_3$–NaCl–KCl eutectic at 150 °C was investigated by e.m.f., voltammetric, and chronopotentiometric techniques. Oxidation states of +2 were observed for these three elements and oxidation states of +1 were observed for cadmium and mercury. Values of equilibrium constants for the reactions $Cd^{2+} + Cd^0 \rightleftarrows Cd_2^{2+}$ and $Hg^{2+} + Hg^0 \rightleftarrows Hg_2^{2+}$ were calculated to be 26 and 36 000 respectively. A standard potential scale for the Zn(II)/Zn, Hg(II)/Hg(I), Hg(I)/Hg(0), Ag(I)/Ag(0), and Al(III)/Al(0) couples was established in the solvent system $AlCl_3$–NaCl–KCl.

Canadian Journal of Chemistry, 46, 1727 (1968)

Introduction

This study is concerned with electromotive force (e.m.f.), voltammetric, and chronopotentiometric measurements of the Group IIB metal ions in the $AlCl_3$–NaCl–KCl eutectic and was initiated by interest in the existence of a subvalent state of cadmium. The divalent oxidation state of cadmium is the most common and standard potentials have been assigned to the Cd^{2+}/Cd^0 couple in several molten salts (1), although no potential values have been assigned to couples such as Cd(II)/Cd(I) or to Cd(I)/Cd(0). However, magnetic (2), cryoscopic (3), and e.m.f. studies (3–5) of the Cd^0–$CdCl_2$ system, and e.m.f. (6), Raman (7), and voltammetric (8) measurements in molten $AlCl_3$–NaCl, indicate the existence of a lower valence cadmium ion, Cd_2^{2+}, in these media. It was therefore considered desirable to investigate the electrochemical behavior of the group IIB elements in a medium in which lower valence ions might be expected.

The ternary eutectic used in this study (66 mole % $AlCl_3$, 20 mole % NaCl, and 14 mole % KCl) has an unusually low melting point of 70 °C (9) as compared with the considerably higher melting points of most fused salts. Electrochemical studies in this melt have included the determination of deposition potentials of metal ions (10–13), conductance measurements (14), and polarography of metal ions (15). Density (9) measurements have also been made.

The eutectic is a solvent for metal chlorides, oxides, and oxychlorides (10–13). It has a useful electrochemical range of 2.6 V, the limiting reactions being the cathodic deposition of aluminium and the anodic evolution of chlorine.

Experimental

Materials

All chemicals were Fisher Certified reagent grade unless otherwise stated. Aluminium chloride was purified by sublimation (16) under a positive pressure of nitrogen into a Pyrex vessel which could be tightly stoppered and then weighed. Aluminium metal turnings were added to the $AlCl_3$ before sublimation to reduce the $FeCl_3$ impurity. Sodium chloride and potassium chloride were dried by heating to 350 °C under vacuum. To prevent contamination of the eutectic by atmospheric moisture and subsequent hydrolysis, an aluminium wire spiral was added to the vessel to reduce any HCl contaminant to hydrogen gas. The vessel containing the eutectic mixture was then heated to 200 °C under a flow of dry nitrogen for 1 h. The fused eutectic was filtered through a 25–50 micron glass frit directly into the electrolytic cell. Further purification was effected by constant-potential electrolysis (2.0 V) between two large (2.0 cm^2) platinum electrodes for several hours, during which time the current decreased by a factor of 5, to about 0.01 mA/cm^2.

Zinc chloride and cadmium chloride (5) were melted under a flow of hydrogen chloride gas; after 3 h they were purged with nitrogen for 1 h and finally filtered through a glass frit. Mercurous chloride was dried over magnesium perchlorate. Reagent grade mercuric chloride (Mallinckrodt) was purified by sublimation.

All material transfers were made in a nitrogen-filled glove box, but weighings were made with an analytical balance outside the box, using tightly stoppered weighing bottles. Moisture in the glove box was eliminated by passing nitrogen over Linde molecular sieves (Union Carbide Corporation) and by storing open P_2O_5 in the glove box.

White heavy paraffin oil (Fisher, viscosity 335/350 USP) was circulated in an oil jacket surrounding the electrolytic cell which was located in the glove box. A type NB-ELE constant temperature bath (Colora, W.

[1]Taken from the Thesis of D. A. Hames submitted to the Faculty of Graduate Studies, University of Alberta, Edmonton, Alberta, in partial fulfillment of the requirements for the degree of Master of Science.

Can. J. Chem. Downloaded from www.nrcresearchpress.com by 210.87.254.5 on 09/05/12
For personal use only.

Germany) was used to maintain the oil temperature. Temperatures for various experimental runs varied from 149 to 159 °C, but the temperature was constant for each individual run to ±0.5 °C. The cell was closed with a machined Teflon stopper which had openings that allowed the electrodes to be inserted into the cell. Half-cells were isolated by glass sealing tubes with 10–20 micron glass frits (D porosity, Ace Glass Inc., Vineland, N.J.) when necessary.

Both tungsten and platinum were found to be inert in the eutectic. Tungsten and platinum indicator electrodes were made by sealing the pure wires into uranium and Pyrex glass tubing respectively, the wire protruding beyond the glass. Zinc and cadmium electrodes were pure wires wound into spirals to increase the area. An aluminium rod was used as the counterelectrode for all experiments. A mercury electrode was made by inserting a tungsten wire into a mercury pool; the eutectic above the pool was connected to the bulk melt through a glass frit.

Apparatus

Potentials were measured with a Type K-3 potentiometer (Leeds and Northrup Co., Phila., Pa.) or a 3440A (Hewlett-Packard, Palo Alto, Calif.) digital voltmeter. Coulometric oxidations and reductions were made using a Model IV coulometric current source (E. H. Sargent and Co., Chicago, Ill.). An Anotrol Model 4100 potentiostat modified to accept a Model 4510 linear scan unit (Magna Electronics) was used for voltammetric scans and for constant potential electrolysis. A Model EUW-20A servo recorder (Heath Co.) with a variable chart speed motor was used for automatic recording of voltammetric scans.

Chronopotentiometric measurements employed a Model 6824A power supply/amplifier in a constant-current configuration controlled by appropiate mercury-wetted relay switching circuitry; measurements were recorded on a Model 175A oscilloscope equipped with 1750B and 1781B plug-in units and a Model 196B camera (Hewlett-Packard) using ASA 3000 Polaroid film.

Reference Electrode

An aluminium reference electrode has been established (12, 17) in this melt and all potentials in this study were measured and are given with respect to the Al(III)/Al(0) couple. This reference electrode would not be expected to be easily polarized because the concentration of Al(III) in the eutectic is large and the activity of both Al(III) and Al(0) is constant (1). Small currents did not significantly alter the potential of the reference electrode (relative to an auxiliary Ag(I)/Ag electrode), and the aluminium electrode returned to its original potential immediately after the passage of larger currents.

This couple assumed its standard potential immediately upon the insertion of an aluminium wire into the eutectic. Other couples were generated by coulometric oxidation or reduction within isolation compartments. The amount of solvent in each isolation compartment was calculated from a Mohr chloride titration. The solute ion concentrations were calculated from these amounts and the moles of metal ion added as a salt or generated coulometically (18). The density data used was that of Midorikawa (9). All reductions unless otherwise stated were carried out at a current density of 3 mA/cm^2; oxidations were carried out at approximately 5 mA/cm^2.

The IUPAC Stockholm sign convention is used throughout. The thermocouple effect was determined between electrodes and found to be negligible (< 0.5 mV). The solute metal ion concentrations were kept below 0.1 *m* so that Henrian behavior would be observed.

Results

Electromotive Force Measurements

If the Zn(II) concentration was varied by oxidation of metallic zinc or reduction of added $ZnCl_2$ the Nernst equation was obeyed and a two-electron change was calculated ($Zn(II) + 2e^- \rightleftarrows Zn^0$). Standard potentials (1) on the molar, molal, and mole fraction scales were calculated as the Zn(II) concentration was varied by oxidation of Zn^0 (Table I); these are denoted by E_M^0, E_m^0, and E_X^0 respectively.

Nernstian behavior was observed for the reduction of added $HgCl_2$ or the oxidation of added Hg_2Cl_2 with a two-electron change being indicated ($2Hg^{2+} + 2e^- \rightleftarrows Hg_2^{2+}$). Standard potentials on the three scales were calculated from the coulometric reduction of Hg^{2+} (Table I). Similarly, the Nernst equation was obeyed as a mercury pool electrode was oxidized and the standard potential of the Hg_2^{2+}/Hg^0 couple was calculated (Table I).

To facilitate comparison of these standard potentials with standard potential series determined in other fused salt media (1) the standard potential of the Ag(I)/Ag(0) couple was also determined in this solvent.

If the logarithm of the equivalents of electricity used to oxidize a cadmium metal rod was plotted against e.m.f., a slope corresponding to a two-electron change is observed. However, if $CdCl_2$ was added to the eutectic and reduced at a platinum or tungsten flag electrode, stable e.m.f. values were not obtained although the potential drift was followed for up to 3 h. This instability was observed regardless of whether the reduction was kept small with respect to the Cd^{2+} concentration or whether it was a significant percentage of the Cd^{2+} concentration. This unstable e.m.f. was an unexpected observation since a previous study (6) reported the quantitative reduction of Cd^{2+} to Cd_2^{2+} in a 95% $NaAlCl_4$ – 5% $AlCl_3$ solvent at 277 °C. Since there is thus uncertainty regarding the oxidation state of cadmium produced anodically, no standard potential was calculated for this system.

Can. J. Chem. Downloaded from www.nrcresearchpress.com by 210.87.254.5 on 09/05/12
For personal use only.

TABLE I

Electromotive force series in $AlCl_3$–NaCl–KCl at 423 °K

Couple	E_M^0, V	E_m^0, V	E_X^0, V	Standard deviation, V
Al^{3+}/Al^0	0.000	0.000	0.000	Defined
Zn^{2+}/Zn^0	+0.254	+0.263	+0.304	0.002
Ag^+/Ag^0	+0.740	+0.759	+0.839	0.001
Hg_2^{2+}/Hg^0	+1.028	+1.037	+1.077	0.001
Hg^{2+}/Hg^0(calcd.)	+1.271	+1.280	+1.321	0.005
Hg^{2+}/Hg_2^{2+}	+1.415	+1.424	+1.464	0.005

For either Cd_2^{2+}/Cd^0 or Cd^{2+}/Cd^0, however, the standard potential would be about +0.35 V. The values obtained in this study are in agreement with those obtained for the Cd(II)/Cd(0) couple in this and other chloride media (1).

Voltammetric Measurements

All voltammetric scans were taken using a tungsten cylindrical electrode with a geometrical area of 1.2×10^{-3} cm^2. Scans were made from oxidizing to reducing potentials. Concentrations of dissolved metal chlorides were 0.03–0.08 *m*. If a voltammetric scan was taken of a solution of $ZnCl_2$, one well-defined wave was obtained indicating a single reduction process, which from the e.m.f. data must be two-electron (B, Fig. 1). The $E_{\frac{1}{4}}$ for this wave was +0.16 V; the plateau current was directly proportional to concentration of $ZnCl_2$, indicating a diffusion-limited process. If the Zn^{2+} concentration was then changed by coulometric reduction, the only change in the voltammogram was a decrease in the height of the diffusion-limited plateau. This indicates that the divalent oxidation state of zinc is the only state present in this eutectic, since formation of a monovalent zinc ion would be expected to increase the anodic current prior to the cathodic wave.

A voltammogram of a solution of $HgCl_2$ (A, Fig. 1) contained two waves of $E_{\frac{1}{4}}$ of +1.36 and +0.85 V. This would correspond to the reduction of Hg^{2+} in two steps: the first to Hg_2^{2+} and the second to Hg^0. If the Hg^{2+} concentration was reduced coulometrically the height of both diffusion-limited plateaus decreased linearly as expected.

If a voltammogram of a solution of $CdCl_2$ was taken, two waves were obtained (C, Fig. 1). The first was small and ill-defined and may correspond to the first step in the reduction Cd(II) → Cd(I) → Cd(0); the second was well-defined and corresponded to reduction to the metal. The $E_{\frac{1}{4}}$ values were approximately +0.3 and +0.22 V and the limiting current for the second wave was directly proportional to $CdCl_2$ concentration. Long scan times of 3 h/V and reduction of the $CdCl_2$ at lower current densities failed to improve the definition of the first wave.

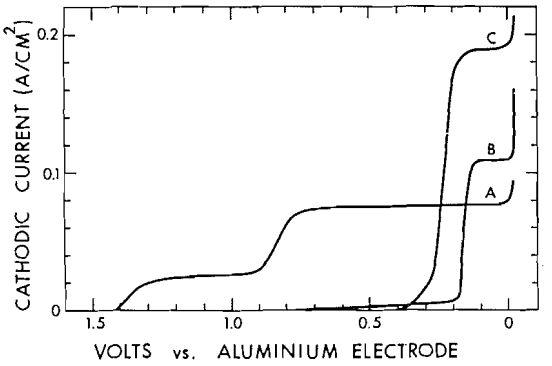

FIG. 1. Voltammetric scans for solutions of metal chlorides. Taken in fused $AlCl_3$–NaCl–KCl eutectic at 150 °C with tungsten microelectrode of area 1.2×10^{-3} cm^2. A, 0.03 *m* $HgCl_2$; B, 0.04 *m* $ZnCl_2$; C, 0.05 *m* $CdCl_2$.

When $CdCl_2$ was reduced coulometrically, successive voltammograms showed an increase in the anodic current prior to the reduction waves as well as a decrease in the height of the well-defined cathodic plateau. Similar behavior was observed if cadmium metal was left in contact with the $CdCl_2$ solution. This increase in anodic current can be explained by the reduction of Cd^{2+} with cadmium metal to form an oxidizable monovalent cadmium species.

Chronopotentiometric Measurements

A tungsten cylindrical electrode whose geometrical area was 1.6×10^{-2} cm^2 was used as the indicator electrode for all chronopotentiometric experiments. The indicator electrode was

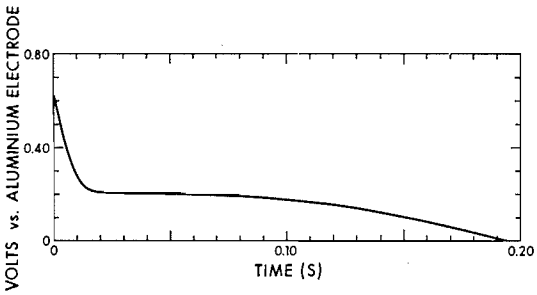

FIG. 2. Chronopotentiogram of 0.06 *m* $ZnCl_2$. Taken in fused $AlCl_3$–NaCl–KCl eutectic at 150 °C with tungsten cylinder electrode of area 1.6×10^{-2} cm^2. Current 6.50 mA.

always driven in the oxidation direction and then allowed 3 min to become quiescent before the reduction chronopotentiogram was recorded.

Chronopotentiometric experiments made on a solution of Zn^{2+} (whether added as the salt or generated coulometrically) showed one well-defined transition (Fig. 2). If the current was reversed during this transition, one transition was obtained in the oxidation direction in which τ_{red} was approximately equal to τ_{ox}. This would correspond to the plating of a metal on the electrode (19).

If the Sand equation is obeyed for the reduction of $ZnCl_2$, $\tau^{\frac{1}{2}}$ should be proportional to A/i for identical concentrations. Thus if log τ is plotted against log i a straight line of slope -2 should be observed. Slopes of -2.0 ± 0.1 were obtained for all determinations. Obedience to this equation for diffusion-limited processes is also indicated by the linearity of a plot of $\tau^{\frac{1}{2}}/C$ against reciprocal current density (Fig. 3). The chronopotentiometric constant ($i\tau^{\frac{1}{2}}/C$) was 0.0325 A $s^{\frac{1}{2}}$ m^{-1} with a relative standard deviation of less than 4% with current densities varying from 0.063 to 0.100 A/cm^2 and concentration of $ZnCl_2$ from 0.064 to 0.144 *m*.

In addition to the main wave a small inflection appeared at approximately +0.4 V. This inflection appeared whether Zn^{2+} was generated coulometrically or added as $ZnCl_2$; it was not well-defined and is believed to be due to a trace of some impurity.

Chronopotentiometric results were also obtained for $CdCl_2$ dissolved in the eutectic. Two well-defined transitions appeared (A, Fig. 4) with a $E_{\tau/4}$ separation of approximately 0.1 V. This small separation in potentials made it

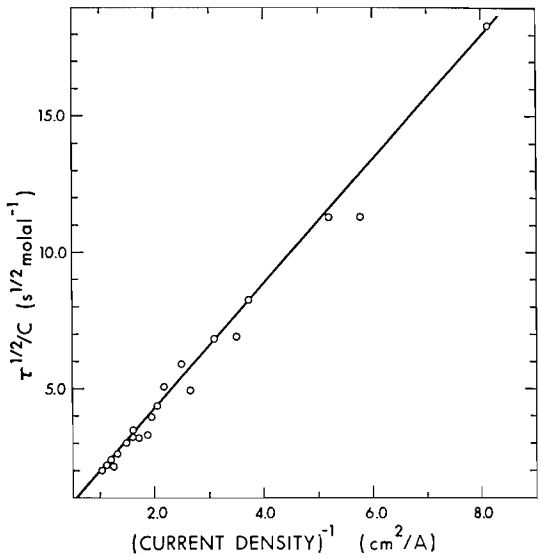

FIG. 3. Plot of $\tau^{\frac{1}{2}}/C$ against reciprocal current density. Various dilute solutions of $ZnCl_2$ in fused $AlCl_3$–NaCl–KCl at 150 °C.

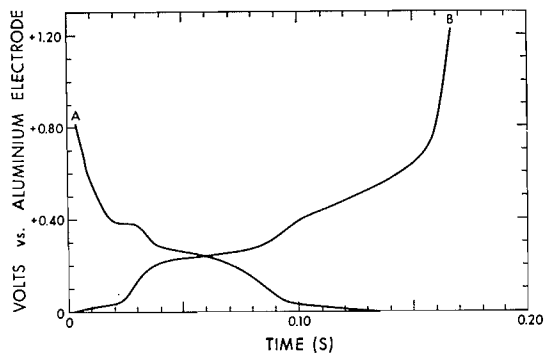

FIG. 4. Chronopotentiograms of 0.03 *m* $CdCl_2$. Taken in fused $AlCl_3$–NaCl–KCl at 150 °C with tungsten cylinder electrode of area 1.6×10^{-2} cm^2. A, reduction curve; B, oxidation curve for Cd metal plated on electrode. Current 2.78 mA anodic, 5.00 mA cathodic.

difficult to obtain results over a large range of current densities. At a suitable current density, several chronopotentiograms could be obtained with a relative standard deviation in $\tau^{\frac{1}{2}}$ of less than 1%.

Berzins and Delahay (20) have shown that if a diffusing substance undergoes multistage oxidation or reduction, a chronopotentiometric curve will show two transitions, and that if the diffusion coefficients of the higher and lower states are nearly equal, then the ratio of tran-

Can. J. Chem. Downloaded from www.nrcresearchpress.com by 210.87.254.5 on 09/05/12
For personal use only.

Can. J. Chem. Downloaded from www.nrcresearchpress.com by 210.87.254.5 on 09/05/12
For personal use only.

sition times will depend only on the number of electrons/stage:

$$\tau_2/\tau_1 = 2n_2/n_1 + n_2^2/n_1^2.$$

Therefore, if n_2 equals n_1, as is expected for the $Cd^{2+}/Cd_2^{2+}/Cd^0$ system, τ_2 should equal $3\tau_1$. The experimental value of τ_2/τ_1 was 3.0 ± 0.3 over the current range used.

Plots of log τ vs. log i gave slopes of −2.0 ± 0.2 for both transitions. The values of $i\tau^{\frac{1}{2}}/C$ were constant and the plots of $\tau^{\frac{1}{2}}/C$ against reciprocal of current density were linear for both transitions (Fig. 5).

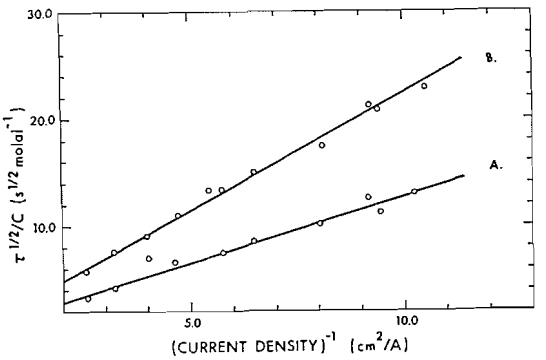

FIG. 5. Plot of $\tau^{\frac{1}{2}}/C$ against reciprocal current density. Various dilute solutions of $CdCl_2$ in fused $AlCl_3$–NaCl–KCl at 150 °C. A, first (Cd^{2+}/Cd_2^{2+}) transition; B, second (Cd_2^{2+}/Cd^0) transition.

If current reversal chronopotentiometry was used, first driving in the reduction direction and then switching to the oxidation direction, two transitions were observed (B, Fig. 4). This two-stage oxidation would correspond to the oxidation of cadmium metal through two separate steps. Values of $i\tau_1^{\frac{1}{2}}$ and $i\tau_2^{\frac{1}{2}}$ were not constant for this oxidation and the τ_2/τ_1 ratio varied from 1.0 to 2.0, with a mean of 1.4. The value of $i\tau_{ox}$ was always significantly less than the value of $i\tau_{red}$ for the second (cathodic) transition ascribed to the Cd_2^{2+}/Cd^0 couple. Even the $i\tau$ product for aluminium oxidation was less than that for reduction in this solution, indicating unusual behavior.

Chronopotentiometric reduction experiments on solutions of $HgCl_2$ showed two transitions with $E_{\tau/4}$ values of +1.3 and +0.93 V, corresponding to the Hg^{2+}/Hg_2^{2+} and Hg_2^{2+}/Hg^0 half-reactions (Fig. 6). The τ_2/τ_1 ratio varied between 1 and 3 and the $i\tau_1^{\frac{1}{2}}/C$ and $i\tau_2^{\frac{1}{2}}/C$ values were not constant. If current reversal

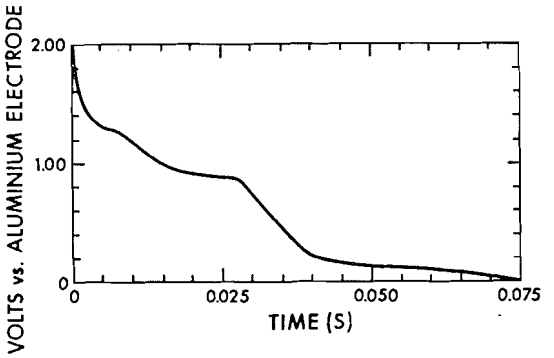

FIG. 6. Chronopotentiogram of 0.03 m $HgCl_2$. Taken in fused $AlCl_3$–NaCl–KCl at 150 °C with tungsten cylinder electrode of area 1.6×10^{-2} cm^2. Current 12.5 mA.

chronopotentiometry was used, first depositing metallic mercury and aluminium on the electrode and then oxidizing the metals to their respective metal ions, the transition time for the oxidation of the metals was shorter than the transition time for their deposition. The decrease in transition time is ascribed to a chemical reaction of the Hg(0) with diffusing Hg(II) thus decreasing the amount of mercury metal available for electrochemical oxidation. The quantity of aluminium would also be less for oxidation than for reduction since it would reduce the diffusing Hg(II) and be oxidized to Al (III).

Diffusion coefficients were calculated for Zn^{2+} and Cd^{2+} from the slopes of Figs. 3 and 5; the values were 6.5×10^{-5} (for Zn^{2+}) and 1.8×10^{-5} (for Cd^{2+}) cm^2/s at 150 °C. These diffusion coefficients are considerably higher than those determined by the less accurate polarographic method (both 1.5×10^{-6} cm^2/s) in fused $LiNO_3$–$NaNO_3$–KNO_3 at 160 °C (21), but that for Cd^{2+} is in agreement with the values of 1.7×10^{-5} cm^2/s determined in fused LiCl–KCl eutectic at 450 °C (22) and 1.8×10^{-5} cm^2/s determined in fused $AlCl_3$–NaCl at 160 °C (23), but lower than the value of 2.7×10^{-5} cm^2/s obtained from voltammetric data in LiCl–KCl at 500 °C (24).

Discussion

Of the three elements of Group IIB, zinc exists only in the divalent oxidation state in this solvent. In the case of cadmium and mercury, both monovalent and divalent species appear, presumably Cd^{2+}, Cd_2^{2+}, Hg^{2+}, and Hg_2^{2+}.

Can. J. Chem. Downloaded from www.nrcresearchpress.com by 210.87.254.5 on 09/05/12
For personal use only.

If the $E_{\tau/4}$ values are taken as approximately equal to standard potentials, the stability of the monovalent cadmium ion can be calculated. The equilibrium constant for $Cd^{2+} + Cd^0 \rightleftarrows Cd_2^{2+}$ is calculated to be 26. The equilibrium constant for the analogous reaction $Hg^{2+} + Hg^0 \rightleftarrows Hg_2^{2+}$ is calculated to be 36 000 using the standard potentials measured in this study (similar results would have been obtained using $E_{\tau/4}$ values). This is considerably larger than the value of 110 calculated for this mercury equilibrium using aqueous standard potentials (25), indicating the greater stabilization of lower valence states in this fused salt medium as compared with water.

The use of these equilibrium constants can explain most of the observations made for the cadmium and mercury systems. Since the equilibrium constant for cadmium is 26, this means that when a cadmium rod is anodized, the product is primarily Cd_2^{2+} but that the generation of Cd_2^{2+} cannot be quantitative; some Cd^{2+} will be formed also. If Cd^{2+} is coulometrically reduced, the reduction to Cd_2^{2+} will proceed, but if the concentration of Cd_2^{2+} in the vicinity of the electrode becomes high, there will be disproportionation into Cd^{2+} and Cd metal; the Cd metal will remain on the electrode. Stable potentials will not be obtained thereafter, since the diffusion of Cd^{2+} toward the electrode will result in generation of more Cd_2^{2+} which must then diffuse away and this process will continue until the supply of Cd metal on the electrode is exhausted. The changing concentrations of Cd^{2+}, Cd_2^{2+}, and Cd metal at the electrode surface will give rise to a potential drift, as observed. This would not be a problem in the mercury system since the equilibrium lies so heavily in favor of Hg_2^{2+} that disproportionation of this species will not occur.

The chronopotentiometric results can be explained in a similar manner. In the cadmium system, two well-defined waves were obtained for both reductive and oxidative chronopotentiometry. In the reductive case the expected τ_2/τ_1 ratio of 3.0 was found. In the oxidative case the ratio would be expected to be 1.0 (or perhaps somewhat lower if much Cd_2^{2+} diffuses away from the electrode) where in fact a higher ratio is obtained, indicating an additional source of Cd_2^{2+}. This additional Cd_2^{2+} could arise from the chemical reaction of Cd^{2+} with Cd^0 on the electrode, as favored by the equilibrium constant. Such a chemical reaction could also explain the fact that the $i\tau$ product for the cathodic metal deposition transition is greater than the $i\tau$ product for the anodic metal stripping transition, although these would be expected to be equal; metal is removed by the chemical reaction and thus is not available for anodic reoxidation. This would hold regardless of whether the metal were cadmium or aluminium.

In the mercury system the expected τ_2/τ_1 ratio of 3.0 for reduction was not obtained nor could the diffusion coefficient be calculated from $\tau^{\frac{1}{2}}/C$ against reciprocal current density plots. A comparison of the reductive transitions for mercury and cadmium (Fig. 6 and A, Fig. 4) shows a long sloping region between the plateaus of the first and second transition in the case of mercury. This sloping region made it difficult to determine the end of the first transition and the start of the second. Although the method of measuring transition times used throughout this work (26) gave the ratios cited, other measurement techniques gave values closer to 3 for the mercury system.

Two similar cases in which mixtures of oxidation states have been produced by electrochemical anodization of metals in fused salts are niobium in fused LiCl–KCl (27), in which the ratio between Nb(IV) and Nb(III) concentrations was approximately equal to 3, and zirconium in the same solvent, in which the proportion of Zr(II) and Zr(IV) obtained is temperature dependent (28).

Acknowledgment

The authors are grateful to the National Research Council of Canada for financial assistance during this work.

1. J. A. PLAMBECK. J. Chem. Eng. Data, **12**, 77 (1967).
2. N. H. NACHTRIEB. J. Phys. Chem. **66**, 1163 (1962).
3. L. E. TOPOL and A. L. LANDIS. J. Am. Chem. Soc. **82**, 6291 (1960).
4. M. OKADA, K. YOSHIDA, and Y. HISAMATSU. J. Electrochem. Soc. Japan, **32**, 99 (1964).
5. L. E. TOPOL. J. Phys. Chem. **67**, 222 (1963).
6. T. C. F. MUNDAY and J. D. CORBETT. Inorg. Chem. **5**, 1263 (1966).
7. J. D. CORBETT. Inorg. Chem. **1**, 700 (1962).
8. YU. K. DELIMARSKII. Zh. Fiz. Khim. **25**, 398 (1951).
9. R. MIDORIKAWA. J. Electrochem. Soc. Japan, **23**, 352 (1955).
10. W. H. WADE, G. O. TWELLMEYER, and L. F. YNTEMA. Trans. Electrochem. Soc. **78**, 77 (1940).

11. E. MARSHALL and L. F. YNTEMA. J. Phys. Chem. **46**, 353 (1942).
12. R. G. VERDIECK and L. F. YNTEMA. J. Phys. Chem. **46**, 344 (1942).
13. R. WEHRMAN and L. F. YNTEMA. J. PHYS. Chem. **48**, 259 (1944); **48**, 268 (1944).
14. R. MIDORIKAWA. J. Electrochem. Soc. Japan, **23**, 83 (1955).
15. R. M. DE FREMONT, R. ROSSET, and M. LEROY. Bull. Soc. Chim. France, 706 (1964).
16. E. D. PARRY. Private communication.
17. V. A. PLOTNIKOV, E. J. KIRICHENKO, and N. S. FORTUNATOV. Zap. Inst. Khim. Akad. Nauk Ukr. R.S.R. **7**, 159 (1940).
18. H. A. LAITINEN and C. H. LIU. J. Am. Chem. Soc. **80**, 1015 (1958).
19. P. DELAHAY. New instrumental methods in electrochemistry. Interscience, New York. 1954. p. 195.
20. T. BERZINS and P. DELAHAY. J. Am. Chem. Soc. **75**, 4205 (1953).
21. M. STEINBERG and N. NACHTRIEB. J. Am. Chem. Soc. **72**, 3558 (1950).
22. H. A. LAITINEN and W. S. FERGUSON. Anal. Chem. **29**, 4 (1957).
23. M. FRANCINI, S. MARTIN, and C. MANFRINI. Electrochim. Metal. **2**, 3 (1967); Chem. Abstr. **67**, 49878 (1967).
24. P. DROSSBACH and P. PETRICK. Z. Elektrochem. **58**, 95 (1954).
25. W. M. LATIMER. Oxidation potentials. 2nd ed. Prentice-Hall, Englewood, N.J. 1952.
26. W. H. REINMUTH. Anal. Chem. **33**, 485 (1961).
27. R. D. CATON, JR. and H. FREUND. Anal. Chem. **36**, 15 (1964).
28. R. BABOIAN, D. L. HILL, and R. A. BAILEY. J. Electrochem. Soc. **112**, 1221 (1965).

Can. J. Chem. Downloaded from www.nrcresearchpress.com by 210.87.254.5 on 09/05/12
For personal use only.

Can. J. Chem. Downloaded from www.nrcresearchpress.com by 210.87.254.5 on 09/05/12
For personal use only.

Mass spectra of some deuterated ethanes. I. The effect of ionizing voltage[1]

Y. AMENOMIYA AND R. F. POTTIE
Division of Applied Chemistry, National Research Council of Canada, Ottawa, Canada

Received December 22, 1967

The mass spectra of seven ethanes (d_0–d_6) have been obtained at various ionizing voltages. For low ionizing voltages (i.v. < 13.4 V), the only remaining ions are the parent molecule ion and that resulting from the loss of two hydrogen atoms (*m/e* 30 and *m/e* 28 in C_2H_6). With the exception of C_2H_5D, the ratio of the ion currents for these species remained reasonably constant below i.v. = 13.0. The sensitivity for detection of the molecule ion was found to decrease continuously as the D atom content was increased, both for high (70 V) and for low (12.8 V) ionizing voltages.

Canadian Journal of Chemistry, 46, 1735 (1968)

Introduction

In general, mass spectrometric analysis of deuterated compounds provides the most convenient and quantitative means of estimation. This technique has been widely used on the assumption of equal sensitivity for detection of molecular ions, both at the normal operating ionizing voltages of 50 or 70 V, and at low ionizing voltages for which interference by fragment ions is reduced. However, it is difficult to apply the latter technique for the analysis of deuterated ethanes because of interference from the ethylene fragment ion whose appearance potential is not significantly above that of the molecule ion. In addition we found in some preliminary studies that there was a considerable variation in the sensitivity of the molecule ion for various degrees of deuteration.

It is particularly important to obtain accurate analysis of mixtures of deuterated ethanes because of the wide interest in the catalytic deuteration of ethylene or in the catalyzed exchange of hydrogen with ethane. Several mass spectral studies of deuterated ethanes (1–7) have been reported, but in no case have all the deuterated isomers been studied, and it is not possible to use the published data to obtain relative sensitivities for mass spectrometric analysis. This work was undertaken to provide such data and to elucidate the mechanism of ion dissociations that lead to the observed mass spectra. In this report (Part I) we shall be concerned mainly with the use of our results for the mass spectrometric analysis of deuterated ethanes.

[1]NRCC No. 9998.

Experimental

The data reported here were taken with two mass spectrometers. Most of the results were obtained from an Atlas CH4 (60° magnetic sector) mass spectrometer at high (70 V) and low (12–15 V) ionizing voltages. This instrument was operated with an ion-accelerating voltage of 3000 V and an ion source temperature of 250°. An electron multiplier was employed for detection of the ions. A second mass spectrometer (90° magnetic sector) was employed to obtain comparison mass spectra at 50 V ionizing voltage. The ion acceleration voltage was 2000 V, and the ion source temperature was about 125°. The ion intensities were measured by means of a Faraday cup collector. In both instruments mass spectra were obtained by variation of the magnetic field, and the i.v. values were uncorrected.

All the ethanes, other than C_2H_6, were obtained from Merck, Sharp and Dohme of Canada, Ltd. and were supplied with a stated minimum isotopic purity of 98 to 99 atom %. The C_2H_6 was Phillips research grade. All samples were repeatedly outgassed over liquid nitrogen. No traces of methane or ethylene were detected by gas chromatographic analysis.

In all instances residual mass spectra were taken before and after the admission of each sample to improve the accuracy of the reported data. However, because of residual ions at M_{16}–M_{18} (M is used here for *m/e* because of convenience), the data for the C_1 fragments are not as precise as those for the C_2 ions.

The sensitivities for the molecular ions were obtained by the method of mixtures and were related to that for $C_2D_6^+$. Mass spectra were first obtained for the individual ethanes and were corrected for isotopic impurities. Mixtures were then composed by manometric techniques and mass spectra of these mixtures were taken. From the known compositions, it was then possible to relate the sensitivities for detection of the molecular ions of all other ethanes to that for $C_2D_6^+$. $C_2D_6^+$ was used as the primary standard since it had the lowest sensitivity of the molecular ions, and the M_{36} ion is free from interference by other ethanes. This technique avoids many of the errors inherent in the absolute method that is conventionally used in mass spectrometric analysis. Thus, a standard mixture, say, of C_2D_6 and C_2H_5D could be used from

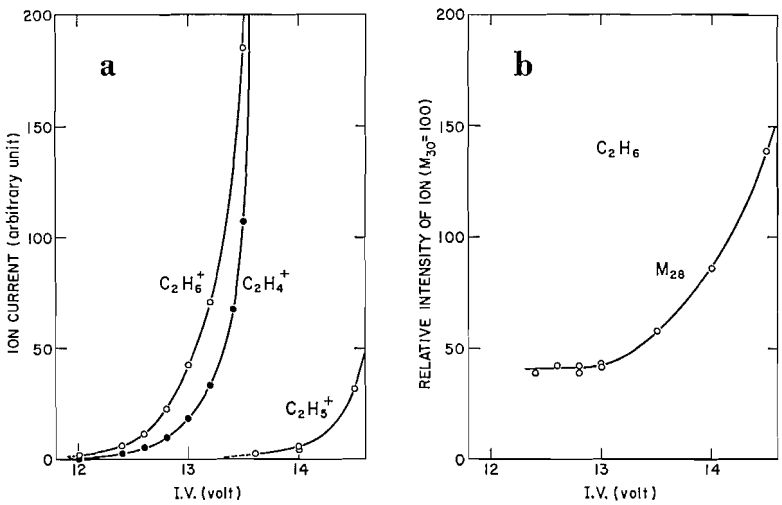

FIG. 1. Mass spectrometry of C_2H_6 at low ionizing voltages. (*a*) Ionization efficiency for the ions from C_2H_6. (*b*) Relative intensity of $C_2H_4^+$ ion ($C_2H_6^+ = 100$).

time to time as a means of calibration for mass spectral variations, or for comparison of different mass spectrometers.

Results and Discussion

(a) Low Ionizing Voltages

Partial ionization efficiency curves are shown for various fragment ions from C_2H_6 in Fig. 1(*a*). Because of the small difference between the ionization potential of C_2H_6 and the appearance potential for $C_2H_4^+$, approximately 0.7 eV (7), it is usually not possible to eliminate completely the ethylene peak from the mass spectrum of ethanes at low i.v. without sacrificing adequate sensitivity for analysis. However, $C_2H_5^+$ disappears below i.v. = 13.4 eV, so that the use of low ionizing voltage does simplify the mass spectrum. Similar results were found for other ethanes, so that corrections could be made for impurities containing one less deuterium atom than the major constituent by using i.v. < 13.4 eV. This was further confirmed by the observed constancy of M_{P-1}/M_P over a wide range of i.v. in the low i.v. region. We define M_P to be the intensity of the molecular ion and M_{P-1} as the intensity for the ion of one mass lower than M_P.

In Fig. 1(*b*), the ratio M_{28}/M_{30} is plotted for C_2H_6 versus i.v., for which the intensity unit of M_{30} is taken as 100. Similar curves are given in Fig. 2 for the other ethanes investigated in this work. In all cases the intensities have been corrected for ^{13}C contributions. In no case were there any impurities of more highly deuterated ethanes than the major constituent. Usually only one correction had to be made, that for the compound at M_{P-1}. Since the fragment ion for M_{P-1} was eliminated below i.v. = 13.4 eV, the corrections were readily made and could then be applied to the mass spectra for both low and high i.v. The impurities thus found were: 3.4% d_0 in d_1, 2.0% d_1 in d_2, 3.7% d_2 in d_3, 5.1% d_3 in d_4, 5.1% d_4 in d_5, and 2.3% d_5 in d_6. The symbols d_0–d_6 refer to the number of deuterium atoms in the ethane of interest.

We see in Figs. 1(*b*) and 2 that the ratios of the ethylene fragments to the molecular ions are reasonably constant in the region of i.v. = 12.8–13.0 V, except for M_{28} of C_2H_5D. Therefore, it is possible to obtain reproducible mass spectra for a i.v. of about 13.0 eV. Mass spectra for i.v. = 12.8 V are summarized in Table I. Also included in this table are relative sensitivities for the molecular ions.

(b) Mass Spectra for Normal Operating Ionizing Voltage (I.V. = 70 V)

Mass spectra of the seven ethanes, obtained at i.v. = 70 V, are summarized in Table II. The mass spectra were corrected for other ethane impurities and for ^{13}C. It was not possible to ascertain the carbon positions of the deuterium atoms for the impurities d_2 in CH_3CD_3, d_3 in CHD_2-CHD_2, and d_4 in CHD_5, so that we used impurity mass spectra as obtained for our d_2, d_3,

Can. J. Chem. Downloaded from www.nrcresearchpress.com by 210.87.254.5 on 09/05/12
For personal use only.

TABLE I

Mass spectra of ethanes (i.v. 12.8 V). Relative sensitivities for molecular ions ($C_2D_6^+ = 1.00$) were smoothed out in Fig. 3

m/e	C_2D_6	C_2HD_5	CHD_2CHD_2	CH_3CD_3	CH_2DCH_2D	C_2H_5D	C_2H_6
36	100						
35		100					
34			100				
33				100			
32	79	27.5	19		100		
31		25.5	27.5	2		100	
30			16	46	36.5		100
29				2.5	20.5	37	
28					5	29	40
Relative sensitivity	1.00	1.09	1.20	1.36	1.55	1.69	1.77

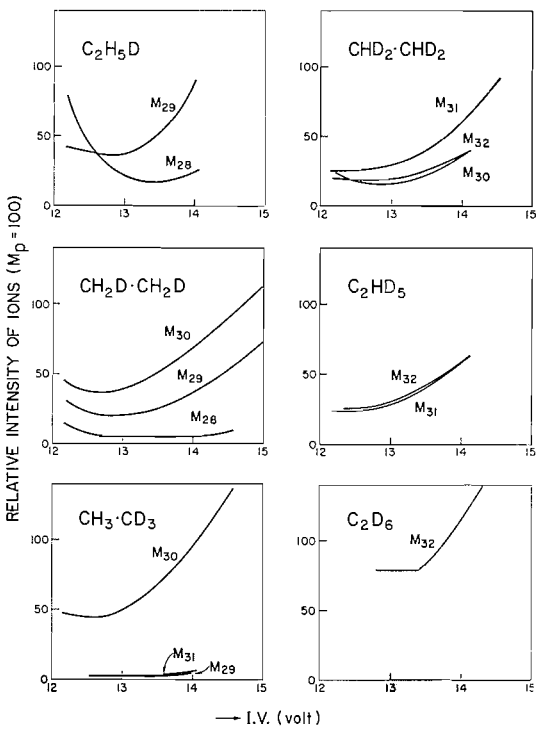

FIG. 2. Relative intensities of ethylene ions for various deuteroethanes (intensity of each molecular ion = 100).

and d_4 ethanes in Table II. However, the errors introduced because of variation in mass spectral ion distributions among isomers of the same D atom content are usually not very large (ref. 8, Part II of this series), and the low impurity contents found here would make these variations of negligible importance.

The results for the compounds listed in Table II differ in some respects from those reported by Quinn and Mohler (5), but are in better agreement with those of other workers (1, 3, 6), with the exception of M_{29} in CH_3CD_3. The relative intensity of our M_{29} for this compound is considerably lower than in some earlier studies (3, 6, 9) but agrees reasonably well with that reported by D'Or *et al.* (7). Therefore our CH_3CD_3 and CHD_2CHD_2 were subjected to analyses by infrared spectroscopy. Very clear spectra were obtained with the absorption bands at 2965, 2240, 1470, 1080, and 680 cm^{-1} for CH_3CD_3 and at 2960, 2220, 1308, and 1068 cm^{-1} for CHD_2CHD_2 respectively. No absorption at 1308 cm^{-1} was found for CH_3CD_3. This band appeared only in the d_4 compound and is presumably the bending frequency for CHD_2. We conclude that our CH_3CD_3 contained none of the isomeric impurity CH_2DCHD_2 within the detection limits of infrared spectroscopy.

As others have pointed out, the mass spectra of the C_1 fragments are complicated by the presence of doubly charged C_2 ions, so that we will not give here a detailed discussion of the C_1 fragments. However, M_{17} in the spectrum of CH_3CD_3 is much larger than is expected from its structure. As already mentioned, no appreciable amount of CH_2DCHD_2 was found in this sample by infrared spectroscopy. Indeed M_{17} was found in $CH_3.CD_3$ spectrum also by previous authors (3, 5–7) and the value 0.27 obtained as the ratio of M_{17}/M_{18} in the present work is comparable to those found by the other authors; 0.48 at 75 V and 0.35 at 17.5 V (1), 0.52 at 70 V (5), 0.27 at 70 V, 0.25 at 25 V and 0.23 at 18 V (6), and 0.30 at 50 V (7).

This fact indicates, as Krauss *et al.* have already suggested (10), that the reshuffling of

Can. J. Chem. Downloaded from www.nrcresearchpress.com by 210.87.254.5 on 09/05/12
For personal use only.

TABLE II

Mass spectra of ethanes (i.v. 70 V). Relative sensitivities for molecular ions ($C_2D_6^+ = 1.00$) were smoothed out in Fig. 3

m/e	C_2D_6	C_2HD_5	CHD_2CHD_2	CH_3CD_3	CH_2DCH_2D	C_2H_5D	C_2H_6
36	100.0						
35		100.0					
34	73.6	18.7	100.0				
33		55.2	36.5	100.0			
32	468.8	197.5	117.4	49.2	100.0		
31		220.0	230.4	71.6	64.2	100.0	
30	99.2	63.6	156.5	337.4	258.1	72.9	100.0
29		41.4	54.3	74.1	201.6	316.7	76.2
28	77.0	52.2	53.3	53.9	98.5	153.1	388.5
27		15.5	28.4	44.3	59.7	78.2	104.3
26	7.0	6.9	7.5	12.9	25.9	44.9	68.1
25			0.8	2.8	4.9	6.7	7.8
24						1.0	1.1
18	13.2	3.6		4.9			
17	1.8	3.9	9.2	1.3	0.4		
16.5		0.9	0.9				
16	8.9	4.6	4.0	3.9	9.3	5.7	
15.5		2.4	2.4	1.8	1.3		
15		1.0	3.4	6.4	5.0	7.7	9.7
14.5				0.7	1.9	2.9	1.9
14	2.5	1.7	1.6	2.0	1.9	3.1	6.3
13		0.2	0.4	0.7	0.8	1.1	1.0
12	0.9	0.8	0.7	0.6	0.8	0.7	0.5
Relative sensitivity	1.00	1.08	1.16	1.24	1.32	1.40	1.48

hydrogen atoms occurs to some extent before or during the C—C bond ruptures as follows:

$$CH_3CD_3^+ \rightarrow CH_2DCHD_2^+.$$

If M_{17}/M_{18} ratio is taken as the degree of this process, about one fifth of the original molecule is reshuffled, but it is still far less than complete randomization. However, it is not yet known whether the whole spectrum would be that of a mixture of the two isomers, or whether most of the reshuffled molecules decompose to C_1 fragments. This matter will be discussed in Part II in somewhat more detail.

(c) Relative Sensitivities

The sensitivities for detection of the molecular ions of the various ethanes were obtained relative to that for $C_2D_6^+$ by the method described in the Experimental section. A similar method involving the use of standard mixtures was employed by Pyper and Long (11) for obtaining the relative sensitivity of deuteroacetylene. The results are shown in Fig. 3. Included also are the sensitivities that were obtained by the second mass spectrometer which employed a Faraday cup detector and for which i.v. = 50 V. The sensitivities for the d_2 and d_4 ethanes were obtained relative to the d_3 and d_5 compounds respectively. The sensitivities for d_3 and d_5 ethanes had previously been obtained relative to d_6 and were used as secondary standards because of much greater interference at the molecular ions

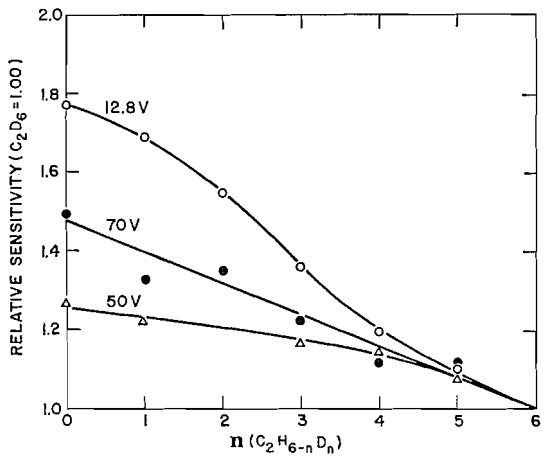

FIG. 3. Relative sensitivities for molecular ions of deuteroethanes ($C_2D_6^+ = 1.00$). The sensitivities for i.v. = 70 V and i.v. = 12.8 V were obtained with an electron multiplier detector in an Atlas mass spectrometer. Those at 50 V were measured on a second instrument that employed a Faraday cup collector.

Can. J. Chem. Downloaded from www.nrcresearchpress.com by 210.87.254.5 on 09/05/12
For personal use only.

Can. J. Chem. Downloaded from www.nrcresearchpress.com by 210.87.254.5 on 09/05/12
For personal use only.

of d_2 and d_4 ethanes from the mass spectrum of C_2D_6.

From Fig. 3 we see that the relative sensitivities decrease continuously as the D atom content increases, both for i.v. = 70 and i.v. = 12.8 V. Ignoring this difference, say, for C_2H_6 vs. C_2D_6 would result in a relative error of some 20% in their relative concentrations for a 1:1 mixture, using i.v. = 70 V. The relative sensitivities listed in Tables I and II were obtained from the smoothed curves of Fig. 3.

We find at low i.v. (12.8 V) that there is somewhat of a variation in the fraction of the total ionization that is retained by the molecular ion. From Table I, these percentages are: $C_2H_6^+$ = 71.4%, $C_2H_5D^+$ = 60.3%, $C_2H_4D_2^+$ = 61.7%, $C_2H_3D_3^+$ = 66.4%, $C_2H_2D_4^+$ = 61.5%, $C_2HD_5^+$ = 65.4%, and $C_2D_6^+$ = 55.7%. The recent results of D'Or *et al.* (7) for C_2H_6, C_2H_5D, $C_2H_3D_3$, and C_2D_6 exhibit less variation in the percentage intensities of the molecular ions, with their values ranging from 62.8% for $C_2D_6^+$ to 66.6% for $C_2H_5D^+$ at an i.v. of 11 V (corrected). Because of the differences between the two instruments (single focusing vs. double focusing) and the apparent lack of a trend with D atom content, we do not consider that there is a fundamental conflict with the earlier results.

However, our observed intensity for M_{28} in C_2H_5D at i.v. = 12.8 V is considerably higher than that of D'Or *et al.*, and from Fig. 2, M_{28} actually increases relative to M_{29} for lower i.v. Although this behavior was not found for ethylene ions in the other ethanes, it was quite reproducible, and we have no explanation for the observation. Also there are no obvious explanations for the large variation in sensitivity between our two instruments. However, in one experiment, a Faraday cup collector was substituted for the electron multiplier as the ion collector in the Atlas mass spectrometer, and mass spectra were obtained at i.v. = 70 V for the standard mixture of C_2H_5D and C_2D_6. We found a relative sensitivity of 1.22 for $C_2H_5D^+$ which agreed exactly with that obtained in the second instrument for i.v. = 50 V. It is not clear why the electron ejection efficiency of the multiplier should be so strongly dependent on D atom content, but this appears to be a sufficiently large effect to account for the discrepancy between the two mass spectrometers. Similar arguments could be advanced to explain the overall lower sensitivities that we find for total ionization (summation of all ion intensities) in C_2D_6 versus C_2H_6.

The wider variations in relative sensitivities at low i.v. would suggest that this region is not as useful as normal operating i.v. for quantitative analysis of deuterated ethanes, despite the simplicity of the mass spectra. However, the intensity ratios of the molecular ions to the ethylene fragments remain reasonably constant in the vicinity of i.v. = 12.8 V, so that some advantage is obtained in estimating the concentrations of mixed ethanes by using low i.v.

Conclusions

We have obtained mass spectra for seven ethanes in two mass spectrometers and find that the molecular ion sensitivities depend strongly on the degree of deuteration both at high (70 V) and low (12.8 V) ionizing voltages. Errors as great as 20% would be introduced into analysis for C_2H_6 vs. C_2D_6 in a 1:1 mixture if their sensitivities would be taken as equal. We suggest the use of a standard mixture, such as C_2H_5D and C_2D_6, as a calibrant for mass spectral sensitivities of the deuterated ethanes.

Acknowledgments

The authors are grateful to Mr. R. Ironside of the Analytical Chemistry Section for the infrared spectroscopy and its interpretation. They also thank Mr. R. Sander for obtaining many of the mass spectra used in this study.

1. J. Turkevich, L. Friedman, E. Solomon, and F. M. Wrightson. J. Am. Chem. Soc. **70**, 2638 (1948).
2. J. Turkevich, D. O. Schissler, and P. Irsa. J. Phys. Colloid Chem. **55**, 1078 (1951).
3. D. O. Schissler, S. O. Thompson, and J. Turkevich. Discussions Faraday Soc. **10**, 46 (1951).
4. C. Kemball. J. Chem. Soc. 735 (1956).
5. E. I. Quinn and F. L. Mohler. J. Res. Natl. Bur. Std. **65A**, 93 (1961).
6. L. J. Stief and P. Ausloos. J. Chem. Phys. **36**, 2904 (1962).
7. L. D'Or, J. E. Collin, and J. Longrée. Bull. Classe Sci. Acad. Roy. Belg. **52**, 518 (1966).
8. Y. Amenomiya and R. F. Pottie. Can. J. Chem. This issue.
9. J. H. Flynn and H. M. Hulburt. J. Am. Chem. Soc. **76**, 3396 (1954).
10. M. Krauss, A. L. Wahrhaftig, and H. Eyring. Ann. Rev. Nucl. Sci. **5**, 241 (1955).
11. J. W. Pyper and F. A. Long. J. Chem. Phys. **41**, 1890 (1964).

Can. J. Chem. Downloaded from www.nrcresearchpress.com by 210.87.254.6 on 09/05/12
For personal use only.

Mass spectra of some deuterated ethanes. II. An empirical method of calculation of the spectra[1]

Y. AMENOMIYA AND R. F. POTTIE
Division of Applied Chemistry, National Research Council of Canada, Ottawa, Canada

Received January 8, 1968

Relative intensities of the C_2 fragment ions in deuterated (d_1–d_5) ethanes have been calculated on a statistical basis from the mass spectrum of C_2H_6 and have been compared with experimental mass spectra previously reported in Part I. For these calculations we have introduced a correction for the relative probabilities of loss of two hydrogen atoms in addition to weighting factors for the loss of H and D atoms. The isotopic weighting factors have been expressed in terms of power series. By this means satisfactory agreement was obtained between the calculated and experimental mass spectra.

This treatment also made it possible to calculate the intensities of doubly charged C_2 fragments that appear in the C_1 mass spectra. We then estimated the degree of reshuffling of hydrogen atoms prior to C—C bond rupture and obtained calculated mass spectra that were in reasonable agreement with the experimental data for the C_1 region of the mass spectrum.

Experimental mass spectra have been newly obtained for 1,1-d_2 ethane and 1,1,1,2-d_4 ethane and are included here for completeness.

Canadian Journal of Chemistry, 46, 1741 (1968)

Introduction

The mass spectra of six deuteroethanes and of C_2H_6 have been reported by the authors in Part I of this series (1), and optimum conditions have been discussed for the mass spectrometric analyses of deuterated ethanes. For analytical purposes it is generally advisable to refer all mass spectra to standard compounds and mixtures. However, for complex mixtures of deuteroethanes this is both costly and inconvenient. It would therefore be preferable to be able to use mass spectra, calculated on a modular basis, that have been shown to give reasonably good agreement with experimental spectra, and that could be obtained for any deuterated isomeric ethane from a convenient standard, such as the mass spectrum of C_2H_6. It is the object of this report to provide such calculations and comparisons. In order to reduce the number of parameters, the calculations were made on a statistical basis in which we used as few empirical rules as possible.

Calculations of a similar nature have been reported for d_1 ethane by Turkevich *et al.* (2) and were later extended for d_2 and d_3 ethanes (3). Weighting factors for loss of H and D were regarded as isotope effects, and good agreement was found with experimental mass spectra for the d_1 and d_2 compounds. However, the calculated mass spectrum of 1,1,1-d_3 ethane was very different from that which was observed for 75 V electrons. At low ionizing voltage (i.v. = 13.0 V), Schissler *et al.* (3) observed the relative ion intensities for losses of H_2:HD:D_2 as 0.04:0.71:0.25 respectively for the CH_3CD_3 compound. At i.v. = 13.0 V, the only ions remaining were those for the parent molecule and for the loss of two hydrogen atoms. Although their intensity for the loss of D_2 is larger than that obtained by Stief and Ausloos (4) and by the present authors (1), the high intensity observed for loss of HD suggests, as they pointed out themselves (3), that there is a much higher probability for removal of two hydrogen atoms from adjacent carbons than from the same carbon atom.

This conclusion was further tested by Flynn and Hulburt (5), who calculated the mass spectrum of CH_3CD_3 for *m/e* 29–33 by assuming that the ethylene ion was the result of (A) loss of two hydrogens from adjacent carbons, or (B) loss from the same carbon, or (C) loss by a random process. Best agreement was found for model (A), although their calculated intensity for *m/e* 29 was less than half the observed value, suggesting that process (B) had occurred to some extent. More recently, Krauss *et al.* (6) and the present authors (1) have shown by analysis of the mass spectra of C_1 fragments that a certain degree of rearrangement of hydrogen atoms must occur before or during C—C bond rupture. It could not be established, however, whether the observed spectra were those of mixed isomers that resulted from the reshuffling of hydrogens or whether most of the rearranged

[1]NRCC No. 10022.

Can. J. Chem. Downloaded from www.nrcresearchpress.com by 210.87.254.6 on 09/05/12
For personal use only.

molecules decomposed to produce C_1 fragments only, without giving rise to rearranged C_2 ions. Thus, mass spectra could be calculated empirically by consideration of the two models: (1) Processes (A) and (B) both occur with a certain ratio of probabilities, but the rearrangement of hydrogen atoms does not further alter the distribution of C_2 ions, or (2) the mass spectrum is that of the original molecule combined with a rearranged isomer, but loss of two hydrogens occurs by process (A) exclusively.

Recently D'Or *et al.* (7) have carefully examined the mass spectra of C_2H_6, C_2H_5D, CH_3CD_3, and C_2D_6 with the purpose of establishing a model for the exchange of hydrogens in CH_3CD_3. Appearance potentials were measured for all major fragment ions; all metastable ions were recorded; and mass spectra were taken over wide ranges in ionizing voltage and in ion residence time in the ion source. Nevertheless, it was not possible to obtain a wholly satisfactory explanation for the mass spectrum of CH_3CD_3 by consideration of hydrogen exchange from any single model.

In this paper we used the first model as the basis for our calculations. We obtained weighting factors for loss of H and D atoms in the usual manner and then calculated the ratio of probabilities for processes (A) and (B). Excepting the process for loss of two hydrogens, all other fragment ion intensities of the C_2 group were calculated on a statistical basis by means of the weighting factors. We will consider later the second model described above.

Notations which will be used in the remainder of this report are as follows: M_i, the relative intensity of an ion of $m/e = i$; $I(n\text{X})$, the relative intensity of the ion that results from the loss of atoms nX from the parent ethane, for example M_{29} (from C_2H_5D) $= I(2\text{H}) + I(\text{D})$; a_n and b_n, the weighting factors for the rupture of C—H and C—D bonds, respectively, in ethane that contains n deuterium atoms; the probabilities for the occurrence of processes (A) and (B) as discussed earlier, are defined as A and B, respectively. In general, the word "hydrogen" will include both isotopes, protium and deuterium, and where necessary, the individual atoms will be designated as H and D. For simplicity, the symbol d_n will be used to indicate the number of deuterium atoms in the parent molecule.

Calculations of C_2 Ions

(a) Isotopic Weighting Factors

We have found, in agreement with previous work (3), that M_{P-1} (P is the mass of the parent molecule ion) is always larger than would be expected from M_{29} of C_2H_6 if hydrogens were removed statistically. We observed further that this discrepancy became larger as the D atom content was increased. We then obtain a weighting factor a_n for the molecule $C_2H_{6-n}D_n$ as the ratio of the observed M_{P-1} to that calculated on a statistical basis, using M_{29} ($M_{29} = 76.2$, cf. Table I) from C_2H_6 as the standard ratio. Thus, the loss of an H atom is a_n times more probable than it is from C_2H_6 for a molecule with n number of D atoms. The average value we obtain for a_n is 1.095^n, so that the individual factors become 1.10, 1.20, 1.31, 1.44, and 1.57 for d_1 to d_5 ethanes. The averaged factor will be used in preference to the experimental a_n of the individual molecule to calculate a particular mass spectrum.

The second weighting factor, b_n, was obtained from M_{27} and M_{29} in 1,1,2,2-d_4 ethane, and from M_{27-30} and M_{33} in C_2HD_5. These ions are all formed by a single process and were selected for that reason. It was first necessary to apply the a_n weighting factors before b_n could be obtained. Other ions, such as M_{25} in the d_1, d_2, d_3, and d_4 ethanes and M_{26} in the d_5 compound, are also derived from a single process, but their intensities are too low to be useful for this calculation. A few examples are given below to illustrate the method for calculating the b_n values. (Intensities are taken from Table I.) For 1,1,2,2-d_4 ethane

$$M_{29} = 54.3 = 104.3 \times 1.44{b_4}^2 \times 3/5$$

and for d_5 ethane

$$M_{27} = 15.5 = 68.1 \times {b_5}^4 \times 1/3.$$

From these and similar equations we obtain average values for b_4 and b_5, and derive the generalized weighting factors as 0.910^{6-n}, namely 0.62, 0.69, 0.75, 0.83, and 0.91 for the d_1 to d_5 ethanes.

Similar formulas were also obtained for weighting factors in terms of power series by Schissler *et al.* (3) and Kandel (8) for deuteromethanes and by Dibeler *et al.* (9) for deuterated ethylenes.

TABLE I

Observed and calculated mass spectra of deuteroethanes at i.v. = 70 V. Observed spectra were obtained with an Atlas CH4 mass spectrometer as reported in Part I (1). Gothic numbers were assigned rather than calculated

	C_2D_6	C_2HD_5		CH_2DCD_3[a]		CHD_2CHD_2		CH_3CD_3	
m/e	Obsd.	Obsd.	Calcd.	Obsd.	Calcd.	Obsd.	Calcd.	Obsd.	Calcd.
36	100.0								
35		100.0	100.0						
34	73.6	18.7	19.9	100.0	100.0	100.0	100.0		
33		55.2	57.8	36.5	36.6	36.5	36.6	100.0	100.0
32	468.8	197.5	185.2	64.6	59.5	117.4	119.6	49.2	49.9
31		220.0	214.9	291.3	289.4	230.4	220.7	71.6	72.0
30	99.2	63.6	67.8	155.2	130.8	156.5	151.0	337.4	344.1
29		41.4	39.1	62.7	62.2	54.3	62.2	74.1	74.6
28	77.0	52.2	53.6	82.1	50.6	53.3	50.6	53.9	57.5
27		15.5	15.7	28.1	29.8	28.4	29.8	44.3	41.5
26	7.0	6.9	7.0	8.5	8.2	7.5	8.2	12.9	12.5
25			0.8	1.7	1.8	0.8	1.8	2.8	2.8
24			1.1	1.1	1.1		1.1		1.0
Statistical deviation			1.88%		4.84%		1.81%		1.09%
18	13.2	3.6	**3.6**	7.0	**7.0**		0.5	4.9	**4.9**
17	1.8	3.9	4.1	2.3	2.3	9.2	**9.2**	1.3	**1.3**
16.5		0.9	1.3	0.5	0.9	0.9	0.9		
16	8.9	4.6	3.2	7.7	9.8	4.0	3.1	3.9	3.6
15.5		2.4	2.4	2.2	3.2	2.4	2.5	1.8	1.2
15		1.0	0.5	3.3	2.3	3.4	2.6	6.4	8.9
14.5								0.7	0.2
14	2.5	1.7	0.7	2.3	1.6	1.6	0.7	2.0	1.7
13		0.2	0.1	0.3	0.6	0.4	0.4	0.7	0.6
12	0.9	0.8	0.4	0.6	0.8	0.7	0.5	0.6	0.6

	CH_2DCHD_2	CH_3CHD_2[a]		CH_2DCH_2D		C_2H_5D		C_2H_6
m/e	Calcd.	Obsd.	Calcd.	Obsd.	Calcd.	Obsd.	Calcd.	Obsd.
36								
35								
34								
33	100.0							
32	49.9	100.0	100.0	100.0	100.0			
31	172.3	64.2	61.0	64.2	61.0	100.0	100.0	
30	229.5	206.6	216.1	258.1	258.0	72.9	69.9	100.0
29	107.3	239.7	236.4	201.6	188.2	316.7	318.7	76.2
28	57.5	100.1	75.6	98.5	89.6	153.1	157.1	388.5
27	41.5	53.3	55.1	59.7	55.1	78.2	71.5	104.3
26	12.5	19.8	22.5	25.9	22.5	44.9	38.9	68.1
25	2.8	2.6	4.3	4.9	4.3	6.7	5.8	7.8
24	1.0		1.1		1.1	1.0	1.1	1.1
Statistical deviation			3.42%		2.14%		1.36%	
18								
17		4.6	**4.6**	0.4	0.4			
16.5								
16		2.4	1.8	9.3	**9.3**	5.7	**5.7**	
15.5		1.4	1.5	1.3	1.5			
15		8.0	8.0	5.0	4.8	7.7	7.7	9.7
14.5		1.6	2.2	1.9	1.7	2.9	3.6	1.9
14		2.5	1.5	1.9	1.3	3.1	2.7	6.3
13		0.7	0.7	0.8	0.7	1.1	0.9	1.0
12		0.6	0.6	0.8	0.5	0.7	0.6	0.5

[a]These samples were prepared from 1,1-d_2 ethylene and were of lower isotopic purity than the remaining compounds.

Can. J. Chem. Downloaded from www.nrcresearchpress.com by 210.87.254.6 on 09/05/12
For personal use only.

Can. J. Chem. Downloaded from www.nrcresearchpress.com by 210.87.254.6 on 09/05/12
For personal use only.

(b) Probabilities of Processes (A) and (B)

In Part I we observed that there was a strong tendency for two hydrogens to be lost from adjacent carbons to produce the ethylene fragment ion. This could be seen most clearly in the low i.v. mass spectrum of CH_3CD_3. However, the ion intensities were low and of insufficient accuracy to be used in the calculation of relative probabilities for loss of two hydrogens from adjacent carbons, process (A), versus loss from the same carbon, process (B). A more accurate estimate of these probabilities, defined as A and B respectively, can now be made by consideration of the mass spectrum for i.v. = 70 V.

We first calculate the contributions of I(D), I(3H), and I(2H + D) to M_{31}, M_{30}, and M_{29}, respectively, in the mass spectrum of CH_3CD_3 by utilizing the mass spectrum of C_2H_6 and by taking into account the statistical and isotope weighting factors derived above. We then subtract these contributions from the observed mass spectrum and obtain the spectrum of ethylene ions only. Thus: I(2H) = 43.0, I(HD) = 325.6, and I(2D) = 13.6. We then have the following equations:

$$388.5Aa_3b_3 = 325.6$$

$$388.5Ba_3^2 \times 1/2 = 43.0$$

$$388.5Bb_3^2 \times 1/2 = 13.6.$$

From these equations we obtain $A = 0.853$ and $B = 0.129$ and 0.125 for good agreement between the two independent equations. Using average B, we obtain $A = 0.87$ and $B = 0.13$. These values will be used in the calculations that are given below.

(c) Calculation of the Mass Spectra

The method of calculation has been described in the Introduction and will be illustrated here by a few examples from the mass spectrum of CH_2DCH_2D. Thus:

$$M_{31} = I(\mathrm{H}) = 76.2a_2 \times 2/3 = 61.0$$

$$\begin{aligned} M_{30} &= I(\mathrm{D}) + I(2\mathrm{H}) \\ &= 76.2b_2 \times 1/3 + 388.5a_2^2[0.87 \times 4/9 \\ &\quad + 0.13 \times 1/3] \\ &= 258.0 \end{aligned}$$

$$\begin{aligned} M_{29} &= I(\mathrm{HD}) + I(3\mathrm{H}) \\ &= 388.5a_2b_2[0.87 \times 4/9 + 0.13 \times 2/3] \\ &\quad + 104.3a_2^3 \times 1/5 \\ &= 188.2 \end{aligned}$$

and

$$\begin{aligned} M_{28} &= I(2\mathrm{D}) + I(2\mathrm{H} + \mathrm{D}) + I(4\mathrm{H}) \\ &= 388.5 \times 0.87b_2^2 \times 1/9 + 104.3a_2^2b_2 \\ &\quad \times 3/5 + 68.1b_2^4 \times 1/15 \\ &= 89.6 \end{aligned}$$

Results and Discussion

The results of our calculations are given in Table I and are compared with the experimental mass spectra (1). Included also are the spectra of CH_2DCD_3 and CH_3CHD_2 which were prepared by the hydrogenation of 1,1-d_2 ethylene on an alumina catalyst at 0° with H_2 or D_2 (10). It has been found that the hydrogenation of ethylene that was preadsorbed on alumina proceeds at low temperature by the symmetrical addition of two hydrogens (11). The unreacted ethylene was removed by gas chromatography.

The two ethanes thus prepared contained 3–4% of the M_{P+1} and 8–9% of the M_{P-1} compounds as the only observable impurities. The contributions of the M_{P+1} impurities to the mass spectra were allowed for by using the observed spectrum of d_5 ethane and that calculated for 1,1,2-d_3 ethane. To obtain the contributions of M_{P-1} we subtracted the corresponding ion intensities of 1,1,2,2-d_4 and 1,2-d_2 ethane from those observed for 1,1,1,2-d_4 and 1,1-d_2 ethane respectively. The residuals thus obtained were in excellent agreement with those found at low ionizing voltage (i.v. = 13 V). The calculated mass spectrum of 1,1,2-d_3 ethane was employed to correct the spectrum of the d_4 compound for the M_{P-1} impurity.

There was no observable M_{28} at low ionizing voltage, indicating the absence of impurities with D atom content lower than M_{P-1}.

From Table I we find good agreement between the calculated and the observed mass spectra for C_2 ions. The statistical deviation was obtained according to the method of Schissler *et al.* (3), by taking the square root of the sum of the squares of the deviations, divided by the total C_2 ion intensities. Despite the somewhat lower isotopic purity of CH_2DCD_3 and CH_3CHD_2, good agreement was also found between the calculated and experimental spectra, indicating that our model correctly accounted for the effect of position of the deuteroatoms on the relative ion intensities.

By further consideration of the details of

Can. J. Chem. Downloaded from www.nrcresearchpress.com by 210.87.254.6 on 09/05/12
For personal use only.

the mass spectra of the C_2 and C_1 fragments, we find it possible to calculate the relative ion intensities in the C_1 region as well. The C_1 spectra are somewhat complicated by the presence of doubly charged C_2 ions. In addition, Schissler *et al.* (3) have reported that the intensity of a doubly charged ion was not proportional to the intensity of the corresponding singly charged ion in various ethanes. However, the results in Table I show that this ratio of intensities is reasonably constant for $M_{14.5}/M_{29}$ in d_0, $M_{15.5}/M_{31}$ in 1,2-d_2, $M_{16.5}/M_{33}$ in 1,1,2,2-d_4 and d_5, and M_{17}/M_{34} in d_6 ethane, the ratios being: 0.025, 0.020, 0.025, 0.016, and 0.025 respectively. Excluding the ratio 0.016 for d_5 ethane, which is unaccountably out of line, we obtain the average ratio 0.024, defined as α_1. These doubly charged ions are all ethyl radical ions.

The absence of $M_{15.5}$ in d_1, $M_{16.5}$ in d_3, and $M_{17.5}$ in d_5 ethane demonstrates conclusively that we do not have to consider doubly charged molecular ions. The similar lack of $M_{13.5}$ in d_0, $M_{14.5}$ in d_4 and d_5, and M_{15} in d_6 ethane also eliminates the possible occurrence of doubly charged ions that have resulted from the loss of three hydrogens. These observations are identical with those previously obtained by D'Or *et al.* (7). Thus, for example, in d_1 ethane, $M_{14.5}$ must consist of contributions from $C_2H_5^{2+}$ and $C_2H_3D^{2+}$ which are derived from $C_2H_5^+$ and $C_2H_3D^+$ respectively, and for which the relative intensities are 7.9 and 310.8. We have already obtained the parameter α_1 as the ratio of the intensities for the doubly charged versus singly charged ethyl radical, and can now calculate the corresponding ratio for the ethylene fragment ion, defined as α_2.

Thus:

$$7.9\alpha_1 + 310.8\alpha_2 = 2.9.$$

Similar equations were set up for $M_{14.5}$ in d_2, $M_{15.5}$ in d_3, d_4, and d_5 ethanes to obtain values for α_2. For these cases they are: 0.0087, 0.013, 0.026, 0.010, and 0.013. The average value $\alpha_2 = 0.011$ was obtained by excluding the exceptionally high value of 0.026 for $M_{15.5}$ in d_3 ethane.

It was then possible to deduct the contributions of doubly charged ions from the C_1 mass spectra by utilizing α_1 and α_2 and the intensities that were calculated for the ethyl radical and ethylene fragment ions in the various ethanes. The resultant experimental mass spectrum for the C_1 fragments in C_2H_6 is:

$$M_{CH_3^+} : M_{CH_2^+} : M_{CH^+} : M_{C^+ \text{ or } C_2^{2+}} = 100:20.6:10.3:5.2.$$

This agrees rather well with that obtained empirically by Flynn and Hulburt (5), namely 100:22.4:10.2:5.4.

We now must account for the effect of rearrangement of hydrogens on the C_1 mass spectra for the d_2, d_3, and d_4 ethanes. We assume that M_{17} in the spectrum of CH_3CD_3 represents the extent of such reshuffling for which the intensity ratios are $1.3/(4.9 + 1.3) = 21\%$ and assume additionally that the degree of rearrangement is the same for all other ethanes. Then the symmetrical and asymmetrical d_2 and d_4 compounds should have respectively $(21 \times 4/9)\%$ and $(21 \times 6/9)\%$ rearranged methyl radical ions.

To obtain the calculated mass spectrum in the C_1 region we first standardize the relative intensities with respect to the methyl radical ion of highest mass, include the doubly charged ions by means of the ratios α_1 and α_2, and calculate the intensities of the methyl, methylene, and methyne ions from the experimental values for the C_2H_6 spectrum, by correcting for the degree of rearrangement as estimated above. The calculated spectra, shown in Table I, are in satisfactory agreement with experiment. The correct prediction of the C_1 spectrum for 1,1,2,2-d_4 versus 1,1,1,2-d_4 and also 1,1-d_2 versus 1,2-d_2 ethane is particularly striking. Failure to observe M_{18} for the former compound is not considered to be a significant deficiency of the theory, since the background intensity was quite high for this mass. We conclude that the C_1 spectra can be of considerable use to determine the carbon positions of the D atoms in the molecule.

We now evaluate the use of the second model, as described in the Introduction, for calculation of the mass spectra. According to this model we would assume a certain degree of reshuffling for both the C_2 and C_1 mass spectra, but would not allow loss of two hydrogens from the same carbon atom to produce the ethylene fragment ion. The degree of rearrangement could be estimated in two ways; firstly, from the intensities M_{31}, M_{30}, and M_{29} in the mass spectrum of CH_3CD_3

by considering that they derive from a rearranged structure rather than from probability ratios of (A) and (B) as discussed above, and secondly, from the M_{17} in CH_3CD_3 by the same manner as already described for the C_1 fragments. These two procedures lead to slightly different estimates for the degree of reshuffling, but the statistical deviations between the calculated and observed mass spectra for the C_2 ions as estimated by these two techniques, 1.82 and 2.23% for CHD_2CHD_2 and 1.68 and 4.10% for CH_3CD_3, are not significantly different from those deviations of 1.81 and 1.09% (Table I) obtained with the first model. Thus we cannot use these calculations for a judgment either in favor of or against the relevancy of either model advanced here.

Summary

Mass spectra have been calculated for a series of deuteroethanes from a statistical model that was standardized to the mass spectrum of C_2H_6. The agreement between the calculated and experimental mass spectra was satisfactory in all cases, for both C_2 and C_1 fragment ions.

The experimental and calculated data were of sufficient accuracy to permit determination of the position of the D atoms in isomers with the same deuterium content. Particularly striking were the large intensity differences between the methyl radical ions of 1,1,2,2-d_4 and 1,1,1,2-d_4 ethane, and those for 1,2-d_2 and 1,1-d_2 ethane.

It was not possible to establish by the empirical procedures used here the exact nature of the model for the decomposing molecule, although information was obtained about the probable degree of rearrangement of hydrogens that will be of some use to future work.

1. Y. Amenomiya and R. F. Pottie. Can. J. Chem. This issue.
2. J. Turkevich, L. Friedman, E. Solomon, and F. M. Wrightson. J. Am. Chem. Soc. **70**, 2638 (1948).
3. D. O. Schissler, S. O. Thompson, and J. Turkevich. Discussions Faraday Soc. **10**, 46 (1951).
4. L. J. Stief and P. Ausloos. J. Chem. Phys. **36**, 2904 (1962).
5. J. H. Flynn and H. M. Hulburt. J. Am. Chem. Soc. **76**, 3396 (1954).
6. M. Krauss, A. L. Wahrhaftig, and H. Eyring. Ann. Rev. Nucl. Sci. **5**, 241 (1955).
7. L. D'Or, J. E. Collin, and J. Longrée. Bull. Classe Sci. Acad. Roy. Belg. **52**, 518 (1966).
8. R. J. Kandel. J. Chem. Phys. **39**, 2581 (1963).
9. V. H. Dibeler, F. L. Mohler, and M. de Hemptinne. J. Res. Natl. Bur. Std. **53**, 107 (1954).
10. Y. Amenomiya, J. H. B. Chenier, and R. J. Cvetanović. J. Catalysis, **9**, 28 (1967).
11. Y. Amenomiya. To be published.

Can. J. Chem. Downloaded from www.nrcresearchpress.com by 210.87.254.6 on 09/05/12
For personal use only.

Can. J. Chem. Downloaded from www.nrcresearchpress.com by 210.87.254.6 on 09/05/12
For personal use only.

Electron spin resonance detection of radicals and electrons condensed from water vapor after irradiation with 1 MeV helium ions[1]

W. A. SEDDON, D. R. SMITH,[2] AND P. E. BINDNER

Atomic Energy of Canada Ltd., Research Chemistry Branch, Chalk River Nuclear Laboratories, Chalk River, Ontario

Received October 24, 1967

A stream of water vapor was irradiated in a "crossed-beam" experiment by 1 MeV He^+ ions. After traversing the He^+ ion beam, the vapor was condensed on a quartz tube at 77 °K. The deposit so formed was then isolated under vacuum and transferred to an electron spin resonance (e.s.r.) spectrometer. E.s.r. spectra were observed that arise from species formed as a consequence of radiolysis in the vapor phase. Species trapped in the deposit were identified as HO_2 radicals and electrons. Addition of CH_3I and N_2O gives results which indicate that hydrogen atoms were also formed although they do not become trapped in the deposit.

The physical parameters of the experiment have been measured or calculated. These include the pressure and velocity of molecules in the vapor stream, and the time between irradiation and deposition on the cold finger.

Canadian Journal of Chemistry, 46, 1747 (1968)

Introduction

In an earlier study (1), it was shown that free radicals were trapped at 77 °K in the deposit condensed from a vapor stream after irradiation of the latter with 40 keV Ar^+ ions. At that time it appeared that such radicals were formed as a result of irradiation in the vapor phase and not as a consequence of any scattered Ar^+ ions striking the condensate. For a more complete understanding of the system it became desirable not only to obtain additional confirmation of this point but also to determine the pressure in the radiation zone. From the latter, one can then estimate the fraction of radicals that may disappear by reaction in the vapor phase during the elapsed time between irradiation and subsequent trapping in the deposit.

Bombardment by 40 keV Ar^+ ions resulted in deposition of energy in the vapor by both atomic collision processes and electronic processes. The ratio of the energy deposited by the two types of processes was about 4 to 1 in favor of collision processes (1). Atomic collision processes involve considerable momentum transfer, which would cause many of the species formed to be ejected in the forward (ion beam) direction. Since this is undesirable from the point of view of trapping the maximum number of species, our experiment was transferred to the target chamber of a 2 MeV Van de Graaff accelerator. The results presented in this paper were all obtained by bombardment of the vapor stream with 1 MeV He^+ ions. Energy deposition by this beam is almost entirely via ionization and electronic excitation processes.

Since the earlier work (1) we have learned of related experiments. Apparatus described by Horani and Leach (2) has been used to irradiate vapors with 100 eV electrons followed by condensation and an e.s.r. study of the deposit. Marx, Leach, and Horani (3) have studied water vapor and Marx and Maruani (4) have studied ammonia vapor.

The first section of this paper describes our improved methods, measurement, and calculation of the physical parameters, and evidence supporting our postulate that the radicals are formed in the vapor phase before becoming trapped in the solid deposit. The second section describes recent work on trapping radicals and electrons from a stream of water vapor after irradiation in the vapor phase.

Experimental

The technique for collecting and transferring the deposit to the e.s.r. spectrometer is the same as described previously (1). Pure samples were obtained in the vapor phase by distillation from the liquid during the experiment. Mixtures were prepared in the vapor phase in a 5 l bulb and used directly. A needle valve (Edwards High Vacuum Ltd.) was used to control the sample flow rates in order to deliver 0.1 g samples in approximately 15 min. H_2O and D_2O were doubly distilled from alkaline permanganate solution, gamma irradiated to about 10^7 rads in a ^{60}Co source, and then distilled a third time from alkaline permanganate. Baker and Adamson CH_3I was

[1]A.E.C.L. No. 3056.

[2]On attachment to Radiation Chemistry Group, Atomic Energy Research Establishment, Harwell, U.K.

Can. J. Chem. Downloaded from www.nrcresearchpress.com by 210.87.254.6 on 09/05/12
For personal use only.

singly distilled. Matheson N_2O was used without further purification. The required amounts of CH_3I and N_2O were metered by a gas burette in a grease-free system. All samples were deaerated by standard vacuum line techniques.

A 100 μA beam of 1 MeV He^+ ions was focussed and collimated to about 1 mm wide and 2 mm high at the point of intersection with the vapor stream. The end of the vapor nozzle was 1.0 cm from the cold finger and the distance between the irradiation zone and the cold finger about 0.8 cm. The ion beam size and position were fixed by focussing with a magnetic quadrupole lens, vertical and horizontal electrostatic steering, and by collimation with a pair of vertical and horizontal current-monitoring slits upstream from the nozzle and cold finger. Since the beam path was bent 15° to reach the target chamber, fluctuations in the terminal voltage of the accelerator cause the beam position to oscillate. To eliminate this, a "feed back" signal derived from the current detected at either horizontal slit was used to stabilize the terminal voltage to ±1.0 keV.

A set of apertures was used to mask the deposit on the cold finger from bombardment by He^+ ions scattered off the collimating slits. These features are shown in Fig. 1. The background pressure in the target chamber was usually about 2×10^{-5} Torr and the accelerator vacuum was protected from stray vapor by an annular liquid nitrogen dewar inside the beam flight tube.

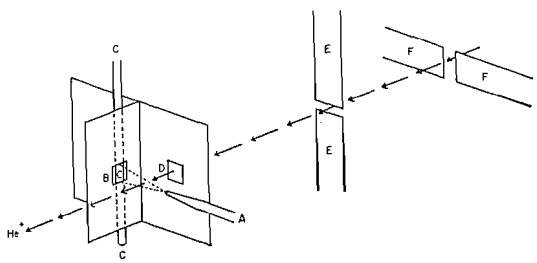

FIG. 1. Schematic diagram of the target assembly and collimating slits: (A) vapor nozzle, (B) vapor aperture, (C) quartz tube filled with liquid nitrogen, (D) He^+ ion beam aperture, (E) vertical collimating slits, (F) horizontal collimating and feed back energy stabilization slits.

Special experiments were performed to measure the pressure of the vapor stream in the radiation zone. In one, a parallel plate ion chamber (copper plates 0.5 cm × 0.5 cm, with 0.5 cm gap), not shown in Fig. 1, was constructed symmetrically about the radiation zone. Electrons and ions formed from the irradiated vapor were collected by applying a positive voltage to one plate with the other plated grounded through a Keithley 414 micro-micro-ammeter. This chamber discharged above 500 V. The other experiment involved measuring the absolute number of He^+ ions deflected through 45° by Rutherford scattering from the vapor atoms. This was done by nuclear counting techniques using conventional equipment consisting of a solid state detector (20 keV resolution, 50 mm^2 area), preamplifier, amplifier, and 100 channel analyzer. The data on punched tape were converted to a graph by an analogue-to-digital converter and a data plotter.

The e.s.r. spectrometer was the Varian model V-4502-04 with Fieldial and dual cavity. The Varian 0.1% pitch standard was used in the second sample position to give a correction factor for fluctuations in spectrometer sensitivity. Relative concentration measurements from different experiments were reproducible to within 5–15%. One source of error in this respect arises from slight differences in the alignment and focussing of the He^+ ion beam at the point of intersection with the vapor stream. The absolute number of spins in a sample was obtained by double integration of the various first derivative e.s.r. spectra and comparison with the previously calibrated 0.1% pitch standard (5). A calculated correction was applied for differences in filling factor and microwave flux distribution at the sample compared with the standard. Quartz concentrates microwaves, resulting in different microwave intensities at the sample and standard in our experiment. The appropriate correction factor for this effect was measured experimentally.

Post irradiation photolysis (photobleaching) of the deposit was done with light from a 500 W tungsten lamp passed through a 0.5 in. water filter to prevent heating the sample.

Results

Physical Parameters

At the cold finger the vapor stream has diverged to about 1 cm. We estimate that about 40% of the vapor is collected giving 0.04 g of deposit and that this remains constant for each experiment. The measured sample flow rate is about 0.4 g/h.

The pressure of the vapor stream in the radiation zone has been both calculated and measured.

A simple calculation of the pressure based on the assumption of thermal velocity, $\upsilon = 5.2 \times 10^4$ cm/s for D_2O at 300 °K, gives a pressure of about 0.05 Torr in the radiation zone.

The results of ion chamber measurements during bombardment of water vapor were inconclusive because a plateau saturation current was not obtained. This may possibly be due to space charge phenomena (6). A rough estimate was obtained by substituting butane for water. Irradiated butane vapor at the same initial reservoir pressure as water vapor gave an ion chamber saturation current of 24 μA at 300 V. From the butane results corrected by the ratio of (molecular weight)$^{3/2}$ to allow for velocity and stopping power (1) the saturation current in water vapor should be about 5.4 μA. Taking $-dE/dx$ (linear energy transfer) = 1.6 keV/μg/cm^2 for 1 MeV He^+ ions in water (7), and W (the average energy required for the formation of one ion pair) = 37.6 eV (8), then the calculated pressure in the radiation zone is about 0.01 Torr.

The most reliable measurement of the pressure

Can. J. Chem. Downloaded from www.nrcresearchpress.com by 210.87.254.6 on 09/05/12
For personal use only.

in the radiation zone was obtained by measuring the absolute number of He^+ ions deflected by Rutherford scattering through a known angle and solid angle. The differential cross section for scattering $d\Phi(\theta)$ (9) was modified to use center of mass coordinates because in our case the mass of the projectile He^+ is not negligible compared with the mass of the scattering nucleus (oxygen). This method determines the density of oxygen nuclei and hence the number of water molecules in the radiation zone. Using the equation

$$N = A/d\Phi(\theta)it,$$

where N = number of O atoms/cm^2, A = number of He^+ scattered through θ in a known solid angle, i = He^+ beam current in ions/s, and t = counting time, this method gave a pressure of 0.045 Torr in the radiation zone, in good agreement with the pressures estimated above.

From the measured values of $N = 6.2 \times 10^{12}$/cm^2, the deposition rate $D \simeq 3.4 \times 10^{18}$ molecules/s, and the width of the radiation zone, $x = 0.1$ cm, it is calculated that the time for water molecules in the vapor stream to travel 0.1 cm $= N/D = 1.8 \times 10^{-6}$ s. Hence the velocity of these molecules is about 5.5×10^4 cm/s, and comparable with thermal velocity. It follows that the water molecules travel the 0.8 cm from the radiation zone to the cold finger in about 1.4×10^{-5} s.

Pure Water Vapor

The deposit from H_2O vapor was colored blue. The e.s.r. spectrum with a cavity input power of 8×10^{-5} W is shown in Fig. 2A. A broad asymmetric spectrum, similar in shape to that calculated for twofold g-factor anisotropy (10), was observed. This spectrum has $g_{\parallel} = 2.032$ and $g_{\perp} = 2.0028$. Photobleaching at 77 °K with visible light removed the blue color, but no change in the e.s.r. spectrum was observed.

D_2O also gave a blue-colored deposit. The e.s.r. spectra at 1.2×10^{-5} and 8×10^{-5} W cavity input power are shown in Figs. 2B and 2C respectively. A broad asymmetric spectrum similar to that observed from H_2O was obtained. However, at the lower power, a narrow singlet of 2.1 G between derivative maxima was superimposed on the high field peak of the broad spectrum. The singlet has $g = 2.0008 \pm 0.0005$. At the higher power, microwave saturation has reduced the intensity of the singlet relative to that of the broad spectrum. The singlet has also become asymmetric presumably due to rapid passage effects (11). Photobleaching removed the blue color and the narrow e.s.r. singlet simultaneously. Figure 2D shows the e.s.r. spectrum, at 8×10^{-5} W cavity input power, obtained from D_2O after photobleaching at 77 °K. Only the broad asymmetric spectrum remains. It is similar to the corresponding spectrum from H_2O except for minor differences in line shape.

FIG. 2. First derivative e.s.r. spectra observed from H_2O and D_2O. The cavity input power is given in parentheses. (A) H_2O (8×10^{-5} W), (B) D_2O (1.2×10^{-5} W), (C) D_2O (8×10^{-5} W), (D) D_2O after photobleaching (8×10^{-5} W).

Effect of Alkyl Iodides and N_2O

A mixture of approximately 5×10^{-3} mole % CH_3I in D_2O was studied. The blue color of the deposit was perceptibly weaker. Figure 3A shows the resultant e.s.r. spectrum. The narrow singlet is reduced by about 30% and four narrow lines ($\Delta H = 23.3$ G) due to CH_3 radicals are superimposed on the broad asymmetric spectrum. No reduction in intensity in the latter spectrum is detected. Photobleaching removed the rest of the blue color and the e.s.r. singlet while the CH_3 radical spectrum increased by 27% (Fig. 3B). The intensity of the CH_3 lines increased with CH_3I concentration up to about 0.14 mole %, beyond which the yield of CH_3

Can. J. Chem. Downloaded from www.nrcresearchpress.com by 210.87.254.6 on 09/05/12
For personal use only.

radicals was constant within experimental error. Figure 3C shows the e.s.r. spectrum obtained when 0.14 mole % CH_3I or greater was added. The limiting CH_3 intensity is about 10 times greater than in Fig. 3A and the broad asymmetric spectrum is almost completely masked. We assume that it is unaffected. Up to 0.14 mole % CH_3I the blue color and the intensity of the singlet decreases with increasing CH_3I concentration. At 0.14 mole % and above, the singlet is absent and the deposit is pale brown in color. Addition of 0.6 mole % *n*-propyl iodide to D_2O gave a pale brown deposit and the e.s.r. spectrum shown in Fig. 3D. Six broad lines ($\Delta H = 21.7$ G) presumably due to *n*-propyl radicals are superimposed on the broad asymmetric spectrum, and the narrow singlet is absent. The addition of a similar amount of *n*-propyl chloride had no such effect.

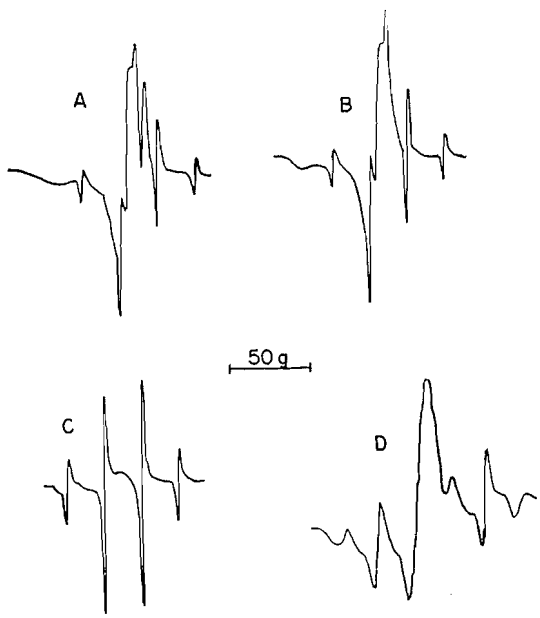

FIG. 3. First derivative e.s.r. spectra observed from D_2O in the presence of alkyl halides at a cavity input power of 8×10^{-5} W. (A) 5×10^{-3} mole % CH_3I, (B) after photobleaching the sample in A, (C) 0.14 mole % CH_3I, (D) 0.6 mole % C_3H_7I.

The normalized yield of CH_3 radicals as a function of CH_3I concentration is shown in Fig. 4A.

Mixtures of 0.14 mole % CH_3I in D_2O with increasing amounts of N_2O were studied. As the ratio N_2O/CH_3I increased, the yield of CH_3 radicals decreased to a new plateau between 55 and 65% of the yield in the absence of N_2O (Fig. 4B) and the brown color of the deposit was visibly diminished.

Relative Yields of Radicals

Yields of radicals in D_2O were obtained under conditions where microwave saturation was absent. Pure D_2O gave relative yields of 1.4 before photobleaching and 1.0 after photobleaching. Hence we assign 1.0 to the species giving rise to the broad asymmetric spectrum and 0.4 to the species giving the narrow singlet. CH_3 radical yields were obtained by doubly integrating the high field line and multiplying by 8. Above 0.14 mole % CH_3I the relative CH_3 yield was 0.97. Addition of increasing amounts of N_2O reduced this yield to between 0.55 and 0.65. The absolute number of paramagnetic species trapped in the pure D_2O deposit was found to be 3.7×10^{15} spins ($\pm 25\%$).

Discussion and Conclusions

Scattering of He^+ Ions by the Vapor Phase

One hazard of this experiment is the possibility that scattered He^+ ions strike the deposit and that the radicals observed were formed by irradiation in the solid phase. This would occur if 1 in 10^7 of the He^+ ions were scattered on to the deposit. The deposit is protected from any ions scattered off the slits, so that the only possible scattering source is the vapor stream itself. Our Rutherford scattering measurements indicate that only 1 in 10^{11} of the He^+ ions are scattered 90° to the cold finger. This intensity of scattered beam is a factor of 10^4 too low to produce the observed number of radicals.

Identification of the Species Formed from Water Vapor

(a) Asymmetric E.S.R. Spectrum

Asymmetric e.s.r. absorption spectra similar to those presented in Figs. 2A and 2D have been reported by various authors using other means of formation and there is considerable controversy over the identity of the free radical. This spectrum has been observed in the condensate from a microwave discharge in H_2O and H_2O_2 vapors (12), from an electric discharge in H_2O and D_2O vapors (13), in frozen aqueous solutions of 5 to 98% H_2O_2 photolyzed by ultraviolet light (14, 15), in frozen aqueous solutions

Can. J. Chem. Downloaded from www.nrcresearchpress.com by 210.87.254.6 on 09/05/12
For personal use only.

of 6 M H_2O_2 irradiated by tritium beta particles (16), and in the condensate from a jet of H_2O or D_2O vapor irradiated by 100 eV electrons (3). The radical must be oxygenated since a similar spectrum is obtained from H_2O or D_2O. These observations have been interpreted on chemical or spectroscopic grounds as evidence for either OH or HO_2 radicals. Either radical would exhibit an e.s.r. spectrum with twofold g-factor anisotropy (13). In the case of the photolysis results (14), HO_2 would be formed according to reaction [1] followed by [3] in competition with [2].

[1] $$H_2O_2 + h\upsilon \rightarrow 2OH$$

[2] $$OH + OH \rightarrow H_2O_2$$

[3] $$OH + H_2O_2 \rightarrow HO_2 + H_2O.$$

Since no effect of H_2O_2 concentration was observed, it was concluded that reaction [3] was not occurring and that the spectrum was due to OH. However, these arguments have been contradicted by evidence that reaction [3] does occur even at low H_2O_2 concentrations (16).

In our experiment kinetic data favor the OH radical. In the vapor phase transient species such as H (D), OH (OD), H_2O^+ (D_2O^+), e^-, and H_2O^* (D_2O)* (electronically excited molecules) are likely to be formed. Based upon the physical parameters it is instructive at this stage to estimate the initial concentration of such species and hence the reaction half-lives, $t_{1/2}$, for possible ion–molecule, radical–radical, or three body processes in the vapor phase. If each portion of the vapor is irradiated for 1.8×10^{-6} s and G(transients) = 16 molecules/100 eV (see later discussion), then we deduce a steady state concentration of transients of $5 \times 10^{11}/cm^3$ in the radiation zone. This represents a maximum concentration which decreases as the vapor stream diverges toward the cold finger. However, assuming this concentration and taking known rate constants for bimolecular and termolecular reactions in the gas phase, e.g. $OH + OH \rightarrow H_2O + O$, $k = 2.5 \times 10^{-12}$ cm^3/molecule^2 s, and $OH + OH + M \rightarrow H_2O_2 + M$ (where $M = H_2O$), $k = 18 \times 10^{-30}$ cm^6/molecule^2 s (17), then $t_{1/2}$ ranges from about 1 to 60 s. Since the transients are condensed in 1.4×10^{-5} s, none of them can disappear by reaction in the vapor phase. Similarly in the presence of 0.14 mole % CH_3I, radical reactions with CH_3I are unlikely in the vapor phase, since using an upper limit for $k = 3 \times 10^{-11}$ cm^3/molecule s gives $t_{1/2} = 1.6 \times 10^{-2}$ s.

On the other hand the ion–molecule reaction

[4] $$H_2O^+ + H_2O \rightarrow H_3O^+ + OH$$

is feasible, since $k_4 = 4.9 \times 10^{-10}$ cm^3/molecule s (18) giving $t_{1/2} \sim 10^{-6}$ s at 0.05 Torr.

Consequently there is insufficient time for reactions [2] and [3] to occur in the vapor stream. It seems probable therefore that the scavenging reactions of CH_3I (or N_2O), discussed below, occur in a transient liquid state which exists for a very short time during the process of condensation. This time interval must be long enough to allow such a reaction in the liquid phase and yet short enough to account for the trapping of at least the observed number of radicals in the absence of a radical scavenger. Taking a typical upper limit, $k = 2 \times 10^{10}$ M^{-1} s^{-1} for diffusion-controlled radical–solute and radical–radical reactions in the liquid phase, we estimate that such a liquid state probably exists for a time 2×10^{-9} s $\leqslant t \leqslant 1 \times 10^{-6}$ s. If this liquid phase were to exist long enough for [2] to occur ($t_{1/2} \sim 5 \times 10^{-6}$ s), it would go essentially to completion before reaction [3] could compete, $k_3 = 4.5 \times 10^7$ M^{-1} s^{-1} (19), $t_{1/2} = 1.4 \times 10^{-4}$ s, and no OH radicals would become trapped. During the cooling process the ratio k_2/k_3 would become larger and less favorable toward HO_2 formation both in a transient liquid phase, and in the solid, since the temperature coefficient for reaction [3] is expected to be greater than that for reaction [2].

On the basis of the earlier e.s.r. data (3, 12–16), it would be hazardous to identify this radical from its e.s.r. spectrum alone. One hazard is illustrated by the fact that the shape of the spectrum varies when ice is formed either by freezing the liquid, or by condensing water vapor, followed by X-ray irradiation. In these cases neither spectrum looks like the one obtained by condensing water vapor after electron irradiation in the vapor phase (3). In addition, previously published examples of this spectrum (12–16), in a water or water – hydrogen peroxide matrix cannot on their own merit be definitely ascribed to the HO_2 radical because of the uncertainty in the process of radical formation.

The identification of the radical can be resolved with some certainty on the basis of

Can. J. Chem. Downloaded from www.nrcresearchpress.com by 210.87.254.6 on 09/05/12
For personal use only.

three recent papers (20–22). Bennett *et al.* (20) have formed HO_2 in an ice matrix (formed by condensing water vapor) by reacting HI with Na in the presence of O_2. For the HO_2 radical they find $g_\parallel = 2.0351$ and $g_\perp = 2.0039$. These values agree fairly well with those measured in our experiment, $g_\parallel = 2.032$ and $g_\perp = 2.0028$. Spectroscopic evidence that our radical is not OH is derived from the g values in the papers by Dibdin (21) and by Brivati *et al.* (22). From these papers one can infer that HO_2 was also formed in the earlier work (3, 12–16).

Although the spectroscopic data show that the radical is HO_2, it is difficult to ignore the kinetic argument that HO_2 is not formed by reactions [2] and [3]. Neither could HO_2 have been formed by combination of H atoms and O_2, since O_2 is not present. Marx, Leach, and Horani (3) suggest that a greater concentration of water vapor molecules exists near the surface of the cold deposit. Possibly in such a region, or in a transient liquid phase, one or more of the reactions [5] (17), [6] (18), or [7] may occur to produce oxygen atoms.

[5] $\quad OH + OH \rightarrow H_2O + O$

[6] $\quad OH^+ + H_2O \rightarrow H_3O^+ + O$

[7] $\quad H_2O^* \rightarrow H_2 + O$

In the condensed phase these may then be followed by reaction [8].

[8] $\quad O + OH \rightarrow HO_2$

Reaction [9], rather than [8], occurs in the gas phase (23), but in our system could result in the formation of HO_2 on condensation.

[9] $\quad O + OH \rightarrow H + O_2$

[10] $\quad H + O_2 \rightarrow HO_2$

It should be noted here that the total concentration of trapped radicals is only about 1% of the estimated number produced initially. With our experimental geometry this difference is almost that expected on the basis of an isotropic flow of radicals from the radiation zone. However, this may be coincidental and does not necessarily support such a model.

(b) Singlet E.S.R. Spectrum

Pure H_2O and D_2O give a blue-colored deposit and, in the case of D_2O, a narrow e.s.r singlet is observed. This singlet and the blue color presumably arise from the same species, since they are both removed by photolysis or by addition of CH_3I. These observations are analogous to those obtained by many authors after the gamma radiolysis of alkaline ice or certain organic glasses at 77 °K, and have been attributed to the presence of trapped electrons. It is highly probable that in this work electrons are also being observed after trapping from the vapor phase. In this respect our conclusions are similar to those of Marx, Leach, and Horani regarding similar observations following the irradiation of D_2O vapor with 100 eV electrons. They actually observed a "doublet", but we conclude from our results in Figs. 2B and 2C that the "doublet" was the result of distortion of a singlet due to rapid passage effects. We observe this in Fig. 2C when the cavity input microwave power was increased to 8×10^{-5} W. Marx *et al.* (3) also observe a very slight absorption associated with the blue color in H_2O. We do not observe this absorption. Apparently in H_2O the electron singlet is broadened and masked by the HO_2 absorption. In D_2O, Marx *et al.* observe that the blue color and the "doublet" disappear on warming to 150 °K.

Formation of $C_3H_7\cdot$ or $CH_3\cdot$ radicals on addition of C_3H_7I or CH_3I supports our proposal that electrons are present. Presumably reaction [11],

[11] $\quad RI + e^- \rightarrow R\cdot + I^-,$

is occurring in the transient liquid phase, k_{11} for C_3H_7I is $1.3 \times 10^{10}\ M^{-1}\ s^{-1}$ and the corresponding value for C_3H_7Cl is $6.9 \times 10^8\ M^{-1}\ s^{-1}$ (24). The 19 times lower rate constant may account for the absence of an effect when C_3H_7Cl is added.

(c) Evidence for Hydrogen Atoms

It was realized that the limiting yield of CH_3 radicals at 0.14 mole % CH_3I need not arise entirely from reaction [11]. The CH_3 radicals could also be formed by reaction [12] with hydrogen atoms.

[12] $\quad CH_3I + D\cdot \rightarrow CH_3 + DI$

Hydrogen atoms would not themselves become trapped in ice at 77 °K, but their temporary existence would be revealed through the formation of CH_3 radicals. The occurrence of reaction [12] is supported by the effect of adding N_2O (Fig. 4B). N_2O would compete via reaction [13] with CH_3I in reaction [11],

[13] $\quad N_2O + e^- \rightarrow N_2 + O^- (\rightarrow OD + OD^-),$

but would not compete with reaction [12]. If all the CH_3 radicals were formed by reaction [11], N_2O would reduce the CH_3 yield to zero. In fact the CH_3 yield is only reduced by slightly less than half at an N_2O/CH_3I ratio of 30. It is concluded that in the absence of N_2O, the yield of CH_3 equals the sum of the yields of electrons and hydrogen atoms. In the presence of N_2O the yield of CH_3 radicals is equivalent to that of hydrogen atoms.

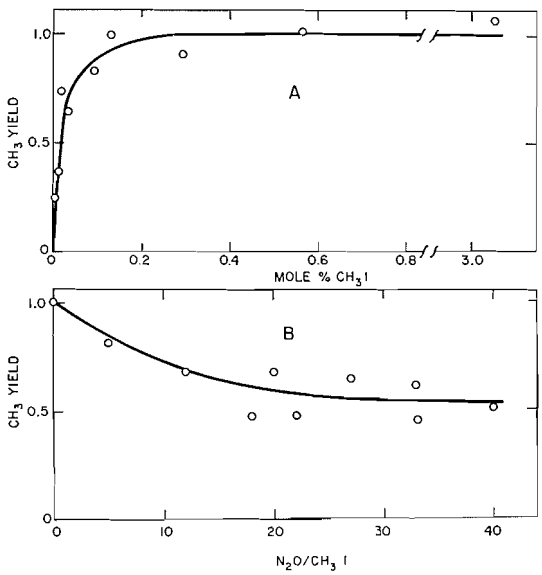

FIG. 4. (A) Dependence of the CH_3 yield on CH_3I concentration in D_2O, (B) effect on the CH_3 yield of increasing amounts of N_2O to D_2O containing 0.14 mole % CH_3I.

This evidence for the presence of hydrogen atoms is supported by the observation of the emission spectrum of hydrogen atoms when water vapor is irradiated by 100 eV electrons (2).

The above results and mechanism are consistent with results obtained by conventional gamma radiolysis of water vapor by Baxendale and Gilbert (25) and by Johnson and Simic (26). Both groups find that the yield of hydrogen atoms and electrons is about 5 and 3 molecules per 100 eV respectively, giving a ratio of yields $D/(e + D) = 0.63$. If we assume for the purposes of our earlier calculations that $G(OD) = G(e + D)$, then $G(total) = 16$. (This may not be strictly true but is adequate for our purpose.)

It must be pointed out that such a close correspondence with the conventional gas phase results may be coincidental, since reactions [14], [15], and [16] may occur to an unknown extent.

[14] $2D \rightarrow D_2$

[15] $D + OD \rightarrow D_2O$

[16] $e^- + H_3O^+ \rightarrow H + H_2O$ (or $2H + OH$)

Furthermore, in the absence of such complicating reactions, there is no way of knowing that the ratio of radicals actually trapped in the deposit is in fact directly related to the number of species produced initially in the radiation zone.

Additional Comments

The observation by ourselves and by Marx *et al.* (3) that electrons can be trapped in neutral ice is interesting. When neutral ice formed by freezing liquid water is gamma irradiated at 77 °K, trapped electrons do not appear: neither are they detected when ice, formed by condensing water vapor, is irradiated with X-rays at 77 °K (3). Electrons are, however, trapped in irradiated alkaline ice (27) (although the e.s.r. line width is greater due to line broadening by hyperfine interaction with alkali metal nuclei (28)). A plausible explanation is that in neutral ice, the positive ion is not neutralized as it is in alkaline ice. When the solid phase is irradiated, the positive ion and the electron never become sufficiently separated to prevent recombination due to coulombic attraction. However, when the ion and the electron are formed in the vapor phase, they are deposited with a homogeneous distribution and must be separated by a distance sufficient to permit trapping. More recent work by Schulte-Frohlinde *et al.* (29–31) suggests that the trapping site is an interstitial or lattice defect which is present initially in the amorphous phase but not in the crystal. If this is so then it may be that the thermal electrons produced in the vapor phase can orient and distort the ice structure during the condensation process and thereby induce their own trap. This process presumably would not be favored for electrons produced at 77 °K within the crystalline ice.

An obvious extension of this work is a study involving the effect of electric and/or magnetic fields on the number of electrons and other species finally detected in the deposit. Preliminary investigations have been made, but the results indicate that this approach is considerably more complex than expected. However, it was

Can. J. Chem. Downloaded from www.nrcresearchpress.com by 210.87.254.6 on 09/05/12
For personal use only.

found that the existence of a magnetic field (about 1000 G perpendicular to the vapor stream) coupled with the presence of a coarse grid in front of the cold finger nearly eliminates both the blue color and the associated e.s.r. signal normally observed in the deposit. This result would be expected if electrons were being removed from the vapor phase by the magnetic field. On the other hand the application of about 100 V potentials to the grid, either negative or positive, does not prevent electrons from being trapped in the deposit.

The detection of 10^{15} electrons in the deposit indicates that a corresponding number of positive ions must also be present, since the negative potential otherwise generated at the cold finger would lead to a field strength of about 10^7 V/cm. This situation is exceedingly unlikely. The irradiated vapor apparently behaves as if it were electrically neutral but any interpretation of electric field effects is complicated by possible space charge phenomena which may, for example, be generated at the cold finger. These results are not entirely understood and must await further investigation.

In conclusion, the validity of this "crossed beam" experiment as a method of studying intermediates generated in vapor phase radiolysis has been confirmed and previous results (1) are validated. The present work has provided physical and chemical evidence for the formation of HO_2 radicals, hydrogen atoms, and electrons on the irradiation of water vapor.

Acknowledgments

We thank Dr. John Davies for several profitable discussions and Dr. Erik Bøgh (visiting scientist from University of Aarhus) for assistance with the Rutherford scattering measurements and for suggesting them as a method of measuring the pressure in the vapor stream. We are also grateful to Mr. G. A. Sims for his competent operation of the accelerator.

1. D. R. Smith and J. C. Tole. Can. J. Chem. **45**, 779 (1967).
2. M. Horani and S. Leach. J. Chim. Phys. **58**, 825 (1961).
3. R. Marx, S. Leach, and M. Horani. J. Chim. Phys. **60**, 726 (1963).
4. R. Marx and J. Maruani. J. Chim. Phys. **61**, 1604 (1964).
5. D. R. Smith and J. J. Pieroni. Can. J. Chem. **43**, 2141 (1965).
6. R. Papoular. Electrical phenomena in gases. Iliffe Books Ltd., London. 1965. pp. 107–108.
7. L. C. Northcliffe. Ann. Rev. Nucl. Sci. **13**, 67 (1963).
8. W. F. Patton, G. S. Hurst, and T. E. Bortner. Oak Ridge National Laboratory-2352 (1957).
9. H. A. Bethe and J. Ashkin. *In* Experimental nuclear physics. Vol. 1. *Edited by* E. Segre. John Wiley and Sons Inc., New York. 1953. p. 249.
10. J. W. Searl, R. C. Smith, and S. J. Wyard. Proc. Phys. Soc. London, **74**, 491 (1959).
11. A. A. Bugai. Soviet Phys.—Solid State, English Transl. **4**, 2218 (1963).
12. C. K. Jen, S. N. Foner, E. L. Cochran, and V. A. Bowers. Phys. Rev. **112**, 1169 (1958).
13. R. Livingston, J. Ghormley, and H. Zeldes. J. Chem. Phys. **24**, 483 (1956).
14. S. D. Kaitmazov and A. M. Prokhorov. Soviet Phys. JETP English Transl. **36**, 1331 (1959).
15. R. C. Smith and S. J. Wyard. Nature, **186**, 226 (1960).
16. J. Kroh, B. C. Green, and J. W. T. Spinks. J. Am. Chem. Soc. **83**, 2201 (1961).
17. J. Caldwell and R. A. Back. Trans. Faraday Soc. **61**, 1939 (1965).
18. J. C. J. Thynne and A. G. Harrison. Trans. Faraday Soc. **62**, 2468 (1966).
19. H. A. Schwarz. J. Phys. Chem. **66**, 255 (1962).
20. J. E. Bennett, B. Mile, and A. Thomas. Intern. Symp. Combust. 11th, Aug. 14–20, 1966. Berkeley, California, Univ. California, 853 (1967).
21. G. H. Dibdin. Trans. Faraday Soc. **63**, 2098 (1967).
22. J. A. Brivati, M. C. R. Symons, D. J. A. Tinling, H. W. Wardale, and D. O. Williams. Trans. Faraday Soc. **63**, 2112 (1967).
23. M. A. A. Clyne and B. A. Thrush. Proc. Roy. Soc. London, Ser. A, **275**, 544 (1963).
24. A. Szutka, J. K. Thomas, S. Gordon, and E. J. Hart. J. Phys. Chem. **69**, 289 (1965).
25. J. H. Baxendale and G. P. Gilbert. Science, **147**, 1571 (1965).
26. G. R. A. Johnson and M. Simic. Nature, **210**, 1356 (1966).
27. D. Schulte-Frohlinde and K. Eiben. Z. Naturforsch. **17a**, 445 (1962); **18a**, 199 (1963).
28. L. Kevan. J. Am. Chem. Soc. **87**, 1481 (1965).
29. K. Eiben and D. Schulte-Frohlinde. Z. Physik. Chem. Frankfurt, **45**, 20 (1965).
30. D. Schulte-Frohlinde. Proc. Radiation Res. Soc. Meeting, Cortina, 1966. North Holland Publ. Co., Amsterdam. 1967. p. 251.
31. H. Barzynski and D. Schulte-Frohlinde. Nature. To be published.

Can. J. Chem. Downloaded from www.nrcresearchpress.com by 210.87.254.6 on 09/05/12
For personal use only.

Can. J. Chem. Downloaded from www.nrcresearchpress.com by 210.87.254.5 on 09/05/12
For personal use only.

Ion–molecule reactions in acetylene and acetylene–methane mixtures

J. J. MYHER[1] AND A. G. HARRISON
Department of Chemistry, University of Toronto, Toronto, Ontario

Received December 1, 1967

The ion–molecule reactions in acetylene have been studied. The reaction of $C_2H_2^+$ with C_2H_2 yields $C_4H_2^+$ and $C_4H_3^+$ in the ratio 0.40:1. C_2H^+ ions also react to form $C_4H_2^+$. Excited states of $C_2H_2^+$ and possibly C_2H^+ are shown to be important in the ion–molecule reactions in acetylene.

In acetylene–methane mixtures the following reactions have been identified and their rates measured.

$$C_2H_2^+ + CH_4 \rightarrow C_3H_5^+ + H$$
$$C_2H_2^+ + CH_4 \rightarrow C_3H_4^+ + H_2$$
$$CH_4^+ + C_2H_2 \rightarrow C_3H_3^+ + H_2 + H$$
$$CH_3^+ + C_2H_2 \rightarrow C_3H_3^+ + H_2$$
$$C_2H^+ + CH_4 \rightarrow C_3H_3^+ + H_2$$
$$C_2H_2^+ + CH_4 \rightarrow C_2H_3^+ + CH_3$$
$$CH_4^+ + C_2H_2 \rightarrow C_2H_3^+ + CH_3$$

By studying the reactions in CH_4–C_2D_2 mixtures the condensation reactions have been shown to involve extensive isotopic scrambling while the hydrogen-transfer reactions occur without isotopic scrambling.

Canadian Journal of Chemistry, 46, 1755 (1968)

Introduction

Several studies have been made of the ionic reactions in gaseous acetylene. The earlier studies (1–4) have elucidated only the ionic reactions of lowest appearance potential while more recent work (5) has been concerned with the higher order reactions occurring at elevated pressures. The present work was undertaken using the ratio plot technique (6) in an attempt to elucidate the possible role of concurrent reactions leading to the same product ion. While this work was in progress both Munson (7) and Derwish *et al.* (8) reported more detailed studies of the ion–molecule reactions in acetylene. The present results will be compared with these studies.

The ion–molecule reactions in methane–acetylene mixtures have been examined by Barker, Hamill, and Williams (2). The secondary ions observed were $C_2H_3^+$, $C_3H_3^+$, $C_3H_4^+$, and $C_3H_5^+$. From appearance potential measurements they identified the following reactions.

[1] $C_2H_2^+ + CH_4 \rightarrow C_2H_3^+ + CH_3$

[2] $CH_4^+ + C_2H_2 \rightarrow C_3H_3^+ + H_2 + H$

[3] $C_2H_2^+ + CH_4 \rightarrow C_3H_4^+ + H_2$

[4] $C_2H_2^+ + CH_4 \rightarrow C_3H_5^+ + H$

In several cases concurrent reactions involving reactant ions of higher appearance potential are thermochemically permitted. The present study was undertaken to establish more clearly all the reactions leading to the observed product ions.

Experimental

The major portion of the study was carried out using the modified MS-2 mass spectrometer described previously (9). All ratio plots with this instrument were obtained at 10 V/cm repeller field corresponding to 3.7 eV ion exit energy. The source concentrations usually were in the range 1 to 4 $\times$ 10^{13} molecules cm^{-3}. The ionizing electron beam was pulsed to reduce the effect of space charge. Since, as we have shown previously (10), the measurement of source concentrations in the MS-2 is subject to rather large errors, runs were also carried out on the medium pressure instrument (10) to obtain more accurate values of absolute rate constants.

The acetylene was obtained from Matheson and Company and showed only a small air impurity which was removed by vacuum distillation. Acetylene-d_2, obtained from Merck, Sharp and Dohme of Canada (98.9% isotopic purity), was used as received. Matheson research grade methane was used without further purification.

Results and Discussion

Acetylene

The major secondary ions in the mass spectrum of acetylene are $C_4H_3^+$ (*m/e* 51) and $C_4H_2^+$ (*m/e* 50) with smaller contributions at *m/e* 49 (C_4H^+), 38 ($C_3H_2^+$), 37 (C_3H^+), and 27 ($C_2H_3^+$).

[1]Present address: Department of Chemistry, Cambridge University, Cambridge, England.

Can. J. Chem. Downloaded from www.nrcresearchpress.com by 210.87.254.5 on 09/05/12
For personal use only.

The dependences of the ion currents at *m/e* 27, 50, and 51 on the $C_2H_2^+$ ion current at constant source pressure are shown in Fig. 1. The $C_2H_2^+$ ion current was varied by variation of the ionizing electron energy. Initially the *m/e* 27 ion current is a linear function of $I_{C_2H_2^+}$ with a slope of 2.2×10^{-2}, indicating that the only contribution to *m/e* 27 in this region is the $^{12}C^{13}CH_2^+$ ion. The upward curvature above approximately 16.5 eV ($I_{C_2H_2^+} \approx 570$) indicates the onset of an ion–molecule reaction, presumably involving an excited $C_2H_2^+$ ion.

[5] $$C_2H_2^{+*} + C_2H_2 \rightarrow C_2H_3^+ + C_2H$$

This reaction also has been suggested by Munson (7) and by Futrell and Sieck (4).

In the initial regions both $C_4H_3^+$ (*m/e* 51) and $C_4H_2^+$ (*m/e* 50) are linear functions of $I_{C_2H_2^+}$, indicating the occurrence of both reactions [6] and [7].

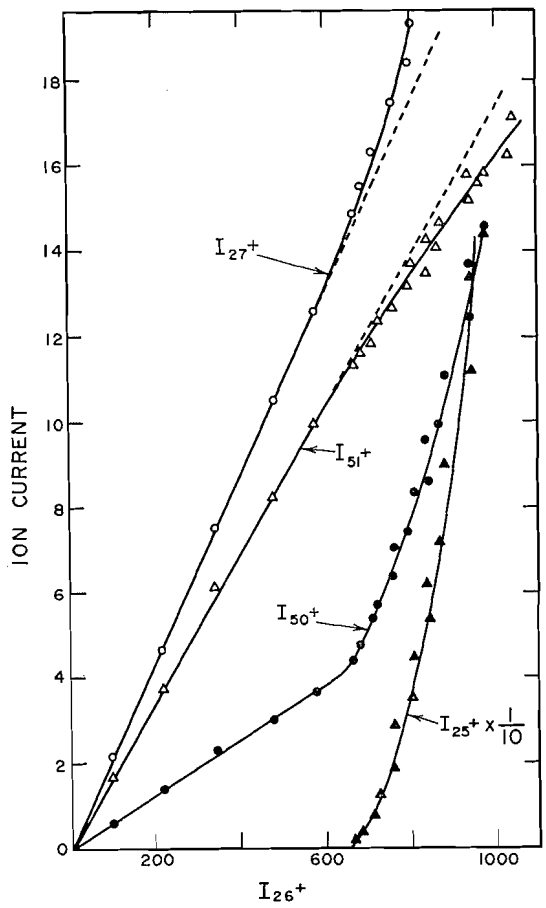

FIG. 1. Secondary ion currents as a function of $I_{C_2H_2^+}$.

[6] $$C_2H_2^+ + C_2H_2 \rightarrow C_4H_3^+ + H$$

[7] $$C_2H_2^+ + C_2H_2 \rightarrow C_4H_2^+ + H_2$$

From the slopes in this linear region we calculate $k_7/k_6 = 0.36 \pm 0.02$ (0.41 ± 0.02 in C_2D_2) in reasonable agreement with the value of 0.44 reported by Munson. Above approximately 16.5 eV the $C_4H_3^+$ intensity deviates in a negative manner from linearity with $I_{C_2H_2^+}$. This drop-off occurs at the same point as the upward curvature of the *m/e* 27 plot and undoubtedly signifies that the excited species $C_2H_2^{+*}$ either does not react to form $C_4H_3^+$ or does so at a lower rate than ground-state $C_2H_2^+$.

Above approximately 17 eV there is a rapid increase in the $C_4H_2^+$ ion current which can be seen to correlate with the onset of C_2H^+ ion formation in the primary spectrum. Therefore, in addition to reaction [7], reaction [8] also leads to $C_4H_2^+$.

[8] $$C_2H^+ + C_2H_2 \rightarrow C_4H_2^+ + H$$

However, as shown in Fig. 2, the ratio plot obtained assuming both reactions [7] and [8] does not lead to the expected linear plot. This can be explained by assuming that $C_2H_2^{+*}$ reacts to form $C_4H_2^+$ at a greater rate than does $C_2H_2^+$. We therefore conclude that k_7/k_6 is greater for $C_2H_2^{+*}$ than for $C_2H_2^+$; however, no quantitative estimate of this difference can be made. From retarding potential difference studies of appearance potentials of primary and secondary ions in acetylene, Melton and Hamill (11) have concluded that $C_2H_2^{+*}$ reacts to give $C_4H_3^+$ and not $C_4H_2^+$. This result is in contrast to that of Lindholm *et al.* (12), who concluded from experiments in a tandem instrument that $C_4H_3^+$ was formed from the ground state ion and $C_4H_2^+$ from the excited ion. Recently, Futrell and Tiernan (13), using a tandem mass spectrometer, have produced $C_2H_2^+$ ions by charge exchange with various ions and observed the $C_4H_2^+/C_4H_3^+$ ratio resulting from reaction of these $C_2H_2^+$ ions with acetylene. When they produced $C_2H_2^+$ by charge exchange with an ion of low recombination energy (e.g. Xe^+) they observed a $C_4H_2^+/C_4H_3^+$ of 0.3_1, while with Ar^+ (r.e. (recombination energy) >15 eV), where presumably the excited $C_2H_2^{+*}$ will be produced, they found $C_4H_2^+/C_4H_3^+ = 1.8_6$. These results

Can. J. Chem. Downloaded from www.nrcresearchpress.com by 210.87.254.5 on 09/05/12
For personal use only.

support the conclusions reached by Lindholm and in the present work.

Munson (7) has attributed the formation of C_4H^+ (*m/e* 49) to the reaction

[9] $$C_2H^+ + C_2H_2 \rightarrow C_4H^+ + H_2,$$

while Derwish *et al.* (8) have considered the reaction to be

[10] $$C_2^+ + C_2H_2 \rightarrow C_4H^+ + H.$$

As shown in Fig. 3, I_{49+} is neither a linear function of I_{25+} (C_2H^+) nor I_{24+} (C_2^+). Furthermore a ratio plot assuming the two reactions does not lead to a straight line. The origin of C_4H^+ remains obscure and possibly may involve excited states of C_2H^+. If an excited state of C_2H^+ is involved, a linear plot versus I_{25+} in Fig. 3 would not be expected.

Munson has attributed formation of both $C_3H_2^+$ and C_3H^+ to the reaction of a single excited state of $C_2H_2^+$. In the present work these ions were studied in C_2D_2 and therefore were observed at *m/e* 40 ($C_3D_2^+$) and *m/e* 38 (C_3D^+). A plot of I_{38+} (C_3D^+) versus I_{40+} ($C_3D_2^+$), Fig. 4, at constant pressure is not linear, indicating different origins for the two ions with C_3D^+ probably having a slightly higher appearance potential. A plot of $I_{C_3D_2^+}$ versus $I_{C_2D^+}$ (Fig. 5) shows that the $C_3D_2^+$ ion has an appearance potential higher than that of C_2D^+. Derwish *et al.* have attributed formation of $C_3D_2^+$ to reaction of C_2^+. However, the ratio $I_{C_3D_2^+}/I_{C_2^+}$ was found to decrease with increasing electron energy, suggesting that $C_3D_2^+$ had an appearance potential lower than C_2^+. The most probable reactant is either an excited state of C_2H^+ or $C_2H_2^+$.

Derwish *et al.* have attributed formation of C_3H^+ to reaction of either C^+ or CH^+. A plot of $I_{C_3D^+}$ versus I_{CD^+} (Fig. 6) shows an initial linear portion followed by upward curvature. It thus appears probable that C_3H^+ is formed

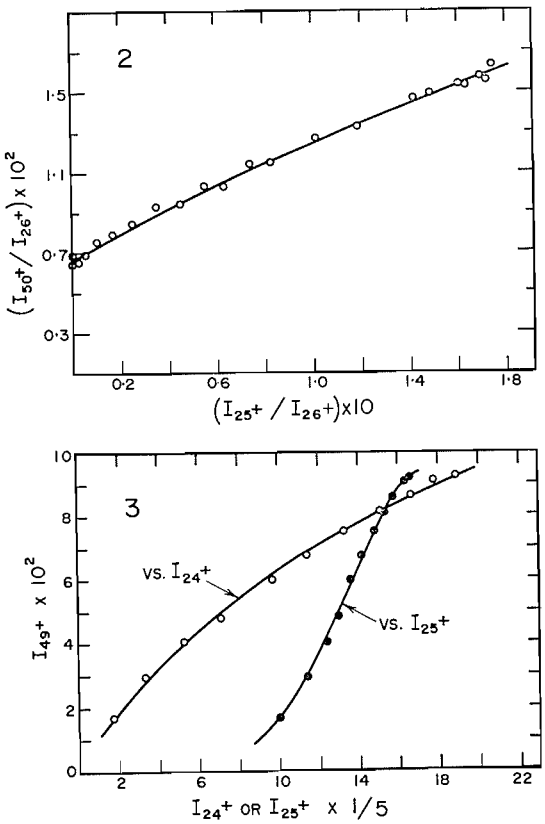

FIG. 2. $I_{C_4H_2^+}/I_{C_2H_2^+}$ versus $I_{C_2H^+}/I_{C_2H_2^+}$, acetylene.
FIG. 3. $I_{C_4H^+}$ versus $I_{C_2H^+}$ and $I_{C_2^+}$, acetylene.

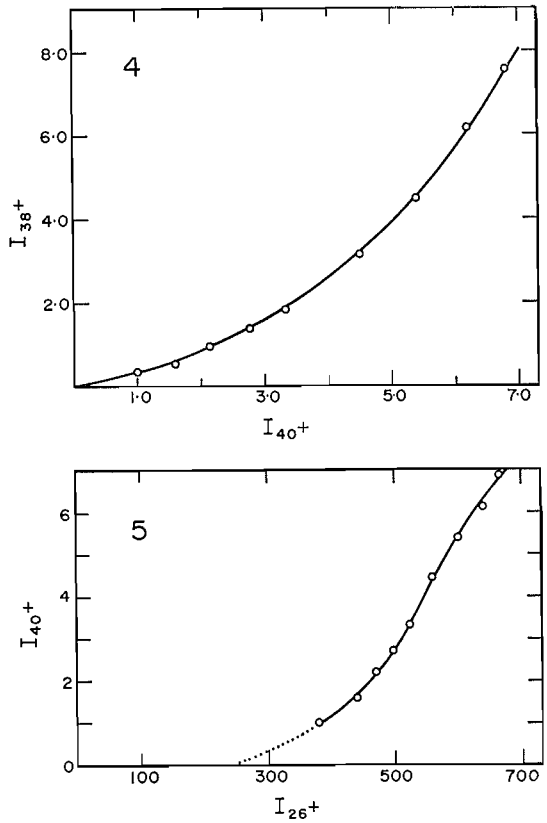

FIG. 4. $I_{C_3D^+}$ versus $I_{C_3D_2^+}$, acetylene-d_2.
FIG. 5. $I_{C_3D^+}$ versus $I_{C_2D^+}$, acetylene-d_2.

Can. J. Chem. Downloaded from www.nrcresearchpress.com by 210.87.254.5 on 09/05/12
For personal use only.

in part from CH^+, the second reactant causing the upward curvature may be C^+.

Effect of Ion Energy on Reaction of $C_2H_2^+$ with C_2H_2

In addition to the studies reported above, which were carried out at 3.7 eV ion exit energy, the reactions of $C_2H_2^+$ with C_2H_2 (and the corresponding reactions in acetylene-d_2) were studied at thermal ion energies on the MS-2 using the pulsing techniques previously described (9). The electron energy was kept below the onset of formation of the $C_2H_2^+$ excited state and below the onset of C_2H^+ formation.

At thermal energies the ratio $k_6/k_7 = 0.41_6$ in C_2H_2 and 0.47_0 in C_2D_2 compared with 0.36_6 and 0.41_0 respectively at 3.7 eV ion exit energy. This small variation probably is not significant. The ratio k_6(thermal)/k_6(3.7 eV) was found to be 1.1, for the C_2H_2 system and 1.2_5 for the C_2D_2 system while the ratio k_7(thermal)/k_7(3.7 eV) was 1.0_3 for C_2H_2 and 1.0_9 for C_2D_2. The results clearly indicate that neither the rate of reaction nor the product distribution is dependent to any significant extent on the kinetic energy of the reactant acetylene ion, although the results discussed above show that the product distribution is dependent on the internal excitation of $C_2H_2^+$.

As pointed out previously (10) absolute rate constants obtained with the MS-2 (although not relative rate constants) are subject to large error due to difficulties in estimating the source pressure accurately. Accordingly the reaction of $C_2H_2^+$ with C_2H_2 was studied using the medium pressure instrument at pressures up to 12 μ and electron energies where only $C_2H_2^+$ was a significant primary ion. From the log plot of the normalized intensity of $C_2H_2^+$ versus pressure at 3.5 and 5.2 eV ion exit energy the total rate constant for the disappearance of $C_2H_2^+$ was found to be $8.0 \pm 0.3 \times 10^{-10}$ cm^3 molecule^{-1} s^{-1} with $C_4H_2^+$ and $C_4H_3^+$ being the major product ions in the ratio $C_4H_2^+/C_4H_3^+ = 0.42_3$, in good agreement with the ratios found using the MS-2. The experimental rate constant is in good agreement with the value of 8.5×10^{-10} cm^3 molecule^{-1} s^{-1} quoted by Munson.

The experimental reaction rate constant is approximately 67% of the collision rate constant calculated on the basis of ion-induced dipole

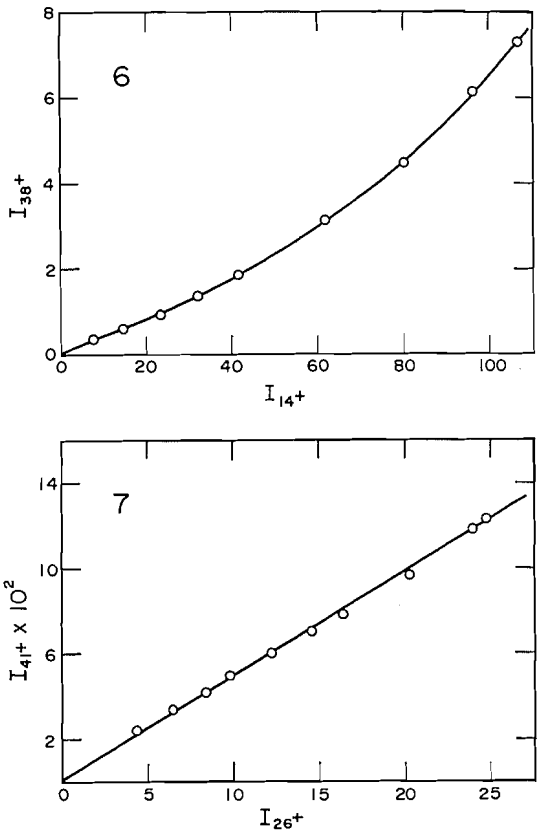

FIG. 6. $I_{C_3D^+}$ versus I_{CD^+}, acetylene-d_2.
FIG. 7. $I_{C_3H_5^+}$ versus $I_{C_2H_2^+}$, acetylene–methane mixture. $[N]_{total} = 1.44 \times 10^{13}$ molecule cm^{-3}.

interactions (14), suggesting the possibility that some fraction of the collisions do not lead to reaction but revert to reactants. In experiments using C_2H_2–C_2D_2 mixtures we found no evidence for isotopically mixed acetylene molecule ions. This result is in agreement with the results obtained by Munson for acetylene, but is in contrast to the ethylene system where it has been found (15) that reversion of the collision complex to reactants occurs with a small amount of isotopic mixing. In further agreement with Munson we have also found that there is no measurable isotope effect on the overall rate of reaction in C_2H_2–C_2D_2 mixtures, although in the mixed collision complex ($C_4H_2D_2^+$) the loss of H was favored to a considerable extent ($k_H/k_D = 1.6$) over loss of D. The loss of H_2 (and isotopic variants) appeared to proceed with essentially complete scrambling and little isotope effect.

Can. J. Chem. Downloaded from www.nrcresearchpress.com by 210.87.254.5 on 09/05/12
For personal use only.

Acetylene–Methane Mixtures

The reactions in acetylene–methane mixtures were studied initially using the MS-2 instrument. With this instrument a mixture containing 33% C_2H_2 and 67% CH_4 was allowed to enter the ionization chamber from the sample inlet system. Since at the pressures used the gas flow both into and out of the ionization chamber is molecular, the composition in the ionization chamber was assumed to be the same as the gas in the inlet system. The correlation between sample line pressure and source concentration was established from separate measurements on the self-reaction in methane carried out over the same period of time. The rate constants reported in Column 4 of Table I are therefore relative to $k = 12.0 \times 10^{-10}$ cm^3 molecule^{-1} s^{-1} for the reaction

[11] $$CH_4^+ + CH_4 \rightarrow CH_5^+ + CH_3.$$

Only the reactions forming $C_3H_5^+$, $C_3H_3^+$, and $C_2H_3^+$ were studied with the MS-2. A plot of $I_{41^+}(C_3H_5^+)$ versus I_{26^+} $(C_2H_2^+)$ is shown in Fig. 7. The good straight line covering the electron energy range from 11 eV to 35 eV (nominal electron energy) indicates that reaction [4] is the only source of $C_3H_5^+$. The rate constant obtained from the slope is given in Table I.

[4] $$C_2H_2^+ + CH_4 \rightarrow C_3H_5^+ + H,$$
$$\Delta H = -12 \text{ kcal/mole}^2,$$

[12] $$CH_4^+ + C_2H_2 \rightarrow C_3H_5^+ + H,$$
$$\Delta H = -62 \text{ kcal/mole},$$

The results eliminate the exothermic reaction [12] as a source of $C_3H_5^+$ although the collision of CH_4^+ with C_2H_2 probably leads to a complex, $C_3H_6^+$, and all C_3H_6 isomers show large $C_3H_5^+$ ions as fragments. A plausible explanation for the failure to observe reaction [12] is that the $C_3H_5^+$ ion retains a sufficient fraction of the exothermicity of the reaction to undergo further decomposition, i.e.

[13] $$C_3H_5^+ \rightarrow C_3H_3^+ + H_2$$
$$\Delta H = +40 \text{ kcal/mole}.$$

In addition to reaction [2], reported by Barker *et al.* (2), reactions [14] and [15], which are of higher appearance potential, are exothermic for formation of $C_3H_3^+$.

[2] $$CH_4^+ + C_2H_2 \rightarrow C_3H_3^+ + H_2 + H,$$
$$\Delta H = -22 \text{ kcal/mole},$$

TABLE I

Ion–molecule reactions in methane–acetylene mixtures

			Rate constant $\times 10^{10}$ (cm^3 molecule^{-1} s^{-1})	
m/e	Secondary ion	Primary ion	MS-2 (3.5 eV*)	Medium pressure (1.7eV*)
27	$C_2H_3^+$	$C_2H_2^+$	9.0	3.3
27	$C_2H_3^+$	CH_4^+	31.	16.7
39	$C_3H_3^+$	$C_2H_2^+$	Not observed	Not observed
39	$C_3H_3^+$	CH_4^+	5.4	1.7
39	$C_3H_3^+$	CH_3^+	21.2	15.4
39	$C_3H_3^+$	C_2H^+	9.8	—
40	$C_3H_4^+$	$C_2H_2^+$	—	0.95
41	$C_3H_5^+$	$C_2H_2^+$	3.8	3.3

*Ion exit energy.

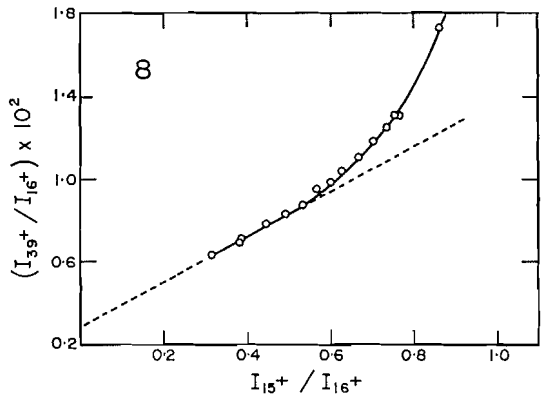

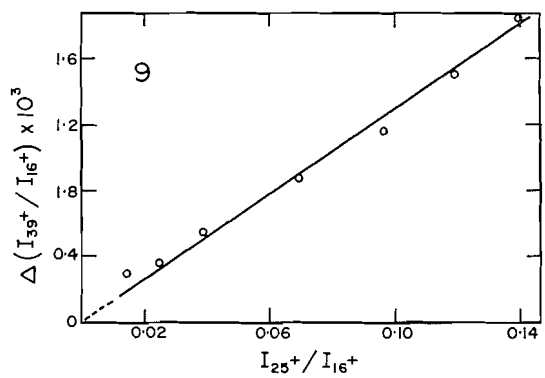

FIG. 8. $I_{C_3H_3^+}/I_{CH_4^+}$ versus $I_{CH_3^+}/I_{CH_4^+}$, acetylene–methane. $[N]_{total} = 1.44 \times 10^{13}$ molecule cm^{-3}.

FIG. 9. $\Delta(I_{C_3H_3^+}/I_{CH_4^+})$ versus $I_{C_2H^+}/I_{CH_4^+}$, acetylene–methane.

[2]All data on which the reaction heats are based have been taken from the compilation of Bernecker and Long (16).

[14] $CH_3^+ + C_2H_2 \rightarrow C_3H_3^+ + H_2$,

$\Delta H = -45$ kcal/mole,

[15] $C_2H^+ + CH_4 \rightarrow C_3H_3^+ + H_2$,

$\Delta H = -131$ kcal/mole.

Attempts to investigate reactions [2] and [14] by the ratio plot method were only partially successful since $I_{CH_3^+}/I_{CH_4^+}$ could be varied only over a small range before C_2H^+ became a significant primary ion. The experimental results are shown in Fig. 8, as a plot of $I_{C_3H_3^+}/I_{CH_4^+}$ versus $I_{CH_3^+}/I_{CH_4^+}$. An apparent initial linearity is evident, as anticipated, followed by an upward curvature whose onset corresponds to the appearance of C_2H^+ in the primary spectrum. The results therefore suggest that all three reactions are occurring. For the three reactions the following expression can be written.

$$\frac{I_{C_3H_3^+}}{I_{CH_4^+}} = k_2\tau_{CH_4^+}[C_2H_2] + k_{14}\tau_{CH_3^+}[C_2H_2]\frac{I_{CH_3^+}}{I_{CH_4^+}} + k_{15}\tau_{C_2H^+}[CH_4]\frac{I_{C_2H^+}}{I_{CH_4^+}},$$

where τ_{X^+} is the residence time for ion X^+, and k_i is the rate constant for reaction $[i]$. On rearrangement eq. [16] gives

[17] $$\frac{I_{C_3H_3^+}}{I_{CH_4^+}} - \left\{k_2\tau_{CH_4^+}[C_2H_2] + k_{14}\tau_{CH_3^+}[C_2H_2]\frac{I_{CH_3^+}}{I_{CH_4^+}}\right\} = k_{15}\tau_{C_2H^+}[CH_4]\frac{I_{C_2H^+}}{I_{CH_4^+}}.$$

The quantity in braces on the left hand side of eq. [17] is given by the straight line of Fig. 8. The difference between the experimental $I_{C_3H_3^+}/I_{CH_4^+}$ and the straight line of Fig. 8, defined as Δ, should be a linear function of $I_{C_2H^+}/I_{CH_4^+}$. This plot is shown in Fig. 9. The satisfactory straight line obtained indicates that the analysis on the basis of these reactions is reasonable. The rate constants obtained from the appropriate slopes and intercepts are given in Table I. The quantitative results obviously are subject to large errors; however, there is little doubt that all three reactions leading to $C_3H_3^+$ are occurring.

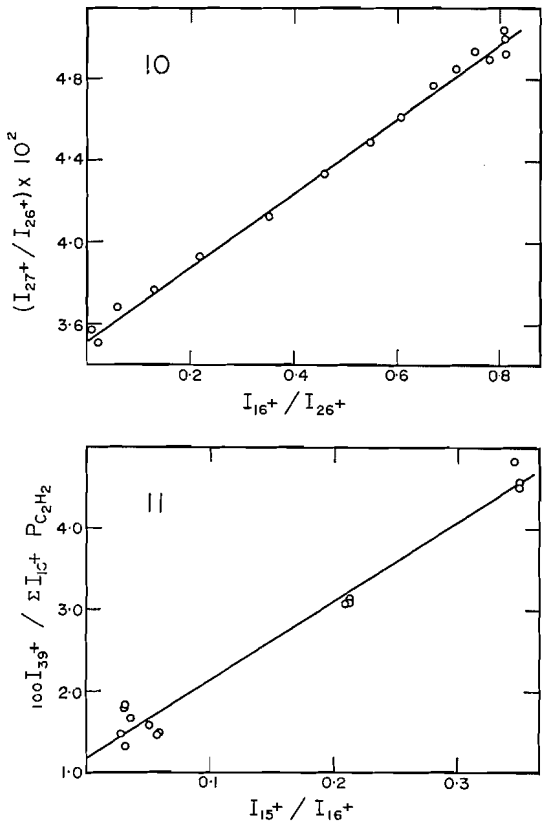

FIG. 10. $I_{C_2H_3^+}/I_{C_2H_2^+}$, acetylene–methane.
FIG. 11. $I_{C_3H_3^+}/\Sigma I_{CH_4^+}P_{C_2H_2}$ versus $I_{CH_3^+}/I_{CH_4^+}$, acetylene–methane.

Figure 10 shows a plot of I_{27^+}/I_{26^+} ($C_2H_3^+/C_2H_2^+$) versus I_{16^+}/I_{26^+} ($CH_4^+/C_2H_2^+$). The good straight line of non-zero slope and intercept indicates that in addition to reaction [1] reaction [8] also contributes to formation of $C_2H_3^+$. The rate constants are given in Table I.

[1] $C_2H_2^+ + CH_4 \rightarrow C_2H_3^+ + CH_3$

[18] $CH_4^+ + C_2H_2 \rightarrow C_2H_3^+ + CH_3$

The reactions in C_2H_2–CH_4 mixtures were also studied on the medium pressure mass spectrometer at various concentration ratios of CH_4 to C_2H_2 (total pressure in the range 1 to 2 μ) and over a range of electron energies (10–15 V nominal energy) chosen so that the ion current ratio $I_{CH_4^+}/I_{C_2H_2^+}$ varied significantly. The rate constants calculated from the experimental results for reactions [3] and [4] were found to be independent of the $I_{CH_4^+}/I_{C_2H_2^+}$ ratio, indicating that only these two reactions were occur-

Can. J. Chem. Downloaded from www.nrcresearchpress.com by 210.87.254.5 on 09/05/12
For personal use only.

Can. J. Chem. Downloaded from www.nrcresearchpress.com by 210.87.254.5 on 09/05/12
For personal use only.

ring. The rate constants obtained are given in the final column of Table I.

With the increased sensitivity of the medium pressure instrument the $I_{CH_3^+}/I_{CH_4^+}$ ratio could be varied in the absence of significant C_2H^+ over a considerably greater range than was possible with the MS-2. Consequently the contributions of reactions [2] and [14] to $C_3H_3^+$ formation could be determined more accurately. For the higher conversions ($> 5\%$) obtained, a modified ratio plot, eq. [19], gives more accurate rate constants.

$$[19]\quad \frac{I_{C_3H_3^+}}{\sum I_{CH_4^+} P_{C_2H_2}} = \kappa k_2 \tau_{CH_4^+} + \kappa k_{14} \tau_{CH_3^+} \frac{I_{CH_3^+}}{\sum I_{CH_4^+}},$$

where $\Sigma I_{CH_4^+}$ is the total ion current for CH_4^+ and products originating from reaction of CH_4^+ and κ is the proportionality constant between source pressure and source concentration. The plot of eq. [19] is shown in Fig. 11. A straight line can reasonably be drawn through the experimental points and leads to the rate constants in Table I. The results are in reasonable agreement with those obtained from the MS-2 experiments which, as noted, are subject to large error.

Abramson and Futrell (17) recently have studied the reaction of $C_2H_2^+$ with CH_4 using a tandem instrument and observed formation of $C_3H_3^+$ (1/3 the abundance of $C_3H_4^+$) by the reaction

$$[20]\quad C_2H_2 + CH_4 \rightarrow C_3H_3^+ + H_2 + H,$$

$$\Delta H = +19 \text{ kcal/mole}.$$

As shown in Fig. 12 our data when plotted as $I_{C_3H_3^+}/I_{C_2H_2^+}$ versus $I_{CH_4^+}/I_{C_2H_2^+}$ extrapolates to $I_{C_3H_3^+}/I_{C_2H_2^+} = 0$, indicating that reaction [20] is not observed in our experiments near the threshold for formation of $C_2H_2^+$. One must conclude that Abramson and Futrell's observed reaction results from ions with considerable internal excitation energy. This is a distinct possibility since they produced their $C_2H_2^+$ ions by impact of 75 eV electrons on acetylene[3].

For the two reactions, [1] and [18], leading

[3]Tiernan and Futrell (personal communication) report that when the $C_2H_2^+$ reactant ions are produced by impact of electrons of 10 eV nominal energy the ratio $C_3H_3^+/C_3H_4^+$ is reduced to about 0.02. This result agrees with our findings.

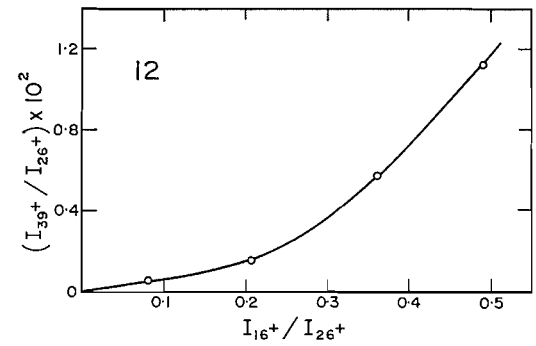

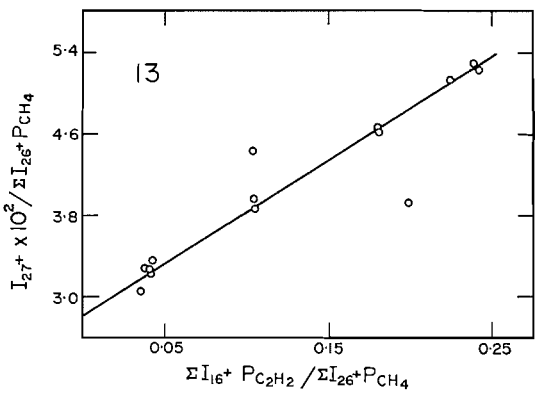

FIG. 12. $I_{C_3H_3^+}/I_{C_2H_2^+}$ versus $I_{CH_4^+}/I_{C_2H_2^+}$, acetylene–methane.

FIG. 13. $I_{C_2H_3^+}/\Sigma I_{C_2H_2^+} P_{CH_4}$ versus $(\Sigma I_{CH_4^+}/\Sigma I_{C_2H_2^+})(P_{C_2H_2}/P_{CH_4})$, acetylene–methane.

to $C_2H_3^+$ formation a modified ratio plot applicable at the higher conversions can be written as follows.

$$[21]\quad \frac{I_{C_2H_3^+}}{\sum I_{C_2H_2^+} P_{CH_4}} = \kappa k_1 \tau_{C_2H_2^+} + k_{18} \tau_{CH_4^+} \frac{\sum I_{CH_4^+}}{\sum I_{C_2H_2^+}} \approx \frac{P_{C_2H_2}}{P_{CH_4}},$$

where ΣI_{X^+} represents the total ion intensity for the ion X^+ and the products derived from that ion. The results obtained are plotted in this form in Fig. 13. The straight line drawn through the experimental points leads to the rate constants given in Table I. The agreement with the MS-2 results is not good; however, since the ion source pressures are measured directly with the medium pressure instrument, we consider the results therefrom to be more reliable.

Isotope Mixing Experiments

The spectrum of a mixture of 1.02 μ CH_4 and 0.50 μ C_2D_2 was recorded at 1.7 eV ion exit

Can. J. Chem. Downloaded from www.nrcresearchpress.com by 210.87.254.5 on 09/05/12
For personal use only.

TABLE II

Secondary ion yields in CH_4–C_2D_2 mixtures

	Electron energy	
m/e	12.7 eV	14.3 eV
27	0.014	0.032
29	1.00	1.00
40	Not meas.	0.018
41	0.106	0.118
42	0.272	0.300
43	0.518	0.563
$I_{CH_4^+}/I_{C_2D_2^+}$	0.016	0.023

TABLE III

Comparison of experimental and calculated ion distribution for $C_2D_2^+ + CH_4$ reaction

m/e	Exp.	Calcd.*
40	0.019	0.015
41	0.117	0.122
42	0.299	0.348
43	0.564	0.513

*On basis of complete isotopic scrambling.

energy and low electron energies to check the extent of isotopic mixing in the product ions. The results, after ^{13}C correction and subtraction of the spectra of the pure components, are given in Table II normalized to unit intensity for the *m/e* 29 ($C_2D_2H^+$) ion. Since the CH_4^+ primary ion current was only about 2% of the $C_2D_2^+$ primary ion current the products observed are almost entirely due to the reaction of $C_2D_2^+$ with CH_4.

The relative abundances in the *m/e* 40–43 region are compared, in Table III, with the relative intensities calculated on the assumption that the $C_3H_4^+$ and $C_3H_5^+$ ions (or partially deuterated analogues) are formed with complete scrambling in the $C_3D_2H_4^+$ complex. The experimental results are consistent with extensive scrambling. On the other hand the formation of the vinyl ion is not consistent with isotopic mixing in the collision complex. The results (Table II) show a $C_2D_2H^+/C_2H_3^+$ ratio of approximately 43.5:1 compared with the ratio 1:1 predicted for scrambling. At somewhat higher electron energies where CH_4^+ was a significant primary ion, $C_3H_3^+$ and deuterated analogues were observed. Owing to the overlap with the $C_3H_4^+$ and $C_3H_5^+$ ions the isotopic distribution could not be accurately determined; however, considerable isotopic scrambling in the complex is indicated.

In summary the isotopic mixing experiments show extensive scrambling in the formation of condensation products, indicating that a complex is formed with sufficient lifetime to permit considerable hydrogen rearrangement. On the other hand the transfer of a hydrogen occurs without isotopic mixing, indicating either that the reaction occurs by a stripping mechanism or through formation of a complex which is either so loosely bound or so short lived that hydrogen rearrangement cannot occur.

Acknowledgments

The authors are indebted to the National Research Council of Canada for financial support and the award of studentships (1963–1966) to J. J. M. They are also indebted to Professor J. H. Futrell for the communication of results prior to publication.

1. F. H. Field, J. L. Franklin, and F. W. Lampe. J. Am. Chem. Soc. **79**, 2665 (1957).
2. R. Barker, W. H. Hamill, and R. R. Williams. J. Phys. Chem. **63**, 825 (1959).
3. R. Fuchs. Z. Naturforsch. **16a**, 1026 (1961).
4. J. H. Futrell and L. W. Sieck. J. Phys. Chem. **69**, 892 (1965).
5. S. Wexler, A. Lifshitz, and A. Quattrochi. Advan. Chem. **58**, 193 (1966).
6. T. W. Shannon and A. G. Harrison. J. Chem. Phys. **43**, 4201 (1965).
7. M. S. B. Munson. J. Phys. Chem. **69**, 572 (1965).
8. G. A. W. Derwish, A. Galli, A. Giardini-Guidoni, and G. G. Volpi. J. Am. Chem. Soc. **87**, 1159 (1965).
9. T. W. Shannon, F. Meyer, and A. G. Harrison. Can. J. Chem. **43**, 159 (1965).
10. S. K. Gupta, E. G. Jones, A. G. Harrison, and J. J. Myher. Can. J. Chem. **45**, 3107 (1967).
11. C. E. Melton and W. H. Hamill. J. Chem. Phys. **41**, 1469 (1964).
12. E. Lindholm, I. Szabo, and P. Wilmenius. Arkiv Fysik, **25**, 417 (1963).
13. J. H. Futrell and T. O. Tiernan. J. Phys. Chem. **72**, 158 (1968).
14. G. Gioumousis and D. P. Stevenson. J. Chem. Phys. **29**, 294 (1958).
15. J. J. Myher and A. G. Harrison. Can. J. Chem. **46**, 101 (1968).
16. R. R. Bernecker and F. A. Long. J. Phys. Chem. **65**, 1565 (1961).
17. F. P. Abramson and J. H. Futrell. J. Chem. Phys. **45**, 1925 (1966).

Isomeric yield ratios of ^{133}Xe in fission of ^{232}Th, ^{233}U, ^{235}U, and ^{238}U with protons of energies 20-85 MeV[1]

J. H. FORSTER[2] AND L. YAFFE

Radiochemistry Laboratory, Department of Chemistry, McGill University, Montreal, Quebec

Received August 8, 1967

The ratio of ^{133}Xe isomers produced in the fission of ^{232}Th, ^{233}U, ^{235}U, and ^{238}U by protons ranging in energy from 20–85 MeV was measured. The Hafner, Huizenga, and Vandenbosch formalism was applied with different sets of input parameters to establish their effect on the relation between initial fragment spin and isomer ratio for three spin-pair classes of isomers. The isomer ratio was found to be independent of the spin and type of fissioning target and only weakly dependent on projectile energy.

Canadian Journal of Chemistry, 46, 1763 (1968)

Can. J. Chem. Downloaded from www.nrcresearchpress.com by 210.87.254.6 on 09/05/12
For personal use only.

Introduction

At present only crude calculations can be made to interpret the experimental ratios of independent yields of the two isomers of a fission product. These moderately successful calculations are based on the statistical model formalism introduced by Vandenbosch and Huizenga (1, 2) and used with only minor modifications (3–7) by numerous other workers to describe the relative formation of isomers in spallation reactions.

Isomer ratio studies for fission have had a different objective from those for spallation. In the latter there was considerable confidence in the model which described the disposition of angular momentum during the reaction. The model has been used with the large number of isomer ratio data from spallation studies (8, 9) to determine parameters describing the nuclear level density, In the more complex process of fission, however, the disposition of angular momentum is less well defined and the isomer ratio studies have been limited by the very few fission products for which isomer ratios can be measured precisely. The following factors determine tthe isomer ratio in fission. [1] The spin distribution of the compound nucleus (if formed). [2] The modification of the spin distribution following emission of pre-fission neutrons. [3] The orbital angular momentum between the two fragments. [4] The disposition of angular momentum between the two fragments immediately after scission. [5] The orientation of the spins of complementary fragments. [6] The modification of the initial spin distribution of the fragments during their de-excitation by emission of several neutrons and a cascade of gamma rays. [7] The effective spin pair for the isomeric species.

Calculations can be made for factors [1] and [2] with parts (1) and (2) of the FORTRAN program of Hafner, Huizenga, and Vandenbosch (10) (the H.H.V. program), which was based on the statistical formalism referred to above. However, these results cannot at present help greatly in the calculation of the isomer ratio, because factors [3]–[5] are not understood. Therefore, the theoretical interpretations of fission isomer ratios used here and in previous work have not attempted to include all of the above factors, but have started by giving the unknown spin of the initial fragments an assumed distribution. Then, factor [6] has been computed by parts (2) and (3) of the H.H.V. program with rather poorly defined input data and level densities assumed from spallation studies of isomer ratios.

Despite their many shortcomings, these fission studies have been pursued because they can provide a powerful method of investigating the angular momentum of fission fragments. Whereas gamma ray studies (11–17) give an estimate of the spin averaged for all fragments, an isomer ratio study estimates the spin of specific initial fragments and such studies could determine the dependence of initial spin on fragment mass (11, 16, 18–20). For example, the spins of fragments from near-symmetric fission have been predicted to be lower than those from asymmetric fission.

Table I surveys fission studies of independent yield ratios and classifies the studies into three

[1]This project received financial assistance from the National Research Council of Canada.

[2]Present address: Imperial Chemical Industries, Central Instrument Research Laboratory, Bozedown House, Whitchurch Hill, Reading, Berks.

TABLE I

Classification and summary of the main studies of isomer ratios in fission

Spin-pair Class	Isomer spin-pair H, L	Isomeric species, half-life				Target ($I = 0$)	Target ($I \neq 0$)	Projectile	energy (MeV)	Isobaric parent, half-life		Ref.
1	9/2, 1/2	^{95}Nb	g	H	35 d	^{238}U, ^{232}Th	^{208}Pb, ^{209}Bi	p	20–160	^{95}Zr	65 d	47
			m	L	90 h							
		^{117}In	g	H	38 m	^{238}U, ^{232}Th	^{209}Bi	p	20–160	^{117}Cd m	3.1 h	
			m	L	1.9 h					g	2.7 h	29
						^{238}U, ^{232}Th		α	33			
								d	18			
		^{131}Te	m	H	30 h							30
							^{235}U	n	Thermal	^{131}Sb	19.4 m	
			g	L	25 m							
							^{233,235}U, ^{239}Pu	n	Thermal			48
2	11/2, 3/2											
		^{133}Te	m	H	53 m	^{238}U, ^{232}Th		α	33			
								d	18	^{133}Sb	3 m	30
			g	L	12.5 m							
		^{133}Xe	m	H	2.3 d	^{238}U, ^{232}Th	^{233}U, ^{235}U	p	20–85	^{133}I	20.8 h	This work
			g	L	5.3 d							
						^{238}U	^{233}U, ^{235}U	α	27, 42			
							^{237}Np	d	21	Both isobaric		
		^{134}Cs	m	8	2.9 h		^{233}U	γ	16	neighbors		31
3	8, (5), 4									are stable		
						^{238}U		p	25–80			49
			g	4	2.1 y							
						^{232}Th		p	20–85			32

spin-pair classes of isomers. Ratios have been measured also for the isomers of ^{80}Br (21), and there have been many studies of the isomers of ^{115}Cd (20, 22). The latter did not give ratios of *independent* yields, so that changes in the observed ratios were partly a result of changes in the charge distribution for chain 115.

Experimental Procedure and Results

Only a brief outline of the experimental procedure is given here. A full description has been published elsewhere (23) along with the formation cross sections of ^{133}Xe^{m} and ^{133}Xe^{g} at various proton energies.

The targets were bombarded for a few minutes in the circulating beam of the McGill synchrocyclotron and then, as quickly as possible (20–30 min), the rare gases were extracted from the target materials and other fission products and were adsorbed on activated charcoal cooled in liquid air. Krypton and xenon were fractionally desorbed and each fraction was collected on activated charcoal in a separate trap cooled in liquid air. The separation was shown to be very efficient by tests made in this and in previous work (24). Finally the xenon fraction was desorbed and transferred to a quartz furnace for purification over titanium at 800 °C; the purified xenon was cooled and its chemical yield measured in a gas burette. A sample was prepared for measurement of gamma activity by condensing and sealing the xenon into a glass vial of standard dimensions.

A second extraction, sweep [*b*], of xenon which had resulted purely from decay of the iodine parents was made after about 30 h.

Radiation Measurements

The gamma spectra and decay curves for ^{133}Xe^{m} and ^{133}Xe^{g} have been discussed previously (23). The composite photo-peak due to 233-keV and 249-keV radiation from 2.3-d ^{133}Xe^{m} and 9.2-h ^{135}Xe^{g} gave a two-component decay curve which was increasingly difficult to resolve for ^{133}Xe^{m} at energies below 30 MeV where the formation cross section of ^{133}Xe decreased rapidly. At the highest proton energies, neutron-deficient xenon isotopes interfered with the analysis of the photo-peak due to ^{133}Xe^{m}, but satisfactory corrections were made.

The measurements of the photo-peaks of the two isomers could be made with good accuracy because they were taken from the same spectrum and errors in background subtraction and peak efficiencies were minimized by calibration with a beta proportional counter.

Results

The isomer ratios of ^{133}Xe are given in Table II and shown in Fig. 1. Only one experimental value, $\alpha_K = 4.4$, has been reported (25) for the 233-keV γ-transition between the ^{133}Xe isomers. This value falls far below the theoretical value of $\alpha_K = 6.2$ (26). Isomer ratios were computed for values of $\alpha_T = 6.2$, 7.3, 8.3, and 9.3, corresponding to α_K values of 4.4, 5.0, 5.7, and 6.4. The ratios are given with and without a simplified correction for growth of ^{133}Xe from ^{133}I. This correction assumes that the precursors of ^{133}I are short-lived, which is not quite

Can. J. Chem. Downloaded from www.nrcresearchpress.com by 210.87.254.6 on 09/05/12
For personal use only.

TABLE II

Effect of α_T for $^{133}Xe^m$ on the isomer ratios of ^{133}Xe (where σ_g' = uncorrected yield of $^{133}Xe^g$ and σ_g'' = "over-corrected" yield of $^{133}Xe^g$)

	Proton energy (MeV)	α_T = 6.3		α_T = 7.3		α_T = 8.3		α_T = 9.3	
		σ_m/σ_g'	σ_m/σ_g''	σ_m/σ_g'	σ_m/σ_g''	σ_m/σ_g'	σ_m/σ_g''	σ_m/σ_g'	σ_m/σ_g''
	30	0.89	1.03	1.28	1.56	1.98	2.62	3.53	5.80
	40	0.88	0.98	1.27	1.46	1.96	2.37	3.46	4.79
^{232}Th	52	0.96	1.01	1.42	1.52	2.29	2.52	4.49	5.37
	65	0.99	1.04	1.48	1.58	2.41	2.67	4.95	6.00
	75	1.05	1.11	1.61	1.73	2.75	3.06	6.41	8.16
	85	1.08	1.13	1.67	1.77	2.90	3.19	7.20	9.00
	15	0.64	—	0.86	—	1.18	—	1.69	—
	17	0.74	—	1.03	—	1.48	—	2.28	—
	20	0.61	0.84	0.82	1.19	1.11	1.80	1.55	3.03
	30	0.95	1.10	1.41	1.70	2.25	2.97	4.36	7.60
^{238}U	42	0.83	0.91	1.18	1.33	1.77	2.09	2.96	3.84
	57	1.09	1.13	1.68	1.76	2.93	3.17	7.33	8.86
	65	0.92	0.97	1.34	1.43	2.11	2.31	3.90	4.59
	75	1.12	1.21	1.76	1.96	3.16	3.77	8.79	14.83
	75	1.14	1.20	1.78	1.92	3.22	3.65	9.24	13.24
	85	0.95	1.01	1.40	1.52	2.23	2.53	4.29	5.41
	20	0.81	0.86	1.15	1.23	1.70	1.87	2.78	3.21
	25	0.88	0.91	1.27	1.33	1.94	2.08	3.42	3.81
	35	1.05	1.10	1.61	1.70	2.74	3.00	6.33	7.75
^{235}U	45	0.95	0.99	1.41	1.47	2.25	2.41	4.37	4.92
	55	1.11	1.17	1.72	1.85	3.05	3.44	8.05	11.08
	70	1.10	1.15	1.71	1.82	3.02	3.33	7.86	10.12
	85	1.02	1.06	1.53	1.62	2.55	2.79	5.50	6.57
	20	0.93	0.95	1.36	1.40	2.16	2.24	4.05	4.33
	30	0.89	0.91	1.28	1.32	1.98	2.06	3.51	3.74
^{233}U	42	1.04	1.06	1.58	1.62	2.27	2.79	6.00	6.58
	55	0.97	—	1.44	—	2.32	—	4.61	—
	70	0.94	0.96	1.38	1.42	2.18	2.29	4.14	4.48

true for ^{133}Te. The correction procedure involves the use of a disintegration rate for the ^{133}I formed cumulatively which is too high and consequently gives independent yields of $^{133}Xe^g$ which are too low and are thus referred to as "over-corrected". Significant errors are introduced by this procedure only when there is a large growth of $^{133}Xe^g$. This was minimized by keeping the time between the end of irradiation and the first xenon separation to a minimum.

It was shown previously (23) that changes in the value used for α_T did not cause serious errors in the measured cross section of ^{133}Xe. The isomer ratios of ^{133}Xe, however, are shown here to be strongly dependent on the value used for α_T. An increase in α_T causes an increase in the experimental isomer ratio and a larger scatter of data.

Excluding the possible large systematic error due to uncertainty in α_K, an uncertainty of 12% has been given to the experimental ratios, corresponding to $\alpha_K = 4.4$. The lowest energy experiments with ^{232}Th and ^{238}U had larger uncertainties. The correction for the growth of $^{133}Xe^g$ from ^{133}I (23) was minimized by a fast sweep [*a*] but could still be large if there was a high ratio of the cumulative yield of ^{133}I to the independent yield of ^{133}Xe. However, this occurred in only a few low-energy experiments. The majority of measured ratios required only small growth corrections which were within the estimated experimental error.

Discussion

[a] Theoretical Isomer Ratios and Fragment Spin

The type of calculation already referred to was made for the de-excitation of fragments leading to ^{133}Xe whose isomers are of the spin-pair class 2 (11/2, 3/2). A full description of the theory for the computation of the disposition of angular momentum during fragment de-excitation to two isomeric states has been given elsewhere (2–4, 27, 28). This method has been used previously to estimate the spin of specific

Can. J. Chem. Downloaded from www.nrcresearchpress.com by 210.87.254.6 on 09/05/12
For personal use only.

TABLE III

Values of B estimated in fission isomer ratio calculations, with initial fragment spin distribution given by eq. [1]

Fission system						
Target		Projectile (MeV)	Isomeric nuclide	Experimental isomer ratio	Estimated B of initial fragment	Ref.
^{238}U, ^{232}Th, ^{209}Bi	p	30	^{117}In	~2.0	~3	29
		100		~10.0	10	
^{235}U	n	Thermal	^{131}Te	1.8±0.4	6±1.5	48
						30
^{232}Th	α	33	^{131}Te	3.3±0.5	~8	31
^{232}Th, ^{238}U, ^{235}U, ^{233}U	p	20–85	^{133}Xe	(*i*) 1.0	4±1.0	This work
				(*ii*) 2.0	6±1.5	
				(*iii*) 3.0	8±1.5	
^{233}U	γ	16	^{134}Cs	0.8±0.2	≲7.5	31
^{232}Th	p	20	^{134}Cs	1.2±0.6	~9	32

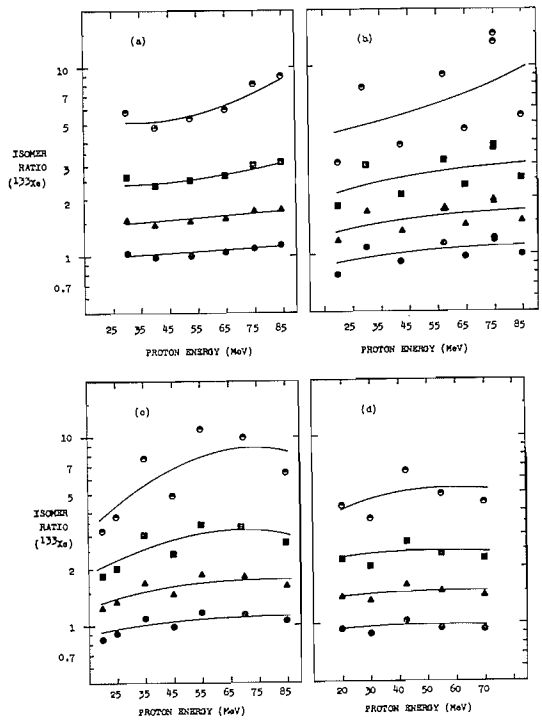

FIG. 1. Experimental isomeric yield ratios for ^{133}Xe from proton-induced fission of (*a*) ^{232}Th, (*b*) ^{238}U, (*c*) ^{235}U, (*d*) ^{233}U. The "over-corrected" values are shown for α_T = (●) 6.3, (▲) 7.3, (▣) 8.3, (◓) 9.3.

fission fragments leading to ^{117}In (29), ^{131}Te (30), and ^{134}Cs (31, 32). Table III summarizes these studies. The symbol B which characterizes the distribution of fragment spin, J_i, in the following expression first suggested by Warhanek and Vandenbosch (31),

$$[1] \quad N(J_i) = (2J_i + 1) \exp [-J_i(J_i + 1)/B^2],$$

was varied until the experimental isomer ratio was reproduced by the calculations.

The relationship of fragment spin to isomer ratio was obtained for a wide variety of input parameters as shown in Table IV. These have a great deal of uncertainty attached to them due to the very limited experimental and theoretical information available. The values of N_n and N_γ, the numbers of neutrons and γ-rays respectively emitted from the excited fragment, cannot be estimated from energy considerations alone, because of the competition between neutron and γ-ray emission (16, 31, 33–35) which is dependent on angular momentum. At best only mean values can be obtained because the isomeric fission product has had several neutron-emitting parents and N_n and N_γ vary with fragment mass (14, 36, 37). From the best available experimental data (36, 38–43) it is estimated that, for fission induced by 30-MeV protons, the predominant neutron parent of ^{133}Xe is ^{136}Xe. There are no available data for N_γ for medium-energy fission and values of 4 ± 1 have been assumed. The multipolarity l of the γ-ray was usually taken to be one. However, since quadrupole radiation has been introduced by some workers into the calculations (5, 11, 12, 14, 16, 29, 31), the effect of quadrupole radiation on the isomeric ratios had to be considered.

Can. J. Chem. Downloaded from www.nrcresearchpress.com by 210.87.254.6 on 09/05/12
For personal use only.

TABLE IV

Input data for stages 1 and 2 of the fragment de-excitation computations

(*a*) For Part 2 of H.H.V. Fortran program (10)

Input parameters \ Neutron emission step		1st	2nd	3rd
Spin distribution		Assumed; formula (1) B = 3,4,6,7,9,11	Output from 1st step	Output from 2nd step
$\bar{E}_{n_l}$ (MeV)		2.0	1.5	1.0
		$T_{l'}(\bar{E}_{n_l})$ (45)		
	l' = 0	0.73	0.70	0.60
	1	0.66	0.60	0.50
	2	0.51	0.40	0.25
	3	0.25	0.14	0.05
	4	0.04	0.01	—
$\sigma_{(n)}$	Trial *i*	6	5	4
	Trial *ii*	7	6	5

(*b*) For Part 3 of H.H.V. Fortran program

Input parameters \ Gamma-cascade step		1st	2nd to 5th
Spin distribution		Output following 3rd neutron emission	Output from previous step
$\sigma_{(\gamma)}$	Trial *i*	3	3
	Trial *ii*	4	4
l	Trial *i*	1	1
	Trial *ii*	2	(2nd, 3rd, = 2: 4th, 5th, = 1)

The only information available to estimate σ, the spin cutoff factor, comes from isomer ratio studies in spallation reactions and simple theory (31, 44) which show that σ is energy dependent.

Table IV summarizes the input data used in the present work for the first two stages of the H.H.V. Fortran program (10). The values for the transmission coefficients, $T_{l'}$ $(\bar{E}_n)$, for emission of a neutron of mean energy $\bar{E}_n$ and angular momentum l' are those of Feld *et al.* (45). Fixed values of 3 and 6 were chosen for N_n and N_γ respectively in order to limit the numerous possible combination of parameters. The distribution for $N_\gamma < 6$ was also contained in the output. Two sets of σ values were used in trials (*i*) and (*ii*). The factor σ was assumed to decrease as fragment excitation energy decreases with successive neutron emission, but was assumed to be constant throughout the γ-cascade where energy changes were only about 1 MeV per emission.

A representative example of the results from stages 1 and 2 is shown in Fig. 2 in which the calculated distributions following each of the three neutron and five γ-ray emissions are characterized by their root mean square angular momentum $(\overline{J_f^2})^{1/2}$, the number above the line is the value of σ used for that step of the computation. The values of B used for the initial spin distribution are given at the right of the figure.

Stages 1 and 2 lead to the following conclusions about the fragment de-excitation process. (*i*) For initial fragments with $B \simeq 6$ there were only small changes in the root mean square angular momentum. (*ii*) For higher B values, $(\overline{J_f^2})^{1/2}$ decreases, and these changes become larger as B is increased, and if the γ-emission is quadrupole,

Can. J. Chem. Downloaded from www.nrcresearchpress.com by 210.87.254.6 on 09/05/12
For personal use only.

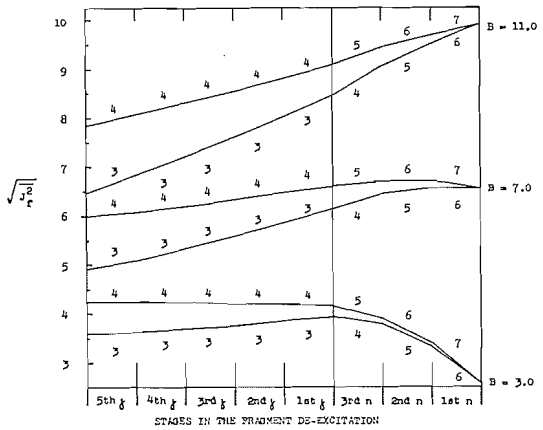

FIG. 2. Values of $(\overline{J_f^2})^{1/2}$ for successive steps in the fragment de-excitation. The first three γ-rays in the cascade had $l = 2$.

not dipole. (*iii*) For lower B values, $(\overline{J_f^2})^{1/2}$ increases.

These trends result simply from the nuclear level density function, used for each neutron emission, which has a maximum at $\sim(\sigma - \frac{1}{2})$. If higher σ values were used, the effect would be to increase the predicted isomer ratio of all classes of isomers, since while the high spin states would decrease to lower values the low spins would increase their spins more. Conversely the predicted ratios are decreased if a lower value of σ is used. The effective converging of spin states during the de-excitation process tends to reduce the sensitivity of the isomer ratio to the spin of the initial fragment.

Stage 3 predicts a value of the isomer ratio from the calculated spin distribution following the penultimate emission in the gamma cascade. The ratio is obtained by adding the probabilities for individual spin states according to the simple prescription that spin states decay to the isomer of nearest spin. This has been done here geometrically using the cumulative spin distribution. Figure 3 gives examples of these curves at different steps in the de-excitation, calculated for $B = 7$ and $\sigma_{(n)} = 6$, 5, 4, and $\sigma_\gamma = 3$. The vertical lines at $J_f = 2$, 3, and 6 intersect the curves at ordinate Y_i. The ratio $(1 - Y_i)/Y_i$ is then the isomer ratio for spin classes 1, 2, and 3 respectively. This type of figure gives a direct representation of the isomer ratios for isomeric pairs of different classes from the distribution calculated at each step of the fragment de-excitation for a particular assumed B value.

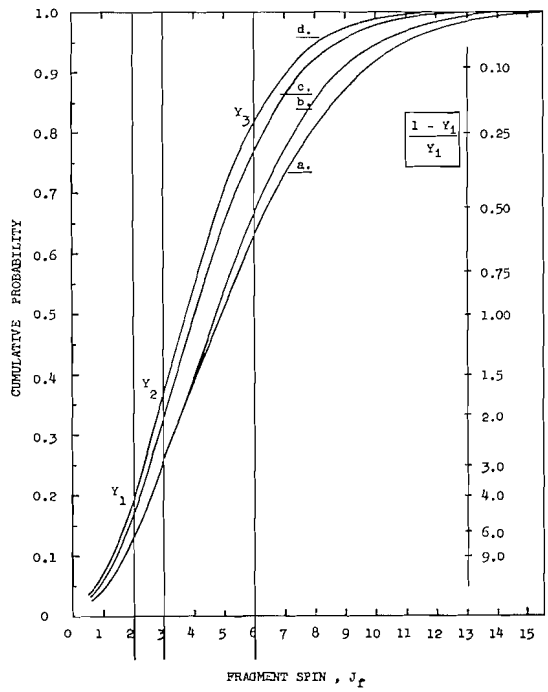

FIG. 3. Theoretical normalized cumulative distributions of the spin of fragments during their de-excitation. The initial spin distribution was given by eq. [1] with $B = 7$. The following modified distributions are shown after the emission of (*a*) 1 neutron, (*b*) 3 neutrons, (*c*) 3 neutrons, and 3 dipole γ-rays, (*d*) 3 neutrons, and 3 quadrupole γ-rays. The intersection points, Y_i, and the corresponding ordinate are described in the text.

Figures similar to Fig. 3 were constructed for 3 values of B in order to obtain functions of the type shown in Fig. 4. This figure shows the predicted isomer ratios for three isomer classes as a function of B. The higher values of B are nearly equal to $(\overline{J_f^2})^{1/2}$. All computations here had $N_n = 3$ and $(N_\gamma - 1) = 3$. Dipole gamma radiation was assumed, except for the long dashed lines which were computed for three quadrupole γ-rays. The short dashed lines show the significant decrease in predicted isomer ratio with a lower set of spin cutoff factors ($\sigma_n = 6$, 5, 4, and $\sigma_\gamma = 3$, whereas the other lines result from $\sigma_n = 7$, 6, 5, and $\sigma_\gamma = 4$).

Unfortunately until α_K of $^{133}Xe^m$ is measured more precisely the present experimental ratios for the ^{133}Xe isomers can give only a range of estimates for the spin of fragments leading to ^{133}Xe. Values for the wide range of input parameters shown in Table IV for isomer ratios of ^{133}Xe equal to 1.0, 2.0, and 3.0 were calculated and were found to correspond to

Can. J. Chem. Downloaded from www.nrcresearchpress.com by 210.87.254.6 on 09/05/12
For personal use only.

Can. J. Chem. Downloaded from www.nrcresearchpress.com by 210.87.254.6 on 09/05/12
For personal use only.

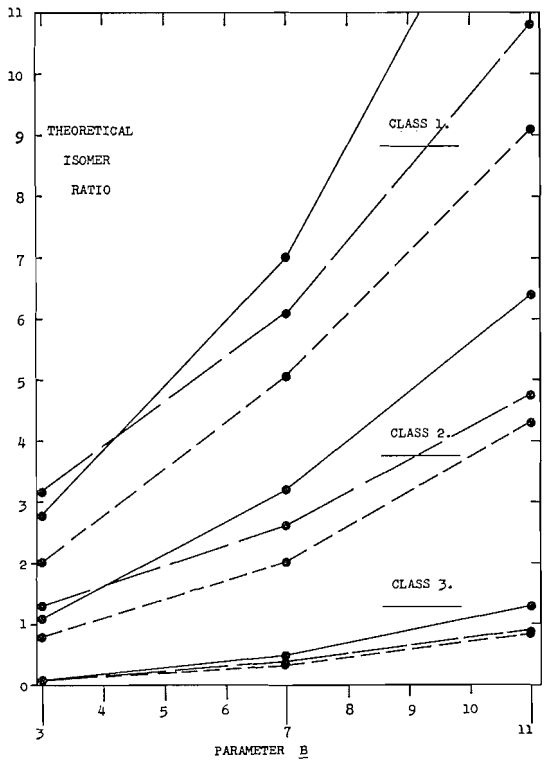

FIG. 4. Theoretical values of the isomer ratio for three spin-pair classes of isomers. The value of B characterizes the initial spin distribution given by eq. [1]. The different lines show the effect of the multipolarity and the spin cutoff factor upon the theoretical ratios. All computations had $N_n = 3$ and $(N_\gamma - 1) = 3$. Dipole radiation was used except for the long dashed lines which were computed for three quadrupole γ-rays. Different sets of spin cutoff factors were used. (— —) $\sigma_n = 6, 5, 4$, and $\sigma_\gamma = 3$; (————) and (—— ——) $\sigma_n = 7, 6, 5$, and $\sigma_\gamma = 4$.

initial fragment spins of 4 ± 1, 6 ± 1.5, and 8 ± 1.5.

Further strong evidence for such high fragment spins has been obtained from isomer ratio measurements of a few species which could be formed either in fission or in a spallation reaction. The measured ratios of high to low spin for an isomeric species formed in fission were much higher than when the isomers were spallation products or formed by neutron capture (31, 46). It would be of some interest to compare the present data for ^{133}Xe with data for the reaction ^{130}Te(α,n)^{133}Xe in the α-energy range 10–25 MeV. In the latter system the initial and modified spin distributions could be rather well defined by calculations similar to those made for other (α,n) reactions (4, 6, 7, 38). It might therefore be possible to obtain a better spin cutoff factor for our fission calculations and to compare the de-excitation process in spallation (and fission) products leading to ^{133}Xe. The spins involved in both types of system should be of about the same magnitude.

Isomer ratio studies have given some evidence for the theoretical prediction that the spin may be less for fission fragments formed in symmetrical fission than that formed in asymmetrical fission. For example, surprisingly low fragment spins were estimated in Hagebo's study (29) of the isomers of ^{117}In formed in the near-symmetric fission of ^{232}Th, ^{238}U, and ^{209}Bi with protons of energy less than 30 MeV. Also relatively low isomeric ratios have been measured for ^{115}Cd in fission, although this is complicated by the decay of ^{115}Ag to ^{115}Cd^g.

[b] Target Effects

For the targets ^{232}Th and ^{238}U ($I = 0$) and for ^{233}U ($I = 5/2$) and ^{235}U ($I = 7/2$) the measured ratios for ^{133}Xe were remarkably constant within the experimental error of 10–20% and behaved in the same way with energy. Thus the spin and type of target do not greatly affect the isomer ratio. This agrees with most of the limited data previously reported which are summarized briefly below for the 3 spin-pair classes.

Class 1—For proton energies up to 115 MeV, Hagebo's (29) ratios of ^{117}In for the targets ^{232}Th and ^{238}U ($I = 0$) were the same as those for ^{209}Bi ($I = 9/2$). In his earlier work (47) on ^{95}Nb, however, the ratio for ^{238}U was lower than for ^{232}Th, ^{209}Bi, and ^{208}Pb.

Class 2—Previous data (31, 48) on the isomers of ^{131}Te gave confusing variations of ratios with various systems. ^{133}Te ratios had larger uncertainties (29) and thus are not very meaningful for such comparisons.

Class 3—The ratios measured for ^{134}Cs (31, 32, 49, 50) like those for ^{133}Xe from this work were the same for fission of ^{233}U, ^{235}U, ^{238}U for medium-energy deuterons and alpha particles and for ^{238}U and ^{232}Th with protons of energy 20–85 MeV. For 20–MeV protons on ^{238}U, Davies and Yaffe (50) obtained a very high value for the ^{134}Cs isomer ratio. This result, obtained from only one experiment, will be repeated since it is inconsistent with the other data.

Simple theoretical considerations confirm the independence of the isomer ratio on type

Can. J. Chem. Downloaded from www.nrcresearchpress.com by 210.87.254.6 on 09/05/12
For personal use only.

and spin of target. Part 1 of the H.H.V. program was used to show that a change of target spin from 0 to 7/2 increases the mean value of the compound nucleus spin distribution by only 1 or 2 units. Many factors in the complex fission and de-excitation processes would probably prevent the small changes in the compound nucleus spin from being reflected in the measured isomer ratio. It can be estimated that changes in initial fragment spin of at least 2 units would be necessary to produce a significant change in the measured isomer ratio.

[c] Projectile Energy Effects

The lower curve in Fig. 1, corresponding to $\alpha_K = 4.4$, shows that the isomer ratios do not change significantly over the proton energy range studied. However, the other curves show that for values of $\alpha_K \geq 5$ the results are consistent with a slight increase of isomer ratio with energy. As discussed above, to cause a detectable change in the isomer ratio, a change in the spin of the initial fragment of about 2 units is necessary. Thus the spin of the initial fragments in all the fission systems investigated here appears to differ by less than 2 units, even though the compound nucleus spin goes from a lower limit of about 5 to a probable value of greater than 10.

All other isomer ratio data that have been determined for a wide range of fission energies are also for proton-induced fission. The ^{134}Cs isomer ratios, like those for ^{133}Xe, show very little energy dependence (with the exception of the 20-MeV result which seems discordant). The isomer ratios (29) for ^{117}In, however, do show a strong energy dependence. The ratios increased from 2 to 10 from 40 MeV to 100 MeV (corresponding to initial fragment spin of less than 3 to at least 10). The ^{95}Nb data are less reliable, but also show a similar increase with energy. Some other fragmentary evidence on the energy dependence on fission ratios does exist. The independent isomer ratio of ^{80}Br increases slightly from 70 to 100 MeV (21). The rapid increase of the cumulative isomer ratio of ^{115}Cd (20, 22) may not be due entirely to the energy dependence of the isobaric distribution in chain $A = 115$. The ^{134}Cs isomer ratios were slightly but significantly higher for medium-energy α-particle and deuteron fission than for low-energy photo-fission (31) and ^{131}Te ratios were similarly higher for this type of medium-energy fission than for thermal neutron fission (30).

The following factors would contribute to the insensitivity of the isomer ratios of ^{134}Cs and ^{133}Xe to projectile energy. (*i*) Direct interactions become more important as the projectile energy increases above about 40 MeV. (*ii*) With the increasing projectile energy there is less transfer of energy and angular momentum to the target and angular momentum is removed by the pre-fission cascade. (*iii*) At higher projectile energies the orbital angular momentum between the fragments may increase leaving less spin available for the initial fragments. (*iv*) Fragments with very high spin will lose relatively large amounts of angular momentum by each neutron emission and by a gamma cascade of high multiplicity and of largely quadrupole radiation. (*v*) This would obviously help to maintain the isomer ratio constant at higher energies if the fragments have a limiting spin value (4). On the other hand, the increase in the ratios of ^{95}Nb and ^{117}In with energy is difficult to explain.

[d] Predictions of Isomer Ratios

Predictions of isomer ratios still contain some uncertainties. The most important factor in determining the ratio is the effective spin pair of the isomeric nuclides. A second factor is the spin assumed for the initial fragments. However, the ratio is not too sensitive to this spin which must be changed by at least 2 units for the isomer ratio to be significantly affected. The fragment spin is believed to be fairly high, but it has not yet been conclusively shown whether it is lower for symmetric than for asymmetric fragments. Furthermore, for increasing energy, it is not clearly understood whether the latter phenomenon would become less important if the fragment spin does reach a limiting value. The variations of the other input parameters are reasonably well defined and cause relatively small changes in the predicted ratios. Most critical amongst the latter is the spin cutoff factor.

An example of the use of theoretical isomer ratios exists in the work of Strom, Grant, and Pappas (51). They used the type of calculations outlined in this paper to predict isomer ratios for the shielded nuclides ^{124}Sb and ^{126}Sb

Can. J. Chem. Downloaded from www.nrcresearchpress.com by 210.87.254.6 on 09/05/12
For personal use only.

(isomeric spins = 3, 5, 8, and 5, 8 respectively) formed in thermal neutron fission of ^{235}U. With activity data for only the ground states and the theoretical isomer ratios, they were able to estimate the total independent yields of these two nuclides. However, these estimated ratios should be regarded as only lower limits, because although no experimental ratios have been measured for Class 3 isomers formed in thermal fission, the theory has predicted too low values for the isomer ratio of ^{134}Cs (isomeric spins = 5, 8) formed in other fission systems.

Conversely, theoretical ratios for Class 1 isomers were too high, particularly for lower-energy fission, if initial fragment spins were assumed to be fairly high (of the order 6–8). Theoretical and experimental ratios for Class 2 isomers were in reasonably good agreement. For Class 2, our experimental ^{133}Xe ratios are consistent with ratios measured in similar fission systems for ^{131}Te and ^{133}Te (30, 48). These data agree reasonably well with ratios predicted for a fairly high initial fragment spin. Therefore, experimental and theoretical results contradict a conclusion by Storms (52) in an earlier study of ^{133}Xe formed in medium-energy fission of thorium and uranium. He concluded that the yield of ^{133}Xe^{m} was negligible. Possible errors in Storms' work have been discussed in our previous paper (23).

1. J. R. Huizenga and R. Vandenbosch. Phys. Rev. **120**, 1305 (1960).
2. R. Vandenbosch and J. R. Huizenga. Phys. Rev. **120**, 1313 (1960).
3. H. K. Vonach, R. Vandenbosch, and J. R. Huizenga. Nucl. Phys. **60**, 70 (1964).
4. N. D. Dudey and T. T. Sugihara. Phys. Rev. **139**, B896 (1965).
5. R. Vandenbosch, L. Haskin, and J. C. Norman. Phys. Rev. **137**, B1134 (1965).
6. C. T. Bishop, H. K. Vonach, and J. R. Huizenga. Nucl. Phys. **60**, 241 (1964).
7. C. T. Bishop, J. R. Huizenga, and J. P. Hummel. Phys. Rev. **135**, B401 (1964).
8. J. Wing. Argonne National Lab. Rept. ANL-6598 (1962).
9. D. R. Sachdev and L. Yaffe. Can. J. Chem. **45**, 2711 (1967).
10. W. L. Hafner, J. R. Huizenga, and R. Vandenbosch. Argonne National Lab. Rept. ANL-662 (1962).
11. J. R. Hoffman and R. Vandenbosch. Phys. Rev. **133**, B714 (1964).
12. G. A. Petrov. Soviet Phys. JETP English Transl. **20**, 1387 (1965).
13. G. Graff, A. Lajtai, and L. Nagy. Symp. on the Physics and Chemistry of Fission, Intern. At. Energy Agency, Salzburg, Paper SM-60/55 (1965).
14. H. Maier-Leibnitz, H. W. Schmitt, and P. Armbruster. Symp. on the Physics and Chemistry of Fission, Intern. At. Energy Agency, Salzburg, Paper SM-60/52 (1965).
15. K. Skarsvag and J. Singstad. Nucl. Phys. **62**, 103 (1965).
16. S. A. E. Johansson. Nucl. Phys. **60**, 378 (1964).
17. S. A. E. Johansson. Nucl. Phys. **64**, 147 (1965).
18. N. T. Porile. Phys. Rev. **108**, 1526 (1957).
19. I. F. Croall and H. H. Willis. J. Inorg. Nucl. Chem. **24**, 221 (1962).
20. T. Sikkeland and G. R. Choppin. J. Inorg. Nucl. Chem. **27**, 13 (1965).
21. I. B. Haller and G. Andersson. J. Inorg. Nucl. Chem. **20**, 12 (1961).
22. R. S. Tilbury and L. Yaffe. Can. J. Chem. **41**, 1956 (1963).
23. J. H. Forster, N. T. Porile, and L. Yaffe. Can. J. Chem. **44**, 2951 (1966).
24. I. Dostrovsky, S. Katcoff, and R. W. Stoenner. Phys. Rev. **136**, B44 (1964).
25. I. Bergstrom, S. Thulin, A. H. Wapstra, and B. Astrom. Arkiv Fysik, 7, 255 (1954).
26. L. H. Sliv and I. M. Band. *In* Alpha, beta, and gamma-ray spectroscopy. *Edited by* K. Siegbahn. North-Holland Publ. Co., Amsterdam. 1965. Appendix 5, p. 1639.
27. J. R. Huizenga and R. Vandenbosch. *In* Nuclear reactions. Vol. 2. *Edited by* P. M. Endt and P. B. Smith. North-Holland Publ. Co., Amsterdam. 1962.
28. C. T. Bishop. Argonne National Lab. Rept. ANL-6405 (1961).
29. E. Hagebo. J. Inorg. Nucl. Chem. **27**, 927 (1965).
30. D. G. Sarantites, C. D. Coryell, and G. E. Gordon. Phys. Rev. **138**, B353 (1965).
31. H. Warhanek and R. Vandenbosch. J. Inorg. Nucl. Chem. **26**, 669 (1964).
32. P. P. Benjamin, N. T. Porile, and L. Yaffe. To be published.
33. J. R. Grover. Phys. Rev. **127**, 2142 (1962).
34. J. F. Mollenauer. Phys. Rev. **127**, 867 (1962).
35. T. D. Thomas. Nucl. Phys. **53**, 577 (1964).
36. J. R. Terrell. Symp. on the Physics and Chemistry of Fission, Intern, At. Energy Agency, Salzburg, Paper SM-60/43 (1965).
37. H. Maier-Leibnitz, H. W. Schmitt, and P. Armbruster. Symp. on Physics and Chemistry of Fission, Intern. At. Energy Agency, Salzburg, Paper SM-60/54 (1965).
38. T. Matsuo, J. M. Matuszek, Jr., N. D. Dudey, and T. T. Sugihara. Phys. Rev. **139**, B886 (1965).
39. J. S. Fraser. Symp. on the Physics and Chemistry of Fission, Intern. At. Energy Agency, Salzburg, Paper SM-60/34 (1965).
40. H. C. Britt and S. L. Whetstone, Jr. Phys. Rev. **133**, B603 (1964).
41. J. A. Wheeler. Intern. Conf. on the Peaceful Uses of At. Energy, U.N., New York, **2**, 155, P/593 (1956).
42. K. Wolfsberg. Phys. Rev. **137**, B929 (1965).
43. R. Batchelor, W. B. Gilboy, and J. H. Towle. Nucl. Phys. **65**, 236 (1965).
44. T. Ericson. Nucl. Phys. **11**, 481 (1959).
45. B. T. Feld, H. Feshbach, M. L. Goldberger, H. Goldstein, and V. F. Weisskopf. U. S. At. Energy Comm. Rept. NYO-636 (1951).
46. I. F. Croall and H. H. Willis. J. Inorg. Nucl. Chem. **25**, 1213 (1963).
47. E. Hagebo. J. Inorg. Nucl. Chem. **25**, 1201 (1963).
48. M. T. Erben, L. E. Glendenin, H. C. Griffin, and E. P. Steinberg. Private communication.

49. J. H. DAVIES and L. YAFFE. Can. J. Phys. **41**, 762 (1963).
50. J. H. DAVIES and L. YAFFE. Can. J. Chem. **41**, 1836 (1963).
51. P. O. STROM, G. R. GRANT, and A. C. PAPPAS. Can. J. Chem. **43**, 2493 (1965).
52. H. A. STORMS. Ph.D. Thesis, Massachusetts Institute of Technology, Cambridge, Mass. 1962.

Can. J. Chem. Downloaded from www.nrcresearchpress.com by 210.87.254.6 on 09/05/12
For personal use only.

Can. J. Chem. Downloaded from www.nrcresearchpress.com by 210.87.254.42 on 09/05/12
For personal use only.

Reactions of iron carbonyls with various ligands in the presence of chloroform. A new method for the preparation of iron halide complexes

P. P. SINGH[1] and R. RIVEST

Département de Chimie, Université de Montréal, Montréal, Québec

Received November 23, 1967

Iron halide complexes of the type $FeCl_2.2L$ ($L = CH_3CONH_2$, $HCONH_2$, $HCONHCH_3$) and $FeCl_3.L$ ($L = (C_6H_5)_3P$, $(C_6H_5)_3As$, $C_6H_5NH_2$, $C_6H_5CONH_2$) have been prepared by the reaction of iron carbonyls with various ligands in chloroform as solvent. The mechanism of the reaction and the effect of other solvents have also been studied. The magnetic susceptibility measurements and infrared spectral study (4000–200 cm^{-1}) suggest that these complexes have tetrahedral configuration. The possible site of bonding in ligands and infrared assignments for Fe—O, Fe—Cl, Fe—N, Fe—P, Fe—As bands have been given. The relative Fe—O bond strengths in various amide complexes have been determined on the basis of metal–oxygen stretching frequency and of shifts in carbonyl stretching frequency.

Canadian Journal of Chemistry, 46, 1773 (1968)

Introduction

Halogenated hydrocarbons have been found to be involved in reactions with metal carbonyls either as oxidizing agents (1–7) or entering as addition molecules (8–10) besides producing substitution products (5, 11). Webb and Borcherdt (12) produced coupling of allyl radicals by treating allyl halides with nickel carbonyl.

Coffey (1) has allowed many metal carbonyls to react with *gem*-dihalides and has found that these reactions lead to the formation of metal chlorides and ethylenic compounds with evolution of carbon monoxide as shown in the following equation.

$$2Fe(CO)_5 + 2(C_6H_5)_2CCl_2 = 2FeCl_2 + 10CO + (C_6H_5)_2C{=}C(C_6H_5)_2$$

He has observed that only *gem*-dihalides can undergo such reactions and chloroform was found to be inert in a similar reaction.

Since halogenated hydrocarbons have been found to react with metal carbonyls in a variety of ways, it was thought to be of interest to carry out a systematic study of this system. This paper describes the reactions of various organic ligands with metal carbonyls in the presence of chloroform and other halogenated hydrocarbons. The structure of the complexes obtained by this method has been elucidated with the help of infrared studies in the range 4000–200 cm^{-1} and magnetic susceptibility measurements.

[1]M.L.K. College, Balrampur (Gonda) U.P., India.

Experimental

Materials and Manipulations

All the solvents were of reagent grade and were purified and dried before use. Reagent grade iron pentacarbonyl was obtained from K and K Laboratories and was used after distillation over molecular sieves. Diiron nonacarbonyl and triiron dodecacarbonyl were obtained from Alfa Inorganics and were used after drying in vacuum. Other metal carbonyls were used without further purification.

Formamide (FA), *N*-methylformamide (MFA), and aniline (AN) were purified by distilling under reduced pressure over molecular sieves. Acetamide (AM) and benzamide (BM) were crystallized from chloroform. Triphenylphosphine (TPP) and triphenylarsine (TPA) were used from fresh bottles without further purifications. Reactions were carried out, where essential, in a dry-box flushed with nitrogen.

Infrared spectra of the complexes and ligands were recorded either in Nujol mulls or in solutions on a Perkin-Elmer Model-621 recording spectrophotometer using sodium chloride optics. For far-infrared measurements cesium iodide optics were used.

The magnetic susceptibility measurements were made by the Gouy method, using mercury(II) tetrathiocyanatocobalt(II) as standard. The diamagnetic corrections were estimated by methods outlined by Figgis and Lewis (25).

Preparation of the Complexes

$FeCl_3.AN$, $FeCl_3.BM$, $FeCl_2.2AM$, $FeCl_2.2FA$, and $FeCl_2.2MFA$ were prepared by refluxing $Fe_3(CO)_{12}$ (2 g) with AN (1.2 g), BM (1.5 g), AM (1.5 g), FA (1.1 g), or MFA (1.5 g) in chloroform (100 ml) till the color of the solution changed from green to light yellow. In each case a white or light-yellow flocculent precipitate separated which was filtered, washed with the solvent, and dried in vacuum. Instead of the trimer, the dimer could be conveniently used. With the monomer $Fe(CO)_5$ the complex was obtained only when the refluxing was continued for about 48 h.

Can. J. Chem. Downloaded from www.nrcresearchpress.com by 210.87.254.42 on 09/05/12
For personal use only.

TABLE I

Melting points and elemental anaylses of complexes

	Melting point (°C)*	Color	Fe (%)		Cl (%)		C (%)		H (%)		N (%)		P (%)	
			Calc.	Obs.	Calc.	Obs.	Calc.	Obs.	Calc.	Obs.	Calc.	Obs.	Calc.	Obs.
$FeCl_2.2AM$	116	White	22.95	22.52	28.70	28.26	19.79	19.62	4.10	4.12	11.06	11.39		
$FeCl_2.2FA$	200d	Yellowish	25.81	25.24	32.72	32.31	11.05	11.71	2.76	2.92	12.90	13.55		
$FeCl_2.2MFA$	140	White	22.95	22.64	28.70	28.52	19.79	19.25	4.10	3.81	11.06	12.01		
$FeCl_2.4FA$	156	Yellowish	18.24	18.16	23.12	23.73	15.64	15.04	3.90	4.23				
$FeCl_3.AN$	—	Yellow	21.96	21.53	42.54	41.97	28.24	27.82	2.69	3.41				
$FeCl_3.TPP$	118	Light yellow	13.19	12.83	25.08	25.60	50.88	50.23	3.57	3.51				
$FeCl_3.TPA$	130	Dark yellow	11.99	12.62	22.48	22.50	46.15	44.99	3.51	3.49				
$(C_6H_5)_2C{=}(C_6H_5)_2$	222	White					93.97	93.66	6.05	5.41				
$FeCl_3.BM$	158	Brown	19.78	19.42	37.63	36.99	29.68	28.94	2.47	2.79	4.94	4.57		
$MoCl_3.TPP$	95	Pink			22.84	22.44	46.67	47.36	3.23	3.89			6.69	6.39

*d = decomposition.

Can. J. Chem. Downloaded from www.nrcresearchpress.com by 210.87.254.42 on 09/05/12
For personal use only.

$FeCl_3$.TPP and $FeCl_3$.TPA were prepared by refluxing $Fe_3(CO)_{12}$ (2 g) and TPP (3.2 g) or TPA (5.6 g) in chloroform (100 ml) for 12 h; the solution was then filtered. The residue was rejected and the filtrate concentrated by vacuum evaporation. To the concentrate *n*-hexane was added and the mixture was vigorously shaken until a dark-yellow viscous mass separated. The supernatant liquid was rejected and the residue treated with small quantities of absolute alcohol. A yellow solid was thus obtained which was washed with *n*-hexane and dried in vacuum. It was recrystallized from absolute alcohol. The complex could also be prepared by refluxing $Fe(CO)_4$.TPP with chloroform, and completing the process as described above.

$MoCl_3$.TPP was also similarly prepared from $Mo(CO)_6$ (2 g) and TPP (2 g) but the refluxing time was 5 days.

Isolation of $(C_6H_5)_2C{=}C(C_6H_5)_2$

$Fe(CO)_4$.TPA (5.3 g) was mixed with 4 ml of diphenyldichloromethane and refluxed in 150 ml of benzene with stirring for 15 h. A viscous layer appeared which was separated from the supernatant liquid. The supernatant liquid was concentrated by vacuum evaporation when a white compound crystallized out; it was filtered, washed several times with acetone, and dried in vacuum. It was recrystallized from an acetone–water mixture and identified as tetraphenylethylene by its melting point, elemental analysis, and infrared spectrum.

Analysis of the Compounds

Iron and chlorine were estimated as oxide and silver halide respectively. Carbon, hydrogen, and nitrogen were analyzed by microtechniques from Galbraith Laboratories Incorporated. The results obtained are given in Table I.

Results

All the three iron carbonyls (monomer, dimer, and trimer) react with various organic ligands in the presence of chloroform and form halide adducts of the type $FeCl_2.2L$ and $FeCl_3.L$. Molybdenum carbonyl also reacts similarly with TPP and forms $MoCl_3.L$. Chromium and tungsten carbonyls under similar conditions do not form any complex. The substituted carbonyl complex $Fe(CO)_4.L$ also forms halide complexes ($FeCl_3.L$) when refluxed with chloroform. The solvents other than chloroform which have been found to lead to similar oxidation reactions are carbon tetrachloride, tetrachloroethane, and benzyl chloride. Dichloroethane and methylene dichloride have been found to lead to some sort of decomposition giving rise to impure compounds.

The organic ligands which have been found to form complexes of the type $FeCl_2.2L$ are formamide, monomethylformamide, and acetamide, whereas those which form the $FeCl_3.L$ type are aniline, benzamide, triphenylphosphine, and triphenylarsine. It has been noticed that all the ligands which have a phenyl group give rise to an iron complex of higher oxidation state.

Acetonitrile, dimethylformamide, and triphenylstibine do not form pure complexes, probably due to the formation of excess $FeCl_2$ during the course of the reaction. Triphenylamine and triphenylbismuthine do not react at all.

This method of preparing halide complexes is an improvement over the direct synthesis from the halides as the latter involves difficulty in dissolution of the halide in nonpolar organic solvents and in its handling. Out of the three forms of iron carbonyls, the dimer and the trimer are best suited for this purpose and can safely be handled even in open air.

Mechanism of the Reaction

The formation of complexes of the type $FeCl_2.2L$ or $FeCl_3.L$ by the reaction of iron carbonyl with various ligands in the presence of halogenated hydrocarbons suggests two possible reaction mechanisms. On the lines of the Coffey (1) mechanism it can be suggested that the halogenated hydrocarbon first reacts with the carbonyl and forms ferrous chloride which further reacts with the ligand and forms the complex. The possibility of this mechanism is ruled out because iron pentacarbonyl does not react with chloroform in the absence of the ligand, and the formation of ferric chloride has never been observed in any kind of reaction in which iron carbonyl reacts with any halogenated hydrocarbon. The second possible mechanism is through the formation of a substituted carbonyl complex of the type $Fe(CO)_4.L$, which reacts with halogenated hydrocarbons to give rise to a halide complex. To verify this, $Fe(CO)_4.L$ was allowed to react with chloroform, and the halide complex was obtained. In order to establish the reaction mechanism we tried to isolate the product formed from chloroform after its involvement in the oxidation reaction but failed to identify or isolate any such compound. We therefore replaced the chloroform with diphenyldichloromethane and allowed this to react with $Fe(CO)_4$.TPA. We could thus isolate tetraphenylethylene besides the halide complex. A possible mechanism of the reaction therefore can be suggested as

$$Fe(CO)_5 + 2L = Fe(CO)_3.L_2 + 2CO$$

$$2Fe(CO)_3.L_2 + 2(C_6H_5)_2CCl_2 = 2FeCl_2.L_2 + (C_6H_5)_2C{=}(C_6H_5)_2 + 6CO.$$

Can. J. Chem. Downloaded from www.nrcresearchpress.com by 210.87.254.42 on 09/05/12
For personal use only.

TABLE II

Assignments of infrared bands of ligands and complexes

Assignments	$FeCl_2$.2FA		$FeCl_2$.2AM		$FeCl_2$.2MFA		$FeCl_3$.BM	
	Ligand ($CHCl_3$ soln.)	Complex (Nujol)	Ligand ($CHCl_3$ soln.)	Complex (Nujol)	Ligand ($CHCl_3$ soln.)	Complex (Nujol)	Ligand ($CHCl_3$ soln.)	Complex (Nujol)
N—H stretch (asym.)	3550 (s)	3400 (s)	3560 (s)	3400 (s)			3555 (s)	3440 (s)
N—H stretch (sym.)	3425 (s)	3280 (s)	3440 (s)	3280 (s)	3483 (s)	3340 (s)	3440 (s)	3340 (s)
Amide I	1710 (s)	1690 (s)	1710 (s)	1670 (s)	1690 (s)	1635 (s)	1675 (s)	1652 (s)
			1685 (s)					
Amide II	1590 (m)	1570 (s)	1605 (s)	1580 (s)			1590 (s)	1560 (s)
C—N stretch	1300 (s)	1335 (m)	1380 (s)	1410 (m)	1410 (s)	1445 (s)		
Fe—Cl stretch		373 (wb)		350 (wb)		380 (sb)		375 (mb)
		330 (mb)				360 (s)		288 (mb)
Fe—O stretch		400 (vw)		420 (vw)		475 (vw)		475 (s)
Fe—O stretch + δNCO		585 (sh)		560 (s)		540 (m)		538 (s)

s = strong, m = medium, w = weak, v = very, b = broad.

TABLE III

Assignments of infrared bands of ligands and complexes

Assignment	$FeCl_3$.AN		$FeCl_3$.TPP		$FeCl_3$.TPA		$MoCl_3$.TPP	
	Ligand ($CHCl_3$ soln.)	Complex (Nujol)	Ligand (Nujol)	Complex (Nujol)	Ligand (Nujol)	Complex (Nujol)	Ligand (Nujol)	Complex (Nujol)
N—H stretch (asym.)	3478 (s)	3360 (sb)						
N—H stretch (sym.)	2400 (s)							
NH_2 bending	1620 (s)	1640 (s)						
Fe—N stretch		462 (s)						
M—Cl stretch		375 (m)		370 (s)		360 (s)		330 (s)
		290 (w)		320 (w)		330 (m)		335 (sh)
Phenyl—P			1095 (s)	1105 (s)				
M—P				525 (s)				522 (s)
Phenyl—As					1072 (s)	1080 (s)		
Fe—As						460 (s)		

s = strong, m = medium, w = weak, b = broad, sh = shoulder, M = Fe, Mo.

Can. J. Chem. Downloaded from www.nrcresearchpress.com by 210.87.254.42 on 09/05/12
For personal use only.

Infrared Study

Amide Complexes

Amides can coordinate either through the nitrogen of the NH_2 group or the oxygen of the C=O group. A reference to Table II shows that there is a negative shift of the carbonyl stretching frequency and a positive shift of the C—N stretching on complex formation, suggesting coordination through the carbonyl oxygen of the amides. A negative shift in NH_2 bending or amide II band on coordination also indirectly supports coordination through oxygen, as coordination through nitrogen would cause a positive shift in this band (20). However, a marked negative shift in the N—H stretching frequency of the amide is also observed. The reason for such a negative shift in N—H stretching frequency is hydrogen bonding between the NH_2 of the amide and chlorine of the metal halide. Such hydrogen bonding has been observed by Chatt *et al.* (13) in a series of amine complexes of platinous chloride. There is also ample evidence (14, 15) for the presence of hydrogen bonding between the hydrogen of amine complexes and anions such as halides. It is worth mentioning that the magnitude of the shift due to hydrogen bonding is even greater than the shift due to coordination, and can be of the order of 200 cm^{-1}. If one makes a molecular model of the complexes one finds quite a good possibility of such a hydrogen bonding. As such, the negative shift in N—H stretching frequency is not due to coordination through nitrogen, but due to hydrogen bonding.

Previous workers on amide and urea complexes (16) have not noticed such a marked shift in N—H stretching frequency when coordination took place through oxygen. Since our observation is the first of its kind it is interesting to explain it in detail. Intermolecular hydrogen bonding between oxygen of the carbonyl group and hydrogen of NH_2 is well known (17) in amides and has a marked effect on the positions of N—H and C—O stretching vibrations. It is therefore essential to record the spectrum of the ligand in very dilute solution so that hydrogen bonding is completely eliminated. We have therefore compared the spectrum of the complexes with that of a very dilute solution of the ligand and have deduced the magnitude of the shift. However, if the spectrum of the complex is compared with that of the ligand in solid phase or in concentrated solution, where hydrogen bonding is not eliminated, no negative shift will be observed, as in ref. 16.

Since the spectrum in the far infrared region provides direct evidence of bonding, we recorded the spectrum in this region also and the assignments are given in Table II. The weak band in the region 400–475 cm^{-1} (for which there are no corresponding ligand bands) is assigned to pure Fe—O stretching vibration. Nakamoto *et al.* (18, 19) also observed a weak band for M—O stretching frequency and gave the assignment for this band in the region 430–490 cm^{-1}. The band in the region 538–585 cm^{-1} has been assigned as a combination band of metal–oxygen stretching frequency and C—C bending vibration (18, 19), or O—C—O bending (34), or N—C—O bending (16). Since the N—C—O bending vibration is present in all the amide complexes, we assign the band in this region to Fe—O stretching vibration plus N—C—O bending vibration.

On the basis of inductive effects, one can fairly well establish that the three amides will have the order of donor ability MFA > AM > FA, because in MFA the methyl group will tend to repel the electrons towards the carbonyl, this effect being absent in FA. Acetamide is intermediate, due to the methyl group on carbon. If coordination takes place through the carbonyl group we should then observe an increase in $\Delta\nu$(C=O) from $FeCl_2$.2FA to $FeCl_2$.2MFA and also an increase in the Fe—O stretching in the same order indicating an increase in bond order. Table IV gives results which confirm these assumptions. A similar relationship has also been elucidated by Nakamoto in acetylacetonate and oxalato complexes (18, 19).

TABLE IV

Infrared spectra assignments

Complex	Position of ν(C=O) (cm^{-1})	Δν(C=O) (cm^{-1})	ν(M—O) (cm^{-1})
$FeCl_2$.2FA	1690	−20	400
$FeCl_2$.2AM	1665	−40	420
$FeCl_2$.2MFA	1635	−55	475

NOTE. The benzamide complex has not been included in this sequence as the metal is in a different oxidation state.

Analine, Triphenylphosphine, and Triphenylarsine Complexes

Since these ligands have only one center of

Can. J. Chem. Downloaded from www.nrcresearchpress.com by 210.87.254.42 on 09/05/12
For personal use only.

coordination, the discussion of the infrared spectrum in the regular region is hardly of any interest. We have therefore confined our discussion to the far infrared region, and the assignments are given in Tables II and III.

In the case of the aniline complex there is a strong band at 462 cm^{-1} corresponding to which there is no ligand band. This band therefore can reasonably be assigned to the Fe—N stretching vibration. Previous workers (21–24) have given M—N assignments in the same region.

In triphenylphosphine complexes of iron and molybdenum there appear bands at 525 cm^{-1} and 522 cm^{-1} respectively, whereas in the triphenylarsine complex a band appears at 450 cm^{-1}. There are no ligand bands corresponding to these bands which can be assigned to Fe—P, Mo—P, and Fe—As stretching vibrations respectively. Assignment for M—P stretching vibration has been given in the same region by Rivest *et al.* (27) and Westland and Westland (35). Coates and Parkins (26) have observed that the Pd—P stretching frequency is higher than the Pd—As stretching frequency in palladium dichloride complexes. A similar observation has been made by Rivest *et al.* (27) in the case of stannic halide complexes of triphenylphosphine and triphenylarsine. Our assignments have a similar relation.

Fe—Cl Bands

The assignments of Fe—Cl vibrations are given in Tables II and III. We find that there are bands at about 375 cm^{-1} in all the iron halide complexes corresponding to which there are no ligand bands. The presence of these bands in all the complexes strongly suggests that they are due to Fe—Cl stretching vibrations. This assignment is in good agreement with the assignments given by Woodward and Taylor (28) and Adams (29) for M—Cl bands.

Magnetic Susceptibility and Structural Studies

It is well known that Cl^- (30) has a weak and TPP a strong ligand field (31). To evaluate the ligand field strength of amides, $FeCl_2.4FA$ was prepared and its magnetic susceptibility measured, which was found to correspond to four unpaired electrons, showing that the ligand field due to amides is weak. A diamagnetic complex ($d_\epsilon^6 d_\gamma^0$) was expected from a strong field.

The number of unpaired electrons in $FeCl_2.2L$ and $FeCl_3.L$ complexes are four and five respectively. These values favor a tetrahedral structure for the complexes. Chatt and Shaw (32) have also observed that in a weak field only a tetrahedral structure is possible and that the field required for a square planar complex must be very high.

The number of bands in the far infrared region also supports the tetrahedral configuration for these complexes. The complexes of the type $FeCl_2.2L$ have a C_2v symmetry and those of $FeCl_3.L$ type have C_3v symmetry, if treated as tetrahedral (33). The number of stretching vibrations expected for $FeCl_2.2L$ is four (two for Fe—L and two for Fe—Cl) and for $FeCl_3.L$ is three (one for Fe—L and two for Fe—Cl). The bending vibrations have not been taken into account as they will appear below 200 cm^{-1}. We observed the expected number of bands (Tables II and III) in the far infrared region of the complexes which is in conformity with the tetrahedral configuration for these complexes.

The molecular weight determinations could not be made because the complexes dissociate in solution; however, the fact that these complexes have a low melting point and are easily soluble with dissociation is indirect evidence of their monomeric nature. If one accepts the hypothesis that they are monomeric, the other data support the tetrahedral configuration for these complexes.

Acknowledgments

The authors gratefully acknowledge financial support from the National Research Council of Canada. P. P. Singh is also grateful to M.L.K. College, Balrampur, India, for grant of leave.

1. C. E. Coffey. J. Am. Chem. Soc. **83**, 1623 (1961).
2. K. K. Joshi. J. Chem. Soc. A, 594 (1966).
3. T. S. Piper and G. Wilkinson. Naturwissenschaften, **42**, 625 (1955).
4. R. Criegee and G. Schroder. Ann. **623**, 1 (1959).
5. G. F. Emerson, L. Watts, and R. Pettit. J. Am. Chem. Soc. **87**, 131 (1965).
6. J. C. Hileman, D. K. Huggins, and H. D. Kaesz. Inorg. Chem. **1**, 933 (1962).
7. I. V. Howell and L. M. Venanzi. J. Chem. Soc. A, 1007 (1967).
8. A. G. Osborne and M. H. B. Stiddard. J. Chem. Soc. 700 (1965).
9. J. Lewis and R. Whyman. J. Chem. Soc. 6027 (1965).
10. D. M. Adams, D. J. Cook, and R. D. W. Kemmitt. Chem. Commun. 103 (1966).
11. W. T. Dent, L. A. Duncanson, R. G. Guy, H. W. B. Reed, and B. L. Shaw. Proc. Chem. Soc. 169 (1961).

12. I. D. WEBB and G. T. BORCHERDT. J. Am. Chem. Soc. **73**, 2654 (1951).
13. J. CHATT, L. A. DUNCANSON, and L. M. VENANZI. J. Chem. Soc. 2712 (1956).
14. A. NAKAHARA, Y. SAITO, and H. KUROYA. Bull. Chem. Soc. Japan, **25**, 331 (1952).
15. K. NAKAMOTO. Infrared spectra of inorganic and coordination compounds. John Wiley and Sons, New York. 1963. p. 145.
16. R. B. PENLAND, S. MIZUSHIMA, C. CURRAN, and J. V. QUAGLIANO. J. Am. Chem. Soc. **79**, 1575 (1957).
17. M. DAVIES and H. E. HALLAM. Trans. Faraday Soc. **47**, 1170 (1951).
18. K. NAKAMOTO, P. J. MCCARTHY, A. RUBY, and A. E. MARTELL. J. Am. Chem. Soc. **83**, 1066 (1961).
19. K. NAKAMOTO, P. J. MCCARTHY, and A. E. MARTELL. J. Am. Chem. Soc. **83**, 1272 (1961).
20. K. NAKAMOTO. Infrared spectra of inorganic and coordination compounds. John Wiley and Sons, New York. 1963. p. 143.
21. K. NAKAMOTO, J. FUJITA, and H. MURATA. J. Am. Chem. Soc. **80**, 4817 (1958).
22. K. NAKAMOTO. Infrared spectra of inorganic and coordination compounds. John Wiley and Sons, New York. 1963. p. 149.
23. T. SHIMANOUCHI and K. NAKAGAWA. Spectrochim. Acta, **18**, 89 (1962).
24. D. B. POWELL and N. SHEPPARD. J. Chem. Soc. 3108 (1956).
25. B. N. FIGGIS and J. LEWIS. *In* Modern coordination chemistry, *Edited by* J. Lewis and R. C. Wilkins. Interscience, New York. p. 403.
26. G. E. COATES and C. PARKIN. J. Chem. Soc. 421 (1963).
27. R. RIVEST, S. SINGH, and C. ABRAHAM. Can. J. Chem. **45**, 3137 (1967).
28. L. A. WOODWARD and M. J. TAYLOR. J. Chem. Soc. 4473 (1960).
29. D. M. ADAMS. Proc. Chem. Soc. 3512 (1961).
30. N. S. GILL. J. Chem. Soc. 3512 (1961).
31. J. CHATT, G. A. GAMLEN, and L. E. ORGEL. J. Chem. Soc. 1047 (1959).
32. J. CHATT and B. L. SHAW. J. Chem. Soc. 285 (1961).
33. K. NAKAMOTO. Infrared spectra of inorganic and coordination compounds. John Wiley and Sons, New York. 1963. p. 111.
34. J. FUJITA, A. E. MARTELL, and K. NAKAMOTO. J. Chem. Phys. **36**, 339 (1962).
35. A. D. WESTLAND and L. WESTLAND. Can. J. Chem. **43**, 426 (1965).

Can. J. Chem. Downloaded from www.nrcresearchpress.com by 210.87.254.42 on 09/05/12
For personal use only.

Can. J. Chem. Downloaded from www.nrcresearchpress.com by 210.87.254.6 on 09/05/12
For personal use only.

Potential parameters and surface areas from third-order gas–solid interactions[1]

ROBERT WOLFE[2] AND JOHN R. SAMS
Department of Chemistry, University of British Columbia, Vancouver, British Columbia

Received October 3, 1966[3]

Values of the effective interaction potential between a pair of adsorbed molecules are evaluated in terms of different potential models for argon adsorbed on two carbon surfaces. The resultant three-body (admolecule–admolecule–solid) energies are not in accord with independent theoretical predictions. It is suggested that the results may be indicative of a saturation phenomenon. The apparent areas of both powders are nearly independent of the assumed interaction model, a fact which lends weight to the quantitative significance of surface areas determined by this method.

Canadian Journal of Chemistry, 46, 1781 (1968)

Introduction

We wish to report an apparent anomaly in values found for the effective pair interaction energy when two gas molecules are adsorbed onto a surface, i.e. the fact that the perturbation of the pair potential is nearly independent of the gas–solid interaction energy. We also comment on surface areas determined from third-order adsorption data.

Considerable insight into the nature of the van der Waals interaction of gas molecules with solid surfaces and the forces acting between adsorbed molecules has been gained from the imperfect gas theory of adsorption developed by Steele and Halsey (1). A recent fruitful approach has been to treat the admolecules as an imperfect two-dimensional gas in an external potential field (2, 3). This approximation appears to be quite satisfactory in the experimental cases to which it has been applied (4), but if desired, corrections to account for nonplanarity of the adsorbed phase can be included without much difficulty (3). These corrections are usually small.

Theoretical studies (5, 6) indicate that when two molecules are adsorbed into a monolayer there should arise an additional repulsion between them which varies as the inverse cube of their separation. Thus, if a Lennard–Jones (L.J.) (12,6) potential is taken for the bulk gas interactions, the potential function for the two-dimensional gas can be written as

$$[1] \qquad u(\tau_{12}) = 4\epsilon[\tau^{*-12} - \tau^{*-6} - \eta\tau^{*-3}],$$

where

$$\tau_{12} = |\tau_1 - \tau_2|, \quad \tau^* = \tau_{12}/\sigma,$$

and where ε and σ are the bulk phase L.J. parameters. τ is a two-dimensional vector in the plane parallel to the surface (assumed to be uniform). The (negative) constant η which measures the three-body energy can be determined in two distinctly different ways. The first of these is to treat η as an empirical parameter to be determined by fitting experimental data to the model (4, 7). Alternatively, two theoretical equations have been proposed for calculating η. Sinanoğlu and Pitzer (5) obtained from third-order perturbation theory the result

$$[2] \qquad -\eta = (1.5\alpha_1\epsilon_{1s}/16\epsilon\sigma^3)\left[\frac{2I_1 + I_s}{I_1 + I_s}\right],$$

where α_1 is the polarizability of the admolecule, I_1 and I_s the respective ionization potentials of admolecule and adsorbent, and ε_{1s} the minimum interaction energy of a single molecule with the surface, obtained from analysis of second-order adsorption data. Yaris (6) has also derived an expression for η employing variational techniques, and finds

$$[3] \qquad -\eta = \frac{1.5\alpha_1\epsilon_{1s}}{16\epsilon\sigma^3}\left[\frac{2\chi_1/\alpha_1 + \chi_s/\alpha_s}{\chi_1/\alpha_1 + \chi_s/\alpha_s}\right],$$

where the χ are diamagnetic susceptibilities. Note that these equations both predict that the perturbation of the lateral pair potential will be greater the more polarizable the admolecule and the stronger the gas–surface interaction.

For all the systems investigated thus far (Ar, Kr, Xe, CH_4, and CD_4 on the highly graphitized carbon P33) it has been found (4) that there is at best only semiquantitative agreement between calculated and empirically determined η values,

[1]Supported in part by the Research Fund of the University of British Columbia.
[2]Present address: Department of Chemistry, University of Toronto, Toronto, Ontario.
[3]Revision received December 19, 1967.

TABLE I

Effective two-dimensional potential parameters and three-body energies. Bulk gas parameters are $\varepsilon/k = 119.8$ °K and $\sigma = 3.41$ Å. The quantity $\delta_{1s} = 42 \times 10^{-2}$

Potential model	ε_2/k (°K)	σ_2 (Å)	η	$\Delta \times 10^2$	$\delta_2 \times 10^2$
	Ar-BP71 system ($\varepsilon_{1s}/k = 1921$ °K)				
(12,6,3)	109	3.43	−0.0318	8.98	7.50
(12,6)	97	3.47	—	19.0	10.5
(∞,6)	216	—	—	38.5	4.4
	Ar-P33 system ($\varepsilon_{1s}/k = 1110$ °K)				
(12,6,3)	109.9	3.43	−0.0290	8.26	7.50
(12,6)	99.4	3.46	—	17.0	10.5
(∞,6)	222	—	—	36.8	4.4

the latter being no more than about half the former. Although one does not necessarily expect experimental measurements to thoroughly substantiate approximate theoretical calculations, one does hope that the measured and calculated values will show the same *trends* as one changes systems, especially so if the theoretical predictions are as intuitively reasonable as those provided by eqs. [2] and [3]. But whereas the calculated η values show a monotonic increase with polarizability of the admolecule, no discernable trend is observed for the experimental ones. It should be noted, however, that for a given adsorbent, all the quantities α_1, ε_{1s}, ε, σ, χ_1, and I_1 change with the adsorbate, and it is virtually impossible to decide just where the difficulty resides.

On the other hand, if one employs data for the same adsorbate on, say, two different carbon surfaces, the η values found should be directly proportional to ε_{1s} (on the basis of eqs. [2] and [3]), since slight changes in α_s and χ_s or I_s will have a very small effect on the calculations. We therefore decided to compare the previous results for the Ar-P33 system with Freeman's measurements (8) for Ar on the carbon black designated as Black Pearls 71 (BP71). The ε_{1s} values for these systems differ by a factor of almost 2, and we anticipated a sizeable increase in η for the Ar-BP71 system.

A further reason for analyzing Freeman's results was to investigate in more detail the apparent insensitivity (4) of surface areas determined from third-order data to the exact form of the potential function chosen to represent the lateral interactions.

The method used to analyze the data, and to determine the effective two-dimensional interaction energy ε_2, collision diameter σ_2, and the surface area A, has been described (4). For purposes of comparison, in addition to eq. [1] we have employed a two-dimensional (12,6) model, for which there is also some theoretical justification (9).

Potential Parameters and Three-Body Energies

Table I lists the effective two-dimensional potential parameters and η values found for the systems Ar-BP71 and Ar-P33. Also included are the (12,6) bulk gas parameters employed and the gas–surface interaction energies. It is immediately obvious that the effective parameters from either model are very nearly the same for both systems, although the differences *between the models* are quite apparent.

We define a reduced three-body energy Δ as

$$[4] \qquad \Delta = (\epsilon - \epsilon_2)/\epsilon,$$

which can be thought of as the fractional nonadditivity of the pair potential. It is more significant and instructive to compare Δ values between the systems than the actual parameters themselves, and these are also given in Table I. For both systems it can be seen that $\Delta(12,6,3)/\Delta(12,6) \simeq 2$. This difference between the models is not difficult to explain. If one employs a (12,6) potential for both bulk gas and adsorbed film, the entire perturbation must be taken up in changing the apparent depth of the well and position of the potential minimum. The introduction of the τ^{-3} term, however, also alters the shape of the potential well. Some of the perturbation is apparently absorbed in altering this shape factor, so that the effective well depth does not decrease by the same amount.

Can. J. Chem. Downloaded from www.nrcresearchpress.com by 210.87.254.6 on 09/05/12
For personal use only.

Can. J. Chem. Downloaded from www.nrcresearchpress.com by 210.87.254.6 on 09/05/12
For personal use only.

The fact that the Δ values for a given model are nearly the same for both systems is not susceptible of such a ready explanation. If we define a quantity δ_2 by

$$[5]\quad \delta_2 = [\Delta(\text{BP71}) - \Delta(\text{P33})]/\Delta(\text{BP71}),$$

then according to eqs. [2] and [3], for a given adsorbate δ_2 should have approximately the same value as

$$[6]\quad \delta_{1s} = [\epsilon_{1s}(\text{BP71}) - \epsilon_{1s}(\text{P33})]/\epsilon_{1s}(\text{BP71}).$$

It is clear from Table I that this is not the case. δ_2 for the (12,6) model is only one-fourth δ_{1s}, and the discrepancy is even larger for the (12,6,3) potential.

These results were quite unexpected. We have examined critically a number of possible deficiencies in the models and experiments which might account for the discrepancy, and these will be considered one by one.

(a) Lack of Planarity of the Adsorbed Phase

One of the crucial assumptions of the treatment is that the admolecules form a strictly two-dimensional layer. The degree to which the systems conform to this model can be estimated as follows. Take the z-axis normal to τ and let z_m be the separation of the admolecule and the surface at the potential minimum of the gas–solid interaction. In terms of the variable $\zeta \equiv z - z_m$ assuming the vibrations in the z-direction to be harmonic, the root-mean-square (r.m.s.) amplitude for motion of the admolecules normal to the surface is

$$[7]\quad z_{\text{r.m.s.}} = \frac{k_z}{kT}\int_{-\infty}^{\infty}\zeta^2\exp(-k_z\zeta^2/2kT)\,d\zeta = (2\pi kT/k_z)^{1/2}.$$

The force constant k_z is proportional to the strength of the gas–solid interaction and inversely proportional to the square of the gas–surface collision diameter z_0, and hence

$$[8]\quad z_{\text{r.m.s.}} \propto z_0(kT/\epsilon_{1s})^{1/2}.$$

z_0 can be computed from ε_{1s} and the Kirkwood-Müller formula (1). If now T is taken as the middle of the temperature range of the experiments for both systems, we find

$$z_{\text{r.m.s.}}(\text{BP71})/z_{\text{r.m.s.}}(\text{P33}) = 0.89.$$

This result implies that the Ar-BP71 system corresponds a bit more closely to the two-dimensional model than does the Ar-P33 system. If one introduces explicit corrections for nonplanarity into the treatment (10) the effective pair energy ε_2 falls slightly, the decrease being greater the larger the corrections. This means that the inclusion of nonplanarity effects would serve to decrease the δ_2 values rather than increase them. Thus, slight deviations from the two-dimensional model cannot account for the observed results.

(b) Deficiencies in the Potential Energy Models

Although neither the (12,6) nor (12,6,3) model fits the data perfectly, in both cases the agreement is certainly adequate (4). It therefore seemed unlikely that the fairly small deficiencies here could account for the very large discrepancy between the theoretical and experimental δ values. However, as a further check we have fitted both sets of data to a Sutherland $(\infty,6)$ model. The effective interaction energies found are listed in Table I. The bulk gas ε for this model was obtained from the (12,6) value and the reduced Boyle temperatures:

$$T_B^*(12,6)/T_B^*(\infty,6) = \epsilon(\infty,6)/\epsilon(12,6).$$

This gave the value $\varepsilon/k(\infty,6) = 351$ °K. The Δ values for this potential are, as one might anticipate, considerably larger than for the other models. It is clear, however, that there is no correlation between the magnitudes of Δ and δ_2.

Of course, what one would really like to do is to fit the data to a model which is more realistic than those employed here, although it is likely that any such function would have to be constructed semiempirically, and probably without much theoretical justification.

(c) Assumed Potential Parameters for the Bulk Gas Phase

This possibility can be dismissed at once as a serious source of discrepancy. Although η, ε_2, and Δ are quite sensitive to the choice of (12,6) bulk parameters (4), the degree of sensitivity for δ_2 is not nearly so great. Furthermore, the energy parameters for argon to be found in the literature are all very similar, differing by no more than about 3%.

(d) Errors in the Experimental Measurements

The results for the Ar-P33 system were obtained with a highly precise apparatus, and are probably the most accurate adsorption measurements in the literature (11, 12). It is a bit

Can. J. Chem. Downloaded from www.nrcresearchpress.com by 210.87.254.6 on 09/05/12
For personal use only.

difficult to estimate the accuracy of Freeman's results (8) as error limits are not given in his paper, but it is unlikely that his measurements are inaccurate by more than $\pm 5\%$. In order to investigate the maximum effect of experimental uncertainties on δ_2, we have doubled this error limit and arbitrarily assumed a $\pm 10\%$ variation in each of the four experimental $B^{(2)}/A$ values for the Ar-BP71 system. We have proceeded as follows. For each point one either adds or subtracts the 10% or leaves the value unchanged. There are thus a total of 3^4 permutations to be tried. The computer time involved in fitting all 81 possibilities to each model is very substantial, but by examining the fit of the original data it is apparent that a large number of the permutations will lead to lower $|\eta|$ and δ_2 values. In many cases, in fact, δ_2 becomes negative. By proceeding in this way it was possible to narrow the choice to about a dozen permutations which would lead to the most significant increases in $|\eta|$. The maximum value of $|\eta|$ obtained was 0.0337, which yields the following results for the (12,6,3)) model:

$$\epsilon_2/k = 108.4\ ^\circ\text{K}, \quad \Delta = 9.51\%, \quad \delta_2 = 13.1\%.$$

The changes from the original results do not lead to substantially improved agreement with the theoretical predictions.

Of course the entire process is quite arbitrary, in that we are trying to adjust the data so as to give the best fit with the calculations, rather than *vice versa*. However, it is interesting to note that in order to obtain a δ_2 value in agreement with the predictions of eqs. [2] and [3], one must impose an error limit of at least $\pm 21\%$ on Freeman's data. We feel the supposition that errors of this magnitude are present in Freeman's work is far-fetched.

(e) Surface Heterogeneity

This is probably the most difficult factor to evaluate because of the absence of much quantitative information on the two solids. Freeman has argued at some length (13) that, by and large, virial treatments of adsorption are not much affected by surface heterogeneity. Although Freeman's view is perhaps a bit sanguine (14), we doubt that heterogeneity can play a very serious role in the present cases. P33 shows all the indications of an extremely uniform surface (15, 16) and even though BP71 is not so homogeneous, the surface area and heat of adsorption data (8) suggest that it is not very heterogeneous. For an extremely heterogeneous surface one expects that the high energy sites will fill preferentially, so that even though the average surface density may be low there are regions in which the adsorbate is quite concentrated. Under these conditions it is unlikely that plots of $\bar{N}a/p$ versus p would be linear (2), since the (Freundlich-type) isotherm does not reduce to Henry's law. There is no apparent indication of this happening with Freeman's data.

(f) Conclusions

With a slight reservation regarding the effects of surface heterogeneity, we conclude that the effect observed here is real, and that the perturbation of the pair interaction by the surface field is not directly proportional to the strength of the field (as measured by ε_{1s}). We suggest that this may be the result of a saturation effect. Not only is the apparent three-body energy smaller than previously supposed, but it also seems quite insensitive to the gas–solid interaction energy. This may indicate that a moderate surface field can perturb the pair interaction only slightly, and that a subsequent large increase in the field induces no more than a small additional perturbation. Of course this surmise is based on data for two systems only and we are not therefore prepared to comment at this time on the possible generality of the effect.

Surface Areas

The apparent surface areas of P33 and BP71 are presented in Table II. It is encouraging that both the (12,6) and (12,6,3) potentials yield the same area, and even the crude (∞,6) function gives values within $\sim 10\%$ of these, indicating that the best-fit value of A is nearly independent of the potential model chosen to represent the two-dimensional interaction. This effective model-independence lends considerable weight to the quantitative significance of areas determined from third-order adsorption data.

The present area values are in good agreement with those found from second-order (Henry's law) data alone (4). However, both second- and third-order areas are about 20% lower than the B.E.T. values, a situation which is generally true for all systems studied thus far. Of course B.E.T. estimates depend strongly upon the assumptions

TABLE II

Surface areas derived from third-order interaction data

System	Potential model	A ($m^2\ g^{-1}$)
Ar-BP71	(12,6,3)	111
	(12,6)	111
	(∞,6)	98
Ar-P33	(12,6,3)	10.4
	(12,6)	10.1
	(∞,6)	9.3

made regarding packing in the monolayer and the effective cross-sectional area of the admolecule. This is the greatest advantage of using low-coverage measurements for determining surface areas: they are unambiguous because they are independent of any estimate of molecular cross-section or monolayer packing. The experiments are somewhat more difficult at the low coverages, but the high degree of consistency found and the fact that it is unnecessary to introduce any external assumptions clearly indicate the value of the method.

1. W. A. Steele and G. D. Halsey. J. Chem. Phys. **22**, 979 (1954).
2. J. R. Sams, G. Constabaris, and G. D. Halsey. J. Chem. Phys. **36**, 1334 (1962).
3. J. A. Barker and D. H. Everett. Trans. Faraday Soc. **58**, 1608 (1962).
4. R. Wolfe and J. R. Sams. J. Chem. Phys. **44**, 2181 (1966).
5. O. Sinanoğlu and K. S. Pitzer. J. Chem. Phys. **32**, 1279 (1960).
6. R. Yaris. Thesis, University of Washington, Seattle, Wash. 1962.
7. J. D. Johnson and M. L. Klein. Trans. Faraday Soc. **60**, 1964 (1964).
8. M. P. Freeman. J. Phys. Chem. **62**, 729 (1958).
9. A. D. McLachlan. Mol. Phys. **7**, 381 (1964).
10. R. Wolfe and J. R. Sams. J. Phys. Chem. **69**, 1129 (1965).
11. G. Constabaris, J. H. Singleton, and G. D. Halsey. J. Phys. Chem. **63**, 1350 (1959).
12. J. R. Sams, G. Constabaris, and G. D. Halsey. J. Phys. Chem. **64**, 1689 (1960).
13. M. P. Freeman. J. Phys. Chem. **62**, 723 (1958).
14. D. H. Everett, J. D. Johnson, and M. L. Klein. Coloquio sobre química física de procesos en superficies sólidas, Librería Científica Medinaceli, Madrid, 1965. p. 73.
15. M. H. Polley, W. D. Schaeffer, and W. R. Smith. J. Phys. Chem. **57**, 469 (1953).
16. J. H. Singleton and G. D. Halsey. J. Phys. Chem. **58**, 330, 1011 (1954).

Can. J. Chem. Downloaded from www.nrcresearchpress.com by 210.87.254.6 on 09/05/12
For personal use only.

Can. J. Chem. Downloaded from www.nrcresearchpress.com by 210.87.254.5 on 09/05/12
For personal use only.

Recherches sur le point isohydrique et les équilibres acido-basiques de condensation ou association en chimie. XXVI. Quelques nouvelles remarques et commentaires théoriques[1]

GEORGES CARPÉNI

Laboratoire de Chimie Minérale A, Faculté des Sciences, Place Victor Hugo, Marseille (3°), France

Reçu le 12 octobre 1967

Les *données expérimentales* acquises à ce jour et relatives aux réseaux de titrage à "points isohydriques" permettent d'affirmer que (*a*) la loi électrochimique qui régit l'ensemble des équilibres acido-basiques n'est valable qu'en milieu "suffisamment dilué" et (*b*) en milieu "suffisamment concentré", les systèmes chimiques acido-basiques dissous sont très généralement le siège d'équilibres de (isopoly-)condensation ou -association, qui se superposent simultanément à ceux de dissociation; la présence des espèces isopolycondensées (sous leurs formes moléculaires et (ou) ioniques) apparaît de façon indubitable dans les réseaux de courbes de titrage, $ph = f(X,c)$, qui sont toujours isohydriques.

L'interprétation théorique du point isohydrique est basée sur un postulat, qui, autour de ce point, accorde un rôle prépondérant à l'espèce la plus condensée dont l'équivalence stoechiométrique correspond approximativement à l'abscisse isohydrique X_i, d'où la relation fondamentale

$$X_i \approx X_{\text{équiv}}^{\text{cond}} = (z/n)_m,$$

l'indice de multiplicité, m, étant fixé après calcul. La relation indiquée est étayée et justifiée par quelques arguments expérimentaux et théoriques.

Jusqu'à nouvel ordre, le postulat avancé paraît licite, car ses critères de validité n'ont jamais été mis en défaut.

On trouvera en Annexe des remarques concernant l'analogie de représentation entre point isohydrique et point isobestique.

The *experimental data* so far obtained relative to titration networks showing isohydric points (i.p.) permit us to affirm that (*a*) the classical electrochemical law which governs all the acid–base equilibria is in fact valid only for "sufficiently diluted" media and (*b*) in "sufficiently concentrated" media, the dissolved acid–base chemical systems always give rise to (isopoly-)condensation or -association equilibria which are simultaneously superposed on those of dissociation; the presence of the isopolycondensed species (under their molecular and (or) ionic forms) appears unquestionably in the titration networks, $ph = f(X,c)$, which are always "isohydric".

The *theoretical interpretation* of the i.p. is based on a postulate that, around the i.p., attributes a prominent importance to the most condensed species which has its stoichiometric equivalence approximately equal to the isohydric abscissa X_i; whence follows the fundamental relation

$$X_i \approx X_{\text{équiv}}^{\text{cond}} = (z/n)_m,$$

the multiplicity index m being found by calculation. The above relation is sustained and justified by several experimental and theoretical arguments.

Until further knowledge is obtained, the above postulate can be held to be true, as its validity has never been known to fail.

Some remarks concerning the analogy in representation between the isohydric and isobestic points can be found in the Appendix.

Canadian Journal of Chemistry, 46, 1787 (1968)

Notations

i ou p.i. Point isohydrique, lieu de convergence des courbes de titrage du réseau $pH = f(X,c)$.

x_i(ou X_i),ph_i Coordonnées du point isohydrique.

h,ph(oh,poh) Concentration (mole/l) des ions H^+, et son cologarithme (concentration des ions OH^-, et son colog.). Dans toutes les recherches présentes, les électrodes à hydrogène ou de verre sont étalonnées directement en "concentrations" des ions H^+, non en "activités".

$P(= \mathrm{d}ph/\mathrm{dlog}.c)$ Pente des courbes de dilution $ph = f(\log.c)_x$ à taux x constant. Entre $x_i - \mathrm{d}x$ et $x_i + \mathrm{d}x$,P change de signe en passant par zéro.

$$[(P < 0)_{x_i - \mathrm{d}x} \rightarrow (P = 0)_{x_i} \rightarrow (P > 0)_{x_i + \mathrm{d}x}]$$

c Concentration analytique (mole/l $\equiv M$) du soluté, supposé "monomère".

[1]Certaines des questions examinées dans le présent article ont déjà été développées par l'auteur, surtout dans la première des deux conférences données, en 1965 et 1966, à l'Institut de Chimie-Physique de Tübingen (A.F.), mais sont néanmoins restées jusqu'à présent inédites.

Can. J. Chem. Downloaded from www.nrcresearchpress.com by 210.87.254.5 on 09/05/12
For personal use only.

c_{nz} ou $c_{n;z}$ Espèce (ou composé), ou sa concentration (mole/l $\equiv M$). Une "*espèce*", définie par son degré de condensation n (nombre entier positif), peut exister sous différentes "*formes*" (molécules ou ions) suivant la valeur de sa charge z, nombre nul (molécule : $c_{n;0}$), positif ou négatif (ion : $c_{n;z}$).

k_{cn} ou $k_{c;n}$ Constante de condensation (ou d'association), exprimée en "concentrations". Exemple, pour l'équilibre $nc_{10} \rightleftharpoons c_{n0}$, on a $k_{cn} = c_{n0}.{c_{10}}^{-n}$.

k_{nz} ou $k_{n;z}$ Constante de dissociation d'ordre z, exprimée en "concentrations". Exemple, pour la dissociation de l'acide $c_{n;z-1} \rightleftharpoons c_{nz} + h$, on a $k_{nz} = c_{nz}.h.{c_{n;z-1}}^{-1}$.

$k_{nz}{}^*$ ou $k_{n;z}{}^*$ Constante de dissociation globale, pour les z premières acidités successives. On a

$$k_{nz}{}^* = k_{n1}.k_{n2} \ldots . k_{nz} = \prod_z k_{nz}.$$

x Taux de neutralisation défini par le rapport du nombre d'équivalents OH^- ajoutés (base forte titrante) au nombre de mole du soluté acide à titrer. On a $x = oh$ ajoutés/c.

X "Taux de neutralisation combiné", défini par $X = x + (h - oh)/c$. Lorsque (cas fréquent) le terme $(h - oh)/c$ est négligeable devant x, X peut être confondu avec x.

$x_{\text{équiv}}^{\text{mono}}$, $x_{\text{équiv}}^{\text{cond}}$ Taux des points d'équivalences des espèces "monomère" et "condensée" (ou "associée"), respectivement.

La définition du point isohydrique (purement expérimentale) et son interprétation théorique (à l'aide d'un postulat) ont été données, pour la première fois, en 1948. Une communication (1), une note (2) et un mémoire (3) sont ainsi à l'origine de toutes les recherches, poursuivies depuis sans interruption, portant sur les multiples problèmes progressivement surgis ou posés par cette nouvelle notion.

Cependant, à l'exception d'une revue d'ensemble, datant de 1960 (4), peu accessible et d'ailleurs volontairement plutôt descriptive, aucun article n'est venu actualiser, en quelque sorte, nos conceptions sur la question. Or, en près de 20 ans, bien que, pour l'essentiel, les bases expérimentales et théoriques n'aient pas changé, une certaine évolution, naturelle, a malgré tout eu lieu, au fur et à mesure que de nouvelles acquisitions sont venues s'ajouter aux anciennes. Le bref développement qui va suivre est destiné à combler cette manifeste lacune, en présentant succinctement l'ensemble du "problème isohydrique" sous son aspect présent.

Données expérimentales

L'électrochimie classique enseigne que, si l'on tient compte des ions H^+ et OH^- libres et éventuellement des coefficients d'activités impliqués, tout acide (ou base)[2] (qu'il soit mono- ou poly-acide, fort ou faible) conduit, par neutralisation, à une courbe de titrage *unique, indépendante de sa concentration*: les différentes courbes représentées par la fonction $ph = f(X,c)$ se réduisent en fait à une seule. La relation mathématique par laquelle la thermodynamique exprime cette loi n'est autre que celle définissant la constante de dissociation.

Or, de multiples systèmes acido-basiques montrent que cette loi n'est en réalité pas toujours valable. C'est le cas, par exemple, et pour ne citer que les principaux connus dès 1948, des acides germanique, chromique et borique. Pour tous ces composés, lorsque la concentration du soluté augmente suffisamment, le réseau $ph = f(X,c)$ forme deux fuseaux, dont les courbes, en se croisant, déterminent un point de convergence I. Comme en ce point *le ph reste constant*, donc indépendant de la concentration du soluté acide considéré, il était logique de l'appeler "point isohydrique", nom que j'ai effectivement proposé dès le début et qui, apparemment, est actuellement adopté.

Il est assez remarquable de constater que, depuis la publication de ce premier résultat, le nombre des réseaux de titrage "isohydriques" trouvés s'est considérablement accru, au point qu'actuellement et depuis déjà plusieurs années, nous cherchons, mais en vain, tant en chimie minérale qu'organique, un système qui, pour ses solutions les plus concentrées, ou saturées, *ne conduise pas* à un tel réseau isohydrique![3]

Soulignons que ce qui précède concerne des *faits expérimentaux*, bien établis, inconstestables et apparemment incontestés, indépendamment de toute interprétation théorique. Les investigations (certaines très poussées, d'autres seulement esquissées, à titre indicatif) faites ces 17 dernières années dans notre laboratoire, ont porté sur:

(1) des anions, ou acides [germanique (3, 5), borique (6*a*, 6*b*), sélénieux (7, 8*a*), arsénieux (8*a*, 8*b*), tellurique (9), molybdique (10), chromique (11), tungstique (12), phosphorique (13), périodique,[4] eau oxygénée (14)];

(2) des cations, hydratés (ou "acides", au sens de Brönsted) [$(Ga.aq)^{3+}$ (15), $(Be.aq)^{2+}$ (16), organo-stanniques $(R_2Sn.aq)^{2+}$ (17)];

(3) des acides carboxyliques, tant homologues que substitués [acides formique (18*a*), acétique (18*b*), propionique (18*c*), mono-, di- et tri-chlor-acétiques (18*d*), oxa-

[2]On sous-entend généralement qu'il s'agit de solutions *aqueuses*, mais cette condition n'est pas impérative, pas plus d'ailleurs, sauf exception (par exemple, pour des solutions *extrêmement concentrées*, etc.), que celle d'une "force ionique" constante, circonstance pourtant favorable par suite du maintien des coefficients d'activité (plus ou moins) constants.

[3]Pour le cas des acides "très forts" ($HClO_4$, HCl . . .) cf. renvoi 11.

[4]Travaux inédits.

Can. J. Chem. Downloaded from www.nrcresearchpress.com by 210.87.254.5 on 09/05/12
For personal use only.

lique (8*a*), succinique,[4] mercapto-succinique,[4] phénylacétique (19), benzoïque (20), acrylique,[4] etc.];

(4) des phénols [phenol(21), pyrocatéchol (22), résorcine,[4] hydroquinone (23)];

(5) un énol [acide ascorbique (= vitamine C) (8*a*)];

(6) un amphotère, amino-acide [glycine (8*a*)].

Au sujet de ces recherches on peut relever:

(1°) la très grande diversité des systèmes, tant au point de vue de la constitution chimique que de leur nature, minérale ou organique;

(2°) le domaine des solubilités, entièrement couvert, depuis les composés très peu solubles [tels les "hydroxydes" $Be(OH)_2$ ou $Ga(OH)_3$] jusqu'à ceux miscibles à l'eau en toutes proportions [tels que les acides phosphorique, formique, acétique].

Remarquons aussi que, suivant les systèmes, les convergences isohydriques peuvent être plus ou moins nettes[5] ou n'avoir lieu que pour des zones plus ou moins restreintes de concentrations (par exemple entre des limites $c_{minimum}$ et $c_{maximum}$).[6]

Interprétation théorique

Les données expérimentales précédentes ont montré que, lorsqu'ils étaient en solution "*suffisamment concentrée*"[7], les systèmes acido–basiques les plus divers fournissaient toujours, sans exception, des réseaux $ph = f(X,c)$ à convergence isohydrique.

La raison de ce fait paraît indubitable: en dehors des équilibres de dissociation normalement envisagés du soluté–acide, *ces* solutions "suffisamment concentrées" sont le siège d'équilibres supplémentaires entre espèces (molécules et (ou) ions) d'une part monomère, d'autre part *isopolycondensées* (ou associées). L'établissement des réseaux $ph = f(X,c)$ permet en fait de déceler immédiatement la présence de ces dernières espèces nouvelles, et nous estimons que cette procédure constitue le test le plus sûr, et le plus rapide, pour prouver l'existence de ce type d'équilibres en solution.

Cependant, dès le début, la question s'est posée: Peut-on attribuer une signification particulière à ce point de convergence?

Remarquons tout d'abord que sa présence dans les réseaux $ph = f(X,c)$ n'est pas du tout fortuite, ni exceptionnelle, mais qu'au contraire, ainsi qu'on l'a vu, il représente un fait expérimental général, au même titre, dans une certaine mesure, que le point d'équivalence, classique, de toute courbe de titrage acido–basique.

Nous basant, essentiellement, sur la *forme* de la courbe de titrage de l'acide germanique en solution pratiquement saturée [réf. 5, Fig. 1][8], nous avons intuitivement déduit que le *point isohydrique résultait, en somme, de l'intersection entre la courbe de titrage de l'acide germanique monomère* (seul présent en solution relativement très diluée ($\approx 0.0004\ M$)) *et celle d'un acide isopolycondensé électrochimiquement "plus fort"*[9]

---

[5]Expérimentalement, étant donné les incertitudes sur les valeurs *mesurées* de x_i et ph_i, le p.i. n'est en fait jamais un point rigoureux mais est défini par un petit rectangle de coordonnées $x_i \pm dx$, $ph_i \pm dph$. En général, plus les fuseaux du réseau $ph = f(X,c)$ sont aplatis, plus la convergence au p.i. est floue et les courbes paraissent confondues sur des tronçons plus ou moins larges. Dans ces cas, une représentation plus adéquate consiste à tracer les courbes "isotaux" c'est-à-dire le réseau $ph = f(c, \text{ou } \log.c)_x$ des courbes de dilution aux différents taux x. Sur de tels graphiques, un p.i. bien défini se traduit par une horizontale unique, au taux x_i. Lorsque le p.i. est flou, plusieurs courbes de taux voisins présentent des tronçons à maxima (ou minima) plus ou moins aplatis.

[6]Bien que ne désirant pas entrer dans les détails, il serait peut-être utile de signaler les quelques particularités expérimentales suivantes:

(1) pour un système donné, le p.i., et en particulier son abscisse x_i, peut se déplacer soit avec la concentration c du soluté lui-même, soit avec la force ionique de la solution, soit avec la température, ou encore, éventuellement, avec la nature du cation antagoniste (Na^+, K^+);

(2) en dehors de la zone de concentration où le réseau $ph = f(x, c_{min} < c < c_{max})$ définit la convergence isohydrique, les courbes relatives aux *autres* concentrations possibles, ne passent plus par le p.i. précédent et sont donc "extra-isohydriques", les ordonnées ph correspondant à x_i étant supérieures ou inférieures à ph_i;

(3) il arrive parfois, mais plutôt rarement, que pour certaines concentrations, x_i soit égal à l'abscisse de l'équivalence du monomère ($x_i = x^{mono}_{équiv}$); dans ce cas, le caractère "anormal" du p.i. est malgré tout manifeste, car la valeur du ph_i est nettement différente de celle du ph à l'équivalence du monomère ($ph_i \neq ph^{mono}_{équiv}$);

(4) lorsqu'il s'agit de systèmes extrêmement peu solubles (tels que par exemple les hydroxydes $Be(OH)_2$ (16) ou $Ga(OH)_3$ (15)) les p.i. apparaissent en milieu *hétérogène*: les réseaux $ph = f(X,c)$ n'en sont pas moins idohydriques, les p.i. étant d'ailleurs bien définis, surtout lorsqu'on opère à force ionique constante.

[7]Il convient de toujours attribuer au terme "concentré" sa signification *relative*, ce qui lui confère une grandeur essentiellement variable avec le système considéré. *Toute solution de concentration voisine de la saturation sera réputée "concentrée"*, quelle que soit sa concentration *effective*: ainsi, la concentration pourra être très forte, si le soluté est par exemple miscible à l'eau, dans tel autre cas, par contre, elle sera relativement très faible, le soluté étant lui-même extrêmement peu soluble.

[8]Celle-ci est en réalité une solution 0.04 *M* seulement, c'est-à-dire plutôt très diluée au sens absolu, mais *relativement* "très concentrée", puisque proche de la saturation, l'oxyde GeO_2 étant peu soluble dans l'eau. Cette remarque justifie ainsi celle qui précède[7].

[9]C'est un fait reconnu et tout à fait général que les acides isopolycondensés sont toujours "plus forts" que ceux monomères dont ils sont issus. Remarquons que s'il n'en était pas ainsi, les courbes de titrage propres aux acides monomère et condensé, supposés à l'état séparé et pur, pourraient parfaitement *ne pas se couper*, et le réseau isohydrique n'existerait plus!

Can. J. Chem. Downloaded from www.nrcresearchpress.com by 210.87.254.5 on 09/05/12
For personal use only.

dont le point d'équivalence aurait une abscisse légèrement supérieure à celle x_i du p.i. Comme, néanmoins, nous n'étions pas sûr que d'autres espèces que celles envisagées n'étaient pas également présentes, nous avons estimé devoir apporter immédiatement quelques réserves restrictives [cf. réf. 3, p. 631, colonne gauche, 1°].

Depuis 1948 cependant, de nouvelles recherches sont venues nous apporter d'autres arguments, à la fois d'ordre expérimental et théorique, tous favorables à notre conception.

En ce qui concerne les *données directes de l'expérience*, relevons:

(1) des composés "isohydriques"[10] (c'est-à-dire ayant une composition correspondant à l'abscisse x_i) sont effectivement connus [exemples: $K_2HB_5O_9$ (24); sel acide potassique du pyrocatéchol (22); disélénites $KHSe_2O_5$ et $NaHSe_2O_5$ (8), etc. .];

(2) des sels "isohydriques"[10] auparavant inconnus ont pu, au cours de nos recherches, être facilement mis en évidence et isolés [exemples: sel acide sodique du pyrocatéchol (22); $K_2Ge_5O_{11}$ (25), etc.];

(3) dans certains cas les courbes de titrage relatives aux solutions les plus concentrées, ou saturées (pour lesquelles les condensations ou associations sont forcément les plus fortes) paraissent être constituées en réalité de deux courbes de titrage distinctes et successives, chacune de forme classique, en S couché. Tout se passe comme si on titrait, d'abord, un acide "plus fort" (celui isopolycondensé) ensuite, un deuxième, "plus faible", qui n'est autre que le monomère restant ou issu du précédent par "dégradation alcaline" [exemples: titrage des acides (*a*) germanique en solution sursaturée (réf. 4, Fig. 6, p. 26), (*b*) propionique (réf. 4, Fig. 4, p. 20), (*c*) phénylacétique en solution saturée à 50 °C (réf. 4, Fig. 8, p. 36), etc.]. Ces nouveaux exemples viennent ainsi renforcer la première observation signalée comme étant à l'origine du postulat.

Quant aux *considérations théoriques*, développons principalement les trois aspects suivants:

(*I*) Au point isohydrique (tout comme au point d'equivalence des acides forts[11]) la pente $P(= \mathrm{d}p\mathit{h}/\mathrm{d}\log.c)$ est nulle, les valeurs de P étant inversées de part et d'autre de ces lieux de convergence: $P < 0$, *avant* X_i et $x_{\text{équiv}}^{\text{mono}}$, et $P > 0$, *après* ces deux points. Les pentes P se comportent donc de façon identique pour le p.i. comme pour le point d'equivalence habituel du monomère, et cette analogie n'est pas sans intérêt pour l'hypothèse faite d'après laquelle le p.i. est en réalité le point d'équivalence, plus ou moins approché, du composé isopoly-condensé ou -associé.

(*II*) Puisque toutes les courbes du réseau expérimental $ph = f(X,c)$ passent par le p.i., en *ce* point la thermodynamique nous autorise à écrire la suite d'égalités évidentes (cf. Notations):

$$[1] \quad h_i = k_{11}.c_{10}.{c_{11}}^{-1} = \ldots\ldots\ldots = k_{nz}.c_{n;z-1}.{c_{nz}}^{-1},$$

ou, en explicitant en fonction de X_i, n et z

$$[2] \quad h_i = k_{11}.(1 - X_i).{X_i}^{-1} = \ldots\ldots\ldots = k_{nz}.(z/n - X_i).[X_i - (z-1)/n]^{-1}.$$

A priori, ces relations incitent à envisager des équilibres fort complexes, puisque au p.i. on peut trouver à côté du monomère des espèces isopolycondensées en nombre considérable, théoriquement même infini. Pour fixer les idées, supposons, par exemple, que le p.i. ait l'abscisse $X_i = 0.4$. En tenant compte des inégalités

$$[3] \quad (z-1)/n < X_i \leqslant z/n,$$

qui relient X_i au degré n de condensation et à la

[10]Ces composés sont forcément des "sels acides", puisque leurs équivalences stoechiométriques correspondent à des taux "plus acides" que ceux où se forment les sels "chimiquement neutres" du monomère. Remarquons aussi que s'il n'est pas du tout nécessaire d'avoir autant d'espèces à l'état solide qu'en solution, il est néanmoins très vraisemblable que *les sels solides en équilibre avec leurs solutions saturées préexistent dans celles-ci*, même si leurs solubilités peuvent être très faibles. On conçoit parfaitement, par contre, des espèces "en solution" qui n'apparaissent pas à l'état solide par suite de produits de solubilités trop élevés.

[11]En réalité, dans le cas des acides très forts ($HClO_4$, HCl, . .) neutralisés par des bases très fortes (KOH, NaOH), le point d'équivalence du *monomère* est *aussi un p.i.* mais son ordonnée ph_i ne dépend que du *solvant* (de son produit ionique). Dans ces solutions, cependant, *il n'y a pas d'espèces isopolycondensées* (ou associées) aussi, si l'on tient compte, comme il se doit, des ions H^+ et OH^- libres en solution, et aussi éventuellement des coefficients d'activité, le réseau $ph = f(x,c)$ se réduit-il à une verticale *unique*, d'abscisse $x_{\text{équiv}}^{\text{mono}}$ précisément. C'est pour tenir compte de ces p.i., observés en milieux suffisamment dilués avec les acides monomères forts, que nous avons proposé (26), en 1953, la classification en p.i. "solvant" et p.i. "soluté". Rappelons que ce dernier étant seul caractéristique des espèces condensées, c'est uniquement lui qui est étudié ici.

Can. J. Chem. Downloaded from www.nrcresearchpress.com by 210.87.254.5 on 09/05/12
For personal use only.

charge z des ions formés au cours du titrage et conditionnent ainsi le passage de toutes les courbes par le p.i., les égalités précédentes deviennent:

$$[4;a] \quad h_i = k_{11}.0.6/0.4 = k_{21}.0.1/0.4 = k_{32}.0.26/0.07 = k_{42}.0.1/0.15 = k_{52}.0/0.2^{12}$$

$$[4;b] \quad h_i = k_{63}.0.1/0.07 = k_{73}.0.03/0.11 = k_{84}.0.1/0.03 = \ldots . k_{10;4}.0/0.1^{13} \ldots .$$

Des relations qui précèdent trois conséquences principales paraissent devoir être dégagées:

(A) Si la complexité envisagée, concrétisée par un nombre d'espèces considérable, est théoriquement possible, pratiquement elle ne paraît guère probable, car *cela impliquerait tout un ensemble de conditions impératives simultanées entre les constantes* k_{nz}. Dans l'exemple choisi, nous devrions en effet avoir: $k_{21}/k_{11} = 6$; $k_{32}/k_{11} = 0.042$; $k_{42}/k_{11} = 2.25$; etc... La simple logique nous incite à estimer que la *plus forte probabilité est celle liée au minimum de conditions*, d'où la limitation (*admise* dans notre postulat) à *deux* espèces, *prépondérantes*.[14]

(B) Chaque séquence *a,b*. . de la "formule [4]" se termine avec le terme relatif à un ion de condensation maximum dont l'équivalence stoechiométrique correspond précisément à l'abscisse isohydrique: $c_{52}, c_{10;4}$. . . Notre relation fondamentale $x_i \approx x_{\text{équiv}}^{\text{cond}}$ est donc retrouvée de façon également logique[15].

(C) Il convient d'écrire généralement

$$x_i \approx x_{\text{équiv}}^{\text{cond}} = (z/n)_m,$$

puisque les *mêmes* conditions d'équivalences stoechiométriques se retrouvent en fin de chaque séquence, *a,b*. . . pour les valeurs entières successives de l'indice de multiplicité m. Dans l'exemple précédent, on a en effet:

$$x_i = 0.4 \begin{cases} m = 1 \rightarrow z = 2;\ n = 5 \\ m = 2 \rightarrow z = 4;\ n = 10, \text{ etc.} . \end{cases}$$

Mais on peut encore ajouter deux observations:

(*a*) étant donné les fortes concentrations [relatives! cf. renvoi 7] des solutions, l'espèce isopolycondensée c_{nz}, de stoechiométrie $x_{\text{équiv}}^{\text{cond}} \approx x_i$, sera probablement celle de condensation n maximum compatible à la fois avec le soluté–solide et sa solution (pratiquement) saturée;

(*b*) l'indice m est toujours précisé après calcul [cf. un exemple d'application (14)].

(*III*) Il nous reste à examiner le côté théorique *quantitatif* du problème. Celui-ci consiste en fait à déterminer: d'une part, les différentes *espèces* en équilibre (sous leurs *formes* moléculaires et (ou) ioniques[16]), d'autre part, les diverses *constantes* de condensation (ou association) k_{cn} et de dissociation k_{nz} (ou des combinaisons de k_{cn} et k_{nz}) des espèces identifiées.

Il est clair que si les constituants et les constantes respectives ont pu être correctement trouvés, le calcul "en retour" du réseau expérimental, $ph = f(X,c)$, sera aisé. Plusieurs exemples de réseaux calculés ont déjà été publiés (7, 14, 17), d'autres sont sous presse (15, 16, 23) ou en cours d'étude. D'ailleurs, dans ce journal même, le mémoire qui suit (et qui porte sur les équilibres de condensation de certains composés organiques de Sn(IV), du type R_pSnCl_{4-p}) indique en détail le mode opératoire, qui est assez classique, rapide et *très général*.

---

[12]Le numérateur étant nul, il y a indétermination, puisque k_{52} doit être infini: x_i est dans ce cas un véritable point d'équivalence.

[13]De nouveau le numérateur est nul et x_i, un point d'équivalence, comme précédemment.

[14](*a*) On peut cependant concevoir que, dans certains cas et de façon éventuellement seulement approchée, *plus de deux conditions* puissent être simultanément remplies entre les constantes k_{nz}: cela constituerait plutôt l'exception, qui confirme la règle [exemples: système borique, arsénieux (?) . . .].

(*b*) Il paraît pratiquement exclu que, du moins dans l'état actuel de nos connaissances, nous puissions (pour un système donné: réseau solide/solution saturée) *démontrer*, ou calculer à priori, quelles sont les espèces thermodynamiquement stables en équilibre! Le caractère "postulat", donc indémontrable, ressort nettement de ce qui précède.

(*c*) Notons enfin que "la réciproque" (si deux espèces sont seules présentes, le réseau est forcément isohydrique) est, elle, évidemment démontrable et immédiatement, puisqu'elle résulte de l'égalité: $h_i = k_{11}(1 - X_i).X_i^{-1} = k_{nz}(z/n - X_i)[X_i - (z-1)/n]^{-1}$. Soulignons cependant, que, comme déjà remarqué [renvoi 9], ceci *implique* une constante d'espèce condensée k_{nz} *plus forte* que celle k_{11} du monomère.

[15]C'est à l'équivalence que l'inflexion au cours du titrage est généralement la plus marquée. Le schéma figurant dans notre premier mémoire [réf. 3, Fig. 2, p. 632] permet aisément de visualiser cette circonstance.

[16]*L'espèce* est essentiellement définie par son degré de condensation n, de sorte qu'elle peut comporter, normalement, à la fois la molécule et tous ses ions possibles, donc plusieurs *formes*, mais sans que ceci soit une nécessité impérative: suivant les conditions (c et ph, en particulier), certaines formes (la molécule ou certains de ses ions) peuvent seuls intervenir.

Can. J. Chem. Downloaded from www.nrcresearchpress.com by 210.87.254.5 on 09/05/12
For personal use only.

Or, les résultats théoriques quantitatifs apportent eux aussi des arguments favorables aux conceptions exposées. En effet:

(*a*) toutes les fois que les conditions d'étude d'un système donné sont suffisamment favorables pour conduire à des conclusions univoques et unanimement acceptées (soit que le système soit relativement simple, ou que les expériences soient aisément reproductibles et interprétables) nos propres résultats, *acquis sur la base des conceptions "isohydriques" générales*, sont toujours en accord avec ceux admis par l'ensemble des auteurs[17];

(*b*) dans les cas litigieux ou controversés, nos conclusions rendent correctement compte des faits et ne conduisent jamais à des incompatibilités avec les données expérimentales. Il serait vraiment étonnant que partout et toujours nos applications bénéficient de coïncidences fortuites et heureuses!

Conclusions

Les faits essentiels qui se dégagent de cette brève présentation d'ensemble du problème isohydrique sous son aspect actuel, peuvent se classer en deux catégories, suivant qu'ils relèvent de l'expérience ou de l'interprétation théorique:

(1) *Les données expérimentales* acquises à ce jour et relatives aux réseaux de titrage à points isohydriques permettent d'affirmer que:

(*a*) la loi électrochimique qui régit l'ensemble des équilibres acido–basiques[18] n'est valable, même si l'on tient compte des coefficients d'activité et des ions H^+ et OH^- libres, qu'en milieu "suffisamment dilué";

(*b*) *en milieu "suffisamment concentré", les systèmes chimiques acido–basiques dissous sont très généralement le siège d'équilibres de condensation (ou association), qui se superposent à ceux de dissociation: la présence d'espèces isopolycondensées (ou associées) (sous leurs formes moléculaires et (ou) ioniques) apparaît de façon sensible dans les réseaux des courbes de titrage* $ph = f(X,c)$, *qui sont toujours "isohydriques".*

(2) *L'interprétation théorique* des p.i. est essentiellement basée sur un postulat, que nous avons discuté et justifié, et qui peut actuellement se définir de la façon suivante: Autour du Point Isohydrique: donc en solution "suffisamment concentrée" (ou saturée) et entre certains p*h*, les équilibres de condensation (ou association) sont principalement dus à *deux* espèces *prépondérantes*, celles dont les équivalences stoechiométriques sont, respectivement, $x_{\text{équiv}}^{\text{mono}}$[19] et ($x_i \approx$) $x_{\text{équiv}}^{\text{cond}} = (z/n)_m$, m étant précisé après calcul du réseau. Si, dans les limites de c et de ph ci-dessus précisées, d'autres espèces coexistent[20], celles-ci sont le plus souvent moins condensées et en proportions moindres ou négligeables. La probabilité d'existence des espèces isohydriques (les plus condensées) diminue au fur et à mesure que les solutions deviennent de plus en plus diluées[21].

Rappelons que les arguments justificatifs présentés au cours de cet article sont soit d'ordre *expérimental* (existence de "sels isohydriques"; forme particulière des courbes de titrage des solutions les plus concentrées) soit *théoriques* (analogie entre pentes des courbes de dilution autour des p.i. et des points d'equivalence du monomère; relations et conditions thermodynamiques au p.i.; résultats quantitatifs obtenus soit en accord avec ceux de la littérature, ou en complète comptabilité avec l'expérience).

Jusqu'à nouvel ordre, le postulat avancé paraît parfaitement licite, car, comme tout postulat acceptable, ses critères de validité ("vérifiable" par ses conséquences et constamment "compatible" avec l'expérience) n'ont jamais été mis en défaut.

Annexe

Sur la comparaison entre point isohydrique (électrochimique) et point isobestique (spectrochimique) [cf. (2)]

L'analogie, visuelle, résulte de la représentation, à points de convergences, d'une part du

[17]Remarquons que, presque toujours, nos conclusions sont quand même plus complètes et présentent, de plus, certains aspects originaux. Quant à nos calculs, ils sont nettement plus simples et rapides que ceux généralement utilisés dans la littérature pour la résolution des *mêmes* problèmes (on fait d'habitude appel à des méthodes de minimisation, à l'aide d'ordinateurs, ou à d'autres techniques, également laborieuses).

[18]"La loi d'action des masses" appliquée aux solutions acido–basiques, d'où découle la définition de la constante de dissociation.

[19]Il n'est pas exclu, pour certains systèmes et entre certaines limites de concentration et de p*h*, que l'espèce monomère soit elle même en quantité négligeable; dans ces cas les équilibres principaux, prépondérants, auraient lieu entre deux espèces toutes deux condensées, de degrés n_1 et n_2 (avec $n_2 > n_1 > 1$).

[20]Cf. renvoi 14*a*.

[21]Dans certains cas, des espèces *plus condensées* que celles isohydriques pourraient également exister, mais alors les courbes ne passeraient pas par le p.i. et seraient relatives à des concentrations *plus fortes* que celles correspondant au domaine isohydrique.

réseau des courbes de titrage $ph = f(X,c)$ d'autre part du réseau des courbes d'absorption $\log.J_0/J = f(\text{pH},\lambda)$.

Cependant, si dans le domaine spectral les faits ont prouvé que la présence du point isobestique indique un équilibre entre *deux constituants* seulement[22], dans le cas du point isohydrique, les conclusions sont généralement compatibles (ainsi que les calculs le montrent) avec des équilibres n'impliquant que *deux espèces prépondérantes*. Exemples: chromates, molybdates, germanates, sélénites, eau oxygénée, hydroxodiméthylétain(IV), etc. . .

1. G. CARPÉNI. Communication, résumé dans Bull. Soc. Chim. France, 505 (1948).
2. G. CARPÉNI. Compt. Rend. **226**, 807 (1948).
3. G. CARPÉNI. Bull. Soc. Chim. France, 629 (1948).
4. G. CARPÉNI. Ann. Fac. Sci. Marseille, **30**, 3 (1960).
5. G. CARPÉNI et A. TCHAKIRIAN. Compt. Rend. **226**, 725 (1948).
6. (*a*) G. CARPÉNI. Bull. Soc. Chim. France, 1327 (1955). (*b*) R. SABBAH. Thèse Doctorat d'Etat, Marseille, France. 1965.
7. R. SABBAH et G. CARPÉNI. J. Chim. Phys. **63**, 1549 (1966).
8. (*a*) G. CARPÉNI *et al.* 7e I.C.C.C., Stockholm. Abstracts. 1962. p. 180. (*b*) P. BIANCO. Diplôme d'Etudes Supérieures, Marseille, France. 1961.
9. CL. PRAT. Diplôme d'Etudes Supérieures, Marseille, France. 1962
10. M. MICHEL et G. CARPÉNI. Travaux inédits. Cf. Ann. Fac. Sci. Marseille, **30**, 15 (1960).
11. (*a*) J. MASPOLI. Diplôme d'Etudes Supérieures, Marseille, France. 1952. (*b*) A. MARTENS. Thèse de Doctorat d'Etat, Marseille, France. 1964.
12. CH. ROQUE. Diplôme d'Etudes Supérieures, Marseille, France. 1961.
13. G. FERRONI. Diplôme d'Etudes Supérieures, Marseille, France. 1962.
14. G. CARPÉNI, J. HALADJIAN et S. POIZE. J. Chim. Phys. **61**, 733 (1964).
15. J. HALADJIAN et G. CARPÉNI. J. Chim. Phys. **64**, 1338 (1967).
16. E. LANZA et G. CARPÉNI. Electrochim. Acta, Sous presse (1967).
17. M. ASSO et G. CARPÉNI. Acad. Rep. Populare Romine, Omagiu Acad. Prof. Raluca Ripan, 81 (1966).
18. G. CARPÉNI *et al.* Congrès Intern. Union Pure Appl. Chem., Zürich, Abstracts p. 7. cf. Ann. Fac. Sci. Marseille, **30** (1960) (*a*) p. 11. (*b*) pp. 21 et 22. (*c*) p. 20. (*d*) p. 17 et tableau p. 14.
19. M. MICHEL. Thèse d'Ing. Dr., Marseille, France. 1959. Cf. Ann. Fac. Sci. Marseille, **30**, 18, 36 (1960).
20. E. FAURE. Diplôme d'Etudes Supérieures, Marseille, France. 1963.
21. G. GEHIN. Diplôme d'Etudes Supérieures, Marseille, France. 1963. Thèse de Doctorat d'Etat, Marseille, France. 1965.
22. G. CARPÉNI et Y. HAMMAN. Compt. Rend. **239**, 1632 (1954).
23. F. SPITALIER, R. SABBAH et G. CARPÉNI. J. Chim. Phys. Sous presse (1968).
24. G. CARPÉNI, J. HALADJIAN et R. PILARD. Bull. Soc. Chim. France, 1634 (1960).
25. (*a*) A. TCHAKIRIAN et G. CARPÉNI. Compt. Rend. **226**, 1094 (1948). (*b*) G. CARPÉNI, Y. HAMANN, J. HALADJIAN et G. PERINET. Bull. Soc. Chim. France, 1903 (1960).
26. G. CARPÉNI. Compt. Rend. **237**, 1088, 1154 (1953).

[22]Avec les réserves:
(1) un troisième constituant en quantité négligeable peut ne pas perturber sérieusement le réseau,
(2) le point isobestique, lui non plus, n'est pas toujours parfaitement déterminable expérimentalement [cf. renvoi 5].

Can. J. Chem. Downloaded from www.nrcresearchpress.com by 210.87.254.5 on 09/05/12
For personal use only.

Can. J. Chem. Downloaded from www.nrcresearchpress.com by 210.87.254.5 on 09/05/12
For personal use only.

Recherches sur le point isohydrique et les équilibres acido-basiques de condensation ou association en chimie. XXVII. Les hydroxocomplexes des sels organostanniques $(CH_3)_3SnCl$ et $(C_2H_5)_2SnCl_2$, en solutions aqueuses, à 25 °C et à différentes forces ioniques

MARCEL ASSO ET GEORGES CARPÉNI

Laboratoire de Chimie Minérale A, Faculté des Sciences, Place Victor Hugo, Marseille (3e), France

Reçu le 12 octobre 1967

L'étude électrométrique du chlorure de triméthylétain et du dichlorure de diéthylétain, à 25 °C et à différentes forces ioniques, conduit à des réseaux $ph = f(x,c)$ présentant, chacun d'eux, un point isohydrique (p.i.), indice de l'existence en solution d'une espèce associée, prépondérante, en équilibre avec le monomère. L'examen théorique a permis de déterminer les différentes constantes d'équilibre. Pour chacun des réseaux précédents, les valeurs des coordonnées isohydriques expérimentales et des constantes calculées sont:

(1°) Système $(CH_3)_3SnCl$–KOH

(a) "Solvant" eau

$x_i = 0.50 \pm 0.01$; $ph_i = 6.16 \pm 0.02$; $pk_e = 13.84 \pm 0.05$; $pk_{c2} + pk_{21} = 5.40 \pm 0.15$; $pk_{11} = 6.16 \pm 0.05$; $pk_{22} = 8.10 \pm 0.40$

(b) "Solvant" $K^+(Cl^-) = 2\ M$

$x_i = 0.50 \pm 0.01$; $ph_i = 6.40 \pm 0.02$; $pk_e = 13.94 \pm 0.05$; $pk_{c2} + pk_{21} = 5.45 \pm 0.20$; $pk_{11} = 6.40 \pm 0.05$; $pk_{22} = 8.40 \pm 0.40$

(2°) Système $(C_2H_5)_2SnCl_2$–KOH

(a) "Solvant" eau

$x_i = 1.50 \pm 0.01$; $ph_i = 4.62 \pm 0.02$; $pk_e = 13.85 \pm 0.05$; $pk_{12} = 4.58 \pm 0.03$; $pk_{23} = 3.30 \pm 0.10$; $pk_{11} = 2.40 \pm 0.05$; $pk_{c2} + pk_{22}^* = 3.40 \pm 0.10$

(b) "Solvant" $K^+(Cl^-) = 1\ M$

$x_i = 1.50 \pm 0.01$; $ph_i = 4.87 \pm 0.02$; $pk_e = 13.90 \pm 0.05$; $pk_{12} = 4.84 \pm 0.03$; $pk_{23} = 3.60 \pm 0.10$; $pk_{11} = 2.65 \pm 0.03$; $pk_{c2} + pk_{22}^* = 4.00 \pm 0.10$

Par ailleurs, le "sel isohydrique" (de taux $x_i = 0.5$) *inconnu* jusqu'à présent a pu être effectivement isolé: $(CH_3)_6Sn_2(OH)Cl$.

The electrometric study of the trimethyltin chloride and diethyltin dichloride, at 25 °C, and at different ionic strengths, leads to $ph = f(x,c)$ networks, each of which shows an isohydric point (i.p.), proof of the existence in solution of an associated preponderant form in equilibrium with the monomeric. The theoretical study permitted us to determine the different equilibrium constants. The values of the experimental isohydric coordinates and of the calculated constants, for each of the previous networks, are:

(1) $(CH_3)_3SnCl$–KOH System

(a) Water "Solvent"

$x_i = 0.50 \pm 0.01$; $ph_i = 6.16 \pm 0.02$; $pk_e = 13.84 \pm 0.05$; $pk_{c2} + pk_{21} = 5.40 \pm 0.15$; $pk_{11} = 6.16 \pm 0.05$; $pk_{22} = 8.10 \pm 0.40$

(b) $K^+(Cl^-) = 2\ M$ "Solvent"

$x_i = 0.50 \pm 0.01$; $ph_i = 6.40 \pm 0.01$; $pk_e = 13.94 \pm 0.05$; $pk_{c2} + pk_{21} = 5.45 \pm 0.20$; $pk_{11} = 6.40 \pm 0.05$; $pk_{22} = 8.40 \pm 0.40$

(2) $(C_2H_5)_2SnCl_2$–KOH System

(a) Water "Solvent"

$x_i = 1.50 \pm 0.01$; $ph_i = 4.62 \pm 0.02$; $pk_e = 13.85 \pm 0.05$; $pk_{12} = 4.58 \pm 0.03$; $pk_{23} = 3.30 \pm 0.10$; $pk_{11} = 2.40 \pm 0.03$; $pk_{c2} + pk_{22}^* = 3.40 \pm 0.10$

(b) $K^+(Cl^-) = 1\ M$ "Solvent"

$x_i = 1.50 \pm 0.01$; $ph_i = 4.87 \pm 0.02$; $pk_e = 13.90 \pm 0.05$; $pk_{12} = 4.84 \pm 0.03$; $pk_{11} = 2.65 \pm 0.03$; $pk_{c2} + pk_{22}^* = 4.00 \pm 0.10$

Furthermore, the "isohydric salt" ($(CH_3)_6Sn_2(OH)Cl$), corresponding to $x_i = 0.50$ but not known until now, was obtained.

Can. J. Chem. Downloaded from www.nrcresearchpress.com by 210.87.254.5 on 09/05/12
For personal use only.

Notations

k_e, pk_e Produit ionique de l'eau, (mole^2 l^{-2}) et son colog.

δ écart $|x_{\text{calculé}} - x_{\text{expérimental}}|$.

Δ écart quadratique moyen $= (\sum\delta^2/N)^{1/2}$, N étant le nombre de mesures.

Pour l'ensemble des autres notations, voir le mémoire précédent.

Introduction

Les diverses études entreprises sur les cations organostanniques, en particulier le cation $[(CH_3)_2Sn\ aq.]^{2+}$, ont montré qu'il existait, en solution, des équilibres entre monomères et espèces associées. Tobias et collaborateurs (1, 2) rendent compte des résultats expérimentaux en considérant aussi bien les espèces dimères et trimères que celles dimères et tétramères. Pour Asso et Carpéni (3), les courbes de titrage conduisent à envisager l'existence surtout d'un dimère, prépondérant au taux isohydrique. Alleston, Davies et Hancock (4), par des déterminations de masses moléculaires et analyses spectrales, estiment que l'hydrolyse des composés du type R_2SnX_2 s'accompagne de la formation des complexes successifs: $R_4Sn_2X_2O$, $R_4Sn_2X(OH)O$ et R_2SnO. Des études concernant l'influence des groupements organiques sur la liaison Sn—Cl ont été faites (5); on observe une décroissance générale d'acidité lorsqu'on passe des dérivés trialkylés aux dérivés monoalkylés. Prince (6) a étudié, par conductimétrie, les dérivés trialkylés. Cet auteur a observé une élévation de la force acide avec l'encombrement stérique des substituants. Janssen et Luijten (7) ont étudié la dissociation des chlorures de trialkylétain dans le mélange eau–éthanol à 44% d'ethanol en poids. Enfin, Kasai *et al.* (8), Luijten et Van der Kerk (9) signalent la grande solubilité de l'hydroxyde de triméthylétain, tandis que Okawara et Yasuda (10) envisagent sa dimérisation. Toutes ces études montrent que les espèces prépondérantes sont essentiellement celles monomère et dimère, sans lesquelles toute interprétation s'avère pratiquement impossible.

Nous nous sommes proposés, au cours du présent travail, d'étendre l'étude entreprise sur le cation diméthylétain, à d'autres systèmes organostanniques tels que le triméthylétain et le diéthylétain.

Comme, dans tous les cas, les courbes de neutralisation $ph = f(x,c)$ se coupent en un point de convergence bien défini, la détermination des différentes constantes d'équilibre a été faite en utilisant la théorie du point isohydrique émise par l'un de nous (11).

Produits et appareillage

Les composés $(CH_3)_3SnCl$ et $(C_2H_5)_2SnCl_2$ nous ont été fournis par la Société Billiton Chemische Industrie (La Haye). Leur pureté a été vérifiée électrométriquement à la fois par titrage acidimétrique (électrode de verre) et chlorométrique (électrode au chlorure d'argent). L'étain est dosé gravimétriquement sous forme de SnO_2, d'après la méthode de Luijten et Van der Kerk (12). Le KCl utilisé est un produit Prolabo, R.P. "Pour analyses".

Les mesures de force electromotrice ont été faites au moyen d'un ph mètre "Radiometer" à ± 0.1 mV près. La pile utilisée est du type "avec transport" et peut être schématisée comme suit:

Electrode indicatrice	solution de sel organo-stannique	siphon de KCl saturé à 25 °C	solution saturée de KCl et Hg_2Cl_2 à 25 °C	Hg

L'électrode indicatrice est une électrode de verre "Radiometer" du type basique, étalonnée en *concentration* des ions H^+, par comparaison avec une électrode à H_2, selon une méthode préconisée au laboratoire (13) et qui permet, en même temps, de déterminer la valeur du produit ionique k_e du "solvant" utilisé.

Toutes les expériences ont été faites dans un thermostat réglé à 25 ± 0.05 °C et à l'abri du CO_2 atmosphérique.

Lorsqu'on a voulu opérer à force ionique sensiblement constante, nous avons ajouté du KCl, à concentration relativement élevée par rapport à celle du soluté, de façon à maintenir la concentration *cationique* constamment égale à $[K^+(Cl^-)] = 2\ M$.[1]

Résultats expérimentaux

(*A*) Les réseaux des courbes de neutralisation, à différentes concentrations, $ph = f(x,c)$, présentent un p.i. d'abscisse $x_i = 0.50$ pour le dérivé triméthylé et $x_i = 1.50$ pour le dérivé diéthylé. Les résultats sont donnés sous formes de "courbes expérimentales" et "points calculés" (Figs. 1, 2). A titre d'exemple, les abscisses expérimentales et calculées ainsi que les écarts quadratiques moyens relatifs à la Fig. 1 sont indiqués dans le Tableau I. Dans les autres cas, nous avons simplement donné les valeurs des constantes d'équilibre.

[1]Il est évidemment impossible d'avoir une concentration constante à la fois en anion *et* en cation. Notre choix a été déterminé:

(1) par le fait que, dans le cas présent, l'isopolyassociation intéresse le *cation*;

(2) parce que le fonctionnement de l'électrode de verre semble meilleur dans ces conditions.

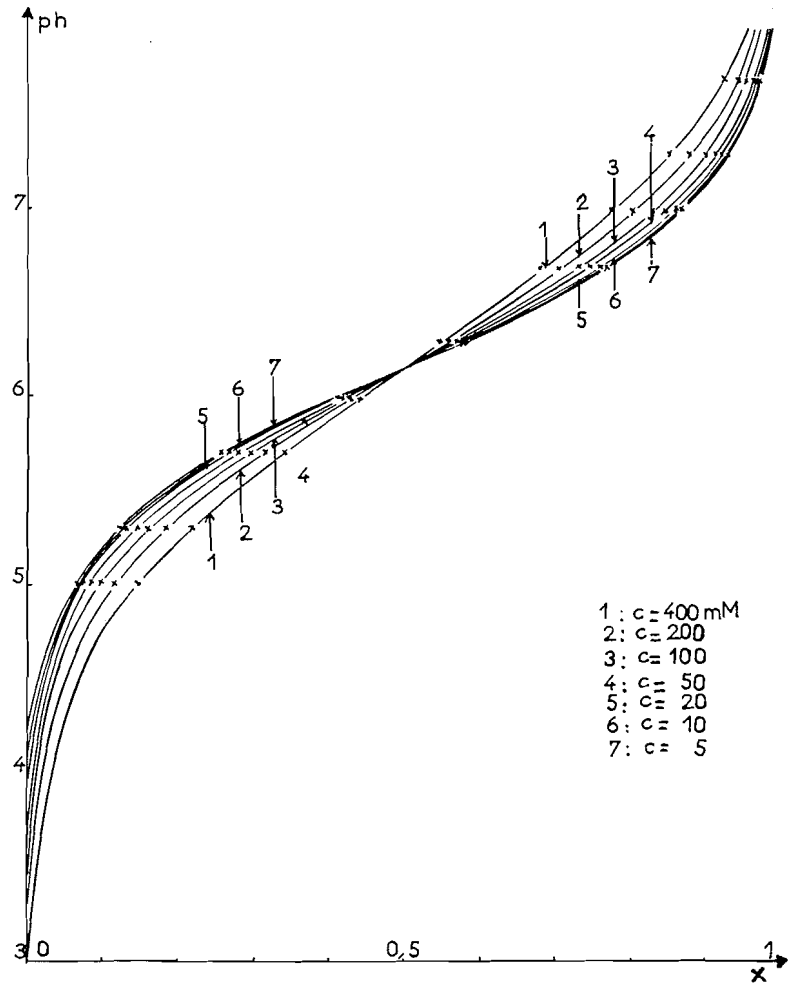

FIG. 1. Réseau des courbes de neutralisation $ph = f(x,c)$ de $(CH_3)_3SnCl$ par KOH, à 25 °C, en milieu "eau": courbes expérimentales en traits plein; points, pour les valeurs calculées.

(*B*) L'étude du système $(CH_3)_3SnCl$–$(CH_3)_3SnOH$–H_2O par la méthode des restes (de Schreinemakers) a permis d'isoler 3 phases solides, dont l'une (celle correspondant au sel acide "isohydrique" $(CH_3)_6Sn_2ClOH$, de taux $x_i = 0.5$) n'était pas jusqu'ici mentionnée dans la littérature.

Interpretation des résultats expérimentaux

La dissolution dans l'eau des sels organostanniques entraîne une dissociation ionique, en même temps qu'une acidification attribuable à la dissociation "acide" (au sens de Brönsted) des cations stanniques hydratés; il apparaît donc, en solution, d'une part, des ions Cl^- et, d'autre part, des cations organométalliques hydratés, plus ou moins "acides".

Pour le chlorure de triméthylétain, peuvent ainsi être envisagées les réactions totales ou équilibrées[2]:

[1] $(CH_3)_3SnCl \rightarrow [(CH_3)_3Sn]^+ + Cl^-$

(dissociation pratiquement totale) et

[2] $[(CH_3)_3Sn]^+ + H_2O \rightleftharpoons (CH_3)_3SnOH + H^+$

ou, symboliquement (cf. Notations)

[3] $c_{10} \rightleftharpoons c_{11} + h$ (avec $k_{11} = c_{11}hc_{10}^{-1}$)

et, éventuellement, aussi des réactions d'association.

[2]Pour simplifier l'écriture, les molécules d'eau d'hydratation (en particulier celles coordinées autour des atomes Sn) ne figurent pas dans les formules. On peut noter, par ailleurs, que l'hydrolyse pourrait être "interne", c'est-à-dire avoir lieu aux dépens de l'eau coordinée précisément.

Can. J. Chem. Downloaded from www.nrcresearchpress.com by 210.87.254.5 on 09/05/12
For personal use only.

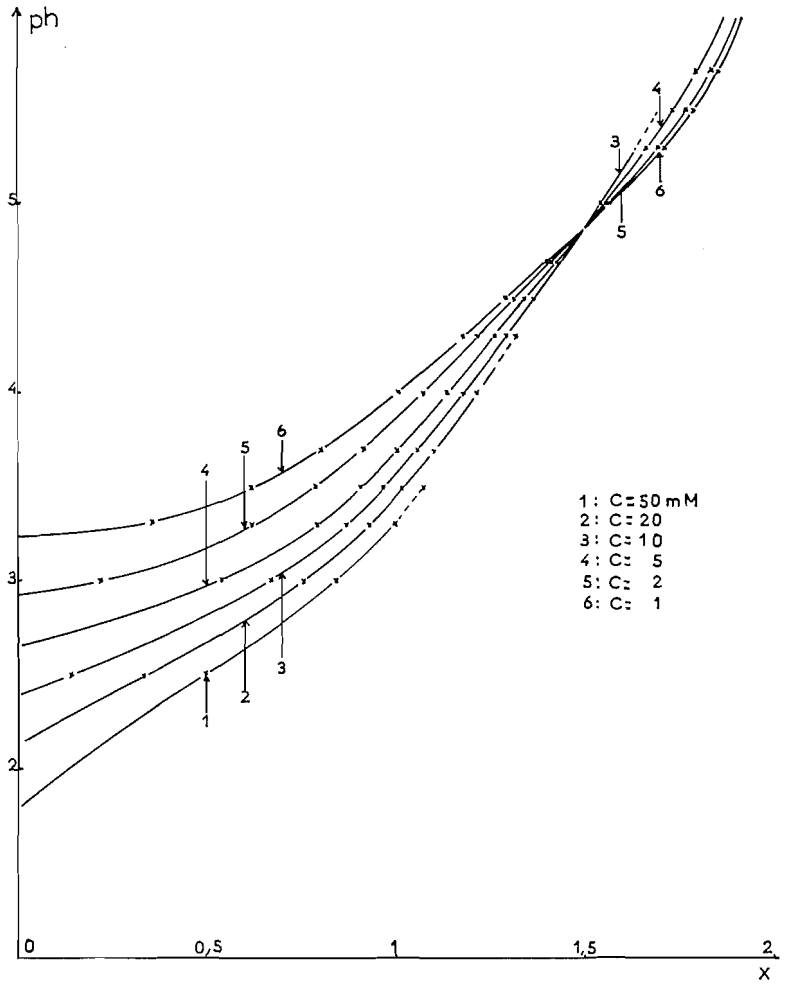

FIG. 2. Réseau des courbes de neutralisation $ph = f(x,c)$ de $(C_2H_5)_2SnCl_2$ par KOH, à 25 °C, en milieu "$K^+(Cl^-)$" = 1 *M*: courbes expérimentales en traits pleins; points, pour les valeurs calculées.

TABLEAU I

Réseau $ph = f(x,c)$ expérimental et calculé: titrage de $(CH_3)_3SnCl$ par KOH à 25 °C ("solvant" eau). Coordonnées isohydriques: $x_i = 0.50$, $ph_i = 6.16$. Constantes: $pk_e = 13.85$; $pk_{11} = 6.16$; $pk_{22} = 8.15$; $pk_{c2} + pk_{21} = 5.40$

	$c = 0.4$		$c = 0.2$		$c = 0.1$		$c = 0.05$		$c = 0.02$		$c = 0.01$		$c = 0.005$	
ph	x_{exp}	x_{cal}	x_{exp}	x_{cal}	x_{exp}	x_{cal}	x_{exp}	x_{cal}	x_{exp}	x_{cal}	x_{exp}	x_{cal}	x_{exp}	x_{cal}
5.00	0.150	0.147	0.117	0.115	0.096	0.092	0.082	0.080	0.074	0.071	0.068	0.068	0.065	0.065
5.30	0.217	0.224	0.183	0.186	0.165	0.160	0.144	0.142	0.135	0.130	0.128	0.125	0.122	0.122
5.70	0.340	0.346	0.315	0.319	0.295	0.296	0.282	0.279	0.265	0.267	0.257	0.262	0.255	0.255
6.00	0.445	0.447	0.430	0.436	0.420	0.426	0.422	0.419	0.415	0.413	0.410	0.411	0.408	0.409
6.16	0.500	0.502	0.500	0.501	0.500	0.501	0.500	0.500	0.500	0.500	0.500	0.500	0.500	0.500
6.30	0.552	0.550	0.560	0.558	0.567	0.565	0.573	0.571	0.578	0.576	0.580	0.578	0.580	0.580
6.70	0.686	0.683	0.710	0.712	0.740	0.736	0.750	0.753	0.765	0.765	0.773	0.769	0.770	0.772
7.00	0.778	0.775	0.805	0.809	0.835	0.836	0.850	0.852	0.860	0.864	0.872	0.868	0.872	0.870
7.30	0.860	0.855	0.880	0.884	0.902	0.906	0.915	0.918	0.920	0.926	0.932	0.930	0.932	0.934
7.70	0.930	0.927	0.945	0.946	0.955	0.957	0.967	0.964	0.973	0.969	0.972	0.970	0.970	0.972
8.00	0.962	0.959	0.972	0.971	0.976	0.978	0.980	0.983	0.988	0.985	0.986	0.986	0.986	0.987
Δ	0.005		0.004		0.004		0.003		0.003		0.002		0.001	

Can. J. Chem. Downloaded from www.nrcresearchpress.com by 210.87.254.5 on 09/05/12
For personal use only.

Can. J. Chem. Downloaded from www.nrcresearchpress.com by 210.87.254.5 on 09/05/12
For personal use only.

Pour le dichlorure de diéthylétain, on aurait de même les équilibres:

[4] $(C_2H_5)_2SnCl_2 \rightarrow [(C_2H_5)_2Sn]^{2+} + 2Cl^-$

[5] $[(C_2H_5)_2Sn]^{2+} + H_2O \rightleftharpoons [(C_2H_5)_2SnOH]^+ + H^+$

soit $c_{10} \rightleftharpoons c_{11} + h$; $(k_{11} = c_{11}hc_{10}^{-1})$

[6] $[(C_2H_5)_2SnOH]^+ + H_2O \rightleftharpoons (C_2H_5)_2Sn(OH)_2 + H^+$

[7] soit $c_{11} \rightleftharpoons c_{12} + h$; $(k_{12} = c_{12}hc_{11}^{-1})$.

La présence, dans un réseau de titrage électrométrique $ph = f(x,c)$, d'un p.i. implique, d'après la théorie de Carpéni (11) les conséquences suivantes:

—l'existence, en solution, d'un équilibre entre 2 espèces principales, ions et molécules *monomères*, d'une part, ions et molécules associés ou condensés, d'autre part;

—l'espèce associée ou condensée, *prépondérante* autour du p.i., possède une courbe de titrage qui doit, elle aussi, passer par ce point;

—le degré n d'association ou de condensation, et le nombre z de liaisons OH, de l'ion c_{nz}, sont liés par la relation: $x_i \approx (z/n)_m$, où m est un facteur de multiplicité. Pour $m = 1$, correspondant à la solution la plus simple du problème, l'abscisse du p.i. $x_i = 0.5 = 1/2$ (cas du triméthyl étain) donne $z = 1$ et $n = 2$ d'où l'ion $c_{21} = [(CH_3)_6Sn_2(OH)]^+$, alors que avec $x_i = 1.50 = 3/2$ (cas du diéthylétain), on aura $z = 3$ et $n = 2$, d'où l'ion $c_{23} = [(C_2H_5)_4Sn_2(OH)_3]^+$.

Dans les deux cas, la théorie conduit ainsi *immédiatement* à des *dimères*. Le calcul ultérieur prouvera si ces conclusions sont compatibles, effectivement, avec l'expérience.

La marche adoptée pour l'analyse quantitative des résultats est la suivante:

On calcule, tout d'abord, (la ou) les constantes de dissociation du *monomère*, en se plaçant sur la courbe expérimentale *la plus diluée*, qui correspond en général aux solutions exemptes d'espèces associées.

On détermine, ensuite, au moyen des équations de "conservation" des masses et des fonctions hydroxydes (cf. Notations)

[8] $$c = \sum_n \sum_z nc_{nz}$$

[9] $$cX = \sum_n \sum_z zc_{nz}$$

les constantes relatives aux différents équilibres de la forme dimère.

Chlorure de triméthylétain

(a) Constante du monomère

Ce système ne présente qu'une seule fonction acide (k_{11}), aussi l'étude de la forme monomère s'effectue-t-elle très simplement, et avec une très bonne approximation, au point de demi-neutralisation, soit à $x = 0.50$. La valeur de la constante k_{11} obtenue est vérifiée en d'autres points de la courbe expérimentale, et, en particulier au p.i. On a, en effet:

[10] $$k_{11} = hx(1 - x)^{-1} = h_i x_i (1 - x_i)^{-1}.$$

Le calcul conduit à:

$pk_{11} = 6.16 \pm 0.05$, dans le "solvant" eau

$pk_{11} = 6.40 \pm 0.05$, dans le "solvant" $K^+(Cl^-) = 2\ M$.

(b) Constantes du dimère

L'hypothèse dimère nous conduit à envisager les équilibres symboliques suivants:

[11] $c_{10} + c_{11} \rightleftharpoons c_{21}$, de constante globale: $k_{c2}k_{21}k_{11}^{-1} = c_{21}c_{10}^{-1}c_{11}^{-1}$

[12] et $c_{21} \rightleftharpoons c_{22} + h$, de constante: $k_{22} = c_{22}hc_{21}^{-1}$

Les équations de "conservations" deviennent:

$$c = c_{10} + c_{11} + 2c_{21} + 2c_{22}$$

$$cX = c_{11} + c_{21} + 2c_{22}$$

soit, en explicitant:

[13] $$c = c_{10}(1 + k_{11}h^{-1}) + c_{10}^2(2k_{c2}k_{21}h^{-1} + 2k_{c2}k_{22}{}^*h^{-2})$$

[14] $$cX = c_{10}k_{11}h^{-1} + c_{10}^2(k_{c2}k_{21}h^{-1} + 2k_{c2}k_{22}{}^*h^{-2}).$$

La résolution de ce système fournit les valeurs des constantes $k_{c2}k_{21}$ et k_{22} cherchées. On peut simplifier les calculs en négligeant la forme $c_{22} \equiv [(CH_3)_6Sn_2(OH)_2]$ dans la première partie du réseau ($0 < x < 0.5$). En calculant au préalable le paramètre c_{10}, une valeur moyenne de $k_{c2}k_{21}$ est obtenue aisément.

On trouve ainsi:

(1°) milieu "eau": $pk_{c2} + pk_{21} = 5.40 \pm 0.15$;

(2°) milieu "$K^+(Cl^-)$" $= 2\ M$: $pk_{c2} + pk_{21} = 5.45 \pm 0.20$.

L'introduction ultérieure de c_{22}, surtout dans les régions de taux élevés ($0.7 < x < 1$), permet finalement d'atteindre les valeurs: $pk_{22} = 8.1$

Can. J. Chem. Downloaded from www.nrcresearchpress.com by 210.87.254.5 on 09/05/12
For personal use only.

$\pm$ 0.4 dans le "solvant" eau, et $pk_{22} = 8.4$ $\pm$ 0.4 dans le "solvant" $K^+(Cl^-) = 2\ M$.

Le calcul des x à partir de ces valeurs, nous a permis de constater qu'elles convenaient réellement, car les écarts entre les x expérimentaux et x calculés, n'excèdent pas 1/100 de taux, précision de l'ordre de l'erreur expérimentale moyenne.

Dichlorure de Diéthylétain

(a) Constantes du monomère

Puisque la forme monomère c_{10} se comporte comme un acide dibasique, dont la courbe de titrage ne présente, pratiquement, pas d'inflexion marquée à la première stoechiométrie, ses constantes de dissociation k_{11} et k_{12} doivent, en fait, intervenir pour toute la zone de $x = 0$ à $x = 2$.

On évalue tout d'abord k_{12} au point de demi-neutralisation de la deuxième fonction acide, soit à $x = 1.50$, qui est pratiquement aussi le p.i. du réseau. On obtient, au moyen de la relation

$$[15] \quad k_{12} = hc_{12}c_{11}^{-1} = h_i(X_i - 1)(2 - X_i)^{-1}$$

dans le "solvant" eau: $pk_{12} = 4.58 \pm 0.03$, dans le "solvant" $K^+(Cl^-) = 1\ M$: $pk_{12} = 4.84 \pm 0.03$.

Ayant k_{12}, on détermine ensuite k_{11}, en se servant des équations de "conservation" relatives au monomère:

$$c = c_{10} + c_{11} + c_{12}$$
$$cX = c_{11} + 2c_{12}$$

et en faisant le calcul en plusieurs points expérimentaux. L'équation

$$[16] \quad k_{11} = X\,[h^{-1}(1 - X) + h^{-2}k_{12}(2 - X)]^{-1}$$

conduit à: $pk_{11} = 2.40 \pm 0.05$, dans le milieu "eau" et $pk_{11} = 2.65 \pm 0.05$, dans le milieu "$K^+(Cl^-)$" $= 1\ M$.

(b) Constantes du dimère

L'espèce dimère prépondérante au point isohydrique serait le complexe $c_{23} \equiv [(C_2H_5)_4Sn_2(OH)_3]^+$ formé d'après l'équilibre:

$$[17] \quad 2[(C_2H_5)_2Sn]^{2+} + 3OH^- \rightleftharpoons [(C_2H_5)_4Sn_2(OH)_3]^+$$

ou, symboliquement, pour séparer l'équilibre de condensation (ou association) proprement dit, de celui de dissociation (neutralisation):

$$[18] \quad 2c_{11} \rightleftharpoons c_{22} \text{ de constante globale } k_{c2}k_{22}^*k_{11}^{-2} = c_{22}c_{11}^{-2}$$

$$[19] \quad c_{22} \rightleftharpoons c_{23} + h, \text{ de constante } k_{23} = c_{23}hc_{22}^{-1}.$$

Une valeur approchée de k_{23} peut être immédiatement obtenue en se servant des coordonnées du p.i. d'après la relation (du type Henderson–Hasselbalch):

$$[20] \quad k_{23} = hc_{23}c_{22}^{-1} = h_i(X_i - 1)(1.5 - X_i)^{-1}.$$

L'abscisse isohydrique (en X) étant $X_i = 1.47$ dans les 2 milieux, on trouve: $pk_{23} = 3.30 \pm 0.10$ dans le "solvant" eau, $pk_{23} = 3.60 \pm 0.10$ dans le "solvant" $K^+(Cl^-)$ 1 M.

On détermine, ensuite, dans la majeure partie du réseau ($0.3 < x < 1.7$), le produit de constantes $k_{c2}k_{22}^*$ relatif à la forme $c_{22} = [(C_2H_5)_4Sn_2(OH)_2]^{2+}$, au moyen des équations:

$$c = c_{10} + c_{11} + c_{12} + 2c_{22} + 2c_{23}$$
$$cX = c_{11} + 2c_{12} + 2c_{22} + 3c_{23},$$

soit, explicitement:

$$[21] \quad c = c_{10}(1 + k_{11}h^{-1} + k_{12}^*h^{-2}) + c_{10}^2(2k_{c2}k_{22}^*h^{-2} + 2k_{c2}k_{23}^*h^{-3})$$

$$[22] \quad cX = c_{10}(k_{11}h^{-1} + 2k_{12}^*h^{-2}) + c_{10}^2(2k_{c2}k_{22}^*h^{-2} + 3k_{c2}k_{23}^*h^{-3}).$$

On obtient ainsi une valeur moyenne du produit $k_{c2}k_{22}^*$: $pk_{c2} + pk_{22}^* = 3.40 \pm 0.10$ dans le milieu "eau", $pk_{c2} + pk_{22}^* = 4.00 \pm 0.10$ dans le milieu "$K^+(Cl^-)$" $= 1\ M$.

On a essayé de déterminer k_{21} (relative à la forme c_{21}) dans la première partie du réseau ($0 < x < 0.50$), et k_{24} (relative à c_{24}) en dernière partie du réseau ($1.5 < x < 2$). N'ayant pu obtenir des valeurs significatives de ces constantes, il semble que les espèces c_{21} et c_{24} soient ou négligeables ou pratiquement absentes en solution. Pour vérifier si les diverses constantes ainsi déterminées convenaient réellement, des réseaux théoriques ont été construits pour les différentes concentrations utilisées dans les expériences. Les valeurs de x calculées ont été portées sur les graphiques (petites croix dans les Figs. 1, 2) et dans le Tableau I.

L'accord est très satisfaisant et les écarts quadratiques moyens (cf. Notations), pour les quatre systèmes calculés, sont de l'ordre de 5×10^{-3}, soit inférieurs aux erreurs moyennes expérimentales.

Les Figs. 3 et 4 représentent graphiquement les pourcentages relatifs des différentes espèces

Can. J. Chem. Downloaded from www.nrcresearchpress.com by 210.87.254.5 on 09/05/12
For personal use only.

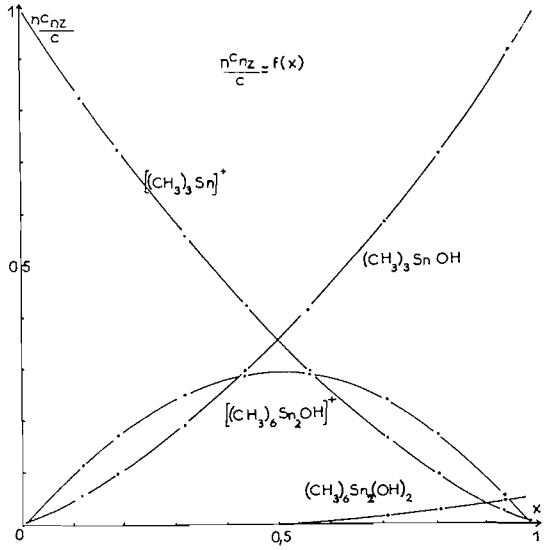

FIG. 3. Concentrations relatives nc_{nz}/c des espèces moléculaires et ioniques monomères et dimères, en équilibre, au cours du titrage d'une solution de $(CH_3)_3SnCl$ 0.2 *M* par KOH, à 25 °C, en milieu "$K^+(Cl^-)$" = 2 *M*.

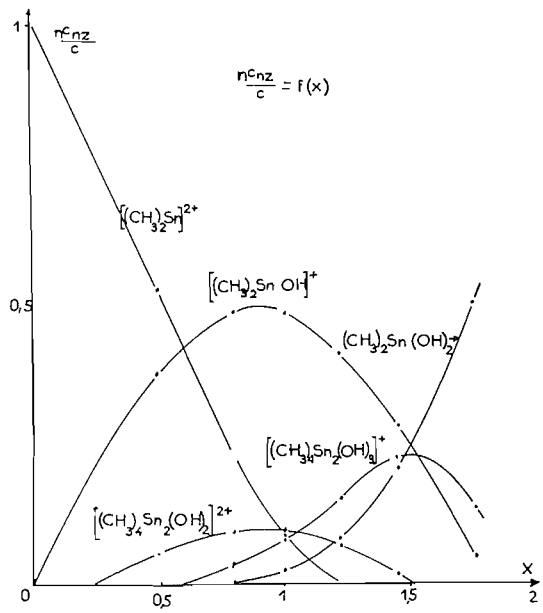

FIG. 4. Concentrations relatives nc_{nz}/c des espèces moléculaires et ioniques monomères et dimères, en équilibre, au cours du titrage d'une solution de $(C_2H_5)_2SnCl_2$ 0.01 *M*, par KOH, à 25 °C, en milieu "$K^+(Cl^-)$" = 1 *M*.

en solution pour des concentrations relativement élevées. Un diagramme ternaire du système $(CH_3)_3SnCl$–$(CH_3)_3SnOH$–H_2O a été également tracé (Fig. 5). On observe que l'addition d'ions OH^- favorise la dimérisation. *La concentration de la forme associée est maximum au taux isohydrique et le solide correspondant précipite également à ce taux* (sa solubilité est donc congruente). On constate ainsi, une fois de plus, que le p.i. permet non seulement de rendre aisément compte des équilibres en solution, mais fourni correctement, en même temps, la composition du solide précipité.

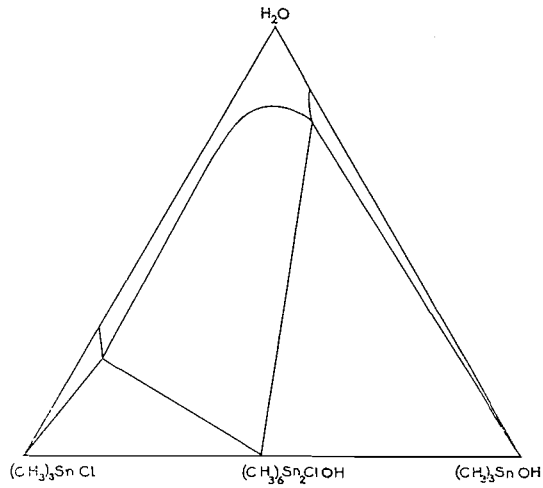

FIG. 5. Diagramme d'équilibre ternaire du système $(CH_3)_3SnCl$–$(CH_3)_3SnOH$–H_2O, à 25 °C, en g %.

Conclusion

L'étude des systèmes $(CH_3)_3SnCl$ et $(C_2H_5)_2SnCl_2$ faite par électrométrie a permis d'obtenir des réseaux de titrage $ph = f(x,c)$ qui, comme toujours, présentent des convergences isohydriques, indice de l'existence d'une espèce associée prépondérante, en équilibre avec le monomère. Les résultats obtenus (en parfaits accords avec la théorie du point isohydrique) font intervenir à côté des espèces monomères, essentiellement les espèces *dimères*: $c_{21} = [(CH_3)_6Sn_2OH]^+$ et $c_{22} = (CH_3)_6Sn_2(OH)_2$ pour le triméthylétain, $c_{22} = [(C_2H_5)_4Sn_2(OH)_2]^{2+}$ et $c_{23} = [(C_2H_5)_4Sn_2(OH)_3]^+$ pour le diéthylétain.

1. R. S. TOBIAS, I. OGRINS et B. A. NEVETT. Inorg. Chem. **1**, 638 (1962).
2. R. S. TOBIAS et M. YASUDA. Can. J. Chem. **42**, 781 (1964).
3. M. ASSO et G. CARPÉNI. Acad. Rep. Populare Romîne, Omagiu Acad. Prof. Raluca Ripan, 81 (1966).
4. D. L. ALLESTON, A. G. DAVIES et M. HANCOCK. J. Chem. Soc. 5744 (1964).
5. R. S. TOBIAS, H. N. FARRER, M. B. HUGHES et B. A. NEVETT. Inorg. Chem. **5**, 2052 (1966).
6. R. H. PRINCE. J. Chem. Soc. 1783 (1959).

7. M. J. JANSSEN et J. G. A. LUIJTEN. Rec. Trav. Chim. **82**, 1008 (1963).
8. N. KASAI, K. YASUDA et R. OKAWARA. J. Organometal. Chem. Amsterdam, **3**, 172 (1965).
9. J. G. A. LUIJTEN et G. J. M. VAN DER KERK. Rec. Trav. Chim. **82**, 1179 (1963).
10. R. OKAWARA et K. YASUDA. J. Organometal. Chem. Amsterdam, **1**, 360 (1964).
11. G. CARPÉNI. (*a*) Compt. Rend. **226**, 807 (1948). (*b*) Bull. Soc. Chim. France, 629 (1948). (*c*) Ann. Fac. Sci. Marseille, **30**, 3 (1960).
12. J. G. A. LUIJTEN et G. J. M. VAN DER KERK. Investigations in the field of organotin chemistry. Tin Research Institute, Columbus, Ohio. p. 83. 1955.
13. G. CARPÉNI, J. HALADJIAN et S. POIZE. J. Chim. Phys. **61**, 733 (1964).

Can. J. Chem. Downloaded from www.nrcresearchpress.com by 210.87.254.5 on 09/05/12
For personal use only.

Can. J. Chem. Downloaded from www.nrcresearchpress.com by 210.87.254.5 on 09/05/12
For personal use only.

Electrocrystallization and surface diffusion: Effect of chemical reaction in the solution

S. K. RANGARAJAN
Central Electrochemical Research Institute, Karaikudi-3, India

Received July 14, 1967

A theoretical solution to the problem of electrochemical crystal growth when (*a*) surface diffusion, (*b*) diffusion in the solution phase, and (*c*) a chemical reaction in the solution are all present is derived. The rate of lattice incorporation is assumed to be finite. A generalized impedance function is derived and its characteristics discussed.

Canadian Journal of Chemistry, **46**, 1803 (1968)

1. Introduction

The theory that surface diffusion can be a slow step in the overall mechanism for electrochemical crystal growth has been proposed (1–5)[1] and experimental evidence from techniques employing faradaic impedance (2, 3) potential step (4), and galvanostatic charging transients (1, 4–6) are advanced. The earlier theories (1, 2, 7, 8) (barring an attempt by Lorenz (3)) were confined to conditions of null-concentration polarization in the solution phase. However, a mathematical formalism developed recently (9, 10) takes into account the diffusion in the solution as well.

The earlier studies (9, 10) treated the diffusion effects in the absence of any prior chemical reaction in solution. We consider in this paper the more general problem of the interaction of bulk diffusion of metal ions with the surface diffusion of adatoms in the presence of a homogeneous reaction. Thus the theory developed here may be useful when a partial dehydration of the metal ions is essential prior to the discharge step or if the oxidant is a complex ion and the concentration polarization for the complexing substance cannot be ignored. The emphasis made by this paper is on the formal, rigorous solution to the mathematical problem. In a subsequent communication, theoretical curves computed on the basis of these results and comparison with the experimental findings of Lorenz and those planned in this Laboratory will be discussed.

In this paper, we present theoretical results concerning the time dependence of the current when the overpotential is kept constant. An expression for the generalized impedance that would formally represent the interface (under certain conditions) is also presented. Some of the earlier results worked out for less general schemes are shown to follow from the solutions given in this paper.

An essential feature characterizing these problems of electrodeposition is the distinction made between the region where the electrochemical charge transfer takes place and sites where the products are to be 'delivered'. The phenomenon linking the two, viz. charge transfer and the adatom incorporation, is the surface diffusion.

Models describing the mechanism of electrochemical crystal growth and the surface structure are both required. The mathematical complexity introduced by even the most elementary description of the 'actual' physical situation limits one to idealizations even if somewhat unsatisfactory.

2. Reaction Schemes

Of the several steps that may constitute the overall scheme of lattice buildup, only the following are considered in this paper: (i) a homogeneous chemical reaction in solution, that is formally monomolecular; (ii) the diffusion of the reactive species to the surface from the bulk of the solution; (iii) the electrochemical charge transfer at the surface; (iv) diffusion of adatoms along the surface to the lattice building sites, viz. edges; (v) lattice incorporation, i.e.

$$\text{metal atom (adsorbed)} \rightleftharpoons \text{metal atom (lattice)}.$$

Though the 'order of events' described here refer to deposition conditions, this scheme and the following discussion could easily be adapted to dissolution conditions as well.

[1]Reference 1 provides a detailed report on the galvanostatic experiments of the Philadelphia School.

Can. J. Chem. Downloaded from www.nrcresearchpress.com by 210.87.254.5 on 09/05/12
For personal use only.

It has been recognized that the lattice incorporation may not be in 'equilibrium', i.e. the rate of adatoms along the surface may be comparable with or less than the rate at which the adatoms lodge themselves in the kinks. The slowness at this incorporation stage may arise from several factors. For example, allowing that adatoms are not wholly desolvated, the reaction (v), viz. adatom (surface) $\rightleftharpoons$ metal atom (lattice), which demands a complete desolvation, can be slow indeed.

Moreover, incorporation of the adatoms into the kinks need not always occur with unit probability (11). Assumption of a finite rate of 'lattice incorporation' is an acknowledgment of the fact that the diffusing species may be either reflected from or reversibly captured at steps. Again, the assumption that the concentration gradient on the surface is one-dimensional and is edge-oriented may become unrealistic if the density of kinks is not too large. A finite incorporation rate postulated at the edge can thus be useful under such conditions which prevent the edges from playing the role of ideal kinks.

3. Model for the Surface

The model assumed for the surface structure, however, is the same as done earlier (1*b*). The surface is composed of a planar region which is 'acceptable' as far as the 'charge transfer' goes but not for the lattice incorporation. The lattice building sites are to be reached by the 'discharged species', adatoms (or adions), by diffusion. The edges provide the lattice-building sites and, in turn, are made available 'continuously' by screw dislocations. Yet another simplification adverted to, primarily to simplify the mathematical apparatus, is that edges form a parallel array with an inter-step distance, $2l$, say. While dealing with a surface not populated by 'fully developed' screw dislocations, $2l$ is to be related to the density of dislocations. The edges are identified with the steps introduced by the pairs of dislocations of opposite sign emerging with screw component perpendicular to the surface (1*c*).

There is no doubt that a uniform distribution of steps (such as that assumed here) does not faithfully reflect the physical picture (1*c*). But in the absence of any reliable information on the frequency distribution of the inter-dislocation distance, it is safer to assume, as has been done elsewhere, that $2l \times N = 1$, where N is the density of 'active' dislocations (1). This is particularly valid in transient studies and near equilibrium conditions. (A satisfactory method of accounting for the spatial distribution of steps would be to assume a distribution of inter-step length and, based on this, to give weightage in evaluating the instantaneous current/potential. The assumed frequency distribution, however, is supposed to be stationary with respect to time).

An attempt to identify the 'growth sites' with the parallel arms of a fully grown spiral (in which case $2l$ is to be equated to the inter-step spacing with the attendant η-dependence, etc.) is indeed more specific, but is less general (8).

4. Formulation of the Problem

Scheme:

[i] $Y + \beta X \rightleftharpoons O$, (chemical reaction in bulk)

[ii] O (bulk) $\rightarrow$ O (pre-electrode layer), (diffusion)

[iii] $O + ne \rightleftharpoons R$ (surface), (charge transfer)

[iv] R (surface) $\rightarrow$ R (edge), (surface diffusion)

[v] R (edge) $\rightleftharpoons$ R (lattice), (lattice incorporation)

A large excess of X, as compared with O and Y, is assumed and, consequently, [i] is formally monomolecular. The concentration changes of Y are not assumed to be negligible but it is assumed that Y and X are not oxidized or reduced at the electrode. It is obvious that if, instead of [i], the reaction $Y \rightleftharpoons O + \beta X$ is considered, the mathematical apparatus that follows is not essentially different. For the overall electrochemical reaction [iii], we assume the usual rate equation in the form

$$i(t) = (ZF/l) \int_0^l (k_1 C_0 - k_2 C_{ad})\, dx,$$

where $ZFk_1C_0^{\,0} = i_0 \exp(\alpha_c F\eta/RT)$

and $ZFk_2C_{ad}^{\,0} = i_0 \exp(-\alpha_a F\eta/RT)$,

the overpotential η being assumed constant. (The integral in the right-hand side (r.h.s.) over the distance variable denotes the averaging process.)

In mathematical terms, we represent this diffusion problem as follows.

[1] $D\nabla^2 C_0 + k_f(C_x^0)^\beta C_y - k_b C_0 = \partial C_0/\partial t,$

[2] $D\nabla^2 C_y - k_f(C_x^0)^\beta C_y + k_b C_0 = \partial C_y/\partial t,$

Can. J. Chem. Downloaded from www.nrcresearchpress.com by 210.87.254.5 on 09/05/12
For personal use only.

[3] $D_a\, d^2C_{ad}/dx^2 + k_1C_0 - k_2C_{ad} = \partial C_{ad}/\partial t$,

[4] $\nabla^2 \equiv \partial^2/\partial x^2 + \partial^2/\partial y^2$,

with the boundary conditions

[5] $y = 0$: $D\partial C_0/\partial y = k_1C_0 - k_2C_{ad}$

$D\partial C_y/\partial y = 0$

[6] $y \to \infty$: $C_0 = C_0^0$

$C_y = C_y^0$

$x = 1$

[7] $D\partial C_0/\partial x = D\partial C_y/\partial x = D_a\partial C_{ad}/\partial x = 0$

$x = 0$

[8] $D\partial C_0/\partial x = D\partial C_y/\partial x = 0$

[9] $D_a\partial C_{ad}/\partial x = k_3(C_{ad} - C_{ad}^0)$

(the x axis is along the surface and perpendicular to the steps; y axis is normal to the electrode and into the solution) and the initial conditions

[10] $t = 0$: $C_0 = C_0^0$, $C_y = C_y^0$, and $C_{ad} = C_{ad}^0$

5. Mathematical Solution

Define

[11] $\bar{f}(p) = p\int_0^\infty e^{-pt}f(t)\,dt = L[f(t)]$

and $f(t) = L^{-1}(f(p))$.

The solution for the boundary value problem [1]–[10] is stated below (refer Appendix I).

[12] $\bar{C}_0^*(x,y,p) = \bar{C}_0(x,y,p) - C_0^0$

$= (K/[K+1])\sum_{m=0}^{\infty} \epsilon_m A_m(p)[1 + (1/K)((p + 1/\tau_m)/(p + \mu + 1/\tau_m))^{1/2}]$

$\cdot \exp(-((p + 1/\tau_m)/D)^{1/2}y)\cos(m\pi x/l)$

[13] $\bar{C}_y^*(x,y,p) = \bar{C}_y(x,y,p) - C_y^0$

$= (1/(K+1))\sum_{m=0}^{\infty} \epsilon_m A_m(p)[1 - ((p + 1/\tau_m)/(p + \mu + 1/\tau_m))^{1/2}]$

$\cdot \exp[-((p + 1/\tau_m)/D)^{1/2}y]\cos(m\pi x/l)$

[14] $\bar{C}_{ad}^*(x,p) = \bar{C}_{ad}(x,p) - C_{ad}^0 = -\sum_{m=0}^{\infty} \epsilon_m A_m(p)[((p + 1/\tau_m)D)^{1/2}/(p + 1/\tau_m^a)]$

$\cdot \cos(m\pi x/l) - [k_3/(k_3s_1^*(p) + pl)](k_1C_0^0 - k_2C_{ad}^0)[(pD)^{1/2}/\psi_0(p)]$

$((p/D_a)^{1/2}l)\cdot \cosh((p/D_a)^{1/2}(l - x))/\sinh((p/D_a)^{1/2}l)$

where

[15] $A_m(p) = -(k_1C_0^0 - k_2C_{ad}^0)\cdot(p/\psi_0(p))\{\delta_{m0} + [k_2(pD)^{1/2}/\psi_m(p)]\cdot[k_3/(k_3s_1^*(p) + pl)]\}$,

[16] $s_1^*(p) = \sum_{m=0}^{\infty}[\epsilon_m p/\psi_m(p)]\cdot[((p + 1/\tau_m)D)^{1/2} + (k_1K/[K+1])\cdot(1 + (1/K)[(p + 1/\tau_m)/(p + \mu + 1/\tau_m)]^{1/2})]$,

[17] $\psi_m(p) = \{((p + 1/\tau_m)D)^{1/2}(p + k_2 + 1/\tau_m^a) + (k_1K/K + 1)[1 + (1/K)(p + 1/\tau_m^a)\cdot((p + 1/\tau_m)/(p + \mu + 1/\tau_m))^{1/2}]\}$

[18] $1/\tau_m = m^2\pi^2D/l^2$

[19] $1/\tau_m^a = m^2\pi^2D_a/l^2$ and

[20] $\delta_{m0} = 1$, $m = 0$; $= 0$, otherwise.

Our primary interest lies in evaluating the current–time behavior.

[21] $i(t) = (ZF/l)\int_0^1 (k_1C_0(x, y, t) - k_2C_{ad}(x, t)\,dx)\,|_{y=0}$

under constant η-conditions. However, it is simpler to obtain the Laplace transform of $i(t)$, viz. $\bar{i}(p)$ as

[22] $\bar{i}(p) = (ZF/l)\int_0^l [k_1\bar{C}_0(x, o, p) - k_2\bar{C}_{ad}(x, p)]\,dx$

$= (ZF/l)\int_0^l D(\partial\bar{C}_0/\partial y)_{y=0}\,dx$

$$= (ZF/l) \int_0^l D(\partial M^*/\partial y)_{y=0}\, dx$$

$$= -ZF\, A_0(p)(pD)^{1/2}.$$

It is proved in Appendix I that

[23] $A_0(p) = -(k_1C^0 - k_2C_{ad}{}^0)(p/\psi_0(p))$
$\cdot [1 + (k_2(pD)^{1/2}k_3/\psi_0(p))/(k_3s_1{}^*(p) + pl)]$

[24] $\psi_0(p) = (pD)^{1/2}(p + k_2) + k_1Kp/(K + 1)$
$\cdot [1 + (1/K)(p/(p + \mu))^{1/2}]$

so that

[25] $\bar{\imath}(p) = ZF(k_1C_0{}^0$
$- k_2C_{ad}{}^0)[p(pD)^{1/2}/\psi_0(p)]$
$\cdot [1 + (k_2k_3(pD)^{1/2}/\psi_0(p))/(k_3s_1{}^*(p) + pl)].$

$s_1{}^*(p)$ is defined through [16]. The solutions [12]–[14] and [22], though exact, are not complete (the time dependence not being explicitly stated). Though inversion of the transforms occurring in [12]–[23] is a formidable task, a formal presentation of these solutions was considered useful because, with [25]:

(i) generalized impedance for small deviations from equilibrium can be given. In particular, for a small sinusoidal input, it is possible to obtain an exact frequency dependence of impedance;

(ii) even if it be heuristic, the relative importance of the relaxation times defined for the various steps can be discussed; and

(iii) numerical inversion of transforms is indeed possible, though usually tedious.[2]

6. Particular Cases

(i) Chemical Reaction (in the Solution) Infinitely Fast

$\mu t \ll 1$ or $K \to \infty$; since

[26] $s_1{}^*(p) \to \sum_{m=0}^{\infty} \epsilon_m p(k_1 + ((p + 1/\tau_m)D)^{1/2})$
$\cdot [(k_1 + ((p + 1/\tau_m)D)^{1/2})(p + 1/\tau_m{}^a)$
$+ k_2(p + 1/\tau_m)D]^{-1}$

[27] $\psi_0(p) \to (k_1 + (pD)^{1/2})p + k_2(pD)^{1/2}.$

A substitution of [26] and [27] in [25] gives an expression for $i(p)$ which is identical with that derived earlier [10]. (A misprint is to be corrected in equation [39] of ref. 10.)

(ii) Surface Diffusion and Lattice Incorporation Fast

[28] $D_at/l^2, k_2l^2/D_a \to 0$ and $k_2l/k_3 \to 0$
$s_1{}^*(p) \to \infty$

[29] $\psi_0(p) \to p(pD)^{1/2} + k_1p(K/K + 1)$
$\cdot [1 + (1/K)(p/p + \mu)^{1/2}]$

[30] $\bar{\imath}(p) \to ZF(k_1C_0{}^0 - k_2C_{ad}{}^0) \cdot [1 + (k_1/$
$K + 1)(K/(pD)^{1/2} + 1/((p + \mu)/D)^{1/2})]^{-1}$

Equation [30] can be seen to be a special case of the result obtained earlier,[3] if one observes that the concentration polarization of the 'reductant' is assumed absent here and $i_0 \neq \infty$.

(iii) Chemical Reaction, Bulk Diffusion: Both Negligible

$Dt/l^2, K, (D/t)^{1/2}/k_1 \to \infty$

[31] $s_1{}^*(p) \to s_{12}{}^*(p) = (p/p + k_2) \cdot ((p$
$+ k_2)/D_a)^{1/2}l \coth ([(p + k_2)/D_a]^{1/2}l)$

[32] $\psi_0(p) \to (p + k_2)(pD)^{1/2}$

so that

[33] $\bar{\imath}(p) \to ZF(k_1C_0{}^0 - k_2C_{ad}{}^0)(p/(p +$
$k_2)) \cdot [1 + (k_2k_3/(p + k_2))(k_3s_{12}{}^*(p) + pl)^{-1}].$

[33] is a familiar result (8, 9).

(iv) A Slow Chemical Reaction

$K \to 0$

[34] $s_1{}^*(p) \to s_{13}{}^*(p) = \sum_{m=0}^{\infty} \epsilon_m p[k_1 + ((p$
$+ \mu + 1/\tau_m)D)^{1/2}] \cdot [((p$
$+ \mu + 1/\tau_m)D)^{1/2}(p$
$+ 1/\tau_m{}^a + k_2)$
$+ k_1(p + 1/\tau_m{}^a)]^{-1},$

[35] $\psi_0(p) \to \psi_{03}(p)$, say $= (p/p + \mu)^{1/2}[k_1p$
$+ (p + k_2)((p + \mu)D)^{1/2}]$

[2] Attempts are being made in this laboratory to obtain numerical inversion of [25] and will be published later.

[3] See, for e.g. ref. 12, eq. [33].

Can. J. Chem. Downloaded from www.nrcresearchpress.com by 210.87.254.5 on 09/05/12
For personal use only.

Can. J. Chem. Downloaded from www.nrcresearchpress.com by 210.87.254.5 on 09/05/12
For personal use only.

$$[36]\quad \bar{\imath}(p) \rightarrow ZF(k_1 C_0^{\,0} - k_2 C_{\mathrm{ad}}^{\,0}) \cdot [(pD)^{1/2}/\psi_{03}(p)][1 + (k_2(pD)^{1/2}/\psi_{03}(p)) \cdot (s_{13}^{*}(p) + pl/k_3)^{-1}]$$

The results derived above refer to the potentiostatic conditions, i.e. k_1 and k_2 are constants.

7. Generalized Impedance

The expression for $i(p)$ when the input, viz. $i(t)$, is small (but time dependent) ($ZF\eta/RT \ll 1$) is

$$[37]\quad \bar{\imath}(p)/i_0 = (ZF\bar{\eta}(p)/RT)(p(pD)^{1/2}/\psi_0'(p)) \cdot [1 + (k_2'(pD)^{1/2}/\psi_0'(p))k_3 (k_3 s_1^{*\prime}(p) + pl)^{-1}]$$

where

$$[38]\quad k_1' = i_0/ZFC_0^{\,0} \text{ and } \quad k_2' = i_0/ZFC_{\mathrm{ad}}^{\,0}.$$

In [37], $\psi_0'(p)$ and $s_1^{*\prime}(p)$ are the same as $\psi_0(p)$ and $s_1^{*}(p)$ *except that* k_1' and k_2' replace k_1 and k_2 respectively in [16] and [17]. Thus, under linearized conditions, the impedance function, $Z_f(p)$, can be introduced.

From [37], it is noted that

$$[39]\quad Z_t(p) = (RT/ZFi_0)[\psi_0'(p)/p(pD)^{1/2}] \cdot [1 + (k_2'(pD)^{1/2}/\psi_0'(p))(s_1^{*\prime}(p) + pl/k_3)^{-1}]^{-1}$$

After some algebraic manipulations, the impedance function can be presented in a more convenient form, viz.

$$[40]\quad Z_t(p) = (RT/ZFi_0)\{1 + k_1 K/(K+1) \cdot [1/(pD)^{1/2} + 1/(K((p+\mu)D)^{1/2})] + [p/k_2 + 1/(s''(p) + k_2 l/k_3)]^{-1}\},$$

where

$$[41]\quad s''(p) = 2\sum_{n=1}^{\infty} [\psi_n'(p)]^{-1} \cdot [k_2'\sqrt{(p + 1/\tau_n)D} + k_1' K/(K+1) \cdot (1 + 1/K \cdot [(p+1/\tau_n)/(p+\mu+1/\tau_n)]^{1/2})]$$

Equation [40] can be rewritten as

$$[42]\quad Z_t(p) = R_t + Z_D(p) + Z_{KD}(p) + [1/C_{SD} + 1/(Z_{SD} + R_L)]^{-1}$$

where

$$[43]\quad R_t = RT/ZFi_0$$

$$[44]\quad Z_D = RT/ZF^2(C_0^{\,0} + C_v^{\,0})(pD)^{1/2}$$

$$[45]\quad Z_{KD} = RT/[KZ^2F^2(C_0^{\,0} + C_v^{\,0})((p+\mu)D)^{1/2}]$$

$$[46]\quad C_{SD} = (1/k_2)(ZFi_0/RT) = Z^2F^2C_{\mathrm{ad}}^{\,0}/RT$$

$$[47]\quad Z_{SD} = (RT/ZFi_0)s''(p)$$

$$[48]\quad R_L = k_2 l/k_3$$

R_t, the familiar transfer resistance, and R_L, a resistance due to finite lattice incorporation, are dependent on i_0 while C_{SD}, termed the 'pseudo-capacitance', is not. R_L, R_t, and C_{SD} are 'constants' and show no frequency dependence. Z_{SD} accounts for the impedance offered by the diffusion on the surface with the interference of the bulk diffusion and kinetic effects in solution properly accounted for. Z_D denotes the Warburg impedance. Thus the faradaic impedance can be analyzed into a series combination of R_t, Z_D, Z_{KD} and an impedance which itself is composed of a capacitance C_{SD} parallel to $(Z_{SD} + R_L)$.

(i) $Z_{SD} \rightarrow$ a pure resistance for $t \rightarrow \infty$ and (ii) for $t \rightarrow 0$, C_{SD} assumes control over $(Z_{SD} + R_L)$ while for $t \rightarrow \infty$, it is vice versa. For a small sinusoidal input, the steady state frequency dependence of impedance is immediate. The complex $Z_f(j\omega)$, $(j = (-1)^{1/2})$ can be easily evaluated for various frequencies and the equivalent circuit elements can be computed. A detailed study of the dependence of $Z_f(j\omega)$ on various non-dimensional parameters, viz. $D/\omega l^2$, $D_a/\omega l^2$, $k_2 l/k_3$, $k_1/\sqrt{\omega D}$, k_2/ω, K, and μ/ω will be reported in a subsequent communication.

The shortcomings inherent in the model postulated for the surface, the lack of generality in the above scheme of reactions for the overall electrochemical crystal growth and the involved nature of the problem reflected through the mathematical solutions given are obvious. Firstly, the possibilities of a potential drop variation along the metal surface and consequent

surface migration effects (ref. 10, p. 1130, comments by Prof. Gerischer) and secondly, the instantaneous time-profile of the surface remain but are ignored in this paper. And a more sophisticated averaging for the current (or the potential) under potentiostatic (or galvanostatic) conditions taking into account the inter-step distance distribution (and various other crystallographic aspects in the case of polycrystalline electrodes) is called for, but not offered here. Investigations on these lines are in progress.

Acknowledgments

The author thanks Professors K. S. G. Doss, H. R. Thirsk, and M. Fleischmann for useful discussions.

Appendix

Transform the variables C_0 and C_y through

[A.1] $M^* = C_0 + C_y - M^0$ and

[A.2] $N^* = (C_y - (1/K)C_0)\exp(\mu t)$, where

[A.3] $M^0 = C_0^0 + C_y^0$

[A.4] $K = (k_t/k_b)(C_x^0)^\beta$

[A.5] $\mu = k_t(C_x^0)^\beta + k_b$.

Equations [1]–[5] and the conditions [5]–[10] become

[A.6] $D\nabla^2 M^* = \partial M^*/\partial t$,

[A.7] $D\nabla^2 N^* = \partial N^*/\partial t$, with

[A.8] $\partial M^*/\partial x = \partial N^*/\partial x = 0$ at $x = 0$ and $x = l$

[A.9] $M^* = N^* = 0$ as $y \to \infty$

[A.10] $D(\partial M^*/\partial y) = k_1 C_0 - k_2 C_{ad}$
$= (k_1 C_0^* - k_2 C_{ad}^*) + k_1 C_0^0 - k_2 C_{ad}^0$
$= k_1(K/(K+1))(M^* - N^* \exp(-\mu t))$
$- K_2 C_{ad}^* + k_1 C_0^0 - k_2 C_{ad}^0$ at $y = 0$

[A.11] $D(\partial N^*/\partial y)\cdot\exp(-\mu t) = -k_1/(K+1)\cdot(M^* - N^*\exp(-\mu t)) - k_2 C_{ad}^* + (k_1 C_0^0 - k_2 C_{ad}^0)/K$ at $y = 0$.

Also

[A.12] $D_a\partial^2 C_{ad}^*/\partial x^2 + D(\partial M^*/\partial y)_{y=0} = \partial C_{ad}^*/\partial t$, with

[A.13] $D_a\partial C_{ad}^*/\partial x = k_3 C_{ad}^*$ at $x = 0$

[A.14] $D_a\partial C_{ad}^*/\partial x = 0$, $x = l$

[A.15] $C_{ad}^* = C_{ad} - C_{ad}^0 = 0$ when $t = 0$.

Defining Laplace transform of a function $f(x,y,t)$ as

[A.16] $f(x,y,p) = p\int_0^\infty \exp(-pt)\cdot f(x,y,t)\,dt = L[f]$

and finite fourier cosine transform of $f(x,y,t)$ in the interval $(0, l)$ through

[A.17] $f_c(n,y,t) = (2/l)\int_0^l f(x,y,t)\cos(n\pi x/l)\,dx$,

one has the simple inversion

[A.18] $f(x,y,t) = L^{-1}[f(x,y,p)] = \sum_{m=0}^{\infty} L^{-1}[\bar{f}_c(m,y,p)]\cos(m\pi x/l)$.

In [A.18]

[A.19] $\epsilon_m = 1$, $m = 0$
$= 2$, otherwise.

Applying the above transforms to the functions $M^*(x,y,t)$, $N^*(x,y,t)$, and $C_{ad}(x,t)$, it can be shown by elementary methods that

[A.20] $\overline{M_c^*}(m,y,p) = A_m(p)\cdot\exp(-((p + 1/\tau_m)/D)^{1/2}y)$

and

[A.21] $\overline{N_c^*}(m,y,p) = B_m(p)\cdot\exp(-((p + 1/\tau_m)/D)^{1/2}y)$

where

[A.22] $1/\tau_m = \pi^2 m^2 D/l^2$

and $A_m(p)$, $B_m(p)$, unknown 'constants'. Thus, with [A.18]

[A.23] $M^*(x,y,p) = \sum_{m=0}^{\infty}\epsilon_m A_m(p)\cdot\exp(-((p + 1/\tau_m)/D)^{1/2}y)\cdot\cos(m\pi x/l)$

Can. J. Chem. Downloaded from www.nrcresearchpress.com by 210.87.254.5 on 09/05/12
For personal use only.

Can. J. Chem. Downloaded from www.nrcresearchpress.com by 210.87.254.5 on 09/05/12
For personal use only.

and

$$[A.24]\quad \overline{N^*}(x,y,p) = \sum_{m=0}^{\infty} \epsilon_m B_m(p) \cdot \exp\,(-((p + 1/\tau_m)/D)^{1/2} y) \cdot \cos\,(m\pi x/l).$$

Since

$$[A.25]\quad (\partial \overline{M^*}/\partial y)_{y=0} = -L[K \partial \bar{N}^*/\partial y \cdot \exp\,(-\mu t)],$$

one obtains

$$[A.26]\quad \epsilon_m A_m(p) \cdot ((p + 1/\tau_m)D)^{1/2} = -\epsilon_m \cdot p \cdot K \cdot B_m(p + \mu) \cdot ((p + \mu + 1/\tau_m)D)^{1/2}/(p + \mu).$$

Substituting for $(\partial M^*/\partial y)_{y=0}$ in [A.12]

$$[A.27]\quad D_a \partial^2 C_{ad}^*/\partial x^2 - pC_{ad}^* - \sum \epsilon_m A_m(p)((p + 1/\tau_m)D)^{1/2} \cos\,(m\pi x/l) = 0$$

from which it is deduced, with the help of [A.14], that

$$[A.28]\quad \bar{C}_{ad}^*(x,p) = E_0(p) \cdot \cosh\,((p/D_a)^{1/2}(l - x)) - \sum_{m=0}^{\infty} \epsilon_m A_m(p)[((p + 1/\tau_m)D)^{1/2}/(p + 1/\tau_m{}^a)] \cdot \cos\,(m\pi x/l).$$

In [A.28], $E_0(p)$ is an unknown constant and

$$[A.29]\quad 1/\tau_m{}^a = m^2\pi^2 D_a/l^2.$$

[A.13] and [A.10] give

$$[A.30]\quad E_0(p) \cdot (pD_a)^{1/2} \sinh\,((p/D_a)^{1/2} l) = -k_3 \cdot E_0(p) \cdot \cosh\,((p/D_a)^{1/2} l) + k_3 \sum_{m=0}^{\infty} \epsilon_m A_m(p)((p + 1/\tau_m)D)^{1/2}/(p + 1/\tau_m{}^a)$$

and

$$[A.31]\quad \sum_{m=0}^{\infty} \epsilon_m A_m(p)((p + 1/\tau_m)D)^{1/2} \cos\,(m\pi x/l) = -(k_1 C_0{}^0 - k_2 C_{ad}{}^0)\delta_{m0} - k_1(K/K + 1)\Big\{ \sum_{m=0}^{\infty} \epsilon_m A_m(p) \cos\,(m\pi x/l) - \sum_{m=0}^{\infty} \epsilon_m (p/p + \mu) B_m(p + \mu) \cos\,(m\pi x/l)\Big\} + k_2 E_0(p) \cosh\,((p/D_a)^{1/2}(l - x)) - k_2 \sum_{m=0}^{\infty} \epsilon_m A_m(p)[((p + 1/\tau_m)D)^{1/2}/(p + 1/\tau_m{}^a)] \cdot \cos\,(m\pi x/l)$$

where

$$[A.32]\quad \delta_{m0} = 1,\ m = 0 = 0,\ \text{otherwise.}$$

We note from [A.26]

$$[A.33]\quad K \cdot B_m(p + \mu)(p/p + \mu) = -A_m(p)((p + 1/\tau_m)D)^{1/2}/((p + \mu + 1/\tau_m)D)^{1/2}$$

and using the identity

$$[A.34]\quad (p/D_a)^{1/2} l \cdot \cosh\,((p/D_a)^{1/2}(l - x))/\sinh\,((p/D_a)^{1/2} l) = \sum_{m=0}^{\infty} [\epsilon_m p/(p + 1/\tau_m{}^a)] \cos\,(m\pi x/l),$$

[A.31] is transformed into

$$[A.35]\quad \epsilon_m A_m(p)\Big\{((p + 1/\tau_m)D)^{1/2} + k_2((p + 1/\tau_m)D)^{1/2}/(p + 1/\tau_m{}^a) + (k_1 K/K + 1)\Big[1 + (1/K) \times \sqrt{(p + 1/\tau_m)/(p + \mu + 1/\tau_m)}\Big]\Big\} = -(k_1 C_0{}^0 - k_2 C_{ad}{}^0)\delta_{m0} + [\sinh\,((p/D_a)^{1/2} l)/(p/D_a)^{1/2} l] \cdot k_2 k_3 S \cdot [k_3 \cosh\,((p/D_a)^{1/2} l) + (pD_a)^{1/2} \sinh\,(p/D_a)^{1/2} l]^{-1}$$

In [A.35], S is defined through

$$[A.36]\quad S = \sum_{m=0}^{\infty} \epsilon_m A_m(p)((p + 1/\tau_m)D)^{1/2}/(p + 1/\tau_m{}^a).$$

Can. J. Chem. Downloaded from www.nrcresearchpress.com by 210.87.254.5 on 09/05/12
For personal use only.

Writing

$$[A.37]\quad \psi_m(p) = [((p + 1/\tau_m)D)^{1/2}(p + 1/\tau_m{}^a + k_2)] + (k_1K/K + 1)(p + 1/\tau_m{}^a)[1 + (1/K)((p + 1/\tau_m)/(p + \mu + 1/\tau_m))^{1/2}]$$

[A.35] is rewritten as

$$[A.38]\quad \epsilon_m A_m(p)\psi_m(p)/(p + 1/\tau_m{}^a) = -(k_1C_0{}^0 - k_2C_{ad}{}^0)\delta_{m0} + [\epsilon_m p/(p + 1/\tau_m{}^a)] \cdot [k_2 \sinh ((p/D_a)^{1/2}l)/((p/D_a)^{1/2}l)] \cdot k_3S \cdot [k_3 \cosh ((p/D_a)^{1/2}l) + (pD_a)^{1/2} \sinh ((p/D_a)^{1/2}l)]^{-1}.$$

[A.38] is an infinite system of linear equations since S is an infinite series involving A_m's. Multiplying [A.38] by $((p + 1/\tau_m)D)^{1/2}/\psi_m(p)$ and summing for $m = 0$ to ∞,

$$[A.39]\quad S\cdot\{1 - k_2k_3s_1(p)[\sinh ((p/D_a)^{1/2}l)/((p/D_a)^{1/2}l)] \cdot [k_3 \cosh ((p/D_a)^{1/2}l) + (pD_a)^{1/2} \sinh ((p/D_a)^{1/2}l)]^{-1}\} = -(k_1C_0{}^0 - k_2C_{ad}{}^0)(pD)^{1/2}/\psi_0(p),$$

where

$$[A.40]\quad s_1(p) = \sum_{m=0}^{\infty} \epsilon_m p((p + 1/\tau_m)D)^{1/2}/(p + 1/\tau_m{}^a) \cdot [\psi_m(p)]^{-1}.$$

Define

$$[A.41]\quad s_1{}^*(p) = \sum_{m=0}^{\infty} p\epsilon_m[\psi_m(p)]^{-1} \cdot \left[((p + 1/\tau_m)D)^{1/2} + (k_1K/K + 1)\left(1 + 1/K\sqrt{(p + 1/\tau_m)/p + \mu + 1/\tau_m}\right)\right].$$

[A.40] and [A.41] together give

$$[A.42]\quad k_2s_1(p) + s_1{}^*(p) = \sum_{m=0}^{\infty} \epsilon_m p/(p + 1/\tau_m{}^a) = ((p/D_a)^{1/2}l) \coth ((p/D_a)^{1/2}l).$$

With a little algebra, [A.39] becomes

$$[A.43]\quad S \cdot [k_3 + (pD_a)^{1/2} \tanh ((p/D_a)^{1/2}l)]^{-1} \cdot [\tanh ((p/D_a)^{1/2}l)/((p/D_a)^{1/2}l)] = -(k_1C_0{}^0 - k_2C_{ad}{}^0) [(pD)^{1/2}/\psi_0(p)][(pD_a)^{1/2}((p/D_a)^{1/2}l) + k_3s_1{}^*(p)]^{-1}.$$

Eliminating S in [A.38] through [A.43]

$$A_m(p)\psi_m(p)/(p + 1/\tau_m{}^a) = -(k_1C_0{}^0 - k_2C_{ad}{}^0)\{\delta_{m0} + [p(pD)^{1/2}/\psi_0(p)][k_2/(p + 1/\tau_m{}^a)] \cdot [s_1{}^*(p) + pl/k_3]^{-1}\}$$

Hence

$$[A.44]\quad A_0(p) = -(k_1C_0{}^0 - k_2C_{ad}{}^0)(p/\psi_0(p)) \cdot \{1 + [k_2(pD)^{1/2}/\psi_0(p)][s_1{}^*(p) + pl/k_3]^{-1}\}$$

and

$$[A.45]\quad A_m(p) = -(k_1C_0{}^0 - k_2C_{ad}{}^0) (p(pD)^{1/2}/\psi_0(p))\cdot [k_2/\psi_m(p)][s_1{}^*(p) + pl/k_3]^{-1}$$

Notations

α_a, α_c: Anodic and cathodic transfer coefficients.

D: Diffusion coefficient of the species O, Y.

D_a: Surface diffusion coefficient of adatoms.

i_0: Exchange current density for the electrochemical reaction $O + Ze \rightleftharpoons R(adatoms)$.

k_f, k_b: Rates of the chemical reaction $Y + \beta X \rightleftharpoons O$.

k_3: Rate of lattice incorporation (cm s^{-1}).

μ: $k_f(C_x{}^0)^\beta + k_b$.

K: $(k_f/k_b)(C_x{}^0)^\beta$.

$2l$: Distance between two adjacent, parallel steps on the electrode.

N: Density of 'active' dislocations.

p: (Laplace) transform variable.

$\eta(t)$: Overpotential as a function of time.

ω: Angular frequency.

Z_f, R_t, Z_D, Z_{KD}, C_{SD}, Z_{SD}, R_L: Impedance elements. Refer to eqs. [42]–[48] in the text.

C_i: Instantaneous concentration of i (i = O, Y, ad).

C_i^0: Bulk concentration of the species i (i = O, X, Y, ad).

C_i^*: $C_i - C_i^0$.

$\bar{C}_i^*$: Laplace transform of $C_i^* = p \int_0^\infty e^{-pt} C_i^* dt$.

M^*: $C_y^* + C_0^*$

N^*: $(C_y^* - 1/K \cdot C_0^*) \exp(\mu t)$.

$A_m(p)$, $s_1^*(p)$, $\psi_m(p)$, $s''(p)$: Please refer to eqs. [15], [16], [17], and [41] respectively.

ϵ_m: 1, $m = 0$; 2 if $m = 1, 2, \ldots$.

δ_{m0}: 1, $m = 0$; zero otherwise.

k_1: $(i_0/ZF C_0^0) \exp(\alpha_c F\eta/RT)$.

k_2: $(i_0/ZF C_{ad}^0) \exp(-\alpha_a F\eta/RT)$.

k_1': $(i_0/ZF C_0^0)$.

k_2': $(i_0/ZF C_{ad}^0)$.

$1/\tau_m$: $m^2\pi^2 D/l^2$.

$1/\tau_m^a$: $m^2\pi^2 D_a/l^2$.

1. (*a*) J. O'M. Bockris and A. Damjanovic. *In* Modern aspects of electrochemistry. No. 3. *Edited by* J. O'M. Bockris and B. E. Conway. Butterworths, London. 1964. B. E. Conway and J. O'M. Bockris. Electrochim. Acta, **3**, 340 (1961). (*b*) Despic and J. O'M. Bockris. J. Chem. Phys. **32**, 389 (1960). (*c*) H. Kita, M. Enyo, and J. O'M. Bockris. Can. J. Chem. **39**, 1670 (1961).
2. W. Lorenz. Z. Naturforsch. **9a**, 716 (1954); Z. Physik. Chem. Frankfurt, **17**, 136 (1958).
3. W. Lorenz. Z. Physik. Chem. Frankfurt, **19**, 377 (1959).
4. H. Gerischer and R. P. Tischer. Z. Elektrochem. **61**, 1159 (1957). H. Gerischer. Z. Elektrochem. **62**, 256 (1958).
5. W. Rojter, W. Juza, and E. Polujnan. Acta Physicochim. URSS, **10**, 389 (1939).
6. T. B. Reddy. J. Electrochem. Soc. **113**, 117 (1966).
7. S. K. Rangarajan. Can. J. Chem. **43**, 1052 (1965).
8. M. Fleischmann and H. R. Thirsk. *In* Advances in electrochemistry and electrochemical engineering. Vol. III. *Edited by* P. Delahay. Interscience, New York. 1963.
9. M. Fleischmann, S. K. Rangarajan, and H. R. Thirsk. Trans. Faraday Soc. **63**, 1240 (1967).
10. J. A. Harrison, S. K. Rangarajan, and H. R. Thirsk. J. Electrochem. Soc. **113**, 1120 (1966); *In* Electrode processes. *Edited by* E. Yeager *et al.* The Electrochemical Society, U.S.A. 1967. p. 104.
11. R. L. Schwoebel and E. J. Shipsey. J. Appl. Phys. **37**, 3682 (1966).
12. R. P. Buck. J. Electroanal. Chem. **5**, 295 (1963).

Can. J. Chem. Downloaded from www.nrcresearchpress.com by 210.87.254.5 on 09/05/12
For personal use only.

Can. J. Chem. Downloaded from www.nrcresearchpress.com by 210.87.254.6 on 09/05/12
For personal use only.

Relative efficiencies of triplet–triplet energy transfer from benzene ($^3B_{1u}$) to monoolefins and 1,3-butadiene[1]

A. MORIKAWA[2] and R. J. CVETANOVIĆ
Division of Applied Chemistry, National Research Council of Canada, Ottawa, Canada

Received December 29, 1967

Relative efficiencies of quenching of the benzene triplet ($^3B_{1u}$) in the gas phase by a number of monoolefins, 1,3-butadiene, and several inorganic gases (SF_6, Xe, CO_2, N_2O) have been determined by a competitive technique. Most of the data have been obtained at room temperature (~ 26 °C) and some measurements have been made at 30 and 70 °C. The latter indicate that the efficiency of the energy transfer to the monoolefins and 1,3-butadiene increases with increasing temperature. The mechanism of the "energy transfer" to the olefins appears to involve a chemical interaction with the benzene ($^3B_{1u}$) molecules. The inert gases are inefficient quenchers.

The kinetic data obtained with 1,3-butadiene indicate that this diolefin quenches also to an appreciable extent the first excited singlet of benzene ($^1B_{2u}$). This has been confirmed by direct fluorescence measurements.

Canadian Journal of Chemistry, 46, 1813 (1968)

Considerable interest has been shown in recent years in the collisional intermolecular transfer of electronic excitation energy. As part of a continuing investigation in this field, we have measured the relative rates of the triplet–triplet energy transfer from the excited molecules of benzene ($^3B_{1u}$) to a number of olefin acceptors. While this work was in progress, a similar study was reported by Haninger and Lee (1). The competitive technique developed earlier by Cundall *et al.* (2) has been used in both studies. Our results agree closely with those of Haninger and Lee: they exhibit a well-defined trend in the rates of energy transfer with the molecular structure of the olefins and thus confirm the difference from the opposite conclusion in the more restricted earlier work (2) that the rate of transfer is independent of olefin structure. Since we have also dealt with some additional olefins and other compounds of interest and have obtained some information on the temperature dependence of the relative rates of energy transfer, we wish to report briefly a summary of our results.

The competitive technique used is based on the following reactions (Be = benzene, Bu = butene-2, Q = another olefin or a quenching substance, superscripts S and T indicate electronically excited molecules in a singlet and a triplet state, respectively).

[1] NRCC No. 9996.
[2] NRCC Postdoctorate Fellow.

[1*a*] $Be + h\nu \rightarrow Be^S$

[1*b*] $Be^S \rightarrow Be^T$

[2] $Be^T + cis\text{-}Bu \rightarrow Be + Bu^T$

[3] $Bu^T \rightarrow \alpha trans\text{-}Bu^{\cdot} + (1-\alpha)cis\text{-}Bu$

[4] $Be^T + Q \rightarrow Be + Q^T$ (or another product)

If the rate of formation of Be^T (benzene $^3B_{1u}$) is $I_a\phi_T$ and the steady state treatment is applied, the rate (R) of formation of the *trans* isomer of butene-2 at negligibly small conversions is given by

$$[1] \qquad 1/R = \frac{1}{\alpha I_a \phi_T}\left\{1 + \frac{k_4}{k_2}\frac{[Q]}{[cis\text{-Bu}]}\right\}$$

At constant light absorption (I_a), the plot of $1/R$ against $[Q]/[cis\text{-Bu}]$ should be linear with the slope to intercept ratio equalling k_4/k_2, i.e. the relative rate of quenching of the benzene triplet ($^3B_{1u}$).

Light from a medium-pressure mercury lamp (Hanovia 673A) or from a homemade low-pressure mercury arc was passed through a Corning 9-54 filter and a KI aqueous solution filter (6.6 mg/100 ml, 10 mm thickness) which absorbed the light of wavelengths below 2400 Å. In view of the absorption spectrum of benzene, although two different light sources were alternatively used, to a good approximation only light close to 2537 Å was absorbed by benzene from either of the two sources. Benzene pressure was kept at 10 or 15 Torr in all experiments and

the ratio of concentrations [Q]/[*cis*-Bu] was varied. Gas chromatographic analyses were carried out and the only reaction product found was *trans*-butene-2 both with and without other olefins added to *cis*-butene-2. Conversion of *cis*-butene-2 did not exceed 5%. In separate experiments, after prolonged irradiation the stationary *trans*- to *cis*-butene ratio was 0.94, in agreement with the value obtained by Tanaka, Terao, and Sato (3) and by Haninger and Lee (1).

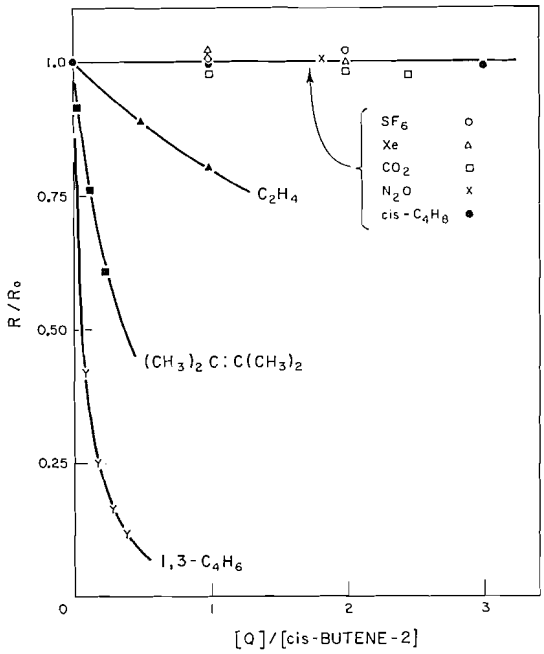

FIG. 1. Relative initial rates of the benzene-photosensitized isomerization of *cis*-butene-2 to *trans*-butene-2 in the presence (R) and absence (R_0) of additives (benzene 10 Torr; *cis*-butene-2 15 Torr in the case of C_2H_4 and $(CH_3)_2C{:}C(CH_3)_2$, 10 Torr in all other cases). Temperature 30 °C.

Examples of the effect of additives (Q) on the rate of isomerization of *cis*-butene-2 are shown in Fig. 1. Inorganic gases, SF_6, Xe, CO_2, and N_2O do not, within the experimental error, affect the rate of isomerization of *cis*-butene-2. In agreement with this, no N_2 production could be detected with N_2O as the additive. Alkenes, on the other hand, have a pronounced effect on the rate of isomerization of *cis*-butene-2, increasing in intensity from C_2H_4 to tetramethyl ethylene and giving at room temperature and at 70 °C good linear plots of $1/R$ (or of R_0/R, where R_0 is the value of R in the absence of Q) in accordance with eq. [1]. Increased pressures of *cis*-butene-2 itself from a standard value of 10 Torr to 20 and 40 Torr, as shown by the filled circles in Fig. 1 at the abscissa values of 0, 1, and 3 respectively, leave the rate of isomerization unaltered. This result agrees with the finding (3) that butene-2 quenches Be^T much more efficiently than does benzene itself and justifies omission of a spontaneous decay of Be^T in the derivation of eq. [1].

Butadiene-1,3 inhibits the isomerization of *cis*-butene-2 much more strongly than do the monoolefins, as is evident from Fig. 1. However, the plots of R_0/R instead of being linear are distinctly curved when the [1,3-C_4H_6]/[*cis*-butene-2] ratio is varied by varying the concentration of butadiene. This is shown in Fig. 2 for experiments at 30 °C. The curvature decreases with the absolute concentration of butadiene at the same [1,3-C_4H_6]/[*cis*-butene-2] ratios. Similar trends are observed at 70 °C as well (not shown in Fig. 2). That the variation in the concentration of 1,3-butadiene is responsible for the deviation from eq. [1] is shown in Fig. 3 (for experiments at 30 °C), which is similar to Fig. 2 except that 1,3-butadiene is kept constant while the *cis*-butene-2 concentration is varied. The curvatures are now absent but two distinct linear plots are obtained at two different butadiene pressures (2.5 Torr, circles, and 5.1 Torr, squares). However, the slope to intercept ratios are, within the experimental error, the same. Similar behavior is found at 70 °C (not shown in Fig. 3).

The distinctive behavior of 1,3-butadiene is apparently due to the fact that, unlike the monoolefins, it is capable of quenching not only the triplet ($^3B_{1u}$) but also the first electronically excited singlet of benzene (Be^S, presumably the $^1B_{2u}$ state). Under such conditions, the following additional reactions have to be considered,

[1*c*] $Be^S \rightarrow Be + h\nu$ (fluorescence)

[1*d*] $Be^S \rightarrow Be$

[5] $Be^S + 1,3\text{-}C_4H_6 \rightarrow Be + 1,3\text{-}C_4H_6^*$,

where reaction [1*d*] indicates all the Be^S consuming processes other than reactions [1*b*], [1*c*], and [5], such as the internal conversion to the ground electronic state, the self-quenching by benzene (constant at constant benzene pressure) and, perhaps also, valence isomerization pro-

Can. J. Chem. Downloaded from www.nrcresearchpress.com by 210.87.254.6 on 09/05/12
For personal use only.

Can. J. Chem. Downloaded from www.nrcresearchpress.com by 210.87.254.6 on 09/05/12
For personal use only.

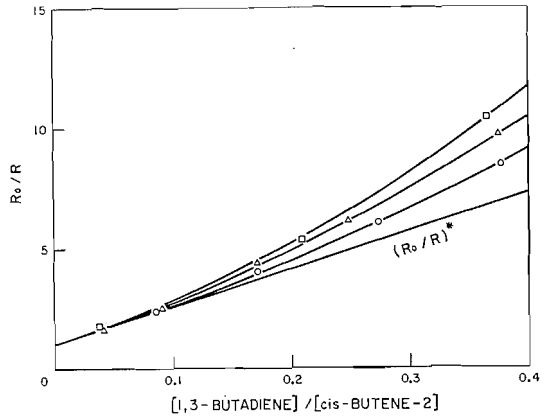

FIG. 2. Plots of (R_0/R) against the [1,3-butadiene]/[*cis*-butene-2] ratios at three different constant pressures of *cis*-butene-2: 10 Torr (circles), 20 Torr (triangles), and 30 Torr (squares). Benzene pressure 10 Torr. Temperature 30 °C.

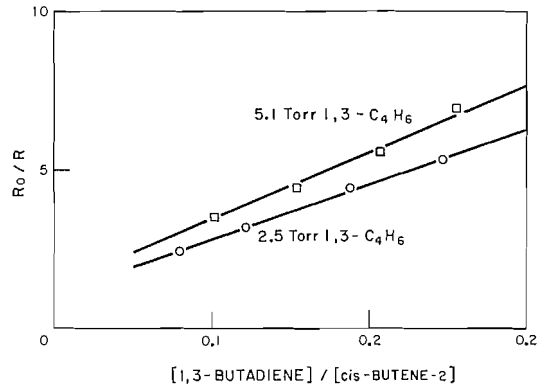

FIG. 3. Plots of (R_0/R) against the [1,3-butadiene]/[*cis*-butene-2] ratios at two different constant pressures of 1,3-butadiene: 2.5 Torr (circles) and 5.1 Torr (squares). Benzene pressure 10 Torr. Temperature 30 °C.

cesses not leading to the formation of Be^T. Steady state treatment gives

$$[2]\quad \frac{R_0}{R} = \left\{1 + \frac{k_4}{k_2}\frac{(1,3\text{-}C_4H_6)}{(cis\text{-}Bu)}\right\} \times \left\{1 + \frac{k_5}{k_{1b} + k_{1c} + k_{1d}}(1,3\text{-}C_4H_6)\right\}.$$

The last term in eq. [2] explains the deviations from linearity of the plots in Fig. 2 and the lack of such deviations in Fig. 3. Moreover, the slope to intercept ratios of the plots in Fig. 3 are equal to k_4/k_2, i.e. to the ratio of the rates of the quenching of benzene triplet by 1,3-butadiene and *cis*-butene-2. The values of k_4/k_2 thus obtained, for 30 °C from Fig. 3 and for 70 ° from analogous plots of the data at 70 °C, have been used to draw the limiting $(R_0/R)^*$ linear plots (shown for 30 °C in Fig. 2) defined as

$$[3]\quad \left(\frac{R_0}{R}\right)^* = 1 + \frac{k_4}{k_2}\frac{(1,3\text{-}C_4H_6)}{(cis\text{-}Bu)}.$$

The latter have been used in turn to evaluate the relative deviations from linearity of the R_0/R plots. Equations [2] and [3] give

$$[4]\quad \left[\frac{R_0}{R} - \left(\frac{R_0}{R}\right)^*\right] \Big/ \left(\frac{R_0}{R}\right)^* = \frac{k_5}{k_{1b} + k_{1c} + k_{1d}}(1,3\text{-}C_4H_6),$$

indicating that the relative deviations from linearity should be directly proportional to the partial pressure of 1,3-butadiene. Figure 4 shows that this is approximately true both at 30 and 70 °C. The appreciable scatter of points is not unexpected for plots of this kind. The slopes of the plots are equal to $k_5/(k_{1b} + k_{1c} + k_{1d})$ and are 1.6×10^{-18} and 3.3×10^{-18} cc/molec at 30 and 70° C respectively. The ratio of about 2 of the values at the two temperatures corresponds to a positive activation energy difference[3] of about 3.8 kcal/mole (with an appreciable margin of uncertainty because of the scatter of points in Fig. 4). The value of $(k_{1b} + k_{1c} + k_{1d})$ is not known precisely, but if it is taken approximately (4) as 1.7×10^6 s^{-1}, then $k_5 = 2.7 \times 10^{-12}$ cc/molec s at 30 °C, i.e. roughly about 1% of collisions at 30 °C lead to the singlet–singlet energy transfer in reaction [5]. As the temperature is raised, the efficiency of this energy transfer becomes greater.

The relative rates of the triplet energy transfer from benzene ($^3B_{1u}$) determined in the present work are summarized in Table I (columns 2–4) and are compared with the results of Haninger and Lee (1) (column 5). The relative rates vary somewhat with the temperature and tend to

[3]Reference to activation energies in this article is necessarily purely formal, indicating the existence of positive temperature coefficients of the ratios of rate constants. To assign the activation energies observed to a particular elementary step, for example to the "energy transfer" reaction [5], a detailed knowledge of the temperature dependence of the rates of the other elementary steps involved, for example of reactions [1*b*], [1*c*], and [1*d*], is required. If $(k_{1b} + k_{1c} + k_{1d})$ increases with temperature, as is probable, the observed activation energy difference is a lower limit for E_5.

TABLE I

Relative rate constants of "energy transfer" and of chemical reactions of several triplets (the value for *cis*-butene-2 is taken as unity)

The quencher (Q)	Energy transfer							Chemical reaction			
	Be^T										
	Present work			HL[c]	Acetone[T]	Hg-	$Cd(^3P_1)$	$O(^3P)$	$S(^3P)$	$Se(^3P)$	$C_2O(^3\Sigma)$
	~26 °C[a]	30 °C[b]	70 °C[b]	23 °C	RA[d]	$(^3P_1)$[e]	TS[f]	C[g] 25 °C	SG[h] 25 °C	CT[i] 25 °C	WB[J] 27 °C
Ethylene	0.22	0.25	0.33	0.16	0.16	0.90	1.03	0.042	0.063	0.042	0.10
Propylene	0.47			0.51	0.33	0.93	1.18	0.24	0.43	0.15	0.62
Butene-1	(0.50)[k]	0.51		0.50	0.33		1.08	0.24	0.63	0.30	0.71
Pentene-1	0.54			0.51		1.00			0.63		
Isobutene	1.27				0.66	0.95	1.11	1.05	3.13	1.87	5.8
2-Methyl-butene-1	0.80								3.50		
cis-Butene-2	1.00	1.00	1.00	1.00	1.00	1.00	1.00	1.00	1.00	1.00	1.00
trans-Butene-2				1.08				1.19	1.25	2.33	1.21
Cyclopentene				1.06				1.25	1.13		1.97
Trimethyl-ethylene	1.61			1.7	1.4		1.02	3.3	5.1		9.9
Tetramethyl-ethylene	2.67	2.75	2.29	3.0	8.7	0.95	0.99	4.3	7.1		25.3
1,3-Butadiene	(16.2)[k]	15.8	13.0		870	0.93	1.13	1.02	5.2	4.1	21.6
Propane				~0	0.015	0.045	~0				
CO_2	(~0)[k]	~0				0.07					
SF_6	(~0)[k]	~0	~0								
Xe	(~0)[k]	~0				~0					
N_2O	(~0)[k]	~0				0.32		v.sm.[l]			

[a]Medium-pressure mercury lamp (Hanovia 673A) used. [b]Low-pressure mercury lamp used. [c]Haninger and Lee (1). [d]Rebbert and Ausloos (5). [e]Taken from ref. 6. [f]Tsunashima and Sato (16). [g]Cvetanović (7). [h]Gunning and Strausz (8). [i]Callear and Tyerman (9). [J]Williamson and Bayes (10). [k]Estimated from the data at 30 and 70 °C. [l]Very small ($k \approx 7.6 \times 10^{-11} \exp(-24100/RT)$ cc molec^{-1} s^{-1}, estimated in ref. 11.

differ less at higher temperatures, indicating that the energy transfer in all probability requires an activation energy. The activation energy differences appear to be small: *cis*-butene-2 has an activation energy about 1 kcal/mole smaller than ethylene and about the same amount larger than tetramethyl ethylene or butadiene. In view of the relatively small temperature interval and the small differences in the relative rates, these values represent only order-of-magnitude estimates.

A comparison is made in Table I of the relative rates of energy transfer from benzene ($^3B_{1u}$) and from the lowest triplets of acetone, mercury, and cadmium with the relative rates of chemical reaction of several triplet reagents ($O(^3P)$, $S(^3P)$, $Se(^3P)$, and $C_2O(^3\Sigma)$). The last four triplets have been recognized as electrophilic reagents (7–10) and there is evidently a close similarity between the trends in their reactivities and the rates of energy transfer from the triplets of benzene and of acetone. It is therefore suggestive that similar electronic interactions come into play in both processes. The "energy transfer" from the triplets of benzene and of acetone to olefins appears to be brought about by a chemical interaction, i.e. formation and subsequent decomposition of a "chemical complex" of limited duration. The need to assume an interaction in the intermediate which is deeper and longer lasting than in a mere "collision complex" comes also from the fact that a non-vertical transition must apparently take place. In the case of the triplet energy transfer from benzene to ethylene a vertical transition would probably be about 22 kcal/mole endothermic (12).

The rates of energy transfer to butadiene from the first triplet of benzene and especially of acetone are very much larger than are the rates of transfer to the monoolefins. In the case of butadiene even a vertical transition is appreciably exothermic and a greater efficiency of energy transfer is therefore strongly favored.

The rates of energy transfer from $Hg(^3P_1)$ and $Cd(^3P_1)$ show very little or no dependence on olefin structure. The pronounced difference in this respect from the triplets of benzene and acetone has been recently pointed out by S. Tsunashima and S. Sato (private communica-

Can. J. Chem. Downloaded from www.nrcresearchpress.com by 210.87.254.6 on 09/05/12
For personal use only.

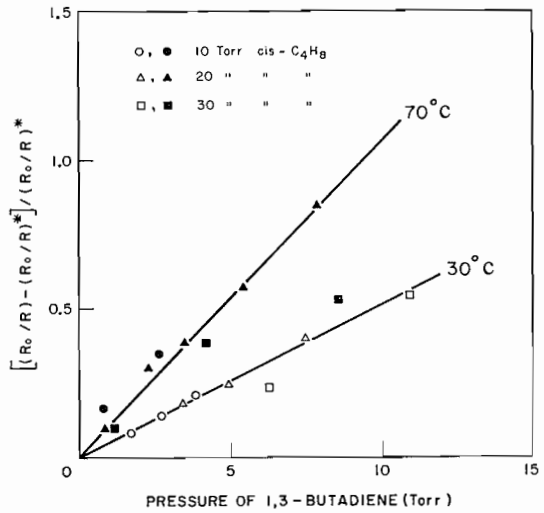

FIG. 4. Plot of $[(R_0/R) - (R_0/R)^*]/(R_0/R)^*$ against the butadiene pressure at three different pressures of *cis*-butene-2: 10 Torr (circles), 20 Torr (triangles), and 30 Torr (squares). Benzene pressure 10 Torr. Temperature 30 °C (open symbols) and 70 °C (filled symbols).

tion, ref. 16). The $Hg(^3P_1)$ data do show an electrophilic trend (13) if expressed as quenching cross sections rather than rate constants but even then the differences between different olefins remain quite small. On the other hand, no electrophilic trend is discernible in the case of $Cd(^3P_1)$ even if the data are expressed as relative quenching cross sections. Another difference of interest is that energy transfer to N_2O occurs readily from $Hg(^3P_1)$ but not from benzene ($^3B_{1u}$) although a chemical decomposition of N_2O into N_2 and $O(^3P)$ would still be quite exothermic. The inefficient interaction of N_2O with the benzene triplet parallels the very slow chemical interaction of N_2O with the $O(^3P)$ atoms. Similarly, paraffins and CO_2 quench at appreciable rates $Hg(^3P_1)$ but apparently not the benzene triplet. Some of the reasons for these differences should no doubt be sought in (1) the large spin-orbit coupling of the heavy atoms Hg and Cd, (2) the more complex molecular structure of the organic triplets (benzene, acetone), and (3) the differences in the available energies. In the case of $Hg(^3P_1)$ the available energy is 112.7 kcal/g atom and vertical triplet–triplet transition to all the alkenes is appreciably exothermic. The quenching cross sections are very large. In the case of $Cd(^3P_1)$ considerably less energy is available (87.7 kcal/g atom) but, for experimental reasons, quenching measurements have to be carried out at higher temperatures, and what effect this may have is not clear. The energy of benzene triplet ($^3B_{1u}$) is about 84.4 kcal/mole (14) and of acetone probably close to 80 kcal/mole (15). The relative rates of energy transfer from benzene triplet are affected by temperature, as shown above.

The present results with 1,3-butadiene are explained assuming that it quenches both the triplet and the excited singlet of benzene while monoolefins quench only the former. A conclusive evidence for this postulate has to be obtained from direct fluorescence measurements. Such experiments are now in progress and the preliminary results show that 1,3-butadiene does indeed quench benzene fluorescence while *cis*-butene-2 does not, or at best quenches it only to a very minor extent.

1. G. A. HANINGER, JR. and E. K. C. LEE. J. Phys. Chem. **71**, 3104 (1967).
2. R. B. CUNDALL, F. J. FLETCHER, and D. G. MILNE. J. Chem. Phys. **39**, 3536 (1963).
3. M. TANAKA, T. TERAO, and S. SATO. Bull. Chem. Soc. Japan, **38**, 1645 (1965).
4. H. ISHIKAWA and W. A. NOYES, JR. J. Chem. Phys. **37**, 583 (1962).
5. R. E. REBBERT and P. AUSLOOS. J. Am. Chem. Soc. **87**, 5569 (1965).
6. R. J. CVETANOVIĆ. Progr. Reaction Kinetics, **2**, 67 (1964)
7. R. J. CVETANOVIĆ. J. Chem. Phys. **30**, 19 (1959); Can. J. Chem. **38**, 1678 (1960); J. Chem. Phys. **33**, 1063 (1960).
8. H. E. GUNNING and O. P. STRAUSZ. Advan. Photochem. **4**, 143 (1966). O. P. STRAUSZ. Private communication.
9. A. B. CALLEAR and W. J. R. TYERMAN. Proc. Chem. Soc. 296 (1964); Trans. Faraday Soc. **62**, 371 (1966).
10. D. WILLIAMSON and K. D. BAYES. J. Am. Chem. Soc. In press.
11. K. SCHOFIELD. Planetary Space Sci. **15**, 643 (1967).
12. R. S. MULLIKEN. J. Chem. Phys. **33**, 1597 (1960).
13. Y. ROUSSEAU, O. P. STRAUSZ, and H. E. GUNNING. J. Chem. Phys. **39**, 962 (1963). A. J. YARWOOD, O. P. STRAUSZ, and H. E. GUNNING. J. Chem. Phys. **41**, 1705 (1964).
14. D. F. EVANS. J. Chem. Soc. 1351 (1957).
15. R. F. BORKMAN and D. R. KEARNS. J. Chem. Phys. **44**, 945 (1966).
16. S. TSUNASHIMA and S. SATO. Bull. Chem. Soc. Japan **40**, 2987 (1967).

Can. J. Chem. Downloaded from www.nrcresearchpress.com by 210.87.254.6 on 09/05/12
For personal use only.

Electron spin resonance studies of radiation damage. Part II. Gamma-irradiated single crystals of sodium chlorate: The ClO_3 radical

P. F. PATRICK AND F. P. SARGENT[1]

Department of Chemistry and Chemical Engineering, University of Saskatchewan, Saskatoon, Saskatchewan

Received September 25, 1967

Single crystals of sodium chlorate were gamma irradiated and examined by e.s.r. at −196 °C. One of the species present was identified as ClO_3.

Canadian Journal of Chemistry, **46**, 1818 (1968)

Can. J. Chem. Downloaded from www.nrcresearchpress.com by 210.87.254.6 on 09/05/12
For personal use only.

The gamma irradiation of single crystals of perchlorates to give several different paramagnetic centers is now reasonably documented and the identity of the centers well established. Cole has observed ClO_3 in both ammonium (1) and potassium (2) perchlorate together with ClO_2 in the latter. These results and assignments were confirmed by Atkins *et al.* (3) for several other perchlorates and chlorine oxide systems. Very recently Morton (4) has detected another paramagnetic species in X-irradiated potassium perchlorate at low temperatures. Although the identity of this species is not as certain, Morton presents a strong argument for identification as ClO_4.

The situation for irradiated chlorates is by no means as settled. Hasty *et al.* (5) examined X-irradiated single crystals of potassium chlorate at room temperature. They interpreted their e.s.r. spectra in terms of two species; namely O_2^- and ClO associated with a chlorate ion. Subbotin (6) found similar spectra from other chlorates and identified the two species in a similar manner. However, Atkins *et al.* (3) disagree with these assignments and propose that the species identified as O_2^- is more likely to be O_3^-. They also dispute the assignment of the species with two non-equivalent chlorine nuclei to ClO---ClO_3^- and tentatively suggest that this species could be a chlorine atom associated with a chlorate ion. Further confusion and ambiguity arose when Gamble observed yet another species in irradiated sodium chlorate crystals (7) which he assigned to ClO_3. This identification was particularly unusual in that the hyperfine electron-nuclear couplings for Cl(35) differed vastly from those reported for ClO_3 in ammonium perchlorate (1); however, the g values agreed quite well.

We wish to report a brief and admittedly qualitative study of gamma-irradiated single crystals of sodium chlorate at liquid nitrogen temperatures.[2] The crystals became blue in color in contrast to the brown color observed on warming to room temperature. We confined our observations to non-annealed crystals at −196 °C which were examined in the dark to preclude the possibility of photo-bleaching. The e.s.r. spectra were exceedingly complex and involved a large number of lines. Under conditions of high sensitivity and high recorder gain the spectrum with H_0 parallel to a crystal 100 direction consisted of four peaks on scale, i.e. A_1B_1 (main spectrum off-scale) B_2A_2. Peaks A_1 and A_2 were of equal intensity as were B_1 and B_2; however, the relative intensities of A_1:B_1 (and A_2:B_2) were almost exactly 3:1. In addition the ratio of the peak separations from A_1 to A_2 and from B_1 and B_2 was 0.832. We assume that these peaks are due to the $M_1 = \pm 3/2$ lines for Cl(35) and Cl(37) in a paramagnetic species with one chlorine nucleus. We cannot completely rule out the possibility of more than one chlorine nucleus being present, but no indication of a small chlorine coupling was observed as in the room temperature spectra (6).

Rotation of the crystal about an [100] axis perpendicular to H_0 caused each of the A and B lines to split into two equally intense lines, demonstrating the presence of at least two equally populated sites in the crystal. For orientations with H_0 neither parallel nor perpendicular to the crystal [100] axis, the presence of four equally populated sites were detected. These sites all became magnetically equivalent when H_0 was parallel to a [100] crystal axis.

When H_0 was parallel to a crystal [100] axis

[1]NRCC Postdoctorate Fellow 1965–1967.

[2]Detailed studies were not possible because of experimental difficulties due to intermittent stability of the magnetic field. However, the spectra reported here were taken at a time of comparatively good stability, this being particularly so for the spectrum recorded with H_0 parallel to the [100] crystal axis.

Can. J. Chem. Downloaded from www.nrcresearchpress.com by 210.87.254.6 on 09/05/12
For personal use only.

the overall width (i.e. A_1 to A_2) of the spectrum was 399.7 G corresponding to a first order coupling constant of 133.2 G (373 Mc/s) for $A(35)$; at this orientation the first order g value was 2.0076. The maximum and minimum values of $A(35)$ (corresponding to the two site splittings) occurred when H_0 was parallel to a [110] crystal direction, giving 151.5 G (425 Mc/s) and 112.3 G (315 Mc/s) respectively. It was also observed that the maximum value of $A(35)$ corresponded to a minimum value of g and the minimum value of $A(35)$ corresponded to a maximum g value. Although experimental difficulties[2] did not permit accurate measurement of these g values they were of the order of 2.007 and 2.008.

Since the crystals are cubic (8), the spectra corresponding to H_0 parallel to the crystallographic axis are all the same. Therefore the diagonal elements of the non-diagonalized A-tensor are all equal to 133 G (373 Mc/s).[3] To determine the relative signs of the off diagonal elements it is necessary to examine the spectra for the orientation with direction cosines of $1/\sqrt{3}$, $1/\sqrt{3}$, $1/\sqrt{3}$, i.e. [1,1,1]. However, we may make some limited deductions from the diagonal values. If these are all of the same sign then the isotropic coupling constant for Cl(35) would be 133 G (373 Mc/s), since the trace of the tensor is not affected by diagonalization. Similarly the isotropic or average g value will be 2.0076. These results are in agreement with the values reported for ClO_3 in perchlorates (1, 3). We therefore feel justified in identifying our species as ClO_3 trapped in sites previously occupied by chlorate ions. Since when H_0 is parallel to a cube edge, i.e. [100] direction, all four sites are equivalent and the ClO_3 must have a symmetry axis along the [111] directions which all make equal angles of 54° 44′ with H_0 at this orientation.

When the crystals are warmed to room temperature the ClO_3 lines are no longer present and the blue color is replaced by a brownish amber coloration. We are at a loss to re-identify the species observed by Gamble (7) but we are convinced that it is not ClO_3. Gamble argues that his species could not be ClO (which also has axial symmetry) because its formation would involve the loss of two oxygen atoms from a chlorate site and the relocation of the Cl—O bond along a body diagonal of the cube. He argues that the distortion required for this process would be too great. We question this reasoning and also dispute the use of the correspondence of g values to support the identification and yet the differences in the observed $A(35)$ values are ignored. In fact Atkins *et al.* (3) have reported variations in the g values for ClO_3 observed in different perchlorates but the isotropic (or average) hyperfine couplings were all of the order of 130 G. We suspect that the species Gamble identifies as ClO_3 is possibly ClO.

The presence of ClO_3 in the samples may be explained by the very simple ionization mechanism

$$ClO_3^- \xrightarrow{\text{gamma}} ClO_3 + e,$$

although the ClO_3 is not necessarily formed in its electronic ground state. The comparatively low yield of this species seems to indicate loss via dissociation, perhaps to give ClO_2 or ClO. Conventional radiation chemical studies of gamma-irradiated chlorates involving dissolution in water after irradiation (9) indicate the formation of perchlorate. We assume that this is derived from the mixed anhydride Cl_2O_6 formed by the dimerization of ClO_3.

Further study of these crystals is contemplated for the near future when we hope to examine and analyze the central field section of the e.s.r. spectra in detail.

[3]This is only true if direct field effects are ignored and if S and I are quantized in the direction of H_0.

Acknowledgments

The National Research Council of Canada is gratefully acknowledged for a Postdoctorate Fellowship to one of us (F. P. S.) and for general equipment grants.

1. T. Cole. J. Chem. Phys. **35**, 1169 (1961).
2. T. Cole. Proc. Natl. Acad. Sci. U.S. **46**, 506 (1960).
3. P. W. Atkins, J. A. Brivati, N. Keen, M. C. R. Symons, and P. A. Tevalion. J. Chem. Soc. 4785 (1962).
4. J. R. Morton. J. Chem. Phys. **45**, 1800 (1966).
5. T. E. Hasty, W. B. Ard, and W. G. Moulton. Phys. Rev. **116**, 1459 (1959).
6. G. I. Subbotin. Opt. Spectr. USSR English Transl. **18**, 98 (1965).
7. F. T. Gamble. J. Chem. Phys. **42**, 3542 (1965).
8. R. W. G. Wyckoff. Crystal structures. Vol. II. Interscience, New York. 1948.
9. G. E. Burchill. M.A. Thesis, University of Saskatchewan, Saskatoon, Saskatchewan. 1960. P. F. Patrick. M.A. Thesis, University of Saskatchewan, Saskatoon, Saskatchewan. 1961.

Relation entre la structure de la kröhnkite et la dissymétrie des spectres de résonance magnétique nucléaire de l'échantillon polycristallin

PIERRE J. VAN TIGGELEN[1]
Laboratoire de Chimie Analytique et Inorganique, Université de Louvain, Louvain, Belgique

Reçu le 22 septembre 1967

Les second et troisième moments ont été obtenus á partir des spectres de résonance magnétique nucléaire du proton d'une poudre cristalline de la kröhnkite. Ces résultats confirment les détails de la configuration atomique proposée antérieurement à partir des spectres d'un monocristal.

Canadian Journal of Chemistry, 46, 1820 (1968)

Can. J. Chem. Downloaded from www.nrcresearchpress.com by 210.87.254.42 on 09/05/12
For personal use only.

Si l'emploi du second moment en résonance magnétique nucléaire des solides est d'usage courant pour étudier certains problèmes structuraux, les moments impairs sont fort peu utilisés par suite de la symétrie de la plupart des spectres. Toutefois, la présence d'ions paramagnétiques dans le réseau provoque, dans le cas d'un monocristal, un glissement de la raie par rapport au champ de résonance H_0 d'un noyau isolé, glissement qui peut être relié à des paramètres structuraux. Dans le cas d'une poudre cristalline au contraire, les orientations au hasard des cristallites annulent le glissement de la raie, tout en faisant apparaître une certaine dissymétrie de la distribution spectrale autour de son centre de gravité.

Dans un article précédent (1), on a déduit une relation qui lie la dissymétrie des raies de résonance magnétique nucléaire (r.m.n.) du proton aux distances internucléaires (ion paramagnétique – proton et proton–proton) qui caractérisent la structure du composé paramagnétique. Par ailleurs, pour la kröhnkite ($Na_2Cu(SO_4)_2 \cdot 2H_2O$), la position des atomes d'hydrogène dans le réseau cristallin a pu être déterminée par l'étude des spectres d'un monocristal (2). Des coordonnées ainsi obtenues et de la position des atomes lourds déterminée par Rao (3), il est possible de calculer

$-\bar{S}_3$, troisième moment théorique (1), à l'aide de la formule:

$$\bar{S}_3 = \frac{1}{N}\sum_i \left[\frac{16}{35}\frac{\bar{\mu}_p^{\,3}}{R_{ip}^{\,9}} + \frac{24}{35}\sum_j \frac{k_{ij}\mu_j^{\,2}\bar{\mu}_p}{r_{ij}^{\,6}R_{ip}^{\,3}}(3\cos^2\lambda_{pij} - 1)\right],$$

où $\bar{\mu}_p$ est le moment magnétique moyen de l'ion cuivre distant de R_{ip} du proton i, et μ_j le moment magnétique nucléaire du noyau j distant de r_{ij} du même proton, $\mu_j = (I_j(I_j+1)/3)^{\frac{1}{2}}g_j\mu_0$, I_j est le nombre de spin du noyau j de facteur de décomposition spectrale g_j et μ_0 le magnéton nucléaire, λ_{pij} est l'angle entre les vecteurs r_{ij} et R_{ip}; enfin k_{ij} est un facteur numérique égal à 3/2 pour des noyaux i et j identiques et 1 dans les autres cas. La somme en j est étendue à tous les noyaux de spin nucléaire I_j non nul et la somme en i porte sur les N protons situés en des sites inéquivalents;

$-\bar{S}_2$, le second moment, à l'aide de la formule de Van Vleck (4):

$$\bar{S}_2 = \frac{1}{N}\frac{4}{5}\sum_i \left[\frac{\bar{\mu}_p^{\,2}}{R_{ip}^{\,6}} + \sum_j \frac{k_{ij}^{\,2}\mu_j^{\,2}}{r_{ij}^{\,6}}\right].$$

Dans la structure de la kröhnkite, il existe deux sites inéquivalents pour les protons ($N = 2$). En outre, les contributions aux second et troisième moments des noyaux situés à une distance supérieure à 4.25 Å du proton envisagé sont négligeables, ceci nous amène donc à utiliser les formules de $\bar{S}_2$ et $\bar{S}_3$ reprises ci-dessus où seule l'influence d'un ion paramagnétique intervient. Avec un moment magnétique moyen de l'ion cuivrique dans la kröhnkite de 34.2 G Å^3 (2), les moments théoriques valent 28.5 ± 0.2 G^2 pour $\bar{S}_2$ et -25.4 ± 3.0 G^3 pour $\bar{S}_3$.

Dans ce travail deux types d'échantillons polycristallins ont été employés: il s'agit en premier lieu d'une poudre préparée par broyage d'un échantillon naturel de kröhnkite et par ailleurs d'un échantillon obtenu par évaporation d'une solution équimolaire des sulfates de cuivre et de sodium dans les conditions décrites par Massink (5). Les deux échantillons fourn ssent des spectres de r.m.n. rigoureusement identiques. Ils

[1]Adresse presente: Laboratoire de Chimie analytique et inorganique, 96, Naamsestraat, Louvain, Belgique.

produisent également un même spectre de diffraction[2] des rayons X (méthode des poudres), qui plus est en parfait accord avec les valeurs citées dans la littérature (6). Les spectres de résonance magnétique du proton furent enregistrés sur un spectromètre Varian V 4300 – 2 dual purpose travaillant à 56.4 MHz. Pour pouvoir mesurer le troisième moment d'une raie de résonance, les conditions à remplir par le spectre sont assez sévères: il faut entre autres:

une intensité du signal suffisante pour déterminer avec précision la forme des ailes du spectre;

une vitesse de balayage lente pour fixer avec précision la position du champ de référence H_0 du proton libre et pour obtenir à partir de mesures effectuées au millimètre près, une précision suffisante des moments en gauss;

une phase correspondant au mode d'absorption à quelques pourcents près. L'erreur de phase s'exprime en pourcent par la différence des surfaces des ailes à haut et à bas champ du signal obtenu à l'enregistreur, rapportée à la surface moyenne des ailes;

une amplitude de modulation assez faible afin que la correction du champ de modulation préconisée par Andrew (7) reste faible.

Sur une série de 30 spectres on a sélectionné ceux remplissant les conditions précitées. Les troisièmes moments mesurés à l'aide de la formule

$$\bar{S}_3 = \frac{\int_{-\infty}^{+\infty} (H - H_0)^3 g(H - H_0) d(H - H_0)}{\int_{-\infty}^{+\infty} g(H - H_0) d(H - H_0)},$$

où $g(H - H_0)$ désigne la fonction de normalisation repérée sur H_0 et H une valeur particulière du champ magnétique, ont permis, par interpolation linéaire dans un diagramme donnant $\bar{S}_3$ en fonction du pourcent d'erreur de phase, de trouver pour un spectre dans le mode d'absorption pure un troisième moment $(\bar{S}_3)_{exp} = -27.0 \pm 5\ G^3$. Les seconds moments des mêmes raies fournissent une valeur de $(\bar{S}_2)_{exp} = 28.22 \pm 1\ G^2$.

Malgré l'imprécision sur la mesure de $\bar{S}_3$, le résultat obtenu confirme bien la structure proposée antérieurement (2) à savoir des liaisons hydrogènes vers des atomes d'oxygène situés à 2.64 et 2.65 Å de l'oxygène de la molécule d'eau. De plus, l'emploi du troisième moment du spectre d'un échantillon de kröhnkite en poudre permet d'exclure la possibilité des liaisons hydrogènes dissymétriques (c'est-à-dire vers des oxygènes à 2.87 et 2.65 Å), pour lesquels le troisième moment serait de $-11.0 \pm 1.5\ G^3$ et le second de $27.7 \pm 0.2\ G^2$. Il faut remarquer que le second moment seul ne permet pas de décider laquelle des deux structures à priori possibles est réalisée effectivement.

Il convient enfin de noter que, si la contribution de la seule interaction dipolaire nucléaire à $\bar{S}_2$ peut être obtenue par extrapolation à champ magnétique nul des seconds moments mesurés sur des spectres pris à des valeurs différentes du champ directeur, l'emploi simultané de $\bar{S}_2$ et de $\bar{S}_3$ pour des spectres d'*un* échantillon à l'état de poudre, enregistrés à *une* valeur du champ magnétique et à *une* température présente dans certain cas un grand avantage.

Remerciements

Nous remercions le Professeur M. Van Meerssche pour les encouragements prodigués, ainsi que le Fonds National de la Recherche Scientifique (Belgique) pour le mandat de chargé de recherches octroyé.

1. P. J. Van Tiggelen. Can. J. Chem. **42**, 246 (1964).
2. P. J. Van Tiggelen. Bull. Soc. Chim. Belges, **75**, 620 (1966).
3. B. Rama Rao. Acta Cryst. **14**, 738 (1961).
4. J. H. Van Vleck. Phys. Rev. **74**, 1168 (1948).
5. A. Massink. Z. Physik. Chem. Leipzig, **92**, 351 (1917).
6. G. L. G. Berry. Index to the powder diffraction file, p. 216. Inorganic Plain Cards No. 11–90. A.S.T.M. Special Publication 48 M2, Philadelphia. 1963.
7. E. R. Andrew. Phys. Rev. **91**, 425 (1953).

[2]Que Monsieur R. de Médicis trouve ici l'expression de nos remerciements pour l'enregistrement des spectres de diffraction de rayon X de poudres.

Can. J. Chem. Downloaded from www.nrcresearchpress.com by 210.87.254.42 on 09/05/12
For personal use only.

Erratum: Sur quelques réactions acide–base dans les solvants fortement basiques anhydres. I. Ethylènediamine

W. R. HEUMANN, A. BOUCHARD ET G. TREMBLAY
Département de Chimie, Université de Montréal, Montréal, Québec

(Ref.: Can. J. Chem. **45**, 3129 (1967))
Reçu le 15 janvier 1968

Canadian Journal of Chemistry, 46, 1822 (1968)

Page 3133, colonne droite, ligne 14:
lire le diphénylméthane au lieu de la diphenylamine.

Can. J. Chem. Downloaded from www.nrcresearchpress.com by 210.87.254.105 on 09/05/12
For personal use only.

Can. J. Chem. Downloaded from www.nrcresearchpress.com by 210.87.254.105 on 09/05/12
For personal use only.

COMMUNICATIONS

Photoinduced paramagnetism in the 1,3,5-trinitrobenzene – cyanide ion system

A. R. NORRIS, A. BRECK, AND J. K. S. WAN
Department of Chemistry, Queen's University, Kingston, Ontario

Received March 25, 1968

Photoinduced paramagnetism has been observed in the 1,3,5-trinitrobenzene – cyanide ion system and evidence is presented to indicate that the radical species is generated via the 1,3,5-trinitrobenzene – cyanide ion σ-complex.

Canadian Journal of Chemistry, 46, 1823 (1968)

Nitroaromatic radical anions can be formed as a result of the interactions of nitro compounds with a number of anions (1–4) and in some instances photoinduced paramagnetism has been observed (5). A simultaneous reaction in many of these systems particularly when the nitroaromatic is 1,3,5-trinitrobenzene is the formation of σ-complexes (6). The extent to which radical anions are present under conditions which lead to significant concentrations of σ-complexes in solution and the role, if any, of the σ-complexes in the formation of the radical anions are uncertain.

As part of a comprehensive study of the equilibrium and kinetic aspects of the cyanide ion – 1,3,5-trinitrobenzene interaction (7–9), we have investigated the paramagnetic species formed by irradiation of this system. We report here evidence which suggests that the paramagnetic species are solvated electrons formed via the one to one, 1,3,5-trinitrobenzene – cyanide ion complex ($TNBCN^-$).

At 25 °C freshly prepared oxygen-free chloroform, carbon tetrachloride, dichloromethane, ethylacetate, *p*-dioxane, or 1,2-dimethoxyethane solutions approximately 10^{-2} *M* in both 1,3,5-trinitrobenzene and tetraphenylarsonium cyanide do not give rise to an electron spin resonance (e.s.r.) spectrum, although they all contain a high concentration of the σ-complex (8).

However, irradiation of these freshly prepared dark-red solutions within the microwave cavity of a Varian e.s.r. spectrometer by light (3500–6500 Å) results in the appearance at $g = 2.002$ of a single symmetrical line of maximum slope width 6 to 7 G. The light source was a Bausch and Lomb high pressure mercury arc equipped with a high intensity monochromator. Tetraphenylarsonium cyanide and 1,3,5-trinitrobenzene alone, in the solvents indicated, do not give rise to an e.s.r. spectrum under similar irradiation. Over the temperature range −30 °C to 30 °C the maximum slope width of the line is apparently both solvent and temperature independent. The photoinduced signal is, however, broadened considerably, sometimes beyond detection, when the solvent is frozen.

Under steady irradiation the intensity of the photoinduced e.s.r. signal remains constant as long as the concentration of σ-complex does not change. The e.s.r. signal rapidly decays to zero intensity when irradiation is discontinued but rapidly returns to its original intensity when irradiation is resumed. The rates of the growth and decay reactions both seem to be solvent and temperature dependent and detailed kinetic studies of these two processes are underway. Over long periods of time secondary dark reactions involving the σ-complex lead to the disappearance of the red color, and the resulting solutions no longer give rise to an e.s.r. signal when irradiated with light in the visible region.

In a given solvent at a fixed temperature and fixed 1,3,5-trinitrobenzene and tetraphenylarsonium ion concentrations the variation in the intensity of the e.s.r. signal with wavelength of the irradiating light parallels the variation with wavelength of the molar extinction coefficient of the σ-complex. In addition, in a series of solvents containing a fixed concentration of 1,3,5-trinitrobenzene and tetraphenylarsonium cyanide and irradiated with the same wavelength of light, the e.s.r. signal intensity varies with solvent as does the equilibrium constant governing complex

formation. These observations strongly suggest the paramagnetic species is generated from the σ-complex upon absorption of light, possibly in the following way.

[1] $TNBCN^- + h\nu \rightarrow (TNBCN)_{solvated} + e^-_{solvated}$

[2] $(TNBCN)_{solvated} + e^-_{solvated} \rightarrow TNBCN^-$

[3] $(TNBCN)_{solvated} + TNBCN^- \rightarrow TNBCN + (TNBCN)^-_{solvated}$

If the exchange reaction [3] is assumed to be rapid, the e.s.r. spectrum of the $(TNBCN)_s$ may be broadened beyond detection. Thus, only the solvated electron is observed which gives an isotropic line (10). Further details of kinetic and mechanistic studies will be forthcoming.

Acknowledgment

Financial support from the National Research Council of Canada and the Ontario Department of University Affairs is gratefully acknowledged.

1. G. A. Russell, E. G. Janzen, and E. T. Strom. J. Am. Chem. Soc. **86**, 1807 (1964).
2. G. A. Russell, A. J. Moye, E. G. Janzen, S. Mak, and E. R. Talaty. J. Org. Chem. **32**, 137 (1967).
3. R. E. Miller and W. F. K. Wynne-Jones. Nature, **186**, 149 (1960).
4. V. Gold and C. H. Rochester. J. Chem. Soc. 1692 (1964).
5. P. B. Ayscough, F. P. Sargent, and R. Wilson. J. Chem. Soc. 5418 (1963).
6. E. Buncel, A. R. Norris, and K. E. Russell. Quart. Rev. London. In press (1968).
7. A. R. Norris. Ph.D. Thesis, University of Chicago, Chicago. (1962).
8. A. R. Norris. Can. J. Chem. **45**, 2703 (1967).
9. E. Buncel, W. Proudlock, A. R. Norris, and K. E. Russell. To be published.
10. P. W. Atkins and M. C. R. Symons. *In* The structure of inorganic radicals. Elsevier, Amsterdam. 1967. pp. 43–77.

Can. J. Chem. Downloaded from www.nrcresearchpress.com by 210.87.254.105 on 09/05/12
For personal use only.

Can. J. Chem. Downloaded from www.nrcresearchpress.com by 210.87.254.105 on 09/05/12
For personal use only.

Canadian Journal of Chemistry

Published by THE NATIONAL RESEARCH COUNCIL OF CANADA

VOLUME 46 JUNE 1, 1968 NUMBER 11

Carbon-13 kinetic isotope effects. IV.[1] The effect of temperature on k_{12}/k_{13} for benzyl halides in bimolecular reactions

JAN BRON AND J. B. STOTHERS

Department of Chemistry, University of Western Ontario, London, Ontario

Received January 10, 1968

The temperature dependence of the ^{13}C kinetic isotope of the α-carbon in benzyl bromide (**1**) and in 1-bromo-1-phenylethane (**2**) has been measured for reaction with alkoxide ion. For these bimolecular displacements, a relatively large temperature effect was found, comparable to that reported for other S_N2 processes. A reexamination of the reaction of **2** with EtO^- has shown an earlier value for k_{12}/k_{13} to be in error.

Canadian Journal of Chemistry, 46, 1825 (1968)

Introduction

Several papers have appeared dealing with carbon isotope effects in bimolecular nucleophilic displacements in aliphatic systems (1–3) and, with a single exception (1), each of the results is relatively large, i.e. in the range, 3–8%, on a ^{13}C basis. For those cases in which the temperature dependence has been examined (2), the expected inverse trend was found such that k_{12}/k_{13} decreases with increasing temperature. This trend is opposite to that found recently for solvolysis (4) and, coupled with the fact that ^{13}C fractionations in S_N1-type reactions tend to be smaller, suggests that ^{13}C kinetic isotope effects may offer a suitable means for distinguishing between transition states for carbonium ion reactions and those for three-center displacements. While this was the original reason for the initial studies (1, 3, 5), the first results have apparently discouraged further work in this area.

As an extension of an earlier study of $^{12}C/^{13}C$ fractionation at the α-carbon of benzylic systems undergoing nucleophilic substitution we have measured k_{12}/k_{13} for (*a*) benzyl bromide (**1**) reacting with methoxide ion at −23 °C and (*b*) 1-bromo-1-phenylethane (**2**) with ethoxide ion at 0° and 25 °C. These systems had been examined previously (1), **1** at 0° and **2** at 25 °C, but an anomalous value for k_{12}/k_{13} was reported for the reaction of **2**. Furthermore, the initial study was conducted at a single temperature and more recent results (2, 4) have shown that a knowledge of the temperature dependence of k_{12}/k_{13} would be valuable.

Experimental

The methods employed were essentially those described previously (5), with some modifications. These included the use of an isotope-ratio, 15 in., Nier-type mass spectrometer with which the carbon dioxide samples derived from the α-carbons were analyzed. A comparison of the mass 45 signal with those for masses 44 and 46 provided a measure of the $^{12}C/^{13}C$ isotopic abundances after correction for ^{17}O and ^{18}O contributions. Kinetic measurements were carried out as before (1) to establish the rates to enable one to quench each experimental run at a known extent of reaction. The purity of the products was confirmed by gas–liquid chromatography after isolation by distillation through an 18 in. Nester Faust platinum spinning-band column. A minor modification in the quenching and isolation stages was the use of 60–80 °C petroleum ether for extraction instead of benzene because of the lower melting point and the reduced solubility of the alcohols.

Results

For the reaction of benzyl bromide (0.5 *M*) with MeO^- (1.0 *M*) in absolute methanol, k_2 was found to be 2.70×10^{-6} l/mole s at

[1]For Part III, see J. Bron and J. B. Stothers, Can. J. Chem. **46**, 1435 (1968).

TABLE I

^{13}C Kinetic isotope effects in the reaction of 1 M MeO^- with benzyl bromide (0.5 M)

Temperature (°C)	Experiment number	Extent of reaction (%)	k_{12}/k_{13}	$(k_{12}/k_{13}-1)100$
−23	1	10	1.0582	5.82
	2	10	1.0581	5.81
	3	10	1.0575	5.75
	4	10	1.0573	5.73
		Mean values	1.0578±0.0002*	5.78±0.02*
0		Mean values†	1.0531±0.0002*	5.31±0.02*

*Standard deviation of the mean.
†Reference 1.

TABLE II

^{13}C Kinetic isotope effects in the reaction of 2 M of EtO^- with 1-bromo-1-phenylethane (0.5 M)

Temperature (°C)	Experiment Number	Extent of reaction (%)	k_{12}/k_{13}	$(k_{12}/k_{13}-1)100$
0	1	5.0	1.0362	3.62
	2	6.0	1.0347	3.47
	3	5.0	1.0378	3.78
	4	5.0	1.0347	3.47
		Mean values	1.0359±0.0007*	3.59±0.07*
25	1	10	1.0332	3.32
	2	10	1.0330	3.30
	3	10	1.0324	3.24
	4	10	1.0297	2.97
		Mean values	1.0321±0.0007*	3.21±0.07*

*Standard deviation of the mean.

−23 °C, while $k_2 = 2.71 \times 10^{-6}$ l/mole s for the reaction of **2** (0.5 M) with EtO^- (2.0 M) in absolute ethanol at 0 °C.

The ^{13}C kinetic isotope effects obtained are collected in Tables I and II for the reactions of **1** and **2**, respectively. As before (5), the measurements for the benzyl systems are the more precise presumably because purification of the ether product is easier and there is little, if any, contamination by side-products.

Discussion

The observed carbon-13 kinetic isotope effects of the reaction of benzyl bromide with methoxide ion show the expected normal temperature dependence, i.e. $k_{12}/k_{13} \propto 1/T$. These results are comparable to those found for bimolecular nucleophilic displacements of methyl halides (2) although the k_{12}/k_{13} values are somewhat smaller, 1.05 *vs.* 1.07. The change in the isotope effect from 5.8 to 5.3% over the temperature interval of 23 °C compares favorably with that, 7.8–6.7% over 45 °C, for the reaction of methyl halides with cyanide ion (2). Although the temperature dependence has not been examined in all of the earlier studies of bimolecular substitution (3), the relatively large fractionations observed in all reported cases, but one, indicate that isotopic mass effects are significantly larger in S_N2 processes than in S_N1-like reactions.

The single exception, 1-bromo-1-phenylethane reacting with ethoxide ion, was reexamined in the present study and the original results were found to be seriously in error. As the data in Table II show, the k_{12}/k_{13} values, although smaller than those found for other bimolecular reactions, are an order of magnitude larger than those previously reported (1). We had originally intended to investigate the temperature dependence of the ^{13}C fractionations for the bimolecular process to compare the results with those for solvolytic reactions of the same reactant (4) but were surprised to find that, at 0 °C, the isotope effect is 3.6%. Since

Can. J. Chem. Downloaded from www.nrcresearchpress.com by 210.87.254.105 on 09/05/12
For personal use only.

Can. J. Chem. Downloaded from www.nrcresearchpress.com by 210.87.254.105 on 09/05/12
For personal use only.

the earlier work (1) gave a value of 0.3% at 25 °C, its reexamination was essential. Initially, reproducible results were not obtained and there was evidence of (*a*) product decomposition during its isolation and purification and (*b*) contamination of the ether with small amounts of the starting material and the corresponding alcohol (presumably formed in small amount during the quenching procedure). In the present work, gas–liquid chromatography was employed to monitor the progress of the purification stages and it was found necessary to carry out the distillations at lower pressures (1–2 mm Hg) than those previously used to avoid contamination. Apparently these modifications are essential for meaningful data although the reproducibility of the earlier results seems remarkable.

Two features of the present data are interesting. Of these, the more significant is the fact that the results for the α-phenylethyl system contrast sharply with those for alcoholysis of the same reactant (4, 5). A plot of the k_{12}/k_{13} values for nucleophilic displacement of various alkyl halides *vs.* temperature is shown in Fig. 1, from which two trends emerge. Processes generally considered to be typical of the S_N2 displacement exhibit relatively large ^{13}C isotope effects which vary inversely with temperature. The α-phenylethyl halides upon solvolysis, however, display very much smaller fractionations at the α-carbon and, furthermore, these vary directly with temperature. Perhaps ^{13}C kinetic isotope effects can serve to distinguish between these two mechanistic extremes.

The second feature of the results for reactions with alkoxide ion, is the smaller k_{12}/k_{13} value for **2** relative to that for **1**. One would not expect that the difference, methoxide *vs.* ethoxide, could affect the fractionation at the α-carbon appreciably in either case and recent work in these laboratories confirms this for the benzyl case.[2] The α-methyl group in **2**, however, will tend to stabilize developing positive charge on the α-carbon and also will tend to inhibit the approach of an attacking nucleophile. These factors can alter the nature of the transition state for **2** + EtO^- relative to that for **1** + MeO^- and the difference may be reflected in the isotope effect for the α-carbon.

If we can assume that three-center displacements at carbon will exhibit isotope effects similar to those predicted for hydrogen isotopes in three-center reactions (6, 7), the maximum fractionation will be observed for systems proceeding through symmetrical transition states. For these, the asymmetric stretching mode involving the nucleophile, N, the leaving group, X, and the carbon at the center of displacement becomes the reaction coordinate and the symmetrical stretching frequency is independent of the mass of the central atom. The transition state, **3**, therefore is symmetrical in the sense that the force constants of the N---C and C----X "bonds" are the same. If these force constants are not equal, the frequency for the "symmetric stretch" will depend on the mass of the central carbon and the observed isotopic fractionation will be less than the maximal value. Several discussions of this phenomenon for hydrogen isotopes have appeared (8), and Fry (3) has discussed the effects predicted for each of the C, N, and X nuclei in terms of a closely-related model.

[N-----C-----X]
3

If this reasoning is valid for carbon isotopes in three-center displacements, the direction in which the transition state is shifted from the symmetric remains to be decided. Is it product-like or reactant-like? This question and its solution have been discussed for hydrogen isotopic fractionations by Thorton (9). In the present system it seems reasonable to suggest, lacking other evidence, that the transition state for the α-phenylethyl system would be carbonium-ion like in the sense that little bond formation is involved with extensive bond rupture, since the α-methyl group and the phenyl ring can stabilize developing charge at the α-carbon. We tentatively conclude, therefore, that the smaller k_{12}/k_{13} for the reaction of **2** with ethoxide ion is indicative of a transition state having some degree of carbonium ion character.

It would be interesting to compare the secondary α-deuterium isotope effect in the α-phenylethyl and benzyl systems undergoing these bimolecular reactions as a test of our interpretation. The former would be predicted to exhibit a k_H/k_D value slightly greater than unity while, for the latter, k_H/k_D should be equal to, or less than, unity (10) if our interpretation of the ^{13}C results is valid.

[2]A. J. McNamara and J. B. Stothers. Unpublished results.

Can. J. Chem. Downloaded from www.nrcresearchpress.com by 210.87.254.105 on 09/05/12
For personal use only.

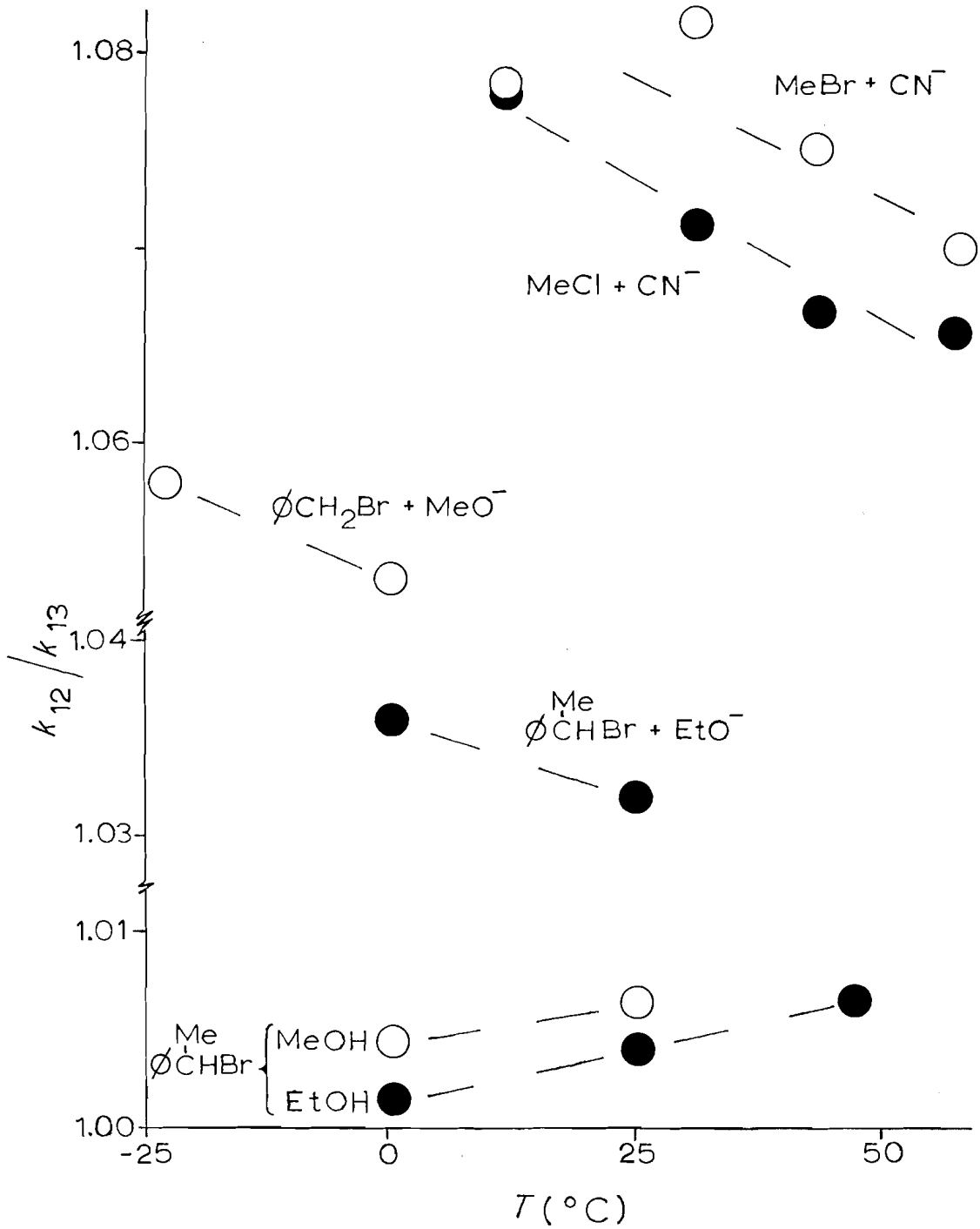

FIG. 1. Plot of k_{12}/k_{13} results for some nucleophilic displacements *vs.* temperature. Methyl halides, ref. (2); α-phenylethyl bromide alcoholyses, ref. (4).

Acknowledgment

We are grateful to the National Research Council of Canada for financial support of this investigation.

1. J. B. STOTHERS and A. N. BOURNS. Can. J. Chem. **40**, 2007 (1962).
2. K. R. LYNN and P. E. YANKWICH. J. Am. Chem. Soc. **83**, 53 (1961); **83**, 790 (1961); **83**, 3220 (1961).
3. M. L. BENDER and D. F. HOEG. J. Am. Chem. Soc. **79**, 5644 (1957); G. J. BUIST and M. L. BENDER. J. Am. Chem. Soc. **80**, 4308 (1958); A. FRY. Pure Appl. Chem. **8**, 414 (1964).
4. J. BRON and J. B. STOTHERS. Can. J. Chem. **46**, 1435, (1968).
5. J. B. STOTHERS and A. N. BOURNS. Can. J. Chem. **38**, 923 (1960).
6. F. H. WESTHEIMER. Chem. Rev. **61**, 265 (1961).
7. L. MELANDER. *In* Isotope effects on reaction rates. The Ronald Press Co., New York. 1960.
8. J. BIGELEISEN. Pure Appl. Chem. **8**, 217 (1964).
9. E. R. THORNTON. J. Org. Chem. **27**, 1943 (1962).
10. E. A. HALEVI. *In* Progress in physical organic chemistry. Vol. 1. Interscience Publishers, Inc., New York. 1963. p. 173.

Can. J. Chem. Downloaded from www.nrcresearchpress.com by 210.87.254.105 on 09/05/12
For personal use only.

Hydroxyl stretching vibration in 2,6-dimethyl- and 2,6-dichloro-4-substituted phenols

GORDON LEARY
Chemistry Division, Department of Scientific and Industrial Research, Petone, New Zealand

Received August 14, 1967

The infrared frequencies and apparent half band widths of the O—H stretching band of a series of 2,6-dimethyl-4-substituted phenols and a series of 2,6-dichloro-4-substituted phenols have been measured in carbon tetrachloride solution. The slopes of the Hammett plots for the frequencies and half band widths of both these series are compared with those calculated from published data for 2,6-di-*t*-butyl-4-substituted phenols and 3- or 4-substituted phenols. Significant differences are found in ρ obtained from the frequency data for the four series. The 2,6-dimethyl-4-substituted phenols, unlike the unhindered phenols, are found to parallel the 2,6-di-*t*-butyl-4-substituted phenols in having a negative ρ for the frequency data and a negative ρ for the half band width correlation. It is concluded that the negative ρ from the half band widths of 2,6-di-*t*-butyl-4-substituted phenols is primarily a result of electronic rather than steric factors.

Canadian Journal of Chemistry, **46**, 1831 (1968)

Can. J. Chem. Downloaded from www.nrcresearchpress.com by 210.87.254.5 on 09/05/12
For personal use only.

Introduction

The infrared frequencies (ν_m) and apparent half band widths $\Delta\nu_{\frac{1}{2}}^a$ of the O—H stretching band in 3- and 4-substituted phenols and in 2,6-di-*t*-butyl-4-substituted phenols have been found to correlate with Hammett σ values for the 3- or 4-substituents (1, 2). Although the slopes of the Hammett plots for the frequency data were very similar for the two series, the slopes for the $\Delta\nu_{\frac{1}{2}}^a$ data were of opposite sign. From a consideration of these two series alone it could not be decided whether this change in sign was a consequence of the steric rather than the polar effect of the *t*-butyl substituent. The methyl substituent normally has a similar electronic effect to the *t*-butyl group, yet it is too small to cause appreciable steric hindrance to solvation of the hydroxy group in 2,6-dimethyl phenol (3). It is thus of interest to examine the dependence of ν_m and $\Delta\nu_{\frac{1}{2}}^a$ on σ_p for 2,6-dimethyl-4-substituted phenols, covering a wide range of 4-substituents.

The changes in ν_m and $\Delta\nu_{\frac{1}{2}}^a$ with σ_p for a series of 2,6-dimethyl-4-substituted phenols are now reported. The corresponding data for a series of 2,6-dichloro-4-substituted phenols are also included.

Experimental

A Beckman DK2A spectrophotometer was used to measure the hydroxyl bands. The instrument was calibrated by the standard absorption lines of water and ammonia. In no case did corrections to the measured O—H frequencies exceed 2 cm^{-1}. The carbon tetrachloride used as solvent (British Drug Houses, "AnalaR" grade) was freshly redistilled through a 12 in. vigreux column. The cells were 10 cm long and phenol concentrations from 0.0025 to 0.0005 *M* were employed. Even at concentrations of 0.01 *M* no association of unhindered phenols is found (1). The preparation and purification of the phenols has been described elsewhere (4, 5).

Results

The frequencies of the band maxima (ν_m) and the apparent half band widths ($\Delta\nu_{\frac{1}{2}}^a$) for the O—H stretching vibration in the phenols examined are given in Table I. Hammett substituent constants for the 4-substituents (σ_p) are included in the table. The σ_p^- values used were considered to be the most accurate available since they were evaluated by Taft's recommended procedure (4). Regression lines were fitted to the ν_m against σ data and the slopes (ρ), correlation coefficients (*r*), standard deviations (*S*) and standard deviations of the slopes (*S*ρ) are given in Table II. Similar calculations using the same σ values for Ingold's data (1) for 2,6-di-*t*-butyl-4-X-phenols (X = OCH_3, *t*-Bu, CH_3, Cl, CN, CHO, NO_2, H) and 3- or 4-X-phenols (X = 4-OCH_3, *t*-Bu, CH_3, Cl, CN, CHO, NO_2, H; 3-CH_3, Cl, NO_2) and also for Cohen and Jones' data (2) for 2,6-di-*t*-butyl-4-X-phenols (X = OCH_3, *t*-Bu, CH_3, H, Br, COOEt, $COCH_3$, CN, CHO, NO_2) are included in Table II. The values used for the 3-CH_3, Cl, and NO_2 substituents were $\sigma^0 s$ (6), that for the 4-Cl substituent was σ^- (5). Ingold's data (1) for multiply-substituted phenols were not included because of the possibility of steric interactions between substituents. His data (1) for 4-OH,—NH_2,—$C_6H_5(CH_3)_2C$, —$C_2H_5(CH_3)CH$,—$C_2H_5(CH_3)_2C$, and Cohen and Jones' data (2) for 4-COO^-,—SO_3^-,—$CONH_2$,—$N(CH_3)_3^+$,—COOH were also omitted because σ values for these substituents are not known with certainty. Plots of $\Delta\nu_{\frac{1}{2}}^a$ against σ_p

TABLE I

Frequencies and apparent half band widths of the O—H band in substituted phenols

Substituents	σ_p	ν_m (cm^{-1})	$\Delta\nu_{\pm}^a$ (cm^{-1})
2,6-Di-(CH_3)-4-CH_3	−0.15†	3628	29
2,6-Di-(CH_3)-4-OCH_3	−0.12†	3630	30
2,6-Di-(CH_3)-4-*t*-Bu	−0.13†	3627	26
2,6-Di-(CH_3)-4-H	0.00†	3626‖	26
2,6-Di-(CH_3)-4-F	0.02‡	3627	26
2,6-Di-(CH_3)-4-Br	0.26‡	3622	26
2,6-Di-(CH_3)-4-CH_3CO	0.85‡	3615	22
2,6-Di-(CH_3)-4-CN	0.89‡	3615	22
2,6-Di-(CH_3)-4-CHO	1.04‡	3612	20
2,6-Di-(CH_3)-4-NO_2	1.25‡	3611	21
2,6-Di-(CH_3)-4-NO*	1.60‡	3583	16
2,6-Di-Cl-4-CH_3	−0.15†	3546	26
2,6-Di-Cl-4-H	0.00†	3540	24
2,6-Di-Cl-4-Br	0.26‡	3540	28.5
2,6-Di-Cl-4-$COOC_2H_5$	0.65§	3527	27
2,6-Di-Cl-4-CH_3CO	0.85‡	3526	26
2,6-Di-Cl-4-CN	0.89‡	3526	27.5
2,6-Di-Cl-4-CHO	1.04‡	3521	26

*Not used in fitting the regression line since it exists in the quinone oxime form (10).
†σ^0 values (6).
‡σ^- values (4, 5).
§ Derived from the pK_a of ethyl 4-hydroxybenzoate (7).
‖Literature values 3622 cm^{-1} (3) and 3620 cm^{-1} (8).

TABLE II

Correlations of ν_m/σ_p for substituted phenols

Phenol series	ρ	*r*	*S*	*S*ρ	Number of phenols in series
4-Substituted	−14.886	0.972	1.963	1.187	11
2,6-Di-*t*-butyl-4-substituted*	−15.897	0.994	1.075	0.694	8
2,6-Di-*t*-butyl-4-substituted†	−16.261	0.999	0.205	0.126	10
2,6-Dimethyl-4-substituted	−13.077	0.990	1.334	0.804	10
2,6-Dichloro-4-substituted	−19.803	0.894	5.127	4.464	7

*Reference 1.
†Reference 2.

for the 2,6-dimethyl-4-substituted phenols and 2,6-dichloro-4-substituted phenols are shown in Fig. 1. With the exception of 2,6-dimethyl-4-nitrosophenol, whose band width is not included in Fig. 1, all the compounds had absorption bands of similar, symmetrical shape. The use of a consistent set of σ values in the calculation of the regression line parameters for each of the phenolic series means that any observed differences in the parameters for different series does not result from fortuitous variations in the choice of σ values.

Discussion

The hydroxyl frequency in 2,6-dimethyl phenol differs from that found by other workers (3, 8). However, the correlation of ν_m with σ_p for the 2,6-dimethyl-4-substituted phenols, including 2,6-dimethyl phenol, is very good, as is that for the 2,6-di-*t*-butyl- and the unhindered 3-, or 4-substituted phenols. The correlation is highest for the di-*t*-butyl series and falls off as the *ortho* groups decrease in size (*t*-Bu > CH_3 > H) and solvation of the hydroxyl group becomes easier. The 2,6-dichloro-4-substituted phenol data gave a relatively low correlation coefficient (0.894) and a relatively high standard deviation of slopes (4.464). This is almost certainly attributable to the presence of an intramolecular hydrogen bond between the O—H group and the *ortho* chloro atom (9). The strength of such a hydrogen bond would not depend solely on σ_p but should also be a function of σ_m for the 4-substituent. Nevertheless, plotting ν_m for the 2,6-dichloro-4-substituted phenols against σ_p

Can. J. Chem. Downloaded from www.nrcresearchpress.com by 210.87.254.5 on 09/05/12
For personal use only.

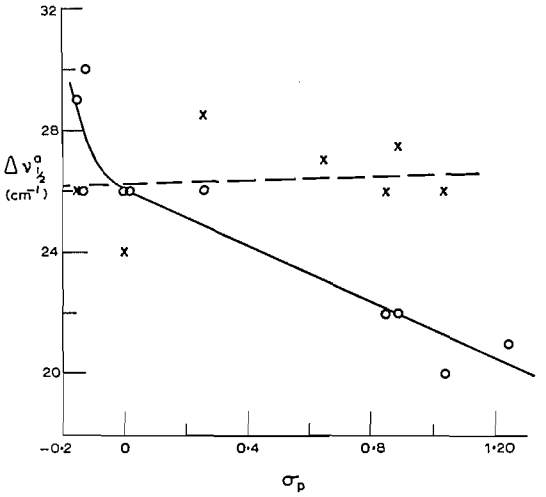

FIG. 1. Apparent half band width of O—H bands against σ_p. *o*-2,6-Dimethyl-4-substituted phenols; X-2,6-dichloro-4-substituted phenols. O represents points for 2,6-dimethyl-4-substituted phenols; X represents points for 2,6-dichloro-4-substituted phenols.

$+ \alpha\sigma_m$, where the constant α was given a wide range of values, did not noticeably improve the correlation.

Comparison of the reaction constant (ρ) for the four series suggests that the agreement in reaction constants previously reported (1) for the plots for the 2,6-di-*t*-butyl-4-substituted phenols and the unhindered phenols is not real but results from the lower correlation found for the latter. Otherwise, the steric and electronic properties of the methyl group would lead to an identical ρ value for the 2,6-dimethyl-4-substituted phenols. Although the precision of the reaction constants is not high enough to be certain that the ρ values for the 2,6-dimethyl-4-substituted phenols and the unhindered phenols are different, ρ for the 2,6-dimethyl-4-substituted phenols is significantly higher (less negative) than that for the 2,6-di-*t*-butyl-4-substituted phenols.

Similarly the low correlation of ν_m with σ_p for the 2,6-dichloro-4-substituted phenols means that the reaction constant for this series is not significantly different from that for the unhindered phenols. It is, however, significantly lower than that for the 2,6-dimethyl-4-substituted phenols. Moreover, the ρ values for the 2,6-dimethyl, unhindered, and 2,6-dichloro series of phenols steadily increase in magnitude (become more negative) as σ_p for the *ortho* substituent becomes more negative. The reaction constant for the ν_m/σ data of the 2,6-di-*t*-butyl-4-substituted phenols does not fit in with this trend and hence seems to be anomalous.

The plots of the $\Delta\nu_{\frac{1}{2}}^{a}/\sigma$ data (Fig. 1) reveal that $\Delta\nu_{\frac{1}{2}}^{a}$ for the 2,6-dichloro-4-substituted phenols does not vary significantly with σ_p, i.e. ρ is roughly zero. On the other hand, $\Delta\nu_{\frac{1}{2}}^{a}$ for the 2,6-dimethyl-4-substituted phenols decreases as σ_p increases. The 2,6-dimethyl-4-substituted phenols thus fall into the same category as the 2,6-di-*t*-butyl-4-substituted phenols which previously were reported (1) as the only known series of benzene derivatives whose frequencies and apparent half band widths vary with σ to give slopes of the same sign. The unhindered phenols have apparent half band widths that increase as σ increases.

Since the value of $\Delta\nu_{\frac{1}{2}}^{a}$ is probably largely dependent upon the degree of association (degree of hydrogen bonding; degree of interaction with solvent or bulky *ortho* groups; etc.) of the phenolic O—H group, it seems that the association of the hydroxy group in 2,6-dichloro-4-substituted phenols is fairly constant. This is not surprising in view of the intramolecular OH....Cl hydrogen bond that is known to be formed. Similarly, the association of the hydroxy group appears to increase with σ in unhindered phenols and to decrease with σ in 2,6-dimethyl-4-substituted phenols and 2,6-di-*t*-butyl-4-substituted phenols. It is difficult to picture how the associations of the hydroxy group of the latter two series can decrease with increase in electron withdrawing power of the 4-substituent, but in view of the great difference in the steric effects of *ortho* methyl and *ortho* *t*-butyl groups, the polar rather than the steric effects of the *ortho* substituents are probalby involved.

1. K. U. INGOLD. Can. J. Chem. **38**, 1092 (1960).
2. L. A. COHEN and W. M. JONES. J. Am. Chem. Soc. **85**, 3402 (1963).
3. L. J. BELLAMY and R. L. WILLIAMS. Proc. Roy. Soc. London, Ser. A, **254**, 119 (1960).
4. A. FISCHER, G. J. LEARY, R. D. TOPSOM, and J. VAUGHAN. J. Chem. Soc. B, 782 (1966).
5. A. FISCHER, G. J. LEARY, R. D. TOPSOM, and J. VAUGHAN. J. Chem. Soc. B, *686 (1967)*.
6. R. W. TAFT. J. Phys. Chem. **64**, 1805 (1960).
7. L. A. COHEN and W. M. JONES. J. Am. Chem. Soc. **85**, 3397 (1963).
8. P. J. KRUEGER and H. W. THOMPSON. Proc. Roy. Soc. London, Ser. A, **250**, 22 (1959).
9. N. A. PUTTNAM. J. Chem. Soc. 5100 (1960).
10. R. K. NORRIS and S. STERNHELL. Australian J. Chem. **19**, 841 (1966).

Can. J. Chem. Downloaded from www.nrcresearchpress.com by 210.87.254.5 on 09/05/12
For personal use only.

Can. J. Chem. Downloaded from www.nrcresearchpress.com by 210.87.254.5 on 09/05/12
For personal use only.

Réactions des époxydes de quelques stéroides avec le glycinate d'éthyle

KRZYSZTOF JANKOWSKI ET CASIMIR BERSE
Département de chimie, Université de Montréal, Montréal, Québec

Reçu le 12 décembre 1967

La réaction d'ouverture de l'hydroxy-3β époxy-16α,17α pregnène-5 one-20, du cétal de l'hydroxy-3β époxy-16α,17α pregnène-5 one-20, de l'hydroxy-3α époxy-5α,6α pregnanone-20 et de l'acétate de l'époxy-5β,6β cholestéryl par le glycinate d'éthyle a été étudiée. La stéréochimie des principaux produits obtenus, les hydroxyaminoesters, a été discutée.

Canadian Journal of Chemistry. 46, 1835 (1968)

La continuation des travaux précédents (1, 2) sur l'ouverture par les acides aminés d'époxydes nous a conduit à examiner les comportements des époxydes des stéroides vis-à-vis des esters des acides aminés. Nous avons voulu obtenir des aminohydroxyesters possédant l'activité physiologique. Nous avons aussi pensé que l'introduction d'un grand substituant sur l'azote des acides aminés peut stabiliser les aminohydroxyesters formés. Nous avons choisi l'hydroxy-3β époxy-16α,17α pregnène-5 one-20 (**1**) et son cétal (**2**) avec l'époxyde sur le cycle D à cause de rigidité moins grande et l'exposition à l'attaque par les acides aminés plus grande. L'hydroxy-3β époxy-5α,6α pregnanone-20 (**3**) et l'acétate de l'époxy-5β,6β cholesteryl (**4**) avec l'époxyde sur le noyau B ont été choisis à cause de leur grande stabilité et de l'empêchement de ce noyau par la présence des noyaux A et C.

Les époxydes utilisés pour les réactions ont été vérifiés par la résonance magnétique nucléaire (r.m.n.). Ils correspondent aux résultats calculés par Tori, Komeno et Nakagawa (3) (Tableau I). L'ouverture de l'hydroxy-3β époxy-16α,17α pregnène-5 one-20 (**1**) avec le glycinate d'éthyle dans le chloroforme a fourni l'amino-hydroxyester, p.f. 220 °C. Le spectre infrarouge (i.r.) montre une large double bande carbonyle entre 1705 et 1693 cm^{-1} et une forte bande carbonyle d'ester à 1725 cm^{-1}. Le spectre r.m.n. montre les signaux des méthyles en 18, 19, 21 vers 1.00, 1.05 et 2.03 p.p.m. de NH—CH_2—CO vers 3.2 p.p.m. et de C_2H_5 vers 4.2 et 1.2 p.p.m. respectivement (Tableau II). Dans les conditions employées, la formation d'une imine par action du groupement aminé du glycinate d'éthyle sur le carbonyle en position-20 (4) a été peu probable et cette réaction n'a pas été observée. En plus, le mélange réactionnel a été traité par l'acide chlorhydrique pour hydrolyser l'imine éventuellement formée.

TABLEAU I

Signal du proton sur le noyau oxirannique

Epoxyde*	δ (p.p.m.)
1	3.67
2	3.70
3	2.85
4	3.07
19	3.29

*Le solvant était $CDCl_3$.

TABLEAU II

Les spectres de résonance magnétique nucléaire des produits d'ouverture* (δ, p.p.m.)

Hydroxyaminoester	Méthyle 18	Méthyle 19	Méthyle 21	CH_3—CH_2	NH—CH_2—CO	Autres
5	1.00	1.05	2.03	1.2 et 4.20	3.20	5.32
8	0.95	0.95	1.32	1.17 et 4.21	3.35	5.35 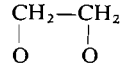 3.93
11	0.58	0.86	2.10	1.20 et 4.18	3.17	—
13	0.68	0.99	0.82	1.25 et 4.20	3.19	méthyle 26 et 27 0.91 (doublet) acétate 2.07

*Le solvant était $CDCl_3$.

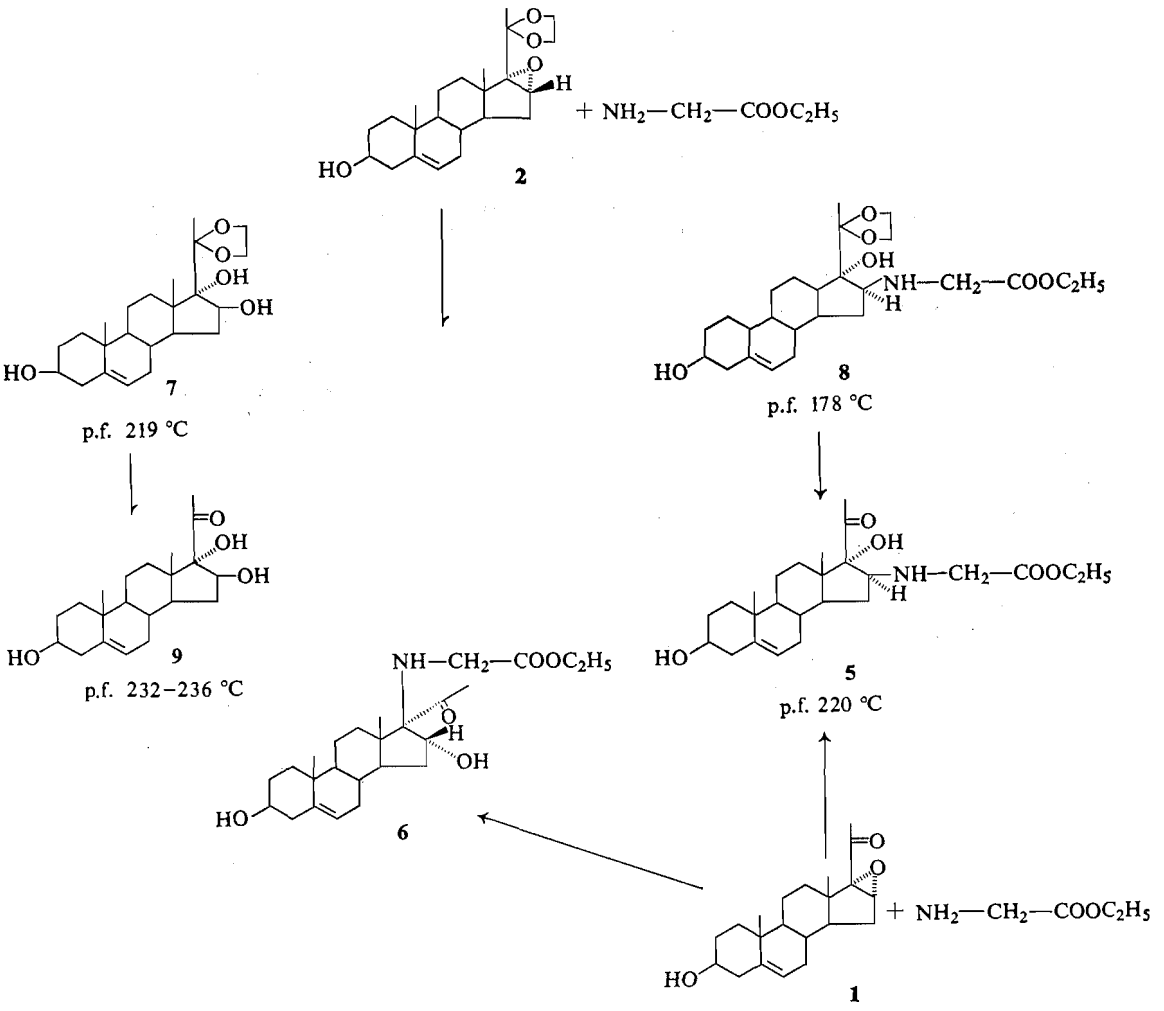

Pour cet aminohydroxyester, on peut attribuer deux structures possibles correspondant à l'attaque du côté du carbone en positions-16 ou -17 donnant le *N*-(oxo-20 dihydroxy-3β,17α pregnène-5 yl)-16β glycinate d'éthyle (**5**) ou le *N*-(oxo-20 dihydroxy-3β,16α pregnène-5 yl)-17β glycinate d'éthyle (**6**) respectivement. La première de ces structures est favorisée par l'effet stérique, règle de Fürst et Plattner (5, 6), la deuxième par l'effet électronique.

Pour résoudre ce problème, nous avons préparé le cétal de l'hydroxy-3β époxy-5α,6α pregnanone-20 (**2**) pour éliminer l'effet électronique.

L'ouverture du cétal de l'hydroxy-3β époxy-16α,17α pregnène-5 one-20 (**2**) avec le glycinate d'éthyle dans le chloroforme a fourni deux produits isolés par la chromatographie: le cétal de la trihydroxy-3β,16β,17α pregnène-5 one-20 (**7**) et le *N*-(cétal de l'oxo-20 dihydroxy-3β,17α pregnène-5 yl)-16β glycinate d'éthyle (**8**).

En plus, on a isolé le produit qui n'a pas réagi. Les deux cétals **7** et **8** ont été décétalisés par l'acide acétique dans le méthanol pendant 2 h à la température de la pièce. Les deux produits ont été isolés et identifiés. Le premier a été identifié par le spectre infrarouge et le point de fusion comme la trihydroxy-3β,16β,17α pregnène-5 one-20 (**9**) identique à celui préparé par Inhoffen *et al.* (7). Le deuxième a été identifié par les spectres infrarouges, r.m.n., point de fusion mixte comme le *N*-(oxo-20 dihydroxy-3β,17α pregnène-5 yl)-16β glycinate d'éthyle (**5**) identique à celui obtenu par l'ouverture de l'hydroxy-3β époxy-16α,17α pregnène-5 one-20 (**1**) par le glycinate d'éthyle.

Can. J. Chem. Downloaded from www.nrcresearchpress.com by 210.87.254.5 on 09/05/12
For personal use only.

TABLEAU III

Les spectres de résonance magnétique nucléaire des dérivés de l'hydroxy-17 pregnanone*

Composé	Méthyle 18	Méthyle 19	Méthyle 21
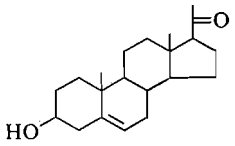 **10**	0.645	1.025	2.15
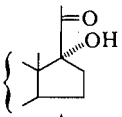 A	0.94	1.02	2.27
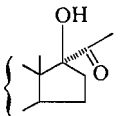 A′	0.93	1.07	2.08
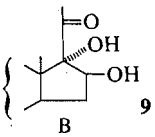 **9** B	1.00 large		2.10
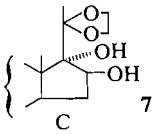 **7** C	1.00 large		1.30
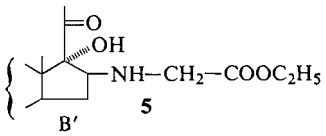 **5** B′	1.00	1.05	2.03
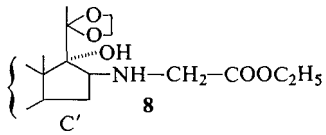 **8** C′	0.95 large		1.32

*Le solvant était $CDCl_3$.

L'absorption du méthyle 19 dans le spectre r.m.n. apparaît très près de celui du méthyle 18 et l'absorption du méthyle 19 reste constante pour toute la série des produits. Cette absorption est influencée par les environnements comme Zürcher (8), Tori (9) et Smith (10) l'ont montré dans leurs travaux. Les calculs ont été faits et les corrections pour les différents substituants ont été rapportées (10). En utilisant l'hydroxy-3β pregnène-5 one-20 (**10**) comme le produit de référence, nous avons calculé les corrections pour les méthyles 18 et 19 du composé **5**, et nous avons trouvé les valeurs suivantes: 0.355 p.p.m. et 0.025 p.p.m. respectivement.

Il faut admettre que l'environnement influence aussi la position du méthyle 21 (c'est-à-dire le

Can. J. Chem. Downloaded from www.nrcresearchpress.com by 210.87.254.5 on 09/05/12
For personal use only.

Can. J. Chem. Downloaded from www.nrcresearchpress.com by 210.87.254.5 on 09/05/12
For personal use only.

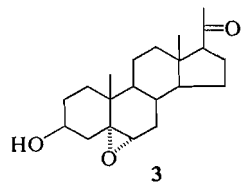

3

$+ NH_2—CH_2—COOC_2H_5$

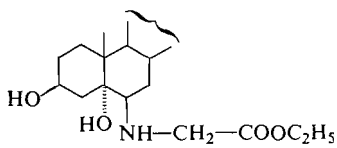

11

p.f. 187 °C

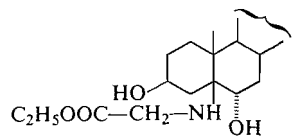

12

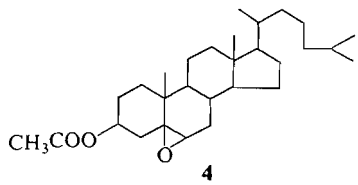

4

$+ NH_2—CH_2—COOC_2H_5$

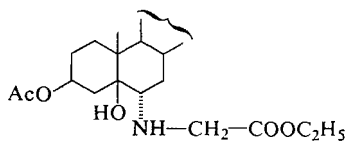

13

p.f. 254 °C

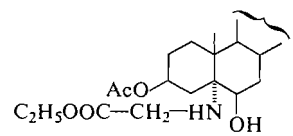

14

méthyle de l'acétyle en position-17). La différence entre l'absorption de 17α-acétyle et de 17β-acétyle est environ 0.19 p.p.m. (A – A′). Nous avons aussi constaté que la différence entre l'absorption des méthyles d'acétyle et de cétal reste presque constante pour les paires des produits (B – B′; C – C′) (Tableau III).

L'ouverture de l'hydroxy-3β époxy-5α,6α pregnanone-20 (**3**) et de l'acétate de l'époxy-5β,6β cholestéryl (**4**) avec le glycinate d'éthyle dans le chloroforme a fourni deux aminohydroxyesters. Le premier avec le p.f. de 187 °C montre le spectre infrarouge pour les bandes carbonyles 1735–1703 cm^{-1} et 1693 cm^{-1}. Le spectre r.m.n. montre les signaux des méthyles en 18, 19, 21 vers 0.58, 0.86 et 2.1 p.p.m.; de C_2H_5 vers 1.2 et 4.18 p.p.m. et de NH—CH_2—CO vers 3.18 p.p.m. respectivement. Le deuxième

aminohydroxyester avec le p.f. de 254 °C montre le spectre infrarouge pour les bandes carbonyles 1730 cm^{-1} et 1715 cm^{-1}. Le spectre r.m.n. montre les signaux des méthyles en 18, 19 et 21, vers 0.68, 0.99, 0.82 respectivement et des méthyles en 26 et 27 vers 0.91.

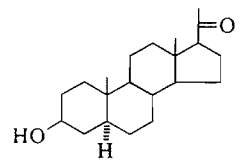

15

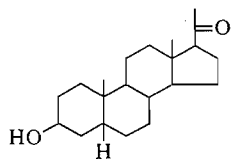

16

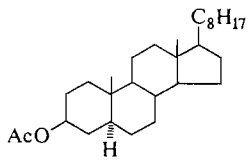

17

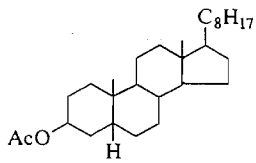

18

Pour chacun de ces aminohydroxyesters, on peut attribuer deux structures possibles correspondant à l'attaque sur le carbone en position-5 ou -6 par le groupement aminé du glycinate d'éthyle. L'attaque en position-6 donne le *N*-(oxo-20 dihydroxy-3β,5α pregnyl)-6β glycinate d'éthyle (**11**) et le *N*-(acétate-3β dihydroxy-3β,5β cholestanyl)-6α glycinate d'éthyle (**13**) respectivement. L'attaque en position-5 donne le *N*-(oxo-20 dihydroxy-3β,6α pregnyl)-5β glycinate d'éthyle (**12**) et le *N*-(acétate-3β dihydroxy-3β,6β cholestanyl)-5α glycinate d'éthyle (**14**) respectivement.

La structure **11** montre que la jonction des noyaux A et B des stéroides est *trans*. L'hydroxy-aminoester **5** se caractérise de la rétention de la configuration du groupement hydroxyle vis-à-vis de l'époxyde de départ. Le produit est diaxial et par conséquence la règle de Plattner est respectée. Dans la structure **12**, la jonction des noyaux A et B des stéroides est *cis*. La structure **13** montre la jonction *cis* pour les noyaux A et B. Dans cette structure, il y a aussi la rétention de la configuration du groupement hydroxyle par rapport à l'époxyde de départ. Même si la structure **13** ne respecte pas la règle de Plattner et Fürst, d'après les examens des spectres r.m.n., les structures **11** et **13** ont été choisies comme les plus probables.

Nous avons calculé l'influence d'environnement sur les méthyles en position-18 et -19 pour les aminohydroxyesters **11** et **13** en utilisant comme références les stéroides ayant les jonctions des noyaux A/B *trans* ou *cis*.

Les valeurs obtenues pour le composé **11** ont été plus proches de celles de l'hydroxy-3β pregnane-5α one-20 avec la jonction *trans* **15** qu'avec celles de l'hydroxy-3β pregnane-5β one-20 avec la jonction *cis* **16**. Les valeurs obtenues pour le composé **12** ont été plus proches de celles de l'acétate de coprostanol avec la jonction *cis* **18** qu'avec celles de l'acétate de cholestanol avec la jonction *trans* **17**.

Il faut souligner que les différences dans les absorptions $\Delta\delta$ calculées pour les méthyles en position-18 et -19 dans le cas des composés **11** et **15** et celles pour les composés **13** et **18** sont de même ordre (Tableau IV).

Nous avons aussi calculé la largeur du pic dans le spectre r.m.n. pour le méthyle en position-19 à sa demi-hauteur. Le méthyle 19 est influencé à cause du couplage à longue distance par les trois hydrogènes sur la jonction *trans* et par un seul pour la jonction *cis* (11). Comme produit modèle, nous avons choisi l'hydroxy-3β pregnanone-20 avec la jonction A/B soit *trans* **15** soit *cis* **16** avec les valeurs pour largeur du pic à demi-hauteur 1.25 c.p.s. et 0.87 c.p.s. respectivement. Le deuxième produit modèle choisi a été le cholestanol-3β avec les valeurs pour largeur du pic 0.72 c.p.s. pour l'isomère *cis* **18** et 0.91 c.p.s. pour l'isomère *trans* **17** (Tableau IV).

La valeur de 1.0 c.p.s. calculée pour le composé **10** indique que la jonction A/B est *trans* et la valeur de 0.8 trouvée pour le composé **13**, montre que la jonction A/B est *cis*. La valeur pour la jonction *trans* du composé **11** est plus petite probablement à cause du fait que l'hydrogène 5α a été substitué par un groupement fonctionnel (Tableau VI). L'ouverture des époxydes stéroidaux avec le glycinate de sodium n'a donné aucune réaction, seulement les époxystéroides ont été récupérés, probablement à cause d'une réaction d'élimination qui suivit la réaction d'ouverture des époxydes en milieu basique. Si on considère le glycinate d'éthyle comme une base faible, cela peut expliquer le faible rendement en produits d'ouvertures de l'époxyde dans la série stéroidale.

Malgré que les époxydes stéroidaux étudiés contiennent les cycles époxycyclopentanique et époxycyclohexanique, nous n'avons pas constaté

Can. J. Chem. Downloaded from www.nrcresearchpress.com by 210.87.254.5 on 09/05/12
For personal use only.

TABLEAU IV

Les résultats de spectres résonance magnétique nucléaire

	δ (p.p.m.)		Δδ		Méthyle 19	*L h*/2 (c.p.s.)
Composé	Méthyle 18	Méthyle 19	Méthyle 18	Méthyle 19	Ce travail	Litt. (11)
11	0.58	0.86	0.032	0.050	1.0	1.25 (*trans*)
15	0.618	0.816				
16	0.618	0.967				
17	0.644	0.823				
13	0.68	0.99	0.027	0.053	0.8	0.72 (*cis*)
18	0.653	0.937				

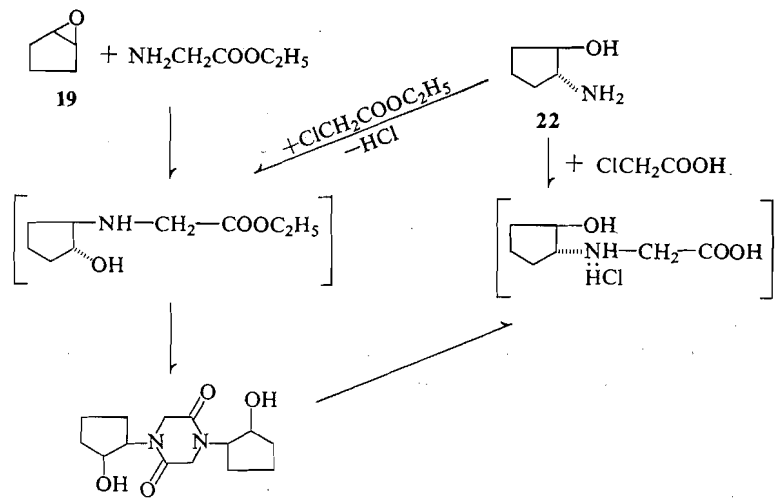

20

p.f. 255 °C

la formation des dérivés de la dicéto-2,5 pipérazine *N*,*N*′-disubstitué ou des morpholones-2 comme pour l'époxycyclohexane (2) comme la formation de la dicéto-2,5 pipérazine dans le cas de l'époxycyclopentane (**19**). L'époxycyclopentane (**19**) dans la réaction avec le glycinate d'éthyle donne le bis-(hydroxy-2 cyclopentyl)-1,4 dicéto-2,5 pipérazine (**20**), p.f. 255 °C. Le produit **20** a été identifié par la comparaison des spectres infrarouges avec celui obtenu pour l'ouverture de l'époxycyclohexane (2) (1635 et 3350 cm^{-1}), par l'hydrolyse et par la synthèse.

L'absence des dérivés de la dicéto-2,5 pipérazine et morpholones-2 dans la série des stéroides peut être expliquée par une plus grande stabilité des hydroxyaminoesters mentionnés comme les produits primaires d'ouverture des époxydes et par la flexibilité des noyaux cyclopentanique et cyclohexanique qui facilite la dimérisation ou la lactonisation. Dans le cas des stéroides, ces transformations sont empêchées.

Partie expérimentale

Les points de fusion ont été déterminés dans l'appareil de Kofler et ne sont pas corrigés. Les spectres infrarouges ont été enregistrés sur un spectrophotomètre BECKMAN IR-8 en Nujol. Les microanalyses ont été effectuées dans les laboratoires Midwest Microlab., Inc., Indianapolis, Indiana, U.S.A. et par nous-mêmes (micro Kjeldahl). Les spectres de résonance magnétique nucléaire ont été enregistrés sur un spectromètre Varian A-60. Le glycinate d'éthyle a été préparé d'après la méthode de E. Fischer (12). Le composé **1**, produit commercial (Sigma Chemical Company) a été purifié par la recristallisation du méthanol (p.f. 191–193 °C). A partir de ce produit, on a préparé son cétal (**2**) (p.f. 171 °C) d'après la méthode décrite par P. L. Julian *et al.* (13) avec le rendement de 37%.

Can. J. Chem. Downloaded from www.nrcresearchpress.com by 210.87.254.5 on 09/05/12
For personal use only.

Can. J. Chem. Downloaded from www.nrcresearchpress.com by 210.87.254.5 on 09/05/12
For personal use only.

Le composé **3** a été séparé du mélange des époxydes α et β obtenus d'après la peroxydation de l'hydroxy-3β pregnène-5 one-20 par l'acide *m*-chloroperbenzoique dans le chloroforme (rendement 17%, p.f. 182–183 °C. Litt. 180–184 °C (14)) ou par l'acide perbenzoique (rendement 12%).

Le composé **4** a été préparé par la peroxydation de l'acétate de cholesteryl avec l'acide *m*-chloroperbenzoique dans le chlorure de méthylène, p.f. 112 °C rendement 21% (Litt. (15), p.f. 112 °C).

Le composé **19** a été préparé à partir du cyclopentène (**21**) par peroxydation avec l'acide *m*-chloroperbenzoique dans le chloroforme p.é. 100 °C, rendement 23% (Litt. (16), p.é. 100–102 °C).

Ouverture de l'hydroxy-3β époxy-16α,17α pregnène-5 one-20 (1) avec le glycinate d'éthyle

La solution du produit **1** (2 g, 7 mmoles) dans le chloroforme anhydre (25 ml) a été chauffée au bain-marie pendant 12 h avec le glycinate d'éthyle (0.8 g, 7 mmoles), puis la solution a été extraite avec l'acide chlorhydrique à 2% (2 × 20 ml) et l'eau. La solution a été séchée avec le carbonate de potassium anhydre et évaporée à sec. Le résidu a été chromatographié sur la colonne de silica gel. Trois fractions ont été séparées: (*a*) p.f. 260 °C (subl.); rendement: 93 mg (21%); (*b*) p.f. 189–191 °C; rendement: 1.35 g (67.5%) et (*c*) p.f. 220 °C; rendement: 26 mg (1%).

Le produit (*a*) a été identifié comme la dicéto-2,5 pipérazine (**23**) par la comparaison des spectres infrarouges et par le point de fusion mixte. Le composé (*b*) a été identifié comme le produit **1** par la comparaison de ses spectres r.m.n., infrarouge et par le point de fusion mixte. Le produit (*c*) cristallisé de l'éthanol absolu a été identifié comme le *N*-(oxo-20 dihydroxy-3β,17α pregnène-5 yl)-16β glycinate d'éthyle (**5**).

Anal. Calc. pour $C_{25}H_{39}O_5N$ (433.6): C, 69.25; H, 9.07; N, 3.23. Trouvé: C, 69.60; H, 8.80; N, 3.01.

Ouverture du cétal de l'hydroxy-3β époxy-16α,17α pregnène-5 one-20 (2) avec le glycinate d'éthyle

La solution du produit **2** (180 mg, 0.5 mmole) dans le chloroforme (50 ml) a été portée à reflux avec le glycinate d'éthyle (50 mg 0.5 mmole) pendant 10 h. Le solvant a été évaporé *in vacuo* et le résidu a été chromatographié sur la colonne de silica gel. Les quatre fractions ont été séparées: (*a*) p.f. 260 °C (subl.); rendement: 5 mg, (17%); (*b*) p.f. 169–171 °C; rendement. 40 mg, (22%); (*c*) p.f. 178 °C; rendement: 45 mg, (19%); (*d*) p.f. 219 °C; rendement: 31 mg, (16%).

Les produits (*a*) et (*b*) sont identiques avec la dicéto-2,5 pipérazine (**23**) et le produit **2**.

Le produit (*c*) recristallisé de l'acétone a été identifié comme étant le *N*-(cétal de l'oxo-20 dihydroxy-3β,17α pregnène-5 yl)-16β glycinate d'éthyle (**8**). Le spectre infrarouge est 1730 et 1095 cm^{-1}.

Anal. Calc. pour $C_{27}H_{43}O_6N$ (477.6): C, 67.90; H, 9.07; N, 2.93. Trouvé: C, 68.23; H, 8.72; N, 2.72.

Le produit (*d*) recristallisé de l'éthanol a été identifié comme le cétal de la trihydroxy-3β,16β,17α pregnène-5 one-20 (7); le spectre infrarouge est 3350 cm^{-1}.

Anal. Calc. pour $C_{23}H_{36}O_5$ (392.5): C, 70.38; H, 9.22. Trouvé: C, 69.70; H, 8.90.

N-(Oxo-20 dihydroxy-3β,17α pregnène-5 yl)-16β glycinate d'éthyle (5)

La solution du produit **8** (26 mg, 0.05 mmole) dans l'acide acétique méthanol 1:1 (5 ml) a été chauffée à 60 °C pendant 4 h puis les solvants ont été évaporés *in vacuo*. Le résidu a été traité deux fois avec le benzène–éthanol absolu 1:1 et évaporé *in vacuo*. Le produit a été chromatographié sur la colonne de silica gel et recristallisée d'éthanol. Le produit **5** a été identifié par le point de fusion mixte, et par la chromatographie sur couches minces, par les spectres infrarouge et r.m.n. Le rendement: 10 mg (45.1%), p.f. 219–220 °C.

Trihydroxy-3β,16β,17α pregnène-5 one-20 (9)

La solution du produit **7** (25 mg, 0.05 mmole) dans l'acide acétique – méthanol 1:1 (3 ml) a été traité à la façon habituelle. Le produit **9** a été identifié par le point de fusion et par les spectres; le rendement: 13 mg (55%), p.f. 232–236 °C. (Litt. (7): p.f. 230–236 °C).

Ouverture de l'hydroxy-3β époxy-5α,6α pregnanone-20 (3) avec le glycinate d'éthyle

La solution du produit **3** (800 mg, 2.5 mmoles) dans le chloroforme anhydre a été chauffée au bain-marie avec le glycinate d'éthyle (250 mg, 2.5 mmoles) pendant 10 h, puis le mélange a été extrait deux fois avec l'acide chlorhydrique à 5%. La solution chloroformique a été séchée avec le carbonate de potassium anhydre et évaporée *in vacuo*. Le résidu a été chromatographié sur la colonne de silica gel et les trois fractions ont été séparées: (*a*) p.f. 260 °C (subl.); rendement: 70 mg (50%); (*b*) p.f. 182–183 °C; rendement: 160 mg (20%) et (*c*) p.f. 187 °C; rendement: 29 mg (1.7%).

Le produit (*a*) cristallisé de l'éthanol a été identifié comme la dicéto-2,5 pipérazine (**23**) par la comparaison des spectres et par le point de fusion mixte. Le produit (*b*) cristallisé de l'acétone a été identifié comme le produit **3** de départ. Le produit (*c*) cristallisé de l'éthanol a été identifié comme le *N*-(oxo-20 dihydroxy-3β,5α pregnyl)-6β glycinate d'éthyle (**11**); le spectre infrarouge est 1735, 1703 et 1693 cm^{-1}.

Anal. Calc. pour $C_{21}H_{41}O_3N$ (435.6): C, 68.93; H, 9.49; N, 3.22. Trouvé: C, 68.71; H, 9.44; N, 3.00.

Ouverture de l'acétate de l'époxy-5β,6β cholesteryl (4) avec le glycinate d'éthyle

La solution du produit **4** (450 mg, 1 mmole) dans le chloroforme (35 ml) a été chauffée avec le glycinate d'éthyle (100 mg, 1 mmole) au bain-marie pendant 14 h. Le solvant a été évaporé et le résidu a été chromatographié sur le silica gel. Les trois fractions ont été séparées: (*a*) p.f. 260 °C (decomp.); rendement: 25 mg (43%); (*b*) p.f. 110–112 °C; rendement: 200 mg (44%) et (*c*) p.f. 254 °C; rendement: 17 mg (3.1%).

Le produit (*a*) recristallisé de l'éthanol a été identifié comme la dicéto-2,5 pipérazine (**23**) par la comparaison des spectres et point de fusion mixte. Le produit (*b*) recristallisé de méthanol a été identifié comme le produit **4** de départ. Le produit (*c*) a été identifié comme le *N*-(acétate-3β dihydroxy-3β,5β cholestanyl)-6α glycinate d'éthyle (**13**); le spectre infrarouge est 1730 et 1715 cm^{-1}.

Anal. Calc. pour $C_{35}H_{57}O_5N$ (547.9): C, 72.35; H, 10.25; N, 2.56. Trouvé: C, 72.10; H, 9.37; N, 2.51.

Ouverture de l'époxycyclopentane (19) avec le glycinate d'éthyle

La solution du produit **19** (4.2 g, 0.05 mmole) dans le chloroforme (45 ml) a été portée à reflux avec le glycinate d'éthyle (5 g, 0.05 mole) au bain-marie pendant 12 h. Le solvant a été évaporé *in vacuo* et le produit a été recristallisé de l'éthanol.

Le bis-(hydroxy-2 cyclopentyl)-1,4 dicéto-2,5 pipérazine (**20**) p.f. 255 °C a été isolé; le rendement 240 mg (3.5%); le spectre infrarouge est 1635 et 3350 cm^{-1}.

Anal. Calc. pour $C_{14}H_{22}O_4N_2$ (282.4): C, 59.56; H, 7.85; N, 9.92. Trouvé: C, 59.84; H, 7.92; N, 9.71.

Le produit **20** hydrolysé avec l'acide chlorhydrique concentré a été comparé avec celui obtenu par la réaction de *trans*-amino-2 cyclopentanol (**22**) (17) avec l'acide chloroacétique. L'identité des deux produits hygroscopiques a été prouvée par la chromatographie sur couches minces dans le système pyridine – eau – acide acétique (1:1:3); le R_f du produit après l'hydrolyse est 0.27 et le R_f du produit synthétisé à partir de *trans*-aminocyclopentanol (**22**): 0.25 – 0.26.

Bis-(hydroxy-2 cyclopentyl)-1,4 dicéto-2,5 pipérazine (20)

Le produit **20** a été synthétisé à partir de l'amino-2 cyclopentanol (**22**) avec le chloroacétate d'éthyle d'après la méthode analogue à celle décrite par l'amino-2 cyclohexanol (2). Après la libération du HCl par le traitement avec la triéthylamine dans le diméthylformamide, les petites quantités du produit **20** ont été séparées; p.f. 255 °C (rendement; 1.4%): le spectre infrarouge est 3350 et 1635 cm^{-1}. Le produit ne donne pas de dépression du point de fusion lorsque mélangé avec le composé **20** déjà obtenu.

Remerciements

Les auteurs remercient le Conseil National de Recherches du Canada pour l'aide financière apportée sous forme d'octroi de recherches.

1. C. BERSE et K. JANKOWSKI. Can. J. Chem. **44**, 1513 (1966).
2. C. BERSE et K. JANKOWSKI. Can. J. Chem. **45**, 2865 (1967).
3. K. TORI, T. KOMENO et T. NAKAGAWA. J. Org. Chem. **29**, 1134 (1964).
4. TH. WAGNER-JAUREGG, L. ZIRNGIBL et H. GÜNTHER. Tetrahedron Letters, **33**, 3123 (1967).
5. A. FÜRST et PL. A. PLATTNER. Intern. Congr. Pure and Appl. Chem. 12th Congr. New York. 1951. Abstr. Papers. p. 405.
6. R. PARKER et N. S. ISAAC. Chem. Rev. **59**, 737 (1959). A. A. AKHREM, A. V. KAMERNITSKII, V. A. DUBROVSKII et A. M. MOISEENKOV. Izv. Akad. Nauk Kaz. S.S.R. Ser. Khim. Nauk, **9**, 1726 (1964). L. VARGHA, E. KASZTREVNER, L. SZPORNY et M. RADOS. Hung. Patent No. 150,213 (May 31, 1963), d'après Chem. Abstr. **60**, 623*f* (1964).
7. H. H. INHOFFEN, F. BROMEYER et K. BRÜCKNER. Ber. **87**, 593 (1954).
8. R. F. ZÜRCHER. Helv. Chim. Acta, **44**, 1380 (1961); Helv. Chim. Acta, **46**, 2054 (1963).
9. K. TORI, T. TOMITA, H. ITAZAKI, M. NARISADA et W. NAGATA. Chem. Pharm. Bull. (Tokyo), **11**, 956 (1963).
10. L. L. SMITH. Steroids, 4, **3**, 395 (1964).
11. K. L. WILLIAMSON, T. HOWELL et T. A. SPENCER. J. Am. Chem. Soc. **88**, 325 (1966).
12. E. FISCHER. Ber. **34**, 436 (1901).
13. P. L. JULIAN, E. W. MEYER et I. RYDEN. J. Am. Chem. Soc. **71**, 756 (1949); J. Am. Chem. Soc. **72**, 367 (1950).
14. M. EHRENSTEIN et T. D. STEVENS. J. Org. Chem. **6**, 908 (1941).
15. L. RUZICKA et L. BOSSHARD. Helv. Chim. Acta, **20**, 244 (1937).
16. W. MEISNER. Ber. **32**, 2052 (1899).
17. M. GODRHOT et M. MOUSSERON. Compt. Rend. **196**, 1680 (1933). J. SICHER, M. HORÁK et M. SVOBODA. Collection Czech. Chem. Commun. **24**, 950 (1959), d'après Chem. Abst. **53**, 21162.

Can. J. Chem. Downloaded from www.nrcresearchpress.com by 210.87.254.5 on 09/05/12
For personal use only.

Can. J. Chem. Downloaded from www.nrcresearchpress.com by 210.87.254.6 on 09/05/12
For personal use only.

Reformatsky reactions with *o*- and *p*-substituted benzophenones

E. H. CHARLESWORTH AND PETER CHARLESON
Department of Chemistry, University of Manitoba, Winnipeg, Manitoba

Received October 26, 1967

Nine new β,β-diarylhydracrylic acids are reported from the condensation of monosubstituted benzophenones with ethyl bromoacetate in Reformatsky reactions. The reaction of 4-nitrobenzophenone which fails to go into classical Reformatsky reactions can be accomplished in excellent yield by the two-step process; however, 2-nitrobenzophenone fails to react under any conditions.

In the case of 2-chlorobenzophenone in benzene–toluene, the hydracrylic acid is not isolated, but rather the unsaturated β-chlorophenyl-β-phenyacrylic acid. Diethyl ether appeared in general to be superior to benzene–toluene as a solvent for the reactions. Anisole under reduced pressure has also been used successfully in two cases.

Canadian Journal of Chemistry, **46**, 1843 (1968)

This research was undertaken largely on the basis of a comment by Klemm and Bower (1) in 1958 that "there has been very little investigation of the Reformatsky reaction employing diaryl ketones".

The four major objectives of the investigation have been: a study of the influence of substituents in the 2- and 4-positions of the benzophenone nucleus on the yield of products; the comparison of the relative effectiveness of two dissimilar reaction solvents namely diethyl ether and benzene–toluene; experiments to see if nitrobenzophenones which previously have failed to go into the classical (one-step) Reformatsky method might react in the two-stage process introduced in 1953 by Siegel and Keckeis (2); the isolation and characterization of the β,β-diarylhydracrylic acids resulting when a variety of 2- and 4-substituted benzophenones are condensed with ethyl bromoacetate under appropriate conditions.

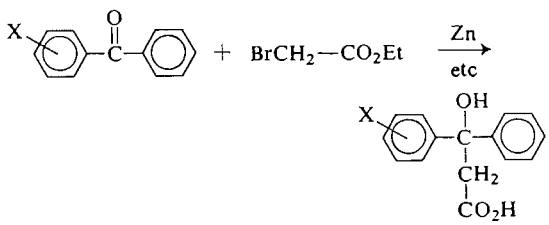

The classical Reformatsky reaction is well reviewed up to 1942 by Shriner (3). The following brief review of the literature since this time may be worth while. Natelson and Gottfried (4) reported that best yields were obtained with a solvent giving a reaction temperature of 95–105 °C and this is best achieved by a benzene–toluene (1:1) solution. Dreiding and Pratt (5) reported a case where different solvents benzene and ether gave different end products. Cason and Fessenden (6) and Evans (7) found that benzene–ether gave better yields than benzene itself. The two-stage process was introduced by Siegel and Keckeis (2) and also used by Vinograd and Vul'fson (8), Grob and Brenneisen (9), and Vaughan *et al.* (10). In general this method has permitted reactions between substances that fail in the one-step process and in other cases has given increased yields.

Fifteen β,β-diarylhydracrylic acids have been synthesized in this investigation, nine of which are new compounds namely: β-(2-aminophenyl)-, β-(4-aminophenyl)-, β-(2-hydroxyphenyl)-, β-(4-hydroxyphenyl)-, β-(2-bromophenyl)-, β-(4-bromophenyl)-, β-(2-chlorophenyl)-, β-(4-fluorophenyl)-, and β-(4-nitrophenyl)-β-phenylhydracrylic acids (see Table II). Twelve of these acids have been characterized by means of their *p*-nitrobenzyl esters as shown in Table III.

TABLE I

Yields with variation of solvent*

X	Solvent	% yield of crude acid
2-CH_3	Benzene–toluene†	32
2-CH_3	Benzene	41
2-CH_3	Benzene–ether‡	53
2-CH_3	Ether	52
4-CH_3	Benzene–toluene	76
4-CH_3	Benzene	62
4-CH_3	Benzene–ether	81
4-CH_3	Ether	84

*Compounds of structure 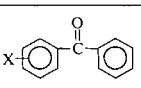

†40:35 v/v.
‡1:1 v/v.

TABLE II

β,β-Diarylhydracrylic acids*

X	% yield of crude acid: In Et_2O	% yield of crude acid: In Benzene–toluene (40:35 v/v)	Melting point† purified acid (°C)	Formula	Analyses: Calculated (%)	Analyses: Found (%)
2-NH_2	20	4	186–189	$C_{15}H_{15}NO_3$	C, 70.0; H, 5.9; N, 5.4	C, 70.1; H, 5.2; N, 5.6
4-NH_2	6	23	ca.171			
2-OH	16	29	109–111	$C_{15}H_{14}O_4$	C, 69.8; H, 5.4	C, 71.3; H, 5.0
4-OH	6	42	154–156	$C_{15}H_{14}O_4$	C, 69.8; H, 5.4	C, 69.7; H, 4.9
2-OCH_3	72	64	139–140.5‡			
4-OCH_3	84	68	154–155§			
2-CH_3	52	32	147–148‖			
4-CH_3	84	76	180–182¶			
H	88	84	210–211**			
4-F	95	77	174–175.5	$C_{15}H_{13}FO_3$	C, 69.2; H, 5.0; F, 7.3	C, 69.4; H, 5.2; F, 8.3
2-Cl	44	40	153–157	$C_{15}H_{13}ClO_3$	C, 65.1; H, 4.7; Cl, 12.8	C, 65.4; H, 4.7; Cl, 12.8
4-Cl	64	76	187–190††			
2-Br	60	32	154–155	$C_{15}H_{13}BrO_3$	C, 56.1; H, 4.1; Br, 24.9	C, 56.7; H, 4.3; Br, 24.8
4-Br	88	80	186–188	$C_{15}H_{13}BrO_3$	C, 56.1; H, 4.1; Br, 24.9	C, 55.8; H, 4.2; Br, 25.0
4-NO_2	0	0	142–143	$C_{15}H_{13}NO_5$	N, 4.9	N, 4.9
2-NO_2	0	0				

*Compounds of structure 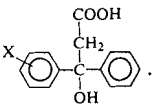 .

†All melted with decomposition (frothing).

‡Literature m.p. 139° (21).
§Literature m.p. 160° (25).
‖Literature m.p. 152° (25).
¶Literature m.p. 187° (25).
**Literature m.p. 212° (26).
††Literature m.p. 180° (24).

In general, diethyl ether proved to be superior to benzene–toluene as a reaction solvent (see Tables I and II). The reaction of 2-chlorobenzophenone in benzene–toluene has resulted in the formation of the unsaturated acid, β-(2-chlorophenyl)-β-phenylacrylic acid rather than the corresponding hydroxyacid isolated from ether.

Resonance and steric effects associated with the substituent groups attached to the benzophenone nucleus, were found to have predictable influences on the yields of the hydroxyacids (Table II). The 4-derivative produces greater yields than the 2-derivative. 4-Nitrobenzophenone which does not react in the classical Reformatsky reaction gives an excellent yield in the two-step process (see Table IV). On the other hand with 2-nitrobenzophenone no yield of acid was obtained by either process. In other cases, the two-step process has given increased yields. (Compare similar substances in Table V and Table II (benzene–toluene).)

Lewis and Wright (11) in their investigation on solvent effects in the Grignard reaction reported that anisole was superior to ether in the reaction of ethyl magnesium bromide with benzophenone. By a reduced pressure technique anisole was successfully used in the present investigation as a Reformatsky solvent (Table V). Due to the relatively high reflux temperature (170°) considerable decomposition occurred at atmospheric pressure and a pressure of 26 mm was employed.

Experimental

Activated Zinc

The zinc used in this investigation was in the form of 20 mesh granules, Fisher Scientific Co. (Z-15) activated by the procedure of Palmer and Reid (12).

Monosubstituted Benzophenones

The sixteen substituted benzophenones employed in this study were all prepared as described in the literature. Syntheses of five of these were sufficiently modified to merit comment.

2-Hydroxybenzophenone

In the past, this appears to have been made by a Friedel–Crafts reaction between 2-methoxybenzoyl chloride and benzene, excess aluminium chloride being used to ensure demethylation as well as aroylation (13). A direct synthesis employing 2-hydroxybenzoyl chloride in the Friedel–Crafts reaction does not appear to have been previously employed.

A suspension of anhydrous aluminium chloride (77 g, 0.58 mole) in benzene (450 ml) was heated under reflux. A solution of 2-hydroxybenzoyl chloride (0.36 mole) prepared by Kirpal's method (14) in benzene (200 ml) was added with stirring to the refluxing solution. The reaction

Can. J. Chem. Downloaded from www.nrcresearchpress.com by 210.87.254.6 on 09/05/12
For personal use only.

TABLE III

p-Nitrobenzyl β,β-diarylhydracrylates*

X	Melting point (°C)	Formula	Analyses	
			Calculated (%)	Found (%)
2-OH	86–89	$C_{22}H_{19}NO_6$	N, 3.6	N, 3.9
4-OH	106–108	$C_{22}H_{19}NO_6$	N, 3.6	N, 3.3
2-OCH_3	106.5–108	$C_{23}H_{21}NO_6$	N, 3.4	N, 3.9
2-CH_3	130–132	$C_{23}H_{21}NO_5$	N, 3.6	N, 3.8
4-CH_3	101–102.5	$C_{23}H_{21}NO_5$	N, 3.6	N, 3.7
4-F	105–106	$C_{22}H_{18}NFO_5$	N, 4.8; F, 3.5	N, 4.2; F, 3.3
2-Cl	108–110	$C_{22}H_{18}NClO_5$	N, 3.4; Cl, 8.6	N, 3.6; Cl, 8.7
4-Cl	111.5–112.5	$C_{22}H_{18}NClO_5$	N, 3.4; Cl, 8.6	N, 3.6; Cl, 8.9
2-Br	122–123	$C_{22}H_{18}NBrO_5$	N, 3.1; Br, 17.5	N, 2.8; Br, 18.2
4-Br	126.5–128	$C_{22}H_{18}NBrO_5$	N, 3.1; Br, 17.5	N, 2.9; Br, 18.4
4-NO_2	139–140.5	$C_{22}H_{18}N_2O_7$	N, 6.6	N, 6.4

*Compounds of structure 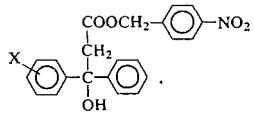 .

TABLE IV

Two-stage reactions*

X	% yield of crude acid
2-NH_2	16
4-NH_2	31
4-OCH_3	82
2-CH_3	56
2-NO_2	0
4-NO_2	100

*Compounds of structure 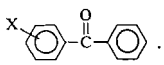 .

TABLE V

Reactions under reduced pressure*

X	Reaction conditions	% yield of crude acid
4-CH_3	Anisole b.p. 64° at 26 mm	76
2-CH_3	Anisole b.p. 62° at 26 mm	58
2-CH_3	Benzene–toluene† b.p. 37° at 82 mm	16
2-CH_3	Benzene–toluene b.p. 92° at atm	32
2-OCH_3	Benzene–toluene b.p. 38° at 84 mm	52
2-OCH_3	Benzene–toluene b.p. 91° at atm	64
2-Br	Benzene–toluene b.p. 38° at 85 mm	24
2-Br	Benzene–toluene b.p. 92° at atm	32

*Reactions involved compounds of structure 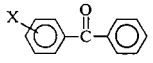 .
†40:35 v/v.

was allowed to continue until the evolution of hydrogen chloride ceased. On cooling, the mixture was poured cautiously onto a mixture of ice and dilute acid. The aqueous layer was separated and extracted with benzene. The benzene extract was washed successively with dilute hydrochloric acid, water, sodium carbonate solution (5%), and water. After drying over magnesium sulfate and removal of the benzene by distillation, the residue was subjected to vacuum distillation. The crude product was collected at 119–138° at 1 mm, as a yellow oil (46.5 g). Recrystallization from aqueous acetone gave a solid (37.2 g) which melted at 39–41 °C. DeTar and Relyea (15) have reported 38.5–39 °C.

2-Aminobenzophenone

This ketone was prepared by the method of Scheifele and DeTar (16) with the following modification.

The benzene reaction mixture after the completion of the Friedel–Crafts reaction was cooled to room temperature and poured onto a mixture of ice and concentrated hydrochloric acid. This hydrolyzed mixture was filtered free of a considerable quantity of light olive-green solid. This solid which was apparently impure 2-toluenesulfonylamidobenzophenone was readily hydrolyzed by hot hydrochloric acid (10%) to 2-aminobenzophenone. The benzene layer from the filtrate was separated from the aqueous phase, washed with water, and dried. Removal of the benzene *in vacuo* afforded a considerable quantity of a brown solid. This solid was heated with concentrated sulfuric acid (200 ml) on a steam bath for 15 min. The resultant solution was cooled, poured into water (500 ml), and filtered free of a solid which was apparently phenyl *p*-tolyl sulfone. The filtrate was neutralized with 6 *N* sodium hydroxide solution. The precipitate of impure 2-aminobenzophenone was collected, combined with the main portion isolated above by hydrochloric acid hydrolysis and recrystallized from aqueous ethanol. The yield of 2-aminobenzophenone was 40.8. g (41% on basis of *p*-toluenesulfonylanthranilic acid). It melted at 105–107 °C.

Can. J. Chem. Downloaded from www.nrcresearchpress.com by 210.87.254.6 on 09/05/12
For personal use only.

Can. J. Chem. Downloaded from www.nrcresearchpress.com by 210.87.254.6 on 09/05/12
For personal use only.

4-Nitrobenzophenone

This ketone was prepared in a Friedel–Crafts reaction by dropwise addition of a solution of 4-nitrobenzoyl chloride in benzene to a well stirred suspension of anhydrous aluminium chloride in benzene at room temperature and then allowing the mixture to stand overnight. A 95% yield of ketone was obtained which melted at 135–137 °C. If the Friedel–Crafts reaction is carried out at the more usual temperature of 50 °C the yield falls to 60%. Schroeter (17) has reported a melting point of 138 °C.

Reduction of this nitroketone with iron and acetic acid according to the directions of Simpson *et al.* (18) for the corresponding 2-nitroketone gave an excellent yield (88%) of 4-aminobenzophenone.

4-Methylbenzophenone

This ketone was prepared in 57% yield by treating 4-methylbenzoyl chloride with diphenyl cadmium according to the directions of Cason and Prout (19) for the preparation of methyl 4-keto-7-methyloctanoate. Purification was accomplished by vacuum distillation, b.p. 127–130° at 1 mm, and recrystallization from alcohol, m.p. 56–59 °C. Blakely and Scarborough (20) have reported a melting point of 56 °C.

2-Nitrobenzophenone

This proved the most difficult of the starting ketones to obtain. A number of syntheses are reported in the literature, but none of these presented a simple method giving a pure product in good yield. Even the diphenyl cadmium method used above for 4-methylbenzophenone gave only an impure product which contained a considerable quantity of biphenyl. The method which was eventually successful was the oxidation of 2-nitrobenzhydrol according to the directions of Stoermer and Fridericji (21) and also used by us in the preparation of 2-methoxybenzophenone.

A solution of potassium dichromate (55.6 g) concentrated sulfuric acid (46 ml) and water (256 ml) was added in one portion, with stirring, to 2-nitrobenzhydrol (30.9 g). The temperature of the mixture was observed to rise quickly to 45° and then slowly dropped back to room temperature. The dark colored liquid was poured into water (500 ml), the crude product isolated by filtration, washed with water and air-dried. Recrystallization of the crude ketone (30.8 g) from methanol afforded a product which melted at 104–106 °C. Hay and Mulley (22) have reported a figure of 103–104 °C.

General Procedures for Synthesis of β,β-*Diarylhydracrylic Acids*

(a) Classical (One-stage) Reaction

Activated zinc granules (3.8 g, 0.058 g-atom) were added to a solution of diarylketone (0.025 mole) and ethyl bromoacetate (4.5 g, 0.027 mole) in anhydrous solvent (30 ml). The reaction mixture was contained in a 100 ml three-necked flask, equipped with a magnetic stirrer, electric heating mantle, thermometer, and an efficient reflux condenser with the outlet protected by a calcium chloride tube.

The mixture was stirred and cautiously heated to the reflux temperature. If, after several minutes of refluxing, the reaction showed no signs of having initiated (a distinct change in clarity and/or color of the solution), one or two small crystals of iodine and/or mercuric chloride were added to reactivate the zinc *in situ*. In the event that the initial exothermic reaction threatened to "froth over", the heating mantle was removed and the flask was cooled as long as it was necessary to keep the reaction under control, but not enough to stop the reaction. Once under control, the reaction was refluxed and stirred for an additional 2 h.

At the end of this period, the reaction mixture was decanted from the unreacted zinc, and both the zinc and the flask were rinsed with additional solvent. The zinc was dried and its weight recorded. The decanted mixture was combined with the solvent and hydrolyzed with 10% sulfuric acid (20 ml). The resultant two-phase system was separated; the aqueous layer was extracted with ether (2 × 25 ml), and then discarded. The combined organic layers were evaporated under reduced pressure and the residue was saponified according to the directions of Palmer and Reid (12) by refluxing with potassium hydroxide solution (13 ml, 2.5 *N*) in ethanol (25 ml) for 4 h. The saponification mixture was diluted with water (25 ml) and most of the alcohol was removed at 60° under reduced pressure.

The residue was extracted with ether (2 × 25 ml, 2 × 10 ml) and the combined ethereal extracts were washed with 5% sodium carbonate solution (these washings were combined with the main aqueous layer). Then the ether layer was dried over magnesium sulfate and filtered into a tared distillation flask. Removal of the ether under reduced pressure left a neutral residue (mainly unreacted ketone) whose weight was recorded.

The combined aqueous layers (above), containing the potassium salt of the hydroxy acid and excess base, were heated on a steam bath to drive off traces of ether, cooled, and acidified with dilute hydrochloric acid. In most instances the precipitated acid was isolated by suction filtration, washed, and dried. In a few cases, it was necessary to extract the acid with ether, with subsequent washing, drying, and removal of the ether. The weight of the crude acid was recorded and the percentage yield calculated on this figure, in general, agreed well with that calculated on the basis of the recovered ketone.

(b) Reaction under Reduced Pressure

This procedure was exactly the same as the above except that the apparatus was connected (via the top of the condenser) to a vacuum pump, manometer, and bleeder valve for adjusting and maintaining a constant low pressure. This setup permitted the reaction mixture to be refluxed at a temperature considerably lower than at atmospheric pressure. The low pressure was maintained throughout the initiation, and the 2 h reflux period.

(c) Two-stage Reaction

As the heading implies, this reaction was carried out in two steps. First, a reaction of activated zinc granules (3.8 g, 0.058 g-atom) with ethyl bromoacetate (4.5 g, 0.027 mole) in anhydrous ether (30 ml) was initiated as in the one-stage procedure and refluxed for 1 h beyond initiation. At the end of this period the ethereal solution was cooled and quickly decanted into another dry reaction flask. Second, a solution of the diarylketone (0.0063 mole[1]) in 30 ml of benzene–toluene (40:35 v/v) was added in one portion to the above ether solution.

The total reaction mixture was refluxed for 2 h, and worked up as in the one-stage procedure.

Purification and Characterization of the β,β-Diarylhydracrylic Acids

The crude acids (Table II) from the Reformatsky reactions and hydrolysis of the esters were crystallized for analysis or for comparison with literature melting points from aqueous alcohol. The 2-hydroxy and the 4-nitro acids were crystallized from benzene. All were colorless except the 2-amino acid which was in the form of yellow needles. The 4-amino compound was not obtained in pure enough condition for analysis. The melting points of the purified acids and the analytical results are reported in Table II.

The *p*-nitrobenzyl esters of these acids were prepared according to the directions of Shriner, Fuson, and Curtin (23). Melting points and analytical results are recorded in Table III.

In the case of the reaction with 2-chlorobenzophenone in benzene–toluene the hydroxy acid was not formed, but rather the corresponding unsaturated β-2-chlorophenyl-β-phenyl acrylic acid. On crystallization from aqueous alcohol this melted at 140–141.5 °C.

Anal. Calcd. for $C_{15}H_{11}O_2Cl$ (neutralization equivalent, 258.5): Cl, 70.0; H, 4.25; Cl, 13.7. Found (neutralization equivalent, 260 ± 3): C, 69.7; H, 4.28; Cl, 13.9.

When a hot alkaline solution of β-4-methoxyphenyl-β-phenylhydracrylic acid, (m.p. 154°) was acidified with dilute hydrochloric acid, carbon dioxide and water were lost and α-methoxyphenyl-α-phenylethylene was produced. After crystallization from aqueous alcohol it melted at 74–76 °C. Hurd and Webb (24) reported 75 °C as the melting point.

Anal. Calcd. for $C_{15}H_{14}O$: C, 85.7; H, 6.7. Found: C, 85.5; H, 6.5.

Acknowledgment

The authors are grateful to the National Research Council of Canada for grants which have aided in this research.

[1]The mole fraction of ketone is reduced from that of the one-step procedure to ensure that it remains the limiting factor in the second stage in spite of self condensation of the Reformatsky reagent during stage one.

1. L. H. KLEMM and G. M. BOWER. J. Org. Chem. **23**, 344 (1958).
2. A. SIEGEL and H. KECKEIS. Monatsh. Chem. **84**, 910 (1953); Chem. Abstr. **48**, 10545 (1954).
3. R. L. SHRINER. Org. Reactions, **1**, 1 (1942).
4. S. NATELSON and S. P. GOTTFRIED. J. Am. Chem. Soc. **61**, 970 (1939).
5. A. S. DREIDING and R. J. PRATT. J. Am. Chem. Soc. **75**, 3717 (1953).
6. J. CASON and R. J. FESSENDEN. J. Org. Chem. **22**, 1326 (1957).
7. F. J. EVANS, JR. Dissertation Abstr. **18**, 1252 (1958).
8. L. KH. VINOGRAD and N. S. VUL'FSON. Dokl. Akad. Nauk SSSR, **123**, 97 (1958); Chem. Abstr. **53**, 5179 (1959).
9. C. A. GROB and P. BRENNEISEN. Helv. Chim. Acta, **41**, 1184 (1958).
10. W. R. VAUGHAN, S. C. BERNSTEIN, and M. E. LORBER. J. Org. Chem. **30**, 1790 (1965).
11. R. N. LEWIS and J. R. WRIGHT. J. Am. Chem. Soc. **74**, 1253 (1952).
12. M. H. PALMER and J. A. REID. J. Chem. Soc. 931 (1960).
13. F. F. BLICKE and O. J. WEINKAUFF. J. Am. Chem. Soc. **54**, 1448 (1932).
14. A. KIRPAL. Ber. **63**, 3190 (1930).
15. D. F. DETAR and D. I. RELYEA. J. Am. Chem. Soc. **76**, 1683 (1954).
16. H. J. SCHEIFELE, JR. and D. F. DETAR. Organic Syntheses. Collective Vol. IV. John Wiley and Sons, Inc., New York. 1963. p. 34.
17. G. SCHROETER. Ber. **42**, 3360 (1909).
18. J. C. E. SIMPSON and (in part) C. M. ATKINSON, K. SCHOFIELD, and O. STEPHENSON. J. Chem. Soc. 653 (1945).
19. J. CASON and F. S. PROUT. Organic Syntheses. Collective Vol. III. John Wiley and Sons, Inc., New York. 1955. p. 601.
20. W. BLAKELY and H. A. SCARBOROUGH. J. Chem. Soc. 2492 (1928).
21. R. STOERMER and E. FRIDERICJI. Ber. **41**, 324 (1908).
22. D. H. HAY and R. D. MULLEY. J. Chem. Soc. 2283 (1952).
23. R. L. SHRINER, R. C. FUSON, and D. Y. CURTIN. The systematic identification of organic compounds. 5th ed. John Wiley and Sons, Inc., New York. 1964. p. 235.
24. C. D. HURD and C. N. WEBB. J. Am. Chem. Soc. **49**, 549 (1927).
25. K. SISIDO, K. KUMAZAWA, and H. NOZAKI. J. Am. Chem. Soc. **82**, 125 (1960).
26. H. RUPE and E. BUSOLT. Ber. **40**, 4538 (1907).

Can. J. Chem. Downloaded from www.nrcresearchpress.com by 210.87.254.6 on 09/05/12
For personal use only.

Etude de quelques dérivés Δ^4-cyclohexèniques

G. M. Brown, P. Dubreuil et E. P. Demers
Département de chimie, Université de Sherbrooke, Sherbrooke, Québec

Reçu le 5 février 1968

Certains dérivés cyclohexènedicarboxyliques de deux séries distinctes sont examinés. Dans une des séries, triméthylée en 3,3,5, les deux monoesters isomères *cis* sont préparés et leurs structures prouvées par lactonisation. L'étude de l'autre série, méthylée en 4, porte sur la lactonisation et l'époxydation. Les spectres résonance magnétique nucléaire de tous ces composés sont donnés.

Canadian Journal of Chemistry, 46, 1849 (1968)

L'anhydride **1** décrit par Diels et Alder (1) et plus tard par Jacquemain (2) provient de la réaction entre l'anhydride maléique et le diméthyl-2,4 pentadiène-1,3. Pour préparer ce produit de départ, nous nous sommes inspirés d'une méthode employée par Ichikizaki (3) qui pourtant, ne chauffe que dix heures et n'isole pas cet intermédiaire; effectivement la conversion de cet anhydride en acide **2** se fait sans purification. Ensuite Ichikizaki lactonise le diacide **2** au moyen de HCl à 20%; il obtient la lactone–acide **3** qu'il nomme comme dérivé bicyclo [2·2·2] octanique. Dans cette publication, nous utilisons la même nomenclature. Nous avons répété la lactonisation en nous servant d'acide formique simplement pour nous assurer de l'efficacité de ce réactif; la détermination de la structure des monoesters **4** et **7** par lactonisation n'aurait pas été possible dans les conditions expérimentales draconiennes d'Ichikizaki.

Le même monoester **4** étant synthétisé à partir des deux composés **1** et **2**, la position de la fonction acide est obligatoirement telle qu'indiquée car la δ-lactone **5** est obtenue par cyclisation. Ichikizaki (3) a préparé cette substance par l'action du diazométhane sur l'acide correspondant **3**; cependant il ne l'a pas obtenue sous forme cristalline. Cette structure du monoester **4** préparé par estérification partielle de l'acide **2** était à prévoir; en effet la fonction équatorielle de l'acide dont la conformation est connue (3) s'estérifie préférentiellement.

Il était donc logique de supposer que le second monoester pourrait être préparé par saponification partielle du diester **6**, lequel est obtenu par une réaction Diels–Alder. Ce produit est rapporté dans la littérature (4) mais les conditions expérimentales de sa préparation ne sont pas divulguées. La saponification partielle conduit au monoester **7**. La lactonisation de **7** donne lieu à la γ-lactone **8**, preuve de la position de la fonction acide. La structure des lactones **5** et **8** est également sans équivoque; la résonance magnétique nucléaire est formelle là-dessus.

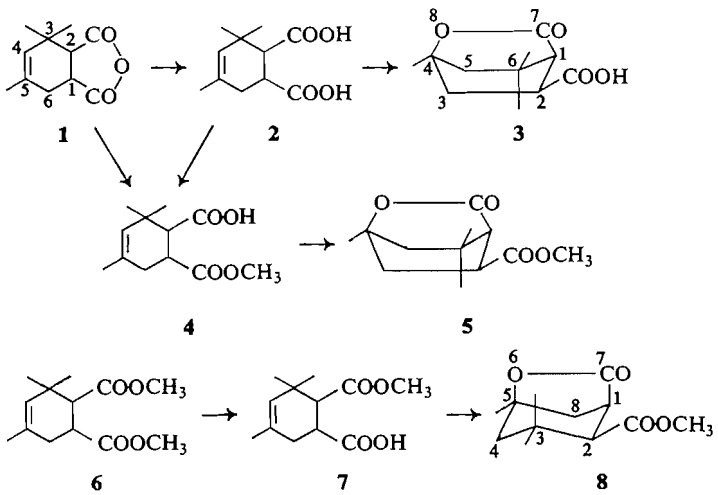

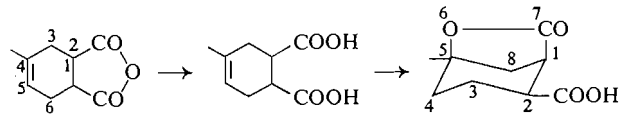

9 10 11

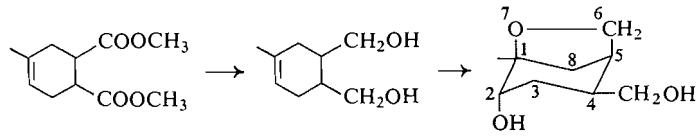

12 13 14

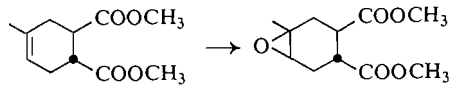

15 16

La deuxième partie de ce travail a été amorcée par la réaction Diels–Alder entre l'isoprène et l'anhydride maléique, ce qui donne l'anhydride **9**. Shabanov et ses collaborateurs (5) ont déjà porté leur attention sur la lactone obtenue par l'action du HCl gazeux en solution acétique sur l'acide **10**. Ils donnent la structure **11** à cette lactone–acide mais la seule preuve apportée est une valeur de 1765 cm^{-1} attribuée à une γ-lactone. Ce chiffre nous semblait peu suffisant pour préciser une formule exacte. Nous avons donc refait la lactonisation au moyen d'acide formique et nous avons mesuré l'emplacement exact de ce pic. Notre valeur plus conforme aux absorptions γ-lactoniques et la résonance magnétique nucléaire confirment cependant la structure avancée par Shabanov.

Le diester **12** est préparé par une réaction Diels–Alder; la méthode générale employée par Petrov et Sopov (6) nous était d'une grande utilité. La réduction du composé **12** en diol **13** s'effectue selon le mode opératoire maintenant classique.

L'époxydation de ce glycol par l'acide *m*-chloroperbenzoïque donne l'éther-alcool **14**. Le produit de la réaction d'époxydation ne subit aucun changement en présence de $LiAlH_4$; preuve que la réaction ne donne pas un époxyde réel.

Sur le spectre résonance magnétique nucléaire (r.m.n.), il y a les pics d'absorption de deux OH différents qui se déplacent avec un changement de température; l'un étant un doublet, donc un OH secondaire et l'autre un triplet du proton hydroxylique d'un alcool primaire. Si le proton de l'hydroxyle en position-2 est un doublet, cela veut dire qu'il est couplé avec un proton qui se trouve sur le même carbone. Alors le méthyle est fixé en 1 sur le carbone qui porte le lien éther. En infrarouge (i.r.), les seules bandes OH présentes sont la bande OH primaire libre à 3638 cm^{-1} et la bande OH secondaire libre à 3623 cm^{-1}. Il n'y a pas sur le spectre de bande OH associé. Cette cyclisation donne obligatoirement un dérivé trans où le lien éther en 1 et la fonction alcool en 2 sont axiaux. La preuve paraît dans une publication où d'autres substances de ce type ont été synthétisées (7).

La préparation du diester trans **15** se fait également par une réaction Diels–Alder selon Walborsky (8). L'époxydation de ce diester mène à un époxyde réel **16**. Nous voulions examiner les produits de réduction du composé **16**, mais nous avons obtenu un mélange de triols et nous n'avons pas réussi à en effectuer la séparation.

Partie expérimentale

Les points de fusion ont été déterminés à l'aide de la plaque chauffante Fisher–Johns et ne sont pas corrigés.

Les spectres infrarouges ont été enregistrés sur le spectrophotomètre Infracord de Perkin–Elmer et, dans les cas où une mesure précise de l'emplacement des bandes était exigée, sur le spectrophotomètre à réseau Perkin–Elmer 125.

Les spectres de résonance magnétique nucléaire ont été pris sur l'appareil Varian A-60 à des concentrations variant de 10 à 15%.

Les microanalyses ont été effectuées par le laboratoire de microanalyse Schwarzkopf à Woodside, New York.

Anhydride de l'acide triméthyl-3,3,5 cyclohexène-4 dicarboxylique-1,2 cis (1)

Un mélange d'anhydride maléique (15.7 g, 0.16 mole), de diméthyl-2,4 pentadiène-1,3 (18.3 g, 0.19 mole), de benzène anhydre (200 ml) et d'hydroquinone (1.0 g) est chauffé 22 h à 90 °C dans un autoclave rempli d'azote. Le benzène est chassé et le résidu obtenu mis au froid où il solidifie. Après traitement au noir animal et recristallisation dans l'éther de pétrole (35–60 °C) on obtient un solide blanc, p.f. = 49–50 °C. Litt. p.f. = 49 °C (1), p.f. = 51.5 °C (2); rendement: 28.0 g (90%).

Infrarouge (CCl_4) en cm^{-1}: 1857, 1785 (carbonyles de l'anhydride); r.m.n. (CCl_4) τ = 4.60 (quadruplet de 1H en 4, J = 1.5 c.p.s.); τ = 6.50 (octuplet de 1H en 1, $J_{1,6}$ = 6.5 et 8.6 c.p.s., $J_{1,2}$ = 10.0 c.p.s.); τ = 7.14 (doublet de 1H en 2, $J_{1,2}$ = 10.0 c.p.s.); τ = 7.56 (2H en 6, résolution imparfaite); τ = 8.24 (doublet de CH_3 en 5, J = 1.5 c.p.s.); τ = 8.74 et 9.04 (deux singulets des CH_3 en 3).

Acide triméthyl-3,3,5 cyclohexène-4 dicarboxylique-1,2 cis (2)

La méthode d'Ichikizaki (3) est employée, p.f. = 191–191.5 °C (acétonitrile). Litt: p.f. = 193–194 °C(3); rendement: 96%.

Infrarouge (KBr) en cm^{-1}: 1706 (carbonyle); r.m.n. (pyridine): τ = −3.78 (singulet de 2H acides); τ = 4.75 (singulet large de 1H en 4); τ = 6.5 à 7.7 (multiplet de 4H en 1,2 et 6 non résolu); τ = 8.24 (singulet du CH_3 en 5); τ = 8.64 et 8.80 (deux singulets des CH_3 en 3).

Acide triméthyl-4,6,6 oxa-8 oxo-7 bicyclo[2·2·2] octane exo-carboxylique-2 (3)

Un mélange de diacide *cis* **2** (2.5 g, 11.8 mmoles) et de 25 ml d'acide formique est agité pendant 3 h à 80 °C. L'acide formique est chassé sous vide et le résidu repris deux fois dans le chloroforme. Après deux recristallisations dans l'acétate d'éthyle, un solide blanc est obtenu, p.f. = 162–163 °C. Litt. p.f. = 166 °C (3); rendement: 1.4 g (56%).

Infrarouge (CCl_4) en cm^{-1}: 1752 (δ-lactone), 1715 (carbonyle de l'acide); r.m.n. (CH_2Cl_2): τ = −0.05 (singulet de 1H acide); τ = 6.70 (octuplet de 1H en 2, $J_{1,2}$ = 2.0 c.p.s., $J_{2,3}$ = 5.7 et 10.5 c.p.s.); τ = 7.39 (doublet 1H en 1, $J_{1,2}$ = 2.0 c.p.s.); τ = 7.99 et 8.05 (pics complexes et mal définis des 2H en 3); τ = 8.43 (singulet large de 2H en 5); τ = 8.58 (singulet du CH_3 en 4); τ = 8.79 et 8.90 (singulets des CH_3 en 6).

Acide triméthyl-3,3,5 carbométhoxy-1 cyclohexène-4 carboxylique-2 cis (4)

Méthode 1

L'anhydride **1** (9.7 g, 49.9 mmoles) est chauffé 5 h sous reflux avec 22 ml de méthanol. Le solvant est chassé et le résidu mis au froid où il solidifie. Après trois recristallisations dans le cyclohexane on obtient un solide blanc, p.f. = 96.5–97.5 °C; rendement: 4.6 g (41%).

Méthode 2

Un mélange du diacide cis **2** (2.5 g, 11.8 mmoles), de méthanol (2.3 g, 72 mmoles), de dichloro-1,2 éthane (8 ml) et de deux gouttes d'acide sulfurique concentré est chauffé 12 h sous reflux. Après l'addition de 20 ml d'eau, le mélange est amené à pH 8 en ajoutant du Na_2CO_3 solide. La couche organique est lavée puis séchée sur $MgSO_4$. Le solvant est chassé et le résidu visqueux solidifie au froid, p.f. et p.f. mixte (méthode 1) = 96.5–97 °C; rendement: 1.5 g (57%).

Infrarouge (CCl_4) en cm^{-1}: 1743 (carbonyle de l'ester), 1710 (carbonyle de l'acide); r.m.n. (CCl_4): τ = −1.60 (singulet de 1H acide); τ = 4.96 (singulet large de 1H en 4); τ = 6.31 (singulet de 3H de l'ester méthylique); τ = 6.81 à 7.28 (pic complexe, superposition des protons en 1 et 2); τ = 7.34 à 8.16 (multiplet mal défini de 2H en 6); τ = 8.29 (doublet de 3H du méthyle en 5, J = 1.1 c.p.s.); τ = 8.89 (singulet de 6H des deux méthyles en 3).

Anal. Calc. pour $C_{12}H_{18}O_4$: C, 63.70; H, 8.02. Trouvé: C, 64.23; H, 8.11.

Triméthyl-4,6,6 oxa-8 oxo-7 bicyclo[2·2·2]octane exo-carboxylate de méthyle-2 (5)

Un mélange du monoacide **4** (3.5 g, 15.5 mmoles) et de 35 ml d'acide formique est agité pendant 4 h à 80 °C. L'acide formique est chassé sous vide et le résidu repris deux fois dans le chloroforme. Le liquide visqueux obtenu est distillé sous pression réduite, $p.e._1$ = 148–150 °C; il cristallise difficilement à la glacière, p.f. = 53.5–54 °C (pentane). Litt: $p.e._{0.8}$ = 131–132 °C (3); rendement: 1.4 g (40%).

Infrarouge (CCl_4) en cm^{-1}: 1764 (δ-lactone), 1747 (ester); r.m.n. (CCl_4), τ = 6.34 (singulet de l'ester méthylique); τ = 6.80 (octuplet de 1H en 2, $J_{2,3}$ = 6.2 et 10.4 c.p.s., $J_{1,2}$ = 2.1 c.p.s.); τ = 7.60 (doublet de 1H en 1, $J_{1,2}$ = 2.1 c.p.s.); τ = 8.00 (quadruplet de 2H en 3, $J_{2,3}$ = 6.2 et 10.4 c.p.s.); τ = 8.45 (2H en 5, résolution imparfaite); τ = 8.64 (singulet du méthyle en 4); τ = 8.81 et 8.95 (singulets des méthyles en 6).

Anal. Calc. pour $C_{12}H_{18}O_4$: C, 63.70; H, 8.02. Trouvé: C, 63.59; H, 7.98.

Triméthyl-3,3,5 cyclohexène-4 dicarboxylate de méthyle-1,2 cis (6)

Un mélange de maléate de méthyle (22.0 g, 0.15 mole), de diméthyl-2,4 pentadiène-1,3 (19.2 g, 0.20 mole), de benzène anhydre (100 ml) et d'hydroquinone (100 mg) est chauffé 72 h à 180 °C dans un autoclave rempli d'azote. Le solvant est chassé et le résidu distillé deux fois sous pression réduite, $p.e._{15}$ = 148–150 °C; n_D^{20} = 1.4717. Litt: 1.4712 (4). Après 2 jours au froid, on obtient un solide blanc, recristallisé dans le pentane, p.f. = 54–54.5 °C Litt. $p.e._{20}$ = 149–151 °C (4); rendement: 16.5 g (46%).

Infrarouge film liquide: 1745 cm^{-1} (carbonyle de l'ester); r.m.n. (CCl_4), τ = 5.08 singulet large de 1H en 4); τ = 6.40 et 6.48 (deux singulets des esters méthyliques); τ = 7.16 (multiplet de 2H en 1 et 2); τ = 7.69 (absorption complexe de 2H en 6); τ = 8.32 (doublet hyperfin de 3H du méthyle en 5, $J \simeq$ 0.6 c.p.s.); τ = 8.94 et 9.03 (deux singulets des méthyles en 3).

Anal. Calc. pour $C_{13}H_{20}O_4$: C, 64.98; H, 8.39. Trouvé: C, 64.85; H, 8.43.

Acide triméthyl-3,3,5 carbométhoxy-2 cyclohexène-4 carboxylique-1 cis (7)

Au diester **6** (5.0 g, 20.8 mmoles) est ajoutée lentement, en agitant, une solution de KOH (4.7 g, 83.2 mmoles) dans 47 ml d'éthanol à 95%. Le mélange est refluë 2 h puis l'alcool est chassé. Après l'addition de 50 ml d'eau, la solution est extraite au chloroforme. La couche aqueuse est acidifiée à froid à l'aide d'une solution de H_2SO_4 2*N*

extraite au chloroforme, lavée à l'eau et finalement séchée sur $MgSO_4$. Le liquide visqueux obtenu solidifie lentement à la température de la pièce. Après traitement au noir animal et recristallisation dans le cyclohexane, on obtient un solide blanc, p.f. = 116.5–117.5 °C; rendement: 4.6 g (97%).

Infrarouge (CCl_4) en cm^{-1}: 1740 (carbonyle de l'ester), 1709 (carbonyle de l'acide); r.m.n. (CCl_4), $\tau = -1.9$ (singulet de 1H acide); $\tau = 4.98$ (singulet large de 1H en 4); $\tau = 6.40$ (singulet de 3H de l'ester méthylique); $\tau =$ 6.72 à 7.27 (superposition des H en 1 et 2); $\tau = 7.27$ à 8.11 (2H en 6, complexe); $\tau = 8.28$ (doublet hyperfin de 3H du méthyle en 5, $J = 1.1$ c.p.s.); $\tau = 8.90$ et 9.00 (deux singulets des méthyles en 3).

Anal. Calc. pour $C_{12}H_{18}O_4$: C, 63.70; H, 8.02. Trouve: C, 63.78; H, 8.24.

*Triméthyl-3,3,5 oxa-6 oxo-7 bicyclo[3·2·1]octane exo-carboxylate de méthyle-2 (**8**)*

Un mélange du monoacide **7** (1.5 g, 6.6 mmoles) et d'acide formique (15 ml) est agité pendant 12 h à 80 °C. L'acide formique est chassé sous vide et le résidu solide repris dans le chloroforme. La solution est amenée à pH alcalin à l'aide d'une solution de Na_2CO_3 à 10%, extraite au chloroforme puis séchée sur $MgSO_4$. Le solvant est chassé et le solide obtenu recristallisé dans le cyclohexane ou mieux dans le tétrachlorure de carbone, p.f. = 93.5–94 °C; rendement: 580 mg (39%).

Infrarouge (CCl_4) en cm^{-1}: 1789 (γ-lactone), 1732 (ester); r.m.n. (CCl_4), $\tau = 6.26$ (singulet de 3H du méthyle de l'ester); $\tau = 7.06$ (quadruplet de 1H en 1 avec également un dédoublement hyperfin, $J_{1,2} = 2.1$ c.p.s., $J_{1,8} = 5.5$ c.p.s.); $\tau = 7.43$ (doublet de 1H en 2, $J_{1,2} =$ 2.1 c.p.s.); $\tau = 7.72$ (octuplet de 2H en 8, $J_{1,8} = 5.5$ et 2.2 c.p.s., $J_{gem} = 11.8$ c.p.s.); $\tau = 8.22$ (quadruplet de 2H en 4, $J_{gem} = 6.5$ c.p.s.); $\tau = 8.57$ (singulet de 3H du méthyle en 5); $\tau = 8.77$ et 8.94 (deux singulets des méthyles en 3).

Anal. Calc. pour $C_{12}H_{18}O_4$: C, 63.70; H, 8.02. Trouvé: C, 63.47; H, 8.21.

*Anhydride de l'acide méthyl-4 cyclohexène-4 dicarboxylique-1,2 cis (**9**)*

Mode opératoire de Diels–Alder (1), p.f. = 63–64 °C (éther de pétrole). Litt p.f. = 63–64 °C (1); rendement: 90%.

Infrarouge (CS_2) en cm^{-1}: 1855 et 1786 (carbonyles); r.m.n. (CCl_4) $\tau = 4.38$ (multiplet de 1H en 5); $\tau = 6.67$ (multiplet de 2H en 1 et 2); $\tau = 7.64$ (multiplet de 4H en 3 et 6) et $\tau = 8.23$ (singulet du méthyle en 4).

*Acide méthyl-4 cyclohexène-4 dicarboxylique-1,2 cis (**10**)*

Préparé à partir de l'anhydride **9** par la méthode employée dans la synthèse de l'acide **2**, p.f. = 154–155 °C (acétonitrile). Litt. p.f. = 154–155 °C (9, 10); rendement: 90%.

Infrarouge ($CHCl_3$) en cm^{-1}: 1709 (carbonyle d'acide); r.m.n. (pyridine) $\tau = -3.38$ (singulet de 2H des protons acides); $\tau = 4.54$ (multiplet de 1H en 5); $\tau = 6.64$ (multiplet de 2H en 1 et 2); $\tau = 7.36$ (multiplet de 4H en 3 et 6) et $\tau = 8.33$ (singulet de 3H du méthyle en 4).

*Acide méthyl-5 oxa-6 oxo-7 bicyclo[3·2·1]octane exo-carboxylique-2 (**11**)*

Un mélange de 3.5 g du diacide **10** et de 25 ml d'acide formique est agité pendant 7 h à la température de la pièce. L'acide formique est chassé sous vide et le produit de la réaction cristallise. Recristallisé plusieurs fois dans l'acétate d'éthyle, la lactone-acide fond à 157–160 °C. Litt. p.f. = 159–161 °C (5); rendement: 1.4 g (40%).

Infrarouge ($CHCl_3$) en cm^{-1}: 1774 (γ-lactone) et 1713 (carbonyle d'acide); r.m.n. (pyridine) $\tau = -3.24$ (singulet de 1H du proton acide); $\tau = 6.56$ (pic mal défini de 1H en 2); $\tau = 7.24$ (pic mal défini de 1H en 1); $\tau =$ de 7.57 à 8.40 (multiplet de 6H des méthylènes en 3, 4 et 8) et $\tau = 8.67$ (singulet de 3H du méthyle en 5).

*Méthyl-4 cyclohexène-4 dicarboxylate de méthyle-1,2 cis (**12**)*

Même mode opératoire général que pour le diester **6**; le chauffage se fait dans un autoclave à 120–125 °C pendant 12 h, $p.e._7$ = 125–126 °C, $n_D^{25} = 1.4703$. Litt. $p.e._{20}$ = 149–150 °C (11), $p.e._{30}$ = 152–154 °C (12); rendement: 46%.

Infrarouge (film liquide) en cm^{-1}: 1742 (carbonyle de l'ester); r.m.n. (CCl_4) $\tau = 4.68$ (multiplet de 1H en 5); $\tau = 6.37$ (singulet de 6H des esters méthyliques); $\tau =$ 7.10 (multiplet de 2H en 1 et 2); $\tau = 7.66$ (multiplet de 4H en 3 et 6); $\tau = 8.33$ (singulet de 3H du méthyle en 4).

*Méthyl-4 cyclohexène-4 diméthylol-1,2 cis (**13**)*

Le diester **12** (6.6 g, 0.042 mole) dans 30 ml de THF sec est ajouté lentement à une suspension de $LiAlH_4$ (2.0 g, 0.053 mole) dans 60 ml de THF sec. Le mélange est agité pendant 4 h à la température de la pièce. Après l'hydrolyse par une solution de tartrate de K et Na 20%, le THF est chassé sous vide et le glycol extrait de l'eau résiduel au chloroforme. Le produit est distillé sous pression réduite, $p.e._{0.3}$ = 118–120 °C. Litt. $p.e._6$ = 155–156 °C (13); rendement: 4.0 g (88%). Le produit cristallise très lentement, p.f. = 37–39 °C (éther).

Infrarouge (CCl_4) en cm^{-1} (concentration du diol 0.002 *M* dans une cellule de 2.5 cm de longueur): 3638 (OH libre) et 3468 (OH associé); r.m.n. (DMSO-d_6) $\tau = 4.74$ (singulet de 1H en 5); $\tau = 5.64$ (triplet de 2H des protons hydroxyliques, $J = 5.0$ c.p.s.); $\tau = 6.66$ (multiplet de 4H des méthylènes en 1 et 2); $\tau = 8.13$ (singulet de 6H en 1, 2, 3 et 6) et $\tau = 8.40$ (singulet de 3H du méthyle en 4).

Anal. Calc. pour $C_9H_{16}O_2$: C, 69.19; H, 10.32. Trouvé: C, 69.10; H, 9.81.

*Méthyl-1 exo-hydroxyméthyl-4 oxa-7 bicyclo[3·2·1] endo-octanol-2 (**14**)*

Une solution d'acide *m*-chloroperbenzoïque (1.95 g, 0.012 mole) dans 15 ml d'éther anhydre est ajoutée à une solution du diol *cis* **13** (1.56 g, 0.01 mole) dans 15 ml d'éther anhydre. La solution est abandonnée une nuit au froid, puis 48 h à la température de la pièce avant d'être de nouveau mise au froid. L'éther-alcool cristallise. Recristallisé dans un mélange chloroforme–éther éthylique 1:1, l'éther-alcool fond à 96.5–97.5 °C; rendement: 700 mg (40%).

Infrarouge (CCl_4) en cm^{-1} (concentration de 0.001 *M* dans une cellule de 2.5 cm de longueur): 3638 (OH libre primaire) et 3623 (OH libre secondaire); r.m.n. (DMSO-d_6) $\tau = 5.36$ (doublet de 1H du proton hydroxylique en 2, $J = 4.0$ c.p.s.); $\tau = 5.62$ (triplet de 1H du proton hydroxylique du méthylol en 4, $J = 5.0$ c.p.s.); $\tau = 6.35$ (doublet de 2H du méthylène en 6, $J = 3.0$ c.p.s.); $\tau = 6.77$ (pic complexe de 3H du méthylène du méthylol et du proton en 2); $\tau = 7.59$ (multiplet de 2H en 4 et 5); $\tau = 8.05$ (multiplet de 2H en 3); $\tau = 8.58$ (doublet de

2H en 8, J = 3.0 c.p.s.) et τ = 8.84 (singulet de 3H du méthyle en 1).

Anal. Calc. pour $C_9H_{16}O_3$: C, 62.76; H, 9.36. Trouvé: C, 63.08; H, 9.06.

*Méthyl-4 cyclohexène-4 dicarboxylate de méthyle-1,2 trans (**15**)*

Mode opératoire selon Walborsky (8), p.e.$_7$ = 122–124 °C, n_D^{25} = 1.4670. Litt. p.e.$_{1.2}$ = 98–100 °C (8); rendement: 92%. Le produit solidifie difficilement, après deux recristallisations dans l'éther de pétrole, p.f. = 33 °C.

Infrarouge (CS_2) en cm^{-1}: 1742 (carbonyle de l'ester); r.m.n. (CCl_4) τ = 4.68 (multiplet de 1H en 5); τ = 6.43 (singulet de 6H des esters méthyliques); τ = 7.33 (multiplet de 2H en 1 et 2); τ = 7.82 (multiplet de 4H en 3 et 6) et τ = 8.33 (singulet de 3H du méthyle en 4).

Anal. Calc. pour $C_{11}H_{16}O_4$: C, 62.25; H, 7.60. Trouvé: C, 62.05; H, 7.05.

*Méthyl-4 époxy-4,5 cyclohexane dicarboxylate de méthyle-1,2 trans (**16**)*

Une solution d'acide perbensoïque (12.4 g, 0.09 mole) dans 185 ml de chloroforme est ajoutée à une solution du diester **15** (16.0 g, 0.07 mole) dans 50 ml de chloroforme. Après avoir été abandonné au froid 3 jours, le mélange est lavé avec une solution de Na_2CO_3 à 20%, puis avec de l'eau et séché sur $MgSO_4$. Le solvant est chassé et le résidu distillé sous pression réduite, p.e.$_{1.5}$ = 86–88 °C. Après trois recristallisations dans un mélange éther–éther de pétrole, p.f. = 81–82 °C; rendement: 5.7 g (33%).

Infrarouge (CS_2) en cm^{-1}: 1739 (carbonyle de l'ester); r.m.n. (CCl_4) τ = 6.35 (singulet de 6H des esters méthyliques); τ = 7.07 (triplet de 1H en 5, J = 2.0 c.p.s.); τ = 7.40 (multiplet de 2H en 1 et 2); τ = 7.89 (multiplet de 4H en 3 et 6) et τ = 8.71 (singulet de 3H du méthyle en 4).

Anal. Calc. pour $C_{11}H_{16}O_5$: C, 57.88; H, 7.07. Trouvé: C, 57.60; H, 6.82.

Remerciements

Nous remercions Monsieur J. R. Martin de l'Université de Sherbrooke d'avoir bien voulu faire les spectres de résonance magnétique nucléaire.

Nous exprimons également notre gratitude envers le Conseil National de Recherches du Canada d'avoir accordé un octroi (G.M.B.) et envers le Ministère de l'Education du Gouvernement du Québec pour une bourse (P.D.).

1. O. Diels, K. Alder, W. Luppert, E. Naujoka, F. Querberitz, K. Roehl et H. Segeberg. Ann. Chem. **470,** 62 (1929).
2. R. Jacquemain. Compt. Rend. **214,** 880 (1942).
3. I. Ichikizaki et A. Arai. Kobayashi Rigaku Kenkyushu Hokoku, **13,** 117 (1963).
4. N. P. Sopov et M. L. Kovner. Zh. Obshch. Khim. **34,** 1496 (1964).
5. A. L. Shabanov, A. S. Onishchenko et V. F. Kucherov. Bull. Acad. Sci. USSR, Div. Chem. Sc. English Transl. 1648 (1963).
6. A. A. Petrov et N. P. Sopov. Sb. Statei Obshch. Khim. **2,** 853 (1953).
7. M. Mousseron-Canet, M. Mousseron et G. Brown. Rev. Chim. Acad. Rep. Populaire Roumaine, **7,** 1089 (1962).
8. H. M. Walborsky, L. Barash et T. C. Davis. Tetrahedron, **19,** 2333 (1963).
9. K. Alder et H. A. Dortmann. Chem. Ber. **85,** 556 (1952).
10. I. N. Nazarov et V. F. Kucherov. Bull. Acad. Sci. USSR, Div. Chem. Sc. English Transl. 265 (1955).
11. N. P. Sopov. J. Gen. Chem. USSR, English Transl. **26,** 1795 (1956).
12. A. P. Terentev, A. N. Kost, E. Kh. Zolotarev, E. N. Vinogradova, T. V. Kalakutskaya et I. A. Yurgenson. Izv. Vysshikh Uchebn. Zavedenii, Khim. i. Khim. Tekhnol. 55 (1958).
13. W. J. Bailey, J. Rosenberg et L. J. Young. J. Am. Chem. Soc. **76,** 2251 (1954).

Preparation of some isothiazolium salts

D. M. McKinnon and E. A. Robak
Department of Chemistry, University of Manitoba, Winnipeg, Manitoba

Received February 5, 1968

Certain 1,2-dithiolium salts react with primary amines in alcoholic solution to provide 1-aminopropene-3-thiones, which can be oxidized by iodine to form isothiazolium salts. These react with sulfur in pyridine to form isothiazole-3-thiones, which react with methyl iodide to form 3-methylthioisothiazolium iodides.

Canadian Journal of Chemistry, 46, 1855 (1968)

Can. J. Chem. Downloaded from www.nrcresearchpress.com by 210.87.254.6 on 09/05/12
For personal use only.

In connection with another study which required certain isothiazolium salts (**1**) as intermediates, we attempted to prepare some of these from readily accessible 1,2-dithiolium salts (**2***a*, *b*, *c*, *d*) (see refs. 1*a*, *b*, and *c*). The versatility of 1,2-dithiolium salts in the preparation of some pyrazole (1*a*, 2) and isothiazole (3, 4) systems by their treatment with hydrazines and ammonia respectively is well known and such nucleophilic attack has been shown to occur at the 3-position of the 1,2-dithiolium salt (see Scheme 1). However, although *N*, *N'*-disubstituted hydrazines react to form *N*-alkyl and *N*-aryl pyrazolium salts (2), primary amines do not give *N*-substituted isothiazolium salts. Instead, disulfide intermediates (**3**) lose one atom of sulfur to generate precursors (**4**) of 1-alkyl- and 1-arylaminopropenethiones (**5***a–e*). This is represented in Scheme 2, reaction (*a*). An alternate reaction path, (*b*), involving the overall loss of a sulfhydride ion to afford the *N*-substituted isothiazolium system is not found, although this is similar to the main pathway in the reaction of ammonia with 1,2-dithiolium salts when isothiazoles are obtained (3, 4).

Although *N*-alkylisothiazolium salts may be prepared by alkylation of suitable isothiazoles (5*a*, *b*) this method is generally inapplicable to the preparation of *N*-arylisothiazolium salts, and ring synthesis is necessary. Consideration of the methods used for the synthesis of certain isothiazolium (6) and *N*-alkyl isothiazolium salts (6, 7) by halogen oxidation of some aminothiones (**5***f* and *g*) indicated that the aminopropenethione products above might be useful precursors of the isothiazolium system, especially of *N*-aryl compounds.

Treatment of the thiones (**5***a–e*) made by the method above (4), in ethanol or methanol solution with iodine, afforded brown precipitates, apparently the triiodides of the required isothiazolium salts. Faust (7) reports obtaining bromides or tribromides depending on the amount of halogen used. Generally the isothiazolium triiodides were converted to the corresponding perchlorates in acetic acid or nitromethane, but in one case (**1***d*, $X = I_3$) a satisfactory analysis was obtained for the triiodide. In certain cases, (**5***a* and *c*) the thiones were not obtained pure and crystalline, but solutions of the crude products oxidized satisfactorily, except in one case. In this case the product was derived by treatment of 4-methyl-3-phenyl-1,2-dithiolium perchlorate (**2***b*, $X = ClO_4$) with aniline, which apparently was unstable.

The structures of the isothiazolium salts prepared follow from the analysis, and from the identity of one of them (**1***a*) with a compound prepared by direct alkylation of 5-phenylisothiazole. The perchlorates were light-colored, usually light-tan or yellow, and more readily purified than the corresponding triiodides.

Klingsberg has shown (2) that 1,2-dithiolium salts (**2**) unsubstituted in positions adjacent to the sulfur atom undergo oxidation by sulfur in boiling pyridine to provide the corresponding 1,2-dithiole-3-thiones (**7***a* and *b*). Similarly, two isothiazolium salts studied (**1***a* and *b*) reacted with sulfur in pyridine to produce isothiazole-3-thiones (**7***c* and *d*), isolated as their methiodides, which may be formulated as the corresponding 3-methylthioisothiazolium iodides (**1***g* and *h*).

One possible scheme for this reaction would proceed via loss of a proton from the isothiazolium cation to form a carbene (**6**) (reaction (*c*) in Scheme 3) which, possibly after dimerization, is oxidized by sulfur to form the thione (**7***c* and *d*). Wanzlick (8) has shown that certain thiazolium salts when treated with bases form carbenes, which after dimerization can be converted to

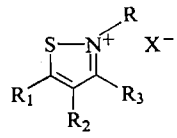

1

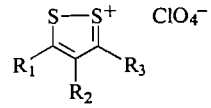

2

a R_1 = Ph,R_2 = R_3 = H,R = Me,X = ClO_4
b R_1 = Ph,R_2 = R_3 = H,R = Ph,X = ClO_4
c R_1 = R_2 = Ph,R_3 = H,R = Ph,X = ClO_4
d R_1 = Ph,R_2 = H,R_3 = Ph,R = Me,X = ClO_4
e R_1 = Ph,R_2 = H,R_3 = R = Ph,X = ClO_4
f R_1 = Ph,R_2 = H,R_3 = Ph,R = Me,X = I_3
g R_1 = Ph,R_2 = H,R_3 = SMe,R = Me,X = I
h R_1 = Ph,R_2 = H,R_3 = SMe,R = Ph,X = I

a R_1 = Ph,R_2 = H,R_3 = H
b R_1 = Ph,R_2 = Me,R_3 = H
c R_1 = R_2 = Ph,R_3 = H
d R_1 = Ph,R_2 = H,R_3 = Ph

SCHEME 1

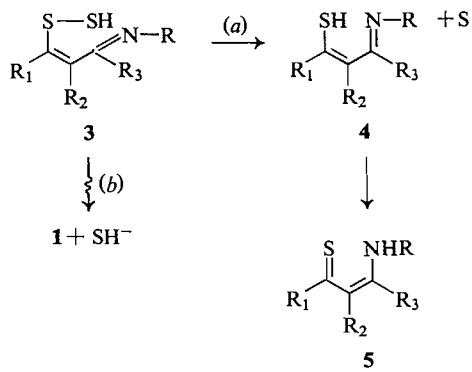

3 4 5

$1 + SH^-$

a R_1 = Ph,R_2 = R_3 = H,R = Me
b R_1 = Ph,R_2 = R_3 = H,R = Ph
c R_1 = R_2 = Ph,R_3 = H,R = Ph
d R_1 = Ph,R_2 = H,R_3 = Ph,R = Me
e R_1 = Ph,R_2 = H,R_3 = R = Ph
f R_1 = NHPh,R_2 = CO_2Et,R_3 = R = Me
g R_1 = SMe,R_2 = R_3 = R = H

SCHEME 2

thiazole-2-thiones. However, yields with isothiazoles are not so high as with 1,2-dithioles or thiazoles. Perhaps an alternate reaction (reaction path (d), Scheme 3) leads to the formation of a thioketoketimine (**8**, X = S), with further decomposition. Woodward (9) has shown that isoxazolium salts treated with tertiary amines form ketoketimines (**8**, X = O). Another possible mechanism would involve direct nucleophilic attack on the 3-position of the isothiazolium cation by polysulfide anion, with subsequent formation of the isothiazole-3-thione. However, at this stage, we are unable to distinguish experimentally between these reaction mechanisms.

Since the overall reaction producing the isothiazolium salts involves loss of a hydride ion from the aminopropenethione precursors, attempts were made to synthesize 2,3,5-triphenylisothiazolium perchlorate (**1***e*) from 1-anilino-1,3-diphenylprop-1-ene-3-thione (**5***e*) directly, using triphenylmethyl perchlorate, a reagent which is known to abstract hydride ions (10). However, this merely gave a compound whose analysis corresponded to an *N*-tritylated product. It was not a simple adduct since it was stable in acetic acid. However, rather unexpectedly, boiling in ethanol regenerated the aminothione. Possibly this reaction is facilitated by the ready loss of the triphenylmethyl cation.

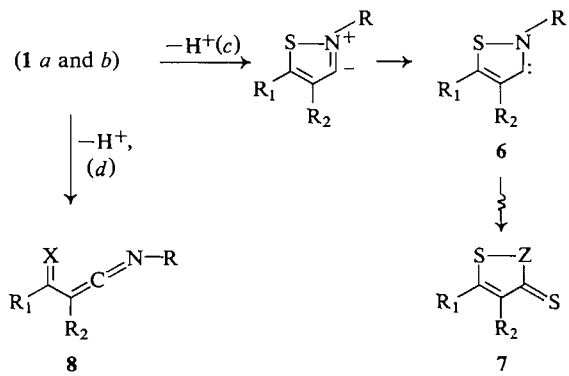

6 7 8

a R_1 = Ph,R_2 = H,Z = S
b R_1 = *p*-NO_2Ph,R_2 = H,Z = S
c R_1 = Ph,R_2 = H,Z = N—Me
d R_1 = Ph,R_2 = H,Z = N—Ph

SCHEME 3

Experimental

1,2-Dithiolium Salts

*3-Phenyl-1,2-dithiolium Perchlorate (**2***a*, X = ClO_4)*

This was prepared (1*a*) from 5-phenyl-1,2-dithiole-3-thione by peracetic acid oxidation.

*3,5-Diphenyl-1,2-dithiolium Perchlorate (**2***d*, X = ClO_4)*

This was prepared by the method of Behringer and Grimm (1*c*).

Can. J. Chem. Downloaded from www.nrcresearchpress.com by 210.87.254.6 on 09/05/12
For personal use only.

Can. J. Chem. Downloaded from www.nrcresearchpress.com by 210.87.254.6 on 09/05/12
For personal use only.

TABLE I

Preparation of isothiazolium salts

Compound	Yield (%)	Melting point °C	Formula	Analysis											
				Calculated (%)						Found (%)					
				C	H	N	S	Cl	I	C	H	N	S	Cl	I
1*a*	19	144–145	$C_{10}H_{10}NSClO_4$	43.65	3.63	5.08	11.99	12.87	—	43.73	3.70	4.92	11.55	12.75	—
1*b*	59	194–196	$C_{15}H_{12}NSClO_4$	53.40	3.56	4.15	9.48	10.50	—	54.63	3.70	3.69	9.25	9.88	—
1*c*	51	208	$C_{21}H_{16}NSClO_4$	60.94	3.90	3.38	7.74	8.67	—	60.84	3.98	3.38	7.82	8.48	—
1*d*	40	162–163	$C_{16}H_{14}NSClO_4$	54.70	4.02	3.98	9.12	10.11	—	54.95	4.05	3.76	10.28	9.57	—
1*e*	53	250–253	$C_{21}H_{16}NSClO_4$	60.94	3.90	3.38	7.74	8.67	—	61.03	3.94	3.25	7.88	8.49	—
1*f*	45	150–151	$C_{16}H_{14}NSI_3$	30.40	2.23	2.21	5.07	60.05	—	30.22	2.18	2.09	5.09	—	60.24
1*g*	42	162–165*	$C_{11}H_{12}NS_2I$	37.65	3.44	4.02	18.38	—	36.15	37.72	3.58	4.04	18.50	—	36.15
1*h*	23	211–214*	$C_{16}H_{14}NS_2I$	46.50	3.39	3.39	15.64	—	30.08	46.47	3.42	3.34	16.10	—	32.11

*Decomposition.

*4-Methyl-5-phenyl-1,2-dithiolium Perchlorate (**2b**, X = ClO_4)*

This was prepared by oxidation of 4-methyl-5-phenyl-1,2-dithiole-3-thione (11) using peracetic acid according to the usual methods (1*a*, *b*). Pale-yellow needles, m.p. 159–160 °C (61%) were formed.

Anal. Calcd. for $C_{10}H_9S_2ClO_4$: C, 41.03; H, 3.08; S, 21.88; Cl, 12.12. Found: C, 40.90; H, 2.91; S, 22.04; Cl, 12.91.

*4,5-Diphenyl-1,2-dithiolium Perchlorate (**2c**, X = ClO_4)*

This was prepared by oxidation of 4,5-diphenyl-1,2-dithiole-3-thione (12) using peracetic acid according to the usual methods (1*a*, *b*). Lemon-yellow needles, m.p. 230–231.5 °C (67%) were formed.

Anal. Calcd. for $C_{15}H_{11}S_2ClO_4$: C, 50.78; H, 3.10; S, 18.06; Cl, 10.00. Found: C, 50.90; H, 3.51; S, 17.69; Cl, 9.70.

1-Alkylamino- and 1-Arylaminoprop-1-ene-3-thiones

The 1,2-dithiolium salts (1 g) suspended in a small quantity of ethanol were treated with a slight excess of the primary amine (methylamine was used as the commercial 40% aqueous solution). The mixtures were heated gently until homogeneous and allowed to cool when the thiones were deposited. The products were recrystallized from ethanol; two of the thiones (**5***b* and *e*) had been made before (4) and one (**5***d*) was new. Tan plates were formed, m.p. 83–84 °C (56%).

Anal. Calcd. for $C_{16}H_{15}NS$: C, 75.85; H, 5.97; N, 12.62; S, 5.52. Found: C, 75.81; H, 5.96; N, 12.73; S, 5.53.

Two other compounds (**5***a* and *d*) were not obtained crystalline, and the ethanolic solution was used directly in the oxidation stage. The treatment of 4-methyl-3-phenyl-1,2-dithiolium perchlorate (**2***b*, X = ClO_4) with aniline by the above method gave a red oil which failed to oxidize satisfactorily.

*Isothiazolium Salts (**1***a–f*)

(i) By Oxidation of 1-Aminoprop-1-ene-3-thiones

A solution of the aminopropenethione (1 g) in ethanol (10 ml) was slowly titrated with a saturated ethanolic iodine solution until precipitation was complete. The brown or dark-red precipitates were removed by filtration, and either recrystallized from nitromethane, or converted to the perchlorates in acetic acid or nitromethane. Cooling or precipitation by dilution with ether afforded the required isothiazolium perchlorates. The results for compounds **1***a* to **1***f* are summarized in Table I.

(ii) By Methylation of 5-Phenylisothiazole

Dimethyl sulfate (1 ml) and 0.5 g of the above were heated at 100 °C for 2 h (3). Dilution of the solution with ether afforded an oily precipitate which was dissolved in acetic acid and treated with perchloric acid (4 drops). Dilution with ether gave 2-methyl-5-phenylisothiazolium perchlorate (**1***a*) as light-tan plates, m.p. 44–45 °C (73%). Infrared analysis and determination of the mixture m.p. showed this to be identical to the compound prepared by method (*i*).

Reaction of Isothiazolium Salts with Sulfur

The isothiazolium salts (1g) (**1***a* and *b*) were slowly added to a saturated solution of sulfur in boiling pyridine (10 ml). The mixtures became deep-red and were refluxed for 30 min. Dilution with water gave precipitates which on ether extraction and evaporation yielded brown pasty solids. The crude isothiazole-3-thiones (*7c* and *d*) were dissolved in methyl iodide and after 1 day the yellow solids were removed by filtration and recrystallized from nitromethane. The results for compounds **1***g* and *h* are summarized in Table I.

Reaction of Triphenylmethyl Perchlorate with 1-Anilino-1,3-diphenylprop-1-ene-3-thione

The thione (0.2 g) in acetone (10 ml) was treated with a slight excess of triphenylmethyl perchlorate (13) with stirring. The red solution became yellow in a few minutes. Dilution with ether and recrystallization from acetic acid containing a drop of perchloric acid gave the *N*-tritylated product as yellow needles, m.p. 188–190 °C (79%).

Anal. Calcd. for $C_{39}H_{32}NSClO_4$: C, 72.4; H, 4.96; N, 2.16; S, 4.98; Cl, 5.49. Found C, 71.30; H, 4.91; N, 2.21; S, 4.76; Cl, 5.04.

Reaction of the N-Triphenylmethyl Perchlorate of 1-Anilino-1,3-diphenylprop-1-ene-3-thione with Ethanol

The yellow salt (0.4 g) dissolved in ethanol (2 ml), was refluxed gently for 2 min. The solution gradually became deep-red and on cooling deposited 1-anilino-1,3-diphenylprop-1-ene-3-thione, m.p. 158 °C.

Acknowledgments

The financial assistance of the National Research Council of Canada, and the Faculty of Graduate Studies of the University of Manitoba is gratefully acknowledged.

1. (*a*) E. KLINGSBERG. J. Am. Chem. Soc. **83**, 2934 (1961). (*b*) D. LEAVER, W. A. H. ROBERTSON, and D. M. MCKINNON. J. Chem. Soc. 5104 (1962). (*c*) C. BEHRINGER and A. GRIMM. Ann. **682**, 188 (1965).
2. E. KLINGSBERG. J. Org. Chem. **28**, 529 (1963).
3. R. A. OLOFSON, J. M. LANDESBERG, R. O. BERRY, D. LEAVER, W. A. H. ROBERTSON, and D. M. MCKINNON. Tetrahedron, **22**, 2119 (1966).
4. D. LEAVER, D. M. MCKINNON, and W. A. H. ROBERTSON. J. Chem. Soc. 32 (1965).
5. (*a*) P. CHAPLEN, R. SLACK, and K. R. H. WOOLRIDGE. J. Chem. Soc. 4577 (1965). (*b*) J. M. LANDESBERG and R. A. OLOFSON. Tetrahedron, **22**, 2135 (1966).
6. J. GOERDELER and H. W. POHLAND. Ber. **94**, 2950 (1961).
7. J. FAUST. Z. Chem. 7, 306 (1967).
8. H. W. WANZLICK, H. J. KLEINER, I. LASCH, H. U. FULDNER, and H. STEINMAUS. Ann. **708**, 155 (1967).
9. R. A. OLOFSON and R. B. WOODWARD. J. Am. Chem. Soc. **83**, 1007 (1961).
10. W. BONTHRONE and D. H. REID. J. Chem. Soc. 2773 (1959).
11. L. LEGRAND and N. LOSAC'H. Bull. Soc. Chim. France, 1130 (1956).
12. M. G. VORONKOV, A. S. BROWN, and G. B. KARPENKO. J. Gen. Chem. USSR Eng. Transl. **19**, 395 (1949); Dokl. Akad. Nauk (SSSR) **59**, 1437 (1948).
13. H. P. DAUBEN, L. R. HONNEN, and K. M. HARMAN. J. Org. Chem. **25**, 1442 (1960).

Can. J. Chem. Downloaded from www.nrcresearchpress.com by 210.87.254.6 on 09/05/12
For personal use only.

Can. J. Chem. Downloaded from www.nrcresearchpress.com by 210.87.254.6 on 09/05/12
For personal use only.

Synthesis of some 1,4-naphthoquinones and reactions relating to their use in the study of bacterial growth inhibition

R. F. Silver and H. L. Holmes

Chemistry Section, Defence Research Establishment Suffield, Defence Research Board, Ralston, Alberta

Received August 8, 1967

A series of 107 1,4-naphthoquinones and related products has been synthesized to study their mode of action in bacterial growth inhibition. The *in vitro* reactions of a number of these with aniline, *n*-butylamine, sodium methoxide, and an *n*-buthanethiol – triethylamine mixture have been examined. A series of epoxides of C-2 monosubstituted and C-2,C-3 disubstituted 1,4-naphthoquinones has been synthesized and their reactions with amines, thiols, and halogen acids have been studied. The ultraviolet absorption maxima of many of these quinones are also tabulated.

Canadian Journal of Chemistry, **46**, 1859 (1968)

A number of 1,4-naphthoquinones were synthesized to determine their growth inhibitory activities against *Staphylococcus aureus* (1) and also the relation of these activities to their partition coefficients in cyclohexane–water (2) and to their polarographic half-wave potentials (3). The inhibitory activities were independent of partition coefficients[1] but exhibited a direct relationship to their polarographic half-wave potentials. The logarithms of the growth inhibitory activities for 1,4-naphthoquinones with unreactive groups at C-2 and C-3, when plotted against their half-wave potentials, gave two maxima, one at −0.23 V and a less pronounced maximum at −0.36 V. The 1,4-naphthoquinones with a free position or a reactive group at C-2 or C-3 gave similar results when the logarithms of the growth inhibitory activities were plotted against the polarographic half-wave potentials of their C-2 or C-3 *n*-butylthio analogues. This was not true when their C-2 or C-3 amine analogues were used.

These results (1) support the postulate (6) that 1,4-naphthoquinones or compounds such as 1,4,4*a*,9*a*-tetrahydroanthraquinone (7) which are readily converted to 1,4-naphthoquinones, function as bacterial growth inhibitors by functioning competitively in electron transport with the endogenous vitamin K or ubiquinone, thus decreasing the effectiveness of the latter as oxidative phosphorylating agents. For 1,4-naphthoquinones with unreactive groups at C-2 or C-3 to be effective growth inhibitors, this requires that their half-wave potentials lie between −0.163 to −0.307 V or −0.314 to −0.536 V (6) and that maximum effectiveness should be intermediate between these limits. The 1,4-naphthoquinones with a free position or a reactive group at C-2 or C-3 may react with a bacterial protein-thiol or protein-amine prior to functioning as growth inhibitors, in which case the half-wave potentials of the derived 1,4-naphthoquinones must lie between these limits with maximum effectiveness intermediate between these limits.

This paper reports the synthesis of a number of 1,4-naphthoquinones along with model *n*-butylthio-, phenylthio-, *n*-butylamino-, and anilino-derivatives. The reactions leading to the model protein analogues were also used to classify substituents at C-2 and/or C-3, at least, *in vitro*, as reactive or unreactive and to demonstrate where these reactions did not follow the normal course.

Anilino derivatives of the 1,4-naphthoquinones were prepared in two ways. The first method involved the addition of aniline to a number of C-2 substituted 1,4-naphthoquinones by the method of Golovanova (8) to give the respective 2-substituted 3-anilino-1,4-naphthoquinones. While most of these give normal products the C-2 substituents of 2-hydroxy-, 2-acetoxy-, and 2-methoxy-1,4-naphthoquinones undergo nucleophilic displacement while 2-bromo-1,4-naphthoquinones, potassium 1,4-naphthoquinone-2-sulfonate, and 2-benzenesulfonyl-1,4-naphthoquinone react in both ways.

[1]Partition coefficients were used to evaluate penetrability into cell-wall and membrane (4, 5). The growth inhibitory activities of the β-nitrostyrenes, β-nitropropenylbenzenes, and β-nitrobutenylbenzenes on the other hand were dependent upon their partition coefficients. (D. J. Currie, C. E. Lough, and G. J. Leahy. Unpublished results.)

Can. J. Chem. Downloaded from www.nrcresearchpress.com by 210.87.254.6 on 09/05/12
For personal use only.

TABLE I

Physical properties and analyses of some 1,4-naphthoquinones*

R	R′	A	B	Reference to method	Melting point (°C)†	Analyses: Calculated C	H	N	S	X	Found‡ C	H	N	S	X	Ultraviolet: λ_{max}	ε
H	H	CH_3	C_6H_5	32	112.0–113.0	82.23	4.87				82.00	4.32					
H	H	CH_3	n-C_4H_9NH	33	75.0–75.4			5.75					5.77 5.73			472 331 235 276 208	3 250 1 500 13 900 24 800 13 900
H	H	C_6H_5	n-C_4H_9NH	34	116.0–116.5			4.59					4.69			472 277 234	3 200 19 200 14 800
H	H	C_6H_5	C_6H_5NH	8,9§	160.0–161.0			4.30					4.25 4.14				
H	H	C_6H_5	n-C_4H_9S	11	74.0–75.0				9.94					9.98 9.92			
H	H	Br	n-C_4H_9NH	34	112.0–113.0					25.93					25.80 25.75	470 276 329 233	3 600 25 800 2 150 14 600
H	H	CH_3CONH	CH_3CONH	35	249.5–250.5			10.29					10.22 10.19			398 332 218 255 196	1 600 2 900 13 300 21 400 31 400
H	H	CH_3CONH	n-C_4H_9NH	10	176.2–177.0 (decomp.)			9.79					9.47 9.40				
H	H	CH_3CONH	n-C_4H_9S	11, 11‖	160.0–161.0			4.61	10.56				4.69 4.61	10.56		433 279.5 332 249	1 620 14 000 3 700 —
H	H	n-C_4H_9NH	n-C_4H_9S	Experimental 11	53.5–54.0			4.41					4.71				
H	H	C_6H_5NH	n-C_4H_9S	Experimental 8, 11	110.5–111.5			4.15					4.26				
H	H	C_6H_5NH	SO_3K	41, Experimental	> 230			3.81					3.66 3.54				
H	H	C_6H_5NH	$C_6H_5SO_2$	8	206.7–207.4			3.60					3.56 3.75				
5-CH_3	H	Cl	Cl	36	159.0–160.0	54.80	2.50				54.72	2.46					
6-CH_3	H	Cl(C_6H_5NH)	C_6H_5NH(Cl)	9	172.0–173.0			4.70		11.90			4.95		11.98		
6-CH_3	7-CH_3	Br	H	37	155.0–156.0	54.36	3.42				53.89	3.34					
6-CH_3	7-CH_3	n-C_4H_9S	H	11	134.0–135.0	70.00	6.61				70.24	6.62				418 323 267 260 227	2 610 9 700 28 400 23 200 13 800
6-CH_3	7-CH_3	C_6H_5S	H	11	173.0–174.0	73.44	4.79				73.25	4.67					
6-CH_3	7-CH_3	$C_6H_5SO_2$	H	38	179.8–180.8	66.22	4.32				66.14 66.37	4.26 4.28					
6-CH_3	7-CH_3	CH_3	CH_3	32	170.0–170.5	78.37	6.57				78.12	6.41					

Can. J. Chem. Downloaded from www.nrcresearchpress.com by 210.87.254.6 on 09/05/12
For personal use only.

TABLE I (*Concluded*)

R	R′	A	B	Reference to method	Melting point (°C)†	Analyses: Calculated C	H	N	S	X	Found‡ C	H	N	S	X	Ultraviolet: λ_{max}		ε	
6-CH_3	7-CH_3	CH_3	Cl	39	178.0–178.8	66.52	4.69				66.38	4.52							
											66.34	4.53							
6-CH_3	7-CH_3	CH_3	Br	39, 37¶	193.0–194.0	55.84	3.96				56.07	3.94							
6-CH_3	7-CH_3	CH_3	OH	40	185.5–186.0	72.20	5.59				72.09	5.43							
6-CH_3	7-CH_3	CH_3	CH_3O	CH_2N_2	138.5–139.0	73.05	6.08				72.99	5.88							
6-CH_3	7-CH_3	CH_3	C_6H_5NH	39	219.0–219.4			4.80					4.40						
6-CH_3	7-CH_3	CH_3	C_6H_5NH	8	217.0–218.0			7.64					7.48						
6-CH_3	7-CH_3	CH_3	Anil of *n*-C_4H_9S	Experimental	90.5–91.0	70.81	6.99				70.51	6.77							
6-CH_3	7-CH_3	CH_3	C_6H_5S	Experimental	112.2–113.2	74.00	5.23				73.78	5.18							
6-CH_3	7-CH_3	C_6H_5	Br	37	164.0–165.0	63.35	3.83				63.17	3.83				334	264.5	5380	16 700
																287	259	8300	?
6-CH_3	7-CH_3	C_6H_5	*n*-C_4H_9NH	34	147.0–148.0			4.21					4.26						
													4.37						
6-CH_3	7-CH_3	C_6H_5	C_6H_5NH	8	>230			3.96					4.20						
6-CH_3	7-CH_3	Cl	NH_2	35	244.0–244.5			5.94					6.18						
6-CH_3	7-CH_3	Cl	CH_3CONH	35	235.0–236.0			5.04					5.04 }						
													5.11 }						
6-CH_3	7-CH_3	Cl	*n*-C_4H_9NH	34	138.0–138.5			4.80					5.04						
6-CH_3	7-CH_3	Cl	C_6H_5NH	9	213.5–214.0			4.89					4.60						
6-CH_3	7-CH_3	Br	C_6H_5NH	8	198.0–198.8			3.93					3.96						
6-CH_3	7-CH_3	CH_3O	CH_3O	11	120.5–121.5	68.28	5.72				68.17	5.47							
6-CH_3	7-CH_3	NH_2	CH_3CONH	35	219.0–220.0	65.07	5.46				65.10	5.38							
6-CH_3	7-CH_3	CH_3CONH	CH_3CONH	35	248.0–249.0	63.98	5.37				64.08	5.38							
6-CH_3	7-CH_3	C_6H_5NH	*n*-C_4H_9S	Experimental	98.8–99.6			3.83					3.69						

*Compounds of the type 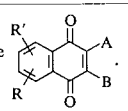

†All melting points are corrected.
‡These analyses were done by Mr. R. P. Hicken of this laboratory.
§The yield was 0% by the method quoted.
||The product obtained by addition of *n*-butanethiol to 2-acetamido-1,4-naphthoquinone proved difficult to purify.
¶The product obtained by method quoted proved difficult to purify.
**This figure was hard to evaluate since it was a shoulder on another curve.

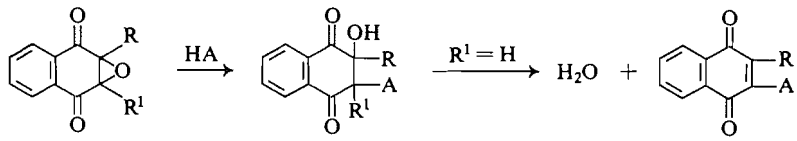

1 2 3

On the other hand, 2-anilino-1,4-naphthoquinone is recovered unchanged from this reaction but the C-2 anilino group can be displaced by *n*-butylamine under forcing conditions. Methyl groups at C-6 and C-7 lead to unexpected results. The compound, 2-methyl-1,4-naphthoquinone, gives a fair yield of 2-anilino-3-methyl-1,4-naphthoquinone while the anil of 2-anilino-3,6,7-trimethyl-1,4-naphthoquinone was the only product isolated from 2,6,7-trimethyl-1,4-naphthoquinone.

These and other 2-substituted 3-anilino-1,4-naphthoquinones were also prepared from 2-substituted 3-halogeno-1,4-naphthoquinones by the method of Calandra and Adams (9). Most of these reactions went as expected and in good yield; however, the chlorine atom of 2-anilino-3-chloro-1,4-naphthoquinone and its 6,7-dimethyl derivative cannot be replaced by aniline. The desired 2,3-dianilino-1,4-naphthoquinone and related quinones were obtained by treating the *N*-nitroso derivative of 2-anilino-3-chloro-1,4-naphthoquinone with aniline or one of its derivatives (10). Generally the C-3 halogen of the 2-amino-3-halogeno-1,4-naphthoquinones is inert towards amines. When 2-anilino-3-chloro-1,4-naphthoquinone is boiled with an ethanolic solution of *n*-butylamine most of the starting material was recovered along with a small amount of 2,*n*-butylamino-3-chloro-1,4-naphthoquinone. Hence, *in vitro*, at least, all the 2-substituted 3-halogeno-1,4-naphthoquinones except the 2-amino-3-halogeno-1,4-naphthoquinones must be classed as quinones with a reactive group towards amines.

While 2-amino- and 2-anilino-1,4-naphthoquinones fail to react with amines by addition, these compounds must be classed as reactive towards *n*-butanethiol and triethylamine. In each case a good yield of the respective 2-amino-3,*n*-butylthio-1,4-naphthoquinone was obtained. Similarly the halogen of the 2-amino-3-halogeno-1,4-naphthoquinones must be classed as reactive towards this reagent and indeed the yields of products are superior to those obtained when sodium ethoxide is used (11). This reagent can be used without fear of formation of 2-amino-3-diethylaminovinyl-1,4-naphthoquinone (12–14) because the oxidation potentials of the 2-amino-3-halogeno-1,4-naphthoquinones, as evaluated by polarographic half-wave potentials (3), are not large enough to permit these quinones to oxidize triethylamine to diethylvinylamine.

Since it is known that methoxyl- (15–19), alkylthio- (20, 21), acetamido- (22), hydroxyl- (17, 23–30), and methyl- (15) groups in quinones are susceptible to nucleophilic displacement, a number of these 1,4-naphthoquinones were treated with boiling ethanolic solutions of aniline and of *n*-butanethiol containing triethylamine. The 2,3-dimethyl-, 2,3-diphenyl-, 2-methyl-3-hydroxy-, and 2,3-diacetamido-1,4-naphthoquinones were recovered unchanged from reaction with aniline while 2,3-diacetamido-1,4-naphthoquinone, 2-anilino-3-methyl-1,4-naphthoquinone, and 2-anilino-6,7-dimethyl-3-phenyl-1,4-naphthoquinone were inert towards *n*-butanethiol – triethylamine reagent. The quinones with abnormal reactions were not used in the plot of the logarithms of the growth inhibitory activities against half-wave potentials.

A number of epoxides, **1**, of C-2 monosubstituted-, and of C-2, C-3 disubstituted-1,4-naphthoquinones were prepared and the epoxide ring opened by such model nucleophiles (HA) as aniline, *n*-butanethiol, and the halogen acids to give the respective 1,4-naphthoquinones, **3**. Yields of 40–50% of the red 2-anilino-3-methyl-1,4-naphthoquinone, **3** ($R = CH_3$; $A = C_6H_5NH$), and 2,*n*-butylthio-3-methyl-1,4-naphthoquinone, **3** ($R = CH_3$; $A = n\text{-}C_4H_9S$), were obtained when 2,3-epoxy-2,3-dihydro-2-methyl-1,4-naphthoquinone, **1** ($R = CH_3$; $R^1 = H$), was boiled respectively with ethanolic solutions of aniline and *n*-butanethiol. As would be expected, no red quinone was formed when 2,3-epoxy-2,3-dihydro-2,3-dimethyl-1,4-naphthoquinone, **1** ($R = R^1 = CH_3$), was treated similarly, with aniline.

4*a*-Methyl-1,4,4*a*,9*a*-tetrahydroanthraquinone

Can. J. Chem. Downloaded from www.nrcresearchpress.com by 210.87.254.6 on 09/05/12
For personal use only.

TABLE II

Summary of reactions of some 1,4-naphthoquinones

Reactants	Conditions	Yields (%)	Products
2-Anilino-1,4-Naphthoquinone and *n*-butylamine	Refluxing in EtOH for 18 h	50	2,*n*-Butylamino-1,4-naphthoquinone
2-Anilino-3-chloro-1,4-Naphthoquinone and *n*-butylamine	Standing in EtOH for 60 h, then refluxed 4 h	15	2,*n*-Butylamino-3-chloro-1,4-naphthoquinone
2-Chloro-1,4-naphthoquinone and bromine	Method used in ref. 42.		2,3-Dibromo-1,4-naphthoquinone
2-Bromo-3-methoxy-1,4-naphthoquinone and aniline	Method used in ref. 9	96	2-Anilino-3-bromo-1,4-naphthoquinone
2-Bromo-3-methoxy-1,4-naphthoquinone and *n*-butylamine	Method used in ref. 9	94	2-Bromo-3,*n*-butylamino-1,4-naphthoquinone
2-Methoxy-3-methyl-1,4-naphthoquinone and aniline	Method used in ref. 9	53	2-Anilino-3-methyl-1,4-naphthoquinone
2-Acetamido-3,*n*-butylthio-1,4-naphthoquinone and aniline	Method used in ref. 9	70	2-Acetamido-3-anilino-1,4-naphthoquinone
2,3-Di-*n*-butylthio-1,4-naphthoquinone and aniline	Method used in ref. 9	55	2-Anilino-3,*n*-butylthio-1,4-naphthoquinone
Potassium 1,4-naphthoquinone-2-sulfonate and aniline	Method used in ref. 41 from aqueous mother liquors	52	Potassium 2-anilino-1,4-naphthoquinone-3-sulfonate
Hydrogen chloride on a glacial acetic acid solution of 2,3-epoxy-2,3-dihydro-2-phenyl-1,4-naphthoquinone		62	2-Hydroxy-3-phenyl-1,4-naphthoquinone
2,3-epoxy-2,3-dihydro-2-alkyl-1,4-naphthoquinones and ethanolic alkanethiols or thiophenols	Reflux	40–60	2-Alkyl-3-alkylthio-(3-arylthio)-1,4-naphthoquinone

was prepared from butadiene and 2-methyl-1, 4-naphthoquinone but it could not be dehydrogenated by air and ethanolic potassium hydroxide under conditions that convert 2,3-dimethyl-1,4,4*a*,9*a*-tetrahydroanthraquinone into 2,3-dimethylanthraquinone (31).

As expected the growth inhibitory activities of neither the 2,3-expoxy-2,3-dihydro-2,3-disubstituted 1,4-naphthoquinones nor of 4*a*-methyl-1, 4,4*a*,9*a*-tetrahydroanthraquinone were of the same order of magnitude as the 2,3-epoxy-2,3-dihydro - 2 - monosubstituted - 1,4 - naphthoquinones or 2-methyl-1,4,4*a*,9*a*-tetrahydroanthraquinone.

Table I lists the new 1,4-naphthoquinones prepared in this work. Similar data for the 1,4-naphthoquinones, previously described, and for related compounds will be found in Tables III and IV.[2]

[2]Photocopies of Tables III and IV may be obtained upon request from The Depository of Unpublished Data, National Science Library, National Research Council of Canada, Ottawa, Canada.

Experimental

Novel features encountered in the synthesis and reactions of some 1,4-naphthoquinones are summarized in Table II. Yields of the order of 85% were obtained when 1 g of the 2-amino-3-halogeno-1,4-naphthoquinone was refluxed for 9 h in 5 ml of ethanol containing 2 g of both *n*-butanethiol and triethylamine. The product separated as a solid when the cold reaction was poured into 5% hydrochloric acid.

1. G. J. LEAHY, D. J. CURRIE, H. L. HOLMES, and J. R. MALTMAN. Can. J. Microbiol. To be published.
2. D. J. CURRIE, C. E. LOUGH, R. F. SILVER, and H. L. HOLMES. Can. J. Chem. **44**, 1035 (1966).
3. D. J. CURRIE and H. L. HOLMES. Can. J. Chem. **44**, 1027 (1966).
4. A. ALBERT. Intern. Congr. Microbiol., 6th. Congr. Rome, 1953. Symposium Growth Inhibition and Chemotherapy, 10. (1953).
5. H. DAVSON and J. F. DANIELLI. The permeability of natural membranes. Cambridge University Press, London. 1943.
6. H. L. HOLMES, D. J. CURRIE, J. R. MALTMAN, R. F. SILVER, C. E. LOUGH, and G. J. LEAHY. Chemotherapia, **9**, 241 (1964).
7. O. DIELS and K. ALDER. Ber. **62**, 2337 (1929).
8. M. Y. GOLOVANOVA. Zh. Obshch. Khim. **18**, 835 (1948).
9. J. C. CALANDRA and E. C. ADAMS. J. Am. Chem. Soc. **72**, 4804 (1950).

Can. J. Chem. Downloaded from www.nrcresearchpress.com by 210.87.254.6 on 09/05/12
For personal use only.

10. K. FRIES and K. BILLIG. Ber. **58**, 1128 (1925).
11. L. F. FIESER and R. H. BROWN. J. Am. Chem. Soc. **71**, 3609 (1949).
12. D. BUCKLEY, H. B. HENBEST, and P. SLADE. J. Chem. Soc. 4891 (1957).
13. D. BUCKLEY, S. DUNSTAN, and H. B. HENBEST. J. Chem. Soc. 4880 (1957).
14. D. BUCKLEY, S. DUNSTAN, and H. B. HENBEST. J. Chem. Soc. 4901 (1957).
15. W. K. ANSLOW and H. RAISTRICK. J. Chem. Soc. 1446 (1939).
16. R. H. THOMPSON. J. Org. Chem. **13**, 870 (1948).
17. L. F. FIESER. J. Am. Chem. Soc. **48**, 2922 (1926).
18. L. F. FIESER and M. T. LEFFLER. J. Am. Chem. Soc. **70**, 3212 (1948).
19. H. O. HUISMAN. Rec. Trav. Chim. **69**, 1130 (1950).
20. K. MIYAKI, N. IKEDA, and D. MIZUNO. Yakugaku Zasshi, **73**, 961 (1953).
21. A. BLACKHALL and R. H. THOMPSON. J. Chem. Soc. 1138 (1953).
22. G. B. BARLIN, K. H. PAUSACKER, and N. V. RIGGS. J. Chem. Soc. 3122 (1954).
23. N. IKEDA. Yakugaku Zasshi, **75**, 649 (1955).
24. E. KNOEVENAGEL and C. BUCKEL. Ber. **34**, 3993 (1901).
25. J. B. LAL and S. DUTT. J. Indian Chem. Soc. **10**, 577 (1933); Chem. Abstr. **28**, 2000 (1934).
26. I. F. VLADIMERTSEV. Zh. Obshch. Khim. **30**, 2670 (1960).
27. C. LIEBERMANN. Ber. **14**, 1664 (1881).
28. I. F. VLADIMERTSEV, I. Y. POSTOVISKII, and L. F. TREFLOVA. Zh. Obshch. Khim. **24**, 181 (1954).
29. R. NIETZKI and F. SCHMIDT. Ber. **22**, 1653 (1889).
30. C. LIEBERMANN and P. JACOBSON. Ann. **211**, 36 (1882).
31. C. F. ALLEN and A. BELL. Org. Synth. Coll. Vol. III, 310.
32. L. F. FIESER and F. C. CHANG. J. Am. Chem. Soc. **64**, 2043 (1942).
33. R. A. COVEY. Belg. Patent No. 614,136 (March 15, 1962); Chem. Abstr. **57**, 15031 (1962).
34. C. E. DALGLEISH. J. Am. Chem. Soc. **71**, 1697 (1949).
35. J. R. E. HOOVER and A. R. DAY. J. Am. Chem. Soc. **76**, 4148 (1954).
36. R. GAERTNER. J. Am. Chem. Soc. **76**, 6150 (1954).
37. R. ADAMS, T. A. GEISSMAN, B. R. BAKER, and H. M. TEETER. J. Am. Chem. Soc. **63**, 528 (1941).
38. D. B. BRUCE and R. H. THOMPSON. J. Chem. Soc. 1428 (1954).
39. J. MADINAVEITA. Anales Real Soc. Españ. Fís. Quím. Madrid, **31**, 750 (1933); Chem. Abstr. **28**, 2708 (1934).
40. L. F. FIESER. J. Biol. Chem. **133**, 391 (1940).
41. M. V. GORELIK, S. V. BOGDANOV, and A. M. RODIONOV. Zh. Obshch. Khim. **30**, 2959 (1960).
42. A. INOUE, N. KUROKI, and N. KONISHI. Yuki Gosei Kagaku Kyokai Shi, **16**, 607 (1958); Chem. Abstr. **53**, 3233 (1959).

Can. J. Chem. Downloaded from www.nrcresearchpress.com by 210.87.254.6 on 09/05/12
For personal use only.

Can. J. Chem. Downloaded from www.nrcresearchpress.com by 210.87.254.5 on 09/05/12
For personal use only.

Synthesis and properties of some formylferrocene thiosemicarbazones[1]

D. M. WILES AND T. SUPRUNCHUK
Division of Applied Chemistry, National Research Council of Canada, Ottawa, Canada

Received February 13, 1968

Twelve new substituted thiosemicarbazones have been prepared from formylferrocene and 2- and 4-monosubstituted and 4,4-disubstituted thiosemicarbazides. The infrared spectra of these compounds are discussed in some detail. Copper complexes of three of them were synthesized and their structures established. They were found to be strongly paramagnetic. The electronic absorption spectra of the thiosemicarbazones and the copper complexes are reported.

Canadian Journal of Chemistry, **46**, 1865 (1968)

Introduction

There have been numerous publications, in recent years, dealing with the chemistry of ferrocene and with the many derivatives which can be prepared from it (e.g. ref. 1). Considerable interest has been shown in the reactions of formylferrocene. It is easy to synthesize and many additional ferrocenes may be derived from it. Both the semicarbazone (1) and the simple thiosemicarbazone (2) of formylferrocene have been synthesized.

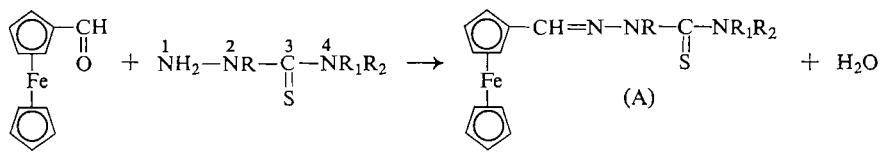

Some benzoylferrocenes have been shown (3) to retard the actinic degradation of polymer films and the photodecomposition of ferrocenes in hydroxylic (4) and alkyl halide (5) solvents has been reported. However, very little use has been made of particular ferrocene derivatives as protective ultraviolet absorbers in spite of the fact that ferrocenes absorb strongly in the important, near-ultraviolet region. The electronic absorption spectra of the new compounds reported here were measured in order to indicate the potential effectiveness of them as photoprotective agents.

It is known that copper will form 1:1 complexes (B) with thiosemicarbazones (6) and a different type of 1:1 complex (C) with dithiosemicarbazones (7). Copper complexes of three of the ferrocene thiosemicarbazones reported here

[1]Issued as NRCC No. 10084.

In the present work, the preparation and some properties of formylferrocene thiosemicarbazones are described. The syntheses involved the reaction of formylferrocene with thiosemicarbazide and substituted thiosemicarbazides. This method produced a set of compounds which have not been reported previously, except for formylferrocene thiosemicarbazone (A; R = R_1 = R_2 = H), mentioned by Boichard *et al.* (2). The structure of A was deduced from infrared spectra and from analytical data.

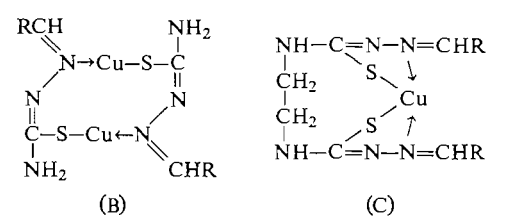

were prepared using cupric acetate. These are interesting organometallic – metal – chelate compounds, somewhat analogous to the copper complexes of diacylferrocenes reported previously (8).

Experimental

Methods and Materials

Formylferrocene was prepared by the method of Broadhead and co-workers (9), and was purified by recrystallizing from aqueous ethanol.

2-Methylthiosemicarbazide was prepared by the method of Greer and Smith (10) and was recrystallized from water.

Can. J. Chem. Downloaded from www.nrcresearchpress.com by 210.87.254.5 on 09/05/12
For personal use only.

4,4-Dimethylthiosemicarbazide was prepared by the method of Jensen (11) and was purified by recrystallizing from water.

Thiosemicarbazide was purchased from commercial sources and purified by recrystallizing from water.

All the alkyl and aryl isothiocyanates were obtained from commercial sources and were used as received.

A series of 4-substituted thiosemicarbazides was synthesized by the following method. Hydrazine hydrate (0.022 mole, 99%) in ethanol (25 ml) was added dropwise to a solution of the required isothiocyanate (0.022 mole) in diethyl ether (50 ml). The resulting mixture was stirred for 1 h with gentle heating and reduced to $\frac{1}{3}$ of the original volume. The precipitate, which formed when the mixture was cooled, was removed by filtration, washed with cold ether, dried, and recrystallized. The compounds listed below were made by this method, and were purified by recrystallization from aqueous ethanol unless otherwise stated.

4(1-Naphthyl)thiosemicarbazide, m.p. 139.5 °C (lit. value (12) 139 °C).

4-Phenethylthiosemicarbazide, m.p. 119 °C (no lit. value).

4(*m*-Nitrophenyl)thiosemicarbazide, m.p. 175.5 °C (lit. value (13) 175 °C).

4(*p*-Nitrophenyl)thiosemicarbazide, m.p. **191** °C (lit. value (14) 190 °C).

4-Phenylthiosemicarbazide, m.p. 141 °C (lit. value (15) 141 °C); recrystallized from water.

4-Methylthiosemicarbazide, m.p. 136 °C (lit. value (16) 137 °C).

4-Ethylthiosemicarbazide, m.p. 84 °C (lit. value (16) 84 °C).

4-Heptylthiosemicarbazide, m.p. 54 °C (lit. value (16) 54 °C).

4-Allylthiosemicarbazide, m.p. 95 °C (lit. value (16) 97 °C).

Preparation of Formylferrocene Thiosemicarbazone

Formylferrocene (0.0047 mole) in ethanol (25 ml) was added dropwise to a solution of thiosemicarbazide (0.0047 mole) in water (40 ml). Glacial acetic acid (1 ml) was then added and the resulting mixture was heated on the steam bath for 15 min. The dark-red precipitate which formed when the mixture cooled was collected, washed with aqueous ethanol, dried, and recrystallized repeatedly from ethanol, until pure, m.p. 183 °C (lit. value (2) 190 °C; an incomplete analysis and no infrared spectrum were reported); yield 71%.

Anal. Calcd. for $C_{12}H_{13}N_3SFe$: C, 50.17; H, 4.53; N, 14.63; S, 11.15; Fe, 19.51. Found: C, 49.60; H, 4.54; N, 14.30; S, 11.03; Fe, 20.0.

Preparation of Formylferrocene-substituted Thiosemicarbazones

A solution of formylferrocene (0.0047 mole) in ethanol (25 ml) was added dropwise to a solution of a substituted thiosemicarbazide (0.0047 mole) in ethanol (40 ml). The mixture was heated for 15 min, and then cooled. Water was added until the onset of precipitation and the precipitate which formed was collected, washed with 50% aqueous ethanol solution, dried, and recrystallized until pure. The compounds prepared in this way are listed in Table I.

Preparation of Ethylene Di(formylferrocene Thiosemicarbazone)

A solution of formylferrocene (0.0047 mole) in ethanol (25 ml) was added dropwise to a solution of ethylene dithiosemicarbazide (7) (0.00235 mole) in dimethylformamide (25 ml). The method was the same as described for the above synthesis and the product was recrystallized repeatedly from dimethylformamide – water mixture, until pure, m.p. 223 °C.

Anal. Calcd. for $C_{26}H_{28}N_6S_2Fe_2$: C, 52.00; H, 4.67; N, 14.00; S, 10.67; Fe, 18.67. Found: C, 51.97; H, 4.63; N, 13.50; S, 10.50; Fe, 19.01.

Preparation of the Copper Complexes of Formylferrocene-substituted Thiosemicarbazones

The general procedure involved the addition of cupric acetate (0.00243 mole) in 25 ml of ethanol, to a warm solution of a formylferrocene-substituted thiosemicarbazone (0.00485 mole) in 30 ml of ethanol. The resulting mixture was refluxed gently for 15 min. The precipitate, which formed after cooling, was removed by filtration, and washed with 3% aqueous hydrochloric acid solution, water, and cold ethanol. The product was dried and recrystallized repeatedly from benzene.

Formylferrocene 4(1-naphthyl)thiosemicarbazone-Cu; m.p. 205 °C.

Anal. Calcd. for $C_{44}H_{36}N_6S_2CuFe_2$: C, 59.49; H, 4.06; N, 9.46; S, 7.22; Cu, 7.21; Fe, 12.53. Found: C, 60.61; H, 4.49; N, 8.96; S, 6.78; Cu, 6.95; Fe, 12.29.

Formylferrocene 4-phenethylthiosemicarbazone-Cu, m.p. 175 °C.

Anal. Calcd. for $C_{40}H_{40}N_6S_2CuFe_2$: C, 56.91; H, 4.74; N, 9.95; S, 7.59; Cu, 7.52; Fe, 13.28. Found: C, 57.03; H, 5.07; N, 10.01; S, 7.43; Cu, 7.36; Fe, 13.78.

Formylferrocene 4-phenylthiosemicarbazone-Cu, m.p. 185 °C.

Anal. Calcd. for $C_{36}H_{32}N_6S_2CuFe_2$: C, 48.58; H, 4.63; N, 12.15; S, 9.26; Cu, 9.20; Fe, 16.19. Found: C, 48.01; H, 3.95; N, 12.26; S, 8.20; Cu, 8.82; Fe, 17.0.

The difficulty experienced in recrystallizing the copper complexes because of their lower solubilities resulted in less satisfactory analyses than were obtained for the parent thiosemicarbazones. Nevertheless, it was felt that these complexes were pure enough for the structural identification purposes for which they were intended.

The infrared spectra of the compounds described in this work were obtained from KBr pellets with a model 21 Perkin–Elmer double-beam spectrophotometer (NaCl prism) over the frequency range 3500 to 700 cm^{-1}. The ultraviolet spectra of the compounds were obtained with either a Cary model 14 or a Beckman DK-1 recording spectrophotometer. All melting points were measured with a Fisher–Johns apparatus and have been corrected. Elemental analyses were performed at the microanalytical laboratory of Drs. Weiler and Strauss in Oxford. The new ferrocene derivatives reported here and the copper complexes of three of them were tested for antifungal activity by a tube dilution method (17). The microorganisms used for this purpose were *Chaetomium globosum*, Strain USDA 1042.4 and *Aspergillus niger*, Strain USDA 215-5373.16.

Results and Discussion

Eleven new formylferrocene-substituted thiosemicarbazones which were prepared in this work are listed in Table I. The general structural formula proposed for this series of compounds (A) represents the accepted structure for

TABLE I

Formylferrocene thiosemicarbazones*

Compound	Substituents	Melting point (°C)	Yield (%)	Formula	Analysis (%) Calculated	Analysis (%) Found
1	$R = CH_3$ $R_1 = R_2 = H$	185	52†	$C_{13}H_{15}N_3SFe$	C, 51.82 H, 4.98 N, 13.95 S, 10.63 Fe, 18.61	C, 52.19 H, 4.98 N, 13.75 S, 10.62 Fe, 19.1
2	$R = H$ $R_1 = R_2 = CH_3$	150	49‡	$C_{14}H_{17}N_3SFe$	C, 53.33 H, 5.39 N, 13.33 S, 10.16 Fe, 17.78	C, 53.91 H, 5.38 N, 13.20 S, 9.94 Fe, 18.1
3	$R = R_1 = H$ $R_2 = C_6H_5$	197	79‡	$C_{18}H_{17}N_3SFe$	C, 59.50 H, 4.68 N, 11.57 S, 8.82 Fe, 15.42	C, 59.59 H, 4.80 N, 11.41 S, 8.52 Fe, 16.0
4	$R = R_1 = H$ $R_2 = 1 - C_{10}H_7$	184	81‡	$C_{22}H_{19}N_3SFe$	C, 63.92 H, 4.60 N, 10.17 S, 7.74 Fe, 13.56	C, 63.66 H, 4.60 N, 9.90 S, 7.80 Fe, 13.7
5	$R = R_1 = H$ $R_2 = (CH_2)_2C_6H_5$	135	76‡	$C_{20}H_{21}N_3SFe$	C, 61.38 H, 5.37 N, 10.74 S, 8.18 Fe, 14.32	C, 61.09 H, 5.38 N, 10.69 S, 8.05 Fe, 14.7
6	$R = R_1 = H$ $R_2 = p\text{-}NO_2C_6H_5$	200	81§	$C_{18}H_{16}N_4O_2SFe$	C, 52.94 H, 3.92 N, 13.73 S, 7.84 Fe, 13.73	C, 52.77 H, 3.98 N, 13.80 S, 8.02 Fe, 14.3
7	$R = R_1 = H$ $R_2 = m\text{-}NO_2C_6H_5$	115	53§	$C_{18}H_{16}N_4O_2SFe$	C, 52.94 H, 3.92 N, 13.73 S, 7.84 Fe, 13.73	C, 52.25 H, 4.07 N, 13.95 S, 7.99 Fe, 14.0
8	$R = R_1 = H$ $R_2 = CH_3$	138	71†	$C_{13}H_{15}N_3SFe$	C, 51.82 H, 4.98 N, 13.95 S, 10.63 Fe, 18.61	C, 52.16 H, 5.05 N, 14.05 S, 10.38 Fe, 18.3
9	$R = R_1 = H$ $R_2 = C_2H_5$	146	73‖	$C_{14}H_{17}N_3SFe$	C, 53.33 H, 5.39 N, 13.33 S, 10.16 Fe 17.78	C, 53.38 H, 5.51 N, 12.94 S, 9.95 Fe, 18.3
10	$R = R_1 = H$ $R_2 = CH_2{=}CHCH_2$	158	51‖	$C_{15}H_{17}N_3SFe$	C, 55.05 H, 5.19 N, 12.84 S, 9.78 Fe, 17.13	C, 55.53 H, 5.43 N, 13.00 S, 9.74 Fe, 17.6
11	$R = R_1 = H$ $R_2 = CH_3(CH_2)_6$	73	75‖	$C_{19}H_{27}N_3SFe$	C, 59.22 H, 7.01 N, 10.91 S, 8.31 Fe. 14.55	C, 58.88 H, 7.09 N, 10.85 S, 8.55 Fe, 14.7

*The structural formula may be represented by:

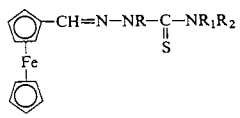

†Recrystallized from ethanol–water.
‡Recrystallized from ethanol.
§Recrystallized from chloroform–hexane.
‖Recrystallized from isooctane.

Can. J. Chem. Downloaded from www.nrcresearchpress.com by 210.87.254.5 on 09/05/12
For personal use only.

Can. J. Chem. Downloaded from www.nrcresearchpress.com by 210.87.254.5 on 09/05/12
For personal use only.

TABLE II

Infrared absorption bands for formylferrocene thiosemicarbazones

Compound number*															
1	**2**	**3**	**4**	**5**	**6**	**7**	**8**	**9**	**10**	**11**	**12**	**13**	**14**	**15**	**16**
	3330w†	3340w	3360m†	3360w	3340m	3340m		3380w	3380w	3350m			3400m	3410m	3410m
3270m									3220vw†		3280w				
3130w	3120w	3140w	3160m	3160m	3160m		3170m	3160m	3140m	3150m	3160m	3100m			
2930w	2960w	2930w	2990w	2990w	2990w	2960w	2980m	2980w	2990w	2940s†	2980w	2960w		2940w	2940w
										2860w					
									1645w			1660w			
1610m	1610m	1600m	1605m	1610m	1600m	1615m	1610m	1610m	1610m	1610m	1600s	1615m	1600s	1595s	1600s
1585s						1595w									
	1535s	1545s	1550s	1550s	1550s	1535s	1555s	1550s	1545s	1550s	1540s	1540s			
		1510m	1500s	1500w	1510s	1510s							1515s	1510s	1505s
1480s	1470m		1470sh†	1475w	1470sh		1475w		1475w	1470m	1465m	1475w	1485s	1450m	1440m
1455w		1455m		1460w		1445m		1460sh					1450m		
1440w			1440w							1445w	1420w	1440w		1435w	
1420w	1400w	1405w	1400m	1415w	1415w	1400m	1415w	1415w	1415br	1410w	1400w	1415w	1400br†	1400w	
					1400vw		1395w				1390w			1385w	1385w
1385w	1375w		1375w					1380w	1375vw	1375w	1375w	1365br			
1360s		1365br	1355w		1340s	1355s	1365w		1355vw	1355w			1350m	1360w	
1325w		1320w			1310sh	1310w	1310w	1310m	1335w	1315w	1335m		1330w	1325w	1315w
	1300m									1300w	1290m	1300m			
		1275m	1280m		1275s				1280br	1280w			1270w		
1255w	1260w		1260m	1255m		1265m	1265m	1260m	1255br	1265m	1255w	1255w	1250m	1245m	1250m
	1230w		1225m					1240m	1225s	1240w			1225m		
1215w	1210w	1200m			1200s	1210s	1210w			1215m	1210w	1215m	1200w	1200m	1210w
1190w			1170m	1185w			1160w	1165w	1190vw	1190w			1170m		
1110m	1110m	1110m	1110w	1110m	1110s	1110m	1110w	1110w	1110m	1110m	1110m	1110m	1110m	1110w	1110w
		1065br	1060w	1060w	1060br	1060w	1085m	1085w	1055m	1050w	1065w		1070w	1090w	1085w
1045w	1030w	1030w	1030w	1030w	1030w	1030m	1035w	1030w	1030w	1035w	1030w	1030w	1030w	1045w	1050w
1000s	1005m	1005m	1005w	1005w	1000w	1010m	1005w	1010m	1005m	1005w	1005w	1005m	1005w	1005w	1005m
940w	945m	955w	945m	945m	950m	945m	940m	935m	940m	935w	940m	935m	945w		940vw
900w						890w						900w	890w		
	865w				850s	845m				865w			850m	855m	870vw
820s	820m	820m	820m	820m	820m	825m	815m	820s	820m	820s	820m	820m	825vw	820vw	820vw
			800w			795w				780w			780m		
			775s	750m	745m	760w	745w	775m	760w	775w	770w	750w		750w	750m
	725w	735m				740m				725w			725w		
				700m	700m									700m	690m

*The numbers 1 to 16 at the head of this table refer to the compounds having the same numbers in Table III.
†The letters following the wave number in the table refer to the band intensity or shape: w, weak; m, medium; vw, very weak; s, strong; sh, shoulder; br, broad.

Can. J. Chem. Downloaded from www.nrcresearchpress.com by 210.87.254.5 on 09/05/12
For personal use only.

substituted thiosemicarbazones. Evidence that this structure does, in fact, represent the products reported here, was obtained from the infrared absorption spectra of these compounds. The bands observed in the 3500 to 700 cm^{-1} frequency region are listed in Table II.

The absorptions characteristic of the expected functional entities for the eleven substituted thiosemicarbazones (Table I), for formylferrocene thiosemicarbazone, and for ethylene di(formylferrocene thiosemicarbazone), are as follows. The bands arising from NH stretching vibrations occur in the 3380 to 3120 cm^{-1} region for all of these compounds. In the 1600 to 1615 cm^{-1} region, the medium to strong band arising from γ(C=N) is observed in all cases. Strong absorption occurs in the 1535 to 1550 cm^{-1} region for compounds **2** to **13** and may be related to the fact that these are *N*-substituted thioamides. The CNH vibration, involving NH bending and C—N stretching (18), gives rise to strong absorption in this region; this has been observed previously in the case of some dithiosemicarbazones of aliphatic and aromatic aldehydes (7). In the spectrum of compound **1**, formylferrocene-2-methylthiosemicarbazone, a strong band appears at 1585 cm^{-1}. This shift to higher frequency has been observed before (19) in a comparison of 2- and 4-substituted thiosemicarbazones. The band which is observed at 1510 or 1500 cm^{-1} in the spectra of compounds **3** to **7** may be attributed to aromatic ring absorptions (see, for example, ref. (20)).

Several absorption bands were observed, in all the spectra shown in Table II, which are characteristic of formylferrocene or other substituted ferrocenes. Peaks in the vicinity of 1460 ($\pm$ 20) cm^{-1} and 1410 ($\pm$ 10) cm^{-1} presumably correspond to the transitions in the ferrocene part of formylferrocene, at 1456 and 1412 cm^{-1}, as described by Rubalcava and Thomson (21). The bands at 1110 cm^{-1} and at 1005 cm^{-1} are also reported for formylferrocene (21) and are described by Rosenblum (22) as characteristic of "ferrocene derivatives possessing an unsubstituted [cyclopentadienyl] ring".

Some of the bands which are observed for the various compounds in the 1030 to 1090 cm^{-1} region presumably represent a contribution from N—C—N stretching vibrations which may be coupled with a small amount of γ(C=S) (23). However, the largest contribution from C=S stretching vibrations gives rise to a band in 830 to 805 cm^{-1} region of the spectra of thiosemicarbazones (23, 24) and presumably accounts for an appreciable proportion of the peaks at 825 to 815 cm^{-1} in the spectra of compounds **1** to **13** (Table II). Superimposed on this in all cases is a contribution from the ferrocene moiety (21).

Collectively, the absorption band assignments described above provide strong evidence that the compounds prepared in this work are indeed the thiosemicarbazones that the analytical data have suggested, and that A represents the correct structure for compounds **1** to **12**. It follows that compound **13**, ethylene di(formylferrocene thiosemicarbazone) could be depicted as

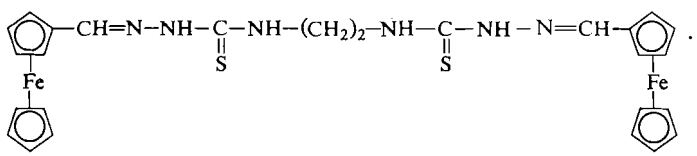

Additional evidence is obtained from the experiments to form copper complexes of some of the thiosemicarbazones. Attempts to prepare copper complexes with 2-substituted thiosemicarbazones failed; only starting materials were recovered from the reaction mixtures. This is in agreement with previous work on copper complex formation with a variety of substituted thiosemicarbazones (19). Copper complexes (2:1) were prepared from compounds **3**, **4**, and **5** (4-substituted compounds) and the infrared spectra of these complexes are given in Table II (spectra **14** to **16**). Comparison with the spectra of the uncomplexed, parent compounds leads to the following observations. The two bands in NH region of the spectrum have been replaced by a single band in the vicinity of 3410 cm^{-1}, on copper complex formation. In addition, the intensity of the C=N band at about 1600 cm^{-1} has increased, whereas the CNH band at 1550 cm^{-1} has disappeared. Finally, the absorption at 820 cm^{-1} has an appreciably lower intensity. It is reasonable to conclude that complex formation is associated with a reduction in the number

TABLE III

Electronic spectra of formylferrocene thiosemicarbazones

Compound*	Absorption band maxima (mμ) (molar extinction coefficient $\times 10^{-3}$)			Solvent
1	270 (9.6)	312 (30.5)	400 (0.8)	Acetonitrile
2	259 (13.9)	303 (15.7)	—	Acetonitrile
3	272 (15.1)	314 (27.8)	390 (1.1)	Acetonitrile
4	272 (14.5)	313 (29.9)	390 (1.1)	Acetonitrile
5	265 (15.1)	311 (30.9)	390 (1.0)	Acetonitrile
6	273 (21.1)	319 (50.6)	462 (1.3)	Acetonitrile
7	267 (11.4)	316 (40.8)	400 (1.9)	Acetonitrile
8	258 (11.8)	303 (42.0)	448 (1.1)	Acetonitrile
9	262 (13.8)	317 (39.1)	455 (0.9)	Isooctane
10	262 (11.4)	316 (41.8)	456 (1.6)	Isooctane
11	255 (13.4)	308 (48.4)	445 (1.1)	Isooctane
12	270 (11.7)	308 (31.9)	390 (1.1)	Acetonitrile
13	253 (22.1)	313 (35.0)	400 (1.1)	*p*-Dioxane
14	270 ⟶	350 (27.2)	444 sh (5.0)	*p*-Dioxane
15	255 (26.3)	300 (25.3)	440 sh (3.8)	*p*-Dioxane

*(1) Formylferrocene-2-methylthiosemicarbazone; (2) formylferrocene-4,4-dimethylthiosemicarbazone; (3) formylferrocene-4-phenylthiosemicarbazone; (4) formylferrocene-4(1-naphthyl)thiosemicarbazone; (5) formylferrocene-4-phenethylthiosemicarbazone; (6) formylferrocene-4(*p*-nitrophenyl)thiosemicarbazone; (7) formylferrocene-4(*m*-nitrophenyl)thiosemicarbazone; (8) formylferrocene-4-methylthiosemicarbazone; (9) formylferrocene-4-ethylthiosemicarbazone; (10) formylferrocene-4-allylthiosemicarbazone; (11) formylferrocene-4-beptylthiosemicarbazone; (12) formylferrocene thiosemicarbazone; (13) ethylene di(formylferrocene thiosemicarbazone); (14) copper complex of compound 4; (15) copper complex of compound 5; (16) copper complex of compound 3.

of NH groups, an increase in the number of C=N groups and elimination of the C=S group.

On the basis of this evidence, and in the context of previously proposed structures for copper complexes of analogous compounds (6, 7), it is reasonable to suggest the following general structure for compounds **14**, **15**, and **16**.

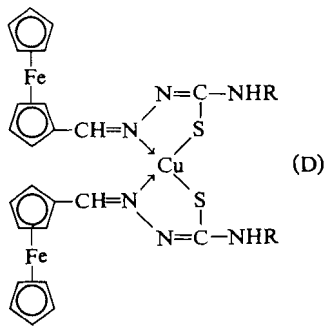

(D)

In such a 2:1 complex, copper would be paramagnetic. The copper complexes prepared in this work are all strongly paramagnetic, having an electron spin resonance signal intensity of the same order of magnitude as that from an equimolar quantity of $CuSO_4 \cdot 5H_2O$. The *g* value for compound **15**, for example, is 2.066. Thus, there is good reason to believe that the Structure D proposed for the copper complexes, and the Structure A proposed for the thiosemicarbazones, are valid.

The important bands in the electronic absorption spectra of most of the compounds prepared in this work are listed in Table III, together with the relevant molar extinction coefficients. The compounds are all colored and many of them absorb strongly in the important, near-ultraviolet region. However, the requirements for a useful ultraviolet protective substance include, in in addition to a high molar extinction coefficient, such considerations as inherent stability, a relatively low volatility and minimal absorption of visible wavelengths. On this simplified basis, it may be suggested that compounds **13**, **6**, and **3** (in that order) could be useful as retarders of the photooxidation of polymeric materials.

Since some organometallic and many thiocarbonyl-containing compounds have antifungal properties, the formylferrocene thiosemicarbazones and the three copper complexes were evaluated as potential fungicides. Below 1000 p.p.m. none was found effective, in tube dilution tests.

Acknowledgments

The authors wish to thank Mr. R. Ironside for measuring the infrared spectra, Miss G. Colin for carrying out the microbiological tests, and Dr. A. M. Tarr and Mr. J. D. Cooney for helpful discussions. Thanks are due Drs. J. R. Morton and L. E. Vannotti for making the electron spin resonance measurements.

Can. J. Chem. Downloaded from www.nrcresearchpress.com by 210.87.254.5 on 09/05/12
For personal use only.

1. M. ROSENBLUM. Chemistry of the iron group metallocenes. Interscience Publishers, Inc., New York. 1965. pp. 91–100, 153–191, and 219–232.
2. J. BOICHARD, J. P. MONIN, and J. TIROUFLET. Bull. Soc. Chim. France, 851 (1963).
3. R. G. SCHMITT and R. C. HIRT. J. Polymer Sci. **7**, 1565 (1963).
4. M. RAUSCH, M. VOGEL, and H. ROSENBURG. J. Org. Chem. **22**, 903 (1957).
5. J. C. BRAND and W. SNEDDEN. Trans. Faraday Soc. **53**, 894 (1957).
6. B. A. GINGRAS and A. F. SIRIANNI. Can. J. Chem. **42**, 17 (1964).
7. D. M. WILES, B. A. GINGRAS, and T. SUPRUNCHUK. Can. J. Chem. **45**, 1735 (1967).
8. C. R. HAUSER and C. E. CAIN. J. Org. Chem. **23**, 1142 (1958).
9. G. D. BROADHEAD, J. M. OSGERBY, and P. L. PAUSON. J. Chem. Soc. 650 (1958).
10. A. H. GREER and G. B. L. SMITH. J. Am. Chem. Soc. **72**, 874 (1950).
11. K. A. JENSEN. J. Prakt. Chem. **159**, 189 (1941).
12. M. BUSCH and TH. ULMER. Ber. **35**, 1710 (1902).
13. M. TIŠLER. Croat. Chem. Acta, **28**, 147 (1956).
14. E. LIEBER and J. RAMACHANDRAN. Can. J. Chem. **37**, 101 (1959).
15. A. G. BAYER. Farbenfabriken. German pat. 832,891 (1952).
16. E. LIEBER, C. N. PILLAI, and R. D. HITES. Can. J. Chem. **35**, 832 (1957).
17. B. G. BENNS, B. A. GINGRAS, and C. H. BAYLEY. Appl. Microbiol. **8**, 353 (1960).
18. N. B. COLTHUP, L. H. DALY, and S. E. WIBERLEY. Introduction to infrared and raman spectroscopy. Academic Press, Inc., New York. 1964.
19. B. A. GINGRAS, R. L. SOMORJAI, and C. H. BAYLEY. Can. J. Chem. **39**, 973 (1961).
20. L. J. BELLAMY. The infrared spectra of complex molecules. 2nd ed. Methuen and Co. Ltd., London. 1958.
21. H. E. RUBALCAVA and J. B. THOMSON. Spectrochim. Acta, **18**, 449 (1962).
22. M. ROSENBLUM. Chem. and Ind. London, 953 (1958).
23. D. M. WILES, B. A. GINGRAS, and T. SUPRUNCHUK. Can. J. Chem. **45**, 469 (1967).
24. D. M. WILES and T. SUPRUNCHUK. Can. J. Chem. **45**, 2258 (1967).

Can. J. Chem. Downloaded from www.nrcresearchpress.com by 210.87.254.5 on 09/05/12
For personal use only.

Acyl derivatives of Hydroxylamine. XIII. Configuration and conformation of hydroxamic acid derivatives containing sulfur[1]

O. EXNER

J. Heyrovsky Institute of Polarography, Czechoslovak Academy of Sciences, Prague, Czechoslovakia

AND

M. H. BENN AND FRANCES WILLIS[2]

Department of Chemistry, University of Calgary, Calgary, Alberta

Received January 18, 1968

The configurations and conformations of *S*-methyl benzothiohydroxamic acid (**3**) and its *S*-oxo and *S*,*S*-dioxo derivatives (**5**) and (**7**) were established by means of a graphical comparison of their dipole moments with those of the corresponding *p*-nitro compounds.

The proton magnetic resonance and infrared spectra of these compounds were also studied.

It is concluded that the relative stability of stereoisomers in the series of compounds $C_6H_5C(NOH)X$ seems to depend more on the electronic nature of the group X than on its steric requirements.

Canadian Journal of Chemistry, **46**, 1873 (1968)

Derivatives of the tautomeric hydroximic form of hydroxamic acids are capable of existing in two geometrically isomeric forms, **1***a* in which the groups X and OH have the *syn* arrangement, and **1***b* in which these groups are *anti* to one another. However, for some hydroxamic acid derivatives both geometrical isomers have not yet been described.

In previous communications in this series (1, 2) it was shown that the configurations originally assigned by Werner (3) to the pair of isomers of the *O*-alkyl hydroxamic acid (**2**) had to be reversed. Subsequently, the stable configurations of some other related compounds, known only in one geometrically isomeric form, were also established (2).

syn (**1***a*) *anti* (**1***b*)

2) R = C_6H_5 and X = OCH_2CH_3 in general formula (**1**).

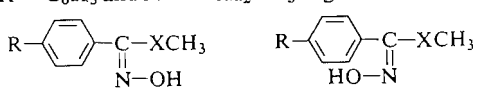

(**3**) R = H, X = S
(**4**) R = NO_2, X = S
(**5**) R = H, X = SO
(**6**) R = NO_2, X = SO
(**7**) R = H, X = SO_2
(**8**) R = NO_2, X = SO_2

(**9**) 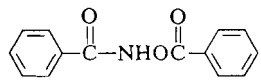

A recent synthesis (4) made *S*-alkyl thiohydroxamic acids (e.g. **3**) readily available, though in every case only one isomer, inferred to be the *anti* form, was isolated.

The initial objective of the present work was to establish the configuration of these *S*-alkyl thiohydroxamic acids; the investigation was then extended to include the oxidized derivatives (**5**–**8**), in order to compare the relative stabilities of stereoisomers **1***a* or **1***b* with various groups X.

The approach which we followed was to measure the dipole moments (μ) of a phenyl and corresponding *p*-nitrophenyl derivative.[3] The experimental and calculated dipole moments were then compared in a simple graph in which μ^2 for the unsubstituted phenyl compound was plotted against μ^2 for the *p*-nitro compound (see Figs. 1–3). This method has been described in detail elsewhere (5).

The dipole moment measurement also enables us to assess the approximate conformation of the N—O and C—S single bonds. We have to consider first eight planar conformations denoted here as *A*1–*D*2; any non-planar conformation can be considered as transitory between planar

[1]For part XII see: O. Exner and W. Simon, Collection Czech. Chem. Commun. **30**, 4078 (1965).

[2]Née Hall.

[3]The proton magnetic resonance and infrared spectra of the compounds **3**–**8** were also recorded and compared with those of stereoisomers **2***a* and **2***b*, the configurations of which are known (1). However, both these approaches are of limited value when, as here, only one isomer form (of **3**–**8**) is available.

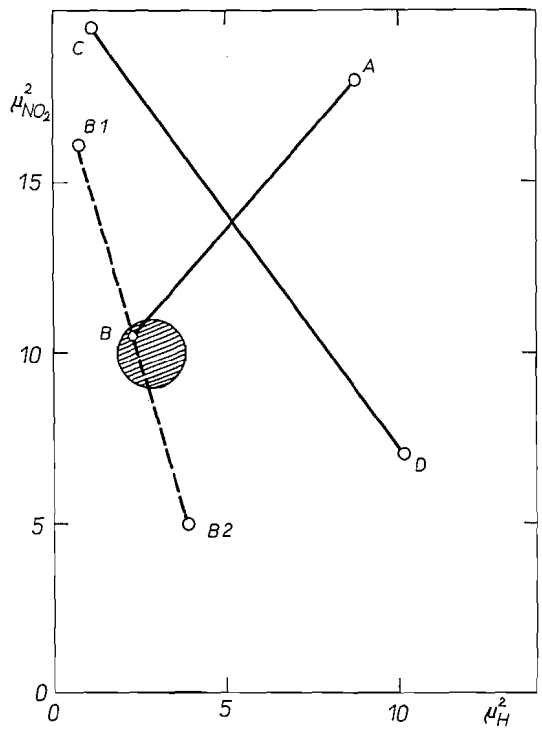

FIG. 1. Comparison of dipole moments of *S*-methyl benzothiodydroxamic acid (**3**) (*x*-Axis) and its 4-nitro derivative (**4**) (*y*-Axis). The experimental moments are expressed by the hatched circle, and the calculated moments by points *A*–*D* and *B*1, *B*2. The full lines represent the rotation about the N—O bond, and the broken line represents rotation around the C—S bond.

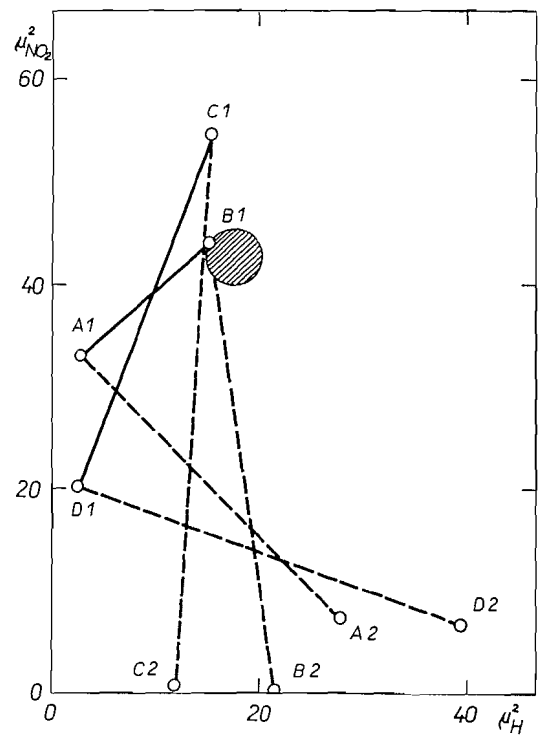

FIG. 2. Comparison of dipole moments of *S*-oxo-*S*-methyl benzothiohydroxamic acid (**5**) and its 4-nitro derivative (**6**). (See Fig. 1 for descriptive details.)

conformations. The conformations *D*1 and *D*2 are improbable for steric reasons, but are included for the sake of completeness.

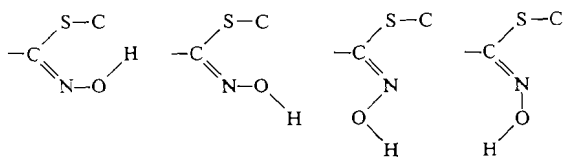

*A*1 *B*1 *C*1 *D*1

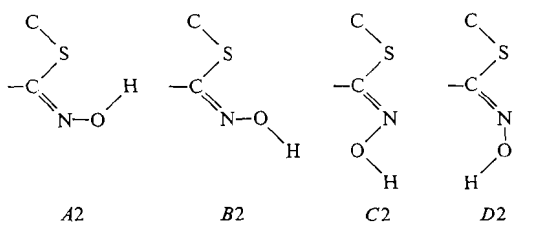

*A*2 *B*2 *C*2 *D*2

Materials

Although the benzothiohydroxamic acids (**3**) and (**4**) were readily prepared and gave the *S*-oxo derivatives (**5**) and (**6**) upon oxidation with hydrogen peroxide – acetic acid, preparation of the *S*,*S*-dioxo derivatives presented some difficulties.

Oxidation of **3** with hydrogen peroxide – acetic acid appeared to stop at the *S*-oxo stage; oxidation with peracetic acid or potassium permanganate gave dibenzohydroxamic acid (**9**), a conversion which has some precedent in the observation that oxidation of benzohydroxamic acid with iodine gives **9** (6).

We then turned to the reaction of benzohydroxamoyl and *p*-nitrobenzohydroxamoyl chlorides with potassium methanesulfinate, and obtained products which analyzed correctly for the desired *S*,*S*-dioxo compounds (**7**) and (**8**).

However, although the reaction of alkyl halides with salts of sulfinic acids is well recognized as a method for preparing sulfones, a recent study has revealed that acyl halides yield sulfin-

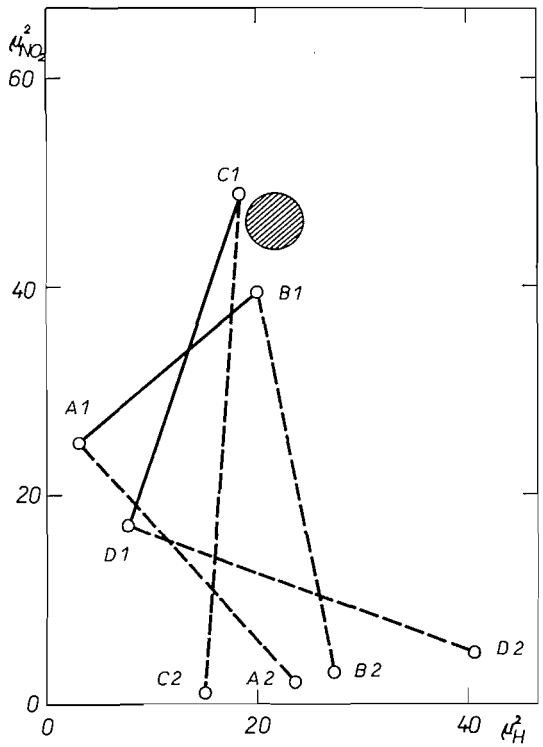

FIG. 3. Comparison of dipole moments of *S,S*-dioxo-*S*-methyl benzothiohydroxamic acid (**7**) and its 4-nitro derivative (**8**). (See Fig. 1 for descriptive details.)

ate ester derivatives, which are usually unstable and react further (7). We therefore have to consider the alternative structures **10** and **11** for our products.

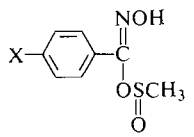

(10) X = H
(11) X = NO_2

Unfortunately, the dipole moments calculated for either **7** and **8**, or **10** and **11** are too close to the observed values to be used to exclude either pair.[4] However the infrared spectra of the products show the intense absorption at 1320 cm^{-1} characteristic of sulfones and absent in sulfinate esters (8). Hence the products are the desired *S,S*-dioxo compounds, **7** and **8**.

[4]Although structures **7** and **8** yield calculated moments that are in fact, closer to the observed values, than those obtained from **10** and **11**.

The products **3–8** were homogeneous as judged by the usual criteria of microanalysis, infrared and proton magnetic resonance spectroscopy, and thin-layer chromatographic analysis. As will be seen later, the stereochemical purity was confirmed, in some cases at least, by the dipole moment measurements.

Experimental

S-Methyl Benzothiohydroxamic Acid (3)

This was prepared as described previously (4).

S-Methyl 4-Nitrobenzothiohydroxamic Acid (4)

p-Nitrobenzaldoxime (3.0 g) was dissolved in dry ether (100 ml); the solution was cooled to 0 °C in an ice–salt bath and a slow stream of chlorine bubbled through it for 30 min. The reaction mixture, which contained a small amount of white solid in suspension, was allowed to warm to room temperature. It was then evaporated under reduced pressure in a fume hood, to a yellow oil of crude *p*-nitrobenzohydroxamoyl chloride, which crystallized from ether – petroleum ether as almost colorless prisms, m.p. 87–88 °C.

Methyl mercaptan (8 ml) in ether (30 ml) was added to a solution of the hydroxamoyl chloride in dry ether (50 ml), followed by triethylamine (8 ml). A copious precipitate of triethylamine hydrochloride separated. After 30 min at room temperature the reaction mixture was poured into ice-cold 1*N* aqueous sulfuric acid (50 ml). The ether layer was separated and the aqueous solution extracted with ether (50 ml). The combined ether extracts were dried ($MgSO_4$) and evaporated to a residual oil which crystallized; this was recrystallized from ether – petroleum ether as lemon-yellow prisms, (0.277g, 7%), m.p. 134–140 °C (determined by open capillary).

Anal. Calcd. for $C_8H_8N_2O_3$ (212.2): C, 45.28; H, 3.79; N, 13.20; S, 15.11. Found: C, 45.19; H, 4.11; N, 13.07; S, 15.22.

In a second preparation the yield from the oxime was 15%.

S-Oxo S-Methyl Benzothiohydroxamic Acid (5)

S-Methyl benzothiohydroxamic acid (1.67 g) was dissolved in glacial acetic acid (15 ml); 30% H_2O_2 (2.2 ml) was added, and the reaction mixture was stored at 0 °C for 24 h. Excess H_2O_2 was still present (indicated by the Starch–KI test) but the reaction mixture was worked up by pouring it into water (100 ml). Neutralization of the solution with $NaHCO_3$ was followed by extraction with ether (3 × 100 ml). The combined dried ($MgSO_4$) extracts were evaporated to a pale-yellow residual oil which crystallized on trituration with ether – petroleum ether. Recrystallization from acetone – petroleum ether gave small colorless prisms, (0.720 g), m.p. 142–143 °C.

Anal. Calcd. for $C_8H_9NO_2S$ (183.2): C, 52.44; H, 4.95; N, 7.64. Found: C, 52.50; H, 5.04; N, 7.07.

S-Oxo S-Methyl 4-Nitrobenzothiohydroxamic Acid (6)

S-Methyl 4-nitrobenzothiohydroxamic acid (1.06 g) was suspended in glacial acetic acid (15 ml) and 30% H_2O_2 (1.25 ml) was added. The reaction mixture was stirred continuously until the crystals had dissolved (*ca.* 10 min).

The solution was kept at room temperature overnight and then poured into water (200 ml). A fine, crystalline precipitate separated and was collected and recrystallized from acetone – petroleum ether to give fine, almost colorless needles, (0.95 g), m.p. 163–164 °C.

Anal. Calcd. for $C_8H_8N_2O_4S$ (228.2): C, 42.10; H, 3.53; N, 12.28; S, 14.05. Found: C, 42.23; H, 3.52; N, 11.81; S, 14.11.

Permanganate Oxidation of S-Methyl Benzothiohydroxamic Acid

S-Methyl benzothiohydroxamic acid (0.81 g) was dissolved in acetone (35 ml) and 6 *N* aqueous sulfuric acid (5 ml) was added. Aqueous permanganate solution (3%) was added from a burette until the permanganate color showed signs of persisting (21 ml). The brownish reaction mixture, containing some suspended solids, was poured into water (250 ml) and extracted with chloroform (3 × 30 ml). The combined, dried ($MgSO_4$) extracts were evaporated and the crystalline residue was recrystallized from acetone–ether as colorless needles, (0.52 g), m.p. 165–166 °C. The melting point was undepressed on admixture with authentic dibenzohydroxamic acid. The infrared spectrum in KBr was also superimposable upon that of authentic dibenzohydroxamic acid.

S,S-Dioxo S-Methyl Benzothiohydroxamic Acid (7)

Benzohydroxamoyl chloride (4.0 g) was added to a solution of potassium methanesulfinate, prepared (9) from methyl methanesulfinate (7.0 g) in ethanol (70 ml). The reaction mixture, which became warm and rapidly deposited a precipitate of KCl, was stirred for 3 h, and the bulk of the ethanol was then removed under reduced pressure. The residue was diluted with water (50 ml) and then extracted with ether (2 × 50 ml). The ether extracts were combined, dried ($MgSO_4$), and evaporated under reduced pressure to yield a pale yellow-brown oil which crystallized in small prisms from chloroform. Recrystallization from benzene–chloroform gave colorless prisms, (2.55 g), m.p. 97–98 °C. This product started to decompose after standing for 18 h.

Concentration of the mother liquors yielded a second crystalline product as fine colorless laths, m.p. 140–142 °C; recrystallization from chloroform–benzene raised the m.p. to 145–146 °C.

Anal. Calcd. for $C_8H_9NO_3S$ (199.2): C, 48.23; H, 4.55. Found: C, 48.21; H, 4.70.

S,S-Dioxo S-Methyl p-Nitrobenzothiohydroxamic Acid (8)

This compound was prepared, as described above, from *p*-nitrobenzohydroxamoyl chloride (2.0 g) and potassium methanesulfinate in ethanol. The product was isolated by pouring the reaction mixture into water, removing the precipitate by filtration and recrystallizing it from ethanol. This method yielded 1.5 g of pale-yellow laths, m.p. 174 °C.

Anal. Calcd. for $C_8H_8N_2O_5S$ (244.2): C, 39.34; H, 3.30; N, 11.47. Found C, 39.32; H, 3.01; N, 11.36.

Results

Measurements of Dipole Moments

Dielectric constants of the benzene or dioxane solutions were measured at 25 °C using a heterodyne apparatus at a frequency of 1.2 Mc.p.s. Usually five measurements were carried out in the concentration range 5×10^{-3}– $5 \times 10^{-2} M$ using the method of Halverstadt and Kumler (10). In the calculations of the dipole moment μ from the overall polarization ${}_\infty P_2$ and molar refraction R_D, an allowance of 5% or 15% of the R_D value was made for the atomic polarization. The molar refraction was calculated using the atomic and group increments of Vogel (11) and the increments for the =NOH group and the exaltations for the conjugation with the benzene nucleus were the same as those used previously (1, 2). The calculation is only approximate, but in fact the errors do not markedly influence the resulting values for the dipole moments. The values found for ${}_\infty P_2$, R_D, and μ are summarized in Table I. In Figs. 1–3 values of μ with a 15% correction are used.

Calculation of Theoretical Dipole Moments

The dipole moments of individual configurations and conformations (*A*1–*D*2) of compounds **3–8** were calculated by vector addition of bond moments in a graphical way with an accuracy of about $\pm 0.3D$. The bond moments used are summarized in Table II. They are mostly based on our previous experience (1, 2, 12). For the bond angles, the values taken were the same as those used previously (2) with the C=NOH group[5] (the angle 120° at the carbon atom being preferred) and with the SO_2 group (12). With the sulfoxyl group the values of 100° for ∠R—S—R and 106° for ∠R—S—O were taken corresponding to values found for some simple sulfoxides (15). The bond moments S—O and μ_m (SO) were derived using these values. For **3** and **4**, the ∠R—S—R was taken as 102°, this being the mean of several values recorded for sulfides (15).

The value of the ∠R—S—R was thus not exactly the same in sulfur compounds of different oxidation level but the differences are not important to the calculations.

The calculated dipole moments are not tabulated but plotted as μ^2 in Figs. 1–3.

[5]From these well-tried values, the value 122° for the angle C=N—O may be somewhat high. It follows from measurements on different oximes (15) that better values should be 114° for the *syn* isomer and 118° for the *anti* isomer. However, this correction does not have a significant influence on further conclusions.

TABLE I

Polarization and dipole moments* of thiohydroxamic acid derivatives†

	Compound	Melting point	Solvent	$_{\infty}P_2(cm^3)$	$R_D(cm^3)$	μ‡(*D*)	μ§(*D*)
3	Where R = H, X = S	85	Benzene	115.8	48.9	1.78	1.71
4	Where R = NO_2, X = S	138	Benzene	266.2	55.7	3.18	3.15
5	Where R = H, X = SO	142	Dioxane	418.9	49.6	4.23	4.20
6	Where R = NO_2, X = SO	163	Dioxane	934.7	56.4	6.54	6.52
7	Where R = H, X = SO_2	145	Dioxane	515.6	49.6	4.75	4.71
8	Where R = NO_2, X = SO_2	174	Dioxane	1012	56.4	6.82	6.80

*Measurements were taken at 25 °C.
†The general formula is 4-R·C_6H_4·C(=NOH)XCH_3.
‡An allowance of 5% of the R_D value is made for the atomic polarization.
§An allowance of 15% of the R_D value is made for the atomic polarization.

TABLE II

Bond moments used in calculation of theoretical dipole moments*

Bond	Bond moment (*D*)	Bond	Bond moment [*D*]
H—C_{al}	0.3	C_{ar}—NO_2	4.2†
H—C_{ar}	0	S—O (in sulfoxides)	3.25‡
H—O	1.51	SO_2	3.0§, ‖
C—S	0.7§	$\mu_m(SO)$	0.55‡, **
C=N	1.4–1.8¶	$\mu_m(SO_2)$	1.0‡, **
N—O	0.3		

*Most values were used and discussed by us previously (1, 2). They are based originally on the values of Smyth (13).
†Including a mesomeric moment for the conjugation with the C=NOH group.
‡Values derived in this work from dipole moments of diethyl sulfoxide, and diphenyl sulfoxide (14).
§Values derived by us previously (12).
‖This value is the vector sum of both SO bonds. it is a vector bisecting the ∠O—S—O and coplanar with C—S—C.
¶The lower value is appropriate to compounds 5–8, the higher value for compounds 3 and 4 (see Discussion).
**These are formal values of the so called mesomeric dipole moments, expressing the conjugation of the SO or SO_2 groups with an unsaturated system.

TABLE III

Some nuclear magnetic resonance and infrared spectral data of the thiohydroxamic acid derivatives

	Nuclear magnetic resonance			Infrared*
	τ (OH)	τ (CH_3)	Solvent	ν_{OH} cm^{-1}
3	0.42†	7.95	$CDCl_3$	3565
4	1.14	7.83	$CDCl_3$	3560
5	−2.65	7.10	DMSO-d_6	—
6	−3.00	7.06	DMSO-d_6	—
7	−2.6	6.85	DMSO-d_6	—
8	−3.65	6.62	DMSO-d_6	—
2 *syn*‡	0.80†	8.55§	CCl_4	3580
2 *anti*‡	1.45§	8.59§	CCl_4	3583

*Measured for dilute solutions in chloroform; compounds 5–8 were insufficiently soluble for this measurement to be made.
†The value is 0.83 in CCl_4. extrapolated to infinite dilution.
‡Data taken from (16).
§Extrapolated to infinite dilution.

Nuclear Magnetic Resonance Spectral Measurements

The spectra of compounds **3** and **4** were taken using $CDCl_3$ as solvent. For compounds **5–8**, DMSO-d_6 was the solvent used. Spectra were taken on a Varian A-60 instrument at a frequency of 60 Mc.p.s; tetramethyl silane was used as an internal standard.

The chemical shifts of the OH and CH_3 protons are summarized in Table III.

Infrared Spectral Measurements

The infrared spectra were measured on $CHCl_3$ solutions using a Perkin–Elmer model 237 spectrometer.

Discussion

Dipole Moments

Our method for determination of configuration and conformation (5) can be illustrated with *S*-methyl benzothiohydroxamic acid (**3**) and its nitro derivative (**4**). This case is the most simple one as there are no difficulties in choosing the appropriate values of bond moments. A basic assumption is that the conformation of the unsubstituted and substituted compounds are the same. (It was in order to make this assumption as reasonable as possible, that a pair of compounds differing only in substitution at the *para* position of a benzene nucleus was chosen.) The dipole moments for all conformations can now be computed and plotted as μ^2 against each other in a graph, (Fig. 1), the unsubstituted compound being on the *x*-axis, the 4-nitro derivative on the *y*-axis. Then each planar limiting conformation is represented by a point (e.g. *B*1 and *B*2 in Fig. 1). Any point on the tie line connecting two such points can be interpreted either as a transitory conformation arising by rotation around the single bond or as a mixture of two forms in a given ratio (5). The mid-point of a tie line (e.g. *B* in

Fig. 1) can also represent unrestricted rotation; the points *A*, *B*, *C*, *D* were calculated assuming such unrestricted rotation about the C—SCH_3 bond. By comparison with experimental values the approximate conformation can be determined and, according to the distances of the other points, the reliability of this conclusion estimated.

It follows from Fig. 1 that the *S*-methyl benzothiohydroxamic acid has the *syn* (**3***a*) configuration and conformation *B* with practically free rotation around the C—S bond (B1 $\rightleftharpoons$ B2). This conclusion is safe within the limits of accuracy of the methods used; the radius of the dashed circle should represent rather the errors in computing the theoretical moments than the experimental uncertainty. This configuration, *syn* (**3***a*), was originally considered by us as most likely, on the basis of arguments concerning the reaction mechanism (4). It was, however, designated as *anti* according to the older nomenclature (see ref. 1).

Both configurations **2***a* and **2***b* of the *O*-ethyl benzohydroxamic acids (**2**) are of comparable stabilities (1, 16), but the conformation of the OH group in the *syn* isomer (**2***a*) is opposite to that of **3***a*, i.e. as in A_1 or A_2. The difference may be due to weak hydrogen bond in the compound **2***a* but we have repeated our older experiments (1) and were unable to detect such an intramolecular hydrogen bond by infrared spectroscopy. A further difference is that there is essentially free rotation of the SCH_3 group in compound **3***a*, whereas rotation of the OC_2H_5 group in **2***a* seemed to be partially restricted (2). The larger size of the sulfur atom as compared to oxygen, and thus the greater distance of the methyl group from the oxime function in **3***a* as compared to **2***a* may be an explanation for this effect.

With the other compounds (**5–8**) the determination of configuration and conformation is more difficult. Firstly some assumptions about the choice of appropriate bond moments must be made; more especially, the C=N bond is highly polarizable so that it has been given various values of bond moments in different compounds (1, 2). The value 1.4*D* has been found most suitable for hydroxamoyl chlorides with respect to the polarization by the adjoining C—Cl bond (2) and we have chosen the same value for the compounds **5–8**, which likewise possess a strongly electron-attracting group. A second assumption concerns the conjugation of the sulfonyl and sulfoxy groups for which a formal mesomeric moment had to be introduced (see (12)) to account for a big difference between moments of aliphatic and aromatic derivatives (12, 14). We have used the same values of mesomeric moments in our compounds **5–8** in which the groups SO_2 or SO are bonded to a sp^2-hybridized carbon atom, too, even though any mesomerism cannot easily be formulated by limiting structures. Both those corrections may seem somewhat arbitrary but they can be checked by comparison with experimental values, using our graphical procedure. In fact, without these corrections it is not possible to obtain computed moments which would be comparable with experimental values. (The computed moments would be much too low.)

In Fig. 2 the calculated and experimental values for the sulfoxy derivatives **5** and **6** are compared. It can be concluded that the sulfoxy group cannot be freely rotating but must have a stable conformation with a nearly maximum dipole moment (conformation *B*1 or *C*1). The same is true for the rotation of the OH group around the N—O bond. On the other hand the configuration about the C=N bond cannot be established from our experiments. Either the *anti* configuration (**5***b*) in an intermediate form (closer to *C*1 than to *C*2), or the *syn* configuration (**5***a*) (in the form *B*1) is possible.

The case of the sulfonyl derivatives **7** and **8** is somewhat better. From Fig. 3 it can be concluded that the conformations of the SO_2CH_3 and NOH groups are the same as in the preceding case and that the *anti* configuration (C_1) is more probable than the *syn* (B_1). This view is further substantiated by nuclear magnetic resonance (n.m.r.) spectral data. The agreement with experiment is only fair with compounds **5–8** but we do not consider it justifiable to improve upon this by making further corrections in the values of bond moments. The most striking and quite reliable result is the restricted rotation of the SO_2CH_3 groups, so that the actual conformation has the largest moment of all conformations possible. (It was believed for some time that in such cases the conformation with a minimum moment is generally preferred (13).) At the same

TABLE IV

Configuration and conformation of hydroxamic acid derivatives*

X	Configuration	Conformation of the OH group	Conformation of the X group	Reference
Cl	*anti*	H away from Ph	—	2
SO_2CH_3	*anti*	H away from Ph	O away from N	This paper
$SOCH_3$	*anti* (?)	H away from Ph	O away from N	This paper
OC_2H_5	*anti*	H away from Ph	"Free rotation"	1, 2
	syn†	H close to O	Somewhat restricted rotation	1, 2
SCH_3	*syn*	H away from S	"Free rotation"	This paper
NH_2	*syn*	H away from N	Unknown‡	2

*The general formula is PhC(NOH)X.
†*Syn* form rearranges to *anti* form upon acylation, but both *syn* and *anti* forms are "stable" under normal conditions.
‡This conformation could be co-planar; there is also a possibility of rotation.

time there is no apparent steric hindrance, or hydrogen bonding. On the contrary, a possible hydrogen bridge would result in the opposite conformation of the SO_2CH_3 grouping.

Nuclear Magnetic Resonance Spectra

The comparison of n.m.r. spectral data is made somewhat difficult because the measurements were not all made in the same solvent. The spectra were consistent with the structures **3**–**8** as they contained the following signals: (*i*) a sharp singlet due to the methyl group, (*ii*) a complex due to aromatic protons, which are separated into two doublets with the 4-nitro derivatives, and (*iii*) a singlet for the hydroxyl group, which is strongly concentration dependent. Some chemical shifts are collected in Table III. The signal due to the OH hydrogen is of some diagnostic value for determination of configuration. With the *S*-methyl benzothiohydroxamic acid (**3**) the extrapolated value for the position of this signal can be compared with the corresponding values for both stereoisomeric *O*-ethyl benzohydroxamic acids (measured in the same solvent) (16). As can be seen from Table III, this comparison confirms the *syn* configuration for **3**. For the sulfonyl derivatives **7** and **8** a direct comparison is not possible due to presence of a strongly electron attracting group in the molecule, and also use of a different solvent. However, the relative position of this peak in both stereoisomers can be compared and the one with a more negative value may be considered as due to a *syn* isomer. This conclusion is supported by the shifts of the methyl hydrogens, the difference of which are however smaller.[6]

Infrared spectra

The infrared spectra of all compounds are also in agreement with the structures assigned to them. Especially noteworthy is the presence of symmetric and asymmetric SO_2 vibrations in compounds **7** and **8** and the absence of such bands in the spectra of **5** and **6**. For comparison purposes only the OH frequency deserves some further comments. Compounds **3** and **4** are strongly associated in chloroform solution, but the frequency of the free OH group can also be observed. There is a small difference in this frequency between both stereoisomers of the *O*-ethyl benzohydroxamic acid **2***a* and **2***b* which may be due to the influence of the adjoining OC_2H_5 group. However, we were unable to detect any signs of an intramolecular hydrogen bridge in a dilute chloroform solution of **2***a* or **3**. If there is any interaction it must be very weak. The difference in frequency of the

[6]All signals are shifted in the expected direction with substitution. The difference between compounds containing the sulfonyl, sulfoxy, or thio group are very marked, the shifts of the signals due to the OH hydrogens being more affected than those due to the CH_3 grouping.

OH absorption band cannot be used for distinguishing the configuration of stereoisomers unless both forms are isolated.

Conclusions

Although the configurations of some of the compounds are not absolutely secure, we can compare the relative stability of stereoisomers **1***a* and **1***b* with various groups X. The present and previous (1, 2) results are summarized in Table IV. In cases when only one isomer was isolated, it was assumed to be the more stable one. This assumption need not be true, as the compounds were prepared by reactions which may be kinetically controlled; however, it is supported by the course of some reactions in which the more stable isomer definitely is produced. Thus chlorination of both stereoisomeric benzaldoximes (17) gives the same benzohydroxamoyl chloride which has the *anti* configuration (2).

From the data of Table IV it follows that the steric requirements of the group X are apparently not the deciding factor, unlike the configuration of ketoximes, $C_6H_5C(=NOH)R$ (18), or methoximes, $C_6H_5C(=NOCH_3)R$ (19), which are controlled by the size of the alkyl group R. With hydroxamic acid derivatives (**1**) the electronic nature of the variable group is evidently more important, the *anti* configuration being more stable as X becomes strongly electron attracting.

The conformation of the NOH group is uniform, with the hydrogen atom remote from other parts of the molecule. There is only one exception, the case of *syn*-O-ethyl benzohydroxamic acid (**2***a*) and the possibility of a very weak hydrogen bridge in this compound has already been discussed.

Acknowledgments

The measurement of dielectric constants and densities has been carried out by Mrs. M. Kuthanova, Department of Physical Chemistry, Institute of Chemical Technology, Prague, under the guidance of Dr. V. Jehlicka; the aid of both is gratefully acknowledged. We also thank Miss Manjit Sihota for assistance in the preparation of some of the compounds used.

1. O. Exner, V. Jehlicka, and A. Reiser. Collection Czech. Chem. Commun. **24**, 3207 (1959).
2. O. Exner. Collection Czech. Chem. Commun. **30**, 652 (1965).
3. A. Werner. Ber. **25**, 27 (1892).
4. M. H. Benn. Can. J. Chem. **42**, 2293 (1964).
5. O. Exner and V. Jehlicka. Collection Czech. Chem. Commun. **30**, 639 (1965).
6. E. Boyland and R. Nery. J. Chem. Soc. (C) 354 (1966).
7. K. Schank. Ann. **702**, 75 (1967).
8. L. J. Bellamy. Infrared spectra of complex molecules. 2nd Ed. Methuen & Co. Ltd., London. 1958. p. 360.
9. I. B. Douglass, F. J. Ward, and R. V. Norton. J. Org. Chem. **32**, 324 (1967).
10. I. F. Halverstadt and W. D. Kumler. J. Am. Chem. Soc. **64**, 2988 (1942).
11. A. I. Vogel. J. Chem. Soc. 1842 (1948).
12. O. Exner, Z. Fidlerova, and V. Jehlicka. Collection Czech. Chem. Commun. To be published.
13. C. P. Smyth. Dielectric behaviour and structure. McGraw-Hill Book Co., Inc., New York. 1955.
14. O. A. Osipov and V. I. Minkin. Tables of dipole moments. Vysshaya shkola Publishing House. Moscow. 1965.
15. L. E. Sutton (*Editor*). Tables of interatomic distances and configurations in molecules and ions. The Chemical Society. London. 1958 and Supplement 1965.
16. D. Snobl and O. Exner. Collection Czech. Chem. Commun. To be published.
17. A. Werner and H. Buss. Ber. **27**, 2193 (1894).
18. R. F. Brown, N. M. van Gulick, and G. H. Schmid. J. Am. Chem. Soc. **77**, 1094 (1955).
19. G. J. Karabatsos and N. Hsi. Tetrahedron, **23**, 1079 (1967).

Structure of pithecolobine. II

K. WIESNER, D. M. MACDONALD, C. BANKIEWICZ, AND D. E. ORR
Natural Product Research Center, University of New Brunswick, Fredericton, New Brunswick
Received March 8, 1968

The alkaloid of *Samanea saman* Merr. Pithecolobine is shown to be a family of closely related analogues of the general formula (**13**). The structure (**9***a*) has been proved for one of these compounds.

Canadian Journal of Chemistry, **46**, 1881 (1968)

Can. J. Chem. Downloaded from www.nrcresearchpress.com by 210.87.254.6 on 09/05/12
For personal use only.

Our first full paper on the alkaloid of *Pithecolobium saman* Benth[1] was published sixteen years ago (1). Since that time we have solved the structure in principle (2, 3) and corroborated the solution by synthetic work (4). All this has been published only in preliminary form. Moreover, owing to its very peculiar nature and experimental difficulties our solution of the "pithecolobine" problem, while essentially correct, represents only a part of the story—the real situation is more complicated. Finally new synthetic work has been performed to render our conclusions as rigorous as possible. For these reasons we have decided to summarize in the present paper, degradative work on pithecolobine not included in our first report (1).

Pithecolobine was purified by chromatography, a twofold countercurrent distribution, and many crystallizations of the picrolonate (1). After these operations it appeared completely homogeneous and many analyses of the picrolonate and free base, while showing fluctuations, fitted best the formula $C_{22}H_{46}N_4O_2$. It was, however, realized from the start that the molecular formula is tentative and had to be corroborated by degradative work and a characterization of all the functions. Consequently the molecular formula has never been used in any structural argument.[2]

Pithecolobine showed, in the infrared (i.r.) spectrum, an amide band at 1650 cm^{-1} and its potentiometric titration curve revealed three basic nitrogens (1). Thus one oxygen and all four nitrogen atoms have been directly proved to be present. The absence of *N*- and *O*-alkyl groups has been originally demonstrated by Zeisel determinations and much later corroborated by nuclear magnetic resonance (n.m.r.) studies.

Reduction of pithecolobine by lithium aluminium hydride yielded desoxypithecolobine, $C_{22}H_{48}N_4$. This compound gave beautifully crystalline salts and its molecular formula was supported by excellent analytical data (1). Nevertheless a molecular formula, richer by two hydrogens, was not excluded and consequently the presence or absence of a ring in desoxypithecolobine, had to be deduced from degradative results.[3]

Potentiometric titration of desoxypithecolobine showed clearly the presence of four basic nitrogen atoms (1). Thus the pithecolobine lactam group has been predictably reduced to a basic nitrogen, and the second elusive oxygen atom has disappeared.

It was first shown (2) that the four nitrogens of desoxypithecolobine are all secondary. Desoxypithecolobine was converted into a glassy, neutral tetraacetyl derivative, which did not show any NH absorption in the i.r. spectrum. This compound was then reduced by lithium aluminium hydride to tetraethyl-desoxypithecolobine, which was characterized by a homogeneous countercurrent distribution and distillation of the peak fraction. An attempt to acetylate this material was negative. This demonstrated conclusively that all the nitrogens in the tetraethyl compound were tertiary, and consequently in desoxypithecolobine they were secondary.

Next the Hofmann degradation of methylated desoxypithecolobine was investigated (1). This reaction gave, in the first stage, tetramethyl-1,4-tetramethylenediamine and a mixture of bases. The second stage performed on this mixture yielded a conjugated diene $C_{12}H_{22}$ (ultraviolet, λ_{max} 227; log $\varepsilon = 4.38$). The molecular formula

[1]The tree has since been renamed *Samanea saman* Merr.

[2]Also, more recent attempts to ascertain the molecular formula by mass spectrometry failed.

[3]Again, much later attempts to determine the molecular formula by mass spectrometry failed.

Can. J. Chem. Downloaded from www.nrcresearchpress.com by 210.87.254.6 on 09/05/12
For personal use only.

of this hydrocarbon was not completely certain but the formula given was compatible with the analytical data.

From the mixture of bases produced in the first stage of the Hofmann reaction it was possible to isolate material which analyzed well for $C_{16}H_{31}N$ (1). It took up two moles of hydrogen and gave a tetrahydro product which by another Hofmann degradation yielded a hydrocarbon $C_{12}H_{24}$ and dimethyl-*n*-propylamine. The hydrogenation of the $C_{12}H_{24}$ hydrocarbon yielded a dihydro derivative $C_{12}H_{26}$ which was practically identical by i.r. spectroscopy with *n*-dodecane. When we first obtained this derivative, we tentatively considered it to be a slightly impure sample of *n*-dodecane, and this conclusion was subsequently fully corroborated (*vide infra*).

It can now be readily shown (2) that the data discussed up to this point enable us to postulate rigorously that desoxypithecolobine is a macrocyclic compound of the type (**1**) or (**2**).

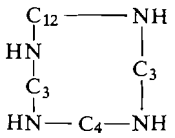

(**1**)

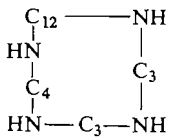

(**2**)

The absence of *N*-alkyl groups in desoxypithecolobine, first postulated (1, 2) on the basis of Zeisel determinations and later corroborated by n.m.r., shows clearly that all the remaining carbon which has not been isolated and characterized in the Hofmann degradation must be present in one fragment. It is now impossible to arrange the four carbon fragments and four secondary nitrogens in any other way than those indicated in the structures (**1**) and (**2**). We note that this conclusion does not require independent knowledge of the molecular formula of desoxypithecolobine. We have further concluded from Kuhn–Roth *C*-methyl determinations performed with desoxypithecolobine, that only one *C*-methyl group is present. (This conclusion was also later corroborated by n.m.r.)

Since the C_{12} fragment can be isolated as a conjugated diene by a double Hofmann degradation, it must be the site of this single carbon methyl group. Thus we may expand the structures (**1**) and (**2**) to the structures (**3**) and (**4**).

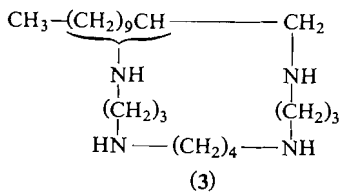

(**3**)

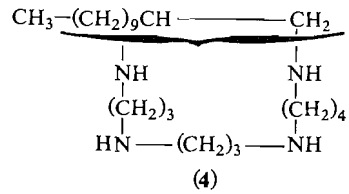

(**4**)

Further clarification of the nature and arrangement of the various pithecolobine fragments, came from the Hofmann degradation of methylated pithecolobine itself (2, 3). The first stage of this procedure yielded a neutral fraction, which was hydrogenated and the individual compounds separated by chromatography. One product turned out to be a primary amide which, after a series of crystallizations, was identified as the amide of *n*-dodecanoic acid. The second compound ($C_{15}H_{31}ON$) was a secondary amide and by hydrolysis yielded *n*-propylamine. From the cold trap used in the Hofmann reaction a good yield of tetramethyl-1,3-trimethylenediamine was obtained. It is clear that the two C_3 compounds identified in this degradation cannot conceivably have a common origin.

Thus we have now isolated all the carbon of pithecolobine in the form of four known compounds. Moreover, the isolation of the secondary amide shows clearly the presence in pithecolobine of the part structure (**5**).

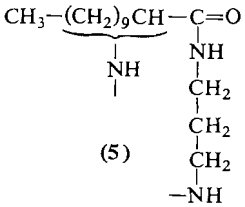

(**5**)

The chromatogram of the neutral hydrogenated Hofmann degradation products of pithecolobine yielded also a liquid δ-lactone, (carbonyl maximum 1732 cm^{-1}) $C_{12}H_{22}O_2$. It was immediately clear that the lactone must possess

the structure (7), and be generated by an internal displacement portrayed in formula (6), followed

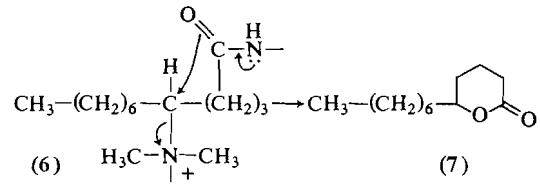

(6) (7)

by hydrolysis of the intermediate imino lactone. The lactone (7) was hydrolyzed to the corresponding hydroxy acid, which was converted into the ketoester (8). This last compound was then identified with an authentic sample as the crystalline 2,4-dinitrophenylhydrazone.

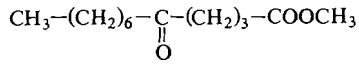

(8)

The isolation and identification of the lactone (7) leaves no doubt about the point of attachment of the second nitrogen in the C_{12} chain. In summary of all the rigorous degradative evidence presented until now, we can write the structures (2, 3) (**9***a*) or (**10***a*) for pithecolobine and (**9***b*) or (**10***b*) for desoxypithecolobine. From the two possibilities, biogenetic considerations strongly favor the formula (**9**) which contains as part structure, the naturally occurring amine, spermine.

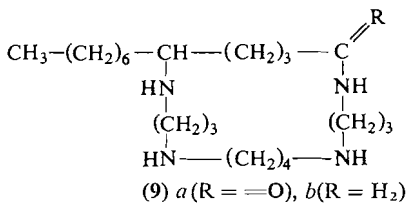

(**9**) *a* (R = =O), *b* (R = H_2)

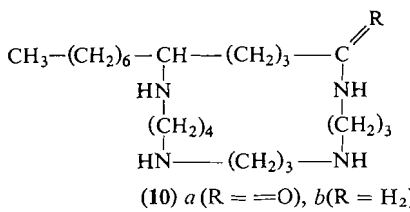

(**10**) *a* (R = =O), *b* (R = H_2)

The next problem to be investigated is the nature of the second oxygen atom, the presence of which is indicated only by the analytical data of pithecolobine. If this oxygen indeed exists, it has to be present in the form of a hydroxylamine hydroxyl to explain the formation of desoxypithecolobine on lithium aluminium hydride reduction. Since pithecolobine clearly is not a hydroxamic acid or aldehyde ammonia, a hydroxylamine group is the only possibility compatible with the facts.

We have stated at the outset that we shall not accept the fluctuating analytical data for pithecolobine until they are corroborated by degradation and direct characterization of all the functional groups. We have, consequently, performed the following experiment designed to prove directly the presence of a hydroxylamine hydroxyl or, in the negative case, to prove directly the presence of three secondary amino groups in pithecolobine. The acetylation of pithecolobine gave a quantitative yield of a glassy peracetyl derivative. This compound showed in the i.r. spectrum a very strong amide band at 1637 cm^{-1} and no ester band. In the n.m.r. spectrum a poorly resolved triplet (3 H) at $\tau = 9.10$ p.p.m. and a broad singlet (9 H) at approximately $\tau = 8.10$ p.p.m. could be distinguished.

The triplet represents the *C*-methyl group of pithecolobine and the singlet may be assigned to three *N*-acetyl groups. This later conclusion was corroborated as follows. Lithium aluminium hydride reduction of peracetyl-pithecolobine followed by acetylation yielded an oily basic acetyl derivative purified by chromatography, which was homogeneous in thin-layer chromatography. Nuclear magnetic resonance spectroscopy revealed a sharp triplet (12 H) at $\tau = 8.95$, 9.05, 9.15 p.p.m. and a sharp singlet (3 H) at $\tau = 8.16$ p.p.m. The triplet must be assigned to three *N*-ethyl groups covering up the *C*-methyl group of pithecolobine. The singlet is clearly one single *N*-acetyl.

None of the compounds discussed yielded crystalline derivatives or a molecular ion, in mass spectrometry. Nevertheless, the experiments described prove that pithecolobine contains three secondary amino groups and a secondary lactam. Since all the carbon of pithecolobine has been identified as known compounds and the entire functionality characterized, we have to conclude that the "second oxygen" of pithecolobine is in fact, not present and the molecular formula of this alkaloid should be $C_{22}H_{46}N_4O$. Thus the structure of pithecolobine must be (**9***a*) or, less likely, (**10***a*) with no hydroxyl group present.

Can. J. Chem. Downloaded from www.nrcresearchpress.com by 210.87.254.6 on 09/05/12
For personal use only.

Can. J. Chem. Downloaded from www.nrcresearchpress.com by 210.87.254.6 on 09/05/12
For personal use only.

In order to corroborate the structure of desoxypithecolobine we have synthesized the tetratosylate of the macrocyclic amine (**9***b*) (4). Since we were unable to detosylate the synthetic material, we prepared the tetratosylate of "natural" desoxypithecolobine and compared it with the synthetic one. The two glassy but chromatographically homogeneous tetratosylates gave *superimposable* i.r. spectra. This most certainly corroborates the structure (**9***b*) for desoxypithecolobine, in principle. For fine detail, however, the rigorous degradation data seem more reliable. It is difficult to assess if, for instance, a change of the ring size by two or three carbons would produce a significant change in the i.r. spectrum.

In spite of the rigorous nature of the degradation data, the apparent identity of the synthetic and "natural" desoxypithecolobine tetratosylates and the fact that pithecolobine was purified by repeated crystallization of a peak fraction from countercurrent distribution, evidence began to accumulate that pithecolobine is a mixture of closely related analogues only one of which possesses the precise structure (**9***a*). The first indication of this came from a more detailed study of the *n*-dodecanoic amide obtained in the Hofmann degradation of pithecolobine (*vide supra*). The crude amide was hydrolyzed and the corresponding acid was analyzed by Dr. Klaus Biemann (Massachusetts Institute of Technology, Cambridge, Massachusetts) by mass spectrometry. Dr. Biemann reported that the main component, *n*-dodecanoic acid, was contaminated by tetradecanoic acid and a trace of tridecanoic acid. Thus certain small amounts of homologous pithecolobines appear to be present.

Furthermore, it turned out that also the 1,5-attachment of the nitrogens in the C_{12} chain is not exclusive.

As discussed above, a mixture of bases analyzing for $C_{16}H_{31}N$, isolated from the first stage of the desoxypithecolobine Hofmann degradation, was subjected to hydrogenation and the tetrahydro derivatives (**11**) and (**12**), on further Hofmann degradation, gave dimethyl propyl amine and a $C_{12}H_{24}$ olefin.

The olefin was ozonized and the mixture of aldehydes obtained by cleaving the ozonides with zinc dust and acetic acid was converted into 2,4-dinitrophenylhydrazones. Paper chromatography of these derivatives proved the presence of formaldehyde, acetaldehyde, propionaldehyde,

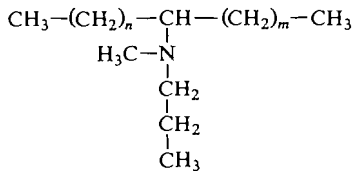

(**11**)

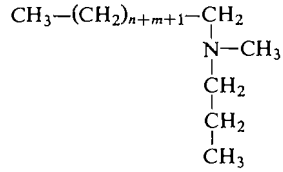

(**12**)

$n + m = 9$ with traces of $n + m = 10$ and 11

and a mixture of higher aldehydes which could not be resolved.

It is clear that the olefin which yielded formaldehyde must come from compound (**12**). On the other hand, the acetaldehyde and propionaldehyde must have been produced by ozonolysis of two olefins originating from the compound (**11**) ($m = 1$).

There is another very important conclusion one can deduce from the experiment just discussed. The paper chromatogram of the dinitrophenylhydrazones reveals that formaldehyde, acetaldehyde, and propionaldehyde were produced in approximately equal quantities. This means that the mixture of (**11**) and (**12**) must have contained the two components in a ratio approximately 2:1. On further Hofmann degradation *pure dimethyl-n-propylamine uncontaminated with dimethyl-n-butylamine* was obtained. This proves that both compounds (**11**) and (**12**) contain a C_3—N—C_{12} junction, and this constitutes our first degradative evidence for the sequence of the fragments shown in formula (**1**). The biogenetically less likely sequence (**2**), may thus be dismissed. It is clear that if the sequence (**2**) was correct, only pure compound (**12**) could yield a C_{12} olefin and pure dimethyl-*n*-propylamine. The C_{12} olefin from pure compound (**12**) however, could yield only formaldehyde, and not acetaldehyde and propionaldehyde, by ozonolysis.

From all these studies we must conclude that besides the rigorously proved pithecolobine (**9***a*) we are dealing with a family of compounds of the general formula (**13**). In this formula $n + m =$

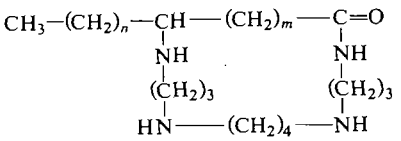

(13)

9, 10, or 11 and there is a considerable proportion of $m = 1$.

This peculiar family of analogues is practically inseparable, and behaves as a homogeneous alkaloid. Thus we are faced with the unusual task of analyzing a mixture and determining the structures of the components without separation. We have consequently decided to extend the studies described in the present communication in order to make our conclusion quantitative and completely rigorous.

The final report will describe the synthesis of both the free and tosylated 1,3- and 1,5-desoxypithecolobines and the mass spectrographic comparison of these compounds with "natural" desoxypithecolobine. We shall also deal in this paper with quantitative gas chromatographic studies of the pithecolobine mixture.

Experimental

Tetraethyldesoxypithecolobine

Desoxypithecolobine (4.2 g) was acetylated with 40 ml of acetic anhydride and 40 ml of pyridine at room temperature. After workup in the usual manner, 6.6 g of a neutral glassy tetraacetyl derivative was obtained. [Infrared (i.r.) spectrum: strong amide band at 1635 cm^{-1}, no NH or OH bands.] This compound was reduced with an excess of lithium aluminium hydride in ether. Workup in the usual manner gave 4.6 g of a liquid base which did not yield crystalline derivatives. The entire amount was consequently subjected to countercurrent distribution in a 50-funnel apparatus between phosphate buffer pH = 6.56 and ether. The distribution curve had the theoretical shape. The peak fraction, number 24, contained 247 mg of material. This was distilled at 0.05 mm/Hg and the middle fraction, b.p. 211–212 °C was analyzed.

Anal. Calcd. for $C_{30}H_{64}N_4$: C, 74.94; H, 13.42; N, 11.64. Found: C, 75.05; H, 13.22; N, 11.6.

The attempt to acetylate this material gave negative results.

Degradation of the $C_{16}H_{31}N$ Bases

The $C_{16}H_{31}N$ bases were obtained by the Hofmann degradation of methylated desoxypithecolobine as described in our first paper (1). They were hydrogenated with platinum oxide in glacial acetic acid. Two moles of hydrogen were taken up in 1 h. Workup yielded a clear basic oil which did not form crystalline derivatives. It was purified by distillation at 0.9 mm/Hg and boiled at 126–131 °C.

Anal. Calcd. for $C_{16}H_{35}N$: C, 79.57; H, 14.61; N, 5.80. Found: C, 80.21; H, 14.81; N, 5.48.

This material (2.9 g) was dissolved in 100 ml of dry methanol and heated under reflux with 20 ml of methyl iodide. Evaporation to dryness yielded 4.5 g of crude methiodides. The methiodides were converted into the methohydroxides by shaking with freshly precipitated silver oxide in aqueous solution. The clear filtered solution of the methohydroxides was evaporated to dryness *in vacuo* and the methohydroxides heated *in vacuo* to 80 °C, at which temperature they decomposed.

The material washed out from the dry ice – acetone trap gave 550 mg of a picrate which after recrystallization melted alone and in admixture with dimethyl-*n*-propylamine picrate at 109–110 °C.

Anal. Calcd. for $C_{11}H_{16}O_7N_4$: C, 41.77; H, 5.10; N, 17.72. Found: C, 41.77; H, 5.16; N, 18.49.

The picrate obtained by degradation and authentic dimethyl-*n*-propylamine picrate gave superimposable i.r. spectra in KBr.

The higher boiling products from the decomposition of the methohydroxides (1.7 g) were dissolved in ether and washed extensively with aqueous sulfuric acid and alkali. Evaporation of the ether and preliminary distillation of the residue at 100–130 °C (10 mm/Hg) gave 846 mg of a clear oil. On redistillation most of the material boiled at 108–113 °C (12 mm/Hg bath temperature).

Anal. Calcd. for $C_{12}H_{24}$: C, 85.64; H, 14.37. Found: C, 85.17; H, 14.24.

The above material (0.24 g) was hydrogenated in glacial acetic acid with platinum oxide. It took up one mole of hydrogen in 30 min. Workup in the usual manner and distillation at 129–132 °C (40 mm/Hg bath temperature) gave the saturated hydrocarbon.

Anal. Calcd. for $C_{12}H_{26}$ (mol. wt., 170): C, 84.63; H, 15.39. Found (mol. wt., 175): C, 84.77; H, 15.09.

The i.r. spectrum of the hydrocarbon was practically identical with the spectrum of *n*-dodecane.

The $C_{12}H_{24}$ olefin (114 mg) was ozonized in 10 ml of glacial acetic acid under cooling with ice. The solution was diluted with 40 ml of water and the ozonides decomposed by the addition of 2 g of zinc dust. The aldehydes were steam distilled into a solution of 250 mg of 2,4-dinitrophenylhydrazine in 33% hydrochloric acid. This reagent has been previously rigorously shown to be free of traces of hydrazones. The hydrazones were extracted with benzene and analyzed by paper chromatography. The descending paper chromatograms were developed with petroleum ether in an air-tight tank, the atmosphere of which was saturated with absolute methanol and petroleum ether. Under these conditions the spots of formaldehyde, acetaldehyde, and propionaldehyde dinitrophenylhydrazones, are widely separated and very distinct. All these three aldehydes were clearly shown to be present in approximately equal quantities.

Hofmann Degradation of Pithecolobine

Pithecolobine (24 g) was dissolved in 47 ml of a 36% formaldehyde solution, and 76 ml of a 88% formic acid solution were added. After 2 h of heating under reflux, additional portions (15.7 ml and 25.5 ml, respectively) of the same solutions were added and the mixture was heated for another 2 h. Finally, the same additions were

Can. J. Chem. Downloaded from www.nrcresearchpress.com by 210.87.254.6 on 09/05/12
For personal use only.

Can. J. Chem. Downloaded from www.nrcresearchpress.com by 210.87.254.6 on 09/05/12
For personal use only.

repeated and the reflux continued for 6 h. Workup in the usual manner gave 25 g (97%) of crude methylated pithecolobine. This material was dissolved in 450 ml of absolute methanol and 80 ml of methyl iodide were added. The solution was refluxed for 90 min and evaporated to dryness *in vacuo*. The yield was 45.6 g (92%) of crude pithecolobine methiodide. The methiodide was dissolved in methanol and filtered through a column (2 kg) of Amberlite IRA-400 anion exchange resin, previously treated with 5% sodium hydroxide and washed to neutrality. The methanol was evaporated at room temperature in high vacuo. The quaternary hydroxide thus obtained was heated *in vacuo* in a round bottom flask equipped with cold-finger and dry ice trap. The decomposition took place between 110–140 °C. The volatile material, condensed in the dry ice trap, yielded 1.2 g of a crystalline picrate, m.p. 215–217 °C.

Anal. Calcd. for $C_{19}H_{24}N_8O_{14}$: C, 38.78; H, 4.11; N, 19.06. Found: C, 38.73; H, 4.12; N, 18.96.

This compound was shown to be identical by mixture melting point and i.r. spectrum (KBr) with authentic tetramethyl-1,3-trimethylenediamine dipicrate.

The less volatile degradation products were collected from the cold finger and the decomposition flask. They were separated in the usual manner into 2.08 g of neutral and 12.4 g of basic material. The neutral material was hydrogenated in glacial acetic acid with 319 mg of prehydrogenated Adam's catalyst. The uptake was 228 ml of hydrogen. From the hydrogenated neutral material, chromatography on 100 g of basic alumina separated three compounds: (*i*) lactone (122 mg) eluted with benzene, (*ii*) secondary amide (257 mg) eluted with ether, (*iii*) primary amide (134 mg) eluted with 5% methanol in chloroform.

The lactone was distilled at 103 °C (0.07 mm/Hg bath temperature) in a collar flask. Infrared: 1732 cm^{-1} (lactone carbonyl).

Mol. Wt. Calcd. for $C_{12}H_{22}O_2$: 198. Mol. Wt. Found: 198 (mass spectrometry).

The lactone was hydrolyzed with an equivalent of methanolic sodium hydroxide and the sodium salt converted into the ketoacid by oxidation with an excess (170 mg) of chromium trioxide in acetic acid. After workup in the usual manner the ketoacid was esterified with diazomethane. The ketoester (45 mg) was converted into a crystalline 2,4-dinitrophenylhydrazone which melted alone and in admixture with the authentic (5) 5-ketododecanoic methyl ester derivative at 207 °C. The i.r. spectra (KBr and $CHCl_3$) of both samples were superimposable.

The primary amide was recrystallized several times from ether and melted at 98–100 °C. The sample was found to be identical by mixture melting point and i.r. spectrum ($CHCl_3$ and KBr) with authentic *n*-dodecanoic acid amide. The once recrystallized amide was hydrolyzed under reflux in 25 ml of concentrated hydrochloric acid for 48 h. The acidic product was separated in the usual manner and the acid (m.p. 33–35 °C) was sublimed in high vacuum for analysis.

Anal. Calcd. for $C_{12}H_{24}O_2$: C, 71.91; H, 12.08; O, 15.97. Found: C, 72.17; H, 12.07; O, 15.62.

Mass spectrometric analysis (performed by Dr. K. Biemann) showed that the material consisted of *n*-dodecanoic acid contaminated with small amounts of the two higher homologues.

The secondary amide was recrystallized from ether to a m.p. 49–50 °C and sublimed for analysis in high vacuum.

Anal. Calcd. for $C_{15}H_{31}ON$: C, 74.63; H, 12.95; N, 5.80. Found: C, 74.74; H, 12.77; N, 5.80.

The above compound (354 mg from two runs) was refluxed in 15 ml of concentrated hydrochloric acid for 36 h. The solution was diluted with water, extracted several times with ether, and evaporated to dryness *in vacuo*. The residue (70 mg) was a crystalline hydrochloride. It was purified by recrystallization under absolutely anhydrous conditions from methanol–ether. The crystals were extremely hygroscopic and they gave an i.r. spectrum (KBr under anhydrous conditions) superimposable with authentic *n*-propylamine hydrochloride.

Peracetylpithecolobine

Pithecolobine (600 mg) was acetylated with 4 ml of acetic anhydride and 4 ml of pyridine for 48 h at room temperature. After workup in the usual manner 630 mg of neutral product were obtained and chromatographed on 30 g of neutral alumina. The peak fractions of the chromatogram, containing 500 mg of clear, glassy material, homogeneous in thin-layer chromatography, (t.l.c.) were used for further work. Infrared: Amide carbonyl (very strong) 1637 cm^{-1}; no ester carbonyl. Nuclear magnetic resonance: see Introduction.

Triethylacetyldesoxypithecolobine

The above compound was reduced with an excess of lithium aluminium hydride in ether and the product, isolated in the usual manner, was acetylated as in the previous case. After workup, 490 mg of a basic acetyl derivative were obtained. This material was chromatographed on 50 g of basic alumina. The peak fractions containing 300 mg were homogeneous in t.l.c., in several systems. Infrared: Amide carbonyl 1735 cm^{-1}; no OH or NH band. Nuclear magnetic resonance: see Introduction.

Acknowledgment

We wish to thank the National Research Council of Canada for the support of these studies.

1. K. Wiesner, D. M. MacDonald, Z. Valenta, and R. Armstrong. Can. J. Chem. **30**, 761 (1952).
2. K. Wiesner, D. M. MacDonald, and C. Bankiewicz. J. Am. Chem. Soc. **75**, 6348 (1953).
3. K. Wiesner and D. E. Orr. Chem. and Ind. London, 672 (1959).
4. K. Wiesner and D. E. Orr. Tetrahedron Letters, **16**, 11 (1960).
5. D. E. Orr. Ph.D. Thesis, University of New Brunswick. 1961. See also forthcoming final communication.

Can. J. Chem. Downloaded from www.nrcresearchpress.com by 210.87.254.105 on 09/05/12
For personal use only.

Reaction of bicyclobutanes with electrophiles[1]

E. LEE-RUFF[2] AND G. JUST
Department of Chemistry, McGill University, Montreal, Quebec

Received January 24, 1968

Reactions of Bicyclobutanes **1** and **1***a*, obtained from the corresponding cholesta-3,5-dienes, with ketones, phosgene, halogens, and tetracyanoethylene gave the A-norcholest-5-ene derivatives **3** – **14**. A possible mechanism for these reactions is postulated.

Canadian Journal of Chemistry, 46, *1887 (1968)*

Recently (1) we reported on the reaction of steroidal bicyclobutanes (**1**) with aldehydes in dilute pentane solution, which were shown to give ketones of type **3**, presumably via an intermediate zwitterion **2** (X = H). No instance of intermediate ether formation was observed, although their presence could not be ruled out. We had also reported that acetone gave no observable reaction under these conditions. We now wish to report on the reaction of bicyclobutanes **1** with ketones, phosgene, halogens, and tetracyanoethylene.

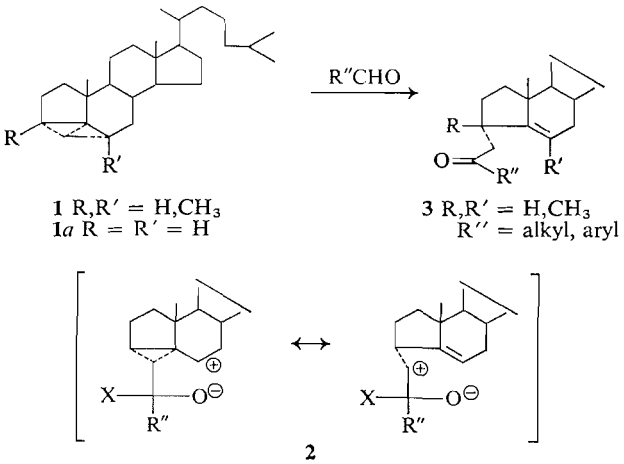

1 R,R′ = H,CH_3
1*a* R = R′ = H

3 R,R′ = H,CH_3
R″ = alkyl, aryl

2

Ketones

Reaction of bicyclobutane **1***a* with a large excess of acetone gave a crystalline product **4** in 50% yield. The nuclear magnetic resonance (n.m.r.) and infrared (i.r.) spectra were consistent with the structure assigned to **4**. Reaction of **1***a* with cyclobutanone gave ketone **5**, ν 1755 cm^{-1}, δ 3.20 p.p.m. (allylic proton), 5.15 p.p.m. (vinyl proton), and a broad 3 proton absorption at 2.30 p.p.m. Similarly, reaction of **1***a* with cyclopentanone and cyclohexanone gave the cyclohexanone derivative **6** (ν 1720 cm^{-1}) and the cycloheptanone derivative **7** (ν 1705 cm^{-1}). All these derivatives showed the appropriate low field signals in the n.m.r.

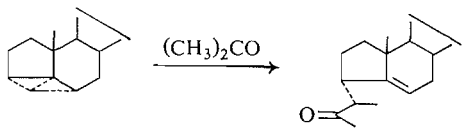

1*a* **4**

These reactions seem to follow the pattern proposed for the aldehydes and presumably proceed via an intermediate of type **2** (X = alkyl).

The reaction of **1***a* with methyl vinyl ketone

[1]This work was supported by the National Research Council of Canada.

[2]Holder of a National Research Council of Canada Bursary, 1964–1965 and Studentship, 1965–1967. Present address: Department of Chemistry, Columbia University, New York, New York 10027.

Can. J. Chem. Downloaded from www.nrcresearchpress.com by 210.87.254.105 on 09/05/12
For personal use only.

gave one major product **8** and two minor ketonic products which were not identified. It may be noted that in the reaction of bicyclobutane **1***a* with acrolein (1), the products of 1,2- and 1,4- addition were formed in equal amounts. This may be due to the larger steric hinderance of the carbonyl group in methyl vinyl ketone as compared to acrolein (2).

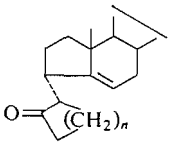

5 $n = 2$
6 $n = 3$
7 $n = 4$

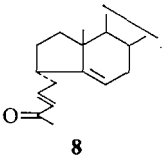

8

Phosgene

When a pentane solution of **1***a* was treated with gaseous phosgene a crystalline compound, $C_{55}H_{88}OCl_2$ was obtained in 30% yield. The spectral data were consistent with structure **9**. Acid chloride **10** is probably an intermediate in this reaction.

Halogens

Reaction of a pentane solution of **1***a* with one equivalent of iodine, gave a crystalline compound, $C_{27}H_{44}I_2$. Its spectral data were consistent with structure **11***a*. The hydrolysis of **11***a* by refluxing for two weeks with 5% methanolic sodium bicarbonate, gave aldehyde **12**, identified by comparison with an authentic sample (3).

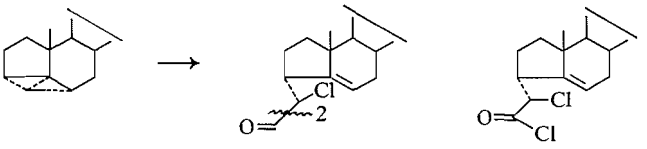

1*a* **9** **10**

Similarly **1***b* gave **11***b*, which, however, could not be obtained in a pure state since it decomposed upon chromatography. Its spectral data left little doubt as to its structure.

Treatment of **1***a* with one equivalent of bromine gave an inseparable mixture. It was evident from the spectral data that the reaction mixture was quite complex.

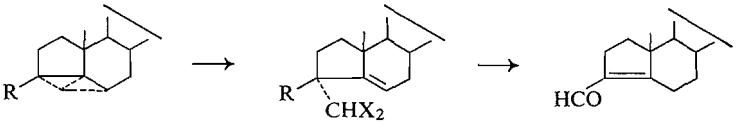

1*a* R = H
1*b* R = CH_3

11*a* R = H, X = I
11*b* R = CH_3, X = I

12

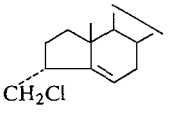

13

When **1***a* was allowed to react with chlorine, chloride **13** and a product $C_{27}H_{43}Cl_3$, were obtained. The formula of the latter indicated addition of two molecules of chlorine, followed by elimination of hydrogen chloride. The reaction of hydrogen chloride with bicyclobutane **1***a* would then give **13**. In a separate reaction involving bicyclobutane **1***a* and hydrogen chloride, the product was chloride **13**. The structure of the compound $C_{27}H_{43}Cl_3$ was not elucidated.

Tetracyanoethylene

Treatment of a pentane solution of bicyclobutane **1***a* with one equivalent of tetracyanoethylene gave a 1:1 adduct which precipitated from the solution after 15 min. The adduct was assigned structure **14**, based on the following

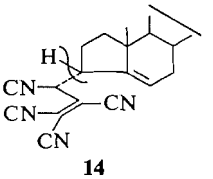

14

evidence. The i.r. spectrum showed nitrile absorption at 2245 cm^{-1} and no absorption in

the carbonyl region. The n.m.r. spectrum showed the appropriate signals at 5.58 (=C_6—H),[3] 2.93 (allylic proton), and 2.90 p.p.m. (*H*C—CN). The mass spectrum showed the molecular ion at 496 and the base peak at 354 *m/e*, corresponding to cleavage and hydrogen transfer as shown in **14**. Hydrolysis with methanolic sodium hydroxide gave a mixture of acids which could not be separated and used for confirmation of the structure.

Hexachloroacetone

Reaction of bicyclobutane **1***a* in pentane with an excess of hexachloroacetone gave a major product **16** and a minor product **17**. Compound **16** absorbed in the i.r. at 1745 cm^{-1}, and showed signals in the n.m.r. at 5.42 (C_6 = CH), 3.50 (allylic proton), and a doublet at 4.90 p.p.m. (J = 4 c.p.s.), corresponding to the proton α to a carbonyl and trichloromethyl groups. Hydrolysis of **16** with methanolic sodium hydroxide gave carboxylic acid, **15**, with methanolic sodium methoxide it gave the ester **15***a*. The identity of **15** was established by comparison with an authentic sample (1). The structure of the minor product **17**, $C_{30}H_{44}Cl_6$, was established by spectroscopic means only. No successful chemical degradation to substantiate the structure could be carried out. Ether **17** showed no absorption in the carbonyl (i.r.) or olefinic region (n.m.r.) region. It had strong ether bands in the i.r. at 1060 cm^{-1}. In the n.m.r. spectrum the only low-field signal was a triplet at 4.85 p.p.m. (H—C_6—O).

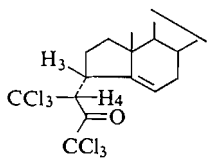

16

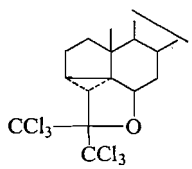

17

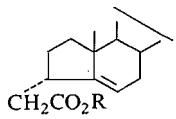

15 R = H
15*a* R = CH_3

The reaction of bicyclobutanes **1** with hexafluoroacetone gave in part, products whose spectral features resembled those of **17**. However, the reaction is considerably more complex and further investigations are being carried out in that area.

Discussion

The reactions of ketones seem to resemble those of aldehydes and most likely proceed via the zwitterion **2**, followed by an intramolecular alkyl shift. The reaction of phosgene, hexachloroacetone, tetracyanoethylene, and iodine can be interpreted to proceed via the same initial addition, with concomitant or subsequent elimination of an anion and recombination of the carbonium ion with the anion. The intermediate ion-pair is probably very closely associated. In one experiment involving **1** and hexachloroacetone, sodium azide was added but no product of recombination with azide could be detected.

By analogy with the reaction of bicyclobutanes with aldehydes, the alkyl shifts to, or additions of nucleophiles at C-4, is most likely stereospecific.[4] The magnitude of the coupling constant $J_{3,4}$ was 2–4 c.p.s., as was the case with the bicyclobutane–deuterioformaldehyde adduct. A recent report (5) suggesting that bicyclobutane **1***a* undergoes nucleophilic attack by ethanol is not substantiated. We have not observed any reaction of bicyclobutane **1***a* with either methyl lithium or sodium methoxide. It would, therefore, be inconceivable that in neutral ethanol, a nucleophilic attack on the bicyclobutane **1***a* would occur.

Experimental

All melting points were taken in a Gallenkamp melting point apparatus and are uncorrected. The infrared (i.r.) spectra were taken in a Perkin-Elmer 337 spectrophotometer. The ultraviolet (u.v.) spectra were measured using a Unicam model SP 800 A spectrophotometer. The nuclear magnetic resonance (n.m.r.) spectra were recorded on a Varian A-60 instrument as CCl_4 solutions using TMS as an external standard. All preparative thin-layer chromatography (t.l.c.)

[3]C_6 refers to carbon number six in the usual steroid numbering system (4).

[4]C-4 refers to that position which originally was C-4 in the steroid nucleus.

Can. J. Chem. Downloaded from www.nrcresearchpress.com by 210.87.254.105 on 09/05/12
For personal use only.

Can. J. Chem. Downloaded from www.nrcresearchpress.com by 210.87.254.105 on 09/05/12
For personal use only.

separations were performed with glass plates (20 × 20 cm) covered with silica gel (0.5 mm, E. Merck A. G.). Bicyclobutanes **1***a* and **1***b* were obtained by irradiating a 0.2% pentane solution of the corresponding cholesta-3,5-diene in a Rayonet photochemical reactor using lamps having a peak intensity at 253 mμ. The photolysis tubes (25 mm internal diameter, 1 ft length) were equiped with drying tubes at the inlet and outlet.

Reaction of Bicyclobutane 1 with Ketones

Reactions of bicyclobutane **1***a* with ketones were carried out using the following general experimental procedures. A pentane solution (90 ml) of 200 mg of cholesta-3,5-diene (6) was irradiated in a helium atmosphere for 15 h. The pentane was evaporated at room temperature under a stream of nitrogen and the residue diluted with 5 ml of anhydrous ether. Excess ketone was added (0.2 ml of acetone, cyclobutanone, cyclopentanone, cyclohexanone, and methyl vinyl ketone) and the solution was stirred at room temperature for 1 h. After evaporation of the solvent and excess reagent, the residue was chromatographed on two t.l.c. plates (benzene–hexane, 6:4).

Acetone

A crystalline product was isolated and identified as ketone **4**, (80 mg), m.p. 126–127 °C (after recrystallization from methanol–ether solution); ν 1725 cm^{-1} (saturated C=O); δ 5.12 p.p.m. (1H, broad signal, C=C—H), 3.07 p.p.m. (1H, broad signal, C_3—H), 2.65 p.p.m. (1H, doublet of quartets, CH—CO—CH_3), and 2.15 p.p.m. (3H, singlet, CH—CO—CH_3).

Anal. Calcd. for $C_{30}H_{50}O$: C, 84.44; H, 11.81. Found: C, 84.31; H, 11.73.

Cyclobutanone

A crystalline product (84 mg) was obtained and identified as ketone **5**, m.p. 134–135 °C (methanol–ether); ν 1755 cm^{-1} (C=O in cyclopentanones); δ 5.15 p.p.m. (1H, broad signal, C=C—H), 3.20 p.p.m. (1H, broad signal, C_3—H), and 2.0–2.4 p.p.m. (3H, complex signals, protons adjacent to carbonyl group).

Anal. Calcd. for $C_{31}H_{50}O$: C, 84.44; H, 11.81. Found: C, 84.49; H, 11.70.

Cyclopentanone

A crystalline material (43 mg) was obtained and identified as ketone **6**, m.p. 115–116 °C (methanol–ether); ν 1720 cm^{-1} (C=O in cyclohexanones); δ 5.00 p.p.m. (1H, broad signal, C=C—H), 3.00 p.p.m. (1H, broad signal, C_3—H) and 2.3–2.6 p.p.m. (3H, complex signals, protons adjacent to carbonyl group).

Anal. Calcd. for $C_{32}H_{52}O$: C, 84.89; H, 11.58. Found: C, 85.15; H, 11.52.

Cyclohexanone

A crystalline product (50 mg) was obtained and identified as ketone **7**, m.p. 68–72 °C (methanol–ether); ν 1705 cm^{-1} (C=O in cycloheptanones); δ 5.05 p.p.m. (1H, broad signal, C=C—H), 3.10 p.p.m. (1H, broad signal, C_3—H), and 2.6–2.2 p.p.m. (3H, complex signals, protons adjacent to carbonyl group).

Anal. Calcd. for $C_{33}H_{54}O$: C, 84.91; 11.66. Found: C, 84.30; H, 11.62.

Methyl Vinyl Ketone

Thin-layer chromatography of the crude reaction mixture showed three bands. The slowest moving band (75 mg) was not obtained crystalline but was identified as the ketone **8**; λ_{max}(EtOH) 225 mμ (ε 10 000); ν 3040 and1680 cm^{-1} (α,β-unsaturated ketone); δ 6.67 p.p.m. (1H, two doublets, J = 6 and 8.5 c.p.s., separations between doublets J = 15.5 c.p.s., vinylic proton adjacent to methylene group), 6.00 p.p.m. (1H, doublet, J = 15.5 c.p.s., vinylic proton adjacent to carbonyl group), 5.22 p.p.m. (1H, broad signal, C-6 vinyl proton), 4.15 p.p.m. (1H, broad signal, C-3 allylic proton), and 2.17 p.p.m. (3H, singlet, methyl adjacent to carbonyl group). The two other bands were not further identified.

Anal. Calcd. for $C_{31}H_{50}O$: C, 84.86; H, 11.49. Found: C, 84.61; H, 11.55.

Reaction of Bicyclobutane 1a with Phosgene

A solution of 200 mg of cholesta-3,5-diene (6) in 90 ml of spectrograde pentane was irradiated for 15 h in a helium atmosphere. Phosgene gas was bubbled through the solution for 10 min and the solution was stirred for a further 2 h. The pentane was evaporated and the residue diluted in 25 ml of ether. The etheral solution was washed to neutrality with water, dried, and evaporated to give 220 mg of an oily residue which was chromatographed on two t.l.c. plates (hexane). A solid material was isolated (50 mg) and identified as the adduct **9**, m.p. 125–130 °C methanol–ether); ν 3030 cm^{-1} (C=C—H), 1730 cm^{-1} (C=O), and 840 cm^{-1} (C—Cl); δ 5.24 p.p.m. (1H, multiplet, C-6 vinyl proton), 5.03 p.p.m. (1H, doublet, —CH(Cl)—), 3.37 p.p.m. (1H, broad signal, C_3—H). Recrystallization from ether–methanol gave an analytical sample, m.p. 129–131 °C.

Anal. Calcd. for $C_{55}H_{86}Cl_2O$ (mol. wt., 833): C, 79.23; H, 10.32; Cl, 8.52. Found (mol. wt., 816, Rast): C, 79.52; H, 10.19; Cl, 8.23.

Reaction of Bicyclobutane 1a with Iodine

A solution of 200 mg of cholesta-3,5-diene in 90 ml of spectrograde pentane was irradiated for 15 h in a helium atmosphere. To the solution was added 100 mg of iodine. The reaction mixture was stirred for 24 h at room temperature. The solution was washed with 2% aqueous sodium thiosulfate and water, dried over anhydrous magnesium sulfate, and evaporated under reduced pressure to give an oily residue which was chromatographed on two t.l.c. plates (hexane). A solid material (110 mg) was isolated and identified as the geminal diiodide **11***a*, m.p. 111–112 °C; ν 3025 cm^{-1} (C=C—H); δ 5.30 p.p.m. (1H, doublet, J = 2 c.p.s., —C*H*I_2), 5.23 p.p.m. (1H, multiplet, C-6 vinyl proton), 2.95 p.p.m. (1H, broad signal, C_3—H). The material was recrystallized from ether–methanol to give an analytical sample.

Anal. Calcd. for $C_{27}H_{44}I_2$: C, 52.09; H, 7.07; I, 40.9. Found: C, 52.12; H, 7.26; I, 40.7.

Hydrolysis of Iodide 11a

A solution of 150 mg of iodide **11***a* in 25 ml ether and 10 ml of methanol containing 200 mg of sodium bicarbonate was heated under reflux for 10 days. The ether solution was washed to neutrality with water, dried, and evaporated to give 145 mg of an oily residue which was chromatographed on two t.l.c. plates (benzene). This yielded 10 mg of the α,β-unsaturated aldehyde **12** which was identical (i.r., u.v., and t.l.c.) with a sample prepared previously (3).

Reaction of Bicyclobutane 1b with Iodine

A solution of 200 mg of 3-methylcholesta-3,5-diene (7)

Can. J. Chem. Downloaded from www.nrcresearchpress.com by 210.87.254.105 on 09/05/12
For personal use only.

in 90 ml of spectrograde pentane was irradiated for 24 h. To this solution was added 100 mg of iodine. The reaction mixture was stirred for 10 h at room temperature. The solution was washed with 2% aqueous sodium thiosulfate and water, dried, and evaporated to give 220 mg of an oily residue. Qualitative t.l.c. (hexane) showed one major spot; ν 3030 cm^{-1} (C=C—H); δ 5.25 p.p.m. (1H, multiplet, C-6 vinyl proton), 5.10 p.p.m. (1H, singlet, —C*H*I_2). The residue decomposed when applied to a t.l.c. plate.

*Reaction of Bicyclobutane **1a** with Chlorine*

A solution of 200 mg of cholesta-3,5-diene in 90 ml of spectrograde pentane was irradiated in a helium atmosphere for 15 h. Chlorine gas was passed through the solution for 10 min at a slow rate. The solution was stirred overnight at room temperature. The solvent was evaporated and the residue (210 mg) was chromatographed on two t.l.c. plates (hexane) giving 76 mg of oily trichloride $C_{27}H_{43}Cl_3$; ν 3010 cm^{-1} (C=C—H), 638, 685, and 770 cm^{-1} (C—Cl); δ 5.02 p.p.m. (1H, doublet, J = 2.5 c.p.s., vinyl proton), 4.30 p.p.m. (1H, triplet), 4.17 p.p.m. (2H, singlet).

Anal. Calcd. for $C_{27}H_{43}Cl_3$: C, 68.49; H, 9.09; Cl, 22.51. Found: C, 68.50; H, 8.73; Cl, 22.83.

The monochloride **13** was also isolated (25 mg) from the reaction mixture, m.p. 71–72 °C; ν 3040 cm^{-1} (C=C—H), 650 cm^{-1} (C—Cl); δ 5.30 p.p.m. (1H, multiplet, C-6 vinyl proton), 3.40 p.p.m. (2H), signals resembling an ABX system, —C*H*$_2$—Cl), 3.00 p.p.m. (1H, broad signal, C_3—H). The chloride **13** was recrystallized from ether–methanol to give an analytical sample.

Anal. Calcd. for $C_{27}H_{45}Cl$: C, 80.20; H, 11.14; Cl, 8.79. Found: C, 79.78; H, 10.98; Cl, 9.09.

*Reaction of Bicyclobutane **1a** with Hydrogen Chloride*

A solution of 200 mg of cholesta-3,5-diene in 90 ml of spectrograde pentane was irradiated for 15 h in a helium atmosphere. Hydrogen chloride was bubbled through the solution for 5 min. The pentane solution was washed to neutrality with water, dried, and evaporated to give 195 mg of an oily residue which was chromatographed on two t.l.c. plates (hexane) giving 130 mg of crystalline monochloride **13**, identical by t.l.c. and i.r. with a sample prepared above.

*Reaction of Bicyclobutane **1a** with Tetracyanoethylene*

A solution of 200 mg of cholesta-3,5-diene in 200 ml of spectrograde pentane was irradiated for 15 h in a helium atmosphere. Tetracyanoethylene (70 mg) was added and the solution stirred for 2 h at room temperature. The resulting precipitate was removed by filtration and identified as the adduct **14**, m.p. 241–243 °C (decomposed); ν 3020 cm^{-1} (C=C—H), 2245 cm^{-1} (nitrile); δ 5.58 p.p.m. (1H, multiplet, C-6 vinyl proton), 2.93 p.p.m. (1H, broad signal, C_3—H), 2.90 p.p.m. (1H, singlet slightly split, —C(CN)*H*—); *m/e* = 550.

Anal. Calcd. for $C_{33}H_{44}N_4$: C, 79.79; H, 8.93; N, 11.28. Found: C, 79.52; H, 8.89; N, 11.63.

*Reaction of Bicyclobutane **1a** with Hexachloroacetone*

A solution of 200 mg of cholesta-3,5-diene in 90 ml of spectrograde pentane was irradiated for 15 h. Hexachloroacetone (0.15 ml) was added and the solution was stirred at room temperature for 48 h. The solvents were evaporated and the residue was chromatographed on two t.l.c. plates (hexane) to give two crystalline products. The less polar material was characterized as the ketone adduct **16**, m.p. 123–124 °C; ν 1745 cm^{-1} (C=O), 3030 cm^{-1} (C=C—H), 850–550 cm^{-1} (C—Cl); δ 5.42 p.p.m. (1H, broad signal, C=C—H), 4.90 p.p.m. (1H, doublet, —C(CCl_3)H—), 3.50 p.p.m. (broad signal, 1H, C_3—H).

Anal. Calcd. for $C_{30}H_{44}Cl_6O$: C, 58.36; H, 7.18; Cl, 34.46. Found: C, 58.37; H, 7.01; Cl, 33.42.

The more polar crystalline product was characterized as the cycloether **17**, m.p. 157–158 °C; ν 3070, 3030, and 1020 cm^{-1} (cyclopropane), 1060 cm^{-1} (ether), 840–650 cm^{-1} (C—Cl); δ 4.85 p.p.m. (1H, unsymmetrical triplet, C_6—H), 2.82 p.p.m. (1H, multiplet, C_3—H) and 2.28 p.p.m. (1H, doublet, C_4—H).

Anal. Calcd. for $C_{30}H_{44}Cl_6O$: C, 58.36; H, 7.18; Cl, 34.46. Found: C, 57.95; H, 7.16; Cl, 33.81.

*Hydrolysis of Ketone **16** with Methanolic Sodium Hydroxide*

A solution of 10 mg of ketone **16** in 5 ml methanol containing 500 mg of sodium hydroxide was refluxed for 10 min. The solution was neutralized with concentrated hydrochloric acid and extracted with 25 ml of ether. The ether extract was washed with water, dried, and evaporated to give 7 mg of carboxylic acid **15** identical in all respects with a sample obtained previously (i.r., m.p., t.l.c.).

*Hydrolysis of Ketone **16** with Methanolic Sodium Methoxide*

A solution of 70 mg of ketone **16** in 5 ml methanol containing 250 mg of sodium methoxide was refluxed for 10 min. The solution was neutralized with concentrated hydrochloric acid and extracted with 25 ml of ether. The ether extract was washed with water, dried, and evaporated to give 55 mg of the methyl ester of carboxylic acid **15**; ν 1730, 1260, and 1130 cm^{-1} (ester); δ 5.20 p.p.m. (1H, multiplet, C=C—H), 3.80 p.p.m. (1H, multiplet, C_3—H) and 3.63 p.p.m. (3H, singlet, —CO_2CH_3).

Hydrolysis of this methyl ester (10 mg) in refluxing methanolic sodium hydroxide (5 ml of 5%) generated after usual workup the carboxylic acid **15** (8 mg) identical by t.l.c., i.r., and m.p. with a previously prepared sample.

*Reaction of Bicyclobutane **1a** with Hexachloroacetone in the Presence of Sodium Azide*

A solution of 200 mg of impure bicyclobutane **1a** in 90 ml of pentane prepared in the usual manner was treated with 0.2 ml of hexachloroacetone and 10 ml of anhydrous ether containing 50 mg of sodium azide. The reaction mixture was stirred for 48 h. Thin-layer chromatography and an infrared spectrum of the residue after workup revealed an identical mixture of products **16** and **17** as previously obtained.

1. E. Lee-Ruff and G. Just. Tetrahedron, **24**, 601 (1968).
2. J. D. Roberts and M. C. Caserio. Basic principles of organic Chemistry. W. A. Benjamin, Inc., New York. 1964. pp. 357.
3. W. G. Dauben and J. A. Ross. J. Am. Chem. Soc. **81**, 6521 (1959).
4. L. F. Fieser and M. Fieser. Steroids. Reinhold Publishing Corp., New York. 1959. p. 1.
5. P. G. Gassman. Chem. Commun. 793, (1967).
6. J. C. Eck, R. L. Van Peursem, and E. W. Hollongsworth. J. Am. Chem. Soc. **61**, 171 (1939).
7. V. diTullio. Ph.D. Thesis. McGill University, Montreal, Quebec. 1964.

Can. J. Chem. Downloaded from www.nrcresearchpress.com by 210.87.254.5 on 09/05/12
For personal use only.

Degradation of wood constituents during the self-agglomeration of an oak sawdust. II. Infrared study of two lignins

HENRY P. NAVEAU
Université de Louvain, Laboratoire Forestier, Heverlee, La Belgique

Received December 27, 1967

Structural changes in lignins isolated from particle-boards are studied by infrared spectrophotometry, in relation to an endothermic trend which characterizes the self-agglomeration process.

Changes in intensity of various infrared bands are reported and are attributed to the following: (*a*) variation in the nature and distribution of substituents of the aromatic ring and conjugation of the aromatic ring with carbonyl C=O or C=C, which indicate an increasing state of condensation of the lignin, (*b*) simultaneous division of the macromolecule of lignin, partially caused by breakage of ether linkages between its lateral chains, (*c*) cleavage of bonds between lignin and carbohydrate material, and (*d*) insolubilization, with the acid lignin, of an increasing amount of carbohydrate material which is also increasingly condensed.

The origin of the endothermic trend cannot be explained in terms of these reactions of lignin.

Canadian Journal of Chemistry, 46, 1893 (1968)

Introduction

The self-agglomeration of woody material to form particle-board can be realized under certain conditions of pressure, temperature, and moisture content (1). A strong endothermic trend accompanies this process and its appearance and development characterize the properties of the resultant product.

In an earlier paper (2), the chemical alterations of wood constituents of oak sawdust (*Quercus pedunculata* Ehrh.) during such self-agglomeration were reported. This paper is a continuation of that work and is concerned with the study by infrared (i.r.) spectrophotometry of structural changes in lignin during this process.

Experimental

Particle-board Manufacture

Sawdust preparation and particle-board formation and subsequent reduction to small fragments were as described in Part I (2). Particle-board made under these same conditions with sawdust extracted with alcohol: benzene (1:1, v/v) was used for the isolation of acidolysis lignin.

Figure 1 indicates the changes in sawdust temperature at the center of the particle-board during its formation. Lignin was isolated at stages S, A, B, C, D, and E of this temperature curve; stage S corresponds to unprocessed sawdust.

Lignin Isolation

Halse lignin was obtained as an insoluble residue in a mixture of concentrated hydrochloric and sulfuric acids (10:1, v/v) (3).

Acidolysis lignin was isolated from milled materials by extraction with dioxane:water (9:1, v/v) 0.2 *N* in hydrochloric acid under nitrogen for 1 h at 87 °C (4). It was assumed that milling does not profoundly alter the structure of the acidolysis lignins, which were considered representative of the lignin *in situ* (5).

Methoxyl group content was determined by the semimicro method of Viebock and Schwappach (6).

Infrared Spectrophotometry

Infrared spectra were obtained with a Grubb Parsons Spectromaster (16 700–400 cm^{-1} (0.6–25 μ), double beam) equipped with grating optics; spectra were recorded proportional to wavelength. KBr pellets with a 1% lignin concentration were used for analysis. To exclude any influence from absorbed water, pellets were prepared under controlled humidity conditions with lignin and KBr samples pre-dried under vacuum. Pertinent absorption band assignments are given in Table I.

Results

The lignin contents of particle-board at designated stages of the temperature curve and the corresponding lignin methoxyl group contents are given in Table II.

Infrared spectra of Halse and acidolysis lignins from 3600–2650 cm^{-1} and 2000–800 cm^{-1} at some of these same stages are shown in Fig. 2, and spectra of acidolysis lignins from 1480–1640 cm^{-1} (aromatic C—C vibration region) are shown in Fig. 3.

Absorbance of individual bands of these spectra are corrected for background absorbance determined at a wavelength at which the samples do not absorb radiation (1900 cm^{-1}) (17). Relative absorbance values are determined in triplicate for all bands by the internal standard method, and compared with corresponding values for lignin isolated at stage S. Mean values for bands with a relative intensity change of over

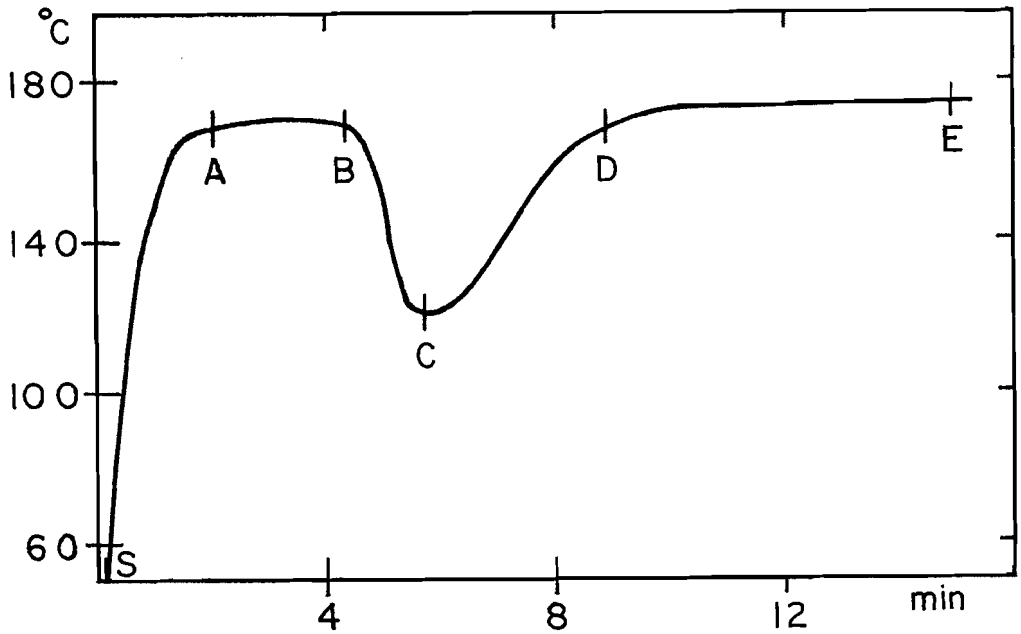

FIG. 1. Changes in the internal temperature of a particle-board during its formation.

TABLE I

Band assignment for the lignin in the infrared region

cm^{-1}	μ	Band origin	References
3435–3425	2.91–2.92	Bonded O—H stretching vibration	(7–9)
2990	3.345	C—H stretching vibration	(7)
2937	3.405	C—H_2 antisymmetric stretching vibration	(7)
2880	3.472	C—H stretching vibration in tertiary C—H groups	(7, 8)
2840	3.521	C—H stretching vibration in methoxyls and C—H_2 symmetric stretching vibration	(7, 8)
1730–1710	5.78–5.85	C=O stretching vibration of aliphatic or β-ketones	(7–12)
1670–1660	5.99–6.02	C=O stretching vibration of α-ketones	(7–10, 12, 13)
1640	6.10	H—O—H deformation vibration of adsorbed water	(7, 14, 15)
1595	6.25	C—C stretching vibration of benzene ring	(7–9, 13–16)
1505	6.65		
1460	6.85	C—H deformation vibration Benzene ring vibration	(7–9) (7, 15)
1425	7.02	C—H bending vibration in methoxyls	(7, 8)
1365	7.32	O—H in plane bending vibration	(7, 8, 13)
1330–1325	7.52–7.55	Aromatic aldehydes	(16)
1270	7.87	Asymmetric stretching vibration of aryl–alkyl ethers	(7–9, 16)
1225	8.16	See text	
1190	8.40	C—O stretching vibration (mixture)	(7)
1150	8.70		
1125	8.89	Asymmetric stretching vibration of dialkyl ethers	(7, 8, 16)
1030	9.71	Symmetric stretching vibration of dialkyl ethers	(7–9)
835	11.97	C—H out of plane bending vibration	(7, 8, 14, 15)

Can. J. Chem. Downloaded from www.nrcresearchpress.com by 210.87.254.5 on 09/05/12
For personal use only.

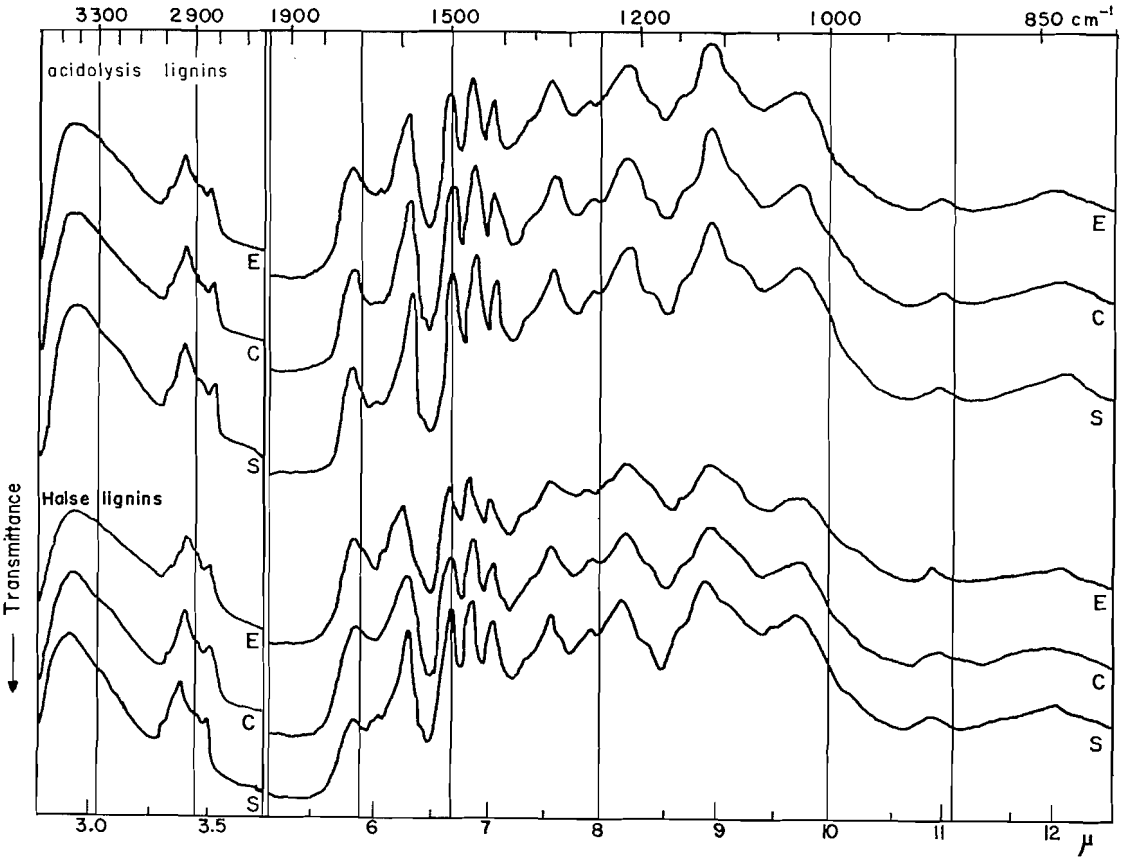

FIG. 2. Infrared spectra of Halse lignins and acidolysis lignins between 3600 and 2650 cm^{-1} and between 2000 and 800 cm^{-1} at different stages of the self-agglomeration.

TABLE II

Amount of Halse and of acidolysis lignins and their methoxyl group contents at each stage of the self-agglomeration

Stage	S	A	B	C	D	E
Halse lignin*	21.5	21.6	22.3	24.5	26.1	27.3
Methoxyls†	20.5	19.6	19.0	18.7	17.7	17.0
Acidolysis lignin*	18.2	18.8	19.5	20.0	22.0	22.1
Methoxyls†	19.0	18.7	18.7	18.6	18.6	18.7

*Expressed as % of wood or designated particle-board.
†Expressed as % of corresponding lignin.

10% in any one of the stages from A to E are given in Figs. 4 and 5 for Halse lignins, and in Fig. 6 for acidolysis lignins. Since these values are related to peak height measurements, only the general trend of each band's relative intensity will be considered.

Discussion

Halse Lignin

The increase in Halse lignin contents and the corresponding decrease in methoxyl group contents of this lignin during agglomeration are caused by the insolubility in acids of some carbohydrate materials which are transformed by thermal action (2, 18). This influences the infrared spectra of Halse lignins in addition to the transformation of lignin itself during the self-agglomeration process.

The internal standard selected for spectrophotometric analysis of these lignins is the sum of the absorbances of the aromatic C—C bands at 1595 and 1505 cm^{-1}. The measure of aromatic group content, considered in terms of the absolute methoxyl group content of the lignin samples, remains fairly constant.

Can. J. Chem. Downloaded from www.nrcresearchpress.com by 210.87.254.5 on 09/05/12
For personal use only.

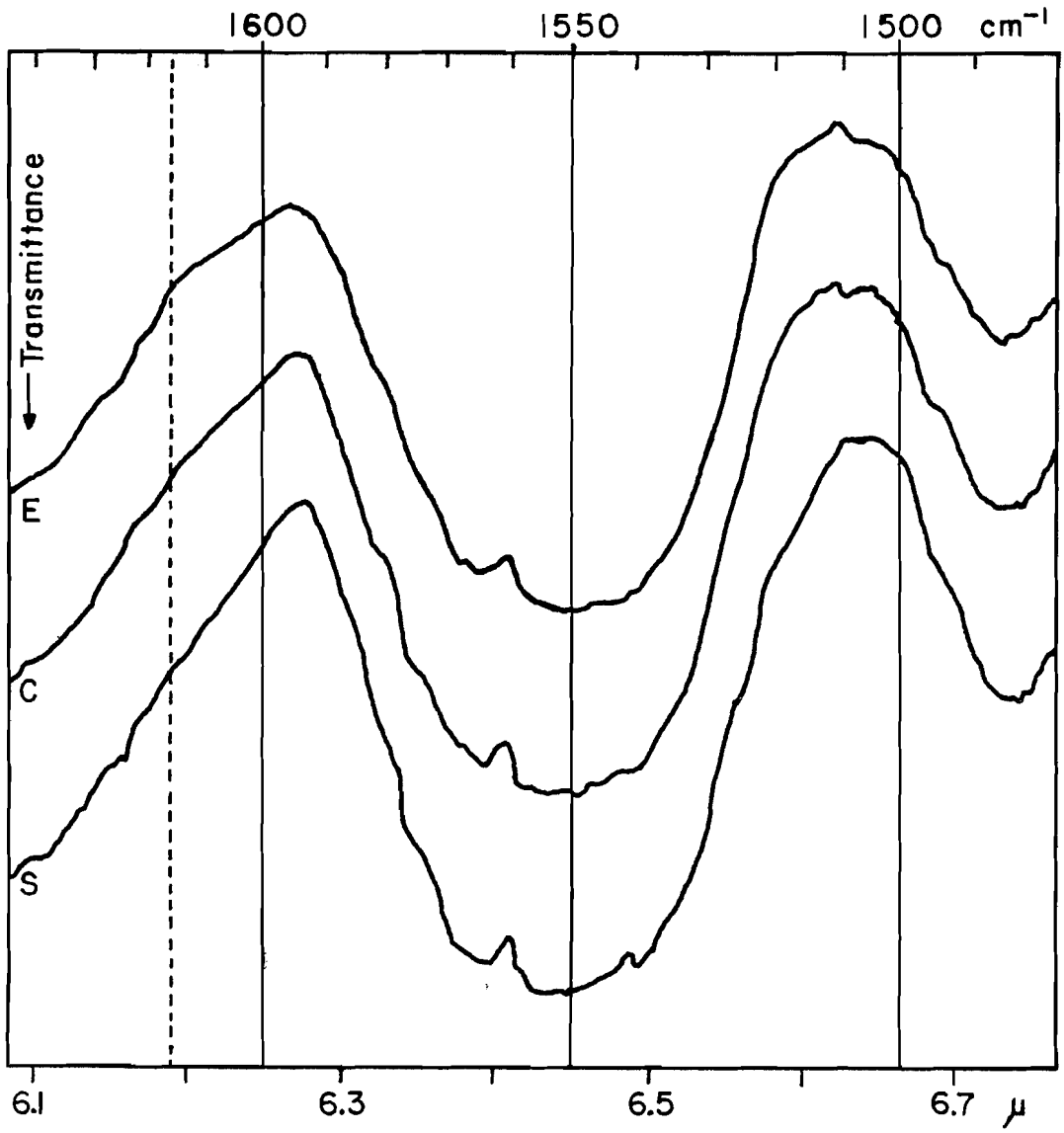

FIG. 3. Infrared spectra of acidolysis lignins between 1640 and 1480 cm^{-1}.

Relative intensity values for individual bands, shown in Fig. 4, are characterized by an increase in C—O band intensities except for the band at 1125 cm^{-1}, attributed to dialkyl ethers, which decreases. A somewhat smaller increase is noted for the band at 1224 cm^{-1} which has been assigned to C—O vibrations of phenols by some authors (8, 9) and to asymmetric C—O vibrations of alkyl–aryl ethers by others (7). The intensity of the carbonyl band at 1724 cm^{-1} increases quite rapidly in contrast to the other C—O bands and more than doubles in magnitude. In addition, a shoulder of increasing intensity on the aromatic C—C band at 1595 cm^{-1} appears at 1610 cm^{-1}.

Similar values for C—H bands display different patterns. The band at 1460 cm^{-1}, which may be partially attributed to aromatic C—H, and the methoxyl C—H band at 1422 cm^{-1} do not change in intensity. In contrast, as shown in Fig. 5, the shoulder at 2996 cm^{-1}, the methylene C—H band at 2932 cm^{-1}, the methylene and

Can. J. Chem. Downloaded from www.nrcresearchpress.com by 210.87.254.5 on 09/05/12
For personal use only.

Can. J. Chem. Downloaded from www.nrcresearchpress.com by 210.87.254.5 on 09/05/12
For personal use only.

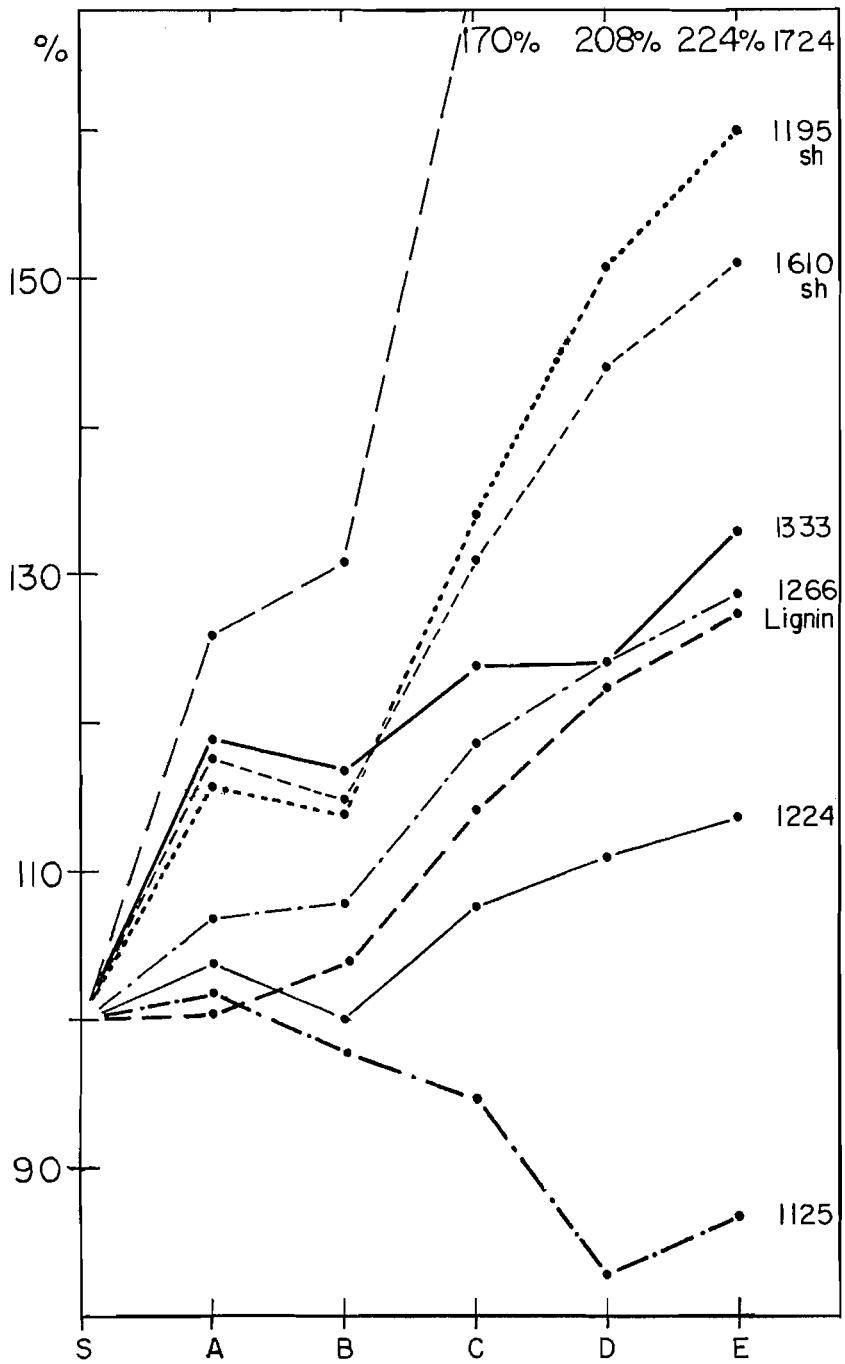

FIG. 4. Relative Halse lignin contents and relative absorbances of bands (cm^{-1}) due to C—O or C—C vibrations in Halse lignins (S = 100%, internal standard: $A_{1595\ cm^{-1}} + A_{1505\ cm^{-1}}$).

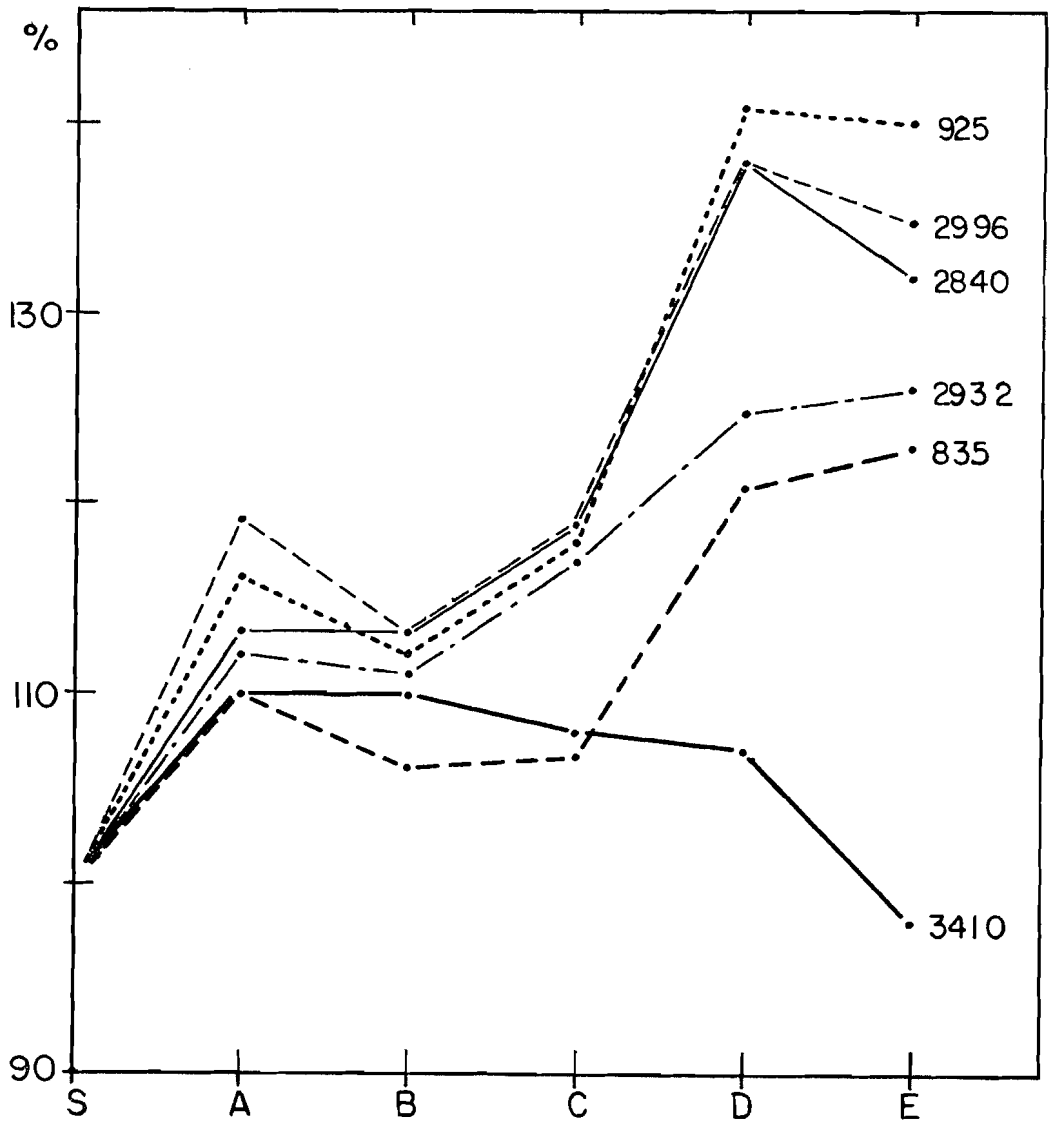

FIG. 5. Relative absorbances of bands (cm^{-1}) due to C—H and O—H vibrations in Halse lignins (S = 100%, internal standard: $A_{1595\ cm^{-1}} + {}_{1505\ cm^{-1}}$).

methoxyl C—H band at 2840 cm^{-1}, and the methenyl C—H shoulder at 2880 cm^{-1}, which is equivalent in magnitude to the band at 2840 cm^{-1}, increase in intensity from stage A to D. The aromatic C—H band at 835 cm^{-1} (adjacent positions on the benzene ring) shows a similar trend from stage C on, and that at 925 cm^{-1} from stage A to D.

The rupture of bonds between carbohydrate material and lignin side chains during agglomeration should be necessary for the plasticization of lignin which is observed in the thermal treatment of wood (19). This rupture could form aromatic ketones (11) which would increase the intensity of the carbonyl band near 1724 cm^{-1}. An increasing amount of aliphatic acid groups in undissolved carbohydrate material and in lignin itself, and of ester groups in hemicellulose,

Can. J. Chem. Downloaded from www.nrcresearchpress.com by 210.87.254.5 on 09/05/12
For personal use only.

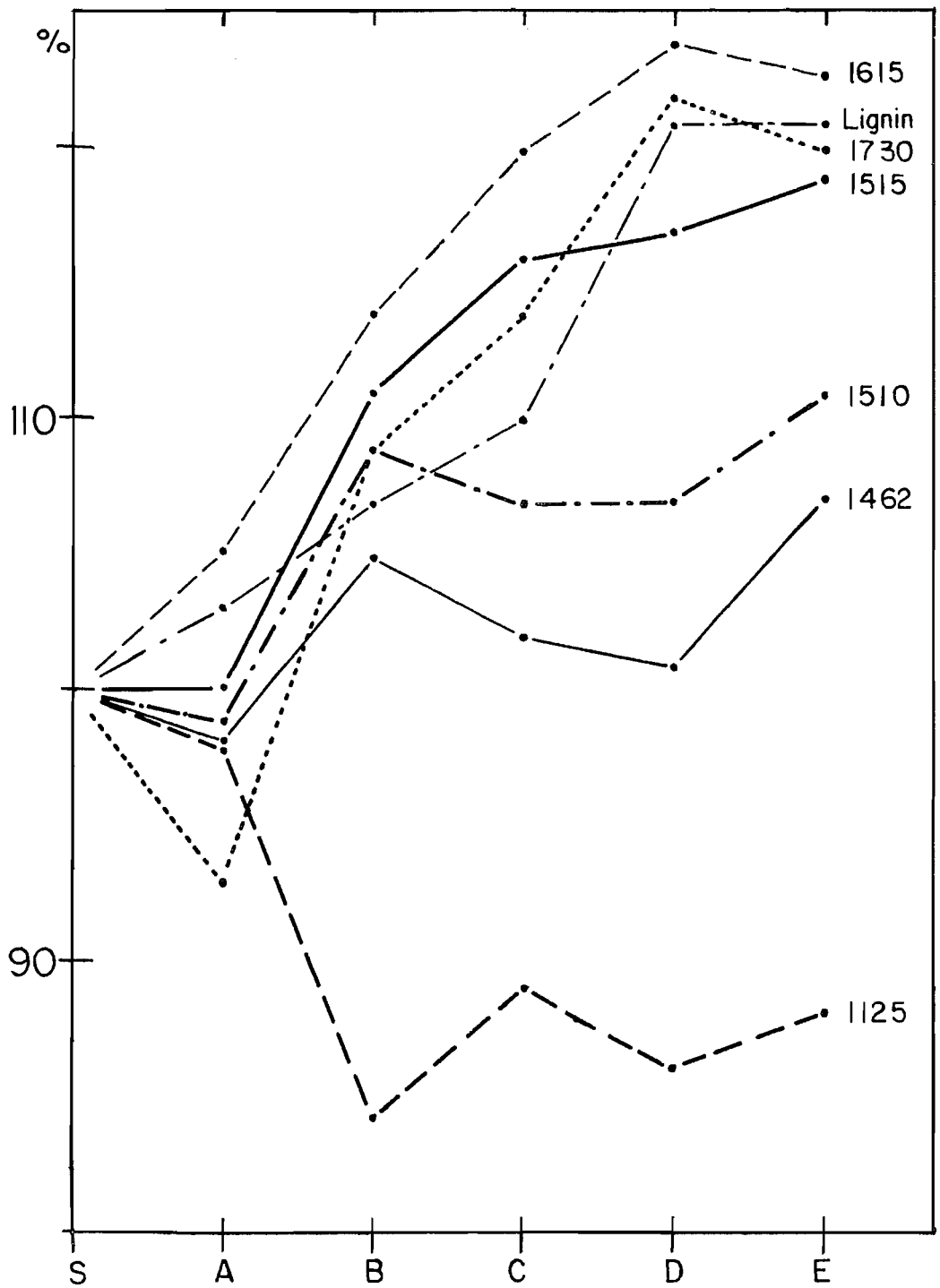

FIG. 6. Relative acidolysis lignin contents and relative absorbances of bands (cm^{-1}) due to C—O and C—C vibrations in acidolysis lignin (S = 100%, internal standard: $A_{1422\ cm^{-1}}$).

Can. J. Chem. Downloaded from www.nrcresearchpress.com by 210.87.254.5 on 09/05/12
For personal use only.

Can. J. Chem. Downloaded from www.nrcresearchpress.com by 210.87.254.5 on 09/05/12
For personal use only.

formed from hydroxyacids under the influence of temperature, could also affect this band in the same manner.

The appearance of a shoulder near 1610 cm^{-1} may be partially or completely attributed to the following: (*a*) the formation of double bonds in conjugation with the benzene ring, e.g. a carbonyl group, (*b*) the changes in number and position of substituents on the benzene ring, and (*c*) the formation of conjugated, C=C in lignin or undissolved carbohydrate material. The division of the lignin macromolecule, discussed elsewhere (2), certainly causes some changes in the substituents of aromatic rings and could explain the increase in intensity of the band at 835 cm^{-1}. Variations in the intensities of the C—H bands are related to the increasing amount of carbohydrate material in the Halse lignin.

The intensity patterns of the bands attributed to C—O should be compared with that of the O—H band at 3410 cm^{-1} shown in Fig. 5. This latter band increases 10% in intensity at stage A, decreases slowly until stage D, and then falls to a level at stage E (in which the Halse lignin has about a 25% carbohydrate content) lower than that at stage S. It is obvious that even if some broadening of the O—H band is conceded, the carbohydrate material is becoming lower in hydroxyl group content, especially between stages D and E, and is in an increasing state of condensation. In this regard, the hydroxyl groups are probably eliminated as water with the formation of C=C or of ether linkages.

The changes in intensity of C—O bands may also be explained by these same reactions; i.e. increase in the number of C=C and adjacent ether linkages with the increasing condensation state of undissolved carbohydrate material. This implies that bands due to these ether linkages should be found in the 1200–1300 cm^{-1} region, whereas those due to preexisting dialkyl ether linkages may be shifted to the alkyl–aryl ether region by the formation of adjacent double bonds. This band shift would explain the decrease in intensity of the dialkyl ether band near 1125 cm^{-1}; however, this band may also be attributed to C—O vibrations of secondary alcohols in lignin which could form ether linkages with phenolic hydroxyl groups. A similar reaction could occur between carbohydrate material and phenolic hydroxyl groups.

Most of the intensity changes of the bands observed in Halse lignins are partially due to the increasing co-precipitation of carbohydrate material. Although this co-precipitation occurs during the isolation process, it is assumed that the structural modifications causing it take place during self-agglomeration since the isolation method remains unchanged. However, it is possible that the acid treatment somewhat accentuates these structural modifications.

Acidolysis Lignin

Acidolysis lignin contents increase until stage D and then remain constant at stage E. Comparison of methoxyl group contents, which are fairly constant, with that of Halse lignin at stage S, indicates an 8% carbohydrate material content since the acidolysis treatment does not induce loss of methoxyls (5). The relative intensity values of individual bands in the spectra of these lignins are calculated using the methoxyl C—H band near 1425 cm^{-1} as the internal standard. The methoxyl group contents in conjunction with Halse lignin results confirm the band assignment cited in the literature.

The intensities of the bands having maxima at 1505 and 1595 cm^{-1} (Fig. 3), do not change although the bands do broaden markedly with the appearance of slight shoulders near 1515 and 1615 cm^{-1}. As shown in Fig. 6, the intensities of these shoulders increase continuously while the intensities at 1510 and 1462 cm^{-1} increase in a less definite manner. The band near 1462 cm^{-1} is generally attributed to coincident C—H and aromatic C—C vibrations (7, 8). This assignment is confirmed by the pattern of intensity changes and the parallelism with the band at 1510 cm^{-1}.

Structural changes are occurring which affect the aromatic ring. The broadening of the bands at 1505 and 1595 cm^{-1} may be attributed to changes in the nature and distribution of substituents of the aromatic ring such as those induced by oxidation or condensation, or to conjugation of aromatic rings with double bonds formed as shown below. The shoulder near 1615 cm^{-1} may also be partially due to the formation of conjugated C=C.

The changes in intensity of bands attributed to C—O are not particularly marked. Conversely, the intensity of the band near 1730 cm^{-1}, attributed to aliphatic or β-keto groups in isolated lignins, increases noticeably as shown in Fig. 6. That of the band near 1660 cm^{-1}, as-

Can. J. Chem. Downloaded from www.nrcresearchpress.com by 210.87.254.5 on 09/05/12
For personal use only.

signed to conjugated keto groups, increases in a similar fashion although the band remains rather weak. These two series of keto groups could be formed when the bonds between carbohydrate material and lignin are broken (11). Such a rupture would permit the isolation of a larger amount of acidolysis lignin which is clearly the case, as indicated in Fig. 6, i.e. the plot of the amounts of acidolysis lignin isolated, expressed as a percentage of its value at stage S, parallels the relative intensity curve of the band at 1730 cm^{-1}. All lignin carbohydrate-bonds susceptible to heat are probably broken from stage D on and the isolated lignin includes the following two complementary classes: (*a*) lignin normally isolable with dioxane – water – hydrochloric acid which is equivalent to the amount of acidolysis lignin at stage S, and (*b*) lignin isolable after thermal treatment, which implies separation from carbohydrate material and is equivalent to the amount of acidolysis lignin in particle-board less that at stage S (4% maximum).

The increase in intensity of the band near 1660 cm^{-1} may also be due to carbonyl C=O vibrations of aromatic acids which have been shown (2) to increase in amount during agglomeration.

The decrease in intensity of the dialkyl ether band near 1125 cm^{-1} can be attributed on one hand to the breaking of ether linkages between the lateral chains of lignin and on the other hand to condensation of the small amount of carbohydrate material remaining in acidolysis lignin. These condensations would produce C=C adjacent to ether bonds and shift the absorption band from the dialkyl to the aryl–alkyl ether region (1200–1300 cm^{-1}). It is also possible that at stage S this carbohydrate material is chemically bound with lignin and later, after these bonds are broken during agglomeration, this material is precipitated with it.

The changes in intensity of other C—O bands below an arbitrary 10% increase in magnitude are not considered.

In summary, the changes noted in the infrared spectra of Halse and acidolysis lignins can be attributed to the following reactions: (*a*) changes in the nature and distribution of substituents of the aromatic ring as caused by formation of acid groups, condensation of alcohols and phenolic hydroxyl groups, and division of the lignin macromolecule which is partially explained by the breaking of ether linkages between its lateral chains, and (*b*) conjugations between the aromatic ring and carbonyl groups, aromatic C—C bonds, or C=C formed by condensation of hydroxyl groups. These results indicate an increasing state of condensation in lignin (20).

The rupture of bonds between lignin and carbohydrate material during agglomeration produces an increase in the amount of acidolysis lignin isolated.

Carbohydrate materials precipitated in increasing amount with Halse lignin are in an increasing state of condensation and show a multiplicity of C=C and adjacent ether linkages. These latter bonds are formed by the condensation of hydroxyl groups with the elimination of water. The number of acid groups increases as well.

Conclusions

The reactions which take place during the self-agglomeration of oak sawdust were studied by infrared spectrophotometry of isolated lignins and by subsequent (2) chemical analysis of particle-boards. On these bases, these reactions may be divided into the following three types: (*a*) scission reactions of macromolecules in the wood, i.e. cleavage within lignin, rupture of bonds between lignin and carbohydrate material, or hydrolysis of carbohydrate material, (*b*) oxidation reactions producing aromatic and aliphatic acids, and (*c*) condensation reactions of lignin and carbohydrate material, often accompanied by the elimination of water, which form hydrophobic, resinous binder materials. Scission reactions take place throughout the entire agglomeration process, oxidation reactions from stage C on, and condensation reactions in stage E although their appearance is delayed by the endothermic trend shown in the earlier stages.

This endothermic trend has been attributed (21) to the formation of bonds in the amorphous zones of cellulose and no one element of this study associates it with other reactions. Accordingly, it seems that the condensation reactions are only slowed by the temperature drop and that their effects prior to stage E are masked by the predominance of the scission reactions. The composite result of these reactions should cause a decrease in the physical properties of particle-board once the minimum in the temperature curve is passed.

Acknowledgments

The author is indebted to the Fonds National de la Recherche Scientifique for a pre-doctoral fellowship (Mandat d'Aspirant) under which this work was carried out. He also wishes to thank Professors R. Antoine and J. J. Fripiat for their assistance and advice, and Mr. J. G. Bicho for his kind help in revising the English text.

1. P. ANDRE. Ministère Agr. Adm. Rech. Agron. C.E.U.S.B. publ. 2–4, Louvain. 1963.
2. H. P. NAVEAU. Holzforschung. To be published.
3. O. M. HALSE. Papir-J. **10**, 121 (1926); *in* E. MERCK. Chemisch-technische Untersuchungsmethoden für die Zellstoff und Papier-Fabrikation. Weinheim. 1957. p. 17.
4. J. M. PEPPER and M. SIDDIQUEULLAH. Can. J. Chem. **39**, 390 (1961); **39**, 1454 (1961).
5. J. M. PEPPER, P. E. T. BAYLIS, and E. ADLER. Can. J. Chem. **37**, 1241 (1959).
6. F. VIEBOCK and A. SCHWAPPACH. Z. Anal. Chem. **91**, 360 (1933).
7. A. J. MICHELL, A. J. WATSON, and H. G. HIGGINS. Tappi, **48**, 520 (1965).
8. H. I. BOLKER and N. G. SOMERVILLE. Pulp Paper Mag. Can. **64**, T187 (1963).
9. H. L. HERGERT. J. Org. Chem. **25**, 405 (1960).
10. J. MARTON, E. ADLER, and K. I. PERSSON. Acta Chem. Scand. **15**, 384 (1961).
11. H. I. BOLKER. Nature, **197**, 489 (1963).
12. J. POLCIN, B. KOSIKOVA, P. SIPOS, M. DANDAROVA-VASATKOVA, and J. SUCHY. Chem. Zvesti, **17**, 891 (1963), *In* Chem. Abstr. **60**, 16 093*h* (1964).
13. S. KOLBOE and Ö. ELLEFSENS. Tappi, **45**, 163 (1962).
14. W. BRUEGEL. Einführung in die Ultrarotspektroscopie. 3rd ed. Steinkopp Verlag, Darmstadt. 1962.
15. L. J. BELLAMY. The infrared spectra of complex molecules. 2nd ed. Methuen and Co. Ltd., London. 1962.
16. A. ROBERT and J. DESMET. Compt. rend. **251**, 430 (1960).
17. L. P. KUHN. Anal. Chem. **22**, 276 (1950).
18. K. KRATZL. Mitt. österr. Ges. Holzforsch. **2**, 135 (1950).
19. D. FENGEL. Holz Roh- Werkstoff, **24**, 529 (1966).
20. J .M. PEPPER. Pulp Paper Mag. Can. **65**, T35 (1964).
21. P. ANDRE. Thèse de Doctorat, Faculty of Agronomical Sciences, Louvain. 1967.

Can. J. Chem. Downloaded from www.nrcresearchpress.com by 210.87.254.5 on 09/05/12
For personal use only.

Can. J. Chem. Downloaded from www.nrcresearchpress.com by 210.87.254.6 on 09/05/12
For personal use only.

Synthesis and properties of some β-diketimines derived from acetylacetone, and their metal complexes

S. G. McGeachin
Department of Chemistry, University of Alberta, Edmonton, Alberta

Received February 13, 1968

The synthesis of a number of diketimine ligands of structure **1** is reported. These give bis-bidentate chelates of type **2** with Cu(II), Ni(II), and Co(II). Optical spectra, magnetic moments and, in a number of instances, solution molecular weights are recorded for these complexes. On the basis of these, it is concluded that the complexes unsubstituted on nitrogen, adopt a square planar stereochemistry in contrast to the others which are all pseudotetrahedral.

Canadian Journal of Chemistry, 46, 1903 (1968)

Introduction

While complexes of β-diketones have enjoyed study for close to one hundred years those of simple analogues in which one or both oxygen atoms are replaced by other elements have only recently received much attention. Worthy of note is the examination of complexes of β-amino-αβ-unsaturated ketones (1), monothio-β-diketones (2), and dithioacetylacetone (3). Insofar as we are aware, no particular attention has been paid to those of β-diketimines, in which both oxygen atoms are replaced by nitrogen, although isolated examples of such complexes do exist (4). This in part may be due to the rarity of the required ligands (5), and to their considerable hydrolytic instability. We herein report the synthesis of several ligands of this type by a mild method of general applicability and record the preparation and properties of their copper, nickel, and cobalt complexes.

Results

The ligands **1** (R = H, Me, Et, *i*-Pr, Ph), which are vinylogous amidinium salts, were synthesized by Reaction Scheme 1 from the readily available corresponding enamino ketones (6). A few examples of this method for the synthesis of such salts have been previously reported (7). It depends on the propensity of triethoxonium fluoborate for *O*-alkylation of the enamino ketone, which renders the carbon of the original carbonyl function readily susceptible to nucleophilic attack in the resulting vinylogous imino ether. Some characteristics of the ligand fluoborate

TABLE I
Characterization of the ligand fluoborate salts

R		Compound analysis %C	%H	%N	Melting point (°C)	Ultraviolet spectrum λ_{max} MeOH(ε)	Nuclear magnetic resonance $(CD_3COCD_3)\tau$
H	Calcd.	32.29	5.96	15.07	79–80	308 mμ (33 500)	7.59(6H),* 4.54(1H),* 1.7–2.6(4H)§
	Found	32.38	6.01	15.35			
Me	Calcd.	39.29	7.06	13.09	123–124	311 mμ (33 700)	7.86(6H),* 7.30(6H, J = 4 c.p.s.),† 5.22(1H),* 1.7–2.7(2H)§
	Found	39.43	7.09	13.34			
Et	Calcd.	44.65	7.91	11.57	159–162	315 mμ (37 200)	8.71(6H, J = 7 c.p.s.),‖ 7.50(6H)* 6.55(4H),‡ 4.74(1H),* 1.35–2.3(2H)§
	Found	44.97	8.26	11.57			
i-Pr	Calcd.	48.90	8.58	10.37	94–97	315 mμ (35 000)	8.71(12H, J = 6.5 c.p.s.),† 7.54(6H),* 6.00(2H),‡ 4.65(1H),* 1.8–2.5(2H)§
	Found	49.10	8.48	10.16			
Ph	Calcd.	60.37	5.66	8.28	160–162	344 mμ (29 700)	7.79(6H),* 4.70(1H),* 3.15(10H),‡ 1.0–1.8(2H)§
	Found	60.75	5.87	7.91			

*Singlet.
†Doublet.
‡Multiplet.
§Broad, unresolved band.
‖Triplet.

TABLE II

Characterization of the free bases from the ligand fluoborate salts **1**

R		Compound analysis %C	%H	%N	Melting point (°C)	Nuclear magnetic resonance $(CDCl_3)\tau$
H**	Calcd.	—	—	—	14–16	8.09(6H),* 5.46(1H),*
	Found	—	—	—		2.33–2.83(3H)§
Me	Calcd.	66.62	11.18	22.20	90	8.16(6H),* 7.05(6H),*
	Found	66.66	11.07	22.03		5.56(1H),* −0.33 – −0.58(1H)§
Et	Calcd.	70.06	11.76	18.16	30–31	8.63(6H, J = 7 c.p.s.),‖ 8.14(6H),*
	Found	70.06	11.65	18.39		6.72(4H, J = 7 c.p.s.),¶ 5.54(H),*
						−1.2 – −0 6(1H)§
Ph	Calcd.	81.56	7.25	11.19	49–50.5	8.08(6H),* 5.26(1H),*
	Found	81.63	7.41	11.05		3.0(10H)‡

*Singlet.
†Doublet.
‡Multiplet.
§Broad, unresolved band.
‖Triplet.
¶Quartet.
**A satisfactory analysis was not obtained, but Mol. Wt. Calcd. for $C_5H_{10}N_2$: 98.0844. Found (mass spectrometry): 98.0844.

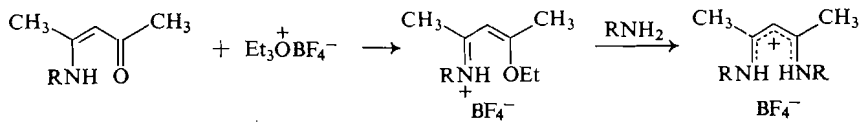

1

REACTION SCHEME 1

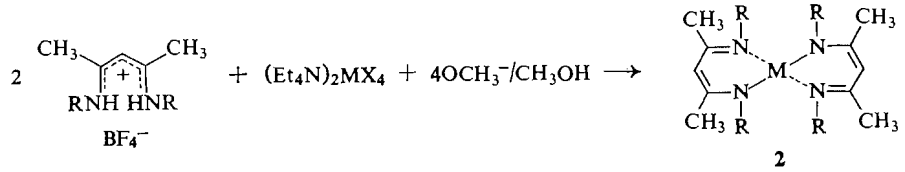

2

REACTION SCHEME 2

salts are given in Table I. They are all stable crystalline substances but are best protected from moisture. The corresponding free bases could be obtained by deprotonation of these salts by methoxide ion in anhydrous methanol. Data concerning these are recorded in Table II.

We chose for study the bis-bidentate copper, nickel, and cobalt complexes of these ligands, as most studies on related species have involved these metals. They were prepared, as shown in Reaction Scheme 2, essentially by the non-aqueous procedure of Everett and Holm (8) but with the use of methanol (in which all of the reactants are freely soluble) in place of *t*-butanol as solvent. Analytical and other data are given in Table III. In the preparation of the nickel and copper complexes **2** (R = H) the isolated products from the above reaction were not the simple bis-bidentate chelates but rather complexes of these with tetraethylammonium halide of the stoicheiometry $Et_4NX(ML_2)_2$. These were decomposed by shaking with water at room temperature to give the simple chelates. By heating them at 220 °/0.01 mm the simple chelates could again be obtained in the form of sublimates. It is likely that the initial product obtained in the preparation of the Co(II) complex in this series is also of this type as it is benzene insoluble. It proved to be too unstable toward air to permit purification and analysis. The nature of these complexes is not known. The ligand field spectra of the solids and their solutions in methanol were the same as those of the simple chelates themselves. The nuclear magnetic resonance (n.m.r.) spectrum of the diamagnetic nickel complex in deuterated dimethyl

Can. J. Chem. Downloaded from www.nrcresearchpress.com by 210.87.254.6 on 09/05/12
For personal use only.

TABLE III

Characterization of the metal complexes **2**

R	Metal	Melting point (°C)	Color	%C		%H		%N	
				Calcd.	Found	Calcd.	Found	Calcd.	Found
H	Cu	145–146*	green	46.93	46.80	7.04	7.22	21.76	22.08
H	Ni	245–255*	red	47.46	47.43	7.17	6.75	22.15	22.11
H	Co†	—*	orange	—	—	—	—	—	—
Me	Cu	150*	purple	53.57	53.55	8.36	8.27	17.85	17.52
Me	Ni	165–166	brown	54.39	54.25	8.48	8.28	18.12	17.94
Me	Co	164–165*	orange	54.36	54.40	8.47	8.46	18.11	18.46
Et	Cu	98–101	blue–black	58.40	58.28	9.26	9.27	15.15	15.43
Et	Ni	65–66	brown	59.20	59.32	9.39	9.35	15.36	15.16
Et	Co	50–51	orange	59.17	58.97	9.37	9.32	15.35	15.15
Ph	Cu	164	green–black	72.62	72.83	6.09	6.05	9.96	9.96
Ph	Ni	167–168	dark green	73.26	73.49	6.15	6.20	10.06	10.08
Ph	Co	143–145	orange–red	73.21	73.05	6.14	5.89	10.05	10.11

*Decomposed at the melting point.
†This compound was too unstable to permit analysis, but Mol. Wt. Calcd. for $C_{10}H_{18}N_4Co$: 253.0864. Found (mass spectrometry): 253.0867.

sulfoxide between 30–100 ° was a superimposition of the spectra of the simple chelate and tetraethylammonium halide in the same solvent. None of the *N*-substituted ligands gave similar complexes.

No chelates of the series with R = *i*-Pr could be obtained by the above method or by the similar but more vigorous conditions utilized by Collman and Kittleman in the synthesis of tris(β-ketoamino)Cr(III) complexes (9). We conclude that these are probably too sterically hindered to exist in either tetrahedral or planar forms, a fact also suggested by an examination of molecular models. For the complexes listed in Table III optical spectra between 5000 and 25 000 cm^{-1} were measured. These were all virtually identical in both the solid state and in non-coordinating solvents. They are recorded in Table IV and graphically in Figs. 1–3. Effective magnetic moments were also obtained as shown in Table V. In addition the solution molecular weights of those complexes of sufficient stability were measured osmometrically and are given in Table VI. A discussion of the data obtained is given below separately for each metal series.

Copper Complexes

The complex with R = H is monomeric in solution. Its ligand field spectrum possesses only one band centered at 15 600 cm^{-1}. This single band is very similar to that observed in known square planar bis(salicylideniminato)copper complexes at around 16 000 cm^{-1} (10–13). We accordingly assign this coordination geometry to the complex. The value of μ_{eff} of 1.86 BM is consistent with the slightly lower orbital contribution expected for this stereochemistry (14), and is to be compared with those of the three *N*-substituted complexes which lie between 1.94 and 1.98 BM. Of these three substituted complexes only one, **2** (R = Me), gave an acceptable value for the molecular weight as a monomer in solution, the remaining two giving values more than 5% below that calculated for the monomeric species. The close resemblance in their electronic spectra, however, strongly suggests that they are all similarly constituted. These spectra are very different from that of the unsubstituted case, and exhibit evidence of three or four bands. In this they bear a resemblance to the spectrum of bis(*N*-*t*-butylsalicylideniminato)-Cu(II) (13) which has been shown by *x*-ray analysis to possess a distorted tetrahedral geometry (15). Splitting of the ground and excited states with a resultant multiplicity in the one transition allowed for perfectly tetrahedral copper has been predicted for the distorted tetrahedral orientation (16). The dangers in assigning extreme square planar or tetrahedral geometries to four-coordinate copper from ligand field spectra have been pointed out (17). We conclude that while the three *N*-substituted complexes are almost certainly of the distorted tetrahedral type there is no evidence to indicate how close to pure tetrahedral they may be individually.

Nickel Complexes

The complex with R = H is diamagnetic in both the solid state and in solution. Its n.m.r. spectrum has absorptions for the methyl and

Can. J. Chem. Downloaded from www.nrcresearchpress.com by 210.87.254.6 on 09/05/12
For personal use only.

Can. J. Chem. Downloaded from www.nrcresearchpress.com by 210.87.254.6 on 09/05/12
For personal use only.

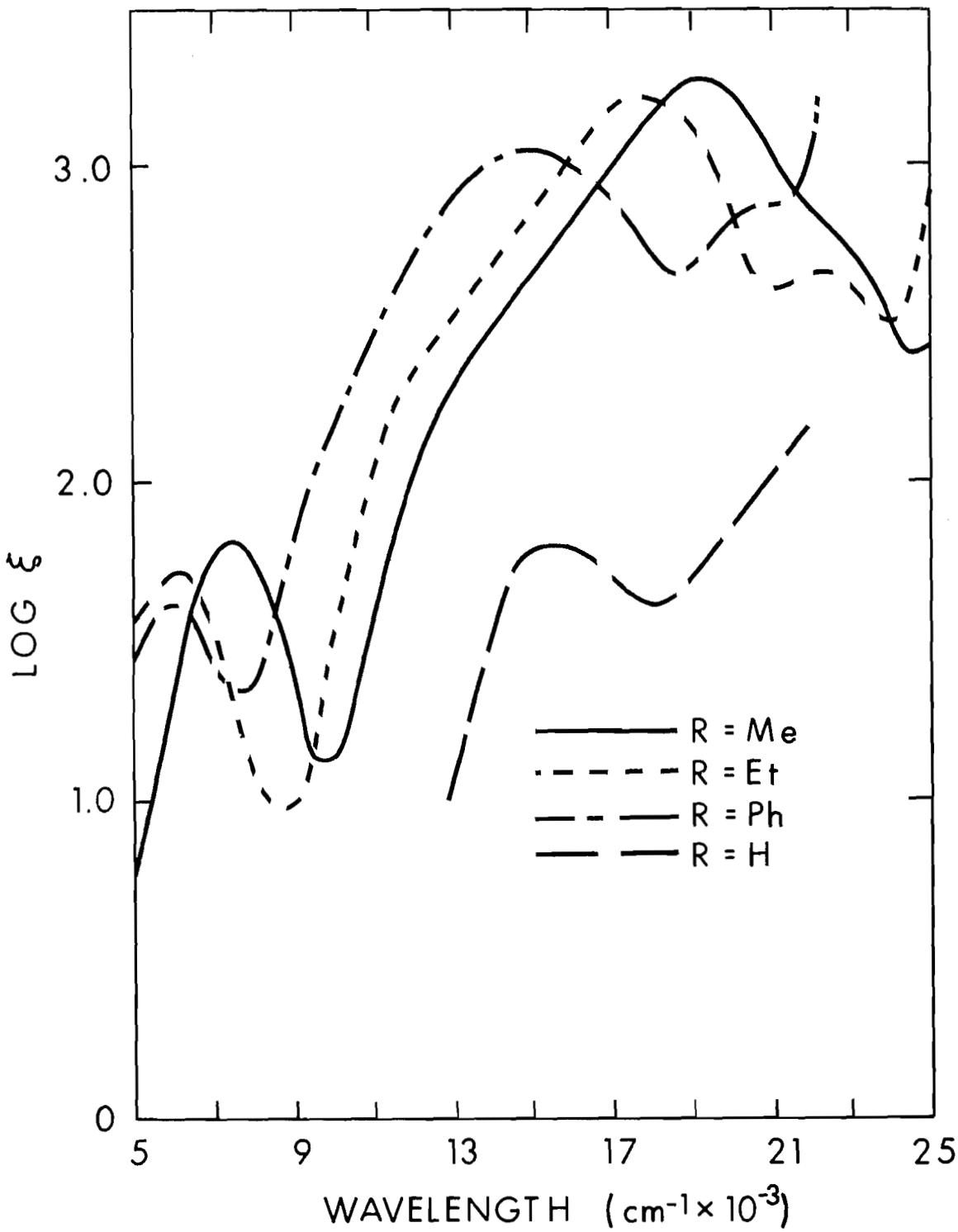

FIG. 1. Optical spectra of the bis-bidentate copper complexes.

Can. J. Chem. Downloaded from www.nrcresearchpress.com by 210.87.254.6 on 09/05/12
For personal use only.

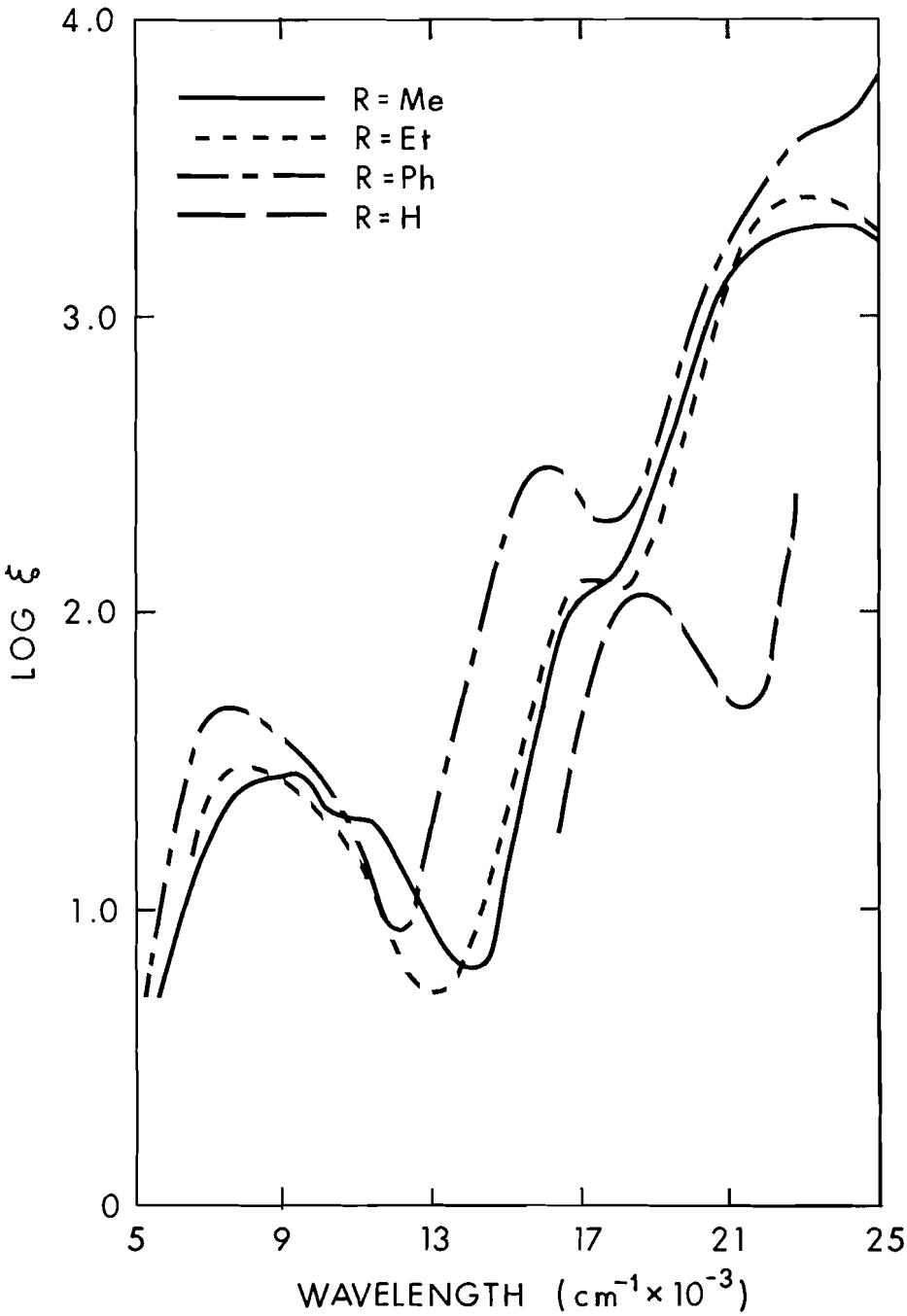

FIG. 2. Optical spectra of the bis-bidentate nickel complexes.

Can. J. Chem. Downloaded from www.nrcresearchpress.com by 210.87.254.6 on 09/05/12
For personal use only.

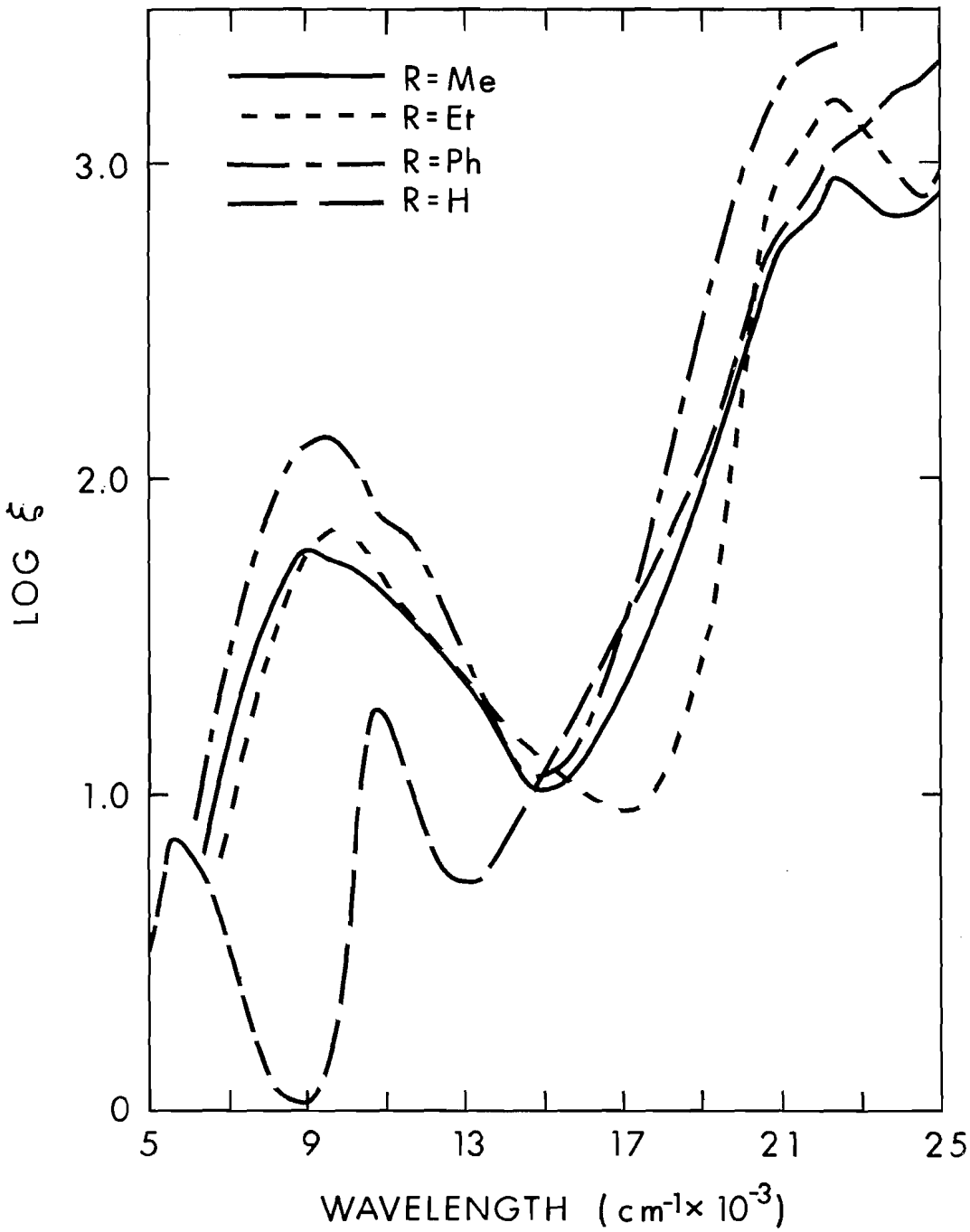

FIG. 3. Optical spectra of the bis-bidentate cobalt complexes.

TABLE IV

Spectral data for complexes **2** between 5000 and 25 000 cm^{-1}

R	Metal	Medium	Spectral maxima and extinction coefficients					
H	Cu	Soln.			15 600 (53)			
		Solid			16 100 (max)			
Me	Cu	Soln.	7400 (66)		12 500 (sh)	19 300 (1850)		23 200 (sh)
		Solid	7400 (max)		12 000 (sh)	19 300 (max)		22 500 (sh)
Et	Cu	Soln.	6060 (51)		12 500 (sh)	17 800 (1620)		22 600 (411)
		Solid	6450 (max)		12 000 (sh)	16 700 (max)		21 800 (sh)
Ph	Cu	Soln.	5900 (41)		—	14 800 (1107)		20 400 (sh)
		Solid	5900 (max)		11 300 (sh)	15 000 (max)		19 600 (sh)
H	Ni	Soln.				18 700 (115)		
		Solid				18 700 (max)		
Me	Ni	Soln.	9100 (sh)	9 500 (28)	10 750 (sh)	17 100 (sh)	22 750 (sh)	24 400 (1900)
		Solid	9100 (sh)	9 500 (max)	10 200 (sh)	17 250 (sh)	22 200 (max)	—
Et	Ni	Soln.	7400–9100 (28)		10 250 (sh)	17 200 (123)	22 200 (sh)	23 700 (2380)
		Solid		10 200 (max)	10 500 (sh)	17 200 (max)	—	—
Ph	Ni	Soln.	7350 (46)		10 000 (sh)	16 000 (310)	—	23 600 (sh)
		Solid	7400 (sh)	8 350 (max)	11 100 (sh)	15 900 (max)	19 500 (sh)	—
H	Co	Soln.	5500–6500 (7)		10 750 (20)	20 400 (sh)	22 200 (sh)	24 100(sh)
		Solid	—	—	10 500 (max)	—	—	—
Me	Co	Soln.	9100 (59)	10 000 (sh)	—	13 300 (sh)	21 000 (sh)	22 500 (880)
		Solid	9000 (max)	10 200 (sh)	10 600 (sh)	13 300 (sh)	21 000 (sh)	22 500 (max)
Et	Co	Soln.	9700 (67)	11 800 (sh)	—	—	21 000 (sh)	22 500 (1600)
		Solid	9700 (max)	10 200 (sh)	13 100 (sh)	14 700 (sh)	—	—
Ph	Co	Soln.	9400 (135)	11 100 (sh)	12 900 (sh)	—	21 800 (sh)	—
		Solid	9350 (max)	11 800 (sh)	12 800 (sh)	—	21 500 (sh)	—

TABLE V

Magnetic moments of the complexes **2**

R	Metal	Solid μ_{eff} BM	Solvent	Solution μ_{eff} BM
H	Cu	1.86	—	—
Me	Cu	1.98	—	—
Et	Cu	1.98	—	—
Ph	Cu	1.94	—	—
H	Ni	dia		dia
Me	Ni	3.13	CH_2Cl_2	3.08
Et	Ni	3.12	$CHCl_3$*	3.11
Ph	Ni	3.21	CH_2Cl_2	3.12
H	Co	2.22	C_6H_6	2.29
Me	Co	4.51	$CHCl_3$	4.45
Et	Co	4.30	$CHCl_3$	4.28
Ph	Co	4.39	$CHCl_3$	4.36

*Freed from ethanol.

TABLE VI

Molecular weights in solution of the complexes **2**

R	Metal	Solvent	Molecular weights Calcd.	Found
H	Cu	PhH	257	250
Me	Cu	PhH	313	323
Me	Ni	CH_2Br_2	309	319
Et	Ni	Me_2CO	365	351
Ph	Ni	Me_2CO	557	555
Et	Co	PhH	365	344
Ph	Co	Me_2CO	557	547

vinylic protons at τ 8.14 and 5.40 (triplet, $J = 2$ c.p.s.), which correspond within 5 c.p.s. to their positions in the free ligand base. The protons on nitrogen appear as a broad band, τ 6.1–6.6, and are responsible through long range coupling for the splitting of the vinylic proton to a triplet. The ligand field spectrum of the complex exhibits one band at 18 700 cm^{-1} which is identical in position with that of known square planar diamagnetic bis(dipivaloylmethanato)Ni(II) (18), and can be assigned to a singlet–singlet transition centered on nickel. This complex is therefore similar to other four-coordinate nickel complexes, with oxygen, sulfur, or nitrogen donor atoms, in preferring to adopt a planar diamagnetic configuration in the absence of significant steric strain. For each of the three *N*-substituted complexes the values of μ_{eff} for the solid and solution are within 2% of each other. These values which range from 3.08 to 3.22 BM lie slightly lower than those, 3.18 to 3.37 BM, observed for fully paramagnetic bis-(β-ketoamino)Ni(II) complexes of proven pseudotetrahedral geometry. Since, however, molecular weight studies on the three, indicated

Can. J. Chem. Downloaded from www.nrcresearchpress.com by 210.87.254.6 on 09/05/12
For personal use only.

absence of association in solution at molarities of the same order of magnitude as those used in the determination of μ_{eff}, one may conclude that they are likewise strictly four-coordinate and adopt a pseudotetrahedral geometry in both the solid and in non-coordinating solvents. This is supported by the ligand field spectra, which are virtually identical in solid and solution phases and show features similar to those of the above-mentioned pseudotetrahedral bis(β-ketoamino)-complexes (8). The evidence does not permit us to exclude 5% or less of the diamagnetic planar form in equilibrium in solution with the tetrahedral, but it is apparent that the latter must greatly predominate. This is to be compared with similarly substituted bis(aminotroponeiminato)Ni(II) complexes **3** which at room temperature are <1% paramagnetic for R = CH_3, 50–75% for R = Ar, and >99% for R = Et (19). It is evident that the greater steric repulsions among the substituents on nitrogen expected for the six membered chelate rings of **2** destabilize the planar form relative to the tetrahedral much more than in the five membered rings of **3**.

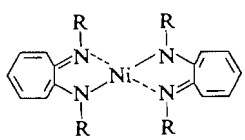

3

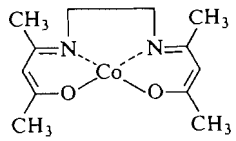

4

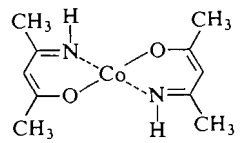

5

Cobalt Complexes

A situation exists with these complexes similar to that for the other two series. The complex with R = H is low spin in both the solid and benzene solution. The two values of μ_{eff} are within 4% of each other and in the range, 2.2 to 2.9 BM, considered characteristic of low spin Co(II) (20). Its ligand field spectrum, identical in the solid and in solution, is characterized by the presence of a narrow band at 11 000 cm^{-1} (ε 20). This band, although shifted to higher frequency, closely resembles in shape and intensity that observed in the spectra of other low spin four-coordinate complexes of cobalt, such as *N,N'*-ethylenebis(4-amino-3-penten-2-onato)-Co(II) (**4**) (21), which have been assigned a square planar configuration. In these latter it is considered characteristic of low spin planar Co(II). We therefore assign this geometry to the complex in question. Holm and Everett have shown for the similarly constituted complex **5** that an equilibrium between low spin planar and high spin tetrahedral forms exists in solution, in which the latter is present to about 70% at room temperature. The evidence presented here does not exclude 5% or less of the tetrahedral form in equilibrium with the planar in solution. The absence, however, of any significant concentration of the tetrahedral form in solution indicates that for this ligand there is a greater free energy difference between the two forms than exists between those of **5**. This difference can scarcely be steric in origin and is probably a consequence of the greater field strength of the diketimine ligand.

The remaining three complexes have μ_{eff} between 4.28 and 4.51 BM and are therefore fully high spin. The adequate stability of two of them toward oxygen permitted molecular weight determinations to indicate their monomeric nature in solution. The near identity of the optical spectra of the complex with R = Et and that with R = Me in solution makes it clear that the latter must also be monomeric under these conditions. In general the ligand field spectra of the three are very similar and feature a broad band at ~10 000 cm^{-1} with a high frequency shoulder at ~12 000 – 13 000 cm^{-1}, and a visible band at ~22 000 cm^{-1} with a low frequency shoulder. These spectra, although shifted to higher frequencies, closely resemble in outline those of bis(*N* - isopropylamino - 3 - penten - 2 - onato)Co(II) (21) which has been convincingly shown to possess a pseudotetrahedral structure. We therefore consider that the three *N*-substituted complexes have this structure.

The cobalt complexes show an increasing lability toward oxygen with decreasing size of the substituent on nitrogen. In the case of the ligand with R = H it proved possible to synthesize the tris(diketimine)Co(III) complex by passing dry air into a solution of the ligand and Co (II) in the ratio of 3:1. This is a deep red diamagnetic complex which has no discrete band in the visible or near infrared portions of the spectrum. Although oxidation clearly took place, attempts to synthesize the corresponding tris-

Can. J. Chem. Downloaded from www.nrcresearchpress.com by 210.87.254.6 on 09/05/12
For personal use only.

Can. J. Chem. Downloaded from www.nrcresearchpress.com by 210.87.254.6 on 09/05/12
For personal use only.

Co(III) complexes of the substituted ligands under the above conditions yielded none of the desired compounds.

Experimental

General

Melting points were taken on a Kofler melting point apparatus and are uncorrected. Analyses were performed by the Microanalytical Laboratory of this department. All measurements on the complexes were performed on freshly purified samples. Optical spectra were obtained on a Cary 14 spectrophotometer. Solution spectra were taken in benzene or chloroform (ethanol free). Solid state spectra were measured by absorption (pressed KBr disk) between 5000 and 10 000 cm^{-1}, and by reflectance between 10 000 and 25 000 cm^{-1}. Magnetic susceptibilities of solids were obtained by the Faraday technique with χ_g for $HgCo(CNS)_4 = 16.44 (\pm 0.08) \times 10^{-6}$ c.g.s. at 293 °K taken as the reference (22). Magnetic susceptibilities of substances in solution were obtained by a nuclear magnetic resonance (n.m.r.) method (23). The solutions for this were prepared under nitrogen, placed in n.m.r. tubes, transferred to a high vacuum line, degassed, and sealed. The Curie Law was used in the evaluation of μ_{eff} from χ_M corrected. Molecular weights in solution were determined on a Mechrolab Osmometer. Accurate molecular weights were obtained on an A.E.I. M.S.9 double focussing mass spectrometer.

Preparation of the Ligands **1**, *(R = H, Me, Et, i-Pr, Ph)*

The preparations of the five ligand salts are very similar and only two are given in detail. Characterizing data are given in Table I.

4-Amino-3-penten-2-immonium Fluoborate **1**, *(R = H)*

Triethoxonium fluoborate (24) (25 g, 0.131 mole) dissolved in dichloromethane (50 ml) was added to a stirred solution of 4-amino-3-penten-2-one (13 g, 0.131 mole) in the same solvent (100 ml). The resulting solution was allowed to stand for 30 min. A solution of anhydrous 3.28 *N* ethanolic ammonia (40 ml) was then added dropwise over a period of 20 min to the stirred reaction mixture. This was allowed to stand a further 10 min, and was then filtered to remove the ammonium fluoborate (3 g). The filtrate, upon concentration at room temperature *in vacuo* to ca. 1/3 of its volume, deposited the crystalline immonium salt (11 g, 45%) in pure form.

The three *N,N'*-dialkyl analogues were prepared by this procedure. In all cases a small amount of amine fluoborate salt had to be removed prior to concentration of the reaction mixture. Yields ranged from 40 to 60%.

N,N'-Diphenyl-4-amino-3-penten-2-immonium Fluoborate **1**, *(R = Ph)*

Triethoxonium fluoborate (4 g, 0.021 mole) in dichloromethane (10 ml) was added dropwise to a stirred solution of 4-*N*-phenylamino-3-penten-2-one (3.68 g, 0.021 mole) in the same solvent (10 ml). The mixture was allowed to stand for 30 min and a solution of aniline (1.96 g, 0.021 mole) in dichloromethane (5 ml) was added. After 1 h the solvent was removed completely *in vacuo* and the residual oil was dissolved in hot ethyl acetate and allowed to crystallize to give the product (5.91 g, 83%).

The ligand salts may all be further purified by recrystallization from acetone – ethyl acetate. The corresponding free bases were obtained from the salts by treatment with an equivalent amount of 0.5 *M* sodium methoxide in methanol. The methanol was removed *in vacuo*, at, or below room temperature, and the residue extracted into benzene. The benzene solution was filtered and taken cautiously to dryness *in vacuo* at room temperature. In the phenyl substituted case the product was crystallized from pentane at 0 °C. The others were sublimed at 50–100 °/0.1 mm on to a cold finger (< 0 °C). Characterizing data are given in Table II.

Bis-bidentate Complexes **2**

These were all generated in the same way by the addition under nitrogen of ca. 1 mmole of Et_4NMX_4 (M = Cu, Ni, Co; $X_4 = Cl_4$ or Br_4) in anhydrous methanol (5–10 ml) to a stirred solution of 2 equivalents of the ligand fluoborate salt in 4 equivalents of anhydrous 0.5 *N* sodium methoxide in methanol. The reaction mixture was then stirred for a further 10 min. The reaction was kept at room temperature throughout and the product was isolated as follows:

2 *(R = H; M = Ni, Cu)*

The precipitate formed was collected and shaken with water and benzene until complete dissolution had occurred. The product was isolated from the benzene layer and recrystallized from benzene–hexane.

2, *(R = H; M = Co)*

The precipitate formed was removed by filtration and dried under nitrogen. It was then transferred rapidly to a sublimation apparatus and the complex isolated by sublimation at 180–220 °C/0.005 mm. It was then sealed *immediately* in a vial under nitrogen.

2, *(R = Ph; M = Cu, Ni, Co; and R = Me; M = Ni)*

The precipitate formed was collected and dissolved in benzene. The solution was then filtered. Crystallization was induced by the addition of methanol to the concentrated solution.

2, *(R = Me; M = Cu, Co)*

The precipitate formed was collected and dissolved in warm hexane. The solution was filtered, concentrated, and allowed to crystallize to give the product.

2, *(R = Et; M = Cu, Ni, Co)*

The reaction mixture was taken to dryness *in vacuo* and the residue washed with warm benzene. The benzene solution was filtered, concentrated, and crystallization induced by the addition of methanol with strong cooling.

The complexes were purified by sublimation at 100–150 °C/0.01 mm except for the phenyl series which were recrystallized from benzene–methanol. These complexes are all sensitive to atmospheric moisture and the cobalt series to oxygen. Therefore, they were stored in sealed vials under nitrogen. Yields ranged from 30 to 80%.

Tris(4-amino-3-penten-2-oneiminato)Co(III)

A solution of Et_4NCoBr_4 (327 mg) in methanol (5 ml) was added under nitrogen to a stirred solution of 4-amino-3-penten-2-immonium fluoborate (285 mg) in 6.1 ml of 0.5 *N* sodium methoxide in methanol. An immediate yellow precipitate of the $[L_2Co(II)]_2Et_4NBr$ complex (see text) formed. Stirring was continued and dry air was passed into the apparatus for 30 min. The

solution darkened and a red precipitate formed. This was collected and crystallized from benzene. The analytical sample had m.p. 215–220 °C (decomp.). It did not give a satisfactory combustion analysis.

Mol. Wt. Calcd. for $C_{15}H_{27}N_6Co$: 350.1629. Found mass spectrometry): 350.1630.

Acknowledgments

The author is grateful to Mr. G. Harvie for technical assistance and to Mr. E. D. Day for his help in obtaining magnetic moments and reflectance spectra. He also wishes to acknowledge financial support accorded him by the National Research Council of Canada.

1. R. H. Holm, A. Chakravorty, and G. W. Everett, Jr. Progr. Inorg. Chem. 7, 83 (1966).
2. S. H. H. Chaston and S. E. Livingstone. Australian J. Chem. **20**, 1065 (1967), and earlier papers; Von E. Uhlemann and Ph. Thomas. J. Prakt. Chem. **34**, 180 (1966).
3. R. L. Martin and I. M. Stewart. Nature, **210**, 522 (1966); R. Beckett and B. F. Hoskins. Chem. Commun. 909 (1967); K. Krauer, P. Hemmerich, and J. D. W. van Voorst. Angew. Chem. Intern. Ed. Engl. **6**, 262 (1967).
4. W. Bradley and I. Wright. J. Chem. Soc. 640 (1956).
5. G. Scheibe. Chem. Ber. **56**, 137 (1923); G. Schwarzenbach and K. Lutz. Helv. Chim. Acta, **23**, 1139 (1940); K. L. Wierzchowski, D. Shugar, and A. R. Katritzky. J. Am. Chem. Soc. **85**, 827 (1963); L. C. Dorman. Tetrahedron Letters, 459 (1966).
6. N. H. Cromwell. Chem. Rev. **38**, 83 (1946).
7. H. Meewein, W. Florian, N. Schon, and G. Stopp. Ann. **641**, 1 (1961); H. Bredereck, F. Effenberg, and D. Zeyfang. Angew. Chem. Intern. Ed. Engl. **4**, 242 (1965).
8. G. W. Everett, Jr. and R. H. Holm. J. Am. Chem. Soc. **87**, 2117 (1965).
9. J. P. Collman and E. T. Kittleman. Inorg. Chem. **1**, 499 (1962).
10. E. C. Lingafelter, G. L. Simmons, B. Morosin, C. Scheringer, and C. Freiburg. Acta Cryst. **14**, 1222 (1961).
11. R. L. Belford and W. A. Yeranos. Mol. Phys. **6**, 121 (1963).
12. J. Ferguson. J. Chem. Phys. **34**, 1609 (1961).
13. L. Sacconi and M. Ciampolini. J. Chem. Soc. 276 (1964).
14. B. N. Figgis. Nature, **182**, 1568 (1958).
15. T. P. Cheeseman, D. Hall, and T. N. Waters. J. Chem. Soc. A, 685 (1966).
16. C. Furlani and G. Morpurgo. Theoret. Chim. Acta, **1**, 102 (1963).
17. T. P. Cheeseman, D. Hall, and T. N. Waters. J. Chem. Soc. 694 (1966).
18. F. A. Cotton and J. P. Fackler. J. Am. Chem. Soc. **83**, 2818 (1961).
19. D. R. Eaton, W. D. Phillips, and D. J. Caldwell. J. Am. Chem. Soc. **85**, 397 (1963).
20. B. N. Figgis and J. Lewis. Progr. Inorg. Chem. **6**, 192 (1965).
21. G. W. Everett, Jr. and R. H. Holm. J. Am. Chem. Soc. **88**, 2442 (1966).
22. B. N. Figgis and R. S. Nyholm. J. Chem. Soc. 4190 (1958).
23. D. F. Evans. J. Chem. Soc. 2003 (1959).
24. H. Meerwein. Org. Syn. **46**, 113 (9166).

Can. J. Chem. Downloaded from www.nrcresearchpress.com by 210.87.254.6 on 09/05/12
For personal use only.

Steroids and steroidases. VII.[1] A unique long-range directing effect exerted by the cholestane C_8H_{17} group on the formation of A-homosteroid ketones

J. Bryan Jones and J. Malcolm Zander
Department of Chemistry, Lash Miller Chemical Laboratories, University of Toronto, Toronto 5, Ontario
Received January 15, 1968

The diazomethane homologation of a broad spectrum of variously C-17-substituted steroid-3-ketones has shown that the C_8H_{17} cholestane side chain exerts a unique influence on the direction of the ring enlargement reaction. This long-range effect is not explicable in terms of polar or conformational transmission.

Canadian Journal of Chemistry, 46, 1913 (1968)

Can. J. Chem. Downloaded from www.nrcresearchpress.com by 210.87.254.6 on 09/05/12
For personal use only.

An earlier study (1), based on literature comparisons, had indicated that a C-17 C_8H_{17} substitutent influenced the direction of ring enlargement of steroid-3-ketones. During the course of a parallel investigation of the related Tiffeneau–Demjanov reaction, the diazomethane homologations of 5α- and 5β-cholestan-3-one were reinvestigated. The results obtained[2] (Table I) confirmed the published data for the 5α-series (2, 3) and further showed that the effect of the C_8H_{17} group was also manifest in the 5β-series.

These observations prompted us to study the homologation of a broad spectrum of variously C-17 substituted 3-ketosteroids. The data obtained (Table I) show that the cholestane C_8H_{17} group exerts a unique influence which cannot be satisfactorily rationalized in terms of the concepts (4) normally invoked to account for long-range directing effects. Furthermore, the observed effect is unusual in that it is reflected in the nature of the products. Relatively few examples of this kind have been documented (5); most steroidal long-range effects manifest themselves in rate differences.

Most of the steroid-3-ketones (1) used in this study were purchased or were obtained by standard procedures from readily available starting materials as indicated in the Experimental section. Real difficulties in obtaining pure starting material were experienced only in the preparation of 17β-hydroxy-5β-estran-3-one (**1***k*).

The preparation of **1***k* has been investigated by several groups (6–9). All of the methods involved hydrogenation of 17β-hydroxyestr-4-en-3-one and, not surprisingly, even the more successful procedures (6, 9) gave mixtures of the 5α and 5β epimers. Separation of the epimers proved to be a difficult process and it is now apparent that complete purification of the 5β-estran **1***k* was not previously achieved.

The most successful of the literature conditions were those of Counsell (9) in which 17β-hydroxyestr-4-en-3-one was hydrogenated in the presence of 5% palladium on charcoal and potassuim hydroxide, and accordingly, this procedure was repeated in the current investigation. The hydrogenation product contained the expected mixture of epimers from which, after repeated chromatographic separations on large quantities of alumina, it proved possible to isolate pure 17β-hydroxy-5β-estran-3-one (**1***k*), albeit in low (25%) yield. Optical rotatory dispersion (o.r.d.) proved to be the only reliable analytical tool and the chromatographic purifications were continued until the samples of **1***k* had constant o.r.d. spectra.

The basic experimental procedure used for the diazomethane homologations of most of the ketones **1***a*–**1***k* was a modification of that developed by Nelson and Schut (2), the diazomethane being generated *in situ* by the addition of *N*-nitrosomethylurea to the steroid-3-ketone and potassium hydroxide in methanol–ether solution. The main exceptions to this general method involved the base-labile acetates **1***d* and **1***h* which were homologated in methanol–ether–water solution by the addition of *ex situ* generated ethereal diazomethane, from which all traces of potassium hydroxide had been removed.

[1]For Part VI of this series, see J. B. Jones and D. C. Wigfield. Can. J. Chem. **46**, 1459 (1968).
[2]J. B. Jones and P. Price. To be published.

TABLE I

Ratios of A-homo-3- and 4-ketones produced by diazomethane homologation of 3-ketosteroids*

Compound	A/B configuration	R	R_1	R_2	Product Ratio (2:3)†
1*a*	5α	CH_3	OH	H	41:59‡ ±3%
1*b*	5α	CH_3	H	OH	45:55 ±3%
1*c*	5α	CH_3	H	H	42:58‡ ±3%
1*d*	5α	CH_3	OAc	H	45:55 ±3%
1*e*	5α	CH_3	OH	CH_3	38:62 ±3%
1*f*	5α	CH_3	C_8H_{17}	H	79:21[2] ±3% (83:17) (2) (95:5) (3)
1*g*	5α	H	OH	H	40:60 ±3%
1*h*	5α	H	OAc	H	45:55 ±3%
1*i*	5β	CH_3	C_8H_{17}	H	22:78[2] ±3%
1*j*	5β	CH_3	OH	H	50:50 ±3%
1*k*	5β	H	OH	H	39:61 ±3%

*The reaction can be represented as:—

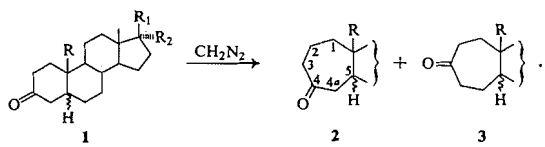

†Overall yields of A-homoketones 60–80%; >95% of total material accounted for.
‡Preferred ratio *cf.* less accurate value quoted in ref. (1) which was obtained prior to the development of the o.r.d. analytical method.

The homologations were monitored by gas–liquid phase chromatography (g.l.c.) and the reactions were terminated when an optimum balance between the disappearance of starting material and the formation of bis-homo products was reached. The isomeric A-homoketones **2** and **3** were then isolated by column chromatography. Optical rotatory dispersion proved to be the best analytical tool since the pairs of A-homoketones were indistinguishable by g.l.c. and differences in their thin-layer chromatographic (t.l.c.) behavior were at best marginal. In some cases the extreme similarity in the chromatographic behavior of the A-homo-isomers resulted in substantial numbers of fractions containing varying proportions of both A-homoketones. In these situations the mixed A-homoketone fractions were combined, evaporated, and the o.r.d. spectrum of the mixture measured; from a knowledge of the o.r.d. amplitudes of the pure A-homoketones the amount of each present was calculated.

For the homologation of 5α-androstan-3-one (**1***c*) it was necessary to rely completely on this latter method to determine the relative proportions of the A-homoketones **2***c* and **3***c* since their complete chromatographic separation was not possible. The authentic samples of **2***c* and **3***c* required for the reference o.r.d. spectra were prepared as indicated in Chart 1.

The product ratios observed for the homologation of **1***a*–**1***k* are summarized in Table I. For the most thoroughly studied compound, **1***a*, the product ratio was insensitive to the amount of diazomethane added (twofold–sevenfold excess) and to variations in the polarity of the solvent used. However, the rates of homologation were very slow when methanol was completely excluded (10). The reaction was unaffected by the presence or absence of potassium hydroxide.[3]

As Table I shows, significant departure from a ~ 40:60 A-homo-4 to 3-ketone ratio occurs only for the 3-ketosteroids possessing the cholestane side chain at C-17. It is of interest to note that the deviations due to the C_8H_{17} group are approximately equal, but in opposite directions, for the 5α- and the 5β-series.

Attempts to explain the role of the C_8H_{17} substituent in terms of polar inductive effects

[3]This observation contrasts inexplicably with the reported potassium hydroxide dependence of the 5α-cholestan-3-one reaction (3).

Can. J. Chem. Downloaded from www.nrcresearchpress.com by 210.87.254.6 on 09/05/12
For personal use only.

Can. J. Chem. Downloaded from www.nrcresearchpress.com by 210.87.254.6 on 09/05/12
For personal use only.

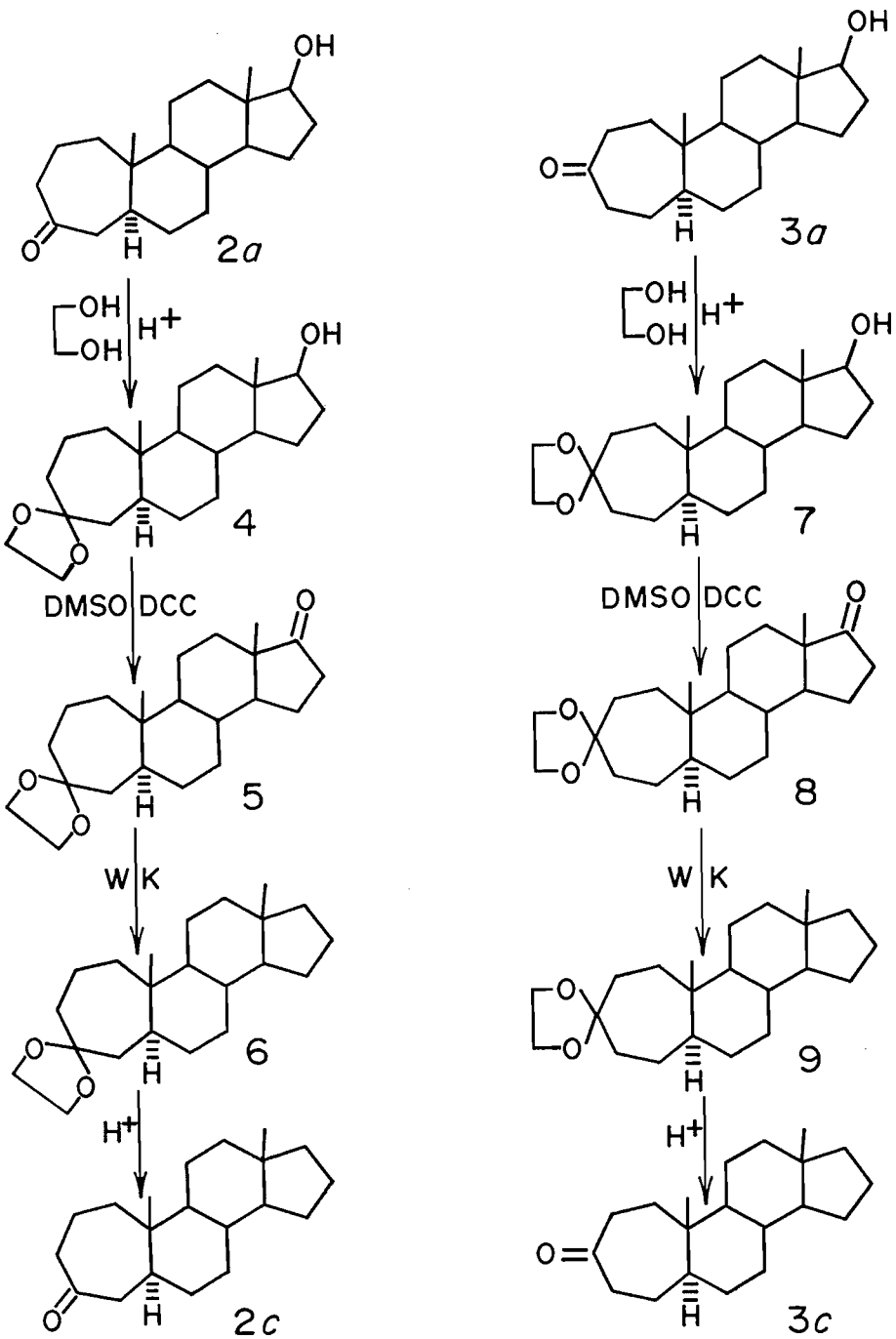

CHART 1

Can. J. Chem. Downloaded from www.nrcresearchpress.com by 210.87.254.6 on 09/05/12
For personal use only.

(4, 11) of the other C-17 groups, are not convincing since compounds bearing C-17 substituents of widely different polarity, such as **1***a*–**1***e* give virtually identical proportions of the corresponding A-homo-4 and 3-ketones.

Alternative explanations involving the through-solvent interaction of C-17 partial cationic charges, with the developing transition state (11) can be ruled out for the same reasons. In addition, such an interaction should be influenced by the solvent polarity whereas, as stated earlier, no solvent dependence of the product ratio from **1***a* was observed.

Any rationale based on conformational transmission (4) is equally unattractive. There is strong circumstantial evidence (12–15) that compounds **1***a*–**1***e* will encompass a range of ring D conformations (including the α- and β-envelopes and half chair) which will induce correspondingly different distortions of the C/D ring junction, and hence dissimilar ring A conformations, whereas again the product ratios are essentially invariant for this group of compounds. That the C-19 angular methyl group has little effect on the course of the reaction, cf. **1***a* and **1***g*, **1***d* and **1***h*, and **1***j* and **1***k*, provides further evidence that conformational transmission is not an important factor.

The manner in which the C_8H_{17} group is able to cause the formation of one of the two possible A-homoketones to be so much preferred is not yet clear. Its presence obviously induces a significant energy difference between the two competing homologation pathways.[4]

The special character of the cholestane side chain also manifests itself in other ways. For example, the chromatographic behaviors of **2***f* and **3***f* are anomalous in that the 3-ketone is eluted from alumina before the 4-one. For all A-homoandrostane and estrane–ketones, the converse is observed. Also, the o.r.d. curves of **2***f*, **3***f*, and **3***i* are atypical, the amplitudes of their Cotton effects being only 30–50% as intense as those of the analogous A-homoandrostane and estrane–ketones.[2] (Abnormal effects due to micellar aggregation in aqueous solution of steroids containing a C_8H_{17} group have also been noted (17), and that micelle formation may be involved in the current long range effect has not yet been ruled out.)

It is hoped that the nature of the C_8H_{17} effect on the homologation reaction, and on the physical properties of A-homoketones, will be clarified by the experiments now in progress which are systematically examining the influence exerted by C-17 hydrocarbon substituents. The direction of addition of diazomethane to the C-3 carbonyl may also be significant and accordingly, the influence of the configuration of the intermediate adduct on the rearrangement is currently under investigation.[2]

[4]For an ~80:20 product ratio to be given, the predominant reaction must be preferred by ~0.8 kcal mole^{-1} (16) whereas the ~40:60 distribution observed for the majority of the ring enlargement reactions represents an almost insignificant free energy difference of only ~0.2 kcal mole^{-1} (16) between the transition states involved.

Experimental

Infrared spectra were obtained on Beckmann IR8 and Perkin–Elmer 237-B spectrophotometers in chloroform solutions, and optical rotations on a Bendix–Ericsson 143A automatic polarimeter. Optical rotatory dispersions (o.r.d.) were measured on a Jasco–Durrum ORD 5 spectropolarimeter at 25 °C. Melting points were determined on a Fisher–Johns block and are corrected. All solvents for column chromatography were distilled before use; the alumina used was British Drug Houses chromatographic grade, which was deactivated by shaking with 5% of its own weight of 10% aqueous acetic acid; Florisil was activated by heating at 140 °C for 24 h prior to use. Gas–liquid phase chromatographic (g.l.c.) analyses were effected with columns containing 3% SE-30 and 1% QF-1 respectively on silanized "Chromosorb G" using an F and M model 400 biomedical unit. Thin-layer chromatography (t.l.c.) was performed on Merck silica gel G with benzene–ether (1:1) as the developing solvent; the spots were detected by spraying the chromatograms with aqueous toluene-*p*-sulfonic acid (1:1 w/w) followed by heating at 100 °C. All compounds described were purified until no impurity was detectable by t.l.c. or by g.l.c. on the two columns, and until a constant o.r.d. spectrum was obtained. Solvent removals were effected with a rotary evaporator at 25 °C.

Steroid-3-ketones

17β-Hydroxy-5α-androstan-3-one (**1***a*) and 17β-hydroxy-5β-androstan-3-one (**1***j*) were prepared as described previously (1). 17β-Hydroxy-17α-methyl-5α-androstan-3-one (**1***e*) was purchased from Searle Chemicals Inc., Chicago.

*17α-Hydroxy-5α-androstan-3-one (**1***b*)*

To a stirred solution of lithium (400 mg) in liquid ammonia (200 ml) was added 17α-hydroxyandrost-4-en-3-one (2 g) in dry dioxane–ether (3:1, 80 ml) during 15 min. Stirring was continued for 1 h and then ammonium chloride (5.2 g) was added. Following overnight evaporation of the ammonia, water (100 ml) was added, and the mixture extracted with chloroform (3 × 50 ml). The combined chloroform extracts were washed successively with 2 *N* hydrochloric acid (50 ml), saturated aqueous

Can. J. Chem. Downloaded from www.nrcresearchpress.com by 210.87.254.6 on 09/05/12
For personal use only.

sodium bicarbonate (50 ml) and water (50 ml). The dried ($MgSO_4$) chloroform solution was evaporated and the residue chromatographed on alumina. Elution with benzene followed by recrystallization from cyclohexane afforded 17α-hydroxy-5α-androstan-3-one (1.47 g) as needles, m.p. 179–180 °C (lit. (18), m.p. 179.5–180 °C); $[\alpha]_D^{24}$ +12.8 ± 0.4° (*c*, 1.2 in $CHCl_3$); ν_{max} 3600 and 1700 cm^{-1}.

*17β-Hydroxy-5α-estran-3-one (**1g**)*

17β-Hydroxyestr-4-en-3-one (3 g) in dry dioxane–ether (1:1, 72 ml) was reduced with lithium (600 mg) in liquid ammonia (300 ml) as described above. 17β-Hydroxy-5α-estran-3-one was obtained as fluffy needles (1.8 g) from hexane, m.p. 132–133 °C, (lit. (19) m.p. 130–131 °C); ν_{max} 1707 cm^{-1}; o.r.d. (*c*, 0.004 in CH_3OH); $[\phi]_{305}$ +4200°; $[\phi]_{270}$ −3500° (*a* = +77).

*5α-Androstan-3-one (**1c**)*

3β-Hydroxy-5α-androstan-17-one was subjected to the modified Wolff–Kishner reduction procedure of Mamlok and Jacques (20) and the 5α-androstan-3β-ol produced was oxidized with Jones' reagent (21). After chromatography on alumina (benzene elution) and recrystallization from acetone 5α-androstan-3-one was obtained in 80% overall yield as needles, m.p. 104–105 °C, $[\alpha]_D^{24}$ +23.3 ± 2° (*c*, 1.1 in $CHCl_3$), (lit. (22) m.p. 104.5–105.5 °C, $[\alpha]_D^{25}$ +25 ± 3°).

*17β-Hydroxy-5β-estran-3-one (**1k**)*

Hydrogenation at atmospheric pressure of 17β-hydroxyestr-4-en-3-one (5 g) in 95% ethanol (50 ml) containing potassium hydroxide (150 mg) and 5% palladium on charcoal (3.5 g) (9) gave a mixture of the 5α- and 5β-epimers **1*g*** and **1*k*** respectively. The crude product (2 g) was chromatographed on alumina (600 g); elution with benzene gave fractions containing the required 5β-compounds as evidenced by the negative Cotton effects of their o.r.d. spectra. These fractions were combined and were successively rechromatographed on alumina (300:1). After four such steps the molecular amplitudes of each of the 5β-fractions had reached the same constant value and the 17β-hydroxy-5β-estran-3-one they contained was then recrystallized from acetone–hexane as fluffy needles[5] (1.25 g), m.p. 125.5–126 °C; ν_{max} 3600 and 1700 cm^{-1}; o.r.d. (*c*, 0.004 in CH_3OH), $[\phi]_{304}$ −800°; $[\phi]_{262}$ +3100° (*a* = −39).

*17β-Acetates **1d** and **1h***

These were prepared in 85–90% yield by treatment of the corresponding 17β-hydroxy compound with pyridine–acetic anhydride for 12 h at 25 °C.

*17β-Acetoxy-5α-androstan-3-one (**1d**)*

This was obtained as needles from hexane, m.p. 159–160 °C, (lit. (24) m.p. 157 °C).

[5]This melting point for **1*k*** is significantly higher than those quoted in the literature viz. 106–108 °C (6) and 108–110 °C (9). (It is now clear that the compound m.p. 133.5 ° reported by Chen (7) is in fact 17β-hydroxy-5α-estran-3-one (cf. ref. (9)). These lower values are presumably due to contamination by the 5α-compound and the o.r.d. data support this view. The molecular amplitude (*a* = −30) (23) of the sample prepared by Counsell (9) indicates the presence of ~8% of **1*g*** (*a* = +77).

*17β-Acetoxy-5α-estran-3-one (**1h**)*

This was obtained as chunky prisms from hexane, m.p. 103–104 °C (lit. (7) m.p. 102–103 °C).

*Homologation of the Steroid-3-ketones **1** with Diazomethane*

General Procedures

(a) With in situ generated diazomethane (2)—The 3-ketosteroid and potassium hydroxide were dissolved in methanol–ether (1:1) and *N*-nitrosomethylurea was added during 15 min to the stirred, cold (0 °C), solution. The reaction mixture was stirred at 0 °C until analysis by g.l.c. showed optimum conversion to A-homoketones (~6 h). The reaction was then acidified by the dropwise addition of 2 *N* hydrochloric acid. The resulting solution was filtered, evaporated, and the residue dissolved in ether. After refiltration, the ether solution was evaporated and the crude product chromatographed on alumina (300–600:1) columns prepared in petroleum ether (b.p. 60–70 °C) or in petroleum ether (b.p. 60–70 °C)–benzene (1:1). Sufficiently careful chromatography was carried out to effect complete separation of the A-homoketones from the starting material remaining and from by-products such as epoxides, A-bishomoketones, etc. The presence of these contaminants was readily detected by g.l.c.; however, the isomeric A-homoketones were indistinguishable by this technique. The fractions containing only the A-homoketones were combined, and were rechromatographed (with benzene–ether elution) until their complete separation was achieved. Generally, the A-homo-4-ketones were eluted prior to the 3-ketones. The 4- to 3-ketones product ratios were then calculated directly from the isolated yields of each. The course of the purifications was monitored by o.r.d. and for the difficultly separable isomers, the composition of the mixed fractions was calculated from their composite o.r.d. spectra and from a knowledge of the o.r.d.'s of each of the pure component A-homoketones.

(b) With ex situ generated diazomethane—This method was applied mainly to the base-labile acetates **1*d*** and **1*h***.

A dried (KOH) ethereal solution of diazomethane (obtained from *N*-nitrosomethylurea, aqueous potassium hydroxide and ether (10)) was added to a cooled (0 °C) solution of the steroid-3-ketone in methanol – ether – water (5:5:1). After ~7 h the reaction was then worked up as described above.

The following compounds were prepared by method (*a*).

*17β-Hydroxy-A-homo-5α-androstan-4-one (**2a**) and -3-one (**3a**)*

These were prepared from 17β-hydroxy-5α-androstan-3-one (1.15 g; 3.9 mmoles), potassium hydroxide (1.54 g), *N*-nitrosomethylurea (1.11 g, 11 mmoles) and ether–methanol (1:1, 110 ml) (1). An overall A-homoketone yield of 81% was obtained, composed of 17β-hydroxy-A-homo-5α-androstan-4-one (30%), as plates from ethyl acetate, m.p. 193.5–194.5 °C, (lit. (25) m.p. 195–196 °C); ν_{max} 3600 and 1695 cm^{-1}; o.r.d. (*c*, 0.004 in CH_3OH) $[\phi]_{302}$ +8850°; $[\phi]_{261}$ −7050°; (*a* = +159); and 17β-hydroxy-A-homo-5α-androstan-3-one (51%), as needles from hexane, m.p. 211–212 °C (lit. (1) m.p. 212–213 °C); ν_{max} 3600 and 1695 cm^{-1}; o.r.d. (*c*, 0.004 in CH_3OH) $[\phi]_{302}$ −4700°, $[\phi]_{259}$ +5100°, (*a* = −98).

Can. J. Chem. Downloaded from www.nrcresearchpress.com by 210.87.254.6 on 09/05/12
For personal use only.

No significant change in the product ratio was observed when the potassium hydroxide free *ex situ* method was used, when the reaction was performed in solvents ranging in composition between methanol–ether (3:1) to methanol – ether – water (3:6:1), or when the diazomethane excess was varied twofold to sevenfold.

17α-Hydroxy-A-homo-5α-androstan-4- (2b) and -3-one (3b)

These were prepared from 17α-hydroxy-5α-androstan-3-one (2.2 g, 7.6 mmoles), potassium hydroxide (2.1 g) and *N*-nitrosomethylurea (1.56 g, 15.2 mmoles) in methanol–ether (1:1, 150 ml). From the A-homoketone fractions (81% overall yield) was obtained 17α-hydroxy-A-homo-5α-androstan-4-one (34%) as needles from hexane, m.p. 173–174 °; ν_{max} 3600 and 1695 cm^{-1}; o.r.d. (*c*, 0.004 in CH_3OH) $[\phi]_{302}$ +8550°, $[\phi]_{263}$ −6950° (*a* = +155).

Anal. Calcd. for $C_{20}H_{32}O_2$: C, 78.90; H, 10.59. Found: C, 79.05; H, 10.65.

17α-Hydroxy-A-homo-5α-androstan-3-one (47%), was obtained as laminae from hexane, m.p. 153.5–154.5 °C; ν_{max} 3600 and 1695 cm^{-1}; o.r.d. (*c*, 0.004 in CH_3OH) $[\phi]_{302}$ −4150°, $[\phi]_{261}$ +4100 (*a* = −82.5).

Anal. Calcd. for $C_{20}H_{32}O_2$: C, 78.90; H, 10.59. Found: C, 79.09; H, 10.52.

A-Homo-5α-androstan-4- (2c) and -3-one (3c)

These were prepared from 5α-androstan-3-one (1 g, 3.7 mmoles), potassium hydroxide (930 mg), and *N*-nitrosomethylurea (660 mg, 6.4 mmoles) in methanol–ether (1:1, 100 ml). The A-homoketone material (60% yield) could only be partly resolved by chromatography and was analyzed by the o.r.d. method using authentic samples of the two ketones prepared as indicated in Chart 1. A-Homo-5α-androstan-4-one and A-homo-5α-androstan-3-one were found to be present in the proportion 42:58 respectively.

17β-Hydroxy-17α-methyl-A-homo-5α-androstan-4- (2e) and -3-one (3e)

These were prepared from 17β-hydroxy-17α-methyl-5α-androstan-3-one (1.5 g, 4.9 mmoles), potassium hydroxide (1.53 g), and *N*-nitrosomethylurea (1.13 g, 11 mmoles) in methanol–ether (1:1, 110 ml). Obtained in an overall yield of 81% were 17β-hydroxy-17α-methyl-A-homo-5α-androstan-4-one (30%) as needles from hexane, m.p. 139–140 °C; ν_{max} 3600 and 1695 cm^{-1}; o.r.d. (*c*, 0.004 in CH_3OH); $[\phi]_{301}$ +8200°, $[\phi]_{262}$ −6800° (*a* = +150).

Anal. Calcd. for $C_{21}H_{34}O_2$: C, 79.19; H, 10.76. Found: C, 79.26; H, 10.83.

17β-Hydroxy-17α-methyl-A-homo-5α-androstan-3-one (51%), was obtained as needles from hexane, m.p. 177.5–178.5 °C; ν_{max} 3600 and 1695 cm^{-1}; o.r.d. (*c*, 0.004 in CH_3OH) $[\phi]_{303}$ −5000°, $[\phi]_{261}$ +4050°, (*a* = −90.5).

Anal. Calcd. for $C_{21}H_{34}O_2$: C, 79.19; H, 10.76. Found: C, 79.22; H, 10.76.

17β-Hydroxy-A-homo-5α-estran-4-(2g and -3-one (3g)

These were prepared from 17β-hydroxy-5α-estran-3-one (910 mg, 3.3 mmoles), potassium hydroxide (1.2 g), and *N*-nitrosomethylurea (950 mg, 9.2 mmoles) in methanol–ether (1:1, 90 ml). The A-homoketone product (74%) was composed of 17β-hydroxy-A-homo-5α-estran-4-one (29%), obtained as needles from hexane, m.p. 164.5–165 °C; ν_{max} 3600 and 1695 cm^{-1}; o.r.d. (*c*, 0.004 in CH_3OH); $[\phi]_{307}$ +7800°; $[\phi]_{267}$ −6250° (*a* = +140.5).

Anal. Calcd. for $C_{19}H_{30}O_2$: C, 78.57; H, 10.41. Found: C, 78.76; H, 11.14.

17β-Hydroxy-A-homo-5α-estran-3-one (45%), was obtained as needles from hexane, m.p. 136–137 °C, ν_{max} 3600 and 1695 cm^{-1}; o.r.d. (*c*, 0.004 in CH_3OH) $[\phi]_{308}$ −6750°, $[\phi]_{265}$ +7000°, (*a* = −137.5).

Anal. Calcd. for $C_{19}H_{30}O_2$: C, 78.57; H, 10.41. Found: C, 78.39; H, 10.82.

17β-Hydroxy-A-homo-5α-androstan-4- (2j) and -3-one (3j)

These were obtained from 17β-hydroxy-5α-androstan-3-one in equal amounts as described previously (1).

The following compounds were prepared by method (*b*).

17β-Hydroxy-A-homo-5β-estran-4- (2k) and -3-one (3k)

These were prepared from 17β-hydroxy-5β-estran-3-one (1.1 g, 4 mmoles) in methanol – ether – water (5:5:1, 70 ml) and ethereal diazomethane (40 ml, from *N*-nitrosomethylurea (1.13 g, 11 mmoles)). An overall yield of 80% was obtained, 39% being 17β-hydroxy-A-homo-5β-estran-4-one, as needles from hexane, m.p. 165.5–166.5 °C; ν_{max} 3600 and 1695 cm^{-1}; o.r.d. (*c*, 0.004 in CH_3OH) $[\phi]_{310}$ −3100°, $[\phi]_{263}$ +5500° (*a* = −86).

Anal. Calcd. for $C_{19}H_{30}O_2$: C, 78.57; H, 10.41. Found: C, 78.74; H, 10.54. 17β-Hydroxy-A-homo-5β-estran-3-one (41%) was obtained as plates from hexane, m.p. 144.5–145.5 °C; ν_{max} 3600 and 1695 cm^{-1}; o.r.d. (*c*, 0.004 in CH_3OH) $[\phi]_{306}$ +4250°, $[\phi]_{268}$ −1850° (*a* = +61).

Anal. Calcd. for $C_{19}H_{30}O_2$: C, 78.57; H, 10.41. Found: C, 78.76; H, 10.53.

17β-Acetoxy-A-homo-5α-androstan-4- (2d) and -3-one (3d)

These were prepared from 17β-acetoxy-5α-androstan-3-one (1g, 3.2 mmoles), methanol – ether – water (5:5:1, 50 ml), and dry, potassium hydroxide-free, ethereal diazomethane (40 ml, from *N*-nitrosomethylurea (1.4 g, 14 mmoles)). The mixture was stirred at 0 °C for 7 h after which time 2 *N* hydrochloric acid was added to terminate the reaction. The pH of the solution was adjusted to 7 with aqueous potassium hydroxide and further potassium hydroxide (150 mg) was then added.[6] The solution was kept overnight at 25 °C, after which time the excess base was neutralized with 2 *N* hydrochloric acid, and the mixture was worked up in the usual way. Chromatographic isolation of the 17β-hydroxy-A-homoketones showed that the overall yield of A-homo-17β-acetates formed in the reaction was 79%, of which 17β-acetoxy-A-homo-5α-androstan-4-one accounted for 37%, and 17β-acetoxy-A-homo-5α-androstan-3-one, 42%.

17β-Acetoxy-A-homo-5α-estran-4- (2h) and -3-one (3h)

These were prepared as described for **2***d* and **3***d*. Again, the 17β-acetoxy-A-homoketones produced were hydrolyzed prior to chromatography, and analysis of the mixture of the corresponding 17β-hydroxy compounds showed the original yield of acetates to be 81%, comprised of 17β-acetoxy-A-homo-5α-estran-4-one (38%) and 17β-acetoxy-A-homo-5α-estran-3-one (43%).

---

[6]This hydrolysis step was introduced since it was found that the 17β-acetates were less amenable to chromatographic separation than the corresponding 17β-hydroxy compounds.

Can. J. Chem. Downloaded from www.nrcresearchpress.com by 210.87.254.6 on 09/05/12
For personal use only.

Preparation of Pure A-Homo-5α-androstan-4- and -3-one

A-Homo-5α-androstan-4-one (2c)

A solution of 17β-hydroxy-A-homo-5α-androstan-4-one (155 mg), toluene-*p*-sulfonic acid monohydrate (15 mg) and ethane-1,2-diol (350 mg) in benzene (12 ml) was refluxed, with magnetic stirring, in a Dean–Stark apparatus for 3 h. The benzene solution was then cooled and was washed with 10% aqueous sodium carbonate (6 ml), followed by water (6 ml), dried ($MgSO_4$) and evaporated. The residue (170 mg) was chromatographed on Florisil (8 g, column packed in hexane); elution with 5% ether–hexane afforded *4,4-ethylenedioxy-A-homo-5α-androstan-17β-ol* (**4**), as prisms (138 mg) from petroleum ether (b.p. 40–60 °C), m.p. 167–168 °C; ν_{max} 3600, 1100, and 965 cm^{-1}.

The above ketal **4** (133 mg), pyridinium trifluoracetate (43 mg), and dicyclohexylcarbodiimide (274 mg) in dimethyl sulfoxide (5 ml) was stirred at 55 °C for 2 h (26). The mixture was then poured into water (50 ml) and extracted with ether (3 × 25 ml). The ether solution was filtered, washed with water (3 × 5 ml), dried ($MgSO_4$), and evaporated. The residue was digested with boiling hexane for 15 min (dicyclohexylurea is insoluble in hexane) and the filtered hexane solution evaporated. The crude product obtained was chromatographed on Florisil (8 g, column packed in hexane); elution with 6% ether–hexane gave *4,4-ethylenedioxy-A-homo-5α-androstan-17-one* (**5**), as needles (80 mg) from petroleum ether (b.p. 40–60 °C), m.p. 184–185 °C; ν_{max} 1725 and 1105 cm^{-1}; o.r.d. (*c*, 0.004 in isooctane) $[\phi]_{318}$ +8700°, $[\phi]_{278}$ −7000° (*a* = +157).

The 4-ketal (**5**) (75 mg), potassium hydroxide (250 mg), 99% hydrazine hydrate (800 mg) in diethylene glycol (2 ml) was refluxed under a nitrogen atmosphere for 3 h (20). The condenser was then removed and the bath temperature raised gradually to 195–200 °C, and maintained at this level until nitrogen evolution ceased (5 h).

The mixture was then poured into water (50 ml), and the solid removed by filtration and washed with water until the washings were neutral. After drying *in vacuo* the crude *4,4-ethylenedioxy-A-homo-5α-androstane* (**6**) (70 mg), m.p. 130.5–131.5 °C was dissolved in methanol–ether (2:1, 20 ml) and 1 *N* hydrochloric acid (1 ml) added. The solution was kept at 25 °C for 2 h, following which it was poured into water (100 ml) and the mixture extracted with ether (3 × 50 ml). The combined ether extracts were washed with water (20 ml), dried ($MgSO_4$), and evaporated to give A-homo-5α-androstan-4-one (60 mg, 99% pure by g.l.c.). Complete purification was effected by low temperature recrystallization from petroleum ether (b.p. 40–60 °C) followed by sublimation at 75 °/0.1 Torr to give prisms, m.p. 85–86 °C; ν_{max} 1695 cm^{-1}; o.r.d. (*c*, 0.004 in isooctane) $[\phi]_{318(sh)}$ +5200°, $[\phi]_{308}$ +5800°, $[\phi]_{299(sh)}$ +3200°, $[\phi]_{271}$ −4200° (*a* = +100); (*c*, 0.004 in CH_3OH); $[\phi]_{302}$ +7600°, $[\phi]_{264}$ −6400°, (*a* = +140).

Anal. Calcd. for $C_{20}H_{32}O$: C, 83.28; H, 11.18. Found: C, 83.27; H, 11.12.

A-Homo-5α-androstan-3-one (3c)

This was prepared from 17β-hydroxy-A-homo-5α-androstan-3-one *via* analogous intermediates, and under exactly similar conditions of reaction and purification, to those described above for **2c**.

17β-Hydroxy-A-homo-5α-androstan-3-one (265 mg), gave *3,3-ethylenedioxy-A-homo-5α-androstan-17β-ol* (**7**), as prisms (260 mg) from petroleum ether (b.p. 40–60 °C), m.p. 108–109 °C; ν_{max} 3600, 1105, and 945 cm^{-1}.

The 17β-hydroxyketal (**7**) (760 mg) was then oxidized to *3,3-ethylenedioxy-A-homo-5α-androstan-17-one* (**8**), which was obtained as needles (680 mg) from petroleum ether (b.p. 40–60 °C), m.p. 113.5–114 °C; ν_{max} 1725, 1105, and 945 cm^{-1}; o.r.d. (*c*, 0.004 in isooctane) $[\phi]_{320}$ +8200° $[\phi]_{277}$ −7700° (*a* = +159).

Anal. Calcd. for $C_{22}H_{34}O_3$: C, 76.26; H, 9.89. Found: C, 76.29; H, 10.00.

The 17-keto-3-ketal (**8**) (395 mg) was reduced to *3,3-ethylenedioxy-A-homo-5α-androstane* (**9**) (336 mg), m.p. 68.5–69 °C, which on treatment with acid yielded A-homo-5α-androstan-3-one (**3c**) (280 mg). Sublimation at 55 °C/0.1 Torr followed by recrystallization from petroleum ether (b.p. 40–60 °C) gave prisms, m.p. 65 °C; ν_{max} 1695 cm^{-1}; o.r.d. (*c*, 0.004 in isooctane) $[\phi]_{323(sh)}$ −3200°, $[\phi]_{312}$ −3800°, $[\phi]_{269}$ +3150 (*a* = −69.5); (*c*, 0.004 in CH_3OH) $[\phi]_{306}$ −5200°, $[\phi]_{262}$ +4700° (*a* = −99).

Anal. Calcd. for $C_{20}H_{32}O$: C, 83.28; H, 11.18. Found: C, 83.14; H, 11.16.

Acknowledgments

We thank the National Research Council of Canada for generous financial support and the University of Toronto for the award (to J. M. Z.) of an Open Fellowship.

1. J. B. Jones and P. Price. Can. J. Chem. **44**, 999 (1966).
2. N. A. Nelson and R. N. Schut. J. Am. Chem. Soc. **81**, 6486 (1959).
3. G. D. Meakins and D. J. Morris. J. Chem. Soc. (C), 394 (1967).
4. E. L. Eliel, N. L. Allinger, S. J. Angyal, and G. A. Morrison. Conformational analysis. Interscience Publishers, Inc., New York. 1965. pp. 345–350.
5. F. Sondheimer, Y. Klibansky, Y. M. Y. Hoddad, G. H. R. Summers, and W. Klyne. J. Chem. Soc. 767 (1961); T. Kubota and F. Hayashi. Tetrahedron, **23**, 995 (1967).
6. A. Bowers, H. J. Ringold, and R. I. Dorfmann. J. Am. Chem. Soc. **79**, 4556 (1957).
7. C. Chen. Tetrahedron, **3**, 43 (1958).
8. R. T. Rapala and E. Farkas. J. Am. Chem. Soc. **80**, 1008 (1958).
9. R. E. Counsell. Tetrahedron, **15**, 202 (1961).
10. C. D. Gutsche. *In* Organic reactions. Vol. VIII. John Wiley and Sons, Inc., New York. 1954. p. 395.
11. H. B. Henbest. Proc. Chem. Soc. 159 (1963).
12. F. V. Brutcher and W. Bauer. J. Am. Chem. Soc. **84**, 2236 (1962); F. V. Brutcher and J. Leopold. J. Am. Chem. Soc. **88**, 3156 (1966).
13. T. Takemoto, Y. Kondo, and H. Mori. Chem. Pharm. Bull. (Tokyo), **13**, 897 (1965).
14. H. J. Geise, C. Altona, and C. Romers. Tetrahedron, **23**, 439 (1967).
15. H. Koyama, M. Shiro, T. Sato, Y. Tsukuda, H. Itazaki, and W. Nagata. Chem. Commun. 812 (1967).
16. E. L. Eliel, N. L. Allinger, S. J. Angyal, and G. A. Morrison. Conformational analysis. Interscience Publishers, Inc., New York. 1965. p. 11.
17. J. B. Jones and D. C. Wigfield. Can. J. Chem. **46**, 1459 (1968).

18. L. RUZICKA and H. KÄGI. Helv. Chim. Acta, **20**, 1557 (1937).
19. A. BOWERS, H. J. RINGOLD, and E. DENOT. J. Am. Chem. Soc. **80**, 6115 (1958).
20. L. MAMLOK and J. JACQUES. Bull. Soc. Chim. France, 484 (1960).
21. K. BOWDEN, I. M. HEILBRON, E. R. H. JONES, and B. C. L. WEEDON. J. Chem. Soc. 39 (1946).
22. L. RUZICKA, V. PRELOG, P. MEISTER, and P. WIELAND. Helv. Chim. Acta, **28**, 618 (1945).
23. C. DJERASSI and W. KLYNE. J. Chem. Soc. 4929 (1962).
24. A. BUTENANDT, K. TSCHERNING, and G. HANISCH. Ber. **68**, 2097 (1935).
25. G. SNATZKE, B. ZEEH, and E. MÜLLER. Tetrahedron, **20**, 2937 (1964).
26. J. B. JONES and D. C. WIGFIELD. Can. J. Chem. **44**, 2517 (1966).

Can. J. Chem. Downloaded from www.nrcresearchpress.com by 210.87.254.6 on 09/05/12
For personal use only.

Can. J. Chem. Downloaded from www.nrcresearchpress.com by 210.87.254.40 on 09/05/12
For personal use only.

Some silicon-containing phenyl and benzyl isoquinoline derivatives, 2-aralkyl imidazolines, and *N*-substituted phenethylamines

IGAL BELSKY, DAVID GERTNER, AND ALBERT ZILKHA
Department of Organic Chemistry, The Hebrew University, Jerusalem, Israel

Received December 14, 1967

Several trimethylsilyl substituted 1-phenyl or 1-benzyl isoquinoline derivatives were synthesized by the Bishler–Napieralsky reaction starting from the corresponding homoveratrylamides, which were cyclized in toluene in the presence of phosphorus pentoxide or phosphorus oxychloride. These conditions were suitable for the homoveratrylamides of *p*- or *o*-trimethylsilylbenzoic acid and *p*-trimethylsilylmethylphenylacetic acid but not for that of *p*-trimethylsilylphenylacetic acid, due to the greater sensitivity of the silicon–aryl bond in the latter to cleavage under acid conditions.

Some 2-aralkyl imidazolines containing a trialkylsilyl group in the para-position were synthesized by condensation of silicon-containing aromatic acids and ethylenediamine.

Several *N*-substituted *p*-trialkylsilyl phenethylamines were prepared by lithium aluminium hydride reduction of the corresponding amides.

Canadian Journal of Chemistry, **46**, 1921 (1968)

As part of a program (1, 2) for the synthesis of analogues of biologically active compounds containing silicon, we have prepared a number of 1-phenyl and 1-benzyl isoquinoline derivatives containing a trimethylsilyl group attached to the phenyl or benzyl ring as well as some 2-aralkyl imidazolines containing a trialkylsilyl group in the para position and some *N*-substituted *p*-trialkylsilylphenethylamines.

Compounds containing the isoquinoline nucleus are interesting from the chemical and pharmacological aspects due to the occurrence of this group in various alkaloids, and the interesting biological activity of some of these alkaloids.

The silicon–aryl bond is sensitive to cleavage under acid conditions, and in the present work the Bischler–Napieralsky cyclization (3) was investigated to find out conditions for cyclizing homoveratrylamides of silicon-containing aromatic acids without causing scission of the silicon–aryl bond.

p-Trimethylsilylbenzhomoveratrylamide (**1**), obtained by reaction of *p*-trimethylsilylbenzoyl chloride and homoveratrylamine in chloroform, was cyclized to 1-*p*-trimethylsilylphenyl-3,4-dihydro-6,7-dimethoxy isoquinoline (**2**) in boiling toluene in the presence of phosphorus pentoxide. Under these conditions no significant cleavage of the silicon–aryl bond occurred. On carrying out the cyclization with *o*-trimethylsilylbenzhomoveratrylamide, the isoquinoline derivative could not be isolated either free or as the picrate or methiodide derivatives. However, using phosphorus oxychloride in toluene, it was possible to isolate the isoquinoline derivative as the methiodide.

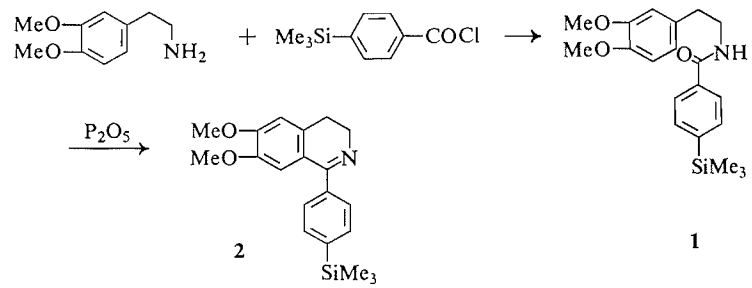

2 **1**

Attempts to cyclize *p*- and *o*-trimethylsilylphenylacethomoveratrylamides using phosphorus pentoxide or phosphorus oxychloride in toluene as well as phosphorus pentachloride in chloroform at room temperature, (4) did not yield a pure product, due to partial cleavage of the silicon–aryl bond. The trimethylsilyl group in these derivatives is in a para or ortho position to a methylene group which is electron releasing as compared to the carbonyl group in (**1**). This makes

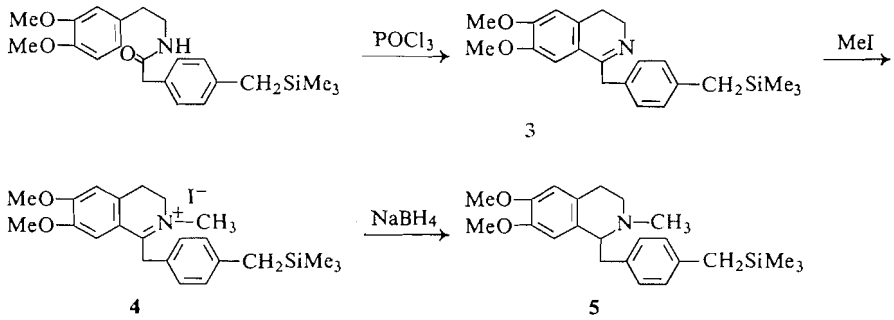

3

4 5

the silicon–aryl bond in these compounds more sensitive to acid conditions. 1-*p*-Trimethylsilylmethylbenzyl-3,4-dihydro-6,7-dimethoxy isoquinoline (**3**) was obtained by cyclization of *p*-trimethylsilylmethylphenylacethomoveratrylamide in toluene in the presence of phosphorus oxychloride. In this case the trimethylsilyl group being separated from the benzene ring by a methylene group is stable to acid conditions (5).

1-*p*-Trimethylsilylmethylbenzyl-1,2,3,4-tetrahydro-2-methyl-6,7-dimethoxy isoquinoline (**5**) was obtained from **3** by reaction with methyl iodide and reduction of the resulting methiodide (**4**) with sodium borohydride.

We investigated the possibility of cyclization under "physiological conditions". *o*-Trimethylsilylphenethylamine hydrochloride and acetaldehyde were kept at room temperature at pH 4 for 10 days, but no cyclization occurred. This is compatible with previous findings of Schopf and Bayerle (6) that cyclization reactions under physiological conditions do not take place if no phenolic groups are present on the phenethylamine skeleton.

Imidazolines substituted at the 2-position by aryl or aralkyl groups have a wide range of pharmacological activities; slight changes in structure may make dominant one or another activity (7, 8). 2-Benzyl imidazoline (Tolazoline, Priscoline) has a sympathomimetic activity and lowers the blood pressure (7).

Some 2-aralkyl imidazolines containing a trialkylsilyl group in the para-position were synthesized by condensation of silicon-containing aromatic acids and ethylenediamine. A modified synthesis in which the components were heated in xylene in the presence of activated alumina, and the water formed removed by azeotropic distillation, gave the substituted imidazolines (**6**) in 35–50% yield.

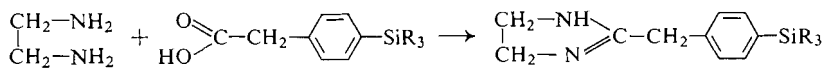

6

The ethylenediamide derivatives of the acids (**7**) were the main by-products in this condensation and could be isolated.

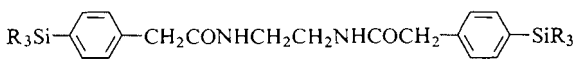

7

Phenethylamine has sympathomimetic activity and increases the blood pressure. Substitution of alkyl groups on the nitrogen causes variation in the extent of this activity, mainly due to various degrees of resistance to enzymatic oxidative degradation (9, 10). Phenethylamines having trialkylsilyl substituents in the para position of the benzene ring (1) were found to lower the blood pressure (11).

We have synthesized some *N*-substituted *p*-trialkylsilyl phenethylamines (**8**) by lithium aluminium hydride reduction of the corresponding amides.

N-*p*-trimethylsilylphenethyl morpholine hydrochloride was found to lower the blood pressure in cats but its effect was of short duration.

Can. J. Chem. Downloaded from www.nrcresearchpress.com by 210.87.254.40 on 09/05/12
For personal use only.

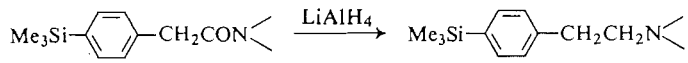

8

Experimental

Melting points were determined on a Fisher–Johns apparatus.

p-Trimethylsilylbenzhomoveratrylamide

A solution of *p*-trimethylsilylbenzoyl chloride (12) (2.12 g; 0.01 mole) in chloroform (10 ml) was dropped into a cooled solution of homoveratrylamine (3.62 g; 0.02 mole) in dry chloroform (30 ml) and stirred for 20 h. The chloroform was evaporated *in vacuo*, and acetone was added to the residue. The precipitated homoveratrylamine hydrochloride was filtered and washed thoroughly with acetone. The combined acetone solutions were evaporated *in vacuo*, water was added and the *p*-trimethylsilylbenzhomoveratrylamide was removed by filtration, washed with 5% hydrochloric acid and then with water; yield 3.03 g (85%), m.p. 117 °C, after recrystallization from aqueous ethanol.

Anal. Calcd. for $C_{20}H_{27}NO_3Si$: C, 67.19; H, 7.61; N, 3.92; Si, 7.85. Found: C, 66.91; H, 7.66; N, 3.84; Si, 7.93.

1-p-Trimethylsilylphenyl-3,4-dihydro-6,7-dimethoxy Isoquinoline

Phosporus pentoxide (16 g) was added in small portions to a well-stirred boiling solution of *p*-trimethylsilylbenzhomoveratrylamide (4 g; 0.011 mole) in dry toluene (100 ml). The addition was performed under nitrogen and the time taken was 30 min. The reaction mixture was heated and stirred for another 30 min, cooled, and the toluene decanted. Crushed ice was added, with stirring, to the residue until it dissolved. The acidic solution was extracted with ether, then cautiously made alkaline with cold dilute sodium hydroxide solution. The separated oil was taken up in ether, washed with water, and dried over magnesium sulfate. The ether was evaporated *in vacuo* and the 1-*p*-trimethylsilylphenyl-3,4-dihydro-6,7-dimethoxy isoquinoline (2.6 g; 70%) crystallized on addition of petroleum ether to the residue, m.p. 95 °C; λ_{max}, 238 mμ (ε 25 500); 315 mμ, (ε 6800).

Anal Calcd. for $C_{20}H_{25}NO_2Si$: C, 70.76; H, 7.42; N, 4.13; Si, 8.27. Found; C, 70.65; H, 7.33; N, 4.36; Si, 8.53.

The methiodide derivative was obtained on addition of methyl iodide (4 ml) to a solution of the 1-*p*-trimethylsilylphenyl-3,4-dihydro-6,7-dimethoxy isoquinoline (0.70 g) in benzene (30 ml). This was left at room temperature for 24 h. The methiodide derivative crystallized out in almost quantitative yield and was recrystallized from benzene – petroleum ether, m.p. with decomposition about 240 °C; λ_{max} 253 mμ (ε 15 500), 316 mμ (ε 10 500), and 373 mμ (ε 1100).

Anal. Calcd. for $C_{21}H_{28}INO_2Si$: C, 52.39; H, 5.86; N, 2.91; I, 26.40. Found: C, 52.18; H, 5.72; N, 3.05; I, 26.72.

1-o-Trimethylsilylphenyl-3,4-dihydro-6,7-dimethoxy Isoquinoline Methiodide

Phosphorus oxychloride (5 ml) was dropped under nitrogen into a solution of *o*-trimethylsilylbenzhomoveratrylamide (13) (3.57 g; 0.01 mole) in toluene (40 ml) and the mixture heated under reflux for 2 h. The toluene and $POCl_3$ were removed *in vacuo* and the residue was taken up in a small quantity of methanol and added to 5% ammonia solution (150 ml). The separated oil was extracted with ether, washed thoroughly with water, and dried over magnesium sulfate. The ether was removed and the residue was taken up in benzene (30 ml). This was gently boiled with methyl iodide (5 ml) for 5 h. Petroleum ether was added until the mixture became cloudy and the methiodide was left to crystallize in the refrigerator, yield 3.2 g (67%); m.p. 193 °C after recrystallization from benzene – petroleum ether; λ_{max}, 254 mμ (ε 16 500), 318 mμ (ε 10 000), 374 mμ (ε 11 300).

Anal. Calcd. for $C_{21}H_{28}INO_2Si$: C, 52.39; H, 5.86; N, 2.91; Si, 5.83; I, 26.40. Found: C, 52.00; H, 6.14; N, 3.14; Si, 6.14; I, 26.57.

p-Trimethylsilylmethylphenylacetyl Chloride

Freshly distilled thionyl chloride (15 ml) was dropped slowly into a solution of *p*-trimethylsilylmethylphenylacetic acid (14) in dry benzene (10 ml) and heated under reflux for 1.5 h. Excess thionyl chloride and benzene were removed *in vacuo* and the *p*-trimethylsilylmethylphenylacetyl chloride (10.5 g; 87%) was distilled at 108–110 °C/1mm.

Anal. Calcd. for $C_{12}H_{17}ClOSi$: C, 59.86; H, 7.12; Cl, 14.73. Found: C, 59.77; H, 7.12; Cl, 14.62.

p-Trimethylsilylmethylphenylacet-homoveratrylamide

The amide was obtained in 90% yield by reaction of *p*-trimethylsilylmethylbenzoyl chloride and homoveratrylamine, b.p. 245–250 °C/1mm; m.p. 54 °C.

Anal. Calcd. for $C_{22}H_{31}NO_3Si$: C, 68.53; H, 8.11; N, 3.63; Si, 7.28. Found: C, 68.42; H, 8.13; N, 3.62; Si, 7.45.

1-p-Trimethylsilylmethylbenzyl-3,4-dihydro-6,7-dimethoxy Isoquinoline Methiodide

Phosphorus oxychloride (10 ml) was dropped into a solution of *p*-trimethylsilylmethylphenylacethomoveratrylamide (4.6 g, 0.012 mole) in toluene (30 ml) and heated under reflux for 3.5 h in an argon atmosphere. Excess oxychloride and toluene were then driven off *in vacuo* and the residue was dissolved in alcohol–water. The solution was made alkaline with dilute sodium hydroxide, and the oil which separated out was extracted with ether, washed with water, and dried over magnesium sulfate. The ether was removed *in vacuo*. Petroleum ether (40–60 °C) (100 ml), benzene (10 ml), and methyl iodide (15 ml) were added and the mixture was heated under reflux for 4 h. The reaction mixture was evaporated *in*

Can. J. Chem. Downloaded from www.nrcresearchpress.com by 210.87.254.40 on 09/05/12
For personal use only.

Can. J. Chem. Downloaded from www.nrcresearchpress.com by 210.87.254.40 on 09/05/12
For personal use only.

vacuo and the residual methiodide was recrystallized from benzene – petroleum ether; yield 4 g (65%); m.p. 206 °C; λ_{max} 256 mμ (ε 14 500), 296 mμ (ε 14 000), 378 mμ (ε 6900).

Anal. Calcd. for $C_{23}H_{32}INO_2Si$: C, 54.22; H, 6.33; N, 2.75; Si, 5.51; I, 24.91. Found: C, 54.60; H, 6.28; N, 2.69; Si, 5.21; I, 24.73.

1-p-Trimethylsilylmethylbenzyl-1,2,3,4-tetrahydro-2-methyl-6,7-dimethoxy Isoquinoline

Sodium borohydride (1.5 g) was added portion-wise with stirring into 1-*p*-trimethylsilylmethylbenzyl-3,4-dihydro-6,7-dimethoxy isoquinoline methiodide (2.55 g, 0.005 mole) in methanol (30 ml). Stirring was continued for 2 h and the solution became yellow. The methanol was removed *in vacuo*, 10% sodium hydroxide (50 ml) was added to the residue, the amine was extracted with ether, washed with water, and dried over magnesium sulfate. The ether was removed *in vacuo* and the amine (1.5 g, 82%) was distilled at 220–225 °C/1mm; λ_{max} 230 mμ (shoulder) (ε 20 000); 283 mμ (ε 4800).

Anal. Calcd. for $C_{23}H_{33}NO_2Si$: C, 72.02; H, 8.67; N, 3.65; Si, 7.32. Found: C, 71.49; H, 8.33; N, 4.01; Si, 7.68.

p-Trimethylsilylphenylacethomoveratrylamide

The amide was obtained in 84% yield from *p*-trimethylsilylphenylacetyl chloride and homoveratrylamine; b.p. 230 °C/1mm; m.p. 45 °C.

Anal. Calcd. for $C_{21}H_{29}NO_3Si$: C, 67.89; H, 7.87; N, 3.77; Si, 7.56. Found: C, 67.92; H, 7.53; N, 3.54; Si, 7.82.

o-Trimethylsilylphenylacethomoveratrylamide

The amide was prepared in 78% yield from *o*-trimethylsilylphenylacetyl chloride and homoveratrylamine; b.p. 232–236 °C/1mm.

Anal. Calcd. for $C_{21}H_{29}NO_3Si$: C, 67.89; H, 7.87; N, 3.77; Si, 7.56. Found: C, 68.03; H, 7.68; N, 3.62; Si, 7.63.

2-(p-Trimethylsilyl)benzyl Imidazoline

A solution of *p*-trimethylsilylphenylacetic acid (1*a*) (4.16 g; 0.02 mole) in benzene (50 ml) was dropped into a solution of ethylenediamine (10 ml) in benzene (50 ml) and stirred for 5 min. The benzene was driven off *in vacuo*. Dry xylene (50 ml) and activated alumina (22 g) (60–200 mesh) were added to the residue and the mixture was heated in an azeotropic distillation apparatus for 3.5 h. The reaction mixture was cooled and the alumina was removed by filtration and washed thoroughly with dry benzene. The xylene and benzene solutions were combined and distilled fractionally *in vacuo*. The 2-(*p*-trimethylsilyl)benzyl imidazoline (1.62 g; 35%) passed at 160–163 °C/1mm and solidified on cooling; m.p. 101 °C on recrystallization from petroleum ether.

Anal. Calcd. for $C_{13}H_{20}N_2Si$: C, 67.19; H, 8.67; N, 12.06; Si, 12.07. Found: C, 67.11; H, 8.34; N, 12.27; Si, 12.35.

From the residue the ethylenediamide of *p*-trimethylsilylphenyl acetic acid (1.85 g, 42%) was isolated; m.p. 126 °C on recrystallization from aqueous ethanol.

Anal. Calcd. for $C_{24}H_{36}N_2O_2Si_2$: C, 65.41; H, 8.24; N, 6.36; Si, 12.73. Found: C, 65.65; H, 8.94; N, 6.48; Si, 12.46.

2-(p-Triethylsilyl)benzyl Imidazoline

p-Triethylsilylphenylacetic acid (11) condensed with ethylenediamine by a similar procedure yielded 2-(*p*-triethylsilyl) benzyl imidazoline in 48% yield, b.p. 189–192 °C/1mm; m.p. 77 °C on recrystallization from petroleum ether.

Anal. Calcd. for $C_{16}H_{26}N_2Si$: C, 70.02; H, 9.55; N, 10.21; Si, 10.22. Found: C, 69.83; H, 9.56; N, 10.50; Si, 10.02.

2-(p-Trimethylsilylmethyl)benzyl Imidazoline

This substituted imidazoline was obtained in 40% yield by the condensation of *p*-trimethylsilylmethylphenyl acetic acid (14) and ethylene diamine, b.p. 174–176 °C/1mm; m.p. 85 °C on recrystallization from petroleum ether.

Anal. Calcd. for $C_{14}H_{22}N_2Si$: C, 68.21; H, 8.99; N, 11.37; Si, 11.38. Found: C, 68.24; H, 8.87; N, 11.56; Si, 11.15.

The ethylenediamide of *p*-trimethylsilylmethylphenyl acetic acid was isolated in 45% yield and melted at 165 °C on recrystallization from aqueous ethanol.

Anal. Calcd. for $C_{26}H_{40}N_2O_2Si_2$: C, 66.62; H, 8.60; N, 5.98; Si, 11.97. Found C, 67.03; H, 8.37; N, 6.44; Si, 11.71.

2-(p-Trimethylsilyl)hydrocinnamyl Imidazoline

The substituted imidazoline was synthesized from *p*-trimethylsilylhydrocinnamic acid (2*c*) and ethylenediamine in 42% yield; b.p. 168–171 °C/1mm; m.p. 105° C.

Anal. Calcd. for $C_{14}H_{22}N_2Si$: C, 68.21; H, 8.99; N, 11.37; Si, 11.38. Found: C, 68.16; H, 9.28; N, 10.95; Si, 11.68.

N-(p-Trimethylsilylphenethyl)piperidine

A solution of *p*-trimethylsilylphenylacetyl piperidine (2*c*) (6.3 g; 0.025 mole) in dry ether (30 ml) was dropped with stirring into a suspension of lithium aluminium hydride (1.9 g; 0.05 mole) in ether (50 ml) under argon, heated to reflux for 3.5 h and stirred overnight. The reaction mixture was cooled in an ice–salt bath and ethyl acetate (6 ml) was dropped in, followed by water (3 ml) and 20% sodium hydroxide solution (4 ml). The precipitated salts were removed by filtration and washed thoroughly with ether. The amine was extracted from the ethereal solutions with dilute hydrochloric acid, made alkaline with sodium hydroxide and taken up again in ether, dried over magnesium sulfate and distilled *in vacuo*. The *N*-(*p*-trimethylsilylphenethyl) piperidine (5.42; 83%) distilled at 130–133 °C/2mm.

Anal. Calcd. for $C_{16}H_{27}NSi$: C, 73.50; H, 10.41; N, 5.36; Si, 10.73. Found: C, 73.77; H, 10.34; N, 5.34; Si, 10.56.

N-(p-Trimethylsilylphenethyl)morpholine

The amine was synthesized as above in 85% yield from *N*-*p*-trimethylsilylphenylacetyl morpholide (2*c*), b.p. 138–140 °C/2mm.

Anal. Calcd. for $C_{15}H_{25}NOSi$: C, 68.39; H, 9.57; N, 5.32; Si, 10.65. Found: C, 68.72; H, 9.25; N, 5.17; Si, 10.84.

N-(p-Trimethylsilylphenethyl)morpholine Hydrochloride

This was obtained by passing dry gaseous hydrogen chloride into a cooled solution of the amine in dry ether; m.p. 240 °C.

Anal. Calcd. for $C_{15}H_{26}ClNOSi$: C, 60.07; H, 8.74; Cl, 11.82. Found: C, 60.04; H, 8.82; Cl, 12.13.

N-Methyl-p-trimethylsilylphenethylamine

This was synthesized as before in 63% yield from *N*-methyl-*p*-trimethylsilylphenylacetamide (2*c*); b.p. 120–122 °C/1mm.

Anal. Calcd. for $C_{12}H_{21}NSi$: C, 69.50; H, 10.21; N, 6.76; Si, 13.53. Found: C, 70.06; H, 10.02; N, 6.63; Si, 13.73.

N-(p-Trimethylsilylbenzyl)p-Trimethylsilylphenethylamine

This amine was prepared similarly in 65% yield by reduction of the appropriate amide; b.p. 190–196 °C/1mm; m.p. 90 °C.

Anal. Calcd. for $C_{21}H_{33}NSi_2$: C, 70.93; H, 9.35; N, 3.94; Si, 15.78. Found: C, 71.16; H, 9.02; N, 4.04; Si, 15.65.

1. (*a*) M. FRANKEL, M. BROZE, D. GERTNER, and A. ZILKHA. J. Chem. Soc. C, 379 (1966); (*b*) M. FRANKEL, I. BELSKY, D. GERTNER, and A. ZILKHA. J. Chem Soc. C, (1966)
2. (*a*) A. ROTMAN, D. GERTNER, and A. ZILKHA. Can. J. Chem. **45,** 1957 (1967); (*b*) **45,** 2469 (1967); (*c*) I. BELSKY. Ph.D. Thesis. Submitted to the Senate of The Hebrew University, Jerusalem, Israel. 1967; (*d*) I. BELSKY, D. GERTNER, and A. ZILKHA. J. Med. Chem. **11,** 92 (1968).
3. W. M. WHALEY and T. R. GOVINDACHARI. *In* Organic reactions. John Wiley & Sons, Inc., New York. Vol. VI. 1951. p.74.
4. J. M. GULLAND and R. D. HAWORTH. J. Chem. Soc. 2083 (1928).
5. C. EABORN. Organosilicon compounds. Butterworth Scientific Publications, London. 1960. p. 145.
6. C. SCHOPF and H. BAYERLE. Ann. **513,** 190 (1934).
7. L. S. GOODMAN and A. GILMAN. The pharmacological basis of therapeutics. 3rd ed. The Macmillan Co., New York. 1965. p. 557.
8. W. H. HARTUNG. Ind. and Eng. Chem. **37,** 127 (1945).
9. C. O. WILSON and O. GISVOLD. Textbook of organic medicinal and pharmaceutical chemistry. 3rd ed. J. B. Lippincott Co., Philadelphia. 1956. p. 302.
10. L. S. GOODMAN and A. GILMAN. The pharmacological basis of therapeutics. 3rd ed. The Macmillan Co., New York. 1965. p. 485.
11. A. ROTMAN. M.Sc. Thesis. The Hebrew University of Jerusalem, 1966.
12. R. S. BENKESER and H. R. KRYSIAK. J. Am. Chem. Soc. **76,** 599 (1954).
13. I. BELSKY, D. GERTNER, and A. ZILKHA. J. Med. Chem. To be published.
14. A. SHENHAR. Ph.D. Thesis. Submitted to the Senate of The Hebrew University, Jerusalem, Israel, 1967.

Can. J. Chem. Downloaded from www.nrcresearchpress.com by 210.87.254.40 on 09/05/12
For personal use only.

Can. J. Chem. Downloaded from www.nrcresearchpress.com by 210.87.254.40 on 09/05/12
For personal use only.

Fischer indole synthesis. The reaction of *N'*-alkyl-2,6-dialkylphenylhydrazines with cyclohexanone[1]

G. S. Bajwa and R. K. Brown
Department of Chemistry, University of Alberta, Edmonton, Alberta

Received January 29, 1968

Condensation of *N'*-methyl-2,6-dimethylphenylhydrazine with cyclohexanone in refluxing benzene gives 8,9-dimethyl-1,2,3,4-tetrahydrocarbazole along with water and ammonia. Yields of the 8,9-dimethyl-1,2,3,4-tetrahydrocarbazole are improved and general decomposition in the reaction mixture minimized if the hydrazine hydrochloride is used. In this case, however, the ammonia is obtained as ammonium chloride contaminated with ~6% of methylammonium chloride. *N'*-Ethyl-2,6-dimethylphenylhydrazine hydrochloride and *N'*-methyl-2,6-diethylphenylhydrazine hydrochloride condense with cyclohexanone to give 9-ethyl-8-methyl-1,2,3,4-tetrahydrocarbazole and 8-ethyl-9-methyl-1,2,3,4-tetrahydrocarbazole respectively along with ammonium chloride contaminated with a very small amount of ethylammonium chloride and methylammonium chloride respectively.

The results are interpreted in terms of the formation first of the intermediate enamine then the dienone–imine.

Canadian Journal of Chemistry, 46, 1927 (1968)

Introduction

Recently (1) this laboratory reported the results of an attempt to isolate the dienone–imine, **3** (Scheme 1) postulated as an intermediate in the mechanism of the Fischer indole synthesis (2, 3). Two innovations had been employed (1). First, to prevent the rapid aromatization of the dienone ring (**3** → **4**, R = H), and thus loss of this diene intermediate, the 2- and 6-positions of the aromatic ring in the phenylhydrazine were blocked by chlorine substituents (**1**, R = Cl). Secondly, since an enamine such as **2** is thought to be a necessary intermediate preceding the dienone–imine (2, 3), it was considered advantageous to condense cyclohexanone with *N'-methyl*-2,6-dichlorophenylhydrazine, rather than with 2,6-dichlorophenylhydrazine and thus obtain the enamine directly. This would avoid the rearrangement of a phenylhydrazone to the enamine, which is considered to be the first step in the formation of indole from a phenylhydrazone.

Two significant results were obtained (1). Although neither the enamine (**2**, R = Cl) nor the dienone–imine (**3**, R = Cl) could be isolated, the products actually obtained, (**5** and **6**, R = Cl, in 14% and 21% yield respectively) were readily explicable only on the basis of both the enamine and dienone–imine intermediates. Also, the condensation, **1** → **2**, and cyclization to **5** and **6** occurred *at room temperature without the aid of an acid catalyst*, the first example of the Fischer reaction under such mild conditions.

Although the 2,6-dichloro substituents in **1** (R = Cl) were expected to retard aromatization (**3** → **4**, R = Cl), their incorporation gave a substance or substances which lost halogen readily at some stage during the formation of **5** or **6** (R = Cl). If one accepts the dienone–imine as an intermediate in the mechanism of the Fischer indole synthesis, then a labile halogen atom is evident in the allylic system present in structures **3** and **7** (Scheme 2), with aromatization as the driving force leading to further reaction.

For the present work it was thought that substitution at positions-2 and -6 by methyl groups rather than by halogen atoms should decrease the tendency towards such elimination and aromatization, and thus improve the stability of the intermediates **3** and **7** (R = CH_3). This paper describes the results obtained when *N'*-methyl-2,6-dimethylphenylhydrazine was condensed with cyclohexanone by azeotropic removal of water.

Results and Discussion

When equimolar quantities of carefully dried *N'*-methyl-2,6-dimethylphenylhydrazine and cyclohexanone were heated under nitrogen in refluxing dry benzene, a 26% yield of 8,9-dimethyl-1,2,3,4-tetrahydrocarbazole was obtained, identical in all respects with an authentic

[1]Taken from the thesis of G. S. Bajwa to be submitted to the Faculty of Graduate Studies, University of Alberta, Edmonton, Alberta, as part of the requirements for the degree of Doctor of Philosophy.

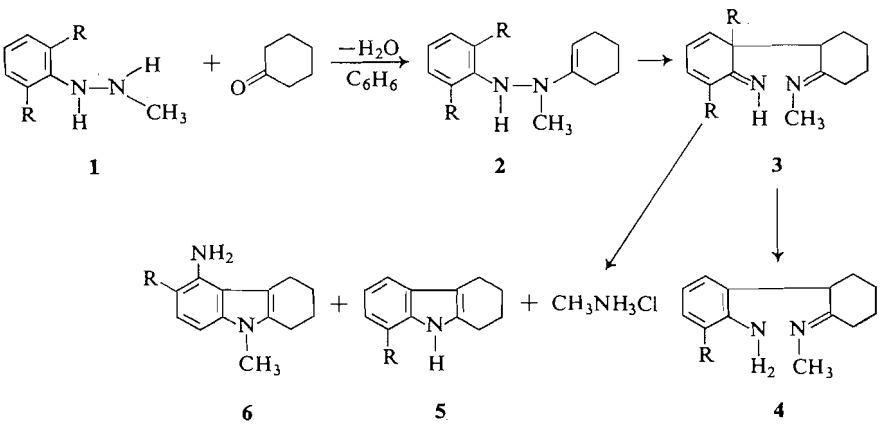

SCHEME 1

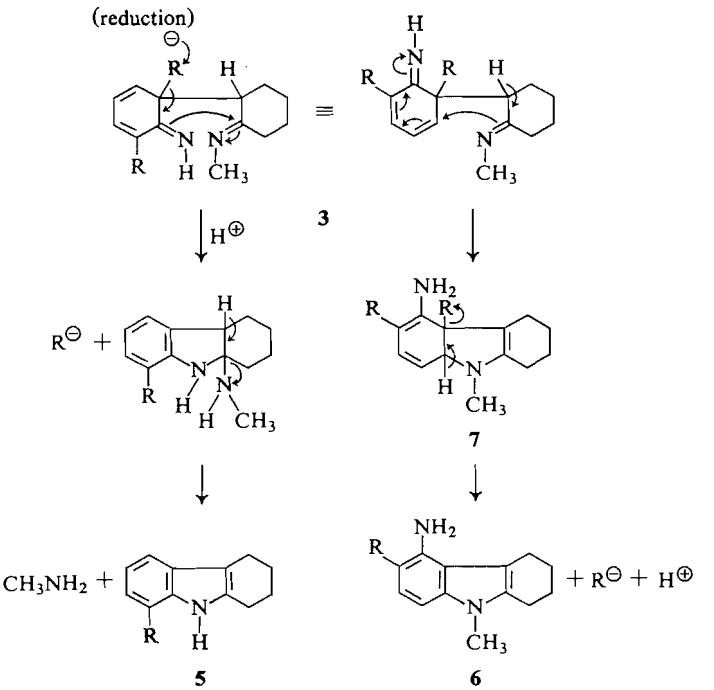

(R = Cl)

SCHEME 2

sample prepared by methylation of 8-methyl-1,2,3,4-tetrahydrocarbazole (4). Water was obtained in a Dean–Stark trap (5). The gases evolved from this reaction were collected in dry ether saturated with dry hydrogen chloride. A precipitate of ammonium chloride was obtained as the only product. The nuclear magnetic resonance (n.m.r.) spectrum in D_2O of the latter material showed only one significant signal, that for DOH. However, the presence of a minute peak at τ 7.3 indicated that a very small amount of methylamine might have been formed. Identification was made by melting point and by n.m.r. spectra obtained in water and in D_2O.

Can. J. Chem. Downloaded from www.nrcresearchpress.com by 210.87.254.40 on 09/05/12
For personal use only.

Can. J. Chem. Downloaded from www.nrcresearchpress.com by 210.87.254.40 on 09/05/12
For personal use only.

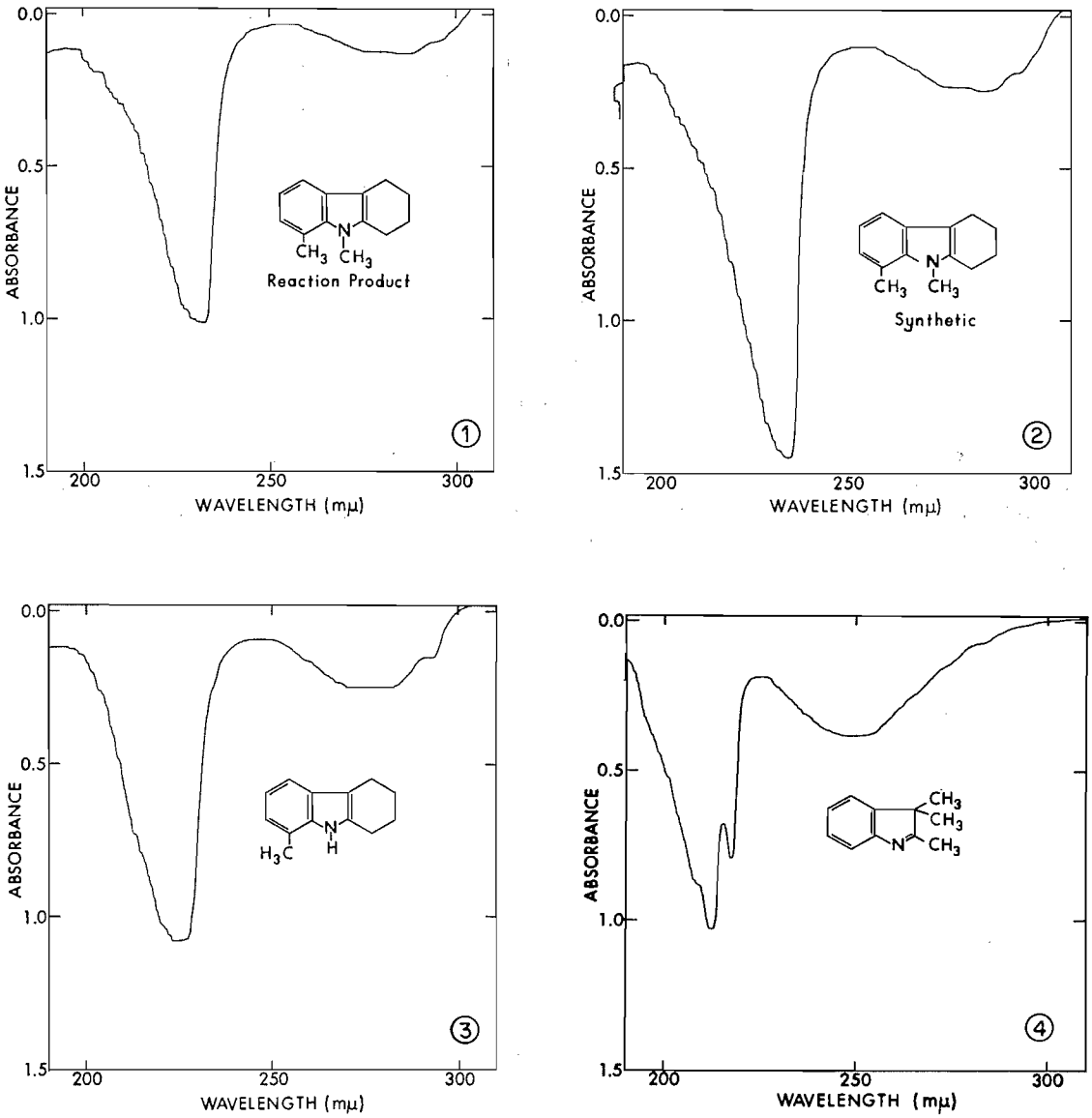

FIG. 1. The ultraviolet spectrum of the reaction product 8,9-dimethyl-1,2,3,4-tetrahydrocarbazole in cyclohexane.
FIG. 2. The ultraviolet spectrum of authentic 8,9-dimethyl-1,2,3,4-tetrahydrocarbazole in cyclohexane.
FIG. 3. The ultraviolet spectrum of authentic 8-methyl-1,2,3,4-tetrahydrocarbazole in cyclohexane.
FIG. 4. The ultraviolet spectrum of 2,3,3-trimethylindolenine in cyclohexane.

When the same condensation was repeated with *N'*-methyl-2,6-dimethylphenylhydrazine hydrochloride and cyclohexanone, the reddish yellow oil which was left after removal of the benzene solvent did not darken, and readily deposited nearly double the yield of 8,9-dimethyltetrahydrocarbazole (44%). In this case, a small amount of methyl ammonium chloride (~6%) was found mixed with the ammonium chloride obtained from the ether trap. The difference in color of the oils is no doubt due to the strong tendency of free *N'*-methyl-2,6-dimethylphenylhydrazine to decompose on standing, whereas its hydrochloride is quite stable and has been kept indefinitely with no apparent decomposition.

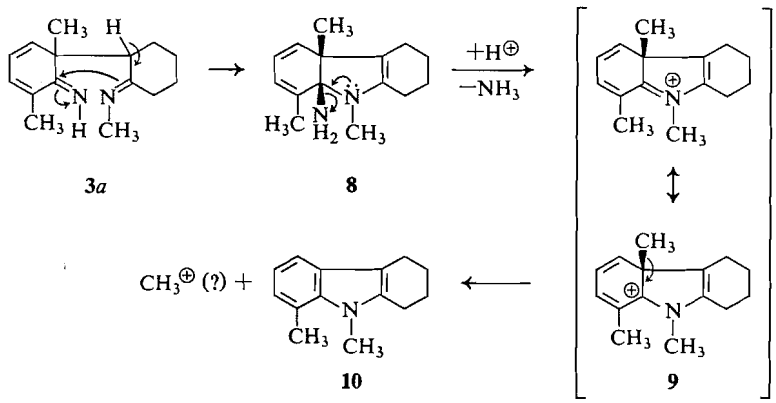

SCHEME 3

In the preparation of authentic 8,9-dimethyl-1,2,3,4-tetrahydrocarbazole it was found that *N*-methylation of 8-methyl-1,2,3,4-tetrahydrocarbazole was difficult and gave at best a poor yield of the 8,9-dimethylated homologue (7% was converted to the *N*-methylated product. Yield, based on the carbazole consumed, is ~20%). Resistance to *N*-methylation might be attributed to steric hindrance due to the methyl group at position-8 since under identical conditions of methylation 1,2,3,4-tetrahydrocarbazole gave the *N*-methyl homologue in at least 45% yield.

That methylation of 8-methyl-1,2,3,4-tetrahydrocarbazole had actually occurred on the nitrogen atom and not elsewhere is indicated by the absence of C=N absorption in the region 1630–1690 cm^{-1} in the infrared (6), and the close similarity of the ultraviolet (u.v.) spectrum of the methylated product (Fig. 2) to that for 8-methyl-1,2,3,4-tetrahydrocarbazole (Fig. 3) and the marked difference from that for 2,3,3,-trimethylindolenine (Fig. 4). Further support for *N*-methylation of 8-methyl-1,2,3,4-tetrahydrocarbazole is shown by its n.m.r. spectrum (in $CDCl_3$ referred to tetramethylsilane). The signals for the methyl group protons in authentic 8-methyl-1,2,3,4-tetrahydrocarbazole and 9-methyl-1,2,3,4-tetrahydrocarbazole are at τ 7.58 and τ 6.57, respectively. The proton signals for the two methyl groups in 8,9-dimethyltetrahydrocarbazole are at τ 7.27 and τ 6.20, in the region expected for the methyl group attached to the benzene ring and to the nitrogen atom, respectively.

The formation of 8,9-dimethyltetrahydrocarbazole by the condensation of cyclohexanone with *N'*-methyl-2,6-dimethylphenylhydrazine can be explained by assuming the intermediacy of the dienone–imine **3***a* (Scheme 3) which cyclizes to **8**. Elimination of NH_2 as ammonia is possible due to the formation of the resonance stabilized imonium–carbonium ion, **9**. Loss of the methyl group as the equivalent of a methyl carbonium ion is facilitated by the stability gained in the conversion of **9** to the aromatic system, **10**.

It is clear that one of the methyl groups of the aromatic ring is lost. However, its fate is as yet unknown. Failure to detect or isolate methyl alcohol or methylamine (except for the small amount of the latter detected when the hydrochloride was used) indicates that the liberated water or ammonia do not provide the chief nucleophile which attacks the labile methyl group. The evolved gases absorbed in ether or in benzene showed no evidence (by mass spectrometry) for the presence of methane, which might arise by a reductive process such as that suggested (1) for the liberation of halogen as halide ion from **3** to give **5** in Scheme 1 (R = Cl).

When equimolar quantities of dry *N'*-methyl-2,6-diethylphenylhydrazine hydrochloride and cyclohexanone were heated under nitrogen for 1.5 to 4 h in refluxing dry benzene a 38% yield of 8-ethyl-9-methyltetrahydrocarbazole was obtained. (If the free hydrazine was used, much decomposition was observed and a yield of only 4% of the 8-ethyl-9-methyltetrahydrocarbazole was obtained.) Ammonia was obtained as the hydrochloride when it was trapped in acidified dry ether. As well, the presence of a small amount of *methyl*ammonium chloride was de-

Can. J. Chem. Downloaded from www.nrcresearchpress.com by 210.87.254.40 on 09/05/12
For personal use only.

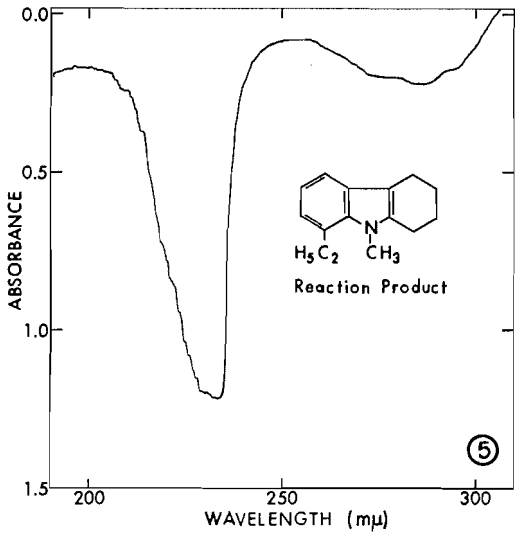

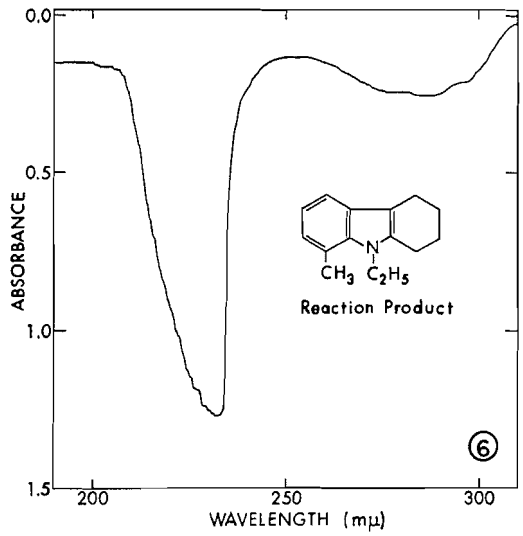

FIG. 5. The ultraviolet spectrum of the reaction product 8-ethyl-9-methyl-1,2,3,4-tetrahydrocarbazole in cyclohexane.

FIG. 6. The ultraviolet spectrum of the reaction product 9-ethyl-8-methyl-1,2,3,4-tetrahydrocarbazole in cyclohexane.

tected by the n.m.r. spectrum of the precipitated salt. No *ethyl*ammonium chloride could be discerned.

The structure of the product 8-ethyl-9-methyl-1,2,3,4-tetrahydrocarbazole was verified by its n.m.r. spectrum and by the similarity of the u.v. absorption spectrum (Fig. 5) to that of 8,9-dimethyl-1,2,3,4-tetrahydrocarbazole (Fig. 2) and to that of 8-ethyl-1,2,3,4-tetrahydrocarbazole (Fig. 7). We were unable to methylate 8-ethyl-1,2,3,4-tetrahydrocarbazole and thus provide an authentic sample for comparison.

Condensation of cyclohexanone and *N'*-ethyl-2,6-dimethylphenylhydrazine hydrochloride under conditions similar to those mentioned above gave a 13% yield of 9-ethyl-8-methyl-1,2,3,4-tetrahydrocarbazole, whose structure was corroborated by the n.m.r. and u.v. (Fig. 6) spectra. Here again, we were unable to ethylate the nitrogen atom of 8-methyl-1,2,3,4-tetrahydrocarbazole to produce an authentic specimen. Of significance was the fact that the gases collected in acidified ether gave a precipitate of ammonium chloride contaminated with a small amount of *ethyl*ammonium chloride but no *methyl*ammonium chloride.

This clearly indicates that the small amount of methylammonium chloride obtained from the condensation of both *N'*-methyl-2,6-dimethylphenylhydrazine hydrochloride and *N'*-methyl-

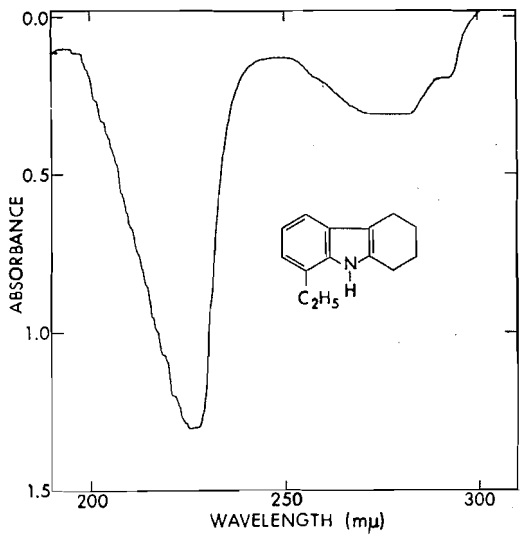

FIG. 7. The ultraviolet spectrum of authentic 8-ethyl-1,2,3,4-tetrahydrocarbazole in cyclohexane.

2,6-diethylphenylhydrazine hydrochloride with cyclohexanone must have come from a side reaction such as shown in Scheme 4 and not from the attack by ammonia on the labile methyl group from the benzene ring. A blank reaction with a solution of the *N'*-methyl (or ethyl)-2,6-dimethylphenylhydrazine hydrochloride in benzene containing no cyclohexanone gave only the

Can. J. Chem. Downloaded from www.nrcresearchpress.com by 210.87.254.40 on 09/05/12
For personal use only.

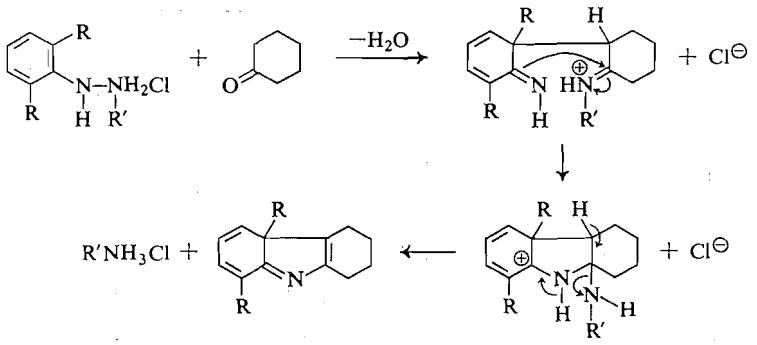

(R = CH_3 or C_2H_5; R′ = CH_3 or C_2H_5)

SCHEME 4

unchanged hydrazine hydrochloride and no methyl (or ethyl) ammonium chloride.

That the chief reaction should be cyclization in the direction shown by Scheme 3 rather than that in Scheme 4 is due to the presence of the proton in *3a* (Scheme 3) which is easily lost to produce the nucleophilic secondary amino group (enamine) attached to the cyclohexene ring system whereas similar formation of a nucleophilic primary amino group from the dienone–imine system is much more difficult.

To date we have been unable to isolate the proposed intermediate enamine, **2** or dienone–imine, **3** (Scheme 1, R = CH_3). However, the results of this work add further support for the accepted mechanism (2, 3) of the Fischer indole synthesis.

Experimental

All melting points and boiling points are uncorrected.

Elemental analyses were made by Mrs. Darlene Mahlow, Department of Chemistry, University of Alberta, and by Dr. C. Daessle, Organic Microanalysis, 5757 Decelles Avenue, Montreal.

Unless otherwise stated, solvents were removed with a rotary evaporator under vacuum produced by a water pump.

Ultraviolet (u.v.) spectra were obtained with a Perkin–Elmer model 202 ultraviolet–visible spectrometer. The solvent in all cases was cyclohexane.

Infrared (i.r.) and nuclear magnetic resonance (n.m.r.) spectra were obtained by Mr. Robert Swindlehurst, Department of Chemistry, University of Alberta, Edmonton. The n.m.r. spectra were taken in $CDCl_3$ solution unless otherwise stated. Signals are referred to tetramethylsilane.

N′-Formyl-2,6-dimethylphenylhydrazine

A solution of 20 g (0.116 mole) of 2,6-dimethylphenylhydrazine hydrochloride (7) in 80 ml of water was made alkaline by the addition of ice-cold concentrated aqueous sodium hydroxide. The liberated oil was extracted with ether and dried ($MgSO_4$). The ether was removed by rotary evaporator and the oily residue was dissolved in 120 ml of glacial acetic acid. Formylation was carried out by a modification of the published directions (1, 8). To the solution was added dropwise 6.6 g (0.147 mole) of formamide and the mixture then stirred for 2 h. It was cooled in an ice bath and made alkaline by the slow addition of 5% aqueous sodium hydroxide, the temperature being kept ~20 °C. The oil which separated was removed by extraction with ether (2 × 150 ml) and dried ($MgSO_4$). The filtered ether solution, when cooled in a refrigerator overnight, deposited needles which were separated and thrice crystallized from ether; yield, 6 g (31%); m.p. 139–140 °C. When the above procedure was modified by dilution of the glacial acetic acid–formamide mixture with water as previously advocated (1, 8), rather than with 5% aqueous sodium hydroxide, the yield was markedly increased (73%).

Anal. Calcd. for $C_9H_{12}N_2O$: C, 65.85; H, 7.31; N, 17.07. Found: C, 66.28; H, 7.52; N, 16.83.

The i.r. spectrum in Nujol showed two strong bands at 3240 cm^{-1} and 3295 cm^{-1} (two different NH) and a strong band at 1670 cm^{-1} (C=O).

The n.m.r. spectrum in $CDCl_3$ possessed two sharp signals at τ 7.62 and τ 7.72 for methyl groups attached to the aromatic ring. These were in the area ratio of 28:11 respectively. In pyridine-d_5 the 100 MHz spectrum showed that they were in the area ratio of ~2:1, but collapsed to a singlet at 100 °C. They reappeared when the temperature was decreased to below ~90 °C, thus indicating that *N′*-formyl-2,6-dimethylphenylhydrazine exists in two forms at temperatures below 90 °C. The other signals of the n.m.r. spectrum in pyridine-d_5 were at τ 2.86–3.24 (multiplet, 3H aromatic + 1 H for NH); τ 1.73 (singlet) and τ 1.20 (doublet, J = 11 Hz) for 1 H for CHO; τ −0.20 (doublet, J = 11 Hz) and τ −0.47, 1 H for NH. The N—H signals were identified by deuterium exchange.

Attempts to introduce a second formyl group, by repetition of the above procedure starting with *N′*-formyl-2,6-dimethylphenylhydrazine, were unsuccessful. Only starting material was recovered in excellent yield.

Raney Nickel Reduction of N′-Formyl-2,6-dimethylphenylhydrazine

N′-Formyl-2,6-dimethylphenylhydrazine was reduced with W-2 Raney nickel according to published directions

Can. J. Chem. Downloaded from www.nrcresearchpress.com by 210.87.254.40 on 09/05/12
For personal use only.

Can. J. Chem. Downloaded from www.nrcresearchpress.com by 210.87.254.40 on 09/05/12
For personal use only.

(9). The oil obtained after removal of the catalyst and solvent was extracted with benzene and dried ($MgSO_4$). Removal of the benzene gave a liquid which, by its i.r. and n.m.r. spectra was identified as 2,6-dimethylaniline. Acetylation gave a derivative which proved to be *N*-acetyl-2,6-dimethylaniline (10) by its melting point and mixture melting point (176–177 °C). The oil left after the extraction with benzene proved to be formamide by comparison of its i.r. spectrum and gas–liquid chromatographic retention time with those of authentic formamide. Chromatography was done on a 100 in. × 0.2 in. (I.D.) column of Apiezon L (8 g) on Gas Chrom P (32 g) with helium as the carrier gas.

This information proved that *mono*formylation had occurred, and only on the nitrogen atom of 2,6-dimethylphenylhydrazine remote from the ring.

Crude N′-Formyl-N′-methyl-2,6-dimethylphenylhydrazine

N′-Formyl-2,6-dimethylphenylhydrazine (4 g) was methylated according to published directions for the preparation of *N′*-methyl-*N′*-formyl-2,6-dichlorophenylhydrazine (1), but using a 2:1 molar ratio of dimethyl sulfate to the hydrazine. The reaction mixture was then diluted with water, extracted with ether, and dried ($MgSO_4$). Removal of the ether gave a yellow oil (3.8 g, 87.5%). The oil was obviously a mixture according to its n.m.r. spectrum. Fractional distillation procedures were prohibitive due to the tendency of the material to decompose. Attempts at purification by chromatography were unsuccessful.

Hydrolysis of N′-Formyl-N′-methyl-2,6-dimethylphenylhydrazine

A solution of 5 g of the crude *N′*-formyl-*N′*-methyl-2,6-dimethylphenylhydrazine in a mixture of 10 ml of concentrated hydrochloric acid in 10 ml of 95% ethyl alcohol was refluxed for 6 h. The cooled mixture was poured into ice cold water (80 ml) and basified with 5% aqueous sodium hydroxide. The mixture was extracted with ether, dried ($MgSO_4$), filtered, and reduced in volume to ~100 ml. Addition of dry hydrogen chloride gave a yellow precipitate (3.85 g) melting at 169–175 °C (addition of a large excess of hydrogen chloride caused some darkening and decomposition). After crystallization from alcohol–ether it melted at 198–199 °C; yield, 2.1 g of *N′-methyl-2,6-dimethylphenylhydrazine hydrochloride.*

Anal. Calcd. for $C_9H_{15}N_2Cl$: C, 57.92; H, 8.04; N, 15.01; Cl, 19.01. Found: C, 58.06; H, 8.09; N, 14.97; Cl, 19.03.

The i.r. spectrum in Fluolube (Hooker Chemicals) showed strong bonds at 3240 cm^{-1} (N—H), 2940 cm^{-1} (CH_3), 2700 cm^{-1} ($NH_2^{\oplus}$), and 1575 cm^{-1} (aromatic C=C).

The n.m.r. spectrum in D_2O showed sharp singlets at τ 2.73 (3H, aromatic), τ 5.20 (DOH, broad singlet), τ 6.98 (3H, for N—CH_3), and τ 7.59 (6H, two CH_3 attached to an aromatic ring).

The *N′*-methyl-2,6-dimethylphenylhydrazine hydrochloride (2.6 g) was dissolved in 50 ml of water and basified with 2% aqueous sodium hydroxide. The ether extract of this mixture was washed with water (3 × 20 ml) and dried ($MgSO_4$). The ether was removed giving crude *N′*-methyl-2,6-dimethylphenylhydrazine $\eta_D^{25.5}$, 1.539. The n.m.r. spectrum agreed with the structure but indicated some decomposition. No evidence of the presence of the solvent, diethyl ether, was observed. The oil darkened rapidly at room temperature, hence further purification was unsuccessful. An elemental analysis of this material gave the following results.

Anal. Calcd. for $C_9H_{14}N_2$: C, 72.00; H, 9.33; N, 18.66. Found: C, 71.08, 71.53; H, 8.53, 8.24; N, 17.63.

The mother liquor obtained from the acidified (HCl) ether solution above was further concentrated to ~50 ml and kept in a refrigerator overnight. A colorless precipitate was obtained (1.5 g) melting at 180–181 °C. Crystallization from ethanol (95%) – ether failed to change the melting point.

Anal. Calcd. for $C_{10}H_{17}N_2Cl$: C, 59.86; H, 8.48; N, 13.99; Cl, 17.68. Found: C, 59.61; H, 8.41; N, 13.72; Cl, 17.77.

This data, along with that shown below, agreed with the structure of the compound as *N′,N′-dimethyl-2,6-dimethylphenylhydrazine hydrochloride.* Apparently some hydrolysis and dimethylation had occurred during the methylation of *N′*-formyl-2,6-dimethylphenylhydrazine.

The i.r. spectrum in Fluolube showed the following bands: 3228 cm^{-1} (NH), 2940 cm^{-1} (CH_3), 2700 cm^{-1} ($NH^{\oplus}$), and 1578 cm^{-1} (aromatic C=C).

The n.m.r. spectrum of the 180–181 °C melting material in D_2O showed signals at τ 2.90 (3H, aromatic, sharp singlet), τ 5.27 (DOH, broad singlet), τ 6.96 (3H) and τ 7.12 (3H) (sharp singlets for two NCH_3 groups) and at τ 7.68 (6H, singlet for two CH_3 groups attached to an aromatic ring).

When *N′*-formyl-2,6-dimethylphenylhydrazine was methylated with an *equimolar* proportion of dimethyl sulfate (1) the product obtained, following the above procedure, was *N′*-methyl-2,6-dimethylphenylhydrazine hydrochloride (42%). No *N′,N′*-dimethyl-2,6-dimethylphenylhydrazine hydrochloride was obtained.

Pure N′-Formyl-N′-methyl-2,6-dimethylphenylhydrazine

A solution of 1 g (0.0053 mole) of *N′*-methyl-2,6-dimethylphenylhydrazine hydrochloride in water (50 ml) was basified with 5% aqueous sodium hydroxide. The ether extract (2 × 50 ml) was washed with water (2 × 20 ml) and dried ($MgSO_4$) for 1 h. The drying agent was separated and the filtrate was freed of solvent. To the residual yellow oil was added 6 ml of glacial acetic acid followed by 0.5 g (0.011 mole) of formamide. The mixture was stirred for 3 h at room temperature, then diluted with 20 ml of water. The benzene extract (2 × 50 ml) of this mixture was washed with 5% aqueous sodium carbonate (4 × 30 ml) and then with water (2 × 50 ml) and dried overnight ($MgSO_4$) in a refrigerator (to minimize decomposition). The filtrate was freed from solvent at room temperature for 6 h. The yellow oil (690 mg) solidified on standing for ~1.5 h. Three crystallizations from petroleum ether (b.p. 60–70 °C) gave 510 mg (53%) of *N′-formyl-N′-methyl-2,6-dimethylphenylhydrazine.*

Anal. Calcd. for $C_{10}H_{14}N_2O$: C, 67.41; H, 7.92; N, 15.73. Found: C, 67.46; H, 7.76; N, 15.74.

The n.m.r. spectrum supported the structure completely. Signals were found at τ 1.44 (1H for CHO, singlet), τ 2.8–3.1 (3H, aromatic, multiplet), τ 3.96, (1H, for NH, broad singlet), τ 7.21 (3H, for NCH_3, singlet), and τ 7.76 (6H, singlet for two aromatic CH_3 groups).

Attempts at hydrogenolysis of *N′*-formyl-*N′*-methyl-2,6-dimethylphenylhydrazine with Raney nickel (9) were

. Lines 11 and 10 shall therefore read: ". . . gave 510 mg (53%) of *N′-formyl-N′-methyl-2,6-dimethylphenylhydrazine*, m.p. 60°."

FOR ERRATA SEE
Vol. 40 1962 p. 347

Can. J. Chem. Downloaded from www.nrcresearchpress.com by 210.87.254.40 on 09/05/12
For personal use only.

unsuccessful. Only unchanged material was recovered. This is not surprising in view of the finding that 1,2-diacetyl-1,2-dimethylhydrazine could not be cleaved by treatment with Raney nickel (11).

2,6-Diethylphenylhydrazine Hydrochloride

This was made by the method described for the preparation of 2,6-dimethylphenylhydrazine hydrochloride (7). From 53 g (0.355 mole) of 2,6-diethylaniline there was obtained 30 g (42%) of 2,6-diethylphenylhydrazine hydrochloride melting at 176–177 °C. An analytical sample, crystallized from a mixture of ether and 95% ethanol melted at 191–192 °C.

Anal. Calcd. for $C_{10}H_{17}N_2Cl$: C, 59.80; H, 8.53; N, 13.95; Cl, 17.68. Found: C, 60.08; H, 8.68; N, 14.22; Cl, 17.70.

N′-Formyl-2,6-diethylphenylhydrazine

N′-Formylation was carried out according to the directions for the *N′*-formylation of phenylhydrazine (8). From 5 g (0.03 mole) of crude 2,6-diethylphenylhydrazine (obtained by evaporation of the solvent from the dried ether extract to which *no* hydrogen chloride had been added (7)) there was obtained an oil which solidified on standing for 0.5 h; yield, 5.5 g, m.p. 61–65 °C. To this solid, dissolved in ether, was added some Skellysolve B (petroleum ether, b.p. 60–70 °C). The amorphous solid which precipitated was separated and washed with petroleum ether (b.p. 60–70 °C) and then with a small amount of ice cold diethyl ether. The residual colorless solid melted at 99–100 °C; yield, 4 g (68%). Two crystallizations from petroleum ether (60–70 °C) raised the melting point to 101 °C.

Anal. Calcd. for $C_{11}H_{16}N_2O$: C, 68.70; H, 8.39; N, 14.57. Found: C, 68.98; H, 8.08; N, 14.78.

The i.r. spectrum in carbon tetrachloride showed absorption bands at 3430 cm^{-1} and 3358 cm^{-1} (medium, for two NH groups), and a strong band at 1700 cm^{-1} (C=O).

The n.m.r. spectrum in $CDCl_3$ agreed with the structure as *N′*-formyl-2,6-diethylphenylhydrazine and showed the following signals: τ 2.06 (1H, broad singlet for CHO), τ 2.25 and τ 4.33 (2H, for two N—H, located by deuterium exchange), τ 8.78 (6H, triplet for two CH_3—CH_2— groups, $J = 7.5$ Hz) and two overlapping quartets centered at τ 7.23 and τ 7.37 (4H, for two CH_3—CH_2— groups, $J = 7.5$ Hz). In pyridine, the 100 MHz spectrum showed two overlapping triplets centered at τ 8.82 and τ 8.85 ($J = 7.5$ Hz) roughly in the ratio 2:1 respectively (methyl protons of the ethyl groups). The methylene protons of the ethyl groups gave *two* overlapping quartets centered at τ 7.02 and τ 7.22 ($J = 7.5$ Hz). The former collapsed to one triplet while two methylene proton quartets merged into one quartet at temperatures above 80 °C thus indicating that *N′*-formyl-2,6-diethylphenylhydrazine exists in two forms at room temperature roughly in the ratio of 2:1.

N′-Formyl-N′-methyl-2,6-diethylphenylhydrazine

Methylation was carried out according to the directions employed for the methylation of *N′*-formyl-2,6-dichlorophenylhydrazine (1) using equimolar proportions of dimethyl sulfate and the hydrazine. From 6 g (0.031 mole) of the *N′*-formyl-2,6-diethylphenylhydrazine there was obtained an oil, after dilution of the reaction mixture with water, which was extracted with ether (2 × 50 ml) and dried ($MgSO_4$). Removal of the ether from the filtered solution gave a yellow oil (4 g, 62%) whose i.r. and n.m.r. spectra supported the structure as *N′*-formyl-*N′*-methyl-2,6-diethylphenylhydrazine. The n.m.r. spectrum showed that *N*-methylation had occurred, by the appearance of two singlets at τ 7.18 and τ 7.22. It was also clear that the material consisted of more than one substance. Since the methylated *N′*-formyl-2,6-dimethylphenylhydrazine had resisted attempts at purification, the methylated 2,6-diethyl homologue was not purified further.

N′-Methyl-2,6-diethylphenylhydrazine Hydrochloride

N′-Formyl-*N′*-methyl-2,6-diethylphenylhydrazine (29 g, 0.14 mole of the crude material) was hydrolyzed by the same procedure used to hydrolyze *N′*-formyl-*N′*-methyl-2,6-dimethylphenylhydrazine above; yield, 6 g (20%) of material melting at 170 °C (from 95% ethanol).

Anal. Calcd. for $C_{11}H_{19}N_2Cl$: C, 61.52; H, 8.92; N, 13.05; Cl, 16.51. Found: C, 61.63; H, 8.73; N, 13.32; Cl, 16.07.

The i.r. spectrum (Fluolube) showed a sharp band at 3240 cm^{-1} (NH) and a medium strength band at 2690 cm^{-1} ($NH_2^{\oplus}$).

The n.m.r. spectrum, in D_2O, agreed with the structure and showed the following signals: τ 2.74 (3H, narrow multiplet, aromatic), τ 5.28 (3H, for $\overset{\oplus}{N}CH_3$ overlapping the DOH signal), τ 7.0 (3H, for NCH_3, singlet), τ 7.25 (4H, for two CH_3—CH_2— groups, quartet, $J = 7.5$ Hz) and τ 8.82 (6H, for two CH_3—CH_2— groups, triplet, $J = 7.5$ Hz).

N′-Ethyl-N′-formyl-2,6-dimethylphenylhydrazine

N′-Formyl-2,6-dimethylphenylhydrazine (5 g, 0.03 mole) was ethylated by the procedure described for the methylation of *N′*-formyl-2,6-dichlorophenylhydrazine (1), using equimolar quantities of diethyl sulfate and the formylated hydrazine. There was obtained a reddish-yellow oil (5 g) whose n.m.r. spectrum indicated that *N*-alkylation had indeed occurred. Signals appeared at τ 2.95–3.2 (aromatic), two overlapping quartets for the methylene protons of the ethyl group centered at τ 6.81 and τ 6.72 and one at τ 5.92, $J = 7$ Hz; at least two overlapping triplets for the methyl moiety of the ethyl group, between τ 8.5 and τ 9.1, $J = 7$ Hz; two prominent singlets at τ 7.63 and τ 7.76 for methyl groups attached to the aromatic ring. These data indicate the presence of more than one ethylated species. No attempt was made to purify this material in view of the lack of success in purification of the *N′*-methyl-*N′*-formyl-2,6-dimethylphenylhydrazine above.

N′-Ethyl-2,6-dimethylphenylhydrazine Hydrochloride

N′-Ethyl-*N′*-formyl-2,6-dimethylphenylhydrazine (30 g crude) was hydrolyzed by the same procedure used to hydrolyze the *N′*-formyl-*N′*-methyl-2,6-dimethylphenylhydrazine above. There was obtained 11 g of *N′*-ethyl-2,6-dimethylphenylhydrazine hydrochloride melting at 181–182 °C. An analytical sample was obtained by three recrystallizations from ethanol(95%) – ether and melted at 189–190 °C.

Anal. Calcd. for $C_{10}H_{17}N_2Cl$: C, 59.86; H, 8.48; N, 13.97; Cl, 17.46. Found: C, 59.89; H, 8.93; N, 14.19; Cl, 17.40.

Can. J. Chem. Downloaded from www.nrcresearchpress.com by 210.87.254.40 on 09/05/12
For personal use only.

The i.r. spectrum (in Fluolube) showed a sharp, strong band at 3245 cm^{-1} (NH) and bands in the region of 2700 cm^{-1} ($\overset{\oplus}{N}H_2$).

The n.m.r. spectrum, in D_2O, agreed with the structure indicated. Signals appeared at τ 2.80 (3H, aromatic, singlet), τ 5.3 (DOH), τ 6.57 (2H, one quartet for N—CH_2—CH_3, J = 7 Hz), τ 8.61 (3H, one triplet for N—CH_2—CH_3, J = 7 Hz), and τ 7.59 (6H, one singlet for two aromatic methyl groups).

o-Methylphenylhydrazine

This compound was prepared by the same method used to make 2,6-dimethylphenylhydrazine (7). From 100 g (0.93 mole) of *o*-toluidine there was obtained 80 g (54%) of *o-methylphenylhydrazine hydrochloride*, m.p. 188–190 °C (from ethanol(95%) – ether).

Anal. Calcd. for $C_7H_{11}N_2Cl$: C, 52.96; H, 6.99; N, 17.67; Cl, 22.38. Found: C. 51.58; H, 7.01; N, 17.98; Cl, 20.35, 20.13.

A more satisfactory purification and analysis eluded us.

The *o*-methylphenylhydrazine was obtained by the addition of base to an aqueous solution of the hydrochloride followed by ether extraction of the mixture and removal of the solvent from the dried ether solution. It crystallized on standing, m.p. 57–58 °C; lit. m.p. 56 °C (12); 59 °C (10, p. 532).

Cyclohexanone o-Methylphenylhydrazone

A solution of 26 g (0.213 mole) of *o*-methylphenylhydrazine and 20.8 g (0.216 mole) of cyclohexanone in 100 ml of 95% ethyl alcohol, containing a small amount of acetic acid, was refluxed for 2.5 h. Removal of the alcohol under vacuum in a rotary evaporator left a residue which quickly deposited needles (35.5 g, crude); m.p., 60–61 °C, lit. m.p. 61–62 °C (13). The hydrazone had a strong tendency to decompose during attempts to crystallize it.

8-Methyl-1,2,3,4-tetrahydrocarbazole

This was prepared according to published directions (5). From 1 g of cyclohexanone *o*-methylphenylhydrazone was obtained 400 mg (44%) of 8-methyl-1,2,3,4-tetrahydrocarbazole; m.p. 95–96 °C, lit. m.p. 98 °C (13, 5). For the u.v. spectrum see Fig. 3.

8,9-Dimethyl-1,2,3,4-tetrahydrocarbazole

To a 250 ml round bottom flask containing 1.84 g (0.0107 mole) of barium hydroxide and 1.84 g (0.012 mole) of barium oxide was added 40 ml of a 1:1 (by volume) solution of *N,N*-dimethylformamide and dimethyl sulfoxide. This was stirred gently and cooled to ~0 °C in a salt–ice bath. To this was added, all at once, 2 g (0.0108 mole) of 8-methyl-1,2,3,4-tetrahydrocarbazole followed by 2.8 g (0.022 mole) of dimethyl sulfate. The reaction mixture was stirred for 3 h at 0 °C, then stirred while it was allowed to come to room temperature, and finally stirred for an additional 12 h at room temperature. To the solution was added 2.8 ml of concentrated ammonium hydroxide and the resulting mixture was then filtered. The filtrate, on standing at room temperature, deposited crystals (100 mg) melting at 152–153 °C. A second crop (50 mg) was obtained when the mother liquor was cooled for 2 days in a refrigerator; yield, 7%.

The i.r. spectrum (in Nujol) showed no absorption in the region > 3100 cm^{-1} (NH).

The n.m.r. spectrum agreed fully with the structure indicated. The following signals were found: τ 2.5–3.3 (3H, aromatic, multiplet), τ 6.18 (3H, for N—CH_3, singlet), τ 7.27 (3H, aromatic methyl, singlet), two characteristic closely spaced multiplets centered at τ 7.35, and τ 8.12 for the 8H of the tetrahydro ring.

The u.v. absorption spectrum is shown in Fig. 2; λ_{max} = 23.4 mμ (ε = 38 000), 28.7 mμ (ε = 3700).

The mother liquor above, diluted with 40 ml of water, was extracted with ether (2 × 50 ml). The dried ($MgSO_4$) extract was freed from ether and gave 1.4 g of solid, unreacted crude 8-methyl-1,2,3,4-tetrahydrocarbazole, m.p. 83–86 °C. The n.m.r. spectrum showed that this was essentially 8-methyl-1,2,3,4-tetrahydrocarbazole contaminated with a small amount of 8,9-dimethyl-1,2,3,4-tetrahydrocarbazole (a very small singlet was found at ~τ 6.2 for the N—CH_3).

Yield of *N*-methylated product based on the 8-methyl-1,2,3,4-tetrahydrocarbazole consumed, ~20%.

The 8,9-dimethyl-1,2,3,4-tetrahydrocarbazole (250 mg) was dehydrogenated by heating with 90 mg of 5% palladium on charcoal for 2.5 h in refluxing mesitylene (3 ml). The hot solution was filtered and the solid was washed with methyl acetate (2 × 10 ml). The washings (filtered) were combined with the mesitylene solution and the whole freed from solvent. The residual solid (200 mg) melted at 110–115 °C. Three crystallizations from ethanol (95%) raised the melting point to 117 °C; yield, 170 mg (69.4%) of *1,9-dimethylcarbazole*.

Anal. Calcd. for $C_{14}H_{13}N$: C, 86.15; H, 6.71; N, 7.17. Found: C, 86.52; H, 6.95; N, 7.37.

The n.m.r. spectrum agreed completely with the structure assigned. The only signals evident were a multiplet between τ 1.8–2.25 (2H) and another between τ 2.4–3.0 (5H), aromatic protons; a singlet at τ 6.0 (3H, for N—CH_3); a singlet at τ 7.23 (3H, for CH_3 attached to an aromatic ring).

o-Ethylphenylhydrazine

This compound was prepared by the method used to synthesize 2,6-dimethylphenylhydrazine (7) with the following modification. The dried ether solution of the *o*-ethylphenylhydrazine was freed from solvent. The residual oil solidified when kept in a refrigerator overnight. From 113 g (0.933 mole) of *o*-ethylaniline there was obtained 18 g (13%) of the product; m.p. 49–50 °C, reported m.p. 49–50 °C (14).

A solution of *o*-ethylphenylhydrazine in dry ether was treated with dry hydrogen chloride gas. The colorless precipitate was removed and washed with dry ether, then dried, m.p. 183–185 °C. Two crystallizations from 95% ethanol gave a melting point of 185–186 °C for *o-ethylphenylhydrazine hydrochloride*.

Anal. Calcd. for $C_8H_{13}N_2Cl$: C, 56.61; H, 7.53; N, 16.23; Cl, 20.05. Found: C, 56.22; H, 7.78; N, 16.53; Cl, 19.95.

The n.m.r. spectrum in D_2O supported the structure assigned.

Cyclohexanone o-Ethylphenylhydrazone

This was prepared by the same method used to synthesize cyclohexanone *o*-methylphenylhydrazone above. From 11 g (0.081 mole) of *o*-ethylphenylhydrazone there was obtained 12 g (69%) of product, m.p. 44–46 °C. The

Can. J. Chem. Downloaded from www.nrcresearchpress.com by 210.87.254.40 on 09/05/12
For personal use only.

hydrazone decomposed rapidly in air at room temperature, hence was not analyzed, but immediately cyclized as below.

The n.m.r. spectrum supported the structure. The signals were at τ 2.5–3.5 (4H, aromatic multiplet); a broad absorption centered at $\sim\tau$ 3.55, (1H for NH, identified by deuterium exchange); τ 7.52 (quartet, 2H for CH_2—CH_3, J = 7.5 Hz); two multiplets at τ 7.5–7.9 and τ 8.0–8.5 (10H for the cyclohexanone moiety); τ 8.78 (3H, triplet for CH_3—CH_2—, J = 7.5 Hz).

8-Ethyl-1,2,3,4-tetrahydrocarbazole

A mixture of 6 g of cyclohexanone *o*-ethylphenylhydrazone and 100 ml of 3 *N* aqueous sulfuric acid was heated under reflux for 1.5 h. The reaction mixture was cooled and then kept overnight at room temperature. The tarry mass was extracted with ether (2 × 200 ml). The ether extract was washed with water (3 × 30 ml) and dried ($MgSO_4$). The filtered solution was freed of solvent and gave a dark yellow oil which was distilled at 168–170 °C at 9 mm (3.6 g). It solidified immediately to a yellow gummy mass melting at 50–52 °C. Crystallization from methanol by the addition of water to faint turbidity followed by cooling of the solution in a refrigerator for 2 h, gave colorless crystals melting at 58–59 °C; yield, 3.4 g, 61%.

Anal. Calcd. for $C_{14}H_{17}N$: C, 84.37; H, 8.60; N, 7.03. Found: C, 83.98; H, 8.35; N, 6.90.

These crystals began to discolor after standing at room temperature for 4–5 h.

The n.m.r. spectrum completely supported this structure. The signals were at τ 2.6–3.2 (3H, aromatic multiplet), τ 2.4–3.2 (1H, for NH, broad, identified by deuterium exchange); τ 7.26 (quartet, 2H for methylene group of the ethyl moiety, J = 7.5 Hz). two multiplets at τ 7.0–7.5 and τ 7.9–8.4 (8H for the tetrahydro ring), τ 8.70 (3H, triplet for CH_3—CH_2—, J = 7.5 Hz).

The i.r. spectrum in CCl_4 showed a sharp strong band at 3480 cm^{-1} (NH).

The u.v. spectrum (Fig. 7) showed two bands: λ_{max} = 227 mμ (ε = 27 000), 277 mμ (ε = 6200).

1-Ethylcarbazole

A quantity of 8-ethyl-1,2,3,4-tetrahydrocarbazole in 3 ml of mesitylene containing 90 mg of 5% palladium on charcoal, was heated under reflux for 2.5 h. The cooled mixture was filtered and the solid washed with methyl acetate (2 × 10 ml). The combined washings and filtrate were freed from solvent. The residual yellow oil solidified when kept in a refrigerator overnight giving 230 mg of material melting at 69–72 °C. This was crystallized by solution in methanol, addition of water to faint turbidity and cooling in a refrigerator; yield, 190 mg of colorless solid melting at 73 °C, reported m.p. 74 °C. (15).

The n.m.r. spectrum agreed with the structure. Signals were at τ 1.8–2.2 and τ 2.5–2.9 (two multiplets for 7H, aromatic), τ 7.11 (2H, quartet for CH_2—CH_3, J = 7.5 Hz), τ 8.62 (3H, triplet for CH_3—CH_2—, J = 7.5 Hz).

This conversion corroborated the structure of 8-ethyl-1,2,3,4-tetrahydrocarbazole.

2,3,3-Trimethylindolenine

A solution of 30 g (0.35 mole) of methyl isopropyl ketone and 37.6 g (0.35 mole) of phenylhydrazine in 100 ml of 95% ethyl alcohol, containing 3 drops of glacial acetic acid, was refluxed for 3 h. The alcohol was removed and the residual oil distilled; b.p. 145 °C at 14 mm; yield, 32 g (52%) of *methyl isopropyl ketone phenylhydrazone*, lit. b.p. 175–176 °C at 47 mm (16).

The i.r. and n.m.r. spectra supported the structure indicated.

The methyl isopropyl ketone phenylhydrazone was converted to 2,3,3-trimethylindolenine according to published directions (16) using an atmosphere of nitrogen rather than hydrogen.

The n.m.r. spectrum agreed with the structure. Signals were found at τ 2.4–3.0 (4H, aromatic, multiplet), τ 7.75 (3H, for CH_3 attached to N=C, singlet) and τ 8.73 (6H, singlet for two aliphatic CH_3 groups).

The i.r. spectrum (film) showed a strong band at 1580 cm^{-1} (C=N); lit., C=N, 1579 cm^{-1} (neat) (17).

The u.v. absorption spectrum in cyclohexane is shown in Fig. 4; λ_{max} = 214 mμ (ε = 11 640), 219 mμ (ε = 10 220), and 252 mμ (ε = 3950), lit., 216 mμ (log ε = 4.27), 255 mμ (log ε = 3.78) in 95% ethanol (17).

Condensation of Cyclohexanone

(a) With N'Methyl-2,6-dimethylphenylhydrazine

A solution of *N'*-methyl-2,6-dimethylphenylhydrazine hydrochloride (1 g, 0.0054 mole) in 20 ml of water was made alkaline with 5% aqueous sodium hydroxide, and the resulting mixture extracted with ether. The ether solution was washed with water (2 × 20 ml), dried ($MgSO_4$), and was freed from solvent. To the residual oil, in 20 ml of dry benzene, was added 0.5 g (0.0052 mole) of freshly distilled (twice) cyclohexanone. The mixture, in an apparatus equipped with a trap to collect the azeotropically distilled water (4), was heated under reflux for 1.5 h in an atmosphere of nitrogen. The solution became dark. Water collected in the Dean–Stark trap and was identified by its reaction with anhydrous copper sulfate (colorless → dark blue) and by its retention time on a gas–liquid chromatogram.

The reaction mixture was then freed from benzene and the residual dark oil allowed to stand at room temperature for 2–3 h. The solid which was deposited was collected and recrystallized from 95% ethanol. Needles were obtained, melting at 152–153 °C, identical in all respects (i.r. and n.m.r. spectra and mixture melting point) with authentic *8,9-dimethyl-1,2,3,4-tetrahydrocarbazole*; yield, 240 mg (22%). Its u.v. spectrum is shown in Fig. 1.

Anal. Calcd. for $C_{14}H_{17}N$: C, 84.42; H, 8.54; N, 7.03. Found: C, 84.83; H, 8.47; N, 6.89.

In a repetition of the above experiment, 2.6 g (0.014 mole) of *N'*-methyl-2,6-dimethylphenylhydrazine, first separated from the hydrogen chloride, was heated with cyclohexanone (1.6 g, 0.016 mole) in refluxing benzene for 1 h, using the same apparatus as above. A current of nitrogen gas was passed through the apparatus to carry away evolved gases into a trap of dry ether saturated with hydrogen chloride gas. A colorless precipitate (~80 mg) accumulated in the acidified ether. This substance decomposed at 350 °C. Its n.m.r. spectrum in D_2O showed only one significant signal, that for DOH at τ 5.28. A minute peak at τ 7.3 suggested the presence and hence the formation of methylamine (as the hydrochloride). Treatment of the solid with aqueous sodium hydroxide liberated ammonia.

Water was obtained from the Dean–Stark trap and identified as such. Gas–liquid chromatography of the

Can. J. Chem. Downloaded from www.nrcresearchpress.com by 210.87.254.40 on 09/05/12
For personal use only.

benzene solution, or the water or benzene obtained from the Dean–Stark trap, showed no evidence of the presence of methyl alcohol.

(b) With N′-Methyl-2,6-dimethylphenylhydrazine Hydrochloride

A mixture of *N′*-methyl-2,6-dimethylphenylhydrazine hydrochloride (1 g, 0.0054 mole) and cyclohexanone (0.7 g, ~0.007 mole) was heated in dry refluxing benzene (30 ml) for 2.5 h in the apparatus used in (*a*) above. The formation of water in the Dean–Stark trap was not at all clear, but that it actually was a product of the reaction was shown in a repetition of this experiment using 3 g rather than 1 g of the hydrochloride. The refluxing solution, which did not darken, but merely changed from red to yellow, deposited a colorless solid. This was separated and air-dried (95 mg). It showed some collapse at 225 °C, then darkened and partly sublimed in the melting point tube and finally completely melted at 300 °C. The n.m.r. spectrum in D_2O showed a very large signal at τ 5.37 for DOH and a small one at τ 7.43 for NCH_3 in the area ratio of ~15:1, indicating that the precipitate was essentially ammonium chloride (~33% yield) contaminated with a small amount of methylammonium chloride (~6%).

The yellow benzene filtrate was freed from solvent, and the residual yellow oil readily deposited crystals (500 mg). Recrystallization from 95% ethanol gave 450 mg (42%) of 8,9-dimethyl-1,2,3,4-tetrahydrocarbazole melting at 151 °C. When 3 g of starting material was used, the yield of the pure 8,9-dimethyltetrahydrocarbazole increased to 55%.

(c) With N′-Ethyl-2,6-dimethylphenylhydrazine Hydrochloride

A mixture of 1 g (0.005 mole) of *N′*-ethyl-2,6-dimethylphenylhydrazine hydrochloride and 0.5 g (0.005 mole) of cyclohexanone in 30 ml of dry benzene was heated under reflux (N_2) for 3 h in an apparatus equipped with a Dean–Stark water trap. No water was apparent in the trap but this again was no doubt due to the small amount of starting material used. The solid precipitate (132 mg) was separated from the reaction mixture. Its n.m.r. spectrum in D_2O showed it to be essentially ammonium chloride contaminated with a small amount of ethylammonium chloride: a large signal (broad singlet) at τ 5.33 (DOH) and small signals for CH_3—CH_2N discernible only under high amplification as a triplet centered at τ 8.80 and a quartet centered at τ 6.93 (J = 8 Hz).

The filtrate was freed from benzene and the residual reddish-yellow oil, under vacuum in the rotary evaporator, was subjected to a temperature of 40–50 °C for 4 h to complete the removal of cyclohexanone. When the residue was cooled in a salt–ice bath, yellow crystals (150 mg) were obtained. Recrystallization from 95% ethanol gave 140 mg (13%) of *9-ethyl-8-methyl-1,2,3,4-tetrahydrocarbazole*, m.p. 55–57 °C.

Anal. Calcd. for $C_{15}H_{19}N$: C, 84.46; H, 8.92; N, 6.57. Found: C, 84.35; H, 8.94; N, 6.65.

The u.v. spectrum is shown in Fig. 6 and supports the assigned structure; λ_{max} = 232 mμ (ε = 36 000), 286 mμ (ε = 7100).

The i.r. spectrum in CCl_4 showed no absorption in the NH region.

The n.m.r. spectrum agreed completely with the structure proposed and showed the following signals: τ 2.6–3.3 (3H, aromatic, multiplet), τ 5.82 (2H, quartet for N—CH_2—CH_3, J = 7 Hz), τ 8.77 (3H, triplet for CH_3—CH_2—N, J = 7 Hz), τ 7.33 (3H, singlet for aromatic CH_3), and two multiplets at τ 7.37 and τ 8.16 for the 8H characteristic of the tetrahydro ring.

Attempts to condense the free *N′*-ethyl-2,6-dimethylphenylhydrazine with cyclohexanone in refluxing benzene with or without catalytic amounts of acetic acid, boron trifluoride etherate or *p*-toluenesulfonic acid resulted in considerable and rapid darkening of the reaction mixture. No product such as 9-ethyl-8-methyl-1,2,3,4-tetrahydrocarbazole could be induced to crystallize out of it. Chromatography of the reaction mixture on neutral alumina was fruitless.

(d) With N′-Methyl-2,6-diethylphenylhydrazine Hydrochloride

N′-Methyl-2,6-diethylphenylhydrazine hydrochloride (1 g, 0.0047 mole) and 0.7 g (0.007 mole) of cyclohexanone were heated for 4 h in refluxing dry benzene (30 ml). The colorless solid (110 mg) obtained from the reaction mixture by filtration proved to be essentially ammonium chloride contaminated with a very small amount of methylammonium chloride. Removal of the benzene and excess cyclohexanone from the filtrate gave a yellow oil which, when cooled, deposited a solid. Crystallization from 95% ethanol gave 380 mg (38%) of *8-ethyl-9-methyl-1,2,3,4-tetrahydrocarbazole*, m.p. 58–59 °C.

Anal. Calcd. for $C_{15}H_{19}N$: C, 84.46; H, 8.98; N, 6.57. Found: C, 84.14; H, 8.99; N, 6.58.

The i.r. spectrum in CCl_4 showed no NH absorption. The u.v. spectrum is shown in Fig. 5 and supports the assigned structure; λ_{max} = 233 mμ (ε = 32 000), 286 mμ (ε = 5900).

The n.m.r. spectrum corroborated the assigned structure and showed the following signals: τ 2.5–3.2 (3H, aromatic, multiplet), τ 6.26 (3H, singlet for NCH_3), τ 6.94 (2H, quartet for CH_2—CH_3 attached to the benzene ring, J = 7.5 Hz), τ 8.70 (3H, triplet for —CH_2—CH_3, J = 7.5 Hz), and two multiplets at τ 7.35 and τ 8.13 (8H, characteristic of the tetrahydro ring).

When cyclohexanone was condensed with the free *N′*-methyl-2,6-diethylphenylhydrazine under the same conditions as above, the dark oil obtained from the benzene filtrate failed to deposit crystals. When this oil was dissolved in benzene, then treated with three drops of glacial acetic acid and the resulting solution heated under reflux for 1 h, workup of the reaction mixture gave 60 mg (~4%) of pure 8-ethyl-9-methyl-1,2,3,4-tetrahydrocarbazole.

Acknowledgment

We thank the National Research Council of Canada for some financial support throughout the course of this work.

1. F. P. Robinson and R. K. Brown. Can. J. Chem **42**, 1940 (1964).
2. R. B. Carlin and E. E. Fisher. J. Am. Chem. Soc. **70**, 3421 (1948).
3. B. Robinson. Chem. Rev. **63**, 373 (1963).
4. S. H. Oakeshott and S. G. P. Plant. J. Chem. Soc. 486 (1927).

5. E. W. DEAN and D. D. STARK. Ind. Eng. Chem. **12**, 486 (1920).
6. L. J. BELLAMY. The infrared spectra of complex molecules. 2nd. ed. John Wiley and Sons, Inc., New York. 1958. p. 267.
7. R. B. CARLIN and D. P. CARLSON. J. Am. Chem. Soc. **81**, 4673 (1959).
8. W. BAKER, W. D. OLLIS, and J. D. POOLE. J. Chem. Soc. 3389 (1950).
9. F. P. ROBINSON and R. K. BROWN. Can. J. Chem. **39**, 1171 (1961).
10. S. I. HEILBRON and H. M. BUNBURY. Dictionary of organic compounds. Vol. IV. Eyre and Spottiswoode Ltd., London. 1953. p. 682.
11. R. L. HINMAN. J. Org. Chem. **22**, 148 (1957).
12. E. FISCHER and M. BÖSLER. Ann. **212**, 338 (1882).
13. B. M. BARCLAY and N. CAMPBELL. J. Chem. Soc. 530 (1945).
14. E. L. CLINE and E. E. EMMET REID. J. Am. Chem. Soc. **49**, 3150 (1927).
15. K. H. PAUSACKER. J. Chem. Soc. 621 (1950).
16. G. PLANCHER. Ber. **31**, 1496 (1898).
17. W. E. NOLAND and C. F. HAMMER. J. Org. Chem. **25**, 1525 (1960).

Can. J. Chem. Downloaded from www.nrcresearchpress.com by 210.87.254.40 on 09/05/12
For personal use only.

Can. J. Chem. Downloaded from www.nrcresearchpress.com by 210.87.254.42 on 09/05/12
For personal use only.

Préparation de quelques nouveaux dérivés de la morpholone-2

KRZYSZTOF JANKOWSKI ET CASIMIR BERSE
Département de chimie, Université de Montréal, Montréal, Québec

Reçu le 19 décembre 1967

Plusieurs morpholones-2 substituées ont été obtenues par la réaction d'ouverture d'époxydes avec la glycine et ses dérivés. Les structures des composés obtenus ont été déterminées par la spectroscopie de résonance magnétique nucléaire.

Canadian Journal of Chemistry, 46, 1939 (1968)

Au cours de travaux précédents (1, 2), nous avons constaté que parmi les produits de l'ouverture des époxydes par les acides aminés, se retrouvaient des morpholones-2. Différentes méthodes de préparation de morpholones-2 ont été rapportées par plusieurs auteurs (3–11). Il nous a donc semblé intéressant de tenter la synthèse de morpholones-2 substituées et d'étudier leurs propriétés (12).

Résultats

Les morpholones-2 obtenues sont très instables, extrêmement sensibles à l'humidité et à l'oxydation (6, 7). Elles se décomposent en quelques heures. Notre travail a donc été limité à la détermination de leurs structures par les méthodes spectroscopiques et analytiques. L'ensemble des résultats observés est résumé dans le Tableau I.

Les synthèses des morpholones-2 ont été réalisées à la suite des réactions suivantes.

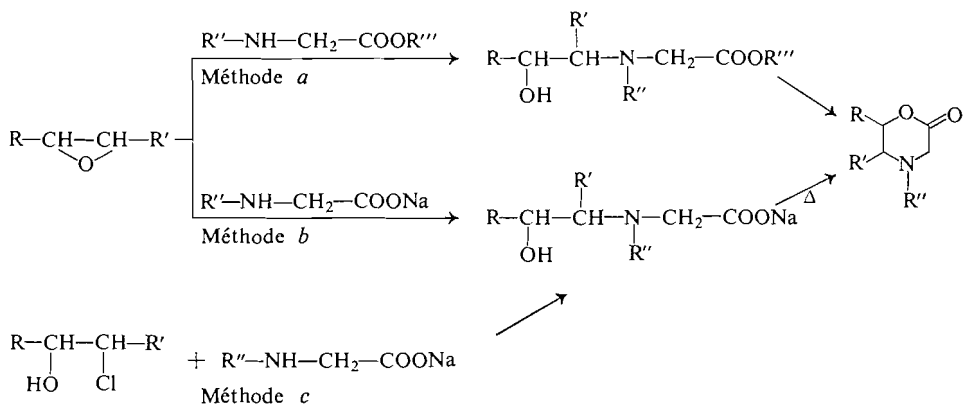

Il faut signaler que les rendements calculés pour les produits purs ont été très faibles. La préparation des morpholones-2 se trouvaient limitée à la fois par la formation des dicéto-2,5 piperazines, des produits de polymérisation des époxydes et par une décomposition importante.

Les spectres de résonance magnétique nucléaire (r.m.n.) des morpholones-2, des *N*-méthylmorpholones-2 et des *N*-phénylmorpholones-2 montrent un déplacement chimique des protons —NH—, $N—CH_3$ et $N—C_6H_5$ qui varie entre 1.60–2.00, 2.05–2.27, 6.27–7.30 p.p.m. et des protons $—CH_2—\overset{\overset{O}{\|}}{C}—$ qui varie entre 2.90–3.30, 2.90–3.13 et 3.45–3.85 p.p.m. respectivement.

Les constantes de couplage des protons

TABLEAU I

Résultats spectroscopiques

Acides aminés	Epoxydes dérivés de	Formule	Nom	p.f. (°C)	p.éb. (°C/mm)	Méthode	Rendement %	Infrarouge C=O cm^{-1}	Résonance magnétique N–R: R=H, CH_3 ou C_6H_5	Résonance magnétique CH_2—CO
Glycine	Ethylène	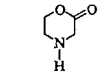	Morpholone-2	—	70/4	a c	3 ~3	1700	1.7	3.22
Glycine	Butène-1,2	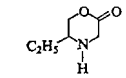	Ethyl-5 morpholone-2	—	80/6	a	0.8	1715	1.6	2.9 (*J*=5 c.p.s.)
Glycine	Cyclopentène	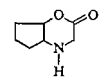	Perhydrocyclopenta-[*b*]-oxazine-1,4 one-2	—	170–173/110	c	0.5	1700	—	—
Glycine	Cyclohexène	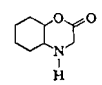	Perhydrobenzoxazine-1,4 one-2 (2)	—	61–65/5	a c	3 1.7	1715	2.0	3.30
Glycine	Styrène	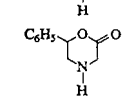	Phényl-6 morpholone-2 (1)	121	—	réf. 1	0.08	1720	2.6 (?)	3.20
Glycine	Stilbène	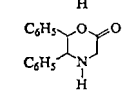	*cis*-diphényl-5,6 morpholone-2 (2)	86	—	réf. 2	1.7	1722	—	3.12
Sarcosine	Ethylène	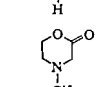	N-méthylmorpholone-2 (3)	—	217	c	14	1720	2.21	3.11
Sarcosine	Butène-1,2	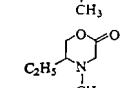	Ethyl-5 *N*-méthylmorpholone-2	—	155/12	a b	0.5 4.2	1717	2.05	2.9 (*J*=5 c.p.s.)
Sarcosine	Butène-2,3	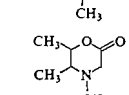	Triméthyl-4,5,6 morpholone-2	—	80–85/5	a b	0.4 7	1715	2.15	2.97
Sarcosine	Cyclohexène	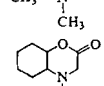	N-méthylperhydrobenzoxazine-1,4 one-2	—	220–224/17	c	3	1720	2.27	3.13
Sarcosine	Styrène	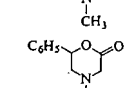	*N*-méthylphényl-6 morpholone-2	—	140–145/5	c	4	1711	2.1	2.9
N-phényl-glycine	Ethylène	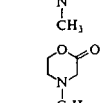	*N*-phénylmorpholone-2 (3)	75	—	c	12	1720	7.20	3.6
N-phényl-glycine	Butène-1,2	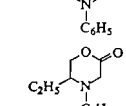	Ethyl-5*N*-méthylmorpholone-2	—	175–178/12	a b	1 1	1720	7.1	3.83
N-phényl-glycine	Cyclohexène	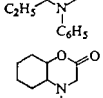	*N*-phénylperhydrobenzoxazine-1,4 one-2	—	240–245/5	b	2	1715	6.77 et 7.30	3.7
N-phényl-glycine	Styrène	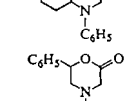	Diphényl-4,6 morpholone-2	—	178/0.2	b	0.5	1720	7.1	3.45 (*J*=6 c.p.s.)
N-phényl-glycine	Butène-2,3	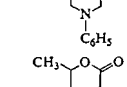	Diméthyl-5,6 *N*-phénylmorpholone-2	—	85/0.1	a b c	1.7 3	1717	6.72 et 7.25	3.68 (*J*=4 c.p.s.)

Can. J. Chem. Downloaded from www.nrcresearchpress.com by 210.87.254.42 on 09/05/12
For personal use only.

et analytiques

nucléaire δ (p.p.m.) dans $CDCl_3$				Analyse					
				Calculé			Trouvé		
CH—O ou CH_2—O	CH—N ou CH_2—N	Autres	Pour les composés	C	H	N	C	H	N
2.4	2.1	—	acide *N*-(hydroxy-2 éthyl) glycine p.f. 141° $C_4H_9O_3N$ (119.2)	40.30	7.52	—	40.33	7.85	—
2.4	2.1	CH_3 0.82 CH_2—CH_3 1.52	$C_6H_{11}O_2N$ (129.2)	55.80	8.58	10.84	54.93	8.58	10.47
—	—	—	$C_7H_{11}O_2N$ (125.2)	59.56	7.85	—	59.49	7.77	—
2.4	2.4	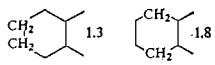 1.3 1.8	$C_8H_{13}O_2N$ (155.2)	—	—	9.03	—	—	8.89
2.45	4.60	C_6H_5 7.2	ref. 1	—	—	—	—	—	—
4.6	3.9	C_6H_5 7.2	ref. 2	—	—	—	—	—	—
4.29	2.57	—	$C_5H_9O_2N$ (115.1)	52.16	7.88	12.17	52.23	7.96	12.00
4.0	3.5	CH_3—CH_2 0.95 CH_3—CH_2 1.45	$C_7H_{13}O_2N$ (143.2)	—	—	9.78	—	—	9.52
3.85	2.47	CH_3 0.97	$C_7H_{13}O_2N$ (143.2)	—	—	9.78	—	—	9.47
2.4	2.4	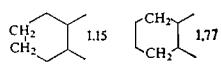 1.15 1.77	sel sodé p.f. 224–225° $C_9H_{17}O_3N$ Na (210.2)	51.68	7.60	—	51.41	7.77	—
3.9	2.3	C_6H_5 7.32	$C_{11}H_{13}O_2N$ (191.2)	—	—	7.32	—	—	6.85
3.9	3.5	—	$C_{10}H_{11}O_2N$ (177.2)	67.78	6.26	7.90	67.75	6.79	7.71
3.7	3.4	CH_3 1.1 CH_3—CH_2 1.65	sel sodé p.f. 175° $C_{12}H_{16}O_3N$ Na (245.2)	58.77	6.53	—	58.40	7.09	—
3.5	3.5	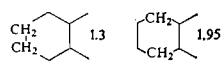 1.3 1.95	$C_{14}H_{17}O_2N$ (231.3)	72.40	7.41	6.06	71.70	6.95	5.81
2.4	3.75	C_6H_5—C 7.3	$C_{16}H_{15}O_2N$ (253.3) *Spectres de masse (m/e)* M^+ 253, $(M - 44)^+$ 209, $(M - 121)^+$ 132	75.87	5.97	5.53	75.18	6.77	5.41
3.86	3.6	CH_3—CH—N 1.07 CH_3—CH—O 1.14	M^+ 205, $(M - 44)^+$ 161, $(M - 121)^+$ 84						

Can. J. Chem. Downloaded from www.nrcresearchpress.com by 210.87.254.42 on 09/05/12
For personal use only.

$-CH_2-\overset{\overset{O}{\|}}{C}-$ varient entre 4-6 c.p.s. Aussi on observe que les déplacements chimiques des protons $-CH_2-\overset{\overset{O}{\|}}{C}-$ des *N*-phénylmorpholones-2 ont lieu vers le champ plus bas par rapport à ceux des morpholones-2 et des *N*-méthylmorpholones-2. On observe aussi que les déplacements chimiques des protons sur le carbone-5 ont les valeurs δ plus basses que ceux du carbone-6.

Les spectres de masse de deux *N*-phénylmorpholones-2 montrent la fragmentation avec perte de CO_2 et de phényle:

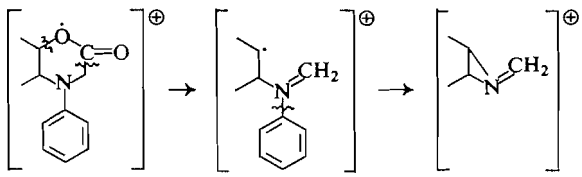

$[M]^{\oplus}$ $[M-44]^{\oplus}$ $[M-121]^{\oplus}$

Remerciements

Les auteurs remercient le Conseil National de Recherches du Canada pour l'aide financière apportée sous forme d'octroi de recherches.

Partie expérimentale

Les points de fusion ont été déterminés dans l'appareil de Kofler et ne sont pas corrigés. Les spectres infrarouges ont été enregistrés sur un spectrophotomètre Beckman IR-8 dans le Nujol. Les microanalyses ont été effectuées dans les laboratoires Midwest Microlab, Inc., Indianapolis, Indiana, U.S.A. et par nous-mêmes (micro Kjeldahl). Les spectres r.m.n. ont été enregistrés sur un spectromètre Varian A-60

Les produits utilisés pour les synthèses ont été soit commerciaux, soit préparés dans nos laboratoires par les méthodes connues (époxydes (14, 15, 17), chlorhydrines (16), dérivés des acides aminés (13, 18, 19)).

Préparation des morpholones-2

Méthode a

Une solution (environ 0.1 *M*) d'un époxyde (0.05 mole) dans l'éthanol absolu ou dans le chloroforme a été portée à reflux avec l'ester d'un acide aminé pendant 12 h. Le solvant a été évaporé *in vacuo* et le résidu a été distillé sous pression réduite. Le produit séparé a été purifié par plusieurs distillations fractionnées.

Méthode b

L'acide aminé (0.1 mole) a été traité par une quantité équimolaire de l'hydroxyde de sodium dissous dans environ 50 ml d'eau. L'époxyde (0.1 mole) a été ajouté sous forte agitation en maintenant la température entre −5 et 0 °C. L'addition terminée, le mélange réactionnel a été agité à la température ambiante pendant 12 h. Après le chauffage au bain-marie pendant 2 h, le mélange a été neutralisé avec l'acide chlorhydrique en présence de méthylorange. Le solvant a été chassé sous vide et le produit de la réaction a été fractionné également sous vide.

Méthode c

La solution d'un acide aminé (0.1 mole) dans l'hydroxyde de sodium (0.1 mole) a été chauffée au bain-marie pendant 1 h. La chlorhydrine d'un alcène (0.1 mole) a été ajoutée goutte à goutte. L'addition terminée, le mélange a été laissé pendant 24 h à la température ambiante, puis chauffé à reflux pendant 2 h. Le solvant a été évaporé *in vacuo* et le résidu a été dissous dans l'éthanol absolu à chaud. Le chlorure de sodium précipité a été séparé par filtration. Le solvant a été chassé sous vide et le résidu a été distillé deux fois sous pression réduite. Le produit a été dissous dans l'éther et la solution éthérée a été séchée avec le carbonate de potassium. Après évaporation de l'éther, le produit a été purifié par la distillation fractionnée sous vide. La *N*-phénylmorpholone-2 a été obtenue suivant la même méthode, mais le produit cristallise après la distillation. La *N*-phénylmorpholone-2 a été recristallisée de l'éthanol–éther.

Dans les trois méthodes, après la distillation, le résidu contient principalement des dicéto-2,5 piperazines et des polymères qui ne contiennent pas d'azote.

1. C. Berse et K. Jankowski. Can. J. Chem. **44**, 1513 (1966).
2. C. Berse et K. Jankowski. Can. J. Chem. **45**, 2865 (1967).
3. E. Knorr. Ann. **307**, 199 (1899); Ber. **32**, 732 (1899).
4. M. L. Pascal. Bull. Soc. Chim. France, 435 (1960).
5. A. T. De Mouilpied. J. Chem. Soc. **87**, 444 (1905). C. A. Bischoff. Ber. **30**, 2927 (1897). R. Vater. J. Prakt. Chem. **29**, 290 (1884).
6. A. I. Kiprianov. Chem. Abstr. **22**, 3134 (1928). A. I. Kiprianov et G. I. Kiprianov. Chem. Abstr. **24**, 1082 (1930). A. I. Kiprianov et D. M. Krasinskaya. Chem. Abstr. **25**, 5143 (1931).
7. N. H. Cromwell *In* Heterocyclic compounds. Vol. VI. *Edited by* R. C. Elderfield. J. Wiley and Sons, New York. 1956. p. 517.
8. E. Fourneau. Bull. Soc. Chim. France, 407, 1145 (1928).
9. M. Tiffneau et E. Fourneau. Bull. Soc. Chim. France, 977 (1913).
10. W. Cocker. J. Chem. Soc. 373 (1943).
11. H. Mosher, M. Frankl, et M. Gregory. J. Am. Chem. Soc. **75**, 5326 (1953). E. Havdeger et H. Ott. Helv. Chim. Acta, **38**, 213 (1955). P. Vièles et J. Séguin. Bull. Soc. Chim. France, 287 (1953); 1210 (1956). M. Izumi. Pharm. Bull. Tokyo, **2**, 275 (1954); **3**, 88 (1955).
12. P. Lebeau et M. M. Janot. Traité de pharm. chimie. Vol. III. Masson et Cie, Paris. 1955–1956. pp. 1270–1302.
13. E. Fischer. Ber. **34**, 436 (1901); **34**, 452 (1901).
14. D. J. Reif et H. O. House. Org. Synth. Coll. Vol. IV, 860 (1963).
15. A. E. Osterberg. Org. Synth. Coll. Vol. I, 185 (1941).
16. G. H. Coleman et H. F. Johnstone. Org. Synth. Coll. Vol. I, 158 (1941).
17. W. Meisner. Ber. **32**, 2052 (1899).
18. H. Biltz et K. Slotte. J. Prakt. Chem. [2] **113**, 252 (1926).
19. C. A. Bischoff et A. Hausdörfer. Ber. **25**, 2270 (1892).

Can. J. Chem. Downloaded from www.nrcresearchpress.com by 210.87.254.42 on 09/05/12
For personal use only.

Partition coefficients of some conjugated heteroenoid compounds in the system cyclohexane–water

C. E. LOUGH, R. F. SILVER, AND F. K. MCCLUSKY
Chemistry Section, Defence Research Establishment Suffield, Ralston, Alberta

Received November 2, 1967

Partition coefficients in cyclohexane–water were determined for 160 conjugated heteroenoid compounds and were used to calculate π constants for several component groupings of molecules.

Canadian Journal of Chemistry, 46, 1943 (1968)

Can. J. Chem. Downloaded from www.nrcresearchpress.com by 210.87.254.6 on 09/05/12
For personal use only.

Substituent and substituent interaction constants (π and π interaction) for some component groupings of molecules have already been developed (1) for the calculation of cyclohexane–water partition coefficients, *K*. Added support is now provided for this concept and π constants for several other component groupings of molecules are presented here for use in eq. [1].

$$[1] \quad \log K = \Sigma\pi + \Sigma\pi \text{ interaction} - 1.30$$

Partition coefficients were determined for 160 of the conjugated heteroenoid compounds prepared by Silver *et al.* (3) and consistent results were obtained even for the readily hydrolyzable compounds (2, 4) when the shaking times were reduced to 5 and 7.5 min and the interval between shakings was reduced to 3 min. The logarithms of these partition coefficients and those derived from eq. [1] using the π values previously reported (1) and the new values listed in Table III are presented in Tables I and II.[1]

The new π values reported here have indirectly permitted refinement of the π values assigned to the phenyl group. Only two values appear to be necessary. The value +2.75 is used in all cases with the following exceptions: for benzene itself and for mono-substituted benzenes when the substituent is alkyl, hydroxyl, hydroxymethyl, nitro, amino, cyano, or cyanomethyl. For each of these cases the value +3.65 is used. This factor improves the calculated values for the partition coefficients of ethyl benzoate, alkyl benzenes, benzyl alcohol, phenylacetonitrile, ethyl phenylacetate, 4-alkylguaiacols, and the acyl derivatives of vanillylamine in comparison to those reported in ref. 1.

Deviations of the calculated values from those observed were noted for the 3-*n*-butoxy derivatives of compounds with the generalized formula **1**. These, as well as the calculated values of the cinnamal analogues of **1** and those of some *p*-phenylene-bis compounds, **2**, are more positive than those measured, and similar anomalies

TABLE III
New π values for the system cyclohexane–water

X	π_x in RCH(X)R, RCH_2X, and CH_3X	π interaction
—COR	—	+0.60
$—CO_2R$	—	−0.30*
$—CONH_2$	−4.95	+1.75
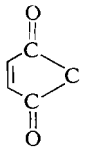	−0.15	—†
	−0.25	—†
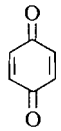	+1.05	—†
	+0.35	0.00‡

*This value is altered from that reported in ref. 1.
†None used.
‡Value when C-3 substituent is present.

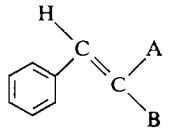

1

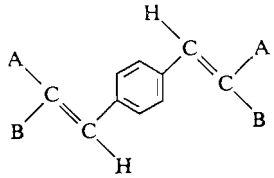

2

[1]Photocopies of Tables I and II may be obtained upon request, from The Depository of Unpublished Data, National Science Library, National Research Council of Canada, Ottawa, Canada.

Can. J. Chem. Downloaded from www.nrcresearchpress.com by 210.87.254.6 on 09/05/12
For personal use only.

have been reported by Hansch and Anderson (5). Work is in progress to relate these results to the conformations of these compounds in solution.

Acknowledgments

The authors thank Dr. D. J. Currie and Dr. H. L. Holmes for their suggestions concerning the π values assigned to the phenyl group.

1. D. J. Currie, C. E. Lough, R. F. Silver, and H. L. Holmes. Can. J. Chem. **44**, 1035 (1966).
2. R. B. Pritchard, C. E. Lough, J. B. Reesor, H. L. Holmes, and D. J. Currie. Can. J. Chem. **45**, 775 (1967).
3. R. F. Silver, K. A. Kerr, P. D. Frandsen, S. J. Kelley, and H. L. Holmes. Can. J. Chem. **45**, 1001 (1967).
4. R. B. Pritchard, C. E. Lough, D. J. Currie, and H. L. Holmes. Can. J. Chem. **46**, 775 (1968).
5. C. Hansch and S. M. Anderson. J. Org. Chem. **32**, 2583 (1967).

Essential oils and their constituents. XLII.[1] Isomerization of epoxides on active alumina

Ishwar C. Nigam and Leo Levi

Research Laboratories, Food and Drug Directorate, Department of National Health and Welfare, Ottawa, Canada

Received May 25, 1967

When chromatographed on active alumina, epoxides isomerize yielding chiefly the corresponding α,β-unsaturated alcohols. Side reactions were observed in some cases. Limonene oxide yielded *cis*-1 (7), 8 *p*-menthadien-ol-2, *cis*- and *trans*-carveol, perillyl alcohol, *trans*-8*p*-menthene-diol-1,2, and *cis*- and *trans*-dihydrocarvone. α-Pinene oxide was converted to pinocarveol, *cis*- and *trans*-pinocamphone, campholenic aldehyde and an unidentified alcohol. Caryophyllene oxide yielded three isomeric unsaturated alcohols which were converted to a ketone of known structure.

Canadian Journal of Chemistry, 46, 1942 (1968)

Recently Nigam and Levi observed that humulene oxide and caryophyllene oxide undergo characteristic isomerizations to unsaturated alcohols during column chromatography on alumina (1, 2). Similar findings were made by Damodaran and Dev (3). Prelog *et al.* observed the rearrangement of *trans*-cyclodecene epoxide to an allylic alcohol during chromatography over strongly activated alumina (4). It is the purpose of this communication to demonstrate the value of the reaction for the preparation of terpene alcohols which serve as valuable raw materials to the perfume, flavor, cosmetic, and pharmaceutical industries.

[1]Presented at the 153rd Meeting of the American Chemical Society, Miami Beach, Florida, April 1967. For the previous paper in this series, see Ishwar C. Nigam and G. A. Neville, J. Chromatog. **24**, 85 (1968).

Experimental

Preparation of Epoxides of Limonene, α-Pinene, and Caryophyllene

The hydrocarbons were allowed to react with equimolar amounts of perphthalic acid in ether solution for 72 h at 5 °C. The reaction mixtures were washed with 10% sodium carbonate solution until free from perphthalic acid (starch-iodine test) and were dried over anhydrous sodium sulfate. Removal of the solvent under reduced pressure gave the crude epoxides which were purified by chromatography on tenfold neutral grade III alumina.

Isomerization of the Epoxides

The purified compounds were dissolved in a small volume of hexane, transferred to a column packed with grade I alumina (1:25 by weight), and eluted with ether. Products of rearrangement were recovered by evaporating the solvent under vacuum.

Analysis of Isomerization Products

The isolates were examined by gas–liquid chromatography (g.l.c.) employing apparatus and procedures pre-

FOR ERRATA SEE
Vol. 46 1968 p. 3419

Can. J. Chem. Downloaded from www.nrcresearchpress.com by 210.87.254.6 on 09/05/12
For personal use only.

have been reported by Hansch and Anderson (5). Work is in progress to relate these results to the conformations of these compounds in solution.

Acknowledgments

The authors thank Dr. D. J. Currie and Dr. H. L. Holmes for their suggestions concerning the π values assigned to the phenyl group.

1. D. J. Currie, C. E. Lough, R. F. Silver, and H. L. Holmes. Can. J. Chem. **44**, 1035 (1966).
2. R. B. Pritchard, C. E. Lough, J. B. Reesor, H. L. Holmes, and D. J. Currie. Can. J. Chem. **45**, 775 (1967).
3. R. F. Silver, K. A. Kerr, P. D. Frandsen, S. J. Kelley, and H. L. Holmes. Can. J. Chem. **45**, 1001 (1967).
4. R. B. Pritchard, C. E. Lough, D. J. Currie, and H. L. Holmes. Can. J. Chem. **46**, 775 (1968).
5. C. Hansch and S. M. Anderson. J. Org. Chem. **32**, 2583 (1967).

Essential oils and their constituents. XLII.[1] Isomerization of epoxides on active alumina

Ishwar C. Nigam and Leo Levi

Research Laboratories, Food and Drug Directorate, Department of National Health and Welfare, Ottawa, Canada

Received May 25, 1967

When chromatographed on active alumina, epoxides isomerize yielding chiefly the corresponding α,β-unsaturated alcohols. Side reactions were observed in some cases. Limonene oxide yielded *cis*-1 (7), 8 *p*-menthadien-ol-2, *cis*- and *trans*-carveol, perillyl alcohol, *trans*-8*p*-menthene-diol-1,2, and *cis*- and *trans*-dihydrocarvone. α-Pinene oxide was converted to pinocarveol, *cis*- and *trans*-pinocamphone, campholenic aldehyde and an unidentified alcohol. Caryophyllene oxide yielded three isomeric unsaturated alcohols which were converted to a ketone of known structure.

Canadian Journal of Chemistry, 46, 1942 (1968)

Recently Nigam and Levi observed that humulene oxide and caryophyllene oxide undergo characteristic isomerizations to unsaturated alcohols during column chromatography on alumina (1, 2). Similar findings were made by Damodaran and Dev (3). Prelog *et al.* observed the rearrangement of *trans*-cyclodecene epoxide to an allylic alcohol during chromatography over strongly activated alumina (4). It is the purpose of this communication to demonstrate the value of the reaction for the preparation of terpene alcohols which serve as valuable raw materials to the perfume, flavor, cosmetic, and pharmaceutical industries.

[1]Presented at the 153rd Meeting of the American Chemical Society, Miami Beach, Florida, April 1967. For the previous paper in this series, see Ishwar C. Nigam and G. A. Neville, J. Chromatog. **24**, 85 (1968).

Experimental

Preparation of Epoxides of Limonene, α-Pinene, and Caryophyllene

The hydrocarbons were allowed to react with equimolar amounts of perphthalic acid in ether solution for 72 h at 5 °C. The reaction mixtures were washed with 10% sodium carbonate solution until free from perphthalic acid (starch-iodine test) and were dried over anhydrous sodium sulfate. Removal of the solvent under reduced pressure gave the crude epoxides which were purified by chromatography on tenfold neutral grade III alumina.

Isomerization of the Epoxides

The purified compounds were dissolved in a small volume of hexane, transferred to a column packed with grade I alumina (1:25 by weight), and eluted with ether. Products of rearrangement were recovered by evaporating the solvent under vacuum.

Analysis of Isomerization Products

The isolates were examined by gas–liquid chromatography (g.l.c.) employing apparatus and procedures pre-

FOR ERRATA SEE
Vol. 46 1968 p. 3419

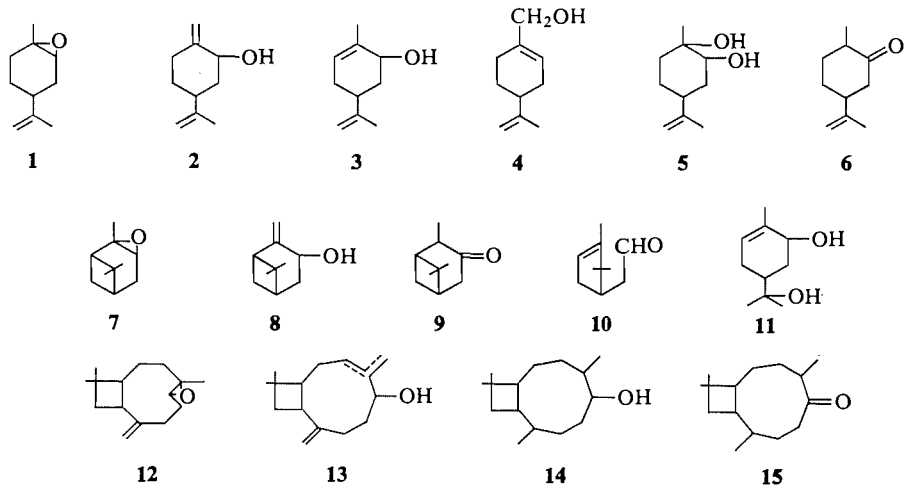

viously described (5, 6). Constituents were identified by comparison of retention times with those of pure reference standards, and by infrared analysis of effluents collected following repeated sample injections and purified by rechromatography under optimal conditions of temperature and carrier gas flow rate.

Conversion of Unsaturated Alcohols from Caryophyllene Oxide to Saturated Ketone

The reaction was carried out in two steps.

Hydrogenation of Unsaturated Alcohols

Each of the three unsaturated alcohols *a*, *b*, and *c* (120 mg, 30 mg, and 30 mg, respectively) was dissolved in glacial acetic acid and hydrogenated at atmospheric pressure in the presence of platinum oxide catalyst until gas absorption ceased. The hydrogenated products were recovered in the usual manner and analyzed by g.l.c. (Column: 20% Reoplex 400 on acid washed Chromosorb W; Temperature 200 °C; Helium: 75 ml/min).

Oxidation of Saturated Alcohols

The crude hydrogenation products obtained from alcohols *a*, *b*, and *c* (Step 1) were dissolved in pyridine (2.0 ml, 0.5 ml, and 0.5 ml, respectively), treated with a solution of 1.5 g of chromium trioxide in 20 ml pyridine (2.0 ml, 0.5 ml, and 0.5 ml, respectively) and the reaction mixtures processed as described previously (2).

Results and Discussion

Product yields obtained by isomerization of limonene oxide (**1**) on basic, neutral, and acidic alumina are shown in Table I. Major products of the reaction were *cis*-1 (7), 8 *p*-menthadiene-ol-2 (**2**), and *cis*- and *trans*-carveol (**3**). Perillyl alcohol (**4**) was formed by allylic rearrangement of (**2**). Side reactions produced *trans*-8*p*-menthene-diol-1,2 (**5**) and *cis*- and *trans*-dihydrocarvone (**6**). These products were also obtained when limonene oxide was isomerized in the

TABLE I

Isomerization products from limonene oxide*

Compound	Retention time†	Product yield (%); type of alumina used: Basic	Neutral	Acidic
trans-Dihydrocarvone	4.9‡	2	3	17
cis-Dihydrocarvone	5.2‡			
cis-1(7),8*p*-Menthadien-ol-2	6.4	33	27	28
trans-Carveol	7.2‡	28	16	17
cis-Carveol	7.7‡			
Perillyl alcohol	8.4	15	11	11
trans-8*p*-Menthene-diol-1,2	26.3	18	40	12
Unidentified	—	4	3	15

*The column used was: Reoplex 400 (20%) on acid washed Chromosorb W. The temperature was 200 °C; and the helium flow rate was 75 ml/min.
†In minutes.
‡Isomers not sufficiently resolved to permit individual estimations.

TABLE II

Isomerization products from α-pinene oxide*

Compound	Retention time†	Product yield (%); type of alumina used: Basic	Neutral	Acidic
Campholenic aldehyde	5.3	7	8	6
trans-Pinocamphone	6.3‡	13	26	53
cis-Pinocamphone	6.9‡			
Pinocarveol	7.9	63	43	22
Alcohol (unidentified)	11.1	13	18	15
Constituents not characterized	—	4	5	4

*The column used was: Reoplex 400 (20%) on acid washed Chromosorb W. The temperature was 170 °C and the helium flow rate was 75 ml/min.
†In minutes.
‡Isomers not sufficiently resolved to permit individual estimations.

Can. J. Chem. Downloaded from www.nrcresearchpress.com by 210.87.254.6 on 09/05/12
For personal use only.

TABLE III

Isomerization products from caryophyllene oxide

				Unsaturated alcohol				
				Infrared		Nuclear magnetic resonance†		
Compound	% yield	Melting point	Retention time*	Band	Assignment	Chemical shift	Assignment	Mass spectrum‡
a	67	—	18.3	3360	—OH	0.98	CH_3, CH_3 >C<	*m/e* = 220
				1020	—OH	4.75	CH_2=C<	
				3080	>C=CH_2	4.96§	CH_2=C<	
				1638	>C=CH_2			
				898	>C=CH_2			
				882	>C=CH_2			
b	18	—	20.6	3350	—OH	—	—	—
				1012	—OH			
				3080	>C=CH_2			
				1630	>C=CH_2			
				880	>C=CH_2			
				825	>C=CH—			
c	15	79–80 °C	23.1	3240	—OH	—	—	*m/e* = 220
				1043	—OH			
				1005	—OH			
				3080	>C=CH_2			
				1625	>C=CH_2			
				880	>C=CH_2			
				827	>C=CH—			
				780	>C=CH—			

*The column used was: Reoplex 400 (20%) on acid washed Chromosorb W. The temperature was 200 °C and the helium flow rate was 75 ml/min. The retention time is given in minutes.
†Nuclear magnetic resonance spectra were recorded using $CDCl_3$ as solvent and TMS as internal standard. Chemical shifts are given as p.p.m.
‡The parent peak in the mass spectrum is given.
§This absorption appeared as a doublet with broad peaks with J = 5.5 c.p.s.

presence of pyridinium bromide (7). The isomerizations reported previously (8, 9) were generally carried out under more drastic conditions and led primarily to the formation of carbonyl compounds. Recently Humbert and Guth isomerized limonene oxide in the presence of alumina at 200 °C and identified carveol, dihydrocarvone, carvone, dihydrocarveol, and a cyclopentanic alcohol as reaction products (10). Formation of the latter three compounds was not observed in the present studies. The facile rearrangement of limonene oxide to alcohols and ketones is of biogenetic significance, since the epoxide has been identified in oil of gingergrass and may be the precursor of several related compounds occurring in this oil (7, 11).

Previous investigations showed that during cleavage of the oxirane ring of α-pinene oxide (7) the pinane carbon skeleton also ruptured leading to the formation of *p*-menthane deriva-

Can. J. Chem. Downloaded from www.nrcresearchpress.com by 210.87.254.6 on 09/05/12
For personal use only.

Can. J. Chem. Downloaded from www.nrcresearchpress.com by 210.87.254.6 on 09/05/12
For personal use only.

tives, e.g. carveol (**3**) and sobrerol (**11**) or of campholenic aldehyde (**10**) (12–16). The present study showed that isomerization of α-pinene oxide on alumina takes place without significant cleavage of the pinane skeleton. Formation of the major reaction products, pinocarveol (**8**) and pinocamphone (**9**) depended on the type of alumina employed (Table II). It has been reported recently that base-catalyzed rearrangement of α-pinene oxide also yields pinocarveol (17).

Caryophyllene oxide (**12**) is known to undergo skeletal rearrangements readily (18–20). However, in the present reaction, the caryophyllane carbon framework remained unchanged and the epoxide yielded three unsaturated alcohols (**13**) (*a*, *b*, and *c*, see Table III), one of which (*c*) was a solid (m.p. 79–80 °C). A mixture of these allylic alcohols was prepared by Holub *et al.* by isomerization of caryophyllene oxide with pyridinium bromide (21). Molecular weights of *a* and *c*, determined by mass spectrometry, agreed with the formula $C_{15}H_{24}O$. Hydrogenation of these alcohols yielded mixtures of corresponding saturated alcohols (**14**), which on chromic acid oxidation formed the same saturated ketone (**15**). The identity of this ketone was established by comparison of its infrared (i.r.) spectrum with that published in literature (21). On the basis of i.r. and nuclear magnetic resonance (n.m.r.) spectral data (Table III), alcohol *a* may be characterized as the isomer containing the double bond, allylic to the hydroxyl group, in the exocyclic position. Both alcohols *b* and *c* possess a trisubstituted double bond and an exocyclic methylene group, and, therefore, appear to be stereoisomers.

The isomerizations of epoxides were brought about by alumina of grade I activity. Only unchanged epoxides were recovered when the catalyst was partially deactivated by the addition of 4–6% of water. Evidently, the isomerizations are initiated at active surface sites of the alumina (22), and one or more of the following three reactions takes place: (*i*) hydration to form a vicinal glycol, (*ii*) rearrangement to allylic alcohols, and (*iii*) rearrangement to a ketone. The glycol was apparently not an intermediate in the formation of the unsaturated alcohol for *trans*-8*p*-menthene-diol-1,2 was recovered unchanged when passed through a column of grade I alumina. Experiments employing different types of alumina indicated that a decrease in the acidity of alumina favors the formation of allylic alcohols and reduces the ketone yield. Of the two unsaturated alcohols, the isomer containing an exocyclic methylene group was formed in preference to that containing an endocyclic double bond.

Acknowledgments

The authors are indebted to Dr. J. L. Holmes and Mr. P. Hanbury for the measurement of mass spectra and n.m.r. spectra, respectively, and to Mrs. C. Radecka for gas chromatographic purification of alcohols derived from caryophyllene oxide. Special thanks are due to Mr. W. G. Strunk, F.M.C. Corporation, New York, for courteously providing samples of limonene oxide and α-pinene oxide.

1. I. C. Nigam and L. Levi. Can. J. Chem. **41**, 1726 (1962).
2. I. C. Nigam and L. Levi. J. Org. Chem. **29**, 2803 (1964).
3. N. P. Damodaran and S. Dev. Tetrahedron Letters, 1941 (1963).
4. V. Prelog, K. Schenker, and H. H. Günthard. Helv. Chim. Acta, **35**, 1598 (1952).
5. I. C. Nigam and L. Levi. Can. J. Chem. **40**, 2083 (1962).
6. I. C. Nigam, W. Skakum, and L. Levi. Perfumery Essent. Oil Record, **54**, 25 (1963).
7. M. C. Nigam, I. C. Nigam, and L. Levi. Can. J. Chem. **43**, 521 (1965).
8. E. E. Royals and L. L. Harrell, Jr. J. Am. Chem. Soc. **77**, 3405 (1955).
9. R. L. Settine, G. L. Parks, and G. L. K. Hunter. J. Org. Chem. **29**, 616 (1964).
10. F. Humbert and G. Guth. Bull. Soc. Chim. France, 2867 (1966).
11. Y. R. Naves and A. V. Grampoloff. Compt. Rend. **249**, 306 (1959); Bull. Soc. Chim. France, 37 (1960).
12. S. S. Nametkin and A. G. Yartzeva. Zh. Russ. Fiz.-Khim. Obshchestva, **55**, 521 (1924).
13. B. A. Arbusov and B. M. Mikhailow. J. Prakt. Chem. **127**, 1 (1930).
14. B. A. Arbusov. Ber. **68**, 1430 (1935).
15. B. A. Arbusov and Z. G. Isaeva. Zh. Obshch. Khim. **24**, 1250 (1954).
16. E. E. Royals and J. C. Leffingwell. J. Org. Chem. **29**, 2098 (1964).
17. J. K. Crandall and L. H. Chang. J. Org. Chem. **32**, 435 (1967).
18. A. Aebi, D. H. R. Barton, and A. S. Lindsay. J. Chem. Soc. 3124 (1953).
19. E. W. Warnhoff. Can. J. Chem. **42**, 1664 (1964).
20. I. C. Nigam and L. Levi. J. Org. Chem. **30**, 653 (1965).
21. M. Holub, V. Herout, M. Horak, and F. Sorm. Collection Czech. Chem. Commun. **24**, 3730 (1959).
22. H. Pines and W. O. Haag. J. Org. Chem. **82**, 2471 (1960).

Thermal condensation of formaldehyde with 3-*p*-menthene, 1-*p*-menthene, and cyclooctene

SHOJI WATANABE, KYOICHI SUGA, AND MASAYUKI KUNIYOSHI
Department of Applied Chemistry, Faculty of Engineering, Chiba University, Yayoicho, Chiba, Japan

Received October 23, 1967

When a mixture of 3-*p*-menthene, paraformaldehyde, and acetic anhydride was heated at 200 °C in an autoclave, an acetate was obtained. By saponification of the acetate with alcoholic potassium hydroxide, 3-hydroxylmethyl-4-*p*-menthene was obtained. Similarly, 2-hydroxymethyl-6-*p*-menthene was produced from 1-*p*-menthene, and 1-hydroxylmethyl-2-cyclooctene was produced from cyclooctene.

Canadian Journal of Chemistry, 46, 1948 (1968)

The addition reaction of formaldehyde with olefins is known as the Prins thermal reaction. The condensation product is mainly the primary alcohol or its acetate, in which the double bond is located at a position adjacent to its original site in the starting olefin (1, 2). This note describes the chemical structures of the Prins alcohols obtained from 3-*p*-menthene (**1**), 1-*p*-menthene (**4**), and cyclooctene (**6**).

From the condensation of 3-*p*-menthene (**1**) with *para*formaldehyde in the presence of acetic anhydride (at 200 °C), an acetate was obtained as the main product. The saponification of the acetate gave an unsaturated alcohol (**2**). The infrared (i.r.) absorption spectrum showed an absorption band at 810 cm^{-1}, indicating the presence of a trisubstituted ethylenic bond. Reduction of the alcohol gave 3-hydroxylmethyl-*p*-menthane (**3**). Therefore, **2** must be 3-hydroxylmethyl-4-*p*-menthene. The structural assignment was further supported by the nuclear magnetic resonance (n.m.r.) spectrum, as will be shown in the Experimental section.

Saponification of the condensation product from 1-*p*-menthene (**4**) with paraformaldehyde gave the corresponding alcohol, 2-hydroxylmethyl-6-*p*-menthene (**5**), as the main product. The structural assignment was supported by i.r. and n.m.r. spectra and also by the catalytic hydrogenation to the corresponding dihydro compound.

From the condensation product of cyclooctene (**6**), an unsaturated alcohol, $C_9H_{16}O$ (**7**), was obtained in ca. 23% yield. The infrared absorption spectrum showed a primary hydroxyl absorption band at 1040 cm^{-1}, and a characteristic band of a *cis* type double bond at 755 cm^{-1}. The dihydro compound obtained by the hydrogenation of **7** was hydroxylmethyl cyclooctane. Therefore, 1-hydroxylmethyl-2-cyclooctene (**7**) is a reasonable assignment for the alcohol.

Experimental

Materials

3-*p*-Menthene (**1**) was prepared as reported previously (3). It was repeatedly distilled until 90% pure. The boiling point at 100 Torr was 102 °C; n_D^{20}, 1.4518.

1-*p*-Menthene (**4**) was prepared by the hydrogenation of *d*-limonene over palladium on carbon: b.p. 68–70 °C at 41 Torr; d_4^{20}, 0.8401; n_D^{20}, 1.4730, infrared: 1360–1380 cm^{-1} (doublet), 800 cm^{-1}.

Commercial cyclooctene (**6**) was fractionally distilled until 95% pure (as shown by gas–liquid chromatographic analysis), b.p. 32 °C at 10 Torr; d_4^{25}, 0.8451; n_D^{25}, 1.4732; infrared: 750 cm^{-1}.

Condensation of 3-p-Menthene (1) with Formaldehyde

A mixture of 180 g of **1**, 60 g of *para*formaldehyde and 75 g of acetic anhydride was heated at 180–220 °C in a stainless steel autoclave for several hours. The reaction mixture was extracted with ether. The ethereal solution was then washed with water and dried over anhydrous sodium sulfate. Fractional distillation gave 102 g of **1** and 60 g of a crude acetate (b.p. 90–110 °C at 5 Torr). Saponification of the product gave 25 g of **2**. This was fractionally distilled until a pure product was obtained, b.p. 100–104 °C at 5 Torr; n_D^{30}, 1.4815; d_4^{30}, 0.9160; hydroxyl group, 10.81% (calcd. for monohydric alcohol, 10.11%); infrared (i.r.): 1050 cm^{-1}, 810 cm^{-1}; nuclear magnetic resonance (n.m.r.): δ 0.97 (two CH_3), δ 1.08 (CH_3), δ 1.72 (two—CH_2), δ 3.60 (—CH_2OH), δ 5.45 (—CH=C—).

Anal. Calcd. for $C_{11}H_{20}O$: C, 78.49; H, 11.98. Found: C, 78.31; H, 11.64.

The 3,5-dinitrobenzoate derivative of **2** was prepared in the usual manner and recrystallized from methanol, m.p. 81 °C.

Anal. Calcd. for $C_{18}H_{22}O_6N_2$: N, 7.73. Found: N, 7.88.

Compound **2** was hydrogenated over a Raney nickel catalyst in methanol solution at 100 °C. An initial hydrogen pressure of 50 kg/cm^2 was used to give 3-hydroxylmethyl-*p*-menthane (**3**), b.p. 91–94 °C at 5 Torr; n_D^{20}, 1.4738; n.m.r.: δ 0.93 (two CH_3), δ 1.02 (CH_3—), δ 1.46 (—CH_2—), δ 2.46 (OH), and δ 3.55 (—CH_2OH).

Anal. Calcd. for $C_{11}H_{22}O$: C, 77.59; H, 13.03. Found: C, 77.12; H, 12.87.

Condensation of 1-p-Menthene (4) with Formaldehyde

From a mixture of 38 g of **4**, 8.5 g of *para*formaldehyde and 14 g of acetic anhydride, 15 g of a crude acetate was obtained. Saponification of this acetate gave 2-hydroxylmethyl-6-*p*-menthene, b.p. 92 °C at 3 Torr; d_4^{20}, 0.9378; n_D^{20}, 1.4850; molecular refraction 52.10 (calcd. for $C_{11}H_{20}O$, F_1 = 51.85); i.r.: 1385 and 1365 cm^{-1} (doublet), 1030 cm^{-1}, 800 cm^{-1}; n.m.r.: δ 0.9 (two CH_3), δ 1.4 (CH_3—C=), δ 1.65 (CH_2—), δ 1.8 (—CH_2—C=), δ 2.2 (O*H*), δ 3.68 (—CH_2OH), δ 5.6 (—CH—C=).

Anal. Calcd. for $C_{11}H_{20}O$: C, 78.49; H, 11.98. Found: C, 78.12; H, 11.36.

The 3,5-dinitrobenzoate derivative of **5** was prepared and recrystallized from methanol, m.p. 138–139 °C.

Anal. Calcd. for $C_{17}H_{22}O_6N_2$: N, 7.73. Found: N, 7.70.

The compound **5** absorbed one equivalent of hydrogen by catalytic hydrogenation to give 2-hydroxylmethyl-*p*-menthane, b.p. 88 °C at 3 Torr.

Anal. Calcd. for $C_{11}H_{22}O$: C, 77.59; H, 13.03. Found: C, 77.36; H, 12.99.

Condensation of Cyclooctene (6) with Formaldehyde

From a mixture of 45 g of **6**, 14.5 g of *para*formaldehyde, and 20.5 g of acetic anhydride, 21 g of a crude acetate was obtained. Saponification of this acetate gave 1-hydroxylmethyl-2-cyclooctene (**7**), b.p. 74–76 °C at 2 Torr; d_4^{20}, 0.9778; n_D^{20}, 1.4950; molecular refraction 41.92 (calcd. for $C_9H_{16}O$, F_1 = 42.15); i.r.: 1040 cm^{-1}, 755 cm^{-1}; n.m.r.: δ 1.6 (—CH_2—), δ 2.2 (—CH_2—C=), δ 3.37 (—CH_2OH), δ 3.4 (O*H*), δ 5.6 (—CH=CH—).

Anal. Calcd. for $C_9H_{16}O$: C, 77.10; H, 11.51. Found: C, 77.01; H, 11.12.

The 3,5-dinitrobenzoate derivative from 7 was prepared in the usual manner, m.p. 72–73 °C.

Anal. Calcd. for $C_{16}H_{18}O_6N_2$: N, 18.17. Found: N, 18.30.

The compound **7** was hydrogenated over palladium on carbon in a methanol solution, under an initial hydrogen pressure of 20 kg/cm² to give hydroxylmethylcyclooctane (**8**), b.p. 125 °C at 40 Torr; i.r.: 1040 cm^{-1}, 1450 cm^{-1}; n.m.r.: δ 1.45 (—CH_2—), δ 1.7 (—CH—), δ 3.48 (—CH_2OH), δ 1.95 (O*H*).

Anal. Calcd. for $C_9H_{18}O$: C, 76.02; H, 12.76. Found: C, 75.98; H, 12.41.

Acknowledgment

The authors are indebted to Dr. Akira Komatsu of Takasago Perfumery Co., Ltd., for providing materials.

1. R. T. Arnold and P. Veeravagu. J. Am. Chem. Soc. **82**, 5411 (1960).
2. S. Watanabe. Bull. Chem. Soc. Japan, **38**, 1231 (1965).
3. W. Hückel, W. Tappe, and G. Legutke. Ann. **543**, 194 (1940).

Deuterated 4-hydroxycoumarin derivatives[1]

Allan R. Knight and J. S. McIntyre
Exploratory Research Laboratory, Dow Chemical of Canada, Limited, Sarnia, Ontario

Received February 13, 1968

4-Hydroxycoumarin exchanges rapidly with heavy water, resulting in deuterium replacing both the 3- and the 4-hydroxy proton. Preparation of the following deuterated coumarin derivatives is described: 4-chlorocoumarin-3-d_1, 4-piperidylcoumarin-3-d_1, and 4-anilinocoumarin-3-d_1.

Canadian Journal of Chemistry, **46**, 1949 (1968)

A number of authors (1–4) have discussed the structure and the tautomers of 4-hydroxycoumarin (**1**) shown below, and suggest that in solution, **1** is the predominant structure. If such tautomerization occurs readily, the 3-proton would be expected to exchange rapidly in protonic solvents, and in D_2O an equilibrium with both the 4-hydroxy proton and the 3-proton would be established. This would then provide a facile method to synthesize coumarin derivatives labelled in the 3-position.

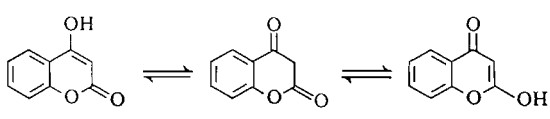

1 **2** **3**

In our investigation of coumarin condensation reactions, we have prepared coumarin derivatives deuterated in the 3-position by reacting 4-hydroxycoumarin (**1**) with D_2O in acetone to

[1]Contribution No. 162 from the Dow Chemical of Canada Exploratory Research Laboratory, Sarnia, Ontario.

Condensation of 1-p-Menthene (4) with Formaldehyde

From a mixture of 38 g of **4**, 8.5 g of *para*formaldehyde and 14 g of acetic anhydride, 15 g of a crude acetate was obtained. Saponification of this acetate gave 2-hydroxylmethyl-6-*p*-menthene, b.p. 92 °C at 3 Torr; d_4^{20}, 0.9378; n_D^{20}, 1.4850; molecular refraction 52.10 (calcd. for $C_{11}H_{20}O$, F_1 = 51.85); i.r.: 1385 and 1365 cm^{-1} (doublet), 1030 cm^{-1}, 800 cm^{-1}; n.m.r.: δ 0.9 (two CH_3), δ 1.4 (CH_3—C(—)=), δ 1.65 (CH_2—), δ 1.8 (—CH_2—C(—)=), δ 2.2 (O*H*), δ 3.68 (—CH_2OH), δ 5.6 (—C*H*—C(—)=).

Anal. Calcd. for $C_{11}H_{20}O$: C, 78.49; H, 11.98. Found: C, 78.12; H, 11.36.

The 3,5-dinitrobenzoate derivative of **5** was prepared and recrystallized from methanol, m.p. 138–139 °C.

Anal. Calcd. for $C_{17}H_{22}O_6N_2$: N, 7.73. Found: N, 7.70.

The compound **5** absorbed one equivalent of hydrogen by catalytic hydrogenation to give 2-hydroxylmethyl-*p*-menthane, b.p. 88 °C at 3 Torr.

Anal. Calcd. for $C_{11}H_{22}O$: C, 77.59; H, 13.03. Found: C, 77.36; H, 12.99.

Condensation of Cyclooctene (6) with Formaldehyde

From a mixture of 45 g of **6**, 14.5 g of *para*formaldehyde, and 20.5 g of acetic anhydride, 21 g of a crude acetate was obtained. Saponification of this acetate gave 1-hydroxylmethyl-2-cyclooctene (**7**), b.p. 74–76 °C at 2 Torr; d_4^{20}, 0.9778; n_D^{20}, 1.4950; molecular refraction 41.92 (calcd. for $C_9H_{16}O$, F_1 = 42.15); i.r.: 1040 cm^{-1}, 755 cm^{-1}; n.m.r.: δ 1.6 (—CH_2—), δ 2.2 (—CH_2—C(—)=), δ 3.37 (—CH_2OH), δ 3.4 (O*H*), δ 5.6 (—C*H*=C*H*—).

Anal. Calcd. for $C_9H_{16}O$: C, 77.10; H, 11.51. Found: C, 77.01; H, 11.12.

The 3,5-dinitrobenzoate derivative from 7 was prepared in the usual manner, m.p. 72–73 °C.

Anal. Calcd. for $C_{16}H_{18}O_6N_2$: N, 18.17. Found: N, 18.30.

The compound **7** was hydrogenated over palladium on carbon in a methanol solution, under an initial hydrogen pressure of 20 kg/cm² to give hydroxylmethylcyclooctane (**8**), b.p. 125 °C at 40 Torr; i.r.: 1040 cm^{-1}, 1450 cm^{-1}; n.m.r.: δ 1.45 (—CH_2—), δ 1.7 (—C*H*—), δ 3.48 (—CH_2OH), δ 1.95 (O*H*).

Anal. Calcd. for $C_9H_{18}O$: C, 76.02; H, 12.76. Found: C, 75.98; H, 12.41.

Acknowledgment

The authors are indebted to Dr. Akira Komatsu of Takasago Perfumery Co., Ltd., for providing materials.

1. R. T. Arnold and P. Veeravagu. J. Am. Chem. Soc. **82**, 5411 (1960).
2. S. Watanabe. Bull. Chem. Soc. Japan, **38**, 1231 (1965).
3. W. Hückel, W. Tappe, and G. Legutke. Ann. **543**, 194 (1940).

Can. J. Chem. Downloaded from www.nrcresearchpress.com by 210.87.254.42 on 09/05/12
For personal use only.

Deuterated 4-hydroxycoumarin derivatives[1]

Allan R. Knight and J. S. McIntyre
Exploratory Research Laboratory, Dow Chemical of Canada, Limited, Sarnia, Ontario

Received February 13, 1968

4-Hydroxycoumarin exchanges rapidly with heavy water, resulting in deuterium replacing both the 3- and the 4-hydroxy proton. Preparation of the following deuterated coumarin derivatives is described: 4-chlorocoumarin-3-d_1, 4-piperidylcoumarin-3-d_1, and 4-anilinocoumarin-3-d_1.

Canadian Journal of Chemistry, **46**, 1949 (1968)

A number of authors (1–4) have discussed the structure and the tautomers of 4-hydroxycoumarin (**1**) shown below, and suggest that in solution, **1** is the predominant structure. If such tautomerization occurs readily, the 3-proton would be expected to exchange rapidly in protonic solvents, and in D_2O an equilibrium with both the 4-hydroxy proton and the 3-proton would be established. This would then provide a facile method to synthesize coumarin derivatives labelled in the 3-position.

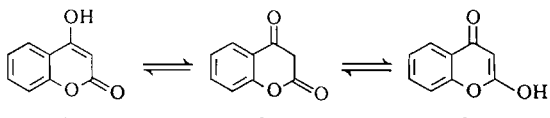

1 **2** **3**

In our investigation of coumarin condensation reactions, we have prepared coumarin derivatives deuterated in the 3-position by reacting 4-hydroxycoumarin (**1**) with D_2O in acetone to

[1]Contribution No. 162 from the Dow Chemical of Canada Exploratory Research Laboratory, Sarnia, Ontario.

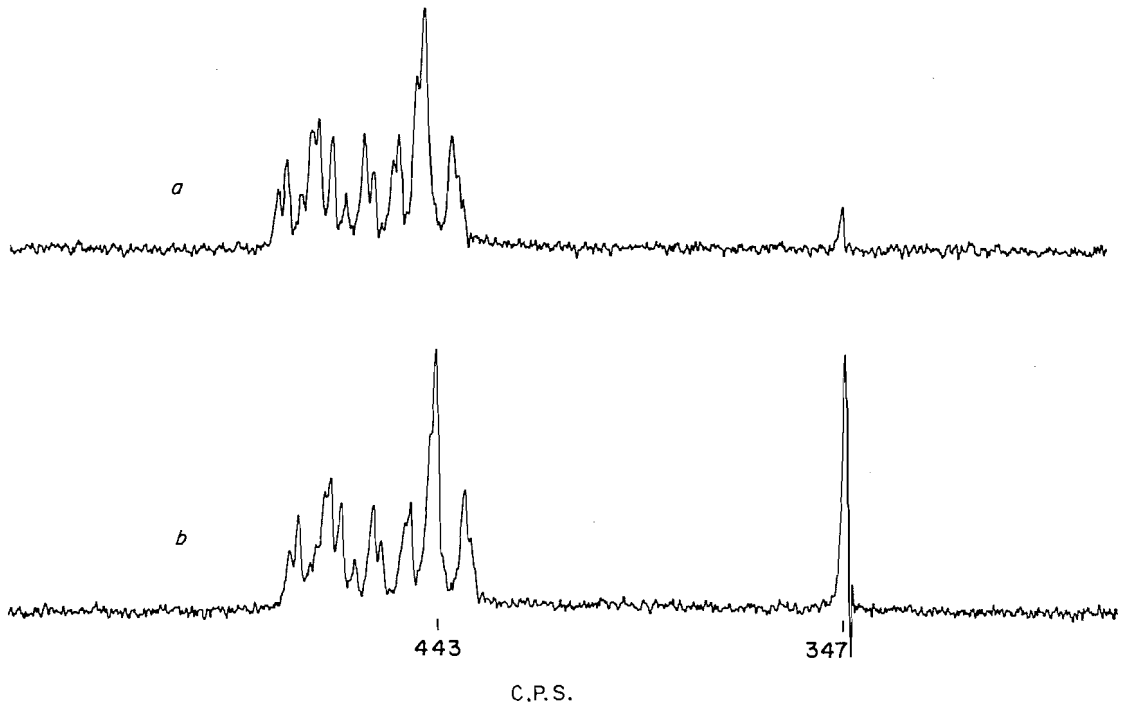

FIG. 1. The nuclear magnetic resonance spectrum of 4-hydroxycoumarin-3,4-d_2 recorded in hexamethylphosphoramide: (*a*) before H_2O was added; (*b*) after H_2O was added.

give 4-hydroxycoumarin-3,4-d_2.[2] The amount of deuteration was determined by nuclear magnetic resonance (n.m.r.) through a comparison of the relative area of the peaks for the 3-proton and the four aromatic protons (Fig. 1). When an acetone solution of this deuterated compound was diluted with a few drops of water, the compound quickly reverted to 4-hydroxycoumarin containing no 3-deuterium as indicated by the area of the 3-proton peak.

Reacting 4-hydroxycoumarin-3,4-d_2 with phosphorous oxychloride (Spalding *et al.* (5)) gives 4-chlorocoumarin-3-*d* (~95% 3-*d*). Retention of this 3-deuterium during the isolation conditions (phosphorous oxychloride diluted with methanol and water) demonstrates that the 3-proton of 4-chlorocoumarin does not exchange in water or acids.

[2]Farmer has investigated the infrared spectra and structures of 4-hydroxycoumarins and also some 4-deuteroxycoumarins. The 4-deuteroxycoumarins were prepared by recrystallizing from dioxane–D_2O or ether–D_2O mixtures; the author explains "although it is to be expected that the labile hydrogen on carbon 3 would also be replaced by deuterium, no spectral changes due to this could be identified" (3).

Treatment of 4-chlorocoumarin with piperidine gives 4-piperidylcoumarin (6). Conducting this reaction with 4-chlorocoumarin-3-d_1 gives primarily deuterium retention.

4-Anilinocoumarin may be prepared from 4-chlorocoumarin and aniline as described by Zagorevski *et al.* (6). When this method is used with the 3-*d* compound, a complete loss of deuterium was obtained. Attempts to prepare the 3-*d* from 4-anilinocoumarin with acetone and D_2O failed, suggesting that under these conditions there is not tautomerization between the amino and imino forms of the 4-anilino compound. However, heating with deuterated aniline resulted in exchange at the 3-position as indicated by the small relative area of the 3-proton in the n.m.r. A similar exchange resulted when 4-piperidylcoumarin-3-d_1, was heated with aniline, the deuterium being replaced by a proton.

In summary the exchange of 4-hydroxycoumarin with heavy water provides a facile starting material, 4-hydroxycoumarin-3,4-d_2 for the preparation of coumarin derivatives with deuterium in the 3-position. Another quite

Can. J. Chem. Downloaded from www.nrcresearchpress.com by 210.87.254.42 on 09/05/12
For personal use only.

satisfactory method to prepare some 3-deuterated derivatives is by base-catalyzed proton exchange at elevated temperatures (i.e. with deuterated aniline at 150 °C).

Experimental

4-Hydroxycoumarin-3,4-d_2

A mixture of 15 g of 4-hydroxycoumarin, 60 g of D_2O, and 50 g of acetone was heated until a solution formed and then stirred for 30 min. The solution was evaporated under vacuum until a dry powder formed; the infrared (i.r.) and nuclear magnetic resonance (n.m.r.) spectra of the powder were recorded immediately. The i.r. spectrum was similar in the carbonyl region but showed considerable differences from 4-hydroxycoumarin at lower frequencies; a broad band occurred at ~2200 cm^{-1} corresponding to O—D vibration.

The n.m.r. spectrum,[3] recorded in hexamethylphosphoramide (Fig. 1*a*), indicated 92% deuteration in the 3-position when the area of the 3-proton peak at 347 c.p.s. was compared to the area of the peaks corresponding to the four aromatic protons. When a drop of H_2O was mixed with the solution in the n.m.r. tube and the spectrum recorded (Fig. 1*b*), a very rapid exchange was noted, with only 47% deuteration remaining in the 3-position. When dioxane was used instead of acetone (3) 4-hydroxycoumarin-3,4-d_2 was also obtained.

4-Chlorocoumarin-3-d_1

Twenty ml of phosphorus oxychloride was added to the 4-hydroxycoumarin-3,4-d_2 prepared above and the mixture was refluxed for 1 h. The solution was cooled, diluted first with methanol and then with water and chloroform and the insoluble precipitate removed by filtration. This precipitate was characterized as a trimer of coumarin (7). The chloroform layer was evaporated and the residue crystallized from methanol to give an orange compound, m.p. 93–94 °C. The n.m.r. spectrum ($CDCl_3$) showed a singlet at 392 c.p.s. having a relative area of 0.05 corresponding to 95% deuteration in the 3-position.

4-Piperidylcoumarin-3-d_1

To 1.0 g of 4-chlorocoumarin (95% 3-d_1) in 15 ml methanol was added 3 ml of piperidine and the methanol solution was boiled for 10 min. The cooled reaction mixture was filtered to give 4-piperidylcoumarin (87% 3-d_1), m.p. 104–107.5 °C; n.m.r. ($CDCl_3$, c.p.s.) 108 broad (area 6), 188–204 broad (area 4), 347 singlet (area 0.13), 439–474 multiplet (area 4).

Reacting 0.3 g of this 4-piperidylcoumarin-3-d_1 with 1 ml of aniline at 150 ° for 1 h, concentration of the solution on a steam bath, and crystallization from methanol, gave 4-piperidylcoumarin with the replacement of the deuterium by a proton.

4-Anilinocoumarin

One gram of 4-chlorocoumarin (95% 3-d_1) and 3 ml of aniline were heated at 150 °C for 1 h. Cooling and dilution with methanol yielded 4-anilinocoumarin. Its i.r. spectrum was identical with that of 4-anilinocoumarin prepared from undeuterated 4-chlorocoumarin. The n.m.r. spectrum in hexamethylphosphoramide showed a peak at 329 c.p.s. corresponding to the 3-proton, area 1.

4-Anilinocoumarin-3-d_1

4-Anilinocoumarin (0.5 g) prepared as above from 4-chlorocoumarin and aniline, was added to 1.5 ml of deuterated aniline[4] and the mixture heated at 150 °C for 1 h. The solution was cooled, diluted with methanol, boiled, cooled, and filtered. Nuclear magnetic resonance showed this compound to be ~92% deuterated in the 3-position, and ~100% protonated at the nitrogen.

When a mixture of 4-anilinocoumarin (0.5 g), 20 ml acetone, and 5 ml D_2O were stirred at room temperature for 1 h, only the undeuterated product was obtained. Similarly when this procedure was repeated with the addition of 10 ml of pyridine and the solution stirred for 15 h, no deuterated 4-anilinocoumarin was obtained.

1. M. E. Perel'son and Yu. N. Sheinker. Zh. Prikl Spektroskopii Akad. Nauk. Belorussk. SSR, **5**, 104 (1966). Chem. Abstr. **65**, 19478*d* (1966).
2. B. K. Sabata and M. R. Rout. J. Indian Chem. Soc. **41**, 74 (1964).
3. V. C. Farmer. Spectrochim. Acta, **10**, 870 (1959).
4. F. Arndt, L. Loewe, R. Un, and E. Ayca. Chem. Ber. **84**, 319 (1951).
5. D. P. Spalding, H. S. Mosher, and F. C. Whitmore. J. Am. Chem. Soc. **72**, 5338 (1950).
6. V. A. Zagorevski and D. A. Zykov. Zhur. Obshchei Khim. **30**, 1378 (1960). (Chem. Abstr. **55**, 524*e* (1961).
7. A. R. Knight and J. S. McIntyre. Can. J. Chem. To be published.

[3]The nuclear magnetic resonance spectra were recorded on a Varian A-60 spectrometer; chemical shifts are reported in c.p.s. downfield from internal tetramethylsilane.

[4]Aniline was treated twice with heavy water, to give deuterated aniline which was shown by nuclear magnetic resonance to be greater than 99% deuterated.

Can. J. Chem. Downloaded from www.nrcresearchpress.com by 210.87.254.42 on 09/05/12
For personal use only.

Synthesis of new chalcone analogues and derivatives

RÉAL LALIBERTÉ, JANE MANSON, HILDA WARWICK, AND GEORGE MEDAWAR

Department of Chemistry, Ayerst Research Laboratories, Ayerst, McKenna, and Harrison Limited, Montréal, Québec

Received December 28, 1967

The synthesis of new derivatives of 2′-hydroxychalcone, such as esters, sulfonates, and thiocarbamates, prepared for evaluation as antiparasitic agents as well as new heterocyclic chalcone analogues prepared for the same purpose, is described.

Canadian Journal of Chemistry, **46**, 1952 (1968)

Can. J. Chem. Downloaded from www.nrcresearchpress.com by 210.87.254.42 on 09/05/12
For personal use only.

In a search for a new gastrointestinal anthelmintic with a broad spectrum of biological activity, a number of chalcones and related compounds were prepared and evaluated as antiparasitic agents (1). In this study a weak anthelmintic activity of chalcone was discovered and the activity has been increased by the addition of a hydroxyl group in position-2′. Derivatives of this phenol have also exhibited increased anthelmintic activity. The new aryl esters, sulfonates, and the thiocarbamate of 2′-hydroxychalcone which were prepared and submitted for testing are herein described.

To establish structure–activity relationship in this series, chemical manipulations to evaluate the importance of the two phenyl groups in the chalcone molecule were made. New chalcone analogues in which one of the phenyl rings is replaced by a heterocyclic ring were prepared by the Claisen–Schmidt condensation of an appropriate aldehyde with a convenient methylketone, using methanol or ethanol as solvent and sodium hydroxide as base.

Experimental

General Procedure (Claisen–Schmidt Condensation)

Two ml of 40% sodium hydroxide was added to a solution of the appropriate aldehyde (0.05 *M*) and the methylketone (0.05 *M*) in methanol. The solution became yellow and generally a solid appeared on standing for a few hours. It was removed by filtration and was crystallized from an appropriate solvent as described in Table I. If no solid formed, the solvent was evaporated under vacuum and the substance was extracted with dichloromethane. The solvent was washed with water and then dried and evaporated. The residue was crystallized from an appropriate solvent (see Table I).

Esters from 2′-Hydroxychalcone

Method a

The technique used has been described by Spasov (2). A benzene solution (300 ml) of 2′-hydroxychalcone (0.03 *M*) and of an appropriate acid chloride (0.04 *M*) was kept under reflux for 4 days in the presence of magnesium turnings (11 g). The mixture was cooled and the magnesium was removed and washed with ether. The solvents were washed to neutrality with 5% NaOH and water. Evaporation yielded a heavy oil that could not be distilled without decomposition. This oil was either crystallized as described in Table II or it was purified by passing it through silicic acid as it was for the cinnamate which did not crystallize.

Method b: the Preparation of Sulfonates

To a solution of 2′-hydroxychalcone (0.01 *M*) in 25 ml of pyridine was added a tenfold excess of a sulfonyl chloride. After 18 h, water was added. The substance was placed in benzene and washed. After evaporation it was crystallized from ether and from methylcyclohexane to give light-yellow solids described in Table II.

2′-Hydroxy-β-N-morpholinoacrylophenone

A mixture of 2′-hydroxy-β-formylacetophenone (3) (0.02 *M*) and morpholine (0.02 *M*) was heated on a steam bath for 1 h. The crude solid crystallized from ethanol to give yellow crystals (85% yield) melting at 107–108 °C; ultraviolet (u.v.), λ_{max} at 256 mμ.

Anal. Calcd. for $C_{13}H_{15}NO_3$: C, 66.93; H, 6.48; N, 6.01. Found: C, 62.17; H, 6.64; N, 5.94.

2′-Hydroxy-β-N(N′-phenyl)piperazinoacrylophenone

A mixture of 2′-hydroxy-β-formylacetophenone (3) (0.02 *M*) and *N*-phenylpiperazine was heated on a steam bath for 1 h. The crude solid obtained was crystallized from ethanol to give yellow crystals (75% yield) melting at 114–115 °C; u.v. λ_{max}, at 230 and 248 mμ.

Anal. Calcd. for $C_{19}H_{20}N_2O_2$: C, 74.00; H, 6.54; N, 9.09. Found: C, 74.20; H, 6.34; N, 8.76.

Di(2′-hydroxychalcone)thiocarbonate

The triethylamine salt of 2′-hydroxychalcone (0.03 *M*) was prepared by adding triethylamine (0.03 *M*) to an equivalent of 2′-hydroxychalcone in benzene (60 ml). This solution was added dropwise with stirring to a cooled solution of thiophosgene (0.03 *M*) in benzene (60 ml). After 2 h, another portion of thiophosgene (0.01 *M*) with an equivalent of triethylamine was added. The reaction mixture was allowed to come to room temperature and it was stirred for a further 2 h. The solvent was removed to give a brown oil which crystallized on addition of ether. Recrystallization from ethanol yielded a pale-yellow solid (65% yield) melting at 131–132 °C; u.v. λ_{max}, at 227 and 306 mμ.

Anal. Calcd. for $C_{31}H_{22}O_4S$: C, 75.91; H, 4.52; S, 6.52. Found: C, 75.54; H, 4.58; S, 6.55.

Can. J. Chem. Downloaded from www.nrcresearchpress.com by 210.87.254.42 on 09/05/12
For personal use only.

TABLE I

Experimental data for new chalcone analogues and derivatives

Compound	Melting point (°C)	Yield (%)	Solvent of crystalization	Molecular formula	Analyses										Infrared† C=O (cm^{-1})
					Calculated					Found					
					C	H	Cl	N	S	C	H	Cl	N	S	
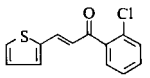	31–32	40	Methylene chloride* and hexane	$C_{13}H_9ClOS$	62.90	3.66	14.25		12.87	62.84	3.70	14.18		12.95	1655
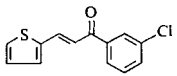	95–96	85	Methanol	$C_{13}H_9ClOS$	62.90	3.66	14.25		12.87	62.98	3.73	14.33		12.96	1658
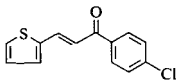	121–122	90	Methanol	$C_{13}H_9ClOS$	62.90	3.66	14.25		12.87	63.11	3.93	14.62		12.86	1655
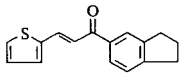	89–90	50	Methanol* and water	$C_{16}H_{14}OS$	75.57	5.55			12.58	75.32	5.67			12.83	1655
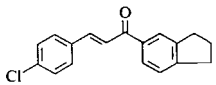	190–191	55	Ethyl acetate	$C_{18}H_{15}ClO$	76.45	5.35	12.54			76.54	5.26	12.55			1662
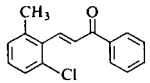	56–57	65	Methanol	$C_{16}H_{13}ClO$	74.87	5.32	13.81			74.63	5.10	13.79			1662

Can. J. Chem. Downloaded from www.nrcresearchpress.com by 210.87.254.42 on 09/05/12
For personal use only.

TABLE I (*Concluded*)

Compound	Melting point (°C)	Yield (%)	Solvent of crystallization	Molecular formula	Analyses										Infrared* C=O (cm^{-1})
					Calculated					Found					
					C	H	Cl	N	S	C	H	Cl	N	S	
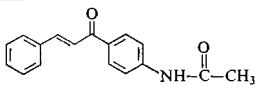	163–164	65	Ethanol	$C_{17}H_{15}NO_2$	76.96	5.70		5.28		76.70	5.71		5.28		1655
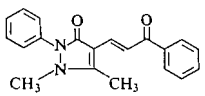	194–196	50	Isopropyl alcoho	$C_{20}H_{18}N_2O_2$	75.45	5.70		8.80		75.77	5.88		8.73		1663
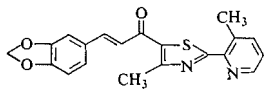	208–209	75	Ethyl acetate	$C_{20}H_{16}N_2O_3S$	65.93	4.43		7.69	8.78	66.09	4.53		7.60	9.16	1648
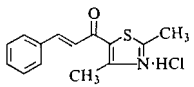	127–130	25	Methanol†	$C_{14}H_{13}NOS{\cdot}HCl$			12.67	5.01	11.45			12.89	4.92	11.92	1660
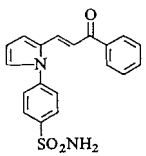	165–167	60	Toluene	$C_{19}H_{16}N_2O_3S$	64.77	4.58		7.95	9.08	65.01	4.67		7.96	9.13	1647

*In chloroform solution.
†These substances were extracted with dichloromethane from the residue after evaporation of the methanol.

Can. J. Chem. Downloaded from www.nrcresearchpress.com by 210.87.254.42 on 09/05/12
For personal use only.

TABLE II

Esters* of 2′hydroxychalcone

R	Method	Melting point (°C)	Solvent of crystallization	Yield (%)	Molecular formula	Analyses: Calculated C	Calculated H	Calculated S	Found C	Found H	Found S	Ultraviolet† λ_{max} (mμ)	Infrared‡ (cm^{-1}) ketone	Infrared‡ (cm^{-1}) ester
$C(=O)-CH=CH_2$	*a*	Oil		60	$C_{18}H_{14}O_3$	77.68	5.07		77.45	4.83		223, 304	1640	1740
$C(=O)-C_6H_5$	*a*	90–91	Benzene and 25% hexane	70	$C_{22}H_{16}O_3$	80.47	4.91		80.23	4.86			1645	1740
$C(=O)-CH_2-C_6H_5$	*a*	118	Benzene	70	$C_{23}H_{18}O_3$	80.35	5.59		80.68	5.30			1645	1757
$C(=O)-CH=CH-C_6H_5$	*a*	71–72	Propanol	65	$C_{24}H_{18}O_3$	81.34	5.12		81.16	5.15		223, 289	1640	1728
	a	92	Ether and 40% hexane	70	$C_{20}H_{14}O_4$	75.46	4.43		75.78	4.65			1645	1740
SO_2CH_3	*b*	98–99	Methylcyclohexane	50	$C_{16}H_{14}O_4S$	63.57	4.67	10.58	63.69	4.85	10.58	228, 305	1650	
$SO_2C_6H_5$	*b*	88	Methylcyclohexane	30	$C_{21}H_{16}O_4S$	69.22	4.43	8.78	69.31	4.65	8.86	221, 308	1646	

*Compounds of structure 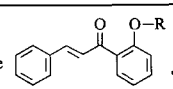 .
†In ethanol solutions.
‡In chloroform solutions.

2,2′-Dicinnamoxychalcone

Triethylamine (0.01 *M*) was added to 2,2′-dihydroxychalcone (0.005 *M*) in hot toluene (20 ml). Cinnamoyl chloride (0.01 *M*) in toluene was added slowly with constant stirring and the mixture was heated under reflux for 90 min. Similar addition is repeated. The mixture was cooled and then it was washed with water and extracted with toluene. After removal of the solvent, the oil was crystallized from propanol to give a yellow solid (65% yield) melting at 126–127 °C; u.v. λ_{max} at 282 mμ.

Anal. Calcd. for $C_{33}H_{24}O_5$: C, 79.18; H, 4.83. Found: C, 79.34; H, 4.96.

2-(N-Phenylcarbamyl)oxy-2′-hydroxychalcone

Phenyl isocyanate (0.01 *M*) was added to 2,2′-dihydroxychalcone (0.005 *M*) in hot toluene (30 ml). Five drops of pyridine were added and the mixture was heated under reflux for 1 h. The solvent was evaporated to give a yellow solid. Recrystallization from acetone by the addition of hexane gave a yellow solid (35% yield) melting at 167–169 °C; u.v. λ_{max} at 237 and 313 mμ.

Anal. Calcd. for $C_{22}H_{17}NO_4$: C, 73.53; H, 4.77; N, 3.90. Found: C, 73.19; H, 4.78; N, 3.82.

1. R. LALIBERTÉ, D. CAMPBELL, and F. BRUDERLEIN. Can. J. Pharm. Sci. **2**, 37 (1967).
2. A. SPASOV. Ber. **75B**, 779 (1942); Chem. Abstr. **36**, 7010.
3. A. SCHÖNBERG and A. SINA. J. Am. Chem. Soc. **72**, 3397 (1950).

Can. J. Chem. Downloaded from www.nrcresearchpress.com by 210.87.254.42 on 09/05/12
For personal use only.

Can. J. Chem. Downloaded from www.nrcresearchpress.com by 210.87.254.6 on 09/05/12
For personal use only.

Canadian Journal of Chemistry

Published by THE NATIONAL RESEARCH COUNCIL OF CANADA

VOLUME 46 JUNE 15, 1968 NUMBER 12

The X-radiolysis of water vapor containing methanol. Effects of some electron and hydrogen atom scavengers[1]

R. S. DIXON AND M. G. BAILEY

Atomic Energy of Canada Limited, Whiteshell Nuclear Research Establishment, Pinawa, Manitoba

Received December 18, 1967

The X-radiolysis of water vapor containing methanol at 125 °C and 1 atm pressure has been studied alone and in the presence of some electron and hydrogen atom scavengers. In water vapor containing methanol only, a plateau value $G(H_2) = 7.9 \pm 0.3$ is obtained at all methanol concentrations above 0.5 mole %. Addition of propylene drastically reduces this yield due to efficient scavenging of hydrogen atoms, and values for the total number of H atoms from all precursors $g(H)_t = 7.5 \pm 0.2$ and $k(H + C_3H_6)/k(H + CH_3OH) \simeq 1600$ are deduced from the competition. An unscavengeable hydrogen yield $g(H_2) \sim 0.5$ is also indicated in mixtures containing propylene. Nitrous oxide and sulfur hexafluoride are found to scavenge electrons efficiently in water vapor containing methanol and the number of hydrogen atoms arising from electron – positive ion recombination is estimated to have a value $G = 2.2 \pm 0.6$. The number of hydrogen atoms arising from processes not involving electrons is $g(H) = 5.2 \pm 0.3$. Carbon tetrachloride reacts efficiently with both electrons and hydrogen atoms, with $k(H + CH_3OH)/k(H + CCl_4) = 0.085$. Values of $g(H) = 4.9 \pm 0.5$ and $g(H_2) = 0.8 \pm 0.2$ are deduced from mixtures containing carbon tetrachloride.

Canadian Journal of Chemistry, 46, 1957 (1968)

Introduction

Pure water vapor undergoes little decomposition when exposed to ionizing radiation (1–3). In the presence of organic additives, however, the hydrogen yield greatly increases and a value for the total reducing species of $G \sim 8$[2] has been obtained in H_2O and D_2O containing various organic additives (2, 4). The contributions of radical and ionic processes towards the yield of reducing species has been the subject of more recent publications (4–6). Irradiation of water vapor containing nitrous oxide gave $G(N_2) = 3.0$, which is thought to represent the yield of scavengeable electrons in water vapor (5, 6). This value agrees well with the reduction in hydrogen yield $\Delta G(H_2) \sim 3$ when nitrous oxide or sulfur hexafluoride is added to H_2O or D_2O vapor containing organic additives (4, 5). However, comparison of $g(e)$ with the total yield of reducing species indicates that a major fraction does not have the electron as a precursor (4, 5). This is in marked contrast to the situation in liquid water, where the major fraction of the reducing species is present as the hydrated electron (see, for example, ref. 7).

The importance of the radical and ion yields in the radiation chemistry of water vapor has led us to study the extent to which electrons and other precursors contribute to the yield of reducing species in water vapor containing methanol. We have done this by looking at the effect of certain electron and hydrogen atom scavengers on the hydrogen yields from this system. The similarities and discrepancies between our results and those from other studies in water vapor are briefly discussed.

Experimental

Water was triply distilled from acid dichromate, from alkaline permanganate, and finally through a quartz tube at 500 °C in a stream of oxygen. Methanol and carbon tetrachloride (Fisher certified), cyclohexane and propylene (Phillips research grade), nitrous oxide and sulfur hexafluoride (Matheson research grade) were used without further purification except for several freeze–pump–thaw cycles.

The irradiation vessels were ~ 450 cc cylindrical quartz

[1]A.E.C.L. No. 3098.

[2]Primary yields are written as $g(x)$ and experimental yields as $G(x)$, molecules per 100 eV absorbed.

Can. J. Chem. Downloaded from www.nrcresearchpress.com by 210.87.254.6 on 09/05/12
For personal use only.

cells fitted with center thermocouple wells and break seals for analysis. The vessels were cleaned as described previously (6). The weighed aqueous methanol sample (~ 0.25 g) was deaerated by several freeze–pump–thaw cycles and distilled into the irradiation vessel immersed in liquid nitrogen. Additives were introduced by condensing a known volume of gas or vapor, at a known temperature and pressure, into the vessel. The vessel and contents were finally evacuated to 10^{-6} Torr at −196 °C before sealing off. Irradiations were carried out at 125 °C and atmospheric pressure using X-rays from a 1.5 MeV Van de Graaff accelerator equipped with a stainless steel target. After irradiation, the gases not condensable at −196 °C were measured volumetrically and the composition determined by gas chromatography.

The dose rate of 3.0×10^{17} eV g^{-1} min^{-1} in H_2O was estimated by the nitrous oxide dosimeter assuming $G(N_2) = 11.0$ (8). The relative dose rate was checked periodically with the Fricke dosimeter. The energy absorbed by each component was calculated assuming it to be directly proportional to the electron density of the gas. Total doses in the samples were generally in the range $10^{19} - 10^{20}$ eV g^{-1}.

All G-values were based on the energy absorbed by water only. Corrections for products produced by direct absorption of energy by methanol were made using the experimentally determined values of $G(H_2) = 11.5$, $G(CH_4) = 0.7$, $G(CO) = 1.8$ for methanol vapor irradiated at 125 °C and 320 Torr. Corrections for other additives were made using $G(N_2)_{N_2O} = 11.0$ (8), $G(H_2)_{cyclohexane} = 5.3$ (9), and $G(H_2)_{propylene} = 1.2$ (10). In correcting, it was assumed that the product yields from each component in a mixture were the same as those in the pure component. This assumption may not be strictly correct, but we estimate that any inaccuracies due to it will not seriously affect our conclusions.

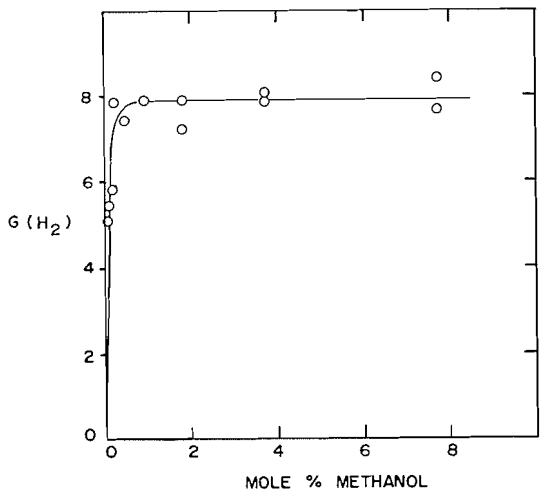

FIG. 1. Effect of methanol concentration on the hydrogen yield from water vapor at 125 °C and atmospheric pressure.

TABLE I

$G(H_2)$ from water vapor containing methanol and propylene

CH_3OH (mole %)	C_3H_6 (mole %)	$G(H_2)$
1.8	1.21	0.35
1.8	0.13	0.49
4.9	0.11	0.52
4.9	0.07	0.85
10.3	0.12	0.73
10.3	0.06	0.96

Results

Water + Methanol

The effect of methanol concentration on the hydrogen yield from water vapor at 125 °C and atmospheric pressure is shown in Fig. 1. $G(H_2)$ increases from 4.6 at 10^{-2} mole % methanol to a plateau value of 7.9 ± 0.3 at about 0.5 mole % methanol, remaining constant up to 7.7 mole % methanol. Small amounts of methane and carbon monoxide were also formed.

A few runs with water vapor containing 2.6 mole % cyclohexane gave $G(H_2) = 7.0 \pm 0.3$.

Water + Methanol + Propylene

Hydrogen yields from water vapor containing various concentrations of methanol and propylene are shown in Table I. In all runs, the methanol concentration was sufficient to have reacted with all available hydrogen atoms in the absence of propylene. Since $G(H_2)$ increased with dose in most of these experiments, presumably due to consumption of the propylene, the values of $G(H_2)$ are initial yields obtained by extrapolation to zero dose.

A few samples of water vapor containing 0.1 and 1.0 mole % propylene (but no methanol) gave $G(H_2) = 0.6$.

Water + Methanol + N_2O (or SF_6)

The effect of nitrous oxide concentration on the hydrogen yield from water vapor containing 2.2 mole % methanol is shown in Fig. 2. $G(H_2)$ falls from 7.9 ± 0.3 to 5.7 ± 0.3 on addition of 0.1 mole % nitrous oxide, followed by a much slower falloff to $G(H_2) = 4.8$ at 10 mole % nitrous oxide. At the same time, the nitrogen yield increases from zero to $G(N_2) = 4.2$ at 0.1 mole % nitrous oxide, then increases slowly to $G(N_2) \sim 4.8$ at 10 mole % nitrous oxide. A few results with water vapor containing various concentrations of methanol (1–10 mole %) and nitrous oxide (1–10 mole %) showed that while $G(N_2)$ depended little on

Can. J. Chem. Downloaded from www.nrcresearchpress.com by 210.87.254.6 on 09/05/12
For personal use only.

N_2O concentration, it increased with increasing methanol concentration to $G(N_2) = 8.0$ at 10.6 mole % methanol. Addition of 1 mole % sulfur hexafluoride reduced $G(N_2)$ to zero at all methanol and nitrous oxide concentrations studied.

Sulfur hexafluoride has a similar effect on $G(H_2)$ from water vapor containing 2.2 mole % methanol, as shown in Fig. 3. $G(H_2)$ falls from 7.9 ± 0.3 to 5.8 ± 0.3 on addition of 0.1 mole % sulfur hexafluoride, then stays approximately constant up to 5 mole % sulfur hexafluoride. Addition of 1 mole % propylene to water vapor

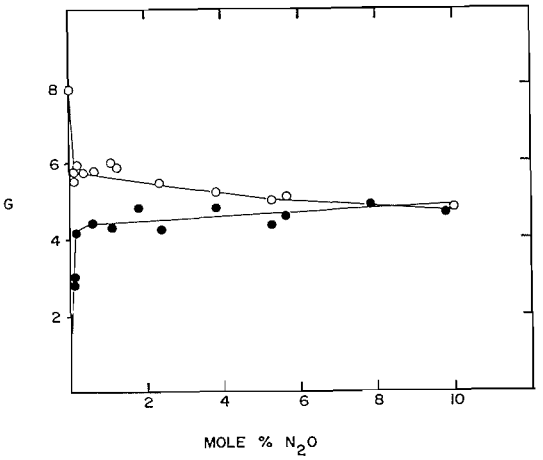

FIG. 2. Hydrogen and nitrogen yields from water vapor containing 2.2 mole % methanol and various concentrations of nitrous oxide: (O) H_2 yields, (●) N_2 yields.

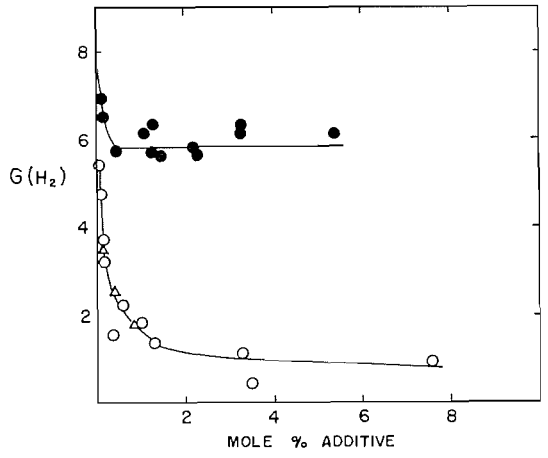

FIG. 3. Effect of sulfur hexafluoride and carbon tetrachloride on the hydrogen yield from water vapor containing 2.2 mole % methanol: (●) sulfur hexafluoride, (O) carbon tetrachloride, (△) carbon tetrachloride + 1 mole % SF_6.

containing 2.2 mole % methanol and 1 to 5 mole % sulfur hexafluoride reduced the hydrogen yield to $G(H_2) = 0.4$.

Water + Methanol + CCl_4

The effect of carbon tetrachloride on the hydrogen yield from water vapor containing 2.2 mole % methanol is shown in Fig. 3. $G(H_2)$ falls rapidly on addition of less than 0.1 mole % carbon tetrachloride, the falloff becoming slower as the carbon tetrachloride concentration increases. A few runs with H_2O–CH_3OH–CCl_4 mixtures containing 1 mole % sulfur hexafluoride gave values of $G(H_2)$ which fall on the same curve as those in the absence of sulfur hexafluoride. $G(H_2)$ does not fall to zero, however, even at 7.7 mole % carbon tetrachloride, but tends to flatten out at a plateau value of ~ 0.8.

Discussion

Water + Methanol

As previously shown (2), even low concentrations of organic additives substantially increase $G(H_2)$ from irradiated water vapor. Figure 1 shows that less than 1 mole % methanol is sufficient to give a limiting value of $G(H_2)$. The major reactions which produce H and OH in water vapor are generally assumed to be

$$H_2O \sim\sim\rightarrow H_2O^+, e^-, H_2O^*$$

[1] $$H_2O^+ + H_2O \rightarrow H_3O^+ + OH$$

[2] $$e^- + H_3O^+ \rightarrow H + H_2O$$

[3] $$H_2O^* \rightarrow H + OH \quad .$$

Recent mass spectrometric investigations (11) have shown that α-particle irradiation of water–methanol vapor mixtures under conditions where ion–molecule reactions occur gives mainly ions of the type $H^+(H_2O)_x(CH_3OH)_y$. Here x and y depend on the temperature and pressure and the concentrations of water and methanol in the mixture. In our experiments, therefore, reaction [2] will be replaced by

[4] $$H_3O^+ + (x-1)H_2O + yCH_3OH \rightarrow H^+(H_2O)_x(CH_3OH)_y$$

[5] $$e^- + H^+(H_2O)_x(CH_3OH)_y \rightarrow H + xH_2O + yCH_3OH,$$

where reaction [4] represents the clustering of the hydronium ion by water and methanol molecules. In the present experiments the cluster will consist mainly of water molecules, except at high methanol concentrations.

Can. J. Chem. Downloaded from www.nrcresearchpress.com by 210.87.254.6 on 09/05/12
For personal use only.

The H and OH radicals produced above will react with methanol,

[6] $$H + CH_3OH \rightarrow H_2 + CH_2OH$$

[7] $$OH + CH_3OH \rightarrow H_2O + CH_2OH,$$

and only when all available H and OH react with methanol will the plateau value be reached. The plateau value of $G(H_2) = 7.9 \pm 0.3$ thus represents the sum of all available H atoms arising via [3] and [5] plus the yield of "molecular" hydrogen, if any. This value (obtained in silica vessels) is in good agreement with Baxendale and Gilbert's value of 7.8 using soda glass vessels (2) but is less than their value of 8.9 in silica vessels (5). The importance of these differences will be discussed later. In view of the possible discrepancies due to different dosimetry methods used by various authors, the experiments with added cyclohexane were carried out for comparitive purposes. The value $G(H_2) = 7.0 \pm 0.3$ found here agrees well with the values found by other workers (2, 12).

Water + Methanol + Propylene

Since propylene is known to add H atoms rapidly giving the isopropyl radical (13),

[8] $$H + C_3H_6 \rightarrow C_3H_7,$$

its effect on $G(H_2)$ from water vapor containing methanol is presumably due to the scavenging of H atoms in competition with reaction [6]. This simple competition for H atoms leads to the relationship

$$\frac{1}{\Delta G} = \frac{1}{g(H)_t}\left[1 + \frac{k_6[CH_3OH]}{k_8[C_3H_6]}\right],$$

where ΔG = the reduction in hydrogen yield on addition of propylene and $g(H)_t$ = the total yield of H atoms from reactions [3] and [5]. The plot of $1/\Delta G$ versus $[CH_3OH]/[C_3H_6]$ is shown in Fig. 4 and although methanol is only reacting with a maximum of about 10% of the total hydrogen atoms, the plot is a reasonable straight line in agreement with the above kinetic scheme. From the slope and intercept we obtain the values $g(H)_t = 7.5 \pm 0.2$ and $k_8/k_6 \simeq 1600$.

These results show that the majority of the hydrogen is formed by H atom abstraction from the methanol. Experiments with water vapor containing propylene (but no methanol) gave $G(H_2) = 0.6$, independent of propylene concentration over a factor of 10. This, together with the kinetic analysis, indicates the presence

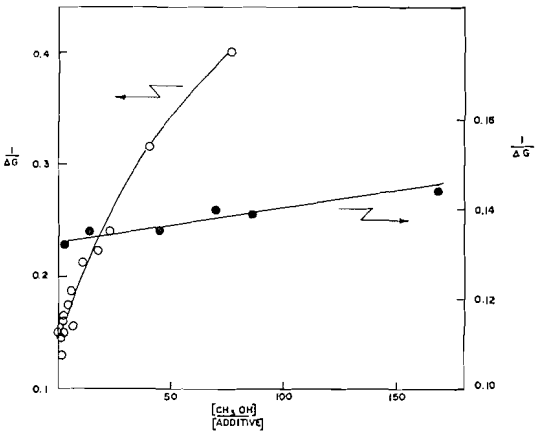

FIG. 4. The reciprocal of the reduction in the hydrogen yield plotted against the ratios of concentrations of methanol and additive in water vapor: (●) propylene, (O) carbon tetrachloride.

of a small yield of hydrogen, $g(H_2) \sim 0.5$, which does not have the H atom as a precursor. The presence of a "molecular" yield of hydrogen is in agreement with that found in other studies in water vapor (14–16).

The above conclusions rest on the assumption that propylene does not interfere with the ionic steps in the mechanism. The simple alkenes, having negative electron affinities, cannot capture electrons and will not interfere with electron reactions. At the pressure of water vapor used, reaction [1] is fast enough to preclude other reactions of H_2O^+ (17). We have also excluded charge or proton transfer to propylene on energetic grounds. Reactions [9] and [10] are both endothermic,

[9] $$CH_3OH_2^+ + C_3H_6 \rightarrow CH_3OH + C_3H_7^+$$
$$\Delta H = +(5\text{–}30) \text{ kcal/mole}$$

[10] $$CH_3OH_2^+ + C_3H_6 \rightarrow H + CH_3OH + C_3H_6^+$$
$$\Delta H = +90 \text{ kcal/mole}$$

(ΔH was calculated using proton affinities: $p(C_3H_6) = 153\text{–}172$ (18), $p(CH_3OH) = 177\text{–}183$ (19) kcal/mole and ionization potentials $I(C_3H_6) = 223$, $I(H) = 313$ kcal/mole). As pointed out earlier, in the absence of propylene the positive ion will actually be present as $H^+(H_2O)_x(CH_3OH)_y$, but since $C_3H_7^+$ and $C_3H_6^+$ will also be present as ion clusters, clustering of the ions will probably not have a marked effect on the enthalpy changes in reactions [9] and [10]. We therefore conclude that propylene does not interfere with the ionic steps

Can. J. Chem. Downloaded from www.nrcresearchpress.com by 210.87.254.6 on 09/05/12
For personal use only.

proposed but merely acts as an H atom scavenger in this system.

Water + Methanol + N_2O (or SF_6)

Previous results (4–6) have shown nitrous oxide and sulfur hexafluoride to be efficient scavengers of electrons in water vapor.

[11] $$e^- + N_2O \rightarrow N_2 + O^-$$

[12] $$e^- + SF_6 \rightarrow SF_6^-$$

In water vapor containing nitrous oxide only, $G(N_2) = 3.0 \pm 0.3$ which was identified with the yield of scavengeable electrons (5, 6) and is in reasonable agreement with the value calculated from the W-value in water vapor (20, 21). Figures 2 and 3, however, show $G(H_2)$ falls by 2.2 ± 0.6 when as little as 0.1 mole % nitrous oxide or sulfur hexafluoride is added to water vapor containing sufficient methanol to capture all available H atoms. Since both nitrous oxide (22, 23) and sulfur hexafluoride (24) react too slowly with H atoms to compete with methanol at low N_2O or SF_6 concentration, their effect on $G(H_2)$ is presumably due to capture of electrons which are precursors to part of the hydrogen yield. Increasing the concentration of nitrous oxide or sulfur hexafluoride from 0.1 to 1 mole % had no noticeable effect on $G(H_2)$; hence we can assume that 0.1 mole % is sufficient to capture all available electrons. In the absence of an electron scavenger, electrons are converted to hydrogen atoms via reaction [5] and the H atoms converted to H_2 via reaction [6]. These results therefore suggest that electron – positive ion neutralization in water vapor containing methanol gives H atoms with a yield corresponding to $G = 2.2 \pm 0.6$, unless ion–ion neutralization results in the formation of H atoms.

It has been shown (6) that O^- probably reacts with water,

[13] $$O^- + H_2O \rightarrow OH + OH^-,$$

and neutralization will therefore proceed via

[14] $$H^+(H_2O)_x(CH_3OH)_y + OH^- \rightarrow (x+1)H_2O + yCH_3OH \ .$$

Reaction [14] is analogous to the reaction

[15] $$D_3O^+ + OD^- \rightarrow D_2O + D_2O$$

proposed in the D_2O–C_3H_8 system (4), where it was found that D atoms were not formed by hydronium ion neutralization. Similarly in alkane gases, positive ion – negative ion neutralization in the gas phase (25) or neutralization at the walls on application of an electric field (26) have been shown not to yield H atoms. In our system nitrous oxide and sulfur hexafluoride have essentially the same effect on $G(H_2)$ at low concentration. If ion–ion recombination yielded H atoms, we would not expect the negative ions from nitrous oxide and sulfur hexafluoride to regenerate H atoms to the same extent. We therefore conclude that ion–ion neutralization does not regenerate H atoms in our system and that the reduction in hydrogen yield on addition of electron scavengers represents the number of H atoms arising from electron – positive ion neutralization.

Our value of $G = 2.2 \pm 0.6$ is slightly less than the values obtained in other studies in water vapor (4, 5). As explained above, we have rejected the possible formation of H atoms by ion–ion neutralization. Similarly we have no evidence for formation of other products in the neutralization reaction [5]. The yields of methane and carbon monoxide were reasonably consistent with those expected from direct absorption by methanol, showing that neither of these products is formed via the neutralization reaction. The difference between our results and those of Baxendale and Gilbert (5) is difficult to explain, since the values of $G(H_2)$ in the presence of electron scavengers are essentially the same in both cases. The discrepancy arises as a result of the different values of $G(H_2)$ in silica vessels in the absence of electron scavengers and we are unable to offer any explanation for these differences and, hence, for the discrepancy.

In the presence of nitrous oxide or sulfur hexafluoride, the total hydrogen which does not have the electron as a precursor is $G(H_2) = g(H_2) + g(H) = 5.7 \pm 0.3$. Since this yield is reduced to $G(H_2) \sim 0.5$, the molecular hydrogen yield, on addition of propylene, then the molecular hydrogen yield does not arise via thermal electron precursors. By subtraction, the number of hydrogen atoms arising from processes not involving the electron is $g(H) = 5.2 \pm 0.3$. This value is in good agreement with the values obtained from other studies in D_2O (4) and H_2O (5) vapors.

In the present work the decrease in $G(H_2)$ on addition of 0.1 mole % nitrous oxide was accompanied by the production of nitrogen with

Can. J. Chem. Downloaded from www.nrcresearchpress.com by 210.87.254.6 on 09/05/12
For personal use only.

$G(N_2) = 4.2$. Since $g(e^-) = 3.0$ (5, 6) we would expect $G(N_2) = 3.0$ from reaction [11], i.e. about 1.2 G units must originate from some other process. The reaction

[16] $$O^- + N_2O \rightarrow N_2 + O_2^-$$

proposed in the radiolysis of propane – nitrous oxide mixtures (25) does not occur in water vapor – nitrous oxide mixtures in the same experimental conditions as the present work (6). Since nitrous oxide is present in the same concentration range as in (6) and since $G(N_2)$ depends little on nitrous oxide concentration, we may discount reaction [16] as a source of nitrogen. The chain propagation reaction

[17] $$N_2O + CH_2OH \rightarrow N_2 + HCHO + OH$$

proposed in pure methanol vapor (27) and in H_2O – methanol vapor (5) does not apparently occur to any extent, since addition of sulfur hexafluoride suppressed the nitrogen yield at all methanol and nitrous oxide concentrations studied. To explain the nitrogen suppression in terms of a competition for CH_2OH radicals between nitrous oxide and sulfur hexafluoride would require the rate of reaction of CH_2OH to be 1000 times faster with sulfur hexafluoride than with nitrous oxide, which seems unlikely. The "extra" nitrogen yield may arise from the following competition

[13] $$O^- + H_2O \rightarrow OH + OH^-$$

[18] $$O^- + CH_3OH \rightarrow P + \ldots,$$

followed by

[19] $$P + 2N_2O \rightarrow 2N_2 + \ldots$$

Reaction [18] has been shown to occur in alkane–methanol – nitrous oxide mixtures, giving some product P which reacts quantitatively with nitrous oxide producing two molecules of nitrogen (28). The complete suppression of the nitrogen yield on addition of sulfur hexafluoride supports a mechanism of this type, since electron capture by sulfur hexafluoride would prevent formation of both N_2 and O^- produced in reaction [11].

As the nitrous oxide concentration increases between 1–10 mole %, the hydrogen yield decreases slowly and the nitrogen yield increases slowly. This may be due to the slow reaction of H atoms with nitrous oxide, $k = 10^6$–10^7 cc mole^{-1} s^{-1} at 150 °C (22, 23),

[20] $$H + N_2O \rightarrow N_2 + OH,$$

competing with reaction [6] at high nitrous oxide concentrations.

Water + Methanol + CCl_4

In this system, the slower falloff in $G(H_2)$ above about 0.1 mole % carbon tetrachloride (Fig. 3) and the nonlinear plot of $1/\Delta G$ versus $[CH_3OH]/[CCl_4]$ shown in Fig. 4 indicate the presence of more than one precursor of hydrogen reacting with carbon tetrachloride. We identify these precursors as the electron and the hydrogen atom, in view of their known reactions with carbon tetrachloride in the vapor phase (6, 29).

[21] $$e^- + CCl_4 \rightarrow CCl_3 + Cl^-$$

[22] $$H + CCl_4 \rightarrow HCl + CCl_3$$

Competition will occur between methanol and carbon tetrachloride for H atoms produced via reactions [3] and [5], the number of H atoms arising via [5] depending on the relative efficiencies of [5] and [21]. Our experiments show that, in the presence of sufficient sulfur hexafluoride to capture all electrons, values of $G(H_2)$ fall on the same curve as those in the absence of SF_6 (Fig. 3). This indicates that $k_{21}[CCl_4] \gg k_5[H^+(H_2O)_x(CH_3OH)_y]$, i.e. that carbon tetrachloride captures all available electrons (in the absence of SF_6) at all CCl_4 concentrations studied. Since the consumption of carbon tetrachloride due to electron capture is negligible at CCl_4 concentrations ≥ 0.1 mole %, the hydrogen yield will therefore be given by

$$G(H_2) = g(H_2) + g(H)\frac{1}{1 + \dfrac{k_{22}[CCl_4]}{k_6[CH_3OH]}},$$

which may be written as

$$G(H_2) = g(H_2) + (g(H_2) + g(H) - G(H_2)) \times \frac{k_6[CH_3OH]}{k_{22}[CCl_4]}.$$

If $g(H_2) + g(H) = 5.7$, as in H_2O–CH_3OH containing either nitrous oxide or sulfur hexafluoride, a plot of $G(H_2)$ vs. $(5.7 - G(H_2)) \times [CH_3OH]/[CCl_4]$ should give a straight line with a slope k_6/k_{22} and an intercept $g(H_2)$. The plot is shown in Fig. 5 and gives $k_6/k_{22} = 0.085$ and $g(H_2) = 0.8 \pm 0.2$. By subtraction, $g(H) = 4.9 \pm 0.5$. The values of $g(H_2)$ and $g(H)$ are a little higher and a little lower, respectively, than those found in H_2O–CH_3OH containing nitrous oxide or sulfur hexafluoride.

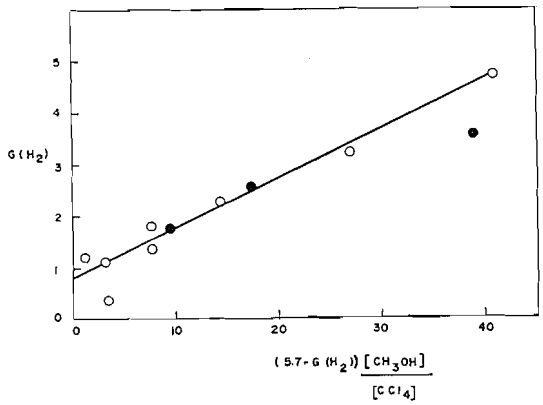

FIG. 5. Plot of $G(H_2)$ versus $(5.7 - G(H_2))[CH_3OH]/[CCl_4]$ from water vapor containing 2.2 mole % methanol and various concentrations of CCl_4: (O) without SF_6, (●) with 1 mole % SF_6.

Since a small yield of hydrogen persists, even at very high carbon tetrachloride concentrations, this is further evidence that this "molecular" hydrogen yield does not arise from either thermal electron or hydrogen atom precursors.

Rates of Reaction of N_2O and SF_6 with Electrons

Figures 2 and 3 show that the concentrations of sulfur hexafluoride and nitrous oxide required to scavenge all available electrons do not differ by more than a factor of 10. This would indicate that sulfur hexafluoride is not greater than a factor of 10 more effective than nitrous oxide in capturing electrons. However, based on the efficiency of sulfur hexafluoride in suppressing the nitrogen yield from water vapor or propane containing nitrous oxide, it appeared that sulfur hexafluoride was reacting at least 10^4 times faster with electrons than was nitrous oxide (6, 25).

In mixtures containing either N_2O or SF_6, the important parameter is the rate of reaction with electrons compared with the rate of electron – positive ion neutralization. When both N_2O and SF_6 are present and compete for electrons, other factors may be important. The electron affinities of N_2O and SF_6 are not known but could be important if the ions formed by electron capture live for any appreciable time. Thus, if the electron affinity of SF_6 is greater than that of N_2O, the reaction

$$[23] \qquad N_2O^- + SF_6 \rightarrow N_2O + SF_6^-$$

would occur if the lifetime of N_2O^- were long enough for it to collide and react with SF_6. In water vapor containing 1 mole % N_2O, the nitrogen yield is completely suppressed by as little as 1.6×10^{-3} mole % SF_6 (6). For this to be due to reaction [23], then N_2O^- would have to live for at least 10^{-5} s, assuming reaction [23] has a collision efficiency less than or equal to unity. Electron transfer of this type has been postulated to account for the effects of certain electron scavengers in methylcyclohexane vapor (30). While not offering direct evidence for reaction [23], the present results suggest that it is not simply the rate of reaction with electrons which is important in water vapor containing more than one electron scavenger.

Acknowledgment

The authors would like to acknowledge the critical comments of Dr. P. J. Dyne during the preparation of this manuscript.

1. R. F. FIRESTONE. J. Am. Chem. Soc. **79**, 5593 (1957).
2. J. H. BAXENDALE and G. P. GILBERT. Discussions Faraday Soc. **36**, 186 (1963).
3. A. R. ANDERSON, B. KNIGHT, and J. A. WINTER. Trans. Faraday Soc. **62**, 359 (1966).
4. G. R. A. JOHNSON and M. SIMIC. J. Phys. Chem. **71**, 1118 (1967).
5. J. H. BAXENDALE and G. P. GILBERT. Science, **147**, 1571 (1965).
6. R. S. DIXON and M. G. BAILEY. Can. J. Chem. **46**, 1181 (1968).
7. A. O. ALLEN. Radiation Res. Suppl. **4**, 54 (1964).
8. J. A. HEARNE and R. W. HUMMEL. Radiation Res. **15**, 254 (1961).
9. J. BLACHFORD and P. J. DYNE. Can. J. Chem. **42**, 1165 (1964).
10. R. A. BACK, T. W. WOODWARD, and K. A. MCLAUCHLAN. Can. J. Chem. **40**, 1380 (1962).
11. P. KEBARLE, R. N. HAYNES, and J. G. COLLINS. J. Am. Chem. Soc. **89**, 5753 (1967).
12. A. R. ANDERSON, B. KNIGHT, and J. A. WINTER. Nature, **209**, 199 (1966).
13. R. J. CVETANOVIC. Advan. Photochem. **1**, 115 (1963).
14. J. H. BAXENDALE and G. P. GILBERT. J. Am. Chem. Soc. **86**, 516 (1964).
15. A. R. ANDERSON, B. KNIGHT, and J. A. WINTER. Nature, **201**, 1026 (1964).
16. J. Y. YANG and I. MARCUS. J. Am. Chem. Soc. **88**, 1625 (1966).
17. F. W. LAMPE, F. H. FIELD, and J. L. FRANKLIN. J. Am. Chem. Soc. **79**, 6132 (1957).
18. V. I. VEDENEYEV *et al.* Bond energies, ionization potentials and electron affinities. Edward Arnold, London. 1966.
19. V. L. TALROZE and E. L. FRANKEVITCH. J. Am. Chem. Soc. **80**, 2344 (1958).
20. C. WINGATE, W. GROSS, and G. FAILLA. Radiation Res. **8**, 411 (1958).
21. J. BOOZ and H. G. EBERT. Z. Angew. Phys. **13**, 376 (1961).

Can. J. Chem. Downloaded from www.nrcresearchpress.com by 210.87.254.6 on 09/05/12
For personal use only.

22. C. P. FENIMORE and G. W. JONES. J. Phys. Chem. **63**, 1154 (1959).
23. G. DIXON-LEWIS, M. M. SUTTON, and A. WILLIAMS. J. Chem. Soc. 5724 (1965).
24. C. P. FENIMORE and G. W. JONES. Combust. Flame, **8**, 231 (1964).
25. G. R. A. JOHNSON and J. M. WARMAN. Trans. Faraday Soc. **61**, 1709 (1965).
26. T. W. WOODWARD and R. A. BACK. Can. J. Chem. **41**, 1463 (1963).
27. M. MEABURN and F. W. MELLOWS. Trans. Faraday Soc. **61**, 1701 (1965).
28. J. M. WARMAN. J. Phys. Chem. **72**, 52 (1968).
29. E. W. R. STEACIE. Atomic and free radical reactions. Vol. 2. Reinhold, New York. 1954. p. 657.
30. W. J. HOLTSLANDER and G. R. FREEMAN. J. Phys. Chem. **71**, 2562 (1967).

Can. J. Chem. Downloaded from www.nrcresearchpress.com by 210.87.254.6 on 09/05/12
For personal use only.

Can. J. Chem. Downloaded from www.nrcresearchpress.com by 210.87.254.105 on 09/05/12
For personal use only.

Thermodynamics of ionization of aqueous toluidinium ions

W. F. O'HARA
Science Department, U.S. Naval Academy, Annapolis, Maryland 21402

Received January 16, 1968

Standard heats of ionization of ortho-, meta-, and para-toluidinium ions in water at 25 °C have been determined in a high precision solution calorimeter. Entropies of ionization have been calculated from these heats and well-defined free energy changes. As predicted by theory, a linear relation is found between ΔS^0_{ion} and ΔG^0_{ion} and between ΔH^0_{ion} and ΔS^0_{ion} for these compounds.

Canadian Journal of Chemistry, 46, 1965 (1968)

Introduction

Current investigations and discussions (1–11, 17) of the effects of molecular structure and solvent effects on the relative strengths of organic acids in water have involved determination and examination of heats and entropies of ionization and their relative effects on standard free energy changes.

Recently we reported the thermodynamics of ionization of aqueous anilinium ion (11) and in continuation of the study of substituted anilines have determined ΔH^0 and calculated ΔS^0 for ionization of the toluidinium ions in water at 25 °C.

Experimental

The reaction calorimeter used in all experiments was of 800 ml capacity and similar to a 900 ml model described before (12). Power for the calorimeter heater was supplied by a Kepco 40–0.5M. d.c. power supply replacing storage batteries. A Fluke 351-A constant current d.c. power supply replaced a low discharge battery as the source of current (0.00277 A) in the transposed Maier bridge thermometer circuit.

The sensitivity of this calorimeter was determined to be 4.3×10^{-5} (deg/μV), the same as the apparatus previously described (12).

All heats of reaction were determined at 25.0 ± 0.15 °C.

Toluidines were obtained from Aldrich Chemical Company. The ortho and meta isomers were vacuum distilled in a micro apparatus with Vigreux column immediately before use. Purity was determined by refractometry, N_d^{20} (ortho) = 1.5731, lit. 1.5728, $N_d^{22.4}$ (meta) = 1.5713, lit. 1.5711. Para-toluidine was sublimed in a Nester/Faust vacuum sublimation apparatus and its purity was ascertained by corrected melting point (42–44°, lit. 43.8°).

Solutions of HCl and $HClO_4$ were prepared and standardized by common procedures. Toluidine solutions were prepared by weight.

The accuracy of the calorimeter has been checked periodically by measuring the heat of solution of KCl(c) in water (13) (endothermic) and the heat of solution of tris(hydroxymethyl)aminomethane, in 0.1 *M* HCl (14) (exothermic).

Results and Discussion

Heats of ionization of ortho-, meta-, and para-toluidinium ions were determined by measuring heats of neutralization of aqueous solutions of the toluidines by 5 ml of 5.498 *N* $HClO_4$ (eight runs for *o*-toluidine, 0.027 to 0.008 *M* final solution, five runs for *m*-toluidine, 0.027 to 0.009 *M* final solution, and nine runs for *p*-toluidine, 0.034 to 0.008 *M* final solution). These reactions are represented by the general equation

$$[1] \quad R\phi NH_2(aq) + H^+(5.498N) \rightarrow R\phi NH_3^+(aq).$$

Seven determinations of the heat associated with breaking the thin pyrex bulb containing the $HClO_4$ solution and dilution of the acid were made. Approximately 5.5 *M* $HClO_4$ was chosen to minimize heat of dilution effects (13) and allow complete neutralization of the aqueous base. Combination of these two heats yields ΔH_2 for the reaction

$$[2] \quad R\phi NH_2(aq) + H^+(aq) \rightarrow R\phi NH_3^+(aq).$$

The values of ΔH_2 were extrapolated to infinite dilution by linear least square treatment to yield ΔH^0_{ion}, the negative of the standard heat of ionization of the aqueous ortho-, meta-, and para-toluidinium ions. These ΔH^0_{ion} values are listed in Table I.

To insure the validity of the heats of ionization so obtained, the following was done. Four measurements of the heat of solution of liquid *m*-toluidine were made. This process is

$$[3] \quad m\text{-}CH_3\phi NH_2(l) \rightarrow m\text{-}CH_3\phi NH_2(aq).$$

The heats obtained were not sensitive to concentration and were extrapolated to zero concentration as before giving ΔH^0_s the standard heat of solution of *m*-toluidine (l).

TABLE I

Thermodynamics of ionization of aqueous toluidinium ions at 25 °C*

Ion	ΔH^0_s	ΔH^0_n	ΔH^0_{ion}	$\Delta H^{0\prime}_{ion}$	ΔG^0_{ion}	ΔS^0_{ion}
Anilinium	0.45 ± 0.03	-6.79 ± 0.09	—	7.24 ± 0.1	6.27 ± 0.02	3.3 ± 0.3
o-Toluidinium	—	—	7.22 ± 0.09	—	6.07 ± 0.02	3.9 ± 0.2
m-Toluidinium	0.30 ± 0.02	-7.06 ± 0.04	7.37 ± 0.06	7.36 ± 0.05	6.44 ± 0.02	3.1 ± 0.2†
p-Toluidinium	—	—	7.60 ± 0.09	—	6.93 ± 0.02	2.2 ± 0.2

*ΔH^0 and ΔG^0 in kcal/mole and ΔS^0 in cal/deg mole.
†ΔH^0_{ion} used to compute ΔS^0_{ion} was 7.37 kcal/mole.

Four heats of neutralization of *m*-toluidine (l) by 0.097 *N* HCl were measured at final concentrations of *m*-toluidinium ion from 0.030 to 0.017 *M*. These reactions are indicated by

[4] $m\text{-}CH_3\phi NH_2(l) + H^+(aq) \rightarrow m\text{-}CH_3\phi NH_3{}^+(aq).$

Extrapolation to infinite dilution as before yields ΔH^0_n, the standard heat of neutralization of *m*-toluidine. Combination of ΔH^0_s and ΔH^0_n gives $\Delta H^{0\prime}_{ion}$, the standard heat of ionization of aqueous *m*-toluidinium ion. This is shown by

$$[5] \qquad \Delta H^{0\prime}_{ion} = \Delta H^0_s - \Delta H^0_n.$$

Values of ΔH^0_s, ΔH^0_n, and $\Delta H^{0\prime}_{ion}$ are in Table I along with ΔH^0_{ion} values obtained by the aforementioned method.

Several investigators (15–17) have determined thermodynamic pK_a values for the toluidinium ions in water at 25 °C, all in excellent agreement. The pK_a values we adopt are ortho 4.45, meta 4.72, and para 5.08. Values of ΔG^0_{ion} are calculated from these pK_a's by

$$[6] \qquad \Delta G^0_{ion} = 1364 pK_a \text{ at } 298.15\ ^\circ K$$

and are listed in Table I. Standard entropies of ionization have been calculated from

$$[7] \qquad \Delta S^0_{ion} = \frac{\Delta H^0_{ion} - \Delta G^0_{ion}}{298.15}$$

and are listed in Table I along with calorimetric data for anilinium ion (11).

Bolton and Hall (17) recently have reported pK_a values for these compounds in water from 10 to 50 °C at 5 deg intervals and have calculated ΔG^0_{ion}, ΔH^0_{ion}, and ΔS^0_{ion} at 25 °C. They also calculate these quantities from the preliminary equilibrium data of Biggs (16). Their data for ΔH^0_{ion} are about 0.1 kcal/mole higher than ours, except in the case of the para isomer where a difference of about 0.4 kcal/mole exists. In addition, their ΔS^0 values are higher than ours. Unfortunately, differences such as these are common when comparing calorimetric values with values from temperature coefficients. For example, the most recent calorimetric heat of ionization of water at 25 °C is 13.34 kcal/mole (18, 19) and the e.m.f. value at 25 °C is 13.53 kcal/mole (20). King (8) and Larson and Hepler (9) discuss to some extent these differences and their causes.

Electrostatic models of solute–solvent interaction (8) predict a linear relation between ΔG^0_{ion} and ΔS^0_{ion} for acids of similar structure. Larson and Hepler (8) show that

$$[8] \qquad \Delta S^0_{ion} = \frac{-(\delta\gamma/\delta T)}{(1+\gamma)} \Delta G^0_{ion}.$$

Here γ is a parameter depending on the particular solvent and on the possible small differences of solute–solvent effects on ΔH^0_{ion} and $T\Delta S^0_{ion}$. Figure 1 is a plot of ΔG^0_{ion} vs. ΔS^0_{ion} using Bolton and Hall's (17) and our data. A similar straight line relation between ΔG^0_{ion} and ΔH^0_{ion} is a consequence of the ΔG^0_{ion} vs. ΔS^0_{ion} linearity, and is not shown here.

Bolton and Hall (17) and Biggs (16) are in excellent agreement on pK_a values in the 10 to 50 °C range. The order of acid strengths is

$$[9] \quad o\text{-}CH_3\phi NH_3{}^+ > \phi NH_3{}^+ > m\text{-}CH_3\phi NH_3{}^+ > p\text{-}CH_3\phi NH_3{}^+$$

at all temperatures in this range. There is little disagreement on ΔG^0_{ion} at 25 °C, but ΔH^0_{ion} and ΔS^0_{ion} at this temperature are not agreed upon. The values calculated by Bolton and Hall from Biggs' (16) preliminary data are significantly different from their own values. Chen and Laidler (4) suggest that the calorimetric heats and entropies of ionization reported by Zawidzki *et al.* (21) are in serious error and should be disregarded. There are no other calorimetric measurements of these heats in the literature.

Can. J. Chem. Downloaded from www.nrcresearchpress.com by 210.87.254.105 on 09/05/12
For personal use only.

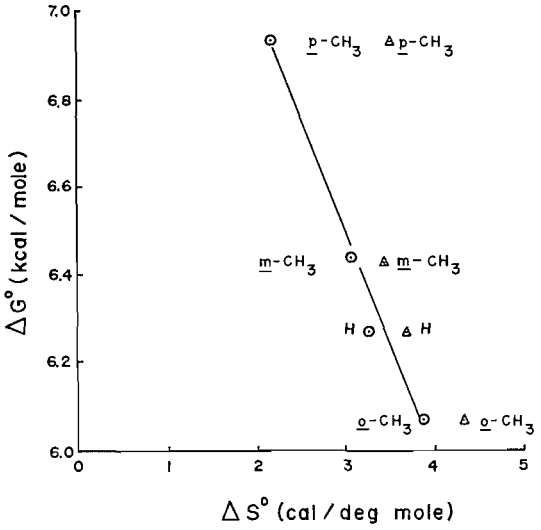

FIG. 1. Correlation between standard free energies and standard entropies of ionization of toluidinium ions and anilinium ion: (○) this paper, (△) data of Bolton and Hall (16).

Larson and Hepler (9) show that

$$[10] \qquad \Delta G^0 \simeq \Delta H_{\text{int}}(1 + \gamma)$$

for symmetrical proton transfer reactions and would apply to the reaction

$$[11] \quad R\phi NH_3^+(aq) + \phi NH_2(aq) \rightarrow R\phi NH_2(aq) + \phi NH_3^+(aq)$$

in which $R\phi NH_3^+$ is the substituted anilinium ion and ϕNH_3^+ is anilinium ion. ΔH_{int} is the "internal" part of the enthalpy change for reaction [11], or this enthalpy change in the absence of solute–solvent effects.

It can be seen from eq. [10] that if $1 \gg \gamma$, which would not be surprising,

$$[12] \qquad \Delta G^0{}_{11} \simeq \Delta H_{\text{int}}.$$

$\Delta G^0{}_{11}$ values from pK_s are: *o*-toluidinium–aniline (−0.20 kcal/mole) *m*-toluidinium–aniline (0.17 kcal/mole), *p*-toluidinium–aniline (0.66 kcal/mole). With γ small compared to 1 for these ions, the relative acid strengths are mainly determined by the ease of proton removal measured by ΔH_{int}. In this case, or in the case where γ is known, solute–solvent interaction enthalpies, or external enthalpies ΔH_{ext}, can be calculated from [10] and

$$[13] \qquad \Delta H^0{}_{11} = \Delta H_{\text{int}} + \Delta H_{\text{ext}},$$

which has been previously discussed (2, 5, 8, 9). $\Delta H^0{}_{11}$ is obtained from heats of ionization such as reported in this paper. These calculations of ΔH_{ext} can be and will be made when more is known about γ.

Acknowledgment

We thank the U.S. Naval Academy Research Council for support of this and related research.

1. L. P. FERNANDEZ and L. G. HEPLER. J. Am. Chem. Soc. **81**, 1783 (1959).
2. L. G. HEPLER and W. F. O'HARA. J. Phys. Chem. **65**, 811 (1961).
3. W. F. O'HARA and L. G. HEPLER. J. Phys. Chem. **65**, 2107 (1961).
4. D. T. Y. CHEN and K. J. LAIDLER. Trans. Faraday Soc. **58**, 480 (1962).
5. L. G. HEPLER. J. Am. Chem. Soc. **85**, 3089 (1963).
6. H. C. KO, W. F. O'HARA, T. HU, and L. G. HEPLER. J. Am. Chem. Soc. **86**, 1003 (1964).
7. D. J. G. IVES and P. D. MARSDEN. J. Chem. Soc. **72**, 649 (1965).
8. E. J. KING. Acid–base equilibria. The Macmillan Co., New York. 1965.
9. J. W. LARSON and L. G. HEPLER. *In* Solvent–solute interactions. *Edited by* C. D. Ritchie. Interscience Publishers, Inc., New York. In press.
10. J. J. CHRISTENSEN, D. P. WRATHALL, R. M. IZATT, and D. O. TOLMAN. J. Phys. Chem. **71**, 3001 (1967).
11. W. F. O'HARA, H. C. KO, M. N. ACKERMANN, and L. G. HEPLER. J. Phys. Chem. **71**, 3107 (1967).
12. W. F. O'HARA, C. H. WU, and L. G. HEPLER. J. Chem. Educ. **38**, 512 (1961).
13. Selected values of chemical thermodynamic properties. Nat. Bur. Std. U.S. Circ. 500. U.S. Government Printing Office, Washington, D.C. 1952.
14. S. R. GUNN. J. Phys. Chem. **69**, 2902 (1965).
15. A. I. BIGGS and R. A. ROBINSON. J. Chem. Soc. **69**, 388 (1961).
16. A. I. BIGGS. J. Chem. Soc. **69**, 495 (1961).
17. P. D. BOLTON and F. M. HALL. Australian J. Chem. **20**, 1797 (1967).
18. J. D. HALE, R. M. IZATT, and J. J. CHRISTENSEN. J. Phys. Chem. **63**, 2605 (1963).
19. C. E. VANDERZEE and J. A. SWANSON. J. Phys. Chem. **65**, 2608 (1963).
20. H. W. HARNED and B. B. OWEN. The physical chemistry of electrolyte solutions. 3rd ed. Reinhold Publishing Corp., New York. 1958.
21. T. W. ZAWIDZKI, H. M. PAPEE, W. J. CANADY, and K. J. LAIDLER. Trans. Faraday Soc. **55**, 1738 (1959).

Can. J. Chem. Downloaded from www.nrcresearchpress.com by 210.87.254.105 on 09/05/12
For personal use only.

Can. J. Chem. Downloaded from www.nrcresearchpress.com by 210.87.254.5 on 09/05/12
For personal use only.

A new simple absolute viscometer for use in experimental systems with limited access to the liquid

M. K. NAGARAJAN[1]

Department of Chemistry, Indian Institute of Technology, Bombay-76, India

Received October 7, 1966

A novel type of vertically oscillating bob viscometer for liquids is described. The mathematical theory of a solid sphere oscillating in a viscous liquid is developed, and results in an exact equation depicting the relationship between the logarithmic decrement of the oscillations of the sphere and the viscosity of the liquid surrounding the bob. The use of this technique for the determination of *absolute* viscosity of liquids is demonstrated. Using five sample liquids, at room temperature, the average error between the absolute viscosities determined and those of previous measurements is $\pm 1.5\%$.

The viscometer consists of a quartz spring, which suspends a solid gold sphere, hanging vertically. The oscillations of the system are sensed by electrically recording the output of a linear variable differential transformer, the core of which forms a part of the oscillating system. The oscillations are stimulated electrically; the positioning of the transducer core is precisely adjustable with the use of an electric motor driven mechanism. Thus, the viscometer can be entirely remotely controlled and is, therefore, recommended for experimental situations which make the liquid not easily accessible, e.g. inside furnaces, pressure vessels, vacuum chambers, etc.

Canadian Journal of Chemistry, 46, 1969 (1968)

Introduction

As an extension of our recent investigation (1) on the effect of pressure on the self-diffusion coefficients in molten salts, it was desired to carry out viscosity measurements in molten salts at high pressures. Such a study requires a *remote-controlled* device capable of measuring the viscosity of liquids at high temperatures and high pressures. The viscometer described here can, in general, be used for measurement of the viscosity of liquids in experimental situations which make the liquid not easily accessible, e.g. inside furnaces, pressure vessels, vacuum chambers, etc.

Among the many methods generally employed for viscosity determination, that which is suitable for electrical recording is some form of logarithmic decrement method. A solid bob oscillating in a liquid will experience a damping force, which is a function of the viscosity of the liquid, resulting in a progressive decrease in amplitude of the oscillations. From the logarithmic decrement (measured as the logarithm of the ratio of successive oscillations), the density of the liquid, and the mass of the system it is generally possible to evaluate the viscosity of the liquid. However, due to the complexity of the exact mathematical relation between the logarithmic decrement and the viscosity of the liquid, many authors (cf. ref. 2) resort to calibration of the apparatus with known liquids. All known oscillational methods (3–8) fall into one of the following two general categories: (i) those involving torsional oscillations of the suspended solid bob and (ii) those involving oscillations in a plane, viz. simple pendulum type. A third possible type of oscillation, solid bob oscillating *vertically* (i.e. in the axis of suspension), has not yet been described in the literature. This communication reports on the theory and the design of a vertically oscillating sphere viscometer.

The main advantages of this new method are: (i) the geometrical arrangement of the components of the viscometer deviates very little from the (often stringent) requirements of the theory, thus allowing *absolute* measurement of viscosity, (ii) the *one dimensional* character of the oscillations eases the mathematical treatment, and (iii) the oscillations can be started and recorded electrically, thus making the method suitable for situations where access to the liquid is limited.

Theory of the Method

A schematic diagram of the experimental assembly is given in Fig. 1. The solid sphere (B) of radius a cm is completely surrounded by a liquid of density ρ g cm^{-3} and viscosity η P. Since the sphere (of mass m_b) is oscillating vertically, in an axis coinciding with the axis of suspension, the system has only one degree of freedom,

[1]This work was performed by the author at The University of Pennsylvania, Philadelphia, Pa., 19104, U.S.A., where he worked as a Postdoctoral Associate.

Can. J. Chem. Downloaded from www.nrcresearchpress.com by 210.87.254.5 on 09/05/12
For personal use only.

i.e. the configuration is completely determined by the vertical displacement (x) from the position of static equilibrium. By a sudden application and removal of an external force the system is set into oscillation, which is now maintained by the elastic force of the spring (S) alone; hence, we are considering only the free vibrations of the system. The viscous drag on the sphere, due to the liquid, acts as the retarding force resulting in the progressive dimunition of amplitude of each successive oscillation.

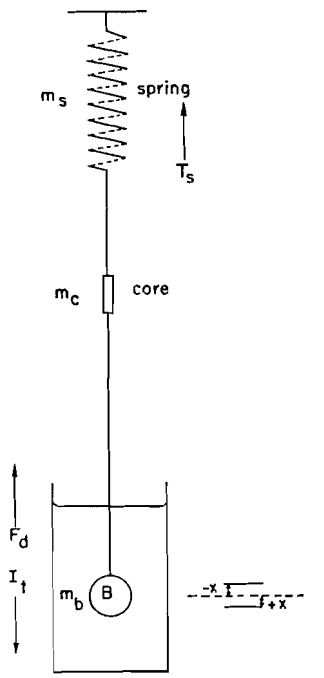

FIG. 1. Schematic diagram of the vertically oscillating sphere viscometer.

(a) Inertial Force of the Sphere

Neglecting the effect of liquid friction and the buoyancy, the inertial force[2] of the sphere is $m_b(d^2x/dt^2)$. However, it is not sufficient to consider only the mass of the sphere, since the transducer core (C) and a part of the spring also belong to the oscillating system. The contribution to the total mass, M, of the system from the spring is (9) $m_s/3$, where m_s is the mass of the spring. The inertial force of the system is, therefore, $(m_b + m_c + \frac{1}{3}m_s)(d^2x/dt^2)$ or $M(d^2x/dt^2)$ (m_c denotes the mass of the transducer core). The buoyancy on the sphere contributes a term $-m'(d^2x/dt^2)$ to the inertial force; where m' is the mass of liquid displaced by the sphere ($m' = \frac{4}{3}\pi\rho a^3$). Stokes (10) has derived the correction (11) to the inertia of a sphere oscillating in a fluid, which is

$$\left(\frac{1}{2} + \frac{9}{4}\mu\right)m'\frac{d^2x}{dt^2},$$

where μ is a dimensionless quantity defined by

$$[1] \qquad \mu = \left[\frac{\eta\tau}{\pi\rho a^2}\right]^{1/2},$$

where τ is the period of oscillation. The effect of this correction term is to increase the inertia of the sphere and hence is denoted positive. Taking into account the buoyancy on the sphere and the correction to the inertia of the sphere given by Stokes, the net inertial force (I_f) of the sphere in the downward direction is

$$[2] \quad I_f = M\frac{d^2x}{dt^2} - m'\frac{d^2x}{dt^2} + \left(\frac{1}{2} + \frac{9}{4}\mu\right)m'\frac{d^2x}{dt^2}$$

$$= \left[M - m'\left(\frac{1}{2} - \frac{9}{4}\mu\right)\right]\frac{d^2x}{dt^2}.$$

(b) The Retarding Force due to the Elasticity of the Spring

Let λ denote the 'spring constant' of the spring; λ is the load necessary to produce unit extension of the spring. When the sphere is displaced by a distance x in the downward direction, the elastic nature of the spring will give rise to a force, T_s, proportional to the displacement and *opposing the motion*. This retarding force is given by

$$[3] \qquad T_s = -\lambda x.$$

Note: The displacement, x, must be in the elastic range. In the experimental arrangement described below, $x = \pm 0.2$ cm and Hooke's law is obeyed by the spring up to an extension of ca. 10 cm.

(c) Damping Force due to the Viscous Drag on the Sphere

The liquid surrounding the oscillating sphere exerts a damping force, F_d, proportional to the velocity of motion. The effect of the force F_d is to hinder the motion of the sphere and hence will

[2]Since the spring hangs vertically, one *may* include gravity in the discussion, in which case the displacement x is measured from the *unstrained* position *or*, as in the present discussion, denote the displacement from the position of static equilibrium (i.e. already *strained*) by x, in which case the term mg cancels out, on writing the differential equation of motion.

Can. J. Chem. Downloaded from www.nrcresearchpress.com by 210.87.254.5 on 09/05/12
For personal use only.

be negative. Stokes (10) has shown that in the case of a sphere oscillating in an unlimited volume of a liquid and in a direction perpendicular to a fixed horizontal plane in the liquid (cf. p. 31 of ref. 10), the damping force is given by

$$[4] \qquad F_d = -\frac{9}{2}\frac{\pi\mu m'}{\tau}(1+\mu)\frac{dx}{dt}.$$

Equation [4] was originally derived by Stokes for the case of periodic laminar flow (Reynold's number lying between 40 and 200). The Reynold's number calculated[3] for the experimental system described below lies within this range. Furthermore, eq. [4] assumes that the liquid is 'unbounded'. The necessary corrections to be applied in the case of a sphere oscillating in a liquid contained in a vessel, with finite boundaries, are discussed in Section (*f*).

(d) Equation of Motion for the Vertically Oscillating Sphere

From eq. [2], [3], and [4], the differential equation of motion of the vertically oscillating sphere is

$$[5] \qquad \left[M - m'\left(\frac{1}{2} - \frac{9}{4}\mu\right)\right]\frac{d^2x}{dt^2} + \frac{9}{2}\frac{\pi\mu m'}{\tau}(1+\mu)\frac{dx}{dt} + \lambda x = 0.$$

We obtain the solution for eq. [5] by the usual procedures. In order to reduce eq. [5] to the 'standard form' we divide the equation by the coefficient of d^2x/dt^2 and write

$$[6] \qquad d^2x/dt^2 + 2K(dx/dt) + n^2 = 0,$$

where

$$[7] \qquad K = \frac{9\pi\mu m'(1+\mu)}{4\tau\left[M - m'\left(\frac{1}{2} - \frac{9}{4}\mu\right)\right]}$$

and

$$[8] \qquad n^2 = \frac{\lambda}{\left[M - m'\left(\frac{1}{2} - \frac{9}{4}\mu\right)\right]}.$$

For the case of under-damped[4] systems (where $K/n \ll 1$), the solution of eq. [6] leads to the normal form for the damped sinusoidal motion of the sphere and the logarithmic decrement (δ) is given (12) by

$$[9] \qquad \delta = \frac{2\pi K}{(n^2 - K^2)^{1/2}}.$$

The amplitudes of successive oscillations on the same side of the origin are considered in this case.

(e) The Relation between the Logarithmic Decrement and the Viscosity[5]

From eq. [9], we can write

$$[10] \qquad \delta^2 = \frac{4\pi^2}{(n^2/K^2) - 1}.$$

In the experimental system described below, $n^2/K^2 \sim 10^5$ for viscosity of the liquid ranging from 0.5 cP to 5 cP and density of unity. Neglecting unity in comparison to n^2/K^2 in eq. [10],

$$[11] \qquad \delta^2 = \frac{4\pi^2K^2}{n^2}.$$

Substituting the values of K and n^2 as defined by eqs. [7] and [8] and simplifying (see Appendix), we get the following relationship between the logarithmic decrement and the viscosity of the liquid,

$$[12] \qquad A\theta\eta^{3/2} + B\theta^2\eta - C\theta\tau\delta^2\eta^{1/2} + \delta^2(D\rho - 1) = 0,$$

where $\theta = (\rho/\tau)^{1/2}$ and the constants, which depend only on the dimensions of the apparatus, are defined by the following equations:

$$[13] \qquad A = \frac{72\pi^{9/2}a^3}{M\lambda} \quad B = \frac{36\pi^5a^4}{M\lambda} \quad C = \frac{3\pi^{1/2}a^2}{M} \quad D = \frac{2\pi a^3}{M}.$$

(f) Correction due to the 'Finite Boundaries' of the Liquid

In the derivation of equations for the net inertial force (eq. [2]) and the damping force (eq. [4]), it has been assumed that the liquid was 'unbounded'. However, in practice the liquid encounters finite boundaries, e.g. the walls and the bottom of the container. Stokes (10) has estimated additive corrections to I_f and F_d by considering a hypothetical spherical boundary

[3]Reynold's number, N_{Re} is defined as $N_{Re} = \bar{v}d\rho/\eta$ where $\bar{v}$ is the linear velocity and d is the diameter of the spherical bob. Substituting typical values, $\bar{v} \sim 1.2$ cm s^{-1}, $d \sim 1$ cm, and $(\eta/\rho) \sim 0.01$, N_{Re} is ~ 120. If $(\eta/\rho) > 0.01$ then N_{Re} is < 120.

[4]Using the following typical values: $\mu \sim 0.04$, $m' \sim 0.8$, $\tau \sim 0.3$, $M \sim 10$, and $\lambda \sim 4 \times 10^3$, the value of K/n is of the order of 10^{-5}.

[5]Although eq. [9] has been arrived at by the use of known principles and well-established methods, the equations derived here are original in respect of their application. There is no reported method which uses the same combination of forces which resulted in eqs. [5] and [9].

Can. J. Chem. Downloaded from www.nrcresearchpress.com by 210.87.254.5 on 09/05/12
For personal use only.

(of radius b cm) concentric with the spherical bob, which are:

[14] $\Delta F_d \simeq 0$ for most low viscosity liquids and

$$\Delta I_f \simeq \frac{3a^3m'}{2(b^3 - a^3)} \frac{d^2x}{dt^2}.$$

Although in actual experiments a cylindrical container is generally employed to contain the liquid, the corrections given in eq. [14] were employed for the following reasons: (i) calculation of the corrections due to the cylindrical walls of the container, with a spherical bob in the liquid, are mathematically tedious and (ii) the ratio b/a can be kept as large as the experimental situation allows thus reducing the magnitude of the correction term; in the experiments reported here the correction to the inertial force was never larger than 1%. Incorporating eq. [14] in eq. [2], we have

$$[15] \quad I_f(\text{corrected}) = \left[M - m' \left\{ \frac{1}{2} - \frac{9}{4}\mu - \frac{3a^3}{2(b^3 - a^3)} \right\} \right] \frac{d^2x}{dt^2}.$$

Using the corrected net inertial force in the differential equation of motion (eq. [5]) one obtains the following modified equation,

$$[16] \quad A\theta\eta^{3/2} + B\theta^2\eta - C\theta\tau\delta^2\eta^{1/2} + \{(D - E)\rho - 1\}\delta^2 = 0,$$

where

$$[17] \qquad E = \frac{2\pi a^6}{m_b(b^3 - a^3)}$$

and the other constants are as defined by eq. [13].

(g) Use of Equation [16]

This equation was used for the *absolute* determination of the viscosity of a number of liquids at room temperature in the following manner. The constants A, B, C, D, and E were calculated using the known parameters of the apparatus, which are: $m_b = 8.7405$ g; $m_c = 0.5932$ g; $m_s = 3.0756$ g; $M = 10.3589$ g; $a = 0.4761$ cm; $b = 1.70$ cm; $\lambda = 3.988 \times 10^3$ g s^{-2}. The apparatus constants calculated according to eqs. [13] and [17] are: $A = 0.03253$; $B = 0.01373$; $C = 0.1163$; $D = 0.06549$; and $E = 0.001743$.

The values of θ were known from density data (13) for the liquids used and from the experimentally observed periods of oscillation.

The resulting cubic equation in $\eta^{1/2}$ was solved by a trigonometric method (14).

Experimental

(a) General

The general schematic view of the apparatus is shown in Fig. 2. It consists, essentially, of a helical quartz spring (S) which suspends a solid gold sphere (B), the latter being immersed in the liquid. Between the gold sphere and the quartz spring there exists a transducer core (made of a specially treated stainless magnetic alloy) (C), which is situated concentric with a linear variable differential transformer (l.v.d.t.).

The system is stimulated into oscillation by the application of a momentary d.c. bias to one of the secondary windings of the l.v.d.t. The amplitude of the resulting oscillations is recorded by sensing the output of the l.v.d.t., which is applied to a fast-response recorder.

The positioning of the core in the l.v.d.t. can be adjusted, as needed, by the use of an electric motorized drive mechanism.

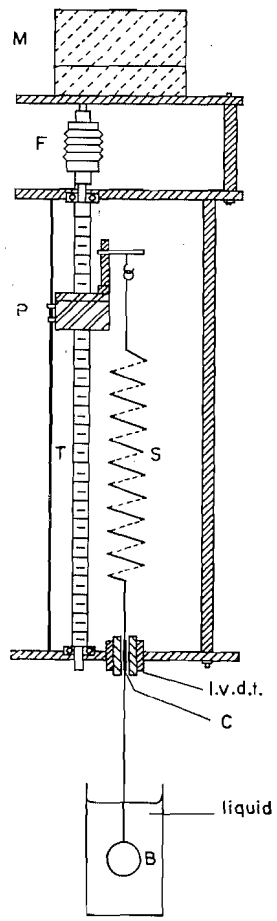

FIG. 2. Experimental assembly. S, quartz spring; B, solid gold sphere; C, transducer core; M, reversible motor with gearbox; T, threaded drive shaft; F, flexible coupling; P, mounting platform.

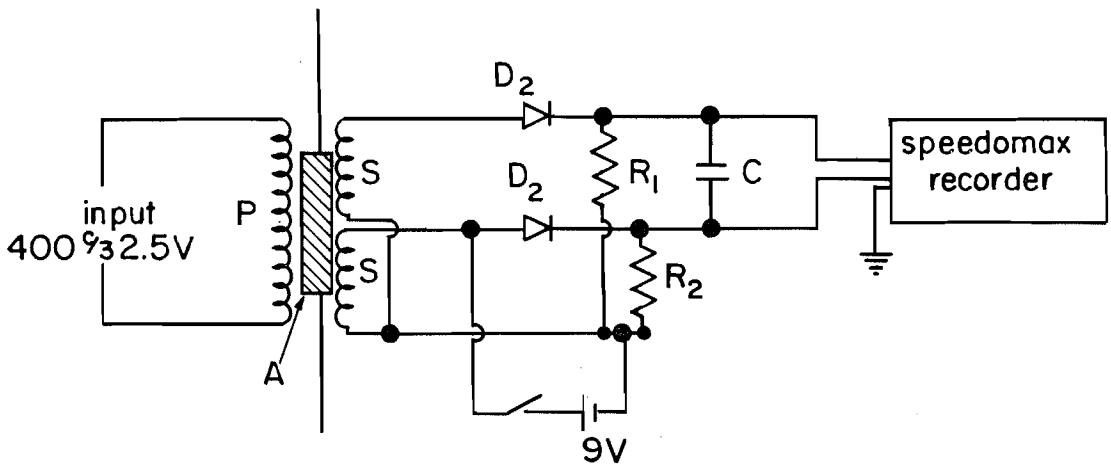

FIG. 3. Circuit for stimulation and recording of oscillations. P, primary winding of l.v.d.t.; S, secondary winding of l.v.d.t.; A, freely moving core; D_1, D_2, germanium rectifiers; C, electrolytic capacitor (30 μF); $R_1 = R_2 = 1000\Omega$.

The apparatus can thus be entirely remotely controlled.

(b) Quartz Spring

Quartz was chosen for its excellent elastic properties; it does not creep. The helical quartz spring used was ca. 1.5 cm in diameter and ca. 7 cm long when unloaded. The maximum capacity of the spring was ca. 40 g; when fully loaded the maximum extension was ca. 10 cm. The quartz spring was supplied by Microchemical Specialties Co., Berkeley, California (Catalogue no. I-2652).

(c) Transducer

The linear variable differential transformer is a linear motion transducer and is essentially an electro-mechanical device, which produces an electrical output proportional to the displacement of the core; the output is also directional.

The l.v.d.t. used was supplied by the International Resistance Co., Philadelphia; model no. 70-3155. The core was about $\frac{1}{2}$ in. long and weighed about 600 mg. The maximum rated input (6 V, 400 c/s) was not used in order to minimize the magnetic field; an input of 3 V, 400 c/s was found to be sufficient. The sensitivity at this input level is 1 mV per 1 V input per 1/1000 in.

The l.v.d.t. used was high temperature wound, capable of withstanding 250 °C.

(d) Circuit for Stimulation and Recording of Oscillations

This is shown in Fig. 3. The circuit serves to convert the a.c. output of the transducer to d.c. The recorder used has a response time of 1/8 s; this response time was quite sufficient to record the oscillations with a frequency of 3 c/s. The recorder was supplied by the Esterline Angus Co., model S-601-S speed servo recorder.

(e) The Bob

A solid gold sphere (0.48 cm radius; 8.7 g) was used in the present experiments. Gold was chosen for use at high temperatures (e.g. molten salts); the results of the high temperature experiments are reported elsewhere.

The sphere was suspended from the free end of the transducer core by means of a fine (0.01 cm diameter) platinum wire.

(f) Motorized Drive Mechanism

A Hurst reversible motor (M) (20 oz-in.) with a built in gear box was used to rotate the threaded drive shaft (T); a flexible coupling (F) between the motor and the threaded shaft helped to overcome any strains that may, otherwise, lead to wobbling. The mechanism was such that by operating the motor one can move a bronze cylindrical mounting platform (P), which is moved vertically on the threaded shaft. The quartz spring was attached to a hook on the mounting platform. With the motor rotating at 6 r.p.m. and a 40 turns/in. threaded shaft, it was possible to precisely locate the core of the transducer in such a way as to produce a minimum null output of the l.v.d.t. The mechanical center of the core with respect to the l.v.d.t. must be adjusted whenever there is a change in the density of the liquid surrounding the bob.

Figure 4 is a photographic reproduction of the experimental assembly used in this work.

Results

The logarithmic decrement was determined from diagrams of the type shown in Fig. 5 and using the relation

$$[18] \qquad \delta = -\frac{2.303}{n}\log_{10}\frac{A_n}{A_0},$$

where A_0 and A_n denote the amplitudes of the 0th and nth oscillations, respectively, and n is the number of oscillations.

The logarithmic decrements obtained in this way were corrected for the air-damping of the oscillating system simply by subtracting from each of the above values the value of the logarithmic decrement of the system when the gold sphere was freely suspended in air. The corrected values of the logarithmic decrement, for five sample liquids, are given in column 4(*a*) of

Can. J. Chem. Downloaded from www.nrcresearchpress.com by 210.87.254.5 on 09/05/12
For personal use only.

Can. J. Chem. Downloaded from www.nrcresearchpress.com by 210.87.254.5 on 09/05/12
For personal use only.

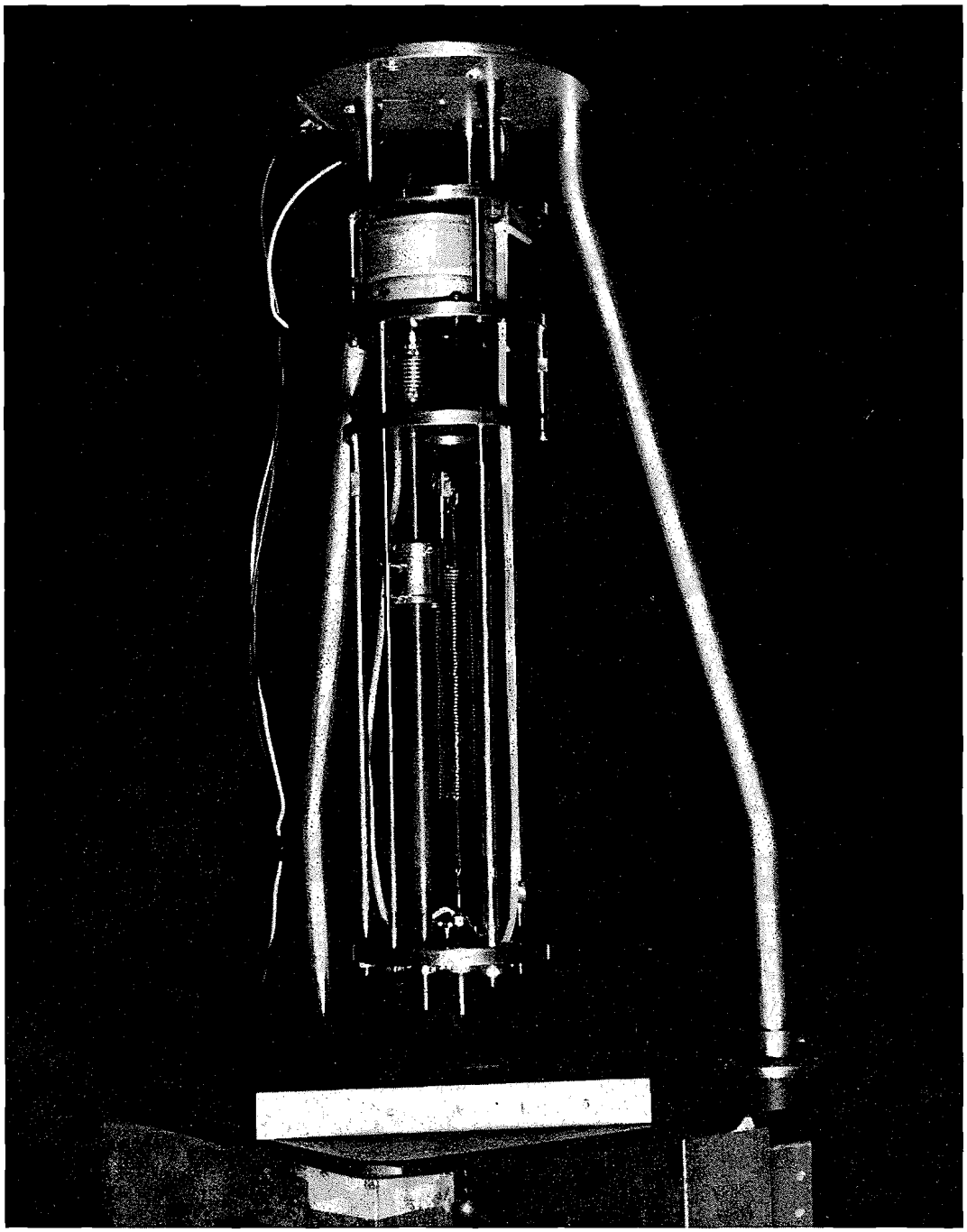

FIG. 4. Photographic view of the apparatus.

Can. J. Chem. Downloaded from www.nrcresearchpress.com by 210.87.254.5 on 09/05/12
For personal use only.

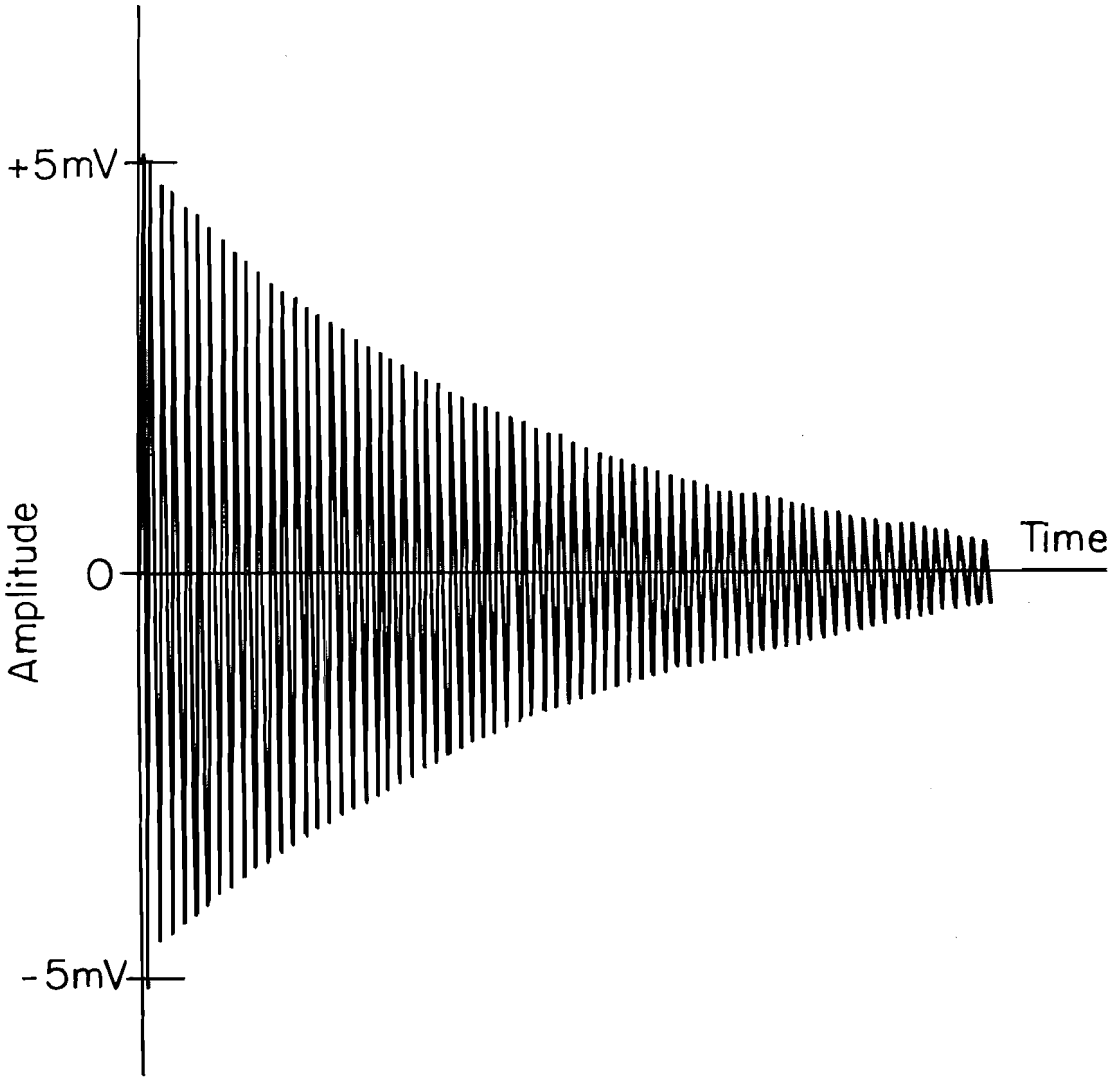

FIG. 5. Typical record of oscillations: CCl_4; chart speed 12 in./min; recorder range 10m V full scale (center zero).

Table I. The period of oscillation was found to vary very little from liquid to liquid; hence one value, $\tau = 0.333$ s, was used.

The theoretically derived eq. [16] was verified in two ways.

(i) Using the theoretical values of the apparatus constants given in eqs. [13] and [17], the measured period of oscillation and the literature values (13) of the density and the viscosity of the five liquids, values of the logarithmic decrement were calculated; these are shown in column 4(*b*) of Table I. The average error in the experimental δ values is $\pm 0.74\%$ (column 4(*c*), Table I).

(ii) Using the apparatus constants, period of oscillation, the known density values, and the experimental δ values, the viscosity of the five liquids were calculated from eq. [16]; these are given in column 5(*b*) of Table I. The average error in the theoretically calculated (absolute) viscosity is $\pm 1.5\%$.

It is seen that a small error (0.74%) in the value of the logarithmic decrement leads to a larger error (1.7%) in the calculated value of the absolute viscosity. If greater accuracy is needed one can calibrate the apparatus with known liquids and then use the calibrated apparatus constants in eq. [16]; in this way the error in the

TABLE I

Verification of eq. [16] using known liquids at room temperature

(1) Liquid	(2) t (°C)	(3) ρ (g cm^{-3})	(4) $\delta^* \times 10^2$ (a) Expt.	(b) Calcd. from eq. [16]	(c) Error (%)	(5) Viscosity (cP) (a) Lit.	Ref.	(b) Determined	(c) Error (%)
1. CCl_4	19	1.5960	2.836	2.814	+0.8	0.985	13	1.001	+1.7
2. $CHCl_3$	23	1.4835	2.013	1.993	+1.0	0.546	13	0.558	+2.2
3. CH_3COCH_3	23	0.7867	1.070	1.076	−0.5	0.313	13	0.310	−1.1
4. C_6H_6	23	0.8756	1.625	1.620	+0.3	0.619	13	0.622	+0.5
5. CS_2	23	1.2587	1.455	1.471	−1.1	0.359	13	0.351	−2.1

*These are corrected values of δ in liquid; $\delta_{air} = 0.00167$.

viscosity values (now no longer absolute) can be reduced to less than 1%.

Appendix

To obtain eq. [12] from eq. [11], we proceed as follows. Substituting for K and n^2 in eq. [11], from eqs. [7] and [8], we have

$$[11a] \quad \delta^2 = \frac{81\pi^4(m')^2\mu^2(1+\mu)^2}{4\lambda\tau^2\left[M - \frac{1}{2}m' + \frac{9}{4}m'\mu\right]}.$$

Now, $\mu \sim 0.04$ in ordinary liquids. If we make an approximation $(1+\mu)^2 \simeq 1 + 2\mu$, the omission of μ^2 in the expansion of $(1+\mu)^2$ results only in a small error of about 0.2%. Using this approximation, eq. [11a] can be written as

$$[11b] \quad \delta^2[4M\lambda\tau^2 - 2m'\lambda\tau^2 + 9m'\mu\lambda\tau^2] = 81\pi^4(m')^2\mu^2 + 162\pi^4(m')^2\mu^3.$$

Dividing both sides by $4M\lambda\tau^2$ and rearranging,

$$[11c] \quad \frac{81\pi^4(m')^2\mu^3}{2\lambda\tau^2M} + \frac{81\pi^4(m')^2\mu^2}{4\lambda\tau^2M} + \frac{m'\delta^2}{2M} - \frac{9m'\mu\delta^2}{4M} - \delta^2 = 0.$$

Substituting for $m' = (4/3)\pi\rho a^3$ and $\mu = (\eta\tau/\pi\rho a^2)^{1/2}$ in eq. [11c] and grouping the constants (cf. eq. [13]), we get eq. [12].

Acknowledgments

The author is grateful to Professor J. O'M. Bockris, Electrochemistry Laboratory, The University of Pennsylvania, Philadelphia, Pa., 19104, U.S.A., for the award of a Postdoctoral Fellowship. The help rendered by Mr. O. R. Shannon in constructing the precision mounting assembly for the viscometer is gratefully acknowledged.

1. M. K. Nagarajan, L. Nanis, and J. O'M. Bockris. J. Phys. Chem. **68**, 2726 (1964). M. K. Nagarajan and J. O'M. Bockris. J. Phys. Chem. **70**, 1854 (1966).
2. J. D. Mackenzie. *In* Physico-chemical measurements at high temperatures. *Edited by* J. O'M. Bockris, J. D. Mackenzie, and J. L. White. Butterworths Publications, London. 1959. Chap. 15.
3. R. S. Dantuma. Z. Anorg. Chem. **175**, 1 (1928).
4. C. E. Fawsitt. Proc. Roy. Soc. London, Ser. A, **80**, 290 (1908).
5. T. P. Yao and C. G. Kondic. J. Inst. Metals, **81**, 17 (1952).
6. J. Towers and R. C. Kay. Trans. Brit. Ceram. Soc. **49**, 341 (1950).
7. Yu. S. Malinin and Z. B. Entin. Russ. J. Phys. Chem. **36**, 207 (1962).
8. R. D. Reeves. Ph.D. Dissertation, Rensselaer Polytechnic Institute, Troy, N.Y. 1964.
9. F. C. Champion and N. Davy. Properties of matter. Blackie and Son, London. 1936, p. 65.
10. R. G. Stokes. Trans. Cambridge Phil. Soc. **9**, 1 (1851).
11. H. Lamb. Hydrodynamics. Cambridge University Press, London. 1932. pp. 124, 644.
12. J. C. Jaeger. Applied mathematics. Clarendon Press, Oxford. 1949. p. 68.
13. International Critical Tables. McGraw-Hill Book Co., Inc., New York. 1928.
14. R. C. Weast (*Editor-in-chief*). Handbook of chemistry and physics. 49th ed. Chemical Rubber Publishing Co., Cleveland, Ohio. 1958–1959. p. 295.

Can. J. Chem. Downloaded from www.nrcresearchpress.com by 210.87.254.5 on 09/05/12
For personal use only.

Can. J. Chem. Downloaded from www.nrcresearchpress.com by 210.87.254.40 on 09/05/12
For personal use only.

Electrical conductivities of quaternary ammonium salts in acetone. Part I. Pressure and temperature effects

W. A. Adams and K. J. Laidler
Department of Chemistry, University of Ottawa, Ottawa, Canada

Received October 20, 1967

The equivalent conductivities of tetramethylammonium iodide, tetraethylammonium iodide, and tetra-*n*-propylammonium iodide in acetone solution were determined at concentrations from 1 to 10 $\times 10^{-4}$ mole/liter and at temperatures of 25 to 55 °C and pressures from atmospheric to 1.1 kbar. The concentration dependence of the equivalent conductivities was analyzed by the Shedlovsky method. Limiting equivalent conductivities and ion-pair dissociation constants are tabulated.

Canadian Journal of Chemistry, 46, 1977 (1968)

Experimental and theoretical research on the thermodynamics of electrolyte solutions has been devoted mainly to aqueous solutions. However, water has many special properties which divert attention from those properties of electrolyte solutions which are common to many solvent systems. The conductivity behavior of salts in acetone solutions over a range of temperature and pressure should reflect a pattern to be found in many solvent systems.

Minc and Werblan (1) have studied several salts in acetonitrile ($\varepsilon = 36.8$ at 25 °C) between 15 and 30 °C and made an analysis of the mechanism of ion-pair formation (2) and conductivity (3) similar to that undertaken for acetone solutions in the present work. The limiting equivalent conductivities were analyzed using the activated-complex theory and the individual ionic activation parameters were estimated (2). It was suggested, on the basis of differences observed in these activation parameters, that the large ClO_4^-, Et_4N^+, and Cs^+ ions undergo translation in solution without the primary solvation layer, the small cations Li^+ and Na^+ with their primary layer. In the latter case, the mechanism of the movement of the ions is determined by the solvent molecules in the second solvation layer. The mechanism of ionic migration for K^+ and Rb^+ ions is intermediate between these two extremes.

Hills (4) has discussed the problem of dividing the activation parameters for conductivity into their ionic contributions. A simple relationship between the ionic and the total activation parameters for conductivity exists only if the transport numbers are independent of temperature and pressure. However, there are few transport number measurements in the literature for non-aqueous solvent systems and the effects of temperature and pressure on transport numbers are uncertain. Some indication of the individual ionic contributions can be estimated by studying a series of salts containing a common ion and noting the effect on the total activation parameters of a variation of either the cation or the anion.

Parker (5) has discussed a number of results in terms of two classes of anionic solvation. In hydrogen-bonding solvents, anions are solvated by ion–dipole interactions upon which is superimposed a strong hydrogen bonding which is strongest for small anions. However, in dipolar aprotic solvents, such as dimethylsulfoxide, N,N-dimethylformamide (DMF), and acetone, anions are solvated by ion-dipole interactions upon which is superimposed only an interaction due to the mutual polarizability of the anion and the solvent molecules; this is greatest for the large anions. The lack of anion solvation in these solvents is indicated by the limiting equivalent conductivity data gathered by Parker (5); these show that anions of the same crystallographic size as cations are much more conducting in acetone or DMF than are these same anions, relative to cations, in methanol or water.

The normal boiling and freezing points of acetone are 56.2 and −95.4 °C respectively. The temperature for acetone which corresponds to 25 °C for water is about −58 °C. The effect of ions in causing a disruption of the structure in acetone at 25 °C will be a minimum, since little structure is present at this temperature and at atmospheric pressure because of the thermal motion of the molecules. However, the ability of external pressure to bring about a change in volume of the solvent is a maximum under these

Can. J. Chem. Downloaded from www.nrcresearchpress.com by 210.87.254.40 on 09/05/12
For personal use only.

circumstances since the solvent is most compressible near its boiling point. Therefore, although ions have a net structure-making effect in acetone at atmospheric pressure, at high pressures the ions must compete with enhanced dipole–dipole interactions between the solvent molecules, and the relative structure-making ability of the ions is reduced.

Mishchenko and Sokolov (6) have studied the thermodynamics of solutions of $NaClO_4$ in acetone. Added $NaClO_4$ results in a marked increase in the ordering of the solvent molecules in acetone solutions and a net disordering in aqueous solutions. Mishchenko and Sokolov (7) have also found that the exothermicity of the integral heat of solution decreases in the order $Mg(ClO_4)_2 > NaI > NaClO_4 > NaCNS > KCNS > NH_4CNS$, suggesting that the heat of solvation is primarily a property of the cations. The integral heat of solution becomes more negative with decreasing concentration because of the solvation of ions released from the more neutral ion-paired state. The heat of dissociation of ion pairs in NaI–acetone solution was estimated to be about -3.0 kcal mole^{-1}.

There is strong evidence to support the view that Na^+ ions in acetone are solvated by four acetone molecules. Below 25.5 – 25.7 °C, NaI is known to separate from saturated solution as $NaI.3CH_3COCH_3$ (8). Mishchenko and Sokolov (7) have determined that the heat of formation of this solvate at 10 °C is -15.67 ± 0.01 kcal mole^{-1}. Also, from steric considerations, the solvation number of the Na^+ ion is four and the ClO_4^- ion is eight. Mishchenko and Sokolov (6) have observed a rapid change in the thermodynamic properties of $NaClO_4$ solutions at a molality of about 1.44 where complete solvation, based on these solvation numbers, would be expected to occur.

Anions are not greatly solvated in dipolar aprotic solvents such as acetone. Cations, on the other hand, interact quite strongly with such solvents. Small cations such as Na^+ favor four coordination in acetone solution. The effect of ions on the solvent structure of acetone at atmospheric pressure between 10 °C and the boiling point is to increase the amount of order.

In a previous paper the compressibility of liquid acetone was measured (9) and several thermodynamic properties of the liquid were evaluated in connection with the present work. In the work described in the present paper the conductivities of the iodide salts of tetramethylammonium ion (Me_4N^+), tetraethylammonium ion (Et_4N^+), and tetra-*n*-propylammonium ion (n-Pr_4N^+) were investigated, at concentrations from 1 to 10×10^{-4} mole/liter, from 25 to 55 °C and 1 to 1100 bar pressure. From measurements of the concentration dependence of the equivalent conductivity, the ion-pair dissociation constants and the limiting equivalent conductivities were calculated. The two papers which follow discuss these results in terms of theories of transport processes and of ion association.

Experimental

Materials

The acetone used was either Fisher Electronic Grade or G.C. Spectrophotometric Quality Baker Analyzed Reagent Grade. Removal of small traces of water was accomplished by drying with Linde 4 Å molecular sieves (10) in a dry nitrogen atmosphere. All operations with acetone, including the preparation of solutions and the filling of conductivity cells, were carried out under dry nitrogen. Confirmation that the removal of water was effective was made by conductance and n.m.r. measurements. According to Muller (11) the chemical shift of water in dilute solutions of water in acetone is -2.8 p.p.m. This peak was reduced in height relative to the ^{13}C satellite peak from 0.87 for untreated acetone to 0.23 for the treated. Since the naturally occurring abundance of ^{13}C is 1.11% (12), this indicates ~0.06% water by weight in the treated acetone. This value is comparable to that obtained by Meeker, Critchfield, and Bishop (10) for sieve-dried acetone.

The water used to prepare the KCl solutions required for determining the conductivity cell constants was purified as described in a previous paper (9).

The tetramethylammonium iodide and the tetra-*n*-propylammonium iodide were purified Eastman Reagent Grade chemicals; the tetraethylammonium iodide was obtained from the Columbia Organic Chemicals Co. All the salts were dried for 24 h or more *in vacuo* at 60 to 100 °C just before the solutions were prepared; they were shielded from direct light to prevent decomposition. The purity was confirmed by Volhard determinations of the percentages of iodine relative to the theoretical. Reagent-grade KCl was dried *in vacuo* at 110 °C for 24 h.

Apparatus

Conductance measurements were carried out with a RC-18 conductivity bridge manufactured by Industrial Instruments, Cedar Grove, New Jersey; the balance detector was a 2-in. oscilloscope and the limit of error was 0.1% of the decade resistance reading over the range 500 – 50 000 Ω.

Figure 1 shows a high-pressure conductivity cell, which is similar to the miniature cells designed by Hills (4). Eight of these cells could be fitted into a cell holder and placed in the high-pressure vessel. This arrangement is shown in Fig. 2. Pressure distortion of the cell and

Can. J. Chem. Downloaded from www.nrcresearchpress.com by 210.87.254.40 on 09/05/12
For personal use only.

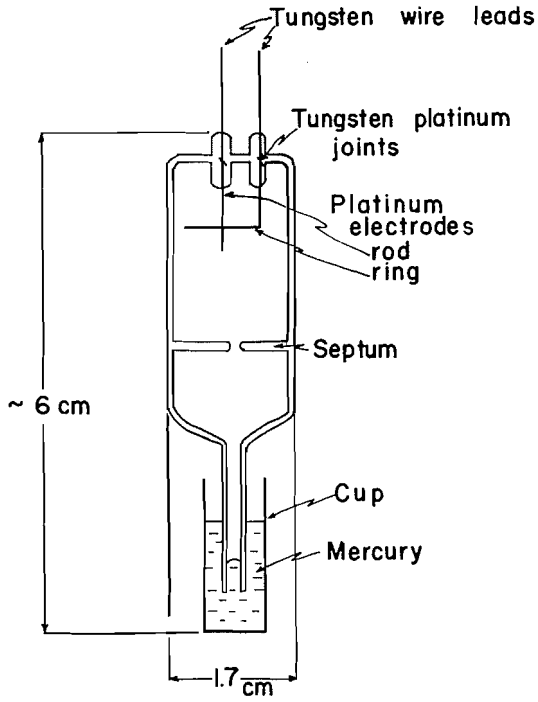

Fig. 1. High-pressure conductivity cell.

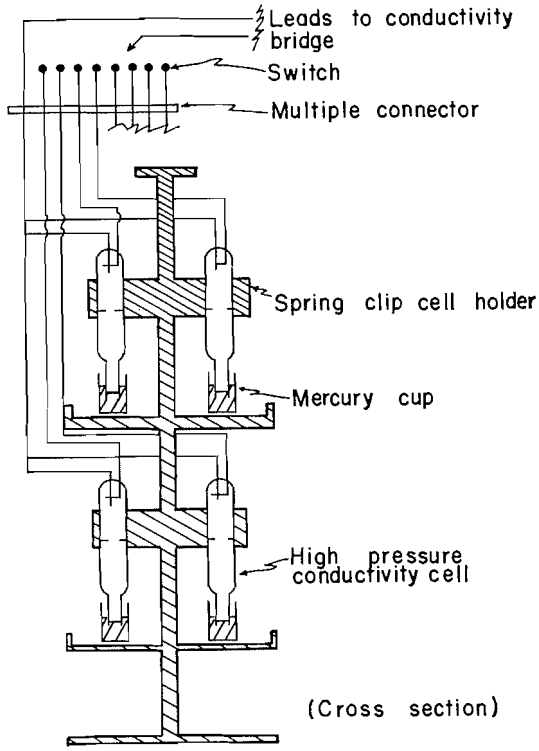

Fig. 2. High-pressure conductivity cell holder.

resultant changes in the cell constant were avoided by a ring and rod arrangement of unplatinized electrodes. Ovenden (13) has shown that this type of cell has a cell constant independent of pressure over a range of 2000 atm. Metal-to-glass seals were made with electrowelded tungsten-to-platinum rods, which were completely sealed in glass so that the solutions would not come in contact with tungsten. Measurements at atmospheric pressure were made using cells of the Shedlovsky type (14), which were filled almost completely with solution to avoid having to make a concentration correction for the acetone vapor in the dead space of the cell. The solvent conductivity cell, used for making a small solvent correction, was constructed from a 1-l flask with large unplatinized electrodes placed close together.

All conductance measurements were made in a 35-gallon oil bath, controlled by a thermoregulator with a sensitivity of ± 0.01 °C. Thermometers used were specially calibrated by the National Research Council of Canada. To ensure temperature equilibrium after compression or decompression, the internal temperature was measured using a bead-type thermistor of about 25 000 Ω resistance; it was placed against the inside of the top of the high-pressure vessel and cemented into position with epoxy resin glue.

The high-pressure system was similar to that used in previous investigations in this laboratory (15) and is shown diagramatically in Fig. 3. The high-pressure vessel was of 2-l capacity, No. OM-2000 manufactured by Autoclave Engineers, Erie, Pennsylvania; it was constructed from 410 stainless steel and had an "O" ring closure. It was modified to accept electrical leads; a 0.030-in. kovar wire was sealed, using a ceramic material, into a thin conical nickel sleeve, which was then force-fitted into a coned 3/32-in. hole in the vessel top. Through another hole passed a 10-wire lead consisting of varnished copper wires; the sealing was done using "Duro" epoxy resin glue, manufactured by the Woodhill Chemical Corporation, Cleveland, Ohio. The total of 11 wires was used for the thermistor and the eight conductivity cells, the arrangement being shown in Fig. 2.

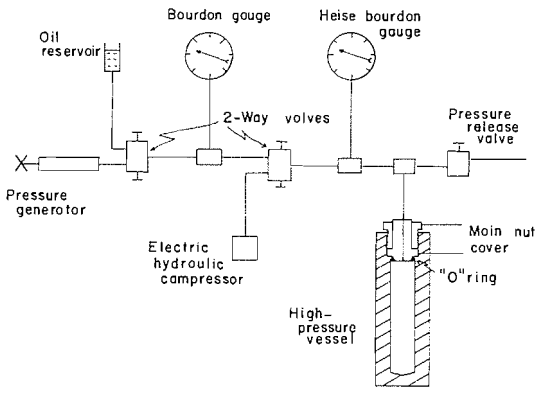

Fig. 3. Diagram of the high-pressure system.

Can. J. Chem. Downloaded from www.nrcresearchpress.com by 210.87.254.40 on 09/05/12
For personal use only.

TABLE I

Properties of acetone (V_{sp}, specific volume (ml g^{-1}); η, viscosity (mg cm^{-1} s^{-1}); ε, dielectric constant)

Pressure (bar)	Temperature (°C)											
	26.6			35.0			45.0			54.8		
	V_{sp}	ε	η	V_{sp}	ε	η	V_{sp}	ε	η	V_{sp}	ε	η
1.0	1.2778	20.54	2.968	1.2938	19.75	2.756	1.3137	18.78	2.530	1.3341	17.82	2.325
137.9	1.2577	20.96	3.272	1.2726	20.17	3.030	1.2899	19.26	2.773	1.3078	18.33	2.541
275.8	1.2405	21.33	3.590	1.2546	20.54	3.316	1.2699	19.65	3.028	1.2861	18.72	2.768
413.7	1.2254	21.65	3.894	1.2389	20.87	3.594	1.2528	20.00	3.277	1.2677	19.08	2.993
551.6	1.2120	21.94	4.191	1.2250	21.17	3.866	1.2378	20.30	3.525	1.2516	19.39	3.218
689.5	1.2000	22.21	4.459	1.2125	21.44	4.116	1.2244	20.58	3.755	1.2375	19.66	3.430
827.4	1.1890	22.47	4.727	1.2018	21.70	4.368	1.2124	20.84	3.990	1.2248	19.92	3.648
965.3	1.1790	22.70	4.976	1.1910	21.93	4.602	1.2014	21.09	4.208	1.2133	20.16	3.851
1103.2	1.1698	22.92	5.235	1.1815	22.15	4.840	1.1914	21.31	4.425	1.2028	20.38	4.050

Can. J. Chem. Downloaded from www.nrcresearchpress.com by 210.87.254.40 on 09/05/12
For personal use only.

Procedure

The dried salt was weighed on a balance enclosed in a dry-nitrogen-filled polyethylene glove bag and placed in a preweighed 500 ml volumetric flask; this operation was carried out in subdued light, since strong light causes slight decomposition. The flasks were filled in another nitrogen-filled glove bag with the dried acetone whose conductivity had just been measured in the solvent conductivity cell. The vacuum-corrected masses of the solutions were used to calculate the molarities at different temperatures and pressures, on the basis that the solution densities were the same as those of acetone given in Table I; these were calculated from the results of the previous paper (9).

Eight solutions prepared the previous day were taken from the refrigerator and placed in a glove bag for transfer to the cells. Small seasoned polyethylene bottles were then filled with the solutions and the appropriate cell was filled through the stem with that solution. Filled cells were then inverted stem down into small cups of triple-distilled mercury, and the complete units then clipped into the cell holder. Enough solution was prepared so that fresh solution could be used to fill the atmospheric cells at each of the four temperatures at which measurements were made. These cells were also filled in a dry-nitrogen atmosphere in a glove bag.

Untreated platinum electrodes were used for the conductivity measurements, since there is a danger that platinized electrodes will bring about catalysis of an undesirable reaction (16). However, when smooth platinum electrodes are used the resistance decreases with increasing frequency (17). The true ohmic resistance of electrolytes is independent of frequency at audio frequencies, the Debye–Falkenhagen effect occurring to a significant extent only at radio frequencies. The true resistance, R_t, should be obtained by extrapolating the resistance, R_f, at frequency, f, against an appropriate function of f. Jones and Christian (17) found that their results for bright platinum electrodes could be expressed by the equation

$$[1] \qquad R_t = R_f + kf^{-\frac{1}{2}}.$$

Bockris and Conway (18) have found this relationship to be obeyed in the electrodeposition of copper, but sometimes it is not obeyed (19, 20). Measurements were made in the present systems, over the frequency range 0.7 to 10 kcycles/s, and the inverse-square-root behavior expressed by eq. [1] was found to be obeyed very satisfactorily. Much less frequency dependence was found when the electrodes were platinized. In all of the results quoted below a frequency correction has been made using eq. [1].

The conductivity cells were calibrated using KCl solutions following the procedure of Lind, Zwolenik, and Fuoss (21).

Results and Calculations

Equivalent Conductivity

Equivalent conductivities, Λ, were calculated from the measured resistances, corrected for the frequency effect; the specific conductance of the solvent was subtracted. The concentration as a function of temperature and pressure was obtained by assuming the solution density to be identical with that of acetone given in Table I. The specific conductances for all the concentrations and conditions studied are given in Table II and the concentrations in Table III.

Dielectric Constant of Acetone

The dielectric constants for the four temperatures at atmospheric pressure were calculated from an equation of Maryott and Smith (22):

$$[2] \quad \log_{10} \epsilon(T) = \log_{10} 20.70 - 0.205 \times (T - 25.00).$$

Measurements of Grimm and Patrick (23) at higher temperatures suggest that this equation gives values that are slightly too high. A correction was therefore applied to the dielectric constant calculated by eq. [2] above 40 °C.

Kyropoulos (24) and Hartmann, Neumann, and Rinck (25) have studied the effect of pressure on the dielectric constant of liquid acetone. Owen and Brinkley (26) successfully fitted Kyropoulos's data at 20 °C to an equation of the form of the Tait equation. Hartmann *et al.*'s data refer to 20, 25, and 50 °C at 12 pressures between atmospheric and 1800 atm. We have used the temperature-dependent constant $B(T)$, obtained from the application of the Tait equation to the compressibility data given in a previous paper (9), to obtain values of the other 'constant' A in the equation

$$[3] \quad \frac{1}{\epsilon(P^0)} - \frac{1}{\epsilon(P)} = A \log_{10} \frac{B(T) + P}{B(T) + P^0}.$$

The A values were plotted first against pressure to obtain the values of A at the pressures of interest, and these were then plotted against temperature. The Tait constants $B(T)$ obtained from the compressibility data were then combined with the dielectric constant values calculated at atmospheric pressure, and the A values, to obtain dielectric constant values for acetone at various temperatures and pressures. The results are given in Table I. The results agree with directly determined values, where available, to within 0.05%.

Viscosity of Acetone

Howard and McAllister (27) measured the viscosity of acetone at atmospheric pressure from room temperature to the boiling point; their interpolated values are included in Table I. Bridgman (28) made measurements at 30 °C and

Can. J. Chem. Downloaded from www.nrcresearchpress.com by 210.87.254.40 on 09/05/12
For personal use only.

TABLE II

Specific conductance, corrected for solvent conductance, calculated from resistance extrapolated to infinite frequency (Λ^{-1} cm^{-1} $\times$ 10^6)

(*a*) High-pressure cells

Solution number	Pressure (bar)	Temperature (°C) 26.61	35.00	45.01	54.83
		$(CH_3)_4NI$			
1	1.0	79.69	83.04	88.68	93.21
	137.9	76.35	80.13	85.22	89.75
	275.8	73.13	76.99	81.91	86.56
	413.7	70.15	74.28	78.87	83.42
	551.6	67.35	71.09	75.82	80.46
	689.5	64.59	68.43	73.26	77.77
	827.4	62.08	65.90	70.66	73.85
	965.3	59.83	63.55	68.18	72.48
	1103.2	57.60	61.37	65.84	69.56
2	1.0	74.16	77.35	82.50	86.79
	137.9	71.00	74.47	79.22	83.50
	275.8	68.01	71.49	76.13	80.47
	413.7	65.25	68.61	73.25	77.52
	551.6	62.68	65.98	70.47	74.74
	689.5	60.16	63.47	68.00	72.07
	827.4	57.84	61.11	65.60	68.59
	965.3	55.73	58.92	63.27	67.23
	1103.2	53.63	56.90	61.12	64.18
4	1.0	52.33	54.46	58.25	61.50
	137.9	49.95	52.29	55.76	58.95
	275.8	47.72	50.10	53.47	56.66
	413.7	45.63	48.00	51.34	54.45
	551.6	43.76	46.08	49.30	52.56
	689.5	41.86	44.28	47.51	50.64
	827.4	40.12	42.59	45.78	47.54
	965.3	38.62	41.03	44.10	47.10
	1103.2	37.15	39.82	42.57	44.68
5	1.0	40.72	42.32	45.37	47.88
	137.9	38.78	40.56	43.34	45.79
	275.8	36.98	38.80	41.48	43.94
	413.7	35.35	37.15	39.79	42.16
	551.6	33.78	35.64	38.19	40.64
	689.5	32.29	34.23	36.78	39.09
	827.4	30.94	32.92	35.42	36.49
	965.3	29.78	31.69	34.13	36.41
	1103.2	28.63	30.57	32.93	34.36
6	1.0	37.91	39.15	41.91	44.16
	137.9	36.07	37.47	40.00	42.18
	275.8	34.40	35.81	38.26	40.45
	413.7	32.86	34.27	36.69	38.82
	551.6	31.43	32.87	35.21	37.43
	689.5	30.02	31.56	33.89	36.16
	827.4	28.74	30.34	32.64	(33.41)
	965.3	27.62	29.20	31.44	33.50
	1103.2	26.53	28.16	30.33	31.51
7	1.0	33.46	34.76	37.21	39.27
	137.9	31.79	33.23	35.50	37.49
	275.8	30.29	31.75	33.95	35.92
	413.7	28.88	30.38	32.54	34.46
	551.6	27.54	29.12	31.22	33.22
	689.5	26.33	27.95	30.04	32.00
	827.4	25.25	26.87	28.92	(29.64)
	965.3	24.29	25.86	27.85	29.73
	1103.2	23.37	24.94	26.87	27.93

TABLE II (*Continued*)

Solution number	Pressure (bar)	Temperature (°C) 26.61	35.00	45.01	54.83
		$(C_2H_5)_4NI$			
1	1.0	162.93	171.69	182.44	190.00
	137.9	156.32	164.28	174.06	182.51
	275.8	149.25	157.29	166.80	175.18
	413.7	142.77	150.47	160.05	168.36
	551.6	137.01	144.31	153.77	161.83
	689.5	131.25	138.84	147.97	155.95
	827.4	126.10	133.78	142.56	149.91
	965.3	121.26	128.78	137.36	144.85
	1103.2	116.69	123.98	132.56	139.98
2	1.0	184.04	193.86	206.29	215.67
	137.9	176.65	185.69	197.30	207.61
	275.8	168.77	177.94	189.38	199.62
	413.7	161.53	170.43	181.93	192.20
	551.6	155.01	163.60	174.89	184.99
	689.5	148.67	157.48	168.45	178.49
	827.4	142.89	151.87	162.31	171.82
	965.3	137.42	146.23	156.54	160.17
	1103.2	132.32	140.92	151.12	160.74
4	1.0	147.14	155.01	165.14	173.11
	137.9	141.00	148.20	157.66	166.16
	275.8	134.28	141.84	151.09	159.23
	413.7	128.63	135.71	144.97	153.35
	551.6	123.32	130.15	139.23	147.46
	689.5	118.16	125.18	134.00	142.14
	827.4	113.50	120.66	129.03	136.75
	965.3	109.08	116.12	124.37	132.16
	1103.2	104.96	111.82	120.00	127.78
6	1.0	62.12	65.16	69.76	73.43
	137.9	59.17	61.97	66.18	70.03
	275.8	56.26	59.06	63.10	66.87
	413.7	53.60	56.32	60.33	64.03
	551.6	51.26	53.87	57.79	61.38
	689.5	48.97	51.69	55.46	58.98
	827.4	46.89	49.69	53.30	56.62
	965.3	44.95	47.75	51.28	54.59
	1103.2	43.16	45.91	49.41	52.68
7	1.0	61.06	64.20	68.74	72.19
	137.9	58.16	61.06	65.25	68.73
	275.8	55.27	58.21	62.21	65.55
	413.7	52.67	55.52	59.49	62.71
	551.6	50.35	53.10	56.97	60.04
	689.5	48.11	50.95	54.67	57.66
	827.4	46.09	49.00	52.54	55.32
	965.3	44.20	47.07	50.56	53.32
	1103.2	42.46	45.27	48.72	51.44
8	1.0	21.15	22.23	23.99	25.34
	137.9	20.11	21.09	22.67	24.09
	275.8	19.06	20.06	21.57	22.95
	413.7	18.11	19.10	20.60	21.95
	551.6	17.29	18.24	19.71	21.01
	689.5	16.47	17.50	18.90	20.07
	827.4	15.77	16.82	18.16	19.36
	965.3	15.12	16.16	17.47	18.67
	1103.2	14.52	15.53	16.83	18.02

Can. J. Chem. Downloaded from www.nrcresearchpress.com by 210.87.254.40 on 09/05/12
For personal use only.

TABLE II (*Continued*)

Solution number	Pressure (bar)	Temperature (°C) 26.61	35.00	45.01	54.83
		n-$(C_3H_7)_4NI$			
1	1.0	162.74	171.72	182.18	189.42
	137.9	155.65	164.09	174.56	181.86
	275.8	148.70	157.02	165.16	175.64
	413.7	142.53	150.79	160.48	168.70
	551.6	136.49	144.64	154.07	162.22
	689.5	130.85	139.15	148.20	156.20
	827.4	126.01	134.04	142.67	150.61
	965.3	121.25	128.87	137.78	145.45
	1103.2	116.69	124.20	132.90	140.44
2	1.0	127.34	134.51	142.91	150.36
	137.9	121.62	128.30	136.81	144.24
	275.8	116.00	122.62	130.89	138.59
	413.7	111.08	117.60	125.61	133.00
	551.6	106.26	112.71	120.51	127.87
	689.5	101.80	108.34	115.90	122.23
	827.4	97.99	104.31	111.55	118.69
	965.3	94.22	100.21	107.73	114.55
	1103.2	90.66	96.55	103.89	110.66
4	1.0	93.41	98.79	105.20	110.99
	137.9	89.02	94.04	100.44	105.28
	275.8	84.80	89.72	95.90	101.72
	413.7	81.11	85.95	91.88	97.48
	551.6	77.52	82.29	88.04	93.60
	689.5	74.20	79.02	84.66	90.00
	827.4	71.34	76.00	81.41	86.68
	965.3	68.55	72.98	78.52	83.58
	1103.2	65.92	70.27	75.68	80.68
6	1.0	63.00	65.96	70.35	74.35
	137.9	59.89	62.64	66.95	70.84
	275.8	57.01	60.55	63.81	67.69
	413.7	54.46	57.90	61.03	64.77
	551.6	52.03	55.39	59.55	62.09
	689.5	49.80	53.17	57.15	59.63
	827.4	47.86	51.10	54.95	57.36
	965.3	45.97	49.08	52.98	55.26
	1103.2	44.20	47.25	51.06	53.30
7	1.0	29.92	31.78	34.04	36.17
	137.9	28.37	30.09	32.30	34.34
	275.8	26.94	28.62	30.71	32.73
	413.7	25.69	27.31	29.33	31.26
	551.6	24.50	26.09	28.07	29.93
	689.5	23.41	25.00	26.90	28.72
	827.4	22.48	24.00	25.83	27.60
	965.3	21.56	23.02	24.88	26.58
	1103.2	20.71	22.14	23.96	25.63
8	1.0	14.68	15.64	16.87	18.05
	137.9	13.90	14.80	15.99	17.12
	275.8	13.19	14.10	15.20	16.30
	413.7	12.57	13.45	14.51	15.57
	551.6	11.99	12.85	13.93	14.90
	689.5	11.46	12.31	13.35	14.31
	827.4	11.00	11.82	12.83	13.76
	965.3	10.56	11.35	12.36	13.26
	1103.2	10.14	10.92	11.91	12.79

TABLE II (*Concluded*)

(*b*) Atmospheric pressure cells

Solution number	Salt	Temperature (°C) 26.61	35.00	45.01	54.83
1	Me_4NI	80.10	84.62	89.53	94.33
	Et_4NI	164.68	173.68	183.25	192.65
	n-Pr_4NI	164.39	173.36	183.48	192.80
2	Me_4NI	74.71	78.88	83.40	87.84
	Et_4NI	187.32	197.41	208.75	219.16
	n-Pr_4NI	129.28	136.40	144.51	152.09
3	Me_4NI	57.64	60.79	64.65	68.78
	Et_4NI	116.67	123.22	131.06	138.23
	n-Pr_4NI	122.59	129.67	137.78	145.15
4	Me_4NI	52.89	55.85	59.30	62.28
	Et_4NI	150.11	158.36	167.00	176.08
	n-Pr_4NI	95.10	100.59	106.73	111.84
5	Me_4NI	41.14	43.68	46.50	49.02
	Et_4NI	102.69	108.44	114.80	121.00
	n-Pr_4NI	80.00	84.64	89.88	94.93
6	Me_4NI	37.59	39.77	42.30	44.97
	Et_4NI	62.34	65.98	70.64	74.58
	n-Pr_4NI	62.71	66.41	70.88	75.11
7	Me_4NI	33.97	36.02	38.25	40.32
	Et_4NI	61.27	64.66	68.89	72.52
	n-Pr_4NI	30.07	31.85	34.04	35.93
8	Me_4NI	21.07	22.34	23.79	25.13
	Et_4NI	20.98	22.24	23.71	25.13
	n-Pr_4NI	14.60	15.54	16.66	17.68

TABLE III

Concentrations of acetone solutions at atmospheric pressure and 26.61 °C (mole l^{-1}) $\times 10^4$

High-pressure cell	Salt* Me_4NI	Et_4NI	n-Pr_4NI
1	4.4682	9.7287	10.669
2	4.2011	11.250	8.1184
3	3.0912	6.5892	7.6156
4	2.8066	8.7703	5.7834
5	2.1695	5.7462	4.7770
6	1.9456	3.3412	3.6471
7	1.7243	3.2916	1.6966
8	1.0707	1.0684	0.8000

*The solvent conductivities for the acetone used to make up these solutions were: Me_4NI, $2.08 \times 10^{-8}\ \Omega^{-1}\ cm^{-1}$; Et_4NI, $2.85 \times 10^{-8}\ \Omega^{-1}\ cm^{-1}$; and n-Pr_4NI, $9.64 \times 10^{-8}\ \Omega^{-1}\ cm^{-1}$.

at pressures up to 12 000 atm. It has sometimes been assumed that η varies with T according to (29)

$$\eta = C\, e^{E/RT}, \qquad [4]$$

where C is independent of T and P and E is

TABLE IV

Onsager slope, S, limiting experimental slope, S_{exp}, and limiting equivalent conductivity, Λ_0, at atmospheric pressure*

	Temperature (°C)											
	26.61			35.00			45.01			54.83		
	S	S_{exp}	Λ_0	S	S_{exp}	Λ_0	S	S_{exp}	Λ_0	S	S_{exp}	Λ_0
Me_4NI	714	1888	218.8	778	2137	236.0	862	2455	256.6	947	3065	276.8
Et_4NI	703	1299	209.9	765	1442	225.6	848	1684	246.0	939	1888	265.0
n-Pr_4NI	677	1188	193.3	737	1342	208.5	817	1570	227.7	905	1780	245.7

*Units in Tables IV and V: S and S_{exp}, $(cm^2\Omega^{-1}\ mole^{-1}) \times (mole\ l^{-1})^{-\frac{1}{2}}$; Λ_0, $cm^2\ \Omega^{-1}\ mole^{-1}$.

independent of T, and that η varies with pressure according to

$$[5] \qquad \eta(P) = \eta^0 e^{\varrho P},$$

where

$$[6] \qquad g = \frac{1}{RT}\left(\frac{\partial E}{\partial P}\right)_T.$$

However, when this procedure was applied to Bridgman's data the activation energy E was found not to be a linear function of pressure, so that C must be considered to be a function of pressure. The procedure employed was to assume E to be independent of T, as found in Howard and McAllister's work. The pressure dependence of E was calculated from Bridgman's results using eq. [4] at each pressure. Pressure-dependent values of $\log_{10} C$ were then calculated from the viscosity data at 30 °C. Graphical interpolation then gave a set of E and $\log_{10} C$ at the pressures of interest, and eq. [4] was then used to calculate viscosities. The results are given in Table I.

Concentration Dependence of Equivalent Conductivity

The Onsager equation, which relates the equivalent conductivity, Λ, to the concentration, c, is

$$[7] \qquad \Lambda = \Lambda_0 - S_{exp}\, c^{1/2},$$

where Λ_0 is the limiting equivalent conductivity at $c = 0$ and S_{exp} is the limiting experimental slope at zero concentration of Λ plotted against $c^{1/2}$. This expression, derived theoretically by Onsager (30), is equivalent to an empirical equation of Kohlrausch (31). For unassociated, symmetrical, 1–1 electrolytes the limiting experimental slope, S_{exp}, is closely approximated by an expression given by Onsager (30):

$$[8] \qquad S = 8204 \times 10^2\, \Lambda_0/(\epsilon T)^{1.5} + 82.5/\eta(\epsilon T)^{0.5},$$

where ε is the dielectric constant of the solvent and η the viscosity in g cm^{-1} s^{-1}.

If the S_{exp} values obtained from a plot of Λ against $c^{1/2}$ are close to those calculated from eq. [8], it would be concluded that the salts were unassociated. This is not the case in the present work. Table IV gives the calculated Onsager slope and the S_{exp} and Λ_0 values for the three salts at atmospheric pressure obtained by least-mean-square (l.m.s.) fitting of the data to eq. [7] on an I.B.M. 360 computer. The calculations were also performed on the Λ data at high pressures, and some of the results are given in Table V. This table also includes the calculated Onsager slopes. It is to be seen that the calculated S values do not agree with the limiting experimental slope, S_{exp}, so that eqs. [7] and [8] do not apply; the conclusion is that there is some ion association.

We have also made use of the Shedlovsky extrapolation method (32, 33) which is an iterative procedure by which successively better estimates of Λ_0 are used to estimate the ion-pair dissociation constant, K_d. Previous applications of the method have been made by Sears, Wilhoit, and Dawson (34) for KCNS and n-Bu_4NI in acetone at various temperatures, and by Savedoff (35) for lithium and n-Bu_4N^+ salts in acetone solution at 25 °C.

The activity coefficients $y_\pm$ are evaluated using the Debye–Hückel formula

$$[9] \qquad \log_{10} f_\pm = -A|z_1 z_2| I^{\frac{1}{2}},$$

where $f_\pm$ is the mean rational activity coefficient, related to $y_\pm$ by

$$[10] \qquad \log f_\pm = \log y_\pm + \log\left[\frac{d}{d_0} + \frac{c(nM_1 - M_2)}{1000 d_0}\right].$$

Here d and d_0 are the densities of solution and

Can. J. Chem. Downloaded from www.nrcresearchpress.com by 210.87.254.40 on 09/05/12
For personal use only.

TABLE V

Onsager slope, S, limiting experimental slope, S_{exp}, and limiting equivalent conductivity, Λ_0, at 45.01 °C

Pressure (bar)	Me_4NI			Et_4NI			n-Pr_4NI		
	S	S_{exp}	Λ_0	S	S_{exp}	Λ_0	S	S_{exp}	Λ_0
1.0	854	2446	253.2	853	1878	250.0	820	1753	230.5
137.9	767	2095	234.9	765	1636	231.0	736	1534	213.8
275.8	696	1839	219.6	693	1454	215.6	669	1424	200.3
413.7	638	1637	206.5	633	1290	201.5	611	1244	187.5
551.6	589	1491	195.0	584	1204	190.4	566	1177	178.2
689.5	548	1339	184.6	543	1087	180.0	526	1087	168.7
827.4	513	1237	175.6	507	1011	171.0	492	1015	160.3
965.3	482	1145	167.1	477	945	162.8	462	951	152.9
1103.2	454	1071	159.6	449	888	155.4	436	898	146.0

solvent, M_1 and M_2 the molecular weights of solvent and solute, c is the concentration of solute, and n is the number of moles of ions produced per mole of solute. For the concentrations studied ($c < 0.001\ M$), $f_\pm \doteq y_\pm$.

The iterations were carried out on an I.B.M. 360 computer using a polynomial-fitting subroutine suggested by Hildebrand (36). The quantities S, Z, $S(Z)$, and $y_\pm^2$ (cf. refs. 32 and 33) were evaluated, starting with the Kohlrausch–Onsager Λ_0 and the Λ values at different concentrations. Then $\Lambda\ S(Z)$ was fitted as a linear function of $cy_\pm^2\Lambda^2S^2(Z)$ and the intercept recorded as the first estimate of Λ_0; K_d calculated from the slope, $-(K_d\Lambda_0)^{-1}$, was also recorded as the first estimate of the dissociation constant. If this new Λ_0 did not agree with the original Λ_0 to better than $\pm 0.05\%$, the new Λ_0 was used to recalculate S, Z, $S(Z)$, and $y_\pm^2$. Three iterations were usually required to give the specified agreement.

Table IV gives the calculated Onsager slopes using the limiting equivalent conductivity which was employed in the final Shedlovsky interation. Table V gives the corresponding results at higher pressures for 45.01 °C.

Table VI contains the limiting equivalent conductivities and dissociation constants calculated by the Shedlovsky method at atmospheric pressure, the errors estimated by the curve-fitting program being shown (cf. later). Table VII contains the limiting equivalent conductivities and dissociation constants calculated by the Shedlovsky method at high pressures.

Errors

The equations upon which the error estimates of Parts I–III are based have been incorporated

TABLE VI

(*a*) Limiting equivalent conductivity at atmospheric pressure ($cm^2\ \Omega^{-1}\ mole^{-1}$)

	Temperature (°C)			
	26.61	35.00	45.01	54.83
Me_4NI	211.9±2.5	228.2±2.6	247.7±2.9	262.9±9.4
Et_4NI	205.5±0.4	220.6±0.6	240.1±1.1	258.4±1.3
n-Pr_4NI	189.9±0.5	204.5±0.7	222.8±1.0	240.1±1.6

(*b*) Dissociation constant at atmospheric pressure ($(mole\ l^{-1}) \times 10^4$)

	Temperature (°C)			
	26.61	35.00	45.01	54.83
Me_4NI	34±6	31±5	28±4	24±11
Et_4NI	79±2	73±3	62±4	58±4
n-Pr_4NI	80±4	72±4	61±4	55±5

Can. J. Chem. Downloaded from www.nrcresearchpress.com by 210.87.254.40 on 09/05/12
For personal use only.

TABLE VII

(*a*) Limiting equivalent conductivity ($cm^2\ \Omega^{-1}\ mole^{-1}$)

Pressure (bar)	Temperature (°C)			
	26.61	35.00	45.01	54.83
		Me_4NI		
1.0	213.3±3.9	222.9±3.4	243.3±3.7	261.8±3.9
137.9	198.0±3.5	207.9±3.2	226.2±3.4	242.9±3.5
275.8	185.1±3.3	194.8±2.9	211.9±3.1	227.5±3.2
413.7	173.6±3.0	182.8±3.0	199.5±2.9	214.1±3.0
551.6	163.1±2.8	173.5±2.5	188.6±2.7	203.7±3.0
689.5	153.7±2.5	164.3±2.4	178.9±2.6	193.5±3.2
827.4	145.4±2.3	156.3±2.2	170.2±2.4	173.7±2.1
965.3	138.4±2.1	148.8±2.1	162.2±2.3	175.5±2.5
1103.2	131.9±2.0	142.3±2.2	155.0±2.1	160.9±2.3
		Et_4NI		
1.0	207.3±1.1	220.4±1.2	243.0±1.7	259.5±1.7
137.9	193.4±1.1	205.1±1.2	224.8±1.4	240.9±1.7
275.8	180.6±1.1	191.9±1.1	210.0±1.3	225.0±1.8
413.7	169.2±0.9	180.2±1.0	196.5±1.2	211.5±1.7
551.6	159.6±0.9	170.7±0.9	185.4±1.7	199.5±1.7
689.5	150.5±0.8	161.3±0.9	175.6±1.2	188.5±1.4
827.4	142.5±0.7	153.9±0.8	166.9±1.1	178.6±2.2
963.3	135.3±0.7	146.3±0.8	158.9±1.1	171.1±1.7
1103.2	128.8±0.7	139.4±0.8	151.7±1.1	163.4±1.7
		n-Pr_4NI		
1.0	190.6±1.8	205.1±1.6	224.3±2.0	244.4±2.1
137.9	177.4±1.7	190.4±1.5	208.3±1.8	226.3±2.5
275.8	165.8±1.6	179.0±1.9	195.2±1.5	211.4±2.0
413.7	155.9±1.5	168.4±1.8	182.9±1.6	198.6±1.9
551.6	146.9±1.5	158.8±1.7	173.8±2.1	187.5±1.8
689.5	138.9±1.4	150.5±1.7	164.7±2.0	177.8±1.8
827.4	132.0±1.3	143.1±1.6	156.5±1.9	168.9±1.7
965.3	125.5±1.3	136.0±1.6	149.3±1.8	161.0±1.7
1103.2	119.6±1.2	129.7±1.5	142.5±1.8	153.8±1.6

into computer programs. The goodness of fit of polynomials to any of the sets of data fitted in the computer programs was estimated by the subroutine from the formula

$$[11] \qquad E_{\text{r.m.s.}} = \left[\frac{\sum_{i=1}^{N} (W_i R_i)^2}{N - K} \right]^{\frac{1}{2}},$$

where R_i is the residual at the ith point, W_i is the weight associated with the ith point, N is the number of points, and K is the number of coefficients (for example K is four for a third-degree polynomial).

The standard error in each coefficient was estimated by the equation

$$[12] \qquad (\Delta a_i)_{\text{r.m.s.}} = A_{ii}^{\frac{1}{2}} E_{\text{r.m.s.}},$$

where $1 < i \leqslant K$ and A_{ii} is the ith diagonal element of the inverse of the matrix of the normal equations.

Where applicable, weighting factors, based on the error estimates of the limiting equivalent conductivity and the dissociation constants generated by the Shedlovsky program, were used. In the curve fitting by the subroutine, a convention according to eq. [12] was adopted:

$$[13] \qquad W_i = \left(\frac{1}{\Delta Y_i} \right)^2,$$

where W_i is the weighting factor for the ith point, Y_i is the ith dependent variable in the set fitted, and ΔY_i is the error estimate in the ith Y above. This convention is similar to that suggested by Young (37).

As an example of how the error estimate was obtained, the error equation for the volume of activation for conductivity (cf. Table IV of Part II) will be derived. This volume parameter was obtained from two separate l.m.s. fittings. The first kind were in the Shedlovsky program, to obtain sets of Λ_0 for each temperature at nine

Can. J. Chem. Downloaded from www.nrcresearchpress.com by 210.87.254.40 on 09/05/12
For personal use only.

TABLE VII (*Concluded*)

(*b*) Dissociation constant ((mole l^{-1}) $\times 10^4$)

Pressure (bar)	Temperature (°C) 26.61	35.00	45.01	54.83
		Me_4NI		
1.0	28±7	32±7	29±6	27±5
137.9	34±9	38±10	34±8	32±7
275.8	38±11	44±12	39±9	37±9
413.7	43±13	53±18	43±11	42±10
551.6	51±17	52±16	46±12	42±11
689.5	58±21	57±18	51±15	45±14
827.4	65±25	60±20	54±16	125±66
965.3	70±27	64±22	57±17	51±14
1103.2	73±29	68±25	59±18	104±55
		Et_4NI		
1.0	60±4	62±4	50±4	47±3
137.9	67±5	69±5	57±4	54±5
275.8	73±6	76±6	63±5	60±6	
413.7	80±7	81±7	71±6	65±7
551.6	86±7	83±7	74±10	70±8
689.5	94±8	88±8	81±8	78±9
827.4	100±9	93±8	84±9	82±15
965.3	106±11	96±9	88±10	82±12
1103.2	111±12	100±10	90±10	85±14
		n-Pr_4NI		
1.0	64±9	58±6	50±6	39±4
137.9	72±11	66±8	57±7	45±6
275.8	78±13	68±11	56±6	52±6
413.7	84±14	74±13	66±9	55±7
551.6	89±16	78±14	65±12	58±8
689.5	93±18	82±16	68±13	59±8
827.4	98±20	87±17	71±13	64±9
965.3	102±21	89±19	73±14	66±10
1103.2	106±23	92±20	75±15	67±10

pressures. Each of these fits resulted in a standard error, defined by eq. [12], for each coefficient of the polynomial fitted. The error in the equivalent conductivity at infinite dilution, $\Delta\Lambda_0$, was obtained directly from the standard error in the intercept. This standard error was then used to weight the dependent variable, ln Λ_0, in the second-order polynomial in pressure which was then fitted:

$$[14] \qquad W_i = \left(\frac{\Lambda_0}{\Delta\Lambda_0}\right)^2.$$

The result of this curve fitting was the polynomial

$$[15] \qquad \ln \Lambda_0 = a_0 + a_1P + a_2P^2,$$

where the standard error in the coefficients are Δa_0, Δa_1, and Δa_2. The coefficient of ln Λ_0 with respect to pressure was obtained by differentiating eq. [15]:

$$[16] \qquad \left(\frac{\partial \ln \Lambda_0}{\partial P}\right)_T = a_1 + 2a_2P.$$

The error in this slope was estimated as follows:

$$[17] \qquad \Delta\left(\frac{\partial \ln \Lambda_0}{\partial P}\right)_T = \Delta a_1 + 2\Delta a_2 P + 2a_2\Delta P.$$

The volume of activation was calculated by substituting the slope given by eq. [16] into the appropriate equation. The error in the volume of activation was then given by the equation

$$[18] \qquad \Delta(\Delta V) = RT\Delta\left(\frac{\partial \ln \Lambda_0}{\partial P}\right)_T + \frac{2}{3}RT\,\Delta\beta.$$

The error in the compressibility was estimated from the errors in the experimentally determined Tait constants (9). Error estimates in other parameters were derived from similar equations.

The error estimates themselves represent the maximum possible estimated error since no factor was used to convert them to a probable error, and positive terms were always taken in the error equations. The curve-fitting procedure results in calculated values for the fitted parameter which

Can. J. Chem. Downloaded from www.nrcresearchpress.com by 210.87.254.40 on 09/05/12
For personal use only.

are more reliable than any of the individual measurements which go into the data set fitted by the curve. This statement is confirmed by a result derived by Young (37),

$$[19] \qquad \sigma_m = \sigma/N^{\frac{1}{2}},$$

where σ_m is the standard deviation of the mean (the "precision" of the mean) and σ is the standard deviation for a set of N points. Therefore, to convert error estimates given in tables to the most probable precision of the measurements, eq. [19] is applied and the result multiplied by 0.674. Comparisons within the data obtained in this work can be made by using the program error estimates in the tables as a guide to the relative precision of the data.

Acknowledgments

The work described in this and the following two papers was supported by a Grant, and a Studentship to W. A. A., from the National Research Council of Canada; this support is much appreciated.

1. S. MINC and L. WERBLAN. Roczniki Chem. **40,** 1537 (1966).
2. S. MINC and L. WERBLAN. Roczniki Chem. **40,** 1753 (1966).
3. S. MINC and L. WERBLAN. Roczniki Chem. **40,** 1989 (1966).
4. G. J. HILLS. *In* Chemical physics of ionic solutions. *Edited by* B. E. Conway and R. G. Barradas. John Wiley and Sons, Inc., New York. 1966. Chap. 23.
5. A. J. PARKER. Quart. Rev. London, **16,** 163 (1962).
6. K. P. MISHCHENKO and V. V. SOKOLOV. Zh. Strukt. Khim. **4,** 184 (1963).
7. K. P. MISHCHENKO and V. V. SOKOLOV. Zh. Strukt. Khim. **5,** 819 (1964).
8. R. MACY and E. W. THOMAS. J. Am. Chem. Soc. **48,** 1547 (1926).
9. W. A. ADAMS and K. J. LAIDLER. Can. J. Chem. **45,** 123 (1967).
10. R. L. MEEKER, F. E. CRITCHFIELD, and E. T. BISHOP. Anal. Chem. **34,** 1510 (1962).
11. N. MULLER. Purdue University, Lafayette, Indiana. Personal communication. cf. N. MULLER and P. I. ROSE. J. Phys. Chem. **69,** 2564 (1965).
12. R. C. WEAST (*Editor-in-chief*). Handbook of chemistry and physics. The Chemical Rubber Publishing Co., Cleveland. 1961. p. 451.
13. P. J. OVENDEN. Thesis, Southampton University, England. 1964.
14. T. SHEDLOVSKY. J. Am. Chem. Soc. **52,** 1806 (1930).
15. K. J. LAIDLER and D. T. Y. CHEN. Trans. Faraday Soc. **54,** 1026 (1958).
16. G. JONES and D. M. BOLLINGER. J. Am. Chem. Soc. **57,** 280 (1935).
17. G. JONES and S. M. CHRISTIAN. J. Am. Chem. Soc. **57,** 272 (1935).
18. J. O'M. BOCKRIS and B. E. CONWAY. J. Chem. Phys. **28,** 707 (1958).
19. R. A. ROBINSON and R. H. STOKES. Electrolyte solutions. Revised 2nd ed. Butterworths, London. 1965. p. 93.
20. T. R. NANNEY and W. R. GILKERSON. J. Phys. Chem. **69,** 1338 (1965).
21. J. E. LIND, JR., J. J. ZWOLENIK, and R. M. FUOSS. J. Am. Chem. Soc. **81,** 1557 (1959).
22. A. A. MARYOTT and E. R. SMITH. Table of dielectric constants of pure liquids. Nat. Bur. Std. U.S. Circ. 514. 1951. p. 10.
23. F. V. GRIMM and W. A. PATRICK. J. Am. Chem. Soc. **45,** 2794 (1923).
24. S. KYROPOULOS. Z. Physik, **40,** 507 (1926).
25. H. HARTMANN, A. NEUMANN, and G. RINCK. Z. Physik. Chem. Frankfurt, **44,** 218 (1965).
26. B. B. OWEN and S. R. BRINKLEY, JR. Phys. Rev. **64,** 32 (1943).
27. K. HOWARD and R. A. MCALLISTER. A.I.Ch.E. J. **4,** 362 (1958).
28. P. W. BRIDGMAN. Proc. Am. Acad. Arts Sci. **61,** 57 (1926).
29. E. KUSS. Z. Angew. Phys. **8,** 372 (1955).
30. L. ONSAGER. Physik. Z. **28,** 277 (1927).
31. H. S. HARNED and B. B. OWEN. The physical chemistry of electrolyte solutions. Reinhold Publishing Corp., New York. 1950. p. 154.
32. T. SHEDLOVSKY. J. Franklin Inst. **225,** 739 (1938).
33. R. M. FUOSS and T. SHEDLOVSKY. J. Am. Chem. Soc. **71,** 1496 (1949).
34. P. G. SEARS, E. D. WILHOIT, and L. R. DAWSON. J. Phys. Chem. **60,** 169 (1956).
35. L. G. SAVEDOFF. J. Am. Chem. Soc. **88,** 664 (1966).
36. F. B. HILDEBRAND. Introduction to numerical analysis. McGraw-Hill Book Co., Inc., New York. 1956. Chap. 7.
37. H. D. YOUNG. Statistical treatment of experimental data. McGraw-Hill Book Co., Inc., New York. 1962. pp. 108, 95.

Can. J. Chem. Downloaded from www.nrcresearchpress.com by 210.87.254.40 on 09/05/12
For personal use only.

Electrical conductivities of quaternary ammonium salts in acetone. Part II. The mechanisms of transport

W. A. ADAMS AND K. J. LAIDLER
Department of Chemistry, University of Ottawa, Ottawa, Canada

Received October 20, 1967

The limiting equivalent conductivities of tetramethylammonium iodide, tetraethylammonium iodide, and tetra-*n*-propylammonium iodide in acetone solution have been interpreted in terms of activated-complex theory; the energies of activation for conductivity at constant pressure and at constant volume, and the volumes of activation for conductivity, were calculated.

The hole free-volume theory of liquids has been discussed and found to give a satisfactory explanation for the observed pressure and temperature coefficients of conductivity, viscosity, and self-diffusion in several solvents. The magnitude of the limiting ionic equivalent conductivity has been shown to depend in a critical way on the ionic radius and on the relative strengths of the ion–solvent and the solvent–solvent interactions.

Canadian Journal of Chemistry, **46**, 1989 (1968)

Can. J. Chem. Downloaded from www.nrcresearchpress.com by 210.87.254.42 on 09/05/12
For personal use only.

Introduction

The present paper is concerned with the interpretation of the limiting equivalent conductivities obtained in Part I (preceding paper) from the standpoint of theories of transport in the liquid state.

Thermodynamic Activation Parameters for Conductivity

The experimental volume of activation for ionic conductivity can be defined as (1)

$$[1] \quad \Delta V_i^{\neq} = -RT\left(\frac{\partial \ln \lambda_i^0}{\partial P}\right)_T - \frac{2}{3}RT\beta,$$

where β is the isothermal solvent compressibility and λ_i^0 the limiting equivalent ionic conductivity. In the present work the combined cationic and anionic conductivities were employed. Calculations of $\Delta V_i^{\neq}$ were made both at finite concentrations, in order to gain some information about the interionic effects, and at zero concentration. The results obtained are given in Tables I–IV. The values are all corrected for solvent compressibility.

The energy of activation for conductivity, at constant pressure, may be defined as (1)

$$[2] \quad E_P = RT^2\left(\frac{\partial \ln \Lambda_0}{\partial T}\right)_P.$$

The logarithms of the Λ_0 values were fitted to a first-order polynomial in temperature by the least-mean-squares method, and E_P was evaluated, at different pressures, from the temperature coefficients. The computed results are given in Table V.

The energy of activation for conductivity at constant volume is (1)

$$[3] \quad E_V = RT^2\left(\frac{\partial \ln \Lambda_0}{\partial T}\right)_V.$$

The logarithms of the Λ_0 values were first fitted to a third-order polynomial in molar volume, at each of the four temperatures. Twelve volumes were then chosen over the pressure range investigated, and $\log_{10} \Lambda_0$ calculated for these volumes from the polynomial. These quantities were then fitted to a first-order polynomial in temperature for each of the 12 volumes, and E_V calculated using eq. [3]. The results are given in Table VI.

Discussion

Summary of Main Results

The main conductivity results obtained in the present work may be summarized as follows:

(1) The limiting equivalent conductivity, Λ_0, decreases with the size of the cation, increases with temperature, and decreases with pressure (Tables V and VI of Part I). Both the dielectric constant and the viscosity of acetone decrease with temperature and increase with pressure (Table I of Part I).

(2) The energy of activation at constant pressure is greater than the energy of activation at constant volume by about 1 kcal/mole (Tables V and VI). Both quantities increase with the size of the cation. E_V increases with decrease in the acetone volume for *n*-Pr_4NI, which has the largest cation, but decreases for the other two salts (Table VI). E_P is independent of the pressure within the precision of the measurements (Table V).

Can. J. Chem. Downloaded from www.nrcresearchpress.com by 210.87.254.42 on 09/05/12
For personal use only.

TABLE I

Volume of activation for conductivity of Me_4NI corrected for solvent compressibility at different salt concentrations (ml $mole^{-1}$)

Temperature (°C)	Pressure (bar)	Concentration at 1.0 bar and 26.61 °C (mole l^{-1}) × 10^4					
		4.468	4.201	2.807	2.170	1.946	1.724
26.61	1.0	8.77	8.64	9.27	9.71	9.69	1.10
	200	8.67	8.56	9.13	9.63	9.50	9.75
	400	8.41	7.03	8.83	9.39	9.16	9.35
	600	8.06	8.01	8.45	9.06	8.74	8.76
	800	7.67	7.64	8.01	8.68	8.26	8.12
	1000	7.24	7.24	7.54	8.27	7.73	7.65
35.00	1.0	8.19	8.42	9.03	9.15	9.33	9.46
	200	8.25	8.41	8.87	9.02	9.17	9.27
	400	8.12	8.22	8.53	8.71	8.83	8.90
	600	7.91	7.94	8.09	8.31	8.39	8.44
	800	7.63	7.60	7.60	7.84	7.90	7.92
	1000	7.32	7.22	7.07	7.34	7.36	7.36
45.01	1.0	8.51	8.86	9.38	9.52	9.42	9.71
	200	8.53	8.74	9.19	9.36	9.31	9.53
	400	8.31	8.38	8.76	8.97	8.97	9.11
	600	7.97	7.90	8.20	8.45	8.49	8.57
	800	7.56	7.33	7.58	7.86	7.96	7.95
	1000	7.10	6.74	7.00	8.22	7.38	7.29
54.83	1.0	8.33	8.53	9.07	9.63	9.55	9.81
	200	8.47	8.64	9.07	9.49	9.45	9.63
	400	8.29	8.42	8.75	9.03	9.02	9.13
	600	7.96	8.06	8.27	8.42	8.44	8.47
	800	7.53	7.60	7.70	7.71	7.76	7.72
	1000	7.08	7.11	7.10	6.97	7.06	6.91

TABLE II

Volume of activation for conductivity of Et_4NI corrected for solvent compressibility at different salt concentrations (ml $mole^{-1}$)

Temperature (°C)	Pressure (bar)	Concentration at 1.0 bar and 26.61 °C (mole l^{-1}) × 10^4					
		11.25	9.729	8.770	3.341	3.292	1.068
26.61	1.0	8.87	8.97	9.14	9.93	10.02	10.63
	200	8.78	8.87	9.01	9.72	9.77	10.28
	400	8.52	8.62	8.72	9.36	9.37	9.77
	600	8.19	8.28	8.34	8.91	8.88	9.17
	800	7.81	7.89	7.91	8.41	8.34	8.53
	1000	7.39	7.46	7.45	7.87	7.77	7.84
35.00	1.0	9.01	9.20	9.29	10.18	9.65	10.64
	200	8.86	9.05	9.10	9.86	9.42	10.22
	400	8.53	8.71	8.73	9.36	9.01	9.63
	600	8.11	8.28	8.27	8.77	8.51	8.93
	800	7.63	7.79	7.75	8.12	7.95	8.19
	1000	7.12	7.27	7.18	7.43	7.35	7.40
45.01	1.0	9.08	10.17	9.77	10.49	11.60	11.05
	200	9.00	9.79	9.51	10.19	11.04	10.62
	400	8.69	9.17	9.01	9.64	10.24	9.94
	600	8.25	8.43	8.39	8.97	9.31	9.14
	800	7.74	7.61	7.70	8.23	8.32	8.26
	1000	7.18	6.75	6.96	7.44	7.28	7.34
54.83	1.0	8.76	9.03	8.97	10.33	10.83	11.06
	200	8.85	9.11	9.04	10.18	10.58	10.72
	400	8.63	8.86	8.80	9.71	10.01	10.06
	600	8.25	8.47	8.40	9.09	9.29	9.25
	800	7.77	7.98	7.91	8.37	8.47	8.34
	1000	7.27	7.46	7.39	7.62	7.63	7.41

TABLE III

Volume of activation for conductivity of n-Pr_4NI corrected for solvent compressibility at different salt concentrations (ml $mole^{-1}$)

Temperature (°C)	Pressure (bar)	Concentration at 1.0 bar and 26.61 °C (mole l^{-1}) × 10^4					
		10.67	8.118	5.783	3.647	1.697	0.8000
26.61	1.0	9.14	9.39	9.67	9.96	10.43	10.31
	200	9.00	9.17	9.42	9.65	10.05	10.02
	400	8.62	8.80	9.02	9.18	9.52	9.58
	600	8.20	8.84	8.53	8.63	8.91	9.06
	800	7.73	7.84	7.98	8.02	8.24	8.48
	1000	7.22	7.29	7.41	7.38	7.54	7.87
35.00	1.0	9.07	9.34	8.67	8.96	10.55	10.55
	200	8.93	9.17	9.45	8.95	10.18	10.17
	400	8.61	8.82	9.05	8.75	9.64	9.61
	600	8.19	8.37	8.56	8.46	8.99	8.95
	800	7.72	7.86	8.01	8.12	8.29	8.23
	1000	7.21	7.31	7.42	7.73	7.55	7.48
45.01	1.0	9.38	9.48	9.91	9.50	10.87	10.86
	200	9.22	9.34	9.70	9.30	10.49	10.45
	400	8.82	8.96	9.25	8.86	9.87	9.80
	600	8.29	8.45	8.67	8.30	9.13	9.02
	800	7.69	7.87	8.02	7.66	8.31	8.17
	1000	7.05	7.25	7.32	6.98	7.45	7.28
54.83	1.0	8.70	9.48	9.59	10.38	10.96	11.15
	200	8.85	9.42	9.56	10.21	10.68	10.79
	400	8.68	9.04	9.21	9.72	10.07	10.11
	600	8.37	8.52	8.71	9.08	9.32	9.29
	800	7.95	7.89	8.11	8.34	8.47	8.36
	1000	7.51	7.24	7.49	7.57	7.59	7.41

(3) The volumes of activation are all positive, and within the precision of the measurements are independent of the cation under all conditions studied. They are also independent of the temperature, but decrease from about 11 to 7 ml $mole^{-1}$ when the pressure is increased from atmospheric to 1.1 kbar (Tables I, II, III, and IV). The volumes of activation all increase with decreasing salt concentration (Tables I, II, and III).

The significance of these results is discussed below.

Walden's Rule

Walden (2) proposed the empirical equation

$$[4] \qquad \Lambda_0\eta_0 = \text{constant},$$

where Λ_0 is the limiting Λ and η_0 is the viscosity of the solvent under the same conditions. Values of the Walden product, calculated on the computer, are given in Table VII. Pressure is seen to bring about an increase in the Walden product in all cases.

The effect of pressure in bringing about an increase in the Walden products of Me_4NBr, NaBr, n-Bu_4NBr, and n-Bu_4NBPh_4 in methanol was found by Skinner and Fuoss (3) to become less in the series of salts from Me_4NBr, where the increase was approximately 10% for about 1 kbar, to n-Bu_4NBPh_4, where no pressure effect was detected. Skinner and Fuoss conclude that the pressure dependence of $\Lambda_0\eta_0$ for the first three salts above must be mostly a property of the bromide ions, since the Walden product for n-Bu_4NBPh_4 is independent of pressure. However, this conclusion is based on results obtained at one temperature only, 31 °C. If the increase in the Walden product was primarily a property of the anion, the behavior of the Walden product as a function of temperature at different pressures would be the same for salts with different cations but a common anion. However, Table VII indicates that in acetone the decrease in the Walden product accompanying a 30 °C increase in the temperature is accentuated by compression to a greater extent for the smaller cation, Me_4N^+, than for n-Pr_4N^+. The conductivity work of Sears, Wilhoit, and Dawson (4) in acetone solutions at atmospheric pressure indicated that the average Walden product for n-Bu_4NI, an iodide salt with a larger cation in the same series of salts studied here, was 0.545 ± 0.001 at temperatures from 25 to −50 °C. It follows from these considerations that the ionic radius is one of the

Can. J. Chem. Downloaded from www.nrcresearchpress.com by 210.87.254.42 on 09/05/12
For personal use only.

Can. J. Chem. Downloaded from www.nrcresearchpress.com by 210.87.254.42 on 09/05/12
For personal use only.

TABLE IV

Volume of activation for conductivity (ml mole^{-1})

Pressure (bar)	Temperature (°C) 26.61	35.00	45.01	54.83
		Me_4NI		
1.0	11.3±0.2	10.7±0.2	10.9±0.3	11±1
137.9	11.0±0.2	10.4±0.3	10.7±0.3	11±3
275.8	10.6±0.2	10.0±0.3	10.3±0.4	11±3
413.7	10.2±0.2	9.6±0.3	9.8±0.4	11±4
551.6	9.7±0.2	9.1±0.4	9.3±0.4	10±4
689.5	9.1±0.2	8.6±0.4	8.8±0.5	10±5
827.4	8.4±0.2	8.1±0.4	8.2±0.5	10±5
965.3	8.0±0.3	7.5±0.5	7.6±0.6	9±6
1103.2	7.4±0.3	7.0±0.5	7.0±0.6	9±6
		Et_4NI		
1.0	11.0±0.1	10.8±0.3	12.0±0.3	11.8±0.3
137.9	10.7±0.2	10.6±0.4	11.6±0.4	11.5±0.3
275.8	10.4±0.2	10.2±0.4	11.1±0.4	11.1±0.3
413.7	10.0±0.2	9.7±0.5	10.5±0.4	10.5±0.3
551.6	9.6±0.2	9.3±0.5	9.8±0.5	9.9±0.3
689.5	9.1±0.2	8.8±0.6	9.1±0.6	9.2±0.4
827.4	8.6±0.2	8.2±0.6	8.4±0.6	8.5±0.4
965.3	8.1±0.2	7.7±0.7	7.6±0.7	7.8±0.4
1103.2	7.6±0.2	7.1±0.8	6.8±0.7	7.0±0.5
		n-Pr_4NI		
1.0	10.9±0.2	10.8±0.3	11.3±0.4	11.8±0.3
137.9	10.6±0.2	10.5±0.3	11.0±0.4	11.5±0.4
275.8	10.2±0.2	10.2±0.4	10.5±0.5	11.0±0.4
413.7	9.8±0.3	9.8±0.4	10.0±0.6	10.5±0.4
551.6	9.3±0.3	9.3±0.5	9.4±0.6	9.8±0.5
689.5	8.8±0.3	8.8±0.5	8.7±0.7	9.2±0.6
827.4	8.2±0.4	8.3±0.6	8.1±0.8	8.4±0.6
965.3	7.7±0.4	7.7±0.6	7.4±0.8	7.7±0.6
1103.2	7.1±0.4	7.2±0.7	6.7±0.9	7.0±0.7

properties of a salt which determines whether or not its conductivity behavior as a function of temperature and pressure can be understood solely in terms of the variation of the viscosity of the solvent.

TABLE V

Energy of activation at constant pressure for conductivity (kcal mole^{-1})

Pressure (bar)	Me_4NI	Et_4NI	*n*-Pr_4NI
1.0 (*a*)	1.58±0.05	1.59±0.02	1.63±0.01
1.0 (*b*)	1.49±0.04	1.60±0.05	1.67±0.02
1.0 (*c*)	1.5 ±0.1	1.59±0.08	1.73±0.03
137.9	1.46±0.08	1.55±0.07	1.69±0.04
275.8	1.47±0.07	1.56±0.06	1.68±0.00
413.7	1.49±0.07	1.55±0.05	1.67±0.02
551.6	1.55±0.05	1.55±0.02	1.69±0.02
689.5	1.60±0.03	1.57±0.02	1.71±0.02
827.4	1.2 ±0.2	1.60±0.04	1.71±0.02
965.3	1.65±0.01	1.63±0.03	1.73±0.03
1103.2	1.4 ±0.2	1.66±0.03	1.75±0.03

To illustrate the relationship which exists between the ionic radius and the limiting equivalent conductivity, Fig. 1 has been constructed from the conductivity data obtained in the present work and in previous work. The ionic radii chosen for the tetraalkylammonium ions are those estimated by Robinson and Stokes (8) from molecular volumes or models; the other ionic radii, with the exception of the ClO_4^-, picrate (Pi^-), and NO_3^- ions were taken from Pauling (9). The ClO_4^- and Pi^- radii were taken to be the van der Waals radii and the NO_3^- radius was taken to be the crystallographic radius. These values were obtained from a critical compilation of ionic radii estimated by various methods described by Stern and Amis (10). The points can be well represented by two straight lines A and B. The vertical line, C, which divides A and B corresponds to the radius of the acetone molecule, 2.8 Å, estimated by

Can. J. Chem. Downloaded from www.nrcresearchpress.com by 210.87.254.42 on 09/05/12
For personal use only.

TABLE VI

Energy of activation at constant volume for conductivity (cal mole^{-1}) $\times 10^{-1}$

Volume of acetone (ml mole^{-1})	Me_4NI	Et_4NI	n-Pr_4NI
77.49	47±5	52±13	50±2
76.30	38±7	46±6	51±2
75.15	33±10	42±6	52±3
74.22	31±10	40±6	53±3
73.63	30±10	40±7	54±3
72.76	30±10	40±7	56±3
71.96	30±9	41±6	58±3
71.17	31±9	43±6	59±3
71.14	31±9	43±5	60±4
70.42	31±11	46±5	62±4
69.80	31±12	50±4	63±5
69.06	30±15	54±4	66±6

TABLE VII

Walden product (g cm Ω^{-1} s^{-1} mole^{-1}) $\times 10^3$

Pressure (bar)	Temperature (°C) 26.61	35.00	45.01	54.83
		Me_4NI		
1.0	633±12	614±9	615±9	609±9
137.9	648±12	630±10	627±9	617±9
275.8	665±12	646±10	641±9	630±9
413.7	676±12	657±11	654±10	641±9
551.6	684±12	671±10	665±9	655±10
689.5	685±11	676±10	672±10	664±11
827.4	687±11	683±10	679±10	634±8
965.3	689±11	685±10	682±10	676±10
1103.2	690±10	689±10	686±9	652±9
		Et_4NI		
1.0	615±3	607±3	615±4	603±4
137.9	633±4	621±4	623±4	612±4
275.8	648±4	636±4	636±4	623±5
413.7	659±4	648±4	644±4	633±5
551.6	669±4	660±4	654±6	642±6
689.5	671±3	666±4	659±4	646±5
827.4	674±3	672±4	666±5	651±8
965.3	673±4	673±4	669±5	659±7
1103.2	674±4	675±4	671±5	662±7
		n-Pr_4NI		
1.0	566±5	565±4	568±5	568±5
137.9	580±6	577±4	577±5	575±6
275.8	595±6	594±6	591±4	585±5
413.7	607±6	605±7	599±5	594±6
551.6	616±6	614±7	613±8	603±6
689.5	619±6	620±7	618±8	610±6
827.4	624±6	625±7	624±8	616±6
965.3	625±6	626±7	628±8	620±6
1103.2	626±7	628±7	631±8	623±7

Zeidler (7). The maximum in the limiting equivalent conductivity at about 2.3 Å illustrates the size factor in determining the extent of solvation and, therefore, the transport behavior of ions.

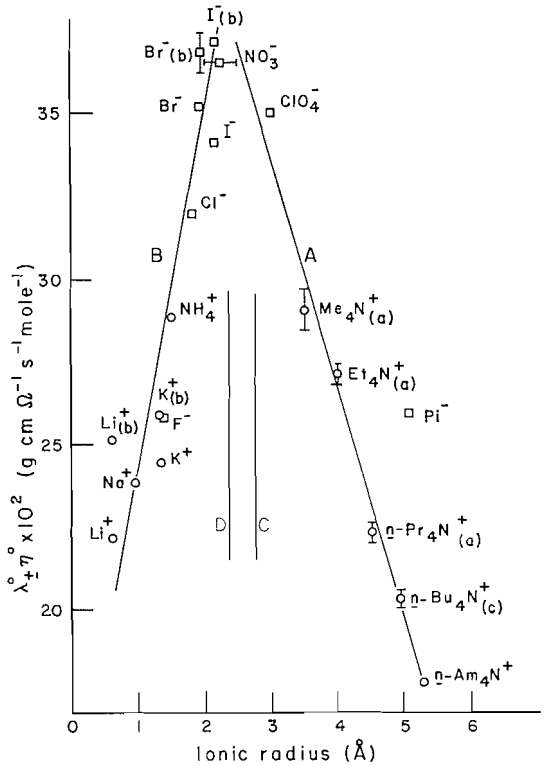

FIG. 1. Walden products in acetone plotted as a function of ionic radii: (*a*) present work, (*b*) Savedoff (5), (*c*) Sears, Wilhoit, and Dawson (4). All unmarked data are from Reynolds and Kraus (6). Vertical lines: C corresponds to the radius of the acetone molecule, 2.8 Å (7). D corresponds to the critical ionic radius, 2.36 Å (see text).

Line A includes the large ions which presumably interact only weakly with the acetone dipoles because of their low surface charge density. The conductivity decreases almost linearly with increasing radius except for Me_4N^+ which falls below curve A; Me_4N^+ interacts more strongly with the acetone dipoles than the other tetraalkylammonium ions. Ions with smaller radii than about 2.3 Å (line B) have decreasing limiting equivalent conductivities as the ionic radius decreases. This indicates that these ions interact strongly with the acetone dipoles producing solvodynamic entities for which effective radii are identical with ions having the same Walden product on line A. For example, the solvated Li^+ ion has approximately the same effective hydrodynamic radius as the n-Pr_4N^+ ion, which is not solvated.

Nightingale (11), in constructing a plot of the crystal radii versus the hydrated radii of ions in

Can. J. Chem. Downloaded from www.nrcresearchpress.com by 210.87.254.42 on 09/05/12
For personal use only.

water, found a broad minimum at about 2.5 Å. This minimum corresponds to a maximum in the Walden product. There is also a break in this curve at about 1.3 Å, which roughly corresponds to the radius of a water molecule. The interpretation of this feature of such plots is that when the radius of an ion approaches the same value as the radius of the solvent molecules, ionic transport can more easily occur by the same mechanism as that of the self-diffusion of the solvent.

If a simple ion–dipole interaction is assumed to hold between an ion and an acetone molecule, for example the ClO_4^- or NO_3^- ions which have approximately the same radius as acetone, it is possible to calculate the ionic radius below which the ion–dipole interaction energy is greater than the heat of vaporization at 25 °C. By use of the procedure given by Gurney (12), with a heat of vaporization of 7.403 kcal $mole^{-1}$ (13), the critical ionic radius can be estimated. The distance r between the center of the ion and the center of the dipole when the dipole axis is oriented along the line joining the centers of the ion and the dipole is given by

$$[5] \qquad r = (\mu eN/\Delta H_v)^{\frac{1}{2}} = 5.14 \text{ Å},$$

where e is the electronic charge, N is Avogadro's number, μ is the dipole moment of acetone, and ΔH_v is the heat of vaporization of acetone at 25 °C. The radius of an acetone molecule is about 2.8 Å; therefore, when ions have a radius of about 5.16 — 2.8 = 2.36 Å or less at 25 °C and atmospheric pressure, solvation by acetone molecules can be expected. Nightingale (11) similarly interpreted the broad minimum in the plot of the hydrated radii of aqueous ions against their crystal radii as indicating the strong hydration of small ions.

Gopal and Rizvi (14), and also Nightingale (11), concluded that the solvated volume of an ion increases with temperature to a greater extent for ions which have minimal solvation at low temperatures. This effect in aqueous media is due to the thermal disruption of the water structure at high temperatures. This permits a greater hydration of these ions at high temperature, because at low temperature the ion–solvent interaction is too weak with respect to the solvent–solvent interaction to bind the water molecules to the ions. The Walden product of ions near the maximum in Fig. 1 would therefore be expected to decrease with temperature. This result was found by Nightingale (11) for those ions in aqueous solution near the minimum in the plot alluded to above. The broadness of the minimum in this plot for water is consistent with a wide range of possible interaction energies between water molecules. In acetone, the primary intermolecular interactions are the dipole–dipole forces which have an inverse cube dependence on the separation of the interacting dipoles. The probability distribution curve of intermolecular energies is probably much narrower than in water, so that the extent of solvation, and hence the mobility, is strongly dependent on the ionic radius; the maximum in Fig. 1 is thus quite sharp.

The effect of pressure on the Walden product will also be a strong function of the ionic radius. Skinner and Fuoss (3) observed an increase in the Walden product of n-Bu_4NBr with pressure but not in that of n-Bu_4NBPh_4. This is probably due to the fact that although the n-Bu_4N^+ ion is not solvated in either salt, and increasing the pressure has little effect on the degree of its solvation, the Br^- ion is somewhat solvated at atmospheric pressure and the extent of its solvation is decreased by pressure. This would not be the case for the BPh_4^- anion which would be expected to remain unsolvated at all pressures because of its large size. Since an increase with pressure in the Walden products was observed for the three salts investigated in acetone, the extent of interaction of these ions with the solvent must be decreased relative to the solvent–solvent interactions by compression. A clearer analysis of this interaction can be obtained by a consideration of conductivity as a process of ions moving between equilibrium positions of low free energy by a jump mechanism.

The decrease in the Stokes radii with pressure is the opposite to that expected from electrostriction considerations. Ions might be expected to cause greater compression of solvent at high pressures where the lower volume of the system is energetically more favorable. However, to counter this effect the attractive intermolecular forces between acetone molecules are enhanced by pressure (15). It therefore becomes more difficult for acetone molecules to be removed from the bulk solvent into the solvation spheres of the ions. Since the Walden products increase with pressure (decrease with temperature), a

Can. J. Chem. Downloaded from www.nrcresearchpress.com by 210.87.254.42 on 09/05/12
For personal use only.

decrease in the extent of solvation of the ions with pressure (increased solvation with temperature) is suggested.

Table VIII shows the Stokes-law ionic radii calculated from the Walden products at 26.61 °C and atmospheric pressure, on the basis of the transport numbers estimated by Reynolds and Kraus (16), using the equation given by Robinson and Stokes (16):

$$[6] \qquad r_i = \frac{0.820}{\lambda_i^0 \eta^0},$$

where r_i is the Stokes radius of the ion in Å.

The Stokes radii increase with the size of the cations estimated by Robinson and Stokes (8): Me_4N^+, 3.47 Å; Et_4N^+, 4.00 Å; and n-Pr_4N^+, 4.52 Å. However, the Stokes radii in acetone are all less than the estimates of the radii of the cations. The average Stokes radius obtained for I^- of 2.45 ± 0.04 Å is in good agreement with both Savedoff (5), 2.40 Å, and Hughes and Hartley (17), 2.36 Å. The Stokes radius of I^- is greater than the crystal radius given by Gourary and Adrian (18) of 2.05 Å or by Pauling (9) of 2.16 Å.

TABLE VIII

Stokes law ionic radius at 26.61 °C and atmospheric pressure (Å)

	Me_4NI	Et_4NI	n-Pr_4NI
Cationic	2.80 ± 0.05	3.00 ± 0.01	3.54 ± 0.02
Anionic	2.44 ± 0.04	2.44 ± 0.01	2.47 ± 0.02
Sum	5.24 ± 0.09	5.44 ± 0.02	6.01 ± 0.04
Sum of crystallographic radii	5.63	6.16	6.68

It is concluded that there is not a permanent primary solvation shell which accompanies these ions as they move through the solution. If this were the case, the Stokes radius would be expected to be much larger than the crystal radius as it is, for example, for Li^+. The crystal radius of Li^+ is 0.60 Å according to Pauling (9), compared to the Stokes radius measured in acetone by Savedoff (5) of 3.16 Å.

Energies of Activation for Conductivity at Constant Volume and at Constant Pressure

In a study of several salts in N,N-dimethylformamide (DMF) Brummer (19) has discussed the interpretation of E_V and E_P on the basis of the theory proposed by Stearn and Eyring (20), in which it is assumed that migration of an ion occurs by a discrete jump over a free-energy barrier to transport between positions of equilibrium in the liquid. An activated-complex treatment (21) which has been applied to proton transfer in hydroxylic solvents has been generalized by Bockris, Kitchener, Ignatowicz, and Tomlinson (22). Bockris, Crook, Bloom, and Richards (23) have elaborated a theory which separates the process of the ion jumping between equilibrium positions and the formation of a hole in the liquid. This discussion employs the equation adopted by Brummer and Hills (24, 25):

$$[7] \qquad \lambda_i^0 = \frac{zeF}{6h} L^2 \exp(-\bar{\mu}_0^{\ddagger}/RT),$$

where L is the jump distance between equilibrium positions and $\bar{\mu}_0^{\ddagger}$ is the change in chemical potential for the ion to reach the activated state. This equation can also be written as

$$[8] \qquad \lambda_i^0 = \frac{zeF}{6h} L^2 \exp(\Delta\bar{S}_0^{\ddagger}/R) \exp(-\Delta\bar{H}_0^{\ddagger}/RT).$$

We then have

$$[9] \qquad RT^2\left(\frac{\partial \ln \lambda_i^0}{\partial T}\right)_P = 2RT^2\left(\frac{\partial \ln L}{\partial T}\right)_P + (\Delta\bar{H}_0^{\ddagger})_P = E_P$$

$$[10] \qquad RT^2\left(\frac{\partial \ln \lambda_i^0}{\partial T}\right)_V = 2RT^2\left(\frac{\partial \ln L}{\partial T}\right)_V + (\Delta\bar{U}_0^{\ddagger})_V = E_V,$$

where $(\Delta\bar{U}_0^{\ddagger})_V$ is the partial molar standard internal energy of activation for conductivity at constant volume. Equation [10] can be further simplified if it is assumed that $(\partial \ln L/\partial T)_V$ is approximately zero, so that E_V is identified with $(\Delta\bar{U}_0^{\ddagger})_V$. E_P, however, is a more complex function involving the isobaric coefficient of expansion of the solvent as well as the enthalpy term $(\Delta\bar{H}_0^{\ddagger})_P$:

$$[11] \qquad E_P = (2/3)RT^2\alpha + (\Delta\bar{H}_0^{\ddagger})_P,$$

since

$$[12] \qquad \left(\frac{\partial \ln L}{\partial T}\right)_P = (1/3)\left(\frac{\partial \ln V}{\partial T}\right)_P = \frac{\alpha}{3}.$$

E_P and E_V are related as follows (25, 26)

$$[13] \qquad E_P - E_V = (\pi + P)\Delta\bar{V}_0^{\ddagger} + (2/3)RT^2\alpha = (\pi + P)((\Delta\bar{V}_0^{\ddagger}) + (2/3)RT\beta),$$

Can. J. Chem. Downloaded from www.nrcresearchpress.com by 210.87.254.42 on 09/05/12
For personal use only.

where $(\partial U/\partial V)_T$ is the internal pressure of the solvent, π, and $\Delta \bar{V}_0^{\pm}$ is the partial molar standard volume of activation for conductivity. Then

$$[14] \quad -RT\left(\frac{\partial \ln \lambda_i^0}{\partial P}\right)_T = -2RT\left(\frac{\partial \ln L}{\partial P}\right)_T + \Delta \bar{V}_0^{\pm}.$$

Since

$$[15] \quad \left(\frac{\partial \ln L}{\partial P}\right)_T = (1/3)\left(\frac{\partial \ln V}{\partial P}\right)_T = -\frac{\beta}{3},$$

where β is the isothermal compressibility of the solvent, eq. [14] can be written as

$$[16] \quad \Delta \bar{V}_0^{\pm} = -RT\left(\frac{\partial \ln \lambda_i^0}{\partial P}\right)_T - (2/3)\,RT\beta.$$

In several systems it has been found that the constant-volume parameters are simpler than the corresponding constant-pressure parameters (27). At constant volume the intermolecular distances remain essentially unchanged as the temperature is varied; the energy of activation at constant volume is thus representative of the process itself and does not contain a term which depends on the variation in the intermolecular potential between the solvent molecules. This view has been put forward for diffusion in liquids by Nagarajan and Bockris (28) and for liquid viscosity by Bondi (29). However, the simplicity of constant-volume parameters over constant-pressure parameters requires that the solvent has no temperature-sensitive structure. The heat capacity of acetone at constant volume has been shown to be a function of temperature, especially at small volumes (15). In acetone, therefore, the constant-volume parameters may not have this simple and more direct interpretation. Furthermore, the nature of the mobile ionic species may be a function of temperature at constant volume; solvent molecules are less bound to each other by dipole–dipole interactions as the temperature is raised. Solvent molecules, are, therefore, more easily bound to the ions at high temperatures, an effect which causes curvature in the Arrhenius plots at either constant pressure or constant volume.

The Hole Theory of Liquids and Transport Properties

There has been some controversy regarding the applicability of a hole theory to liquids. Hildebrand and Scott (30, 31) have presented several arguments against the reality of holes of a molecular size and the use of the concept of free volume to calculate thermodynamic properties of liquids, stressing that "all liquids with fairly symmetrical molecules possess equal amounts of configurational entropy under the conditions of comparison, a situation quite unlikely to exist if the molecular disorder in them were less than maximum". However, there need be no postulate of a pseudo-lattice structural model of the liquid state for a theory of holes to be developed. Bockris and Richards (32), on the basis of an earlier treatment of a hole theory of liquids by Fürth (33), suggested that the holes have sizes that are thermally distributed and that they arise from density fluctuations in the liquid. Brummer (19) has suggested that the view of Watts, Alder, and Hildebrand (34), that movement of a molecule occurs by a weakening of the cage surrounding the molecule, differs only semantically from a hole model of the liquid where a hole is supposed to arise near a molecule by a density fluctuation. However, there is more than a semantic difference between the two views. Hildebrand and Scott (30) strongly support the views of Alder and Wainwright (35) which are based on the computed trajectories of hard-sphere molecules in which diffusion is found to occur by a process of random walk with very small steps. Nagarajan and Bockris (28), in studies of the self-diffusion in molten salts at constant volume, do not support a micro-jump model such as that described above, or the model of Swalin (36) in which small random movements of about 0.1 Å of the diffusing species occur. Their observations can be best interpreted in terms of a hole model of the liquid. If a liquid contained no holes of the size of the diffusing particles, the diffusing particle must open a hole of its own size when it moves in such a liquid, and the energy of activation at constant volume would have to contain the energy of hole formation as well as the energy of activation for jumping. However, Nagarajan and Bockris (28) find that E_V is about 15–20% of E_P. This indicates that E_V does not contain the energy of hole formation. This relation between E_V and E_P is observed for conductivity in acetone as can be seen in Tables V and VI. Fukuda and Kobayashi (42) state that the hole theory is a reasonable qualitative model for the liquid state after testing the theory's predictions against the experimental behavior of liquid isochores. These observations lend strong support to the impor-

Can. J. Chem. Downloaded from www.nrcresearchpress.com by 210.87.254.42 on 09/05/12
For personal use only.

tant part that holes in the liquid must play in the mechanism of transport.

Near the melting point or at high pressure the Arrhenius equation does not hold in its simple form. An equation in which $\exp(E_{act}/RT)$ is replaced by $\exp(E_{act}/R(T - T_0))$, where T_0 is a constant, has been found by Angell (37) to represent the viscosity results more accurately. Hogenboom, Webb, and Dixon (38) have used a free volume approach to interpret the pressure and temperature dependence of liquid hydrocarbon viscosity. In connection with the effect of volume on the temperature dependence of the viscosity of associated liquids or of van der Waals liquids at small volume, Bridgman (39) has reported that the viscosity varies markedly with temperature at constant volume. Contrary to the view of Hildebrand and Scott (30), these observations are thought to be best interpreted by a model of the liquid state which emphasizes the importance of free volume. In the non-Arrhenius region of liquids, according to Angell (37, 40) and Davies and Matheson (41), a free-volume parameter should be considered. Free volume, v_f, is defined as the expansion volume $(v - v_0)$, where v is the specific volume of the liquid at temperature T and v_0 is the specific volume of the liquid at temperature T_0 at which the mobility of the molecules is effectively zero. Angell (40) suggests that T_0 corresponds to the theoretical glass transition temperature where $v_f \to 0$ and, therefore, $\Lambda_0 \to 0$, $D \to 0$, and $\eta \to \infty$. In the liquid range of a substance, a discontinuity often occurs in the temperature dependence of the viscosity which divides Arrhenius behavior from non-Arrhenius behavior. According to Davies and Matheson (41, 43), the temperature at which such a discontinuity is found should correspond to a second-order thermodynamic transition. In the temperature range investigated in acetone at atmospheric pressure, the behavior of the viscosity is Arrhenius. However, in a compressed condition in this temperature range, acetone shows some evidence that the heat capacity at constant volume, as a function of temperature, goes through a minimum (15). This effect would constitute a second-order thermodynamic transition. It is, therefore, thought that at high pressures a free-volume theory should describe the transport properties observed in acetone.

The physical model treated by Davies and Matheson (41, 43) involves restriction of rotational modes of freedom as the amount of free volume is reduced. In the Arrhenius region the molecules have sufficient rotational freedom to reorientate several times between translational jumps. However, in the non-Arrhenius region, reorientation between translational jumps is hindered because one or more rotational degrees of freedom is lost. A molecule may possess sufficient energy to jump, but may not be capable of jumping. It may lose the ability to reorientate itself in order to move into a position where surrounding molecules have momentarily opened up sufficient free volume. The viscosity of liquids at high pressures has been treated by a free-volume formulation by Matheson (44).

Angell (40) states that measurements of the effect of pressure on relaxation properties have not been in accord with free-volume model predictions. This assertion was based on a statement by Brummer (19) that his conductivity results did not support the Cohen and Turnbull (45) free-volume theory. According to Cohen and Turnbull, the diffusion coefficient, D, for free-volume-limited transport should vary as $T^{\frac{1}{2}}$ at constant volume. The Nernst–Einstein equation (46)

$$[17] \qquad \lambda_i^0 = \frac{F^2}{RT} z_i D_i^0,$$

where λ_i^0 is the limiting equivalent ionic conductivity and D_i^0 is the limiting ionic diffusion coefficient, relates the diffusion coefficient and the limiting equivalent conductivity for cases where the moving species translate under identical local conditions $(\lambda_+^0 = \lambda_-^0)$. On the assumption that this equation holds, Λ_0 should be a linear function of $T^{-\frac{1}{2}}$ at constant volume, under conditions where the process is free-volume-limited. Within the experimental error Λ_0 varies linearly with $T^{-\frac{1}{2}}$.

The free energy of activation for conductivity at constant pressure, E_P, is assumed to contain a partial free-energy term for hole formation, $\Delta\bar{G}_h$, as well as a partial free energy of activation for jumping, $\Delta\bar{G}_j^{\neq}$, in the theory of conductivity outlined below. Application of the equation given by Nagarajan and Bockris (28) for diffusion in fused salts gives the following conductance equation which refers to constant-pressure conditions:

$$[18] \qquad \Lambda_0 = \text{constant} \times \exp[(\Delta\bar{S}_h + \Delta\bar{S}_j^{\neq})/R] \times \exp[-(\Delta\bar{H}_h + \Delta\bar{H}_j^{\neq})/RT],$$

where the subscripts h and j refer to parameters

Can. J. Chem. Downloaded from www.nrcresearchpress.com by 210.87.254.42 on 09/05/12
For personal use only.

of hole formation and jump respectively. This equation is based on the concept developed by Frenkel (47) for crystal defects. The number of holes per mole of liquid, N_h, in equilibrium with the number of molecules per mole of liquid is given by the relationship

$$[19] \qquad N_h/N = \exp(-\Delta\bar{G}_h/RT).$$

To obtain eq. [18], eq. [19] has been combined with a probability factor, $\exp(-\Delta\bar{G}_j^{\ddagger}/RT)$, which predicts the probability of a collision between a hole and an ion, that is the probability for a jump to take place. Comparison of eqs. [18] and [2] gives

$$[20] \qquad E_P = (\Delta\bar{H}_h)_P + (\Delta\bar{H}_j^{\ddagger})_P.$$

In the formulation by Nagarajan and Bockris (27), $(\Delta\bar{H}_j^{\ddagger})_P$ is written as an energy of activation for jumping, but it is preferable to write it as an enthalpy of activation following Brummer (24). Further, for constant-volume conditions, the enthalpy function becomes an internal-energy function, so that comparing eqs. [18] and [3] the following relationship can be written:

$$[21] \qquad E_V = (\Delta\bar{U}_h)_V + (\Delta\bar{U}_j^{\ddagger})_V.$$

In order to identify E_V with an energy associated solely with the jump process in liquid transport, it must be demonstrated that $(\Delta\bar{U}_h)_V$ is negligible compared with $(\Delta\bar{U}_j^{\ddagger})_V$. Nagarajan and Bockris (28) assume that change in the volume of a liquid with temperature is largely a result of an increase in the free volume or the total volume of holes:

$$[22] \qquad V_{T_2} - V_{T_1} = (N_h v_h)_{T_2} - (N_h v_h)_{T_1},$$

where v_h represents the most probable volume of the holes. It is assumed that v_h is independent of temperature at constant volume. From eqs. [22] and [19]

$$[23] \qquad \exp(-\Delta\bar{G}_h/RT_2) - \exp(-\Delta\bar{G}_h/RT_1) = 0,$$

since $V_{T_2} = V_{T_1}$ at constant volume. This means that $(\Delta\bar{U}_h)_V$ is zero. Therefore, if we assume that the most probable volume of holes is not affected by a variation in the temperature at constant volume, the energy of activation at constant volume, E_V, may be equated to $(\Delta\bar{U}_j^{\ddagger})_V$. The two quantities $(\Delta\bar{H}_j^{\ddagger})_P$ and $(\Delta\bar{U}_j^{\ddagger})_V$ are identical if the movement of an ion into a hole is not accompanied by a volume change. This problem is discussed in connection with the volume of activation parameter associated with conductivity. A hole theory of liquids based on density fluctuations in the liquid has been used by Bockris and Richards (32) to derive an equation which gives a rough correlation between the melting point, T_m, at atmospheric pressure and $\Delta\bar{H}_h$ for the viscous flow of a wide variety of liquid gases, hydrocarbons, simple organic liquids, and fused salts:

$$[24] \qquad (\Delta\bar{H}_h)_P \doteq 3.74\,RT_m.$$

The predicted enthalpy of hole formation in acetone is 1.32 kcal mole^{-1}. The difference $E_P - E_V$ at atmospheric pressure, based on the results in Tables V and VI, are 1.16, 1.17, and 1.21 kcal mole^{-1} for Me_4NI, Et_4NI, and n-Pr_4NI respectively. The constancy of this number for the three salts suggests that the same process is being measured for each salt and that this is indeed the enthalpy of hole formation in eq. [20]. The results of Howard (48) in methanol solutions also tend to support the view that $E_P - E_V$ is nearly independent of the ionic species as would be expected if it represented the energy of hole formation.

The results in Table VI show that the usual increase with decreasing volume is found for n-Pr_4NI and Et_4NI. This increase in E_V is associated with the enhanced solvent–solvent interactions present when the solvent is more densely packed. In contrast to the results reported by Brummer (19), which indicated that E_V was inversely proportional to the ion size, it was found that E_V increased with the ion size. The Me_4NI results appear to show a decrease in E_V with compression. This observation suggests that condition-variable solvation effects associated with smaller ions, which are near the peak of plots such as that in Fig. 1, would somewhat limit the applicability of the simple hole theory. However, the decrease in E_V with pressure could also be interpreted as a lessening with pressure, of the solvation binding, relative to the solvent–solvent interaction, such that the energy of activation for the jump process is reduced. From the results of E_V as a function of volume reported by Brummer (19), particularly for KPi, where the solvation should be most important, there appears to be some indication of a minimum in E_V at the higher volume side of the plot.

The pre-exponents of the isochoric plots between $\ln \Lambda_0$ and T^{-1} have been plotted against

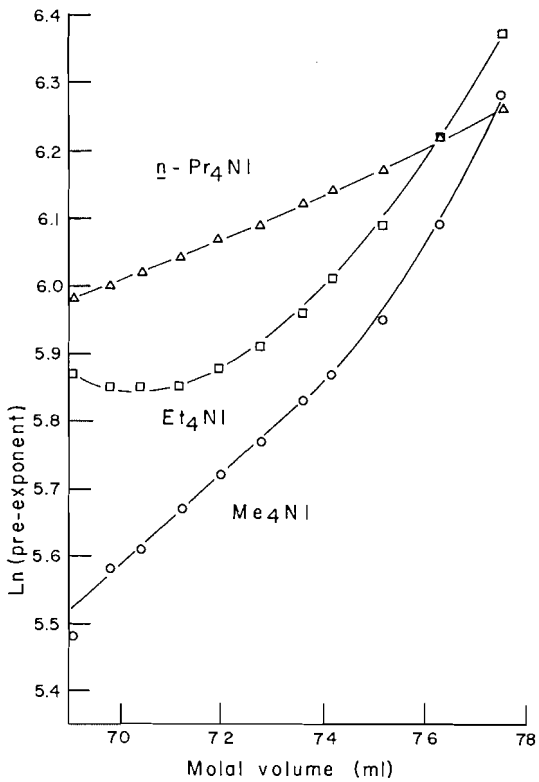

FIG. 2. Semi-logarithmic plot of the pre-exponent of the isochoric plots of ln Λ_0 versus T^{-1} against the molal volume.

the volume in Fig. 2. The pre-exponent decreases with decreasing volume throughout the range of volumes studied, except for Et_4NI, which shows evidence of a minimum at about 71 ml. The results presented by Brummer (19) indicate that such minima are present in all of the salts he studied in DMF. There are two unknowns in the pre-exponent, L, the jump distance, and $\Delta\bar{S}_0^{\ddagger}$, the partial molar entropy of activation. Brummer (19) has discussed the problem of estimating the pre-exponent. A transmission factor included in this term has been assumed to be unity. Estimates of the jump distance, L, have been made by Brummer from the equation

$$[25] \qquad L \doteq (V/N)^{1/3},$$

where V is the molar volume of the liquid. With the L parameter calculated from eq. [25], Brummer found that the calculated entropies, when plotted against the volume, paralleled the pre-exponent vs. volume curves. The entropies were negative and had values from 7.5 to 6.5 e.u. Negative entropies of activation indicate that the activated state is more ordered than the initial state. Equation [25] is not thought to give an adequate estimate of the volume dependence of L, especially since there are indications, from the volume dependence of the pre-exponent, that L may not be a monotonic function of the solvent volume. In a study of n.m.r. spin-lattice relaxation times of protons and deuterons by pulse methods in mixtures of proton-containing and fully deuterated acetone molecules in the liquid state, Zeidler (7) has estimated the mean jump distance from the self-diffusion coefficient of acetone. If this mean jump distance, estimated for acetone at 25 °C and atmospheric pressure to be 10.5 Å, is taken to be equivalent to the ionic jump distance, L, then $\Delta\bar{S}_0$ is estimated to be -8.7 e.u. from the pre-exponent of eq. [8]. This jump distance is slightly less than two molecular diameters, which certainly does not support the micro-jump mechanism of transport in liquids. In order to interpret a negative entropy of activation in conjunction with the positive volumes of activation observed (see Tables I–IV), the volume of activation measured is considered to be largely determined by the volume of hole formation in the liquid, which is independent of the species being studied. In acetone, in contrast to the findings of Brummer (19), over most of the volume range studied the entropy of activation is more negative for the smaller ions. This observation is taken to indicate (i) the greater ordering influence of the ions with larger charge to surface-area ratios, and (ii) that larger ions produce a greater degree of disruption in the solvent when the jump occurs. The reversal of the ion-size trend observed by Brummer (19) is probably due to the solvation of K^+ and Me_4N^+. The presence of solvation effects in the case of K^+ is indicated by the decrease in Λ_0 in the order Me_4N^+, K^+, and n-Bu_4N^+.

McCall, Douglas, and Anderson (49) have used n.m.r. spin-echo techniques to measure the pressure and temperature dependence of self-diffusion in acetone. The energy of activation at constant pressure was 2.03 kcal mole^{-1} for the self-diffusion of acetone, and was independent of temperature to within 5–10%. The energy of activation for self-diffusion at constant volume was 1.00 kcal mole^{-1}. Within the experimental errors of these two energies, the difference, 1.03

Can. J. Chem. Downloaded from www.nrcresearchpress.com by 210.87.254.42 on 09/05/12
For personal use only.

Can. J. Chem. Downloaded from www.nrcresearchpress.com by 210.87.254.42 on 09/05/12
For personal use only.

kcal mole^{-1}, is close to the predicted enthalpy of hole formation of 1.32 kcal mole^{-1}. This is the same result found in the acetone conductivity work. Such a close similarity in these values suggests a common mechanism to both ionic conductivity and self-diffusion in acetone.

The importance of the ionic size in connection with the limiting equivalent conductivity has been emphasized in the discussion of Fig. 1. Cohen and Turnbull (45) have made a similar correlation between the size of a diffusing species with respect to the solvent molecules and the rate of diffusive transport. If the species is smaller than or about the same size as the solvent, but larger than the average hole size, then the diffusion process is controlled by the rate of self-diffusion of the solvent and such species will diffuse at the same rate as the solvent. This condition corresponds to that of ions with radii approaching that of the solvent molecule. In Fig. 1, such ions have a maximum ionic mobility. Smaller ions do not have a higher mobility, because they are solvated. Larger species than the solvent molecules diffuse more slowly and, therefore, larger ions or ion–solvent complexes also have lower mobilities.

Calculations have been made by Mackenzie (50) on the ratio of the energy of activation for viscosity of liquid acetone at constant volume to the energy at constant pressure; this ratio increases with decreasing volume from 0.2 to 0.6. This increase is a result of an increase in E_V with decrease in volume. He suggests that E_P is the energy of activation for jumping plus the energy of hole formation. In addition, on the basis of a review of the viscosity data for many liquids, he concluded that, in general, E_V is always much less than E_P, except at very high pressures. The energy of activation for viscosity at constant volume for acetone is about 0.5 kcal mole^{-1}, whereas at constant pressure this energy is 1.70 kcal mole^{-1}. These activation energies closely resemble those obtained for conductivity in acetone (Tables V and VI). In addition, the difference between E_P and E_V for viscosity, 1.2 kcal mole^{-1}, is approximately equal to the energy of hole formation, 1.32 kcal mole^{-1}. Viscosity, as well as self-diffusion, appears to depend on the same molecular processes as conductivity in dilute solution. The nature of this fundamental process seems to be closely related to the amount of free volume in the system.

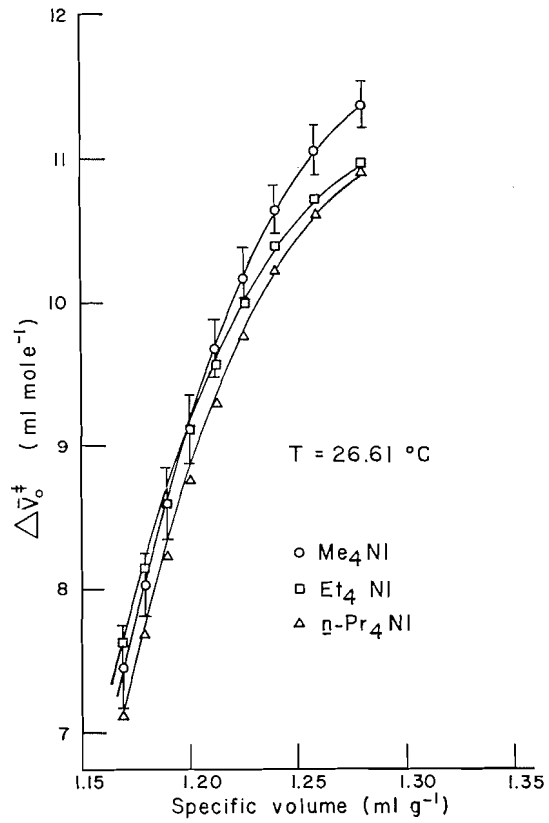

FIG. 3. Volume of activation for conductivity, corrected for solvent compressibility, plotted against specific volume of acetone.

Volume of Activation for Conductivity

Volumes of activation are given in Tables I–IV. The decrease in $\Delta\bar{V}_0^{\ddagger}$ with pressure is similar to the decreases observed by Brummer (19) in DMF, by Brummer and Hills (25) in methanol and nitrobenzene, and by Howard (48) in methanol solutions. This decrease is related to the reduced free volume in the solvent at high pressures.

The most striking observation in connection with the volumes of activation is their independence, within the experimental error of about 1–2%, from the ionic species (see Fig. 3). This observation confirms the results of Brummer (19), using DMF, that the volumes of activation of *n*-Bu_4NPi, Me_4NPi, HPi, KPi, and KBr, over a 10% range of volume, differ by less than 10%. Neglecting KBr in this comparison, the volumes of activation are found to be identical to within about 5%. The effect of different sized anions on

TABLE IX

Comparison between the volume of activation for conductivity, self-diffusion, and viscosity and the average volume of holes estimated by Fürth's equation

Liquid	Dielectric constant (25 °C)	Surface tension (27 °C) (dyn cm^{-1})	$(\Delta V_h)_{av}$	$\Delta \bar{V}_{\Lambda 0}^{\neq}$ (ml mole^{-1})	$\Delta V_D^{\neq}$	$\Delta V_\eta^{\neq}$
Acetone	20.7	23.2	30	13[a]	13[b]	15.9[b]
Methanol	32.63	21.7	34	7[c]		8[d]
Water	78.54	71.2	6	−2[e]	0.0[b]	1.3[b]
N,N-Dimethylformamide	36.7	35.2[f]	16	11[g]		
Nitrobenzene	34.82	42.2	13	15[e]		
Benzene	2.274	28.0	23		20.0[b]	20.4[b]
Cyclohexane	2.015	25.3	27		28[b]	30.8[b]
Nitromethane	39.5	35.5	16		13.6[b]	
Isopentane	2	15.8	50		34[b]	23.8[b]

[a]Present work.
[b]McCall, Douglas, and Anderson (49).
[c]Howard (48).
[d]Bondi (29).
[e]Hills (51).
[f]Blankenship and Clampitt (52).
[g]Brummer (19).

$\Delta \bar{V}_0^{\neq}$ is of the same order of magnitude as the effect that different sized cations have on $\Delta \bar{V}_0^{\neq}$. KBr and KPi have $\Delta \bar{V}_0^{\neq}$ values which differ by about 4% at high volumes and become almost identical when the system is compressed by 10%. This independence of $\Delta \bar{V}_0^{\neq}$ from the nature of the ionic species has also been observed by Brummer and Hills (25) in methanol and nitrobenzene solutions.

This behavior can be related to the dual nature of the proposed mechanism for transport in liquids and is expressed by the equation

$$[26] \qquad \Delta \bar{V}_0^{\neq} = \Delta \bar{V}_j^{\neq} + \Delta \bar{V}_h,$$

where $\Delta \bar{V}_h$ is the most probable volume of holes. The volume of activation for jumping, $\Delta \bar{V}_j^{\neq}$, can be understood in terms of the equation

$$[27] \quad \Delta \bar{V}_j^{\neq} = (\bar{V}_i^{\neq} + \bar{V}_h^{\neq}) - (\bar{V}_i + \bar{V}_h),$$

where $\bar{V}_i$ and $\bar{V}_i^{\neq}$ are the partial molar volumes of the ions before jumping and in the activated state, and $\bar{V}_h$ and $\bar{V}_h^{\neq}$ are the most probable volumes of the holes without and with an ion at the activated state. The term $\bar{V}_j^{\neq}$ is the result of distortion of the holes when the ion jumps and is likely to be small. In fact, since the other term, $\Delta \bar{V}_h$, in eq. [26], is independent of the ionic species at infinite dilution, the small differences observed in $\bar{V}_0^{\neq}$, of about 10%, indicate that if there is a large distortion volume, it does not depend strongly on the charge-to-volume ratio of the ions.

The most probable volume of holes in a liquid, ΔV_h, has been theoretically derived by Fürth (33), in whose model the holes are analogous to clusters of molecules in a dense gas or vapor and which perform a kind of Brownian movement. A test of this simple theory is to assume that $\Delta \bar{V}_j^{\neq}$ is small compared to ΔV_h. This comparison is made in Table IX. The agreement between $\Delta V_h^{\neq}$ and $\Delta \bar{V}_{\Lambda 0}^{\neq}$, $\Delta V_D^{\neq}$, and $\Delta V_\eta^{\neq}$ for DMF, nitrobenzene, benzene, cyclohexane, and nitromethane is very good. The volumes of activation for isopentane show fair agreement. However, the liquids acetone, methanol, and water have volumes of activation for transport which are much smaller than the estimated $\Delta V_h^{\neq}$ values. This lack of agreement can be interpreted in terms of the following ideas. The volume of activation for jumping may be negative, such that $\Delta \bar{V}_0^{\neq}$ is reduced to a value much less than ΔV_h in these liquids. This interpretation is commonly made to explain the negative volumes of activation for conductivity in water (see Horne, Courant, and Johnson (53)). A negative $\Delta \bar{V}_j^{\neq}$ implies that the short-range liquid structure in the environment of the ion is destroyed when the ion jumps. This explanation correctly correlates the negative entropies of activation with negative volume changes on jumping, if it is assumed that there is more dense packing around the ion at the col, resulting in an increase in order in the activated over the initial state. A second possibility is that the model upon which this treatment is based is not adequate to treat highly polar solvents and that the bulk

Can. J. Chem. Downloaded from www.nrcresearchpress.com by 210.87.254.42 on 09/05/12
For personal use only.

Can. J. Chem. Downloaded from www.nrcresearchpress.com by 210.87.254.42 on 09/05/12
For personal use only.

liquid surface tension is not a good parameter for estimating the volume of holes when the liquid possesses more than a minimum of short-range order. The significant result is that the similarities in the volumes of activation for ionic conductivity at high dilution, self-diffusion, and viscosity in a wide range of liquids indicate that these processes are related in a fundamental way. The mechanism of transport appears to involve the formation of holes as a separate process from the movement of the mobile species.

At finite concentrations, the effect of different ionic species on the activation parameters of conductivity is more pronounced. This quantity is quite complex because the equivalent conductivity at finite concentrations depends on both the mobility and extent of ion association. However, Tables I, II, and III indicate that the volume of activation for conductance increases approximately linearly with concentration to its limiting value at infinite dilution. The slope becomes progressively less negative at higher pressures. The salt with the smallest cation has the most negative slope with concentration, the increase in $\Delta \overline{V}^{\ddagger}$ being about 3 ml for a decrease from 5×10^{-4} to 0×10^{-4} mole l^{-1} for Me_4NI. This variation can be correlated with the effect that added solutes have on the surface tension in liquids, in view of Fürth's theory. However, this is not a large enough change to explain the strong concentration dependence of $\Delta \overline{V}^{\ddagger}$, especially at low concentrations, although it is in the correct direction. The smallest ions show the strongest dependence on the concentration, suggesting that the explanation for this effect should involve electrostriction.

Equation [13] suggests that the major expenditure of energy in the jump of an ion is the work done in the change in volume, $\Delta \overline{V}_0^{\ddagger}$, against the internal pressure of the liquid, π. Combining the experimental values of π and β for 40 °C and atmospheric pressure with the average measured difference $E_P - E_V$ of 1.18 kcal mole^{-1} at atmospheric pressure, the value of $\Delta \overline{V}_0^{\ddagger}$ predicted by eq. [13] is 12 ml mole^{-1}. This is in excellent agreement with the experimental activation volumes of Table IV. Therefore, the pressure dependence of the limiting equivalent conductivity is seen to be largely a volume property of the solvent. This follows because the internal pressure is the rate of change of the internal energy of the liquid with volume at constant temperature. The internal-pressure function, therefore, relates the intermolecular solvent forces to the volume. That this agreement is so satisfactory suggests that the activated-complex theory gives an adequate account of the limiting equivalent conductivity. The agreement between the calculated and the experimental $\Delta \overline{V}_0^{\ddagger}$ for acetone, using the internal-pressure correlation, is better than the treatment involving the surface tension. This probably reflects the fact that the simple assumptions in this version of the hole theory are not adequate for a dipolar liquid. The internal-pressure function is more characteristic than the surface tension of the intermolecular forces which determine the energetics of hole formation.

Summary of Conclusions

1. There is a sharp maximum in the correlation between ionic radius and limiting ionic equivalent conductivity in acetone solution at a radius close to the acetone molecular radius. This value has a significance in terms of the ion–dipole and dipole–dipole forces in the solution. For ions with radii which are greater than the radius at this break, the ionic equivalent conductivity decreases with increasing ion size. For ions with radii less than this value, increasing solvation of the ions with decreasing radius brings about a decrease in the limiting ionic equivalent conductivity.

2. An increase observed in the Walden product with pressure is a result of a decrease in the extent of ionic solvation at high pressure.

3. None of the quaternary ammonium ions studied is accompanied by a primary solvation layer when it moves in the solution, whereas the Li^+ ion moves in acetone with its primary solvation shell intact.

4. The energies of activation for conductivity at constant pressure and at constant volume observed in acetone solution are consistent with predictions of the hole theory of liquid structure and transport processes in liquids.

5. The volume of activation for conductivity, which is found experimentally to be almost independent of the ionic species, is closely related to the distribution of free volume in the liquid. The distortion volume change accompanying the jump process is small compared with the most probable volume of holes.

6. Activated-complex theory offers a conve-

nient framework in terms of which the temperature and pressure coefficients of conductivity can be interpreted. However, maximum insight into the mechanism of ionic conductivity is obtained at the present time when hydrodynamic and activated-complex theory are both used. There is a lack of a large body of data from pressure and temperature studies of conductivity into which the results of a single investigation can be fitted, but the conductivity results at 25 °C and atmospheric pressure are extensive for many solvents.

1. S. B. BRUMMER and G. J. HILLS. Trans. Faraday Soc. **57**, 1823 (1961).
2. P. WALDEN. Z. Physik. Chem. Leipzig, **55**, 207, 246 (1906).
3. J. F. SKINNER and R. M. FUOSS. J. Phys. Chem. **70**, 1426 (1966).
4. P. G. SEARS, E. D. WILHOIT, and L. R. DAWSON. J. Phys. Chem. **60**, 169 (1956).
5. L. G. SAVEDOFF. J. Am. Chem. Soc. **88**, 664 (1966).
6. M. B. REYNOLDS and C. A. KRAUS. J. Am. Chem. Soc. **70**, 1707 (1948).
7. M. D. ZEIDLER. Ber. Bunsenges. Physik. Chem. **69**, 659 (1965).
8. R. A. ROBINSON and R. H. STOKES. Electrolyte solutions. Revised 2nd ed. Butterworths, London. 1965. p. 125.
9. L. PAULING. The nature of the chemical bond. Cornell University Press, Ithaca. 1939. Chap. 10.
10. K. H. STERN and E. S. AMIS. Chem. Rev. **59**, 1 (1959).
11. E. R. NIGHTINGALE, JR. J. Phys. Chem. **63**, 1381 (1959).
12. R. W. GURNEY. Ionic processes in solution. Dover Publications, New York. 1953. p. 51.
13. R. E. PENNINGTON and K. A. KOBE. J. Am. Chem. Soc. **79**, 300 (1957).
14. R. GOPAL and S. A. RIZVI. J. Indian Chem. Soc **43**, 104 (1966).
15. W. A. ADAMS and K. J. LAIDLER. Can. J. Chem. **45**, 123 (1967).
16. R. A. ROBINSON and R. H. STOKES. Electrolyte solutions. Revised 2nd ed. Butterworths, London. 1965. p. 44.
17. O. L. HUGHES and G. S. HARTLEY. Phil. Mag. **15**, 610 (1933).
18. B. S. GOURARY and F. J. ADRIAN. Solid State Phys. **10**, 127 (1960).
19. S. B. BRUMMER. J. Chem. Phys. **42**, 1636 (1965).
20. A. E. STEARN and H. EYRING. J. Chem. Phys. **5**, 113 (1937).
21. S. GLASSTONE, K. J. LAIDLER, and H. EYRING. The theory of rate processes. McGraw-Hill, New York. 1941. pp. 552, 563.
22. J. O'M. BOCKRIS, J. A. KITCHENER, S. I. IGNATOWICZ, and J. W. TOMLINSON. Trans. Faraday Soc. **48**, 75 (1952).
23. J. O'M. BOCKRIS, E. H. CROOK, H. BLOOM, and N. E. RICHARDS. Proc. Roy. Soc. London, Ser. A, **255**, 588 (1960).
24. S. B. BRUMMER. Ionic conductance at constant volume. Ph.D. Thesis, University of London. 1960.
25. S. B. BRUMMER and G. J. HILLS. Trans. Faraday Soc. **57**, 1816, 1823 (1961).
26. M. G. EVANS and M. POLANYI. Trans. Faraday Soc. **31**, 875 (1935).
27. D. M. NEWITT and A. WASSERMAN. J. Chem. Soc. 735 (1940).
28. M. K. NAGARAJAN and J.O'M. BOCKRIS. J. Phys. Chem. **70**, 1854 (1966).
29. A. BONDI. J. Chem. Phys. **14**, 591 (1946).
30. J. H. HILDEBRAND and R. L. SCOTT. Regular solutions. Prentice-Hall, Englewood Cliffs, New Jersey. 1962. Chap. 5.
31. J. H. HILDEBRAND. Proc. Natl. Acad. Sci. U.S. **57**, 542 (1967).
32. J. O'M. BOCKRIS and S. R. RICHARDS. J. Phys. Chem. **69**, 671 (1965).
33. R. FÜRTH. Proc. Cambridge Phil. Soc. **37**, 252 (1941).
34. H. WATTS, B. J. ALDER, and J. H. HILDEBRAND. J. Chem. Phys. **23**, 657 (1955).
35. B. J. ALDER and T. E. WAINWRIGHT. Molecular dynamics by electronic computers. Transport properties in statistical mechanics. Interscience Publishers, Inc., New York. 1958.
36. R. A. SWALIN. Acta Met. **7**, 736 (1959).
37. C. A. ANGELL. J. Phys. Chem. **69**, 399, 2137 (1965).
38. D. L. HOGENBOOM, W. WEBB, and J. A. DIXON. J. Chem. Phys. **46**, 2586 (1967).
39. P. W. BRIDGMAN. The physics of high pressure. Bell and Sons, Ltd., London. 1931. p. 352.
40. C. A. ANGELL. J. Phys. Chem. **70**, 2793 (1966).
41. D. B. DAVIES and A. J. MATHESON. J. Chem. Phys. **45**, 1000 (1966).
42. Y. FUKUDA and R. KOBAYASHI. J. Chem. Phys. **46**, 2661 (1967).
43. D. B. DAVIES and A. J. MATHESON. Trans. Faraday Soc. **63**, 596 (1967).
44. A. J. MATHESON. J. Chem. Phys. **44**, 695 (1966).
45. M. H. COHEN and D. TURNBULL. J. Chem. Phys. **31**, 1164 (1959).
46. R. A. ROBINSON and R. H. STOKES. Electrolyte solutions. Revised 2nd ed. Butterworths, London. 1965. Chap. 11.
47. J. FRENKEL. Kinetic theory of liquids. Dover Publications, New York. 1955. Chap. 1.
48. B. HOWARD. Ph.D. Thesis, University of London. 1963.
49. D. W. MCCALL, D. C. DOUGLAS, and E. W. ANDERSON. J. Chem. Phys. **31**, 1555 (1959).
50. J. D. MACKENZIE. J. Chem. Phys. **28**, 1037 (1958).
51. G. J. HILLS. *In* Chemical physics of ionic solutions. *Edited by* B. E. Conway and R. G. Barradas. John Wiley and Sons, Inc., New York. 1966. p. 521.
52. F. BLANKENSHIP and B. CLAMPITT. Proc. Oklahoma Acad. Sci. **31**, 106 (1950).
53. R. A. HORNE, R. A. COURANT, and D. S. JOHNSON. Electrochim. Acta, **11**, 987 (1966).

Can. J. Chem. Downloaded from www.nrcresearchpress.com by 210.87.254.42 on 09/05/12
For personal use only.

Electrical conductivities of quaternary ammonium salts in acetone. Part III. Ion-pair formation

W. A. ADAMS AND K. J. LAIDLER
Department of Chemistry, University of Ottawa, Ottawa, Canada

Received October 20, 1967

The ion-pair dissociation constants determined from a Shedlovsky analysis of conductivity (see Part I) were used to calculate the enthalpy, the internal energy at constant volume, the entropy, and the volume of dissociation of tetramethylammonium iodide, tetraethylammonium iodide, and tetra-*n*-propylammonium iodide ion pairs in acetone solution. The sign and magnitude of these parameters over the range of conditions investigated, temperature 25 to 55 °C and atmospheric to 1.1 kbar pressure, indicated that the free ions in acetone solution are extensively solvated and that, depending on the conditions, solvent-shared or solvent-separated ion pairs are formed.

Canadian Journal of Chemistry, **46**, 2005 (1968)

Introduction

Part I of this series (1) gives results for ion-pair dissociation constants in acetone. The present paper is concerned with a thermodynamic analysis of these results and a discussion of the derived parameters in relation to the molecular nature of ion pairs.

Thermodynamic Parameters for Ion-Pair Dissociation

The standard Gibbs free energies for the dissociation are given by the equation

$$[1] \qquad \Delta G_d^0 = -RT \ln K_d.$$

The volume changes on dissociation are defined by

$$[2] \qquad \Delta V_d^0 = -RT\left(\frac{\partial \ln K_d}{\partial P}\right)_T + RT\beta.$$

The log K_d values were fitted to a second-order polynomial by the least-mean-squares method; the resulting values are given in Table I.

The standard enthalpy of dissociation is defined by

$$[3] \qquad \Delta H_d^0 = RT^2\left(\frac{\partial \ln K_d}{\partial T}\right)_P + RT^2\alpha.$$

The log K_d values were fitted to a first-order polynomial in temperature. The ΔH_d^0 values obtained are given in Table II.

The standard entropy changes for dissociation, calculated from the ΔG_d^0 and ΔH_d^0 values, are listed in Table III.

The standard change in the internal energy of dissociation at constant volume is defined by the equation

$$[4] \qquad (\Delta U_d^0)_V = RT^2\left(\frac{\partial \ln K_d}{\partial T}\right)_V.$$

The logarithms of the dissociation constants were first fitted to a third-order polynomial in the molal volume at each of the four temperatures. Twelve volumes were then chosen over the range of pressure investigated, and the logarithms of K_d calculated for these volumes from the polynomial. These quantities were then fitted to a first-order polynomial in temperature for each one of the 12 volumes and $(\Delta U_d^0)_V$ was calculated using eq. [4]. Computed results are reported for the three salts studied in Table IV.

Discussion

Summary of Results

The ion-pair dissociation behavior of the three tetraalkylammonium halides studied has the following general features:

(i) All of the K_d values increase with pressure and decrease with temperature (Tables VI and VII of Part I).

(ii) The K_d values increase in the order $Me_4NI < Et_4NI \doteq n\text{-}Pr_4NI$ (Tables VI and VII of Part I).

(iii) The ΔG_d^0 values are about 3 kcal mole^{-1}; they decrease with pressure and increase with temperature.

(iv) The ΔG_d^0 values decrease in the order $Me_4NI > Et_4NI \doteq n\text{-}Pr_4NI$.

(v) The ΔH_d^0 values are negative (the dissociation process is exothermic), the values being about -2 kcal mole^{-1} (Table II).

TABLE I

Volume of dissociation (ml mole^{-1})

Pressure (bar)	Temperature (°C) 26.61	35.00	45.01	54.83
		Me_4NI		
1.0	−27±2	−28±4	−25±2	−19±12
137.9	−26±3	−25±4	−22±2	−19±15
275.8	−24±3	−22±5	−20±2	−19±18
413.7	−22±3	−18±6	−18±2	−19±21
551.6	−20±4	−15±6	−15±2	−19±24
689.5	−18±4	−11±7	−12±3	−18±28
827.4	−16±5	− 8±8	− 9±3	−18±31
965.3	−14±5	− 4±9	− 6±3	−17±34
1103.2	−12±6	− 0±9	− 4±4	−17±37
		Et_4NI		
1.0	−17±1	−14±2	−22±2	−22±2
137.9	−16±1	−13±2	−19±2	−20±2
275.8	−15±1	−12±3	−17±2	−18±2
413.7	−14±1	−10±3	−14±2	−15±3
551.6	−12±1	− 9±4	−12±3	−12±3
689.5	−11±1	− 7±4	− 9±3	−10±3
827.4	−10±2	− 6±4	− 6±3	− 7±4
965.3	− 8±2	− 4±5	− 4±4	− 4±4
1103.2	− 7±2	− 3±5	− 1±4	− 1±4
		n-Pr_4NI		
1.0	−15±1	−13±2	−13±4	−20±3
137.9	−14±2	−12±2	−12±5	−18±3
275.8	−12±2	−11±2	−10±6	−16±4
413.7	−10±2	−10±3	− 9±7	−11±4
551.6	− 9±2	− 8±3	− 7±8	−10±4
689.5	− 7±2	− 7±3	− 6±9	− 7±5
827.4	− 6±2	− 6±4	− 4±10	− 4±6
965.3	− 4±3	− 4±4	− 2±11	− 1±6
1103.2	− 2±3	− 2±4	− 1±12	+ 1±6

(vi) The ΔH_d^0 values do not show any significant change with pressure, but tend to become more negative in the order $Me_4NI < Et_4NI < n$-Pr_4NI (Table II).

(vii) The ΔS_d^0 values are strongly negative and are independent of the temperature; they become more negative in the order $Me_4NI < Et_4NI < n$-Pr_4NI (Table III).

(viii) The ΔS_d^0 values for Me_4NI and Et_4NI become significantly larger (less negative) as the pressure increases, whereas the ΔS_d^0 values for n-Pr_4NI show little or no increase with pressure (Table III).

(ix) The ΔV_d^0 values are all strongly negative. They tend to become more negative as the temperature increases. The ΔV_d^0 values vary with the salt in the order $Me_4NI < Et_4NI < n$-Pr_4NI (Table I).

(x) The $(\Delta U_d^0)_V$ values all become significantly larger (less negative) as the pressure increases (Table IV).

(xi) The $(\Delta U_d^0)_V$ values decrease with decreasing volume and are increasingly negative in the order $Me_4NI < Et_4NI < n$-Pr_4NI (Table IV).

General Discussion

A comparison of the K_d values obtained with the literature is only possible for n-Pr_4NI at 25 °C and atmospheric pressure. McDowell and Kraus (2) obtained a value of 4.98×10^{-3} mole l^{-1}, which agrees within the experimental error limits with the values given in Tables VI and VII of Part I (1).

The negative ΔV_d^0 and ΔS_d^0 values indicate that there is considerably more solvation in the dissociated than in the ion-pair state. The variation of ΔV_d^0 with the salt (point (ix)) suggests that there is more ionic solvation in the case of the smaller cations.

The small K_d values and positive ΔG_d^0 values are largely due to the strongly negative ΔS_d^0 values; the dissociated state is one of low entropy,

TABLE II

Enthalpy of dissociation (kcal $mole^{-1}$)

Pressure (bar)	Me_4NI	Et_4NI	n-Pr_4NI
1.0	−0.4±0.7	−1.6±0.6	−3.2±0.4
137.9	−0.4±0.7	−1.5±0.6	−3.1±0.5
275.8	−0.2±0.7	−1.4±0.6	−2.7±0.4
413.7	−0.4±0.9	−1.3±0.4	−2.6±0.3
551.6	−1.3±0.4	−1.3±0.2	−2.7±0.1
689.5	−1.6±0.3	−1.1±0.1	−3.0±0.1
827.4	−1.8±0.9	−1.4±0.2	−2.9±0.2
965.3	−2.05±0.09	−1.7±0.1	−2.9±0.2
1103.2	0±2	−1.8±0.2	−3.0±0.2

and is reached only with difficulty. The solvation of the ions causes their enthalpy to be low, so that the ΔH_d^0 values are negative; the enthalpy effect is, however, offset by the entropy effect.

The pressure effects on K_d reflect negative ΔV_d^0 values. The fact that ΔS_d^0 values become less negative as pressure increases (point (viii)) reflects the greater difficulty that the field of the ion has in orienting solvent dipoles when the solvent is compressed. The decrease in the volume change ΔV_d^0 with pressure is also related to this effect.

The effect of variation of the temperature and pressure on ion-pair dissociation in water has been investigated for $[Co(III)\ (NH_3)_6]\ (SO_4)^+$ going to $[Co(III)\ (NH_3)_6]^{3+}$ and SO_4^{2-} by Shimizu, Takizawa, and Osugi (3). They reported that, at 25 °C, ΔV_d^0 went from a value of −2.0 to −12 ml $mole^{-1}$ for a rise from 1 to 600 kg cm^{-2} in pressure. This decrease in ΔV_d^0 with pressure was not observed at 40 °C, where an increase in ΔV_d^0 with pressure, similar to that observed in acetone, was found. The entropy of dissociation was found to be strongly negative and to increase (become less negative) with pressure. The enthalpy of dissociation showed complicated temperature and pressure dependence. At 25 °C, ΔH_d^0 was negative at all pressures, while it was found to become positive at 40 °C and 600 kg cm^{-2}.

Osugi, Shimizu, and Takizawa (4) found that the pressure dependence of the dissociation in water of $[Co(III)\ (NH_3)_6]\ Cl^{2+}$, to give $[Co(III)\ (NH_3)_6]^{3+}$ and Cl^-, gave a positive volume change at low pressures, the values becoming negative at higher pressures. These anomalous results in aqueous solutions are attributed to the structural effects.

Fisher and Davis (5) have studied the pressure dependence of the dissociation of $MnSO_4$ in aqueous solutions, and have found that ΔV_d^0 increases from about −7 to −5 ml $mole^{-1}$ for an increase of 2000 atmospheres in the pressure. The pressure and temperature dependence of the thermodynamic parameters of ion-pair formation in water are not the same as those found in acetone, but the entropy and volume changes observed are generally negative and show in most cases a similar, although smaller, pressure dependence than that observed in acetone.

TABLE III

Entropy of dissociation (cal deg^{-1} $mole^{-1}$)

Pressure (bar)	Me_4NI	Et_4NI	n-Pr_4NI
1.0	−13±2	−15±2	−21±2
137.9	−12±3	−15±2	−20±2
275.8	−12±3	−14±2	−19±1
413.7	−12±4	−14±2	−18±1
551.6	−15±2	−13.8±0.9	−18.5±0.8
689.5	−16±2	−13.1±0.6	−19.2±0.7
827.4	−16±3	−14.0±0.8	−19±1
965.3	−16.7±0.9	−12.7±0.5	−19±1
1103.2	− 8±9	−14.9±0.7	−19±1

TABLE IV

Internal-energy change of dissociation at constant volume (kcal mole^{-1})

Volume of acetone (ml mole^{-1})	Me_4NI	Et_4NI	n-Pr_4NI
77.49	0±2	0.3±0.4	0±1
76.30	1.5±0.7	0.1±0.3	−0.8±0.6
75.15	1.9±0.4	0.1±0.6	−1.2±0.4
74.22	1.7±0.9	0.1±0.6	−1.5±0.3
73.63	1±1	0.1±0.6	−1.6±0.2
72.76	1±1	0.0±0.5	−1.8±0.2
71.96	1±1	0.0±0.4	−1.9±0.1
71.17	0.7±0.8	−0.1±0.3	−2.0±0.1
71.14	0.7±0.7	−0.2±0.3	−2.0±0.1
70.42	0.9±0.6	−0.4±0.2	−2.2±0.2
69.80	1.4±0.9	−0.6±0.1	−2.3±0.2
69.06	3±2	−1.0±0.1	−2.5±0.3

Variation of K_d with Changes in the Ionic Radius

It is not possible to give an adequate interpretation of the different K_d values solely in terms of the electrostatic interactions between the cation and the anion using the crystallographic radii. This can be inferred from the solvation effects observed in the ionic-radius dependence of the limiting equivalent conductivity. When the ionic radius falls below a certain value which will depend on temperature and pressure the ion becomes solvated and the effective charge to volume ratio is reduced. If the counter-ion cannot displace the molecules in the solvation sheath the observed K_d will be greater than predicted on the basis of an electrostatic theory using the crystallographic radii. Also, Hughes and Price (6) have found evidence that there is penetration between the ethyl groups in the ion pairs formed between some tetraalkylammonium ions and halides in ethyl methyl ketone. With the lithium halides, whose conductivities have been studied by Savedoff (7), there is a 2000-fold increase in the dissociation constant in going from LiCl to LiI. This increase is far larger than that predicted by the electrostatic theory based on the increase in the anionic radii from Cl^- to I^-. These results suggest that there is a drastic difference in the ion pair formed between Li^+ and Cl^- from that formed between Li^+ and I^-. Furthermore, the enthalpy of dissociation for LiCl ion pairs is much more negative than that for either LiBr or LiI ion pairs (8).

Four classes of ion pairs were defined by Griffiths and Symons (9): (i) Complexes: two or more ions, in contact, held together by covalent bonds; (ii) Contact ions pairs: ions in contact, but with no covalent bonding between them; (iii) Solvent-shared ion pairs: pairs of ions, linked electrostatically, by a single (oriented) solvent molecule; and (iv) Solvent-separated ion pairs: pairs of ions, linked electrostatically, but separated by more than one solvent molecule. They used the general term "ion pairs" to include classes (ii), (iii), and (iv) when a distinction between them can not be made. Ions in solvents of low bulk dielectric constants but large dipole moments such as acetone are predicted to form solvent-separated ion pairs of class (iv) as well as some class-(iii) ion pairs.

Recently, Griffiths and Scarrow (10) have presented spectroscopic evidence that ion-pair interactions are important in acetone solutions of a series of alkylammonium bromides. The Br^-:Ni^{2+} ratio for conversion of $NiBr_2$ to $NiBr_4^{2-}$ was found to be quite sensitive to the radius of the cation.

The sensitivity, with respect to pressure and temperature, of the ultraviolet spectrum of iodide ions in various organic solvents has been studied by Griffiths and Wijayanayake (11) up to about 160 bar pressure and 300 °C. It was found that the charge-transfer-to-solvent spectrum was sensitive to the temperature and pressure. Solvents with dielectric constants greater than 23 are expected to contain only solvent-separated ion pairs. From dielectric constants of 23 down to 11, solvents are expected to contain solvent-shared ion pairs as well. It is interesting, therefore, that the dielectric constant of acetone increases from about 20 to 23 at 26.6 °C when the pressure is raised from 1 atm to 1.1 kbar.

The solvation of the iodide ion in acetone is expected to be symmetrical, even in the ion-paired state, if the dielectric constant is such as

to prohibit the formation of solvent-shared ion pairs. The measured values of the temperature dependence of the absorption maximum position over a wide temperature range agree with the correlation predicted for pure solvation. When the dielectric constant is less than about 20 (in acetone this corresponds to low pressures and temperatures greater than 35 °C [see Table I, Part I (1)]), the spectrum becomes cation-dependent. This is interpreted as an indication of the formation of some solvent-shared ion pairs in addition to the solvent-separated ion pairs already present. On the basis of a study of band shapes, the excited orbital of iodide in these ion pairs is concluded to be ellipsoidal. In solvent-shared ion pairs, a single solvent molecule is polarized and oriented differently from the other solvent molecules, so that an excited electron is now no longer in a spherically symmetrical orbital as it would be in the case of the class-(iv) ion pair. The temperature dependence of the solvent-shared ion-pair absorption maximum position is greatly reduced from that of the solvent-separated ion pair.

This spectroscopic evidence indicates that the class of ion pair formed depends critically on the solvent and the temperature and pressure. Acetone, because of the variation of its dielectric constant over the present range of temperature and pressure (Table I, Part I (1)), should contain solvent-shared ion pairs at the higher temperatures and lower pressures, and solvent-separated ion pairs at the lower temperatures and higher pressures. Because of the nature of the charge transfer in these two classes of ion pairs, a difference in the extent of electrostriction of the solvent is predicted. In a solvent-shared ion pair, the residual charge on the ions is thought to be negligible. This implies that two full charges are developed on the dissociation of a neutral ion pair for class-(iii) ion pairs, with a large electrostriction of solvent to be expected. Table II indicates that a large negative volume change results under the dielectric conditions thought to favor solvent-shared ion pairs. Solvent-separated ion pairs, however, do not result in a charge neutralization, since the charge of the anion is not neutralized by the cation. This implies that there is only a small increase in the charge developed when a class-(iv) ion pair dissociates. The increased electrostriction of the solvent that results from the dissociation of this kind of ion pair should be small. Table I indicates that a small negative volume change is found under conditions thought to favor class-(iv) ion-pair formation.

The values of the dissociation constants themselves also support this explanation involving two classes of ion pairs. At low pressures, the salt with the largest cation, *n*-Pr_4NI, is most dissociated (see summary point (ii)). However, at high pressure, the dissociation constants approach one another in value. The radius of the cation is less important under these conditions, a characteristic of class-(iv) ion pairs.

The internal-energy change at constant volume, shown in Table IV, indicates that there is a significant difference in the volume dependence of this function for the three salts investigated. $(\Delta U_d^0)_V$ decreases with decreasing volume in each case. The trend is not well delineated for Me_4NI, but is very definite for Et_4NI and *n*-Pr_4NI. Work must be done to separate the ions forming an ion pair, which implies that $(\Delta U_d^0)_V$ should be positive. At large volumes, $(\Delta U_d^0)_V$ is either positive, or small and negative, for the three salts studied. This suggests that the dominant interaction in the ion pair under these conditions is the electrostatic interaction between the two ions. These results suggest that a negative $(\Delta U_d^0)_V$ could be used as a diagnostic test to indicate the formation of solvent-separated ion pairs.

Fuoss Theory of Ion-Pair Dissociation

In the theory developed by Fuoss (12) the cations are represented by charged spheres of radius a in a continuum having the bulk dielectric constant of the solvent. Ion pairs are said to be present when anions, considered to be charged point masses, are a distance $r \leqslant a$ from the center of a cation. Hamann, Pearce, and Strauss (13) have derived the equation.

$$[5] \quad \Delta V_d^0 = \frac{-Nz_1z_2e^2}{a\epsilon^2}\left(\frac{\partial \epsilon}{\partial P}\right)_T + RT\beta.$$

This equation holds if the contact distance a is not a function of pressure.

The enthalpy of dissociation can similarly be calculated from the Fuoss theory by taking the temperature derivative of ln K_F; the resulting equation is

$$[6] \quad \Delta H_d^0 = \frac{TN|z_1z_2|e^2}{a\epsilon^2}\left(\frac{\partial \epsilon}{\partial T}\right)_P + \frac{N|z_1z_2|e^2}{a\epsilon} + RT^2\alpha.$$

A computer program was written which calculated the dissociation constants from the Fuoss

TABLE V

Average ion-size parameters for nine pressures (Å)

	Temperature (°C)			
	26.61	35.00	45.01	54.83
Me_4NI	3.33±0.04	3.38±0.05	3.35±0.07	3.4±1.0
Et_4NI	3.75±0.04	3.8±0.1	3.74±0.09	3.8±0.1
n-Pr_4NI	3.79±0.08	3.7±0.1	3.6±0.2	3.6±0.1

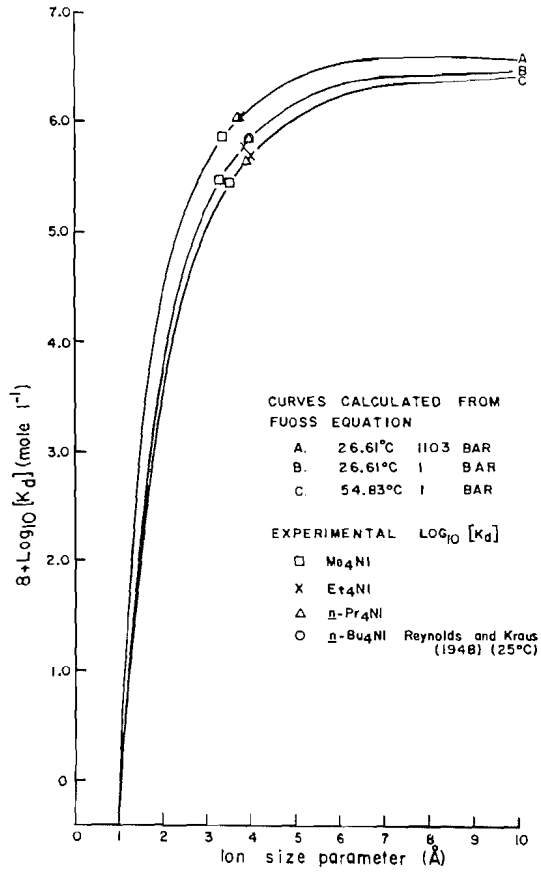

FIG. 1. Logarithm of the dissociation constant calculated from the Fuoss equation plotted against the ion-size parameter.

equation for values of the ion-size parameter from 0.05 to 10.00 Å, for the 36 conditions of temperature and pressure studied. Calculations to obtain the dissociation constants at 25 °C and atmospheric pressure for ion-size parameters from 0.05 to 20.00 Å were also completed. The dependence of $\log_{10} K_F$ on the ion-size parameter is shown graphically for three conditions in Fig. 1. The results obtained for the ion-size parameter at the nine pressures were averaged for each temperature and the values are shown in Table V.

The experimental volumes of dissociation and enthalpies of dissociation were used in conjunction with eqs. [5] and [6] to compute the ion-size parameters associated with these pressure and temperature derivatives. The average values are shown in Table VI.

The average values of the ion-size parameter shown in Table VI(*a*) are seen to increase with the ion size. This result is expected and is found when the ion-size parameter is calculated from ΔV_d^0. However, the ion-size parameter calculated from ΔH_d^0 decreases with the ion size. The model upon which the Fuoss equation rests is crude and it is therefore not unexpected that physically unreasonable ionic separations are found. For example, the sum of the Stokes radii for n-Pr_4NI is 6.01 ± 0.04 Å, the Fuoss–Onsager conductance equation predicts an ion-size parameter of 5.2 ± 0.6 Å, while the sum of the crystallographic radii is 6.68 Å. A comparison of these values, which refer to 26.6 °C, to the ion-size parameters given in Table V shows that the Fuoss equation predicts separations that are too small to be physically realistic. Also, the large standard deviations in the average ion-size parameters given in Table VI(*a*) and the large variation with temperature of the average ion-size parameters in Table VI(*b*) indicate that it is not a good assumption that the contact distance be considered to be independent of pressure and temperature in the derivation of eqs. [5] and [6] respectively.

Summary of Conclusions

1. Solvation of the free ions determines the sign and magnitude of the thermodynamic parameters of ion-pair dissociation in acetone.

2. Theories of ion-pair formation advanced on the basis of spectroscopic observations are consistent with the results obtained in the present work.

TABLE VI

Average ion-size parameters calculated at several temperatures (Å)

	Temperature (°C)			
	26.61	35.00	45.01	54.83
(*a*) Values based on the experimental volumes of dissociation and the pressure derivative of the Fuoss equation				
Me_4NI	2.8±0.2	6±3	5.1±0.7	4±1
Et_4NI	4.4±0.2	6.8±0.7	7±2	7±2
n-Pr_4NI	6.3±0.8	7.2±0.6	9±1	14±7
(*b*) Values based on the experimental enthalpy of dissociation and the temperature derivative of the Fuoss equation				
Me_4NI	3.8±4.1	5.3±5.6	7.4±8.0	10±11
Et_4NI	2.1±0.7	3.1±0.8	4.5±1.1	6.2±1.3
n-Pr_4NI	1.1±0.5	1.6±0.4	2.4±0.5	3.3±0.6

3. Acetone solutions are thought to contain solvent-shared and solvent-separated ion pairs; the proportion of each class present depends on the conditions of temperature and pressure.

4. The ion-size parameters calculated by continuous dielectric theory are generally a function of pressure and temperature and have smaller values than would be expected from other considerations.

1. W. A. ADAMS and K. J. LAIDLER. Can. J. Chem. This issue.
2. M. J. MCDOWELL and C. A. KRAUS. J. Am. Chem. Soc. **73**, 3293 (1951).
3. K. SHIMIZU, H. TAKIZAWA, and J. OSUGI. Rev. Phys. Chem. Japan, **33**, 1 (1963).
4. J. OSUGI, K. SHIMIZU, and H. TAKIZAWA. Rev. Phys. Chem. Japan, **36**, 1 (1966).
5. F. H. FISHER and D. F. DAVIS. J. Phys. Chem. **69**, 2595 (1965).
6. S. R. C. HUGHES and D. H. PRICE. J. Chem. Soc. 1093 (1967).
7. L. G. SAVEDOFF. J. Am. Chem. Soc. **88**, 664 (1966).
8. P. C. BLOKKER. Rec. Trav. Chim. **54**, 975 (1935).
9. T. R. GRIFFITHS and M. C. R. SYMONS. Mol. Phys. **3**, 90 (1960).
10. T. R. GRIFFITHS and R. K. SCARROW. International Conference on Non-Aqueous Solvent Chemistry, McMaster University, Hamilton, Ontario, June 1967.
11. T. R. GRIFFITHS and R. W. WIJAYANAYAKE. XIII Colloquium Spectroscopicum Internationale, Ottawa, Canada, June 1967.
12. R. M. FUOSS. J. Am. Chem. Soc. **80**, 5059 (1958).
13. S. D. HAMANN, P. J. PEARCE, and W. STRAUSS. J. Phys. Chem. **68**, 375 (1964).

Can. J. Chem. Downloaded from www.nrcresearchpress.com by 210.87.254.5 on 09/05/12
For personal use only.

Etude par diffusion de la lumière de la polydispersité résiduelle des polymères fractionnés[1]

ELIE AHAD, JACQUES PRUD'HOMME[2] ET YVON SICOTTE
Laboratoire de Chimie Physique, Département de Chimie, Université de Montréal, Montréal, Québec

Reçu le 5 décembre 1967

Les résultats expérimentaux confirment l'allure générale des résultats théoriques obtenus par Tung sur des fractionnements simulés et montrent que la polydispersité résiduelle et la variation de cette polydispersité résiduelle d'une fraction à l'autre dépendent des conditions de fractionnement et particulièrement de la concentration initiale en polymère. A la limite, pour des fractionnements effectués à partir de concentrations très faibles en polymère, on peut obtenir des fractions médianes de polydispersité négligeable au niveau de précision des mesures. Le paramètre $\langle\overline{S_0^2}\rangle_z/\overline{M}_p$ mesuré pour ces fractions sert de point de référence dans la caractérisation de la polydispersité d'autres échantillons. La comparaison avec ce paramètre des grandeurs $\langle\overline{S_0^2}\rangle_z/\overline{M}_p$ obtenues sur des échantillons polydispersés permet d'en mesurer l'indice de polydispersité $\overline{M}_z/\overline{M}_p$. Les résultats ainsi obtenus sur des fractions provenant d'un fractionnement à efficacité moyenne confirment pleinement les calculs de Tung.

The general trend of the theoretical results obtained by Tung on simulated fractionations is verified experimentally, showing that the sharpness of the fractions and the variation of the sharpness in the different fractions of a given fractionation are very much dependent on the fractionation conditions and especially on the polymer starting concentration. For very low starting concentration, the middle fractions can be considered as being monodisperse as far as polydispersity detection by light scattering is concerned. The ratio $\langle\overline{S_0^2}\rangle_z/\overline{M}_w$ for these fractions can be used as a reference for polydispersity characterization of other samples of the same polymer. The comparison of this ratio to the same ratio obtained on a polydisperse sample yields $\overline{M}_z/\overline{M}_w$. Results obtained in this way for a moderately sharp fractionation are in good accord with the theoretical predictions of Tung.

Canadian Journal of Chemistry, 46, 2013 (1968)

Introduction

On sait que l'on peut obtenir des données de diffusion lumineuse un certain nombre de moyennes des grandeurs moléculaires dont les valeurs relatives constituent des informations sur la polydispersité de l'échantillon. L'extrapolation à angle d'observation nul donne la moyenne en poids, $\overline{M}_p$, de la masse moléculaire,

$$[1] \qquad \overline{M}_p = \frac{\sum c_i M_i}{\sum c_i},$$

où c_i est la concentration en poids de l'espèce ayant la masse moléculaire M_i.

Dans le cas des macromolécules en chaînes, Benoît a montré (1, 2) que l'on peut tirer du comportement asymptotique de la fonction $P(\theta)$, c'est-à-dire la variation de l'intensité de diffusion en fonction de l'angle d'observation, θ, la moyenne en nombre de la masse moléculaire et le carré moyen du rayon de giration d'une molécule ayant cette masse. En pratique, cependant, cette région n'est accessible pour les longueurs d'onde visibles que pour les très grands rayons de giration, correspondant à des masses moléculaires de plusieurs millions.

D'utilisation plus courante, la pente à l'origine de la fonction $P(\theta)$ donne la moyenne suivante pour le carré moyen du rayon de giration (3),

$$[2] \qquad \langle\overline{S_0^2}\rangle_z = \frac{\sum c_i M_i \langle S_0^2\rangle_i}{\sum c_i M_i},$$

que l'on dénote z par analogie avec la moyenne z de la masse moléculaire:

$$[3] \qquad \overline{M}_z = \frac{\sum c_i M_i^2}{\sum c_i M_i}.$$

Dans le cas d'une macromolécule en chaîne en solvant thèta, le carré moyen du rayon de giration d'une chaîne isolée est proportionnel à sa masse moléculaire:

$$[4] \qquad \langle S_0^2\rangle = CM.$$

Dans le cas d'un milieu polydispersé, nous aurons la relation simple:

$$[5] \qquad \langle\overline{S_0^2}\rangle_z/\overline{M}_p = C\overline{M}_z/\overline{M}_p$$

[1]Les résultats utilisés dans le présent travail sont tirés de la thèse de Ph.D. en Chimie de Jacques Prud'homme, Université de Montréal (1967), et du mémoire de Maîtrise en Chimie de Elie Ahad, Université de Montréal (1967).

[2]Présentement boursier post-doctoral au Conseil National de Recherches du Canada, Ottawa.

Can. J. Chem. Downloaded from www.nrcresearchpress.com by 210.87.254.5 on 09/05/12
For personal use only.

On dispose donc ici d'une méthode simple de détermination de la quantité $\overline{M}_z/\overline{M}_p$, méthode qui ne fait intervenir qu'une seule méthode expérimentale. Bien qu'elle soit connue depuis très longtemps (3), cette méthode n'a guère été utilisée parce qu'elle repose sur la connaissance de la grandeur C. On pourra effectuer la détermination de cette grandeur sur un échantillon aussi monodispersé que possible, mais l'échantillon en question conservera toujours une polydispersité résiduelle qu'il sera souvent difficile d'évaluer.

Pour éviter ce problème, et également pour étendre la méthode aux bons solvants où l'éq. [4] n'est plus utilisable, Badley (4) propose d'évaluer la relation entre le rayon de giration et la masse moléculaire à l'aide de la théorie de Fox et Flory. Malheureusement cette théorie n'est pas rigoureuse à cet égard et peut introduire des erreurs importantes. En fait la mesure de C peut sembler délicate à prime abord mais, en examinant le mécanisme du fractionnement, nous verrons qu'on peut espérer obtenir des échantillons dont la polydispersité résiduelle soit assez faible pour ne pas introduire d'erreurs importantes.

Considerations theoriques sur le fractionnement

La séparation d'un échantillon polydispersé, par précipitation fractionnée à partir d'une solution, repose évidemment sur la variation de l'enthalpie libre molaire partielle de mélange avec la masse moléculaire. Comme on peut le voir par exemple dans la théorie de Flory et Huggins (5), cette grandeur est fonction de plusieurs variables dont on peut considérer les trois suivantes comme indépendantes au point de vue expérimental: la masse moléculaire évidemment, la concentration en molécules ayant cette masse moléculaire et enfin la concentration globale en polymère.

Il en résulte que la séparation d'un échantillon polydispersé en deux phases, qui n'est jamais une fonction discontinue au point de vue masse moléculaire, pourra cependant, selon les conditions expérimentales, s'approcher plus ou moins de cette fonction discontinue. De plus, au cours du fractionnement d'un échantillon en plusieurs fractions par appauvrissement progressif du solvant, on doit s'attendre à ce que la fonction en question évolue puisque les trois variables impliquées changent de valeur. Par conséquent, dans les fractions successives ainsi obtenues, on observera une variation monotone de la polydispersité résiduelle.

Pour notre besoin, il est intéressant de suivre l'évolution de cette variation de la polydispersité résiduelle des fractions successives en fonction des conditions expérimentales, spécialement en fonction de la concentration initiale globale en polymère. Nous nous en tiendrons au cas des échantillons présentant une courbe de distribution à un seul maximum. A la suite des travaux de Schulz et Dinglinger (6), et en se basant sur la théorie de Flory et Huggins, Tung a montré (7) par des fractionnements simulés que, pour des concentrations initiales de polymère assez élevées (2% dans l'exemple de Tung), on doit s'attendre à ce que la polydispersité résiduelle soit la plus grande pour les hautes masses moléculaires, qui correspondent aux premières fractions dans ce cas, et diminue graduellement pour les fractions de masses moléculaires plus faibles. La polydispersité résiduelle des fractions est alors fortement influencée par la concentration totale du polymère et par sa variation au cours du fractionnement. Nous excluons de cette discussion la fraction de masse moléculaire la plus faible qui constitue un cas particulier (7). Pour une concentration initiale de polymère de 0.5%, la polydispersité résiduelle des fractions diminue globalement, mais sa variation pour les fractions successives garde la même allure. Nous verrons d'ailleurs que dans un cas comparable nous avons retrouvé expérimentalement le même phénomène.

Par contre, pour des dilutions encore plus grandes (fractionnement double, concentration initiale de 1% et refractionnement à partir d'une solution à 0.2% selon le schéma de Flory), non seulement la polydispersité résiduelle calculée par Tung continue à diminuer, mais la concentration initiale des espèces contenues dans chacune des fractions commence à intervenir. La polydispersité résiduelle des fractions successives commence à refléter l'allure de la courbe de distribution et présente un minimum (l'indice $\overline{M}_p/\overline{M}_n$ est de 1.05) dans le voisinage du maximum de la courbe de distribution pour ensuite augmenter aussi bien pour les fractions plus basses que pour les fractions plus hautes.

Cet effet, qui ne fait que commencer à se manifester à cette concentration, est cependant assez marqué pour que l'on puisse extrapoler de là et prévoir, pour une concentration initiale

Can. J. Chem. Downloaded from www.nrcresearchpress.com by 210.87.254.5 on 09/05/12
For personal use only.

beaucoup plus faible, que la polydispersité résiduelle des fractions successives présentera pour les fractions médianes un plateau marqué, correspondant à un indice $\overline{M}_p/\overline{M}_n$ encore plus voisin de l'unité. A toutes fins pratiques par conséquent on pourra alors considérer ces fractions comme étant monodispersées.

Partie expérimentale

Nous avons fractionné deux échantillons de polystyrène. Le premier a été obtenu par polymérisation thermique et nous a été fourni par la maison Dow-Corning sous le numéro B-25. Le second, que nous dénoterons 60-1, a été obtenu dans ce laboratoire, sous vide, en présence de 2,2′-azobis(2-méthyl propionitrile) comme initiateur, à 60 °C, avec un taux de conversion de 13%.

L'échantillon B-25 a été fractionné en ajoutant à une solution à 1% dans la butanone des quantités croissantes de méthanol. Les fractions ainsi obtenues ont été redissoutes par élévation de température puis reprécipitées par retour lent à la température initiale, 25 °C. Seize fractions ont ainsi été obtenues dont les poids, variant irrégulièrement, représentaient de 1 à 12% de l'échantillon de départ. Ces fractions ont été numérotées B-25-1 à B-25-16. Trois de ces fractions, B-25-3, B-25-6 et B-25-8, représentant chacune environ 8% de l'échantillon de départ, ont été refractionnées selon le même procédé, en partant d'une solution à 0.1%. Dans chacun de ces trois cas une des fractions médianes a de nouveau été fractionnée en partant d'une solution à 0.05% pour donner entre autres les fractions B-25-3-4-2, B-25-6-3-2 et B-25-8-3-2, représentant chacune environ 1% de l'échantillon de départ et ayant été triplement fractionnées.

L'échantillon 60-1 a été soumis à un fractionnement double, en utilisant la même paire de solvants, selon un schéma utilisé depuis de nombreuses années dans ce laboratoire (8) et qui est très voisin du schéma de refractionnement de Flory. De façon à partir d'une concentration en polymère qui soit assez faible, tout en obtenant des fractions assez importantes, nous avons dû nous contenter d'un nombre de fractions plus faible dans ce cas, sept en l'occurence, représentant de 7 à 20% de l'échantillon de départ et numérotées 60-1-D-1 à 60-1-D-7. Dans la première étape du fractionnement la concentration originale était de 0.05% et de l'ordre de 0.02% dans la seconde étape. La fraction 60-1-D-3, représentant 19% de l'échantillon de départ a été de nouveau soumise à un fractionnement double, pour donner, entre autres, la fraction 60-1-D-3-D-2, représentant environ 5% de l'échantillon de départ et obtenue à partir d'une solution à 0.01%.

Les mesures de diffusion lumineuse, en raie verte du mercure, 5461 Å, ont été effectuées dans le cyclohexane à 35 °C (température thèta) sur un photogoniodiffusomètre de Wippler et Scheibling, fabriqué par Sofica. Les solutions ont été dépoussiérées par centrifugation dans un appareil Lourdes (LCA 1, 37 000 *g*) durant 1 h.

Comme valeur de dn/dc pour le polystyrène dans le cyclohexane à 35 °C, nous avons utilisé 0.171_5, c'est-à-dire la moyenne de plusieurs valeurs très cohérentes (9). Le benzène a été utilisé comme standard pour calibrer le photogoniodiffusomètre, en prenant comme valeur du rapport de Rayleigh pour ce liquide, à 5461 Å et à 25 °C, 17.2×10^{-6} (10) valeur qui passe à 17.9×10^{-6} à 35 °C (11).

Résultats et discussion

Etant donné le grand nombre de fractions obtenues, il n'était pas question de les caractériser toutes par diffusion de la lumière. D'ailleurs, comme nous allons le voir, il suffisait d'en caractériser quelques unes pour voir très nettement l'allure du phénomène.

Puisque l'évaluation du paramètre C, éq. [4], requiert la mesure de la masse moléculaire de fractions monodispersées, la valeur que l'on obtiendra pour ce paramètre contiendra les erreurs de calibration de l'appareil (basée sur l'intensité de diffusion d'un solvant) ainsi que les erreurs contenues dans la grandeur dn/dc, la variation d'indice de réfraction de la solution avec la concentration Par contre ces erreurs seront systématiques et joueront tout aussi bien pour l'éq. [5], de sorte que l'évaluation de la polydispersité d'un échantillon, c'est-à-dire dans ce cas l'indice $\overline{M}_z/\overline{M}_p$, sera indépendante de ces erreurs.

L'évaluation du rayon de giration par diffusion des radiations électromagnétiques est absolue et ne requiert aucune connaissance sur la structure de l'objet diffractant, du moins dans les cas où la pente à l'origine de la fonction $P(\theta)$ est accessible à l'expérience: c'est la loi de Guinier (12). Toutefois, dans le cas de la diffusion de la lumière par les macromolécules en chaînes, nous avons montré (13) que, dans les intervalles angulaires généralement explorés, ce comportement limite de la fonction $P(\theta)$ n'est accessible à l'expérience que pour les rayons de giration inférieurs à 300 Å environ. Au delà de cette limite, la détermination précise du rayon de giration nécessite la connaissance à priori de la fonction $P(\theta)$.

Les échantillons monodispersés

Dans le cas d'un échantillon monodispersé de macromolécules en chaînes, en solvant thèta, on sait qu'on peut utiliser l'équation maintenant classique de Debye,

$$[6] \qquad P(\theta) = 2(e^{-u} - 1 + u)/u^2,$$

où u représente $4\pi^2\sigma^2\langle S_0^2\rangle$, σ est la quantité $(2/\lambda)\sin(\theta/2)$, λ est la longueur d'onde de la

TABLEAU I

Caractérisation des fractions quasi monodispersées

	$c_i/\Sigma c_i$	$\overline{M}_p \times 10^{-6}$	$\langle\overline{S_0^2}\rangle_z \times 10^{-6}$ (Å^2)	$\langle\overline{S_0^2}\rangle_z/\overline{M}_p$ (Å^2)
B-25-3-4-2	0.007	0.96_5	0.071	0.073
B-25-6-3-2	0.013	0.66_0	0.045_5	0.069
B-25-8-3-2	0.011	0.44_0	0.030_5	0.069
60-1-D-3	0.19	2.28	0.168	0.073
60-1-D-5	0.19	1.35	0.097	0.071
60-1-D-3-D-2	0.05	2.55	0.180	0.070

lumière incidente mesurée dans le milieu. On pourra dans ce cas obtenir la masse moléculaire et le rayon de giration, par exemple en superposant les courbes théorique et expérimentale selon la méthode décrite précédemment (13).

A titre d'exemple, nous avons reproduit à la Fig. 1, pour la fraction 60-1-D-3, la superposition, par translation x–y, de la courbe théorique (log $P(\theta)$ en fonction de log u) à l'ensemble des points expérimentaux (log-$[c/I(\theta)]_{c\to 0}$ en fonction de log $4\pi^2\sigma^2$). La superposition des abcisses donne $\langle S_0^2\rangle_z$ et la superposition des ordonnées donne $\overline{M}_p$. La grandeur $I(\theta)$ est l'intensité de diffusion normée,

$$[7]\quad I(\theta) = \frac{\lambda_0^4 N_A \sin\theta R_{st}^0}{2\pi^2(dn/dc)^2(1+\cos^2\theta)n_{st}^2} \times \left(\frac{\Delta_{sln} - \Delta_{solvt}}{\Delta_{st}}\right),$$

où N_A est le nombre d'Avogadro, R_{st}^0 le rapport de Rayleigh du liquide utilisé comme standard de calibration, n_{st} l'indice de réfraction de ce liquide; les Δ sont les lectures galvanométriques pour la solution (sln.), le solvant (solvt.) et le liquide utilisé comme standard (st.).

Nous avons rassemblé au Tableau I les résultats ainsi obtenus pour les fractions quasi monodispersées. Les résultats indiquent clairement qu'on a, dans les deux cas, atteint un plateau au point de vue indice de polydispersité. Cette concordance des résultats obtenus par deux expérimentateurs différents, sur des échantillons de polystyrène d'origines différentes, par des méthodes de fractionnement différentes mais caractérisées toutes les deux par une dilution extrême, cependant que la dilution n'est pas la même dans les deux cas, de même que le fait qu'un fractionnement double ultérieur de 60-1-D-3 n'amène pas de changement important, tout cela indique que le plateau de polydispersité en question doit correspondre à une valeur de $\overline{M}_z/\overline{M}_p$ très voisine de l'unité, l'unité constituant évidemment la limite théorique pour cette grandeur. A ces évidences s'ajoute d'ailleurs le fait que ces valeurs de $\langle\overline{S_0^2}\rangle_z/\overline{M}_p$ pour le polystyrène sont précisément les plus basses parmi celles qui ont été obtenues à date (14–17).

Bien qu'elles aillent dans le sens prévu théoriquement au point de vue efficacité du fractionnement, les variations de $\langle\overline{S_0^2}\rangle_z/\overline{M}_p$ dans les résultats du Tableau I ne semblent pas significatives, puisqu'elles sont de l'ordre de grandeur de l'erreur expérimentale. Quoiqu'il en soit nous choisirons comme valeur du paramètre C, c'est-à-dire le rapport $\langle\overline{S_0^2}\rangle_z/\overline{M}_p$ pour un milieu monodispersé, la valeur 0.070 Å^2, correspondant au plateau prévu théoriquement. Il est intéressant de noter que des fractions représentant près de

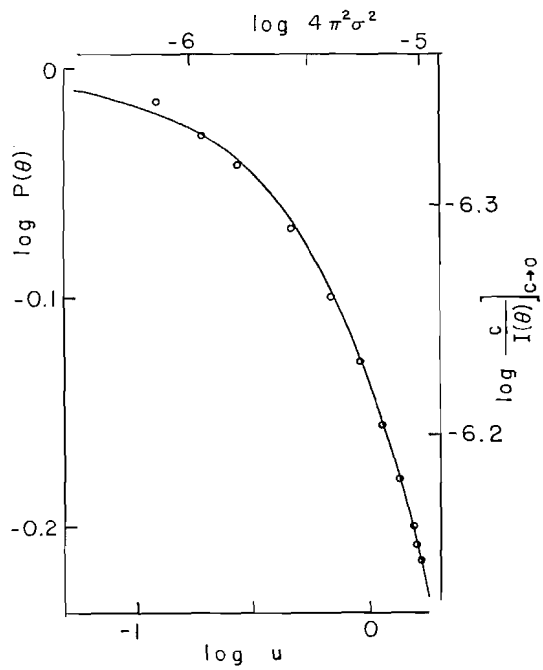

FIG. 1. Superposition de la courbe théorique, éq. [6], et des données expérimentales pour la fraction 60-1-D-3.

Can. J. Chem. Downloaded from www.nrcresearchpress.com by 210.87.254.5 on 09/05/12
For personal use only.

Can. J. Chem. Downloaded from www.nrcresearchpress.com by 210.87.254.5 on 09/05/12
For personal use only.

20% de l'échantillon de départ présentent dans ces conditions de fractionnement une polydispersité résiduelle négligeable à ce niveau de précision.

En plus de l'utilité qu'il présente dans les études de polydispersité, le paramètre C présente beaucoup d'intérêt dans les théories des solutions macromoléculaires, puisqu'il est relié aux interactions à courte distance et par là à la structure de la chaîne. De très nombreux chercheurs ont mesuré ce paramètre pour le polystyrène en solution dans le cyclohexane à 35 °C. Les valeurs obtenues présentent des écarts considérables, allant de 0.075 (14, 15) à 0.093 Å^2 (16, 17). Les valeurs voisines de 0.075 pour C sont en bon accord avec nos propres résultats, compte tenu des erreurs normales, des erreurs systématiques et des erreurs dans l'estimation de la polydispersité résiduelle des échantillons utilisés. Par ailleurs l'écart entre cette valeur basse et 0.093 est apparemment plus importante que toute erreur vraisemblable et nous nous proposons d'étudier si cet écart ne révélerait pas des différences structurales dans les échantillons utilisés.

Les échantillons polydispersés

Dans le cas d'un échantillon polydispersé, en solvant thèta toujours, il faudra utiliser (3) la moyenne z de la fonction $P(\theta)$ donnée par l'éq. [6],

$$[8] \qquad \bar{P}_z(\theta) = \frac{\sum c_i M_i P_i(\theta)}{\sum c_i M_i} = \frac{\int_0^\infty MP(\theta)P(M)\mathrm{d}M}{\int_0^\infty MP(M)\mathrm{d}M},$$

où $P(M)$ est la fonction de distribution en poids des masses moléculaires dans l'échantillon polydispersé. En développant la fonction $P(\theta)$ en série de puissances positives de u, on peut facilement voir que $\bar{P}_z(\theta)$ s'exprime finalement en fonction des différents moments de la fonction $P(M)$, c'est-à-dire M_p, M_z, M_{z+1}, etc, et que les moments d'ordre élevé n'interviennent que pour les puissances correspondantes de u. Il en résulte que dans l'intervalle de valeurs de u que nous avons exploré (u inférieur à 2, correspondant à des valeurs de $P(\theta)$ supérieures à 0.6), la fonction $\bar{P}_z(\theta)$ dépend très peu de la forme exacte de la fonction $P(M)$, mais presqu'exclusivement des valeurs relatives de ses premiers moments. Par conséquent, la valeur de $\langle \overline{S_0^2} \rangle_z$ qu'on tirera des résultats expérimentaux à l'aide de la fonction $\bar{P}_z(\theta)$ dépendra très peu de la forme de la fonction $P(M)$ utilisée pour calculer $\bar{P}_z(\theta)$, pour peu évidemment que la fonction $P(M)$ en question ne s'écarte pas grossièrement de la fonction de distribution réelle. Dans les cas étudiés dans le présent travail, nous avons utilisé la fonction de Zimm (3), qui a une forme assez générale et qui se prête bien au calcul,

$$[9] \qquad P(M) = \frac{y^{h+1}}{h!} M^h \mathrm{e}^{-yM},$$

où y et h représentent deux paramètres ajustables qu'on peut facilement relier aux différents moments de la fonction. Entre autres, le rapport $\overline{M}_z/\overline{M}_p$ devient $(h + 2)/(h + 1)$.

Il est bien évident que cette façon de procéder est limitée aux valeurs relativement basses de u, c'est-à-dire à la région qui ne contient que très peu de renseignements sur la forme de la fonction $P(M)$. Il n'en sera plus ainsi dans la région des valeurs plus élevées de u, plus riche en renseignements sur $P(M)$, et où on pourra tenter d'obtenir ces renseignements sur la forme de $P(M)$, comme Carpenter l'a fait (18). Malheureusement, dans le cas étudié par Carpenter, l'effet de solvant vient compliquer l'interprétation des résultats. En effet il s'agit d'un bon solvant et non seulement Carpenter néglige l'influence de l'effet solvant sur le $P(\theta)$, mais également, ce qui est vraisemblablement plus important, il néglige le fait que dans ce cas le rayon de giration et la masse moléculaire ne sont plus reliés aussi simplement que dans l'éq. [4].

Dans les cas que nous avons étudiés, la situation est plus simple, tant par le fait que le polymère est en solvant thèta que par le fait que la quantité d'informations est plus restreinte. Nous sommes dans des conditions telles que la seule donnée à propos de laquelle les informations sont présentes en quantité appréciable, c'est $\overline{M}_z/\overline{M}_p$ c'est-à-dire finalement la variance, le carré moyen de l'écart à la moyenne. On sait en effet que:

$$[10] \qquad \frac{\overline{M}_z}{\overline{M}_p} = 1 + \frac{1}{(\overline{M}_p)^2} \times \int_0^\infty (M - \overline{M}_p)^2 P(M)\mathrm{d}M = 1 + \frac{\overline{(M - \overline{M}_p)^2}}{(\overline{M}_p)^2}.$$

TABLEAU II

Caractérisation d'échantillons polydispersés

	$c_i/\Sigma c_i$	$\overline{M}_p \times 10^{-6}$	$\langle\overline{S_0^2}\rangle_z \times 10^{-6}$ (Å²)	$\langle\overline{S_0^2}\rangle_z/\overline{M}_p$ (Å²)	$\overline{M}_z/\overline{M}_p$
B-25	1	0.53_0	0.059	0.111	1.59
B-25-2	0.019	1.20_0	0.109	0.091	1.30
B-25-4	0.104	0.83_5	0.071	0.085	1.21
B-25-5	0.025	0.78_0	0.063	0.081	1.16
B-25-7	0.126	0.56_0	0.043	0.077	1.11
B-25-9	0.021	0.41_5	0.031	0.075	1.07

Dans les cas où nous ne connaissions pas à priori la polydispersité des échantillons, il a fallu évidemment procéder par approximations successives. On se donne d'abord une valeur approchée de $\overline{M}_z/\overline{M}_p$; on en tire une fonction $\overline{P}_z(\theta)$ dont on se sert pour déterminer $\langle\overline{S_0^2}\rangle_z$ et $\overline{M}_p$ à partir des données expérimentales de diffusion lumineuse. L'équation [5] permet alors de calculer une première approximation pour $\overline{M}_z/\overline{M}_p$, à l'aide de laquelle on recommence le cycle. La méthode converge évidemment plus ou moins rapidement selon la valeur de $\overline{M}_z/\overline{M}_p$ choisie au départ. Pour les échantillons faiblement polydispersés, on choisit l'unité pour cette grandeur. Pour les échantillons non fractionnés, il vaut mieux partir de 1.5. Dans ces conditions, deux cycles suffisent généralement. La Fig. 2 représente les résultats obtenus pour la fraction B-25-2.

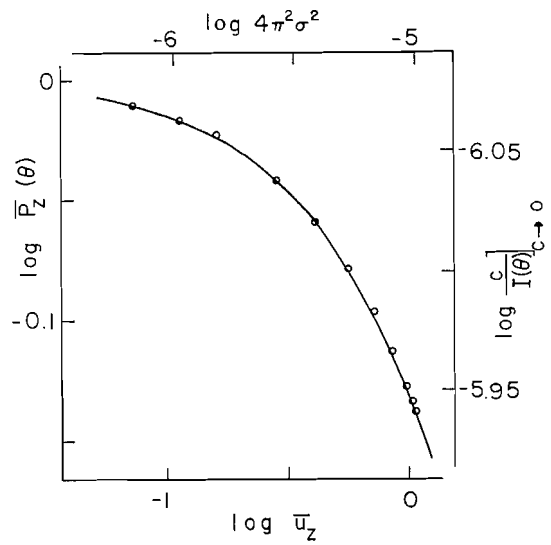

FIG. 2. Superposition de la courbe théorique, éq. [6], [8] et [9], pour $h = 6$, et des données expérimentales pour la fraction B-25-2.

Le Tableau II montre les résultats obtenus pour l'échantillon B-25 brut et pour quelques unes de ses fractions[3]. La variation de la polydispersité résiduelle pour les fractions successives se superpose très bien aux cas calculés par Tung (7), même si le calcul n'a pas été fait pour le système que nous avons étudié expérimentalement. L'allure générale est tout à fait semblable et confirme le genre de calcul de Tung. Il est intéressant de noter par ailleurs, comme on peut le prévoir théoriquement, qu'à cette concentration de départ pour le fractionnement, 1%, la polydispersité résiduelle dépend fort peu de l'importance de la fraction. Nous avons porté au Tableau II la fraction en poids correspondant à chaque fraction, $c_i/\sum c_i$; on voit que les fractions étudiées sont alternativement fortes et faibles et que la polydispersité résiduelle évolue cependant de façon monotone d'une fraction à l'autre. Par ailleurs la fraction B-25-2, qui représente moins de 2% de l'échantillon de départ, est beaucoup moins monodispersée que la fraction 60-1-D-5 qui est 10 fois plus importante par rapport à l'échantillon de départ. Cet exemple illustre bien l'effet des conditions de fractionnement sur la polydispersité résiduelle des fractions.

Conclusion

Il semble donc, comme on pouvait le prévoir en extrapolant aux basses concentrations les résultats des fractionnements simulés de Tung, qu'on puisse obtenir dans ces conditions des fractions de polydispersité très faible. Ces échantillons permettent d'évaluer le rapport $\langle\overline{S_0^2}\rangle_z/$

[3]Les mêmes fractions B-25 avaient déjà été utilisées dans un travail antérieur (13) et caractérisées dans le toluène. Les différences de masses moléculaires qu'on observera entre le Tableau II du présent mémoire et le Tableau I du mémoire précédent (13) proviennent d'une valeur trop grande utilisée dans (13) pour le dn/dc du polystyrène dans le toluène (J. Prud'homme et Y. Sicotte, a paraître).

Can. J. Chem. Downloaded from www.nrcresearchpress.com by 210.87.254.5 on 09/05/12
For personal use only.

$\overline{M}_p$, pratiquement en absence des effets de polydispersité, ce que nous avons appelé le paramètre C.

Une fois ce paramètre connu, on peut évaluer la polydispersité d'un échantillon quelconque, c'est-à-dire le rapport $\overline{M}_z/\overline{M}_p$, en utilisant seulement les données de diffusion lumineuse en solvant thèta.

Par ailleurs les résultats obtenus pour la série des fractions B-25 confirment les calculs de Tung sur la variation de la polydispersité résiduelle des fractions successives obtenues à partir d'une concentration de départ assez élevée.

Remerciements

Nous tenons à exprimer nos remerciements au Docteur H. W. McCormick et à la maison Dow Chemical pour nous avoir fourni des échantillons de polystyrène.

Nous remercions l'Hydro-Québec pour l'octroi de bourses à l'un de nous (J. P.). Nous remercions également le Conseil National de Recherches du Canada pour l'octroi d'une subvention de recherches (Y. S.) et de bourses (E. A.).

1. H. BENOÎT. J. Polymer Sci. **11**, 507 (1953).
2. C. LOUCHEUX, G. WEILL et H. BENOÎT. J. Chim. Phys. **55**, 540 (1958).
3. B. H. ZIMM. J. Chem. Phys. **16**, 1099 (1948).
4. J. H. BADLEY. J. Polymer Sci. Pt. C, **8**, 305 (1965).
5. P. J. FLORY. Principles of polymer chemistry. Cornell University Press, Ithaca, N.Y. 1953.
6. G. V. SCHULZ et A. DINGLINGER. Z. Physik. Chem. Leipzig, **B43**, 47 (1939).
7. L. H. TUNG. J. Polymer Sci. **61**, 449 (1962).
8. M. PARENT. Thèse de Ph.D. en chimie, Université de Montréal, Montréal, Québec. 1954.
9. J. BRANDRUP et E. W. IMMERGUT. Polymer handbook. Interscience, New York. 1966.
10. Y. SICOTTE et M. RINFRET. Trans. Faraday Soc. **58**, 1090 (1962).
11. J. EHL, C. LOUCHEUX, C. REISS et H. BENOÎT. Makromol. Chem. **75**, 35 (1964).
12. A. GUINIER. Ann. Phys. Paris **12**, 161 (1939).
13. J. PRUD'HOMME et Y. SICOTTE. Can. J. Chem. **42**, 2078 (1964).
14. W. R. KRIGBAUM et D. K. CARPENTER. J. Phys. Chem. **59**, 1166 (1955).
15. G. C. BERRY. J. Chem. Phys. **44**, 4550 (1966).
16. T. A. OROFINO et J. W. MICKEY. J. Chem. Phys. **38**, 2512 (1963).
17. J. M. G. COWIE et S. BYWATER. Polymer, **6**, 197 (1965).
18. D. K. CARPENTER. J. Polymer Sci. Pt. A-2, 4, 923 (1966).

Can. J. Chem. Downloaded from www.nrcresearchpress.com by 210.87.254.5 on 09/05/12
For personal use only.

Can. J. Chem. Downloaded from www.nrcresearchpress.com by 210.87.254.6 on 09/05/12
For personal use only.

Influence des effets inductifs et stériques sur la basicité des amines tertiaires. Détermination et interprétation des ΔH et des ΔS[1]

GUY PERRAULT
Centre Canadien de Recherches et Perfectionnement des Armes, Québec, Québec

Reçu le 26 décembre 1967

Les pK_a d'une série d'amines tertiaires dihydroxylées ont été mesurés dans l'eau à differentes températures afin de calculer des ΔH et les ΔS de la réaction. Les facteurs thermodynamiques semblent confirmer la théorie d'empêchement frontal à la solvatation combinée à une sorte de tension arrière pour expliquer la diminution de basicité introduite par les substituants à longue chaîne carbonée. Pour les substituants à courte chaîne, l'effet de formation de liaisons hydrogènes intramoléculaires peut être noté grâce aux variations du facteur entropique.

ΔH and ΔS were obtained by pK_a measurements in water at different temperatures for a series of dihydroxylated tertiary amines. The thermodynamic factors seem to confirm that the diminution in basicity introduced by long chain substituents is caused by frontal hindrance to solvation, accompanied by a new type of back-strain. With short chain substituents, the formation of intramolecular hydrogen bonds can be seen by the variations of the entropy factor.

Canadian Journal of Chemistry, 46, 2021 (1968)

Introduction

Grâce à une famille d'amines tertiaires dihydroxylées (**1**) dont le chlorhydrate est soluble dans l'eau, il a été confirmé (1) que la relation de Hall (2), reliant la basicité des amines tertiaires aux seuls effets inductifs (σ^*), s'appliquait à tous les produits qui ne comporte pas de substituants à chaîne plus longue que cinq atomes de carbone.

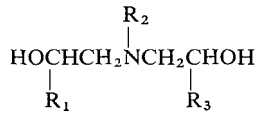

(**1**)

Pour les amines avec un substituant à longue chaîne (6 C et plus), une série d'équations a été déduite pour calculer l'effet stérique (E_s) de ces groupes (1). Ces équations étaient basées sur deux hypothèses. En premier lieu, les longues chaînes diminuaient la basicité des amines en créant de l'empêchement frontal à la solvatation. En second lieu, le degré d'empêchement frontal d'une chaîne de longueur donnée est déterminé par la nature des deux substituants voisins sur l'azote. Cette interaction des substituants sur l'azote a été nommée tension arrière, en comprenant qu'il s'agissait d'une tension arrière qui influencait le nombre de conformations de la chaîne ne provoquant pas d'empêchement frontal.

Afin d'obtenir plus de précision sur les effets stériques impliqués, il a été décidé de déterminer les ΔH et les ΔS de neutralisation.

Partie expérimentale

La synthèse des produits et la technique de mesure des pK_a ont déjà été rapportées (1). La quantité d'acide ajouté au départ a été calculée pour obtenir une force ionique d'environ 0.06 au point stoichiométrique. Les pK_a ont été déterminés dans un bain à température constante. La température de la réaction est déterminée par un thermomètre qui plongeait dans la solution à titrer. Cette température était constante à ± 0.2 °C. Les pK_a sont reproductibles à ± 0.1 et chaque valeur est la moyenne d'au moins deux déterminations. Le Tableau I donne les pK_a mesurés avec la température entre parenthèses.

Les ΔH et les ΔS ont été calculés grâce aux équations usuelles en prenant la meilleur concordance obtenue par la méthode des moindres carrés pour la droite du ln K en fonction de l'inverse de la température absolue ($1/T$). Les valeurs obtenues sont compilées aux Tableaux II et III pour les produits à effets inductifs et aux Tableaux IV et V pour les amines à effets inductifs et stériques.

La précision des ΔH et des ΔS est encore sujette à discussion. Un article récent (3) porte à croire qu'avec la précision sur les pK_a et l'écart de température utilisé, les ΔH devraient être précis à ± 1 kcal/mole et les ΔS à ± 3 cal/deg mole si les erreurs introduites sont dues au hasard au lieu d'être consistantes. Toutefois, la précision des ΔH et des ΔS peut être, jusqu'à un certain point, vérifiée expérimentalement. En effet, les résultats obtenus avec le propyl-N(hydroxy-2 propyl, hydroxy-2 butyl)-amine (cf. Tableaux II et III, C_3H_7 *B*) peuvent être comparés à ceux du propyl-N bis-(hydroxy-2 propyl)-amine (cf. Tableaux II et III, C_3H_7 *E*) vu que la somme des constantes σ^* de ces deux produits est pratiquement égale, soit respectivement 0.19 et 0.205. Or les deux ΔH

[1]Cet article a été présenté en partie au congrès de l'ACFAS en novembre 1967.

TABLEAU I

pK_a des alkyl-N bis-(hydroxy-2 alkyl)amines (**1**)

R_1	R_2	R_3	pK_a (Température, °C)						
C_2H_5	CH_3	C_2H_5	9.0(25),*	8.9(32),	8.65(38),	8.7(42),	8.3(58.5)		
,,	,,	CH_3	8.9(25),	8.5(40),	8.1(58),	8.2(58.5)			
,,	,,	H	8.7(25),	8.2(39),	8.3(40),	8.1(56),	7.9(58)		
CH_3	,,	H	8.7(25),	8.1(39),	8.15(40),	7.8(57),	7.7(58)		
C_2H_5	C_2H_5	C_2H_5	9.2(25),	8.7(39),	8.4(58),	8.2(68)			
,,	,,	CH_3	9.2(25),	8.7(39),	8.3(58)				
,,	,,	H	9.1(25),	8.6(39),	8.2(58)				
CH_3	,,	H	8.9(25),	8.75(31),	8.4(39),	8.45(44.5),	8.1(58)		
C_2H_5	C_3H_7	C_2H_5	9.0(25),	8.7(39),	8.3(58)				
,,	,,	CH_3	9.0(25),	8.6(39),	8.2(58)				
,,	,,	H	9.0(25),	8.5(39),	8.1(58)				
CH_3	,,	H	8.9(25),	8.6(31),	8.4(40),	8.0(58)			
,,	,,	CH_3	8.9(25),	8.4(39),	8.1(58)				
C_2H_5	C_5H_{11}	C_2H_5	9.2(25),	8.7(39),	8.3(58)				
,,	,,	CH_3	9.1(25),	8.6(39),	8.2(58)				
,,	,,	H	9.1(25),	8.6(39),	8.2(58)				
CH_3	,,	H	8.9(25),	8.4(39),	8.0(58)				
C_2H_5	t-C_4H_9	C_2H_5	9.6(25),	9.0(39),	8.5(58)				
,,	,,	CH_3	9.5(25),	8.9(39),	8.4(58)				
,,	,,	H	9.4(25),	8.8(39),	8.3(58),	8.0(68)			
CH_3	,,	H	9.2(25),	9.0(31),	8.8(40),	8.2(58)			
,,	,,	CH_3	9.4(25),	8.8(39),	8.3(58)				
CH_3	$C_6H_5CH_2$	CH_3	7.5(25),	7.2(39),	6.9(58)				
CH_3	CH_2=$CHCH_2$	CH_3	8.2(25),	7.9(39),	7.5(58)				
C_2H_5	C_6H_{13}	C_2H_5	8.6(25),	8.2(39),	7.7(58)				
,,	,,	CH_3	8.9(25),	8.5(39),	8.0(58)				
,,	,,	H	9.0(25),	8.7(39),	8.4(47),	8.1(58)			
CH_3	,,	,,	9.0(25),	8.5(39),	8.1(58)				
C_2H_5	C_8H_{17}	C_2H_5	7.5(25),	7.0(39),	6.6(58),	6.4(68)			
,,	,,	CH_3	7.7(25),	7.65(31),	7.3(39),	7.2(40),	6.95(48),	6.8(58),	6.5(68)
,,	,,	H	8.3(25),	7.8(39),	7.1(58),	6.8(68)			
CH_3	,,	H	7.95(36),	7.8(39),	7.5(58),	7.2(68)			
C_2H_5	$C_{10}H_{21}$	C_2H_5	6.6(25),	6.1(39),	5.6(58),	5.4(68)			
,,	,,	CH_3	6.7(25),	6.4(39),	5.8(58),	5.6(68)			
,,	,,	H	7.2(25),	6.6(39),	6.1(58),	5.8(68)			
CH_3	,,	H	7.5(25),	7.0(39),	6.6(58),	6.5(68)			
C_2H_5	$C_{12}H_{25}$	C_2H_5	5.6(25),	5.3(39),	4.6(58),	4.35(68)			
,,	,,	CH_3	6.2(25),	5.6(39),	5.1(58),	4.8(68)			
,,	,,	H	6.4(25),	6.1(39),	5.7(58)				
CH_3	,,	H	6.5(25),	6.3(39),	5.8(58),	5.6(68)			
C_2H_5	$C_{14}H_{29}$	C_2H_5	5.7(25),	4.9(39),	4.5(58),	4.1(68)			
,,	,,	CH_3	6.1(25),	5.4(39),	4.9(58),	4.4(68)			
,,	,,	H	6.1(25),	6.0(35),	5.85(40),	5.6(48.5),	5.2(58),	4.8(68)	
CH_3	,,	H	6.3(25),	5.6(39),	5.2(58),	4.8(68)			
C_2H_5	$C_{16}H_{33}$	C_2H_5	5.6(25),	5.3(35),	4.95(39),	4.9(48),	4.8(50),	4.4(58)	
,,	$C_{18}H_{37}$	,,	5.6(25),	4.95(39),	4.4(58),				

*Dans l'article précédent, le pK_a n'avait pas été mesuré à température constante ce qui explique certaines modifications dans les valeurs rapportées.

ne diffèrent que par 0.2 kcal/mole et les ΔS, 0.2 cal/deg mole. La même observation peut être faite entre le *t*-butyl-N(hydroxy-2 propyl, hydroxy-2 butyl)amine (cf. Tableaux II et III, t-C_4H_9 *B*) et le *t*-butyl-N bis-(hydroxy-2 propyl)amine (cf. Tableaux II et III, t-C_4H_9 *E*), où la somme des σ^* est respectivement égale à 0.05 et 0.20. Dans ce cas, les deux ΔH sont égaux et les ΔS varient de 0.4 cal/deg mole. Cette concordance entre les valeurs indiquent une bonne précision sur les ΔH et les ΔS.

Résultats et discussion

Amines tertiaires à effets inductifs

En général, pour les amines tertiaires où ne devraient se manifester que des effets inductifs le ΔH a tendance à augmenter à mesure que l'effet inductif négatif des substituants en R_2 est augmenté en gardant R_1 et R_3 constants (cf. Tableau II, σ^* $CH_3 = 0$ jusqu'à σ^* t-C_4H_9 $= -0.300$). Ceci est en accord avec l'explication classique d'une plus grande disponibilité du doublet d'électrons de l'azote à mesure que l'effet inductif devient plus négatif. Un des produits, le méthyl-N (hydroxy-2 éthyl, hydroxy-2 propyl)amine (cf. Tableau II, CH_3 *D*) s'éloigne de façon anormale de la tendance générale, sans

Can. J. Chem. Downloaded from www.nrcresearchpress.com by 210.87.254.6 on 09/05/12
For personal use only.

TABLEAU II

$+\Delta H$ kcal/mole des amines (**1**) à effets inductifs

R_2	*A* $R_1 = C_2H_5$ $R_3 = C_2H_5$	*B* $R_1 = C_2H_5$ $R_3 = CH_3$	*C* $R_1 = C_2H_5$ $R_3 = H$	*D* $R_1 = CH_3$ $R_3 = H$	*E* $R_1 = CH_3$ $R_3 = CH_3$
CH_3	9.8	10.1	9.4	12.6	
C_2H_5	10.3	11.1	12.3	10.8	
C_3H_7	9.6	11.0	12.2	11.8	10.8
C_5H_{11}	12.2	12.2	12.2	12.2	
t-C_4H_9	15.0	15.0	14.7	13.6	15.0
$C_6H_5CH_2$					8.2
$CH_2{=}CHCH_2$					9.6

qu'il y ait d'explication apparente. Tel qu'attendu, les substituants à effet inductif positif (σ^* $C_6H_5CH_2 = 0.22$ et σ^* $CH_2 = CHCH_2 = 0.13$) donnent les ΔH les plus bas.

Les variations de ΔS (Tableau III) sont en général assez faibles. Leur apport à la basicité n'est pas déterminant pour ce groupe de produits. Toutefois, le sens de ces variations est significatif. Il est remarquable que toutes les amines avec un $\Delta H \simeq 12.2$ donnent un $\Delta S \simeq 0$. Toutes les amines qui ont un $\Delta H < 12.2$ ont un $\Delta S < 0$ et toutes celles qui ont un $\Delta H > 12.2$ ont un $\Delta S > 0$.

Si le ΔH est pris comme étant une mesure de la disponibilité du doublet d'électrons tel que suggéré plus haut, il devient possible d'identifier cette valeur de 12.2 kcal/mole comme étant le seuil à partir duquel une liaison hydrogène intramoléculaire commence à se manifester (cf. Fig. 1). Cette liaison hydrogène ralentit le mouvement d'inversion de l'azote dans l'amine tertiaire libre ce qui change l'entropie de l'état fondamental. Lorsque le $\Delta H < 12.2$, le doublet d'électron n'est pas disponible à la liaison hydrogène. L'observation expérimentale indique que dans ce cas, le ΔS est positif rendant l'amine plus basique. Par contre, lorsque le

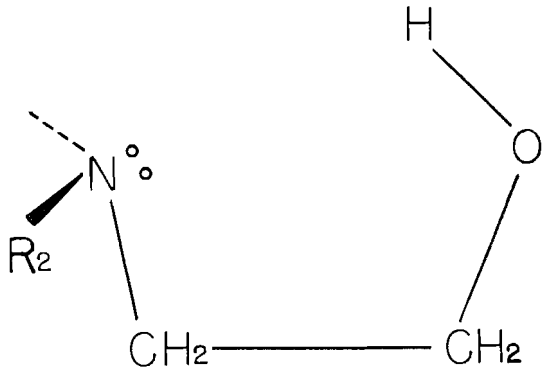

FIG. 1. Liaison hydrogène intramoléculaire.

$\Delta H > 12.2$, le doublet d'électron est assez disponible pour permettre la formation du lien N---H; en perdant de sa mobilité, l'amine devient semblable au chlorohydrate ce qui se manifeste par un ΔS négatif et une légere diminution de basicité.

Mais l'influence de ce facteur, particulier à cette série d'amines, est minime. Il reste que la basicité des amines tertiaires ne comportant pas de substituants à chaîne plus longue que cinq atomes de carbone, est surtout influencé par les effets inductifs.

TABLEAU III

$+\Delta S$ cal/deg mole des amines (**1**) à effets inductifs

R_2	*A* $R_1 = C_2H_5$ $R_3 = C_2H_5$	*B* $R_1 = C_2H_5$ $R_3 = CH_3$	*C* $R_1 = C_2H_5$ $R_3 = H$	*D* $R_1 = CH_3$ $R_3 = H$	*E* $R_1 = CH_3$ $R_3 = CH_3$
CH_3	−8.3	−6.8	−8.0	2.8	
C_2H_5	−7.2	−4.7	−0.4	−4.2	
C_3H_7	−9.0	−4.3	0	0.7	−4.1
C_5H_{11}	0.9	0.4	0.4	0.5	
t-C_4H_9	6.4	6.9	6.5	3.4	7.3
$C_6H_5CH_2$					−6.8
$CH_2{=}CHCH_2$					−5.4

Can. J. Chem. Downloaded from www.nrcresearchpress.com by 210.87.254.6 on 09/05/12
For personal use only.

TABLEAU IV

$+\Delta H$ kcal/mole des amines (1) à effets inductifs et stériques

R_2	Courbe (Fig. 2)	*A* $R_1 = C_2H_5$ $R_3 = C_2H_5$	*B* $R_1 = C_2H_5$ $R_3 = CH_3$	*C* $R_1 = C_2H_5$ $R_3 = H$	*D* $R_1 = CH_3$ $R_3 = H$
C_6H_{13}	1	12.3	12.3	12.5	12.2
C_8H_{17}	2	11.6	13.4	16.3	10.2
$C_{10}H_{21}$	3	12.9	12.3	14.7	10.8
$C_{12}H_{25}$	4	14.0	15.2	9.6	10.0
$C_{14}H_{29}$	5	16.2	17.3	14.5	15.2
$C_{16}H_{33}$		15.4			
$C_{18}H_{37}$		15.4			

Amines tertiaires à effets inductifs et stériques

La clef de l'interprétation des variations de ΔH et de ΔS pour ce groupe d'amines réside dans l'observation des diminutions brusques dans les valeurs. Ainsi, en passant de l'octyl-N(hydroxy-2 éthyl, hydroxy-2 butyl)amine (cf. Tableaux IV et V, C_8H_{17} *C*) à l'octyl-N(hydroxy-2 éthyl, hydroxy-2 propyl)amine (cf. Tableau IV et V, C_8H_{17} *D*), le ΔH passe de -16.3 kcal/mole à -10.2, tandis que le ΔS passe de -16.6 cal/deg mole à $+3.0$. De la même façon, entre le décyl-N(hydroxy-2 éthyl, hydroxy-2 butyl)amine ($C_{10}H_{21}$ *C*) et le décyl-N(hydroxy-2 éthyl, hydroxy-2 propyl)amine ($C_{10}H_{21}$ *D*), le ΔH passe de -14.7 à -10.8 et le ΔS de -16.5 à -2.1. Les même baisses subites se retrouvent respectivement entre le dodécyl-N(hydroxy-2 propyl, hydroxy-2 butyl)amine ($C_{12}H_{25}$ *B*) et le dodécyl-N(hydroxy-2 éthyl, hydroxy-2 butyl)amine ($C_{12}H_{25}$ *C*) de même qu'entre le tétradécyl-N (hydroxy-2 propyl, hydroxy-2 butyl)amine ($C_{14}H_{29}$ *B*) et le tétradécyl-N(hydroxy-2 éthyl, hydroxy-2 butyl)amine ($C_{14}H_{29}$ *C*). De cette façon les amines à effet inductifs et stériques peuvent être séparées en cinq groupes de produits et dans chacun de ces groupes les effets stériques (E_s), tels que calculés grâce aux équations issues des hypothèses de départ, sont du même ordre de grandeur (cf. Tableau VI).

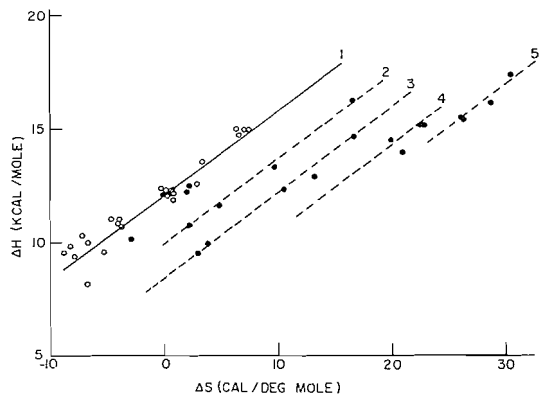

FIG. 2. Relation ΔH vs. ΔS.

De plus, si la relation enthalpie–entropie[2] est tracée, cinq droites parallèles sont obtenues (cf. Fig. 2) qui correspondent aux cinq groupes du Tableau VI. La première courbe se superpose sur celle qui serait obtenue à partir des produits à effets inductifs seulement.

Or quel est l'explication impliquée par une serie de droites enthalpie–entropie parallèles? Tel qu'énoncé par Leffler (3), des lignes parallèles

[2]Si, tel que suggéré par Exner (4), le graphiques des pK_a à 25°C en fonction des pK_a à 58 °C est tracé, une droite est obtenue qui relie tous les produits.

Can. J. Chem. Downloaded from www.nrcresearchpress.com by 210.87.254.6 on 09/05/12
For personal use only.

TABLEAU V

$+\Delta S$ cal/deg mole des amines (**1**) à effets inductifs et stériques

R_2	Courbe (Fig. 2)	*A* $R_1 = C_2H_5$ $R_3 = C_2H_5$	*B* $R_1 = C_2H_5$ $R_3 = CH_3$	*C* $R_1 = C_2H_5$ $R_3 = H$	*D* $R_1 = CH_3$ $R_3 = H$
C_6H_{13}	1	2.0	0.6	2.1	−0.1
C_8H_{17}	2	4.8	9.6	16.6	−3.0
$C_{10}H_{21}$	3	13.2	10.3	16.5	2.1
$C_{12}H_{25}$	4	20.9	22.6	2.9	3.6
$C_{14}H_{29}$	5	28.6	30.4	19.9	22.5
$C_{16}H_{33}$		26.1			
$C_{18}H_{37}$		26.1			

proviennent de différentes valeurs d'un vecteur constant qui caractérise soit un effet de substituant, soit un effet de solvant. Dans le cas présent, cette observation expérimentale s'explique bien par de l'empêchement frontal à la solvatation qui introduit un vecteur entropie–enthalpie constant. Chacun des cinq groupes de produits correspondrait à un état de solvatation donné.

TABLEAU VI

Partage des effets stériques (E_s)

R_2	*A*	*B*	*C*	*D*
C_6H_{13}	0.14	0.07	0.07	0
C_8H_{17}	0.42	0.28	0.21	0.07
$C_{10}H_{21}$	0.70	0.50	0.42	0.28
$C_{12}H_{25}$	0.98	0.84	0.70	0.56
$C_{14}H_{29}$	1.26	1.12	0.98	0.84
$C_{16}H_{33}$	1.26*			
$C_{18}H_{37}$	1.26			

*La somme des E_s a été considérée constante à partir de C_{14} pour la série *A*, dans l'optique de l'empêchement frontal ou il est normal de s'attendre à ce que l'allongement de la chaîne mène à un palier d'effet stérique.

A l'intérieur d'un même groupe, le ΔS positif augmente à mesure que l'empêchement frontal diminue tel qu'attendu. Toutefois, le ΔH augmente indiquant qu'une diminution d'empêchement frontal introduit de l'énergie du point de vue enthalpie entre l'amine et le chlorhydrate.

D'autres phénomènes, tels la formation de liaisons hydrogènes intramoléculaires et l'association des longues chaînes en solution, exercent sûrement une certaine influence sur la diminution de basicité des amines à longue chaîne. Toutefois, avec les mesures d'enthalpie et d'entropie, il apparaît que le degré d'empêchement frontal à la solvatation tel que déterminé par la tension arrière des substituants voisins sur l'azote, tient compte à lui seul des variations des données thermodynamiques.

Remerciements

Tous mes remerciements s'addressent à Mlle M. Talbot et Yves Giguère pour leur assistance technique.

1. G. PERRAULT. Can. J. Chem. **45**, 1063 (1967).
2. H. K. HALL, JR. J. Am. Chem. Soc. **79**, 2570 (1956).
3. J. E. LEFFLER. J. Org. Chem. **31**, 533 (1966).
4. O. EXNER. Nature, **201**, 488 (1964).

Can. J. Chem. Downloaded from www.nrcresearchpress.com by 210.87.254.6 on 09/05/12
For personal use only.

Can. J. Chem. Downloaded from www.nrcresearchpress.com by 210.87.254.42 on 09/05/12
For personal use only.

Accurate heats of atomization and accurate bond lengths. I. Benzenoid hydrocarbons

DONALD H. LO AND M. A. WHITEHEAD
Quantum Chemistry Laboratory, Department of Chemistry, McGill University, Montreal, Quebec

Received October 5, 1967

A semi-empirical P.P.P. type s.c.f.m.o. method has been developed to calculate, with practical accuracy, heats of atomization (at 25 °C), bond lengths, and resonance energies of benzenoid hydrocarbons. Sigma bond energies $E_{\sigma b}$ are estimated simultaneously with the pi bond energies $E_{\pi b}$ in this method. Self-consistent field bond lengths are obtained, by minimization of the total bond energy, $E_{\sigma b} + E_{\pi b}$, with respect to each individual bond length. The empirical resonance energies are calculated and a new term, the stabilization energy per CC bond, is introduced.

Canadian Journal of Chemistry, 46, 2027 (1968)

(I) Introduction

Although the P.P.P.–s.c.f.–m.o. (Pople–Pariser–Parr – self-consistent field – molecular orbital) theory of pi electron systems (1, 2) has been successfully applied to the prediction of transition energies (2, 3), comparatively little work has been done either in the realm of chemical reactivity or on ground state properties of conjugated systems. Traditionally, complete sigma and pi separation has been assumed, and the sigma electrons have been treated as if they were an inert core of non-polarizable electrons. A set of semi-empirical parameters for the Hamiltonian matrix elements have generally been adopted, so as to fit each particular chemical problem (4, 5). It is difficult to find one general set that can predict all chemical properties. Many of these semi-empirical parameters, such as the *resonance integral* (β_{ij}) and the *two center repulsion integral* (γ_{ij}), depend arbitrarily on a convenient function form (3, 6) rather than on a sound theoretical basis. Therefore a comparative study of the different parameters has been carried out, and both the pi and sigma bond energies have been considered simultaneously on a variable geometry basis.

The heats of atomization (at 25 °C) of the benzenoid hydrocarbons have been calculated, with the *CC sigma bond energy* taken into consideration *explicitly* for *each* bond. Bond lengths have been estimated by minimizing the total electronic energy. The empirical resonance energy and the newly established *stabilization energy per CC bond* have been calculated without any additional (5) auxiliary assumptions.

(II) Thermochemistry

The experimental heat of combustion (ΔH_c) data permit the empirical calculation of the heats of atomization (ΔH_a). The standard energies (7) shown in Table I have been used, in which C_aH_b represents a conjugated hydrocarbon. Equation [1] represents the heat of combustion reaction, and eqs. [2] through [5] represent the standard energy reactions. The heat of atomization is given by eq. [7]:

$$[7]\quad \Delta H_a = [a(264.944) + b(86.2607) - \Delta H_c] \pm [(\Delta H_c) \times 0.0002 + a(0.4608) + b(0.0648)] \text{ kcal/mole.}$$

The heat of combustion is the change in heat content per mole, when the compound reacts with oxygen in its standard state to form gaseous CO_2 (at 1 atm) and liquid water at 25 °C. The "best" experimental measurement of ΔH_c, using the bomb calorimeter technique, has an uncertainty of $\pm 0.02\%$ (8). Equation [7] therefore generates the *minimum* uncertainty in the measurements. The heat of atomization is the heat content change necessary to dissociate the isolated gaseous molecule into isolated gaseous atoms in their ground state.

(III) Theory

(A) Theoretical Approach to ΔH_a

Using Pople's (1) s.c.f. pi theory, diagonal F_{ii} and off-diagonal F_{ij} Hamiltonian matrix elements are systematically simplified to the following:

$$[8]\quad F_{ii} = W_{Pi} + \tfrac{1}{2}q_i\gamma_{ii} + \sum_{j(\neq i)} (q_j - 1)\gamma_{ij}$$

and

$$[9]\quad F_{ij} = \beta_{ij} - \tfrac{1}{2}P_{ij}\gamma_{ij},$$

where W_{Pi} is the core integral, q_i is the charge,

TABLE I

Heat of combustion (ΔH_c), standard energies, and heat of atomization (ΔH_a) reactions and energies

	Reaction	Heat content change (kcal/mole)	Error
[1]	$C_aH_b(gas) + (a + \frac{1}{4}b)O_2(gas) \rightarrow aCO_2(gas) + \frac{1}{2}bH_2O(gas)$	$-\lvert\Delta H_c\rvert$*	$\pm 0.02\%$
[2]	$aCO_2(gas) \rightarrow aC(graphite) + aO_2(gas)$	$a(94.054)$†	$\pm a(0.0108)$†
[3]	$aC(graphite) \rightarrow aC(gas)$	$a(170.89)$†	$\pm a(0.45)$†
[4]	$\frac{1}{2}bH_2O(gas) \rightarrow \frac{1}{2}bH_2(gas) + \frac{1}{4}bO_2(gas)$	$b(34.1587)$†	$\pm b(0.0048)$†
[5]	$\frac{1}{2}bH_2(gas) \rightarrow bH(gas)$	$b(52.102)$†	$\pm b(0.06)$†
	Overall		
[6]	$C_aH_b(gas) \rightarrow aC(gas) + bH(gas)$ (at 1 atm and 25 °C)	ΔH_a	

*Reference 37.
†Reference 7.

and P_{ij} is the bond order. The total pi bond energy is given by

$$[10]\quad E_{\pi b} = -\left\{ \sum_i \frac{q_i^2}{4}\gamma_{ii} + 2\sum_{i<j} P_{ij}\beta_{ij} + \sum_{i<j}[(q_i - 1)(q_j - 1) - \tfrac{1}{2}P_{ij}^2]\gamma_{ij} \right\}.$$

If the total sigma bond energy $E_{\sigma b}$ can be represented by a sum of all individual sigma bond energies, $\sum_k E_k^{CC}$, then the heat of atomization of a conjugated hydrocarbon, ΔH_a (25 °C), is the sum of three independent contributions,

$$[11]\quad \Delta H_a\ (25\ °C) = E_{\pi b} + E_{\sigma b} + N^{CH}E^{CH},$$

where E^{CH} is the CH bond energy and N^{CH} is the number of CH bonds.

These various parameters will be discussed in (*B*). Since more thermochemical data are available for comparison at 25 °C, ΔH_a (25 °C) is used instead of ΔH_a (0 °K) in this work. It is assumed that vibrational energy is an additive property, which can be transferred from molecule to molecule.

(B) Parameters

(1) The q_i and P_{ij} are respectively the relative measures of the pi electron distribution on the atom and in the bond. The W_{Pi} ($\equiv \int \phi_i^*(1) H^{0\,core} \phi_i(1)\, d\tau_1$) represents the kinetic and potential energies of an electron in an atomic orbital ϕ_i of the core. Semi-empirically, this is the negative of the valence state ionization potential.

The

$$\gamma_{ii}\left(\equiv \int \phi_i^*(1)\phi_i(1)\frac{e^2}{R_{12}}\phi_i^*(2)\phi_i(2)\, d\tau_1\, d\tau_2\right)$$

is the electrostatic repulsion energy between two electrons, both distributed within the same atomic orbital ϕ_i. The neglect of electronic correlation causes the direct theoretical evaluation of γ_{ii}, using, for example, a Slater 2p atomic orbital ($\gamma_{ii} = 5.324 \times Z^*$ (9), where Z^* is the effective nuclear charge) to give a much higher value than that estimated semi-empirically from the difference between valence state ionization potential and electron affinity (10). The semi-empirical estimation will be followed, using Hinze and Jaffe's (11) valence state energies. For carbon (tr tr tr π), the semi-empirical value for W_{Pi} is -11.16 eV and for γ_{ii} is 11.134 eV.

(2) The

$$\gamma_{ij}\left(\equiv \int \phi_i^*(1)\phi_i(1)\frac{e^2}{R_{12}}\phi_j^*(2)\phi_j(2)\, d\tau_1\, d\tau_2\right)$$

represents the two center repulsion integral.

(a) Theoretical γ_{ij}—Explicit formulas have been devised by Roothaan (9) for the theoretical evaluation of γ_{ij}, using Slater-type atomic orbitals, with arbitrary effective nuclear charge Z^*, which can be estimated using the classical Slater's rule (12). However, new rules for determining Z^* have been developed by Clementi and Raimondi (13), who optimized the orbital exponent of an atomic orbital to give minimum energy, by Burns (14), who compared the moments $\langle R^q \rangle$ of Slater-type atomic orbitals to previously calculated Hartree–Fock wave functions, and by Paoloni (15), who used the analytical relation $\gamma_{ii} = 5.324\, Z^*$ and the semi-empirical value for γ_{ii} to develop a parallel set of Z^* values. These values for a carbon 2p atomic orbital are:

Can. J. Chem. Downloaded from www.nrcresearchpress.com by 210.87.254.42 on 09/05/12
For personal use only.

Z^*, the effective nuclear charge for carbon 2p atomic orbital

Slater's rule (12)	Clementi and Raimondi (13)	Burns (14)	Paoloni (15)
3.25	3.0887	2.65	2.052

Using Roothaan's formula (9) together with these Z^*, different sets of γ_{ij} are evaluated as a function of distance. Their functional dependences are illustrated in Fig. 1.

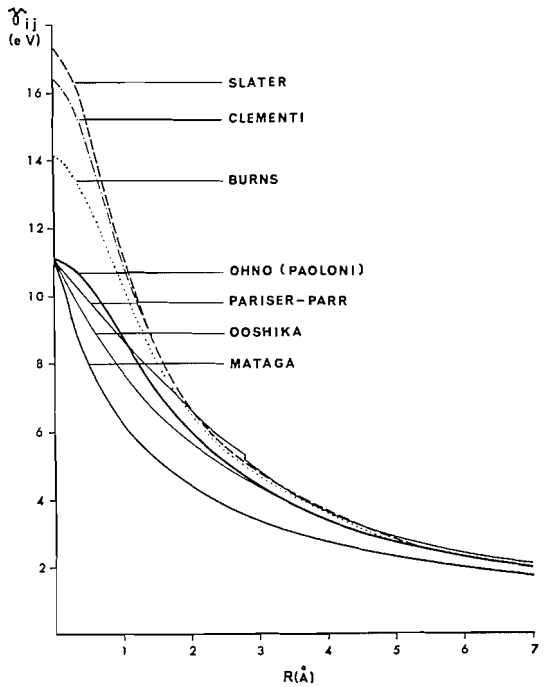

FIG. 1. Theoretical and semi-empirical γ_{ij} evaluated as a function of R_{ij}.

(b) Semi-empirical γ_{ij}—Several simple but arbitrary relations are in the literature (16–18). They all satisfy two basic conditions: when $R_{ij} \rightarrow \infty$, then $\gamma_{ij} \rightarrow 0$, and when $R_{ij} \rightarrow 0$, then $\gamma_{ij} \rightarrow \gamma_{ii}$. However, there are no further restrictions on their functional behavior at intermediate distances, and it is especially necessary to know how the functions behave at bond distances and nearby. Consequently, it is difficult to justify any of these different approximate forms. Several of the current semi-empirical schemes are shown below.

[12] $\gamma_{ij} = 1/(R_{ij}^2 + a^2)^{1/2}$ Ohno (16)

[13] $\gamma_{ij} = [1 - \exp(-aR_{ij})]/R_{ij}$ Ooshika (17)

[14] $\gamma_{ij} = 1/[R_{ij} + a]$ Mataga and Nishimoto (18)

Pariser and Parr (2) use a uniform charged sphere (u.c.s.) model to approximate the effect of electrostatic repulsion γ_{ij} when $R_{ij} > 2.8$ Å, but when $R_{ij} \leq 2.8$ Å, an adjusted polynomial with two parameters A and B is employed.

[15] $\gamma_{ij} = a + AR_{ij} + BR_{ij}^2$ Pariser and Parr (2)

Lorquet (19) follows the same line of argument and develops a modified form:

[16] $\gamma_{ij} = a + CR_{ij}^2 + DR_{ij}^3$ Lorquet (19).

In all these cases, the parameter "a" is adjusted so that in the limit as R_{ij} approaches zero, γ_{ij} approaches γ_{ii}, the one center repulsion energy.

As a further extension of the u.c.s. model, Dewar *et al.* (5) propose a split-p-orbital (s.p.o.) method, where two pi electrons may exert significantly different electrostatic repulsions, if they are located with respect to each other in different lobes from the nodal plane. To some extent, this is expected to take into consideration the effect of electronic correlation.

The first four semi-empirical relations are shown in Fig. 1 together with the theoretical relations.

As shown in Fig. 1, the semi-empirical values of γ_{ij} are, in general, lower than the theoretical estimates. However, when $R_{ij} > 3.0$ Å, all the forms, except Mataga, approximately converge. It is interesting to note that the theoretical γ_{ij} line, using Paoloni's Z^*, coincides exactly with the line of Ohno's formulation. Paoloni's Z^* is semi-empirically adjusted at $R_{ij} = 0$, and "if" this Z^* value is equally valid for regions where $R_{ij} > 0$, this coincidence may be taken as a verification of Ohno's semi-empirical form. Mataga and Nishimoto's and Ooshika's γ_{ij}'s are much lower in magnitude. Pariser and Parr's γ_{ij} are slightly higher than even the theoretical γ_{ij} when $R_{ij} > 3.0$ Å, and there is a discontinuity of about 0.14 eV at $R_{ij} = 2.8$ Å, due to the two approximations used at this point.

Can. J. Chem. Downloaded from www.nrcresearchpress.com by 210.87.254.42 on 09/05/12
For personal use only.

Can. J. Chem. Downloaded from www.nrcresearchpress.com by 210.87.254.42 on 09/05/12
For personal use only.

Because of the coincidence of Paoloni's theoretical curve and Ohno's semi-empirical curve, Ohno's γ_{ij} have been used in this work.

(3) The final parameters to be considered are β_{ij} ($\equiv \int \phi_i^*(1) H^{0\ \mathrm{core}} \phi_j(1)\ d\tau_1$), the resonance integral, and $E_{\sigma b}{}^{CC}$, the CC sigma bond energy.

In calculating atomization energies, a widely accepted scheme for evaluating β_{ij} is that due to Dewar *et al.* (5), which is based on a hypothetical thermocycle:

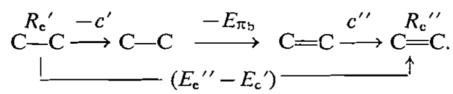

R_e', R_e'', E_e', and E_e'' are the equilibrium bond lengths and bond energies of CC single and double bonds respectively. c' and c'' are compression energies involved in the two processes, and evaluated using a Morse potential function. $E_{\pi b}$ is the pi bond energy given by eq. [10], in which the only unknown is β_{ij}. However, despite the theoretical beauty of the thermocycle, a critical and highly controversial point is the "*valid*" properties of a single sigma C(sp^2)—C(sp^2) bond. Since R_e', E_e', and k_e' (the force constant) are all purely hypothetical estimates associated with this bond, the validity of β_{ij}, derived in this manner, is open to question. For example, Lorquet (19) uses 1.517 Å for R_e' and 92.19 kcal/mole for E_e' (0 °K), while Dewar *et al.* (5) adopt 1.485 Å for R_e' and 96.674 kcal/mole for E_e' (25 °C). The logic behind this scheme is completely obscure, when this thermocycle is applied to a bond C—X, where X contributes *two* pi electrons (20). First, it is difficult to visualize the formal meaning of an equilibrium double bond between C and X, and secondly, it is difficult to associate any valid physical properties with this bond.

Consequently, it was necessary to develop a completely different scheme, in which all the input parameters are based on experimental observables.

The bond energy $E_b{}^{C=C}$ of "a" C=C bond is partitioned into pi and sigma bond energies as follows.

$$[17]\quad E_b{}^{C=C}(R_{ij}) = E_{\pi b}(R_{ij}) + E_{\sigma b}(R_{ij})$$

By assuming that the CH bond energy at 25 °C is a constant property, that is E(C—H) = 102.13 kcal/mole (5), then from the experimental ΔH_a (25 °C) values for ethylene and benzene, the *equilibrium* bond energies $E_e{}^{C=C}$ for both compounds can be determined. The dependence of $E_b{}^{C=C}$ on distance R_{ij} in ethylene and benzene can be expressed by a Morse potential function, in which the k_e (the force constant) and the R_e (the equilibrium bond length) are experimentally determined.

Hence,

$$[18]\quad E_b{}^{C=C}(R_{ij}) = E_e{}^{C=C}[2\exp\{-a(R_{ij}-R_e)\} - \exp\{-2a(R_{ij}-R_e)\}],$$

for which the experimental parameters are:

	E(CH) (kcal/mole)	$E_e{}^{C=C}$ (kcal/mole)	R_e (Å)	k_e (21) (dyn/cm)	$a = [k_e/(2E_e{}^{C=C})]^{1/2}$ (Å^{-1})
Ethylene	102.13	129.172	1.334 (22)	9.57×10^5	2.309
Benzene	102.13	117.558	1.397 (23)	7.50×10^5	2.142

Therefore, the total pi bond energy, according to eq. [10], in which the density matrix elements q_i and P_{ij} are predetermined by symmetry in these compounds, reduces to

$$[19]\quad E_{\pi b}{}^{\mathrm{ethylene}} = -\left[\frac{1}{2}\gamma_{11} + 2\beta - \frac{1}{2}\gamma_{12}\right]$$

C^1=C^2

and

$$[20]\quad E_{\pi b}{}^{\mathrm{benzene}} = \frac{1}{6}[E_{\pi b}{}^{\mathrm{benzene}}\ (\mathrm{total})]$$

$$= -\left[\frac{1}{4}\gamma_{11} + \frac{4}{3}\beta - \frac{2}{9}\gamma_{12} - \frac{1}{36}\gamma_{14}\right]$$

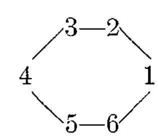

in the case of ethylene and benzene respectively.

Substituting eqs. [19] and [18] into [17] for ethylene, and eqs. [20] and [18] into [17] for benzene, the following expressions are obtained

Can. J. Chem. Downloaded from www.nrcresearchpress.com by 210.87.254.42 on 09/05/12
For personal use only.

for $\beta_{ij}(R_{ij})$ and $E_b(R_{ij})$, as all other parameters are previously determined.

$$[21]\quad \beta_{ij}(R_{ij}) = \frac{3}{2}\Big[-(E_b{}^{C=C}(R_{ij})_{ethylene} - E_b{}^{C=C}(R_{ij})_{benzene} - \frac{1}{4}\gamma_{11} + \frac{5}{18}\gamma_{12} - \frac{1}{36}\gamma_{14}\Big]$$

and

$$[22]\quad E_{\sigma b}(R_{ij}) = \frac{1}{2}\Big[E_b{}^{C=C}(R_{ij})_{ethylene} + E_b{}^{C=C}(R_{ij})_{benzene} + \frac{3}{4}\gamma_{11} + \frac{10}{3}\beta_{ij}(R_{ij}) - \frac{13}{18}\gamma_{12} - \frac{1}{36}\gamma_{14}\Big]$$

Their functional dependences on distances are shown in Fig. 2 for β_{ij} and in Fig. 3 for $E_{\sigma b}(R_{ij})$ against R_{ij}. Of special importance is the maximum in Fig. 3, the plot of $E_{\sigma b}(R_{ij})$ vs. R_{ij}. This establishes, without any auxiliary assumptions or any extrapolations, that the *equilibrium single bond distance* between *two trigonally* hybridized carbons is *1.505 Å*.

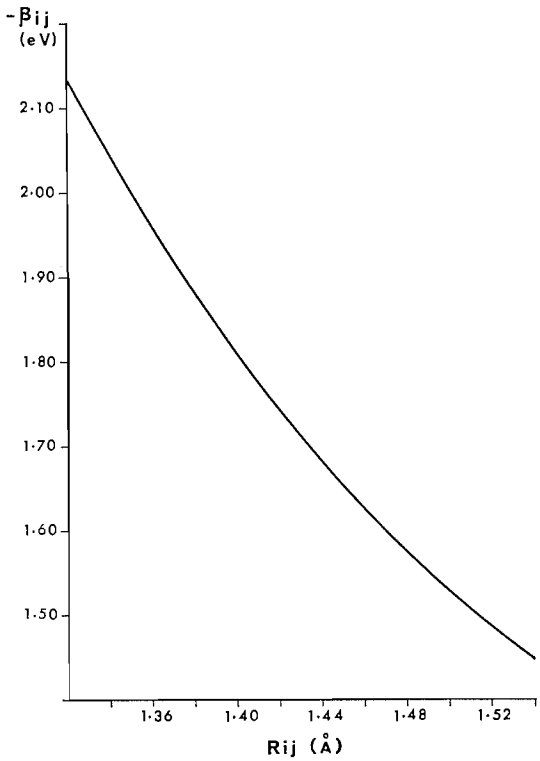

FIG. 2. The resonance integral β_{ij} evaluated as a function of R_{ij}.

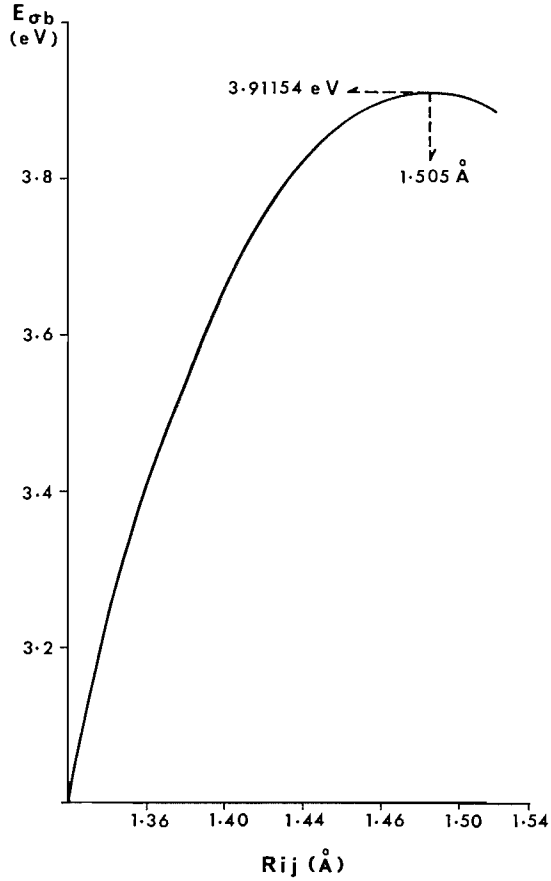

FIG. 3. A plot of the sigma bond energy $E_{\sigma b}$ of a C=C bond against interatomic separation R_{ij}.

The present theory is of fundamental value because it is based entirely on experimental observables. The only limitation on its validity lies in the partitioning of energies, and the use of the Morse potential function, but they are both known to be extremely satisfactory approximations (24, 25).

(c) The S.C.F. Bond Lengths R_{ij}—The pi bond order is generally used (26) as a relative measure of the pi electron distribution between atoms in a molecule. By minimizing the total electronic energy of a molecule with respect to R_{ij}, using the molecular orbital theory, it can be shown that there is a direct relation between P_{ij} and R_{ij} (26); the variation of bond length is attributed to the delocalization of the pi electrons.

Can. J. Chem. Downloaded from www.nrcresearchpress.com by 210.87.254.42 on 09/05/12
For personal use only.

Many linear relationships (5, 27, 30) between P_{ij} and R_{ij} have been suggested, as typified by

$$[23] \qquad R_{ij} = 1.504 - 0.166\,P_{ij},$$

due to Dewar and Gleicher (5), and

$$[24] \qquad R_{ij} = 1.517 - 0.18\,P_{ij},$$

due to Coulson and Golebiewski (27).

These approaches depend upon the arbitrary selection of several molecules, such as benzene, ethylene, and graphite, as fixed points on the calibration line. Unfortunately, the bond distances calculated for molecules other than the calibration molecules show a wide scatter from such calibration lines.

An alternate approach is to directly minimize the total energy with respect to *each* bond length R_{ij} in a molecule for a given P_{ij} for the bond. Although P_{ij} is an explicit function of R_{ij}, the exact form of this function is unknown, consequently the pi bond order has been considered to be a molecular property, where $\partial P_{ij}/\partial R_{ij} = 0$.

With the total bond energy given by eq. [11], a second minimization of the total energy can be performed with respect to R_{ij} (the first minimization (28) is that involving the coefficients of the atomic orbitals in the variation method, used to establish eqs. [8] and [9]):

$$[25] \qquad \frac{\partial E_b\ (\text{total})}{\partial R_{ij}} = \frac{\partial E_{\pi b}}{\partial R_{ij}} + \frac{\partial E_{\sigma b}}{\partial R_{ij}} = 0.$$

Furthermore,

$$[26] \qquad \frac{\partial E_{\pi b}}{\partial R_{ij}} = -\left[2P_{ij}\frac{\partial \beta_{ij}}{\partial R_{ij}} + \{(q_i - 1)(q_j - 1) - \tfrac{1}{2}P_{ij}^{\,2}\}\frac{\partial \gamma_{ij}}{\partial R_{ij}}\right].$$

Using Ohno's version of γ_{ij}, and two third degree polynomial fits to the established relations for β_{ij} and $E_{\sigma b}$ respectively, then

$$[27] \qquad \frac{\partial \gamma_{ij}}{\partial R_{ij}} = -\frac{R_{ij}}{[R_{ij}^{\,2} + a]^{3/2}}$$

$$[28] \qquad \frac{\partial \beta_{ij}}{\partial R_{ij}} = 41.199202 - 40.241434R_{ij} + 9.494283R_{ij}^{\,2}$$

and

$$[29] \qquad \frac{\partial E_{\sigma b}}{\partial R_{ij}} = 367.63581 - 452.66920R_{ij} + 138.46111R_{ij}^{\,2}.$$

(d) Method of Calculation—In all the conjugated molecules considered, an arbitrary planar geometry with standard bond lengths of 1.400 Å is initially assumed to start the calculation. A simple Huckel m.o. treatment is performed on the pi electrons in a molecule to give the q_i and P_{ij}'s which are used as input data, together with the assumed geometry for the s.c.f. program of eqs. [8] and [9]. A new density matrix is generated, and subsequently *new bond lengths*, corresponding to the modified P_{ij}'s, are obtained from eq. [25], by using a numerical method (regula-falsi). The roots R_{ij} of eq. [25] are obtained to a tolerance of 10^{-5}. With the *new* R_{ij}'s, new neighboring γ_{ij}, β_{ij}, and $E_{\sigma b}$ are generated. These modified parameters are then used as input for the second iteration of the s.c.f. program. In general, 5 or 6 iterations suffice to give self-consistency.

The final results for R_{ij} and ΔH_a, corresponding to the real molecule, are found to be insensitive to the input geometry of the molecule. Numerical computations are programmed in Fortran IV, and executed by an IBM 7044 computer at the McGill Computing Centre.

(e) Resonance Energy—The single and double bond energies of a CC bond are now known. The double bond energy is from the experimental results for ethylene,

$$[30] \quad E(\text{C=C}) = 5.6033 \text{ eV at } R = 1.334 \text{ Å (eq. [18] parameters),}$$

and the single bond energy from Fig. 3:

$$[31] \quad E(\text{C—C}) = 3.91154 \text{ eV at } R = 1.505 \text{ Å.}$$

With these quantities known, the total sigma and pi bond energies can be determined, corresponding to the most stable reference valence-bond structure, while in the s.c.f. procedure the total bond energy is calculated, corresponding to the *real* molecule. Hence, it can easily be estimated that the empirical resonance energy (ERE) is

$$[32] \quad \text{ERE} = (E_{\sigma b}^{\,\text{tot}} + E_{\pi b}^{\,\text{tot}})_{\text{calcd}} - N_{C=C}E(\text{C=C}) - N_{C-C}E(\text{C—C}),$$

where $N_{C=C}$ and N_{C-C} are the number of isolated double and single bonds in the reference valence-bond structure. Physically, ERE is a measure of the stability difference between a *real* molecule and a most stable hypothetical reference structure. As the number of pi electrons

Can. J. Chem. Downloaded from www.nrcresearchpress.com by 210.87.254.42 on 09/05/12
For personal use only.

increases in these systems, the total resonance energy generally exhibits a parallel increase. Consequently, it is difficult to carry out a "sensitive" comparison between different classes of conjugated hydrocarbons, using these ERE quantities. Therefore, a new term, the *stabilization energy per CC bond* (*SECC*) is introduced and defined by

[33] SECC = ERE/total number of CC bonds in the molecule.

The introduction of the SECC common basis permits the analysis of the energies with respect to the type of molecule and its degree of aromaticity.

The Huckel m.o. theory stabilization energy *per pi electron* has been previously established (29), in a similar way to the newly defined SECC. The Huckel m.o. method is a purely pi electron theory, the sigma bonds being treated as a nonpolarizable core, which is assumed not to have any effect on the pi bond energy. Hence, it is not logical to use a term corresponding to the SECC in the Huckel m.o. theory stabilization energy, since all the bonds of a molecule are *not* explicitly considered.

In the s.c.f. method used in this paper, the total resonance energy is dependent on both the pi delocalization and the sigma bond compression. Consequently, all the CC bonds, whether formally single or double bonds, are involved in generating the total resonance energy, and an "average" measure of the stabilization of the real molecule relative to the hypothetical localized structure will be given by the SECC. The stabilization per pi electron would not be a good measure since the number of pi electrons does *not* always equal the number of CC bonds. An example of this discrepancy occurs in hexatriene (C_6H_8) and fulvene (C_6H_6), both of which have six pi electrons, but five and six CC bonds respectively. The SECC is therefore a more illustrative term than the stabilization energy per pi electron.

Although the concept of aromaticity is traditionally connected with definite patterns of chemical reactivity, the ERE and SECC are purely ground state properties, characteristic of an isolated molecule in an ideal gaseous state; nevertheless, qualitative patterns of reactivity are discussed in terms of these quantities and the s.c.f. bond lengths.

The thermochemical ERE are not considered, because they usually suffer from the defect of using the same bond energies for a CC, or CH bond, no matter what the hybridization state of the carbon atom may be. Further, these thermochemical ERE values include many different effects which are specifically excluded in the theoretical treatment, such as changes in hybridization, nonbonded interactions, ring strain, etc. The theoretical treatment only considers the significance of pi electron delocalization and sigma bond compressions, and the validity of the ERE and SECC can only be judged by comparing their values with experimental ground state measurements, such as bond length, total energy, ionization potential, and dipole moments. The SECC can then be used as a measure of the stability of the ground state, and this is related to the chemical reactivity of the molecule; it is *not* a direct measure of the reactivity (31).

(IV) Results and Discussions

(A) ΔH_a *and* R_{ij}

The calculated heats of atomization for benzenoid hydrocarbons are well in accord with the available experimental data, Table II. The difference between the ΔH_a calculated and observed, δ, Table II, is within the experimental uncertainties in eq. [7]. In cases where severe steric hindrance occurs, due to substantial nonbonded H,H van der Waal's interactions, nonplanarity is imposed on the systems, as in 3,4-benzphenanthrene (**6**) (32), yet agreement between the calculated and the experimental ΔH_a is still within the limits of experimental accuracy. This suggests that a planar configuration may be a satisfactory description of the actual state of the molecule.

In these molecules, the total sigma bond energy, $E_{\sigma b}$, is two to three times as large as the pi bond counter part, $E_{\pi b}$ (Table II, $E_{\sigma b}$ and $E_{\pi b}$ columns), thus justifying the use of a variable sigma bond energy in the work.

By minimizing the total energy E_b (eq. [25]) at 25 °C, bond lengths are obtained which are averaged over the vibrational motions of the nuclei and which are *not* the equilibrium distances between two nuclei in a hypothetical vibrationless state. The s.c.f. bond lengths, Table III, are compared with experimental bond lengths, whenever possible, and also with Dewar

TABLE II

Values of the heats of atomization (25 °C) and resonance energies (in eV)

Compound		Code	$E_{\pi b}$	$E_{\sigma b}$	ΔH_a Calcd.	ΔH_a Obsd.*	ΔH_a δ	Resonance energy Total	Resonance energy SECC
C_6H_6	Benzene	**1**	8.624	21.971	57.177	57.178	−0.001	2.050	0.3417
$C_{10}H_8$	Naphthalene	**2**	14.600	40.576	90.618	90.653	−0.035	3.690	0.3355
$C_{14}H_{10}$	Anthracene	**3**	20.422	59.178	123.902	124.050	−0.148	5.173	0.3233
$C_{14}H_{10}$	Phenanthrene	**4**	20.783	59.164	124.250	124.354	−0.104	5.520	0.3450
$C_{16}H_{10}$	Pyrene	**5**	23.886	70.456	138.644	138.855	−0.211	6.489	0.3415
$C_{18}H_{12}$	3,4-Benzphenanthrene	**6**	26.877	77.767	157.807	157.534	+0.273	7.276	0.3465
$C_{18}H_{12}$	1,2-Benzanthracene	**7**	26.716	77.734	157.612	157.651	−0.039	7.082	0.3372
$C_{18}H_{12}$	Chrysene	**8**	26.869	77.774	157.805	157.824	−0.019	7.275	0.3464
$C_{18}H_{12}$	Naphthacene	**9**	26.161	77.791	157.114	157.615	−0.501	6.584	0.3135
$C_{18}H_{12}$	Triphenylene	**10**	26.971	77.843	157.977	157.885	+0.092	7.446	0.3546
$C_{20}H_{12}$	Perylene	**11**	29.877	89.134	172.173	172.100	+0.073	8.216	0.3423
$C_{22}H_{12}$	1,12-Benzperylene	**12**	33.345	100.404	186.911			9.528	0.3529
$C_{22}H_{12}$	Anthanthrene	**13**	32.951	100.326	186.440			9.056	0.3354
$C_{22}H_{14}$	Pentacene	**14**	31.766	96.477	190.266			7.934	0.3051
$C_{22}H_{14}$	Picene	**15**	32.983	96.382	191.388			9.056	0.3483
$C_{22}H_{14}$	1,2;5,6-Dibenzanthracene	**16**	32.867	96.376	191.267			8.934	0.3436
$C_{22}H_{14}$	1,2;3,4-Dibenzanthracene	**17**	32.909	96.446	191.378			9.046	0.3479
$C_{22}H_{14}$	Pentaphene	**18**	32.674	96.310	191.007			8.675	0.3336
$C_{24}H_{12}$	Coronene	**19**	36.604	111.743	201.510			10.700	0.3566
$C_{24}H_{12}$	1,2;6,7-Dibenzopyrene	**20**	36.335	107.796	206.154			10.395	0.3584
$C_{24}H_{14}$	Zethene	**21**	35.537	107.654	205.215			9.455	0.3260
$C_{26}H_{16}$	Hexacene	**22**	37.322	115.183	223.389			9.254	0.2985
$C_{30}H_{18}$	1,2;3,4;5,6;7,8-Tetrabenzo-anthracene	**23**	45.294	133.725	258.764			12.827	0.3563
$C_{32}H_{14}$	Ovalene	**24**	49.061	152.938	264.022			14.558	0.3551

*Obtained from Table I.

and Gleicher's calculated bond lengths (5). These are given for nine benzenoids in Table III.

In Dewar and Gleicher's calculations (5), the two center repulsion integrals are formulated by the split-p-orbital method, and bond lengths are estimated from the linear relation $R_{ij} = 1.504 - 0.166P_{ij}$. The split-p-orbital method is believed to compensate for the effect of correlation, and the linear relationship between R_{ij} and P_{ij} has been widely used in many s.c.f. or Huckel calculations of bond lengths (26, 29). It is of interest to compare the significance and accuracy of the results from the present procedure with those from experiment and s.p.o. calculations.

Because of the systematic errors in diffraction data (33), which result in undetermined inaccuracies of the individual bond length in a molecule, it was necessary to carry out root mean square (r.m.s.) tests for *all* bond lengths of a molecule between the experimental and various different calculated values. In nearly all cases, Table III, the s.c.f. bond distances predicted by the minimization of the total electronic energy are well within the experimental error, and they prove to be more satisfactory than the s.p.o. values.

*(B) Linear Polyacenes (Benzene (**1**), Naphthalene (**2**), Anthracene (**3**), Naphthacene (**9**), Pentacene (**14**), Hexacene (**22**))*

The s.c.f. bond lengths estimated for this set of molecules are in excellent agreement with experiment, especially for the first three molecules, whose experimental results are most accurately known. In naphthalene (**2**), the r.m.s. values of the experimental bond lengths obtained from electron diffraction technique, and between these experimental bond lengths and those predicted by s.p.o. calculations and this work (l.w.), are respectively ε: .00925, s.p.o.: .01319, and l.w.: .00682, Table III. The corresponding r.m.s. values from X-ray data are X: .006, s.p.o.: .01207, and l.w.: .0096. In anthracene (**3**), the respective r.m.s. values are X: .008, s.p.o.: .01414, and l.w.: .00648, Table III. In all these cases, the lower magnitudes of the r.m.s. of this work compared with s.p.o. calculations illustrate that, in the prediction of bond lengths, the

Can. J. Chem. Downloaded from www.nrcresearchpress.com by 210.87.254.42 on 09/05/12
For personal use only.

Can. J. Chem. Downloaded from www.nrcresearchpress.com by 210.87.254.42 on 09/05/12
For personal use only.

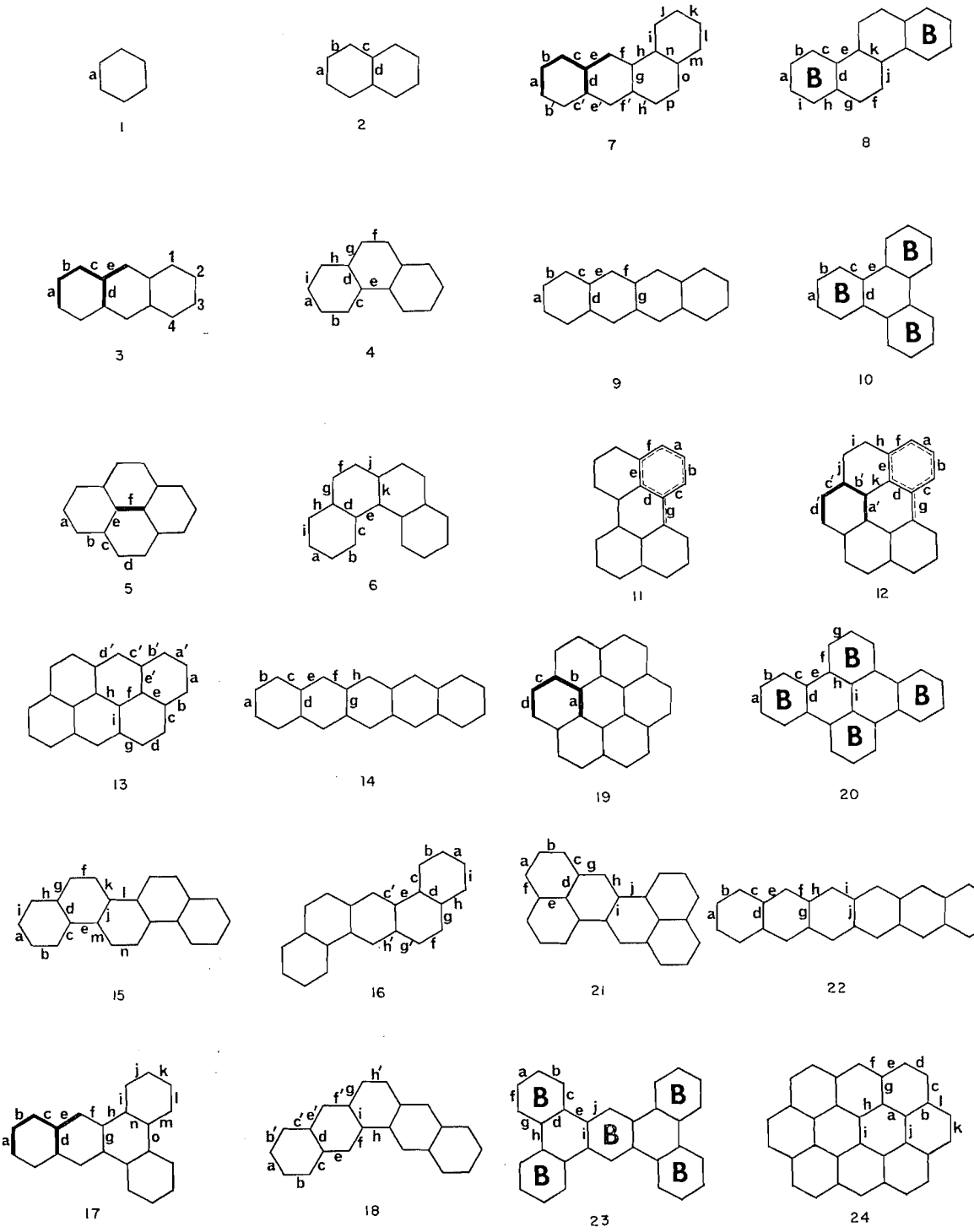

FIG. 4. Geometries of the benzenoid hydrocarbons.

Can. J. Chem. Downloaded from www.nrcresearchpress.com by 210.87.254.42 on 09/05/12
For personal use only.

TABLE III*

Bond lengths (Å) and r.m.s. of the benzenoid hydrocarbons

Compound		R_{ij} (Å)											
		a	*b*	*c*	*d*	*e*	*f*	*g*	*h*	*i*	*j*	*k*	r.m.s.
1	R (23)	1.397											.001
	l.w.	1.400											.003
2	X (38)	1.415	1.364	1.421	1.418								.006
	ε (39)	1.412	1.371	1.422	1.420								.00925
	s.p.o.	1.422	1.369	1.426	1.396								X .01207
													ε .01319
	l.w.	1.419	1.382	1.426	1.420								X .00960
													ε .00682
3	X (33)	1.418	1.375	1.444	1.433	1.405							.008
	ε (39)	1.419	1.390	1.420	1.425	1.404							
	s.p.o.	1.432	1.362	1.437	1.409	1.402							X .01414
													ε .01752
	l.w.	1.428	1.374	1.436	1.427	1.408							X .00648
													ε .01107
4	X (35)	1.398	1.383	1.405	1.404	1.448	1.372	1.390	1.457	1.381			.0155
	s.p.o.	1.410	1 378	1.413	1.394	1.447	1.356	1.445	1.413	1.378			.0248
	l.w.	1.414	1.388	1.418	1.412	1.448	1.365	1.443	1.419	1.387			.0232
5	X (40)	1 380	1.420	1.442	1.320	1.417	1.417						.0179
	s.p.o.	1 393	1.398	1.449	1.354	1.406	1.438						.0201
	l.w.	1 399	1.409	1.446	1.363	1.421	1.434						.0210
6	X (32)	1.409	1.378	1.433	1.431	1.446	1.342	1.443	1.391	1.374	1.430	1 412	.0210
	s.p.o.	1.415	1.375	1.417	1.394	1.439	1.361	1.438	1 418	1.374	1.436	1 382	.0185
	l.w.	1 416	1.385	1.421	1.414	1.441	1.370	1.438	1.422	1.385	1.437	1 402	.0154
7	l.w.	1.428	1.375	1.434	1.421	1.417	1.396	1.427	1.455	1.415	1.390	1.412	
			(*b'*)1.375	(*c'*)1.434		(*e'*)1.417	(*f'*)1.397		(*h'*)1.451				
								(*l*)1 389	(*m*)1 416	(*n*)1.409	(*o*)1.450	(*p*)1.359	
8	X (41)	1.394	1.381	1 409	1.409	1.468	1.369	1.421	1.428	1.363	1 428	1.401	.0150
	s.p.o.	1.415	1 375	1.418	1.394	1.439	1.361	1.437	1.418	1.374	1.436	1.383	.0152
	l.w.	1.416	1.385	1.421	1.414	1.442	1.371	1.438	1.422	1.385	1.435	1.402	.0141
9	X (42)	1 479	1.385	1 431	1.439	1.398	1.409	1.475					.0280
	s.p.o.	1 440	1.358	1.445	1.422	1.385	1.415	1.413					.0311
	l.w.	1.434	1.369	1.442	1.432	1.400	1.419	1.432					.0247
10	X (43)	1.402	1.377	1.416	1.415	1.447							.0108
	s.p.o.	1.402	1.384	1.405	1.396	1.455							.0109
	l.w.	1.408	1.393	1.412	1.410	1.456							.0091

Can. J. Chem. Downloaded from www.nrcresearchpress.com by 210.87.254.42 on 09/05/12
For personal use only.

TABLE III* (*Concluded*)

Compound			R_{IJ} (Å)											r.m.s.
			a	*b*	*c*	*d*	*e*	*f*	*g*	*h*	*i*	*j*	*k*	
11	X	(44)	1.370	1.418	1.397	1.425	1.424	1.400	1.471					.0180
	s.p.o.		1.371	1.419	1.375	1.426	1.397	1.425	1.462					.0166
	l.w.		1.383	1.417	1.391	1.429	1.418	1.427	1.461					.0125
12	l.w.		1.392	1.408	1.399	1.423	1.417	1.417	1.458	1.441	1.368	1.439	1.437	
			(*a'*)1.431	(*b'*)1.411	(*c'*)1.426	(*d'*)1.380								
13	l.w.		1.409	1.399	1.453	1.357	1.426	1.428	1.453	1.413	1.437			
			(*a'*)1.390	(*b'*)1.420	(*c'*)1.430	(*d'*)1.386	(*e'*)1.422							
14	X	(45)	1.441	1.358	1.428	1.453	1.381	1.409	1.464	1.396				.0420
	l.w.		1.435	1.368	1.443	1.434	1.397	1.424	1.436	1.411				.0166
15	l.w.		1.415	1.386	1.420	1.413	1.444	1.369	1.440	1.421	1.386	1.406	1.437	
			(*l*)1.435	(*m*)1.429	(*n*)1.378									
16	l.w.		1.412	1.389	1.416	1.411	1.451	1.363	1.446	1.417	1.389	1.421		
					(*c'*)1.405				(*g'*)1.446	(*h'*)1.407				
17	l.w.		1.423	1.378	1.430	1.420	1.422	1.392	1.428	1.451	1.410	1.395	1.407	
			(*l*)1.394	(*m*)1.410	(*n*)1.410	(*o*)1.459								
18	l.w.		1.426	1.376	1.433	1.419	1.420	1.393	1.455	1.458	1.427			
				(*b'*)1.376	(*c'*)1.433		(*e'*)1.420	(*f'*)1.394		(*h'*)1.356				
19	ε	(39)	1.438	1.381	1.444	1.362								.0135
	l.w.		1.431	1.416	1.430	1.377								.0206
20	l.w.		1.408	1.393	1.411	1.410	1.457	1.406	1.400	1.416	1.447			
21	l.w.		1.385	1.414	1.396	1.430	1.418	1.426	1.453	1.368	1.457	1.461		
22	l.w.		1.436	1.368	1.443	1.435	1.396	1.425	1.438	1.408	1.416	1.439		
23	l.w.		1.408	1.394	1.411	1.410	1.457	1.394	1.411	1.457	1.416	1.405		
24	X	(46)	1.426	1.416	1.433	1.345	1.441	1.404	1.435	1.428	1.461	1.442	1.383	
	l.w.		1.434	1.414	1.440	1.367	1.442	1.408	1.424	1.419	1.441	1.429	1.383	
	X		(*l*)1.403											
	l.w.		(*l*)1.423											.0122

*Experimental bond lengths obtained from (X) X-ray diffraction, (ε) electron diffraction, (R) Raman spectroscopy; s.p.o.: s.c.f. bond lengths calculated by $R_{IJ} = 1.504 - 0.166\ P_{IJ}$; γ_{IJ} by split-p-orbital method, ref. 5; l.w.: this work.

present treatment is more satisfactory than the s.p.o. method.

In these systems the SECC decrease with increase in ring size, whereas there is an increase in the average[1] calculated CC bond lengths, Fig. 5. The "calculated" bond length averages are used, and not the "experimental" bond length averages, because experimental data are not available for hexacene. The averages of the known "experimental" CC bond lengths, Table III, in this series of molecules also show this increase (**1**, 1.400 Å; **2**, 1.460 Å; **3**, 1.412 Å; etc.) with increased ring size. Thus pi electron delocalization is less favorable in an elongated linear polyacene.

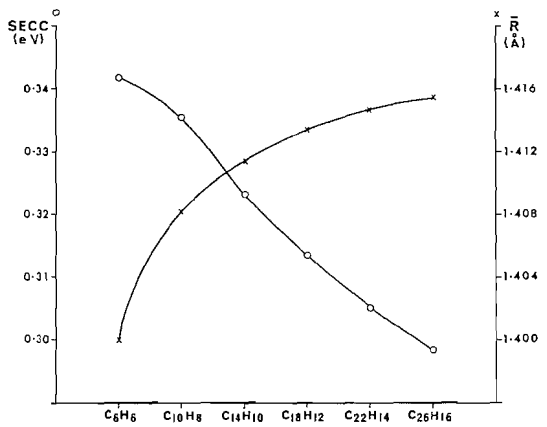

FIG. 5. Plot of the stabilization energy per CC bond, SECC, and the calculated bond length averages, $\bar{R}$, as a function of ring size n of linear polyacenes.

In these compounds, the number of pi electrons satisfies Huckel's $4n + 2$ rule (29), where $n = 1, \ldots 6$. Dewar and Gleicher (5) have shown that the total resonance energy of the monocyclic polyenes, with $4n + 2$ pi electrons, decreases with the increase in n. If the periphery bonds of these linear polyacenes are treated as if they were monocyclic polyenes, slightly perturbed by the bridging bonds, then the decrease of SECC in the linear polyacenes parallels the decrease in total resonance energy of the monocyclic polyenes.

The bridge linkages, bond *d*, in these linear polyacenes (Fig. 4, Table III) are quite long: 1.420 Å (**2**), 1.427 Å (**3**), 1.432 Å (**9**), 1.434 Å (**14**), and 1.435 (**22**); they therefore increase in length as the number of joined rings increases. The same trend occurs for bonds *g*. Thus, as the ring size increases linearly, the central bridge CC bonds tend to elongate, so that the linear polyacene increasingly resembles a compressed monocyclic ring. In the peripheral CC bonds, bond *b* is always shorter (1.37 Å), Table III, and bond alternations always occur, becoming more pronounced as the ring size increases.

(C) Clar and Zander's Benzenoids

Clar and Zander (34) noted that many benzenoids appear to be composed of unperturbed benzene nuclei, linked together by psuedo single CC bonds. Three of these, triphenylene (**10**), 1,2;6,7-dibenzopyrene (**20**), and 1,2;3,4;5,6;7,8-tetrabenzoanthracene (**23**), have been examined.

On a simple resonance model, pi electron delocalization would be expected to occur over the whole molecule. Chemical evidence (34) of their unusually low reactivities, such as their inertness to attack by sulfuric acid, and their very small spectral shifts towards violet, similar to biphenyl, strongly suggest that isolated pi electron ring sextets occur, as in biphenyl, preferentially to a symmetrical distribution of pi electrons over the whole molecule. The calculated bond lengths for the bonds in these benzene "islands", marked "B" in **10**, **20**, and **22**, Fig. 4, are all approximately 1.4 Å (bonds *a*, *b*, *c*, *d*, *g*, and *f* in Table III for these compounds). The interbenzene linkages, such as bond *e*, are long, about 1.457 Å. Thus the calculations are in good agreement with Clar and Zander's empirical deductions. Moreover, the SECC are comparatively high, which reflects their relative inertness. In the case of triphenylene (**10**) the calculated bond lengths are well within the experimental X-ray measurement accuracy.

(D) Other Benzenoidal Rings

In Phenanthrene (**4**), the calculated s.c.f. bond lengths are more satisfactory than those previously calculated by the s.p.o. method; for bonds *g* and *h* (Table III), while there is an improvement, there is still a major discrepancy with X-ray data. The calculations predict $g = 1.443$ Å and $h = 1.419$ Å, respectively lower and higher than the s.p.o. results, but X-ray measurements give $g = 1.390$ Å and $h = 1.457$ Å. None of extant m.o. methods (5, 35) can correctly

[1]The average calculated or experimental CC bond length $\bar{R}$ is obtained by $\bar{R} = \sum R_{ij}$(all CC bonds)/total number of CC bonds in a molecule.

Can. J. Chem. Downloaded from www.nrcresearchpress.com by 210.87.254.42 on 09/05/12
For personal use only.

Can. J. Chem. Downloaded from www.nrcresearchpress.com by 210.87.254.42 on 09/05/12
For personal use only.

predict *g* and *h* relative to each other, let alone individually; whether this is because *g* and *h* are in fact interchanged in the X-ray analysis or because the gaseous state free molecule calculations cannot account for the solid state situation remains to be seen. It seems, however, that in the free molecule *g* and *h* will be 1.443 Å and 1.419 Å respectively. In pyrene (**5**), the experimental bond length for the peripheral bond *d* is very short, 1.320 Å, Table III, which is even shorter than the experimental bond length of ethylene, 1.334 Å. The s.c.f. value for *d* is distinctly shorter than all other bonds with a value of 1.363 Å but is nowhere near the 1.320 Å experimental measurement. Thus, since there is no inherent reason within the present theory for such a discrepancy, and since it does not seem possible that a double bond can be shorter than an ethylenic bond and still stable, it appears the experimental measurement is in error, or that crystallographic effects are peculiar.

Extensions of Huckel's $4n + 2$ rule to polycyclic aromatics have been attempted (36) by decomposing a whole molecule into constituent structural units. The linkages between these units are treated as mild perturbations to the whole system. For example, pyrene (**5**) ($C_{16}H_{10}$) can be considered as a peripheral C_{14} ring, with an isolated C_2 unit inside, connected by bridge linkages, *e*, both of which satisfy the $4n + 2$ condition.

Perylene (**11**) ($C_{20}H_{12}$) can be analyzed in terms of two C_{10} naphthalene-like components (36), connected by bridge linkages, *g*.

An analysis of the predicted s.c.f. structures is helpful in considering the validity of such an approach. In pyrene (**5**), bond *e* is 1.421 Å and bond *f* is 1.434 Å, Table III, which is not only indicative of C_{14} and C_2 separation, but also shows that *f* has less double bond character than *e*.

However, in perylene (**11**), such a decomposition of the molecule is satisfactory: thus bonds *a* to *f* in **11** compared with *a* to *d* in **2**, Fig. 4 (dark lines in **11** and **2**), show that the distances (Table III) in the C_{10} unit are very similar to those in a free naphthalene molecule. Bonds *c* and *d* are slightly modified, because of the inter-naphthalene linkage *g*, but bonds *a*, *b*, *e*, *f* are basically unperturbed, and show the free naphthalene bond lengths. Bond *g* is found to be 1.461 Å, which is much longer than the benzenoidal 1.400 Å, but still shorter than the single bond value of 1.505 Å. Thus some pi bond delocalization occurs across *g*.

Fused rings such as coronene (**19**) and ovalene (**24**) usually possess higher SECC values than benzene, and increase in the series perylene (**11**), 0.3423 eV; 1,12-benzperylene (**12**), 0.3529 eV; and coronene (**19**), 0.3566 eV (Table II). **12** demonstrates some properties intermediate between those displayed by **11** and **19**. Thus the lengths of bond *a'* to *d'* in **12** are very similar to the corresponding coronene bond lengths *a* to *d* in **19**, Table III, while the bond lengths *a* to *g* in **12** are similar to those of *a* to *g* in perylene **11** (follow dark lines in **11**, **12**, and **19**, Fig. 4, for comparison).

The pattern of the bond lengths for bonds *a* to *e* between anthracene (**3**), 1,2-benzanthracene (**7**), and 1,2;3,4-dibenzanthracene (**27**) are very similar, showing that the additional ring fusions at the 1,2 and 3,4 (Fig. 4) positions do not cause the bond lengths at the other extreme of the molecule to differ from those present in the anthracene molecule with no such ring fusion.

Chrysene (**8**) can be pictured as a quasi-molecule of 1,6-diphenylhexatriene from the calculated bond lengths, Table III; bonds *f* and *k* are short, while bond *e* is comparatively long; nevertheless, the benzene rings marked "B" have significant bond alternations.

Conclusion

The success of the present method in predicting the heats of atomization and bond lengths of the benzenoids indicates that it can be applied to other classes of conjugated hydrocarbons. Moreover, because of the reliability of the predicted s.c.f. bond lengths, it is possible to make detailed structural analyses of many new sets of molecules. Results on non-benzenoid hydrocarbons are given in Part II of this series.

1. J. A. POPLE. Trans. Faraday Soc. **49**, 1375 (1953).
2. R. PARISER and R. G. PARR. J. Chem. Phys. **21**, 466, 767 (1953).
3. J. E. BLOOR, B. R. GILSON, and N. BREARLEY. Theoret. Chim. Acta, **8**, 35 (1967).
4. K. NISHIMOTO and L. S. FORSTER. Theoret. Chim. Acta, **3**, 407 (1965).
5. A. L. H. CHUNG and M. J. S. DEWAR. J. Chem. Phys. **42**, 756 (1965). M. J. S. DEWAR and G. J. GLEICHER. J. Am. Chem. Soc. **87**, 685 (1965).
6. K. OHNO. Advan. Quantum Chem. **3**, 239 (1967).
7. JANAF INTERIM THERMOCHEMICAL TABLES. The Dow Chemical Company, Midland, Michigan. December 31, 1960.

8. T. L. COTTRELL. The strengths of chemical bonds. Butterworths Scientific Publications, London. 1958.
9. C. C. J. ROOTHAAN. J. Chem. Phys. **19**, 1445 (1951).
10. R. PARISER. J. Chem. Phys. **21**, 568 (1953).
11. J. HINZE and H. H. JAFFE. J. Am. Chem. Soc. **84**, 540 (1962).
12. J. C. SLATER. Phys. Rev. **36**, 57 (1930).
13. E. CLEMENTI and D. L. RAIMONDI. J. Chem. Phys. **38**, 2686 (1963).
14. G. BURNS. J. CHEM. Phys. **41**, 1521 (1964).
15. L. PAOLONI. Nuovo Cimento, **4**, 410 (1956).
16. K. OHNO. Theoret. Chim. Acta, **2**, 219 (1964).
17. Y. OOSHIKA. J. Phys. Soc. Japan, **12**, 1246 (1957).
18. N. MATAGA and K. NISHIMOTO. Z. Physik. Chem. Frankfurt, **13**, 140 (1957).
19. A. J. LORQUET. Theoret. Chim. Acta, **5**, 192 (1966).
20. M. J. S. DEWAR and G. J. GLEICHER. J. Chem. Phys. **44**, 759 (1966).
21. G. HERZBERG. Molecular spectra and molecular structure. Vol. II. D. Van Nostrand Co. Inc., New York. 1945.
22. L. S. BARTELL and R. A. BONHAM. J. Chem. Phys. **27**, 1414 (1957). B. P. STOICHEFF. Current Sci. India, **27**, 1 (1958).
23. B. P. STOICHEFF. Can. J. Phys. **32**, 339 (1954).
24. P. G. LYKOS and R. G. PARR. J. Chem. Phys. **24**, 1166 (1956).
25. C. A. COULSON and W. T. DIXON. Tetrahedron, **17**, 215 (1962).
26. L. SALEM. Molecular orbital theory of conjugated systems. W. A. Benjamin Inc., New York. 1966.
27. C. A. COULSON and A. GOLEBIEWSKI. Proc. Phys. Soc. London, **78**, 1310 (1961).
28. C. C. J. ROOTHAAN. Rev. Mod. Phys. **23**, 69 (1951).
29. A. STREITWIESER. Molecular orbital theory. John Wiley & Sons, New York. 1961.
30. G. V. BOYD and N. SINGER. Tetrahedron, **22**, 3383 (1966).
31. D. P. CRAIG. *In* Non-benzenoid aromatic compounds. *Edited by* D. Ginsburg. Interscience Publishers, New York. 1959.
32. F. L. HIRSHFELD, S. SANDLER, and G. M. J. SCHMIDT. J. Chem. Soc. 2108 (1963).
33. R. MASON. Acta Cryst. **17**, 547 (1964).
34. E. CLAR and M. ZANDER. J. Chem. Soc. 1861 (1958).
35. J. TROTTER. Acta Cryst. **16**, 605 (1963).
36. D. PETERS. J. Chem. Soc. 1023 (1958).
37. G. W. WHELAND. Resonance in organic chemistry. John Wiley & Sons Inc., New York. 1955.
38. D. W. J. CRUICKSHANK and R. A. SPARKS. Proc. Roy. Soc. London, Ser. A, **258**, 270 (1960).
39. O. BASTIANSEN and P. N. SKANCKE. Advan. Chem. Phys. **3**, 323 (1961).
40. A. CAMERMAN and J. TROTTER. Acta Cryst. **18**, 636 (1965).
41. D. M. BURNS and J. IBALL. Proc. Roy. Soc. London, Ser. A, **257**, 491 (1960).
42. J. ROBERTSON, V. C. SINCLAIR, and J. TROTTER. Acta Cryst. **14**, 697 (1961).
43. F. R. AHMED and J. TROTTER. Acta Cryst. **16**, 503 (1963).
44. A. CAMERMAN and J. TROTTER. Proc. Roy. Soc. London, Ser. A, **279**, 129 (1964).
45. R. B. CAMPBELL, J. M. ROBERTSON, and J. TROTTER. Acta Cryst. **14**, 705 (1961).
46. A. J. BUZEMAN. Proc. Phys. Soc. London, **A63**, 827 (1950).

Can. J. Chem. Downloaded from www.nrcresearchpress.com by 210.87.254.42 on 09/05/12
For personal use only.

Can. J. Chem. Downloaded from www.nrcresearchpress.com by 210.87.254.105 on 09/05/12
For personal use only.

Accurate heats of atomization and accurate bond lengths. II. Polyenes and polyphenyls

DONALD H. LO AND M. A. WHITEHEAD
Quantum Chemistry Laboratory, Department of Chemistry, McGill University, Montreal, Quebec

Received October 26, 1967

Accurate heats of atomization and bond lengths are calculated for several polyenes and polyphenyls, using the s.c.f.–l.c.a.o.–m.o. method described in Part I (1). Localization of π and σ bonds is found in the linear polyenes and in the diphenyl-substituted polyenes. The estimated stabilization energy per CC bond (SECC) gives a direct measure of the π electron conjugation and σ bond compression. Conjugation stabilization and steric hindrance are analyzed in 1,3-butadiene and biphenyl; the predicted geometries are in good agreement with experimental results. The minimum energy for any planar structure is found to be associated with the s.c.f. calculated bond lengths. The validity of pi bond order as a measure of molecular stability in the polyphenyls is discussed.

Canadian Journal of Chemistry, **46**, 2041 (1968)

(I) Introduction

In the pi theory of conjugated systems (2, 3), the sigma electrons are either treated as a non-polarizable core, or else some average property is adopted, such as the CC sigma bond energy, from which a collective property such as the total sigma bond energy can be deduced. While the pi theory (3) is successful in predicting heats of atomization, and bond lengths of benzenoid hydrocarbons, it is less satisfactory when applied to other classes of conjugated hydrocarbons, since averaging the sigma property is invalid unless all the bonds are of approximately the same length.

The simultaneous treatment of pi and sigma bond energies in a semi-empirical s.c.f.–l.c.a.o.–m.o. method was developed in Part I, in order to improve the calculation of the heats of atomization and bond lengths of the benzenoid hydrocarbons, and is now extended to the polyenes and polyphenyls.

Theoretical Method

Pople's original s.c.f.–l.c.a.o.–m.o. method (2) is extended by the following modifications (1):

(i) The core integrals and the one center repulsion integrals are estimated from valence state energies (4).

(ii) The two center repulsion integrals are expressed by Ohno's functional form (5).

(iii) The resonance integrals and the CC sigma bond energies are estimated from thermochemical data (6) together with the experimental force constants and bond lengths of ethylene and benzene (7–9).

The s.c.f. bond lengths are calculated by a direct minimization of the total electronic energy, with respect to each bond length. The heat of atomization ΔH_a of the real molecule is

$$[1] \qquad \Delta H_a = E_{\pi b} + E_{\sigma b} + N_{CH}E_{CH},$$

where $E_{\pi b}$, the total pi bond energy, is estimated by the s.c.f.–l.c.a.o.–m.o. method; $E_{\sigma b}$, the total sigma bond energy, is the sum of all the individual CC sigma bond energies, corresponding to the respective s.c.f. bond lengths; N_{CH} is the number of CH bonds and E_{CH} is the CH bond energy.

The stabilization energy per CC bond (SECC) is evaluated by dividing the calculated empirical resonance energy (ERE) by the total number of CC bonds present in the system. This SECC is an average property, characteristic of the specific molecule.

Results and Discussion[1]

The calculated values for ΔH_a at 25 °C, ERE, and SECC for the polyenes and vinyl compounds are tabulated in Table I, and the corresponding bond lengths in Table II; the results for the polyphenyls are in Tables III and IV. Experimental data are also shown in these tables and the accuracy of the calculation examined. The trends are discussed in terms of the importance of conjugation, internal rotation, localization of π and σ bonds, and modification of the molecular geometry by phenyl substitution.

[1]Molecules **1** to **24** (benzenoids) are contained in Part I (1).

Can. J. Chem. Downloaded from www.nrcresearchpress.com by 210.87.254.105 on 09/05/12
For personal use only.

(II) Polyenes and Vinyl Compounds

1,3-Butadiene **26** is shown by electron-diffraction measurements to be planar and to exist 99% in the *trans* conformation at room temperature (12). The bond lengths R_{12} and R_{23} in this molecule reflect the significance of conjugation throughout the molecule. The s.c.f. bond lengths calculated by the present minimization procedure are more accurate than those obtained from the conventional linear relation between bond length and pi bond order (3, 11), the bond lengths R_{23} and R_{12} being herein 1.470 and 1.338 Å compared with 1.465 and 1.344 Å in ref. 10 and 1.483 and 1.337 Å from experimental measurements (12). However, the central pi bond order P_{23} is 0.2534, which is within the extreme values of P_{23}, 0.23 and 0.28, calculated by conventional m.o. methods (14); the Huckel m.o. value of 0.447 for P_{23} is much higher.

The effect of hybridization, π electron delocalization, σ bond compression, steric hindrance due to H—H interaction, hyperconjugation, and non-bonded electrostatic repulsion on the overall stability and the equilibrium geometry of the molecule has been critically investigated by Dewar and Schmeising (15) and Mulliken (14). The first four effects are considered in this work.

The carbon atoms are assumed to be trigonally (sp^2) hybridized, and no variation of geometry is attributed to this effect. The combined effects of π electron delocalization and σ bond compression to the stability of a molecule is illustrated by the ERE of *cis*- and *trans*-1,3-butadiene. The reference structure used to determine the ERE is a *trans* structure with bond (R_{12}) at 90° to the molecular plane. The geometry is $R_{12} = R_{34} = 1.334$ Å and $R_{23} = 1.505$ Å, corresponding to the equilibrium CC double and single bonds respectively (1). The *cis* structure with ERE equal to 0.404 eV is the more stable form since the *trans* structure ERE is 0.370 eV (Table I). This result contradicts experiment.

The effect of steric hindrance, which causes internal rotation about the central bond, is included by using Bartell's intramolecular potentials (16) for the interaction through space of the H and C atoms. The van der Waal's interaction energies, corresponding to molecular conformations of 0, 90, and 180° twist angles have been calculated by Fisher-Hjalmars (17) using Bartell's potentials. These values were used for 1,3-butadiene. The combined effect of π electron delocalization, σ bond compression, and van der Waal's interaction in 1,3-butadiene gives total stabilization energies of 0.361, 0.028, and 0.163 eV for twist angles of 0, 90, and 180° respectively. Thus, *trans*-1,3-butadiene is the most stable conformation, the difference in energy between the *cis* and the *trans* conformations being 0.198 eV. Further discussion on internal rotation will be given in Section (III) for biphenyl.

It is interesting to note that the calculated ΔH_a is 42.069 eV for a strain-free model which is higher than the experimental ΔH_a of 42.052 eV by +0.017 eV. Since the van der Waal's repulsion energy, calculated using Bartell's intramolecular potential, is +0.009 eV (17) and since steric hindrance destabilizes the total bond energy, then the remaining error in ΔH_a calculated is only +0.008 eV.

The series of linear polyenes will be considered next with respect to the increase in chain length N. The length of the double bond at the center of these chains (1.331 Å, **25**; 1.338 Å, **26**; 1.347 Å, **29**; 1.348 Å, **30**; and 1.350 Å, **31**) shows that there is a definite increase in conjugation as the chain length increases. The SECC increases in the same direction (0.0 eV, **25**; 0.1233 eV, **26**; 0.1512 eV, **29**; 0.1637 eV, **30**; 0.1706 eV, **31**).

In the diphenyl-substituted linear polyenes (e.g. stilbene **40**, etc.), the central double bond lengths (1.348 Å, **40**; 1.349 Å, **42**; 1.350 Å, **43**; 1.349 Å, **44**; and 1.350 Å, **45**) are essentially constant and, moreover, as the bridge CC chain lengthens, the SECC gradually decreases (0.3257 eV, **40**; 0.3103 eV, **42**; 0.2983 eV, **43**; 0.2884 eV, **44**; and 0.2803 eV, **45**). The terminal benzene rings become less effective in stabilizing the linear polyene unit in these molecules, when the bridge chain lengthens. To illustrate this point, the SECC over the polyene unit[2] are derived, treating the benzene rings as isolated units. The SECC (linear polyene unit) are 0.262 eV, **40**; 0.235 eV, **42**; 0.223 eV, **43**; 0.217 eV, **44**; and 0.213 eV, **45**.

Dewar and Gleicher (13) showed that the bond energies for these classical polyenes are additive, when the pi bond contribution is

[2]SECC (linear polyene unit) = $[(E_{\pi b} + E_{\sigma b}) - (2E_{CC}^{benzene} - N''_{CC}E'' - N'_{CC}E')]/[N'_{CC} + N''_{CC}]$, where $E'' = 5.603$ eV (the ethylenic double bond energy, Table I) and $E' = 3.911$ eV (the equilibrium single bond energy (1)). Other symbols are defined in the text.

TABLE I

The heats of atomization (eV) and resonance energies (eV) for polyenes and vinyl compounds

Compound		Code	$E_{\pi b}$	$E_{\sigma b}$	ΔH_a Calcd.	ΔH_a Obsd. (1)	ΔH_a δ	ERE	SECC
C_2H_4	Ethylene	**25**	2.464	3.139	23.324	23.324	0	0	0
C_4H_6	1,3-Butadiene (*trans*)	**26**	5.182	10.306	42.069	42.052	+0.017	0.370	0.1233
C_4H_6	1,3-Butadiene (*cis*)	**27**	5.192	10.330	42.103			0.404	0.1346
C_6H_8	2-Vinylbutadiene	**28**	7.903	17.492	60.836			0.762	0.1524
C_6H_8	Hexatriene	**29**	7.895	17.494	60.831			0.756	0.1512
C_8H_{10}	Octatetraene	**30**	10.622	24.672	79.596			1.146	0.1637
$C_{10}H_{12}$	Decapentaene	**31**	13.330	31.868	98.361			1.535	0.1706
C_8H_8	Styrene	**32**	11.379	29.113	75.934	75.896	+0.038	2.433	0.3041
$C_{10}H_{10}$	*o*-Divinylbenzene	**33**	14.133	36.264	94.699			2.823	0.2823
$C_{10}H_{10}$	*m*-Divinylbenzene	**34**	14.134	36.255	94.691			2.815	0.2815
$C_{10}H_{10}$	*p*-Divinylbenzene	**35**	14.133	36.259	94.694			2.818	0.2818
$C_{12}H_{12}$	1,3,5-Trivinylbenzene	**36**	16.889	43.396	113.448			3.196	0.2663
$C_{10}H_{10}$	2-Phenylbutadiene	**37**	14.095	36.272	94.669			2.793	0.2793
$C_{12}H_{12}$	8,8-Divinylstyrene	**38**	16.845	43.477	113.484			3.233	0.2694
$C_{14}H_{12}$	1,1-Diphenylethylene	**39**	20.298	55.072	128.534			4.855	0.3236
$C_{14}H_{12}$	Stilbene	**40**	20.313	55.088	128.563	128.523	+0.040	4.885	0.3257
$C_{22}H_{18}$	Bis-triphenylene	**41**	31.997	88.218	199.959			7.728	0.3220
$C_{16}H_{14}$	1,4-Diphenylbutadiene	**42**	23.037	62.269	147.329			5.276	0.3103
$C_{18}H_{16}$	1,6-Diphenylhexatriene	**43**	25.748	69.463	166.094			5.666	0.2982
$C_{20}H_{18}$	1,8-Diphenyloctatetraene	**44**	28.480	76.636	184.860			6.056	0.2884
$C_{22}H_{20}$	1,10-Diphenyldecapentaene	**45**	31.192	83.829	203.625			6.446	0.2803

absorbed into the empirical single and double bond energies. Thus, a non-resonating localized model, with alternating single and double bonds, can satisfactorily account for the collective properties of these molecules, such as ΔH_a and the bond length. The ΔH_a of a linear polyene is

$$[2] \quad \Delta H_a = N_{CH}E_{CH} + N'_{CC}E'_{CC} + N''_{CC}E''_{CC},$$

where N'_{CC} and N''_{CC} are the number of 'single' and 'double' CC bonds with bond energies E'_{CC} and E''_{CC} respectively.

In the present s.c.f. method, ΔH_a is obtained from eq. [1]. Therefore, combining eqs. [1] and [2], and with N''_{CC} equal to $(N'_{CC} + 1)$ in the non-resonating model:

$$[3] \quad E_b(\text{tot}) = (E'_{CC} + E''_{CC})\,N'_{CC} + E''_{CC},$$

where

$$[4] \quad E_b(\text{tot}) = E_{\pi b} + E_{\sigma b}.$$

Using the calculated results of $E_{\pi b}$ and $E_{\sigma b}$ in columns 2 and 3 of Table I for the molecules **25**, **26**, **29**, **30**, and **31**, E_b(tot) is plotted against N'_{CC} in Fig. 2. The linear relationship [5] is obtained for eq. [3].

$$[5] \quad E_b(\text{tot}) = (9.904)N'_{CC} + 5.584,$$

from which E'_{CC} is 4.320 eV and E''_{CC} is 5.584 eV. The E''_{CC} (5.584 eV) is very close to 5.603 eV, the E''_{CC} value for ethylene. The calculated bond lengths of the '*s*ingle' and '*d*ouble' bonds vary very little in the series (s = 1.338 Å to 1.340 Å and d = 1.464 Å to 1.470 Å). The results demonstrate the success of this localized bond model in representing the linear polyenes.

An extension of the above approach can be applied to the diphenyl-substituted linear polyenes. If these compounds are treated as non-resonating localized bond molecules, the ΔH_a is

$$[6] \quad \Delta H_a = N_{CH}E_{CH} + N'_{CC}E'_{CC} + N''_{CC}E''_{CC} + 2E_{CC}^{\text{benzene}}$$

where E_{CC}^{benzene} is the sum of the total sigma and pi CC bond energies of an 'isolated' benzene ring, which is reasonable since the bond lengths in the rings 'B' are close to 1.400 Å. Since N'_{CC} equals $(N''_{CC} + 1)$ in these systems, then equating eqs. [1] and [6] gives

$$[7] \quad E_b(\text{tot}) = (E'_{CC} + E''_{CC})N''_{CC} + (E'_{CC} + 2E_{CC}^{\text{benzene}}).$$

On plotting the calculated results of $(E_{\pi b} + E_{\sigma b})$ for the molecules **40**, **42**, **43**, **44**, and **45**, the linear relation of eq. [7] is established in Fig. 3 as

$$[8] \quad E_b(\text{tot}) = (9.905)N''_{CC} + 65.496,$$

Can. J. Chem. Downloaded from www.nrcresearchpress.com by 210.87.254.105 on 09/05/12
For personal use only.

Can. J. Chem. Downloaded from www.nrcresearchpress.com by 210.87.254.105 on 09/05/12
For personal use only.

TABLE II

Bond lengths of polyenes and vinyl compounds

Compound		R_{ij} (Å)									r.m.s.
		a	*b*	*c*	*d*	*e*	*f*	*g*	*h*	*i*	
25	R[1]	1.334									
	l.w.	1.331									.003
26	ε[2]	1.337	1.483								.00791
	P[3]	1.344	1.465								.01235
	l.w.	1.338	1.470								.00922
27	l.w.	1.340	1.466								
28	l.w.	1.347	1.470	1.338							
			(*b'*)1.466	(*c'*)1.340							
29	l.w.	1.339	1.467	1.347							
30	l.w.	1.339	1.468	1.348	1.465						
31	l.w.	1.340	1.467	1.348	1.464	1.350					
32	l.w.	1.340	1.468	1.405	1.400	1.400					
33	l.w.	1.340	1.467	1.410	1.404	1.400					
34	l.w.	1.339	1.468	1.404	1.406	1.399					
35	l.w.	1.340	1.468	1.406	1.400	1.406					
36	l.w.	1.339	1.468	1.407	1.403						
37	l.w.	1.346	1.470	1.469	1.404	1.399	1.400				
		(*a'*)1.338			(*d'*)1.405	(*e'*)1.398	(*f'*)1.401				
38	l.w.	1.341	1.465	1.357	1.463	1.407	1.397	1.402			
		(*a'*)1.339	(*b'*)1.469			(*e'*)1.405	(*f'*)1.399	(*g'*)1.400			
39	l.w.	1.347	1.469	1.405	1.398	1.401					
				(*c'*)1.404	(*d'*)1.400	(*e'*)1.400					
40	X[4]	1.33	1.45	1.39	1.39	1.39					
	l.w.	1.348	1.467	1.406	1.398	1.402					
41	l.w.	1.349	1.465	1.405	1.399	1.402	1.400	1.400	1.405	1.411	
			(*b'*)1.466	(*c'*)1.406	(*d'*)1.398	(*e'*)1.402					
42	l.w.	1.349	1.467	1.406	1.402	1.402	1.465				
				(*c'*)1.405	(*d'*)1.400	(*e'*)1.400					
43	l.w.	1.349	1.466	1.406	1.398	1.402	1.464	1.350			
				(*c'*)1.405	(*d'*)1.400	(*e'*)1.400					
44	l.w.	1.348	1.467	1.406	1.398	1.402	1.465	1.349	1.464		
				(*c'*)1.404	(*d'*)1.404	(*e'*)1.404					
45	l.w.	1.349	1.466	1.406	1.398	1.402	1.465	1.350	1.464	1.350	
				(*c'*)1.405	(*d'*)1.400	(*e'*)1.400					

*R = Raman spectroscopic data; ε = electron-diffraction data; X = X-ray data; l.w. = this work.
[1]References 9*a*, 24. [2]Reference 12. [3]Reference 10. [4]Reference 25.

TABLE III

The heats of atomization (eV) and resonance energies (eV) of polyphenyls and related compounds

	Compound	Code	$E_{\pi b}$	$E_{\sigma b}$	ΔH_a Calcd.	ΔH_a Obsd. (1)	δ	ERE	SECC
(A)									
$C_{12}H_{10}$	Biphenyl	**46**	17.577	47.904	109.784	109.671	+0.113	4.480	0.3446
$C_{18}H_{13}$	*m*-Terphenyl	**47**	26.529	73.838	162.390			6.910	0.3455
$C_{18}H_{14}$	*p*-Terphenyl	**48**	26.532	73.838	162.393			6.913	0.3457
$C_{24}H_{18}$	*p,p'*-Diphenylbiphenyl	**49**	35.487	99.773	215.004			9.347	0.3462
$C_{24}H_{18}$	1,3,5-Triphenylbenzene	**50**	35.480	99.771	214.995	214.998	−0.003	9.338	0.3459
(B)									
$C_{16}H_{12}$	1-Phenylnaphthalene	**51**	23.574	66.505	143.242			6.137	0.3409
$C_{16}H_{12}$	2-Phenylnaphthalene	**52**	23.583	66.491	143.236			6.132	0.3407
$C_{20}H_{14}$	2,2′-Binaphthalene	**53**	29.596	85.074	176.693			7.787	0.3385
$C_{20}H_{14}$	1,2′-Binaphthalene	**54**	29.586	85.089	176.698			7.792	0.3388

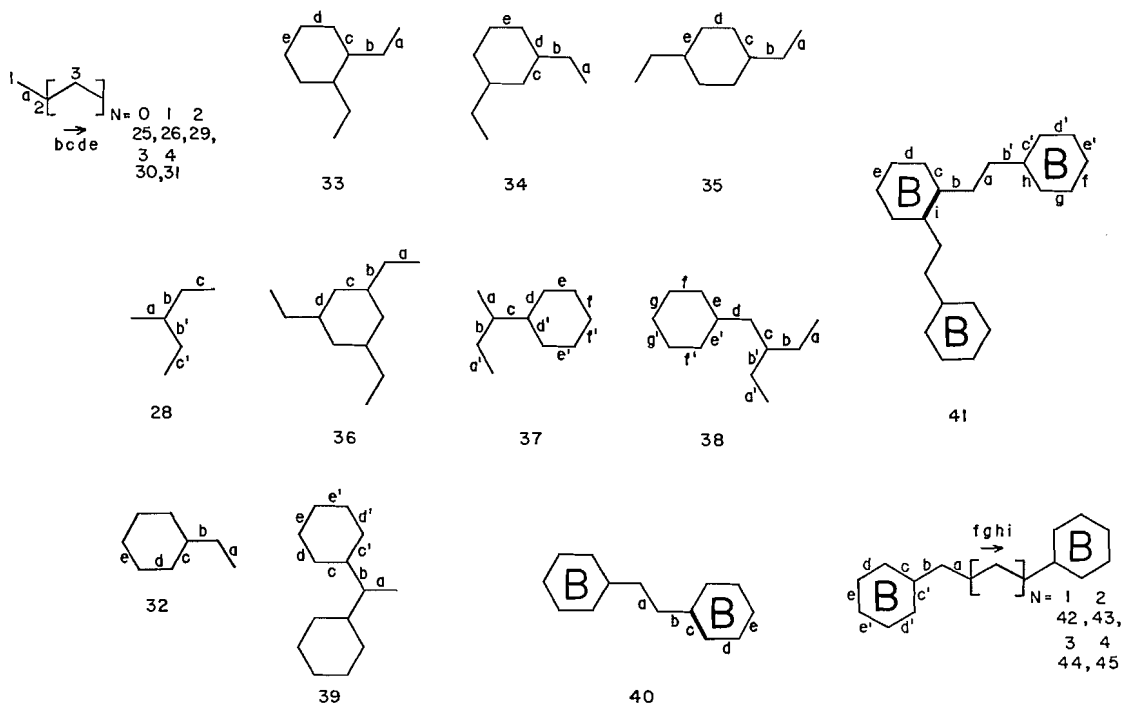

FIG. 1. Geometries of polyenes and vinyl compounds.

from which E'_{CC} is 4.305 eV and E''_{CC} is 5.600 eV. Equations [5] and [8] have the same slopes, since ($E'_{CC} + E''_{CC}$) equals 9.904 eV and 9.905 eV respectively. The estimates for E'_{CC} from both eqs. [5] (4.320 eV) and [8] (4.305 eV) agree closely with each other. The same is true for the two estimates of E''_{CC} (5.584 eV and 5.600 eV). Since eqs. [5] and [8] are empirical results for two different types of molecules, the agreements of the different estimates of E'_{CC} (and E''_{CC}) strongly suggest that in the diphenyl-substituted linear polyenes pi delocalizations

Can. J. Chem. Downloaded from www.nrcresearchpress.com by 210.87.254.105 on 09/05/12
For personal use only.

Can. J. Chem. Downloaded from www.nrcresearchpress.com by 210.87.254.105 on 09/05/12
For personal use only.

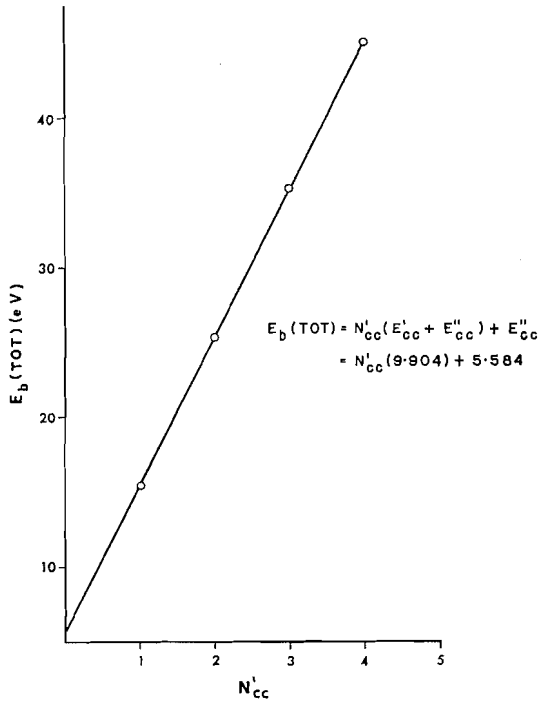

FIG. 2. Plot of E_b(tot) versus chain length (N) of linear polyenes.

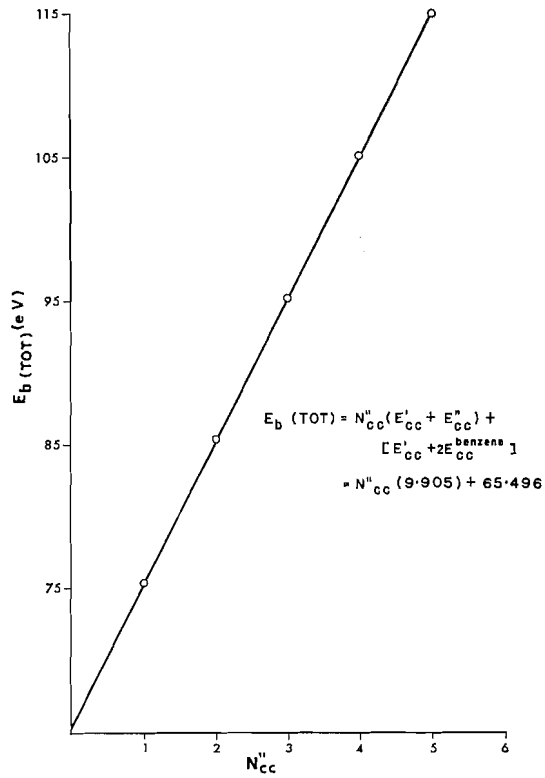

FIG. 3. Plot of E_b(tot) versus chain length (N) of diphenyl-substituted linear polyenes.

from the benzene rings to the bridge chain are relatively unimportant. Also, the linear plot of Fig. 3 further confirms that these substituted polyenes can be treated as molecules with localized bonds which are "non-resonating".

The above results are very reliable because the calculated heats of atomization for these systems are very accurate. (The deviations of ΔH_a between the calculated values and experimental data are only 0.017 eV for **26**, 0.038 eV for **32**, and 0.040 eV for **40**, which is within the experimental uncertainty (1)).

Though the variations of bond lengths in the benzene ring are small, it is possible to see how the pi electron delocalization has actually participated in these systems. For example, bond *i* in bis-triphenylene **41**, from which two linear chains originate, has increased to 1.411 Å, as compared with 1.406 Å for bond *c* in **40** with one bridging CC chain and 1.400 Å for a normal benzenoidal distance.

(III) Polyphenyls and Related Compounds

(A) Biphenyl

The structures of biphenyl **46** in the solid, liquid, and vapor states show interesting variations in the twist angle and bond lengths which prove to be characteristic of polyphenyls.

(i) The solid state structure of biphenyl (18) is a planar molecule, with the inter-benzene bond length *d* of 1.506 Å. The ortho-hydrogen atoms on the two rings are separated by 2.07 Å. These ortho-hydrogens would be 1.80 Å apart in a totally flat molecule in which bond *d* is 1.506 Å. The displacement of 0.27 Å presumably reduces the steric strain by making the H non-planar. Intermolecular forces of packing are responsible for the planarity of the ring.

(ii) Spectroscopic data for biphenyl in solution suggest that the twist angle is about 20° from planarity (19) and the two benzene rings are only weakly interacting (20).

(iii) Vapor phase electron-diffraction data (21) indicate that biphenyl is non-planar, with a twist angle of 42°, bond *d* being 1.49 Å and the ortho-hydrogen separation being 2.35 Å.

The separation of the ortho-hydrogens in the

Can. J. Chem. Downloaded from www.nrcresearchpress.com by 210.87.254.105 on 09/05/12
For personal use only.

solid (2.07 Å), liquid, and vapor (2.35 Å), and the corresponding twist angles (0, 20, and 42°), suggest that van der Waal's interactions (essentially repulsive destabilization) are important and comparable in magnitude to conjugation stabilization. Mulliken (14) estimated the ortho-hydrogen overlap to be 0.28, and concluded that the observed twist in biphenyl was due to steric hindrance. The total bond energy can be analyzed in terms of the geometries of a planar molecule. Conventional pi theory (22) depends on assuming an initial fixed geometry for the calculation, which is not the minimum energy planar structure. The present method calculates all individual bond lengths, and the final s.c.f. planar geometry is the one associated with the minimum energy. Consider three different planar geometries for biphenyl: model I, the X-ray solid state structure described earlier; II, 2 normal benzene rings linked by a bridge bond $d = 1.506$ Å; III, the s.c.f. geometry calculated for biphenyl, **46**, Table IV, then the energies of interest for the 3 models are shown in Table V.

Several conclusions can be drawn:

(1) Model III with the s.c.f. geometry possesses the highest total bond energy (and SE). It is, therefore, the most stable planar structure. This serves as a direct justification of the present method of calculating all individual bond lengths of a molecule, rather than to adopt an arbitrary geometry (22) for the calculations.

(2) An obvious contradiction is obtained, if *only* the pi quantities $E_{\pi b}$ and π-SE are used as measures of stability, I is more stable than II which is more stable than III. In general, the stabilization gained by pi conjugation is insufficient to balance the comparable amount of sigma destabilization, and it is only by treating *both* the sigma and pi bond energies, that the energy of the whole molecule can be estimated and compared (Table V). In this case, only III gives both positive π-SE and σ-SE.

(3) The pi bond order is used as a semi-quantitative measure of conjugation and molecular stability and the inter-benzene pi bond order $P_{1,1'}$ in biphenyl is 0.22 in I, 0.24 in II, and 0.26 in III. It is a fortunate coincidence that in biphenyl the total bond energy, E_b(tot), and the pi bond order, $P_{1,1'}$, both vary as III > II > I. $P_{1,1'}$ is simply the pi electronic property of one bond in a molecule and since the collective properties of the pi electrons, $E_{\pi b}$ and π-SE, give a reverse order of stability, III < II < I, then $P_{1,1'}$ alone must be used with reserve in considering the stability of a molecule, because the bond order P_{ij} for any one bond need not necessarily reflect the behavior of the E_b(tot) for a conjugated system.

In order to investigate the effect of steric hindrance, and consequently internal rotation, about the bridge bond in biphenyl, van der Waal's interactions are included as in 1,3-butadiene (Section II). The interaction energies, calculated by Fisher-Hjalmars (17), using Bartell's intramolecular potentials (16), are used here for the various conformations of biphenyl. The angular dependence of the total stabilization energy is expressed as (SE) × $\cos^2\theta$ (17). θ is the twist angle of one phenyl group from planarity about the bridge bond, and (SE) is the maximum stabilization energy of +0.380 eV as calculated for model III. The combined effect of van der Waal's interaction energies (VW) and total stabilization energies (SE) are shown below for various twist angles.

Thus the equilibrium conformation of biphenyl is non-planar with a twist angle of about 40° and with a barrier to internal rotation of about 0.174 eV (4 kcal/mole). The potential minimum in the region between θ equal to 30 and 40° is very shallow, which is consistent with the experimental result of $\theta = 42 \pm 10°$ (21); the molecule has a large amplitude of rotational oscillations about the bridge bond.

(B) Polyphenyls

The SECC in biphenyl **46**, *p*-terphenyl **48**, and *p,p'*-diphenylbiphenyl **49** are 0.3446 eV, 0.3457

Twist angle θ (°)	0	30	40	50	60	90
VW = van der Waal's interaction energy* (17) (eV)	−.3595	−.0924	−.0286	+.0087	+.0243	+.0284
SE = total stabilization energy* (π conjugation + σ compression) (eV)	+.3795	+.2846	+.2227	+.1568	+.0949	0
Combined effect* (VW + SE) (eV)	+.0200	+.1922	+.1941	+.1655	+.1192	+.0284

*Positive energy is stabilization.

Can. J. Chem. Downloaded from www.nrcresearchpress.com by 210.87.254.105 on 09/05/12
For personal use only.

TABLE IV

Bond lengths of polyphenyls and related compounds

Compound		R_{IJ} (Å)									
		a	*b*	*c*	*d*	*e*	*f*	*g*	*h*	*i*	*j*
(A)											
46	ε[1]	1.400	1.400	1.400	1.490						
	l.w.	1.401	1.399	1.405	1.469						
47	l.w.	1.401	1.399	1.405	1.469	1.406	1.400	1.404			
48	l.w.	1.401	1.399	1.405	1.468	1.406	1.398				
49	l.w.	1.401	1.399	1.405	1.468	1.406	1.397	1.406	1.467		
50	l.w.	1.401	1.399	1.405	1.469	1.404					
(B)											
51[2]	l.w.	1.419	1.387	1.432	1.417	1.382	1.428	1.466	1.406	1.399	1.401
		(*a*′)1.421	(*b*′)1.381	(*c*′)1.426		(*e*′)1.380	(*f*′)1.428				
52[2]	l.w.	1.426	1.386	1.427	1.417	1.378	1.429	1.467	1.405	1.399	1.401
		(*a*′)1.421	(*b*′)1.380	(*c*′)1.428		(*e*′)1.381	(*f*′)1.427				
53	l.w.	1.426	1.386	1.427	1.417	1.378	1.429	1.467			
		(*a*′)1.421	(*b*′)1.380	(*c*′)1.428		(*e*′)1.381	(*f*′)1.425				
54	l.w.	1.427	1.387	1.426	1.417	1.378	1.429	1.465			
		(*a*′)1.421	(*b*′)1.380	(*c*′)1.428		(*e*′)1.381	(*f*′)1.427				
		(a_1)1.419	(b_1)1.388	(c_1)1.432	(d_1)1.417	(e_1)1.381	(f_1)1.428				
		(a_1′)1.421	(b_1′)1.381	(c_1′)1.426		(e_1′)1.380	(f_1′)1.428				

[1]Reference 21.
[2]The s.c.f. (l.w.) bond lengths of naphthalene (in part I) are: a = 1.419 Å, b = 1.382 Å, c = 1.426 Å, d = 1.420 Å.

TABLE V

Bond lengths, bond energies, stabilization energies, and pi bond order for models I, II, and III

	Biphenyl		Models I	Models II	Models III (s.c.f.)
I	Geometries (Å)	*a*	1.361	1.400	1.401
		b	1.421	1.400	1.399
		c	1.383	1.400	1.405
		d	1.506	1.506	1.469
II	Energies (eV)				
	A. Bond energies (for all CC bonds)				
	$E_{\pi b}$		18.558	17.626	17.577
	$E_{\sigma b}$		46.676	47.830	47.904
	E_b(tot)		65.234	65.456	65.481
	B. Stabilization energies* (SE in eV)				
	πSE		+1.310	+0.378	+0.329
	σSE		−1.177	−0.023	+0.051
	Tot. SE		+0.133	+0.355	+0.380
III	Pi bond order $P_{1,1'}$ (inter-benzene bond)		0.22	0.24	0.26

*The reference structure consists of two orthogonal benzene rings (treated as isolated units, E_{π_b} = 8.624 eV and E_{σ_b} = 21.971 eV (1)) joined by bridge bond 1.505 Å which is the equilibrium single CC bond length with E_{σ_b} of 3.911 eV (1). A positive (+) SE is stabilizing.

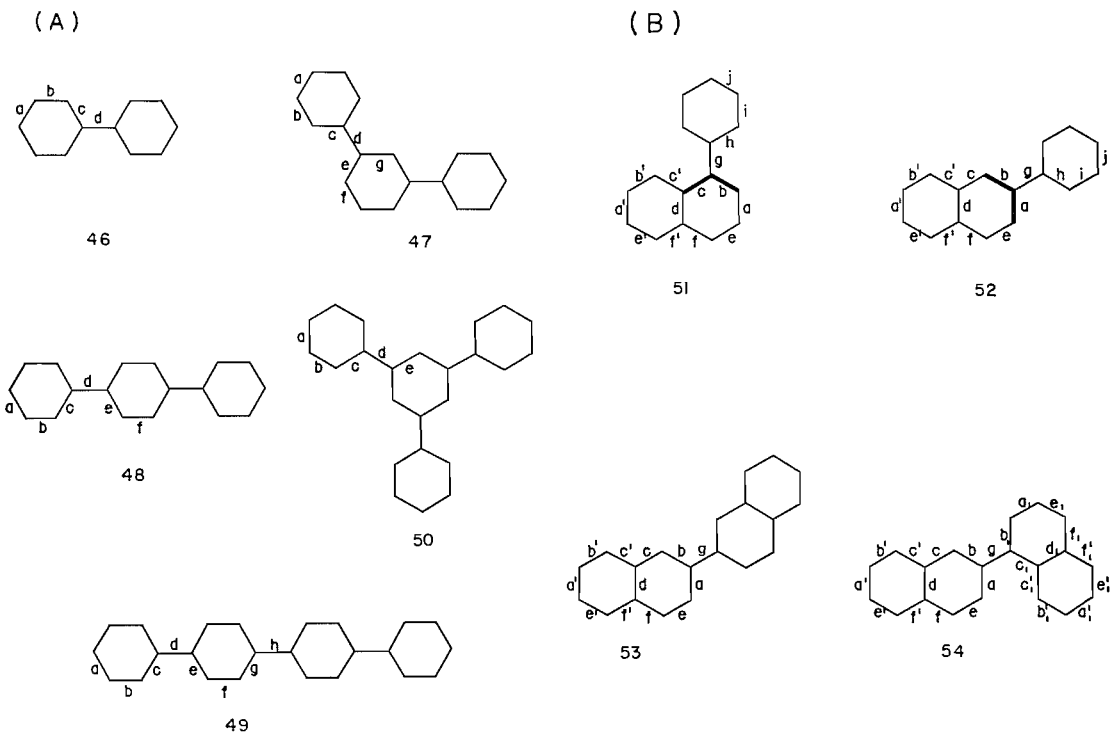

FIG. 4. Geometries of polyphenyls and related compounds.

Can. J. Chem. Downloaded from www.nrcresearchpress.com by 210.87.254.105 on 09/05/12
For personal use only.

Can. J. Chem. Downloaded from www.nrcresearchpress.com by 210.87.254.105 on 09/05/12
For personal use only.

eV, and 0.3462 eV, compared with 0.3417 eV in benzene (1). Therefore, additional phenyl substitutions provide further stabilization. The cumulative van der Waal's interaction might easily override the established stabilization energy of a planar conformation. However, as the benzene rings increase, the conjugation band in the ultraviolet absorption spectra (19) of *p*-polyphenyls (in solution) is shifted towards longer wavelength with increased absorption intensity. This is attributed to the increasing extent of conjugation due to elongation of the conjugation system, which is of course consistent with the increase of SECC mentioned above. Such comparisons are dangerous since the present calculations give the same energy for *m*-terphenyl **47** and *p*-terphenyl **48**, for which the absorption spectra are quite different (19).

In the solid phase, the three phenyl rings of 1,3,5-triphenylbenzene **50** are twisted out of the plane of the central ring by 24, 27, and 34° (23). The van der Waal's interactions in **50** are more complicated than those in biphenyl, because the hydrogens at the central ring are acted upon simultaneously by the hydrogens of the two adjacent phenyl rings. It is encouraging to note that the predicted ΔH_a calculated using a model of 4 planar rings is precisely the same as the experimental value of the non-planar conformation ($\delta = 0.003$ eV).

(C) Phenyl Substitution and Molecular Geometry

The effect of phenyl substitution in the naphthalenes **51** and **52** can be discussed in terms of the variations from the free naphthalene bond lengths, Table IV. 1-Phenylnaphthalene **51** and 2-phenylnaphthalene **52** are considered. The two bonds that are adjacent to the point of phenyl substitution, *b* and *c* in **51**, and bonds *a* and *b* in **52**, change by +0.006 Å, while the rest of the molecule is basically unchanged, ±0.001 Å. The SECC are 0.3409 eV (**51**) and 0.3407 eV (**52**), both of which are higher than 0.3355 eV in free naphthalene SECC. This result indicates there is an additional stabilization by the phenyl groups.

In 2,2′-binaphthalene **53** and 1,2′-binaphthalene **54**, the same geometrical variations are observed; that is, the bonds that are adjacent to the position of phenyl substitution are modified, where additional conjugation is enforced, and results in significant geometrical change. Distant points are basically unperturbed.

(IV) Conclusion

Accurate heats of atomization and accurate bond lengths of many classes of conjugated hydrocarbons have been obtained. The calculated heats of atomization can be used as accurate thermochemical energies in systems for which the experimental heats of combustion are difficult to obtain. The calculated bond lengths will be practically useful in experimental diffraction studies. The degree of aromaticity is quantitatively illustrated by the SECC values.

The present method has been extended to apply to open shell ground states of radicals, and radical ions, of the conjugated hydrocarbons, and to calculate the unpaired spin densities of π electrons, the total bond energies, and the s.c.f. bond lengths.

(V) Acknowledgments

We wish to thank the National Research Council of Canada for support of this Research, the Canadian Industries Limited for the award of a Fellowship to D. H. Lo, the McGill Computing Centre for Facilities, and Miss A. Chan for drawing the figures. We are indebted to the Referees and Editor for their criticism and advice.

1. D. H. Lo and M. A. Whitehead. Can. J. Chem. This issue.
2. J. A. Pople. Trans. Faraday Soc. **49**, 1375 (1953).
3. A. L.-H. Chung and M. J. S. Dewar. J. Chem. Phys. **42**, 756 (1965). M. J. S. Dewar and G. J. Gleicher. J. Am. Chem. Soc. **87**, 685 (1965).
4. H. H. Jaffe and J. Hinze. J. Phys. Chem. **67**, 1501 (1963).
5. K. Ohno. Theoret. Chim. Acta, **2**, 219 (1964).
6. JANAF Interim Thermochemical Tables. The Dow Chemical Company, Midland, Michigan. December 31, 1960.
7. G. Herzberg. Molecular spectra and molecular structure. Vol. II. D. Van Nostrand Co. Inc., New York. 1945.
8. C. A. Coulson and W. T. Dixon. Tetrahedron, **17**, 215 (1962).
9. (*a*) B. P. Stoicheff. Current Sci. India, **27**, 1 (1958). (*b*) A. Langseth and B. P. Stoicheff. Can. J. Phys. **34**, 350 (1956).
10. L. Salem. Molecular orbital theory of conjugated systems. Benjamin, Inc., New York. 1966. p. 139.
11. C. A. Coulson and A. Golebiewski. Proc. Phys. Soc. London, **78**, 1310 (1961).
12. A. Almenningen, O. Bastiansen, and M. Traetteberg. Acta Chem. Scand. **12**, 1221 (1958).
13. M. J. S. Dewar and G. J. Gleicher. J. Am. Chem. Soc. **87**, 692 (1965).
14. R. S. Mulliken. Tetrahedron, **6**, 68 (1959).
15. M. J. S. Dewar and H. N. Schmeising. Tetrahedron, **5**, 166 (1959); **11**, 96 (1960).
16. L. S. Bartell. J. Chem. Phys. **32**, 827 (1960); Tetrahedron, **17**, 265 (1962).

17. I. FISHER-HJALMARS. Tetrahedron, **19**, 1805 (1963).
18. A. HARGREAVES and S. H. RIZVI. Acta Cryst. **15**, 365 (1962).
19. H. SUZUKI. Bull. Chem. Soc. Japan, **32**, 1340 (1959); **33**, 109 (1960).
20. D. STEELE and E. R. LIPPINCOTT. J. Mol. Spectry. **6**, 238 (1961).
21. A. ALMENNINGEN and O. BASTIANSEN. Kgl. Norske Videnskab. Selskabs, Skrifter, No. 4, 1 (1958).
22. T. NAKAMURA, S.-I. KWUN, and H. EYRING. Molecular orbitals in chemistry, physics and biology. Academic Press, New York. 1964. p. 421.
23. M. S. FARAG. Acta Cryst. **7**, 117 (1954).
24. L. S. BARTELL and R. A. BONHAM. J. Chem. Phys. **27**, 1414 (1957).
25. Tables of interatomic distances. Chem. Soc. London Spec. Publ. No. 11 (1958).

Can. J. Chem. Downloaded from www.nrcresearchpress.com by 210.87.254.105 on 09/05/12
For personal use only.

Kinetics of disproportionation of chlorous acid

C. C. HONG[1] AND W. H. RAPSON

Department of Chemical Engineering and Applied Chemistry, University of Toronto, Toronto, Ontario

Received December 15, 1967

A mechanism involving HOCl, Cl—ClO_2, and Cl_2 as intermediates is proposed for the disproportionation of chlorous acid. In the absence of chloride, the reaction is controlled by two simultaneous processes, $2HClO_2 \rightarrow H^+ + HOCl + ClO_3^-$ and $HClO_2 + ClO_2^- \rightarrow HOCl + ClO_3^-$. Chloride has a catalytic effect and an inhibiting effect as well on the formation of chlorine dioxide. The initial reaction rate passes through a minimum at a certain concentration of chloride at low acidities, which can be interpreted by the postulated mechanism. Under chloride catalysis, the reaction is controlled by the process $H^+ + Cl^- + HClO_2 \rightarrow 2HOCl$.

Canadian Journal of Chemistry, 46, 2053 (1968)

Can. J. Chem. Downloaded from www.nrcresearchpress.com by 210.87.254.5 on 09/05/12
For personal use only.

The first kinetic investigation of the disproportionation of chlorous acid was carried out in 1935 by Barnett (1), who showed that the rate of formation of chlorine dioxide varied with the square of the chlorous acid concentration. The second-order rate law was also observed by Launer *et al.* (2) and Nabar *et al.* (3). However, in 1954, several authors (4, 5) found that the reaction forming chlorine dioxide was second order with respect to total chlorite concentration rather than the equilibrium concentration of chlorous acid.

If the second-order dependence on the equilibrium concentration of chlorous acid is correct, it would be expected that the reaction order with respect to the equilibrium hydrogen ion concentration is 2. Nevertheless, Stitt *et al.* (5) found that the order was definitely less than 2. The reaction appeared to be nearer to first order with respect to the equilibrium concentration of hydrogen ions than second order, the numerical values falling between 1.0 and 1.2. Buser and Hänisch (6) found that the rate of formation of chlorine dioxide in dilute chlorite solution is not a simple function of pH. They observed a maximum reaction rate at pH 1.70 for a solution of 3.18×10^{-3} *M* $NaClO_2$. A similar dependence of the reaction rate on pH was found by Hefti (7).

The published literature about the effect of chloride on the rate of disproportionation of chlorous acid is meager. The catalytic effect of chloride was first observed by Barnett (1), who found that the catalyzed disproportionation reaction was first order with respect to chloride and first order with respect to chlorous acid. He also found that in the presence of chloride and after long standing, the reaction was probably complicated by the chloride-catalyzed decomposition of chlorine dioxide.

Several intermediates have been proposed for the formation of chlorine dioxide from the disproportionation of chlorous acid. These include $H_2Cl_2O_4$, H_2ClO_2, Cl_2O_3, ClO, HOCl by Barnett (1), and Cl—ClO_2 or Cl—O—Cl—O by Taube and Dodgen (8).

An extensive investigation of the disproportionation of chlorous acid both in the absence and presence of chloride has been carried out in the present work. It is hoped that the mechanism postulated from the experimental results will explain many contradictory observations published in the literature.

The parameters investigated include ionic strength, effect of chlorate, and the reaction order with respect to the concentration of each reactant. All experiments were carried out at 25 °C.

A brief investigation on the reaction between chlorous acid and hypochlorous acid was made in order to justify the postulated mechanism.

Experimental

(a) Reagents

Chlorous acid was prepared by the acidification of sodium chlorite containing 97.8% $NaClO_2$ with nitric acid in most of the kinetic studies. The equilibrium between chlorous acid and chlorite ions is rapidly established upon acidification. The equilibrium concentration of chlorous acid is calculated from the equation (9)

$$[1]\quad 2(HClO_2) = (a + b + K_c) - [(a + b + K_c)^2 - 4ab]^{\frac{1}{2}},$$

where a and b are respectively the concentrations of nitric acid and sodium chlorite after mixing and K_c is the dissociation constant of chlorous acid expressed in terms of concentrations. K_c depends on the ionic strength of the solution, as shown in Fig. 1 (9).

[1]Present address: Research Department, Imperial Oil Enterprises, Ltd., Sarnia, Ontario.

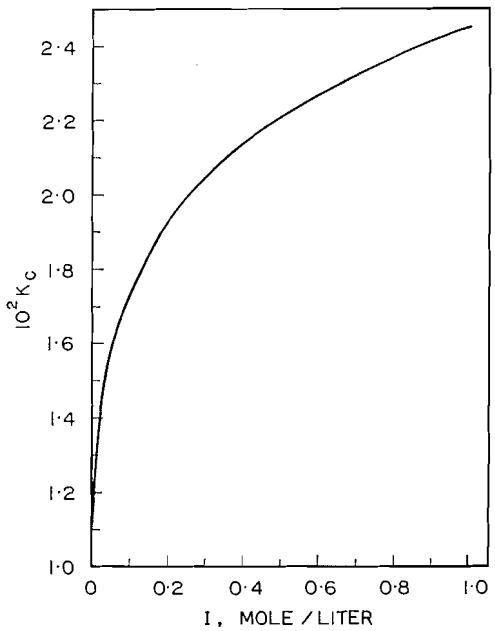

FIG. 1. Effect of ionic strength on the dissociation constant of $HClO_2$ in terms of concentrations at 25 °C.

Hypochlorous acid solutions, which were used in some experiments, were prepared by adding excess mercuric oxide to a chlorine solution and distilling off the hypochlorous acid.

(b) Experimental Procedure

Separate solutions of nitric acid and sodium chlorite, either in the absence or presence of added chloride, were contained in volumetric flasks and brought to the reaction temperature by immersion in a thermostat for over an hour. The reaction was started by adding 10 ml of nitric acid solution with a pipet into a 10-ml sodium chlorite solution contained in a 25-ml volumetric flask immersed in the thermostat. Zero time was taken when the pipet containing nitric acid solution had half-emptied into the sodium chlorite solution. Immediately after mixing, the flask was shaken vigorously. The reacting solution was filled into a 10-mm glass-stoppered absorption cell after rinsing three times. The cell was wiped with tissue paper and placed in the cell compartment of a Beckman DB spectrophotometer. The reaction was followed by measuring the absorbance of chlorine dioxide produced at 360 mμ with an automatic chart recorder. The reaction time was calculated from the speed of the recorder.

The initial rates of reaction were calculated from the slopes of absorbance vs. time curves, obtained from the chart recorder, together with the measured molar absorptivity of chlorine dioxide at 360 mμ.

Results and Discussions

(A) Disproportionation in the Absence of Chloride

The disproportionation of chlorous acid in the absence of chloride follows the stoichiometry (1, 3, 9)

$$[2]\quad 2H^+ + 4ClO_2^- \rightarrow 2ClO_2 + Cl^- + ClO_3^- + H_2O.$$

(a) Ionic Strength Dependence

The ionic strength of the solution was varied by adding sodium nitrate of analytical reagent grade. It was found that the initial reaction rate is independent of ionic strength.

For an ionic reaction, the rate constant is related to ionic strength by the following expression (10, 11),

$$[3]\quad \log k_2 = \log k_0 + 1.018 z_A z_B I^{1/2},$$

where k_2 is the rate constant at ionic strength I, k_0 is the rate constant at zero ionic strength, and z_A, z_B are the ionic charges of ions.

The independence of the reaction rate from ionic strength in the disproportionation of chlorous acid leads to the conclusion that at least one of the reactants is an uncharged species of chlorous acid. The stoichiometric equation (eq. [2]) as such represents only the net change of the reaction.

(b) Reaction Orders

If the reaction is assumed to occur as a result of the interactions of the undissociated molecules of chlorous acid, the initial rate equation can be written as

$$[4]\quad r_0 = \frac{d(ClO_2)}{dt} = k(HClO_2)^n,$$

where n is the reaction order with respect to the concentration of chlorous acid, or

$$[5]\quad \log r_0 = \log k + n \log(HClO_2).$$

A plot of $\log r_0$ against $\log(HClO_2)$ should yield a straight line whose slope is equal to the reaction order.

The reaction is second order with respect to the equilibrium concentration of chlorous acid, as shown in Fig. 2. It is of interest to note that as the acidity is decreased, the observed reaction order with respect to chlorous acid decreases slightly. This can be attributed to the dependence of the rate constant of eq. [4] on hydrogen ion concentration rather than the actual change in the reaction order. This result in conjunction with the fact that the four lines in Fig. 2 do not coincide with one another suggests that a reaction occurs between chlorous acid and chlorite ions in parallel with the bimolecular reaction of

Can. J. Chem. Downloaded from www.nrcresearchpress.com by 210.87.254.5 on 09/05/12
For personal use only.

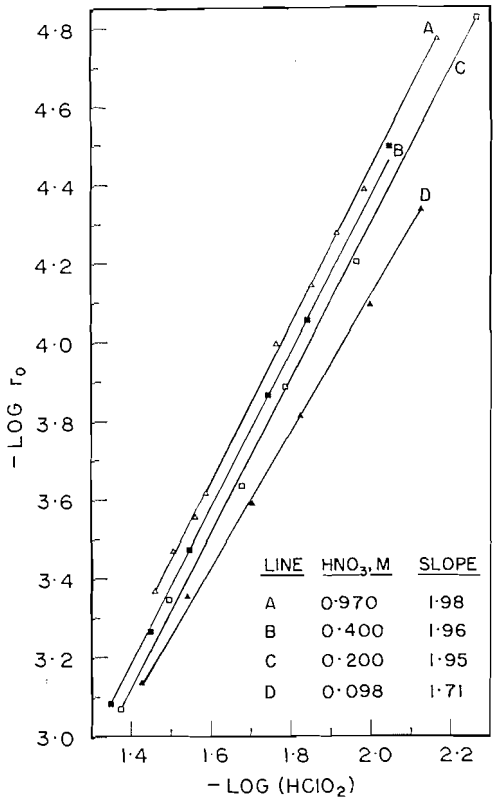

FIG. 2. Determination of reaction order with respect to chlorous acid.

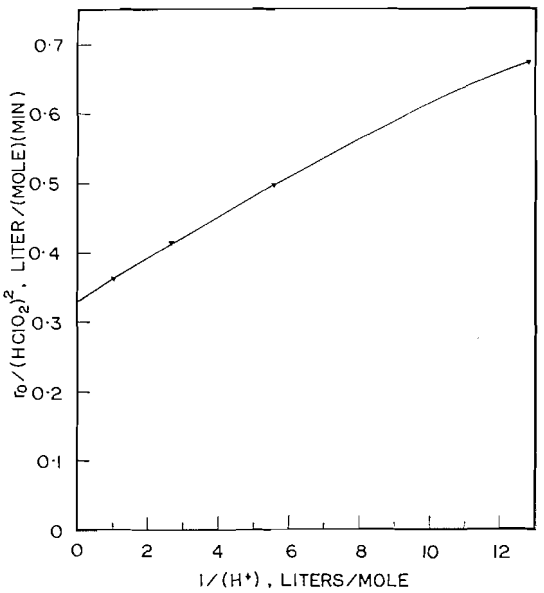

FIG. 3. Calculation of second-order rate constants at 25 °C.

chlorous acid. The overall reaction is the composite of the two reactions, and its rate can be represented by

$$[6] \quad r_0 = k(HClO_2)^2 + k'(HClO_2)(ClO_2^-).$$

The equilibrium concentration of chlorite ions can be expressed by

$$[7] \quad (ClO_2^-) = \frac{K_c(HClO_2)}{(H^+)}.$$

Substitution of eq. [7] into eq. [6] and rearranging gives

$$[8] \quad \frac{r_0}{(HClO_2)^2} = k + \frac{k'K_c}{(H^+)}.$$

If K_c is constant, a plot of $r_0/(HClO_2)^2$ against $1/(H^+)$ should yield a straight line with an intercept equal to k and a slope equal to $k'K_c$. The values of k and k' at 25 °C, as calculated from Fig. 3, are 0.330 and 1.37 l/(mole) (min), respectively. The line in Fig. 3 levels off slightly at low acidity due to the decrease in the dissociation constant of chlorous acid with ionic strength (Fig. 1).

Equation [6] can also be written as

$$[9] \quad r_0 = k(HClO_2)^2 + k'(HClO_2) \times [b - (HClO_2)],$$

where b is the total concentration of sodium chlorite. Differentiation of eq. [9] with respect to the concentration of chlorous acid gives

$$[10] \quad \frac{dr_0}{d(HClO_2)} = bk' - 2(k' - k)(HClO_2)$$

and

$$[11] \quad \frac{d^2r_0}{d(HClO_2)^2} = -2(k' - k).$$

Since k' is greater than k, the second derivative is negative. It is therefore expected that a plot of the initial reaction rate against the equilibrium concentration of chlorous acid will have a maximum, as observed by Buser and Hänisch (6).

Barnett (1) found that the rate law for the disproportionation of chlorous acid was

$$[12] \quad r = k(HClO_2)^2$$

and the value of k at 25 °C was 1.4 l/(mole)(min). His experiments were for conditions of fairly low

Can. J. Chem. Downloaded from www.nrcresearchpress.com by 210.87.254.5 on 09/05/12
For personal use only.

Can. J. Chem. Downloaded from www.nrcresearchpress.com by 210.87.254.5 on 09/05/12
For personal use only.

acidity, (ClO_2^-) > ($HClO_2$). In view of the low equilibrium concentrations of chlorous acid investigated by him, the bimolecular reaction of chlorous acid may be neglected, and the rate he measured may be mainly due to the reaction between chlorous acid and chlorite ions. The rate constant for the latter reaction is 1.37 l/(mole)(min) as determined in the present work. Barnett's rate law cannot explain why there is a maximum reaction rate at a certain pH.

It was found that at the same equilibrium concentration of $HClO_2$ the initial rate due to the reaction of $HClO_2$ with ClO_2^- is approximately directly proportional to the equilibrium concentration of ClO_2^-. Thus, this reaction is first order with respect to ClO_2^-.

The rate law represented by eq. [6] explains the contradictory observations published in the literature. When the concentration of sodium chlorite is in excess, the reaction between $HClO_2$ and ClO_2^- will be predominant, and the reaction order with respect to H^+ will be close to 1, as observed by Stitt *et al.* (5). On the other hand, if the acid used for the acidification of sodium chlorite is in excess, the bimolecular reaction of $HClO_2$ will be predominant and the reaction order with respect to total chlorite is close to 2, as observed by Launer *et al.* (4) and Stitt *et al.* (5), since most of sodium chlorite is converted to chlorous acid.

(c) Effect of Chlorate

Chlorate and chloride are the coproducts of chlorine dioxide in the disproportionation of chlorous acid. It will be of interest to know the effects of these products on the rate of production of chlorine dioxide.

It was found that the addition of 0.324 *M* $NaClO_3$ into a solution containing 0.0207 *M* $NaClO_2$ and 0.0375 *M* H_2SO_4 only increased the initial reaction rate by approximately 6.7%. This implies that the oxidation of chlorite by chlorate also gives chlorine dioxide, but its reaction rate is smaller than that of the disproportionation of chlorous acid (8). It also implies that chlorate does not have an inhibiting effect on the reaction rate.

(B) Disproportionation in the Presence of Chloride

In the presence of chloride, stoichiometric results (9) are compatible with the following two reactions

$$[13]\quad 4H^+ + 5ClO_2^- \rightarrow 4ClO_2 + Cl^- + 2H_2O$$

$$[14]\quad 3ClO_2^- \rightarrow Cl^- + 2ClO_3^-$$

occurring in conjunction with reaction [2]. The contribution of reaction [13] increases with increasing concentration of chloride. Reaction [14] does not give chlorine dioxide and is responsible for the observed inhibiting effect of chloride.

(a) Ionic Strength Dependence

In the presence of chloride, the disproportionation of chlorous acid is also independent of ionic strength. Consequently, the reaction is expected to proceed through $HCl + HClO_2$ and/or $H^+ + Cl^- + HClO_2$ and/or $HCl + H^+ + ClO_2^-$, in which at least one of the reactants is the uncharged species. However, since HCl is a much stronger acid than $HClO_2$, the reaction is more likely to proceed through $H^+ + Cl^- + HClO_2$, which is a third-order reaction. The relationship between the rate constant and ionic strength for a third-order ionic reaction has the same expression as eq. [3].

(b) Effect of Chlorate

In the presence of added chloride, it was found that the addition of sodium chlorate also increases the reaction rate slightly, due to the oxidation of chlorous acid by chlorate to give chlorine dioxide.

(c) Catalytic Effect vs. Inhibiting Effect

In contrast to the relatively simple effect of chlorate the presence of chloride affects the disproportionation of chlorous acid in a complex manner. Figure 4 shows that at low acidities, the initial rate of production of chlorine dioxide passes through a minimum as the concentration of added chloride is increased (curves A and B). At high acidities, however, the minimum reaction rate disappears (curve C).

In view of the fact that a minimum reaction rate occurs as the concentration of chloride is increased, it may be concluded that chloride has a catalytic effect and an inhibiting effect as well on the formation of chlorine dioxide. The overall reaction rate is the summation of these two opposing effects and the uncatalyzed disproportionation of chlorous acid.

The solid lines in Fig. 4 are the experimental initial rates as a function of chloride concentration. The calculated values (see the sections on Treatment of Data and Mechanism) are represented by the broken lines.

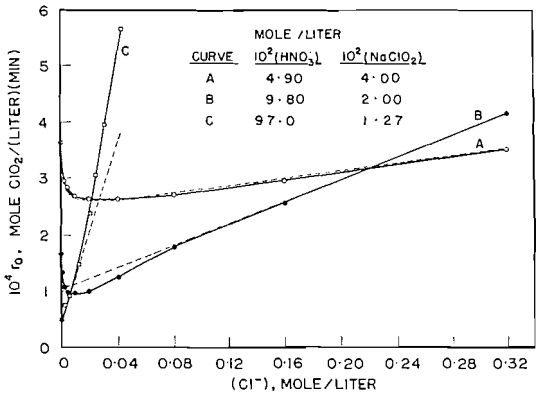

FIG. 4. Effect of chloride as a function of acidity.

(d) Reaction Orders

Figure 4 shows that at high concentrations of chloride, there exists a linear relationship between the initial reaction rate and the concentration of chloride. This suggests that the catalytic disproportionation of chlorous acid is first order with respect to the concentration of chloride.

When the concentrations of nitric acid and sodium chloride are maintained constant, the reaction order with respect to chlorous acid can be determined for the chloride-catalyzed reaction. In Fig. 5, r_0 denotes the overall initial rate of both the chloride-catalyzed and uncatalyzed reactions, and r_0' the initial reaction rate of the uncatalyzed reaction calculated from the rate constant already determined. The difference between the two reaction rates, or $r_0 - r_0'$, represents the initial rate due to the chloride-catalyzed reaction, and has approximately a linear relationship with the equilibrium concentration of chlorous acid. This confirms Barnett's results (1) that the chloride-catalyzed

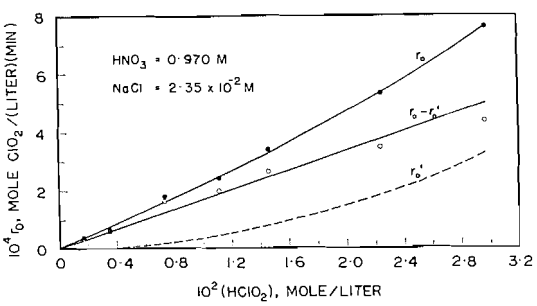

FIG. 5. Determination of reaction order with respect to chlorous acid under chloride catalysis.

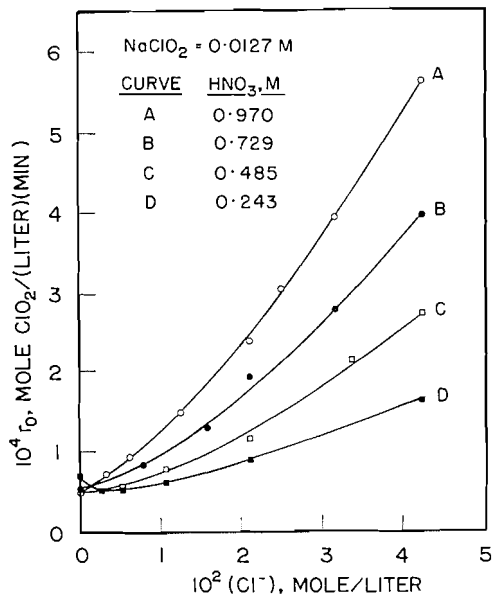

FIG. 6. Effect of acidity on chloride-catalyzed reaction at 25 °C.

reaction is first order with respect to chlorous acid.

The effect of acidity on the chloride-catalyzed reaction is shown in Fig. 6. At a given concentration of chloride, the variation in the slopes of different curves is a measure of the effect of hydrogen ion concentration. Therefore, the reaction order with respect to H^+ can be determined from the slopes of different curves at a given concentration of chloride. The concentration of chloride may be taken arbitrarily at any value, but it is better to choose higher values than lower ones, since the catalytic effect of chloride preponderates over the inhibiting effect at high concentrations of chloride. Thus, at 3.50×10^{-2} *M* NaCl, the slope of each curve, $\Delta r_0/\Delta(Cl^-)$, can be estimated from Fig. 6. A plot of log $[\Delta r_0/\Delta(Cl^-)]$ against log (H^+) gives a straight line with slope equal to 0.962, indicating first order with respect to H^+ under chloride catalysis.

(e) Treatment of Data

The data on the initial rate of formation of chlorine dioxide in the presence of chloride were found to fit the rather complicated expression

$$[15] \qquad r_0 = (m + nx)\left(1 - \frac{x}{p + qx}\right),$$

Can. J. Chem. Downloaded from www.nrcresearchpress.com by 210.87.254.5 on 09/05/12
For personal use only.

TABLE I

The four constants of curves A and B in Fig. 4

	m	n	p	q
Curve A	3.62×10^{-4}	5.05×10^{-4}	5.21×10^{-3}	3.02 (3.35)
Curve B	1.65×10^{-4}	1.62×10^{-3}	1.12×10^{-3}	2.53 (2.28)

where x is the concentration of chloride and m, n, p, and q are positive constants independent of the concentration of chloride but dependent on the equilibrium concentrations of H^+, $HClO_2$, and ClO_2^-. The function has a minimum provided that $mq > np$.

When $x = 0$, eq. [15] is reduced to $r_0 = m$, which is the initial reaction rate in the absence of chloride. Other constants of eq. [15] can be calculated by making some approximations. When x is large, $qx \gg p$ so that p is negligible, and eq. [15] becomes

$$[16] \qquad r_0 = (m + nx)\left(1 - \frac{1}{q}\right),$$

which is the equation of the straight line extended from high values of x. The intercept and the slope of the line are $m(1 - (1/q))$ and $n(1 - (1/q))$ respectively. The intercept can be used to calculate q, which in turn can be used to calculate n from the slope. On the other hand, when x is small, $m \gg nx$, and eq. [15] is reduced to

$$[17] \qquad r_0 = m\left(1 - \frac{x}{p + qx}\right),$$

which can be rearranged to

$$[18] \qquad \frac{1}{1 - (r_0/m)} = \frac{p}{x} + q.$$

A plot of $1/(1 - (r_0/m))$ vs. $1/x$ should give a straight line with slope equal to p, and intercept equal to q, which can be checked against the value obtained from eq. [16].

The four constants for curves A and B in Fig. 4 as fitted by eq. [15] are given in Table I. The values of q in parentheses are those calculated from eq. [18]. The approximations which have been made to calculate these four constants are justified from the relative values of these constants.

The calculated initial reaction rates for curves A and B are shown by the broken lines of Fig. 4. For curve C the range of the concentrations of chloride investigated does not justify the evaluation of the four constants by the same approximations made for curves A and B. However, the four constants for curve C can be evaluated from the concentrations of H^+, $HClO_2$, and ClO_2^-, and will be dealt with in the section of Mechanism.

(C) Reaction between $HClO_2$ and HOCl

In the oxidation of chlorous acid by hypochlorous acid, stoichiometric results (9) are compatible with the following two parallel reactions:

$$[19] \quad HOCl + 2HClO_2 \rightarrow 2ClO_2 + Cl^- + H^+ + H_2O$$

$$[20] \quad HOCl + HClO_2 \rightarrow 2H^+ + Cl^- + ClO_3^-.$$

In the absence of nitric acid, the dilute solutions of $NaClO_2$ and HOCl give measurable reaction rates so that the reaction orders can be determined. It was found that reaction [19] which produces chlorine dioxide is first order with respect to the concentrations of both chlorous acid and hypochlorous acid (9).

Mechanism

From the experimental results obtained, a reaction mechanism for the disproportionation of chlorous acid can be proposed.

(A) Disproportionation in the Absence of Chloride

(step 1) $2HClO_2 \rightarrow H^+ + HOCl + ClO_3^-$

(step 2) $ClO_2^- + HClO_2 \rightarrow HOCl + ClO_3^-$

(step 3) $HOCl + HClO_2 \rightarrow H_2O + Cl{-}ClO_2$

(step 4) $Cl{-}ClO_2 + HClO_2 \rightarrow H^+ + Cl^- + 2ClO_2$

The reaction is initiated by hypochlorous acid produced from the disproportionation of two molecules of chlorous acid or one molecule of chlorous acid with one chlorite ion, according to steps 1 and 2 which occur simultaneously. The sequence of reactions is propagated by step 3 to form another intermediate, $Cl{-}ClO_2$, which then reacts with chlorous acid to give chlorine

Can. J. Chem. Downloaded from www.nrcresearchpress.com by 210.87.254.5 on 09/05/12
For personal use only.

Can. J. Chem. Downloaded from www.nrcresearchpress.com by 210.87.254.5 on 09/05/12
For personal use only.

dioxide according to step 4. The observed stoichiometry, eq. [2], can be obtained by the summation of steps 1, 3, and 4, or 2, 3, and 4.

Using the steady-state hypothesis for the concentrations of the two intermediates, HOCl and Cl—ClO_2, gives

$$[21]\quad \frac{d(ClO_2)}{dt} = 2k_1(HClO_2)^2 + 2k_2(ClO_2^-)(HClO_2),$$

which agrees exactly with the empirical expression (eq. [6]). The same rate expression is obtained if ClO_2^- is written instead of $HClO_2$ in steps 3 and 4.

Steps 1 and 2 are slow processes which control the overall reaction rate. Step 3 has been shown to be fast and of second order, being first order with respect to both $HClO_2$ and HOCl. Step 4 is also expected to be fast, since it involves the reaction with a reactive intermediate.

Steps 1 and 2 are irreversible, since chlorate does not inhibit the reaction, and the equilibrium constants for these two reactions are as high as 3.78×10^{14} and 1.87×10^{17} respectively. If step 3 is written in reversible form, it does not make any difference to the derived kinetic law. Step 4 is irreversible, since it was experimentally observed that the absorbance of a mixed solution of chlorine dioxide and chloride does not decrease with time.

Since the controlling steps 1 and 2 involve at least one uncharged molecule as reactants, the reaction is independent of ionic strength.

The possible existence of the intermediate Cl—ClO_2, first proposed by Taube and Dodgen (8), may be justified partly by the fact that the congeners of oxygen form similar compounds with chlorine, such as S_2Cl_2, Se_2Cl_2, $SOCl_2$, and $SeOCl_2$. Lenzi (12) demonstrated spectrophotometrically the presence of an intermediate in the chloric – hydrochloric acid reaction, which may be Cl—ClO_2. In addition to these, it is reasonable to write Cl—ClO_2 as the product, with water as its coproduct, in the bimolecular reaction between chlorous acid and hypochlorous acid, as shown in step 3.

Strictly speaking, the reaction is not taking place in the absence of chloride even if chloride is not added, since chloride is one of the products. However, as the reaction rates were measured only at the initial stages of the reaction, the concentration of chloride produced would be too low to have any significant effect on the reaction.

(B) Disproportionation in the Presence of Chloride

In addition to those elementary steps cited for the disproportionation of chlorous acid in the absence of chloride, the following steps also occur in the present case.

(step 5) $H^+ + Cl^- + HClO_2 \rightarrow 2HOCl$

(step 6) $H^+ + Cl^- + HOCl \rightarrow H_2O + Cl_2$

(step 7) $Cl_2 + HClO_2 + H_2O \rightarrow 3H^+ + 2Cl^- + ClO_3^-$

(step 8) $Cl_2 + HClO_2 \rightarrow H^+ + Cl^- + Cl—ClO_2$

Step 5 is introduced to account for the catalytic effect of chloride, and step 6 for the observed inhibition by chloride. Chlorine produced by step 6 is another intermediate in the present system and reacts with chlorous acid in two different paths, one giving the intermediate Cl—ClO_2 which is favorable for the formation of chlorine dioxide and the other giving chloride and chlorate.

The summations of (step 3 + step 4) × 2 + step 5, and step 1 + step 6 + step 7, give respectively the stoichiometric eqs. [13] and [14], both of which occur in parallel with reaction [2].

Steps 5, 6, and 7 are all irreversible, since their equilibrium constants are 1.24×10^5, 2.29×10^3, and 1.34×10^6 respectively. Step 8 is written as irreversible to simplify the rate expression derived from the mechanism.

Applying the steady-state hypothesis again to the concentrations of the three intermediates, HOCl, Cl—ClO_2, and Cl_2, gives the following rate expression:

$$[22]\quad \frac{d(ClO_2)}{dt} = 2[k_1(HClO_2)^2 + k_2(ClO_2^-)(HClO_2) + 2k_5(H^+)(Cl^-)(HClO_2)] \times \left\{1 - \frac{k_6k_7(H^+)(Cl^-)}{(k_7 + k_8)[k_3(HClO_2) + k_6(H^+)(Cl^-)]}\right\}.$$

To visualize the effect of chloride, the following quantities are defined.

$$[23]\quad r_0 = \frac{d(ClO_2)}{dt}$$

$$[24]\quad m = 2[k_1(HClO_2)^2 + k_2(ClO_2^-)(HClO_2)]$$

TABLE II

Calculations of average rate constants or their ratios at 25 °C

				$q(=1+k_8/k_7)$	
$10^2(H^+)$	$10^2(HClO_2)$	k_5	$10^3k_3(k_7+k_8)/k_6k_7$	Eq. [16]	Eq. [18]
2.22	2.68	0.212	4.32	3.02	(3.35)
8.04	1.76	0.286	5.11	2.53	(2.28)
3.39	1.51	0.278	2.10	2.17	(2.30)
3.16	2.10	0.324	5.26	2.46	(2.46)
3.47	1.52	0.351	3.52	2.15	(2.14)
Average		0.290	4.06	2.47	(2.51)

[25] $n = 4k_5(H^+)(HClO_2)$

[26] $p = \dfrac{k_3(k_7+k_8)(HClO_2)}{k_6k_7(H^+)}$

[27] $q = \dfrac{k_7+k_8}{k_7}$

[28] $x = (Cl^-)$.

The substitution of these definitions into eq. [22] gives

[15] $$r_0 = (m+nx)\left(1-\frac{x}{p+qx}\right),$$

which is the same as the empirical expression.

The values of m, n, and p are dependent on the equilibrium concentrations of H^+, $HClO_2$, and ClO_2^-. However, q is independent of these concentrations.

The calculated rate constants or their ratios by the method given in the section of Treatment of Data are summarized in Tables II and III. The

TABLE III

Individual rate constants or their ratios at 25 °C

k_1	k_2	k_3/k_6	k_5	k_8/k_7
0.165	0.685	1.65×10^{-3}	0.290	1.47

rate constants k_1 and k_2 are those determined from the reaction in the absence of chloride. The rate constants k_1, k_2, k_3, and k_8 are second-order rate constants with units of l/(mole)(min), k_7 is a pseudo second-order rate constant, and k_5 and k_6 are third-order rate constants with units of $l^2/(mole)^2(min)$.

By use of the rate constants or their ratios evaluated, the calculated initial rate of formation of chlorine dioxide as a function of the concentration of chloride at high acidity for curve C in Fig. 4 is shown by the broken line in the same figure.

Conclusion

The proposed reaction mechanism for the disproportionation of chlorous acid in the presence or absence of chloride are in good agreement with the experimental results. Although the calculated reaction rates in the presence of chloride at high acidity are somewhat smaller than the experimental values, the calculated results do show that the minimum in the initial reaction rate gradually disappears as the acidity is increased. This is consistent with the experimental observations.

Acknowledgments

The fellowship presented by Rayonier Canada Ltd. (B.C.) in 1963–1964 and the studentship awarded by the National Research Council of Canada in 1964–1966 to C. C. Hong are gratefully acknowledged.

1. B. Barnett. Ph.D. Thesis, University of California. 1935.
2. H. F. Launer, W. K. Wilson, and J. H. Flynn. J. Res. Natl. Bur. Std. **51**, 237 (1953).
3. G. M. Nabar, V. A. Shenai, and S. Sundaram. Indian J. Technol. **2**, 7 (1964).
4. H. F. Launer and Y. Tomimatsu. J. Am. Chem. Soc. **76**, 2591 (1954).
5. F. Stitt, S. Friedlander, H. L. Lewis, and F. E. Young. Anal. Chem. **26**, 1478 (1954).
6. W. Buser and H. Hänisch. Helv. Chim. Acta, **35**, 2547 (1952).
7. H. Hefti. J. Text. Res. **30**, 861 (1960).
8. H. Taube and H. Dodgen. J. Am. Chem. Soc. **71**, 3330 (1949).
9. C. C. Hong. Ph.D. Thesis, University of Toronto, Toronto, Ontario. 1966.
10. J. N. Brönsted. Z. Phys. Chem. **102**, 169 (1922); **115**, 337 (1925).
11. N. Bjerrum. Z. Phys. Chem. **108**, 82 (1924); **118**, 251 (1925).
12. F. Lenzi. Ph.D. Thesis, University of Toronto, Toronto, Ontario. 1965.

Can. J. Chem. Downloaded from www.nrcresearchpress.com by 210.87.254.5 on 09/05/12
For personal use only.

Analyses of chlorine dioxide, chlorous acid, chlorite, chlorate, and chloride in composite mixtures

C. C. HONG[1] AND W. H. RAPSON

Department of Chemical Engineering and Applied Chemistry, University of Toronto, Toronto, Ontario

Received December 15, 1967

An analytical procedure was devised to determine chlorine dioxide, chlorous acid, and chlorite, chlorate, and chloride ions in composite mixtures. Chlorine dioxide was determined spectrophotometrically at 360 mμ. After the removal of chlorine dioxide by passing air through the solution, the total concentration of chlorous acid and chlorite ion in the solution was determined spectrophotometrically at 250 mμ where the two species have the same molar absorptivity. The total concentration of chlorous acid, chlorite ion, and chlorate ion was determined by iodimetric titration. Chloride ion was determined by the Mohr titration in neutral solution.

Canadian Journal of Chemistry, **46**, 2061 (1968)

Can. J. Chem. Downloaded from www.nrcresearchpress.com by 210.87.254.105 on 09/05/12
For personal use only.

To find the stoichiometric equations for the disproportionation of chlorous acid, it was necessary to analyze composite mixtures of $HClO_2$, ClO_2^-, ClO_2, ClO_3^-, and Cl^-. Other oxidation states of the chlorine system, namely Cl_2, HOCl (OCl^-), and ClO_4^- have been excluded, since Cl_2 and HOCl (OCl^-) undergo rapid reactions (1) with chlorous acid, and the published stoichiometric equations, though often conflicting, agree at least in not showing ClO_4^- as a product, and ClO_4^- has not been found as a product under the conditions used in these experiments.

In addition to analytical complications caused by components of closely related chemical properties, the analysis is further complicated by the possible interactions of some components in the solution.

Prince (2) used an indirect method by which chlorite and chlorine dioxide were determined spectrophotometrically at 350 mμ by absorbance of triiodide produced from iodide oxidation at the appropriate pH. Chlorate was determined spectrophotometrically at 305 mμ by ferric ion absorbance after chlorate reduction by ferrous ion in sulfuric acid solution. Chloride was determined either by the Mohr titration at pH 9 or the Volhard titration. Several empirical corrections were made by Prince (2) in order to get satisfactory results.

Harrison and Rosenblatt (3) achieved separation of chloride, chlorate, and chlorite by use of paper partition chromatography. However, this method took 16 h to obtain good chromatograms by the development of each strip with a mixture of 2-propanol, water, pyridine, and concentrated ammonium hydroxide.

The procedure devised in the present work permits a simple and accurate determination of composite mixtures of chlorine dioxide, total chlorite (including $HClO_2$ and ClO_2^-), chlorate, and chloride in much shorter time without empirical corrections. It consists of spectrophotometric determinations of chlorine dioxide and total chlorite, iodimetric titration for total concentration of chlorite and chlorate, and the Mohr titration for chloride.

The procedure is based on the following considerations:

(*a*) Chlorine dioxide in aqueous solution has an absorption maximum at 360 mμ (4) with a high molar absorptivity in the order of 1100 l/(mole)(cm). At this wavelength, the molar absorptivity of sodium chlorite in water is only 1.2 l/(mole)(cm), which can be neglected. Chlorate and chloride do not interfere with the analysis at this wavelength.

(*b*) In the four components to be analyzed, only chlorine dioxide is a gas which can readily be removed from the solution by bubbling air through it. The solution free from chlorine dioxide can be analyzed for total chlorite ($HClO_2$ and ClO_2^-) spectrophotometrically. The absorption spectra of these two species intersect at 250 mμ (4), where the molar absorptivities of the two species are the same. This particular wavelength was chosen for the analysis of the total concentration of $HClO_2$ and ClO_2^-.

(*c*) After the removal of chlorine dioxide with air, the two oxidizing agents, total chlorite and chlorate, in the solution may be determined

[1]Present address: Research Department, Imperial Oil Enterprises Ltd., Sarnia, Ontario.

iodimetrically. In strong acid solution, both chlorite and chlorate are reduced by iodide to chloride:

[1] $ClO_2^- + 4H^+ + 4e^- \rightarrow Cl^- + 2H_2O$

[2] $ClO_3^- + 6H^+ + 6e^- \rightarrow Cl^- + 3H_2O.$

It follows that

[3] $$N_1V_1 = (4M_i + 6M_a)\,V_2,$$

where N_1 and V_1 are the normality and the volume of the standard sodium thiosulfate solution used for titration, V_2 the volume of the unknown solution, and M_i and M_a the molarities of total chlorite and chlorate respectively. This equation, in conjunction with the concentration of total chlorite already determined spectrophotometrically at 250 mμ, may be used to calculate the concentration of chlorate.

Alternatively, chlorite and chlorate may be determined separately by iodimetric titration in different acidities. In moderately acid solution, only chlorite is reduced to chloride by iodide. In strong acid solution, both chlorite and chlorate are reduced to chloride.

(*d*) The solution free from chlorine dioxide is analyzed for chloride by the Mohr titration.

[4] $Ag^+ + Cl^- \rightarrow AgCl$

Experimental

Apparatus

The spectrophotometric analyses were carried out with a Beckman DB spectrophotometer, equipped with an automatic recorder. The temperature was controlled by circulating water through coils molded into the sample compartment. The temperature of the water bath was maintained constant at 25 ± 0.1 °C by a thermoregulator.

Materials

All the chemicals employed were reagent grade. Sodium chlorite is very stable and not hygroscopic (5). Sodium chlorite, chlorate, and chloride used were all supplied by British Drug Houses Limited. All these chemicals were dried in an oven at 120 °C for 2 h and then stored in desiccators before use.

The sodium chlorite reagent employed was found by iodimetric titration in strong acid solution to contain 97.8 ± 0.7% sodium chlorite. Since the analysis in moderately acid solution did not make any significant difference, no appreciable chlorate was present in the chlorite as an impurity. With a silver nitrate solution, sodium chlorite and chlorate were tested to be free from chloride. The dried sodium chlorate and chloride on analysis were found to be essentially 100% pure.

Pure chlorine dioxide was prepared from sodium chlorite in sulfuric acid solution. After a few hours, air was passed through the solution to transfer chlorine dioxide into distilled water. The chlorine dioxide prepared was free from chlorine, since the addition of a silver nitrate solution did not give any white precipitate of silver chloride. If chlorine were present in the solution, chloride would be formed by the equilibrium

$$Cl_2 + H_2O \rightleftharpoons H^+ + Cl^- + HOCl.$$

Experimental Details

To determine the molar absorptivity of chlorine dioxide, some solutions were prepared by dissolving pure chlorine dioxide in distilled water. The concentration of chlorine dioxide in each solution was determined by iodimetric titration. To 25.0 ml of chlorine dioxide solution contained in a glass-stoppered conical flask, about 1.0 g of iodate-free potassium iodide and 25 ml of concentrated hydrochloric acid were added. The flask was stoppered, and the contents were shaken and allowed to stand for 10 min in the dark. The iodine produced by the reaction

[5] $2ClO_2 + 10I^- + 8H^+ \rightarrow 2Cl^- + 5I_2 + 4H_2O$

was titrated with standard sodium thiosulfate solution, using starch solution as indicator. A blank was run on the same volume of distilled water. The absorbance corresponding to the concentration of chlorine dioxide in each solution was measured in a 10-mm absorption cell with the Beckman DB spectrophotometer at 360 mμ. If the concentration of chlorine dioxide was too high to be measured spectrophotometrically, the solution was diluted to a suitable volume. Distilled water was used as reference in the absorbance measurements. The molar absorptivity of chlorite in distilled water was determined by the same procedure at 250 mμ. Since chlorite undergoes decomposition in acid solution, the spectrophotometric analyses were carried out in netural solution.

After the determinations of the molar absorptivities of chlorine dioxide and chlorite at 360 mμ and 250 mμ respectively, some synthetic samples containing chlorine dioxide, chlorite, chlorate, and chloride were prepared in 100-ml volumetric flasks. Some samples were prepared without the addition of chloride or chlorine dioxide.

The concentration of chlorine dioxide was determined from the direct measurement of the absorbance at 360 mμ after suitable dilution. Chlorine dioxide was then removed by passing air through the solution contained in a gas-washing bottle for 10–15 min. The complete removal of chlorine dioxide was confirmed by the absorbance measurements at 360 mμ.

After the removal of chlorine dioxide, the solution contained only three components, chlorite, chlorate, and chloride. The concentration of total chlorite was determined by the absorbance measurement at 250 mμ. The concentration of chlorate was found by the same iodimetric titration mentioned previously for chlorine dioxide, in conjunction with the concentration of total chlorite determined spectrophotometrically. Equation [3] was used for this calculation.

Chloride was analyzed by the Mohr titration (6), using a mixed indicator of potassium chromate and potassium dichromate. To 25.0 ml of the solution in a 250 ml conical flask resting upon a large white porcelain crucible, 1 ml of the indicator solution was added with a pipette. The solution was titrated with a standard silver nitrate solution with constant swirling until a faint but distinct change in color occurred. The faint reddish brown color

Can. J. Chem. Downloaded from www.nrcresearchpress.com by 210.87.254.105 on 09/05/12
For personal use only.

TABLE I

Molar absorptivity of ClO_2 at 360 mμ and 25 °C

$10^3(ClO_2)$, moles/l (before dilution)	Dilution	Absorbance (after dilution)	Molar absorptivity, l/(mole)(cm)
5.20	20 times	0.278	1070
9.26	20 times	0.518	1120
12.4	20 times	0.680	1100
			Average 1100

TABLE II

Molar absorptivity of total chlorite at 250 mμ and 25 °C

$10^3(NaClO_2)$, moles/l	Absorbance	Molar absorptivity, l/(mole)(cm)
1.10	0.151	137
2.15	0.303	141
3.22	0.452	141
4.40	0.604	137
4.83	0.682	141
6.44	0.900	140
		Average 140

TABLE III

Analyses of synthetic samples

		10^2(concentration), moles/l			
Sample	Added or Found	ClO_2	ClO_2^-	ClO_3^-	Cl^-
1	Added	—	1.63	1.09	4.73
	Found	—	1.63	1.08	4.74
2	Added	—	0.606	2.49	8.34
	Found	—	0.603	2.42	8.35
3	Added	—	0.450	11.5	9.26
	Found	—	0.445	11.2	9.23
4	Added	—	0.450	1.36	33.9
	Found	—	0.445	1.37	33.9
5	Added	1.07	1.56	0.963	3.49
	Found	1.04	1.57	0.958	3.51
6	Added	0.477	1.23	9.23	8.80
	Found	0.468	1.24	9.36	8.96
7	Added	0.415	0.440	1.13	26.2
	Found	0.404	0.447	1.15	26.7
8	Added	0.354	1.92	1.65	—
	Found	0.347	1.87	1.69	—
9	Added	0.291	0.673	3.77	—
	Found	0.287	0.678	3.82	—

should persist after brisk shaking. A blank was run on a volume of distilled water equal to the final volume in the titration.

Results and Discussion

The molar absorptivity of chlorine dioxide at 360 mμ and 25 °C measured by Lenzi (7) was 1100 ± 50 l/(mole)(cm). This value was checked by the three runs in Table I. Lenzi (7) also showed that the molar absorptivity of chlorine dioxide is independent of the acidity of the solution.

The molar absorptivity of total chlorite (including $HClO_2$ and ClO_2^-) at 250 mμ and 25 °C was determined to be 140 ± 2 l/(mole)(cm) (Table II).

Can. J. Chem. Downloaded from www.nrcresearchpress.com by 210.87.254.105 on 09/05/12
For personal use only.

The accuracy of the analytical procedure proposed can be judged from the experimental data of Table III for some synthetic samples.

This method proved to be excellent for the determinations of chlorite and chloride in neutral solutions. The slight negative discrepancy in the chlorine dioxide determination can be attributed to the possible loss of chlorine dioxide to the atmosphere during the preparation of synthetic samples. Another possible reason is that the addition of the solids sodium chlorite, chlorate, and chloride may increase the volume of chlorine dioxide solution and, accordingly, the concentration of chlorine dioxide is decreased. For chlorine dioxide and chlorate the maximum deviation was 2.8%.

Acknowledgments

C. C. Hong wishes to express appreciation to Rayonier Canada Ltd. for a fellowship granted in 1963–1964 and to the National Research Council of Canada for a studentship award in 1964–1966.

1. H. TAUBE and H. DODGEN. J. Am. Chem. Soc. **71**, 3330 (1949).
2. L. A. PRINCE. Anal. Chem. **36**, 613 (1964).
3. B. L. HARRISON and D. H. ROSENBLATT. J. Chromatog. **13**, 271 (1964).
4. W. BUSER and H. HÄNISCH. Helv. Chim. Acta, **35**, 2547 (1952).
5. M. C. TAYLOR, J. F. WHITE, C. P. VINCENT, and G. L. CUNNINGHAM. Ind. Eng. Chem. **32**, 899 (1940).
6. A. I. VOGEL. A text-book of quantitative inorganic analysis. 3rd ed. Longmans, Green and Co., Ltd., London. 1961.
7. F. LENZI. Ph.D. Thesis. University of Toronto, Toronto, Ontario. 1965.

Can. J. Chem. Downloaded from www.nrcresearchpress.com by 210.87.254.105 on 09/05/12
For personal use only.

Can. J. Chem. Downloaded from www.nrcresearchpress.com by 210.87.254.42 on 09/05/12
For personal use only.

Vapor–liquid equilibrium studies of *n*-propanol–*n*-decanol mixtures[1]

JASWANT SINGH[2] AND G. C. BENSON
Division of Pure Chemistry, National Research Council of Canada, Ottawa, Canada

Received January 5, 1968

Static vapor pressure measurements were made on mixtures of *n*-propanol with *n*-decanol over the temperature range 20–50 °C. From the results, the molar excess Gibbs free energies were calculated. The applicability of the principle of congruence to these values and to similar data published previously for methanol–decanol and ethanol–decanol systems was examined.

Canadian Journal of Chemistry, 46, 2065 (1968)

I. Introduction

Vapor–liquid equilibrium studies on mixtures of methanol–*n*-decanol (MeOH–DeOH) and ethanol–*n*-decanol (EtOH–DeOH) were reported in a previous communication (1). We have now extended these studies of binary alcohol systems by measurements on *n*-propanol–*n*-decanol (PrOH–DeOH) mixtures over the temperature range 20–50 °C.

II. Experimental

The vapor pressure assembly and experimental procedure used in the present investigation have been described in ref. 1. Measurements of vapor pressures were made for 12 different (total) compositions and at 6 temperatures (20.0, 25.0, 30.0, 35.0, 40.0, and 50.0 °C) for each mixture. Generally the temperatures were within ±0.1 °C of the standard set and values at the rounded temperatures were interpolated by fitting the data with an Antoine form of equation

$$[1] \qquad \log_{10} p(\text{Torr}) = A - \frac{B}{C + t(^\circ\text{C})} .$$

An iterative calculation similar to that outlined in ref. 1 was used to obtain the compositions of the liquid and vapor phases from the known volumes of the various parts of the apparatus, the overall composition, and the total vapor pressure. In the present work the equation of state employed was

$$[2] \qquad V^g = n^g \left(\frac{RT}{p} + B \right) ,$$

where V^g is the vapor volume, n^g is the number of moles in the vapor, and B is the second virial coefficient. For mixtures, it was assumed:

(i) that the second virial coefficient of the vapor (mole fraction y_1 of propanol) could be approximated by that of pure propanol B_{11} and

(ii) that the partial pressure of decanol could be estimated by the Raoult's law expression

$$[3] \qquad p_2 = x_2 p_2^0 ,$$

where x_2 is the mole fraction of decanol in the liquid phase and p_2^0 is the vapor pressure of decanol at the same temperature as the mixture.

These assumptions should provide reasonable estimates, since p_2^0 is relatively small over the temperature range studied and $y_2 < 0.03$ for all the mixtures.

Purification of the decanol used in the present work has been described in ref. 1. The *n*-propanol (Eastman Organic Chemicals) was purified in a model 775 F & M preparative gas chromatograph with a column containing PEG 4000 supported on Chromosorb W. Chromatographic analyses of the materials indicated an impurity content < 0.1 mole %. Density measurements at 25 °C on samples of the alcohols yielded the values 0.79962 and 0.82687 g cm^{-3} for the propanol and decanol respectively.

III. Results

Properties of the pure alcohols at rounded temperatures are given in Table I. The vapor pressures for *n*-propanol (listed under heading p_1^0) are calculated from eq. [1] with the values $A = 8.36512$, $B = 1777.23$, and $C = 227.388$, which represents our experimental pressures with an estimated standard error of 0.029 Torr. Over most of the temperature range studied, our results for propanol are higher than the vapor pressures tabulated by the American Petroleum Institute (2). At the 6 standard temperatures from 20 to 50 °C, the deviations amount to 0.62, 0.58, 0.50, 0.35, 0.14, and −0.44 Torr respectively.

The molar volumes at 25 °C in Table I were obtained from the densities stated in the preceding section; in estimating values at other temperatures, coefficients of expansion based on observations by Costello and Bowden (3) were used. The values of the second virial coefficient B_{11} for propanol were calculated from the equation

$$[4] \qquad \log_{10}(-B_{11}) = 12.491 - 3.7 \log_{10} T$$

which represents the measurements of Cox (4) over the range 105 to 150 °C.

[1]Issued as NRCC No. 10053.
[2]NRCC Postdoctorate Fellow 1965–1967.

TABLE I

Properties of pure component liquids

Temp. (°C)	Propanol p_1^0 (Torr)	Propanol V_1^0 (cm^3 mole^{-1})	Propanol B_{11} (cm^3 mole^{-1})	Decanol p_2^0 (Torr)	Decanol V_2^0 (cm^3 mole^{-1})
20	15.18	74.780	−2301	0.016	190.644
25	21.06	75.156	−2163	0.026	191.428
30	28.86	75.541	−2037	0.042	192.207
35	39.07	75.934	−1910	0.060	192.980
40	52.30	76.337	−1807	0.089	193.748
50	90.81	77.172	−1607	0.210	195.278

Table II summarizes the vapor–liquid equilibrium measurements on PrOH–DeOH mixtures. p is the measured value of the vapor pressure; x_1 and y_1 are the mole fractions of propanol in the liquid and vapor phases respectively. Also included in the table are values of the natural logarithm of the activity coefficient of propanol in the liquid phase calculated from the formula

$$[5]\quad \ln \gamma_1 = \ln\left(\frac{p_1}{x_1 p_1^0}\right) + \frac{(p - p_1^0)(B_{11} - V_1^0)}{RT}.$$

IV. Discussion

(a) Molar Excess Functions

The expression

$$[6]\quad \ln \gamma_1 = \frac{x_2^2}{RT} \sum_{r=1}^{n} C_r(1 - 2rx_1)(x_2 - x_1)^{r-2}$$

was fitted to the experimental results for $\ln \gamma_1$ by a least squares procedure. At each temperature the use of 4 coefficients (i.e. $n = 4$ in eq. [6]) led to a satisfactory fit of the data. The values of the coefficients are listed in Table III along with $\sigma_{\ln\gamma}$, the standard error for each fit, and σ_G the statistical estimate of the root mean square error of G^E (the molar excess Gibbs free energy) as calculated from the formula

$$[7]\quad G^E = x_1 x_2 \sum_{r=1}^{n} C_r(x_2 - x_1)^{r-1}.$$

At all mole fractions G^E for PrOH–DeOH mixtures decreases with increasing temperature, indicating a positive molar excess entropy.

$$[8]\quad S^E = -\left(\frac{\partial G^E}{\partial T}\right)_p$$

At 25 °C this appears to be similar in magnitude to that of the system EtOH–DeOH (1). However, the numerical values of S^E obtained in this way are questionable, since the corresponding molar excess enthalpies calculated from

$$[9]\quad H^E = G^E + TS^E$$

do not agree with values determined calorimetrically. For an equimolar mixture the excess free energy data lead to a value of 344 J mole^{-1} for H^E at 25 °C, which is considerably higher than the calorimetric result 252 J mole^{-1} (5). The reason for this discrepancy is not clear.

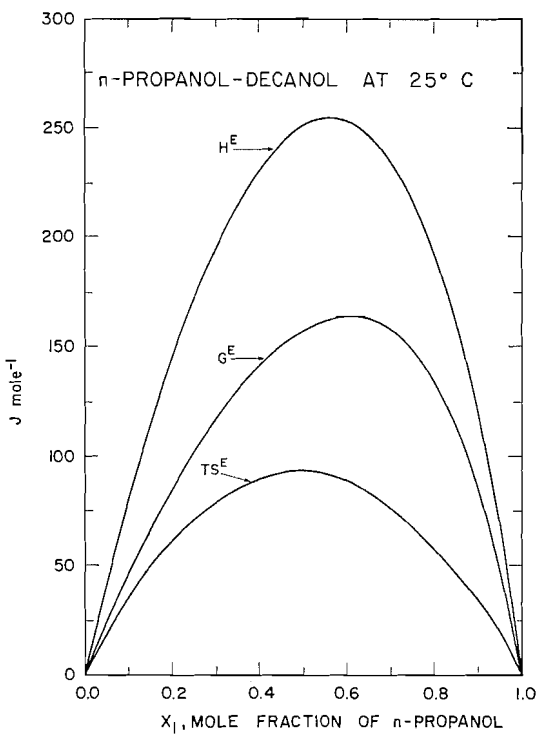

FIG. 1. Excess thermodynamic properties of propanol–decanol mixtures at 25 °C: G^E from vapor pressures; H^E calorimetric results from ref. 5; TS^E calculated from eq. [9].

Can. J. Chem. Downloaded from www.nrcresearchpress.com by 210.87.254.42 on 09/05/12
For personal use only.

Can. J. Chem. Downloaded from www.nrcresearchpress.com by 210.87.254.42 on 09/05/12
For personal use only.

TABLE II

Vapor–liquid equilibrium for propanol–decanol mixtures (p in Torr)

x_1	p	y_1	$\ln \gamma_1$	x_1	p	y_1	$\ln \gamma_1$
	20 °C				25 °C		
0.0652	1.20	0.9876	0.1901	0.0652	1.66	0.9854	0.1812
0.1381	2.50	0.9945	0.1732	0.1381	3.45	0.9935	0.1662
0.1902	3.38	0.9962	0.1576	0.1902	4.67	0.9955	0.1523
0.2517	4.41	0.9973	0.1420	0.2516	6.09	0.9968	0.1374
0.2673	4.66	0.9975	0.1380	0.2672	6.44	0.9970	0.1334
0.3654	6.26	0.9984	0.1203	0.3653	8.65	0.9981	0.1165
0.4454	7.49	0.9988	0.1016	0.4454	10.35	0.9986	0.0986
0.5650	9.25	0.9992	0.0758	0.5650	12.80	0.9991	0.0733
0.6565	10.55	0.9995	0.0566	0.6564	14.60	0.9994	0.0547
0.7669	12.04	0.9997	0.0339	0.7669	16.70	0.9996	0.0331
0 8469	13.10	0.9998	0.0194	0.8469	18.16	0.9998	0.0186
0.8811	13.56	0.9999	0.0139	0.8811	18.80	0.9998	0.0135
	30 °C				35 °C		
0.0652	2.27	0.9827	0.1724	0.0651	3.05	0.9816	0.1659
0.1381	4.70	0.9923	0.1593	0.1380	6.32	0.9918	0.1534
0.1901	6.37	0.9947	0.1468	0.1901	8.58	0.9943	0.1420
0.2516	8.30	0.9962	0.1329	0.2515	11.19	0.9960	0.1290
0.2671	8.78	0.9965	0.1288	0.2670	11.83	0.9963	0.1248
0.3652	11.80	0.9977	0.1126	0.3650	15.90	0.9976	0.1089
0.4453	14.13	0 9984	0.0955	0.4451	19.07	0.9983	0.0924
0.5649	17.50	0.9990	0 0709	0.5648	23.62	0.9989	0.0685
0.6564	19.96	0.9993	0.0528	0.6563	26.97	0.9992	0.0510
0.7669	22.85	0 9996	0.0321	0.7669	30.89	0.9995	0.0312
0.8468	24.88	0.9997	0.0179	0.8468	33.65	0.9997	0.0173
0.8811	25.75	0.9998	0.0130	0.8811	34.85	0.9998	0.0124
	40 °C				50 °C		
0.0651	4.05	0.9795	0.1591	0.0650	6.97	0.9718	0.1438
0.1380	8.41	0.9909	0.1475	0.1378	14.41	0.9874	0.1352
0.1900	11.42	0.9937	0.1370	0.1898	19.62	0.9913	0.1267
0.2515	14.92	0.9955	0.1251	0.2512	25.68	0.9939	0.1175
0.2668	15.76	0.9959	0.1209	0.2663	27.09	0.9943	0.1132
0.3649	21.19	0.9973	0.1051	0.3644	36.45	0.9963	0.0977
0.4450	25.43	0 9981	0 0893	0.4445	43.80	0.9973	0 0829
0.5647	31.53	0.9988	0 0662	0.5644	54.42	0.9983	0.0615
0.6562	36.03	0.9992	0 0493	0.6560	62.29	0.9988	0.0460
0.7668	41.31	0.9995	0.0302	0.7667	71.54	0.9993	0.0281
0.8468	45 01	0 9997	0 0167	0.8468	78.06	0.9996	0.0158
0.8810	46.62	0 9998	0.0119	0.8810	80.82	0.9997	0.0108

The change in G^E (at $x_1 = 0.5$) between 20 and 30 °C is only about 6 J mole^{-1}, but this would have to be reduced to 3 J mole^{-1} to bring about agreement with the calorimetric result. The virial coefficients used in the present work were obtained by a rather lengthy extrapolation of Cox's data (4) and uncertainty in these values might account for some of the difference (but only a small fraction of it).

The thermodynamic functions G^E, H^E, and TS^E for PrOH–DeOH mixtures at 25 °C are plotted in Fig. 1. The values of G^E were calculated from eq. [7] with the coefficients given in Table III; results of direct calorimetric determinations (5) were used in constructing the curve for H^E, and TS^E was obtained from these two sets of data by means of eq. [9]. Graphs constructed in the same way for the systems MeOH–DeOH and EtOH–DeOH are given in ref. 1. Comparison with these shows that the behavior of the present system is similar to that of EtOH–DeOH. However, although both G^E and H^E have been decreased by the change from ethanol to propanol, the difference between these values (i.e. TS^E) has increased over most of the concentration range.

The magnitudes of G^E for the three systems at 25 °C are illustrated by the solid curves in Fig. 2. These are all skewed towards low mole fractions of decanol, with the asymmetry less for

TABLE III

Coefficients for eqs. [6] and [7] (C_r and σ_G in J mole^{-1})

Temp. (°C)	C_1	C_2	C_3	C_4	$\sigma_{\ln\gamma}$	σ_G
20	644.5	−233.3	158.4	−68.5	0.0018	0.98
25	632.1	−232.9	151.5	−70.3	0.0017	0.95
30	618.7	−231.5	144.6	−72.8	0.0016	0.89
35	607.9	−228.5	139.7	−72.6	0.0015	0.83
40	595.9	−225.2	134.2	−73.9	0.0013	0.76
50	568.4	−218.9	120.5	−81.2	0.0011	0.64

systems having a smaller difference in chain length of the components. The maxima occur at mole fractions of decanol equal to 0.352, 0.383, and 0.395 for the systems containing methanol, ethanol, and propanol respectively. It can be shown from the coefficients in Table III that there is a tendency for the curves to become more symmetric at higher temperatures, but this is so slight that for practical purposes the mole fraction at the maximum can be treated as independent of temperature over the range investigated.

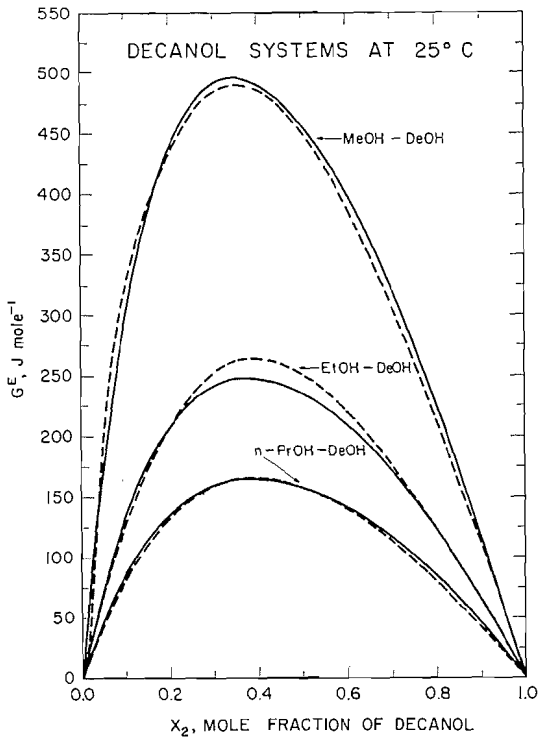

FIG. 2. Excess free energy of decanol systems. Solid curves represent experimental results from vapor pressure data (MeOH–DeOH and EtOH–DeOH from ref. 1; PrOH–DeOH present investigation). Dashed curves calculated from principle of congruence.

(b) Congruence Calculations

The principle of congruence (6) has been applied with significant success to the thermodynamic properties of *n*-alkane mixtures (7–10). Application to the excess enthalpies (11, 12) and excess volumes (13) of binary *n*-alcohol systems has shown that the principle is also useful in correlating these data, but that estimates of the excess enthalpy and excess volume based on the principle are subject to relatively larger errors than in the case of the *n*-alkanes. The congruence of the present free energy results for PrOH–DeOH mixtures with those published previously (1) for MeOH–DeOH and EtOH–DeOH was investigated following the method described in ref. 12.

If a set of component materials characterized by their "chain length" are congruent, the thermodynamic properties of a binary mixture are the same (at constant temperature and pressure) as those of the member with chain length equal to the mean in the mixture, as defined by

$$[10] \qquad n = x_1 n_1 + x_2 n_2.$$

In this expression n_1 and n_2 are the chain lengths of the two components (by convention, $n_1 < n_2$), and x_1 and x_2 are their mole fractions in the mixture. The molar excess free energy can then be written in the form

$$[11] \quad G^E(n_1, n_2, x_1) = f(n) - x_1 f(n_1) - x_2 f(n_2),$$

where $f(n)$ is a suitable function.

In our considerations of the excess enthalpies and excess volumes of alcohol systems (12, 13) a four term polynomial in reciprocal powers of the chain length was employed. A similar function could also be used in fitting the free energy data. However, Bellemans and Mat (14) have pointed out that in the limit of long chain lengths,

Can. J. Chem. Downloaded from www.nrcresearchpress.com by 210.87.254.42 on 09/05/12
For personal use only.

TABLE IV

Results of congruence calculations (all units J mole^{-1})

Temp. (°C)	B_0	B_1	B_2	B_3	σ^{MeOH}	σ^{EtOH}	σ^{PrOH}	σ
20	−24 205	37 798	−33 823	12 015	12.7	9.4	4.0	9.4
25	−24 498	38 395	−34 523	12 316	14.2	9.3	3.2	10.0
30	−24 712	38 771	−34 965	12 512	15.5	9.2	2.8	10.6
35	−24 936	39 149	−35 392	12 697	16.7	9.2	2.9	11.2
40	−25 090	39 335	−35 598	12 793	17.9	9.2	3.4	11.8
50	−25 147	39 006	−35 182	12 645	20.0	8.9	5.4	13.0

the combinatorial entropy of chain molecules should contribute a term of the form

$$RT(x_1 \ln n_1 + x_2 \ln n_2 - \ln n)$$

to the excess free energy. Therefore in the analysis of our G^E results, the form

$$[12] \quad f(n) = -RT \ln n + \frac{B_0}{n} + \frac{B_1}{n^2} + \frac{B_2}{n^3} + \frac{B_3}{n^4}$$

was assumed, and the values of the four coefficients were determined to minimize the value of

$$[13] \quad \sigma^2 = \frac{1}{N} \sum_{s=1}^{N} (\sigma^s)^2,$$

where

$$[14] \quad (\sigma^s)^2 = \int_0^1 (G^E_{calcd}(n_1^s, n_2^s, x_1) - G^E_{obsd})^2 \, dx_1.$$

G^E_{calcd} (n_1^s, n_2^s, x_1) indicates the value of the excess free energy calculated for system s from eq. [11] with the form of $f(n)$ substituted from eq. [12], and G^E_{obsd} is the corresponding experimental value obtained from eq. [7]. The sum in eq. [13] is taken over the N systems of the set considered. ($N = 3$ in the present application and the name of the shorter chain component in each of the three systems is used for the identifying label s in eq. [14].)

Table IV contains the results of the calculations. There the values of the coefficients at each temperature and the resulting minimum value of σ are given; in addition, the standard errors (σ^{MeOH}, σ^{EtOH}, σ^{PrOH}) for the individual systems are shown. Although the deviations are too large to be attributed entirely to experimental error, the principle does provide a useful approximation to the data. This is illustrated by the dashed curves in Fig. 2 which are calculated with the coefficients for 25 °C from Table IV. However, the temperature variation of G^E, as represented by the coefficients in Table IV, is not satisfactory and leads to positive excess entropies for all three systems in contrast to the negative entropy values found for MeOH–DeOH mixtures (1). It can be seen from Table IV that the fit of the MeOH–DeOH system is poorer at higher temperatures. Deviations from congruence which increase with increasing temperature have also been reported for the excess enthalpies of *n*-alkane mixtures (10).

V. Acknowledgment

We are indebted to Mr. C. J. Halpin for invaluable technical assistance throughout the course of this investigation.

1. J. Singh and G. C. Benson. Can. J. Chem. **46**, 1249 (1968).
2. American Petroleum Institute. Research Project 44. Selected values of properties of hydrocarbons and related compounds. Carnegie Press, Carnegie Inst. of Technology, Pittsburgh. 1953 and later revisions.
3. J. M. Costello and S. T. Bowden. Rec. Trav. Chim. **77**, 36 (1958).
4. J. D. Cox. Trans. Faraday Soc. **57**, 1674 (1961).
5. H. D. Pflug and G. C. Benson. J. Chem. Eng. Data. In press.
6. J. N. Brønsted and J. Koefoed. Kgl. Danske Videnskab. Selskab, Mat.Fys. Medd. **22**, 17 (1946).
7. J. Hijmans. Mol. Phys. **1**, 307 (1958).
8. M. L. McGlashan. Mol. Phys. **4**, 87 (1961).
9. Th. Holleman. Physica, **29**, 585 (1963).
10. Th. Holleman and J. Hijmans. Physica, **31**, 64 (1965).
11. M. Díaz Pena and F. Fernández Martín. Anales Real Soc. Espan. Fis. Quim. Madrid, Ser. B, **60**, 9 (1964).
12. A. E. Pope, H. D. Pflug, B. Dacre, and G. C. Benson. Can. J. Chem. **45**, 2665 (1967).
13. H. D. Pflug and G. C. Benson. Can. J. Chem. **46**, 287 (1968).
14. A. Bellemans and P. Mat. Mol. Phys. **6**, 637 (1963).

Can. J. Chem. Downloaded from www.nrcresearchpress.com by 210.87.254.42 on 09/05/12
For personal use only.

Can. J. Chem. Downloaded from www.nrcresearchpress.com by 210.87.254.40 on 09/05/12
For personal use only.

Nuclear magnetic resonance studies of tertiary phosphine hydrobromides

SAMUEL O. GRIM AND WILLIAM MCFARLANE
Department of Chemistry, University of Maryland, College Park, Maryland 20740

Received January 18, 1968

Phosphorus and proton magnetic resonance data are presented for hydrobromides of 15 tertiary phosphines, of which 5 are trialkylphosphines, 5 are dialkylphenylphosphines, and 5 are diphenylalkylphosphines. The ^{31}P chemical shifts of each of these series of phosphonium compounds are linearly related to the sum of the group contributions (g.c.) of the organic groups on the respective phosphines.

Canadian Journal of Chemistry, 46, 2071 (1968)

Introduction

Recently some quantum mechanical treatments which illustrate *a priori* calculations of phosphorus-31 chemical shifts have been published (1–5). These studies add considerably to the understanding of various factors influencing chemical shifts, although their predictive utility is rather limited because the parameters, such as bond angles, electronegativities, and average electron excitation energies, which are necessary for the calculations, are generally more tedious to obtain than the chemical shifts.

In order to develop a predictive basis for phosphorus chemical shifts, we (6–9) have been engaged in phosphorus magnetic resonance measurements of various series of closely related organophosphorus compounds, whose chemical shifts are predicted rather accurately by group contributions, which were originally devised to be useful in predicting the chemical shift of any trivalent phosphorus compound (10), but are especially useful for primary phosphines (11), secondary and tertiary phosphines (6, 8), and quaternary phosphonium salts (7).

We report in this work ^{31}P chemical shifts for 15 tertiary phosphine hydrobromides, as well as proton chemical shifts and coupling constant data.

Experimental

The tertiary phosphines, R_3P, R_2PhP, and RPh_2P, were prepared by the reaction between PCl_3, $PhPCl_2$, or Ph_2PCl and a 10–20% excess of the appropriate Grignard reagent in ether at −23°. They were isolated by hydrolysis of NH_4Cl solution, followed by distillation under reduced pressure. The solutions of the tertiary phosphine hydrobromides were made by bubbling anhydrous HBr into ca. 30% solution of the phosphines in CH_2Cl_2 for a few minutes, and then by passing dry N_2 through the solution for about a minute. The solutions, which are saturated in HBr, probably contain HBr_2^- (12) and more complex anions in addition to Br^-, since in several cases it was observed that a precipitate would form on first addition of gaseous HBr, but would redissolve on continued addition of HBr.

The ^{31}P magnetic resonance measurements were performed at 24.3 MHz on a Varian DP60 spectrometer. The solutions were contained in 13 mm o.d. tubes which were stationary and the 85% H_3PO_4 reference was placed in a 5 mm o.d. tube fixed concentrically within the specimen tube. Line positions were determined by visual superposition on the oscilloscope of the signal and of a sideband of H_3PO_4 generated by a Hewlett Packard wide range oscillator, model No. 200CD. The chemical shift values are accurate to ±5 Hz (0.2 p.p.m.).

The ^1H magnetic resonance spectra were determined on the same spectrometer at 56.4 MHz using ca. 10% solutions in CH_2Cl_2 contained in a spinning 5 mm o.d. tube with tetramethylsilane (TMS) as the internal reference.

Results and Discussion

Table I lists the ^{31}P chemical shifts of 15 tertiary phosphonium compounds. A plot of these chemical shifts against the sum of the group contributions (8) for the three organic groups (methyl, 21; ethyl, 7; *n*-butyl, 11; isopropyl, −6; cyclohexyl, −2; phenyl, 3) does not yield a

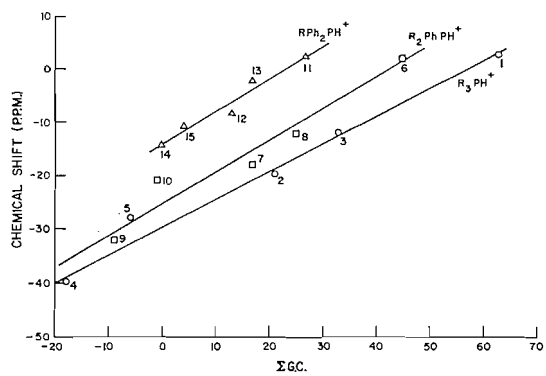

FIG. 1. The chemical shift of tertiary phosphonium compounds vs. the sum of the group contributions for the three organic groups. The number associated with each point identifies the compound listed in Table I.

Can. J. Chem. Downloaded from www.nrcresearchpress.com by 210.87.254.40 on 09/05/12
For personal use only.

TABLE I

^{31}P chemical shifts in phosphine hydrobromides

Phosphine	No.	Chemical shift (p.p.m.)		
		Free phosphine	Hydrobromide	Difference
$(CH_3)_3P$	1	62	2.9*	−59.1
$(C_2H_5)_3P$	2	20.4	−19.7	−40.1
$(n\text{-}C_4H_9)_3P$	3	32.3	−11.9	−44.2
$(i\text{-}C_3H_7)_3P$	4	−19.4	−39.6	−20.2
$(C_6H_{11})_3P$	5	−7	−27.9	−20.9
$(CH_3)_2(C_6H_5)P$	6	46	2.1	−43.9
$(C_2H_5)_2(C_6H_5)P$	7	16	−18.3	−34.3
$(n\text{-}C_4H_9)_2(C_6H_5)P$	8	26.2	−12.2	−38.4
$(i\text{-}C_3H_7)_2(C_6H_5)P$	9	−10	−32.0	−22.0
$(C_6H_{11})_2(C_6H_5)P$	10	−2.5	−20.8	−18.3
$(CH_3)(C_6H_5)_2P$	11	28	2.2	−25.8
$(C_2H_5)(C_6H_5)_2P$	12	12	−8.3	−20.3
$(n\text{-}C_4H_9)(C_6H_5)_2P$	13	17.1	−2.1	−19.2
$(i\text{-}C_3H_7)(C_6H_5)_2P$	14	−0.2	−14.0	−13.8
$(C_6H_{11})(C_6H_5)_2P$	15	4.4	−10.5	−14.9

*In aqueous solution.

straight line, but rather a series of three lines of similar slope (Fig. 1). The correlation is fairly good except for the cyclohexyl compounds, which have been noticeably out of line in other work (13). The correlation coefficients for the lines are 0.96, 0.96, and 0.97, respectively. These lines represent the three classes of compounds, trialkylphosphonium salts, dialkylphenylphosphonium salts, and alkyldiphenylphosphonium salts. The number labels in Fig. 1 are identified in Table I.

The equations for the three lines are:

$$\delta(\text{p.p.m.}) = -28.5 + 0.50 \sum \text{g.c. for } R_3PH^+$$

$$\delta(\text{p.p.m.}) = -25.0 + 0.57 \sum \text{g.c. for } (C_6H_5)R_2PH^+$$

$$\delta(\text{p.p.m.}) = -13.2 + 0.57 \sum \text{g.c. for } (C_6H_5)_2RPH^+.$$

Since it has been shown that the change in the phenyl group contribution to the ^{31}P chemical shift in going from phosphines to phosphonium salts is quite different from the change in the alkyl group contributions in phosphines relative to phosphonium salts (7), it is understandable that the different number of phenyl groups in the phosphonium compound would lead to different intercepts.

The last column in Table I lists the change in chemical shift on protonation of the tertiary phosphines. It was hoped that this chemical shift on protonation might be a measure of basicity of the phosphine, reflecting the extent of electron donation by phosphorus and thus the decrease in shielding.

Comparison of the chemical shift on protonation in the series R_3P, $R_2(C_6H_5)P$, and $R(C_6H_5)_2P$ with the basicities gives the expected results, i.e. both values decrease in the series as listed in order of increasing number of phenyl groups. However, comparison of the values within a particular series, e.g. $R_2(C_6H_5)P$ as R varies, gives no correlation between basicity and chemical shift on protonation. The same observation was noted for the chemical shifts of the phosphines themselves, viz. the group contributions of the alkyl groups are not linearly related to the Taft σ^* values (6).

It is reasonable that the chemical shift on protonation is related to change in bond angles upon protonation. Assuming that all the protonated species have approximately tetrahedral configuration, then the phosphines with the smallest groups (e.g. methyl) would have the

TABLE II

J_{P-H} (Hz) in tertiary phosphonium compounds, $[R_{3-n}Ph_nPH]^+$

R	$n = 0$	$n = 1$	$n = 2$
CH_3	505	525	525
C_2H_5	500	490	515
$n\text{-}C_4H_9$	475	490	520
$i\text{-}C_3H_7$	455	485	510
C_6H_{11}	455	485	510

TABLE III

Proton n.m.r. data in tertiary phosphines and tertiary phosphonium compounds*

Phosphine	$\tau_{H\alpha}$		$\tau_{H\beta}$		$J_{P-H\alpha}$		$J_{P-H\beta}$		$J_{H\alpha-H\beta}$		$J_{H-H\alpha}$,	J_{P-H},
	x	y	x	y	x	y	x	y	x	y	y	y
$(CH_3)(C_6H_5)_2P$	8.49	7.35	—	—	5.0	15.0	—	—	—	—	?	525
$(CH_3)_2(C_6H_5)P$	8.83	6.50	—	—	3.4	15.8	—	—	—	—	5.8	520
$(C_2H_5)(C_6H_5)_2P$	7.99	6.88	9.00	8.62	~1.5	?	~15	22.1	7.2	7.3	?	517
$(C_2H_5)_2(C_6H_5)P$	8.46	7.16	9.07	8.62	<1.5	~14	~14	21.5	7.2	7.5	6.0	492
$(i\text{-}C_3H_7)(C_6H_5)P$	7.66	?	8.96	8.54	~1.5	?	15.2	20.6	7.0	7.1	?	510
$(i\text{-}C_3H_7)_3P$	8.27	?	8.88	8.43	~1.5	?	11.5	18.0	6.6	6.8	?	455

*x is the value in the free phosphine. y is the value in the phosphonium compound. τ in p.p.m.; J in Hz. $J_{H-H\alpha}$ is the coupling between the acidic proton and Hα.

smallest angles in the unprotonated species and would change most on protonation, resulting in the largest chemical shift on protonation. This idea was presented earlier with respect to chemical shifts on coordination of tertiary phosphines with chromium carbonyl (9). This concept does explain the difference in the chemical shifts on protonation between the series (constant R with a different number of phenyl groups) and within a series (constant number of phenyls with variable R).

Table II lists the coupling constants between phosphorus and the directly bound proton. Two of these have been reported previously (14–16). Proton–carbon-13 coupling constants have been shown to depend linearly on the s-character in the bond (17), in addition to other factors (18, 19). Proton–phosphorus-31 couplings are qualitatively (but not linearly) related to the amount of s-character (20) in the bond and the large value of J_{P-H} (ca. 500 Hz) for approximately sp^3 bonding by phosphorus in the phosphonium salt is reasonable compared to the smaller value (ca. 200 Hz) for P—H bonds in trivalent compounds (15, 20) in which the bonding is largely p^3 with a small amount of s-character.

J_{P-H} couplings in these compounds increase with the number of phenyl groups and decrease with R in the order shown in Table II.

Triphenylphosphine, diphenylphosphine, and phenylphosphine are so weakly basic that proton exchange in solution of their hydrobromides in dichloromethane solution prevented any determination of the coupling constants or ^{31}P chemical shifts. The lifetime of $(C_6H_5)_3PH^+$ must be less than about 3×10^{-3} s, since J_{P-H} would be expected to be about 500 Hz and $T = \sqrt{2}/J$ (21), where T is the lifetime.

Proton magnetic resonance data are given in Table III. Of particular interest here are $J_{H-H\alpha}$, the coupling between the methyl hydrogens and the acidic hydrogen, in methyl compounds. This coupling is observed to be 5.8 Hz in dimethylphenylphosphine, which means the mean lifetime of the phosphonium salt must be of the order of 0.2 s or longer. On the other hand, under approximately the same conditions (the concentration of HBr in solution was not known, but the solutions were prepared similarly) $J_{H-H\alpha}$ is not observed for diphenylmethylphosphine, which is less basic than dimethylphenylphosphine. However, J_{P-H} is observed, so that the mean lifetime of dimethylphenylphosphonium cation is in the range of approximately 3×10^{-3} to 0.2 s. In the series triphenylphosphine, diphenylmethylphosphine, and dimethylphenylphosphine, as the phosphine becomes more basic, the respective phosphonium ion becomes longer-lived, as would be intuitively predicted. Proton magnetic resonance studies of trimethylphosphonium cation in aqueous solution under controlled pH have been used to determine the kinetics of proton exchange in that system (14), but it is not possible to compare the totally different solvent systems.

The increase of $J_{P-H\alpha}$ and $J_{P-H\beta}$ and changes in τ values on phosphonium salt formation have been discussed previously (22, 23).

Acknowledgment

We are grateful to the National Science Foundation for support of this work under Grant No. GP4483.

1. H. S. GUTOWSKY and J. LARMANN. J. Am. Chem. Soc. **87**, 3815 (1965).

Can. J. Chem. Downloaded from www.nrcresearchpress.com by 210.87.254.40 on 09/05/12
For personal use only.

2. J. H. LETCHER and J. R. VAN WAZER. J. Chem. Phys. **44**, 815 (1966).
3. J. H. LETCHER and J. R. VAN WAZER. J. Chem. Phys. **45**, 2916 (1966).
4. J. H. LETCHER and J. R. VAN WAZER. J. Chem. Phys. **45**, 2926 (1966).
5. D. PURDELA. Rev. Chim. Acad. Rép. Populaire Roumaine, **10**, 949 (1965).
6. S. O. GRIM and W. MCFARLANE. Nature, **208**, 995 (1965).
7. S. O. GRIM, W. MCFARLANE, E. F. DAVIDOFF, and T. J. MARKS. J. Phys. Chem. **70**, 581 (1966).
8. S. O. GRIM, W. MCFARLANE, and E. F. DAVIDOFF. J. Org. Chem. **32**, 781 (1967).
9. S. O. GRIM, D. A. WHEATLAND, and W. MCFARLANE. J. Am. Chem. Soc. **89**, 5573 (1967).
10. J. R. VAN WAZER, C. F. CALLIS, J. N. SHOOLERY, and R. C. JONES. J. Am. Chem. Soc. **78**, 5715 (1956).
11. L. MAIER. Helv. Chim. Acta, **49**, 1718 (1966).
12. M. VAN DEN AKKER and F. JELLINEK. Rec. Trav. Chim. **86**, 275 (1967).
13. S. O. GRIM, E. F. DAVIDOFF, and W. MCFARLANE. Unpublished results.
14. B. SILVER and Z. LUZ. J. Am. Chem. Soc. **83**, 786 (1961).
15. K. MOEDRITZER, L. MAIER, and L. C. D. GROENWEGHE. J. Chem. Eng. Data, 7, 307 (1962).
16. W. MCFARLANE. Chem. Commun. 58 (1967).
17. C. JUAN and H. S. GUTOWSKY. J. Chem. Phys. **37**, 2198 (1962).
18. D. M. GRANT and W. M. LITCHMAN. J. Am. Chem. Soc. **87**, 3994 (1965).
19. D. S. BARLOW and J. W. RICHARDSON. J. Chem. Phys. **42**, 4018 (1965).
20. S. L. MANATT, G. L. JUVINALL, R. I. WAGNER, and D. D. ELLEMAN. J. Am. Chem. Soc. **88**, 2689 (1966).
21. C. S. JOHNSON, JR. *In* Advances in magnetic resonance. Vol. I. *Edited by* J. S. Waugh. Academic Press, New York. 1965. p. 65.
22. J. B. HENDRICKSON, M. L. MADDOX, J. J. SIMS, and H. D. KAESZ. Tetrahedron, **20**, 449 (1964).
23. S. R. JAIN, W. S. BREY, JR., and H. H. SISLER. Inorg. Chem. **6**, 515 (1967).

Can. J. Chem. Downloaded from www.nrcresearchpress.com by 210.87.254.40 on 09/05/12
For personal use only.

Can. J. Chem. Downloaded from www.nrcresearchpress.com by 210.87.254.105 on 09/05/12
For personal use only.

Radiolysis in the adsorbed state. II. N_2O adsorbed on silica gel and zirconia[1,2]

N. H. SAGERT AND R. W. ROBINSON
Research Chemistry Branch, Chalk River Nuclear Laboratories, Chalk River, Ontario

Received January 11, 1968

The ^{60}Co γ-radiolysis of N_2O adsorbed on silica gel and zirconia has been studied. In both systems a large fraction of the energy absorbed in the solid is able to cause decomposition of the N_2O. For the silica gel – N_2O system, studies with electron scavengers have shown that on gels degassed at low temperatures, electrons are precursors for a large fraction of the yield and about 1 *G* unit of nitrogen is produced by other processes. The total nitrogen yield is smaller for gels degassed at high temperatures, but the yield of nitrogen produced by direct excitation stays constant at 1 *G* unit.

Experiments using electron scavengers with the zirconia–N_2O system have shown that direct excitation of the solid is responsible for most of the nitrogen yield at 7 *G* units on high surface zirconia. Studies of nitrogen yields on a number of zirconias showed that the range over which energy is transferred is about 50 Å.

Canadian Journal of Chemistry, 46, 2075 (1968)

Introduction

In a recent paper (1), we showed that N_2O could reduce hydrogen yields when perdeuterocyclohexane was irradiated adsorbed on silica gel and suggested that this decrease arose because the N_2O captures free electrons. Early work has shown that large yields of N_2 and nitrogen oxides are obtained when N_2O is irradiated by fission fragments or γ-rays when adsorbed on silica and silica–alumina (2). Recent results of Sutherland and Goodrich (3) have shown that nitrogen and oxygen are the major products from the γ-radiolysis of N_2O on silica gel. These authors suggested that electrons formed in the solid are precursors of nitrogen. Wong and Willard (4) observed anions when silica gel was irradiated with adsorbed naphthalene or biphenyl. Their data indicates that electrons are produced in silica gel by ionizing radiation, with $G(e^-)$ greater than unity. We therefore examined the nitrogen yields in the presence of other electron scavengers and studied the yield as a function of degassing temperature as done by Kohn (5) in order to see if electrons actually were precursors of the nitrogen yield.

It has been shown that cyclohexane adsorbed on zirconia does not decompose to a much greater extent than can be accounted for by energy absorbed in the cyclohexane (6). This is probably because the band gap in zirconia, which is the maximum energy which can be transferred, is 5.0 eV; approximately one-half that of silica (7). Hence it was of interest to see if N_2O would decompose when irradiated over zirconia. It was also of interest to study the effects of other electron scavengers on this system, since it has been reported that electron irradiation does not induce changes in the electrical conductivity of anodic zirconia (8) and therefore no measurable increase in charge carriers is produced. We also studied the radiolysis of N_2O adsorbed on zirconia particles of varying size, in order to get an estimate of the range of the observed interactions.

Experimental

The silica gel was the same as that used previously (1). Its surface area was 760 ± 50 m^2/g. Zirconia was usually prepared by the slow neutralization of 0.1 to 1.0 *M* solutions of $ZrO(NO_3)_2 \cdot 2HNO_3 \cdot 4H_2O$ (Anachemia), or $ZrO(NO_3)_2 \cdot 2H_2O$ (Fisher), by dilute ammonium hydroxide. All solutions were made from doubly distilled water. Precipitates were filtered, washed, and dried at 110 °C. They were then ground and heated to 550–580 °C. The low surface area samples were Fisher zirconia. The zirconia was monoclinic, with a small admixture of the cubic form, as shown by X-ray diffraction patterns. Surface areas were measured as before (1).

Adsorption isotherms for N_2O and SF_6 on silica gel and zirconia were measured at 0 °C using the Sor-Bet surface area apparatus (Aminco) and the helium carrier technique. The N_2O (Canadian Liquid Air), SF_6 (Matheson), and CCl_4 (Anachemia) were used as received.

Samples of 4 to 6 g were weighed out into cylindrical vessels fitted with Hoke valves (1). The vessels were evacuated and raised to the desired temperature. They were kept overnight at this temperature while being evacuated to 10^{-6} Torr. Most zirconia samples were evacuated at 400 °C, while the silica gel samples were evacuated at various temperatures.

Small amounts of N_2O, SF_6, and CCl_4 were measured out, degassed, and transferred to the solid on a mercury-free grease-free vacuum line. Samples were irradiated at

[1]Issued as A.E.C.L. No. 3097.
[2]Presented in part at the 51st Chemical Institute of Canada Conference, Vancouver, B.C., June 1968.

Can. J. Chem. Downloaded from www.nrcresearchpress.com by 210.87.254.105 on 09/05/12
For personal use only.

0 °C in a ^{60}Co γ-source at a dose rate of 7.3×10^{17} eV/g min in silica gel. The dose rate was determined by Fricke dosimetry using $G(Fe^{3+}) = 15.6$ molecules/100 eV. With a high atomic number material such as zirconium and the highly shielded source used (Atomic Energy of Canada Limited, Gammacell 220), there is some energy absorption by the photoelectric effect, not only from the primary γ-rays of about 1.25 MeV, but also from the small reflected component of 100–200 keV. The dose rate was therefore determined by ion chamber dosimetry using ion chambers of various materials, following the procedure of Ritz and Attix (9) and interpolating for zirconium. The details of this dosimetry in our source have been described by Stone (10). The dose rate in zirconia was $8.0_6 \times 10^{17}$ eV/g min.

Products volatile at −196 °C were measured volumetrically and analyzed mass spectrometrically. In order to measure NO_2, all the material degassed from the gel was collected at −196 °C and 3 ml of 0.1 *N* NaOH were added. Nitrogen dioxide was then determined as nitrite by the method of Rider and Mellon (11, 12).

Results

(a) Silica Gel

The major product from the irradiation of the N_2O silica gel system is nitrogen. We obtained very little oxygen, even when the gel was heated above 600 °C to collect strongly adsorbed products, and saw no evidence for any yield of NO. Sutherland and Goodrich (3) noted almost stoichiometric yields of oxygen. However, as the total dose given our samples was only about 2.5% that given theirs, our smaller amounts of oxygen could be chemisorbed irreversibly, or could react with carbon impurities in the gel (13). A yield of NO_2 has been noted (2), but for our system NO_2 was a very minor product, with $G(NO_2) < 0.2$. Typical nitrogen yields as a function of surface coverage for a gel degassed at 140 °C are shown in Fig. 1. The fraction of a monolayer adsorbed on the surface (θ) was calculated taking the area of N_2O to be 16.8 Å^2/molecule (14) and correcting for the N_2O not adsorbed at 0 °C. The *G* values are molecules produced for every 100 eV of energy absorbed in the entire system. This energy was about 2.5×10^{19} eV/g. No nitrogen whatsoever was produced when N_2O was adsorbed on the silica gel and the system allowed to stand for several hours. Only small amounts of nitrogen ($G(N_2) \sim 0.3$) were produced when N_2O was added to irradiated silica gel, although the blue color of the irradiated gel was bleached.

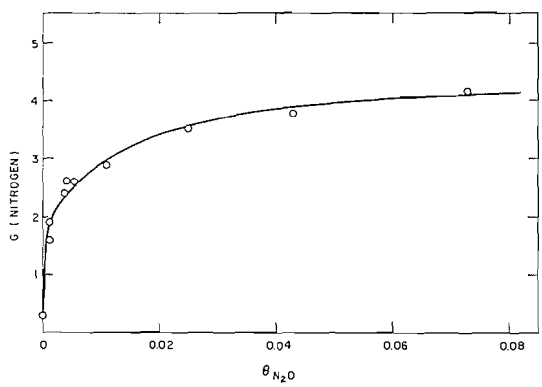

FIG. 1. Nitrogen yields from the silica gel – N_2O system. Dose = 2.5×10^{19} eV/g. Gel degassed at 140 °C.

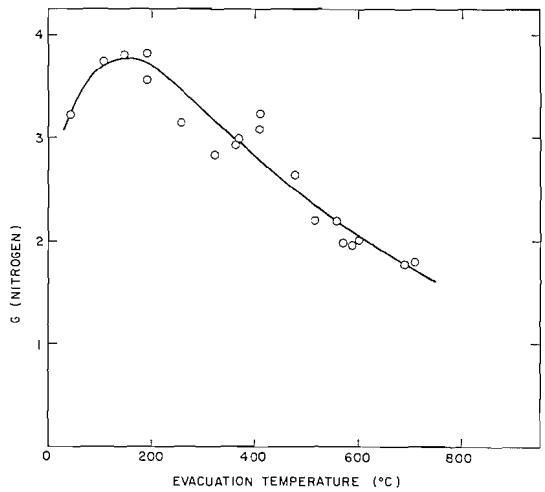

FIG. 2. The effect of degassing temperature on the nitrogen yield from the silica gel – N_2O system. $\theta_{N_2O} = 0.03$. Dose = 2.4×10^{19} eV/g.

Nitrogen yields as a function of evacuation temperature are shown in Fig. 2. These results were obtained at a surface coverage of 3% of a monolayer and with an absorbed dose of 2.4×10^{19} eV/g. The nitrogen yields decrease with increasing evacuation temperature, as has been noted by Kohn (5). These yields parallel the decrease in surface OH as a function of evacuation temperature, which have been given previously for this silica gel (1).

In an attempt to see if species resembling electrons were responsible for the nitrogen yield, electron scavengers were added to the system. Nitrogen yields as a function of the surface coverage of scavenger are shown in Fig. 3 for a gel degassed at 400 °C. The SF_6 coverage is corrected for SF_6 not adsorbed at 0 °C. Both

Can. J. Chem. Downloaded from www.nrcresearchpress.com by 210.87.254.105 on 09/05/12
For personal use only.

SF_6 and CCl_4 appear to reduce these yields to about 1 G unit. Over a gel degassed at 150 °C and one degassed at 750 °C, this same limiting yield of 1 G unit was obtained. It should be noted that a gel degassed at 750 °C is not strictly comparable to one degassed at temperatures below 600 °C, as its surface area has been reduced to 600 m^2/g.

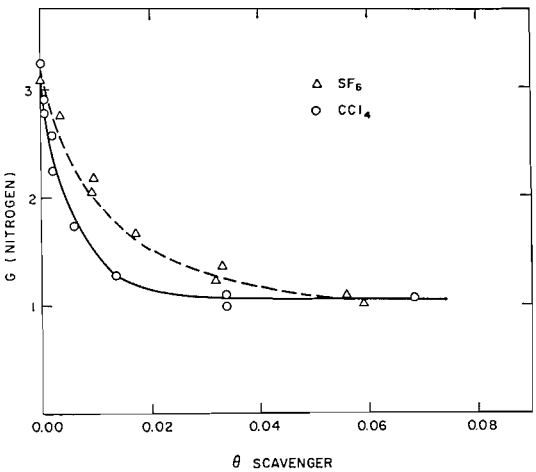

FIG. 3. Effect of electron scavengers on the nitrogen yield from the silica gel – N_2O system. $\theta_{N_2O} = 0.11$. Gel degassed at 410 °C. Dose = 2.5×10^{19} eV/g.

The 0.3 G units of nitrogen produced when N_2O was added to the irradiated gel has not been subtracted from any yields. It was observed that the blue color centers were bleached when SF_6 was added to irradiated silica gel, and therefore a large portion of these 0.3 G units is probably included in the scavengeable nitrogen.

(b) Zirconia

Nitrogen was the major product observed when the N_2O–zirconia system was irradiated. No NO was noted in the products and $G(NO_2)$ was < 0.2. Yields of nitrogen for a number of zirconia samples of varying surface area are shown in Fig. 4 as a function of surface coverage of N_2O. These surface coverages were corrected for the N_2O not adsorbed at 0 °C, which, although negligible at the lower coverages, consisted of over half the total N_2O at the highest coverages. The total dose given was about 2.5×10^{19} eV/g and the amounts of nitrogen produced were linear with dose to at least 4×10^{19} eV/g. Initially $G(N_2)$ rises very

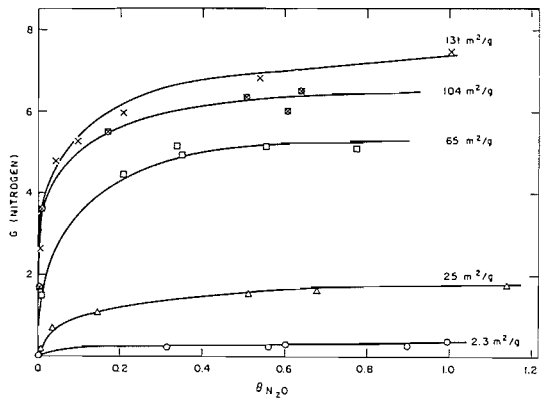

FIG. 4. Nitrogen yields from the zirconia–N_2O system for several zirconias of varying surface area. Dose = 2.5×10^{19} eV/g.

sharply with coverage, but at coverages greater than 30% of a monolayer little additional increase in yield is observed. As with N_2O on silica gel, blank experiments indicated that most of the phenomena observed are radiation effects which occur during irradiation. Nitrogen yields when N_2O was added to irradiated zirconia (65 m^2/g) were about 0.02 G units. On a few samples of zirconia accidently formed in the cubic modification, yields were only about 60% of those obtained over monoclinic zirconia.

It would appear from Fig. 4 that the higher the surface area of the gel the larger the "limiting" yield of nitrogen. Figure 5 shows nitrogen yields at one monolayer coverage plotted as a function of the surface area of the oxide. The yields rise almost linearly at first, but then much more slowly for areas larger than 90 m^2/g.

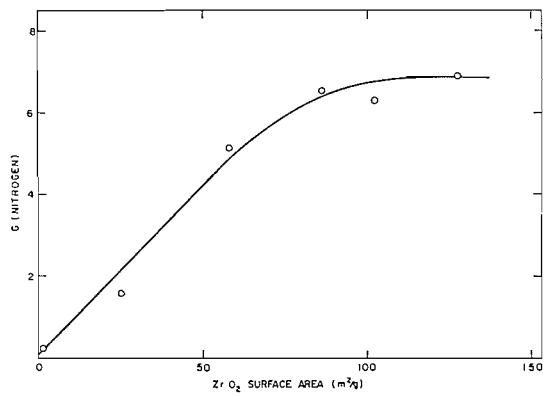

FIG. 5. Nitrogen yields at one monolayer coverage as a function of the surface area of the zirconium oxide.

To remove the last traces of air from the zirconia, we had to evacuate it at 400 °C at least. Hence it was impossible to study the behavior of zirconia samples evacuated at temperatures less than 400 °C, and therefore no extensive study of the effect of degassing temperature was attempted.

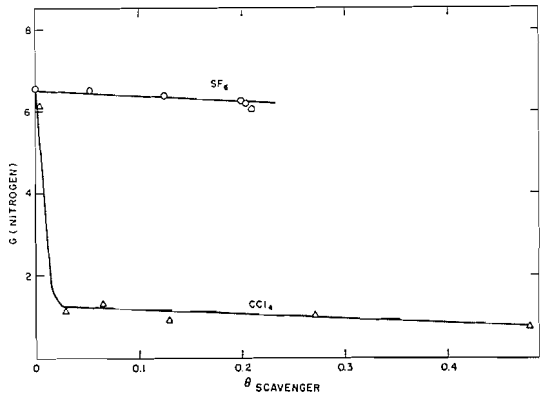

FIG. 6. Effect of electron scavengers on the nitrogen yield from the zirconia–N_2O system. $\theta_{N_2O} = 1.1$. Dose = 2.4×10^{19} eV/g.

As with the N_2O – silica gel system, other electron scavengers were added to the N_2O–zirconia system. The results using a zirconia sample 104 m^2/g and an N_2O surface coverage of 1.1 monolayers are shown in Fig. 6. Small additions of carbon tetrachloride reduce the nitrogen yield to about 1.2 G units, whereas SF_6 hardly reduces the yield at all. The coverages shown in Fig. 6 are calculated from adsorption isotherms of individual components, not allowing for mixed adsorption effects (ref. 14, chapter 11). Therefore the possibility exists that less SF_6 is adsorbed than indicated. If the Langmuir isotherm is assumed to hold, then

$$[1] \qquad \frac{\theta_{N_2O}}{\theta_{SF_6}} = \frac{b_{N_2O}\, P_{N_2O}}{b_{SF_6}\, P_{SF_6}}$$

where the constants have the form $b = b_0\, e^{\Delta H/RT}$, ΔH being the heat of adsorption. The heat of adsorption for SF_6 would not be expected to be less than that of N_2O, and the b_0 terms should be comparable. Hence sufficient SF_6 should be adsorbed to act as a scavenger. Experimental evidence that sufficient SF_6 was adsorbed was considered necessary, however, and several irradiations were done at −78 °C. At this temperature N_2O and SF_6 are certainly adsorbed completely. Although the results were rather scattered, probably because of the difficulty of obtaining uniform coverages, adding up to 0.2 of a monolayer of SF_6 reduced the nitrogen yield by only 1 G unit.

Discussion

(a) Silica Gel

Some of the energy absorbed in the silica gel is transferred to the N_2O and causes decomposition. This is clearly shown by the results given in Fig. 1. If the gas phase value of $G(N_2)$ from N_2O is taken as 10 (12), it is easily shown that the nitrogen yield from energy absorbed in the N_2O alone, calculated on the basis of energy absorbed in the entire system, is 0.2 at a surface coverage of 7% of a monolayer. Since the measured value at this surface coverage is about 4.1, most of the nitrogen is produced by energy absorbed in the gel. This "energy transfer" is quite effective at the lowest coverages, but beyond 3% of a monolayer little increase in yield is noted, except that accounted for by direct radiolysis of the additional N_2O. Since $G(N_2)$ is 10 for the gas phase radiolysis of N_2O, the energy absorbed in the gel decomposes N_2O with only ~1/3 the efficiency of the gas phase decomposition.

The experiments with electron scavengers indicate that a large portion of the energy is transferred from the solid by a mechanism involving electrons and 1 G unit is transferred by some other mechanism. Following our earlier suggestions (1), we may write

$$[2a] \qquad \text{solid} \rightsquigarrow \ominus + \oplus$$

$$[2b] \qquad \rightsquigarrow \text{solid}^*$$

$$\text{solid}^{**}$$

$$[3a] \qquad \ominus + \oplus \nearrow$$

$$[3b] \qquad \searrow \text{recombination}$$

$$[4] \qquad \ominus + N_2O \rightarrow [N_2O]^- \rightarrow N_2 + O^-,$$

where solid* and solid ** are unspecified excited states of the solid which may or may not be distinguishable from each other. Electrons and positive holes are denoted by ⊖ and ⊕ respectively. The "unscavengeable" yield of N_2 may result from

$$[5] \qquad \text{solid}^* + N_2O \rightarrow N_2 + O + \text{solid}.$$

Can. J. Chem. Downloaded from www.nrcresearchpress.com by 210.87.254.105 on 09/05/12
For personal use only.

Can. J. Chem. Downloaded from www.nrcresearchpress.com by 210.87.254.105 on 09/05/12
For personal use only.

Since the species identified as solid* may have energies as large as the 10 eV band gap in silica, whereas the dissociation energy of the N_2—O bond is 1.7 eV, reaction [5] may be very exothermic. The O^- and O appear to be strongly adsorbed on the silica gel and no NO and only small amounts of O_2 and NO_2 are produced. Reaction [6],

$$[6] \qquad O^- + N_2O \rightarrow N_2 + O_2^-,$$

proposed by Johnson and Warman (15) for the gas phase radiolysis of the propane–N_2O system and often considered for the thermal decomposition of N_2O over semiconducting catalysts (16), may occur to some extent. Hence the reduction in nitrogen yield should not be equated with $G(\ominus)$ for silica gel.

The nitrogen yield is lower the higher the degassing temperature of the gel. The electron scavenger results indicate that electrons make a smaller contribution to the yield for gels degassed at higher temperatures and that, in fact, the "unscavengeable nitrogen yield" is virtually constant at about 1 *G* unit. The "electron yield" thus appears to parallel the water content measured previously for these gels, indicating that some form of "solvation" may be important in stabilizing these electrons (5).

It might well be that some of the "unscavengeable nitrogen yield" is unscavengeable because the N_2O molecule is smaller than either the CCl_4 or the SF_6 molecules, and thus the CCl_4 and SF_6 cannot penetrate into pores of the gel accessible to the N_2O. However, the ratio of the "scavengeable" yield to the "unscavengeable" yield changes greatly over the range of evacuation temperatures, whereas the surface area, and hence the pore structure, does not change greatly (1). Hence it is unlikely that a molecular sieve effect is responsible for most of the "unscavengeable yield".

(b) Zirconia

Calculations of the same type as used in the silica gel case above show that energy originally deposited in the zirconia decomposes nitrous oxide adsorbed on its surface. For the 131 m^2/g oxide, the contribution to the nitrogen yield of 7 *G* units from energy absorbed directly in the N_2O is 0.33 *G* units at a coverage of 70% of a monolayer. Contributions from direct radiolysis over lower surface area zirconias will, of course, be less in direct proportion to the surface area for a given coverage. Apparently the energy absorbed in the zirconia decomposes N_2O with about 2/3 the efficiency of the gas phase decomposition.

The "energy transfer" from the zirconia to the adsorbed layer will only operate over some finite range, or, more probably, some distribution of ranges. For low surface area solids, this range may be very much smaller than the average particle radius. A large fraction of the energy deposited in the solid will then be unable to cause decomposition of the adsorbate, so $G(N_2)$ will be small. As the surface area is raised a greater fraction of the energy will be able to cause decomposition, so $G(N_2)$ will rise. Then, when the average range of interaction is equal to the particle radius, most of the energy deposited will be capable of interacting with the adsorbate and $G(N_2)$ will stop rising. An examination of Fig. 5 shows that such a levelling off of $G(N_2)$ occurs at a surface area of 90–100 m^2/g. Assuming a unique range for energy transfer processes and a spherical particle shape, the range is about 50 Å. This is smaller than the migration distance found by Kohn (17) in silica samples for D_2 exchange over silica gel, and is of the order of the migration distance found in MgO by Rabe, Rabe, and Allen (18) for azoethane decomposition as calculated by Kohn (17). The larger migration distance in silica gel is consistent with our observation that the limiting yield of nitrogen is obtained at much lower coverages over silica gel than over zirconia.

The mechanism by which the energy is transferred from the solid is somewhat obscure and we do not have a completely satisfactory one. Sulfur hexafluoride does not appear to reduce the nitrogen yields even though it is known to react with electrons much more efficiently than N_2O in the gas phase (15). Thus it may be concluded either that the usual assumptions about dissociative electron capture by N_2O are wrong, or that the radiolysis of N_2O adsorbed on zirconia is a very special case. Although the first possibility should not be discarded outright, only the second will be seriously discussed here. The inability of SF_6 to drastically reduce nitrogen yields will be taken as evidence that electrons are not involved in the rate-controlling step for the radiolysis of N_2O on zirconia. Electron transfer from O^- may be the rate-controlling step, as discussed by Winter (19)

Can. J. Chem. Downloaded from www.nrcresearchpress.com by 210.87.254.105 on 09/05/12
For personal use only.

for the thermal decomposition of N_2O on doped nickel oxides, particularly since zirconia may be a p-type semiconductor at oxygen pressures greater than 10^{-6} atmosphere (8, 20, 21). In this case SF_6 would not lower the nitrogen yield since its electron affinity is higher than that of an oxygen atom (22, 23). Therefore O^- would probably give up its electron more easily than SF_6^-. However, the evidence from CCl_4 scavenger experiments tends to refute this mechanism. Carbon tetrachloride probably captures electrons by a dissociative process and since chlorine atoms have a much higher electron affinity than oxygen atoms (22), it is difficult to see why Cl^- should give up its electrons more easily than O^-, as it would have to do in order to interfere with the nitrogen yield. As shown in Fig. 6, CCl_4 competes quite successfully for precursors of nitrogen. Thus electron transfer from O^- is probably not the rate-controlling step under our conditions. Any mechanisms involving positive charge transfer from the zirconia to the N_2O can probably be excluded because the ionization potential of N_2O is 12.9 eV (22), much larger than the 5.0 eV band gap of zirconia.

It appears that, with zirconia, the results may be best explained by a mechanism involving reactions [1] and [2], followed by reaction [4]. The species identified as solid* may be of two sorts, one quenchable by CCl_4 and one not. On the other hand, it may not be necessary to postulate two species. The reason that CCl_4 does not reduce the yield of nitrogen to zero may be that N_2O can penetrate into pores and crevices in the oxide from which the larger CCl_4 molecule is partially excluded. The fact that the concentration of charge carriers is not increased, relatively speaking, by electron irradiation (6) supports a mechanism which does not involve charge separation. If such a mechanism applies, it seems likely that $G(N_2)$ is a measure of the excitation, since N_2O is known to be relatively inert to ground state oxygen atoms (24).

Acknowledgments

We wish to thank Dr. B. Cox for a discussion of the electronic properties of zirconia, and our colleagues for fruitful discussions.

1. N. H. Sagert and P. J. Dyne. Can. J. Chem. **45**, 615 (1967).
2. R. Coekelbergs, A. Crucq, and A. Frennet. Advan. Catalysis, **13**, 55 (1962).
3. J. W. Sutherland and R. Goodrich. J. Am. Chem. Soc. **89**, 6779 (1967).
4. P. K. Wong and J. E. Willard. 154th Meeting, American Chemical Society, Chicago, Ill. Abstr. Papers, V 79 (1967).
5. H. W. Kohn. O.R.N.L. Rept. No. 3994. Oak Ridge National Laboratory, Oak Ridge, Tenn. p. 49.
6. G. M. Zhabrova, V. B. Kazanskii, V. L. Vladmirova, B. M. Kadenatsi, and G. B. Pariiskii. Neftekhimiya, **4**, 753 (1964).
7. J. G. Bendoraitis and R. E. Salomon. J. Phys. Chem. **69**, 3666 (1965).
8. P. J. Harrop and J. N. Wanklyn. Brit. J. Appl. Phys. **16**, 155 (1965).
9. V. H. Ritz and F. H. Attix. Radiation Res. **16**, 401 (1962).
10. J. A. Stone. Can. J. Chem. **46**, 1267 (1968).
11. B. F. Rider and M. G. Mellon. Ind. Eng. Chem. Anal. Ed. **18**, 96 (1946).
12. F. T. Jones and T. J. Sworski. J. Phys. Chem. **70**, 1546 (1966).
13. Z. L. Krylova and P. I. Dolin. Kinetika i Kataliz, **7**, 977 (1966).
14. D. M. Young and H. D. Crowell. Physical adsorption of gases. Butterworths, London. 1962. p. 226.
15. G. R. A. Johnson and J. M. Warman. Trans. Faraday Soc. **61**, 1709 (1965).
16. F. S. Stone. Advan. Catalysis, **13**, 1 (1962).
17. H. W. Kohn. J. Am. Chem. Soc. **87**, 3521 (1965).
18. J. G. Rabe, B. Rabe, and A. O. Allen. J. Phys. Chem. **76**, 1098 (1966).
19. E. R. S. Winter. Discussions Faraday Soc. **28**, 183 (1959).
20. R. W. Vest, N. M. Tallan, and W. C. Tripp. J. Am. Ceramic Soc. **47**, 635 (1964).
21. P. Kofstad and D. J. Ruzicka. J. Electrochem. Soc. **110**, 181 (1963).
22. V. I. Vedeneyev, L. V. Gurvich, V. N. Kondrat'yev, V. A. Medvedev, and Ye. L. Frankevich. Bond energies, ionization potentials, and electron affinities. Edward Arnold (Publishers), London. 1965.
23. J. Kay and F. M. Page. Trans. Faraday Soc. **60**, 1042 (1964).
24. H. Yamazaki and R. J. Cvetanović. J. Chem. Phys. **39**, 1902 (1963).

Can. J. Chem. Downloaded from www.nrcresearchpress.com by 210.87.254.6 on 09/05/12
For personal use only.

Infrared spectra of triphenylboron and triphenylborate

H. F. SHURVELL AND J. A. FANIRAN
Department of Chemistry, Queen's University, Kingston, Ontario

Received December 27, 1967

The infrared spectra of triphenylboron and triphenylborate have been obtained in the region 4000 to 300 cm^{-1}. The analysis of the spectra supports a propeller-shaped structure with symmetry D_3 for triphenylboron and a planar structure with symmetry C_{3h} for triphenylborate. The Urey–Bradley force field has been applied to the calculation of approximate vibrational force constants for the BC_3 and BO_3 groups.

Les spectres infrarouges du triphénylbor et triphénylborate ont été enregistrés entre 4000 et 300 cm^{-1}. L'analyse des spectres indique une structure helice avec symétrie D_3 pour triphénylbor et une structure plane avec symétrie C_{3h} pour triphénylborate. Le champs de force Urey–Bradley a été utilisé pour calculer des constantes de force pour les groupes BC_3 et BO_3.

Canadian Journal of Chemistry, 46, 2081 (1968)

Introduction

In continuation of our study of the infrared spectra of triphenyl derivatives (1–3) we have investigated the infrared spectra of triphenylboron and triphenylborate. The infrared spectrum of triphenylboron has been previously reported by Sharp and Sheppard (4) while that of triphenylborate was reported by Werner and O'Brien (5). However, no detailed assignments or discussion of the observed frequencies were given. The present study was therefore undertaken to record the infrared spectra over a larger frequency range than that covered by the previous workers and to present as far as possible complete frequency assignments for the two molecules.

As in previous studies of polyphenyl compounds (1–3, 6), the spectra are interpreted in terms of monosubstituted benzene derivatives (point group C_{2v}) and the central BC_3 or BO_3 groups. For a monosubstituted benzene, there are $11a_1 + 6b_1 + 10b_2$ vibrations active in the infrared while for the BC_3 and BO_3 skeletons (point group D_{3h}) we expect $2e' + 1a_2''$ infrared active vibrations.

We have made the assignments of the observed frequencies by analogy with the spectra of other monosubstituted benzenes (7, 8), triphenyl derivatives (1–3, 6), alkylborates (9, 10), and boric acid (11, 12). The notations used for the vibrations of the monosubstituted benzenes are those of Whiffen (7).

The Urey–Bradley force field has been used in calculations involving the BC_3 and BO_3 group vibrations. The calculated force constants are only approximations to the true force constants, since the phenyl groups are either treated as groups of mass equal to that of the carbon atom (triphenylboron) or ignored (triphenylborate). However, the results provide an approximate value for the B—C force constant and enable the strength of the B—O bonds in triphenylborate and the BO_3^{3-} ion (13) to be compared. From these force constants it is also possible to estimate approximate frequencies of the infrared inactive B—C and B—O symmetric stretching vibrations.

Experimental

Because of the ease with which both triphenylboron and triphenylborate are hydrolyzed, precautions were taken to avoid exposure of the samples to the atmosphere.

The triphenylboron sample obtained from Aldrich Chemical Company was used without further purification. The results of an analysis and a melting point determination showed that the material was pure.

Triphenylborate was prepared from boron trichloride and phenol (14) under dry nitrogen, and the product was recrystallized from methylene dichloride: m.p. 89–90°.

The spectra were obtained in the solid phase as Nujol and Fluorolube mulls between CsBr windows and in solution in carbon tetrachloride at different concentrations using 0.05 mm sodium chloride cells. All spectra were recorded with a Beckman IR 10 spectrophotometer which was calibrated against a polystyrene film (15). The frequencies reported in Tables I and II are believed to be correct to within ± 2 cm^{-1}.

Symmetry and Structure

We have assumed a propeller-shaped structure with symmetry D_3 for triphenylboron and a planar structure of symmetry C_{3h} for triphenylborate. Our assumptions are based on the following arguments.

TABLE I

Infrared absorption (frequencies in cm^{-1}) and assignments for triphenylboron

Present work*		Reference 4,*	Assignments†		
Nujol	CCl_4	Nujol			
3090 w	3091 w	—	νCH	b_1	(z_4)
3070 w	3070 w	—	νCH	a_1	(z_1)
—	3054 vw	3050 w	νCH	a_1	(z_2)
3040 vw	3040 vw	—	νCH	a_1	(z_3)
3023 vw	3023 vw	—	νCH	b_1	(z_5)
1614 w	1614 w	—		c	
1600 s	1600 s	1600 w, sh	νCC	a_1	(*k*)
1570 w	1572 w	1588 s	νCC	b_1	(*l*)
—	1500 w	1492 w	νCC	a_1	(*m*)
—	1485 w				
1440 s	1440 s	1430 s	νCC	b_1	(*n*)
1372 w	1372 w	—		c	
1355 w	1355 w	—		c	
1320 m	1320 m	1315 s	νCC	b_1	(*o*)
1285 m	1285 m	1280 s	βCH	b_1	(*e*)
1270 w	1270 w	—		c	
1242 s	1242 s	1240 s	ν_{as}BC	e'	—
1190 m	1190 m	1189 w, sh	βCH	a_1	(*a*)
1160 w	1160 w	1158 w, sh	βCH	b_1	(*c*)
1075 w	1074 w	1075 w	βCH	b_1	(*d*)
1035 m	1035 m	1032 m	βCH	a_1	(*b*)
1000 m	1000 m	1000 m	Ring	a_1	(*p*)
980 w	986 w	976 w	γCH	b_2	(*j*)
940 w	—	—		c	
901 w	910 w	900 w	γCH	b_2	(*i*)
889 s	889 s	885 s	X-sens.	a_1	(*r*)
828 (calculated)			ν_sBC	a_1'	—
775 m	—	774 m			
—	—	749 m	γCH	b_2	(*f*)
742 s	—	742 m			
700 vs	700 vs	697 s	φCC	b_2	(*v*)
675 w	675 w	—		c	
657 w	658 w	—		c	
641 m	642 m	—	$\delta'BC_3$	a_2''	—
616 vw	616 vw	—	αCCC	b_1	(*s*)
599 s	—	—	δBC_3	e'	—
460 w	—	—	X-sens.	b_2	(*y*)
400 w	—	—	φCC	a_2	(*w*)

*In this and subsequent tables, relative intensities are denoted by: vs = very strong, s = strong, m = medium, w = weak, vw = very weak, and sh = shoulder.

†In this table and in Table II, the letters in parentheses after the assignments identify the corresponding vibrations in monosubstituted benzenes according to Whiffen (7). *c* denotes a combination band.

A cryoscopic molecular weight determination (16) showed that triphenylboron is unimolecular and an electron diffraction study (17) showed that the BC_3 group is planar with the B—C bonds single. The orientation of the phenyl groups about these bonds will therefore determine the structure of triphenylboron. An all-planar D_{3h} structure is unlikely, because the overlap of the Van der Waals' spheres of the ortho hydrogen atoms would be expected to give rise to twisting of the phenyl groups out of the plane of the BC_3 group, so that a propeller-shaped molecule with symmetry D_3 would result. Sharp and Sheppard (4) concluded that the D_3 model was reasonable on the basis of the number of components into which well-defined absorption bands of a single phenyl group split in the spectrum of triphenylboron. Each of the b_1, b_2, and a_2 vibrations of the local point group C_{2v} are split into doublets for overall point groups D_3 or D_{3h}. For D_3 both of the components from the b_1 and b_2 vibrations, and one of the a_2 vibrations, become infrared (i.r.) active; for D_{3h} only one of the components of b_1 and b_2 vibrations is i.r. active, and both components of the a_2 vibrations remain inactive.

Can. J. Chem. Downloaded from www.nrcresearchpress.com by 210.87.254.6 on 09/05/12
For personal use only.

Can. J. Chem. Downloaded from www.nrcresearchpress.com by 210.87.254.6 on 09/05/12
For personal use only.

Some of these predictions have been observed in the spectrum of triphenylboron. Thus, the peak assigned to the b_2 γCH vibration is split into two components at 775 and 742 cm^{-1} and the infrared inactive a_2 ϕCC vibration at 400 cm^{-1} has been observed. The infrared spectrum therefore supports the propeller-shaped model for triphenylboron.

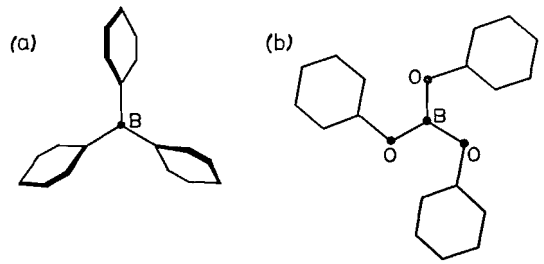

FIG. 1. Structures of (*a*) triphenylboron and (*b*) triphenylborate.

We assume that triphenylborate like the alkylborates exists as a monomer (18) and that the BO_3 skeleton is planar (19, 20). Examination of molecular models of triphenylborate shows that the most symmetrical configuration is the one in which all the benzene rings are coplanar with the BO_3 plane. No steric interactions occur in this model and with this structure triphenylborate belongs to the point group C_{3h}.

The proposed structures of both molecules are illustrated in Fig. 1.

Results and Discussion

The spectra obtained from Nujol mulls and from solutions in CCl_4 were similar. The infrared spectrum of triphenylboron is shown in Fig. 2, while the observed fundamentals and their assignments are summarized in Table I, together with those reported by Sharp and Sheppard (4). The strongest combination bands are also included in Table I. The frequencies and assignments of the observed fundamentals of triphenylborate with the results of Werner and O'Brien (5) are listed in Table II, together with the strongest combination bands, and the spectrum is shown in Fig. 3.

Triphenylboron

BC_3 Skeletal Vibrations

The BC_3 group of symmetry D_{3h} has six fundamental vibrations. Two of these are B—C stretching vibrations, a totally symmetric a_1' vibration and an antisymmetric e_1' vibration. The latter is infrared active and we have assigned the strong peak at 1242 cm^{-1} to this vibration. Stewart (21) assigned a band at 1309 cm^{-1} in the spectrum of trimethylboron to the antisymmetric B—C stretching vibration, while Lehmann *et al.* (22) for the same molecule assigned a band at 1150 cm^{-1} to this vibration. A similar disagreement is found for triethylboron. Bands at 1298 and 1120 cm^{-1} were assigned to this vibration by Blau and Mulligan (23) and Lehmann *et al.* (24) respectively. Our assignment supports the work of Stewart (21) and Blau and Mulligan (23). From a normal coordinate calculation, we have estimated the frequency of the symmetric B—C stretching vibration to be 828 cm^{-1}.

TABLE II

Infrared absorption (frequencies in cm^{-1}) and assignments for triphenylborate

Present work	Reference 5	Assignments		
3100 vw	—	νCH	b_1	(z_4)
3080 vw	—	νCH	a_1	(z_1)
3052 w	—	νCH	a_1	(z_2)
3042 vw	—	νCH	a_1	(z_3)
3020 vw	—	νCH	b_1	(z_5)
1956 w	—		*c*	
1870 w	—		*c*	
1795 w	—		*c*	
1734 w	—		*c*	
1600 s	1593 s	νCC	a_1	(*k*)
1565 vw	—	νCC	b_1	(*l*)
1491 s	1486 s	νCC	a_1	(*m*)
1456 w	—	νCC	b_1	(*n*)
1402 s, sh	1400 s	νCC	b_1	(*o*)
1350 vs	1350 vs	$\nu_{as}BO$	*e'*	—
1300 w	—		*c*	
1285 vw	—	βCH	b_1	(*e*)
1214 s	1217 s	νCO	a_1	—
1199 vw	1196 w	βCH	a_1	(*a*)
1164 w	1153 w	βCH	b_1	(*c*)
1068 m	1071 m	βCH	b_1	(*d*)
1020 w	1024 w	βCH	a_1	(*b*)
1000 vw	—	Ring	a_1	(*p*)
974 w	—	γCH	b_2	(*j*)
904 m	—	γCH	b_2	(*i*)
860 (calculated)	—	ν_sBO	a_1'	—
830 m	—		*c*	
805 vw	—	X-sens.	a_1	(*r*)
760 s	767 s	γCH	b_2	(*f*)
710 m	—		*c*	
685 s	692 s	ϕCC	b_2	(*v*)
635 m	—	αCCC	b_1	(*s*)
598 m	—	$\delta'BO_3$	a_2''	—
522 w	—		*c*	
505 s	—	δBO_3	*e'*	—
450 vw	—	X-sens.	b_1	(*y*)
430 m	—	X-sens.	a_1	(*t*)
380 vw	—	X-sens.	b_1	(*u*)
350 vw	—	X-sens.	b_2	(*x*)

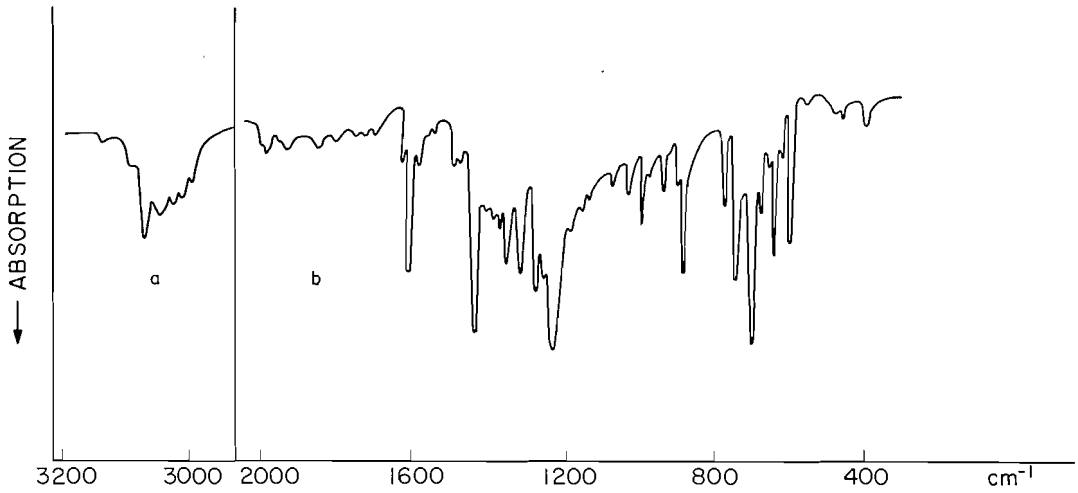

FIG. 2. The infrared spectrum of triphenylboron: (*a*) in CCl_4 solution in a 0.05 mm NaCl cell, (*b*) in a Nujol mull between CsBr windows.

The BC_3 in-plane and out-of-plane deformations have been assigned to the absorption bands at 599 and 641 cm^{-1} respectively. These assignments are different from those of previous workers on trialkylborons (21–24). However, the normal coordinate analysis supports our assignment, since a reasonable set of force constants was obtained using these frequencies. It is probable that the frequencies previously assigned to these vibrations, 336 and 320 cm^{-1}, correspond to BC_3 rocking vibrations, which are expected to give rise to absorptions in this lower frequency range. In the spectrum of triphenylboron the corresponding vibrations are likely to occur at still lower frequencies, below the range of our instrument.

Benzene Ring Vibrations

The assignments of the fundamentals associated with the benzene rings are listed in Table I. The notation of Whiffen (7) for monosubstituted benzenes has been used to describe these vibrations. A weak peak at 400 cm^{-1} has been assigned to an out-of-plane ring deformation (ϕCC) of species a_2. It is suggested that this mode has been made allowed by the overall D_3 symmetry of the molecule. The out-of-plane CH deformation (γCH) near 760 cm^{-1} is split into two components at 775 and 742 cm^{-1}. This supports the D_3 structure for triphenylboron (4).

The correlation of the benzene ring vibrations in triphenylboron with corresponding modes in other monosubstituted benzenes and triphenyl compounds is good both in frequency and intensity.

Triphenylborate

BO_3 Skeletal Vibrations

Two of the six vibrations of the BO_3 group are the symmetric and antisymmetric B—O stretching modes. The absorption band associated with the latter is readily identified at 1350 cm^{-1}. It is the strongest band in the spectrum of triphenylborate. In the spectrum of boric acid, this vibration was assigned by Bethel and Sheppard (11) to a band at 1450 cm^{-1} and by Servoss and Clark (12) to an absorption at 1428 cm^{-1}. A band near 1355 cm^{-1} in the infrared spectra of some trialkylborates (5, 9) was attributed to this vibration. The B—O symmetric stretching vibration is of species a_1' which is infrared inactive. From a normal coordinate analysis, we have estimated a frequency of 860 cm^{-1} for this mode. In the spectrum of the borate ion BO_3^{3-} (25) this vibration has been observed at 910 cm^{-1}. The decrease in frequency of both the symmetric and antisymmetric stretching vibrations of the BO_3 group in triphenylborate compared with similar vibrations of the BO_3^{3-} ion is not unexpected, since the B—O bond strength in the borate ion should be greater than in the BO_3 skeleton of triphenylborate.

A strong peak at 505 cm^{-1} is assigned to the symmetric in-plane deformation (δBO_3) by com-

Can. J. Chem. Downloaded from www.nrcresearchpress.com by 210.87.254.6 on 09/05/12
For personal use only.

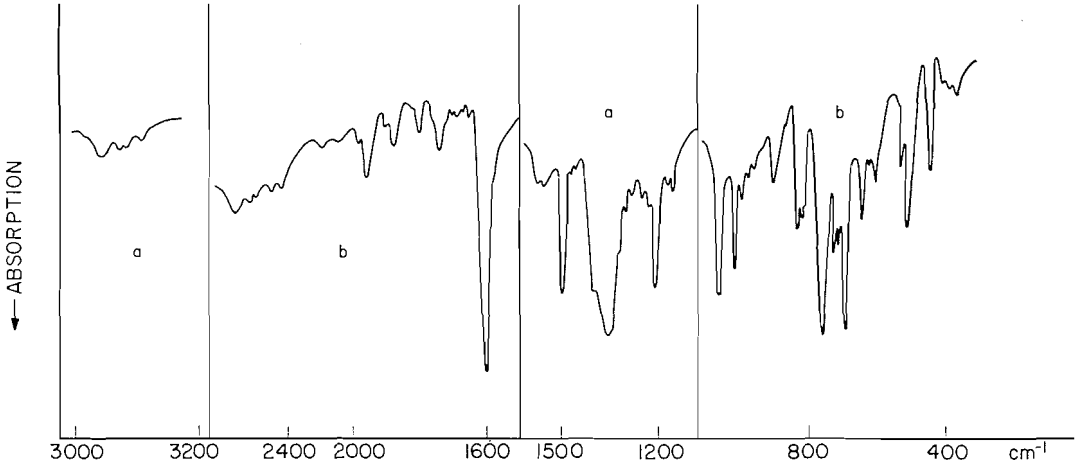

FIG. 3. The infrared spectrum of triphenylborate: (*a*) in CCl_4 solution in a 0.05 mm NaCl cell, (*b*) in a Nujol mull between CsBr windows.

parison with the spectra of boric acid (11) and the alkyl borates (5), where the corresponding frequencies were 544 and 525 cm^{-1} respectively. Bands due to the out-of-plane BO_3 deformation ($\delta'BO_3$) were located by Servoss and Clark at 639 and 667 cm^{-1} in the infrared spectra of boric acid (12) and trimethylborate (9) respectively. In each case isotopically labelled boron ^{10}B compounds were used to identify the peaks, since the vibration in question involves movement of the boron atom along the axis of symmetry. We might expect to find the corresponding band in the spectrum of triphenylborate at a lower frequency and have therefore assigned the band at 598 cm^{-1} to this vibration.

The C—O Stretching Vibration

The C—O stretching vibration in triphenylborate has been assigned to the peak at 1214 cm^{-1}. Although this frequency is within the range of the in-plane CH deformation vibrations of the benzene ring, it is the only prominent band in the region. Our assignment is in agreement with that of Werner and O'Brien (5).

Benzene Ring Vibrations

The assignments of the vibrations of the phenyl groups in triphenylborate given in Table II are again based on previous work on monosubstituted benzenes (7, 8) and triphenyl derivatives (1–3, 6).

The C—H stretching vibrations in triphenylborate give rise to much weaker absorption than for triphenylboron. The in-plane ring deformation (αCCC) is assigned to a peak at 635 cm^{-1}, somewhat higher than the usual frequency range for this mode.

Calculation of BC_3 and BO_3 Skeletal Vibrations

We have applied the Wilson *F–G* matrix method (26) to calculate Urey–Bradley force constants (27, 28) from the observed frequencies for the BC_3 and BO_3 groups. Both groups belong to the point group D_{3h} and hence the normal modes of vibration shown in Fig. 4 are of species $a_1' + 2e' + a_2''$. For this calculation, the symmetry coordinates as well as the *F* and *G*

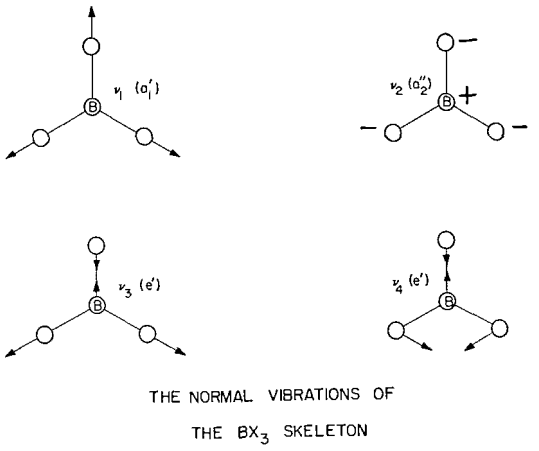

FIG. 4. The normal vibrations of a planar BX_3 group.

Can. J. Chem. Downloaded from www.nrcresearchpress.com by 210.87.254.6 on 09/05/12
For personal use only.

Can. J. Chem. Downloaded from www.nrcresearchpress.com by 210.87.254.6 on 09/05/12
For personal use only.

matrices used have the same form as those reported by Janz and Mikawa (13). The geometry and internal coordinates for these groups are shown in Fig. 5. The following molecular parameters were used (29): r(B—O) = 1.38 Å, r(B—C) = 1.56 Å, and all bond angles = 120°. All calculations were carried out with an IBM 1620 computer. The program was designed so that the elements of the F matrix could be varied independently until the best fit is obtained with the frequencies.

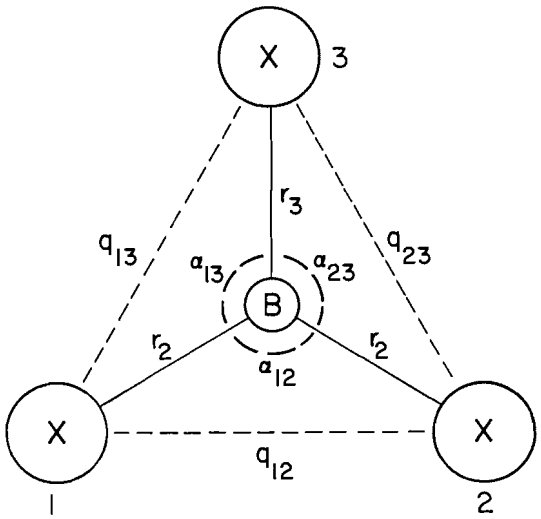

FIG. 5. Geometry and internal coordinates of the BX_3 group (X = O or C).

The calculated force constants for the BC_3 and BO_3 groups are given in Table III. The values obtained for the BO_3^{3-} ion (13) are included for comparison. In Table IV the calculated and observed frequencies are summarized.

TABLE III

Calculated Urey–Bradley force constants (mdyn/Å) for the BC_3 and BO_3 groups and the BO_3^{3-} ion

Force constant	BC_3	BO_3	BO_3^{3-} (13)
Bond stretching K_{BX}	3.5	3.8	4.64
Angle bending H_{XBX}	0.43	0.733	0.744
Interaction F_{XX}	0.45	1.05	1.05

For the BO_3 skeleton, our calculated force constants are similar to those of Janz and Mikawa (13) for the BO_3^{3-} ion. It seems, therefore, that the calculated value of 860 cm^{-1} for the symmetric B—O stretching frequency and our assignment of the 505 cm^{-1} to the in-plane BO_3 deformation are reasonable. Although the reliability of the force constants obtained for the BC_3 group cannot be ascertained, since there are no force constants with which they can be compared, the set appears fairly satisfactory. In both skeletons, the symmetric B—C and B—O stretching frequencies calculated at 828 and 860 cm^{-1} respectively must be considered to be only approximate, since drastic assumptions were made in the calculations.

TABLE IV

Observed and calculated frequencies (cm^{-1}) for the BC_3 and BO_3 groups

		Observed	Calculated
BC_3	a_1'	—	828
	e'	599	594
		1242	1249
BO_3	a_1'	—	860
	e'	505	505
		1350	1347

Conclusions

Two features in the infrared spectrum of triphenylboron support a propeller-shaped D_3 structure for this molecule. A forbidden a_2 ϕCC deformation of the monosubstituted benzene ring was observed at 400 cm^{-1} and one of the b_2 γCH vibrations was split into two peaks at 775 and 742 cm^{-1}. An approximate value of 828 cm^{-1} has been calculated for the infrared inactive symmetric BC_3 stretching vibration in this molecule.

Reasonable assignments of the observed frequencies have been made for both triphenylboron and triphenylborate in terms of monosubstituted benzene derivatives and central BC_3 and BO_3 groups.

Acknowledgments

The authors gratefully acknowledge the financial support of the National Research Council of Canada and the Department of University Affairs of the Province of Ontario.

1. H. F. SHURVELL, J. A. FANIRAN, and H. DODSWORTH. Spectrochim. Acta, **23**, 1313 (1967).
2. H. F. SHURVELL. Spectrochim. Acta, **24**, 2925 (1968).
3. H. F. SHURVELL. J. Chim. Phys. **62**, 1027 (1965).
4. D. W. A. SHARP and N. SHEPPARD. J. Chem. Soc. 674 (1957).

5. R. L. WERNER and K. G. O'BRIEN. Australian J. Chem. **8**, 355 (1955).
6. R. E. WESTON, JR., A. TSUKAMOTO, and N. N. LICHTIN. Spectrochim. Acta, **22**, 433 (1966).
7. D. H. WHIFFEN. J. Chem. Soc. 1350 (1956).
8. N. FUSON, C. GARRIGOU-LAGRANGE, and M. L. JOSIEN. Spectrochim. Acta, **16**, 106 (1960).
9. R. R. SERVOSS and H. M. CLARK. J. Chem. Phys. **26**, 1179 (1957).
10. R. L. WERNER and K. G. O'BRIEN. Australian J. Chem. **9**, 137 (1956).
11. D. E. BETHEL and N. SHEPPARD. Trans. Faraday Soc. **51**, 9 (1957).
12. R. R. SERVOSS and H. M. CLARK. J. Chem. Phys. **26**, 1175 (1957).
13. G. J. JANZ and Y. MIKAWA. J. Mol. Spectry. **5**, 92 (1960).
14. T. COLCLOUGH, W. GERRARD, and M. F. LAPPERT. J. Chem. Soc. 907 (1955).
15. E. K. PLYLER, A. DANTI, L. R. BLAINE, and E. D. TIDWELL. J. Res. Natl. Bur. Std. A, **64**, 1 (1960).
16. E. KRAUS. Ber. **57**, 815 (1924).
17. H. LEWIS and L. C. BROCKWAY. J. Am. Chem. Soc. **59**, 2085 (1937).
18. M. F. LAPPERT. Chem. Rev. 959 (1956).
19. G. L. LEWIS and G. P. SMYTH. J. Am. Chem. Soc. **62**, 1529 (1940).
20. S. H. BAUER and J. Y. BEACH. J. Am. Chem. Soc. **63**, 1394 (1941).
21. J. E. STEWART. J. Res. Natl. Bur. Std. **56**, 337 (1956).
22. W. J. LEHMANN, C. O. WILSON, JR., and I. SHAPIRO. J. Chem. Phys. **28**, 777 (1958).
23. E. J. BLAU and B. W. MULLIGAN. J. Chem. Phys. **26**, 1085 (1957).
24. W. J. LEHMANN, C. O. WILSON, and I. SHAPIRO. J. Chem. Phys. **28**, 781 (1958).
25. LANDOLT-BORNSTEIN. Zahlenwerte und Funktionen. 6th ed. Vol. I. Part II. Springer-Verlag, Berlin. 1951.
26. E. B. WILSON, JR. J. Chem. Phys. **7**, 1047 (1939); **9**, 76 (1941).
27. H. C. UREY and C. A. BRADLEY. Phys. Rev. **38**, 1969 (1931).
28. T. SHIMANOUCHI. J. Chem. Phys. **17**, 245, 734, 848 (1949).
29. L. E. SUTTON (*Editor*). Tables of interatomic distances in molecules and ions. Chem. Soc. London. Publ. No. 11. 1958.

Can. J. Chem. Downloaded from www.nrcresearchpress.com by 210.87.254.6 on 09/05/12
For personal use only.

Can. J. Chem. Downloaded from www.nrcresearchpress.com by 210.87.254.6 on 09/05/12
For personal use only.

Infrared spectra of phenylboronic acid (normal and deuterated) and diphenyl phenylboronate

J. A. FANIRAN AND H. F. SHURVELL
Department of Chemistry, Queen's University, Kingston, Ontario

Received January 25, 1968

The infrared spectra of phenylboronic acid, normal and deuterated, and diphenyl phenylboronate have been recorded in the range 4000–300 cm^{-1} and assignments of the observed frequencies have been made. The spectrum of the acid in the OH stretching region shows evidence of intramolecular hydrogen bonding. The spectrum of diphenyl phenylboronate has been interpreted by analogy with monosubstituted benzene derivatives. The two different environments of the phenyl groups in this molecule give rise to splitting of two of the characteristic vibrations of the benzene ring near 760 and 680 cm^{-1}.

Canadian Journal of Chemistry, 46, 2089 (1968)

Introduction

Our interest in the study of phenylboronic acid and diphenyl phenylboronate arose during our investigation of the infrared spectrum of triphenylboron $(C_6H_5)_3B$ (1). It was found that triphenylboron can be easily contaminated through various stages of hydrolysis that give phenylboronic anhydride $(C_6H_5BO)_3$, phenylboronic acid $C_6H_5B(OH)_2$, and diphenyl phenylboronate $C_6H_5B(OC_6H_5)_2$ (2, 3). Therefore, in conjunction with our spectral study of triphenylboron (1), a detailed spectroscopic investigation on these contaminants seemed worthwhile. The infrared spectrum of phenylboronic anhydride has been studied (4). Although phenylboronic acid has been known for a long time, only a brief reference to part of its infrared spectrum has appeared in the literature as a means of distinguishing the acid from its anhydride (5–7). Burch *et al.* (8) in their study of the infrared spectra of dialkyl phenylboronates discussed a few of the bands in the infrared spectrum of dibenzyl phenylboronate without any tabulation of the observed frequencies.

In this work, we present the infrared spectroscopic data on phenylboronic acid, normal and deuterated, and diphenyl phenylboronate. The spectra of phenylboronic anhydride (4), boric acid (9, 10), and dialkyl phenylboronates (8) have been useful in making our assignments. In addition, the spectrum of diphenyl phenylboronate is interpreted in terms of a monosubstituted benzene derivative and a central CBO_2 skeleton. We have applied Wilson's *F–G* matrix method in an attempt to calculate the Urey–Bradley force constants from the observed frequencies involving the CBO_2 group. However, the results of this calculation were unsatisfactory and are not reproduced here.

Symmetry Consideration

Cryoscopic molecular weight determinations (11, 12) and dipole moment measurement (13) indicate that phenylboronic acid is a monomer. By analogy with boric acid (14, 15), we have assumed a planar structure of symmetry *Cs* for phenylboronic acid. Under the *Cs* point group, all the 42 normal vibrations of phenylboronic acid will be infrared active. These comprise $29a'$ in-plane and $13a''$ out-of-plane vibrations.

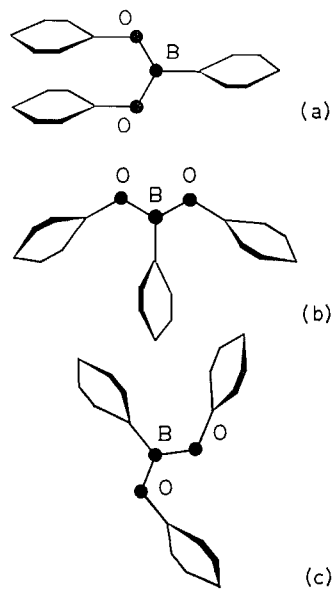

FIG. 1. Three possible structures of diphenyl phenylboronate, $C_6H_5B(OC_6H_5)_2$.

Can. J. Chem. Downloaded from www.nrcresearchpress.com by 210.87.254.6 on 09/05/12
For personal use only.

Examination of the molecular models of diphenyl phenylboronate shows that no planar structure is feasible for this compound due to the overlap of the benzene rings. Three possible structures for this molecule, considered from molecular models, are shown in Fig. 1. It is likely that the true structure is intermediate between these. However, treating the phenyl groups as monosubstituted benzenes and the CBO_2 skeleton separately, we expect $11a_1 + 3a_2 + 6b_1 + 10b_2$ vibrations for the monosubstituted benzene and $3a_1 + 2b_1 + b_2$ vibrations for the CBO_2 group. Only the $3a_2$ vibrations will be inactive in the infrared. This treatment assumes that all the phenyl groups in this molecule are identical. The actual differences in the environments of the phenyl groups are expected to give rise to small splittings of some of the monosubstituted benzene vibrations.

Experimental

Phenylboronic acid was prepared by two methods: (*a*) from a Grignard reagent and *n*-butylborate (3, 7) and (*b*) by the hydrolysis of phenylboron dichloride with water (16, 17). The products were crystallized from petroleum ether. Determination of an accurate melting point was difficult due to the ease of dehydration of the acid to form the anhydride, m.p. 214–215 °C, literature m.p. 215–216 °C (2, 11, 12, 18).

Deuterated phenylboronic acid was prepared by the exchange reaction between D_2O and phenylboronic acid containing about 0.1 g of K_2CO_3 and by the hydrolysis of phenylboron dichloride with D_2O. The products were crystallized from petroleum ether. The hydrogen–deuterium exchange reaction was not complete, however. The last method gave a better product.

Because diphenyl phenylboronate is easily hydrolyzed, its preparation was carried out in an inert atmosphere of dry nitrogen. The compound was prepared by the esterification of phenylboron dichloride with phenol (3, 17, 18) under dry nitrogen. The absence of any absorption band between 3300–3200 cm^{-1} due to an O—H stretching vibration or near 1000 cm^{-1} due to a B—O—H deformation mode in the spectrum indicated the absence of O—H bonds and was thus a proof of the purity of the sample.

The infrared spectra of the acids were obtained from KBr pressed discs, as mulls between CsBr windows and in solution in CCl_4 at various concentrations using 0.05 mm NaCl cells. No differences were observed in the spectra obtained in solution and in the solid state. The spectrum of diphenyl phenylboronate was obtained as a Fluorolube mull between 4000 and 1350 cm^{-1} and as a Nujol mull between 1600 and 300 cm^{-1}. All spectra were recorded on a Beckman IR10 grating spectrophotometer which was calibrated against a polystyrene film (19). The frequencies given in Tables I–III are believed to be accurate to ± 3 cm^{-1} between 2000 and 300 cm^{-1} and ± 5 cm^{-1} between 4000 and 2000 cm^{-1}.

Results and Discussion

We shall use the usual symbols to describe monosubstituted benzene vibrations. We shall also use δ to denote a deformation mode. The fundamental frequencies of phenylboronic acid, normal and deuterated, and diphenyl phenylboronate are listed in Table I which includes corresponding frequencies for phenylboronic anhydride (4). Tables II and III contain assignments of the combination and overtone bands of phenylboronic acids and diphenyl phenylboronate respectively. The spectra of the acids are shown in Fig. 2 and that of diphenyl phenylboronate in Fig. 3. Splitting of the γCH vibration at 755 and 745 cm^{-1} and the ϕCC vibration at 692 and 682 cm^{-1} occurs in the spectrum of diphenyl phenylboronate. It is likely that the splitting arises from the different environments of the phenyl groups in the molecule

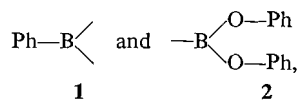

1 **2**

where Ph = phenyl group.

O—H and O—D Vibrations

One of the two very strong and broad bands in the spectrum of phenylboronic acid occurs at 3280 cm^{-1}. This shifts to 2440 cm^{-1} upon deuteration. The assignment of these bands to νOH and νOD stretching vibrations is straightforward. In the spectra of the boric acids, normal and deuterated, absorption bands at 3200 and 2400 cm^{-1} (9) and 3150 and 2380 cm^{-1} (10) have been assigned to these vibrations. The strength, broadening, and frequencies of these bands suggest that intramolecular hydrogen bonding occurs in phenylboronic acid.

B—O Vibrations

The second strong band in the spectrum of phenylboronic acid occurs at 1350 cm^{-1} and in the deuterated acid as a doublet at 1344 and 1330 cm^{-1}. The doublet at 1360 and 1340 cm^{-1} is the strongest band in the spectrum of diphenyl phenylboronate. We have assigned these bands to the asymmetric ^{10}B—O and ^{11}B—O (νBO asym.) stretching vibrations. Treating the B—O group as a diatomic molecule, then assuming harmonic frequencies, one predicts that the ratio $\nu^{10}BO:\nu^{11}BO$ is 1.01:1. The observed isotopic splitting fits this ratio remarkably well. Stretching vibrations of double bonds usually give rise

Can. J. Chem. Downloaded from www.nrcresearchpress.com by 210.87.254.6 on 09/05/12
For personal use only.

TABLE I

Fundamental frequencies in cm^{-1} of phenylboronic acids, normal and deuterated, and diphenyl phenylboronate with the corresponding data for phenylboronic anhydride*

$C_6H_5B(OH)_2$	$C_6H_5B(OD)_2$	$C_6H_5B(OC_6H_5)_2$	$(C_6H_5BO)_3$, Ref. 4	Assignment†
3280 vs	2440 vs	—	—	νOH,νOD
3095 vw	3090 w	3100 vw	—	νCH b_1
3080 vw	3069 w	3080 vw	—	νCH a_1
3070 vw	3050 sh	3050 vw	—	νCH a_1
3040 vw	3040 w	3032 vw	3031	νCH a_1
3020 vw	—	—	—	νCH b_1
1608 s	1608 s	1608 s	1605	νCC a_1
1580 vw	1580 vw	1575 vw	—	νCC b_1
1500 m	1498 m	1492 m	—	νCC a_1
1444 ms	1444 ms	1440 s	—	νCC b_1
1375 s	1370 s	—	—	νCC b_1
1350 vs	1344, 1330 d,vs	1360, 1340 d,vs	1370	νBO asym.
1310 vw	1305 vw	1308 w	1312(νCC)	βCH b_1
1270 mw	1269 mw	—	1295	βCH b_1
—	—	1205 w	—	νCO asym.
1186 s	1186 s	1178 w	1182	βCH a_1
1160 sh	1160 vw	1164 vw	1163	βCH b_1
—	—	1149 vw	—	νCO sym.
1089 s	1085 s	1084 mw	1104, 1087 d	νBC
—	—	1065 m	—	βCH b_1
1025 ms	1024 ms	1022 m	—	βCH a_1
—	1000 vw	994 vw	1000	Ring a_1
1002 ms	910 s	—	—	δBOH,δBOD
966 vw	970 vw	894 w	927	γCH b_2
850 vw	850 vw	850 w	—	νBO sym.
			778	Boroxole ring
758 m	755 m	755, 745 d,ms	761	γCH b_2
691 s	685 s	692, 682 d,s	698	φCC b_2
			670	Boroxole ring
631 ms	644 ms	650 w	—	δ′BO_2 (out-of-plane)
615 vw	610 vw	630 w		αCCC b_1
570 ms	568 ms	508, 494 d,mw		δBO_2 (in-plane)
450 vw	452 vw	397, 384 d,vw		BO_2 rock
465 w	430 vw	805 w		X-sens.
	385 vw	566 m		X-sens.
		425 mw		X-sens.

*Relative intensities in this and subsequent tables are denoted by : vs = very strong, s = strong, m = medium, ms = medium strong, w = weak, vw = very weak, d = doublet, sh = shoulder.
†The notation employed is described in the text.

to very strong absorption bands (20). It is possible, therefore, that the high intensity of the B—O asymmetric stretching vibration could indicate some double bond character for the B—O bonds in phenylboronic acid. This is consistent with a calculation of a bond order of 1.58 in the BO_3^{3-} ion (21). Our observed frequencies for the asymmetric B—O stretching vibration in diphenyl phenylboronate are higher than those reported by Burch *et al.* for this vibration in the spectra of dialkyl phenylboronates (8).

The assignment of the B—O symmetric stretching vibration (νBO sym.) is not simple. In the spectrum of dialkyl phenylboronates (8) a peak at 1123 ± 3 cm^{-1} has been assigned to this mode. One might expect to find a band in phenylboronic acid in a similar spectral region and at lower frequencies in diaryl phenylboronates. A possible assignment would be the shoulder at 1070 cm^{-1} in the spectrum of the undeuterated acid and the band at 1065 cm^{-1} in the spectrum of diphenyl phenylboronate. However, no corresponding frequency has been found in the deuterated acid and the peak at 1065 cm^{-1}

TABLE II

Assignment of the combination and overtone bands in the spectra of phenylboronic acids (normal and deuterated). Frequencies in cm^{-1}

$C_6H_5B(OH)_2$	Assignment		$C_6H_5B(OD)_2$	Assignment	
3110 vw	1500+1608=3108	$(a_1 \times a_1 = A_1)$	3110 vw	1498+1608=3106	$(a_1 \times a_1 = A_1)$
2950 vw	1375+1580=2955	$(b_1 \times b_1 = A_1)$	2940 vw	1370+1580=2950	$(b_1 \times b_1 = A_1)$
2860 vw	1580+1270=2850	$(b_1 \times b_1 = A_1)$	2220 vw	610+1608=2218	$(b_1 \times a_1 = B_1)$
2800 vw	1188+1608=2796	$(a_1 \times a_1 = A_1)$	1920 vw	610+1305=1915	$(b_1 \times b_1 = A_1)$
2155 vw	570+1580=2150	$(a_1 \times b_1 = B_1)$	1840 vw	568+1269=1837	$(a_1 \times b_1 = B_1)$
2060 vw	615+1444=2059	$(b_1 \times b_1 = A_1)$	1791 vw	610+1186=1796	$(a_1 \times b_1 = B_1)$
1978 vw	966+1002=1968	$(b_1 \times a_1 = B_1)$	1700 vw	2× 850=1700	$(a_1 \times a_1 = A_1)$
1926 vw	2× 966=1932	$(b_2 \times b_2 = A_1)$	1690 vw	610+1085=1695	$(a_1 \times b_1 = B_1)$
1835 vw	570+1270=1840	$(a_1 \times b_1 = B_1)$	1560 vw	644+ 910=1554	$(a_1 \times b_2 = B_2)$
1790 vw	758+1025=1783	$(b_2 \times a_1 = B_2)$	1540 vw	568+ 970=1538	$(a_1 \times b_1 = B_1)$
1734 vw	570+1160=1730	$(a_1 \times b_1 = B_1)$	1323 vw	568+ 755=1323	$(a_1 \times b_2 = B_2)$
1700 vw	2× 850=1700	$(a_1 \times a_1 = A_1)$	1110 vw	430+ 685=1115	$(a_1 \times b_2 = B_2)$
1669 vw	570+1089=1659	$(a_1 \times a_1 = A_1)$	1110 vw	451+ 644=1095	$(b_2 \times b_2 = A_1)$
1560 vw	570+1002=1572	$(a_1 \times a_1 = A_1)$	800 vw	385+ 430= 815	$(a_1 \times b_1 = B_1)$
1070 sh	450+ 615=1065	$(b_1 \times b_1 = A_1)$			
920 vw	2× 450= 900	$(b_1 \times b_1 = A_1)$			
720 vw	—				
650 vw	—				

is more likely to be due to one of the in-plane CH deformations (βCH) of the monosubstituted benzene ring. It is then likely that the symmetric B—O stretching vibration does not occur in this region. A strong polarized Raman line at 726 cm^{-1} in trimethylborate (22) and at 910 cm^{-1} in the borate ion BO_3^{3-} (23) was assigned to this vibration. It is therefore possible that the weak absorption bands at 850 cm^{-1} in the spectra of phenylboronic acid, normal and deuterated, and diphenyl phenylboronate correspond to the B—O symmetric stretching vibration.

The B—C Vibration

Santucci *et al.* (5) associated an absorption band between 1080 and 1110 cm^{-1} with a B—C stretching mode (νBC) in arylboronic acids. We have assigned the band at 1089 and 1085 cm^{-1} in the spectra of the normal and deuterated phenylboronic acids respectively and at 1084 cm^{-1} in diphenyl phenylboronate to the B—C stretching vibration. This corresponds to the doublet at 1104 and 1087 cm^{-1} in the infrared spectrum of phenylboronic anhydride (4). The band is weaker in diphenyl phenylboronate.

TABLE III

Combination and overtone bands in diphenyl phenylboronate. Frequencies in cm^{-1}

Frequency	Assignment	
1556 vw	395+1164=1559	$(b_1 \times b_1 = A_1)$
1278 sh	630+ 650=1280	$(b_1 \times b_1 = A_1)$
1250 sh	2× 630=1260	$(b_1 \times b_1 = A_1)$
1100 vw	425+ 682=1107	$(b_2 \times a_1 = B_2)$
820 vw	395+ 425= 820	$(a_1 \times b_1 = B_1)$
715 vw	—	
600 vw	—	
365 vw	—	
345 vw	—	

B—O—H and B—O—D Deformation Vibrations

The B—O—H deformation (δBOH) is easily recognized in the spectrum of phenylboronic acid, since upon deuteration, its frequency is significantly lowered. A strong band at 1002 cm^{-1} in the spectrum of phenylboronic acid which shifts to 910 cm^{-1} upon deuteration is identified with this vibration. Bands located at 1197 and 929 cm^{-1} (9) and at 1183 and 914 cm^{-1} (10) have been assigned to δBOH, δBOD respectively in normal and deuterated boric acids. The absence of this peak in the spectra of phenylboronic anhydride (4) and diphenyl phenylboronate further supports our assignment.

BO_2 Deformations

By comparing our spectra with those of dialkyl phenylboronates (8) and boric acid (9, 10), we have placed the BO_2 out-of-plane deformation mode (δ′BO_2) at 631 and 644 cm^{-1} in normal and deuterated phenylboronic acids and at 650 cm^{-1} in diphenyl phenylboronate. Burch *et al.* (8) assigned a band at 652 cm^{-1} to this mode in dialkylamino and dialkyl phenylboronates. The

Can. J. Chem. Downloaded from www.nrcresearchpress.com by 210.87.254.6 on 09/05/12
For personal use only.

Can. J. Chem. Downloaded from www.nrcresearchpress.com by 210.87.254.6 on 09/05/12
For personal use only.

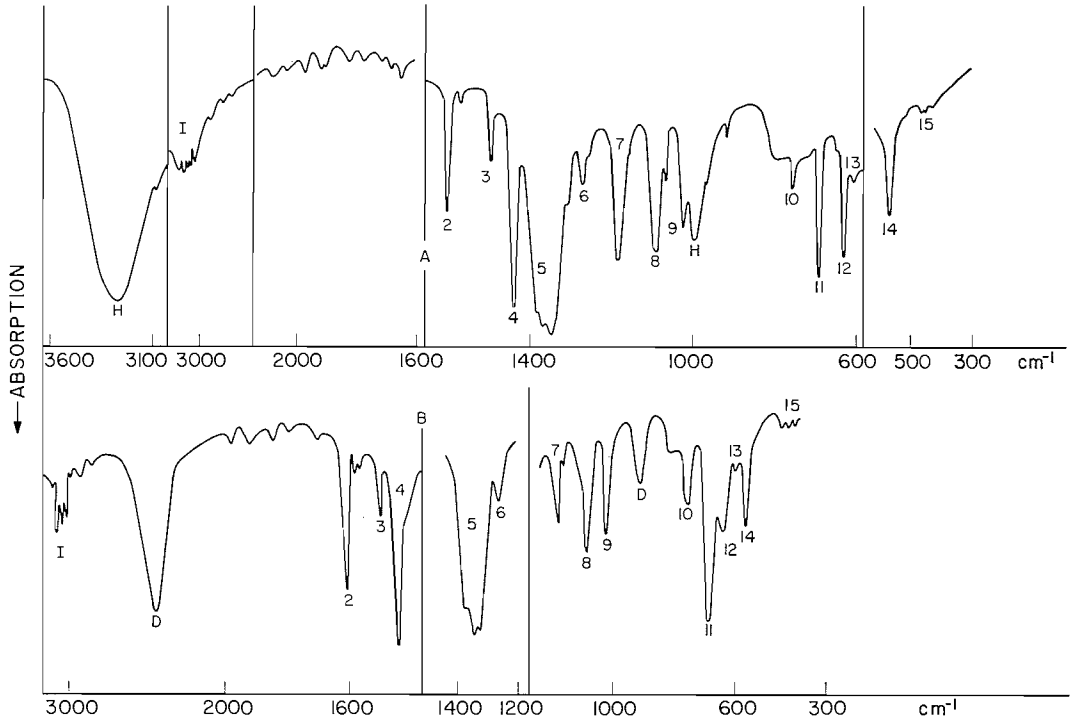

FIG. 2. The infrared spectra of KBr discs of the phenylboronic acids: (A) $C_6H_5B(OH)_2$ and (B) $C_6H_5B(OD)_2$.

in-plane BO_2 deformation mode (δBO_2) gives rise to an absorption band at a lower frequency. Bands at 570 and 568 cm^{-1} in the spectra of the phenylboronic acids are assigned to this mode. These values are higher than previously reported for the δBO_3 vibration in the boric acids (9, 10). In the spectrum of diphenyl phenylboronate, a doublet at 508, 494 cm^{-1} is assigned to $\delta^{10}BO_2$ and $\delta^{11}BO_2$ respectively.

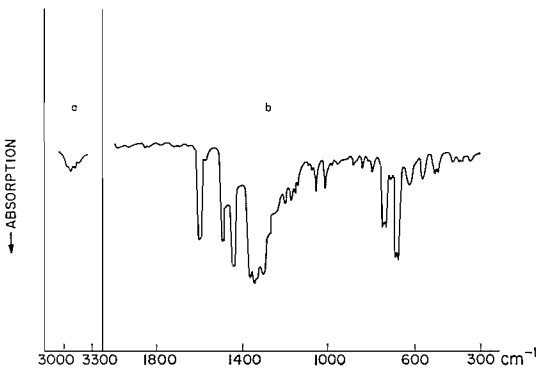

FIG. 3. The infrared spectrum of diphenyl phenylboronate, $C_6H_5B(OC_6H_5)_2$. A scale expansion device was used to record (*a*).

The absorption bands arising from the rocking deformation modes are generally observed in the low frequency region and, in these molecules, are expected to be very weak. The weak peaks found at 450 and 452 cm^{-1} in normal and deuterated acids, respectively, and the doublet at 397 and 384 cm^{-1} in diphenyl phenylboronate are therefore attributed to BO_2 rocking vibrations.

C—O Vibrations

In the spectrum of diphenyl phenylboronate, the asymmetric C—O stretching vibration (νCO asym.) is observed at 1205 cm^{-1}. Bands at 1238 and 1214 cm^{-1} were assigned respectively to this mode in arylboronates (24) and triphenylboronate (1). The frequency of the symmetric C—O vibration (νCO sym.) has been shown to depend upon the nature of the substituents on the carbon atom (25). The assignment of the band at 1149 cm^{-1} to this mode is made by analogy with those of dialkyl phenylboronates (8).

C—H Vibrations

The absorption bands in the aromatic CH

Can. J. Chem. Downloaded from www.nrcresearchpress.com by 210.87.254.6 on 09/05/12
For personal use only.

stretching region of these compounds are very weak. We have resolved the absorption in this region into five peaks in the case of phenylboronic acid, and four peaks for the deuterated acid and diphenyl phenylboronate. The assignments to symmetry species a_1 and b_1 are arbitrary.

In the spectra of the three compounds, five peaks have been assigned to the in-plane C—H deformations (βCH). These are located at 1310, 1270, 1186, 1160, and 1025 cm^{-1} in the spectrum of phenylboronic acid, at 1305, 1269, 1186, 1160, and 1024 cm^{-1} in the deuterated acid, and at 1308, 1178, 1164, 1065, and 1022 cm^{-1} in diphenyl phenylboronate. These agree well with similar assignments in monosubstituted benzenes (25).

Bands at 966 and 758 cm^{-1} in the spectrum of phenylboronic acid and at 970 and 755 cm^{-1} in the deuterated acid are assigned to out-of-plane CH deformation modes (γCH). In diphenyl phenylboronate, the strong γCH absorption near 750 cm^{-1} splits into two peaks at 755 and 745 cm^{-1}. Since there are two kinds of phenyl groups in different environments in this molecule, such splitting is not unexpected. The out-of-plane ring deformation (ϕCC) also shows a splitting of a similar magnitude. The band at 894 cm^{-1} is also assigned to a γCH vibration in this molecule. A third γCH mode for a monosubstituted benzene derivative is expected near 980; however, it has not been observed in the spectrum of diphenyl phenylboronate.

Benzene Ring Vibrations

In the aromatic C—C stretching region (1320–1620 cm^{-1}) the assignments of five bands in the spectra of phenylboronic acids (normal and deuterated) and four in diphenyl phenylboronate to νCC modes is straightforward. The fifth band in diphenyl phenylboronate near 1370 cm^{-1} probably has been obscured by the broad asymmetric B—O stretching band.

The out-of-plane ring deformation (ϕCC) usually observed near 680 cm^{-1} in the spectra of monosubstituted benzenes (26), has been assigned to the strong peaks at 691 and 685 cm^{-1} in the spectra of the phenylboronic acids (normal and deuterated respectively). As mentioned previously, the ϕCC vibration in the spectrum of diphenyl phenylboronate is split into a doublet at 692 and 682 cm^{-1}.

In the spectra of normal and deuterated phenylboronic acids, the in-plane ring deformation (αCCC) is located at 615 and 610 cm^{-1} respectively. A peak of medium intensity at 630 cm^{-1} in the spectrum of diphenyl phenylboronate is also assigned to an αCCC vibration.

The symmetric ring breathing mode usually found near 1000 cm^{-1} in the spectra of monosubstituted benzenes (26) could not be identified in phenylboronic acid due to the presence of the δBOH band at 1002 cm^{-1}. However, weak peaks at 1000 cm^{-1} in the spectrum of the deuterated acid and at 994 cm^{-1} in diphenyl phenylboronate are respectively assigned to this vibration.

X-Sensitive Vibrations

In monosubstituted benzenes, C_6H_5X, vibrations in which the substituent X moves with an appreciable amplitude have been described as X-sensitive (26). In this study, the substituent X is $—B(OH)_2$ and $—B(OD)_2$ in phenylboronic acids, normal and deuterated respectively, and $—B(OC_6H_5)_2$ in diphenyl phenylboronate. Thus, the B—C vibration in these three compounds is really one of the X-sensitive vibrations. These vibrations are not easy to identify, since in many cases bands that could be due to X-sensitive vibrations have possible alternative assignments as combinations and overtones of unobserved fundamentals. We have tentatively assigned a band at 465 cm^{-1} in the spectrum of phenylboronic acid, bands at 430 and 485 cm^{-1} in the deuterated acid, and bands at 805, 566, and 425 cm^{-1} in diphenyl phenylboronate to X-sensitive vibrations.

Combinations and Overtones

Most of the weak absorption bands which are not assigned to fundamental modes are accounted for in terms of combinations and overtones of the fundamentals. However, the weak bands below 750 cm^{-1} which could not be accounted for are probably combination and overtone bands of the fundamentals outside the spectral range covered.

Conclusion

The *Cs* symmetry assumed for phenylboronic acid seems to be satisfactory. We have found evidence of intramolecular hydrogen bonding between the two hydroxyl groups in this molecule. It is not possible to decide which of the three structures of Fig. 1 are most likely for diphenyl phenylboronate. The phenyl groups in

this molecule are not planar, however. Our interpretation of the observed spectrum in terms of a monosubstituted benzene derivative and a central CBO_2 group seems reasonable. The spectrum also indicates that there are two sets of phenyl groups in the molecule; the small differences in frequencies of their vibrations result in the observed splitting of the γCH and ϕCC vibrations observed in the infrared spectrum near 760 and 680 cm^{-1}.

Acknowledgments

The authors wish to acknowledge the financial support of the National Research Council of Canada and the Department of University Affairs of the Province of Ontario.

1. H. F. SHURVELL and J. A. FANIRAN. Can. J. Chem. This issue.
2. R. M. ADAMS. Advan. Chem. Ser. **23**, 87 (1959).
3. H. F. LAPPERT. Chem. Rev. 959 (1956).
4. D. W. AUBREY, M. F. LAPPERT, and H. PYSZORA. J. Chem. Soc. 1931 (1961).
5. L. SANTUCCI and H. GILMAN. J. Am. Chem. Soc. **80**, 193 (1958).
6. H. R. SNYDER, M. S. KONECKY, and W. J. LENNARZ. J. Am. Chem. Soc. **80**, 3611 (1958).
7. R. M. WASHBURN, E. LEVENS, C. F. ALBRIGHT, F. A. BILLIG, and E. S. CERNAK. Advan. Chem. Ser. **23**, 102 (1959).
8. J. E. BURCH, W. GERRARD, M. GOLDSTEIN, E. F. MOONEY, and H. A. WILLIS. Spectrochim. Acta, **18**, 1403 (1962).
9. D. E. BETHEL and N. SHEPPARD. Trans. Faraday Soc. **51**, 9 (1955).
10. R. R. SERVOSS and H. M. CLARK. J. Chem. Phys. **26**, 1175 (1957).
11. H. E. FRENCH and S. D. FINE. J. Am. Chem. Soc. **60**, 352 (1938).
12. C. R. KINNEY and D. F. PONTZ. J. Am. Chem. Soc. **58**, 196 (1936).
13. M. M. OTTO. J. Am. Chem. Soc. **57**, 1476 (1935).
14. J. M. COWLEY. Nature, **171**, 440 (1953).
15. W. H. ZACHARIASEN. Acta Cryst. **7**, 305 (1954).
16. E. W. ABEL, W. GERRARD, and M. F. LAPPERT. J. Chem. Soc. 112 (1957).
17. S. H. DANDEGAONKER, W. GERRARD, and M. F. LAPPERT. J. Chem. Soc. 2872 (1957).
18. F. R. BEAN and J. R. JOHNSON. J. Am. Chem. Soc. **54**, 4415 (1932).
19. E. K. PLYER, A. DANTI, L. R. BLAINE, and E. D. TIDWELL. J. Res. Natl. Bur. Std. A, **64**, 1 (1960).
20. M. ST. C. FLETT. Characteristic frequencies of chemical groups in the infrared. Elsevier Publ. Co., Inc., Amsterdam. 1963.
21. C. A. COULSON. Proc. Roy. Soc. London, Ser. A, **207**, 91 (1951).
22. R. R. SERVOSS and H. M. CLARK. J. Chem. Phys. **26**, 1179 (1957).
23. LANDÖLT-BÖRNSTEIN. Zahlenwerte und Funktionen. 6th ed. Vol. I. Part II. Springer-Verlag, Berlin. 1951.
24. F. K. BUTCHER, W. GERRARD, M. HOWARTH, E. F. MOONEY, and H. A. WILLIS. Spectrochim. Acta, **20**, 79 (1964).
25. R. L. WERNER and K. G. O'BRIEN. Australian J. Chem. **8**, 355 (1955).
26. D. H. WHIFFEN. J. Chem. Soc. 1360 (1956).

Can. J. Chem. Downloaded from www.nrcresearchpress.com by 210.87.254.6 on 09/05/12
For personal use only.

Association of perchlorate, fluoroborate, and fluorophosphate ions with complex ions of palladium and platinum

A. D. WESTLAND AND J. PLUŠČEC
Department of Chemistry, University of Ottawa, Ottawa, Canada

Received October 27, 1967

Perchlorate, tetrafluoroborate, and hexafluorophosphate salts containing the ions $(PhSC_3H_4SPh)_2M^{2+}$ where M = Pd or Pt are extensively associated as 1:1 electrolytes in nitromethane. Association is preceded by loss of one of the ligand molecules.

Canadian Journal of Chemistry, **46**, 2097 (1968)

Can. J. Chem. Downloaded from www.nrcresearchpress.com by 210.87.254.5 on 09/05/12
For personal use only.

Perchlorate and fluoro-ions are notable for their poor donor ability. Consequently, perchlorate which occurs as a ligand in a solid complex is dissociated as an ion when the complex is dissolved. Electrostatic interaction in the solid state between perchlorate and a central ion can lead to deformation of the perchlorate ion (1). The lifting of degeneracy in the vibrational spectra of such coordinated ions does not necessarily indicate the occurrence of decidedly covalent bonding.

There is some evidence of the association of perchlorate ion with certain cations in aqueous solution. It is probable that in a given case, the phenomenon is due to solvent-separated or outer sphere ion-pairing. Evidence of possible association between Tl^+, Mg^{2+}, and Mn^{2+} and ClO_4^- was obtained by Raman studies of aqueous solutions (2). Hester and Plane failed to observe any Raman line splittings with solutions of $Mg(ClO_4)_2$, while under similar conditions a variety of metal nitrates gave positive evidence of association (3). There is a broadening of the ^{35}Cl n.m.r. resonance line in $HClO_4$ solutions containing Mn^{2+} (4). This was attributed to the exchange of ^{35}Cl between different sites via an inner sphere $Mn–ClO_4$ complex. Polarographic studies by Blazej and Svancer (5) were interpreted as showing complex formation between $Cr(H_2O)_6^{3+}$ and ClO_4^- (5). There have been reports of complexes between perchlorate and ZrO^{2+} (6), Fe^{3+} (7), and Ce^{3+} (8).

Inner sphere coordination should be more easily attained in a solvent whose molecules are poorer donors than water. Thus, Barker *et al.* observed weak electrolyte behavior with $Cu(bipy)_2(ClO_4)_2$ in nitrobenzene and this was shown to be due to coordination of ClO_4^- to the copper atom (9).

In the course of work on solutions of nitrate and perchlorate salts in nonaqueous solvents, we encountered weak electrolyte behavior in nitromethane. The compounds which showed this behavior are $L_2Me(ClO_4)_2$, where L = $PhSC_3H_6SPh$ and Me = Pd or Pt. It would be misleading not to point out immediately that it is not these compounds themselves which are weak electrolytes but rather the monochelated derivatives which form by the loss of one ligand molecule when the bis-chelated compounds are dissolved. This is represented by the equation:

$$[1] \qquad L_2Me^{2+} \rightleftharpoons LMe^{2} + L.$$

The weak electrolyte association is believed to be

$$[2] \quad LMe(O_2NCH_3)_2^{2+} + ClO_4^- \rightleftharpoons LMe(ClO_4)(O_2NCH_3)^+ + CH_3NO_2.$$

The occurrence of [1] was indicated in three ways. (1) The conductivity increased upon the addition of excess dithioether. (2) Essentially strong electrolyte behavior, unaffected by addition of excess ligand, was shown by the platinum perchlorate complex containing $PhSC_2H_4SPh$ which forms a five-membered chelate ring. Chugaeff and Kobljansky have shown that dithioethers which form six-membered chelate rings with platinum form much less stable complexes than dithioethers which form five-membered rings (10). These authors established that dissociation according to an equilibrium such as [1] occurs to an appreciable extent at the concentrations used in the present work. The palladium perchlorate complex of $PhSC_2H_4SPh$ exhibited a slightly lower conductivity in nitromethane than the platinum analogue and the conductivity was raised by the addition of excess ligand. Palladium complexes are generally a little less stable than platinum complexes. (3) The absorption maximum of the palladium perchlorate complex of

Can. J. Chem. Downloaded from www.nrcresearchpress.com by 210.87.254.5 on 09/05/12
For personal use only.

$PhSC_3H_6SPh$ at 384 mμ was shifted to 390 mμ and its intensity was increased by more than a factor of three when a large excess of ligand was added. A spectrophotometric study of the palladium complex showed the stability constant for eq. [1] to be 2×10^4. The platinum complex could not be so examined because it absorbs strongly in the near ultraviolet region where nitromethane shows strong absorption.

We have reported the conductivity behavior of the palladium perchlorate complexes with $PhSC_2H_4SPh$ and $PhSC_3H_6SPh$ in a brief communication (11).

Fluoroanion complexes, because of the rarity of two-coordination for fluorine (12), seemed to be even less likely than perchlorates to show evidence of ionic association, so we proceeded to examine the salts containing the BF_4^- and the PF_6^- ions. Tetrafluoroborate appears to be coordinated to the central atom in trimethyltin tetrafluoroborate (13) and in bis-ethylenediaminecopper(II) tetrafluoroborate (14), but only in the crystalline state. There is a report of the coordination of BF_4^- and ClO_4^- in ethyl acetate and methyl cyanide solutions with the ion $Cu(solvent)_4^{2+}$ (15). The conclusions were based upon the visible absorption spectrum. However, the compounds behaved as strong 2:1 electrolytes in CH_3CN.

Experimental

Conductivity Measurements

Conductivities were measured at 25.00 ± 0.05° in purified dimethylformamide and nitromethane, using an Industrial Instruments model RC16B2 conductivity bridge and a solution cell of the Washburn type with platinized electrodes. The cell was calibrated with 0.1000 *N* potassium chloride and it had a cell constant of 0.761.

Preparation of Complexes

Bis-1,3-di(phenylthio)propanepalladium(II) perchlorate, bis-1,3-di(phenylthio)propaneplatinum(II) perchlorate, and di-(1,2-bisdiphenylphosphinoethane)platinum perchlorate were prepared as described previously (3, 16).

Bis-1,2-di(phenylthio)ethanepalladium(II) Perchlorate

Dichloro-1,2-di(phenylthio)ethanepalladium (1.87 g) was suspended in hot CH_3NO_2 (100 cc) and silver perchlorate (1.78 g, 2 equiv) was added. A precipitate formed which was allowed to age for 0.5 h on the steam bath. The solvent was removed on a rotary evaporator and a yellow oil was obtained. This was triturated three times with acetone and a mustard-yellow powder was formed (1.31 g) which exploded at 251°.

Anal. Calcd. for $C_{28}H_{28}Cl_2O_8PdS_4$: C, 42.1; H, 3.55. Found: C, 42.5; H, 3.55.

Bis-1,2-di(phenylthio)ethaneplatinum(II) Perchlorate

This was prepared in 40% yield from bis-1,2-di-(phenylthio)ethaneplatinum(II) chloride by a procedure similar to the foregoing. The product was a white solid which decomposed at 185°.

Anal. Calcd. for $C_{28}H_{28}Cl_2O_8PtS_2$: C, 37.9; H, 3.19. Found: C, 37.0; H, 3.43.

Bis-1,3-di(phenylthio)propanepalladium(II) Tetrafluoroborate

Dichloro-1,3-di(phenylthio)propanepalladium (1.0 g) was suspended in CH_2Cl_2 (100 cc) and additional ligand (0.60 g, 1 mole equiv) and silver tetrafluoroborate (0.89 g, 2 mole equiv) added. The mixture was shaken for 12 h after which the resulting precipitate was separated and washed with a solution consisting of methanol (50 cc) and 49% aqueous hydrofluoric acid (5 cc). The washings were evaporated in a Teflon beaker on the steam bath to a volume of ca. 15 ml. The evaporation was continued thereafter at room temperature to produce crystals which were recrystallized from methanol – hydrofluoric acid solution. The product (76% yield, glistening amber crystals) had m.p. 255–257°.

Anal. Calcd. for $C_{30}H_{32}B_2F_8PdS_4$: C, 40.38; H, 3.58; S, 14.20. Found: C, 40.51; H, 3.62; S, 14.42.

Bis-1,3-di(phenylthio)propaneplatinum(II) Tetrafluoroborate

This was prepared in a manner identical with that used for the palladium analogue. The product (79% yield, light grey powder) had m.p. 255–258°.

Anal. Calcd. for $C_{30}H_{32}B_2F_8PtS_4$: C, 45.00; H, 4.01; S, 16.01. Found: C, 44.76; H, 4.04; S, 15.93.

Bis-1,3-di(phenylthio)propanepalladium(II) Hexafluorophosphate

Dichloro-1,3-di(phenylthio)propanepalladium (0.449 g) was suspended in acetone (20 cc) and additional ligand (0.244 g) and a filtered solution of $AgPF_6$ (0.476 g) in acetone (25 cc) added. The mixture was shaken for 5 h after which the precipitate of silver chloride was separated. The filtrate was evaporated under reduced pressure and the resulting crystals were recrystallized from acetone. The product (76% yield, yellowish green powder) was heated at 60° in a drying pistol for 6 h and it had m.p. 215–218°. The various operations were carried out in the dark.

Anal. Calcd. for $C_{30}H_{32}F_{12}P_2PdS_4$: C, 39.28; H, 3.50; S, 14.00. Found: C, 39.47; H, 3.69; S, 14.26.

Bis-1,3-di(phenylthio)propaneplatinum(II) Hexafluorophosphate

This was prepared in a manner identical with that used for the palladium analogue. The product (69% yield, white powder) had m.p. 220–222°.

Anal. Calcd. for $C_{30}H_{32}F_{12}P_2PtS_4$: C, 35.82; H, 3.20; S, 12.76. Found: C, 36.05; H, 3.31; S, 13.05.

Results

The conductivities of the perchlorate salts in nitromethane and N,N-dimethylformamide (DMF) are given in Table I. Measurements in

Can. J. Chem. Downloaded from www.nrcresearchpress.com by 210.87.254.5 on 09/05/12
For personal use only.

methanol were attempted, but in this solvent the compounds were not sufficiently soluble.

TABLE I

Molar conductivity of perchlorate salts in CH_3NO_2 and DMF

Compound	Conductivity at concentration $c = 5 \times 10^{-4}$ M in ohm^{-1}	
	CH_3NO_2	DMF
$\{(Ph_2P)_2C_2H_4\}_2Pt(ClO_4)_2$	194	139
$\{(PhS)_2C_2H_4\}_2Pt(ClO_4)_2$	194	
$\{(PhS)_2C_2H_4\}_2Pd(ClO_4)_2$	180	134
$\{(PhS)_2C_3H_6\}_2Pt(ClO_4)_2$	166	144
$\{(PhS)_2C_3H_6\}_2Pd(ClO_4)_2$	169	148

The molar conductivities of the complexes of $(PhS)_2C_3H_6$ in DMF were just as great as that for $\{(Ph_2P)_2C_2H_4\}_2Pt(ClO_4)_2$ at a concentration of 5×10^{-4} M. This suggests that the sulfur-containing complexes are strong electrolytes in DMF. Previous work (16) has established that the phosphorus-containing compound is a strong electrolyte.

Plots of molar conductivities against $\sqrt{c}$ for the various perchlorate compounds in nitromethane are shown in Figs. 1 and 2. The linear plots illustrate the Onsager relation for 1:1 and 2:1 strong electrolytes. The conductivity curves for complexes of $PhSC_3H_6SPh$ show a sharp drop in molar conductivity with increasing concentration such that at high concentrations the conductivity approaches a value suggestive of a 1:1 electrolyte.

One cannot expect the conductance curves to approach that of Et_4NClO_4 asymptotically because (*a*) the mobilities of the complex metal ion and of ammonium ion may differ considerably and (*b*) a conductance minimum resulting from a conflict between the Ostwald dilution effect and the decrease in activity coefficients may occur at the higher concentrations (17) and indeed appears in the case of the palladium compound to lie close to the upper end of the concentration range.

The conductivities in nitromethane of the palladium and the platinum salts were raised to upper limits of 169 ohm^{-1} mole^{-1} and 166 ohm^{-1} mole^{-1} respectively upon adding a large molar excess of $PhSC_3H_6SPh$. The establishment of equilibrium was somewhat slow with the platinum salts and 20 min standing at 25 °C was required in order to permit the conductivity to reach a steady value.

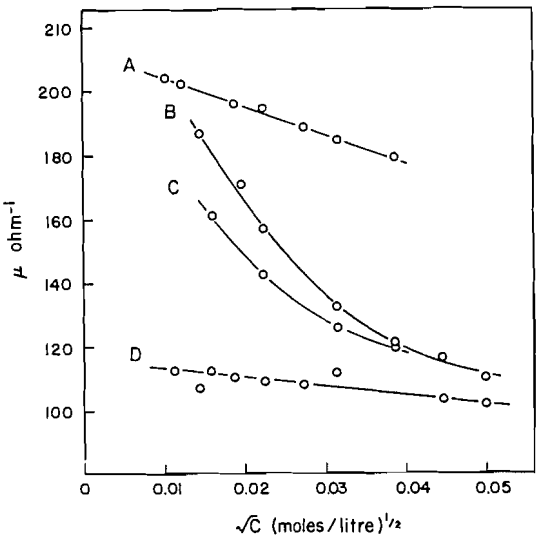

FIG. 1. Plot of molar conductivity vs. (concentration)$^{1/2}$ of perchlorate salts in nitromethane: (A) $[(Ph_2P)_2C_2H_4]_2Pt(ClO_4)_2$, (B) $[(PhS)_2C_3H_6]_2Pd(ClO_4)_2$, (C) $[(PhS)_2C_3H_6]_2Pt(ClO_4)_2$, (D) $[Et_4N]ClO_4$.

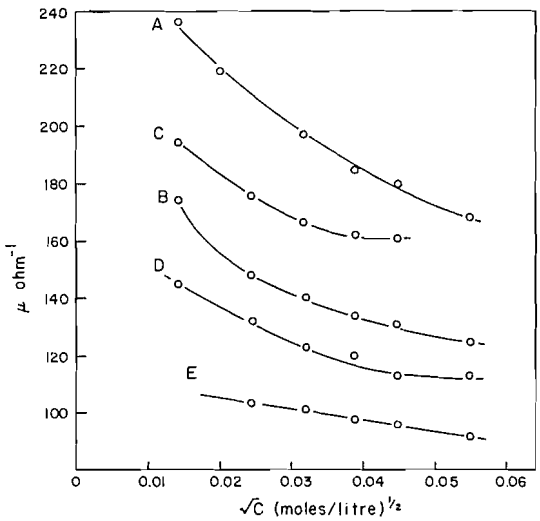

FIG. 2. Plot of molar conductivity vs. (concentration)$^{1/2}$ of tetrafluoroborate and hexafluorophosphate salts in nitromethane: (A) $[(PhS)_2C_3H_6]_2Pd(PF_6)_2$, (B) $[(PhS)_2C_3H_6]_2Pd(BF_4)_2$, (C) $[(PhS)_2C_3H_6]_2Pt(PF_6)_2$, (D) $[(PhS)_2C_3H_6]_2Pt(BF_4)_2$, (E) $AgBF_4$.

The tetrafluoroborate and hexafluorophosphate salts were examined in nitromethane only. The conductivities of these compounds are plotted against $\sqrt{c}$ in Fig. 2. The behavior of these salts is qualitatively similar to that of the

Can. J. Chem. Downloaded from www.nrcresearchpress.com by 210.87.254.5 on 09/05/12
For personal use only.

perchlorate salts but we may note the following features:

1. The hexafluorophosphate salts are the strongest electrolytes among those under study.
2. The perchlorate and tetrafluoroborate salts are somewhat alike in appearing to behave almost like 1:1 electrolytes at the higher concentrations under study.
3. The platinum compounds are weaker electrolytes than the corresponding palladium analogues.

A solution of $(PhSC_3H_6SPh)_2Pd(ClO_4)_2$ in nitromethane at a concentration of 1.7×10^{-4} *M* was studied spectrophotometrically. Addition of $AgClO_4$ in about 10-fold excess caused an increase in absorption intensity at $\lambda_{max} = 384$ mμ of 207%. Addition of $AgBF_4$ caused an increase in λ_{max} of 300%. Chloride and nitrite ions, added as the lithium salts, caused a slight decrease in intensity. The value of λ_{max} was not noticeably influenced. However, halide produced an increase in relative intensity at longer wavelengths with the result that the absorption curve became slightly more skewed.

Discussion

The complexes of $PhSC_3H_6SPh$ all show a marked tendency to be incompletely dissociated in nitromethane, a solvent of moderately strong polar character ($\varepsilon = 35.9$), while no evidence was found for association in more strongly polar media. It is of interest to consider whether the ion-pair association is of the outer sphere type with a solvent molecule interposing between the central metal atom and the anion, or whether the anion enters the first coordination sphere of the metal. In the latter situation, the various anions ClO_4^-, BF_4^-, and PF_6^- would be serving as ligands.

The observation that the fluoroborate salts are associated to about the same extent as the perchlorate salts seems to indicate that it is not necessary for the donor atom to have a free valence as has the oxygen atom in an oxyanion. If the free valence of the oxygen atom were a factor in the coordination, we should expect a greater difference in behavior between the ions ClO_4^- and BF_4^-. The similarity is very understandable in electrostatic terms because the structures of the two ions are almost identical.

We feel that the evidence supports the hypothesis of inner sphere coordination. The observation that one of the thiodiether ligands must be lost in order for ion association to take place supports this view. Further support is provided by a calculation of the degree of association using Bjerrum's theory and also Fuoss' theory of ion-pairing (18, 19). In order to carry out the calculations we must make, in addition to the assumptions already embodied in the respective treatments, the assumption that for inner sphere coordination the anion and the central metal atom approach one another to within about 3.2 Å. This figure was obtained by adding the thermochemical radius of the perchlorate ion (20) to 0.80 Å, the apparent radius of the Pd^{2+} and Pt^{2+} ions. If a solvent molecule is located between the ions, their closest distance of approach cannot be less than 7.5 Å. This figure was arrived at by measurement of a space-filling model. We have used these two assumed distances of closest approach to calculate the theoretical degree of association.

The degree of association may be written as $1 - \alpha$ where α is the degree of dissociation. The values of $1 - \alpha$ given by Bjerrum's treatment are 0.32 and 0.058 for the inner and outer sphere models respectively. Activity coefficients were assumed to be unity and the free ion concentration 5×10^{-4} *M*. The Fuoss treatment gives 0.33 and 0.03 respectively, in good agreement with the former values.

The inner sphere model thus leads to the prediction that the perchlorate salt should be 32% associated to $[LMeClO_4]^+ClO_4^-$. The outer sphere model indicates that about 3–6% of the cations should be associated as ion-pairs. The conductivity at a concentration of 5×10^{-4} *M* ($\sqrt{c} = 0.0236$) is in fact approximately halfway between the values for the 2:1 and the 1:1 electrolytes and is thus in agreement with the calculations for the inner sphere model. It is likely that there is some 5 to 10% ion-pairing of the reference compound $\{(Ph_2P)_2C_2H_4\}_2Pt(ClO_4)_2$ at 5×10^{-4} *M* concentration.

It is not possible with our present knowledge of nonaqueous solutions to obtain more information from the shape of the conductance plots. Moreover, there is no entirely satisfactory theory available for the conductivity of unsymmetrical electrolytes.

The results of Barker *et al.*, who obtained evidence of inner sphere coordination from the visible spectrum of a copper complex (9), lend

support to our view of the bonding. Our experience with the visible spectra of the palladium complex led to negative results, however. Although the large changes in intensity which occurred upon adding additional ClO_4^- or BF_4^- ion indicated that an association equilibrium was involved, the position of the absorption maximum was invariant. It should be noted, however, that the absorption band for Pd^{2+} is generally affected very little by changes of the ligands if the donor atoms are oxygen (21). Fluoride is very close to oxygen in the spectrochemical series. Most important is our observation that even upon replacement of two sulfur donor atoms by solvent molecules (presumably an oxygen of the nitro group), there is a shift in λ_{max} of only 6 mμ. It appears that the two residual sulfur donors dominate the ligand field conditions so that substitutions at the other two coordination sites have little effect on the position of λ_{max}.

Acknowledgments

The authors wish to acknowledge the financial assistance of the National Research Council of Canada and to express their appreciation for helpful discussions with Dr. B. E. Conway.

1. B. J. HATHAWAY and A. W. UNDERHILL. J. Chem. Soc. 3091 (1961).
2. M. M. JONES, E. A. JONES, D. F. HARMON, and R. T. SEMMES. J. Am. Chem. Soc. **83**, 2038 (1961).
3. R. E. HESTER and R. A. PLANE. Inorg. Chem. **3**, 769 (1964).
4. F. KLANBERG, J. P. HUNT, and H. W. DODGEN. Inorg. Chem. **2**, 139 (1963).
5. A. BLAZEJ and J. SVANCER. Veda Vyzkum Prumyslu Kozedelnem, **7**, 157 (1963).
6. P. R. MURTHY and C. C. PATEL. Naturwiss. **48**, 693 (1961).
7. F. SUTTON. Nature, **169**, 71 (1952).
8. L. H. SUTCLIFFE and J. R. WEBER. Trans. Faraday Soc. **52**, 1225 (1956).
9. N. T. BARKER, C. M. HARRIS, and E. D. MCKENZIE. Proc. Chem. Soc. 335 (1961).
10. L. A. CHUGAEFF and A. G. KOBLJANSKY. Z. Anorg. Chem. **83**, 8 (1913); **83**, 159 (1913).
11. J. PLUŠČEC and A. D. WESTLAND. J. Chem. Soc. 5371 (1965).
12. D. W. A. SHARP. Advances in fluorine chemistry. Vol. I. Butterworths, London. 1960. p. 83.
13. B. J. HATHAWAY and D. E. WEBSTER. Proc. Chem. Soc. 14 (1963).
14. D. S. BROWN, J. D. LEE, B. G. A. MELSOM, B. J. HATHAWAY, I. M. PROCTOR, and A. A. G. TOMLINSON Chem. Commun. 369 (1967).
15. B. J. HATHAWAY and A. W. UNDERHILL. J. Chem. Soc. 2257 (1962).
16. A. D. WESTLAND. J. Chem. Soc. 3060 (1965).
17. C. W. DAVIES. Ion association. Butterworths, London. 1962. p. 108.
18. N. BJERRUM. K. Danske Vidensk. Selskab. **7**, 108 (1926).
19. R. M. FUOSS. J. Am. Chem. Soc. **80**, 5059 (1958).
20. K. B. JAZIMIRSKI. Thermochemie von Komplex Verbindungen. Akademie Verlag GmbH., Berlin. 1956. p. 25.
21. C. K. JØRGENSEN. Absorption spectra and chemical bonding in complexes. The Pergamon Press, Ltd., Oxford. 1962. p. 122.

Can. J. Chem. Downloaded from www.nrcresearchpress.com by 210.87.254.5 on 09/05/12
For personal use only.

Can. J. Chem. Downloaded from www.nrcresearchpress.com by 210.87.254.105 on 09/05/12
For personal use only.

Méthode directe de mesure d'intensité intégrée d'une bande d'absorption infrarouge en phase liquide. Application à la bande ν_1 de quelques haloformes en solution dans le CCl_4 et dans le CS_2

I. Rossi, A. Levy et C. Haeusler[1]

Laboratoire d'Infrarouge, Chimie Physique, Equipe de Recherche Associée au C.N.R.S., Faculté des Sciences de Paris, Bâtiment 350 – (91) Orsay (France)

Reçu le 12 décembre 1967

Nous nous sommes proposés de montrer que, dans le cas où le rapport $\Delta\nu/2\gamma$ est inférieur ou égal à 1/20 ($\Delta\nu$, largeur de la fonction d'appareil; 2γ, largeur à mi-hauteur de la bande) on peut obtenir directement A (intensité intégrée) sans effectuer de correction, et que dans ces conditions, le spectre obtenu représente sensiblement la forme exacte de la bande. Nous avons déterminé à partir d'un seul spectre les grandeurs A, 2γ et ν_{max} des bandes ν_1 des haloformes $CHCl_3$, $CHBr_3$ et CHI_3 en solution dans le CCl_4 et dans le CS_2. Les résultats des mesures d'intensité sont en accord satisfaisant avec ceux obtenus par les méthodes habituelles.

Canadian Journal of Chemistry, 46, 2103 (1968)

I. Introduction

Les mesures de nombre d'onde ν_{max} des bandes en solution sont nombreuses; la situation est différente en ce qui concerne les mesures de largeur et la détermination de la forme des bandes.

Diverses méthodes de mesure des intensités ont récemment été décrites (1). Il faut noter de suite que la méthode très utilisée de Wilson et Wells (2) repose sur l'extrapolation à épaisseur nulle, ce qui entraîne des erreurs expérimentales importantes. Mais les résultats obtenus par différents auteurs sur la même bande et par la même méthode diffèrent bien plus que par l'erreur expérimentale normalement admise et qui est de l'ordre de 5%. Il pourrait donc être utile de disposer de l'étude d'une bande standard afin de connaître les écarts entre les valeurs de A obtenues dans des laboratoires différents. Nous envisageons donc l'étude d'une bande étalon d'intensité, proposée par Shimozawa et Wilson (3) dans la région spectrale de 3 μ; et nous nous proposons comme application de mesurer également A et 2γ dans le cas des haloformes dissous.

Soit $I_t(\nu)$ l'intensité lumineuse vraie transmise par l'échantillon, l'intensité transmise apparente $I_t'(\nu)$ est différente de I_t, du fait des déformations qu'introduit le spectromètre.

La loi de Beer–Lambert (valable dans un domaine de concentration où les interactions entre molécules de soluté sont suffisamment faibles pour pouvoir être négligées) s'écrit

$$I_t(\nu) = I_0(\nu) \exp[-\alpha(\nu)cl]$$

et l'intensité intégrée A est définie par la relation:

$$A = \int_{\nu_1}^{\nu_2} \alpha(\nu)d\nu = \frac{1}{cl} \int_{\nu_1}^{\nu_2} \mathrm{Ln}\left[\frac{I_0(\nu)}{I_t(\nu)}\right]d\nu.$$

Il s'agit donc d'évaluer A à partir des grandeurs accessibles à l'expérience, soit $I_0'(\nu)$ et $I_t'(\nu)$.

ν_1 et ν_2 désignent les nombres d'onde qui délimitent l'étendue de la bande. L'expression précédente suppose en particulier que la diffusion de la lumière soit négligeable, ce qui n'est pas toujours le cas.

De plus, le bruit de fond dans le spectre empêche des mesures suffisamment étendues dans les ailes de la bande, de sorte qu'une correction d'ailes s'impose le plus souvent.

II. Rappel théorique

Le spectromètre fournit une distribution approchée $I_t'(\nu)$ donnée par la relation

$$I_t'(\nu) = \int_{\nu-\Delta\nu}^{\nu+\Delta\nu} D(\nu - \nu_i) I_t(\nu)d\nu,$$

où $2\Delta\nu$ est la largeur totale de la fonction $D(\nu - \nu_i)$, dite fonction d'appareil, souvent symétrique par rapport à ν_i.

L'expérience nous permet donc d'atteindre une valeur de la transmission apparente,

$$\eta' = \frac{I_t'(\nu)}{I_0'(\nu)} = \frac{\int_{\nu_i-\Delta\nu}^{\nu_i+\Delta\nu} D(\nu - \nu_i) \cdot I_t(\nu)d\nu}{\int_{\nu_i-\Delta\nu}^{\nu_i+\Delta\nu} D(\nu - \nu_i) \cdot I_0(\nu)d\nu},$$

[1]Adresse actuelle: Faculté des Sciences de Rennes.

Can. J. Chem. Downloaded from www.nrcresearchpress.com by 210.87.254.105 on 09/05/12
For personal use only.

et l'on se propose d'évaluer numériquement l'intégrale $\int_{\nu_1}^{\nu_2} \alpha'(\nu)d\nu$ en se fixant certains paramètres.

Les méthodes de mesures les plus souvent utilisées à l'heure actuelle sont les suivantes:

(A) Méthode de mesure directe de Ramsay (4)

Cette méthode suppose que $\alpha(\nu)$ est une fonction de Lorentz (la hauteur au maximum de la courbe correspondante est a/γ^2 et la largeur à mi-hauteur 2γ).

Les phénomènes de diffraction et d'aberration étant négligés, la fonction d'appareil est représentée par une fonction triangle de base égale à $2\Delta\nu$ (5, 6).

η' a alors été évaluée par intégration numérique pour diverses valeurs de a, γ et $\Delta\nu$.

Les rapports

$$r = \frac{\text{Ln } (I_0/I_t)_{\nu_{max}}}{\text{Ln } (I_0'/I_t')_{\nu_{max}}} \text{ et } r' = \frac{2\gamma}{2\gamma'}$$

ont ensuite été évalués comme fonctions de Ln $[I_0'/I_t']$ et de $\Delta\nu/2\gamma'$.

On peut alors écrire A sous la forme

$$A = \frac{K}{cl} \text{ Ln} \left[\frac{I_0'}{I_t'}\right]_{\nu_{max}} 2\gamma',$$

avec $K = rr'$. K pouvant alors être tabulé en fonction de Ln $[I_0'/I_t']$ et de $\Delta\nu/2\gamma'$.

Le calcul de A est complété par l'évaluation de la contribution des ailes.

Notons enfin que Kostkowski et Bass (7) ont évalué numériquement l'intégrale $\eta'(\nu_i)$ pour une fonction d'appareil de Gauss et pour un coefficient d'absorption défini soit par la loi de Lorentz (effet de collision) soit par celle de Gauss (effet Doppler).

(B) Méthode de Wilson et Wells (2)

Cette méthode est basée sur l'utilisation de la grandeur

$$B' = A'cl$$

$$= \int_{\nu_1}^{\nu_2} \left\{ \text{Ln} \frac{\int_{\nu_i-\Delta\nu}^{\nu_i+\Delta\nu} D(\nu - \nu_i) I_0(\nu) d\nu}{\int_{\nu_i-\Delta\nu}^{\nu_i+\Delta\nu} D(\nu - \nu_i) I_t(\nu) d\nu} \right\} d\nu_i.$$

Si $I_0(\nu)$ reste constant dans l'intervalle spectral $2\Delta\nu$ et si $\alpha(\nu)$ est sensiblement constant dans l'intervalle allant de $(\nu_i - \Delta\nu)$ à $(\nu_i + \Delta\nu)$, on montre (8) que

$$\frac{\partial B'}{\partial (cl)} = \int_{\nu_1}^{\nu_2} \alpha(\nu) d\nu = A$$

d'où la méthode de mesure.

On trace la courbe B' en fonction des valeurs du produit cl, la pente de cette courbe est égale à A. En fait, il résulte de l'expérience qu'il faut utiliser la pente au voisinage de l'origine, car c'est seulement pour de faibles absorptions que $\alpha(\nu)$ est sensiblement constant dans l'intervalle spectral $2\Delta\nu$.

Une variante consiste à tracer la courbe $A' = B'/cl$ en fonction du produit cl; l'ordonnée à l'origine représente une bonne valeur de A.

Signalons enfin la mise au point récente d'une méthode de déconvolution (9); mais une telle méthode nécessite de connaître avec suffisamment de précision la fonction d'appareil.

Les méthodes sont donc dans l'ensemble d'un maniement long et délicat, soit qu'elles nécessitent l'étude de plusieurs spectres, soit qu'elles conduisent à des calculs laborieux.

III. Méthode utilisée dans le présent travail

Nous nous proposons d'étudier le cas d'une bande d'absorption symétrique ou non, explorée par une fonction d'appareil symétrique, quasi triangulaire. On montre que si le rapport $\Delta\nu/2\gamma' \leqslant 1/20$, une seule mesure d'intensité fournit une valeur de $A_{solution}$ (et ceci sans effectuer de corrections) en excellent accord avec celles obtenues par les méthodes d'extrapolation.

L'intérêt d'une bonne méthode pour l'obtention des valeurs des grandeurs telles que A, 2γ et ν_{max} réside dans le fait que les théories relatives aux effets de solvant, en particulier celle de Buckingham (10), reliant les grandeurs A_{gaz} et $A_{solution}$, ν_{gaz} et $\nu_{solution}$ n'ont encore pu être vérifiées expérimentalement de façon suffisamment systématique.

Dans le travail présent, nous appliquons la méthode directe aux bandes parallèles CH de $CHCl_3$, $CHBr_3$ et CHI_3 dans le tétrachlorure de carbone et sulfure de carbone.

IV. Conditions expérimentales

(*a*) Nous disposions d'un spectromètre de type Pfund à réseau échelette de 240 traits/mm fonctionnant dans le premier ordre, la largeur utile du réseau étant de 102 mm.

Can. J. Chem. Downloaded from www.nrcresearchpress.com by 210.87.254.105 on 09/05/12
For personal use only.

Le pouvoir de résolution théorique est voisin de 25.000. Le détecteur est une cellule photorésistante au sulfure de plomb refroidie à la carboglace.

(*b*) L'amplificateur est linéaire à la précision de nos observations près, ainsi que l'ensemble de la chaine amplification-détection.

(*c*) L'étalonnage du domaine spectral en nombre d'onde se fait par la méthode de Poggendorff. Nous avons utilisé les raies de rotation du gaz chlorhydrique comme repères de nombre d'onde. La dispersion est linéaire dans le domaine spectral délimité par ν_1 et ν_2 (de 60 à 80 cm^{-1}).

(*d*) Nous avons enregistré la raie d'émission de l'isotope ^{198}Hg à 1.53 μ dans le deuxième ordre. La source utilisée est un tube sans électrodes contenant 1 mg de mercure et de l'argon sous une pression de 3 mm de mercure. La source est alimentée par un générateur haute fréquence. Elle est maintenue à basse température par un courant d'air comprimé, refroidi par un mélange réfrigérant acétone-carboglace.

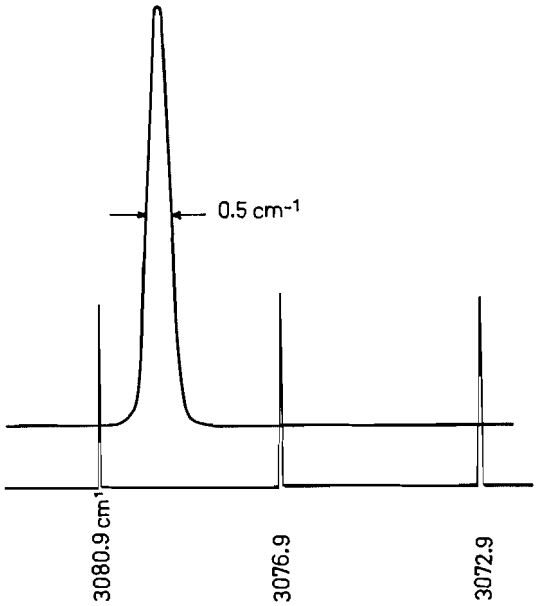

FIG. 1. Raie d'èmission du mercure 198.

La raie reproduite (Fig. 1) représente selon toute vraisemblance la fonction d'appareil approximativement dans le domaine d'utilisation du spectrographe de 3 μ à 4 μ. La fonction d'appareil apparait comme étant sensiblement une fonction triangle (la largeur à mi-hauteur $\Delta\nu$ est de 0.5 cm^{-1} à 3000 cm^{-1}). En effet, nous avons préféré nous placer dans des conditions où le rapport signal/bruit soit aussi bon que possible. Nous avons donc été amenés à utiliser des ouvertures de fentes relativement importantes.

(*e*) Les cuves circulaires utilisées d'épaisseur 1 cm et 5 mm sont munies de faces en F_2Ca et les concentrations de solutions étudiées ont été de l'ordre de 10^{-5} à 10^{-6} mole/cm^3. Dans ces conditions le pourcentage d'absorption a toujours été maintenu à une valeur inférieure à 50% (11, 12). Il est couramment admis en effet que les mesures pour avoir une précision suffisante doivent se faire aux moyennes absorptions.

De plus, dans ce domaine de concentration, on peut admettre que les interactions soluté-soluté sont pratiquement nulles et la loi de Beer-Lambert peut être appliquée de façon valable.

V. Résultats

Nous nous sommes proposés en premier lieu de vérifier la validité de notre méthode de mesure directe. Pour cela, nous avons effectué des mesures préliminaires relatives à une bande parfaitement symétrique d'une part, et d'une bande nettement dissymétrique d'autre part. La bande symétrique est celle dûe au vibrateur CH du trichloréthylène, bande située à 3084.6 cm^{-1} lorsqu'on opère en solution dans le CCl_4. Récemment Shimozawa et Wilson (3) en ont déterminé l'intensité intégrée, par deux méthodes différentes en vue de la proposer comme étalon. Les valeurs de A ainsi obtenues s'écartent de 4%, alors que l'imprécision des mesures est estimée par les auteurs égale à 5%, ils trouvent $A = 1.723 \times 10^6$ cm $mole^{-1}$ par la méthode de Ramsay. Nous avons mesuré A directement et la valeur obtenue est de 1.781×10^6 cm $mole^{-1}$ sans effectuer de corrections, car si nous avions opéré par la méthode de Ramsay, la correction dûe à la largeur finie de la fente aurait été nulle. L'accord est excellent, puisque ces deux déterminations diffèrent de moins de 4%. Nous avons également mesuré A pour la bande ν_1 très dissymétrique (l'absorption est plus prononcée du côté des fréquences élevées) de CHI_3 dans le CS_2 en fonction du produit cl, qui varie entre 2 et 6×10^{-6} mole cm^{-2}. Cette bande est située à 2999.0 cm^{-1}.

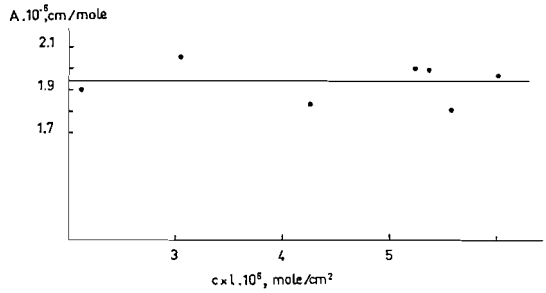

FIG. 2. Bande ν_1 de CHI_3 en solution dans le tetrachlorure de carbone; courbe $A' = f(cl)$.

TABLEAU I

Couple	Nos valeurs, ν (cm^{-1})(± 0.2)	Autres valeurs, ν (cm^{-1})	2γ (cm^{-1}) (± 0.2)	Nos valeurs, A (cm $mole^{-1}$) ($\pm 5\%$)	Autres valeurs, A (cm $mole^{-1}$)
$CHCl_3$–CCl_4	3018.2	3017 (13)	14.6	5.602×10^5	6.030×10^5 (13) 6.300×10^5 (14)
$CHCl_3$–CS_2	3007.1		10.6	4.868×10^5	5.96×10^5 (14)
$CHBr_3$–CCl_4	3029.8	3030 (13)	14.4	1.341×10^6	1.447×10^6 (13)
$CHBr_3$–CS_2	3018.2		10.4	1.290×10^6	
CHI_3–CCl_4	3011.4	3011 (13)	16.5	1.964×10^6	1.910×10^6 (13)
CHI_3–CS_2	2999.0		10.9	1.818×10^6	

Pour le chloroforme pur: $2\gamma = 12.5\ cm^{-1}$. Pour le bromoforme pur: $2\gamma = 11.9\ cm^{-1}$.

Si l'on porte la quantité A' en fonction du produit cl, on peut constater que les différents points représentatifs se répartissent autour d'une droite horizontale. La valeur moyenne de A' est ainsi immédiatement obtenue (Fig. 2).

On voit que pour la plupart des points obtenus, l'écart à la valeur moyenne est inférieur à 3%, et pour deux points seulement il atteint à peine 6%.

On peut donc dire que dans les conditions expérimentales qui ont été réalisées, une seule mesure permettrait pratiquement d'atteindre la valeur de A sans qu'aucune correction soit nécessaire, ceci quelle que soit la forme de la bande étudiée. En fait, il sera toujours plus indiqué d'effectuer un petit nombre de mesures à des épaisseurs différentes et d'en prendre la valeur moyenne.

Ayant ainsi éprouvé la méthode de mesure, nous avons procédé à l'évaluation de A, de $\nu_{solution}$, et de 2γ pour $CHCl_3$, $CHBr_3$ et CHI_3 dans les deux solvants non polaires cités précédemment. Certaines valeurs de A obtenues par des méthodes d'extrapolation ont été signalées récemment (13, 14). Ces résultats sont rassemblés dans le Tableau I.

Nous remarquons que CS_2 perturbe de façon systématique la molécule de soluté davantage que ne le fait CCl_4, en effet $\nu_{CS_2} < \nu_{CCl_4}$ pour les trois haloformes. La largeur 2γ des bandes ν_1 est toujours plus grande en solution CCl_4 qu'en solution CS_2. Dans la mesure où l'on admet (13) que l'élargissement des bandes en solution est dû au mouvement brownien (collision suivie d'une rotation) le coefficient $\alpha(\nu) = f(\nu)$ est une fonction de Lorentz. Le temps de relaxation, c'est-à-dire le temps pendant lequel la molécule maintient une orientation donnée, est alors égal à

$$\tau = \frac{1}{2\pi c\gamma}$$

Ceci implique que $\tau_{CCl_4} < \tau_{CS_2}$, donc que les molécules de soluté peuvent effectuer un mouvement de rotation plus facilement en solution CCl_4 qu'en solution CS_2. Le phénomène est lié à la forme de la molécule du solvant; la molécule de CCl_4 est de symétrie sphérique, tandis que la molécule de CS_2, linéaire, pourrait offrir davantage de résistance au mouvement de rotation.

Les mesures de largeurs de raies relatives au chloroforme et au bromoforme pur montrent que la rotation est plus aisée dans $CHCl_3$ que dans $CHBr_3$, car $2\gamma_{CHCl_3}$ est égal à 12.5 cm^{-1} et $2\gamma_{CHBr_3}$ vaut 11.9 cm^{-1}.

Signalons enfin que la théorie de Rakov (15) a été appliquée avec succès à la vibration ($\nu_1 + \nu_4$) de CCl_4 dans CS_2 et pur (16) et pour les vibrations ν_1, ν_2 et ν_3 de CS_2 dans CCl_4 et pur (17).

En ce qui concerne la valeur de A, il y a pour les trois haloformes en solution une faible augmentation lorsqu'on passe de CS_2 à CCl_4. Nous reviendrons dans un travail ultérieur sur cette question.

VI. Conclusion

L'utilisation d'un spectromètre résolutif nous a permis d'enregistrer sensiblement le profil vrai de bandes d'absorption infrarouge relatives à la phase liquide.

A partir d'un seul spectre nous obtenons rapidement de bonnes valeurs des grandeurs A, 2γ et $\nu_{solution}$ donnant des renseignements intéressants sur les forces intermoléculaires en milieu dense.

1. K. S. Seshadri et R. N. Jones. Spectrochim. Acta, **19**, 1013 (1963).
2. E. B. Wilson et A. J. Wells. J. Chem. Phys. **14**, 578 (1946). A. H. Thorndike, A. J. Wells et E. B. Wilson. J. Chem. Phys. **15**, 157 (1947).
3. J. T. Shimozawa et M. K. Wilson. Spectrochim. Acta, **22A**, 1591 (1966).
4. D. A. Ramsay. J. Am. Chem. Soc. **74**, 72 (1952).

Can. J. Chem. Downloaded from www.nrcresearchpress.com by 210.87.254.105 on 09/05/12
For personal use only.

5. D. M. DENNISON. Phys. Rev. **31**, 503 (1928).
6. V. Z. WILLIAMS. Rev. Sci. Instr. **19**, 151 (1948).
7. H. J. KOSTKOWSKI et A. BASS. J. Opt. Soc. Am. **46**, 1060 (1956).
8. S. S. PENNER. Quantitative molecular spectroscopy and gas emittivities. Addison-Wesley Publishing Company Inc., Reading, Mass. 1959.
9. R. N. JONES, R. VENTAKATARAGHAVAN et J. V. HOPKINS. Spectrochim. Acta, **23A**, 925 (1967).
10. A. D. BUCKINGHAM. Proc. Roy. Soc. London, **238**, 235 (1956); **248**, 169 (1958); **255**, 32 (1960).
11. G. AMAT. Thèse de Doctorat ès Sciences, Paris. 1951. p. 105.
12. J. VINCENT-GEISSE. Thèse de Doctorat ès Sciences, Paris. 1954. p. 6.
13. C. C. ROBINSON, S. A. TARE et H. W. THOMPSON. Proc. Roy. Soc. London, **269**, 492 (1962).
14. M. M. DENARIEZ. Thèse Doctorat 3ème cycle, Paris. 1962.
15. A. V. RAKOV. Opt. Spectry. USSR English Transl. **13**, 203 (1962).
16. B. LEFRANC, J. JACOB et J. VINCENT-GEISSE. Spectrochim. Acta, **22**, 1057 (1966).
17. J. VINCENT-GEISSE et J. JACOB. Compt. Rend. **264**, 864 (1967).

Can. J. Chem. Downloaded from www.nrcresearchpress.com by 210.87.254.105 on 09/05/12
For personal use only.

Can. J. Chem. Downloaded from www.nrcresearchpress.com by 210.87.254.5 on 09/05/12
For personal use only.

Radiolysis of methylcyclopentane. II. Effects of benzene and 1,3-cyclohexadiene in the liquid phase

E. DIANE STOVER[1] AND GORDON R. FREEMAN
Chemistry Department, University of Alberta, Edmonton, Alberta

Received January 29, 1968

The inhibiting effects of benzene and of 1,3-cyclohexadiene (CHD) on the formation of hydrogen during the radiolysis of methylcyclopentane (MCP) have been analyzed according to the nonhomogeneous kinetics of charge scavenging. The results are consistent with the following suggestions: CHD is an efficient scavenger of electrons; benzene is not an efficient scavenger of electrons but it may scavenge positive ions. These reactions offer alternatives to the hydrogen atom scavenging mechanism that has often been postulated in the past. They can decrease the hydrogen yield from MCP by 2.0 g units (based upon the energy absorbed only in MCP). In addition to the above scavenging mechanisms, which occur at relatively low solute concentrations ($\sim$ 1 mole %), benzene and CHD can each take part in a less efficient hydrogen inhibition reaction that can decrease $g(H_2)$ by another 1.6 units. This confirms the earlier suggestion (J. Chem. Phys. **33**, 71 (1960)) that two different, inhibitable hydrogen forming processes occur during the radiolysis of saturated hydrocarbons.

The yields of other products are also reported.

Canadian Journal of Chemistry, 46, 2109 (1968)

Introduction

Earlier studies of the effects of unsaturated hydrocarbons on the radiolysis of saturated hydrocarbons involved the use of homogeneous kinetics. It was concluded from such studies that in the radiolysis of saturated hydrocarbons there were two major reactive species that form hydrogen from the saturated hydrocarbons and that react at different rates with unsaturated hydrocarbons to inhibit hydrogen formation (see, for example, ref. 1). The recent development of a nonhomogeneous kinetics model of charge scavenging (2) makes it necessary to reconsider the effects of unsaturated hydrocarbons and to check the conclusion about two kinetically distinguishable, inhibitable hydrogen forming reactions. (To simplify the presentation, aromatics are included in the classification of unsaturated hydrocarbons.)

The present article reports and analyzes the effects of benzene and of 1,3-cyclohexadiene (CHD) on the γ-radiolysis of methylcyclopentane (MCP). Benzene was chosen as an additive because it has been used so often in the past, and CHD was chosen because it is a more efficient inhibitor of radiolysis reactions than is benzene (3).

[1]Holder of NRCC Studentships, 1963–1966.

Experimental

Phillips Pure Grade MCP was purified as described elsewhere (4). The purified material contained < 0.001 mole % olefin, < 0.1% n-hexane, and < 0.1% cyclohexane.

Aldrich Chemical Co. CHD was distilled at atmospheric pressure and purified by gas chromatography. The impurities remaining in it were 0.36 mole % cyclohexene, 0.55% benzene, and a trace of 1,4-cyclohexadiene.

Phillips Research Grade benzene was distilled before use, the center fraction being retained.

The samples (2 ml volume) were prepared by standard techniques and were sealed under vacuum in Pyrex cells (4 ml volume). They were irradiated in a Gammacell-220 (Atomic Energy of Canada Ltd.) at 25°. The dose given the samples was 1.9×10^{20} eV/g and the dose rate was 4.6×10^{19} eV/g h.

The products volatile at −196°, namely hydrogen and methane, were separated from the sample by vacuum distillation. They were then measured in a Toepler–McLeod apparatus and analyzed by gas chromatography. Liquid products were also measured by gas chromatography. The gas chromatograph was calibrated with standard samples containing known radiolysis products.

Results

Hydrogen and Methane

Benzene and CHD each inhibited the formation of hydrogen and methane from MCP (Fig. 1). At low concentrations CHD was a more efficient inhibitor than was benzene.

Liquid Products from MCP

The yields of 1-methylcyclopentene (1-MC)

Can. J. Chem. Downloaded from www.nrcresearchpress.com by 210.87.254.5 on 09/05/12
For personal use only.

and 3-methylcyclopentene (3-MC) were decreased by either CHD or benzene, although CHD was the more efficient inhibitor (Fig. 2A). The products referred to as 1-MC and 3-MC were probably mixtures of (1-MC and methylenecyclopentane) and (3-MC and 4-MC), respectively. It was found in an earlier study that the analogous gas chromatographic peaks in the methylcyclohexane system represented the corresponding sums of products (5). The 1-MC and 3-MC could not be measured in the higher solute concentration solutions, due to overlap of the product and solute gas chromatographic peaks.

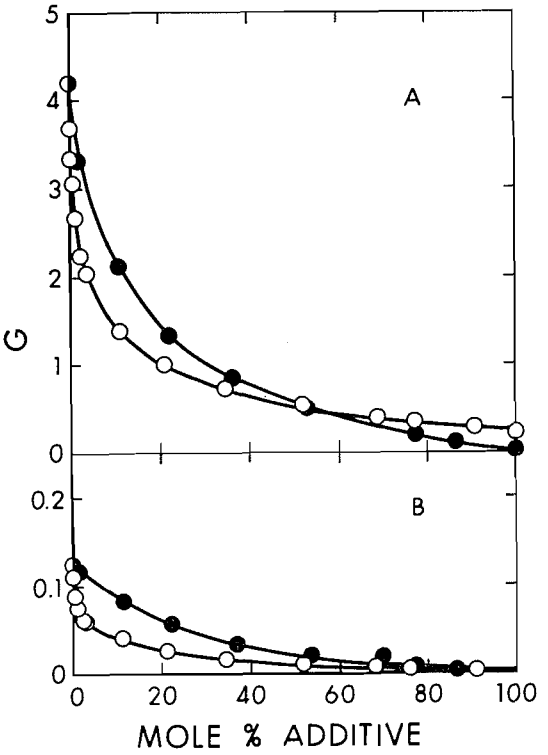

FIG. 1. Yields of hydrogen and methane as functions of additive concentration. A, hydrogen; B, methane; ○, 1,3-cyclohexadiene added; ●, benzene added.

The product identified as hexene was measured with two different chromatographic columns. The two sets of measured yields differed by less than 5% and the averages are shown in Fig. 2B. Hexene formation was greatly inhibited by both CHD and benzene.

The MCP "dimer" yield was also measured on two different chromatographic columns. One column resolved only bimethylcyclopentyl (BMCP) in the presence of the solutes. The other column resolved several minor MCP dimers, in addition to BMCP; the yields were summed to give the total MCP dimer yield. The addition of CHD rapidly decreased the yield of MCP dimers to a limiting value of 0.16 G units (Fig. 3A). Benzene also inhibits dimer formation (Fig. 3B), but less readily than does CHD.

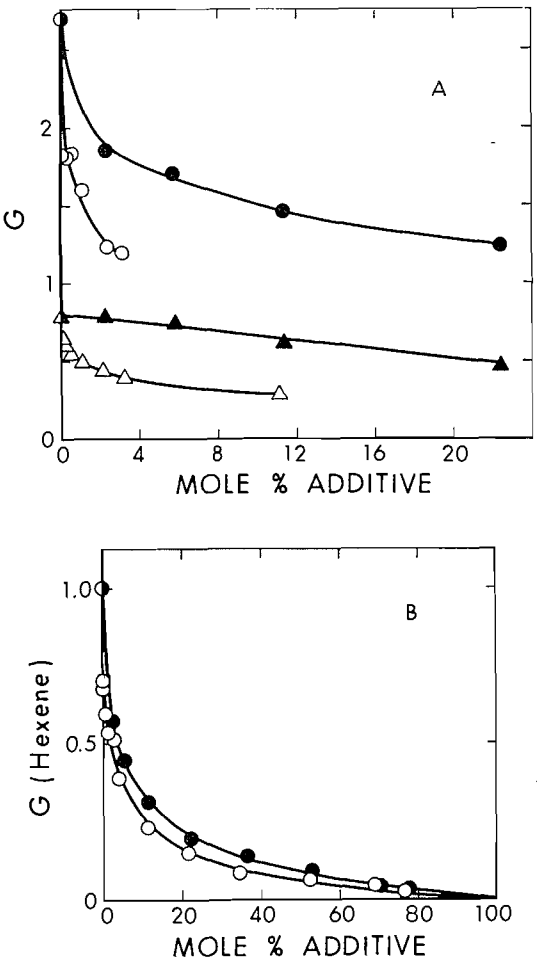

FIG. 2. Yields of C_6 olefins as functions of additive concentration. A: circles, 1-MC; triangles, 3-MC. B: hexene. Open points, CHD added; filled points, benzene added.

Liquid Products from the Solutes

Dimers of CHD were formed during the radiolysis of the MCP–CHD solutions. The variation of the total yield of these dimers with CHD concentration is shown in Fig. 4A. The yield goes

Can. J. Chem. Downloaded from www.nrcresearchpress.com by 210.87.254.5 on 09/05/12
For personal use only.

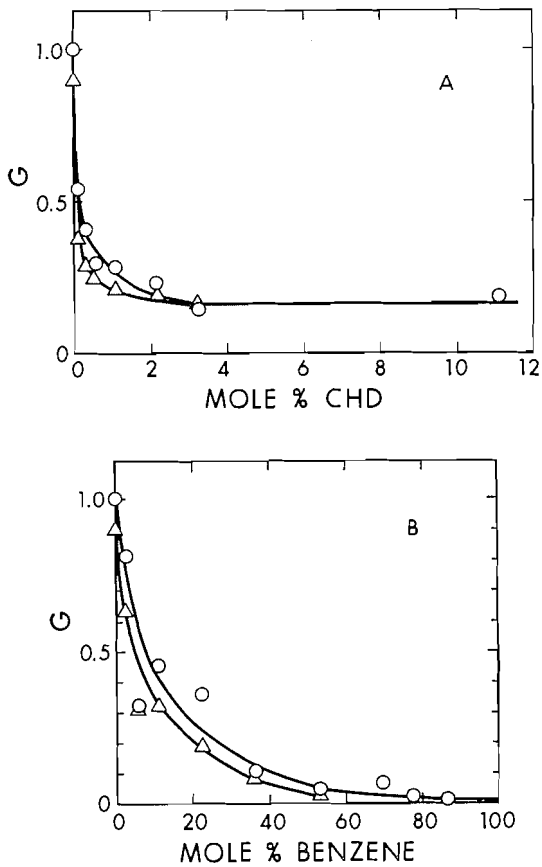

FIG. 3. Yields of bimethylcyclopentyl (△) and total MCP "dimer" (○) as functions of additive concentration. A, CHD added; B, benzene added.

through a maximum value of about 6.5 G units at about 10 mole % CHD.

The rate of disappearance of CHD could be measured in the solutions of up to about 3% concentration. The rate increased rapidly with increasing CHD concentration, reaching a value of $G(-\text{CHD}) = 38$ at 3.3 mole % CHD.

In the MCP–benzene solutions, four minor products were found in the region of the C_{12} product peaks on the gas chromatogram. Only one of the minor products, namely biphenyl, was identified, but the others are also assumed to be C_{12} hydrocarbons. Their yields are very low and are shown in Fig. 4B. The products D_1 and D_2 are presumably cross products between MCP and benzene, such as phenylmethylcyclopentane and methylcyclopentylcyclohexadiene (by analogy with the cyclopentane–benzene system (6)).

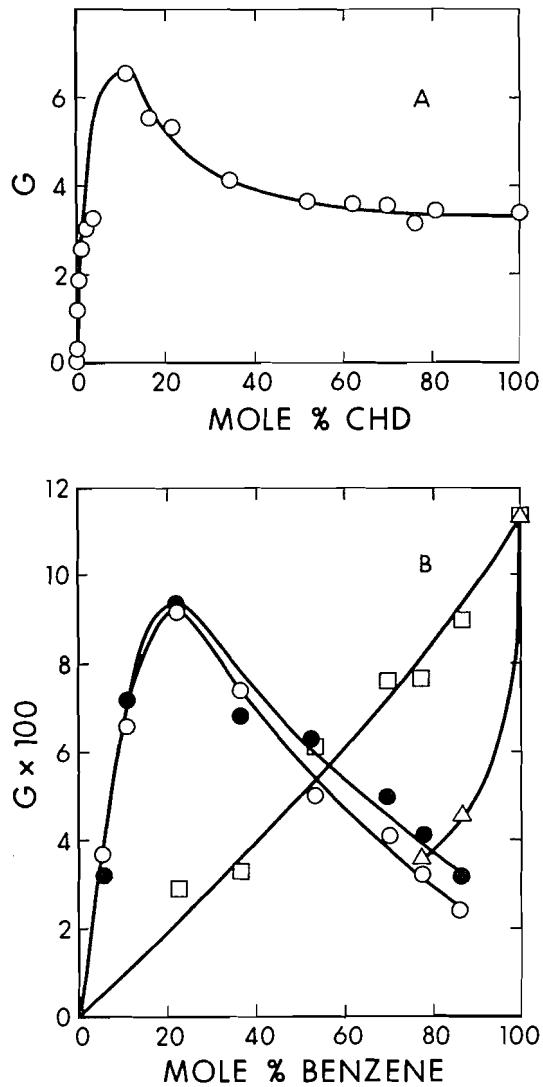

FIG. 4. Yields of liquid products from additives. A, dimer from CHD. B, dimers from benzene: ○, D_1; ●, D_2; △, biphenyl; □, D_3.

Discussion

1. Hydrogen

For the kinetic analysis, the hydrogen yields will be expressed in g units, based upon the energy absorbed in MCP and corrected for hydrogen formed by direct radiolysis of the solute.

$$[i] \qquad g(H_2) = \frac{G(H_2) - G(H_2)_s \epsilon_s}{\epsilon_{MCP}},$$

Can. J. Chem. Downloaded from www.nrcresearchpress.com by 210.87.254.5 on 09/05/12
For personal use only.

where $G(H_2)$ is the observed hydrogen yield from the solution (based upon the total energy absorbed by the solution), $G(H_2)_s$ is the yield of hydrogen from pure solute (0.23 for CHD and 0.035 for benzene), and ε_s and ε_{MCP} are the electron fractions of solute and of MCP, respectively, in the solution.

Furthermore,

[*ii*] $$\Delta g(H_2) = G(H_2)_0 - g(H_2),$$

where $G(H_2)_0$ is the yield from pure MCP.

(a) MCP–CHD Solutions

CHD has been shown to capture electrons in methyltetrahydrofuran (MTHF) solvent during radiolysis at − 196 ° (7). Nonconjugated diolefins apparently do not capture electrons in MTHF at −196 ° (7). In view of the recent evidence that even a mono-olefin (propylene) might be able to associate with solvated electrons in liquid cyclohexane (8), it would be useful to see whether the present inhibition of hydrogen by CHD fits the electron scavenging model.

The model is described in detail (2) and summarized (4) elsewhere. Only three relevant equations will be given here:

[*iii*] $$\Delta g'(H_2) = \frac{\sum N(y)\Phi_-}{\sum N(y)} \Delta g'(H_2)_{max}$$

[*iv*] $$\Phi_- = \phi_{fi} + \phi_-(1 - \phi_{fi})$$

[*v*] $$\phi_- = 1 - (1 - f_- N_s)^{\beta_-/\nu}$$

where $\Delta g'(H_2)$ is the decrease in hydrogen yield caused by electron scavenging, $N(y)$ is the relative number of ion pairs that have an initial separation distance y between the positive ion and the "thermalized" electron, Φ_- is the total probability of scavenging a thermalized electron that is initially separated by a distance y from its parent ion, ϕ_{fi} is the fraction of electrons which escape geminate neutralization, and ϕ_- is the probability that a thermalized electron is scavenged before it undergoes geminate neutralization. In eq. [*v*], N_s is the mole fraction of solute in the solution and f_-, β_-, and ν are parameters, of which only β_- is taken to be freely adjustable.

For the known electron scavengers N_2O and SF_6 in MCP, it has been found that $\beta_- = 5 \times 10^{14}$ V/cm^2 and $\Delta g'(H_2)_{max} = 2.0$ (4). If CHD is an electron scavenger, $\Delta g'(H_2)_{max}$ for ion scavenging in MCP–CHD solutions should also be equal to 2.0 and β_- should be close to 5×10^{14} V/cm^2. The $N(y)$ vs. y distribution was obtained as described elsewhere (2), the values of y in MCP being 1.28 times greater than those in water at 25°. The calculated values of $\Delta g'(H_2)$ for electron scavenging, using the above-mentioned quantities, are represented by the dashed curve in Fig. 5. Although agreement between calculation and experiment is satisfactory at low CHD concentrations, it is clear that another process contributes to the inhibition of hydrogen formation at high concentrations. The maximum decrease in hydrogen yield caused by CHD is actually 3.5 units (Fig. 5), of which the second process contributes 1.5 units.

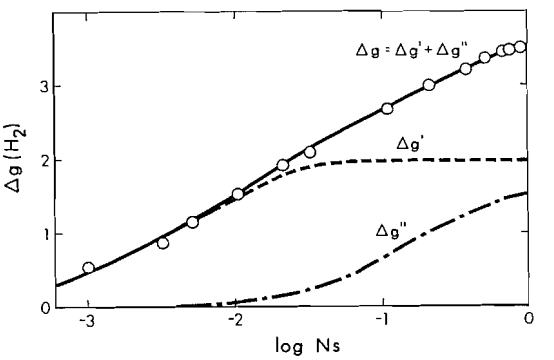

FIG. 5. Dependence of hydrogen yield on CHD concentration. (- -), calculated ion scavenging curve; (- .), calculated H atom scavenging or energy transfer curve; (—), sum of the two calculated curves; ○, experimental points. N_S is the mole fraction of CHD. $\Delta g(H_2)$ is the decrease in H_2 yield, corrected for H_2 from CHD radiolysis, and is based on the energy absorbed by MCP only.

Two additional possible inhibition processes are hydrogen atom scavenging and energy transfer, both of which may be treated by homogeneous kinetics. The scavenging of positive ions would obey nonhomogeneous kinetics and any such reaction would not increase $\Delta g(H_2)$ beyond that caused by electron scavenging.

In the hydrogen atom mechanism, the relevant reactions would be

[1] $$H + MCP \rightarrow H_2 + C_5H_{11}$$

[2] $$H + CHD \rightarrow C_6H_9$$

and the decrease in the hydrogen yield, $\Delta g''(H_2)$, would be given by

[*vi*] $$\Delta g''(H_2) = G''(H)\left\{1 + \frac{k_1[MCP]}{k_2[CHD]}\right\}^{-1},$$

Can. J. Chem. Downloaded from www.nrcresearchpress.com by 210.87.254.5 on 09/05/12
For personal use only.

where $G''(H)$ is the yield of hydrogen atoms from reactions other than ion neutralization in pure MCP. The dot–dashed line in Fig. 5 was calculated from eq. [*vi*], using $G''(H) = 1.5$ and $k_2/k_1 = 7$. The sum of the two calculated lines is represented by the full line in Fig. 5, and it passes satisfactorily through the experimental points.

In the energy transfer mechanism the relevant reactions would be

[3] $$MCP^* \rightarrow H_2 + \text{products}$$

[4] $$MCP^* + CHD \rightarrow MCP + CHD^*$$

[5] $$CHD^* \rightarrow \text{no } H_2$$

The decrease in the hydrogen yield caused by reaction [4] would be

[*vii*] $$\Delta g''(H_2) = G(MCP^*)\left\{1 + \frac{k_3}{k_4[CHD]}\right\}^{-1},$$

where $G(MCP^*)$ is the yield of MCP* in the radiolysis of pure MCP. The same dot–dashed line in Fig. 5 can be calculated from eq. [*vii*] by using $G(MCP^*) = 1.7$ and $k_3/k_4 = 1.4$ mole/*l*. Thus the energy transfer mechanism also fits the results.

Unfortunately there is no reliable independent source of information about the value of k_2/k_1 or of k_3/k_4 that allows a choice to be made between the atom scavenging and energy transfer mechanisms. A value of $k_2/k_1 = 7$ seems improbably low for thermal hydrogen atoms, but the unsatisfactory state of information from traditional free radical studies is indicated by the uncertain methods that were used to estimate hydrogen atom reaction rate parameters in a recent review (ref. 9, Table 2). Furthermore, the hydrogen atoms that take part in reactions [1] and [2] might be epithermal.

(b) MCP–Benzene Solutions

The values of $\Delta g(H_2)$ at low benzene concentrations could not be fit by using the previously mentioned values of the electron scavenging parameters in eq. [*iii*]–[*v*], so benzene is not an efficient scavenger of solvated electrons in MCP. For positive ion scavenging, the value of $\Delta g'(H_2)_{max}$ should be the same as that for electron scavenging, but the value of β_+ for an efficient positive ion scavenger should be an order of magnitude smaller than that of β_- for an efficient electron scavenger (4). Hence, to test the present results against a positive ion scavenging mechanism, $\Delta g'(H_2)_{max} = 2.0$ and $\beta_+ \approx 5 \times 10^{13}$ V/cm^2 should be used. The dashed line in Fig. 6 was obtained by using $\Delta g'(H_2)_{max} = 2.0$ and $\beta_+ = 6 \times 10^{13}$ V/cm^2.

As in the CHD solutions, an additional mechanism must be applied to explain the continuing decrease in hydrogen yield caused by the higher concentrations of benzene ($\Delta g''(H_2)_{max} = 3.7 - 2.0 = 1.7$, see Fig. 6). The dot–dashed line in Fig. 6 can be calculated from eq. [*vi*] using $G''(H) = 1.7$ and $k_2/k_1 = 3$, or from eq. [*vii*] using $G(MCP^*) = 2.3$ and $k_3/k_4 = 4$ mole/*l*.

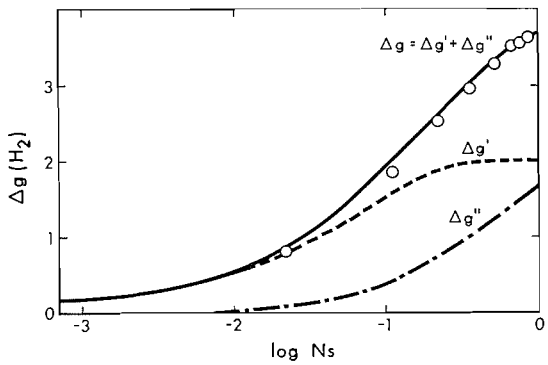

FIG. 6. Dependence of hydrogen yield on benzene concentration. (- -), calculated ion scavenging curve; (- .), calculated H atom scavenging or energy transfer curve; (—), sum of the two calculated curves; ○, experimental points. N_S is the mole fraction of benzene. $\Delta g(H_2)$ is the decrease in H_2 yield, corrected for H_2 from benzene radiolysis, and is based on the energy absorbed by MCP only.

The sum $(\Delta g'(H_2) + \Delta g''(H_2))$ is represented by the full line in Fig. 6, and it passes satisfactorily through the experimental points.

(c) Summary

It is not possible to explain the hydrogen results from either the CHD or the benzene solutions by any single inhibition mechanism that has been proposed, whether it involves homogeneous or nonhomogeneous kinetics. It has previously been suggested that the effects of low concentrations of unsaturated compounds in alkanes are consistent with a hydrogen atom scavenging mechanism (10). The present work demonstrates that charge scavenging mechanisms are also consistent with the results at low solute concentration.

The occurrence of an additional inhibition mechanism at high solute concentrations, that

Can. J. Chem. Downloaded from www.nrcresearchpress.com by 210.87.254.5 on 09/05/12
For personal use only.

was proposed earlier (1), but which has usually been neglected (e.g. ref. 10), is confirmed by the present work.

It should be noted that some hydrogen was unscavengeable even at the highest scavenger concentrations. In the MCP–CHD solutions the unscavengeable hydrogen amounted to 0.7 *g* units and in the MCP–benzene solutions it was 0.5 units. This unscavengeable hydrogen has many possible sources and speculation on the subject is too uncertain to be offered here.

2. Other Products from MCP

As with hydrogen, approximately half of the methane, 1-MC, 3-MC, and hexene have precursors (ions and free radicals) that are *readily scavengeable*. As a rule of thumb, the *readily scavengeable* yield of a product from a pure compound may be taken as the decrease in yield caused by the addition of ~ 3 mole % of an efficient inhibitor to the compound (see Figs. 1–3).

Eighty-four percent of the dimer from MCP is *readily scavengeable* (Fig. 3A), and the remaining 16% is presumably formed in spur reactions. The same fraction of the dimer formed in the γ-radiolysis of liquid cyclohexane was *readily scavengeable* (11).

3. Liquid Products from the Solutes

The CHD dimer reached a maximum yield of 6.5 *G* units at about 10 mole % CHD, from which it decreased to a constant value of 3.3 units above 70 mole % CHD (Fig. 4A). Similar behavior was observed in the cyclohexene–CHD system (3) and the dimerization reaction is currently being studied in other solvents.[2] The general shape of the curve in Fig. 4A indicates reactivity transfer from MCP to CHD.

The value $G(-\text{CHD}) = 38$ at 3.3 mole % CHD indicates that an appreciable amount of polymerization occurs in the system. If only trimers and higher molecular weight products are considered as polymers, then at 3.3 mole % CHD, $G(\text{CHD} \rightarrow \text{polymer}) \approx 30$.

In contrast to the CHD system, the yields of dimers that involved the benzene solute were very small (Fig. 4B).

Acknowledgments

We are grateful to the National Research Council of Canada for partial financial support of this project.

1. G. R. Freeman. J. Chem Phys. **33**, 71 (1960); **36**, 1542 (1962).
2. G. R. Freeman. J Chem. Phys. **46**, 2822 (1967).
3. B. R. Wakeford and G. R. Freeman. J. Phys. Chem. **68**, 2992 (1964).
4. E. D. Stover and G. R. Freeman. J. Chem. Phys. In press.
5. G. R. Freeman. J. Chem. Phys. **36**, 1534 (1962).
6. L. G. Walker. Ph.D. Thesis, University of Alberta, Edmonton, Alberta. 1967. p. 187.
7. T. Shida and W. H. Hamill. J. Am. Chem. Soc. **88**, 5371 (1966).
8. M. G. Robinson and G. R. Freeman. J. Chem. Phys. **48**, 983 (1968).
9. A. F. Trotman-Dickenson. Advan. Free-Radical Chem. **1**, 1 (1965).
10. T. J. Hardwick. J. Phys. Chem. **66**, 291 (1962).
11. S. K. Ho and G. R. Freeman. J. Phys. Chem. **68**, 2189 (1964).

[2]R. Schutte, private communication.

Can. J. Chem. Downloaded from www.nrcresearchpress.com by 210.87.254.6 on 09/05/12
For personal use only.

Preparation and reactions of sulfoxides and phosphine oxides containing silicon and germanium

A. G. Brook and D. G. Anderson
Department of Chemistry, University of Toronto, Toronto, Ontario

Received December 12, 1967

The preparation of several sulfoxides containing silicon or germanium is reported. The thermal rearrangement of the silicon-containing sulfoxides has been observed but neither germanium-containing sulfoxides nor silicon-containing phosphine oxides were found to rearrange thermally at a detectable rate.

Canadian Journal of Chemistry, 46, 2115 (1968)

Recently the first example of a thermal rearrangement of a β-functional organosilane, the isomerization of a β-ketosilane to its isomeric siloxyalkene, was reported (1).

Related rearrangements with other similarly substituted compounds appeared to be a possibility. In order to test this hypothesis members of several previously unreported classes of compounds were prepared: silylmethyl sulfoxides, $R_3SiCH_2\overset{O}{\uparrow}SR'$; germylmethyl sulfoxides, $R_3GeCH_2\overset{O}{\uparrow}SR'$; and silylmethylphosphine oxides, $R_3SiCH_2\overset{O}{\uparrow}PR'_2$. Of these, only the silylmethyl sulfoxides were found to rearrange, yielding siloxymethyl sulfides.

The silylmethyl sulfoxides were prepared in high yield by the reaction of methyl arylsulfinate esters with the Grignard reagents prepared from halomethyltrialkylsilanes.

$$R_3SiCH_2MgX + ArSO_2Me \rightarrow R_3SiCH_2\overset{O}{\uparrow}SAr + MeOMgX$$

1, R = Me, Ar = Ph

2, R = Et, Ar = *p*-MeC_6H_4—

As outlined below, there was difficulty in obtaining pure sulfoxides and their structures were assigned primarily on the basis of spectroscopic data. The methylene group adjacent to the asymmetric sulfoxide group appeared as an AB system in the n.m.r. spectrum, and strong absorption characteristic of sulfoxides occurred at 9.67 μ in the infrared spectrum. A minor peak in the n.m.r. spectra of silylmethyl sulfoxides at δ = 5 p.p.m. was assigned to the methylene group of the rearrangement product, the silyloxymethyl sulfide.

The polar character of the silylmethyl sulfoxides together with their tendency to rearrange thermally (vide infra) prevented preparation of pure samples. The sulfoxides could not be isolated in good yield from the magnesium halides present in a nonaqueous workup, and it was exceedingly difficult to free the sulfoxides from traces of water introduced by aqueous workup. This water led to hydrolysis of the sulfoxide, yielding hexaalkyldisiloxanes and methyl aryl sulfoxides.

$$2R_3SiCH_2\overset{O}{\uparrow}SR' + H_2O \rightarrow R_3SiOSiR_3 + 2MeS\overset{O}{\uparrow}R'$$

Very careful drying of the crude silylmethyl sulfoxide prior to distillation, using desiccant grade silica gel, gave much lower yields of hydrolysis products and much higher yields of rearrangement products. The fact that the silylmethyl sulfoxides are readily cleaved by water is consistent with the generally observed tendency of β-functional silanes to undergo silicon–carbon bond cleavage: the closely related silylmethyl sulfones also readily undergo cleavage (2).

In the hope of being able to avoid aqueous workups with the attendant problems, attempts were made to prepare trimethylsilylmethyl phenyl sulfoxides from trimethylsilylmethyllithium and benzene sulfinyl chloride, but only uncharacterized gum, and chloromethyltrimethylsilane, the product of halogen–metal exchange, were isolated.

Two additional routes for the preparation of silylmethyl sulfoxides were investigated. The oxidation of silylmethyl sulfides with a variety of standard oxidizing agents showed some evidence

Can. J. Chem. Downloaded from www.nrcresearchpress.com by 210.87.254.6 on 09/05/12
For personal use only.

of the formation of sulfoxides based on the infrared spectra, but upon workup only starting materials and silanols or disiloxanes were isolated. The second route investigated was the reaction between a halosilane and sodium methylsulfinyl carbanion in dimethyl sulfoxide (3).

$$R_3SiCl + Na^+CH_2^-\text{—}\overset{\overset{\displaystyle O}{\uparrow}}{S}\text{—}R' \rightarrow R_3SiCH_2\overset{\overset{\displaystyle O}{\uparrow}}{S}R' + NaCl$$

The only characterizable products isolated from this very complex reaction were disiloxanes or silanols. These products probably arose from the reaction of the chlorosilane with dimethyl sulfoxide, since it has been shown that hexaphenyldisiloxane is the major product found when triphenylchlorosilane is dissolved in dimethyl sulfoxide (4).

The silylmethyl sulfoxides **1** and **2** could be converted essentially quantitatively into the isomeric siloxymethyl sulfides **3** and **4**.

$$R_3SiCH_2\overset{\overset{\displaystyle O}{\uparrow}}{S}R' \rightarrow R_3SiOCH_2SR'$$

1, R = Me, R′ = Ph **3**, R = Me, R′ = Ph

2, R = Et, R′ = *p*-MeC_6H_4 **4**, R = Et, R′ = *p*-MeC_6H_4

That the rearrangement products were siloxymethyl sulfides was verified by the alternative synthesis shown below:

$$PhSH + n\text{-}BuLi \xrightarrow[0\ ^\circ C]{Et_2O} PhSLi + n\text{-}BuH$$

$$PhSLi \xrightarrow{CH_2O(g)} PhSCH_2OLi \xrightarrow{Me_3SiCl} PhSCH_2OSiMe_3$$

$$PhSLi \xrightarrow{Me_3SiCl} PhSSiMe_3$$

The product, trimethylsiloxymethyl phenyl sulfide, **3**, had the same spectral and physical properties as the product obtained from the rearrangement of **1**. Trimethylsilyl phenyl sulfide was a major by-product.

Triethylsilyl *p*-tolyl sulfoxide was also shown to undergo an analogous rearrangement yielding **4**. Hexaethyldisiloxane and methyl *p*-tolyl sulfoxide were also isolated from the rearrangement.

The thermal rearrangement of trialkylsilylmethyl aryl sulfoxides may be represented mechanistically as follows:

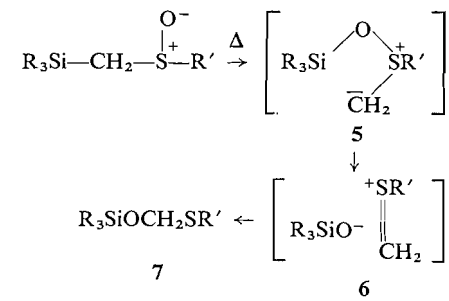

The first step, attack on silicon by oxygen, is common to several previously studied rearrangements of oxygen-containing organosilicon compounds, such as the silylcarbinol to silyl ether rearrangement (5, 6) and the β-ketosilane to siloxyalkene rearrangement (1). The formation of the strong silicon–oxygen bond would appear to provide a powerful driving force for these rearrangements. The intermediate formed in this process, **5**, a sulfur ylid, is related to that proposed by Parham *et al.* (7, 8) or Oae *et al.* (9) for the Pummerer reaction and it may reasonably be expected to similarly dissociate into an ion pair, **6**, which recombines giving the observed product, **7**, the siloxymethyl sulfide. An attempt to study the rearrangement kinetically failed since the impure silylmethyl sulfoxide gave unreproducible and uncharacterized results so that the order of the reaction could not be established.

Trimethylgermylmethyl phenyl sulfoxide, **8**, which was synthesized in a similar way to its silicon analog, **1**, was prepared in order to compare the rates of rearrangement of related silylmethyl and germylmethyl sulfoxides. Many reactions which involve nucleophilic attack on metalloid atoms proceed much more slowly, if at all, when germanium is substituted for silicon in the molecule (1,10–14). The germyl sulfoxide, **8**, was unchanged after heating for 6 days at 60 °C, whereas **1** was totally decomposed after 1 h at 60 °C. However, the germylmethyl sulfoxide underwent hydrolysis to hexamethyldigermoxane and methyl phenyl sulfoxide at 60 °C over 50 days, in the presence of about 1 mole equivalent of water.

In view of the ready rearrangement of silylmethyl sulfoxides to siloxymethyl sulfides, a reaction which essentially results in the reduction of a sulfoxide to a sulfide, it appeared of interest to investigate whether silylmethylphosphine oxides would undergo a similar rearrangement.

Can. J. Chem. Downloaded from www.nrcresearchpress.com by 210.87.254.6 on 09/05/12
For personal use only.

It was hoped that such a rearrangement would provide a simple, clean, and stereospecific pathway for the reduction of phosphine oxides to carbon-functional phosphines. The stereospecific reduction of phosphine oxides to phosphines using trichlorosilane has been reported by Horner and Balzer (15).

Trimethylsilylmethyldiphenylphosphine oxide, **9**, prepared by metalation of diphenylmethylphosphine oxide, followed by coupling with trimethylchlorosilane, did not rearrange when heated at 180° for 21 h, but because of traces of water in the samples used, some cleavage of the silicon–carbon bond occurred, presumably by a reaction analogous to those observed with other β-functional silanes, e.g. the sulfones (2), sulfoxides, and ketones (16). Diphenylmethylphosphine oxide, **10**, hexamethyldisiloxane, and recovered starting material were identified by their n.m.r. spectra as components of the reaction product. That **9** was, however, essentially unchanged was shown by its recovery in 57% yield along with **10** in 37% yield when a sample to which water had been added purposely was heated to 180° for 21 h.

Experimental

General Methods

The infrared spectra reported were recorded using a Perkin-Elmer model 257 or model 237B instrument. The n.m.r. spectra of the compounds were recorded on a Varian model A60 or A100 instrument. The data reported for the AB systems observed in the sulfoxides are the calculated chemical shifts of the two protons, which were obtained from the relationship $\Delta\nu = (Q^2 - J^2)^{\frac{1}{2}}$, where J is the coupling constant, Q is the distance in Hz between the first and third peaks of the AB system, and $\Delta\nu$ is the difference in chemical shift between the two protons. A Varian Aerograph 202-1B dual column instrument was used for the purification of some of the compounds by gas–liquid chromatography. All melting points are uncorrected.

*Trimethylsilylmethyl Phenyl Sulfoxide, **1***

A solution of 14.0 g (0.09 mole) of methyl benzenesulfinate (17) in 25 ml of tetrahydrofuran was added to 72 ml of a stirred solution of trimethylsilylmethylmagnesium bromide (18) (0.1 mole) in dry ether at 0 °C. After stirring at 0 °C for 2 h, the reaction mixture was hydrolyzed with dilute aqueous hydrochloric acid and the aqueous layer was extracted with ether. After very careful drying of the ethereal extracts with sodium sulfate (anhyd.), and removal of the ether by evaporation at room temperature *in vacuo*, 17.5 g (90%) of trimethylsilylmethyl phenyl sulfoxide was obtained. This product was shown by n.m.r. to be ca. 90% pure, the main impurity being a small amount of rearrangement product **2**.

The material was further dried by dissolving it in dry ether and passing it through a short column (1″ × 2″) containing desiccant grade silica gel. After removal of the ether, 12.5 g of reasonably dry **1** was isolated, but since it could not be freed of the rearrangement product an analytical sample could not be obtained. N.m.r. (CCl_4): δ 0.14 (s, 9H, Me_3Si), 2.28 and 2.36 (AB, 2H, J = 13.5 Hz, CH_2SO), and 7.2–7.8 p.p.m. (m, 5H, C_6H_5); infrared (neat): 9.67 (S → 0), 8.0, and 11.75 μ (Si—Me).

*Thermal Rearrangement of **1***

A 10.5 g sample of the above material was placed in a small scale fractional distillation apparatus and heated in a nitrogen atmosphere at 60 °C for 1 h at atmospheric pressure. The reaction mixture was then distilled *in vacuo* to give 8.25 g (79%) of trimethylsiloxymethyl phenyl sulfide, **3**, 0.4 g (10%) of hexamethyldisiloxane, collected in a trap cooled with dry ice/acetone, and undistillable gum. The crude **3** was shown by n.m.r. to contain about 10% methyl phenyl sulfoxide. Redistillation of the crude sulfide at 67° (0.55 mm) gave pure material. n_D^{23} 1.5242; n.m.r. (CCl_4) δ 0.11 (s, 9H, Me_3Si), 5.07 (s, 2H, SCH_2O), and 7.05–7.6 p.p.m. (m, 5H, C_6H_5); infrared (neat): 9.3 (C—O—Si), 8.0, and 11.7 μ (Si—Me).

Anal. Calcd. for $C_{10}H_{16}OSSi$: C, 56.56; H, 7.60; S, 15.1; mol. wt., 212.4. Found: C, 56.80; H, 7.63; S, 15.4; mol. wt. (osmometer), 211.5.

*The Preparation of **3** from Thiophenol, Formaldehyde, and Trimethylchlorosilane*

n-Butyllithium (0.1 mole) in 65 ml of hexane was added to a solution of 11.0 g (0.101 mole) of thiophenol in 100 ml of dry ether. Formaldehyde gas was bubbled through the solution until the reaction was complete (1½ h). Trimethylchlorosilane (11 g, 0.101 mole) was added to the above solution at 0°, and the mixture was stirred at room temperature for 1 h. After filtration of the precipitated lithium chloride, distillation of the filtrate gave 11 g (60%) of trimethylsilyl phenyl sulfide (b.p. 37° (0.75 mm), lit. (19) 72° (8 mm)) and 4.9 g (23%) of **3**, which was identical with the material obtained from the rearrangement of **1**.

*Triethylsilylmethyl p-Tolyl Sulfoxide, **2***

Using similar techniques to those used in the preparation of **1**, the reaction of triethylsilylmethylmagnesium chloride with methyl *p*-toluenesulfinate gave an 80% yield of **2**, again slightly contaminated with rearrangement product so that a pure sample for analysis could not be obtained. N.m.r. (CCl_4) δ 0.33–1.22 (m, 15H, Et_3Si), 2.23 and 2.38 (AB, 2H, J = 13.5 Hz, CH_2SO), 2.34 (s, 3H, p-MeC_6H_4), 7.22, and 7.46 (AA′BB′ analyzed as AB, 4H, J = 8.5 Hz, p-MeC_6H_4); infrared (neat): 9.68 (S → 0), 8.05, and 11.60 μ (Si—Et).

*The Rearrangement of **2***

Using similar techniques as were applied to the thermolysis of trimethylsilylmethyl phenyl sulfoxide, the thermolysis of **2** gave triethylsiloxymethyl *p*-tolyl sulfide **4** (50%), hexaethyldisiloxane (12%), methyl *p*-tolyl sulfoxide (12%), and undistillable gums. The yields of hexaethyldisiloxane (δ 0.3–1.2 p.p.m., Et_3Si) and methyl

Can. J. Chem. Downloaded from www.nrcresearchpress.com by 210.87.254.6 on 09/05/12
For personal use only.

p-tolyl sulfoxide (δ 2.28 p.p.m., *p*-MeC_6H_4) were estimated from the n.m.r. spectrum of the fraction containing both materials. Gas–liquid chromatography of a small amount of the impure **4** using a 20′ × 3/8″ aluminium column packed with 20% SE 30 (silicone gum rubber) on Chromosorb W (60–80 mesh) at 265°, flow rate 150 ml/min with helium as carrier gas, gave a sample which after distillation gave **4**: b.p. 120° (0.01 mm) (Kugelrohr); n_D^{23} 1.5280; n.m.r. (CCl_4) δ 0.3–1.3 (m, 15H, Et_3Si); 2.28 (s, 3H, *p*-MeC_6H_4), 5.01 (s, 2H, SCH_2O), 7.02, and 7.30 p.p.m. (AA′BB′ analyzed as AB, 4H, J = 8.5 Hz, *p*-MeC_6H_4); infrared (neat): 8.0 and 11.7 (Si—Et), and 9.3 μ (C—O—Si).

Anal. Calcd. for $C_{14}H_{24}OSSi$: C, 62.63; H, 9.01. Found: C, 62.72; H, 8.96.

Trimethylgermylmethyl Phenyl Sulfoxide, 8

Using techniques similar to those used in the preparation of **1**, the reaction of trimethylgermylmethylmagnesium chloride (20, 21) with methyl benzenesulfinate gave a 78% yield of **8**. Distillation of this material gave pure trimethylgermylmethyl phenyl sulfoxide: b.p. 120° (0.01 mm) (Kugelrohr); n_D^{22} 1.5528; n.m.r. (neat) δ 0.27 (s, 9H, Me_3Ge), 2.48 and 2.56 (AB, 2H, J = 12.5 Hz, CH_2SO), 7.34–7.84 p.p.m. (m, 5H, C_6H_5); infrared (neat): 9.67 (S → 0), 8.07, and 12.00 μ (Ge—Me).

Anal. Calcd. for $C_{10}H_{16}GeOS$: C, 46.76; H, 6.28. Found: C, 46.85; H, 6.33.

Trimethylsilylmethyldiphenylphosphine Oxide, 9

n-Butyllithium (0.06 mole) in hexane (35 ml) was added to a solution of 9.3 g (0.043 mole) of diphenylmethylphosphine oxide, **10**, in 50 ml of tetrahydrofuran at 10° (22). The mixture was left at 10° for 10 min before 6.5 g (0.06 mole) of trimethylchlorosilane in hexane (10 ml) was added dropwise. The resulting solution was stirred at room temperature for ½ h. Workup gave 10 g of crude product. Chromatography of this material on silica gel gave 6.5 g (53%) of trimethylsilylmethyldiphenylphosphine oxide, m.p. 118–119° after recrystallizations from 1:1 cyclohexane and *n*-hexane: n.m.r. (acetone-d_6) δ 0.02 (s, 9H, Me_3Si), 2.01 (d, 2H, J = 15 Hz, CH_2P), and 7.3–8.2 p.p.m. (m, 10H, $(C_6H_5)_2P$); infrared (Nujol mull): 6.98 (P—C_6H_5), 8.51 (P=O), 8.02, and 11.80 μ (Si—Me).

Anal. Calcd. for $C_{16}H_{21}OPSi$: C, 66.64; H, 7.34. Found: C, 66.53; H, 7.42.

Also recovered was 2.8 g (30%) of diphenylmethylphosphine oxide, m.p. 108–111°, identified by a mixed melting point.

The Attempted Thermolysis of Trimethylsilylmethyldiphenylphosphine Oxide, 9

A 0.2 g sample of **9** was heated at 180° for 21 h. The n.m.r. spectrum of the product showed only starting material (76%), diphenylmethylphosphine oxide (24%), and hexamethyldisiloxane (20%). A further experiment was carried out by heating **9** (1.25 g) (0.00435 mole) containing water (ca. 0.05 g) in a sealed tube at 180° for 21 h. The mixture was estimated to contain 60% of **9** and 40% of diphenylmethylphosphine oxide, **10**. Chromatography of this sample gave 0.38 g (37%) of **10**, m.p. 110–112° (mixed melting point undepressed), and 0.71 g (57%) of **9**, m.p. 118–119° (mixed melting point undepressed). The n.m.r. and infrared spectra of both of these samples were identical with the respective spectra of authentic samples.

Acknowledgments

The research was supported by the National Research Council of Canada. The authors are grateful to Professor Kurt Mislow of Princeton University for stimulating discussions and suggestions.

1. A. G. Brook, D. M. MacRae, and W. W. Limburg. J. Am. Chem. Soc. **89**, 5493 (1967).
2. G. D. Cooper. J. Am. Chem. Soc. **76**, 3713 (1954).
3. E. J. Corey and M. Chaykovsky. J. Am. Chem. Soc. **87**, 1345 (1965).
4. A. G. Brook and J. M. Duff. Unpublished results.
5. A. G. Brook, G. E. LeGrow, and D. M. MacRae. Can. J. Chem. **45**, 239 (1967).
6. A. G. Brook, C. M. Warner, and W. W. Limburg. Can. J. Chem. **45**, 1231 (1967).
7. W. E. Parham and S. H. Groen. J. Org. Chem. **30**, 728 (1965).
8. W. E. Parham and M. D. Bhavsar. J. Org. Chem. **28**, 2686 (1963).
9. S. Oae, T. Kitao, S. Kawamura, and Y. Kitaoka. Tetrahedron, **19**, 817 (1963).
10. R. W. Bott, C. Eaborn, and T. W. Swaddle. J. Chem. Soc. 2342 (1963).
11. G. Schott and C. Harzdorff. Z. Anorg. Allgem. Chem. **307**, 105 (1960).
12. A. G. Brook, W. W. Limburg, D. M. MacRae, and S. A. Fieldhouse. J. Am. Chem. Soc. **89**, 704 (1967).
13. D. A. Nicholson and A. L. Allred. Inorg. Chem. **4**, 1751 (1965).
14. D. G. Anderson, M. A. M. Bradney, and D. E. Webster. Intern. Symp. Organosilicon Chem. Prague, 1965, Abstracts, p. 270.
15. L. Horner and W. D. Balzer. Tetrahedron Letters, **17**, 1157 (1965).
16. C. R. Hauser and C. R. Hance. J. Am. Chem. Soc. **74**, 5091 (1952).
17. R. Otto and A. Rössing. J. Prakt. Chem. **47**, 152 (1893).
18. F. C. Whitmore and L. H. Sommer. J. Am. Chem. Soc. **68**, 481 (1946).
19. A. Berger and J. P. Magnuson. Anal. Chem. **36**, 1156 (1964).
20. D. Seyferth and E. G. Rochow. J. Am. Chem. Soc. **77**, 907 (1955).
21. D. Seyferth. J. Am. Chem. Soc. **79**, 2738 (1957).
22. D. J. Peterson. J. Organometal. Chem. **8**, 199 (1967).

Can. J. Chem. Downloaded from www.nrcresearchpress.com by 210.87.254.42 on 09/05/12
For personal use only.

Bis(metalloidal)ketones

A. G. Brook and Peter F. Jones
Department of Chemistry, University of Toronto, Toronto, Ontario

and

G. J. D. Peddle
Department of Chemistry, University of Alberta, Edmonton, Alberta

Received January 8, 1968

A number of bis(silyl)- and bis(germyl)-ketones have been prepared by the oxidation of the corresponding carbinol or by the hydrolysis of the dithiane precursor. The ketones are all highly colored and their spectral properties are consistent with inductive interaction of both metalloid atoms with the carbonyl group. The reactions of bis(triphenylgermyl)ketone under various conditions have been studied and the results obtained are consistent with the intermediacy of triphenylgermyl radicals.

Canadian Journal of Chemistry, 46, 2119 (1968)

Research (1–6) in these laboratories over a number of years has resulted in the preparation of a large number of acylsilanes and acylgermanes.[1] The most striking features of these compounds are their remarkable spectral properties, both in the infrared and ultraviolet regions. Thus the carbonyl n → π* transitions of the acyl-silanes and -germanes show a marked bathochromic shift compared with those of their carbon counterparts, and the infrared carbonyl stretching wavelength in the metalloidal compounds is also significantly longer than in the analogous carbon compounds. In addition it has recently been shown (7, 8) that acylsilanes undergo unusual photochemical transformations.

$Ph_3SiCOSiPh_3$ (1) $Ph_3GeCOGePh_3$ (2)

In view of the above results, it appeared of interest to synthesize compounds where the carbonyl group was flanked by two metalloid atoms, in order to gain further insight into the effect of adjacent metalloid atoms on the chemical and spectral properties of the carbonyl group. A preliminary account of the preparation and spectral properties of bis(triphenylsilyl)ketone, **1**, and its germanium analog **2**, has appeared (9) and in the present communication we wish to give full details of this work, together with an account of the synthesis and spectral properties of additional ketones, and a study of the chemical reactions of bis(triphenylgermyl)ketone, **2**.

[1]We now favor usage of the term acylsilane instead of the formerly used α-silyl ketone to describe compounds with the structure Si—CO—.

Preparation of Bis(metalloidal)ketones

Bis(triphenylgermyl)ketone, **2**, was prepared by the route shown in Fig. 1. Addition of

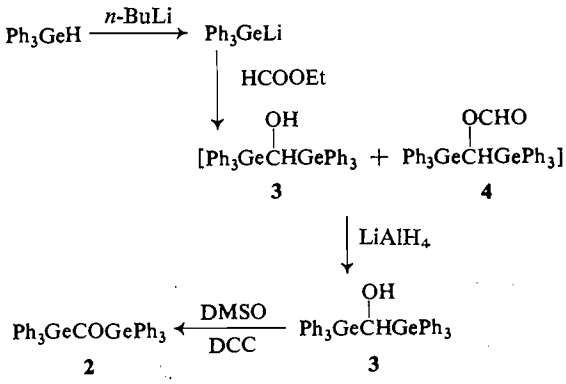

FIG. 1.

ethyl formate to the germyllithium reagent gave apart from the desired carbinol, **3**, some formate ester, **4**, which presumably arose by ester interchange. Reduction of this mixture with lithium

$$(Ph_3Ge)_2CHO^- + H{-}\overset{\overset{O}{\|}}{C}{-}OEt \rightarrow (Ph_3Ge)_2CH\overset{\overset{O}{\|}}{C}H + OEt^-$$

4

aluminium hydride gave pure carbinol in 68% yield. This could be oxidized to the ketone **2** in yields of up to 70%, using the dimethyl sulfoxide – dicyclohexylcarbodiimide – pyridinium trifluoroacetate reagent (10). The ketone is an orange-red solid, m.p. 152°, which is extremely light sensitive, especially in solution.

A similar procedure was used to synthesize bis(triphenylsilyl)ketone, **1**.

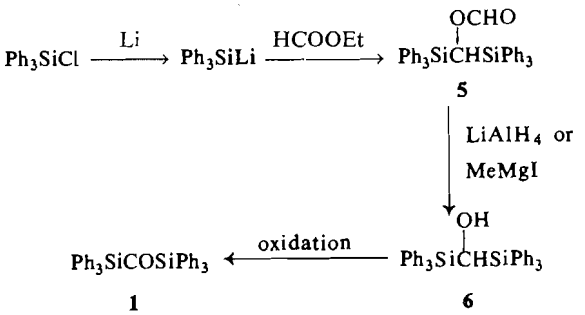

In this case, the preparation of the intermediate carbinol, **6**, from triphenylsilyllithium and ethyl formate was complicated by the formation of substantial quantities of triphenylsilyltriphenylsiloxymethane, **7**, which is the expected product of the well-studied "silylcarbinol to silyl ether" rearrangement (11, 12).

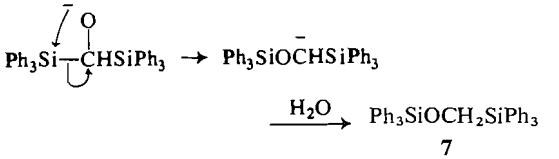

No carbinol at all could be isolated, but the formate ester, **5**, formed in low yield, could be reduced by lithium aluminium hydride or methyl Grignard reagent to the carbinol **6**.

It was further found that the yield of formate ester depended upon the method used to prepare the silyllithium reagent. When it was formed by cleavage of hexaphenyldisilane, no formate ester was obtained and the major

$$Ph_3SiSiPh_3 + 2Li \rightarrow 2Ph_3SiLi$$

product was the silyl ether, **7**. Only when the silyllithium was prepared by treatment of triphenylchlorosilane with excess lithium was some formate ester, **5**, isolated. Although the reason for this difference is not fully understood at present, it seems possible that when the silyllithium reagent was prepared from triphenylchlorosilane, the lithium chloride formed catalyzed the ester interchange of the intermediate alkoxide ion with the ethyl formate, thereby diminishing the isomerization of the anion to the silyl ether, **7**.

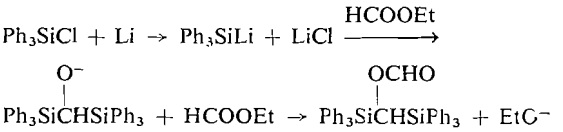

Kollonitsch (13) has shown that the related reaction of organocadmium reagents with acyl halides is greatly influenced by the presence or absence of metal halides.

The carbinol, **6**, could be successfully oxidized to the ketone, **1**, by two alternative methods. Oxidation using chromium trioxide – sulfuric acid gave a 36% yield of **1**, while the dimethyl sulfoxide – dicyclohexylcarbodiimide – pyridinium trifluoroacetate method gave the ketone in 26% yield. Both these methods have previously been used successfully for the preparation of acylsilanes (5). A third method, using N-bromosuccinimide, gave halosilanes as the major products. The ketone, **1**, is a pinkish red solid, m.p. 155–158°, which, like its germanium counterpart, is extremely light sensitive.

The above route was also used to prepare bis(diphenylmethylsilyl)ketone, $Ph_2MeSiCOSiMePh_2$, **8**. A sample of pure ketone could not be obtained in this case, oxidation of the carbinol giving pink solutions which decolorized on attempted workup. However, the presence of the ketone was clearly indicated by the ultraviolet spectrum of the solution, which showed the characteristic absorption bands exhibited by bis(metalloidal)ketones.

A further route to bis(metalloidal)ketones from the hydrolysis of 2,2-dimetalloidal-1,3-dithianes was explored, since the general method had been found useful for the synthesis of acyl-silanes and -germanes (6, 14).

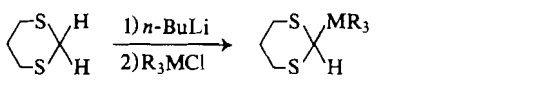

	R_3M	R'_3M'
a)	Ph_3Si	Ph_3Si
b)	Me_3Si	Me_3Si[2]
c)	Ph_3Si	Me_3Si
d)	Et_3Ge	Me_3Si
e)	Et_3Ge	Et_3Ge

[2]Professor E. J. Corey, private communication, has indicated that he too obtained unstable pink solutions on hydrolysis of this dithiane.

Can. J. Chem. Downloaded from www.nrcresearchpress.com by 210.87.254.42 on 09/05/12
For personal use only.

TABLE I

Spectral properties of the bis(metalloidal)ketones

Ketone	λ_{max} (ε) mμ	Solvent
$Me_3SiCOSiMe_3$	472, 505, 537	C_6H_6–Me_2CO–H_2O
$Ph_3SiCOSiMe_3$	480, 517, 550	C_6H_{12}
$Ph_3SiCOSiPh_3$	518(47), 548(63)	C_6H_6
	524(30), 554(47)	CCl_4
	517(41), 545(64)	EtOH
$Ph_2MeSiCOSiMePh_2$	524, 554	Heptane
$Et_3GeCOSiMe_3$	535	C_6H_6
$Et_3GeCOGeEt_3$	464, 495, 527	MeOH-THF
$Ph_3GeCOGePh_3$	455(18), 485(43), 515(66)	C_6H_6
	451, 483, 513	C_6H_{12}

With the exception of 2,2-bis(triphenylsilyl)-1,3-dithiane, ***9a***, each of the disubstituted dithianes hydrolyzed in a benzene–acetone–water solvent mixture containing mercuric chloride and cadmium carbonate to give pink solutions containing bis(metalloidal)ketones, as shown by their characteristic ultraviolet absorption spectra. However, as with the bis(silyl)ketone, **8**, these solutions decolorized on attempted workup, rendering impossible the investigation of properties other than their electronic spectra.

Other brief investigations of possible routes to bis(metalloidal)ketones were made. The hydrolysis of benzylic *gem*-dihalides has been found (1–3) to be a convenient route to benzoylsilanes. Therefore the route shown in Fig. 2 appeared to be a possible approach to bis(triphenylsilyl)-ketone, **1**.

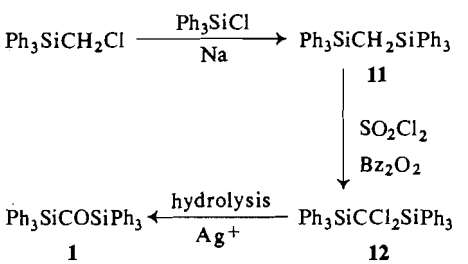

FIG. 2.

Bis(triphenylsilyl)methane, **11**, was prepared in 50% yield by the mixed Wurtz reaction. Although it was inert to bromination using N-bromosuccinimide, it could be chlorinated using sulfuryl chloride and benzoyl peroxide to give bis(triphenylsilyl)dichloromethane, **12**. However the *gem*-dihalide could not be hydrolyzed using silver nitrate, even when heated under reflux in a benzene–ethanol mixture for 2 days. This behavior obviously parallels the inertness of the corresponding dithiane, ***9a***, to hydrolysis. The reaction of triphenylsilyllithium with carbonyl compounds as a route to bis(silyl)ketones was also unsuccessful. Addition of the silyllithium reagent to phosgene gave an immediate precipitate of hexaphenyldisilane, $Ph_3SiSiPh_3$, but no bis(silyl)ketone could be detected. The similar formation of hexaphenyldigermane, $Ph_3GeGePh_3$, from the reaction of triphenylgermyllithium with phosgene has been reported (15).

Another possible route to **1** investigated was the reaction of triphenylsilyllithium with methyl triphenylsilanecarboxylate, **13**.

$$Ph_3SiLi + Ph_3SiCOOMe \rightarrow Ph_3SiCOSiPh_3 + LiOMe$$

13

Treatment of the ester with triphenylsilyllithium gave triphenylmethoxysilane as the major product, presumably from the attack on the ester by methoxide ions formed in the reaction (16).

Spectral Properties

Table I lists the positions of the $n \rightarrow \pi^*$ transitions observed for the bis(metalloidal)ketones.

All compounds absorb far into the visible, and all the visible transitions were strongly banded, as has been observed previously with acylmetalloid compounds (4, 6). The extinction coefficients reported cannot be considered to be very accurate because of the demonstrable instability of the solutions, especially in light, but in all cases the band intensities are progressively larger, the longer the wavelength. The benzenoid bands in the 250–270 mμ region were also studied in the case of bis(triphenylsilyl)ketone and its germanium analog. The former exhibited maxima at

Can. J. Chem. Downloaded from www.nrcresearchpress.com by 210.87.254.42 on 09/05/12
For personal use only.

Can. J. Chem. Downloaded from www.nrcresearchpress.com by 210.87.254.42 on 09/05/12
For personal use only.

255, 262, 267, and 273 mμ in cyclohexane, while the latter had bands at 248, 254, 260, 265, and 271 mμ in the same solvent. However, it is not certain whether these bands are characteristic of the metalloidal ketones or of their oxidation products which show identical fine structure, since it is likely that the extremely dilute solutions required for the ultraviolet measurements are readily photolyzed. There is no such doubt, however, about the identity of the bands in the $n \rightarrow \pi^*$ region, since the more concentrated solutions used are visibly pink throughout the measurements, and some ketone is recoverable from them.

The only infrared spectra of bis(metalloidal)-ketones which have been obtained are those of bis(triphenylsilyl)ketone and bis(triphenylgermyl)ketone. The former showed carbonyl stretching absorption at 6.42 μ (1558 cm^{-1}) in KBr or 6.44 μ (1553 cm^{-1}) in ethylene dichloride and the intensity of the band was low. The latter compound absorbed with medium intensity at 6.19 μ (1619 cm^{-1}) in either KBr or carbon tetrachloride.

From the above data it is evident that these ketones display remarkable spectral properties when compared with analogous carbon compounds; for example hexamethylacetone, $Me_3CCOCMe_3$, has λ_{max} 296 mμ, with a carbonyl infrared band at 5.91 μ. The figures in Table I show that when a second silicon or germanium atom is attached to the carbonyl group of an acylmetalloid, this causes a similar lowering of the $n \rightarrow \pi^*$ transition energy to that caused by the introduction of the first metalloid atom. A similar result is found in the carbonyl infrared position. The unusually long wavelength infrared absorption for the bis(silyl)ketone relative to the bis(germyl)ketone would seem to be explainable, at least in part, as due to steric hindrance between the two triphenylsilyl groups, as appears obvious from consideration of a Fischer–Hirschfelder–Taylor model. Similar shifts to longer wavelength have also been observed (17) for such strained ketones as hexamethylacetone and triptyl *t*-butyl ketone. Additional evidence of steric interaction is found in the low intensity of the carbonyl absorption in this bis(silyl)ketone (18)

Reactions of Bis(metalloidal)ketones

These ketones appear to react normally with metallic reagents, since bis(triphenylgermyl)-ketone, **2**, was reduced to its carbinol precursor, bis(triphenylgermyl)methanol, in 71% yield by lithium aluminium hydride, and bis(triphenylsilyl)ketone, **1**, reacted with methyl Grignard reagent to give 1,1-bis(triphenylsilyl)ethanol, **14**, in 82% yield.

$$\underset{\mathbf{1}}{Ph_3SiCOSiPh_3} \xrightarrow{MeMgI} \underset{\mathbf{14}}{Ph_3SiC(OH)(Me)SiPh_3}$$

Both bis(metalloidal)ketones are rapidly decolorized, and evolve carbon monoxide, at their melting points, the major products formed in air being the disilane (or digermane) and the disiloxane (or digermoxane). The results are consistent with a radical pathway:

$$Ph_3MCOMPh_3 \xrightarrow{\Delta} Ph_3MCO^{\cdot} + Ph_3M^{\cdot}$$

$$Ph_3MCO^{\cdot} \rightarrow Ph_3M^{\cdot} + CO$$

$$Ph_3M^{\cdot} + Ph_3MCOMPh_3 \rightarrow Ph_3MMPh_3 + Ph_3MCO^{\cdot}$$

The disiloxane (or digermoxane) can be explained as arising from the reaction of the $Ph_3M^{\cdot}$ radical either with atmospheric oxygen, or with unreacted ketone. Eaborn *et al.* (19) have shown that the trimethylsilyl radical, $Me_3Si^{\cdot}$, in addition to forming disilane, abstracts oxygen atoms readily from oxygen-containing species: with the ketones acetophenone or benzophenone, hexamethyldisiloxane was the major product.

The photolysis of bis(triphenylgermyl)ketone, **2**, under various conditions has been studied. When **2** was photolyzed under nitrogen in benzene or methanol, decarbonylation occurred, forming hexaphenyldigermane in high yield. The reaction presumably proceeds via a Norrish type I cleavage (20).

$$Ph_3GeCOGePh_3 \xrightarrow[PhH \text{ or } MeOH]{h\nu, N_2} Ph_3GeCO^{\cdot} + Ph_3Ge^{\cdot}$$

$$Ph_3GeCO^{\cdot} \rightarrow Ph_3Ge^{\cdot} + CO$$

$$Ph_3Ge^{\cdot} + Ph_3GeCOGePh_3 \rightarrow Ph_3GeGePh_3 + Ph_3GeCO^{\cdot}$$

Further evidence in favor of a radical pathway was found when **2** was photolyzed under nitrogen in chloroform. The major product in this case was found to be triphenylchlorogermane, Ph_3GeCl. This result can be rationalized in terms of the abstraction of $Cl^{\cdot}$ radicals from the solvent by the triphenylgermyl radical.

$$Ph_3Ge^{\cdot} + CHCl_3 \rightarrow Ph_3GeCl + {}^{\cdot}CHCl_2$$

Can. J. Chem. Downloaded from www.nrcresearchpress.com by 210.87.254.42 on 09/05/12
For personal use only.

Similar behavior has been reported for triethylgermyl radicals generated from bis(triethylgermyl)mercury (21, 22).

When the photolysis of bis(triphenylgermyl)-ketone was carried out in the presence of oxygen in carbon tetrachloride a different process evidently occurred, since the major products were the known triphenylgermyl triphenylgermanecarboxylate, $Ph_3GeCOOGePh_3$, and triphenylchlorogermane, Ph_3GeCl. With benzene as solvent, the photolysis gave the ester and hexaphenyldigermane, $Ph_3GeGePh_3$. It is clear that again triphenylgermyl radicals are formed, but in what way they combine with other species and oxygen to yield the ester is not yet known.

Experimental

Preparation of 1,1-Bis(triphenylgermyl)methanol

To a solution of 12.0 g (0.0396 mole) of triphenylgermane in 150 ml of anhydrous THF at −23° was added 24.8 ml (0.0396 mole) of *n*-butyllithium solution. The resulting green solution was stirred for a further 30 min at −23°. A solution of 1.47 g (0.0198 mole) of freshly distilled ethyl formate in 100 ml of THF was added dropwise, the green color of the germyllithium reagent being absent at the end of the addition. The resulting colorless solution was stirred for a further 5 min, hydrolyzed with 5% hydrochloric acid, and extracted with ether. The organic layer was dried over anhydrous magnesium sulfate, filtered, and solvent removed under reduced pressure. An infrared spectrum of the solid obtained showed the presence of bands for both —OH at 2.80 μ and —OCHO at 5.81 μ. The crude product, dissolved in anhydrous THF, was added to a suspension of 1.0 g (0.0264 mole) of lithium aluminium hydride in 150 ml of anhydrous ether. After the mixture had been stirred for 60 min at room temperature, normal acid workup, followed by recrystallization from a 9:1 ethanol:benzene mixture, gave 8.48 g (68%) of 1,1-bis(triphenylgermyl) methanol, m.p. 138–139°.

Anal. Calcd. for $C_{37}H_{32}Ge_2O$: C, 69.66; H, 5.05. Found: C, 69.47; H, 5.18.

Infrared spectrum: λ_{max} (CCl_4), 2.80(w), 3.26(m), 3.27(m), 6.73(m), 7.00(s), 9.15(s), 9.70(m), 10.00(m), 14.35(s), 14.85(m) μ.

N.m.r. spectrum: δ (CCl_4), 7.08 to 7.43 (30H, complex), 5.29 (1H, singlet), 1.28 (1H, singlet, removed by the addition of D_2O) p.p.m.

Preparation of Bis(triphenylgermyl)ketone

To a solution of 2.7 g (0.00426 mole) of 1,1-bis-(triphenylgermyl)methanol in 25 ml of anhydrous ether was added successively 2.07 g (0.01 mole) of dicyclohexylcarbodiimide and 0.99 g (0.00514 mole) of pyridinium trifluoroacetate. On the addition of 1.2 ml (0.0169 mole) of dimethyl sulfoxide, the mixture turned an orange-pink color. After stirring the mixture for 14 h in the dark the supernatant red liquor was drawn off by means of a syringe, and the solvent was removed under reduced pressure. The resulting red solid was recrystallized from a 4:1 methanol:benzene mixture to give 2.08 g (77%) of crude ketone, m.p. 135–141°. Several recrystallizations gave the analytical sample, m.p. 152–154°, in 37% yield.

Anal. Calcd. for $C_{37}H_{30}Ge_2O$: C, 69.88; H, 4.75. Found: C, 70.18; H, 4.95.

Infrared spectrum: λ_{max} (KBr pellet) 3.25(m), 6.19(m) (carbonyl absorption; the same value was found in carbon tetrachloride), 6.75(m), 7.00(s), 9.20(s), 10.02(m), 12.60(m), 13.66(s), 14.30(s), 14.80(m) μ.

Ultraviolet spectrum: (*a*) n → π* region: λ_{max} (C_6H_6), 455(18), 485(43), 515(66) mμ; (C_6H_{12}) 451, 483, 513 mμ. The solution used was visibly pink, both before and after taking the spectrum. A spectrum taken on the same solution after 2 h was identical with the above, with the exception that the intensities of the 3 bands had fallen to 11, 24, and 36 respectively. (*b*) π → π* region: λ_{max} (C_6H_{12}), 248(1590), 254(1952), 260(2290), 265(2180), and 271(1590) mμ. Evaporation of this solution, after being allowed to stand for 30 min, gave a white solid, whose infrared spectrum indicated the presence of triphenylgermyl triphenylgermanecarboxylate, $Ph_3GeCOOGePh_3$, as shown by infrared bands at 6.04 and 8.60 μ. A cyclohexane solution of this solid gave an ultraviolet spectrum identical with the above. A cyclohexane solution of authentic $Ph_3GeCOOGePh_3$ (23) also gave ultraviolet bands identical with the above in this region.

Triphenylsilyllithium with Formate Esters

(*A*) A solution containing 2.3 g (0.032 mole) of ethyl formate in 25 ml of tetrahydrofuran was rapidly added to 125 ml (0.062 mole) of 0.5 *M* triphenylsilyllithium prepared by the cleavage of hexaphenyldisilane with lithium in tetrahydrofuran. After stirring for 3 h, normal acid workup gave 2.1 g (13%) of hexaphenyldisilane, m.p. 360°, and a yellow oil. Chromatography of the oil on silica gel eluted with benzene gave 2.5 g (15%) of triphenylsilane, m.p. 43–44°, 9.9 g (58%) of triphenylsiloxytriphenylsilylmethane (24), m.p. 129–130°, and 0.3 g (2%) of triphenylsilanol, m.p. 148–151°.

(*B*) A solution of 24 ml (0.4 mole) of methyl formate in 50 ml of tetrahydrofuran was rapidly added to the triphenylsilyllithium prepared from 29.6 g (0.1 mole) of triphenylchlorosilane and 2.8 g (0.4 g atom) of lithium in 250 ml of tetrahydrofuran. After stirring for 20 min, normal acid workup gave 0.3 g (1%) of hexaphenyldisilane, m.p. 356–360°, and a yellow oil. Chromatography of the oil on silica gel eluted with benzene gave 6.4 g (22%) of bis(triphenylsilyl)methyl formate, m.p. 187–189°. Recrystallization from benzene raised the melting point to 189–191°.

Anal. Calcd. for $C_{38}H_{32}O_2Si_2$: C, 79.1; H, 5.59; Si, 9.74. Found: C, 79.2; H, 5.66; Si, 9.86.

Infrared spectrum: λ_{max} (CCl_4), 3.24(m), 3.26(m), 3.40(w), 5.80(s), 6.72(w), 7.00(s), 8.68(s, broad), 9.00(s), 14.35(s, broad) μ.

N.m.r. spectrum: δ (CCl_4), 7.58 (1H, singlet), 6.97 to 7.42 (30H, complex), 6.65 (1H, singlet) p.p.m.

In addition 8.2 g (30%) of triphenylsiloxytriphenylsilylmethane, m.p. 129–131°, and 11.3 g (41%) of triphenylsilanol, m.p. 150–152°, were obtained.

Several additional reactions were run involving the addition of ethyl formate to triphenylsilyllithium prepared from hexaphenyldisilane, and in no instance was any

Can. J. Chem. Downloaded from www.nrcresearchpress.com by 210.87.254.42 on 09/05/12
For personal use only.

evidence of the formation of bis(triphenylsilyl)methyl formate found.

1,1-Bis(triphenylsilyl)methanol

A solution of 0.4 g (0.7 mmole) of bis(triphenylsilyl)methyl formate in 10 ml of ether was added to 20 ml (10 mmoles) of 0.5 *M* methylmagnesium iodide in ether. After stirring for 1 h, normal acid workup, followed by recrystallization of the product from methanol, gave 0.34 g (69%) of 1,1-bis(triphenylsilyl)methanol, m.p. 154–156°.

Anal. Calcd. for $C_{37}H_{32}OSi_2$: C, 80.98; H, 5.88. Found: C, 80.88; H, 5.97.

Infrared spectrum: λ_{max} (CCl_4), 2.80(m), 3.24(m), 3.26(m), 3.32(w), 6.73(w), 7.00(s), 8.40(m), 9.00(s), 14.35(s, broad) μ.

N.m.r. spectrum: δ (CCl_4), 6.89 to 7.80 (30H, complex), 4.90 (1H, doublet, J = 4 c.p.s., becomes a singlet on addition of D_2O), 1.07 (1H, doublet, J = 4 c.p.s., removed on addition of D_2O) p.p.m.

A similar reduction was effected using excess lithium aluminium hydride in ether although in one run, carried out on a large scale, complete rearrangement of the carbinol to the silyl ether occurred.

Bis(triphenylsilyl)ketone

(*A*) A solution of 0.055 g (0.1 mmole) of 1,1-bis(triphenylsilyl)methanol in 10 ml of ether was stirred for 45 min with 0.5 ml (0.25 mmole) of 0.5 *M* chromium trioxide in 0.1 *M* sulfuric acid. The reaction mixture was then added to water and extracted with ether. The pink ether layer was dried with sodium sulfate and then concentrated under reduced pressure. Chromatography of the resulting oil on silica gel gave 0.019 g (35%) of triphenylsilanol, m.p. 149–150°, 0.012 g (20%) of triphenylsilylcarboxylic acid, m.p. 177–179°, and a pink solid. Following recrystallization from a 1:4 benzene:pentane mixture, 0.020 g (36%) of bis(triphenylsilyl)ketone, m.p. 155–158°, was obtained.

Anal. Calcd. for $C_{37}H_{30}OSi_2$: C, 81.3; H, 5.53; mol. wt., 546.1836. Found: C, 80.3; H, 5.52; mol. wt., 540 (osmometry), 546.1838 (mass spectrometry).[3]

Infrared spectrum: λ_{max} (KBr), 3.25(m), 3.26(m), 3.30(w), 6.28(w), 6.42(m) (carbonyl absorption, found at 6.44 μ in 1,2-dichloroethane), 6.72(m), 6.99(s), 9.00(s), 10.00(m), 13.58(s), 14.05(s), 14.30(s) μ.

Ultraviolet spectrum: (*a*) n → π* region: λ_{max} (PhH), 518(47), 548(63) mμ. (CCl_4), 524(30), 554(47) mμ. (95% EtOH), 517(41), 545(64) mμ. All solutions were visibly pink, both before and after taking the spectra. In the case of the benzene solution, evaporation of the solvent, followed by addition of methanol, gave recovered ketone, m.p. 156°. (*b*) π → π* region: A freshly made cyclohexane solution showed a broad band with indistinct shoulders at 250 and 266 mμ. When a spectrum was retaken on the same solution after 2 h the broad band had been replaced by a series of distinct shoulders, λ_{max} 255, 262, 267, 273 mμ. Evaporation of the solution gave a white solid, whose infrared spectrum indicated the presence of triphenylsilyl triphenylsilanecarboxylate (23) by the presence of bands at 5.96 and 8.80 μ. When redissolved in cyclohexane this gave an ultraviolet spectrum identical with the above in this region.

(*B*) To a solution of 0.197 g (0.000358 mole) of 1,1-bis(triphenylsilyl)methanol in 2.0 ml of anhydrous ether was added successively 0.172 g (0.000864 mole) of dicyclohexylcarbodiimide and 0.082 g (0.000425 mole) of pyridinium trifluoroacetate. On the addition of 0.1 ml (0.00142 mole) of dimethyl sulfoxide the mixture turned pink. After stirring the mixture for 12 h, the supernatant liquor was drawn off by means of a syringe, and solvent was removed under reduced pressure. The orange-red solid obtained was recrystallized from a 1:4 benzene:pentane mixture to give 19 mg (10%) of hexaphenyldisiloxane, m.p. 232–234°. The addition of methanol to the orange-red filtrate caused the precipitation of pink needles. These were filtered off to give 50.8 mg (26%) of bis(triphenylsilyl)ketone, m.p. 155–159°.

(*C*) To a solution of 0.055 g (0.1 mmole) of 1,1-bis(triphenylsilyl)methanol and 0.05 ml (0.005 mmole) of a 0.01 *M* carbon tetrachloride solution of benzoyl peroxide in 5 ml of carbon tetrachloride 0.040 g (0.22 mmole) of N-bromosuccinimide was added and the resultant mixture was slowly warmed. At 65° a faint yellow color developed in the solution, but it was immediately replaced by an intense pink color. The reaction mixture was immediately cooled in an ice bath and then filtered to remove the succinimide. Chromatography of the filtrate on silica gel gave 0.004 g (7%) of bis(triphenylsilyl)ketone, m.p. 153–154°.

In a second reaction where the filtrate was not chromatographed it decolorized within 20 min. Addition of pentane gave 0.042 g of what appeared to be a mixture of triphenylchlorosilane and triphenylbromosilane, m.p. 100–105°, mixture melting point with triphenylchlorosilane 99–103°.

Treatment of the mixture with excess lithium aluminium hydride in ether followed by normal workup gave 0.031 g (60%) of triphenylsilane, m.p. 41–44°.

Preparation of Bis(diphenylmethylsilyl)ketone

Under the same conditions as those used with triphenylsilyllithium, addition of methyl formate to a solution of diphenylmethylsilyllithium, prepared from diphenylmethylchlorosilane and lithium metal, gave on chromatography 19% of 1,1-bis(diphenylmethylsilyl)methyl formate, m.p. 105–107°.

Anal. Calcd. for $C_{28}H_{28}O_2Si_2$: C, 74.3; H, 6.23. Found: C, 74.6; H, 6.16.

Infrared spectrum: λ_{max} (CCl_4), 3.25(m), 3.28(m), 3.33(w), 3.38(w), 3.43(w), 5.85(s), 7.00(s), 8.00(s, broad), 8.62(s, broad), 9.00(s, broad), 14.30(s) μ.

N.m.r. spectrum: δ 7.67 (1H, singlet), 7.59 to 7.12 (20H, complex), 6.05 (1H, singlet), 0.29 (6H, singlet) p.p.m. (external TMS).

This was reduced by methylmagnesium iodide to 1,1-bis(diphenylmethylsilyl)methanol, m.p. 60–63°, in 74% yield.

Anal. Calcd. for $C_{27}H_{28}OSi_2$: C, 76.4; H, 6.64. Found: C, 76.3; H, 6.65.

Infrared spectrum: λ_{max} (CCl_4), 2.80(m), 3.24(m), 3.26(m), 6.99(s), 7.95(m, broad), 8.20(m), 8.98(s, broad), 14.11(s) μ.

N.m.r. spectrum: 7.68 to 7.12 (20H, complex), 4.24 (1H, singlet), 0.87 (1H, singlet, removed on addition of D_2O), 0.20 (6H, singlet) p.p.m.

[3]Analysis of this compound has proved difficult, presumably because of its instability.

Can. J. Chem. Downloaded from www.nrcresearchpress.com by 210.87.254.42 on 09/05/12
For personal use only.

Attempts to oxidize the carbinol under a variety of conditions gave pink solutions, λ_{max} (heptane) 524, 554 mμ. The solutions decolorized during workup, and no meaningful infrared spectra were obtained.

The Dithiane Route to Bis(metalloidal)ketones

Since the majority of the dithianes and their hydrolyses have been reported elsewhere (6), they will not be further considered here. Only those reactions previously unreported will be described.

Preparation of 2-Trimethylsilyl-2-triphenylsilyl-1,3-dithiane

To a solution of 7.58 g (0.02 mole) of 2-triphenylsilyl-1,3-dithiane in 125 ml of anhydrous THF, cooled to −23°, was added 17.3 ml (0.02 mole) of *n*-butyllithium. The resulting solution was stirred for 3 h at −23°. The temperature was raised to 0° and a solution of 2.18 g (0.02 mole) of trimethylchlorosilane in 100 ml of anhydrous THF was added dropwise. The resulting mixture was stirred at 0° for 2 h, then at room temperature for 20 h, after which it was hydrolyzed with 5% hydrochloric acid and extracted with ether. The organic layer was dried over anhydrous magnesium sulfate, filtered, and the solvent was removed under reduced pressure. The resulting oil was recrystallized from benzene by the addition of methanol to give 2.8 g (31%) of 2-trimethylsilyl-2-triphenylsilyl-1,3-dithiane, m.p. 148°.

Infrared spectrum: λ_{max} (CCl_4), 3.24(m), 3.26(m), 3.38(m), 3.41(m), 3.43(m), 6.78(m), 7.00(s), 8.05(m), 8.40(m), 9.10(s), 10.98(m), 11.25(m), 14.40(s, broad), 14.80(s) μ.

N.m.r. spectrum: δ ($CDCl_3$, CH_2Cl_2 as internal reference at 5.30 p.p.m.), 7.22 to 8.16 (15H, 2 complex peaks), 2.30 to 2.60 (4H, complex), 1.50 to 2.00 (2H, complex), 0 (9H, singlet) p.p.m.

Anal. Calcd. for $C_{25}H_{30}S_2Si_2$: C, 66.61; H, 6.71. Found: C, 66.65; H, 6.83.

Hydrolysis of 2-Trimethylsilyl-2-triphenylsilyl-1,3-dithiane

A mixture of 0.50 g (0.0011 mole) of 2-trimethylsilyl-2-triphenylsilyl-1,3-dithiane, 1.36 g (0.005 mole) of mercuric chloride, and 0.34 g (0.002 mole) of cadmium carbonate in 40 ml of 3:1 acetone:benzene containing 5% water was heated under reflux for 8 h. Some of the mixture was taken, and the solvent was removed under reduced pressure. The solid obtained was extracted with cyclohexane, filtered, and the ultraviolet spectrum of the pink filtrate was determined. An attempt was made to trap the bis(silyl)ketone by reduction of the remainder of the mixture after it had been shaken with anhydrous magnesium sulfate, filtered, and the filtrate evaporated under reduced pressure. The product was dissolved in anhydrous ether and 0.25 g (0.0066 mole) of lithium aluminium hydride was added. The mixture was allowed to stand for 60 min when it was hydrolyzed with 5% hydrochloric acid and extracted with ether. The organic layer was dried over anhydrous magnesium sulfate, filtered, and the solvent was removed under reduced pressure. The solid obtained was chromatographed on silica gel. Elution with carbon tetrachloride gave 0.12 g (24%) of starting dithiane, m.p. 148°. The mixed melting point with an authentic sample was not depressed.

Elution with benzene gave 100 mg of a mixture of a silanol and what was presumed to be the desired carbinol, as shown by absorption in the infrared region at 2.70 and 2.80 μ. However, these products could not be separated either by chromatography or by crystallization.

Hydrolysis of 2,2-Bis(trimethylsilyl)-1,3-dithiane

A mixture of 1.32 g (0.005 mole) of 2,2-bis(trimethylsilyl)-1,3-dithiane (14), 6.75 g (0.025 mole) of mercuric chloride, and 1.72 g (0.01 mole) of cadmium carbonate, in 80 ml of a 3:1 acetone:benzene solution containing 5% water, was stirred in the dark at room temperature for 5 h, the mixture gradually becoming pink. Some of the liquid was removed, filtered, and its ultraviolet spectrum was taken, using benzene in the reference cell. The rest of the mixture was filtered and the solvent was removed under reduced pressure to leave a pink-orange solid. This was extracted with anhydrous ether and filtered to give a pink filtrate, considerably lighter in color than the original solution. An attempt was made to trap the remaining bis(silyl)ketone by reduction. Excess lithium aluminium hydride was added to the ether filtrate and the mixture was allowed to stand for 1 h. The addition of 5% hydrochloric acid and extraction with ether left a colorless organic layer. This was dried over anhydrous magnesium sulfate, filtered, and the solvent removed under reduced pressure to give 0.42 g of colorless liquid, identified as starting dithiane (32% recovery) on the basis of its identical infrared spectrum and refractive index.

Ultraviolet spectrum: λ_{max} ($PhH/Me_2CO/H_2O$), 472, 505, 537 mμ.

Bis(triphenylsilyl)methane

A solution of 2.0 g (6.5 mmoles) of triphenylsilylchloromethane and 2.0 g (6.8 mmoles) of triphenylchlorosilane in 15 ml of toluene was added over 90 min to 0.3 g (13 mmoles) of sodium in 5 ml of refluxing toluene. After heating under reflux for 2 h the purple precipitate which had formed was filtered off and added slowly to ethanol to yield 0.49 g (28%) of hexaphenyldisilane, m.p. 360°. The toluene filtrate was concentrated under reduced pressure and chromatographed on silica gel which was eluted with benzene to obtain 1.8 g (52%) of bis(triphenylsilyl)methane, m.p. 138–142°. Recrystallization from heptane sharpened the m.p. to 141–142°.

Anal. Calcd. for $C_{37}H_{32}Si_2$: C, 83.41; H, 6.06; Si, 10.53. Found: C, 82.64; H, 5.88; Si, 10.49.

Bis(triphenylsilyl)dichloromethane

A solution of 0.6 g (1.1 mmoles) of bis(triphenylsilyl)methane and 0.2 ml (2.5 mmoles) of sulfuryl chloride in 5 ml of benzene was heated under reflux for 6 h with five small additions of benzoyl peroxide. As the reaction proceeded, crystals formed in the solution. Recrystallization from benzene gave 0.6 g (88%) of bis(triphenylsilyl)dichloromethane, m.p. 255–257°.

Anal. Calcd. for $C_{37}H_{30}Cl_2Si_2$: C, 73.78; H, 5.03. Found: C, 74.02; H, 5.30.

Bis(triphenylsilyl)dichloromethane with Silver Nitrate

A solution of 0.1 g (0.16 mmole) of bis(triphenylsilyl)dichloromethane and 5 ml (0.5 mmole) of 0.1 *M* silver nitrate in 90% ethanol in 100 ml of benzene and 30 ml of ethanol was refluxed for 48 h. The reaction mixture was extracted with water, dried with sodium sulfate, and concentrated under reduced pressure to

Can. J. Chem. Downloaded from www.nrcresearchpress.com by 210.87.254.42 on 09/05/12
For personal use only.

yield 0.09 g (90%) of recovered bis(triphenylsilyl)dichloromethane, m.p. 253–256°.

Triphenylsilyllithium with Phosgene

Solutions of 0.58 g (5.8 mmoles) of phosgene in 30 ml of tetrahydrofuran and 32 ml (11.7 mmoles) of 0.37 *M* triphenylsilyllithium in tetrahydrofuran were run slowly and simultaneously down a long tubular stirrer into 100 ml of tetrahydrofuran cooled in a dry ice – acetone mixture. Following normal acid workup, 1.9 g (62%) of hexaphenyldisilane, m.p. 360–363°, was obtained. In addition 0.26 g (8%) of triphenylsilane, m.p. 47°, 0.11 g (3%) of tetraphenylsilane, m.p. 224–226°, and 0.45 g (14%) of triphenylsilanol, m.p. 149–152°, were obtained by chromatography on silica gel eluted with benzene.

Triphenylsilyllithium with Methyl Triphenylsilanecarboxylate

A solution of 2.0 g (6.3 mmoles) of methyl triphenylsilanecarboxylate in 20 ml of tetrahydrofuran was cooled to 0 °C and 7.1 ml (3.1 mmoles) of a 0.44 *M* triphenylsilyllithium solution in tetrahydrofuran was added over 90 min. The mixture was allowed to warm to room temperature and stirred for 11 h. Following normal acid workup, 0.36 g (12%) of hexaphenyldisilane, m.p. 360–362°, was filtered off. The following products were obtained by chromatography on silica gel eluted with benzene: 1.1 g (60%) of methoxytriphenylsilane, m.p. 52–55°, b.p. 168–172° (0.6 mm); 0.53 g (30%) of triphenylsilanol, m.p. 150–152°; and 0.93 g of but-3-enol, b.p. 128–130° (760 mm), m.p. of 3,5-dinitrobenzoate 60–61°, lit. (25) m.p. 59°.

The Lithium Aluminium Hydride Reduction of Bis(triphenylgermyl)ketone

To 7 mg (0.000185 mole) of lithium aluminium hydride dissolved in 20 ml of anhydrous ether was added 95 mg (0.000150 mole) of bis(triphenylgermyl)ketone and the mixture was stirred together in the dark for 30 min. Following normal acid workup, recrystallization from a 9:1 ethanol:benzene mixture gave 68 mg (71%) of 1,1-bis(triphenylgermyl)methanol, m.p. 138–140°. The mixed melting point with an authentic sample was not depressed.

1,1-Bis(triphenylsilyl)ethanol

To a solution of 17 mg (0.031 mmole) of bis(triphenylsilyl)ketone in 5 ml of ether was added 10 ml (0.1 mole) of 0.01 *M* methylmagnesium iodide in ether and the mixture was stirred for 2 h. Following normal acid workup, chromatography of the resultant oil on silica gel eluted with benzene gave 14 mg (82%) of 1,1-bis(triphenylsilyl)-ethanol (26), m.p. 215°. A mixed melting point with an authentic sample was not depressed.

The Pyrolysis of Bis(triphenylsilyl)ketone

A glass tube containing 20 mg of the pink ketone was heated in an oil bath at 200° for 3 h. The pink solid melted and bubbles of gas were evolved from the liquid formed. The gas evolved blackened a piece of filter paper, moistened with acidified palladium dichloride solution, which was positioned in the mouth of the tube. An infrared spectrum was run on the solid after cooling and showed Si—Ph absorptions at 7.0 and 8.95 μ, together with a broad band at 9.35 μ, characteristic of the Si—O—Si system. The solid was dissolved in boiling carbon tetrachloride, from which a small amount of hexaphenyldisilane, m.p. 350°, precipitated on cooling. Addition of pentane to the filtrate precipitated crystals of hexaphenyldisiloxane, m.p. 230–233°. The mixed melting point with an authentic sample was not depressed.

The Pyrolysis of Bis(triphenylgermyl)ketone

A glass tube containing 20 mg of the pink ketone was heated in an oil bath at 200° for 3 h. The orange-red solid melted and bubbles of gas were evolved from the liquid formed. The gas evolved blackened a piece of filter paper, moistened with acidified palladium dichloride solution, which was positioned in the mouth of the tube. An infrared spectrum (KBr pellet) was run on the solid after cooling and showed the presence of Ge—Ph absorptions at 7.0 and 9.15 μ, together with a broad band at 11.8 μ, characteristic of the Ge—O—Ge system. Thin layer chromatography of the residue, with carbon tetrachloride as the developing solvent, gave 2 spots, which were shown to be hexaphenyldigermane and hexaphenyldigermoxane by comparison with the distances moved by authentic samples of these two substances on the same plate.

A similar experiment was performed with the pyrolysis being carried out *in vacuo*. Hexaphenyldigermane and hexaphenyldigermoxane were similarly shown to be present.

The Photolysis of Bis(triphenylgermyl)ketone in Dry Benzene under N_2

A pink solution of 99 mg (0.000157 mole) of bis(triphenylgermyl)ketone in 15 ml of dry benzene was stirred under nitrogen. Irradiation using a General Electric "PAR-38" spot lamp caused the solution to decolorize within 15 min. The solvent was removed under reduced pressure to give 97 mg (102%) of hexaphenyldigermane, m.p. 338°. A mixed melting point with an authentic sample was not depressed. Thin layer chromatography on the product showed only one compound present, which travelled the same distance as an authentic sample of hexaphenyldigermane.

The Photolysis of Bis(triphenylgermyl)ketone in Dry Methanol under N_2

A suspension of 99.6 mg (0.000158 mole) of fine orange-pink crystals of bis(triphenylgermyl)ketone in 20 ml of dry methanol was stirred under nitrogen. Irradiation using a General Electric "PAR-38" spot lamp for 45 min caused the removal of the pink color and the gradual deposition of a thick white precipitate. This was filtered off, washed with methanol, and dried *in vacuo* to give 70 mg (74%) of hexaphenyldigermane, m.p. 343–345°. The mixed melting point with an authentic sample was not depressed. The filtrate was taken and solvent was removed under reduced pressure to give 11.8 mg of an oil whose infrared spectrum showed the presence of a strong GeOH band at 2.72 μ.

The Photolysis of Bis(triphenylgermyl)ketone in Dry Chloroform under N_2

A pink solution of 91 mg (0.000145 mole) of bis(triphenylgermyl)ketone in 15 ml of dry chloroform was stirred under nitrogen. Irradiation using a General Electric "PAR-38" spot lamp for 2 min caused the

disappearance of the pink color. The irradiation was continued for a further 5 min when the solvent was removed to give 83 mg of a white solid. Chromatography on acid-washed alumina gave, on elution with carbon tetrachloride, 63 mg (64%) of triphenylchlorogermane, m.p. 112–115°. The mixed melting point with an authentic sample was not depressed.

The Photolysis of Bis(triphenylgermyl)ketone in Carbon Tetrachloride in Air

A pink solution of 103 mg (0.000162 mole) of bis(triphenylgermyl)ketone in 20 ml of carbon tetrachloride was allowed to stand in light. After 5 min the solution had decolorized. The solvent was removed under reduced pressure to give an oil which solidified on standing. Chromatography on a silica gel column on elution with 50:50 benzene:carbon tetrachloride gave 28 mg (25%) of triphenylchlorogermane, m.p. 112–115°. The mixed melting point with an authentic sample was not depressed. The column was rapidly flushed with ether to give 20 mg (19%) of triphenylgermyl triphenylgermanecarboxylate, m.p. 162–164°, which had absorptions in the infrared region at 6.04 μ and 8.60 μ. The mixed melting point with an authentic sample was not depressed.

The Photolysis of Bis(triphenylgermyl)ketone in Dry Benzene in Air

A pink solution of 95 mg (0.000150 mole) of bis(triphenylgermyl)ketone in 20 ml of dry benzene was irradiated with a General Electric "PAR-38" spot lamp for 5 min, after which time it had decolorized. The solvent was removed under reduced pressure to give a white solid, which was chromatographed on a silica gel column. Elution with 50:50 benzene:carbon tetrachloride gave 13 mg (15%) of hexaphenyldigermane, m.p. 354°. The mixed melting point with an authentic sample was not depressed. The column was rapidly flushed with ether to give 34 mg of a mixture of what was presumed to be triphenylgermanol and triphenylgermyl triphenylgermanecarboxylate, as indicated by bands in the infrared spectrum at 2.72, 6.04, and 8.60 μ. This behavior was found in several runs. When the column was eluted slowly, separation of the ester from the hexaphenyldigermane was achieved but the ester fraction contained some germanol. Rapid elution gave no germanol but poor separation of the ester from the hexaphenyldigermane. When a pure sample of triphenylgermyl triphenylgermanecarboxylate was slowly chromatographed on a silica gel column, triphenylgermanol, as shown by its infrared band at 2.72 μ, was eluted in the later fractions.

Acknowledgments

We are grateful for the support of this research by the National Research Council of Canada and by Dow-Corning Silicones of Canada through the award of a Fellowship to P. F. J. in 1966–1967.

1. A. G. Brook. J. Am. Chem. Soc. **79**, 4373 (1957).
2. A. G. Brook, M. A. Quigley, G. J. D. Peddle, N. V. Schwartz, and C. M. Warner. J. Am. Chem. Soc. **82**, 5102 (1960).
3. A. G. Brook and G. J. D. Peddle. Can. J. Chem. **41**, 2351 (1963).
4. A G. Brook, R. Kivisikk, and G. E. LeGrow. Can. J. Chem. **43**, 1175 (1965).
5. A. G. Brook and J. B. Pierce. J. Org. Chem. **30**, 2566 (1965).
6. A. G. Brook, J. M. Duff, P. F. Jones, and N. R. Davis. J. Am. Chem. Soc. **89**, 431 (1967).
7. A. G. Brook and J. M. Duff. J. Am. Chem. Soc. **89**, 454 (1967).
8. A. G. Brook and J. B. Pierce. To be published.
9. A. G. Brook and G. J. D. Peddle. J. Organometal. Chem. **5**, 105 (1966).
10. K. E. Pfitzner and J. G. Moffat. J. Am. Chem. Soc. **87**, 5661 (1965).
11. A. G. Brook, G. E. LeGrow, and D. M. McRae. Can. J. Chem. **45**, 239 (1967).
12. A. G. Brook, C. M. Warner, and W. W. Limburg. Can. J. Chem. **45**, 1231 (1967).
13. J. Kollonitsch. Nature, **188**, 140 (1960).
14. E. J. Corey, D. Seebach, and R. Freedman. J. Am. Chem. Soc. **89**, 434 (1967).
15. D. A. Nicholson and A. L. Allred. Inorg. Chem. **4**, 1747 (1965).
16. A. G. Brook and H. Gilman. J. Am. Chem. Soc. 77, 2322 (1955).
17. P. D. Bartlett and M. Stiles. J. Am. Chem. Soc. 77, 2806 (1955).
18. R. Cetina and J. L. Mateos. J. Org. Chem. **25**, 704 (1960).
19. C. Eaborn, A. G. Beaumont, R. A. Jackson, and R. W. Walsingham. J. Organometal. Chem. **5**, 297 (1966).
20. R. W. Norrish and M. E. S. Appleyard. J. Chem. Soc. 874 (1934).
21. N. S. Vyazankin, G. A. Razuvaev, and E. N. Gladyshev. Dokl. Akad. Nauk SSSR, **151**, 1326 (1963).
22. K. Kühnlein, W. P. Neumann, and H. P. Becker. Angew. Chem. **79**, 870 (1967).
23. A. G. Brook. J. Am. Chem. Soc. 77, 4827 (1955).
24. A. G. Brook and B. Iachia. J. Am. Chem. Soc. **83**, 827 (1961).
25. L. W. J. Newan and H. N. Rydon. J. Chem. Soc. 261 (1936).
26. A. G. Brook, C. M. Warner, and M. E. McGriskin. J. Am. Chem. Soc. **81**, 981 (1959).

Can. J. Chem. Downloaded from www.nrcresearchpress.com by 210.87.254.42 on 09/05/12
For personal use only.

Can. J. Chem. Downloaded from www.nrcresearchpress.com by 210.87.254.42 on 09/05/12
For personal use only.

Group vibrations and the vibrational analysis of molecules containing methylene groups. Part I. The basic equations and the application of the method to methylene dichloride and cyclopropane[1]

J. M. FREEMAN AND T. HENSHALL
University of Salford, Salford 5, England

Received November 1, 1967

The vibrations of the methylene group first considered by King have been reexamined; and the group factorization procedure previously applied to molecules containing methyl groups has now been extended to molecules containing methylene groups. The vibrational analysis of such molecules can be simplified by factoring from the secular determinant those frequencies that are characteristic of the symmetric and antisymmetric CH_2 stretching, and the $\widehat{HCH}$ angle bending modes. Corrections are then applied to the **G** and **F** matrices to account for the interactions with the molecular framework of the CH_2 'rocking', and $\widehat{XCX}$ angle deformation modes where the atoms X may form part of a ring system.

Canadian Journal of Chemistry, 46, 2129 (1968)

King and Crawford (1) have applied the concept of group vibrations to simplify the vibrational analysis of molecules containing methyl groups. They have developed a method whereby the frequencies characteristic of the methyl group are factored from the vibrational problem, leaving only those atomic displacements to be considered that involve the direct interaction of the methyl group and the framework to which it is attached, and of the framework itself.

King (2) has also considered the similar problem of the vibrations of the methylene group, but the results are rather inconclusive. It was therefore considered to be desirable to reexamine the problem in the hope that the method may be of value in our studies of ring systems containing methylene groups.

In this paper, we present the basic equations in the same notation as that used previously (1, 3), together with the results obtained by the application of the method to methylene dichloride and to cyclopropane.

To establish the nature of the methylene group vibrations, a 'standard molecule' CH_2X_2 was first considered, in which the X atoms were assigned masses of 10^6 a.m.u. The basis set of internal displacement coordinates from which symmetry coordinates were constructed in symmetry point group C_{2v} is shown in Fig. 1.

In his choice of symmetry coordinates, King (2) preferred to retain the redundancy condition in the A_1 species which arises from the angles at the carbon atom and to remove it from the secular determinant (ref. 2, eq. [35]). In this study, it was considered to be desirable to remove this difficulty at the outset by constructing a redundant coordinate, and thereby creating a corresponding row of zeros in the **G** matrix.

The first calculations were made with the symmetry coordinates of Table I and the force field of Tables II and III. The normal coordinate matrices obtained, taken with experimental evidence, indicated that ν_1 and ν_2 in the A_1 species, and ν_6 in the B_1 species, could be regarded as group frequencies. Symmetry species A_2 and B_2 contained no group frequencies within the scope and requirements of the method (2), and so were not considered further.

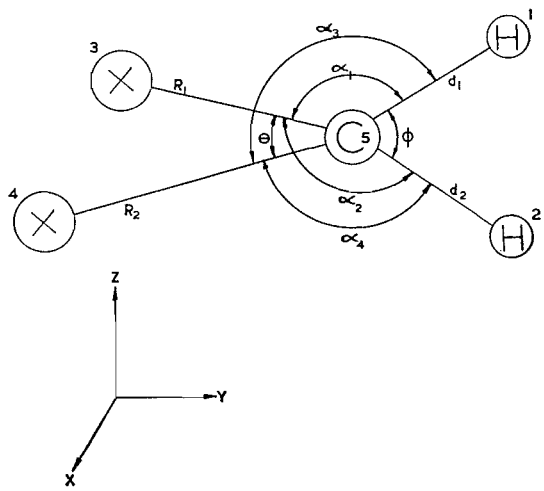

FIG. 1.

[1]All correspondence should be addressed to: Dr. T. Henshall, Department of Chemistry and Applied Chemistry, The University of Salford, Salford 5, England.

Can. J. Chem. Downloaded from www.nrcresearchpress.com by 210.87.254.42 on 09/05/12
For personal use only.

TABLE I

First trial symmetry coordinates

A_1 species	
$S_r = (\phi + \Theta + \alpha_1 + \alpha_2 + \alpha_3 + \alpha_4)/\sqrt{6}$	Redundant coordinate
$S_1 = (d_1 + d_2)/\sqrt{2}$	Group coordinate
$S_2 = (2\phi + 2\Theta - \alpha_1 - \alpha_2 - \alpha_3 - \alpha_4)/\sqrt{12}$	Group coordinate
$S_3 = (R_1 + R_2)/\sqrt{2}$	
$S_4 = (\Theta - \phi)/\sqrt{2}$	
A_2 species	
$S_5 = (\alpha_1 - \alpha_2 - \alpha_3 + \alpha_4)/2$	
B_1 species	
$S_6 = (d_1 - d_2)/\sqrt{2}$	Group coordinate
$S_7 = (\alpha_1 - \alpha_2 + \alpha_3 - \alpha_4)/2$	
B_2 species	
$S_8 = (R_1 - R_2)/\sqrt{2}$	
$S_9 = (\alpha_1 + \alpha_2 - \alpha_3 - \alpha_4)/2$	

TABLE II

The valence force field*

	d_1	d_2	$d_0\phi$	$d_0\alpha_1$	$d_0\alpha_2$	$d_0\alpha_3$	$d_0\alpha_4$	R_1	R_2	$R\Theta$
d_1	K_d	F_d	0	0	0	0	0	0	0	0
d_2		K_d	0	0	0	0	0	0	0	0
$d_0\phi$			H_ϕ	0	0	0	0	0	0	0
$d_0\alpha_1$				H_α	F_α	$F_{\alpha\alpha}$	0	$F_{R\alpha}$	$f_{R\alpha}$	0
$d_0\alpha_2$					H_α	0	$F_{\alpha\alpha}$	$F_{R\alpha}$	$f_{R\alpha}$	0
$d_0\alpha_3$			(sym.)			H_α'	F_α'	$f_{R\alpha}'$	$F_{R\alpha}'$	0
$d_0\alpha_4$							H_α'	$f_{R\alpha}'$	$F_{R\alpha}'$	0
R_1								K_R	F_R	$F_{R\Theta}$
R_2									K_R'	$F_{R\Theta}'$
R_Θ										H_Θ

*d_0, R are C—H and C—X equilibrium bond lengths respectively.

TABLE III

Force constants*

	Standard molecule	Methylene dichloride
K_d	4.95	5.04
$K_R = K_R'$	4.50	3.38
d^2H_ϕ	0.526	0.526
$d^2H_\alpha = d^2H_\alpha'$	0.729	0.693
R^2H_0	0.949	1.592
F_d	0	0
F_R	0.27	0.33
$dF_{R\alpha} = dF_R'{}_\alpha$	0.339	0.339
$df_{R\alpha} = df_R'{}_\alpha$	−0.164	−0.175
$RF_{R\alpha} = RF_R'{}_\alpha$	0.185	0.385
$d^2F_\alpha = d^2F_\alpha'$	−0.036	−0.036
$d^2F_{\alpha\alpha}$	−0.036	−0.072

*K_d, F_d, K_R, F_R are in mdyn Å^{-1}; H_α, H_ϕ, H_θ, F_α, $F_{\alpha\alpha}$ are in mdyn Å rad^{-2}; $F_{R\alpha}$, $f_{R\alpha}$ are in mdyn rad^{-1}.

TABLE IV

Frequencies for the standard methylene molecule and for methylene dichloride

	Standard molecule (cm^{-1})	Methylene dichloride (cm^{-1})		
		Complete soln.	Approximate soln.	
			1st set	2nd set
A_1 species				
ν_1	2974	3000	3001	3001
ν_2	1446	1429	1431	1431
ν_3	711	726	731	726
ν_4	0	327	268	327
B_1 species				
ν_6	3050	3076	3076	3076
ν_7	874	818	818	818

Using the force constants for the 'standard molecule' in ref. 2, the frequencies in column 1 of Table IV were obtained. Then, following the procedure described in refs. 1 and 3, a set of approximate equations was constructed to calculate the group frequencies of methylene dichloride. These are given in Table IV, column 3, and compared with the values obtained by a complete analysis of the molecule using the data of Decius (4). The agreement is seen to be satisfactory.

However, when the **A*** matrices required for the group factorization procedure were con-

Can. J. Chem. Downloaded from www.nrcresearchpress.com by 210.87.254.42 on 09/05/12
For personal use only.

structed, that for the A_1 species was found to carry large off-diagonal elements (Table V). This was considered to be a potential source of difficulty in applying the method to larger molecules (ref. 2, p. 85), and is reflected here in the poor agreement for ν_4.

TABLE V

The $\mathbf{A}^*$ matrix for the transformation $D = \mathbf{A}^* S$ in the A_1 species. (First set of symmetry coordinates.)

$\mathbf{A}_{A_1}{}^*$	S_1	S_2	S_3	S_4
D_1	−0.9986	0.0016	0.0501	−0.0175
D_2	0.0221	0.7245	0.1848	−0.6635
D_3	−0.0029	−0.6029	−0.2965	−0.7408
D_4	0.0481	−0.3340	0.9355	−0.1029

It was therefore decided to construct new symmetry coordinates for S_2 and S_4 to approximate more closely to normal modes in an effort to overcome this difficulty. The new coordinates, S_2' and S_4' given below, were constructed on the basis of the $\mathbf{L}^{-1}$ matrix of the A_1 species of methylene dichloride and the requirements of orthogonality (cf. ref. 5).

$$S_2' = \frac{1}{\sqrt{30}}(5\phi - \Theta - \alpha_1 - \alpha_2 - \alpha_3 - \alpha_4)$$

$$S_4' = \frac{1}{\sqrt{20}}(4\Theta - \alpha_1 - \alpha_2 - \alpha_3 - \alpha_4)$$

Using this new set, and the same force field as before, the transformation matrix $\mathbf{A}^*$ in $D = \mathbf{A}^* S$ for the A_1 species now assumes the form of Table VI.

TABLE VI

The $\mathbf{A}^*$ matrix in the A_1 species. (Second set of symmetry coordinates.)

$\mathbf{A}_{A_1}{}^*$	S_1	S_2'	S_3	S_4'
D_1	−0.9986	0.0146	0.0501	−0.0098
D_2'	0.0221	0.9723	0.1855	0.1411
D_3	0.0358	−0.2300	0.8667	0.4416
D_4'	−0.0324	−0.0401	−0.4612	0.8860

The matrix $\bar{\mathbf{H}} = \overline{\mathbf{GF}}$ was then calculated; the submatrix $\bar{\mathbf{H}}_{gf}$ was found to be null as required by the method, whilst $\bar{\mathbf{H}}_{gg}$ was lower triangular with the group frequency parameters, λ_g, along the diagonal.

The corrections, $\mathbf{\Phi}_{ff}$, to the force field for the framework vibrations are given in Table VII. The entries, unlike those based on the first symmetry coordinates of Table I, are relatively small.

TABLE VII

The corrections Φ_{ff} to the force field for the framework vibrations

Φ_{ff} (A_1)	S_3	S_4'
S_3	0.0843 (mdyn Å^{-1})	0.0418 (mdyn rad^{-1})
S_4'	0.0418	0.0262 (mdyn Å rad^{-2})

Φ_{ff} (B_1)	S_7
S_7	0.0026 (mdyn Å rad^{-2})

The effective mass tensor, $(\mathbf{M}^{-1})_{cc}{}^+$, whose elements are the effective inverse masses in (a.m.u.)$^{-1}$ of the carbon atoms of the methylene group required for the reduced kinetic matrix $\mathbf{G}_{ff}{}^+$, is calculated to be:

$(\mathbf{M}^{-1})_{cc}{}^+$	X_c	Y_c	Z_c
X_c	0.08326	0	0
Y_c	0	0.07097	0
Z_c	0	0	0.07438

Hence the inverse carbon masses in (a.m.u.)$^{-1}$ associated with the methylene group to be used in constructing $\mathbf{G}_{ff}{}^+$ are $\mu_{C_x}{}^+ = \mu_C = 0.08326$, $\mu_{C_y}{}^+ = 0.07097$, $\mu_{C_z}{}^+ = 0.07438$, and no correction is therefore necessary to the inverse carbon mass for motion in the x-direction in Fig. 1.

The $\widehat{\mathrm{XCX}}$ 'scissors' mode, S_4', and the 'rocking' mode, S_7, describe displacements of both the methylene carbon and hydrogen atoms. The effective inverse mass matrix $(\mathbf{M}^{-1})^+$ therefore contains cross-terms involving carbon and hydrogen atoms. The elements $(G^+)_{ii}$ of the reduced kinetic matrix with $i = 4'$ and 7 therefore require effective hydrogen masses; and the procedure for their calculation follows the description of ref. 1, p. 437, leading to the values:

$$(G^+)_{4',4'} = \frac{\mu_H{}^+}{10d^2} + \frac{2}{15}\left(\frac{5}{R} - \frac{1}{d}\right)^2 \mu_{C_y}{}^+ + \frac{5}{2R^2}\mu_X,$$

where $$\frac{\mu_H{}^+}{10d^2} = \left(\frac{5}{R} - \frac{1}{d}\right)\left(\frac{0.0186}{d} + \frac{0.0088}{R}\mu_X\right) + \frac{0.0093}{d^2} - \frac{0.0932}{Rd}\mu_X$$

$$(G^+)_{7,7} = \frac{\mu_H{}^+}{2d^2} + \frac{3\mu_R}{2R^2} + 3\left(\frac{1}{R} + \frac{1}{3d}\right)^2 \mu_{C_z}{}^+,$$

where $$\frac{\mu_H{}^+}{2d^2} = \frac{0.4958}{d^2} - \frac{0.0028}{d}\left(\frac{1}{R} + \frac{1}{3d}\right).$$

Can. J. Chem. Downloaded from www.nrcresearchpress.com by 210.87.254.42 on 09/05/12
For personal use only.

For the off-diagonal elements involving the interactions S_i ($i = 4', 7$) with any framework coordinate S_j, and for which $(G^+)_{ij} = B_i(\mathbf{M}^{-1})^+B_j^*$, the required row vectors are:

	X_3			X_4			C_5		
$B_i(\mathbf{M}^{-1})^+$	x	y	z	x	y	z	x	y	z
$B_4(\mathbf{M}^{-1})^+$	$-\mu_X\sqrt{5/2}\sqrt{3R}$	$\mu_X\sqrt{10/2}\sqrt{3R}$	0	$\mu_X\sqrt{5/2}\sqrt{3R}$	$\mu_X\sqrt{10/2}\sqrt{3R}$	0	0	a	0
$B_7(\mathbf{M}^{-1})^+$	0	0	$-\mu_X\sqrt{3/2R}$	0	0	$-\mu_X\sqrt{3/2R}$	0	0	b

$$a = \frac{-2}{\sqrt{30}}\left[\frac{5}{R} - \frac{0.0141}{d}\right]\mu_{C_y}{}^+ - \frac{0.0120}{R}\mu_X$$

$$b = \sqrt{3}\left[\frac{1}{R} + \frac{0.3404}{d}\right]\mu_{C_z}{}^+ + \frac{0.0020}{R}\mu_X$$

On this basis, it is to be noted that when the terms

$$\left(\frac{5}{R} - \frac{1}{d}\right) \quad \text{and} \quad \left(\frac{1}{3d} + \frac{1}{R}\right)$$

arise in the **G** matrix elements for the interactions between methylene group and framework vibrations, they are to be replaced respectively by

$$\left(\frac{5}{R} - \frac{0.0141}{d}\right) \quad \text{and} \quad \left(\frac{0.3404}{d} + \frac{1}{R}\right).$$

Solution of the reduced secular equation $|\mathbf{G}^+\mathbf{F}^+ - \lambda\,\mathbf{E}| = 0$ gave the values of ν_3, ν_4, and ν_7 for the framework vibration frequencies of methylene dichloride listed in Table IV, in excellent agreement with those obtained by the complete solution.

The following approximate equations apply to the group frequencies of molecules containing methylene groups.

Species A_1

$$\lambda_1 = 1.0469\Delta F_{11} + 0.0202\Delta F_{2'2'} + 5.2103$$

$$\lambda_2 = 2.1959\Delta F_{2'2'} + 0.2042\Delta F_{2'3} + 0.6002\Delta F_{2'4'} + 0.0410\Delta F_{4'4'} + 1.2322$$

Species B_1

$$\lambda_6 = 1.1027\Delta F_{66} + 0.0405\Delta F_{77} + 5.4786$$

($\Delta F_{ij} = F_{ij} - F_{ij}{}^0$, etc., where $F_{ij}{}^0$ refers to the standard methylene molecule, and $\lambda_i = 4\pi^2c^2\nu^2{}_i$). In these equations, the relevant symmetry force constants for molecules containing methylene groups are:

$$F_{11} = K_d + F_d$$

$$F_{2'2'} = \frac{1}{30}[d_0{}^2(H_\phi + 2F_\alpha + 2H_\alpha + 4F_{\alpha\alpha} + 2H_\alpha' + 2F_\alpha') + R^2H_\Theta]$$

$$F_{4'4'} = \frac{1}{10}[d_0{}^2(F_\alpha + H_\alpha + 2F_{\alpha\alpha} + H_\alpha' + F_\alpha') + 8R^2H_\Theta]$$

$$F_{2'4'} = \frac{1}{5\sqrt{6}}[d_0{}^2(F_\alpha + H_\alpha + 2F_{\alpha\alpha} + H_\alpha' + F_\alpha') - 2R^2H_\Theta]$$

$$F_{66} = K_d - F_d$$

$$F_{77} = \frac{d_0{}^2}{2}(H_\alpha + H_\alpha' - F_\alpha - F_\alpha' + 2F_{\alpha\alpha}).$$

The symmetry force constants for the standard methylene molecule are (2):

$$F_{11}{}^0 = 4.95; \quad F_{2'2'}{}^0 = 0.5572;$$
$$F_{2'4'}{}^0 = -0.0476; \quad F_{4'4'}{}^0 = 0.8903;$$
$$F_{66}{}^0 = 4.95; \quad F_{77}{}^0 = 0.7281.$$

These equations give the values for the group frequencies of methylene dichloride that are entered in the last column of Table IV; and again the agreement with the values obtained by a complete solution is extremely good.

Although the bond angles subtended at the carbon atoms in methylene dichloride and cyclopropane are very different, the results of preliminary calculations on the effect of changes in the $\widehat{HCH}$ angle on those frequencies of the methylene group that are involved in the framework vibrations indicated that the group frequency procedure might be profitably applied to the cyclopropane molecule.

Can. J. Chem. Downloaded from www.nrcresearchpress.com by 210.87.254.42 on 09/05/12
For personal use only.

TABLE VIII

Methylene group frequencies in cyclopropane

Species	Approximate description	Observed frequencies, ω (cm^{-1})	Calculated frequencies (cm^{-1})	
			Approximate	Exact
A_1'	Sym. CH stretch	3301	3339	3311
	CH_2 deformation	1479	1462	1477
A_2''	CH stretch	3194	3167	3194
E'	CH stretch	3196	3203	3198
	CH_2 deformation	1478	1475	1477
E''	CH stretch	3221	3192	3232

A normal coordinate analysis of cyclopropane has been reported (6). These authors tabulated the **G** matrices and calculated symmetry force constants, but do not give any frequencies obtained from them. Using their **G** and **F** matrices on an English-Electric KDF-9 computer gave the results of Table IX; the agreement with the observed frequencies after corrections for anharmonicity is good.

TABLE IX

Skeletal frequencies for the cyclopropane molecule*

Approximate description	ω (cm^{-1})	Calculated frequencies (cm^{-1})		
		Approximate calculation		Exact calculation
A_1' symmetric C—C stretch (ring breathing)	1188	1203	(1294)	1185
A_2'' CH_2 'rocking'	867	874		866
E' ring deformation	1051	1051	(960)	1050†
E' CH_2 'wagging'	884	868		884
E'' CH_2 'twisting'	1212	1232		1207
E'' CH_2 'rocking'	750	753		750

*Figures in parentheses correspond to the point-mass model.
†The potential energy distribution reverses this assignment due to Cyvin (6), see text.

The group frequencies for cyclopropane calculated on the basis of eq. [1] are compared with those from a complete solution in Table VIII. The framework vibrations were treated by the factorization method with the results of Table IX, which also lists the results of a complete calculation and the observed values corrected for anharmonicity. However, because the ring stretching, methylene 'wag' and 'twisting' vibrations in the cyclopropane molecule involve movements of the carbon atoms having components in both the x and y directions (Fig. 2), a more sophisticated method of introducing μ_{C_x} and μ_{C_y} into the reduced **G** matrix than that described previously (1, 3) was required. To this end, local cartesian axes were constructed on each carbon atom in the same positions as those in the "standard molecule". The inverse masses relative to these local axes are known. The inverse mass tensor, M_T^{-1}, for each methylene group in the non-local coordinate system (i.e. the reference system for the whole molecule) was then obtained from the transformation

$$M_T^{-1} = RM^{-1}R^*,$$

where R is the rotation operator which brings the local axes for a particular methylene group

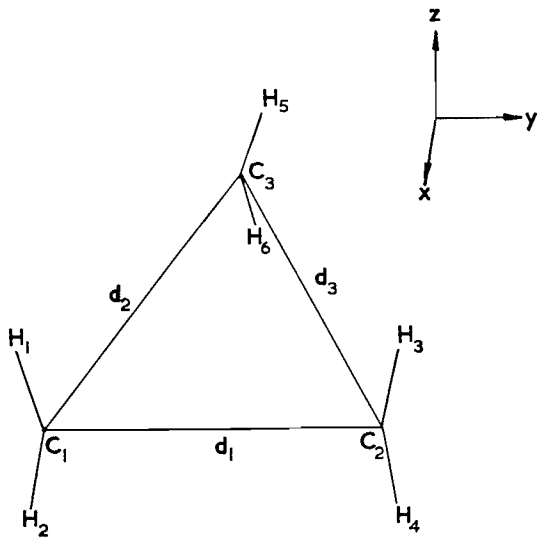

FIG. 2.

into coincidence with the directions of the axes of the molecular framework. Each carbon atom therefore has its own inverse mass tensor, and this will generally carry non-zero off-diagonal elements. The computer program for the calculation of **G** matrices described in ref. 7 has been modified to perform the required rotations on the inverse mass tensor and to calculate the reduced **G** matrix from the equation

$$G_{ij} = \sum_{n=1}^{N} B_n{}^{i} M_n{}^{-1} B_n{}^{j*},$$

where n refers to a particular atom of the N present in the molecule, and $M_n{}^{-1}$ is the 3×3 inverse mass tensor for the atom n.

The corrections to the **B** matrix elements that are necessary in the consideration of the interactions between group and skeletal vibrational modes have also been introduced into the program in a general form. The reduced hydrogen masses were subsequently introduced after inspection of the **B** matrices obtained from the computer. This overcame the need to use different hydrogen masses for different symmetry coordinates.

The **L** matrices calculated by the approximation method showed close agreement with those obtained from the complete calculation. However, it is interesting to note that a calculation of the potential energy distribution for the E' species indicates that the absorption at 1050 cm^{-1} is due almost entirely (> 99%) to the "wagging" vibration, and that at 884 cm^{-1} arises almost entirely from an antisymmetric ring deformation vibration. This is quite contrary to Cyvin's assignment (6). The "rocking" and "twisting" frequencies in the E'' species show an almost equal extent of mixing so that no assignment can be made with certainty.

Considering that no attempt has been made to account for the effect of changes in the molecular geometry on the reduced masses, the results are sufficiently encouraging for us to proceed with the application of the methods to larger ring systems containing methylene groups.

Acknowledgments

The authors thank the Council of the University of Salford for the award of a Research Demonstratorship to J. M. F., and the Staff of the Computations Laboratory for assistance with the calculations.

1. W. T. KING and B. L. CRAWFORD. J. Mol. Spectry. **5**, 421 (1960); **8**, 58 (1962).
2. W. T. KING. Ph.D. Thesis, University of Minnesota, Minneapolis, Minnesota. 1956.
3. J. H. CARTER, J. M. FREEMAN, and T. HENSHALL. J. Mol. Spectry. **20**, 402 (1966); **22**, 18 (1967).
4. J. C. DECIUS. J. Chem. Phys. **16**, 214 (1948).
5. H. TAKAHASHI, T. SHIMANOUCHI, K. FUKUSHIMA, and T. MIYAZAWA. J. Mol. Spectry. **13**, 43 (1964).
6. S. J. CYVIN. Spectrochim. Acta, **16**, 1022 (1960).
7. J. H. CARTER, J. M. FREEMAN, and T. HENSHALL. Spectrochim. Acta, **23A**, 1463 (1967).

Can. J. Chem. Downloaded from www.nrcresearchpress.com by 210.87.254.42 on 09/05/12
For personal use only.

Group vibrations and the vibrational analysis of molecules containing methylene groups. Part II. Ethylene oxide, d_4-ethylene oxide, and ethylene sulfide

J. M. FREEMAN AND T. HENSHALL[1]

Department of Chemistry and Applied Chemistry, University of Salford, Salford 5, England

Received January 19, 1968

Vibrational analyses, based on the group frequency factorization procedure of King and Crawford, are reported for ethylene oxide, d_4-ethylene oxide, and ethylene sulfide in an attempt to decide between two possible vibrational assignments for these molecules.

The results, whilst not providing an unequivocal decision between the assignments, nevertheless do suggest that the higher frequencies in the A_2 and B_2 species may be preferentially assigned to the methylene rocking modes.

Canadian Journal of Chemistry, **46**, 2135 (1968)

Can. J. Chem. Downloaded from www.nrcresearchpress.com by 210.87.254.6 on 09/05/12
For personal use only.

The infrared and Raman spectra of ethylene oxide have been extensively investigated, the most recent study being that reported by Potts (1), whose results have been used in this work and whose paper should be consulted for earlier references.

The calculations on d_4-ethylene oxide are based on the assignments by Lord and Nolin (2); those on ethylene sulfide use the most recent study by Guthrie (3).

These molecules belong to the symmetry point group C_{2v}, and the structure of the representation of the vibration frequencies other than the characteristic frequencies of the methylene group is:

$$\Gamma_v = 3A_1 + 2B_1 + 2A_2 + 2B_2.$$

There appears to be little doubt about the assignments in the A_1 and B_1 species, but those of the A_2 and B_2 modes are still controversial. Earlier workers, including Thompson and Cave (15), assigned the higher frequencies in these modes to the methylene rocking vibrations and the lower frequencies to the methylene twisting vibrations (Table IV, assignment I). These assignments have since been reversed on the basis of considerations involving group frequencies (Table IV, assignment II). A complication arises in that the A_2 fundamentals are inactive in the infrared and are difficult to observe in the Raman spectra. The band at 1300 cm^{-1} in ethylene oxide has been estimated by Potts (1) from thermodynamic data, whilst for ethylene sulfide, the band at 660 cm^{-1} observed in the Raman spectrum by Thompson and Cave (15) and assigned by them to an A_2 species has since been reassigned by Guthrie (3) to an asymmetric ring deformation mode of species B_1. There are therefore no frequencies available for the A_2 vibrational species of this compound.

It is because of the uncertainty in the vibrational assignments for these molecules that we decided to calculate a force field and potential energy distribution for the two assignments indicated in Table IV. In our iterative calculations (4) on ethylene oxide and ethylene sulfide, the frequencies of the A_2 species were included for the former, but given zero weight for the latter. No iterations were performed on d_4-ethylene oxide.

To simplify the calculations, King and Crawford's (5) group frequency factorization procedure was used to factor from the secular equations those frequencies characteristic of the methylene and deutero-methylene group vibrations. However, it has been shown (6) that whilst the factorization of the CD_2 group frequencies gives good results for the CD_2Cl_2 molecule, application of the method to d_6-cyclopropane is unsatisfactory and indicates that the method will be without success for such small ring systems as those under consideration having vibrational species which involve a CD_2 deformation and a 'ring breathing' mode. This is due mainly to the large correction, Φ_{ff}, to the force constant for the 'ring breathing' mode, and to the high degree of mixing involved in the A_1 species of d_6-cyclopropane between the 'ring breathing' and CD_2 deformational modes. The results for d_4-ethylene oxide are therefore

[1]All correspondence should be addressed to: Dr. T. Henshall, Department of Chemistry and Applied Chemistry, University of Salford, Salford 5, England.

confined to the A_2, B_2, and B_1 vibrational species.

The information necessary to construct the G_{ff}^{+} matrices for the B_1, A_2, and B_2 species for d_4-ethylene oxide is

$$(M^{-1})_{cc}^{+} = \begin{pmatrix} 0.0833 & 0 & 0 \\ 0 & 0.0546 & 0 \\ 0 & 0 & 0.0665 \end{pmatrix};$$

for the methylene rocking mode in the B_1 species (S_7) the correction to the F matrix is

$$\Phi_{ff(7,7)} = \frac{S_7}{S_7 \quad 0.0090 \text{ mdyn Å rad}^{-2}};$$

for $G_{7,7}^{+}$, $\mu_D^{+}/2d^2 = 0.2482/d^2 - 0.0028\sqrt{3}((1/R) + (1/3d))/d$; and wherever the quantity $((1/R) + (1/3d))$ occurs in an off-diagonal element of G_{ff}^{+} involving the coordinate S_7, it is to be replaced by $((1/R) + (0.9636/3d))$. The reduced G_{ff}^{+} matrices were calculated using a computer program based on that described in ref. 7.

The symmetry coordinates were similar to those described for cyclopropane by Cyvin (8) and are presented in Table I. The relevant internal coordinates are given in Fig. 1.

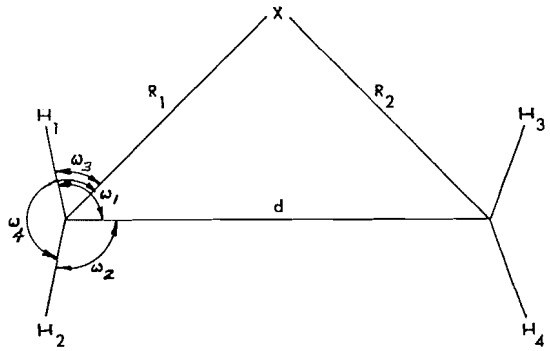

FIG. 1. The internal displacement coordinates (X = O, S).

Force field calculations on ethylene oxide have been reported by Gunthard, Messikommer, and Kohler (9), based only on the A_2 and B_2 species and a simple valence force field, and by Stone (10), using a more elaborate force field with interaction constants. The most recent calculations by Venkateswarlu and Thyagarajan (11) on ethylene oxide, d_4-ethylene oxide, and ethylene sulfide are suspect on two counts:

TABLE I

Symmetry coordinates

Vibrational species	Symmetry coordinate	Approximate description of mode
A_1	$S_1=(d+R_1+R_2)/\sqrt{3}$	Ring 'breathing'
	$S_2=(\mathcal{S}_\omega^{1}-\mathcal{S}_\omega^{2})/\sqrt{2}$	Methylene 'wag'
	$S_3=(2d-R_1-R_2)/2$	Symmetric ring deformation
B_1	$S_4=(\mathcal{S}_\omega^{1}+\mathcal{S}_\omega^{2})/\sqrt{2}$	Methylene 'wag'
	$S_5=(R_1-R_2)/\sqrt{2}$	Asymmetric ring deformation
A_2	$S_6=(\mathcal{S}_T^{1}+\mathcal{S}_T^{2})/\sqrt{2}$	Methylene 'twist'
	$S_7=(\mathcal{S}_R^{1}-\mathcal{S}_R^{2})/\sqrt{2}$	Methylene 'rock'
B_2	$S_8=(\mathcal{S}_T^{1}-\mathcal{S}_T^{2})/\sqrt{2}$	Methylene 'twist'
	$S_9=(\mathcal{S}_R^{1}+\mathcal{S}_R^{2})/\sqrt{2}$	Methylene 'rock'

one, their choice of symmetry coordinates, in which they have overlooked the linear dependence of the C—C stretching coordinate on the change in the ring angles; and the other, the large differences reported between the force constants of ethylene oxide and its deutero-analogue.

TABLE II

Group coordinates

$$\mathcal{S}_T^{i} = \tfrac{1}{2}(\omega_1^{i} - \omega_2^{i} - \omega_3^{i} + \omega_4^{i})$$
$$\mathcal{S}_\omega^{i} = \tfrac{1}{2}(\omega_1^{i} + \omega_2^{i} - \omega_3^{i} - \omega_4^{i})$$
$$\mathcal{S}_R^{i} = \tfrac{1}{2}(\omega_1^{i} - \omega_2^{i} + \omega_3^{i} - \omega_4^{i})$$
$$(i = 1,2)$$

Two definitions of force field have been used in the present work. One involved the use of valence force constants,[2] with due allowance for some degree of correlation between the four symmetry species in respect of the force constants governing methylene 'rocking', 'twisting', and 'wagging' modes; the other involved the group coordinates (12) defined in Table II, and in this case the A_2 and B_2 modes are isolated from the others.

It was found to be convenient in our calculations to apply the corrections, Φ_{ff}, to the valence force field in a slightly different, yet entirely equivalent, way to that used in ref. 13. The corrections for the CH_2 group: (1) to H_ω, H_ω', $f_{\omega\omega}$ are given by $\Phi_{ff(7,7)}/2 = 0.0013$ and (2) to f_R, f_R', f_d, f_{Rd} by $\Phi_{ff(33)}/2 = 0.042$. No correction is required for f_ω'. The force

[2]Taken from Snyder and Zerbi (14) and the force field for the standard molecule CH_2X_2 (13).

Can. J. Chem. Downloaded from www.nrcresearchpress.com by 210.87.254.6 on 09/05/12
For personal use only.

Can. J. Chem. Downloaded from www.nrcresearchpress.com by 210.87.254.6 on 09/05/12
For personal use only.

TABLE III

Force fields

Force constants		Interacting coordinates	Ethylene oxide			Ethylene sulfide		
			Assign. I and II	Assign. I	Assign. II	Assign. I and II	Assign. I	Assign. II
(1)	f_R	R_1,R_2 mdyn Å^{-1}	4.861			2.842		
	f_d	d,d ,,	4.567			4.524		
	f_R'	R_1,R_2 ,,	0.235			−0.333		
	f_{Rd}	R,d ,,	−0.314			0.086		
(2)	H_ω	ω_1^t,ω_1^t mdyn Å rad^{-2}		1.054			0.767	
	H_ω'	ω_3^t,ω_4^t ,,		0.627			0.466	
	f_ω'	ω_1^t,ω_2^t ,,		0.427			0.154	
	$f_{\omega\omega}$	ω_1^t,ω_3^t ,,		−0.073			−0.088	
	$f_{R\omega}$	R_1,ω_3^1 mdyn rad^{-1}		0.308			−0.007	
	$f_{d\omega}$	d,ω_t^t mdyn rad^{-1}		0.216			0.175	
	f_t	ω_1^1,ω_4^2 mdyn Å^{-2}		Assumed 0			0.058	
(3)	f_{rock}	$\mathcal{S}_R^t,\mathcal{S}_R^t$ mdyn Å rad^{-2}		0.554	0.259		0.421	0.333
	f'_{rock}	$\mathcal{S}_R^1,\mathcal{S}_R^2$,,		Assumed 0	0.069		Assumed 0	?
	f_{twist}	$\mathcal{S}_T^t,\mathcal{S}_T^t$,,		0.701	1.513		0.620	0.782
	f'_{twist}	$\mathcal{S}_T^1,\mathcal{S}_T^2$,,		Assumed 0	0.241		Assumed 0	?
	f_{wag}	$\mathcal{S}_\omega^t,\mathcal{S}_\omega^t$,,	1.128			0.781		
	f'_{wag}	$\mathcal{S}_\omega^1,\mathcal{S}_\omega^2$,,	−0.003			0.029		
	$f_{d,\text{wag}}$	$d,\mathcal{S}_\omega^t$ mdyn rad^{-1}	0.432			−0.392		
	$f_{R,\text{wag}}$	$R_1,\mathcal{S}_\omega^1$ mdyn rad^{-1}	−0.624			0.014		

NOTES: (1) Constants common to both force fields. (2) Constants peculiar to the valence force field. (3) Constants peculiar to group force field.

Can. J. Chem. Downloaded from www.nrcresearchpress.com by 210.87.254.6 on 09/05/12
For personal use only.

TABLE IV

Calculated and observed frequencies and potential energy distribution (p.e.d.)

	Species	Frequency (cm^{-1})	Ethylene oxide			d_4-Ethylene oxide			Ethylene sulfide		
			Obsd.	Calcd.	P.e.d.	Obsd.	Calcd.	P.e.d.	Obsd.	Calcd.	P.e.d.
	A_1	ν_1	1270	1269	$1.00S_1$	1013	—	—	1112	1120	$0.53S_1+0.33S_3$
		ν_2	1130	1128	$0.79S_2+0.21S_3$	970	—	—	1025	1024	$0.24S_1+0.77S_2$
		ν_3	877	873	$0.21S_2+0.79S_3$	755	—	—	625	635	$0.23S_1+0.68S_3$
	B_1	ν_4	1151	1152	$0.99S_1$	952	944	$0.69S_1$	1051	1067	$0.92S_1$
		ν_5	890	906	$0.99S_2$	809	823	$0.69S_2$	660	635	$0.92S_2$
	A_2	ν_6	807	799	$0.97S_1$	581	569	$0.96S_1$	?	788†(819*)	$0.81S_1$
(I)		ν_7	1300	1293	$0.97S_2$	1083	1034	$0.96S_2$	?	1216†(1082*)	$0.81S_2$
	B_2	ν_8	821	826	$0.96S_1$	577	601	$0.92S_1$	824	815†(824*)	$1.00S_1$
		ν_9	1142	1151	$0.96S_2$	896	876	$0.92S_2$	943	935†(943*)	$1.00S_2$
	A_2	ν_6	1300	1302	$0.98S_1$	1083	965	$0.92S_1$	?	—	—
(II)		ν_7	807	802	$0.98S_2$	581	621	$0.92S_2$	?	—	—
	B_2	ν_8	1142	1142	$0.96S_1$	896	867	$0.91S_1$	943	943	$0.93S_1$
		ν_9	821	819	$0.96S_2$	577	600	$0.91S_2$	824	824	$0.93S_2$

NOTE: I, II refer to the two assignments.
*Value from group force field.
†Value from valence force field.

Can. J. Chem. Downloaded from www.nrcresearchpress.com by 210.87.254.6 on 09/05/12
For personal use only.

constants $f_t, f'_{twist}, f'_{rock}$ were constrained at zero unless, by so doing, it was found to be impossible to reach good agreement with the observed frequencies.

The values of the force constants obtained from these calculations are presented in Table III, from which it is apparent that assignment I requires smaller values of interaction force constants between the methylene twisting and rocking modes. Since they necessarily involve both methylene groups, such interaction would be expected to be small. This result, taken with the impossibility in finding *valence* force constants which will simultaneously satisfy the *symmetry* force constants of both the A_2, B_2 vibrations from assignment II and the A_1 B_1 vibrations on assignment I (the assignments lead to identical results in the A_1, B_1 species), lends support to the correctness of assignment I.

The frequencies and potential energy distributions calculated from the two assignments are presented in Table IV. No calculated frequencies are given for the A_2 species of ethylene sulfide on the basis of assignment II because of the uncertainty in the force constants for this mode as obtained by simple transfer from the B_1 species. This would have assumed that the group constants, f'_{twist} and f'_{rock}, were zero, which is far from true in ethylene oxide for which more data is available.

The frequencies of d_4-ethylene oxide were not used in the iterative calculations of force constants; hence the frequencies calculated for this molecule can be used to assess the accuracy of the force field. Although it must be borne in mind that King and Crawford's method may carry quite different errors for the two isotopic species, nonetheless the frequencies calculated for d_4-ethylene oxide using the force field of ethylene oxide based on assignment I are considerably more accurate than that based on assignment II, again supporting the former.

Although the calculations do not decide unequivocally between the two possibilities, they do indicate which of the two is preferable; and, perhaps equally important, they emphasize the caution that vibrational assignments using group frequency arguments should be supported by vibrational analyses whenever possible.

Acknowledgments

The authors wish to thank the Council of the University of Salford for the award of a Demonstratorship to J. M. F., and the staff of the Computations Laboratory for help with the calculations.

1. W. J. Potts. Spectrochim. Acta, **21**, 511 (1965).
2. R. C. Lord and B. Nolin. J. Chem. Phys. **24**, 656 (1956).
3. G. B. Guthrie, Jr., D. W. Scott, and G. Waddington. J. Am. Chem. Soc. **74**, 2795 (1952).
4. J. M. Freeman and T. Henshall. J. Mol. Spectry. **25**, 101 (1968).
5. W. T. King and B. L. Crawford, Jr. J. Mol. Spectry. **5**, 421 (1960).
6. J. M. Freeman and T. Henshall. Unpublished results.
7. J. H. Carter, J. M. Freeman, and T. Henshall. Spectrochim. Acta, **23A**, 1463 (1967).
8. S. J. Cyvin. Spectrochim. Acta, **16**, 1022 (1960).
9. H. H. Gunthard, B. Messikommer, and M. Kohler. Helv. Chim. Acta, **33**, 1809 (1950).
10. S. A. Stone. J. Chem. Phys. **22**, 925 (1954).
11. K. Venkateswarlu and G. Thyagarajan. Proc. Indian Acad. Sci. Sect. A, **62**, 159 (1965).
12. H. Takahashi, T. Shimanouchi, K. Fukushima, and T. Miyazawa. J. Mol. Spectry. **13**, 43 (1964).
13. J. M. Freeman and T. Henshall. Can. J. Chem. This issue.
14. R. G. Snyder and G. Zerbi. Spectrochim. Acta, **23A**, 391 (1967).
15. H. W. Thompson and W. T. Cave. Trans. Faraday Soc. **47**, 951 (1951).

Can. J. Chem. Downloaded from www.nrcresearchpress.com by 84.22.46.98 on 09/08/12
For personal use only.

Ion–molecule reactions in formic-*d* acid and methyl formate[1]

HOWARD PRITCHARD, J. C. J. THYNNE,[2] AND A. G. HARRISON
Department of Chemistry, University of Toronto, Toronto 5, Ontario

Received January 2, 1968

The following ion–molecules reactions have been found to occur in DCOOH for ions produced by bombardment with electrons of 10–15 eV energy (all rate constants in cm^3 $molecule^{-1}$ units).

$$[a]\ DCO_2H^+ + DCO_2H \rightarrow DCO_2HD^+ + CO_2H \quad k = 1.0 \times 10^{-9}$$
$$[b]\ DCO_2H^+ + DCO_2H \rightarrow DCO_2H_2^+ + DCO_2 \quad k = 0.5_9 \times 10^{-9}$$
$$[c]\ DCO_2^+ + DCO_2H \rightarrow DCO_2HD^+ + CO_2 \quad k = 1.7_2 \times 10^{-9}$$
$$[d]\ CO_2H^+ + DCO_2H \rightarrow DCO_2H_2^+ + CO_2 \quad k = 1.9_3 \times 10^{-9}$$
$$[e]\ DCO^+ + DCO_2H \rightarrow DCO_2HD^+ + CO \quad k = 1.3_2 \times 10^{-9}$$

In methyl formate the following reactions have been identified and rate constants measured for ions formed by bombardment with electrons of 10–15 eV energy.

$$[f]\ HCO_2CH_3^+ + HCO_2CH_3 \rightarrow HCO_2CH_3H^+ + ? \quad k = 1.5_7 \times 10^{-9}$$
$$[g]\ CH_3OH^+ + HCO_2CH_3 \rightarrow HCO_2CH_3H^+ + ? \quad k = 2.5_4 \times 10^{-9}$$
$$[h]\ CH_2OH^+ + HCO_2CH_3 \rightarrow HCO_2CH_3H^+ + CH_2O \quad k = 2.0 \times 10^{-9}$$

Experiments using DCO_2CH_3 show that reaction [*f*] involves transfer of the methyl hydrogen at a rate 1.5 times that of the formyl hydrogen while reaction [*g*] involves transfer from only the methyl position of CH_3OH^+. The rate constants for all reactions are considerably higher than predicted on the basis of ion – induced dipole interactions only but are in good agreement with values calculated by including ion–dipole interactions.

Canadian Journal of Chemistry, 46, 2141 (1968)

Introduction

Although Munson (1) has shown recently that the gaseous ion–molecule reactions of oxygenated molecules lead predominately to solvated protons, little information is available on the details of the reactions occurring and their rates. Indeed, with the exception of the extensive (2–5) studies of methyl alcohol and some partial studies (5, 6) of dimethyl ether no exhaustive examination of the rates of ion–molecule reactions in oxygenated molecules has been undertaken. The present work reports a detailed study of the ionic reactions in formic-*d* acid, methyl formate, and methyl formate-*d*. The use of isotopic labelling has permitted evaluation of the relative importance of reactions involving hydrogens in the different functional positions of the molecule and/or ion.

[1]This work was supported in part by the Defence Research Board of Canada, Grant No. 9530-58, and in part by the National Research Council of Canada.

[2]Permanent address: Department of Chemistry, University of Edinburgh, Edinburgh, Scotland.

Experimental

Preliminary studies were carried out using the modified MS-2 instrument (7) to elucidate the reactions occurring. The pressure studies and the ratio plot studies reported below were carried out using the medium pressure instrument recently described (5). The pertinent operating conditions were a source temperature of approximately 100 °C, a primary ion travel distance of 0.54 cm, and a constant repeller field corresponding to 2.4 eV ion exit energy. The electron beam was pulsed and primary ion residence times were measured by the deflection technique previously described (5). The source pressures were measured directly with an MKS Baratron micromanometer.

The methyl formate used was a commercial sample of high purity while the methyl formate-*d* and formic-*d* acid were obtained from Merck, Sharp and Dohme of Canada. Low energy analysis showed the isotopic purity of the methyl formate-*d* to be ~99.5% and that of the formic-*d* acid to be ~98%.

Results and Discussion

Formic-d Acid (DCOOH)

Figure 1 shows a typical pressure plot obtained for formic-*d* acid at 12 eV nominal electron energy and 2.4 eV ion exit energy. At the reduced electron energy only the DCO^+, DCO_2^+,

Can. J. Chem. Downloaded from www.nrcresearchpress.com by 84.22.46.98 on 09/08/12
For personal use only.

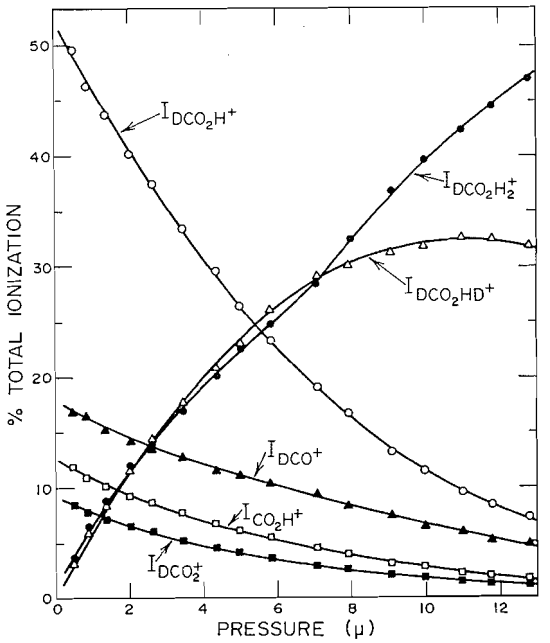

FIG. 1. Fractional ion intensities versus pressure, DCOOH.

and CO_2H^+ ions are significant fragment ions.[3] All fragment ions in addition to the parent ion are reactive, the only detectable products being $DCO_2H_2^+$ and DCO_2HD^+. These results are in agreement with Munson (1) who reported that in HCO_2H all ions reacted to give the protonated species. The rate constants for the individual reactions [1] to [4] were obtained from the slopes of the appropriate log $I/\sum$ versus [M] plots, where $I/\sum$ is the normalized ion current (fraction of total ionization) and [M] is the molecular concentration (molecules cm^{-3}) in the ion source. The rate constants (units: cm^3 $molecule^{-1}$ s^{-1}) are the average of four separate determinations.

$$[1]\quad DCO_2H^+ + DCO_2H \begin{cases} \rightarrow DCO_2HD^+ + COOH \\ \rightarrow DCO_2H_2^+ + DCO_2 \end{cases}$$

$$k_{total} = 1.5_9 \pm 0.1 \times 10^{-9}$$

$$[2]\quad DCO_2^+ + DCO_2H \rightarrow DCO_2HD^+ + CO_2$$

$$k = 1.7_2 \pm 0.1 \times 10^{-9}$$

$$[3]\quad CO_2H^+ + DCO_2H \rightarrow DCO_2H_2^+ + CO_2$$

$$k = 1.9_3 \pm 0.1 \times 10^{-9}$$

[3]The appearance potentials of the DCO_2^+ and CO_2H^+ ions were found to be 12.4 ± 0.1 and 12.8 ± 0.1 eV, respectively, leading to $\Delta H_f(DCO_2^+) = 143$ kcal/mole and $\Delta H_f(CO_2H^+) = 153$ kcal/mole.

$$[4]\quad DCO^+ + DCO_2H \rightarrow DCO_2HD^+ + CO$$

$$k = 1.3_2 \pm 0.1 \times 10^{-9}$$

Reaction [1] may lead to either the $DCO_2H_2^+$ or DCO_2HD^+ ions. To establish the relative importance of the two reactions we need note that reactions [2] to [4] involve no ambiguity in the products, since each can lead only to a specific product. The contribution of each of these reactions was subtracted from the overall yield of the DCO_2HD^+ and $DCO_2H_2^+$ ions. The resultant yields are plotted in Fig. 2 as a function of the DCO_2H^+ reacted. Each plot is linear in the initial region, the slope giving the fractional yield of the secondary ion from reaction [1]. Four determinations gave the average yields 63 ± 1% $DCO_2H_2^+$ and 37 ± 1% DCO_2HD^+, indicating a preference for transfer of the hydroxyl hydrogen over the formyl hydrogen. It is also noted both from Fig. 1 and Fig. 2 that at higher conversions the yield of DCO_2HD^+ decreases while that of $DCO_2H_2^+$ increases. This is presumably due to the rapid proton transfer reaction

$$[5]\quad DCO_2HD^+ + DCO_2H \rightarrow DCOOD + DCO_2H_2^+.$$

The net effect of this reaction is to convert the DCO_2HD^+ ion to the $DCO_2H_2^+$ ion. (The equivalent reaction [5] involving D^+ transfer leads to the same ionic species as the reactant and is therefore not detectable.) A similar reaction is considered (4) to be responsible for the decrease in the yield of CD_3OHD^+ in CD_3OH at high pressures.

Methyl Formate and Methyl Formate-d

Figure 3 shows a typical pressure plot obtained at 2.4 eV ion exit energy and 10 eV nominal

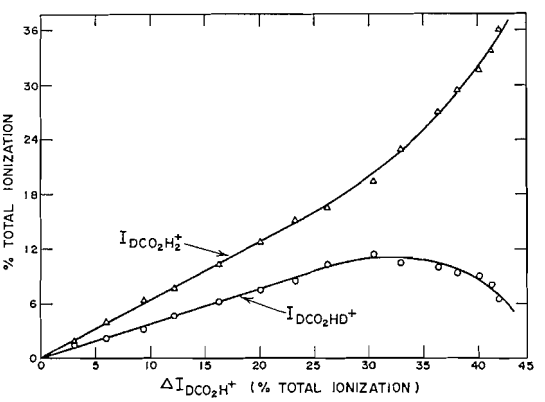

FIG. 2. Yield of DCO_2HD^+ and $DCO_2H_2^+$ as a function of $DCOOH^+$ reacted.

Can. J. Chem. Downloaded from www.nrcresearchpress.com by 84.22.46.98 on 09/08/12
For personal use only.

electron energy for the methyl formate system. The molecule ion, $HCO_2CH_3^+$, and the fragment ion CH_3OH^+ intensities decrease rapidly with pressures while that for the CH_2OH^+ ion shows initially a slight increase followed by a decrease, indicating that an ion of *m/e* 31 is formed in the initial reactions in minor yield. The major product is the protonated species $HCO_2CH_3H^+$ with $CH_3OH_2^+$ being formed to a minor extent and reacting further. The reaction forming $CH_3OH_2^+$ was not positively identified but presumably involves hydrogen abstraction from the neutral molecule by CH_3OH^+. From the semi-logarithmic plots the following rate constants for disappearance of the primary ions were determined, each value being the average of three determinations.

[6] $HCO_2CH_3^+ + HCO_2CH_3 \rightarrow HCO_2CH_3H^+ + ?$
$k = 1.5_7 \pm 0.1 \times 10^{-9}$ cm^3 molecule^{-1} s^{-1}

[7] $CH_3OH^+ + HCO_2CH_3 \rightarrow HCO_2CH_3H^+ + ?$
$k = 2.5_4 \pm 0.1 \times 10^{-9}$ cm^3 molecule^{-1} s^{-1}

[8] $CH_2OH^+ + HCO_2CH_3 \rightarrow HCO_2CH_3H^+ + CH_2O$
$k = 2.0 \pm 0.2 \times 10^{-9}$ cm^3 molecule^{-1} s^{-1}

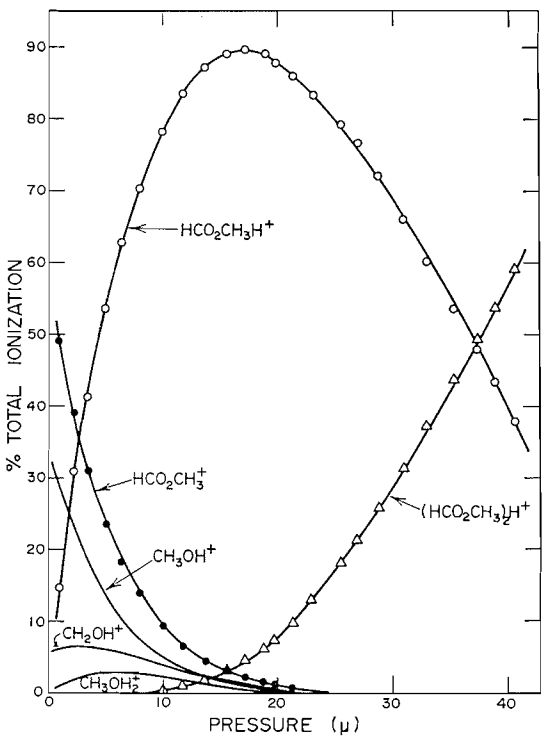

FIG. 3. Fractional ion intensities versus pressure, HCO_2CH_3.

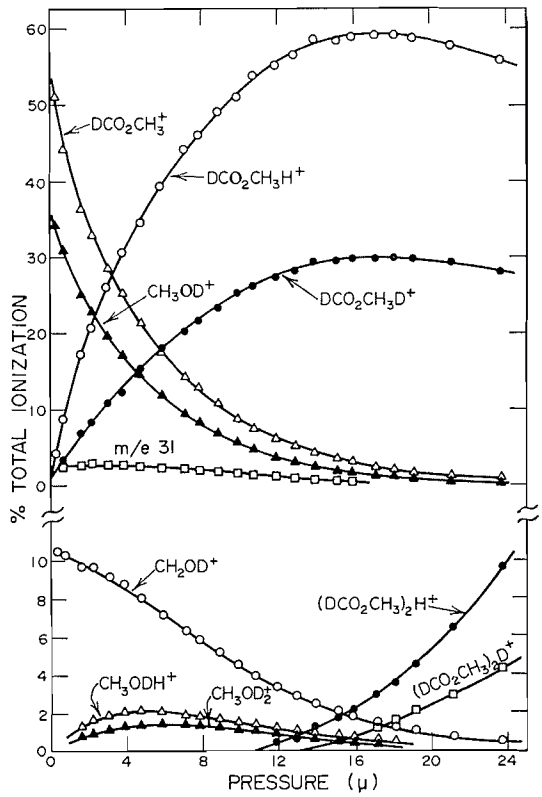

FIG. 4. Fractional ion intensities versus pressure, DCO_2CH_3.

Due to the formation of CH_2OH^+ to a minor extent the initial regions of the semi-log plot were not linear and the rate constant was calculated from the linear region at higher pressures. The protonated species reacts further to form the disolvated proton $(HCO_2CH_3)_2H^+$ (see Fig. 3) and it was confirmed that the fractional abundance of this ion depended on the third power of the source pressure, as expected since the product requires collisional stabilization.

Reaction [6] may involve transfer of either the methyl hydrogen or the formyl hydrogen (either as a proton or neutral species) while reaction [7] may involve transfer (as a proton) of either the hydroxyl or methyl hydrogen. By analogy with the reaction of CH_2OH^+ with methanol (3) one would expect reaction [8] to involve transfer of only the hydrogen (i.e. proton) bound to oxygen. To determine the relative importance of the reactions involving transfer of the differing hydrogens the ion–molecule reactions were studied in DCO_2CH_3. Figure 4 shows a typical plot of the ionic intensities (% total ionization) as a

Can. J. Chem. Downloaded from www.nrcresearchpress.com by 84.22.46.98 on 09/08/12
For personal use only.

function of pressure for the ions present at approximately 10 eV nominal electron energy. At this electron energy the only significant primary ions are $DCO_2CH_3^+$, CH_3OD^+, and CH_2OD^+. As expected both the $DCO_2CH_3H^+$ and $DCO_2CH_3D^+$ ions (and similar disolvated ions) are found as products, while the $CH_3OH_2^+$ ions of the unlabelled system appears as both CH_3ODH^+ and $CH_3OD_2^+$. There is definite evidence for formation of an ion at *m/e* 31 in minor yield and also at *m/e* 32 since the shape of the CH_2OD^+ curve is abnormal in the initial region. The overall rate constants for disappearance of the primary ions were found to be as follows (average of three runs).

[9] $DCO_2CH_3^+ + DCO_2CH_3 \rightarrow$ products

$k = 1.6_5 \pm 0.1 \times 10^{-9}$ cm^3 molecule^{-1} s^{-1}

[10] $CH_3OD^+ + DCO_2CH_3 \rightarrow$ products

$k = 2.4_1 \pm 0.1 \times 10^{-9}$ cm^3 molecule^{-1} s^{-1}

[11] $CH_2OD^+ + DCO_2CH_3 \rightarrow$ products

$k = 1.9 \pm 0.2 \times 10^{-9}$ cm^3 molecule^{-1} s^{-1}

As for the similar ion in HCO_2CH_3 the logarithmic plot for CH_2OD^+ was not linear in the initial regions and the rate constant was evaluated from the linear portion at higher pressures. The total disappearance rate constants are in good agreement with those found for the similar reactions in the undeuterated system.

It was not possible with the present instrumentation to work under conditions where only the $DCO_2CH_3^+$ ion was present as a primary ion. Consequently the relative contributions of D versus H transfer in reactions [9] and [10] were determined from ratio plots at constant pressure. It has been observed (3) that the CD_2OH^+ ion reacts with CD_3OH to transfer only H^+. A similar specificity would be expected in the present case and would result in reaction [11] producing only $DCO_2CH_3D^+$ as a product. Consequently we may conclude that $DCO_2CH_3H^+$ is produced in significant amounts only by the following reactions.

[9*a*] $DCO_2CH_3^+ + DCO_2CH_3 \rightarrow DCO_2CH_3H^+ + DCO_2CH_2$

[10*a*] $CH_3OD^+ + DCO_2CH_3 \rightarrow DCO_2CH_3H^+ + CH_2OD$

For the higher pressures used in the medium pressure instrument the usual ratio plot equations (8) must be modified since significant conversion of reactants to products occurs. It can be shown that for the two concurrent reactions [9] and [10] the product ion intensity is given by

$$[12]\quad I_{DCO_2CH_3H^+} = \frac{k_{9a}}{k_9}(e^{-k_9[M]t_9} - 1) \times I_{DCO_2CH_3^+} + \frac{k_{10a}}{k_{10}}(e^{-k_{10}[M]t_{10}} - 1)I_{CH_3OD^+},$$

where I_{X^+} is the measured current for ionic species X^+, k_{9a} and k_{10a} are the rate constants for reactions [9*a*] and [10*a*] respectively, and k_9 and k_{10} are the total disappearance rate constants for $DCO_2CH_3^+$ and CH_3OD^+ respectively, where t_9 and t_{10} are the ion source residence times for the two ions and [M] is the concentration of neutral species. Equation [12] may be divided by either $I_{DCO_2CH_3^+}$ or $I_{CH_3OD^+}$ to give two complimentary ratio plot eqs. [13] and [14] similar to those derived for the case of low conversion.

$$[13]\quad \frac{I_{DCO_2CH_3H^+}}{I_{DCO_2CH_3^+}} = \frac{k_{9a}}{k_9}(e^{-k_9[M]t_9} - 1) + \frac{k_{10a}}{k_{10}}(e^{-k_{10}[M]t_{10}} - 1)\frac{I_{CH_3OD^+}}{I_{DCO_2CH_3^+}}$$

$$[14]\quad \frac{I_{DCO_2CH_3H^+}}{I_{CH_3OD^+}} = \frac{k_{9a}}{k_9}(e^{-k_9[M]t_9} - 1) \times \frac{I_{DCO_2CH_3^+}}{I_{CH_3OD^+}} + \frac{k_{10a}}{k_{10}}(e^{-k_{10}[M]t_{10}} - 1)$$

Equations [13] and [14] predict straight lines when the appropriate ion current ratios are plotted, the slope of one plot being equal to the intercept of the other. Typical results are shown in Fig. 5 for a constant ion source concentration $[M] = 7.0_4 \times 10^{13}$ molecules cm^{-3}. The primary ion current ratios were varied by changing the electron energy in the range 10 to 15 V nominal. Satisfactory straight lines are obtained, the slopes and intercepts of the complementary plots being in good agreement. Since k_9, k_{10}, t_9, t_{10}, and [M] are all known, k_{9a} and k_{10a} may be evaluated. Three separate determinations led to $k_{9a} = 0.84 \pm 0.06 \times 10^{-9}$ cm^3 molecule^{-1} s^{-1} and $k_{10a} = 2.4_9 \pm 0.1 \times 10^{-9}$ cm^3 molecule^{-1} s^{-1}. Since k_{10a} is, within experimental error, equal to the total rate constant for disappearance of CH_3OD^+, k_{10}, one must conclude that reaction [10] involves transfer of H^+ only, i.e. the rate of the competing reaction [10*b*] is negligibly small.

[10*b*] $CH_3OD^+ + DCO_2CH_3 \rightarrow DCO_2CH_3D^+ + CH_3O$

Can. J. Chem. Downloaded from www.nrcresearchpress.com by 84.22.46.98 on 09/08/12
For personal use only.

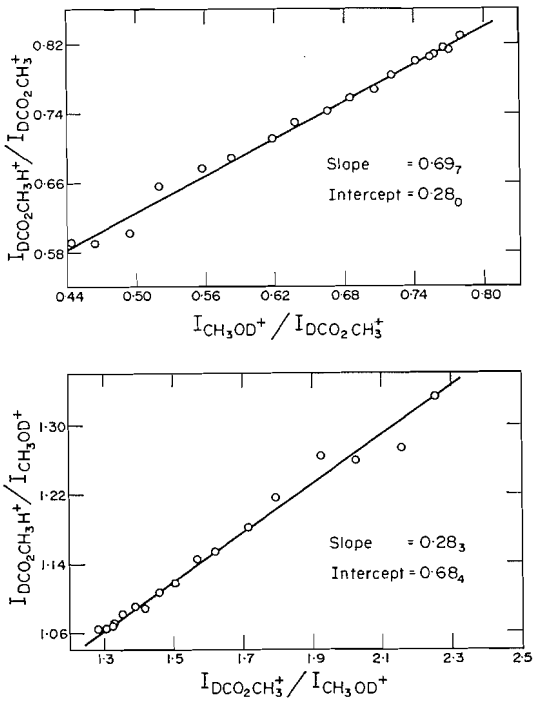

FIG. 5. Ratio plot for formation of $DCO_2CH_3H^+$.

Consequently we may assume that only the two reactions [9*b*] and [11] contribute significantly to formation of $DCO_2CH_3D^+$.

[9*b*] $DCO_2CH_3^+ + DCO_2CH_3 \rightarrow DCO_2CH_3D^+ + CO_2CH_3$

[11] $CH_2OD^+ + DCOOCH_3 \rightarrow DCO_2CH_3D^+ + CH_2O$

The ratio plot equations for these two concurrent reactions (assuming reaction of CH_2OD^+ leads only to $DCO_2CH_3D^+$) may be written as follows.

$$[15]\quad \frac{I_{DCO_2CH_3D^+}}{I_{DCO_2CH_3^+}} = \frac{k_{9b}}{k_9}(e^{-k_9[M]t_9} - 1) + (e^{-k_{11}[M]t_{11}} - 1)\frac{I_{CH_2OD^+}}{I_{DCO_2CH_3^+}}$$

$$[16]\quad \frac{I_{DCO_2CH_3D^+}}{I_{CH_2OD^+}} = \frac{k_{9b}}{k_9}(e^{-k_9[M]t_9} - 1) \times \frac{I_{DCO_2CH_3^+}}{I_{CH_2OD^+}} + (e^{-k_{11}[M]t_{11}} - 1)$$

A typical plot of the data obtained at a constant molecular concentration of 7.38×10^{13} molecules cm^{-3} is shown in Fig. 6. Satisfactory straight lines are obtained, the slopes and intercepts of the complementary plots being in good agreement. The average of three separate runs gave $k_{11} = 1.8_6 \pm 0.1 \times 10^{-9}$ cm^3 $molecule^{-1}$ s^{-1} and $k_{9b} = 0.56 \pm 0.06 \times 10^{-9}$ cm^3 $molecule^{-1}$ s^{-1}. The value of k_{11} determined from the ratio plot is in good agreement with the value of $1.9 \pm 0.2 \times 10^{-9}$ cm^3 $molecule^{-1}$ s^{-1} determined from the pressure plots. The sum $k_{9a} + k_{9b} = 1.4 \pm 0.12 \times 10^{-9}$ cm^3 $molecule^{-1}$ s^{-1} is in reasonable agreement with $k_9(\text{total}) = 1.6_5 \pm 0.1 \times 10^{-9}$ cm^3 $molecule^{-1}$ s^{-1} determined from the pressure plots.

In summary the ratio plots show that CH_3OD^+ transfers exclusively an H^+ to the formate while the reaction of $DCOOCH_3^+$ with $DCOOCH_3$ involves both H transfer and D transfer in the ratio 1.5:1. The results for reaction [10] are in contrast to the methanol self-reaction where transfer of both the methyl and hydroxyl hydrogen occur; however, the self-reaction may involve both atom abstraction and hydron transfer reactions, whereas in the present case the reaction of CH_3OD^+ involves hydron transfer only. The results obtained indicate that the ion transfer and hydrogen transfer

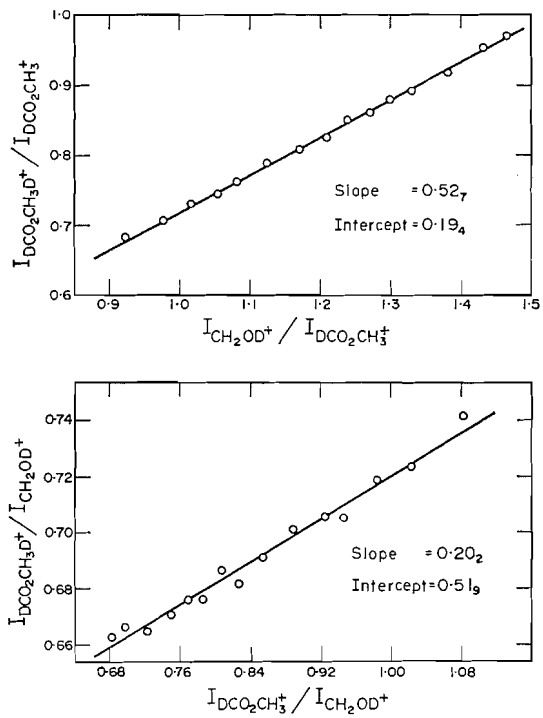

FIG. 6. Ratio plot for formation of $DCO_2CH_3D^+$.

TABLE I

Comparison of experimental and calculated rate constants (2.4 eV ion exit energy)

Reaction	k(expt.) ($\times 10^9$ cm^3 molecule^{-1} s^{-1})	k(calcd.) ($\times 10^9$ cm^3 molecule^{-1} s^{-1}) Ion – induced dipole	Ion – dipole included
$DCO_2H^+ + DCO_2H$	1.5_9	0.86	1.63
$DCO_2^+ + DCO_2H$	1.7_2	0.86	1.64
$CO_2H^+ + DCO_2H$	1.9_3	0.87	1.64
$DCO^+ + DCO_2H$	1.3_2	0.97	1.79
$HCO_2CH_3{}^+ + HCO_2CH_3$	1.5_7	0.97	1.77
$CH_3OH^+ + HCO_2CH_3$	2.5_4	1.16	2.05
$CH_2OH^+ + HCO_2CH_3$	2.0	1.17	2.07

reactions involving methanol will show considerable difference in the selectivity of the hydrogens involved. The reaction involving the parent ion in the methyl formate-*d* clearly can occur by both the ion transfer and atom transfer mechanism, with the result that no information can be obtained as to the specificity in the separate types of reactions.

Comparison with Theory

Table I compares the experimental rate constants for the formic-*d* acid and methyl formate systems with rate constants calculated from the simple collision theory considering ion–induced dipole interactions only (9) and including ion–dipole interactions (5). The experimental rate constants are approximately a factor of two greater than those calculated on the basis of the induced dipole interaction only, indicating that ion – permanent dipole interactions are important. Indeed the rate constants calculated from the simple theory including dipole terms are in good agreement with the experimental at least in this energy range. However, as pointed out previously (5) such agreement does not extend to thermal ion energies.

Acknowledgment

J. C. J. T. gratefully acknowledges financial support from the Ramsey Memorial Fellowship Trust.

1. M. S. B. Munson. J. Am. Chem. Soc. **87**, 5313 (1965).
2. K. R. Ryan, L. Sieck, and J. H. Futrell. J. Chem. Phys. **41**, 111 (1964).
3. J. C. J. Thynne, F. K. Amenu-Kpodo, and A. G. Harrison. Can. J. Chem. **44**, 1655 (1966).
4. D. J. Hyatt, E. A. Dodman, and M. J. Henchman. Advan. Chem. Ser. **58**, 131 (1966).
5. S. K. Gupta, E. G. Jones, A. G. Harrison, and J. J. Myher. Can. J. Chem. **45**, 3107 (1967).
6. A. G. Harrison, A. Ivko, and T. W. Shannon. Can. J. Chem. **44**, 1351 (1966).
7. T. W. Shannon, F. Meyer, and A. G. Harrison. Can. J. Chem. **43**, 159 (1965).
8. T. W. Shannon and A. G. Harrison. J. Chem. Phys. **43**, 4201 (1965).
9. G. Giomousis and D. P. Stevenson. J. Chem. Phys. **29**, 294 (1958).

Can. J. Chem. Downloaded from www.nrcresearchpress.com by 84.22.46.98 on 09/08/12
For personal use only.

Can. J. Chem. Downloaded from www.nrcresearchpress.com by 210.87.254.40 on 09/05/12
For personal use only.

Nuclear magnetic resonance studies of ketone.BF_3 complexes. I. Exchange reactions in methylene chloride solution

R. J. GILLESPIE AND J. S. HARTMAN[1]
Department of Chemistry, McMaster University, Hamilton, Ontario

Received December 12, 1967

^1H and ^{19}F n.m.r. studies of BF_3 adducts of some simple methyl ketones in methylene chloride solution have led to the following conclusions. (1) Only 1:1 adducts are formed which are not appreciably dissociated. (2) The down-field shifts of the proton resonances caused by complexation with BF_3 are essentially independent of the ketone and depend only on the distance of the proton from the carbonyl group. (3) BF_3 exchange is rapid on the n.m.r. time scale at room temperature, but the exchange process can be slowed sufficiently by lowering the temperature that separate signals due to free and complexed species can be observed. (4) Collapse of the ^{10}B–^{11}B isotope shift with increasing temperature showed that a second chemical exchange process, which exchanges fluorine among boron atoms, occurs in addition to the process of rapid breaking and re-forming of donor–acceptor bonds. A possible mechanism for this fluorine scrambling reaction is discussed.

Canadian Journal of Chemistry, 46, 2147 (1968)

Introduction

High-resolution nuclear magnetic resonance spectroscopy is a convenient and versatile technique for the study of donor–acceptor complexes of boron trifluoride in solution. Complexation shifts, resulting from changes in screening of ^1H, ^{19}F, or ^{11}B nuclei, provide a measure of changes in electronic structure on complex formation. Changes in charge density should be greatest at the site of the donor–acceptor bond but can be significant at other sites in the complex due to inductive and mesomeric effects. Thus proton complexation shifts in a saturated Lewis base normally attenuate rapidly with increasing distance from the donor site (1, 2), but are still observable even for protons which are several bonds removed. Complexation shifts have been used as a measure of relative strengths of the donor–acceptor interaction in series of donor and acceptor molecules (3–8). In a number of cases room temperature spectra of mixtures of oxygen donors and BF_3, in which [base] $>$ [BF_3], have only a single set of peaks rather than separate sets arising from free and complexed base, indicating rapid breaking and re-forming of donor–acceptor bonds (1, 2, 6, 8–10). Similar exchange averaging has been observed in room temperature ^{19}F spectra of solutions in which [base] $<$ [BF_3] (11) and of solutions containing more than one species of base (12, 13). In some cases the separate sets of peaks have been observed at low temperatures and the relative areas of the peaks then allow a direct determination of the relative amounts of species in solution, and hence of the equilibrium distribution of Lewis acid among donors (12, 13). Even when separate resonances arising from the different species are not visible as a result of rapid exchange, it may be possible to obtain equilibrium constants from chemical shift data (1, 6, 13). In several cases kinetic studies have been carried out in the temperature range in which signal shapes are dependent on donor–acceptor bond lifetimes, and activation energies for BF_3 rearrangement calculated (2, 9, 11, 13). Such studies by Rutenberg and co-workers (13) have shown that different mechanisms of exchange predominate in mixtures of different relative proportions of ethers and BF_3.

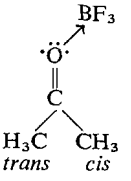

1

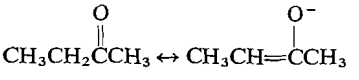

2*a* 2*b*

The first reported n.m.r. investigation of a complex between a ketone and a boron trihalide was an attempt by Lappert (14) to observe separate methyl resonances of the acetone.BF_3 complex due to methyl groups *cis* and *trans* to BF_3, as in **1**. He was unable to observe separate signals even at $-60°$ and postulated a rapid

[1]Present address: Physical Chemistry Laboratory, South Parks Road, Oxford, England.

Can. J. Chem. Downloaded from www.nrcresearchpress.com by 210.87.254.40 on 09/05/12
For personal use only.

exchange of BF_3 to account for this. An attempt to study ketone.BF_3 complexes by n.m.r. was abandoned because of difficulties in obtaining pure adducts (1). Gates and Mooney (15) investigated the small coupling between α- and α′-protons across the carbonyl group in methyl ethyl ketone and reported that this coupling increases by a factor of three when the ketone is complexed with BF_3. This increase was attributed to an increased contribution from mesomeric structures such as **2***b*. Gates, McLauchlan, and Mooney (7) have claimed that the relative acid strengths of the boron trihalides towards complexation with benzophenone correspond to the relative magnitudes of the ^{11}B complexation shifts of the trihalides. Taft and co-workers (16) have recently utilized ^{19}F n.m.r. to study complexation of *p*-fluoro-*m*′- and *p*′-substituted benzophenones with the boron trihalides. The chemical shift of the *p*-fluorine atom was used to measure π-charge density at the carbonyl carbon; in some cases the complexation shifts were used to successfully predict enthalpies of complexation.

Kaplan and Weisleder have reported the proton spectra of adducts of α-chloropinacolone (**3**) and α-bromopinacolone with the boron trihalides (17). The 1:1 BF_3 adduct, which gave a simple proton spectrum in which the ketone resonances were shifted to low field, was postulated to be a normal donor–acceptor complex. The adducts with BCl_3 and BBr_3, however, gave an AB coupling pattern for the methylene resonance. This requires the presence of an asymmetric center in the molecule, which can only be explained readily if the adducts have the structure **4**. Collapse of the AB pattern at higher temperatures was interpreted in terms of reversible addition of boron trihalide across the double bond.

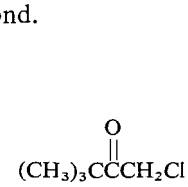

3

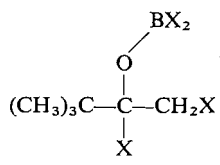

4

The low-temperature ^1H and ^{19}F spectra of acetone.BF_3 have been reported in connection with our recent study of $H_2O.BF_3$ in which acetone was used as the solvent (18). The ^{19}F spectrum of acetone.BF_3 was found to be split by a ^{10}B–^{11}B isotope shift of 0.066 p.p.m.; this splitting was clearly visible as there were no interfering splittings due to coupling with protons or boron. In that study we observed that BF_3 causes decomposition of acetone at room temperature, and hence the work was carried out entirely at low temperatures. Solutions of simple ketones and BF_3 in methylene chloride have been found to be much more stable and show little decomposition even over extended periods of time at room temperature. The stability of the complexes in this solvent facilitated the present n.m.r. study of the complexes and their exchange reactions.

Results and Discussion

BF_3 Exchange: Breaking and Re-forming of Donor–Acceptor Bonds

Proton Spectra

Room temperature proton spectra of methylene chloride solutions of simple ketones and BF_3, in various molar ratios, contain a single set of resonances corresponding to the spectrum of the ketone. The chemical shifts of the ketone peaks with respect to internal tetramethylsilane (TMS) vary linearly with the ratio [BF_3]/[ketone] as the relative proportion of BF_3 is increased up to the ratio 1:1, as is shown in Fig. 1 for the four ketones studied. Since separate resonances were not observed for free and complexed ketone in mixtures in which [ketone] > [BF_3], in spite of the considerable chemical shift differences between these species, it is evident that a rapid exchange of BF_3 occurs among donor molecules. The absence of further changes in chemical shifts as BF_3 is added beyond 1:1 proportions indicates that the additional BF_3 does not complex; in accord with previous studies it appears that only 1:1 complexes are formed between ketones and BF_3. The linearity of the plots, with a sharp break corresponding to 1:1 proportions, shows that there can be no more than a small degree of dissociation of the complex. For methyl isopropyl ketone and pinacolone the break in the plot appears to occur when somewhat more BF_3 than ketone is present. This may arise from nonideal behavior of the vapor of these ketones, leading to condensation into the n.m.r. sample tubes of greater amounts than those recorded.

Table I shows that the low-field complexation shift is almost three times as large for α- as for

Can. J. Chem. Downloaded from www.nrcresearchpress.com by 210.87.254.40 on 09/05/12
For personal use only.

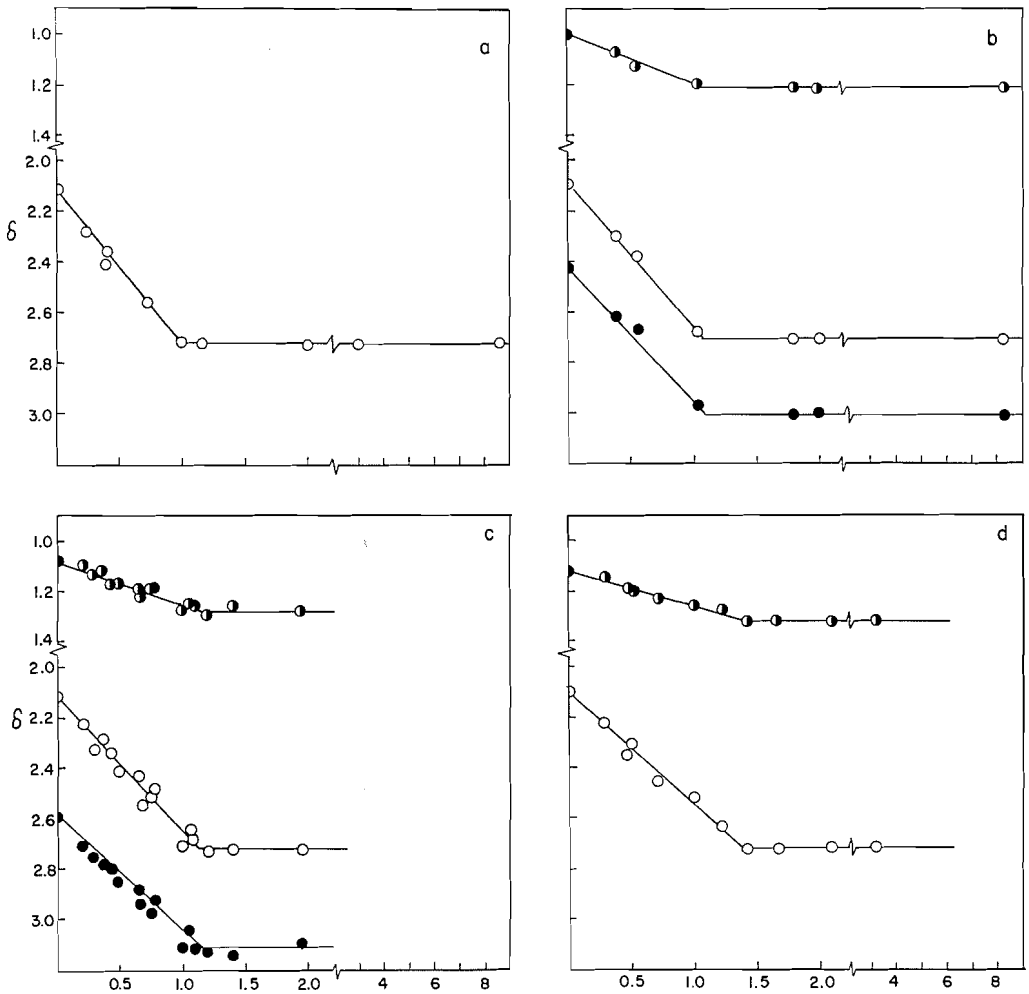

FIG. 1. Variation of ketone ^1H chemical shifts with the BF_3/ketone ratio: (*a*) acetone, (*b*) methyl ethyl ketone, (*c*) methyl isopropyl ketone, (*d*) pinacolone. (◑) β-Methyl, (○) α-methyl, (●) α-methylene and α-methine.

β-protons, and is essentially independent of the ketone. This is consistent with the shift being due simply to a decrease in electron density at the protons arising from inductive withdrawal of electrons into the carbonyl group by the boron trifluoride. The coupling constant within the ethyl and isopropyl groups, $J_{\alpha\beta}$, is practically unaffected by complexation. This contrasts with the behavior of the small coupling between α- and α′-protons across the carbonyl carbon which in methyl ethyl ketone increases by a factor of three on complex formation with BF_3 (15). The 0.59 p.p.m. complexation shift of acetone, which was found to be essentially independent of temperature, does not agree with the value of 0.32 p.p.m. at −70° previously reported by Lappert (14) for a solution in the same solvent. However, the complexation shifts obtained for methyl ethyl ketone agree with the values obtained by Gates and Mooney (15).

Only a single set of ketone resonances could be observed at −50° in any of the samples studied. At −90°, however, each sample which contained fewer moles of BF_3 than of ketone yielded a spectrum containing one set of peaks with chemical shifts corresponding to those of the free ketone and a second set with chemical shifts corresponding to those of the 1:1 complex

TABLE I

Proton shifts to low field, and changes in $J_{\alpha\beta}$, on complexation of ketones with BF_3

	Proton complexation shifts (p.p.m.)				$J_{\alpha\beta}$ (Hz)	
	α-CH_3	α-CH_2	α-CH	β-CH_3	Free	Complexed
Acetone	0.59	—	—	—	—	—
Methyl ethyl ketone	0.60	0.60		0.21	7.0	6.6
Methyl isopropyl ketone	0.61	—	0.54	0.21	7.0	7.1
Pinacolone	0.61	—	—	0.21	—	—

(Fig. 2). The relative areas of the two sets of peaks varied in the expected manner, the "free ketone" set decreasing in size as the relative concentration of BF_3 increased towards 1:1 proportions. Integration of the peak areas obtained from acetone and methyl ethyl ketone solutions having a BF_3/ketone ratio of 0.5 showed that the areas of corresponding "free" and "complexed" peaks were equal, within experimental error.

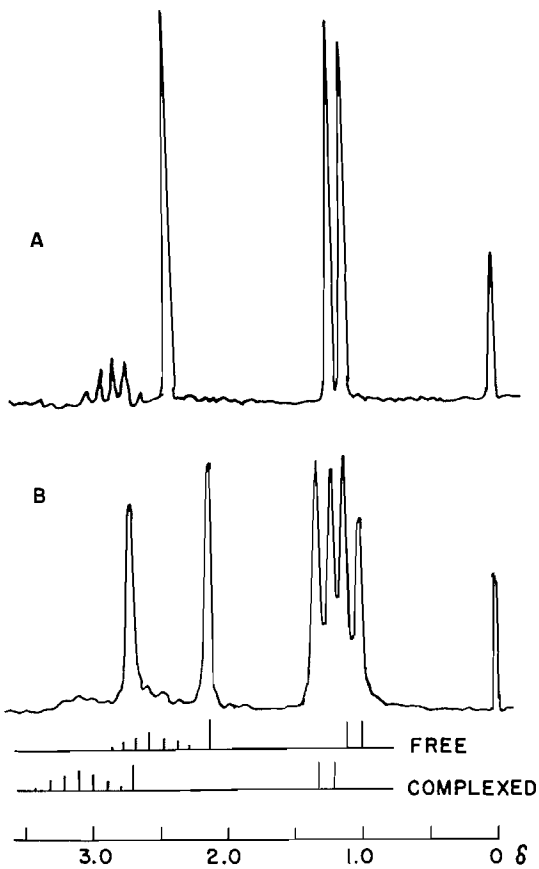

FIG. 2. Proton spectra of a methylene chloride solution of methyl isopropyl ketone and BF_3, in the molar ratio 2:1: (A) room temperature; (B) −90°.

No peaks due to free ketone were observed at −90° for samples in which [ketone] ≤ [BF_3]. These results confirm that dissociation of the 1:1 complexes is negligible.

At temperatures above −90°, samples in which [ketone] > [BF_3] yielded spectra in which the separate peaks due to free and complexed ketone were partially collapsed due to moderately rapid chemical exchange. Similar samples containing different ketones gave very similar coalescence temperatures. Since the magnitudes of the complexation shifts are also similar (Table I), it seems that the rate of BF_3 exchange is similar for all the ketones studied.

The changes in signal shape with temperature were utilized over almost the entire range of signal shapes in a kinetic study of BF_3 exchange in a solution of acetone and BF_3 of relative proportions 2:1 (0.30 *M* and 0.15 *M*). A least squares calculation of the activation energy gave a value of 11.1 kcal/mole, but the error in this value may be as large as ±3 kcal/mole; the Arrhenius plot (Fig. 3) does not give a good straight line. A broadening of all the peaks arising from protons in α-positions in the ketone.BF_3 complexes was observed at −90°; this contributes to the uncertainty in the value of the Arrhenius activation energy for the acetone–BF_3 sample. In samples in which [ketone] = [BF_3] the broadening was visible at temperatures up to −40°, but in no case could it be observed at room temperature. It might arise from a small coupling of the α-protons to boron or to fluorine, the effects of which would disappear as exchange of BF_3 becomes rapid. Alternatively the broadening could result from *cis–trans* isomerism about the double bond of the complexed carbonyl group. *Cis–trans* interconversion is likely to be slow on the n.m.r. time scale at low temperatures, as it is in the closely analogous protonated ketones (19). In protonated acetone separate *cis* and *trans* methyl peaks are not observed even in the slow-exchange

Can. J. Chem. Downloaded from www.nrcresearchpress.com by 210.87.254.40 on 09/05/12
For personal use only.

Can. J. Chem. Downloaded from www.nrcresearchpress.com by 210.87.254.40 on 09/05/12
For personal use only.

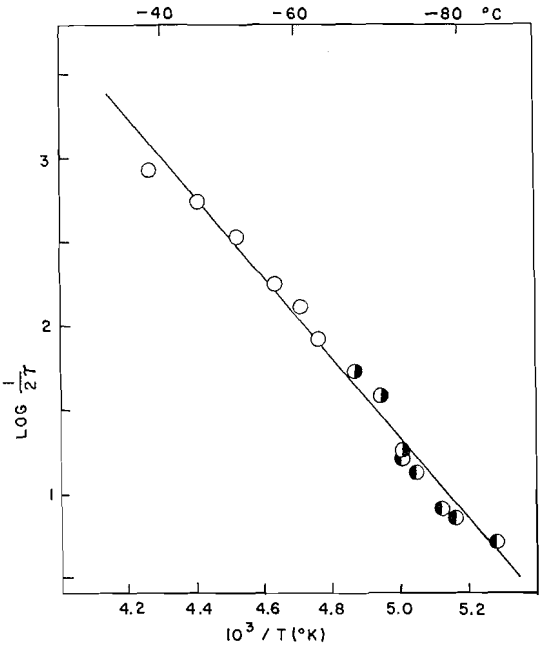

FIG. 3. Arrhenius plot for BF_3 exchange among donor sites in a solution of acetone (0.30 *M*) and BF_3 (0.15 *M*) in methylene chloride. Methods of calculation: (○) from width at half-height of the coalesced single peak, assuming infinite T_2; (◑) from separation of peak maxima below the coalescence temperature, assuming infinite T_2; (◐) from width at half-height in the slow-exchange limit of a peak which is not seriously broadened by effects other than chemical exchange.

limit, but instead a complex multiplet is observed for the methyl resonance; this is because the methyl chemical shifts are quite similar, and the spectrum is complicated by long-range proton–proton coupling between the methyl groups, and by coupling of one of the methyl groups with the OH proton. The broad methyl resonance of acetone.BF_3, and the similarly broadened α-proton resonances of the other ketone.BF_3 complexes, are likely due to similar effects. Since broadening is also found in the spectrum of pinacolone.BF_3, in which α,α′-coupling is not possible and the isomer with BF_3 *cis* to the α-methyl group is probably strongly preferred, it would appear that coupling to boron or to fluorine contributes to the observed broadening of the α-proton resonances in the ketone.BF_3 complexes.

Fluorine Spectra

Samples in which [ketone] > [BF_3] gave a single major ^{19}F peak at about 148 p.p.m. to high field of trichlorofluoromethane. Below about −20° the peak was split by an isotope shift of 0.066 p.p.m. The absence of additional splittings arising from boron–fluorine coupling can be attributed to rapid quadrupole relaxation of boron, as has been proposed previously for other complexes of BF_3 with oxygen donors (11, 18). The sharpness of the main peak at temperatures between −20° and −90° provides evidence that essentially all the BF_3 is complexed, since in this temperature range it was found that free BF_3, if present, exchanges with the 1:1 complex rapidly enough to cause considerable peak broadening.

The ^{19}F chemical shifts of the BF_3 complexes of the four ketones appear to be almost identical; the variations of up to 1 p.p.m. which were observed in different samples did not appear to depend on the ketone used. Further evidence of very similar chemical shifts was provided by a solution of BF_3 with both acetone and pinacolone, such that [acetone]:[pinacolone]:[BF_3] = 1:1.08:1.82. This gave only a single ^{19}F resonance, split by the usual isotope shift, at −80° despite the presence of sufficient BF_3 to complex with most of both ketones. Since the proton spectrum at the same temperature showed separate peaks due to the free and complexed ketones, indicating that BF_3 exchange is slow, the single ^{19}F peak is apparently due to very similar ^{19}F chemical shifts of the two complexes rather than to exchange averaging. The near identity of the ^{19}F chemical shifts is a further indication that the number of β-methyl groups in this series of methyl ketones has very little effect on the donor–acceptor bond.

Solutions in which [ketone] < [BF_3] gave a single ^{19}F peak at room temperature. At −90° two peaks, still slightly broadened by exchange, could be detected at about 124 and 148 p.p.m. The high-field peak can with confidence be assigned to the 1:1 complex, since its chemical shift agrees closely with that of the single peak obtained in the presence of excess ketone. The low-field peak must then be assigned to free BF_3; its chemical shift is in agreement with that of a solution of BF_3 in methylene chloride when no ketone is present (122.2 p.p.m. at −90°). In confirmation of this assignment an increase in the relative proportion of BF_3 caused an increase in the relative size of the low-field peak. Similar ^{19}F complexation shifts of BF_3 have been observed previously (11).

A kinetic study based on changes in ^{19}F signal shape was carried out on a sample of

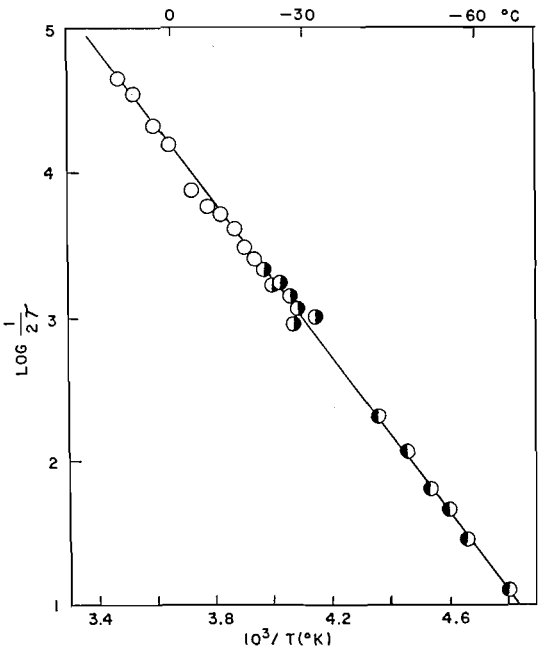

FIG. 4. Arrhenius plot for BF_3 exchange between 1:1 complex and free BF_3 in a solution of pinacolone (0.9 *M*) and BF_3 (1.8 *M*) in methylene chloride. Method of calculation: see legend to Fig. 3.

pinacolone (0.9 *M*) and excess BF_3 in which the peaks arising from free BF_3 and from the 1:1 complex were approximately the same size. The Arrhenius plot of the results gave a good straight line, corresponding to an activation energy of 12.1 ± 1.0 kcal/mole (Fig. 4). The substitution of pinacolone for acetone and the increase in reagent concentrations in the ^{19}F kinetic study limit the value of a comparison with the previously described ^1H kinetic study. However, it is of interest that similar activation energies for exchange are obtained in the presence of excess ketone and of excess BF_3. This result contrasts with results of Rutenberg and co-workers (13) which indicate that exchange in ether.BF_3 complexes becomes much faster, and the activation energy much less, in the presence of excess BF_3. A mechanism involving participation of the second of the oxygen donor's two lone pairs in the transition state might be involved in the especially rapid exchange of excess BF_3 with the ether complexes:

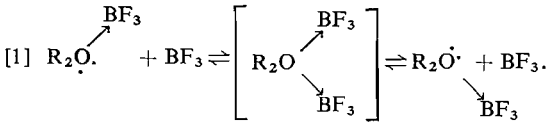

This mechanism, which might provide a transition state of lower energy, would become important only in the presence of excess BF_3, and might allow exchange to occur more readily than either of the two competing mechanisms postulated by Rutenberg and co-workers to occur in the presence of excess ether. The lower Lewis basicity of ketones with respect to ethers (20) suggests that the second lone pair of the carbonyl oxygen may be too unreactive towards a second molecule of BF_3 to allow even transitory formation of the 1:2 complex required in the above mechanism. Alternatively the differences in behavior found in the two studies may be related to the presence of methylene chloride as solvent in the present work. Rutenberg and co-workers did not use a solvent for their mixtures.

Exchange of Fluorine among Boron Atoms

Evidence for Fluorine Scrambling

A ^{10}B–^{11}B isotope shift of 0.066 p.p.m., as has been previously observed for the acetone.BF_3 complex in excess acetone (18), was observed in low-temperature ^{19}F spectra of methylene chloride solutions in which [ketone] ≥ [BF_3]. However, the isotope splitting collapsed above −20° and in no case could it be observed at room temperature although it reappeared on cooling to −20°. The room temperature ^{19}F spectra of all solutions studied consisted of a single rather broadened peak, having widths at half-height of 2–8 Hz in different samples. The degree of broadening did not appear to be dependent on the ketone used, on the concentration, or on the ketone–BF_3 ratio, provided [ketone] ≥ [BF_3]. Spectra obtained at high temperatures consisted of a single peak, sufficiently sharp at 80° in all cases that an isotope shift of 0.066 p.p.m., if present, would have been clearly visible. It can be concluded that a rapid chemical exchange process occurs which averages the environments of the fluorine atoms. This implies a rapid scrambling of fluorine atoms among different boron atoms, and thus that a second exchange process occurs in these solutions in addition to the previously discussed process of breaking and re-forming of ketone donor–acceptor bonds, which causes the temperature dependence of the proton spectra of the same solutions at much lower temperatures.

Figure 5 shows the collapse of the isotope shift in a solution of pinacolone (1.3 *M*) and

Can. J. Chem. Downloaded from www.nrcresearchpress.com by 210.87.254.40 on 09/05/12
For personal use only.

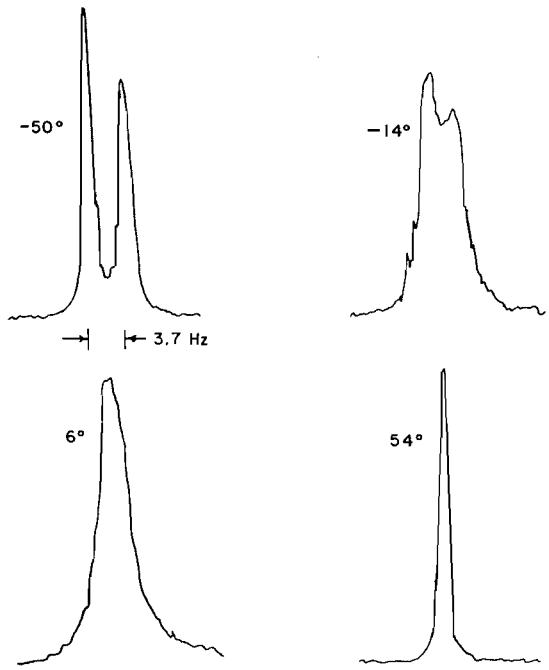

FIG. 5. Collapse of the isotope shift in a methylene chloride solution of pinacolone (1.3 *M*), and BF_3 (1.15 *M*), of isotope ratio $^{10}B:^{11}B = 52:48$.

BF_3 (1.15 *M*) containing isotopically substituted boron of approximately 52% ^{10}B and 48% ^{11}B. The spectra of the isotopically substituted sample show the coalescence of the peaks more clearly than spectra of natural abundance samples. It is evident from the spectrum at 54° that the isotope splitting is indeed absent at high temperatures. In this sample, unlike several others, there is little excess broadening of the signal in the coalescence region and the spectrum closely approximates the series of signal shapes expected for the collapse of two chemically shifted peaks.

The excess broadening found in the ^{19}F spectra of many samples in the temperature range of isotope shift coalescence is most easily explained by chemical exchange between the main ketone.BF_3 species and a second species which gives rise to a chemically shifted resonance. It has been pointed out (21) that the presence of a second species undergoing chemical exchange with the main species may cause a marked broadening of the resonance of the main species even if the second species is present in such small amount that its own resonance absorption is not readily seen, even under conditions of slow exchange. The presence of a second species was confirmed, in all samples studied, by the detection at low temperatures and high radio-frequency power levels of a very small peak to high field of the ketone.BF_3 peak. The samples in which this peak was larger were those which showed the greater degree of broadening of the ketone.BF_3 resonance near room temperature. At about −20° the small peak broadened to such an extent that it could not be observed above the base line; it did not reappear at higher temperatures. This behavior is in accord with a rapid chemical exchange of the fluorines of this species with those of the ketone.BF_3 complex. In the few samples in which this peak was of a sufficient size to allow its area relative to that of the main peak to be determined, it was found that the coalescence pattern agreed quite well with that calculated for chemical exchange collapse.

It is evident that a fluorine-containing impurity is present, sometimes in very small amount, in the samples studied. Since the small peak collapses in the same temperature range as the ketone.BF_3 isotope shift, it appears that a fairly general fluorine scrambling reaction occurs in solution. In a few samples in which the additional peak was especially large it was possible to detect a skewed quartet fine structure very similar to that of Fig. 1*c* of ref. 18. In that paper it was shown that the peak with this fine structure arises from $H_2O.BF_3$. The presence of differing amounts of moisture in different samples can explain the variable size of the peak. The assignment of the peak was confirmed by the proton spectrum at −44° of one of the samples, which gave a small 1:3:3:1 quartet of splittings 2.78 ± 0.1 Hz and chemical shift 12.0 δ, in good agreement with the values previously reported for $H_2O.BF_3$ (18). The presence of $H_2O.BF_3$ in these solutions, prepared under "anhydrous" conditions on a high-vacuum system using dried reagents, emphasizes the difficulty in obtaining truly anhydrous conditions. The very small amounts of water present in these solutions can be detected as $H_2O.BF_3$ by ^{19}F n.m.r. because of the strong preference of BF_3 to complex with water rather than with ketones (18).

The collapse of the ketone.BF_3 and $H_2O.BF_3$ ^{19}F peaks affects the spectra in a much higher temperature range than the collapse of ^1H peaks

Can. J. Chem. Downloaded from www.nrcresearchpress.com by 210.87.254.40 on 09/05/12
For personal use only.

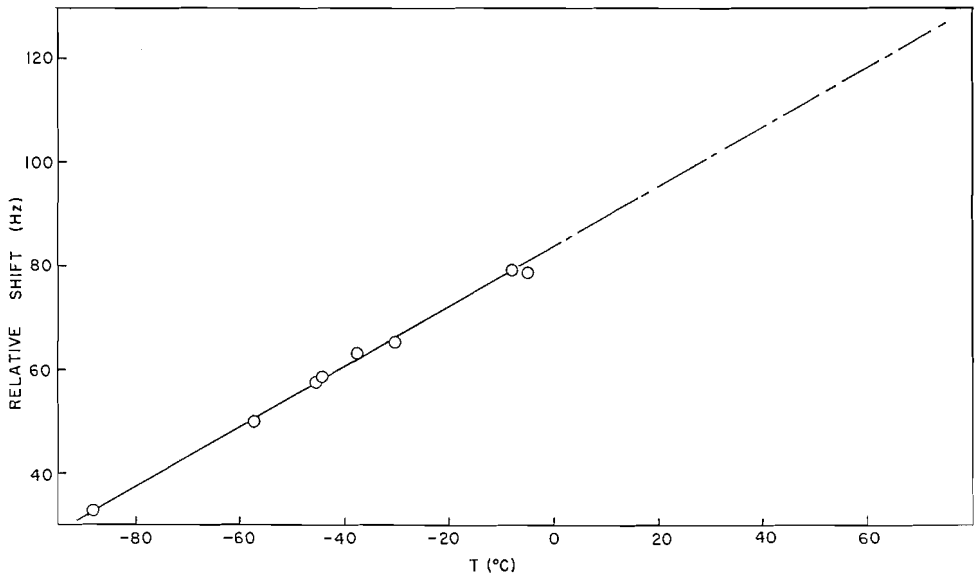

FIG. 6. Variation of the relative ^{19}F chemical shift of (methyl isopropyl ketone).BF_3 and $H_2O.BF_3$ with temperature in methylene chloride solutions.

arising from free and complexed ketone, observed in the same samples and discussed previously. Since the frequency separations of the collapsing peaks differ by a factor of less than three in the two cases (^1H, 36 Hz; ^{19}F, 80–100 Hz), processes occurring at similar rates would give rise to ^1H and ^{19}F coalescence temperatures differing by not much more than 10°. In order to account for the observed difference in coalescence temperatures of about 70°, it must be assumed that BF_3 exchange among ketone donor sites is a much faster process than the exchange of fluorine between ketone.BF_3 and $H_2O.BF_3$. Thus at least two distinct chemical exchange processes occur in solution.

Since the isotope shift collapse occurs in a temperature range similar to that of the collapse of the ketone.BF_3 and $H_2O.BF_3$ ^{19}F peaks, the same exchange process may be responsible for both effects on the ^{19}F spectra. Fluorine scrambling in the ketone.BF_3 complexes does not appear to require the presence of $H_2O.BF_3$, since the collapse of the isotope shift occurs at about the same temperature regardless of the amount of $H_2O.BF_3$ in solution. It seems likely, instead, that a general rearrangement of fluorine among boron atoms occurs. The collapse of the $H_2O.BF_3$ peak could thus be caused by the fluorine scrambling process, rather than by BF_3 exchange. This would be in accord with a much greater donor–acceptor bond strength in $H_2O.BF_3$ than in ketone.BF_3.

Kinetic Studies of Fluorine Scrambling

In a sample of methyl isopropyl ketone (0.7 *M*) and BF_3 (0.3 *M*), which gave an exceptionally large $H_2O.BF_3$ peak consisting of 17 ± 4% of the total fluorine-on-boron peak area, approximate rates of fluorine exchange between the ketone.BF_3 and $H_2O.BF_3$ species were determined by comparison of observed and calculated spectra. The calculations were complicated by the variation of the relative chemical shift of the peaks with temperature as shown in Fig. 6. A very similar temperature dependence of the relative shift between ketone.BF_3 and $H_2O.BF_3$ was found in all the methylene chloride solutions studied. Relative chemical shifts in the coalescence region, required for the rate calculations, were obtained by extrapolation from Fig. 6. The Arrhenius plot of the kinetic data is shown in Fig. 7. The activation energy for the exchange process was found to be 15.6 kcal/mole; an error of ±2 kcal/mole seems likely as a result of the approximations involved. Comparison with the data for BF_3 exchange among different ketone donor sites in a solution of acetone.BF_3 and excess acetone shows that the rate of the reaction exchanging fluorine between

Can. J. Chem. Downloaded from www.nrcresearchpress.com by 210.87.254.40 on 09/05/12
For personal use only.

Can. J. Chem. Downloaded from www.nrcresearchpress.com by 210.87.254.40 on 09/05/12
For personal use only.

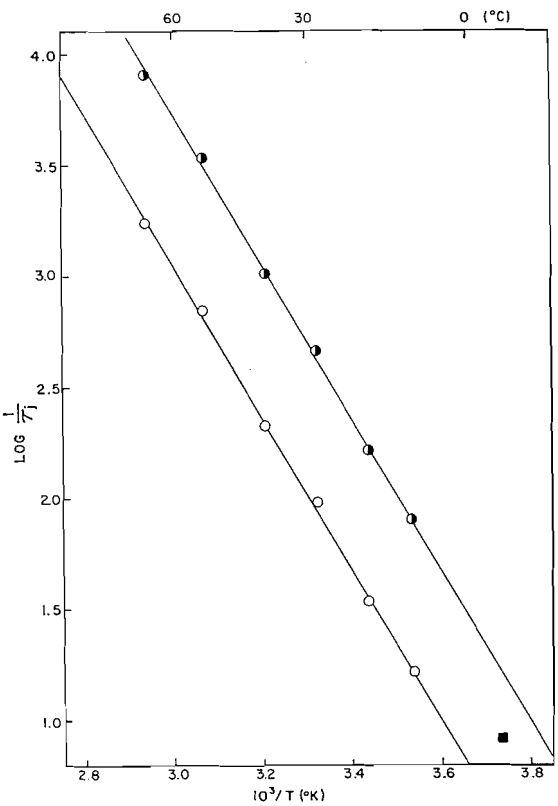

FIG. 7. Arrhenius plot for fluorine exchange between (methyl isopropyl ketone).BF_3 (0.25 *M*) and $H_2O.BF_3$ (0.05 *M*) in methylene chloride: (◑) τ_j = mean lifetime on $H_2O.BF_3$; (○) τ_j = mean lifetime on (methyl isopropyl ketone).BF_3; (■) τ_j = mean lifetime of fluorine on ^{10}B or ^{11}B in the isotopically substituted sample of Fig. 5.

ketone.BF_3 and $H_2O.BF_3$ is less at a given temperature by a factor of about 1600, in spite of the similar concentrations of the exchanging species.

The spectra of Fig. 5, which illustrate the collapse of the isotope shift in a solution of pinacolone and BF_3, are negligibly affected by broadening due to collapse of the ketone.BF_3 resonance with the $H_2O.BF_3$ resonance, since very little $H_2O.BF_3$ is present in this solution. Thus the signal shapes obtained should approximate to those expected for the chemical exchange collapse of two peaks of equal areas and of relative chemical shift 3.7 Hz. The calculated lifetime of a fluorine atom attached to either ^{10}B or ^{11}B at the coalescence temperature, assuming infinite T_2 and equal populations of F-on-^{10}B and F-on-^{11}B, is shown in Fig. 7; the point falls between the two parallel lines obtained for fluorine exchange between (methyl isopropyl ketone).BF_3 and $H_2O.BF_3$, at about the position through which the single line of the Arrhenius plot would pass if the concentration of (methyl isopropyl ketone).BF_3 were equal to that of $H_2O.BF_3$. Thus the average lifetime of fluorine on a boron nucleus at this temperature in the isotopically substituted sample is quite similar to the average lifetime of fluorine exchange between ketone.BF_3 and $H_2O.BF_3$ at the same temperature. Since different concentrations and different ketones are involved in the two samples compared, an exact fit to the Arrhenius plot is not expected; however, the good qualitative agreement found supports our suggestion that the mechanism of fluorine exchange could be the same in both cases.

Possible Mechanisms for Fluorine Scrambling

The above evidence establishes the existence of a fluorine scrambling reaction in methylene chloride solution. This may be analogous to the reported scrambling of halogen atoms of tetrahaloborate anions in methylene chloride solution (22) and to a similar scrambling of fluorine atoms in the tetrafluoroborate anion in acetonitrile solution observed in this laboratory (23).

A rapid equilibration of the simple ketone.BF_3 complex with the ionic form $(R_2CO)_2BF_2^+.BF_4^-$ (**5**) would cause fluorine scrambling. This reaction might occur through a preliminary dissociation of a molecule of complex to give free BF_3, as in the following reaction scheme.

[2] $R_2CO.BF_3 \rightleftharpoons R_2CO + BF_3$

$R_2CO.BF_3 + BF_3 \rightleftharpoons$ 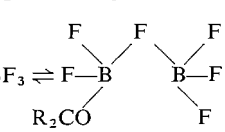

6

$\rightleftharpoons R_2CO.BF_2^+ + BF_4^-$

$R_2CO.BF_2^+ + R_2CO \rightleftharpoons (R_2CO)_2BF_2^+$

Such a scheme seems especially likely since the proposed intermediate fluorine-bridged species **6** is an analogue of the $B_2F_7^-$ ion for which there is good evidence (24). Moreover the reaction

[3] $BF_3 + BF_4^- \rightleftharpoons B_2F_7^-$

could also contribute to the fluorine exchange. Mixed species (donor)(donor′)$BF_2^+.BF_4^-$, very

Can. J. Chem. Downloaded from www.nrcresearchpress.com by 210.87.254.40 on 09/05/12
For personal use only.

similar to **5**, should also be capable of existence so that the above mechanism would allow a general scrambling of fluorine among all BF_3 complexes. This would explain the collapse of the $H_2O.BF_3$ peak. The presence of a small amount (e.g. $< 1\%$) of the ionic species would probably not be detected by n.m.r., even in the slow-exchange limit. Structures analogous to **5** have been proposed previously. Greenwood and Wade (25) have proposed, on the basis of electrical conductivity measurements, that the fused complexes pyridine.BCl_3 and piperidine.BCl_3 are dissociated to the extent of about 1% to yield $(donor)_2BCl_2^+.BCl_4^-$. The structure **7** has been proposed by Wiberg and Buchler (26) on the basis of n.m.r. studies for the adduct of BF_3 with tetrakis(dimethylamino)ethylene.

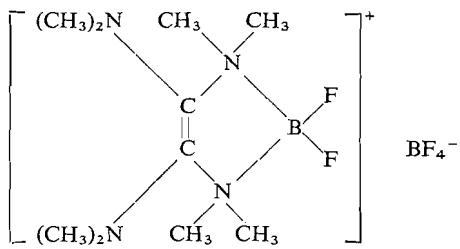

7

Ludman and Waddington have reported that tetrafluoroborate ion precipitates as the potassium salt when potassium methoxide is reacted with an excess of BF_3 in methanol (27); this illustrates the lability of ligand groups about boron. We have previously proposed a mechanism somewhat analogous to [2] for the exchange of fluorine among boron atoms in solutions of silver tetrafluoroborate (23).

Complexes of other Lewis acid fluorides apparently undergo similar reactions; n.m.r. studies have shown that solutions of niobium pentafluoride in dimethylformamide (28), ethanol (29), and dimethylsulfoxide (30) contain the NbF_6^- ion rather than the simple donor–acceptor complex. It is of interest that Tebbe and Muetterties (31) have reported fluorine exchange between phosphorus atoms in acetonitrile solutions of $CH_3CN.PF_5$; at about 80° the ^{19}F doublet arising from P—F coupling collapses to a single broad peak. This exchange process may be analogous to that which collapses the ^{10}B–^{11}B isotope shift in the ^{19}F spectra of ketone.BF_3 solutions. Tebbe and Muetterties have attributed the exchange to the presence of a trace of PF_6^- rather than to autoionization, since addition of PF_6^- greatly increases the exchange rate. In any case dissociation of $CH_3CN.PF_5$ would probably give rise to a series of reactions analogous to [2], as we have suggested previously (23).

Experimental

Materials

Reagent grade acetone, methyl ethyl ketone, methyl isopropyl ketone, and pinacolone were dried over calcium chloride and magnesium sulfate and fractionated; the fractions of boiling ranges 55.9–56.2°, 78.8–79.1°, 92.0–92.5°, and 104.5–105.5°, respectively, were used. The amounts required for the n.m.r. samples were allowed to stand over Linde 4A molecular sieves immediately prior to use. Methylene chloride (Fisher spectranalysed) and practical grade tetramethylsilane were allowed to stand over Linde 4A molecular sieves, and trichlorofluoromethane (Matheson) was allowed to stand at 0° over phosphorus pentoxide, before use. The purification of natural abundance boron trifluoride, and the preparation of isotopically substituted boron trifluoride, were carried out as described previously (18).

Preparation of Samples

The samples were prepared by standard high-vacuum techniques. Known amounts of BF_3 and ketone were condensed from a calibrated volume directly into 5 mm o.d. pyrex sample tubes into which suitable amounts of solvent had previously been distilled. Small amounts of tetramethylsilane and trichlorofluoromethane were added in the same fashion. In the case of the less volatile ketones pinacolone and methyl isopropyl ketone some error in calculation of the amounts added was introduced by the nonideality of the vapors. The samples were sealed off under vacuum with the contents at liquid nitrogen temperature and allowed to warm slowly to room temperature. Approximate volumes of the solutions were determined by measuring the height of liquid in the sample tube and comparing this with the height of a known volume of liquid which had been added to the tube prior to the preparation of the sample. Since the number of moles of solute had been determined by condensation from a calibrated volume, it was possible to calculate approximate solution concentrations in moles per liter.

N.M.R. Spectra

Spectra were obtained on a Varian Associates HR-60 n.m.r. spectrometer operating at 60 MHz for protons and 56.4 MHz for fluorine-19. The spectra were calibrated by the audio sideband method using a Muirhead-Wigan D-890-A decade oscillator. Proton chemical shifts (δ) are given in p.p.m. to low field of internal tetramethylsilane; ^{19}F chemical shifts are given in p.p.m. to high field of internal trichlorofluoromethane.

A Varian V-4340 variable-temperature n.m.r. probe was used to adjust the spinning sample tube to the required temperature. Low temperatures were obtained by passing cold air from a liquid air boiler into the Dewar-jacketed assembly; high temperatures were obtained by passing heated air. The sample temperature was moni-

tored by a copper–constantan thermocouple placed inside the jacket and attached to a Leeds and Northrup temperature potentiometer. Corrections for the difference between the monitored temperature and the true sample temperature were determined by placing a second thermocouple directly in a sample tube containing a suitable solvent.

Calculations

An IBM 7040 computer was used for the calculation of exchange rates and Arrhenius activation energies. In cases involving coalescence of two peaks of equal areas, approximate methods of calculation based on equations given by Pople, Schneider, and Bernstein (32) were used; these made use of three different spectral parameters, as indicated in the legend to Fig. 3. Exchange rates were determined from the coalescence of two peaks of unequal areas by calculating theoretical spectra from eq. [10–23] to [10–25] of ref. 32 and matching calculated and experimental widths at half-height of the larger peak.

Acknowledgments

We wish to thank the National Research Council of Canada and the United States Air Force Office of Scientific Research for financial support of this work and the Department of University Affairs, Province of Ontario, for the award of an Ontario Graduate Fellowship (to J. S. H.).

1. R. A. Craig and R. E. Richards. Trans. Faraday Soc. **59**, 1962 (1963).
2. P. Diehl. Helv. Phys. Acta, **31**, 685 (1958).
3. J. M. Miller and M. Onyszchuk. Can. J. Chem. **44**, 899 (1966); **42**, 1518 (1964).
4. S. J. Kuhn and J. S. McIntyre. Can. J. Chem. **43**, 375 (1965); **43**, 995 (1965).
5. E. Gore and S. S. Danyluk. J. Phys. Chem. **69**, 89 (1965).
6. R. W. Taft and J. W. Carten. J. Am. Chem. Soc. **86**, 4199 (1964).
7. P. N. Gates, E. J. McLauchlan, and E. F. Mooney. Spectrochim. Acta, **21**, 1445 (1965); P. G. Davies and E. F. Mooney. Spectrochim. Acta, **22**, 953 (1966); E. J. McLauchlan and E. F. Mooney. Spectrochim. Acta, **23A**, 1227 (1967).
8. R. E. Schuster, A. Fratiello, and T. P. Onak. Chem. Commun. 1038 (1967).
9. J. Paasivirta and S. Brownstein. J. Am. Chem. Soc. **87**, 3593 (1965).
10. R. J. Gillespie and J. S. Hartman. Can. J. Chem. **45**, 2243 (1967).
11. S. Brownstein, A. M. Eastham, and G. A. Latremouille. J. Phys. Chem. **67**, 1028 (1963).
12. R. A. Ogg and P. Diehl. J. Inorg. Nucl. Chem. **8**, 468 (1958).
13. A. C. Rutenberg, A. A. Palko, and J. S. Drury. J. Am. Chem. Soc. **85**, 2702 (1963); J. Phys. Chem. **68**, 976 (1964); A. C. Rutenberg and A. A. Palko. J. Phys. Chem. **69**, 527 (1965).
14. M. F. Lappert. J. Chem. Soc. 817 (1961).
15. P. N. Gates and E. F. Mooney. J. Chem. Soc. 4648 (1964).
16. R. G. Pews, Y. Tsuno, and R. W. Taft. J. Am. Chem. Soc. **89**, 2391 (1967); C. S. Giam and R. W. Taft. J. Am. Chem. Soc. **89**, 2397 (1967).
17. F. Kaplan and D. Weisleder. J. Am. Chem. Soc. **88**, 4103 (1966).
18. R. J. Gillespie and J. S. Hartman. Can. J. Chem. **45**, 859 (1967).
19. G. A. Olah, M. Calin, and D. H. O'Brien. J. Am. Chem. Soc. **89**, 3586 (1967).
20. N. N. Greenwood and R. L. Martin. Quart. Rev. London, **8**, 1 (1954).
21. S. Meiboom. J. Chem. Phys. **34**, 375 (1961).
22. R. D. W. Kemmitt, R. S. Milner, and D. W. A. Sharp. J. Chem. Soc. 111 (1963).
23. R. J. Gillespie, J. S. Hartman, and M. Parekh. Can. J. Chem. **46**, 1601 (1968).
24. S. Brownstein and J. Paasivirta. Can. J. Chem. **43**, 1645 (1965); P. J. Burchill, S. Brownstein, and A. M. Eastham. Can. J. Chem. **45**, 17 (1967); J. J. Harris. Inorg. Chem. **5**, 1627 (1966).
25. N. N. Greenwood and K. Wade. J. Chem. Soc. 1130 (1960).
26. N. Wiberg and J. W. Buchler. J. Am. Chem. Soc. **85**, 243 (1963).
27. C. J. Ludman and T. C. Waddington. J. Chem. Soc. A, 1816 (1966).
28. K. J. Packer and E. L. Muetterties. J. Am. Chem. Soc. **85**, 3035 (1963).
29. J. V. Hatton, Y. Saito, and W. G. Schneider. Can. J. Chem. **43**, 47 (1965).
30. U. R. K. Rao. Ph.D. Thesis. McMaster University, Hamilton, Ontario. 1966.
31. F. N. Tebbe and E. L. Muetterties. Inorg. Chem. **6**, 129 (1967).
32. J. A. Pople, W. G. Schneider, and H. J. Bernstein. High-resolution nuclear magnetic resonance. McGraw-Hill Book Co., Inc., New York. 1959. Chap. 10.

Can. J. Chem. Downloaded from www.nrcresearchpress.com by 210.87.254.40 on 09/05/12
For personal use only.

Can. J. Chem. Downloaded from www.nrcresearchpress.com by 210.87.254.40 on 09/05/12
For personal use only.

Crystal structures of $RuSe_2$, $OsSe_2$, $PtAs_2$, and α-$NiAs_2$

W. N. STASSEN[1] AND R. D. HEYDING
Department of Chemistry, Queen's University, Kingston, Ontario

Received January 5, 1968

The atom positions in $RuSe_2$, $OsSe_2$, $PtAs_2$, and α-$NiAs_2$ have been determined from X-ray powder diffraction data. In the pyrite-type compounds (*Pa*3), the metal atoms are in 4(*a*), the face-centered positions, and the nonmetal atoms in 8(*c*), with $x = 0.381 \pm 3$ ($RuSe_2$, $a = 5.935$ Å); $x = 0.382 \pm 4$ ($OsSe_2$, $a = 5.946$ Å); and $x = 0.385 \pm 4$ ($PtAs_2$, $a = 5.967$ Å).

In orthorhombic α-$NiAs_2$ (*Pbca*, $a = 5.770$, $b = 5.838$, $c = 11.419$ Å), the atom positions are

Ni in 8(*c*): $x = 0.020$, $y = 0.823$, $z = 0.135$ (± 5);

As_I in 8(*c*): $x = 0.865$, $y = 0.194$, $z = 0.069$ (± 5);

As_{II} in 8(*c*): $x = 0.123$, $y = 0.447$, $z = 0.182$ (± 5).

As in the marcasite and pyrite structures, the nonmetal atoms in α-$NiAs_2$ are paired, and the metal atoms have six nearest nonmetal neighbors at the corners of a distorted octahedron. Between metal atom layers these octahedra are coordinated alternately by corner sharing only, as in the pyrite lattice, and by a combination of corner and edge sharing, as in the marcasite lattice. The mean Ni—As distance is 2.38 Å, with minimum and maximum distances of 2.25 and 2.46 Å. The As—As distance is 2.46 Å, and the shortest Ni—Ni distance is 3.72 Å.

Canadian Journal of Chemistry, 46, 2159 (1968)

Introduction

The great majority of the MY_2 and MZ_2 compounds formed by the Group VIII transition metals (M) and the chalcogens (Y) and the pnigogens (Z) crystallize in pyrite-, marcasite-, $CoSb_2$-, or CdI_2-type structures. The most common of these is the pyrite lattice (1, 2). The atomic positional parameters of the nonmetal atom in several of these pyrites have been reported recently by Sutarno *et al.* (3) and Furuseth *et al.* (4); nevertheless a remarkable number of these compounds have yet to be examined in detail.

Three of these pyrite-type compounds ($RuSe_2$, $OsSe_2$, $PtAs_2$) were prepared recently in our laboratory by J. J. Murray for thermodynamic studies (5). These specimens have been used to obtain the X-ray diffraction intensity data required in the calculation of atom positions. Although the atom positions in $PtAs_2$ have been reported (4), it was included to check our procedures.

The low temperature modification of nickel diarsenide, α-$NiAs_2$, is one of the MZ_2 compounds which does not crystallize in one of the four common structure types. Bennett and Heyding prepared this compound synthetically and confirmed the similarity in lattice dimensions to the mineral pararammelsbergite (6). Studies on single crystals of the mineral have shown it to be orthorhombic *Pbca* (7). Bennett's specimen of α-$NiAs_2$ has been used to obtain Debye–Scherrer patterns for a detailed crystallographic study.

Experimental

The preparation of the specimens has been reported in detail by Murray and Heyding (5) and Bennett and Heyding (6) and need not be repeated here.

Debye-Scherrer photographs were obtained in 11.46 cm cameras with nickel-filtered copper radiation. The relative intensities of the diffraction lines were obtained by microphotometer recordings, using an intensity (film density) wedge as a standard. The wedge was prepared using the same film, radiation, and development techniques used in obtaining the diffraction patterns. Multiple film techniques were employed to check the intensities of very strong reflections.

The relative intensities were corrected for absorption as well as Lorentz and polarization effects (8). The corrected relative intensities were used in full matrix least squares refinement programs specifically written for the two types of structure involved (9). Thomas–Fermi–Dirac atomic scattering factors were taken from the International Tables (10). Only one temperature factor was employed for each structure. Atomic form factors were not corrected for anomalous dispersion. The simple weighting scheme of one for all observed reflections and zero for unobserved reflections was used. Overlapping reflections were included in the refinement, the observed quantity being divided among the possible reflections in proportions equal in ratio to the corresponding calculated quantities. The refinement adjusted all positional parameters, the scaling factor, and the temperature parameter.

[1]Present address: Division of Applied Chemistry, National Research Council of Canada, Ottawa, Canada.

TABLE I

Nonmetal coordinates and interatomic distances in $RuSe_2$, $OsSe_2$, and $PtAs_2$. ($Pa3$, FeS_2)

Compound	a (Å)	x	R[1]	Metal/nonmetal distance (Å)	Nonmetal/nonmetal distance (Å)
$RuSe_2$	5.935 ± 1[2]	0.381 ± 3	0.04	2.473 ± 6[4]	2.44 ± 6[4]
$OsSe_2$	5.946 ± 1[2]	0.382 ± 4	0.06	2.478 ± 8	2.43 ± 8
$PtAs_2$	5.968 ± 1[2]	0.385 ± 4	0.06	2.494 ± 8	2.38 ± 8
	5.9665 ± 4[3]	0.383 ± 2		2.490 ± 4	2.42 ± 4

[1]Reliability factor, $\Sigma(|F_o| - |F_c|)/\Sigma|F_o|$.
[2]Murray (5).
[3]Furuseth (4).
[4]Uncertainty, 2.5σ.

The IBM 360 computer in the Computing Centre at Queen's University was used in these calculations.

Initial values of the temperature parameter B and the scaling factor k used in refining the $PtAs_2$ data were estimated using Wilson's method (11). Similar values of B and k were used for the other structures, since these parameters were readily adjusted by the program over a large range of values, and only very approximate initial values were required.

For the pyrite-type structures, the initial value of x, the nonmetal parameter, was taken as 0.380. This value is simply the average of all known positional parameters in MY_2 and MZ_2 pyrite structures. The intensities of 31 reflections were used in the pyrite programs.

We have assumed that α-$NiAs_2$ and the mineral pararammelsbergite are isostructural. Only four 1:2 compounds, TiO_2 (12), TeO_2 (13), $AuSn_2$ (14), and α-$NiAs_2$ are known to crystallize in this space group. The Au/Sn and Ni/As atomic radius ratios are very similar. Accordingly, Schubert's values (14) for the atom positions in $AuSn_2$ were assumed for α-$NiAs_2$, and structure factor maps prepared. Corrections based on these maps led to the initial parameters used in the refinement program: Ni, x,y,z: 0.010, 0.820, 0.110; As_I, x_1,y_1,z_1: 0.845, 0.200, 0.082; As_{II}, x_2,y_2,z_2: 0.130, 0.450, 0.190. The intensities of 39 reflections ($\theta \leqslant 40°$) were used in the program.

Results and Discussion

The results of the refinement program for the pyrite-type compounds are given in Table I. The reliability factor, R, quoted in this table is given by $\Sigma(|F_o| - |F_c|)/\Sigma|F_o|$. Uncertainties in the fractional coordinates were estimated by Luzzati's method (15). A table of observed and calculated intensities for the various planes in all three compounds has been submitted to the Depository of Unpublished Data.[2] Agreement of the crystallographic data for $PtAs_2$ with those published by Furuseth (4) is within experimental error (Table I).

[2]Photocopies may be obtained upon request to: The Depository of Unpublished Data, National Science Library, National Research Council of Canada, Ottawa, Canada.

Knop and his colleagues have already discussed the sensitivity of interchalcogen distances in the pyrite lattice to the value of the positional parameter for these atoms (3). Indeed, as far as the Se—Se distances in these compounds are concerned, the calculations leave us with values which are scarcely more reliable than those we might have estimated on the basis of an average positional parameter of 0.380. The inter-selenium distance is slightly greater than that observed in hexagonal selenium (2.32 Å), and, within uncertainty, equal to the distance of 2.50 ± 10 Å observed in the marcasite lattice of $FeSe_2$ (16). The nonmetal interatomic distances in RuY_2 and OsY_2 pyrites are: for sulfides, 2.19 ± 3; for selenides, 2.44 ± 8; and for tellurides, 2.81 ± 4 Å.

Again using the values recorded by Sutarno, Knop, and Reid for the disulfides and ditellurides of ruthenium and osmium, and the mean values for the chalcogen radii implied in the nonmetallic interatomic distances, the radii of ruthenium and osmium are found to be identical regardless of the chalcogen forming the compound. The metal atom radii are 1.26 ± 2 Å in the disulfides and ditellurides and 1.26 ± 4 Å in the diselenides.

TABLE II

Crystal structure data for α-$NiAs_2$

Space group: orthorhombic D_{2h}^{15} – $Pbca$ (No. 61)
Unit cell dimensions: a 5.770 ± 1 Å; b 5.838 ± 1; c 11.419 ± 1; V 384.6 ± 2 Å^3
Cell content: $M = 8$, $Z = 24$
Densities: $D_x = 7.20\pm1$, $D_m = 7.25\pm7$ g cm^{-3}
Atom positions: all atoms in general positions, 8(c):
$\pm(x,y,z)$; $(\frac{1}{2}+x, \frac{1}{2}-y, -z)$;
$(-x, \frac{1}{2}+y, \frac{1}{2}-z)$; $(\frac{1}{2}-x, -y, \frac{1}{2}+z)$

	x	y	z
Ni	0.020	0.823	0.135 ± 5
As_I	0.865	0.194	0.069 ± 5
As_{II}	0.123	0.447	0.182 ± 5

Can. J. Chem. Downloaded from www.nrcresearchpress.com by 210.87.254.40 on 09/05/12
For personal use only.

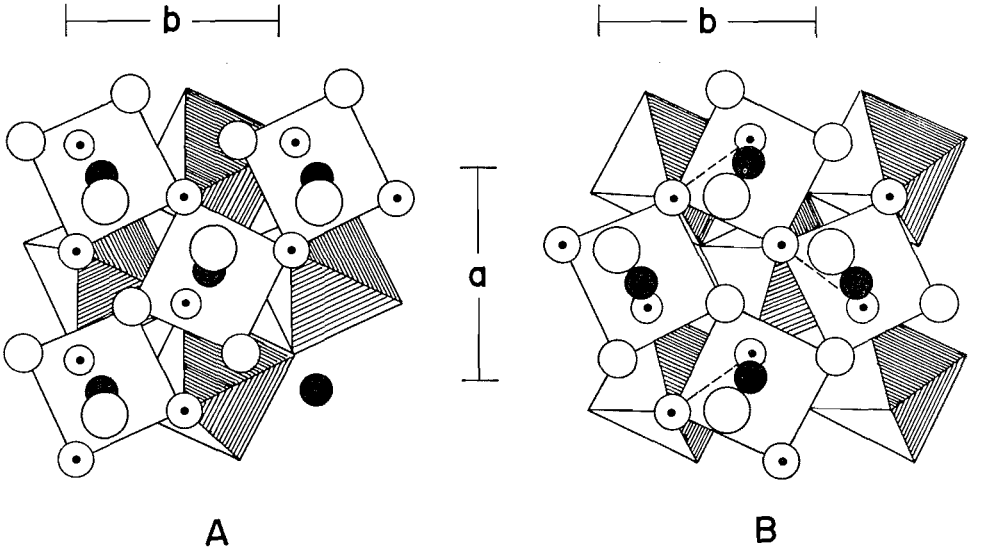

FIG. 1. Projections of atom positions in α-$NiAs_2$ along the *c* axis. The black circles represent Ni, the white circles As. The white circles containing a black dot lie below the plane of the nickel atoms. In A, the Ni atoms shown are at $z = -0.135$; in B, at $z = -0.365$; the origin is at the center of the unit cell. The lower octahedra in A are identical with the upper (open) octahedra in B. Shared octahedral edges in B are indicated by broken lines.

TABLE III

Nearest neighbor interatomic distances in α-$NiAs_2$

Atom	Neighbor	Distance (Å, ±0.10)[1]
Ni	2 As_I	2.46
	1 As_I	2.42
	1 As_{II}	2.36
	1 As_{II}	2.34
	1 As_{II}	2.25
	1 Ni	3.72
As_I	2 Ni	2.46
	1 Ni	2.42
	1 As_{II}	2.46
As_{II}	1 Ni	2.36
	1 Ni	2.34
	1 Ni	2.25
	1 As_I	2.46

[1]Uncertainty, 2.5σ.

The crystallographic data for α-$NiAs_2$ are given in Table II. The calculated interatomic distances are given in Table III, while the values of the observed and calculated intensities and structure factors for all possible reflections up to 40° θ are summarized in Table IV.

The pyrite structure contains a metal sublattice which consists of sets of face-centered square planar nets parallel to the (100) planes and separated from one another by $a_0/2$. Similar nets exist in the marcasite lattice parallel to the (101) plane, but are face-centered rectangular rather than face-centered square. In both structures pairs of nonmetal atoms can be recognized, as well as more-or-less distorted octahedra of nonmetal atoms about each metal atom. The important difference in the two structures is that in the pyrite structure each octahedron shares corners only with 12 other octahedra, while in the marcasite structure both corners and edges are shared with 10 octahedra.

Projections along the *c* axis of two double sets of Ni planes in the α-$NiAs_2$ structure are shown in Fig. 1. The nickel atoms form planar nets which are neither square nor face centered; nevertheless the similarity to the metal atom nets in the pyrite and marcasite structures is obvious. The existence of pairs of arsenic atoms is also clear in both projections. The octahedra are distorted in that the body diagonals do not pass through the metal atom site and are not mutually perpendicular. The magnitude of the distortion is indicated in the table of interatomic distances (Table III).

In Fig. 1A, the solid octahedra in the bottom layer surround Ni atoms which lie in a plane perpendicular to the *c* axis and 4.17 Å ($z = -0.365$) below the origin (center of unit cell). The open octahedra in the top layer show the pseudo-face-centered square net of nickel atoms parallel to the bottom net and 1.54 Å ($z = -0.135$) below the origin. The arsenic atoms between these two nets are shared by three

Can. J. Chem. Downloaded from www.nrcresearchpress.com by 210.87.254.40 on 09/05/12
For personal use only.

TABLE IV

Observed and calculated Debye–Scherrer intensities and structure factors for α-$NiAs_2$. (R = 0.057) (Threshold for photometrically observed intensities, 3)

hkl	I_{obsd}	I_{calcd}	F_{obsd}	F_{calcd}	*hkl*	I_{obsd}	I_{calcd}	F_{obsd}	F_{calcd}
002	0	0	0	−29	117	0	2	0	25
102	0	0	0	−12	233, 323	27	22, 8 (30)	87	−91
111	11	12	35	37				52	−55
112	0	1	0	20	040	0	0	0	18
020	11	13	86	−92	041, 400	21	6, 9 (15)	81	70
								142	−122
200	26	27	132	135	135	4	3	40	34
004	65	62	211	−207	008, 315, 027	19	8, 7, 1 (16)	124	−117
021	61	64	145	149				57	54
113	48	32	92	75				33	31
022, 210, 202	123	73, 50, 35 (158)	167	−169	042	0	0	0	−2
			137	140	234, 141, 410, 324	7	1, 5, 0, 0 (6)	22	21
			36	−37				47	−44
104	183	168	270	258				8	8
								11	11
121, 211	237	70, 133 (203)	128	119	402	0	0	0	−6
			178	164					
122, 212, 114	217	79, 80, 40 (199)	138	−132	226	0	1	0	−23
			139	133	411	0	0	0	−11
			98	−94	108, 127, 217	29	2, 5, 21 (28)	44	−43
								46	−45
023	11	12	70	−72				95	92
123	8	12	44	−54	142	0	0	0	−1
213	0	0	0	1	043	0	0	0	20
220, 024	13	6, 11 (17)	48	−55	412	0	1	0	−17
			67	76	331	0	2	0	28
					306	0	0	0	14
204, 221	39	24, 23 (47)	102	−113	118	0	4	0	44
			71	78	332	0	0	0	−3
115	55	59	121	−126	143, 136	13	10, 0 (10)	75	−67
222	0	1	0	16				2	−2
124	0	0	0	−5					
					316, 235, 325, 413	22	0, 24, 0, 1 (25)	9	−9
214	0	5	0	−39				95	−101
006	0	1	0	40				7	7
131, 302	88	87, 5 (92)	158	−162				16	−17
			55	−57					
223, 106, 311, 025	60	11, 0, 3, 60 (74)	52	57	240	0	0	0	−19
			11	13	044	0	0	0	13
			27	30	241	0	6	0	−50
			172	−191	420	0	2	0	−41
132	6	7	44	−47	404	0	1	0	−35
312	100	106	179	183	333	0	3	0	39
116	56	63	135	143	421	0	0	0	11
125	0	0	0	7	028, 208, 227	7	2, 5, 0 (7)	39	−39
215	0	1	0	−16				65	64
224	6	9	45	55				15	−15
133	25	33	92	106	242	0	0	0	1
313	34	39	108	−116	144	0	1	0	22
230	34	35	155	−158	422	14	16	79	83
					414	0	1	0	−23
231, 026, 304, 321, 206	77	3, 22, 33, 16, 3 (77)	31	32	128	0	0	0	5
			126	126	218	0	0	0	−32
			153	154					
			75	76	334, 243, 045, 236, 326, 423, 137	49	11, 4, 7, 1, 6, 15, 0 (44)	74	−70
			49	50				45	−43
								81	77
232, 134, 322	54	2, 30, 11 (43)	30	27				24	−22
			117	105				56	−53
			71	−63				88	83
314, 126, 216, 225	57	4, 14, 31, 8 (57)	41	41				9	−9
			71	−72					
			107	−108	317	0	3	0	37
			55	−55	119	0	1	0	24
					145	10	12	68	75
					415	0	0	0	4

Can. J. Chem. Downloaded from www.nrcresearchpress.com by 210.87.254.40 on 09/05/12
For personal use only.

Can. J. Chem. Downloaded from www.nrcresearchpress.com by 210.87.254.40 on 09/05/12
For personal use only.

octahedra; i.e. the octahedra share corners only between these two planes of nickel atoms. The coordination of the octahedra between these planes and the relative positions of the nickel and arsenic atoms are almost identical with the coordination and relative positions of metal and nonmetal atoms between any two metal atom face-centered square nets in the pyrite structure.

In Fig. 1B, the open octahedra in the top layer correspond to the solid octahedra in Fig. 1A. This plane of Ni atoms is 4.17 Å below the origin, while the bottom plane represented by the solid octahedra in Fig. 1B is 7.25 Å below the origin. Between these nets each arsenic atom is again shared by three octahedra, but each octahedron shares one edge with another. The coordination of the octahedra between these planes corresponds to the coordination of octahedra between any two metal atom face-centered rectangular nets parallel to the (101) plane in the marcasite structure.

Viewed in this way, the structure of α-$NiAs_2$ can be described as a combination of the pyrite and marcasite structures. Nickel atoms, in distorted face-centered rectangular nets perpendicular to the *c* axis, are surrounded by six arsenic atoms at the corners of distorted octahedra. The coordination of the octahedra between the metal atom planes is alternately pyrite type (p) and marcasite type (m). The separation between p-coordinated nets is 2.63 Å, and between m-coordinated nets is 3.08 Å. The unit cell *c* dimension spans the stacking sequence m/p/m/p/m. Each octahedron is coordinated to 10 other octahedra by corner sharing, and to one other octahedron by edge sharing.

The atoms forming arsenic pairs in the crystal are 2.46 Å apart. This distance is roughly the mean of As—As separations in marcasite-type diarsenides (β-$NiAs_2$, 2.55 Å; $FeAs_2$, 2.47 Å) and pyrite-type diarsenides ($PtAs_2$, 2.38 Å; $PdAs_2$, 2.43 Å). The nickel–arsenic distances show a variation (2.25–2.46 Å) not encountered in pyrites and marcasites, although the mean metal/nonmetal distance (2.38 Å) is, within error, equal to the nickel arsenic distance in β-$NiAs_2$ (2.36 Å). The molar volume of α-$NiAs_2$ is ca. 1.5% less than that of β-$NiAs_2$.

Each metal atom in α-$NiAs_2$ has one metal nearest neighbor at 3.72 Å across the shared edge of two arsenic octahedra. This distance is somewhat greater than the intermetallic distance in β-$NiAs_2$, in which each nickel atom has two nearest neighbors at 3.54 Å, also across shared edges of arsenic octahedra. The distance is too large to suggest that pairs of metal atoms exist (as, for example, in the $CoSb_2$ lattice) or that metal–metal bonds may exist. In spite of the distortions in the arsenic octahedra, we regard the α-$NiAs_2$ structure as more closely related to the pyrite structure than the 'anomalous' marcasite structure (17) exhibited by β-$NiAs_2$ and $NiSb_2$.

Very recently Munson reported the synthesis of a cubic pyrite-type modification of $NiAs_2$ at 1400 °C and 60 kbar which, quenched to normal conditions of temperature and pressure, has a cell dimension of 5.77 Å (18).

Acknowledgments

We are indebted to Dr. L. D. Calvert of the National Research Council of Canada for many helpful discussions. Awards to W. N. Stassen of a Reuben Wells Leonard Resident Fellowship by Queen's, and, subsequently, of Studentships by the National Research Council of Canada, are gratefully acknowledged. This study was supported by Operating Grants from the National Research Council of Canada.

1. R. W. G. Wyckoff. Crystal structures. 2nd ed. Vol. 1. Interscience Publishers, Inc., New York. 1963.
2. W. B. Pearson. A handbook of lattice spacings and structures of metals and alloys. Vol. 2. The Pergamon Press, Ltd., Oxford. 1967.
3. Sutarno, O. Knop, and K. I. G. Reid. Can. J. Chem. **45**, 1391 (1967).
4. S. Furuseth, K. Selte, and A. Kjekshus. Acta Chem. Scand. **19**, 735 (1965).
5. J. J. Murray and R. D. Heyding. Can. J. Chem. **45**, 2675 (1967).
6. S. L. Bennett and R. D. Heyding. Can. J. Chem. **44**, 3017 (1966).
7. L. G. Berry and R. M. Thompson. X-ray powder data file. 8th set. Card 9–8. Special Technical Publication 480G. A.S.T.M., Philadelphia, Penn. 1958.
8. J. S. Kasper and K. Lonsdale (*Editors*). International tables for X-ray crystallography. Vol. II. The Kynoch Press, Birmingham. 1959.
9. W. N. Stassen. Ph.D. Thesis. Queen's University, Kingston, Ontario. 1967.
10. C. H. MacGillavry and G. D. Rieck (*Editors*). International tables for X-ray crystallography. Vol. III. The Kynoch Press, Birmingham. 1962.
11. A. J. C. Wilson. Nature, **150**, 152 (1942).
12. R. Weyl. Z. Krist. **111**, 401 (1959).
13. T. Ito and H. Sawada. Z. Krist. **102A**, 13 (1939).
14. K. Schubert, H. Breiner, and R. Gohle. Z. Metallk. **50**, 152 (1959).
15. V. Luzzati. Acta Cryst. **5**, 802 (1952).
16. G. Fischer. Can. J. Phys. **36**, 1435 (1958).
17. F. Hulliger and E. Mooser. *In* Progress in solid state chemistry. Vol. 2. *Edited by* H. Reiss. The Pergamon Press, Ltd., Oxford. 1964. p. 361.
18. R. A. Munson. Inorg. Chem. **7**, 389 (1968).

Can. J. Chem. Downloaded from www.nrcresearchpress.com by 210.87.254.105 on 09/05/12
For personal use only.

Reactions of organotin compounds. IX. The reactions of tin hydrides with perfluorovinyl germanium and tin compounds

M. Akhtar and H. C. Clark
Department of Chemistry, University of Western Ontario, London, Ontario

Received December 18, 1967

The formation of addition products $(CH_3)_3MCFHCF_2Sn(CH_3)_3$ and $(CH_3)_3MCF[Sn(CH_3)_3]CF_2H$ where M = Ge or Sn has been observed in reactions involving the ultraviolet irradiation of $(CH_3)_3MCF{=}CF_2$ with trimethyltin hydride. The former type of addition product is more stable than the latter, and the stability of both types decreases in the order M = Si, Ge, or Sn. Evidence is presented that decomposition occurs in all cases by a β-fluorine elimination with the formation of fluorovinyl derivatives of M and trimethyltin fluoride. Similar reactions occur between $(CH_3)_3GeCF{=}CF_2$ and dimethyltin dihydride and between $(CH_3)_2Ge(CF{=}CF_2)_2$ and dimethyltin dihydride or trimethyltin hydride. The evidence indicates that a free radical process is involved. Spectroscopic data are presented for new organogermanium compounds.

Canadian Journal of Chemistry, 46, 2165 (1968)

Introduction

We have previously described some reactions of organotin hydrides with fluoro-olefins (1–3) and have presented evidence in favor of a free radical mechanism, with the formation of radicals from the tin hydrides being probably the rate-determining step. Such evidence for the free radical nature of these and other reactions of organotin hydrides arises from observations of the accelerating effect of catalysts (4), free radical sources (4) (e.g. azobisisobutyronitrile), and ultraviolet irradiation (1–3, 5, 6), and the retardation caused by efficient scavengers (e.g. galvinoxyl (4, 5)). We have also described the reactions of trimethyltin hydride and dimethyltin dihydride (5) with $(CH_3)_3SiCF{=}CF_2$ and $(CH_3)_2Si(CF{=}CF_2)_2$, where conclusive evidence for a free radical mechanism was obtained again by the use of such a scavenger and initiators. The course of such reactions can be influenced, firstly by the organic group on tin, e.g. in R_nSn where R can be an alkyl or an aryl group (7), and secondly by the inductive effects of R_3M on the vinylic —C=C bond, caused by the nature of M and by the $d\pi$–$p\pi$ interactions in the R_3M—C=C group (8, 9). The present investigation describes the reactions of organotin hydrides with perfluorovinyl germanium and tin compounds. The variation in the nature of the reaction and in the stability of the reaction products, in going from silicon to germanium to tin perfluorovinyl groups, is also discussed.

Discussion

Trimethyltin hydride reacted with $(CH_3)_3SiCF{=}CF_2$ in the presence of free radical sources (5) to form two addition products, $(CH_3)_3SiCFHCF_2Sn(CH_3)_3$ and $(CH_3)_3SiCF[Sn(CH_3)_3]CF_2H$. These deposit trimethyltin fluoride at room temperature by β-fluorine elimination to give $(CH_3)_3SiCH{=}CF_2$ and *cis*-$(CH_3)_3SiCF{=}CFH$ respectively. However, under thermal conditions, fluorovinyl–silicon compounds containing —CH=CF_2, *cis*-CF=CFH, *trans*-CF=CFH, and —C_2H_2F groups were obtained, with the —CH=CF_2 and *cis*-CF=CFH derivatives being the major reaction products. We have now found that trimethyltin hydride does not react with $(CH_3)_3GeCF{=}CF_2$ at room temperature, even over long periods, but at 55° reaction occurs readily with the deposition of trimethyltin fluoride and formation of fluorovinyl germanes, notably $(CH_3)_3GeCF{=}CFH$ (*cis*), $(CH_3)_3GeCH{=}CF_2$, $(CH_3)_3GeC_2H_2F$, and $(CH_3)_3GeCF{=}CFH$ (*trans*), these being listed in the order of decreasing yield. When the hydride and $(CH_3)_3GeCF{=}CF_2$ were irradiated at room temperature, a high yield of a mixture containing the two addition products $(CH_3)_3GeCFHCF_2Sn(CH_3)_3$ and $(CH_3)_3GeCF[Sn(CH_3)_3]CF_2H$ was obtained. This mixture is unstable at room temperature and eliminates trimethyltin fluoride with the preferential formation of $(CH_3)_3GeCF{=}CFH$ (*cis*) and with the more rapid disappearance of $(CH_3)_3GeCF[Sn(CH_3)_3]CF_2H$. A sample of the mixture of addition products containing $(CH_3)_3GeCF[Sn(CH_3)_3]CF_2H$ and $(CH_3)_3GeCFHCF_2Sn(CH_3)_3$ in the ratio 2:5 is completely decomposed at 55° after 24 h to give $(CH_3)_3GeCF{=}CFH$ (*cis*) and $(CH_3)_3GeCH{=}CF_2$ in the ratio of 1:2, with the simultaneous formation of trimethyltin fluoride. This confirms

Can. J. Chem. Downloaded from www.nrcresearchpress.com by 210.87.254.105 on 09/05/12
For personal use only.

the formation of $(CH_3)_3GeCF{=}CFH$ (*cis*) from $(CH_3)_3GeCF[Sn(CH_3)_3]CF_2H$, and of $(CH_3)_3GeCH{=}CF_2$ from $(CH_3)_3GeCFHCF_2Sn(CH_3)_3$ by β-fluorine elimination. The facile nature of this type of elimination can be readily ascertained by the use of molecular models, from which it can be seen that the p-orbitals of the β-fluorine are directed more towards the tin than are the p-orbitals of the α-fluorine, and that the $Sn{-}F_\beta$ distance is the smaller. The alternative process would be an α-elimination followed by a fluoride ion migration (10), which seems less likely from energetic grounds alone.

The reaction of trimethyltin hydride with $(CH_3)_3SiCF{=}CF_2$ (5) was shown to proceed by a free radical mechanism under ultraviolet irradiation as well as in the presence of free radical sources, e.g. azobisisobutyronitrile. The reaction was completely inhibited by the free radical inhibitor "galvinoxyl". In the present case, the addition of trimethyltin hydride to $(CH_3)_3GeCF{=}CF_2$ apparently occurred at 55° in the presence of azobisisobutyronitrile, but the thermal instability of the addition products at 55° probably explains why only $(CH_3)_3GeCF{=}CFH$ (*cis*), $(CH_3)_3GeCH{=}CF_2$, and $(CH_3)_3GeC_2H_2F$ were obtained. It certainly seems reasonable to assume that here, and in the reactions under ultraviolet irradiation, a free radical process is again involved.

Trimethyltin hydride and $(CH_3)_2Ge(CF{=}CF_2)_2$ do not react at room temperature, and at 55° only a limited reaction takes place. However, the reaction does take place easily under ultraviolet irradiation at room temperature, with the formation of an involatile addition product which was identified spectroscopically as a mixture of the addition products **1**, **2**, and **3**.

The mixture was unstable at room temperature, slowly eliminating trimethyltin fluoride accompanied by the formation of $-CF{=}CFH$ (*cis*) and $-CH{=}CF_2$ groups, thus again supporting a β-fluorine elimination process. It was not possible to separate individual compounds from the mixture chromatographically because of their instability.

In the reactions of trimethyltin hydride (11) with $(CH_3)_3SnCF{=}CF_2$, the main reaction product was always $(CH_3)_3SnCF{=}CFH$ (*cis*), and the possibility of addition followed immediately by trimethyltin fluoride elimination was

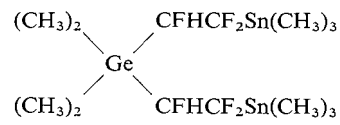

1

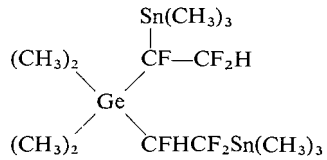

2

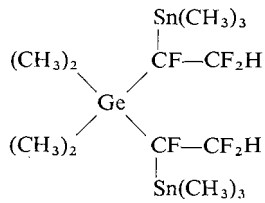

3

suggested. These reactions have now been repeated and in the reaction of trimethyltin hydride with an excess of $(CH_3)_3SnCF{=}CF_2$ in cyclohexane, under ultraviolet irradiation at 25°, the formation of addition products $[(CH_3)_3Sn]_2CFCF_2H$ and $(CH_3)_3SnCFHCF_2Sn(CH_3)_3$ has been established. The addition products could not be isolated because of their instability. At room temperature they quickly eliminate trimethyltin fluoride with the formation of $(CH_3)_3SnCF{=}CFH$ (*cis*), this again being consistent with a β-fluorine elimination, whereby both the products $[(CH_3)_3Sn]_2CFCF_2H$ and $(CH_3)_3SnCFHCF_2Sn(CH_3)_3$ can give $(CH_3)_3SnCF{=}CFH$ (*cis*). The reason that these addition products were not observed previously (11) is apparently due to the long irradiating period of 18 h then involved, in contrast to only 1 h in the present study. In the former case, decomposition had obviously occurred by the end of the irradiation period.

It is interesting to note the difference in the stability of the addition products of trimethyltin hydride with $(CH_3)_3SiCF{=}CF_2$ (5), $(CH_3)_3GeCF{=}CF_2$, and $(CH_3)_3SnCF{=}CF_2$. The addition products with $(CH_3)_3SiCF{=}CF_2$ are the most stable, although $(CH_3)_3SiCF[Sn(CH_3)_3]CF_2H$ decomposes more easily than its isomer $(CH_3)_3SiCFHCF_2Sn(CH_3)_3$. This mixture can be handled for short periods under vacuum without

Can. J. Chem. Downloaded from www.nrcresearchpress.com by 210.87.254.105 on 09/05/12
For personal use only.

decomposition and can even be prepared at 55° using azobisisobutyronitrile, while the analogous addition products with $(CH_3)_3GeCF{=}CF_2$ start decomposing at room temperature after a short time and decompose even while handling under vacuum and cannot be prepared under thermal conditions, even in the presence of azobisisobutyronitrile. Here again $(CH_3)_3GeCF[Sn(CH_3)_3]CF_2H$ decomposes more quickly than $(CH_3)_3GeCFHCF_2Sn(CH_3)_3$. The greater steric requirements for the molecules $(CH_3)_3SiCF[Sn(CH_3)_3]CF_2H$ and $(CH_3)_3GeCF[Sn(CH_3)_3]CF_2H$, where the two heavy groups are attached to one carbon atom, may be responsible for their comparative instability. The addition products of trimethyltin hydride with $(CH_3)_3SnCF{=}CF_2$ are the least stable; they cannot even be separated from the other reaction products and decompose quickly at room temperature. The differences in the metal–carbon bond energies for group IV elements (12), which are in the order Si—C > Ge—C > Sn—C, and the variations of the $d\pi$–$p\pi$ interactions within the R_3M—C=C group, where M varies from Si, Ge to Sn, could be responsible for the above-mentioned order of stabilities of addition products.

Under *thermal* conditions trimethyltin hydride (5, 11) does not add to $(CH_3)_3MCF{=}CF_2$ compounds, where M is Si, Ge, and Sn. However, reactions (9) of the type

$$C_6H_5SnH + (C_6H_5)_3MCH{=}CH_2 \xrightarrow{\text{heat}} C_6H_5MCH_2CH_2Sn(C_6H_5)_3$$

are known, although $(C_6H_5)_3MCH_2CH_2Sn(C_6H_5)_3$ and $[(C_6H_5)_3Sn]_2CHCH_3$ have not been differentiated. This may be due to the difference in stabilities of the vinyl M—C=C bond compared with the perfluorovinyl M—C=C bond (8) and also due to the greater stabilizing effects of C_6H_5 groups compared with CH_3 groups (7). The formation of $(CH_3)_3SnCF{=}CFH$ (*trans*) and $(CH_3)_3SnC_2H_2F$ has been suggested (11) as due to secondary reactions of the type

$$(CH_3)_3SnCF{=}CFH\ (cis) + (CH_3)_3SnH \xrightarrow{\text{u.v.}} (CH_3)_3SnC_2H_2F + (CH_3)_3SnCF{=}CFH\ (trans) + (CH_3)_3SnF.$$

This type of reaction has now also been observed, though under thermal conditions, for the germanium series:

$$(CH_3)_3GeCF{=}CFH\ (cis) + (CH_3)_3SnH \xrightarrow{55^\circ} (CH_3)_3SnC_2H_2F + (CH_3)_3SnF + (CH_3)_3SnCF{=}CFH\ (trans).$$

The behavior of dimethyltin dihydride with $(CH_3)_3GeCF{=}CF_2$ and also with $(CH_3)_2Ge(CF{=}CF_2)_2$ has also been investigated. In each case little reaction occurred at room temperature, but by heating at 55° and also under ultraviolet irradiation considerable reaction took place with the formation of fluorovinyl germanes having *cis* and *trans* —CF=CFH, —CH=CF_2, and —C_2H_2F groups, and the formation of dimethyltin difluoride. In view of the greater reactivity of dimethyltin dihydride compared with trimethyltin hydride, and also of their probable structures, it is not too surprising that the addition products were not isolated.

We have described in detail the characterization of the fluorovinyl compounds of tin (11) and silicon (5) by spectroscopic methods, based on their characteristic infrared and n.m.r. features. The trimethyl- and dimethyl-fluorovinyl germanes are completely analogous to the fluorovinyltin and fluorovinylsilicon compounds described previously (11, 5) and it is only necessary to list the data in Tables I and II. The characterization of the addition products of trimethyltin hydride with $(CH_3)_3GeCF{=}CF_2$ and $(CH_3)_3SnCF{=}CF_2$ is based on their n.m.r. spectra, which are completely analogous to those of the addition products of trimethyltin hydride with $(CH_3)_3SiCF{=}CF_2$ (5). The general pattern of the proton spectrum of these addition products is given in Fig. 1. The complete spectroscopic data is given in Tables III, IV, and V. The proton spectrum clearly shows that each addition product gives a complex pattern of 8 lines in addition to signals from the methyl protons. The two sets of 8 lines can be attributed to the two ethane protons of $AC^{\alpha}F_2C^{\beta}FHB$ and $ABC^{\beta}FC^{\alpha}F_2H$ molecules, where the non-equivalence of the two α-fluorine atoms arises from the fact that there are three different substituents on the β-carbon atom. Hence the proton spectrum for each proton is of the ABX pattern, where the signal of the ethane proton is split successively three times into doublets by coupling with the three non-equivalent fluorine nuclei. The values of the coupling constants obtained are consistent

TABLE I

Proton n.m.r. assignments for perfluorovinyl and fluorovinyl germanes*

$(CH_3)_3Ge$, X_1, X_2, X_3	δCH_3	δH vinyl	J_{12}	J_{23}	J_{13}
$X_1=X_2=X_3=F$	−0.52	—	—	—	—
$X_1=H$, $X_2=X_3=F$ (*cis*)	−0.51	−6.1 quartet	76	—	23
$X_1=X_2=F$, $X_3=H$ (*trans*)	−0.38	−7.5 quartet	74	15	—
$X_1=X_3=F$, $X_2=H$	−0.45	−3.72 quartet	—	9	42
$X_1=F$, $X_2=H_b$, $X_3=H_a$	Not distinguished	−6.5 (H_b) quartet −4.8 (H_a) quartet	78	6	96
$(CH_3)_2Ge(X_1=X_2=F, X_3=F)_2$	−0.45	—	—	—	—
$(CH_3)_2Ge(X_1=H, X_2=X_3=F)_2$ (*cis*)	−0.42	−6.12 quartet	75	—	22
$(CH_3)_2Ge(X_1=X_2=F, X_3=H)_2$ (*trans*)	−0.28	−7.42 quartet	73	15	—
$(CH_3)_2Ge(X_1=X_3=F, X_2=H)_2$	−0.30	−3.82 quartet	—	7	42
$(CH_3)_2Ge(X_1=F, X_2=H_b, X_3=H_a)_2$	−0.32	−6.8 (H_b) quartet −4.88 (H_a) quartet	78	7	95

*Chemical shifts are in p.p.m. with respect to external $CHCl_3$. Coupling constants are in c.p.s.

Can. J. Chem. Downloaded from www.nrcresearchpress.com by 210.87.254.105 on 09/05/12
For personal use only.

TABLE II

Characteristic C=C stretching and C—F frequencies observed in trimethyl and dimethyl perfluorovinyl and fluorovinyl germanes (gas phase, KBr windows)

Compound	C=C region (± 2 cm^{-1})	C—F region (± 2 cm^{-1})
$(CH_3)_3GeCF{=}CF_2$	1730 vs	1290 vs, 1255 m, 1135 vs, 1025 vs
$(CH_3)_3GeCF{=}CFH$ (*cis*)	1700 vs	1280 m, 1250 m, 1110 vs, 1080 m, 930 w
$(CH_3)_3GeCF{=}CFH$ (*trans*)	1725 s	1270 w, 1250 s, 1070 s, 1025 w
$(CH_3)_3GeCH{=}CF_2$	1665 s	1245 m, 1120 vs, 1070 6, s, 1020 w
$(CH_3)_3GeC_2H_2F$	1625 s	1245 m, 1180 m, 1120 w, 1060 vs, 975 m, 925 w
$(CH_3)_2Ge(CF{=}CF_2)_2$	1730 vs	1291 vs, 1254 s, 1139 s, 1028 vs
$(CH_3)_2Ge(CF{=}CFH)_2$ (*cis*)	1700 vs	1280 s, 1252 m, 1125 s, 1065 m, 940 m
$(CH_3)_2Ge(CF{=}CFH)_2$ (*trans*)	1722 s	1250 w, 1050 s, 920 w
$(CH_3)_2Ge(CH{=}CF_2)_2$	1665 s	1250 m, 1130 vs, 1085 s, 1070 s, 930 vw
$(CH_3)_2Ge(C_2H_2F)_2$	1628 s	1255 m, 1170 s, 1080 m, 1000 m, 940 w

with those observed for $—CF_2H$ group (13) and also for the $—CFHCF_2$ groups respectively. The spectra of closely related compounds have been discussed in considerable detail (14, 15), hence a full analysis of the proton and ^{19}F spectrum is not given here. The ^{19}F spectrum of the addition products of trimethyltin hydride with $(CH_3)_3GeCF{=}CF_2$ is quite analogous to those of the addition products with $(CH_3)_3Si$-$CF{=}CF_2$ (5), consisting of 24 lines for each molecule. From closely coincident values of H—F coupling constants the proton and ^{19}F spectra were matched. The normal first-order analysis then gave the values shown in Table III.

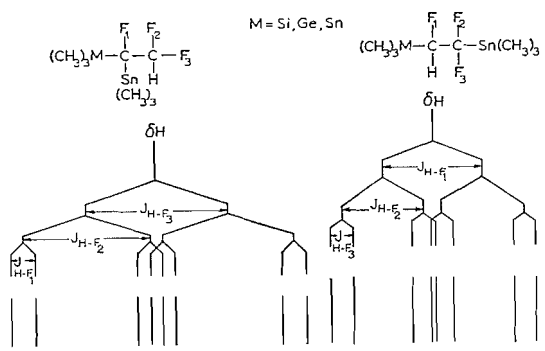

FIG. 1. General pattern of the proton spectra of the addition products of $(CH_3)_3SnH$ with $(CH_3)_3MCF{=}CF_2$ compounds.

The involatile liquid obtained from the ultraviolet irradiation of trimethyltin hydride and $(CH_3)_2Ge(CF{=}CF_2)_2$ was shown from spectroscopic evidence to be a mixture containing three molecules: (**1**) $(CH_3)_2Ge[CFHCF_2Sn(CH_3)_3]_2$, (**2**) $(CH_3)_2Ge[CF(Sn(CH_3)_3)CF_2H][CFHCF_2$-$Sn(CH_3)_3]$, and (**3**) $(CH_3)_2Ge[CF(Sn(CH_3)_3)$-$CF_2H]_2$. The numerical data is given in Tables IV and VI. The proton n.m.r. spectrum, although complex, was completely consistent with the data already given for other addition products. The spectrum of $—CF(Sn(CH_3)_3)CF_2H$ groups in molecules (**2**) and (**3**) and that of $—CFHCF_2$-$Sn(CH_3)_3$ groups in molecules (**1**) and (**2**), though closely spaced, did not overlap. The possible assignments are given in Table VI.

Experimental

All general techniques have been described previously (5). Trimethyltin hydride and dimethyltin dihydride were prepared by the procedure of Finholt *et al.* (16) using *n*-butyl ether as solvent. Trimethyl(perfluorovinyl)germane and dimethylbis(perfluorovinyl)germane were prepared (17) by the reaction of trimethylgermanium bromide and dimethylgermanium dichloride respectively with perfluorovinylmagnesium bromide in anhydrous tetrahydrofuran. Most of the tetrahydrofuran was separated by fractional distillation, and final purification was achieved by gas chromatography on a silicone QF-1 column at 150°. Thus trimethyl(perfluorovinyl)germane was obtained in 36% yield and dimethylbis(perfluorovinyl)germane in 33% yield. The spectroscopic data is given in Tables I and II. Trimethyl(perfluorovinyl)tin was prepared by the method described by Beveridge *et al.* (11).

In all of the reactions described below, the reaction mixture was worked up as follows. The reaction tube was opened to the vacuum system and all volatile components were separated by conventional trap-to-trap fractionation. Further purification was achieved by gas chromatography

Can. J. Chem. Downloaded from www.nrcresearchpress.com by 210.87.254.105 on 09/05/12
For personal use only.

TABLE III

Nuclear magnetic resonance data* for the addition products of $(CH_3)_3SnH$ with $(CH_3)_3GeCF{=}CF_2$ in cyclohexane

	$(CH_3)_3Ge{-}\underset{\underset{(CH_3)_3}{Sn}}{\overset{\overset{F_1}{\vert}}{C}}{-}\overset{\overset{F_2}{\vert}}{\underset{\underset{H}{\vert}}{C}}{-}F_3$		$(CH_3)_3Ge{-}\underset{\underset{H}{\vert}}{\overset{\overset{F_1}{\vert}}{C}}{-}\overset{\overset{F_2}{\vert}}{\underset{\underset{F_3}{\vert}}{C}}{-}Sn(CH_3)_3$	
	^1H spectrum	^{19}F spectrum	^1H spectrum	^{19}F spectrum
$\delta Ge{-}CH_3$	−0.15		−0.15	
δH	−6.12		−4.6	
$\delta Sn{-}CH_3$	−0.2		−0.2	
$J^{119}_{Sn-CH_3}$	56		56	
$J^{117}_{Sn-CH_3}$	55		55	
δF_1		217.7		229
δF_2		118		111.2
δF_3		108		98.6
J_{H-F_1}	10	9.7	45	46.3
J_{H-F_2}	63	62.4	40	39.4
J_{H-F_3}	58	58	8	8
$J_{F_1-F_2}$		19.2		11
$J_{F_1-F_3}$		24		13
$J_{F_2-F_3}$		277.6		271.3

*Chemical shifts (p.p.m.) are relative to internal cyclohexane and internal CCl_3F for ^1H and ^{19}F spectrum respectively. Coupling constants in c.p.s.

TABLE IV

Infrared spectra of the addition products as liquid films

$(CH_3)_3SnH$ + $(CH_3)_3GeCF{=}CF_2$	$(CH_3)_3SnH$ + $(CH_3)_2Ge(CF{=}CF_2)_2$	Assignment
508 (m)	510 (s)	Sn—C stretch
530 (s)	530 (vs)	
562 (w)	570 (m)	Ge—C asym. stretch
600 (s)	605 (m)	
715 (sh, w)	730 (vs)	CH_3—Sn and CH_3—Ge rock
770 (b, s)	770 (vs, b)	
825 (s)	825 (s, sh)	
	840 (s, sh)	
945 (s)	945 (s)	
985 (s)	985 (s)	
1030 (s)	1030 (s)	C—F stretch
1060 (m)	1060 (s)	
1110 (sh, m)	1110 (sh, s)	
1125 (s)	1130 (vs)	
1190 (w)	1190 (m)	
1215 (w)	1210 (sh, w)	
1240 (m)	1240 (m)	Sym. CH_3—Ge deformation
1260 (w)		
1300 (vw)	1305 (w)	
1330 (w)	1335 (m)	
1355 (w)	1355 (m)	
1390 (vw)	1385 (w)	
1410 (m)	1410 (m)	Asym. CH_3—Ge deformation
2910 (m)	2910 (s)	C—H stretch
2990 (s)	2990 (s)	

Can. J. Chem. Downloaded from www.nrcresearchpress.com by 210.87.254.105 on 09/05/12
For personal use only.

TABLE V

^{1}H n.m.r. data* for the addition products of $(CH_3)_3SnH$ with trimethyl perfluorovinyl compounds of group IV elements

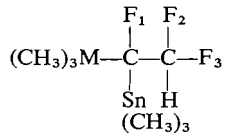

M	Si	Ge	Sn
δH	−6.5	−6.12	−6.3
δM—CH_3	−0.08	−0.15	−0.22
δSn—CH_3	−0.15	−0.2	−0.22
$J^{119}_{Sn-CH_3}$	57	56	55
$J^{117}_{Sn-CH_3}$	55	55	54
J_{H-F_1}	10	10	12
J_{H-F_2}	62	63	62
J_{H-F_3}	56	58	60

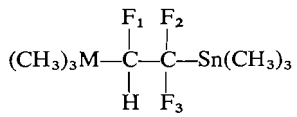

M	Si	Ge	Sn
δH	−4.72	−4.6	−5.0
δM—CH_3	−0.08	−0.15	−0.22
δSn—CH_3	−0.15	−0.2	−0.22
$J^{119}_{Sn-CH_3}$	57	56	55
$J^{117}_{Sn-CH_3}$	55	55	54
J_{H-F_1}	44	45	47
J_{H-F_2}	37	40	45
J_{H-F_3}	10	8	6

*Chemical shifts (p.p.m.) are relative to external $CHCl_3$ for silicon compounds, while those for germanium and tin compounds are relative to internal cyclohexane. Coupling constants in c.p.s.

TABLE VI

Proton n.m.r. data* for the addition products of $(CH_3)_3SnH$ with $(CH_3)_2Ge(CF{=}CF_2)_2$ in cyclohexane

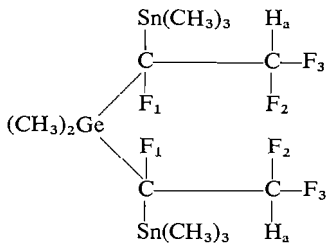

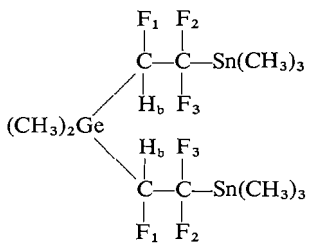

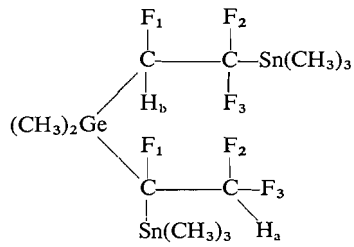

δGe—CH_3	−0.58	−0.58	−0.58
δSn—CH_3	−0.35	−0.35	−0.35
δH_a	−6.36		−6.3
δH_b		−4.98	−4.92
$J^{119}_{Sn-CH_3}$	56	56	56
$J^{117}_{Sn-CH_3}$	55	55	55
$J_{H_a-F_1}$	10		10
J_{H_a-F2}	65		60
$J_{H_a-F_3}$	58		56
$J_{H_b-F_1}$		45	45
$J_{H_b-F_2}$		42	42
$J_{H_b-F_3}$		5	5

*Chemical shifts (p.p.m.) are relative to internal cyclohexane. Coupling constants in c.p.s.

and each fraction was identified from its infrared spectrum, and for pure compounds ultimately by their n.m.r spectra. Any involatile material remaining in the reaction tube was examined spectroscopically.

Reactions of Trimethyl(perfluorovinyl)germane with Organotin Hydrides

(*a*) Trimethyltin hydride (0.225 g, 1.36 mmoles) and $(CH_3)_3GeCF{=}CF_2$ (0.27 g, 1.36 mmoles) were allowed to react at 25° for 10 days. There was no visible reaction and vacuum fractionation gave the starting materials quantitatively.

(*b*) Trimethyltin hydride (0.33 g, 2 mmoles) and $(CH_3)_3GeCF{=}CF_2$ (0.395 g, 2 mmoles) were heated at 55° for 30 h. A white solid was deposited, which was identified spectroscopically as trimethyltin fluoride (0.145 g, ca. 40% yield). Examination of the infrared spectrum of the gas phase mixture showed the presence of both reactants and at least four reaction products. The proton n.m.r. spectrum (Table I) of this mixture was recorded and from its integration the following percentage of each component in the total reaction mixture was obtained: *cis*-CFH=CFGe$(CH_3)_3$ (45%), *trans*-CFH=CFGe$(CH_3)_3$ (6%), $CF_2{=}CHGe(CH_3)_3$ (40%), and

Can. J. Chem. Downloaded from www.nrcresearchpress.com by 210.87.254.105 on 09/05/12
For personal use only.

Can. J. Chem. Downloaded from www.nrcresearchpress.com by 210.87.254.105 on 09/05/12
For personal use only.

$(CH_3)_3GeC_2H_2F$ (9%). Gas chromatography on a silicone QF-I column at 150° gave pure products which were identified by their characteristic infrared spectra (Table II).

(*c*) Trimethyltin hydride (0.45 g, 2.7 mmoles) and $(CH_3)_3GeCF{=}CF_2$ (0.54 g, 2.7 mmoles) were exposed to ultraviolet irradiation (silica tube) at 25° for 8 h. A trace of trimethyltin fluoride, identified spectroscopically, was deposited, as well as a small amount of metallic tin. Vacuum fractionation gave, at −78°, a small amount of $(CH_3)_3GeCF{=}CFH$ (*cis*) and trimethyltin hydride and a high yield (0.72 g, 73%) of a slightly volatile liquid at −23°. This was identified unambiguously, from infrared and n.m.r. studies (Tables III, IV), as a mixture of two addition products $(CH_3)_3GeCF[Sn(CH_3)_3]CF_2H$ and $(CH_3)_3GeCFHCF_2Sn(CH_3)_3$ in the ratio 2:5.

This mixture of addition products is unstable at room temperature. A small amount was sealed into a 5 mm pyrex tube with 1 ml of cyclohexane and left at room temperature for 24 h. Then its proton n.m.r. spectrum was recorded in the same glass tube. This showed a very small amount of $(CH_3)_3GeCF[Sn(CH_3)_3]CF_2H$ still to be present along with a considerable amount of $(CH_3)_3GeCF{=}CFH$ (*cis*) and some $(CH_3)_3SnF$. The original amount of $(CH_3)_3GeCFHCF_2Sn(CH_3)_3$ remained unchanged. A similar sample of the addition products was left at 55° for 2 h. Its proton n.m.r. spectrum showed the complete disappearance of $(CH_3)_3GeCF[Sn(CH_3)_3]CF_2H$ with the formation of $(CH_3)_3GeCF{=}CFH$ (*cis*) and elimination of $(CH_3)_3SnF$. But this time a small amount of $(CH_3)_3GeCH{=}CF_2$ also appeared with a decrease in the amount of $(CH_3)_3GeCFHCF_2Sn(CH_3)_3$. Another sample of the addition products $(CH_3)_3GeCF[Sn(CH_3)_3]CF_2H$ and $(CH_3)_3GeCFHCF_2Sn(CH_3)_3$ in the ratio 2:5 was sealed into a glass tube with 1.5 ml of cyclohexane and left at 55° for 24 h. A considerable amount of $(CH_3)_3SnF$ was deposited in the tube. The volatiles were transferred to a 5 mm glass tube under vacuum, and the proton n.m.r. spectrum showed $(CH_3)_3GeCF{=}CFH$ (*cis*) and $(CH_3)_3GeCH{=}CF_2$ in the ratio of 1:2. Molecular weight (in benzene osmometrically) was 365. Further characterization was obtained by alkaline hydrolysis of the products. A sample (0.3063 g, 0.844 mmole) was hydrolyzed with 20% potassium hydroxide alcoholic solution. The only volatile product was trifluoroethylene (0.068 g, 0.84 mmole) characterized spectroscopically (18).

In the following experiments (*d–g*), the products were separated by trap-to-trap distillation and identified by their infrared and proton n.m.r. spectra as in (*b*) above.

(*d*) Trimethyltin hydride (0.45 g, 2.7 mmoles) and $(CH_3)_3GeCF{=}CF_2$ (0.54 g, 2.7 mmoles) were sealed with 50 mg of azobisisobutyronitrile and allowed to react at 55° for 8 h. Examination of the reaction mixture gave a small amount of a noncondensable gas, presumably a mixture of hydrogen and nitrogen, along with $(CH_3)_3GeCF{=}CFH$ (*cis*) as the main product, and $(CH_3)_3GeCH{=}CF_2$ and $(CH_3)_3GeC_2H_2F$ in about equal amounts, these being identified by their characteristic C=C stretching frequencies at 1700, 1665, and 1625 cm^{-1} respectively. A mixture of trimethyltin fluoride, metallic tin, and azobisisobutyronitrile remained in the reaction tube.

(*e*) Trimethyltin hydride (0.112 g, 0.68 mmole) and $(CH_3)_3GeCF{=}CFH$ (*cis*) (0.123 g, 0.68 mmole) were allowed to react at 55° for 10 h. Vacuum fractionation of the volatile products gave $(CH_3)_3GeC_2H_2F$ as the main reaction product with a characteristic C=C stretching frequency at 1665 cm^{-1}. Another band was observed at 1725 cm^{-1} (C=C stretch) characteristic of $(CH_3)_3GeCF{=}CFH$ (*trans*). Trimethyltin fluoride remained in the reaction tube and was identified spectroscopically.

(*f*) Dimethyltin dihydride (0.204 g, 1.36 mmoles) and $(CH_3)_3GeCF{=}CF_2$ (0.27 g, 1.36 mmoles) were allowed to react at room temperature for 10 days. The infrared spectrum of the volatile products showed a strong band at 1625 cm^{-1} (C=C stretch), characteristic of $(CH_3)_3GeC_2H_2F$, and two other medium bands at 1700 and 1665 cm^{-1}, characteristic of (C=C stretch) $(CH_3)_3GeCF{=}CFH$ (*cis*) and $(CH_3)_3GeCH{=}CF_2$ respectively. However, the amounts were so small that the proton n.m.r. spectrum showed only $(CH_3)_2SnH_2$ and $(CH_3)_3GeCF{=}CF_2$. From the reaction tube a small amount (0.008 g) of $(CH_3)_2SnF_2$ was recovered, from which it could be calculated that the reaction was about 3% complete.

(*g*) Dimethyltin dihydride (0.204 g, 1.36 mmoles) and $(CH_3)_3GeCF{=}CF_2$ (0.27 g, 1.36 mmoles) were irradiated at 25° for 6 h, leading to the extensive formation of a white solid. A mixture of methane and hydrogen present in the reaction tube was pumped off. The infrared spectrum (gas phase) of the volatiles showed the presence of $(CH_3)_3GeCF{=}CFH$ (*cis*), $(CH_3)_3GeCH{=}CF_2$, $(CH_3)_3GeC_2H_2F$, and $(CH_3)_3GeCF{=}CFH$ (*trans*), based on the observed C=C stretching frequencies and listed in the order of decreasing concentration. From the reaction tube, dimethyltin difluoride (0.125 g) was recovered, corresponding to 50% complete reaction.

Reactions of Dimethylbis(perfluorovinyl)germane with Organotin Hydrides

(*a*) Trimethyltin hydride (0.33 g, 2 mmoles) and $(CH_3)_2Ge(CF{=}CF_2)_2$ (0.264 g, 1 mmole) were allowed to react at 25° for 10 days. There was no visible reaction and vacuum fractionation led to complete recovery of the reactants.

(*b*) Trimethyltin hydride (1.29 g, 7.8 mmoles) and $(CH_3)_2Ge(CF{=}CF_2)_2$ (0.875 g, 3.3 mmoles) were allowed to react at 55° for 20 h. A considerable amount of white solid was deposited and a trace of a noncondensable gas was pumped off. Infrared and ^1H n.m.r. spectra of the volatiles showed the presence of —CF=CFH (*cis*), —CH=CF_2, —C_2H_2F, and —CF=CFH (*trans*) groups, with characteristic infrared C=C stretching frequencies at 1700, 1665, 1628, and 1722 cm^{-1} respectively, these groups being listed in the order of decreasing amounts. Complete spectroscopic data are listed in Tables I and II. From the residue in the reaction tube 0.9023 g of $(CH_3)_3SnF$ was extracted, corresponding to 63% reaction.

(*c*) Trimethyltin hydride (0.898 g, 5.4 mmoles) and $(CH_3)_2Ge(CF{=}CF_2)_2$ (0.719 g, 2.72 mmoles) were irradiated (silica tube) at 25° for 5 h, at the end of which time a very small amount of metallic tin and a white solid had deposited. Other than a small amount of a noncondensable gas, the only volatile product was a negligible amount of trimethyltin hydride. There remained in the reaction tube an involatile liquid, which was washed out with cyclohexane and examined spectroscopically after

Can. J. Chem. Downloaded from www.nrcresearchpress.com by 210.87.254.105 on 09/05/12
For personal use only.

removal of the solvent. The infrared and proton spectra (Tables III and VI) showed the material to be a mixture of three addition products of $(CH_3)_3SnH$ and $(CH_3)_2Ge(CF{=}CF_2)_2$, listed in Table VI; these could not be separated chromatographically due to instability. On standing at 25° decomposition occurred slowly with the deposition of $(CH_3)_3SnF$ and formation of —CF=CFH (*cis*) and —CH=CF_2 groups with characteristic C=C stretching frequencies at 1700 and 1665 cm^{-1} respectively.

(*d*) Dimethyltin dihydride (0.29 g, 2 mmoles) and $(CH_3)_2Ge(CF{=}CF_2)_2$ (0.53 g, 2 mmoles) were allowed to react at room temperature for 10 days. A white-to-yellow solid appeared in the reaction tube. The infrared spectrum (gas phase) of the volatile reaction products showed the presence of —CF=CFH, —CH=CF_2, and —C_2H_2F groups, in addition to considerable amounts of the starting materials. The residue (0.003 g) in the reaction tube was washed out, examined, and found to be mainly dimethyltin difluoride with a little metallic tin.

(*e*) Dimethyltin dihydride (0.76 g, 5 mmoles) and $(CH_3)_2Ge(CF{=}CF_2)_2$ (1.32 g, 5 mmoles) were allowed to react at 55° for 8 h. A considerable amount of white-to-black solid was deposited. Noncondensable gas, a mixture of hydrogen and methane, was pumped off. The ^1H n.m.r. spectrum of the total volatile products (Table I) confirmed the presence of four reaction products, in addition to some unidentified peaks, these being listed with the percentage of each component in the total reaction mixture, as determined by integration of the ^1H n.m.r. spectrum. The products were $(CH_3)_2Ge(CF{=}CFH)_2$ (*cis*) (33.3%), $(CH_3)_2Ge(CH{=}CF_2)_2$ (41.7%), $(CH_3)_2Ge(CF{=}CFH)_2$ (*trans*) (13.8%), and $(CH_3)_2Ge(C_2H_2F)_2$ (11.1%). Gas chromatography on a silicone QF-1 column at 150° gave pure products, in addition to unreacted $(CH_3)_3SnH_2$ and $(CH_3)_2Ge(CF{=}CF_2)_2$, which were identified by their characteristic infrared and proton n.m.r. spectra (Tables I and II). From the reaction tube 0.552 g of $(CH_3)_2SnF_2$ with some metallic tin was recovered.

(*f*) Dimethyltin dihydride (0.29 g, 2 mmoles) and $(CH_3)_2Ge(CF{=}CF_2)_2$ (0.53 g, 2 mmoles) were irradiated at 25° for 1 h. A white solid was deposited and the noncondensable gas was pumped off. The infrared spectrum (gas phase) of the volatile products confirmed the presence of $(CH_3)_2Ge$— derivatives containing —CF=CFH, —CH=CF_2, and —C_2H_2F groups, based on their C=C stretching frequencies (Table II), but the amounts were so small that the proton n.m.r. spectrum showed only $(CH_3)_2SnH_2$ and $(CH_3)_2Ge(CF{=}CF_2)$. From the reaction tube 0.061 g of dimethyltin difluoride containing a trace of metallic tin was recovered.

Reactions of Trimethyl(perfluorovinyl)tin with Trimethyltin Hydride

(*a*) Trimethyltin hydride (0.45 g, 2.8 mmoles) and $(CH_3)_3SnCF{=}CF_2$ (0.682 g, 2.8 mmoles) were irradiated at 25° for 1 h. A considerable amount of white solid was deposited. A negligible amount of noncondensable gas was pumped off. The infrared spectrum of the volatile reaction products confirmed (11) the presence of $(CH_3)_3SnCF{=}CFH$ (*cis*) and $(CH_3)_3SnCF{=}CFH$ (*trans*), in addition to some unreacted $(CH_3)_3SnCF{=}CF_2$. This mixture was sealed in a 5 mm glass tube and its ^1H n.m.r. spectrum was recorded. This again confirmed the presence of $(CH_3)_3SnCF{=}CFH$ (*cis*) and $(CH_3)_3SnCF{=}CFH$ (*trans*), from the available spectroscopic data (11). The amounts of the reaction products in the total reaction mixture were determined by integration of the ^1H n.m.r. spectrum, which gave $(CH_3)_3SnCF{=}CFH$ (*cis*) (78%) and $(CH_3)_3SnCF{=}CFH$ (*trans*) (18%). Trimethyltin fluoride (0.406 g) was recovered from the reaction tube, corresponding to 80% complete reaction.

(*b*) Trimethyltin hydride (0.22 g, 1.4 mmoles) and $(CH_3)_3SnCF{=}CF_2$ (0.682 g, 2.8 mmoles) and 1 ml of cyclohexane were irradiated at 25° into a 5 mm pyrex glass tube. After 1 h, a considerable amount of white solid [$(CH_3)_3SnF$] was visible in the reaction tube. Immediately the ^1H n.m.r. spectrum of the reaction mixture was recorded in the same 5 mm reaction tube, and this confirmed the presence of the addition products $[(CH_3)_3Sn]_2CFCF_2H$ and $(CH_3)_3SnCFHCF_2Sn(CH_3)_3$, spectroscopic data being given in Table V. From the integration of the proton n.m.r. spectrum the ratio of $[(CH_3)_3Sn]_2CFCF_2H$ to $(CH_3)_3SnCFHCF_2Sn(CH_3)_3$ was 1:1. The tube containing the reaction mixture was left at room temperature for 6 h, after which time extensive elimination of $(CH_3)_3SnF$ had taken place. The proton n.m.r. spectrum of the reaction products in the same reaction tube confirmed the presence of only one reaction product, i.e. $(CH_3)_3SnCF{=}CFH$ (*cis*).

1. H. C. Clark, S. G. Furnival, and J. T. Kwon. Can. J. Chem. **41**, 2889 (1963).
2. C. Barnetson, H. C. Clark, and J. T. Kwon. Ind. Chemist, 458 (1964).
3. H. C. Clark and J. T. Kwon. Can. J. Chem. **42**, 1288 (1964).
4. W. P. Neuman. Angew. Chem. **76**, 849 (1964).
5. M. Akhtar and H. C. Clark. Can. J. Chem. **46**, 633 (1968).
6. J. C. Pommier and J. Valade. Bull. Soc. Chim. France, 951 (1963).
7. W. P. Neuman, H. J. Abert, and W. Kaise. Tetrahedron Letters, 2041 (1967).
8. D. Seyferth. Progress in inorganic chemistry. Vol. 3. *Edited by* F. A. Cotton. Interscience Publishers, Inc., New York. 1962. p. 129.
9. M. C. Henry and J. C. Noltes. J. Am. Chem. Soc. **82**, 558 (1960).
10. R. N. Haszeldine and J. C. Young. Proc. Chem. Soc. 394 (1959).
11. A. D. Beveridge, H. C. Clark, and J. T. Kwon. Can. J. Chem. **44**, 179 (1966).
12. H. A. Skinner. Advances in organometric chemistry. Vol. 2. *Edited by* F. A. Stone and Robert West. Academic Press, Inc., New York. 1964. p. 49.
13. H. C. Clark, J. T. Kwon, L. W. Reeves, and E. J. Wells. Can. J. Chem. **41**, 3005 (1963).
14. D. Seyferth, T. Wada, and G. E. Maciel. Inorg. Chem. **1**, 232 (1962).
15. H. C. Clark, N. Cry, and J. H. Tsai. Can. J. Chem. **45**, 1073 (1967).
16. A. E. Finholt, A. C. Bond, Jr., K. E. Wilzbach, and H. I. Schlesinger. J. Am. Chem. Soc. **69**, 2692 (1947).
17. S. L. Stafford and F. G. A. Stone. Spectrochim. Acta, **17**, 412 (1961).
18. D. G. Weiblen. *In* Fluorine chemistry. Vol. 2. *Edited by* J. H. Simons. Academic Press, Inc., New York. 1954.

Can. J. Chem. Downloaded from www.nrcresearchpress.com by 210.87.254.42 on 09/05/12
For personal use only.

Group vibrations and the vibrational analysis of molecules containing the CD_3 group[1]

J. M. FREEMAN AND T. HENSHALL
University of Salford, Salford 5, England

Received November 15, 1967

The procedure introduced by King and Crawford for the simplification of the molecular vibrational problem by factorization from the secular determinant of characteristic group frequencies, and applied by them to the CD_3 group, has been reexamined and programmed in English-Electric KDF-9 Algol. A few small corrections have been made to their results, and equations are given for the calculation of CD_3 group frequencies in molecules bearing such groups.

The group factorization procedure has also been applied to the calculation of the skeletal frequencies of $\alpha\alpha\alpha$-d_3-dimethyl sulfide and d_6-dimethyl selenide.

Canadian Journal of Chemistry, **46**, 2175 (1968)

King and Crawford (1) have shown how the concept of group vibrations (i.e. vibrations associated with certain molecular functional groups whose frequencies are relatively insensitive to their molecular environments) can lead to a simplification of the vibrational problem. In this method, the order of the secular determinant is reduced by factoring from it those frequencies that are characteristic of the group under consideration.

After correcting small arithmetical errors in King and Crawford's paper, we successfully applied the method to dimethyl sulfoxide (2); dimethyl sulfone (3); dimethyl sulfide, selenide, and telluride (4).

We have now programmed King and Crawford's procedure in English-Electric KDF-9 Algol, have applied it first to a reexamination of the vibrations of the CD_3 group, and quote the following slight amendments to the results quoted for this group by King and Crawford (5), whose paper should be consulted for details of the method.

Whilst, as King and Crawford assert, no correction to μ_D is required for the symmetric CD_3 deformation, they omit a small, though necessary, correction to the corresponding row of the B matrix when calculating off-diagonal elements of the reduced kinetic G_{ff}^{+} matrix for the framework modes, viz.

	C_x	C_y	C_z	R_x	R_y	R_z
$B_2(M^{-1})^+$:	0	0	b	0	0	0

$$\left(b = -0.986 \times 4\frac{\sqrt{3}}{3}\mu_{C_z}{}^{+}\right).$$

Thus whenever an entry $-4\sqrt{3}\,u_{C_z}{}^{+}/3$ appears in an off-diagonal element of the $G_{ff}{}^{+}$ matrix associated with the coordinate S_2, it is to be replaced by this corrected value b.

The corresponding corrections for the E species of vibration are

	C_x	C_y	C_z	R_x	R_y	R_z
$B_{6x}(M^{-1})^+$:	b'	0	0	$\frac{-\sqrt{6}}{2}a\mu_R$	0	0

($a = r/R$, the ratio of CD to CR bond lengths; $b' = \frac{1}{2}\sqrt{6}\,(a + \frac{1}{3} + g)\,\mu_{C_x}{}^{+}$; $g = 0.258$).

Hence whenever a term $(a + \frac{1}{3})$ occurs in an off-diagonal element of $G_{ff}{}^{+}$ associated with symmetry coordinate S_6, it must be replaced by $(a + \frac{1}{3} + g)$; and the diagonal element $G_{66}{}^{+}$ assumes the form

$$G_{66}{}^{+} = \mu_D{}^{+} + \tfrac{3}{2}(a + \tfrac{1}{3})^2\mu_{C_x}{}^{+} + \tfrac{3}{2}a^2\mu_R,$$

with $\mu_D{}^{+} = 0.4118 + (0.0480 - 0.1506\mu_R)a + 0.0273\,a^2\mu_R$. This is a more complete form than that quoted by King and Crawford (5).

The corrections, Φ_{ff}, to the force constant matrices, F_{ff}, for the framework modes to give the matrix, $F_{ff}{}^{+}$, for the reduced vibrational problem of any CD_3R molecule [R = a single atom or an atomic grouping] are:

[1]All correspondence should be addressed to: Dr. T. Henshall, Department of Chemistry and Applied Chemistry, The University of Salford, Salford 5, England.

Species A

Φ_{ff} (mdyn Å^{-1}):	S_2	S_5
S_2	0.002	0.008
S_5	0.008	0.030

Species E

Φ_{ff} (mdyn Å^{-1})	S_6
S_6	0.042

These corrections are in reasonable agreement with the values quoted in ref. 5, except for the change of sign of $\Phi_{ff\ (2,\ 5)}$ in the A species.

The reduced secular determinant $|G_{ff}{}^{+}F_{ff}{}^{+} - \lambda E_{ff}| = 0$ was first solved for the CD_3Cl molecule using the force constants for methyl chloride given in ref. 2. The results are presented in Table I.

TABLE I

CD_3Cl skeletal frequencies

CD_3Cl	$\nu_{approx}(cm^{-1})$	$\nu_{exact}(cm^{-1})$
ν_2	1020	1025
ν_5	692	690
ν_6	788	782

The values of the force constants in mdyn Å^{-1} used in calculations on the 'standard molecule' CD_3R ($R = 10^6$ a.m.u.) were

$$F_{11} = 4.95,\ F_{22} = 0.495,\ F_{33} = 4.95,$$
$$F_{44} = 0.44,\ F_{66} = 0.64,$$

and the approximate equations for the group frequencies for the CD_3 group were calculated to be

$$\lambda_1 = 2.6244 + 0.5224\Delta F_{11} + 0.0453\Delta F_{22} + 0.0064\Delta F_{55};$$

$$\lambda_3 = 3.0462 + 0.6059\Delta F_{33} + 0.062\Delta F_{44} + 0.0310\Delta F_{66};$$

$$\lambda_4 = 0.6358 + 1.3575\Delta F_{44} + 0.0548\Delta F_{66}.$$

($\lambda_i = 4\pi^2c^2\nu_i^2$; $\Delta F_{ij} = F_{ij} - F_{ij}{}^0$, where $F_{ij}{}^0$ refers to the standard molecule and F_{ij} to the corresponding force constant in a molecule carrying a CD_3 group).

Application of these equations to the CD_3 group vibrations in CD_3Cl gave the results of Table II.

The group factorization procedure was then applied to ααα-d_3-dimethyl sulfide and d_6-dimethyl selenide for which the spectra have been reported in refs. 6 and 7 respectively.

TABLE II

CD_3Cl group frequencies

CD_3Cl	$\nu_{approx}(cm^{-1})$	$\nu_{exact}(cm^{-1})$
ν_1	2126	2127
ν_3	2293	2293
ν_4	1038	1039

TABLE III

d_6-Dimethylselenide group and skeletal frequencies

	d_6-Dimethylselenide (C_{2v}): skeletal frequencies		
Species	$\nu_{obsd}(cm^{-1})$	$\nu_{calcd}(cm^{-1})$	Assignment (7)
A_1	983	986	CD_3 sym. deformation
	744	718	CD_3 'rock'
	548	549	CX sym. stretch
	201	207	$\widehat{CXC}$ bend
B_1	968	952	CD_3 sym. deformation
	658	631	CD_3 'rock'
	563	562	CX antisym. stretch
A_2	684	666	CD_3 'rock'
B_2	692	674	CD_3 'rock'

	Group Frequencies (average values)	
	$\nu_{calcd}(cm^{-1})$	$\nu_{obsd}(cm^{-1})$
CD sym. stretch	2098	2140
CD antisym. stretch	2231	2256
CD_3 antisym. deformation	1026	1048

The symmetry coordinates for $(CD_3)_2Se$ are the same as those already used for $(CH_3)_2Se$ in ref. 4, except that the symmetrical CD_3 deformation frequencies are now included in both the A_1 and B_1 vibration species under C_{2v}, viz.

$$S^{A_1}(CD_3\,\text{defn.}) = \frac{1}{\sqrt{12}}(\alpha_1 + \alpha_2 + \alpha_3 + \alpha_4 + \alpha_5 + \alpha_6 - \delta_1 - \delta_2 - \delta_3 - \delta_4 - \delta_5 - \delta_6)$$

and

$$S^{B_1}(CD_3\,\text{defn.}) = \frac{1}{\sqrt{12}}(\alpha_1 + \alpha_2 + \alpha_3 - \alpha_4 - \alpha_5 - \alpha_6 - \delta_1 - \delta_2 - \delta_3 + \delta_4 + \delta_5 + \delta_6)\,.$$

ααα-d_3-Dimethyl sulfide, however, has the lower symmetry of point group C_s. The following symmetry coordinates were constructed from the internal displacement coordinates described in ref. 4.

Can. J. Chem. Downloaded from www.nrcresearchpress.com by 210.87.254.42 on 09/05/12
For personal use only.

TABLE IV

ααα-d_3-Dimethylsulfide group and skeletal frequencies

	ααα-d_3-Dimethylsulfide (C_s): skeletal frequencies		
	ν_{obsd} (cm^{-1})	ν_{calcd} (cm^{-1})	P.E.D.
Species A'	1013	997	$0.47S_1 + 0.50S_4$
	961	933	$0.44S_1 + 0.44S_4$
	740	768	$0.49S_5 + 0.36S_6 + 0.11S_3$
	705	695	$0.53S_6 + 0.37S_5$
	656	654	$0.83S_3 + 0.1S_5$
	—	268	$0.96S_2$
Species A''	—	946	
	725.5	735	

Group frequencies

CD_3 group			CH_3 group		
	ν_{calcd} (cm^{-1})	ν_{obsd} (cm^{-1})		ν_{calcd} (cm^{-1})	ν_{obsd} (cm^{-1})
CD sym. stretch	2096	2128	CH sym. stretch	2916	2917
CD antisym. stretch	2220	2231	CH antisym. stretch	2981	2970
CD_3 deformation	1026	1045	CH_3 sym. stretch	1331	1322
			CH_3 antisym. deformation	1428	1433

TABLE V*

d_6-Dimethylselenide

A_1	S_1	S_2	S_3	S_4	B_1	S_5	S_6	S_7	A_2, B_2	$S_{8,9}$
S_1	0.6744	−0.0129	0	−0.0339	S_5	2.7205	0	0.4061	$S_{8,9}$	0.6095
S_2	−0.0129	0.8867	0.0853	0.0064	S_6	0	0.5417	0.0339		
S_3	0	0.0853	2.7053	−0.4061	S_7	0.4061	0.0339	0.5124		
S_4	−0.0339	0.0064	−0.4061	0.5463						

ααα-d_3-Dimethylsulfide

A'	S_1	S_2	S_3	S_4	S_5	S_6	A''	S_7	S_8
S_1	0.7059	0.0232	0	−0.0456	0	0.0913	S_7	0.7059	0
S_2	0.0232	0.9713	0.1505	−0.0115	0	0.0232	S_8	0	0.7059
S_3	0	0.1505	3.1008	−0.2871	0	0			
S_4	−0.0456	−0.0115	−0.2871	0.5584	−0.2871	0			
S_5	0	0	0	−0.2871	3.2682	0			
S_6	0.0913	0.0232	0	0	0	0.7059			

*The force field used in these calculations: Units: stretching force constants in mdyn Å^{-1}, bending force constants in mdyn Å rad^{-2}, stretch–bend interaction force constants in mdyn rad^{-1}.

Symmetry coordinate	Approximate description
Species A'	
$S_1 = (2\delta_4 - \delta_5 - \delta_6)/6$	CH_3 'rock'
$S_2 = \beta$	$\widehat{CX}C$ deformation
$S_3 = (d_1 + d_2)/2$	CX sym. stretch
$S_4 = (\alpha_1 + \alpha_2 + \alpha_3 - \delta_1 - \delta_2 - \delta_3)/6$	CD_3 deformation
$S_5 = (d_1 - d_2)/2$	CX antisym. stretch
$S_6 = (2\delta_1 - \delta_2 - \delta_3)/6$	CD_3 'rock'
Species A''	
$S_7 = (\delta_2 - \delta_3 + \delta_5 - \delta_6)/2$	Admixture of CH_3 and
$S_8 = (\delta_2 - \delta_3 - \delta_5 + \delta_6)/2$	CD_3 rocking modes

The G_{ff}^{+} matrices for these molecules were calculated using a computer program based on that described in ref. 8. The F^{+} matrices in Table V followed easily from those quoted in ref. 4 by applying the corrections quoted above.

The calculated frequencies for both the group and skeletal modes of d_6-dimethyl selenide are presented in Table III; those for ααα-d_3-dimethyl sulfide in Table IV, which also includes the potential energy distributions calculated according to eq. [16.4] of ref. 9, since there is some

Can. J. Chem. Downloaded from www.nrcresearchpress.com by 210.87.254.42 on 09/05/12
For personal use only.

measure of doubt concerning the vibrational assignments for the A' modes in this case.

The potential energy distribution makes meaningless the assignment of the two highest frequencies and also suggests that the assignments in ref. 6 of the bands at 740 cm^{-1} and 705 cm^{-1} to the CD_3 rocking mode (S_6) and CX antisymmetric stretching mode (S_5) are oversimplified.

Acknowledgments

The authors wish to thank the Council of the University for the award of a Demonstratorship to J. M. F., and the staff of the Computations Laboratory for their help.

1. W. T. KING and B. L. CRAWFORD, JR. J. Mol. Spectry. **5**, 421 (1960).
2. J. H. CARTER, J. M. FREEMAN, and T. HENSHALL. J. Mol. Spectry. **20**, 402 (1966).
3. J. H. CARTER, J. M. FREEMAN, and T. HENSHALL. J. Mol. Spectry. **22**, 18 (1967).
4. J. M. FREEMAN and T. HENSHALL. J. Mol. Structure, **1**, 31 (1967).
5. W. T. KING and B. L. CRAWFORD, JR. J. Mol. Spectry. **8**, 58 (1962).
6. J. A. PERCHARD, M. T. FOREL, and M. L. JOSIEN. J. Chim. Phys. **61**, 645 (1964).
7. J. R. ALLKINS and P. J. HENDRA. Spectrochim. Acta, **23A**, 1671 (1967).
8. J. H. CARTER, J. M. FREEMAN, and T. HENSHALL. Spectrochim. Acta, **23A**, 1466 (1967).
9. K. NAKAMOTO. Infrared spectra of inorganic and coordination compounds. John Wiley & Sons, New York. 1963.

Can. J. Chem. Downloaded from www.nrcresearchpress.com by 210.87.254.42 on 09/05/12
For personal use only.

Longitudinal spin-lattice relaxation in aqueous solutions of dysprosium(III) and copper(II) ions as an indicator of complex formation

E. BOCK

Parker Chemistry Laboratory, University of Manitoba, Winnipeg, Manitoba

Received January 25, 1968

Spin-lattice relaxation times of aqueous solutions of Dy(III) and Cu(II) in the presence of acetate ions were determined. The experimental results suggest that the coordination number with respect to the acetate ion appears to be 3 and 2 for the Dy(III) and Cu(II) ion respectively.

Canadian Journal of Chemistry, **46**, 2178 (1968)

Introduction

In a recent paper Reuben and Fiat (1) reported on the proton chemical shifts in aqueous solutions of a number of rare-earth ions in the presence of different amounts of added acetate ions. They concluded that the observed shifts could be successfully interpreted, with the exception of the Gd(III) ion, as resulting from pseudo-contact interaction. They also concluded, on the basis of the observed acetate protons shifts, that the acetate ion ". . . is bound in the first coordination sphere of the rare-earth ions definitely forming an "inner sphere" complex", and that the probable coordination number with respect to the acetate ion was 3 to 1 in the acetate–rare-earth ion complex.

It occurred to the author that a simple way of testing the suggestions of Reuben and Fiat regarding the complex-forming propensities of the acetate ions with the rare-earth ions in aqueous solutions would be to determine the spin-lattice relaxation time, T_1, of the water protons as a function of the acetate ion concentration in dilute aqueous rare-earth ion solutions. Since the most pronounced chemical shift observed by Reuben and Fiat occurred in Dy(III) solutions, it was decided to determine the spin-lattice relaxation time for solutions of this ion. In addition, for the purpose of comparison, the spin-lattice relaxation times for $Cu(NO_3)_2$ solution were also determined.

Experimental

The longitudinal spin-lattice relaxation times, T_1, were determined on a PS-60A NMR Specialties pulsed NMR spectrometer, equipped with a variable temperature probe, at 15 MHz using the now well-established "null technique", i.e. 180°–90° pulse sequence (2). The solutions were prepared from distilled water, of conductance water quality, $K = 1.0 \times 10^{-6}$ mhos, and Fisher Certified Reagent $Cu(NO_3)_2$, NaCl, NH_4Cl, CH_3COONa, and CH_3COONH_4, respectively. The $DyCl_3$ was obtained from the Lindsay Chemical Co. The concentration of all solutions was established by ion-exchange techniques, i.e. exchanging of cation by protons and subsequent titration with standard NaOH. A total of 10

measure of doubt concerning the vibrational assignments for the A' modes in this case.

The potential energy distribution makes meaningless the assignment of the two highest frequencies and also suggests that the assignments in ref. 6 of the bands at 740 cm^{-1} and 705 cm^{-1} to the CD_3 rocking mode (S_6) and CX antisymmetric stretching mode (S_5) are oversimplified.

Acknowledgments

The authors wish to thank the Council of the University for the award of a Demonstratorship to J. M. F., and the staff of the Computations Laboratory for their help.

1. W. T. KING and B. L. CRAWFORD, JR. J. Mol. Spectry. **5**, 421 (1960).
2. J. H. CARTER, J. M. FREEMAN, and T. HENSHALL. J. Mol. Spectry. **20**, 402 (1966).
3. J. H. CARTER, J. M. FREEMAN, and T. HENSHALL. J. Mol. Spectry. **22**, 18 (1967).
4. J. M. FREEMAN and T. HENSHALL. J. Mol. Structure, **1**, 31 (1967).
5. W. T. KING and B. L. CRAWFORD, JR. J. Mol. Spectry. **8**, 58 (1962).
6. J. A. PERCHARD, M. T. FOREL, and M. L. JOSIEN. J. Chim. Phys. **61**, 645 (1964).
7. J. R. ALLKINS and P. J. HENDRA. Spectrochim. Acta, **23A**, 1671 (1967).
8. J. H. CARTER, J. M. FREEMAN, and T. HENSHALL. Spectrochim. Acta, **23A**, 1466 (1967).
9. K. NAKAMOTO. Infrared spectra of inorganic and coordination compounds. John Wiley & Sons, New York. 1963.

Can. J. Chem. Downloaded from www.nrcresearchpress.com by 210.87.254.40 on 09/05/12
For personal use only.

Longitudinal spin-lattice relaxation in aqueous solutions of dysprosium(III) and copper(II) ions as an indicator of complex formation

E. BOCK

Parker Chemistry Laboratory, University of Manitoba, Winnipeg, Manitoba

Received January 25, 1968

Spin-lattice relaxation times of aqueous solutions of Dy(III) and Cu(II) in the presence of acetate ions were determined. The experimental results suggest that the coordination number with respect to the acetate ion appears to be 3 and 2 for the Dy(III) and Cu(II) ion respectively.

Canadian Journal of Chemistry, **46**, 2178 (1968)

Introduction

In a recent paper Reuben and Fiat (1) reported on the proton chemical shifts in aqueous solutions of a number of rare-earth ions in the presence of different amounts of added acetate ions. They concluded that the observed shifts could be successfully interpreted, with the exception of the Gd(III) ion, as resulting from pseudo-contact interaction. They also concluded, on the basis of the observed acetate protons shifts, that the acetate ion ". . . is bound in the first coordination sphere of the rare-earth ions definitely forming an "inner sphere" complex", and that the probable coordination number with respect to the acetate ion was 3 to 1 in the acetate–rare-earth ion complex.

It occurred to the author that a simple way of testing the suggestions of Reuben and Fiat regarding the complex-forming propensities of the acetate ions with the rare-earth ions in aqueous solutions would be to determine the spin-lattice relaxation time, T_1, of the water protons as a function of the acetate ion concentration in dilute aqueous rare-earth ion solutions. Since the most pronounced chemical shift observed by Reuben and Fiat occurred in Dy(III) solutions, it was decided to determine the spin-lattice relaxation time for solutions of this ion. In addition, for the purpose of comparison, the spin-lattice relaxation times for $Cu(NO_3)_2$ solution were also determined.

Experimental

The longitudinal spin-lattice relaxation times, T_1, were determined on a PS-60A NMR Specialties pulsed NMR spectrometer, equipped with a variable temperature probe, at 15 MHz using the now well-established "null technique", i.e. 180°–90° pulse sequence (2). The solutions were prepared from distilled water, of conductance water quality, $K = 1.0 \times 10^{-6}$ mhos, and Fisher Certified Reagent $Cu(NO_3)_2$, NaCl, NH_4Cl, CH_3COONa, and CH_3COONH_4, respectively. The $DyCl_3$ was obtained from the Lindsay Chemical Co. The concentration of all solutions was established by ion-exchange techniques, i.e. exchanging of cation by protons and subsequent titration with standard NaOH. A total of 10

Can. J. Chem. Downloaded from www.nrcresearchpress.com by 210.87.254.40 on 09/05/12
For personal use only.

different solutions for each paramagnetic ion were investigated. The concentration of paramagnetic ion was identical in each sample and was 1.8×10^{-2} M in $DyCl_3$ and 2.8×10^{-2} M in $Cu(NO_3)_2$ respectively. The concentration of the acetate ion and other salts was varied from 0 to 1.0 M. The solutions were prepared from stock solutions by dilution with distilled water. The overall volume of the solution was 1.00 ml. All measurements were carried out at 25.0 ± 0.2 °C on non-degassed samples.

Results and Discussion

The experimental results are summarized in Fig. 1 and Fig. 2 respectively. From the figures it is apparent that addition of acetate ions, in the form of sodium or ammonium acetate, increases the spin-lattice relaxation time, T_1, of the water protons in the dysprosium and copper ion solution, whereas the addition of sodium chloride or ammonium nitrate has no effect on

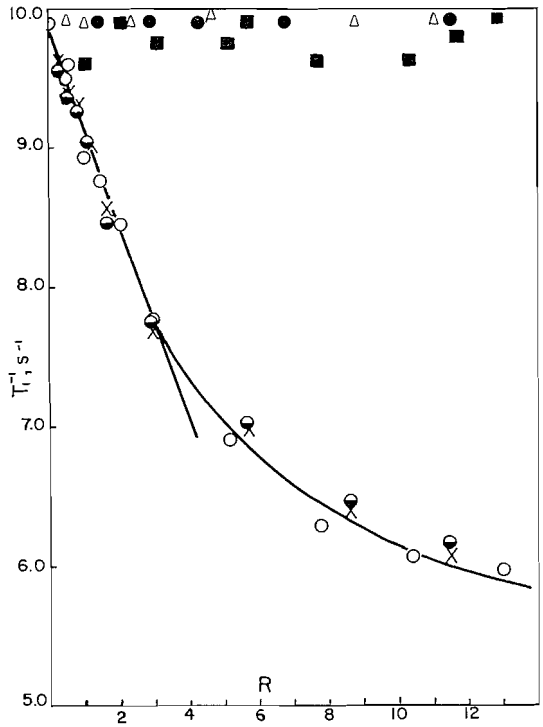

FIG. 1. T_1^{-1} (in s^{-1}) of the water protons as a function of the ratio, R, of anion to dysprosium ion concentration (in moles per liter). (◒) Sodium acetate; (■) solution containing sodium or ammonium acetate acidified with strong HCl; (●) solutions containing sodium chloride; (○) ammonium acetate; (×) acidified solutions after being neutralized with concentrated NH_4OH; (△) solutions containing ammonium nitrate. T_1 for pure water 2.9 s.

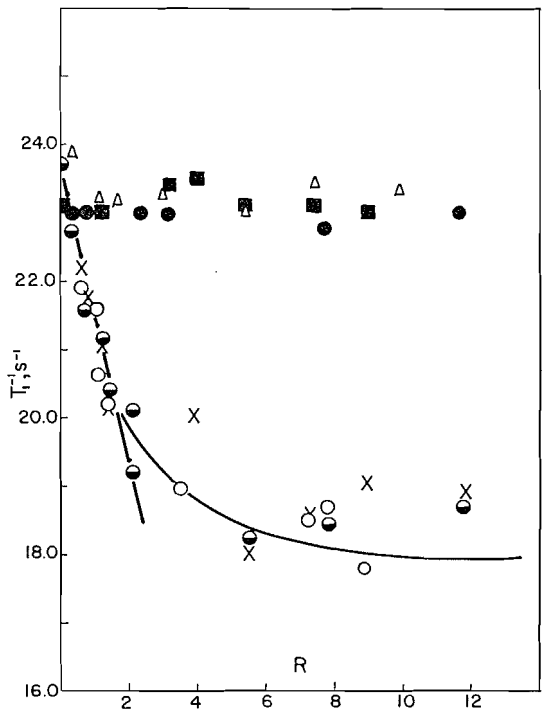

FIG. 2. T_1^{-1} (in s^{-1}) of the water protons as a function of the ratio, R, of anion to copper ion concentration (in moles per liter). (◒) Sodium acetate; (■) solutions containing sodium or ammonium acetate acidified with strong HCl; (●) solutions containing sodium chloride; (○) ammonium acetate; (×) acidified solutions after being neutralized with concentrated NH_4OH; (△) solutions containing ammonium nitrate.

the relaxation time. It is also apparent from the figures that the decrease in T_1^{-1}, a quantity proportional to τ, the residence time of the protons in a particular magnetic environment, is at first directly proportional to the ratio of acetate to paramagnetic ions concentration, R. Moreover the form of the curve changes for $R > 2$ for copper ion solutions and $R > 3$ for dysprosium ion solutions. One may interpret the different behavior of T_1^{-1} in the two different regions, viz. in region $0 < R < 2$, and $R > 2$ for copper ion solutions, and $0 < R < 3$, and $R > 3$ for dysprosium ion solutions, in terms of two different kinetic processes. In region I, $0 < R < 2$ or $0 < R < 3$ for Cu(II) or Dy(III) respectively, the magnitude of T_1 is determined by the competition between the water molecules and acetate ions for the sites in the first coordination sphere of the paramagnetic ions. Such a process would lead to a linear dependence of τ for the water

protons, since the number of acetate ions in the coordination sphere of the paramagnetic ion would be directly proportional to the number of acetate ions added to the solution. After saturation of the first coordination sphere of the paramagnetic ion by acetate ions, 2 per Cu(II) ion and 3 per Dy(III) ion, the magnitude of T_1 will depend on the exchange of acetate ions in the coordination sphere of the paramagnetic ion and acetate ions and water molecules in the bulk of the solution respectively. On the basis of this explanation and the observed results one would conclude that the coordination number of the acetate ions in the coordination sphere of the Cu(II) ion and Dy(III) ion is 2 and 3 respectively. Both numbers are quite reasonable in the light of the known structures of other complexes for the two ions. The coordination number 3 for the Dy(III) ions is in agreement with the conclusions of Reuben and Fiat (1).

The formation of the complex between the acetate ion and paramagnetic ion was further confirmed by the addition of strong HCl, $\simeq 12$ M, to each of the solutions. After the addition of 0.03 ml of 12 M HCl, the relaxation time, T_1, of each solution became equal, within experimental error, to the value of T_1 in the absence of acetate ions. Addition of the same amount of HCl to pure water or a solution containing paramagnetic ions only had no effect on the value of T_1 of either system. On the other hand, careful neutralization of the acidified solution with strong NH_4OH restored the original value of T_1 for each solution, and again had no effect on the T_1 of pure water or blank solutions containing paramagnetic ions only. The addition of HCl and subsequent neutralization with NH_4OH was accomplished with the aid of an Agla micrometer syringe capable of an accuracy of $\pm 5 \times 10^{-5}$ ml (3). The use of the precision syringe was necessary for two reasons: (*a*) to avoid excessive dilution of sample which is reflected in an increase in T_1, and (*b*) to avoid excess addition of base. Excess base precipitated the metal hydroxide, especially in the case of $DyCl_3$, which vastly increased the T_1 of the solution. The effects of the addition of strong acid and subsequent addition of strong base to the solutions on the T_1 of the latter is in complete agreement with the results discussed above. The addition of HCl strips the paramagnetic ion of all acetate ions by forming the much more stable acetic acid molecule. This in turn opens the sites in the coordination sphere of the paramagnetic ion to occupancy by water molecules, which in turn leads to a restoration of the original value of T_1, i.e. identical with that of the blank solution. Neutralization of the acid by NH_4OH removes the protons from the acetate ions, and these in turn displace the water molecules in the coordination sphere of the paramagnetic ion, which leads to a restoration of the T_1 value which now is identical with the value measured before the addition of strong acid.

Acknowledgments

The author thanks Dr. H. D. Gesser for the sample of $DyCl_3$. The financial assistance of the National Research Council of Canada is deeply appreciated.

1. J. Reuben and D. Fiat. Chem. Commun. 729 (1967).
2. A. Laukien. Handbuch der Physik. Vol. XXXVIII. Springer-Verlag, Berlin. 1958. p. 120.
3. Anonymous. The Wellcome Research Laboratories, Beckenham, Kent, England. Biochem. J. **19**, 1111 (1925).

Can. J. Chem. Downloaded from www.nrcresearchpress.com by 210.87.254.40 on 09/05/12
For personal use only.

Dielectric studies. Part XIX. Molecular relaxation of some rigid molecules

J. CROSSLEY AND W. F. HASSELL
Chemistry Department, University of Aston in Birmingham, England

AND

S. WALKER[1]
Chemistry Department, Lakehead University, Port Arthur, Ontario

Received November 27, 1967

The dielectric absorption at five microwave frequencies of solutions of seven rigid polar molecules in nonpolar solvents has been examined as also has cyclohexanone. Furan, pyridine, and thiophene have their dipole moments along the major axis and their dielectric absorption should be characterized by a single relaxation time. Unlike the monohalobenzenes, camphor, pentamethylene sulfide, tetrahydropyran, and *s*-trioxan, however, furan, pyridine, and thiophene have non-zero distribution coefficients at 25 °C, whereas for pyridine at 50 °C and cyclohexanone at 25 °C the value is zero. The non-zero distribution coefficients are to be related to either weak solute-solute or solute–solvent interactions, resulting in the polar molecule experiencing a variety of local environments. The observed relaxation times of furan, pyridine, and thiophene are comparable with those of other rigid molecules of similar shape and size. For such cases, even though the distribution parameters are not zero, it is not feasible to analyze the dielectric data into contributions from more than one relaxation process.

Canadian Journal of Chemistry, **46**, 2181 (1968)

Dielectric absorption measurements of pyridine in cyclohexane at 25 °C gave a Cole–Cole plot (2) with a significant distribution parameter. For pyridine and the monohalobenzenes the dipole moment lies along the major axis of a rigid molecule and, further, the pyridine molecule is not too dissimilar in shape and size from, for example, fluorobenzene. However, all four monohalobenzenes in inert solvents at 15–50 °C have distribution coefficients of zero (1), which is in harmony with the Perrin theory (3), since for such molecules only one relaxation time is to be expected even though relaxation may occur about two axes. Thus the non-zero distribution parameter of pyridine seemed worth more detailed examination, especially since the distribution parameter (α) is of importance in the study of systems with more than one relaxation time.

Experimental Methods

The apparatus and techniques employed have been described previously (4, 5) and the errors discussed (6). The dielectric constant (ε') and loss factor (ε'') were determined by a bridge method (4). The frequencies employed were 70.00, 34.86, 23.98, 16.20, and 9.313 GHz. The static dielectric constant (ε_0) was measured with a heterodyne beat apparatus at 2 MHz.

The compounds used were available commercially. Cyclohexanone, furan, pyridine, pentamethylene sulfide, tetrahydropyran, and thiophene were treated with a suitable drying agent followed by fractional distillation employing a 30 theoretical plate spinning band column. A small center fraction was collected and the purity checked by gas–liquid chromatography.

Camphor was purified by sublimation and *s*-trioxan was recrystallized from *p*-xylene.

Experimental Results

The majority of the experimental points lay to the low frequency side of ε''_{max} on the Cole–Cole arcs and the dielectric constant at very high frequency (ε_∞) was obtained by graphical extrapolation. The ε' and ε'' data are presented in Table I and the static and high frequency dielectric constant, ε_0 and ε_∞ respectively, and the observed relaxation time (τ_0) are given in Table II together with the distribution parameter as evaluated from the Cole–Cole graphical method. The accuracy of α is dependent on the distribution of points on the Cole–Cole plot and for pyridine in cyclohexane the value is repeatable to about 0.02.

The dipole moments of thiophene in carbon tetrachloride and *p*-xylene and of furan in cyclohexane were obtained from the equation

$$[1] \quad \mu = 0.012812\left[\frac{3T(\epsilon_0 - \epsilon_\infty)}{c(\epsilon_0 + 2)(\epsilon_\infty + 2)}\right]^{1/2},$$

in which c is the concentration in mole/cc and T the absolute temperature. For the other solutions

[1]Correspondence to: Dr. S. Walker, Chemistry Department, Lakehead University, Port Arthur, Ontario, Canada.

Can. J. Chem. Downloaded from www.nrcresearchpress.com by 210.87.254.5 on 09/05/12
For personal use only.

Can. J. Chem. Downloaded from www.nrcresearchpress.com by 210.87.254.5 on 09/05/12
For personal use only.

TABLE I

Dielectric constant and loss data for the polar solutes in nonpolar solvents at various microwave frequencies

Solute	Solvent	t (°C)	Frequency (Gc/s)	ε'	ε''
Pyridine	Cyclohexane	25	34.86	2.089	0.043_4
$w_2 = 0.01998$			23.98	2.104	0.035_0
			16.20	2.114	0.027_2
			9.313	2.123	0.015_8
Pyridine	Cyclohexane	25	70.00	2.063	0.040_1
$w_2 = 0.01790$			34.86	2.085	0.038_8
			23.98	2.099	0.031_5
			16.20	2.104	0.023_6
			9.313	2.112	0.014_5
Pyridine	Cyclohexane	50	70.00	2.036	0.042_9
$w_2 = 0.02093$			34.86	2.063	0.035_9
			23.98	2.075	0.027_6
			16.20	2.073	0.020_8
			9.313	2.063	0.013_0
Pyridine	Cyclohexane	50	70.00	2.036	0.041_1
$w_2 = 0.02014$			34.86	2.058	0.034_4
			23.98	2.068	0.026_7
			16.20	2.070	0.018_3
			9.313	2.066	0.011_3
Pyridine	Benzene	25	70.00	2.307	0.055_1
$w_2 = 0.01962$			34.86	2.352	0.061_4
			23.98	2.379	0.057_5
			16.20	2.399	0.045_6
			9.313	2.413	0.028_1
Pyridine	*p*-Xylene	25	70.00	2.312	0.048_4
$w_2 = 0.01989$			34.86	2.337	0.055_8
			23.98	2.357	0.050_5
			16.20	2.372	0.041_1
			9.313	2.387	0.027_9
Pyridine	Carbon tetrachloride	25	70.00	2.260	0.059_4
$w_2 = 0.01180$			34.86	2.302	0.072_8
			23.98	2.332	0.068_6
			16.20	2.360	0.059_5
			9.313	2.382	0.040_5
Thiophene	*p*-Xylene	25	70.00	2.382	0.066_2
$w_2 = 0.48826$			34.86	2.413	0.062_8
			23.98	2.434	0.054_9
			16.20	2.446	0.045_2
			9.313	2.462	0.026_9
Thiophene	Carbon tetrachloride	25	70.00	2.378	0.079_2
$w_2 = 0.4211$			34.86	2.437	0.081_6
$d = 1.1334$			23.98	2.459	0.069_5
			16.20	2.478	0.049_3
			9.313	2.492	0.034_6
Furan	Cyclohexane	25	70.00	2.272	0.160_8
$w_2 = 0.52997$			34.86	2.365	0.117_0
$d = 0.8385$			23.98	2.395	0.089_8
			16.20	2.417	0.065_1
			9.313	2.421	0.032_8
Pentamethylene sulfide	Cyclohexane	25	70.00	2.072	0.054_2
$w_2 = 0.05255$			34.86	2.100	0.061_0
			23.98	2.123	0.055_4
			16.20	2.144	0.042_6
			9.313	2.159	0.226_6
Tetrahydropyran	Cyclohexane	25	70.00	2.075	0.048_9
$w_2 = 0.04823$			34.86	2.09_2	0.049_1
			23.98	2.111	0.040_4
			16.20	2.122	0.031_5
			9.313	2.131	0.020_7
s-Trioxan	Cyclohexane	25	70.00	2.070	0.036_8
$w_2 = 0.02031$			34.86	2.083	0.034_3
			23.98	2.093	0.027_9
			16.20	2.101	0.022_4
			9.313	2.107	0.013_3

TABLE I (*Concluded*)

Solute	Solvent	t (°C)	Frequency (Gc/s)	ε'	ε''
s-Trioxan	Cyclohexane	25	70.00	2.063	0.043_3
$w_2 = 0.02297$			34.86	2.095	0.040_6
			23.98	2.103	0.037_7
			16.20	2.117	0.024_1
			9.313	2.119	0.015_7
Camphor	Cyclohexane	25	70.00	2.031	0.032_4
$w_2 = 0.02136$			34.86	2.050	0.048_0
			23.98	2.065	0.052_1
			16.20	2.090	0.052_2
			9.313	2.118	0.038_8
Cyclohexanone	Cyclohexane	25	70.00	2.046	0.035_7
$w_2 = 0.01241$			34.86	2.066	0.046_2
			23.98	2.082	0.043_8
			16.20	2.105	0.039_0
			9.313	2.114	0.024_8

(more dilute) ε_0 and ε_∞ were taken to equal the static dielectric constant of the solvent.

Discussion

The dipole moments obtained agree fairly well with literature values (8) in Table II; this supports the ε_∞ values and the validity of the Cole–Cole plots.

The Cole–Cole plots of Holland and Smyth (9) for pyridine in *n*-heptane had distribution parameters of 0.05, 0.04, and 0.06 at 1, 20, and 40 °C respectively. In contrast Miller and Smyth (10) reported zero distribution parameters for solutions of pyridine in benzene at 20, 40, and 60 °C. Their results for benzene conflict with those in Table II, and the divergence may be attributed to their lack of data at high frequency, such as 70 GHz, since the flattening of the Cole–Cole plot is difficult to detect from lower frequency data, as is apparent also from our early measurements on pyridine (4) for which only three wavebands were employed with a deficiency of points on the high frequency side of the Cole–Cole plot. Similarly, the significant distribution parameters for furan and thiophene (Table II) are to be contrasted with values indistinguishable from zero, which have been reported for these two molecules in cyclohexane solution at 20 °C (11). These discrepancies may also be attributed to insufficient high frequency data, however; Garg and Smyth (12) using a 2 mm apparatus confirmed a zero distribution parameter for thiophene, as the pure liquid at 20 and 40 °C, and their results may be significant in the interpretation of the results presented in Table II (see later).

The Cole–Cole plots of pentamethylene sulfide, tetrahydropyran, and *s*-trioxan in cyclohexane at 25 °C showed zero distribution parameters and their relaxation times (Table II) may be ascribed to molecular relaxation. On comparison of their values with those of furan, pyridine, and thiophene it follows for the latter group of molecules that the τ_0 values are of the order for molecular reorientation. Furthermore, the shortening of the relaxation time along the series pyridine, thiophene, and furan is consistent with the decrease in molecular size. Thus the non-zero distribution parameters reported in Table II are probably due to a distribution of relaxation times about a mean value rather than contributions from, for example, two discrete processes.

The lengthening of the pyridine relaxation time, in passing from cyclohexane to *p*-xylene to carbon tetrachloride solution, can probably be accounted for by solute–solvent interaction (13, 14). Crossley (15) found such interaction for isoquinoline and phthalazine with *p*-xylene, manifested by longer relaxation times in this solvent than in cyclohexane, whereas for quinoline and acridine, where the nitrogen atom is shielded from the approach of the π-electrons of *p*-xylene, it was not possible to detect any interaction. Furthermore, all these aromatic amines showed non-zero distribution parameters in cyclohexane at 25 °C but had zero values at 50 °C, which is comparable with the behavior of pyridine. With camphor in cyclohexane at 25 °C $\alpha = 0$ and the adequacy of the Cole–Cole concept is demonstrated for this system in which no significant interaction would be expected. Thus

Can. J. Chem. Downloaded from www.nrcresearchpress.com by 210.87.254.5 on 09/05/12
For personal use only.

TABLE II

Static dielectric constant, dielectric constant at very high frequency, observed relaxation time, distribution coefficient, and dipole moment (in debyes) data for solutions of weight fraction w_2. The relaxation times (in seconds) have been multiplied by 10^{12}

Solute	Solvent	w_2	t (°C)	ε_0	ε_∞	τ_0	α	μ	μ_{lit}
Pyridine	Cyclohexane	0.01998	25	2.127	2.02_1	3.1	0.11	2.22	2.22–2.28
		0.01790	25	2.115	2.02_0	2.9	0.09	2.22	
		0.02093	50	2.077	0.97_0	2.1	0	2.23	
		0.02014	50	2.071	1.97_7	2.0	0	2.22	
	Benzene	0.01962	25	2.422	2.28_3	4.6	0.08	2.26	2.20–2.28
	p-Xylene	0.01989	25	2.401	2.26_8	4.3	0.13	2.23	
	Carbon tetrachloride	0.01180	25	2.400	2.23_3	5.0	0.09	2.40	2.35–2.39
Thiophene	*p*-Xylene	0.4883	25	2.471	2.31_2	2.8	0.11	0.47	
	Carbon tetrachloride	0.4211	25	2.513	2.29_8	3.2	0.15	0.54	0.54–0.56
Furan	Cyclohexane	0.5300	25	2.426	2.05_0	1.9	0.08	0.69	0.63–0.71
Pentamethylene sulfide	Cyclohexane	0.05255	25	2.162	2.03_8	4.0	0	1.68	1.71
Tetrahydropyran	Cyclohexane	0.04823	25	2.134	2.03_0	3.3	0	1.44	1.55
s-Trioxan	Cyclohexane	0.02031	25	2.109	2.03_3	3.0	0	1.99	2.16
		0.02297	25	2.123	2.03_2	3.1	0	2.04	
Camphor	Cyclohexane	0.2136	25	2.131	2.01_1	7.4	0	3.02	2.91
Cyclohexanone	Cyclohexane	0.01241	25	2.120	2.02_7	5.0	0	2.94	2.75–3.07

the available evidence indicates that the non-zero distribution parameters at 25 °C probably result from solute–solute and/or solute–solvent interactions giving rise to a variety of local environments and a range of free-energy barriers opposing reorientation.

The relaxation time of thiophene in *p*-xylene (2.8×10^{-12} s) is significantly longer than in cyclohexane (2.1×10^{-12} s (11)), and its apparent dipole moment in carbon tetrachloride is greater. Thus the molecular interaction of the solute with the solvent seems more appreciable in the last solvent. Relatively high concentrations were employed for furan and thiophene in order to obtain accurate loss factors. Such concentrations may result in weak molecular interaction between the solute molecules and lead to the solute molecules experiencing a variety of local environments which would account for the non-zero distribution parameters. In the pure liquid, owing to local structure, a more homogeneous environment could exist which would account for the zero distribution parameter for liquid thiophene at 20 and 40 °C (12).

In general, for systems which have a non-zero distribution parameter, analysis of the dielectric data into two (or more) contributing relaxation times is only justified if the observed relaxation time differs significantly from that of a rigid molecule of similar shape and size in a similar environment. In view of this conclusion, we became concerned as to whether an analysis on cyclopentanone in cyclohexane ($w_2 = 0.0144$) was justifiable (16). This solute exhibited a definite distribution parameter value at 25, 40, and 60 °C (unlike pyridine in cyclohexane) which seemed a point against the non-zero α of cyclopentanone being related to weak molecular interaction. However, to test whether the α values resulted from molecular association, cyclohexanone was also examined in cyclohexane at a similar concentration ($w_2 = 0.01241$). An $\alpha = 0$ resulted and the relevant data are given in Tables I and II. Thus it seems unlikely that the non-zero α for cyclopentanone is to be ascribed to weak association owing to the presence of the highly polar keto-group bringing about dipole–dipole association. This is also borne out by the camphor in cyclohexane result where $\alpha = 0$ also. Further, when the ε'_v ε''_ω plot (17) is made for the cyclopentanone at 25 °C the initial slope yields a lower value for the relaxation time of 6.1×10^{-12} s which is longer than that of 5.0×10^{-12} s for the molecular relaxation of the larger molecule cyclohexanone. Further such a plot yields only a lower limit for that relaxation time (17). Thus there is some justification for analyzing the dielectric data for cyclopentanone into contributions from two (or more) relaxation times (16) in which the non-molecular process has the longer value. It is

Can. J. Chem. Downloaded from www.nrcresearchpress.com by 210.87.254.5 on 09/05/12
For personal use only.

also interesting to note that thiacyclopentane in cyclohexane ($w_2 = 0.0561$) had a non-zero α at 5, 25, and 50 °C (16), whereas pentamethylene sulfide in the same solvent at 25 °C and a similar concentration ($w_2 = 0.05255$) has $\alpha = 0$. If there is a relaxation process in addition to that of molecular relaxation, it would seem, in view of the present work, that its origin is to be sought in an intramolecular (16) rather than an intermolecular process for such saturated five-membered ring systems.

1. W. F. HASSELL and S. WALKER. Trans. Faraday Soc. **62**, 2695 (1966).
2. K. S. COLE and R. H. COLE. J. Chem. Phys. **9**, 341 (1941).
3. F. PERRIN. J. Phys. Radium, **5**, 497 (1934).
4. W. F. HASSELL, M. D. MAGEE, S. W. TUCKER, and S. WALKER. Tetrahedron, **20**, 2137 (1964).
5. D. B. FARMER and S. WALKER. Tetrahedron, **22**, 111 (1965).
6. M. D. MAGEE and S. WALKER. Trans. Faraday Soc. **62**, 3093 (1966).
7. C. P. SMYTH. Dielectric behavior and structure. McGraw-Hill Book Co. Inc., New York. 1955. p. 69.
8. A. L. MCCLELLAN. Tables of experimental dipole moments. W. H. Freeman & Co., San Francisco. 1963.
9. R. S. HOLLAND and C. P. SMYTH. J. Phys. Chem. **59**, 1088 (1955).
10. R. C. MILLER and C. P. SMYTH. J. Am. Chem. Soc. **79**, 308 (1957).
11. F. HUFNAGEL and H. KILP. Z. Naturforsch. **18a**, 769 (1963).
12. S. K. GARG and C. P. SMYTH. J. Chem. Phys. **42**, 1397 (1965).
13. A. N. SHARPE and S. WALKER. J. Chem. Soc. 157 (1962).
14. K. W. MORCOM and D. N. TRAVERS. Trans. Faraday Soc. **62**, 2063 (1966).
15. J. CROSSLEY. Ph.D. Thesis, University of Aston in Birmingham, England. 1967.
16. J. CROSSLEY, S. W. TUCKER, and S. WALKER. Trans. Faraday Soc. **62**, 576 (1966).
17. W. P. PURCELL, K. FISH, and C. P. SMYTH. J. Am. Chem. Soc. **69**, 2483 (1947).

Can. J. Chem. Downloaded from www.nrcresearchpress.com by 210.87.254.5 on 09/05/12
For personal use only.

Can. J. Chem. Downloaded from www.nrcresearchpress.com by 210.87.254.5 on 09/05/12
For personal use only.

Strongly hindered rotation in α,α,2,6-tetrachlorotoluene. Stereospecific five-bond coupling. Hyperconjugative contributions to long-range sidechain–ring proton coupling constants

T. SCHAEFER, R. SCHWENK, AND C. J. MACDONALD
Chemistry Department, University of Manitoba, Winnipeg, Manitoba

AND

W. F. REYNOLDS
Chemistry Department, University of Toronto, Toronto, Ontario

Received April 8, 1968

At −40 °C the C—H bond of the dichloromethyl group of α,α,2,6-tetrachlorotoluene lies in the plane of the ring. The proton resonance spectrum demonstrates a stereospecific five-bond coupling between the C—H proton and the ring proton in the meta position. The coupling to the para proton is essentially zero as expected from a hyperconjugative mechanism. The free energy of activation of rotation of the dichloromethyl group is about 15 kcal/mole at 25 °C.

Canadian Journal of Chemistry, 46, 2187 (1968)

At −40 °C the proton magnetic resonance (60 Mc/s) of α,α,2,6-tetrachlorotoluene in toluene-d_8 consists of an ABC spectrum ($\sigma_C > \sigma_B > \sigma_A$) for the ring protons and a doublet (J = 0.5 c/s) for the dichloromethyl proton. The peaks of the ring proton resonating at lowest field are split by 0.5 c/s. The spectrum is consistent with a locked conformation **1** resulting in a stereo-

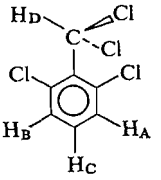

1

specific five-bond coupling $J_{AD} \equiv J_m^{H,CHCl_2}$ = 0.5 c/s. The dichloromethyl proton resonance occurs at −7.5 p.p.m. to low field of internal tetramethylsilane. The low shielding may be attributed to conformation **1**. The C—H bond lies in the plane of the ring and is deshielded strongly by the magnetic anisotropy of the ring as well as by the interaction with the ortho chlorine atom. The steric interaction between the chlorine atoms on the sidechain and the ortho chlorine atom deshields H_A relative to H_B in **1**.

At 30 °C in benzene-d_6 the meta ring proton peaks (H_A and H_B) are strongly broadened as the dichloromethyl group begins to rotate at a rate comparable to the reciprocal of the shift between H_A and H_B, effectively interchanging the αβ and βα spin states of the meta protons. The resonance of the dichloromethyl proton is a triplet (J = 0.25 c/s) arising from an averaged coupling, (0.5 + 0.0)/2 c/s, to H_A and H_B. At 80 °C the ring protons yield an A_2B spectrum due to rapid rotation of the dichloromethyl group.

No coupling between the para (H_C) and dichloromethyl proton is evident between −40 and 80 °C. Thus the two para proton peaks corresponding to αα and ββ spin states of the meta protons have a line width of 0.1 c/s at 30 °C and hence $J_p^{H,CHCl_2} < 0.05$ c/s. The hyperconjugative mechanism[1] of the long-range methyl proton – ring proton coupling has a $\cos^2\theta$ dependence, where θ is the dihedral angle between the C—H bond in the dichloromethyl group and the p_z orbital on the bonded ring carbon. Hence if the sidechain C—H bond flips between the two equivalent planar conformations represented by **1** and the time taken for the flip is

[1]See ref. 1 for a collection of the pertinent literature citations.

short compared with its mean lifetime in the planar site (as is assumed in the treatments of rate-dependent nuclear magnetic resonance spectra), the essentially zero magnitude of $J_p^{H,CHCl_2}$ is expected.[2]

The stereospecific coupling to the meta protons, following the so-called zig-zag rule (5), implies a substantial σ contribution to J_m^{H,CH_3}. Spin polarization via a σ–π mechanism (6) would here appear to be less important. The five-bond stereospecific couplings involving aldehydic (7), hydroxyl (8), and amino protons (9) in aromatic systems may thus not depend primarily on the nature or the hybridization state of the sidechain atoms.[3]

From the rate of collapse with increase in temperature of the ABC to an A_2B spectrum, as well as from the change in the five-bond coupling above, a free energy of activation of 15 ± 1 kcal/mole at 25 °C can be estimated. This large value may result from a cooperative combination of steric hindrance between the sidechain and ring chlorine atoms and of hydrogen bonding[4] between the polar C—H bond and the ortho chlorine atom; hyperconjugation between the sidechain chlorine atoms and the π system may also contribute to the barrier (12).

The separation of σ and π contributions to the long-range coupling in systems of this kind and the elucidation of the origin of the high barrier to rotation about an essentially single C—C bond (the barrier in toluene itself is 0.014 kcal/mole (13)) in this and related molecules is now under extensive investigation.

Acknowledgments

We are grateful to the National Research Council of Canada for financial support.

1. D. J. Blears, S. S. Danyluk, and T. Schaefer. Can. J. Chem. **46**, 564 (1968).
2. G. Kotowycz. Ph.D. Thesis, University of Manitoba, Winnipeg, Manitoba. 1967.
3. G. Kotowycz and T. Schaefer. Can. J. Chem. **44**, 2743 (1966).
4. J. M. Read, Jr., R. W. Crecely, R. S. Butler, J. E. Loemker, and J. H. Goldstein. Tetrahedron Letters, No. 10, 1215 (1968).
5. C. N. Banwell and N. Sheppard. Discussions Faraday Soc. **34**, 115 (1962).
6. M. K. Carter and G. Vincow. J. Chem. Phys. **47**, 302 (1967).
7. G. J. Karabatsos and F. M. Vane. J. Am. Chem. Soc. **85**, 3886 (1963).
8. S. Forsén and R. A. Hoffman. J. Mol. Spectry. **20**, 168 (1966).
9. J. A. Weil, A. Blum, A. H. Heiss, and J. K. Kinnaird. J. Chem. Phys. **46**, 3132 (1967).
10. N. Muller. J. Chem. Phys. **42**, 4309 (1965).
11. D. M. Grant and W. M. Litchman. J. Am. Chem. Soc. **87**, 3994 (1965).
12. K. Kimura and S. Nagakura. J. Chem. Phys. **47**, 2916 (1967).
13. H. Rudolph, H. Dreizler, A. Jaeschke, and P. Wendling. Z. Naturforsch. **22a**, 940 (1967).

[2] J_p^{H,CH_3} in a number of substituted toluenes is independent of substituent and solvent (2) and of opposite sign (3) but within 10% of the magnitude of $J_p^{H,H}$ = 0.66 ± 0.04 c/s in benzene (4). The two chloro substituents on the methyl group are here assumed not to substantially affect hyperconjugation, which depends more on the symmetry of the system than on the polarity of the C—H bond.

[3] $J(^{13}C—H)$ = 179 c/s in the dichloromethyl group (10). This value can be adequately explained on the basis of the polarity of the C—H bond, without the need of a substantial rehybridization of the sp^3 hybridized carbon atom (11).

[4] In **1** the distance between the proton of the dichloromethyl group and the ortho chlorine is about 0.5 Å less than the sum of the van der Waals radii of chlorine and hydrogen.

Can. J. Chem. Downloaded from www.nrcresearchpress.com by 210.87.254.5 on 09/05/12
For personal use only.

Can. J. Chem. Downloaded from www.nrcresearchpress.com by 210.87.254.5 on 09/05/12
For personal use only.

Canadian Journal of Chemistry

Published by THE NATIONAL RESEARCH COUNCIL OF CANADA

VOLUME 46 JULY 1, 1968 NUMBER 13

Chemical and biological properties of some oxindolidyl-3-methines[1]

R. HODGES

Biochemistry Department, Massey University of Manawatu, Palmerston North, New Zealand

AND

J. S. SHANNON

Commonwealth Scientific and Industrial Research Organization Division of Coal Research, Chatswood, New South Wales, Australia

AND

W. D. JAMIESON AND A. TAYLOR

Atlantic Regional Laboratory, National Research Council of Canada, Halifax, Nova Scotia

Received January 15, 1968

Several 1-methyloxindolidyl-3-methines have been synthesized, either by condensation of 1-methyloxindole with an aldehyde, or by a Wittig reaction of a chloromethylene compound with a 1-methylisatin. When examined in the mass spectrometer the expected ion reactions were observed and, in addition, a reaction involving expulsion of the carbonyl group of the oxindole moiety and rearrangement of the residual fragment, to give a 1-methylbenzo[*b*]azepinium ion was observed. The anions of the oxindolidyluracilmethines **4** and **5**, (R = Me, R′ = OH) had an absorption band near 380 mμ but the corresponding neutral molecules absorbed at 325–350 mμ. The 5-nitrofuran derivatives **3** were the only compounds that inhibited the growth of *Bacillus subtilis*.

Canadian Journal of Chemistry, 46, 2189 (1968)

It has been shown (1) that isosporidesmin-B (**7**) inhibits the growth of *Bacillus subtilis* at lower concentrations than sporidesmin-B **6**; this result is in accord with reports (2) of changes in activity following the conversion of certain indole alkaloids to their oxindole analogues. As isosporidesmin-B is readily converted (3) to the oxindolidylmethine **8** which has some structural resemblance to the antibacterial agent, **3**, (R = H) (4) it was of interest to find whether antibacterial properties were confined to 5-nitrofuran derivatives, or whether such properties resided in oxindolidylmethines generally. A further objective of the present work was to examine the spectroscopic and mass spectroscopic properties of some model oxindolidylmethines because some of the properties of the degradation product **8** were unexpected (3).

The model oxindoles (**1–5**) were synthesized by three methods. Excellent yields were obtained using Hull's method (4), the methine often crystallizing directly from the reaction mixture. Some of the compounds were obtained by a Wittig reaction of a 1-methylisatin with a triphenylphosphonium chloride. In compounds like **2** geometrical isomers were obtained but one of the isomers (5) was isolated in yields too low to permit characterization. Geometrical isomers were not obtained when the product had an acidic proton capable of tautomerism. Presumably such products were complex mixtures of tautomers. When oxindole was methylated oily products were obtained from which only 1-methyloxindole was isolated after chromatography. Hirst and his co-workers (6), in the case of isatin, similarly observed only *N*-methylation. However, methylation and ethylation of the oxindole, **3**, (R = H) gave two isomeric products

[1]Issued as NRCC No. 10072.

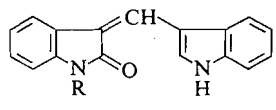

1

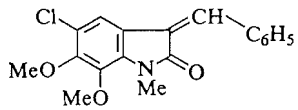

2

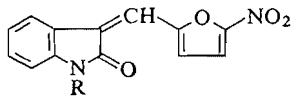

3

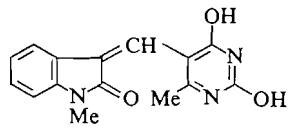

4

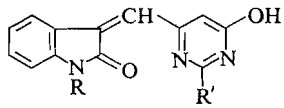

5

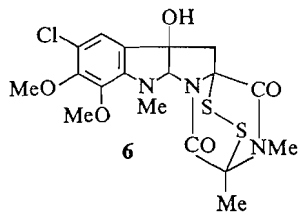

6

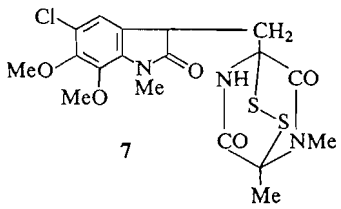

7

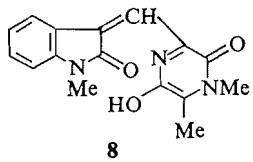

8

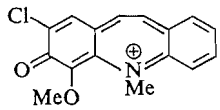

10

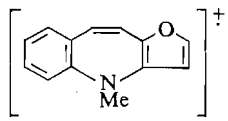

11

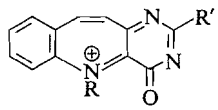

12

in each case. One of each pair was neutral and was therefore assigned the *N*-alkyl structure, **3**, (R = Me, Et) whilst the other one of each pair was basic and is regarded as the *O*-alkyl derivative. The OEt derivative of **3** was unstable and satisfactory analytical data for this material have not been obtained.

The compounds thus prepared were stable high-melting solids, the uracil derivatives, **5**, (R = Me, R′ = OH; R = C[$^2H_3$], R′ = SH) were unchanged when heated in air to 350 °C. The compounds having analogous chromophoric groups to the degradation product **8** (i.e. **2**, **4**, and **5**) similarly had an absorption band between 320–350 mμ which was also shifted bathochromically in alkaline solution in the case of the uracil derivatives **4** and **5** (R = Me, R′ =OH). Such shifts are unusual in heterocyclic compounds where (e.g. in the case of **5**, R = C[$^2H_3$], R′ = SH) a hypsochromic shift is observed when the spectrum of the neutral molecule is compared with that of its anion. There are many other examples of such hypsochromic shifts in simple pyrimidines, (7) pyridines (8), and quinolines (9). A possible way of explaining these results is to assume that in the anions of the uracil derivatives **4** and **5** (R = Me, R′ = OH), and the anion of **8**, the charge is located on the oxindole carbonyl oxygen atom. Such a structure in classical terms requires the pyrimidine moiety of **4** to be stabilized in the ketonic form and the pyrazine moiety of **8** in the quinonoid form and hence to absorb at lower frequencies. In support of this assumption the mercaptan derivative **5**, (R = C[$^2H_3$], R′ =SH) where the charge on the anion is unlikely to be located on the oxindole carbonyl oxygen atom because of the greater acidity of the mercaptan group behaves analogously to all other mercaptopyrimidines (7). It is also noteworthy that the bathochromic shift observed in the case of the uracil, **5** (R = Me, R′ = OH) where the charge cannot be located formally on the oxygen atom of the oxindole carbonyl group, is smaller (353–385 mμ).

Can. J. Chem. Downloaded from www.nrcresearchpress.com by 210.87.254.5 on 09/05/12
For personal use only.

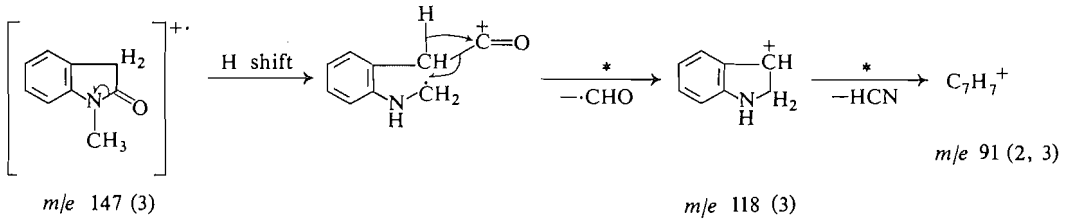

SCHEME 1[2]

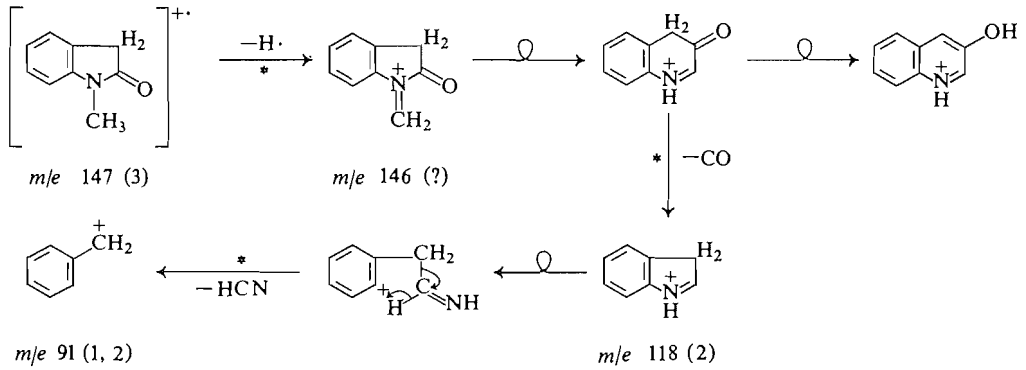

SCHEME 2[2]

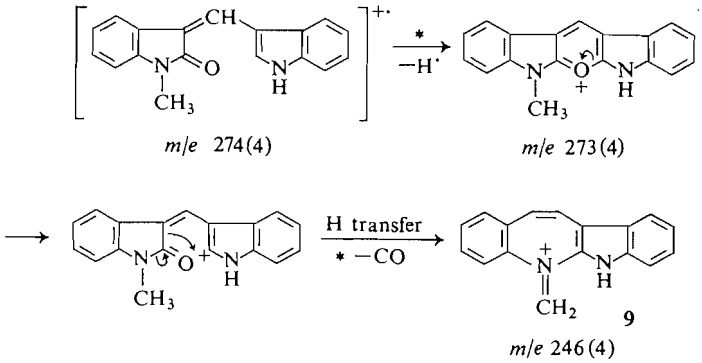

SCHEME 3[3]

The main reactions in the mass spectrometer of 1-methyloxindole are shown in Schemes 1 and 2. Metastable peaks show that the ion at *m/e* 118 is formed by two different processes. These involve direct loss of ·CHO from the molecular ion, in one case and successive loss of H· and CO in the other. Study of the spectrum of 1-methyloxindole indicated that in the formation of the ion at *m/e* 118 by the latter two-step pathway one of the hydrogen atoms of the N—Me group was lost. The ion at *m/e* 118 further fragments by the loss of HCN to produce the $C_7H_7^+$ ion at *m/e* 91.

The spectra of the oxindoles **1**–**5** differed from that of 1-methyloxindole because the molecular ion was by far the most abundant ion in the spectrum; in some cases the doubly charged molecular ion was the next most abundant species. The relative abundances of the $M - X - 28^+$ ions are given in Table I. The ion reactions substantiated by the occurrence of metastable ions are as follows.

[2]Figures in brackets are shifts observed in the mass spectrum of the N—C^2H_3 analogue.

[3]Figures in brackets are shifts observed in the mass spectrum of the N—C^2H_3 and N—^2H analogues.

Can. J. Chem. Downloaded from www.nrcresearchpress.com by 210.87.254.5 on 09/05/12
For personal use only.

1 (R = CH_3)	274	272 ⟶	273	219.5 ⟶	245		
1 (R = $C[^2H_3]$)	277	275 ⟶	276	223 ⟶	248		
2	329	299.5 ⟶	314	260.7 ⟶	286	256.5 ⟶	271
3 (R = CH_3)	270	185.5 ⟶	224	171.3 ⟶	196	142.3 ⟶	167
4	283	249.5 ⟶	266	143 ⟶	195		
5 (R = CH_3, R′ = OH)	269	235.5 ⟶	252				
	269	215.5 ⟶	241	239.5 ⟶	240		
	269	145.9 ⟶	198				
5 (R = $C[^2H_3]$, R′ = SH)	288	241.5 ⟶	259				

TABLE I

The relative abundances of the M − X − 28⁺ions

Compound	Abundance*
1	14
2	27
3	60
5 (R = CH_3; R′ = OH)	23
5 (R = $C[^2H_3]$, R′ = SH)	16
4	3

*Molecular ion = 100.

In these reactions the figures above the arrows refer to *m/e* values of the metastable peaks associated with the indicated reactions. In three cases (**1**; **5**, R = Me, R′ = OH; R = $C[^2H_3]$, R′ = SH) the molecular formulas of the product ions were established by precise mass measurement. Scheme 3 shows proposed formulations of the two main reactions of the molecular ion of the compound **1**, (R = Me), the most abundant involving ring closure to form a stable M − 1^+ ion. These reactions are modified by the introduction of substituents and ions of the type **10**, **11**, and **12** may be formed from the molecular ions of **2**, **3**, **4**, and **5**. In the spectrum of **3** the formation of the M − 46^+ ion may involve the loss of $\cdot NO_2$ followed by hydrogen transfer in the furanyl ring which would permit ring-closure involving the oxindole oxygen atom. In the spectra of compounds of the type **5** ions are found which represent the fragmenting and product species of the reaction M − 29^+ → M − 29 − 71^+, a reaction typical of 2,4-dihydroxypyrimidines (10). Similarly in the deuteriated thio compound **5**, (R = $C[^2H_3]$, R′ = SH) ions are observed at M − 29^+ and M − 29 − 87^+. This may be evidence in favor of the formula **12**. In the mass spectrum of **4** the M − 29^+ ion is of low abundance which may be associated with substitution on all carbon atoms in the pyrimidine ring.

Only the 5-nitrofuryl derivatives were biologically active and alkylation of the oxindole resulted in little change in activity (11).

Experimental

Infrared (i.r.) spectra were determined using a Perkin–Elmer 237 instrument and ultraviolet (u.v.) spectra were taken on a Beckmann DK-2 spectrophotometer. Nuclear magnetic resonance (n.m.r.) spectra were obtained with Varian A60A instruments; chemical shifts are quoted in p.p.m. downfield from the signal of tetramethylsilane which was always used as an internal standard. Mass spectra were measured on an Atlas CH4 spectrometer and also on a Consolidated Electrodynamics Corporation 110B instrument using electrical detection. Precise masses were obtained on the latter instrument by reference to fragments of known mass in the spectrum of perfluorokerosene. The mass spectra are presented as follows: *m/e* value of the ion, followed in brackets by (*a*) the number of hydrogen atoms exchanged by deuterium in the inlet system (12), (*b*) the relative abundance of the ion; the most intense ion in the mass spectrum was assigned an arbitrary value 100, and (*c*) the theoretical value for the mass of the ion which agrees best with the experimentally determined value, (usually within 10 p.p.m.) together with the required elemental composition of that ion. In general the accuracy of these measurements was within 5 p.p.m. All samples for mass spectrometry were inserted directly into the source of the instrument. Alumina was obtained from Merck (West Germany) and was Brockmann grade II. Silica gel was 100–200 mesh and was obtained from Mallinckrodt.

1-Methyloxindole

Oxindole (Aldrich, 5 g), tetrahydrofuran (100 ml) and potassium *t*-butoxide (prepared by lyophilizing a solution of potassium in *t*-butanol, 4.2 g) were shaken together at 20 °C until most of the butoxide had dissolved. Methyl iodide (5.4 g) was added and the exothermic reaction was shaken at 20 °C for 18 h. The mixture was filtered, the filtrate evaporated, and the residue distributed between ice-cold sodium hydroxide solution (2%,

Can. J. Chem. Downloaded from www.nrcresearchpress.com by 210.87.254.5 on 09/05/12
For personal use only.

Can. J. Chem. Downloaded from www.nrcresearchpress.com by 210.87.254.5 on 09/05/12
For personal use only.

100 ml) and benzene (50 ml). The benzene soluble products were adsorbed from light petroleum (b.p. 40–60 °C) on alumina (50 g). 1-Methyloxindole (2.2 g, m.p. 86–87 °C) was eluted with benzene.

Mass Spectrum: *m/e* 147 (89), 132 (9), 118 (100), 104 (5), 91 (18), 78 (14.5).

ν_{max} (CS_2) 3440, 3150 1725, (KBr) 1705, 1605, 1260, 1125, 1075, 910, 745 cm^{-1}.

τ ($C[^2H]Cl_3$), 6.68 (intensity 2) and 6.89 (intensity 3) p.p.m.

The 1-[$^2H_3$]methyl derivative was prepared as described above on the same scale using [$^2H_3$]methyl iodide (isotopic purity > 99% by mass spectroscopic analysis, obtained from Merck, Sharp & Dohme, Canada). The oxindole had the following properties: m.p. 88–89 °C.

Mass spectrum: *m/e* 150 (90), 132 (25), 121 (100), 104 (16), 94 (12), 93 (16), 92 (17), 78 (40).

ν_{max} (KBr) 1695, 1610, 1330, 1250, 1205, 1100, 1005, 840, 750 cm^{-1}.

τ ($C[^2H]Cl_3$) 2.5–3.3 (complex multiplet intensity 4) and 6.48 (intensity 2) p.p.m.

1-Methyloxindolidene-3-(indolyl-3')-methine

1-Methyloxindole (150 mg), indole-3-aldehyde (Aldrich, 150 mg), acetic acid (40 ml), and acetic anhydride (10 ml) were heated together under reflux for 3 h and then allowed to stand at 20 °C for 18 h. The solution was concentrated, diluted with water (100 ml), and neutralized with sodium bicarbonate. The precipitate was adsorbed from benzene on silica gel; a red band which eluted with ether–benzene (1:99) was discarded and a bright yellow band which eluted with ether–benzene (1:9) was collected. The *indole* separated from ethanol as yellow prisms, m.p. 274 °C.

Anal. Calcd. for $C_{18}H_{14}N_2O$: C, 78.9; H, 5.1; N, 10.2. Found: C, 79.3; H, 5.3; N, 10.0.

Mass spectra: *m/e* 274 (d_1, 100), 273 (d_1, 27), 258 (d_0, 5), 245 (d_1, 14), 231 (d_1, 4), 217 (d_1, 6), 204 (d_1, 4), 189 (2), 176 (2), 158 (3), 147 (6), 137 (14), 130 (7), 128 (3), 122 (6), 118 (7), 117 (7), 115 (5), 102 (9), 91, 89 (6), 44 (52), 28 (100).

λ_{max} (MeOH) 262, 274 (shoulder), 395 mμ (log ε 4.22, 4.16, 4.54).

ν_{max} (KBr) 1670, 1620, 1610, 1510, 1495, 1475, 1420, 1395, 1350, 1270, 1255, 1235, 1210, 1130, 1090, 1030, 930, 925, 790, 745, 735, 710 cm^{-1}.

1-[$^2H_3$]Methyloxindolidene-3-(indolyl-3')-methine

3-Formylindole (60 mg), 1-[$^2H_3$]methyloxindole (60 mg), acetic acid (4 ml), and acetic anhydride (50 mg) were heated under reflux for 18 h. The mixture was diluted with a saturated solution of sodium hydrogen carbonate and the neutral mixture extracted (×4) with benzene. The dried (Na_2SO_4) extract was concentrated (20 ml), adsorbed on silica gel (20 g, 1 cm diameter), and the column developed with ether–benzene (1:50, 400 ml). The 1-[$^2H_3$]methyl derivative was eluted with ether–benzene (1:9) and separated from ethanol as orange prisms, m.p. 271–273 °C.

Mass spectrum: *m/e* 277.1293 (100, $C_{18}H_{11}[^2H_3]N_2O$ requires 277.1295); 276 (20), 261 (4), 259 (4), 249.1334 (5, $C_{17}H_9[^2H_4]N_2$ requires 249.1331); 248.1262 (7, $C_{17}H_{10}[^2H_3]N_2$ requires 248.1268); 231 (5), 219 (3), 204 (5), 191 (1), 176 (2), 161 (2), 150 (4), 138.5 (15), 130 (21), 125, 124, 123, 120, 102 (6).

ν_{max} (KBr) 1675, 1610, 1490, 1470, 1400, 1365, 1250, 1205, 1135, 1120, 1000, 780, 745, 710 cm^{-1}.

2,4-Dihydroxy-5-formyl-6-methylpyrimidine

Potassium hydroxide (5.6 g), water (50 ml) and 6-methyluracil (12.6 g) at 70 °C were diluted with ethanol (40 ml) and then treated with chloroform (18 g) and a solution of potassium hydroxide (28 g) in water (30 ml), as described by Hull (13). The solution was heated under reflux for 50 min, chloroform (25 ml) was added, and the reaction mixture was boiled until it was concentrated to a syrup. This was left standing overnight, and then water (150 ml) was added and the stirred solution was neutralized (pH 6) with concentrated hydrochloric acid. A yellow precipitate (7.8 g) slowly separated over the next 4 days. The *aldehyde* separated from water–ethanol (1:4) as needles.

Anal. Calcd. for $C_6H_5N_2O_3K$, $0.25H_2O$: C, 36.6; H, 2.8; N, 14.25; O, 26.5. Found: C, 36.6; H, 3.2; N, 14.0; O, 26.0.

λ_{max} (H_2O) 237, 296 mμ (log ε 3.50, 4.04); λ_{max} (0.27 *N* HCl) 232, 283 mμ (log ε 4.01, 4.07).

ν_{max} (KBr) 1725, 1700, 1575, 1525, 1115, 775, 700 cm^{-1}.

1-Methyloxindolidene-3-(2',4'-dihydroxy-6'-methylprimidinyl-5')methine (4)

1-Methyloxindole (0.3 g), the above 5-formyluracil (0.3 g), acetic acid (20 ml), and acetic anhydride (1 ml) were heated together under reflux for 18 h. The solution was evaporated, the residue treated with water (30 ml), and the mixture continuously extracted with ethyl acetate for 24 h. The extract was cooled, the precipitate collected, and the *oxindole* (0.13 g) recrystallized from acetic acid.

Anal. Calcd. for $C_{15}H_{13}N_3O_3$, CH_3CO_2H: C, 59.6; H, 5.0; N, 12.3. Found: C, 60.2; H, 5.45; N, 12.8.

Mass spectra: *m/e* 283.0965 (d_2, 100, $C_{15}H_{13}N_3O_3$ requires 283.0957); 266.0909 (d_2, 38, $C_{15}H_{12}N_3O_2$ requires 266.0930); 254 (d_2, 3), 239 (d_1, 8), 223 (d_2, 3), 212 (d_1, 17), 195 (d_1, 16), 183 (d_1, 8.5), 171 (d_1, 12), 142 (d_1, 8), 115 (13), 101 (3), 42 (17), 28 (100).

λ_{max} (MeOH) 251, 273, 328 mμ (log ε 4.59, 4.07, 4.21); λ_{max} (0.25 *N* NaOH) 257, 288, 375 mμ (log ε 4.34, 4.05, 4.29).

ν_{max} (KBr) 1726, 1700, 1660, 1615, 1475, 780, 765 cm^{-1}.

1-Methyloxindolidene-3-(2',4'-dihydroxypyrimidinyl-6')-methine

6-Formyl-2,4-dihydroxypyrimidine (0.3g) [λ_{max} (H_2O) 260 mμ (log ε 3.92); λ_{max} (0.01 *N* NaOH) 286, 335 mμ (log ε 3.79, 2.68); ν_{max} (KBr) 3230, 2930, 2850, 1712, 1675, 1115, 1095, 1065, 1040, 1010, 830 cm^{-1}; (14)], 1-methyloxindole (0.3 g), acetic acid (20 ml), and acetic anhydride (1 ml) were heated together under reflux for 24 h. The reaction mixture was cooled and the beautiful scarlet needles collected. The *oxindole*, (0.4 g) separated from acetic acid.

Anal. Calcd. for $C_{14}H_{11}N_3O_3$, $0.5CH_3CO_2H$: C, 60.5; H, 4.35; N, 14.1; O, 21.4. Found: C, 61.0; H, 4.35; N, 14.5; O, 20.2.

Mass Spectra: *m/e* 269 (d_2, 100), 252.0777 (d_2, 10.5, $C_{14}H_{10}N_3O_2$ requires 252.0772); 241.0859 (d_2, 8, $C_{13}H_{11}N_3O_2$ requires 241.0851); 240.0771 ($d_{1(2)}$, 15, $C_{13}H_{10}N_3O_2$ requires 240.0772); 225 (d_1, 10), 213 (d_2, 3), 198 (d_1, 39), 185 (d_1, 3), 171 (6), 169 (d_1, 6), 158 (19), 143 (5), 130 (10.5), 128 (6), 115 (8), 99 (5), 89 (5), 77 (8), 28 (34).

Can. J. Chem. Downloaded from www.nrcresearchpress.com by 210.87.254.5 on 09/05/12
For personal use only.

λ_{max} [635 μg in HOAc (1 ml) diluted to 25 ml with MeOH, and further dilutions with MeOH] 263, 270, 353 mμ (log ε 4.56, 4.58, 4.45); λ_{max} (1 ml of the above solution diluted to 2 ml with 2 *N* NaOH) 385 mμ (log ε 3.48).

ν_{max} (KBr) 1725, 1675, 1610, 1480, 1390, 1105, 790, 750, 660 cm^{-1}.

1-[$^2H_3$]Methyloxindolidene-3-(4'-hydroxy-2'-mercapto-pyrimidinyl-6')-methine

6-Formyl-4-hydroxy-2-mercaptopyrimidine (14) (50 mg) and 1-[$^2H_3$]methyloxindole (50 mg) were heated under reflux with acetic acid (3 ml) and acetic anhydride (0.1 ml). After 7 h the red crystals that had separated were collected and recrystallized from formamide, 45 mg, m.p. > 350 °C. The *1-[$^2H_3$]methyloxindolylpyrimidine* separated from boiling formamide as orange-red needles.

Anal. Calcd. for $C_{14}H_8[^2H_3]N_3O_2S$: C, 58.5; H, 4.9; O, 11.1. Found: C, 58.7; H, 4.0; O, 13.4.

Mass Spectrum: *m/e* (290), 288 (100), 277 (12), 260.0797 (10, $C_{13}H_6[^2H_4]N_3OS$ requires 260.0795); 259.0733 (16, $C_{13}H_7[^2H_3]N_3OS$ requires 259.0733); 245 (10), 244 (15.5), 227 (35), 202 (15), 201 (15), 188 (13), 174 (10), 172 (8), 161 (54), 150 (25), 149 (30), 133, 132, 130, 129, 128, 127, 121, 120, 119, 118, 117, 116, 115, 114, 113, 102 (10), 93 (10).

λ_{max} (1.089 mg in formamide (1 ml) diluted with methanol) 277, 339 mμ (log ε 4.49, 4.24); λ_{max} (0.1 *N* NaOH) 260, 305 mμ (log ε 4.21, 4.01).

ν_{max} (KBr) 1660, 1590, 1470, 1395, 1190, 890, 780, 745, 700 cm^{-1}.

5-Chloro-6,7-dimethoxy-1-methyloxindolidene-3-(phenyl)-methine (2)

Benzyl chloride (2 g), triphenylphosphine (2.62 g), and benzene (20 ml) were refluxed together for 18 h. The product (0.2 g, m.p. 313–316 °C) in methanol (10 ml) was added to a solution (0.54 *N*, 2.5 ml) of sodium methoxide in methanol. The solution was stirred for 30 min at 20 °C, then treated with a solution of 5-chloro-6,7-dimethoxy-1-methylisatin (15) (0.1 g) in methanol (10 ml). This was heated under reflux for 30 min and evaporated. The benzene soluble products were adsorbed from benzene on silica gel (20 g, 1 × 12 cm) and the yellow benzene eluate (95 mg, m.p. 147–160 °C) collected. The *chlorodimethoxyoxindole* (2) separated from ethanol as yellow needles m.p. 179 °C (subliming above 150 °C).

Anal. Calcd. for $C_{18}H_{16}ClNO_3$: C, 65.7; H, 4.85; N, 4.3. Found: C, 65.8; H, 4.85; N, 4.2.

Mass Spectra: *m/e* 331, 329 (d_0); 316, 314; 288, 286; 273, 271.

λ_{max} (EtOH) 216, 271, 335 mμ (log ε 4.40, 4.12, 4.06).

ν_{max} (KBr) 1699, 1635, 1601, 809, 764, 702 cm^{-1}.

τ (C[^{2}H]Cl_3) 6.09 (intensity 6) and 6.47 (intensity 3).

Methylation of Oxindolidene-3-(5'-nitrofuryl-2')-methine (3)

Oxindolidene-3-(5'-nitrofuryl-2')-methine (4) (1.2 g), potassium *t*-butoxide (3 g) and tetrahydrofuran (100 ml) were shaken together 0.5 h when a black solution was obtained. Methyl iodide (20 ml) was added and the mixture shaken at room temperature for 18 h. The mixture was filtered, the filtrate was evaporated, and the benzene soluble products were adsorbed on silica gel (50 g, 25 × 3 cm). *2-Methoxy-3H-indolidene-3-(5'-nitrofuryl-2')-methine*, eluted with benzene, separated as crimson plates m.p. 230–231 °C, from ethanol.

Anal. Calcd. for $C_{14}H_{10}N_2O_4$: N, 10.35. Found: N, 10.2.

λ_{max} (EtOH) 261, 315, 397 mμ (log ε 4.41, 4.06, 4.28); λ_{max} (0.1 *N* ethanolic HCl) 264, 382 mμ (log ε 4.25, 4.40).

ν_{max} (KBr) 1685, 1600, 1560, 1505, 890, 709 cm^{-1}.

Further elution of the silica gel column with benzene–ether (4:1) gave *1-methyloxindolidene-3-(5'-nitrofuryl-2')-methine* as dark red prisms m.p. 215–216 °C, from ethanol. Found: N, 10.1.

Mass spectra: *m/e* 270 (d_0 100), 240 (2), 224 (19), 196 (60), 184 (7), 170 (4), 167 (11), 158 (2), 153 (5), 139 (6), 130 (1), 127 (5), 115 (5), 101 (2), 89 (2), 28 (2).

λ_{max} (EtOH or 0.1 *N* ethanolic HCl) 260, 310, 386 mμ (log ε 4.46, 4.01, 4.19).

ν_{max} (KBr) 1705, 1595, 1505, 745, 739, 729, 679 cm^{-1}.

1-Ethyloxindolidene-3-(5'-nitrofuryl-2')-methine

This compound was prepared as described above for the 1-methyl derivative. The *oxindole* was eluted with benzene–ether (19:1) from silica gel and separated from ethanol as needles m.p. 210 °C.

Anal. Calcd. for $C_{15}H_{12}N_2O_4$: C, 63.4; H, 4.25; N, 9.85. Found: C, 63.4; H, 4.2; N, 9.9.

λ_{max} (EtOH or 0.1 *N* ethanolic HCl) 260, 310, 386 mμ (log ε 4.47, 3.99, 4.15).

ν_{max} (KBr) 1710, 1605, 1515, 750, 730, 680 cm^{-1}.

Acknowledgments

We thank D. G. Smith and S. Sternhell for the nuclear magnetic resonance spectra and Miss D. E. Hannah for the biological assays.

1. D. Brewer, D. E. Hannah, and A. Taylor. Can. J. Microbiol. **12**, 1187 (1966).
2. Raymond-Hamet. Compt. Rend. Soc. Biol. **128**, 777 (1938); **134**, 459 (1940); **146**, 1042 (1952); **154**, 2037 (1960). Bull. Sci. Pharmacol. **47**, 33 (1940). N. Finch and W. I. Taylor. J. Am. Chem. Soc. **84**, 3871 (1962).
3. R. Hodges, J. S. Shannon, and A. Taylor. J. Chem. Soc. 1803 (1966).
4. R. Hull. U. S. Patent No. 2,872,372.
5. R. L. Autrey and F. C. Tahk. Tetrahedron, **23**, 901 (1967).
6. R. G. Ault, E. L. Hirst, and R. A. Morton. J. Chem. Soc. 1653 (1935).
7. S. F. Mason. *In* S. F. Mason and D. J. Brown. The pyrimidines. John Wiley and Sons, Inc., New York. 1962. p. 493.
8. R. A. Jones and A. R. Katritzky. J. Chem. Soc. 3610 (1958).
9. A. Albert and G. B. Barlin. J. Chem. Soc. 2384 (1959).
10. J. M. Rice, G. O. Dudek, and M. Barber. J. Am. Chem. Soc. **87**, 4569 (1965).
11. D. J. Bauer and P. W. Sadler. Brit. J. Pharmacol. **15**, 101 (1960); R. G. Johnston and D. Kidd. J. Chem. Soc. 4734 (1964).
12. J. S. Shannon. Tetrahedron Letters, 1229 (1962).
13. R. Hull. J. Chem. Soc. 4845 (1957).
14. T. B. Johnson and E. F. Schroeder. J. Am. Chem. Soc. **53**, 1989 (1931); C. Heidelberger and R. B. Hurlbert. J. Am. Chem. Soc. **72**, 4704 (1950).
15. R. Hodges, J. W. Ronaldson, A. Taylor, and E. P. White. J. Chem. Soc. 5332 (1963).

Can. J. Chem. Downloaded from www.nrcresearchpress.com by 210.87.254.40 on 09/05/12
For personal use only.

Proton chemical shifts of polyhalobenzenes in cyclohexane and carbon tetrachloride. An additivity scheme based on pairwise parameters

B. RICHARDSON[1] AND T. SCHAEFER
Department of Chemistry, University of Manitoba, Winnipeg, Manitoba

Received February 26, 1968

An additivity scheme which takes into account the interactions between ortho substituents is applied to 39 proton shifts in 22 tri-, tetra-, and pentasubstituted halobenzenes as 3 mole % solutions in cyclohexane and carbon tetrachloride. The shift of any proton can be written as the sum of two parameters $D(X,Y)$ and one parameter d_p. $D(X,Y)$ refers to a pair of substituents placed ortho (X) and meta (Y) to the proton and d_p refers to a substituent placed para to the proton. The mean deviation between observed and calculated shifts is found to be 0.010 p.p.m. for the cyclohexane solutions and 0.012 p.p.m. for the carbon tetrachloride solutions. The scheme also works reasonably well for mono and dihalobenzenes. The parameter $D(X,Y) - D(H,Y)$ is a measure of the steric interaction between the X and Y substituents. It is also suggested that the steric environment of a proton is important in determining the shift in carbon tetrachloride solution.

Canadian Journal of Chemistry, 46, 2195 (1968)

Introduction

The ultimate goal of the study of the chemical shifts of aromatic protons is their prediction by molecular quantum mechanics. There is little evidence that this goal will soon be reached. Some progress has been made in correlating the proton shifts in substituted benzenes with electron densities at the bonded carbon atoms (1–3) or with Hammett substituent constants (4, 5). But there are also contributions[2] to the shifts arising from substituent magnetic anisotropy, local van der Waals interactions, field effects introduced by substituent dipole moments, and from rather subtle ortho effects (7, 8). Substituent-induced changes in ring currents also contribute (9). Their disentanglement is difficult and perhaps impossible (6).

Under these circumstances empirical schemes, based on additivity relationships, for the prediction and correlation of proton shifts still have their place, particularly when their accuracy is considerably better than the correlations referred to above. Perhaps one of the first additivity schemes was that of Diehl (5) who evaluated characteristic ortho, meta, and para constants for eleven substituents in meta and para disubstituted benzenes. These constants failed to predict the shifts in ortho disubstituted benzenes. Smith (10) extended the measurements to 50 more substituents and van Meurs (11) gave a scheme for alkyl substituted benzenes. Brey and Lawson (12), using a procedure similar to that of Diehl, were unable to find an additivity scheme in polysubstituted benzenes; especially when halogens were present. The Diehl procedure was refined by Martin and Dailey (13). They were able to predict the chemical shift to within 0.02 p.p.m. in para disubstituted benzenes by the formula "proton shift ortho to R_1" $= d_o(R_1) + \gamma(R_1)\, d_m(R_4)$. Here d_o and d_m are ortho and meta substituent constants and γ is a measure of the susceptibility of the position ortho to R_1 to a perturbation by the substituent para to R_1; γ decreases as d_o increases. A precision of about 0.1 p.p.m. was found in predicting shifts additively in meta disubstituted benzenes but deviations as large as 0.5 p.p.m. occurred for protons next to the substituents in ortho disubstituted benzenes.

In more highly substituted benzenes there must be at least one pair of substituents situated ortho to one another (except of course for 1,3,5-trisubstituted benzenes). Therefore large deviations of observed shifts from those calculated by existing additivity schemes are to be expected. In this paper we propose a somewhat different scheme which is applicable to proton shifts in a variety of polyhalo-substituted benzenes. The polyhalobenzenes were chosen because many of the mono- and dihalobenzenes have already been studied and because the deviations from additivity appear to be largest

[1]Holder of an NRCC Bursary, 1966–1967.
[2]See ref. (6) for a discussion of the various factors contributing to the shifts.

Can. J. Chem. Downloaded from www.nrcresearchpress.com by 210.87.254.40 on 09/05/12
For personal use only.

for halogen substituents (12, 14). The shifts relative to benzene of 39 protons in 22 tri-, tetra-, and penta-substituted halobenzenes are reported for 3 mole % solutions in cyclohexane and carbon tetrachloride.

Experimental

The chemicals were of commercial origin and were used without further purification. Spurious peaks were found in two cases but were easily identified. Samples were prepared as 3 mole % solutions in carbon tetrachloride or cyclohexane. If the solubility was less than 3 mole % the saturated solution was used. Concentration studies on benzene and 1,3,5-tribromobenzene showed that from 3 mole % downward, there is a relative shift of less than 0.005 p.p.m. The solutions were degassed by the freeze – pump – thaw technique.

Spectral measurements were done on a DA-60-I spectrometer using internal tetramethylsilane (TMS) as a reference. Line positions were found by reading the sweep oscillator frequencies or periods at appropriate intervals. The sample temperature was 28.5 °C as determined by an ethylene glycol sample (Varian Associates). Peak positions were found with a typical r.m.s. error of ± 0.03 c.p.s.

Results and Discussion

Spectral Analysis

Many of the proton resonance spectra were analyzed by standard methods (15). The ABC spectra were solved by a computer program[3] based on the algebraic method of Castellano and Waugh (16). Subspectral methods (17) were found useful and some deceptively simple spectra were also found (18). The resultant chemical shifts relative to benzene are thought to be accurate to 0.005 p.p.m. and are given in Table I. Some of the coupling constants have already been reported in another connection (19) and the remainder will be published in a study of benzene solvent effects on these compounds (20).

A Pairwise Additivity Scheme for Polyhalobenzenes

As discussed above, the substituent constants derived by Martin and Dailey (13) are not in general expected to give a good prediction of the observed proton shifts for the compounds in Table I. In fact, a comparison between the 39 observed shifts in cyclohexane and those calculated using d_o, d_m, and d_p (13) yielded an average deviation of 0.184 p.p.m. or 16% of the observed range of 1.175 p.p.m. The maximum deviation was 0.507 p.p.m. for symtetrabromobenzene. Such large deviations are probably caused by a steric interaction between the ortho substituents (see below).

The interaction can be accommodated in an empirical scheme by assigning a parameter $D(X_o - Y_m) \equiv D(X,Y)$ to a pair of substituents placed ortho (X) and meta (Y) to the proton whose chemical shift is required. It is then assumed that the shift of any proton can be found as the sum of two parameters D and one para parameter d_p. This assumption is consistent with the fact that in a 1,2-disubstituted benzene the ortho interaction is not such as to interfere with the additive effect at protons 4 and 5 (3, 8). It is also consistent with the evidence (6) that in a 1-X-2-Y-benzene the shift of proton-4 is linearly related to the shift of proton-3 in the 1-Y-benzene.

The D and d_p parameters should be strictly applicable to compounds in which only pairs of substituents are placed ortho to each other. Thus, 1,2,3- or 1,2,3,4- or 1,2,3,4,5-substituted benzenes would fall outside the validity of the present scheme. However, we find that 1,2,3- and some 1,2,3,4-substituted benzenes can be accommodated within the present scheme (see further discussion below).

The D and d_p values were derived from the data in Table I, excluding any 1,2,3,4- or penta-substituted compounds (the latter can be used to test the validity of the scheme when applied to such a substitution pattern). Table II gives the D and d_p values found for the two solvents.[4] It was possible to evaluate 17 of the 25 possible D values involved in such a scheme for the halogens.

Cyclohexane Solutions

The parameters in Table II reproduce the 35 observed shifts in Table I (compounds **1 – 19**) with a mean deviation of 0.010 p.p.m. or 0.9% of the observed range of 1.175 p.p.m. (This represents a considerable improvement over existing additivity schemes.) However, there are nine deviations of 0.02 p.p.m. or greater and two of these are greater than 0.03 p.p.m.

These parameters were also used to calculate

[3]We are grateful to Dr. J. Cavanaugh for a listing of this program and to Dr. H. M. Hutton for the adaptation to an IBM System 360/65.

[4]Simultaneous equations in D, d_p, and the observed shifts were solved for D and d_p; minimizing the disagreement among overdetermined sets of equations.

TABLE I

Proton chemical shifts* in some polyhalosubstituted benzenes in cyclohexane and carbon tetrachloride

	Compound	Proton	Shift (p.p.m. relative to 3 *M* % benzene)			
			Cyclohexane (3 *M* %)		Carbon tetrachloride (3 *M* %)	
			Calculated	Observed	Calculated	Observed
1	1,3,5-tribromobenzene	H-2,4,6	−0.314	−0.310	−0.323	−0.332
2	1,3,5-trichlorobenzene	H-2,4,6	0.057	0.048	0.022	0.014
3	1,2,4,5-tetrabromobenzene	H-3,6	−0.556	−0.557	−0.558	−0.558
4	1,2,4,5-tetrachlorobenzene	H-3,6	−0.220	−0.220	−0.290	−0.289
5	1,2,4,5-tetrafluorobenzene	H-3,6	0.324	0.324	0.206	0.207
6	1,3,4,5-tetrafluorobenzene	H-2,6	0.622	0.618	0.522	0.523
7	1,4-dibromo-2,5-difluorobenzene	H-3,6	−0.030	0.006	−0.057	−0.073
8	1,3,5-tribromo-2-iodobenzene	H-4,6	−0.394	−0.394	−0.420	−0.420
9	1,2,3-trichlorobenzene	H-4,6	−0.003	−0.014	−0.059	−0.074
		H-5	0.303	0.266	0.174	0.174
10	1,3-difluoro-5-iodobenzene	H-2	0.553	0.563	0.478	0.484
		H-4,6	0.083	0.047	0.036	0.012
11	1,2,4-trichlorobenzene	H-3	−0.135	−0.144	−0.177	−0.188
		H-5	0.180	0.169	0.098	0.090
		H-6	−0.012	−0.012	−0.101	−0.084
12	1-bromo-2,5-dichlorobenzene	H-3	−0.016	−0.016	−0.091	−0.091
		H-4	0.151	0.125	0.063	0.056
		H-6	−0.337	−0.322	−0.354	−0.354
13	1-bromo-3,4-dichlorobenzene	H-2	−0.306	−0.301	−0.332	−0.332
		H-5	0.051	0.053	−0.026	−0.026
		H-6	0.009	0.018	−0.057	−0.026
14	1,2-dichloro-4-fluorobenzene	H-3	0.139	0.128	0.086	0.056
		H-5	0.454	0.430	0.361	0.340
		H-6	−0.057	−0.057	−0.132	−0.132
15	1,2,4-tribromobenzene	H-3	−0.474	−0.471	−0.481	−0.493
		H-5	0.043	0.063	−0.017	0.001
		H-6	−0.117	−0.120	−0.175	−0.186
16	2,4-dibromo-1-fluorobenzene	H-3	−0.404	−0.401	−0.408	−0.424
		H-5	0.065	0.050	−0.123	−0.158
		H-6	0.387	0.384	0.283	0.283
17	1,2-dichloro-4-iodobenzene	H-3	−0.487	−0.487	−0.528	−0.504
		H-5	−0.172	−0.168	−0.253	−0.214
		H-6	0.182	0.202	0.130	0.130
18	1-Br-3,5-dichlorobenzene	H-2,6	−0.114	−0.112	−0.133	−0.126
		H-4	0.028	0.008	−0.013	−0.034
19	1,2,3,4-tetrafluorobenzene	H-5,6	0.426	0.450	0.304	0.351
	.....					
20	1,2,3,4-tetrachlorobenzene	H-5,6	0.095	0.049	−0.015	−0.029
21	pentafluorobenzene	H-6	0.535	0.492	0.394	0.373
22	pentachlorobenzene	H-6	−0.113	−0.190	−0.214	−0.268

*There is an uncertainty of up to 0.005 p.p.m. in the observed shifts.

the nine shifts in the para disubstituted benzenes measured by Martin and Dailey at infinite dilution in cyclohexane (13). The mean deviation of the observed from the calculated values was 0.006 p.p.m. If the eleven shifts involving meta and ortho disubstituted benzenes (13) are included the mean deviation rises to 0.02 p.p.m. or about 1.5% of the observed range of 1.361.

Read and Goldstein (21) have recently measured the proton shifts in the four monohalobenzenes as 10 mole % solutions in tetramethylsilane. The mean deviation of our calculated from their observed values is 0.018 p.p.m. In this comparison as with those involving the data of Spiesecke and Schneider (4) (mean deviation of 0.03 p.p.m.) and the data of Martin and Dailey, the error attributable to the use of different solvents, concentrations and internal references is not known.

Consideration of compounds **20–22** in Table I indicates that for the two penta and the 1,2,3,4-tetrachloro compound the scheme is much less accurate. The mean deviation for these three compounds is 0.055 p.p.m., i.e., greater than five times the average deviation for the other compounds in Table I. The deviation gets larger in

Can. J. Chem. Downloaded from www.nrcresearchpress.com by 210.87.254.40 on 09/05/12
For personal use only.

Can. J. Chem. Downloaded from www.nrcresearchpress.com by 210.87.254.40 on 09/05/12
For personal use only.

TABLE II

Derived ortho–meta constants, $D(X,Y)$, and para constants, d_p, for halogen substituents in polysubstituted benzenes

$D(X,Y)$ or d_p (p.p.m.)	Cyclohexane	Carbon tetrachloride
H,H	0.000	0.000
H,F	0.053	0.013
H,Cl	0.098	0.044
H,Br	0.161	0.119
H,I	0.292	0.275
F,H	0.249	0.231
F,F	0.162	0.103
F,Br	0.226	0.164
Cl,H	−0.025	−0.032
Cl,Cl	−0.110	−0.145
Cl,Br	−0.114	−0.135
Br,H	−0.196	−0.187
Br,F	−0.208	−0.221
Br,Cl	−0.312	−0.322
Br,Br	−0.278	−0.294
Br,I	−0.276	−0.284
I,H	−0.377	−0.383
H	0.000	0.000
F	0.211	0.188
Cl	0.107	0.086
Br	0.078	0.051
I	0.055	0.016

magnitude as the degree of substitution and the size of the substituents increase (but four fluoro substituents next to each other appear not to show an anomalous low-field shift). It may be predicted, therefore, that most 1,2,3,4- or 1,2,3,4,5-substituted halobenzenes will display anomalous low-field shifts within the present scheme.

Carbon Tetrachloride Solutions

The mean deviation of the observed from the calculated shifts for the first 19 compounds (36 values) is 0.012 p.p.m. or 1.1% of the observed range. Ten deviations are greater than 0.02 p.p.m. and three of these are greater than 0.03 p.p.m. For compounds **20–22** only one value (pentachlorobenzene) displays an excess low-field shift equal to about five times the mean deviation. In this connection it may be relevant to note that all the shifts in carbon tetrachloride lie to low-field of those in cyclohexane, that the excess low-field shifts vary between 0.00 and 0.12 p.p.m. and that the size of the excess shift depends on the size of the substituents ortho to the proton.[5] Carbon tetrachloride and, for that matter, chloroform are perhaps to be avoided as solvent whenever possible.[6]

Smith, Cole, and Roark (6, 8) have measured a number of ortho dihalobenzenes in dilute carbon tetrachloride solution. The 14 shift comparisons with our parameters give a mean deviation of 0.022 p.p.m. but there are three values near 0.05 p.p.m. The twelve proton shifts in the monohalobenzenes in 10 w/w % concentration in carbon tetrachloride (25) yield a mean deviation of 0.019 p.p.m. from our calculated values (using −7.253 p.p.m. as the shift of benzene). Again, concentration effects may be significant in both of these comparisons.

The D(X,Y) Parameters

It is clear that $D(X,Y) - D(H,Y)$, keeping X constant, is a measure of the effect of the interaction between X and Y on the proton shift ortho to X. A plot of $D(X,Y) - D(H,Y)$ where X = Br; Y = H,F,Cl,Br,I, vs. the van der Waals radius of Y is fairly smooth and shows an algebraic decrease of $D(X,Y) - D(H,Y)$ as the size of Y increases. The ortho interaction between X and Y is therefore indicated to be steric in origin. Increased perturbation due to crowding of the ortho C—H bond is expected to lead to an increased low-field shift, as observed. (The $D(Br,Y)$ values do not vary regularly with the van der Waals radius of Y because the meta shift due to Y increases algebraically in going from F to I and partly cancels the algebraic decrease in $D(Br,Y)$, naively expected on steric grounds).

Acknowledgment

This work was supported by the National Research Council of Canada.

1. T. K. Wu and B. P. Dailey. J. Chem. Phys. **41**, 2796 (1964).
2. J. C. Schug. J. Chem. Phys. **46**, 2447 (1967).
3. J. C. Schug and B. P. Smith. J. Chem. Phys. **47**, 849 (1967).
4. H. Spiesecke and W. G. Schneider. J. Chem. Phys. **35**, 731 (1961).
5. P. Diehl. Helv. Chim. Acta, **44**, 829 (1961).
6. W. B. Smith and J. L. Roark. J. Am. Chem. Soc. **89**, 5018 (1967).
7. F. Hruska, H. M. Hutton, and T. Schaefer. Can. J. Chem. **43**, 2392 (1965).
8. W. B. Smith and G. M. Cole. J. Phys. Chem. **69**, 4413 (1965).
9. H. P. Figeys and R. Flamming. Mol. Phys. **12**, 581 (1967).
10. G. W. Smith. J. Mol. Spectry. **12**, 146 (1964).

[5]Reaction field models (22) do not appear to be applicable. Thus, the maximum shift of −0.12 p.p.m. for a proton placed between two fluorine atoms is of opposite sign to that predicted by the reaction field theory (22). See ref. (23) for further examples of the inadequacy of reaction field theory.

[6]The steric environment of a solute proton is important when carbon tetrachloride is used as solvent (24).

11. N. VAN MEURS. Rec. Trav. Chim. **86**, 111 (1967)
12. W. S. BREY and K. D. LAWSON. Private communication to J. W. Emsley, J. Feeney, and L. H. Sutcliffe. High resolution nuclear magnetic resonance. Vol. 2. The Pergamon Press, Ltd., London. 1965. p. 759.
13. J. S. MARTIN and B. P. DAILEY. J. Chem. Phys. **39**, 1722 (1963).
14. J. NIWA. Bull. Chem. Soc. Japan, **40**, 1512 (1967).
15. J. W. EMSLEY, J. FEENEY, and L. H. SUTCLIFFE. *Editors*. High resolution nuclear magnetic resonance. Vol. 1. The Pergamon Press, Ltd., London. 1965.
16. S. CASTELLANO and J. S. WAUGH. J. Chem. Phys. **34**, 295 (1961).
17. P. DIEHL, R. K. HARRIS, and R. G. JONES. *In* Progress in nuclear magnetic resonance. *Edited by* J. W. Emsley, J. Feeney, and L. H. Sutcliffe. Vol. 3. The Pergamon Press, Ltd., London. 1967.
18. R. J. ABRAHAM and H. J. BERNSTEIN. Can. J. Chem. **39**, 216 (1961).
19. H. M. HUTTON, B. RICHARDSON, and T. SCHAEFER. Can. J. Chem. **45**, 1795 (1967).
20. R. J. SCHWENK and T. SCHAEFER. To be published.
21. J. M. READ and J. H. GOLDSTEIN. J. Mol. Spectry. **23**, 179 (1967).
22. A. D. BUCKINGHAM. Can. J. Chem. **38**, 300 (1960).
23. P. LASZLO. *In* Progress in nuclear magnetic resonance spectroscopy. Vol. 3. *Edited by* J. W. Emsley, J. Feeney, and L. H. Sutcliffe. The Pergamon Press, Ltd., London. 1967.
24. D. H. WILLIAMS, J. RONAYNE, and R. G. WILSON. Chem. Commun. p. 1089 (1967).
25. S. CASTELLANO, R. KOSTELNIK, and C. SUN. Tetrahedron Letters, **46**, 4635 (1967).

Can. J. Chem. Downloaded from www.nrcresearchpress.com by 210.87.254.40 on 09/05/12
For personal use only.

Can. J. Chem. Downloaded from www.nrcresearchpress.com by 210.87.254.42 on 09/05/12
For personal use only.

Steroids and related products. XXVIII.[1] Cardiotonic steroids. III.[2] The synthesis of 3β-hydroxy steroids of the A/B-*cis* series[3]

R. BOUCHARD AND CH. R. ENGEL
Department of Chemistry, Laval University, Quebec, Quebec

Received November 30, 1967

In the course of the synthesis of 3β-hydroxy-21,21-dimethoxy-5β-pregnan-20-one (**8**), a method was developed for the preferential reduction of steroid 3-ketones of the A/B-*cis* series to the axial 3β-alcohols, the stereochemistry in positions-3 and -5 of which corresponds to that of the truly active steroid cardiotonics. This method, which seems the best available to date, consists of a Meerwein–Ponndorf reduction carried out over a very short reaction period.

Canadian Journal of Chemistry, 46, 2201 (1968)

It is well known that the highly active steroid cardiotonics show a *cis* fusion of rings A and B and that their 3-hydroxy substituent has a β-configuration which presents itself in the thermodynamically unfavorable axial conformation (1–3).[4] Because of this situation, the synthesis of such products presents certain difficulties, since for the majority of suitable starting materials, the 3-hydroxy function is equatorial, and since the chemical reduction and the catalytic reduction in neutral and alkaline media of suitable 3-ketones lead predominantly to equatorial alcohols (cf., *inter alia*, refs. 4, 5).

It is true that Butenandt and Müller (6) have reported the catalytic reduction of 5β-pregnane-3,20-dione in ether – acetic acid, in very good yield, to the axial 3β-alcohol (cf. also 4*a*) but, as already reported (7), in our hands, even in acidic media, such catalytic reductions gave rise predominantly to the equatorial 3α-alcohols. We also have already reported (7) that the use of aged Raney nickel (8) for the reduction of 3-ketones of the A/B-*cis* series to axial alcohols (compare also ref. 9) may be regarded as an improvement over catalytic reduction, but that it still does not represent a satisfactory solution to the problem.

We have now found that the best results for the production of 3β-hydroxy steroids of the A/B-*cis* series could be obtained by subjecting a 3-ketone to a Meerwein–Ponndorf reduction. The characteristic feature of the procedure consists of the limitation of the reaction time. This approach had seemed logical since the accepted mechanisms for the Meerwein–Ponndorf reduction (10–15) would be consistent with the assumption that an axial hydroxy derivative would be formed, if the reaction were to take place under kinetic control (compare refs. 11–13, 16), but that equilibration to the equatorial alcohol could and did occur under the actual reaction conditions.

We elaborated the procedure in the course of the synthesis of a steroid glyoxal derivative, 3β-hydroxy-21,21-dimethoxy-5β-pregnan-20-one(**8**), which we used in connection with synthetic work in the field of butadienolides.

In a first series of experiments we had synthesized this product from Reichstein's Compound S (**1**).[5] This readily available starting material[6] (18–21)[7] was transformed in the usual fashion (23, 24) to its bismethylenedioxy derivative **2** which was then reduced in high yield, with

[1]For paper XXVII of this series, see Ch. R. Engel and M. N. Roy Chowdhury. Tetrahedron Letters, 2107 (1968).

[2]For the preceding paper in this series, see G. Bach, J. Capitaine, and Ch. R. Engel, Can. J. Chem. **46**, 733 (1968).

[3]Abbreviated from part of the D.Sc. Thesis of R. Bouchard, to be presented to the School of Graduate Studies, Laval University. The synthetic work described in this paper was first presented as part of an invited lecture on the synthesis of cardiotonics at the Steroid Symposium of the VIth Pan-American Congress of Pharmacy and Biochemistry, Mexico City, December 1963. The general method for the synthesis of 3β-hydroxy steroids of the A/B-*cis* series was reported in a communication to the 49th Annual Conference of the Chemical Institute of Canada, Saskatoon, June 1966.

[4]Only a selection of references is given.

[5]The synthesis of this product from another starting material, by an entirely different route, was reported by Ruzicka *et al.* (17).

[6]We express very sincere thanks to Dr. E. B. Hershberg from the Schering Corp., Bloomfield, New Jersey, for kindly providing us with this product.

[7]Only a small selection of references is given. Compare also with ref. 22.

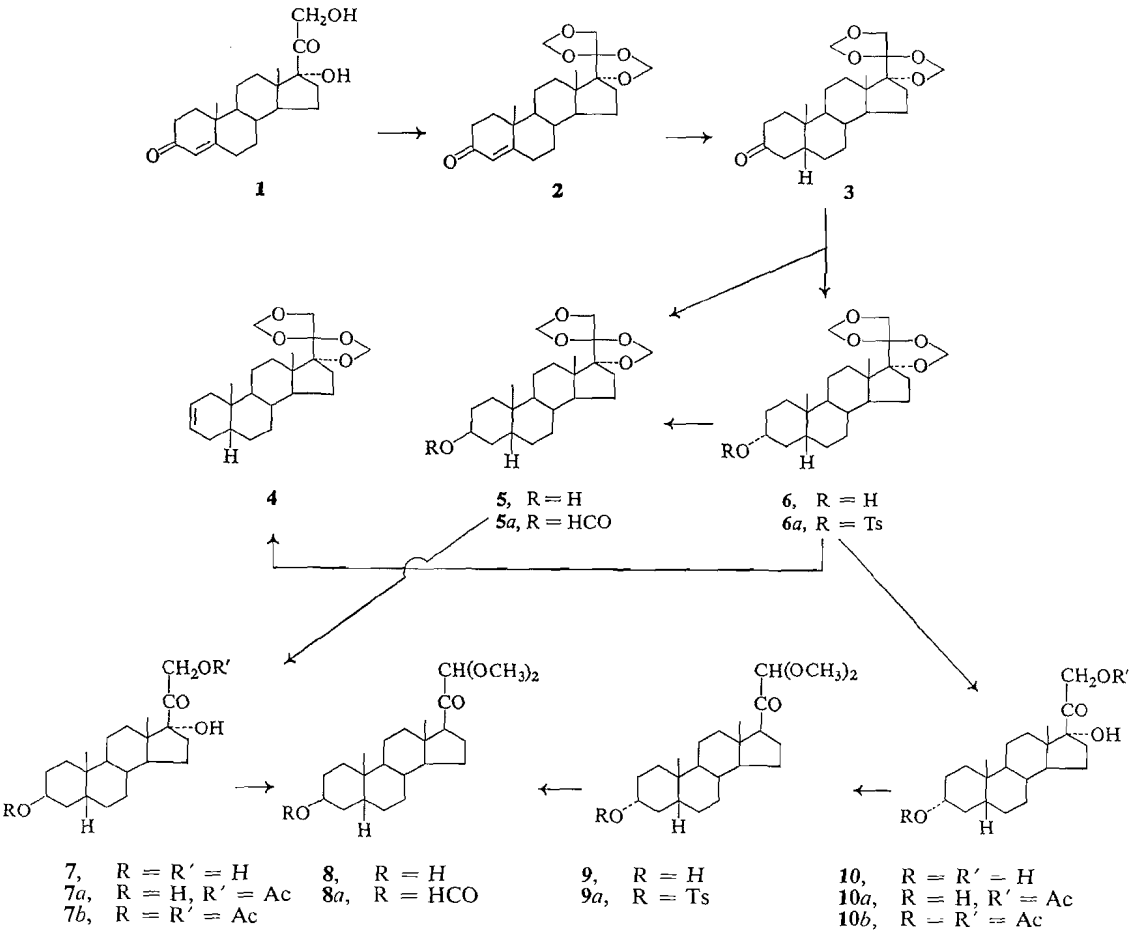

palladium on calcium carbonate in the presence of potassium hydroxide, to the 5β-pregnanone **3**. This ketone was now reduced with lithium aluminium hydride, predominantly (in 88% yield) to the equatorial alcohol **6**, the axial alcohol **5** representing a minor side product. The equatorial alcohol **6** was converted via its tosylate **6***a* and the formate **5***a* to the axial alcohol **5**. In this sequence of reactions, some starting material, the tosylate **6***a*, was recovered and some 2,3-unsaturated material (**4**), arising from an elimination reaction, was isolated (in 22% yield). Even when taking into account the recovery of starting material the yield of the desired axial alcohol **5** amounted only to 47%.

For the completion of the synthesis the dihydroxyacetone side chain was liberated in the usual fashion (23, 24) by treatment with acetic acid and the resulting triol **7** was acetylated to the hydroxy diacetate **7***b*. This product was now subjected to the Mattox rearrangement (25) with methanolic hydrogen chloride which gave in 60% yield the desired glyoxal derivative **8**.

In a modified pathway, the equatorial 3α-hydroxy derivative **6** was transformed via the triol **10** to the hydroxy diacetate **10***b* and thence, by rearrangement with hydrochloric acid, to the 3α-hydroxy glyoxal derivative **9**. This product was then converted through its tosylate **9***a* and the formate **8***a* to the 3β-hydroxy derivative **8**. Again, the yield of the inversion of the equatorial to the axial alcohol was, for practical purposes, not satisfactory (24% from alcohol **9**).

Independently, Harnik (9) had isomerized in a similar fashion alcohol **10***a* to alcohols **7** and **7***a*, using the same method; also in this case, the yield of the inversion reaction had not been satisfactory.

Can. J. Chem. Downloaded from www.nrcresearchpress.com by 210.87.254.42 on 09/05/12
For personal use only.

TABLE I

Relationship between the reaction time and the yields of the axial and equatorial alcohols **5** and **6** in the Meerwein–Ponndorf reduction of ketone **3**

Reaction time (min)	Starting material **3** (g)	Yield of axial alcohol **5** (g)	(%)	Yield of equatorial alcohol **6** (g)	(%)	Yield of recovered starting material **3** (g)	(%)	Yield of reduction (%)
120	1	0.430	43	0.56	56	0	0	99
50	2	0.968	48.4	1.00	50	0	0	98.4
35	10	5.7	57	4.1	41	0	0	98
15	10.4	6.14	59	4.0	38.5	0	0	97.5
8	5.6	2.91	52 (56)*	2.24	40 (43)*	0.403	7.2	92

*The figures in parentheses correspond to the yields of the alcohols when the recovery of starting material is taken into account.

These not very encouraging results of a relatively lengthy and cumbersome procedure prompted us to investigate, as intimated, the Meerwein–Ponndorf reduction of ketone **3** and we were able to show that, according to our expectations, the yield of the axial alcohol increased with the diminution of the reaction period. Table I gives the relation between reaction time and the yields of the epimeric alcohols **5** and **6**. The reaction was carried out with *sec*-butyl alcohol and aluminium *t*-butylate in absolute benzene at reflux temperature.

The first observation of interest was that the Meerwein–Ponndorf reduction was practically complete in 15 min, a fact which becomes significant if one considers that usually Meerwein–Ponndorf reductions are carried out over prolonged periods. Furthermore, we could establish that the yield of the thermodynamically unfavored axial alcohol could indeed be raised to approximately 60% by reducing the reaction time to 15 min. In the previous paper in this series on cardiotonic steroids (7), we have shown that this method proved superior to any other known method for the preparation of an axial 3α-hydroxy steroid of the A/B-*cis* series from the corresponding 3-keto derivative.[8]

[8]It is evident that this method is particularly attractive if the equatorial alcohol formed along with the axial alcohol is reoxided in a simple and rapid manner, for instance with Jones' reagent (26), to the ketone which is then subjected to another Meerwein–Ponndorf reduction, carried out over a very short period (cf. ref. 7). Such a recyclization is, of course, not practical in the case of the inversion sequence involving the tosylate, since the reaction product contains, apart from the desired alcohol and starting material, a dehydrated product, and since, furthermore, the procedure would be lengthy.

Experimental[9]

17,20;20,21-Bismethylenedioxy-4-pregnen-3-one (2)

Following the procedure of Beyler *et al.* (23, cf. also 24), 980 mg of Reichstein's Compound S (17α,21-dihydroxy-4-pregnen-3,20-dione) (**1**) was transformed with 16 ml of a 37% aqueous formaldehyde solution and 16 ml of concentrated hydrochloric acid, at room temperature in 54 ml of dichloromethane, to its bismethylenedioxy derivative **2**. The crude reaction product (1.404 g) gave, by chromatography on aluminium oxide, 920 mg (83.6% yield) of pure 17,20;20,21-bismethylenedioxy-4-pregnen-3-one (**2**), m.p. 254–255°. A sample was recrystallized three times from dichloromethane–ether for analysis; shiny prisms, m.p. 254–255°, $[\alpha]_D^{25}$ −7.8° (*c*, 1.000 in $CHCl_3$); λ_{max}(EtOH) 235 mμ (log ε 4.27); ν_{max}(KBr) 1683 cm^{-1} (ketone), 1625 cm^{-1} (double bond), 1100 cm^{-1} (ether bonds).

Anal. Calcd. for $C_{23}H_{34}O_5$: C, 71.11; H, 8.30. Found: C, 71.05; H, 8.48.

17,20;20,21-Bismethylenedioxy-5β-pregnan-3-one (3)

To a solution of 4.98 g of the above-described bismethylenedioxy derivative **2** of Reichstein's Compound S, m.p. 254–255°, in 250 ml of 95% ethanol, there were added 600 mg of potassium hydroxide in 50 ml of 95% ethanol and 1 g of a 4% palladium on calcium carbonate catalyst. The mixture was hydrogenated at room temperature. After 3 h, 270 ml of hydrogen had been taken up. The mixture was filtered through sodium sulfate and the filtrate was reduced to 200 ml and poured into 500 ml of cold water. The precipitate was extracted with ether, the ethereal solution was washed with water, dried over sodium sulfate, and the solvent was removed. The

[9]The melting points were taken in evacuated capillaries and the temperatures were corrected. If not otherwise stated, non-alkaline aluminium oxide Woelm, activity III, and Davison's silica gel No. 923 were used for chromatography. The infrared spectra were recorded on a Beckman IR-4 spectrophotometer and the ultraviolet spectra on a Beckman DK-1A spectrophotometer. The microanalyses were performed by Mr. A. Bernhardt, Mülheim (Ruhr), Germany, and Dr. C. Daesslé, Montreal, to whom we express our sincere appreciation.

Can. J. Chem. Downloaded from www.nrcresearchpress.com by 210.87.254.42 on 09/05/12
For personal use only.

Can. J. Chem. Downloaded from www.nrcresearchpress.com by 210.87.254.42 on 09/05/12
For personal use only.

crystalline residue (5.283 g) was recrystallized from ether–hexane to give 3.446 g of 17,20;20,21-bismethylenedioxy-5β-pregnan-3-one (**3**), m.p. 180–181°. The residue of the mother liquors (1.9 g) was chromatographed on 60 g of aluminium oxide. Elutions with petroleum ether – benzene (4:1 and 1:1) afforded another 1.15 g of the pure 5β-pregnane derivative **3**, m.p. 180–181° (total yield, 92%). A sample was recrystallized three times from ether–hexane for analysis; colorless needles, m.p. 180.5–181.5°; $[\alpha]_D^{25}$ −69° (*c*, 1.000 in $CHCl_3$); ν_{max}(KBr) 1718 cm^{-1} (ketone), 1100 cm^{-1} (ether bonds).

Anal. Calcd. for $C_{23}H_{36}O_5$: C, 70.74; H, 8.78. Found: C, 70.68; H, 8.71.

3β-Hydroxy-17,20;20,21-bismethylenedioxy-5β-pregnane (5) and 3α-Hydroxy-17,20;20,21-bismethylenedioxy-5β-pregnane (6) by Lithium Aluminium Hydride Reduction of 17,20;20,21-Bismethylenedioxy-5β-pregnan-3-one (3)

To a slurry of 2.2 g of lithium aluminium hydride in 30 ml of absolute tetrahydrofuran were added, over a period of 50 min, dropwise and with stirring, 2 g of the above-described bismethylenedioxy derivative **3** of 17α,21-dihydroxy-5β-pregnane-3,20-dione, m.p. 180–181°, in 100 ml of absolute tetrahydrofuran. The mixture was refluxed for 1 h, with stirring, and was then left at room temperature for 16 h. Subsequently, there were added, at 0°, 10 ml of ethyl acetate and a small quantity of ice, followed by 25 ml of an aqueous ammonium chloride solution. The mixture was poured into 1.5 l of cold water, and the precipitate was extracted with ether. The ethereal layer was washed with a saturated ammonium chloride solution and with water and was dried over sodium sulfate. The evaporation of the solvent gave 2.04 g of white needles, melting between 160 and 170°. The product was chromatographed on 60 g of aluminium oxide. Elutions with petroleum ether – benzene (1:1) gave 150 mg (7.5%) of *3β-hydroxy-17,20;20,21-bismethylenedioxy-5β-pregnane (5)*, m.p. 151–158°. A sample was recrystallized three times from ether–hexane for analysis; colorless needles, m.p. 157.5–158.5°; $[\alpha]_D^{25}$ −99.5° (*c*, 1.000 in $CHCl_3$); ν_{max}(KBr) 3490 cm^{-1} (small band, hydrogen-bonded hydroxyl, absent in the 3α-isomer), 3250 cm^{-1} (hydroxyl), 1100 cm^{-1} (ether bonds).

Anal. Calcd. for $C_{23}H_{38}O_5$: C, 70.37; H, 9.24. Found: C, 70.32; H, 9.49.

Elutions in the above-described chromatogram with petroleum ether – benzene (1:4) gave 1.757 g (87.8%) of *3α-hydroxy-17,20;20,21-bismethylenedioxy-5β-pregnane* (*6a*), m.p. 177–178°. A sample was recrystallized three times from ether–hexane for analysis; colorless needles, m.p. 180.5°; $[\alpha]_D^{25}$ −80° (*c*, 1.000 in $CHCl_3$); ν_{max}(KBr) 3225 cm^{-1} (sharp hydroxyl band), 1310 cm^{-1} (characteristic band of the 3α-hydroxy isomer, absent in the 3β-hydroxy isomer), 1110 cm^{-1} (ether bonds).

Anal. Calcd. for $C_{23}H_{38}O_5$: C, 70.37; H, 9.24. Found: C, 70.37; H, 9.35.

3α-Tosyloxy-17,20;20,21-bismethylenedioxy-5β-pregnane (6a)

Following the experimental procedure of Fukushima and Daum (26), 11.3 g of the bismethylenedioxy derivative **6** of 3α,17α,21-trihydroxy-5β-pregnan-20-one, m.p. 177–178°, was transformed with 11.3 g of *p*-toluenesulfonyl chloride in 125 ml of pyridine into its tosylate *6a*. There was obtained 15.5 g (98% yield) of crystalline product, m.p. 140–144°. A sample was recrystallized three times from acetone–hexane for analysis; colorless needles, m.p. 151–152°; $[\alpha]_D^{25}$ −39° (*c*, 1.000 in $CHCl_3$); λ_{max}(EtOH) 225 mμ (log ε 4.04); ν_{max}(KBr) 1600, 1185, and 1175 cm^{-1} (tosylate), 1100 cm^{-1} (ether bonds).

Anal. Calcd. for $C_{30}H_{42}O_7S$: C, 65.91; H, 7.74; S, 5.86. Found: C, 65.96; H, 7.50; S, 5.73.

3β-Hydroxy-17,20;20,21-bismethylenedioxy-5β-pregnane (5) and17,20;20,21-Bismethylenedioxy-5β-pregn-2-ene (4) from 3α-Tosyloxy-17,20;20,21-bismethylenedioxy-5β-pregnane (6a)

A solution of 15.5 g of crude tosylate *6a*, m.p. 140–144°, in 130 ml of unpurified *N,N*-dimethylformamide was heated to 80–82° for 72 h, cooled, and poured into ice-water. The precipitate was extracted with ether, the ethereal layer was washed with water and was dried over sodium sulfate. The solvent was removed and the oily residue, containing crude *3β-formoxy-17,20;20,21-bismethylenedioxy-5β-pregnane (5a)*, was treated for 4 h at room temperature with 1.5 l of a 5% methanolic potassium hydroxide solution. The solution was reduced *in vacuo* and then extracted with ether. The ethereal layer was washed with water, dried over sodium sulfate, and taken to dryness. The residue (11.1 g) crystallized from hexane. The product was chromatographed on 340 g of aluminium oxide. Elutions with petroleum ether – benzene (9:1) gave 2.3 g (21.7%) of *17,20;20,21-bismethylenedioxy-5β-pregn-2-ene (4)*, m.p. 117–123°. A sample was recrystallized three times from methanol for analysis: colorless prisms, m.p. 129–130°; ν_{max}(KBr) 3025 cm^{-1} (double bond), 1100 cm^{-1} (BMD-protection).

Anal. Calcd. for $C_{23}H_{34}O_4$: C, 73.76; H, 9.15. Found: C, 73.98; H, 9.07.

Elutions in the above-described chromatogram with petroleum ether – benzene (1:1) gave 3.3 g (25%) of starting material, *tosylate 6a*, m.p. 149–151°. Elutions with petroleum ether – benzene (1:4) and with pure benzene gave 4.1 g (36.8% yield) of *3β-hydroxy-17,20;20,21-bismethylenedioxy-5β-pregnane (5)*, m.p. 154–155°. The identity of the product with an authentic sample (compare above) was established by the comparison of the infrared spectra and by the determination of a mixture melting point. Considering the recovery of starting material, the yield of the 3β-hydroxy derivative **5** amounted to 47%, that of the dehydrated product **4** to 27.5%.

3β,17α,21-Trihydroxy-5β-pregnan-20-one (7) from 3β-Hydroxy-17,20;20,21-bismethylenedioxy-5β-pregnane (5)

Following the experimental procedure of the Merck group (23, 24), 486 mg of 3β-hydroxy-17,20;20,21-bismethylenedioxy-5β-pregnane (**5**), m.p. 154–155°, was hydrolyzed under nitrogen with 40 ml of acetic acid and 40 ml of water at 90° for 8 h. After having been left for another 16 h at room temperature, the mixture was neutralized with 35 g of sodium hydroxide in 75 ml of water and was worked up in the usual fashion. There were obtained 435 mg of colorless small crystals, m.p. 230–232° (yield 98.5%). A sample was recrystallized three times from acetone for analysis; m.p. 240–243°; $[\alpha]_D^{25}$ +53° (*c*, 1.000 in ethanol) [Lit. m.p. 224–226° (28), 232–234° (9);

Can. J. Chem. Downloaded from www.nrcresearchpress.com by 210.87.254.42 on 09/05/12
For personal use only.

$[\alpha]_D$ (ethanol) +54° (28), +50° (9)]; ν_{max}(KBr) 3450 and 3390 cm^{-1} (hydroxyls), 1715 cm^{-1} (20-ketone).

Anal. Calcd. for $C_{21}H_{34}O_4$: C, 71.94; H, 9.87. Found: C, 71.82; H, 9.69.

Diacetate 7b

The diacetate was prepared in the usual way from 53 mg of the diol **7** with 0.5 ml of acetic anhydride in 1 ml of pyridine. The reaction product (65 mg), m.p. 143–148°, was recrystallized twice from ethyl acetate – ether for analysis; m.p. 152–154°; $[\alpha]_D^{25}$ +50.3° (*c*, 1.000 in $CHCl_3$) [Lit. m.p. 149–151° (29); 154–157° (30); 152–154° (9); $[\alpha]_D$ (ethanol) +51° (9, 30); $[\alpha]_D$ (dioxane) +49° (29)]; ν_{max}(KBr) 3475 cm^{-1} (17α-hydroxyl), 1745 and 1722 cm^{-1} (21-acetoxy-20-keto doublet) (the peak at 1745 cm^{-1} is enlarged by the 3-acetate band), 1250 cm^{-1} (acetates).

Anal. Calcd. for $C_{25}H_{38}O_6$: C, 69.09; H, 8.82. Found: C, 69.23; H, 8.93.

*3α,21-Diacetoxy-17α-hydroxy-5β-pregnan-20-one (**10b**)*

A quantity of 180 mg of 3α-hydroxy-17,20;20,21-bismethylenedioxy-5β-pregnane (**6**) was hydrolyzed as described for the 3β-hydroxy derivative **5**, to 160 mg of *3α,17α,21-trihydroxy-5β-pregnan-20-one (**10**)*, m.p. 222–230°; ν_{max}(KBr) 3450 cm^{-1} (large hydroxyl band), 1720 cm^{-1} (20-ketone). This product was acetylated without further purification with 1 ml of acetic anhydride in 2 ml of pyridine. The reaction product (200 mg), representing *3α,21-diacetoxy-17α-hydroxy-5β-pregnan-20-one (**10b**)*, melted at 186–192°. A sample was recrystallized three times from ether–hexane for analysis; colorless pellets, m.p. 199–201°; $[\alpha]_D^{25}$ +83°(*c*, 1.000 in ethanol) [Lit. m.p. 201–206° (28); 205° (Kofler block) (30); $[\alpha]_D$ (ethanol) +77° (28), +88° (30)]; ν_{max}(KBr) 3450 cm^{-1} (sharp 17α-hydroxyl band), 1740 and 1732 cm^{-1} (21-acetoxy-20-ketone doublet and 3-acetate), 1265 and 1245 cm^{-1} (acetates).

Anal. Calcd. for $C_{25}H_{38}O_6$: C, 69.09; H, 8.82. Found: C, 69.09; H, 8.72.

*3β-Hydroxy-21,21-dimethoxy-5β-pregnan-20-one(**8**)*

(a) From 3β,21-Diacetoxy-17α-hydroxy-5β-pregnan-20-one (7b)

Following the procedure of Mattox (25), 700 mg of the 3β,21-diacetate **7b** was treated with 40 ml of a dry 0.5 *N* methanolic hydrogen chloride solution and with 20 ml of chloroform at room temperature. After 3 h, the steroid was dissolved and the solution was allowed to stand for 48 h at 25°. After addition of 2.2 g of sodium acetate in 10 ml of water, the mixture was concentrated *in vacuo* and water was added. The precipitate was extracted with ether, the ethereal layer was washed with water, saturated sodium bicarbonate solution, and water, and was dried over sodium sulfate. The solvent was evaporated and the residue (660 mg of a yellow oil) was chromatographed on 25 g of aluminium oxide. Elutions with petroleum ether – benzene (1:4) gave 360 mg (59% yield) of the glyoxal derivative **8**, m.p. 102–104°. A sample was recrystallized once from ether–hexane for analysis; long needles, m.p. 104–106°; $[\alpha]_D^{26}$ +143° (*c*, 1.000 in $CHCl_3$) [Lit. (17): m.p. 126–129° (recrystallization from ligroin, followed by sublimation); $[\alpha]_D$ ($CHCl_3$) +132°(± 10°)]; ν_{max}(KBr) 3340 cm^{-1} (3β-hydroxyl), 1725 cm^{-1} (20-ketone), 1090 cm^{-1} (ketal).

Anal. Calcd. for $C_{23}H_{38}O_4$: C, 72.98; H, 10.12. Found: C, 73.20; H, 10.18.

*(b) From 3α,21-Diacetoxy-17α-hydroxy-5β-pregnan-20-one (**10b**)*

As described for the 3β-acetoxy epimer **7b**, 7.8 g of 3α,21-diacetoxy-17α-hydroxy-5β-pregnan-20-one (**10b**) m.p. 199–201°, was transformed in 220 ml of chloroform with 460 ml of a dry 0.5 *N* methanolic hydrogen chloride solution to 7.27 g of a product representing the crude glyoxal derivative **9**. Chromatography on 250 g of aluminium oxide gave 5.8 g (85.2% yield) of crystalline *3α-hydroxy-21,21-dimethoxy-5β-pregnan-20-one (**9**)*, m.p. 114–117°, eluted with petroleum ether – benzene (4:1 and 1:1). Recrystallization from ether–hexane raised the melting point to 121.5–122.5°; $[\alpha]_D^{25}$ +130° (*c*, 1.000 in $CHCl_3$); ν_{max}(KBr) 3390 cm^{-1} (strong band, 3α-hydroxyl), 1735 cm^{-1} (20-ketone), 1100, 1085, 1035 cm^{-1} (ether bands). The product was transformed without further purification into the tosylate **9a**, as described in the following paragraph.

A quantity of 7.5 g of the 3α-hydroxy-21,21-dimethoxypregnanone **9**, m.p. 120–122°, was converted, as above, with a solution of 7.5 g of *p*-toluenesulfonyl chloride in 120 ml of pyridine to crude *tosylate* **9a**. This product (8.8 g), which showed the ultraviolet (31) and infrared absorptions typical of a tosylate, was dissolved in 300 ml of *N,N*-dimethylformamide. The solution was heated for 72 h at 82° and was then poured into ice-water. The usual work-up gave a crude product, consisting mainly of *formate* **8a**, which was dissolved in 300 ml of a 5% methanolic potassium hydroxide solution. The mixture was kept for 4 h at room temperature and was worked up in the usual fashion (see above). Chromatography of the crude reaction product (5 g) on 150 g of aluminium oxide gave 1.6 g (21%) of pure *3β-hydroxy-21,21-dimethoxy-5β-pregnan-20-one(**8**)*, eluted with petroleum ether – benzene (1:1) and melting at 103–105°. The product proved to be identical with the product obtained by Mattox rearrangement of 3β,21-diacetoxy-17α-hydroxy-5β-pregnan-20-one (**7b**) (see above), as established by the determination of a mixture melting point and the comparison of the infrared spectra.

*Meerwein–Ponndorf Reductions of 17,20;20,21-Bismethylenedioxy-5β-pregnan-3-one(**3**)*

The various Meerwein–Ponndorf reductions summarized in Table I were carried out under identical conditions with the exception of a variation of the reaction period and the quantities of materials used.[10] Our experimental procedure was adopted from that described by Miescher and Fischer (32). We report here, as an example, the reduction carried out over a period of 2 h.

To a solution of 1 g of 17,20;20,21-bismethylenedioxy-5β-pregnan-3-one (**3**), m.p. 180–181°, in 5 ml of absolute benzene, 25 ml of *sec*-butyl alcohol and 1 g of aluminium *t*-butoxide were added. The mixture was refluxed for 2 h, diluted with 2 ml of benzene, and then poured into ice-water. The precipitate was extracted with a 1:3 mixture of dichloromethane and ether, the organic layer was washed with a saturated cold ammonium chloride solution and

[10]While the quantities varied, the proportions of reagents and solvent remained identical.

with water, and was dried over sodium sulfate. Evaporation of the solvent gave 1.116 g of an oil which crystallized upon trituration with ether. This product was chromatographed on 35 g of aluminium oxide. Elutions with petroleum ether – benzene (4:1) gave 432 mg (43%) of *3β-hydroxy-17,20;20,21-bismethylenedioxy-5β-pregnane (5)*, m.p. 150–152°. Elutions with petroleum ether – benzene (1:1 and 1:4) gave 560 mg (56% yield) of *3α-hydroxy-17,20;20,21-bismethylenedioxy-5β-pregnane (6)*, m.p. 175–177°.

The identity of the products with authentic samples (see above) was established by the determination of mixture melting points and the comparison of the infrared spectra.

As apparent from Table I, in the case of the experiment carried out over a reaction period of 8 min, 7.2% of starting material, *17,20;20,21-bismethylenedioxy-5β-pregnan-3-one (3)*, m.p. 180–181°, eluted from the chromatogram with petroleum ether – benzene (9:1), was isolated in addition to the isomeric alcohols **5** and **6**.

Acknowledgments

We wish to express our sincerest thanks to Mrs. J. Capitaine for her expert cooperation in a number of the experiments described in this paper, and to Mr. D. Capitaine and Mrs. G. Pelletier for their devoted technical assistance. Once again we thank Dr. E. B. Hershberg from the Schering Corporation, Bloomfield, New Jersey, for the generous gift of starting material. We are greatly indebted to the National Research Council of Canada and to the Quebec Heart Foundation for financial support. One of us (R. B.) acknowledges gratefully the award of a NRCC scholarship.

1. H. HEUSSER. *In* Progress in the chemistry of organic natural products. Vol. 7. *Edited by* L. Zechmeister. Springer Verlag, Vienna. 1950. pp. 87–166.
2. CH. TAMM. *In* Progress in the chemistry of organic natural products. *Edited by* L. Zechmeister. Springer Verlag, Vienna. Vol. 13. 1956. pp. 137–231; Vol. 14. 1957. pp. 71–140.
3. J. HOCH. A survey of cardiac glycosides and genins. University of South Carolina Press. Charleston. 1961.
4. (*a*) L. F. FIESER and M. FIESER. Natural products related to phenanthrene. 3rd ed. Reinhold Publishing Corp., New York. 1949. p. 99. (*b*) L. F. FIESER and M. FIESER. Steroids. Reinhold Publishing Corp., New York. 1959. p. 268.
5. H. O. HOUSE. Modern synthetic reactions. W. A. Benjamin Inc., New York. 1965. p. 54.
6. A. BUTENANDT and G. MÜLLER. Ber. **71**, 191 (1938).
7. G. BACH, J. CAPITAINE, and CH. R. ENGEL. Can. J. Chem. **46**, 733 (1968).
8. C. DJERASSI, A. J. MANSON, and M. GORMAN. J. Am. Chem. Soc. **77**, 4925 (1955).
9. M. HARNIK. Steroids, **3**, 359 (1964).
10. E. S. GOULD. Mechanism and structure in organic chemistry. Holt, Rinehart, and Winston, New York. 1959. p. 545, and references quoted therein.
11. E. L. ELIEL. Stereochemistry of carbon compounds. McGraw-Hill Book Company Inc., New York. 1962. p. 72, also p. 69.
12. W. N. MOULTON, R. E. VAN ATTA, and R. R. RUCH. J. Org. Chem. **26**, 290 (1961).
13. V. J. SHINER, JR. and D. WHITTAKER. J. Am. Chem. Soc. **85**, 2337 (1963).
14. B. J. YAGER and C. K. HANCOCK. J. Org. Chem. **30**, 1174 (1965).
15. L. OTVOS, L. GRUBER, and J. MEISEL-AGOSTON. Acta Chim. Acad. Sci. Hung. **43** (2), 149 (1965).
16. E. L. ELIEL. Stereochemistry of carbon compounds. McGraw-Hill Book Company Inc., New York. 1962. p. 244.
17. L. RUZICKA, V. PRELOG, and P. WIELAND. Helv. Chim. Acta, **26**, 2050 (1943).
18. T. REICHSTEIN and J. VON EUW. Helv. Chim. Acta, **23**, 1258 (1940).
19. J. VON EUW and T. REICHSTEIN. Helv. Chim. Acta, **24**, 401 (1941).
20. P. L. JULIAN, E. W. MEYER, W. J. KARPEL, and I. R. WALLER. J. Am. Chem. Soc. **72**, 5145 (1950).
21. CH. MEYSTRE, E. VISCHER, and A. WETTSTEIN. Helv. Chim. Acta, **37**, 1548 (1954).
22. C. DJERASSI and C. T. LENK. J. Am. Chem. Soc. **76**, 1722 (1954).
23. R. E. BEYLER, R. M. MORIARTY, F. HOFFMAN, and L. H. SARETT. J. Am. Chem. Soc. **80**, 1517 (1958).
24. D. TAUB, R. D. HOFFSOMMER, H. L. SLATES, C. H. KUO, and N. L. WENDLER. J. Am. Chem. Soc. **82**, 4012 (1960).
25. V. R. MATTOX. J. Am. Chem. Soc. **74**, 4340 (1952).
26. K. BOWDEN, I. M. HEILBRON, E. R. H. JONES, and B. C. L. WEEDON. J. Chem. Soc. 39 (1946).
27. D. F. FUKUSHIMA and S. DAUM. J. Org. Chem. **26**, 520 (1961).
28. F. UNGAR and R. I. DORFMAN. J. Am. Chem. Soc. **76**, 1197 (1954).
29. R. B. WAGNER and J. A. MOORE. J. Am. Chem. Soc. **72**, 5301 (1950).
30. B. A. KOECHLIN, T. H. KRITCHEVSKY, and T. F. GALLAGHER. J. Am. Chem. Soc. **73**, 189 (1951).
31. CH. R. ENGEL, K. F. JENNINGS, and G. JUST. J. Am. Chem. Soc. **78**, 6153 (1956).
32. K. MIESCHER and W. H. FISCHER. Helv. Chim. Acta, **22**, 158 (1939).

Can. J. Chem. Downloaded from www.nrcresearchpress.com by 210.87.254.42 on 09/05/12
For personal use only.

Can. J. Chem. Downloaded from www.nrcresearchpress.com by 210.87.254.5 on 09/05/12
For personal use only.

Studies on the azidolysis of 4-arylidene and 4-alkylidene 5(4)-oxazolones. Part II

WILLIAM IBRAHIM AWAD AND AMEEN FAROUK MOHAMED FAHMY
Faculty of Science, Ain Shams University, Abbassia, Cairo, Egypt, United Arab Republic

Received August 9, 1967

4-Alkylidene-5(4)-oxazolones (**1**) react with sodium azide in acetic acid in 5 min, or with hydrazoic acid in benzene to give the diazide **2**. The latter gives by thermolysis the oxadiazine (**4**), which forms on hydrolysis the diamide (**5**). The corresponding monoazides (**3**) react with sodium azide – acetic acid mixture to give the corresponding diazides.

4-Arylidene-5(4)-oxazolones (**8**) react under the same conditions to give α-[tetrazolyl-(1)]-acrylic acid derivatives (**9**).

The work of Deorha and Gupta (6) is reinvestigated. The constitution of the products is discussed chemically and spectroscopically.

Canadian Journal of Chemistry, **46**, 2207 (1968)

In a previous publication (1) it was stated that 4-arylidene-5(4)-oxazolones react with sodium azide in acetic acid to give α-[tetrazolyl-(1)]-acrylic acid derivatives, while in the case of 4-alkylidene-5(4)-oxazolone, a neutral compound was obtained, benzamide (**5***a*). A mechanism was proposed for the formation of the latter compound.

In this study we attempted to discern the possible intermediates involved in both reactions.

When 4-isopropylidene-2-phenyl-5(4)-oxazolone (**1***a*) is allowed to react with sodium azide and acetic acid for 3 h, **5***a* is obtained (1) together with a small quantity of **6***a*; while permitting short reaction time (5 min) an azido compound (**2***a*) ($\nu N_3 = 2125\ cm^{-1}$), m.p. 146 °C is obtained. Analytical data prove that the above azido compound is a diazide. Isopropylidene hippuric azide (**3***a*) is known (2) (m.p. 92 °C) to be obtained via the hydrazide – sodium nitrite route. In addition to the azidolysis of the oxazolone ring, the azido group adds to the double bond of α,β-unsaturated carbon atoms. This is also known to be true of acrylates (3). It is also known that the *exo*-double bond of 4-isopropylidene-2-phenyl-5(4)-oxazolone adds ammonia or mercaptans (4). Thermolysis of both azides **2***a* and **3***a* gives the same product, 3,4-dihydro-4-isopropylidene-6-phenyl-2-oxo-1,3,5-oxadiazine (**4***a*), m.p. 186 °C via the Curtius rearrangement and cyclization. Hydrolysis of the latter by water or dilute acetic acid gives *N*-isobutyroyl benzamide (**5***a*). The monoazide (**3***a*) gives the diazide (**2***a*) when treated with sodium azide and acetic acid mixture.

The diazide (**2***a*), when treated with aqueous sodium azide in acetic acid at (100 °C), gives mainly **5***a* and some **6***a*. Similarly the oxadiazine (**4***a*) gives mainly **5***a* and a little **6***a*.

The only difference between the monoazide and the diazide is their behavior on pyrolysis. The monoazide gives the oxadiazine (**4***a*) whereas the diazide gives 5-phenyltetrazole (**6***a*).

A mixture of hydrazoic acid and 4-isopropylidene-2-phenyl-5(4)-oxazolone (**1***a*) in benzene solution at room temperature precipitated the diazide (**2***a*) after one week, and the solution proved to contain 5-phenyltetrazole (**6***a*). When (**4***a*) is refluxed with glacial acetic acid the oxazolone (**1***a*) is formed.

Similarly, when 2-*p*-chlorophenyl-4-isopropylidene-5(4)-oxazolone (**1***b*) and 2-anisyl-4-isopropylidene-5(4)-oxazolone (**1***c*) were treated with sodium azide and acetic acid and were allowed to stand for a long time, a mixture of *N*-isobutyroyl-*p*-chlorobenzamide (**5***b*) and 5-*p*-chlorophenyltetrazole (**6***b*); *N*-isobutyroylanisamide (**5***c*) and 5-anisyltetrazole (**6***c*), respectively were obtained together. 4-Cyclohexylidene-2-phenyl-5(4)-oxazolone (**1***d*) behaves similarly (see Scheme 1).

2-Aryl-4-fluorenylidene (**7***a* and *b*) failed to react with hydrazoic acid. This may be attributed to their insolubility in the reaction medium.

Can. J. Chem. Downloaded from www.nrcresearchpress.com by 210.87.254.5 on 09/05/12
For personal use only.

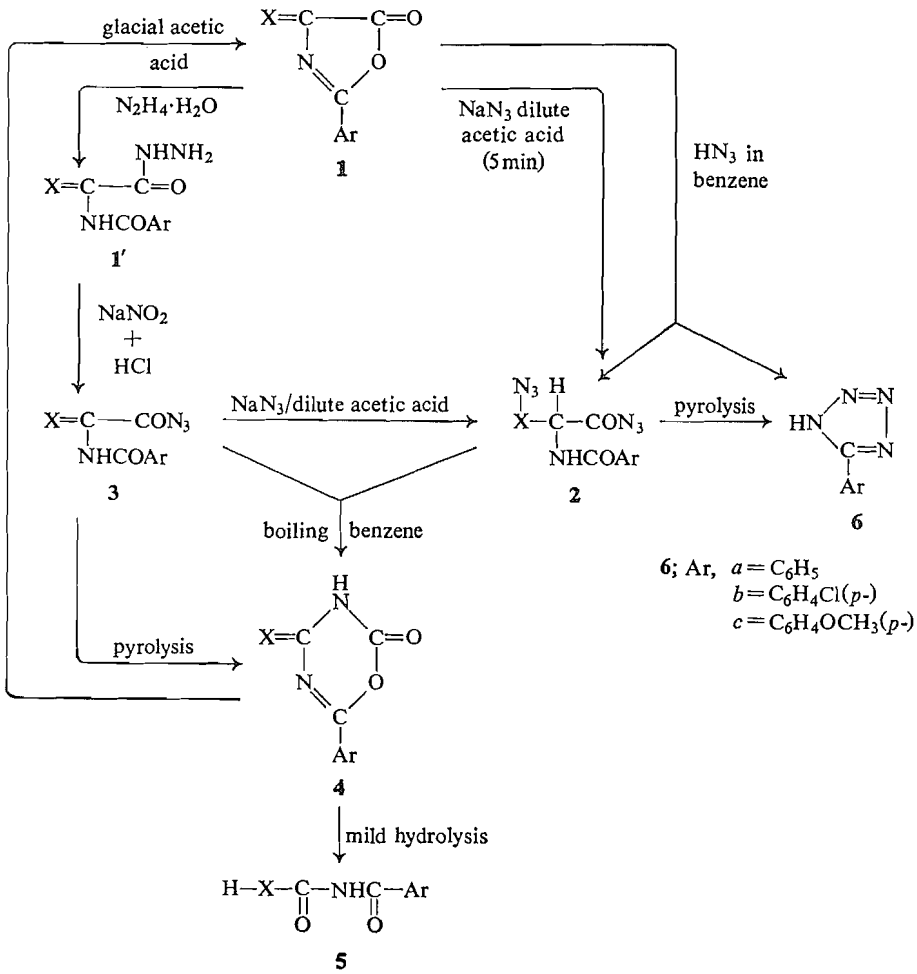

a, X = $\begin{matrix} CH_3 \\ CH_3 \end{matrix}$C, Ar = C_6H_5; b, X = $\begin{matrix} H_3C \\ H_3C \end{matrix}$C, Ar = $C_6H_4Cl(p\text{-})$;

c, X = $\begin{matrix} H_3C \\ H_3C \end{matrix}$C, Ar = $C_6H_4OCH_3(p\text{-})$; d, X = HC, Ar = C_6H_5

SCHEME 1

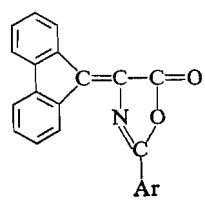

7a; Ar = C_6H_5
b; Ar = $C_6H_4OCH_3(p\text{-})$

2-Aryl-4-arylidene-5(4)-oxazolones (**8***a–d*), when treated with sodium azide in acetic acid or hydrazoic acid in benzene, gave only the corresponding tetrazolyl acrylic acid derivatives (**9**).

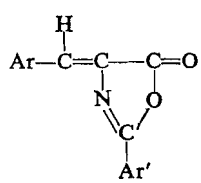

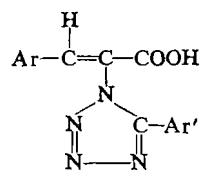

8 **9**

a; Ar = $C_6H_4Cl(p\text{-})$; Ar′, $C_6H_4OCH_3(p\text{-})$
b; Ar = $C_6H_4OCH_3(p\text{-})$; Ar′, C_6H_5
c; Ar = $CH_2O_2C_6H_3$—; Ar′, C_6H_5
d; Ar = $C_6H_5 \cdot CH{=}CH$—; Ar′, C_6H_5

Can. J. Chem. Downloaded from www.nrcresearchpress.com by 210.87.254.5 on 09/05/12
For personal use only.

We have prepared the corresponding hydrazides (**10**) from which the corresponding azides (**11**) were obtained by treatment with sodium nitrite and hydrochloric acid. These azides do not react with sodium azide and acetic acid mixture and no diazide could be isolated. When these azides (**11**) are heated in benzene, oxadiazines of type **12** are obtained.

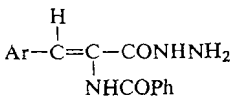

10

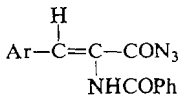

11

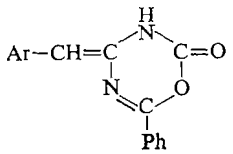

12

a; Ar = $C_6H_4OCH_3(p\text{-})$,
b; Ar = $CH_2O_2C_6H_3$,
c; Ar = $C_6H_5CH{=}CH{-}$

It may be noted that, in contrast to acrylates, cinnamic acid and cinnamate do not react with hydrazoic acid (3). It is also known that oxadiazines give by alkaline hydrolysis the corresponding phenylacetic acid (5).

From our investigation it is clear that 4-arylidene oxazolones differ from the 4-alkylidene derivatives towards hydrazoic acid. However, Deorha and Gupta (6) reportedly obtained from sodium azide – acetic acid mixture using 2-phenyl-4-(3′-methylbenzfurfurylidene)-5(4)-oxazolone (**13**), the corresponding azide which they failed to identify. They heated these products and obtained the corresponding oxadiazine (**21**).

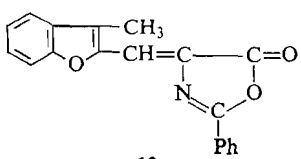

13

In contrary, it was found in the present investigation that 4-furfurylidene-2-phenyl-5(4)-oxazolone and 2-phenyl-4-(3′-methylbenzfurfurylidene)-5(4)-oxazolone (**13**) gave, with sodium azide – acetic acid mixture, only the tetrazolyl acids (**14**) and (**15**), regardless of whether the reaction was carried out in the cold for a prolonged time (**6**), or as described here.

The analytical data of these compounds do not assist in distinguishing between the tetrazolyl acid and the azide structure; however, the region of the νN_3 in the infrared (i.r.) spectra of these compounds is devoid of any absorption. This excludes the azide structure for these compounds.

The tetrazolyl acid structure of **14** and **15** is further confirmed by the ultraviolet (u.v.) spectra which shows for **14** λ_{max} 235 mμ; ε_{max} 11 760, λ_{max} 229 mμ; ε_{max} 16 120 and for **15** λ_{max} 237 mμ; ε_{max} 17 280, λ_{max} 237 mμ; ε_{max} 37 800. Similar absorption was recorded in our previous work (1).

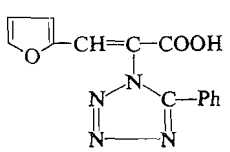

14

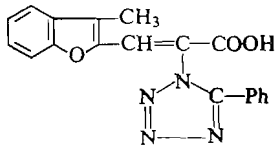

15

The corresponding hydrazides (**16** and **17**) and azides (**18** and **19**) were prepared, which, by heating gave the corresponding oxadiazine (**20** and **21**). These oxadiazines do not show νNH.

It seems that the reaction of alkylidene oxazolones with hydrazoic acid or sodium azide – acetic acid mixture starts by 1,4-addition of hydrazoic acid to the α,β-unsaturated system.

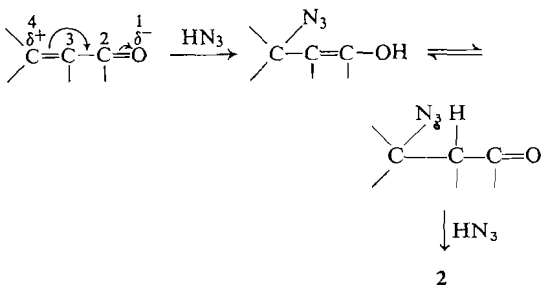

2

For arylidene oxazolones, the fractional positive charge on C-4 is dissipated on the aromatic ring.

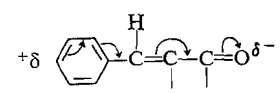

This may be the reason for the fact that alkylidene oxazolones behave differently from arylidene oxazolones towards hydrazoic acid.

The u.v. spectra of 4-alkylidene hippuric hydrazides show one band (225–258 mμ) depending upon the nature of the benzamido group;

Can. J. Chem. Downloaded from www.nrcresearchpress.com by 210.87.254.5 on 09/05/12
For personal use only.

TABLE I

Alkylidene and arylidene hippuric hydrazides

Compound	Yield* %	Melting point °C	Formula	C% Calculated	C% Found	H% Calculated	H% Found	N% Calculated	N% Found	Ultraviolet λ_{max} mμ	Ultraviolet ε_{max}	Infrared νNH cm^{-1}	Infrared νC=O cm^{-1}
1′*a*(2)										225–235	23664		
1′*b*	68	163	$C_{12}H_{14}N_3O_2Cl$	53.83	54.11	5.23	5.01	15.70	15.24	237.5	22344	3250	1640
1′*c*	67	162	$C_{13}H_{17}N_3O_3$	59.30	59.20	6.51	5.98	15.96	15.63	254–258	21868	3200	1625
1′*d*	79	174–176	$C_{15}H_{19}N_3O_2$	65.91	65.02	7.01	7.33	15.37	14.56	227.5	14508	3300	1650
10*a*	71	174	$C_{17}H_{17}N_3O_3$	65.58	65.09	5.50	5.69	13.50	12.60	226.5, 302.5	23690, 27600	3250	1640
10*b*	77	166–170	$C_{17}H_{15}N_3O_4$	62.71	62.54	4.65	5.01	12.92	11.30	227–237, 320	13386, 10476	3300	1640
10*c*	80	170–172	$C_{18}H_{17}N_3O_2$	70.34	69.47	5.58	6.02	13.67	13.15	228–234; 320–335	24640, 26880	3300	1670
16	61	171–172	$C_{14}H_{13}N_3O_3$	61.98	62.89	4.83	4.88	15.49	14.71	230, 310	17920, 29680	3300	1650
17(12)										223; 330–338	22320, 33480	3300	1670

*The time of reaction was in all cases 1 h.

TABLE II

Alkylidene and arylidene oxadiazine

Compound	Reaction time*	Yield %	Melting point (°C)	Formula	C% Calculated	C% Found	H% Calculated	H% Found	N% Calculated	N% Found	Ultraviolet λ_{max} mμ	Ultraviolet ε_{max}	Infrared† νNH	Infrared† νC=O δ-lactone (14)
4*a*(13)‡											237	17762	3325	1750
4*b*	15 min	55	165	$C_{12}H_{11}N_2O_2Cl$	57.48	57.08	4.43	4.03	11.17	10.04	237	15368	3225	1775
4*c*‡	15 min	66	180	$C_{13}H_{14}N_2O_3$	63.40	63.17	5.73	6.05	11.38	11.64	256	18816	3300	1750
4*d*‡	15 min	55	162–164	$C_{15}H_{16}N_2O_2$	70.29	70.69	6.29	6.66	10.93	10.63	223–230	16400	3300	1750
12*a*	30 min	54	171	$C_{17}H_{14}N_2O_3$	69.37	65.15	4.80	5.67	9.52	8.72	224–230, 276–286, 289	31600, 25520 2640	3300	1760
12*b*	1 h	64	over 360	$C_{17}H_{12}N_2O_4$	66.23	66.06	3.92	4.62	9.09	8.68	227.5, 268, 274–282	13440, 11760 12432	3300	1750
12*c*	1 h	65	235–237	$C_{18}H_{14}N_2O_2$	74.47	75.02	4.86	5.14	9.65	9.26	227.5, 284–298	19760, 18620	3325	1760
20	30 min	66	165–166	$C_{14}H_{10}N_2O_3$	66.13	66.86	3.96	4.46	11.02	10.86	239.5, 278	15960, 21000	—	1800
21(12)											224–231, 317.5	13200, 18040	—	1790

*The reported time and yields are for the experiments using the corresponding monoazide.
†In cm^{-1}.
‡Using the corresponding diazide (2*a*, *c*, and *d*) the corresponding oxadiazine (4*a*, *c*, and *d*) was obtained after 1 h in the yields 39, 38, and 25% respectively.

Can. J. Chem. Downloaded from www.nrcresearchpress.com by 210.87.254.5 on 09/05/12
For personal use only.

TABLE III

Alkylidene and arylidene hippuric monoazides

Compound	Yield* %	Melting point °C	Formula	2N available		Ultraviolet		Infrared		
				Calculated	Found	λ_{max} mμ	ε_{max}	νNH cm^{-1}	νN_3 cm^{-1}	νC═O cm^{-1}
3*a*(2)						236, 243, 297, 310	19440, 19880, 23976, 24300	3125	2125	1675, 1625
3*b*	48	86–87 (decomp.)	$C_{12}H_{14}N_4O_2Cl$	10.05	9.86	225, 236, 242, 248, 302.5, 310	11524, 13400, 16080, 16616, 23852, 24254	3250	2125	1690, 1630
3*c*	47	84–85 (decomp.)	$C_{13}H_{14}N_4O_3$	10.21	9.99	256, 320	28880, 29260	3300	2125	1690, 1630
3*d*	48	72 (decomp.)	$C_{15}H_{16}N_4O_2$	9.86	9.82	226, 241, 296, 310	12480, 11440, 3120, 2600	3300	2125	1690, 1650
11*a*	62	107–110 (decomp.)	$C_{17}H_{14}N_4O_3$	8.69	8.65	226–232, 246, 260, 300–310, 384 393, 397	13080, 13360, 12426, 13516, 19184, 17876, 17440	3450	2150	1650
11*b*	67	74 (decomp.)	$C_{17}H_{12}N_4O_4$	8.28	8.37	264, 392	12792, 20336	3250	2150	1680, 1650
11*c*	57	116–117 (decomp.)	$C_{18}H_{14}N_4O_2$	8.80	8.76	240.5, 274, 383	5400, 5130, 15930	3300	2150	1700, 1650
18	62	110 (decomp.)	$C_{14}H_{10}N_4O_3$	9.92	9.80	262, 385, 399	9996, 18156, 16932	3250	2150	1700 1650
19	57	94 (decomp.)	$C_{19}H_{14}N_4O_3$	8.20	7.90	355, 405, 425	20680, 23760, 24200	3325	2175	1700, 1640

*The time of reaction in all cases was 30 min.

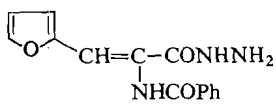

16

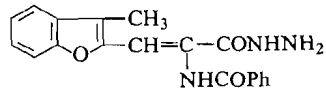

17

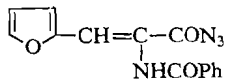

18

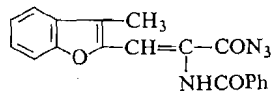

19

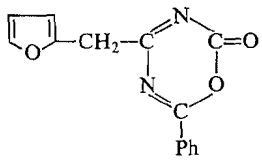

20

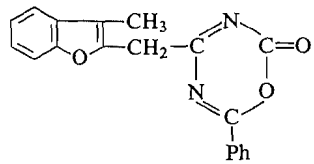

21

however, the 4-arylidene analogues show two bands at (225–258 mμ) and (300–335 mμ) (see Table I). The oxadiazines behave similarly (see Table II). The known value of the azido (7) (285 mμ) is shifted to longer wavelength in the case of compounds under investigation (see Table III). Similar observations have been reported (7).

The electronic spectra of the alkylidene azides are similar with the expected bathochromic shift according to the substituent. The diazides show identical spectra.

All the azides and diazides show in the i.r. spectra the characteristic stretching frequency of the azido group (8) (see Table III).

Addendum

The azides and diazides are difficult to analyze by the normal procedure since they are easily decomposed. We have devised a micro method by which they can be analyzed by heating in dilute acetic acid and collecting the nitrogen evolved on a micro scale. For monoazides, N_2/mole is obtained while for diazides, in addition to the evolved nitrogen, hydrazoic acid was obtained. This required us to use a potassium permanganate or ceric sulfate trap to oxidize the liberated hydrazoic acid and 5N/mole were obtained, in this case. This work has been published elsewhere (9).

Experimental

Melting points are not corrected. Analyses were carried out by National Research Center, Microanalytical Unit, Doki, Cairo and by Alfred Bernhard, Max Planck Institute, Mulheim, Germany. Infrared spectra were measured on a Perkin–Elmer Infracord model 137 spectrophotometer using KBr wafer technique. Ultraviolet spectra were measured on a Perkin–Elmer Spectracord model 4000A spectrophotometer using ethyl alcohol solutions.

Preparation of Some New 5(4)-Oxazolones

2-Anisyl-4-fluorenylidene-5(4)-oxazolone (7b)

A mixture (10 g) anisuric acid, fluorenone (9 g), fused sodium acetate (8 g), and acetic anhydride (30 ml) was heated on a hot plate until all the solid liquefied, then heating was continued on a boiling water-bath for 1 h after which the mixture was cooled and filtered. The yellow crystalline precipitate (yield 47%) was crystallized from glacial acetic acid, m.p. 226–227 °C.

Anal. Calcd. for $C_{23}H_{15}NO_3$: C, 78.18; H, 4.25; N, 3.97. Found: C, 77.60; H, 4.44; N, 4.01.

2-Anisyl-4-(p-chlorobenzylidene)-5(4)-oxazolone (8a)

A mixture of anisuric acid (10 g), *p*-chlorobenzaldehyde (7.3 g), sodium acetate (8 g), and acetic anhydride (30 ml) was heated on a hot plate until all the solid liquefied, then heating was continued on a boiling water-bath for 1 h after which the mixture was cooled and filtered. The yellow crystalline precipitate (yield 53%) was crystallized from ethyl acetate, m.p. 211 °C.

Anal. Calcd. for $C_{17}H_{12}NO_3Cl$: C, 64.96; H, 3.82; N, 4.45. Found: C, 64.85; H, 3.87; N, 4.76.

2-Anisyl-4-isopropylidene-5(4)-oxazolone (1c)

A mixture of anisuric acid (10 g), acetone (170 ml), acetic anhydride (16 ml), and sodium bicarbonate (4.6 g) was refluxed for 6 h after which the mixture was allowed

Can. J. Chem. Downloaded from www.nrcresearchpress.com by 210.87.254.5 on 09/05/12
For personal use only.

Can. J. Chem. Downloaded from www.nrcresearchpress.com by 210.87.254.5 on 09/05/12
For personal use only.

to cool. The mixture was filtered and poured on crushed ice (500 g) and diluted with ice-cold water to 1.5 l. The precipitated solid (yield, 54%) was removed by filtration and recrystallized from light petroleum ether, m.p. 108 °C.

Anal. Calcd. for $C_{13}H_{13}NO_3$: C, 67.52; H, 5.67; N, 6.06. Found: C, 67.33; H, 5.56; N, 5.45.

Action of Aqueous Sodium Azide Solution and Acetic Acid on

*(a) 4-Isopropylidene-2-phenyl-5(4)-oxazolone (**1a**)*

A mixture of sodium azide (1 g in the least amount of water) and **1***a* (1 g in the least amount of glacial acetic acid) was heated on a water-bath for 5 min. The mixture was then poured on crushed ice, to give **2***a*, m.p. 145–146 °C (decomp.); (yield, 69%). It decomposed upon crystallization from most common solvents (e.g. ethyl acetate, alcohol, benzene).

Anal. Calcd. for $C_{12}H_{13}N_7O_2$(5N): N, 24.46. Found: N, 24.70.

When this reaction was carried out for 3 h and the reaction mixture poured on crushed ice, the product was removed by filtration digested in sodium bicarbonate solution, and again removed by filtration. The insoluble part proved to be **5***a* (yield 83%) (1), m.p. 154 °C. The above filtrates were mixed together and concentrated to a small volume (~2 ml), acidified with HCl, filtered while hot, and allowed to cool. After scratching, the crystalline product was removed by filtration and proved to be **6***a* by melting point and mixture melting point (10), yield 5%.

*(b) 2-p-Chlorophenyl-4-isopropylidene-5(4)-oxazolone (**1b**)*

The reaction was carried out as above and after 15 min the starting material was recovered unchanged (m.p. and mixture m.p.). When the reaction was carried out for 3 h and the reaction mixture poured on crushed ice, the product was removed by filtration, digested in sodium bicarbonate solution, and again removed by filtration. The insoluble part proved to be **5***b* (1), m.p. 134 °C, yield 83%. The filtrate was acidified with cold dilute HCl and the precipitated product was removed by filtration and recrystallized from light petroleum (b.p. 100–120 °C) as colorless needles, m.p. 253 °C, yield 16%. The latter proved to be 5-*p*-chlorophenyltetrazole (**6***b*) identified by melting point and mixture melting point experiment with an authentic sample (10).

*(c) 2-Anisyl-4-isopropylidene-5(4)-oxazolone (**1c**)*

The reaction was carried out as in (*a*). After 10 min **2***c* was obtained and removed by filtration, m.p. 134 °C (decomp.); yield 58%. It decomposes upon crystallization from most common solvents (e.g. ethyl acetate, alcohol).

Anal. Calcd. for $C_{13}H_{15}N_7O_3$(5N): N, 22.09. Found: N, 22.00.

When the reaction was carried out for 1 h and the reaction mixture poured on crushed ice, the product was removed by filtration, digested in sodium bicarbonate solution, and again removed by filtration. The insoluble part (**5***c*) was crystallized from light petroleum (b.p. 60–80 °C) as colorless needles, m.p. 121 °C, yield 31%.

Anal. Calcd. for $C_{12}H_{15}NO_3$: C, 65.15; H, 7.78; N, 6.33. Found: C, 65.79; H, 7.35; N, 6.51.

The filtrate was acidified with cold dilute HCl and the precipitated product (**6***c*) was removed by filtration and recrystallized from ethyl acetate as colorless needles, m.p. 233 °C, yield 52%.

Anal. Calcd. for $C_8H_8N_4O$: C, 54.54; H, 4.54; N, 31.75. Found: C, 54.71; H, 4.87; N, 31.75.

*(d) 4-Cyclohexylidene-2-phenyl-5(4)-oxazolone (**1d**)*

The reaction was carried out as in (*a*). After 10 min (**2***d*) yield, 73% was obtained, m.p. 126–127 °C (decomp.). It decomposes upon crystallization from most common solvents.

Anal. Calcd. for $C_{15}H_{17}N_7O_2$(5N): N, 21.43. Found: N, 21.25.

The reaction was carried out for 1 h and the reaction mixture poured on crushed ice. The product was removed by filtration, digested in sodium bicarbonate solution, and again removed by filtration. The insoluble part, yield, 73% m.p. 157 °C, was previously identified as (**5***d*) (1). The filtrate was acidified with cold dilute HCl and the precipitated product was removed by filtration and recrystallized from ethyl acetate as colorless needles, m.p. 212–213 °C, yield, 24%. The latter proved to be 5-phenyltetrazole (**6***a*) identified by melting point and mixture melting point experiment with authentic sample (10).

Anal. Calcd. for $C_7H_6N_4$: C, 57.60; H, 4.11; N, 37.75. Found: C, 58.1; H, 4.64; N, 37.32.

*(e) 4-Fluorenylidene-2-phenyl-5(4)-oxazolone (**7a**)*

The reaction was carried out as in (*a*). After 15 min or 3 h the starting material was recovered unchanged (m.p. and mixture m.p.). Similarly 2-anisyl-4-fluorenylidene-5(4)-oxazolone (**7***b*) was recovered unchanged.

*(f) 2-Anisyl-4(p-chlorobenzylidene)-5(4)-oxazolone (**8a**)*

The reaction was carried out as in (*a*). After 15 min the starting material was recovered unchanged (m.p. and mixture m.p.). The reaction was carried out for 1 h and the reaction mixture poured on crushed ice. The product was removed by filtration and digested in sodium bicarbonate. The unchanged oxazolone was extracted with ether and aqueous layer was acidified with cold dilute HCl. The precipitated product (**9***a*) was removed by filtration and recrystallized from ethyl acetate as colorless crystals, m.p. 185 °C, yield 90%.

Anal. Calcd. for $C_{17}H_{13}N_4O_3Cl$: C, 57.17; H, 3.64; N, 15.86. Found: C, 57.08; H, 3.89; N, 15.91.

Similarly 4-anisylidene-2-phenyl-5(4)-oxazolone (**8***b*), 2-phenyl-4-piperonylidene-5(4)-oxazolone (**8***c*), and 4-cinnamylidene-2-phenyl-5(4)-oxazolone (**8***d*) were recovered unchanged, after 15 min.

(g) 4-Furfurylidene-2-phenyl-5(4)-oxazolone

The reaction was carried out as in (*a*). After 15 min the starting material was recovered unchanged (as shown by m.p. and mixture m.p.). When the reaction was carried out as in (*a*) for 1 h, the precipitated product (**14**) was removed by filtration and recrystallized from ethyl acetate as greenish-yellow crystals, m.p. 184–185 °C (decomp.), yield 85%.

Anal. Calcd. for $C_{14}H_{10}N_4O_3$: C, 59.57; H, 3.57; N, 19.85. Found: C, 59.64; H, 3.64; N, 19.74.

*(h) 2-Phenyl-4-(3'-methylbenzfurfurylidene)-5(4)-oxazolone (**13**)*

The reaction was carried out as in (*a*), after 15 min the starting material was recovered unchanged (as shown by

TABLE IV

Action of hydrazoic acid solution in benzene on 4-alkylidene and arylidene oxazolones

Oxazolone	Product	Reaction time	Solvent of crystallization	Melting point °C	Yield %	Reference
1*a*	Isopropylidene hippuric diazide (**2***a*)	1 week	—	145–147	34	—
	5-Phenyltetrazol* (**6***a*)	3 weeks	—†	212–213	26	10
1*b*	5-*p*-Chlorophenyltetrazol (**6***b*)	3 weeks	—†	253	78	10
1*c*	Isopropylidene anisuric diazide (**2***c*)	1 week	—	134	37	—
	5-Anisyltetrazol* (**6***c*)	3 weeks	—‡	233	39	10
1*d*	Cyclohexylidene hippuric diazide (**2***d*)	1 week	—	127–128	29	—
	5-Phenyltetrazol* (**6***a*)	3 weeks	—†	212–213	48	10
8*a*	α-[Tetrazolyl(1)]-5-anisyl-*p*-chlorocinnamic acid (**9***a*)	3 days	—‡	185	90	—
8*b*	α-[Tetrazolyl(1)]-5-phenyl-*p*-methoxycinnamic acid (**9***b*)	3 days	—§	185	69	1
8*c*	α-[Tetrazolyl(1)]-5-phenyl-3,4-methylenedioxycinnamic acid (**9***c*)	3 days	—§	183	70	1
8*d*	α-[Tetrazolyl(1)]-5-phenylbenzylidenecrotonic acid (**9***d*)	3 days	—‡	225	65	1
4-Furfurylidene-5-phenyl-5(4)-oxazolone	α-[Tetrazolyl(1)]-5-phenylfurfurylacrylic acid (**14**)	3 days	—‡	184–185	93	—

*The reaction was completed using the mother liquors.
†Light petroleum ether (b.p. 100–120 °C).
‡Ethyl acetate.
§Ethyl acetate – light petroleum ether (b.p. 40–60 °C).

m.p. and mixture m.p.). When the reaction was carried out as in (*g*) for 1 h, the precipitated product was removed by filtration and recrystallized from ethyl acetate – light petroleum (b.p. 40–60 °C) as colorless crystals of **15**, m.p. 194 °C (decomp.), yield 71%.

Anal. Calcd. for $C_{19}H_{14}N_4O_3$: C, 65.89; H, 4.07; N, 16.10. Found: C, 65.14; H, 4.34; N, 15.27.

Action of Aqueous Sodium Azide Solution and Acetic Acid on

(a) 4-Furfurylidene-2-phenyl-5(4)-oxazolone

To a suspension of 4-furfurylidene-2-phenyl-5(4)-oxazolone (0.15 mole) in distilled acetic acid (75 ml) was added sodium azide (0.15 mole in least amount of water). The mixture was vigorously stirred at room temperature till the color of the oxazolone became very faint. The solid product was removed by filtration, digested in sodium bicarbonate solution, and removed by filtration. The insoluble part proved to be unchanged (as shown by m.p. and mixture m.p.). The filtrate was acidified with cold dilute HCl and the precipitated product was removed by filtration and recrystallized from ethyl acetate to give greenish-yellow crystals, m.p. 184–185 °C (decomp.), yield 50%.

It proved to be identical (as shown by m.p. and mixture m.p.). with **14** obtained via action of sodium azide and acetic acid for 1 h on the title compound.

*(b) 2-Phenyl-4(3'-methylbenzfurfurylidene)-5(4)-oxazolone **13***

The reaction was carried out as above, the precipitated product (**15**) was crystallized from ethyl acetate – light petroleum (b.p. 40–60 °C), m.p. 194 °C (decomp.), yield 40%. It was identical with the product obtained by heating a mixture of an aqueous sodium azide, acetic acid, and **13** for 1 h (m.p. and mixture m.p.).

Action of Hydrazoic Acid Solution (11) in Benzene on 4-Alkylidene and 4-Arylidene Oxazolones: General Procedure

A mixture of hydrazoic acid solution in benzene (20 ml) and oxazolone (1 g in 20 ml dry benzene) was left at room temperature for the times specified in Table 1 and the resulting products were crystallized from suitable solvents (see Table IV).

Action of Hydrazine Hydrate on Oxazolones: General Procedure

Hydrazine hydrate (100%) (4 ml) was added dropwise with occasional shaking to a suspension of the oxazolone (3 g) in methanol. After the addition had been completed, the reaction mixture was left for 1 h, whereby a crystalline precipitate was formed. It was removed by filtration and crystallized from a suitable solvent (see Table I).

Action of Aqueous Sodium Nitrite and Hydrochloric Acid on Alkylidene and Arylidene Hippuric Hydrazides: General Procedure

A solution of sodium nitrite (1 g in least amount of ice-cold water) was added dropwise with shaking to an ice-cold solution or the hydrazide (2 g in least amount *N*-hydrochloric acid) so that the temperature did not rise above 5 °C. After the addition was completed, the reaction mixture was left at room temperature for 30 min, the product was then removed by filtration, dried, and its

Can. J. Chem. Downloaded from www.nrcresearchpress.com by 210.87.254.5 on 09/05/12
For personal use only.

TABLE V

Action of glacial acetic acid on 1,3,5-oxadiazines

Oxadiazine	Oxazolone	Solvent of crystallization	Melting point °C	Yield %	Reference
4*a*	4-Isopropylidene-2-phenyl (**1***a*)	—*	96	43	13
4*b*	2-*p*-Chlorophenyl-4-isopropylidene (**1***b*)	—†	170–172	53	1
4*c*	2-Anisyl-4-iso-propylidene (**1***c*)	—†	108	71	Inter alia
4*d*	4-Cyclohexylidene-2-phenyl (**1***d*)	—‡	136	31	15
12*a*	4-Anisylidene-2-phenyl (**8***b*)	—§	160	42	16
12*b*	2-Phenyl-4-piperonylidene (**8***c*)	—§	197	39	17
12*c*	4-Cinnamylidene-2-phenyl (**8***d*)	—§	150	42	18
20	4-Furfurylidene-2-phenyl	—‡	179	31	19
21	2-Phenyl-4(3′-methylbenzfurfurylidene (**13**))	—‖	159–161	52	12

*Ethyl alcohol – water.
†Light petroleum ether (100–120 °C).
‡Ethyl acetate.
§Ethyl acetate – light petroleum ether (100–120 °C).
‖Glacial acetic acid.

m.p. was recorded. It decomposed upon crystallization from most common solvents (e.g. ethyl alcohol, ethyl acetate, benzene). (See Table III.)

Thermolysis of Alkylidene and Arylidene Hippuric Azides in Benzene: General Procedure

A suspension of the azide (mono- or diazides) in dry benzene (25 ml) was refluxed for 15 min on a boiling water-bath and cooled. The oxadiazine was removed by filtration and recrystallized from benzene (see Table II).

Action of Boiling Water on

(a) 4-Isopropylidene-6-phenyl-2-oxo-1,3,5-oxadiazine (4a)

A suspension of **4***a* (1 g in 25 ml water) was refluxed for 2 h and was cooled and filtered; **5***a* was obtained in colorless needles (yield, 34%) from absolute ethanol, m.p. 154 °C, undepressed on admixture with an authentic sample (1).

(b) 6-p-Chlorophenyl-4-isopropylidene-2-oxo-1,3,5-oxadiazine (4b)

The reaction was carried out as above, **5***b* was obtained (yield, 55%), m.p. 132–134 °C, undepressed on admixture with an authentic sample (1).

(c) 6-Anisyl-4-isopropylidene-2-oxo-1,3,5-oxadiazine (4c)

The reaction was carried out as in (*a*). *N*-Isobutyroylanisamide was obtained, m.p. 121 °C, yield 66%. It proved to be identical with the product obtained by the action of sodium azide and acetic acid for 1 h on 2-anisyl-4-isopropylidene-5(4)-oxazolone.

(d) 4-Cyclohexylidene-6-phenyl-2-oxo-1,3,5-oxadiazine (4d)

The reaction was carried out as in (*a*). *N*-Hexahydrobenzoylbenzamide was obtained, m.p. 157 °C, yield 44%. It proved to be identical with the product obtained by the action of sodium azide and acetic acid for 1 h on 4-cyclohexylidene-2-phenyl-5(4)-oxazolone (1).

Action of Glacial Acetic Acid on 1,3,5-Oxadiazines

When a solution of the oxadiazine (1 g) in glacial acetic acid (25 ml) was refluxed for 30 min and the mixture cooled; the corresponding oxazolone was obtained and was identified by m.p. and mixture m.p. (see Table V).

Action of Aqueous Sodium Azide and Acetic Acid on

(a) Isopropylidene Hippuric Azide (3a)

A mixture of sodium azide (1 g in least amount of water) and **3***a* (1 g in 14 ml dilute acetic acid) was left at room temperature for 4 h. The precipitated product (**2***a*) was removed by filtration and dried, m.p. 145–146 °C (decomp.), yield 85%. It proved to be identical with the product obtained by the action of hydrazoic acid in benzene on **1***a*. Comparison was made by m.p., mixture m.p., and infrared spectrum.

(b) Isopropylidene Anisuric Azide (3c)

The reaction was carried out as in (*a*), **2***c* was obtained, m.p. 134° C (decomp.), yield 60%. It proved to be identical with the product obtained by action of hydrazoic acid in benzene on **1***c*. Comparison was made by melting point, mixture melting point, and infrared spectrum.

(c) Cyclohexylidene Hippuric Azide (3d)

The reaction was carried out as in (*a*), **2***d* was obtained (yield 69%), m.p. 126–127 °C (decomp.). It proved to be identical (by melting point and mixture melting point) with the product obtained by action of hydrazoic acid in benzene on 4-cyclohexylidene-2-phenyl-5(4)-oxazolone (**1***d*). Similarly the reaction was carried out on **11***a* and 3-methylbenzfurfurylidene azide **19** and the reactants were recovered (identification was made by m.p. and mixture m.p.).

Action of Aqueous Sodium Azide and Acetic Acid on

(a) Isopropylidene Hippuric Diazide (2a) or 3,4-Dihydro-6-phenyl-4-isopropylidene-2-oxo-1,3,5-oxadiazine (4a)

A mixture of sodium azide (1 g in least amount of water) and **2***a* or **4***a* (1 g in 20 ml dilute acetic acid) was heated on a boiling water bath for 1 h. The reaction mixture was cooled and the product was removed by filtration. It was recrystallized from absolute ethanol as colorless needles, m.p. 154 °C (1); yield 90% in the case of **2***a* and 75% in the case of **4***a*. The product proved to be *N*-iso-butyroylbenzamide (**5***a*). Identification was made by m.p. and mixture m.p. The filtrate was concentrated to a

Can. J. Chem. Downloaded from www.nrcresearchpress.com by 210.87.254.5 on 09/05/12
For personal use only.

small volume (~2 ml), acidified with HCl, filtered while hot, and allowed to cool. The crystalline product was removed by filtration, m.p. 213 °C; yields, 5% in the case of **2***a* and 10% in the case of **4***a*. It proved to be 5-phenyltetrazole (**6***a*). Identification was made by m.p. and mixture m.p.

(b) Isopropylidene Anisuric Diazide (2c) or 3,4-Dihydro-6-anisyl-4-isopropylidene-2-oxo-1,3,5-oxadiazine (4c)

The reaction was carried out as in (*a*), the insoluble part, m.p. 121 °C, yields 57% in the case of **2***c* and 70% in the case of **4***c*. It proved to be *N*-isobutyroylanisamide (**5***c*). Identification was made by m.p. and mixture m.p.

The filtrate was concentrated, was cooled, and the precipitate was removed by filtration. It was crystallized from ethylacetate as colorless needles; m.p., 233 °C (decomp.) (10); yields, 41% in the case of **2***c* and 20% in the case of **4***c*. It proved to be 5-anisyltetrazole (**6***c*). Identification was made by m.p. and mixture m.p.

(c) Cyclohexylidene Hippuric Diazide (2d) or 3,4-Dihydro-6-phenyl-4-cyclohexylidene-2-oxo-1,3,5-oxadiazine

The reaction was carried out as in (*a*), the insoluble part, m.p. 157 °C, yields 42% in the case of **2***d* and 70% in the case of **4***d*. It proved to be *N*-hexahydrobenzoylbenzamide (**5***d*). Identification was made by m.p. and mixture m.p.

The filtrate gave **6***a*; m.p., 212–213 °C (decomp.) (10); yields, 66% in the case of **2***d* and 20% in the case of **4***d*. It was identified as 5-phenyltetrazole by m.p. and mixture m.p.

Pyrolysis of Monoazides and Diazides

(a) Alkylidene and Arylidene Hippuric Azide

Isopropylidene hippuric azide **3***a* (1 g) was heated at its melting point under vacuum (10 mm) for a few minutes till it solidified, **4***a* was obtained, m.p. 174 °C (decomp.), yield 50%. It proved to be identical with 4-isopropylidene-6-phenyl-2-oxo-1,3,5-oxadiazine (**4***a*) obtained by thermolysis of **3***a* (13) (m.p. and mixture m.p.). Similarly isopropylidene-*p*-chlorohippuric azide (**3***b*) gave **4***b*, m.p. 165° (decomp.), yield 55% (decomposition time 30 min), isopropylidene anisuric azide (**3***c*) gave **4***c*, m.p. 180°, yield 55%, cyclohexylidene hippuric azide; (**3***d*) gave **4***d*, m.p. 162–164°, yield 55%, anisylidene hippuric azide **11***a* gave **12***a*, m.p. 171°, yield 43%, and furfurylidene hippuric azide (**18**) gave **20**, m.p. 166°, yield 44%.

(b) Alkylidene Hippuric Diazides

The reaction was carried out as above using **2***a* to give 6*a*, m.p. 211–213° (decomp.), yield 48%. The latter proved to be 5-phenyltetrazole by melting point and mixture melting point with an authentic specimen (10). Similarly isopropylidene anisuric diazide **2***c* gave 5-anisyltetrazole **6***c*, m.p. 233° (10), yield 54%, and cyclohexylidene hippuric diazide (**2***d*) gave 5-phenyltetrazole, m.p. 211–213 °C, yield 67%.

1. W. I. AWAD, A. F. M. FAHMY, and A. M. A. SAMOUR. J. Org. Chem. **30**, 2222 (1965).
2. H. T. CLARKE, J. R. JOHNSON, and R. ROBINSON. The chemistry of penicillin. Princeton University Press, Princeton, New Jersey. 1949. p. 780.
3. J. H. BOYER. J. Am. Chem. Soc. **73**, 5248 (1951).
4. H. T. CLARKE, J. R. JOHNSON, and R. ROBINSON. The chemistry of penicillin. Princeton University Press, Princeton, New Jersey. 1949. p. 737.
5. K. F. JENNINGS. J. Chem. Soc. 1512 (1957).
6. D. S. DEORHA and P. GUPTA. J. Indian Chem. Soc. **42**, (3), 199 (1965).
7. E. LIEBER, C. N. RAMACHANDRA RAO, T. S. CHAO, and W. H. WAHL. J. Sci. Ind. Res. India, **16B**, 95 (1957).
8. C. N. RAMACHANDRA RAO, T. S. CHAO, and C. W. W. HOFFMAN. Anal. Chem. **29**, 916 (1957).
9. W. I. AWAD, Y. A. GAWARGIOUS, and S. S. M. HASSAN. Talanta, **14**, 1441 (1967).
10. R. M. H. HERBST and K. R. WILSON. J. Org. Chem. **22**, 1142 (1957).
11. W. L. GARBRECHT and R. M. HERBST. J. Org. Chem. **18**, 1003 (1953).
12. D. S. DEORHA and P. GUPTA. Ber. **97**, (12), 3577 (1964).
13. H. T. CLARKE, J. R. JOHNSON, and R. ROBINSON. The chemistry of penicillin. Princeton University Press, Princeton, New Jersey. 1949. p. 788.
14. L. J. BELLAMY. The infrared spectra of complex molecules. Methuen and Co., Ltd., London. 1959. p. 179.
15. V. BACKELHEID and L. M. SCHRAMM. J. Org. Chem. **19**, 298 (1949).
16. H. D. DAKIN. J. Biol. Chem. **8**, 11 (1910).
17. J. B. NIEDERL and A. ZIERING. J. Am. Chem. Soc. **64**, 885 (1942).
18. E. ERLENMEYER and J. KUNLIN. Ber. **35**, 384 (1902).
19. E. ERLENMEYER and W. STADLIN. Ann. **337**, 283 (1904).

Can. J. Chem. Downloaded from www.nrcresearchpress.com by 210.87.254.5 on 09/05/12
For personal use only.

Can. J. Chem. Downloaded from www.nrcresearchpress.com by 210.87.254.40 on 09/05/12
For personal use only.

Thermal rearrangement of methyl *cis*-2-alkylcyclopropanecarboxylates[1]

DONALD E. MCGREER AND NORMAN W. K. CHIU
Department of Chemistry, University of British Columbia, Vancouver, British Columbia

Received January 17, 1968

Seven alkyl substituted methyl cyclopropanecarboxylates with an alkyl group *cis* to the ester group have been found to ring open to the isomeric γ,δ-unsaturated ester through a 1,5-hydrogen shift upon heating to 259.4 °C in a sealed tube. Methyl cyclopropanecarboxylates which do not have a *cis* 2-alkyl group are unaffected when heated for longer periods at this or higher temperatures and thus a simple method for determining geometrical isomers in this series is now available. The reactions are first-order, with $\Delta H\dagger$ between 25 and 38 kcal/mole and $\Delta S\dagger$ between −8 and −37 e.u. This and other information fully supports a cyclic hydrogen transfer mechanism.

Canadian Journal of Chemistry, 46, 2217 (1968)

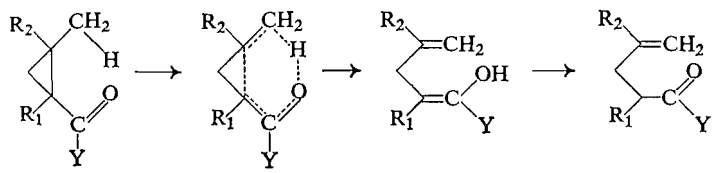

1 **2** **3** **4**

In an earlier communication (1) we described a thermal rearrangement of methyl *cis*-2-alkylcyclopropanecarboxylates[2] which did not take place for the isomeric *trans* esters. A number of other systems which are directly related to the ester rearrangement can be represented by the reaction **1** → **4**. Anhydrides (2), ketones (3–6), aldehydes (7), vinyl cyclopropanes (8), *N*-acylaziridines (9), and possibly phenylcyclopropanes (10) are known to react in this manner. The most extensive mechanistic study to date has been on a series of ketones (4) and from this work enolene intermediates (**3**) are strongly indicated. Kinetic studies on the vinylcyclopropanes (8) and ketones (4) show good first-order plots and suggest a highly organized intermediate (large negative entropy) compatible with the description shown in **2**. The fact that hydrogen migration occurs only when the carbonyl or vinyl group is *cis* to an alkyl group on the vicinal ring carbon has been noted in several studies (3–8).

In the present study we have determined the kinetics for the rearrangement of several alkyl substituted methyl cyclopropanecarboxylates. From the data presented we are able to standardize the conditions of the reaction so that *cis* and *trans* stereochemical evaluations can be made with only one isomer at hand and we have been able to verify the mechanism proposed earlier.

The compounds studied and the products isolated from the rearrangement are shown in Table I. Most of the starting materials were available from earlier work in this laboratory and the others were prepared by standard methods as described in the Experimental. The products were all isolated in a pure state by vapor-phase chromatography and identified as described in the Experimental. These reactions yielded γ,δ-unsaturated esters free of any by-products and as such are an excellent synthetic method. In the case where the alkyl group vicinal to the ester is an ethyl group two products were formed (*cis*- and *trans*- γ,δ-unsaturated esters) depending on which of the hydrogens migrates. These could be readily distinguished due to the fact that the *trans* isomer gave the characteristic infrared band at 970 cm^{-1} for the *trans vicinal* hydrogens on a carbon double bond.

[1]Taken in part from the Ph.D. Thesis of N. W. K. Chiu, September, 1967.

[2]Throughout this paper *cis* will refer to the structure having the alkyl group on C-2 *cis* to the carbomethoxy group.

Can. J. Chem. Downloaded from www.nrcresearchpress.com by 210.87.254.40 on 09/05/12
For personal use only.

TABLE I

Parameters for the thermal rearrangement of a number of methyl cyclopropanecarboxylates[a]

Methyl 1-cyclopropanecarboxylates		R^1	R^2	R^3	R^4	Methyl 4-pentenoate (**18**)	$t_{1/2}$[b] (259.4°) (h)	$\Delta H\dagger$ (kcal/mole)	$\Delta S\dagger$ (e.u.)
1,2,2-Trimethyl (**5**)		CH_3	H	CH_3	H	2,4-Dimethyl (**12**)	2.26	37.5	−8
1-Methyl-2-ethyl (**6**)	(11)	CH_3	H	H	CH_3	Methyl *cis*- and *trans*-2-methyl-4-hexenoate (**13** and **14**)	12.62	33.9	−18
2,2-Dimethyl (**7**)		H	H	CH_3	H	4-Methyl (**15**)	15.16	36.1	−14
1,2-Dimethyl (**8**)	(12)	CH_3	H	H	H	2-Methyl (**16**)	16.30	30.2	−25
2,3-Dimethyl (**9**)	(12)	H	CH_3	H	H	3-Methyl (**17**)	28.46	32.5	−22
2-Methyl (**10**)	(13)	H	H	H	H	(**18**)	31.39	35.9	−17
1,2,3-Trimethyl (**11**)	(14)	CH_3	CH_3	H	H	2,3-Dimethyl (**19**)	45.00	25.2	−37

[a]The structural configuration can be represented by:

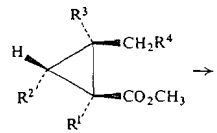

$\rightarrow R^4CH{=}CR^3CHR^2CHR^1CO_2CH_3$.

[b]Maximum error is estimated to be ±5% for k corresponding to ±2 kcal/mole for $\Delta H\dagger$ and ±4 e.u. for $\Delta S\dagger$.

Can. J. Chem. Downloaded from www.nrcresearchpress.com by 210.87.254.40 on 09/05/12
For personal use only.

Mechanism

First-order plots of the kinetics, determined on samples in sealed tubes where each point is a different sample and where the composition of the reaction mixture was determined by vapor-phase chromatography, gave good straight lines as illustrated in Fig. 1. The low degree of scatter of the points and the fact that the plots pass through the origin fully support the first-order kinetics observed and exclude a free radical chain process.

The half-lives at 259.4 °C, the heat of activation, and the entropy of activation were calculated and are listed in Table I.

As a further test of the mechanism the *trans* isomers corresponding to structures **6**, **8**, **9**, and **10** and the isomeric nitriles *cis*- and *trans*-1,2-dimethyl-1-cyanocyclopropane were heated for prolonged periods at 258 °C or higher and in all cases no evidence for rearrangement could be found.

The values of $\Delta H\dagger$ and $\Delta S\dagger$ are in line with the thermodynamic parameters reported for *cis*-2-methyl-1-vinylcyclopropane (8, $E_a = 31$ kcal/mole and $\Delta S\dagger = -11.6$ e.u.) and 1-acetyl-2,2-dimethylcyclopropane (4, $\Delta H\dagger = 30$ kcal/mole, $\Delta S\dagger = -10$ e.u.). The large negative entropy of activation in all examples fully supports an ordered transition state as illustrated by structure **2**. The high stability of the *trans* isomers of **6**, **8**, **9**, and **10** and of the nitriles also supports this transition state, for in these compounds the multiple bonds are no longer in the proximity of the alkyl group from which a hydrogen must migrate. Clearly this proximity is a necessary requirement.

It is therefore possible to discuss the reaction in light of this mechanism. The 2-ethyl derivative (**6**) gave two γ,δ-derivatives. Examination of Dreiding models of the transition states expected for migration of each of the methylene hydrogens shows that one (the one that would give the *cis* double bond in the product) has a major steric interaction between the methyl of the ethyl group and the ring carbons. This or an equivalent steric factor is not present for the transition state that leads to the *trans* product. The ratio of *trans*:*cis* in the product of 4.7:1 can therefore be rationalized.

We can now compare the rate of formation of the *trans* product ($t_{1/2}$ at 259.4 °C is 15.3 h) from **6** with that for the formation of **16** from **8** with corrections for the statistically faster rate due to the three available hydrogens ($t_{1/2}$ at 259.4 °C is 48.9 h per hydrogen). A faster rate of reaction is obtained for migration of a secondary hydrogen over that of a primary hydrogen as would be expected if bond breaking of the C—H bond were important in the transition state as proposed by Frey (8) and illustrated by intermediate **2**.

The alkyl substituted cyclopropanecarboxylates studied give a 20-fold variation in rate at 259.4 °C. Factors which influence this variation may be steric or electronic. It is significant that in the series **10**, **9**, **8**, **6**, and **5** increasing substitution on C-1 and C-2 increases the rate. Substitution on C-1 to C-2 would be expected to weaken that bond and thus the breaking of the C-1 and C-2 bond must also be an important feature of the transition state as indicated by structure **2**.

The presence of a substituent on C-3 as in **11** where it is *cis* to the methyl at C-1 clearly creates a steric factor in the transition state which is unfavorable. This would suggest that for the transition state from **11** the *cis* methyls are closer to being fully eclipsed, than in **11**, contributing to a slower rate and larger negative entropy. As a corollary we might therefore suggest, that for cyclopropanes in general, the presence of bulky groups can cause the structure to twist away from a fully eclipsed conformation.

Finally it should be noted that when the unsaturated group in **1** is a ketone the reaction is faster (compare 1-acetyl-2,2-dimethylcyclopropane with $t_{1/2}$ of 4.8 h at 152 °C (4) with compound **7**). This order suggests ionic character in the reaction, related to the greater nucleophilic nature of a ketone oxygen than the oxygen of an ester carbonyl. The facile rearrangement of methyl 2,2-dimethyl-1-cyanocyclopropanecarboxylate (1) and 2-methyl-1,1-diacetylcyclopropane (5) may also reflect easier bond breaking of the C-1 to C-2 bond in an ionic sense which fits an alternating pattern of −,+,−,+,−,+ for the 6 atoms in the transition state, beginning at the oxygen.

Conclusions

In conclusion we can state that the cyclic unimolecular mechanism is fully supported for the series of *cis*-2-alkyl-1-cyclopropanecarboxylates described herein. The lack of reaction for

Can. J. Chem. Downloaded from www.nrcresearchpress.com by 210.87.254.40 on 09/05/12
For personal use only.

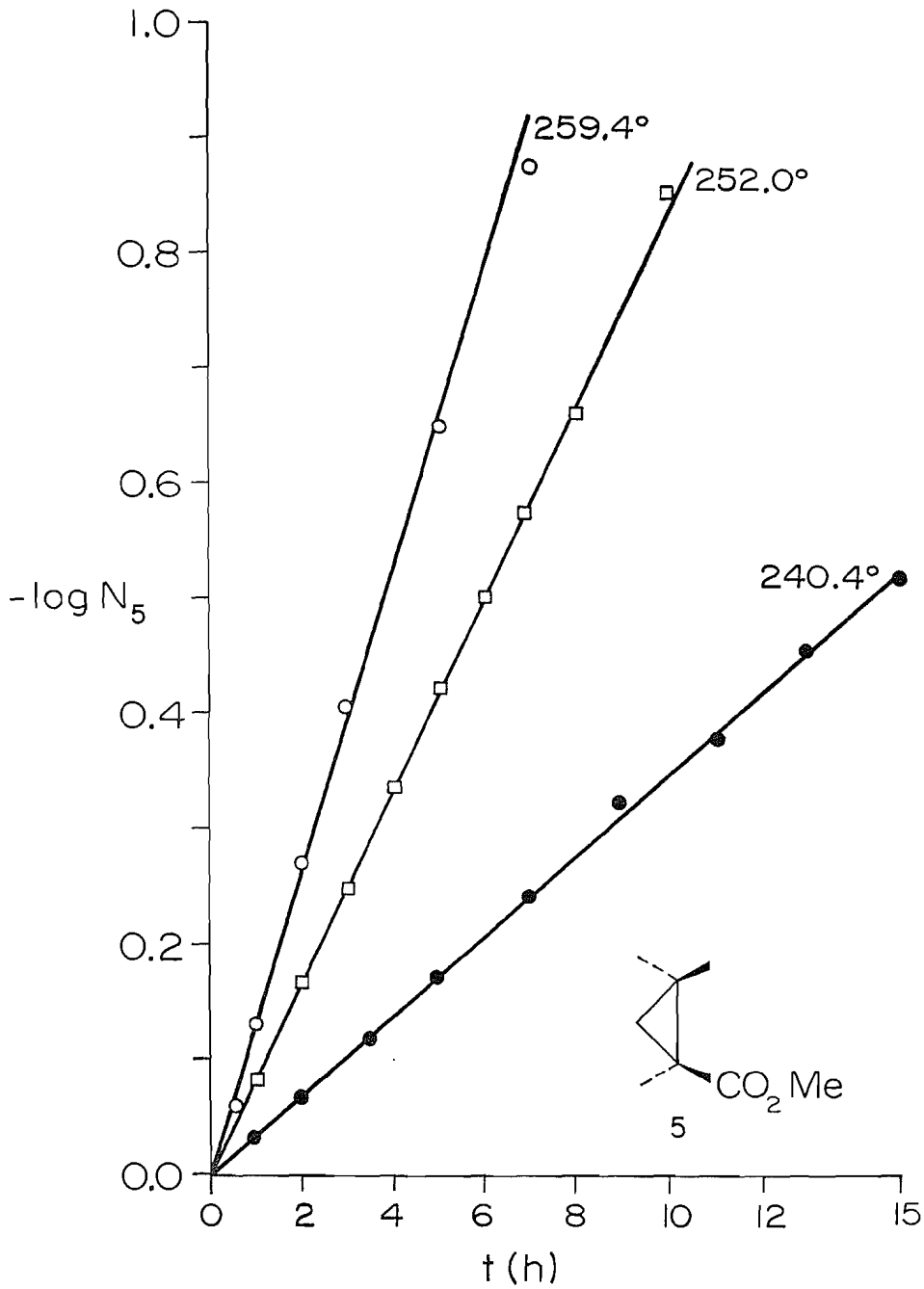

FIG. 1. First-order rate plots for the thermal isomerization of **5**.

Can. J. Chem. Downloaded from www.nrcresearchpress.com by 210.87.254.40 on 09/05/12
For personal use only.

the corresponding *trans* isomers under more vigorous reaction conditions clearly makes this reaction useful for determining the stereochemistry directly when only a single isomer is at hand. Indeed we have based the structural assignments for **6** (11), **8** (1), and **11** (14) and their *trans* isomers on this reaction. Similarly *cis*-1,2-dimethyl-1-acetylcyclopropane has been distinguished from the *trans* isomer (6).

The most useful method to date for determining geometry of cyclopropane derivatives has been based on the cyclic anhydride formation possible only from a *cis*-1,2-dicarboxylic acid (15). This reaction has been applied in some extensive studies recently (16). Cyclopropanecarboxylic acids with a hydrogen on the α-carbon can be equilibrated in base or thionyl chloride to give the more stable configuration (17, 18). Steric factors also influence the rate of hydrolysis of cyclopropanecarboxylate esters and this has been used to distinguish **8** from its *trans* isomer (19). The use of nuclear magnetic resonance (n.m.r.) is promising as the coupling constants for vicinal ring hydrogens are greater for the *cis* orientation (8–11 Hz) than for the *trans* (5–8 Hz) (see refs. 20–22 for further discussion). Although n.m.r. has been used (14, 17) successfully it is frequently limited by the complexity of the spectra which often have overlapping signals. We anticipate therefore that our new method of assigning stereochemical configuration will be most useful.

Experimental

Boiling points recorded are not corrected and were determined by the micro-inverted capillary method. Infrared spectra were recorded on a Perkin–Elmer model 21DB spectrophotometer and were calibrated using the 1603 cm^{-1} band of a polyethylene film. The nuclear magnetic resonance (n.m.r.) spectra were determined on 20% by volume solutions in carbon tetrachloride using a Varian A-60 and/or a Varian HA-100 spectrometer. All samples were separated by a Varian aerograph model A-90-P chromatograph and integrations of the peak areas were achieved using a disk integrator fitted to a Honeywell electronic 15 recorder.

Compounds prepared or identified elsewhere are described in the references cited in Table I. The following procedures were used to prepare the remaining cyclopropanes.

Methyl 1,2,2-Trimethyl-1-cyclopropanecarboxylate (5)

The 3,5,5-trimethyl-3-carbomethoxy-1-pyrazoline used to prepare **5** was obtained from the reaction of 2-diazopropane (23) with methyl methacrylate. A mixture of 58 g (0.25 mole) of silver oxide, 25 g (0.25 mole) of methyl methacrylate, and 300 ml of anhydrous ether was cooled to −60 °C. While the reaction medium was stirred 18 g (0.25 mole) of acetone hydrazone were added over a 10 min period. The mixture was stirred at −25 °C for 1 h and then slowly warmed to room temperature. The residual solids were filtered off and the filtrate evaporated and distilled to give 15 g of the pyrazoline, b.p. 55–56 °C at 0.1 mm.

Anal. Calcd. for $C_8H_{14}O_2N$: C, 56.47; H, 8.23; N, 16.47. Found: C, 56.30; H, 8.13; N, 16.35.

The n.m.r. spectrum confirmed the structure showing peaks at τ 6.27 (ester methyl), τ 8.03 and τ 8.79 (doublets with J_{gem} = 13.1 Hz for the AB system of the hydrogens on C-4) and τ 8.46, τ 8.60, and τ 8.64 (ring methyls on C-3 and C-5). Pyrolysis of 12.5 g of 3,5,5-trimethyl-3-carbomethoxy-1-pyrazoline at 90–100 °C gave 9.5 g of product which when analyzed by v.p.c. using a dinonyl phthalate column at 158 °C gave two products:

(*i*) Methyl 1,2,2-trimethyl-1-cyclopropanecarboxylate (**5**), 85%, b.p. 148.5 °C, n_D^{25} 1.4280 with n.m.r. (20% in benzene) peaks at τ 6.57 (ester methyl), τ 8.74, τ 8.87, and τ 9.01 (ring methyls) and τ 8.58 and τ 9.74 (doublets with J_{gem} = 4.6 Hz for the AB system of the hydrogens on C-3).

Anal. Calcd. for $C_8H_{14}O_2$: C, 67.57; H, 9.93. Found: C, 67.69; H, 9.88.

(*ii*) Methyl *trans*-2,4-dimethyl-2-pentenoate, 15%, b.p. 164.5 °C, n_D^{25} 1.4366 (lit. (24), b.p. 49–50 °C at 10 mm, n_D^{20} 1.4383). The *trans* geometry is based on comparison with the *cis* isomer available by an independant synthesis (25).

Anal. Calcd. for $C_8H_{14}O_2$: C, 67.57; H, 9.93. Found: C, 67.85; H, 9.71.

Methyl 2,2-Dimethyl-1-cyclopropanecarboxylate (7)

The 5,5-dimethyl-3-carbomethoxy-1- and 2-pyrazoline used to prepare **7** were obtained from the reaction of 2-diazopropane with methyl acrylate. The crude pyrazoline which was clearly a mixture of the 1- and 2-pyrazolines as indicated by n.m.r. was not further purified but was pyrolyzed directly to give a pyrolysis mixture which was separated on a dinonyl phthalate column at 165 °C to give two components.

Methyl 2,2-dimethyl-1-cyclopropanecarboxylate (**7**), 26%, was the major compound in the more volatile component. However methyl *cis*-4-methyl-2-pentenoate, 4%, was also present and could not be removed. This component however did not interfere with the identification of **7** nor the kinetics on **7**.

Anal. Calcd. for the mixture $C_7H_{12}O_2$: C, 65.49; H, 9.45. Found: C, 65.37; H, 9.62.

The n.m.r. spectrum of **7** showed peaks at τ 6.37 (ester methyl), τ 8.81, and τ 8.86 (ring methyls), τ 8.50, τ 9.21, and about τ 8.95 (ring hydrogens on C-1, C-2 *cis*, and C-2 *trans* showing J_{gem} = 4.0 Hz, J_{cis} = 8.1 Hz, and J_{vic} = 5.1 Hz) in accord with that of the corresponding acid (22).

Methyl *trans*-4-methyl-2-pentenoate, 70%, b.p. 150 °C, n_D^{22} 1.4298 had the expected n.m.r. spectrum (25) in addition to the infrared band at 990 cm^{-1} characteristic of a *trans* H—C=C—H unit.

Anal. Calcd. for $C_7H_{12}O_2$: C, 65.49; H, 9.45. Found: C, 65.39; H, 9.44.

cis- and trans-1,2-Dimethyl-1-cyanocyclopropane

Addition of a solution of diazoethane in ether to methacrylonitrile gave on evaporation of the solvent a

Can. J. Chem. Downloaded from www.nrcresearchpress.com by 210.87.254.40 on 09/05/12
For personal use only.

mixture of *cis*- and *trans*-3,5-dimethyl-3-cyano-1-pyrazoline. Pyrolysis of 10 g of this pyrazoline mixture at 100 °C gave a product which showed three components when analyzed on a dinonyl phthalate column at 145 °C. The components were assigned structures by comparison of the physical data with those found for the corresponding esters isolated from an analogous reaction (14).

trans-1,2-Dimethyl-1-cyanocyclopropane, 53%, b.p. 137.5 °C, n_D^{26} 1.4179 showed no n.m.r. signals below τ 8.65.

Anal. Calcd. for C_6H_9N: C, 75.74; H, 9.54; N, 14.72. Found: C, 75.82; H, 9.67; N, 14.92.

cis-1,2-Dimethyl-1-cyanocyclopropane, 44%, b.p. 149 °C, n_D^{26} 1.4238 showed no n.m.r. signals below τ 8.50.

Anal. Calcd. for C_6H_9N: C, 75.74; H, 9.54; N, 14.72. Found: C, 75.72; H, 9.80; N, 14.82.

γ,δ-Unsaturated Esters

Samples of the cyclopropane esters **5** to **11** were heated at 280 °C until n.m.r. or v.p.c. showed rearrangement to be nearly complete. Separation by v.p.c. from any remaining starting material gave the pure γ,δ-unsaturated ester.

Methyl 2,4-dimethyl-4-pentenoate (**12**), b.p. 155 °C, n_D^{24} 1.4228 (lit. (26), b.p. 51 °C at 12 mm, n_D^{20} 1.4270) from **5** was separated on a didecyl phthalate column at 150 °C to give a relative retention time of 1.13 with respect to **5**.

Anal. Calcd. for $C_8H_{14}O_2$: C, 67.57; H, 9.93. Found: C, 67.42; H, 10.14.

The n.m.r. spectrum was consistent with this assignment showing peaks at τ 5.31 (terminal olefinic hydrogens), τ 6.41 (ester methyl), τ 7.20–8.10 (multiplet for hydrogens on C-2 and C-3), τ 8.31 (methyl on C-4), τ 8.91 (doublet for the methyl on C-2 with $J = 6.5$ Hz).

Methyl *cis*-2-methyl-4-hexenoate (**13**), b.p. 164.5 °C, n_D^{26} 1.4261, 17.5% from **6** was separated on a diethylene glycol succinate column at 153 °C and gave a relative retention time of 1.41 with respect to the *trans* isomer (**14**).

Anal. Calcd. for $C_8H_{14}O_2$: C, 67.57; H, 9.93. Found: C, 67.33; H, 9.97.

The n.m.r. spectrum showed peaks at τ 4.25 to τ 4.95 (multiplet for the olefinic hydrogens), τ 6.40 (ester methyl), τ 7.35 to τ 8.05 (multiplet for the hydrogens on C-2 and C-3), τ 8.39 (doublet for the hydrogens on C-6 with $J = 5.7$ Hz) and τ 8.88 (doublet for the methyl on C-2 with $J = 6.3$ Hz).

Methyl *trans*-2-methyl-4-hexenoate (**14**), b.p. 161 °C, n_D^{26} 1.4225, 82.5% from **6**, was distinguished from the *cis* isomer **13** by the presence in its infrared spectrum of a band at 973 cm^{-1} characteristic of *trans* vicinal disubstituted olefins.

Anal. Calcd. for $C_8H_{14}O_2$: C, 67.57; H, 9.93. Found: C, 67.36; H, 10.00.

The n.m.r. spectrum showed peaks at τ 4.50 to τ 5.00 (multiplet for the olefinic hydrogens), τ 6.41 (ester methyl), τ 7.50 to τ 8.10 (multiplets for the hydrogens on C-2 and C-3), τ 8.36 (doublets for the hydrogens on C-6 with $J = 4.7$ Hz) and τ 8.96 (doublet for the methyl on C-2 with $J = 6.5$ Hz).

The final ratio of *trans*:*cis* of 4.7:1 corresponded well with the ratio observed after partial reaction during kinetic runs where values of 4.5, 5.0, 5.2, 4.8, 4.0, and 5.3 were observed. Heating of **13** and **14** at 296 °C for 20 h gave only about 5% conversion of each isomer into the other. It is interesting to note that this *cis* ⇄ *trans* isomerization is not accompanied by any double bond migration (25).

Methyl 4-methyl-4-pentenoate (**15**), b.p. 149 °C, n_D^{23} 1.4230 was prepared from **7**. This experiment was complicated by the fact that **7** contained 15% of methyl *cis* 4-methyl-2-pentenoate which under the reaction conditions isomerized to methyl 4-methyl-3-pentenoate (25). On a dinonyl phthalate column at 155 °C the starting material **7**, the product **15** and the 3-pentenoate had retention times of 14.7, 18.9, and 23.3 respectively.

Anal. Calcd. for **15**, $C_7H_{12}O_2$: C, 65.49; H, 9.45. Found: C, 65.67; H, 9.53.

The n.m.r. spectrum of **15** showed peaks at τ 5.20 (broad singlet for the terminal olefinic hydrogens), τ 6.35 (ester methyl), τ 7.64 (singlet for the hydrogens on C-2 and C-3), and τ 8.25 (broad singlet for the methyl on C-4).

Methyl 2-methyl-4-pentenoate (**16**), b.p. 137.5 °C, n_D^{22} 1.4156 from **8** was isolated using a dinonyl phthalate column at 140 °C.

Anal. Calcd. for $C_7H_{12}O_2$: C, 65.49; H, 9.45. Found: C, 65.68; H, 9.57.

The n.m.r. spectrum showed peaks at τ 4.15 to τ 4.85 (multiplet for the C-4 olefinic hydrogen), τ 5.05 and τ 5.26 (broadened multiplets for the terminal olefinic hydrogens), τ 6.49 (ester methyl), τ 7.35 to τ 8.10 (multiplet for the hydrogens on C-2 and C-3), and τ 8.97 (doublet for the methyl on C-2 with $J = 6.5$ Hz).

Methyl 3-methyl-4-pentenoate (**17**), b.p. 137.5 °C, n_D^{24} 1.4152 from **9** was isolated using a dinonyl phthalate column at 150 °C.

Anal. Calcd. for $C_7H_{12}O_2$: C, 65.49; H, 9.45. Found: C, 65.58; H, 9.45.

The n.m.r. spectrum showed peaks at τ 4.22, τ 4.95, and τ 5.18 (broad multiplets for the olefinic hydrogens), τ 6.41 (ester methyl), τ 7.35 (multiplet for the hydrogen on C-3), τ 7.76 and τ 7.76 (overlapping doublets for the nonequivalent methylene at C-2 with $J = 8.6$ and 5.8 Hz respectively), and τ 8.97 (doublet for the methyl on C-3 with $J = 5.3$ Hz).

Methyl 4-pentenoate (**18**), b.p. 125.5 °C, n_D^{22} 1.4148 was obtained from a mixture of **10** and its *trans* isomer, determined by the OCH_3 peak of the n.m.r. at 100 MHz to be in the proportions 28:72 respectively (the OCH_3 of the *cis* ester appears at lower field). Attempts to separate these isomers have been unsuccessful except on capillary columns. The methyl 4-pentenoate was separated from the methyl *trans*-2-methylcyclopropanecarboxylate on a Ucon polar column at 92 °C and had a relative retention time of 0.85 and gave the following analysis.

Anal. Calcd. for $C_6H_{10}O_2$: C, 63.11; H, 8.84. Found: C, 62.90; H, 8.81.

The n.m.r. spectrum showed peaks at τ 4.09, τ 4.84, and τ 5.08 (multiplets for the olefinic hydrogens), τ 6.45 (ester methyl) and τ 7.62 and τ 7.67 (singlets for the hydrogens on C-2 and C-3).

Methyl 2,3-dimethyl-4-pentenoate (**19**), b.p. 151.5 °C, n_D^{23} 1.4212 was obtained by heating a mixture of methyl *cis,trans*-1,2,3-trimethylcyclopropanecarboxylate and its isomer with the methyls all *cis* (14). Separation on a didecyl phthalate column at 168 °C gave pure **19** with a relative retention time of 0.93 with respect to the unchanged isomer with all methyls *cis*.

Can. J. Chem. Downloaded from www.nrcresearchpress.com by 210.87.254.40 on 09/05/12
For personal use only.

Anal. Calcd. for $C_8H_{14}O_2$: C, 67.57; H, 9.93. Found: C, 67.71; H, 9.91.

The n.m.r. spectrum of **19** showed peaks at τ 4.31, τ 4.92 and τ 5.14 (multiplets for the olefinic hydrogens), τ 6.38 (ester methyl), τ 7.64 (multiplets for the hydrogens on C-2 and C-3), τ 8.94 and τ 9.01 (doublets for the methyls on C-2 and C-3 with J = 6.7 and 6.6 Hz respectively).

Kinetics

Cyclopropane samples for the kinetic runs were estimated to be better than 99.9% pure by v.p.c. except in the case of **10** which was mixed with methyl *trans*-2-methylcyclopropanecarboxylate (*cis*:*trans* ratio of 28:72). For each run 10–15 samples of about 7 μl each were sealed in pyrex tubes 4 × 120 mm in size (approximate volume 500 μl) at atmospheric pressure and placed in a vertical cylindrical induction furnace. At appropriate time intervals samples were removed and quenched in ice–water and analyzed by vapor chromatography. The disk integrator method of analysis yielded less than ±1% error for known samples in a ratio of 1:1 and 1:2 and thus corrections for thermal conductivity differences between samples were not made. The furnace temperature was controlled to ±0.5 °C by means of Temcometer input controller. The thermometer used to record the temperature, which was placed level with the samples in the furnace, had 1 ° subdivisions and was calibrated in the range 240 to 340 °C against a N.B.S. calibrated thermometer. No corrections were made for thermal variations within this static system.

First-order plots of all kinetic data taken to over 70% completion gave good straight lines as illustrated in Fig. 1.

TABLE II

First-order rate constants[a]

Compound	Rate constant ($s^{-1} \times 10^5$)	Temperature (°C)
5	2.21	240.4
	5.35	252.0
	8.53	259.4
6	1.53	259.4
	3.25	272.2
	6.50	283.7
7	1.27	259.4
	2.95	272.2
	5.92	283.7
8	1.18	259.4
	2.41	272.2
	4.31	283.7
9	0.68	259.4
	1.37	272.2
	2.68	283.7
	5.46	297.4
10	0.61	259.4
	1.45	272.2
	2.98	283.7
	6.29	294.4
11	0.43	259.4
	0.85	272.2
	1.35	283.7
	1.26	283.7
	2.23	297.4

[a]Values used for calculation of $\Delta H\dagger$ and $\Delta S\dagger$.

The first-order rate constant at various temperatures used for calculation of $\Delta H\dagger$ and $\Delta S\dagger$ are listed in Table II.

The major factor contributing to errors is believed to be in the control of the temperature which with a ±0.5 ° range can amount to as much as ±5% error in the rates. The low degree of scatter in the plots suggests that other errors are minimal.

Acknowledgments

The authors gratefully appreciate the support received for this work from the National Research Council of Canada and from the Committee on Research of the University of British Columbia.

1. D. E. McGREER, N. W. K. CHIU, and R. S. McDANIEL. Proc. Chem. Soc. 415 (1964).
2. K. VON AUWERS and O. UNGEMACH. Ann. Chem. **511**, 152 (1934).
3. R. M. ROBERTS and R. G. LANDOLT. J. Am. Chem. Soc. **87**, 2281 (1965).
4. R. M. ROBERTS, R. G. LANDOLT, R. N. GREENE, and E. W. HEYER. J. Am. Chem. Soc. **89**, 1404 (1967).
5. K. ICHIKAWA, O. ITOH, T. KAWAMURA, M. FUJIWARA, and T. UENO. J. Org. Chem. **31**, 447 (1966).
6. D. E. McGREER, N. W. K. CHIU, and M. G. VINJE. Can. J. Chem. **43**, 1398 (1965).
7. G. OHLOFF. Tetrahedron Letters, 3795 (1965).
8. R. J. ELLIS and H. M. FREY. J. Chem. Soc. 5578 (1964).
9. P. E. FANTA and M. K. KATHAN. J. Heterocyclic Chem. **1**, 293 (1964).
10. H. KRISTINSSON and G. W. GRIFFIN. Tetrahedron Letters, 3259 (1966).
11. D. E. McGREER and W. S. WU. Can. J. Chem. **45**, 461 (1967).
12. D. E. McGREER, P. MORRIS, and G. CARMICHAEL. Can. J. Chem. **41**, 726 (1963).
13. D. E. McGREER, W. WAI, and G. CARMICHAEL. Can. J. Chem. **38**, 2410 (1960).
14. D. E. McGREER, N. W. K. CHIU, M. G. VINJE, and K. C. K. WONG. Can. J. Chem. **43**, 1407 (1965).
15. E. BUCHNER. Ber. **36**, 1085 (1903).
16. G. BONAVENT, N. CAUSSE, M. GUITARD, and R. FRAISSE-JULLIEN. Bull Soc. Chim. France. 2462 (1964).
17. L. L. McCOY and G. W. NACHTIGALL. J. Org. Chem. **27**, 4312 (1962).
18. I. A. D'YAKONOV and R. R. KOSTIKOV. Zh. Organ. Khim. **2**, 823 (1966).
19. T. V. VAN AUKEN and K. L. RINEHART, JR. J. Am. Chem. Soc. **84**, 3736 (1962).
20. K. L. WILLIAMSON, C. A. LANFORD, and C. R. NICHOLSON. J. Am. Chem. Soc. **86**, 762 (1964).
21. H. M. HUTTON and T. SCHAEFER. Can. J. Chem. **41**, 684 (1963).
22. D. J. PATEL, M. E. H. HOWDEN, and J. D. ROBERTS. J. Am. Chem. Soc. **85**, 3218 (1963).
23. D. E. APPLEQUIST and H. BABAD. J. Org. Chem. **27**, 288 (1962).
24. S. G. BATRAKOV and L. D. BERGELSON. Izvest. Akad. Nauk. Kazakh. S.S.R. Ser. Khim. 1640 (1964).
25. D. E. McGREER and N. W. K. CHIU. Can. J. Chem. This issue.
26. J. B. ROGAN. J. Org. Chem. **27**, 3910 (1962).

Can. J. Chem. Downloaded from www.nrcresearchpress.com by 210.87.254.42 on 09/05/12
For personal use only.

Thermal rearrangement of α,β- to β,γ-unsaturated esters. Evidence for a 1,5-hydrogen transfer mechanism[1]

DONALD E. MCGREER AND NORMAN W. K. CHIU
Department of Chemistry, University of British Columbia, Vancouver, British Columbia

Received January 17, 1968

Methyl *cis*-4-methyl-2-pentenoate (**1**) has been found to rearrange at 252 °C by a simple first-order and presumably unimolecular mechanism to methyl 4-methyl-3-pentenoate (**3**) with a rate constant k of 4.28×10^{-5} s^{-1}. The heat of activation $\Delta H\dagger$, was determined to be 37.5 ± 2 kcal/mole and the entropy of activation, $\Delta S\dagger$, was determined to be −8.2 ± 4 e.u. These activation parameters and the steric requirements of the reaction support a mechanism involving a cyclic 1,5-transfer of hydrogen. Studies on the isomerization of methyl *cis*-2-pentenoate, methyl *cis*-2,4-dimethyl-2-pentenoate, and methyl *cis*-2-methyl-2-pentenoate to the corresponding 3-pentenoates suggest that the 1,5-hydrogen transfer mechanism could well be general for the equilibration of α,β- and β,γ-unsaturated esters.

An isopropyl group *cis* to a methyl or a carbomethoxy group on a double bond is shown by nuclear magnetic resonance to prefer a conformation with the methyls of the isopropyl group held away from the methyl or carbomethoxy group. A *cis* hydrogen does not restrict the conformation of the isopropyl group.

Canadian Journal of Chemistry, 46, 2225 (1968)

The equilibrium and kinetics of *cis–trans* olefin interconversions in the gas phase and in solution have received much attention in recent years (1). Equilibrium is normally established in the presence of a catalyst and under such conditions positional isomers, where possible, are also formed (2, 3). This feature of catalyzed equilibrations has been exploited by many workers to evaluate steric factors and the conjugative effects due to alkyl, carbalkoxy, and related groups on olefin stability (3–5). In many cases, however, the positional isomerization is an interfering side reaction. This is particularly so in kinetic studies on *cis–trans* interconversions which are expected to be unimolecular (6, 7). The positional isomerization reaction is usually catalyzed on the wall or by free radicals, acids, or bases.

α,β-Unsaturated esters when heated to about 300 °C equilibrate to give *cis* and *trans* α,β-isomers and β,γ-isomers (8). Possible reaction paths can be represented by reactions 1, 2, and 3. Although reactions 2 and 3 might be catalyzed

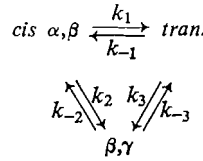

reactions, we have found little evidence for decomposition or catalytic effects below 300 °C. On the other hand the positional isomerism might well be expected to occur by a unimolecular 1,5-transfer of hydrogen as illustrated by reaction 4. This would be possible for the *cis*

[4]

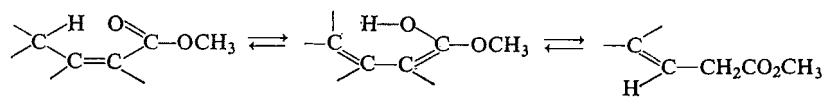

α,β-isomer (reaction 2) but not for the *trans* α,β-isomer (reaction 3). Analogous reactions in the literature support 4 as a possible reaction path. Stereochemical evidence has been presented for the reversible isomerization of 1,3-dienes that requires that an alkyl group and a vinyl group must be *cis*, suggesting a 1,5-hydrogen transfer mechanism (9). Similarly *cis*-2-methylvinylcyclo-

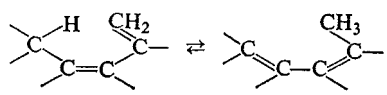

propane ring opens by a 1,5-transfer of hydrogen while the *trans* isomer does not (10). The reaction

[1]Taken in part from the Ph.D. Thesis of N. W. K. Chiu, September, 1967.

Can. J. Chem. Downloaded from www.nrcresearchpress.com by 210.87.254.42 on 09/05/12
For personal use only.

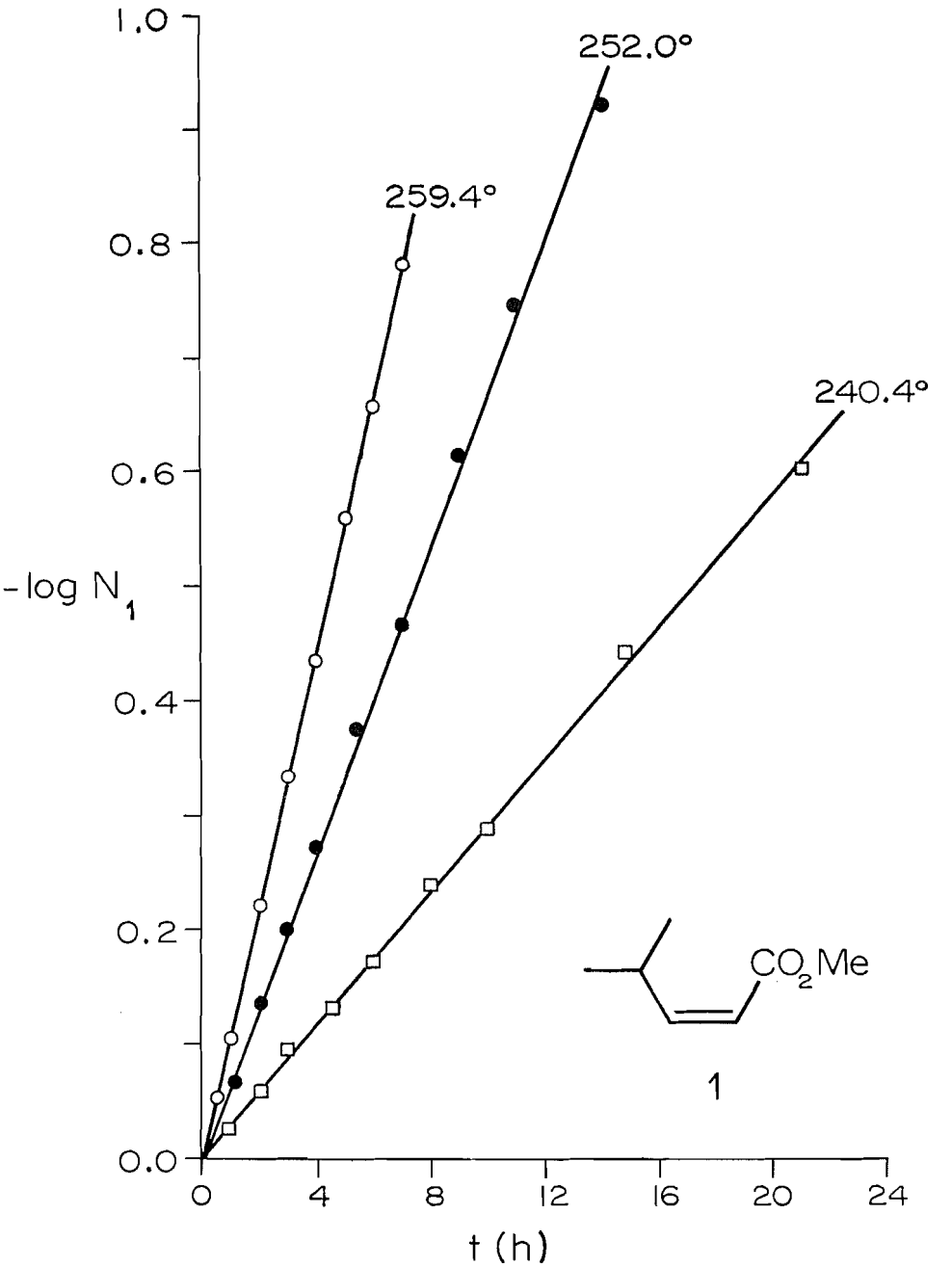

FIG. 1. First-order rate plots for the thermal isomerization of **1**.

Can. J. Chem. Downloaded from www.nrcresearchpress.com by 210.87.254.42 on 09/05/12
For personal use only.

of methyl *cis*-2-alkylcyclopropanecarboxylates is now known to follow a similar path (11).

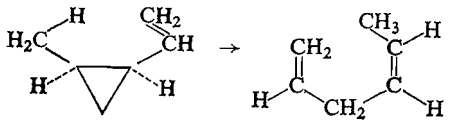

To our knowledge the 1,5-transfer of hydrogen as illustrated by reaction 4 has not been demonstrated for esters or ketones although the related photochemical reaction has been observed (12, 13). The reason for this is that it is difficult to isolate reaction 2 from reaction 1. We have now studied some systems that verify the existence of reaction 4 for the positional isomerization of unsaturated esters.

Results

Methyl 4-Methyl-2- and 3-pentenoates

Methyl *cis*- and *trans*-4-methyl-2-pentenoate (**1** and **2**) were prepared in 46% yield by a modified Wittig procedure using trimethyl phosphonoacetate and isobutyraldehyde which gave **1** and **2** in the ratio of 31:69. The β,γ-isomer, methyl 4-methyl-3-pentenoate (**3**) was prepared by heating **1** at 297 °C for 3 h and thereby converting it to a mixture of **1**, **2**, and **3** containing over 97% of **3**.

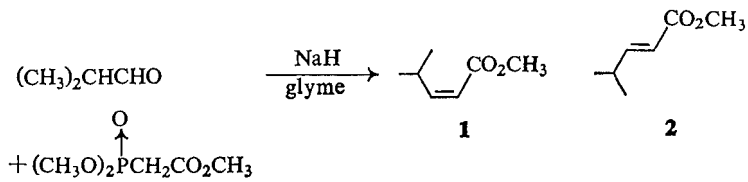

Equilibration studies were carried out on **1**, **2**, and **3** by heating small samples sealed at atmospheric pressure in 4 mm O.D. pyrex tubes. The results are listed in Table I. Equilibrium was reached from **1** and **2** and at 297 °C the equilib-

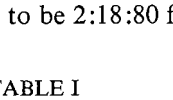

3

rium ratio was found to be 2:18:80 for **1**, **2**, and **3** respectively.

TABLE I

Thermal rearrangement of methyl 4-methyl-2- and 3-pentenoates (**1**, **2**, and **3**) at 297 °C

Initial olefin	Time (h)	Products 1	2	3
1*	7	16	5	79
1	4	2	2	96
1	24	2	5	93
1	40	2	7	91
1	259	2	18	80
1	336	2	18	80
2	4	—	92	8
2	24	—	82	18
2	40	—	78	22
2	259	2	18	80
2	336	2	18	80
3	4	2	2	96
3	40	2	9	89

*Temperature 259 °C.

Two features of the preequilibrium analyses are of note. **1** and **3** rapidly reach equilibrium while **2** isomerizes slowly when it is heated and builds up slowly when **1** or **3** is heated. Clearly for this system k_2 and k_{-2} are fast compared to k_1 and k_{-1} or k_3 and k_{-3}. Prolonged heating of this system gave little decomposition and good recovery of the isomeric components. This encouraged us to follow reaction 2 kinetically.

Samples sealed at atmospheric pressure were heated at 240.4, 252.0, and 259.4 °C and were removed as required for analysis by vapor-phase chromatography. The reaction **1** → **3** was treated as an irreversible reaction in which the side reactions due to **1** → **2** and **3** → **2** are assumed negligible. The resulting data when plotted according to first-order kinetics gave good straight lines (Fig. 1) to over 70% reaction. The rate constants found were 1.86×10^{-5} s^{-1} at 240.4 °C, 4.28×10^{-5} s^{-1} at 252.0 °C, and 7.06×10^{-5} s^{-1} at 259.4 °C. Inclusion of the back reaction **3** → **1** in the calculation of k_2 at 259.4 °C raised k_2 to 7.22×10^{-5} s^{-1}. The maximum error in k_2 is expected to be in the control of the temperature which was to ±0.5 °C leading to a maximum error of 5% for k_2. The heat of activation, $\Delta H\dagger$, obtained from a three point straight line plot was 37.5 ± 2 kcal/mole and the entropy of activation, $\Delta S\dagger$, was found to be −8.2 ± 4 e.u.

Can. J. Chem. Downloaded from www.nrcresearchpress.com by 210.87.254.42 on 09/05/12
For personal use only.

In the reaction **1** → **3** reaction 2 is essentially complete before reaction 1 and 3 become important. Reaction 2 is first order and presumably unimolecular. The absence of decomposition and the absence of induction even in the presence of oxygen sealed in with the air are consistent with a unimolecular process. The fact that $k_2 \gg k_3$ supports the postulate that **1** → **3** occurs by a 1,5-transfer of hydrogen as illustrated in reaction 4. This is also supported by the activation parameters which are quite similar in magnitude to those found in the analogous 1,5-transfer of hydrogen in methyl *cis*-2-alkylcyclopropanecarboxylates (11). It is not clear from these results whether k_1 is particularly small, however comparison with further results below suggests that it is.

Methyl 2- and 3-Pentenoates

Methyl *cis*-2-pentenoate (**4**) and methyl *trans*-2-pentenoate (**5**) were isolated from the product from pyrolysis of 5-methyl-3-carbomethoxy-1-pyrazoline as reported earlier (8). Methyl *trans*-3-pentenoate (**6**) was isolated from equilibrium mixtures of **4**, **5**, and **6** obtained by heating **4** at 270 °C for 50 h.

Equilibration studies were carried out on **4**, **5**, and **6** and these results are presented in Table II. Equilibrium was reached from **4**, **5**, and **6** and

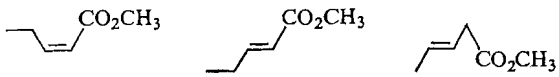

4 **5** **6**

at 259 °C the equilibrium ratio was found to be 6:42:52 for **4**, **5**, and **6** respectively. Although a *cis* β,γ-unsaturated ester is possible here it was not detected.

It is not possible to separate reaction 2 from reactions 1 and 3 in this case as they have similar rates. It is apparent however that $k_2 > k_1$ since **4** and **6** reach equilibrium with each other earlier than **5** reaches equilibrium with either **4** or **6**. This permits **6** to reach a maximum when **4** is used as the starting material which then falls off as **5** increases. This is illustrated graphically in Fig. 2. On the other hand isomer **5** reacts slowly enough that it gives directly a near equilibrium mixture of **4** and **6**. These results are compatible with **5** giving **4** in a slow step followed by conversion to **6** in a fast step.

Compared with the reaction of **2** (8% reacted in 24 h at 297.4 °C), **5** more readily undergoes

TABLE II

Thermal rearrangement of methyl 2- and 3-pentenoates (**4**, **5**, and **6**) at 259 °C

Initial olefin	Time (h)	Products		
		4	**5**	**6**
4	5	86	2	12
4	22	46	6	48
4	45	17	11	72
4	61	14	12	74
4	84	10	18	73
4	106	9	20	71
4	135	9	25	66
4	180	8	30	62
4	328	6	42	52
5	17	1	90	9
5	26	2	81	17
5	64	4	61	35
5	328	6	42	52
6	17	9	12	79
6	26	9	16	75
6	41	8	27	65
6	64	8	31	61
6	328	6	42	52

trans–cis isomerization (19% reacted in 26 h at 259.4 °C). At the same time the conversion of **4** to **6** (14% reacted in 5 h at 259.4 °C) is slower than the conversion of **1** to **3** (73% reacted in 5 h at 259.4 °C). This latter fact follows in line with the observation that a secondary hydrogen is more readily transferred to the ester carbonyl than is a primary hydrogen in the 1,5-hydrogen transfer ring opening of methyl *cis*-2-alkylcyclopropanecarboxylates (11). In this case the tertiary hydrogen of **1** is more readily transferred than the secondary hydrogen of **4**.

Methyl 2,4-Dimethyl-2- and 3-pentenoates

Methyl *cis*- and *trans*-2,4-dimethyl-2-pentenoate (**7** and **8**) were prepared in 83% yield by the procedure used to prepare **1** and **2** except that an α-phosphonopropionate was used. Methyl 2,4-dimethyl-3-pentenoate (**9**) was prepared by heating **7** for 5 days at 281 °C. The resulting mixture contained over 90% of **9**.

Examination of the equilibrium data in Table III shows that both reactions 1 and 2 are slower

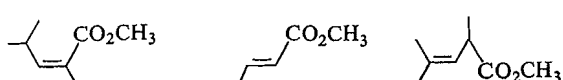

7 **8** **9**

than experienced in the series **1**, **2**, and **3**. Above 300 °C decomposition and polymerization becomes extensive. To obtain equilibrium values it

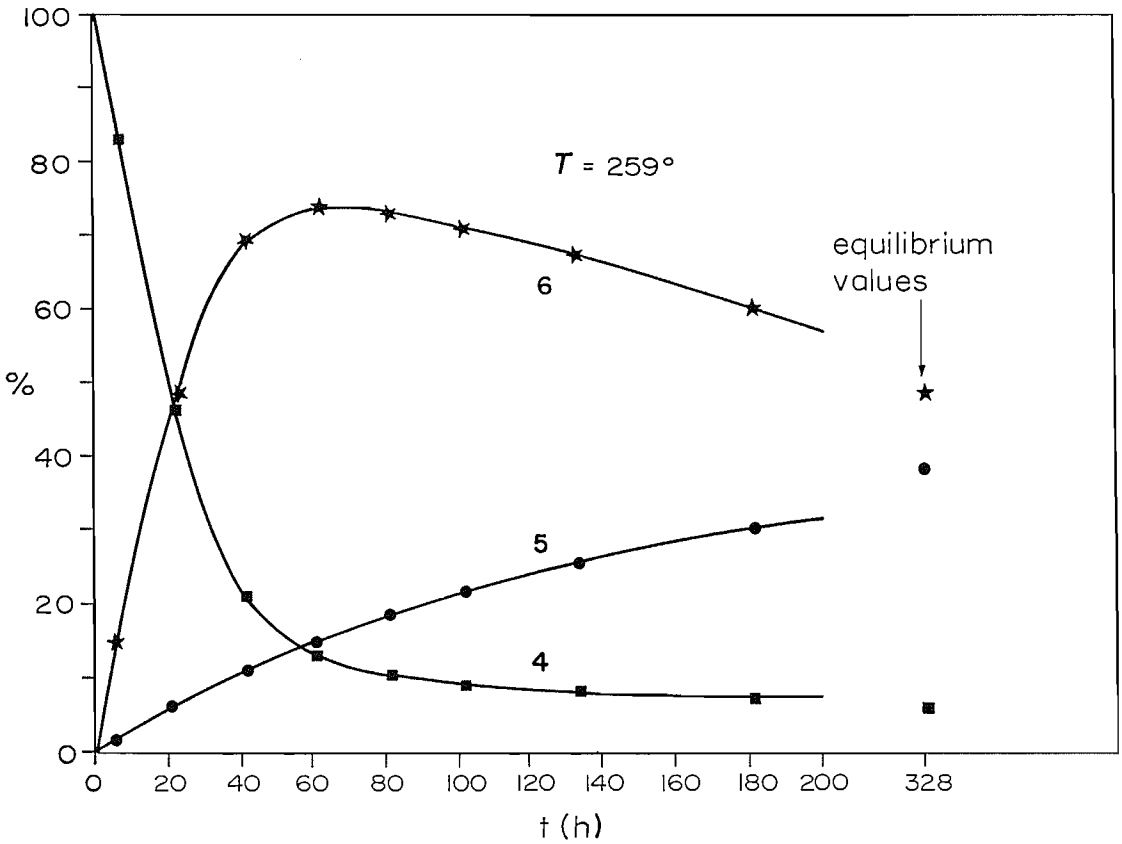

FIG. 2. Isomerization of methyl *cis*-2-pentenoate (**4**).

TABLE III

Thermal rearrangement of methyl 2,4-dimethyl-2- and 3-pentenoates (**7**, **8**, and **9**) at 297 °C

Initial olefin	Time (h)	Products		
		7	**8**	**9**
7*	30	28	2	70
7	17	17	2	81
7	83	10	4	86
7	151	9	7	84
7:8 (70:30)	360	8	33	59
7:8 (60:40)	360	7	39	54
ref. (14)		7	38	55
8	83	3	75	22
8	151	3	70	27
8	174	4	68	28
9*	36	2	—	98
9*	155	6	—	94
9	83	7	—	93
9	151	8	trace	92

*Temperature 284 °C.

was necessary to observe the trends for mixtures containing varying amounts of the *trans* isomer **8**. The equilibrium was found to be near a ratio of 7:39:54 for **7**, **8**, and **9** respectively. Kinstle (14) has obtained a similar value of 6:38:56 by equilibrating this system in ethylene glycol in the presence of sodium glycolate at 195 °C for 87 h. During the base-catalyzed equilibration by Kinstle a fourth isomer 2,4-dimethyl-4-pentenoate which is a γ,δ-unsaturated ester builds up to 17% of the total product. No evidence for such an isomer was found in our work.

Since $k_1 \ll k_2$ it was again possible to determine k_2 from the first-order plot of the disappearance of **7** and k_2 was found to be $0.91 \times 10^{-5}\ s^{-1}$ at 272.2 °C, $1.27 \times 10^{-5}\ s^{-1}$ at 283.7 °C and $2.98 \times 10^{-5}\ s^{-1}$ at 297.4 °C. These constants however did not yield a linear activation energy plot and calculations based on pairs of points gives $\Delta H\dagger$ anywhere from 16 to 38 kcal/mole. Possibly side reactions are inter-

Can. J. Chem. Downloaded from www.nrcresearchpress.com by 210.87.254.42 on 09/05/12
For personal use only.

Can. J. Chem. Downloaded from www.nrcresearchpress.com by 210.87.254.42 on 09/05/12
For personal use only.

fering at the high temperatures required making the data less reliable, however this is not apparent in the rate plots.

Qualitatively, however, it is interesting to note the effect of additional substitution on the α-carbon. The value of k_2 for the reaction of **1** when extrapolated to 272.2 °C is 16.5×10^{-5} s^{-1} corresponding to an 18-fold increase when compared with the k_2 value of 0.91×10^{-5} s^{-1} for the reaction of **7**. This fact may reflect a steric hindrance in the reaction of **7** due to the α-methyl which would affect the ease with which the methoxyl of the ester might assume planarity with the double bond as required by reaction 4.

Methyl 2-Methyl-2- and 3-pentenoates

Methyl *cis*- and *trans*-2-methyl-2-pentenoate (**10** and **11**) and methyl *trans*-2-methyl-3-pentenoate (**12**) have also been studied qualitatively.

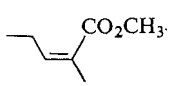

10

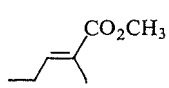

11

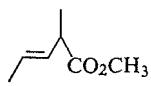

12

Equilibrium could not be reached satisfactorily at 297 °C but the equilibrium ratio approached the value of 15:55:30 for **10**, **11**, and **12**. The rate constants k_2 and k_1 at 297.4 °C are sufficiently close to each other that conversion of **10** to **12** followed with time gives a maximum value for **12** of 42% only slightly above the equilibrium value. This implies a reduction in k_2 due to the methyl on the α-carbon similar to that noted above for the reaction of **7**.

Nuclear Magnetic Resonance Results

The n.m.r. spectra of all new compounds are recorded in the Experimental. The data provide an extension to some data originally assembled by Jackman and Wiley (15) which form the bases of much useful stereochemical work. Of particular interest in the present series of compounds is the magnitude of the vicinal coupling constant between the methine hydrogen of a β-isopropyl group and the β-hydrogen illustrated in structure **13**. When Y is hydrogen (**2**) this coupling is 6.5 Hz which is a normal value when compared with

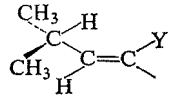

13

the corresponding values of 6.9 and 7.3 Hz found in *cis*- and *trans*-crotonate respectively (16). If however Y is CH_3 (**8**) or CO_2CH_3 (**1** and **7**) then the coupling constants are 9.6, 9.2, and 9.6 Hz respectively. These values clearly reflect a conformational preference by the isopropyl group towards the form with the coupled hydrogens *trans* and indicate some steric interaction between the methyls of the isopropyl group and Y. This steric interaction however is expected to be small and to have little influence on the ground state energy of systems where it exists. Evaluation of the steric factor due an isopropyl group *cis* to a methyl compared with a methyl *cis* to a methyl showed little difference between these groups (17).

The effect of the conformational preference of an isopropyl group is also noticeable from the chemical shift of the methine hydrogen which for **1** is 1.19 τ to lower field than in **2** and for **7** is 0.61 τ to lower field than **8**. The corresponding shift in methyl *cis*- and *trans*-crotonates is 0.26 Δτ (16). This difference is undoubtedly due to the closer net distance between the methine hydrogen and the carbonyl group in **1** and **7**, than the net distance between the hydrogens on the methyl and the carbonyl in *cis*-crotonate. A steric interaction between the α-methyl and the carbomethoxy group has been suggested above, for kinetic reasons, in discussing the reaction **7** → **9** and may also be the factor contributing towards the difference between the values of 1.19 Δτ and 0.61 Δτ found for these related systems.

Conclusions

Equilibrium

Many studies have attempted to correlate olefin stability with conjugative or steric factors (3–5, 18, 19). Our data cannot add much to the previous arguments. Some comments, however, are in order. In all such discussions the amount of *cis* α,β-unsaturated isomer is assumed negligible. The present data and the data from earlier work on esters (8) show however that the *cis* isomer can be an important member of the equilibrium mixture and this is particularly so when there is an α-methyl group. The series provided by compounds **7**, **8**, and **9** is of particular interest for between each, with three similar groups attached to the carbons of the double bond, we might expect to find negligible free energy differences due to steric factors. The

Can. J. Chem. Downloaded from www.nrcresearchpress.com by 210.87.254.42 on 09/05/12
For personal use only.

predominance of the β,γ-isomer **9** at equilibrium suggests that conjugation with a carbomethoxy group need not be considered more important for stabilization than conjugation with an alkyl group by the double bond. There is also no apparent reason why the *cis:trans* ratio of the α,β-unsaturated esters should not be 1:1 rather than 1:5.5. This problem is discussed further elsewhere (20).

Kinetics

The kinetic results have provided evidence that formation of a β,γ-isomer from a *cis* α,β-isomer is a unimolecular process and is favored over the direct conversion of a *trans* α,β-isomer into a β,γ-isomer. This process is undoubtedly a cyclic 1,5-transfer of hydrogen and is faster when the hydrogen to be transferred is tertiary than when it is secondary. The case where the hydrogen to be transferred is primary (methyl crotonate) has been studied in the gas phase (21) but it was not possible from that study to isolate reaction 2 and the mechanism for the formation of methyl vinylacetate was left in doubt. Two facts suggest to us that reaction 4 is general for esters and ketones. The first is the ease by which equilibrium is achieved between α,β- and β,γ-unsaturated systems. At the same time positional isomerism further along the chain appears to require a catalyst. For example the ethyl esters corresponding to **7**, **8**, and **9** on treatment with sodium glycolate in ethylene glycol yield up to 17% of a γ,δ-isomer (14). We have also found that heating γ,δ-isomers does not lead to positional isomers (11). We therefore conclude, that although reaction 4 has been proven in a limited number of cases, that it may in fact be the general mode of thermal isomerization for these systems.

Experimental

The techniques used for compound isolation and identification as well as the method for carrying out kinetics and equilibrium measurements are described in the accompanying paper (11). Preparation and properties of new compounds are given below.

*Methyl cis- and trans-4-Methyl-2-pentenoate (**1** and **2**)*

Trimethyl phosphonoacetate—A mixture of 77 g (0.5 mole) of methyl bromoacetate and 87 g (0.7 mole) of trimethyl phosphite was heated in a 500 ml two-necked, round-bottom flask equipped with a thermometer and a condenser which was connected to a dry-ice acetone trap. As the temperature was increased above 80 °C methyl bromide began to distill from the reaction and ceased when the reaction temperature reached 160 °C after 2 h. Distillation of the resulting solution gave 73 g (80%) of trimethyl phosphonoacetate, b.p. 85–86 °C at 0.08 mm.

Anal. Calcd. for $C_5H_{11}O_5P$: C, 32.97; H, 6.09. Found: C, 32.63; H, 6.37.

To a suspension of 14.4 g (0.3 mole) of sodium hydride (49% dispersion in oil) in 300 ml of glyme (distilled from sodium hydride) was added with stirring at 15–20 °C 54.6 g (0.3 mole) of trimethyl phosphonoacetate. After addition was complete it was stirred at 15 °C for 1 h, then warmed to 35 °C for 5 min and cooled to 15 °C. To the stirred solution was added 22 g (0.3 mole) of isobutyraldehyde over a 15 min interval. After 20 min stirring at room temperature 200 g of ice was added and the solution was extracted with ether. The ether extracts were washed with water and dried over anhydrous sodium sulfate. The crude product 17.6 g (46%) isolated from the ether was shown to contain **1** and **2** in the ratio of 31:69. Fractional distillation through a spinning band column gave 5.2 g, b.p. 138–140 °C and 9.2 g, b.p. 148–150 °C. Methyl *cis*-4-methyl-2-pentenoate (**1**), b.p. 140 °C, n_D^{22} 1.4225, showed infrared bands at 1723, 1650, and 1417 cm^{-1}. The nuclear magnetic resonance (n.m.r.) spectrum had peaks at τ 4.03 (two doublets with J_{cis} = 11.4 Hz and $J_{1,2}$ = 9.2 Hz for the hydrogen on the β-carbon), τ 4.43 (doublet with J = 11.4 Hz for the hydrogen on the α-carbon), τ 6.36 (ester methyl), τ 6.35 (multiplet for the methine hydrogen), and τ 8.99 (doublet with J = 6.6 Hz for the terminal methyls).

Anal. Calcd. for $C_7H_{12}O_2$: C, 65.59; H, 9.44. Found: C, 65.60; H, 9.56.

Methyl *trans*-4-methyl-2-pentenoate (**2**), b.p. 150 °C, n_D^{22} 1.4298, showed infrared bands at 1723, 1657, and 990 cm^{-1}. The n.m.r. spectrum had peaks at τ 3.14 (two doublets with J_{trans} = 15.8 Hz and $J_{1,2}$ = 6.5 Hz for the hydrogen on the β-carbon) τ 4.32 (two doublets with J_{trans} = 15.8 Hz and $J_{1,3}$ = 1.4 Hz), τ 6.34 (ester methyl), τ 7.54 (multiplet for the methine hydrogen), and τ 8.91 (doublet with J = 6.7 Hz for the terminal methyls).

*Methyl 4-Methyl-3-pentenoate (**3**)*

A sample of 1 ml of methyl *cis*-4-methyl-2-pentenoate (**1**) was heated for 3 h in a sealed tube at 294 °C to give a mixture containing over 97% of **3** (analyzed by vapor-phase chromatography (v.p.c.) using a dinonyl phthalate column at 160 °C). A purified sample of **3**, b.p. 153.5 °C, n_D^{22} 1.4298 (lit (22), b.p. 145–148 °C at 640 mm, n_D^{25} 1.4302) showed n.m.r. peaks at τ 4.75 (multiplet for the vinyl hydrogen), τ 7.08 (doublet with J = 7.2 Hz for the C-2 methylene hydrogens), τ 6.40 (ester methyl), τ 8.26 and 8.37 (for the C-4 methyls).

Anal. Calcd. for $C_7H_{12}O_2$: C. 65.59; H, 9.44. Found: C, 65.49; H, 9.55.

*Methyl cis- and trans-2,4-Dimethyl-2-pentenoate (**7** and **8**)*

The procedure used to make **1** and **2** was followed except that triethylphosphite was reacted with methyl α-bromopropionate to give the Wittig reagent methyl *C*-methyl-*P*-diethyl-α-phosphonopropionate, b.p. 62–65 °C at 0.15 mm which was reacted with isobutyraldehyde. The conditions of the reaction gave *trans* esterification and thus yielded both ethyl and methyl ester products. The combined ester product was hydrolyzed with 30% potassium hydroxide solution and the acidified solution was extracted with ether. The dried ether solution was

Can. J. Chem. Downloaded from www.nrcresearchpress.com by 210.87.254.42 on 09/05/12
For personal use only.

treated with diazomethane to give on evaporation a good yield of a mixture of **7** and **8** in the ratio of 71:29.

Methyl *cis*-2,4-dimethyl-2-pentenoate (7), b.p. 149.5 °C, n_D^{25} 1.4308 (lit. (23), b.p. 58–59 °C at 23 mm, n_D^{20} 1.4328) had n.m.r. peaks at τ 4.38 (two quartets with $J_{1,2} = 9.6$ Hz and $J_{1,3} = 1.4$ Hz for the hydrogen on the β-carbon), τ 6.32 (ester methyl), τ 6.75 (multiplet for the methine hydrogen), τ 8.18 (doublet with $J = 1.4$ Hz for the methyl on the α-carbon), and τ 9.04 (doublet with $J = 6.7$ Hz for the terminal methyls).

Anal. Calcd. for $C_8H_{14}O$: C, 67.57; H, 9.93. Found: C, 67.38; H, 10.00.

Methyl *trans*-2,4-dimethyl-2-pentenoate (**8**), b.p. 165 °C n_D^{25} 1.4365 (lit. (23), b.p. 49–50 °C at 10 mm, n_D^{20} 1.4383) had n.m.r. peaks at τ 3.51 (two quartets with $J_{1,2} = 9.6$ Hz and $J_{1,3} = 1.4$ Hz for the hydrogen on the β-carbon), τ 6.33 (ester methyl), τ 7.36 (multiplet for the methine hydrogen), τ 8.20 (doublet with $J = 1.4$ Hz for the methyl on the α-carbon), and τ 8.98 (doublet with $J = 6.7$ Hz for the terminal methyls).

Anal. Calcd. for $C_8H_{14}O$: C, 67.47; H, 9.93. Found: C, 67.85; H, 9.71.

*Methyl 2,4-Dimethyl-3-pentenoate (**9**)*

A sample of 2 ml of methyl *cis*-2,4-dimethyl-2-pentenoate (**7**) was heated for 5 days in a sealed tube at 281 °C to give a mixture containing over 90% of **9** (analyzed by v.p.c. using a dinonyl phthalate column at 160 °C). A purified sample of **9**, b.p. 159.5 °C, n_D^{27} 1.4280, showed n.m.r. peaks at τ 4.89 (multiplet for the vinyl hydrogen), τ 6.38 (ester methyl), τ 6.76 (multiplet for the C-2 methine hydrogen), τ 8.28 and 8.34 (doublets with $J = 1.4$ Hz for the terminal methyls) and τ 8.48 (doublet with $J = 7.1$ Hz for the methyl on C-2).

Anal. Calcd. for $C_8H_{14}O$: C, 67.57; H, 9.93. Found: C, 67.74; H, 9.92.

*Methyl trans-2-Methyl-3-pentenoate (**12**)*

A sample of 1 ml of methyl *cis*-2-methyl-2-pentenoate (**10**) (8) was heated in a sealed tube for 85 h at 294 °C and yielded a mixture of **9**, **10**, and **12** in the ratio of 18:40:42 (analyzed on a dinonylphthalate column at 152 °C). Methyl *trans*-2-methyl-3-pentenoate (**12**), b.p. 140 °C, n_D^{23} 1.4217, (lit. (8), b.p. 139 °C, n_D^{23} 1.4229) had n.m.r. peaks at τ 4.51 (multiplet for the vinyl hydrogens), τ 6.39 (ester methyl), τ 7.00 (multiplet for the hydrogen on C-2), τ 8.31 (doublet with $J = 6.5$ Hz for the terminal methyl), and τ 8.98 (doublet with $J = 7.1$ Hz for the methyl on C-2).

Anal. Calcd. for $C_7H_{12}O_2$: C, 65.59; H, 9.44. Found: C, 65.77; H, 9.68.

Acknowledgments

The authors gratefully appreciate the support received for this work from the National Research Council of Canada and from the Committee on Research of the University of British Columbia. A University Microfilms Inc. copy of the Thesis of Dr. T. H. Kinstle entitled "Equilibration of Unsaturated Esters" University of Illinois 1963 has been used and was of particular help throughout. Correspondence with Professor S. J. Rhoads has been stimulating and helpful.

1. R. B. CUNDALL. Progress in reaction kinetics. Vol. 2. The Macmillan Co., New York. 1964. Chap. 4.
2. H. H. VOGE and N. C. MAY. J. Am. Chem. Soc. **68**, 550 (1946).
3. K. L. RINEHART, JR. and L. J. DOLBY. J. Org. Chem. **22**, 13 (1957).
4. H. ADKINS. Organic chemistry. 2nd ed., Vol. I. *Edited by* H. Gilman. John Wiley and Sons, Inc., New York. 1943. p. 1042.
5. L. BATEMAN and J. I. CUNNEEN. J. Chem. Soc. 2283 (1951).
6. B. S. RABINOVITCH and K. W. MICHEL. J. Am. Chem. Soc. **81**, 5065 (1959).
7. R. B. CUNDALL and T. F. PALMER. Trans. Faraday Soc. **57**, 1936 (1961).
8. D. E. MCGREER, W. WAI, and G. CARMICHAEL. Can. J. Chem. **38**, 2410 (1960).
9. J. WOLINSKY, B. CHOLLAR, and M. D. BAIRD. J. Am. Chem. Soc. **84**, 2775 (1962).
10. R. J. ELLIS and H. M. FREY. J. Chem. Soc. 5578 (1964).
11. D. E. MCGREER and N. W. K. CHIU. Can. J. Chem. This issue.
12. N. C. YANG and M. J. JORGENSON. Tetrahedron Letters, **19**, 1203 (1964).
13. M. J. JORGENSON. Chem. Commun. 137 (1965).
14. T. H. KINSTLE. Ph.D. Thesis. The University of Illinois. 1963.
15. L. M. JACKMAN and R. H. WILEY. J. Chem. Soc. 2881 (1960).
16. R. R. FRASER and D. E. MCGREER. Can. J. Chem. **39**, 505 (1961).
17. R. B. TURNER, D. E. NETTLETON, JR., and M. PERELMAN. J. Am. Chem. Soc. **80**, 1430 (1958).
18. J. W. BAKER. Hyperconjugation. The Clarendon Press, Oxford. 1952. p. 58.
19. P. B. DE LA MARE, E. D. HUGHES, and C. K. INGOLD. J. Chem. Soc. 22 (1948).
20. D. E. MCGREER and B. D. PAGE. To be published.
21. J. N. BUTLER and G. J. SMALL. Can. J. Chem. **41**, 2492 (1963).
22. J. B. ROGAN. J. Org. Chem. **27**, 3910 (1962).
23. S. G. BATRAKOV and L. D. BERGELSON. Izvest. Akad. Nauk Kazakh S.S.R. Ser. Khim. 1640 (1964); Chem. Abst. **62**, 429*f* (1965).

Can. J. Chem. Downloaded from www.nrcresearchpress.com by 210.87.254.6 on 09/05/12
For personal use only.

Reaction of chloral with naphthalene, and the synthesis of α-methoxynaphthylacetic acids from naphthyl(trichloromethyl)carbinols

WILKINS REEVE, JOHN C. HOFFSOMMER, AND PATRICK F. ALUOTTO
Department of Chemistry, University of Maryland, College Park, Maryland
Received November 20, 1967

From the Friedel–Crafts reaction of chloral and naphthalene, others have reported the isolation of only 2-naphthyl(trichloromethyl)carbinol. Our reexamination of this reaction has shown that a mixture of 1- and 2-naphthyl(trichloromethyl)carbinols is obtained and that 80 to 90% of the product consists of the 1-naphthyl(trichloromethyl)carbinol. The 1- and 2-naphthyl(trichloromethyl)carbinols, their acetates, and their methyl ethers differ in their nuclear magnetic resonance (n.m.r.) spectra in that the signal of the α-hydrogen of the side chain of the 1-naphthyl isomer always occurs 0.8 p.p.m. downfield compared to the signal of the α-hydrogen of the corresponding 2-naphthyl isomer. This is because the α-hydrogens in the 1-naphthyl series of these compounds are in the region between the 1- and 8-positions of the naphthalene ring and subject to the ring currents of both benzenoid rings.

The mixture of crude naphthyl(trichloromethyl)carbinols was converted to the mixture of α-methoxynaphthylacetic acids, and these were separated. A small amount of α,α′-dimethoxy-1,5-naphthalenediacetic acid was also obtained, demonstrating that a certain amount of 1,5-substitution occurred in the Friedel–Crafts reaction of naphthalene and chloral.

Canadian Journal of Chemistry, 46, 2233 (1968)

The study of the reaction of chloral with naphthalene is of some interest because substitution might occur in either the 1- or 2-positions. For instance, acetyl chloride in a Friedel–Crafts reaction with naphthalene gives predominantly the 1-isomer when carbon disulfide is the solvent; but with nitrobenzene as the solvent the 2-isomer is formed preferentially, presumably because the solvent forms a larger complex with the oxocarbonium ion and steric considerations strongly favor attack of this larger complex on the more open 2-position (for a review, consult ref. 1). Since the chloral molecule is certainly larger than the acetyl group, one might expect that substitution in the 2-position would be favored.

In the aluminium chloride catalyzed reaction of naphthalene with chloral, the amount of aluminium chloride employed is a critical factor in determining the nature of the products formed. Under optimum conditions, a mixture of the 1- and 2-naphthyl(trichloromethyl)carbinols is formed. With more aluminium chloride, or under more severe reaction conditions, the reaction proceeds beyond the carbinol stage to form a mixture of trichlorodinaphthylethanes and dehydrohalogenated products; with less aluminium chloride, the reaction is incomplete. The first studies on the reaction of naphthalene with chloral were carried out with excessive amounts of aluminium chloride and none of the naphthyl(trichloromethyl)carbinols were obtained (2). More recently, two groups have studied this reaction and worked out the conditions for obtaining the naphthyl(trichloromethyl)carbinols in 24 to 28% yields and they reported the isolations of only the 2-naphthyl isomer (3–5). This was contrary to the results we were obtaining at about the same time which showed the reaction product to be a mixture of the 1-naphthyl and 2-naphthyl isomers with the 2-naphthyl(trichloromethyl)carbinol the minor component.

Our work had involved the reaction of naphthalene with chloral and aluminium chloride, with nitrobenzene or carbon disulfide as solvents, and the conversion of the naphthyl(trichloromethyl)carbinols to the corresponding mixture of α-methoxy-1- and 2-naphthylacetic acids. These could be separated semiquantitatively and formed the basis for our conclusion that the reaction occurred predominantly at the 1-position of naphthalene. We have now repeated our work and the work of the French workers, analyzed the carbinol mixture obtained under their and our experimental conditions by nuclear magnetic resonance (n.m.r.) spectra, and shown conclusively that under all reaction conditions, the major product is the 1-naphthyl(trichloromethyl)carbinol. Our results are summarized in Table I.

It is apparent that under all conditions, the substitution occurs between 80 and 90% in the 1-position, and that the choice of solvent does play a real but minor role within this range.

The n.m.r. spectra are of unusual interest

TABLE I

Friedel–Crafts reaction of chloral with naphthalene to form 1- and 2-$C_{10}H_7$—CHOH—CCl_3

Naphthalene (mole)	Chloral (mole)	$AlCl_3$ (mole)	Solvent	Reaction temperature	Carbinol mixture Yield (%)	Carbinol mixture Ratio 1-/2-substitution	Carbinol mixture Method of analysis
0.2	0.4	0.06	Nitrobenzene	0°	61	7 to 1	*
0.2	0.4	0.06	Nitrobenzene	0°	61	6 to 1	†
0.2	0.4	0.06	Carbon disulfide	0°	56	9 to 1	*
0.2	0.4	0.04‡	Cyclohexane	0°	39‡	4 to 1	†

*By conversion to a mixture of α-methoxy(1- and 2-naphthyl)acetic acids, and by separation of these.
†By nuclear magnetic resonance.
‡Reaction conditions followed Broquet-Borgel (5) including the use of freshly sublimed aluminium chloride.

because of certain consistent and pronounced differences in the spectra of the 1- and 2-substituted naphthalene compounds. Considering first the naphthyl(trichloromethyl)carbinols, the side chain α-hydrogen for the 1-substituted naphthalene (**1**) is found to be shifted almost 0.8 p.p.m. downfield relative to the α-hydrogen in the 2-substituted naphthalene (**2**). The same downfield shift is observed with the acetates and also the methyl ethers of the two carbinols; in each of these cases the α-hydrogen signal occurs slightly over 0.8 p.p.m. downfield in the 1-substituted naphthalene relative to the 2-substituted naphthalene. This also occurs in the isomeric α-methoxynaphthylacetic acids to the extent of 0.4 p.p.m. This consistent behavior can be explained by placing the hydrogen attached to the side chain α-carbon of the 1-substituted naphthalenes in the region between the 1- and 8-positions of the naphthalene ring where the ring currents from both rings have a maximum effect and cause the larger downfield shift. A study of models shows that the 1-substituted naphthalenes must have this conformation since the larger groups are excluded from this position by steric considerations.

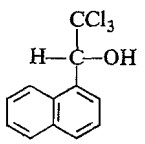

1

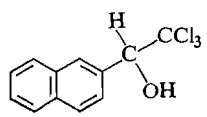

2

The isomeric methylnaphthalenes exhibit a similar pattern of chemical shifts (6), but the differences in the chemical shifts of the two methyl groups is less than one quarter of that observed with the carbinols and their derivatives.

With the 1- and 2-naphthyl(trichloromethyl)-carbinols showing such different chemical shifts for the side chain hydrogen, mixtures of the isomeric carbinols could be unambiguously and accurately analyzed by comparing areas under these two peaks.

Our study of the naphthalene–chloral Friedel–Crafts reaction was originally undertaken in the expectation of forming the 2-naphthyl(trichloromethyl)carbinol and converting this to α-methoxy-2-naphthylacetic acid by reaction with methanolic potassium hydroxide (7). This methoxy acid might serve as a source of additional 2-naphthyl compounds difficult to obtain by other methods. The sodium hydrogen di-(α-methoxy-2-naphthylacetate) is the least soluble of the known sodium acid salts of the α-methoxy acids (8) and was being studied as a reagent for sodium. While the composition of the mixture of isomeric carbinols was not as expected, the positive achievements of this part of the work were the elucidation of the reaction conditions so that the mixture of carbinols could be obtained in 61% yield, the conversion of the mixture of carbinols to the corresponding mixture of the isomeric α-methoxynaphthylacetic acids, and the semiquantitative separation of these isomeric acids.

The optimum conditions for the reaction of naphthalene with chloral involved treating a nitrobenzene solution of 1 mole of naphthalene and 2 mole of chloral with 0.3 mole of aluminium chloride at 0 °C. The conversion of the carbinol mixture to the mixture of isomeric α-methoxynaphthylacetic acids was accomplished by the usual procedure involving treatment with methanolic potassium hydroxide at 50 °C (7) (Reaction Scheme 1). Their separation was accomplished semiquantitatively by taking advantage

Can. J. Chem. Downloaded from www.nrcresearchpress.com by 210.87.254.6 on 09/05/12
For personal use only.

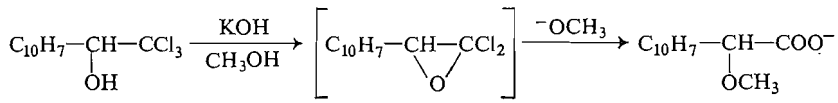

of the fact that the α-methoxy-2-naphthylacetic acid forms a *normal* sodium salt insoluble in 2.3 *N* sodium hydroxide solution; under the same conditions, the isomeric 1-naphthyl salt remains in solution. The compositions of the carbinol mixtures determined by this two-step chemical method are in agreement with the later n.m.r. analyses.

Although the α-methoxy-2-naphthylacetic acid forms an insoluble sodium *acid* salt and the pure 1-naphthyl isomer does not (8), this difference could not be used in their separation. When both acids were present, they coprecipitated as a non-stoichiometric sodium acid salt mixture from which acetone would extract the 1-naphthyl isomer only incompletely. Repeated reprecipitation of the sodium acid salt mixture only partially eliminated the 1-naphthyl isomer.

Since the sulfonation of naphthalene is a reversible reaction, and some Friedel–Crafts reactions are reversible, attempts were also made to convert the 1-naphthyl(trichloromethyl)carbinol into its 2-naphthyl isomer by heating at 200 °C for 2 h both with and without hydrogen chloride being present. No isomerization was detected. Likewise, no isomerization was detected on stirring a carbon disulfide solution of the 2-naphthyl(trichloromethyl)carbinol (0.0036 mole) with aluminium chloride (0.001 mole) for 24 h at 25 °C.

From a large scale run with 5 moles of naphthalene, 15 g of a crude high-melting acid crystallized from a benzene extract of the mixture of isomeric acids, and from this by repeated recrystallization from several solvents, 1.5 g of pure α,α′-dimethoxy-1,5-naphthalenediacetic acid was obtained. The structure was assigned on the basis of analytical data, the infrared spectrum which agrees with that of disubstituted naphthalenes having a symmetrical structure with three adjacent unsubstituted positions in each ring (9), and the n.m.r. spectrum which clearly showed both side chain α-hydrogens to be equivalent in that they give only a single signal at δ 5.57. For comparison purposes, the α-hydrogen of α-methoxy-1-naphthylacetic acid gives a signal at δ 5.5 and the corresponding signal for the α-methoxy-2-naphthylacetic acid occurs at δ 5.05. It clearly follows from this and from the infrared spectra that the disubstituted acid must have the naphthalene ring symmetrically substituted in the α-positions, and must therefore be either 1,5 or 1,8. The latter can be eliminated because 1,8 substitution does not occur with 1-substituted naphthalenes; also, two side chain α-hydrogens could not both fit into the same region between the 1- and 8-positions and the n.m.r. signals observed would be therefore either a singlet or a doublet upfield from the characteristic δ 5.5 position.

Tetralin has been reported to condense with chloral exclusively in the 2-position (3, 5) and our work confirms this. Treatment of the 5,6,7,8-tetrahydro-2-naphthyl(trichloromethyl)carbinol with methanolic potassium hydroxide yielded the oily α-methoxy-1,2,3,4-tetrahydronaphthalene-6-acetic acid which formed an insoluble sodium acid salt. Attempts to dehydrogenate the carbinol and also the sodium salt of the methoxy acid to the naphthalene analogues were unsuccessful.

Experimental

All melting points are corrected. Nuclear magnetic resonance (n.m.r.) spectra were recorded with a Varian A-60A. Analyses were performed by Mrs. Kathryn G. Baylouny, Mrs. Jane R. Ratka, and Dr. Franz J. Kasler.

1-Naphthyl(trichloromethyl)carbinol

To an ether–benzene solution of 1-naphthylmagnesium bromide, prepared from 100 g (0.48 mole) of 1-bromonaphthalene and 12 g of magnesium, were added 73 g (0.48 mole) of anhydrous chloral over a 3 h period. The reaction mixture was maintained at ice-bath temperature during the addition and then stirred at room temperature for 4 h before working up in the usual way. There was obtained 77 g (58% of theory) of the crude carbinol as a yellow-orange oil, b.p. 170–190 °C at 6 mm. It was purified by conversion to the acetate.

The acetate was prepared by refluxing 10 g of the crude carbinol with 75 ml of acetic anhydride for 3 h, after which the reaction mixture was poured into 400 ml of an ice and water mixture and stirred vigorously for 30 min. The oily layer was separated and allowed to dry; it then solidified. Recrystallization from ethanol–water gave 8 g of white crystalline *1-naphthyl(trichloromethyl)methyl acetate*, m.p. 82–83 °C. The infrared (i.r.) spectrum (KBr pellet) showed absorption bands at 3045, 2980, 1730, 1360, 1190, 1025, 920, 875, 770, 725, 665, 625, and 605 cm^{-1}. Signals in the n.m.r. spectrum (in CCl_4) appeared

Can. J. Chem. Downloaded from www.nrcresearchpress.com by 210.87.254.6 on 09/05/12
For personal use only.

Can. J. Chem. Downloaded from www.nrcresearchpress.com by 210.87.254.6 on 09/05/12
For personal use only.

at δ 8.5 to 7.1, multiplet (7 ring protons); 7.28, singlet (—C*H*(OAc)—); 2.13, singlet (3 protons, —CH_3).

Anal. Calcd. for $C_{14}H_{11}O_2Cl_3$: C, 52.93; H, 3.49; Cl, 33.49. Found: C, 53.09; H, 3.40; Cl, 33.20.

The acetate was hydrolyzed by refluxing for 8 h a solution of 3 g of the acetate in 10 ml of ethanol, 15 ml of water, and 10 ml of concentrated hydrochloric acid. After separating and drying the yellow-brown oil in a vacuum oven, it slowly solidified; 2 g were obtained. Recrystallization from cyclohexane gave white *1-naphthyl(trichloromethyl)carbinol*, m.p. 59 °C in agreement with the literature value (4, 5). The infrared spectrum of the oil showed absorption bands at 3525 (shoulder), 3340, 3055, 2920, 2845, 1600, 1510, 1395, 1350, 1260, 1230, 1205, 1165, 1075, 1015, 975, 870, 820, 790, 770, 730, 660, 635, and 600 cm^{-1}. Signals in the n.m.r. spectrum (in CCl_4) appeared at δ 8.2 to 7.1, multiplet (7 ring protons); 5.97, singlet (—C*H*OH—); 3.42, broad singlet (—CHO*H*—).

The carbinol was converted to its methyl ether by treating 5 g of the crude product dissolved in 25 ml of methyl iodide with 5 g of silver oxide (for preparation, see ref. 10) at 0 °C for 20 h. The oily product solidified; recrystallization from aqueous ethanol gave 3 g of *methyl 1-naphthyl(trichloromethyl)methyl ether* melting at 76 °C. The infrared spectrum (KBr pellet) showed absorption bands at 3060, 2990, 2910, 2820, 1590, 1510, 1440, 1225, 1190, 1160, 1100, 1010, 875, 800, 775, 730, 675, 640, 615, and 550 cm^{-1}. Signals in the n.m.r. spectrum (compound dissolved in CCl_4) appeared at δ 8.33 to 7.27, multiplet (7 ring protons); 5.52, singlet (—C*H*=); 3.40, singlet (3 protons of —OCH_3).

Anal. Calcd. for $C_{13}H_{11}OCl_3$: C, 53.91; H, 3.83; Cl, 36.72. Found: C, 53.70; H, 3.70; Cl, 36.60.

2-Naphthyl(trichloromethyl)carbinol

This was prepared in the same way as the above carbinol. From 45 g of 2-bromonaphthalene, there was obtained 22 g (37% of theory) of the oily carbinol, b.p. 180–190 °C at 2 mm. This solidified and was recrystallized from petroleum ether giving 14 g of the pure carbinol, m.p. 101–102 °C in agreement with the literature value (4, 5). The infrared spectrum (KBr pellet) showed absorption bands at 3470 (broad), 1590, 1355, 1290, 1230, 1160, 1120, 1070, 990, 950, 905, 880, 860, 810 to 840, 745, 720, 660, 615, 565, 515, and 475 cm^{-1}. Signals in the n.m.r. spectrum (in CCl_4) appeared at δ 8.0 to 7.3, multiplet (7 ring protons); 5.2, doublet (J = 4 c.p.s.) (—C*H*OH—); and 3.37, doublet (J = 4 c.p.s.) (—CHO*H*—).

The acetate was prepared by refluxing 4 g of the carbinol with 40 ml of acetic anhydride for 12 h. On pouring into ice-water, 5.5 g of the solid acetate was obtained. The *2-naphthyl(trichloromethyl)methyl acetate* melted at 110–112 °C after recrystallization from aqueous ethanol. The infrared spectrum (KBr pellet) showed absorption bands at 3050, 2940, 1750, 1370, 1210, 1170, 1125, 1060, 930, 905, 865, 840, 820, 790, 740, and 675 cm^{-1}. Signals in the n.m.r. spectrum (in CCl_4) appeared at δ 8.2 to 7.3, multiplet (7 ring protons); 6.43, singlet (1 proton of —C*H*OAc); 2.18, singlet (3 protons of —CH(OCOC*H*$_3$)—).

Anal. Calcd. for $C_{14}H_{11}O_2Cl_3$: C, 52.93; H, 3.49; Cl, 33.49. Found: C, 52.75; H, 3.62; Cl, 33.30.

The methyl ether was prepared from the carbinol by methylation with excess methyl iodide and silver oxide as in the previous case. The *methyl 2-naphthyl(trichloromethyl)methyl ether* melted at 49–50 °C after crystallization from ethanol. The infrared spectrum (KBr pellet) showed absorption bands at 1600, 1450, 1330, 1265, 1190, 1100, 1000, 905, 880, 865, 840, 810, 750, 725, 670, 625, 570, 510, and 475 cm^{-1}. Signals in the n.m.r. spectrum (in CCl_4) appeared at δ 7.9 to 7.2, multiplet (7 ring protons); 4.70, singlet (1 proton of —C*H*(OCH$_3$)—); 3.43, singlet (3 protons of —CH(OC*H*$_3$)—).

Anal. Calcd. for $C_{13}H_{11}OCl_3$: C, 53.91; H, 3.83; Cl, 36.72. Found: C, 54.20; H, 3.97; Cl, 36.43.

Mixture of 1- and 2-Naphthyl(trichloromethyl)carbinols

To a solution of 25.6 g (0.20 mole) of naphthalene and 60 g (0.40 mole) of anhydrous chloral in 50 ml of nitrobenzene, there was added with stirring over a 3 h period a solution of 7.8 g (0.06 mole) of aluminium chloride in 50 ml of nitrobenzene. The temperature was maintained near 0 °C by means of an ice-bath. After standing overnight, the reaction mixture was washed three times with 6 *N* hydrochloric acid to remove the aluminium chloride, then twice with 5% sodium carbonate solution to remove chloral polymers, and finally with water. The nitrobenzene was removed by distillation under reduced pressure. Five g of calcium carbonate were added to the residue to lessen decomposition, and the residue was rapidly distilled at 1 to 2 mm. The carbinol mixture distilled at 150–180 °C/2 mm as a pale-yellow, viscous oil weighing 34 g (61% yield). The literature b.p. is 180 °C at 1.5 mm (5). The areas of the peaks in the n.m.r. spectrum at δ 5.97 (1-naphthyl isomer) and 5.2 (2-naphthyl isomer) were in the ratio of 85 to 14. This indicates the mixture contained the 1-naphthylcarbinol and the 2-naphthylcarbinol in the ratio of 6:1. Another large peak at δ 6.45 showed the presence of an unidentified impurity. Since the carbinol mixture was converted into the isomeric α-methoxynaphthylacetic acids (see below) in 76% yield, the amount of impurities was probably under 20%.

The experiments with carbon disulfide as a solvent were carried out in an analogous manner except that the aluminium chloride was added portionwise as a solid since it is insoluble in the solvent.

The experiments with cyclohexane followed the published experimental procedures (5). To a solution of 26 g (0.20 mole) of naphthalene and 60 g (0.40 mole) of anhydrous chloral in 150 ml of cyclohexane, there was added with stirring over a 3 h period, 5 g (0.04 mole) of freshly sublimed aluminium chloride. The temperature was maintained at 0 °C throughout the entire addition period. After the addition, the mixture was allowed to warm up to room temperature and stirring was continued for 8 h before decomposing the reaction mixture with cold 6 *N* hydrochloric acid. There was obtained 22 g (39% yield) of the mixture of carbinols as a yellow viscous oil distilling at 170 °C at 1 mm. The areas of the singlet peaks at δ 5.97 and 5.2 of the 1- and 2-naphthylcarbinols, measured as before, were in the ratio of 43:11, indicating these isomers to be present in the reaction mixture in the ratio of 4:1.

α-Methoxynaphthylacetic Acids

To 27 g (0.1 mole) of the mixture of carbinols, prepared using nitrobenzene as the solvent, dissolved in 100 ml of methanol was added with stirring over a 3 h period 22.5 g (0.4 mole) of potassium hydroxide dissolved in 100 ml of methanol. The temperature was maintained between 45

Can. J. Chem. Downloaded from www.nrcresearchpress.com by 210.87.254.6 on 09/05/12
For personal use only.

and 50 °C during the addition, and then allowed to cool slowly to room temperature while stirring was continued. The reaction mixture was allowed to stand overnight and then diluted with an equal volume of water. It was filtered to remove potassium chloride and some neutral material, and the filtrate was clarified by two treatments with activated carbon. The clear filtrate was then acidified with hydrochloric acid to a pH of 3.3, and enough sodium chloride added to half saturate the water present. After stirring and then standing overnight, 21 g of a light-brownish solid were filtered off. Acidification and evaporation of the filtrate yielded only a trace of acidic material. The precipitate was triturated with three 50 ml portions of acetone and filtered. Upon evaporation of the acetone, 8 g of crude α-methoxy-1-naphthylacetic acid, m.p. 130–145 °C, were collected. The white, insoluble material from the acetone trituration weighed 9 g and consisted of a mixture of the sodium acid salts of the α-methoxy-1- and 2-naphthylacetic acids.

After further working up as described in the following sections, a total of 14.2 g (66% yield) of α-methoxy-1-naphthylacetic acid, and 2.2 g (10% yield) of α-methoxy-2- naphthylacetic acid was obtained. This approximates a 7:1 ratio of the two acids.

Separation of α-Methoxy-1- and 2-naphthylacetic Acids

The 9 g mixture of sodium acid salts obtained above was dissolved in 36 ml of 20% potassium hydroxide solution. It was warmed on the steam bath to effect solution and then filtered to remove traces of alkali-insoluble material. Enough water was added to the filtrate to make the concentration of the solution exactly 5.0% with respect to the mixture of 1-naphthyl and 2-naphthyl salts. Exactly 10.0 *N* sodium hydroxide was then added with stirring to precipitate the sodium α-methoxy-2-naphthylacetate. For each ml of the 5% solution, 0.30 ml of the sodium hydroxide solution was used. (An excess causes the isomeric 1-naphthyl sodium salt to precipitate.) After the addition, the solution was allowed to stand for 10 min, and the insoluble sodium salt was then filtered off on a large Buchner funnel. The salt was washed with acetone, stirred with more acetone in a beaker, and filtered to yield 5 g of the crude sodium salt of α-methoxy-2-naphthylacetic acid.

The filtrate from the sodium salt precipitation was cooled in an ice-bath and acidified with 6 *N* hydrochloric acid to yield the crude α-methoxy-1-naphthylacetic acid.

α-Methoxy-2-naphthylacetic Acid

The above crude sodium salt was dissolved in 225 ml of hot water, the solution filtered and then cooled to 0 °C. The solution was poured into an excess of cold 6 *N* hydrochloric acid, seeded, and allowed to stand two days at 0 °C. The crystals (3 g) were filtered off, air-dried, and recrystallized from benzene. The yield was 2.2 g melting at 97–98 °C in agreement with the literature value of 99° (8). Signals in the n.m.r. spectrum (in $DCCl_3$) appeared at δ 9.37, singlet (1 proton of —COO*H*); 7.93 to 7.17, multiplet (7 protons of ring); 4.9, singlet (1 proton of —C*H*(OCH_3)—); 3.42, singlet (3 protons of —OCH_3). In dimethyl sulfoxide, the last two signals were shifted slightly to δ 5.05 and 3.46 respectively.

Anal. Calcd. for $C_{13}H_{12}O_3$: C, 72.20; H, 5.59; —OCH_3, 14.34. Found: C, 71.95; H, 5.80; —OCH_3, 14.18.

α-Methoxy-1-naphthylacetic Acid

The crude acid was obtained from the acetone extraction of the sodium acid salt precipitate and also by acidifying the filtrate after precipitating the sodium α-methoxy-2-naphthylacetate as described above. It was purified by recrystallization from benzene. A preliminary trituration with a small amount of cold ethyl acetate was necessary to remove colored material when undistilled carbinol was used in the reaction with the methanolic potassium hydroxide. The acid melted at 148–149 °C in agreement with the literature value (8). Signals in the n.m.r. spectrum (in $DCCl_3$) appeared at δ 10.43, singlet (1 proton of —COO*H*); 8.4 to 7.1, multiplet (7 protons of ring); 5.35, singlet (1 proton of —C*H*(OCH_3)—); 3.4, singlet (3 protons of —OCH_3). In dimethyl sulfoxide, the last two signals were shifted slightly to δ 5.50 and δ 3.47.

Anal. Calcd. for $C_{13}H_{12}O_3$: C, 72.20; H, 5.59; —OCH_3, 14.34. Found: C, 72.17; H, 5.54; —OCH_3, 14.30.

α,α′-Dimethoxynaphthalene-1,5-diacetic Acid

A condensation of chloral and naphthalene was carried out in a manner similar to the one described above using nitrobenzene as solvent, but scaled up 25-fold. During the workup, the nitrobenzene was distilled at 16 to 20 mm until the temperature of the liquid reached 180 °C, and the residual crude carbinol was used in the undistilled form. After reaction with methanolic potassium hydroxide, the aqueous alkaline solution was clarified by several treatments with activated carbon, acidified, and the oily acids which separated were extracted with benzene. From this benzene extract α,α′-dimethoxynaphthalene-1,5-diacetic acid crystallized on washing the extract with water. The crude acid (15 g) was crystallized from acetone–water, ethyl acetate, and finally benzene. The 1.5 g of acid obtained melted at 233–234 °C. The infrared spectrum (Nujol mull) showed absorption bands at 2900, 1725, 1670, 1450, 1165, 1110, 794, 781, and 763 cm^{-1}. Assignment of the 1,5 structure was based on the peaks at 781 and 763 cm^{-1} (9) and on the n.m.r. spectrum. Signals in the n.m.r. spectrum (in DMSO-d_6) appeared at δ 8.6 to 8.2, multiplet (2 ring protons); 7.8 to 7.5, multiplet (4 ring protons); 5.55, singlet (2 protons, —C*H*-(OCH_3)—); and 3.5, singlet (6 protons, —CH(OCH_3)—).

Anal. Calcd. for $C_{16}H_{16}O_6$ (neutralization equivalent 152): C, 63.15; H, 5.30; —OCH_3, 20.40. Found (neutralization equivalent, 154): C, 63.22; H, 5.62; —OCH_3, 19.95.

α-Methoxy-1,2,3,4-tetrahydronaphthalene-6-acetic Acid

The preparation of the carbinol from chloral and tetralin using carbon disulfide as the solvent was analogous to the procedure given above for naphthalene. The *5,6,7,8-tetrahydro-2-naphthyl(trichloromethyl) carbinol* distilled at 188–190 °C/2 mm and was obtained in 51% yield.

Reaction of the carbinol with methanolic potassium hydroxide was carried out in the same way as described for the naphthyl(trichloromethyl)carbinols. The methoxy acid was isolated as *sodium hydrogen di(α-methoxy-1,2,3,-4-tetrahydronaphthalene-6-acetate)*. After washing with water and acetone, the material had a neutralization equivalent of 460; the theoretical value is 462. The *free acid* was an oil. Signals in the n.m.r. spectrum (free acid in $DCCl_3$) appeared at δ 10.4, singlet (—COO*H*); 7.3 to 6.9, four peaks (3 protons of aromatic ring); 4.7, singlet (1

proton of —C*H*(OCH_3)—); 3.38, singlet (3 protons of —OCH_3); 2.73, multiplet (4 protons of carbons 1 and 4); and 1.75, multiplet (4 protons of C-2 and C-3).

Anal. Calcd. for $C_{13}H_{16}O_3$: C, 70.88, H, 7.31. Found: C, 70.82; H, 7.36.

1. F. RADT (*Editor*). Elsevier's encyclopaedia of organic chemistry. Series III. Vol. 12B. Elsevier Publ. Co., Inc., New York. 1950. p. 2211. G. BADDELEY. J. Chem. Soc. S99 (1949).
2. G. B. FRANKFORTER and W. KRITCHEVSKY. J. Am. Chem. Soc. **37**, 385 (1915).
3. G. CAQUILL and J. BOYER-HOUARD. Bull. Soc. Chim. France, 1391 (1955).
4. R. QUELET, C. BORGEL, and R. DURAND. Compt. Rend. **240**, 1900 (1955).
5. C. BROQUET-BORGEL. Ann. Chim. Paris, **3**, 204 (1958).
6. P. DURAND, J. PARELLO, and N. P. BUU-HOI. Bull. Soc. Chim. France, 2438 (1963). F. F. YEW, R. J. KURLAND, and B. J. MAIR. Anal. Chem. **36**, 843 (1964).
7. W. REEVE, J. P. MUTCHLER, and C. L. LIOTTA. Can. J. Chem. **44**, 575 (1966).
8. W. REEVE and E. L. COMPERE. J. Am. Chem. Soc. **83**, 2755 (1961).
9. J. G. HAWKINS, E. R. WARD, and D. H. WHIFFEN. Spectrochim. Acta, **10**, 105 (1958).
10. W. REEVE, R. S. HUDSON, and C. W. WOODS. Tetrahedron, **19**, 1243 (1963).

Can. J. Chem. Downloaded from www.nrcresearchpress.com by 210.87.254.6 on 09/05/12
For personal use only.

Can. J. Chem. Downloaded from www.nrcresearchpress.com by 210.87.254.40 on 09/05/12
For personal use only.

Reaction of anhydro sugars with sodium cobalt tetracarbonyl and carbon monoxide

ALEX ROSENTHAL AND J. N. C. WHYTE
Department of Chemistry, University of British Columbia, Vancouver 8, British Columbia

Received December 12, 1967

5,6-Anhydro-1,2-*O*-isopropylidene-α-D-glucofuranose reacts with sodium cobalt tetracarbonyl and carbon monoxide in methanol to afford methyl 6-deoxy-1,2-*O*-isopropylidene-α-D-*gluco*-heptofuranouronate (**3**) in 82% yield. Treatment of tri-*O*-acetyl-1,2-anhydro-D-glucopyranose with sodium cobalt tetracarbonyl in ether gives 3,4,6-tri-*O*-acetyl-D-glucal. The 2,3-anhydro sugars are resistant to cleavage by cobalt tetracarbonyl anion in ether or in methanol. Sugar acetates are de-*O*-acetylated by treatment with sodium cobalt tetracarbonyl in ether–methanol.

Canadian Journal of Chemistry, 46, 2239 (1968)

This investigation was undertaken in an attempt to provide a new route to the synthesis of branched-chain sugars. Previous workers (1, 2) have shown that cobalt tetracarbonyl anion in methanol reacts with epoxides at elevated temperatures and at high pressure of carbon monoxide to afford esters of β-hydroxyacids. Part of the epoxide was found to rearrange to a ketone.

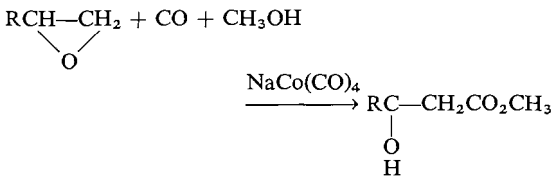

When 5,6-anhydro-1,2-*O*-isopropylidene-α-D-glucofuranose (**1**) was allowed to react with sodium cobalt tetracarbonyl in ether and 10 atm of carbon monoxide at 25° for 2 days, and the resulting complex was cleaved *in situ* with iodine in methanol, a mixture of 6-deoxy-1,2-*O*-isopropylidene-α-D-*xylo*-hexofuranose-5-ulose (**2**) and methyl 6-deoxy-1,2-*O*-isopropylidene-α-D-*gluco*-heptofuranouronate (**3**) was formed. This mixture was readily separated by column chromatography on silica gel using chloroform:acetone (95:5) as developer.

Compound **2**, isolated in 8% yield, showed a strong peak at 1720 cm^{-1} in its infrared spectrum indicating the presence of a carbonyl group, while its nuclear magnetic resonance (n.m.r.) spectrum exhibited a sharp singlet (3 hydrogens) at τ 7.75 attributed to an isolated methyl group. Its mass spectrum gave a molecular weight of 202 and microanalysis agreed with the formula $C_9H_{14}O_5$.

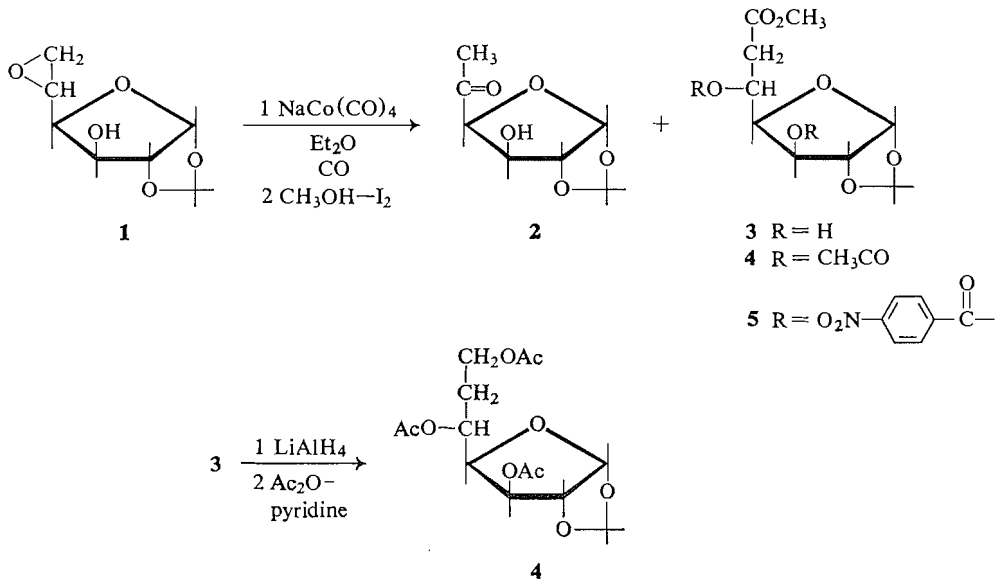

TABLE I

Proton chemical shifts and coupling constants for furanose ring hydrogens

First-order proton chemical shifts (in τ values)								
Compound	1H	2H	3H	4H	5H	6_1H	6_2H	$7_{1,2}$H
4	4.12	5.53	4.71	5.62	4.65	7.13	7.42	
5	3.98	5.33	4.42	5.29	4.24	6.9	7.13	
6	4.11	5.57	4.71	5.75	4.85	7.8	8.1	5.89
7*	4.06	5.49	4.64	5.59	4.81	5.51	5.94	

Proton coupling constants (Hz)							
Compound	$J_{1,2}$	$J_{2,3}$	$J_{3,4}$	$J_{4,5}$	$J_{5,6}$	$J_{5,6_2}$	$J_{6_1,6_2}$
4	3.6	<0.5	3.0	9.0	3.8	7.5	15
5	3.6	<0.5	3.1	9.3	4.2	7.2	16
7	3.5	<0.5	3.0	9.0	2.0	6.3	12.3

*7 is 3,5,6-Tri-*O*-acetyl-1,2-*O*-isopropylidene-α-D-glucofuranose.

The melting point, but not the optical rotation, agreed with the literature values (3). On the basis of the above evidence, especially the n.m.r., it is certain that compound **2** is 6-deoxy-1,2-*O*-isopropylidene-α-D-*xylo*-hexofuranose-5-ulose. Undoubtedly, **2** arose from the rearrangement of the anhydro ring to a ketose. Its presence was not surprising since it had been reported previously (2, 4) that aliphatic epoxides rearranged to ketones when treated with cobalt carbonyl anion.

Compound **3**, isolated in 82% yield, was characterized as its acetyl (**4**) and *p*-nitrobenzoyl (**5**) derivatives, respectively. When compound **3** was reduced with lithium aluminium hydride in tetrahydrofuran, followed by acetylation, compound **6** was obtained which was identical (by n.m.r.) to that obtained by the sodium borohydride reduction (followed by acetylation) of 6-deoxy-1,2-*O*-isopropylidene-α-D-*gluco*-heptodialdo-1,4-furanose-3,7-pyranose (5).

As shown in Table I, the chemical shifts and coupling constants of the furanose ring hydrogens of compounds **4** and **6** are in excellent agreement with the corresponding values quoted for the known 3,4,6-tri-*O*-acetyl-1,2-*O*-isopropylidene-α-D-glucofuranose (6) showing that compounds **4** and **6** had retained the furanose ring. Nuclear magnetic resonance spectroscopy of the *p*-nitrobenzoate (**5**) clearly demonstrated the presence of two methylenic hydrogens at τ 6.9–7.13 and three methyl ester hydrogens (singlet) at τ 6.36. Therefore, compound **3** is undoubtedly methyl 6-deoxy-1,2-*O*-isopropylidene-α-D-*gluco*-heptofuranouronate.

When methyl 5-*O*-acetyl-2,3-anhydro-β-D-ribofuranoside was allowed to react with sodium cobalt tetracarbonyl in ether and 10 atm of carbon monoxide for 24 h at 25° no reaction occurred. Raising the temperature of the reaction mixture to 50° led to no scission of the epoxide ring. Surprisingly, when methanol was added to the reactants and the reaction mixture heated at 100° for 6 h, then complete de-*O*-acetylation occurred with the exclusive formation of methyl 2,3-anhydro-β-D-ribofuranoside. If deacetylation is due to the formation of sodium methoxide from the catalyst and methanol, then some scission of the epoxide should have occurred. Under the same conditions, α-D-glucopyranose pentaacetate was also deacetylated.

An equally surprising result was obtained when 3,4,6-tri-*O*-acetyl-1,2-anhydro-D-glucopyranose (Brigl's anhydride) was allowed to react with sodium cobalt tetracarbonyl in ether and carbon monoxide at room temperature. Deoxygenation of the anhydride occurred to give predominately 3,4,6-tri-*O*-acetyl-D-glucal.

The epoxide ring of methyl 2,3-anhydro-4,6-*O*-benzylidene-α-D-allopyranoside was not opened when the substrate was treated with sodium cobalt tetracarbonyl in ether and carbon monoxide at room temperature. At 80°, however, in the presence of methanol, part of the substrate rearranged to a ketose and part underwent methanolysis (as shown by n.m.r. spectroscopy). Since no insertion of carbon monoxide occurred, as indicated by mass spectral studies, further work on the complex mixture of products was abandoned.

Can. J. Chem. Downloaded from www.nrcresearchpress.com by 210.87.254.40 on 09/05/12
For personal use only.

Can. J. Chem. Downloaded from www.nrcresearchpress.com by 210.87.254.40 on 09/05/12
For personal use only.

Experimental

General Procedures

The reactions were performed in an Aminco Autoclave (having a glass liner) of 200 ml internal capacity. The autoclave was fitted with an injector septum from an Aerograph vapor-phase chromatography (v.p.c.) instrument. After the autoclave was sealed, it was removed from a nitrogen-filled dry box, flushed three times with 9 atm of Matheson C.P. carbon monoxide (gas passed through a gas purifier), and finally pressurized with 1 atm of carbon monoxide. Ether solutions of sodium cobalt tetracarbonyl (7, 8) were prepared by treating an ether solution of preformed dicobalt octacarbonyl (Alfa Inorganics Inc.) with sodium amalgam and the resultant solution was injected into the autoclave through the inlet system by means of a Hamilton syringe. The autoclave was then pressurized with the required amount of carbon monoxide.

Thin-layer chromatography (t.l.c.) and column chromatography were performed with silica gel G (E. Merck A. G. Darmstadt (Germany)) with the following solvents: *a*, chloroform:acetone (95:5 v/v); *b*, chloroform; *c*, petroleum ether (30–60° b.p.):ethyl ether (4:1); *d*, butanone – water azeotrope.

Rotations were performed at room temperature, melting points were determined on a Leitz hot-stage microscope, and nuclear magnetic resonance (n.m.r.) spectra were obtained on deuterio-chloroform solutions with tetramethylsilane as the internal standard (set at τ 10) using a Jeolco 60, a Varian A-60, or Varian HA 100 spectrometers. Mass spectroscopy was obtained with an A.E.I. M.S.9 spectrometer. Elemental analyses were performed by the Micro-analytical Laboratory, University of British Columbia.

Reaction of 5,6-Anhydro-1,2-O-isopropylidene-α-D-glucofuranose[1] with Sodium Cobalt Tetracarbonyl and Carbon Monoxide to Yield 6-Deoxy-1,2-O-isopropylidene-α-D-xylo-hexofuranose-5-ulose (2) and Methyl 6-Deoxy-1,2-O-isopropylidene-α-D-gluco-heptofuranouronate (3)

An amount of 500 mg of 5,6-anhydro-1,2-*O*-isopropylidene-α-D-glucofuranose (9, 10) in 20 ml of anhydrous ether was allowed to react with an ether solution of sodium cobalt tetracarbonyl (7, 8) (50 ml of about 0.2 *M*) and 10 atm of carbon monoxide at 25° for 48 h (with rocking until gas absorption had ceased). The gas was then vented until the residual gas pressure was about 1 atm and the autoclave then cooled to −5°. A solution of 0.5 *M* iodine in anhydrous methanol (30 ml) was then injected and the vessel rocked for a further 12 h at room temperature. After the solvent was removed by distillation under reduced pressure at room temperature, the residue was extracted with chloroform. The combined extracts were washed successively with aqueous sodium thiosulfate, aqueous sodium bicarbonate, then dried over anhydrous sodium sulfate, and evaporated to dryness. The residue was again extracted with ether and the solvent evaporated to yield 550 mg of a syrup, which by t.l.c. (solvent *a*) was shown to consist of two components having an R_f of 0.24 and 0.14 respectively. Column chromatography of the residue on silica gel G (50 g), using solvent *a* as developer, gave compound **2** (0.04 g) and compound **3** (0.450 g, 82% yield).

Compound **2** was crystallized from benzene – petroleum ether, m.p. 99–100°, $[\alpha]_D^{22}$ −47° (*c*, 1 in chloroform) (lit. (3) m.p. 99–100°, $[\alpha]_D^{18}$ −107° (chloroform)). Nuclear magnetic resonance ($CDCl_3$): 4.0 (doublet equal to 1H), 5.4–5.6 (multiplet equal to 3H), 6.45 (1H or OH), 7.78 (singlet equal to 3H), 8.52, and 8.70 (two singlets each equal to 3H). Infrared: sharp peak at 1720 cm^{-1}.

Anal. Calcd. for $C_9H_{14}O_5$ (mol. wt., 202): C, 53.50; H, 6.94. Found (mol. wt., 202 (*m/e* 187, loss of CH_3)): C, 53.28; H, 6.93.

It was converted into a phenyl hydrazone derivative in the usual way. 6-Deoxy-1,2-*O*-isopropylidene-α-D-*xylo*-hexofuranose-5-ulose phenylhydrazone was crystallized from chloroform – light petroleum ether, m.p. 200–204°, $[\alpha]_D^{22}$ −12° (*c*, 0.5 in chloroform).

Anal. Calcd. for $C_{15}H_{20}O_4N_2$: C, 61.60; H, 6.85. Found: C, 61.54; H, 6.78.

Compound **3** was obtained as a syrup, $[\alpha]_D^{22}$ −5° (*c*, 3.5 in chloroform).

Anal. Calcd. for $C_{11}H_{18}O_7$: C, 50.40; H, 6.87. Found: C, 50.59; H, 6.90.

Compound **3** was acetylated in the usual way using acetic anhydride and pyridine to yield a syrup, $[\alpha]_D^{22}$ +8° (*c*, 1.9 in chloroform), R_f 0.73.

Anal. Calcd. for $C_{15}H_{22}O_9$ (mol. wt., 346): C, 52.00; H, 6.36. Found (mol. wt., *m/e* 331 (loss of CH_3)): C, 52.24; H, 6.52.

Preparation of Methyl 6-Deoxy-1,2-O-isopropylidene-3,5-di-O-p-nitrobenzoyl-α-D-gluco-heptofuranouronate (5)

Compound **3** (0.05 g) was allowed to react with *p*-nitrobenzoyl chloride (0.40 g) in 10 ml pyridine for 18 h at 0°. The reaction mixture was poured into ice water and the solution extracted with chloroform. The chloroform extracts were washed successively with cold dilute hydrochloric acid and saturated aqueous sodium bicarbonate, dried over sodium sulfate, and evaporated under reduced pressure. Preparative t.l.c. purification on silica gel using solvent *b* gave a crystalline product, R_f 0.8, which was recrystallized from ether – light petroleum ether, m.p. 68°, $[\alpha]_D^{22}$ −111° (*c*, 1 in chloroform).

Anal. Calcd. for $C_{25}H_{24}O_{13}N_2$: C, 53.50; H, 4.28. Found: C, 53.38; H, 4.50.

Reaction of Tri-O-acetyl-1,2-anhydro-D-glucopyranose with Sodium Cobalt Tetracarbonyl and Carbon Monoxide

To the autoclave, containing 500 mg of the anhydride (11) and 20 ml of carbon monoxide-saturated ether, was injected 50 ml of approximately 0.2 *M* sodium cobalt tetracarbonyl in ether. The vessel was pressurized with 10 atm of carbon monoxide and rocked at 24° until absorption of gas had ceased (about 24 h), then cooled to −5°, and 20 ml 0.5 *N* iodine in anhydrous methanol solution was added followed by 6 h of further shaking. The resultant solution was evaporated and the residue extracted with ether, filtered, and evaporated to yield a syrup, 280 mg, which on t.l.c. indicated a major component, R_f 0.80 in solvent *a*, and several minor components. The infrared (i.r.) and n.m.r. spectra were identical to those given by tri-*O*-acetyl-D-glucal. The syrup was applied to a column of silica (30 g) and eluted with solvent *a*. The eluate was fractionally collected and examined by chromatography, the like fractions being bulked. The

[1]This compound was prepared by Mr. Gordon Kan.

Can. J. Chem. Downloaded from www.nrcresearchpress.com by 210.87.254.40 on 09/05/12
For personal use only.

fraction, R_f 0.80 in solvent *a*, was recrystallized several times from ether – petroleum ether to give 80 mg of a solid, m.p. and mixture m.p. 54.5–55° which was chromatographically indistinguishable from 3,4,6-tri-*O*-acetyl-D-glucal.

Reaction of Methyl 5-O-Acetyl-2,3-anhydro-β-D-ribofuranoside with Sodium Cobalt Tetracarbonyl and Carbon Monoxide

To the autoclave, containing 1 g of the sugar (10, 12) and 30 ml of carbon monoxide-saturated ether, was injected 100 ml of approximately 0.3 *M* sodium cobalt tetracarbonyl in ether, then 10 atm of carbon monoxide. The vessel was rocked for 24 h at 24° but no absorption of gas was noted. The gas was released from the autoclave until 30 p.s.i. pressure was reached and, employing a long needle syringe, a portion of the reaction mixture, 1 ml, was removed and examined by t.l.c. in solvents *a*, *b*, and *c* using the starting material as standard. The product of the reaction was found to be chromatographically identical to the starting material. The autoclave was repressurized to 10 atm and heated at 50° for 5 h. Chromatographic examination of a 1 ml portion of the reaction mixture indicated that no reaction had occurred. Anhydrous methanol, 20 ml, was injected into the reaction mixture and the autoclave pressurized to 10 atm and heated at 60° for 5 h, then using the long needle syringe a 1 ml sample of the reaction mixture was removed from the autoclave and chromatographed by t.l.c. The examination indicated that the products of the reaction were a small yield of a compound, R_f 0.35 in solvent *a*, together with the major component, starting material, R_f 0.72 in solvent *a*. Conversion of the latter to the former was accomplished by reheating the pressurized, 10 atm, autoclave at 100° for 6 h. A solution of 0.5 *N* iodine in anhydrous methanol, 30 ml, was added to the reaction mixture and after rocking the vessel for a further 6 h at 24° the reaction solution was removed and evaporated to a residue which was extracted with ethyl ether, filtered, and evaporated to a syrup, 700 mg, R_f 0.35 in solvent *a*, $[\alpha]_D^{22} = -106°$ (*c*, 1 in water), which was chromatographically identical with and had identical i.r. and n.m.r. spectra to those of authentic methyl 2,3-anhydro-β-D-ribofuranoside.

Anal. Calcd. for $C_6H_{10}O_4$: C, 49.3; H, 6.85. Found: C, 48.9; H, 6.53.

Reaction of Methyl 2,3-Anhydro-4,6-O-benzylidene-α-D-allopyranoside with Sodium Cobalt Tetracarbonyl and Carbon Monoxide

To the autoclave, containing 2.5 g sugar (10, 13) and 20 ml carbon monoxide saturated ether, was injected 100 ml of approximately 0.5 *M* sodium cobalt tetracarbonyl in ether, followed by 10 atm of carbon monoxide. The vessel was rocked for 4 days and the contents inspected by removing a 1 ml portion with the use of a long needle syringe. A t.l.c. in solvents *a*, *b*, and *c* indicated that no reaction had occurred, since the product was chromatographically indistinguishable from the starting material together with the fact that the sample freed from catalyst crystallized and gave a m.p. and mixture m.p. identical with the starting material (199°). The autoclave was repressurized to 10 atm and heated at 80° for 6 h. Thin-layer chromatography inspection of the reaction mixture indicated a number of products had been formed. Iodine, 10 ml (0.5 *N* solution in anhydrous methanol), was injected into the reaction mixture, the vessel shaken for 24 h, and the products isolated and evaporated to a residue which was dissolved in chloroform and applied to a column of silica gel, 100 g, which was eluted with solvent *a*. The eluate was fractionated and the bulked sugar-containing fractions, 950 mg, gave an i.r. spectrum showing hydroxy and strong carbonyl peaks and an n.m.r. spectrum indicating methoxyl peaks in the τ 6–7 region. The product after column chromatography was identical chromatographically on t.l.c. to the reaction mixture removed from the bomb prior to the addition of iodine. The mass spectrum of the product mixture showed that no carbomethoxy group had been added to the starting material.

Reaction of α-D-Glucopyranose Pentaacetate with Sodium Cobalt Tetracarbonyl and Carbon Monoxide at 24° in Different Solvents

The pentaacetate, 200 mg, was added to 20 ml anhydrous dioxane and another portion, 200 mg, was added to 20 ml anhydrous methanol. To both these solutions was added under carbon monoxide 25 ml of approximately 0.5 *M* sodium cobalt tetracarbonyl in ether. The resultant mixtures were shaken for 24 h at 24° and then carbon dioxide was bubbled through the solutions which were evaporated to dryness. The residues thus isolated were examined by chromatography in solvent *d*. The pentaacetate which was allowed to react in dioxane and ether was unchanged, but the sample of pentaacetate in methanol and ether was shown to have undergone deacetylation as most of the reaction product had a chromatographic mobility identical to glucose in solvent *d* and no pentaacetate was found.

Acknowledgments

The authors gratefully acknowledge financial assistance from the United States Public Service Research Grant No. CA-08382, National Cancer Institute and from the National Research Council of Canada.

1. R. F. HECK and D. S. BRESLOW. J. Am. Chem. Soc. **83**, 4023 (1961).
2. R. F. HECK. J. Am. Chem. Soc. **85**, 1460 (1963).
3. H. OHLE and R. DEPLANGUE. Ber. **66**, 12 (1933). M. G. BLAIR. Methods Carbohydrate Chem. **2**, 415 (1963).
4. J. L. EISENMANN. J. Org. Chem. **27**, 2706 (1962).
5. A. ROSENTHAL and G. KAN. Tetrahedron Letters, **5**, 477 (1967).
6. R. J. ABRAHAM, L. D. HALL, L. HOUGH, and K. A. MCLAUCHLAN. J. Chem. Soc. 3699 (1962).
7. W. HIEBER and G. WAGNER. Z. Naturforsch. **12b**, 478 (1957); **13b**, 192 (1958); **13b**, 339 (1958).
8. J. EISCH and R. B. KING. Organometallic Syn. **1**, 153 (1965).
9. H. OHLE and L. VON VARGHA. Ber. **62**, 2435 (1929).
10. L. F. WIGGINS. Methods Carbohydrate Chem. **2**, 188 (1963).

11. P. BRIGL. Z. Physiol. Chem. **122**, 245 (1922). R. U. LEMIEUX and J. HOWARD. Methods Carbohydrate Chem. **2**, 400 (1963).
12. P. W. KENT, M. STACEY, and L. F. WIGGINS. J. Chem. Soc. 1232 (1949). C. D. ANDERSON, L. GOODMAN, and B. R. BAKER. J. Am. Chem. Soc. **80**, 5247 (1958).
13. N. K. RICHTMEYER and C. S. HUDSON. J. Am. Chem. Soc. **63**, 1727 (1941). H. R. BOLLINGER and D. A. PRINS. Helv. Chim. Acta, **28**, 465 (1945).

Can. J. Chem. Downloaded from www.nrcresearchpress.com by 210.87.254.40 on 09/05/12
For personal use only.

Can. J. Chem. Downloaded from www.nrcresearchpress.com by 210.87.254.105 on 09/05/12
For personal use only.

Reaction of halogenated carbohydrates with sodium cobalt tetracarbonyl and carbon monoxide. A new novel synthesis of unsaturated sugars

ALEX ROSENTHAL AND J. N. C. WHYTE
Department of Chemistry, University of British Columbia, Vancouver 8, British Columbia

Received December 18, 1967

Methyl tri-*O*-acetyl-2-deoxy-2-iodo-β-D-glucopyranoside reacted at room temperature with sodium cobalt tetracarbonyl and carbon monoxide in ether to give in high yield methyl 4,6-di-*O*-acetyl-2,3-dideoxy-β-D-*erythro*-hex-2-enoside (**5**). Under the same reaction conditions the corresponding 2-iodo-α-D-mannopyranoside failed to react, but at 100° it was smoothly converted into the anomeric α-D-*erythro*-hex-2-enoside (**7**). When methanol was used in place of ether no appreciable ester formation took place but elimination of iodine and an acetoxy group occurred, accompanied by complete deacetylation of the remaining ester groups.

Canadian Journal of Chemistry, **46**, 2245 (1968)

This investigation was undertaken to find a new route for preparing branched-chain sugars. Renewed interest in the chemistry of these unusual sugars has arisen partly because of their presence in some recently discovered antibiotics (1–3).

The great difficulty in introducing branched-chains into carbohydrates by classical chemical reactions led us to explore the possibility of using transition metal catalysts for inserting carbon monoxide into the carbon chain. One attractive route is based on the finding (4) that cobalt tetracarbonyl anion can displace active halogen from an alkyl halide to yield an unstable alkylcobalt tetracarbonyl (**1**). Under an atmosphere of carbon monoxide, the latter undergoes carbonyl insertion (5, 6) to afford an acylcobalt tetracarbonyl (**2**) as shown in eq. [2]. The addi-

[1] $$RX + NaCo(CO)_4 \longrightarrow \underset{\mathbf{1}}{RCo(CO)_4} + NaX$$

[2] $$RCo(CO)_4 \longrightarrow RCOCo(CO)_3 \xrightarrow{CO} \underset{\mathbf{2}}{RCOCo(CO)_4}$$

tion of triphenylphosphine (7) to (**2**) results in the displacement of a carbonyl ligand by triphenylphosphine to yield a stable acylcobalt tricarbonyl triphenylphosphine complex (**3**). Cleavage of the

[3] $$RCOCo(CO)_4 + PPh_3 \longrightarrow \underset{\mathbf{3}}{RCOCo(CO)_3PPh_3} + CO$$

latter is readily effected by treatment with sodium methoxide to yield an ester. Alternatively, the alkyl halide has been allowed to react with carbon monoxide and sodium cobalt tetracarbonyl in methanol (addition of a tertiary amine facilitates the reaction) under elevated temperature and pressure to yield the ester directly (8), as shown in eq. [5].

[4] $$RCOCo(CO)_3PPh_3 + NaOCH_3 \longrightarrow RCO_2CH_3$$

[5] $$RX + NaCo(CO)_4 + CO + CH_3OH \xrightarrow[60°]{} RCO_2CH_3$$

In the carbohydrate field it has been shown that tetra-*O*-acetyl-α-D-glucopyranosyl bromide readily reacted with sodium cobalt tetracarbonyl and carbon monoxide in ether at room temperature to afford alkyl and acylcobalt derivatives of carbohydrates which could be readily isolated as their triphenylphosphine complexes (9). It therefore seemed feasible to allow the readily available 2-halogenated carbohydrates to react under similar conditions to afford sugars containing a branched-chain on C-2 as shown in structure **9**.

When methyl 3,4,6-tri-*O*-acetyl-2-deoxy-2-iodo-β-D-glucopyranoside (**4**) was allowed to react with sodium cobalt tetracarbonyl and carbon monoxide in ether at room temperature, both halogen and the acetoxy group on the adjoining carbon were readily removed to afford in almost quantitative yield an unsaturated sugar, namely, methyl 4,6-di-*O*-acetyl-2,3-dideoxy-β-D-*erythro*-hex-2-enoside (**5**). Although the latter has not been previously isolated in the pure state, a mixture of it and its α anomer (**7**) has been synthesized by treatment of 3,4,6-tri-*O*-acetyl-D-glucal with methanol at elevated temperature (10). Repeated attempts in our laboratory to separate the α and β anomeric mixture by vapor-phase chromatography (v.p.c.) or thin-layer chromatography (t.l.c.) have failed. Direct

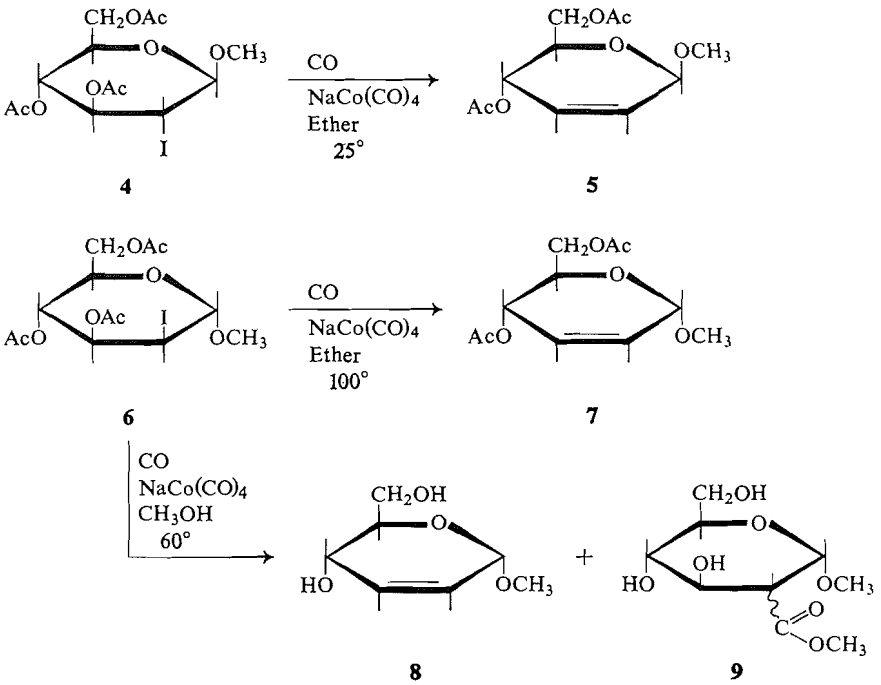

comparison by nuclear magnetic resonance (n.m.r.) of **5** with the α and β mixture conclusively showed that **5** was identical to the β anomer obtained from 3,4,6-tri-*O*-acetyl-D-glucal. Similar treatment of methyl 3,4,6-tri-*O*-acetyl-2-deoxy-2-iodo-α-D-mannopyranoside (**6**) with sodium cobalt tetracarbonyl and carbon monoxide in ether at room temperature (even for 8 days) gave only unreacted starting material. However, when **6** was allowed to react at 100° for 8 h, then it was converted in high yield into the pure unsaturated sugar (**7**). Again, direct comparison (by n.m.r.) of **7** with the α and β anomeric mixture showed conclusively its identity. Both of the unsaturated sugars (**5** and **7**) had the same v.p.c. retention time. Mass spectrometry of **5** and **7** showed that both the allylic hydrogen and methoxyl group on C-1 were removed to afford ions of *m/e* 243 and 213. In the n.m.r. spectrum of **5** the vinyl protons occurred as a multiplet at τ 4.04, whereas those of **7** resonated at τ 4.10. The methoxyl protons also differed in their resonances by 1.5 Hz.

When the unsaturated carbohydrates (**5** and **7**) were de-*O*-acetylated with sodium methoxide in methanol the resulting unsaturated sugars were unstable at room temperature. However, deacetylation of **5** with barium methoxide in the cold, followed by immediate benzoylation with *p*-nitrobenzoyl chloride and pyridine at 0°, gave a stable crystalline bis-*p*-nitrobenzoate derivative. Attempts to prepare a similar derivative of **7** were unsuccessful.

Attempts to isolate the expected cobalt derivative of **4** as the triphenylphosphine complex were unsuccessful. Injection of methanol and iodine during the course of the reaction failed to lead to the production of the anticipated branched-chain ester.

Direct treatment of methyl tri-*O*-acetyl-2-deoxy-2-iodo-α-D-mannopyranoside with sodium cobalt tetracarbonyl and carbon monoxide in methanol at 60° gave predominately the deacetylated elimination product (**8**) and what was presumed to be (on the basis of n.m.r. evidence only), in less than 3% yield, the branched-chain ester (**9**) (both isolated as the acetates). It is possible that, in the presence of methanol, the sodium cobalt tetracarbonyl dissociates to yield sodium methoxide and the latter leads to deacetylation of the substrate.

When methyl tri-*O*-acetyl-2-bromo-2-deoxy-β-D-*gluco*- (and 2-bromo-α-D-*manno*-) pyranoside were allowed to react with sodium cobalt tetra-

Can. J. Chem. Downloaded from www.nrcresearchpress.com by 210.87.254.105 on 09/05/12
For personal use only.

Can. J. Chem. Downloaded from www.nrcresearchpress.com by 210.87.254.105 on 09/05/12
For personal use only.

carbonyl and carbon monoxide in ether at 100° for 8 h, no reaction occurred.

Although methyl tri-*O*-acetyl-2-deoxy-2-iodo-β-D-glucopyranoside failed to undergo a carbonyl insertion reaction, it is interesting to consider the possible mechanism of formation of the unsaturated compound because such a consideration might help give a better insight into carbonyl insertion reactions. In this connection, it is interesting to consider the carbonyl insertion products obtained by the treatment of ethyl α-bromopropionate with potassium cobalt tetracarbonyl and carbon monoxide at 0°, followed by cleavage of the products with iodine and ethanol (11). Orchin (12), in his discussion of the probable mechanism to account for the formation of a mixture of esters, has suggested two possibilities. In the first suggestion, one can consider the displacement of bromine by cobalt tetracarbonyl anion to give an alkylcobalt tetracarbonyl (see eq. [6]), followed by an elimination (see eq. [7]), and readdition of $HCo(CO)_4$ (see eq. [8]) to give a mixture of alkylcobalt tetracarbonyls. Cleavage of these with ethanol and iodine might be expected to afford the isolable mixture of esters (see eq. [9]). An alternative

[6] $CH_3\underset{\displaystyle Br}{\underset{|}{C}}HCO_2Et + KCo(CO)_4 \rightarrow CH_3\underset{\displaystyle Co(CO)_4}{\underset{|}{C}}HCO_2Et$

[7] $CH_3\underset{\displaystyle Co(CO)_4}{\underset{|}{C}}HCO_2Et \rightleftarrows CH_2{=}CHCO_2Et + HCo(CO)_4$

[8] $\downarrow\uparrow$

$CH_2\underset{\displaystyle Co(CO)_4}{\underset{|}{C}}H_2CO_2Et$

[9] $\downarrow I_2$ EtOH

Mixture of Esters

mechanism also considered (12) was the possibility of an initial dehydrohalogenation of the ester to acrylate, followed by subsequent addition of $HCo(CO)_4$ (see eq. [10]). The second

[10] $CH_3\underset{\displaystyle Br}{\underset{|}{C}}HCO_2Et + [Co(CO)_4]^- \rightarrow CH_2{=}CHCO_2Et + HCo(CO)_4 + Br^-$

mechanism (prior elimination) in all probability could not apply to the 2-iodo compound (**4**) because there exists no secondary hydrogen in a *trans* position to the iodine. If the first suggestion applies, then the resulting sugar cobalt tetracarbonyl might be expected to have the D-*manno*-configuration (**10**). A *trans* elimination of $HCo(CO)_4$ from **10**, as envisaged by Orchin (12) would not give the 2,3-ene (**5**). Although the

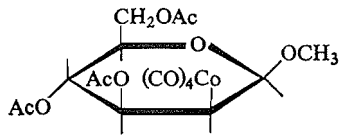

10

evidence thus far adduced rules out the mechanisms suggested by Orchin, it merely shows that no single mechanism applies for the elimination of iodine and acetate which are either *cis* or *trans* oriented. To the best knowledge of the authors this is the first recorded instance of such an elimination, although elimination of iodine and a tosyl group from adjacent carbons to form a 2,3-ene is well known (13).

Experimental

General Considerations

The reactions were performed in an Aminco autoclave fitted with an injector septum. Ether solutions of sodium cobalt tetracarbonyl (14, 15) were prepared by treating an ether solution of dicobalt octacarbonyl (Alfa Inorganics, Inc., Beverley, Massachusetts) with sodium amalgam. Nuclear magnetic resonance spectra were performed on a 100-MHz HA spectrometer, using tetramethylsilane as the internal standard set at $\tau = 10$. Mass spectra were measured with an A.E.I. M.S.9 spectrometer. Vapor-phase chromatography (v.p.c.) was performed on a Varian Aerograph model 1525 instrument operated at 215° using 5% butanediol succinate or 10% SE 52 on Chromosorb W.

Reaction of Methyl 3,4,6-Tri-O-acetyl-2-deoxy-2-iodo-β-D-glucopyranoside with Sodium Cobalt Tetracarbonyl to Yield Methyl 4,6-Di-O-acetyl-2,3-dideoxy-β-D-erythro-hex-2-enoside (5)

Procedure A

A solution of methyl 3,4,6-tri-*O*-acetyl-2-deoxy-2-iodo-β-D-glucopyranoside (16) (1 g) dissolved in 30 ml of anhydrous ether was placed in a glass liner contained in a shaking autoclave of 200 ml internal capacity. The autoclave was then sealed with the pressure head which was fitted with an injector septum (from an Aerograph v.p.c. instrument) and a gauge. After the autoclave was flushed three times with 100 p.s.i. of anhydrous carbon monoxide it was pressurized with 1 atm of carbon monoxide. An ether solution of sodium cobalt tetracarbonyl (100 ml of 0.25 *M*) was then injected through the septum with a syringe. After the autoclave was again flushed with carbon monoxide, it was filled with 150 p.s.i. of carbon monoxide and then rocked at 60° for about 2 h. The contents of the liner were placed in a beaker and allowed to stand in a hood until the ether had evaporated. The resultant residue was extracted with 100 ml of ether and on evaporation this extract gave 490 mg of syrup which was distilled, b.p.

Can. J. Chem. Downloaded from www.nrcresearchpress.com by 210.87.254.105 on 09/05/12
For personal use only.

78–85°/0.04 mm. The product was homogeneous by thin-layer chromatography (t.l.c.) and by v.p.c., and absorbed 1.05 moles hydrogen per mole sugar: $[\alpha]_D^{20}$ +142° (*c*, 3.0 in benzene); n_D^{23} 1.4617.

Anal. Calcd. for $C_{11}H_{16}O_6$ (mol. wt., 244): C, 54.1; H, 6.56. Found *m/e* 243 (loss of H) and 213 (loss of OCH_3): C, 53.8; H, 6.80.

Nuclear magnetic resonance (deuteriochloroform): multiplet at τ 4.04 equal to 2 vinyl protons; singlet at τ 6.54 equal to 3 methoxyl protons; singlet at τ 7.90 equal to 6 acetyl H; in deuteriobenzene the acetyl protons appeared at τ 8.30 and 8.36.

Preparation of methyl 2,3-dideoxy-4,6-di-O-p-nitrobenzoyl-β-D-erythro-hex-2-enoside—Methyl 4,6-di-*O*-acetyl-2,3-dideoxy-β-D-erythro-hex-2-enoside was first de-*O*-acetylated with barium methoxide in methanol at 0° (17). The residual syrup, which was unstable at room temperature, was immediately converted into a *p*-nitrobenzoate derivative by treatment with *p*-nitrobenzoyl chloride and pyridine at 0° for 1 day. The product was worked up in the usual way and recrystallized from methanol, m.p. 130–132°. A trace of a contaminant was present (t.l.c.) which could not be removed.

Anal. Calcd. for $C_{21}H_{18}O_{10}N_2$: mol. wt. 458. Found: *m/e* 457 (loss of H) and *m/e* 427 (loss of OCH_3).

Procedure B

To the autoclave, filled with 1.5 sugar and 20 ml carbon monoxide-saturated ether, were injected 100 ml of approximately 0.25 *M* sodium cobalt tetracarbonyl in ether. The vessel was pressurized with 10 atm of carbon monoxide and heated, with rocking, at 60° for 2 h. After the vessel was cooled, 3 g of triphenylphosphine in 15 ml ether were injected into the vessel. The contents of the autoclave were filtered in an atmosphere of nitrogen. The residue was extracted with water, the extracts filtered, and on evaporation a red, velvety material remained which was quite deliquescent. This residue gave positive tests for cobalt, sodium, iodine, and acetate ions. To the filtrate 20 ml of methyl iodide were added and the mixture allowed to stand at 0° for 10 h. The mixture was filtered under nitrogen, the filtrate evaporated to a syrup which was extracted with boiling petroleum ether (30–60° b.p.), and, on cooling the extracts, a crystalline solid, m.p. 156°, was obtained which was shown by n.m.r. and mass spectroscopy to be triphenylphosphine oxide. The crystals were removed by filtration and the resultant solution evaporated to afford 700 mg of a syrup which was identical to methyl 4,6-di-*O*-acetyl-2,3-dideoxy-β-D-*erythro*-hex-2-enoside obtained from the previous reaction.

Procedure C

The halogenated sugar (1 g) was allowed to react with sodium cobalt tetracarbonyl in ether and 10 atm of carbon monoxide for 3 days at 24°. After the autoclave was cooled to −3°, 20 ml of 0.5 *N* iodine in anhydrous methanol solution was added, and the reactants were shaken for a further 12 h at room temperature. The contents of the autoclave were removed and allowed to stand in an open beaker until all ether and methanol had evaporated. The resultant residue was extracted with ether and on evaporation of the ether gave 490 mg of syrup (homogeneous by t.l.c.) which was identical to that obtained in the previous two procedures.

Reaction of Methyl 3,4,6-Tri-O-acetyl-2-deoxy-2-iodo-α-D-mannopyranoside (6) with Sodium Cobalt Tetracarbonyl and Carbon Monoxide to Yield Methyl 4,6-Di-O-acetyl-2,3-dideoxy-α-D-erythro-hex-2-enoside (7)

Procedure A

Methyl 3,4,6-tri-*O*-acetyl-2-deoxy-2-iodo-α-D-mannopyranoside (16) (0.5 g) was allowed to react with 50 ml of an ether solution of 0.25 *M* sodium cobalt tetracarbonyl and 10 atm of C.P. carbon monoxide at 100° for 6 h. Work-up of the product, as described previously in Experimental Procedure A, afforded 200 mg of a syrup, $[\alpha]_D^{21}$ +126° (*c*, 1.2 in benzene), n_D^{23} 1.4580.

Anal. Calcd. for $C_{11}H_{16}O_6$: C, 54.1; H, 6.56. Found: C, 53.9, H, 6.50.

Nuclear magnetic resonance: singlet with shoulders at τ 4.10 equal to 2 vinyl protons; singlet at τ 6.55 equal to 3 methoxyl protons; singlet at τ 7.88 equal to 6 acetyl H.

Procedure B

When the same sugar (**6**) was allowed to react with sodium cobalt tetracarbonyl in ether and carbon monoxide at 25° for 8 days no reaction occurred.

Procedure C

Treatment of sugar (**6**) with sodium cobalt tetracarbonyl in methanol and carbon monoxide at 60° for 2 h yielded methyl 2,3-dideoxy-α-D-*erythro*-hex-2-enoside which was too unstable to be characterized. It was immediately acetylated using acetic anhydride and pyridine to yield methyl 4,6-di-*O*-acetyl-2,3-dideoxy-α-D-*erythro*-hex-2-enoside. Nuclear magnetic resonance of the latter compound revealed the presence of an additional singlet at τ 6.25 which might be due to the presence of a trace (less than 3%) of a compound containing a carbomethoxy group.

Treatment of methyl 3,4,6-tri-O-acetyl-2-bromo-2-deoxy-β-D-gluco- (and α-D-manno-) pyranoside with sodium cobalt tetracarbonyl and carbon monoxide—Under similar conditions to those described in I-A (except at a temperature of 100° for 8 h), both methyl 3,4,6-tri-*O*-acetyl-2-bromo-2-deoxy-β-D-gluco- (and α-D-manno-) pyranoside (16) underwent no appreciable reaction.

Preparation of Methyl 4,6-Di-O-acetyl-2,3-dideoxy-α,β-D-erythro-hex-2-enoside

3,4,6-Tri-*O*-acetyl-D-glucal (2 g) (18) was allowed to react with methanol in a rocking autoclave (previously flushed with nitrogen) at 180° for 4 h. After the methanol and acetic acid were removed from the unsaturated sugars by evaporation under reduced pressure, the residual syrup was distilled; yield 1.4 g, b.p. 80–83° (0.04 mm), $[\alpha]_D^{21}$ +136° (*c*, 1.2 in benzene), n_D^{23} 1.4565. Attempts to separate the mixture of unsaturated sugars by v.p.c. were unsuccessful. Nuclear magnetic resonance: vinyl protons at τ 4.04 and τ 4.10 (ratio of β:α anomer 5:9).

Acknowledgments

The authors gratefully acknowledge financial assistance from the U.S. Public Service Research Grant No. CA-08382, National Cancer Institute, and from the National Research Council of Canada.

1. R. U. LEMIEUX and M. L. WOLFROM. Advan. Carbohydrate Chem. **3**, 337 (1948).
2. F. SHAFIZADEH. Advan. Carbohydrate Chem. **11**, 263 (1956).
3. W. G. OVEREND. Chem. Ind. London, 342 (1963).
4. W. HIEBER, O. BOHLER, and G. BRAUN. Z. Naturforsch. **13b**, 192 (1958). W. HIEBER and E. LINDNER. Ber. **94**, 1417 (1961).
5. R. F. HECK and D. S. BRESLOW. J. Am. Chem. Soc. **83**, 4023 (1961).
6. R. F. HECK. J. Am. Chem. Soc. **85**, 1460 (1963).
7. R. F. HECK. J. Am. Chem. Soc. **85**, 651 (1963); **85**, 3387 (1963).
8. R. F. HECK and D. S. BRESLOW. J. Am. Chem. Soc. **85**, 2779 (1963).
9. A. ROSENTHAL and H. J. KOCH. Tetrahedron Letters, 871 (1967).
10. R. J. FERRIER. J. Chem. Soc. 5443 (1964).
11. Y. TAKEGAMI, C. YOKOKAWA, Y. WATANABE, and Y. OKUDA. Bull. Chem. Soc. Japan, **37**, 181 (1964).
12. M. ORCHIN. Advan. Catalysis, **16**, 2 (1966).
13. R. J. FERRIER. Advan. Carbohydrate Chem. **20**, 67 (1965).
14. W. HIEBER and G. WAGNER. Z. Naturforsch. **12b**, 478 (1957); **13b**, 192 (1958); **13b**, 339 (1958).
15. J. EISCH and R. B. KING. Organometallic Syn. **1**, 153 (1965).
16. R. U. LEMIEUX and B. FRASER-REID. Can. J. Chem. **42**, 532 (1964).
17. H. S. ISBELL. J. Res. Natl. Bur. Std. **5**, 1179 (1930). A. THOMPSON and M. L. WOLFROM. Methods Carbohydrate Chem. **2**, 215 (1963).
18. B. HELFERICH, E. N. MULCAHY, and H. Ziegler. Ber. **87**, 233 (1954).

Can. J. Chem. Downloaded from www.nrcresearchpress.com by 210.87.254.105 on 09/05/12
For personal use only.

Can. J. Chem. Downloaded from www.nrcresearchpress.com by 210.87.254.42 on 09/05/12
For personal use only.

Reaction of 1,2,3-thiadiazoles with base. II. Thioneesters from thioketene intermediates

R. RAAP
R & L Molecular Research, Ltd., 8045 Argyll Road, Edmonton, Alberta

Received March 26, 1968

Alkynethiolates, generated from 1,2,3-thiadiazoles by a strong base, react with alcohols and alkanethiols to give thioneesters and dithioesters respectively. In this manner were prepared: dimethyl monothionemalonate, (methoxythiocarbonyl)acetamide, methyl phenylthioneacetate, and ethyl phenyldithioacetate. 2,ω-Diphenyl-1,4-dithiafulvene results from the reaction between lithium 2-phenylethynethiolate and water.

Canadian Journal of Chemistry, 46, 2251 (1968)

In a previous publication (1) we reported on the cleavage of 1,2,3-thiadiazoles (**1**) by strong base to give alkynethiolates (**2**), which could subsequently be alkylated or acylated to 1-alkynyl thioethers (**3**). An alkynethiolate **2** can possibly abstract a proton from protic substances to give an alkynethiol or its tautomer, the thioketene **4**. It thus seemed possible to obtain some additional insight into the behavior of thioketenes[1] by either decomposing 1,2,3-thiadiazoles in protic solvents, such as alcohols or alkanethiols, or by addition of these substances to an alkynethiolate solution.

When methyl 1,2,3-thiadiazole-4-carboxylate

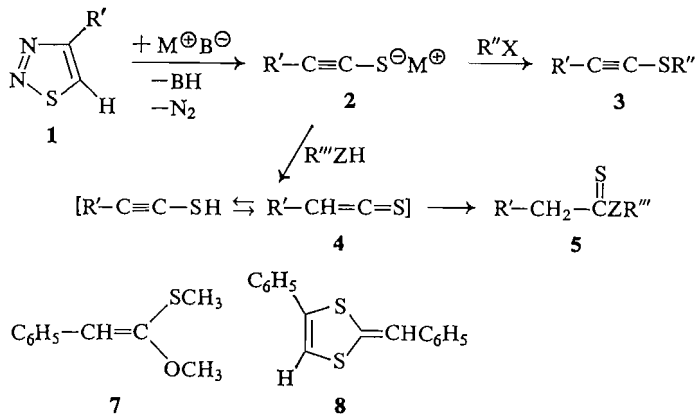

a R′ = CH_3O_2C; Z = O; R‴ = CH_3
b R′ = H_2NCO; Z = O; R‴ = CH_3
c R′ = C_6H_5; Z = O; R‴ = CH_3
d R′ = C_6H_5; Z = S; R‴ = C_2H_5

SCHEME 1

was added to a threefold excess of methanolic sodium methoxide at 0°, a rapid gas evolution took place and dimethyl monothionemalonate[2]

[1]Reactions described in the literature which are believed to involve thioketenes as intermediates include the thermal decomposition of diphenyldithioacetic acid (2), 1-alkynyl thioethers (3,4) and 1,3-dithietanes (5). Thioketene, a very unstable substance polymerizing at temperatures above −80°, was prepared by Howard (4) by pyrolysis of *t*-butylthioethyne. A stable thioketene, bis(trifluoromethyl)thioketene, was recently reported by Raasch (6). Arens and co-workers obtained dithioesters in 30–50% yield by adding alkanethiols to ethereal solutions of lithium alkynethiolates (7); they also studied the reactions of alkynethiolates generated in the presence of proton donors from acetylthioalkynes by the action of nucleophiles (8,9).

[2]A brief resume of reactions leading to thioneesters has been given by Renson and Bidaine (10). Since then, a superior method, involving the reaction of iminoester hydrochlorides with H_2S in pyridine, has been described by Schmidt, Heymann, and Kabitzke (11). By employing this latter procedure Scheithauer and Mayer (12) and, independently, Barnikow and Strickmann (13) have recently prepared some dialkyl monothionemalonates.

(**5***a*) was isolated from the reaction mixture in 71% yield. This product was identical with that synthesized from the iminoester hydrochloride **6** according to recently described procedures (11–13).

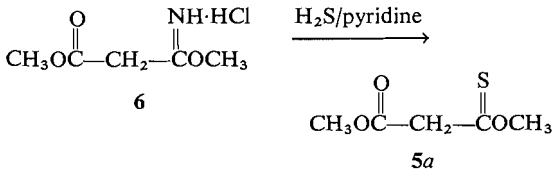

6 **5***a*

Equally rapid was the reaction of methanolic sodium methoxide with 1,2,3-thiadiazole-4-carboxamide to give (methoxythiocarbonyl)-acetamide (**5***b*, 59%). 4-Phenyl-1,2,3-thiadiazole did not react with sodium methoxide in the cold, but when the methanolic solution was heated under reflux, the gas evolution ceased within 1 h and methyl phenylthioneacetate (**5***c*) was obtained (69%). When prior to work-up the latter reaction mixture was treated with dimethyl sulfate, β-methoxy-β-methylthiostyrene (**7**) was the only product isolated (62%). Apparently the reaction medium is sufficiently basic for the product to be present as the anion, which preferentially alkylates on the sulfur.

Next, lithium 2-phenylethynethiolate in tetrahydrofuran was treated with some protic substances. When water was carefully added at −60° a quantitative amount of 2,ω-diphenyl-1,-4-dithiafulvene (**8**) was formed. The addition of ethanethiol at −60° resulted in a mixture of dithiafulvene **8** (45%) and ethyl phenyldithioacetate (**5***d*, 50%).[3] When the lithium 2-phenylethynethiolate solution was added dropwise to methanol at 0°, a mixture of methyl phenylthioneacetate (**5***c*, 18%) and **8** (48%) was obtained. A surprising 82% yield of the dithiafulvene was isolated when the 2-phenylethynylthiolate solution was added to refluxing methanol. The predominant formation of **8** in these reactions can be explained by a rapid reaction of phenylthioketene with lithium 2-phenylethynylthiolate. Kirmse and Horner (14) obtained 2,ω-diphenyl-1,4-dithiafulvene by photochemical decomposition of 4-phenyl-1,2,3-thiadiazole in benzene, a reaction which is also believed to involve phenylthioketene as an intermediate.

[3]The yield of the latter product could be increased to 61% by inverse addition.

Experimental

All melting points and boiling points are uncorrected. Nuclear magnetic resonance (n.m.r.) spectra were measured using a Varian Associates model A-60 spectrometer, with tetramethylsilane as a reference. Microanalyses were performed by Dr. G. Weiler and Dr. F. B. Strauss, Microanalytical Laboratory, Oxford, England.

Dimethyl Monothionemalonate (5a)

Methyl 1,2,3-thiadiazole-4-carboxylate (200 g, 1.39 mole) (1, 15) was added in portions to a stirred solution of sodium methoxide (from 96 g, 4.17 g-atom, of sodium) in 2 l of methanol, cooled in an ice-salt bath. Immediately a vigorous gas evolution took place. The addition was completed in approximately 30 min, during which time the temperature of the reaction mixture was maintained at 0–15°. The ice bath was removed and the reaction mixture was left at ambient temperature for 15 min whereafter the methanol was removed under reduced pressure. To the residue were added 2.5 l of ice-water. The resultant solution was washed with ether then acidified with 6 *N* hydrochloric acid and extracted with three 500 ml portions of ether. The combined extracts were dried, the ether removed and the residue distilled *in vacuo* to give 146 g (71%) of a yellow-colored liquid, b.p. 59–60° (2.5 mm). The n.m.r. spectrum (CCl_4) contained methyl singlets at τ 5.89 and 6.29 and a methylene singlet at τ 6.25.

Anal. Calcd. for $C_5H_8O_3S$: C, 40.52; H, 5.44; S, 21.64. Found: C, 40.71; H, 5.44; S, 21.35.

The same product was also prepared in 72% overall yield from methyl cyanoacetate by the procedure given by Barnikow and Strickmann (13) for diethyl monothionemalonate. The material, b.p. 55–56° (2.0 mm), was shown to be identical with the above prepared product by comparison of the infrared and n.m.r. spectra.

(Methoxythiocarbonyl)acetamide (5b)

1,2,3-Thiadiazole-4-carboxamide, (25.8 g, 0.20 mole) (15) was added in portions to a stirred ice-cooled solution of sodium methoxide (from 13.8 g, 0.60 g-atom, of sodium) in 200 ml of methanol, at such a rate that the temperature of the reaction mixture did not exceed 15°. When the addition was completed the reaction mixture was kept at room temperature for 15 min whereafter the solvent was removed under reduced pressure. The residue was dissolved in 150 ml of ice-water and the resultant solution was carefully acidified, under cooling, with concentrated hydrochloric acid. The product was immediately extracted with six 75 ml portions of ethyl acetate. The combined extracts were dried and passed through a short silica gel column. The eluate was concentrated to a volume of 50 ml, treated with 25 ml of warm *n*-hexane and cooled. The yellow needles, m.p. 62–65°, were collected by filtration and amounted to 15.6 g (59%). An analytical sample, m.p. 68–69°, was obtained by two recrystallizations from ethyl acetate–*n*-hexane.

Anal. Calcd. for $C_4H_7NO_2S$: C, 36.08; H, 5.30; N, 10.52; S, 24.07. Found: C, 36.19; H, 5.23; N, 10.24; S, 23.80.

Methyl Phenylthioneacetate (5c)

To a solution of sodium methoxide (from 13.8 g, 0.60 g-atom, of sodium) in 300 ml of methanol was added

Can. J. Chem. Downloaded from www.nrcresearchpress.com by 210.87.254.42 on 09/05/12
For personal use only.

Can. J. Chem. Downloaded from www.nrcresearchpress.com by 210.87.254.42 on 09/05/12
For personal use only.

4-phenyl-1,2,3-thiadiazole (32.4 g, 0.20 mole) (16). The reaction mixture was heated under reflux for 1 h whereafter the methanol was removed under reduced pressure. The residue was poured into 200 ml of ice-water and the product was extracted with four 75 ml portions of ether. The combined ether extracts were dried followed by removal of the ether and vacuum distillation of the residue to give 22.9 g (69%) of pale-yellow liquid, b.p. 70–71° (0.8 mm); reported (17) b.p. 145–149° (83 mm).

Anal. Calcd. for $C_9H_{10}OS$: C, 65.05; H, 6.07; S, 19.29. Found: C, 65.10; H, 6.18; S, 19.45.

The infrared and n.m.r. spectra were superimposable with the corresponding spectra of an authentic sample prepared from benzyl cyanide by the method of Schmidt, Heymann, and Kabitzke (11).

β-Methoxy-β-methylthiostyrene (7)

A mixture of 4-phenyl-1,2,3-thiadiazole (8.1 g, 0.050 mole) sodium methoxide (from 3.44 g, 0.150 g-atom, of sodium) and 90 ml of methanol was heated under reflux for 45 min. The reaction mixture was cooled to room temperature and dimethyl sulfate (12.6 g, 0.10 mole) was added in one portion. After the mixture had been worked up in the usual manner there was obtained 5.6 g (62%) of product, b.p. 81–82° (0.2 mm). The n.m.r. spectrum (CCl_4) contained a multiplet at τ 2.4 – 2.9 (phenyl) and singlets at τ 4.14 (olefinic H), 6.27 (OCH_3) and 7.76 (SCH_3) with an integrated area ratio of 5:1:3:3 respectively.

Anal. Calcd. for $C_{12}H_{12}OS$: C, 66.61; H, 6.71; S, 17.78. Found: C, 66.72; H, 6.67; S, 17.95.

Reactions of Lithium 2-Phenylethynethiolate with Water, Methanol, and Ethanethiol

A 1.6 *M* solution of *n*-butyllithium in *n*-hexane (34 ml, 0.055 mole of butyllithium) was added to a stirred suspension of 4-phenyl-1,2,3-thiadiazole (8.1 g, 0.050 mole) in 75 ml of anhydrous tetrahydrofuran, cooled in dry ice – acetone, at such a rate that the temperature did not exceed −60°. The addition was carried out in a nitrogen atmosphere. When the addition was completed the reaction mixture was stirred at −60° an additional 10 min. The following reactions were carried out with the thus prepared lithium 2-phenylethynethiolate solutions:

(a) With Water

Water (50 ml) was carefully added at −60° to the thiolate solution. The temperature of the mixture was allowed to rise to 10° and the two layers were separated. The organic solution was dried and the solvent removed, leaving 6.7 g (103%) of a yellow-colored solid. Upon heating, the solid partly melted at approximately 130° then solidified again completely and melted to a red-colored liquid at 185–190°. A 3.0 g sample was recrystallized from toluene (40 ml) to give 1.5 g of pure *2,ω-diphenyl-1,4-dithiafulvene* (**8**) as a yellow solid, m.p. 198–199°, identical in all respects (infrared spectra superimposable, mixture melting point undepressed) with an authentic sample, m.p. 197–198°, prepared by photolysis of 4-phenyl-1,2,3-thiadiazole (14). The solid residue obtained from the filtrate was heated *in vacuo* at 140–145° for 15 min (no significant change in the infrared spectrum was observed by this treatment) and then recrystallized from toluene (40 ml) to give an additional 0.9 g of the pure dithiafulvene, m.p. 198–199°. The behavior of the product suggests that in the reaction both isomeric forms of the dithiafulvene **8** are produced and that one of these forms isomerizes to the more stable form at approximately 130°.

(b) With Methanol

The lithium thiolate solution was placed in a dropping funnel and added dropwise in 10 min to 50 ml of methanol at 0°. The methanol was removed, the residue added to 200 ml of ice-water and this solution extracted with five 60 ml portions of ether. The combined ether extracts were dried and the ether removed, leaving a mixture of *methyl phenylthioneacetate* (1.5 g, 18%; b.p. 78–79° (1.5 mm)) and 2,ω-diphenyl-1,4-dithiafulvene (3.2 g, 48%) which could be separated by treatment with *n*-hexane in which the dithiafulvene was not soluble. When the 2-phenylethynylthiolate solution was added to refluxing methanol an 82% yield of the dithiafulvene was isolated and only a trace of methyl phenylthioneacetate was formed.

(c) With Ethanethiol

To the lithium 2-phenylethynylthiolate solution, at −60°, was added a solution of ethanethiol (8.4 g, 0.13 mole) in 30 ml of tetrahydrofuran, in one portion. The reaction mixture was worked up in the usual manner to give 3.0 g (45%) of 2,ω-diphenyl-1,4-dithiafulvene, m.p. 193–195°, and 4.9 g (50%) of *ethyl phenyldithioacetate* (**5***d*) an orange-colored liquid with b.p. 100–101° (0.6 mm); reported (18) b.p. 140–144° (45 mm).

Anal. Calcd. for $C_{10}H_{12}S_2$: C, 61.18; H, 6.16; S, 32.67. Found: C, 61.51; H, 6.21; S, 32.49.

When the thiolate solution was added dropwise in 15 min to the ethanethiol solution, at −20 to −30°, a 61% yield of ethyl phenyldithioacetate was obtained whereas only a 15% yield of the dithiafulvene was isolated.

Acknowledgments

The author is indebted to Mr. V. R. Baker and Mr. P. K. Wolfert for their technical assistance and to Professor R. U. Lemieux for his advice and interest in this work.

1. R. Raap and R. G. Micetich. Can. J. Chem. **46**, 1057 (1968).
2. A. Schönberg, A. Stephenson, H. Kaltschmitt, E. Petersen, and H. Schulten. Chem. Ber. **66**, 237 (1933).
3. H. J. Boonstra and J. F. Arens. Rec. Trav. Chim. **79**, 866 (1960).
4. E. G. Howard, Jr. U. S. Patent 3,035,030 to E. I. duPont de Nemours and Company; Chem. Abstr. **57**, 13617 (1962).
5. K. Dickoré and R. Wegler. Angew. Chem. Intern. Ed. Engl. **5**, 970 (1966).
6. M. S. Raasch. Chem. Commun. 577 (1966).
7. P. J. W. Schuijl, L. Brandsma, and J. F. Arens. Rec. Trav. Chim. **85**, 889 (1966).
8. H. E. Wijers, L. Brandsma, and J. F. Arens. Rec. Trav. Chim. **86**, 670 (1967).
9. H. W. Wijers, C. H. D. Van Ginkel, L. Brandsma, and J. F. Arens. Rec. Trav. Chim. **86**, 907 (1967).
10. M. Renson and J. Bidaine. Bull. Soc. Chim. Belges. **70**, 519 (1961).

11. U. SCHMIDT, E. HEYMANN, and K. KABITZKE. Chem. Ber. **96**, 1478 (1963).
12. S. SCHEITHAUER and R. MAYER. Chem. Ber. **100**, 1413 (1967).
13. G. BARNIKOW and G. STRICKMANN. Chem. Ber. **100**, 1428, 1661 (1967).
14. W. KIRMSE and L. HORNER. Ann. Chem. **614**, 4 (1958).
15. D. L. PAIN and R. SLACK. J. Chem. Soc., 5166 (1965).
16. C. D. HURD and R. I. MORI. J. Am. Chem. Soc. **77**, 5359 (1955).
17. Y. SAKURADA. Mem. Coll. Sci. and Eng., Kyoto Imp. Univ., Ser. A, **10**, 67 (1926); Chem. Zentr. I, 1300 (1927).
18. Y. SAKURADA. Mem. Coll. Sci. and Eng., Kyoto Imp. Univ., Ser. A, **10**, 79 (1926); Chem. Abstr. **21**, 3609 (1927).

Can. J. Chem. Downloaded from www.nrcresearchpress.com by 210.87.254.42 on 09/05/12
For personal use only.

Can. J. Chem. Downloaded from www.nrcresearchpress.com by 210.87.254.105 on 09/05/12
For personal use only.

Some syntheses with dimethyl monothionemalonate

R. RAAP
R & L Molecular Research, Ltd., 8045 Argyll Road, Edmonton, Alberta

Received March 26, 1968

Reactions are described in which the *S*-alkylation products of dimethyl monothionemalonate and the reaction products with amino compounds have been employed to prepare compounds such as 3-hydroxythiophenes, 1-tetrazolylacetates, 1,3,4-oxadiazolylacetates, and methyl 3,3-di-*N*-morpholinoacrylate.

Canadian Journal of Chemistry, 46, 2255 (1968)

The syntheses of various dialkyl monothionemalonates from cyanoacetic esters via the iminoester hydrochlorides were reported in recent publications by Scheithauer and Mayer (1) and Barnikow and Strickmann (2, 3). Apart from undergoing Michael additions and Knoevenagel condensations (1) these compounds reacted with amino compounds to give structures such as Δ^2-imidazolinyl- and Δ^2-oxazolinylacetic esters and 3-alkoxypyrazol-5-ones (3). In a previous publication we reported on the synthesis of dimethyl monothionemalonate (**1**) from methyl 1,2,3-thiadiazole-4-carboxylate (4). We had similarly explored some of the synthetic possibilities of this compound and the results described in the present paper further emphasize the value of monothionemalonates for organic syntheses (Scheme 1).

The sodio derivative of **1** reacted with alkyl halides to give the *S*-alkylated products **2***a–d* in 60–80% yield. Compounds **2***b–d* readily underwent a Dieckmann cyclization to the 3-hydroxythiophenes **3** upon treatment with base. Even the hydrolysis of **2***b* and **2***c* with methanolic sodium hydroxide at room temperature gave rise to both the expected acid (**2**, R = CH_2CO_2H) and the cyclization products **3***a* and **3***b*. This cyclization is mechanistically related to the preparation of 3-hydroxythiophenes from thioglycolic ester and β-keto esters or acetylene carboxylic esters in the presence of base (5). Compounds **3***a* and **3***b* were quantitatively converted to the 3,5-dimethoxythiophenes **4** upon reaction with diazomethane. Compound **3***c* on the other hand reacted with diazomethane to give predominantly 5-methoxy-2-methoxybenzylidene-4-thiolen-3-one (**5**)[1], a readily crystallizable white solid, m.p. 85–87°. A small amount (approximately 15% yield) of **4***c* was also formed and could be separated from **5** by elution chromatography on silica gel.

When *N,N*-dimethylhydrazine was added to dimethyl monothionemalonate at room temperature an instantaneous reaction took place, with evolution of H_2S. Distillation of the reaction mixture afforded pure methyl (methoxy-*N,N*-dimethylcarbhydrazino) acetate (**6**, R = $(CH_3)_2N$-) in 87% yield. This reaction appears to be an example of a general reaction between thionemalonates and amino compounds (Table I; cf. reference 3) and even a relatively unreactive amino compound such as aniline reacted smoothly. The same reaction could be applied to methyl phenylthioneacetate, although this compound reacted more slowly. A direct application of this reaction consisted of the addition of acetylhydrazine to a solution of **1** in dimethylformamide and heating the resulting mixture at 100° for 4 h without isolating the intermediate **7**. Methyl 5-methyl-1,3,4-oxadiazolylacetate (**8**, R = CH_3) was readily isolated

TABLE I

Yield and boiling point data for the reaction* of thione esters with amino compounds

Compound†		Yield	Boiling point, °C
R	R′	%	(mm Hg)
CH_3O_2C	C_2H_5	77	62–63 (0.7)
CH_3O_2C	CH_3O	75	43–45 (0.5)
CH_3O_2C	$(CH_3)_2N$	87	82–84 (12)
CH_3O_2C	C_6H_5	76	92–93 (0.4)
C_6H_5	$(CH_3)_2N$	86	67–68 (0.5)
C_6H_5	C_6H_5	41	115–116 (0.4)

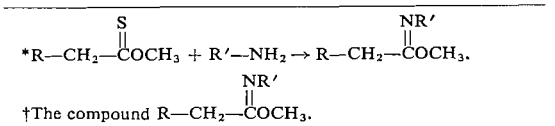

[1]The structural assignment is primarily based on the infrared and nuclear magnetic resonance spectra. The minor reaction product contains a strong carbonyl band in the infrared spectrum at 1650 cm^{-1}; the major product does not absorb in the 1600–1800 cm^{-1} region.

Can. J. Chem. Downloaded from www.nrcresearchpress.com by 210.87.254.105 on 09/05/12
For personal use only.

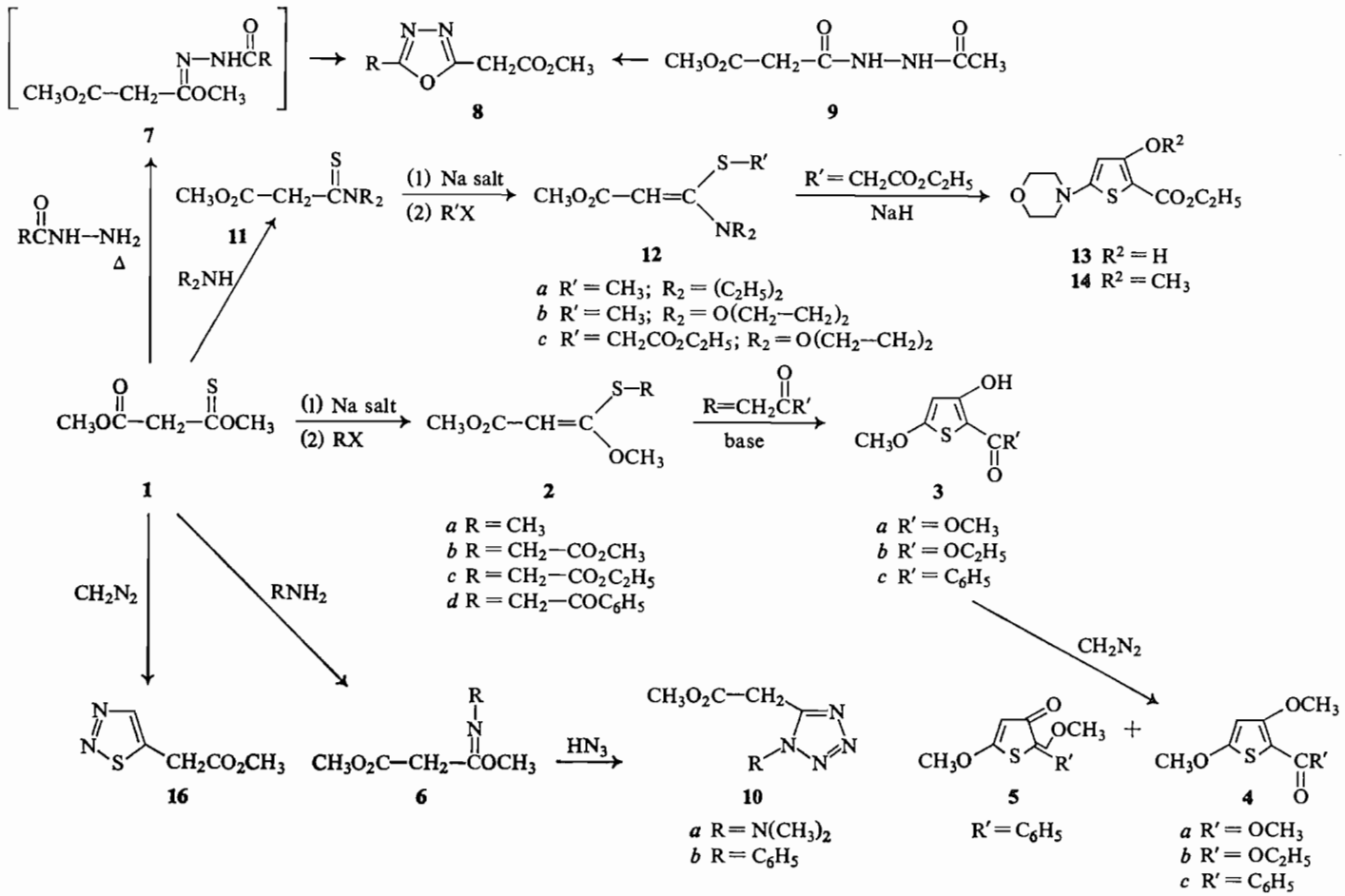

SCHEME 1

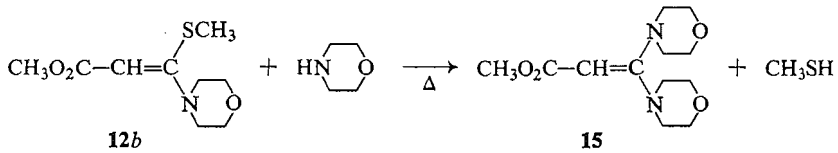

12*b* 15

by distillation in 64% yield and was identical with a sample prepared by dehydration of the monohydrazide **9**, according to the procedure of Quelet and Milcent (6). Methyl 5-phenyl-1,3,4-oxadiazolylacetate (**8**, R = C_6H_5) was similarly prepared from **1** and benzoylhydrazine.[2]

When the iminoesters **6** were treated with sodium azide in glacial acetic acid, according to conditions described by Hagedorn and Winkelmann (7), the 1-substituted 5-tetrazolylacetic esters **10** were obtained in fair yields.

Dimethyl monothionemalonate reacted readily with the secondary amines diethylamine and morpholine to give almost quantitative yields of the thioamides **11** which could subsequently be *S*-alkylated to compounds **12**. Ethyl 3-hydroxy-5-*N*-morpholinothiophene-2-carboxylate (**13**) was prepared from **12***c* by a Dieckmann cyclization with sodium hydride in tetrahydrofuran. This product could be methylated to compound **14** upon treatment with diazomethane. When **12***b* was heated with morpholine, methanethiol evolved and methyl 3,3-di-*N*-morpholinoacrylate (**15**), m.p. 115–116°, was isolated in 77% yield.

Upon reaction of **1** with diazomethane in a methanol–ether mixture methyl 5-(1,2,3-thiadiazolyl)acetate (**16**; 74%) was obtained. Methanol clearly acts as a catalyst in this reaction as in the absence of methanol **16** was not isolated and the product mixture decomposed vigorously upon distillation (cf. references 1, 8, 9).

Experimental

All melting points and boiling points are uncorrected. The infrared spectra were recorded on a Perkin–Elmer model 137 "Infracord" spectrophotometer. Nuclear magnetic resonance (n.m.r.) spectra were measured using a Varian Associates model A-60 spectrometer, with tetramethylsilane as a reference. Ultraviolet spectra were obtained using a Perkin–Elmer model 202 recording spectrophotometer. Microanalyses were performed by Dr. G. Weiler and Dr. F. B. Strauss, Microanalytical Laboratory, Oxford, England.

Methyl 3-Methoxy-3-methylthioacrylate (2a)

Sodium (1.38 g, 0.060 g-atom) was allowed to react with 60 ml of methanol. To the sodium methoxide solution were successively added, at 0°, dimethyl monothionemalonate (7.4 g, 0.050 mole) and methyl iodide (9.9 g, 0.070 mole). The solvent was removed, the residue diluted with 50 ml of water and extracted with ether. Drying and removal of the ether, followed by recrystallization of the residue from *n*-hexane yielded 6.0 g (75%) of white crystals, m.p. 52–54°. The n.m.r. spectrum ($CDCl_3$) contained methyl singlets at τ 6.17, 6.33, and 7.71 and a singlet for the olefinic proton at τ 4.79. An analytical sample, m.p. 62–63°, was obtained by two additional recrystallizations from *n*-hexane.

Anal. Calcd. for $C_{10}H_{10}O_3S$: C, 44.42; H, 6.22; S, 19.76. Found: C, 44.71; H, 6.35; S, 19.80.

An n.m.r. spectrum revealed that the crude material (2 g) that was recovered when the solvent was removed from the filtrate, existed almost exclusively of the same acrylic ester, indicating that the isomeric dimethyl methylmonothionemalonate was either not formed at all or only in trace amounts.

Methyl 3-Carbomethoxymethylthio-3-methoxyacrylate (2b)

Dimethyl monothionemalonate (7.4 g, 0.050 mole) was added dropwise in 15 min to a stirred suspension of sodium hydride (1.25 g, 0.052 mole) in 75 ml of anhydrous tetrahydrofuran, cooled in ice. When the addition was completed the mixture was stirred for an additional 15 min followed by the addition of methyl chloroacetate (6.0 g, 0.055 mole) in one portion. The reaction mixture was heated under reflux for 1 h, then poured into 100 ml of ice-water and extracted with two 100 ml portions of ethyl acetate. The residue obtained after drying and removal of the ethyl acetate was recrystallized from a mixture of benzene (20 ml) and *n*-hexane (40 ml) to give 6.7 g (61%) of white crystals, m.p. 73–74°. The n.m.r. spectrum ($CDCl_3$) contained sharp singlets at τ 4.78, 6.22, 6.30, 6.33, and 6.43 with an integrated area ratio of 1:3:3:3:2 respectively.

Anal. Calcd. for $C_8H_{12}O_5S$: C, 43.62; H, 5.49; S, 14.56. Found: C, 43.51; H, 5.71; S, 14.71.

When the material was treated with a slight excess of 3 *N* methanolic sodium hydroxide at room temperature for 10 min there was obtained, after work-up, a mixture of methyl 3-carboxymethylthio-3-methoxyacrylate (53%, m.p. 111–112°) and methyl 3-hydroxy-5-methoxythiophene-2-carboxylate (*3a*) (18%, m.p. 71–73°). The former product crystallized readily from ethyl acetate whereas the thiophene compound was obtained by cooling a concentrated methanolic solution of the residue.

[2]Methyl 1,3,4-oxadiazolylacetate (**8**, R = H) was formed in very low yield from **1** and formylhydrazine. However, attempts to isolate this compound by either chromatography on silica gel or distillation resulted almost invariably in complete decomposition.

Can. J. Chem. Downloaded from www.nrcresearchpress.com by 210.87.254.105 on 09/05/12
For personal use only.

Can. J. Chem. Downloaded from www.nrcresearchpress.com by 210.87.254.105 on 09/05/12
For personal use only.

Anal. Calcd. for $C_7H_{10}O_5S$ (mol. wt., 206): C, 40.77; H, 4.89; S, 15.55. Found (neutralization equivalent, 197): C, 41.21; H, 5.17; S, 15.72.

Methyl 3-Carbethoxymethylthio-3-methoxyacrylate (2c)

This compound, m.p. 88–90° (ethyl acetate – *n*-hexane), was prepared in 79% yield from sodium dimethyl monothionemalonate and ethyl bromoacetate by the preceding procedure. Treatment of this product with a slight excess of 2 *N* ethanolic sodium hydroxide yielded a mixture of methyl 3-carboxymethylthio-3-methoxyacrylate (32%) and ethyl 3-hydroxy-5-methoxythiophene-2-carboxylate (*3b*; 48%), m.p. 28–31°.

Methyl 3-Methoxy-3-(phenacylthio)acrylate (2d)

A solution of sodium dimethyl monothionemalonate in tetrahydrofuran was prepared from dimethyl monothionemalonate (7.4 g, 0.050 mole) as described above. To this solution, cooled in ice, was added a solution of 2-bromoacetophenone (11.0 g, 0.055 mole) in 25 ml of tetrahydrofuran, in one portion. The reaction mixture was stirred at room temperature for 30 min, then concentrated and diluted with 150 ml of water. The product precipitated and was taken up in ethyl acetate (200 ml). The ethyl acetate solution was dried and concentrated to a volume of 50 ml. To the hot ethyl acetate solution was added 50 ml of boiling *n*-hexane and the mixture was allowed to cool. There was obtained 10.0 g (75%) of white needles, m.p. 94–96°. The n.m.r. spectrum ($CDCl_3$) showed absorption at τ 2.2–2.9 (phenyl H's), τ 4.96 (singlet; olefinic H), τ 5.90 (singlet; CH_2), and τ 6.47 (overlapping methoxy groups) with an integrated area ratio of 5:1:2:6 respectively.

Anal. Calcd. for $C_{13}H_{14}O_4S$: C, 58.63; H, 5.30; S, 12.04. Found: C, 58.64; H, 5.24; S, 12.20.

Methyl 3-Hydroxy-5-methoxythiophene-2-carboxylate (3a)

Methyl 3-carbomethoxymethylthio-3-methoxyacrylate (6.6 g, 0.030 mole) was added to a stirred suspension of sodium hydride (0.96 g, 0.040 mole) in 75 ml of anhydrous tetrahydrofuran, cooled in ice. The reaction mixture was allowed to warm up slowly. At approximately 10° an exothermic reaction started which necessitated occasional cooling. When the reaction subdued, the reaction mixture was stirred at room temperature for an additional 30 min and was then diluted with 150 ml of ice-water. The mixture was washed with ether and then acidified with dilute sulfuric acid. The product was extracted with two 75 ml portions of ether. The combined ether extracts were dried and the ether removed, leaving 5.1 g (90%) of white solid residue m.p. 67–71°. The melting point could be raised to 72–73° by recrystallization from methanol; λ_{max}(MeOH) 287 mμ (log ε 4.17). The infrared spectrum (Nujol mull) contained sharp bands at 1650 and 1565 cm^{-1} ascribed to the carboxyl group and the thiophene ring respectively. The n.m.r. spectrum ($CDCl_3$) contained singlets at τ 0.15, 4.12, 6.13, and 6.21 with an integrated area ratio of 1:1:3:3 respectively. A methanol solution of the compound obtained an intense purple color upon addition of ferric chloride.

Anal. Calcd. for $C_7H_8O_4S$ (mol. wt., 188): C, 44.67; H, 4.29; S, 17.04. Found (mol. wt., 183, osmometric): C, 44.15; H, 4.27; S, 16.91.

The product could also be obtained, in 80% yield, when the cyclization was carried out in methanol with a slight excess of sodium methoxide (1 h at 25°).

Ethyl 3-Hydroxy-5-methoxythiophene-2-carboxylate (3b)

This product, m.p. 32–33° (after recrystallization from methanol), was prepared in 86% yield from methyl 3-carbethoxymethylthio-3-methoxyacrylate (7.0 g, 0.030 mole) in the same manner as described above. The n.m.r. spectrum (CCl_4) showed absorption at τ 0.12 (broad singlet), 4.19 (singlet), 5.76 (quartet), 6.15 (singlet), and 8.68 (triplet) with an integrated area ratio of 1:1:2:3:3 respectively.

Anal. Calcd. for $C_8H_{10}O_4S$: C, 47.51; H, 4.99. Found: C, 47.57; H, 4.96.

2-Benzoyl-3-hydroxy-5-methoxythiophene (3c)

To a slightly warm solution of methyl 3-methoxy-3-(phenacylthio)acrylate (9.0 g, 0.034 mole) in 75 ml of methanol were added 13 ml of a 3 *N* methanolic sodium hydroxide solution. The mixture was left at room temperature for 5 min, then the methanol was removed, followed by the addition of ether (100 ml) to the residue. The pale-yellow colored sodium salt (8.7 g, 100%) was collected by filtration. Part of this salt (5.1 g, 0.020 mole) was dissolved in 50 ml of water and acidified with dilute sulfuric acid. The product was extracted with two 50 ml portions of ethyl acetate. The combined extracts were dried and the solvent removed to give 3.8 g (81%) of yellow crystalline residue, m.p. 55–59°. The product could be recrystallized from methanol (20 ml) to give 3.5 g of yellow needles, m.p. 58–60°; λ_{max}(MeOH) 339 mμ (log ε 4.16). The infrared spectrum (Nujol mull) did not show any carbonyl absorption in the 1600–1800 cm^{-1} region. The n.m.r. spectrum (CCl_4) contained a broad singlet at τ 0.1, complex absorption at τ 2.2–2.9 and singlets at τ 4.23 and 6.20 with an integrated area ratio of 1:5:1:3 respectively. A methanolic solution of the compound obtained an intense green color upon addition of ferric chloride.

Anal. Calcd. for $C_{12}H_{10}O_3S$ (mol. wt., 234): C, 61.50; H, 4.30; S, 13.68. Found (mol. wt., 232, osmometric): C, 61.44; H, 4.50; S, 13.85.

The product could also be prepared with sodium hydride in tetrahydrofuran in the manner described above (63% yield).

Methyl 3,5-Dimethoxythiophene-2-carboxylate (4a)

To a solution of methyl 3-hydroxy-5-methoxythiophene-2-carboxylate (2.1 g, 0.011 mole) in 25 ml of ether was added an excess of an ethereal solution of diazomethane. The reaction mixture was left at room temperature for 2 h whereafter the ether and excess diazomethane were removed to give 2.3 g (100%) of white solid residue, m.p. 61–65°. Recrystallization from benzene – *n*-hexane (1:2) raised the melting point to 67–68°; λ_{max}(MeOH) 291 mμ (log ε 4.18). The infrared spectrum (Nujol mull) contained sharp bands at 1670 and 1550 cm^{-1}. The n.m.r. spectrum (CCl_4) contained sharp singlets at τ 3.92, 6.07, and 6.22 with an integrated area ratio of 1:6:3 respectively.

Anal. Calcd. for $C_8H_{10}O_4S$ (mol. wt., 202): C, 47.51; H, 4.99; S, 15.86. Found (mol. wt., 202, osmometric): C, 47.10; H, 4.75; S, 16.23.

Can. J. Chem. Downloaded from www.nrcresearchpress.com by 210.87.254.105 on 09/05/12
For personal use only.

Ethyl 3,5-Dimethoxythiophene-2-carboxylate (4b)

This compound, m.p. 42–45°, was prepared in the same manner as the methyl ester.

Anal. Calcd. for $C_9H_{12}O_4S$: C, 49.98; H, 5.60; S, 14.83. Found: C, 50.03; H, 5.55; S, 14.92.

Reaction of 2-Benzoyl-3-hydroxy-5-methoxythiophene with Diazomethane

A solution of 2-benzoyl-3-hydroxy-5-methoxythiophene (4.0 g, 0.017 mole) in 75 ml of ether was treated with an excess of an ethereal solution of diazomethane. The reaction mixture was left at room temperature for 2 h. The residue obtained after removal of the ether was recrystallized from a benzene – *n*-hexane (1:2) mixture to give 2.6 g (62%) of 5-methoxy-2-methoxybenzylidene-4-thiolen-3-one (**5**) as white needles, m.p. 85–87°; λ_{max}(MeOH) 334 mμ (log ε 4.19). The infrared spectrum (Nujol mull) contained bands at 1590 and 1540 cm^{-1}, but no carbonyl absorption in the 1600–1800 cm^{-1} region. The n.m.r. spectrum ($CDCl_3$) showed a complex band at τ 2.2–2.8 and singlets at τ 3.97, 6.13, and 6.33, with an integrated area ratio of 5:1:3:3 respectively. The same product was obtained (in low yield) from the reaction of the sodium salt of the starting material with methyl iodide.

Anal. Calcd. for $C_{13}H_{12}O_3S$ (mol. wt., 248): C, 62.88; H, 4.87; S, 12.91. Found (mol. wt., 247, osmometric): C, 63.04; H, 4.77; S, 12.70.

The filtrate was concentrated to dryness to give 1.5 g of yellow oil, approximately a 1:1 mixture of the above isolated product and a product believed to be 2-benzoyl-3,5-dimethoxythiophene (**4c**). The mixture could be separated by elution chromatography on silica gel, most of the former product being eluted with ether, the latter with ethyl acetate. The ethyl acetate fraction was again chromatographed, and in this manner 0.3 g of 2-benzoyl-3,5-dimethoxythiophene was obtained as a viscous oil with a purity of approximately 90%; λ_{max}(MeOH) 339 (log ε 4.14). The infrared spectrum of the neat liquid contained strong bands at 1650, 1585, and 1550 cm^{-1}, ascribed to the carbonyl group and the phenyl and thiophene ring respectively. The n.m.r. spectrum ($CDCl_3$) showed singlets at τ 2.54, 4.54, 6.08, and 6.47 with an integrated area ratio of 5:1:3:3 respectively.

Methyl (Methoxy-N,N-dimethylcarbhydrazino)acetate (6, R = $(CH_3)_2N$)

N,N-Dimethylhydrazine (3.0 g, 0.050 mole) was added carefully to dimethyl monothionemalonate (7.4 g, 0.050 mole), resulting in an immediate reaction. The mixture was left at room temperature for 30 min, then distilled *in vacuo* to give 7.6 g (87%) of colorless liquid, b.p. 82–84° (12 mm). The n.m.r. spectrum (CCl_4) contained sharp singlets at τ 6.32, 6.36, 6.59, and 7.69 with an integrated area ratio of 3:3:2:6 respectively. The infrared spectrum of the neat liquid shows strong bands at 1725 and 1635 cm^{-1}.

Anal. Calcd. for $C_7H_{14}N_2O_3$: C, 48.26; H, 8.10; N 16.09. Found: C, 48.48; H, 8.34; N, 16.49.

Methyl (Methoxy-N-ethylcarbimino)acetate (6, R = C_2H_5)

A solution of ethylamine (4.5 g, 0.10 mole) in 30 ml of methanol was added dropwise in 15 min to a stirred solution of dimethyl monothionemalonate (14.8 g, 0.10 mole) in 50 ml of methanol at 0–10°. Removal of the solvent and fractional distillation of the residue yielded 12.2 g (77%) of a colorless liquid, b.p. 62–63° (0.7 mm). The infrared spectrum (neat liquid) of a center distillation cut contained a weak band at 3250 cm^{-1} and strong bands at 1740, 1650, and 1605 cm^{-1} suggesting the presence of both the tautomeric imino and enamine forms. The n.m.r. spectrum also pointed to a mixture of these tautomers.

Anal. Calcd. for $C_7H_{13}NO_3$: C, 52.81; H, 8.04; N, 8.80. Found: C, 52.54; H, 8.00; N, 8.53.

Methyl (Methoxy-O-methylcarboximino)acetate (6, R = OCH_3)

Methoxyamine hydrochloride (8.4 g, 0.10 mole) was added to 50 ml of a cold 2 *N* methanolic sodium hydroxide solution. The sodium chloride was filtered off and the filtrate added dropwise in 15 min to a stirred solution of dimethyl monothionemalonate (14.8 g, 0.10 mole) in 50 ml of methanol, cooled in ice. When the addition was completed the mixture was kept at 0° for an additional 1 h. Most of the methanol was removed under reduced pressure and 150 ml of ice-water was added to the residue. The product was extracted with three 75 ml portions of ether. The combined ether extracts were dried, the ether removed and the residue distilled *in vacuo* to give 12.0 g (75%) of colorless liquid, b.p. 43–45° (0.5 mm). The infrared spectrum of the neat liquid contained strong bands at 1740 and 1640 cm^{-1}.

Anal. Calcd. for $C_6H_{11}NO_4$: C, 44.71; H, 6.88; N, 8.69. Found: C, 44.84; H, 6.64; N, 8.42.

Methyl (Methoxy-N-phenylcarbimino)acetate (6, R = C_6H_5)

Aniline (4.7 g, 0.050 mole) was added to dimethyl monothionemalonate (7.4 g, 0.050 mole). The evolution of hydrogen sulfide became apparent immediately. The mixture was left at room temperature overnight, then distilled *in vacuo* to give 7.8 g (76%) of a yellow-colored liquid, b.p. 92–93° (0.4 mm). The infrared spectrum of the neat liquid showed strong absorption at 1740 and 1675 cm^{-1}.

Anal. Calcd. for $C_{11}H_{13}NO_3$: C, 63.75; H, 6.32; N, 6.76; Found: C, 63.79; H, 6.42; N, 7.01.

α-(Methoxy-N-phenylcarbimino)toluene

A mixture of aniline (4.7 g, 0.050 mole) and methyl phenylthioneacetate (8.4 g, 0.050 mole) (4) was heated at 35–45° for 40 h, whereafter the mixture was fractionally distilled *in vacuo* to give 4.6 g (41%) of product, b.p. 115–116° (0.4 mm). The infrared spectrum of the neat liquid contained a strong band at 1660 cm^{-1}.

Anal. Calcd. for $C_{15}H_{15}NO$: C, 79.94; H, 6.71; N, 6.22. Found: C, 79.76; H, 6.55; N, 6.35.

α-(Methoxy-N,N-dimethylcarbhydrazino)toluene

N,N-Dimethylhydrazine (3.0 g, 0.050 mole) was added to methyl phenylthioneacetate (8.4 g, 0.050 mole) (4). The reaction mixture was left at room temperature for 2 h and was then distilled *in vacuo* to give 8.3 g (86%) of colorless product, b.p. 67–68° (0.5 mm). The infrared spectrum of the neat liquid contained a strong band at 1630 cm^{-1}.

Anal. Calcd. for $C_{11}H_{16}N_2O$: C, 68.70; H, 8.39; N, 14.57. Found: C, 68.79; H, 8.07; N, 14.27.

Can. J. Chem. Downloaded from www.nrcresearchpress.com by 210.87.254.105 on 09/05/12
For personal use only.

Methyl 5-Methyl-1,3,4-oxadiazolylacetate (8, R = CH_3)

A mixture of dimethyl monothionemalonate (8.9 g, 0.060 mole), acetylhydrazine (4.8 g, 0.065 mole) and dimethylformamide (40 ml) was slowly heated to 100° in an oil bath. The reaction mixture was kept at this temperature for 5 h. The initial dark color disappeared after approximately 2 h. The solvent was removed under reduced pressure and the residue distilled *in vacuo* to give 6.0 g (64%) of pale-yellow product, b.p. 112–114° (1.5 mm), m.p. 12–16°. The n.m.r. spectrum ($CDCl_3$) consisted of singlets at τ 6.04, 6.23, and 7.46 with an integrated area ratio of 2:3:3 respectively. The n.m.r. and infrared spectra were superimposable with the corresponding spectra of an authentic sample, prepared by the procedure of Quelet and Milcent for the ethyl ester (6).

5-Methyl-1,3,4-oxadiazolylacetic Acid

To a solution of 5-methyl-1,3,4-oxadiazolylacetate (8.0 g, 0.051 mole) in 50 ml of methanol were added 20 ml of a 3 *N* methanolic sodium hydroxide solution. The reaction mixture was left at room temperature for 30 min, then the methanol was removed and the residue dissolved in 25 ml of water. The aqueous solution was washed with ether, then cooled and acidified with 12 ml of 6 *N* hydrochloric acid. The product (water-soluble) was extracted with eight 40 ml portions of ethyl acetate. The combined ethyl acetate extracts were dried and concentrated to a volume of 25 ml, followed by addition of 25 ml of *n*-hexane, and cooling. There was obtained 5.6 g (77%) of white solid, decarboxylating sharply at 84–85°; neutralization equivalent, 143 (calculated 142).

The analyses were obtained on the amide, m.p. 112–113°.

Anal. Calcd. for $C_5H_7N_3O_2$: C, 42.55; H, 5.00; N, 29.78. Found: C, 42.46; H, 5.14; N, 29.47.

5-Phenyl-1,3,4-oxadiazolylacetic Acid

The methyl ester was obtained from benzoylhydrazine (6.8 g, 0.050 mole) and dimethyl monothioneacetate (7.4 g, 0.050 mole) by the preceding procedure. The ester was, without purification, hydrolyzed (in 33% overall yield) to the acid, m.p. 95–96° (decomp.); neutralization equivalent, 199 (calculated 204). The analysis was performed on the amide which was obtained as follows: the crude ester obtained in the above experiment was treated with 45 ml 6 *M* methanolic ammonia. The mixture was left at room temperature overnight, cooled, and filtered to give 4.0 g (40%) of white platelets, m.p. 216–218° (after recrystallization from dioxane).

Anal. Calcd. for $C_{10}H_9N_3O_2$: C, 59.10; H, 4.47; N, 20.68. Found: C, 58.89; H, 4.68; N, 20.29.

1,3,4-Oxadiazolylacetic Acid

The methyl ester was formed in low yield from formylhydrazine and dimethyl monothioneacetate. The isolation, however, presented difficulties as in most runs the product completely polymerized both by distillation *in vacuo* (0.5 mm Hg) and by chromatography on silica gel. In a few instances the material was isolated by distillation in 10–20% yield; b.p. 100–105° (1.5 mm). The n.m.r. spectrum ($CDCl_3$) consisted of singlets at τ 1.44, 5.93, and 6.22 with an integrated area ratio of 1:2:3 respectively. The ester could be hydrolyzed in the same manner as described for the 5-methyl derivative to give an unstable solid, decarboxylating at 78–83°; neutralization equivalent, 128.5 (calculated 128).

Methyl 1-N,N-Dimethylamino-5-tetrazolylacetate (10a) and 1-N,N-Dimethylamino-5-tetrazolylacetic Acid

A mixture of methyl (methoxy-*N*,*N*-dimethylcarbhydrazino)acetate (5.5 g, 0.032 mole), sodium azide (9.7 g, 0.15 mole), and glacial acetic acid (75 ml) was heated at 60° for 18 h. The reaction mixture was poured into 150 ml of ice-water and the product extracted with ethyl acetate (4 times with 75 ml). The ethyl acetate extract was dried, the solvent removed, and the residue distilled *in vacuo* to give 3.0 g (51%) of product, b.p. 120–125° at 0.5 mm. The elemental analyses were performed on the acid which could be obtained from the ester by hydrolysis with methanolic sodium hydroxide followed by acidification and recrystallization from ethyl acetate – *n*-hexane, m.p. 115–117° (decomp.).

Anal. Calcd. for $C_5H_9N_5O_2$ (mol. wt., 171): C, 35.08; H, 5.30; N, 40.92. Found (neutralization equivalent, 170): C, 35.29; H, 5.38; N, 41.16.

1-Phenyl-5-tetrazolylacetic Acid

A mixture of methyl (methoxy-*N*-phenylcarbimino)-acetate (5.0 g, 0.024 mole), sodium azide (7.8 g, 0.12 mole), and glacial acetic acid (60 ml) was heated at 40° for 48 h and then poured into 150 ml of ice-water. The ester (5.0 g) was extracted with ether and, without purification, hydrolyzed with 3 *N* methanolic sodium hydroxide at room temperature (1 h). The acid could be recrystallized from ethyl acetate; yield, 1.3 g (26%); m.p. 134–135° (decomp.).

Anal. Calcd. for $C_9H_8N_4O_2$ (mol. wt., 204): C, 52.94; H, 3.95; N, 27.44. Found (neutralization equivalent, 198): C, 52.38; H, 3.98; N, 27.82.

Methyl (N,N-Diethylaminothiocarbonyl)acetate (11, R = C_2H_5)

Diethylamine (16.0 g, 0.22 mole) was added in one portion to dimethyl monothionemalonate (29.6 g, 0.20 mole) at 0°. The mixture was allowed to come to room temperature in 1 h and distilled *in vacuo* to give 32.0 g (85%) of a pale-yellow liquid, b.p. 106–108° (0.3 mm). The n.m.r. spectrum ($CDCl_3$) contained singlets at τ 6.04 and 6.25, a quartet at τ 6.38, and a triplet at τ 8.69 with an integrated area ratio of 2:3:4:6 respectively.

Anal. Calcd. for $C_8H_{15}NO_2S$: C, 50.76; H, 7.99; N, 7.40; S, 16.94. Found: C, 50.80; H, 7.88; N, 7.50; S, 17.10.

Methyl (N-Morpholinothiocarbonyl)acetate (11, $R_2 = O(CH_2CH_2)_2$)

Morpholine (8.7 g, 0.10 mole) was added in one portion to dimethyl monothionemalonate (14.8 g, 0.10 mole) at 0°. An immediate reaction took place and the temperature rose to approximately 40°. To the mixture, which solidified, were added 150 ml of ether and, after cooling, the white crystalline product was collected by filtration; yield, 17.5 g (86%); m.p. 99–101°.

Anal. Calcd. for $C_8H_{13}NO_3S$: C, 47.26; H, 6.44; N, 6.89; S, 15.77. Found: C, 47.49; H, 6.13; N, 6.69; S, 15.95.

Methyl (3-N,N-Diethylamino-3-methylthio)acrylate (12a)

A solution of methyl (*N*,*N*-diethylaminothiocarbonyl)-acetate (7.9 g, 0.042 mole) in 20 ml of anhydrous tetrahydrofuran was added dropwise with stirring to an ice-cooled suspension of sodium hydride (1.06 g, 0.044 mole) in 35 ml of tetrahydrofuran, followed by the addition of methyl iodide (6.4 g, 0.045 mole) in one portion. The mixture was allowed to come to room temperature. The

Can. J. Chem. Downloaded from www.nrcresearchpress.com by 210.87.254.105 on 09/05/12
For personal use only.

solvent was removed and ethyl acetate and water were added to the residue. The ethyl acetate layer was dried, followed by removal of the solvent and distillation of the residue *in vacuo* to give 7.2 g (85%) of almost colorless liquid, b.p. 83–84° at 0.3 mm. The n.m.r. spectrum ($CDCl_3$) contained singlets at τ 5.08, 6.36, and 7.58, a methylene quartet at τ 6.53 and a methyl triplet at τ 8.85 with an integrated area ratio of 1:3:3:4:6 respectively.

Anal. Calcd. for $C_9H_{17}NO_2S$: C, 53.17; H, 8.43; N, 6.89; S, 15.77. Found: C, 53.09; H, 8.34; N, 7.00; S, 16.02.

Methyl (3-Methylthio-3-N-morpholino)acrylate (12b)

This product was prepared from methyl (*N*-morpholinothiocarbonyl)acetate (18.7 g, 0.092 mole), sodium hydride (2.2 g, 0.092 mole), and methyl iodide (14.2 g, 0.10 mole) by the above outlined procedure; yield, 18.7 g (94%); b.p. 108–110° at 0.2 mm.

Anal. Calcd. for $C_9H_{15}NO_3S$: C, 49.74; H, 6.96; N, 6.45; S, 14.75. Found: C, 50.11; H, 7.19; N, 6.66; S, 14.42.

Ethyl 3-Hydroxy-5-N-morpholinothiophene-2-carboxylate (13)

Methyl (*N*-morpholinothiocarbonyl)acetate (10.2 g, 0.050 mole) was added in portions with stirring to an ice-cooled suspension of sodium hydride (1.2 g, 0.050 mole) in 75 ml of tetrahydrofuran, followed by the addition of ethyl bromoacetate (8.4 g, 0.050 mole). The reaction mixture was left at ambient temperature for 45 min, then the usual procedure was employed to give 13.0 g of crude methyl 3-carbethoxymethylthio-3-*N*-morpholinoacrylate (**12***c*) as an oil. A solution of this material in 25 ml of tetrahydrofuran was added in one portion to a stirred suspension of sodium hydride (1.1 g, 0.046 mole) in 75 ml of tetrahydrofuran. The temperature of the mixture was allowed to rise. A vigorous reaction, which necessitated cooling, started at approximately 15°. When the gas evolution ceased most of the solvent was removed and the residue dissolved in 200 ml of water. The aqueous solution was washed with ether, then acidified with hydrochloric acid. The white solid precipitate was taken up in ether and the aqueous layer extracted with an additional 100 ml of ether. The combined ether solutions were dried, concentrated, and cooled to give 7.8 g (61%) of white solid, m.p. 115–116° (after recrystallization from ethyl acetate). The infrared spectrum (Nujol mull) contained bands at 1620 and 1570 cm^{-1} ascribed to the carboxyl group and the thiophene ring respectively. The n.m.r. spectrum ($CDCl_3$) contained a broad singlet at τ 1.1, a sharp singlet at τ 4.29, a methylene quartet at τ 5.72, complex absorption at τ 6.1–6.3 and τ 6.7–6.9 and a methyl triplet at τ 8.68 with an integrated area ratio of 1:1:2:4:4:3 respectively.

Anal. Calcd. for $C_{11}H_{15}NO_4S$: C, 51.35; H, 5.88; N, 5.45; S, 12.46. Found: C, 51.08; H, 6.00; N, 5.44; S, 12.52.

Ethyl 3-Methoxy-5-N-morpholinothiophene-2-carboxylate (14)

Ethyl 3-hydroxy-5-*N*-morpholinothiophene-2-carboxylate (1.1 g, 0.0043 mole) was treated with an excess of an ethereal diazomethane solution for 5 h at room temperature. The product was filtered off as a white solid after the solution had been concentrated and cooled; yield, 1.05 g (91%); m.p. 116–118°. The melting point could be raised to 119–120° by recrystallization from ethyl acetate. The infrared spectrum (Nujol mull) contained sharp bands at 1675 and 1545 cm^{-1}.

Anal. Calcd. for $C_{12}H_{17}NO_4S$: C, 53.11; H, 6.32; N, 5.16; S, 11.82. Found: C, 52.86; H, 6.44; N, 4.98; S, 12.05.

Methyl 3,3-Di-N-morpholinoacrylate (15)

A mixture of methyl (3-methylthio-3-*N*-morpholino)-acrylate (17.5 g, 0.081 mole) and morpholine (7.0 g, 0.081 mole) was heated at 120° for 8 h. After cooling, ether (200 ml) was added and the white solid was filtered off; yield, 18.8 g (77%); m.p. 115–116° (after recrystallization from ethyl acetate). The infrared spectrum (Nujol mull) contained a sharp carbonyl band at 1665 cm^{-1}. The n.m.r. spectrum ($CDCl_3$) consisted of sharp singlets at τ 5.89 and 6.35 and broad absorption at τ 6.1–6.4 and τ 6.6–6.9 with an integrated area ratio of approximately 1:3:8:8.

Anal. Calcd. for $C_{12}H_{20}N_2O_4$: C, 56.23; H, 7.87; N, 10.93. Found: C, 56.42; H, 7.69; N, 11.21.

Methyl 5-(1,2,3-Thiadiazolyl)acetate

A solution of dimethyl monothionemalonate (14. 8 g, 0.10 mole) in 150 ml of methanol was added to 340 ml of a 0.38 *M* ethereal diazomethane (0.13 mole) solution. The reaction mixture was left in the dark for 18 h. Removal of the solvent and distillation of the residue *in vacuo* yielded 11.8 g (74%) of a yellow liquid boiling at 101–105° (0.8 mm). The n.m.r. spectrum ($CDCl_3$) contained singlets at τ 1.48, 5.84, and 6.22 with an integrated area ratio of 1:2:3 respectively.

5-(1,2,3-Thiadiazolyl)acetic Acid

This acid was obtained in 60% yield as white platelets, m.p. 179–180° (decomp.), by treatment of the methyl ester with methanolic sodium hydroxide at room temperature, followed by acidification of the salt. The product could be recrystallized from ethyl acetate.

Anal. Calcd. for $C_4H_4N_2O_2S$ (mol. wt., 144): C, 33.31; H, 2.80; N, 19.43; S, 22.24. Found (neutralization equivalent, 140): C, 33.85; H, 3.32; N, 19.60; S, 21.85.

Acknowledgments

The author is indebted to Mr. V. R. Baker and Mr. P. K. Wolfert for their technical assistance and to Professor R. U. Lemieux for his advice and interest in this work.

1. S. Scheithauer and R. Mayer. Chem. Ber. **100**, 1413 (1967).
2. G. Barnikow and G. Strickmann. Chem. Ber. **100**, 1428 (1967).
3. G. Barnikow and G. Strickmann. Chem. Ber. **100**, 1661 (1967).
4. R. Raap. Can. J. Chem. This issue.
5. H. Fiesselmann, P. Schipprak, W. Böhm, and F. Thoma. Chem. Ber. **89**, 1897, 1902, 1907 (1956).
6. R. Quelet and R. Milcent. Compt. Rend. **261**, 5520 (1965).
7. I. Hagedorn and H. D. Winkelmann. Chem. Ber. **99**, 850 (1966).
8. U. Schmidt, E. Heymann, and K. Kabitzke. Chem. Ber. **96**, 1478 (1963).
9. U. Schmidt. Chem. Ber. **100**, 3825 (1967).

Can. J. Chem. Downloaded from www.nrcresearchpress.com by 210.87.254.105 on 09/05/12
For personal use only.

Synthesis and chemistry of 1-methyl-3-imino-4-hydroxy-4-phenyl-6-chloro-1,2,3,4-tetrahydroquinoline-2-one

C. PODESVA, K. VAGI, AND C. SOLOMON
Delmar Chemicals Limited, LaSalle, Quebec

Received February 21, 1968

Reaction between 2-(*N*-methyl)dichloroacetamido-5-chlorobenzophenone and aqueous ammonia yields 1-methyl-3-amino-3,4-dihydroxy-4-phenyl-6-chloro-1,2,3,4-tetrahydroquinoline-2-one which dehydrates readily to give the title compound. Structural proof of this substance is reported and several of its transformation products are described.

Canadian Journal of Chemistry, 46, 2263 (1968)

When a solution of 2-(*N*-methyl)-dichloroacetamido-5-chlorobenzophenone in dimethylformamide was allowed to stand overnight at room temperature in presence of concentrated aqueous ammonia, a crystalline precipitate formed which analyzed for $C_{16}H_{15}Cl\ N_2O_3$ and whose infrared spectra in Nujol exhibited peaks at 3430, 3360, 3280, 3185, 1660, and 1585 cm^{-1}. When stored at room temperature, this product lost after some time one molecule of water giving another crystalline substance, whose infrared spectra in Nujol contained a sharp peak at 3215 with an inflection at 3150, a strong peak at 1685, and a peak of medium intensity at 1670 cm^{-1} together with aromatic absorption at 1600 and 1580 cm^{-1}. This transformation was practically immediate when the first reaction product was heated in an inert solvent or even in suspension. On reduction with sodium borohydride the second product added one molecule of hydrogen while losing another molecule of water. The infrared spectra in Nujol of this last compound (3460, 3305, 1645, 1605, and 1595 cm^{-1}) suggested that a structure of aminoquinolone **3** should be considered. We have therefore undertaken an unambiguous synthesis of **3** in the following way: 2-(*N*-methyl)-chloroacetamido-5-chlorobenzophenone was allowed to react with sodium nitrite whereby nitroquinolone **4** was readily formed by spontaneous cyclization. Reduction of the nitro product with zinc in hydrochloric acid yielded the aminoquinolone **3**, which was found to be identical with the product obtained from the sodium borohydride reduction by comparing the physical properties and infrared spectra. On this basis the precursor of **3** has to be formulated as ketimine **2** and structure **1** has to be accepted for the precursor of **2**. The above mentioned infrared spectra are also in excellent agreement with both structures as are the reactions and transformations described below.

Acetylation of the ketimine **2** afforded two distinct products depending on the conditions used. When it was carried out at room temperature using acetic anhydride in pyridine, an *O*-acetate **5** (ν_{max} (KBr) 3205 (sharp), 1730, 1670, 1630, and 1580 cm^{-1}) was formed. Mild alkaline hydrolysis of the latter recovered the starting ketimine **2**, thus excluding any possibility of a rearrangement whereas controlled acid hydrolysis yielded the acetylated ketol **6** (ν_{max} (KBr) 1750 (inflection), 1740, 1680, and 1590 cm^{-1}), which in turn yielded the known ketol **7** (1) on heating with aqueous inorganic bases. When, however, the ketimine **2** was acetylated in boiling acetic anhydride in presence of anhydrous sodium acetate, the *N*-acetate **8** (ν_{max} (KBr) 3320, 1705, 1650, and 1600 cm^{-1}) was the reaction product. Its structure was established as follows: sodium borohydride reduction yielded the alcohol **9** (ν_{max} (KBr) 3340, 3160, 1680, 1630, and 1595 cm^{-1}) which in turn could be acetylated to give the *N,O*-diacetate **10** (ν_{max} (KBr) 3375, 1740, 1690, 1660, and 1595 cm^{-1}) thus proving the presence of a ketone conjugated with an aromatic ring in compound **8**. Furthermore, when the ultraviolet spectra of **8** were compared with those of the recently reported 1-methyl-3-acetoxy-3-phenyl-6-chloro-1,2,3,4-tetrahydroquinoline-2,4-dione (1), they were found to be superimposable exhibiting maxima at 239 mμ with a shoulder at 260 mμ. When **8** was refluxed overnight in aqueous–alcoholic hydrochloric acid, the α-aminoketone **11** was isolated as the reaction product (ν_{max} (KBr) 3365, 3285, 1700, 1665, 1655 (inflection), and 1600 cm^{-1}).

Can. J. Chem. Downloaded from www.nrcresearchpress.com by 210.87.254.105 on 09/05/12
For personal use only.

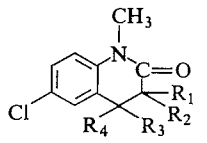

1 $R_1 = NH_2$, $R_2 = OH$, $R_3 = OH$, $R_4 = Ph$
9 $R_1 = NHAc$, $R_2 = Ph$, $R_3 = H$, $R_4 = OH$
10 $R_1 = NHAc$, $R_2 = Ph$, $R_3 = H$, $R_4 = OAc$
12 $R_1 = OH$, $R_2 = OH$, $R_3 = OH$, $R_4 = Ph$

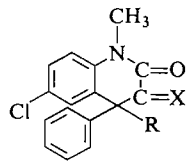

2 R = OH, X = NH
5 R = OAc, X = NH
6 R = OAc, X = O
15 R = OH, X = N—OH

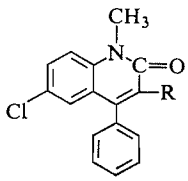

3 $R = NH_2$
4 $R = NO_2$
16 R = NO

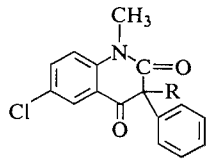

7 R = OH
8 R = NHAc
11 $R = NH_2$

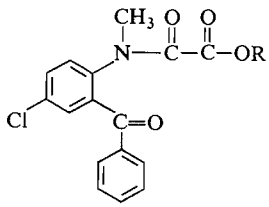

13 R = H
14 R = Et

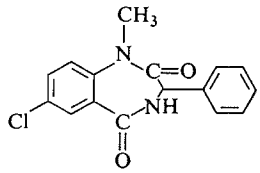

17

Mechanistically, the migration of the phenyl group during treatment of **2** with acetic anhydride is readily conceivable and can be represented as follows.

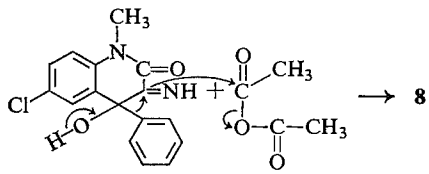

On contact with dilute acids **2** was transformed into the triol **12** (ν_{max} (KBr) 3440, 3415, 3365, 3305, 1670, and 1590 cm^{-1}) which in contrast to **1** was stable when heated in solvents and did not show any tendency to lose water on storage. Its reactions were typical for an α-hydroxy ketone. It was readily oxidized by periodic acid to the keto acid **13** (ν_{max} 1740, 1670, 1620, and 1590 cm^{-1}) which on treatment with ethanolic HCl yielded the keto ester **14** (ν_{max} (KBr) 1730, 1680, 1670, 1595, and 1585 cm^{-1}). We have also obtained the same ester by a direct condensation of 2-methylamino-5-chlorobenzophenone with ethyloxalylchloride whereby the structures of **12**, **13**, and **14** are rigorously established.

When the triol **12** was allowed to react with ammonia in methanolic solution containing catalytic amount of triethylamine, it afforded a mixture of the ketimine **2** and of the recently reported 1-methyl-3-hydroxy-3-phenyl-4-imino-6-chloro-1,2,3,4-tetrahydroquinoline-2-one (1), which clearly was formed by a ketol rearrangement of **12** preceding the reaction with ammonia. On acetylation of **12** the above mentioned ester **6** was obtained. It is noteworthy that in contrast to **12** this ester showed no tendency to exist as a geminal diol. A mixture of oxime **15** (ν_{max} (KBr) 3500 (sharp), 3090, 1640, 1590, and 1570 cm^{-1}) and its dehydration product **16** (ν_{max} (KBr) 3160, 1645, 1615 (short), and 1560

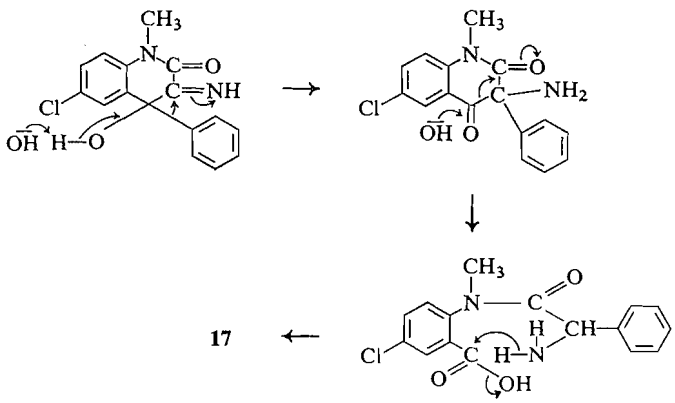

cm^{-1}) was isolated from the reaction mixture resulting from the condensation of the imine **2** with hydroxylamine. The same oxime **15** resulted also from a reaction between the triol **12** and hydroxylamine and it could be easily dehydrated to the nitroso product **16**. Attempted reduction of this last compound with zinc in hydrochloric acid yielded only trace quantities of the expected aminoquinolone **3** and most of the starting material was recovered unchanged. Aqueous inorganic bases transformed on heating both the imine **2** and the triol **12** into the recently reported 1-methyl-3-hydroxy-3-phenyl-6-chloro-1,2,3,4-tetrahydroquinoline-2,4-dione (**7**) thus confirming the correctness of the mechanism postulated for the formation of this compound (1). (The first step in this mechanism is also applicable for the explanation of the formation of the aminoalcohol **1**.)

An interesting rearrangement took place when the imine **2** was heated in anhydrous methanol in presence of a catalytic amount of trimethylbenzylammonium hydroxide (Triton B). The crystalline reaction product was shown by elemental analysis to be isomeric with the starting material but it lacked its basic character. Its infrared spectra in KBr exhibited maxima at 3165, 1680, 1665 (the last two peaks of equal intensity), and at 1610 cm^{-1}. On the basis of these data as well as on the basis of mechanistic considerations, structure **17** was tentatively assigned to this substance. This structure was proven to be correct by an independent synthesis consisting of (*a*) condensation of *N*-methyl-5-chloroanthranilic acid with D,L-phthalimidophenylacetyl chloride, (*b*) removing the phthaloyl group by means of hydrazine hydrate, (*c*) esterification of the carboxyl, and (*d*) cyclization of the resulting amino ester by refluxing in anhydrous methanol in presence of triethylamine.

The following mechanism accounts fully for the transformation of **2** into **17**.

As the first intermediate postulated in the above mechanism is identical with the aminoketone **11**, we subjected this last compound to the same treatment as the imine **2**, whereby a fair yield of the cyclic diamide **17** was obtained.

When 2-(*N*-methyl)-dichloroacetamido-5-chlorobenzophenone was kept overnight in ethanol–dimethylformamide solution saturated with ammonia gas, a neutral crystalline substance was isolated whose elemental analysis corresponded to a formula of $C_{16}H_{12}ClNO_3$. The product was isolated in two crystalline modifications, one melting at 177–178°, the other at 212°, both having the same infrared spectra in chloroform solution (ν_{max} 3430, 1700, 1675, and 1600 cm^{-1}). The nuclear magnetic resonance (n.m.r.) spectrum in deuteriochloroform with tetramethylsilane as internal reference standard exhibited two *N*-methyl peaks at τ 6.42 and 6.89 and two one proton singlets at τ 4.00 and 5.22 plus a multiplet (16 protons) in the aromatic region with the strongest peak appearing at τ 2.80. Both spectra suggested that the product in question must be a dimer, which was confirmed by molecular weight determination. As the most obvious structure satisfying the elemental analysis, infrared, and n.m.r. spectra would correspond to formula **18**, we reasoned that it should be possible to prepare this compound by dehydration of the triol **12**. Refluxing of the latter in benzene solution with azeotropic removal of water yielded indeed the expected product thus

Can. J. Chem. Downloaded from www.nrcresearchpress.com by 210.87.254.105 on 09/05/12
For personal use only.

Can. J. Chem. Downloaded from www.nrcresearchpress.com by 210.87.254.105 on 09/05/12
For personal use only.

confirming the correctness of structure **18**. Subsequently we were able to obtain the same dimer by treatment of the ketimine **2** with glacial acetic acid. The chemical reactions of the dimer **18** resembled those of the triol **12**.

It is interesting to speculate about the stereochemistry of the dimer **18**. The four asymmetric centers present in the molecule would suggest eight possible stereoisomers due to the fact that identical substituents are present on both sides of the dioxane ring. Closer examination of the models, however, reveals that this is not the case. The quinolone moiety has to be flat due to the presence of the amide grouping and therefore one substituent on C-3 has to be in the same plane as one of the substituents on C-4, the same requirement being valid for the second pair of substituents. From that follows further, (and the study of models confirms it) that in a strain free molecule the dioxane moiety has to be in a boat conformation, with the oxygen atoms as flagpoles. Now, if the above reasoning is accepted, one is still left with three possible stereomers in which the quinolone moieties would be endo–endo, exo–exo, or endo–exo with respect to the dioxane ring. The fact, however, that the infrared spectra of this product exhibit two distinct amide absorptions and that in the n.m.r. spectra the chemical shift is different for the two hydroxyl protons as well as for the two *N*-methyls strongly suggests that these protons are situated in a different environment and therefore the endo–exo form would appear to be the most likely one. However, as the models built for this structure reveal a considerable degree of steric interference and as at the same time it is not possible to bring a chemical proof for the proposed conformation, the above suggestion based on spectral evidence has to be treated with extreme caution.

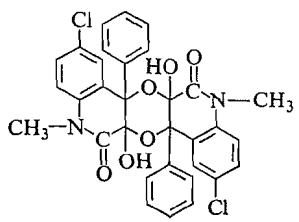

18

Experimental

The infrared spectra were taken on Perkin–Elmer 237 and 237B instruments. The ultraviolet spectra were obtained with a Unicam SP 800 apparatus. The nuclear magnetic resonance (n.m.r.) spectra were recorded on Varian model HR-60 spectrometer. The melting points were determined in capillaries on a Mel-Temp apparatus and are uncorrected. Microanalyses were performed by Organic Microanalysis, Dr. C. Daesslé, Montreal.

1-Methyl-3-amino-3,4-dihydroxy-4-phenyl-6-chloro-1,2,3,4-tetrahydroquinoline-2-one (1)

To a solution of 2-(*N*-methyl)-dichloroacetamido-5-chlorobenzophenone (1) (17 g, 0.478 mole) in dimethylformamide (120 ml) was added concentrated aqueous ammonia (80 ml) and the mixture stirred at room temperature overnight. The crystalline precipitate was collected by filtration (10 g, 65.9%), washed with water, then with acetone and dried for analysis at room temperature in high vacuum; m.p. 171–174°.

Anal. Calcd. for $C_{16}H_{15}ClN_2O_3$: C, 60.28; H, 4.74; Cl, 11.12; N, 8.79. Found: C, 60.53; H, 4.92; Cl, 11.39; N, 8.89.

1-Methyl-3-imino-4-hydroxy-4-phenyl-6-chloro-1,2,3,4-tetrahydroquinoline-2-one (2)

When **1** was kept in an oven at about 80° for approximately 2 h, a quantitative yield of **2** was obtained. The analytical sample was purified by crystallization from dimethylformamide–ether mixture, m.p. 182–183°.

Anal. Calcd. for $C_{16}H_{13}ClN_2O_2$: C, 63.90; H, 4.35; Cl, 11.79; N, 9.32. Found: C, 63.86; H, 4.35; Cl, 11.44; N, 9.42.

The same product was obtained when **1** was heated in acetone suspension or when stored for several weeks at room temperature.

1-Methyl-3-nitro-4-phenyl-6-chloro-2(1H)-quinolone (4)

To a solution of 2-(*N*-methyl)-chloroacetamido-5-chlorobenzophenone (2) (6.44 g, 0.02 mole) in ethanol (50 ml) was added a solution of $NaNO_2$ (1.52 g, 0.022 mole) in water (15 ml) and the mixture was refluxed overnight. After cooling to room temperature the crystalline precipitate was collected by filtration (3 g, 47.7%) and recrystallized from ethyl acetate, m.p. 208–210°.

Anal. Calcd. for $C_{16}H_{11}ClN_2O_3$: C, 61.06; H, 3.52; Cl, 11.27; N, 8.90. Found: C, 61.02; H, 3.54; Cl, 11.23; N, 9.06.

1-Methyl-3-amino-4-phenyl-6-chloro-2(1H)-quinolone (3)

(*a*) To a solution of **2** (2 g, 0.00665 mole) in a mixture of methanol (100 ml) and dimethylformamide (20 ml) was added a solution of $NaBH_4$ (0.2 g, 0.00528 mole) in water (5 ml) and the mixture was left standing at room temperature overnight. After further dilution with water the crystalline precipitate was collected by filtration (1.22 g, 64.5%) and recrystallized from methanol, m.p. 134–136°.

Anal. Calcd. for $C_{16}H_{13}ClN_2O$: C, 67.49; H, 4.60; Cl, 12.45; N, 9.84. Found: C, 67.32; H, 4.92; Cl, 12.50; N, 9.48.

(*b*) To a suspension of **4** (2 g, 0.00635 mole) in a mixture of ethanol (100 ml) and water (50 ml) was added zinc dust (2 g) and the pH was adjusted to about 3.0 by means of

Can. J. Chem. Downloaded from www.nrcresearchpress.com by 210.87.254.105 on 09/05/12
For personal use only.

5% HCl. After stirring at room temperature for 90 min the unchanged starting material (1 g) was filtered off, the filtrate was basified with aqueous sodium hydroxide, and the crystalline precipitate was collected by filtration (0.5 g, 27.7%). It was recrystallized from methanol to a m.p. of 134–135°. This product was found to be identical with the one obtained by the process (*a*) by mixture m.p. determination and by comparison of infrared spectra.

1-Methyl-3-imino-4-phenyl-4-acetoxy-6-chloro-1,2,3,4-tetrahydroquinoline-2-one (5)

A solution of **2** (2.5 g, 0.0083 mole) in dry pyridine (25 ml) containing acetic anhydride (3 ml) was left standing at room temperature overnight. After removal of the solvent *in vacuo* the residue was treated with ether and then collected by filtration (2 g, 70.1%). The product was purified by crystallization from benzene, m.p. 224–226°.

Anal. Calcd. for $C_{18}H_{15}ClN_2O_3$: C, 63.07; H, 4.41; Cl, 10.34; N, 8.18. Found: C, 63.42; H, 4.40; Cl, 10.21; N, 7.97.

A solution of this product in methanolic ammonia containing catalytic amount of sodium methoxide after standing at room temperature overnight yielded the starting **2**, identified by a mixture m.p. determination and comparison of infrared spectra.

1-Methyl-4-acetoxy-4-phenyl-6-chloro-1,2,3,4-tetrahydroquinoline-2,3-dione (6)

Into a solution of **5** (1.5 g, 0.0044 mole) in chloroform (15 ml) containing water (1 ml) HCl gas was introduced at room temperature. The organic phase was separated from the aqueous phase, the solvent distilled off *in vacuo*, and the residue was crystallized from ether, then from ethyl acetate. The yield was 1.35 g (90%), m.p. 210–212°.

Anal. Calcd. for $C_{18}H_{14}ClNO_4$: C, 62.88; H, 4.10; Cl, 10.32; N, 4.08. Found: C, 63.20; H, 4.34; Cl, 10.49; N, 4.12.

1-Methyl-3,3,4-trihydroxy-4-phenyl-6-chloro-1,2,3,4-tetrahydroquinoline-2-one (12)

A suspension of **2** (3 g, 0.00997 mole) in water (30 ml) acidified with glacial acetic acid (2 ml) was refluxed for 30 min. After cooling to room temperature the crystalline substance was collected by filtration and washed with water. The yield was 3 g (94.1%), m.p. 131–133 °C and the product was analyzed without further purification.

Anal. Calcd. for $C_{16}H_{14}ClNO_4$: C, 60.10; H, 4.41; Cl, 11.09; N, 4.38. Found: C, 60.04; H, 4.54; Cl, 11.11; N, 4.49.

When this product (2 g, 0.00625 mole) was allowed to stand at room temperature overnight in a mixture of pyridine (10 ml) and acetic anhydride (3 ml), 1.8 g (83.7%) of **6**, m.p. 210–212° was obtained after the work-up of the reaction mixture and purification by recrystallization from ethyl acetate. Its identity was established by m.p. and mixture m.p. as well as by comparison of the infrared spectra.

1-Methyl-3-hydroxy-3-phenyl-6-chloro-1,2,3,4-tetrahydroquinoline-2,4-dione (7)

A solution of **12** (0.15 g, 0.0005 mole) in methanol (5 ml) was basified with 35% aqueous NaOH and left standing for some time at room temperature. After dilution with water the reaction product was extracted into chloroform, the solvent distilled off *in vacuo*, and the residue recrystallized from ether. The yield was 0.1 g (71%), m.p. 170–172°, undepressed on admixture of an authentic sample (1). The infrared spectra of the two samples were superimposable. The same product was obtained when **5** was refluxed for 15 min in aqueous methanol in presence of some KOH (28% yield), when **6** was allowed to stand at room temperature for two days in aqueous–ethanolic solution containing some NaOH (50% yield) and when **2** was heated for 90 min in cellosolve–water mixture in presence of sodium acetate (45% yield).

1-Methyl-3-acetamido-3-phenyl-6-chloro-1,2,3,4-tetrahydroquinoline-2,4-dione (8)

A solution of **2** (15 g, 0.05 mole) in acetic anhydride (100 ml) containing some anhydrous sodium acetate was heated under reflux for 1 h. After cooling to room temperature the unreacted anhydride was decomposed by a careful addition of methanol, the reaction mixture was then further diluted with water and extracted with chloroform. Removal of the solvent *in vacuo* and treatment of the residue with methanol yielded 9 g (52.6%) of crystalline material, which was recrystallized from methanol – ethyl acetate mixture, m.p. 231–232°.

Anal. Calcd. for $C_{18}H_{15}ClN_2O_3$: C, 63.07; H, 4.41; Cl, 10.34; N, 8.18. Found: C, 63.41; H, 4.59; Cl, 10.49; N, 7.98.

1-Methyl-3-acetamido-3-phenyl-4-hydroxy-6-chloro-1,2,3,4-tetrahydroquinoline-2-one (9)

To a solution of **8** (3 g, 0.0087 mole) in methanol (100 ml) a solution of $NaBH_4$ (0.2 g, 0.00528 mole) in water (5 ml) was added and the mixture allowed to stand at room temperature for 3 h. After dilution with water the crystalline precipitate was collected by filtration and recrystallized from isopropanol. The yield was 2.8 g (93%), m.p. 191–193°.

Anal. Calcd. for $C_{18}H_{17}ClN_2O_3$: C, 62.70; H, 4.97; Cl, 10.28; N, 8.13. Found: C, 62.64; H, 4.93; Cl, 10.47; N, 7.98.

1-Methyl-3-acetamido-3-phenyl-4-acetoxy-6-chloro-1,2,3,4-tetrahydroquinoline-2-one (10)

A solution of **9** (2 g, 0.0058 mole) in acetic anhydride (10 ml) containing some anhydrous sodium acetate was heated under reflux for 1 h. After cooling to room temperature some methanol was added, the reaction mixture was then diluted with water and the crystalline precipitate collected by filtration (1.5 g, 67%). The analytical sample had a m.p. of 247–248° after recrystallization from isopropanol.

Anal. Calcd. for $C_{20}H_{19}ClN_2O_4$: C, 62.10; H, 4.95; Cl, 9.17; N, 7.24. Found: C, 61.96; H, 5.04; Cl, 8.91; N, 6.99.

1-Methyl-3-amino-3-phenyl-6-chloro-1,2,3,4-tetrahydroquinoline-2,4-dione (11)

A solution of **8** (2.5 g, 0.0073 mole) in ethanol (100 ml) containing 17% aqueous HCl (50 ml) was refluxed overnight. After cooling to room temperature the reaction mixture was diluted with water, basified to pH 8.0–9.0 with aqueous NaOH, and extracted with chloroform. The solvent was distilled off *in vacuo* and the residue recrystallized from ether, then from benzene. The yield was 1 g (45.6%), m.p. 154–156°.

Anal. Calcd. for $C_{16}H_{13}ClN_2O_2$: C, 63.90; H, 4.35; Cl, 11.79; N, 9.32. Found: C, 64.13; H, 4.35; Cl, 11.55; N, 9.07.

Can. J. Chem. Downloaded from www.nrcresearchpress.com by 210.87.254.105 on 09/05/12
For personal use only.

*2-(N-Methyl)-oxalylamido-5-chlorobenzophenone (**13**)*

To a solution of **12** (1 g, 0.0031 mole) in ethanol (50 ml) a solution of periodic acid (0.76 g, 0.0033 mole) in water (5 ml) was added and the mixture allowed to stand for 2 h at room temperature. After dilution with water the reaction mixture was extracted with chloroform in order to remove the unchanged starting material (0.25 g). The aqueous layer was allowed to stand overnight at room temperature, whereby the reaction product separated in a crystalline form. It was collected by filtration (0.35 g, 35.3%) and recrystallized from ethyl acetate – hexane mixture, m.p. 122–124°.

Anal. Calcd. for $C_{16}H_{12}ClNO_4$: C, 60.48; H, 3.80; Cl, 11.16; N, 4.41. Found: C, 60.67; H, 3.59; Cl, 11.43; N, 4.64.

*2-(N-Methyl)-ethyloxalylamido-5-chlorobenzophenone (**14**)*

A solution of **13** (5 g, 0.0157 mole) in absolute ethanol (25 ml) was saturated with HCl gas and left standing overnight at room temperature. The reaction mixture was concentrated to a small volume, some ether was added and the crystalline precipitate collected by filtration (2.1 g, 38.6%). It was purified by recrystallization from methanol–water mixture, m.p. 80–81°.

Anal. Calcd. for $C_{18}H_{16}ClNO_4$: C, 62.52; H, 4.66; Cl, 10.26; N, 4.05. Found: C, 62.80; H, 4.70; Cl, 10.61; N, 4.11.

The same product was obtained in the following way: a solution of 2-methylamino-5-chlorobenzophenone (7.4 g, 0.03 mole) in dry chloroform (100 ml) was refluxed for 3 h in presence of ethyloxalyl chloride (4.1 g, 0.03 mole) (3). After removal of the solvent *in vacuo* the residue was crystallized first from ether–hexane, then from methanol–water mixture. The yield was 7 g (67.5%), m.p. 80–81°, unchanged on admixture of the product from the first experiment. Also the infrared spectra of both samples were superimposable.

*Reaction of **12** with Ammonia*

A solution of **12** (1 g, 0.00312 mole) in anhydrous methanol (40 ml) containing a few drops of triethylamine was saturated with NH_3 gas and left standing at room temperature for 3 days. 1-Methyl-3-hydroxy-3-phenyl-4-imino-6-chloro-1,2,3,4-tetrahydroquinoline-2-one (1) (identified by m.p., mixture m.p. with the authentic sample, and comparison of infrared spectra) was removed by filtration (0.15 g, 16%), the mother liquors were concentrated to a small volume, whereby 0.5 g (51.1%) of **2** identified by comparison with the authentic sample in the above described way separated.

*1-Methyl-3-isonitroso-4-hydroxy-4-phenyl-6-chloro-1,2,3,4-tetrahydroquinoline-2-one (**15**)*

A solution of **12** (2 g, 0.0063 mole), hydroxylamine hydrochloride (0.5 g, 0.0072 mole) and triethylamine (0.73 g, 0.0072 mole) in benzene (30 ml) was heated under reflux for 20 h, using water trap. After cooling to room temperature the triethylamine hydrochloride was removed by filtration, the filtrate evaporated to dryness *in vacuo* and the residue crystallized by treatment with ethyl acetate, then recrystallized from dimethylformamide–water mixture. The yield was 0.7 g, (35%), m.p. 195–197°.

Anal. Calcd. for $C_{16}H_{13}ClN_2O_3$: C, 60.68; H, 4.14; Cl, 11.19; N, 8.85. Found: C, 61.03; H, 4.18; Cl, 11.42; N, 8.80.

*1-Methyl-3-nitroso-4-phenyl-6-chloro-2(1H)-quinolone (**16**)*

A solution of **2** (4 g, 0.0133 mole), hydroxylamine hydrochloride (1 g, 0.0144 mole), and triethylamine (2.9 g, 0.028 mole) in a mixture of benzene (50 ml) and dimethylformamide (10 ml) was heated under reflux for 20 h. After cooling to room temperature the precipitated triethylamine hydrochloride was removed by filtration and the filtrate evaporated to dryness *in vacuo*. Treatment of the residue with ethyl acetate yielded 0.3 g (7.7%) of **16**, which was recrystallized for analysis from benzene, m.p. 225–227°.

Anal. Calcd. for $C_{16}H_{11}ClN_2O_2$: C, 64.33; H, 3.71; Cl, 11.87; N, 9.38. Found: C, 64.58; H, 3.74; Cl, 12.06; N, 9.19.

The filtrate deposited on standing 2.2 g (52.4%) of the oxime **15**, identified by comparison with the authentic sample in the usual way.

When a solution of **15** (1 g, 0.0031 mole) in dry toluene (25 ml) was refluxed for 1 h in presence of a small amount of PCl_5, a crystalline precipitate of **16** separated on cooling of the reaction mixture (0.5 g, 53.2%).

*Reduction of **16***

To a suspension of **16** (0.15 g, 0.0005 mole) and zinc dust (0.15 g) in a mixture of ethanol (10 ml) and dimethylformamide (10 ml) 5% aqueous HCl was added dropwise until the pH of 3.0 was reached. After stirring at room temperature for 2 h the insolubles were removed by filtration, the filtrate was basified with aqueous NaOH, diluted with water, and extracted with chloroform. Evaporation of the chloroform *in vacuo* and dilution of the remaining dimethylformamide with water caused precipitation of a small amount of crystalline material, which was identified as **3** by m.p. and mixture m.p. determination and by comparison of the infrared spectra.

*1-Methyl-3-phenyl-7-chloro-3,4-dihydro-2H-1,4-benzodiazepine-2,5(1H)-dione (**17**)*

A solution of **2** (10 g, 0.033 mole) in a mixture of dimethylformamide (60 ml) and anhydrous methanol (120 ml) was refluxed for 3 h, in presence of 40% methanolic solution of Triton B (1 ml). After cooling to room temperature the reaction mixture was diluted with water and extracted with chloroform. Removal of the solvent *in vacuo* left a residue which crystallized on treatment with ether. It was collected by filtration and recrystallized from methanol. The yield was 5.1 g (51%), m.p. 234–235°.

Anal. Calcd. for $C_{16}H_{13}ClN_2O_2$: C, 63.90; H, 4.35; Cl, 11.79; N, 9.32. Found: C, 63.73; H, 4.48; Cl, 11.82; N, 9.56.

The same product was obtained in 18% yield when a solution of **11** (0.55 g) in anhydrous methanol containing a few drops of a 40% methanolic solution of Triton B was refluxed for 3 h. It was isolated in the usual way and its identity was established by m.p. and mixture m.p. determination and by comparison of the infrared spectra.

*Synthesis of **17** from N-Methyl-5-chloroanthranilic Acid*

A solution of *N*-methyl-5-chloroanthranilic acid (1, 4) (3.1 g, 0.016 mole) and D,L-phthalimidophenylacetyl chloride (5) (5 g, 0.016 mole) in dry chloroform (70 ml)

Can. J. Chem. Downloaded from www.nrcresearchpress.com by 210.87.254.105 on 09/05/12
For personal use only.

was heated under reflux for overnight. The solvent was distilled off *in vacuo*, the residue dissolved in methanol (80 ml), and refluxed in presence of decolorizing carbon. The solution was filtered, the methanol was distilled off *in vacuo*, and the residue was crystallized from ethyl acetate. The yield of crystalline 2-(*N*-methyl)-phthalimidophenylacetamido-5-chlorobenzoic acid was 2.8 g (77%), m.p. 235–236°.

Anal. Calcd. for $C_{24}H_{17}ClN_2O_5$: C, 64.23; H, 3.82; Cl, 7.90; N, 6.24. Found: C, 64.09; H, 4.09; Cl, 8.01; N, 6.33.

The solution of the above product (2.64 g, 0.0058 mole) in ethanol (26 ml) containing hydrazine hydrate (0.6 g, 0.012 mole) was heated under reflux for 2½ h. After cooling in an ice bath the precipitate was collected on a Buchner filter funnel and put aside. The filtrate was evaporated to dryness, the crystalline residue was combined with the solid separated previously and suspended into 5% aqueous HCl (80 ml). After stirring at room temperature for 15 min the insolubles were removed by filtration and the filtrate was extracted with *n*-butanol. Removal of the solvent *in vacuo* left a residue which solidified on addition of ether (1.3 g). As we were unable to prepare an analytically pure sample of that product we proceeded with the preparation of the methyl ester: the above product (0.7 g, 0.0022 mole) was dissolved in anhydrous methanol (25 ml) and the solution saturated with HCl gas. After standing overnight at room temperature the methanol was distilled off *in vacuo* and the crystalline 2-(*N*-methyl)-phenylglycylamido-5-chlorobenzoic acid methyl ester hydrochloride was recrystallized from methanol – ethyl acetate mixture. The yield was 0.4 g (57.1%), m.p. 209–211°.

Anal. Calcd. for $C_{17}H_{18}Cl_2N_2O_3$: C, 55.30; H, 4.91; Cl, 19.21; N, 7.59. Found: C, 54.92; H, 4.83; Cl, 19.28; N, 7.73.

A solution of the above product (0.3 g, 0.00081 mole) in anhydrous methanol (5 ml) containing triethylamine (0.13 ml, 0.00094 mole) was refluxed for 2½ h. After cooling to room temperature the reaction mixture was diluted with water, extracted with chloroform, the solvent removed *in vacuo*, and the residue was treated with ether. The crystalline product was separated and recrystallized from methanol. It was found to be identical with **17** by m.p. and mixture m.p. determination and by comparison of the infrared spectra.

Dimer ***18***

A solution of 2-(*N*-methyl)-dichloroacetamido-5-chlorobenzophenone (10 g, 0.028 mole) in dimethylformamide (70 ml) was added to 95% ethanol (140 ml) previously saturated with NH_3 gas. After standing overnight at room temperature the solvent mixture was removed by distillation *in vacuo* and the semicrystalline residue was triturated with ether. The crystalline precipitate was collected on a Buchner filter funnel, suspended in ethyl acetate, the ammonium chloride was removed by filtration, and the filtrate was diluted with *n*-hexane. The crystalline precipitate (2.6 g, 30.7%) was collected by filtration and recrystallized from ethyl acetate – hexane mixture, m.p. 177–178°. Sometimes another crystalline modification m.p. 212° was obtained. The infrared spectra in chloroform solution of both polymorphs were superimposable.

Anal. Calcd. for $C_{32}H_{24}Cl_2N_2O_6$ (mol. wt., 603.44): C, 63.70; H, 4.01; Cl, 11.74; N, 4.64. Found (mol. wt., 632.9 Rast): C, 63.32; H, 4.12; Cl, 11.79; N, 5.01.

The same product was obtained in the following way: a solution of **12** (2.5 g, 0.0782 mole) in benzene (40 ml) was refluxed overnight with azeotropic removal of water. On concentration the solution deposited a crystalline product, which was identified as **18** by m.p. and mixture m.p. determination and by comparison of the infrared spectra (1.1 g, 46.5%).

Finally, when a suspension of **2** (2.5 g, 0.0083 mole) in glacial acetic acid (10 ml) was stirred at room temperature for 4 h, the work-up of the reaction mixture yielded 1.9 g (76%) of **18**, characterized by determination of m.p., mixture m.p., and by comparison of infrared spectra.

Acknowledgments

The authors thank Professor Z. Valenta from the University of New Brunswick for stimulating discussions and for the nuclear magnetic resonance spectrum. Thanks are also due to Miss Lise Lacasse who carried out the four step synthesis of **17** and who efficiently assisted in the preparation of a number of intermediates.

1. C. Podesva, C. Solomon, and K. Vagi. Can. J. Chem. **46**, 435 (1968).
2. L. H. Sternbach, R. Ian Fryer, W. Metlesics, E. Reeder, G. Sach, G. Saucy, and A. Stempel. J. Org. Chem. **27**, 3788 (1962).
3. D. A. Shirley. Preparation of organic intermediates. John Wiley & Sons, Inc., New York. 1951. p. 160.
4. O. Keller. Arch. Pharm. **246**, 37 (1908).
5. A. McKenzie and F. Barrow. J. Chem. Soc. **103**, 1331 (1913).

Can. J. Chem. Downloaded from www.nrcresearchpress.com by 210.87.254.105 on 09/05/12
For personal use only.

Anomalous reaction products from the alkylation of the disodium adduct of benzophenone anil

JAMES G. SMITH
Department of Chemistry, University of Waterloo, Waterloo, Ontario

Received February 26, 1968

Treatment of the disodium adduct of benzophenone anil with isopropyl bromide produced substantial amounts of a by-product as well as the previously reported product, 2-methyl-*N*,1,1-triphenylpropylamine. This by-product is shown to be *N*(*o*-isopropylbenzhydryl)aniline, formed by alkylation of the adduct on the aromatic ring.

The structural proof relies both upon the synthesis of the unknown amine and upon the oxidation of the unknown amine to *o*-isopropylbenzophenone.

Canadian Journal of Chemistry, 46, 2271 (1968)

We have recently reported (1) that treatment of the sodium adduct of benzophenone anil with alkyl halides effected alkylation of the adduct at the benzylic carbon atom. We have now found that during this reaction substantial amounts of alkylation occur on the aromatic ring attached to the benzylic carbon.

In the particular example chosen for study, the reaction of isopropyl bromide with the disodium adduct of benzophenone anil, the two products are 2-methyl-*N*,1,1-triphenylpropylamine (**1**) and *N*(*o*-isopropylbenzhydryl)aniline (**2**).

Results

From the crude reaction mixture, the "normal" C-alkylated product (**1**) was isolated by crystallization. The remainder of the material, which contained large amounts of the second amine (**2**), was purified by column chromatography. An examination of the nuclear magnetic resonance (n.m.r.) spectrum showed the presence of a benzylic proton and an isopropyl group. On the basis of the splitting of the isopropyl group (a double doublet), the structure (**2**) was assigned to this amine.

Its identity was established both by degradative and by synthetic means. Oxidation of the amine (**2**) with dichromate (2) produced *o*-isopropylbenzophenone, isolated and identified by its 2,4-dinitrophenylhydrazone derivative. Synthesis of the amine (**2**) was accomplished according to Scheme 1. *o*-Isopropylbenzoic acid (**4**), obtained by hydrogenolysis of α,α-dimethylphthalide (**3**), was converted, by treatment of its acid chloride with phenylcadmium chloride, to *o*-isopropylbenzophenone (**5**). After converting this ketone to its anil (**6**), the latter was reduced by lithium aluminium hydride to *N*(*o*-isopropylbenzhydryl)aniline (**2**).

The synthesized amine had the same n.m.r. spectrum as the unknown amine, and the benzamides of the known and unknown amine were identical.

Discussion

The formation of ring alkylated products from benzyl-type organometallic reagents appears to be a general phenomenon. Such products have been observed with benzylmagnesium chloride (3, 4) and have recently been reported for the benzophenone sodium ketyl (5). The factors controlling the extent of ring substitution are not fully established but a solvent effect has been noted both for the benzyl Grignard and for the benzophenone ketyl. A concentration effect has also been reported (3) and our preliminary results indicate that the halide involved may also be a contributing factor. Further studies are planned with the system described here.

Experimental

Melting points are uncorrected and were determined in an open capillary using a Mel-Temp melting point apparatus. Infrared (i.r.) spectra were recorded on a Beckmann

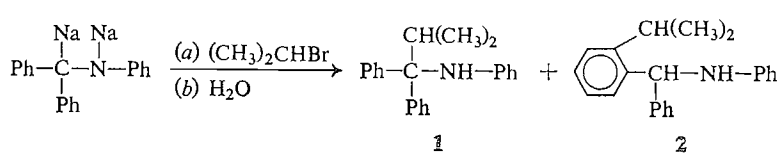

1 **2**

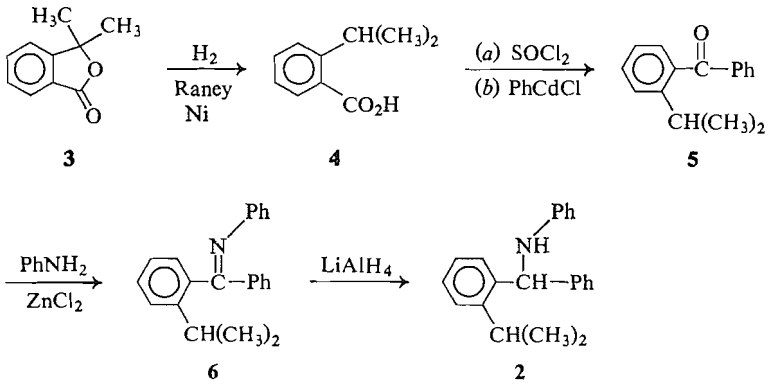

SCHEME 1

IR-10 spectrophotometer using carbon tetrachloride solutions. Nuclear magnetic resonance (n.m.r.) spectra were recorded on a Jeol C-60 spectrometer using deuterated chloroform solutions with tetramethylsilane (TMS) as an internal standard. Chemical shifts are reported in p.p.m. downfield from TMS. Thin-layer chromatography (t.l.c.) was carried out with Eastman Chromagram 6060 (silica gel) sheets using a 1% solution of *p*-nitrobenzenediazonium tetrafluoroborate as a detecting spray. Microanalyses are by Mr. A. B. Gygli, Toronto.

The benzophenone anil and its disodium adduct were prepared as described previously (1).

Reaction with Isopropyl Bromide

The adduct prepared from 5.7 g (0.022 moles) of benzophenone anil, 2.0 g (0.089 g-atoms) of sodium, and 100 ml of dry tetrahydrofuran was drained from the excess sodium, into a nitrogen filled flask and cooled in dry ice. The mixture was stirred and treated with 4.1 g (0.033 moles) of isopropyl bromide. After stirring for 1 h at dry ice temperatures, the mixture was allowed to warm to room temperature overnight.

The final bright orange reaction mixture was treated with 25 ml of water and 50 ml of ether. After washing the ether layer three times with water, the ether solution was dried over magnesium sulfate, filtered, and evaporated. The residue, 7.5 g of a yellow partially crystalline oil, was dissolved in 25 ml of warm methanol and cooled to 5 °C. The 2-methyl-*N*,1,1-triphenylpropylamine (**1**) which crystallized amounted to 2.57 g (38% yield), m.p. 104–110 °C.

The filtrate was concentrated to a gum and placed on a column of 100 g of Woelm grade II basic alumina and eluted with hexane containing 10% benzene. The fractions collected were examined by t.l.c. using 10:2:5 benzene – tetrahydrofuran – 98% formic acid as a developing solvent. The fractions first collected were found to contain an unknown amine (R_f 0.77), some 2-methyl-*N*,1,1-triphenylpropylamine (R_f 0.54), and small amounts of *N*-benzhydryl aniline (R_f 0.68). Later fractions showed increasing amounts of the last compound.

Examination by n.m.r. of the best sample of the unknown amine showed the presence of a benzylic proton at 5.82, an NH at 4.0 and the methyl protons of the isopropyl group appeared as a double doublet at 1.0, 1.12, 1.17, and 1.28. The structure *N*(*o*-isopropylbenzhydryl)-aniline was assigned to this compound, total weight 4.00 g (60% crude yield).

A 1.56 g sample of the amine was converted to its benzamide derivative by refluxing with 30 ml of pyridine and 1.5 ml of benzoyl chloride. The crude product, 2.28 g was purified by recrystallizing from 50 ml of 1:1 cyclohexane–hexane and treatment with charcoal giving 1.44 g, m.p. 152.5–154 °C.

Anal. Calcd. for $C_{29}H_{27}NO$: C, 85.90; H, 6.71; N, 3.45. Found: C, 86.07; H, 6.89; N, 3.50.

Oxidation of Unknown Amine

The procedure follows that described by Neumann and Gould (2). Under the conditions described here, *N*-benzhydryl aniline was converted to benzophenone in 57% yield (isolated as the 2,4-dinitrophenylhydrazone).

A 0.54 g sample of the unknown amine was stirred with 3.0 ml of 2 *M* sulfuric acid and 6.0 ml of a 1 *M* solution of chromium trioxide in 1.5 *M* sulfuric acid, and warmed on a hot plate for 15 min at 60–70 °C. Oxidation occurred with formation of a black precipitate.

After standing overnight, the mixture was diluted with water, extracted with ether, and the ether layer washed with water, dilute sodium hydroxide, and again with water. After drying over magnesium sulfate and evaporating, the residue was boiled with a solution of 0.40 g of 2,4-dinitrophenylhydrazine in 10 ml of methanol and 3 ml of concentrated hydrochloric acid for 2 h. After cooling, the brownish-red solid was removed by filtration and dried, 0.40 g (56% yield), m.p. 162–185 °C. Recrystallization from glacial acetic acid raised the melting point to 200–206 °C but subsequent recrystallizations effected no further improvement.

The 2,4-dinitrophenylhydrazone was dissolved in benzene, placed on a column of 50 g of alumina and eluted with benzene containing 20% chloroform. The material which eluted was recrystallized from glacial acetic acid giving 0.14 g, m.p. 207–209.5 °C and mixture m.p. with authentic 2,4-dinitrophenylhydrazone of *o*-isopropylbenzophenone was 207–210 °C.

Can. J. Chem. Downloaded from www.nrcresearchpress.com by 210.87.254.105 on 09/05/12
For personal use only.

Can. J. Chem. Downloaded from www.nrcresearchpress.com by 210.87.254.105 on 09/05/12
For personal use only.

α,α-Dimethylphthalide (3)

This was prepared by adding phthalic anhydride in tetrahydrofuran to an excess of methylmagnesium iodide in ether. Essentially this is the procedure of Bauer (7) except for the use of tetrahydrofuran as a solvent for phthalic anhydride. This modification eliminates the inconveniently large volumes of ether which would be necessary to dissolve the anhydride.

The phthalide was obtained in 77% yield, m.p. 69–70 °C after one recrystallization from cyclohexane (2 ml/g).

o-Isopropylbenzoic Acid (4)

The Raney nickel catalyst, freshly prepared from 32 g of alloy, was added to a solution prepared from 19.44 g (0.12 mole) of α,α-dimethylphthalide dissolved in a hot solution of 9.60 g (0.24 moles) of sodium hydroxide in 125 ml of water.

The mixture was shaken on a Parr hydrogenator initially pressurized to 50 p.s.i.g. for 8 h at 50–60 °C. After cooling, the reaction mixture was filtered, acidified with concentrated hydrochloric acid, and extracted twice with ether. The ether extract was washed once with water and extracted four times with 100 ml portions of 5% sodium carbonate solution.

Acidification of the sodium carbonate extract precipitated the *o*-isopropylbenzoic acid as an oil which rapidly crystallized, 12.62 g (64% yield), m.p. 54–58 °C (reported m.p. (8) 61–62 °C). This material was used without further purification.

The carbonate insoluble material, recovered by evaporation of the ether, proved to be a low melting solid, 5.70 g (29% yield), m.p. 35–48 °C. Repeated recrystallization from 50% methanol–water gave material of m.p. 61–62.5 °C.

Anal. Calcd. for $C_{10}H_{16}O_2$: C, 71.38; H, 9.59. Found: C, 71.62; H, 9.69.

The n.m.r. spectrum showed only aliphatic protons in the region 1–3 p.p.m. The methyl protons appeared as two doublets, one centered at 1.25, the other at 1.34. The i.r. spectrum showed a carbonyl absorption at 1790 cm^{-1}. As a possible structure, the lactone of 2-isopropyl-X-hydroxycyclohexanecarboxylic acid is suggested.

o-Isopropylbenzoyl Chloride

The *o*-isopropylbenzoic acid was converted to its acid chloride by refluxing with excess thioryl chloride and distilling the reaction product, b.p. 57–59 °C at 0.4 mm.

A sample of the acid chloride was converted to its anilide, m.p. 137–139 °C (reported (9) m.p. 137 °C).

o-Isopropylbenzophenone (5)

Phenylmagnesium bromide was prepared from 12.6 g (0.080 moles) of bromobenzene and 1.94 g (0.08 g-atoms) of magnesium in 90 ml of ether. The ether was then distilled and 70 ml of dry benzene followed by 7.3 g (0.04 mole) of anhydrous cadmium chloride were added. The mixture was stirred and refluxed for 1 h and then the solvent again distilled until the vapor temperature reached 75 °C.

After cooling, a solution of 9.7 g (0.053 moles) of *o*-isopropylbenzoyl chloride in 50 ml of benzene was added with stirring, and the mixture was refluxed for 2 h. The reaction mixture was poured onto a mixture of ice and 15 ml of concentrated hydrochloric acid, the benzene phase separated and the aqueous phase extracted once with 25 ml of ether. The combined benzene and ether phases were washed with water and evaporated. The residue was refluxed with 50 ml of 5% sodium hydroxide solution for 3 h, cooled, and extracted twice with ether. The ether extracts were combined, washed twice with water, dried, and evaporated. Distillation of the residue afforded 8.06 g (68% yield) of *o*-isopropylbenzophenone, b.p. 106–111 °C at 0.5 mm, n_D^{25} 1.5735.

The 2,4-dinitrophenylhydrazone was prepared and found as reported (6), to have a broad melting range, 139–185 °C. Recrystallization from glacial acetic acid afforded a bright orange-red derivative, m.p. 207.5–209 °C (reported (6) m.p. 204–206.8).

o-Isopropylbenzophenone Anil (6)

The procedure of Reddelien (10) was followed. A mixture of 47 g (0.5 mole) of aniline, 1.0 g of aniline–zinc chloride salt, and 10.97 g (0.049 mole) of *o*-isopropylbenzophenone were refluxed for 3 h and then approximately 25 ml of aniline was permitted to distil. The residue was cooled and treated with 25 ml of chloroform. The aniline – zinc chloride salt was removed by filtration and the filtrate concentrated and distilled under vacuum to give 5.20 g consisting largely of unreacted ketone, b.p. 110–145 °C at 0.4 mm., and 6.81 g of the anil (42% yield), b.p. 150–160 °C at 0.4 mm. The crude anil was dissolved in 50 ml of 90% isopropanol – 10% water, cooled, and seeded. The anil which crystallized out amounted to 6.11 g, m.p. 87.5–89.5 °C.

Anal. Calcd. for $C_{22}H_{21}N$: C, 88.23; H, 7.07; N, 4.68. Found: C, 88.04; H, 7.28; N, 4.74.

The i.r. spectrum showed the absence of any characteristic functional groups except a weak band at 1620 cm^{-1} due to the C=N group. The n.m.r. spectrum showed the aromatic protons in a broad band from 6.1 to 7.9 (14.0 H), the CH of isopropyl group, a multiplet centered at 2.77 (0.8 H) and the methyl protons as two doublets centered at 0.86 and 0.97 (6.0 H).

N(o-Isopropylbenzhydryl)aniline (2)

o-Isopropylbenzophenone anil (6.00 g, 0.02 mole) was dissolved in 50 ml of ether and added to a suspension of 1.5 g (0.04 mole) of lithium aluminium hydride in 50 ml of ether. The mixture was stirred and refluxed for 1½ h. A deep red color developed. Excess hydride was destroyed by the addition of ethyl acetate, and the final reaction product was poured onto ice and 16 ml of concentrated hydrochloric acid. The ether phase was separated, washed three times with water, dried, and evaporated. The residue was distilled under vacuum in a Kontes – Bantam – Ware distillation apparatus giving 5.29 g (88% yield) of a very viscous yellow oil, b.p. 160–168 °C at 0.25 mm.

Anal. Calcd. for $C_{22}H_{23}N$: C, 87.64; H, 7.69; N, 4.65. Found: C, 87.48; H, 7.66; N, 4.52.

The i.r. spectrum showed an NH band at 3420 cm^{-1} and the n.m.r. spectrum showed the aromatic H in a complex band 6.2–7.5 (14.0 H), the benzylic proton a singlet at 5.81 (1.1 H), the NH singlet at 4.02 (1.0 H), the CH of isopropyl a multiplet centered at 3.26 (1.1 H), and the methyl protons as two doublets centered at 1.08 and 1.23 (5.8 H), $J = 6.6$.

A sample was converted to its benzamide by refluxing in pyridine with benzoyl chloride. The benzamide after

recrystallization from 1:1 hexane–cyclohexane and treatment with charcoal had a m.p. 154–156 °C and mixture m.p. with the benzamide of the unknown amine of 153–155 °C. Infrared spectra of the known and unknown benzamides were identical. The n.m.r. spectrum showed the benzylic proton at 7.65 (1.1 H), the aromatic protons in a complex band 6.5–7.5 (19.0 H), the tertiary proton of the isopropyl group as a multiplet centered at 3.39 (0.75 H), and the methyl protons as a triplet at 1.26 (6.0 H, $J = 6.6$).

Acknowledgment

The author is indebted to the National Research Council of Canada for financial support of this research.

1. J. G. Smith and C. D. Veach. Can. J. Chem. **44**, 2245 (1966).
2. F. W. Neumann and C. W. Gould. Anal. Chem. **25**, 751 (1953).
3. R. A. Benkeser and T. E. Johnston. J. Am. Chem. Soc. **88**, 2220 (1966).
4. R. A. Benkeser and W. DeTalvo. J. Am. Chem. Soc. **89**, 2141 (1967).
5. G. O. Schenck and G. Matthias. Tetrahedron Letters, 699 (1967).
6. P. A. S. Smith and E. P. Antoniades. Tetrahedron, **9**, 210 (1960).
7. P. Bauer. Ber. **37**, 735 (1904).
8. A. L. J. Beckwith and J. E. Goodrich Australian J. Chem. **18**, 1023 (1965).
9. B. B. Elsner, H. E. Strauss, and E. J. Forbes. J. Chem. Soc. 578 (1957).
10. G. Reddelien. Ann. Chem. **388**, 165 (1912).

Can. J. Chem. Downloaded from www.nrcresearchpress.com by 210.87.254.105 on 09/05/12
For personal use only.

Can. J. Chem. Downloaded from www.nrcresearchpress.com by 210.87.254.6 on 09/05/12
For personal use only.

Stereospecificity of the Curtius rearrangement[1]

MARTIN B. HOCKING
Exploratory Research Laboratory, Dow Chemical of Canada, Limited, Sarnia, Ontario

Received December 12, 1967

Jones and Mason claimed a number of years ago (1) that rearrangement of *cis*-olefinic acyl azides gave *trans*-olefinic isocyanates. However, several other workers have found that rearrangement of an acyl azide group attached to an optically active carbon gives configurationally identical products, a discovery which apparently conflicts with Jones and Mason's findings. We have reexamined the rearrangement of *cis*-crotonyl azide with stringent checks at each reaction step and found perfect retention of geometry in the product. Details of this finding are discussed.

Canadian Journal of Chemistry, 46, 2275 (1968)

Introduction

The Curtius rearrangement of an acyl azide to an isocyanate with loss of nitrogen has, with saturated aliphatic acyl azides, no special stereochemical involvement. However, with the rearrangement of unsymmetrical olefinic acyl azides, two possible courses are open. A number of years ago, Jones and Mason (1) reported that the rearrangement of *cis* olefinic acyl azides, at least for *cis*-cinnamyl (**3***b*, R = C_6H_5) and *cis*-crotonyl (**3***b*, R = CH_3) azides, gave *trans*-olefinic isocyanates (**4***a*), the same as those obtained from *trans*-olefinic acyl azides. This finding has been mentioned with reservations by review authors (2).

While trying to prepare *cis*-crotonyl chloride from *cis*-crotonic acid by the method of Jones and Mason (1, 3) we obtained largely the *trans* isomer (4). This experimental result has made us question their finding.

There are examples in the literature of optically active azido acyl compounds which have been rearranged to optically active isocyanates (5) (probably with retention of configuration (6)), of *cis* and *trans* cyclic 1,2-diacyl azides rearranged with retention of geometry (7), of retention of *endo* or *exo* configuration on rearrangement of the corresponding 2-azidoacyl norbornanes (8), and an example of an analogous cyclic 1,3-diacylazide rearrangement which was not stereospecific (9). Consequently, we felt that the question of the stereospecificity of the rearrangement of olefinic acyl azides had not as yet been adequately answered and for us, use of the crotonyl azide as the starting point was the obvious choice.

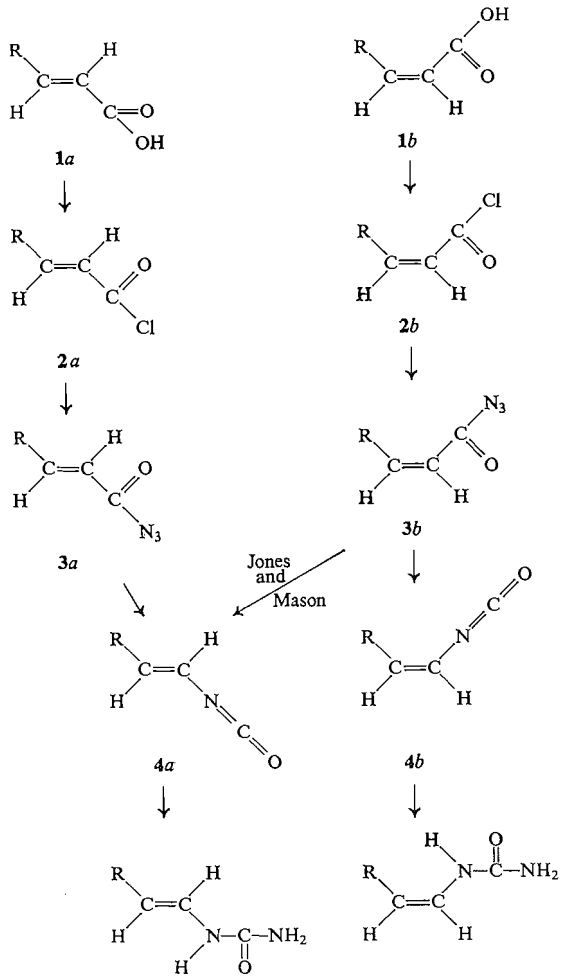

Reaction Scheme 1

R = C_6H_5 for cinnamic acid sequences.
R = CH_3 for crotonic acid sequences.

[1]Contribution No. 157 from the Exploratory Research Laboratory.

TABLE I

Nuclear magnetic resonance data for crotonyl azides and propenyl isocyanates*

Compound†	Double doublets CH_3— Shift	Double doublets CH_3— Coupling	Overlapping quartet pairs —CH= Shift	Overlapping quartet pairs —CH= Coupling	Quartet pairs =CH—X Shift	Quartet pairs =CH—X Coupling
cis-Crotonyl azide	2.85	$J_{ab}=7.35$ $J_{ac}=1.8$	6.50	$J_{ba}=7.3$ $J_{bc}=11.0$	5.75	$J_{ca}=1.8$ $J_{cb}=11.0$
trans-Crotonyl azide	1.91	$J_{ab}=6.7$ $J_{ac}=1.6$	7.10	$J_{ba}=6.8$ $J_{bc}=15.0$	5.83	$J_{ca}=1.6$ $J_{cb}=15.0$
cis-Propenyl isocyanate	1.68	$J_{ab}=6.8$ $J_{ac}=1.7$	5.23	$J_{ba}=6.8$‡ $J_{bc}=7.2$‡	5.89	$J_{ca}=1.7$ $J_{cb}=7.2$
trans-Propenyl isocyanate	1.64	$J_{ab}=6.2$ $J_{ac}=1.2$	5.50	$J_{ba}=6.2$ $J_{bc}=12.6$	5.69	$J_{ca}=1.2$ $J_{cb}=12.6$

*In the formula CH_3—CH=CH—X; CH_3—, —CH=, and =CH—X are represented by *a*, *b*, and *c* respectively.
†The solvent used was deuteriochloroform.
‡Resultant, a broad quintet.

Experimental

Trans-crotonyl chloride, containing about 2% of the *cis* isomer, was purchased from Eastman Organic Chemicals. The unambiguous preparation of *cis*-crotonyl chloride has been described previously (4). Melting points and boiling points are not corrected. Infrared (i.r.) spectra were obtained on a Perkin–Elmer model 337 grating spectrophotometer using thin films between rock salt plates.

Azide Preparations and Decompositions

trans-Crotonyl Azide

trans-Crotonyl chloride (104 g, 1 mole) was added to a well-stirred slurry of dry, finely-ground sodium azide (130 g, 2 moles) in dry ether (400 ml). Stirring, with protection from atmospheric moisture, was continued for 64 h while thermostatting in a water bath at 25 °C. The sodium chloride and unreacted sodium azide were then filtered off, and the ether was removed from the filtrate by raising the bath temperature to 30 °C and applying aspirator vacuum. The residual yellow oil (95.5 g) contained a substantial amount of the azide (i.r. maximum at 2148 cm^{-1}) and a lesser amount of the isocyanate (i.r. maximum at 2265 cm^{-1}) in addition to some (about 30%) unreacted acid chloride.

Azide preparations which were carried out in an aqueous medium were very much quicker and gave better yields. *trans*-Crotonyl chloride (52 g, 0.5 mole) in acetone (25 ml) was added dropwise over 15 min to a well-stirred solution of sodium azide (37 g, 0.5 mole) in water (100 ml) at room temperature. After the first 2 min of addition the remainder of the reaction was carried out with cooling in an ice-water bath, and stirring was continued for a further 5 min after completion of the addition. The organic phase was separated and dried ($MgSO_4$) yielding 47 g (85% yield) of pale-yellow oil. By nuclear magnetic resonance (n.m.r.) and i.r. this was found to be essentially *trans*-crotonyl azide free of isocyanate or acid chloride, and containing only a trace of acetone The azide effervesced very slowly at room temperature.

trans-Propenyl Isocyanate

Azide prepared in ether could not be separated from isocyanate by cold (25 °C bath) distillation so the crude mixture obtained from the azide preparation was decomposed without isolation. The mixture (92 g) diluted with dry *m*-xylene (125 ml), was heated under a reflux condenser on a boiling water bath for 1 h when decomposition was complete (no azide band in i.r.). This solution was distilled through a 30 cm high Widmer column to recover the isocyanate which was collected in two fractions: 11 4 g (b.p. 80–84 °C) and 12.0 g (b.p. 84–101 °C); followed by 30 g (b.p. 101–130 °C; most at 126 °C) of recovered *trans*-crotonyl chloride. Redistillation of the first two fractions through the same column gave 10.1 g of *trans*-propenyl isocyanate (b.p. 78–82 °C, n.m.r. in Table I) containing a trace of *cis*, and 10.8 g of slightly less pure material. They were colorless, highly lachrymatory mobile oils. The yield based on crotonyl chloride consumed was 35%.

When purer azide (prepared by aqueous method) was decomposed as described above better yields of isocyanate were expected. However, while isocyanate was being distilled over, white solids (probably polymeric) formed in the still pot and only 10 g of monomeric isocyanate could be recovered from 45–50 g of azide, the same overall yield as previously.

trans-Propenyl Urea

Dry ammonia gas was played onto the surface of a stirred, ice-cold solution of *trans*-propenyl isocyanate (1.2 g) in dry ether (25 ml) until precipitation ceased. The white solid (1.2 g) was removed by filtration and dried, m.p. 106–111 °C. Two recrystallizations of this precipitate from ethyl acetate – chloroform (1:7 by volume) with a minimum of heating (very susceptible to polymerization) sharpened but simultaneously lowered the melting point to 99–101 °C (lit. (1) m.p. 122 °C), after final drying at 0.01 mm pressure for 8 h.

Anal. Calcd. for $C_4H_8N_2O$: C, 48.0; H, 8.1; N, 28.0. Found: C, 47.4, 47.2; H, 8.2, 8.1; N, 27.3, 27.4.

cis-Crotonyl Azide

cis-Crotonyl chloride (51 g, 0.49 mole) was added to a well-stirred slurry of dry finely-ground sodium azide (52 g, 0.80 mole) in dry ether (250 ml) kept in a thermostat bath at +9 °C. After stirring for 24 h an aliquot was

Can. J. Chem. Downloaded from www.nrcresearchpress.com by 210.87.254.6 on 09/05/12
For personal use only.

TABLE II

Nuclear magnetic resonance data for propenyl ureas*

	trans-Propenyl urea			*cis*-Propenyl urea		
Assignment†	Shift	Multiplicity	Coupling	Shift	Multiplicity	Coupling
CH_3—	1.58	Double doublet	J_{ab}= 6.8 J_{ac}= 1.6	1.53	Double doublet	J_{ab}= 7.1 J_{ac}= 1.6
—CH=	4.80	Overlapping quartet pair	J_{ba}= 6.8 J_{bc}=14.4	4.57	Overlapping quartet pair	J_{ba}= 7.1 J_{bc}= 9.0
=CH—	6.43	Three multiplet groups	complex	6.44	Two multiplet groups	complex
—NH—	8.12	Broad doublet	J_{dc}=10.5	7.95	Broad doublet	J_{dc}=11.1
—NH_2	3.57	Singlet		3.64	Singlet	

*The solvent used was dimethylsulfoxide-d_6
†In the formula CH_3—CH=CH—NH—CO—NH_2; CH_3—, —CH=, =CH—, —NH—, and —NH_2 are represented by *a*, *b*, *c*, *d*, and *e* respectively.

withdrawn, the ether was evaporated. The residual oil contained only a very slight trace of azide and no isocyanate (by i.r.). The bath temperature was raised to 31 °C and stirring continued for a further 14 h when another aliquot was checked and found to be as before. The temperature was then raised to 42 °C and stirring continued for 24 h more with no progress evident. The sodium azide was then filtered off and 35 g of *cis*-crotonyl chloride (now containing about 5% *trans*) were recovered by distillation at 20 mm. Attempted preparation of *cis* azide at 65 °C in diethyl triethylene glycol was as unpromising as the diethyl ether reaction.

Aqueous preparations were successful. 97% *cis*-Crotonyl chloride (52 g, 0.5 mole) in acetone (25 ml) at 0 °C was added over 15 min to a vigorously stirred solution of sodium azide (39 g, 0.6 mole) in water (105 ml) kept at +4 to +7 °C in an ice–salt bath. Preparations where the reaction temperature was allowed to run as high as 15–20 °C gave significantly lower retention of *cis* geometry. Stirring was continued for 5 min after completion of the addition, and then the organic layer was separated, washed with ice-water (120 ml), and dried ($MgSO_4$) yielding 48 g of colorless oil. Infrared analysis indicated this material was predominantly azide though traces of isocyanate, the *cis* acid, and acetone were present. Nuclear magnetic resonance integrals established that 85% of the azide present was *cis*. After 17 h at 25 °C, 8% of a sample of azide had decomposed to isocyanate, but another sample kept one week at −24 °C showed no decomposition. A wash of 23.5 g of the crude azide with weak brine (2 × 100 ml) at −5 °C and two dryings (Na_2SO_4) reduced the quantity of recovered azide to 10.2 g and simultaneously eliminated the acetone and the *cis* acid that were present.

cis-Propenyl Isocyanate

Preliminary preparations showed that decomposition of *cis*-crotonyl azide at temperatures above 45–50 °C gave some concomitant isomerization of *cis*-isocyanate to the *trans* configuration. Also, it was found that temperatures below 40 °C were low enough to prevent significant decomposition of *trans*-crotonyl azide. Apart from preparative reactions three decompositions carried out in a thermostat bath at 33(±0.1) °C and protected from atmospheric moisture, were carefully followed by n.m.r., after a rough preliminary run in ether. Three grams of about 85% *cis*-crotonyl azide were placed in each of three test tubes. To one was added ether (12 ml), another deuteriochloroform (12 ml), and a third was left without solvent. All three were placed in the thermostat and aliquots were withdrawn at intervals and analyzed by n.m.r.; the presence of ether did not interfere. The results of these runs are summarized in Table IV and Fig. 2.

cis-Propenyl Urea

The remainder of the *cis*-crotonyl azide decomposition in deuteriochloroform was diluted with ether (25 ml) and treated with ammonia in the same way as the corresponding *trans* isomer to yield 1.2 g of cream-colored crystals, m.p. 100–108 °C. One recrystallization brought the m.p. to 111–114 °C, mixture m.p. with once recrystallized *trans* 94–98 °C. After two recrystallizations the m.p. was 117–118 °C and the mixture m.p. with twice recrystallized *trans* 92–111 °C. Nuclear magnetic resonance also confirmed its dissimilarity from the *trans* isomer (see Table II).

Anal. Calcd. for $C_4H_8N_2O$: C, 48.0; H, 8.1; N, 28.0. Found: C, 46.7, 47.1; H, 8.2, 8.2; N, 27.5, 27.8.

Nuclear Magnetic Resonance Analyses

The n.m.r. data reported were obtained using a Varian A60 instrument fitted with a phase detector integrator, and a Hewlett–Packard wide range oscillator (model 200CD) for sweep width calibration. Monitoring the oscillator was an electronic counter of the same make (model 5212A). All spectra were run at room temperature and shifts are reported in p.p.m. from internal tetramethyl silane corrected for sweep width variations. Coupling constants were measured on appropriate portions of spectra expanded to 50 cycles sweep width, and are reported in c.p.s. Integrals were all consistent with the assignments indicated.

(a) Curtius Rearrangements

Determination of the proportions of *cis*- and *trans*-crotonyl azides and *cis*- and *trans*-propenyl isocyanates was accomplished by integration of the respective methyl

Can. J. Chem. Downloaded from www.nrcresearchpress.com by 210.87.254.6 on 09/05/12
For personal use only.

TABLE III

Nuclear magnetic resonance data for methyl propenyl ureas*

	N-Methyl-*N'-trans*-propenyl urea (R = H)			*N,N*-Dimethyl-*N'-trans*-propenyl urea (R = CH_3)		
Assignment†	Shift	Multiplicity	Coupling	Shift	Multiplicity	Coupling
CH_3—	1.57	Double doublet	J_{ab}= 6.7 J_{ac}= 1.7	1.58	Double doublet	J_{ab}= 6.8 J_{ac}= 1.6
—CH=	4.80	Overlapping quartet pair	J_{ba}= 6.7 J_{bc}=14.1	5.03	Overlapping quartet pair	J_{ba}= 6.8 J_{bc}=14.0
=CH—	6.48	Three multiplet groups	Complex	6.57	Complex, ranging over 27 c.p.s.	
—NH—	8.08	Broad doublet	J_{dc}=10.0	8.25	Broad doublet	J_{dc}=10.5
—N(CH_3)	2.59	Two overlapping doublets‡	Ambiguous	2.82	Singlet	
R	5.93	Eight probable	Signal too weak			

*The solvent used was dimethylsulfoxide-d_6.
†In the formula CH_3—CH=CH—NH—CO—N(CH_3)R; CH_3—, —CH=, =CH—, —NH—, —N(CH_3), and R are represented by *a*, *b*, *c*, *d*, *e*, and *f* respectively.
‡Three peaks visible, ratio 1:2:1, spacing 2.7 and 2.1 cycles.

resonances (see Table I). Isocyanate methyl identity was double checked by adding small portions of the geometrically opposite analogous isocyanate. The methyl integrals on spectra expanded to 50 or 100 cycles sweep width were then totalled, and the proportion of each compound found by dividing its integral by the total.

(b) Preparation of Model Compounds

The N—H, and NH_2 assignments in the n.m.r. spectra obtained for *cis*- and *trans*-propenyl ureas were not completely unequivocal but the n.m.r. spectra of a number of new propenyl ureas of greater substitution eliminated any doubt. Description of the preparations of these model compounds follows and the n.m.r. data obtained for them in dimethylsulfoxide-d_6 are given in Table III.

N,N-Dimethyl-N'-trans-propenyl urea—An ice-cold solution of dimethylamine (2.5 ml) in dry ether (8 ml) was added with stirring and protection from atmospheric moisture to a solution of *trans*-propenyl isocyanate (1.6 g) in ether (25 ml). The white precipitate formed was filtered off, washed with a small portion of chilled ether, and dried yielding 1.8 g white crystals m.p. 142–149 °C. Recrystallization, once from ethyl acetate and once from acetone yielded 0.3 g of feathery plates m.p. 144–148 °C.

Anal. Calcd. for $C_6H_{12}N_2O$: C, 56.2; H, 9.4; N, 21.9. Found: C, 56.3; H, 9.9; N, 21.9, 21.7.

N-Methyl-N'-trans-propenyl urea—Using the method of the preceding preparation on *trans*-propenyl isocyanate (0.6 g) and adding gaseous methylamine above the solution yielded a precipitate which went back into solution on addition of further methylamine. Leaving the solution overnight with protection from atmospheric moisture yielded 0.49 g of rosettes of crystals m.p. 112–123 °C which were used as such.

Anal. Calcd. for $C_5H_{10}N_2O$: C, 52.6; H, 8.8; N, 24.5. Found: C, 52.6, 52.6; H, 9.0, 9.3; N, 24.5, 24.4.

N,N-Dimethyl-N'-cis-propenyl urea—Dimethylamine (4.5 ml) in ether (10 ml) was added in the same way as the analogous *trans* derivative, to *cis*-propenyl isocyanate obtained from the decomposition of 2.9 g of *cis*-crotonyl azide. The first crop of crystals (0.4 g) was rapidly made useless by deliquescense, but a second crop, (0.4 g) obtained by cooling the mother liquor to −22 °C, melted at 60–65 °C (sealed tube) and this was used for analysis.

Anal. Calcd. for $C_6H_{12}N_2O$: C, 56.2; H, 9.4; N, 21.9. Found: C, 56.5, 56.1; H, 9.7, 10.0; N, 22.0, 21.8.

(c) Study of D_2O Exchange with the Propenyl Ureas

The D_2O exchange experiments were carried out with *cis*- and *trans*-propenyl ureas with the same effects being observed with each. Initially spectra were run in dimethylsulfoxide-d_6 alone. Then gradually increasing amounts of D_2O were added to the DMSO solution with new spectra run each time. The changes observed for *cis*-propenyl urea are described and discussed later with our conclusions.

Results and Discussion

The sequence of reactions starting with *trans*-crotonic acid through to *trans*-propenyl isocyanate was carried out straightforwardly by us according to the methods of Jones and Mason (1, 3) and each stage was carefully followed by nuclear magnetic resonance (n.m.r.) and infrared (i.r.) spectroscopy.

In this work the strongest n.m.r. signal in the spectra of all four compounds primarily involved in this series, the *cis*- and *trans*-crotonyl azides and *cis*- and *trans*-propenyl isocyanates, was that

Can. J. Chem. Downloaded from www.nrcresearchpress.com by 210.87.254.6 on 09/05/12
For personal use only.

Can. J. Chem. Downloaded from www.nrcresearchpress.com by 210.87.254.6 on 09/05/12
For personal use only.

of the methyl group of the four compounds. Very conveniently for the purposes of this work nearly all of the double doublets representing the methyls of these four compounds were sufficiently well separated from each other to be used for the analysis of mixtures (Fig. 1 and Table I). While there was an overlap of one of the peaks in the *cis*-propenyl isocyanate methyl pattern with one for the methyl of *trans*-propenyl isocyanate, it was possible to use satisfactorily the remaining three unencumbered bands of each of the two compounds. This permitted easy direct determination of the proportions of each of the components present in aliquots removed from the main reaction solution, with minimal disturbance of conditions (for *cis* determinations the n.m.r. probe was at the same temperature as that of the thermostat being used for the decompositions).

With the *cis*-crotonic acid sequence it had already been discovered (4) that the preparation of acid chloride according to the method of Jones and Mason (1, 3) resulted in a significant proportion of *trans*-crotonyl chloride. That this source of loss of geometry was at least partly responsible for the latter authors' conclusions about the stereochemistry of the azide rearrangement was evident from the next step, conversion to the acyl azide. It had already been ascertained by us that treatment of *trans*-crotonyl chloride in ether with finely ground sodium azide was sufficient to obtain the azide, conditions which the earlier workers (3) had not only found adequate for the preparation of *trans*-crotonyl azide, but had also found sufficient with *cis*-crotonyl chloride. We could not react the *cis* acid chloride with sodium azide in ether even at temperatures 15 °C higher than the earlier work or, to a significant extent, in diethyl triethylene glycol at 65 °C.

Hence, it is felt that this lack of reactivity of unequivocal *cis*-crotonyl chloride with sodium azide under these conditions is an additional indication that a significant loss of geometry had already been incurred by Jones and Mason in their preparation of *cis* acid chloride. Therefore, it is postulated that the azide obtained by them was almost certainly largely the *trans* isomer.

Possibly the much greater solubility of a tetralkyl ammonium azide (10) in ether would have given improved results with the *cis* acid chloride but since aqueous preparation of the *cis* azide led to good yields of material with good retention of geometry these less accessible azides were not considered further. Both stereochemical and yield objectives were improved by carrying out the aqueous reaction with strong cooling; chloride hydrolysis, isomerization, and decomposition to the isocyanate were all reduced to negligible levels. *cis*-Crotonyl azide of 85–90% correct geometry in 80% or better yields could regularly be obtained by this method.

TABLE IV

Decomposition of *cis*-crotonyl azide at 33 °C

Solvent	Time (h)	Mole percent of total: *cis* Azide	*trans* Azide	*cis* Isocyanate	*trans* Isocyanate
Deuteriochloroform	0	84.4	15.6	0	0
	4	62.8	15.6	21.6	0
	21	20.2	15.4	64.4	Trace
	45	4.3	14.6	77.8	3.3
None	0	84.4	15.6	0	0
	6	69.2	16.0*	14.8	0
	25	39.0	16.5*	43.0	1.5
	54	15.3	18.2*	63.1	3.4
Ether	0	84.4	15.6	0	0
	6	71.7	17.2*	11.1	0
	25	50.3	18.1*	31.5	Trace
	71	21.9†	25.1†	52.0†	Trace
Ether‡	0	84.4	15.6	0	0
	18	65.0	18.5*	16.5	0
	42	32.1†	24.0†	43.3†	0

*These give some indication of the extent of loss of the other three components in the run by volatilization or hydrolysis.
†The nuclear magnetic resonance samples were very dilute, consequently the integrals are not very accurate.
‡Most of the ether was carefully boiled off the aliquots before nuclear magnetic resonance analysis.

Important to side-step ambiguity in the final rearrangement step of the sequence was the significantly lower decomposition temperature of *cis*-crotonyl azide over the *trans* isomer. The temperature that was necessary to stop the decomposition of the *cis* isomer was −20 °C whereas, with the *trans* isomer, 0 °C was sufficient and even at room temperature its rate of decomposition was negligible. In this work decompositions were carried out at 33 °C since at this temperature the *cis* azide rearranged at an easily measurable rate and the *trans* azide was still more or less stable. Table IV summarizes these results. The rate of appearance of *cis*-propenyl isocyanate was found to be the same as the rate of loss of *cis*-crotonyl azide, within experimental error. In spite of precautions against the intrusion of

Can. J. Chem. Downloaded from www.nrcresearchpress.com by 210.87.254.6 on 09/05/12
For personal use only.

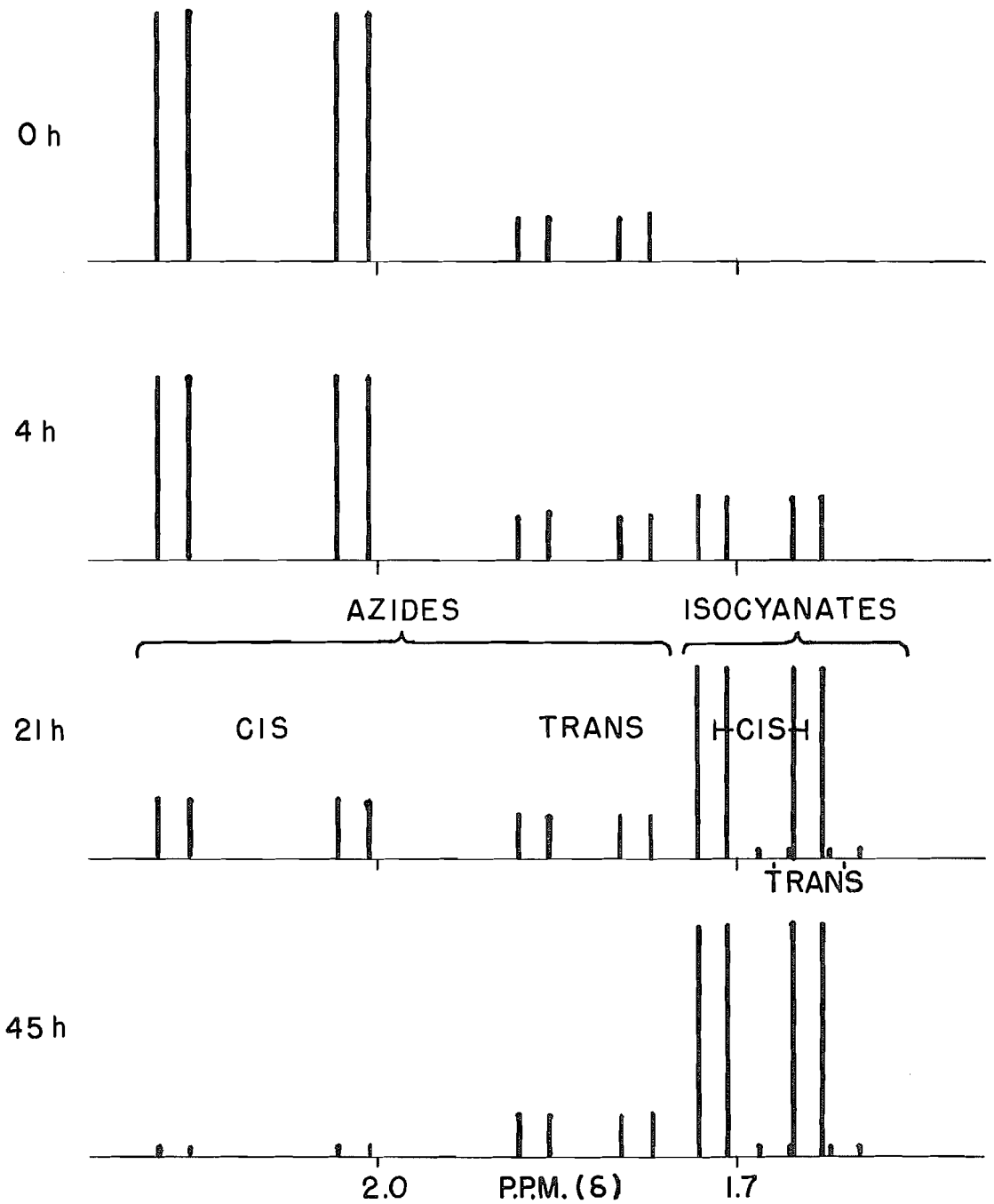

FIG. 1. The nuclear magnetic resonance spectra of the decomposition of *cis*-crotonyl azide at 33 °C in $CDCl_3$.

Can. J. Chem. Downloaded from www.nrcresearchpress.com by 210.87.254.6 on 09/05/12
For personal use only.

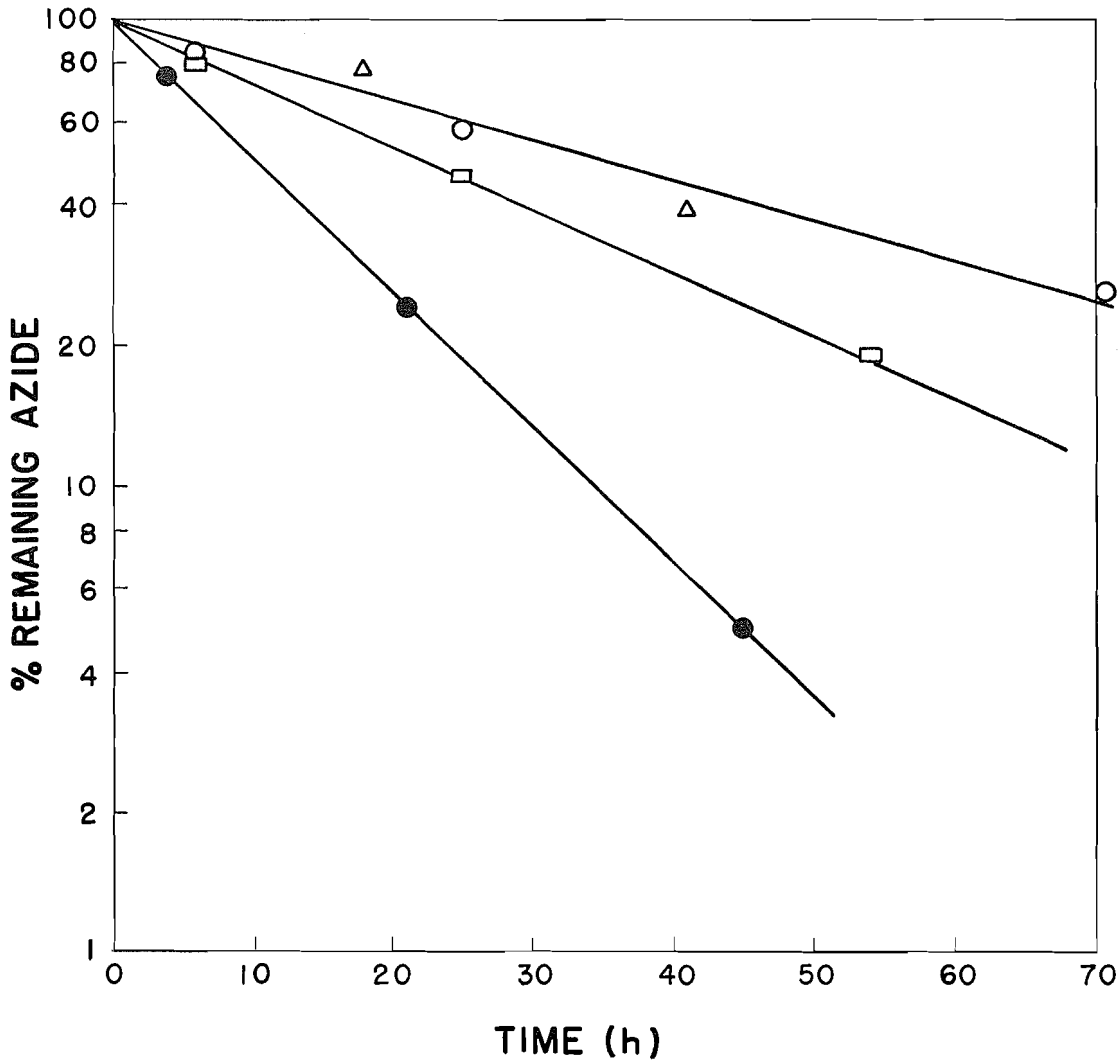

FIG. 2. The decomposition of *cis*-crotonyl azide at 33 °C: ○, Ether; △, Ether (rough); □, neat; ●, $CDCl_3$.

atmospheric moisture some could have entered when aliquots for analysis were being withdrawn. Hydrolysis of a small portion of the isocyanate to amine with this moisture is probably the explanation for the gradual apparent rise in the proportion of the *trans* azide reported for some of the runs. However, these results show quite conclusively that the rearrangement of *cis*-olefinic acyl azides is stereospecific, at least for *cis*-crotonyl azide.

The effect of solvent on the decomposition of *cis*-crotonyl azide was tested while azide was still available. It was thought quite possible that the stereospecificity of the rearrangement might be affected, but no significant effect on the rate was expected (2). Referring to Table IV, again, one can see no noticeable effect of solvent polarity or lack of solvent altogether on stereospecificity, but even our crude (kinetically speaking) runs show quite a noticeable enhancement of rate in going from a decomposition run in ether, to a run without solvent, to a run in

deuteriochloroform (see Fig. 2). This is a somewhat surprising result since the Curtius rearrangement is thought to proceed via a unimolecular path (2, 5) but perhaps an azide half-life difference of a factor of 3.7 between the slowest and the fastest reactions is not considered large.

We have no explanation for one apparent anomaly. As traditional confirmation of our n.m.r. findings, conversion with ammonia of portions of the two isomeric isocyanates to the corresponding *cis*- and *trans*-propenyl ureas was undertaken. Jones and Mason (1) had found a value of 122 °C for the melting point of *trans*-propenyl urea. Through a number of preparations and recrystallizations we could not duplicate this melting point, even though reasonable analyses were obtained. Perhaps of more importance though, at any stage of the crystallization of either isomeric urea, significant mixture melting point depressions were consistently observed. Also, n.m.r. spectra of the two compounds showed the expected differences (Table II).

Two methods were used to confirm the n.m.r. spectral assignments of the *cis*- and *trans*-propenyl ureas. The first was by checking the n.m.r. spectra of the urea when one or both of the NH_2 hydrogens were replaced by methyls; this confirmed all the N—H assignments (Table III). The second was addition of D_2O to a hexadeuteriodimethylsulfoxide solution of *trans*-propenyl urea to see if sufficient exchange of the single N—H hydrogen with deuterium could be induced to eliminate the assigned allylic hydrogen coupling with it. About 30% D_2O in the solution brought about the collapse of the allylic hydrogen multiplet from at least 14 visible peaks (theoretical = 16) to the 8 seen for allylic hydrogen in spectra of the isocyanates, and a simultaneous loss of the propenyl N—H resonance. This result must be ascribed to elimination of the allylic hydrogen N—H coupling by exchange of the N—H with deuterium, serving as confirmation for the assignment of the single N—H doublet.

Acknowledgments

The author thanks Mr. H. D. Mak of this laboratory for obtaining the nuclear magnetic resonance spectra required for this work, and for suggesting the D_2O exchange experiments. He is also grateful to Dr. L. E. Swim and his associates, The Dow Chemical Company, Midland, Michigan, for performing the elemental microanalyses.

1. L. W. JONES and J. P. MASON. J. Am. Chem. Soc. **49**, 2528 (1927).
2. E. S. WALLIS and J. F. LANE. The Hofmann reaction. *In* Organic reactions. Vol. III. John Wiley and Sons, Inc., New York. 1946. p. 273.
3. J. P. MASON. Ph.D. Thesis. Princeton University. (1927). p. 12.
4. M. B. HOCKING. Can. J. Chem. **46**, 466 (1968).
5. L. W. JONES and E. S. WALLIS. J. Am. Chem. Soc. **48**, 169 (1926).
6. C. K. INGOLD. Structure and mechanism in organic chemistry. Cornell Univ. Press, Ithaca, New York. (1953). p. 500. J. S. HINE. Physical organic chemistry. McGraw-Hill Book Co., Inc., New York. 1962. p. 337.
7. E. R. BUCHMAN, A. O. REIMS, T. SKEI, and M. J. SCHLATTER. J. Am. Chem. Soc. **64**, 2696 (1942).
8. K. ALDER and G. STEIN. Ann. **514**, 211 (1934).
9. A. SKITA and R. RÖSSLER. Ber. **72B**, 461 (1939).
10. V. GUTMANN, G. HAMPEL, and O. LEITMANN. Monatsh. Chem. **95**, 1034 (1964).

Can. J. Chem. Downloaded from www.nrcresearchpress.com by 210.87.254.6 on 09/05/12
For personal use only.

Can. J. Chem. Downloaded from www.nrcresearchpress.com by 210.87.254.42 on 09/05/12
For personal use only.

Synthesis of methyl 2,3-anhydro-4-deoxy-6-*O*-methyl-α-DL-*lyxo*-hexopyranoside[1]

F. SWEET AND R. K. BROWN
Department of Chemistry, University of Alberta, Edmonton, Alberta

Received February 15, 1968

Bromomethoxylation of 2-methoxymethyl-3,4-dihydro-2*H*-pyran, **1**, at −55° gave in 87% yield a 9:1 mixture of 3α-bromo-2β-methoxy-6α-methoxymethyltetrahydropyran (**2**) and 3β-bromo-2α-methoxy-6α-methoxymethyltetrahydropyran (**3**) respectively. Of the mixture of **2** and **3**, in refluxing methanol containing sodium methoxide, **2** is dehydrohalogenated much more readily than is **3**, giving a product that contains at least 95% of the *trans*-2-methoxy-6-methoxymethyl-5,6-dihydro-2*H*-pyran, **4**. The identity and configuration of **4** was established by its hydrogenation to the known *trans*-2-methoxy-6-methoxymethyltetrahydropyran, **5**. *m*-Chloroperoxybenzoic acid slowly and selectively converts **4**, in 80% yield, to a mixture of methyl 2,3-anhydro-4-deoxy-6-*O*-methyl-α-DL-*lyxo*-hexopyranoside (**6**) (>95%) and methyl 2,3-anhydro-4-deoxy-6-*O*-methyl-α-DL-*ribo*-hexopyranoside, (**7**) (<5%).
A rationalization is given for the selectivity observed.

Canadian Journal of Chemistry, 46, 2283 (1968)

Introduction

A recent report from this laboratory (1) has described the synthesis of methyl 4-deoxy-3-*O*-methyl-αβ-DL-*threo*-pentopyranoside by a series of stereoselective reactions starting with 3,4-dihydro-2*H*-pyran. The present work describes the application of a similar rationale to the preparation of methyl 2,3-anhydro-4-deoxy-6-*O*-methyl-α-DL-*lyxo*-hexopyranoside (methyl 2,3-anhydro-4-deoxy-6-*O*-methyl-α-DL-manno-pyranoside) from 2-methoxymethyl-3,4-dihydro-2*H*-pyran.

Results and Discussion

The sequence of reactions for this synthesis is shown in Scheme 1.

When bromine was added to a cold (−50 to −55°) solution of 2-methoxymethyl-3,4-dihydro-2*H*-pyran (**1**) in a mixture of methanol and liquid ammonia, an oil was obtained in 87% yield (by distillation) which according to gas–liquid chromatography (g.l.c.) and nuclear magnetic resonance (n.m.r.) analysis consisted of only two isomeric products in the ratio 9:1. These were assigned the structures 3α-bromo-2β-methoxy-6α-methoxymethyltetrahydropyran (**2**) and 3β-bromo-2α-methoxy-6α-methoxymethyltetrahydropyran (**3**) respectively, for the following reasons. The elemental analysis of the oil was correct for the structures **2** and **3**. Previous work involving bromomethoxylation of 3,4-dihydro-2*H*-pyran under similar conditions (2) gave a very high proportion of the isomer 3-bromo-2-methoxytetrahydropyran in which the Br and OCH_3 substituents are *trans* (*trans*:*cis* = 99:1). Bromomethoxylation of 3,4-dihydro-2*H*-pyran with Br_2, CH_3OH, and Ag_2CO_3 at 0° has been shown to provide a 9:1 mixture of *trans*- and *cis*-3-bromo-2-methoxy-tetrahydropyran (3). Accordingly, because of the greater selectivity in producing the *trans* isomer under our conditions (2), a *trans* relation of Br and CH_3O was assigned for *both* **2** and **3**.

The n.m.r. spectrum of the mixture of **2** and **3** in $CDCl_3$ showed two sets of signals in the anomeric proton region, one at τ 5.28 (an envelope, $w/2 = 3$Hz) and the other at τ 5.71 (doublet, $J = 9.2$ Hz) with the integrated areas in the ratio of 9:1. The higher field signal, with the larger coupling, was assigned to the minor isomer (**3**) in which the C-2 and C-3 protons are *trans* diaxial (4). The signal at τ 5.28 was due to the C-2 proton in **2**. In both isomers, **2** and **3**, it is assumed that the most favorable conformation is that in which the C-6 CH_3OCH_2— group is equatorial, thus avoiding strong 1,3-diaxial interaction involving this group in the alternate chair form.

The 9:1 mixture of **2** and **3**, when heated with sodium methoxide in refluxing methanol, gave in 70% yield an olefinic product which g.l.c. indicated to be composed of only one product. However the n.m.r. spectrum (Fig. 1) did show the presence of an impurity (≤5%) as indicated by the small signal at τ 5.46 which could be due to the anomeric proton of the *cis* isomer. The

[1]From the thesis of F. Sweet to be presented to the Faculty of Graduate Studies, University of Alberta, Edmonton, Alberta, as part of the requirements for the degree of Doctor of Philosophy.

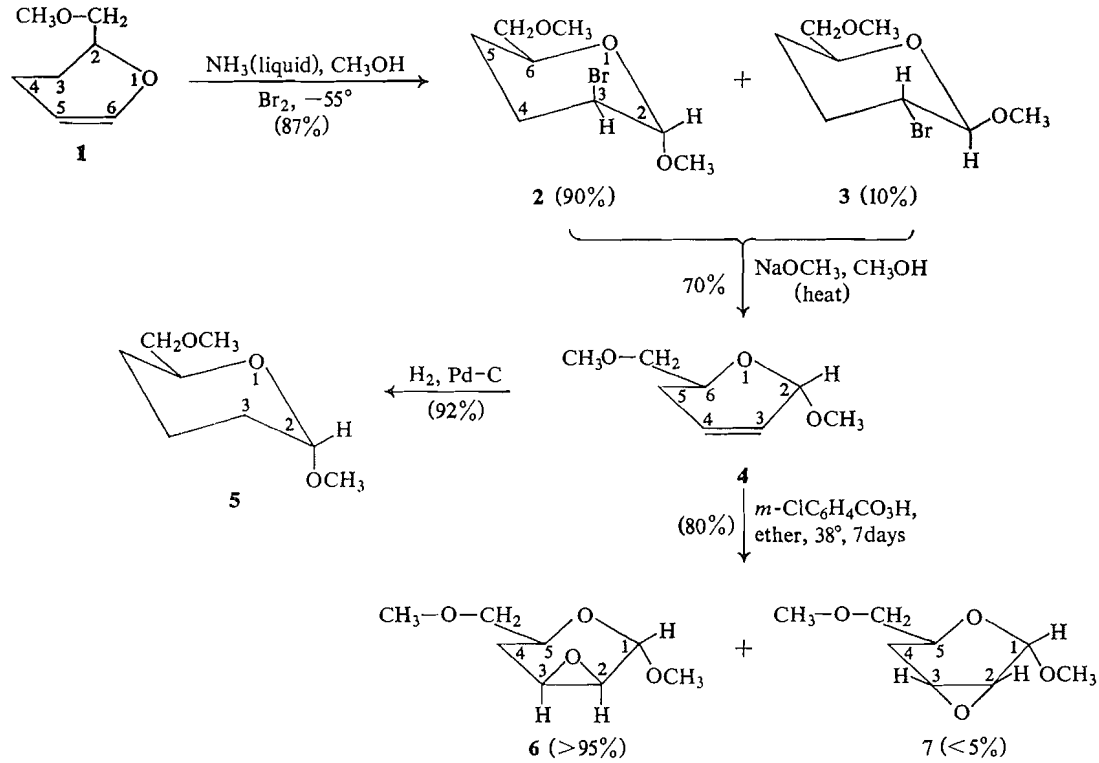

SCHEME 1

main product was assigned the structure *trans*-2-methoxy-6-methoxymethyl-5,6-dihydro-2*H*-pyran (**4**) on the basis of the following experiment. Catalytic hydrogenation (Pd–C) of **4**, under alkaline conditions to avoid isomerization, gave a nearly quantitative yield of *trans*-2-methoxy-6-methoxymethyltetrahydropyran (**5**) identical in all respects (infrared, n.m.r., g.l.c.) with an authentic sample (5). No evidence for the presence of the *cis* isomer or any other compound was found in either the g.l.c. or the n.m.r. spectrum of **5**. Since no rearrangement of the substituents is expected to occur during the conversion of **4** to **5** under the conditions of hydrogenation, it follows that **4** must be the *trans* isomer.

Treatment of an ether solution of **4**, at 38°, with *m*-chloroperoxybenzoic acid for 7 days gave an 80% yield of epoxidized product which both g.l.c. and n.m.r. showed to be composed of two substances in the ratio of $>95:<5$. These have been assigned the structures **6** and **7** respectively because of the following information. Elemental analysis agreed with that expected for the mixture of structures **6** and **7**. The n.m.r. (Fig. 2, cf. Fig. 2 in ref. 7) of this mixture clearly supports the assignment of structure **6** as indicated. The signal for H-1[2] is a singlet at τ 5.18 and that for H-2 is a doublet at τ 7.10 ($J = 4.0$ Hz). It has been shown (6) that epoxides of the general structure of **6**, wherein the C-2, C-3 epoxy group and the C-1 methoxy substituent are *trans* to each other, exhibit a "singlet" ($J_{1,2} \sim 0$) for H-1 while the *cis* isomer shows a distinct doublet for H-1 with a coupling $J_{1,2} = 2.5$–4.5 Hz. A recent report from this laboratory (7) has corroborated this finding and in addition has shown that for the *trans* isomer, the signal for H-2 appears as a distinct doublet at τ 7.0–7.1, well up-field from the more complicated signal for H-3. The "singlet" for H-1 and the doublet for H-2 (at τ 7.0) are thus quite characteristic of a *trans* configuration. Hence the major isomeric epoxide is considered to have the structure shown by **6**

[2]In structures **1**–**5** the accepted tetrahydrofuran numbering system has been used. For structures **6** and **7**, the numbering system is that used for carbohydrates, since these two structures are now being considered as such.

Can. J. Chem. Downloaded from www.nrcresearchpress.com by 210.87.254.42 on 09/05/12
For personal use only.

Can. J. Chem. Downloaded from www.nrcresearchpress.com by 210.87.254.42 on 09/05/12
For personal use only.

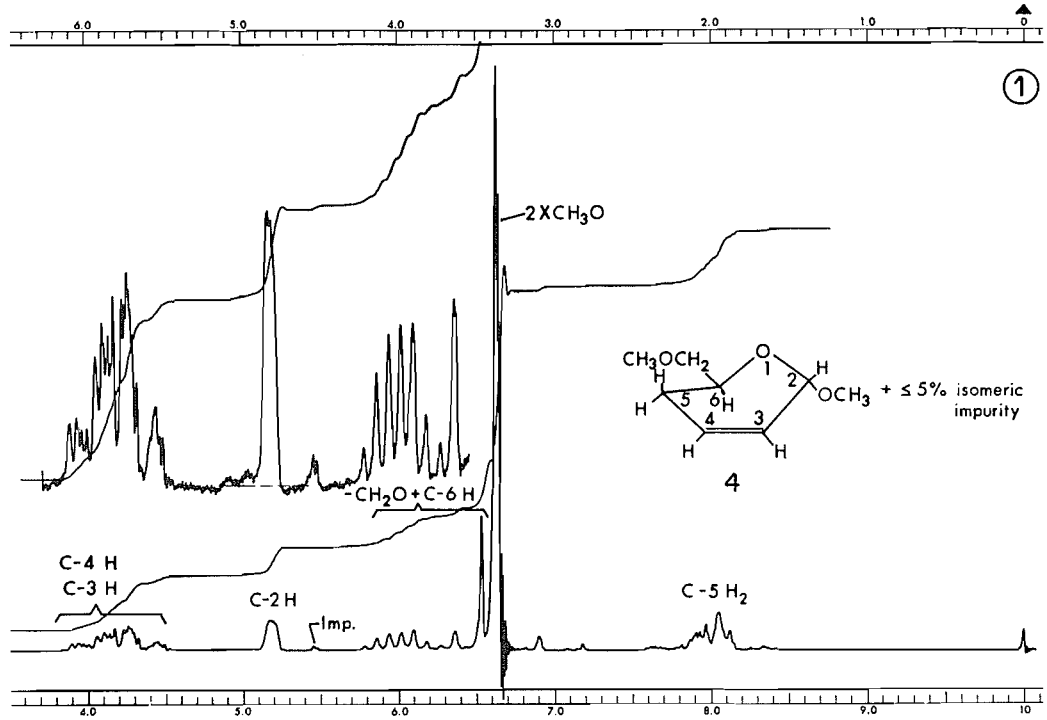

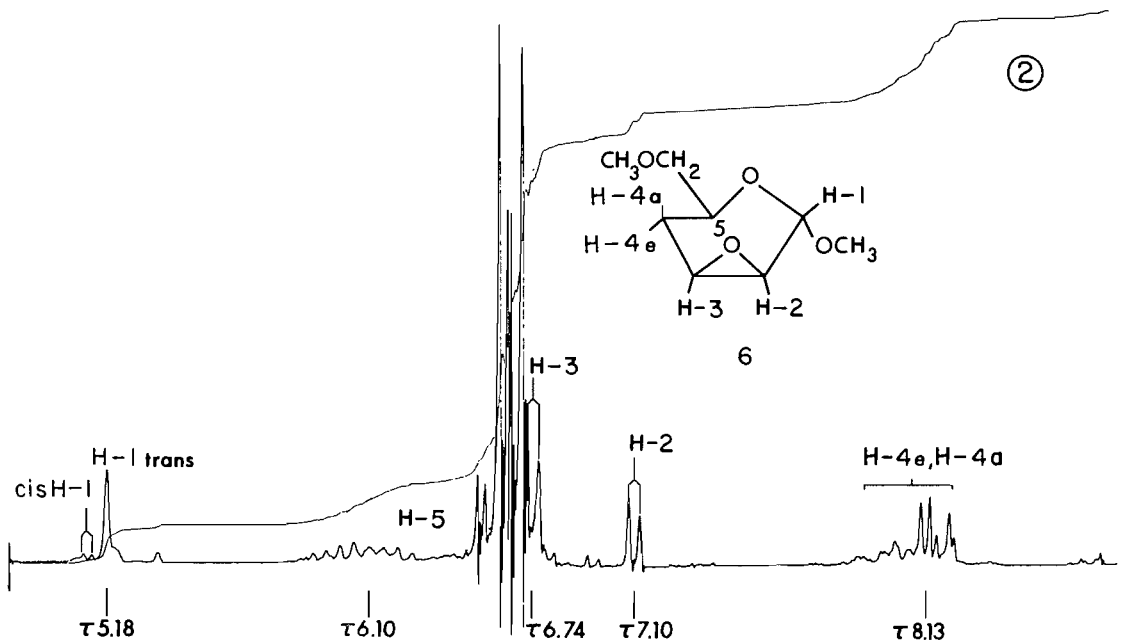

FIG. 1. The 60 MHz nuclear magnetic resonance spectrum of *trans*-2-methoxy-6-methoxymethyl-5,6-dihydro-2*H*-pyran in $CDCl_3$ solution.

FIG. 2. The 100 MHz nuclear magnetic resonance spectrum of *trans* methyl 2,3-anhydro-4-deoxy-6-*O*-methyl-α-DL-*lyxo*-hexopyranoside (with some *cis*) in $CDCl_3$ solution.

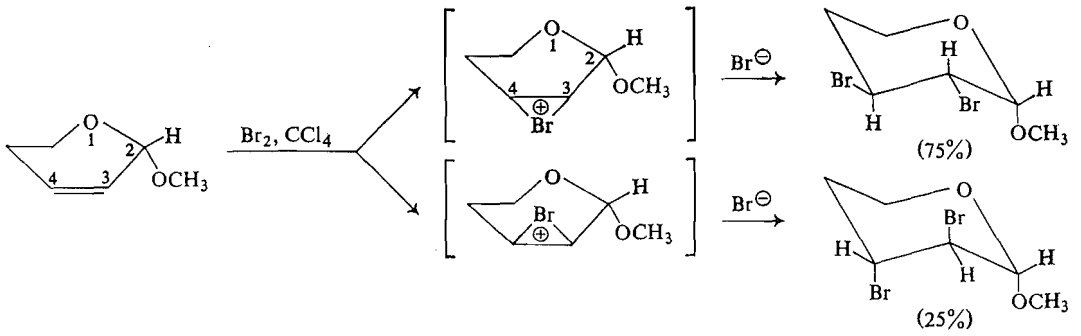

SCHEME 2

(methyl 2,3-anhydro-4-deoxy-6-*O*-methyl-α-DL-*lyxo*-hexopyranoside), while the minor isomer is assigned structure **7** (methyl 2,3-anhydro-4-deoxy-6-*O*-methyl-α-DL-*ribo*-hexopyranoside).[3]

Three aspects of the stereochemical sequence of this synthesis require some comment.

(*i*) *The Bromomethoxylation of* **1**

A report from this laboratory (8) has explained the preponderance of the dibromo isomer, 3β,4α-dibromo-2β-methoxytetrahydropyran, obtained from bromination of 2-methoxy-5,6-dihydro-2*H*-pyran as due to considerable initial complex formation of bromine with the oxygen atom of the C-2 methoxy group. In this way a $Br^{\oplus}$ could be readily transferred to the double bond *on the same side as is occupied by the C-2 methoxy substituent* (Scheme 2). The C-3, C-4 epibromonium moiety is then attacked by $Br^{\ominus}$ with preferred *epi* ring breaking at the C—Br bond remote from the anomeric center (C-2). The same rationale can be applied to the bromomethoxylation of 2-methoxymethyl-3,4-dihydro-2*H*-pyran. The results indicate that bromine attack of the double bond takes place preferentially on the same side of the ring as is occupied by the methoxymethyl group. Models show that the $Br^{\oplus}$—O< complex with the methoxymethyl group can assume a position directly over and very near to the double bond when the methoxymethyl group is in the *quasi*-axial position. This is an ideal arrangement to permit intramolecular transfer of the $Br^{\oplus}$ species from oxygen to the π bond. In this way the C-2, C-3 epibromonium ion is formed predominantly *cis* to the C-6 methoxymethyl substituent. Subsequent attack by methanol would then be at C-2 to yield 3α-bromo-2β-methoxy-6α-methoxymethyltetrahydropyran. That Br—C_2 rather than Br—C_3 bond breaking should be preferred nearly completely is understandable since the ring oxygen electron pair would stabilize the positive charge on C-2 made by incipient Br—C_2 bond breaking very much more than a similar charge on C-3.

(*ii*) *Selective Dehydrohalogenation of the 9:1 Mixture of* **2** *and* **3**

Since only *trans*-2-methoxy-6-methoxymethyltetrahydropyran was obtained in apparently quantitative yield from the catalytic reduction of the product obtained from the sodium methoxide dehydrohalogenation of the 9:1 mixture of **2** and **3**, it is clear that under the reaction conditions (sodium methoxide in refluxing methanol) the major isomer, **2**, was dehydrohalogenated with high selectivity. The *trans* diaxial orientation of the H and Br moieties required for facile base catalyzed dehydrohalogenation (9), is present in the preferred conformation of **2** but absent in the preferred conformation of **3**, hence would explain the selectivity observed.

(*iii*) *Selective Epoxidation of* **4**

The preferential epoxidation of **4** to **6** rather than to **7** is interesting. Of the two important

[3]That the assignment of the signals in the anomeric proton region (τ 5.0–5.2) to the *cis* and *trans* isomers **7** and **6**, is correct is supported by the findings (7) that for the isomeric 1-alkoxy-2,3-epoxytetrahydropyrans the anomeric proton signal for the *cis* isomer is a doublet and is found invariably at slightly lower field than is the signal (singlet) for the anomeric proton of the *trans* isomer. The small signal at ~τ 5.2–5.3 (Fig. 2) may be due to an impurity (isomeric) which could arise from a small amount of epoxide obtained from contaminating 4,5 olefins (8) since the position of the signal is at somewhat higher field than is expected for a substance arising from epoxidation of a contaminant such as *cis*-**4**.

Can. J. Chem. Downloaded from www.nrcresearchpress.com by 210.87.254.42 on 09/05/12
For personal use only.

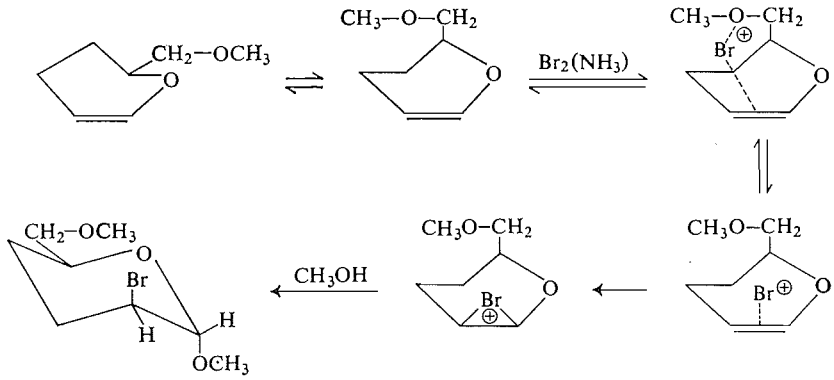

SCHEME 3

conformations (A and B) shown below, A should be preferred not only because of the *quasi*-

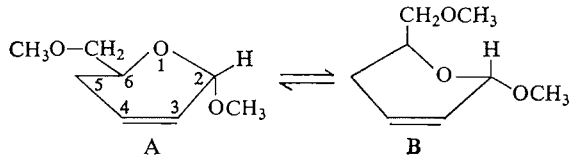

equatorial arrangement of the $CH_3—O—CH_2$- group but also because of the *quasi*-axial position of the C-2 methoxyl substituent, an arrangement stabilized by the *anomeric effect* (10). It has been shown that both alkyl and alkoxy substituents in the cyclohexene ring (11, 12) sterically hinder the approach of the peroxy acid to the double bond on that side occupied by the substituent. A similar steric effect has been observed in epoxidation of 2-alkoxy-5,6-dihydro-2*H*-pyrans (2). In the present work, the preponderance (>95%) of the isomer **6** in which the epoxy group is *trans* to the methoxy substituent clearly shows that either (*a*) the chief reacting species is conformer A in which the *quasi*-axial C-2 methoxy group blocks approach to the double bond or (*b*) that a group situated α to the double bond (at C-2) is sterically more effective than is a group situated β to the double bond (at C-6). A combination of both factors may be involved. That β-situated groups do exert steric hindrance to epoxidation of double bonds is known (12).

Experimental

All melting points and boiling points are uncorrected. The elemental analyses were performed by Mrs. Darlene Mahlow of the Microanalytical Laboratory, Department of Chemistry, University of Alberta.

The nuclear magnetic resonance (n.m.r.) spectra were obtained with Varian Associates A60 and HR100 spectrometers by Mr. R. N. Swindlehurst and Mr. Glen Bigam, Department of Chemistry, University of Alberta, Edmonton.

Gas–liquid chromatography analyses were made with an F and M model 700 Chromatograph using a column (1/8 in. × 12 ft) of 20% butanediol succinate on Gas-Chrom P(60–80 mesh) at a helium flow rate of 40 ml/min.

Solvents were usually removed in a rotary evaporator under vacuum unless otherwise stated.

3-Bromo-2-methoxy-6-methoxymethyltetrahydropyran (2 and 3)

To a stirred, cold (−60°) mixture of 52 g (0.41 mole) of 2-methoxymethyl-3,4-dihydro-2*H*-pyran (13) in 500 ml of dry methyl alcohol and 50 ml of anhydrous liquid ammonia, were added 65.6 g (0.41 mole) of bromine in 100 ml of methylene chloride. The bromine was added dropwise, over a period of 1 h, at a rate which maintained the reaction temperature in the range −55 to −50° (dry ice – acetone bath). The cooling bath was then removed and the solution was stirred overnight and was allowed to come to room temperature. Removal of the bulk of the solvent left a mixture of ammonium bromide and pale-yellow oil. This was extracted with ether. The residual solid was taken up in water and this aqueous solution extracted with ether. The combined ether extracts were washed with 50 ml of saturated aqueous sodium carbonate solution, then with 50 ml of water. If the water wash was acidic (pH paper) the aqueous sodium carbonate wash was repeated. The ether solution was dried (Na_2SO_4), was filtered, and was freed from solvent. The oily residue was distilled and gave 85.3 g (87%) of colorless liquid boiling at 70° at 0.6 mm; n_D^{25}, 1.4745.

Anal. Calcd. for $C_8H_{15}BrO_3$: C, 40.18; H, 6.28; Br, 33.42. Found: C, 40.32; H, 6.38; Br, 33.40.

The n.m.r. spectrum in $CDCl_3$ referred to tetramethylsilane showed the presence of two isomers (**2** and **3**) in the ratio of 9:1 (see Results and Discussion). Gas–liquid chromatography (column temperature, 195°) showed only two slightly overlapping peaks in the area ratio of 9:1.

Can. J. Chem. Downloaded from www.nrcresearchpress.com by 210.87.254.42 on 09/05/12
For personal use only.

Can. J. Chem. Downloaded from www.nrcresearchpress.com by 210.87.254.42 on 09/05/12
For personal use only.

trans-2-Methoxy-6-methoxymethyl-5,6-dihydro-2H-pyran (4)

A quantity (47.8 g, 0.2 mole) of 3-bromo-2-methoxy-6-methoxymethyltetrahydropyran (**2** and **3**) was added slowly, via an addition funnel, to a stirred mixture of 32.4 g (0.6 mole) of sodium methoxide in 250 ml of methyl alcohol. During the addition, the temperature of the reaction mixture rose to the boiling point of the methanol, and a precipitate of sodium bromide appeared. After the addition was completed, the mixture was heated under reflux for 24 h. The volume of the solution was then reduced to 100 ml by fractional distillation. The cooled residue was diluted with 200 ml of ether and shaken to promote further precipitation of sodium bromide. The organic layer was decanted and sufficient water was added to the solid residue to effect its solution. This aqueous material was extracted with ether (2 × 50 ml). The combined ether solutions were washed with water (3 × 25 ml), were dried (Na_2SO_4), were filtered and were freed from solvent by distillation through a fractionating column. The residue was distilled at reduced pressure and gave 22.3 g (70%) of colorless liquid; b.p., 84° at 20 mm, n_D^{25}, 1.4466.

Anal. Calcd. for $C_8H_{14}O_3$: C, 60.74; H, 8.92. Found: C, 60.77; H, 8.68.

The g.l.c. showed only one peak. The n.m.r. spectrum (Fig. 1) in $CDCl_3$ showed two signals in the anomeric proton region—τ 5.20 (broad singlet $w/2$ = 5 Hz) and τ 5.46 (narrow multiplet) in the ratio, respectively, of $\geq 95 : \leq 5$. The remainder of the spectrum agreed with the structure (**4**).

trans-2-Methoxy-6-methoxymethyltetrahydropyran (5)

A solution of 2.0 g (0.013 mole) of 2-methoxy-6-methoxymethyl-5,6-dihydro-2*H*-pyran (**4**) in 75 ml of methyl alcohol containing 1 g of sodium methoxide (to prevent acid-catalyzed isomerization) and 100 mg of 5% palladium-on-charcoal (Coleman, Matheson, and Bell), all contained in a 500 ml heavy wall hydrogenation bottle, was shaken for 24 h under 60 p.s.i. of hydrogen. The mixture was then filtered and the filtrate freed from solvent (at 45°). The residue was shaken with 100 ml of ether and the liquid filtered. The solvent was removed from the filtrate by fractional distillation and the residual oil distilled in a semimicro distillation apparatus under reduced pressure; yield, 1.85 g (92%) of **5**; b.p., 108° at 75 mm; n_D^{24}, 1.4312; lit. b.p. of a 7:3 *trans/cis* mixture, 110° at 75 mm, n_D^{25}, 1.4320 (5).

The g.l.c. showed the presence of only one product. (The *cis* and *trans* disubstituted tetrahydropyrans are usually well separated by g.l.c. on the columns employed, in contrast to the corresponding dihydropyrans which show two poorly resolved peaks.)

The n.m.r. spectrum in $CDCl_3$ was identical to that obtained from an authentic specimen of **5** (5) (anomeric proton, broad singlet at τ 5.27, $w/2$ = 5 Hz) and showed no evidence of the presence of the *cis* isomer whose anomeric proton signal is found at τ 5.65 (multiplet) (5).

Epoxidation of 4

To a 250 ml, 3-neck round bottom flask, equipped with a magnetic stirrer and a condenser fitted with a drying tube, containing a solution of 4 g (0.025 mole) of *trans*-2-methoxy-6-methoxymethyl-5,6-dihydro-2*H*-pyran in 50 ml of dry ether, were added 6.6 g of 80% (~0.03 mole) *m*-chloroperoxybenzoic acid. The solution was stirred for several days at ~38° (heated by the stirring motor). After 4 days, a white precipitate of *m*-chlorobenzoic acid appeared and accumulated. After a total of 7 days of reaction under these conditions, the mixture was cooled and filtered under gentle suction. The solid was washed with cold ether (2 × 25 ml) and the combined ether filtrate and washings were washed with saturated aqueous sodium carbonate solution (2 × 25 ml) then with 25 ml of water. The combined water washings in turn were extracted with ether (2 × 20 ml). The combined extracts and solutions were dried (Na_2SO_4), were filtered and were freed from solvent by fractional distillation in a spinning band column. The residual oil was distilled under reduced pressure; yield, 3.5 g (80%) of pure epoxide; b.p., 64–66° at 0.5 mm; 78–80° at 2.5 mm; n_D^{25}, 1.4495.

Anal. Calcd. for $C_8H_{14}O_4$: C, 55.16; H, 8.10. Found: C, 54.93; H, 7.80.

Gas–liquid chromatography showed a large peak with a very small shoulder.

The 100 MHz n.m.r. spectrum in $CDCl_3$ is shown in Fig. 2 and supports the structure **6** contaminated by a small amount of 7 ($\leq 5\%$) (see Results and Discussion).

Acknowledgments

The authors are grateful to the National Research Council of Canada for financial assistance during the course of this work.

1. F. Sweet and R. K. Brown. Can. J. Chem. To be published.
2. F. Sweet and R. K. Brown. Can. J. Chem. To be published.
3. R. U. Lemieux and B. Fraser-Reid. Can. J. Chem. **43**, 1460 (1965).
4. R. U. Lemieux, R. K. Kullnig, H. J. Bernstein, and W. G. Schneider. J. Am. Chem. Soc. **80**, 6098 (1958).
5. U. E. Diner and R. K. Brown. Can. J. Chem. **45**, 2547 (1967).
6. D. H. Buss, L. Hough, L. D. Hall, and J. F. Manville. Tetrahedron, **21**, 69 (1965).
7. F. Sweet and R. K. Brown. Can. J. Chem. To be published.
8. F. Sweet and R. K. Brown. To be published.
9. E. L. Eliel. Stereochemistry of carbon compounds. McGraw-Hill Book Co., Inc., New York. 1962. p. 228.
10. R. U. Lemieux. *In* Molecular rearrangements. *Edited by* P. de Mayo. John Wiley and Sons, Inc., New York. 1964. pp. 738–741.
11. H. B. Henbest and R. A. L. Wilson. J. Chem. Soc. 1958 (1957).
12. H. B. Henbest and B. Nicholls. J. Chem. Soc. 221 (1959).
13. U. E. Diner, F. Sweet, and R. K. Brown. Can. J. Chem. **44**, 1591 (1966).

Synthesis of 1,6-anhydro-4-deoxy-β-DL-*xylo*-hexopyranose[1]

F. SWEET AND R. K. BROWN
Department of Chemistry, University of Alberta, Edmonton, Alberta

Received February 29, 1968

6,8-Dioxabicyclo[3·2·1]octane (**2**), obtained from acid-catalyzed cyclization of the $NaBH_4$ reduction product of acrolein dimer, has been converted to 4-bromo-6,8-dioxabicyclo[3·2·1]octane **3**. Epoxidation of the base-catalyzed dehydrohalogenated product of **3**, 6,8-dioxabicyclo[3·2·1]oct-3-ene (**4**), gave stereoselectively 1,6:2,3-dianhydro-4-deoxy-β-DL-*ribo*-hexopyranose (**5**) contaminated with <5% of the isomeric 1,6:2,3-dianhydro-4-deoxy-β-DL-*lyxo*-hexopyranose (**6**). Compound **5**, with the contaminating **6**, subjected to treatment with aqueous KOH, gave 1,6-anhydro-4-deoxy-β-DL-*xylo*-hexopyranose (**7**) whose di-*p*-nitrobenzoate (**8**) gave a 100 MHz nuclear magnetic resonance (n.m.r.) spectrum superimposable on that obtained from an authentic sample of 1,6-anhydro-4-deoxy-β-D-*xylo*-hexopyranose di-*p*-nitrobenzoate.

A first order analysis of the n.m.r. spectrum of **5** showed that the anomeric proton was coupled to all other protons except H-4 *exo*. Long range coupling over five bonds, as well as over four bonds, is observed. Couplings between H-1 and H-6 or H-5 illustrate that such effects can be obtained when an oxygen atom replaces carbon as in the structural feature 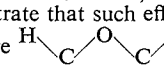 .

Canadian Journal of Chemistry, 46, 2289 (1968)

Can. J. Chem. Downloaded from www.nrcresearchpress.com by 210.87.254.42 on 09/05/12
For personal use only.

Introduction

Recently, by a series of stereoselective reactions involving bromomethoxylation, dehydrobromination, epoxidation of the resulting olefin, and then epoxide ring cleavage, we have converted 3,4-dihydro-2*H*-pyran to methyl 4-deoxy-3-*O*-methyl-α,β-DL-*threo*-pentopyranoside (1), and 2-methoxymethyl-3,4-dihydro-2*H*-pyran to methyl 2,3-anhydro-4-deoxy-6-*O*-methyl-α-DL-*lyxo*-hexopyranoside (2). The present paper describes the preparation of 1,6-anhydro-4-deoxy-β-DL-*xylo*-hexopyranose from acrolein dimer, by application of the rationale previously employed (1, 2).

Results and Discussion

The sequence of reactions for this synthesis is shown in Chart 1.

Acrolein dimer[2] (3,4-dihydro-2*H*-pyran-2-carboxaldehyde) was reduced by sodium borohydride (3) to 2-hydroxymethyl-3,4-dihydro-2*H*-pyran[3] (3,4-dihydro-2*H*-pyran-2-methanol), **1**. When this alcohol was heated in refluxing benzene containing a catalytic amount of *p*-toluenesulfonic acid, the previously reported (4, 5) compound, 6,8-dioxabicyclo[3·2·1]octane, **2**, was formed in 40–65% yield.

Bromination of acyclic acetals is known to occur on the carbon atom α to the functional group (6). Accordingly, **2** was brominated similarly to give a distillable liquid whose elemental analysis agreed with that expected for the structure 4-bromo-6,8-dioxabicyclo[3·2·1]octane, **3**. The product showed only one (symmetrical) peak on the gas–liquid chromatogram (g.l.c.), indicative of the presence of only one compound. The same g.l.c. column of butanediol succinate on Gas–Chrom P had readily separated the *cis* and *trans* isomers of 2-alkoxy-3-bromotetrahydropyran. The nuclear magnetic resonance (n.m.r.) spectrum (Fig. 1) also agreed with the structure **3** and with the presence of one isomer, since only one signal (a singlet at τ 4.6) was found in the anomeric proton region. The orientation of the bromine substituent is not certain, but it is believed to occupy a position on C-4 which is *cis* to the C-5, C-7 anhydro ring.[4]

Dehydrohalogenation of **3** with hot alcoholic potassium hydroxide was sluggish and gave in 24 h only a 30% conversion to the olefin, 6,8-dioxabicyclo[3·2·1]oct-3-ene, **4**, along with

[1]Taken from the thesis of F. Sweet, submitted to the Faculty of Graduate Studies, University of Alberta, Edmonton, Alberta, as part of the requirements for the degree of Doctor of Philosophy.

[2]Acrolein dimer was kindly donated by Dr. G. H. Segall and the Canadian Industries Limited, Montreal, Quebec.

[3]At the beginning of this work, the 2-hydroxymethyl-3,4-dihydro-2*H*-pyran had been obtained as a gift from J. A. Craig and Shell of Canada Ltd., Winnipeg, Manitoba. Later it became available commercially from K and K Laboratories, Plainview, New York and Hollywood, California. During the latter portions of this work it could no longer be obtained commercially, hence had to be made by reduction of acrolein dimer.

[4]The evidence for this, and a discussion of the interesting α-bromination of acetals will appear in a later communication from this laboratory.

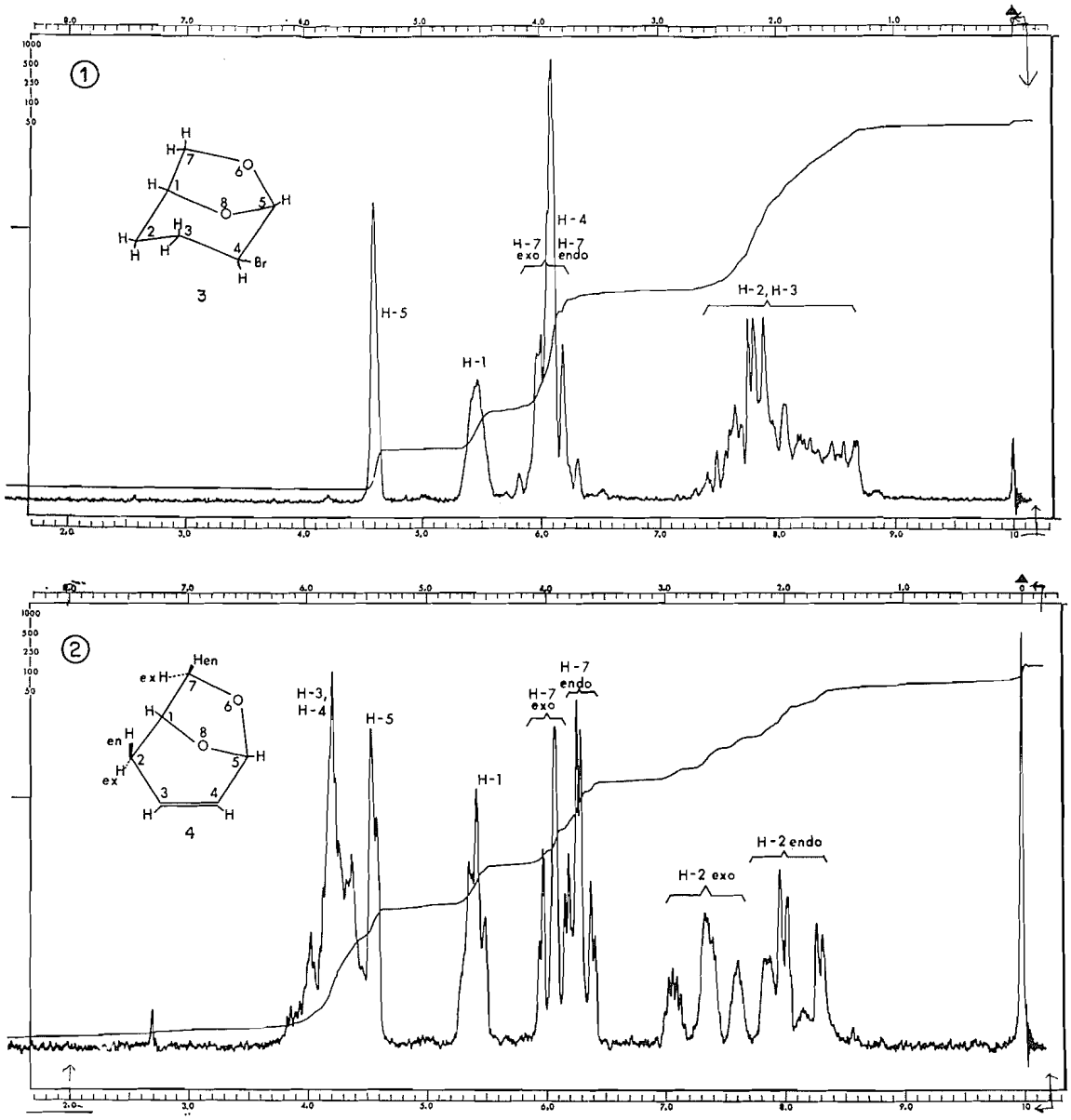

FIG. 1. The 60 MHz n.m.r. spectrum of 4-bromo-6,8-dioxabicyclo[3·2·1]octane, **3**, in $CDCl_3$, referred to tetramethylsilane.

FIG. 2. The 60 MHz n.m.r. spectrum of 6,8-dioxabicyclo[3·2·1]oct-3-ene, **4**, in $CDCl_3$, referred to tetramethylsilane.

much (50%) unchanged **3**. The g.l.c. analysis showed the presence of only one compound (one symmetrical peak). The elemental analysis, as well as the infrared and n.m.r. spectrum (Fig. 2) supported the structure.

The reaction of the bicyclo olefin, **4**, with *m*-chloroperoxybenzoic acid proceeded very slowly ($\sim$ 10 days) to give an 80% yield of an epoxide, **5**, contaminated with $<5\%$ of an impurity. This impurity is believed to be the isomeric epoxide, **6**, on the basis of the elemental analysis which agreed well with **5** (or **6**), and because previous work (7, 8) has shown that, while epoxidation of the double bond in a cycloolefin occurs preferably

Can. J. Chem. Downloaded from www.nrcresearchpress.com by 210.87.254.42 on 09/05/12
For personal use only.

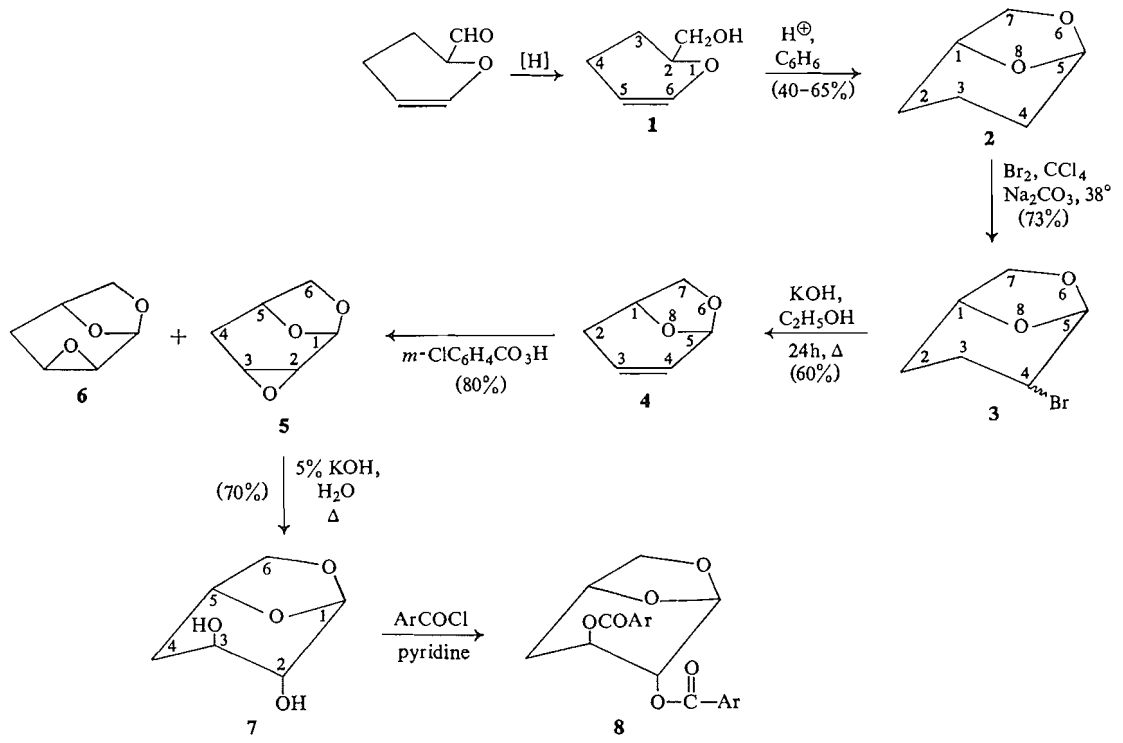

CHART 1

trans to the alkyl or alkoxy substituent on the carbon adjacent to the double bond, some *cis* epoxidation also occurs. The n.m.r. (Fig. 3) of **5**, completely supports the structure assigned, as well as the presence of contaminating **6** indicated by the low intensity doublet at τ 4.25 ($J_{1,2}$ = 3.3 Hz) close to the high intensity singlet at τ 4.36 for the anomeric proton of **5**. The n.m.r. spectrum of **5** and the assignment of signals by decoupling is discussed more fully in the Experimental section since it provides a good example of a carbohydrate whose proton signals are nearly all well separated and in which the anomeric proton is coupled to all other protons in the molecule except H-4 *exo*. In addition, long range coupling is found to occur over five bonds (H-1 to H-4 *endo*), and over four bonds when an oxygen atom replaces carbon as in the structural feature 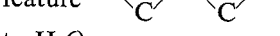 (H-1 to H-5 and H-1 to H-6).

Černý *et al.* (9, 10) had converted 1,6:2,3-dianhydro-4-deoxy-β-D-*ribo*-hexopyranose exclusively to 1,6-anhydro-4-deoxy-β-D-xylo-hexopyranose, and 1,6:2,3-dianhydro-4-deoxy-β-D-*lyxo*-hexopyranose to a mixture[5] of 1,6-anhydro-4-deoxy-β-D-*xylo*-hexopyranose and 1,6-anhydro-4-deoxy-β-D-*arabino*-hexopyranose by heating the dianhydro compounds in boiling 5% aqueous potassium hydroxide solution. When the same procedure was employed with our compound **5**, there was obtained in 70% yield a substance believed to be 1,6-anhydro-4-deoxy-β-DL-*xylo*-hexopyranose, **7**, apparently uncontaminated by another isomer. This was a solid, melting at 155–156°. The compound 1,6-anhydro-4-deoxy-β-D-*xylo*-hexopyranose obtained by Černý melted at 155–157° (9). The apparent agreement between these melting points, however, must be treated with caution since it is not possible to state *a priori* whether the DL mixture is a racemic *compound* or a racemic *mixture* and thus what the melting point will be relative to that of the D or L isomer. The di-*p*-nitrobenzoate (**8**) melted at 198° while the melting point of

[5]Unfortunately, no indication was given concerning the relative amounts of these two isomers.

Can. J. Chem. Downloaded from www.nrcresearchpress.com by 210.87.254.42 on 09/05/12
For personal use only.

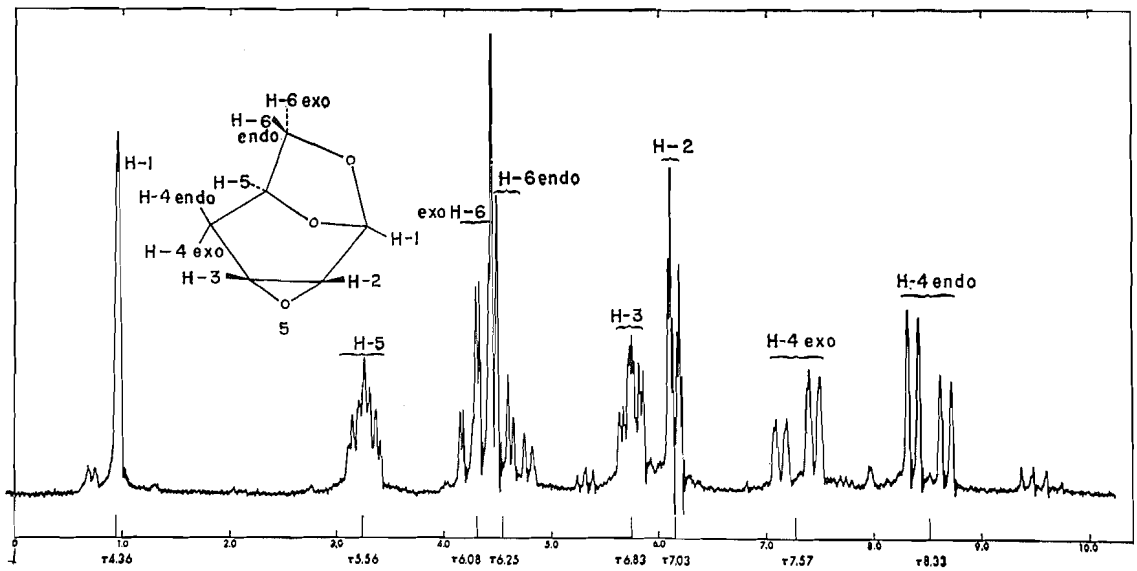

FIG. 3. The 100 MHz n.m.r. spectrum of 1,6:2,3-dianhydro-4-deoxy-β-DL-*ribo*-hexopyranose, **5**, in $CDCl_3$, referred to tetramethylsilane (expanded and offset).

1,6-anhydro-4-deoxy-β-D-*xylo*-hexopyranose di-*p*-nitrobenzoate was 218° (9).

Both the elemental analyses and the n.m.r. spectrum (Fig. 4 and Fig. 5) fully agreed with the structures assigned to **7** and **8**. However, convincing evidence was obtained from the fact that the 100 MHz n.m.r. spectrum of an authentic sample of the di-*p*-nitrobenzoate of 1,6-anhydro-4-deoxy-β-D-*xylo*-hexopyranose[6] (9) is completely superimposable on the 100 MHz spectrum of the di-*p*-nitrobenzoate of 1,6-anhydro-4-deoxy-β-DL-*xylo*-hexopyranose, **8**. The 100 MHz spectrum of 1,6-anhydro-4-deoxy-β-D-*arabino*-hexopyranose di-*p*-nitrobenzoate is quite different from that of the β-D-*xylo* isomer.

Experimental

All melting points and boiling points are uncorrected.

Elemental analyses were performed by Mrs. Darlene Mahlow of the Microchemical Laboratory, Department of Chemistry, University of Alberta, Edmonton.

Nuclear magnetic resonance (n.m.r.) spectra were obtained with Varian Associates 60 MHz and 100 MHz spectrometers, by Mr. R. N. Swindlehurst and Mr. G. Bigam, Department of Chemistry, University of Alberta, Edmonton, Alberta.

Gas–liquid chromatographic (g.l.c.) analyses were made with an F and M model 700 chromatograph equipped with a column (1/8 in. × 12 ft) containing 20% butanediol succinate on Gas-Chrom P (60–80 mesh) at a helium flow rate of 40 ml/min.

Solvents were usually removed in a rotary evaporator under vacuum unless otherwise stated.

2-Hydroxymethyl-3,4-dihydro-2H-pyran (1) was prepared by a modification of the published procedure (3). To a stirred, cold (5°) solution of 33.6 g (0.3 mole) of 3,4-dihydro-2*H*-pyran-2-carboxaldehyde (see footnote 2) in 300 ml of methanol was added, in small portions of ~1 g, a total of 8.3 g (0.3 mole) of sodium borohydride. After each addition, the temperature rose ~10°, but was allowed to return to 5° before a subsequent 1 g portion of reducing agent was added. Following complete addition of the hydride, the reaction mixture was stirred overnight while it came to room temperature. The solvent was removed and then 30 ml of water were added to the residual syrup. The methylene chloride extract (2 × 200 ml) of this mixture was dried (Na_2SO_4), filtered, and freed from solvent. The oily residue was distilled under reduced pressure and gave 31.4 g (92%) of pure **1**; b.p., 102° at 45 mm; n_D^{25}, 1.4772; lit. b.p., 100–103° at 47 mm; n_D^{25}, 1.4764 (3).

6,8-Dioxabicyclo[3·2·1]octane, 2

To a stirred solution of 500 mg of *p*-toluenesulfonic acid in 500 ml of dry benzene was slowly added 68 g (0.6 mole) of 2-hydroxymethyl-3,4-dihydro-2*H*-pyran (**1**). After the initial heat of reaction had subsided the mixture was heated under reflux for 2 h, then cooled to room temperature. A slight excess of sodium methoxide (2 g) was added to neutralize the acid and the reaction mixture was then stirred for 30 min. The solvent was removed by fractional distillation and the residue was distilled

[6]We are deeply indebted to Dr. M. Černý for providing us with authentic samples of the di-*p*-nitrobenzoates of 1,6-anhydro-4-deoxy-β-*xylo*-hexopyranose and 1,6-anhydro-4-deoxy-β-D-*arabino*-hexopyranose.

Can. J. Chem. Downloaded from www.nrcresearchpress.com by 210.87.254.42 on 09/05/12
For personal use only.

Can. J. Chem. Downloaded from www.nrcresearchpress.com by 210.87.254.42 on 09/05/12
For personal use only.

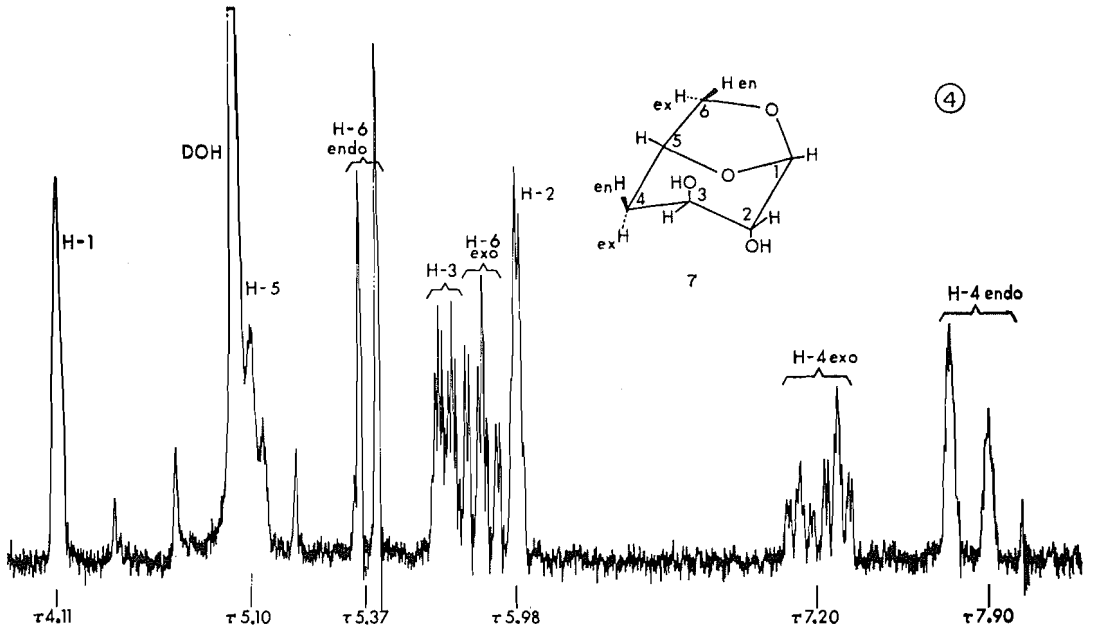

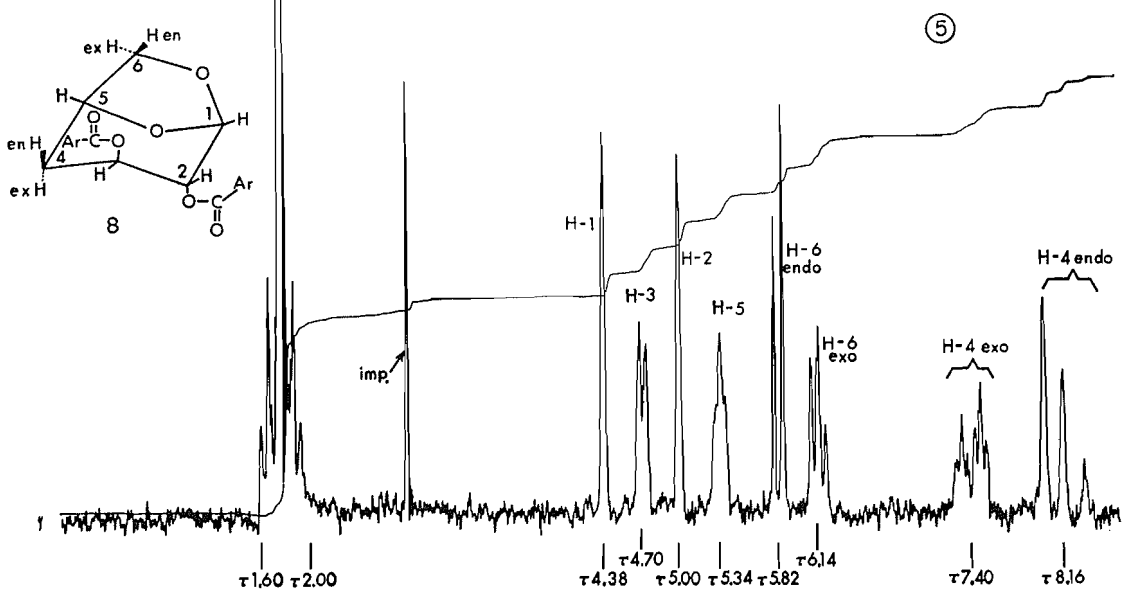

FIG. 4. The 100 MHz n.m.r. spectrum of 1,6-anhydro-4-deoxy-β-DL-*xylo*-hexopyranose, **7**, in D_2O referred to tetramethylsilane.

FIG. 5. The 100 MHz n.m.r. spectrum of 1,6-anhydro-4-deoxy-β-DL-*xylo*-hexopyranose di-*p*-nitrobenzoate, **8**, in $CDCl_3$ referred to tetramethylsilane. The impurity (imp.) is $CHCl_3$.

Can. J. Chem. Downloaded from www.nrcresearchpress.com by 210.87.254.42 on 09/05/12
For personal use only.

under reduced pressure in an apparatus equipped with an air condenser and a receiver immersed in a dry ice–acetone bath. A heat lamp or hot air stream was necessary to avoid solidification of the product in the air condenser; yield, 40–65%; b.p., 65° at 30 mm; m.p., 47–49°; lit. b.p., 64–66° at 38 mm; m.p., 46–48° (5); b.p., 68–70° at 39 mm; m.p., 50° (4).

4-Bromo-6,8-dioxabicyclo[3·2·1]octane (3)

A modification of the procedure used for acyclic acetals (6) was employed.

To a well-stirred mixture of 100 g (0.87 mole) of **2** in 1 l of anhydrous carbon tetrachloride (dried over calcium chloride) containing 300 g of powdered, anhydrous sodium carbonate, was added dropwise a solution of 139 g (0.87 mole) of bromine in 200 ml of dry carbon tetrachloride. Consumption of the bromine occurred rapidly, though still under control, when the reaction mixture was kept at 35–40° with a cold water bath. During the bromine addition, a vigorous evolution of carbon dioxide took place. After the addition was completed, the solution was stirred for 0.5 h and then filtered under vacuum. The solid was washed with methylene chloride (2 × 100 ml). The combined washings and filtrate were washed with 300 ml of saturated aqueous sodium carbonate solution, then with 200 ml of water. The combined washings were extracted in turn with 100 ml of methylene chloride. The combined organic layers were dried ($MgSO_4$), filtered, and freed from solvent at 45°. The residual, light-amber oil was distilled under reduced pressure providing 115 g (73%) of pure colorless oil, b.p., 90° at 4.5 mm, 68° at 1 mm; n_D^{27}, 1.5176.

Anal. Calcd. for $C_6H_9O_2Br$: C, 37.33; H, 4.69; Br, 41.39. Found: C, 37.53; H, 4.60; Br, 41.02.

Gas–liquid chromatography (column temperature, 190°) showed only one symmetrical peak.

The 60 MHz n.m.r. spectrum (Fig. 1) shows only one peak (singlet τ 4.60, $w/2 = 3.5$ Hz) in the anomeric proton region (H-5) indicating the presence of only one isomer. The tentative assignments for H-1, H-4, and H-7 were made on the basis of the first order analysis of the structure of **5** and the similarity of features in **5** and **3**.

6,8-Dioxabicyclo[3·2·1]oct-3-ene (4)

A stirred mixture of 70 g (0.36 mole) of 4-bromo-6,8-dioxabicyclo[3·2·1]octane (**3**) and 120 g of potassium hydroxide in 600 ml of 95% ethanol was heated under reflux for 24 h. The volume of the mixture was then reduced to one-half by fractional distillation of the solvent through a 30 cm Vigreux column. The cooled mixture was filtered under vacuum and the solid washed with ether (2 × 100 ml). The combined filtrate and washings were washed with water (2 × 50 ml), were dried (Na_2SO_4) and were then filtered and freed from solvent by fractional distillation. The residual oil was distilled under reduced pressure and gave 12 g (30%) of pure **4** along with 35 g (50%) of unreacted **3**; yield, based on **3** consumed, 60%; b.p., 54° at 9 mm, 84° at 50 mm; n_D^{25}, 1.4772.

Anal. Calcd. for $C_6H_8O_2$: C, 64.27; H, 7.19. Found: C, 64.07; H, 7.46.

Gas–liquid chromatography (column at 150°) showed only one peak which was quite symmetrical.

The 60 MHz n.m.r. spectrum in $CDCl_3$ (Fig. 2) clearly supported the assigned structure. The signal assignments are shown in Fig. 2 and are based in part on the results of the first order analysis of the n.m.r. of **5** which is structurally similar to **4**.

The infrared spectrum (neat) shows weak absorption at 1630 cm^{-1} indicative of C=C.

1,6:2,3-Dianhydro-4-deoxy-β-DL-ribo-hexopyranose (5)

A quantity (14.2 g, 0.066 mole) of 80% *m*-chloroperoxybenzoic acid was added to a solution of 7.4 g (0.065 mole) of 6,8-dioxabicyclo[3·2·1]oct-3-ene (**4**) in 150 ml of anhydrous ether. The solution was stirred and kept at 35–38° (reflux condenser) by the heat of the magnetic stirrer motor for 4.5 days when a colorless precipitate began to appear. After a total of 10 days under these conditions, when precipitation of the solid had apparently ceased, the mixture was diluted with 100 ml of ether (the precipitate dissolved) and then washed with saturated aqueous sodium carbonate solution (2 × 50 ml), then with 50 ml of water. The combined aqueous washings were retained. The ether layer was dried (Na_2SO_4), was filtered, and was freed from solvent by fractional distillation, giving 1.5 g of colorless oil. The combined aqueous washings (above) were continuously extracted with chloroform (250 ml) for 48 h. The chloroform extract was dried (Na_2SO_4), was filtered, and was freed from solvent by fractional distillation. The oil remaining (5.8 g) was found to be identical (by g.l.c.) with that obtained from the ether solution. The g.l.c. showed the presence of two components by two, slightly overlapping peaks in the ratio of > 95: < 5. The combined oils were distilled under vacuum giving 6.05 g (80%) of a colorless oil which solidified spontaneously in the receiver; b.p., 62° at 0.8 mm; m.p., 24–26°; n_D^{25}, 1.4809.

Anal. Calcd. for $C_6H_8O_2$: C, 56.25; H, 6.29. Found: C, 56.38; H, 6.60.

The g.l.c. as well as the n.m.r. spectrum showed that this material was still composed of two substances in the proportion of > 95: < 5 (no doubt **5** and **6** respectively). This material (**5**) is readily soluble in water, chloroform, ether or alcohol.

The n.m.r. spectrum (Fig. 3) agrees well with the structure. Its first order analysis is described at the end of the Experimental section.

1,6-Anhydro-4-deoxy-β-DL-xylo-hexopyranose (7)

1,6:2,3-Dianhydro-4-deoxy-β-DL-*ribo*-hexopyranose (**5**) (1.20 g, 0.0093 mole) was heated for 24 h in a refluxing solution (50 ml) of 5% aqueous potassium hydroxide. To the cooled reaction mixture was added a solution of 2.5 ml of concentrated hydrochloric acid in 10 ml of water. The resulting solution, which was slightly alkaline (pH ~9), was extracted with 150 ml of chloroform continuously for 48 h. The chloroform extract was dried (Na_2SO_4), was filtered, and was freed from solvent at 45°. The syrupy residue was dissolved in a minimum quantity of ethyl acetate (~15 ml) and the solution heated to boiling and then filtered while still hot. The filtrate was diluted with 30 ml of Skellysolve B and reduced in volume, by distillation, to ~15 ml. This addition of Skellysolve B and subsequent reduction in volume was repeated twice in order to remove the ethyl acetate. Finally, the 15 ml residue now diluted with 25 ml of Skellysolve B, was heated just to boiling, then allowed

TABLE I

Observed chemical shifts of protons in **5** referred to tetramethylsilane (τ units)*

H-1	H-2	H-3	H-4 *exo*	H-4 *endo*	H-5	H-6 *exo*	H-6 *endo*
4.36s	7.03d	6.83m	7.57q	8.33q	5.56m	6.08m	6.25m
			A B System			A B System	

*Obtained in $CDCl_3$ at 100 MHz.

to stand overnight and come to room temperature. The hygroscopic crystals were collected by filtration and then dried at room temperature overnight under vacuum (0.5 mm) over anhydrous calcium sulfate. The weight was 0.60 g. When the filtrate was concentrated to half its volume and then cooled to room temperature an additional 0.35 g was obtained; total yield, 70%; m.p., 155–156°; lit. m.p. of the D enantiomer, 155–157° (9).

Anal. Calcd. for $C_6H_{10}O_4$: C, 49.31; N, 6.70. Found: C, 48.90; H, 6.90.

The n.m.r. spectrum (Fig. 4) in D_2O supports the structure of **7**. Signal assignments are made on the basis of the first order analysis of the n.m.r. spectrum of **5** and decoupling experiments.

1,6-Anhydro-4-deoxy-β-DL-xylo-hexopyranose di-p-Nitrobenzoate, 8

To a solution of 300 mg of **7** in 5 ml of pyridine was added 1.12 g of *p*-nitrobenzoyl chloride. The mixture was heated, (with frequent shaking) just to boiling and then poured onto 25 g of crushed ice. When the ice had all melted, the solid was separated by filtration under vacuum and washed with 5% aqueous sodium carbonate solution, then with water. The crude product was added to 15 ml of boiling methanol, the solution heated to boiling and sufficient ethyl acetate added dropwise to effect solution. The solution was cooled slightly and decolorized with charcoal. The filtrate, on cooling, deposited pale-yellow needles. Two recrystallizations from the same solvent mixture, followed by drying under vacuum, gave 800 mg of pure **8**; m.p., 196–198°; lit. m.p. for the D enantiomer, 218–219° (9).

Anal. Calcd. for $C_{20}H_{16}O_{10}N_2$: C, 54.06; H, 3.63; N, 6.31. Found: C, 54.05; H, 3.87; N, 6.21.

The 100 MHz spectrum in $CDCl_3$ (Fig. 5) supports the structure proposed (**8**). The assignment of proton signals was made on the basis of the first order analysis of **5** and decoupling experiments.

The 100 MHz spectrum of an authentic sample of 1,6-anhydro-4-deoxy-β-D-*xylo*-hexopyranose di-*p*-nitrobenzoate was completely superimposable on that obtained from **8**.

First Order Analysis of the Nuclear Magnetic Resonance Spectrum of 5

The presence of the small amount of isomeric contaminant, **6**, offered no complication in the first order analysis of the spectrum of **5** (Fig. 3). That the intense *singlet* at τ 4.36 is due to the anomeric proton of **5**, while the low intensity *doublet* at τ 4.25 is due to the anomeric proton of **6**, is in accordance with the finding that when H-2 of the epoxy ring of 1-alkoxy-2,3-epoxy-tetrahydropyrans[7] is *trans* to H-1, the anomeric (H-1) signal is a singlet with H-1, H-2 coupling ~0, while if H-1 and H-2 are *cis*, the coupling $J_{1,2}$ = 2.5–4.5 Hz (11, 12).

The obvious signal assignment is that of the "singlet" at τ 4.36 for the anomeric proton H-1. The two quartets at high field centered at τ 7.57 and τ 8.33 can be assigned reasonably to the two protons on C-4. Using the C-1 and C-4 protons as reference points, signal assignments (Table I) can be made by decoupling experiments. These are described below.

Irradiation of H-1 gave a small but definite collapse of the multiplets at τ 7.03 and τ 6.83, tentatively identifying these as due to H-2 and H-3. On the basis of previous work (12), the higher field signal is due to H-2. Irradiation at τ 7.03 (H-2) gave some sharpening of the H-1 signal at τ 4.36. A collapse of a small coupling occurred at the low field C-4 proton quartet (τ 7.57), but there was no effect on the high field C-4 proton quartet (τ 8.33). On the other hand, irradiation at τ 6.83 (tentatively assigned to H-3), changed the high field quartet (H-4, τ 8.33) to a doublet of 15.8 Hz, but left the low field H-4 quartet intact. This information clearly shows that the H-3 signal is the multiplet at τ 6.83 since we would expect strong coupling between H-3 and H-4 *(endo)*. Thus the signal at τ 7.03 is due to H-2.

A tentative assignment of the two high field quartets to the two protons on C-4 can now be made by using the Karplus relation between the size of the dihedral angle and the magnitude of the coupling (13). From the rigid structure of **5**, it is seen that the H-3, H-4 *exo* dihedral angle is very nearly 90° while that for H-3, H-4 *endo* is nearly 30°. Thus a larger coupling is expected for H-3, H-4 *endo* than for H-3, H-4 *exo*. On this basis, in keeping with the above information, the high-field quartet at τ 8.33 is assigned to H-4 *endo* and therefore that at τ 7.57 is due to H-4 *exo*.

Irradiation at τ 7.57 (H-4 *exo*) causes a pronounced change of the multiplet at τ 5.56, identifying this as due to H-5. As well, small couplings disappear in the τ 6.08 region, but little if any change occurs at τ 6.25. Since one expects a long range coupling between protons which

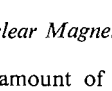

have the configuration (14), the clearly noticeable small change at τ 6.08 indicates that this

[7]Here we are numbering the tetrahydropyran ring so that the carbon atom adjacent to the ring oxygen and attached to the alkoxy group is number 1, in accordance with the practice for the pyranosides. This is done as a matter of convenience.

Can. J. Chem. Downloaded from www.nrcresearchpress.com by 210.87.254.42 on 09/05/12
For personal use only.

Can. J. Chem. Downloaded from www.nrcresearchpress.com by 210.87.254.42 on 09/05/12
For personal use only.

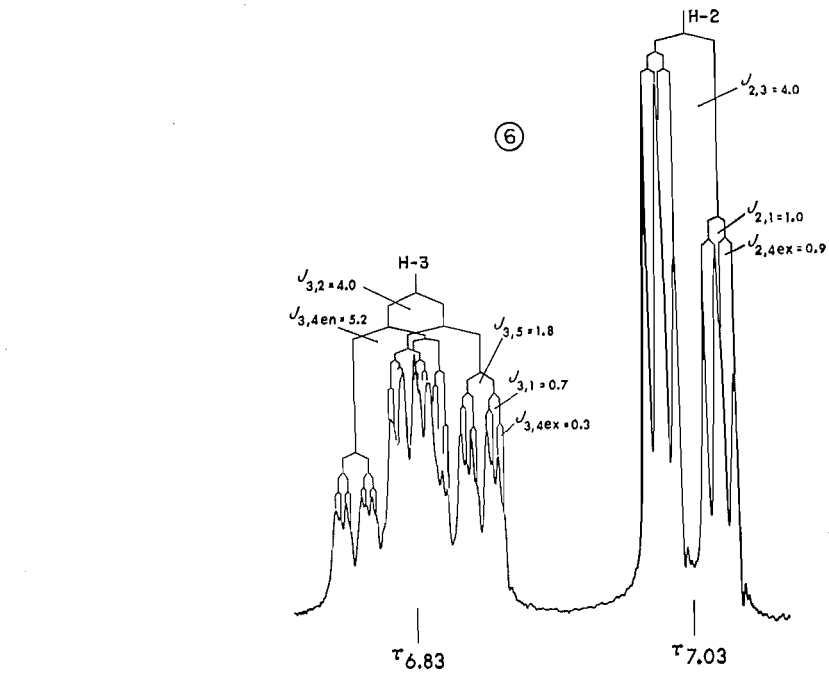

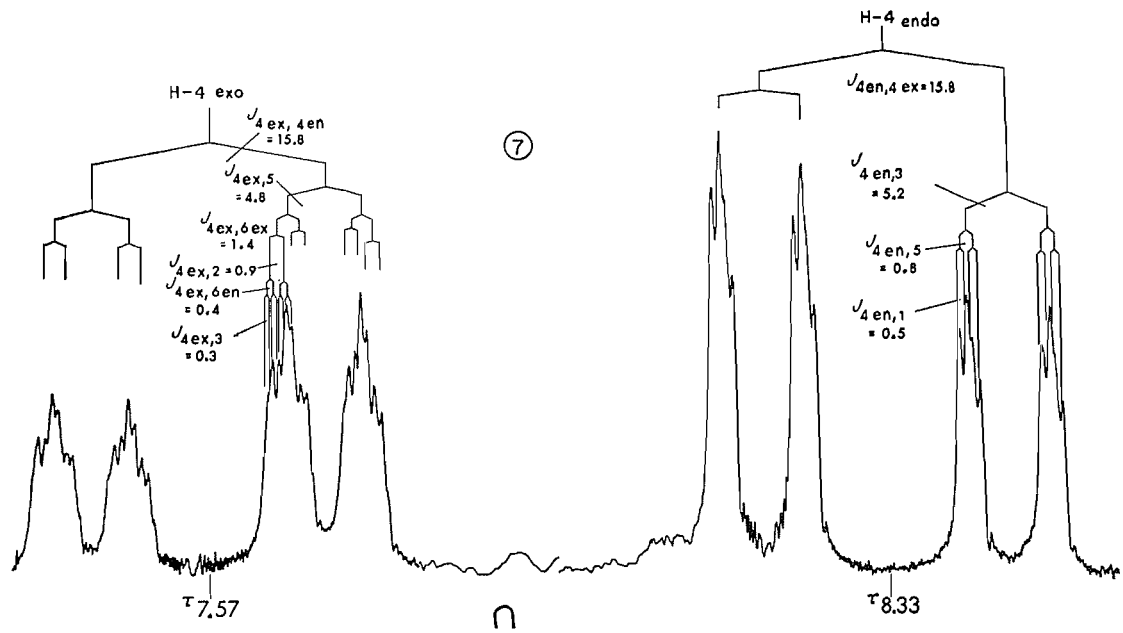

FIG. 6. The partial 100 MHz spectrum of 1,6-anhydro-4-deoxy-β-DL-*xylo*-hexopyranose, **5**, in $CDCl_3$ referred to tetramethylsilane.

FIG. 7. The partial 100 MHz spectrum of 1,6-anhydro-4-deoxy-β-DL-*xylo*-hexopyranose, **5**, in $CDCl_3$ referred to tetramethylsilane.

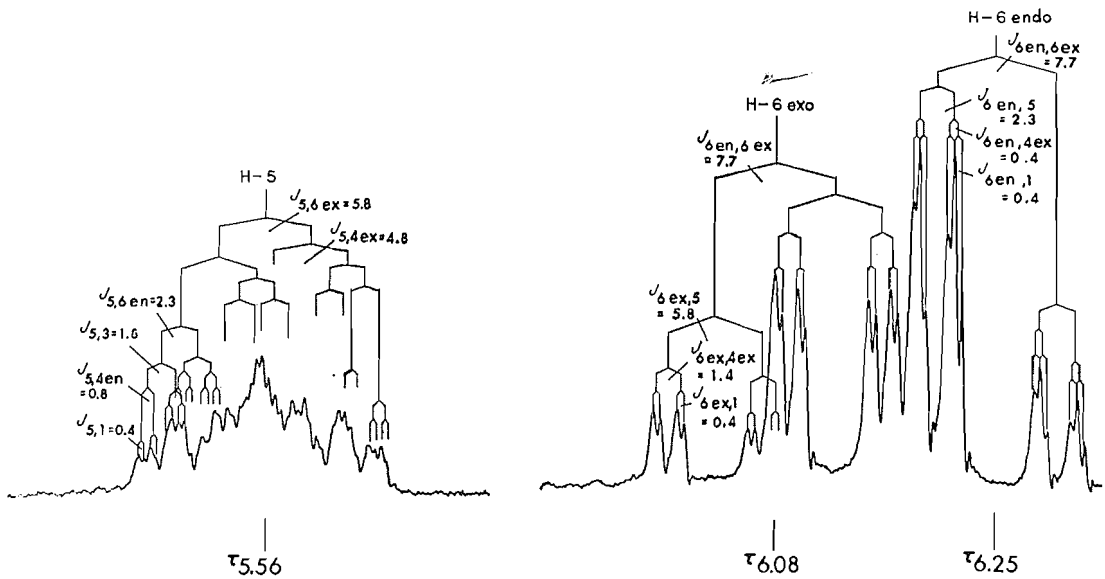

FIG. 8. The partial 100 MHz spectrum of 1,6-anhydro-4-deoxy-β-DL-*xylo*-hexopyranose, **5**, in $CDCl_3$ referred to tetramethylsilane.

TABLE II

Observed coupling constants (Hz) of protons in **5**

	H-1	H-2	H-3	H-4 *exo*	H-4 *endo*	H-5	H-6 *exo*	H-6 *endo*
H-1	—	1.0	0.7	0	0.5	0.4	0.4	0.4
H-2	—	—	4.0	0.9	0	—	—	—
H-3	—	—	—	0.3	5.2	1.8	—	—
H-4 *exo*	—	—	—	—	15.8	4.8	1.4	0.4
H-4 *endo*	—	—	—	—	—	0.8	0	0
H-5	—	—	—	—	—	—	5.8	2.3
H-6 *exo*	—	—	—	—	—	—	—	7.7

multiplet is due to H-6 *exo*, leaving the τ 6.25 region for H-6 *endo*. Some observable change also occurred at τ 6.83 (H-3).

Irradiation at τ 5.56 (H-5) caused a collapse of the quartet at τ 7.57 (H-4 *exo*) to a doublet, but relatively little change at τ 8.33 (H-4 *endo*). The former confirms the assignment of the multiplet at τ 5.56 to H-5. The larger coupling of H-5 to H-4 *exo*, but apparently little coupling of H-5 to H-4 *endo* agrees with the prediction from the Karplus relation (13), since the dihedral angle for H-5, H-4 *exo* ~40° while that for H-5, H-4 *endo* ~80°.

Irradiation of the region τ 6.15 (H-6 *exo*) gave collapse of the small couplings at τ 7.57 (H-4 *exo*). This corroborates the view that the signal at τ 6.08 is due to H-6 *exo*.

To determine the degree of coupling between the protons, 100 cycle sweeps were made of portions of the spectrum while suitably chosen protons were irradiated. In this manner it was possible to obtain coupling constants for nearly all of the protons. These are shown in Table II. The expanded signals and the first order couplings are shown in Figs. 6–8.

The data in Table II show that H-1 is coupled to all other protons with the exception of H-4 *exo*. The H-4 *endo* and H-6 *endo* protons are at slightly higher field, and thus subjected to more shielding, than are H-4 *exo* and H-6 *exo*. The expected long range coupling between

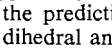

protons which have the C C structure is clearly discernible, but in addition, such long range coupling is found when oxygen replaces one of the carbon atoms (15)

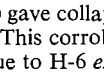

in this structural feature i.e. C C . An example of unusual long range coupling over 5 bonds (15) is shown in the coupling between H-1 and H-4 *endo*.

Can. J. Chem. Downloaded from www.nrcresearchpress.com by 210.87.254.42 on 09/05/12
For personal use only.

Acknowledgment

The authors are grateful for financial support from the National Research Council of Canada.

1. F. SWEET and R. K. BROWN. Can. J. Chem. To be published.
2. F. SWEET and R. K. BROWN. Can. J. Chem. To be published.
3. R. ZELIŃSKI, A. VERBISCAR, and W. J. EICHEL. J. Org. Chem. **23**, 184 (1958).
4. R. R. WHETSTONE. U.S. Patent 2,511,891. 1950. Chem. Abstr. **44**, 8961 (1950).
5. E. L. ELIEL, B. E. NOWAK, R. A. Daignault, and V. G. BADDING. J. Org. Chem. **30**, 2441 (1965).
6. S. M. MCELVAIN, R. L. CLARKE, and G. D. JONES. J. Am. Chem. Soc. **64**, 1966 (1942).
7. F. SWEET and R. K. BROWN. Can. J. Chem. To be published.
8. H. B. HENBEST and R. A. WILSON. J. Chem. Soc. 1958 (1957).
9. M. ČERNÝ, J. PACÁK, and J. STANĚK. Chem. and Ind. London, 945 (1961).
10. M. ČERNÝ and J. PACÁK. Collection Czech. Chem. Commun. **27**, 94 (1962).
11. D. H. BUSS, L. HOUGH, L. D. HALL, and J. F. MANVILLE. Tetrahedron, **21**, 69 (1965).
12. F. SWEET and R. K. BROWN. Can. J. Chem. To be published.
13. M. KARPLUS. J. Chem. Phys. **30**, 11 (1959).
14. E. W. GARBISCH, JR. Chem. and Ind. London, 1715 (1964).
15. J. C. JOCHIMS, G. TAIGEL, and W. MEYER ZU Reckendorf. Tetrahedron Letters, **33**, 3227 (1967).

Can. J. Chem. Downloaded from www.nrcresearchpress.com by 210.87.254.42 on 09/05/12
For personal use only.

Can. J. Chem. Downloaded from www.nrcresearchpress.com by 210.87.254.105 on 09/05/12
For personal use only.

Galactomannans of *Trichosporon fermentans* and other yeasts; proton magnetic resonance and chemical studies[1]

P. A. J. Gorin and J. F. T. Spencer
National Research Council of Canada, Prairie Regional Laboratory, Saskatoon, Saskatchewan

Received February 15, 1968

A survey of the alkali soluble polysaccharides of yeast cells shows that galactomannans are formed by certain species of the genera *Trichosporon*, *Schizosaccharomyces*, and *Nadsonia*. Different species of *Trichosporon* form galactomannans, pentosylmannans, and a mannan. The galactomannans are distinguishable from those of *Schizosaccharomyces* by the H-1 region of their proton magnetic resonance spectra (recorded at 70° in D_2O using an HA-100 Varian spectrometer), but the spectra of *Trichosporon hellenicum* and *Nadsonia fulvescens* galactomannans are virtually indistinguishable.

The proton magnetic resonance spectrum of the *Trichosporon fermentans* galactomannan contains fewer signals than those of other *Trichosporon* galactomannans. The polymer consists predominantly of a main-chain containing a high proportion of (1 → 6)-mannopyranosyl units substituted in their 2-positions by *O*-α-D-galactopyranosyl-(1 → 2)-*O*-α-D-mannopyranosyl side-chains (**1**).

Canadian Journal of Chemistry, 46, 2299 (1968)

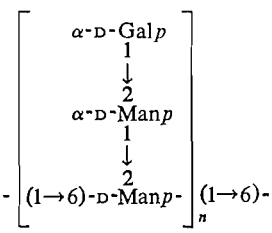

1

The classification of yeasts is based partly on morphological characteristics, which are used largely to distinguish genera, and partly on biochemical behavior which serve to distinguish species. Yeast taxonomists have relied heavily on the ability of yeasts to utilize different sugars, to a lesser extent on the ability to utilize different forms of inorganic and organic nitrogen and occasionally on the property of some yeasts to synthesize a particular compound, such as starch or carotenoid pigments, for the differentiation of yeast species. Knowledge of the structures of the extracellular or intracellular polysaccharides of yeasts is sometimes useful in classification and identification of the parent organisms. For example, yeasts of the genus *Rhodotorula* form β-D-linked mannans (1) which distinguish them from *Cryptococcus* spp., which form starch and a heteropolysaccharide containing xylose, mannose, and glucuronic acid (2–7). Previously the two genera were distinguished by the ability of *Rhodotorula* to form red, pink, orange, or yellow carotenoid pigments, but this criterion has been considered inadequate by Phaff and Spencer (8). The polysaccharide–chemotaxonomic technique has necessitated the reclassification of *Rhodotorula peneaus* (9), *Rhodotorula infirmo-miniata*, and *Rhodotorula macerans*[2] as *Cryptococcus*. This reclassification is in agreement with the ability of *Cryptococcus* spp. to utilize inositol as a sole carbon source and the inability of *Rhodotorula* to do so (8). *Lipomyces lipoferus* may readily be distinguished from *Lipomyces starkeyi* by the sugars formed on hydrolysis of their extracellular polysaccharides (10).

The yeasts of the genus *Trichosporon* lend themselves particularly well to the polysaccharide–chemotaxonomic approach. *Trichosporon cutaneum* is known to form extracellular starch (11), a glucan, and a pentosylmannan with an α-D-(1 → 3)-linked mannopyranosyl main-chain and D-mannopyranosyl, D-xylopyranosyl, and 4-*O*-α-L-arabinopyranosyl-D-xylopyranosyl side-chains (12). In the present investigation, the cells of *T. cutaneum* and eight other *Trichosporon* spp. were extracted with hot aqueous alkali to give, from each organism, a glucan and a mannose-containing polysaccharide. The latter was purified through its insoluble copper complex formed with Fehling solution. Each regenerated polysaccharide appeared to be homogeneous on ultracentrifugation and on electrophoresis in aqueous sodium tetraborate. The

[1]Issued as NRCC No. 10101.

[2]P. A. J. Gorin and J. F. T. Spencer. Unpublished results.

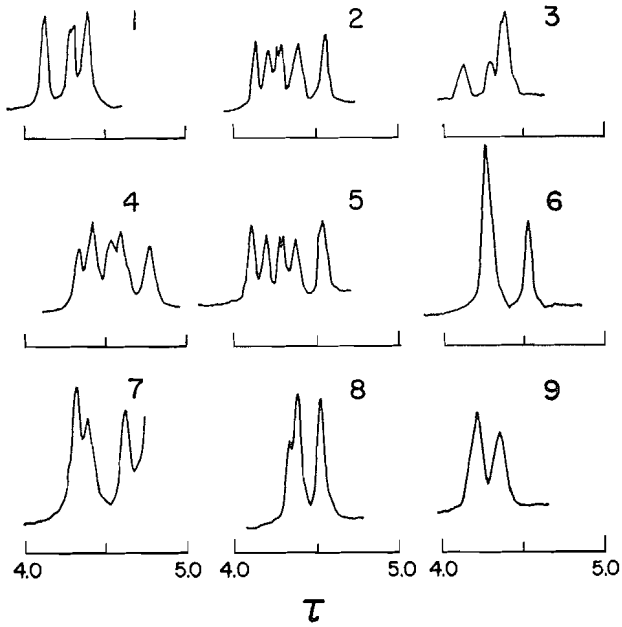

FIG. 1. The proton magnetic resonance spectra of some fungal galactomannans. Source of galactomannan: **1**, *Trichosporon fermentans*; **2**, *Trichosporon hellenicum*; **3**, *Trichosporon penicillatum*; **4**, *Nadsonia elongata*; **5**, *Nadsonia fulvescens*; **6**, *Schizosaccharomyces malidevorans*, *Schizosaccharomyces octosporus*, *Schizosaccharomyces pombe*, *Schizosaccharomyces versatilis*; **7**, *Schizosaccharomyces* spp. measured at 25°; **8**, *Trichophyton ferrugineum* galactomannan I[4]; **9**, *Trichophyton ferrugineum* galactomannan II[4].

sugars formed on hydrolysis of each polysaccharide showed that *Trichosporon* yeasts can be sub-classified into three groups (Table I). Whereas galactomannans occur as cell components of *Trichosporon fermentans*, *T. hellenicum*, and *T. penicillatum*, pentosylmannans are formed by *T. cutaneum*, *T. inkin*, *T. pullulans*, *T. undulatum*, and *T. sericeum*. *T. aculeatum* cells, on the other hand, contain a mannan.

The galactomannans[3] from *T. fermentans*, *T. hellenicum*, and *T. penicillatum* are distinguishable by their proton magnetic resonance (p.m.r.) spectra in deuterium oxide (Fig. 1). The H-1 protons give complex signals in the τ 4.0 to τ 5.0 region and these are generally better defined and are further removed from the DOH signal on warming the solution to 70°. Proton magnetic resonance spectral examination of this 'fingerprint region' shows that *Trichosporon* galactomannans differ markedly in structure from galactomannans of four yeasts of *Schizosaccharomyces* and *Nadsonia* genera and galactomannans I and II of the fungus *Trichophyton ferrugineum*.[4] However, the complex spectrum of the *Trichosporon hellenicum* polymer is identical to that of the galactomannan of *Nadsonia fulvescens*, one of two *Nadsonia* species examined. The probable structural similarity of the cell-wall components suggests at least an evolutionary relationship between the two yeasts.

The choice of a representative galactomannan, on which to carry out structural studies, was made by comparing the H-1 region of the various p.m.r. spectra. The chemical shifts of the H-1 proton signals should depend largely on (*a*) the structure of the parent anhydrohexose unit, (*b*) the position(s) substituted in the unit, (*c*) the structure of the substituent unit, (*d*) the structure of the aglycone unit, and (*e*) the position(s) substituted in the aglycone unit. The *T. fermentans* polymer was investigated since

[3]Proton magnetic resonance spectra of the pentosylmannans could not be measured since the solutions were very viscous at working concentrations.

[4]C. T. Bishop. Unpublished results. See C. T. Bishop, M. B. Perry, and F. Blank. Can. J. Chem. **44**, 2291 (1966), and preceding references.

Can. J. Chem. Downloaded from www.nrcresearchpress.com by 210.87.254.105 on 09/05/12
For personal use only.

Can. J. Chem. Downloaded from www.nrcresearchpress.com by 210.87.254.105 on 09/05/12
For personal use only.

it appeared to have the simplest structure, having a minimum of three signals.

Acid hydrolysis of the galactomannan gave mannose and galactose in 13:7 ratio, as estimated by gas–liquid chromatography (g.l.c.) of the derived alditol hexaacetates. The galactomannan was methylated by the Haworth method and then by the Purdie procedure. Formolysis of the methylated polysaccharide gave a mixture which was fractionated by cellulose column chromatography. 2,3,4,6-Tetra-*O*-methyl-D-galactose was isolated and characterized as its *N*-phenylgalactosylamine derivative, and 3,4,6-tri-*O*-methyl-D-mannose and 3,4-di-*O*-methyl-D-mannose were also identified and each component estimated gravimetrically. Seven percent of 2,3,4-tri-*O*-methylmannose was also detected in the tri-*O*-methyl fraction by g.l.c. of derived trimethylsilylated methyl mannosides (13). The molar proportion of the methyl sugars obtained from the galactomannan, 2,3,4,6-tetra-*O*-methylgalactose, 2,3,4,6-tetra-*O*-mannose, 3,4,6- and 2,3,4-tri-*O*-methylmannose, and 3,4-di-*O*-methylmannose, based on the gravimetric analysis and g.l.c. of the derived methyl glycosides was 10.0:0.6:9.7:0.8:8.5 (average values). The strong positive specific rotation of the polysaccharide, +115°, indicated predominant α-D-linkages.

The galactomannan consumed 1.30 moles of sodium periodate with formation of 0.33 mole of formic acid per mole of anhydroaldose unit. On a larger scale, oxidized polysaccharide was reduced with sodium borohydride to a polyalcohol. In agreement with the methylation data, hydrolysis of the polyalcohol gave only glycerol.

The galactomannan was partly acetolyzed and the resulting acetates were deacetylated. The mixture was fractionated by cellulose column chromatography to give a trisaccharide in 25% yield and smaller amounts of disaccharides and mannose. The amorphous trisaccharide fraction, which gave mannose and a smaller amount of galactose on hydrolysis was reduced with sodium borohydride and the resulting alditol gave known 2-*O*-α-D-mannopyranosyl-D-mannitol on partial hydrolysis. Bromine oxidation of the trisaccharide gave an aldonic acid, which was oxidized as its sodium salt with 3 *M* proportions of lead tetraacetate. The tartronic acid semialdehyde derivative thus formed was partly hydrolyzed to a disaccharide (14), which gave mannose and galactose on hydrolysis. Since the disaccharide was inert to lead tetraacetate and the reduced disaccharide gave galactose and hexitol on hydrolysis, a 2-*O*-D-galactopyranosyl-D-mannose structure was indicated (15). The configuration of the disaccharide is α, since the molecular rotation of the disaccharide alditol, +28 000°, is closer to the value of +38 040° for methyl-α-D-galactopyranoside than +140°, quoted for the β-isomer (16). A methylation–fragmentation experiment was carried out on the trisaccharide and 2,3,4,6-tetra-*O*-methyl-D-galactose and 3,4,6-tri-*O*-methyl-D-mannose were formed in a ratio of 1:2.1, according to g.l.c. of the derived methyl glycosides and their trimethylsilyl ethers. The trisaccharide therefore has an *O*-α-D-galactopyranosyl-(1 → 2)-*O*-α-D-mannopyranosyl-(1 → 2)-*O*-α-D-mannose structure arising from preferential splitting of the (1 → 6)-mannosidic linkages.

Partial hydrolysis of the galactomannan removed most of the galactosyl units and a smaller proportion of the mannosyl units to yield a polysaccharide with a specific rotation of +92°. It consumed 1.55 moles of sodium periodate with formation of 0.59 mole of acid per mole of anhydrohexose unit. A methylation–fragmentation analysis was carried out on the degraded polysaccharide and methyl glycosides of the 2,3,4,6-tetra-*O*-methyl derivatives of mannose and galactose, 2,3,4- and 3,4,6-tri-*O*-methylmannose and 3,4-di-*O*-methylmannose were detected by g.l.c. in a molar ratio of 10:2.4:3.8:4.3:13.0. The branched structure of the degraded polysaccharide, the methylation–fragmentation data on the galactomannan, the isolation of the galactosylmannobiose via acetolysis, and the p.m.r. spectrum of the galactomannan are consistent with a higher proportion of structure **1**.

Experimental

The proton magnetic resonance spectra of the polysaccharides were obtained from 20% solutions in D_2O at 70° using an HA-100 Varian spectrometer. The chemical shifts are based on an external tetramethylsilane standard.

Cultures were obtained from the National Collection of Yeast Cultures, Brewing Industry Research Foundation, Nutfield, Surrey (NCYC), the Centraalbureau voor Schimmelcultures, Delft, The Netherlands (CBS), from Dr. Lidia do Carmo-Sousa of the Gulbenkian Institute of Science, Oerias, Portugal (IGC) and from the culture collection of the Prairie Regional Laboratory (PRL).

Paper chromatography was carried out using *n*-butanol – ethanol – water (40:11:19 v/v/v) (solvent *a*)

TABLE I

Polysaccharide cell-wall components of yeasts of the genera *Trichosporon*, *Schizosaccharomyces*, and *Nadsonia*

Yeast	Dry weight of cells from 3 l of medium (g)	Yield of extracted polysaccharides* (based on cells)	Yield (based on cells) and components of purified polysaccharides
T. inkin IGC 3727	25.2	8%	4%; Man, Xyl
T. sericeum CBS 2545	26.4	12%	<1%;† Man, Xyl
T. undulatum CBS 2546	41.4	31%	<1%;† Man, Xyl
T. cutaneum PRL, RS1	26.4	11%	2%; Man, Xyl, Ara
T. pullulans NCYC 477	38.4	9%	5%; Man, Xyl, tr. Fuc, Gal
T. fermentans PRL 2263	18.0	18%	6%; Man, Gal
T. hellenicum CBS 4099	27.9	18%	6%; Man, Gal
T. penicillatum IGC 3716	34.2	16%	4%; Man, Gal
T. aculeatum IGC 3551	32.1	12%	7%; Man
S. malidevorans NCYC 683	20.7	16%	2%; Man, Gal
S. octosporus PRL F2	14.4	17%	1%; Man, Gal
S. pombe PRL Y30	7.8	27%	2%; Man, Gal
S. versatilis CBS 103	20.7	16%	2%; Man, Gal
N. fulvescens CBS 2596	2.8	14%	3%; Man, Gal
N. elongata CBS 2593	4.9	12%	1%; Man, Gal

*Hydrolysis of these crude polysaccharides gives the same sugars as obtained from purified polysaccharides plus glucose.
†The copper complex of the xylomannan is relatively water soluble, resulting in low yield.

and ethyl acetate – acetic acid – water (9:2:2 v/v/v) (solvent *b*).

Cultural Methods for Production of Yeast Cells

The yeasts were grown in a medium containing yeast–nitrogen base (Difco), glucose (5%), casamino acids (0.25%), and a vitamin mixture (0.2 ml/100 ml) (17), either in 5 l New Brunswick stirred fermentors containing 3 l medium or in 2 l Erlenmeyer flasks containing 500 ml medium. The flasks were incubated on a rotary shaker, eccentricity 1 in., at 230 r.p.m. for 3 or 4 days, the fermentors were operated at 400 r.p.m. air flow 1 l/min/fermentor, for 3 days. The temperature of incubation was 25°. Inoculum for the fermentor, 100 ml/fermentor, was grown in 500 ml Erlenmeyer flasks containing 100 ml medium, incubated at 22° on a rotary shaker for 2 or 3 days. The 2 l flasks were inoculated directly from the slants.

The cells were recovered by centrifugation and washed twice with distilled water. The dry weight of the cells was obtained either by freeze-drying or by weighing the wet cells and drying a small aliquot of cells.

Isolation of Polysaccharides from Cells

Yeast cells were suspended in 2% aqueous potassium hydroxide (200 ml) and extracted for 2 h at 100°. The solutions were neutralized with acetic acid centrifuged at 9000 r.p.m. and the supernatants evaporated to 50 ml. Methanol (200 ml) was added and the precipitates were centrifuged off, resuspended in methanol, isolated by filtration and dried. The yields of crude polysaccharides are given in Table I.

The polysaccharides were dissolved in water (50 ml) by heating at 100° for 2 h. The insoluble material was removed either by filtration or centrifugation and Fehling solution (50 ml) was added. The solution was stored overnight in a refrigerator and the insoluble copper complexes were filtered off, washed with 2% aqueous potassium hydroxide and then methanol. Remaining alkali was removed from the complex by trituration with methanol and refiltration. The copper complexes were decomposed by shaking in water with Amberlite IR120 and after 1 h the resin was filtered off. The solutions were evaporated to approximately 10 ml and methanol (100 ml) added followed by 3 drops of concentrated hydrochloric acid. The precipitates were centrifuged off, washed with methanol, and isolated by filtration.

The polysaccharides were hydrolyzed at 100° in *N* sulfuric acid for 18 h, the solutions neutralized ($BaCO_3$), filtered, and evaporated to syrups. They were analyzed by paper chromatography by running for 2 days with solvent *a* and using *p*-anisidine hydrochloride as spray reagent.

The p.m.r. spectra of the polymers were obtained using an HA-100 Varian spectrometer, from 20% solutions in D_2O at 70° with tetramethylsilane as the external standard. The H-1 'fingerprint regions' are recorded in Fig. 1.

Sedimentation coefficients of the polymer were measured at concentrations of 0.15% to 0.6% in 0.5% aqueous sodium chloride at 59 000 r.p.m. and electrophoretic mobilities as 0.5% solutions in 0.05 *M* sodium tetraborate.

Hydrolysis Products and Periodate Oxidation Characteristics of Trichosporon fermentans Galactomannan

The *T. fermentans* galactomannan had $[\alpha]_D$ +115° (*c*, 0.9 H_2O). Its hydrolysis products were reduced with sodium borohydride and the resulting polyols were analyzed as their acetates by g.l.c. on 2% LAC-1-R-296 on Chromosorb W in an 8 ft × $\frac{1}{4}$ in. outside diameter copper tube at 218° with helium (40 p.s.i.) as carrier gas. The unit was of conventional design with thermal conductivity detectors. The peak ratio of the galactitol and

Can. J. Chem. Downloaded from www.nrcresearchpress.com by 210.87.254.105 on 09/05/12
For personal use only.

Can. J. Chem. Downloaded from www.nrcresearchpress.com by 210.87.254.105 on 09/05/12
For personal use only.

mannitol acetates (retention times 17.6 min and 20 min respectively) were 35:65 based on an equal detector response.

Oxidation of the galactomannan with sodium periodate resulted in the consumption of 1.27 and 1.30 moles of oxidant per mole of anhydroaldose unit with the formation of 0.32 and 0.33 mole of acid after 16 h and 40 h, respectively. The oxidized polysaccharide was isolated by dialysis, reduced with sodium borohydride and the resulting polyalcohol hydrolyzed with acid to glycerol (paper chromatography in solvent *a*).

Methylation of T. fermentans Galactomannan and Analysis of Fragments from Methylated Polysaccharide

The galactomannan was methylated by the Haworth procedure (18) and the partially methylated product was further methylated for 1 week by the method used by Purdie and Irvine (19). The product was isolated in 80% yield and had —OCH_3 44.1%.

The methylated galactomannan (0.85 g) was hydrolyzed overnight in 90% formic acid (20 ml at 100°). The hydrolyzate was evaporated to a syrup and formate esters were decomposed by heating in water. A small portion of the product was converted to mixed methyl glycosides with methanolic hydrogen chloride and examined by g.l.c. using 2% neopentylglycol succinate on Chromosorb W in an 8 ft × ¼ in. outside diameter copper tube at 134° with helium (40 p.s.i.) as the carrier gas. The methyl glycosides of 2,3,4,6-tetra-*O*-methylgalactose (32%), 2,3,4,6-tetra-*O*-methylmannose (2%), 2,3,4- and 3,4,6-tri-*O*-methylmannose (34%), and 3,4-di-*O*-methylmannose (32%) were detected on a molar basis. The percentage composition is corrected on the basis of detector responses arising from an equimolar mixture of the above methyl glycoside fractions. These are 0.98, 1.0, 0.86, 0.90, and 0.72 respectively.

The *O*-methylaldose mixture was fractionated on a cellulose column. Benzene – ethanol – water (1000:50:1 v/v/v) eluted 2,3,4,6-tetra-*O*-methyl-D-galactose (183 mg) characterized as its *N*-phenylgalactosylamine derivative with m.p. and mixture m.p. 194–195° and $[\alpha]_D$ −134° (*c*, 0.6 pyridine) (20).

Benzene – ethanol – water (500:50:1 v/v/v) eluted a mixture of 3,4,6- and 2,3,4-tri-*O*-methyl-D-mannose (179 mg). Gas–liquid chromatography of the TMS derivatives of derived methyl glycosides at 110° (13) showed a ratio of 12:1 (each derivative gave a similar detector response). 3,4,6-Tri-*O*-methyl-D-mannose was crystallized from ether and had m.p. and mixture m.p. 103–105° and $[\alpha]_D$ +36° (*c*, 0.9 MeOH) (21). 3,4-Di-*O*-methyl-D-mannose (120 mg) was eluted and on crystallization from EtOAc had m.p. and mixture m.p. 107–108° and $[\alpha]_D$ +35° (*c*, 1.1 MeOH) (22, 23).

Partial Hydrolysis of T. fermentans Galactomannan

Galactomannan (8.0 g) was partially hydrolyzed in 0.33 *N* sulfuric acid (200 ml) at 100° for 6 h. The solution was neutralized ($BaCO_3$), filtered, and chromatographed on a charcoal column. Monosaccharides were eluted with water and higher molecular weight material removed with 30% aqueous ethanol. The polysaccharide component (2.5 g) was precipitated from aqueous solution with excess ethanol. It gave mainly mannose on acid hydrolysis and had $[\alpha]_D$ +92° (*c*, 0.9 H_2O).

Oxidation of the degraded polymer with sodium periodate resulted in consumption of 1.36, 1.55, and 1.59 moles/mole of oxidant per anhydrohexose unit with formation of 0.51, 0.59, 0.62 mole of acid after 20, 44, and 68 h, respectively.

Methylation of the degraded polymer via the route described earlier in the section gave a product that did not exhibit infrared hydroxyl absorption at 3600–3640 cm^{-1} when examined as a 0.8% chloroform solution in a 5 mm cell. The methylated polymer was converted to a methyl glycosidic mixture which was examined by g.l.c. in the free form and as their TMS derivatives. The methyl glycosides of 2,3,4,6-tetra-*O*-methylmannose (10 pts), 2,3,4,6-tetra-*O*-methylgalactose (2.4 pts), 2,3,4-tri-*O*-methylmannose (3.8 pts), 3,4,6-tri-*O*-methylmannose (4.3 pts), and 3,4-di-*O*-methylmannose (13.0 pts) were detected.

Partial Acetolysis of Galactomannan

The galactomannan (8.0 g) was shaken for 5 days in acetic anhydride (50 ml) – acetic acid (50 ml) containing sulfuric acid (5 ml). The resulting solution was poured into excess aqueous sodium bicarbonate and after 3 h the acetates were extracted with chloroform, which was evaporated to dryness. The product was deacetylated in chloroform–methanol (100 ml:100 ml) containing a catalytic amount of 0.1 *N* methanolic sodium methoxide. Examination of a paper chromatogram (solvent *b*; spray *p*-anisidine hydrochloride) showed that two oligosaccharides running at 1.34 and 0.79 times the rate of lactose (R_{Lact}) were present in addition to mannose. The mixture was fractionated on a cellulose column using acetone–water (6:1 v/v) as eluent and a disaccharide mixture (R_{Lact} 1.34; 0.32 g) was obtained which gave mannose and a smaller amount of galactose on hydrolysis (*N* H_2SO_4 at 100° for 18 h). Elution with acetone–water (4:1 v/v) gave a trisaccharide (2.04 g) with R_{Lact} 0.79.

Characterization of Trisaccharide from Galactomannan

The trisaccharide had $[\alpha]_D$ +110° (*c*, 1.0 H_2O), gave mannose and a smaller amount of galactose on hydrolysis and consumed 0.01, 0.05, and 0.14 mole/mole of lead tetraacetate after 2, 5, and 15 min (15) respectively. The derived alditol obtained by sodium borohydride reduction had $[\alpha]_D$ +77° (*c*, 1.7 H_2O), gave galactose and mannose on hydrolysis and consumed 5.78 and 5.86 moles/mole of sodium periodate with formation of 2.46 and 2.60 moles/mole of acid after 16 and 40 h, respectively. The alditol (0.32 g) was partly hydrolyzed in 0.33 *N* sulfuric acid (10 ml) at 100° for 6 h and the resulting mixture fractionated on a cellulose column using acetone–water (6:1 v/v) as eluent. 2-*O*-α-D-Mannopyranosyl-D-mannitol (83 mg) was isolated, recrystallized twice from EtOH–MeOH, and had m.p. and mixture m.p. 135–136° and $[\alpha]_D$ +42° (*c*, 1.0 H_2O) (24).

The trisaccharide (0.32 g) was dissolved in water (20 ml), containing bromine (1 ml). After 3 days excess bromine was removed by evaporation, the solution neutralized (Ag_2CO_3), filtered, treated with Amberlite IR120, and evaporated to a small volume. Conversion to the sodium salt of the aldonic acid was effected by addition of sodium hydroxide (0.10 g) and heating at 100° for 1 h. The volume of water was adjusted to 5 ml, acetic acid (200 ml) added, followed by lead tetraacetate

(2.7 *M* equivalents). After 18 h the solution was evaporated to a residue which was treated with an aqueous suspension of Amberlite IR120. The resin was removed by filtration and the solution (50 ml) adjusted to pH 2 with dilute sulfuric acid. The solution was heated at 100° for 1 h, neutralized ($BaCO_3$), filtered, and evaporated. The hydrolyzate gave a yellow spot on a paper chromatogram with the *p*-anisidine hydrochloride spray with R_{Lact} 1.75 in solvent *a* and R_{Lact} 1.55 in solvent *b*. Fractionation of the product on a cellulose column (eluent: acetone–water 6:1 v/v) gave syrupy 2-*O*-α-D-galactopyranosyl-D-mannose (69 mg) with $[\alpha]_D$ +84° (*c*, 0.9 H_2O). It gave galactose and mannose on hydrolysis and was not appreciably oxidized by lead tetraacetate. The derived alditol, obtained by sodium borohydride reduction, had $[\alpha]_D$ +81° (*c*, 0.9 H_2O) and gave galactose and a hexitol on hydrolysis.

Methylation of the trisaccharide by the methods described previously gave a product, which did not show infrared hydroxyl absorption. Formolysis followed by glycosidation with methanolic hydrogen chloride provided fragments which corresponded on g.l.c. to the methyl glycosides of 2,3,4,6-tetra-*O*-methylgalactose and 3,4-tri-*O*-methylmannose in a ratio of 1:2.1. Methyl 2,3-tri-*O* methylmannoside was not detectable as its TMS ether.

Acknowledgments

The authors thank Mr. M. Mazurek for preparation of proton magnetic resonance spectra. Thanks are also due to Mr. R. J. Magus and Mr. N. Gardner for technical assistance and to Mr. W. C. Haid for infrared determinations. The illustrations were kindly drawn by Mr. E. Knapp and Mr. A. Lutzko.

1. P. A. J. GORIN, K. HORITSU, and J. F. T. SPENCER. Can. J. Chem. **43**, 950 (1965).
2. E. E. EVANS and J. W. MEHL. Science, **114**, 10 (1951).
3. E. DROUHET, G. SEGRATAIN, and J.-P. AUBERG. Ann. Inst. Pasteur, **79**, 891 (1950).
4. E. E. EVANS and R. J. THERIAULT. J. Bacteriol. **65** 571 (1953).
5. M. J. ABERCROMBIE, J. K. N. JONES, M. V. LOCK, M. B. PERRY, and R. J. STOODLEY. Can. J. Chem **38**, 1617 (1960).
6. J. MAGER. Biochem. J. **41**, 603 (1947).
7. M. E. SLODKI, L. J. WICKERHAM, and R. J. BANDONI. Can. J. Microbiol. **12**, 489 (1966).
8. H. J. PHAFF and J. F. T. SPENCER. Proc. 2nd Int. Symp. on Yeasts, Bratislava. July 16–21, 1966.
9. P. A. J. GORIN, J. F. T. SPENCER, and S. L. MCKENZIE. Can. J. Chem. **44**, 2087 (1966).
10. M. E. SLODKI and L. J. WICKERHAM. J. Gen. Microbiol. **42**, 381 (1966).
11. M. ASCHNER and A. CURY. J. Bacteriol. **62**, 350 (1951).
12. P. A. J. GORIN and J. F. T. SPENCER. Can. J. Chem. **45**, 1543 (1967).
13. Y.-C. LEE and C. E. BALLOU. Biochemistry, **4**, 257 (1965).
14. P. A. J. GORIN and A. S. PERLIN. Can. J. Chem. **35**, 262 (1957).
15. A. J. CHARLSON and A. S. PERLIN. Can. J. Chem. **34**, 1200 (1956).
16. J. K. DALE and C. S. HUDSON. J. Am. Chem. Soc. **52**, 2534 (1930).
17. D. W. S. WESTLAKE and F. J. SIMPSON. Can. J. Microbiol. **7**, 33 (1961).
18. W. N. HAWORTH. J. Chem. Soc. 8 (1915).
19. T. PURDIE and J. C. IRVINE. J. Chem. Soc. 1021 (1903).
20. I. EHRENTHAL, M. C. RAFIQUE, and F. SMITH. J. Am. Chem. Soc. **74**, 1341 (1952).
21. H. G. BOTT, W. N. HAWORTH, and E. L. HIRST. J. Chem. Soc. 1395 (1930).
22. W. N. HAWORTH, R. L. HEATH, and S. PEAT. J. Chem. Soc. 833 (1941).
23. W. N. HAWORTH, E. L. HIRST, and F. A. ISHERWOOD. J. Chem. Soc. 784 (1937).
24. P. A. J. GORIN and A. S. PERLIN. Can. J. Chem. **34**, 1796 (1956).

Can. J. Chem. Downloaded from www.nrcresearchpress.com by 210.87.254.105 on 09/05/12
For personal use only.

Can. J. Chem. Downloaded from www.nrcresearchpress.com by 210.87.254.42 on 09/05/12
For personal use only.

Proton magnetic resonance spectra of *Trichosporon aculeatum* mannan and its borate complex and their relationship to chemical structure[1]

P. A. J. Gorin, M. Mazurek, and J. F. T. Spencer
National Research Council of Canada, Prairie Regional Laboratory, Saskatoon, Saskatchewan

Received February 15, 1968

Methylation–fragmentation and periodate oxidation studies show that the mannan of *Trichosporon aculeatum* is branched with 2-*O*- and 6-*O*-monosubstituted units and 2,6-di-*O*-substituted D-mannopyranosyl units. It contains up to five consecutive α-D-(1 → 2)-linkages. The proton magnetic resonance spectrum of the mannan (recorded in D_2O at 70° using a Varian HA-100 spectrometer) indicates structural differences from other yeast mannans. It contains four distinct H-1 signals, but more than four H-1 environments are present since addition of sodium tetraborate shifts two signals downfield so that six signals are observed (Fig. 1). Two of the four signals in the mannan spectrum at τ 4.40, and τ 4.20 can be assigned to chemical structures. The former signal arises from nonreducing end units attached to the 2-positions of adjacent mannopyranose units and from 2,6-di-*O*-substituted units and the latter from 2-*O*-substituted mannopyranose units. These assignments are based on the above chemical evidence, comparison with H-1 chemical shifts of known compounds, and the magnitudes of the H-1 shifts on borate addition. Downfield shifts of H-1 proton signals on borate addition to known mannopyranosides vary from a maximum with compounds that can form 2,3-borate complexes to virtually none with 2-*O*-substituted derivatives. The magnitude of the downfield shifts observed with α-D-linked mannopyranose derivatives is greater than that of their β-linked counterparts.

Canadian Journal of Chemistry, 46, 2305 (1968)

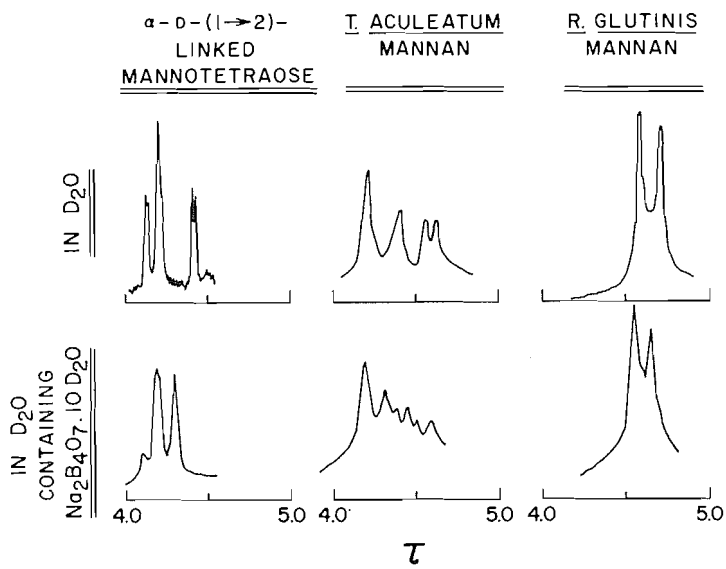

FIG. 1. Effect of sodium tetraborate on H-1 signals of mannopyranose derivatives.

Cells of yeasts of the genus *Trichosporon* contain either galactomannan, pentosylmannan, or a mannan depending upon the individual species. Structural studies on representatives of two of the polysaccharide types, the pentosylmannan of *Trichosporon cutaneum* (1) and the galactomannan of *Trichosporon fermentans* (2), have previously been described. Attention has now been given to the mannan of *Trichosporon aculeatum* and some of its structural features and proton magnetic resonance (p.m.r.) properties have been related.

The mannan was isolated from the alkali extractable cell-wall polysaccharides, which also contain glucan, *via* the insoluble copper complex formed with Fehling solution. The p.m.r. spectrum of a 20% solution in deuterium oxide at 70° (2) contained four signals in the H-1

[1]Issued as NRCC No. 10102.

TABLE I

Properties of α-(1 → 2)-linked D-mannopyranosyl oligosaccharides

α-D-(1 → 2)-Linked oligosaccharide and yield	R_{Lact}	Acetone:water v/v ratio used in cellulose chromatography	Specific rotation (1% in H_2O)	Ratio of derived methyl 2,3,4,6-tetra-*O*- and 3,4,6-tri-*O*-methylmannosides	Ratio of proton magnetic resonance signals at		
					τ 4.10	τ 4.40	τ 4.18
Mannotriose (5%)	0.80	5:1	+52°	1:1.9	0.9	1	1.1
Mannotetraose (14%)	0.42	4:1	+53°	1:3.0	1.0	1	2.0
Mannopentaose (8%)	0.22	7:2	+58°	1:3.6	0.9	1	3.15
Mannohexaose (6%)	0.14	3:1	+54°	1:4.6	1.2	1	4.1

'fingerprint region', representing a minimum of four different H-1 environments. (The clarity of the spectrum was only slightly improved at 110° with sodium acetate or *n*-octadecanol as standard.) The spectrum is clearly distinguishable from those of the mannans of the yeasts *Saccharomyces cerevisiae* (3–5), *Saccharomyces rouxii* (6, 7), *Hansenula* spp. (8–13), several *Candida* spp. (14–17), and *Rhodotorula* spp. (18) on which structural data are available. It also differs from the spectra of approximately 200 other yeast mannans, on which structural studies have not been carried out. A number of examples of p.m.r. spectra of yeast mannans are presented in Fig. 2. Although the spectra of some mannans arising from the same genus are similar, most of them are sufficiently different that they can be used as a means of distinguishing between and identifying the parent yeasts (2). This investigation is being continued and full reports on it will appear elsewhere.

The mannan of *T. aculeatum* appeared to be homogeneous on ultracentrifugation and on electrophoresis in borate buffer. It gave only D-mannose on hydrolysis and the specific rotation of the polysaccharide, +59°, indicated predominant α-D-glycosidic linkages. A methylation–fragmentation analysis gave 2,3,4,6-tetra-*O*-, 3,4,6-tri-*O*-, and 3,4-di-*O*-methyl-D-mannose, which were isolated by cellulose column chromatography and characterized. Gas–liquid chromatography (g.l.c.) of the derived methyl glycosides and their trimethylsilyl (TMS) ethers (5) indicated the presence of 2,3,4-tri-*O*-methylmannose. A molar ratio of 10:7:32:7 of 2,3,4,6-tetra-*O*-, 2,3,4-, 3,4,6-tri-*O*-, and 3,4-di-*O*-methylmannose was calculated on the basis of cellulose column chromatography and gravimetric analysis of the various fractions and by g.l.c. comparison of the TMS ethers of the methyl glycosides of the two tri-*O*-methylmannose fragments. In reasonable agreement with these data, the mannan consumed 1.37 moles of periodate with formation of 0.34 mole of acid per anhydromannose unit. (Calculated 1.32 mole/mole $NaIO_4$, 0.30 mole/mole HCO_2H.) The oxidized mannan was reduced with sodium borohydride on a preparative scale, the resulting

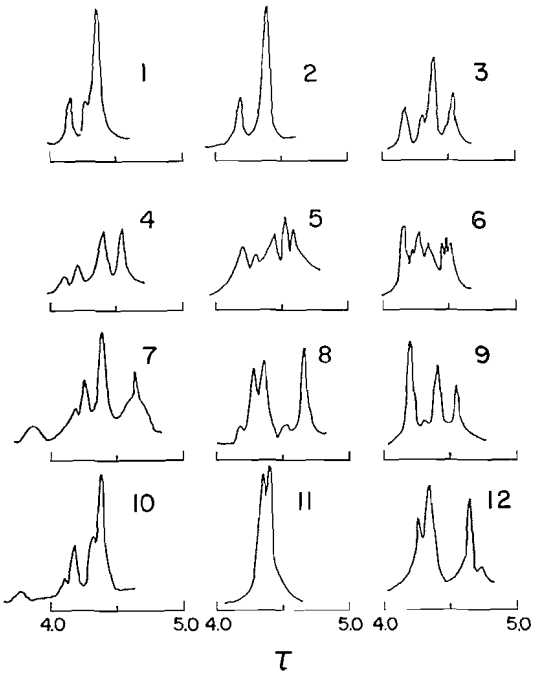

FIG. 2. Proton magnetic resonance spectra of some yeast mannans. Source of mannan: **1**, *Saccharomyces cerevisiae*; **2**, *Saccharomyces rouxii* PRL 411-64; **3**, *Saccharomyces aestuarii* PRL Y117; **4**, *Candida albicans* serotype B; **5**, *Candida albicans* serotype A; **6**, *Candida utilis* NRRL Y900; **7**, *Hansenula capsulata* NRRL Y1842; **8**, *Hanseniaspora vineae* JPV 72; **9**, *Trichosporon aculeatum* IGC 3551 (acid degraded mannan); **10**, *Hansenula holstii* NRRL Y2155; **11**, *Endomycopsis selenospora* CBS 2562; **12**, *Kloeckera africana* CBS 277.

Can. J. Chem. Downloaded from www.nrcresearchpress.com by 210.87.254.42 on 09/05/12
For personal use only.

TABLE II

Composition of acid degraded mannans of *Trichosporon aculeatum* and *Saccharomyces cerevisiae*

Degradation time	Yield (%) of degraded mannan	Percentage of linkage types in mannans				
		End unit	6-*O*-	2-*O*-	3-*O*-	2,6-Di-*O*-
T. aculeatum mannan						
0 h	—	18	12	58	—	13
6 h	82	21	12	48	—	19
18 h	61	21	17	43	—	19
66 h	8	31	16	25	—	28
S. cerevisiae mannan						
0 h (4)	—	33	2	16	16	31
6 h	70	38	6	12	8	36
20 h	37	36	20	10	2	32
68 h	36	35	28	6	—	31

polyalcohol was hydrolyzed, and glycerol was detected on a paper chromatogram as the only product.

Partial acetolysis of the mannan split (1 → 6)-linkages preferentially (5, 6) giving acetates of linear α-D-(1 → 2)-linked mannose oligosaccharides of up to 6 units in length. The oligosaccharides, following deacetylation, were isolated by cellulose column chromatography and with the exception of mannobiose which was converted to crystalline 2-*O*-α-D-mannopyranosyl-D-mannitol, they were analyzed by the methylation–fragmentation technique. In each analysis 2,3,4,6-tetra-*O*- and 3,4,6-tri-*O*-methylmannose were characterized and compared quantitatively by g.l.c. of derived free and trimethylsilylated methylmannosides. The specific rotations of the oligosaccharides were consistent with α-D-linkages. The chain lengths of the oligosaccharides were confirmed by quantitative p.m.r. spectroscopy, by comparison of the H-1 proton signals of reducing end, the nonreducing end, and the internal units which are at τ 4.10 ($J = 1.2$ c.p.s.), τ 4.40 ($J = 2.0$ c.p.s.) and τ 4.18, respectively[2] (Table I). The H-1 signals of both end units are split, except in the penta- and hexasaccharide spectra, which exhibit splitting only on heating the solution to 70°. By analogy with the spectra of the oligosaccharides the major signal (45%) at τ 4.20 in the mannan spectrum (Fig. 1) should arise from the H-1 protons of the predominant internal α-(1 → 2)-linked D-mannopyranosyl units.

[2]Reaction of the reducing end-unit with methoxyamine at a slightly alkaline pH (A. S. Perlin. Unpublished results.) resulted in disappearance of the signal at lowest field.

To ascertain whether the (1 → 2)-linked chains are present in the main chains and/or side chains of the mannan an attempt was made to cleave the (1 → 2)-linkages preferentially under the hydrolytic conditions used by Peat and co-workers in their study on the structure of the cell-wall mannan of *Saccharomyces cerevisiae* (3). However, partial hydrolysis of the mannan of *T. aculeatum* did not give oligosaccharides, instead the residual degraded mannans were isolated at intervals by ethanol precipitation and some of their structural features determined. The p.m.r. spectrum of a mannan obtained after degradation for 18 h did not differ markedly from that of undegraded mannan, except that the minor signal at highest field had disappeared and the proportion of the H-1 protons of (1 → 2)-linked mannopyranosyl units had decreased. Methylation–fragmentation analysis of the degraded mannans gave 2,3,4,6-tetra-*O*-, 2,3,4-tri-*O*-, 3,4,6-tri-*O*-, and 3,4-di-*O*-methylmannoses, which were identified and quantitatively measured by g.l.c. The relative proportions of each linkage type are given in Table II. Although these figures indicate some preferential cleavage of (1 → 2)-linkages in the side chains, the residual mannans were still highly branched and a well-defined structure could not be assigned to the main chain. Similarly, application of the hydrolytic technique to baker's yeast mannan, which is reported to contain a (1 → 6)-linked main-chain and (1 → 2)- and (1 → 3)-linkages in the side chains (3–5), resulted in formation of a branched-chain mannan (see Table II).

It has been found that H-1 p.m.r. signals of mannopyranoside derivatives at 70° in D_2O are

Can. J. Chem. Downloaded from www.nrcresearchpress.com by 210.87.254.42 on 09/05/12
For personal use only.

TABLE III

H-1 Proton signals in mannose derivatives; chemical shifts and downfield shifts on borate addition

Location of H-1 proton	Chemical shift, τ	Downfield shift on borate addition, c.p.s.
Methyl α-D-mannopyranoside	4.71	14
Methyl 4,6-*O*-ethylidene α-D-mannopyranoside	4.71	11
α-D-(1 → 3)-Linked mannopyranosyl units in linear polymer	4.35	5
Nonreducing end of 6-*O*-α-D-mannopyranosyl-D-mannose	4.57	—
Units of 3-*O*-α-D-mannopyranosyl-D-mannose	4.33, 4.35	—
Nonreducing end of α-(1 → 2)-linked-D-mannopyranosyl oligosaccharides	4.40	10
Internal units of above	4.20	2
2,6-Di-*O*-Substituted D-mannopyranose units in mannans from *S. cerevisiae*, *S. rouxii*, and *T. aculeatum*	4.38, 4.40	< 5
Methyl β-D-mannopyranoside	4.92	6
β-(1 → 3)-Linked units in *Rhodotorula glutinis* mannan	4.58	4
β-(1 → 4)-Linked units in above	4.69	7

shifted downfield on addition of excess $Na_2B_4O_7 \cdot 10D_2O$. Various derivatives were tested, analogous to structures that may be present in yeast mannans. For example, the split H-1 signal of methyl α-D-mannopyranoside was, on borate addition, converted to a relatively broad singlet at 14 c.p.s. lower field. Similarly the H-1 doublet of methyl 4,6-*O*-ethylidene-α-D-mannopyranoside was shifted downfield by 11 c.p.s. Addition of borate to a linear polysaccharide containing α-(1 → 3)-D-mannopyranose units (obtained by successive Smith degradations of *Candida bogoriensis* heteropolysaccharide[3]) resulted in a downfield shift of 5 c.p.s. of the H-1 signal. A downfield shift of 10 c.p.s. was observed in the H-1 signal of the non reducing end of an α-D-(1 → 2)-linked mannotetraose, but the H-1 signals of the internal (1 → 2)-linked units were virtually unaffected on borate addition (Fig. 1).

In the β-D-mannopyranoside series borate addition causes smaller downfield shifts of H-1 signals than with comparable α-linked derivatives. For example, a shift of 6 c.p.s. occurs with methyl β-D-mannopyranoside without loss of splitting. Addition of borate to the *Rhodotorula glutinis* mannan, which gives two H-1 signals arising from alternate β-D-(1 → 3)-linked and β-D-(1 → 4)-linked D-mannopyranosyl units, resulted in downfield shifts of 4 c.p.s. and 7 c.p.s., of the signals at τ 4.58 and 4.69 respectively (Fig. 1).

From the foregoing results it appears that the size of the downfield shift can be correlated with structure. The greatest shifts occur with mannosides that can form 2,3-borate complexes and a smaller shift occurs with a derivative which has a free C-2 hydroxyl group. Little shift of H-1 occurs on addition of borate to a 2-*O*-substituted mannopyranoside derivative. These generalizations have now been applied to the mannan from *T. aculeatum*.

Although the mannan spectrum contains four major H-1 signals, more than four H-1 protons with different environments (2) are present since six signals were detected after borate addition (Fig. 1). The spectrum of the borate complex was less well defined, but several features could still be observed. The major H-1 signal at τ 4.20 assigned to (1 → 2)-linked units was shifted downfield only 2 c.p.s. On the other hand, the two middle signals, previously at τ 4.40 and τ 4.54, were shifted downfield by 8 c.p.s. and 9 c.p.s., respectively. These signals presumably arise from 2,3-borate-complexed units and correspond to nonreducing end-units or possibly 6-*O*-linked mannopyranosyl units. The former structure could well give rise to the signal at

[3]P. A. J. Gorin and J. F. T. Spencer. Unpublished results.

Can. J. Chem. Downloaded from www.nrcresearchpress.com by 210.87.254.42 on 09/05/12
For personal use only.

Can. J. Chem. Downloaded from www.nrcresearchpress.com by 210.87.254.42 on 09/05/12
For personal use only.

τ 4.40 since its chemical shift is closest to that (τ 4.40) of H-1 of the nonreducing end of the α-D-(1→2)-linked mannotetraose. Another component of the τ 4.40 signal in the *T. aculeatum* mannan spectrum appeared to be shifted downfield only a few cycles on borate addition. This signal likely arises from H-1 of 2,6-di-*O*-substituted units and is probably analogous to components of the signals at τ 4.38 in the p.m.r. spectra of *Saccharomyces cerevisiae* and *Saccharomyces rouxii* mannans (Fig. 2).

Assignment of part of the τ 4.40 signal to H-1 of nonreducing end units in the *Trichosporon* mannan is important since it means that the end unit is 2-*O*-linked to the adjacent unit. If it were 6-*O*-linked, it would give a signal at τ 4.57, similar to the chemical shift of H-1 of the nonreducing end-unit of 6-*O*-α-D-mannopyranosyl-D-mannose. The mannan signal at τ 4.54 could perhaps arise from the protons of end units 6-*O*-linked to the adjacent unit.

The chemical shifts of various H-1 protons in known structures and their downfield shifts on borate addition are summarized in Table III.

Experimental

The proton magnetic resonance (p.m.r.) spectra of the mannans were obtained from 20% solutions in D_2O at 70° using an HA-100 Varian spectrometer. The chemical shifts are based on an external tetramethylsilane standard.

Purification of Mannans and Determination of Proton Magnetic Resonance Spectra of Free and Borate-complexed Mannose Derivatives

Cultural conditions for production of yeast cells and the method of isolation of purified component mannans via their copper complexes has been described previously (2).

A lower concentration was used in determining the p.m.r. spectra of borate-complexed mannans or mannose derivatives. Fifteen percent of $Na_2B_4O_7 \cdot 10D_2O$ was dissolved in a 7% carbohydrate solution in D_2O by heating to 100° with agitation. At higher concentrations of mannan the solutions often became extremely viscous.

Physical Properties of Trichosporon aculeatum Mannan

The *Trichosporon aculeatum* mannan was isolated from cells (2). It had $[\alpha]_D$ +59° (0.9, H_2O). The polymer appeared to be homogeneous giving single peaks on ultracentrifugation (59 000 r.p.m.) as 0.15% to 0.6% solutions in 0.5% aqueous sodium chloride and on moving boundary electrophoresis as a 0.5% solution in 0.05 *M* aqueous sodium tetraborate. The p.m.r. spectra of the mannan contained signals at τ 4.20 (45%), τ 4.40 (26%), τ 4.54 (16%), and τ 4.62 (13%). The borate complex gave six signals at τ 4.18, τ 4.31, τ 4.35, τ 4.43, τ 4.51, and τ 4.58 (Fig. 1).

Hydrolysis, Periodate Oxidation Characteristics, and Methylation–Fragmentation Analysis of T. aculeatum Mannan

The mannan was hydrolyzed (*N* H_2SO_4 at 100° for 18 h) and the product examined by paper chromatography (solvent: *n*-butanol–ethanol–water 40:11:19 v/v/v; spray: *p*-anisidine hydrochloride). Mannose was the only product and it crystallized from ethanol as the D-form with m.p. and mixed m.p. 133° and $[\alpha]_D$ +30° → 14° (*c*, 1.0 H_2O).

The mannan consumed 1.28, 1.37, and 1.37 moles of sodium periodate per mole of anhydromannose unit with concomitant formation of 0.30, 0.34, and 0.34 mole of acid after 19, 43, and 67 h, respectively. Only glycerol was detected (paper chromatogram) on hydrolysis of the polyalcohol formed by sodium borohydride reduction of the periodate-oxidized mannan.

The mannan was partially methylated by the Haworth procedure (19) and the product was further methylated by the Purdie method (20). The methylated mannan was obtained in 78% yield and had —OCH_3 43.8%.

The methylated mannan (1.00 g) was hydrolyzed for 18 h at 100° in 90% formic acid (20 ml) and the solution evaporated to a syrup. Formate esters were destroyed by repeatedly heating in water and then evaporating the solution. One-third of the hydrolyzate was fractionated on a cellulose column. Benzene – ethanol – water (1000:50:1 v/v/v) eluted 2,3,4,6-tetra-*O*-methyl-D-mannose (55 mg), followed by a mixture of 2,3,4- and 3,4,6-tri-*O*-methyl-D-mannose (177 mg). The latter component crystallized from ether and had m.p. and mixed m.p. 104–105° and $[\alpha]_D$ +36° (*c*, 1.0 MeOH) (21). Benzene – ethanol – water (500:50:1 v/v/v) eluted 3,4-di-*O*-methyl-D-mannose (58 mg), which crystallized from EtOAc and had m.p. and mixed m.p. 106–108° and $[\alpha]_D$ +34° (*c*, 1.0 MeOH) (22, 23).

A small portion of the hydrolyzate of the methylated mannan was converted to a methyl glycosidic mixture and examined by g.l.c. An 8 ft × 1/4 in. outside diameter copper tube was used with 2% neopentylglycol succinate on Chromosorb W at 142°, with helium (40 p.s.i.) as carrier gas. The methyl glycosides of 2,3,4,6-tetra-*O*-methylmannose (1 part), a mixture of 2,3,4-, and 3,4,6-tri-*O*-methylmannose (3.90 parts) and 3,4-di-*O*-methylmannose (0.70 part) were detected (5). The ratio is corrected on the basis of detector responses arising from an equimolar mixture of the methylmannoside fractions. These are 1.0, 0.86, 0.90, and 0.72, respectively. The tri-*O*-methyl fraction obtained by cellulose column chromatography was converted to the trimethylsilyl methyl mannosides (5). Gas–liquid chromatographic examination at 110° showed that the derivatives of 2,3,4- and 3,4,6-tri-*O*-methylmannoses were present in a ratio of 1:4.8.

Acetolysis of T. aculeatum Mannan

The mannan (2.8 g) was shaken in acetic acid (17.5 ml) and acetic anhydride (17.5 ml) containing sulfuric acid (1.75 ml) for 5 days. The reaction mixture was added to excess ice-cold aqueous sodium bicarbonate and the acetates were extracted with chloroform which was evaporated. The mixture (5.14 g) was deacetylated with methanolic sodium methoxide in chloroform–methanol. The solution was neutralized, the solvent evaporated to a crust, and salts were removed by addition of an aqueous

Can. J. Chem. Downloaded from www.nrcresearchpress.com by 210.87.254.42 on 09/05/12
For personal use only.

suspension of mixed-bed resins. Examination of the product on a paper chromatogram (solvent: ethyl acetate – acetic acid – water 2:1:1 v/v/v); spray: *p*-anisidine hydrochloride) showed spots with rates relative to lactose (R_{Lact}) of 1.31, 0.80, 0.42, 0.22, and 0.14 in addition to mannose.

The mixture was fractionated on a cellulose column. The chromatographic eluants, yields of each oligosaccharide, their specific rotations and the ratios of H-1 p.m.r. signals at τ 4.10, τ 4.40, and τ 4.18 are presented in Table I. Attempts to crystallize the oligosaccharides, the polyols obtained by sodium borohydride reduction or the acetates of these materials, were unsuccessful. The disaccharide fraction was reduced with sodium borohydride to 2-*O*-α-D-mannopyranosyl-D-mannitol with m.p. and mixed m.p. 135–136° (from EtOH–MeOH) and $[\alpha]_D$ +41° (*c*, 1.0 H_2O) (6). The remaining oligosaccharides were each methylated by the methods described earlier in the section. The methylated oligosaccharides did not absorb at 3600–3640 cm^{-1} in the infrared when examined as 0.8% carbon tetrachloride solutions in a 5 mm cell. Formolysis of the methylated oligosaccharides gave tri-*O*- and tetra-*O*-methylmannoses which were detected on paper chromatograms. Gas–liquid chromatography of the derived methyl glycosides and their TMS ethers showed that methyl 3,4,6-tri-*O*- and methyl 2,3,4,6-tetra-*O*-methylmannosides were formed. The ratios of each fragment (estimated by g.l.c. of the methyl glycosides) are presented in Table I.

Partial Hydrolysis of Mannans from T. aculeatum and Saccharomyces cerevisiae

Ten percent solutions of mannans of *T. aculeatum* and *Saccharomyces cerevisiae* in 0.33 *N* sulfuric acid were heated at 100° and aliquots were added at intervals to a 16-fold excess of ethanol. The precipitates which formed were centrifuged off, washed three times with ethanol, and dried. The yields of isolated degraded mannans are given in Table II. The p.m.r. spectrum of *T. aculeatum* mannan, degraded for 18 h, is shown in Fig. 2 as spectrum **9**. The degraded mannans were analyzed by the methylation–fragmentation technique using methods described in an earlier publication (2). The linkage types present in the mannans were determined qualitatively and quantitatively (see Table II).

Acknowledgments

Polysaccharides from *Candida albicans* were kindly supplied by Dr. C. T. Bishop. The authors thank Mr. R. J. Magus and Mr. N. Gardner for technical assistance, Mr. W. C. Haid for infrared determinations, and Mr. E. Knapp and Mr. A. Lutzko for drafting the figures.

1. P. A. J. GORIN and J. F. T. SPENCER. Can. J. Chem. **45**, 1543 (1967).
2. P. A. J. GORIN and J. F. T. SPENCER. Can. J. Chem. **46**, 2299 (1968).
3. S. PEAT, W. J. WHELAN, and T. E. EDWARDS. J. Chem. Soc. 29 (1961).
4. S. PEAT, J. R. TURVEY, and D. DOYLE. J. Chem. Soc. 3918 (1961).
5. Y-C LEE and C. E. BALLOU. Biochem. **4**, 257 (1965).
6. P. A. J. GORIN and A. S. PERLIN. Can. J. Chem. **34**, 1796 (1956).
7. P. A. J. GORIN and A. S. PERLIN. Can. J. Chem. **35**, 262 (1957).
8. M. E. SLODKI. Biochim. et Biophys. Acta, **57**, 525 (1962).
9. M. E. SLODKI. U.S. Pat. 3,002,966 (1959); Chem. Abstr. **56**, 3927 (1962).
10. A. E. JEANES, J. E. PITTSLEY, P. R. WATSON, and R. J. DIMLER. Arch. Biochem. Biophys. **92**, 343 (1961).
11. A. JEANES and P. R. WATSON. Can. J. Chem. **40**, 1318 (1962).
12. A. JEANES, J. E. PITTSLEY, P. R. WATSON, and J. H. SLONEKER. Can. J. Chem. **40**, 2256 (1962).
13. M. E. SLODKI. Biochim. et Biophys. Acta, **69**, 96 (1962).
14. C. T. BISHOP, F. BLANK, and P. E. GARDNER. Can. J. Chem. **38**, 869 (1960).
15. T. MIYAZAKI. Yakugaku Zasshi, **82**, 1678 (1962).
16. D. SIKL, L. MASLER, and S. BAUER. Chem. Zvesti, **19**, 21 (1965).
17. R. J. YU, C. T. BISHOP, F. P. COOPER, H. F. HASENCLEVER, and F. BLANK. Can. J. Chem. **45**, 2205 (1967).
18. P. A. J. GORIN, K. HORITSU, and J. F. T. SPENCER. Can. J. Chem. **43**, 950 (1965).
19. W. N. HAWORTH. J. Chem. Soc. 8 (1915).
20. T. PURDIE and J. C. IRVINE. J. Chem. Soc. 1021 (1903).
21. H. G. BOTT, W. N. HAWORTH, and E. L. HIRST. J. Chem. Soc. 1395 (1930).
22. W. N. HAWORTH, R. L. HEATH, and S. PEAT. J. Chem. Soc. 833 (1941).
23. W. N. HAWORTH, E. L. HIRST, and F. A. ISHERWOOD. J. Chem. Soc. 784 (1937).

Can. J. Chem. Downloaded from www.nrcresearchpress.com by 210.87.254.42 on 09/05/12
For personal use only.

NOTES

Isolation of two arabinobioses from *Acacia nilotica* gum

R. C. CHALK,[1] J. F. STODDART, W. A. SZAREK, AND J. K. N. JONES
Department of Chemistry, Queen's University, Kingston, Ontario

Received February 2, 1968

A new, crystalline arabinobiose, 2-*O*-β-L-arabinofuranosyl-L-arabinose has been isolated from *A. nilotica* gum. Another arabinobiose, 3-*O*-β-L-arabinopyranosyl-L-arabinose, found previously in other *Acacia* gums, was also present.

Canadian Journal of Chemistry, 46, 2311 (1968)

Previous investigations (1) on the structural features of *Acacia nilotica* gum have shown it to contain galactose, arabinose, rhamnose, and four aldobiouronic acids, 6-*O*-(β-D-glucopyranosyluronic acid)-D-galactose, 6-*O*-(4-*O*-methyl-β-D-glucopyranosyluronic acid)-D-galactose, 4-*O*-(α-D-glucopyranosyluronic acid)-D-galactose, and 4-*O*-(4-*O*-methyl-α-D-glucopyranosyluronic acid)-D-galactose. More recently, a structural investigation of *Acacia arabica* gum (2) led to the isolation and characterization of 3,5-di-*O*-methyl-L-arabinose from the *O*-methyl derivative of the gum. There is similar evidence for the existence of 2-*O*-substituted L-arabinofuranose residues in the arabinose-containing side chains of other *Acacia* gums (3, 4), mesquite gum (5), lemon gum (6), and of *Agave americana* gum (7) as well as in the arabinogalactan from gum tragacanth (8). We report now the isolation and characterization from *A. nilotica* gum of a new crystalline arabinobiose, 2-*O*-β-L-arabinofuranosyl-L-arabinose, in addition to 3-*O*-β-L-arabinopyranosyl-L-arabinose, which has been characterized from other *Acacia* gums (2, 9).

The purified sample of *A. nilotica* gum, which was treated with 1,1,2-trichloro-1,2,2-trifluoroethane (Genetron) (10) to remove most of the proteinaceous material, gave one peak on free-boundary electrophoresis in borate and veronal buffers. Autohydrolysis of the acid form of the gum resulted in the release of rhamnose, arabinose, a trace of galactose, and the two arabinobioses mentioned above. The first was characterized as the crystalline hemihydrate of 2-*O*-β-L-arabinofuranosyl-L-arabinose. The facile acid hydrolysis of the disaccharide indicated the presence of a furanosyl linkage, and a negative colorimetric test with triphenyltetrazolium chloride reagent (11) suggested that the reducing arabinose residue was 2-*O*-substituted. These indications were confirmed by the isolation and characterization of 3,4- and 3,5-di- as well as 2,3,5-tri-*O*-methyl-L-arabinose from the hydrolyzate of the methylated disaccharide. In accordance with the structure proposed for the derived glycitol, periodate oxidation yielded 0.94 mole/mole of formic acid and 0.97 mole/mole of formaldehyde, and consumed 3.06 mole/mole of periodate. The values for the specific optical rotations of the disaccharide (+148°) and of the reduced disaccharide (+69°) suggest that the configuration of the 1→2-linkage is β. Further evidence for this assignment follows from the fact that the synthetically prepared α isomer has $[\alpha]_D$ −8.5°. Although an attempted condensation of 2,3,5-tri-*O*-benzoyl-α-L-arabinofuranosyl bromide (12) with 1,3,5-tri-*O*-benzoyl-β-L-arabinofuranose (12) was unsuccessful, the former compound did condense with benzyl 3,4-*O*-isopropylidene-β-L-arabinopyranoside (13) in anhydrous benzene in the presence of silver oxide, iodine, and a drying agent to give benzyl 2-*O*-(2,3,5-tri-*O*-benzoyl-α-L-arabinofuranosyl)-3,4-*O*-isopropylidene-β-L-arabinopyranoside, which was characterized as a crystalline compound after chromatography on silica gel. Some cleavage of the isopropylidene group occurred during fractionation on silica gel[2] to give a syrupy product, benzyl 2-*O*-(2,3,5-tri-*O*-benzoyl-α-L-arabinofuranosyl)-β-L-arabinopyranoside, which was de-*O*-benzoylated to crystalline

[1]Present address: Organic Chemistry Laboratory, Pioneering Research Division, U.S. Army Natick Laboratories, Natick, Massachusetts 01762.

[2]R. C. Chalk, D. H. Ball, and L. Long, Jr. Unpublished results.

benzyl 2-*O*-α-L-arabinofuranosyl-β-L-arabinopyranoside. Catalytic de-*O*-benzylation of the glycoside yielded 2-*O*-α-L-arabinofuranosyl-L-arabinose.

The second arabinobiose from *A. nilotica* gum was characterized as the crystalline phenylosazone of 3-*O*-β-L-arabinopyranosyl-L-arabinose (14). Since both arabinobioses were released under mild conditions of acid hydrolysis, the reducing arabinose residue in each case was probably originally present in the furanose form in the polysaccharide.

Experimental

Melting points are uncorrected and were determined with a Fisher–Johns apparatus. Optical rotations were measured in water at 21 ± 2 °C unless otherwise stated. Paper chromatography was carried out on Whatman No. 1 paper using the following solvent systems (v/v): (*a*) ethyl acetate – acetic acid – formic acid – water (18:3:1:4); (*b*) butan-1-ol – ethanol – water (4:1:5, upper layer). Sugars were detected with either *p*-anisidine hydrochloride (15) or alkaline silver nitrate (16). R_G values of *O*-methyl sugars refer to distances moved relative to that of 2,3,4,6-tetra-*O*-methyl-D-glucose. Gas–liquid partition chromatography (g.l.c.) (F and M chromatograph, type 402) of mixtures of methyl glycosides of *O*-methyl sugars (17) was carried out at nitrogen flow rates of ca. 100 ml/min on a column of 15% by weight of butan-1,4-diol succinate polyester on 60–80 mesh acid washed Chromosorb W (110 × 0.4 cm) at 175 °C. Retention times, *T*, are quoted relative to methyl 2,3,4,6-tetra-*O*-methyl-β-D-glucopyranoside as standard. Thin-layer chromatography (t.l.c.) was carried out on glass microplates (40 × 90 mm) coated with silica gel (Camag).

Purification of A. nilotica Gum

Five separate nodules of *A. nilotica* gum were purified by dissolving in water, filtering, precipitating with acidified ethanol, washing with ethanol and ether, and drying. Since all samples had similar values for their specific optical rotations, they were combined by redissolving and reprecipitating to give a product (228 g), $[\alpha]_D$ +98° (*c*, 1.0) (Found: N, 0.69%). Free-boundary electrophoresis on a Tiselius apparatus (Perkin–Elmer model 38-A) in a borate buffer at pH 9.2 and in a veronal buffer at pH 10.0 showed the presence of a fast moving major component and a slow moving minor component. A sample (4 g) of the polysaccharide was dissolved in water (20 ml) and homogenized for 10 min with 1,1,2-trichloro-1,2,2-trifluoroethane (Genetron) (10). After centrifugation, the mixture was separated into a lower layer of Genetron, a middle gelatinous layer composed mainly of denatured protein, and an upper aqueous layer containing protein-depleted polysaccharide (3.2g), $[\alpha]_D$ +86° (*c*, 1.0) (Found: ash (sulfated), 2.9%; equivalent weight, 2037; OCH_3, 1.7; N, 0.13%). Free-boundary electrophoresis showed the presence of the fast moving component only. The remainder of the polysaccharide sample was treated with Genetron as described above.

Autohydrolysis of A. nilotica Gum

A sample (50g) of the free acid form of the gum was dissolved in water (835 ml) and heated for 57 h under reflux. The extent of hydrolysis was followed by paper chromatography and by the change in specific optical rotation which was as follows: $[\alpha]_D$ +83° (1 h); +84° (2.5 h); +84° (5 h); +87° (11 h); +87° (22 h); +82° (31 h); +75° (46 h); +75° (57 h), constant value. The cooled solution was filtered and concentrated to a syrup, a portion (ca. 12 g) of which was fractionated on a Dowex 50W (Li^+ form) column (18) using water as eluent to give four fractions. The first fraction contained mainly degraded polysaccharide and the other three fractions, a mixture of oligo- and monosaccharides. The third fraction (2.6 g) was rechromatographed on a cellulose column using initially butan-1-ol half-saturated with water, then butan-1-ol saturated with water, and then finally butan-1-ol – ethanol – water (40:11:19) as eluents to give four new fractions.

Fraction 1 was rhamnose monohydrate (10 mg), m.p. and mixture m.p. with an authentic sample 93 °C.

Fraction 2 was L-arabinose (110 mg), m.p. and mixture m.p. with an authentic sample 157 °C, $[\alpha]_D$ +96° (*c*, 1.0). A crystalline benzoylhydrazone was prepared, m.p. 196 °C.

Fraction 3 (357 mg) was recrystallized twice from butan-1-ol – methanol to give a crystalline arabinobiose (130 mg), m.p. 103 °C, $[\alpha]_D$ +148° (*c*, 1.0).

Anal. Calcd. for $C_{10}H_{18}O_9 \cdot \frac{1}{2} H_2O$: C, 41.2; H, 6.5. Found: C, 41.4; H, 6.3.

Hydrolysis with 0.01 *N* sulfuric acid at 100 °C for 3 h gave only arabinose, and addition of triphenyltetrazolium chloride reagent (11) to an aqueous solution of the disaccharide failed to give the red color given by arabinose itself. No red color was produced by 2-*O*-methyl-L-arabinose. A portion (137 mg) of the syrupy disaccharide was methylated with methyl iodide and silver oxide in *N,N*-dimethyl formamide (19) to give a product (140 mg), $[\alpha]_D$ +114° (*c*, 1.0 in chloroform).

Anal. Calcd. for $C_{16}H_{30}O_9$: OCH_3, 50.8. Found: OCH_3, 49.9.

The methylated product was heated at 100 °C with 60% formic acid for 12 h and then with *N* sulfuric acid for 1 h. Paper chromatographic examination of the hydrolyzate in solvents (*a*) and (*b*) showed the presence of three components, which were separated on a small cellulose column with light petroleum – butan-1-ol (7:3, saturated with water) as eluent (light petroleum, b.p. 100–120 °C). Fraction (*i*) (23 mg) had $[\alpha]_D$ −32° (*c*, 1.0) and the same paper chromatographic mobility [R_G 1.00 in solvent (*a*) and 0.98 in solvent (*b*)] as an authentic sample of 2,3,5-tri-*O*-methyl-L-arabinose. It was characterized by conversion into 2,3,5-tri-*O*-methyl-L-arabonamide, m.p. 134–135 °C, not depressed on admixture with an authentic specimen. Fraction (*ii*) (10 mg) had $[\alpha]_D$ −2° (*c*, 1.0), gave a positive test with the triphenyltetrazolium chloride reagent, and had the same paper chromatographic mobility [R_G 0.87 in solvent (*a*) and 0.81 in solvent (*b*)] as 3,5-di-*O*-methyl-L-arabinose. Conversion of a small portion to the methyl glycosides followed by g.l.c. examination confirmed the presence of 3,5-di-*O*-methyl-L-arabinose (*T*, 1.07, 2.46). Fraction (*iii*) (8 mg) had $[\alpha]_D$ +98° (*c*, 1.0), gave a positive test with the triphenyltetrazolium chloride reagent, and had the same paper

Can. J. Chem. Downloaded from www.nrcresearchpress.com by 210.87.254.42 on 09/05/12
For personal use only.

Can. J. Chem. Downloaded from www.nrcresearchpress.com by 210.87.254.42 on 09/05/12
For personal use only.

chromatographic mobility [R_G 0.68 in solvent (*a*) and 0.54 in solvent (*b*)] as 3,4-di-*O*-methyl-L-arabinose. Conversion of a small portion to the methyl glycoside(s) followed by g.l.c. examination confirmed the presence of 3,4-di-*O*-methyl-L-arabinose (*T*, 1.96). The crystalline disaccharide (25 mg) was reduced with sodium borohydride and isolated in the usual way to give a syrupy product (24 mg), $[\alpha]_D$ +69° (*c*, 1.7). The consumption of periodate during oxidation of this reduced disaccharide, determined spectrophotometrically by the method of Aspinall and Ferrier (20), was 3.06 mole/mole. The amounts of formic acid (21) and formaldehyde (22) released during periodate oxidation were 0.94 and 0.97 mole/mole, respectively.

Fraction 4 (1.3 g) had $[\alpha]_D$ +210° (*c*, 1.0) and the same paper chromatographic mobility as an authentic sample of 3-*O*-β-L-arabinopyranosyl-L-arabinose. It was characterized as its crystalline phenylosazone, m.p. 233 °C, not depressed on admixture with an authentic specimen (23).

Synthesis of 2-O-α-L-Arabinofuranosyl-L-arabinose

Methyl 2,3,5-tri-*O*-benzoyl-α-L-arabinofuranoside (30 g) was converted (12) into 2,3,5-tri-*O*-benzoyl-α-L-arabinofuranosyl bromide (11.8 g), m.p. 103 °C, $[\alpha]_D$ −81° (*c*, 1.0 in chloroform) by treatment with hydrogen bromide in glacial acetic acid. Benzyl 3,4-*O*-isopropylidene-β-L-arabinopyranoside (13) (1.5 g) was dissolved in anhydrous benzene (20 ml), silver oxide (4 g) and Drierite were added, and the mixture was shaken at room temperature. After 1 h, iodine (780 mg) and a solution of 2,3,5-tri-*O*-benzoyl-α-L-arabinofuranosyl bromide (2.78 g) were added. After shaking for 3 days, the reaction mixture was filtered and the filtrate concentrated to a syrup (3.76 g). Thin-layer chromatographic examination of the syrupy mixture with benzene–ethanol (97:3) as solvent showed the presence of four main spots, two of which corresponded to the starting materials. Fractionation of this mixture on a column of silica gel (350 g) with benzene – ethyl acetate (1:1) as eluent yielded the following: (*i*) Benzyl 2-*O*-(2,3,5-tri-*O*-benzoyl-α-L-arabinofuranosyl)-3,4-*O*-isopropylidene-β-L-arabinopyranoside (305 mg), m.p. 95–97 °C after recrystallization from ether – petroleum ether (b.p. 60–80 °C), $[\alpha]_D$ +28° (*c*, 0.5 in chloroform).

Anal. Calcd. for $C_{41}H_{40}O_{12}$: C, 67.9; H, 5.5. Found: C, 68.0; H, 5.3.

De-*O*-benzoylation followed by hydrolysis with 50% aqueous acetic acid for 3 h at 100 °C gave only arabinose. (*ii*) 1,3,5-Tri-*O*-benzoyl-β-L-arabinofuranose (12). (*iii*) 2,3,5-Tri-*O*-benzoyl-α-L-arabinofuranosyl bromide. (*iv*) Benzyl 3,4-*O*-isopropylidene-β-L-arabinopyranoside. (*v*) Benzyl 2-*O*-(2,3,5-tri-*O*-benzoyl-α-L-arabinofuranosyl)-β-L-arabinopyranoside (800 mg). This product did not crystallize, but was homogeneous on t.l.c. De-*O*-benzoylation gave benzyl 2-*O*-α-L-arabinofuranosyl-β-L-arabinopyranoside (175 mg) which on recrystallization from ethyl acetate had m.p. 144–145 °C, $[\alpha]_D$ +91° (*c*, 1.0).

Anal. Calcd. for $C_{17}H_{24}O_9$ (mol. wt., 372): C, 54.8; H, 6.5. Found (mol. wt., 370): C, 54.5; H, 6.3.

Hydrolysis gave only arabinose. After 30 h, the consumption of periodate was constant at 2.03 mole/mole $C_{17}H_{24}O_9$. The benzyl glycoside (40 mg) was hydrogenated in ethanol (5 ml) at room temperature for 36 h over 10% palladium on carbon (20 mg). The syrupy de-*O*-benzylated product (27 mg) had $[\alpha]_D$ −8.5° (*c*, 1.4), and paper chromatographic examination in solvent (*a*) showed it to have the same mobility as the β isomer. The disaccharide was not detected on paper chromatograms on spraying them with 2,5-diphenyl-3-(4-styrylphenyl)-tetrazolium chloride solution (24) under conditions in which arabinose was clearly distinguishable.

Acknowledgments

The authors thank Dr. H. O. Fowler for the gift of the *Acacia nilotica* gum and the National Research Council of Canada for financial assistance (N.R.C. T-19).

1. D. M. W. Anderson and K. A. Karamalla. J Chem. Soc. C, 762 (1966); Carbohydrate Res. **2**, 403 (1966).
2. D. M. W. Anderson, Sir Edmund Hirst, and J. F. Stoddart. J. Chem. Soc. C, 1476 (1967).
3. G. O. Aspinall, E. L. Hirst, and A. Nicolson. J. Chem. Soc. 1697 (1959).
4. M. Kaplan and A. M. Stephen. Tetrahedron, **23**, 193 (1967). A. M. Stephen and D. C. Vogt. Tetrahedron, **23**, 1473 (1967).
5. E. V. White. J. Am. Chem. Soc. **68**, 272 (1946). I. J. Cunneen and F. Smith. J. Chem. Soc. 1146 (1948).
6. J. F. Stoddart and J. K. N. Jones. Carbohydrate Res. To be published.
7. A. M. Stephen, M. Kaplan, G. L. Taylor, and E. C. Leisegang. Tetrahedron, Suppl. No. 7, 233 (1966).
8. G. O. Aspinall and J. Baillie. J. Chem. Soc. 1714 (1963).
9. F. Smith and R. Montgomery. The chemistry of plant gums and mucilages. Reinhold Publishing Corp., New York. 1959.
10. A. S. Markowitz and J. R. Henderson. Nature, **181**, 771 (1958).
11. K. Wallenfels. Naturwissenschaften, **37**, 491 (1950).
12. R. N. Ness and H. G. Fletcher, Jr. J. Am. Chem. Soc. **80**, 2007 (1958).
13. C. E. Ballou. J. Am. Chem. Soc. **57**, 165 (1957).
14. R. W. Bailey. Oligosaccharides. Pergamon Press, Ltd., New York. 1965. p.42.
15. L. Hough, J. K. N. Jones, and W. H. Wadman. J. Chem. Soc. 1702 (1950).
16. W. E. Trevelyan, D. P. Proctor, and J. S. Harrison Nature, **166**, 444 (1950).
17. G. O. Aspinall. J. Chem. Soc. 1676 (1963).
18. J. K. N. Jones, R. A. Wall, and A. O. Pittet. Can. J. Chem. **38**, 2285 (1960).
19. R. Kuhn, H. Trischmann, and I. Löw. Agew. Chem. **67**, 32 (1955).
20. G. O. Aspinall and R. J. Ferrier. Chem. and Ind. (London), 1216 (1957).
21. E. H. Sloane-Stanley. Biochem. J. **73**, 8P (1959).
22. J. F. O'Dea and R. A. Gibbons. Biochem. J. **55**, 580 (1953).
23. P. A. Andrews, D. H. Ball, and J. K. N. Jones. J. Chem. Soc. 4090 (1953).
24. J. S. D. Bacon. Biochem. J. **73**, 507 (1959).

Rearrangement studies with ^{14}C. XXXII. Solvent effects in the solvolyses of 2-phenyl-1-^{14}C-ethyl tosylate and 2-phenyl-1-^{14}C-ethylmercuric perchlorate

C. C. Lee and R. J. Tewari

Department of Chemistry and Chemical Engineering, University of Saskatchewan, Saskatoon, Saskatchewan

Received February 19, 1968

The extents of isotope position rearrangement accompanying the solvolyses of 2-phenyl-1-^{14}C-ethyl bromide (I–Br), 2-phenyl-1-^{14}C-ethyl tosylate (I–OTs), and 2-phenyl-1-^{14}C-ethylmercuric perchlorate (I–$HgClO_4$), in three aqueous dioxane solvent pairs with different ionizing power Y were determined. No rearrangement was found for I–Br. For I–OTs and I–$HgClO_4$ the results are considered together with similar data previously obtained from ethanolysis, acetolysis, and formolysis. Linear correlations between log % rearrangement and Y are found for the solvolyses in ethanol and the aqueous dioxane solvent pairs. The mechanistic implications of these observations are discussed.

Canadian Journal of Chemistry, 46, 2314 (1968)

Can. J. Chem. Downloaded from www.nrcresearchpress.com by 210.87.254.40 on 09/05/12
For personal use only.

The isotope position rearrangements accompanying solvolyses of 2-phenyl-1-^{14}C-ethyl tosylate (I–OTs) and of 2-phenyl-1-^{14}C-ethylmercuric perchlorate (I–$HgClO_4$) in ethanol, acetic acid, and formic acid have been reported (1, 2). The solvents employed differed in both ionizing power and nucleophilic character. It is known that the Grunwald–Winstein mY correlation of solvolysis rates with "ionizing power" Y gave best fitting linear plots for solvent pairs of similar nucleophilic character (3, 4). In order to assess the effects of changes in ionizing power on the extent of isotopic rearrangements, solvolytic studies were carried out on I–OTs, I–$HgClO_4$, and 2-phenyl-1-^{14}C-ethyl bromide (I–Br) in three dioxane–water solvent pairs with different Y values.

The 2-phenylethanol obtained from solvolyses of I–OTs, I–$HgClO_4$, or I–Br in aqueous dioxane was oxidized to benzoic acid. The ^{14}C-activity in the benzoic acid measured the extent of rearrangement of the ^{14}C-label from C-1 to C-2. The solvolysis of I–Br in 30–70% dioxane gave a product which showed an essentially negligible amount of ^{14}C-position rearrangement of less than 0.2% in all cases. Apparently under these conditions, the reaction of I–Br likely has taken place by direct displacement. The results from the experiments with I–OTs and I–$HgClO_4$ are summarized in Table I. It is seen from Table I that for a given set of experimental conditions, the solvolysis of I–$HgClO_4$ gave more rearrangement than the solvolysis of I–OTs. As concluded earlier (2), in the heterolysis of the carbon–mercury bond of the 2-phenylethylmercuric ion,

TABLE I

Data from solvolyses of 2-phenyl-1-^{14}C-ethyl tosylate (I–OTs) and 2-phenyl-1-^{14}C-ethylmercuric perchlorate (I–$HgClO_4$) in aqueous dioxane

Compound solvolyzed	Solvent (% dioxane*)	Compound assayed†	Specific activity (c.p.m./mmole)‡		Rearrangement (%)	
			Run 1	Run 2	Run 1	Run 2
I–OTs	70, 50, 30	$PhCH_2CH_2OTs$	758 700	758 700		
	70	PhCOOH	21 240	24 280	2.8	3.2
	50	PhCOOH	53 870	51 590	7.1	6.8
	30	PhCOOH	155 500	160 800	20.5	21.2
I–$HgClO_4$	75	$PhCH_2CH_2HgOAc$	19 900	72 700		
	75	PhCOOH	2 800	10 900	14.1	15.0
	50, 30	$PhCH_2CH_2HgOAc$	65 340	65 340		
	50	PhCOOH	20 910	20 950	32.0	32.1
	30	PhCOOH	26 170	26 040	40.0	39.8

*X% dioxane means X volumes of dioxane plus 100 − X volumes of water at room temperature before mixing.

†Except in the solvolysis of I–$HgClO_4$ in 75% dioxane, the same batch of $PhCH_2{}^{14}CH_2OTs$ or $PhCH_2{}^{14}CH_2HgOAc$ was used in all experiments. In a number of runs, samples of the solvolysis product, 2-phenylethanol, were converted to the phenylurethan and found to have essentially the same specific activities as the corresponding starting materials.

‡Measured by a liquid scintillation counter.

TABLE II

Averaged ^{14}C-rearrangements observed in solvolyses of I–OTs and I–$HgClO_4$ in solvents of different ionizing power Y

Solvent	Y*	Rearrangement (%) I–OTs	Rearrangement (%) I–$HgClO_4$
C_2H_5OH	−2.03	0.3†	6.8‡
CH_3COOH	−1.64	5.5†	44.1‡
HCOOH	2.05	44.8†	45.0‡
90% HCOOH	2.22	40.5†	—
75% Dioxane	−0.40§	—	14.6
70% Dioxane	0.01	3.0	—
50% Dioxane	1.36	7.0	32.0
30% Dioxane	2.46	20.9	39.9

*From ref. 5.
†From Ref. 1.
‡From Ref. 2.
§Interpolated value, calculated from equation given in ref. 5.

metallic mercury is apparently a better leaving group than the tosylate ion in the solvolysis of 2-phenylethyl tosylate.

Collected in Table II are the mean values of known isotope position rearrangements observed in the various solvolytic studies on I–OTs and I–$HgClO_4$. The values of ionizing power Y for the solvents employed (5) are also included in Table II. When log % rearrangement is plotted against Y for I–OTs or I–$HgClO_4$, the data from solvolyses in ethanol and aqueous dioxane fit fairly well into a straight line, while the results for acetolysis and formolysis fall well outside of this linear plot. The slopes of these lines, to be designated m_R, would measure the sensitivity of isotope position rearrangements to changes in Y in ethanol and the aqueous dioxane solvent systems. The values of m_R are 0.40 and 0.17, respectively, for I–OTs and I–$HgClO_4$.

The linear correlation observed between log % rearrangement and Y for ethanol and aqueous dioxane is somewhat analogous to the Grunwald–Winstein mY correlation for solvolysis rates. The present findings, however, relate strictly not the reaction rates, but the amount of rearranged products formed, with changes in Y in ethanol and the aqueous dioxane solvent systems. The correlation can hold only up to the theoretical maximum rearrangement of 50%, whether the rearrangement is assumed to result from reaction proceeding through the ethylenephenonium ion or a pair of rapidly equilibrating 2-phenylethyl cations. The similarity between the presently observed relationship and the Grunwald–Winstein correlation of solvolysis rates suggest that the isotope position rearrangements observed in solvolyses of 2-phenyl-l-^{14}C-ethyl derivatives likely arose from kinetically controlled processes and is unlikely to have included, for example, any changes in the products resulting from such effects as the subsequent heating of the reaction mixture.

From the discussion of Streitwieser on solvolytic reactions (3) and from the work of Fainberg and Winstein (4), it is not surprising to note that the data from the acidic solvents, acetic acid and formic acid, do not fit into the same correlation line with those from ethanol and aqueous dioxane. Possibly, another straight line correlation might be obtained if results were available from studies with varying amounts of acetic acid and formic acid as a solvent pair with different Y values (4).

In solvolyses involving the 2-phenyl-l-^{14}C-ethyl system, as far as product formation is concerned the net results may be considered as arising from a unimolecular process with rate constant k_Δ *via* the ethylenephenonium ion, or its equivalent of a pair of rapidly equilibrating 2-phenylethyl cations, which would give rise to 50% ^{14}C-rearrangement, and a direct displacement process with specific rate constant k_s which would give a product without rearrangement (1, 6). When the contribution from the k_Δ component is high, much of the reaction would lead to products accompanied by rearrangement and the overall extent of rearrangement would be relatively insensitive to changes in Y. This is the case for acetolysis and formolysis of I–$HgClO_4$. For the solvolyses of I–$HgClO_4$ in the more nucleophilic ethanol and aqueous dioxane, k_s plays a more important role and the k_Δ component is found to show more variations as the ionizing power is changed ($m_R = 0.17$). In the solvolyses of I–OTs, the relative contribution of k_Δ is less than in the solvolyses of I–$HgClO_4$, as indicated by the greater extents of rearrangement in the latter system. The value of m_R for I–OTs is 0.40, greater than the corresponding m_R of 0.17 for I–$HgClO_4$. Apparently, when the k_Δ contribution is relatively low, an increase in Y would exert a relatively larger effect on the overall % rearrangement. Thus the rearrangement accompanying solvolyses of I–OTs in ethanol and aqueous dioxane is more sensitive to changes in Y than the solvolyses of I–$HgClO_4$ in these solvents.

Can. J. Chem. Downloaded from www.nrcresearchpress.com by 210.87.254.40 on 09/05/12
For personal use only.

Can. J. Chem. Downloaded from www.nrcresearchpress.com by 210.87.254.40 on 09/05/12
For personal use only.

Experimental

Preparations of the compounds solvolyzed were carried out as previously described for I–OTs (1), I–HgOAc (2), and I–Br (7).

The solvolyses were effected by placing 12.5 mmole of I–Br, I–OTs, or I–HgOAc plus an equimolar quantity of $HClO_4$ in 50 ml of the appropriate aqueous dioxane solvent-pair and then subjecting the solution to heating under reflux for 2 h in the reactions with I–OTs or I–$HgClO_4$ and for 12 h in the case of I–Br. The resulting reaction mixture was poured into ice-water, made alkaline by the addition of solid K_2CO_3 and then repeatedly extracted with ether. After drying over anhydrous $MgSO_4$, the ether was removed and the 2-phenylethanol recovered by distillation under reduced pressure, b.p. 100° at 10 mm, phenylurethan, m.p. 79–80° (lit. (8), m.p. 79–80°). The yield of alcohol obtained from the various runs ranged between 40 and 65%.

Degradation of the 2-phenylethanol to benzoic acid was effected by oxidation in alkaline $KMnO_4$ (8).

Acknowledgment

The financial support given by the National Research Council of Canada is gratefully acknowledged.

1. C. C. Lee, G. P. Slater, and J. W. T. Spinks. Can. J. Chem. **35**, 1417 (1957).
2. C. C. Lee and R. J. Tewari. Can. J. Chem. **45**, 2256 (1967).
3. A. Streitwieser, Jr. Chem. Rev. **56**, 571 (1956).
4. A. H. Fainberg and S. Winstein. J. Am. Chem. Soc. **79**, 1597, 1602, 1608 (1957).
5. A. H. Fainberg and S. Winstein. J. Am. Chem. Soc. **78**, 2770 (1956).
6. J. W. Clayton and C. C. Lee. Can. J. Chem. **39**, 1510 (1961).
7. D. P. Thornhill and C. C. Lee. Can. J. Chem. **41**, 2482 (1963).
8. C. C. Lee and J. W. T. Spinks. Can. J. Chem. **31**, 761 (1953).

Decomposition of a phosphoryl azide adduct of norbornylene

R. S. McDaniel and A. C. Oehlschlager[1]
Department of Chemistry, Simon Fraser University, Burnaby 2, British Columbia

Received March 4, 1968

The thermal decomposition of the diethyl phosphoryl azide adduct of norbornylene has been shown to proceed directly to the phosphoryl amidate, **5***a*. The aziridine **4***a* has been shown to be stable under the reaction conditions. Contrary to an earlier report, the product of the photolytic decomposition of the diethyl phosphoryl azide – norbornylene adduct is aziridine **4***a*.

Canadian Journal of Chemistry, **46**, 2316 (1968)

Organic azides **1** react readily with bicyclo-[2·2·1]heptene **2** via 1,3-dipolar cycloadditions (see refs. 1 and 2). The initial products of these reactions are usually 1,2,3-Δ^2-triazolines **3**; however, in cases where the reacting azide possesses a strong electron-withdrawing group the products of the thermal decomposition of the initially formed triazolines are isolated (3). The thermally induced decomposition of triazoline adducts of bicyclo[2·2·1]heptene gives predominantly aziridine **4** and imine **5** products (4). A few triazoline adducts have yielded, in addition, minor amounts of Wagner–Meerwein rearranged products (4*b*).

A survey of the literature reveals that the electron-withdrawing ability of the N-1 substituent also influences the proportion of aziridine product formed during the thermal decomposition. The data in Table I indicate that, in general, the stronger the electron-withdrawing ability of this group, the higher the proportion of aziridine product formed. The most apparent exception to this trend is the diethyl phosphonate substituent which is reported (4*d*) to give only the phosphorylated amidate **5***a*. A possible explanation for this observation is that the decomposition of the phosphorylated triazoline **3***a* leads initially to aziridine **4***a* which isomerizes under the reaction conditions to give the observed product. We have checked this possibility by independent synthesis of the phosphorylated aziridine **4***a* by two routes. Reaction of diethyl phosphorochloridate with the known (3*c*) aziridine (**4***b*) gave the desired product. The phosphorylated aziridine **4***a* was also produced in high yield by the photolysis (5) of the corresponding triazoline **3***a*.[2] The phosphorylated aziridine

[1]To whom inquiries should be addressed.

[2]K. D. Berlin and L. A. Wilson (5) previously encountered tars upon the exposure of **3***a* to ultraviolet light. The present photolysis appears to parallel Scheiner's (4*c*) results in similar systems, (R = *p*-Br—C_6H_4) in that the aziridine was produced cleanly.

Experimental

Preparations of the compounds solvolyzed were carried out as previously described for I–OTs (1), I–HgOAc (2), and I–Br (7).

The solvolyses were effected by placing 12.5 mmole of I–Br, I–OTs, or I–HgOAc plus an equimolar quantity of $HClO_4$ in 50 ml of the appropriate aqueous dioxane solvent-pair and then subjecting the solution to heating under reflux for 2 h in the reactions with I–OTs or I–$HgClO_4$ and for 12 h in the case of I–Br. The resulting reaction mixture was poured into ice-water, made alkaline by the addition of solid K_2CO_3 and then repeatedly extracted with ether. After drying over anhydrous $MgSO_4$, the ether was removed and the 2-phenylethanol recovered by distillation under reduced pressure, b.p. 100° at 10 mm, phenylurethan, m.p. 79–80° (lit. (8), m.p. 79–80°). The yield of alcohol obtained from the various runs ranged between 40 and 65%.

Degradation of the 2-phenylethanol to benzoic acid was effected by oxidation in alkaline $KMnO_4$ (8).

Acknowledgment

The financial support given by the National Research Council of Canada is gratefully acknowledged.

1. C. C. Lee, G. P. Slater, and J. W. T. Spinks. Can. J. Chem. **35**, 1417 (1957).
2. C. C. Lee and R. J. Tewari. Can. J. Chem. **45**, 2256 (1967).
3. A. Streitwieser, Jr. Chem. Rev. **56**, 571 (1956).
4. A. H. Fainberg and S. Winstein. J. Am. Chem. Soc. **79**, 1597, 1602, 1608 (1957).
5. A. H. Fainberg and S. Winstein. J. Am. Chem. Soc. **78**, 2770 (1956).
6. J. W. Clayton and C. C. Lee. Can. J. Chem. **39**, 1510 (1961).
7. D. P. Thornhill and C. C. Lee. Can. J. Chem. **41**, 2482 (1963).
8. C. C. Lee and J. W. T. Spinks. Can. J. Chem. **31**, 761 (1953).

Decomposition of a phosphoryl azide adduct of norbornylene

R. S. McDaniel and A. C. Oehlschlager[1]

Department of Chemistry, Simon Fraser University, Burnaby 2, British Columbia

Received March 4, 1968

The thermal decomposition of the diethyl phosphoryl azide adduct of norbornylene has been shown to proceed directly to the phosphoryl amidate, **5***a*. The aziridine **4***a* has been shown to be stable under the reaction conditions. Contrary to an earlier report, the product of the photolytic decomposition of the diethyl phosphoryl azide – norbornylene adduct is aziridine **4***a*.

Canadian Journal of Chemistry, 46, 2316 (1968)

Organic azides **1** react readily with bicyclo-[2·2·1]heptene **2** via 1,3-dipolar cycloadditions (see refs. 1 and 2). The initial products of these reactions are usually 1,2,3-Δ^2-triazolines **3**; however, in cases where the reacting azide possesses a strong electron-withdrawing group the products of the thermal decomposition of the initially formed triazolines are isolated (3). The thermally induced decomposition of triazoline adducts of bicyclo[2·2·1]heptene gives predominantly aziridine **4** and imine **5** products (4). A few triazoline adducts have yielded, in addition, minor amounts of Wagner–Meerwein rearranged products (4*b*).

A survey of the literature reveals that the electron-withdrawing ability of the N-1 substituent also influences the proportion of aziridine product formed during the thermal decomposition. The data in Table I indicate that, in general, the stronger the electron-withdrawing ability of this group, the higher the proportion of aziridine product formed. The most apparent exception to this trend is the diethyl phosphonate substituent which is reported (4*d*) to give only the phosphorylated amidate **5***a*. A possible explanation for this observation is that the decomposition of the phosphorylated triazoline **3***a* leads initially to aziridine **4***a* which isomerizes under the reaction conditions to give the observed product. We have checked this possibility by independent synthesis of the phosphorylated aziridine **4***a* by two routes. Reaction of diethyl phosphorochloridate with the known (3*c*) aziridine (**4***b*) gave the desired product. The phosphorylated aziridine **4***a* was also produced in high yield by the photolysis (5) of the corresponding triazoline **3***a*.[2] The phosphorylated aziridine

[1]To whom inquiries should be addressed.

[2]K. D. Berlin and L. A. Wilson (5) previously encountered tars upon the exposure of **3***a* to ultraviolet light. The present photolysis appears to parallel Scheiner's (4*c*) results in similar systems, (R = *p*-Br—C_6H_4) in that the aziridine was produced cleanly.

Can. J. Chem. Downloaded from www.nrcresearchpress.com by 210.87.254.105 on 09/05/12
For personal use only.

TABLE I

Products of decomposition of azide norbornylene adducts

N-1 Substituent (R)	Triazoline decomposition temperature (°C)	Yield of products (%) Aziridine	Imine	Reference
C_6H_5	160	60	20	4*a*
p-Br—C_6H_4	171	53	20	4*c*
$(C_2H_5O)_2P(=O)$—	108	Trace*	95	4*d*
$CH_3OC(=O)$—	71	40	55	4*b*
$C_6H_5C(=O)$—	40	‡		4*a*
N≡C—	†	‡		3*b*
p-$CH_3C_6H_4SO_2$	†	88	6–9	4*a*
$C_6H_5SO_2$	†	79	Some	3*c*
2,4,6$(NO_2)_3C_6H_2$	†	‡		3*e*

*See Experimental.
†The decomposition occurred spontaneously at room temperature.
‡Only the aziridine was isolated and no imine was detected.

is stable in benzene solution at temperatures above 200 °C (sealed tube) for two days. These conditions are much more drastic than those necessary for the thermal decomposition of the phosphorylated triazoline. Thus the phosphoryl amidate **5***a* is not derived from rearrangement of initially formed phosphorylated aziridine **7***a*. The decomposition of a phosphoryl azide adduct of norbornylene can be represented as follows.

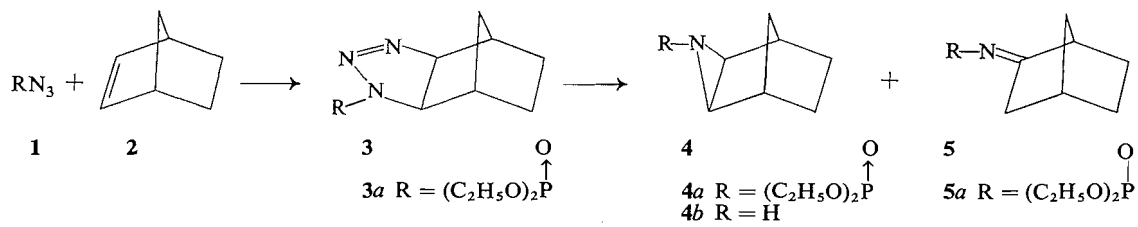

1 **2** **3** **4** **5**

3*a* R = $(C_2H_5O)_2P(=O)$—

4*a* R = $(C_2H_5O)_2P(=O)$—
4*b* R = H

5*a* R = $(C_2H_5O)_2P(=O)$—

Experimental

Carbon, hydrogen, and nitrogen analyses were performed by Alfred Bernhardt, Microanalytical Laboratory, Mulheim, West Germany. Infrared (i.r.) spectra were obtained with a Unicam SP-200 or a Beckman IR-12 spectrophotometer. Deuteriochloroform was used as the solvent and line positions are reported as δ units using tetramethylsilane as an internal standard (δ = 0). Boiling points are uncorrected.

Synthesis of 3-Diethyl Phosphoryl-3-azatricyclo-(3·2·1·0^{2,4})-octane 4a

A solution of 0.5 g of **4***b*, prepared as previously described (3*c*) in 5 ml of triethylamine, was treated with 0.5 ml of diethyl phosphorochloridate. The solution was refluxed for 20 min after which time water and ether were added. The ether layer was separated, dried ($MgSO_4$), and evaporated to give 0.74 g of oil. The ether extract was chromatographed on 15 g of silica gel. Elution with ether gave 0.632 g (56%) of **4***a*; b.p. 110 °C (0.1 mm); i.r. (film) 1260 (P = O), 1160, and 1050 cm^{-1} (P—O—C); n.m.r. δ 4.02 (m, 4, O—*CH*—CH_3), 2.52 (d, 2H, *J* = 11.3, N—C—*H*)[3], 2.15 (m, 2, bridgehead), 1.50 (d, 1H, *J* = 9.7, *syn* C-8), 1.14 (6, O—CH_2—CH_3), 1.03 m, 4, C-6, C-7) and 0.47 (d, 1H, *J* = 9.7, *anti* C-8).

Anal. Calcd. for $C_{11}H_{20}NPO_3$: C, 53.83; H, 8.22; N, 5.71. Found: C, 53.76; H, 8.08; N, 5.92.

Photolysis of the Phosphorylated Triazoline 3a

A solution of 1 g of triazoline, **3***a* in 200 ml of dry ether was photolyzed under nitrogen for 2 h with a 250 W Hanovia medium pressure mercury lamp (quartz vessel). Analysis of the reaction mixture obtained after evaporation of the ether, revealed that the conversion of triazoline to aziridine **4***a* occurred in high yield (>90%). The aziridine was identified by comparison of its i.r. and nuclear magnetic resonance (n.m.r.) spectra with the sample prepared as described above.

[3]This coupling is that expected for P—N—C—H coupling for a phosphorylated aziridine (6).

Can. J. Chem. Downloaded from www.nrcresearchpress.com by 210.87.254.105 on 09/05/12
For personal use only.

Detection of Aziridine 4a in the Pyrolysis Mixture of the Triazoline 3a

A solution of 1.0 g of the phosphoryl triazoline (4*d*) **3***a* in xylene was heated at reflux for 7 h. The reaction mixture remaining after removal of the xylene was analyzed by thin-layer chromatography. Two components were detected, one of which was identical to the phosphoryl amidate **5***a*, and the other to the aziridine **4***a*.

Attempted Pyrolysis of the Phosphorylated Aziridine 4a

A solution (15 w/w) of the aziridine **4***a* in benzene was heated in a sealed n.m.r. tube for two days at temperatures between 200 and 220 °C. The sample was periodically cooled to room temperature and the n.m.r. spectra of the solution recorded. No change in intensity or chemical shift of the protons was noted during this time.

Acknowledgments

We wish to thank the Simon Fraser University Research Fund and the National Research Council of Canada for generous financial support. We also wish to thank Dr. K. D. Berlin of Oklahoma State University, Stillwater, Oklahoma, for several discussions.

1. R. Huisgen, R. Grashey, and J. Saver. *In* The chemistry of alkenes. Chapt. 11. *Edited by* S. Pataai. Interscience Publishers, Inc., New York. 1964.
2. A. S. Bailey and J. E. White. J. Chem. Soc. (B) 819 (1966).
3. (*a*) A. C. Oehlschlager and L. H. Zalkow. J. Org. Chem. **30**, 4205 (1965); (*b*) A. G. Anastassiou, H. E. Simmons, and F. D. Marsh. J. Am. Chem. Soc. **87**, 2296 (1965); (*c*) L. H. Zalkow, A. C. Oehlschlager, G. A. Cabat, and R. L. Hale. Chem. and Ind. London, 1556 (1964); (*d*) L. H. Zalkow and A. C. Oehlschlager. J. Org. Chem. **28**, 3303 (1963); (*e*) A. S. Bailey and J. E. White. Chem. and Ind. London, 1628 (1965).
4. (*a*) R. Huisgen, L. Moebius, G. Mueller, H. Stangl, G. Szeimes, and J. M. Vernon. Chem. Ber. **98**, 3992 (1965); (*b*) A. C. Oehlschlager, P. Tillman, and L. H. Zalkow. Chem. Commun. 596 (1965); (*c*) P. Scheiner. J. Org. Chem. **30**, 7 (1965); (*d*) K. D. Berlin, L. A. Wilson, and L. M. Raff. Tetrahedron, **23**, 965 (1967).
5. K. D. Berlin and L. A. Wilson. Chem. Commun. 280, (1965).
6. F. A. L. Anet, R. D. Trepka, and D. J. Cram. J. Am. Chem. Soc. **89**, 357 (1967).

Synthesis of oxytocin using the solid phase technique

D. A. J. Ives

Connaught Medical Research Laboratories, University of Toronto, Toronto, Ontario

Received February 2, 1968

This communication reports the synthesis of oxytocin using the Merrifield solid phase technique. For the synthesis, both the *o*-nitrophenyl sulfenyl and *t*-butyloxycarbonyl blocking groups were used for masking the amino function. The oxytocin precursor obtained gave the same yield of hormone when subjected to the usual procedures as that obtained from a nonapeptide synthesized by conventional methods.

Canadian Journal of Chemistry, 46, 2318 (1968)

The solid phase method of peptide synthesis was first introduced by Merrifield (1) and has been successfully used to obtain a number of biologically active peptides (e.g. 2, 3) of varying size, the most interesting being the synthesis of the A & B chains of insulin (4). So far the syntheses of the hormonal peptide oxytocin has not been reported and this communication describes the solid phase synthesis of the protected nonapeptide Z-(S-Bzl)-Cys-Tyr(Bzl)-Ile-Gln-Asn-(S-Bzl)-Cys-Pro-Leu-GlyNH_2, a precursor to oxytocin.

Because of their relative ease of preparation, it was decided to use the *o*-nitrophenyl sulfenyl (NPS) derivatives of the amino acids rather than the *t*-butyloxycarbonyl (*t*-BOC) compounds. The NPS derivatives were made according to Zervas *et al.* (5) and stored as their dicyclohexylamine (DCHA) salts because of the instability of the free compounds. The melting point found for NPS-L-proline DCHA salt was 176–178 °C, rather than the 151–154 °C reported by Zervas; however, the rotation of $[\alpha]_D = -43$ was identical with the value found by the previous workers.

The normal method of coupling the amino acids to the peptide chain in the solid phase method is by the use of dicyclohexylcarbodiimide; however, this reagent cannot be used with glutamine or asparagine derivatives because of excess side reactions. Thus the NPS derivatives of these two amino acids were converted to their *p*-nitrophenyl esters by a modification of the

Can. J. Chem. Downloaded from www.nrcresearchpress.com by 210.87.254.105 on 09/05/12
For personal use only.

Detection of Aziridine 4a in the Pyrolysis Mixture of the Triazoline 3a

A solution of 1.0 g of the phosphoryl triazoline (4*d*) **3***a* in xylene was heated at reflux for 7 h. The reaction mixture remaining after removal of the xylene was analyzed by thin-layer chromatography. Two components were detected, one of which was identical to the phosphoryl amidate **5***a*, and the other to the aziridine **4***a*.

Attempted Pyrolysis of the Phosphorylated Aziridine 4a

A solution (15 w/w) of the aziridine **4***a* in benzene was heated in a sealed n.m.r. tube for two days at temperatures between 200 and 220 °C. The sample was periodically cooled to room temperature and the n.m.r. spectra of the solution recorded. No change in intensity or chemical shift of the protons was noted during this time.

Acknowledgments

We wish to thank the Simon Fraser University Research Fund and the National Research Council of Canada for generous financial support. We also wish to thank Dr. K. D. Berlin of Oklahoma State University, Stillwater, Oklahoma, for several discussions.

1. R. Huisgen, R. Grashey, and J. Saver. *In* The chemistry of alkenes. Chapt. 11. *Edited by* S. Pataai. Interscience Publishers, Inc., New York. 1964.
2. A. S. Bailey and J. E. White. J. Chem. Soc. (B) 819 (1966).
3. (*a*) A. C. Oehlschlager and L. H. Zalkow. J. Org. Chem. **30**, 4205 (1965); (*b*) A. G. Anastassiou, H. E. Simmons, and F. D. Marsh. J. Am. Chem. Soc. **87**, 2296 (1965); (*c*) L. H. Zalkow, A. C. Oehlschlager, G. A. Cabat, and R. L. Hale. Chem. and Ind. London, 1556 (1964); (*d*) L. H. Zalkow and A. C. Oehlschlager. J. Org. Chem. **28**, 3303 (1963); (*e*) A. S. Bailey and J. E. White. Chem. and Ind. London, 1628 (1965).
4. (*a*) R. Huisgen, L. Moebius, G. Mueller, H. Stangl, G. Szeimes, and J. M. Vernon. Chem. Ber. **98**, 3992 (1965); (*b*) A. C. Oehlschlager, P. Tillman, and L. H. Zalkow. Chem. Commun. 596 (1965); (*c*) P. Scheiner. J. Org. Chem. **30**, 7 (1965); (*d*) K. D. Berlin, L. A. Wilson, and L. M. Raff. Tetrahedron, **23**, 965 (1967).
5. K. D. Berlin and L. A. Wilson. Chem. Commun. 280, (1965).
6. F. A. L. Anet, R. D. Trepka, and D. J. Cram. J. Am. Chem. Soc. **89**, 357 (1967).

Synthesis of oxytocin using the solid phase technique

D. A. J. Ives

Connaught Medical Research Laboratories, University of Toronto, Toronto, Ontario

Received February 2, 1968

This communication reports the synthesis of oxytocin using the Merrifield solid phase technique. For the synthesis, both the *o*-nitrophenyl sulfenyl and *t*-butyloxycarbonyl blocking groups were used for masking the amino function. The oxytocin precursor obtained gave the same yield of hormone when subjected to the usual procedures as that obtained from a nonapeptide synthesized by conventional methods.

Canadian Journal of Chemistry, 46, 2318 (1968)

The solid phase method of peptide synthesis was first introduced by Merrifield (1) and has been successfully used to obtain a number of biologically active peptides (e.g. 2, 3) of varying size, the most interesting being the synthesis of the A & B chains of insulin (4). So far the syntheses of the hormonal peptide oxytocin has not been reported and this communication describes the solid phase synthesis of the protected nonapeptide Z-(S-Bzl)-Cys-Tyr(Bzl)-Ile-Gln-Asn-(S-Bzl)-Cys-Pro-Leu-GlyNH_2, a precursor to oxytocin.

Because of their relative ease of preparation, it was decided to use the *o*-nitrophenyl sulfenyl (NPS) derivatives of the amino acids rather than the *t*-butyloxycarbonyl (*t*-BOC) compounds. The NPS derivatives were made according to Zervas *et al.* (5) and stored as their dicyclohexylamine (DCHA) salts because of the instability of the free compounds. The melting point found for NPS-L-proline DCHA salt was 176–178 °C, rather than the 151–154 °C reported by Zervas; however, the rotation of $[\alpha]_D = -43$ was identical with the value found by the previous workers.

The normal method of coupling the amino acids to the peptide chain in the solid phase method is by the use of dicyclohexylcarbodiimide; however, this reagent cannot be used with glutamine or asparagine derivatives because of excess side reactions. Thus the NPS derivatives of these two amino acids were converted to their *p*-nitrophenyl esters by a modification of the

Can. J. Chem. Downloaded from www.nrcresearchpress.com by 210.87.254.5 on 09/05/12
For personal use only.

Can. J. Chem. Downloaded from www.nrcresearchpress.com by 210.87.254.5 on 09/05/12
For personal use only.

method of Elliot & Russel (6) and the resulting active esters used in the synthesis. The glutamine derivative could not be obtained crystalline and was used as an oil.

The methodology used in the solid phase synthesis of the nonapeptide was essentially that of Merrifield in the synthesis of bradykinyl-bradykinin (7), except that the active ester couplings were performed in dimethylformamide rather than chloroform and were run overnight. To increase stability, the *N*-terminal cysteine was added as its *N*-carbobenzoxy (*N*-CBZ) derivative rather than the *N*-NPS compound. The protected nonapeptide was removed from the resin by ammonolysis in dimethylformamide/methanol overnight, the solution precipitated with ethyl acetate and the precipitate washed free of contaminants. When the resulting material was treated with sodium in liquid ammonia, the ammonia removed under vacuum, and the product oxidized by passing air through a solution at pH 7 (8), the final solution gave an oxytocic activity comparable to that obtained from protected nonapeptide synthesized by the active ester technique (9).

The crude oxytocin obtained from freeze-drying the oxidized solution had an activity of approximately 100 u/mg and, when purified by gel filtration on G.25 followed by partition chromatography also on G.25 (10), a material with a potency of 508 u/mg could be obtained. Synthetic oxytocin by other methods has been found to have a potency in the range of 510–520 u/mg.

Using essentially the same technique, the same protected nonapeptide was obtained using the *t*-BOC derivatives rather than the NPS materials. Again the *N*-terminal cysteine was added as the *N*-CBZ derivative. On reduction and oxidation as before, an equally active solution was obtained.

Experimental

O-Nitrosulfenyl Amino Acids

The amino acid (0.02 mole) was dissolved in 2 *N* sodium hydroxide (10 ml) and dioxane (25 ml). NPS-Chloride (11) (4.2 g) and 2 *N* sodium hydroxide (11 ml) were added slowly over 15 min. The solution was stirred for a further 5 min, then diluted with water (200 ml) and filtered. The filtrate was acidified to pH 3.5–4.0 with 4 *N* HCl. At this point, the asparagine and glutamine derivatives were removed by filtration, washed, and dried. For the remaining derivatives, the acid mixture was extracted with ethyl acetate (120 ml); then, the organic layer was washed, dried, and evaporated to approximately 40 ml. Dicyclohexylamine (4 ml) was added and the solutions left in the refrigerator for a few hours. The melting points and rotations after filtering and recrystallization were the same as those recorded by Zervas, apart from NPS proline DCHA salt with m.p. = 176–178 °C rather than 151–154 °C.

NPS-Asparagine p-Nitrophenyl Ester

NPS-Asparagine (16.2 g) and *p*-nitrophenol (8.3 g) were dissolved in DMF (44 ml) and the solution cooled in ice. A solution of dicyclohexylcarbodiimide (12.9 g) in tetrahydrofuran (78 ml) was added slowly over a period of 1 h to the cooled solution with stirring. After the addition, the mixture was stirred for a further hour at 0 °C, then filtered and the precipitate was washed with a little tetrahydrofuran. The combined filtrates were reduced in volume, under vacuum, to approximately 80 ml and cooled in ice. Water (16 ml) was added and the mixture was stirred for 10 min in ice, then filtered. Water (80 ml) was added to the filtrate and the mixture left in the refrigerator overnight. The resulting precipitate was removed by filtration and recrystallized from methanol (approximately 500 ml) to give a light-yellow crystalline solid m.p. 152–154 °C, $[\alpha]_D = -116$, ($c = 1.8$ dimethylformamide); yield = 7.2 g.

NPS-Glutamine was treated similarly but would only give an oil.

Solid Phase Synthesis

NPS-Glycine was attached to the chlormethylated resin (1) as detailed by Merrifield. Analysis indicated that the resin had 0.71 mmole of glycine/g of resin. The amino acids were introduced onto the peptide-resin using the following schedule.

The peptide-resin was washed with chloroform, then shaken 10 min with a mixture of approximately 4 *N* HCl in dioxane (to remove the NPS group), then washed three times each with chloroform, dimethylformamide, ethanol, and chloroform. The resin was then treated with 10% triethylamine in chloroform to convert the peptide to the free base and washed three times with chloroform. The procedure thus far was the same whichever method was used to effect the peptide bond. Using dicyclohexylcarbodiimide, the resin was equilibrated with a chloroform solution (3 mole excess) of the NPS-amino acid for 10 min, then a solution of dicyclohexylcarbodiimide (equimolar to the NPS-derivative) was added to the mixture and was shaken for 2 h. The resin was then washed with chloroform, dimethylformamide, ethanol, and chloroform and was ready for the next cycle. For the active esters the resin was washed three times with dimethylformamide and then a dimethylformamide solution of the active ester (3 mole excess) was added and the mixture was shaken overnight. It was then washed with dimethylformamide, ethanol, and chloroform and was ready for the next cycle.

Removal of Nonapeptide from Resin

After the addition of the *N*-terminal Z-(S-Bzl)-cysteine, the resin (5 g) was shaken overnight with a mixture of dimethylformamide (20 ml) and methanol saturated with ammonia at 10 °C (20 ml). The mixture was filtered

and the resin was washed three times with dimethylformamide (20 ml). The combined filtrates were reduced under vacuum to approximately 50 ml and then ethyl acetate (400 ml) was added. The solution was left in the refrigerator for a few hours, then it was centrifuged. The resulting precipitate was washed with ethyl acetate and methanol (centrifuging after each wash) and finally it was suspended in ether (100 ml) and filtered. The precipitate was dried to give the protected nonapeptide (1.8 g) with m.p. = 234–238 °C $[\alpha]_D = -45$ ($c = 2$, dimethylformamide).

Purification of Oxytocin

The nonapeptide (0.5 g) was subjected to reduction with sodium and liquid ammonia, followed by oxidation at pH 7 (9) and the solution was freeze-dried. The product (0.6 g) was dissolved in 0.2 *N* acetic acid (10 ml) and was filtered through a Sephadex G.25 column, equilibrated with 0.2 *N* acetic acid and, using the same solvent as eluent, 5 ml fractions were collected and 0.1 ml samples used for the Folin–Lowry test. One major and several minor peptide peaks were observed. The contents of the tubes making up the fractions containing the major peak were lyophilized to give 0.4 g of white powder.

A Sephadex G.25 column was equilibrated with the aqueous phase of a mixture of 3.5% acetic acid (containing 1.5% pyridine): 1-butanol: benzene (2:1:1) and then the organic phase was run through. A solution of the partially purified oxytocin (100 mg) in the aqueous phase (2 ml) was added to the column, and then eluted with the organic phase. The fractions containing the major peptide peak (as determined by the Folin–Lowry reaction) were combined, diluted with twice their volume of water, and evaporated to a small volume. The solution was then freeze-dried to give a white powder (20 mg) having an activity of 508 u/mg.

Acknowledgments

The author would like to thank Dr. A. L. Tosoni for his interest and encouragement, and the Quality Control Department of the Connaught Laboratories for the biological assays.

Note added in proof—The author notes that M. Manning of McGill University has independently achieved the synthesis of oxytocin using the solid phase technique and has published the results in J. Am. Chem. Soc. **90**, 1348 (1968). (See also Takashima, du Vigneaud and Merrifield, J. Am. Chem. Soc. **90**, 1323 (1968) for the synthesis of deamino oxytocin.)

1. R. B. MERRIFIELD. J. Am. Chem. Soc. **85**, 2149 (1963).
2. R. B. MERRIFIELD. J. Am. Chem. Soc. **86**, 304 (1964).
3. M. BODANSZKY and J. T. SHEENAN. Chem. and Ind. 1597 (1966).
4. A. MARGLIN and R. B. MERRIFIELD. J. Am. Chem. Soc. **88**, 5051 (1966).
5. L. ZERVAS, D. BOROVAS, and E. GAZIS. J. Am. Chem. Soc. **85**, 3660 (1963).
6. D. F. ELLIOT and D. W. RUSSEL. Biochem. J. **66**, 49*P* (1957).
7. V. A. NAJJAR and R. B. MERRIFIELD. Biochemistry, **5**, 3765 (1966).
8. V. DU VIGNEAUD, C. RESSLER, J. M. SWAN. C. W. ROBERTS, P. G. KATSOYANNIS, and S. GORDON. J. Am. Chem. Soc. **75**, 4879 (1953).
9. V. DU VIGNEAUD and M. BODANSZKY. J. Am. Chem. Soc. **81**, 5688 (1959).
10. D. YAMASHIRO. Nature, 201, **76**, (1964).
11. M. H. HUBACHER. Org. Syntheses. Coll. Vol. II. John Wiley & Sons, Inc., New York. 1943. p. 455.

Synthesis of 5-methyl-8-hydroxy-1-tetralone

JOSEPH P. JOHN, R. K. NATARAJAN, S. SWAMINATHAN, AND P. S. VENKATARAMANI
Department of Organic Chemistry, University of Madras, Madras 25, India

Received September 19, 1967

The tetralone **2***a* has been obtained in 45% overall conversion from the dione **3** by the sequence **3** → **4***a* → **4***b* → **5***b* → **5***a* → **2***a*.

Canadian Journal of Chemistry, 46, 2320 (1968)

The title compound (**2***a*) has been reported (1) as a liquid obtained in low yields by prolonged reflux of the enol ketone (**1**) in xylene. We have obtained it as a crystalline solid, m.p. 47–48.5 °C by the following method, which has been studied previously by Newman and Mekler (2).

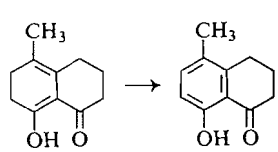

1 **2***a*

Can. J. Chem. Downloaded from www.nrcresearchpress.com by 210.87.254.5 on 09/05/12
For personal use only.

and the resin was washed three times with dimethylformamide (20 ml). The combined filtrates were reduced under vacuum to approximately 50 ml and then ethyl acetate (400 ml) was added. The solution was left in the refrigerator for a few hours, then it was centrifuged. The resulting precipitate was washed with ethyl acetate and methanol (centrifuging after each wash) and finally it was suspended in ether (100 ml) and filtered. The precipitate was dried to give the protected nonapeptide (1.8 g) with m.p. = 234–238 °C $[\alpha]_D = -45$ ($c = 2$, dimethylformamide).

Purification of Oxytocin

The nonapeptide (0.5 g) was subjected to reduction with sodium and liquid ammonia, followed by oxidation at pH 7 (9) and the solution was freeze-dried. The product (0.6 g) was dissolved in 0.2 *N* acetic acid (10 ml) and was filtered through a Sephadex G.25 column, equilibrated with 0.2 *N* acetic acid and, using the same solvent as eluent, 5 ml fractions were collected and 0.1 ml samples used for the Folin–Lowry test. One major and several minor peptide peaks were observed. The contents of the tubes making up the fractions containing the major peak were lyophilized to give 0.4 g of white powder.

A Sephadex G.25 column was equilibrated with the aqueous phase of a mixture of 3.5% acetic acid (containing 1.5% pyridine): 1-butanol: benzene (2:1:1) and then the organic phase was run through. A solution of the partially purified oxytocin (100 mg) in the aqueous phase (2 ml) was added to the column, and then eluted with the organic phase. The fractions containing the major peptide peak (as determined by the Folin–Lowry reaction) were combined, diluted with twice their volume of water, and evaporated to a small volume. The solution was then freeze-dried to give a white powder (20 mg) having an activity of 508 u/mg.

Acknowledgments

The author would like to thank Dr. A. L. Tosoni for his interest and encouragement, and the Quality Control Department of the Connaught Laboratories for the biological assays.

Note added in proof—The author notes that M. Manning of McGill University has independently achieved the synthesis of oxytocin using the solid phase technique and has published the results in J. Am. Chem. Soc. **90**, 1348 (1968). (See also Takashima, du Vigneaud and Merrifield, J. Am. Chem. Soc. **90**, 1323 (1968) for the synthesis of deamino oxytocin.)

1. R. B. MERRIFIELD. J. Am. Chem. Soc. **85**, 2149 (1963).
2. R. B. MERRIFIELD. J. Am. Chem. Soc. **86**, 304 (1964).
3. M. BODANSZKY and J. T. SHEENAN. Chem. and Ind. 1597 (1966).
4. A. MARGLIN and R. B. MERRIFIELD. J. Am. Chem. Soc. **88**, 5051 (1966).
5. L. ZERVAS, D. BOROVAS, and E. GAZIS. J. Am. Chem. Soc. **85**, 3660 (1963).
6. D. F. ELLIOT and D. W. RUSSEL. Biochem. J. **66**, 49*P* (1957).
7. V. A. NAJJAR and R. B. MERRIFIELD. Biochemistry, **5**, 3765 (1966).
8. V. DU VIGNEAUD, C. RESSLER, J. M. SWAN. C. W. ROBERTS, P. G. KATSOYANNIS, and S. GORDON. J. Am. Chem. Soc. **75**, 4879 (1953).
9. V. DU VIGNEAUD and M. BODANSZKY. J. Am. Chem. Soc. **81**, 5688 (1959).
10. D. YAMASHIRO. Nature, 201, **76**, (1964).
11. M. H. HUBACHER. Org. Syntheses. Coll. Vol. II. John Wiley & Sons, Inc., New York. 1943. p. 455.

Synthesis of 5-methyl-8-hydroxy-1-tetralone

JOSEPH P. JOHN, R. K. NATARAJAN, S. SWAMINATHAN, AND P. S. VENKATARAMANI
Department of Organic Chemistry, University of Madras, Madras 25, India

Received September 19, 1967

The tetralone **2***a* has been obtained in 45% overall conversion from the dione **3** by the sequence **3** → **4***a* → **4***b* → **5***b* → **5***a* → **2***a*.

Canadian Journal of Chemistry, 46, 2320 (1968)

The title compound (**2***a*) has been reported (1) as a liquid obtained in low yields by prolonged reflux of the enol ketone (**1**) in xylene. We have obtained it as a crystalline solid, m.p. 47–48.5 °C by the following method, which has been studied previously by Newman and Mekler (2).

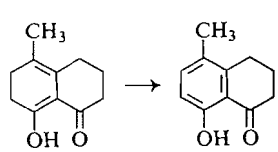

1 **2***a*

Can. J. Chem. Downloaded from www.nrcresearchpress.com by 210.87.254.105 on 09/05/12
For personal use only.

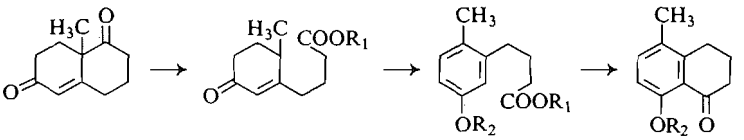

3 4*a*, $R_1 = H$ 4*b*, $R_1 = CH_3$ 5*a*, $R_1 = H$; $R_2 = H$ 5*b*, $R_1 = CH_3$; $R_2 = H$ 5*c*, $R_1 = CH_3$; $R_2 = —Ac$ 5*d*, $R_1 = H$; $R_2 = —Ac$ 2*a*, $R_2 = H$ 2*b*, $R_2 = —Ac$

The above authors obtained the acetate ester (**5***c*) from the dione (**3**) by a sequence of steps involving cleavage of **3** to the acid (**4***a*), esterification, enol acetylation of **4***b*, bromination and dehydrobromination. We have obtained the desired acid (**5***a*) by saponification of the ester (**5***c*) but the overall yields were unsatisfactory. We find now that the ester (**4***b*) can be catalytically dehydrogenated to the phenolic ester (**5***b*) directly and then saponified to give 50% overall yield of **5***a* based on **3**. Several reagents were tried to effect the cyclization of the acid (**5***a*), and polyphosphoric acid proved singularly effective giving 85–90% yield of the tetralone (**2***a*) which had the expected spectral absorptions. The structure of **2***a* was also confirmed by a Wolff–Kishner reduction to the known 4-methyl-ar-1-tetralol (3). This gave excellent yields.

Experimental

γ-(3-Keto-6-methyl-1-cyclohexen-1-yl)butyric Acid (4a)

The following procedure for cleavage of the dione (**3**) to the acid (**4***a*) proved superior to the one described in the literature (2).

The dione (**3**) (40 g) (4) was mixed with a saturated solution of barium hydroxide (1500 ml) in an atmosphere of nitrogen, the mixture was kept overnight and then extracted with ether to remove any unreacted dione. The aqueous solution was acidified and extracted with ether. After usual work-up, an oil was obtained which soon solidified. It was triturated with ether and collected; yield, 40–41 g; m.p. 78–79 °C. (ether – petroleum ether).

The crude acid was converted to the methyl ester (**4***a*) as described in ref. 2.

Methyl-γ-(2-methyl-5-hydroxyphenyl) butyrate (5b)

The ester (**4***a*) (15g) was heated at 280–300 °C with a 10% Pd/C catalyst (1g) for 1h. After usual work-up, 11 g (94%) of the phenolic ester (**5***b*) was obtained; m.p. 80–81 °C (petroleum ether) and undepressed by a sample prepared according to Newman and Mekler (2). Below 280 °C, the above dehydrogenation was incomplete and gave a mixture **4***a* and **5***b*.

γ-(2-Methyl-5-hydroxyphenyl)butyric Acid (5a)

The ester (**5***b*) (30g) was saponified with 5% aqueous sodium hydroxide and after usual work-up yielded 22 g (50% yield based on the dione **3**) of crude acid (**5***a*), m.p. 90–93 °C. The analytical sample prepared by four crystallizations from ether – petroleum ether had m.p. 99–100 °C. λ_{max} ($CHCl_3$) 2.75 and 5.85 μ; λ_{max} (EtOH) 279 mμ (log ε 3.4).

Anal. Calcd. for $C_{11}H_{14}O_3$: C, 68.0; H, 7.2. Found: C, 67.9; H, 7.4.

The same acid could be obtained by saponification of the ester (**5***c*) (2) but only in 30% yield based on the dione (**3**).

γ-(2-Methyl-5-acetoxyphenyl)butyric Acid (5d)

This was obtained in 60% yield by treatment of **5***a* with acetic anhydride and *p*-toluenesulfonic acid; m.p. 60–61.5 °C (petroleum ether); λ_{max} (EtOH) 216, 266, and 273 mμ (log ε 3.66, 2.70, 2.70); λ_{max} ($CHCl_3$) 5.71 and 5.85 μ nuclear magnetic resonance (CCl_4): τ −1.67 (s, —COOH), τ 7.73 and 7.8 (s, ar—CH_3 and —$OCOCH_3$) τ 2.92–3.33 (m, 3 aromatic protons) τ 7.37 to 7.63 (t, Ar—CH_2).

Anal. Calcd. for $C_{13}H_{16}O_4$: C, 66.1; H, 6.8. Found: C, 66.3; H, 6.9

The acetoxy acid (**5***d*) furnished a liquid acid chloride which was characterized as the amide m.p. 117–118 °C (ethylacetate). λ_{max} (KBr) 2.975, 3.125, 6.025, and 6.25μ.

Anal. Calcd. for $C_{11}H_{15}O_2N$: C, 68.4; H, 7.8. Found: C, 68.3; H, 8.0.

5-Methyl-8-hydroxy-1-tetralone (2a)

A mixture of phosphorus pentoxide (30 g) and phosphoric acid (30 ml) was heated on a steam bath for 2 h. The acid (**5***a*) (8 g) was added and the resulting mixture was heated for an additional 1 h and poured onto crushed ice. The yellow product was collected, dried, and crystallized from petroleum ether after treatment with decolorizing charcoal. This method yielded 6.2 g (86%) of the tetralone **2***a* as pale-yellow needles; m.p. 45–47 °C. An analytically pure sample prepared by three more crystallizations had m.p. 47–48.5 °C; λ_{max} ($CHCl_3$) 6.15 (hydrogen bonded C=O) and 6.25μ (aromatic) and no absorption for —OH due to hydrogen bonding. λ_{max} (EtOH) 262, 345 mμ (log ε 4.0, 3.5) [cf.: with absorptions of 8-hydroxy-1-tetralone (5)] nuclear magnetic resonance ($CDCl_3$): τ – 2.4 (s, —OH), τ 2.70 and 3.25 (d, 2 adjacent aromatic protons), τ 7.1–7.5 (m, 2 benzylic protons and 2 protons α to carbonyl) τ 7.8 (s, Ar—CH_3) and τ 7.92 (m, 2 protons β to carbonyl).

Anal. Calcd. for $C_{11}H_{12}O_2$: C, 75.0; H, 6.9. Found: C, 74.9; H, 7.2

The 2,4-dinitrophenylhydrazone had m.p. 285–286 °C (EtOAC—$CHCl_3$).

Can. J. Chem. Downloaded from www.nrcresearchpress.com by 210.87.254.105 on 09/05/12
For personal use only.

Anal. Calcd. for $C_{17}H_{16}N_4O_5$: C, 57.3; H, 4.5. Found: C, 57.0; H, 4.2.

The tetralone (**2***a*) furnished 5-methyl-8-acetoxy-1-tetralone (**2***b*) on treatment with acetic anhydride and *p*-toluenesulfonic acid; m.p. 121.4–122.4 °C (benzene–petroleum ether); λ_{max} ($CHCl_3$) 5.70 (—OAC), 5.975 (ketone C=O), 6.3 (aromatic), and 6.85 μ.

Anal. Calcd. for $C_{13}H_{14}O_3$: C, 71.5; H, 6.5. Found: C, 71.8; H, 6.7.

Acknowledgments

The authors wish to thank Mr. R. Balasubramanian for analysis and infrared spectra and Dr. T. R. Govindachari for providing the nuclear magnetic resonance spectra. R. K. Natarajan is grateful to the Council of Scientific and Industrial Research, New Delhi for financial support. J. P. John and P. S. Venkataramani thank the University Grants Commission, New Delhi for the award of fellowships.

1. M. S. NEWMAN and A. B. MEKLER. J. Am. Chem. Soc. **82**, 4039 (1960).
2. M. S. NEWMAN and A. B. MEKLER. J. Org. Chem. **26**, 336 (1961).
3. R. B. WOODWARD and T. SINGH. J. Am. Chem. Soc. **72**, 500 (1950).
4. M. S. NEWMAN and S. RAMACHANDRAN. Org. Syntheses, **41**, 38 (1961).
5. F. A. HOCHSTEIN, C. R. STEPHENS, L. H. CANOVER, P. R. REGNA, R. PASTERNACK, P. N. GORDON, F. J. PILGRIM, K. J. BRUNINGS, and R. B. WOODWARD, J. Am. Chem. Soc. **75**, 5455 (1953).

Oxidative fragmentation of 3-pyrazolidinones to olefins

R. H. KENT AND J.-P. ANSELME[1]

Department of Chemistry, University of Massachusetts, Boston, Massachusetts 02116

Received January 22, 1968

The oxidation of 5-aryl-3-pyrazolidinones with mercuric oxide to the corresponding olefins is reported. Diethyl azodicarboxylate also converts 4,5-diphenyl-3-pyrazolidinone to *trans*-stilbene. The fragmentation of the intermediate cyclic α-carbonyl azo compounds is suggested to account for the observed products.

Canadian Journal of Chemistry, **46**, 2322 (1968)

The chemistry of l-pyrazolines has been the subject of increased investigation over the last few years (1). As part of our own interest in this general area, we have examined the oxidation of 3-pyrazolidinones (**1**) and we should like to report briefly our initial results.

When 5-phenyl-3-pyrazolidinone (**1**, Ar = C_6H_5, R = H) was oxidized with yellow mercuric oxide, the grayish color of mercury was observed along with vigorous evolution of gas. After removal of mercury and evaporation of the solvent, a thick greenish oil, having the odor of styrene, was obtained. Bromination of this oil gave a 42% yield of styrene dibromide, m.p. 71–73 °C. The oxidation of 4,5-diaryl-3-pyrazolidinones (**1**, R = Ar) gave the corresponding *trans*-stilbenes (**3**, R = Ar) in fair to good yields (see Table I). No attempts were made to obtain the highest possible yields.

In a recent review (2), Fahr and Lind have emphasized the extreme instability of cyclic α-carbonyl azo compounds. We believe that the initial step in our reaction is the oxidation of the 3-pyrazolidinones (**1**) to the corresponding α-carbonyl azo compounds (**2**). These highly reactive intermediates then undergo fragmentation (3) with the loss of carbon monoxide and nitrogen to give the olefins.[2] The formation of metallic mercury and a positive carbon monoxide test from the evolved gases, lend support to this view.

A related fragmentation has been previously observed by Rosenblum and his students (4). They reported the formation of *trans*-stilbene and tolan, from the oxidation of 5,6-diphenyltetrahydroöxadiazinone (**4**) and 5,6-diphenyl-1,2-dihydroöxadiazinone (**5**) with lead tetraacetate.

Presumably, similar azo compounds were formed and underwent fragmentation with loss of carbon dioxide and nitrogen. Although the

[1]To whom all correspondence should be addressed.

[2]Approximately nine months after our initial discovery of the oxidation of 3-pyrazolidinones with mercuric oxide, the lead tetraacetate oxidation of 4,5-diphenyl-3-pyrazolidinone to *trans*-stilbene was reported (12).

Can. J. Chem. Downloaded from www.nrcresearchpress.com by 210.87.254.105 on 09/05/12
For personal use only.

Anal. Calcd. for $C_{17}H_{16}N_4O_5$: C, 57.3; H, 4.5. Found: C, 57.0; H, 4.2.

The tetralone (**2***a*) furnished 5-methyl-8-acetoxy-1-tetralone (**2***b*) on treatment with acetic anhydride and *p*-toluenesulfonic acid; m.p. 121.4–122.4 °C (benzene–petroleum ether); λ_{max} ($CHCl_3$) 5.70 (—OAC), 5.975 (ketone C=O), 6.3 (aromatic), and 6.85 μ.

Anal. Calcd. for $C_{13}H_{14}O_3$: C, 71.5; H, 6.5. Found: C, 71.8; H, 6.7.

Acknowledgments

The authors wish to thank Mr. R. Balasubramanian for analysis and infrared spectra and Dr. T. R. Govindachari for providing the nuclear magnetic resonance spectra. R. K. Natarajan is grateful to the Council of Scientific and Industrial Research, New Delhi for financial support. J. P. John and P. S. Venkataramani thank the University Grants Commission, New Delhi for the award of fellowships.

1. M. S. NEWMAN and A. B. MEKLER. J. Am. Chem. Soc. **82**, 4039 (1960).
2. M. S. NEWMAN and A. B. MEKLER. J. Org. Chem. **26**, 336 (1961).
3. R. B. WOODWARD and T. SINGH. J. Am. Chem. Soc. **72**, 500 (1950).
4. M. S. NEWMAN and S. RAMACHANDRAN. Org. Syntheses, **41**, 38 (1961).
5. F. A. HOCHSTEIN, C. R. STEPHENS, L. H. CANOVER, P. R. REGNA, R. PASTERNACK, P. N. GORDON, F. J. PILGRIM, K. J. BRUNINGS, and R. B. WOODWARD, J. Am. Chem. Soc. **75**, 5455 (1953).

Oxidative fragmentation of 3-pyrazolidinones to olefins

R. H. KENT AND J.-P. ANSELME[1]

Department of Chemistry, University of Massachusetts, Boston, Massachusetts 02116

Received January 22, 1968

The oxidation of 5-aryl-3-pyrazolidinones with mercuric oxide to the corresponding olefins is reported. Diethyl azodicarboxylate also converts 4,5-diphenyl-3-pyrazolidinone to *trans*-stilbene. The fragmentation of the intermediate cyclic α-carbonyl azo compounds is suggested to account for the observed products.

Canadian Journal of Chemistry, **46**, 2322 (1968)

The chemistry of l-pyrazolines has been the subject of increased investigation over the last few years (1). As part of our own interest in this general area, we have examined the oxidation of 3-pyrazolidinones (**1**) and we should like to report briefly our initial results.

When 5-phenyl-3-pyrazolidinone (**1**, Ar = C_6H_5, R = H) was oxidized with yellow mercuric oxide, the grayish color of mercury was observed along with vigorous evolution of gas. After removal of mercury and evaporation of the solvent, a thick greenish oil, having the odor of styrene, was obtained. Bromination of this oil gave a 42% yield of styrene dibromide, m.p. 71–73 °C. The oxidation of 4,5-diaryl-3-pyrazolidinones (**1**, R = Ar) gave the corresponding *trans*-stilbenes (**3**, R = Ar) in fair to good yields (see Table I). No attempts were made to obtain the highest possible yields.

In a recent review (2), Fahr and Lind have emphasized the extreme instability of cyclic α-carbonyl azo compounds. We believe that the initial step in our reaction is the oxidation of the 3-pyrazolidinones (**1**) to the corresponding α-carbonyl azo compounds (**2**). These highly reactive intermediates then undergo fragmentation (3) with the loss of carbon monoxide and nitrogen to give the olefins.[2] The formation of metallic mercury and a positive carbon monoxide test from the evolved gases, lend support to this view.

A related fragmentation has been previously observed by Rosenblum and his students (4). They reported the formation of *trans*-stilbene and tolan, from the oxidation of 5,6-diphenyltetrahydroöxadiazinone (**4**) and 5,6-diphenyl-1,2-dihydroöxadiazinone (**5**) with lead tetraacetate.

Presumably, similar azo compounds were formed and underwent fragmentation with loss of carbon dioxide and nitrogen. Although the

[1]To whom all correspondence should be addressed.

[2]Approximately nine months after our initial discovery of the oxidation of 3-pyrazolidinones with mercuric oxide, the lead tetraacetate oxidation of 4,5-diphenyl-3-pyrazolidinone to *trans*-stilbene was reported (12).

Can. J. Chem. Downloaded from www.nrcresearchpress.com by 210.87.254.42 on 09/05/12
For personal use only.

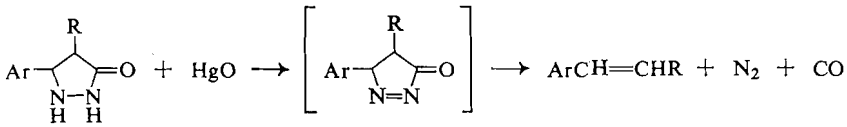

1 2 3

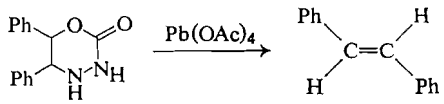

4

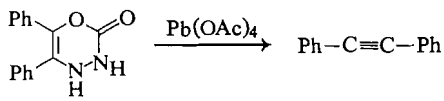

5

unstable α-carbonyl azo compounds **6** and **7** have been trapped as Diels–Alder adducts with dienes, (5, 6) neither benzyne (5) nor tolan[3]

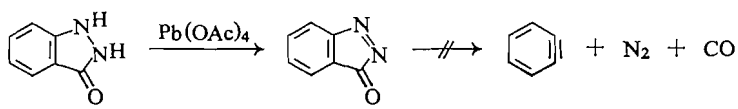

6

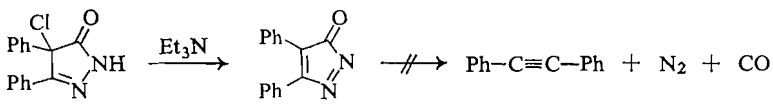

7

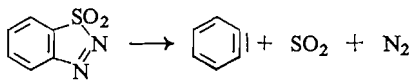

8

cases of **6** and **7** such an alternate path was not available. Evidently, the elimination of nitrogen and carbon monoxide to give aryl conjugated olefins is more rapid than the tautomerization to the 2-pyrazolin-5-ones. We found that, with mercuric oxide, 3-phenyl-2-pyrazolin-5-one reacted rapidly to give a white, highly insoluble solid, m.p. > 300 °C. This compound is possibly the mercury derivative of the pyrazolinone (9). None of the starting 3-pyrazolidinones was recovered in these oxidations. Tautomerization of **2** to the 2-pyrazolinones (**9**), followed by reaction with mercuric oxide to give the mercury adducts, may account for the balance of unrecovered starting material. Owing to the insolubility of these mercury derivatives, this point could not be ascertained. These reactions may be rationalized as shown in the following scheme.

Diethyl azodicarboxylate also oxidized 4,5-diphenyl-3-pyrazolidinone (**1**, Ar = R = Ph) to *trans*-stilbene over a period of three days in refluxing benzene.

[3]L. A. Carpino. Private communication.

Experimental

All the 3-pyrazolidinones reported were prepared by heating for 6 h to reflux the appropriate methyl cinnamates with an excess of hydrazine hydrate in dioxane. The properties of new compounds prepared in this series will be described at a later date.

Can. J. Chem. Downloaded from www.nrcresearchpress.com by 210.87.254.42 on 09/05/12
For personal use only.

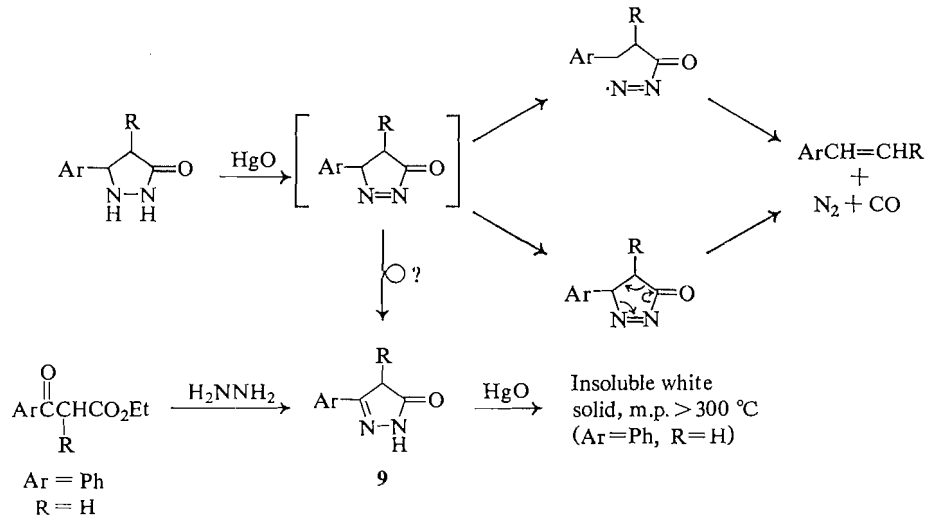

TABLE I

Oxidation of aryl-3-pyrazolidinones to olefins

3-Pyrazolidinone (**1**)	% yield of **3**	Melting point (°C)
Ar = C_6H_5, R = H	42*	71–73†
Ar = C_6H_5, R = C_6H_5	73	122–124
Ar = *p*-ClC_6H_4, R = *p*-$CH_3OC_6H_4$‡	48 (41)	173–175.5 (177.5–179.5)§
Ar = *p*-ClC_6H_4, R = C_6H_5	79	124–126‖

*Based on the weight of the dibromide; a pinch of hydroquinone was added.
†Dibromide.
‡Numbers in parenthesis refer to yield and melting point of product of second run.
§Reference 10.
‖Reference 11.

Oxidation Procedure

Fifty mmole of the 3-pyrazolidinones in 100 ml of methylene chloride containing anhydrous sodium sulfate were heated under reflux with 50 mmole of yellow mercuric oxide until the orange color had changed to a dark gray color. The mixture was then filtered through a pad of diatomaceous earth and the filtrate evaporated under vacuum. The residue was crystallized from ethanol to give the products indicated in Table I.

Acknowledgments

The authors wish to acknowledge the partial support of this work by a grant from the Graduate Research Council of the University of Massachusetts. Financial aid to R. H. K. by the Office of Economic Opportunity is hereby gratefully acknowledged.

1. R. J. Crawford and A. Mishra. J. Am. Chem. Soc. **88**, 3963 (1966); R. J. Crawford and G. L. Erickson. J. Am. Chem. Soc. **89**, 3907 (1967); R. J. Crawford and L. H. Ali. J. Am. Chem. Soc. **89**, 3908 (1967); C. G. Overberger, N. Weinshenker, and J.-P. Anselme. J. Am. Chem. Soc. **87**, 4119 (1965); E. L. Allred and R. L. Smith. J. Am. Chem. Soc. **89**, 7133 (1967); D. E. McGreer and W. S. Wu. Can. J. Chem. **45**, 461 (1967).
2. E. Fahr and H. Lind. Angew Chem. Intern. Ed. Engl. **5**, 372 (1966).
3. C. A. Grob and P. W. Schiess. Angew Chem. Intern. Ed. Engl. **6**, 1 (1967).
4. M. Rosenblum, A. Longroy, M. Neuveu, and C. Steel. J. Am. Chem. Soc. **87**, 5716 (1965).
5. E. F. Ullman and E. A. Bartkus. Chem. and Ind. London, 93 (1962).
6. L. A. Carpino, P. H. Terry, and S. D. Thatte. J. Org. Chem. **31**, 2867 (1966).
7. R. Breslow and E. Mohacsi. J. Am. Chem. Soc. **83**, 4100 (1961).
8. G. Wittig and R. W. Hoffmann. Angew Chem. **73**, 435 (1961).
9. W. Schrauth and H. Bauerschmidt. Ber. **47**, 2736 (1914).
10. L. Horner, P. Breck, and V. B. Toscano. Ber. **94**, 1323 (1961).
11. H. Meerwein, E. Buchner, and K. van Emster. J. prakt. Chem. **152**, 237 (1939).
12. B. T. Gillis and R. Weinkam. J. Org. Chem. **32**, 3321 (1967).

Can. J. Chem. Downloaded from www.nrcresearchpress.com by 210.87.254.42 on 09/05/12
For personal use only.

22-Dihydrostigmasterol from *Saussurea lappa* Clarke

TIKAM C. JAIN AND CALVIN M. BANKS[1]
Department of Chemistry, University of Victoria, Victoria, British Columbia

Received January 31, 1968

The identity of a natural product, erroneously reported as a diterpene alcohol from *Saussurea lappa* Clarke, has been established as 22-dihydrostigmasterol.

Canadian Journal of Chemistry, 46, 2325 (1968)

Can. J. Chem. Downloaded from www.nrcresearchpress.com by 210.87.254.42 on 09/05/12
For personal use only.

Paul and his co-workers (1) had reported the isolation of a diterpene alcohol, $C_{20}H_{34}O$, m.p. 135–136 °C, $[\alpha]_D$ — 40.55°, from hexane extract of the roots of *Saussurea lappa* Clarke. As a part of our projected program on diterpenoids,[2] we were interested in elucidating the structure of this diterpene alcohol. By essentially following the reported procedure, we isolated the same alcohol, m.p. 137.5–138 °C, $[\alpha]_D$ — 34.34°. The nuclear magnetic resonance (n.m.r.) spectrum of this alcohol described in sequel, at first sight, indicated that it was characteristic of a steroid rather than a diterpenoid skeleton. This led us to reexamine its elementary composition prior to elucidation of its structure. High resolution mass measurement on the parent alcohol as well as on its several derivatives (see Table I) clearly established its molecular formula as $C_{29}H_{50}O$.

Sterol **1** contains one double bond as it absorbs one mole of hydrogen during catalytic hydrogenation. It gives positive coloration with tetranitromethane and Liebermann–Burchard reaction. The trisubstituted nature of the olefinic linkage was revealed by a pair of bands at 797 and 834 cm^{-1} in its infrared (i.r.) spectrum, further supported by its ultraviolet (u.v.) spectrum (λ_{max} 200.4 mμ, ε 5930, ε_{210} 1986, ε_{215} 552, and ε_{220} 135) typical of Δ^5-steroids (2). The broad signal due to olefinic proton at τ 4.56 had disappeared in the n.m.r. spectrum of dihydro compound **4**. The i.r. spectrum of **1** exhibited absorption bands at 3440 and 1053 cm^{-1} due to the hydroxyl group, confirmed by an acetate **2** (i.r. spectrum: 1727, 1255, and 1039 cm^{-1}) and a benzoate **3** (i.r. spectrum: 1712, 1276, 1256, and 1112 cm^{-1}). The n.m.r. spectrum of **1** shows an 18-proton multiplet ranging from τ 9.02 to 9.30 which accounts for six methyl groups. The hydroxyl proton resonates as a sharp singlet at τ 8.46 which is removed by exchange with D_2O.

The mass spectrum of the parent alcohol **1** was very informative. The principal peak in the mass range 205–245 corresponded to *m/e* 213 (Σ_{40} = 0.84%) which led to the formulation of $C_{10}H_{21}$ side chain at C-17 in D ring (3). This also eliminated the possibility of an unsaturation in the side chain. The presence of an intense peak at *m/e* 119 (Σ_{40} = 0.98%) suggested it to be Δ^5-3β-sterol (4). In addition, fragments characteristic of stigmastane skeleton (5, 6) were observed at *m/e* 273 (M — side chain), 255 (M — side chain — H_2O), 231 [M — side chain — 42 (ring D fragment)], and 213 (231 — H_2O). These fragments shifted by two units in the mass spectrum of dihydro compound **4**. It is worth mentioning that the molecular ion peaks for acetate **2** and benzoate **3** constitute only 4.4% and 0.8% respectively of the base peak at *m/e* 396, even when using direct inlet system. All

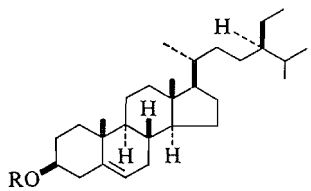

1, R = —H

2, R = —C(=O)—CH_3

3, R = —C(=O)—C_6H_5

these chemical and spectroscopic properties can be accounted for if the parent alcohol has structure **1**, which then should be identical with 22-dihydrostigmasterol. This was confirmed by comparing its i.r., n.m.r., and mass spectra

[1]Recipient of a University of Victoria Bursary, 1967–1968.
[2]R. J. Striha and T. C. Jain. Unpublished results.

TABLE I

Exact masses and composition of ions

	m/e		
	Observed	Calculated	Composition
Sterol **1**	414.3865	414.3862	$C_{29}H_{50}O$
Acetate **2**	456.3968	456.3967	$C_{31}H_{52}O_2$
Benzoate **3**	396.3756	396.3756	$C_{29}H_{48}$ ($M - C_6H_5COOH$)
Dihydro compound **4**	416.4018	416.4018	$C_{29}H_{52}O$

with the corresponding spectra of 22-dihydrostigmasterol and they were identical in all respects. Besides this, R_f values of **1**, **2**, **3**, and **4** in several thin-layer chromatographic systems (silica gel, silica gel – $AgNO_3$ and alumina) were comparable with those of corresponding authentic specimens.

Experimental

Melting points were determined on a Kofler hot-stage microscope and are uncorrected. Infrared (i.r.) spectra were recorded in KBr pellets on a Perkin–Elmer model 337 grating spectrophotometer calibrated with polystyrene film; ultraviolet (u.v.) spectrum was measured in cyclohexane on a Unicam model SP-700 spectrophotometer. Nuclear magnetic resonance (n.m.r.) spectra were obtained in $CDCl_3$ with Varian A-60 spectrometer using TMS as an internal standard. Unless otherwise stated, specific rotations were determined in chloroform on a Perkin–Elmer model 141 polarimeter. The mass spectra were obtained with an AEI-MS9 mass spectrometer, using direct insertion technique. The ionizing energy was maintained at 70 eV.

Sterol 1

This was isolated from the hexane extract of the roots of *Saussurea lappa* Clarke following essentially the procedure described in the literature (1); overall yield, 0.4% based on crude extract. Crystallization from ether–ethanol afforded sterol **1** as colorless plates, m.p. 137.5–138 °C, $[\alpha]_D^{31} - 34.34°$ (*c*, 1.03); dark-yellow coloration with tetranitromethane; Liebermann–Burchard reaction (7) positive; u.v. spectrum: λ_{max} 200.4 mμ, ε 5930, ε_{210} 1986, ε_{215} 552, and ε_{220} 135; i.r. spectrum: ν_{max} 3440, 1053 cm^{-1} (equatorial hydroxyl group (8)), 1665, 834, and 797 cm^{-1} (trisubstituted olefinic linkage); n.m.r. spectrum: τ 9.02–9.30 (multiplet, 18H, 6x—C*H*$_3$), τ 8.46 (sharp singlet, —O*H*, disappeared after exchange with D_2O), τ 4.56 (broad multiplet, 1H, $>C=\underset{|}{C}-H$); mass spectrum[3]: *m/e* ($\%\Sigma_{40}$)[4]: 43 (4.79, base peak), 119 (0.98), 231 (0.21, M – side chain – 42 [ring *D* fragment]), 213 (0.84, 231 – H_2O), 255 (1.26, M – side chain – H_2O), 273 (0.33, M – side chain), 381 (0.84, M – CH_3 – H_2O), 396 (4.30, M – H_2O), 399 (0.42, M – CH_3), and 414 (1.90, M^+).

Anal. Calcd.[5] for $C_{29}H_{50}O \cdot 1/2H_2O$: C, 82.24; H, 12.13. Found: C, 81.99; H, 12.06.

Acetate 2

A solution of compound **1** (20.5 mg) dissolved in anhydrous pyridine (5 ml) was treated with acetic anhydride (0.5 ml) and was allowed to stand overnight at room temperature. The mixture was then decomposed with water and the solvent was removed *in vacuo* and dried over Na_2SO_4. The crystalline material, obtained after removal of solvent, was chromatographed on neutral alumina (500 mg). Elution with petroleum ether gave acetate **2**, crystallized from ether–ethanol as white rectangular plates, m.p. 127–129 °C, $[\alpha]_D^{30}$ −39.90° (*c*, 1.06); i.r. spectrum: ν_{max} 1727 cm^{-1} (aliphatic ester carbonyl), 1255, and 1039 cm^{-1} (C—O—C stretching of ester). The i.r. spectrum was superimposable with that of authentic specimen. Mass spectrum: *m/e* ($\%\Sigma_{40}$): 255 (1.95, M – CH_3COOH – side chain), 381 (1.04, M – CH_3COOH – CH_3), 396 (7.58, base peak, M – CH_3COOH), 456 (0.30, M^+).

Benzoate 3

Sterol **1** (20 mg), dissolved in dry pyridine (5 ml), was treated with freshly distilled benzoyl chloride (0.25 ml) and the mixture was stirred magnetically overnight. It was worked up in the same manner as described above for acetate. Crystallization of the product from ethanol–ether furnished shining flakes of benzoate, m.p. 144–146 °C; i.r. spectrum: ν_{max} 1712 cm^{-1} (aromatic ester carbonyl), 1276, 1256, and 1112 cm^{-1} (C—O—C stretching of ester). It was superimposable with the i.r. spectrum of authentic specimen. Mass spectrum: *m/e* ($\%\Sigma_{186}$): 255 (4.49, M – C_6H_5COOH – side chain), 381 (2.78, M – C_6H_5COOH – CH_3), 396 (23.90, base peak, M – C_6H_5COOH), and 518 (0.19, M^+).

Dihydro Compound 4

Sterol **1** (50 mg) was added to a prereduced PtO_2 catalyst (25 mg) in glacial acetic acid (100 ml). The solution was stirred magnetically at room temperature whereupon it absorbed one mole equivalent of hydrogen

[3]For the sake of brevity, peaks relevant to structural assignment are described. Complete mass spectra will be presented in the M.Sc. Thesis of C. M. Banks, University of Victoria.

[4]The symbol Σ_{40} denotes the percentage of total ionization over the range *m/e* 40 to M^+.

[5]Crystals with $\frac{1}{2}H_2O$ have been observed by various investigators (9, 10).

Can. J. Chem. Downloaded from www.nrcresearchpress.com by 210.87.254.42 on 09/05/12
For personal use only.

in 12 h. The reaction mixture was worked up in the customary manner to give a solid (46 mg). This was chromatographed on neutral alumina (2.0 g). Elution with petroleum ether gave a trace of oily material and further elution with petroleum ether – benzene (1:1) afforded dihydro compound **4**, which crystallized from ether–ethanol as plates, m.p. 139–140 °C, $[\alpha]_D^{31}$ +20.70° (*c*, 0.57); no coloration with tetranitromethane; i.r. spectrum: ν_{max} 3406, 1043 cm^{-1} (equatorial hydroxyl), no band in 790–840 cm^{-1} region. It was identical with the infrared spectrum of authentic sample. The n.m.r. spectrum had τ 9.03–9.33 (multiplet, 18H, 6x—C*H*$_3$), τ 8.52 (sharp singlet, —O*H*), and no signal in olefinic region. Mass spectrum (%Σ_{40}): 233 (3.69, M − side chain − 42 (ring D fragment)), 215 (3.33, 233 − H_2O), 257 (0.32, M − side chain − H_2O), 275 (0.12, M − side chain), 383 (0.58, M − CH_3 − H_2O), 398 (0.18, M − H_2O), 401 (1.42, M − CH_3), and 416 (5.08, M^+, base peak).

Acknowledgments

The authors wish to express their gratitude to National Research Council of Canada and U.VIC Research Committee for financial support of this work. Tikam C. Jain is indebted to Professors A. C. Riddiford and L. J. Clark for their encouragement and interest in this work.

Added in proof—Because of the unavailability of the original sample described in reference (1), a direct comparison with our sample was not possible. We thank Professor Bhattacharyya for this information.

1. A. Paul, A. S. Bawdekar, R. S. Joshi, G. H. Kulkarni, A. S. Rao, G. R. Kelkar, and S. C. Bhattacharyya. Perfumery Essent. Oil Record, **51**, 115 (1960).
2. P. Bladon, H. B. Henbest, and G. W. Wood. J. Chem. Soc. 2737 (1952).
3. H. J. M. Fitches. Advances in mass spectrometry. Vol. II. *Edited by* R. M. Elliott. The Pergamon Press, New York. 1963. p. 433.
4. S. S. Friedland, G. H. Lane, Jr., R. T. Longman, K. E. Train, and M. J. O'Neal, Jr. Anal. Chem. **31**, 169 (1959).
5. J. W. Clark-Lewis and I. Dainis. Australian J. Chem. **20**, 1961 (1967).
6. P. Reichstein, H. Kaufmann, W. Stöcklin, and T. Reichstein. Helv. Chim. Acta, **50**, 2114 (1967).
7. K. H. Overton. Technique of organic chemistry. Vol. XI. Part I. *Edited by* A. Weissberger. Interscience Publishers, Inc., New York. 1963. p. 42.
8. K. Nakanishi. Infrared absorption spectroscopy. Holden-Day, San Francisco. 1964. p. 33.
9. P. Crabbé, E. A. Azpeitia, and C. Djerassi. Bull. Soc. Chim. Belges. **70**, 168 (1961).
10. Elsevier's encyclopaedia of organic chemistry. Series III. Vol. 14. Supp. Elsevier Publ. Co., Inc., Amsterdam. 1954. p. 1808 *s*.

Can. J. Chem. Downloaded from www.nrcresearchpress.com by 210.87.254.42 on 09/05/12
For personal use only.

Can. J. Chem. Downloaded from www.nrcresearchpress.com by 210.87.254.40 on 09/05/12
For personal use only.

Electron spin resonance study of the interaction of *tert*-butyl hydroperoxide with zinc oxide

MAURICE CODELL and HENRY GISSER
Pitman-Dunn Research Laboratories, Frankford Arsenal, Philadelphia, Pennsylvania

AND

R. D. IYENGAR
Center for Surface and Coatings Research, Lehigh University, Bethlehem, Pennsylvania

Received May 7, 1968

The complexity of the electron spin resonance signal, appearing at $g = 1.96$ on ZnO vacuum outgassed at higher temperatures, has been examined by adsorption of tertiary butyl hydroperoxide (TBHP). Two individual signals with g values 1.961 and 1.965 observed following TBHP adsorption have been attributed to Zn^+ ions and oxygen vacancies with trapped electrons.

Canadian Journal of Chemistry, 46, 2329 (1968)

The complexity of the electron spin resonance signal which appears in the vicinity of $g = 1.96$ in samples of zinc oxide vacuum outgassed at high temperatures was first noted by Schneider and Raüber (1). Kasai (2) suggested that the complexity results from the presence of two signals caused by anionic vacancies (trapped electrons) and halogen ions present in substitutional positions. Subsequent investigations have emphasized only the effects of adsorbed oxygen on the electron spin resonance spectrum of zinc oxide, with little or no attention given to factors contributing to the complexity of the signal at $g = 1.96$.

In an attempt to understand the mechanism of hydroperoxide participation in the catalysis of oxidation of organic lubricants, the electron spin resonance spectra of *tert*-butyl hydroperoxide (TBHP) adsorbed on ZnO have been investigated. Surprising and interesting observations have been made which lead to a better understanding of the nature of the complex signal occurring at $g = 1.96$.

Zinc oxide which is vacuum outgassed for 2 h at temperatures above 375° gives primarily a signal at $g = 1.96$ (peak to peak width = 7.6 G). Adsorption of TBHP not only produces an overall decrease in signal intensity but also renders possible the observation of two signals with g values of 1.965 and 1.961, in place of the somewhat broad signal at $g = 1.96$ (Fig. 1). The spectrum shows no hyperfine structure attributable to free radicals resulting from the decomposition of TBHP. Power variation studies as well as observations on intensity changes on subsequent oxygen and vacuum treatment show

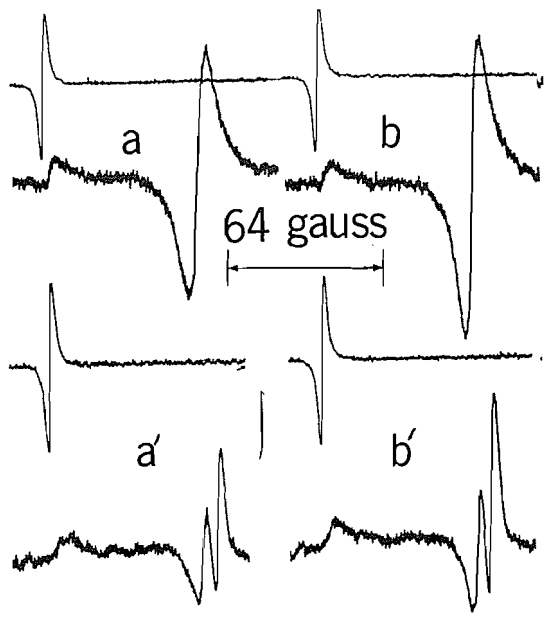

FIG. 1. Electron spin resonance (X-band) spectra of zinc oxide outgassed for 2 h at (*a*) 375° and (*b*) 400°. (*a'*) and (*b'*) are spectra after the addition of TBHP. Diphenylpicrylhydrazyl (upper spectra) is used as a standard for g value. The field increases from left to right.

Can. J. Chem. Downloaded from www.nrcresearchpress.com by 210.87.254.40 on 09/05/12
For personal use only.

that the two signals are independent of each other and cannot result from a single species. Further, neither of the signals exhibits saturation in the power range 2 to 25 mW and hence the possibility of either signal being caused by chloride ions present as impurity in interstitial positions in ZnO (2) can be eliminated.

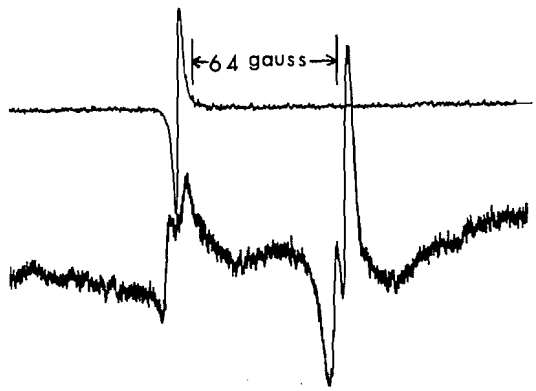

FIG. 2. Electron spin resonance (X-band) spectrum of zinc oxide outgassed at 500° and treated with methane containing 2% oxygen.

The addition of hydrocarbons containing 2% oxygen to zinc oxide, which has been vacuum outgassed at 500°, leads to an immediate formation of the same two signals observed on treatment with TBHP (Fig. 2). The use of a pure hydrocarbon does not produce the two signals. On the other hand, the addition of oxygen to zinc oxide outgassed at 500° leads to the formation of an O_2^- triplet with g values of 2.002, 2.008, and 2.047. The signals at $g = 1.96$ are not observed immediately. If the sample is allowed to stand for more than 24 h, the intensity of the O_2^- signal is observed to diminish with the simultaneous appearance of two signals (Fig. 3), with g values comparable to those obtained following treatment with TBHP.

The delay observed in the formation of the two signals in experiments with oxygen (instead of TBHP or hydrocarbons containing oxygen) indicates a different mechanism for the formation of the species responsible for the signals. If the observed decrease in the intensity of the O_2^- signal is due to desorption of oxygen, then the resulting enhancement in electron concentration at the surface provides a clue for the identity of the signals observed at $g = 1.965$ and 1.961. It is likely that these signals are caused by electrons

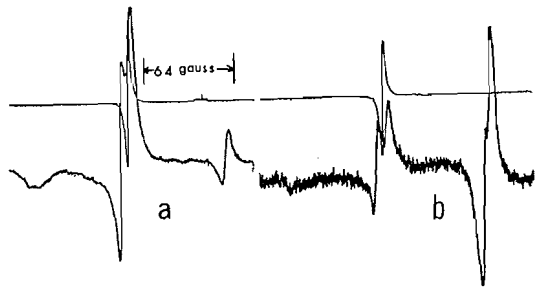

FIG. 3. Electron spin resonance (X-band) spectra of zinc oxide vacuum outgassed for 2 h at 500°: (*a*) 100 mm of oxygen added and re-outgassed 10 min at 25°; (*b*) after standing for 70 h following treatment (*a*).

trapped either at the Zn^{++} ions or at oxide ion vacancies.

Our experiments also suggest that the signals at $g = 1.965$ and 1.961 preexist within the broad signal at $g = 1.96$ (in vacuum-outgassed ZnO), and become observable due to decrease in signal widths and relative differences in their ability to interact with some oxygen species provided by the adsorbing TBHP or hydrocarbon–oxygen mixtures. The absence of O_2^- ions during adsorption of TBHP would mean that the oxygen species involved in this interaction is O^-. In fact, the formation of hydroperoxide in hydrocarbon–oxygen mixtures and the decomposition of hydroperoxide to yield O^- ions have been reported (3).

Further, according to Thomas (4) most of the interstitial zinc in ZnO should be removed by oxygen treatment at 500° for a few minutes. It is observed in our experiments that heating in oxygen at 500° for 2 h eliminates the signal at $g = 1.965$ completely, while the signal at $g = 1.961$ is partially affected. On this basis the signal at $g = 1.965$ can be assigned to interstitial Zn^+ ions and the signal at $g = 1.961$ to oxide ion vacancies.

It appears, therefore, that the complexity of the signal observed at $g = 1.96$ in vacuum-outgassed high purity ZnO is caused by the presence of two signals corresponding to $g = 1.965$ and $g = 1.961$. The close proximity of the two signals in addition to a broadening associated with the signals especially at the higher outgassing temperature is responsible for the apparently one signal observed. The small fluctuations in g values observed for the signal appearing at $g = 1.96$ in vacuum-outgassed ZnO

is then explained as due to relative differences in intensities of the two constituent signals at $g = 1.965$ and $g = 1.961$.

Details of this investigation will be published elsewhere.

Acknowledgment

R. D. Iyengar wishes to acknowledge the support by the Advanced Research Projects Agency of the Department of Defense, monitored by the Naval Research Laboratory under contract No. NONR 610(09).

1. J. SCHNEIDER and A. RAÜBER. Z. Naturforsch. **16a**, 712 (1961).
2. P. H. KASAI. Phys. Rev. **130**, 989 (1963).
3. K. U. INGOLD. Chem. Rev. **61b**, 563 (1961).
4. D. G. THOMAS. J. Phys. Chem. Solids, **3**, 229 (1957).

Can. J. Chem. Downloaded from www.nrcresearchpress.com by 210.87.254.40 on 09/05/12
For personal use only.

Can. J. Chem. Downloaded from www.nrcresearchpress.com by 210.87.254.105 on 09/05/12
For personal use only.

Canadian Journal of Chemistry

Published by THE NATIONAL RESEARCH COUNCIL OF CANADA

VOLUME 46 JULY 15, 1968 NUMBER 14

Partial molal volumes of tetraalkylammonium chlorides in ethanol–water mixtures

IKCHOON LEE AND J. B. HYNE

Department of Chemistry, University of Calgary, Calgary, Alberta

Received July 18, 1967

The partial molal volumes of four tetraalkylammonium chlorides, Me_4NCl, Et_4NCl, Pr_4NCl, and Bu_4NCl, in a series of ethanol–water mixtures have been determined. The experimental results are discussed in terms of the varying size and surface charge of the ions and the structure of the binary solvent mixtures. The results indicate that at 0.1 mole fraction ethanol the maximum structuredness of water causes a minimum in the partial molal volumes, while at 0.3 mole fraction the solvent structure is such that the free volume is a minimum but the effect of surface charge on the salts is a maximum.

Canadian Journal of Chemistry, 46, 2333 (1968)

Introduction

In 1945, Frank and Evans (1) proposed that tetraalkylammonium ions should promote water structure as the hydrophobic nature of the ions increases with the size. Since then, numerous studies have shown that the idea was essentially correct. For example conductivity (2), osmotic and activity coefficients (3), viscosity (4), enthalpy and entropy of dilution (5), infrared spectra (6), molal heat capacity (7), partial molal volume and compressibility (8), and heats of mixing (9) of aqueous solutions of tetraalkylammonium salts have been reported. The results of these studies provide evidence that tetrapropyl and tetrabutylammonium ions are indeed strong hydrophobic structure makers while tetramethylammonium ion is a weak structure breaker, and tetraethylammonium ion falls on the border line of the two opposing effects. No systematic work of a similar nature has been done in aqueous solvent mixtures (10). In this paper we report a study of partial molal volumes of four tetraalkylammonium chlorides in a series of ethanol–water mixtures at 50.25°. Our interest was to obtain more information about the structural changes accompanying the addition of ethanol to liquid water, using the hydrophobic and electrostrictive effects of these salts as an experimental probe.

Experimental

Eastman reagent grade quaternary ammonium salts were purified by recrystallization and dried *in vacuo* as described by Conway *et al.* (11). Magnesium-dried ethanol and double-distilled water mixtures were prepared by weight.

Salt solutions were made up in calibrated 100 ml volumetric flasks and for each salt concentration three replicate density measurements were made using 25 ml Weld-type pycnometers. Pycnometers were thermostated at 50.250 ± 0.002 °C and weighed after 1½ h standing at room temperature. This standardization of procedure improved reproducibility. Average reproducibility of density was ±0.00003 and in no case was it greater than ±0.00005.

Apparent molal volumes ϕ were calculated using the equation

$$[1] \qquad \phi = \frac{M_2}{d_0} - \frac{1000}{d_0}\frac{(d - d_0)}{C},$$

where M_2 is the molecular weight of the salt, C is the concentration in moles per liter, and d and d_0 are the density of solution and solvent respectively. ϕ values were determined for each salt in each solvent composition over a concentration range of approximately 0.02 M to 0.60 M. Partial molal volumes $\bar{V}^0$ were then obtained from ϕ and its concentration dependence using the relation

$$[2] \qquad \phi = \bar{V}^0 + SC^{1/2},$$

where S is the limiting slope. The precision of apparent molal volumes, $\delta\phi$, was ±0.1 ml/mole at $C = 0.04$ M using the equation of Redlich and Bigeleisen (12).

$$[3] \qquad \delta\phi = \frac{1000\delta d}{d_0 C} + \frac{1000(d - d_0)\delta C}{C^2 d_0},$$

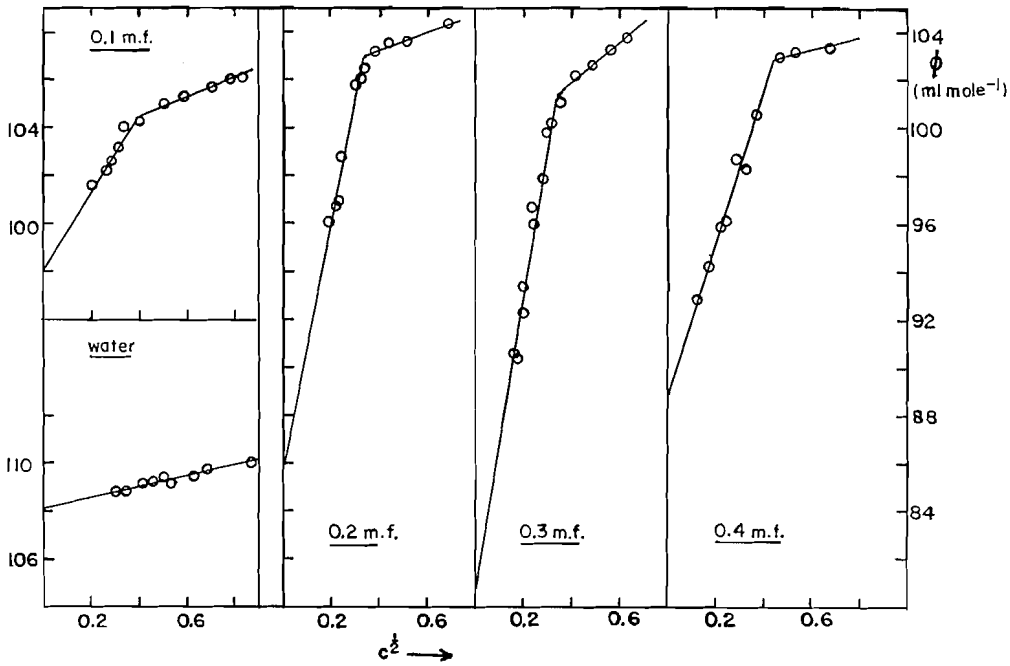

FIG. 1. The limiting law plots for Me_4NCl in various ethanol–water mixtures at 50.25° (m.f. = mole fraction ethanol).

where δd and δC are the uncertainties in density and concentration. All the density and apparent molal volume data[1] obtained in this work has been filed with The Depository of Unpublished Data, National Science Library, National Research Council of Canada, Ottawa.

Results and Discussion

Concentration Dependence of Apparent Molal Volumes

Illustrative examples of the plots of apparent molal volumes, ϕ, against the square root of the salt concentration are shown for Me_4NCl in various solvents in Fig. 1. These plots show a sharp transition region at approximately $C^{1/2} = 0.35$ connecting two straight-line sections of different slope S. The same type of transition has been observed in the region of 1 N concentration of alkali metal chlorides in water and has been discussed by Vaslow (20). This author suggested that the observed transition may be due to a change from dilute to concentrated solution types of solvent reorganization. It is of interest to note that the transition is sharper and at lower concentration for the mixed solvents than for water. It has been suggested (21) that the positive concentration dependence of the apparent molal volume is primarily due to the salting out effect of ionic electrostriction. However, the experimental slopes as drawn contain contributions from other important effects such as ion–ion interactions and changes in hydrophobic structural effects on the solvent as the solute concentration varies. As Vaslow (20) has noted a detailed explanation of this change in slope of the ϕ versus $C^{1/2}$ plot must await further study of the problem. It is, however, perhaps worth noting that the low concentration region slopes in mixed solvents are considerably greater than for water and that the slope has a maximum positive value for Me_4NCl at 0.3 mole fraction ethanol in the ethanol–water binary solvent mixture. This observation of a maximum in the solvent composition dependence of the slope S further suggests that at least some of the contributing factors that determine the S value, probably electrostriction and structural effects, have an extremum in their influence at this solvent composition.

[1]Photocopies of this data may be obtained free of charge, upon request, from: Depository of Unpublished Data, National Science Library, National Research Council of Canada, Ottawa, Canada.

Can. J. Chem. Downloaded from www.nrcresearchpress.com by 210.87.254.105 on 09/05/12
For personal use only.

Can. J. Chem. Downloaded from www.nrcresearchpress.com by 210.87.254.105 on 09/05/12
For personal use only.

TABLE I

Partial molal volumes of various salts at 50.25 °C

Solvent (mole fraction EtOH)	$\bar{V}^0$ (ml mole^{-1})			
	Me_4NCl	Et_4NCl	Pr_4NCl	Bu_4NCl
0.00	108.1	170.0	237.2	301.0
0.10	98.1	156.0	219.0	286.8
0.20	85.7	153.7	218.3	286.4
0.30	80.7	152.0	219.5	288.5
0.40	88.7	152.8	214.7	277.7

The data presented in Table II also show that in water the S value decreases as the size of the tetraalkylammonium ion increases. For Me_4NCl, it is close to the theoretical value of 2.333 at 50° for 1:1 electrolytes (22); for the other three salts, S values are negative as has been shown by other workers (23).

The partial molal volumes, $\bar{V}_s^0$ (Table I), obtained from extrapolation to zero concentration of the low concentration linear portion of the ϕ versus $C^{1/2}$ plots are considered to be accurate to ± 0.5 ml mole^{-1}.

Ionic Partial Molal Volumes

The additivity of individual ionic partial molal volumes has been the subject of many recent investigations (11, 15, 16) in view of the importance of the individual ionic contribution in understanding ion–solvent interactions. The individual ionic partial volume seems to differ according to the method used for its determination. For example, $\bar{V}_{Cl^-}{}^0$ values in water range from 18.0 to 37.0 ml/mole, as shown in Table III. Conway and co-workers (11) in their recent report proposed a new method of obtaining ionic partial molal volumes for tetraalkylammonium salts with a common anion in water. In this method, anionic partial molal volumes are obtained by extrapolation of $\bar{V}_{R_4NX}{}^0$ values to zero cation weight in a linear plot of $\bar{V}_{R_4NX}{}^0$ versus molecular weight of the cations, R_4N^+. The method was applied to the present system of salts, in mixed solvents, as shown in Fig. 2. The linearity is good for all solvent systems. The $\bar{V}_{Cl^-}{}^0$ values obtained from intercepts of these plots are illustrated in Fig. 3. The only literature value available is for water at 25° (Table III). Our value agrees well with those of Mukerjee (15) and Glueckauf (16). Although our measurement was done at 50.25°, the temperature dependence of the $\bar{V}_{Cl^-}{}^0$ value seems to be small enough so

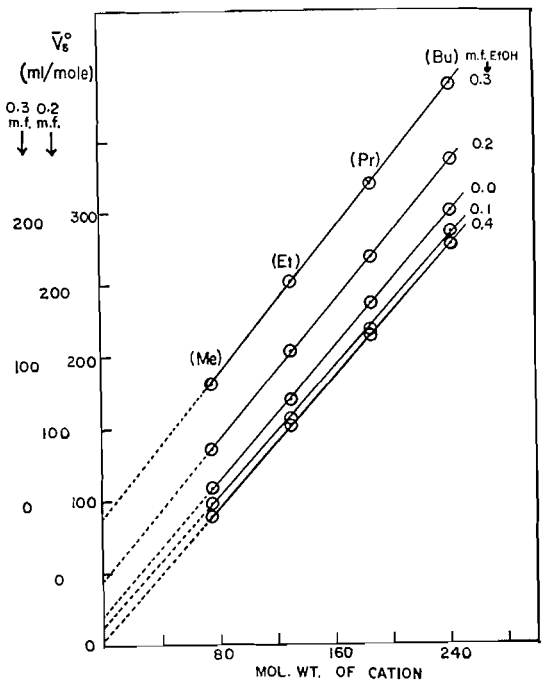

FIG. 2. Partial molal volumes of tetraalkylammonium chlorides as a function of the molecular weight of cation in various ethanol–water mixtures at 50.25°.

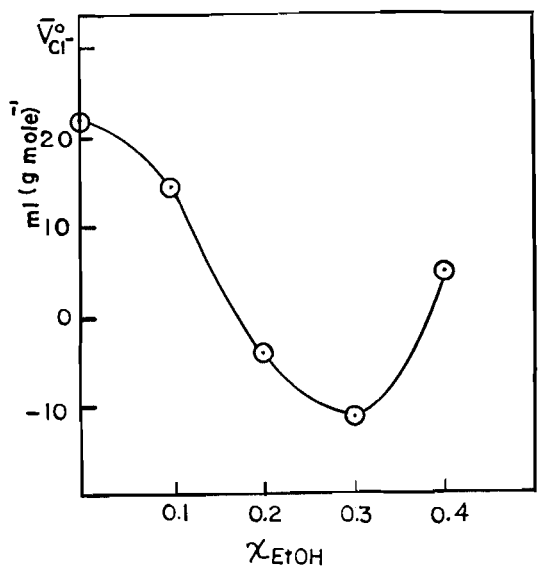

FIG. 3. Ionic partial molal volumes of chloride ion as a function of solvent composition (mole fraction ethanol) at 50.25°.

that the difference in $\bar{V}_{Cl^-}{}^0$ is well within the experimental accuracy (13).

Figure 3 shows a deep minimum in $\bar{V}_{Cl^-}{}^0$ at 0.3 mole fraction ethanol, and $\bar{V}_{Cl^-}{}^0$ values for 0.2 and 0.3 mole fractions are negative. Since chloride ion has a high charge to surface ratio, the minimum at 0.3 mole fraction is probably due to the maximum in electrostriction effect, which agrees with the conclusion derived from the maximum value of the limiting slope at the same composition.

The ionic partial molal volumes of the cations were determined by subtracting the $\bar{V}_{Cl^-}{}^0$ value from the partial molal volumes of salt $\bar{V}_{R_4NCl}{}^0$.

$$[4] \qquad \bar{V}_{R_4N^+}{}^0 = \bar{V}_{R_4NCl}{}^0 - \bar{V}_{Cl^-}{}^0$$

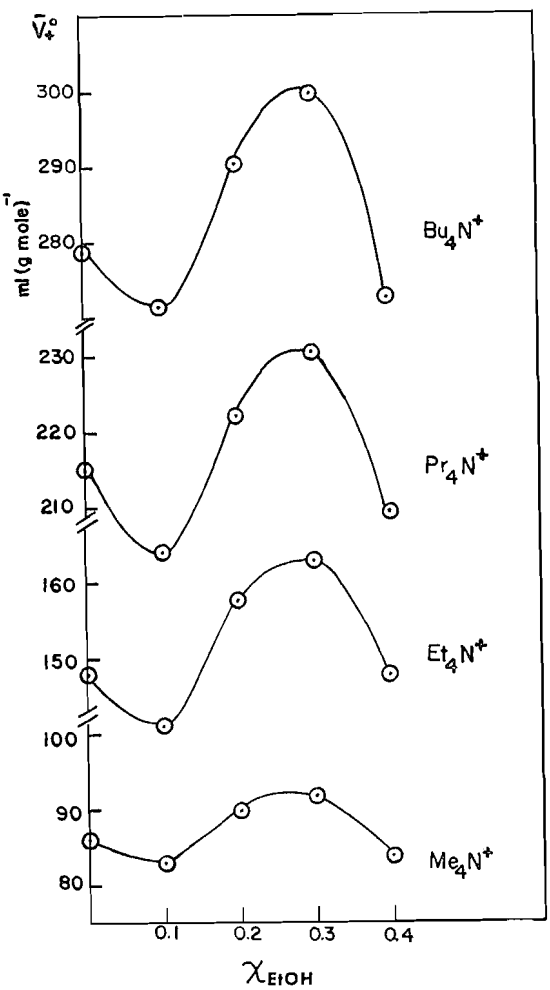

FIG. 4. Ionic partial molal volumes of the tetraalkylammonium cations as a function of solvent composition (mole fraction ethanol) at 50.25°.

TABLE II

Limiting slope, S, for various salts at 50.25 °C

Solvent (mole fraction EtOH)	S (ml mole$^{-1}C^{-1/2}$)			
	Me_4NCl	Et_4NCl	Pr_4NCl	Bu_4NCl
0.00	2.3	−2.0	−4.6	−5.3
0.10	16.7	23.0	36.7	36.7
0.20	52.7	19.0	45.0	51.0
0.30	62.7	24.3	36.0	51.0
0.40	31.5	18.0	40.7	53.2

TABLE III

Comparison of the ionic partial molal volume of chloride, $\bar{V}_{Cl^-}{}^0$ (ml/mole), in water at 25° determined by various workers

Author	$\bar{V}_{Cl^-}{}^0$	Reference
Present work	22.0*	
Fajans and Johnson	18.0	(13)
Padova	18.6	(14)
Mukerjee	22.3	(15)
Glueckauf	22.3	(16)
Conway *et al.*	23.6	(11)
Zana and Yeager	23.7	(17)
Stokes and Robinson	25.3	(18)
Bernal and Fowler	37.0	(19)

*At 50.25°.

The individual ionic partial molal volumes of the cations obtained in this manner are plotted against solvent composition in Fig. 4. All the cations show a minimum at 0.1 mole fraction and a maximum at 0.3 mole fraction. The marked similarity between the curves in Fig. 4 for the four tetraalkylammonium ions suggests that the same effects are operating, although to varying degrees, in all cases. The observed enhancement of the extremum effect as the alkyl function is varied from methyl to *n*-butyl supports the claim that the common effects are those of hydrophobic interaction and size. It is interesting to note that even the smallest and least hydrophobic of the cations, Me_4N^+, shows the double extremum characteristic of predominant hydrophobic and size effects.

When the combined effects of cation and anion are considered, however, the partial molal volume picture changes considerably. The electrostriction effect of the chloride anion, which manifests itself as a minimum at 0.3 mole fraction ethanol (see Fig. 3), is then in competition with the hydrophobic and size effect of the ammonium cation, which is characterized by a maximum at the same solvent composition. The

Can. J. Chem. Downloaded from www.nrcresearchpress.com by 210.87.254.105 on 09/05/12
For personal use only.

Can. J. Chem. Downloaded from www.nrcresearchpress.com by 210.87.254.105 on 09/05/12
For personal use only.

balance between these two competing effects is illustrated in Fig. 5, where the partial molal volumes of the salt species are plotted against solvent composition. The maximum at 0.3 mole fraction observed for the Me_4N^+ ion has now become a minimum, indicating that the electrostriction effect of the chloride ion more than compensates for the small hydrophobic and size effect of the tetramethylammonium cation. As the cation effects become larger the chloride ion electrostriction is exactly compensated in tetraethylammonium and is outweighed by the hydrophobic and size effects in tetrapropyl- and tetrabutyl-ammonium salts.

Structure of the Binary Solvent

The behavior of the partial molal volume of quaternary ammonium salts and their component ions as a function of solvent composition can be used as a probe to investigate the varying structure of the binary solvent system. Three characteristic features may be identified:

I. A minimum in partial molal volume of the ammonium cations (Fig. 4) and of the larger salts at or near 0.1 mole fraction ethanol.

II. A maximum in partial molal volume of ammonium cations (Fig. 4) and of the larger salts at or near 0.3 mole fraction ethanol.

III. A minimum in partial molal volume of the chloride anion at or near 0.3 mole fraction ethanol.

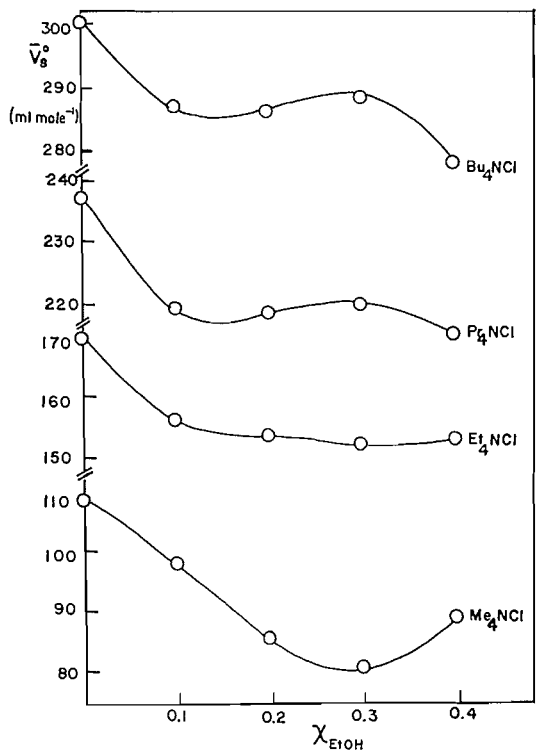

FIG. 5. Partial molal volumes of tetraalkylammonium chlorides as a function of solvent composition (mole fraction ethanol) at 50.25°.

These three observations may be explained on the basis of variation of the structure of the binary solvent with composition.

I. The 0.1 mole fraction minimum. The characteristic extremum behavior of many of the physicochemical properties of alcohol–water mixtures near the pure water end of the composition range has been well documented (24). It is now generally accepted that this behavior is a reflection of structure promotion in the water by initial addition of the cosolvent, probably as a result of hydrophobic interactions between the cosolvent and the water. The enhanced structure has been described as "ice-berg" (25) implying an open lattice work having the structural order of ice itself but differing from the "soft ice" (25) character of water around a small, fully charged ion exerting electrostriction effects on the solvent medium. At the binary solvent composition where "ice-berg" structure promotion is a maximum (circa 0.1 mole fraction in ethanol–water), there will be a maximum of preformed "holes" into which the third component solute molecule (alkylammonium) may fit without the prerequisite of hole formation prior to dissolution. Accordingly the partial molal volume of the solute species will be a minimum at this solvent composition. This phenomenon is clearly demonstrated in Fig. 4 and to a lesser extent in Fig. 5 where the additional complication of the competing effect of the chloride ion (see III which follows) tends to reduce this effect.

II. The 0.3 mole fraction maximum. As the proportion of nonaqueous cosolvent in the mixture increases the simple bulk effect of the cosolvent will begin to break down the characteristic water structure. At 0.3 mole fraction alcohol the competition between pure water and pure cosolvent structure results in the mixture having essentially a close-packed structure with consequent minimum free volume. Franks (26) has pointed out that the first derivative of the viscosity – solvent composition curve for ethanol water shows a maximum at 0.1 and a minimum

at 0.3 mole fraction corresponding to maximum and minimum structure. Franks further notes that the first derivative behavior, i.e. $d\eta/dc$ versus c, may be more revealing as far as structure is concerned than the simple plot of η versus c which shows a single maximum at 0.2 mole fraction. At 0.3 mole fraction, therefore, there are no preformed holes in the binary solvent and dissolution of the third component solute requires maximum expansion of the solvent to accommodate the solute. A maximum in partial molal volume of the quaternary ammonium salts should therefore be observed. The plots in Fig. 4 demonstrate such behavior and, in addition, show that the height of the partial volume maximum is strictly size dependent, as would be expected if the dissolution mechanism involved simple expansion of the solvent to accommodate the solute.

III. The 0.3 mole fraction minimum. The partial molal volume of the chloride ion passes through a minimum at 0.3 mole fraction and, furthermore, is distinctly negative at this composition. Clearly electrostriction by the small, fully charged chloride ion is a maximum at 0.3 mole fraction. While it was suggested that at this composition the solvent was closest to close packed, it is clearly not strictly close packed, and under the influence of the strong charge field of the chloride ion, solvent molecules can be electrostricted to form solvation shells, previously described as "soft ice" to distinguish such structural ordering from that characteristic of hydrophobic interaction at 0.1 mole fraction. Such electrostriction contraction of the solvent leads to the minimum in partial molal volume of the chloride ion at 0.3 mole fraction. The observation of maximum electrostriction (minimum volume) at this composition results from the fact that here the electrostriction or "soft ice" promoting effect of the ion is no longer in competition with the hydrophobic "ice-berg" promoting effect of the alcohol cosolvent. Indeed at 0.3 mole fraction the binary solvent system is as unstructured as it can be and the solvent molecules are relatively most available for electrostriction around the ion. While it can be considered nothing more than an indication, it should also be noted (Fig. 3) that the partial molal volume of the chloride ion only begins to decrease rapidly (onset of dominant electrostriction) beyond 0.1 mole fraction ethanol after the hydrophobic structure making of the cosolvent has passed its maximum and the electrostriction effect of the ion is essentially without competition.

Acknowledgments

The authors acknowledge with thanks general financial support of this work by the National Research Council of Canada and The University of Calgary for a Postdoctoral Fellowship to I. L. during the tenure of which this work was carried out.

1. H. S. Frank and M. W. Evans. J. Chem. Phys. **13** 507 (1945).
2. D. F. Evans and R. L. Kay. J. Phys. Chem. **70**, 366 (1966). D. F. Evans, G. P. Cunningham, and R. L. Kay. J. Phys. Chem. **70**, 2974 (1966). R. L. Kay and D. F. Evans. J. Phys. Chem. **70**, 2325 (1966).
3. G. E. Boyd, A. Schwarz, and S. Lindenbaum. J. Phys. Chem. **70**, 821 (1966). W-Y. Wen, S. Saito, and C-M. Lee. J. Phys. Chem. **70**, 1244 (1966).
4. R. L. Kay, T. Vituccio, C. Zawoyski, and D. F. Evans. J. Phys. Chem. **70**, 2336 (1966).
5. S. Lindenbaum. J. Phys. Chem. **70**, 814 (1966). G. E. Boyd, J. W. Chase, and F. Vaslow. J. Phys. Chem. **71**, 573 (1967).
6. K. W. Bunzl. J. Phys. Chem. **71**, 1358 (1967).
7. H. S. Frank and W-Y. Wen. Discussions Faraday Soc. **24**, 133 (1957).
8. L. G. Hepler, J. M. Stokes, and R. H. Stokes. Trans. Faraday Soc. **61**, 20 (1965). B. E. Conway and R. E. Verrall. J. Phys. Chem. **70**, 3952 (1966). R. E. Verrall and B. E. Conway. J. Phys. Chem. **70**, 3961 (1966).
9. R. H. Wood and H. L. Anderson. J. Phys. Chem. **71**, 1871 (1967).
10. B. E. Conway. Ann. Rev. Phys. Chem. **17**, 481 (1966).
11. B. E. Conway, R. E. Verrall, and J. E. Desnoyers. Trans. Faraday Soc. **62**, 2738 (1966).
12. O. Redlich and J. Bigeleisen. J. Am. Chem. Soc. **64**, 758 (1942).
13. K. Fajans and O. Johnson. J. Am. Chem. Soc. **64**, 668 (1942).
14. J. Padova. J. Chem. Phys. **39**, 1552 (1963).
15. P. Mukerjee. J. Phys. Chem. **65**, 740 (1961); **65**, 744 (1961).
16. E. Glueckauf. Trans. Faraday Soc. **61**, 914 (1965).
17. R. Zana and E. Yeager. J. Phys. Chem. **71**, 521 (1967).
18. R. Stokes and R. Robinson. Trans. Faraday Soc. **53**, 301 (1957).
19. J. Bernal and R. Fowler. J. Chem. Phys. **1**, 515 (1933).
20. F. Vaslow. J. Phys. Chem. **70**, 2286 (1966).
21. G. W. Stewart. J. Chem. Phys. **7**, 869 (1939). H. E. Wirth. J. Am. Chem. Soc. **62**, 1129 (1940).
22. O. Redlich and D. M. Meyer. Chem. Rev. **64**, 221 (1964).
23. W-Y. Wen and S. Saito. J. Phys. Chem. **68**, 2639 (1964).

Can. J. Chem. Downloaded from www.nrcresearchpress.com by 210.87.254.105 on 09/05/12
For personal use only.

24. F. FRANKS and D. J. G. IVES. Quart. Rev. London, **20**, 1 (1966). E. M. ARNETT, W. G. BENTRUDE, J. J. BURKE, and P. M. DUGGLEBY. J. Am. Chem. Soc. **87**, 1541 (1965).
25. J. L. KAVANAU. Water and solute-water interactions. Holden-Day, Inc., San Francisco. 1964. pp. 22 and 28.
26. F. FRANKS (*Editor*). Physico-chemical processes in mixed aqueous solvents. W. Heinemann Educational Books, Ltd., London. 1967. pp. 66–67.

Can. J. Chem. Downloaded from www.nrcresearchpress.com by 210.87.254.105 on 09/05/12
For personal use only.

Can. J. Chem. Downloaded from www.nrcresearchpress.com by 210.87.254.42 on 09/05/12
For personal use only.

Methods of preparation of sulfanes

E. MULLER AND J. B. HYNE

Fundamental Sulphur Research Group, Alberta Sulphur Research Ltd., and Department of Chemistry, The University of Calgary, Calgary, Alberta

Received July 26, 1967

Sulfane crude oils obtained by acidification of aqueous sodium polysulfide solutions vary little in composition with varying sulfur content of the solution. Evidence presented suggests that the distribution of the sulfanes in such crude oils reflects the equilibrated distribution of the various polysulfide anions in the aqueous solution before acidification. The sulfane distribution in mixtures obtained by reaction of liquid H_2S with Br_2, SCl_2, and S_2Cl_2 respectively varies over a wide range, depending on the molar ratio of the reactants. Liquid H_2S reacts with Br_2 or SCl_2 to yield essentially the same products. These reactions, however, differ in the nature of their intermediates. By using a large excess of liquid H_2S, H_2S_3 was directly synthesized in over 90% purity. Liquid H_2S reacts with S_2Cl_2 to yield H_2S_4 in over 90% purity. Gaseous HCl catalyzes the reaction of H_2S with the chlorosulfanes and a mechanism is suggested involving HCl as a proton transfer agent in the formation of the reactive intermediates.

Canadian Journal of Chemistry, 46, 2341 (1968)

Introduction

Hydrogen polysulfides have been synthesized by a variety of methods each of them yielding a mixture of sulfanes rather than a single species. The preparation of sulfane crude oils from aqueous sodium polysulfide solutions has been reported previously (1–4). Butler and Maass reported the isolation of H_2S_2 and H_2S_3 in good yield from crude oils, suggesting the existence of substantial amounts of these sulfanes in the parent crude oil. Feher, however, reported that crude oils from aqueous polysulfide solutions did not contain H_2S_2 and H_2S_3, but did contain H_2S_4 and the higher sulfanes. He further pointed out that the average sulfur chain length of the crude oil decreased with decreasing average sulfur chain length of the sodium polysulfide solutions. Though contradictory, these observations indicate that the synthesis of a crude oil containing only one or two major sulfane species may be accomplished under suitable conditions.

In addition, differing results have been reported for the reaction of liquid H_2S with halogens and chlorosulfanes (5–7). While Feher and Kruse found H_2S_3 and H_2S_4 to be the main components of the reaction of liquid H_2S with halogens (6), Schmidt reported the formation of considerable amounts of H_2S_2 and H_2S_3 (7). Bromine was reported to react less vigorously than chlorine, although yielding the same reaction products. In order to gain a deeper understanding of these reactions we investigated them in greater detail, particularly with respect to the direct synthesis of single sulfane species.

Experimental

Materials

H_2S: Matheson of Canada Ltd., used without further purification.

Bromine: Analytical reagent grade, the British Drug Houses Ltd., used without further purification.

Chlorosulfanes: SCl_2 and S_2Cl_2, Hooker Electro Chemical Co., distilled before use, b.p. (SCl_2) = 59–60 °C, b.p. (S_2Cl_2) = 24–25 °C at 10 mm.

Synthesis

Sodium Polysulfides

Two molar aqueous Na_2S_x solutions with $x = 2$ to 4.7 (saturation) were prepared by dissolving the required amount of elemental sulfur in a 2 *M* aqueous Na_2S solution by stirring and gentle heating.

Sulfane Mixtures ("Crude Oils")

The various 2 *M* aqueous polysulfide solutions were acidified with a 10-fold excess of 6 *M* HCl by slowly adding the polysulfide solution to the hydrochloric acid and cooling the reaction mixture to 0 °C. The separated crude oil was dissolved immediately in CCl_4 or CS_2.

Sodium polysulfide solutions with an average sulfur content of $x = 2$ gave a very poor percent yield of total hydrogen polysulfides based on conversion of sodium polysulfides, the main product upon acidification being H_2S. An increase of the sulfur content up to $x = 4.7$ (saturation) increased the overall yield of hydrogen polysulfides. A similar dependence of the yield on the average sulfur chain length of the sodium polysulfide solution was observed by Feher and Laue (3).

H_2S_3 and H_2S_4

Gaseous H_2S was liquified and simultaneously saturated with HCl under anhydrous conditions. 0.01 mole of one of Br_2, SCl_2, and S_2Cl_2 respectively were dissolved in CCl_4 or CS_2 and slowly added to the liquified H_2S while stirring. The reaction mixture was kept at −70 °C for 1 to 2 h before the excess of H_2S was allowed to evaporate slowly. The remaining sulfane solution was then brought to a standard concentration of 2 moles H_2S_x per 1000 ml solvent, assuming a 100% yield. The

Can. J. Chem. Downloaded from www.nrcresearchpress.com by 210.87.254.42 on 09/05/12
For personal use only.

molar ratio of H_2S to the added reactants was varied from 30:1 to 660:1.

The reaction of SCl_2 and S_2Cl_2 with a 440 molar excess of liquid H_2S yielded 86% and 94% sulfanes, respectively. Under the same conditions bromine was converted into 72% sulfanes.

Results

1. Hydrogen Polysulfides from Sodium Polysulfides

Sodium polysulfides were converted upon acidification with hydrochloric acid into hydrogen polysulfides according to

[1] $$Na_2S_x + 2HCl \rightarrow H_2S_x + 2NaCl$$

The n.m.r. analysis showed that the reaction products were a mixture of sulfane homologues. A small variation of sulfane distribution within a crude oil as a function of the sulfur content of the starting material was observed but may not be significant in view of the experimental uncertainties in the n.m.r. analytical method (Fig. 1). The points shown in Fig. 1 are considered to be accurate to within $\pm 5\%$ of the value shown. H_2S_4 was the predominant single species regardless of the initial sulfur content of the sodium polysulfide solution. H_2S_3 and H_2S_5 were present in considerable amounts, whereas H_2S_2 was present only in traces. By increasing the sulfur content of the starting material the relative proportion of the combined higher sulfanes ($x \geqslant 6$) was increased at the expense of the lower sulfanes.

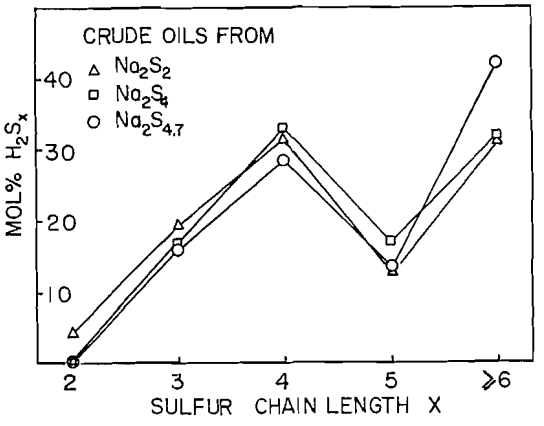

FIG. 1. The distribution of sulfanes in crude oils from acidification of polysulfide solutions with varying sulfur content. *Note*: Mole % yields shown are relative to other sulfanes and are not absolute yields based on % conversion of the sodium polysulfides.

2. Hydrogen Polysulfides by the Reaction of Liquid H_2S with Br_2

Under careful exclusion of moisture an excess of liquid H_2S reacted with bromine at -70 °C to yield a sulfane mixture according to

[2] $$xH_2S + (x-1)Br_2 \rightarrow H_2S_x + 2(x-1)HBr$$

$x = 2$ to 6 and higher.

The composition of the sulfane mixture was found to be largely dependent on the molar ratio of H_2S to Br_2. H_2S_3 was the main component (Fig. 2). An increase of the molar ratio of H_2S:Br_2 increased the relative occurrence of H_2S_3 and decreased the occurrence of the higher sulfanes accordingly. The formation of small amounts of H_2S_2 is favored by an increase of the H_2S:Br_2 ratio. When pure bromine rather than a bromine–CS_2 mixture is allowed to react with the liquid H_2S, the sulfane distribution changed considerably in favor of H_2S_4 and the higher sulfanes.

3. Hydrogen Polysulfides by the Reaction of Liquid H_2S with SCl_2 and S_2Cl_2

Under careful exclusion of moisture an excess of liquid H_2S was allowed to react with SCl_2 and S_2Cl_2 dissolved in CCl_4 or CS_2. Neither SCl_2 nor S_2Cl_2 reacted with H_2S at -70 °C before the greater part of the H_2S had evapo-

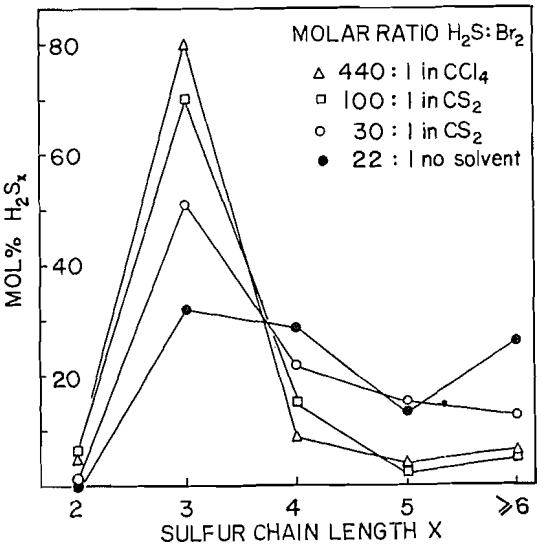

FIG. 2. The distribution of sulfanes from H_2S plus Br_2 as a function of the molar ratio of the reactants.

Can. J. Chem. Downloaded from www.nrcresearchpress.com by 210.87.254.42 on 09/05/12
For personal use only.

rated. Then a violent reaction took place yielding HCl and polymeric sulfur according to

[3] $$n\mathrm{S}_y\mathrm{Cl}_2 + n\mathrm{H}_2\mathrm{S} \rightarrow m\mathrm{S}_x + 2n\mathrm{HCl}$$

$y = 1, 2$; S_x = polymeric sulfur.

It appeared that the developing HCl autocatalyzed the reaction such that the reaction went out of control. As this reaction took place when only little H_2S was left, the conditions for the formation of sulfanes were unfavorable. To avoid the initial delay of the reaction, advantage was taken of the catalytic effect of HCl by saturating the liquid H_2S with HCl *previous* to the addition of the chlorosulfanes. H_2S saturated with HCl reacted immediately with the chlorosulfanes to yield a mixture of hydrogen polysulfides according to

[4] $$2n\mathrm{H}_2\mathrm{S} + n\mathrm{S}_y\mathrm{Cl}_2 \rightarrow n\mathrm{H}_2\mathrm{S}_x + 2n\mathrm{HCl}$$

$y = 1, 2$; $x = 2$ to 6 and higher.

The composition of the mixture was found to be dependent on the nature of the chlorosulfane and the molar ratio H_2S:chlorosulfane. H_2S and SCl_2 yielded a sulfane mixture with H_2S_3 being the main component (Fig. 3). An increase of the H_2S:SCl_2 ratio increased the relative occurrence of H_2S_3 in the sulfane mixture and decreased the yield of the higher sulfanes accordingly. Since the proton n.m.r. signal of H_2S_4 overlaps the broad base of the H_2S_3 signal the relative occurrence of H_2S_4 when present in small amounts can only be estimated. H_2S_2 is present only in trace amounts.

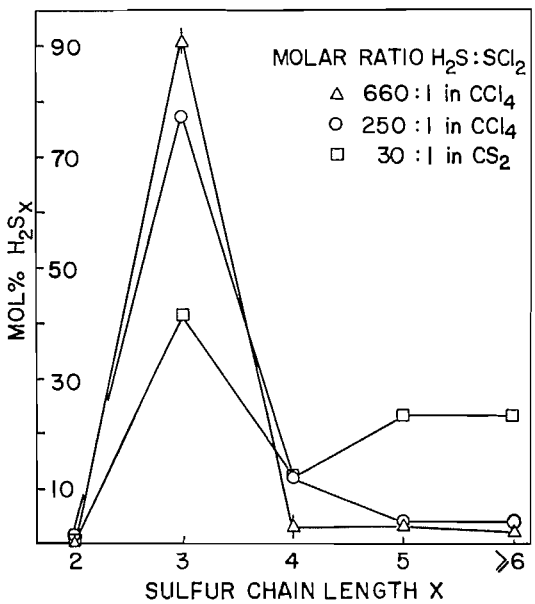

FIG. 3. The distribution of sulfanes from H_2S plus SCl_2 as a function of the molar ratio of the reactants.

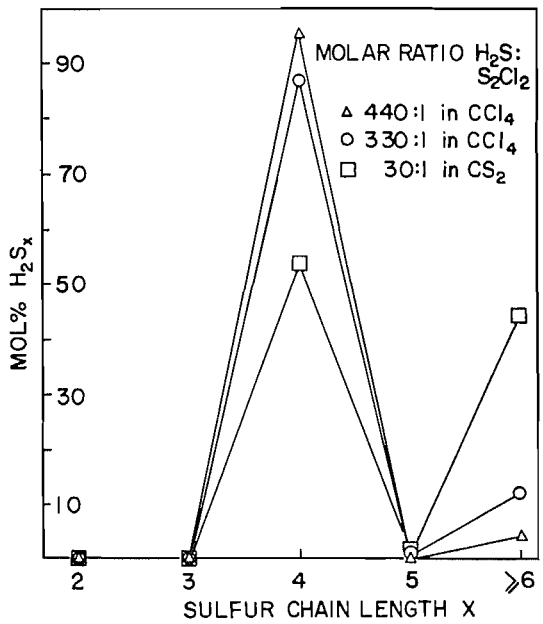

FIG. 4. The distribution of sulfanes from H_2S plus S_2Cl_2 as a function of the molar ratio of the reactants.

S_2Cl_2 reacted with H_2S to yield a sulfane mixture with H_2S_4 being the main component (Fig. 4). Increase of the H_2S:S_2Cl_2 ratio increased the relative occurrence of H_2S_4, as was observed in the case of H_2S_3 production from H_2S and SCl_2. The distribution of the higher sulfanes next to the main sulfane, however, is somewhat different. While the relative occurrence of H_2S_5 is low and is affected only very slightly by a change of the molar ratio of the reactants, the relative occurrence of sulfanes with a sulfur chain length of 6 or greater increased with decreasing H_2S:S_2Cl_2 ratio in a more pronounced manner than was observed in the case of H_2S plus SCl_2 (Figs. 3 and 4). The proton signal for H_2S_x ($x \geqslant 6$) from H_2S and S_2Cl_2 was also found to be narrower than that for H_2S_x ($x \geqslant 6$) from H_2S and SCl_2, suggesting a narrower composition range for the higher sulfanes from S_2Cl_2 compared with SCl_2.

Discussion

In the investigation of the qualitative and quantitative composition of a sulfane mixture,

Can. J. Chem. Downloaded from www.nrcresearchpress.com by 210.87.254.42 on 09/05/12
For personal use only.

n.m.r. has been found to be very useful (4, 8). All sulfanes up to a sulfur chain length of 5 are characterized by a single resolvable proton signal for the terminal hydrogens; the position of this signal was found to be dependent on the sulfur chain length of the sulfanes. For H_2S_6 and the higher sulfanes a broad n.m.r. signal was found, thus limiting the qualitative n.m.r. analysis to the lower members of the sulfanes with a sulfur chain length of 1 to 5.

When aqueous sodium polysulfide solutions of a given average sulfur chain length are converted to hydrogen polysulfides by reaction [1], the question arises as to whether the sulfane distribution in the crude oils reflects the polysulfide anion distribution in the aqueous solution or whether the observed sulfane distribution is a consequence of an equilibration among the sulfanes after formation.

Feher attributed the absence of H_2S_2 and H_2S_3 in the crude oils to secondary disproportionation reactions according to

[5] $$H_2S_4 \rightarrow H_2S + 3S$$
$$2H_2S_2 \rightarrow H_2S + H_2S_3$$
$$2H_2S_3 \rightarrow H_2S + H_2S_5 \quad .$$

In the present work, however, it was found that all crude oils did contain considerable amounts of H_2S_3 and H_2S_4 (Fig. 1). It was further observed that both pure H_2S_3 and H_2S_4 are relatively stable for several hours at room temperature, indicating that the observed H_2S_3/H_2S_4 ratios in mixtures are not necessarily the equilibrated values. Sulfanes, therefore, do not equilibrate after their formation at a rate fast enough to invalidate the n.m.r. analytical technique.

We, therefore, conclude that the distribution of the sulfanes in crude oils shows the distribution of the various polysulfide anions in the aqueous solution prior to acidification, provided that the n.m.r. analysis is made immediately after the preparation of the crude oils. By converting the equilibrated polysulfide anions [6] into the corresponding hydrogen polysulfides according to [7] the equilibrium [6] can be made evident in a "quasi-frozen" state by taking the n.m.r. spectrum of the hydrogen polysulfides.

[6] $$S_x^{2-} \rightleftharpoons S_{x-y}^{2-} + S_y^{2-}$$

$x = 2$ to 6 and higher; $y = 1$ to $x - 1$.

[7] $$S_x^{2-} + 2H^+ \rightarrow H_2S_x$$

Feher attributed his observations that the average sulfur chain length of the crude oils was higher than the average sulfur chain length of the parent polysulfide solution to secondary reactions of the type [5]. As S^{2-} ions upon acidification will be converted into H_2S which will escape out of the hydrogen polysulfide mixture, the apparent higher average sulfur chain length of the hydrogen polysulfide mixture with respect to the parent polysulfide solution may well be explained.

The observed increase in yield of hydrogen polysulfides with increasing sulfur content of the sodium polysulfide solution may be due to the fact that an increase of the sulfur content of the polysulfide solutions will decrease the S^{2-} ion concentration by removing the S^{2-} ions out of equilibrium [6] by

[8] $$S^{2-} + xS \rightarrow S_{x+1}^{2-},$$

thus reducing the formation of H_2S. As H_2S_4 was found to be the main component of the sulfane mixture, it is suggested that the tetrasulfide anion is the most stable polysulfide anion in the aqueous solution under the prevailing conditions. This agrees with the findings of Pearson and Robinson, who found the stability of sodium tetrasulfides to be significant (9).

The first step of the reaction of excess liquid H_2S with the halogen most likely will be the formation of a reactive monohalogenated intermediate according to [9], as was suggested by Schmidt (7). The reactive intermediate will subsequently react with H_2S to form H_2S_2 by [10]. An increase of the molar ratio of H_2S:Br_2 is expected to enhance the reaction of HSBr with H_2S and consequently to yield H_2S_2 in increasing amounts. However, H_2S_2 was found only in relatively small amounts (Fig. 2), whereas H_2S_3 was found to be the main component. This would suggest that H_2S_2 is far more reactive than H_2S and is competing favorably with H_2S for HSBr according to [11]. The formation of H_2S_3 as main component and the fact that sulfanes higher than H_2S_3 were found in decreasing amounts with increasing sulfur chain length suggest that sulfanes higher than H_2S_2 are relatively stable with respect to the reaction with HSBr as shown in [12].

[9] $$H_2S + Br_2 \rightarrow HSBr + HBr$$

[10] $$HSBr + H_2S \rightarrow H_2S_2 + HBr$$

Can. J. Chem. Downloaded from www.nrcresearchpress.com by 210.87.254.42 on 09/05/12
For personal use only.

[11] $HSBr + H_2S_2 \xrightarrow{\text{fast}} H_2S_3 + HBr$

[12] $HSBr + H_2S_x \rightarrow H_2S_{x+1} + HBr, x = 3, 4, 5, \ldots$

[13] $Br_2 + H_2S_x \rightarrow HS_xBr + HBr$

[14] $HS_xBr + H_2S \rightarrow H_2S_{x+1} + HBr$

Alternatively, H_2S_3 may have been formed via SBr_2 as one of the reactive intermediates according to

[15] $HSBr + Br_2 \xrightarrow{\text{fast}} SBr_2 + HBr$

[16] $SBr_2 + H_2S \rightarrow HSSBr + HBr$

[17] $HSSBr + H_2S \rightarrow H_2S_3 + HBr$.

A clear differentiation between the two possible reaction pathways cannot be made at present. The observed small increase of the H_2S_2 yield with the increase of the H_2S:Br_2 ratio (see Fig. 2), however, supports the view of the intermediate formation of H_2S_2 rather than of SBr_2.

The observed increase of the yield of sulfanes higher than H_2S_3 when pure bromine is added rather than a solution of bromine is probably due to a slower distribution of the added bromine and the primarily formed reactive intermediates and reaction products in the liquid H_2S. Br_2, HSBr, and its reaction products might become locally concentrated, thus enhancing the formation of higher polysulfides by reactions [12], [13], and [14]. If a solution of Br_2 is added, a faster distribution in the liquid hydrogen sulfide will occur and consequently reactions leading to higher polysulfides will be suppressed. The effect of bromine dilution on the composition of the products levelled off quickly. A dilution of bromine to less than 2 moles Br_2 per 1000 ml solvent had no further noticeable effect on the composition of the products.

The first step of the reaction of H_2S with SCl_2 is likely to be the formation of an S—S bond yielding a reactive intermediate according to equation [18] which subsequently will react by equation [19] to yield essentially the same reaction products as the reaction of liquid H_2S with bromine. The reactions differ, however, in the nature of their intermediates. Accordingly, no H_2S_2 is expected from the reaction of liquid H_2S with SCl_2. The trace amounts of H_2S_2 actually found are probably due to the formation of chlorine (eq. [20]) and subsequent reaction with H_2S. Sulfanes higher than H_2S_3 can be formed by the further reaction of lower sulfanes with HSSCl according to eq. [21].

[18] $HSH + ClSCl \rightarrow HSSCl + HCl$

[19] $HSSCl + HSH \rightarrow H_2S_3 + HCl$

[20] $2SCl_2 \rightleftharpoons S_2Cl_2 + Cl_2$

[21] $HSSCl + H_2S_x \rightarrow H_2S_{x+2} + HCl$

$x = 2, 3, 4, 5, \ldots$

The mechanism of the observed catalytic effect of HCl is not fully understood. HCl may participate in the formation of a six-membered transition state to act as a proton transfer agent in the formation of HSSCl from H_2S and the chlorosulfane.

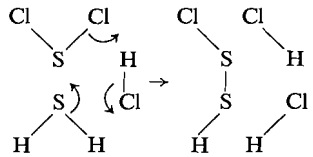

The reaction of liquid H_2S with S_2Cl_2 most likely proceeds via a similar monohalogenated intermediate formed by reaction [22], which then subsequently reacts with H_2S to form H_2S_4 by reaction [23]. The formation of sulfanes with a sulfur chain length of 6 and greater was suppressed by an increase of the H_2S:S_2Cl_2 ratio (Fig. 4). Sulfanes higher than H_2S_4, therefore, are most likely formed by secondary reactions of the primary H_2S_4 with the reactive intermediate according to [24].

[22] $HSH + ClSSCl \rightarrow HSSSCl + HCl$

[23] $HSH + ClSSSH \rightarrow H_2S_4 + HCl$

[24] $H_2S_4 + ClSSSH \rightarrow H_2S_7 + HCl$

According to this reaction sequence, H_2S_4 is expected to be the main component in the reaction mixture and H_2S_7 is expected to be the main component of the sulfanes with a sulfur chain length of 6 or greater. As mentioned previously, H_2S_4 indeed was found to be the main sulfane. Unfortunately, the n.m.r. analysis does not resolve signals of sulfanes with a sulfur chain length of 6 or greater. The proton signal of these sulfanes, however, is much narrower than that observed for the higher sulfanes prepared by other methods and could well indicate a predominance of H_2S_7.

1. I. BLOCH and F. HOHN. Ber. Deut. Chem. Ges. **41**, 1961 (1908).
2. K. H. BUTLER and O. MAASS. J. Am. Chem. Soc. **52**, 2184 (1930).

3. F. FEHER and W. LAUE. Z. Anorg. Allgem. Chem. **288**, 104 (1956).
4. H. SCHMIDBAUR, M. SCHMIDT, and W. SIEBERT. Chem. Ber. **97**, 3374 (1964).
5. F. FEHER and W. KRUSE. Z. Anorg. Allgem. Chem. **288**, 123 (1956).
6. F. FEHER and W. KRUSE. Z. Anorg. Allgem. Chem. **293**, 302 (1957).
7. M. SCHMIDT. Inorganic polymers. *Edited by* F. G. Stone and W. A. Graham. Academic Press, Inc., New York. 1962. Chap. 3.
8. J. B. HYNE, E. MULLER, and T. K. WIEWIOROWSKI. J. Phys. Chem. **70**, 3733 (1966).
9. T. G. PEARSON and P. L. ROBINSON. J. Chem. Soc. 1473 (1930).

Can. J. Chem. Downloaded from www.nrcresearchpress.com by 210.87.254.42 on 09/05/12
For personal use only.

Can. J. Chem. Downloaded from www.nrcresearchpress.com by 210.87.254.6 on 09/05/12
For personal use only.

Complexes of alkyl and aryl cyanides. Part VI.[1] The vibrational spectra of $MX_2.2RCN$, where M = Pd or Pt, X = Cl or Br, and R = Me or Ph, and the assignment of the metal–nitrogen stretching frequency

R. A. WALTON

Department of Chemistry, University of Reading, Whiteknights Park, Reading, Berkshire, England

Received January 25, 1968

A careful examination of the Raman and infrared spectra of the crystalline planar complexes *cis*- and *trans*-$MX_2.2RCN$, where M = Pd or Pt, X = Cl or Br, and R = Me or Ph, reveals intense absorption bands in the 125–80 cm^{-1} region which can be assigned to modes involving stretching of the metal–nitrogen bonds. Alternative assignments for ν(M—N) are also discussed. These results are compared with those for other metal halide – RCN systems. The complexes *trans*-$PtBr_2.2RCN$ are described for the first time.

Canadian Journal of Chemistry, 46, 2347 (1968)

Introduction

In a previous paper (Part III in this series) (2) it was concluded from far-infrared spectral measurements (500–200 cm^{-1}) that ν(M—N) occurs below 200 cm^{-1} in methyl and phenyl cyanide complexes of palladium(II), platinum(II), and rhodium(III). Previously, ν(Zn—N) had been assigned (3) to a band at 174 cm^{-1} in the spectrum of $ZnCl_2.2MeCN$. Since this time, various workers have reported metal–nitrogen stretching frequencies in a variety of alkyl and aryl cyanide complexes viz. ~300 cm^{-1} in $MX_4.NC.CH_2CONH_2$, where M = Ti or Sn (4); ~175 cm^{-1} in silver(I)–succinonitrile complexes (5); 550–500 cm^{-1} in $M(CO)_3(MeCN)_3$, where M = Cr, Mo, or W (6); 250–195 cm^{-1} in $SnCl_4.2RCN$, where R = Me, CH_2=CH—, or Ph (7). The most convincing results to date are those of Farona and Grasselli (7), who assigned two ν(Sn—N) modes in the infrared spectra of *cis*-$SnCl_4.2RCN$, consistent with the *cis*-stereochemistry. The above assignments have been based exclusively upon infrared spectral measurements. Unfortunately these are rarely unambiguous and in the assignment of metal–ligand stretching vibrations (other than metal–halogen) a certain amount of "band picking" is usually necessary. It should also be borne in mind that ν(M—L) may be masked by the intense bands due to ν(M—X), and that the former could in some instances be confused with bands arising from overtone and combination vibrations.

In the present paper detailed Raman and infrared spectral studies on several complexes of the type $MX_2.2RCN$ are reported, and these results, taken in conjunction with earlier work (2, 8), are compared with the results and interpretations of others (3–7) on the assignment of ν(M—N) in related systems. Complexes of the palladium(II) and platinum(II) halides have been used as model compounds in this and other spectral investigations (2, 8) because of the wealth of data already reported in the literature on the M—X stretching and bending modes of complexes of the type $MX_2.2L$ (8–15). This should aid the assignment of the spectra of $MX_2.2RCN$.

Results and Discussion

A. Coordinated Ligand Spectra (4000–500 cm^{-1})

The infrared spectra of *trans*-$PdCl_2.2PhCN$ and *cis*-$PtX_2.2PhCN$ have been reported previously (8). *Trans*-$PtBr_2.2PhCN$ which is reported here for the first time has an infrared spectrum (see Experimental) very similar to that of *trans*-$PdCl_2.2PhCN$, with ν(C≡N) at 2280 cm^{-1} and strong absorptions at 757 and 683 cm^{-1}, associated with the out-of-plane C—H deformation vibrations of the phenyl groups.

Of the methyl cyanide complexes, only *trans*-$PtBr_2.2MeCN$ does not appear to have been isolated previously (16–18). A comparison of the hexachlorobutadiene mull spectra of *trans*- and *cis*-$MX_2.2MeCN$ (Fig. 1) suggests that the regions 3100–2800 and 1500–1300 cm^{-1} may be used to establish the stereochemistry of a planar complex of the type $MX_2.2MeCN$.

B. Far-Infrared and Raman Spectra of $MX_2.2MeCN$

The spectral data for the methyl cyanide

[1]Part V, ref. 1.

Can. J. Chem. Downloaded from www.nrcresearchpress.com by 210.87.254.6 on 09/05/12
For personal use only.

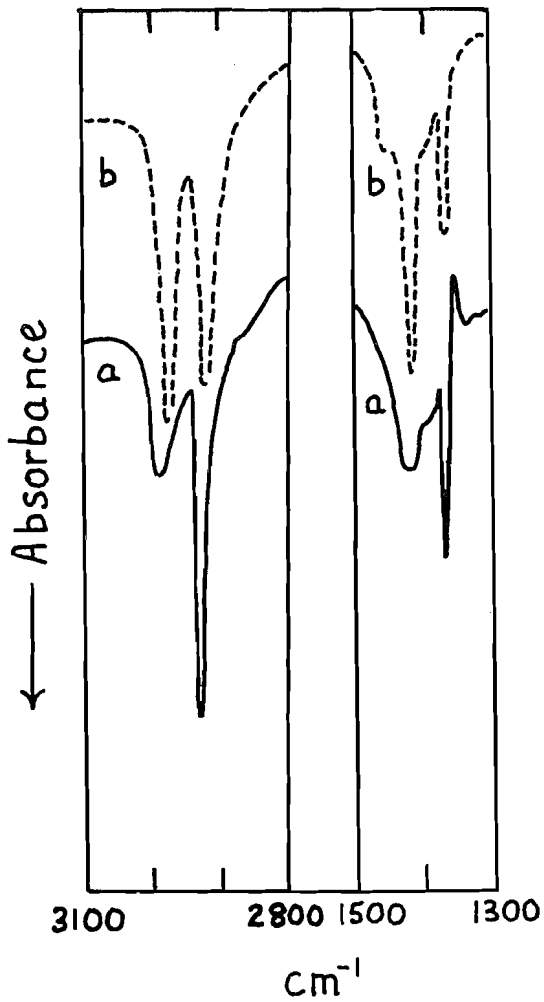

FIG. 1. Hexachlorobutadiene mull spectra of *trans*- and *cis*-MX_2.2MeCN: (*a*) *trans*-$PdCl_2$.2MeCN and *trans*-$PtBr_2$.2MeCN (*b*) *cis*-$PtCl_2$.2MeCN and *cis*-$PtBr_2$.2MeCN.

complexes are shown in Table I. The fluorescence of $PdCl_2$.2MeCN prevented the measurement of its Raman spectrum. For *trans*-$PdCl_2$.2MeCN, *cis*-$PtCl_2$.2MeCN, and *trans*-$PtBr_2$.2MeCN ν(M—X) are immediately obvious from a comparison with other work (8–15), and confirm the stereochemistry of these species. Thus, *trans*-$PtBr_2$.2MeCN should have two ν(M—X) modes, one of which is Raman active (A_{1g} symmetry) and the other infrared active (B_{3u} symmetry) as a consequence of the mutual-exclusion principle. *Cis*-$PtCl_2$.2MeCN, on the other hand, has two ν(M—X) modes (symmetry $A_1 + B_1$) which are both infrared and Raman active. One unusual feature of the spectra of *cis*-$PtCl_2$.2MeCN is the splitting (~ 10 cm^{-1}) of the highest ν(Pt—Cl) frequency. This may be a solid-state effect or, alternatively, arise from the presence of an overtone (2×170?) or combination band with enhanced intensity, possibly by Fermi resonance.

The infrared spectrum of *cis*-$PtBr_2$.2MeCN has two intense bands at 246 and 220 cm^{-1}, which could be assigned to ν(Pt—Br). However, the Raman spectrum of this complex reveals a strong band at 245 cm^{-1} and weaker bands at 258 and 212 cm^{-1}, which suggests that the band at ~ 215 cm^{-1} is not ν(Pt—Br), since the A_1 metal–halogen stretching mode is invariably at a lower frequency than B_1 and more intense than the latter in the Raman spectrum. The band at ~ 215 cm^{-1} may correspond to that at 226 cm^{-1} in the infrared spectrum of *cis*-$PtCl_2$.2MeCN.

Rather more difficulty is encountered in the unambiguous assignment of the metal–halogen bending modes; in these particular complexes these modes will not exclusively involve the metal–halogen bonds. However, *trans*-$PdCl_2$.2MeCN and *cis*-$PtCl_2$.2MeCN have bands in the 180–160 cm^{-1} region (Table I) which are assigned to modes involving bending of the MCl_2 groups.

This then leaves the problem of the metal–nitrogen stretching vibrations which will be discussed in terms of three spectral regions.

(a) 500–300 cm^{-1}

The group of bands which are observed around 400 cm^{-1} in these and other complexes of alkyl and aryl cyanides (19–22) are assigned to δ(C—C≡N) of the coordinated RCN molecules. Since their frequencies do not appear to be dependent upon the stereochemistry or oxidation state of the central metal atom, it seems unlikely that this group of bands also contains absorptions due to ν(M—N).

The complexes *cis*- and *trans*-$PtBr_2$.2MeCN show medium–weak absorptions at ~ 320 and ~ 350 cm^{-1}, respectively, which do not apparently appear in the spectra of *cis*-$PtCl_2$.2MeCN, although they could be obscured by ν(Pt—Cl). The weakness of these bands (see Table I and Figs. 2 and 3) and the failure for more than one band to be observed (symmetry requires two ν(M—N) modes for *cis*-$PtBr_2$.2MeCN) suggest that they are not associated with the metal–nitrogen stretching vibrations.

TABLE I

Vibrational spectra and assignments for $MX_2.2MeCN$*

Trans-$PdCl_2.2MeCN$, infrared	*Cis*-$PtCl_2.2MeCN$		*Trans*-$PtBr_2.2MeCN$		*Cis*-$PtBr_2.2MeCN$		Assignment
	Infrared	Raman	Infrared	Raman	Infrared	Raman	
449 m	432 w	444 w	436 m–w	420 m–w	434 m–w	439 m	
413 m	417 w	422 w		388 m	404 m–w	406 m	δ(C—C≡N)
	406 w	409 w					
		389 s					
361 s	358 sh	362 m	231 s	232 w†		258 m	
	347 s	354 m		211 s	246 s	245 s	ν(M—X)
	330 sh	336 s					
160 m	175 m	177 m					$\delta(MCl_2)$
	160 m–s						
125 m–s	120 m–s	124 vs	117 m–s		116 s	117 vs	ν(M—N)?
	100 m–s			107 m–s	95 m–s	104 sh	
253 m	264 w		282 m–s	350 w	315 m–s	322 m–w	
240 m	251 m–w		251 m–w		279 vw		
~105 m,br	226 m	232 w†	134 sh	~140 w,br	220 m–s	212 w	Unassigned
~72 m–w		201 w	102 sh			194 m–w	
		90 m–s		83 m–s		78 m	
	73 w			58 m			
	68 m						

*Except for a band at 380 cm^{-1}, which is infrared and Raman active, methyl cyanide is transparent below 400 cm^{-1}.
†Spurious absorption.

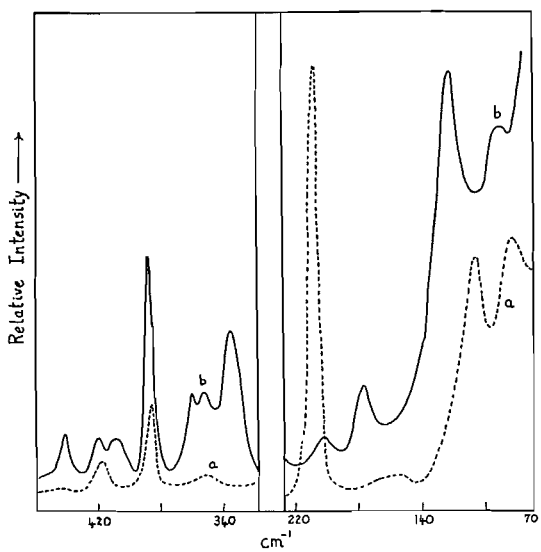

FIG. 2. Raman spectra of crystalline (*a*) *trans*-$PtBr_2.2MeCN$ and (*b*) *cis*-$PtCl_2.2MeCN$.

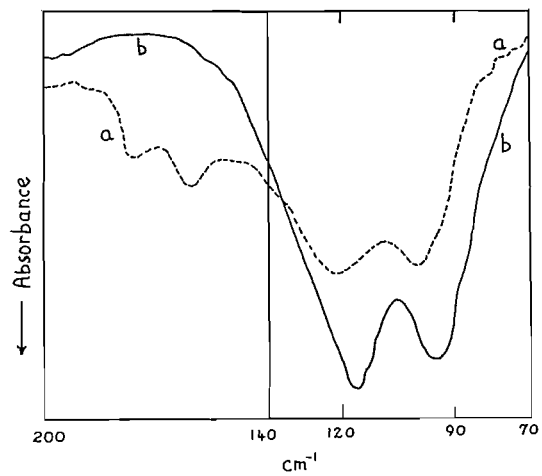

FIG. 3. Far-infrared spectra of (*a*) *cis*-$PtCl_2.2MeCN$ and (*b*) *cis*-$PtBr_2.2MeCN$.

(b) 300–200 cm^{-1}

As was remarked in a previous paper (2), the infrared spectra of $MX_2.2RCN$ in this region shows, in addition to ν(M—X), several absorptions which cannot on symmetry grounds be assigned to ν(M—N). Complimentary Raman data in the present investigation would seem to confirm this. Thus *cis*-$PtCl_2.2MeCN$ has infrared-active absorptions at 264, 251, and 226 cm^{-1} which are absent in the Raman spectrum of this crystalline complex. Therefore, unless ν(Pt—N) are unusually weak in the Raman spectra, they do not appear to occur in this spectral region.

(c) Below 200 cm^{-1}

As can be seen from Figs. 2 and 3 and Table I, the spectra in this region are dominated by intense absorptions between 125 and 80 cm^{-1}.

Can. J. Chem. Downloaded from www.nrcresearchpress.com by 210.87.254.6 on 09/05/12
For personal use only.

TABLE II

Vibrational spectra and assignments for $MX_2.2PhCN$

Trans-$PdCl_2$.2PhCN		*Cis*-$PtCl_2$.2PhCN		*Trans*-$PtBr_2$.2PhCN		*Cis*-$PtBr_2$.2PhCN, infrared	Assignment
Infrared	Raman	Infrared	Raman	Infrared	Raman		
420 m–w		415 w	422 w		400 w	393 w	
393 w	392 w	402 w	406 w				δ(C—C≡N)
		395 w					
368 s		355 s	369 m	243 s	234 w*	247 s	ν(M—X)
	306 s	344 s	340 s		204 vs	238 s	
104 m–s		109 sh					
	92 vs	104 m			90 m†		ν(M—N)?
		100 m–w					
312 m		306 s	310 w		176 w	293 w	
287 m–s		270 w	275 w		134 w	~228 sh?*	
250 w	255 w		234 m		~70 sh	~188 m–w,br	
	209 w		202 sh			~137 w	Unassigned
160 s	~160 w,br		183 m				
		165 s	163 s			121 w?	
130 m	~130 w	151 w				113 m–w	
72 w	~78 sh	135 m–w	138 m			~93 w?	
56 m		128 m?	~125 sh				
		~72 m					
		~62 m					

*Spurious absorption.
†Alternatively assigned to $\delta(PtBr_2)$.

The bands at ~ 170 cm^{-1} in the chloro complexes are assigned to δ(Cl—M—Cl), while the weak absorptions between 200 and 150 cm^{-1} in all the complexes are of unknown origin.

One problem of making spectral assignments below 150 cm^{-1} is the likely occurrence of absorption bands due to "lattice modes". These might not only obscure ν(M—L) but in some instances be incorrectly assigned to the latter. For $PtBr_2$.2MeCN, δ(Br—Pt—Br) should also be observed below 150 cm^{-1}, but since the corresponding absorption bands in the chloride complexes are only medium–weak in intensity, they are most likely obscured, at least in the *cis*-isomer (see Table I), by the very intense band between 120–80 cm^{-1}.

The intensity of the 120–80 cm^{-1} bands and their presence in both the Raman and infrared spectra of the chloride *and* bromide complexes would be consistent with their assignment as ν(M—N).

C. Far-Infrared and Raman Spectra of $MX_2.2PhCN$

For these complexes, the increased complexity of the ligand spectra (23) makes spectral assignments more difficult. As before (see *B*) the bands due to δ(C—C≡N), ν(M—X), and δ(Cl—M—Cl) are readily assigned (Table II).

During attempts to re-prepare samples of *cis*-$PtBr_2$.2PhCN, it was found that the reaction products had infrared spectra (500–200 cm^{-1}) different from that of the sample originally believed to be the *cis*-isomer (2, 8). Five samples were prepared by the same procedure and had identical spectra (Table II). During a further preparation, the *trans*-isomer was isolated, but attempts to repeat this preparation were not successful; the exact conditions under which the *trans*-isomer crystallizes in preference to the *cis* are as yet unknown. The *trans*-isomer does not appear to have been isolated before. The Raman spectrum of the "*cis*"-isomer (2, 8), which had an intense band at 206 cm^{-1}, similar to that observed in the *trans*-isomer (Table II) and assigned to $\nu_{sym}(Pt—Br)$, indicates that the original sample (8) was a mixture of isomers. Attempts to obtain the Raman spectrum of the authentic *cis*-isomer were frustrated by the fluorescence of the sample. In view of the complexity of the infrared and Raman spectra of *cis*-$PtCl_2$.2PhCN and *cis*-$PtBr_2$.2PhCN, detailed assignments will not be attempted. Indeed, the Raman spectrum of *cis*-$PtCl_2$.2PhCN was not accessible below ~ 120 cm^{-1} and the infrared spectra of the *cis*-isomers (200–33 cm^{-1}) were poorly defined, compared with those of the *trans*-isomers.

Can. J. Chem. Downloaded from www.nrcresearchpress.com by 210.87.254.6 on 09/05/12
For personal use only.

Can. J. Chem. Downloaded from www.nrcresearchpress.com by 210.87.254.6 on 09/05/12
For personal use only.

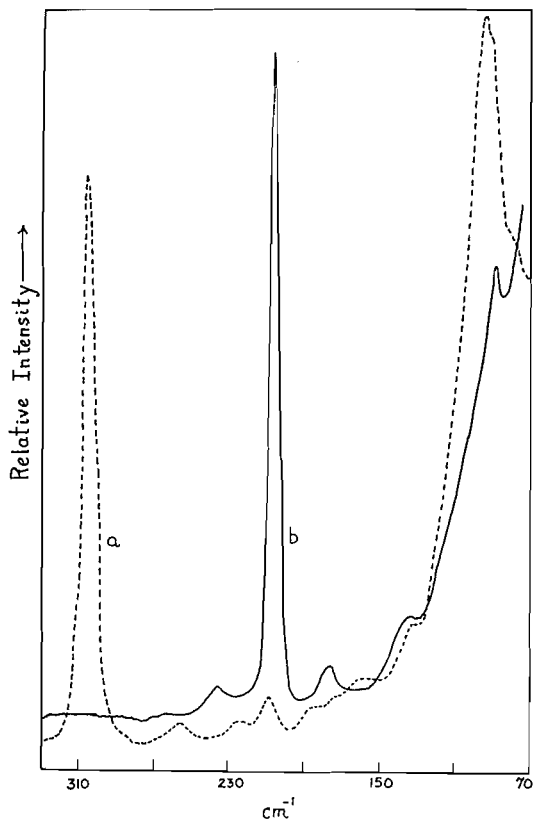

FIG. 4. Raman spectra of crystalline (*a*) *trans*-$PdCl_2$.2PhCN and (*b*) *trans*-$PtBr_2$.2PhCN.

The Raman spectra of *trans*-$PdCl_2$.2PhCN and *trans*-$PtBr_2$.2PhCN (Table II and Fig. 4) are each dominated by two intense absorptions. The higher frequency one is assigned to ν_{sym}-(M—X) and that at ~ 90 cm^{-1} to ν(M—N), being similar in position to that tentatively assigned to this mode in *trans*-$PtBr_2$.2MeCN. The band at 104 cm^{-1} in the infrared spectrum of *trans*-$PdCl_2$.2PhCN could be due to $\nu_{antisym}$-(Pd—N). The corresponding infrared spectrum of *trans*-$PtBr_2$.2PhCN could not be measured owing to lack of sufficient sample.

The Raman spectrum of phenyl cyanide (23) has its lowest energy band at 172 cm^{-1}, so the bands at ~ 100 cm^{-1} in the spectra of *trans*-MX_2.2PhCN cannot be assigned to ligand modes.

D. Other Alkyl Cyanide Complexes

The complexes $RhCl_3$.3MeCN and $RhCl_3$.3-EtCN (20) were re-prepared and their infrared spectra (500–200 cm^{-1}) remeasured. The former complex was previously reported (20) to have bands at 350(s), 340(s), and 300(sh) cm^{-1} assignable to ν(Rh—Cl) of the *trans*-isomer. In the present work, this complex (two separate preparations) was found to have a strong absorption at 350 cm^{-1}, with the possibility of an ill-defined shoulder at ~ 355 cm^{-1}, and a broad weak band at 300 cm^{-1}. The previous assignment (20) is therefore revised, and the complex assigned a *cis*-stereochemistry. δ(C—C≡N) is observed at the unusually high frequency of 454 cm^{-1}, with a weak absorption at 427 cm^{-1}.

The complex *trans*-$PdCl_2$.2EtCN, prepared by the direct reaction of palladium(II) chloride with ethyl cyanide, has infrared absorption bands at 395(s) and 351(s) cm^{-1}, assigned to δ(C—C≡N) and ν(Pd—Cl) respectively; a band at 314(m–s) cm^{-1} is the only other prominent absorption between 500 and 200 cm^{-1}.

E. General Discussion

It is clear from the above results that the 125–80 cm^{-1} spectral region is the only one in which absorption bands could be assigned to vibrational modes involving the stretching of the metal–nitrogen bonds of σ-bonded RCN molecules. Even so, these assignments cannot be regarded as unambiguous, even for the relatively simple planar MX_2.2MeCN molecules. However, the present work does raise some doubt regarding the assignments of ν(M—N) in other systems (3–7), since these were only based upon infrared measurements.

Although MX_2.2MeCN show several bands in the 300–200 cm^{-1} region, these are not assignable to ν(M—X) or ν(M—N) but may be due to overtone or combination vibrations. Bending modes of the MX_2N_2 skeleton should also occur in the region below 200 cm^{-1}, and this might therefore further complicate the assignment of ν(M—N). It is also interesting to note that although detailed infrared and Raman measurements have been made on TiX_4.2MeCN (24), where X = Cl or Br, the assignment of ν(Ti—N) remains in doubt.

At first sight we might have anticipated ν(M—N) at ~ 500 cm^{-1} in these complexes, by comparison with the much studied metal–ammine complexes (10, 12, 13), since mass effects alone are unlikely to cause such a drastic drop in metal–nitrogen stretching frequencies (compare ν(Pt—N) in methylamine complexes of platinum(II) with those of the

related ammonium complexes (25)). If the intense bands in the 125–80 cm^{-1} region are correctly assigned to ν(M—N), then they are at an unusually low frequency, compared to other platinum(II) and palladium(II)–ligand stretching frequencies (10–15, 25). This may be a reflection on the existence of rather long weak metal–nitrogen bonds in these complexes. Crystallographic data for several of these systems would seem to be desirable.

Experimental

Cis-$PtX_2.2RCN$, *trans*-$PdCl_2.2RCN$, and $RhCl_3.3EtCN$ were prepared as described previously (2, 8, 20). $RhCl_3.3MeCN$ was isolated by a slight modification of the original procedure (20); the preparation was carried out in the presence of ethyl orthoformate, to ensure anhydrous reaction conditions.

Anal. Found: C, 21.0; H, 2.9; N, 12.5. $C_6H_9N_3Cl_3Rh$ requires C, 21.7; H, 2.7; N, 12.6.

During the preparation of *cis*-$PtBr_2.2PhCN$ (8), in one instance the *trans*-isomer crystallized from the solution. The exact conditions under which the *trans*-isomer is formed in preference to the *cis*- could not be ascertained since attempts to repeat the preparation of the *trans*-isomer were unsuccessful.

Anal. Found: C, 29.8; H, 1.8; N, 4.8. $C_{14}H_{10}N_2Br_2Pt$ requires C, 30.0; H, 1.8; N, 5.0.

Infrared absorption bands (2300–1500 and 1300–400 cm^{-1}) of the *trans*-isomer are as follows: 2280 s; 1598 s; 1292 m–w; 1198 s; 1172 s; 1093 w; 1067 w; 1021 w; 998 m; 968 vw; 929 m; 843 vw; 757 vs; 683 vs; 625 vw; 555 sh; 550 vs; 537 s.

Trans-$PtBr_2.2MeCN$ was prepared by exactly the same procedure used previously (8) to obtain the *cis*-isomer. In one instance a mixture of isomers was obtained (far-infrared spectra) but the pure *cis*-isomer (8) could not be re-prepared.

Anal. Found: C, 10.95; H, 1.45; N, 6.4. $C_4H_6N_2Br_2Pt$ requires C, 11.0; H, 1.4; N, 6.4.

Principal infrared absorption bands (Nujol mull) were observed at 2320(m); 2305(sh); ~1400(m,br); 1358(s); 1020(s); 960(w) cm^{-1}.

Trans-$PdCl_2.2EtCN$ was prepared by refluxing a suspension of palladium(II) chloride in ethyl cyanide and evaporating the resulting yellow solution to dryness (ν(C≡N) 2320(s) cm^{-1}).

Anal. Found: C, 24.5; H, 3.5; N, 9.6. $C_6H_{10}N_2Cl_2Pd$ requires C, 25.1; H, 3.5; N, 9.75.

The complexes *cis*-$PtCl_2.2MeCN$, *cis*-$PtCl_2.2PhCN$, and *cis*-$PtBr_2.2PhCN$ were slightly soluble in acetone in which they formed nonconducting solutions.

Physical Measurements

Infrared spectra were recorded as Nujol mulls on Grubb–Parsons DM4 (500–200 cm^{-1}) and Beckman IR11 (250–33 cm^{-1}) spectrophotometers. The Raman spectra of the crystalline complexes were obtained using a Cary 81 spectrometer with He–Ne laser excitation; the instrument used has been described in detail elsewhere (26). Measurements were restricted to the solid state because the complexes were insufficiently soluble in suitable solvents.

Acknowledgments

The author is most grateful to Professor I. R. Beattie for allowing the use of the Beckman IR11 and Cary 81 spectrometers. Dr. G. A. Ozin kindly measured several of the Raman spectra described in the present paper. The assistance of Mr. P. J. Jones is also gratefully acknowledged.

1. R. A. Walton and R. Whyman. J. Chem. Soc. A. In press (1968).
2. R. A. Walton. Can. J. Chem. **44**, 1480 (1966).
3. J. C. Evans and G. Y. S. Lo. Spectrochim. Acta, **21**, 1033 (1965).
4. S. C. Jain and R. Rivest. Can. J. Chem. **45**, 139 (1967).
5. M. Kubota, D. L. Johnston, and I. Matsubara. Inorg. Chem. **5**, 386 (1966).
6. M. F. Farona, J. G. Grasselli, and B. L. Ross. Spectrochim. Acta, **23A**, 1875 (1967).
7. M. F. Farona and J. G. Grasselli. Inorg. Chem. **6**, 1675 (1967).
8. R. A. Walton. Spectrochim. Acta, **21**, 1795 (1965).
9. D. M. Adams, J. Chatt, J. Gerratt, and A. D. Westland. J. Chem. Soc. 734 (1964).
10. P. J. Hendra. Spectrochim. Acta, **23A**, 1275 (1967).
11. J. R. Durig, B. R. Mitchell, D. W. Sink, J. N. Willis, Jr., and A. S. Wilson. Spectrochim. Acta, **23A**, 1121 (1967).
12. C. H. Perry, D. P. Athans, E. F. Young, J. R. Durig, and B. R. Mitchell. Spectrochim. Acta, **23A**, 1137 (1967).
13. P. J. Hendra and N. Sadasivan. Spectrochim. Acta, **21**, 1271 (1966).
14. J. R. Durig, R. Layton, D. W. Sink, and B. R. Mitchell. Spectrochim. Acta, **21**, 1367 (1965).
15. J. R. Allkins and P. J. Hendra. J. Chem. Soc. **A**, 1325 (1967).
16. K. A. Hofmann and G. Bugge. Ber. **40**, 1772 (1907).
17. L. Ramberg. Ber. **40**, 2578 (1907).
18. V. V. Lebedinskii, P. V. Simanovskii, and O. D. Slutsker. Izvest. Sektora. Platiny i Drug. Blagorodn. Metal. Inst. Obshch. i Neorgan. Khim. Akad. Nauk SSSR, **21**, 43 (1948).
19. R. J. H. Clark. Spectrochim. Acta, **21**, 955 (1965).
20. B. F. G. Johnson and R. A. Walton. J. Inorg. Nucl. Chem. **28**, 1901 (1966).
21. M. Kubota and D. L. Johnston. J. Inorg. Nucl. Chem. **29**, 769 (1967).
22. I. R. Beattie and M. Webster. J. Chem. Soc. 3507 (1964).
23. J. H. S. Green. Spectrochim. Acta, **17**, 607 (1961).
24. R. E. Collis. Private communication (November 1967).
25. G. W. Watt, B. B. Hutchinson, and D. S. Klett. J. Am. Chem. Soc. **89**, 2007 (1967).
26. I. R. Beattie. Chem. Brit. **3**, 347 (1967).

Can. J. Chem. Downloaded from www.nrcresearchpress.com by 210.87.254.6 on 09/05/12
For personal use only.

Can. J. Chem. Downloaded from www.nrcresearchpress.com by 210.87.254.42 on 09/05/12
For personal use only.

Photolysis of ketene. I

A. N. STRACHAN AND D. E. THORNTON
Department of Chemistry, Loughborough University of Technology, Loughborough, Leicestershire, England

Received March 28, 1968

Ketene has been photolyzed at 3660 and 3130 Å both alone and in the presence of the inert gases C_4F_8 and SF_6. The quantum yield of carbon monoxide has been determined at both wavelengths as a function of pressure and temperature. At 3660 Å the quantum yield decreases with increasing pressure but increases with increasing temperature. At 3130 Å the quantum yield with ketene alone remains 2.0 at both 37 and 100 °C at pressures up to 250 mm. At higher pressures of ketene or with added inert gas the quantum yield decreases with increasing pressure. The results are interpreted in terms of a mechanism in which intersystem crossing from the excited singlet state to the triplet state occurs at both wavelengths, and collisional deactivation of the excited singlet state by ketene is single stage at 3660 Å but multistage at 3130 Å.

Canadian Journal of Chemistry, **46**, 2353 (1968)

Introduction

The photolysis of ketene appears to provide data that can be used to test the predictions of unimolecular reaction theories regarding the dependence of the rate of decomposition of a molecule on its total energy. Previous work on the photolysis has shown that the carbon monoxide quantum yield at 3660, 3340, and 3130 Å is pressure dependent (1–3). If a simple mechanism is assumed in which decomposition of the excited singlet state competes with collisional deactivation, estimates can be made of the values of the decomposition rate constant at different wavelengths and temperatures and hence at different total energies of the excited singlet state molecule. Several comparisons of theory with experiment have been made on the basis of this assumption (3–5).

However, evidence has been mounting that triplet methylene as well as singlet methylene is formed during the photolysis at all wavelengths, the proportion increasing as the wavelength is lengthened (6–12). This has necessitated postulating the formation of triplet ketene as the precursor of triplet methylene and thrown doubts on the validity of the simple mechanism upon which the comparisons of reaction rate theory with experiment have been based. Several new mechanisms for the photolysis have recently been proposed (12–14).

In the present work more extensive data on the pressure dependence of the carbon monoxide quantum yield at 3660 and 3130 Å have been obtained. Inert gases have been used, in addition to ketene itself, as quenching agents, and the photolysis has been carried out over a wider temperature range than that covered in previous work. The objects have been, firstly, to provide a larger body of data on which to base conclusions regarding the probable mechanism of the photolysis and, secondly, to obtain information on energy transfer, by ascertaining whether, as in the case of hexafluoroacetone (15), there is any evidence that deactivation is a two- or multi-stage process at the shorter wavelengths.

Experimental

Ketene was prepared by the method of Jenkins (16). The vapor of acetic anhydride was passed through an evacuated tube maintained at 500 °C. Acetic acid and unreacted anhydride were condensed by two dry ice traps and the ketene collected in a third trap immersed in liquid nitrogen. Any more volatile gases were removed continuously by a diffusion pump. The ketene was further purified by several trap to trap distillations. It was stored in a reservoir at −196 °C. Prior to each run the small quantity of ketene required was thoroughly outgassed by further trap to trap distillations.

Octafluorocyclobutane and sulfur hexafluoride were both Matheson products stated to be 99.99% and 98% pure respectively. Noncondensables were removed at −196 °C and before each run the quantity of gas to be used was thoroughly outgassed by trap to trap distillation.

British Drug Houses diethyl ketone was fractionally distilled. A constant boiling middle third (b.p. 102.5° uncorrected; lit. b.p. 102.7° (17)) was thoroughly outgassed in the vacuum line and stored in a reservoir at −196 °C.

A cylindrical quartz reaction cell of length 20 cm and internal diameter 3 cm was used. It was enclosed in an electrically heated aluminium block whose temperature could be controlled to within ±0.5 °C. For the work at 3660 Å, the light source was a Philips 125-watt black glass mercury vapor lamp. For the 3130 Å runs, a Hanovia 220-watt medium pressure arc was employed. In both cases a fairly parallel and uniform light beam, filling the cell, was achieved by the use of a quartz lens and a stop.

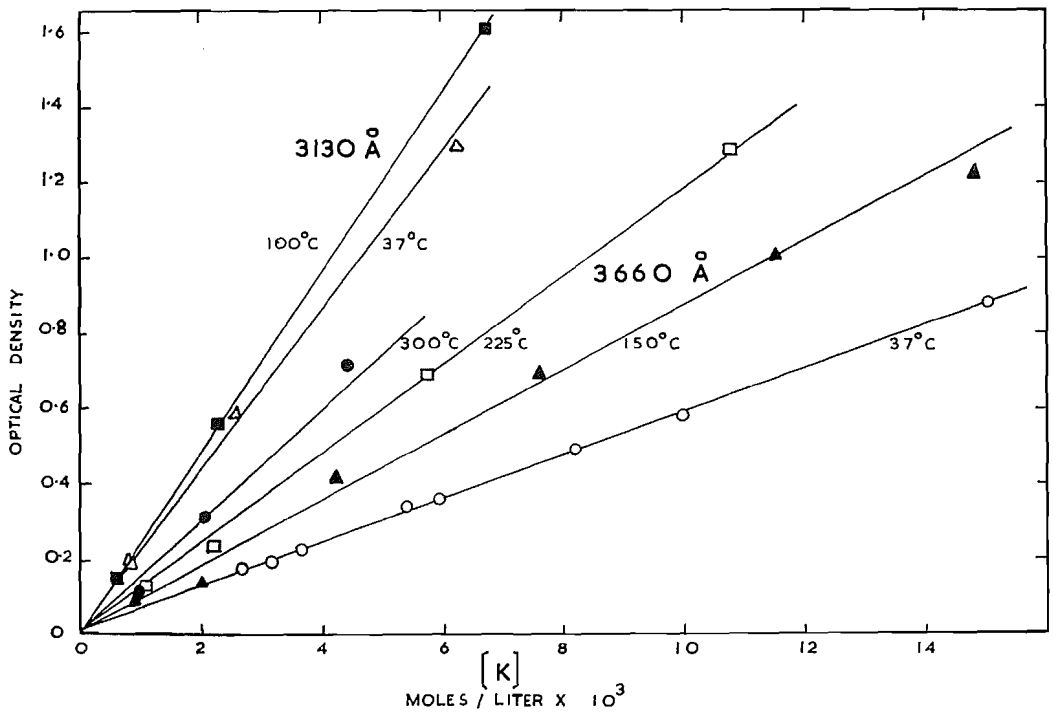

FIG. 1. Optical density versus ketene concentration at 3130 and 3660 Å and various temperatures.

To isolate 3660 Å, two Chance–Pilkington glass filters, OX1 and OV1, each 2 mm in thickness, were placed between the lens and the cell. Their combined transmission extends from 3400 Å to 4200 Å with a maximum at 3750 Å. The 3130 Å filter combination was that recommended by Hunt and Davies (18), except that the strength of the potassium chromate solution was halved. Light intensities were monitored by means of a photocell, mounted behind the reaction cell, in combination with a microammeter.

In the runs with added inert gas, appropriate quantities of ketene and the gas were introduced in turn into the reaction cell. The two were then mixed by opening the cell to an adjoining 250 ml volume and lowering and raising the mercury in this a number of times. At the end of each run, all products other than carbon monoxide were retained by two traps, the first at −196 °C and the second at −210 °C. The carbon monoxide was collected and measured with a McLeod–Toepler gauge (1). Conversions were kept below 2% in all cases.

The absolute magnitudes of the quantum yields at 3660 Å were based on the work of Taylor and Porter (3) at this wavelength. Using a ferrioxalate actinometer, they obtained a value of 4.029×10^{-5} mole l^{-1} for the inverse slope of the plot of twice the reciprocal of the carbon monoxide quantum yield versus ketene concentration at 23 °C. Strachan and Noyes, Jr. (1) found that the inverse slopes of such plots increase with temperature with an activation energy of 4500 cal $mole^{-1}$. Utilizing this finding, the inverse slope of the same plot at 37 °C was estimated to have the value 5.656×10^{-5} mole l^{-1}. The assignment of this value to the experimentally determined inverse slope at 37 °C enabled relative quantum yields to be converted into absolute ones. At 3130 Å diethyl ketone, which at this wavelength and 100 °C has a carbon monoxide quantum yield of unity (19), was used as an internal actinometer.

Results

Plots of optical density versus ketene concentration are shown in Fig. 1.[1] Beer's law is obeyed within experimental error for each temperature at both wavelengths. The extinction coefficients found are, at 3660 Å, 2.91, 4.33, 5.95, and 7.49 $mole^{-1}\,l\,cm^{-1}$ at 37, 150, 225, and 300 °C respectively, and, at 3130 Å, 10.7 and 11.9 $mole^{-1}\,l\,cm^{-1}$ at 37 and 100 °C respectively.

Figures 2, 3, and 4 show the variation in the quantum yield of carbon monoxide at 3660 Å with increasing pressure of ketene or inert gas.[1]

[1]Tables of the data from which these plots were made have been placed in the Depository of Unpublished Data. Photocopies may be obtained free of charge, upon request, from: Depository of Unpublished Data, National Science Library, National Research Council of Canada, Ottawa, Canada.

Can. J. Chem. Downloaded from www.nrcresearchpress.com by 210.87.254.42 on 09/05/12
For personal use only.

Can. J. Chem. Downloaded from www.nrcresearchpress.com by 210.87.254.42 on 09/05/12
For personal use only.

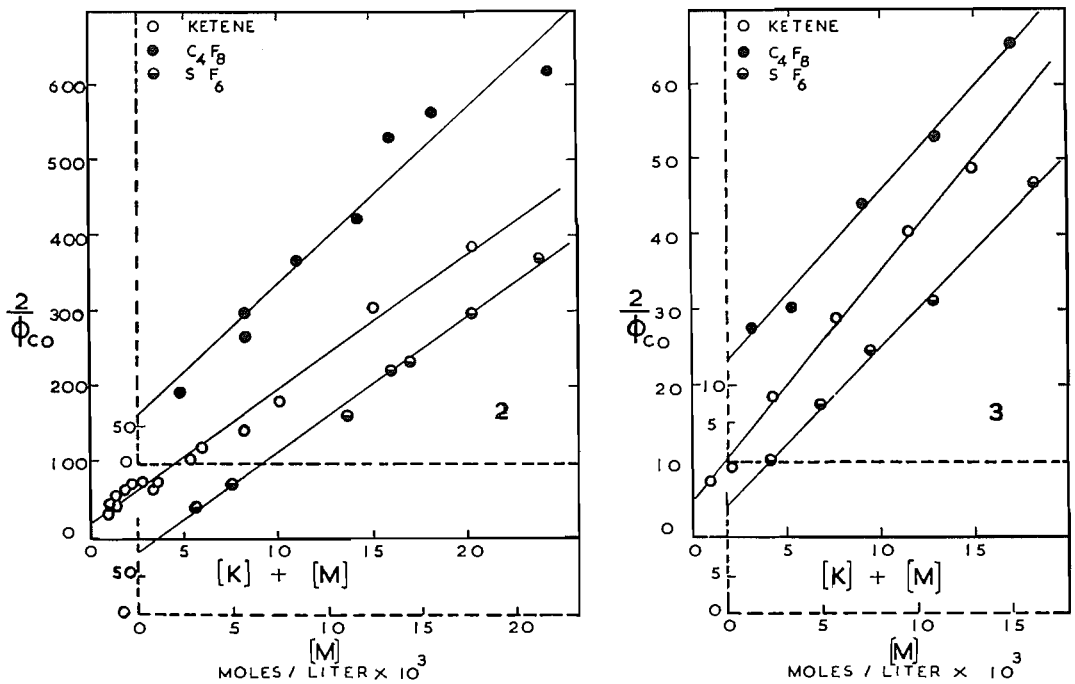

FIG. 2. Twice the reciprocal of the carbon monoxide quantum yield versus concentration at 3660 Å and 37 °C. For clarity the ordinate origin has been displaced upwards by 100 units for the C_4F_8 points and downwards by 100 units for the SF_6 points.

FIG. 3. Twice the reciprocal of the carbon monoxide quantum yield versus concentration at 3660 Å and 150 °C. For clarity the ordinate origin has been displaced upwards by 10 units for the C_4F_8 points and downwards by 10 units for the SF_6 points.

In the runs with C_4F_8 and SF_6 a constant pressure of 50 mm of ketene was used at all four temperatures. It can be seen that at each temperature reasonable linearity is obtained when twice the reciprocal of the quantum yield of carbon monoxide is plotted against concentration of ketene or inert gas. The slopes of the lines in Figs. 2, 3, and 4, calculated by the method of least squares, are shown in Table I along with the intercepts of the plots for ketene alone.

Figures 5 and 6 show the results at 3130 Å.[1] With ketene on its own the quantum yield of carbon monoxide remains 2, within experimental error, at both 37 and 100 °C at pressures up to 250 mm. At higher pressures it starts to fall. At 37 °C the addition of C_4F_8 or SF_6 to 50 mm of ketene brings about an immediate decrease in the carbon monoxide quantum yield. In contrast at 100 °C, at least 100 mm of inert gas have to be added before a significant decrease occurs. At both temperatures the decrease continues up to the highest pressures of inert gas used. The values of the slopes of the lines in Figs. 5 and 6, calculated by the method of least squares from the C_4F_8 and SF_6 points combined, are 19.6 and 18.2 $mole^{-1}$ l at 37 and 100 °C respectively.

TABLE I

Slopes and intercepts of $2/\phi_{CO}$ vs. concentration at 3660 Å

Temp. (°C)	Slopes ($mole^{-1}$ l)			Intercept, ketene
	Ketene	C_4F_8	SF_6	
37	17 680	23 330	17 940	20.0
150	3 050	2 810	2 588	4.6
225	1 131	530	—	3.3
300	966	158	—	0.8

Discussion

The results are best explained in terms of the reactions and transitions shown in Fig. 7. Spectroscopic evidence and theoretical calculations place the triplet state and the first excited singlet state of ketene 61 and 74 kcal $mole^{-1}$, respectively, above the ground state (20).

Can. J. Chem. Downloaded from www.nrcresearchpress.com by 210.87.254.42 on 09/05/12
For personal use only.

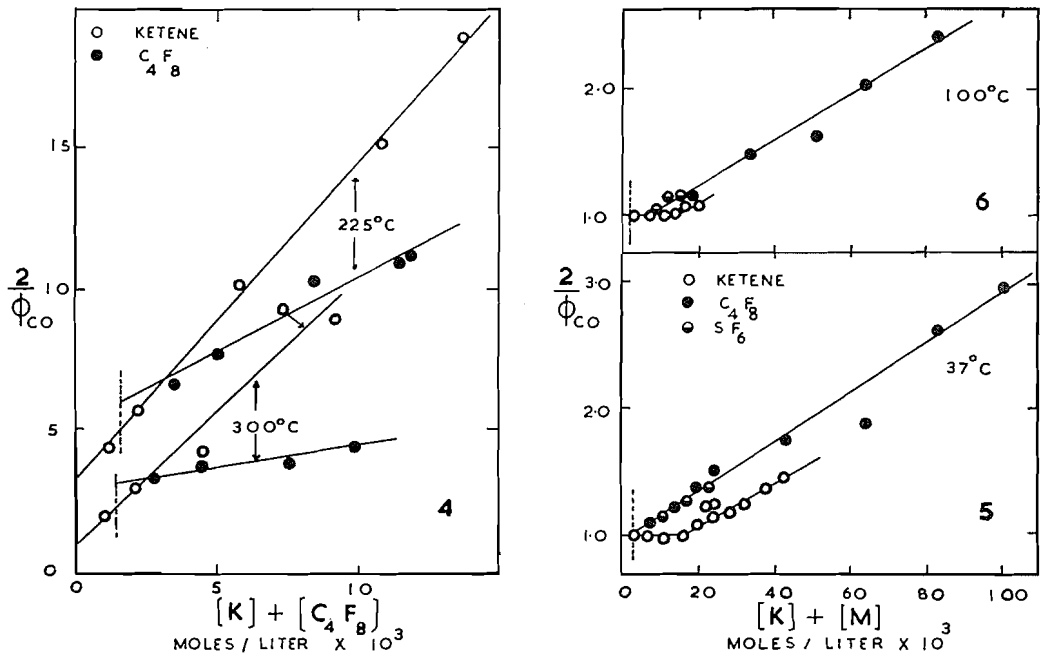

FIG. 4. Twice the reciprocal of the carbon monoxide quantum yield versus concentration at 3660 Å and 225 and 300 °C. The vertical broken line denotes the concentration of ketene used in the runs with C_4F_8.

FIG. 5. Twice the reciprocal of the carbon monoxide quantum yield versus concentration at 3130 Å and 37 °C. The broken vertical line denotes the concentration of ketene used in the runs with C_4F_8 and SF_6.

FIG. 6. Twice the reciprocal of the carbon monoxide quantum yield versus concentration at 3130 Å and 100 °C. The broken vertical line denotes the concentration of ketene used in the runs with C_4F_8 and SF_6.

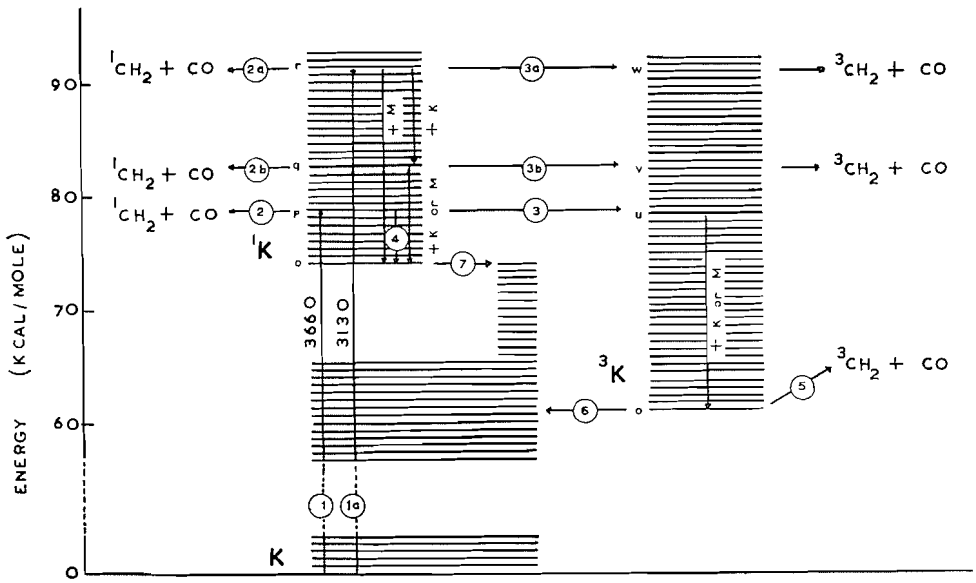

FIG. 7. Energy diagram of the electronic states of ketene.

Can. J. Chem. Downloaded from www.nrcresearchpress.com by 210.87.254.42 on 09/05/12
For personal use only.

3660 Å

On the above basis, absorption at 3660 Å results in the formation of excited singlet state molecules with ~ 4 kcal mole^{-1} of vibrational energy. These may then undergo the three alternative processes [2], [3], and [4]. Reaction [2] is decomposition into singlet methylene ($^1CH_2$) and carbon monoxide. There is evidence that some singlet methylenes are formed at 3660 Å, although estimates of the percentage of the total methylenes which are singlet at this wavelength vary (7, 8, 10, 12).

Step [3] is intersystem crossing to the triplet state. Other workers (8, 10) support the view that this is an intramolecular process and is not collision induced. The triplet state formed by [3] is assumed to live long enough to reach thermal equilibrium. It then either decomposes into triplet methylene ($^3CH_2$) and carbon monoxide [5], or undergoes intersystem crossing to the ground state [6]. The fate of both singlet and triplet methylene is assumed to be reaction with ketene to form ethylene and carbon monoxide.

Competing with [2] and [3] is collisional deactivation [4]. Since the average vibrational energy transferred per collision to polyatomic deactivators in other systems has been found to be of the order of 10 kcal mole^{-1} (21), it is probable that a single collision with either ketene or one of the two gases added is sufficient to deactivate the excited singlet state molecule to its lowest vibrational level. Figures 2 and 3 confirm the findings of previous workers (1, 3) that, in contrast to the behavior of hexafluoroacetone (22), there is no tendency for the carbon monoxide quantum yield ϕ_{CO} to reach a limiting value at high concentrations. It appears that, from the lowest vibrational level of the excited singlet state, internal conversion to the ground state [7] is considerably faster than either decomposition or intersystem crossing, and takes place to the exclusion of both. A fast internal conversion process [7] would also explain why no fluorescence from ketene has ever been observed, despite several attempts to find it (see ref. 23).

The above processes may be written

[1] $\quad K + h\nu\,(3660\text{ Å}) \rightarrow {}^1K_p$

[2] $\quad {}^1K_p \rightarrow {}^1CH_2 + CO$

[3] $\quad {}^1K_p \xrightarrow{+\,K\text{ or }M} {}^3K_u \rightarrow {}^3K_0$

[4a] $\quad {}^1K_p + K \rightarrow {}^1K_0 + K$

[4b] $\quad {}^1K_p + M \rightarrow {}^1K_0 + M$

[5] $\quad {}^3K_0 \rightarrow {}^3CH_2 + CO$

[6] $\quad {}^3K_0 \rightarrow K$

[7] $\quad {}^1K_0 \rightarrow K$

[8] $\quad {}^1CH_2 + K \rightarrow C_2H_4 + CO$

[9] $\quad {}^3CH_2 + K \rightarrow C_2H_4 + CO,$

where K represents a ground state molecule of ketene, M a molecule of added gas, ${}^1K_m$ a molecule of ketene in the mth vibrational level of the excited singlet state, and ${}^3K_n$ a molecule of ketene in the nth vibrational level of the triplet state.

Application of the usual steady-state assumption leads to

$$\frac{2}{\phi_{CO}} = \frac{k_2 + k_3}{A} + \frac{k_{4a}[K]}{A} + \frac{k_{4b}[M]}{A},$$

where $A = k_2 + k_3k_5/(k_5+k_6)$. Figures 2, 3, and 4 show how, at all temperatures, in agreement with this expression, $2/\phi_{CO}$ increases linearly with ketene concentration [K] in the absence of added gas, and linearly with inert gas concentration [M] at constant concentration of ketene. In addition, at each of the two lower temperatures, the slopes for the three different gases (Table I) are all of similar magnitude, a result which would be expected if [4*a*] and [4*b*] occur on every collision.

Appreciable thermal polymerization of ketene occurs at the higher temperatures. In consequence, the experimental results at 225 and 300 °C (Fig. 4) are less reliable than those at 37 and 150 °C. However, the differences between the slopes for ketene and those for C_4F_8 (Fig. 4 and Table I) appear too large to be accounted for by experimental error. As the temperature is raised, C_4F_8 seems to remove energy from the excited singlet state increasingly less efficiently than ketene. One possible explanation is that some of the collisions at the higher temperatures result in energy transfer to, rather than from, the excited singlet state (24). If, because of the greater number of its vibrational modes, the average energy transferred from C_4F_8 were larger than from ketene, a fraction of the excited singlet state molecules could, on collision, be acquiring sufficient energy from C_4F_8 to decompose, but insufficient to do so from ketene. In this way C_4F_8 would become less effective at lowering the carbon monoxide quantum yield than ketene, as observed.

Can. J. Chem. Downloaded from www.nrcresearchpress.com by 210.87.254.42 on 09/05/12
For personal use only.

On the basis of [1]–[9], the fraction of methylenes formed which are singlet is $\alpha = k_2/A$ and should therefore be independent of pressure. Other workers (8, 12), while disagreeing on the exact value of α at this wavelength, agree that it shows little variation with pressure. The slopes listed in Table I decrease with increasing temperature. Assuming k_{4a} and k_{4b} do not vary greatly with temperature, A must increase with temperature. Hence α would be expected to decrease if k_2 is fairly constant. This could account for the much lower value of α found by DeGraff and Kistiakowsky (10) at 50 °C as compared with the values reported by others (8, 12) working at 24 and 27 °C.

Without a knowledge of α, it is impossible to assign values to all the individual rate constants. But some assignments can be made and conclusions drawn. Assuming a collision diameter for ketene of 4.0 Å and that [4*a*] occurs on every collision, the value of k_{4a} is calculated to be $9.61 \times 10^9 \sqrt{T}$ mole^{-1} l s^{-1}. Multiplication of k_{4a} by the ketene intercepts divided by the ketene slopes in Table I gives $k_2 + k_3$ whose value at 37 °C is therefore 1.92×10^8 s^{-1}. The value increases slightly with temperature. The absence of fluorescence and the lack of evidence for decomposition or intersystem crossing from the lowest vibrational level of the excited singlet state suggest that k_7 has a value greater than 10^9 s^{-1}. An activation energy for [5] is required in order to explain the decrease in the slopes of $2/\phi_{CO}$ vs. [K] or [M] with temperature (Table I). If α is zero, this activation energy must be around 3500 cal mole^{-1} (14). If α is not zero, the value will be greater.

3130 Å

Absorption at 3130 Å leads to the formation of excited singlet state molecules with $\sim$ 17 kcal mole^{-1} of vibrational energy (Fig. 7). The constancy and value (2.0) of the carbon monoxide quantum yield at low ketene pressures and its steady decrease at pressures greater than 250 mm (Fig. 5) are in reasonable agreement with previous work where either filter solutions have also been used (25, 2), or a monochromator has been employed (10), to isolate the 3130 Å region. But Taylor and Porter (3), using an interference filter, found considerably lower quantum yields. The disagreement between their results and those of all other workers makes it probable that their interference filter was not isolating 3130 Å efficiently and was transmitting some light of longer wavelength. Support for this explanation is to be found in the curvature which these authors observed in their Beer's law plot.

A carbon monoxide quantum yield of 2.0 implies that every molecule which absorbs a quantum ultimately decomposes. But from the evidence of other work (8–11) not all the methylenes formed at this wavelength are singlet. Thus intersystem crossing [3*a*] followed by decomposition from a high vibrational level of the triplet state must be competing with direct decomposition [2*a*].

The most probable explanation of the departure from linearity of the $2/\phi_{CO}$ vs. [K] plot (Fig. 5) is that collisional deactivation is multistage (4), and that the excited singlet state molecule does not lose the whole of its 17 kcal mole^{-1} of vibrational energy on its first collision with ketene. It still retains sufficient vibrational energy to decompose ([2*b*]) or undergo intersystem crossing to the triplet state ([3*b*]) from which it then decomposes. Only after one or more additional collisions does the excited singlet state lose all its excess vibrational energy. The data are not sufficiently accurate to allow any of the methods for determining the number of deactivation stages (15) to be applied. But calculations show that a two stage process with $k_{2b} + k_{3b}$ equal to $(k_{2a} + k_{3a})/4$ will adequately account for the data.

The linearity of the $2/\phi_{CO}$ vs. [M] plot (Fig. 5) implies that deactivation by C_4F_8 and SF_6 is still single stage and that most of the 17 kcal mole^{-1} of vibrational energy of the excited singlet state is lost as a result of a single collision with either of these two gases. This is not unexpected in view of the larger number of vibrational modes of these gases in comparison with ketene, and in the light of the observations of other workers on the amounts of energy transferred per collision during the deactivation of vibrationally excited molecules (21).

At 100 °C the difference between the deactivation behavior of the two gases and that of ketene is less pronounced than at 37 °C (Fig. 6). It seems probable that at the higher temperature deactivation by the two gases is becoming multistage. This might be because, as the tempera-

Can. J. Chem. Downloaded from www.nrcresearchpress.com by 210.87.254.42 on 09/05/12
For personal use only.

ture is raised, more vibrational modes of C_4F_8 and SF_6 become active and as a result less vibrational energy can be absorbed on collision.

The processes occurring at 37 °C may be written

[1a] $K + h\nu\,(3130\text{ Å}) \rightarrow {}^1K_r$

[2a] ${}^1K_r \rightarrow {}^1CH_2 + CO$

[3a] ${}^1K_r \rightarrow {}^3K_w \rightarrow {}^3CH_2 + CO$

[4a] $\begin{cases} {}^1K_r + K \rightarrow {}^1K_q + K \\ {}^1K_q + K \rightarrow {}^1K_0 + K \end{cases}$

[4b] $\begin{cases} {}^1K_r + M \rightarrow {}^1K_0 + M \\ {}^1K_q + M \rightarrow {}^1K_0 + M \end{cases}$

[2b] ${}^1K_q \rightarrow {}^1CH_2 + CO$

[3b] ${}^1K_q \rightarrow {}^3K_v \rightarrow {}^3CH_2 + CO.$

Singlet and triplet methylene are again assumed to react by [8] and [9] to form ethylene and carbon monoxide. Application of the steady-state assumption leads to

$$\frac{2}{\phi_{CO}} = \frac{k_{2a} + k_{3a} + k_{4a}[K] + k_{4b}[M]}{k_{2a} + k_{3a} + k_{4a}[K](k_{2b} + k_{3b})/B}$$

and $$\alpha = \frac{k_{2a} + k_{4a}[K]k_{2b}/B}{k_{2a} + k_{3a} + k_{4a}[K](k_{2b} + k_{3b})/B},$$

where $B = k_{2b} + k_{3b} + k_{4a}[K] + k_{4b}[M]$.

These expressions are cumbersome but simplify in limiting cases. When [M]=0 and [K] is small such that $k_{4a}[K] \ll (k_{2b} + k_{3b})$, $B \simeq (k_{2b} + k_{3b})$ and $2/\phi_{CO}$ remains constant and equal to unity; when [K] is large such that $B \simeq k_{4a}[K]$, $2/\phi_{CO}$ becomes equal to $(k_{2a} + k_{3a} + k_{4a}[K])/(k_{2a} + k_{3a} + k_{2b} + k_{3b})$ and hence increases linearly with [K]. When [M] $\neq 0$ and [K] is small and constant, $2/\phi_{CO} = 1 + k_{4b}[M]/(k_{2a} + k_{3a})$ and hence increases linearly with [M]. Thus the mechanism satisfactorily accounts for the experimental behavior shown in Fig. 5. The experimental slope, 19.6 mole^{-1} l, of the plot of $2/\phi_{CO}$ vs. [M] may be equated with $k_{4b}/(k_{2a} + k_{3a})$. Assuming $k_{4b}/k_{4a} = 1.32$, this being the ratio of the C_4F_8 and ketene slopes of the corresponding plots at 3660 Å and 37 °C (Table I), $k_{2a} + k_{3a}$ is calculated to have the value 1.14×10^{10} s^{-1}. Extrapolation of the linear portion of the plot of $2/\phi_{CO}$ vs. [K] back to [K]=0 leads to a value of ~ 0.8 for $(k_{2a} + k_{3a})/(k_{2a} + k_{3a} + k_{2b} + k_{3b})$. Hence $k_{2b} + k_{3b}$ must be approximately $\frac{1}{4}$ of $k_{2a} + k_{3a}$.

When [M] is large or zero and [K] is small, $\alpha = k_{2a}/(k_{2a} + k_{3a})$. When [M]=0 and [K] is large, $\alpha = (k_{2a} + k_{2b})/(k_{2a} + k_{2b} + k_{3a} + k_{3b})$ which, since k_{2b} and k_{3b} are considerably smaller than k_{2a} and k_{3a} respectively, will not differ greatly from $k_{2a}/(k_{2a} + k_{3a})$. Thus no significant variation of α with pressure would be expected. While different authors (8–11) report values ranging from 0.59 to 0.86 for α at this wavelength, all are agreed that α varies little with pressure.

At 100 °C, if a two-stage deactivation process is included for the inert gases as well as for ketene, the expressions for $2/\phi_{CO}$ and α become even more cumbersome and will not be given here. But the plot of $2/\phi_{CO}$ vs. [M] is again expected to become linear at high [M], as observed (Fig. 6), with a slope close to $k_{4b}/(k_{2a} + k_{3a})$. The fact that the slope is similar in magnitude to the slope of the same plot at 37 °C (Fig. 5) indicates that $k_{2a} + k_{3a}$ does not vary greatly with temperature. This is to be expected. As the temperature is raised, excitation to the excited singlet state will take place from a higher vibrational level of the ground state. But the resulting increase in the vibrational energy of the excited singlet state will be very slight in comparison with its total vibrational energy, and hence only a marginal change in $k_{2a} + k_{3a}$ will occur.

The separation of the decomposition and intersystem crossing rate constants and a knowledge of their variation with the total vibrational energy of the excited singlet state must await agreement on the values of α at different wavelengths and temperatures.

1. A. N. Strachan and W. A. Noyes, Jr. J. Am. Chem. Soc. **76**, 3258 (1954).
2. B. T. Connelly and G. B. Porter. Can. J. Chem. **36**, 1640 (1958).
3. G. A. Taylor and G. B. Porter. J. Chem. Phys. **36**, 1353 (1962).
4. G. B. Porter and B. T. Connelly. J. Chem. Phys. **33**, 81 (1960).
5. P. G. Bowers. J. Chem. Soc. A, 466 (1967).
6. J. W. Simons and B. S. Rabinovitch. J. Phys. Chem. **68**, 1322 (1964).
7. S. Ho, I. Unger, and W. A. Noyes, Jr. J. Am. Chem. Soc. **87**, 2297 (1965).
8. R. W. Carr, Jr. and G. B. Kistiakowsky. J. Phys. Chem. **70**, 118 (1966).
9. C. McKnight, E. K. C. Lee, and F. S. Rowland. J. Am. Chem. Soc. **89**, 469 (1967).
10. B. A. DeGraff and G. B. Kistiakowsky. J. Phys. Chem. **71**, 1553, 3984 (1967).

11. D. E. THORNTON and A. N. STRACHAN. J. Phys. Chem. **71**, 4583 (1967).
12. S. HO and W. A. NOYES, JR. J. Am. Chem. Soc. **89**, 5091 (1967).
13. B. S. RABINOVITCH, K. W. WATKINS, and D. F. RING. J. Am. Chem. Soc. **87**, 4960 (1965).
14. A. N. STRACHAN and D. E. THORNTON. J. Phys. Chem. **70**, 952 (1966).
15. A. N. STRACHAN, R. K. BOYD, and K. O. KUTSCHKE. Can. J. Chem. **42**, 1345 (1964).
16. A. D. JENKINS. J. Chem. Soc. 2563 (1952).
17. D. R. STULL. Ind. Eng. Chem. **39**, 517 (1947).
18. R. E. HUNT and W. DAVIES. J. Am. Chem. Soc. **69**, 1415 (1947).
19. W. DAVIES. J. Am. Chem. Soc. **70**, 1868 (1948).
20. R. N. DIXON and G. H. KIRBY. Trans. Faraday Soc. **62**, 1406 (1966).
21. B. S. RABINOVITCH and M. C. FLOWERS. Quart. Rev. **18**, 122 (1964).
22. P. G. BOWERS and G. B. PORTER. J. Phys. Chem. **70**, 1622 (1966).
23. W. A. NOYES, JR. and I. UNGER. Pure Appl. Chem. **9**, 461 (1964).
24. R. B. CUNDALL and A. S. DAVIES. Progr. Reaction Kinetics, **4**, 163 (1967).
25. G. B. KISTIAKOWSKY and B. H. MAHAN. J. Am. Chem. Soc. **79**, 2412 (1957).

Can. J. Chem. Downloaded from www.nrcresearchpress.com by 210.87.254.42 on 09/05/12
For personal use only.

Can. J. Chem. Downloaded from www.nrcresearchpress.com by 210.87.254.42 on 09/05/12
For personal use only.

Infrared and electronic spectral studies of 2-thiazolidinethione complexes of Co(II) halides

P. P. SINGH[1] AND R. RIVEST
Département de Chimie, Université de Montréal, Montréal, Québec

Received January 24, 1968

Cobalt(II) halide complexes $[CoX_2.2L]$ (X = Cl, Br, I and L = 2-thiazolidinethione) and $[CoL_4](ClO_4)_2$ have been prepared. The infrared spectral study suggests that the probable site of bonding in the ligand is nitrogen. The results of electronic spectral study and magnetic susceptibility measurements indicate that the complexes are tetrahedral in structure. The various ligand field parameters *Dq*, *B'*, and β show about 80% covalency in the complexes and suggest a weak ligand field.

Des complexes d'halogénures de cobalt(II) $[CoX_2.2L]$ (X = Cl, Br ou I et L = 2-thiazolidinethione) et $[CoL_4](ClO_4)_2$ ont été préparés. L'étude des spectres infrarouges semble indiquer que l'azote sert de site pour la liaison du ligand au métal. Les résultats de l'étude des spectres électroniques et des mesures de susceptibilité magnétique suggèrent que les complexes sont de structure tétraédrique. Les différents paramètres du champ du ligand *Dq*, *B'* et β indiquent un haut degré de covalence (environ 80%) et un champ du ligand faible.

Canadian Journal of Chemistry, 46, 2361 (1968)

Introduction

Recently Madan *et al.* (1–3) studied the complexes of metal halides with a number of thioamides and concluded on the basis of infrared spectral evidence that the site of bonding is probably sulfur. The complexes of thiazolidinethione (L), which has an additional sulfur as a site of coordination besides the thioamide group —C(=S)—NH, has not been reported.

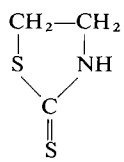

Cobalt(II) halide and perchlorate complexes with this ligand were therefore prepared to investigate the possible site of bonding in the ligand and to derive various ligand field parameters *Dq*, *B'*, and β from which the halides and the ligand could be placed in the spectrochemical and the nephelauxetic series.

In order to study the nature of the complexes, magnetic susceptibility and conductivity measurements were also made.

Experimental

Materials and Manipulations

All the solvents were of reagent grade and were purified before use. Reagent grade cobalt halides and perchlorate (Alfa Inorganics) were used without further purification. 2-thiazolidinethione "L" (Eastman Organic Chemicals) was used after recrystallization from benzene. Reactions, where essential, were carried out in a dry box flushed with nitrogen.

Infrared Spectra

The spectra of the complexes and the ligand were recorded on a Perkin–Elmer model-621 recording spectrophotometer using sodium chloride optics. For the far infrared region, cesium iodide optics were used.

Visible and Near Infrared Absorption Spectra

The spectra of the complexes in the 350–2250 mu region were obtained on a Beckman model DK-1 recording spectrophotometer using nitromethane as solvent in cells of 1 cm light path. The spectra in the solid phase were obtained in Nujol mulls by the technique described by Lee *et al.* (4) and are given in Fig. 1.

Magnetic Susceptibility Measurements

The measurements were made by the Gouy method using mercury(II) tetrathiocyanato-cobalt(II) as standard. The diamagnetic corrections were estimated by the method outlined by Figgis and Lewis (5).

Electrolytic Conductance Measurements

The measurements were made with a Radiometer direct-reading conductivity meter type CDM 2d No. 47501 and the Radiometer conductivity cell type CDC 114.

Preparation of the Complexes

The complexes $(CoX_2.2L)$ [X = Cl, Br, I and L = 2-thiazolidinethione] were prepared by refluxing the anhydrous cobalt halides and the ligand in 1:2 molar ratio in chloroform for 48 h. After filtering the solution, the residue obtained in each case was washed with the solvent and dried in vacuum. Complexes were recrystallized from 1-butanol.

[1]Present address: M. L. K. College, Balrampur, (Gonda) U.P., India.

Can. J. Chem. Downloaded from www.nrcresearchpress.com by 210.87.254.42 on 09/05/12
For personal use only.

TABLE I
Analytical results

Complexes	Color	Melting point (°C)	Cobalt (%)		Halogen (%)		Carbon (%)		Hydrogen (%)		Sulfur (%)	
			Calcd.	Obsd.	Calcd.	Obsd.	Calcd.	Obsd.	Calcd.	Obsd.	Calcd.	Obsd.
$CoCl_2.2L$	Dark blue	142	16.04	15.61	19.30	18.92	19.56	19.82	2.71	2.78	34.78	34.52
$CoBr_2.2L$	Bluish green	175	12.93	12.32	15.54	15.06	15.75	15.96	2.18	2.14	28.00	27.55
$CoI_2.2L$	Light green.	164	10.71	10.05	46.09	46.49	13.06	13.25	1.81	2.34	23.23	23.01
$[CoL_4].(ClO_4)_2$	Dark green	192	8.04	8.25	9.67	10.15	19.62	19.66	2.72	2.95	34.87	34.63

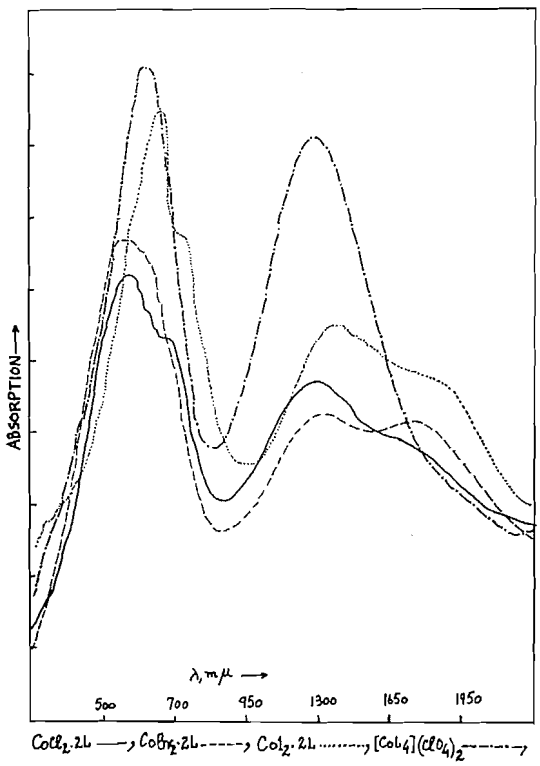

FIG. 1. Electronic spectra of the complexes in Nujol.

The perchlorate complex $[CoL_4].(ClO_4)_2$ was similarly prepared, but the starting material was $Co(ClO_4)_2.6H_2O$ and the perchlorate and ligand molar ratio was 1:4. The complex was recrystallized from nitromethane.

Analysis of the Complexes

Complexes were analyzed for carbon, hydrogen, sulfur, and halogen by Organic Microanalysis, Montreal, and cobalt was determined gravimetrically as sulfate using 1-nitroso-2-naphtol as precipitant. The results obtained are given in Table I.

Selection of Bands and Calculations

In the visible and the near infrared region there appears either a broad band or many peaks for ν_2 and ν_3 bands, causing considerable difficulty in selecting a single value for these energies. As outlined by Cotton *et al.* (6) we have based our method of finding the single values for these bands upon the center of gravity of the total intensity with an accuracy of ± 200 cm^{-1}.

The various ligand field parameters Dq, B', and β have been calculated from ν_2 and ν_3 values using the matrix of Tanabe and Sugano (7).

Results and Discussion

Electronic Spectral Study

The spectral data and the values chosen for the energies of ν_2 and ν_3, along with the values of parameters Dq, B', and β derived from them, are presented in Table II and Table III, respectively. Though there is no significant difference between the spectra of the complexes in solution and those in solid phase, to avoid any effect of solvolysis, spectra in Nujol have been preferred for selecting ν_2 and ν_3 bands. The spectra in solution have been used to evaluate the molar extinction coefficient (ε max) of the complexes in the visible region. The spectra of the complexes in solution in the near infrared region gave scattered peaks which were not found suitable for determination of ε max. The complex $CoL_4(ClO_4)_2$ changed its color from green to brown in solution, hence its spectrum in solution was not recorded.

The various ligand field parameters (Table III), magnetic susceptibility data (Table IV), molar extinction coefficient (Table II), and the color of the complexes indicate that these are tetrahedral in configuration (1, 8). The lower value of the ε max value for the complex $CoCl_2.2L$ is possibly due to the presence of a fraction of Co(II) in an octahedral environment.

The Dq values (Table III) for the complexes suggest the order $Cl^- > Br^- > I^-$ for the halides in the spectrochemical series. This order is consistent with the previous observations from relative values of magnetic moments (9, 10) and the generally accepted sequence of ligands in the spectrochemical series (11). In order to find out the position of the ligand "L" in the spectrochemical series, the Dq values of the complexes were compared with the Dq values of known tetrahedral halide complexes of Co(II). Table V, which lists the Dq and B' values of the complexes, suggests the following order for the ligand in the spectrochemical series.

$$\varepsilon\text{-Thiocaprolactam} > \text{thiazolidinethione} > \text{triphenylphosphine oxide} > \text{triphenylarsine oxide} > \text{dimethylacetamide}$$

A reference to Table III shows that the B' values for all the complexes studied by us are of the order of 76–86% of the free ion value (971 cm^{-1}) (7), which suggests that there is considerable orbital overlap. The nephelauxetic parameter β shows a decrease in the order $Cl^- > Br^- > I^-$. The lowest value of β for iodide suggests that it has the highest covalency. The nephelauxetic sequence is in the expected order (13, 14). Similarly the ligand 'L' can also be

Can. J. Chem. Downloaded from www.nrcresearchpress.com by 210.87.254.42 on 09/05/12
For personal use only.

TABLE II

Electronic spectral data

Complexes	Medium	ν_3 mμ	ν_3 cm^{-1}	ε ($l\ mole^{-1}\ cm^{-1}$)	ν_2 mμ	ν_2 cm^{-1}
$CoCl_2.2L$	Nitromethane	580	17 200	146		
		612	16 300	197		
		635	15 700	200		
	Nujol mull	589	17 000	—	1700	5900
		660	15 100	—	1256	8000
$CoBr_2.2L$	Nitromethane	594	16 800	276		
		626	16 000	440		
		650	15 400	471		
	Nujol mull	610	16 400	—	1740	5700
					1340	7500
$CoI_2.2L$	Nitromethane	626	16 000	255		
		657	15 200	430		
		693	14 400	481		
	Nujol mull	660	15 100	—	1830	5500
		700	14 300	—	1422	7000
$[CoI_4].(ClO_4)_2$	Nujol mull	642	15 600	–	1274	7800

TABLE III

Selected bands, assignments, and spectral parameters

Complexes	State	Assignments: $4A_2g \rightarrow 4T_1g$ (F) ν_2 (cm^{-1})	Assignments: $4A_2g \rightarrow 4T_1g$ (P) ν_3 (cm^{-1})	Dq (cm^{-1})	B' (cm^{-1})	β (obsd.)
$CoCl_2.2L$	Nujol mull	6700	16 800	364	838	.86
$CoBr_2.2L$	Nujol mull	6600	16 500	362	815	.84
$CoI_2.2L$	Nujol mull	6000	15 000	326	741	.76
$[CoL_4](ClO_4)_2$	Nujol mull	6100	15 400	338	756	.78

placed in the nephelauxetic series in order of their decreasing B' values. Thiazolidinethione > dimethylacetamide > triphenylphosphine oxide > triphenylarsine oxide > ε-thiocaprolactam. It is interesting to note that ε-thiocaprolactam is placed first in the spectrochemical series and last in the nephelauxetic series. This is quite possible because the former is a measure of the electrical field produced by the ligand while the latter is a measure of the orbital overlap or of covalency. Jorgensen and Schäffer (14, 15) have also given a different sequence for a set of ligands in the spectrochemical and the nephelauxetic series.

Magnetic and Conductance Study

The magnetic susceptibility data (Table IV) of the complexes fall within the normal range for tetrahedral complexes of divalent cobalt (6). The spectrochemical series and the magnetic moments (9, 10) require the μ eff. to increase in the order Cl > Br > I, and our observation has a similar relation.

The molar conductance data for the halide complexes as presented in Table IV suggest that these complexes are not ionized in solution and are true molecular addition compounds, whereas the perchlorate complex has a very high conductance value suggestive of a 1:2 electrolyte (1).

Infrared Spectral Study

The spectra of the ligand in solid and in solution phase (Table VI) show a marked difference in the positions of N—H and C=S stretching frequencies, clearly indicating intermolecular hydrogen bonding between hydrogen of the NH and sulfur of the C=S, whereas the

Can. J. Chem. Downloaded from www.nrcresearchpress.com by 210.87.254.42 on 09/05/12
For personal use only.

Can. J. Chem. Downloaded from www.nrcresearchpress.com by 210.87.254.42 on 09/05/12
For personal use only.

TABLE IV

Magnetic susceptibility and molar conductance

	Magnetic susceptibility at 295 °K			Molar conductance in nitromethane at 25 °C		
	$\chi m \times 10^{-6}$	Corr. $\times 10^{-6}$	μ eff. (B.M)	Concentration (M)	Molar conductance (cm^2 mhos/mole)	Ionic nature
$[CoCl_2.2L]$	9 854	175.18	4.88	$M/256$	14.3	—
				$M/512$	17.0	
				$M/1024$	20.9	
$[CoBr_2.2L]$	10 200	197.58	4.97	$M/256$	14.5	—
				$M/512$	16.4	
				$M/1024$	21.0	
$[CoI_2.2L]$	10 340	229.58	5.01	$M/256$	14.8	—
				$M/512$	18.3	
				$M/1024$	23.2	
$[CoL_4](ClO_4)_2$	10 150	320.76	4.98	$M/256$	148.0	1:2
				$M/512$	164.0	1:2
				$M/1024$	195.0	1:2

TABLE V

D_q and B' values of the complexes

	ε-Thiocaprolactam (1)		Thiazolidinethione (L)		Triphenylarsine oxide (12)		Triphenyl-phosphine oxide (6)		Dimethyl-acetamide (13)	
	Dq	*B'*	*Dq*	*B'*	*Dq*	*B'*	*Dq*	*B'*	*Dq*	*B'*
$CoCl_2.2L$	387	651	364	838	327	753	327	760	322	797
$CoBr_2.2L$	366	656	362	815	325	727	318	754	303	788
$CoI_2.2L$	340	640	326	741	321	717	305	—	307	745

sharp peak of NH in the spectra of the complexes indicates that no hydrogen bonding is present in the complexes (3). To avoid the effect of hydrogen bonding we have compared the spectra of the complexes in Nujol with the spectrum of the ligand in dilute solution. Comparison of the spectrum of the ligand with that of the complexes (Table VI) shows a negative shift of the order of 200 cm^{-1} in NH stretching frequency, clearly suggesting coordination through the nitrogen. The negative shift in NH stretching frequency may also be due to hydrogen bonding between the hydrogen of the NH and halogen of the metal halide (16, 17). If the shift is due to hydrogen bonding its magnitude should differ considerably from chloride to iodide and should become negligible for the perchlorate complex (18). Since we do not observe considerable change in the magnitude of the shifts in various halide and perchlorate complexes we believe that the shift is not due to hydrogen bonding but is due to coordination through the nitrogen.

Since coordination through the nitrogen will have some effect upon the C=S stretching frequency, it is essential to examine the changes in this band also. Unfortunately there has been great indefiniteness with regard to the assignment of the C=S stretching frequency in nitrogen-containing compounds and the assignments in these compounds vary in the wide range of 850–1510 cm^{-1} (19). Elmore (20) has shown that the band which is generally assigned to C=S stretching vibration results from the coupling of the C—N and C=S stretching vibrations. The band at 1490 cm^{-1} in thiazolidinethione has been assigned to thioamide I (19); and there is ample evidence (21) that the thioamide I band shows positive shift when coordination takes place through nitrogen. We observe a positive shift in the thioamide I band on complex formation, which supports our postulate of linkage through the nitrogen of NH. Besides this, the band at 1295 cm^{-1} assigned to ν(C=S) + (NCS) shows a positive shift, which strongly indicates that sulfur of C=S is not involved in coordination. On the other hand this is indirectly suggestive of coordination through nitrogen.

The bands at 697 and 652 cm^{-1} assigned to symmetrical and antisymmetrical C—S stretching frequencies show a positive shift on coordination. This observation coupled with a marked negative shift in N—H stretching frequency completely rules out any possibility of coordination through the sulfur of the ring. Though the final confirmation for the site of bonding will have to await a complete single crystal X-ray analysis, on the basis of our infrared evidence we can reasonably suggest that the probable site of bonding in the ligand is nitrogen.

To have further confirmation of our assumption of coordination through the nitrogen and have direct evidence for the Co—N bond, we recorded the spectrum in the far infrared region also. Though the assignment for Co—N stretching frequency is still a subject of discussion (22), the majority of the workers have given the assignment in the region 308–328 cm^{-1} (22). In all the spectra of our complexes a band appears in the range 341–325 cm^{-1} (Table VI) for which there is no ligand band. The band in this range can reasonably be assigned to Co—N stretching mode.

Various authors (23, 24) have deduced the relative bond order in a number of complexes using the magnitude of shift of the stretching frequency of the coordinating group, and have related it with the metal–ligand vibration. Table VII gives such a relation for our halide complexes, suggesting the following bond order of the halide complexes: Cl > Br > I.

Madan and Goldstein (1) have concluded that in the ε-thiocaprolactam complexes of cobalt(II)

Can. J. Chem. Downloaded from www.nrcresearchpress.com by 210.87.254.42 on 09/05/12
For personal use only.

Can. J. Chem. Downloaded from www.nrcresearchpress.com by 210.87.254.42 on 09/05/12
For personal use only.

TABLE VI

Assignments of infrared bands in the ligand and the complexes

Assignments (refs. 1, 19, 28–30)	Ligand = L ($CHCl_3$.soln.)	L (Nujol–emuls.)	$CoCl_2.2L$ (Nujol–emuls.)	$CoBr_2.2L$ (Nujol–emuls.)	$CoI_2.2L$ (Nujol–emuls.)	$CoL_4.(ClO_4)_2$ (Nujol–emuls.)
ν(N—H)	3425 (s)	3120 (s)	3160 (s)	3200 (s)	3250 (s)	3175 (s)
Thioamide I	1490 (s)	1512 (s)	1535 (s)	1536 (s)	1508 (s)	1535 (s)
			1522 (s)	1522 (s)		
				1518 (s)		
Thioamide II	1335 (s)	——	1350 (w)	1348 (m)	1348 (m)	——
ν(C═S) + δ(NCS)	1295 (s)	1294 (s)	1310 (s)	1307 (s)	1295 (s)	1311 (s)
ν(Cl—O)	——	——	——	——	——	1071 (s,b)
ν(C—N) + δ(NCN)	1050	1048 (s)	1040 (s)	1044 (s)	1040 (s)	1048 (s)
$\nu(CH_3)$ + ν(C—N) + ν(C—S)	990	996 (s)	995 (s)	999 (s)	989 (s)	994 (s)
Thioamide III	——	932 (s)	932 (s)	931 (s)	925 (s)	930 (s)
ν(C—S) sym.	——	697 (s)	705 (s)	715 (m)	718 (m)	697 (sh)
ν(C—S) asym.		652 (s)	662 (s)	655 (m)	669 (m)	660 (w)
$\nu(ClO_4)^-$	——	——	——	——	——	621 (s)
δ(NCS)		585 (s)	580 (s)	580 (sh)	582 (s)	575 (m)
η(CC′)		544 (s)	540 (m)	529 (s,b)	526 (s)	——
δ(NCN) + ν(CN) + δ(CNC)		436 (s)	432 (s)	428 (s)	428 (s)	428 (s)
ν(Co—N)			341 (m)	330 (m)	326 (s)	325 (w)
Co—X			318 (s)	260 (s)	——	——
δ(NCS) + δ(CNC)		281 (m)	291 (m)	315 (m)	275 (w)	——

ABBREVIATIONS: s = strong; m = medium; w = weak; b = broad; X = Cl, Br.

TABLE VII

Bathochromic effects of ν(N—H) and the values of ν(M—N)

Complexes	Position of ν(N—H) (cm^{-1})	Δν(N—H) (cm^{-1})	ν(M—N) (cm^{-1})
$CoCl_2.2L$	3160	265	341
$CoBr_2.2L$	3200	225	338
$CoI_2.2L$	3250	175	326

halide the site of coordination in the ligand is sulfur. Since ε-thiocaprolactam and thiazolidinethione are very similar in their structures, it is quite surprising to have different results in the same type of complexes. It is therefore essential to compare critically the two cases. Intermolecular hydrogen bonding between hydrogen of NH and sulfur of C=S is well known in thioamides. ε-Thiocaprolactam will also have hydrogen bonding which will have a marked effect upon the positions of NH and C=S stretching frequencies. On the other hand, hydrogen bonding in the complexes is absent, and Madan *et al.* have also mentioned this fact. It is therefore not justified to deduce the shifts in various bands without eliminating hydrogen bonding in the ligand. No allowance for the effect of hydrogen bonding has been given (1) while comparing the spectrum of the ligand with the spectra of the complexes. Besides this the positive shift observed by them in NH is indicative of coordination through the nitrogen (25). The evidence on which they have based their assumption of coordination through the sulfur is the negative shift of the order of 1 to 3 cm^{-1} in C=S stretching frequency. The shift of this magnitude is insignificant for any conclusion. The assignment proposed by Madan *et al.* for Co—S stretching frequency (390 cm^{-1}) is also not in conformity with the recent assignments (205 cm^{-1}) proposed by Adams and Cornell (26) for the thiourea complexes of cobalt(II) chloride.

Metal-Halogen Bands

The bands at 318 cm^{-1} in $CoCl_2.2L$ and at 258 cm^{-1} in $CoBr_2.2L$ (Table VI) are assigned to Co—Cl and Co—Br stretching frequencies, respectively. The Co—I band is not observed in our spectrum and will probably appear below 250 cm^{-1}. Our assignments for cobalt–halogen frequencies are in good agreement with the recent observations of Adams and Cornell (26) and of Bradbury *et al.* (27).

Acknowledgments

The authors gratefully acknowledge the financial support from the National Research Council of Canada. P. P. Singh is also grateful to MLK College, Balrampur (India), for grant of leave.

1. S. K. Madan and C. Goldstein. J. Inorg. Nucl. Chem. **28**, 1251 (1966).
2. S. K. Madan and D. Mueller. J. Inorg. Nucl. Chem. **28**, 177 (1966).
3. S. K. Madan and M. Sulich. Inorg. Chem. **5**, 1662 (1966).
4. R. H. Lee, G. Griswold, and J. Kleinberg. Inorg. Chem. **3**, 1278 (1964).
5. B. N. Figgis and J. Lewis. Modern coordination chemistry. *Edited by* J. Lewis and R. C. Wilkins. Interscience Publishers, Inc., New York. 1960. p.403.
6. F. A. Cotton, D. M. L. Goodgame, and M. Goodgame. J. Am. Chem. Soc. **83**, 4690 (1961).
7. Y. Tanabe and S. Sugano. J. Phys. Soc. Japan, **9**, 753 (1954).
8. N. S. Gill and R. S. Nyholm. J. Chem. Soc. 3997 (1959).
9. F. A. Cotton, O. D. Faut, D. M. L. Goodgame, and R. H. Holm. J. Am. Chem. Soc. **83**, 1780 (1961).
10. R. H. Holme and F. A. Cotton. J. Am. Chem. Soc. **82**, 2983 (1960).
11. T. M. Dunn. Modern coordination chemistry. *Edited by* J. Lewis and R. G. Wilkins. Interscience Publishers, Inc., New York. 1960. p. 266.
12. D. M. L. Goodgame, M. Goodgame, and F. A. Cotton. Inorg. Chem. **1**, 239 (1962).
13. S. K. Madan and A. M. Donohue. J. Inorg. Nucl. Chem. **28**, 1617 (1966).
14. C. E. Schäffer and C. K. Jorgensen. J. Inorg. Nucl. Chem. **8**, 143 (1958).
15. C. E. Schäffer. J. Inorg. Nucl. Chem. **8**, 150 (1958).
16. J. Chatt, L. A. Duncanson, and L. M. Venanzi. J. Chem. Soc. 2712 (1956).
17. A. Nakahara, Y. Saito, and H. Kuroya. Bull. Chem. Soc. Japan, **25**, 331 (1952).
18. K. Nakamoto. Infrared spectra of inorganic and coordination compounds. John Wiley and Sons, Inc., New York. 1963. p. 145.
19. C. N. R. Rao and R. Venkataraghavan. Spectrochim. Acta, **18**, 541 (1962).
20. D. T. Elmore. J. Chem. Soc. 3489 (1958).
21. S. C. Jain and R. Rivest. J. Inorg. Nucl. Chem. **29**, 2787 (1967).
22. K. Nakamoto. Infrared spectra of inorganic and coordination compounds. John Wiley and Sons, Inc., New York. 1963. p. 148 and 149.
23. K. Nakamoto, P. J. McCarthy, A. Ruby, and A. E. Martell. J. Am. Chem. Soc. **83**, 1066 (1961).
24. K. Nakamoto, P. J. McCarthy, and M. E. Martell. J. Am. Chem. Soc. **83**, 1272 (1961).
25. K. Nakamoto. Infrared spectra of inorganic and coordination compounds. John Wiley and Sons, Inc., New York. 1963. p. 143.
26. D. M. Adams and J. B. Cornell. J. Chem. Soc. A, 884 (1967).
27. J. Bradbury, K. P. Forest, R. H. Nuttal, and D. W. A. Sharp. Spectrochim. Acta, **23A**, 2704 (1967).
28. G. A. Rodley and P. W. Smith. J. Chem. Soc. A, 1580 (1967).
29. R. K. Gosavi, U. Agarwala, and C. N. R. Rao. J. Am. Chem. Soc. **89**, 235 (1967).
30. I. Suzuki. Bull. Chem. Soc. Japan, **35**, 1456 (1962).

Can. J. Chem. Downloaded from www.nrcresearchpress.com by 210.87.254.42 on 09/05/12
For personal use only.

Can. J. Chem. Downloaded from www.nrcresearchpress.com by 210.87.254.5 on 09/05/12
For personal use only.

Dielectric studies. Part XX. Molecular relaxation of some heterocyclic amines in dilute solution

J. CROSSLEY
The University of Aston in Birmingham, England

AND

S. WALKER[1]
Chemistry Department, Lakehead University, Port Arthur, Ontario

Received February 1, 1968

Dielectric constant and loss data have been obtained at microwave frequencies for acridine, 4-methylpyridine, phthalazine, quinoline, and isoquinoline in both cyclohexane and *p*-xylene solution. The data have been used to calculate relaxation times and apparent dipole moments. For phthalazine, quinoline, and isoquinoline in cyclohexane at 50 °C the distribution coefficient is zero and their relaxation times are very similar. Although the axes about which these three molecules may relax lead to different volumes being swept out, no variation in relaxation behavior has been detected, and each system can be characterized by one relaxation time. The relaxation times for all the heterocyclic molecules except quinoline and acridine in *p*-xylene are appreciably longer than in cyclohexane. Relaxation time values appear a sensitive means of detecting the weak molecular interaction between the amine and the *p*-xylene. The difference in behavior between the quinoline and acridine as opposed to isoquinoline could be attributed to a more appreciable steric effect in the former two, hindering the approach of the π-electrons of the *p*-xylene molecules to the hybridized lone pair on the nitrogen atom. No interaction is, in fact, detectable in the case of quinoline and acridine. The importance of allowing for weak intermolecular forces, even in dilute solution, when relaxation values are being anticipated, is emphasized.

Canadian Journal of Chemistry, 46, 2369 (1968)

In dilute solution, where the internal field and viscosity effects are comparatively small, any relationship between the molecular relaxation time and the direction of the molecular dipole within the molecule may be examined for rigid molecules of the same shape and size, such as phthalazine, quinoline, and isoquinoline.

The relaxation times of quinoline as the pure liquid at 40 °C and in naphthalene solution at 85 °C have been found to be 29.7 and 9.5×10^{-12} s respectively (1). For isoquinoline, a molecule of identical shape and size, in the same conditions, values of 44.6 and 12.5×10^{-12} s were obtained (2). The difference in values between quinoline and isoquinoline was attributed to additional molecular reorientation around the axis in the carbon–carbon bond held in common by the two rings of isoquinoline, a motion not feasible for quinoline. However, measurements of these two molecules in cyclohexane (3) and Nujol solutions (4) at 20 °C show them to have very similar relaxation times of ~ 10 and $\sim 46 \times 10^{-12}$ s respectively in the two solvents. Thus, this set of results appeared opposed to those for pure quinoline and isoquinoline and further study of the influence of the direction of the dipole on the molecular relaxation time seemed appropriate in a molecule of similar shape and size.

Experimental Methods

The apparatus and procedure for determining the dielectric constant and loss have been described previously (5, 6).

Commercially available 4-methylpyridine, quinoline, and isoquinoline were dried over potassium hydroxide prior to distillation from a column of 35 theoretical plates. Acridine and phthalazine were recrystallized from a *p*-xylene–cyclohexane mixture and dried in a vacuum oven over phosphorous pentoxide.

Experimental Results

The mean relaxation time (τ_0), high frequency dielectric constant (ε_∞), and distribution coefficient (α) were obtained from the measured static dielectric constant (ε_0), dielectric constant (ε'), and dielectric loss (ε'') by the procedure previously described (7, 8), and the dipole moment estimated from the Debye equation as applied to dilute solutions (8).

The dielectric constant and loss data are presented in Table I. The mean relaxation times,

[1]Correspondence to: Dr. S. Walker, Chemistry Department, Lakehead University, Port Arthur, Ontario.

Can. J. Chem. Downloaded from www.nrcresearchpress.com by 210.87.254.5 on 09/05/12
For personal use only.

TABLE I

Dielectric constant and loss data for some rigid molecules in cyclohexane and *p*-xylene solution at specified weight fractions and temperatures

Solute	Solvent	w_2	t (°C)	Freq. (GHz)	ε'	ε''
Quinoline	Cyclohexane	0.03866	50	70.00	2.00_6	0.028_4
				35.09	2.03_5	0.042_8
				23.98	2.04_7	0.047_5
				16.20	2.06_7	0.044_1
				9.313	2.06_9	0.031_7
Quinoline	*p*-Xylene	0.03780	25	70.00	2.28_8	0.026_6
				34.86	2.30_7	0.047_7
				23.98	2.31_5	0.058_7
				16.20	2.34_9	0.063_9
				9.313	2.38_0	0.056_0
Quinoline	*p*-Xylene	0.03582	50	35.09	2.25_6	0.049_7
				23.98	2.29_4	0.056_7
				16.20	2.31_4	0.052_3
				9.313	2.33_2	0.042_2
Isoquinoline	Cyclohexane	0.03582	25	35.09	2.05_5	0.052_1
				23.98	2.06_1	0.062_7
				16.20	2.11_0	0.068_7
				9.313	2.14_1	0.062_0
				6.697	2.15_0	0.051_4
Isoquinoline	Cyclohexane	0.03328	50	70.00	1.99_8	0.031_0
				35.09	2.03_1	0.051_4
				23.98	2.04_7	0.058_6
				16.20	2.07_4	0.055_4
				9.313	2.08_4	0.043_6
Isoquinoline	*p*-Xylene	0.03647	25	70.00	2.28_5	0.028_2
				34.86	2.29_7	0.048_5
				23.98	2.31_9	0.065_3
				16.20	2.35_0	0.080_4
				9.313	2.39_0	0.082_7
Isoquinoline	*p*-Xylene	0.03088	50	70.00	2.25_5	0.025_8
				35.09	2.27_1	0.046_6
				16.20	2.30_7	0.060_8
				9.313	2.33_5	0.056_5
Phthalazine	Cyclohexane	—	50	35.09	1.99_0	0.029_0
				23.98	2.01_5	0.031_0
				16.20	2.03_1	0.027_5
				9.313	2.03_7	0.022_0
Phthalazine	*p*-Xylene	0.01301	25	70.00	2.29_6	0.029_6
				34.86	2.30_2	0.056_1
				23.98	2.32_1	0.075_5
				16.20	2.34_6	0.096_8
				9.313	2.39_5	0.114_1
Phthalazine	*p*-Xylene	0.01301	50	35.09	2.28_2	0.063_9
				23.98	2.29_3	0.082_7
				16.20	2.31_6	0.097_8
				9.313	2.37_3	0.097_3
Acridine	Cyclohexane	0.02608	50	35.09	1.99_7	0.011_9
				23.98	1.99_7	0.015_0
				16.20	2.00_8	0.018_1
				9.313	2.01_2	0.020_4
Acridine	*p*-Xylene	0.05807	25	34.86	2.31_3	0.030_0
				23.98	2.32_2	0.041_2
				16.20	2.33_2	0.055_6
				9.313	2.36_0	0.069_0
Acridine	*p*-Xylene	0.04802	50	70.00	2.25_5	0.013_3
				35.09	2.25_6	0.027_8
				23.98	2.26_8	0.036_7
				16.20	2.28_6	0.047_5
				9.313	2.31_3	0.049_9
4-Methyl-pyridine	Cyclohexane	0.02380	50	70.00	2.00_0	0.043_8
				35.09	2.04_0	0.061_4
				23.98	2.06_1	0.061_5
				16.20	2.08_2	0.049_6
				9.313	2.09_6	0.033_7
4-Methyl-pyridine	*p*-Xylene	0.02310	25	70.00	2.29_3	0.036_2
				35.09	2.31_4	0.060_3
				23.98	2.33_4	0.073_4
				16.20	2.36_6	0.076_6
				9.313	2.40_3	0.067_6

TABLE II

Dipole moment (in debyes), dielectric constant at high frequency (ε_∞), static dielectric constant (ε_0), distribution parameter (α), mean relaxation time (τ_0), and weight fraction (w_2) in cyclohexane and *p*-xylene solutions at t °C. The relaxation times (in seconds) have been multiplied by 10^{12}

Solute	Solvent	w_2	t (°C)	ε_0	ε_∞	τ_0	α	μ
Quinoline	Cyclohexane	0.03866	50	2.089	1.99_6	6.6	0.00	2.04
Quinoline	*p*-Xylene	0.03780	25	2.417	2.28_5	10.4	0.03	2.06
Quinoline	*p*-Xylene	0.03780	50	2.349	2.23_0	6.7	0.02	2.08
Isoquinoline	Cyclohexane	0.03582	25	2.180	2.03_5	10.5	0.03	2.48
Isoquinoline	Cyclohexane	0.03328	50	2.109	1.99_3	7.5	0.00	2.45
Isoquinoline	*p*-Xylene	0.03647	25	2.471	2.28_7	15.4	0.05	2.48
Isoquinoline	*p*-Xylene	0.03088	50	2.371	2.24_4	10.3	0.01	2.38
Phthalazine	Cyclohexane	*	50	2.044	1.98_2	6.7	0.00	—
Phthalazine	*p*-Xylene	0.01301	25	2.539	2.28_6	19.9	0.06	4.88
Phthalazine	*p*-Xylene	0.01301	50	2.452	2.24_8	12.9	0.06	4.67
Acridine	Cyclohexane	0.02608	50	2.033	1.99_1	15.1	0.02	1.97
Acridine	*p*-Xylene	0.05807	25	2.456	2.30_9	21.9	0.00	2.06
Acridine	*p*-Xylene	0.04802	50	2.351	2.25_1	14.7	0.00	2.00
4-Methylpyridine	Cyclohexane	0.02380	50	2.107	1.98_4	5.2	0.00	2.54
4-Methylpyridine	*p*-Xylene	0.02310	25	2.446	2.28_3	9.8	0.03	2.78

*Owing to the insolubility of phthalazine in cyclohexane a saturated solution of unknown weight fraction was used.

apparent dipole moments, distribution coefficients, and the static and high frequency dielectric constants are shown in Table II.

Discussion

The relaxation times of quinoline and isoquinoline in *p*-xylene at 25 °C are 10.4 and 15.4 $\times 10^{-12}$ s, whereas in the relatively inert solvent cyclohexane at 20 °C they are 10^{-11} s and 10.5 $\times 10^{-12}$ s respectively (3). Since the macroscopic viscosity of *p*-xylene is less than that of cyclohexane (e.g. at 25 °C these are 0.898 cP and 0.605 cP respectively), then such behavior suggests that the appreciable lengthening of the relaxation time in *p*-xylene at 25 °C may be attributed to the isoquinoline interacting more appreciably with the *p*-xylene than the quinoline. The results at 50 °C (Table II) in these two solvents bear this out.

The behavior of phthalazine bears out the concept of molecular interaction of the aromatic amine with the *p*-xylene, since its relaxation time in cyclohexane at 50 °C is virtually identical with that of quinoline, whereas its values in *p*-xylene at both 25 and 50 °C differ significantly from those of quinoline and isoquinoline under identical conditions. Evidently the extent of interaction with *p*-xylene at 25 °C is

phthalazine > isoquinoline > quinoline,

and since the basicities of these solutes are very similar, then this order may be accounted for in terms of the phthalazine having two nitrogens which can act as donors, while the quinoline is sterically hindered from interacting with presumably the π-electrons of the *p*-xylene.

Sharpe and Walker (9) have shown that the difference in dipole moment of pyridine in cyclohexane and carbon tetrachloride can be attributed to a weak form of donor–acceptor interaction which was confirmed by thermochemical measurements (10), whereas the sterically hindered nitrogen atom in 2,6-diphenylpyridine shows no evidence of such interactions. Recent dielectric absorption studies (11) have shown the relaxation time of pyridine in cyclohexane and *p*-xylene at 25 °C to be 3.1 and 4.3 $\times 10^{-12}$ s respectively. Rampolla and Smyth (12) in a study of several methylquinolines in the pure liquid state observed somewhat shorter critical wavelengths for 2- and 8-methylquinoline and attributed these anomalies to "the partial shielding of the nitrogen atom by the methyl group with its attendant reduction of intermolecular attractions".

Additional support for the conclusions relating to steric effects is given by the results for acridine and 4-methylpyridine (Table II). The latter molecule, in which the nitrogen atom is unshielded, has relaxation times in cyclohexane and *p*-xylene solutions at 25 °C of 7.2 and 9.8 $\times 10^{-12}$ s respectively. Conversely, in acridine, the relaxation time is virtually the same in both

Can. J. Chem. Downloaded from www.nrcresearchpress.com by 210.87.254.5 on 09/05/12
For personal use only.

Can. J. Chem. Downloaded from www.nrcresearchpress.com by 210.87.254.5 on 09/05/12
For personal use only.

solvents at 50 °C, the nitrogen atom being effectively shielded by the two adjacent hydrogen atoms, and this is to be contrasted with the behavior of phthalazine under these conditions.

The evidence indicates that both isoquinoline and phthalazine are capable of acting as donors in donor–acceptor interactions while no such interaction is detectable for quinoline from relaxation time values. It thus becomes understandable why the relaxation times of quinoline and isoquinoline differ when naphthalene is the solvent, since only the isoquinoline would be expected to interact with the π-electrons of the naphthalene.

The difference in relaxation time of pure liquid quinoline and isoquinoline cannot be accounted for solely in terms of macroscopic viscosity (e.g. at 30 °C their viscosities are 2.97 and 3.34 cP respectively). Another factor which could lead to a longer observed relaxation time for the isoquinoline is that its dipole moment is about 0.4 D greater and this would result in a stronger internal field effect which could be pronounced in the closely packed pure liquid but might have a negligible influence on the relaxation time in dilute solution.

TABLE III

Volumes (V_x, V_y, V_z) swept out in molecular reorientation around the molecular axes (X, Y, Z) and molecular volumes (V), obtained from measurements using Courtauld models*

	V_x	V_y	V_z	V
Quinoline	355	—	217	116
Isoquinoline	355	447	217	116
Phthalazine	—	413	201	111

*The volumes are expressed as Å^3.

A comparison of the volumes swept out by reorientation about different axes for quinoline, isoquinoline, and phthalazine is given in Table III. The volume swept out has been evaluated for a cylinder of length equal to the length of the longest axis of rotation and diameter equal to the length of the longest axis perpendicular to it. For all the molecules the Z-axis was taken to be that perpendicular to the plane of the rings, and for acridine, phthalazine, quinoline, and isoquinoline the short and long axes in the plane of the ring were designated as Y and X respectively.

Quinoline and phthalazine have identical relaxation times in cyclohexane solution at 50 °C. Since they have only one common axis of rotation one possibility is that both predominantly reorientate about the common Z-axis which involves the smallest volume swept out and presumably the least energy barrier. If, however, relaxation occurred about their two possible axes, on the assumption that the frictional coefficients are the same about the different axes, it follows from Table III that the relaxation time of phthalazine should be longer than that of quinoline. This, however, is not detectable in cyclohexane at 50 °C. Further the distribution coefficients for phthalazine, quinoline, and isoquinoline in cyclohexane at 50 °C are all zero, indicating that only one relaxation process is detectable.

In conclusion, a study of the relaxation times of phthalazine, quinoline, and isoquinoline, when the molecular interaction is minimized, indicates there is hardly any variation of relaxation time by varying the direction of the molecular dipole in these three molecules of almost identical size and shape. It would perhaps be unwise to draw any definite conclusions as to whether the reorientation is solely about the Z-axis, since the value of the frictional coefficient may vary for relaxation about each axis and might lead fortuitously to similar relaxation time values for these three molecules. Clearly, further work is required on groups of molecules, each group containing molecules of similar shape and size and differing from the other groups by having different axial ratios.

1. R. S. Holland and C. P. Smyth. J. Phys. Chem. **59**, 1088 (1955).
2. R. C. Miller and C. P. Smyth. J. Am. Chem. Soc. **79**, 308 (1957).
3. F. Hufnagel and H. Kilp. Z. Naturforsch. **18a**, 769 (1963).
4. E. N. DiCarlo and C. P. Smyth. J. Phys. Chem. **66**, 1105 (1962).
5. W. F. Hassell, M. D. Magee, S. W. Tucker, and S. Walker. Tetrahedron, **20**, 2137 (1964).
6. D. B. Farmer and S. Walker. Tetrahedron, **22**, 111 (1965).
7. J. Crossley, W. F. Hassell, and S. Walker. J. Chem. Phys. **48**, 1261 (1968).
8. J. Crossley and S. Walker. J. Chem. Phys. **45**, 4733 (1966).
9. A. N. Sharpe and S. Walker. J. Chem. Soc. 157 (1962).
10. K. W. Morcom and D. N. Travers. Trans. Faraday Soc. **62**, 2063 (1966).
11. J. Crossley, W. F. Hassell, and S. Walker. Can. J. Chem. **46**, 2181 (1968).
12. R. W. Rampolla and C. P. Smyth. J. Am. Chem. Soc. **80**, 1057 (1958).

Can. J. Chem. Downloaded from www.nrcresearchpress.com by 210.87.254.40 on 09/05/12
For personal use only.

Proton magnetic resonance spectra of vinylmetallic compounds. Part I. Tetravinyl and triphenylvinyl derivatives of Group IVB elements

SEÁN CAWLEY[1] AND STEVEN S. DANYLUK[2]
Department of Chemistry, University of Toronto, Toronto, Ontario

Received January 25, 1968

A study has been made of the proton magnetic resonance spectra for all of the Group IVB derivatives of the series MVi_4 and ϕ_3MVi (ϕ = phenyl group and Vi = vinyl group). The spectra were measured at 60 MHz as accurately as possible and the assignment of transitions was checked with a variety of supplemental aids including double irradiation, multiple quantum transitions, and medium effects. Final, accurate spectral parameters were derived using both iterative and exact computational methods for solution of the three-spin problem. Excellent agreement was obtained between the sets of parameters determined by the two methods.

The chemical shifts for both series of compounds display a number of characteristic trends of which the most notable is a displacement of the vinyl proton signals to low field with increasing atomic number of the M atom. In each series the largest shift change is noted in going from the carbon to the silicon derivative. These deshieldings have been attributed to the enhanced possibility of d_π–p_π interaction between the central M atom and the vinyl group in higher members of the series. Marked changes are also noted for the internal shifts of the vinyl protons down both series of compounds. It is concluded that these changes are principally due to the effects of the M—C bond diamagnetic anisotropy. The trends in internal shifts can be satisfactorily reproduced by the dipole approximation using $\Delta\chi$ values of 4, 6, 8, 12, and 18 $\times$ 10^{-6} cm^3 $mole^{-1}$ for the C, Si, Ge, Sn, and Pb–carbon bonds respectively.

The signals for the vinyl protons of the ϕ_3MVi series are all located to low field relative to the MVi_4 series. This deshielding is satisfactorily accounted for by the effects of the phenyl ring diamagnetic anisotropy in the former series.

A linear correlation is observed between the sums of the coupling constants and the electronegativities, E_m, of the central M atom for both series of compounds. However, the ΣJ values for the ϕ_3MVi series are all slightly lower than the corresponding sums for the MVi_4 series, indicating that the electronegativity of the phenyl group is somewhat larger than for the vinyl group.

A significant solvent and concentration dependence is only noted for compounds belonging to the ϕ_3MVi series. For example, the *trans* proton of ϕ_3GeVi shifts up-field by 4 Hz while the *cis* proton is displaced down-field by 4 Hz as the concentration of ϕ_3GeVi is increased to 50 mole % in carbon tetrachloride. These changes have been interpreted on the basis of a solute–solute interaction scheme of the type proposed previously for phenyl proton shifts.

Canadian Journal of Chemistry, 46, 2373 (1968)

Introduction

The usefulness of chemical shifts and coupling constants in providing an insight into electron distribution and bonding characteristics in molecules is well established (1, 2). With the advent of sophisticated computer techniques and more stable spectrometer systems, more precise determinations of these parameters are possible. Nevertheless, relatively few attempts have been made to carry out such studies for closely related series of compounds under conditions where intermolecular solvent and solute effects are minimized. Accordingly, as part of a continuing n.m.r. study of vinylmetallic compounds we have measured and accurately analyzed the high-resolution proton resonance spectra for the series of compounds[3] X_nMVi_{4-n}, where M represents the Group IVB elements from carbon to lead and X represents a wide range of substituent groups (ϕ, CH_3, Cl, etc.). Of particular interest were the effects of (i) the central metal atom and (ii) the nature and location of the substituent group upon the chemical shifts and coupling constants of the vinyl protons.

In this communication (Part I) the results are presented for the MVi_4 and ϕ_3MVi series of compounds. Although the spectra for some of these compounds have been reported previously by other workers (3–8) the derived parameters are open to question in several cases. For example, the *gem* and *cis* proton couplings reported at 40 MHz for $SnVi_4$ by Moore and

[1]Present address: Department of Applied Mathematics, Queen's University, Belfast.

[2]Present address: Department of Biological and Medical Research, Argonne National Laboratory, Argonne, Illinois.

[3]Abbreviations used: Vi = vinyl group; ϕ = phenyl group.

Can. J. Chem. Downloaded from www.nrcresearchpress.com by 210.87.254.40 on 09/05/12
For personal use only.

Happe (6) are roughly 40% higher and 20% lower respectively than the corresponding coupling constants reported by Brügel and co-workers (3). Considerable difficulties have also been encountered in obtaining an unambiguous analysis of the $SiVi_4$ spectrum (3–5). The problem in the latter case has been largely resolved by determining the proton couplings from the ^{13}C satellite spectra (5). We have re-investigated the spectra for these compounds with emphasis on obtaining unambiguous assignments and an increased accuracy of the parameters. In order to achieve unique assignments, use was made of a variety of supplementary aids including solvent and concentration effects, double irradiation (9, 10), and multiple quantum transitions (11, 12). The final parameters were calculated by the iterative method of Swalen and Reilly (13) and by the "exact" method of Castellano and Waugh (14). In all cases agreement between the final parameters obtained by the two computational procedures was well within experimental error.

Experimental

Materials

All of the tetravinyl compounds were obtained from commercial sources and were used without further purification. Impurities were estimated to be less than 1%, based upon the n.m.r. spectra for concentrated solutions. The triphenylvinyl derivatives of C, Si, and Ge were kindly supplied by Prof. A. G. Brook. Triphenylvinyl stannane was obtained from Metallomer Labs. Triphenylvinylplumbane was prepared according to procedures described in the literature (15). The melting point and i.r. spectrum for the purified compound agreed with the literature values (15). Commercially available spectroscopic grade solvents were used after further drying over calcium sulfate. The solutions were contained in precision bore 5 mm spinning tubes with a drop of tetramethylsilane (TMS) added to serve as internal reference.

N.M.R. Spectra

The spectra of the MVi_4 series were recorded on a Varian A60 spectrometer at ambient temperatures, 25 ± 2 °C Line positions were determined by superposition of TMS side bands, generated with a Krohn-Hite 440A audio oscillator. This procedure was further checked by bracketting the signals with TMS side bands and interpolating the line positions. A Hewlett-Packard 5245 L counter was used to monitor the audio-side-band frequencies. The final line positions, representing an average of four forward and reverse scans of the spectrum, are precise to better than ±0.03 Hz.

The spectra of the ϕ_3MVi compounds were recorded with a Varian DP 60 spectrometer at a probe temperature of 23 ± 1 °C. Calibration of the spectra was carried out in the same manner as for the MVi_4 spectra and the line frequencies are precise to ±0.03 Hz.

Analysis

In certain cases the iterative method of solving the Hamiltonian matrix for a three-spin system can lead to an incorrect set of n.m.r. parameters (14). The "exact" algebraic method of Castellano and Waugh (14) purports to remove any possible ambiguities by solving the three-spin problem without the use of an iteration at any stage of the calculation. However, the latter method generally yields more than one solution equally consistent with the observed transition frequencies and within experimental error of the measured intensities. Thus, without careful scrutiny both methods can yield ambiguous results. The problem is particularly acute in tightly coupled ABC systems where the assignment of transition frequencies to an energy level scheme is not straightforward. A striking example of such a system is the spectrum of $SiVi_4$. Despite a number of attempts (3–5) to determine a correct set of parameters by iterative and exact methods (4) at two different frequencies (40 and 60 MHz) the parameters were still in question until accurate values of the coupling constants were obtained from the ^{13}C satellite spectra (5).

Similar problems in assignment arose in the present work in the case of the $GeVi_4$ spectrum (and also for $SiVi_4$ which was further re-investigated in order to test the procedure used in this work). To resolve any ambiguities, an extensive study was made of the effects of solvent (concentration), spin-tickling (10), saturation, and double-quantum transitions (11, 12) upon the spectrum. After unequivocal assignment of the transitions, the chemical shifts and coupling constants were then calculated by both the iteration and "exact" methods. The NMREN II and NMRIT programs of Swalen and Reilly (13) were used in the iteration method, while a sub-routine QORTIC, based upon the exact method and coded in Fortran for an IBM 7094 computer, was incorporated into a modified NMREN II program to calculate the parameters by the exact method.[4]

Results

Tetravinyl Series

The protons of both series of compounds have been labelled as follows.

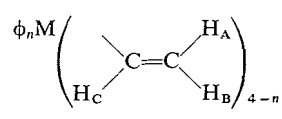

The spectrum for $SiVi_4$, at low concentration in CCl_4 (5 mole %), was essentially the same

[4]In the exact method of Castellano and Waugh (14) the fourth degree polynomial was solved analytically by the Ferrari method. In QORTIC, however, the polynomial is solved by two independent iteration methods. The first method finds all the zeros while the second finds only the real zeros of the quartic. Both methods gave identical real solutions of the quartic.

TABLE I

Chemical shifts and coupling constants for the tetravinyl series obtained by the iterative and exact methods

Compound		Chemical shifts*			Coupling constants†				Average errors	
		δ_A	δ_B	δ_C	J_{AB}	J_{AC}	J_{BC}	ΣJ	δ	J
CVi_4 (19)		300.3	306.0	349.0	2.0	18.5	8.75	29.25	—	—
$SiVi_4$	Iteration	346.160	363.436	367.067	3.622	20.397	14.670	38.689	0.01	0.025
	Quartic	−12.686	4.500	8.185	3.601	20.402	14.685	38.688	0.01	0.025
$GeVi_4$	Iteration	340.988	361.766	372.721	3.084	20.066	13.446	36.596	0.02	0.047
	Quartic	−17.504	3.290	14.214	3.068	20.072	13.456	36.596	0.02	0.047
$SnVi_4$	Iteration	345.144	372.568	383.307	3.147	20.686	13.778	37.611	0.03	0.053
	Quartic	−21.862	5.569	16.292	3.138	20.691	13.782	37.611	0.03	0.053
$PbVi_4$	Iteration	344.965	383.529	419.096	2.024	19.569	12.127	33.768	0.06	0.025
	Quartic	−37.565	0.999	36.566	2.025	19.569	12.174	33.768	0.06	0.025

*Chemical shifts are in hertz; for the iteration method the shifts are relative to internal TMS, while for the quartic they are relative to the center of gravity.
†Coupling constants are in hertz.

(apart from minor differences in intensities) as the spectra reported by previous workers (4, 5). Assignment of the lines was based upon the effects of concentration and radio-frequency (r.f.) power level upon the signals. An increase in concentration of the solute from 5 mole % to 100 mole % resulted in an up-field shift of approximately 1 Hz for the set of signals assigned to the B proton. This change was accompanied by a down-field shift of the same amount for the combination line at the center of the spectrum. No shift changes were noted for the other signals.[5] The combination transitions were then determined from the saturation behavior of the spectrum. It was observed that the three combination lines are readily detected under conditions which saturate the normal transitions, i.e. at r.f. power levels of 0.1 to 1.0 mG on the A-60. Identification of the combination transitions permitted a tentative assignment of the remaining transitions. A spin-tickling experiment, carried out on the spectrum at 100 MHz by Dr. R. Freeman, confirmed the assignment and also indicated that the couplings were all of the same sign (assumed positive). A summary of the chemical shifts and coupling constants calculated by the iterative and exact (quartic) methods is given in Table I. Also included are the calculated errors for these parameters. Convergence in the iterative method was found to be dependent upon the trial values used for the starting parameters. No satisfactory convergence was obtained if the trial values differed markedly (> 1 Hz) from the correct values. The final parameters listed in Table I were obtained using the coupling constants reported for trimethylvinylsilane (10) as the starting parameters. The "exact" method was somewhat unsatisfactory since no real zeroes were obtained for the polynomial in the defined range. The difficulty presumably arises because of the small shift difference between the B and C protons (~3.6 Hz at 60 MHz) and is similar in nature to that encountered by Cavanaugh (16) for other three-spin systems. A plot of the polynomial showed that the function approached but did not cross the X axis. A real solution was therefore approximated by extrapolation of the function minimum to the X axis. The resultant parameters are listed in Table I.

The spectrum of neat $GeVi_4$, illustrated in Fig. 1A, is less tightly coupled than $SiVi_4$. An assignment of the transitions was carried out following the procedures used for $SiVi_4$. As in the latter case only the B proton transitions were found to be solvent and concentration dependent. The assignment was further checked by studying the double-quantum spectrum. Such measurements are of considerable usefulness in analysis and in sign determination of moderately coupled spectra (11, 12, 17, 18). In the present system satisfactory agreement was observed between the observed and calculated double-quantum transitions, Table II thus confirming the assignment and also indicating that the signs of the couplings were all the same (+ve). A summary of chemical shifts and coupling constants calculated by iterative and exact methods is given in Table I. Satisfactory solutions were obtained in both cases.

[5]Similar concentration effects were observed in acetonitrile and acetone.

Can. J. Chem. Downloaded from www.nrcresearchpress.com by 210.87.254.40 on 09/05/12
For personal use only.

Can. J. Chem. Downloaded from www.nrcresearchpress.com by 210.87.254.40 on 09/05/12
For personal use only.

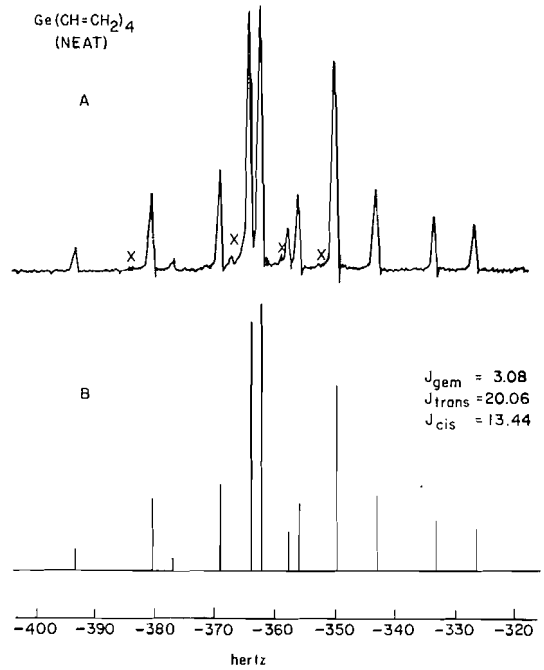

FIG. 1. 60 MHz spectrum of neat $GeVi_4$; shifts are in hertz to low field relative to internal TMS.

TABLE II

Calculated and experimental multiple quantum transitions for the $GeVi_4$ spectrum

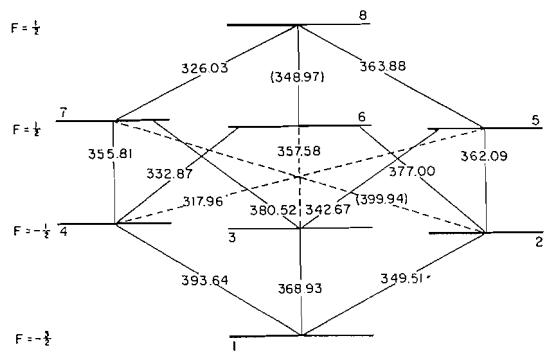

Transition*	Calculated	Observed†
4–8	340.9	341.0
3–8	348.3	349.0
1–5	355.3	353.0
1–6	358.3	
1–8	358.5	
2–8	363.0	363.1‡
1–7	374.7	374.5

*The eight energy levels are labelled according to the scheme in the diagram.
†In hertz; correct ± 1.0 Hz.
‡Uncertain because of superimposed single quantum transitions.

The spectra of $SnVi_4$ and $PbVi_4$ in CCl_4 (~ 5 mole %) were both less tightly coupled than for other members of this series and unambiguous analyses were obtained more readily. The parameters for both compounds are listed in Table I. The parameters listed for CVi_4 are those reported at 60 MHz by Berger and coworkers (19).

Triphenyl Vinyl Series

The vinyl proton spectra for compounds in this series were all close to first order at low concentration in CCl_4. The spectrum for ϕ_3GeVi is typical of the series and is illustrated in Fig. 2. Assignment of the signals was relatively straightforward for all of the compounds, and the parameters derived by iterative and exact methods are listed in Table III. For ϕ_3PbVi the quartet at lowest field was obscured by the ring proton signals and the chemical shift of the proton was therefore taken as the mid-point of the corresponding ^{207}Pb satellite spectrum. The limits of errors for the parameters of the triphenyl vinyl series are somewhat larger than for the tetravinyl series because the line positions measured with the DP-60 spectrometer were slightly less accurate.

A marked solvent and concentration dependence was noted for the two β protons in all of the compounds. In contrast, little medium effect was noted for the α proton. Figure 3 illustrates the concentration dependence for ϕ_3GeVi in CCl_4. Proton A, located *cis* to the germyl group, is observed to shift *down-field* by approximately 4 Hz, while proton B (*trans* to ϕ_3Ge) shifts 4 Hz *up-field* when the concentration is increased from 6 mole % to 50 mole % (saturation). Proton C (*gem* to ϕ_3Ge) shows only a slight, ~0.2 Hz, shift over the same concentration range.

Discussion

Comparison with Earlier Parameters

A summary of the most recent MVi_4 parameters reported in the literature is given for comparative purposes in Table IV. A close inter-comparison of the chemical shifts is not feasible because the spectra were not all measured under the same solvent and concentration conditions. Although the medium effects are generally quite small they are significant enough in the case of $SiVi_4$ to affect the analysis. The excellent agreement of the coupling constants

TABLE III

Chemical shifts and coupling constants for the triphenylvinyl series obtained by iterative and exact (quartic) methods

Compound		Chemical shifts*			Coupling constants†				Average errors	
		δ_A	δ_B	δ_C	J_{AB}	J_{AC}	J_{BC}	ΣJ	δ	J
ϕ_3CVi	Iteration	292.233	321.968	409.984	1.156	16.993	10.436	28.585	0.16	0.31
	Quartic	−49.137	−19.461	68.597	1.159	17.003	10.423	28.585	—	—
ϕ_3SiVi	Iteration	346.127	377.617	399.131	3.604	20.203	14.568	38.375	0.06	0.13
	Quartic	−28.176	3.365	24.812	3.580	20.212	14.583	38.375	—	—
ϕ_3GeVi	Iteration	342.909	374.157	398.403	2.459	19.990	13.776	36.225	0.10	0.42
	Quartic	−29.067	2.313	26.754	2.342	19.745	13.749	35.836	—	—
ϕ_3SnVi	Iteration	353.965	385.273	404.455	3.105	20.536	13.520	37.161	0.10	0.20
	Quartic	−27.283	4.118	23.710	3.048	20.561	13.551	37.160	—	—
ϕ_3PbVi	Iteration‡	354.99	392.76	436.62	1.866	19.824	11.952	33.438		

*Shifts are given in hertz relative to TMS for the iteration method, and to the center of gravity for the quartic method.
†Coupling constants are in hertz.
‡Only eight lines were detectable for the vinyl protons.

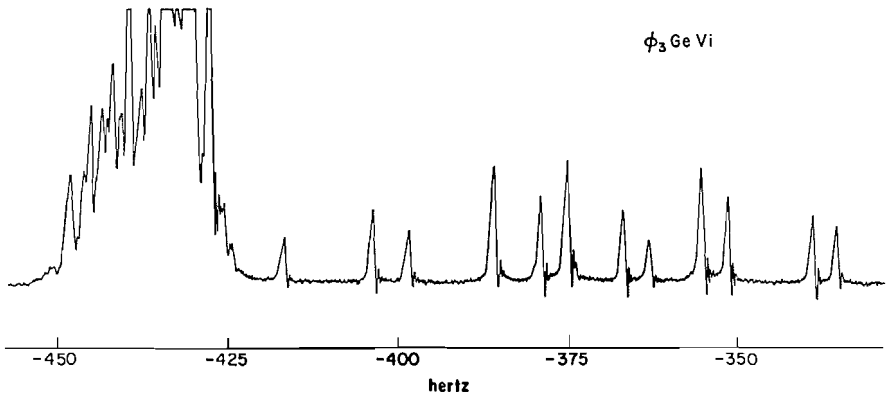

FIG. 2. 60 MHz spectrum of ϕ_3GeVi; 12 mole % in CCl_4; shifts are in hertz to low field relative to internal TMS.

derived for $SiVi_4$ by the iterative and exact methods with the values reported by Hobgood, Mayo, and Goldstein (5), using the ^{13}C method, confirms that the set is correct. The possible reasons for earlier ambiguities have been commented upon in a preceding section. Such ambiguities can be minimized by appropriate supplementary measurements, i.e. ^{13}C satellite spectra, "tickling" experiments, and judicious use of solvent effects.

The coupling constants for $GeVi_4$ are in close agreement with the values reported for Ge_2Vi_6 (20). However, the shifts for the $GeVi_4$ protons are all slightly lower (3–7 Hz) than the corresponding shifts for Ge_2Vi_6. The origin of this effect is not clear although it is possible that the deshieldings arise from anisotropy effects involving the vinyl groups. Both sets of parameters reported earlier (3, 6) for $SnVi_4$ at 40 MHz differ significantly from the present values. These discrepancies are probably the result of a combination of factors including larger errors and different computational procedures used in the earlier work. In view of the excellent agreement between the iterative and exact solutions the parameters reported in this work are considered to be more satisfactory.

The only parameters reported previously for the ϕ_3MVi series were those for the silyl compound at 40 MHz (7, 8). Although the errors were larger than in the present case the agreement between the different sets of coupling constants is quite satisfactory.

Chemical Shifts

MVi_4 Series

A schematic illustration of the chemical shifts for the complete series of compounds is given

Can. J. Chem. Downloaded from www.nrcresearchpress.com by 210.87.254.40 on 09/05/12
For personal use only.

TABLE IV

Summary of coupling constants* for MVi_4 compounds reported in the literature

Compound	Solvent	J_{AB}	J_{AC}	J_{BC}	ΣJ	Ref.
$SiVi_4$	Neat	2.70	20.47	15.33	38.5	4
	Neat	4.38	19.95	14.17	38.5	4
	C_6H_{12}	3.63	20.36	14.63	38.69	5
	C_6H_{12}	3.68	20.4	14.6	38.6	3
	Neat†	3.68	20.29	14.55	38.51	Present
$SnVi_4$	Neat	3.7	13.2	20.3	37.2	6
	Neat	2.6	16.1	20.7	39.4	3
$PbVi_4$	Neat	2.0	12.1	19.6	33.7	3

*Coupling constants are given in hertz.
†From 100 MHz spectrum run by Dr. R. Freeman.

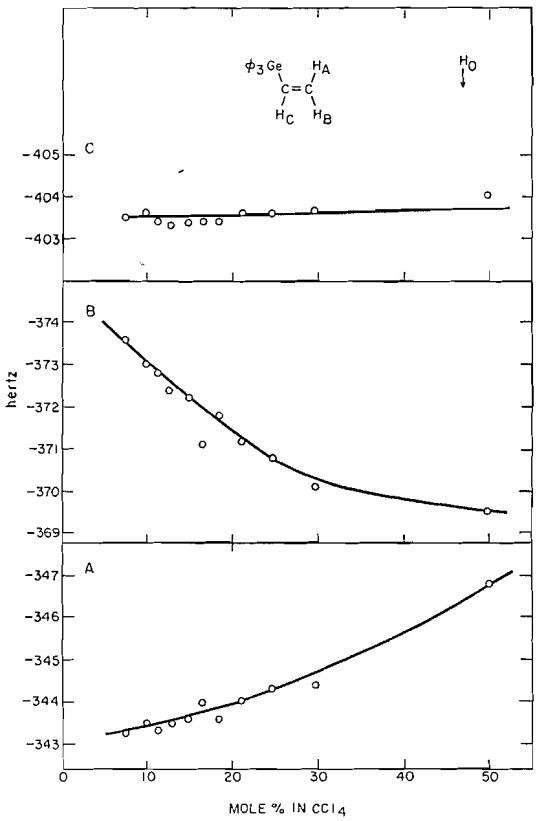

FIG. 3. Concentration dependence of the chemical shifts of ϕ_3GeVi in CCl_4 at room temperature; shifts are in hertz to low field relative to internal TMS.

in Fig. 4. Several points of interest can be noted: (1) The centers of gravity of the spectra for all of the compounds, from $SiVi_4$ to $PbVi_4$, are shifted to low field relative to the carbon analogue and to other ethylene derivatives (1, 2). The incremental changes are most pronounced in going from the carbon to the silicon derivative and the largest low-field shift (relative to ethylene) occurs for the $PbVi_4$ protons. (2) In each case the shieldings vary in the order *gem* < *trans* < *cis*,[6] in contrast with the order generally observed in other vinyl compounds, i.e. *gem* < *cis* < *trans* (1, 2). (3) A surprising constancy in shielding is noted for the *cis* proton over the entire series. The *gem* and *trans* protons, on the other hand, are progressively deshielded down the series with the largest change observed for the *gem* proton.

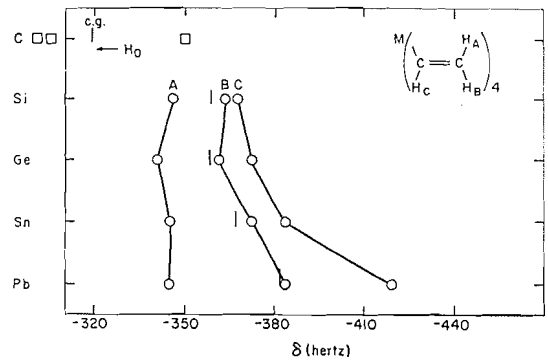

FIG. 4. Schematic illustration of the shift trends for the vinyl protons of the MVi_4 series; c.g. denotes the center of gravity of the spectrum.

Since the tetravinyls are nonpolar and show a minimal solvent and concentration dependence, it can be concluded that the observed shift changes are intramolecular in origin. A number of comprehensive reviews (1, 2, 21, 22) have been given of shift contributions from such sources. In the present compounds the most likely possibilities are (i) inductive effects due to the

[6]The designations are given relative to the substituent (M).

Can. J. Chem. Downloaded from www.nrcresearchpress.com by 210.87.254.40 on 09/05/12
For personal use only.

Can. J. Chem. Downloaded from www.nrcresearchpress.com by 210.87.254.40 on 09/05/12
For personal use only.

M atom, (ii) resonance interaction between the π electron system of the vinyl group and appropriate orbitals of the M atom (e.g. d_π–p_π interaction), and (iii) diamagnetic anisotropy of the bonds, in particular the M—C bond.

It is convenient to consider first the trend in the center of gravity of the spectra (in terms of (i)–(iii)). Inductive effects, arising primarily from electronegativity differences of substituent groups and operating via the σ electron system, are known to exert an appreciable influence upon proton shifts (2, 3, 24, 25). For example, low-field shifts amounting to 1.4 p.p.m. per unit increase in electronegativity are noted (25) for the methyl protons in a series of methyl halides. However, inductive effects drop off very rapidly with the number of intervening bonds and shift changes for β protons are approximately 1/10 those of α protons in saturated compounds (1–3). On this basis little shift change would be expected for the *cis* and *trans* protons of the tetravinyls while the *gem* proton could show a shielding of up to 50 Hz in $PbVi_4$ relative to CVi_4. The observed changes are in the wrong direction, however, and it can be concluded that some factor other than (i) is responsible.

A number of attempts have been made recently to rationalize the deshieldings of vinyl protons in allyl and aryl silanes, germanes, and stannanes in terms of a resonance interaction between d_π orbitals of the M atom and the p_π orbitals of the vinyl group (7, 8, 20, 26–28). The deshieldings, i.e. shift of the center of gravity, relative to alkenes, are presumed to result from a back donation of p_π electrons on the trigonal C atom to suitable low-lying d_π orbitals on the M atom. This back donation is assumed to be strong enough to overcome any inductive effects acting in the opposite direction. The effect of any d_π–p_π interaction should decrease with the number of intervening bonds and should increase with a greater availability of d orbitals on the M atom (i.e. at higher atomic numbers).[7] Both of these trends are noted in the MVi_4 series and it is tempting to conclude that the shifts of the centers of gravity are primarily due to d_π–p_π interaction. Such a conclusion is tentative, however, and further confirmatory spectroscopic studies are essential. In this connection, it can be noted that Si d orbital interaction with the π electron system of benzene rings has been definitively established in a recent ultraviolet (u.v.) study (29). More recent u.v. measurements suggest that a similar conjugation is also possible for phenyl derivatives of other Group IV elements (30).

Although d_π–p_π interaction would account for the low-field shifts relative to alkenes, it is more difficult to attribute the trends in the internal *cis*, *trans*, and *gem* shift changes in the series solely to such an interaction. A more likely source of the changes is the diamagnetic anisotropy of the $M(sp^3)$—$C(sp^2)$ bond.[8,9] The effect of bond anisotropies upon the shift can be estimated from the dipole approximation (31)

$$[1] \qquad \Delta\sigma = \frac{\Delta\chi}{3NR^3}(1 - 3\cos^2\Theta),$$

where $\Delta\chi$ is the difference between the longitudinal χ_L and transverse χ_T susceptibilities and Θ is the angle between the dipole axis and the radius vector R joining the dipole and the given proton. It should be noted that shifts calculated using the dipole approximation may have a considerable error when R is less than 3 Å, as in the case of the *gem* proton. Nevertheless, eq. [1] should provide a qualitative test of the influence of bond anisotropy upon the shifts. In the present compounds the M—C bond susceptibilities are not known and the shift trends were therefore estimated by using trial values of $\Delta\chi$ and assuming that the shift difference, δ_A–δ_B, is due mainly to the diamagnetic anisotropy of the nearest[10] M—C bond. The $\Delta\chi$ value which gave the best fit of δ_A–δ_B, using reasonable R and Θ values, was then used to calculate δ_C. Vinyl bond angles were assumed to be the same as those reported for vinylsilane (32) while bond distances were obtained from the literature (33). The bond dipole origin was taken as the mid-point of the M—C bond in each case. Little variation was

[7]It is also likely that the *trans* proton would be more influenced by the resonance interaction than the *cis* proton.

[8]A rough estimate of shift changes due to the C=C bond anisotropy (assuming free rotation) indicates that these will be quite small, i.e. −5 to 5 Hz, because of averaging between shielding and deshielding regions of the double bond and will decrease down the series.

[9]In view of the tetrahedral symmetry of the central M atom no anisotropic magnetic effects would be expected from this source.

[10]It can be shown, on the basis of the dipole approximation, that contributions from the other M—C bonds (3) total up to less than 5 Hz for the β protons.

Can. J. Chem. Downloaded from www.nrcresearchpress.com by 210.87.254.40 on 09/05/12
For personal use only.

noted for the calculated shifts with small changes in the bond distances (0.10 Å) and dipole origin. A schematic illustration of the calculated shift trends is given in Fig. 5 along with the final $\Delta\chi$ values. Several points can be noted: (1) Reasonable agreement between the calculated and observed trends is only obtained for the case where $\chi_T > \chi_L$. This order is consistent with (22, 34, 35) theoretical and experimental results for other bonds (22, 36). (2) $\Delta\chi$ increases by threefold in going from Si to Pb. Although no experimental measurements are available for comparison, it is interesting to note that the atom susceptibilities for Si, Ge, and Sn increase in the order 20.7, 31.5, and 49.2 c.g.s. units respectively (37). Also, the value of 6×10^{-6} cm^3 mole^{-1} for $\Delta\chi$(Si—C) is very close to the value of the total molar susceptibility for the Si—C bond reported by Pacault (38). (3) The calculated α proton shifts lie to lower field than the β protons, in agreement with the observed trend. However, the calculated shift difference δ_B–δ_C is appreciably greater down the entire series. This result is probably due to a progressive breakdown of the dipole approximation at small R values (i.e. for the *gem* proton).[11] It has been shown theoretically that the dipole model (eq. [1]) will lead to excessive low-field shifts at low R values (39). (4) The calculated *cis* proton shift is effectively constant in the series. The constancy is expected on the dipole model since Θ is close to 54.5° for the *cis* proton. (5) A linear correlation is noted between the final $\Delta\chi$(M—C) values and the atomic number of the M atom. Similar correlations with atomic number have previously been reported for the atomic susceptibilities of Si, Ge, and Sn (37) and also for the bond susceptibilities, $\Delta\chi$, of C—X bonds, where X represents halogen atoms (38). The linearity is consistent with theoretical predictions for related systems. According to the theory of Van Vleck (40) the diamagnetic susceptibility of an atom is directly proportional to the effective atomic number of the atom. This relationship has been confirmed experimentally for a number of systems including the series of Group IVB atoms (37). For molecules the situation is considerably more complicated and the total molar diamagnetic susceptibility is generally considered to be made up of contributions from inner electrons, lone-pair electrons of outer shells, and bonding electrons in each bond (38). Of these the last contribution is by far the most important. Calculations by Pacault and co-workers (38) indicate that bonding electrons contribute up to 80–90% of the total susceptibility; moreover, this contribution increases with the atomic number of the bonding atoms. It is therefore reasonable to expect that the principal components of the bond susceptibilities will change in a similar manner and hence a linear variation of $\Delta\chi$ versus Z should result. The excellent linearity in Fig. 6 provides a confirmation of the assumption that the internal shift changes are primarily due to the anisotropy of the M—C bond.

It is interesting to note that extrapolation of the line in Fig. 6 to $Z = 6$ yields a value of $\Delta\chi = 4.0 \times 10^{-6}$ cm^3 mole^{-1} for the C—C bond, in excellent agreement with the value deduced by

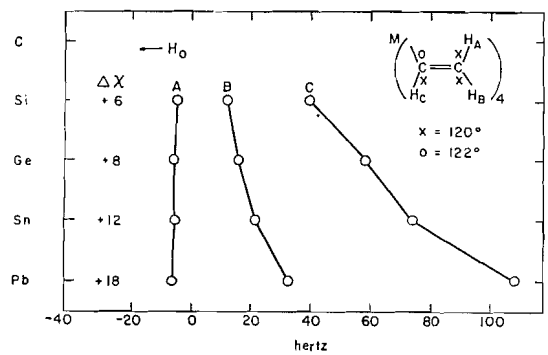

FIG. 5. Shift trends for the MVi_4 series calculated using the dipole approximation.

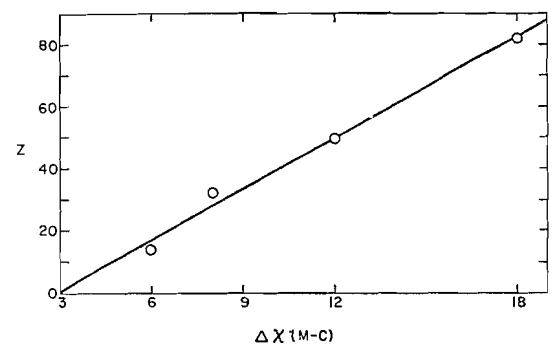

FIG. 6. Plot of the atomic number of the M atom versus the diamagnetic bond susceptibilities used in calculating the shift trends in Fig. 5.

[11]The discrepancy is even greater when one considers that the observed $\delta_B - \delta_C$ value includes a possible deshielding contribution from d_π–p_π interaction.

Can. J. Chem. Downloaded from www.nrcresearchpress.com by 210.87.254.40 on 09/05/12
For personal use only.

Davies (36) from a consideration of various experimental and theoretical results. However, in view of the assumptions involved in the present work and the difficulties encountered in relating shifts to bond anisotropies, the agreement is probably fortuitous.

ϕ_3MVi Series

Figure 7 illustrates schematically the proton shifts for the complete series. Comparison of the shifts in Figs. 4 and 7 shows a number of similarities and differences in trends for the two series. In both series the shieldings increase in the order $\delta_{gem} < \delta_{trans} < \delta_{cis}$; also, the centers of gravity of the spectra for the ϕ_3MVi compounds shift to low field with increasing Z as in the first series. Again, the largest change is noted in going from the carbon to the silicon derivative. It is interesting to note that the δ—M trend for the *trans* proton of the ϕ_3MVi series (Fig. 7) is almost exactly superimposable upon the corresponding curve for the MVi_4 series.[12] A similar correlation is also observed for the trends in the centers of gravity for the two series.

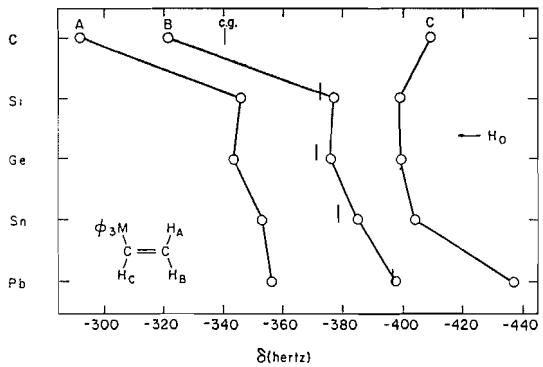

FIG. 7. Schematic illustration of the shift trends of the vinyl protons of the ϕ_3MVi series.

The chief differences between the two series are the appreciably lower shieldings for all of the protons of the ϕ_3MVi series, except for the *cis* proton of ϕ_3CVi, and the progressively larger internal shift differences, $\delta_A - \delta_B$ and $\delta_B - \delta_C$,[13] with decreasing Z. Thus $(\delta_A - \delta_B)$ and $(\delta_B - \delta_C)$ are almost the same in $PbVi_4$ and ϕ_3PbVi, but are approximately 4 Hz and 21 Hz larger in ϕ_3SiVi than in $SiVi_4$. The deshieldings for individual pairs of compounds vary in the order $\Delta\delta_C > \Delta\delta_B > \Delta\delta_A$ in all cases,[14] Table V. Both $\Delta\delta_C$ and $\Delta\delta_B$ decrease in magnitude down the series while $\Delta\delta_A$ increases; the largest change is noted for $\Delta\delta_C$. Of additional interest is the surprising constancy in the shift of the centers of gravity for the spectra down the series, relative to the corresponding tetravinyl derivatives.

TABLE V

Comparison of vinyl proton shifts in MVi_4 and ϕ_3MVi

	$\Delta\delta_A$*	$\Delta\delta_B$*	$\Delta\delta_C$*
C	+8.1	−16.0	−61.0
Si	0	−14.2	−32.1
Ge	−1.9	−12.3	−25.7
Sn	−8.8	−12.7	−21.2
Pb	−10.0	−9.3	−17.5

*$\Delta\delta_A = \delta_A(\phi_3MVi) - \delta_A(MVi_4)$.
$\Delta\delta_B = \delta_B(\phi_3MVi) - \delta_B(MVi_4)$.
$\Delta\delta_C = \delta_C(\phi_3MVi) - \delta_C(MVi_4)$.
Shift differences are in hertz.

The most reasonable explanation of the main differences between the two series is the effect of the phenyl ring anisotropy upon the ϕ_3MVi shifts. A detailed quantitative calculation of the shielding changes is not feasible because of the complexity of the systems. However, a consideration of the angles subtended by the lines joining the vinyl protons with the centers of the phenyl rings, along with the corresponding distances for a variety of representative configurations, shows qualitatively that all of the protons, *except* the *cis* proton of ϕ_3CVi, are predominantly located (on the average) in the deshielding regions[15] of the neighboring phenyl rings.[16] Furthermore, the largest deshieldings are expected for the *gem* and *trans* protons, in that order. The *cis* proton, in contrast, initially lies in a *shielding* region for

[12]Apart from the overall down-field shifts of the ϕ_3MVi protons.

[13]Relative to the corresponding MVi_4 compounds.

[14]$\Delta\delta = \delta(\phi_3MVi) - \delta(MVi_4)$.

[15]Angles and distances were approximated with the aid of Fisher-Taylor-Hirschfelder models and ring anisotropy effects were estimated from the shielding values reported by Johnson and Bovey (41).

[16]Free rotation of the vinyl and phenyl groups about the C—M bonds is assumed for each compound. Recent microwave and infrared measurements (32, 42) indicate that the vinyl group is freely rotating in H_3SiVi (32) and that the energy barriers to rotation about the M—C bond in MEt_4 compounds (42) are less than 1 kcal $mole^{-1}$. Free rotation is also indicated by the approximately constant additive phenyl ring contribution to the shift of the *gem* proton in the series ϕ_nSiVi_{4-n} with increasing n (7, 43).

Can. J. Chem. Downloaded from www.nrcresearchpress.com by 210.87.254.40 on 09/05/12
For personal use only.

the carbon derivative, but then as the bond distances increase down the series the influence of the phenyl rings becomes increasingly one of deshielding. The ring deshielding effect upon the *gem* and *trans* protons is expected to decrease with increasing Z because of the accompanying increase in R. The largest overall change should occur for the *gem* proton as observed, i.e. $\Delta\delta_C$ changes by 43.5 Hz while $\Delta\delta_B$ changes by 6.7 Hz from ϕ_3CVi to ϕ_3PbVi. The neighbor-ring anisotropy also accounts satisfactorily for the changes in internal shift down the series. It is apparent that the internal shift differences in the ϕ_3MVi series will approximate those in the MVi_4 series as the bond distances increase (i.e. Z increase). Finally, it can be noted that a plot of $\Delta\delta_C$ versus R^{-3} (M—C vinyl) gives a satisfactory straight line. Since the average distance from proton C to the phenyl ring dipole is proportional to the M—C bond length, the linear relationship provides an additional confirmation that the observed deshieldings are largely due to the phenyl ring anisotropy.

In an earlier n.m.r. study of the series ϕ_nSiVi_{4-n} at 40 MHz Hobgood and Goldstein (7) observed that introduction of a phenyl group led to a significant deshielding of the *gem* (α) vinyl proton but had little effect upon the β protons. The shift changes reported by these authors, $\Delta\delta_A = +1.2$ Hz, $\Delta\delta_B = -9.1$ Hz, and $\Delta\delta_C = -31.5$ Hz, are in reasonable agreement with the present results, Table V. Based on the constancy of the shift changes for the vinyl protons with increase in n from one member of the phenylvinyl silane series to the next, Hobgood and Goldstein suggest that the deshielding effects are mainly due to the phenyl ring anisotropy. The present results indicate that similar trends will be observed in all of the phenylvinyl Group IVB derivatives.

Although the deshieldings relative to the MVi_4 series are satisfactorily accounted for by the phenyl ring anisotropy, it is highly unlikely that the down-field shift in the centers of gravity with increasing Z is due to the same source. In view of the similarity of the trends in the two series, in particular the large change from the carbon to the silicon derivative, it is more reasonable to attribute the changes within the series to a d_π–p_π interaction analogous to that suggested for the MVi_4 series. The similarity of the trends for the individual *cis*, *trans*, and *gem*

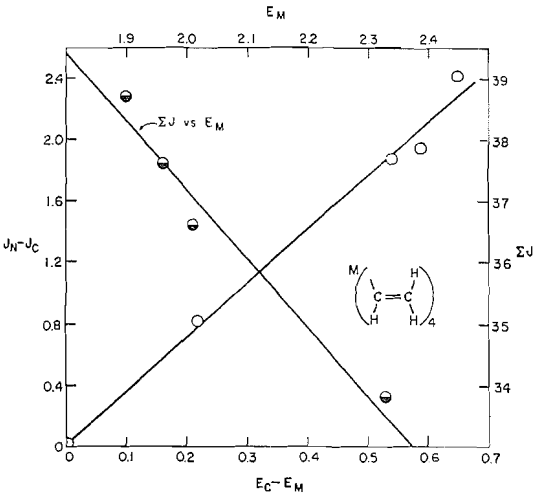

FIG. 8. Plot of the coupling constants (sum) for the MVi_4 series versus the electronegativity of the M atom.

protons with increasing Z in both series also indicates that the adjacent M—C bond anisotropy is operative in the ϕ_3MVi series.

Coupling Constants

The coupling constants for all of the compounds vary in the same order, i.e. $J_{trans} > J_{cis} > J_{gem}$, as observed for most vinyl compounds (1, 2). In addition the relative signs of the three couplings (all positive) conform to the trend generally noted for vinyl derivatives having a substituent group with an electronegativity less than ~ 3.0.

A plot of the sum of the coupling constants versus the electronegativity[17] of the M atom (E_M) yields straight lines[18] for both series of compounds, Figs. 8 and 9. Linear correlations have previously been reported for a wide variety of vinyl compounds over a broad range of substituent electronegativities (44–46). The present results indicate that a similar trend holds for a series of vinyl derivatives of elements belonging to the same group in the periodic table.

The electronegativities of Group IVB atoms have been the subject of some controversy recently. On the basis of an extensive analysis of a wide range of chemical and spectroscopic data

[17]The electronegativity values reported by Allred (47) have been used in the plot.

[18]Straight lines are also obtained for plots of the individual couplings versus electronegativity.

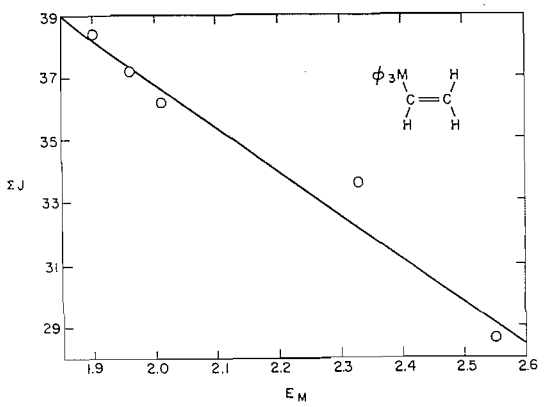

FIG. 9. Plot of the coupling constants (sum) for the ϕ_3MVi series versus the electronegativity of the M atom.

for a series of Group IVB derivatives Allred and Rochow (48) concluded that the electronegativities for the Group IVB atoms varied in the order $E_C > E_{Pb} > E_{Ge} > E_{Sn} > E_{Si}$. This differs from earlier conclusions (49) which favored the order $E_C > E_{Si} > E_{Ge} \simeq E_{Sn} \simeq E_{Pb}$. Assuming that the linear trends of coupling constant versus E_N are general for vinyl derivatives, then the present coupling constant data provide additional confirmation of the electronegativity scheme proposed by Allred and Rochow (48).

A comparison of the plots in Figs. 8 and 9 shows that the curve for the ϕ_3MVi series lies slightly below that of the MVi_4 series. Although the differences in $\sum J$ values are small and range from 0.65 Hz to 0.30 Hz from C to Pb, the trend is outside the limits of errors. The smaller $\sum J$ for the phenyl derivatives suggests that E_N of the M atom is increased upon phenyl substitution, i.e. the ϕ_3M group is more electronegative than the Vi_3M group. This is in agreement with the order suggested by Webster (26) on the basis of chemical shift measurements of R_3SiH compounds.

Medium Effects

The lack of any significant solvent or concentration effect for the MVi_4 series is not unexpected. In contrast, the ϕ_3MVi compounds show a significant concentration dependence but little solvent effect. The concentration dependence is undoubtedly related to the presence of the anisotropic phenyl rings. Striking concentration effects have previously been noted for the ring proton spectra of ϕ_3SiVi and ϕ_3GeVi (50). It was found that an increase in solute concentration led to a down-field shift of the ortho protons and an up-field shift of the meta and para protons. These changes were interpreted on the basis of a solute–solute interaction model in which the up-field shifts result because of the greater probability of out-of-plane (shielding) contacts for meta and para protons with neighboring solute rings than for ortho protons. In the latter case steric hindrance favors in-plane contacts with neighboring solute rings, thereby leading to a down-field shift. A similar interaction model can account for the shift changes of the vinyl protons. The *trans* proton, which is the most exposed of the three protons to external contact, would be expected to shift up-field with increasing solute concentration because of the higher probability of out-of-plane contacts with the rings of other solute molecules. The *cis* proton, in contrast, is in a more protected region of the molecule, and the most favored contacts with phenyl rings of other molecules are those which are in-plane. Little contact of the *gem* proton with solute and/or solvent molecules is possible. Thus the solute interaction model predicts up-field shifts for the *trans* protons and down-field shifts of the *cis* protons in agreement with the observed results.

Acknowledgments

The financial support of the National Research Council of Canada in the form of a grant, and studentship to S. C., is gratefully acknowledged. We also wish to express our thanks to Professor A. G. Brook for kindly supplying a number of triphenylvinyl compounds and to Dr. R. Freeman for recording the 100 MHz and double resonance spectra of $SiVi_4$. Acknowledgment is also made to the Ontario Research Foundation for permitting us to use their A-60 spectrometer for several measurements.

1. J. A. POPLE, W. G. SCHNEIDER, and H. J. BERNSTEIN. High resolution nuclear magnetic resonance. McGraw-Hill Book Co., Inc., New York. 1959. Chaps. 7 and 8.
2. J. W. EMSLEY, J. FEENEY, and L. H. SUTCLIFFE. High resolution nuclear magnetic resonance spectroscopy. Vols. I and II. The Pergamon Press, Ltd., Oxford. 1965.
3. W. BRÜGEL, TH. ANKEL, and F. KRÜCKEBERG. Z. Elektrochem. **64**, 1121 (1960).
4. S. CASTELLANO and J. S. WAUGH. J. Chem. Phys. **37**, 1951 (1962).
5. R. T. HOBGOOD, R. E. MAYO, and J. H. GOLDSTEIN. J. Chem. Phys. **39**, 2501 (1963).

Can. J. Chem. Downloaded from www.nrcresearchpress.com by 210.87.254.40 on 09/05/12
For personal use only.

6. D. W. Moore and J. A. Happe. J. Phys. Chem. **65**, 224 (1961).
7. R. T. Hobgood and J. H. Goldstein. Spectrochim. Acta, **19**, 321 (1963).
8. R. Summitt, J. J. Eisch, J. T. Trainor, and M. T. Rogers. J. Phys. Chem. **67**, 2362 (1963).
9. R. Freeman and D. H. Whiffen. Mol. Phys. **4**, 321 (1961).
10. R. Freeman and W. A. Anderson. J. Chem. Phys. **37**, 2053 (1962).
11. A. D. Cohen and D. H. Whiffen. Mol. Phys. **7**, 449 (1963).
12. W. A. Anderson, R. Freeman, and C. A. Reilly. J. Chem. Phys. **39**, 1518 (1963).
13. J. D. Swalen and C. A. Reilly. J. Chem. Phys. **37**, 21 (1962).
14. S. Castellano and J. S. Waugh. J. Chem. Phys. **34**, 295 (1961).
15. E. C. Juenge and S. E. Cook. J. Am. Chem. Soc. **81**, 3578 (1959).
16. J. R. Cavanaugh. J. Chem. Phys. **39**, 2378 (1963).
17. A. D. Cohen and K. A. McLauchlan. Discussions Faraday Soc. **34**, 132 (1962).
18. J. I. Musher. J. Chem. Phys. **40**, 983 (1964).
19. J. G. Berger, E. L. Stogryn, and A. A. Zimmerman. J. Org. Chem. **29**, 950 (1964).
20. S. Cawley and S. S. Danyluk. Can. J. Chem. **41**, 1850 (1963).
21. A. A. Bothner-By and C. J. Naar-Colin. J. Am. Chem. Soc. **83**, 231 (1961).
22. A. A. Bothner-By and J. A. Pople. Ann. Rev. Phys. Chem. **16**, 43 (1965).
23. J. N. Shoolery and B. P. Dailey. J. Am. Chem. Soc. **77**, 3977 (1955).
24. A. A. Bothner-By and C. J. Naar-Colin. Ann. N.Y. Acad. Sci. **70**, 833 (1958).
25. A. L. Allred and A. L. Hensley. J. Inorg. Nucl. Chem. **17**, 43 (1961).
26. D. E. Webster. J. Chem. Soc. 5132 (1960).
27. R. T. Hobgood, J. H. Goldstein, and G. S. Reddy. J. Chem. Phys. **35**, 2038 (1961).
28. D. J. Blears, S. Cawley, and S. S. Danyluk. J. Organometal. Chem. Amsterdam, **6**, 284 (1966).
29. L. Goodman, A. H. Konstam, and L. H. Sommer. J. Am. Chem. Soc. **87**, 1012 (1965).
30. J. Nagy, J. Reffy, A. Kuszmann-Borbely, and K. Palossy-Becker. J. Organometal. Chem. Amsterdam, **7**, 393 (1967).
31. H. McConnell. J. Chem. Phys. **27**, 226 (1957).
32. J. M. O'Reilly and L. Pierce. J. Chem. Phys. **34**, 1176 (1961).
33. A. F. Wells. Structural inorganic chemistry. 3rd ed. Oxford University Press, London. 1962. p. 696.
34. J. Guy and J. Tillieu. J. Chem. Phys. **24**, 1117 (1956).
35. J. Tillieu. Ann. Phys. **2**, 471 (1957); **2**, 631 (1957).
36. D. W. Davies. Mol. Phys. **6**, 481 (1963).
37. E. W. Abel, R. P. Bush, C. R. Jenkins, and T. Zobel. Trans. Faraday Soc. **60**, 1214 (1964).
38. A. Pacault, J. Hoarau, and A. Morebond. Advances in chemical physics. Vol. III. *Edited by* I. Prigogine. Interscience Publishers, Inc., New York. 1961.
39. J. I. Musher. J. Chem. Phys. **40**, 2399 (1964).
40. J. H. Van Vleck. Theory of electric and magnetic susceptibilities. The Clarendon Press, Oxford. 1932.
41. C. E. Johnson, Jr. and F. A. Bovey. J. Chem. Phys. **29**, 1012 (1958).
42. P. Tarmsabe and J. L. Wood. Trans. Faraday Soc. **59**, 1754 (1963).
43. S. Cawley and S. S. Danyluk. To be published.
44. S. Castellano and J. S. Waugh. J. Chem. Phys. **35**, 1900 (1961).
45. C. N. Banwell, N. Sheppard, and J. J. Turner. Spectrochim. Acta, **16**, 794 (1960).
46. T. P. Schaefer. Can. J. Chem. **40**, 1 (1962).
47. A. L. Allred. J. Inorg. Nucl. Chem. **17**, 215 (1961).
48. A. L. Allred and E. G. Rochow. J. Inorg. Nucl. Chem. **5**, 269 (1958).
49. L. Pauling. The nature of the chemical bond. Cornell Univ. Press, Ithaca, New York. 1939. Chap. 2.
50. S. Cawley and S. S. Danyluk. J. Chem. Phys. **38**, 285 (1963).

Can. J. Chem. Downloaded from www.nrcresearchpress.com by 210.87.254.40 on 09/05/12
For personal use only.

Constraints on the determination of stability constants for metal complexes. II. The iron(III) phenolates

W. A. E. McBryde
Department of Chemistry, University of Waterloo, Waterloo, Ontario
Received May 30, 1967

Stability constants have been measured spectrophotometrically for the 1:1 complexes of iron(III) with phenol and five derivatives in background solutions having two different compositions, 0.027 *M* $NaClO_4$ and 0.5 *M* KNO_3. Conditional acidity constants for these phenols in the second of these media were also determined. The experimental results were treated in two different ways to obtain values of the equilibrium constants and the molar extinction coefficients of the complexes. It is apparent that the equilibrium in these cases must be studied under conditions, such as low pH and low concentration of iron, which militate against good precision in the results.

Canadian Journal of Chemistry, 46, 2385 (1968)

Can. J. Chem. Downloaded from www.nrcresearchpress.com by 210.87.254.6 on 09/05/12
For personal use only.

Introduction

The following investigation arose out of an attempt to measure the first-stage stability constant for the complex formed by the reaction of iron(III) with phenol sulfonic acid. Because of the nature of our findings with this ligand, we were led to extend our investigation to a series of iron(III)–phenol complexes previously studied by Milburn (1).

A problem with these phenol complexes is that under conditions appropriate for their study by spectrophotometric methods they behave as weak complexes. The essential reaction is

$$[1] \qquad Fe + HL \rightleftarrows FeL + H$$

(charges having been omitted for the sake of simplicity and generality). The equilibrium constant is approximated by a concentration quotient which we call κ, and which in this study is of the form

$$[2] \qquad \frac{[FeL]H}{[Fe][HL]} = \kappa,$$

in which [] denotes molar concentrations and H = antilog (−pH).

In general κ is rather small, and since measurements must be made in moderately acidic solutions to minimize hydrolysis of iron(III), the degree of conversion to FeL is low. For all phenolic ligands FeL has an absorption band in the visible spectral region so that, in principle, the position of equilibrium should be capable of measurement if the optical density and pH of the solutions containing iron(III) and phenol are known. In practice, however, ε, the molar extinction coefficient of FeL, is not directly obtainable, so that the experiments must be designed to secure values of both ε and κ. This is by no means a new problem, and a number of methods have been described for arranging data from experimental measurements in such a way as to extract values of ε and κ when dealing with the formation of weak complexes (2–6).

These methods share the common feature that a linear relationship is sought among the experimental quantities, from which ε and κ may be extracted by measuring slope and intercept when the data are suitably plotted. As will be subsequently shown, in the iron(III) phenolates ε and κ are related approximately inversely (εκ ∼ constant), so that an uncertainty in the estimate of one of these is matched in the opposite direction by an uncertainty in the other.

When this work began the principal spectrophotometric study of the iron(III) phenolates was that of Milburn (1). This has subsequently been extended (7), and other measurements have been reported by Ernst and Herring (8). We encountered difficulties with the method of treatment of experimental results described by Milburn (1, 7), which are discussed in some detail later in this paper. Accordingly we resorted to other ways of extracting ε and κ from our experimental results, and in particular sought a method that freed the determination of one of these from the other.

Determination of ε and κ

The methods to be described were adapted from procedures developed for other systems by making appropriate allowance for the ionization of the phenolic ligand and for hydrolysis of the metal ion. Two independent applications of the data were possible.

1(a). Measurement of κ *(9)*

Suppose that two solutions, 1 and 2, are prepared having the same pH and C_{Fe}, but differing in C_L. Also, suppose that in both solutions $C_L \gg C_{Fe}$. The concentration of complex [FeL] = D/ε may be represented by x. The following relationships apply,

$$[3] \qquad x_2 = \frac{C_{Fe}(D_2C_{L1} - D_1C_{L2})}{D_1(C_{L1} - C_{L2})}$$

$$[4] \qquad \kappa = \frac{x_2H}{(C_{Fe} - x_2)C_{L2}}(1 + K_h/H),$$

where K_h is a first stage hydrolysis constant for the metal ion.

Equation [4] gives an estimate of κ independent of ε. If several such solutions are prepared and their optical densities measured, the results may be combined in pairs according to eq. [3], and the data from n solutions can, in principle, generate $\frac{1}{2}n\ (n-1)$ values of κ from eq. [4]. In practice x_2 is defined in eq. [3] by the difference of two like magnitudes, and it was considered justifiable to retain only those values that could be defined with reasonable certainty; thus values of x_2 in which the uncertainties in the experimental quantities generated an uncertainty of 20% (relative) or greater were discarded. This reduced the number of useful estimates of κ, but in practice 25 to 35 separate evaluations of κ were obtained from 9 or 10 samples.

1(b). Measurement of ε

Equation [2] may be adapted to

$$[5] \qquad \frac{DH(1 + K_h/H)}{(C_{Fe} - D/\epsilon)(C_L - D/\epsilon)} = \epsilon\kappa.$$

For a low degree of conversion to complex this becomes

$$[5a] \qquad DH(1 + K_h/H)/C_{Fe}C_L \sim \epsilon\kappa.$$

It was observed for solutions containing fixed C_L and C_{Fe}, but differing in H, that the expression on the left-hand side of eq. [5*a*] was reasonably constant. About 10 values of εκ were obtained in this way and averaged. Given a value of κ from the application of eq. [4] it was possible to estimate ε. This could be applied in the left-hand side of eq. [5] to derive an improved value of εκ, and the whole cycle repeated until constant values of ε were obtained. Different combinations of C_L and C_{Fe} could be taken to obtain independent evaluations of εκ.

2. Slope–Intercept Method (4)

For solutions in which $C_L \gg C_{Fe}$, eq. [5] may be modified and rearranged to

$$[6] \qquad DH(1 + K_h/H)/C_L = C_{Fe}\epsilon\kappa - D\kappa.$$

For solutions with fixed C_{Fe} and H the expression on the left side is a linear function of D. A plot of this against D will have slope = −κ and intercept = $C_{Fe}\varepsilon\kappa$, from which ε can be derived. A straight line was fitted through the experimental points by a computer-based least squares program.

In practice, however, this method failed in a few cases to give a well-defined straight line. These instances were always linked to sets of solutions in which the ratio C_L/C_{Fe} was not maintained very high.

Experimental

All of the compounds examined as ligands were purchased from the British Drug Houses, Ltd., with the exception of phenol which was purchased from Mallinckrodt Chemical Works. Phenol and *p*-cresol were purified by vacuum distillation and the purity of the latter checked by a refractive index measurement. *p*-Nitrophenol was recrystallized from chloroform. Each phenol was assayed for purity by titration of a weighed portion with standard alkali, the end-point of the titration being determined by pH meter. Phenol was also assayed by the bromate method as a check on the acidity titration. The two phenols not specially purified proved to be 98–100% pure. The molarity of solutions of the phenols were corrected in accordance with the purity found for each compound.

All other chemicals used were reagent grade and solutions of these were prepared when possible by direct weighing. All solutions were prepared with distilled deionized water.

Stock solutions of ferric perchlorate in dilute perchloric acid and of ferric nitrate in dilute nitric acid were standardized gravimetrically. The stock solution of sodium perchlorate was standardized by passing measured volumes through a cation exchanger previously loaded with acid and titrating the liberated acid. The acid concentration of the stock iron solutions was obtained in this way also.

All pH measurements were made with a Radiometer model pH M 4b meter with glass and calomel electrodes, calibrated by two buffers of N.B.S. specifications. Adjustment of the pH of samples was made by the addition of measured volumes of standard acid, and the background electrolyte was adjusted accordingly to maintain constant ionic strength. No buffers were used to maintain constant pH during the determination of κ.

Optical densities were measured with a Beckman model DU spectrophotometer after selecting the wavelength of maximum absorption from spectra recorded by a Cary model 14 spectrophotometer. Milburn (1) had reported fading in samples of iron(III) phenolate or cresolate. We also observed this with *p*-cresol and with some phenol

Can. J. Chem. Downloaded from www.nrcresearchpress.com by 210.87.254.6 on 09/05/12
For personal use only.

TABLE I

Conditional acidity constants for phenols (25 °C)

Phenol	Our results, 0.5 *M* KNO_3		Bordwell and Cooper ($\mu < 0.02$ *M*)	
	K_a	pK_a	K_a	pK_a
p-CH_3	$9.45(\pm 0.39)\times 10^{-11}$	10.02	5.62×10^{-11}	10.25
—H	$1.64(\pm 0.06)\times 10^{-10}$	9.79	1.05×10^{-10}	9.98
	$1.45(\pm 0.05)\times 10^{-10}$*	9.85		
p-Br	$6.79(\pm 0.17)\times 10^{-10}$	9.17	4.57×10^{-10}	9.34
m-NO_2	$6.62(\pm 0.17\times 10^{-9}$	8.18	4.17×10^{-9}	8.38
p-NO_2	$1.10(\pm 0.02)\times 10^{-7}$	6.96	6.92×10^{-8}	7.16
p-SO_3H	$2.76(\pm 0.06)\times 10^{-9}$	8.56	—	—

*0.027 *M* $NaClO_4$.

solutions; in these cases optical densities were measured with the Cary instrument set at fixed wavelength, and plots of absorbance vs. time were extrapolated back to zero time. Absorbance measurements appeared to be unaffected by small variations in temperature, and so for many of the solutions no special precautions for temperature control were taken, since the laboratory temperature remained fairly constant around 23 °C. Recently Milburn has studied the temperature dependence of the iron(III)–phenol reaction (7), and in view of his findings a second series of measurements were made with solutions prepared and absorbances measured at 25.0 °C (or 20.0 °C in a few cases). The solutions were made up from previously thermostatted reagents, and the spectrophotometer provided with thermospacers through which water was circulated.

Measurements of κ by method 1(*a*) were carried out in backgrounds of essentially constant ionic strength, one series maintained at 0.5 *M* with potassium nitrate, the other maintained at 0.027 *M* with sodium perchlorate (for comparison with the work of Milburn (1)). For method 1(*b*) the same backgrounds were employed, but the solutions were adjusted with acid over a range of pH.

Acidity and Hydrolysis Constants

To correct values of κ to values of K, the formation constant of FeL, required dividing values of the former by the acidity constant of the phenol in question. For values of κ applying to 0.027 *M* $NaClO_4$ background, we used values of K_a obtained by Bordwell and Cooper (10). These are based on pH measurements during titration of phenol solutions by alkali without control of the ionic strength, but apply to an ionic strength of about 0.01. For want of data appropriate to 0.5 *M* KNO_3 background we determined conditional acidity constants in this medium. These are mixed (Brönsted) acidity constants in the sense that they are of the form H[L]/[HL]. However, to obtain these from the results of pH titrations it was necessary to use the relationship [HL] = C_H − [H], and for this an empirical relationship between H and [H] was measured in each salt background. Our results, together with those of Bordwell and Cooper for comparison, are given in Table I.

In applying eq. [4] to [6], values of the first-stage hydrolysis constants of Fe(III) appropriate to the background solution must be inserted. For the concentrations of iron in the solutions taken it is probably sufficient to limit consideration to one step of hydrolysis. The "choice" of hydrolysis constant used, however, makes an appreciable difference in the values of κ obtained. To keep our values in 0.027 *M* $NaClO_4$ as compatible as possible with those of Milburn (1) we used his value for K_h, except that we adjusted it by our observed ratio H/[H] to be consistent with our other data. For solutions 0.5 *M* in KNO_3 we took the value of K_h from Taube and Wilson (11), but again adjusted from a concentration quotient to a "mixed" quotient in the same way.

Hydrolysis constants are appreciably temperature dependent, and to allow for a number of measurements of κ made at about 23 °C and at 20 °C we attempted to estimate values for K_h appropriate to this temperature by assuming that the same temperature coefficient (d log K_h/dT) applied to the constants chosen above as that observed by Turner and Miles (12) between 15 and 35 °C at an ionic strength of 0.01. The values resulting from these adjustments are given in Table II.

Results and Discussion

By method 1(*a*) four sets of solutions, each differing in C_L but with constant C_{Fe} and pH

Can. J. Chem. Downloaded from www.nrcresearchpress.com by 210.87.254.6 on 09/05/12
For personal use only.

TABLE II

Summary of hydrolysis constants, Fe^{3+} (perchlorate background)*

Temperature (°C)	Turner and Miles (μ = 0.01)		Milburn and Vosburgh (μ = 0.027)		Taube and Wilson (μ = 0.5)	
	$K_H \times 10^3$	$K_h \times 10^3$	$K_H \times 10^3$	$K_h \times 10^3$	$K_H \times 10^3$	$K_h \times 10^3$
15		1.942				
20			2.96	2.31		
23				2.66		1.16
25		3.433	3.83	2.98	1.58	1.28
35		5.175				

*K_H = concentration quotient; K_h = mixed (Bronsted) quotient.

TABLE III

Stability constant for iron(III)–phenolate (medium 0.027 M ClO_4^-; temperature for 1–4, 25 °C; for 5–7, 20 °C; K_h used = 2.98×10^{-3} (25 °C), 2.31×10^{-3} (20 °C); K_a used = 1.42×10^{-10})

Number	$\kappa \times 10^2$		$\varepsilon\kappa$ (final)	ε	$K \times 10^{-7}$
1	0.998±0.016	(i)	14.39±0.38	1441	7.03
		(ii)	14.77±0.31	1480	
		(iii)	14.37±0.58	1440	
2	1.01 ±0.06	(i)	14.40±0.47	1426	7.11
		(ii)	14.78±0.31	1464	
		(iii)	14.40±0.59	1426	
3	1.33 ±0.06	(i)	14.88±0.63	1118	9.37
		(ii)	15.24±0.47	1146	
		(iii)	15.32±1.00	1152	
4	1.38 ±0.14	(i)	14.95±0.67	1083	9.72
		(ii)	15.32±0.50	1110	
		(iii)	15.47±1.06	1121	
Mean 25 °C	1.18 ±0.18			1284±162	8.31±1.24
5	0.902±0.13	(iv)	15.53±0.21	1722	6.35
6	1.00 ±0.09	(iv)	15.72±0.19	1572	7.04
7	1.06 ±0.12	(iv)	15.84±0.19	1491	7.46
Mean 20 °C	0.99 ±0.06			1595±85	6.95±0.40

Solutions			
1(*a*)	$C_{Fe}=3.00\times10^{-3}$ M,	$C_L=2.74\times10^{-1}-5.5\times10^{-2}$ M,	pH=1.87
2(*a*)	$C_{Fe}=3.00\times10^{-3}$ M,	$C_L=2.74\times10^{-1}-5.5\times10^{-2}$ M,	pH=2.14
3(*a*)	$C_{Fe}=4.00\times10^{-3}$ M,	$C_L=3.29\times10^{-1}-3.29\times10^{-2}$ M,	pH=1.87
4(*a*)	$C_{Fe}=1.00\times10^{-3}$ M,	$C_L=6.62\times10^{-1}-6.62\times10^{-2}$ M,	pH=1.87
5(*a*)	$C_{Fe}=2.00\times10^{-3}$ M,	$C_L=2.42\times10^{-1}-6.93\times10^{-2}$ M,	pH=1.87
6(*a*)	$C_{Fe}=1.00\times10^{-3}$ M,	$C_L=5.15\times10^{-1}-6.44\times10^{-2}$ M,	pH=1.84
7(*a*)	$C_{Fe}=2.00\times10^{-3}$ M,	$C_L=4.34\times10^{-1}-4.82\times10^{-2}$ M,	pH=1.84
1–4(*b*) (i)	$C_{Fe}=2.00\times10^{-3}$ M,	$C_L=1.097\times10^{-1}$ M,	pH=1.80–2.44
(ii)	$C_{Fe}=1.00\times10^{-3}$ M,	$C_L=1.097\times10^{-1}$ M,	pH=1.75–2.46
(iii)	$C_{Fe}=1.00\times10^{-3}$ M,	$C_L=2.484\times10^{-1}$ M,	pH=1.74–2.45
5–7(*b*) (iv)	$C_{Fe}=1.00\times10^{-3}$ M,	$C_L=1.61\times10^{-1}$ M,	pH=1.68–2.35

within each set, led to four independent estimates of κ for iron(III)–phenolate at 25 °C and three estimates at 20 °C. These were all in a background made 0.027 M in ionic strength by the addition of sodium perchlorate. The values are recorded in Table III. Estimates of κ for the reaction of iron(III) with phenol and four substituted phenols at about 23 °C and in two media of different ionic strength are given in Table IV. Experimental data for the same solutions may be treated by method 2 and representative results are shown in Table IV as well. A representative

Can. J. Chem. Downloaded from www.nrcresearchpress.com by 210.87.254.6 on 09/05/12
For personal use only.

TABLE IV

Stability constants Fe(III) phenolates (~ 23 °C) (first group 0.5 *M* KNO_3 background; second group 0.027 *M* $NaClO_4$ background)

Phenol	Method 1(*a*) and 1(*b*)			Method 2		
	$\kappa \times 10^2$	ε^*	$K \times 10^{-6}$	$\kappa \times 10^2$	ε^*	$K \times 10^{-6}$
p-CH_3	2.03±0.41	422	215	2.55	363	270
−H	1.05±0.18	747, 662	64	1.23	647	75
p-Br	3.53±1.05	519, 440	52	4.04	453	59.5
m-NO_2	3.25±0.40	682, 682	4.9	3.23	781	4.9
p-NO_2	4.48±0.67	751, 744	0.41	4.08	861	0.37
	4.32±0.72	777, 769	0.39	7.40	507	0.67
p-SO_3H	1.57±0.22	1033 (av.)	5.7	1.47	941	5.3
	1.45±0.21	1480 (av.)	5.3	1.34	1396	4.9
	1.61±0.10	1160 (av.)	5.8	1.43	1146	5.2
p-CH_3	3.00±0.45	643	534	2.74	696	488
−H	1.34±0.08	1012, 1159	128	1.45	991	138
p-Br	3.58±1.02	951	78	4.03	859	88
m-NO_2	4.62±0.34	1039	11.1	5.87	797	14
p-NO_2	4.91±0.52	1271	0.71	4.38	1454	0.63
	5.08±0.57	1232	0.73	5.17	1235	0.75

*Wavelengths: *p*-CH_3, λ_{max} 550 mμ; −H, λ_{max} 550 mμ; *p*-Br, λ_{max} 560 mμ; *m*-NO_2, λ_{max} 520 mμ; *p*-NO_2, λ_{max} 520 mμ; *p*-SO_3H, λ470, λ_{max} 530, λ 580.

set of experimental numbers is given in Table V; complete sets of observations have been placed in the Depository of Unpublished Data.[1]

By method 1(*b*) three sets of solutions, differing in pH but with constant C_{Fe} and C_L within each set, led to three independent first estimates of εκ at 25 °C and a single estimate at 20 °C for the iron(III)–phenol reaction in 0.027 *M* $NaClO_4$. These preliminary estimates of εκ were refined as described previously to produce the values of εκ and ε given in Table III. Similar estimates of εκ and ε were made with phenol and four substituted phenols at *about* 23 °C and in two media of differing ionic strength and are given in Table IV. A representative set of experimental numbers is given in Table VI.

The values of *K*, the first-stage formation constant, shown in Tables III and IV are obtained from the relationship $K = \kappa/K_a$. Values of log *K* in the two media for which they apply are shown in Table VII together with comparable values obtained by Milburn (1). Of the latter, those in 0.027 *M* $NaClO_4$ background differ from the values in the original paper by about 0.24 log units, the amount of his correction for zero ionic strength.

TABLE V

Representative data for calculation of κ ($Fe(ClO_4)_3$ = 2.66 × 10^{-3} *M*; ClO_4^- = 2.7 × 10^{-2} *M*; phenol = (2.875 to 28.75) × 10^{-2} *M*; temperature ~ 23 °C)

$C_L \times 10^2$	*D* (550 mμ)*	pH
5.75	0.207	2.15
8.63	0.298	2.15
11.50	0.383	2.15
14.38	0.461	2.15
17.25	0.529	2.15
20.13	0.600	2.14
23.00	0.660	2.13
25.88	0.723	2.12

*1 cm cells, 1 min after mixing. These led to 27 usable values of κ. κ = 1.34 (±0.08) × 10^{-2}.

TABLE VI

Representative data for calculation of εκ ($Fe(ClO_4)_3$ 4.078 × 10^{-3} *M*; perchlorate 2.7 × 10^{-2} *M*; phenol 1.457 × 10^{-1} *M*)

pH	*D* (550 mμ)*	εκ
1.57	0.289	15.35
1.62	0.316	15.38
1.66	0.351	15.69
1.74	0.392	14.66
1.80	0.443	15.27
1.88	0.515	15.46
1.99	0.602	15.02
2.10	0.723	15.29
2.17	0.815	16.38
2.29	1.003	16.79

*1 cm cells, 1 min after mixing. These led to ε = 1159 after 5 approximations.

[1]Photocopies of this material may be obtained free of charge, upon request, from: Depository of Unpublished Data, National Science Library, National Research Council of Canada, Ottawa, Canada.

Can. J. Chem. Downloaded from www.nrcresearchpress.com by 210.87.254.6 on 09/05/12
For personal use only.

TABLE VII

Formation constants for iron(III) phenolates (log K_1 (~ 23 °C))

Phenol	This study*		Milburn (1), 0.027 *M* $NaClO_4$
	0.5 *M* KNO_3	0.027 *M* $NaClO_4$	
p-CH_3	8.33 (8.43)	8.73 (8.69)	8.96
−H	7.81 (7.87)	8.11 (8.14)	7.96
p-Br	7.72 (7.77)	7.89 (7.94)	7.87
m-NO_2	6.69 (6.69)	7.05 (7.15)	6.98
p-NO_2	5.60 (5.72)	5.86 (5.84)	5.51
p-SO_3H	6.72 (6.71)		

*Values in parentheses determined by our method 2.

We have endeavored to convey the precision of our results by adding values for the mean deviation within a set of measurements. The deviations illustrate the difficulty, mentioned at the beginning of this paper, of precisely evaluating κ. Some of the constraints in this case can now be discussed in the light of the experimental results. The data of Table V show a degree of conversion in reaction [1] between 8 and 27%; this is the consequence of having to work at low pH to suppress hydrolysis of the iron(III) ion. But in order to simplify the evaluation of the extent of the latter it was necessary to work with small values of C_{Fe}, and this in turn imposed a limit on the optical density attainable. (We frequently had to use long-path optical cells.) At higher pH and higher iron(III) concentration, hydrolysis leads to other products beyond first stage.

We noted in all cases that the estimate of εκ, even by eq. [5*a*], tended to be more reproducible than estimates of κ by eqs. [3] and [4]. The nature of eq. [3] is such that very small uncertainties in D lead to much amplified uncertainties in the estimate of x_2, and hence of κ. What is not clear is why the uncertainties in κ at 25 °C within a set (shown best in Table III) are smaller than the discrepancies among the values of κ between sets.

It may appear that our method (1) for extracting κ from the experimental results is incapable of yielding precise results. However, many observations on the system in question have convinced us that this method yields more satisfactory values for this equilibrium constant than methods, such as our method (2), based on evaluating slopes and intercepts. It is easy for a single experimental point to introduce a bias in the position of a straight line sought in such cases. In this connection a few observations concerning Milburn's method (1, 7) for extracting values for ε and κ seem indicated.

The slope and intercept are sought from a plot of $1/D$ (reciprocal of optical density) vs. [H] for solutions containing known concentrations of iron and phenol (with the latter in great excess) at various values of [H]. Milburn defined κ and ε in this case by the following relationships:

$$[7] \quad \kappa = \frac{\text{intercept/slope} - K_h}{C_L}$$

$$[8] \quad \epsilon = \frac{1}{C_{Fe}(\text{intercept} - K_h \times \text{slope})}.$$

In applying these equations to our data we found poor agreement among results derived from different sets of solutions containing the same ligand. The magnitudes of the measured quantities and the nature of the above equation are such that significant variations in κ and ε are introduced by small uncertainties in the measured slopes and intercepts. Thus, while a 1% uncertainty in slope will produce a 1% uncertainty in κ in the application of eq. [6] to plotted data, the same uncertainty in slope may lead to greater uncertainties in κ by the application of eq. [7]. This is because the ratio slope/intercept is about the same magnitude as K_h, and for this reason also the estimate of ε by eq. [8] is subject to uncertainties greater than those in the observed slopes and intercepts.

To illustrate this point we show values for κ and ε (Table VIII) obtained graphically by the use of eqs. [7] and [8] with the data for solutions 1–4(*b*) recorded in Table III.

Note that the products of the corresponding values of ε and κ obtained by the use of eqs. [7] and [8] are reasonably constant in spite of a

Can. J. Chem. Downloaded from www.nrcresearchpress.com by 210.87.254.6 on 09/05/12
For personal use only.

TABLE VIII

Values of κ and ε obtained from eqs. [7] and [8]

	Temperature (°C)	First approximation to εκ, [5*a*]†	$\kappa \times 10^3$, [7]*	ε, [8]*	εκ
i	25	12.93	3.98	4539	18.06
ii	25	13.36	5.29	3455	18.28
iii	25	11.60	7.34	2347	17.23
iv	20	13.79	9.87	1761	17.38

*Final values, allowing for hydrolysis and phenolysis.
†Cf. final values in Table III.

good deal of variation among the replicate measurements of each. The value of κ from eq. [7] is a pure concentration quotient and must be multiplied by our observed ratio $H/[H] = 0.78$ to be compared with values in Table III. It is clear that Milburn's procedure and ours give values of the product εκ that are consistent and in reasonable agreement, but that there is unsatisfactory agreement between values of κ obtained by the two methods of treating the data. The effect of a 1% change in the value assigned to the slope of the plot of $1/D$ vs. [H] was to change the value of κ by 9.8%, 7.6%, and 3.1% for solutions *i*, *ii*, and *iii* respectively, and this evidence bears out our previous comment on the use of eq. [7].

There was one other aspect of the use of Milburn's procedure that caused us some concern. In this, values of [H] were taken to be the stoichiometric concentration of acid in the solution augmented by the hydrogen-ion concentration derived from hydrolysis and phenolysis. This leads to an iterative approach to estimating κ and ε, input to which includes the previous trial value of κ and the previous estimate of [H]. Throughout our work we have used a pH meter, calibrated by solutions of known hydrogen-ion concentration and equivalent ionic strength, as a hydrogen-ion concentration probe. We must acknowledge that values of [H] in our solutions based on values of H determined by a pH meter did not agree particularly well with values of [H] derived in the manner described by Milburn and outlined above. It is obviously a question of preference which method of estimating [H] is used in this procedure, but if the methods are not concordant neither will be the ultimate values of κ.

The effect of change in medium on log K is seen in Table VII to lower values in 0.5 M KNO_3 by about 0.3 log unit. Since a change of anion and of ionic strength are involved, the shift in log K cannot be simply interpreted. Unexpectedly, the values of ε in 0.5 M KNO_3 are about two thirds of the corresponding values in 0.027 M $NaClO_4$. We presume this is indicative of some interaction with the medium, but again it is impossible to distinguish among two variables.

The value of K appears to be lower at lower temperature (see Table III). However, the precision of the measurements in this study does not invite comparison with Milburn's study of the temperature dependence of the equilibrium in this reaction.

There have been many published efforts to relate formation constants of metal complexes to properties such as the acid dissociation constant or Hammett σ-function of the ligand acid. Ernst and Herring (8) and Jabalpurwala and Milburn (13) have each published plots of log K for a substantial number of mono-substituted phenol complexes of iron(III) vs. pK_a for the corresponding phenol. These are of the form $\log K = ap K_a + b$. In Table IX we give a comparison of our results with those of previous workers in the form of values of a and b when the experimental results are fitted by a least-squares treatment to this linear equation. The significance to be attached to these attempted correlations is by no means clear. It is widely held that values of a less than unity are symptomatic of π-bonding between metal and ligand. However, the iron(III) ion is not usually regarded as a π-donor, so that this interpretation may not be appropriate in this case. It is also known that the phenols sometimes fail to give normal correlations with Hammett σ-functions (14).

In this particular set of complexes $\log K = pK_a + \log \kappa$, so that unit slope in the plot of log K vs. pK_a may be interpreted as evidence that log κ is independent of pK_a. But a slope of less than unity must mean that log κ becomes more negative the greater is pK_a (implying that the weaker the acidic properties of the particular phenol the smaller is κ). Since κ is the equilibrium constant for eq. [1], which depicts the competition between iron(III) ions and hydrogen ions for the phenolate ion, it is really in the plot of log κ vs. pK_a that we should look for trends suggestive of structural factors affecting the position of this competitive equilibrium. When such plots are drawn for the data given or cited in this paper it

Can. J. Chem. Downloaded from www.nrcresearchpress.com by 210.87.254.6 on 09/05/12
For personal use only.

TABLE IX

Parameters in equation $\log K = ap K_a + b$

Source and medium	a	b	Mean deviation in $\log K$
This paper, 0.5 M NO_3^-	0.862	−0.425	0.147
This paper, 0.027 M ClO_4^-	0.868	−0.304	0.120
Milburn, 0.027 M ClO_4^-	0.998	−1.544	0.216
Jabalpurwala and Milburn, 0.1 M ClO_4^-	1.012	−1.256	0.077
Ernst and Herring, 0.05 M ClO_4^-	0.752	1.174	0.320

is found that our results as well as those of Ernst and Herring show a general trend toward lower values of log κ with increasing pK_a, whereas those of Milburn do not support such a trend. However, the precision with which values of κ can be determined, to judge from the author's experience, does not appear to be great enough to permit interpretive conclusions to be drawn. In our own studies and those of Milburn the behavior of phenol, and perhaps of *p*-cresol, is sufficiently different from that of the phenols bearing electronegative substituents so as to make comparisons inappropriate, and certainly it is clear that phenol itself cannot be used as a standard for comparisons of log κ (14).

Acknowledgments

The author gratefully acknowledges the technical assistance of Miss Janet Rohr, and a research grant from the National Research Council of Canada.

1. R. M. Milburn. J. Am. Chem. Soc. **77**, 2064 (1955).
2. E. Rabinowitch and W. H. Stockmayer. J. Am. Chem. Soc. **64**, 335 (1942).
3. H. S. Frank and R. L. Oswalt. J. Am. Chem. Soc. **69**, 1321 (1947).
4. H. A. Benesi and J. H. Hildebrand. J. Am. Chem. Soc. **71**, 2703 (1949).
5. M. W. Lister and D. E. Rivington. Can. J. Chem. **33**, 1572 (1955).
6. N. J. Rose and R. S. Drago. J. Am. Chem. Soc. **81**, 6138 (1959).
7. R. M. Milburn. J. Am. Chem. Soc. **89**, 54 (1967).
8. Z. L. Ernst and F. G. Herring. Trans. Faraday Soc. **61**, 454 (1965).
9. S. M. Edmonds and N. Birnbaum. J. Am. Chem. Soc. **63**, 1471 (1941).
10. F. G. Bordwell and G. D. Cooper. J. Am. Chem. Soc. **74**, 1058 (1952).
11. A. S. Wilson and H. Taube. J. Am. Chem. Soc. **74**, 3509 (1952).
12. R. C. Turner and K. E. Miles. Can. J. Chem. **35**, 1002 (1957).
13. K. E. Jabalpurwala and R. M. Milburn. J. Am. Chem. Soc. **88**, 3224 (1966).
14. J. J. R. F. Da Silva and J. G. Calado. J. Inorg. Nucl. Chem. **28**, 125 (1966).

Can. J. Chem. Downloaded from www.nrcresearchpress.com by 210.87.254.6 on 09/05/12
For personal use only.

Can. J. Chem. Downloaded from www.nrcresearchpress.com by 210.87.254.5 on 09/05/12
For personal use only.

Molecular force field for bromine pentafluoride

M. G. KRISHNA PILLAI AND P. PARAMESWARAN PILLAI
Department of Physics, Shivaji University, Kolhapur, India

Received January 16, 1968

An attempt has been made to study the influence of lone pair electrons on the potential constants of BrF_5 with a modified Urey–Bradley force field. It is found that the lone pair – bond pair repulsion is greater than the bond pair – bond pair repulsion. It is also concluded from a study of other molecules containing halogen atoms that the ratio of lone pair – bond pair interaction to bond pair – bond pair interaction is very nearly 1.23.

Canadian Journal of Chemistry, 46, 2393 (1968)

Introduction

Recently Begun *et al.* (1) re-investigated the infrared and the Raman spectra of bromine pentafluoride and some other molecules having similar structure. They have confirmed the vibrational assignments of the fundamental frequencies made by previous workers with minor modifications. They have also reported the result of normal coordinate analysis of this molecule, assuming a square pyramidal structure with all FBrF angles equal to 90°. Earlier, Stephenson and Jones (2) made a similar analysis of this molecule on the following assumptions: (i) the bromine atom is located at the center of mass of the molecule and (ii) the five interbond distances are equal to the sum of the single covalent bond radii as given by Pauling (3). Later Khanna (4) made a similar attempt with two models, one with the interbond angles suggested by Lord *et al.* (5) and the other with that of Pauling (3). He showed that the set of parameters suggested by the former is preferable.

In AX_5 type molecules the central atom A has six electron pairs in the valence shell with one unshared pair. Infrared and Raman spectra strongly suggest a C_{4v} symmetry for this type of molecule. According to Pauling (3) the square pyramidal structure can be derived from an octahedral structure. This is easily explained, assuming that the central atom uses a set of sp^3d^2 octahedral hybrid orbitals with one containing an unshared pair. In such a case it is assumed that the bond angles are less than 90° from the fact that lone pair – bond pair repulsion exceeds bond pair – bond pair repulsion. X-ray diffraction data reported by Burbank and Bensey (6) supports this point of view. Hence it seems to be reasonable to assume that the deviation of bond angles from 90° is due to the influence of the unpaired electron. If this is accepted then one should expect that this unpaired electron will have its own influence on molecular force constants. Previous work (7–12) for molecules having unpaired electrons gave more consistent and chemically meaningful force constants, and many ambiguities in the explanation of the results of normal coordinate analysis of these molecules vanished. As such it is thought worthwhile to extend this modified approach to the BrF_5 molecule.

Procedure

Bromine pentafluoride has a square pyramidal structure and it belongs to the point group C_{4v}.

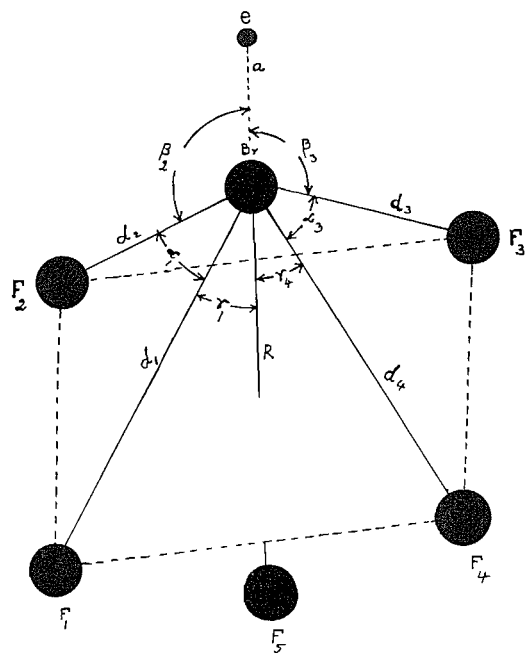

FIG. 1. Internal coordinates for BrF_5.

Can. J. Chem. Downloaded from www.nrcresearchpress.com by 210.87.254.5 on 09/05/12
For personal use only.

The lone pair electron occupies a position on the symmetry axis as shown in Fig. 1. The internuclear distances (d, R, and a) and the interbond angles (α, β, and γ) used for the construction of F and G matrices are as defined in Fig. 1.

In terms of the internal coordinates defined in Fig. 1 the expression for the potential energy based on the Urey–Bradley model was written in the usual way (12) and the following expressions for the valence force constants were obtained.

[1]
$$f_a = K_a + 4(t_{ey}^2 F_{ey}' + S_{ey}^2 F_{ey})$$
$$f_d = K_d + 2(t_{yy}^2 F_{yy}' + S_{yy}^2 F_{yy}) + (t_{yz}^2 F_{yz}' + S_{yz}^2 F_{yz}) + (t_{ye}^2 F_{ye}' + S_{ye}^2 F_{ye})$$
$$f_R = K_R + 4(t_{zy}^2 F_{zy}' + S_{zy}^2 F_{zy})$$
$$f_\beta = H_\beta - S_{ey}S_{ye}F_{ey}' + t_{ey}t_{ye}F_{ey}$$
$$f_\alpha = H_\alpha - S_{yy}^2 F_{yy}' + t_{yy}^2 F_{yy}$$
$$f_\gamma = H_\gamma - S_{zy}S_{yz}F_{zy}' + t_{zy}t_{yz}F_{zy}$$
$$f_{dd} = S_{yy}^2 F_{yy} - t_{yy}^2 F_{yy}'$$
$$f_{ad} = S_{ey}S_{ye}F_{ye} - t_{ey}t_{ye}F_{ey}'$$
$$f_{Rd} = S_{zy}S_{yz}F_{yz} - t_{zy}t_{yz}F_{yz}'$$
$$f_{d\alpha} = t_{yy}S_{yy}F_{yy}' + t_{yy}S_{yy}F_{yy}$$
$$f_{d\gamma} = t_{yz}S_{zy}F_{yz}' + t_{zy}S_{yz}F_{yz}$$
$$f_{R\gamma} = t_{zy}S_{yz}F_{ye}' + t_{yz}S_{zy}F_{zy}$$
$$f_{a\beta} = t_{ye}S_{ey}F_{ye}' + t_{ey}S_{ye}F_{ye}$$
$$f_{a\beta} = t_{ey}S_{ye}F_{ey}' + t_{ye}S_{ey}F_{ey},$$

where $S_{ij} = (r_i - r_j \cos\alpha_{ij})/q_{ij}$

and $t_{ij} = r_j \sin\alpha_{ij}/q_{ij}$.

y stands for F atoms other than the axial F atom which is represented by z. Here the subscripts refer to pairs of atoms. The qs represent the non-bonded distances; the symbols K, H, and F have their usual meaning. The constants F' are set equal to -0.1 times the corresponding F values, assuming that the energies associated with the qs are proportional to q^{-9} (13).

The following set of symmetry coordinates was then defined.

A_1 Species

$$S_1 = \tfrac{1}{2}(\Delta d_1 + \Delta d_2 + \Delta d_3 + \Delta d_4)$$
$$S_2 = \Delta R$$
$$S_3 = \tfrac{1}{2}N_2(\Delta\alpha_1 + \Delta\alpha_2 + \Delta\alpha_3 + \Delta\alpha_4) + \tfrac{1}{2}N_1(\Delta\gamma_1 + \Delta\gamma_2 + \Delta\gamma_3 + \Delta\gamma_4)$$
$$S_4 = \Delta a$$
$$S_5 = \tfrac{1}{2}N_1(\Delta\alpha_1 + \Delta\alpha_2 + \Delta\alpha_3 + \Delta\alpha_4) - \tfrac{1}{2}N_2(\Delta\gamma_1 + \Delta\gamma_2 + \Delta\gamma_3 + \Delta\gamma_4)$$
$$S_6 = (1/\sqrt{12})(\Delta\alpha_1 + \Delta\alpha_2 + \Delta\alpha_3 + \Delta\alpha_4 + \Delta\gamma_1 + \Delta\gamma_2 + \Delta\gamma_3 + \Delta\gamma_4 + \Delta\beta_1 + \Delta\beta_2 + \Delta\beta_3 + \Delta\beta_4)$$

B_1 Species

$$S_7 = \tfrac{1}{2}(\Delta d_1 - \Delta d_2 + \Delta d_3 - \Delta d_4)$$
$$S_8 = \tfrac{1}{2}(\Delta\gamma_1 - \Delta\gamma_2 + \Delta\gamma_3 - \Delta\gamma_4)$$
$$S_9 = (1/\sqrt{8})(\Delta\gamma_1 - \Delta\gamma_2 + \Delta\gamma_3 - \Delta\gamma_4 + \Delta\beta_1 - \Delta\beta_2 + \Delta\beta_3 - \Delta\beta_4)$$

B_2 Species

$$S_{10} = \tfrac{1}{2}(\Delta\alpha_1 - \Delta\alpha_2 + \Delta\alpha_3 - \Delta\alpha_4)$$

E Species

[2]
$$S_{11} = \tfrac{1}{2}(\Delta d_1 + \Delta d_2 - \Delta d_3 - \Delta d_4)$$
$$S_{12} = (1/\sqrt{2})(\Delta\alpha_1 - \Delta\alpha_3)$$
$$S_{13} = \tfrac{1}{2}(\Delta\gamma_1 + \Delta\gamma_2 - \Delta\gamma_3 - \Delta\gamma_4)$$
$$S_{14} = \tfrac{1}{2}(\Delta\beta_1 + \Delta\beta_2 - \Delta\beta_3 - \Delta\beta_4)$$
$$S_{15} = \tfrac{1}{2}(\Delta d_1 - \Delta d_2 - \Delta d_3 + \Delta d_4)$$
$$S_{16} = (1/\sqrt{2})(-\Delta\alpha_2 + \Delta\alpha_4)$$
$$S_{17} = \tfrac{1}{2}(\Delta\gamma_1 - \Delta\gamma_2 - \Delta\gamma_3 + \Delta\gamma_4)$$
$$S_{18} = \tfrac{1}{2}(\Delta\beta_1 - \Delta\beta_2 - \Delta\beta_3 + \Delta\beta_4),$$

where $N_1 = C/(1 + C^2)^{1/2}$,

$N_2 = 1/(1 + C^2)^{1/2}$,

and $C = (\cos\alpha/2)/(2^{1/2}\cos\gamma)$.

Here the coordinates S_3 and S_5 are not orthogonal with coordinate S_6. Coordinates S_5, S_6, and S_9 are kept redundant in accordance with the following assumptions: (i) the total change in the angles in a plane is equal to zero, and (ii) the total change in the angles around a point is equal to zero.

The above set of symmetry coordinates gives a non-orthogonal U matrix. The unsymmetrized G matrix is constructed by standard methods. Then the matrices are symmetrized by the following transformations.

$$F = (U^{-1})'fU^{-1}$$
$$\mathcal{G} = UGU'$$

Some of the $\mathcal{G}$ elements are infinite, owing to the presence of the atom (electron) of negligible

Can. J. Chem. Downloaded from www.nrcresearchpress.com by 210.87.254.5 on 09/05/12
For personal use only.

mass. The rows and columns containing these elements are now dropped from $\mathscr{G}$ and the residue $\mathscr{G}^0$ is taken with a modified F^0 to give for each symmetry block a reduced secular equation (14).

The F matrix is modified to F^0 by the method suggested by Pariseau *et al.* (7) and the elements are given below.

A_1 Species

$$[3]\quad \begin{vmatrix} f_d + 2f_{dd} - \frac{4f_{d\alpha}^2}{f_\alpha} & 2f_{dR} & M \\ & f_R & \frac{2N_1}{A} f_{R\gamma} \\ & & P \end{vmatrix},$$

where $M = \frac{2N_2}{A} f_{d\alpha} + \frac{N_1}{A} f_{d\gamma} - \frac{B}{A} f_{d\beta} + \frac{4B}{A} \frac{f_{d\alpha} \cdot f_{\alpha\beta}}{f_\alpha}$

$$P = \frac{1}{A^2}(N_2^2 f_\alpha + N_1^2 f_\gamma + B^2 f_\beta) - \frac{4B^2}{A^2} \frac{f_{\alpha\beta}^2}{f_\alpha}$$

$$A = N_1^2 + N_2^2$$

$$B = N_1 + N_2$$

and $F_{ij} = F_{ji}$ (this is applicable to the following matrices also).

B_1 Species

$$[4]\quad \begin{vmatrix} f_d - 2f_{dd} & f_{d\gamma} - f_d \\ & f_\gamma + f_\beta \end{vmatrix}$$

B_2 Species

$$[5]\quad |f_\alpha|$$

E Species

$$[6]\quad \begin{vmatrix} f_d - \frac{f_{d\beta}^2}{f_\beta} & 2^{1/2} f_{d\alpha} & f_{d\gamma} \\ & f_\alpha & 0 \\ & & f_\gamma \end{vmatrix}$$

For the convenience of calculation the F^0 matrix obtained above is modified to a new F matrix through the transformation

$$F = U' F^0 U,$$

where U is the matrix of transformation from real internal coordinates (excluding the lone pair) to the symmetry coordinates.

The modified F elements thus obtained are

$$[7]\quad \bar{f}_d = f_d - \frac{f_{d\alpha}^2}{f_\alpha} - \frac{f_{d\beta}^2}{2f_\beta}$$

$$\bar{f}_R = f_R$$

$$\bar{f}_{dd} = f_{dd} - \frac{f_{d\alpha}^2}{f_\alpha}$$

$$\bar{f}_{dR} = f_{dR}$$

$$\bar{f}_\alpha = f_\alpha - \frac{f_{\alpha\beta}}{f_\alpha} + \frac{f_\beta}{4}$$

$$\bar{f}_\gamma = f_\gamma - \frac{f_{\alpha\beta}^2}{f_\alpha} + \frac{f_\beta}{2}$$

$$\bar{f}_{d\alpha} = f_{d\alpha} - \frac{f_{d\beta}}{4} + \frac{f_{d\alpha} \cdot f_{\alpha\beta}}{f_\alpha}$$

$$\bar{f}_{d\gamma} = f_{d\gamma} - \frac{f_{d\beta}}{2} + \frac{f_{d\alpha} \cdot f_{\alpha\beta}}{f_\alpha}$$

$$\bar{f}_{R\gamma} = f_{R\gamma}.$$

Then the problem is treated as a simple U.B.F.F. calculation with the following modified U.B.F.C.

$$[8]\quad \bar{K}_d = K_d + (t_{ye}^2 F_{ye}' + S_{ye}^2 F_{ye}) - \frac{f_{d\alpha}^2}{f_\alpha} - \frac{f_{d\beta}^2}{2f_\beta}$$

$$[9]\quad \bar{K}_R = K_R$$

$$[10]\quad \bar{H}_\alpha = H_\alpha - \frac{f_{\alpha\beta}^2}{f_\alpha} + \frac{f_\beta}{4}$$

$$[11]\quad \bar{H}_\gamma = H_\gamma - \frac{f_{\alpha\beta}^2}{f_\alpha} + \frac{f_\beta}{2}$$

$$[12]\quad \bar{F}_{yy} = F_{yy}$$

$$[13]\quad \bar{F}_{yz} = F_{yz}$$

and with the additional non-Urey–Bradley cross terms

$$[14]\quad \bar{F}_{dd} = \frac{-f_{d\alpha}^2}{f_\alpha}$$

$$[15]\quad \bar{F}_{dR} = 0$$

$$[16]\quad \bar{F}_{d\alpha} = \frac{-f_{d\beta}}{4} + \frac{f_{d\alpha} \cdot f_{\alpha\beta}}{f_\alpha}$$

$$[17]\quad \bar{F}_{R\gamma} = 0.$$

The force constants in eqs. [8]–[17] were adjusted in the usual way using the molecular

TABLE I

Molecular parameters and vibrational frequencies of BrF_5

Molecular parameters		Ref.	Frequency (cm^{-1})		Ref.
Br—Y distance	1.79 Å	15		682	1
Br—Z distance	1.68 Å		A_1	570	
				365	
Y—Br—Y angle	89° 48′	*	B_1	535	
				281	
Y—Br—Z angle	86° 30′	6	B_2	312	
				644	
Y—Br—e angle	93° 30′	*	E	414	
				237	

*These angles were calculated from the geometry of the molecule using the Y—Br—Z angle.

TABLE II

Force constants of BrF_5

F^0 matrix elements in symmetry coordinates	Modified U.B.F.F. constant in internal coordinates	Modified U.B.F.F. constants
$F_{11}{}^0=3.4595$†	$\bar{f}_d=3.3596$	$\bar{K}_d=2.3104$
$F_{12}{}^0=0.6514$	$\bar{f}_R=4.1120$	$\bar{K}_R=4.1120$
$F_{13}{}^0=-0.7550$	$\bar{f}_{dd}=0.0623$	$\bar{H}_\alpha=0.8897$
$F_{22}{}^0=4.1120$	$\bar{f}_{Rd}=0.3257$	$\bar{H}_\gamma=1.8550$
$F_{23}{}^0=0.5120$	$\bar{f}_\alpha=1.2258$	$\bar{F}_{yy}=0.6093$
$F_{33}{}^0=2.6500$	$\bar{f}_\gamma=2.2150$	$\bar{F}_{yz}=0.6248$
$F_{44}{}^0=3.2104$	$\bar{f}_{d\alpha}=0.1109$	$\bar{F}_{ye}=0.7501$
$F_{45}{}^0=-0.3667$	$\bar{f}_{d\gamma}=-0.0272$	
$F_{55}{}^0=2.9036$	$\bar{f}_{R\gamma}=0.2575$	
$F_{66}{}^0=0.8816$	$\bar{F}_{yy}=0.6093$	
$F_{77}{}^0=3.4580$	$\bar{F}_{yz}=0.6248$	
$F_{78}{}^0=0.3878$	$\bar{F}_{ye}=0.7501$	
$F_{79}{}^0=0.3038$		
$F_{88}{}^0=0.8816$		
$F_{89}{}^0=0$		
$F_{99}{}^0=1.5265$		

*The F^0 matrix elements containing only stretching constants are in mdyn Å, those containing only angle–angle constants are in mdyn Å/rad², and those containing bond–angle interaction are in mdyn Å/rad.

†This number of significant figures is retained to secure internal consistency in the calculations and to obtain the best agreement with the observed wavenumbers.

parameters and frequencies given in Table I and with the assumption that the lone pair electrons are located at a point 0.54 Å, which is the average radii of the outer electronic orbits of M and N shells, from the nucleus.

The set of force constants which gave the best reproduction of frequencies was obtained.

The results thus obtained are shown in detail in Table II.

The calculated frequencies are in agreement with the observed frequencies within $\pm 0.1\%$. Hence they are not reproduced here.

Discussion

The main results obtained in the present investigation are presented in Table II. Quantitative comparison of these results with those of previous authors (2, 4) is not possible due to several reasons. The presence of an unpaired electron is taken into account only in the present work. As indicated in the introductory part of this report, the parameters used and the assumptions made by previous investigators were not identical. In addition to the small differences in line positions the assignment made by Begun

Can. J. Chem. Downloaded from www.nrcresearchpress.com by 210.87.254.5 on 09/05/12
For personal use only.

et al. (1) is slightly different from that reported by Stephenson and Jones (2). The assignment given by Begun *et al.* (1) is more acceptable from more than one point of view and as such the same is used in the present work. As is to be expected, the results obtained are comparable to those reported by these authors, even though they used the G.V.F.F. method. A slightly higher ratio $\overline{K}_R/\overline{K}_d$ obtained here is probably due to the fact that the unpaired electrons influence only BrF_y bonds and not BrF_z bonds. Additional significant results obtained in our calculation are the relative values of the repulsive force constants between bond pair – bond pair and lone pair – bond pair. These values are in conformity with the electron pair repulsion theory of Gillespie and Nyholm (16). Moreover it is also found that the lone pair – bond pair repulsion bears very nearly the same constant ratio, viz. 1.23, to the bond pair – bond pair repulsion, as is concluded from our previous results (12) ($PF_3 = 1.242$, $PCl_3 = 1.237$, $PBr_3 = 1.146$, $AsF_3 = 1.231$, and $AsCl_3 = 1.277$).

1. G. M. Begun, W. H. Fletcher, and D. F. Smith. J. Chem. Phys. **42**, 2236 (1965).
2. C. V. Stephenson and E. A. Jones. J. Chem. Phys. **20**, 1830 (1952).
3. L. Pauling. The nature of the chemical bond. Cornell Univ. Press, Ithaca, New York. 1960.
4. R. K. Khanna. J. Sci. Ind. Research, India, **21B**, 352 (1962).
5. R. C. Lord, M. A. Lynch, W. C. Schumb, and E. J. Slowinski. J. Am. Chem. Soc. **72**, 522 (1950).
6. R. D. Burbank and F. N. Bensey. J. Chem. Phys. **27**, 982 (1957).
7. M. Pariseau, E. Wu, and J. Overend. J. Chem. Phys. **39**, 217 (1963).
8. E. C. Curtis and J. S. Murihead. J. Phy. Chem. **70**, 3330 (1966).
9. M. G. K. Pillai, K. Ramaswamy, and R. Pichai. Australian J. Chem. **18**, 261 (1965).
10. M. G. K. Pillai, K. Ramaswamy, and R. Pichai. Can. J. Chem. **43**, 463 (1965).
11. R. Pichai, M. G. K. Pillai, and K. Ramaswamy. Australian J. Chem. **20**, 1055 (1967).
12. M. G. K. Pillai and P. P. Pillai. Indian J. Pure Appl. Phys. To be published.
13. D. E. Mann, T. Shimanouchi, J. H. Meal, and L. Fano. J. Chem. Phys. **27**, 51 (1957).
14. E. B. Wilson, J. C. Decius, and P. C. Cross. Molecular vibrations. McGraw-Hill Book Co., Inc., New York. 1955. p. 75.
15. J. Gaunt. Trans. Faraday Soc. **49**, 1122 (1953).
16. R. J. Gillespie and R. S. Nyholm. Quart. Rev. **9**, 339 (1957).

Can. J. Chem. Downloaded from www.nrcresearchpress.com by 210.87.254.5 on 09/05/12
For personal use only.

Partially miscible liquid systems: The density, change of volume on mixing, vapor pressure, surface tension, and viscosity in the system: aniline–hexane

A. N. CAMPBELL, E. M. KARTZMARK, S. C. ANAND, Y. CHENG, H. P. DZIKOWSKI, AND S. M. SKRYNYK

Department of Chemistry, University of Manitoba, Winnipeg, Manitoba

Received December 12, 1967

The following properties have been investigated experimentally: density, change of volume on mixing, vapor pressure, surface tension, and viscosity, at temperatures above and below the critical solution temperature. The question at issue is: How does the chemical potential, or any property dependent on chemical potential, change, at constant temperature, over a range of composition, just above the critical solution temperature? In the present case, the vapor pressure and surface tension, properties directly dependent on chemical potential, are constant within the range of experimental accuracy (which, however, may not be sufficient) over a range of concentration. The viscosity is complicated by the occurrence of anomalous viscosity. The change of volume on mixing is negative, and this is usually associated with compound formation. In all other systems investigated by us, except the system triethylamine–water, ΔV is positive. We have shown elsewhere, however, that a very stable chemical compound is formed between water and triethylamine.

Canadian Journal of Chemistry, 46, 2399 (1968)

Can. J. Chem. Downloaded from www.nrcresearchpress.com by 210.87.254.6 on 09/05/12
For personal use only.

Subsequent to the classical work of the last century, interest in the subject of critical phenomena waned to zero, and the subject was relegated to the textbooks, where it unfortunately still remains in this form. The observation of Maass and his co-workers (1) that differences of density may exist at different heights in a vertical tube containing a fluid above its critical temperature, created a renewal of interest in the subject. These differences are now attributed to the effect of gravitational potential on a fluid which is highly compressible in its critical state (2).

Theories of the critical state by Mayer and Harrison (3) and by Rice (4), according to which the upper boundary of the heterogeneous region for $L \rightleftarrows V$ or $L_1 \rightleftarrows L_2$ critical phenomena is, or may be, a horizontal straight line, appeared between 1938 and 1949.

In the last 20 years the problem has been subjected to quantum statistical treatment (5). Recent work of Dunlap and Furrow (6) and by Myers, Smith, Katz, and Scott (7) deals with volume of mixing and enthalpy of mixing as a function of composition and with the effect of pressure on the critical solution temperature.

The question of the horizontality of the upper boundary is somewhat academic. Beyond question, the two-liquid boundaries are frequently very flat at the apex (8). Recently, it has been recognized (9) that many properties of the two-liquid system (e.g. congruent concentrations) can be represented as straight line functions of $(T_c - T)^{1/3}$ or $(T_c - T)$ to some other fractional power. This means that the nose of the curve representing, say, congruent concentration is necessarily very flat and the question reduces to whether or not the curve is flatter than the cubic relation requires. In recent work on the triethylamine–water system Kohler and Rice (10) have controlled the temperature to 0.001°. Above this temperature, the system is heterogeneous, below it homogeneous. This, however, does not necessarily prove that the nose of the curve is a horizontal straight line. Recent work by Campbell and Kartzmark (8) might be taken to demonstrate that some systems yield two straight lines intersecting at the critical solution temperature, while others, which also present two straight lines, show a gap at the critical solution temperature, when the two congruent concentrations are plotted against $(T_c - T)^{1/3}$. On this basis, the systems showing a gap on the $(T_c - T)^{1/3}$ plot should represent those systems having a horizontal nose on the usual composition versus temperature plot. We are doubtful, however, whether this conclusion is justified.

Avoiding then the question of whether or not the nose of the curve is truly horizontal, we thought it of interest to investigate the shape of the curves of chemical potential versus composition, slightly above the critical temperature. Since the nose of the composition curve is sometimes very flat, the question arises of how

Can. J. Chem. Downloaded from www.nrcresearchpress.com by 210.87.254.6 on 09/05/12
For personal use only.

flat is the chemical potential curve just above the critical solution temperature.

We chose as a system suitable for this work the aniline–*n*-hexane system, since it is possible that here the nose of the curve is really horizontal. The most obvious property related to chemical potential is vapor pressure. It would have been desirable to obtain the partial pressures of both components, from total pressure and vapor composition. For the latter purpose we intended to use the air-saturation method but we soon found that the partial pressure of aniline is so low and therefore the content of aniline in the vapor so small, that the error of determination is very great. We confined ourselves therefore to the determination of total vapor pressure and this is, of course, also a measure of chemical potential. Because of the occurrence of anomalous viscosity on the curves of viscosity versus composition, at temperatures just above the critical solution temperature, we also investigated the viscosity isotherms. We also investigated surface tension, for the obvious reason that the so-called critical temperature is determined as the temperature of disappearance of the meniscus, that is, the temperature at which the interfacial tension becomes zero. We also determined the change of volume on mixing, in the homogeneous region. For such nonideal systems, ΔV would be expected to be large and positive.

Experimental and Results

Materials

Certified (ACS) aniline was distilled over zinc dust to reduce any oxidized impurity. The normal boiling point was found to be 184.1° and the refractive index $n_D^{25°} = 1.5837$. Spectro-analyzed *n*-hexane was used without further purification (normal b.p. = 68.60°, $n_D^{25°} = 1.3754$).

Density

Density measurements were made on a given solution by the dilatometer method, at different temperatures. Solutions were made up by weighing and not subsequently analyzed. It was therefore necessary to prevent completely evaporation during filling of the dilatometer. Moreover, when working at temperatures just above the critical solution temperature (c.s.t.) (66.5° to 68.0°) with solutions of the gap composition, very slight cooling would produce heterogeneity. For both these reasons an apparatus was devised, consisting of filling apparatus and dilatometer, which was completely immersed in the thermostat. The solution was then forced over from storage flask to dilatometer. The weight of solution in the dilatometer was obtained at the end of the experiment. The dilatometer was calibrated with mercury for each temperature. We estimate the precision of our density measurements to be $\pm 2 \times 10^{-4}$.

Results

Density as a function of composition, at constant temperature, was found to be expressed by the quadratic equation $d = a + bm + cm^2$, where d = density of solution at $t°$ and a = density of hexane at $t°$; b and c are constants and m the mole % aniline. The equation represents the experimental densities to an accuracy of ± 1 to $\pm 3 \times 10^{-4}$. Table I gives the densities of hexane and the values of b and c as functions of temperature.

TABLE I

Density of hexane and values of b and c in the equation $d = a + bm + cm^2$

Temperature	a (density of hexane in g ml^{-1})	$b \times 10^3$	$c \times 10^5$
62.00	0.6264	2.450	1.140
63.00	0.6255	2.480	1.108
64.00	0.6245	2.509	1.081
65.00	0.6235	2.515	1.077
65.50	0.6229	2.513	1.082
66.00	0.6224	2.520	1.074
67.00	0.6212	2.528	1.070
68.00	0.6202	2.533	1.065

These densities were used in surface tension and viscosity measurements. They can also be used to calculate molar volumes and change of volume on mixing but, while they give the algebraic sign of ΔV, they are not sufficiently accurate to give the numerical values of ΔV with any certainty. Indeed, no density figures are sufficiently accurate for this purpose. It is necessary to determine this quantity directly and this we did using the apparatus of Brown and Smith (11).

Determination of Change of Volume on Mixing

Campbell and Chatterjee (12) had previously modified the Brown and Smith apparatus. The accuracy of the method is approximately ± 0.003 cc/mole. The mercury was highly purified and

Can. J. Chem. Downloaded from www.nrcresearchpress.com by 210.87.254.6 on 09/05/12
For personal use only.

the hexane was kept on the side remote from the stopcock to prevent its attacking the stopcock lubricant

Results

Table II gives a summary of extreme values for temperatures of 25, 60, and 65°. The work could not be carried beyond 65° because of bubble formation which seemed to be induced by the presence of the mercury plug. Figure 1 is a plot of the data versus mole fraction hexane.

TABLE II

Range of ΔV values

Temperature (°C)	Range of ΔV (cc/mole)	Range of concentration (wt. % hexane)
25	0 to −0.159	0 to 7.28
	+0.042 to 0	92.44 to 100
60	0 to −0.726	0 to 19.7
	−0.423 to 0	73.21 to 100
65	0 to −0.736	0 to 23.63
	−0.120 to 0	88.99 to 100

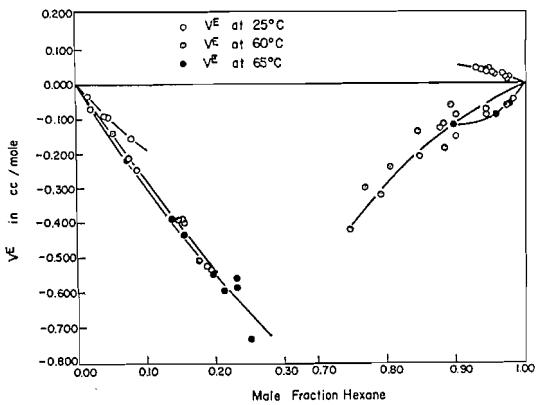

FIG. 1. Excess volume of mixing for system aniline–hexane.

Vapor Pressure

Total vapor pressures were measured by means of a mercury manometer and cathetometer, reading to 0.05 mm: solutions were stirred magnetically. The whole assembly was immersed in a thermostat, controlled to ±0.01°. Correction for surface tension (which was extremely small) was applied to the narrower limb and the mercury column was reduced to 0 °C. As the degassing procedure was prolonged, it gave rise to changes in composition and this made it necessary to analyze the solution after the determination of vapor pressure: this was done by density determination at 25°. The liquid volume was so large (50 ml) that the composition was essentially unaffected by the formation of the equilibrium vapor. Solutions within the miscibility gap were rendered homogeneous, before analysis, by addition of weighed amounts of one of the components. The vapor pressure of each solution was determined at temperatures of 55, 60, 62, 64, 65, 65.5, 66.0, 66.5, 67.0, 67.5, and 68.6°.

Results

Table III gives total vapor pressure as a function of composition and temperature.

The isothermals are plotted in Fig. 2, the outline of the miscibility gap being shown dotted. The data of each isopleth were plotted in the form $\log_{10}P$ vs. $1/T$. Two distinct curves were obtained, one for the temperature range lying within the miscibility gap and the other for the

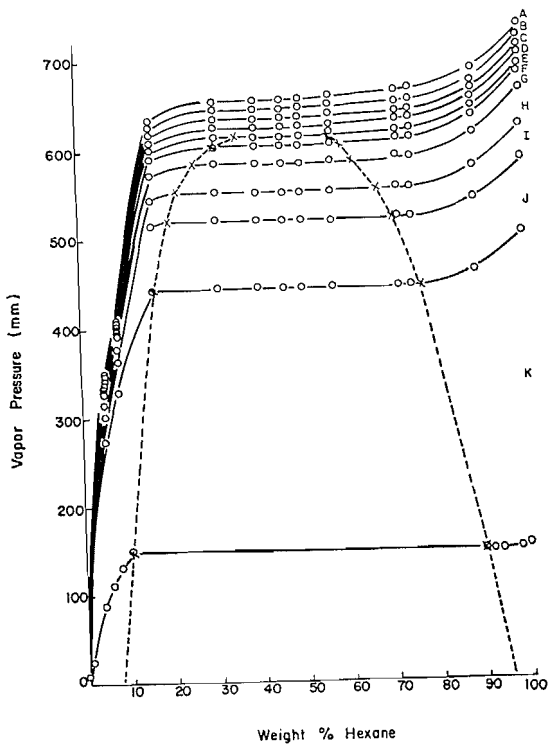

FIG. 2. Vapor pressure isotherms: A = 67.5 °C, B = 67.0 °C, C = 66.5 °C, D = 66.0 °C, E = 65.5 °C, F = 65.0 °C, G = 64.0 °C, H = 62.0 °C, I = 60.0 °C, J = 55.0 °C, K = 25.0 °C.

Can. J. Chem. Downloaded from www.nrcresearchpress.com by 210.87.254.6 on 09/05/12
For personal use only.

TABLE III

Vapor pressures of system: aniline–hexane

I, 25° isotherm

Mole % hexane	0.0	1.1	4.3	6.4	8.6	10.7	90.7	92.6	94.4	98.1	100
Wt. % hexane	0.0	1.0	4.0	6.0	8.0	10.0	90.0	92.0	94.0	98.0	100
Pressure in mm Hg	0.4	23.1	81.3	109.5	129.7	146.3	146.2	146.4	146.5	148.0	151.0

II, other temperatures

	Mole % hexane		5.4%	8.6%	17.3%	32.5%	41.9%	47.9%	52.0%	58.9%	63.7%	67.0%	89.9%	
t (°C)	Wt. % hexane	0.0%	5.0%	8.0%	16.2%	30.8%	40.0%	46.0%	50.1%	57.0%	61.9%	65.3%	89.2%	100%
55.0		4.8	273.3	327.7	445.4	445.6	445.6	445.1	445.1	445.8	446.3	446.1	459.3	503.6
60.0		6.2	303.4	361.7	517.2	522.3	522.6	521.6	522.3	523.0	524.9	523.4	541.1	584.8
62.0		6.6	316.4	375.5	546.3	554.6	554.3	553.3	552.9	555.1	559.3	557.1	577.2	624.7
64.0		7.0	329.6	389.8	574.9	587.0	587.4	587.0	586.6	589.7	593.0	591.6	614.4	665.8
65.0		7.3	336.4	397.1	592.4	606.4	606.7	607.3	607.4	610.3	614.5	613.5	639.7	683.5
65.5		7.5	340.6	400.7	601.3	616.6	616.5	617.8	617.7	621.3	623.9	624.5	644.8	693.3
66.0		7.7	343.9	404.4	610.8	627.2	626.2	628.1	629.4	631.9	635.5	635.9	655.2	706.3
66.5		7.9	347.9	408.3	619.9	637.1	637.3	638.4	640.3	642.5	644.0	647.1	664.9	716.0
67.0		8.2	350.6	411.8	628.1	647.4	648.2	648.6	650.4	654.7	654.4	656.9	674.5	725.5
67.5		8.5	354.4	415.5	636.9	657.4	657.9	658.5	660.4	663.8	666.8	669.2	687.0	738.5
68.6														760.9

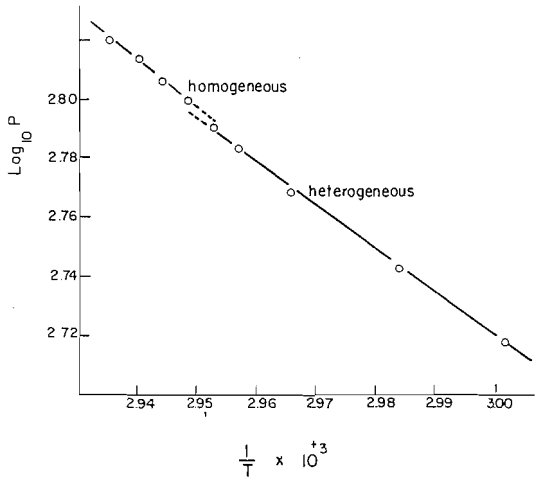

FIG. 3. Log P vs. $1/T$.

range outside the gap, as shown in Fig. 3 for the mixture containing 47.9 mole % hexane. The difference in slope is real: for a given isopleth lying within the gap the compositions of the congruent layers change with temperature and therefore the vapor pressure varies with temperature in a manner different from the homogeneous region where the composition of the condensed phase is constant. For mixtures of compositions lying within the gap the temperature range of homogeneity is quite small.

Surface Tension

The stalagmometer method was used (13) for the 25° isotherm but the method was unsuitable for higher temperatures, because a single determination required 45 min and considerable evaporation from the drop of the more volatile constituent occurred in that time. For higher temperatures, we used the capillary rise method, as modified by Sugden (14). Sugden's modification uses two capillary tubes. The difference in height in the two tubes can be measured very accurately (± 0.01 mm) with a travelling microscope, and this method does not require the level of the bulk surface to be known: both capillaries are simultaneously in the field of vision. The system was completely closed to prevent evaporation. To prevent the formation of heterogeneity during filling, both cell and filler flasks were completely immersed in the thermostat. The method was checked with highly purified benzene, at 25°. Our figure of 28.17 dyn/cm compares with the literature figure of 28.28 dyn/cm (15).

Results

Measurements were made at various concentrations at the temperatures 25°, 55°, and 60° to 68° at 1° intervals. The experimental data are given in Table IV. The 25° and 66° isotherms are reproduced in Fig. 4. Figure 5 shows the 66° and 68° isotherms on an enlarged scale. It is of interest that these isotherms cross at about 40% hexane. The scale of plotting would imply that our results are accurate to ± 0.01 dyn but we make no such claim; nevertheless this crossover is real. For instance, a solution containing 54.09 wt. % hexane has apparent surface tensions of 16.00, 16.07, 16.20, and 16.35 at temperatures of 65, 66, 67, and 68°. This corresponds to differences in height, measured in the same apparatus with the same solution, of 3.003, 3.013, 3.040, and 3.072 cm. Such differences could be read with an accuracy of ± 0.001 cm. Hence there is no doubt that, for this solution, the surface

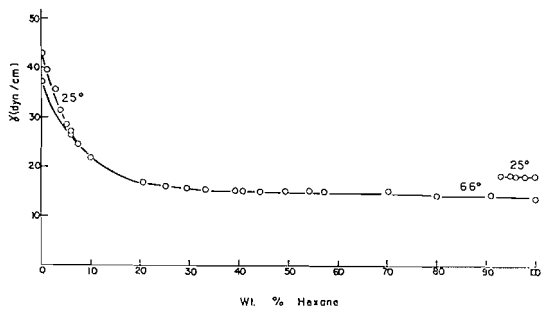

FIG. 4. Surface tension vs. composition.

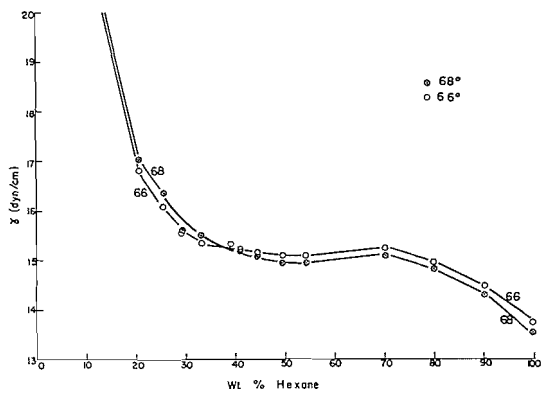

FIG. 5. Surface tension vs. composition.

Can. J. Chem. Downloaded from www.nrcresearchpress.com by 210.87.254.6 on 09/05/12
For personal use only.

TABLE IV

Surface tension (dyn cm^{-1}) versus composition (wt. % hexane) at various temperatures

Wt. % hexane	Surface tension at temperatures of:									
	55 °C	60 °C	61 °C	62 °C	63 °C	64 °C	65 °C	66 °C	67 °C	68 °C
100	14.83	14.35	14.22	14.12	14.04	13.97	13.86	13.73	13.62	13.52
90.07	15.47	15.07	14.95	14.86	14.76	14.67	14.58	14.46	14.37	14.29
79.91	15.84	15.48	15.40	15.31	14.23	15.16	15.05	14.93	14.87	14.81
70.26			15.62	15.54	15.47	15.39	15.30	15.21	15.16	15.07
57.21								15.27	15.21	15.16
54.09								15.08	15.02	14.95
49.37								15.10	15.06	14.94
44.37								15.16	15.14	15.11
40.79								15.22	15.21	15.18
39.24								15.32	15.31	15.34
33.16								15.34	15.45	15.49
29.36							15.49	15.54	15.57	15.59
25.06						15.98	16.00	16.07	16.20	16.35
20.63			16.56	16.59	16.62	16.66	16.76	16.81	16.85	17.03
9.99	20.44	21.20	21.32	21.38	21.46	21.59	21.69	21.75	21.95	22.01
0	39.13	38.51	38.42	38.29	38.19	37.91	37.52	37.31	37.19	37.10

25° isotherm

Wt. % hexane	0	1.00	2.99	3.77	5.05	5.12	5.81
Surface tension	42.89	39.57	35.90	31.47	28.66	28.49	27.12
Wt. % hexane	5.97	7.44	93.03	95.06	96.02	97.94	100
Surface tension	26.54	24.58	18.41	18.32	18.19	18.20	18.13

tension increases with rising temperature (presumably for a few degrees only).

The following derived quantities were plotted: molecular surface energy, Fig. 6; surface heat ($H_s = \gamma - T(d\gamma/dT)$), Fig. 7; and excess hexane in surface layer (Gibbs adsorption isotherm), Fig. 8.

Viscosity

The viscometer was of the type designed by Cannon and Fenske (16) modified for filling with a volatile mixture near its boiling point. Filling flask and viscometer were completely

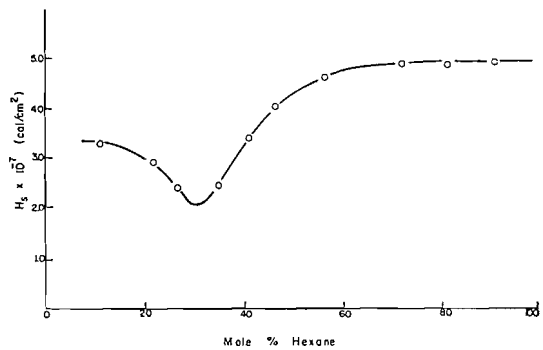

FIG. 7. Surface heat vs. composition.

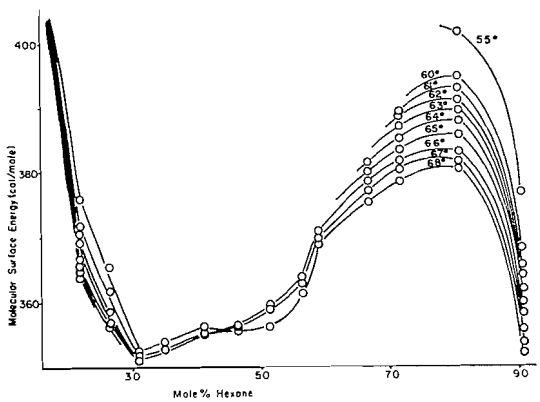

FIG. 6. Molecular surface energy vs. composition.

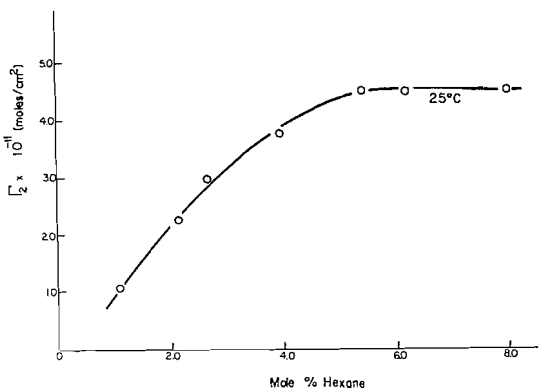

FIG. 8. Gibbs adsorption isotherm.

Can. J. Chem. Downloaded from www.nrcresearchpress.com by 210.87.254.6 on 09/05/12
For personal use only.

closed to prevent change of composition from evaporation. As we worked very close to the c.s.t. it was necessary that at no stage of the operation should the temperature be allowed to fall, because should separation into two layers occur, gravitation would separate the two layers and the viscosity determination would become meaningless. The viscometer was calibrated with carbon dioxide free water: run times were reproducible to $\pm 0.1\%$. Details of design and manipulation may be found in ref. 22. The overall accuracy of a determination was about $\pm 1.0\%$.

Results

Viscosities were measured at 25, 55, 60, 61, 62, 63, 64, 65, 65.7, 65.8, 65.9, 66.0, 67.0, 68.0°. Isotherms are plotted in Fig. 9 for temperatures of 55, 66, 67, and 68°.

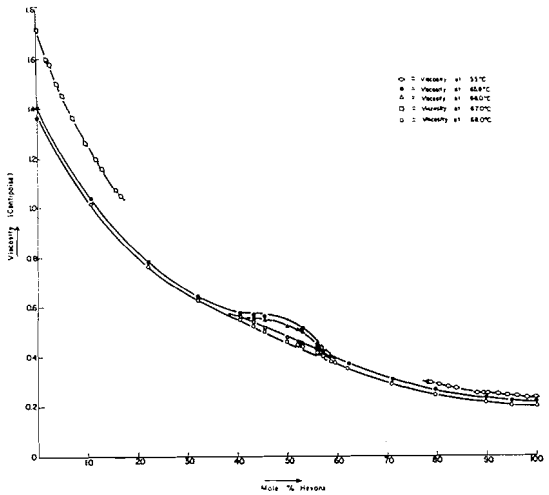

FIG. 9. Viscosity isotherms.

Discussion

Except for solutions rich in hexane, at 25°, the change in volume on mixing is negative. This is unusual in a partially miscible system where positive deviations from Raoult's law are observed and where the heat of mixing is positive. (Work in progress in this laboratory shows a maximum value of $\Delta H_{mix} = +700$ cal/mole.) Both ΔV and ΔH were shown to be negative in the system triethylamine–water, but this could be readily explained as due to the formation of a compound (17). No evidence of compound formation has been found between aniline and hexane but there is evidence of association in aniline due to hydrogen bonding (18). The theory of Prigogine and Mathot (19), for association in an inert solvent, predicts positive and negative values of ΔV.

For those compositions and temperatures lying within the heterogeneous region, the vapor pressures are of necessity constant, at constant temperature. Our figures at 55° show a mean deviation of ± 0.3 mm for mixtures lying within the gap. Above 65.5° (the c.s.t.), the isotherms appear to be horizontal over the critical region, within the experimental error of 1 mm. No matter how accurate the measurements, the statement can always be made that, though apparently horizontal, there is actually a slope less than the experimental error.

As would be expected, if the isothermal vapor pressures are plotted against mole fraction hexane, marked positive deviation from Raoult's law is observed. Such behavior is common to systems which form two liquid layers.

We use the term terminal vapor pressure to describe the vapor pressure of a solution which is on the point of becoming heterogeneous (at constant temperature) or, in other words, the vapor pressure of either of the congruent solutions. If these figures are plotted in the form of $(T_c - T)^{1/3}$ versus terminal vapor pressure, a straight line is not obtained. On the other hand, if congruent concentrations are plotted against $(T_c - T)^{1/3}$ two straight lines are obtained (8).

If surface tension is plotted against weight % hexane, using a scale of 0.5 dyn as unit, the graph appears completely horizontal between 40 and 70% hexane (Fig. 4). If, however, 0.1 dyn is used as the unit, the graph appears to go through a minimum, between 40 and 50% hexane, the minimum lying about 0.2 dyn below the values for 40 and 70% (Fig. 5). We are not prepared to say that this minimum is real, because though the sensitivity of determination for any mixture is greater than this, errors may arise for different mixtures. It may well be that the surface tension graph presents a true horizontal or that the slope is so slight that it cannot be detected with certainty by any experimental method. Rice (4) points out the very small temperature coefficient of interfacial tension and the same may well be true of surface tension. Measurements could not be made above 68°, because hexane boils at this temperature, nor below 66° (within the heterogeneous region), because of the liability of the solution to become heterogeneous.

Can. J. Chem. Downloaded from www.nrcresearchpress.com by 210.87.254.6 on 09/05/12
For personal use only.

Can. J. Chem. Downloaded from www.nrcresearchpress.com by 210.87.254.6 on 09/05/12
For personal use only.

Addition of hexane up to 30% hexane causes a rapid decrease in the surface tension of aniline, while addition of aniline to hexane in the range 0 to 40% aniline produces only a slight increase in the surface tension of hexane. Keyes and Hildebrand previously observed this (20). Similar behavior is observed with the viscosity. It seems obvious that the aniline molecules have a large mutual attraction and this pushes the hexane molecules to the surface. In other words, the aniline molecules resist dispersion by the hexane until a relatively large amount of hexane has been added.

In the region between 40 and 100% hexane, the surface tension increases with falling temperature: this is normal behavior. Between 4 and 40%, however, the surface tension decreases with falling temperature. The decrease is only slight but there is no doubt of the reality of the phenomenon. On the other hand, the temperature dependence of the surface tension of aniline is normal, i.e. it decreases with rising temperature. It follows therefore that the composition isotherms of surface tension must cross twice, since the surface tension of pure hexane is also normal with respect to temperature.

Figure 6 is the plot of molecular surface energy ($\gamma(M/d)^{2/3}$) versus mole % hexane. The curve exhibits a pronounced minimum and a pronounced maximum. The minimum no doubt corresponds to the formation of an outer layer consisting almost entirely of hexane molecules. Further addition of hexane causes aniline molecules to appear in the surface layer, with consequent rise in the molecular surface energy. Finally, with large addition of hexane, the molecular surface energy drops to the low value of pure hexane. If this explanation is correct, however, it is difficult to see why the surface tension does not show a similar behavior. If there is a maximum in surface tension it is a very slight one. Molecular surface energy involves the molar volume, however, and this is much larger for hexane than for aniline. The m.s.e. isotherms also cross in the same manner as the surface tension isotherms.

Figure 7 shows the behavior of the surface heat, $H_s = \gamma - T(d\gamma/dT)$, as a function of molar composition. If $d\gamma/dT$ is constant, as we assume it to be over the small range of temperature under consideration, then H_s is also constant: this is not obvious but the derivation of the expression shows it to be true. A minimum is observed at 30.5 mole % hexane. The surface heat then rises to a constant value of 4.89 cal/cm^2, at 71.8 mole % hexane.

The Gibbs adsorption isotherm was used to calculate the excess concentration of hexane in the surface layer of an aniline-rich solution, at 25°. The results are represented in Fig. 8 in which Γ is plotted against mole % hexane. The excess concentration of hexane in the surface layer increases with addition of hexane until a value of 5.43 mole % hexane is reached. At this point, a constant value of 4.46×10^{-11} mole/cm^2 is maintained up to the heterogeneous region of the coexistence curve. This constant value means that the surface layer has become saturated with hexane. On the high hexane side, the excess concentration of hexane in the surface layer remains constant at 18.36×10^{-11} mole/cm^2, throughout the composition range, from pure hexane to the heterogeneous region.

Several relations have been suggested connecting surface tension of a liquid in air with its viscosity. We used the relation of Pelovsky (21), according to which the plot of $\log \gamma$ versus $1/\eta$ should give a straight line. This plot of our results (Fig. 10) for pure aniline, pure hexane, and two solutions, does indeed give straight lines, on the scale used by Pelovsky, but if a finer scale is used the curves are seen not to be straight lines.

The viscosity of aniline falls rapidly with addition of hexane, at constant temperature, while the viscosity of hexane increases only slightly on addition of aniline. The same behavior was observed with surface tension and the explanation may be the same in both cases, viz. formation of a surface layer of almost pure hexane. Outside of the region of anomalous viscosity, there is neither maximum nor minimum on the viscosity isotherms.

The activation energies of viscous flow, obtained from the plots of $\log \eta$ versus $1/T$ are given in Table V.

The phenomenon of anomalously high viscosity was observed over a temperature range of 2.4° above the critical solution temperature and over the concentration range of 37 to 58.5 mole % hexane. Isotherms near the critical solution temperature show a greater relative increase in viscosity than isotherms farther removed. This range of concentration is about the same as that found by Campbell and Kartzmark (8) for the critical region.

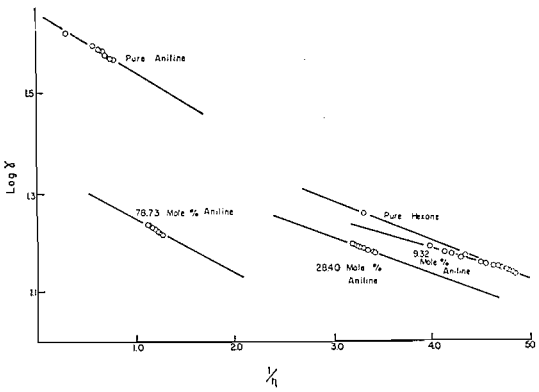

FIG. 10. Log γ vs. 1/η.

TABLE V

Activation energies of viscous flow

Mole % aniline	Activation energy (cal/mole)	Mole % aniline	Activation energy (cal/mole)
0.00	1830	40.29	4730
4.73	1975	41.00	4840
10.03	2300	67.88	2750
20.13	2550	77.67	2600
28.83	2700	89.22	3500
37.59	2975	100.00	4520

1. J. R. DACEY, R. L. MACINTOSH, and O. MAASS. Can. J. Res. B, **17**, 206 (1939). R. L. MACINTOSH, J. R. DACEY, and O. MAASS. Can. J. Res. B, **17**, 241 (1939). S. G. MASON, S. N. NALDRETT, and O. MAASS. Can. J. Res. B, **18**, 103 (1940). S. N. NALDRETT and O. MAASS. Can. J. Res. B, **18**, 118 (1940).
2. R. GOUY. Compt. Rend. Acad. Sci. Paris, **115** 720 (1892); M. A. WEINBERGER and W. G. SCHNEIDER. Can. J. Chem. **30**, 422 (1952).
3. J. E. MAYER and S. F. HARRISON. J. Chem. Phys. **6**, 87 (1938); S. F. HARRISON and J. E. MAYER. J. Chem. Phys. **6**, 101 (1938).
4. O. K. RICE. Chem. Rev. **44**, 69 (1949).
5. CRITICAL PHENOMENA. Natl. Bur. Std. (U.S.) Misc. Publ. No. 273. Washington. 1966.
6. R. D. DUNLAP and S. D. FURROW. J. Phys. Chem. **70**, 1331 (1966).
7. D. B. MYERS, R. A. SMITH, J. KATZ, and R. L. SCOTT. J. Phys. Chem. **70**, 3341 (1966).
8. A. N. CAMPBELL and E. M. KARTZMARK. Can. J. Chem. **45**, 2433 (1967).
9. J. S. ROWLINSON. Liquids and liquid mixtures. Butterworths, London. 1959. p. 165.
10. F. KOHLER and O. K. RICE. J. Chem. Phys. **26**, 1614 (1957).
11. R. BROWN and F. SMITH. Australian J. Chem. **15**, 1 (1962).
12. A. N. CAMPBELL and R. M. CHATTERJEE. Can. J. Chem. **44**, 1183 (1966).
13. W. D. HARKINS and E. C. HUMPHREY. J. Am. Chem. Soc. **38**, 228 (1916).
14. S. SUGDEN. J. Chem. Soc. **119**, 1483 (1921).
15. R. E. DONALDSON and O. R. QUAYLE. J. Am. Chem. Soc. **72**, 35 (1950).
16. M. J. CANNON and M. R. FENSKE. Ind. Eng. Chem. Anal. Ed. **10**, 299 (1938).
17. E. M. KARTZMARK. Can. J. Chem. **45**, 1089 (1967).
18. J. LAURANSAN, P. PINEAU, and M. L. JOSIEN. Ann. Chim. **9**, 213 (1964); J. H. LADY and K. B. WHETSEL. J. Phys. Chem. **64**, 1001 (1964); G. PANNETIER, L. ABELLO, and P. MIGNOTTE. Bull. Soc. Chim. France, 2048 (1965); G. PANNETIER, and L. ABELLO. Bull. Soc. Chim. France, **5**, 1645 (1966).
19. I. PRIGOGINE and V. MATHOT. J. Chem. Phys. **20**, 56 (1952).
20. D. H. KEYES and J. H. HILDEBRAND. J. Am. Chem. Soc. **39**, 2126 (1917).
21. A. H. PELOVSKY. J. Chem. Eng. Data, **11**, 394 (1966).
22. S. C. ANAND. M.Sc. Thesis, University of Manitoba, Winnipeg, Manitoba. 1967.

Can. J. Chem. Downloaded from www.nrcresearchpress.com by 210.87.254.6 on 09/05/12
For personal use only.

Can. J. Chem. Downloaded from www.nrcresearchpress.com by 210.87.254.6 on 09/05/12
For personal use only.

Oligomeric stannoxanes

SHMUEL MIGDAL, DAVID GERTNER, AND ALBERT ZILKHA
Department of Organic Chemistry, The Hebrew University, Jerusalem, Israel

Received February 5, 1968

The controlled basic hydrolysis of tetrabutyl-1,3-dichlorodistannoxane under interfacial conditions was found to lead to α,ω-dichlorooligostannoxanes, $Cl(SnBu_2O)_nSnBu_2Cl$, *n* being controlled by the molar ratio of base to distannoxane. These oligostannoxanes were identical with those prepared by other methods. They were used in the preparation of oligostannoxane dicarboxylates and organotin polyesters, having stannoxane recurring units in their backbone, by reaction with the sodium salts of mono- or dicarboxylic acids under interfacial conditions.

Canadian Journal of Chemistry, **46**, 2409 (1968)

Polymeric dibutyltin oxide is the last product in the exhaustive hydrolysis of dibutyltin dichloride under basic conditions, which was assumed to proceed as follows (1–4).

$$Bu_2SnCl_2 \rightarrow \underset{\mathbf{1}}{ClSnBu_2OSnBu_2Cl} \rightarrow \underset{\mathbf{2}}{ClSnBu_2OSnBu_2OH} \rightarrow Bu_2SnO$$

Tetrabutyl-1,3-dichlorodistannoxane (**1**) is a known intermediate which may be hydrolyzed under controlled conditions to a product which has been given the structure (**2**) (1, 2). Other intermediates were not isolated.

In the present work we have investigated the structure of the products formed under controlled basic hydrolysis of tetrabutyl-1,3-dichlorodistannoxane (**1**). It seemed that oligostannoxanes of the type $Cl(SnBu_2O)_nSnBu_2Cl$ may be formed, and since recently such compounds were prepared (5–7), it would be possible to elucidate the structure of intermediate products formed.

The controlled basic hydrolysis of **1** was carried out under interfacial conditions. Aqueous alkali was reacted with the organotin compound dissolved in methylene chloride, and the hydrolysis product was recovered on evaporation of the organic solvent. Different molar ratios of alkali to **1** were used. In all cases the amount of chloride ion liberated into the aqueous phase equalled the amount of alkali added. Assuming that oligostannoxanes were formed, the reactions carried out may be formulated as follows.

[1] $3ClSnBu_2OSnBu_2Cl + 2NaOH \rightarrow 2Cl(SnBu_2O)_2SnBu_2Cl + 2NaCl + H_2O$

[2] $2ClSnBu_2OSnBu_2Cl + 2NaOH \rightarrow Cl(SnBu_2O)_3SnBu_2Cl + 2NaCl + H_2O$

[3] $3ClSnBu_2OSnBu_2Cl + 4NaOH \rightarrow Cl(SnBu_2O)_5SnBu_2Cl + 4NaCl + 2H_2O$

The structure of the compounds formed was elucidated as follows: The analytical data were in accordance with the formation of dichlorooligostannoxanes. The infrared spectra showed the presence of Sn—O—Sn bonds. The compounds were crystalline, and their melting points were the same as those obtained by other methods, e.g.

$$Bu_2SnCl_2 + nBu_2SnO \rightarrow Cl(SnBu_2O)_nSnBu_2Cl \quad \text{(refs. 5, 7)}$$

$$2HCl + (n+1)Bu_2SnO \rightarrow Cl(SnBu_2O)_nSnBu_2Cl + H_2O \quad \text{(ref. 6),}$$

and were not depressed by authentic samples of dichlorooligostannoxanes prepared according to these methods.

To prove further the structure of the dichlorooligostannoxanes obtained by the controlled hydrolysis, ester derivatives with carboxylic acids were prepared (Table I) utilizing the interfacial method developed by us previously for the preparation of organotin esters and polyesters (8, 9). The dichlorooligostannoxanes containing reactive Sn—Cl bonds were dissolved in dichloromethane or petroleum ether and reacted with an aqueous solution of the sodium salt of a carboxylic acid such as acetic acid or *p*-nitrobenzoic acid. The reaction proceeds as follows.

[4] $Cl(SnBu_2O)_nSnBu_2Cl + 2RCOONa \rightarrow RCOO(SnBu_2O)_nSnBu_2OOCR + 2NaCl$

The ester derivatives were crystalline and were identified by analysis, infrared spectrum (absorption for Sn—O—Sn at 610–680 cm^{-1} and for carboxylate at 1590–1620 cm^{-1}), melting point,

Can. J. Chem. Downloaded from www.nrcresearchpress.com by 210.87.254.6 on 09/05/12
For personal use only.

TABLE I

Oligomeric stannoxanes $R(SnBu_2O)_nSnBu_2R$[a]

R	n	Yield (%)	Melting point (° C)	Carbon (%)		Hydrogen (%)		Nitrogen (%)		Titration equiv	
				Calcd.	Found	Calcd.	Found	Calcd.	Found	Calcd.	Found
m-$NO_2C_6H_4COO$—	2	67	83	42.9	43.2	5.8	5.7	2.6	2.9	531	540
p-$NO_2C_6H_4COO$—	3	98	83[c]	42.1	42.3	6.1	6.3	2.1	2.4	656	662[d]
p-$NO_2C_6H_4COO$—[b]		70	83	42.1	41.8	6.1	6.4	2.1	2.3	656	655
m-$NO_2C_6H_4COO$—	3	99	78					2.1	2.4	656	645
CH_3COO—	3	57	119–122[e]	39.3	38.9	7.1	6.9			549	550
CH_3COO—[b]		76	119–122[e]	39.3	38.9	7.1	7.0			549	555
$CHCl_2COO$—	3	64	131[f]	34.9	34.7	6.0	5.7			618	630[g]
$HOOCC\equiv CCOO$—	3	89	250	39.8	39.8	6.1	5.9				
—$OOC(CH_2)_4COO$—	3	96	158–168[h]	40.6	40.5	7.1	6.9			562	550[i]
—$OOC(CH_2)_4COO$—[b]		79	158–168[h,j]	40.6	40.0	7.1	7.3			562	540
—$OOC(CH_2)_2COO$—	3	85	205–220[k]	39.4	38.8	6.9	6.7			548	570[i]
—$OOC(CH_2)_2COO$—[b]		97	203–215[k]	39.4	39.6	6.9	6.9			548	548[i]
p-$OOCC_6H_4COO$—	3	84	> 300	42.0	41.1	6.6	7.1			572	570[i]
p-$OOCC_6H_4COO$—[b]		94	> 300	42.0	41.7	6.6	6.5				
—$OOCC\equiv CCOO$—	3	25	145–150	39.6	39.7	6.5	6.9			546	555[i]
—$OOC(CH_2)_4COO$—	5	74	160–170	40.0	39.9	7.2	7.3				

[a]Carboxylic acid was dissolved or suspended in water (5 ml) and neutralized with 1 *N* sodium hydroxide. An equivalent amount of α,ω-dichlorooligostannoxane in dichloromethane was added (50 ml) and the reaction mixture was stirred at room temperature for several hours. The oligomer was obtained by evaporation of the organic solvent and was recrystallized from toluene–heptane or heptane. In the case of dicarboxylic acids, polymers, —[$OOCR'COO(SnBu_2O)_mSnBu_2$]—$_n$, were formed.

[b]The oligomers were prepared under the above interfacial conditions using intermediate 2 obtained according to the literature (2). The analytical data are to be compared with the respective compounds having $n=3$.

[c]Lit. (6), 83°.

[d]Molecular weight determined by v.p.o. in chloroform at 37°, 1340 (calcd. 1312).

[e]Lit. (2), 122° after recrystallization from benzene.

[f]Lit. (6), 131°.

[g]Chlorine, calcd: 11.5, found: 11.6. Molecular weight (v.p.o. in benzene at 20° 1190 (calcd. 1238)).

[h]Lit. (6), 158–168°.

[i]Molecular weight of half of a recurring unit.

[j]Molecular weight of some soluble samples by v.p.o. in chloroform: 3160; 2700.

[k]Lit. (6), 210–225°.

Can. J. Chem. Downloaded from www.nrcresearchpress.com by 210.87.254.6 on 09/05/12
For personal use only.

and mixed melting point with authentic samples prepared by other methods, e.g.

$$2p\text{-}NO_2C_6H_4COOH + (n+1)Bu_2SnO \rightarrow p\text{-}NO_2C_6H_4COO(SnBu_2O)_nSnBu_2OOCC_6H_4NO_2\text{-}p + H_2O \text{ (ref. 6)}$$

$$p\text{-}NO_2C_6H_4COO(SnBu_2O)_nSnBu_2OOCC_6H_4NO_2\text{-}p + Bu_2SnO \rightarrow p\text{-}NO_2C_6H_4COO(SnBu_2O)_{n+1}SnBu_2OOCC_6H_4NO_2\text{-}p \text{ (ref. 5)}$$

The molecular weight (m.w.) of some of the soluble oligostannoxane dicarboxylates, as determined by vapor-pressure osmometry, was as calculated.

The fact that the compounds obtained by hydrolysis were bifunctional α,ω-dichlorooligostannoxanes was also proved by the formation of polyorganotin esters as follows.

[5] $$nCl(SnBu_2O)_mSnBu_2Cl + nNaOOCR'COONa \xrightarrow[\text{conditions}]{\text{interfacial}} -[(SnBu_2O)_mSnBu_2OOCR'COO]-_n + 2nNaCl$$

These polymers had the same melting point range, infrared (i.r.) spectra, and solubility as those prepared either from authentic dichlorooligostannoxanes by the same reaction, or by the reaction of dicarboxylic acids with dibutyltin oxide at appropriate molar ratios.

It may be noted that although short dichlorooligostannoxanes may be uniquely formed in the controlled basic hydrolysis under interfacial conditions, it is very probable that mixtures of oligomers are obtained at further stages of hydrolysis.

The dichlorooligostannoxanes were converted to polymeric dibutyltin oxide on addition of an equivalent amount or excess of alkali. The amount of dibutyltin oxide isolated was compatible with the structure of the oligomers, e.g.

[6] $$Cl(SnBu_2O)_3SnBu_2Cl + 2NaOH \rightarrow 4Bu_2SnO + 2NaCl + H_2O.$$

The oligomeric stannoxane dicarboxylates were converted to dibutyltin dicarboxylates by reaction with a free carboxylic acid under azeotropic conditions in toluene, e.g.

[7] $$p\text{-}NO_2C_6H_4COO(SnBu_2O)_3SnBu_2OOCC_6H_4NO_2\text{-}p + 6p\text{-}NO_2C_6H_4COOH \rightarrow 4Bu_2Sn(OOCC_6H_4NO_2\text{-}p)_2 + 3H_2O.$$

In view of the fact that it was possible to obtain α,ω-dichlorooligostannoxanes by the interfacial method using appropriate molar ratios of alkali to dichlorodistannoxanes, we investigated the controlled hydrolysis in the presence of tertiary amines. It was found that on reacting tetrabutyl-1,3-dichlorodistannoxane with an equivalent of pyridine or triethylamine under interfacial conditions, the same α,ω-dichlorooligostannoxanes were formed. On using excess of triethylamine, exhaustive hydrolysis to dibutyltin oxide occurred. Previously the hydrolysis of dialkyltin dihalides by excess (4 equiv) of triethylamine in ethanol, or of tetralkyl dichloro distannoxanes by excess pyridine in methanol, was reported (1, 2) to lead to compounds which were given the structure $XR_2SnOSnR_2OH$. This shows that the medium of the hydrolysis is important and that in alcoholic solvents using tertiary amines the hydrolysis stops at an intermediate stage, not as in an aqueous medium.

The compounds given the structure $XR_2SnOSnR_2OH$ were reported to have a wide range of melting points even after several recrystallizations; the melting point of the respective *n*-butyl derivative was 109–121°. The properties and the i.r. spectra of those compounds were identical (1) with the compounds reported as $H(R_2SnO)_3OH.R_2SnX_2$ by Harada (10), which were prepared by refluxing R_2SnX_2 and polymeric R_2SnO in 1:3 molar ratio in a wet organic solvent. The molecular weights of these compounds as determined by thermistor vapor-pressure osmometry were double those given from the simple formula $R_4Sn_2X(OH)O$ and this was attributed to dimerization (2). Dimerization of these distannoxanes was thought to result by the pairing of two Sn—O—Sn bonds to form a four-membered ring, in which two kinds of tin atoms, tetra- and penta-coordinated, are involved (1).

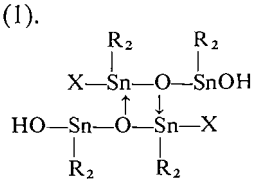

These compounds were reported to be unexpectedly stable towards condensation or reaction with carbon dioxide in which the Sn—OH might have been involved (1). This stability was assumed to be due to an additional weak intramolecular coordination from the hydroxyl oxygen to the four-coordinated tin atom in the dimeric distannoxane.

Can. J. Chem. Downloaded from www.nrcresearchpress.com by 210.87.254.6 on 09/05/12
For personal use only.

The most important evidence given in favor of the structure $XR_2SnOSnR_2OH$ was the absorptions in the infrared at 3420 (CS_2 solution) – 3660 cm^{-1} attributed to the hydroxyl group attached to the tin atom (1, 2).

It seems that the i.r. absorptions in this region are not reliable enough to prove the presence of Sn—OH bonds. Thus it was shown by Davies *et al.* (2) that the initial product of hydrolysis of Bu_2SnCl_2 (obtained by adding water to a methanolic solution of the dichloride), which was claimed (11) to be $Bu_2SnCl(OH)$, based on the i.r. absorption at 3509 cm^{-1} which was taken as indicating an OH group, was actually tetrabutyl-1,3-dichlorodistannoxane. Published spectra of various organotin compounds (12, 13) show absorptions in this region, although they have no OH groups attached to the tin atom. Recent studies of the i.r. absorption for Sn—OH bonds have proved (13–14) that these bonds have a characteristic absorption at 890–910 cm^{-1}.

In view of the results of our work and the above discussion and the fact that it is very difficult to isolate compounds having Sn—OH bonds, due to their great tendency to lose water and pass to the oxide or to absorb CO_2 (14–16), we wanted to look again into the structure of intermediate **2** and we repeated its synthesis as described (2). The compound melted at 102°, and was found to be identical as regards melting point, mixed melting point, i.r. spectrum, and formation of ester and polyester derivatives (Table I) with the compound obtained by the controlled basic hydrolysis under interfacial conditions. The i.r. spectrum did not show an absorption at 890–910 cm^{-1} for the Sn—OH bond. The stability of the intermediate **2** to carbon dioxide, and its molecular weight as reported, are in conformation with the 1,7-dichlorooctabutyltetrastannoxane structure.

It may be mentioned that in the hydrolysis of di-*o*-phenoxy phenyltin dichloride, a compound having the structure $(o\text{-}PhOC_6H_4)_4Sn_2(OH)_2O$, was isolated in which the presence of the Sn—OH groups was demonstrated chemically (17).

Experimental

Melting points were determined on a Fisher-Johns apparatus and are uncorrected.

The titration equivalent of the derivatives of the oligostannoxanes was determined by suspending the compound in alcohol (1 ml) and titrating with 0.1 *N* aqueous sodium hydroxide, using an "Agla" micrometer syringe in the presence of thymol blue as indicator. The titration was carried out until the blue color of the indicator persisted for more than 5 min. By this method the Sn—X bonds but not the Sn—O bonds were titrated.

A typical procedure for the preparation of the oligomers or polymers is given below.

Hexabutyl-1,5-dichlorotristannoxane

To a solution of tetrabutyl-1,3-dichlorodistannoxane (1.66 g, 3 mmoles) in dichloromethane (50 ml), aqueous 0.1 *N* sodium hydroxide (20 ml, 2 mmoles) was added at room temperature and the mixture was stirred for 4 h. The dichloromethane layer was separated, dried over sodium sulfate, and evaporated, yielding the tristannoxane (1.4 g, 88%), m.p. 97° after recrystallization from heptane (lit. (5), 97°, lit. (7), 89–90°). The aqueous layer contained 1.92 mmoles chloride ions.

Anal. Calcd. for $C_{24}H_{54}Cl_2O_2Sn_3$: C, 35.9; H, 6.7; Cl, 8.9; titration equiv, 401; m.w., 801. Found: C, 36.0; H, 6.9; Cl, 9.0; titration equiv, 398; m.w., 900 (v.p.o. in benzene at 20°).

Octabutyl-1,7-dichlorotetrastannoxane

This was obtained as before by reacting tetrabutyl-1,3-dichlorodistannoxane (20 mmoles) with 0.1 *N* sodium hydroxide (20 mmoles); yield 98%, m.p. 102° after recrystallization from heptane (lit. (5, 6) 102°, lit. (7), 94–95°).

Anal. Calcd. for $C_{32}H_{72}Cl_2O_3Sn_4$: C, 36.4; H, 6.9; Cl, 6.8; titration equiv, 525; m.w., 1050. Found: C, 36.2; H, 7.2; Cl, 6.9; titration equiv, 522; m.w., 1140 (v.p.o. in benzene at 20°).

This oligomer was also obtained in almost quantitative yield by reaction of the distannoxane (3.1 mmoles) in dichloromethane (50 ml) with aqueous pyridine (5 ml, 3.1 mmoles), m.p. and mixed m.p. 102° (heptane).

Preparation of the Intermediate 2 (2)

Dibutyltin dichloride (25.3 g, 8.32 mmoles) in ethanol (125 ml) was added slowly to a solution of triethylamine (33.6 g, 33.28 mmoles) in ethanol (125 ml). The mixture was stirred for 1 h, water (5 ml) was added, and the precipitate was filtered off, dissolved in hot acetone (100 ml), and reprecipitated by the addition of water (200 ml); yield 14.7 g (69%), m.p. 102° (lit. (1), 109–121°), mixed m.p. with octabutyl-1,7-dichlorotetrastannoxane 102°.

Anal. Calcd. for $C_{32}H_{72}Cl_2O_3Sn_4$: C, 36.4; H, 6.9; Cl, 6.8. Found: C, 36.3; H, 7.0; Cl, 6.5.

Dodecabutyl-1,11-dichlorohexastannoxane

This was obtained as before by reacting the distannoxane (1.5 mmoles) with 0.1 *N* sodium hydroxide (2 mmoles); yield 78%, m.p. 110° after recrystallization from heptane (lit. (7), 100–102°).

Anal. Calcd. for $C_{48}H_{108}Cl_2O_5Sn_6$: C, 37.2; H, 7.0; Cl, 4.6; titration equiv, 774. Found: C, 37.4; H, 7.1; Cl, 4.5; titration equiv, 755.

Hexabutyl-1,5-di-p-nitrobenzoyloxytristannoxane

A suspension of *p*-nitrobenzoic acid (0.9 g, 5.3 mmoles) in water (10 ml) was neutralized with sodium hydroxide (1 *N*) to phenolphthalein. Hexabutyl-1,5-dichlorotristannoxane (2 g, 2.49 mmoles) in dichloromethane (50 ml) was added and the mixture stirred at 0° for several hours. The organic layer was separated, washed with water, dried (Na_2SO_4), and evaporated. The solid residue was recrystallized from toluene–heptane, m.p. 85° (lit. (5), 85°; yield 2.4 g (91%)).

Anal. Calcd. for $C_{38}H_{62}N_2O_{10}Sn_3$: C, 42.9; H, 5.8; N, 2.6; titration equiv, 531. Found: C, 43.3; H, 6.0; N, 2.6; titration equiv, 540.

Poly(hexabutyl adipoyloxy)tristannoxane —$[OOC(CH_2)_4COO(SnBu_2O)_2SnBu_2]$—$_n$

A suspension of adipic acid (0.364 g, 2.49 mmoles) in water (10 ml) was neutralized with sodium hydroxide (1 *N*). Hexabutyl-1,5-dichlorotristannoxane (2 g, 2.49 mmoles) in dichloromethane (50 ml) was added and the mixture stirred at 0° for 6 h. The precipitated polymer was filtered and washed with water, acetone, and dichloromethane; yield 1.5 g (69%), m.p. 170–180°.

Anal. Calcd. for $(C_{30}H_{62}O_6Sn_3)_n$: C, 41.1; H, 7.1; titration equiv, 437. Found: C, 40.9; H, 7.2; titration equiv, 437.

The titration equiv in this case gives half of the molecular weight of the recurring unit.

Reaction of p-Nitrobenzoic Acid with Octabutyl-1,7-di-p-nitrobenzoyloxytetrastannoxane

Octabutyl-1,7-di-*p*-nitrobenzoyloxytetrastannoxane (1.248 g, 0.95 mmoles) was dissolved in toluene (80 ml), *p*-nitrobenzoic acid (0.96 g, 5.75 mmoles) was added, and the mixture was refluxed for 9 h under azeotropic distillation. The toluene solution was concentrated, heptane was added, and the precipitated di-*p*-nitrobenzoyloxy dibutyltin (2.14 g, 3.79 mmoles) was collected; m.p. 218° (lit. (8), 218°), which was not depressed by an authentic sample.

1. R. OKAWARA and M. WADA. J. Organometal. Chem. Amsterdam, **1**, 81 (1963).
2. D. L. ALLESTON, A. G. DAVIES, and M. HANCOCK. J. Chem. Soc. 5744 (1964).
3. D. L. ALLESTON, A. G. DAVIES, and B. N. FIGGIS. Proc. Chem. Soc. 457 (1961).
4. R. C. POLLER. J. Organometal. Chem. Amsterdam, **3**, 321 (1965).
5. D. WAGNER. Ph.D. Thesis submitted to the Hebrew University of Jerusalem, Israel. 1967.
6. S. MIGDAL, D. GERTNER, and A. ZILKHA. European Polymer J. In press.
7. A. G. DAVIES, P. G. HARRISON, and R. R. PALAN. J. Organometal. Chem. Amsterdam, **10**, 33 (1967).
8. M. FRANKEL, D. GERTNER, D. WAGNER, and A. ZILKHA. J. Organometal. Chem. Amsterdam, **9**, 83 (1967).
9. M. FRANKEL, D. GERTNER, D. WAGNER, and A. ZILKHA. J. Appl. Polymer Sci. **9**, 3383 (1965).
10. T. HARADA. Sci. Papers Inst. Phys. Chem. Res. Tokyo, **35**, 290 (1939); R. K. INGHAM, S. D. ROSENBERG, and H. GILMAN. Chem. Rev. **60**, 459 (1960).
11. A. J. GIBBSONS, A. K. SAWYER, and A. ROSS. J. Org. Chem. **26**, 2304 (1961).
12. R. C. CUMMINS and P. DUNN. The infrared spectra of organotin compounds. Report 266. Department of Supply. Australian Defence Scientific Service, Maribyrnong, Victoria. October 1963.
13. B. KUSHLEFSKY, I. SIMMONS, and A. ROSS. Inorg. Chem. **2**, 187 (1963).
14. E. FRIEBE and H. KELKER. Z. Anal. Chem. **192**, 267 (1963).
15. D LOHMANN. J. Organometal. Chem. Amsterdam, **4**, 382 (1965).
16. W. P. NEUMANN. Die organische Chemie des Zinns. Ferdinand Enke Verl. Stuttgart. 1967. pp. 129 and 181.
17. R. C. POLLER. J. Chem. Soc. 706 (1963).

Can. J. Chem. Downloaded from www.nrcresearchpress.com by 210.87.254.6 on 09/05/12
For personal use only.

Can. J. Chem. Downloaded from www.nrcresearchpress.com by 210.87.254.40 on 09/05/12
For personal use only.

Kinetics of the thermal reactions of ethylene. Part I

M. L. Boyd,[1] T-M. Wu, and M. H. Back
Chemistry Department, University of Ottawa, Ottawa, Canada

Received November 21, 1967

The pyrolysis of ethylene has been studied in the temperature range 500–600 °C and the pressure range 15–60 cm. The main products were ethane, propylene, butene, butadiene, and a polymer of molecular weight corresponding to C_8 or higher. Small amounts of methane, butane, unsaturated C_5, unsaturated C_6, and benzene were also measured. Of the main products, propylene, butene, and butadiene showed an induction period, as long as several minutes at the lowest temperature. The order with respect to ethylene of ethane, propylene, and butene was close to two and the activation energy of the rates was approximately 40 kcal/mole. The results have been interpreted in terms of a free radical chain polymerization. It is suggested that the polymer formed is unstable and decomposes to yield the products for which an induction period was observed.

Canadian Journal of Chemistry, **46**, 2415 (1968)

Introduction

The reactions occurring during the pyrolysis of olefins are much less well understood than those involved in the decomposition of the paraffins. The kinetics of the olefin systems have been found to be complex and few entirely satisfactory mechanisms have been suggested (1). The simplest olefin, ethylene, has received less attention than the higher members and, as is often the case with the first member of a series, provides some unique mechanistic problems.

One of these is the initiation process. Because the bonds are all very strong, bond rupture may be a relatively slow process and initiation may occur by the formation of the triplet state, the interaction of two molecules to form two radicals or one diradical, or the simple condensation of double bonds to form high molecular weight products. Another problem is the importance of free radicals in the mechanism. Although free radical reactions frequently are important in thermal decompositions, olefins may also undergo molecular reactions, and the relative importance of the two may not always be simply determined.

These questions were not entirely resolved by previous studies of the pyrolysis of ethylene in the temperature range 500–600 °C (2–5), although the results were, in general, consistent. The main products were propylene and butene with considerable amounts of higher olefins, including benzene and toluene. The disappearance of ethylene was a second order process with an activation energy of about 40 kcal/mole. There was some uncertainty regarding the distinction between primary and secondary products partly because of the detection of a small induction period. The approach of the present study therefore, using improved analytical techniques, was the measurement of the initial rates of formation of all the important products in order to distinguish primary from secondary and thus establish a better basis for a discussion of the mechanism.

The decomposition of ethylene in a shock tube at temperatures of 1500–2000 °K has been rather thoroughly studied (6–8) and the kinetics are also complex in this region. The products formed are almost entirely acetylene and hydrogen with none of the higher olefins, except butadiene, which are observed at lower temperatures. The order and activation energy of the reaction are also in marked contrast to those observed in the region 500–600 °C and a different set of reactions is undoubtedly involved (9).

Experimental

Apparatus

The pyrolysis was studied in a conventional static system. The course of the reaction was followed by two methods. In the principal series of experiments, product analyses were made at various time intervals. In a second series, the reaction was followed by measuring the pressure changes in the system with a fused quartz spiral pressure gauge.

The reaction vessel was a quartz cylinder of 266.4 ml capacity fabricated from 40 mm o.d. quartz tubing, about 200 mm in length and having a surface/volume (S/V) ratio of 1.0 cm^{-1}. The vessel was enclosed in an electrically heated steel cylinder, 2 in. thick, whose temperature was controlled to within ± 1 °C with a Thermoelectric thermoregulator. A second quartz vessel, of 157.5 ml

[1]Mines Branch, Department of Energy, Mines and Resources, Ottawa, Canada.

Can. J. Chem. Downloaded from www.nrcresearchpress.com by 210.87.254.40 on 09/05/12
For personal use only.

capacity, packed with tubes and having a S/V ratio of 8.5 cm^{-1} was also used.

Reagents

Phillips research grade ethylene labelled 99.98% pure was used in all experiments. The ethane impurity was consistently 0.005%. Since the lowest conversions were between 0.05 and 0.1%, no correction was made. No higher molecular weight impurities were detected by the gas chromatographic techniques described later. At the time the storage flask was filled, the ethylene was degassed at −196 °C.

Procedure

Before each experiment, the apparatus was evacuated to a pressure of at most 5×10^{-5} mm. Ethylene was admitted to the reaction vessel from a section of the apparatus which consisted of a 1 l flask with an inner cold finger, a manometer, and a trap leading to the vacuum line. Immediately prior to each experiment the ethylene was condensed in the cold finger and then slowly distilled with continuous pumping into the trap maintained at −196 °C. Evacuation was continued for 15 min. This procedure was followed in an attempt to ensure the absence of oxygen in the reactant. The 1 l flask with the inner cold finger also served as a mixing flask for experiments in which gases were added to ethylene before pyrolysis.

The analytical portion of the system consisted of a LeRoy still, a conventional trap, two removable sample containers, a mercury diffusion pump, a spiral trap filled with copper turnings, a Toepler pump, and a gas burette. Sealed to the burette was a palladium thimble maintained at 280 °C. At the conclusion of each experiment the reactant and condensable products were collected in the LeRoy still maintained at −196 °C, and the noncondensables collected and measured in the gas burette. The trap filled with copper turnings maintained at −196 °C prevented ethylene from being collected in the gas burette. The noncondensable gases were found, on the basis of their mass spectrum, to consist of only hydrogen and methane. The methane was taken to be the amount of noncondensable gas remaining after the removal of hydrogen through the palladium thimble. The hydrogen yield was obtained by subtracting the methane from the total noncondensable gas.

In the majority of experiments the contents of the LeRoy still were analyzed directly on the gas chromatograph. When the initial concentration of ethylene was greater than 45 cm, the contents of the LeRoy still were separated into two or three fractions by raising the temperature to −170 °C. Each fraction was then analyzed separately. This was found necessary in order to reduce the ethylene–ethane ratio and thus facilitate the analysis of ethane.

The analyses were made with an F & M model 720 dual-column, temperature-programmed gas chromatograph, equipped with a thermal conductivity detector. All analyses were made with a column (32 in. × ¼ in.) packed half its length with silica gel and half with alumina (60–80 mesh), the sample passing first through the silica gel. Three hundred and thirty-six seconds after the sample entered the gas chromatograph the temperature programmer was turned on and the column temperature was increased linearly at the rate of 4 °C/min up to a maximum of 300 °C. By this technique, it was found possible to analyze all the condensable products up to and including C_7.

The condensable products were identified by the mass spectrum of the individual chromatographic peaks, comparison of retention times with authentic samples, and in some cases analysis on a second column. The following products were identified and measured: ethane, propane, propylene, n-butane, butene (> 80% butene 1, the remainder almost equally divided between *cis*- and *trans*-butene-2), butadiene, unsaturated C_5, unsaturated C_6, benzene, and toluene. All calibrations were made with pure substances and were reproducible to within 5%. For all product analyses except ethane duplicate reaction mixtures agreed to within 10%. In the case of ethane, the scatter was 2 to 3 times greater. This lower accuracy was probably due to the short retention time in the gas chromatographic analysis.

Pressure changes were measured with a Texas Instrument Company fused quartz pressure gauge, model 141, sealed directly to the reaction vessel. One digit on the counter was equal to 0.025 mm. Conversions from degrees rotation to mm were made using the calibration table provided with the instrument. During these experiments, temperature readings were made simultaneously with pressure readings and the pressure measurements were corrected for temperature fluctuations. The gauge was operated so that balance was obtained within a few seconds after the reaction had started.

A few experiments were made at 503 °C with a 50:50 mixture of C_2H_4 and C_2D_4. Mass spectrometric analyses were made of the ethylene, ethane, and butene resulting from the pyrolysis of this mixture.

Results

Product yields were measured as a function of time at four temperatures in the range 500–600 °C and at four or five pressures in the range 15–60 cm. Those products whose yield–time curves showed a well-defined linear portion were ethane, propylene, butene, butadiene, and butane. Of these all except ethane and possibly butane showed an induction period. At the lowest temperature studied, 503 °C, this difference in initial behavior was most pronounced and is illustrated in Figs. 1–3 for the three main products, ethane, propylene, and butene. The induction periods decreased with increasing temperature and increasing pressure, as illustrated in Figs. 2 and 4. There seems little doubt that this difference in initial behavior was real. At 503 and 541 °C, several analyses of the reaction products obtained at reaction times shorter than the observed induction period revealed no propylene, butene, or butadiene, but no such analysis failed to reveal ethane. Although from Fig. 6 it appears that butane has a finite initial

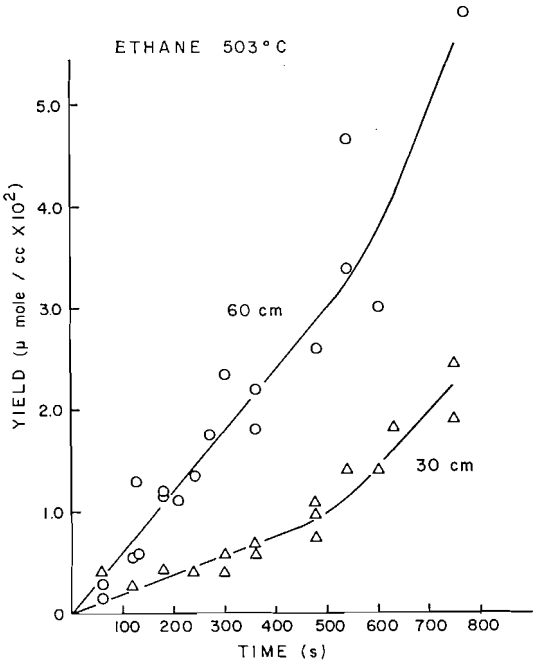

FIG. 1. Yield of ethane as a function of time.

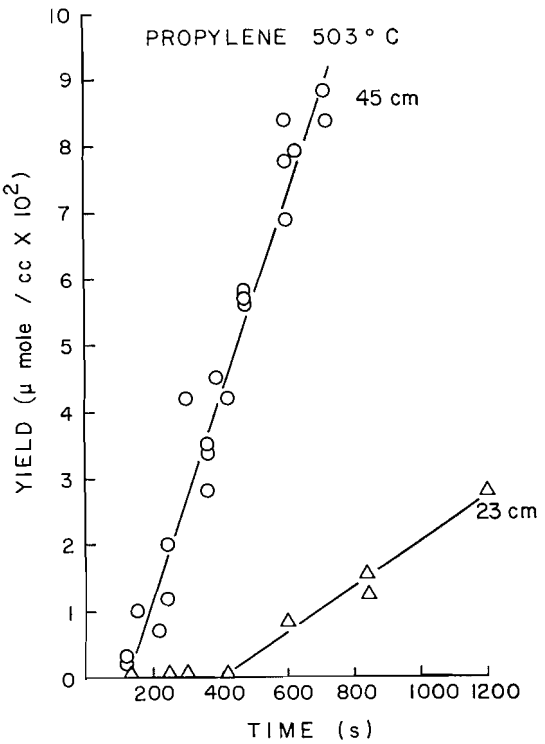

FIG. 2. Yield of propylene as a function of time.

rate the quantities measured were so small that the evidence is not conclusive.

At all temperatures the ethane yield increased very rapidly beyond the initial linear portion. At higher temperatures and pressures, this rapid secondary rise obscured the true initial rate. Yields of butane showed a similar behavior. The yield of propylene increased linearly at all temperatures while the yields of butene and butadiene levelled off after the initial linear rise and approached a maximum at the higher temperatures. Rates obtained from the initial linear portion of the yield–time curves for these products are summarized in Table I. The orders of these rates with respect to ethylene and the activation energies of the rates are given in Table II. These values have been obtained by least squares analysis of the data. The error limits quoted therefore merely represent the standard deviation and do not assess the reliability of the values. The temperature dependence of the initial rates, measured at an initial ethylene pressure of 30 cm, is illustrated in Fig. 7.

The order plots for butene gave some indication of curvature and if interpreted as such, the order would be close to two above 30 cm, but decreasing at lower pressures. Similarly, the Arrhenius plots for propylene and butene might be interpreted as indicating a decreasing activation energy with decreasing temperature. Because of the uncertainty of the data, however, we have treated all these curves by least squares analysis.

A second group of products were those whose rates increased continuously from a vanishingly small amount. These were methane, hydrogen, propane, unsaturated C_5, unsaturated C_6, benzene, and toluene. A typical yield–time plot of methane is shown in Fig. 8. Methane was by far the most important product in this group. Most of the others appeared only after relatively long reaction times and did not constitute an appreciable fraction of the total products.

Acetylene was not detected among the products. Careful checks of the lower limit of detection of acetylene were made by analyzing mixtures of large amounts of ethylene with small amounts of acetylene. It was estimated that 0.075 μmole of acetylene could be detected, corresponding to a yield of 2.8×10^{-4} μmole/cc. Its rate of formation was therefore negligible compared with the other products. Cyclobutane and allene were also shown to be absent.

Can. J. Chem. Downloaded from www.nrcresearchpress.com by 210.87.254.40 on 09/05/12
For personal use only.

Can. J. Chem. Downloaded from www.nrcresearchpress.com by 210.87.254.40 on 09/05/12
For personal use only.

TABLE I

Initial rates of product formation (moles $cc^{-1}\ s^{-1} \times 10^{11}$)

Temperature (°C)	$P^{0}_{C_2H_4}$ (cm)	$R^{0}_{C_2H_6}$	$R^{0}_{C_3H_6}$	C_3H_6 induction period (s)	$R^{0}_{C_4H_{10}}$	$R^{0}_{C_4H_8}$	C_4H_8 induction period (s)	$R^{0}_{C_4H_6}$	C_4H_6 induction period (s)
503±2	15.2	0.23	1.58	1100		0.64	1450	Not detected	
	22.7	0.74	3.52	410		1.33	600	"	
	30.2	1.80	6.35	270		1.42	490	"	
	46.7	4.00	15.20	120	0.16	2.90	210	"	
	60.3	6.16	34.60	70	0.44	8.70	150	"	
541±1	15.33	0.76	2.51	380	0.027	0.81	240	0.20	480
	22.98	2.25	6.74	190	0.057	1.48	160	0.41	380
	30.32	4.02	11.86	140	0.096	2.93	130	0.53	200
	45.39	38.59	25.97	60	0.24	5.72	65	0.93	100
563±1	15.00	2.30	6.62	220	—	—	—	—	—
	22.93	5.71	13.48	130	—	—	—	—	—
	30.35	14.85	21.42	88	0.57	7.09	85	1.37	118
	60.35	66.03	90.73	30	—	—	—	—	—
600±1	15.14	7.01	15.04	70	0.66	7.98	37	5.13	50
	22.82	16.11	29.68	42	1.02	8.92	25	8.36	38
	30.22	31.91	52.99	32	1.76	17.34	18	13.02	37
	45.30	135.0	117.4	20	5.26	41.59	15	20.64	19

TABLE II

Summary of orders (with respect to ethylene) and activation energies for the initial rates

Product	Temperature range (°C)	E (kcal/mole)	Order with respect to C_2H_4			
			503 °C	541 °C	563 °C	600 °C
Ethane	503–600	41.6±4.1	2.4±.1	2.4±.1	2.4±.1	2.2±.1
Propylene	503–600	29.4±2.1	2.2±.07	2.1±.02	1.9±.06	1.9±.04
n-Butane	541–600	70	—	2.1±.05	—	2.4±.1
Butene	503–600	35.4±2.5	1.7±.2	1.8±.08	—	1.6±.25
Butadiene	541–600	77	None detectable	1.4±.07	—	1.3±.06

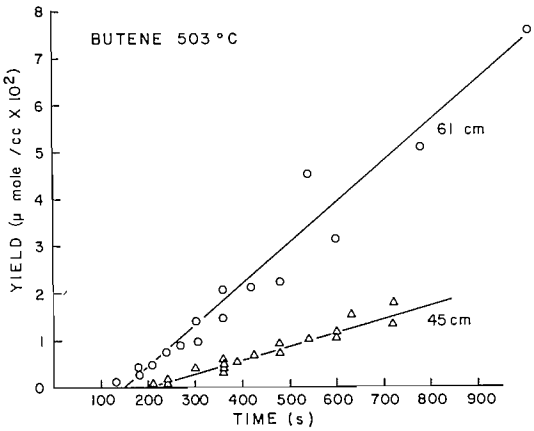

FIG. 3. Yield of butene as a function of time.

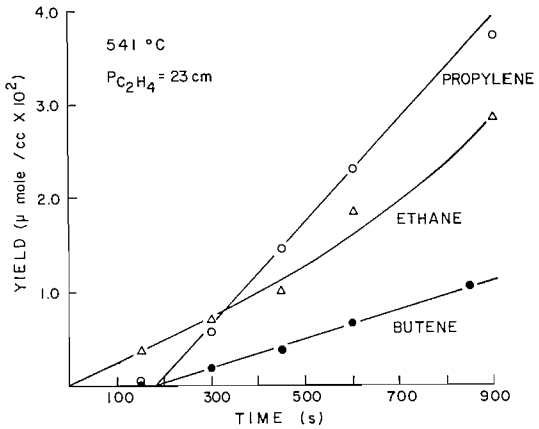

FIG. 4. Yield of ethane, propylene, and butene as a function of time.

Pressure Measurements

The absence of an induction period in the production of ethane and the presence of an appreciable one for butadiene indicated an anomalously high hydrogen content for the products measured in the early stages of the pyrolysis. This suggested that an unsaturated product was formed which was not detected in the analysis. To test this possibility, the reaction was followed by the measurement of the pressure change under the same conditions for which product analyses had been made. Pressure–time curves were determined at 503, 541, 563, and 600 °C. A typical curve is shown in Fig. 9. Duplicate or triplicate experiments were made for each set of initial conditions and in most cases the pressure–time curves were superimposable upon one another. The initial pressure was obtained by extrapolation of the pressure–time curve to zero time. Also shown is the ΔP curve calculated from the product analyses. These ΔP values were normalized to the P^0 obtained by the extrapolation. This adjustment was necessary because the gauge was not calibrated in an absolute sense, that is, with respect to P^0. From graphs such as Fig. 9, 'difference' pressure curves were obtained by subtracting the experimental pressure curve from the calculated curve. These difference curves were calculated from data obtained at 503, 541, and 600 °C and over the pressure range 15–60 cm.

In general, the experimental pressure–time curves were characterized by a rapid initial decrease in pressure, followed by a period where the rate of change was comparatively small, which in turn was followed by a linear portion where the pressure decreased more rapidly. The lag in the pressure curves corresponded approximately to the induction period observed for propylene, butene, and butadiene formation. Blank experiments with air were performed to ensure that this initial rapid decrease was not the result of non-equilibration of the temperature. No such rapid initial change of the pressure was observed with air; only a slow fluctuation which

Can. J. Chem. Downloaded from www.nrcresearchpress.com by 210.87.254.40 on 09/05/12
For personal use only.

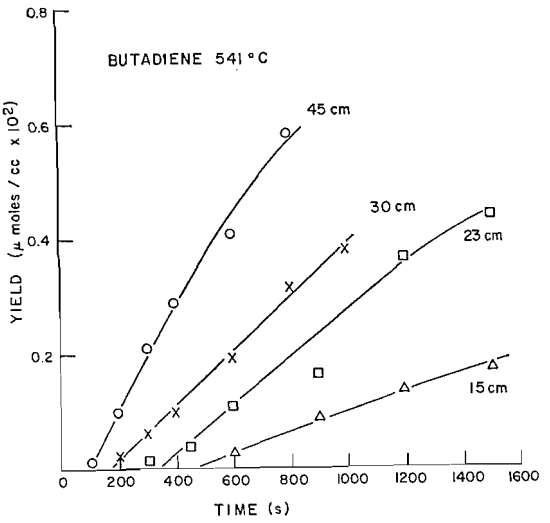

FIG. 5. Yield of butadiene as a function of time.

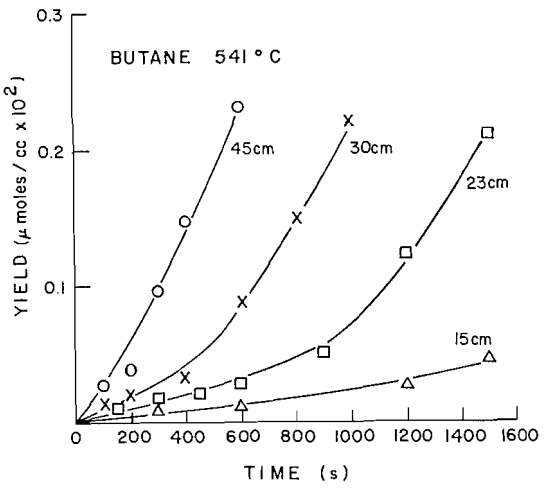

FIG. 6. Yield of butane as a function of time.

correlated with the fluctuation of the temperature of the furnace about its equilibrium position was noted. Since the initial pressure decrease was very rapid and the uncertainties in P^0 large, it is possible that the initial rate of pressure decrease may have been considerably underestimated. This is suggested by the low value obtained for the order (~ 1.0) for these initial rates and the correspondingly low activation energy (30–12 kcal/mole over the range 600–500 °C). Even so, except for experiments at the highest initial pressure, the initial rate of pressure decrease was always much in excess of (about 5–20 times) the initial rate of ethane formation. There seems no doubt that considerably more ethylene is consumed than the analyzed products would indicate.

The second portion of the pressure–time curve was linear for a considerable period and the rate was found to be second order with respect to ethylene and to correspond to an activation energy of 36 kcal/mole. These values agree with those previously reported from pressure measurements (1), which suggests that it is this secondary drop in pressure which has been measured previously. The data obtained from the pressure measurements are given in Table III. The difference between the pressure calculated from the products measured and that observed from the gauge is given in units of mole cc^{-1}. This represents the decrease in the concentration of ethylene resulting from the formation of polymer, assuming that the number of moles of polymer is small compared with the number of moles of ethylene consumed.

In brief, the comparison of experimental pressure–time curves with those calculated from the products analyzed suggested the formation of two products not detected by the analysis. These will subsequently be referred to as polymers, probably having molecular weights corresponding to C_8 or higher, since the analytical procedure should have detected lighter products. The first relates to the formation of ethane, since no induction period was observed, while the second parallels the behavior of the other major products, showing an induction period of comparable size.

Deuterated Ethylene Experiments

The experiments with mixtures of C_2H_4 and C_2D_4 were undertaken to test the hypothesis that some form of C_4H_8 might be an intermediate in the course of the reaction. Analysis of the butene showed that the D and H atoms were thoroughly mixed and there was no evidence for the preponderance of $C_4H_4D_4$. Therefore, if C_4H_8 is an intermediate it is not subsequently stabilized as butene-1. Analysis of the unreacted ethylene showed only a very small amount of mixing and no large amount of $C_2H_2D_2$. It was considered that had cyclobutane been an intermediate some mixing of the unchanged ethylene into $C_2H_2D_2$ would have occurred and this possibility may therefore be

Can. J. Chem. Downloaded from www.nrcresearchpress.com by 210.87.254.40 on 09/05/12
For personal use only.

TABLE III

Rates of formation of polymer II

Temperature (°C)	Pressure (cm)	d/dt [$P_{calcd} - P_{obsd}$] (mole cc^{-1} s$^{-1} \times 10^{11}$)	Order with respect to ethylene	E (kcal/mole)
503	15.15	0.58		
	30.48	1.92		
	46.47	4.36	1.8	
	60.63	9.29		
541	15.33	1.47		
	22.98	5.02		
	30.32	5.90	1.8	35.5
	45.39	14.75		
600	15.14	7.78		
	22.82	18.75		
	30.22	22.75	1.8	
	45.30	54.6		

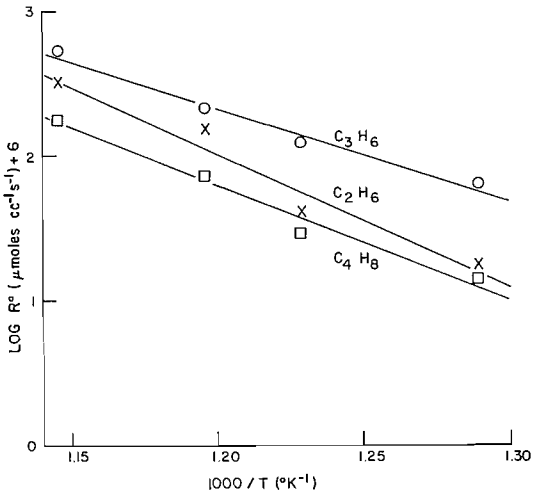

FIG. 7. Arrhenius plot of the rates of formation of the three main products measured at an initial ethylene pressure of 30 cm.

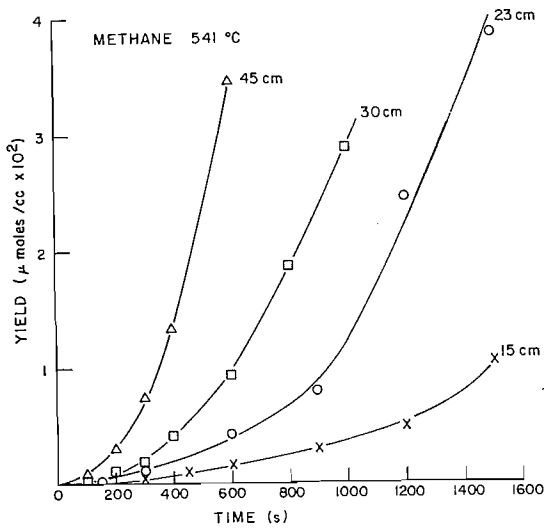

FIG. 8. Yield of methane as a function of time.

rejected. The product ethane showed a variety of D and H contents and this observation helped to rule out the possibility of a bimolecular reaction of ethylene to give ethane and acetylene, which is discussed in a later section. In brief, the mixing of the H and D atoms observed in the products is consistent with a free radical mechanism.

Surface Effects

Pressure–time curves were determined at 541 °C and 15, 23, 30, and 45 cm pressure using the reaction vessel of S/V ratio 8.5 cm^{-1}. These curves were practically superimposable upon the corresponding ones obtained with the unpacked vessel. Ethane, propylene, and butene production were determined using both the packed and unpacked vessels at 530 and 584 °C in the range 15–60 cm pressure. The changes in rate observed were very small, the largest being for ethane where the error is greater than in the other cases. It may be concluded that the surface effects are not very important and, if any exist, ethane is the most likely product to be so affected.

Discussion

The main features of the reaction which a mechanism must account for may be summarized as follows:

Can. J. Chem. Downloaded from www.nrcresearchpress.com by 210.87.254.40 on 09/05/12
For personal use only.

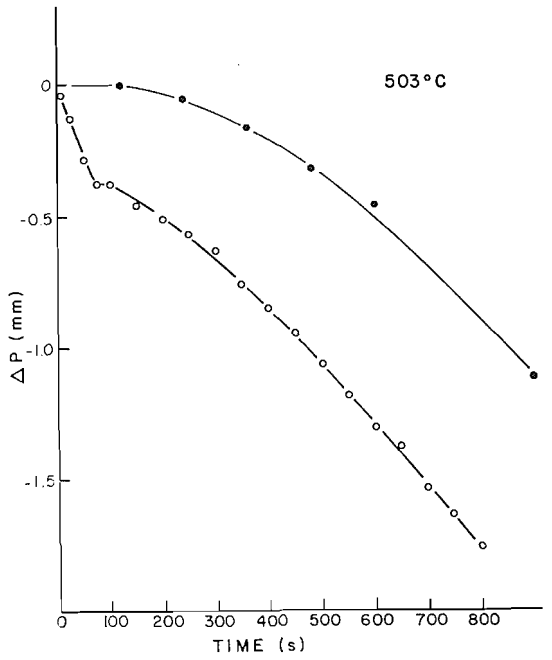

FIG. 9. Comparison between the pressure calculated from the products analyzed and that measured by the gauge as a function of time. Initial pressure of ethylene 30 cm. (●) Calculated; (○) measured.

(1) The two main products, ethane and a polymer, and the minor product butane do not show an induction period.

(2) The products whose yield rises linearly with time after an induction period are propylene, butene, butadiene, and a second polymer, probably different from the first polymer.

(3) The rate of all other products increased continuously with time from a vanishingly small amount.

(4) The rate of production of the main products is approximately second order with respect to ethylene, with the exception of butadiene which is about 1.3.

(5) The activation energy for the formation of ethane, propylene, and butene, about 40 kcal/mole, is much lower than that observed for the rate of product formation from the decomposition of most simple hydrocarbons.

The last two points suggest that the main chain-propagating step is not the dissociation of a radical. In particular, failure to find acetylene in the products is direct evidence that dissociation of the vinyl radical is not important under the present conditions. The mechanism which we suggest may be briefly described as follows: a free radical chain polymerization, initiated by the interaction of two ethylene molecules to form a vinyl and an ethyl radical, yields as products ethane and a polymer, called polymer I. Polymer I is a relatively unstable product and itself decomposes to yield propylene, butene, butadiene, and a second polymer, called polymer II. The time taken for polymer I to reach a steady state concentration is the induction period observed for these products. Since the steady state concentration is reached at very low conversions of ethylene, the yields of these products are observed to increase linearly with time over a fairly wide interval.

The Free Radical Chain Polymerization

The following reactions represent a simplified version of the polymerization process:

$$[1] \quad C_2H_4 + C_2H_4 \rightarrow C_2H_3 + C_2H_5$$

$$[2a] \quad C_2H_5 + C_2H_4 \rightarrow C_2H_6 + C_2H_3$$

$$[2b] \quad \rightarrow C_4H_9$$

$$[3] \quad C_2H_3 + C_2H_4 \rightarrow C_4H_7$$

$$[4] \quad C_4H_7 + C_2H_4 \rightarrow C_6H_{11}$$

$$\cdots\cdots\cdots$$

$$[5] \quad C_nH_{2n-1} + C_2H_4 \rightarrow C_2H_5 + C_nH_{2n-2}$$

$$[6a] \quad C_4H_9 + C_2H_4 \rightarrow C_4H_{10} + C_2H_3$$

$$[6b] \quad \rightarrow C_6H_{13}$$

$$\cdots\cdots\cdots$$

$$[7] \quad C_nH_{2n+1} + C_2H_4 \rightarrow C_2H_5 + C_nH_{2n}$$

$$[t] \quad 2C_2H_5 \rightarrow C_4H_{10}.$$

There are several conditions necessary in order that this type of polymerization take place. Addition of the radicals, vinyl, butyl, and higher, to ethylene must be much faster than abstraction. Thus the higher molecular weight products build up and the lower products formed by abstraction are produced in amounts too small to be observed. The fact that ethane is a major product of this reaction indicates that the ethyl radical must be one of the chain-carrying radicals. The chain transfer steps [5] and [7] allow ethyl radicals, but no other alkyl radicals, to be regenerated. This chain transfer process must also be rather inefficient since unsaturated products of low molecular weight were not observed during the induction period.

For purposes of applying the steady-state treatment the combination of ethyl radicals was chosen as the chain termination step. Whether

Can. J. Chem. Downloaded from www.nrcresearchpress.com by 210.87.254.40 on 09/05/12
For personal use only.

Can. J. Chem. Downloaded from www.nrcresearchpress.com by 210.87.254.40 on 09/05/12
For personal use only.

in fact termination occurs by combination of ethyl or vinyl radicals does not affect the conclusions. The following expressions were obtained:

rate of formation of ethane

$$= k_{2a}(k_1/k_t)^{1/2}[C_2H_4]^2$$

rate of formation of polymer I

$$= (k_{2a} + k_{2b})(k_1/k_t)^{1/2}[C_2H_4]^2.$$

The rate constant k_{2a} was calculated at four temperatures and several pressures using the following values:

$k_1 = 10^{14.82}\, e^{-64000/RT}$ cc mole^{-1} s^{-1} (ref. 10)

$k_t = 10^{13.361}$ cc mole^{-1} s^{-1} (ref. 11).

The following expression was obtained:

$$k_{2a} = 10^{11.5\pm1.0}\, e^{-13000\pm3000/RT}.$$

The uncertainties arise mainly because the rate of formation of ethane was not exactly second order, as required by the mechanism. Nevertheless, this is a reasonable value for a hydrogen abstraction reaction. The underlying assumption in this treatment is that the propagation steps [2*a*] and [2*b*] are rate controlling. If in fact reactions [5] and [7] are slower than reaction [2] then termination will occur by combination of higher molecular weight radicals. The activation energy of the slow step must, however, not exceed about 13 kcal/mole. Such a low value probably excludes a radical decomposition reaction as an important propagation step.

The fate of the butyl radical as described by the mechanism is the formation of butane by abstraction or addition to ethylene to begin the formation of polymer. The kinetic parameters measured for butane, however, suggest that it is not formed mainly by the abstraction reaction [6*b*]. The activation energy for butane, about 70 kcal/mole, suggests that it may be a measure of the termination step, which would thus be the combination of ethyl radicals. We have therefore neglected reaction [6*b*] in obtaining the expression for the rate of formation of the polymer. The dissociation reaction of butyl radicals, which is the reverse of [2*b*], has also been neglected. It is very likely that this occurs to some extent, and if so, may reduce k_{2b} in the expression for the rate of formation of polymer by some factor. The information on the rate constants involved is not sufficiently precise to make an accurate assessment of this factor.

This mechanism predicts that the rate of ethane formation should be exactly second order with respect to ethylene. Although the observed order was greater than two, we feel this is probably not significant in view of the difficulties involved in the measurement of the initial rates of ethane. The rate of formation of polymer, which was measured by the initial rate of pressure decrease, must have the same kinetic parameters as the rate of formation of ethane. The difficulties involved in the measurement of this initial rate have already been discussed and the results do not, we feel, provide a reliable test of the mechanism.

The Decomposition of Polymer I

Since the present results give no information about the structure or molecular weight of polymer I, a detailed description of its mode of decomposition is not possible. A general mechanism may nevertheless be formulated:

[8] polymer I → propylene + polymer II

[9] polymer I → butene + polymer II

[10] polymer I → $R_1 + R_2$

[11] $R_1 + C_2H_4 \rightarrow R_3$

[12] $R_1 \rightarrow$ butadiene + R_4.

Free radicals may or may not be involved in the formation of butene and propylene and the one-step reaction is written for simplicity. Results obtained from the pyrolysis of mixtures of ethane and ethylene, which are discussed in Part II, suggest that radicals are involved in the formation of butadiene and that the butadiene is probably formed by decomposition of the radical rather than by abstraction.

When the rate of decomposition of polymer I becomes equal to its rate of formation its steady state concentration is achieved and the rate of formation of propylene, butene, and butadiene may be expressed as follows:

$$R_{C_3H_6} = \frac{k_8(k_{2a} + k_{2b})(k_1/k_t)^{1/2}[C_2H_4]^2}{k_8 + k_9 + k_{10}}$$

$$R_{C_4H_8} = \frac{k_9(k_{2a} + k_{2b})(k_1/k_t)^{1/2}[C_2H_4]^2}{k_8 + k_9 + k_{10}}$$

$$R_{C_4H_6} = \frac{k_{12}k_{10}(k_{2a} + k_{2b})(k_1/k_t)^{1/2}[C_2H_4]^2}{(k_8 + k_9 + k_{10})(k_{11}[C_2H_4] + k_{12})}.$$

Can. J. Chem. Downloaded from www.nrcresearchpress.com by 210.87.254.40 on 09/05/12
For personal use only.

This type of mechanism predicts that the rates of formation of propylene and butene will be second order (or equal to that of ethane) and that of butadiene will be between one and two, depending on the relative importance of k_{12} and $k_{11}[C_2H_4]$. This condition is adequate for propylene and butadiene but the order of the rate of formation of butene was significantly less than two. It is probable that a radical mechanism of the type proposed for butadiene may account for some of the butene formed and act to lower the order for butene.

The ratio butene/propylene, which equals k_9/k_8, was approximately 0.3 and was unchanged within the experimental error over the temperature range studied. Since reaction [10] does not contribute greatly to the sum of reactions [8], [9], and [10], the difference in the activation energy for the formation of butene and propylene from that for ethane should be accounted for by the temperature coefficient of $(k_{2a} + k_{2b})/k_{2a}$. The differences are 6.2 and 12.2 kcal/mole respectively, which is roughly what might be expected. The fact that the activation energies for propylene and butene are not the same again points out that other processes are making some contribution.

The ratio of the rates of (propylene + butene + butadiene) to that of ethane should, according to the mechanism, equal $k_{12}/(k_{12} + k_{11}[C_2H_4])$. Again this ratio showed very little dependence on temperature and it may be concluded that the process giving rise to the high activation energy for formation of butadiene is reaction [10], the dissociation of the polymer into radicals.

The rate of formation of polymer I may be expressed by the equation

$$\frac{d}{dt}[I] + k_d[I] = k_f[C_2H_4]^2,$$

where [I] = concentration of polymer I and k_d and k_f are the composite rate constants for decomposition and formation of the polymer respectively. Solution of this equation yields the following expression for [I],

$$[I] = \frac{k_f}{k_d}[C_2H_4]^2[1 - e^{-k_d t}].$$

The induction period may be defined as the time required to reach a concentration of I approaching as close as required to that of the steady state value, so that the fraction $e^{-k_d t}$ takes an arbitrary value, for example 0.01. From the equation above, this time is independent of the ethylene concentration and will therefore be a constant for any particular temperature. The induction period was not, however, independent of the ethylene concentration but decreased as the concentration of ethylene increased. This may be accounted for if the decomposition of the polymer is a bimolecular process involving a molecule of ethylene and not a unimolecular process as written in reactions [8]–[10]. The equation for the concentration of polymer I as a function of time then becomes

$$[I] = \frac{k_f}{k_d}[C_2H_4][1 - e^{-k_d[C_2H_4]t}].$$

The time required to achieve a certain value for the fraction $e^{-k_d[C_2H_4]t}$ will thus be inversely proportional to the concentration of ethylene. This proportionality was observed within the rather wide errors involved in estimating the induction period. It is therefore concluded that dissociation of the polymer involves a bimolecular interaction with a molecule of ethylene. Inclusion of this process leaves unchanged the expressions for the rates of formation of butene and propylene.

In presenting this general mechanism for the reaction we have not dealt with the many possible reactions which were considered and finally rejected. One such reaction which deserves mention is the bimolecular interaction of two ethylene molecules to give ethane and acetylene:

$$2C_2H_4 \rightarrow C_2H_2 + C_2H_6.$$

If the acetylene reacted rapidly with ethylene to yield a polymer, then ethane and polymer would still be primary products. Since acetylene was not observed in the products it was necessary to suggest that its rate of disappearance was sufficiently fast that its steady state concentration was kept below the minimum amount detectable. Experiments in which small amounts of acetylene were added showed that acetylene was consumed but that the rate of consumption was too slow by almost a factor of 10 to meet the requirements. The induction period also was hardly reduced, although the amounts added should have been sufficient to remove it altogether, if in fact acetylene were the precursor of the polymer I. Taking into account also the results of the experiments with mixtures of C_2H_4 and C_2D_4,

Can. J. Chem. Downloaded from www.nrcresearchpress.com by 210.87.254.40 on 09/05/12
For personal use only.

this reaction was therefore rejected in favor of the free radical mechanism.

Secondary Products

Most of the secondary products are present in such small quantities that their mechanism of formation is not very important in the initial stages of the reaction. Methane, however, is a fairly important product, especially at high temperatures. Because its yield rises from zero time, rather than from the end of the induction period, it is probably secondary with respect either to ethane or to the polymer I. The unimolecular dissociation of ethane is too slow by a factor of about 10^4 to yield the amounts of methane found (12) and it must therefore be formed by the dissociation of polymer I, probably through the intermediate formation of a methyl radical.

Comparison with Previous Results

The difference between the present mechanism and those previously reported can for the most part be attributed to the smaller conversions at which rates were measured in the present work. Silcocks (3), for example, suggested that a species of formula C_4H_8, which he tentatively identified as butene-1, was an intermediate in the formation of methane, propylene, and a polymer. This idea was based on measurements of the yields of these products at 600 °C, where the yield of butene-1 rapidly reached a maximum while those of the other products continued to increase with the course of the reaction. The present results also show that the yield of butene-1 does tend to a maximum at 600 °C but it cannot, however, be an intermediate in the formation of the other products. Similarly Tanieski (5) suggested that ethane was a secondary product from the decomposition of the polymer, but again the results of the present study, which were obtained at conversions lower than his, show that this cannot be the case.

One of the important questions concerning the mechanism was whether a free radical chain was involved. Although we have suggested that the reaction is initiated by a free radical chain polymerization, the evidence for the presence of free radicals is indirect, except for the results from the experiments with mixtures of C_2H_4 and C_2D_4. Previous studies of the effect of additions of nitric oxide were somewhat ambiguous but could be interpreted to indicate the presence of free radicals. The effect of nitric oxide on the thermal reactions of olefins has not been studied in detail (13) and the interpretation of a few experiments without complete analysis may not be straightforward. Dahlgreen and Douglas (4) found that addition of H_2S increased the yield of ethane and reduced the yield of propylene, while the addition of oxygen increased the yield of both of these. These results are consistent with the proposed free radical polymerization.

Dahlgreen and Douglas proposed a diradical intermediate C_4H_8* and suggested that ethane and butadiene might be formed by the reaction of this diradical with ethylene. The present results show that this cannot be the case since the rates of formation of ethane and butadiene have quite different characteristics. In fact the diradical hypothesis, while attractive in some respects, was rejected because it does not account for the production of ethane and also would not be expected to give the induction period observed.

After this paper was submitted, a paper on the pyrolysis of ethylene was published by Halstead and Quinn (14). There are important differences in the two sets of results which lead to differences in the mechanism proposed. We believe the differences are largely due to the different range of pressures in which the reaction was studied. In order to clarify the situation the present authors are extending their measurements to cover the pressure range studied by Halstead and Quinn. These results will form the basis of a further discussion on the relation of the two mechanisms to the particular conditions of temperature and pressure.

Acknowledgments

The authors wish to thank Dr. R. A. Back of the National Research Council of Canada and Dr. V. I. Vedeneev of the Institute of Chemical Physics, Moscow, for many helpful discussions. They are also indebted to Dr. Back for the use of his quartz spiral pressure gauge and to Dr. J. L. Holmes for the mass spectral analyses. M. L. B. wishes to thank Dr. J. Convey, Director of the Mines Branch, for the opportunity to participate in this work. The authors are grateful to the National Research Council of Canada and the Department of University Affairs of the Province of Ontario for continued financial assistance.

1. E. W. R. STEACIE. Atomic and free radical reactions. 2nd ed. Vol. I. Reinhold Publishing Corp., New York. 1954. p. 175–182.
2. J. E. DOUGLAS, B. S. RABINOVITCH, and F. S. LOONEY. J. Chem. Phys. **23**, 315 (1955).
3. C. G. SILCOCKS. Proc. Roy. Soc. London, Ser. A, **233**, 465 (1956).
4. G. DAHLGREEN and J. E. DOUGLAS. J. Am. Chem. Soc. **80**, 5108 (1958).
5. M. TANIEWSKI. Proc. Roy. Soc. London, Ser. A, **265**, 519 (1962).
6. G. B. SKINNER and E. M. SOKOLOSKI. J. Phys. Chem. **64**, 1028 (1960).
7. G. I. KOZLOV and V. G. KNORRE. Combust. Flame, **6**, 253 (1962).
8. I. D. GAY, R. D. KERN, G. B. KISTIAKOWSKY, and H. NIKI. J. Chem. Phys. **45**, 2371 (1966).
9. S. W. BENSON and G. R. HAUGEN. J. Phys. Chem. **71**, 1735 (1967).
10. M. L. BOYD and M. H. BACK. Can. J. Chem. This issue.
11. A. SHEPP and K. O. KUTSCHKE. J. Chem. Phys. **19**, 326 (1951).
12. M. C. LIN and M. H. BACK. Can. J. Chem. **44**, 505 (1966).
13. B. G. GOWENLOCK. Progress in reaction kinetics. Vol. III. The Pergamon Press, Ltd., London. 1965. p. 171.
14. M. P. HALSTEAD and C. P. QUINN. Trans. Faraday Soc. **64**, 103 (1968).

Can. J. Chem. Downloaded from www.nrcresearchpress.com by 210.87.254.40 on 09/05/12
For personal use only.

Kinetics of the thermal reactions of ethylene. Part II. Ethylene–ethane mixtures

M. L. BOYD[1] AND M. H. BACK
Chemistry Department, University of Ottawa, Ottawa, Canada

Received November 21, 1967

Mixtures of ethane and ethylene have been pyrolyzed in the temperature range 563–600 °C and at pressures from 30–60 cm. The products were similar to those obtained from the pyrolysis of ethylene by itself, described in Part I, with a marked increase in the yields of the saturated products. The initial rates of product formation and the dependence of these rates on the concentration of ethane suggest that the initiation step is the same as that proposed in the pyrolysis of ethylene alone, viz.

$$2C_2H_4 \rightarrow C_2H_3 + C_2H_5$$

and that the reaction

$$C_2H_4 + C_2H_6 \rightarrow 2C_2H_5$$

is not an important source of radicals. A simplified mechanism is outlined to account for the main effects of ethane on the free radical chain polymerization.

Canadian Journal of Chemistry, 46, 2427 (1968)

Introduction

The results of the study of the pyrolysis of ethylene reported in Part I (1) were interpreted in terms of a free radical chain polymerization. The initiation step postulated was the bimolecular reaction of two ethylene molecules to form a vinyl and an ethyl radical. It seemed of interest to look for the occurrence of an analogous reaction between ethane and ethylene, and for this purpose the pyrolysis of mixtures of ethane and ethylene was studied in the temperature range 563 to 600 °C.

The pyrolysis of mixtures of ethane and ethylene at 600 °C has been studied by Silcocks (2). In several respects, such as the products formed and their relative importance, the present results are in agreement with the earlier work.

In the present work the rates of formation of the products were measured at an earlier stage of the reaction and this has allowed a clearer definition of the induction period and the changes observed in it on addition of ethane. Differences in interpretation can for the most part be attributed to this distinction.

Experimental

The apparatus, procedure, and analytical methods were identical with those described in Part I. The ethane and ethylene used were Phillips Research Grade, degassed at −196 °C. The trap-to-trap distillation *in vacuo* prior to each experiment, as described previously, was also made here. The reaction vessel used in all experiments was the quartz cylinder of 266.4 ml capacity with a surface/volume ratio of 1.0 cm^{-1}. Homogeneous gaseous mixtures of ethane and ethylene were obtained by condensing both gases in the central cold finger of the 1 l flask described in Part I. On warming, convection currents were generated and complete mixing occurred in a short time.

Results

Mixtures containing 15 cm ethylene and varying amounts of ethane (15–45 cm) were pyrolyzed at 563, 584, and 600 °C. Yields of the following products were measured as a function of time: *n*-butane, methane, hydrogen, propylene, butene, butadiene, propane, and benzene. Figures 1–5 show representative yield–time plots for the main products, from which initial rates were obtained. Figure 6 shows the initial rates of the main products as a function of ethane pressure. The order of these rates with respect to ethane was determined by least squares analysis of log rate against log pressure curves. These orders are given in Table I.

In brief, the main effects of the addition of ethane upon the pyrolysis of ethylene may be summarized as follows: (1) The yields of *n*-butane, methane, and hydrogen, each considerably increased, were linear with time in the initial stages. The rates of each were first order with respect to ethane. (2) The initial rates of propylene and butene were scarcely affected, but the induction periods observed in both cases were markedly reduced, usually to the point when their existence was doubtful. (3) The initial rate

[1]Mines Branch, Department of Energy, Mines and Resources, Ottawa, Canada.

Can. J. Chem. Downloaded from www.nrcresearchpress.com by 84.22.46.98 on 09/08/12
For personal use only.

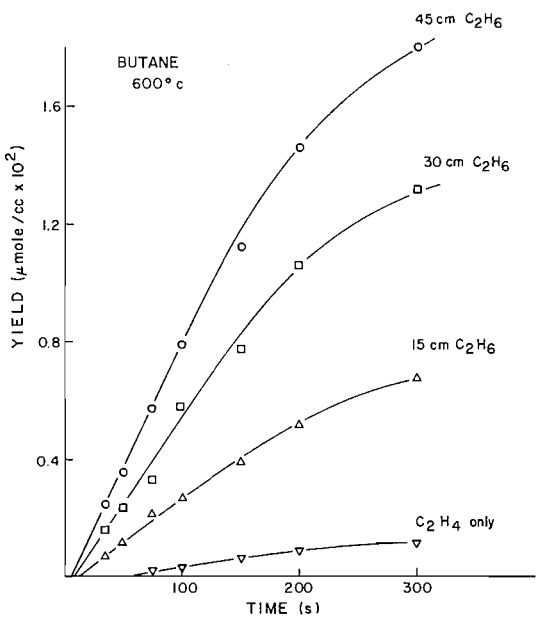

FIG. 1. Yield of butane as a function of time.

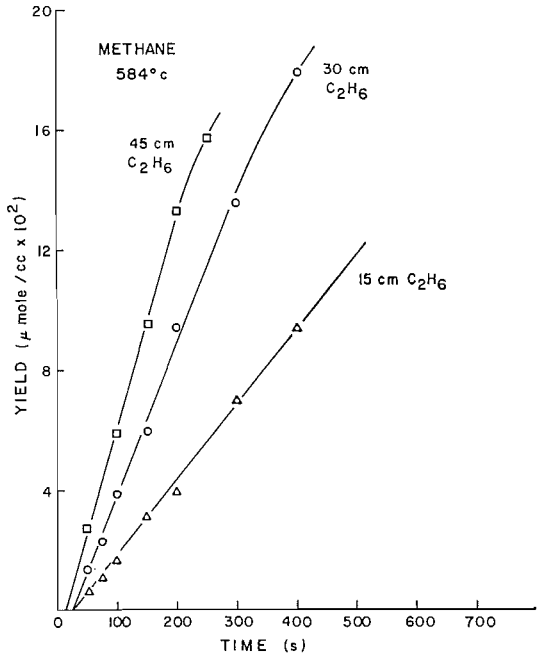

FIG. 2. Yield of methane as a function of time.

of formation of butadiene was inversely proportional to the concentration of ethane.

The yield plots for butane and methane suggested a small induction period, but since it was less than 20 s its existence is questionable. The rate of production of propylene as a function of temperature is shown in Fig. 7 along with the rates obtained in the absence of ethane. A similar plot was obtained for the rate of formation of butene. Ethane clearly has a negligible effect on the rates of production of propylene and butene.

Secondary Products

The shape of the yield–time plots for propane and benzene were unchanged upon addition of ethane and in both cases the yields were not appreciably altered. The propane yield increased from zero time whereas benzene appeared to rise from the end of the induction period.

Discussion

The Initiation Step

One of the objects in the study of the mixtures of ethane and ethylene was a search for the occurrence of the bimolecular initiation step

[1] $$C_2H_4 + C_2H_6 \rightarrow C_2H_5 + C_2H_5$$

analogous to that suggested in the pyrolysis of ethylene alone,

[2] $$C_2H_4 + C_2H_4 \rightarrow C_2H_3 + C_2H_5.$$

A third reaction which it is necessary to consider is the dissociation of ethane.

[3] $$C_2H_6 \rightarrow 2\,CH_3.$$

TABLE I

Activation energies and order with respect to ethane of the initial rates

Temperature (°C)	Butane	Methane	Hydrogen	Propylene	Butene	Butadiene
563±1	1.0 ±.3	0.99±.16	0.85±.3	−0.31±.05	0.18±.1	−1.4±.4
584±1	0.91±.1	0.94±.02	0.71±.06	0.10±.2	0.17±.2	
600±1	0.95±.1	0.87±.14	1.2±.3	0.14±.2	0.0±.1	0.77±.3
Activation energy	50±4	78±1	64±6	29±2	35±2	100±6

Can. J. Chem. Downloaded from www.nrcresearchpress.com by 84.22.46.98 on 09/08/12
For personal use only.

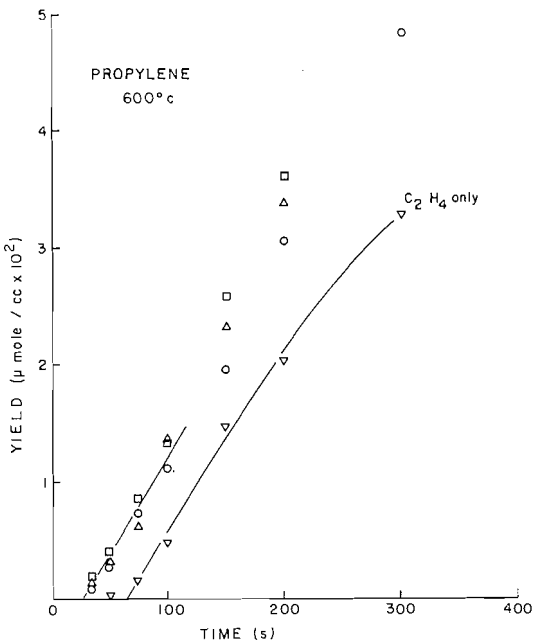

FIG. 3. Yield of propylene as a function of time: (○) 15 cm C_2H_6; (△) 30 cm C_2H_6; (□) 45 cm C_2H_6.

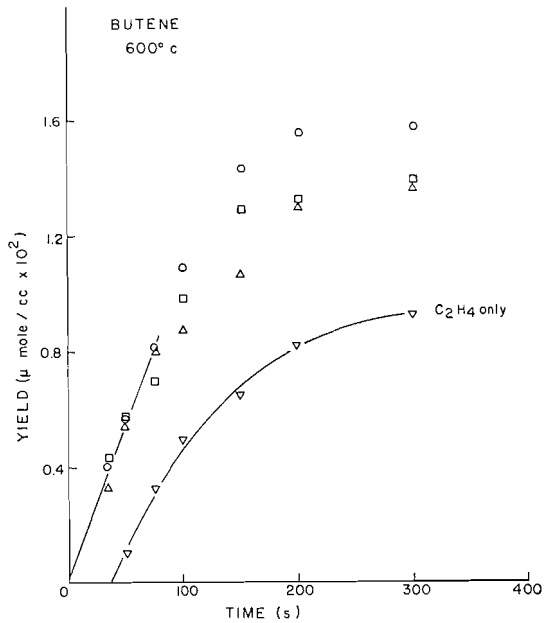

FIG. 4. Yield of butene as a function of time: (△) 15 cm C_2H_6; (□) 30 cm C_2H_6; (○) 45 cm C_2H_6.

A summary of the relevant rate parameters is given in Table II. The frequency factors and rate constants for reactions [1] and [2] have been calculated on the assumption that the rate constant for the reverse disproportionation of radicals is in both cases equal to 3×10^{12} cc mole^{-1} s^{-1} at 298 °K (3). For comparison, the general expressions for the rate constants have been obtained using data at 298 °K (4). The rate constant for reaction [3] has been discussed by Lin and Laidler (5). We use the following average value suggested by them,

$$k_3 = 3.2 \times 10^{16} e^{-88000/RT} s^{-1}.$$

The last column of Table II lists the rates for the three reactions for equal pressures of ethane and ethylene. Reactions [1] and [3] would therefore be expected to be the main initiation processes. Nevertheless the evidence from the measurement of the initial rates of formation of the main products is against the occurrence of these steps.

Initiation by reaction [1] and termination by mutual combination of radicals would give a radical concentration proportional to $[C_2H_4]^{1/2}$ $[C_2H_6]^{1/2}$. Initiation by reaction [3] and termination by mutual combination of radicals would give a radical concentration proportional to $[C_2H_6]^{1/2}$. If the products were then formed through a series of radical addition and abstraction reactions similar to those outlined in Part I, the order with respect to ethane of the rates of formation of these products should be either 0.5 or 1.5. None of the rates measured showed this dependence. The orders with respect to ethane of the rates of methane and butane were very close to one and were constant over the range of pressure and temperature studied. The rates of formation of propylene and butene were essentially independent of ethane concentration.

Since the activation energy for reaction [3] is 22 kcal/mole greater than that for reaction [2], initiation by reaction [3] should raise the activation energy for the rates of formation of the products by about 11 kcal/mole, assuming the activation energy for the propagation steps remains the same. This was not observed for any of the products. The activation energy for butene and propylene was unchanged while that for butane decreased by about 20 kcal/mole. We conclude, therefore, that in the mixtures of ethane and ethylene, ethane is not involved in the initiation process.

The question remains of why reaction [2] appears to be the predominant initiation reaction. The measurements and the data pertaining

Can. J. Chem. Downloaded from www.nrcresearchpress.com by 84.22.46.98 on 09/08/12
For personal use only.

Can. J. Chem. Downloaded from www.nrcresearchpress.com by 84.22.46.98 on 09/08/12
For personal use only.

TABLE II

Thermodynamic data and reaction rate parameters

	S^0(298 °K)* (cal/deg mole)	Ref.	ΔH_f(298 °K) (kcal/mole)	Ref.	Reaction	ΔH(298 °K) (kcal/mole)	ΔS(298 °K)* (cal/deg mole)	log A (cc mole^{-1} s^{-1} or s^{-1})	K(857 °K) (cc mole^{-1} s^{-1} or s^{-1})	Rate at 857 °K (C_2H_4 = 15 cm) (mole cc^{-1} s^{-1} $\times 10^{12}$)
C_2H_4	52.45	4	12.5	4	1	59.7	11.28	14.95	0.51	4.03
C_2H_6	54.85	4	−20.2	4	2	64.0	10.69	14.82	0.030	0.237
C_2H_5	59.29	7	26	6	3			16.505	1.08×10^{-6}	3.03
C_2H_3	56.3	8	63	6						

*Standard state: 1 atm of ideal gas.

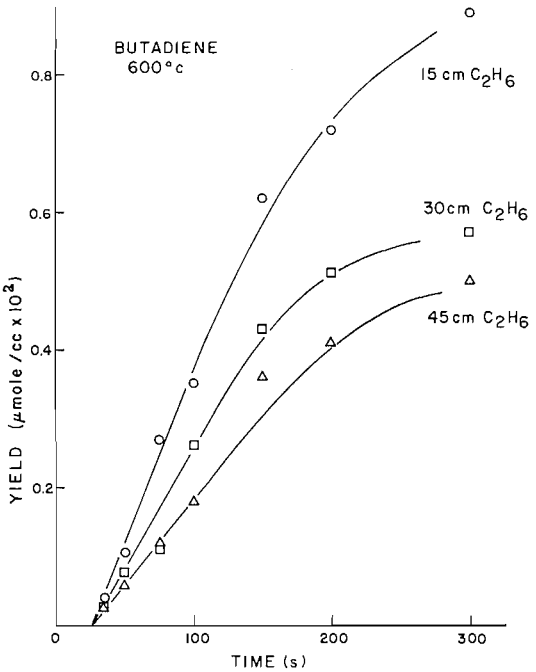

FIG. 5. Yield of butadiene as a function of time.

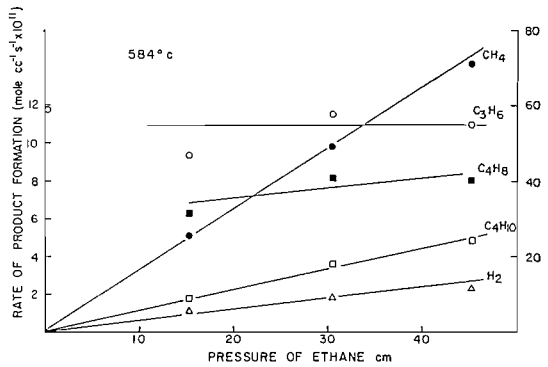

FIG. 6. Rate of product formation as a function of ethane pressure. Left-hand scale applies to all products except methane. Right-hand scale applies to methane.

to reactions [1] and [3] are the most reliable and the simplest explanation lies in the possibility of errors in the thermodynamic data used to calculate k_2. The most uncertain quantities are those of the vinyl radical. An error of 5 kcal/mole in the heat of formation of the vinyl radical would raise k_2 to the same value as k_1 at 857 °K. This would, however, require a C—H bond dissociation energy in ethylene 5 kcal/mole lower than the current value of 103 kcal/mole (9, 10). Less uncertainty is probably involved in the entropy of the vinyl radical but a combination of errors in both quantities might change k_2 considerably. Another uncertainty is the reverse radical disproportion rate constants. k_{-2} could be greater than k_{-1} by a factor of about 5 or 10 (11, 12). It thus appears probable that k_2 has been underestimated.

The Mechanism

The proposed mechanism may be briefly summarized in general terms. The presence of ethane provides a more readily abstractable hydrogen atom than is available from ethylene. The polymer will tend to be more saturated and probably of a shorter length. More radicals may be diverted into lower molecular weight products by abstraction from ethane which may now compete successfully with addition to ethylene. It is suggested, in fact, that the four main products, butane, methane, butene, and propylene, arise during the polymerization by abstraction of hydrogen from ethane by the corresponding radical. In the case of the unsaturated radicals, C_4H_7 and C_3H_5, this abstraction process must be faster than the addition to ethylene, since the rate of formation of butene and propylene is essentially independent of ethane concentration. The rates of formation of butene and propylene will then be practically unchanged from the rates observed in pure ethylene. In the latter system the rates of formation of butene and propylene were essentially the rate of propagation of the free radical polymerization,

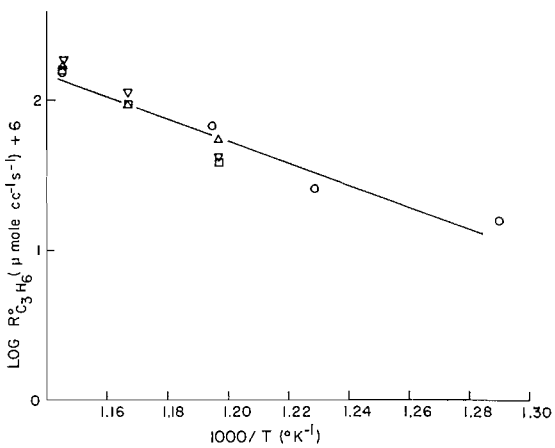

FIG. 7. Arrhenius plot of the rate of propylene formation. Pressure of ethylene = 15 cm. Pressure of ethane: (○) 0 cm; (△) 15 cm; (▽) 30 cm; (□) 45 cm.

Can. J. Chem. Downloaded from www.nrcresearchpress.com by 84.22.46.98 on 09/08/12
For personal use only.

since after the induction period the rate of decomposition of the polymer was equal to its rate of formation. In the mixtures of ethane and ethylene the radical abstraction reaction will be comparable to the rate of propagation of the free radical polymerization. However, since the abstraction occurs during the polymerization process no induction period will be observed.

In the case of methane and butane it must be assumed that the abstraction from ethane by the saturated radical is slow compared with the addition to ethylene in order to give the first order dependence on ethane. The *n*-butyl radical is probably formed largely by addition of ethyl radicals to ethylene, since the activation energy for butane formation is close to that for butene and propylene. The methyl radical, on the other hand, probably arises from decomposition of radicals formed during the polymerization, since the activation energy for methane formation is large. The rate of methane formation is greatly increased in the mixtures and it may be that the saturated polymer radical tends to lose a methyl group more readily than the unsaturated polymer formed in pure ethylene. Since the rates of methane and propylene are not equal, decomposition of the *n*-butyl radical is not an important source of methyl radicals.

The characteristics of the rate of formation of butadiene were rather different from the other products and it is suggested that the mechanism for formation of butadiene in the mixtures is the same as in pure ethylene. The negative order with respect to ethane is accounted for by reaction of its precursor radical with ethane to form products other than butadiene.

A summary of the most probable reactions is presented as a guide but is not intended to be comprehensive. For simplicity the termination step is again taken as the combination of ethyl radicals. The general term R denotes any radical higher than C_4 and R′ represents an unsaturated polymer molecule.

[2] $C_2H_4 + C_2H_4 \rightarrow C_2H_3 + C_2H_5$

[4] $C_2H_3 + C_2H_4 \rightarrow C_4H_7$

[5] $C_2H_3 + C_2H_6 \rightarrow C_2H_4 + C_2H_5$

[6] $C_2H_5 + C_2H_4 \rightarrow C_4H_9$

[7] $C_2H_5 + C_2H_4 \rightarrow C_2H_6 + C_2H_3$

[8] $C_4H_7 + C_2H_4 \rightarrow R$

[9] $C_4H_7 + C_2H_6 \rightarrow C_4H_8 + C_2H_5$

[10] $C_4H_9 + C_2H_4 \rightarrow R$

[11] $C_4H_9 + C_2H_6 \rightarrow C_4H_{10} + C_2H_5$

[12] $R \rightarrow CH_3 + R$

[13] $CH_3 + C_2H_4 \rightarrow C_3H_7$

[14] $CH_3 + C_2H_6 \rightarrow CH_4 + C_2H_5$

[15] $R + C_2H_6 \rightarrow RH + C_2H_5$

[16] $R + C_2H_4 \rightarrow R' + C_2H_5$

[t] $2C_2H_5 \rightarrow C_4H_{10}$

Making the assumptions already discussed, the radical concentrations may be expressed as follows,

$$[C_2H_5] = (k_2/k_t)^{1/2}[C_2H_4]$$

$$[C_2H_3] = \frac{k_7}{k_4}[C_2H_5]$$

$$[C_4H_7] = \frac{k_4[C_2H_3][C_2H_4]}{k_9[C_2H_6]}$$

$$[C_4H_9] = \frac{k_6}{k_{10}}[C_2H_5]$$

$$[CH_3] = \frac{k_{12}k_5[C_2H_5]}{k_{13}(k_{15}[C_2H_6] + k_{16}[C_2H_4] + k_{12})},$$

and the steady state expressions for the rates of formation of products are then given as

$$R_{C_4H_8} = k_7(k_2/k_t)^{1/2}[C_2H_4]^2$$

$$R_{C_4H_{10}} = \frac{k_{11}k_6}{k_9}(k_2/k_t)^{1/2}[C_2H_4][C_2H_6]$$

$$R_{CH_4} = \frac{k_{14}k_{12}k_5}{k_{13}}(k_2/k_t)^{1/2}[C_2H_4][C_2H_6].$$

The activation energy for butene will thus be close to that observed in pure ethylene. The activation energy for butane will be similar to that for butene while the activation energy for methane may be much larger because of reaction [12], the decomposition of the polymer radical.

The weaknesses of the assumptions necessary to account for the orders of the rates with respect to ethane are apparent. The results, however, are not easy to tie together in a consistent mechanism. The disappearance of the induction period is the fact which suggests the products are formed during the free radical polymerization. Otherwise a change in the induction period must arise by a change in k_d, the composite rate

Can. J. Chem. Downloaded from www.nrcresearchpress.com by 84.22.46.98 on 09/08/12
For personal use only.

constant for decomposition of the polymer, or by participation of ethane in the decomposition process. This may be seen from the equation given in Part I for the concentration of polymer as a function of time.

$$[\mathrm{I}] = \frac{k_\mathrm{f}}{k_\mathrm{d}}[\mathrm{C_2H_4}][1 - \mathrm{e}^{-k_\mathrm{d}[\mathrm{C_2H_4}]t}]$$

Although it was suggested in Part I that decomposition of the polymer did involve reaction with ethylene, reaction with ethane is much less likely. An increase in k_d, due possibly to the larger degree of saturation of the polymer formed in the presence of ethane, is an alternative explanation. This in fact may be a more reasonable mechanism for the formation of propylene, since the induction period for this product did not disappear entirely as it did for butene. There is, however, a further difficulty in suggesting a change in k_d. The rates of butene and propylene were essentially unchanged in the mixtures, but a decrease in k_d would lower the steady state concentration of polymer I and hence lower the rate of formation of product which arises from its decomposition.

Acknowledgments

The authors wish to thank the National Research Council of Canada and the Department of University Affairs of the Province of Ontario for financial support. M. L. B. thanks Dr. J. Convey, Director of the Mines Branch, for the opportunity to participate in this work.

1. M. L. Boyd, T-M. Wu, and M. H. Back. Can. J. Chem. This issue.
2. C. G. Silcocks. Proc. Roy. Soc. London, Ser. A, **233**, 465 (1956).
3. A. Shepp and K. O. Kutschke. J. Chem. Phys. **26**, 1020 (1957).
4. Selected values of physical and thermodynamic properties of hydrocarbons. American Petroleum Institute Research Project. Carnegie Press, Carnegie Inst. of Technology, Pittsburgh 13. 1953.
5. M. C. Lin and K. J. Laidler. Trans. Faraday Soc. **64**, 79 (1968).
6. S. W. Benson. J. Chem. Educ. **42**, 502 (1965).
7. J. H. Purnell and C. P. Quinn. J. Chem. Soc. 4049 (1964).
8. S. W. Benson and G. R. Haugen. Private communication.
9. A. G. Harrison and F. P. Lossing. J. Am. Chem. Soc. **82**, 519 (1960).
10. A. F. Trotman-Dickenson and G. J. O. Verbeke. J. Chem. Soc. 2580 (1961).
11. A. G. Sherwood and H. E. Gunning. J. Phys. Chem. **69**, 2323 (1965).
12. N. A. Weir. J. Chem. Soc. 6870 (1965).

Can. J. Chem. Downloaded from www.nrcresearchpress.com by 84.22.46.98 on 09/08/12
For personal use only.

Can. J. Chem. Downloaded from www.nrcresearchpress.com by 210.87.254.42 on 09/05/12
For personal use only.

Reactions of triplet methylene radicals with alkanes[1]

D. F. RING[2] AND B. S. RABINOVITCH
Department of Chemistry, University of Washington, Seattle, Washington, 98105

Received December 21, 1967

Studies have been made of the products resulting from reaction between triplet methylene and several alkanes, propane, *n*-butane, and isobutane. Triplet methylene was produced by photolysis of diazomethane in the presence of a large excess of inert nitrogen gas. Complicating side reactions involving diazomethane were encountered.

Observation of higher products allowed the determination of the relative rates of 1°:2°:3° H abstraction from C—H bonds; these are ~ 1:14:150. The rate of addition of $^3CH_2$ to the C=C bond in ethylene appears to proceed ~ 3.5 times faster than H abstraction from a 3° C—H bond. The possible occurrence of insertion by $^3CH_2$ into C—H bonds is discussed and relative rates of insertion for 1°:2°:3° bonds are deduced to be ~ 1:2:7. Comparisons of the relative rates of insertion:abstraction are also given. Studies with propane-d_6 indicated an isotope effect for abstraction of H:D from the 1° position of ~ 3.9; insertion by $^3CH_2$ into the same position showed an isotope effect of ~ 2.

Canadian Journal of Chemistry, **46**, 2435 (1968)

Introduction

Methylene chemical activation systems have been used for the quantitative study of the collisional deactivation and unimolecular reactions of vibrationally excited molecules (1). In this and other connections it is of importance to clarify the chemical characteristics of methylene systems.[3] It has been the hallmark of such systems that new data has frequently occasioned reinterpretation of the old. An ever-increasing list of properties has been assigned to methylene. Singlet methylene ($^1CH_2$) appears to insert nearly statistically into C—H bonds (2), and possibly into C—O bonds (3), and to add stereospecifically to C=C bonds (1*a*, 4). It has also been suggested that in some systems $^1CH_2$ may abstract H from a C—H bond (5). Triplet methylene ($^3CH_2$) is now known to abstract H from C—H bonds (2*c*, 2*d*, 6), may insert into these (7), and also adds non-stereospecifically to C=C bonds (1*a*, 4*b*, 8). The present study was undertaken in order to elucidate the interactions between $^3CH_2$ and the various C—H bonds in alkanes and to conduct a gas phase investigation of these interactions in a chemical environment in which the C=C competition is absent.

The mechanism for the production of singlet and triplet methylene on photolysis of diazomethane and ketene is still open to speculation (9, 10). The mechanisms of photolysis are of no concern for the systems which are studied here in the presence of a large excess of inert gas. No matter which state of methylene is preferentially formed on photolysis, the inert gas brings about collisional deactivation to the triplet ground state (11).

Since this work was completed, Ho and Noyes (12) have published results on the reaction of methylene with propane in systems that were preponderantly triplet in nature.[4]

Experimental

Materials

Propane and isobutane were Matheson instrument grade; *n*-butane was Matheson C.P. grade. These gases were further purified by gas chromatography so that no reaction products were present.

Ethylene (Phillips research grade) was used without further purification.

Diazomethane (DM) was prepared by the reaction between N-nitrosomethylurea and 12 *M* KOH and was purified by trap-to-trap distillation (−78 °C to −196 °C);

[1]This work was supported by the Office of Naval Research. Abstracted in part from the Ph.D. Thesis of David F. Ring.

[2]Present address: Division of Applied Chemistry, National Research Council of Canada, Ottawa, Canada.

[3]Carr reported that insertion by $^1CH_2$ (ketene source) was non-statistical and that CH_2 inserted into 1°:2°:3° CH bonds of isopentane at ~ 1:1.3:1.5 (radicals were removed by O_2); for $^3CH_2$ abstraction he listed ~ 1:1.5:9. Herzog and Carr found no difference between relative rates of insertion by $^1CH_2$ from DM and from ketene, though $^3CH_2$ from DM appeared to be less discriminatory. However, Halberstadt and McNesby reported nearly indiscriminate insertion by $^1CH_2$ when NO was employed to scavenge radicals. In ref. 2*c*, it is pointed out that a correction to singlet insertion due to triplet abstraction in a propane system gave back nearly statistical ratios.

[4]An example of variation of $^3CH_2$ concentration, either with change in photolyzing wavelength or with addition of a photosensitizing agent, for systems in which the production of $^3CH_2$ is important, has been studied by Ho and Noyes. We appreciate the favor of a preprint of this work.

Can. J. Chem. Downloaded from www.nrcresearchpress.com by 210.87.254.42 on 09/05/12
For personal use only.

TABLE I

Experimental conditions and major product ratios for propane + $^3CH_2$

System	Propane / DM	N_2 / propane	C_2H_4 / propane	O_2 / propane	Press. (atm)	Temp. (°C)	Radiation	iB / nB	iP / nP	DMB / 2MP	DMB / iP	2MP / iP	iB / DMB	nB / 2MP	iB / iP	nB / nP
1[a]	6.9	814	0.0	0.0	1.6	23	4358 Å	1.11	3.45	1.72	0.57	1.16	15.1	22.8	8.60	26.5
2[b]	68	800	0.0	0.0	3.0	23	4358 Å	1.48	3.66	2.22	2.07	3.45	4.80	7.17	9.94	24.8
3[c]	68	800	0.0	0.0	3.0	23	4358 Å	1.74	12.30	9.73	1.37	1.73	5.76	32.2	7.90	55.5
4	68	800	0.0	0.0	2.9	−12	Unfiltered	1.97	3.44	2.82	1.54	1.87	8.85	12.6	13.7	23.6
5	62	800	0.0	0.0	2.8	−20	Unfiltered	2.26	3.47	3.07	1.66	1.87	10.9	14.8	18.1	27.6
6	6.7	800	0.10	0.0	1.6	23	4358 Å	1.04	3.72	1.30	0.44	1.24	12.3	15.5	5.4	19.2
7	7.3	728	0.18	0.0	1.6	23	4358 Å	0.97	4.03	1.74	0.42	0.97	12.8	22.9	5.37	22.2
8	6.0	890	0.33	0.0	1.6	23	4358 Å	0.77	3.52	1.78	0.20	0.39	17.4	40.2	3.48	16.4
9	7.3	728	0.18	0.0	1.6	0	4358 Å	0.88	2.54	1.40	0.33	0.61	22.4	35.4	7.47	21.6
10	7.3	728	0.18	0.0	1.6	−50	4358 Å	0.67	2.59	1.43	0.16	0.29	99.5	212	16.0	44.3
11[d]	31	800	0.0	5.51	3.0	23	4358 Å	0.50 (1.50)[f]								
12	6.0[e]	1110	0.0	0.0	2.0	23	Unfiltered	1.55								

[a]Ratios are averages of six experiments, all of nearly the same pressure and dilution.
[b]Ratios are averages of two experiments.
[c]Propane-d_6 was used in this experiment.
[d]An average of three experiments; no products above C_4 were formed in the presence of O_2.
[e]Ketene, not DM, was used as the methylene precursor in this experiment. Complete product analysis was not obtained.
[f]Parenthetic number is ratio per bond.

TABLE II

Relative variation of major and minor products for propane + $^3CH_2$ with change in experimental conditions

	iB	iB	iB	iB	iB	iB	iB
System[a]	▽	B1	3MB1	14P	P1	2MB2	4MP1
1	5.30	0.55	15.06	6.56	4.62	7.63	4.81
2	44.2	5.16	26.0	140	38.5	119	12.8
3	28.2	4.44	26.8	119	30.4	[b]	11.6
5	33.4	4.80	21.6	84.4	150	[b]	30.0
7	1.05	0.52	17.8	7.44	1.96	7.58	3.78
10	1.17	0.30	13.5	4.57	3.31	4.36	14.7
	iP	iP	iP	iP	iP	iP	iP
System[a]	▽	B1	3MB1	14P	P1	2MB2	4MP1
1	0.74	0.07	1.88	0.86	0.56	0.95	0.60
2	4.44	0.52	2.62	14.2	3.88	12.10	1.29
3	3.57	0.50	3.39	15.1	3.85	[b]	1.47
5	1.44	0.21	1.20	4.68	8.35	[b]	1.66
7	0.21	0.10	3.44	1.44	0.38	1.46	0.73
10	0.14	0.04	1.53	0.52	0.38	0.49	1.66
	DMB	DMB	DMB	DMB	DMB	DMB	DMB
System[a]	▽	B1	3MB1	14P	P1	2MB2	4MP1
1	0.46	0.05	1.19	0.54	0.36	0.60	0.38
2	9.19	1.08	5.43	29.4	8.03	25.14	2.68
3	4.89	0.69	4.64	20.7	5.28	[b]	2.00
5	2.39	0.34	1.99	7.76	13.8	[b]	2.76
7	0.10	0.05	1.69	0.71	0.18	0.72	0.36
10	0.02	0.006	0.21	0.07	0.05	0.07	0.23

[a]For the same experiment(s) as listed in Table I. See Table I for experimental conditions.
[b]No 2MB2 was observed.

the diazomethane was stored in a dibutylphthalate matrix at −196 °C. Upon warming of the dibutylphthalate–diazomethane solution, the initial gas fractions were discarded in order to eliminate low boiling impurities (ethane or ethylene). At no time was the diazomethane exposed to light. Ketene (K) was prepared by the decomposition of acetone on a hot wire; it was purified by trap-to-trap distillation and by gas chromatography on a Fluoropak column at −78 °C and stored at −196 °C.

Nitrogen (Airco purified N_2) was employed as the inert gas in these systems. It was passed through a copper-packed tube at 400 ° and then through two liquid nitrogen traps to remove oxygen and other impurities.

Apparatus and Procedure

A standard greaseless gas-handling system was employed. The diazomethane was measured out in a well-seasoned (with diazomethane) standard volume which was kept isolated from the rest of the system.

A diazomethane-seasoned 1 l pyrex bulb was used as the reactor for all experiments; it was pumped to $< 10^{-4}$ mm prior to loading with reactants. Several ratios of reactants were used; N_2:alkane ranged between the extremes 728:1 to 2000:1 while alkane:DM (or K) varied from 6:1 to 110:1. Systematic variation of the product yields with pressure was not a primary concern of this study, but the reaction pressures ranged in any case from a minimum of 1.6 atm to a maximum of 4.0 atm. In several experiments carbon monoxide and/or oxygen was added to the reaction mixture; the CO:alkane ratio employed was 10:1 while O_2:alkane was varied from 4:1 to 8:1. The light source for photolysis of DM was a GE AH-6 high pressure mercury arc. Two light filters (Dow-Corning No. 5543 and No. 3389) housed in a Pyrex water-cooled jacket were used; the wavelength issuing from this combination was centered at 4358 Å. Ketene was photolyzed by means of the unfiltered radiation from the AH-6. Photolysis times for DM or K runs were usually 1 to 3 h.

Analysis

Reaction products were usually divided and analyzed by gas chromatography on two instruments; one employed a standard thermistor detector, the other a flame detector. Several chromatographic columns were utilized. They were a 300 ft squalane capillary; a 35 ft 40% mineral oil on Chromosorb-P column; a 20 ft $AgNO_3$ – ethylene glycol on firebrick column in series with a 10 ft 40% mineral oil on Chromosorb-P column; and an 8 ft 15% hexamethylphosphoramide on Chromosorb-P column. These columns resolved all compounds of interest. Most products were identified with authentic samples.

Can. J. Chem. Downloaded from www.nrcresearchpress.com by 210.87.254.42 on 09/05/12
For personal use only.

Can. J. Chem. Downloaded from www.nrcresearchpress.com by 210.87.254.42 on 09/05/12
For personal use only.

Results

Nitrogen Dilution

Earlier results have shown that generation of CH_2 in a gas mixture in which the ratio N_2:*cis*-butene was > 1200:1 effectively produced a 100% $^3CH_2$ reaction system. In the present alkane systems a lower dilution of substrate, N_2:alkane = 750:1, was found adequate because the insertion of $^1CH_2$ into C—H bonds is approximately 8 times slower than addition to the C=C. Experiments in which the dilution was increased to 1500:1 resulted in no significant change in the product ratios.

Propane

The following principal products which were formed in the propane–$^3CH_2$ reaction system are most directly linked to the initial products of reaction: ethane, isobutane (iB), *n*-butane (nB), isopentane (iP), *n*-pentane (nP), 2,3-dimethylbutane (DMB), 2-methylpentane (2MP), and *n*-hexane (nH); the latter compound was only produced in small amount. The experimental conditions and various product ratios are shown in Tables I and II.[5]

Additional secondary or minor compounds observed were ethylene, cyclopropane (∇), butene-1 (B1), 3-methylbutene-1 (3MB1), 1,4-pentadiene (14P), pentene-1 (P1), 2-methylbutene-2 (2MB2), 4-methylpentene-1 (4MP1), and 4-methyl-*trans*-pentene-2 (4MP2). The identity of the latter two compounds is still open to question. All of these products were reduced drastically in amount relative to the "principal" C_4, C_5, and C_6 alkane products upon increase of the propane/DM ratio by a factor of 10. However, not all of them decreased by the same factor; the following is the sequence for relative decrease in yield: 14P > 2MB2 > P1 $\cong$ B1 > ∇ > 4MB1 $\gtrsim$ 3MB1. The first two compounds in this series decreased by a factor of about 20, the next three by about 8, and the last two by a factor of around 2; we will return to this matter in the Discussion. The relative change in ethane and ethylene yields was not determined. However, in early experiments ethylene was found to be more than 5 times as abundant as ethane and nearly 3 times as abundant as isobutane.

The relative amounts of some of the minor products with respect to the principal alkane products are given in Table II for all the experimental conditions.[5]

Seven other compounds were observed in this system. Four of these were trace components; two (*cis*-pentene-2 and hexene-1) were very minor (nearly as abundant as nP); the seventh compound, an unidentified C_6, or C_7 compound, was 3 times as abundant as nP. These compounds also decreased in relative abundance upon increase of the ratio propane/DM: four trace compounds were completely eliminated, the two minor products decreased by a factor of 10–15, and the seventh unidentified compound fell in relative amount by more than a factor of 100. It is evident that the formation of many secondary products depends intimately on the proportions of DM present and that side reactions which increase the complexity of the system may be greatly reduced by high ratios of propane/DM.

n-Butane

The reaction between *n*-butane and $^3CH_2$ produced as the primary products, ethane, iP, nP, 3-methylpentane (3MP), nH, 3,4-dimethylhexane (DMH), 3-methylheptane (3MH), and *n*-octane (the latter compound was produced in very small amounts). Tables III and IV[5] exhibit ratios of products and list the experimental conditions under which they were obtained.

Secondary and (usually) minor compounds observed were ethylene, propane, propylene, $\tilde{\nabla}$, B1, *cis*-butene-2 (CB2), *trans*-butene-2 (TB2), 14P, P1, and 1,5-hexadiene (15H). The result of the increase of the *n*-butane/DM ratio upon the minor compounds relative to the main alkane products is shown in Table IV[5]. The relative amount of decrease among these products is C_2H_4 (by a factor of 6) > C_3H_6 > ∇ > B1 > C_3H_8 > C_2H_6 > CB2 > TB2 (virtually unchanged). Ten other compounds were also observed at low ratios (7:1) of *n*-butane/DM; upon increase of this ratio to at least 30:1 the yield of eight of these (one of them was *n*-heptane), as well as the yield of 14P, P1, and 15H, decreased to nearly zero while one of the compounds (2-methylbutene-2) fell by a factor of $\sim$ 5 and the other (3-methylhexane) decreased by about 2/3.

Isobutane

The principal products from the reaction between isobutane and $^3CH_2$ were ethane, neopentane (neP), iP, 2,2-dimethylbutane (22DMB),

[5]The ratios in this table are derived from experimentally observed product amounts. These represent original data, before correction as described in the text.

Can. J. Chem. Downloaded from www.nrcresearchpress.com by 210.87.254.42 on 09/05/12
For personal use only.

2-methylpentane (2MP), 2,2,3,3-tetramethylbutane (TMB), 2,2,4-trimethylpentane (TMP), and 2,5-dimethylhexane. The latter compound was present in very small amount. Experimental conditions and ratios of these products are given in Tables V and VI.[5] *n*-Butane could not be determined in the presence of swamping amounts of isobutane.

Several additional products were formed. They were ethylene, propane, propylene, B1, isobutene (iBene), 14P, and P1. Table VI[5] gives various ratios of these products. Nearly 20 additional compounds (ranging from C_5 to C_8) were found at minimum ratio of isobutane/DM; of these only five persisted upon increase of the ratio by a factor of 6; of the remaining five, three (2 unidentified and 2-methylhexane) had fallen to about 1/20 of their previous level of abundance, one (3,3-dimethylbutene-1) fell by a factor of $\sim$ 5, and one (2,2-dimethylpentane) decreased to 1/3 of its previous level.

The complexity of these systems in the presence of high levels of DM is thus reemphasized.

Discussion

Reaction Scheme

The photolysis of diazomethane in the presence of excess nitrogen may be written as (11):

$$[I] \qquad DM + h\nu \xrightarrow{\text{excess } N_2} {}^3CH_2 + N_2.$$

Primary reaction of $^3CH_2$ with an alkane may be represented by

$$[1] \qquad {}^3CH_2 + RH \rightarrow \cdot CH_3 + \cdot R \quad \text{(primary H abstraction)}$$

$$[2] \qquad \rightarrow \cdot CH_3 + \cdot R' \quad \text{(secondary or tertiary H abstraction)}$$

$$[3] \qquad \rightarrow RCH_3^* \quad \text{(primary insertion)}$$

$$[4] \qquad \rightarrow R'CH_3^* \quad \text{(secondary or tertiary insertion).}$$

The excited, (*), species in [3] and [4] are assumed to be collisionally stabilized at these reaction pressures, which were at least 1.6 atm. Subsequent combination reactions of the initial radical species are

$$[5] \qquad 2\cdot R \rightarrow R_2$$

$$[6] \qquad 2\cdot R' \rightarrow R_2'$$

$$[7] \qquad \cdot R + R' \rightarrow RR'$$

$$[8] \qquad 2\cdot CH_3 \rightarrow C_2H_6$$

$$[9] \qquad \cdot CH_3 + \cdot R \rightarrow RCH_3$$

$$[10] \qquad \cdot CH_3 + \cdot R' \rightarrow R'CH_3.$$

Ethyl radicals are formed in these systems; they undergo the following combinations.

$$[11] \qquad 2C_2H_5\cdot \rightarrow n\text{-}C_4H_{10}$$

$$[12] \qquad \cdot CH_3 + C_2H_5\cdot \rightarrow C_3H_8$$

$$[13] \qquad C_2H_5\cdot + \cdot R \rightarrow RC_2H_5$$

$$[14] \qquad C_2H_5\cdot + \cdot R' \rightarrow R'C_2H_5$$

Disproportionation can occur among the radical species,

$$[15] \qquad \cdot CH_3 + \cdot R \rightarrow CH_4 + O$$

$$[16] \qquad \cdot CH_3 + \cdot R' \rightarrow CH_4 + O',$$

where O and O′ may or may not be the same olefin. For example, for $\cdot R = n$-butyl, O′ could be either butene-1 or butene-2.

$$[17] \qquad \cdot CH_3 + C_2H_5\cdot \rightarrow CH_4 + C_2H_4$$

$$[18a] \qquad C_2H_5\cdot + \cdot R \rightarrow C_2H_6 + O$$

$$[18b] \qquad \rightarrow C_2H_4 + RH$$

$$[19a] \qquad C_2H_5\cdot + \cdot R' \rightarrow C_2H_6 + O'$$

$$[19b] \qquad \rightarrow C_2H_4 + RH$$

$$[20] \qquad 2C_2H_5\cdot \rightarrow C_2H_4 + C_2H_6$$

$$[21] \qquad 2\cdot R \rightarrow RH + O$$

$$[22] \qquad 2\cdot R' \rightarrow RH + O'$$

$$[23a] \qquad \cdot R + \cdot R' \rightarrow RH + O'$$

$$[23b] \qquad \rightarrow O + RH$$

Insertion Reactions

Reactions [3] and [4] account for a common feature which was observed in all systems: with a substrate of carbon number n, more of the next higher C_{n+1} alkane products were found than could be accounted for by conventional radical processes. The major alkane products for each system may be grouped into three classes, C_{n+1}, C_{n+2}, and C_{2n}. For example, in the propane system these were *n*-butane and isobutane (C_{n+1}), *n*-pentane and isopentane (C_{n+2}), and 2,3-dimethylbutane, 2 methylpentane, and *n*-hexane (C_{2n}). A comparison in each alkane system of the ratio of the total amount of radicals formed, $(\cdot R')/(\cdot R)$ (based on reactions [5]–[7], [13], [14], disproportionation being taken into account) revealed reasonable agreement between the ratios from classes C_{n+2} and C_{2n}. However, the C_{n+1} class indicated a different (smaller) $(\cdot R')/(\cdot R)$ ratio. There appeared to exist an additional source of the C_{n+1} products

Can. J. Chem. Downloaded from www.nrcresearchpress.com by 210.87.254.42 on 09/05/12
For personal use only.

TABLE III

Experimental conditions and major product ratios for *n*-butane + $^3CH_2$

System	nB/DM	N_2/nB	C_2H_4/nB	O_2/nB	Press. (atm)	Temp. (°C)	Radiation	iP/nP	3MP/nH	DMH/3MH	DMH/3MP	3MH/nH	iP/DMH	nP/3MH	iP/3MP	nP/nH
13[a]	7.1	837	0.0	0.0	1.6	23	4358 Å	2.89	7.89	3.68	1.00	2.13	8.38	10.6	8.38	22.6
14	31	800	0.0	0.0	2.0	23	4358 Å	3.76	9.65	3.22	2.06	6.16	4.80	4.11	9.89	25.3
15	50	800	0.0	0.0	2.0	23	4358 Å	3.44	14.50	3.31	2.76	12.1	3.74	3.56	10.3	43.1
16	62	800	0.0	0.0	2.0	23	4358 Å	2.81	9.43	3.12	3.87	11.7	3.90	4.32	15.1	50.5
17	94	800	0.0	0.0	3.0	23	4358 Å	3.00	5.83	3.59	7.18	11.6	3.32	3.66	23.8	42.4
18	110	800	0.0	0.0	3.5	23	4358 Å	3.67	11.70	3.74	4.22	13.2	3.66	3.74	15.4	49.4
19	50	800	0.0	0.0	2.9	0	Unfiltered	3.81	11.53	2.75	2.19	9.18	7.01	5.06	15.4	46.4
20	50	800	0.0	0.0	2.8	−20	Unfiltered	4.34	19.35	4.41	2.56	11.2	8.27	8.42	21.2	94.4
21	6.2	855	0.123	0.0	1.6	23	4358 Å	2.63	7.64	3.21	0.47	1.11	11.1	13.6	5.22	15.1
22	6.7	800	0.20	0.0	1.6	23	4358 Å	2.39	9.46	4.70	0.37	0.74	20.8	41.2	7.70	30.5
23[b]	31	800	0.0	4.14	3.0	23	4358 Å	0.89[c] (1.34)[d]								
24[b]	27	1200	0.0	9.9	2.5	−20	Unfiltered	0.89[c] (1.33)[d]								
25[e]	31	800	0.0	4.0	3.0	23	4358 Å	0.83[c] (1.25)[d]								
26	60[f]	1000	0.0	0.0	1.8	23	Unfiltered	3.04								

[a]Ratios are averages of seven experiments performed under very similar conditions.
[b]An average of two experiments; no products above C_5 were formed in the presence of O_2.
[c]No products above C_5 were formed in the presence of O_2.
[d]The parenthetic number is the ratio of reaction per bond for the formation of the C_{n+1} compounds.
[e]Carbon monoxide was also present in this experiment; CO/nB was 9.5.
[f]An average of two experiments in which ketene, not DM, was used as the methylene precursor. Complete product analysis was not obtained.

TABLE IV

Relative variation of major and minor products for *n*-butane + $^3CH_2$ with change in experimental conditions

System	C_2H_4/C_2H_6	C_3H_6/C_3H_8	TB2/CB2
13[a]	4.02	1.17	3.80
14–18[b]	1.42	0.97	5.70
21–22[c]			

System	iP/C_2H_6	iP/C_3H_8	iP/TB2	iP/▽	iP/B1
13[a]	0.70	3.57	6.37	21.2	1.13
14–18[b]	1.11	7.07	4.22	70.7	3.04
21–22[c]				3.46	1.11

System	3MP/C_2H_6	3MP/C_3H_8	3MP/TB2	3MP/▽	3MP/B1
13[a]	0.09	0.48	0.86	3.08	0.16
14–18[b]	0.08	0.47	0.33	6.94	0.23
21–22[c]				0.59	0.18

System	DMH/C_2H_6	DMH/C_3H_8	DMH/TB2	DMH/▽	DMH/B1
13[a]	0.09	0.48	0.82	2.89	0.15
14–18[b]	0.29	1.91	1.07	17.1	0.76
21–22[c]				0.29	0.08

[a]These data concern the same experiments as in Table III.
[b]An average of system 14 through 18 in Table III. The average of *n*-butane/DM is ~ 70/1.
[c]An average of system 21 and 22 in Table III. C_2H_4, C_2H_6, C_3H_6, C_3H_8, TB2, or CB2 were not analyzed for in these experiments.

(especially of the least branched one); these were *n*-butane, *n*-pentane, and isopentane in the propane, *n*-butane, and isobutane systems, respectively. For several reasons (see *Results* and discussion below) the percent of $^1CH_2$ in each reaction system was very low and should not have been a significant source of these excess C_{n+1} products. It is postulated that $^3CH_2$ can insert into C—H bonds (or in any case that some processes occur which do not involve conventional long-lived radical intermediates). The quantitative treatment of the data on which this conclusion was based is described below but first we note that insertion by $^3CH_2$ into C—H bonds is not eliminated in oxygen experiments (Tables I, III, and V) in which C_{n+1} products were still formed although all C_{n+2} and C_{2n} products of conventional long-lived radical intermediates were eliminated. Furthermore, the ratio of these C_{n+1} products does not lend support to a statistical process such as insertion by $^1CH_2$; the secondary and tertiary positions are favored but not to so great an extent as abstraction. At −20 ° and 23 °, the average ratios of reactivity on a per bond basis were closely similar and were, for *n*-butane, 2 °/1 ° = 1.33, and for isobutane, 3 °/1 ° = 4.4. These ratios, however, differ somewhat from the normal relative rates of insertion in the absence of O_2 (given below), so that some complication exists which weakens, but by no means vitiates, our deductions. Relative to the normal yield, the yield of C_{n+1} products in the presence of oxygen were reduced, although more for the more-branched products (10–20% of normal yield) than for the less-branched product (30–60% of normal yield). Unfortunately, independent information on the extent to which oxygen might reduce the amount of products is not available.

Calculations

The data were treated as follows. The C_{2n} product, R_2', which was formed from $2\cdot R'$ was combined with an appropriate rate constant (k_6) to determine a number proportional to the steady-state concentration $\cdot R_{ss}'$ in the system. The RR′ product was then used with $\cdot R_{ss}'$ and an assumed value of k_7 to determine the relative steady-state concentration of $\cdot R_{ss}$. This ratio was in reasonable agreement with that determined independently from the ratio of the C_{n+2} products. The principal sources of methyl radicals were reactions [1] and [2]. It follows that the $\cdot CH_{3ss}$, $\cdot R_{ss}$, and $\cdot R_{ss}'$ radical concentrations in the reaction system are interrelated. A reasonable estimate of the relative steady-state concentration of $\cdot CH_3$ is given by the sum, $\cdot R_{ss}' + \cdot R_{ss}$; this estimate will be supported below. The amounts of the C_{n+1} products formed by reactions [9] and [10] were calculated with use of the values of $\cdot R_{ss}$, $(\cdot R' + \cdot R)_{ss}$, and k_9, and of $\cdot R_{ss}'$, $(\cdot R' + \cdot R)_{ss}$, and k_{10}. The excess amount of C_{n+1} is attributed to $^3CH_2$ insertion.

The relative rate of apparent insertion to abstraction at a particular reaction site was readily calculated from the total amount of $\cdot R'$ (or of $\cdot R$) produced in the system to the appropriate net insertion product. In the propane system the experimentally observed *n*-butane was corrected for an amount which arose via ethyl combination (reaction [11]). The relative amount of ethyl radical was determined from the amounts of C_{n+2} products in

Can. J. Chem. Downloaded from www.nrcresearchpress.com by 210.87.254.42 on 09/05/12
For personal use only.

Can. J. Chem. Downloaded from www.nrcresearchpress.com by 210.87.254.42 on 09/05/12
For personal use only.

TABLE V

Experimental conditions and major product ratios for isobutane + $^3CH_2$

System	iB/DM	N_2/iB	C_2H_4/iB	O_2/iB	Press. (atm)	Temp. (°C)	Radiation	neP/iP	22DMB/2MP	TMB/TMP	TMB/22DMB	TMB/2MP	neP/TMB	iP/TMP	neP/22DMB	iP/2MP
27[a]	7.4	774	0.0	0.0	1.7	23	4358 Å	1.69	5.16	4.50	1.59	1.82	6.02	16.0	9.57	29.1
28[a]	5.6	1560	0.0	0.0	2.0	23	4358 Å	2.09	6.96	4.72	0.96	1.44	8.06	19.4	7.74	27.9
29[a]	48	800	0.0	0.0	2.0	23	4358 Å	2.52	9.90	5.38	3.86	7.53	4.50	7.59	17.4	57.2
30[a]	101	800	0.0	0.0	3.5	23	4358 Å	2.46	7.71	5.15	5.29	8.12	4.00	7.86	21.2	63.8
31[b]	50	800	0.0	0.0	2.9	0	Unfiltered	2.74	8.22	7.22	4.02	4.80	6.20	16.1	24.9	77.5
32	50	800	0.0	0.0	2.8	−20	Unfiltered	4.70	12.10	8.05	5.94	8.92	8.73	14.9	51.6	133.2
33[b]	7.0	762	0.14	0.0	1.6	23	4358 Å	1.40	7.26	3.41	0.86	1.50	7.91	22.3	6.80	33.4
34[b]	31	800	0.0	4.0	3.0	23	4358 Å	0.48[c] (4.33)[e]								
35[c]	31	933	0.0	8.8	2.3	−20	Unfiltered	0.49[c] (4.45)[e]								
36[d]	31	800	0.0	4.0	3.0	23	4358Å	0.53[c] (4.79)[e]								
37	6.0[f]	1000	0.0	0.0	1.8	23	Unfiltered	2.18	8.51	4.11	9.45	22.1	3.98	7.48	37.6	165.3
38	7.0	762	0.0	7.18[g]	1.6	23	4358 Å	1.89	7.15	4.15	1.68	2.89	6.39	14.1	10.7	40.8

[a]An average of three experiments.
[b]An average of two experiments.
[c]No products above C_5 were formed in the presence of O_2.
[d]Carbon monoxide was also present in this experiment; CO/iB was 10.
[e]The parenthetic expression is the ratio of reaction per bond for the formation of the C_{n+1} compounds.
[f]Ketene was used as the precursor for methylene. An average of two experiments.
[g]This number is the ratio of CO/iB.

Can. J. Chem. Downloaded from www.nrcresearchpress.com by 210.87.254.42 on 09/05/12
For personal use only.

TABLE VI

Relative variation of major alkane and minor products for isobutane + $^3CH_2$ with change in experimental conditions

System[a]	C_2H_4/C_2H_6	C_3H_6/C_3H_8	neP/C_2H_6	neP/C_3H_8	neP/∇	neP/B1	neP/iBene
27	3.01	0.92	0.47	3.67	23.5	0.50	1.01[b]
28	3.12	0.70	0.38	2.47	21.0	0.80	0.73[b]
29	1.12	0.49	0.69	6.26	[c]	7.13[d]	0.44
30	1.99	0.54	0.90	7.26	[c]	[c]	0.48
33	7.47	1.04	0.28	1.96	3.22	0.57	[c]
34	[c]	0.72	[c]	23.7	[c]	[c]	[c]
37	1.57	2.09	0.79	6.68	41.6[d]	0.59[d]	[c]
38	2.64	0.85	0.55	4.17	42.6	[c]	[c]

System[a]	22DMB/C_2H_6	22DMB/C_3H_8	22DMB/∇	22DMB/B1	22DMB/iBene
27	0.04	0.30	2.48	0.05	0.10[b]
28	0.05	0.32	2.56	0.14	0.13
29	0.043	0.38	[c]	0.50	0.032
30	0.058	0.45	[c]	[c]	0.032
33	0.041	0.29	0.48	0.085	[c]
34	[c]	[c]	[c]	[c]	[c]
37	0.021	0.18	1.04[d]	0.015[d]	[c]
38	0.05	0.39	3.97	[c]	[c]

System[a]	TBM/C_2H_6	TBM/C_3H_8	TBM/∇	TBM/B1	TBM/iBene
27	0.08	0.62	3.90	0.08	0.18[b]
28	0.05	0.34	2.83	0.10	0.11[b]
29	0.15	1.40	[c]	1.66	0.10
30	0.34	2.41	[c]	[c]	0.14
33	0.036	0.25	0.41	0.10	[c]
34	[c]	[c]	[c]	[c]	[c]
37	0.20	1.68	10.7[d]	0.15[d]	[c]
83	0.09	0.65	6.67	[c]	[c]

[a]These data are from the same experiments as in Table V.
[b]Isobutene was not observed in all of the experiments; this number is not averaged on the same number of runs as the other ratios.
[c]The compound in the denominator was not measured.
[d]The denominator was observed in only one of the experiments, thus the ratio is not an average.

TABLE VII

Relative rate constants and disproportionation:combination ratios employed in the calculations

Quantity	Set 1[a]	Set 2[b]	Quantity	k_d/k_c Propane[c]	k_d/k_c *n*-Butane[d]	k_d/k_c Isobutane[e]
k_5	4.0	1.0	k_{21}/k_5	0.14	—	0.18
k_6	2.5	1.0	k_{22}/k_6	0.64	0.64	2.20
k_7	6.0	2.0	$(k_{23a} + k_{23b})/k_7$	0.40	0.41	1.19
k_9	12.0	2.0	k_{15}/k_9	0.05	0.05	0.09
k_{10}	9.0	2.0	k_{16}/k_{10}	0.20	0.32	1.10
k_{11}	5.1	1.0	k_{20}/k_{11}	0.13	0.13	0.13
k_{13}	9.5	2.0	$(k_{18a} + k_{18b})/k_{13}$	0.14	0.15	0.14
k_{14}	7.5	2.0	$(k_{19a} + k_{19b})/k_{14}$	0.40	0.40	1.17

[a]These relative rate constants are from ref. 2*a*.
[b]These are the statistical relative constants mentioned in *Calculations*.
[c]k_d/k_c for the propane calculations in Tables VIII and IX from ref. 2*c*.
[d]k_d/k_c for the *n*-butane calculation in Tables X and XI from ref. 2*c*.
[e]k_d/k_c for the isobutane calculations in Tables XII and XIII. They are best estimates from data in the literature.

TABLE VIII

Results of calculations for propane + $^3CH_2$[a]

System[b]	Methyl[c] / Ethyl	·R′/·R[d]	iB_{ins}[e] / iB_{tot}	nB_{ins}[f] / nB_{tot}	$2°_{ins}$[g] / $1°_{ins}$	$2°_{abs}$[h] / $1°_{abs}$	$2°_{ins}$[i] / $2°_{abs}$	$1°_{ins}$[j] / $1°_{abs}$
1	2.10	4.12	0.68	0.83	2.74	11.6	0.86	3.64
2	6.89	5.31	0.11	0.65	0.74	14.7	0.06	1.06
3	3.43	23.4	0.35	0.88	2.08	58.6	0.22	6.34
4	4.15	6.77	0.53	0.78	4.03	17.7	0.49	2.14
5	4.23	7.37	0.62	0.81	5.19	19.0	0.71	2.62
6	2.07	3.13	0.62	0.76	2.51	9.75	0.57	2.22
7	1.70	4.17	0.65	0.81	2.33	12.3	0.65	3.41
8	0.75	4.28	0.74	0.70	2.48	12.0	0.79	3.83
9	1.27	3.36	0.79	0.84	2.49	9.33	1.26	4.71
10	0.62	3.34	0.95	0.93	2.07	9.30	5.15	23.1

[a]Calculations employ rate constants from set 1 and k_d/k_c (propane) in Table VII.
[b]These numbers correspond to those in Tables I and II.
[c]Methyl is from ·R′ + ·R as indicated by the C_{2n} compounds; ethyl is an average of ethyl from each of the two C_{n+2} compounds.
[d]·R′ and ·R are both deduced from the C_{2n} compounds.
[e]iB_{ins} means isobutane formed by insertion; iB_{exp} means experimental isobutane.
[f]nB_{ins} means *n*-butene formed by insertion; nB_{exp} means experimental *n*-butane.
[g]Insertion into secondary C—H per insertion into primary C—H.
[h]Abstraction from secondary C—H per abstraction from primary C—H.
[i]Total insertion into secondary C—H relative to total abstraction from secondary C—H.
[j]Total insertion into primary C—H relative to total abstraction from primary C—H.

combination with $\cdot R_{ss}'$ and k_{14}, or with $\cdot R_{ss}$ and k_{13}. Disproportionation corrections were made to C_{2n}, C_{n+2}, and to calculated C_{n+1}, and from these quantities the ratio of (total ·R′): (total ·R) was obtained; this ratio, when combined with the number ratio of primary: secondary (or tertiary) C—H bonds gave the relative rate of abstraction (per bond) of H by $^3CH_2$. The calculational detail is illustrated in the Appendix at the request of a referee.

Four sets of rate constants were employed in the above calculations, of which the two most disparate and complete sets of calculations are those presented here. The first set was reported earlier by Whitten and Rabinovitch (*2c*) for the propane–methylene system, and was extended to the *n*-butane and isobutane calculations with similar reactions receiving the appropriate rate constants. A second non-selective set of constants was used in which the relative magnitudes of the rate constants for radical combination reactions were simply set equal to 1 or 2, depending on the symmetry number for the reaction. A list of both the rate constants and the disproportionation to combination ratios employed in the calculations is given in Table VII. A summary of the calculational results is presented for the first set of rate constants in Tables VIII, X, and XII, and in Tables IX, XI, and XIII for the second set. In these tables the columns labelled $C_{n+1\,(ins)}/C_{n+1\,(tot)}$ indicate the fraction of the experimental yield of C_{n+1} product which was formed by other than radical processes. All ratios for the least-branched C_{n+1} product, and virtually all studies for the most-branched product under conditions of high RH/DM, and *all* studies at lower temperatures or with isotopic substitution wherein radical processes were inhibited gave positive indications of substantial amounts of C_{n+1} product in excess of estimated radical-related sources. The wide range of relative rate constants for the two sets appears to rule out any dependence of this conclusion upon fortuitous selection of the constants.

Only the ratios determined at large values of RH/DM are considered reliable and free of chemical complications.

Additional Reactions

Two reactions with DM which could cause complications for the proposed interpretation of experimental data were not included in the reaction scheme. The first reaction involves other sources of methyl, notably

[24] $$^3CH_2 + DM \rightarrow \cdot CH_3 + CHN_2.$$

A consequence of reaction [24] would be that $\cdot CH_{3ss} > (\cdot R' + \cdot R)_{ss}$ and its estimation would be very difficult. However, it appears that reaction [24] is only significant when a relatively high proportion of DM is present; an increase in RH/DM in each alkane system was accompanied by a two- to three-fold decrease of the

Can. J. Chem. Downloaded from www.nrcresearchpress.com by 210.87.254.42 on 09/05/12
For personal use only.

TABLE IX

Results of calculations for propane + $^3CH_2$[a]

System[b]	Methyl[c] / Ethyl	·R′/·R[d]	iB_{ins}[e] / iB_{tot}	nB_{ins}[f] / nB_{tot}	$2°_{ins}$[g] / $1°_{ins}$	$2°_{abs}$[h] / $1°_{abs}$	$2°_{ins}$[i] / $2°_{abs}$	$1°_{ins}$[j] / $1°_{abs}$
1	1.48	3.43	0.81	0.87	3.11	12.4	1.26	5.03
2	4.60	4.43	0.49	0.81	2.70	15.6	0.31	1.82
3	2.23	19.5	0.64	0.90	3.69	60.4	0.53	8.59
4	2.74	5.64	0.73	0.87	5.03	18.4	0.86	3.17
5	2.78	6.14	0.79	0.88	6.03	19.8	1.16	3.81
6	1.42	2.61	0.78	0.83	2.90	10.6	0.88	3.22
7	1.15	3.48	0.80	0.85	2.73	13.1	0.97	4.64
8	0.51	3.57	0.85	0.68	2.88	12.5	1.05	4.55
9	0.86	2.80	0.88	0.86	2.70	9.78	1.68	6.07
10	0.42	2.86	0.97	0.92	2.12	9.58	6.02	27.2

[a]Calculations employ rate constants from set 2 and k_d/k_c (propane) in Table VII.
[b]These numbers refer to the same experiments as in Tables I and II.
[c]Methyl is from ·R′ and ·R as indicated by the C_{2n} compounds; ethyl is an average of ethyl from each of the two C_{n+2} compounds.
[d]·R′ and ·R are both deduced from the C_{2n} compounds.
[e]Isobutane formed by insertion relative to total experimental isobutane.
[f]*n*-Butane formed by insertion relative to total experimental *n*-butane.
[g]Insertion into secondary C—H per insertion into primary C—H.
[h]Abstraction from secondary C—H per abstraction from primary C—H.
[i]Total insertion into secondary C—H relative to total abstraction from secondary C—H.
[j]Total insertion into primary C—H relative to total abstraction from primary C—H.

C_{n+1}:C_{2n} ratios which presumably resulted from a decrease in $\cdot CH_{3ss}$ concentration relative to both $\cdot R_{ss}'$ and $\cdot R_{ss}$. Convincing evidence that no extra source of $\cdot CH_3$ arose at low DM proportions is demonstrated by a comparison of the $\cdot CH_3$ steady-state proportions calculated as the sum of $(\cdot R' + \cdot R)_{ss}$ with that calculated from the ethane product. At low RH/DM ratios, the sum $(\cdot R' + \cdot R)_{ss}$ was ~ 0.6 of the $\cdot CH_{3ss}$ estimate based on ethane by taking the overestimate that *all* ethane arose by methyl recombination. When the DM proportion was decreased, $(\cdot R' + \cdot R)_{ss}$ rose to 1.1 and 0.9 of the $\cdot CH_{3ss}$ in the *n*-butane and isobutane systems, respectively (measurement of ethane was not accurate in the propane system). Similarly, the propane product, which was assumed to result from recombination of methyl and ethyl, gave like agreement. This supports the assumption that $\cdot CH_{3ss} \simeq (\cdot R' + \cdot R)_{ss}$, at least at higher ratios of RH/DM.

A second set of possible complicating reactions could be higher analogs of the methyl reaction.

[25] $\cdot CH_3 + DM \rightarrow CH_3CH_2\cdot + N_2$

such as

[26] $CH_3CH_2 + DM \rightarrow CH_3CH_2CH_2\cdot + N_2$

[27] $\cdot R + DM \rightarrow RCH_2\cdot + N_2$

[28] $\cdot R' + DM \rightarrow R'CH_2\cdot + N_2$

$RCH_2\cdot + DM \rightarrow RCH_2CH_2\cdot + N_2$, etc.

These reactions are followed by combination and disproportionation of all such radical species. Some of the major and minor products reported could arise from these chain-lengthening processes; however, many other products, both alkenes and alkanes, should also arise (uniquely) from such a mechanism and, indeed, at low values of RH/DM many of these products were observed. The propane system is not a good diagnostic one since no *unique* alkanes (below C_6) could arise in this manner; the unique alkenes B1, P1, 3MB1, and 4MP1 did appear, but B1 and P1 are ubiquitous species and not good indicators. In the *n*-butane and isobutane systems, the presence of (unique) 3-methylhexane and *n*-heptane product in the former study and 2-methylhexane and 2,2-dimethylpentane in the latter appear to establish that chain lengthening does occur. Indeed, upon increase of RH/DM, these products which were diagnostic of chain lengthening decreased drastically (by a factor of ~ 5) in all systems (see *Results*). In general, the amounts of ordinary products altered with decrease of DM proportion in the manner expected for inhibition of reactions [24]–[28] (for propane compare systems 1 and 2, Table I; for *n*-butane systems 13 through 18, Table III; and for isobutane systems 28, 31, and 32, Table V).

1,1,1,3,3,3-Propane-d_6

The results for deuterated propane warrant specific mention. Comparison with the light

Can. J. Chem. Downloaded from www.nrcresearchpress.com by 210.87.254.42 on 09/05/12
For personal use only.

TABLE X

Results of calculations for *n*-butane + $^3CH_2$[a]

System[b]	Methyl[c]/Ethyl	·R′/·R[d]	iP_{ins}[e]/iP_{tot}	nP_{ins}[f]/nP_{tot}	$2°_{ins}$[g]/$1°_{ins}$	$2°_{abs}$[h]/$1°_{abs}$	$2°_{ins}$[i]/$2°_{abs}$	$1°_{ins}$[j]/$1°_{abs}$
13	3.55	8.82	0.50	0.77	2.84	12.8	0.41	1.85
14	8.51	7.73	0.15	0.45	1.92	11.4	0.08	0.45
15	13.0	7.95	−0.08[k]	0.37	−1.19[k]	11.8	−0.03[k]	0.33
16	16.2	7.48	−0.05[k]	0.47	−0.43[k]	11.0	−0.02[k]	0.51
17	22.4	8.62	−0.21[k]	0.39	−2.63[k]	12.3	−0.08[k]	0.36
18	17.7	8.98	−0.09[k]	0.40	−1.27[k]	13.1	−0.04[k]	0.38
19	10.4	6.61	0.41	0.54	4.30	9.96	0.29	0.67
20	11.7	10.6	0.52	0.74	4.60	15.6	0.46	1.57
21	1.76	7.70	0.64	0.83	3.01	11.5	0.59	2.24
22	1.22	11.3	0.81	0.95	3.06	16.0	1.35	7.02

[a]Calculations employ rate constants from set 1 and k_d/k_c (*n*-butane) in Table VII.
[b]These numbers refer to the same experiments as in Tables III and IV.
[c]Methyl is from ·R′ + ·R as derived from the C_{2n} compounds; ethyl is an average of ethyl from the two C_{n+2} compounds.
[d]The ratio of *sec*-butyl/*n*-butyl.
[e]Isopentane from insertion relative to total experimental isopentane.
[f]*n*-Pentane from insertion relative to total experimental *n*-pentane.
[g]Insertion into secondary C—H per insertion into primary C—H.
[h]Abstraction from secondary C—H per abstraction from primary C—H.
[i]Total insertion into secondary C—H relative to total abstraction from secondary C—H.
[j]Total insertion into primary C—H relative to total abstraction from primary C—H.
[k]A negative quantity signified incompatible data.

system (systems 2 and 3 in Table I) reveals that products derived from ·R′ increased in relation to those from ·R. It is reasonable that $^3CH_2$ abstracts deuterium less readily than hydrogen. Also, steady-state concentrations of ethyl radicals increased relative to $\cdot R_{ss}'$ and $\cdot R_{ss}$, as might be expected from the decreased total reaction probability between $^3CH_2$ and propane-d_6. Systems 2 and 3 in Table I reveal further support for the occurrence of $^3CH_2$ insertion: whereas on going to propane-d_6, the C_{n+1} ratio iB/nB increased by only 20%, that for C_{n+2} and C_{2n} products, iP/nP, and DMB/2MP, increased by much larger factors (3.4 and 4.4 respectively) due to the changed steady-state concentration ratio of $\cdot R_{ss}'$ and $\cdot R_{ss}$.

Production of C_{n+1} and C_{n+2} alkenes relative to the most-branched, major alkane products was nearly unchanged (systems 2 and 3 in Table II). Since many of these alkenes were produced uniquely by processes like [27] and [28], it is apparent that chain lengthening is as unimportant for this deuterated substrate as for the light substrate, at high ratios of RH/DM.

Decrease in Temperature

This experimental change (systems 2, 4, and 5 in Table I, systems 15, 19, and 20 in Table III, and systems 29, 31, and 32 in Table V) enhanced the yield of the ·R′ products relative to those from ·R, due to enhanced abstraction at the secondary (or tertiary) position compared with that at the primary. The experimental product ratios further show that the proportion of C_{n+1} products which is due to other than radical recombination reactions (Tables VIII–XIII, columns $C_{n+1\,(ins)}/C_{n+1\,(tot)}$) increases at lower temperatures and is the preponderant part of these products.

Addition of Ethylene

Studies were made in the presence of ethylene in order to obtain a measure of the rates of $^3CH_2$ reaction with alkane relative to double bond addition. Comparison of systems 1, 6, 7, and 8 in Table I, of systems 13, 21, and 22 in Table III, and of systems 27 and 33 in Table V reveals a clear-cut increase in $\cdot CH_2CH_{3ss}$ relative to $\cdot CH_{3ss}$, while both increased relative to $\cdot R_{ss}'$ and $\cdot R_{ss}$. This could be due to the reaction sequence recently proposed by Cvetanović (13):

[29] $C_2H_4 + {}^3CH_2 \rightarrow \cdot CH_2CH_2CH_2\cdot{}^*$

[30] $\cdot CH_2CH_2CH_2\cdot{}^* \rightarrow H + \cdot CH_2{-}CH{=}CH_2$

[31] $C_2H_4 + H \rightarrow C_2H_5\cdot$

[32] $\cdot CH_2CH_2CH_2\cdot{}^* + M \rightarrow \nabla + M.$

In some experiments at low RH/DM, the proportion of 1,5-hexadiene product, which was ordinarily half the amount of 3MP in the *n*-butane system, and was nearly 9/10 of 22DMB in the isobutane system, rose to ~ 1.5 of these products upon introduction of ethylene. This supports the occurrence of [29]–[32].

Can. J. Chem. Downloaded from www.nrcresearchpress.com by 210.87.254.42 on 09/05/12
For personal use only.

TABLE XI

Results of calculations for *n*-butane + $^3CH_2$[a]

System[b]	Methyl[c] / Ethyl	·R′/·R[d]	iP_{ins}[e] / iP_{tot}	nP_{ins}[f] / nP_{tot}	$2°_{ins}$[g] / $1°_{ins}$	$2°_{abs}$[h] / $1°_{abs}$	$2°_{ins}$[i] / $2°_{abs}$	$1°_{ins}$[j] / $1°_{abs}$
13	2.38	7.36	0.72	0.88	3.55	12.6	0.76	3.22
14	5.72	6.44	0.52	0.72	4.07	12.1	0.33	1.00
15	8.73	6.63	0.38	0.68	2.97	12.6	0.20	0.84
16	10.8	6.23	0.40	0.73	2.33	11.6	0.22	1.10
17	14.7	7.18	0.31	0.69	2.23	13.0	0.15	0.88
18	11.6	7.48	0.38	0.70	3.00	13.8	0.20	0.92
19	7.00	5.51	0.66	0.77	4.95	10.6	0.62	1.32
20	7.81	8.82	0.73	0.87	5.47	16.6	0.85	2.58
21	1.17	6.41	0.79	0.91	3.42	12.0	0.90	3.19
22	0.81	9.41	0.89	0.97	3.28	16.4	1.80	9.04

[a]Calculations employ rate constants from set 2 and k_d/k_e (*n*-butane) in Table VII.
[b]These numbers refer to the same experiments as in Tables III and IV.
[c]Methyl is derived from the C_{2n} compounds, and ethyl is an average of ethyl from each C_{n+2} product.
[d]The ratio of *sec*-butyl/*n*-butyl.
[e]Isopentane from insertion relative to total experimental isopentane.
[f]*n*-Pentane from insertion relative to total experimental *n*-pentane.
[g]Insertion into secondary C—H per insertion into primary C—H.
[h]Abstraction from secondary C—H per abstraction from primary C—H.
[i]Total insertion into secondary C—H relative to total abstraction from secondary C—H.
[j]Total insertion into primary C—H relative to total abstraction from primary C—H.

In an early propane study the temperature was lowered in an ethylene reaction system. The effect upon the product ratios may be seen by comparing systems 7, 9, and 10 in Table I. Unfortunately, the experiments were performed at low values of RH/DM, and the side reactions render detailed interpretation difficult.

Addition of CO

Carbon monoxide is known to selectively remove $^3CH_2$ from methylene reaction systems (14). Thus addition of sevenfold amounts of CO relative to substrate should alter the experimental product ratios if both spin states of methylene were present as reactive species. The results with CO showed scarcely any change in product proportions so that $^1CH_2$ must have been present only in very minor amounts. (Compare systems 27 and 38 in Tables V and VI and XII and XIII.)

Various Rate Relations

On the basis of the data in Tables VIII–XIII some rate ratios were calculated for systems having high values of RH/DM. Two values are presented for each ratio corresponding, respectively, to the two sets of rate constants. All values in this section are on a "per bond" basis. At room temperature the relative rates of abstraction of 1 °:2 ° hydrogen by $^3CH_2$ are, propane, 1:14.7, 15.6; *n*-butane, 1:11.9, 12.6; and for 1 °:3 ° hydrogen in isobutane, 1:148, 148. For 1 °:2 °:3 ° abstraction the averages (with estimated uncertainties) are 1:13.7 ± 2.0:148 ± 20. These results compare favorably to those reported by Whitten and Rabinovitch (2*c*) for 1 °:2 ° abstraction by $^3CH_2$ of 1:9, and by Ho and Noyes (12) of 1:14. At the lower temperatures, the relative rates of abstraction are slightly altered: propane, 1:18.4, 19.1; *n*-butane, 1:12.8, 13.6; isobutane 1:210, 210. These values correspond to averages of 1:16 ± 3:210 ± 40. For the propane-d_6 system, the abstraction ratios were 1 $°_D$:2 $°_H$ equal to 1:58.6, 60.4, which indicates an (average) isotope effect for abstraction of primary D of 3.9.

The relative rates of H abstraction to addition to the double bond by $^3CH_2$ were (for 1 °:2 ° (or 3 °):C=C)[6]: propane, 1:10.4, 12.1:354, 452; *n*-butane, 1:13.9, 14.5:381, 489; isobutane, 1:113, 116:324, 406. Averages of the rates of $^3CH_2$ reaction for 1 °:2 °:3 °:C=C are 1:12.7 ± 2:114 ± 18:401.[7]

[6]In order to determine the amount of reaction between $^3CH_2$ and C_2H_4 it was necessary to correct the amount of cyclopropane observed for decomposition [cf. the data of ref. 15]. The data for *n*-butane indicated that cyclopropane should be corrected by a factor of 1.61, while data from the isobutane system suggested that "no" correction was required. The product proportions observed for $^3CH_2$ with pure C_2H_4 at 1.5–2.2 atm were cyclopropane:propylene = 2.2:1 at 23 °C.

[7]Disagreement between these relative rates of abstraction and those obtained in the previous room temperature system is not large and is rather encouraging when one considers that the addition of ethylene introduces many other reaction species.

Can. J. Chem. Downloaded from www.nrcresearchpress.com by 210.87.254.42 on 09/05/12
For personal use only.

TABLE XII

Results of calculations for isobutane + $^3CH_2$[a]

System[b]	Methyl[c]/Ethyl	·R′/·R[d]	neP_{ins}[e]/neP_{tot}	iP_{ins}[f]/iP_{tot}	$3°_{ins}$[g]/$1°_{ins}$	$3°_{abs}$[h]/$1°_{abs}$	$3°_{ins}$[i]/$3°_{abs}$	$1°_{ins}$[j]/$1°_{abs}$
27	4.01	10.41	0.34	0.86	6.06	121.	0.13	2.48
28	2.87	10.6	0.49	0.86	10.60	125.	0.23	2.80
29	12.6	12.9	0.13	0.77	3.97	151.	0.04	1.49
30	15.3	12.4	−0.93[k]	0.68	−10.2[k]	144.	0.01	1.13
31	9.47	17.3	0.38	0.86	11.0	197.	0.16	2.79
32	16.6	19.3	0.57	0.86	27.9	224.	0.33	2.65
33	2.73	8.99	0.49	0.89	6.92	111.	0.21	3.54
37	37.8	8.83	−0.03[k]	0.59	−1.77[k]	107.	−0.005[k]	0.92
38	5.37	9.82	0.38	0.84	7.64	119.	0.15	2.28

[a]Calculations employ rate constants from set 1 and k_a/k_c (isobutane) in Table VII.
[b]These numbers refer to the same experiments as in Tables V and VI.
[c]Methyl is from the C_{2n} compounds, and ethyl is an average of ethyl from each C_{n+2} product.
[d]The ratio of *t*-butyl/isobutyl.
[e]Neopentane from insertion relative to total experimental neopentane.
[f]Isopentane from insertion relative to total experimental isopentane.
[g]Insertion into tertiary C—H per insertion into primary C—H.
[h]Abstraction from tertiary C—H per abstraction from primary C—H.
[i]Total insertion into tertiary C—H relative to total abstraction from tertiary C—H.
[j]Total insertion into primary C—H relative to total abstraction from primary C—H.
[k]A negative quantity signified incompatible data.

Relative rates of insertion, at room temperature, by $^3CH_2$ for 1 °:2 ° (or 3 °) bonds were: propane, 1:0.74, 2.7; *n*-butane, 1:1.9, 2.9; isobutane, 1:4.0, 10.4. An average of these values is 1:2.1 ± 1.1:7.2 ± 3.8.[8] At low temperature the corresponding quantities were: propane, 1:4.6, 5.5; *n*-butane, 1:4.5, 5.2; isobutane, 1:19.4, 25.9, for an average of 1:5.0 ± 0.6:22.6 ± 2.7. The deuterated propane system indicated relative insertion by $^3CH_2$ for 1 °:2 ° to be 1:2.08, 3.69; this indicates an isotope effect of ~ 2.1.

A comparison of the rate of insertion relative to abstraction by $^3CH_2$ (given as $1°_{ins}$:$1°_{abs}$, $2°_{ins}$:$2°_{abs}$) at room temperature can also be made: propane, 1.06, 1.82:1 and 0.06, 0.31:1; *n*-butane, 0.41, 0.95:1 and 0.08, 0.22:1; isobutane, 1.31, 1.98:1 and 0.03, 0.17:1. These ratios increase upon decrease in temperature: propane, 2.38, 3.49:1 and 0.60, 1.01:1; *n*-butane, 1.12, 1.95:1 and 0.38, 0.74:1; isobutane, 2.72, 3.81:1 and 0.25, 0.45:1. Uncertainties in correct rate constants introduce considerable uncertainty into these values.

An isotope effect is again observed in the propane-d_6 system for $1°_{ins}$:$1°_{abs}$ and $2°_{ins}$:$2°_{abs}$; the values of these ratios were 6.34, 8.59:1 and 0.22, 0.53:1 which correspond to composite primary isotope effect at the primary position of 5.98, 4.72 and to a secondary isotope effect at the secondary position (non-deuterated) of 3.67, 1.71.

Finally, we have not proposed a transition state or structure for the insertion process. Insofar as a repulsive triplet state may first be formed, then dissociation to methyl + R (or R′) radicals corresponds to overall abstraction of H by $^3CH_2$, while spin inversion, whatever its mechanism, and at whatever stage it occurs, leads to insertion products.

Appendix

The calculational technique may be illustrated for the propane system for which

$$\text{isopropyl}_{ss} = (\text{DMB}_{expt}/k_6)^{1/2},$$

$$n\text{-propyl}_{ss} = 2\text{MP}_{expt}/k_7(\text{isopropyl}_{ss}),$$

and $$\text{methyl}_{ss} \simeq \text{isopropyl}_{ss} + n\text{-propyl}_{ss}.$$

The amount of iso- and *n*-butane formed by radical combination is found by

$$\text{iB}_{abs} = k_{10}(\text{methyl}_{ss})(\text{isopropyl}_{ss})$$

and $$\text{nB}_{abs} = k_9(n\text{-propyl}_{ss})(\text{methyl}_{ss}),$$

from which the amounts of iso- and *n*-butane formed by insertion may be found,

$$\text{iB}_{ins} = (\text{iB}_{expt} - \text{iB}_{abs});$$

$$\text{nB}_{ins} = (\text{nB}_{expt} - \text{nB}_{abs} + k_{11}(\text{ethyl}_{av})^2)$$

[8]Data from O_2 experiments in Tables II, III, and V indicate relative rates of insertion for 1°:2°:3° C—H bonds of 1:1.33:4. These values may reflect the presence of small amounts of $^1CH_2$.

Can. J. Chem. Downloaded from www.nrcresearchpress.com by 210.87.254.42 on 09/05/12
For personal use only.

TABLE XIII

Results from calculations for isobutane + $^3CH_2$[a]

System[b]	Methyl[c] / Ethyl	·R′/·R[d]	$\frac{neP_{ins}}{neP_{tot}}$[e]	$\frac{iP_{ins}}{iP_{tot}}$[f]	$\frac{3°_{ins}}{1°_{ins}}$[g]	$\frac{3°_{abs}}{1°_{abs}}$[h]	$\frac{3°_{ins}}{3°_{abs}}$[i]	$\frac{1°_{ins}}{1°_{abs}}$[j]
27	2.69	8.45	0.62	0.92	10.3	121.	0.29	3.40
28	1.91	8.72	0.71	0.93	14.4	126.	0.41	3.75
29	8.24	10.8	0.51	0.88	13.1	152.	0.19	2.22
30	10.1	10.3	0.26	0.84	7.71	145.	0.15	1.74
31	5.55	14.4	0.65	0.93	17.3	196.	0.34	3.88
32	10.8	16.1	0.76	0.93	34.5	225.	0.57	3.74
33	1.84	7.31	0.71	0.94	9.48	113.	0.40	4.72
37	25.8	7.28	0.41	0.78	10.4	109.	0.13	1.51
38	5.37	9.82	0.38	0.84	7.64	119.	0.15	2.28

[a]Calculations were performed with rate constants from set 2 and k_d/k_e (isobutane) in Table VII.
[b]These numbers refer to the same experiments as in Tables V and VI.
[c]Methyl is calculated from the C_{2n} compounds; ethyl is an average of ethyl from each C_{n+2} product.
[d]The ratio of *t*-butyl/isobutyl.
[e]Neopentane from insertion relative to total experimental neopentane.
[f]Isopentane from insertion relative to total experimental isopentane.
[g]Insertion into tertiary C—H per insertion into primary C—H.
[h]Abstraction from tertiary C—H per abstraction from primary C—H.
[i]Total insertion into tertiary C—H relative to total abstraction from tertiary C—H.
[j]Total insertion into primary C—H relative to total abstraction from primary C—H.

where

$$\text{ethyl}_{av} = (\text{ethyl}_{np} + \text{ethyl}_{ip})/2,$$

$$\text{ethyl}_{np} = \text{nP}_{expt}/k_{13}(n\text{-propyl}_{ss}),$$

and $$\text{ethyl}_{ip} = \text{iP}_{expt}/k_{14}(\text{isopropyl}_{ss}).$$

The relative amount of abstraction from primary and secondary positions may be calculated after correcting for disproportionation:

$$\text{nB}_{corr} = 1.05(\text{nB}_{abs});$$
$$\text{iB}_{corr} = 1.20(\text{iB}_{abs});$$
$$\text{nP}_{corr} = 1.14(\text{nP}_{expt});$$
$$\text{iP}_{corr} = 1.40(\text{iP}_{expt});$$
$$\text{nH}_{corr} = 1.14(\text{nH}_{expt});$$
$$\text{DMB}_{corr} = 1.64(\text{DMB}_{expt});$$
$$\text{2MP}_{corr} = 1.40(\text{2MP}_{expt});$$

thus,

$$\frac{\text{(total secondary abstraction)}}{\text{(total primary abstraction)}} = \frac{(\text{iB}_{corr} + \text{iP}_{corr} + 2(\text{DMB}_{corr}) + 2\text{MP}_{corr})}{(\text{nB}_{corr} + \text{nP}_{corr} + 2(\text{nH}_{corr}) + 2\text{MP}_{corr})}.$$

The relative amount of insertion and abstraction may be found by

$$\frac{\text{prim. ins.}}{\text{prim. abs.}} = \frac{\text{nB}_{ins}}{\text{(total prim. abs.)}}$$

and $$\frac{\text{sec. ins.}}{\text{sec. abs.}} = \frac{\text{iB}_{ins}}{\text{(total sec. abs.)}}.$$

1. (*a*) K. H. Sauer and G. B. Kistiakowsky. J Am. Chem. Soc. **78**, 5447 (1956); H. M. Frey and G. B. Kistiakowsky. J. Am. Chem. Soc. **79**, 6373 (1957); J. N. Butler and G. B. Kistiakowsky. J. Am. Chem. Soc. **82**, 759 (1960). (*b*) B. S. Rabinovitch and M. C. Flowers. Quart. Rev. London, **18**, 122 (1964). (*c*) D. W. Setser, B. S. Rabinovitch, and J. W. Simons. J. Chem. Phys. **40**, 1751 (1964); J. W. Simons, B. S. Rabinovitch, and D. W. Setser. **41**, 800 (1965); J. W. Simons and B. S. Rabinovitch. J. Phys. Chem. **68**, 1322 (1964).
2. (*a*) W. von E. Doering, R. G. Buttery, R. G. Laughlin, and N. Chaudhuri. J. Am. Chem. Soc. **78**, 3224 (1956). W. von E. Doering and L. H. Knox. J. Am. Chem. Soc. **83**, 1989 (1961). (*b*) H. M. Frey. Proc. Roy. Soc. London, Ser. A, **250**, 409 (1959). (*c*) G. Z. Whitten and B. S. Rabinovitch. J. Phys. Chem. **69**, 4348 (1965). (*d*) R. W. Carr. J. Phys. Chem. **70**, 1920 (1966). (*e*) B. M. Herzog and R. W. Carr. J. Phys. Chem. **71**, 2688 (1967). (*f*) M. L. Halberstadt and J. R. McNesby. J. Am. Chem. Soc. **89**, 3417 (1967).
3. H. M. Frey and M. A. Voisey. Chem. Commun. **454** (1966).
4. (*a*) W. von E. Doering and P. LaFlamme. J. Am. Chem. Soc. **78**, 5447 (1956). (*b*) R. C. Woodworth and P. S. Skell. J. Am. Chem. Soc. **78**, 4496 (1956); **81**, 3383 (1959). (*c*) K. H. Sauer and G. B. Kistiakowsky. J. Am. Chem. Soc. **78**, 5699 (1956).
5. D. W. Setser, R. Littrell, and J. C. Hassler. J. Am. Chem. Soc. **87**, 2062 (1965).
6. (*a*) R. W. Carr and G. B. Kistiakowsky. J. Phys. Chem. **70**, 118 (1966). (*b*) H. M. Frey. Proc. Chem. Soc. London, 318 (1959).
7. D. F. Ring and B. S. Rabinovitch. J. Am. Chem. Soc. **88**, 4285 (1966).
8. (*a*) K. R. Kopecky, G. S. Hammond, and P. A. Leermakers. J. Am. Chem. Soc. **84**, 1015 (1962). (*b*) F. J. Duncan and R. J. Cvetanović. J. Am. Chem. Soc. **84**, 3593 (1962).
9. B. S. Rabinovitch, K. W. Watkins, and D. F. Ring. J. Am. Chem. Soc. **87**, 4960 (1965); D. F. Ring and B. S. Rabinovitch. J. Phys. Chem. **72**, 191 (1968).

Can. J. Chem. Downloaded from www.nrcresearchpress.com by 210.87.254.42 on 09/05/12
For personal use only.

10. (*a*) S. Ho, I. UNGER, and W. A. NOYES. J. Am. Chem. Soc. **87**, 2297 (1965). (*b*) A. N. STRACHAN and D. E. THORNTON. J. Phys. Chem. **70**, 952 (1966).
11. (*a*) G. HERZBERG and J. SHOOSMITH. Nature, **183**, 1801 (1959). (*b*) G. HERZBERG. Proc. Roy. Soc. London, Ser. A, **262**, 291 (1961). (*c*) H. M. FREY. J. Am. Chem. Soc. **82**, 5947 (1960).
12. S. Y. Ho and W. A. NOYES. J. Am. Chem. Soc. **89**, 5091 (1967).
13. R. J. CVETANOVIĆ, H. E. AVERY, and R. S. IRWIN. J. Chem. Phys. **46**, 1993 (1967).
14. B. A. DEGRAFF and G. B. KISTIAKOWSKY. J. Phys. Chem. **71**, 1553 (1967).
15. D. W. SETSER and B. S. RABINOVITCH. Can. J. Chem. **40**, 1425 (1962).

Can. J. Chem. Downloaded from www.nrcresearchpress.com by 210.87.254.42 on 09/05/12
For personal use only.

Can. J. Chem. Downloaded from www.nrcresearchpress.com by 210.87.254.105 on 09/05/12
For personal use only.

Radical displacement reactions: The vapor phase reaction of methyl radicals with allyl formate

G. GREIG
Chemistry Department, University of Alberta, Edmonton, Alberta

AND

J. C. J. THYNNE
Department of Chemistry, The University, Edinburgh

Received November 7, 1967

Trideuteromethyl radicals have been reacted in the vapor phase with allyl formate and the principal reaction over the temperature range 100–250 °C has been shown to be the displacement reaction

$$CD_3 + HCOOCH_2—CH=CH_2 \rightarrow (HCOOCH_2CHCH_2CD_3)$$
$$(HCOOCH_2CHCH_2CD_3) \rightarrow H + CO_2 + CH_2=CHCH_2CD_3.$$

Hydrogen atoms generated by this decomposition also react readily to produce propylene by the reaction

$$H + HCOOCH_2—CH=CH_2 \rightarrow H + CO_2 + CH_2=CHCH_3.$$

Canadian Journal of Chemistry, 46, 2451 (1968)

Allyl radicals play important roles in the decomposition of many olefins and cyclic alkyl radicals and at temperatures below about 300 °C they have been shown to react predominantly by combination, either with themselves or with other free radicals present in the reacting system. The production of allyl radicals is somewhat difficult since the usual free radical sources such as the photolysis of aldehydes, ketones, and azocompounds (1) are not practicable either because of the low yield of radicals (e.g. 3-butenal) (2) or because of the unavailability of the starting product (e.g. azopropene).

Thynne (3, 4) has shown that the methyl-radical-sensitized decomposition of alkyl formates is a useful source of alkyl radicals, the reaction sequence being predominantly the abstraction of the formyl hydrogen atom by the methyl radical yielding an alkoxycarbonyl radical which then decarboxylates quantitatively to form carbon dioxide and an alkyl radical, i.e.

$$CH_3 + HCOOR \rightarrow CH_4 + COOR$$
$$COOR \rightarrow CO_2 + R.$$

Allyl formate might so be used to produce thermalized allyl radicals. However, James and Troughton (5) have shown that allyl compounds react readily with ethyl radicals in the vapor phase by addition to the double bond followed by dismutation of a proportion of the adduct radicals, e.g.

$$CH_3CH_2 + CH_2=CHCH_2X \rightarrow (CH_3CH_2CH_2CHCH_2X)$$
$$(CH_3CH_2CH_2CHCH_2X) \rightarrow CH_3CH_2CH_2CH=CH_2 + X.$$

They have suggested that the temperature at which this dismutation occurs is governed by the nature of the substituent X and increases as the enthalpy of the dismutation reaction increases, e.g. where X = OH, the reaction occurs at temperatures above 140 °C, whereas for $X = COOH_3$, it occurs at 35 °C. In the case where $X = HCO_2$, i.e. allyl formate, it might be expected to occur with similar ease to the acetate. Consequently, we have studied the reactions of trideuteromethyl radicals, generated by the photolysis of acetone-d_6 at wavelengths > 3000 Å (where the formate is transparent), with allyl formate over the temperature range 101–252 °C.

Experimental

Materials

Acetone-d_6 was obtained from Merck, Sharp and Dohme. It was dried, distilled, and stored in a blackened bulb at liquid nitrogen temperature. Its isotopic purity was reported as being 99%.

TABLE I

Ethane-d_6 (E), propylene (P), butene-1 (B), and 1,5-hexadiene (H) formation in the reaction of methyl radicals with allyl formate*

T (°C)	t (s)	A	F	E	P	B	H	X	Y
101.5	3600	2.262	1.285	0.912	7.47	1.75	N.A.†	1.43	—
101.5	3600	2.827	1.285	1.39	5.41	1.77	0.013_5	1.17	12.8
101.5	7200	2.904	1.259	1.28	4.59	1.75	0.013_7	1.23	11.4
126.8	3600	2.824	1.212	1.22	13.4	3.92	0.033_1	2.93	19.5
152.3	3600	2.730	1.109	1.07	20.9	6.36	0.105	5.55	18.8
152.3	3600	2.737	1.116	1.04	20.7	6.35	0.147	5.59	16.2
176.5	1800	2.648	1.035	1.50	41.4	9.78	0.422	7.71	12.3
202.2	1800	2.539	1.033	1.76	47.9	11.3	0.262	8.22	16.6
202.2	1800	2.540	1.040	1.78	48.1	10.8	0.433	7.79	12.3
252.5	900	2.399	0.879	4.11	84.5	N.A.	2.49	—	—
252.5	900	2.258	0.952	4.30	80.4	13.50	2.83	6.84	3.87

*A = concentration of acetone, 10^6 mole cm^{-3}.
F = concentration of allyl formate, 10^6 mole cm^{-3}, E, P, B, and H in 10^{12} mole cm^{-3} s^{-1}.
$X = R_{C_4H_5D_3}/R^{1/2}_{C_2D_6}(F)$.
$Y = C_4H_5D_3/(C_2D_6)^{1/2}(C_6H_{10})^{1/2}$.
†N.A. = not analyzed.

Allyl formate (Koch–Light) was dried and distilled several times, narrow boiling ranges being retained each time. It was further purified by preparative gas chromatography.

Procedure

The selective photolysis of acetone at $\lambda > 3000$ Å was used as the methyl radical source. A Mazda 250 watt ME/D lamp in conjunction with a Chance–Pilkington filter OX1A was used. Blank runs with the formate present showed no photodecomposition of the formate to occur throughout the temperature range.

The experiments were performed in the vapor phase in a quartz cylindrical cell, volume 159 cm^3. Mixtures of the acetone and formate were made up in a 1 l bulb before being expanded into the reaction cell. The cell was housed in a heavy aluminium block furnace, fitted with quartz side-windows. The temperature of the furnace was controlled to better than ±0.2 °C by a Fielden–Bikini relay. The reaction cell was fitted with a short side-arm and connected to the usual type of high vacuum apparatus, containing cold traps and a gas burette. After reaction the contents of the reaction cell were expanded into the analytical train and the fraction noncondensable in liquid nitrogen collected and measured in the gas burette. It was then analyzed using an AEI Ltd. MS 10 mass spectrometer and was shown to contain hydrogen, carbon monoxide, trideuteromethane, and tetradeuteromethane. In a typical analysis at 202 °C the proportions of these components were 20.3, 64.4, 13.1, and 2.1% respectively.

The condensable fraction was analyzed gas chromatographically using a hydrogen flame detector and a mixed column of diethyl adipate and dinonyl phthalate on celite. The C_6 product was analyzed on a 9 ft dinonyl phthalate column maintained at 45 °C. A typical analysis at 252 °C of the reaction products (expressed in terms of rates of formation of product × 10^{12} mole cm^{-3} s^{-1}) was hydrogen (4.8_3), trideuteromethane (2.3_0), tetradeuteromethane (0.6_0), carbon monoxide (11.6), ethane-d_6 (4.3_0), propylene (80.4), butene-1 (13.5), and 1,5-hexadiene (2.8_3). In addition small amounts of propane, allene, and isobutane were observed.

Results and Discussion

When acetone-d_6 is photolyzed alone CD_4 and CD_3H are formed, the latter being formed because of the isotopic impurity of the ketone. Their formation may be described in terms of the following reactions.

[1] $CD_3COCD_3 + h\nu \rightarrow 2CD_3 + CO$

[2] $CD_3 + CD_3COCD_3 \rightarrow CD_4 + CD_2COCD_3$

[3] $CD_3 + HCD_2COCD_3 \rightarrow CD_3H + CD_2COCD_3$

[3′] $CD_2H + CD_3COCD_3 \rightarrow CD_3H + CD_2COCD_3$

[4] $2CD_3 \rightarrow C_2D_6$

Some of the trideuteromethane can arise by reaction [3′]; we were not able to estimate the individual contributions of reactions [3′] and [3], though since reaction [3′] involves abstraction of deuterium atom and consequently will have a larger activation energy than reaction [3′], then it is likely that the major contribution to trideuteromethane formation will involve reaction [3].

When acetone-d_6 is selectively photolyzed in the presence of allyl formate the noncondensable products comprise H_2, CD_4, and CD_3H, the latter being formed in larger amounts than indicated by reaction [3]. The 'extra' amount CD_3H formed where measured was consistent with the reactions:

[5] $CD_3 + HCOOCH_2CH{=}CH_2 \rightarrow CD_3H + COOCH_2CH{=}CH_2$

[6] $COOCH_2CH{=}CH_2 \rightarrow CO_2 + CH_2CH{=}CH_2$,

if it is assumed that reaction [5] has a rate similar to that reported for other formates (3).

Can. J. Chem. Downloaded from www.nrcresearchpress.com by 210.87.254.105 on 09/05/12
For personal use only.

Can. J. Chem. Downloaded from www.nrcresearchpress.com by 210.87.254.105 on 09/05/12
For personal use only.

The observation that methane-d_3 is formed to only a limited extent suggests that few allyl radicals are produced by reactions [5] and [6] and hence the considerable yields of propylene and butene-1 (see Table I) cannot be completely explained by such reactions as [7] and [8].

[7] $CD_3 + CH_2{=}CHCH_2 \rightarrow CD_3CH_2CH{=}CH_2$

[8] $CH_2{=}CHCH_2 + RH \rightarrow CH_2{=}CHCH_3 + R$

It is possible that the small yield of allene may be explained by the disproportionation of allyl and allyl and allyl and methyl radicals, since values of 0.023 and 0.07 may be predicted for k_9/k_7 and k_{10}/k_{11} respectively from the equation

$$\log(k_{dis}/k_{comb}) = 0.131(S^0_{dis} - S^0_{comb}) - 5.47$$

suggested by Holroyd and Klein (6).

[9] $CD_3 + CH_2{=}CHCH_2 \rightarrow CD_3H + CH_2{=}C{=}CH_2$

[10] $2CH_2{=}CHCH_2 \rightarrow CH_2{=}C{=}CH_2 + CH_3CH{=}CH_2$

[11] $\rightarrow CH_2{=}CHCH_2CH_2CH{=}CH_2$

Also if allyl radicals are generated in appreciable yields, then since methyl radicals are also present in the reacting system, auto- and cross-combination of these radicals will lead to the formation of ethane, butene, and hexadiene in such proportions that the following relation should hold over the whole temperature range,

$$\frac{R_{C_4H_5D_3}}{R^{1/2}_{C_2D_6}R^{1/2}_{C_6H_{10}}} = 2,$$

since Kerr and Trotman-Dickenson (7) have shown this relation to hold for many alkyl radicals. In the final column of Table I we have tabulated this ratio and clearly it is considerably higher than 2 under our experimental conditions. We consider that this result implies that the butene and the hexadiene are formed by other reactions, and that these products, together with propylene, are formed by a mechanism not involving allyl radicals. The reaction sequence we propose begins with the addition of a methyl radical to allyl formate (reaction [12a]).

[12a] $CD_3 + HCOOCH_2CH{=}CH_2 \rightarrow (HCOOCH_2CHCH_2CD_3)$,

followed by a decomposition of the adduct radical (reaction [12b])

[12b] $(HCOOCH_2CHCH_2CD_3) \rightarrow H + CO_2 + CH_2{=}CHCH_2CD_3$.

The hydrogen atom formed in this decomposition may react with the formate by hydrogen atom abstraction to produce molecular hydrogen (reaction [13]).

[13] $H + HCOOCH_2CH{=}CH_2 \rightarrow H_2 + CO_2 + CH_2{=}CHCH_2$

Since, however, the hydrogen yield is much less than that of butene (typically 10–30%), this is clearly not the major fate of the hydrogen atoms. We consider this to be their reaction by addition to the formate, reaction [14a], followed by decomposition of the adduct radical, reaction [14b], yielding propylene and a further HCO_2 radical or hydrogen atom. This continues the chain process, which is, however, of fairly short length since there are several convenient chain termination steps and also probably not all of the adduct radicals decompose. Among the minor reaction products are propane and isobutane, which are probably formed by a series of reactions, the first of which is the addition of a hydrogen atom to propylene, since the latter is a major reaction product.

[14a] $H + HCOOCH_2CH{=}CH_2 \rightarrow (HCOOCH_2CHCH_3)$

[14b] $(HCOOCH_2CHCH_3) \rightarrow H + CO_2 + CH_2{=}CHCH_3$

The possibility exists that not all of the propylene is formed by the reaction involving hydrogen atom addition to the formate, but that some may be formed by the non-terminal addition of the methyl radical to the formate, reaction [15a], followed by decomposition of the adduct radical to yield propylene. Since we used trideuteromethyl radicals, such a series of reactions would yield propylene-d_3. Mass spectrometric analysis of the propylene formed showed it to contain no deuterium and we therefore conclude that methyl radicals play no part in the production of propylene, and that reaction [14] is the precursor to propylene formation.

[15a] $CD_3 + HCOOCH_2CH{=}CH_2 \rightarrow (HCOOCH_2CD_3CHCH_2)$

[15b] $(HCOOCH_2CD_3CHCH_2) \rightarrow HCOOCH_2 + CD_3CH{=}CH_2$

1,5-Hexadiene formation is mainly attributed to allyl radicals reacting with the formate by addition and subsequent decomposition of the adduct radical, i.e.

[16a] $CH_2{=}CHCH_2 + HCOOCH_2CH{=}CH_2 \rightarrow (HCOOCH_2CHCH_2CH_2CH{=}CH_2)$

[16b] $(HCOOCH_2CHCH_2CH_2CH{=}CH_2) \rightarrow H + CO_2 + CH_2{=}CHCH_2CH_2CH{=}CH_2.$

Allen and Pitts (8) studied the reactions of methyl radicals with crotonaldehyde and have concluded that the following reaction is important in butene-2 formation.

[17a] $CH_3 + HCOCH{=}CHCH_3 \rightarrow (HCOCH(CH_3)CHCH_3)$

[17b] $(HCOCH(CH_3)CHCH_3) \rightarrow HCO + CH_3CH{=}CHCH_3$

Assuming that this reaction is solely responsible for the butene-2, they calculated the ratio $R_{C_4H_8}/R^{1/2}{}_{C_2H_6}(\text{aldehyde}) = k_{17}/k_4{}^{1/2}$, and deduced values of 7.5 (kcal mole^{-1}) and 11.8 (mole^{-1} cm^3 s^{-1}) as the Arrhenius parameters for reaction [17].

In column 9, Table I, we have calculated the corresponding ratio $C_4H_5D_3/R^{1/2}{}_{C_2D_6}$(formate) for the reaction of methyl radicals with allyl formate. This is equivalent to assuming that reaction [12] is the sole source of butene-1. As can be seen from Table I, the ratio $k_{12}/k_4{}^{1/2}$ increases steadily up to about 200 °C and then decreases. An Arrhenius plot of our data shows appreciable curvature, particularly above 150 °C, and Arrhenius parameters may not be derived. This curvature may reflect the increasing competition of reactions [5] and [12], since a falloff in the ratio $C_4H_5D_3/R^{1/2}{}_{C_2D_6}$(formate) with increasing temperature is to be expected if reaction [5] becomes increasingly important with respect to reaction [12]. This might also reflect the decrease in the cross-combination ratio at 252 °C, since more allyl radicals will be generated as a result of reactions [5] and [6].

The principal reactions of the trideuteromethyl radicals generated by the photolysis of acetone-d_6 are [2], [3], [4], [5], and [12]. The following material balance relationship might therefore be expected to hold.

$$2R_{CO} = R_{CD_3H} + R_{CD_4} + 2R_{C_2D_6} + R_{C_4H_5D_3}$$

The data reported above for 252 °C indicate that this equation is obeyed within experimental error and lend support to the validity of our general scheme.

Acknowledgments

We thank the referee for helpful comments and Esso Research Ltd., for their support of this work.

1. J. G. CALVERT and J. N. PITTS, JR. Photochemistry. John Wiley and Sons, Inc., New York. 1966. Chap. 5.
2. R. S. TOLBERG and J. N. PITTS, JR. J. Am. Chem. Soc. **80**, 1304 (1958).
3. J. C. J. THYNNE. Trans. Faraday Soc. **58**, 676 (1962).
4. J. C. J. THYNNE. Trans. Faraday Soc. **58**, 1394 (1962).
5. D. G. L. JAMES and G. E. TROUGHTON. Trans. Faraday Soc. **62**, 120 (1966).
6. R. A. HOLROYD and G. W. KLEIN. J. Phys. Chem. **67**, 2273 (1963).
7. J. A. KERR and A. F. TROTMAN-DICKENSON. Progress in reaction kinetics. Vol. 1. The Pergamon Press, Ltd., London. 1961. p. 105.
8. E. R. ALLEN and J. N. PITTS, JR. J. Phys. Chem. **70**, 1691 (1966).

Thermal decomposition of propylene oxide

T. J. HARDWICK

Gulf Research & Development Company, Pittsburgh, Pennsylvania 15230

Received March 8, 1968

In the temperature range 402–425 °C, propylene oxide in a toluene medium decomposes to form propionaldehyde (60–70%), acetone (14%), and free radicals (25%). The ratio of products is invarient with temperature, suggesting a common precursor to all three products. Propionaldehyde further decomposes into free radicals. The first order rate expression for propylene oxide disappearance is

$$3.7 \times 10^{12}\, e^{-51900/RT}\, s^{-1}.$$

Canadian Journal of Chemistry, 46, 2454 (1968)

The thermal decomposition of propylene oxide has previously been studied in the gas phase at moderate (20–600 mm) pressures in the temperature range 445–499 °C by Thompson and Meissner (1). The inhibited reaction (several mm of NO) was first order in propylene oxide. Measurements were made of the pressure increase, and these were related to the oxide

Can. J. Chem. Downloaded from www.nrcresearchpress.com by 210.87.254.105 on 09/05/12
For personal use only.

[16a] $CH_2{=}CHCH_2 + HCOOCH_2CH{=}CH_2 \rightarrow (HCOOCH_2CHCH_2CH_2CH{=}CH_2)$

[16b] $(HCOOCH_2CHCH_2CH_2CH{=}CH_2) \rightarrow H + CO_2 + CH_2{=}CHCH_2CH_2CH{=}CH_2.$

Allen and Pitts (8) studied the reactions of methyl radicals with crotonaldehyde and have concluded that the following reaction is important in butene-2 formation.

[17a] $CH_3 + HCOCH{=}CHCH_3 \rightarrow (HCOCH(CH_3)CHCH_3)$

[17b] $(HCOCH(CH_3)CHCH_3) \rightarrow HCO + CH_3CH{=}CHCH_3$

Assuming that this reaction is solely responsible for the butene-2, they calculated the ratio $R_{C_4H_8}/R^{1/2}{}_{C_2H_6}(\text{aldehyde}) = k_{17}/k_4{}^{1/2}$, and deduced values of 7.5 (kcal mole^{-1}) and 11.8 (mole^{-1} cm^3 s^{-1}) as the Arrhenius parameters for reaction [17].

In column 9, Table I, we have calculated the corresponding ratio $C_4H_5D_3/R^{1/2}{}_{C_2D_6}$(formate) for the reaction of methyl radicals with allyl formate. This is equivalent to assuming that reaction [12] is the sole source of butene-1. As can be seen from Table I, the ratio $k_{12}/k_4{}^{1/2}$ increases steadily up to about 200 °C and then decreases. An Arrhenius plot of our data shows appreciable curvature, particularly above 150 °C, and Arrhenius parameters may not be derived. This curvature may reflect the increasing competition of reactions [5] and [12], since a falloff in the ratio $C_4H_5D_3/R^{1/2}{}_{C_2D_6}$(formate) with increasing temperature is to be expected if reaction [5] becomes increasingly important with respect to reaction [12]. This might also reflect the decrease in the cross-combination ratio at 252 °C, since more allyl radicals will be generated as a result of reactions [5] and [6].

The principal reactions of the trideuteromethyl radicals generated by the photolysis of acetone-d_6 are [2], [3], [4], [5], and [12]. The following material balance relationship might therefore be expected to hold.

$$2R_{CO} = R_{CD_3H} + R_{CD_4} + 2R_{C_2D_6} + R_{C_4H_5D_3}$$

The data reported above for 252 °C indicate that this equation is obeyed within experimental error and lend support to the validity of our general scheme.

Acknowledgments

We thank the referee for helpful comments and Esso Research Ltd., for their support of this work.

1. J. G. Calvert and J. N. Pitts, Jr. Photochemistry. John Wiley and Sons, Inc., New York. 1966. Chap. 5.
2. R. S. Tolberg and J. N. Pitts, Jr. J. Am. Chem. Soc. **80**, 1304 (1958).
3. J. C. J. Thynne. Trans. Faraday Soc. **58**, 676 (1962).
4. J. C. J. Thynne. Trans. Faraday Soc. **58**, 1394 (1962).
5. D. G. L. James and G. E. Troughton. Trans. Faraday Soc. **62**, 120 (1966).
6. R. A. Holroyd and G. W. Klein. J. Phys. Chem. **67**, 2273 (1963).
7. J. A. Kerr and A. F. Trotman-Dickenson. Progress in reaction kinetics. Vol. 1. The Pergamon Press, Ltd., London. 1961. p. 105.
8. E. R. Allen and J. N. Pitts, Jr. J. Phys. Chem. **70**, 1691 (1966).

Thermal decomposition of propylene oxide

T. J. Hardwick

Gulf Research & Development Company, Pittsburgh, Pennsylvania 15230

Received March 8, 1968

In the temperature range 402–425 °C, propylene oxide in a toluene medium decomposes to form propionaldehyde (60–70%), acetone (14%), and free radicals (25%). The ratio of products is invarient with temperature, suggesting a common precursor to all three products. Propionaldehyde further decomposes into free radicals. The first order rate expression for propylene oxide disappearance is

$$3.7 \times 10^{12}\, e^{-51900/RT}\, s^{-1}.$$

Canadian Journal of Chemistry, 46, 2454 (1968)

The thermal decomposition of propylene oxide has previously been studied in the gas phase at moderate (20–600 mm) pressures in the temperature range 445–499 °C by Thompson and Meissner (1). The inhibited reaction (several mm of NO) was first order in propylene oxide. Measurements were made of the pressure increase, and these were related to the oxide

Can. J. Chem. Downloaded from www.nrcresearchpress.com by 210.87.254.42 on 09/05/12
For personal use only.

Can. J. Chem. Downloaded from www.nrcresearchpress.com by 210.87.254.42 on 09/05/12
For personal use only.

disappearance. Products included ethylene, carbon monoxide, propionaldehyde; both isomerization and free radical formation were postulated.

We have reexamined the thermal decomposition of propylene oxide in the temperature range 402–459 °C using as a radical scavenger (inhibitor) a large excess (100/1) of toluene. This served the additional purpose of acting as an inert carrier for both the initial propylene oxide and the liquid products.

Pyrolyses were made in small stainless steel pressure vessels (7.35 ml) equipped with two capillary tubes leading to removable valves. Liquid was added to the vessel prior to installing the valves, and air was removed by evacuation while the solution was chilled to −78 °C. Decomposition took place when the vessels were immersed in a 6 l salt bath maintained at high temperature to ±0.3 °C. The cooled liquid was removed from the reaction vessels and analyzed by gas–liquid chromatography on a column suitable for quantitative separation of propylene oxide, propionaldehyde, toluene, and acetone. This last product had not been observed previously.

As the pyrolyses temperatures were above the critical temperatures of both reactants and products, the original liquid in the vessel expanded to fill the volume uniformly. The estimated gross pressure was 4000–5000 p.s.i.

In the range 402–459 °C, propylene oxide disappeared in a first order reaction (at least 80% of its loss). The acetone formed decomposed slowly and its initial rate of formation was obtained with good accuracy. Propionaldehyde decomposed rather rapidly and, in fact, reached a maximum concentration when some 50–60% of the propylene oxide had disappeared (cf. ref. 1). Its initial rate of formation was not easy to establish with desirable accuracy. A typical plot of product formation versus time is shown in Fig. 1.

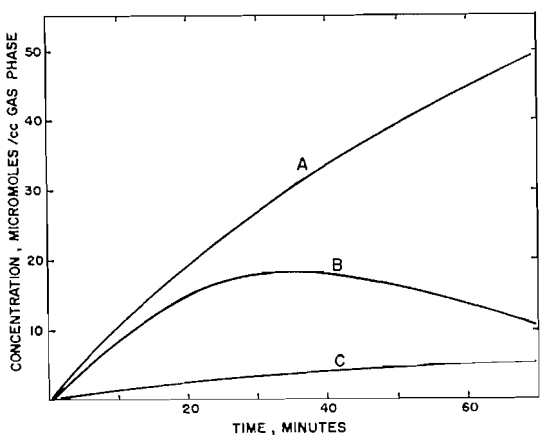

FIG. 1. Propylene oxide decomposition at 428 °C: (A) loss of propylene oxide, (B) formation of propionaldehyde, (C) formation of acetone.

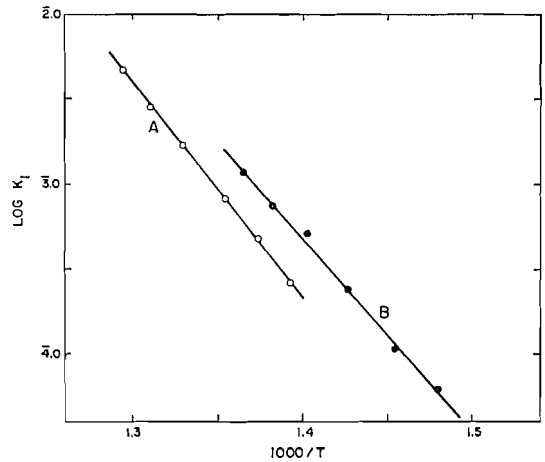

FIG. 2. Arrhenius plot of first order rate constants for propylene oxide decomposition: (A) data of Thompson and Meissner, (B) present data.

TABLE I

First order rate constants for propylene oxide decomposition

T (°C)	k_1 (s^{-1})
459	1.13×10^{-3}
450	7.28×10^{-4}
440	5.04×10^{-4}
428	2.39×10^{-4}
414.5	1.05×10^{-4}
402	6.0×10^{-5}

First order rate constants for the measured disappearance of propylene oxide were determined at six temperatures (Table I). An Arrhenius plot (Fig. 2) gave the rate expression

$$k_1 = 3.7 \times 10^{12}\ e^{-51900/RT}\ s^{-1}.$$

The fraction decomposing into acetone was constant over the whole temperature range

(0.14 ± 0.02). The fraction decomposing to propionaldehyde could not be determined with as great precision, but was 0.60 ± 0.10 with no significant variation over the temperature range studied. The balance of the propylene oxide lost (about 25%) was assumed to have decomposed into free radicals.

As all three modes of decomposition occur with the same relative probability, regardless of temperature, it appears that the rate-governing step is a unimolecular rearrangement of propylene oxide into some intermediate form, which in turn decomposes by three different routes.

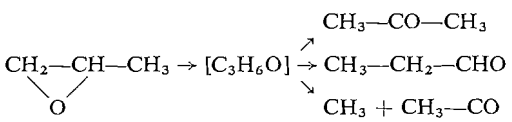

Our rate data do not agree with those of Thompson (1) (Fig. 2), although he, too, found no change in mechanism over the range studied. One suggestion to account for the higher activation energy is that at higher temperature the propionaldehyde decomposed to a greater extent in Thompson's case, giving more gas, and hence an apparent increase in decomposition. In the earlier work the loss in propylene oxide was calculated from the assumed stoichiometry of the reaction, whereas in the present work the propylene oxide concentration was measured directly. Rearrangement into acetone and propionaldehyde involves no change in pressure; the increase in pressure observed by Thompson arose from reactions subsequent to the breakdown of propylene oxide and propionaldehyde into free radicals.

As propionaldehyde decomposes homogeneously with an activation energy of 50.3 kcal (2), the behavior of the concentration–time curve for its production is readily explained. Acetone, on the other hand, requires 68 kcal activation energy for thermal decomposition (3) and would not decompose significantly under the conditions of our experiments.

1. H. W. THOMPSON and M. MEISSNER. Trans. Faraday Soc. 34, 1222 (1938).
2. A. F. BOYER and M. NICLAUSE. Compt. Rend. 233, 687 (1951).
3. E. W. R. STEACIE. Atomic and free radical reactions. Vol. 1. Reinhold Publishing Corp., New York. 1954. p. 220.

Can. J. Chem. Downloaded from www.nrcresearchpress.com by 210.87.254.42 on 09/05/12
For personal use only.

Détermination de la température thêta pour le système polyméthacrylate de méthyle – tétrachlorure de carbone

NGA HO-DUC ET HUBERT DAOUST
Département de Chimie, Université de Montréal, Montréal, Québec

Reçu le 21 juillet 1967

La température thêta pour le système polyméthacrylate de méthyle – tétrachlorure de carbone a été déterminée par la diffusion de la lumière et par la viscosimétrie. On a obtenu 43.5 ± 1 °C par la première méthode et 48 ± 1 °C par la deuxième méthode.

The theta temperature for the conventional polymethylmethacrylate – carbon tetrachloride system has been determined by light scattering and by viscometry. It is found to be 43.5 ± 1 °C by the first method and 48 ± 1 °C by the second.

Canadian Journal of Chemistry, 46, 2456 (1968)

Introduction

La viscosimétrie offre une méthode simple pour la détermination de la température thêta pour un système polymère–solvant. La théorie de Fox et Flory (1) permet de relier la viscosité intrinsèque d'un polymère dans un solvant donné et le coefficient d'expansion linéaire intramoléculaire α_η. Cette relation s'écrit

$$[1] \qquad [\eta] = KM^{1/2}\alpha_\eta{}^3,$$

où $K = \Phi(\overline{R_0{}^2}/M)^{3/2}$, M étant la masse molaire du polymère, Φ, une constante universelle et $\overline{R_0{}^2}$, la distance quadratique moyenne entre les bouts de la chaîne dans un solvant thêta. Alors

(0.14 ± 0.02). The fraction decomposing to propionaldehyde could not be determined with as great precision, but was 0.60 ± 0.10 with no significant variation over the temperature range studied. The balance of the propylene oxide lost (about 25%) was assumed to have decomposed into free radicals.

As all three modes of decomposition occur with the same relative probability, regardless of temperature, it appears that the rate-governing step is a unimolecular rearrangement of propylene oxide into some intermediate form, which in turn decomposes by three different routes.

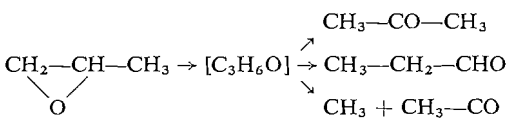

Our rate data do not agree with those of Thompson (1) (Fig. 2), although he, too, found no change in mechanism over the range studied. One suggestion to account for the higher activation energy is that at higher temperature the propionaldehyde decomposed to a greater extent in Thompson's case, giving more gas, and hence an apparent increase in decomposition. In the earlier work the loss in propylene oxide was calculated from the assumed stoichiometry of the reaction, whereas in the present work the propylene oxide concentration was measured directly. Rearrangement into acetone and propionaldehyde involves no change in pressure; the increase in pressure observed by Thompson arose from reactions subsequent to the breakdown of propylene oxide and propionaldehyde into free radicals.

As propionaldehyde decomposes homogeneously with an activation energy of 50.3 kcal (2), the behavior of the concentration–time curve for its production is readily explained. Acetone, on the other hand, requires 68 kcal activation energy for thermal decomposition (3) and would not decompose significantly under the conditions of our experiments.

1. H. W. THOMPSON and M. MEISSNER. Trans. Faraday Soc. 34, 1222 (1938).
2. A. F. BOYER and M. NICLAUSE. Compt. Rend. 233, 687 (1951).
3. E. W. R. STEACIE. Atomic and free radical reactions. Vol. 1. Reinhold Publishing Corp., New York. 1954. p. 220.

Can. J. Chem. Downloaded from www.nrcresearchpress.com by 210.87.254.42 on 09/05/12
For personal use only.

Détermination de la température thêta pour le système polyméthacrylate de méthyle – tétrachlorure de carbone

NGA HO-DUC ET HUBERT DAOUST
Département de Chimie, Université de Montréal, Montréal, Québec

Reçu le 21 juillet 1967

La température thêta pour le système polyméthacrylate de méthyle – tétrachlorure de carbone a été déterminée par la diffusion de la lumière et par la viscosimétrie. On a obtenu 43.5 ± 1 °C par la première méthode et 48 ± 1 °C par la deuxième méthode.

The theta temperature for the conventional polymethylmethacrylate – carbon tetrachloride system has been determined by light scattering and by viscometry. It is found to be 43.5 ± 1 °C by the first method and 48 ± 1 °C by the second.

Canadian Journal of Chemistry, 46, 2456 (1968)

Introduction

La viscosimétrie offre une méthode simple pour la détermination de la température thêta pour un système polymère–solvant. La théorie de Fox et Flory (1) permet de relier la viscosité intrinsèque d'un polymère dans un solvant donné et le coefficient d'expansion linéaire intramoléculaire α_η. Cette relation s'écrit

$$[1] \qquad [\eta] = KM^{1/2}\alpha_\eta{}^3,$$

où $K = \Phi(\overline{R_0{}^2}/M)^{3/2}$, M étant la masse molaire du polymère, Φ, une constante universelle et $\overline{R_0{}^2}$, la distance quadratique moyenne entre les bouts de la chaîne dans un solvant thêta. Alors

une série de mesures de viscosités intrinsèques de plusieurs fractions d'un polymère dans un solvant à différentes températures nous permettent de tracer les graphiques de la quantité $[\eta]/M^{1/2}$ en fonction de la température. Ces graphiques se croisent à température thêta car alors α_η est égal à l'unité.

La détermination de la température thêta peut aussi se faire par l'étude de la variation du second coefficient du viriel A_2, en fonction de la température, et à la température thêta, A_2 s'annule. Cette étude peut se faire par la mesure de la lumière diffusée par une solution diluée de polymère. Les grandeurs qu'on mesure habituellement en diffusion de la lumière sont les intensités des rayons lumineux émergents et l'équation de la variation de l'intensité diffusée en fonction de la concentration est donnée par (2)

$$[2]\quad kc(1 + \cos^2\theta)/(R_\theta - R_\theta^0) = 1/MP(\theta) + 2A_2c,$$

où k est une constante pour un système donné dans la mesure où l'incrément de l'indice de réfraction est indépendant du poids moléculaire du soluté, ce qui est généralement le cas. Elle est définie par

$$[3]\quad k = 2\pi^2 n_0^2 (dn/dc)^2/N_0\lambda_0^4,$$

où n_0 est l'indice de réfraction du solvant, dn/dc, l'incrément d'indice de réfraction dû à la présence du soluté, N_0, le nombre d'Avogadro et λ, la longueur d'onde de la lumière incidente. Les quantités R_θ et R_θ^0 sont les rapports de Rayleigh de la solution et du solvant mesurés sous un angle d'observation θ; c est la concentration en g/ml. Il s'agit donc de mesurer l'intensité de la lumière diffusée par des solutions de différentes concentrations et celà, à différentes températures.

Partie expérimentale

Les fractions de masses molaires moyennes viscosimétriques ($\bar{M}_v$) égales à 3.91×10^5, 6.75×10^5 et 1.34×10^6 ont été obtenues à partir d'un échantillon préparé selon la méthode suggérée par Fox *et coll.* (3). Le fractionnement a été fait dans l'acétone par addition d'heptane; 12 fractions ont été obtenues à partir d'une solution de 100 g de polymère dans 5 l d'acétone.

Les masses molaires des fractions obtenues ont été déterminées par viscosimétrie en utilisant le benzène comme solvant à 30° (4).

Les viscosités intrinsèques des différentes fractions en solution dans le tétrachlorure de carbone ont été déterminées à 35, 45, 50 et 55 °C.

Les mesures d'intensités de la lumière diffusée par rapport au toluène utilisé comme standard de référence ont été effectuées à des températures allant de 30 à 55 °C à l'aide d'un photo-gonio-diffusiomètre Sofica. Le liquide utilisé dans la cuve de l'appareil était du xylène. Le dépoussiérage du solvant et des solutions-mères préparées par gravimétrie a été réalisé par filtration à travers un filtre de verre fritté de porosité ultra fine. Le dispositif de filtrage a déjà été décrit ailleurs (5). Les dilutions furent préparées par gravimétrie également. Ces opérations se sont passées à l'intérieur d'une boîte à gants maintenue à 40 °C. Tous les solvants utilisés dans ce travail étaient de qualité réactif analytique.

Résultats et discussion

La Fig. 1 représente les diagrammes de Zimm, pour un angle de 90°, obtenus à partir de l'éq. [2] pour les trois fractions étudiées. Les rapports de Rayleigh sont exprimés en termes d'intensités relatives I et I_0 de la lumière diffusée par la solution et le solvant respectivement, en unités arbitraires. La Fig. 2 représente la variation de la pente des droites de la Fig. 1 en fonction de la température.

Bien que les droites de la Fig. 2 ne se croisent pas au point d'ordonnée zéro, les résultats nous

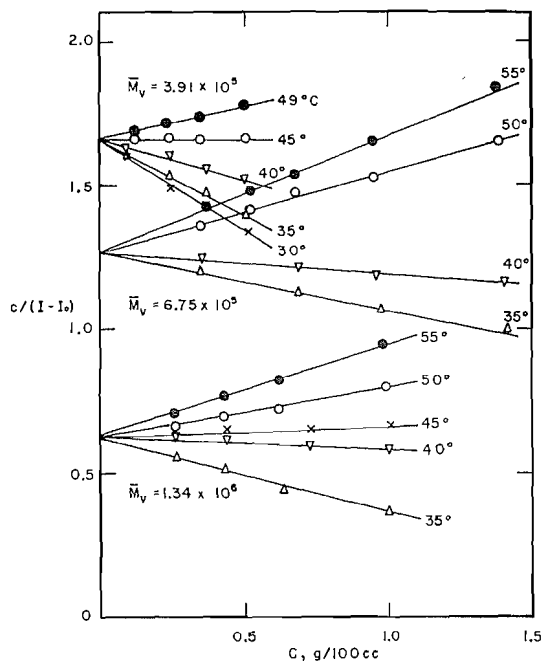

FIG. 1. Diagrammes de Zimm pour $\theta = 90°$, à différentes températures pour chacune des fractions.

Can. J. Chem. Downloaded from www.nrcresearchpress.com by 210.87.254.42 on 09/05/12
For personal use only.

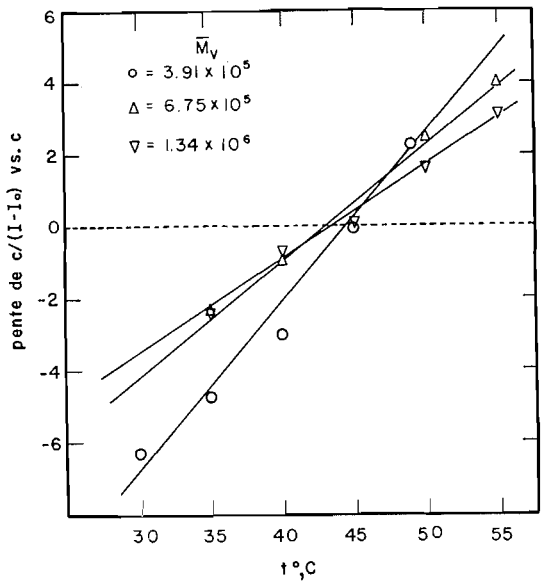

FIG. 2. Variation de la pente des diagrammes de Zimm en fonction de la température.

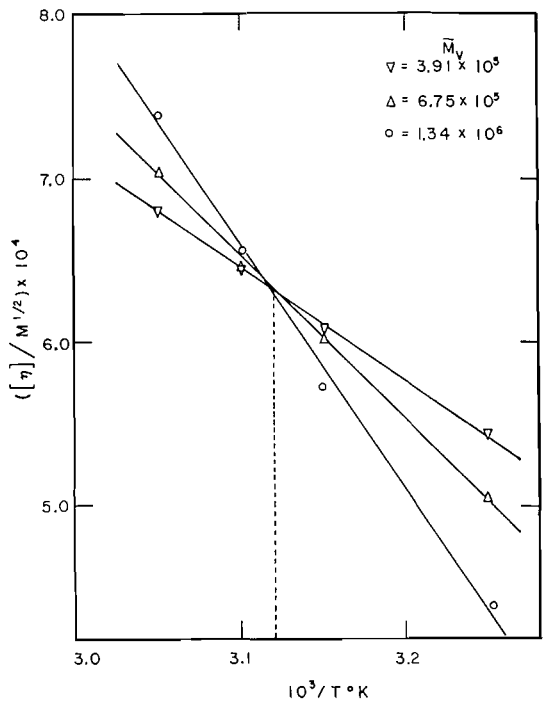

FIG. 3. Vérification de la valeur du point thêta par viscosité.

permettent de déterminer sans ambiguité que la température thêta se situe aux environs de 43.5 ± 1 °C.

La Fig. 3 représente la variation de $[\eta]/M^{1/2}$ en fonction de la température pour les trois fractions. Les résultats indiquent que la température thêta se trouve aux environs de 48 ± 1 °C. La différence entre les deux valeurs rapportées dans ce présent travail pour la température thêta peut venir de l'hétérogénéité des fractions utilisées mais dans les deux cas, elle est beaucoup plus élevée que celle donnée par Fox (6) soit 27 °C. La différence dans la tacticité des échantillons de polyméthacrylate de méthyle utilisés dans les deux travaux ne saurait expliquer la divergence des résultats. Ordinairement la différence dans les températures thêta entre un échantillon de polymère atactique et des ses isomères isotactique et syndiotactique n'est que quelques degrés (7). Une autre explication pourrait se trouver dans une différence du degré de ramification ou de réticulation des deux séries d'échantillons de polymères. Cependant, une étude de la diffusion de la lumière par la fraction de masse molaire 6.75×10^5 en solution dans l'heptanone-4 à 34 °C, la température thêta pour ce système (6), indique que notre polymère possède une structure qui se compare bien à celle du polymère préparé par Fox *et coll.* (3) car la pente du graphique de $c/(I - I_0)$ vs. c est bien nulle dans ce cas. Par ailleurs, la constante structurale $(\overline{R_0^2}/M)^{1/2}$ telle que calculée à partir de la valeur moyenne trouvée pour K, soit 6.32×10^{-4}, et en utilisant 2.87×10^{21} pour la valeur de Φ à la température thêta, est de 610×10^{-11} en unités c.g.s., une valeur qui se compare très bien avec celles rapportées par Kurata et Stockmayer (8). La littérature rapporte des valeurs de K allant de 4.8×10^{-4} à 7×10^{-4} (6, 8, 9); le polyméthacrylate de méthyle est un des polymères pour lesquels les valeurs de la constante K s'étalent sur une gamme aussi étendue.

Remerciements

Nous remercions le Conseil National de Recherche pour son aide financière au cours de ce travail. Mme Ho-Duc le remercie également pour les bourses d'études qui lui ont été octroyées.

1. P. J. FLORY. Principles of polymer chemistry. Cornell Univ. Press, Ithaca, N.Y. 1953.
2. B. H. ZIMM. J. Chem. Phys. **16**, 1093 (1948).

Can. J. Chem. Downloaded from www.nrcresearchpress.com by 210.87.254.42 on 09/05/12
For personal use only.

3. T. G. Fox, J. B. Kinsinger, H. F. Mason et E. M. Schuele. Polymer, **3**, 71 (1962).
4. E. Cohn-Ginsberg, T. G. Fox et H. F. Mason. Polymer, **3**, 97 (1962).
5. J. Duranceau. Thèse de Doctorat. Université de Montréal, Montréal, Québec. 1966.
6. T. G. Fox. Polymer, **3**, 111 (1962).
7. W. R. Krigbaum. Newer methods of polymer characterization. Interscience Publishers, Inc., New York. 1964. Chap. I.
8. M. Kurata et W. H. Stockmayer. Fortschr. Hochpolymer Forsch. **3**, 196 (1963).
9. G. V. Schulz et R. Kirste. Z. Physik. Chem. **30**, 171 (1961).

Role of the triplet state in the benzene-sensitized decomposition of chloroform[1]

S. H. Ng, G. P. Semeluk, and I. Unger
Chemistry Department, University of New Brunswick, Fredericton, New Brunswick

Received January 22, 1968

A study has been made of the effect of increasing chloroform pressure on benzene and biacetyl emission under various conditions. No quenching of benzene fluorescence by chloroform is observed when excitation is by 2570 Å radiation, whether or not biacetyl is present. On the other hand, quenching of the sensitized biacetyl phosphorescence is pronounced. However, it is demonstrated that chloroform does not quench biacetyl phosphorescence when excitation occurs at 3660 Å, from which it can be concluded that chloroform preferentially accepts energy from the benzene triplet rather than the excited singlet. Therefore it is probably the triplet which is responsible for the benzene-photosensitized decomposition of chloroform previously reported.

Canadian Journal of Chemistry, **46**, 2459 (1968)

Can. J. Chem. Downloaded from www.nrcresearchpress.com by 210.87.254.42 on 09/05/12
For personal use only.

Introduction

The increasing popularity of organic sensitizers as initiators of a large variety of photochemical reactions in both gas and liquid phases (1–3) is related to the many advantages these have over the traditional inorganic sensitizers. The more important among these are no doubt due to the greater range of energies and states available in regions of interest to chemists. Thus, it is often possible to excite an acceptor molecule selectively to a triplet state and then study the resulting chemistry (3–5). This is particularly useful for molecules such as ketones and aldehydes where more than one primary mode of decomposition is observed on direct excitation (6, 7). Recently Lee and co-workers (8, 9) have used benzene sensitization as a diagnostic tool in mechanism studies.

In the case of chlorine-containing acceptor molecules mercury sensitization cannot be used because of a chemical reaction between excited mercury and the chloride (10). Relatively few studies of organic-sensitized decomposition of such chlorides have been reported. Oster and Kallmann (11) used benzene to sensitize the decomposition of CCl_4 in solution, attributing the sensitization to the "first excited state" of benzene. Van Dusen and Hamill (12) examined the benzene-sensitized decomposition of several alkyl halides in solution and suggested the possibility of triplet benzene sensitization. It has been shown that the direct photolysis of $CHCl_3$ vapor at 1849 Å leads to a carbon–chlorine bond cleavage, whereas the benzene-sensitized decomposition at 2537 Å results in a carbon–hydrogen bond break (13, 14). In the first of these reports (13) we commented on the unexpected result that the sensitized process which involved an energy input much lower than the direct photolysis nevertheless broke the stronger of the two bonds in chloroform, while the direct photolysis involved the weaker bond. We interpreted this to mean that these dissociations took place in different excited electronic states of the chloroform, and speculated that while the photolysis involved an $n_{Cl} \rightarrow \sigma^*_{C-Cl}$ transition, the sensitized reaction involved a $\sigma_{C-H} \rightarrow \sigma^*_{C-H}$ transition with spin inversion in which the required energy was transferred from the benzene triplet in a manner analogous to the mercury-photosensitized decomposition of hydrocarbons. The mechanism of this decomposition was fully discussed in the second report (14). It was not possible, however, to present any evidence in support of our speculation. We report here some spectrofluorometric results which strongly suggest that the benzene triplet is the energy donor.

[1]This note is Part II of "Spectrofluorometric Studies".

3. T. G. Fox, J. B. Kinsinger, H. F. Mason et E. M. Schuele. Polymer, **3**, 71 (1962).
4. E. Cohn-Ginsberg, T. G. Fox et H. F. Mason. Polymer, **3**, 97 (1962).
5. J. Duranceau. Thèse de Doctorat. Université de Montréal, Montréal, Québec. 1966.
6. T. G. Fox. Polymer, **3**, 111 (1962).
7. W. R. Krigbaum. Newer methods of polymer characterization. Interscience Publishers, Inc., New York. 1964. Chap. I.
8. M. Kurata et W. H. Stockmayer. Fortschr. Hochpolymer Forsch. **3**, 196 (1963).
9. G. V. Schulz et R. Kirste. Z. Physik. Chem. **30**, 171 (1961).

Role of the triplet state in the benzene-sensitized decomposition of chloroform[1]

S. H. Ng, G. P. Semeluk, and I. Unger
Chemistry Department, University of New Brunswick, Fredericton, New Brunswick

Received January 22, 1968

A study has been made of the effect of increasing chloroform pressure on benzene and biacetyl emission under various conditions. No quenching of benzene fluorescence by chloroform is observed when excitation is by 2570 Å radiation, whether or not biacetyl is present. On the other hand, quenching of the sensitized biacetyl phosphorescence is pronounced. However, it is demonstrated that chloroform does not quench biacetyl phosphorescence when excitation occurs at 3660 Å, from which it can be concluded that chloroform preferentially accepts energy from the benzene triplet rather than the excited singlet. Therefore it is probably the triplet which is responsible for the benzene-photosensitized decomposition of chloroform previously reported.

Canadian Journal of Chemistry, **46**, 2459 (1968)

Can. J. Chem. Downloaded from www.nrcresearchpress.com by 210.87.254.42 on 09/05/12
For personal use only.

Introduction

The increasing popularity of organic sensitizers as initiators of a large variety of photochemical reactions in both gas and liquid phases (1–3) is related to the many advantages these have over the traditional inorganic sensitizers. The more important among these are no doubt due to the greater range of energies and states available in regions of interest to chemists. Thus, it is often possible to excite an acceptor molecule selectively to a triplet state and then study the resulting chemistry (3–5). This is particularly useful for molecules such as ketones and aldehydes where more than one primary mode of decomposition is observed on direct excitation (6, 7). Recently Lee and co-workers (8, 9) have used benzene sensitization as a diagnostic tool in mechanism studies.

In the case of chlorine-containing acceptor molecules mercury sensitization cannot be used because of a chemical reaction between excited mercury and the chloride (10). Relatively few studies of organic-sensitized decomposition of such chlorides have been reported. Oster and Kallmann (11) used benzene to sensitize the decomposition of CCl_4 in solution, attributing the sensitization to the "first excited state" of benzene. Van Dusen and Hamill (12) examined the benzene-sensitized decomposition of several alkyl halides in solution and suggested the possibility of triplet benzene sensitization. It has been shown that the direct photolysis of $CHCl_3$ vapor at 1849 Å leads to a carbon–chlorine bond cleavage, whereas the benzene-sensitized decomposition at 2537 Å results in a carbon–hydrogen bond break (13, 14). In the first of these reports (13) we commented on the unexpected result that the sensitized process which involved an energy input much lower than the direct photolysis nevertheless broke the stronger of the two bonds in chloroform, while the direct photolysis involved the weaker bond. We interpreted this to mean that these dissociations took place in different excited electronic states of the chloroform, and speculated that while the photolysis involved an $n_{Cl} \rightarrow \sigma^*_{C-Cl}$ transition, the sensitized reaction involved a $\sigma_{C-H} \rightarrow \sigma^*_{C-H}$ transition with spin inversion in which the required energy was transferred from the benzene triplet in a manner analogous to the mercury-photosensitized decomposition of hydrocarbons. The mechanism of this decomposition was fully discussed in the second report (14). It was not possible, however, to present any evidence in support of our speculation. We report here some spectrofluorometric results which strongly suggest that the benzene triplet is the energy donor.

[1]This note is Part II of "Spectrofluorometric Studies".

Can. J. Chem. Downloaded from www.nrcresearchpress.com by 210.87.254.42 on 09/05/12
For personal use only.

Experimental

Materials

Hartmann–Ledden "Fluorometric Grade" benzene was shown by vapor phase chromatography to have a negligible impurity content, and was therefore used without further treatment. Chloroform was purified according to the method already described (14). Biacetyl from the Aldrich Chemical Company was stored in a blackened bulb and used without purification.

Apparatus and Procedure

All emission measurements were made with a modified Aminco–Bowman spectrophotofluorometer (s.p.f.). The techniques and most of the other experimental details were as described previously (15). The s.p.f. cell, a quartz cuvette-type, 1 cm × 1 cm × 4.6 cm, was attached to a mercury- and grease-free handling system equipped with Hoke packless diaphragm metal valves. In the present investigation mixing was effected with an all-glass circulating pump constructed at the National Research Council of Canada laboratories in Ottawa. Adequate mixing was indicated by constant absorption and emission.

With the excitation monochromator set for 2540 Å, and using a 200 watt xenon–mercury compact arc source, the exciting light was analyzed with the help of a Jarrel Ash 1/2 m grating monochromator and a Hilger-Watts Schwartz vacuum thermopile. Because of reversal at 2537 Å, the exciting light was asymmetrically distributed about the maximum at 2570 Å, and extended from 2548 Å to 2580 Å. With this monochromator setting benzene absorbs entirely in the region where constant triplet and singlet yields are observed (16). We may therefore consider the present study and the previous one (14) to have been carried out at essentially the same excitation wavelength.

TABLE I

Dependence of benzene fluorescent yield on chloroform pressure (excitation wavelength 2570 Å; benzene pressure 22 Torr)

$CHCl_3$ pressure (Torr)	Fluorescent yield, Φ_f
0	0.183*
2.37	0.187
5.82	0.188
11.8	0.199
17.7	0.193
28.2	0.177
38.8	0.175
54.6	0.174
70.7	0.177
93.0	0.182
	Mean value 0.183 ± 0.007

*Reference value (17).

TABLE II

Dependence of biacetyl emission yield on chloroform pressure (excitation wavelength 3660 Å; biacetyl pressure 20.3 Torr)

$CHCl_3$ pressure (Torr)	Yield relative to pure biacetyl
0	1
11.5	1.03 ± 0.03
23.0	1.02 ± 0.03
40.1	1.07 ± 0.03
57.1	1.05 ± 0.03

Results and Discussion

Three types of experiments were performed:

(1) An investigation of the effect of chloroform pressure on the fluorescent yield of 22.0 Torr benzene excited by 2570 Å radiation. The yields are based on the value given by Noyes *et al.* (17), and are listed in Table I.

(2) An investigation of the effect of chloroform pressure on the emission yield of 20.3 Torr of biacetyl excited by 3660 Å radiation. The relative phosphorescent yields are summarized in Table II.

(3) An investigation of the effect of chloroform pressure on the benzene (22 Torr) sensitized emission yield of biacetyl (0.17 Torr) excited by 2570 Å. The yield, which is based on the values given by Noyes and Harter (16), is depicted in Fig. 1*a*. These particular benzene and biacetyl partial pressures were chosen in order to obtain the maximum sensitized emission yield of biacetyl (18), and to use it as reference point. The yield of benzene fluorescence as a function of chloroform partial pressure was monitored simultaneously. This yield, uncorrected for biacetyl absorption and sensitized decomposition, is shown in Fig. 1*b*.

Table I illustrates the significant fact that chloroform does not quench benzene fluorescence, which indicates that it is not the excited benzene singlet which is responsible for the photosensitized decomposition of chloroform.

From the results given in Table II it can be concluded that chloroform does not quench biacetyl phosphorescence (a result which is not surprising since it is unlikely that chloroform would have an energy state close to the first triplet of biacetyl). We may conclude also that no chemical reaction takes place between excited biacetyl and ground state chloroform.

Figure 1 illustrates the contrasting situation which occurs in a system containing all three compounds when it absorbs 2570 Å radiation: sensitized biacetyl emission is quenched by chloroform, but the benzene fluorescence is little

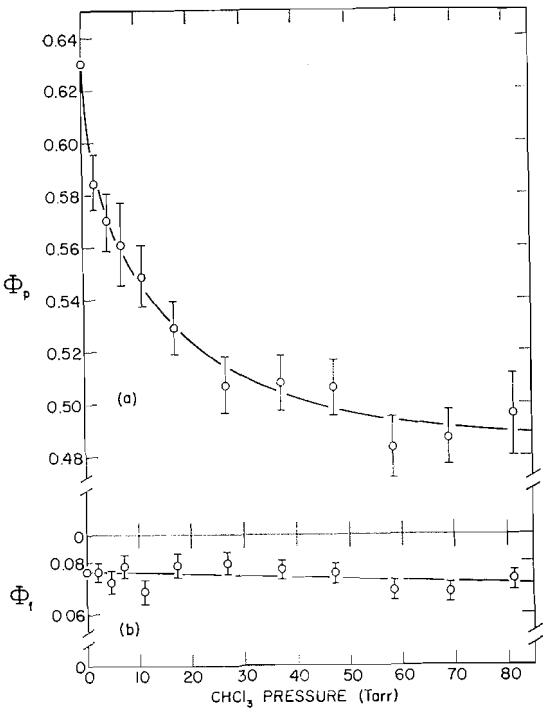

FIG. 1. Variation of emission yields with chloroform pressure: biacetyl pressure = 0.17 Torr, benzene pressure = 22 Torr. (*a*) Sensitized biacetyl emission yield (Φ_p), normalized to benzene triplet yield (16) at zero chloroform pressure. (*b*) Benzene fluorescent yield (Φ_f). The line is the best-fit straight line resulting from a least squares treatment.

affected. Since chloroform does not directly quench the biacetyl triplet emission (Table II), it must be quenching that species (benzene triplet) which is exciting the biacetyl triplet. This means that chloroform more readily accepts energy from the benzene triplet than from the benzene singlet, and it is therefore likely that it is the triplet which is responsible for the sensitized decomposition of chloroform previously reported.

In terms of the mechanism previously discussed (14), the reaction

[26] $$^3B_v^1 + CHCl_3 \rightarrow B + \cdot CCl_3 + H$$

applies, rather than

[26*a*] $$^1B^1 + CHCl_3 \rightarrow B + \cdot CCl_3 + H.$$

Acknowledgments

The authors gratefully acknowledge a grant from the Associated Alumni of the University of New Brunswick towards the purchase of instrumentation used in this study, and operating grants from the National Research Council of Canada. We wish to thank Mr. S. Stevens for assistance in collecting some of the data.

NOTE ADDED IN PROOF: Dr. O. P. Strausz has commented on the apparent inability of chloroform to completely quench the sensitized emission (Fig. 1*a*). He suggests that this may be interpreted to mean that chloroform is not able to accept energy from triplet benzene which has been vibrationally deactivated below some definite fairly high energy level, and is additional evidence for reaction [26].

1. G. S. HAMMOND, P. A. LEERMAKERS, and N. J. TURRO. J. Am. Chem. Soc. **83**, 2395 (1961).
2. G. S. HAMMOND, C. A. STOUT, and A. A. LAMOLA. J. Am. Chem. Soc. **86**, 3103 (1964).
3. R. E. REBBERT and P. AUSLOOS. J. Am. Chem. Soc. **86**, 4803 (1964).
4. G. S. HAMMOND and N. J. TURRO. Science, **142**, 1541 (1963).
5. P. BORREL. J. Am. Chem. Soc. **86**, 3156 (1964).
6. R. G. W. NORRISH and M. E. S. APPLEYARD. J. Chem. Soc. 874 (1934).
7. R. SRINIVASAN. J. Am. Chem. Soc. **81**, 1546 (1959).
8. E. K. C. LEE and N. E. LEE. J. Phys. Chem. **71**, 1167 (1967).
9. E. K. C. LEE, G. A. HANINGER, and H. O. DENSCHLAG. International Conference on Photochemistry, Munich, September 6–9, 1967.
10. H. E. GUNNING and O. P. STRAUSZ. Advan. Photochem. **1**, 209 (1963).
11. G. K. OSTER and H. P. KALLMAN. Nature, **194**, 1033 (1962).
12. W. VAN DUSEN and W. H. HAMILL. J. Am. Chem. Soc. **84**, 3648 (1962).
13. G. P. SEMELUK and I. UNGER. Nature, **198**, 853 (1963).
14. I. UNGER and G. P. SEMELUK. Can. J. Chem. **44**, 1427 (1966).
15. F. W. AYER, F. GREIN, G. P. SEMELUK, and I. UNGER. International Conference on Photochemistry, Munich, September 6–9, 1967. Ber. Bunsenges. Physik. Chem. **72**, 282 (1968).
16. W. A. NOYES, JR. and D. A. HARTER. J. Chem. Phys. **46**, 674 (1967).
17. W. A. NOYES, JR., W. A. MULAC, and D. A. HARTER. J. Chem. Phys. **44**, 2100 (1966).
18. H. ISHIKAWA and W. A. NOYES, JR. J. Chem. Phys. **37**, 583 (1962).

Can. J. Chem. Downloaded from www.nrcresearchpress.com by 210.87.254.42 on 09/05/12
For personal use only.

Reactions of thiyl radicals. V. The gas phase photolysis of methyl disulfide and ethyl disulfide mixtures in the presence of ethylene[1]

P. M. RAO AND A. R. KNIGHT

Department of Chemistry and Chemical Engineering, University of Saskatchewan, Saskatoon, Saskatchewan

Received November 27, 1967

The gas phase photolysis of methyl disulfide and ethyl disulfide and their mixtures, in the presence and absence of ethylene, has been studied at 25 °C and λ = 2300–2800 Å. The pure substrates give predominantly the corresponding thiol, whereas co-photolysis yields methyl ethyl disulfide in appreciably larger yields.

When ethylene is added, the substrates individually show a reduction in RSH rate and the formation of relatively small amounts of sulfides. In their co-photolysis, added C_2H_4 does not appreciably alter the rate of methyl ethyl disulfide formation, indicating a low efficiency of RS scavenging by the olefin in this system.

Isopropanol and 2,3-dimethyl butane do not increase the thiol yield from the pure substrates.

Canadian Journal of Chemistry, 46, 2462 (1968)

Can. J. Chem. Downloaded from www.nrcresearchpress.com by 210.87.254.105 on 09/05/12
For personal use only.

It has been established previously that in both the vapor (1) and liquid (2) phase, thiyl radicals, whose principal fate is recombination, are formed in the photolysis of methyl disulfide. Co-photolysis of liquid methyl disulfide and ethyl disulfide yields $CH_3SSC_2H_5$ predominantly via the chain step

[1] $$R'S + RSSR \rightarrow R'SSR + RS,$$

which leads to a photochemical equilibrium. Reactions yielding products other than disulfides are negligible. The attack of methylthiyl radicals in the gas (3, 4) and liquid (5, 6) phase on olefinic double bonds involves the reversible formation of a thiaalkyl radical. With disulfides as substrates the absence of a labile hydrogen prevents chain propagation, and product yields should indicate the effectiveness of attack on the olefin as an alternative to RS recombination.

We report here the results of a further investigation of disulfide photolyses to determine if a photochemical equilibrium characterizes the system in the gas phase, and to examine the effects of added olefin and two addends potentially providing a site for H-atom abstraction.

In the first series of experiments,[2] 3 Torr each of CH_3SSCH_3 and $C_2H_5SSC_2H_5$ were photolyzed. Product yields are given in Fig. 1. As observed in the liquid phase (2) the yield of methyl ethyl disulfide is appreciable even after relatively short exposure times. In the gas phase, however, CH_3SH and C_2H_5SH are also formed, and this decomposition mode becomes increasingly important.

When methyl disulfide is photolyzed with added ethylene, the yield of methanethiol, the major product of pure substrate decomposition, decreases with increasing $P(C_2H_4)$. A new product, methyl ethyl sulfide, in yields directly proportional to olefin pressure, is also formed.

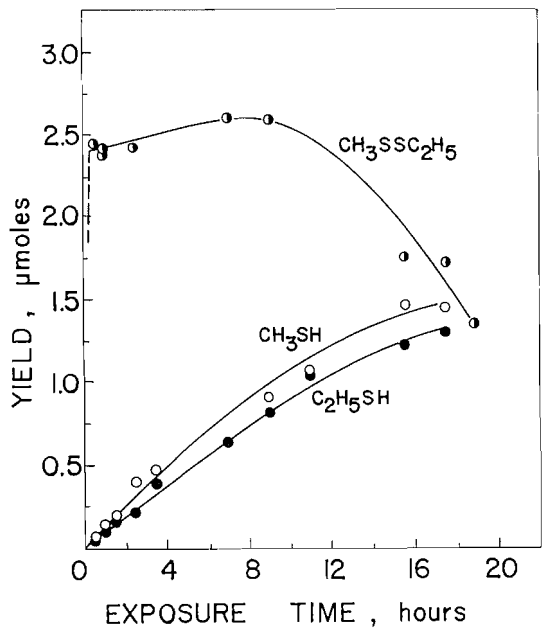

FIG. 1. Yield of $CH_3SSC_2H_5$ (◑), CH_3SH (○), and C_2H_5SH (●) as a function of exposure time for the photolysis of 3 Torr each of CH_3SSCH_3 and $C_2H_5SSC_2H_5$.

[1]From the thesis to be submitted by P. M. Rao in partial fulfilment of the requirements of the Ph.D. Degree, University of Saskatchewan, Saskatoon. Part IV, R. P. Steer and A. R. Knight, J. Phys. Chem., in press.

[2]The apparatus and general procedures have been described previously (1).

Can. J. Chem. Downloaded from www.nrcresearchpress.com by 210.87.254.105 on 09/05/12
For personal use only.

The results are given in Fig. 2. Figure 3 shows the results of a similar series of experiments with ethyl disulfide, at the maximum practical working pressure at room temperature of 3 Torr. In contrast to methyl disulfide, the yield of the sulfide from $C_2H_5SSC_2H_5$, formed in small quantities from the pure substrate, does not increase as rapidly with olefin pressure.

The rates of product formation when 3 Torr each of methyl disulfide and ethyl disulfide are photolyzed in the presence of C_2H_4 are shown in Fig. 4. When allowance is made for the different disulfide pressures employed, comparison of Figs. 2 and 3 with Fig. 4 shows that the decomposition of each substrate leading to RSH production, or reaction with ethylene, is virtually independent of the presence of the other. Unsymmetrical disulfide formation, however, dominates the photolysis both in the presence and absence of ethylene. The slight decrease in its yield at higher pressures is within experimental error.

Finally, the systems methyl disulfide – isopropanol and ethyl disulfide – 2,3-dimethyl butane were examined and the rate of mercaptan formation followed as a function of addend pressure. In both cases the rate decreases as the addend pressure is raised in the same manner as previously observed for other addends (1). Thus, even in the presence of a species possessing a relatively labile hydrogen, the recombination mode evidently remains the principal fate of thiyl radicals.

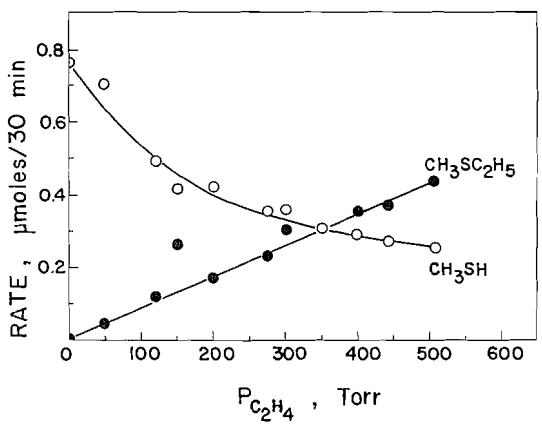

FIG. 2. Rate of formation of CH_3SH (○) and $CH_3SC_2H_5$ (●) from the photolysis of 6 Torr of methyl disulfide for an exposure time of 30 min as a function of ethylene pressure.

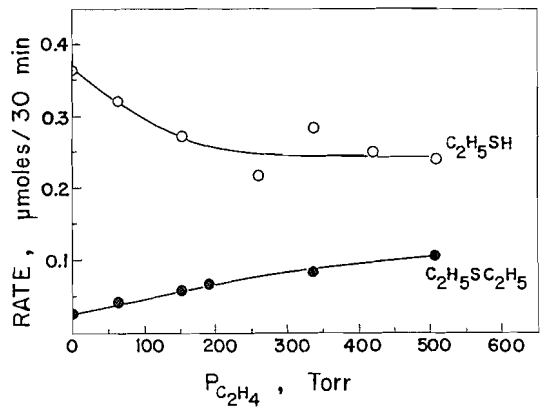

FIG. 3. Rate of formation of C_2H_5SH (○) and $C_2H_5SC_2H_5$ (●) from the photolysis of 3 Torr of ethyl disulfide for an exposure time of 30 min as a function of ethylene pressure.

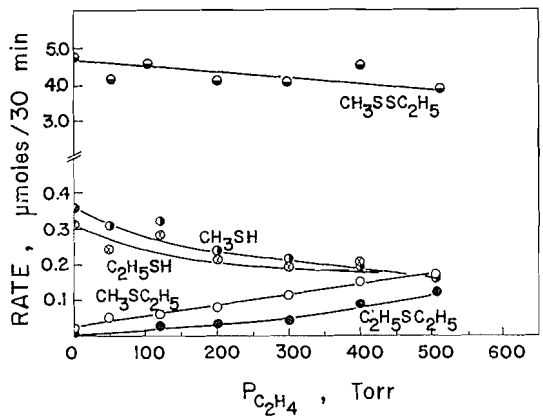

FIG. 4. Rate of formation of $CH_3SSC_2H_5$ (◒), $CH_3SC_2H_5$ (○), CH_3SH (◑), C_2H_5SH (⊗), and $C_2H_5SC_2H_5$ (●) as a function of pressure of ethylene from the photolysis of 3 Torr each of methyl disulfide and ethyl disulfide for an exposure time of 30 min.

On the basis of the mechanism previously suggested for the liquid phase system (2), the production of methyl ethyl disulfide from mixtures of CH_3SSCH_3 and $C_2H_5SSC_2H_5$ should be through the sequence

[2] $CH_3SSCH_3 + h\nu \rightarrow 2CH_3S$

[3] $C_2H_5SSC_2H_5 + h\nu \rightarrow 2C_2H_5S$

[4] $CH_3S + C_2H_5S \rightarrow CH_3SSC_2H_5$

[5] $CH_3SSC_2H_5 + h\nu \rightarrow CH_3S + C_2H_5S$

and reaction [1]. It is apparent from Fig. 1, however, that a photochemical equilibrium is not attained in the gas phase because thiyl

radicals are being removed in mercaptan-forming reactions. These results constitute further evidence for the role of an excited species not completely deactivated in the gas phase as the precursor of RSH.

The fact that with added C_2H_4 the yields of sulfides are small and that mercaptan formation persists is consistent with a minor contribution from RSC_2H_5 formation via a chain mechanism through consumption of product mercaptan. RSH formation accounts for only a small fraction of total thiyl radical yield and the failure of the sulfide yields to exceed that of mercaptan also indicates a low net efficiency for RS scavenging. The predominant fate of the thiaalkyl radical formed is thus regeneration of RS and C_2H_4.

$$[6] \qquad RS + C_2H_4 \underset{k_{-6}}{\overset{k_6}{\rightleftharpoons}} RSC_2H_4$$

$$[7] \qquad RSC_2H_4 + RSSR \rightarrow RSC_2H_5 + CH_2R''SSR$$

In the CH_3SH–2-butene liquid phase system, the rate constant ratio analogous to k_6/k_{-6} is 80 (6). If RSC_2H_4 were to lead to product formation, it must be removed efficiently from the equilibirum represented by [6], since otherwise reactions [6] and [7] could not compete effectively with rapid RS recombination.

RSC_2H_4 radicals could also participate in radical–radical reactions, but if these were important there should be at least some production of methyl vinyl sulfide, or ethyl vinyl sulfide, via disproportionation. Neither of these products is formed in detectable quantities.

The data in Figs. 2, 3, and 4 show that ethylene reduces mercaptan yields in the same manner as the "inert" addends studied previously, and as isopropanol and 2,3-dimethyl butane in this work. The rate of formation of the sulfides, however, increases linearly with $P(C_2H_4)$, indicating that their formation is not directly related to the decrease in the yield of mercaptan. The pressure dependence of the mercaptan yield is evidence against a *direct* radical–radical disproportionation, but is consistent with the formation of this product through decomposition of CH_3SSCH_3 (4). The role of disproportionation through a relatively long-lived excited molecule is currently being further studied in an investigation of CH_3SCH_3, where the relative importance of CH_3S recombination is more easily determined, since this process results in a measureable product rather than substrate reformation.

Acknowledgments

The authors express their thanks to the National Research Council of Canada and Imperial Oil Limited for financial support of this research.

1. P. M. Rao, J. A. Copeck, and A. R. Knight. Can. J. Chem. **45**, 1369 (1967).
2. K. Sayamol and A. R. Knight. Can. J. Chem. **46**, 999 (1968).
3. C. Siverts, W. Andrews, E. Eldson, and K. Graham. J. Polymer Sci. **19**, 587 (1956).
4. R. P. Steer and A. R. Knight. J. Phys. Chem. In press.
5. C. Sivertz. J. Phys. Chem. **63**, 34 (1959).
6. C. Walling and W. Helmreich. J. Am. Chem. Soc. **81**, 1144 (1959).

Thermal analysis of germanium(II) sulfide

L. Ross and M. Bourgon
Department of Chemistry, Université de Montréal, Montréal, Québec

Received November 24, 1967

Germanium(II) sulfide has been studied by the technique of differential thermal analysis. The results show that the reported Ge—S phase diagram may be in error: no evidence has been found for a solid-state transition at 590 °C and GeS appears to undergo peritectic disproportionation at approximately 650 °C.

Canadian Journal of Chemistry, 46, 2464 (1968)

Pashinkin *et al.* (1) investigated the Ge—S system over the whole composition range. The main features of the reported phase diagram are:

The existence of two sulfides of germanium, GeS and GeS_2, which melt congruently at 665 °C and 840 °C respectively.

The existence of a Ge–GeS eutectic at 650 °C (48 at. % S).

Can. J. Chem. Downloaded from www.nrcresearchpress.com by 210.87.254.105 on 09/05/12
For personal use only.

radicals are being removed in mercaptan-forming reactions. These results constitute further evidence for the role of an excited species not completely deactivated in the gas phase as the precursor of RSH.

The fact that with added C_2H_4 the yields of sulfides are small and that mercaptan formation persists is consistent with a minor contribution from RSC_2H_5 formation via a chain mechanism through consumption of product mercaptan. RSH formation accounts for only a small fraction of total thiyl radical yield and the failure of the sulfide yields to exceed that of mercaptan also indicates a low net efficiency for RS scavenging. The predominant fate of the thiaalkyl radical formed is thus regeneration of RS and C_2H_4.

$$[6] \qquad RS + C_2H_4 \underset{k_{-6}}{\overset{k_6}{\rightleftharpoons}} RSC_2H_4$$

$$[7] \qquad RSC_2H_4 + RSSR \rightarrow RSC_2H_5 + CH_2R''SSR$$

In the CH_3SH–2-butene liquid phase system, the rate constant ratio analogous to k_6/k_{-6} is 80 (6). If RSC_2H_4 were to lead to product formation, it must be removed efficiently from the equilibirum represented by [6], since otherwise reactions [6] and [7] could not compete effectively with rapid RS recombination.

RSC_2H_4 radicals could also participate in radical–radical reactions, but if these were important there should be at least some production of methyl vinyl sulfide, or ethyl vinyl sulfide, via disproportionation. Neither of these products is formed in detectable quantities.

The data in Figs. 2, 3, and 4 show that ethylene reduces mercaptan yields in the same manner as the "inert" addends studied previously, and as isopropanol and 2,3-dimethyl butane in this work. The rate of formation of the sulfides, however, increases linearly with $P(C_2H_4)$, indicating that their formation is not directly related to the decrease in the yield of mercaptan. The pressure dependence of the mercaptan yield is evidence against a *direct* radical–radical disproportionation, but is consistent with the formation of this product through decomposition of CH_3SSCH_3 (4). The role of disproportionation through a relatively long-lived excited molecule is currently being further studied in an investigation of CH_3SCH_3, where the relative importance of CH_3S recombination is more easily determined, since this process results in a measureable product rather than substrate reformation.

Acknowledgments

The authors express their thanks to the National Research Council of Canada and Imperial Oil Limited for financial support of this research.

1. P. M. Rao, J. A. Copeck, and A. R. Knight. Can. J. Chem. **45**, 1369 (1967).
2. K. Sayamol and A. R. Knight. Can. J. Chem. **46**, 999 (1968).
3. C. Siverts, W. Andrews, E. Eldson, and K. Graham. J. Polymer Sci. **19**, 587 (1956).
4. R. P. Steer and A. R. Knight. J. Phys. Chem. In press.
5. C. Sivertz. J. Phys. Chem. **63**, 34 (1959).
6. C. Walling and W. Helmreich. J. Am. Chem. Soc. **81**, 1144 (1959).

Thermal analysis of germanium(II) sulfide

L. Ross and M. Bourgon
Department of Chemistry, Université de Montréal, Montréal, Québec

Received November 24, 1967

Germanium(II) sulfide has been studied by the technique of differential thermal analysis. The results show that the reported Ge—S phase diagram may be in error: no evidence has been found for a solid-state transition at 590 °C and GeS appears to undergo peritectic disproportionation at approximately 650 °C.

Canadian Journal of Chemistry, 46, 2464 (1968)

Pashinkin *et al.* (1) investigated the Ge—S system over the whole composition range. The main features of the reported phase diagram are:

The existence of two sulfides of germanium, GeS and GeS_2, which melt congruently at 665 °C and 840 °C respectively.

The existence of a Ge–GeS eutectic at 650 °C (48 at. % S).

Can. J. Chem. Downloaded from www.nrcresearchpress.com by 210.87.254.40 on 09/05/12
For personal use only.

The existence of a GeS–GeS_2 eutectic at approximately 610 °C (60 at. % S).

The existence of a transition point at 590 °C. By analogy with tin sulfide (2) and selenide (3, 4) the above authors assume this transition to be a second order transformation.

Several observations made in our laboratory could not be reconciled with the reported thermal properties of GeS, and it was found necessary to study this compound further by the technique of differential thermal analysis.

Experimental

Germanium Sulfide

The germanium sulfide used in this work was prepared by direct synthesis from pure germanium and sublimed sulfur in evacuated quartz or Pyrex vials. The germanium was obtained in powder form by hydrogen reduction of high purity GeO_2. In order to determine the reaction temperature, germanium and sulfur were introduced into an evacuated vial with a reentrant thermocouple well. On slow heating, a large exothermal effect was observed at 350 °C. It is thus quite unnecessary to react the elements at temperatures as high as 1000 °C as has been done by other investigators (5). Consequently, the general technique of preparation adopted was to react the elements at 350 °C for 3 h, in the presence of a small excess of germanium (approximately 3%), and to bake the product at 500 °C for 24 h to insure completeness of reaction. The product was then cooled to room temperature in the furnace.

The sulfide was purified by successive sublimations under vacuum (10^{-3} mm Hg). It was often observed that, after a first sublimation to eliminate the excess germanium and a small amount of GeS_2 formed during reaction, further sublimations yielded a residue of germanium and GeS_2 (yellow), if carried out at temperatures above 400 °C. If, on the other hand, the sublimations are carried out slowly at temperatures between 375–400 °C, no residue is left and no GeS_2 can be detected visually in the sublimate. For this reason, all the GeS used in this work was sublimed at a temperature lower than 400 °C. The product so obtained is beautifully crystallized and possesses a strong metallic sheen.

Chemical analyses on the sublimed sulfide to determine possible deviations from stoichiometric proportions were not performed, since previous work (6) had shown that the deviations, if any, are within the experimental errors of the analytical methods.

A mass spectrographic analysis performed on the sublimed sulfide at 350 °C (the upper temperature limit of the instrument) showed the presence of GeS molecules only in the vapor. Since the GeS used in this work was sublimed at temperatures close to the above temperature, it can be concluded that the composition is very near to stoichiometric proportions.

The spacings of the lattice planes calculated from the X-ray diagram of the sublimed sulfide are identical with those reported in the literature (1, 7, 8). No lines corresponding to Ge could be detected.

It should be mentioned at this point that the presence of GeS_2 can often be observed visually in quenched GeS samples although no lines corresponding to this phase can be detected on the X-ray diagram. It was verified that pure GeS_2 crystals obtained by sublimation, when powdered for Guinier sample mounting, do not give an X-ray diagram. Debye–Scherrer photographs can be obtained, however, by careful mounting of clusters of crystals on a capillary. Since all the GeS samples used in this work were powdered for X-ray work, the absence of GeS_2 lines is not an indication that GeS_2 is not present.

Differential Thermal Analysis

(a) Instrumentation

The d.t.a. instrument used in this work (semi-micro head) is the one designed by Mazières and is described fully elsewhere (9). The main feature of the instrument is that the platinum sample and reference cups constitute the junctions of the differential thermocouple, thus increasing sensitivity and resolving power. The maximum sample size permissible is 6 μl.

The d.t.a. instrument is coupled to a two-pen spot-follower recorder ("Graphispot", Sefram, Paris). The temperature signal is fed directly to a galvanometer–spot-follower system incorporated in the recorder while the differential temperature signal is fed to an external galvanometer ("Verispot", Sefram, Paris), with 62.5 μV full-scale sensitivity, which is read by a second spot-following device also incorporated in the recorder.

(b) Preparation of Samples

Because of the corrosive nature and high vapor pressure of germanium sulfide, it is essential that the samples be enclosed. The powdered samples (400 mesh) were introduced into small vials made from fused silica tubing (2 mm o.d.) and compacted by mechanical vibration: the vials were then sealed after evacuation (10^{-3} mm Hg). For reasons that will become clear later the samples must not melt during the sealing operation. To insure this, the vials were soaked in liquid nitrogen prior to sealing with a small hydrogen flame. Samples which have undergone fusion show a characteristic peak at 590 °C on a d.t.a. heating curve: this fact was used for controlling the sealing operation.

In order to determine the loss of sensitivity on enclosing the samples, the α–β quartz transition temperature was determined with both open and enclosed samples. The sample in a platinum crucible gave a 12 μV peak at 573 °C; the enclosed sample, smaller in size, gave a 6 μV peak at the same temperature.

(c) Reporting of Data

All d.t.a. traces reported in this work were obtained during heating cycles from undiluted samples (2–3 mg) at a heating rate of 4–5 °C/min unless otherwise stated. Small GeS samples are subject to severe supercooling; for this reason not much information on equilibrium freezing temperatures can be obtained from cooling curves. Platinel thermocouples were used. Reported temperatures are those of the maximum of the peaks since they proved to be the most reproducible. The ordinate scale gives the values of $\Delta T/T$, as recommended by the Committee on Standardization of the International Conference on Thermal Analysis (I.C.T.A.) (10).

Calcined Al_2O_3 or PbS was used as a reference material: no essential difference between the two sets of results was

Can. J. Chem. Downloaded from www.nrcresearchpress.com by 210.87.254.40 on 09/05/12
For personal use only.

noted. The calibration curves of the thermocouples provided by the manufacturer of the d.t.a. instrument were used as such. We believe that the temperatures reported are precise to ± 2 °C.

X-ray diagrams were taken with a Philips instrument (Cu Kα radiation, Ni filter) using a Guinier camera; exposure time was 4 h.

Results

Differential thermal analysis traces were obtained from both annealed and unannealed samples.

Annealed Samples (Fig. 1)

Trace "a"

This is the actual trace of a sample annealed at 500 °C: the endothermal peak at 667 °C corresponds to melting of the sample. The sample was annealed for a period of 3 days in the d.t.a. instrument. At the end of this period the thermogram was traced starting from the annealing temperature. Similar traces were obtained for samples annealed at 525, 550, 575, 625, and 640 °C: these traces are identical with the ones obtained from unannealed sublimed samples. Samples annealed at these temperatures and cooled to 500 °C again gave the same trace on heating. No thermal effects other than freezing were observed on cooling curves.

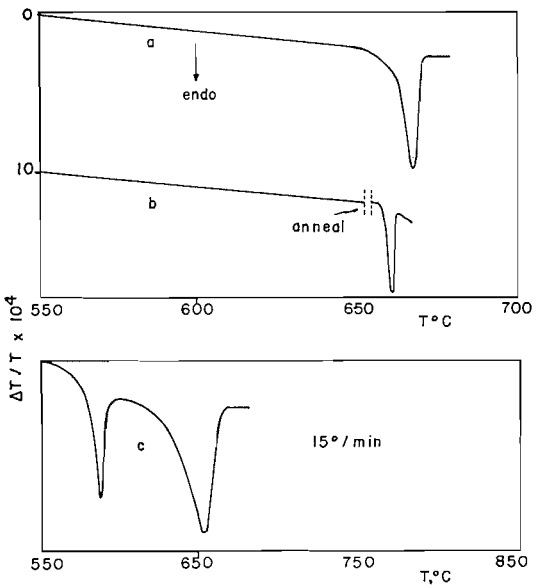

FIG. 1. Differential thermal analysis traces (heating) of GeS: (*a*) sample annealed at 500 °C, (*b*) sample annealed at 652 °C: the thermogram was traced from room temperature then interrupted at 652 °C for annealing, (*c*) sample annealed at 652 °C, cooled, and reheated.

Several samples were annealed at different temperatures for 7 days and quenched in liquid nitrogen; X-ray diagrams of the quenched samples were taken. The diagrams of the samples annealed at temperatures below 640 °C were identical and showed the same lines as the diagram of the freshly sublimed sample.

Trace "b"

Samples annealed at 652 °C for a few hours show a different behavior. On heating from the annealing temperature trace "*b*" is obtained due to crossing of the liquidus; as can be seen, the area of the peak is smaller. Samples cooled from 652 °C show a relatively large exothermal peak at approximately 630 °C; the shape of the peak clearly shows the occurrence of supercooling. X-ray diagrams of samples quenched from 652 °C show the presence of germanium lines in addition to the GeS lines.

Trace "c"

Samples annealed at 652 °C when cooled give trace "*c*" on reheating. As can be observed, a second endothermal peak appears at approximately 590 °C.

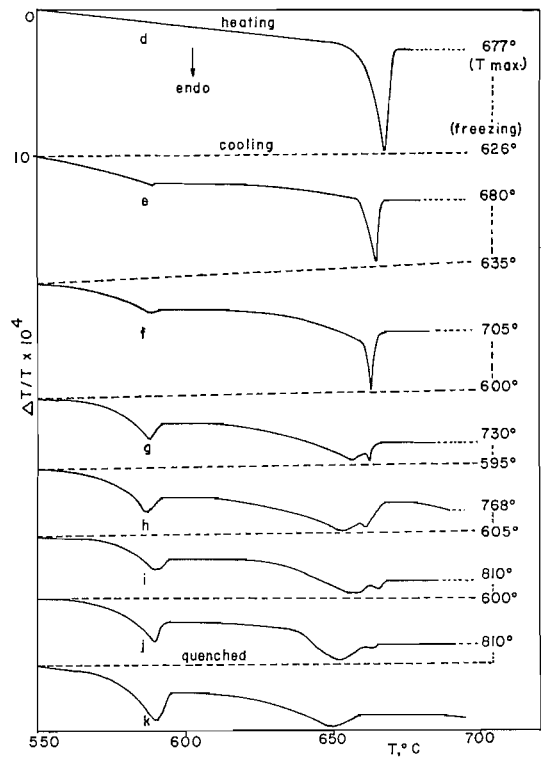

FIG. 2. Differential thermal analysis traces (heating) of a GeS sample heated at different temperatures above the melting point.

Can. J. Chem. Downloaded from www.nrcresearchpress.com by 210.87.254.40 on 09/05/12
For personal use only.

Unannealed Samples

In Fig. 2 are shown d.t.a. traces obtained from a sample heated successively at different temperatures above the melting point. Other samples, from different batches and different sublimations, gave essentially the same results. The sample was heated at different temperatures above the melting point (T max.), cooled to a temperature between 400 and 500 °C, and reheated in order to trace the thermogram. The temperatures indicated on the traces below T max. are the temperatures at which the sample solidified. Trace "*d*" corresponds to the fresh sample.

Discussion

The presence of Ge and GeS_2 in residues of samples sublimed above 400 °C is an indication that the reaction

$$GeS\ (s) \rightarrow x Ge\ (s) + Ge_{1-x}S\ (s)$$

takes place in the solid, where the phase $Ge_{1-x}S$ can be considered as a solid solution of GeS_2 in GeS. Since the X-ray diagrams of samples annealed at temperatures below 640 °C and quenched show no germanium lines, it can be concluded that, under equilibrium conditions, the change in the stoichiometry of GeS as a function of temperature is light. It is probable, as in the case of SnS (11), that the existence region of GeS lies entirely on the sulfur-excess side.

The thermal accident which was observed by Pashinkin *et al.* (1) at 590 °C on the thermograms of all samples with 55 at. % S or less never appears on the d.t.a. traces of freshly sublimed samples or of sublimed samples annealed at temperatures below 640 °C. This is a clear indication that this thermal accident does not correspond to a solid-state transition.

The peak at 590 °C appears consistently on d.t.a. traces of all samples which were previously melted and cooled (see Fig. 1, trace "*c*", and Fig. 2). This peak can be made to disappear by annealing the samples for a few hours at 620 °C or a few days at 500–550 °C; the d.t.a. traces of these annealed samples are then quite similar to the traces of the freshly sublimed samples. This indicates that the peak at 590 °C occurs because of non-equilibrium conditions. The temperature at which this peak appears is quite close to the reported temperature of the GeS–GeS_2 eutectic (1). Furthermore, the presence of GeS_2 and Ge can be observed in samples cooled or quenched from the liquid state, indicating that in the liquid state, germanium(II) sulfide disproportionates partially according to:

$$2GeS\ (l) \rightleftharpoons Ge\ (solution) + GeS_2\ (solution).$$

It is therefore highly probable that the peak at 590 °C is due to melting of the GeS–GeS_2 eutectic. It is significant that the amount of Ge in samples quenched from above the liquidus (as judged from the intensity of the X-ray lines) increases as the maximum temperature to which the samples are taken increases; this increase in the germanium content runs parallel to the increase in the area of the peak at 590 °C (see Fig. 2).

The thermograms of sublimed samples annealed at 652 °C, i.e. just above the temperature of the reported Ge–GeS eutectic, show an endothermal effect on heating (Fig. 1, trace "*b*") and a rather large exothermal effect on cooling from the annealing temperature: this is indicative of a two-phase region which, however, can hardly be due to the existence of a Ge–GeS eutectic, since there is no evidence for the presence of reasonable amounts of free germanium in samples annealed just below 650 °C. Furthermore, samples quenched from 652 °C contain free germanium and the thermogram obtained on heating the quenched sample (trace "*c*", Fig. 1) shows the presence of the peak at 590 °C. These facts are easily explained if GeS melts incongruently at 650 °C because of the peritectic disproportionation

$$GeS\ (s) \rightarrow x Ge\ (s) + Ge_{1-x}S\ (l),$$

where the phase $Ge_{1-x}S$ can be considered as a liquid solution of GeS_2 in GeS. This peritectic reaction is quite slow since it cannot be observed on fresh samples at the normal heating rates of the d.t.a. instrument. However, the double peak which appears on some of the thermograms of Fig. 2 can be interpreted as being due to the crossing of the peritectic and liquidus lines: it can be observed that the double peak appears only when the peak at 590 °C is important.

Although the evidence for incongruent melting presented above is somewhat indirect, we believe that it is of sufficient strength to justify re-examination of the Ge—S phase diagram.

The boiling Point of GeS

Boiling of GeS or, rather, boiling of a liquid solution of composition GeS, at atmospheric

Can. J. Chem. Downloaded from www.nrcresearchpress.com by 210.87.254.40 on 09/05/12
For personal use only.

pressure, under a helium atmosphere, was observed visually and the boiling point was recorded as a plateau at 750 °C. A d.t.a. trace was obtained from a sample of the distillate; it showed two small peaks at 590 °C and 645 °C and a large one at 676 °C. Although no further work was performed on the composition of the vapor, this variety of peaks is an indication that the vapor over GeS at high temperature contains a good amount of GeS_2.

Acknowledgments

The financial support of the National Research Council of Canada is gratefully acknowledged. Thanks are due to Professor Guy Perreault of the Ecole Polytechnique for assistance in the determination of the X-ray diagrams.

1. A. S. PASHINKIN and LIU CHUN-HUA. Dokl. Akad. Nauk SSSR, **151**, 1335 (1963).
2. R. L. ORR and A. V. CHRISTENSEN. J. Phys. Chem. **62**, 124 (1958).
3. V. V. ZHDANOVA. Fiz. Tverd. Tela, **3**, 1619 (1961).
4. S. A. DEMBOVSKII, B. N. EGOROV, A. S. PASHINKIN, and YU. A. POLYAKOV. Russ. J. Inorg. Chem. English Transl. **8**, 530 (1963).
5. T. YABUMOTO. J. Phys. Soc. Japan, **13**, 559 (1958).
6. M. D'AMBOISE, G. HANDFIELD, and M. BOURGON. Can. J. Chem. **44**, 853 (1966).
7. E. SHIMASAKI and T. WADA. Bull. Chem. Soc. Japan, **29**, 294 (1956).
8. W. H. ZACHARIASEN. Phys. Rev. **40**, 917 (1932).
9. C. MAZIÈRES. Anal. Chem. **36**, 602 (1964).
10. H. G. MCADIE. Anal. Chem. **39**, 543 (1967).
11. W. ALBERS, C. HAAS, H. J. VINK, and J. D. WASSCHER. J. Appl. Phys. **32**, 2220 (1961).

Can. J. Chem. Downloaded from www.nrcresearchpress.com by 210.87.254.40 on 09/05/12
For personal use only.

Can. J. Chem. Downloaded from www.nrcresearchpress.com by 210.87.254.5 on 09/05/12
For personal use only.

Protonation of conjugated carbonyl groups in sulfuric acid solution. I. Adaptation of the amide acidity function H_A for protonation of the carbonyl group in non-Hammett bases

R. I. ZALEWSKI[1] AND G. E. DUNN
Department of Chemistry, University of Manitoba, Winnipeg, Manitoba

Received May 10, 1968

The protonation of a number of aromatic and α,β-unsaturated aliphatic aldehydes, ketones, and carboxylic acids in sulfuric acid has been found to obey the H_A acidity function, rather than H_0.

Canadian Journal of Chemistry, 46, 2469 (1968)

In 1964 Yates, Stevens, and Katritzky (1) reported a new acidity function, H_A, for sulfuric acid solutions. This function was defined in the same way as the Hammett H_0 function, but was based upon primary amides as indicators. Later they proved its validity for other amides (2). Earlier measurements of the basicity of amides indicated that most of them do not follow (3) the conventional acidity function H_0 proposed by Hammett (4); these compounds are called "non-Hammett" bases. The class "non-Hammett" bases included as well typical organic compounds in which the carbonyl group is conjugated to an aromatic ring: aromatic acids, aldehydes (5), and ketones (6), or to an olefinic bond: α,β-unsaturated acids (7) and α,β-unsaturated ketones (8).

The protonation of these classes of organic compounds has been intensively investigated in recent years, mostly by spectrophotometric methods. From spectral data it is generally possible to determine pK values in two ways:

(1) a plot of absorptivity against H_0 gives a titration curve (at the inflection point $H_0 = pK$);

(2) by calculating

$$\frac{[B]}{[BH^+]} = \frac{\varepsilon_{BH^+} - \varepsilon}{\varepsilon - \varepsilon_B}$$

and computing pK_{BH^+} from the equation

$$pK_{BH^+} = H_0 - \log \frac{[B]}{[BH^+]} .$$

Necessary conditions for the base to be a Hammett base are that pK values computed from this equation be independent of acidity and that log ([B]/[BH^+]) vs. H_0 give a straight line with unit slope. One of us (R. I. Z.) was interested in protonation of α,β-unsaturated ketones (steroids) (8) and concluded that those substances do not follow the H_0 function. We have now measured the protonation of simple α,β-unsaturated ketones. They do not follow the H_0 function, but obey very well the new H_A function (9). For this reason it was very interesting to reinvestigate the protonation of other non-Hammett bases and use the H_A function for calculating pK.

In Table I we present absorption characteristics of the bases and their conjugate acids as well as pK_{BH^+} values and slopes of the plots log ([B]/[BH^+]) vs. H_A. The slopes were calculated using the Stewart–Granger procedure (10). These data indicate that all reported bases fit the H_A function in their ionization. In Table I we also present pK_{BH^+} data and φ calculated by the Bunnett and Olsen procedure (11). These pK_{BH^+} values are smaller by about 0.3 unit and the coefficient φ takes values near 0.5. These same differences in pK_{BH^+} and similar mean values of φ were reported by Bunnett and Olsen for amides.

Generally, in all the substances investigated, the carbonyl group was conjugated to a double bond or to an aromatic ring, and the carbon atom of the carbonyl group was bound to another substituent: OH, CH_2, CH_3, Ar, H. The substituents affected the strength of the base, but had no influence on the slope of log ([B]/[BH^+]) vs. H_A. From other sources we know that the

[1]University of Manitoba Postdoctorate Fellow, 1967–1968.

TABLE I

Absorption characteristics and pK_{BH^+} values of the bases

Base	λ_{BH^+}	ε_{BH^+}	λ_B	ε_B	$-pK_{BH^+}$	Slope	Bunnett–Olsen procedure pK_{BH^+}	Bunnett–Olsen procedure ϕ
Aromatic								
Benzaldehyde	298	19 300	254	10 100	4.87± .04	0.97	4.40	0.52
p-Methylbenzaldehyde	310	23 200	265	13 500	4.18± .04	0.97	3.85	0.52
Benzoic acid	258	10 200	230	7 200	4.60± .03	0.97	4.20	0.52
Anthranilic acid	239	15 200	—	—	3.92± .15	1.02	3.75	0.52
Acetophenone	291	18 400	254	10 900	4.12± .03	0.99	3.65	0.57
Benzophenone	340	24 400	265	18 800	4.01± .04	0.98	3.90	0.48
4-Methylacetophenone	310	18 600	262	11 800	3.61± .06	0.96	3.50	0.50
Aliphatic								
Crotonic aldehyde	256	20 400	230	15 600	4.32± .06	1.00	4.35	0.47
Acrylic acid	216	12 100	197	9 700	4.41± .04	1.02	4.15	0.52
Crotonic acid	235	17 700	209	13 200	4.03± .03	0.99	3.85	0.48
3-Methyl-3-penten-2-one	274	12 800	250	11 400	3.42± .03	0.98	3.10	0.52
Alicyclic								
2-Cyclohexen-1-one	271	9 400	231	7 500	3.59± .04	1.00	3.25	0.55
1-Methyl-$\Delta^{1,9}$-octalone	297	11 300	258	11 000	2.47± .04	0.98	2.25	0.49
2-Cyclopentylidenocyclopentanone	305	10 000	270	6 900	2.56± .03	0.97	2.30	0.57

protonation of a carbonyl group holding similar substituents, but unconjugated, obeys the H_0 function (12) very well. From our investigation we conclude that the H_A function describes the protonation of α,β-unsaturated carbonyl groups in typical organic compounds.[2] The separate classes of bases are under further examination.

1. K. YATES, J. B. STEVENS, and A. R. KATRITZKY. Can. J. Chem. **42**, 1957 (1964).
2. K. YATES and J. B. STEVENS. Can. J. Chem. **43**, 529 (1965).
3. A. R. KATRITZKY. Tetrahedron, **19**, 465 (1963). C. D. JOHNSON, A. R. KATRITZKY, and N. SHAKIR. J. Chem. Soc. 1235 (1967).
4. L. P. HAMMETT. Chem. Rev. **16**, 67 (1935).
5. K. YATES and H. WAI. Can. J. Chem. **43**, 2131 (1965).
6. L. A. FLEXER, L. P. HAMMETT, and A. DINGWALL. J. Am. Chem. Soc. **57**, 2103 (1935).
7. T. SORENSEN. Can. J. Chem. **42**, 724 (1964).
8. R. I. ZALEWSKI. Ph.D. Thesis, University of Poznań, Poznań, Poland. 1967.
9. R. I. ZALEWSKI and G. E. DUNN. Abstract of papers 51st Canadian Chemical Conference, Vancouver, B.C., June 3–5, 1968.
10. R. STEWART and M. GRANGER. Can. J. Chem. **39**, 2508 (1961).
11. J. F. BUNNETT and F. P. OLSEN. Can. J. Chem. **44**, 1899 (1966).
12. S. HOSHINO, H. HOSOYA, and S. NAGAKURA. Can. J. Chem. **44**, 1961 (1966). H. J. CAMPBELL and J. T. EDWARD. Can. J. Chem. **38**, 2109 (1960).

[2]Dr. T. Sorensen informs us that by the nuclear magnetic resonance technique he has found the protonation of a variety of α,β-unsaturated acids, aldehydes, and ketones to fit the H_A function. His pK_{BH^+} values agree with ours in the few cases where the same compounds were investigated.

Can. J. Chem. Downloaded from www.nrcresearchpress.com by 210.87.254.5 on 09/05/12
For personal use only.

Lapachol

GEORGE R. PETTIT AND LEONARD E. HOUGHTON
Department of Chemistry, Arizona State University, Tempe, Arizona 85281

Received May 21, 1968

A practical total synthesis of hydroxyhydrolapachol and lapachol has been summarized.

Canadian Journal of Chemistry, 46, 2471 (1968)

In a remarkable series of investigations (e.g. ref. 1), Hooker succeeded in completing the structural assignment for lapachol (**1**), a yellow pigment isolated from Bethabarra and Surinam greenheart woods.[1] The Fieser synthesis (3*a*) of lapachol in 1927 helped confirm the structural assignment. The early approach employed as terminal step (5% yield) alkylation of 2-hydroxy-1,4-naphthaquinone silver salt[2] with 2-methyl-4-bromo-2-butene. Currently lapachol and certain related quinones are of interest in antimalarial and cancer chemotherapeutic programs (4*a*). We now wish to report a new synthetic route to lapachol which potentially allows large scale preparation and also readily provides the well-characterized derivative hydroxyhydrolapachol (**2**).

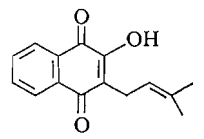

1

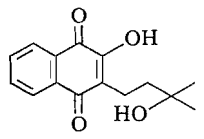

2

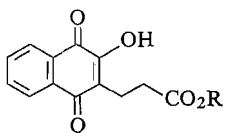

3 *a*, R = H
b, R = CH_2CH_3

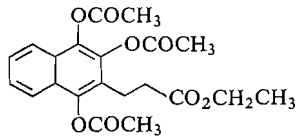

4

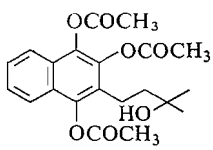

5

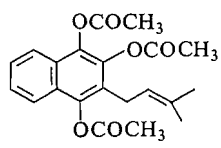

6

[1]At the time lapachol was also known to occur in a number of South American trees such as the Argentine lapacho. Subsequently, the yellow quinone has been found in a variety of trees from other locations (2).

[2]The yield was later improved using the potassium salt (3*b*). A more recent synthetic approach to lapachol involved condensing (in ca. 3% yield) leucoisonaphthazarin with isoprene as final step (3*c*).

Reaction between 2-hydroxy-1,4-naphthaquinone[3] and the half-peracid from succinic anhydride, in acetic acid, followed by esterification (of acid 3*a*) afforded (35% overall) the previously reported ethyl ester 3*b* (5). Zinc dust reduction (2 h) of quinone 3*b* in acetic anhydride containing 10% triethylamine gave (78%) triacetate **4** as colorless prisms, m.p. 112–113° (methanol).[4] Treating (22 h) a benzene solution of ester **4** with methylmagnesium iodide in diethyl ether and subsequent reprecipitation (using 1 *N* hydrochloric acid) of product from 2% sodium bicarbonate solution provided an orange oil which crystallized from benzene as brilliant-yellow prisms (**2**). Hydroxyhydrolapachol (**2**) melted at 125–125.5° (ref. 1 reports m.p. 125°), 63% yield. Applying the zinc – acetic anhydride step (cf. **4**) to quinone **2** led to triacetate **5** (colorless needles from diethyl ether, m.p. 151–152°, 87% yield).[5] Heating (40 min) tertiary alcohol **5** (1.6 g) in refluxing xylene (30 ml) with iodine (0.12 g) yielded (1.0 g, 66%) colorless olefin **6**, m.p. 122–123° (methanol). Stirring (30 min) triacetate **6** with 1 *N* sodium hydroxide in dioxane easily provided lapachol, yellow plates (83% yield) from ethanol–water, m.p. 135–137°. An authentic specimen[6] had the same melting point

[3]The quinone was obtained by *t*-butoxide-catalyzed oxidation of α-tetralone (4*b*) and commercially (Aldrich Chemical).

[4]Satisfactory spectral (ultraviolet, infrared, and proton magnetic resonance) data and elemental analyses were recorded for each new substance.

[5]Protracted attempts, using a variety of methods, to directly dehydrate hydroxyhydrolapachol to lapachol (**2** → **1**) proved impractical. The major product (cf. ref. 1) in each case was β-lapachone (**i**).

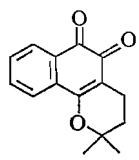

i

[6]We are indebted to Dr. Robert Engle for this sample.

and also exhibited identical thin layer chromatographic and infrared spectral values.

Acknowledgments

This investigation was supported in part by PHS Research Grant CA-10612-01 from the National Cancer Institute and in part by the U.S. Army Medical R and D Command under Contract DA-49-193-MD-3010. The manuscript represents contribution number 417 from the Army Research Program on Malaria.

1. S. C. HOOKER. J. Chem. Soc. **61**, 611 (1892); **69**, 1355 (1896).
2. A. R. BURNETT and R. H. THOMSON. J. Chem. Soc. C, 850 (1968).
3. (*a*) L. F. FIESER. J. Am. Chem. Soc. **49**, 857 (1927). (*b*) R. G. COOKE. Australian J. Sci. Res. Ser. A, **3**, 481 (1950). (*c*) M. GATES and D. L. MOESTA. J. Am. Chem. Soc. **70**, 614 (1948).
4. (*a*) G. R. PETTIT, W. C. FLEMING, and K. D. PAULL. J. Org. Chem. **33**, 1089 (1968). G. R. PETTIT and L. E. HOUGHTON. J. Med. Chem. To be published. 1968. (*b*) T. R. KASTURI and T. ARUNACHALAM. Can. J. Chem. **44**, 1086 (1966).
5. L. F. FIESER *et al.* J. Am. Chem. Soc. **70**, 3206 (1948).

Vibrational absorption of the trapped diazomethyl radical

J. F. OGILVIE

Department of Chemistry, Memorial University of Newfoundland, St. John's, Newfoundland

Received May 28, 1968

Vibrational absorption lines newly discovered after the photolysis, with a low-pressure mercury lamp, of isotopic diazomethanes in inert-gas matrices at 4 °K have been assigned to the diazomethyl radical, HCNN and DCNN.

Canadian Journal of Chemistry, 46, 2472 (1968)

Despite much effort (1; 2; 3 and references therein) devoted to the study of the photolysis products of diazomethane in noble gas matrices at cryogenic temperatures, no conclusive absorption spectrum of the methylene radical has yet been obtained. However, a new vibrational spectrum has been recorded following photolysis, using radiation from an unfiltered low-pressure mercury lamp, of diazomethane isolated in several matrices at 4 °K. Conventional apparatus and procedures were employed in these experiments, as previously described (4, 5). The new absorption lines (with absorbance) are listed in Table I. These lines can be distinguished from other, minor absorptions also appearing after photolysis, both because the former appear, and increase in intensity, only during resonance-lamp irradiation, and because only they decrease in intensity during subsequent irradiation of the sample in argon with an unfiltered high-pressure mercury lamp. When a mixture of deuterium-substituted diazomethanes (H_2CNN, D_2CNN, and HDCNN) is used at a matrix ratio of argon to total diazomethane of 250, at 4 °K, only two sets of absorptions with intensity behavior as above, labeled A and B in Fig. 1, appear after resonance-lamp photolysis. The principal A line, at 861 cm^{-1}, coincides with the experimental bending vibration of the methylene radical, 861 $\pm$ 7 cm^{-1}, deduced as follows from the vibronic data of Herzberg (6, 7): $\nu_2' = 71383$ cm^{-1} (1400.9 Å) $-$ 70696 cm^{-1} (1414.5 Å) $=$ 686 cm^{-1}; $\nu_2' - \nu_2'' = 70522$ cm^{-1} (1418.0 Å) $-$ 70696 $cm^{-1} = -175$ cm^{-1}; therefore $\nu_2'' =$ 861 cm^{-1} (only frequency differences have meaning in this calculation). Bending frequencies of HCD and CD_2 are calculated (8) to be 763 and 654 cm^{-1} respectively. Therefore, the A and B lines cannot be assigned to methylene radicals. The A lines are observed in other experiments when pure H_2CNN is used, whereas *only* the B lines are present when almost pure D_2CNN is in the matrix. Thus the carrier of these absorption lines contains only one hydrogen atom. In diazomethyl lithium, Li^+HCNN^-, the CH stretching frequency is 3215 cm^{-1}, and a skeletal stretching frequency is 1898 cm^{-1} (9). The bending frequency of HCN is 712 cm^{-1}, which changes to 569 cm^{-1} in DCN. On the basis of conditions of formation and resemblance of vibration frequencies with those of similar molecules, these lines may be assigned to the diazomethyl radical, A = HCNN and B = DCNN.

The mechanism of formation is believed to be

and also exhibited identical thin layer chromatographic and infrared spectral values.

Acknowledgments

This investigation was supported in part by PHS Research Grant CA-10612-01 from the National Cancer Institute and in part by the U.S. Army Medical R and D Command under Contract DA-49-193-MD-3010. The manuscript represents contribution number 417 from the Army Research Program on Malaria.

1. S. C. HOOKER. J. Chem. Soc. **61**, 611 (1892); **69**, 1355 (1896).
2. A. R. BURNETT and R. H. THOMSON. J. Chem. Soc. C, 850 (1968).
3. (*a*) L. F. FIESER. J. Am. Chem. Soc. **49**, 857 (1927). (*b*) R. G. COOKE. Australian J. Sci. Res. Ser. A, **3**, 481 (1950). (*c*) M. GATES and D. L. MOESTA. J. Am. Chem. Soc. **70**, 614 (1948).
4. (*a*) G. R. PETTIT, W. C. FLEMING, and K. D. PAULL. J. Org. Chem. **33**, 1089 (1968). G. R. PETTIT and L. E. HOUGHTON. J. Med. Chem. To be published. 1968. (*b*) T. R. KASTURI and T. ARUNACHALAM. Can. J. Chem. **44**, 1086 (1966).
5. L. F. FIESER *et al.* J. Am. Chem. Soc. **70**, 3206 (1948).

Vibrational absorption of the trapped diazomethyl radical

J. F. OGILVIE

Department of Chemistry, Memorial University of Newfoundland, St. John's, Newfoundland

Received May 28, 1968

Vibrational absorption lines newly discovered after the photolysis, with a low-pressure mercury lamp, of isotopic diazomethanes in inert-gas matrices at 4 °K have been assigned to the diazomethyl radical, HCNN and DCNN.

Canadian Journal of Chemistry, 46, 2472 (1968)

Despite much effort (1; 2; 3 and references therein) devoted to the study of the photolysis products of diazomethane in noble gas matrices at cryogenic temperatures, no conclusive absorption spectrum of the methylene radical has yet been obtained. However, a new vibrational spectrum has been recorded following photolysis, using radiation from an unfiltered low-pressure mercury lamp, of diazomethane isolated in several matrices at 4 °K. Conventional apparatus and procedures were employed in these experiments, as previously described (4, 5). The new absorption lines (with absorbance) are listed in Table I. These lines can be distinguished from other, minor absorptions also appearing after photolysis, both because the former appear, and increase in intensity, only during resonance-lamp irradiation, and because only they decrease in intensity during subsequent irradiation of the sample in argon with an unfiltered high-pressure mercury lamp. When a mixture of deuterium-substituted diazomethanes (H_2CNN, D_2CNN, and HDCNN) is used at a matrix ratio of argon to total diazomethane of 250, at 4 °K, only two sets of absorptions with intensity behavior as above, labeled A and B in Fig. 1, appear after resonance-lamp photolysis. The principal A line, at 861 cm^{-1}, coincides with the experimental bending vibration of the methylene radical, 861 $\pm$ 7 cm^{-1}, deduced as follows from the vibronic data of Herzberg (6, 7): $\nu_2' = 71383$ cm^{-1} (1400.9 Å) $-$ 70696 cm^{-1} (1414.5 Å) $=$ 686 cm^{-1}; $\nu_2' - \nu_2'' = 70522$ cm^{-1} (1418.0 Å) $-$ 70696 $cm^{-1} = -175$ cm^{-1}; therefore $\nu_2'' =$ 861 cm^{-1} (only frequency differences have meaning in this calculation). Bending frequencies of HCD and CD_2 are calculated (8) to be 763 and 654 cm^{-1} respectively. Therefore, the A and B lines cannot be assigned to methylene radicals. The A lines are observed in other experiments when pure H_2CNN is used, whereas *only* the B lines are present when almost pure D_2CNN is in the matrix. Thus the carrier of these absorption lines contains only one hydrogen atom. In diazomethyl lithium, Li^+HCNN^-, the CH stretching frequency is 3215 cm^{-1}, and a skeletal stretching frequency is 1898 cm^{-1} (9). The bending frequency of HCN is 712 cm^{-1}, which changes to 569 cm^{-1} in DCN. On the basis of conditions of formation and resemblance of vibration frequencies with those of similar molecules, these lines may be assigned to the diazomethyl radical, A = HCNN and B = DCNN.

The mechanism of formation is believed to be

Can. J. Chem. Downloaded from www.nrcresearchpress.com by 210.87.254.6 on 09/05/12
For personal use only.

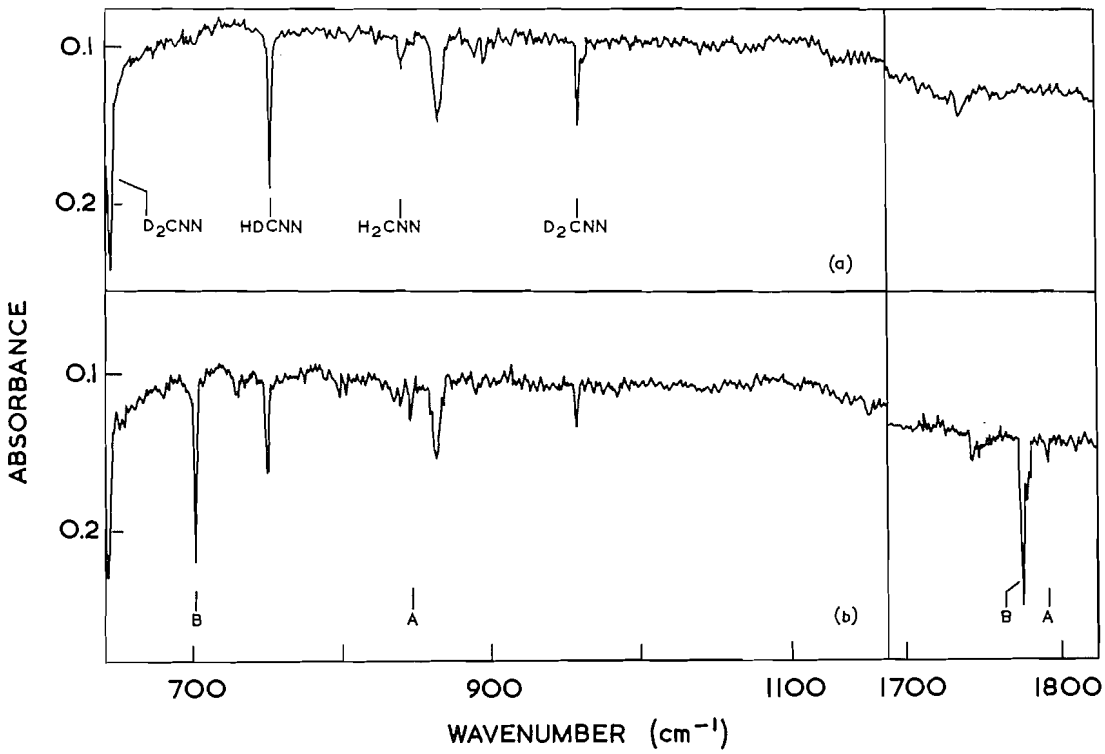

FIG. 1. Vibrational absorption of isotopic diazomethanes and products in argon (*a*) before and (*b*) after irradiation with a low-pressure mercury lamp.

TABLE I

Observed absorptions (cm^{-1}) for HCNN and DCNN in various matrices

HCNN (Ar)	HCNN (Kr)	HCNN (N_2)	DCNN (Ar)
861 (0.28)	860 (0.15)	863 (0.035)*	725 (0.125)
863 (0.13)	866 (0.04)	871 (0.025)*	
1787 (0.145)	1784 (0.07)	1789 (0.035)	1771 (0.125)
1792 (0.04)	1790 (0.03)	1800 (0.085)	1775 (0.04)
3233 (0.02)		3229 (0.035)	

*Interference by other bands makes these absorbances uncertain; otherwise absorbance accuracy is ±.01; wavenumber accuracy, ±2 cm^{-1}.

photodissociation from diazomethane of a hydrogen atom, which, unlike the methylene radical, can escape from the site of production within the matrix lattice:

$$H_2CNN + h\nu \rightarrow H + HCNN.$$

The photodecomposition of the diazomethyl radical during exposure to the high-pressure mercury lamp can proceed via dissociation to molecular nitrogen and the methylidene radical, the latter absorbing too weakly in the infrared to be directly detected:

$$HCNN + h\nu \rightarrow CH + N_2.$$

In a recent investigation (10) of the extreme ultraviolet photolysis of methane in nitrogen matrices, there have been reported several (unassigned among many others) vibrational absorptions of very similar wavenumbers to those in Table I. The methyl radical was detected (10)

Can. J. Chem. Downloaded from www.nrcresearchpress.com by 210.87.254.6 on 09/05/12
For personal use only.

and resulted from photoejection of a hydrogen atom from methane:

$$CH_4 + h\nu \rightarrow CH_3 + H.$$

Diazomethane was also detected and was formed from reaction of methylene (produced according to the reaction well established from gaseous phase experiments (11):

$$CH_4 + h\nu \rightarrow CH_2 + H_2)$$

with the available nitrogen (12):

$$CH_2 + N_2 \rightarrow H_2CNN.$$

The diazomethane was then subject to secondary photolysis, as in the present experiments, to produce a hydrogen atom and what is now identified as the diazomethyl radical.

Further results of studies of the diazomethane system will be reported soon. The original experiments were performed in the Department of Physical Chemistry, University of Cambridge.

1. W. B. DeMore, H. O. Pritchard, and N. Davidson. J. Am. Chem. Soc. **81**, 5874 (1959).
2. G. W. Robinson and M. McCarty. J. Am. Chem. Soc. **82**, 1859 (1960).
3. C. B. Moore, G. C. Pimentel, and T. D. Goldfarb. J. Chem. Phys. **43**, 63 (1965).
4. J. F. Ogilvie. Spectrochim. Acta, **23A**, 737 (1967).
5. J. F. Ogilvie. Spectrovision, **16**, 1 (1966).
6. G. Herzberg. Proc. Roy. Soc. London, Ser. A, **262**, 291 (1961).
7. G. Herzberg and J. W. C. Johns. Proc. Roy. Soc. London, Ser. A, **295**, 107 (1966).
8. G. Herzberg. Molecular spectra and molecular structure. Vol. II. Van Nostrand, Princeton. 1945. pp. 172–173.
9. E. Müller and W. Rundel. Chem. Ber. **90**, 2673 (1957); personal communication.
10. D. E. Milligan and M. E. Jacox. J. Chem. Phys. **47**, 5146 (1967).
11. P. Ausloos, R. Gorden, and S. G. Lias. J. Chem. Phys. **40**, 1854 (1964).
12. C. B. Moore and G. C. Pimentel. J. Chem. Phys. **41**, 3504 (1964).

Can. J. Chem. Downloaded from www.nrcresearchpress.com by 210.87.254.6 on 09/05/12
For personal use only.

Can. J. Chem. Downloaded from www.nrcresearchpress.com by 210.87.254.42 on 09/05/12
For personal use only.

Canadian Journal of Chemistry

Published by THE NATIONAL RESEARCH COUNCIL OF CANADA

VOLUME 46 AUGUST 1, 1968 NUMBER 15

Infrared spectra of 2-pyridone-^{16}O and 2-pyridone-^{18}O[1]

G. H. KELLER,[2] L. BAUER, AND C. L. BELL

Department of Chemistry, College of Pharmacy, University of Illinois (Medical Center), P.O. Box 6998, Chicago, Illinois 60680

Received February 29, 1968

A comparison of the infrared spectra of natural 2-pyridone with that of the oxygen-18 labelled compound indicated modest shifts not only for the CO stretching mode (8.3–17.8 cm^{-1}) for the various species in solution, but also for ring modes (0–13 cm^{-1}) indicating a considerable mixing of the vibrations. The infrared spectrum of 2-pyridone at high concentrations revealed a new absorption band in chloroform solutions at 1685.0 and 1667.2 cm^{-1} for the unlabelled and labelled compound, respectively. In addition, absorption at 1614.9 cm^{-1} in the spectrum of 2-pyridone-^{18}O in chloroform was found to be concentration dependent.

Canadian Journal of Chemistry, 46, 2475 (1968)

Introduction

In the vapor state 2-pyridone has been shown to consist of a mixture of tautomers (1). However, in the solid state and in solution, 2-pyridone exists predominantly as the lactam (**1**, **2**) rather than as 2-pyridinol (4).[3]

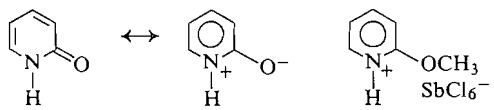

1 **2** **3**

Although the predominant tautomeric form of 2-pyridone has been established, there remains to be settled the question concerning the electron distribution about the heteroatoms since a zwitterionic form, **2**, would gain aromatic stabilization. This project addresses itself to the problem of assessing the relative contributions of **1** and **2** to the structure of the molecule.

Previously, the main evidence cited in favor of the simple lactam formulation of 2-pyridone has been the assignment of a band in the infrared (i.r.) spectrum near 1650 cm^{-1} to a carbonyl stretching mode (5). This assignment has been questioned (6) on the basis that this band could be a high frequency ring mode shifted to a higher than usual frequency due to the dipolar nature of the molecule (7). For example, 2-methoxypyridinium hexachloroantimonate, **3**, which does not possess a carbonyl function and is related electronically to **2** has a strong ring mode absorption at 1638 cm^{-1} (7). Moreover, a comparison of integrated absorption intensities for CO stretching modes in different types of molecules and 2-pyridone indicates a very high polarity in the CO bond of 2-pyridone and its intensity compared well with that found in sydnones (8, 9). These authors (8) concluded that 2-pyridone is best considered as an aromatic compound "in the same way as done for tropones, sydnones, and diphenylcyclopropenone."

More recently, it has been pointed out (3) that a pure C—O stretching mode of **2** should absorb with a frequency no higher than 1380 cm^{-1}. An appreciable contribution from this form to the structure would dictate a lower frequency absorption for the carbonyl than that assigned.

In order to establish without ambiguity the vibrational modes which involve the oxygen atom, 2-pyridone-^{18}O was prepared and the isotopic shifts in the i.r. spectrum determined.

[1]This work was supported, in part, by funds from the Research Board of the Graduate College at the University of Illinois, at the Medical Center.

[2]Present address: Sinclair Oil Co., Harvey, Illinois. Taken in part from the M.Sc. thesis of G. H. Keller, University of Illinois at the Medical Center, Chicago, Illinois, June 1967.

[3]Some substituted 2-pyridones have been found to be tautomeric mixtures (see refs. 2 and 3).

Can. J. Chem. Downloaded from www.nrcresearchpress.com by 210.87.254.42 on 09/05/12
For personal use only.

Results

The infrared absorption bands found for 2-pyridone-^{16}O and 2-pyridone-^{18}O in chloroform solution (0.527 *M*) are listed in Table I. In addition, the bands in the region between 1300–1700 cm^{-1} for the two isotopic species in carbon tetrachloride (0.026 *M*) are listed in Table II.

TABLE I

Vibration frequencies (cm^{-1}) and isotopic shifts in chloroform solution*

Band	2-Pyridone-^{16}O	2-Pyridone-^{18}O	Isotopic shift†
1	3402	3402	0
2	3289	3287	2
3	3242	3241	1
4	3132	3121	11
5	3075	3072	3
6	3032	3033	−1
7	2996	2996	0
8	2919	2915	4
9	2873	2866	7
10	2828	2828	0
11	1685.0	1667.2	17.8
12	1674.5	1661.8	12.7
13	1657.5	1649.2	8.3
14	1618.0	1614.9	3.1
15	1615.0‡	1603.1	12
16	1542.0	1534.3	7.7
17	1471.7	1469.0	2.7
18	1442.3	1434.0	8.3
19	1378.3	1376.5	1.8
20	1155	1155	0
21	1100	1098	2
22	1049	1049	0
23	993	992	1
24	924	924	0
25	848	848	0
26	709	700	9
27	665	665	0
28	618	615	3
29	565	555	10
30	516	516	0
31	496	483	13

*Bands 1–10, ±2 cm^{-1}; bands 11–19, ± 0.3 cm^{-1}; bands 20–31, ± 1.5 cm^{-1}.
†$\nu(^{16}O) - \nu(^{18}O)$.
‡Shoulder.

In studying the effect of concentration changes on the spectrum between 1300 and 1700 cm^{-1}, a previously unreported band was detected at 1685.0 cm^{-1} in the spectrum of 2-pyridone-^{16}O in chloroform. Figure 1 shows the change in relative intensity of this band, along with those observed for the bands at 1674.5 and 1657.5 cm^{-1} as a function of concentration. In dilute chloroform solution a pair of bands is observed at 1674.5 and 1657.5 cm^{-1} with an indistinct shoulder on the higher frequency band. As the concentration is increased, the 1674.5 cm^{-1} band becomes less intense *relative* to the band at 1657.5 cm^{-1} and the high frequency shoulder. At yet higher concentration, the shoulder is resolved as a separate peak at 1685.0 cm^{-1}.

TABLE II

Vibration frequencies (cm^{-1}) and isotopic shifts in carbon tetrachloride solution*

Band	2-Pyridone-^{16}O	2-Pyridone-^{18}O	Isotopic shift†
12	1682.8	1666.7	16.1
13	1660.1	1650.0	10.1
14	1619.4	1617.0	2.4
16	1542.5	1535.8	6.7
17	1476.2	1471.9	4.3
18	1443.4	1436.5	6.9

*Band frequencies accurate to ±0.3 cm^{-1}.
†$\nu(^{16}O) - \nu(^{18}O)$.

The limited solubility of 2-pyridone in carbon tetrachloride prevented the observation of this new high-frequency absorption band and only a pair of bands at 1682.8 and 1660.1 cm^{-1} is found in this region.

In the same spectral region, the 2-pyridone-^{18}O spectrum in chloroform exhibited exactly analogous behavior as shown in Fig. 2. The bands corresponding to 1674.5 and 1657.5 now appear at 1661.8 and 1649.2 cm^{-1} with the new high-frequency absorption developing near 1667.2 cm^{-1} in more concentrated solutions.

In addition to the frequency shifts for the bands just discussed in the oxygen labelled compound, an ^{18}O isotopic shift and concentration dependence is found for the shoulder at 1615.0 cm^{-1} in the spectrum of 2-pyridone-^{16}O. 2-Pyridone-^{18}O exhibits a band at 1614.9 cm^{-1} corresponding to the one at 1618.0 cm^{-1} in the normal spectrum as well as a band at 1603.1 which corresponds to the shoulder at 1615.0 cm^{-1} in the spectrum of the ^{16}O compound. Moreover, it is evident from Fig. 2, that these bands alter their relative intensities with concentration changes. No similar behavior could be noted in the spectrum of 2-pyridone-^{16}O, since only a single absorption band representing close to coincident absorptions (a shoulder 3 cm^{-1} from peak maximum) can be seen.

The assignments for the bands numbered 1 through 10 in Table I for 2-pyridone-^{16}O in solution have been made by Shindo (10) and by Bellamy and Rogasch (11). Assignments for bands numbered 12 through 25 have been given by both Katritzky and Jones (12) and more recently by Spinner and White (3). However, the

Can. J. Chem. Downloaded from www.nrcresearchpress.com by 210.87.254.42 on 09/05/12
For personal use only.

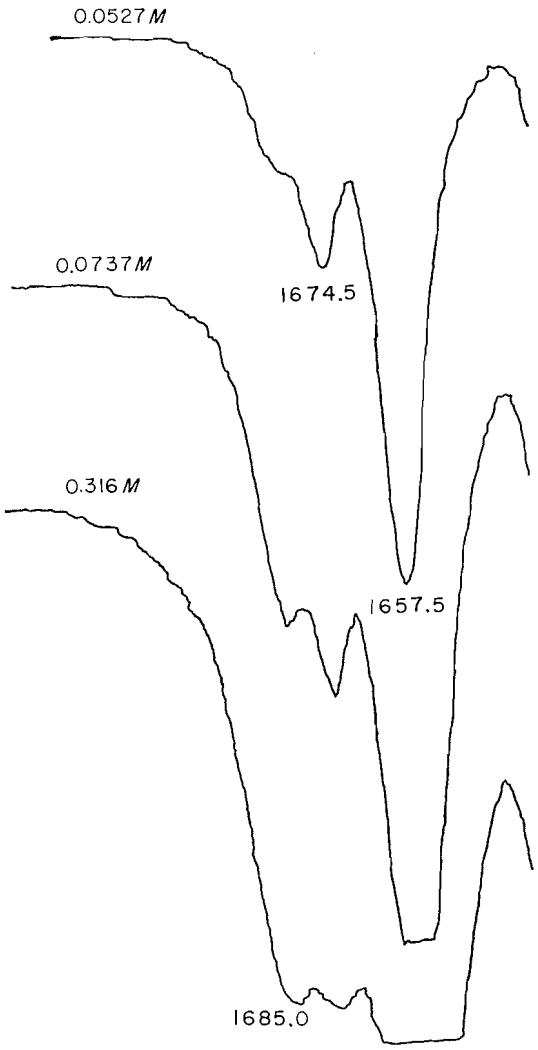

FIG. 1. Concentration dependence in the infrared spectrum of 2-pyridone-^{16}O in chloroform solution (cm^{-1}).

two assignments are not in complete agreement. The far infrared spectrum of 2-pyridone-^{16}O has been reported previously (13) but no vibrational assignments have been made.

The band numbered 11 has not been reported previously for 2-pyridone-^{16}O in solution although a shoulder in the solid state spectrum at 1680 cm^{-1} has been reported (14).

Discussion

1300–1700 cm^{-1} Region

The shifts to lower frequency with oxygen-18

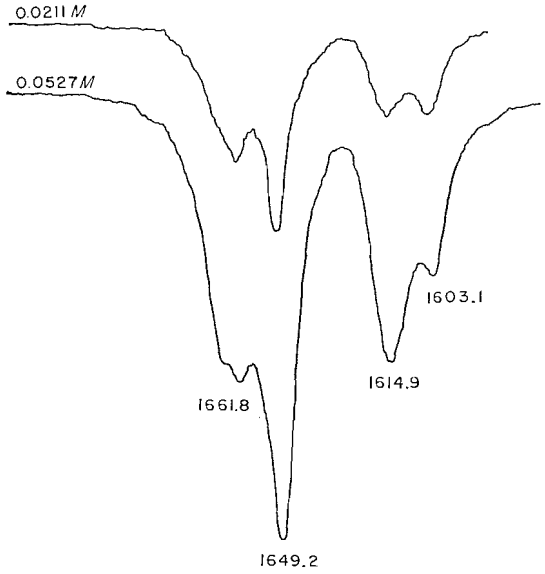

FIG. 2. Concentration dependence in the infrared spectrum of 2-pyridone-^{18}O in chloroform solution (cm^{-1}).

labelling observed for bands 11, 12, and 13 are 17.8, 12.7, and 8.3 cm^{-1}, respectively in chloroform solution (Table I). In the more dilute carbon tetrachloride solution only bands corresponding to 12 and 13 are found (Table II) and these shift 16.1 and 10.1 cm^{-1}, respectively, with the inclusion of the heavier oxygen isotope. The magnitude of these shifts, although less than those previously reported for isotopic shifts of carbonyl absorptions (17–22), and far below the calculated value for a pure CO stretching mode ($\sim$30 cm^{-1}), indicate that the oxygen atom is indeed involved in these vibrations and the lactam description for the molecule (**1**) is better than the dipolar one (**2**).

The concentration dependence found for the three bands in the 1640–1690 cm^{-1} portion of the infrared spectrum can be attributed to an equilibrium existing between different hydrogen bonded species. The frequencies assigned to these species in the spectrum of 2-pyridone-^{16}O are 1674.5 cm^{-1} for the monomer, 1657.5 cm^{-1} for the dimer and the weak 1685.0 cm^{-1} again to the dimer or possibly a polymer species.

At low concentrations, the monomer and cyclic dimer are favored to exist predominantly and relatively little of the species causing the shoulder at 1685 cm^{-1} is present. As the concentration of 2-pyridone is increased, less monomer

Can. J. Chem. Downloaded from www.nrcresearchpress.com by 210.87.254.42 on 09/05/12
For personal use only.

is present and a relative increase in the 1685 cm^{-1} band is observed.

No polymeric species has ever been postulated for 2-pyridone in solution; however, evidence has been reported from X-ray studies for a polymer in the solid state (15). The solid state spectrum does contain an absorption near 1680 cm^{-1} (14) which suggests, but by no means proves, that a polymer species could be the cause of the 1685 cm^{-1} absorption reported here at high concentrations in solution. The molecular weight measurements reported on 2-pyridone (16) in benzene and dioxane solutions were made at concentrations too low to reveal polymer formation.

The differences in isotopic shift for the CO absorptions of the monomer and dimer species are in the same direction as reported for the benzoic acid system (17).

Moreover, the isotopic shift is larger in carbon tetrachloride than in chloroform and follows the same trend reported in the literature for carbonyl compounds (17, 18). Five of the six remaining absorptions (bands 14 to 19) in the mid-frequency region (1300–1700 cm^{-1}) have been assigned to ring mode vibrations by Katritzky and Jones (12); however, more recently, Spinner and White (3) have reassigned several of these absorptions. From an investigation of substituted 2-pyridones (3), it was reported that considerable coupling of vibrations takes place and, in the solid state, the four vibrations at (1649, 1641), 1607, 1577, and 1540 cm^{-1} are intermixed. The isotopic shifts do indeed indicate considerable coupling with the CO group since larger shifts than expected for ring modes are observed.

The absorption at 1607 cm^{-1} was reported to be principally an NH in-plane bending mode (3) and would correspond to the 1615 cm^{-1} absorption in chloroform solution reported here and shows the expected large 12 cm^{-1} isotopic shift due to CO intermixing.

In addition, a second fundamental occurs in the same region (1618.0 cm^{-1}) and from the concentration dependence observed for the corresponding bands in the 2-pyridone-^{18}O spectrum (Fig. 2), it appears that the amount of mixing of these two modes in the labelled compound changes with the degree of association. No concentration dependence for these bands was found in the 2-pyridone-^{16}O spectrum.

In carbon tetrachloride, where solubility limited the investigation to only very dilute solution, only one band at 1619.4 cm^{-1} is found, and only a modest frequency shift (2.4 cm^{-1}) is observed. The large 8.3 cm^{-1} shift for the 1442.3 cm^{-1} band indicates that this ring mode is strongly coupled to the CO group in addition to those at 1542.0 and 1615.0 cm^{-1}. The other modes at 1618.0, 1471.7, and 1378.3 cm^{-1} produce much smaller shifts and, therefore, do not involve extensive oxygen movement.

2000–4000 cm^{-1} Region

Table I lists only ten peaks found in this region along with their ^{18}O isotopic shifts, although broad absorption occurs over a much wider frequency range. The free NH and CH stretching is assigned to the 3402 and 2996 cm^{-1} absorptions, respectively, and shows no isotope effect, as expected. In addition, the NH stretching frequency (associated) is at 2828 cm^{-1} and verifies the reported value of 2825 cm^{-1} in carbon tetrachloride solution deduced from deuterium labelling (11). Oxygen-18 labelling did not affect this absorption. The other bands in this region show varying shifts as expected since they arise from a Fermi interaction of the NH stretching mode with overtones and combination bands which would be affected by ^{18}O labelling.

1300–400 cm^{-1} Region

The spectrum of 2-pyridone-^{16}O has been assigned by Katritzky (12) between 1300 and 800 cm^{-1} and the region between 650 and 300 cm^{-1} has been reported by Sternglanz *et al.* (13) but was not assigned. A band reported at 1254 cm^{-1} was not observed since the solvent, chloroform, absorbs in this region. Spinner (3) questions the assignment of the 850 cm^{-1} band as a CH out-of-plane bending on the basis of Raman results and attributes the absorption to a ring stretching mode.

Of the six bands found between 400–800 cm^{-1}, three show relatively large shifts for the ^{18}O-labelled compound (Table I). The four strongest absorptions in this region are at 618, 565, 516, and 496 cm^{-1} with the 565 and 496 cm^{-1} bands shifting 10 and 13 cm^{-1} to lower frequency in the ^{18}O-labelled compound.

Experimental

Infrared Spectra

The infrared (i.r.) spectra were obtained on a Perkin–Elmer model 337 grating spectrophotometer using

abscissa expansion with an auxiliary Sargent SR strip chart recorder. The scanning speed was 72 min for the region 4000–1200 cm^{-1} and 72 min for the region 1300–400 cm^{-1} with a recorder chart speed of $\frac{1}{2}$ in. per min. The slit program was normal.

The absorption band frequencies were determined from a calibration curve constructed from the spectrum of indene containing 4.0 weight percent each of camphor and cyclohexanone (23). Three calibration curves were constructed for the regions 4000 to 1700 cm^{-1}, 1700 to 1300 cm^{-1}, and 1300 to 400 cm^{-1}. Repeated scans of the sample were taken (minimum of four) in each region with at least one scan having a superposition of the spectrum of the reference mixture as a further check on the calibrating procedure. The accuracies for the band positions in each region were ± 2, ± 0.3, and ± 1.5 cm^{-1} respectively.

All solvents were spectroscopic quality and used without further purification. The solutions were made by weighing the samples and pipetting in the solvent. The infrared cells used were a carefully matched pair with potassium bromide windows and a path length of 0.103 mm.

2-Pyridone-^{18}O

The synthesis was adapted for the one described by Bradlow and Vanderwerf (24) for the acid-catalyzed hydrolysis of 2-fluoropyridine. A fine stream of hydrogen chloride gas (dried over P_2O_5) was led through $H_2{}^{18}O$ (1 ml, 97.18% labelled, purchased from Yeda Research and Development Co., Ltd., Weizman Institute of Science, Rehovoth, Israel) for 1 h and the concentration of the acid was determined to be about 6 *N* (several runs on water under identical conditions were titrated, and the solution was found to be about 6 *N*). Freshly distilled 2-fluoropyridine (110 mg, purchased from Aldrich Chemical Co.) was dissolved in the isotopically labelled HCl solution and the solution heated under reflux (protected by freshly prepared $CaCl_2$ drying tube) in an oil bath at 110 °C for 24 h. The cold solution was withdrawn by means of a capillary pipette and quickly dropped onto anhydrous potassium carbonate (800 mg). The mixture was shaken with chloroform (50 ml), filtered, and the solid residue washed with small quantities of chloroform (an additional 200 ml). Evaporation of the chloroform filtrate furnished a solid which was recrystallized from hot cyclohexane to yield 2-pyridone-^{18}O (93.2 mg, 86%), m.p. 102–103 °C; lit. (24), m.p. 101–102 °C. It was shown to be 91.7% labelled by ^{18}O from a detailed analysis of the *m/e* 95, 97 peaks in the mass spectrum obtained using a Hitachi – Perkin–Elmer model RMU-6D instrument.

1. E. S. Levin and G. N. Rodionova. Dokl. Akad. Nauk SSSR, **164**, 584 (1965).
2. A. R. Katritzky, J. D. Rowe, and S. K. Roy. J. Chem. Soc. 758B (1967).
3. E. Spinner and J. C. B. White. J. Chem. Soc. 991B (1966).
4. A. R. Katritzky. Chem. and Ind. London, 331 (1965).
5. S. F. Mason. J. Chem. Soc. 4874 (1957).
6. A. R. Katritzky and R. E. Reavill. J. Chem. Soc. 753 (1963).
7. J. P. Shoffner. Ph.D. Thesis, University of Illinois at the Medical Center, Chicago, Illinois. 1965.
8. B. E. Zaitsev and Yu. N. Sheinker. Bull. Acad. Sci. USSR, Div. Chem. Sci. **11**, 2070 (1962).
9. B. E. Zaitsev and Yu. N. Sheinker. Bull. Acad. Sci. USSR, Div. Chem. Sci. **3**, 407 (1962).
10. H. Shindo. Chem. Pharm. Bull. Tokyo, **7**, 407 (1959).
11. L. J. Bellamy and P. E. Rogasch. Proc. Roy. Soc. (London), Ser. A, **257**, 98 (1960).
12. A. R. Katritzky and A. R. Jones. J. Chem. Soc. 2947 (1960).
13. H. Sternglanz, W. C. Coburn, C. V. Stephenson, and W. S. Wilcox. Appl. Spectry. **17**, 90 (1963).
14. J. A. Gibson, W. Kynaston, and A. S. Lindsey. J. Chem. Soc. 4340 (1955).
15. B. R. Penfold. Acta Cryst. **6**, 591 (1953).
16. M. H. Krackov, C. M. Lee, and H. G. Mautner. J. Am. Chem. Soc. **87**, 892 (1965).
17. S. Pinchas, D. Samuel, and M. Weiss-Broday. J. Chem. Soc. 1688 (1961).
18. S. Pinchas, D. Samuel, and M. Weiss-Broday. J. Chem. Soc. 2666 (1961).
19. S. Pinchas, D. Samuel, and M. Weiss-Broday. J. Chem. Soc. 2382 (1961).
20. G. J. Karabatsos. J. Org. Chem. **25**, 315 (1960).
21. M. Halman and S. Pinchas. J. Chem. Soc. 703 (1958).
22. R. Stewart, L. J. Muenster, and J. T. Edward. Chem. and Ind. London, 1906 (1961).
23. Intern. Union Pure Appl. Chem. Comm. Mol. Struct. Spectry. *Tables of wavenumbers for the calibration of infrared spectrometers.* Butterworths, Washington. 1961. pp. 678–682.
24. H. L. Bradlow and C. A. Vanderwerf. J. Org. Chem. **14**, 509 (1949).

Can. J. Chem. Downloaded from www.nrcresearchpress.com by 210.87.254.42 on 09/05/12
For personal use only.

Can. J. Chem. Downloaded from www.nrcresearchpress.com by 210.87.254.105 on 09/05/12
For personal use only.

Synthesis of 2-amino-2-deoxy-D-talose and 2-amino-2-deoxy-D-galactose[1]

M. B. PERRY AND ANN C. WEBB
Division of Biosciences, National Research Council of Canada, Ottawa, Canada

Received March 8, 1968

Treatment of D-lyxose with nitromethane in the presence of sodium methoxide gave 1-deoxy-1-nitro-D-galactitol which, after conversion to 2,3,4,5,6-penta-*O*-acetyl-1-deoxy-1-nitro-D-galactitol, reacted with saturated methanolic ammonia solution to yield 2-acetamido-1,2-dideoxy-1-nitro-D-talitol and 2-acetamido-1,2-dideoxy-1-nitro-D-galactitol. 2-Acetamido-1,2-dideoxy-1-nitro-D-talitol and 2-acetamido-1,2-dideoxy-1-nitro-D-galactitol were converted by a modified Nef reaction to 2-acetamido-2-deoxy-D-talose and 2-acetamido-2-deoxy-D-galactose which on hydrolysis with hydrochloric acid afforded 2-amino-2-deoxy-D-talose hydrochloride and 2-amino-2-deoxy-D-galactose hydrochloride. The properties and derivatives of the aminoglycoses are described.

Canadian Journal of Chemistry, 46, 2481 (1968)

The increasing importance of aminoglycoses as components of biological systems and the frequent occurrence of new compounds in microbial products have, in connection with the work of this laboratory, made it desirable to have available many aminoglycoses and their derivatives for use as reference standards and as biological substrates. We have prepared six 2-amino-2-deoxy-D-aldohexoses from D-ribose, D-xylose, and D-lyxose by treatment of the aldopentoses with nitromethane to yield 1-deoxy-1-nitrohexitols (1). This was followed by treatment of the derived penta-*O*-acetyl-1-deoxy-1-nitrohexitols or corresponding 3,4,5,6-tetraacetoxy-1-nitro-1-hexenes with ammonia to yield epimeric pairs of 2-acetamido-1,2-dideoxy-1-nitrohexitols which were converted to 2-acetamido-2-deoxyhexoses *via* the Nef (2) reaction. The method has been previously applied to two aldopentoses; 2-amino-2-deoxyglucose and 2-amino-2-deoxymannose were obtained from arabinose (3–6) and 2-amino-2-deoxy-D-gulose was obtained from D-xylose (7). This paper records the successful application of the synthetic method to D-lyxose to prepare 2-amino-2-deoxy-D-talose and 2-amino-2-deoxy-D-galactose.

2-Amino-2-deoxy-D-galactose may be obtained from chondroitin sulfate (8–11). It may be synthesized from D-lyxose by reduction of 2-amino-2-deoxy-D-galactononitrile prepared by the addition of hydrogen cyanide to 1-amino-1-deoxy-D-lyxose (D-lyxosylamine) (12), and by a method involving addition of ammonia to 2,3:1,6-dianhydro-β-D-talopyranose (13). 2-Amino-2-deoxy-D-talose has been synthesized from D-lyxose by the action of aniline (14), or 9-aminofluorene (15) and hydrogen cyanide, followed by reduction of the product having the D-talo configuration, and from 2-acetamido-4,6-*O*-benzylidene-2-deoxy-α-D-idopyranoside by Walden inversion of its 3-*O*-(methylsulfonyl) derivative and subsequent hydrolysis (16). Recently, Lemieux and coworkers (17, 18) have synthesized 2-amino-2-deoxy-D-galactose and 2-amino-2-deoxy-D-talose from tri-*O*-acetyl-D-galactal by reactions involving the addition of nitrosyl chloride, followed by conversion of the adduct to the acetylated 2-oximinohexose and reduction of the oxime to amine.

In the present work D-lyxose was condensed with nitromethane in the presence of sodium methoxide and the resulting precipitated sodium salts of 1-deoxy-1-nitro-D-galactitol (96%) and 1-deoxy-1-nitro-D-talitol (4%) were deionized with hydrogen form ion-exchange resin to remove sodium, and the product afforded pure 1-deoxy-1-nitro-D-galactitol. The 1-deoxy-1-nitro-D-galactitol gave only D-galactose with sulfuric acid (2). The optical rotary dispersion (o.r.d.) curve for the 1-deoxy-1-nitro-D-galactitol showed a positive Cotton effect centered at 310 mμ in agreement with the rules proposed by Satoh, Kiyomoto, and Okuda (19, 20) for *C*-nitro glycitols which stated that derivatives having groups at C-2 in the S-configuration show positive Cotton effects in the 310 mμ region.

The 2,3,4,5-penta-*O*-acetyl-1-deoxy-1-nitro-D-galactitol obtained on acetylation of the 1-deoxy-1-nitro-D-galactitol with saturated methanolic ammonia (6) afforded a mixture of

[1]Issued as NRCC No. 10134.

Can. J. Chem. Downloaded from www.nrcresearchpress.com by 210.87.254.105 on 09/05/12
For personal use only.

2-acetamido-1,2-dideoxy-1-nitro-D-talitol and 2-acetamido-1,2-dideoxy-1-nitro-D-galactitol which were separated in pure form by fractional crystallization from ethanol solution. The o.r.d. curves for the compounds showed a positive Cotton effect for the 2-acetamido-1,2-dideoxy-1-nitro-D-galactitol and a negative Cotton effect for the 2-acetamido-1,2-dideoxy-1-nitro-D-talitol, both centered about 310 mμ, in agreement with the proposed rules of Satoh *et al.* (19, 20).

The 2-acetamido-1,2-dideoxy-1-nitrohexitols were treated separately with barium hydroxide solution and on treatment with 5 *N* sulfuric acid (6) gave the corresponding derivatives 2-acetamido-2-deoxy-D-talose and 2-acetamido-2-deoxy-D-galactose. Under the mild conditions used to effect the Nef reaction (2) it was observed that the D-talose derivative was hydrolyzed in part to the free aminoglycose and the product was therefore treated with aqueous acetic anhydride in the presence of basic ion-exchange resin to reconvert it to the *N*-acetyl derivative.

The 2-acetamido-2-deoxy-D-talose and 2-acetamido-2-deoxy-D-galactose obtained in the above synthesis had chemical and physical properties identical with those of authentic glycoses. The 2-acetamido-2-deoxyglycoses were each hydrolyzed with hot dilute hydrochloric acid to yield 2-amino-2-deoxy-D-talose hydrochloride and 2-amino-2-deoxy-D-galactose hydrochloride. Reduction of the 2-acetamido-2-deoxyglycoses with aqueous sodium borohydride afforded crystalline 2-acetamido-2-deoxy-D-talitol and 2-acetamido-2-deoxy-D-galactitol in good yield, and the glycitols appear to be convenient derivatives for the characterization of the aminoglycoses.

The synthesis of the aminoglycoses from 2,3,4,5,6-penta-*O*-acetyl-1-deoxy-1-nitro-D-galactitol as described above, but without the isolation of intermediates, afforded a mixture of the 2-acetamido-2-deoxyglycoses which were separated by cellulose column chromatography to yield pure 2-acetamido-2-deoxy-D-talose and 2-acetamido-2-deoxy-D-galactose in 41% and 28% yield respectively from D-lyxose. The preparative method provides a convenient three-step procedure for the synthesis of 2-acetamido-2-deoxy-D-talose and 2-acetamido-2-deoxy-D-galactose in good yield and provides a method for the synthesis of the 1-^{14}C aminoglycoses by condensation of D-lyxose with $^{14}CH_3NO_2$.

Experimental

Paper chromatography was performed by the descending method (21) on Whatman No. 1 filter paper using pyridine – ethyl acetate – water (2:5:5 v/v, top layer) as the mobile phase. Glycose derivatives were detected with either 1% silver nitrate in acetone, followed by 2% sodium hydroxide in ethanol (22), or by 2% *p*-anisidine hydrochloride in butan-1-ol (23). The rates of movement of the glycoses on the paper chromatograms are quoted relative to D-galactose (R_{Gal}).

Gas–liquid partition chromatography was carried out at 200 °C using a Hewlett–Packard model 402 chromatograph with a hydrogen flame detector and fitted with glass U tubes (4 ft × 6 mm × 3 mm internal diameter) packed with 10% neopentylglycol sebacate polyester on 80–100 mesh acid-washed Chromosorb W. Retention times of the compounds are quoted relative to 2-acetamido-2-deoxy-1,3,4,5,6-penta-*O*-(trimethylsilyl)-D-glucitol (T_{GN}) (24).

Melting points were determined on a Fisher–Johns apparatus and are corrected. Solutions were concentrated under reduced pressure, below 40 °C.

Optical rotations were determined at 20 °C using a Perkin–Elmer 141 polarimeter. Optical rotary dispersion (o.r.d.) measurements were made using a JASCO model ORD/UV-5 automatically recording spectropolarimeter.

*2-Amino-2-deoxy-*D*-talose and 2-Amino-2-deoxy-*D*-galactose*

*1-Deoxy-1-nitro-*D*-galactitol*

To a suspension of D-lyxose (10 g) in absolute methanol (50 ml) and nitromethane (50 ml), contained in a 500 ml flask, was added a solution of sodium (2.2 g) in absolute methanol (75 ml), and the mixture was shaken at room temperature for 24 h. Following the addition of ether (60 ml), the precipitated product was collected by filtration, washed with cold methanol, ether, and light petroleum (b.p. 30–60 °C) and dried under vacuum. The product was dissolved in cold water (200 ml) and passed down a column of Rexyn 101 (H^+) ion-exchange resin (200 ml) and the eluate and water washings were concentrated to a syrup. This was dissolved in hot methanol (50 ml) and on keeping at 5 °C successive crops of crystalline 1-deoxy-1-nitro-D-galactitol (12.2 g), m.p. 141 °C were collected. After three recrystallizations from methanol pure 1-deoxy-1-nitro-D-galactitol had m.p. 143 °C; $[\alpha]_D$ +1.7 ° (*c*, 0.8 in water); o.r.d. (*c*, 0.3 in water) $[\phi]_{342-344}$ + 833 °.[2]

Anal. Calcd. for $C_6H_{13}O_7N$: C, 34.13; H, 6.21; N, 6.63. Found: C, 33.9; H, 5.94; N, 6.6.

A portion of the 1-deoxy-1-nitro-D-galactitol (0.2 g) was dissolved in 2 *N* sodium hydroxide (2 ml) and the solution was added dropwise to 6 *N* sulfuric acid (2.5 ml) at 0 °C. After 2 h at room temperature the mixture was diluted with water (10 ml) and neutralized ($BaCO_3$). The filtered solution was passed down Rexyn 101 (H^+)

[2]The molecular rotation $[\phi]$ is defined by $[\phi] = \frac{[\alpha]M}{100} = \frac{M\alpha_r Sc}{cl}$ where α_r is the reading of the rotation in degrees, M is the molecular weight, *c* is the concentration in g per 100 ml of solution, *l* is the path length in dm, and Sc is the scale setting.

Can. J. Chem. Downloaded from www.nrcresearchpress.com by 210.87.254.105 on 09/05/12
For personal use only.

(4 ml) and Rexyn RG6 (OH^-) (4 ml) ion-exchange resins and the eluate and washings were concentrated to a syrup (150 mg). Paper chromatographic examination of the product showed a single spot corresponding to galactose and from ethanol solution crystalline D-galactose (90 mg) having m.p. and mixture m.p. 170 °C and $[\alpha]_D$ +80 ° (*c*, 0.5 in water) was obtained.

2,3,4,5,6-Penta-O-acetyl-1-deoxy-1-nitro-D-galactitol

1-Deoxy-1-nitro-D-galactitol (10 g) in acetic anhydride (90 ml) was treated with two drops of concentrated sulfuric acid and the mixture was heated for 40 min on a boiling water bath. The cooled reaction mixture was poured into an ice and water mixture (500 ml), and the product was extracted with chloroform in the usual way. After removal of the solvent the residual syrup was dissolved in hot methanol (50 ml) and on cooling crystalline 2,3,4,5,6-penta-*O*-acetyl-1-deoxy-1-nitro-D-galactitol (15.8 g) having m.p. 130 °C was obtained. After three recrystallizations from methanol the product had m.p. 130 °C and $[\alpha]_D$ +6° (*c*, 1.5 in chloroform).

Anal. Calcd. for $C_{16}H_{23}O_{12}N$: C, 45.62; H, 5.50; N, 3.32. Found: C, 45.43; H, 5.3; N, 3.3.

2-Acetamido-1,2-dideoxy-1-nitro-D-talitol and 2-Acetamido-1,2-dideoxy-1-nitro-D-galactitol

2,3,4,5,6-Penta-*O*-acetyl-1-deoxy-1-nitro-D-galactitol (12 g) dissolved in absolute methanol (140 ml), was cooled to 0 °C, and anhydrous ammonia gas was passed into the solution for 1 h. The saturated solution was then allowed to stand for 18 h at room temperature. The reaction mixture was concentrated to a syrup which was triturated with hot chloroform (3 × 100 ml) to remove acetamide. The light-brown syrup remaining was dissolved in hot ethanol, treated with charcoal, filtered, and after concentration to about 60 ml, was kept at 5 °C. Successive crops of 2-acetamido-1,2-dideoxy-1-nitro-D-talitol (3.9 g) were first obtained. After two recrystallizations from ethanol these gave a product (3.2 g), m.p. 158 °C; $[\alpha]_D$ +20 ° (*c*, 1.8 in water); o.r.d. (*c*, 0.3 in water) $[\phi]_{344-348}$ −288 °.

Anal. Calcd. for $C_8H_{16}O_7N_2$: C, 38.10, 6.39; N, 11.11. Found: C, 38.3; H, 6.5; N, 11.1.

Following the removal of the 2-acetamido-1,2-dideoxy-1-nitro-D-talitol, concentration of the mother liquors and cooling to 2 °C yielded 2-acetamido-1,2-dideoxy-1-nitro-D-galactitol (2.0 g), which after two recrystallizations from ethanol gave the pure compound (1.7 g), m.p. 168 °C; $[\alpha]_D$ −25.7 ° (*c*, 1 in water); o.r.d. (*c*, 0.3 in water) $[\phi]_{348-350}$ +277 °.

Anal. Calcd. for $C_8H_{16}O_7N_2$: C, 38.10; H, 6.39; N, 11.11. Found: C, 37.6; H, 6.5; N, 11.0.

2-Acetamido-2-deoxy-D-talose

2-Acetamido-1,2-dideoxy-1-nitro-D-talitol (3 g) was dissolved in a solution of $Ba(OH)_2 \cdot 8H_2O$ (3.7 g) in water (60 ml) and the solution was added dropwise to a cooled, stirred solution of concentrated sulfuric acid (3.4 ml) in water (35 ml). The mixture was stirred for 4 h at 20 °C and was then left at 24 °C for 18 h. The reaction mixture was neutralized with barium carbonate, the filtered solution was concentrated to about 50 ml, and following the addition of Dowex-1 ($CO_3^=$) ion-exchange resin (30 ml), methanol (10 ml), and acetic anhydride (0.4 ml), the mixture was shaken for 20 min. The filtered solution, after passage down columns of Rexyn 101 (H^+) (10 ml) and Rexyn RG6 (OH^-) (10 ml) ion-exchange resins, was concentrated to a syrup (2.1 g) which on paper chromatographic analysis, showed a single spot (R_{Gal} 1.92), having the same mobility as authentic 2-acetamido-2-deoxy-D-talose. The syrup, which could not be induced to crystallize had, $[\alpha]_D$ −8.8 ° (*c*, 2 in water) (lit. $[\alpha]_D$ −11 ° (16)).

Anal. Calcd. for $C_8H_{15}O_6N$: C, 43.44; H, 6.82; N, 6.33. Found: C, 43.22; H, 6.9; N, 6.3.

The fully trimethylsilylated (24) 2-acetamido-2-deoxy-D-talose on gas–liquid partition chromatography showed three peaks having T_{GN} 0.85, 1.04, and 1.66.

2-Amino-2-deoxy-D-talose Hydrochloride

2-Acetamido-2-deoxy-D-talose (0.5 g) in 2 *N* hydrochloric acid (15 ml) was heated on a boiling water bath for 2 h and then concentrated to dryness. The residue was co-distilled with ethanol and benzene to remove the last trace of water and acetic acid, and on keeping the product moistened with a little ethanol, it gave crystalline 2-amino-2-deoxy-D-talose hydrochloride (0.37 g) which had m.p. 150 °C (decomposed) and $[\alpha]_D$ −6 ° (*c*, 1.5 in water).

Anal. Calcd. for $C_6H_{14}O_5$ NCl; C, 33.26; H, 6.84; Cl, 16.44. Found: C, 33.0; H, 6.8; Cl, 16.5.

Paper chromatographic analysis of the 2-amino-2-deoxy-D-talose hydrochloride revealed a single spot having R_{Gal} 0.56.

2-Acetamido-2-deoxy-D-talitol

2-Acetamido-2-deoxy-D-talose (0.2 g) in water (5 ml) was reduced by the addition of sodium borohydride (80 mg), and after 2 h at room temperature, the excess borohydride was destroyed by the addition of acetic acid. The reaction mixture was passed down a column of Rexyn 101 (H^+) ion-exchange resin (5 ml) and the concentrated eluate and washings were repeatedly evaporated with absolute methanol to remove boric acid. The final residue was taken up in hot methanol (2–3 ml) and filtered. On cooling the methanol solution, crystalline 2-acetamido-2-deoxy-D-talitol (0.17 g) was obtained, which after two recrystallizations from methanol had m.p. 153 °C and $[\alpha]_D$ +33 ° (*c*, 0.8 in water).

Anal. Calcd. for $C_8H_{17}O_6N$: C, 43.05; H, 7.68; N, 6.27. Found: C, 42.9; H, 7.8; N, 6.2.

On paper chromatographic analysis the 2-acetamido-2-deoxy-D-talitol gave a single spot having R_{Gal} 1.30.

2-Acetamido-2-deoxy-D-galactose

2-Acetamido-1,2-dideoxy-1-nitro-D-galactitol (1.7 g) was converted to 2-acetamido-2-deoxy-D-galactose (1.2 g) using the conditions described above for the conversion of 2-acetamido-1,2-dideoxy-1-nitro-D-talitol to 2-acetamido-2-deoxy-D-talose. The 2-acetamido-2-deoxy-D-galactose, obtained crystalline from ethanol–water mixture, gave a single spot on paper chromatograms with R_{Gal} 1.43 and had m.p. and mixture m.p. 110 °C and $[\alpha]_D$ +84 ° (*c*, 2 in water). The trimethylsilylated (24) derivative on gas–liquid partition chromatography gave a single peak (T_{GN} 1.72) having the same retention time as an authentic sample of trimethylsilyl 2-acetamido-2-deoxy-3,4,5-tri-*O*-(trimethylsilyl)-α-D-galactopyranoside.

2-Amino-2-deoxy-D-galactose Hydrochloride

2-Acetamido-2-deoxy-D-galactose (0.3 g) after hydrolysis with 2 *N* hydrochloric acid for 2 h at 100 °C, afforded crystalline 2-amino-2-deoxy-D-galactose hydrochloride (0.21 g), having $[\alpha]_D$ +124° → +94° (*c*, 1.2 in water).

Anal. Calcd. for $C_6H_{14}O_5NCl$: C, 33.26; H, 6.84; Cl, 16.44. Found: C, 33.1; H, 6.7; Cl, 16.4.

On paper chromatography the 2-amino-2-deoxy-D-galactose hydrochloride gave a single spot having R_{Gal} 0.43.

2-Acetamido-2-deoxy-D-galactitol

2-Acetamido-2-deoxy-D-galactose (0.2 g) on borohydride reduction gave 2-acetamido-2-deoxy-D-galactitol (0.17 g), having m.p. and mixture m.p. 174 °C and $[\alpha]_D$ −44 ° (*c*, 0.5 in water) (25). On paper chromatography the derivative gave a single spot having R_{Gal} 1.96.

Anal. Calcd. for $C_8H_{17}O_6N$: C, 43.05; H, 7.68; N, 6.27. Found: C, 43.0; H, 7.6; N, 6.15.

Direct Synthesis of 2-Acetamido-2-deoxy-D-talose and 2-Acetamido-2-deoxy-D-galactose

2,3,4,5,6-Penta-*O*-acetyl-1-deoxy-1-nitro-D-galactitol (10 g) was treated with methanolic ammonia as described above and the product was treated with sulfuric acid to convert the mixed resulting 2-acetamido-1,2-dideoxy-1-nitrohexitols to the corresponding 2-acetamido-2-deoxy-D-hexoses. These were separated on a cellulose column (4.5 × 40 cm) using butan-1-ol half-saturated with water as the mobile phase (26) and yielded chromatographically pure 2-acetamido-2-deoxy-D-galactose (1.9 g) and 2-acetamido-2-deoxy-D-talose (2.9 g).

Acknowledgments

We thank Mr. A. E. Castagne for the microanalyses and Drs. P. Morand and H. H. Baer for the optical rotary dispersion facilities.

1. J. C. Sowden. Advan. Carbohydrate Chem. **6**, 315 (1951).
2. J. U. Nef. Ann. Chem. **280**, 263 (1894).
3. A. N. O'Neill. Can. J. Chem. **37**, 1747 (1959).
4. J. C. Sowden and M. L. Oftedahl. J. Am. Chem. Soc. **82**, 2303 (1960).
5. S. D. Gero and J. Defaye. Compt. Rend. **261**, 1555 (1965).
6. C. Satoh and A. Kiyomoto. Chem. Pharm. Bull. Tokyo, **12**, 615 (1964).
7. J. C. Sowden and M. L. Oftedahl. J. Org. Chem. **26**, 2153 (1961).
8. P. Karrer and J. Mayer. Helv. Chim Acta, **20**, 407 (1937).
9. M. Stacey. J. Chem. Soc. 272 (1944).
10. S. Gardell. Acta Chem. Scand. **5**, 195 (1951).
11. M. L. Wolfrom and K. Onodera. J. Am. Chem. Soc. **79**, 4737 (1957).
12. R. Kuhn and W. Kirschenlohr. Ann. Chem. **600**, 126 (1956).
13. S. P. James, F. Smith, M. Stacey, and L. F. Wiggins. J. Chem. Soc. 625 (1946).
14. R. Kuhn and H. Fischer. Ann. Chem. **612**, 65 (1958).
15. R. Kuhn and J. C. Jochims. Ann. Chem. **641**, 143 (1961).
16. R. W. Jeanloz, Z. T. Glazer, and D. A. Jeanloz. J. Org. Chem. **26**, 532 (1961).
17. R. U. Lemieux and T. L. Nagabhushan. Tetrahedron Letters, **26**, 2143 (1965).
18. R. U. Lemieux and T. L. Nagabhushan. Can. J. Chem. **46**, 401 (1968).
19. C. Satoh and A. Kiyomoto. Carbohydrate Res. **3**, 248 (1966).
20. C. Satoh, A. Kiyomoto, and T. Okuda. Carbohydrate Res. **5**, 140 (1967).
21. S. M. Partridge. Biochem. J. **42**, 238 (1948).
22. W. E. Trevelyan, D. D. Procter, and J. S. Harrison. Nature, **166**, 444 (1950).
23. L. Hough, J. K. N. Jones, and W. H. Wadman. J. Chem. Soc. 1702 (1950).
24. M. B. Perry. Can. J. Biochem. **42**, 451 (1964).
25. W. R. C. Crimmin. J. Chem. Soc. 2838 (1957).
26. L. Hough, J. K. N. Jones, and W. H. Wadman. J. Chem. Soc. 2511 (1949).

Can. J. Chem. Downloaded from www.nrcresearchpress.com by 210.87.254.105 on 09/05/12
For personal use only.

Synthesis and nuclear magnetic resonance spectra of some partially acylated β-D-glucopyranosides[1]

A. P. TULLOCH AND A. HILL[2]
Prairie Regional Laboratory, National Research Council of Canada, Saskatoon, Saskatchewan
Received February 19, 1968

The synthesis of ten new partially acylated derivatives of methyl β-D-glucopyranoside, all with an acyl group at C-6, is described. The nuclear magnetic resonance spectra of these compounds, and of a number of related derivatives, have been measured using pyridine, acetone-d_6, and deuteriochloroform as solvents. When OH-4 is acylated, the H-6 signals are at higher field (by 0.1–0.3 p.p.m.) than when OH-4 is not acylated, but this effect is not observed when OH-3 is acylated. When a trimethylsilyl ether group is introduced at C-4 the difference between the chemical shifts of the H-6 protons (δA − δB) increases markedly. Estimation of J_{BX} and J_{AX} (where B is the H-6 proton at higher field and X is H-5), from spectra obtained using acetone-d_6 and pyridine as solvents, shows that $J_{BX} < J_{AX}$ when there is an acyl group at C-4 but $J_{BX} > J_{AX}$ when there is no acyl group at C-4.

Canadian Journal of Chemistry, 46, 2485 (1968)

Can. J. Chem. Downloaded from www.nrcresearchpress.com by 210.87.254.105 on 09/05/12
For personal use only.

During an investigation of the structure of a partially acylated sophoroside (1), we wished to determine the positions of acyl groups by nuclear magnetic resonance (n.m.r.) spectroscopy. We, therefore, decided to examine the n.m.r. spectra of some methyl β-D-glucopyranoside diesters which would serve as simple model compounds. When we realized that useful correlations between the n.m.r. spectra and the structure of partially acylated glucosides existed, we extended the investigation to a number of related derivatives.

No partially acylated glucosides had been studied in this way though n.m.r. spectra of methyl 2,3,4,6-tetra-*O*-acetyl-β-D-glucopyranoside (**9**) (2), of β-glucose pentaacetate (3, 4), of 1,3,4,6- and 2,3,4,6-tetra-*O*-acetyl-β-D-glucopyranose (5, 6) had been discussed previously.

Synthesis of Partly Acylated Methyl β-D-Glucopyranosides

All four methyl β-D-glucopyranoside triacetates have been synthesized, but only the 3,4,6-triacetate (**6**) (7) was used in the present work. It appears that diacetates other than the 2,3-diacetate, and monoacetates other than the 6-acetate (**3**) (8), have not been prepared before.

The 6-acetate (**3**) was first prepared by Frohwein (8), by partial hydrolysis of the tetraacetate, but the yield was very low. We therefore examined the method used by Hurst and McInnes (9) to synthesize methyl 6-*O*-acetyl-α-D-glucopyranoside, in which a trimethylsilyl group at the 6-position of methyl 2,3,4,6-tetra-*O*-trimethylsilyl-α-D-glucopyranoside is selectively removed, the product acetylated, and the remaining trimethylsilyl groups taken off. When this method was used with β-methyl glucoside, 6-acetate (**3**) and 6-stearate (**4**) were readily prepared.

Methyl 4,6-di-*O*-acetyl-β-D-glucopyranoside (**8**) was prepared by hydrogenolysis of the 4,6-diacetate (**7**), which had been obtained by acetylation of methyl 2,3-di-*O*-benzyl-β-D-glucopyranoside. In addition to the 6-stearate (**4**), above, we also prepared the 6-acetate-4-stearate (**14**) to compare the effects of the long chain stearoyl group with those of the short chain acetyl group. Methyl 6-*O*-acetyl-2,3-di-*O*-benzyl-β-D-glucopyranoside (**12**) was prepared using the trimethylsilyl ether derivative (**10**) as intermediate. Treatment of **12** with stearoyl chloride and hydrogenolysis of the benzyl groups yielded methyl 6-*O*-acetyl-4-*O*-stearoyl-β-D-glucopyranoside (**14**); acetylation gave methyl 2,3,6-tri-*O*-acetyl-4-*O*-stearoyl-β-D-glucopyranoside (**15**).

To compare the effect of an acetate group at C-3 with that of an acetate at C-4 the 3,6-diacetate (**18**) was prepared. Partial acetylation of methyl 4,6-*O*-benzylidene-β-D-glucopyranoside (cf. ref. 10) with one mole of acetic anhydride in pyridine, gave a mixture of products which were separated by column chromatography into 3-acetate (22%), 2-acetate (34%), and 2,3-diacetate (15%). A number of other conditions were tried, including the use of acetyl chloride, but all resulted in lower yields of 3-acetate. Methyl 3-*O*-acetyl-β-D-glucopyranoside (**16**) was obtained by removing the benzylidene group with

[1]Issued as NRCC No. 10133.
[2]NRCC Postdoctorate Fellow, 1965–1967.

Can. J. Chem. Downloaded from www.nrcresearchpress.com by 210.87.254.105 on 09/05/12
For personal use only.

TABLE I

Chemical shifts (in p.p.m.) of acetoxy, H-6, and H-1 protons of β-methyl glucoside derivatives in pyridine, acetone-d_6, and deuteriochloroform

	Acetoxy			H-6			H-1		
Compound	Pyridine	Acetone-d_6	Deuterio-chloroform	Pyridine	Acetone-d_6	Deuterio-chloroform	Pyridine	Acetone-d_6	Deuterio-chloroform
6-*O*-Acetyl (**3**)	1.95	2.03	—	4.79	4.30	—	4.57	4.22	—
6-*O*-Stearoyl (**4**)	—	—	—	4.73	4.29	4.36	4.53	4.18	4.19
4,6-Di-*O*-acetyl (**8**)	2.00, 2.01	1.99, 2.03	2.07, 2.10	4.41	4.10	4.20	4.58	4.24	4.20
3,6-Di-*O*-acetyl (**18**)	1.94, 1.96	2.02, 2.04	2.10, 2.16	4.70	4.30	4.37	4.57	4.28	4.25
6-*O*-Acetyl-4-*O*-stearoyl (**14**)	2.01	1.97	2.06	4.45	4.06	4.14	4.59	4.21	4.20
3,4,6-Tri-*O*-acetyl (**6**)	1.97, 2.01 (2)*	1.96 (2),* 1.98	2.04, 2.07, 2.09	4.40	4.16	4.20	4.60	4.36	4.31
2,3,6-Tri-*O*-acetyl-4-*O*-stearoyl (**15**)	2.00 (2)*, 2.02	1.92,1.96, 2.00	1.97, 2.02, 2.07	4.42	4.15	4.18	4.75	4.60	4.42
2,3,4-Tri-*O*-acetyl-6-*O*-stearoyl (**5**)	1.97, 2.00 (2)*	1.92, 1.97, 1.98	1.97, 1.99, 2.01	4.46	4.20	4.22	4.66	4.61	4.41
2,3,4,6-Tetra-*O*-acetyl (**9**)	1.95, 1.97, 1.99 (2)*	1.93, 1.98 (2),* 2.01	2.00, 2.02, 2.04, 2.08	4.38	4.17	4.19	4.71	4.60	4.42

*Denotes number of coincident signals.

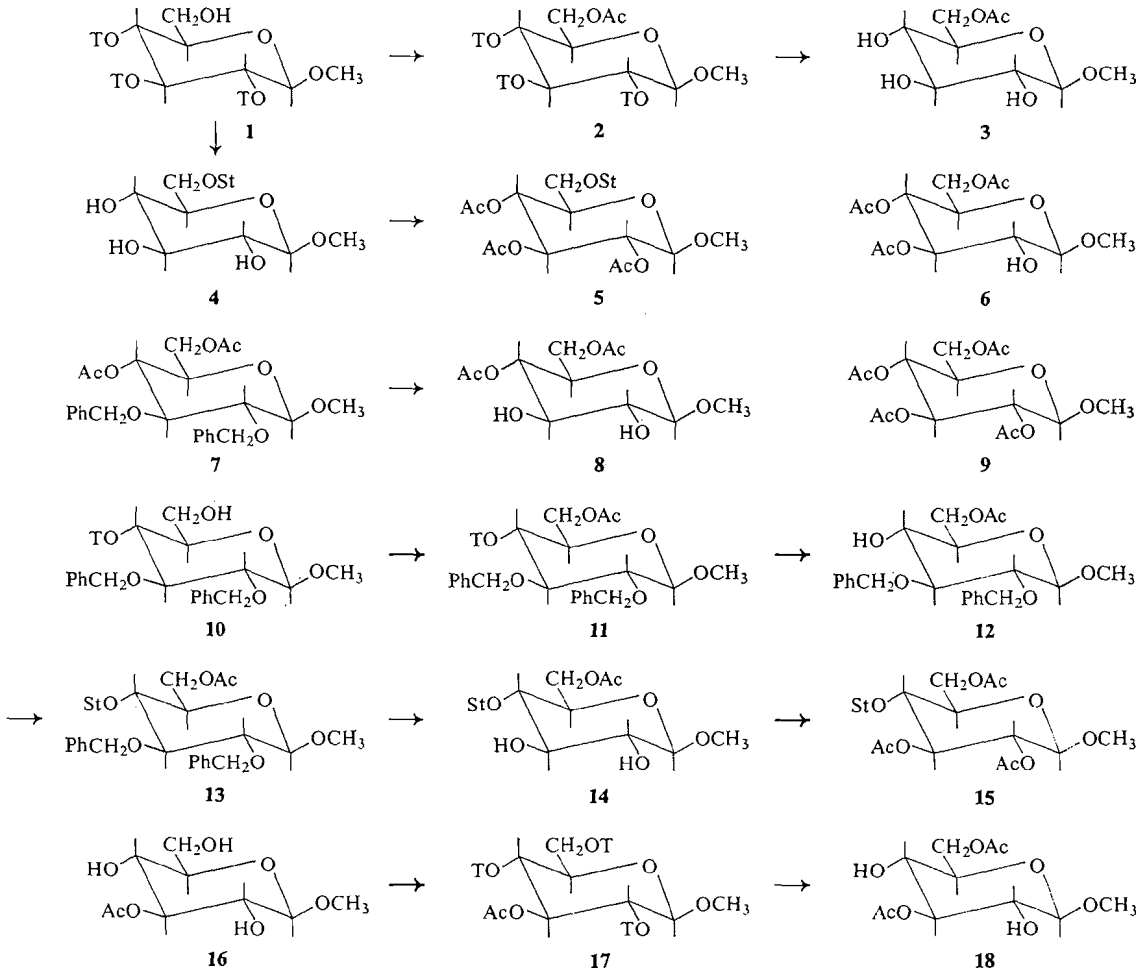

50% acetic acid. Application of the method of Hurst and McInnes (9) to **16** led to the synthesis of the 3,6-diacetate (**18**). The yield was very low, apparently because the presence of the acetate group increased the rate of hydrolysis of the secondary trimethylsilyl groups. The positions of the acyl groups in the new compounds were confirmed by spin decoupling experiments.

Nuclear Magnetic Resonance Spectra

Spectra of all the compounds were recorded using pyridine as solvent, and also, when they were sufficiently soluble, using acetone-d_6 and deuteriochloroform as solvents. We have been concerned with the chemical shifts of the signals due to H-6, H-1 and the acetoxy groups because they can be related to the structure of the compounds under investigation. For the present purpose it was satisfactory to take the center of the H-6 multiplet as the chemical shift of the H-6 protons, except in the case of the trimethylsilyl ether derivatives discussed below.

The chemical shifts of the acetoxy, H-6, and H-1 protons of some β-methyl glucoside derivatives are shown in Table I; those assigned to H-6 will be considered first. The spectra of **3**, **4**, and **18**, compounds, in which OH-4 is not acylated, have H-6 signals at lower field than the spectra

Can. J. Chem. Downloaded from www.nrcresearchpress.com by 210.87.254.105 on 09/05/12
For personal use only.

of **8**, **14**, and the fully acetylated compounds. The difference in chemical shift of H-6 using pyridine is at least 0.3 p.p.m. and using the other two solvents is 0.1–0.2 p.p.m. The spectra of **3**, **18**, and **8**, shown in Fig. 1, illustrate this observation.

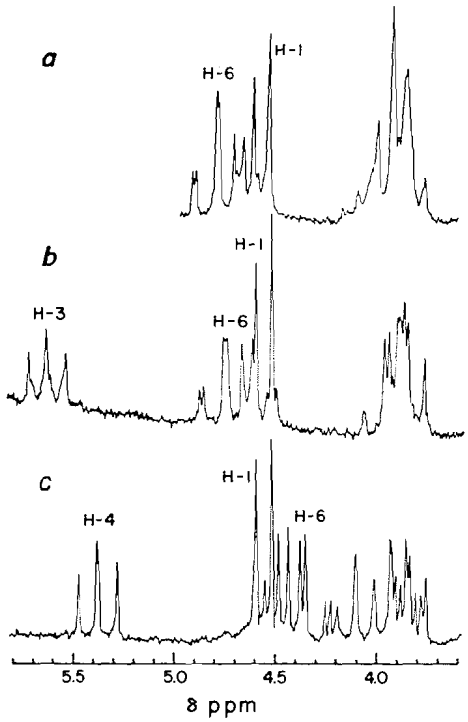

FIG. 1. Nuclear magnetic resonance spectra of: (*a*) methyl 6-*O*-acetyl-β-D-glucopyranoside (**3**); (*b*) methyl 3,6-di-*O*-acetyl-β-D-glucopyranoside (**18**); (*c*) methyl 4,6-di-*O*-acetyl-β-D-glucopyranoside (**8**); in pyridine, (3.5–5.8 p.p.m. region).

The differences in chemical shift are probably the result of interaction between the solvent and OH-4. Pyridine, which could form a hydrogen bond with OH-4, has the greatest effect on the spectra. The deshielding of neighboring protons resulting from complex formation between a hydroxyl group and pyridine has already been noted (11).

Acylation of a hydroxyl group might be expected to have a small deshielding effect on the protons γ to the OH group (see effect of acylation of OH-3 on H-1 in Table I). However, any such deshielding effect resulting from acylation of OH-4 is apparently more than counteracted by the prevention of interaction between OH-4 and the solvent.

TABLE II

Chemical shifts (in p.p.m.) of H-6 protons of β-D-glucopyranoses in pyridine, acetone-d_6, and deuteriochloroform

Compound	H-6		
	Pyridine	Acetone-d_6	Deuteriochloroform
1,2,3,6-Tetra-*O*-acetyl	4.63	4.28	4.36
1,2,4,6-Tetra-*O*-acetyl	4.37	4.12	4.18
1,2,3,4,6-Penta-*O*-acetyl	4.39	4.14	4.09

This effect may be peculiar to H-6 in the glucopyranose ring. However, in the spectrum of methyl 4-hydroxystearate the chemical shift of the methylene protons α to the carboxyl group, which are γ to the OH group, is 2.33 p.p.m. (11), but in the spectrum of methyl 4-acetoxystearate the α methylene signal appears at 2.22 p.p.m. (spectra were taken in carbon tetrachloride).

Table I also shows that the H-1 signal is displaced to lower field when 3 or 4 acyl groups are present. The effect is most noticeable in acetone-d_6 and least noticeable in pyridine. A similar deshielding of H-5 was also observed (using acetone-d_6); the signal appears at about 3.4–3.5 p.p.m. in the spectrum of **3**, but at 3.75–3.90 p.p.m. in the spectra of compounds in which OH-4 is acylated.

Signals due to the acetoxy groups of β-methylglucoside tetraacetate (9), using dimethyl formamide as solvent, were discussed by Barker *et al.* (2) who concluded that the signal at highest field was that of acetate at C-2. This assignment is probably true for spectra using acetone-d_6 and deuteriochloroform since the signal at 1.95–1.97 p.p.m. in the fully acylated compounds is absent from the spectra of those which lack an acetate at C-2. The spectra of the fully acylated compounds (using deuteriochloroform as solvent), except that of **5**, show an acetoxyl signal at relatively low field (2.07–2.09 p.p.m.) which is apparently due to acetate at C-6.

The spectra of β-glucopyranose pentaacetate and of two β-glucopyranose tetraacetates were also examined and the chemical shifts of the H-6 signals are listed in Table II. Here also the absence of an acyl group at C-4 results in the appearance of H-6 at appreciably lower field.

The spectra of some partially acylated deriva-

Can. J. Chem. Downloaded from www.nrcresearchpress.com by 210.87.254.105 on 09/05/12
For personal use only.

Can. J. Chem. Downloaded from www.nrcresearchpress.com by 210.87.254.105 on 09/05/12
For personal use only.

tives containing benzyl and trimethylsilyl groups were then investigated, with the results shown in Table III. Again H-6 is at lower field when OH-4 is not acylated, but H-1 is not affected by acylation of OH-4 when there are benzyl ether groups at C-2 and C-3. The spectra of compounds with a trimethylsilyl group at C-4, **2** and **11**, show an H-6 signal at higher field than do the spectra of the parent compounds, but the displacement is smaller than that shown by spectra of compounds with an acyl group at C-4. However, when the spectra are examined carefully (see Table IV below) the H-6 signal is seen to be more spread out and sometimes (particularly using acetone-d_6) only the high field H-6 proton has been shielded. Thus if the center of the H-6 multiplet is taken as the chemical shift of H-6, only a small displacement seems to have occurred.

The H-6 portion of the spectra of a representative selection of compounds (using acetone-d_6) was next examined in detail. H-6 can be considered as the AB portion of an ABX system (4, 9), where B is the H-6 proton at higher field and X is H-5 and, by the method of Bernstein *et al.* (12), the n.m.r. parameters in Table IV can be determined. In every case J_{AB} is about 12 c.p.s. In the spectra of the four acetylated derivatives $\delta A - \delta B$ is 13.5–16.6 c.p.s., but is much larger in the spectra of the trimethylsilyl ethers **11** and **2**. When $\delta A - \delta B$ becomes larger compared to J_{AB} the appearance of the spectrum changes and the intensities of the outer pairs increase.

Also $J_{BX} < J_{AX}$ when OH-4 is acetylated, but when OH-4 is free, or combined as a trimethylsilyl ether, $J_{BX} > J_{AX}$. Bernstein *et al.* (12) showed that when $J_{AX} + J_{BX}$ is positive and the splitting of the two highfield B pairs is larger than that of the two lowfield A pairs, $J_{BX} > J_{AX}$. Therefore, it can be seen by simple inspection of the spectra whether $J_{BX} > J_{AX}$. The spectra of all the compounds were then examined and in those of compounds with an OH or trimethylsilyl group at C-4, in pyridine solution, $J_{BX} > J_{AX}$; this was also true in acetone-d_6 solution though the spectrum of **12** was insufficiently resolved for measurement of the splitting of the H-6 pairs. In deuteriochloroform solution, $J_{BX} > J_{AX}$ in the spectra of the two trimethylsilyl ether derivatives **2** and **11**; the spectra of **4** and **18** were not well enough resolved; however, in those of **12** and of β-glucose 1,2,3,6-tetraacetate $J_{BX} < J_{AX}$. In the spectra of all the other compounds $J_{BX} < J_{AX}$ no matter which solvent was used.

The observations made here have already been useful in locating acyl groups in naturally occurring sophorosides (1, 13). Nuclear magnetic resonance spectral measurement of partly acylated glucose derivatives before and after conversion to trimethylsilyl ethers should help to locate free hydroxyl groups. Such measurements could be useful in studies of partial esterification of glucosides, and in investigations of migrations of acyl groups.

Experimental

Nuclear magnetic resonance (n.m.r.) spectra were measured at 32 °C using a Varian HA-100 spectrometer. Chemical shifts are in parts per million (p.p.m.) from tetramethylsilane (internal standard). Silicic acid (Bio-Sil A from Bio-Rad Laboratories, Richmond, California) was used for column chromatography. Specific rotations in chloroform solution were measured at 25 °C in a 1 dm cell using a Perkin–Elmer model 141 polarimeter.

Methyl 6-O-Acetyl-β-D-glucopyranoside (3)

Methyl β-D-glucopyranoside (9.6 g) was converted to the tetra-*O*-trimethylsilyl ether (21 g) by the method used with the α anomer (9). The ether was taken up in methanol (100 ml) and cooled to 0 °C; a solution of potassium carbonate (0.055 g) in methanol (12 ml) was added and the mixture kept at 0 °C for 45 min. Acetic acid (0.06 g) was then added and the solution poured into water; the product was extracted with light petroleum and the extract dried over sodium sulfate. Solvent was removed and the residue was crystallized from acetone containing 5% water (50 ml) at −40 °C and then from hexane at −30 °C to give methyl 2,3,4-tri-*O*-trimethylsilyl-β-D-glucopyranoside (**1**), (7.3 g), m.p. 72 °C and $[\alpha]_D$ −8.6° (*c*, 0.5 in chloroform).

Anal. Calcd. for $C_{16}H_{38}O_6Si_3$: C, 46.83; H, 9.27 Found: C, 47.20; H, 9.28.

Acetylation of **1** (6.7 g) with acetic anhydride and pyridine gave **2**, (b.p. 105 °C/0.1 mm), $[\alpha]_D$ −3.4° (*c*, 1.5 in chloroform).

Anal. Calcd. for $C_{18}H_{40}O_7Si_3$: C, 47.75; H, 8.91. Found: C, 47.56; H, 8.77.

Compound **2** was then refluxed for 4 h in methanol–water 4:1 (50 ml), the reagents removed, and the residual gum taken up in ethanol (15 ml) to give **3** (3 g), m.p. 132–134 °C, (lit. (8) gives m.p. 129 °C).

Methyl 6-O-Stearoyl-β-D-glucopyranoside (4)

Compound **1** (3.1 g) was dissolved in a mixture of methylene chloride (10 ml) and pyridine (3 ml) and a solution of stearoyl chloride (2.4 g) in methylene chloride added. After 18 h methylene chloride (15 ml) was added, the solution washed with water and dried over sodium sulfate. Solvent was removed and the trimethylsilyl

Can. J. Chem. Downloaded from www.nrcresearchpress.com by 210.87.254.105 on 09/05/12
For personal use only.

TABLE III

Chemical shifts (in p.p.m.) of acetoxy, H-6, and H-1 protons of some acylated β-methyl glucoside derivatives containing benzyl and trimethylsilyl groups in pyridine, acetone-d_6, and deuteriochloroform

Compound	Acetoxy			H-6			H-1		
	Pyridine	Acetone-d_6	*Deuterio*-chloroform	Pyridine	Acetone-d_6	*Deuterio*-chloroform	Pyridine	Acetone-d_6	*Deuterio*-chloroform
6-*O*-Acetyl-2,3-di-*O*-benzyl (**12**)	1.93	2.03	2.09	4.65	4.29	4.33	4.52	4.35	4.32
6-*O*-Acetyl-2,3-di-*O*-benzyl-4-*O*-trimethylsilyl (**11**)	2.04	2.06	2.08	4.47	4.24	4.25	4.52	4.38	4.32
6-*O*-Acetyl-2,3-di-*O*-benzyl-4-*O*-stearoyl (**13**)	2.00	1.99	2.04	4.36	4.08	4.13	4.54	4.44	4.30
4,6-Di-*O*-acetyl-2,3-di-*O*-benzyl (7)	1.97	1.96	1.94						
	2.02	2.01	2.06	4.35	4.10	4.14	4.53	4.43	4.32
6-*O*-Acetyl-2,3,4-tri-*O*-trimethylsilyl (**2**)	2.02	2.04	2.09	4.46	4.18	4.22	4.25	4.14	4.06

TABLE IV

Nuclear magnetic resonance parameters (in c.p.s.) of H-6 protons of some partially acylated β-methyl glucosides in acetone-d_6

Compound	J_{AB}	δA−δB	J_{AX}	J_{BX}
6-*O*-Acetyl (**3**)	12.0	16.6	1.45	5.05
3,6-Di-*O*-acetyl (**18**)	12.0	13.5	1.76	5.24
4,6-Di-*O*-acetyl (**8**)	12.0	15.6	5.90	2.40
4,6-Di-*O*-Acetyl-2,3-di-*O*-benzyl (7)	12.0	14.8	5.60	2.10
6-*O*-Acetyl-2,3-di-*O*-benzyl-4-*O*-trimethylsilyl (**11**)	11.5	25.15	1.98	4.52
6-*O*-Acetyl-2,3,4-tri-*O*-trimethylsilyl (**2**)	12.0	33.95	1.70	4.90

groups were taken off as before. Product (**4**) (2 g) crystallized from acetone and had m.p. 102–103 °C and $[\alpha]_D$ −35.9° (*c*, 1.6 in chloroform).

Anal. Calcd. for $C_{25}H_{48}O_7$: C, 65.18; H, 10.50. Found: C, 65.38; H, 10.52.

Methyl 2,3,4-Tri-O-acetyl-6-O-stearoyl-β-D-glucopyranoside (5)

Compound **4** (1.3 g) was acetylated with acetic anhydride and pyridine giving **5** (1.4 g) which was crystallized from acetone; it melted at 55–57 °C and had $[\alpha]_D$ −5.6° (*c*, 1.8 in chloroform).

Anal. Calcd. for $C_{31}H_{54}O_{10}$: C, 63.45; H, 9.28. Found: C, 63.50; H, 9.30.

Methyl 4,6-Di-O-acetyl-β-D-glucopyranoside (8)

Acetylation of methyl 2,3-di-*O*-benzyl-β-D-glucopyranoside (14) (4 g) yielded **7** (4.1 g), which was crystallized from ether–hexane (1:1). The m.p. was 41–43 °C and $[\alpha]_D$ −17.2° (*c*, 1.3 in chloroform).

Anal. Calcd. for $C_{25}H_{30}O_8$: C, 65.49; H, 6.60. Found: C, 65.40; H, 6.48.

Product **7** (1 g) was hydrogenated twice in glacial acetic acid (10 ml) over 10% palladium charcoal (0.3 g), for 5 h each time, when the benzyl groups were completely removed. The solvent was taken off and the residue crystallized from benzene to give **8** (0.4 g) with m.p. 92–95 °C and $[\alpha]_D$ −40.2° (*c*, 2.0 in chloroform). Nuclear magnetic resonance: H-4 at 4.89 p.p.m. ($CDCl_3$), 4.78 p.p.m. (acetone-d_6) and 5.40 p.p.m. (pyridine). Spin-decoupling experiments were carried out in D_2O as the best resolution of the signals was obtained in this solvent, tetramethylsilane was used as an external standard. Irradiation of H-2 at 3.82 p.p.m. affected H-1 (4.88 p.p.m.) but did not affect H-4 (5.32 p.p.m.), irradiation at the center of H-5 (4.33 p.p.m.) affected H-4 and H-6 (center at 4.70 p.p.m.) and irradiation at H-4 affected H-5 and H-3 (4.17 p.p.m.). The spacings of the affected signals were reduced to about two-thirds of the original and the intensities to about one-fifth.

Anal. Calcd. for $C_{11}H_{18}O_8$: C, 47.48; H, 6.52. Found: C, 47.46; H, 6.57.

Methyl 6-O-Acetyl-2,3-di-O-benzyl-β-D-glucopyranoside (12)

Methyl 2,3-di-*O*-benzyl-β-D-glucopyranoside (25 g) was converted to the syrupy trimethylsilyl ether and the crude product taken up in methanol (65 ml) at 0 °C. A solution of potassium carbonate (0.057 g) in methanol (13 ml) was added and, after 75 min at 0 °C, the methanol was removed at 20 °C and 0.5 mm. The residue was extracted with hexane (100 ml) leaving insoluble methyl 2,3-di-*O*-benzyl-β-D-glucopyranoside (13 g) which had lost both trimethylsilyl groups. Methyl 2,3-di-*O*-benzyl-4-*O*-trimethylsilyl-β-D-glucopyranoside (**10**) (11.7 g) crystallized from the hexane extract and had m.p. 77–79 °C and $[\alpha]_D$ +36.5° (*c*, 5.0 in chloroform).

Anal. Calcd. for $C_{24}H_{34}O_6Si$: C, 64.55; H, 7.67. Found: C, 64.46; H, 7.67.

Compound (**10**) (10 g) was allowed to stand overnight in pyridine (60 ml) and acetic anhydride (30 ml); the reagents were then removed at 30 °C and 1 mm and the product crystallized from hexane (50 ml) giving 6-*O*-acetyl-2,3-di-*O*-benzyl-4-*O*-trimethylsilyl-β-D-glucopyranoside (**11**) (11 g). The melting point was 96–97 °C and $[\alpha]_D$ +34.8° (*c*, 2.6 in chloroform).

Anal. Calcd. for $C_{26}H_{36}O_7Si$: C, 63.91; H, 7.43. Found: C, 63.86; H, 7.36.

Compound (**11**) (10 g) was refluxed overnight with methanol (100 ml) and water (20 ml), after removal of the solvents, crystallization from benzene–hexane 1:1 (100 ml) gave **12** (4.7 g) with m.p. 123–124 °C and $[\alpha]_D$ −22.5° (*c*, 1.9 in chloroform).

Anal. Calcd. for $C_{23}H_{28}O_7$: C, 66.33; H, 6.78. Found: C, 66.22; H, 6.69

Methyl 6-O-Acetyl-4-O-stearoyl-β-D-glucopyranoside (14)

Compound **12** (2.5 g) was dissolved in methylene chloride (10 ml) and pyridine (2 ml), and after addition of stearoyl chloride (2.72 g) in methylene chloride (4 ml), the mixture was left overnight at room temperature. Methylene chloride (20 ml) was added and the solution washed with water; removal of the solvent gave a solid (4.6 g) which crystallized from hexane (20 ml) giving methyl 6-*O*-acetyl-2,3-di-*O*-benzyl-4-*O*-stearoyl-β-D-glucopyranoside (**13**) (3.5 g); m.p. 55–56 °C and $[\alpha]_D$ −7.3° (*c*, 2.1 in chloroform).

Anal. Calcd. for $C_{41}H_{62}O_8$: C, 72.10; H, 9.15. Found: C, 71.80; H, 9.01.

Removal of the benzyl groups from **13** (2 g) by the method used to prepare **8** gave a crude material still containing some monobenzyl derivative. This product was chromatographed on a silicic acid column and the monobenzyl compounds were eluted with hexane–chloroform (1:1); elution with chloroform gave **14** (0.65 g); m.p. 80–82 °C and $[\alpha]_D$ −17.7° (*c*, 3.5 in chloroform) (after crystallization from benzene–hexane (1:1)). Nuclear magnetic resonance: H-4 at 4.88 p.p.m. ($CDCl_3$), 4.82 p.p.m. (acetone-d_6), and 5.45 p.p.m. (pyridine).

Anal. Calcd. for $C_{27}H_{50}O_8$: C, 64.51; H, 10.03. Found: C, 64.31; H, 9.85.

Can. J. Chem. Downloaded from www.nrcresearchpress.com by 210.87.254.105 on 09/05/12
For personal use only.

Can. J. Chem. Downloaded from www.nrcresearchpress.com by 210.87.254.105 on 09/05/12
For personal use only.

Methyl 2,3,6-Tri-O-acetyl-4-O-stearoyl-β-D-glucopyranoside (15)

Compound (**15**), obtained by acetylation of **14**, was crystallized from acetone and had m.p. 60–62 °C and $[\alpha]_D$ −14.7° (*c*, 1.1 in chloroform).

Anal. Calcd. for $C_{31}H_{54}O_{10}$: C, 63.45; H, 9.28. Found: C, 63.45; H, 9.17.

Partial Acetylation of Methyl 4,6-O-Benzylidene-β-D-glucopyranoside

Fractions obtained during partial acetylation experiments were analyzed by thin-layer chromatography (t.l.c.) on silica gel in ether; the products had the following R_f values: 2,3-diacetate, 0.7; 2-acetate, 0.53; 3-acetate, 0.34; starting material, 0.16.

A mixture of methyl 4,6-*O*-benzylidene-β-D-glucopyranoside (25 g), pyridine (100 ml), and acetic anhydride (9.1 g) was kept at 25 °C for 6 days when the reagents were removed at 20 °C and 0.2 mm. The gummy product was heated with hexane (25 ml) and chloroform (25 ml) and filtered from starting material (7.6 g); on standing 1.3 g of 2-acetate crystallized from the filtrate. The remaining solution was then applied to a silicic acid column (200 g) and eluted with hexane–chloroform (1:1); 2,3-diacetate (0.95 g) was eluted first, followed by a mixture of diacetate and 2-acetate (2.7 g), then pure 2-acetate (0.54 g), then fractions with increasing proportions of 3-acetate (4.9 g). Elution with chloroform gave fairly pure 3-acetate (1.5 g) and finally unacetylated material (1.6 g). The 2-acetate was much less soluble in hexane–chloroform (1:1) than the 3-acetate or the diacetate, but was much more soluble in ethanol than these two compounds. By crystallization of the above fractions from the appropriate solvents, all three products were almost completely separated. The yields and percentage yields, based on unrecovered starting material, were as follows: 2,3-diacetate, 2.8 g, 15%; 2-acetate, 5.4 g, 34%; 3-acetate, 3.5 g, 22%.

Methyl 2,3-di-*O*-acetyl-4,6-*O*-benzylidene-β-D-glucopyranoside had m.p. 177–178 °C and $[\alpha]_D$ −87.7° (*c*, 1.6 in chloroform). Nuclear magnetic resonance ($CDCl_3$): H-2 at 4.98 p.p.m. (quartet), H-3 at 5.31 p.p.m. (triplet), H-1 at 4.51 p.p.m.

Anal. Calcd. for $C_{18}H_{22}O_8$: C, 59.01; H, 6.05. Found: C, 58.96; H, 5.95.

Methyl 2-*O*-acetyl-4,6-*O*-benzylidene-β-D-glucopyranoside had m.p. 174–177 °C and $[\alpha]_D$ −74.4° (*c*, 1.7 in chloroform). Nuclear magnetic resonance ($CDCl_3$): H-2 at 4.88 p.p.m. (quartet) and H-1 at 4.35 p.p.m.

Anal. Calcd. for $C_{16}H_{20}O_7$: C, 59.25; H, 6.22. Found: C, 59.31; H, 6.19.

Methyl 3-*O*-acetyl-4,6-*O*-benzylidene-β-D-glucopyranoside had m.p. 162–163 °C and $[\alpha]_D$ −55.2° (*c*, 2.1 in chloroform). Nuclear magnetic resonance ($CDCl_3$): H-3 at 5.22 p.p.m. (triplet), H-1 at 4.34 p.p.m.

Anal. Calcd. for $C_{16}H_{20}O_7$: C, 59.25; H, 6.22. Found: C, 59.11; H, 6.15.

Methyl 3-O-Acetyl-β-D-glucopyranoside (16)

Methyl 3-*O*-acetyl-4,6-*O*-benzylidene-β-D-glucopyranoside (2.53 g) was refluxed for 10 min with 50% acetic acid (100 ml), the solvent taken off at 80 °C/0.2 mm, and the residue crystallized from acetone giving **16** (1.43 g). The m.p. was 137–139 °C and $[\alpha]_D$ −9.8° (*c*, 3.8 in acetone). Nuclear magnetic resonance (acetone-d_6): H-3 at 4.92 p.p.m., irradiation at 3.30 p.p.m. (H-2) reduced the spacing and intensity of both H-3 and H-1 (4.26 p.p.m.) and irradiation of H-1 changed H-2 to a doublet.

Anal. Calcd. for $C_9H_{16}O_7$: C, 45.76; H, 6.83. Found: C, 45,78; H, 6.80.

Methyl 3,6-Di-O-acetyl-β-D-glucopyranoside (18)

Compound **16** (2 g) was converted to methyl 3-*O*-acetyl-2,4,6-tri-*O*-trimethylsilyl-β-D-glucopyranoside (**17**) as before. The crude product was distilled giving pure **17** (2.4 g), with b.p. 108–111 °C/0.1 mm and $[\alpha]_D$ −1.0° (*c*, 1.0 in chloroform).

Anal. Calcd. for $C_{18}H_{40}O_7Si_3$: C, 47.75; H, 8.91. Found: C, 47.76; H, 8.80.

Compound (**17**) (1.94 g), in methanol (5 ml), was treated with a solution of potassium carbonate (0.012 g) in methanol (60 ml) and the mixture kept at 0 °C for 1 h. After removal of the solvent the residue was extracted with hexane giving a gum (0.28 g), which was acetylated and then refluxed with methanol (20 ml) and water (7 ml) for 4 h. The solvents were removed leaving a viscous syrup (0.24 g), which combined with material from previous preparations (total 0.31 g), was chromatographed on silicic acid and eluted with chloroform containing 5% methanol. After elution of by-products, apparently containing more than one acetate group, **18** (0.12 g) was obtained. It was crystallized from methylene chloride and had m.p. 45–47 °C, but appeared to retain traces of solvent very tenaciously; $[\alpha]_D$ −17.2° (*c*, 1.8 in chloroform).

Anal. Calcd. for $C_{11}H_{18}O_8$: C, 47.48; H, 6.52. Found: C, 46.85; H, 6.35.

Nuclear magnetic resonance (acetone-d_6): H-3 at 4.94 p.p.m., irradiation of H-2 (3.32 p.p.m.) reduced the intensity and spacing of both H-1 and H-3; in $CDCl_3$: H-3 at 4.92 p.p.m.; in pyridine: H-3 at 5.64 p.p.m.

Previously described methods were used to prepare methyl 3,4,6-tri-*O*-acetyl-β-D-glucopyranoside (**6**) (7), 1,2,3,6-tetra-*O*-acetyl-β-D-glucopyranose (15) and 1,2,4,6-tetra-*O*-acetyl-β-D-glucopyranose (16).

Acknowledgments

The authors are indebted to Dr. P. A. J. Gorin for a number of very helpful discussions, to Mr. L. L. Hoffman for experimental assistance, to Mr. M. Mazurek for n.m.r. measurements, and to Mr. W. C. Haid for microanalyses.

1. A. P. Tulloch, A. Hill, and J. F. T. Spencer. Chem. Commun. 584 (1967).
2. S. A. Barker, J. Homer, M. C. Keith, and L. F. Thomas. J. Chem. Soc. 1538 (1963).
3. R. U. Lemieux, R. K. Kullnig, H. J. Bernstein, and W. G. Schneider. J. Am. Chem. Soc. **80**, 6098 (1958).
4. R. U. Lemieux and J. D. Stevens. Can. J. Chem. **43**, 2059 (1965).
5. R. U. Lemieux and A. R. Morgan. Can. J. Chem. **43**, 2190 (1965).
6. O. Arndt. Ann. Chem. **695**, 176 (1966).
7. E. K. Gladding and C. B. Purves. J. Am. Chem. Soc. **66**, 153 (1944).

8. Y. Z. FROHWEIN and J. LEIBOWITZ. Bull. Res. Council Israel, Sect. A, **11**, 330 (1963).
9. D. T. HURST and A. G. MCINNES. Can. J. Chem. **43**, 2004 (1965).
10. R. W. JEANLOZ and D. A. JEANLOZ. J. Am. Chem. Soc. **79**, 2579 (1957).
11. A. P. TULLOCH. J. Am. Oil Chemists' Soc. **43**, 670 (1966).
12. H. J. BERNSTEIN, J. A. POPLE, and W. G. SCHNEIDER. Can. J. Chem. **35**, 65 (1957).
13. A. P. TULLOCH, J. F. T. SPENCER, and M. H. DEINEMA. Can. J. Chem. **46**, 345 (1968).
14. J. C. DENNISON and D. I. MCGILVRAY. J. Chem. Soc. 1616 (1951).
15. W. A. BONNER. J. Am. Chem. Soc. **80**, 3697 (1958).
16. K. FREUDENBERG and E. PLANKENHORN. Ann. Chem. **536**, 257 (1938).

Can. J. Chem. Downloaded from www.nrcresearchpress.com by 210.87.254.105 on 09/05/12
For personal use only.

Can. J. Chem. Downloaded from www.nrcresearchpress.com by 210.87.254.40 on 09/05/12
For personal use only.

Isolation and characterization of 4-chloro-3,4′;3′,4″-tercoumarin

ALLAN R. KNIGHT AND JOHN S. MCINTYRE
Exploratory Research Laboratory, Dow Chemical of Canada, Limited,[1] *Sarnia, Ontario*

Received February 19, 1968

The products from the reaction of 4-hydroxycoumarin with phosphorous oxychloride are the reported 4-chlorocoumarin and an additional compound of high molecular weight. This latter compound was characterized by substitution, degradation, and deuteration reactions as 4-chloro-3,4′;3′,4″-tercoumarin, a trimer corresponding to condensations between three coumarin molecules.

Canadian Journal of Chemistry, 46, 2495 (1968)

Introduction

The preparation of 4-chlorocoumarin derivatives from their 4-hydroxycoumarin analogues through neat reaction with phosphorous oxychloride with moderate yields has been reported by several authors (1–5). Following the method of Spalding *et al.* (1) we have obtained 4-chlorocoumarin in 49% yield along with a large amount of a highly insoluble, high-melting orange by-product. Ziegler and Maier (5) reported a similar by-product resulting from the reaction of 6,8-dimethyl-4-hydroxycoumarin with phosphorous oxychloride. On the basis of analytical data he assigned the structure to the trimer resulting from a double intermolecular condensation at the 3- and 4-positions.

This report describes substitution, degradation, and deuteration reactions of the by-product from the chlorination of 4-hydroxycoumarin. These reactions show the by-product to be 4-chloro-3,4′;3′,4″-tercoumarin (**1***a*), the unsubstituted analogue of the compound described by Ziegler and Maier (5). Also a number of 4-substituted coumarins and 3-(4-coumarinyl) coumarins have been prepared to confirm the proposed structures, shown in Scheme 1.

Results and Discussion

The orange by-product (**1***a*) obtained in the preparation of 4-chlorocoumarin (**3**) from 4-hydroxycoumarin and phosphorous oxychloride was analyzed for a molecular formula $C_{27}H_{13}ClO_6$. Mass spectroscopy showed a molecular weight of 468 which was consistent with the elemental analysis. These results suggest that the compound is composed of three coumarin molecules and one atom of chlorine.

The infrared (i.r.) spectra of **1***a*, 4-chlorocoumarin (**3**), and 4-chloro-3-(4-coumarinyl)coumarin (**7**) are quite similar in the carbonyl regions (Table I), suggesting that there is a correspondence between the structure of (**1***a*) and those of the characterized monomer (**3**) and dimer (**7**). The mass spectral fragmentation patterns also show definite similarities.

Furthermore the i.r. spectra of the 4-piperidyl derivatives of **3** and **7** are also similar to that of the piperidyl derivative of **1***a* (Table I). The nuclear magnetic resonance (n.m.r.) spectral data (Table II) show that in the derivatives of the dimer and **1***a*, the 3-proton occurs in the aromatic region, whereas in the monomer the 3-proton is at 347 c.p.s.; integration confirms the assigned structures. The mass spectral fragmentation pattern is also consistent with the proposed structure **1***b*.

Attempted chlorination of **1***a* in acetic acid yields 4-chloro-3-(4-coumarinyl)coumarin (**7**) and some oily residues which were not characterized. Thus at least two of the coumarin molecules are intact and joined by a 3,4-carbon-to-carbon linkage.

Reaction of **1***a* with aniline did not yield 4-anilino-3,4′;3′,4″-tercoumarin contrary to the piperidine reaction. Temperatures were ≈150 °C and 65 °C respectively. Instead 4-anilinocoumarin (**4**) and 4-anilino-3-(4-coumarinyl)coumarin (**8**) were obtained. The n.m.r. spectra of these two compounds in hexamethylphosphoramide show the protons in 3-positions to have a shift difference of 31 c.p.s. (Fig. 1). Integration of these peaks presents a very facile method of determining their respective molar concentrations, which were found to be approximately 50:50 for the above reaction.

It was also shown that reaction of 4-chloro-3-(4-coumarinyl)coumarin with aniline under rigorous conditions (i.e. 160 °C for $2\frac{1}{2}$ h) yields only

[1]Contribution No. 161.

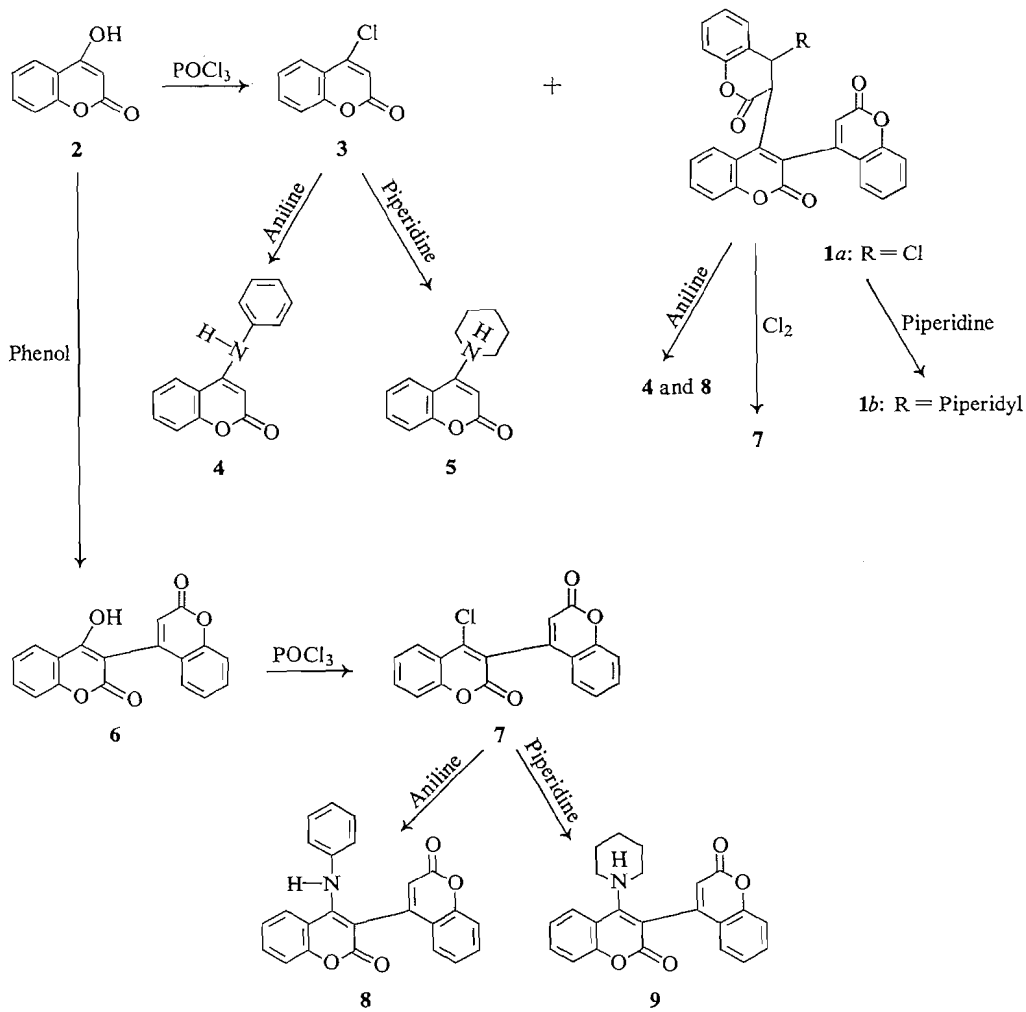

SCHEME 1

4-anilino-3-(4-coumarinyl)coumarin; no 4-anilinocoumarin could be detected by n.m.r. Thus 4-anilinocoumarin must result directly from the fragmentation of the by-product, and these results suggest that the chlorine atom is originally in the 4-position of a coumarin molecule. This is also conclusive evidence that **1***a* is composed of three intact coumarin molecules and further supports the conclusion that two coumarins are bonded by a 3,4-carbon-to-carbon linkage.

This cleavage of the by-product on reaction with chlorine and aniline is in agreement with the fragmentation pattern. The mass spectrum of the by-product shows an *m/e* of 289 corresponding to cleavage of a 4-chlorocoumarin fragment. This type of fragmentation does not occur in 4-chloro-3-(4-coumarinyl)coumarin.

4-Chlorocoumarin-3-d_1 was prepared with 95% deuteration (6). Attempted chlorination of the by-product **1***a*-d_1 from this preparation yielded 4-chloro-3-(4-coumarinyl-3-d_1)coumarin. The product experienced no m.p. depression with 4-chloro-3-(4-coumarinyl)coumarin, but the n.m.r. spectrum showed the absence of the peak at 418 c.p.s., indicating deuteration at the 3-position. Reaction of the deuterated dimer with aniline yields the deuterated 4-anilino-3-(4-coumarinyl-3-d_1)coumarin which was verified by the absence of the 3-proton at 360 c.p.s. This indicates that the deuterium of the dimer does not exchange with aniline, as does the

Can. J. Chem. Downloaded from www.nrcresearchpress.com by 210.87.254.40 on 09/05/12
For personal use only.

TABLE I

Infrared spectral data

Compound	Characteristic absorptions* (cm^{-1})				
4-Hydroxycoumarin	1690	1660	1600	1550	750 770
4-Hydroxy-3-(4-coumarinyl)coumarin	1700	1680	1600		750 760
4-Chlorocoumarin	1710 1750(sh)		1596 1608(sh)	1550	749 775
4-Chloro-3-(4-coumarinyl)coumarin	1720		1600	1550	765
4-Chloro-3,4′;3′,4″-tercoumarin	1718	1628	1590	1540	755
4-Piperidylcoumarin	1710		1600	1550	770
4-Piperidyl-3-(4-coumarinyl)coumarin	1710	1620	1600(sh)	1560(w)	750
4-Piperidyl-3,4′;3′,4″-tercoumarin	1718	1620	1600	1570	745 755
4-Anilinocoumarin	3300	1660	1615 1605(sh)	1585 1530	760
4-Anilino-3-(4-coumarinyl)coumarin	3325	1685	1600 1580	1520	745 760(sh)

*The spectra were recorded on a Perkin–Elmer 221 spectrometer with Nujol–fluorolube mulls (sh, shoulder; w, weak).

TABLE II

Nuclear magnetic resonance data

Compound	Solvent	Peak position, splitting pattern, and area*			
4-Piperidylcoumarin	$CDCl_3$	(102–118)b6	(188–204)b4	347sl	439–74m4
4-Piperidyl-3-(4-coumarinyl)coumarin	$CDCl_3$	(92–108)b6	(214–233)b4		439–95m9 (sharp at 464)
4-Piperidyl-3,4′;3′,4″-tercoumarin	$CDCl_3$	(112–130)b6	(230–245)b2 (249–265)b2		425–95m13
4-Chlorocoumarin	$CDCl_3$			392sl	430–77m4
4-Anilinocoumarin	HMPA†			329sl	428–79m8 (sharp at 446) 521dl, 615bl
4-Acetoxy-3-(4-coumarinyl)coumarin	$CDCl_3$	134s3		386sl	430–75m8
4-Anilino-3-(4-coumarinyl)coumarin	HMPA†			360sl	408s5, 418–483m7 528dl, 628bl
4-Chloro-3-(4-coumarinyl)coumarin	HMPA†			418sl	439–93m8

*Shifts are in c.p.s. downfield from internal tetramethylsilane; b, broad, d, doublet; m, multiplet; s, singlet. Relative areas are shown after the peak designations. Spectra were recorded at room temperature on a Varian A-60 spectrometer.
†Hexamethylphosphoramide.

deuterium in 4-chlorocoumarin-3-d_1 on reaction with aniline (6).

Reaction of the deuterated by-product (**1***a*) with aniline yielded a mixture of 4-anilinocoumarin and 4-anilino-3-(4-coumarinyl-3-d_1) coumarin. Deuteration in the dimer was shown by the absence of the singlet at 360 c.p.s. while the singlet of the monomer remained at 329 c.p.s. A comparison of the integral of this singlet with that of the anilino aromatic protons of the dimer indicated a 53:47 mole ratio of monomer to dimer respectively. This firmly establishes that the deuterium is located on the 3-position of coumarin and that the original by-product (**1***a*) must have a 3-proton.

The evidence presented above indicates that the by-product **1***a* has: (*a*) 3 coumarin molecules, (*b*) 2 coumarin molecules joined in the 3,4-position, (*c*) a hydrogen atom in a 3-position, (*d*) chlorine in a 4-position. We conclude from these experimental results that compound **1***a* is 4-chloro-3,4′;3′,4″-tercoumarin.

Experimental

Melting points were determined with a Mel-Temp block and are uncorrected. The nuclear magnetic resonance (n.m.r.) spectra were recorded on a Varian A-60 spectrometer; shifts are reported in c.p.s. downfield from internal tetramethylsilane. The mass spectral data were obtained by Nier peak matching method (CEC 21-110B spectrometer). The microanalysis was performed by A. B. Gygli, Toronto.

Reaction of 4-Hydroxycoumarin with Phosphorous Oxychloride

The method of Spalding *et al.* (1) was followed. 4-Hydroxycoumarin (50 g) and 75 ml of $POCl_3$ were refluxed for 1 h, cooled, and slowly diluted with water.

Can. J. Chem. Downloaded from www.nrcresearchpress.com by 210.87.254.40 on 09/05/12
For personal use only.

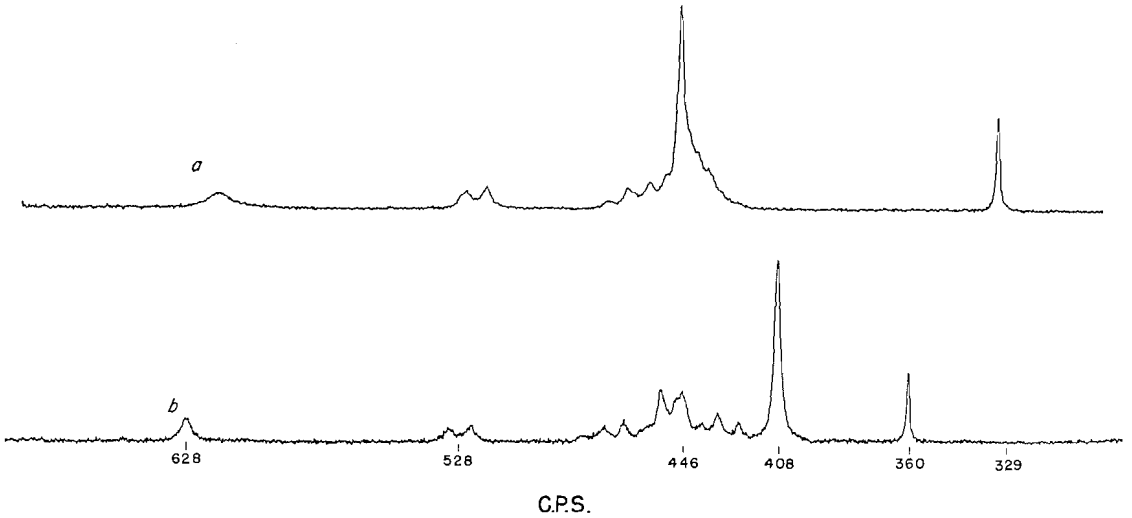

FIG. 1. Nuclear magnetic resonance spectra of (*a*) 4-anilinocoumarin and (*b*) 4-anilino-3-(4-coumarinyl)coumarin. The spectra were recorded in hexamethylphosphoramide; shifts are in c.p.s. downfield from internal tetramethylsilane.

The mixture was extracted with chloroform and filtered. The chloroform layer yielded 26.3 g, 49% of 4-chlorocoumarin (**3**), m.p. 93–94 °C, from *n*-heptane, lit. 89–91 °C (1).

The precipitate from the above filtration was washed with methanol and dried to yield 20.1 g. After crystallization, once from a large volume of acetic acid and once from nitrobenzene, the melting point was 324–327 °C. This product has been identified as 4-chloro-3,4′; 3′,4″-tercoumarin.

Anal. Calcd. for $C_{27}H_{13}ClO_6$ (mol. wt., 468.5): C, 69.16; H, 2.78; Cl, 7.58. Found (mass spectrum, parent ions: 468, 470): C, 69.37; H, 2.76; Cl, 7.54.

4-Chlorocoumarin-3-d_1

The preparation of this compound has been described previously (6).

*3-(4-Coumarinyl)-4-hydroxycoumarin (**6**) and 4-Acetoxy-3-(4-coumarinyl)coumarin*

These compounds were prepared by the method of Junek and Ziegler (7); their melting points are 298–300 °C and 220–222 °C respectively.

*4-Chloro-3-(4-coumarinyl)coumarin (**7**)*

A mixture of 8.0 g of 3-(4-coumarinyl)-4-hydroxycoumarin, 20 ml of $POCl_3$ and 1 drop of pyridine was refluxed for 1 h, diluted with methanol and water, and extracted with chloroform. Concentration of the chloroform layer, followed by boiling with benzene and a hot filtration, yielded 6.6 g, of 4-chloro-3-(4-coumarinyl)-coumarin, m.p. 274–276 °C.

Anal. Calcd. for $C_{18}H_9ClO_4$: C, 66.56; H, 2.77; Cl, 10.94. Found: C, 66.41; H, 2.80; Cl, 10.52.

*4-Piperidylcoumarin (**5**)*

A mixture of 2.0 g of 4-chlorocoumarin, 10 ml of piperidine and 16 ml of methanol was boiled for 10 min and then added to 50 g of ice. Filtration and crystallization of the precipitate from methanol yielded 1.4 g of 4-piperidylcoumarin, m.p. 104–107.5 °C, lit. 105.5–106 °C (3).

Anal. Calcd. for $C_{14}H_{15}NO_2$: C, 73.36; H, 6.55; N, 6.11. Found: C, 73.19; H, 6.59; N, 6.27.

4-Piperidylcoumarin-3-d_1

The preparation of this compound has been described previously (6).

*3-(4-Coumarinyl)-4-piperidylcoumarin (**9**)*

This compound was prepared as 4-piperidylcoumarin, m.p. 259–261.5 °C.

Anal. Calcd. for $C_{23}H_{19}NO_4$: C, 74.00; H, 5.09; N, 3 75. Found: C, 74.08; H, 5.08; N, 3.86.

*4-Piperidyl-3,4′;3′,4″-tercoumarin (**1b**)*

This compound was prepared as 4-piperidylcoumarin, m.p. 261–263 °C.

Anal. Calcd. for $C_{32}H_{23}NO_6$: C, 74.27; H, 4.45; N, 2.71. Found: C, 74.21; H, 4.19; N, 2.83.

*4-Anilinocoumarin (**4**)*

4-Chlorocoumarin (8.5 g) and 15 ml of aniline were heated for 1 h at 150 °C. Cooling and dilution with methanol yielded 9.8 g of 4-anilinocoumarin, m.p. 267–269 °C from nitrobenzene, (lit. 268–269 °C (3)).

Anal. Calcd. for $C_{15}H_{11}NO_2$: C, 75.95; H, 4.64; N, 5.91. Found: C, 75.77; H, 4.65; N, 5.63.

*4-Anilino-3-(4-coumarinyl)coumarin (**8**)*

1.0 g of 4-chloro-3-(4-coumarinyl)coumarin and 5 ml of aniline were heated at 160 °C for 2 h. Cooling and dilution with methanol yielded 0.96 g of 4-anilino-3-(4-coumarinyl)coumarin, m.p. 287–291 °C, from nitrobenzene.

Anal. Calcd. for $C_{24}H_{15}NO_4$: C, 75.59; H, 3.94; N, 3.67. Found: C, 75.95; H, 4.06; N, 3.89.

Can. J. Chem. Downloaded from www.nrcresearchpress.com by 210.87.254.40 on 09/05/12
For personal use only.

Can. J. Chem. Downloaded from www.nrcresearchpress.com by 210.87.254.40 on 09/05/12
For personal use only.

An n.m.r. investigation of both this sample and the residues showed no peak corresponding to 4-anilinocoumarin.

Reaction of 4-Chloro-3,4′;3′,4″-tercoumarin with Aniline

4-Chloro-3,4′;3′,4″-tercoumarin (3.0 g) and 10 ml of aniline were heated at 160 °C for 1½ h. The reaction mixture was cooled, diluted with methanol, boiled for a few minutes, and then evaporated on a steam bath. The residue was washed with methanol and filtered to yield 2.67 g (70%) of a mixture consisting of 46% 4-anilino-3-(4-coumarinyl)coumarin and 54% 4-anilinocoumarin. The percentage composition was determined from the n.m.r. spectrum obtained in hexamethylphosphoramide.

Chlorination of 4-Chloro-3,4′;3′,4″-tercoumarin

Chlorine was passed through a mixture of 1.5 g of 4-chloro-3,4′;3′,4″-tercoumarin in 10 ml acetic acid until the orange color of the starting material disappeared. Evaporation of the solution, followed by a methanol wash yielded 0.9 g of 4-chloro-3-(4-coumarinyl)coumarin. The n.m.r. and i.r. spectra were identical to those of the above preparation. Evaporation of the methanol yielded only a tarry unidentified material.

Chlorination of 4-Chloro-3,4′;3′,4″-tercoumarin Prepared from 4-Hydroxycoumarin-3,4-d_2

Following the above chlorination procedure, the compound obtained had a m.p. 272–275 °C, mixture m.p. with 4-chloro-3-(4-coumarinyl)coumarin 272–275 °C. The i.r. spectrum differs from that of 4-chloro-3-(4-coumarinyl)coumarin in the region below 1400 cm^{-1}. The n.m.r. spectrum in hexamethylphosphoramide showed the absence of the peak at 418 c.p.s., indicating deuteration in the 3-position of a coumarin molecule.

4-Anilino-3-(4-coumarinyl-3-d_1)coumarin

4-Anilino-3-(4-coumarinyl-3-d_1)coumarin was prepared from 4-chloro-3-(4-coumarinyl-3-d_1)coumarin as described for the nondeuterated compound. The mixture melting point showed no depression, but the i.r. spectrum showed differences in the region below 1400 cm^{-1}. The n.m.r. spectrum in hexamethylphosphoramide showed the absence of the peak at 360 c.p.s. indicating deuteration.

Reaction of Aniline with 4-Chloro-3,4′;3′,4″-tercoumarin-d_1 Obtained from 4-Hydroxycoumarin-3,4-d_2

Reaction conditions were identical with those for the nondeuterated 4-chloro-3,4′;3′,4″-tercoumarin. A mixture of 4-anilinocoumarin and 4-anilino-3-(4-coumarinyl-3-d_1)coumarin containing 53 and 47 mole % respectively was obtained. The absence of a peak at 360 c.p.s. indicates deuteration of the latter compound. Relative concentrations were determined from the areas of the aromatic peak for 4-anilino-3-(4-coumarinyl-3-d_1)coumarin occurring at 408 c.p.s. and that at 329 c.p.s. corresponding to the 3-proton of 4-anilinocoumarin.

Acknowledgments

The authors wish to thank H. D. Mak for the recording of the nuclear magnetic resonance spectra and L. A. Shadoff for recording and interpreting the mass spectral fragmentation patterns.

1. D. P. SPALDING, H. S. MOSHER, and F. C. WHITMORE. J. Am. Chem. Soc. **72**, 5338 (1950).
2. N. S. VUL'FSON and R. B. ZHURIN. Zh. Obshch. Khim. **31**, 875 (1961). (Chem. Abstr. **55**, 24759 (1961).)
3. V. A. ZAGOREVSKI and D. A. ZYKOV. Zh. Obshch. Khim. **30**, 1378 (1960). (Chem. Abstr. **55**, 524 (1961).)
4. V. A. ZAGOREVSKI, D. A. ZYKOV, and E. K. ORLOVA. Zh. Obshch. Khim. **31**, 568 (1961). (Chem. Abstr. **55**, 25938*a* (1961).)
5. E. ZIEGLER and H. MAIER. Monatsh. Chem. **89**, 143 (1958).
6. A. R. KNIGHT and J. S. MCINTYRE. Can. J. Chem. **46**, 1949 (1968).
7. H. JUNEK and E. ZIEGLER. Monatsh. Chem. **87**, 218 (1956).

Can. J. Chem. Downloaded from www.nrcresearchpress.com by 210.87.254.5 on 09/05/12
For personal use only.

Mass spectra and proton magnetic resonance spectra of some tetrahydroprotoberberine alkaloids

C.-Y. CHEN AND D. B. MACLEAN
Department of Chemistry, McMaster University, Hamilton, Ontario

Received February 23, 1968

The mass spectra and the proton magnetic resonance spectra of tetrahydroprotoberberine alkaloids, oxygenated at the 9- and 10-positions, show marked differences from the spectra of those oxygenated at the 10- and 11-positions. These differences may be useful in structural studies on new members of this group of alkaloids.

Canadian Journal of Chemistry, 46, 2501 (1968)

The tetrahydroprotoberberines are a group of alkaloids biogenetically related to benzylisoquinolines and occur in a wide variety of botanical families. The basic skeleton (**1**) can be identified (1) by its characteristic ultraviolet (u.v.) spectrum; however, no information regarding the oxygenation pattern of the alkaloids in question can be secured by this method. Recently, in the course of structural studies (2) on two tetrahydroprotoberberine alkaloids, substituted

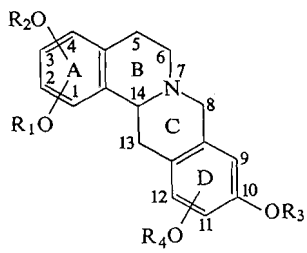

1

at 1-, 2-, 10-, and 11-positions, namely, caseamine and caseadine, we examined the mass spectra and the proton magnetic resonance (p.m.r.) spectra of ten tetrahydroprotoberberine alkaloids. Our results show that there is a systematic way to characterize this group of alkaloids which should be useful to others engaged in structural studies on the tetrahydroprotoberberines.

Mass Spectra of Tetrahydroprotoberberine Alkaloids

The main fragment ions observed in the mass spectra of tetrahydroprotoberberines are given in Fig. 1. The formation of ions *b*, *c*, and *d* has been discussed by Ohashi *et al.* (3). Ion *c* is derived by a retro Diels–Alder opening of ring C and ion *d* by loss of R_3 or R_4 from ion *c*. Loss of a single hydrogen from the neutral nitrogen-containing fragment formed in retro Diels–Alder fragmentation results in ion *b*. Ions of type *a* were of negligible intensity in the spectra of the alkaloids examined by Ohashi *et al.*, but have been detected in the mass spectra of other alkaloids in this family (4, 5). The formation of ions of type *a* requires the transfer of a hydrogen from either of rings C or D to ring B. The origin of the hydrogen in this transfer process has not been investigated.

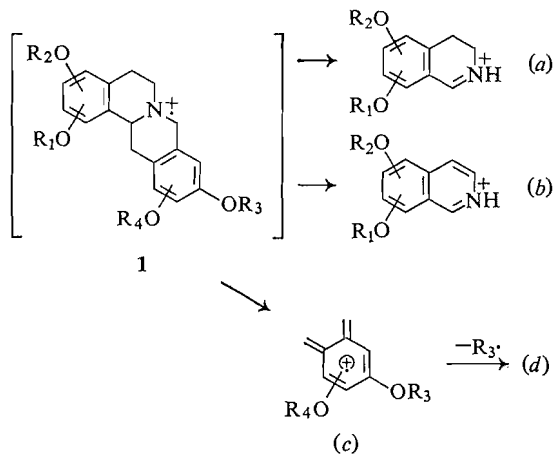

FIG. 1. Main fragment ions of tetrahydroprotoberberine alkaloids.

The mass spectra of the ten tetrahydroprotoberberine alkaloids which we have examined are found in Figs. 2 and 3 and the pertinent data derived from them are summarized in Table I. With the exclusion of stylopine, the alkaloids may be divided into three groups; (*i*) those with a hydroxyl group in ring D, *dl*-scoulerine, capaurimine, and caseamine, (*ii*) those with 9,10-dimethoxy substitution, *dl*-canadine, *dl*-tetrahydropalmatine, capaurine, and, (*iii*) those with 10,11-dimethoxy substitution, caseadine, caseadine-*O*-methyl ether and norcoralydine.

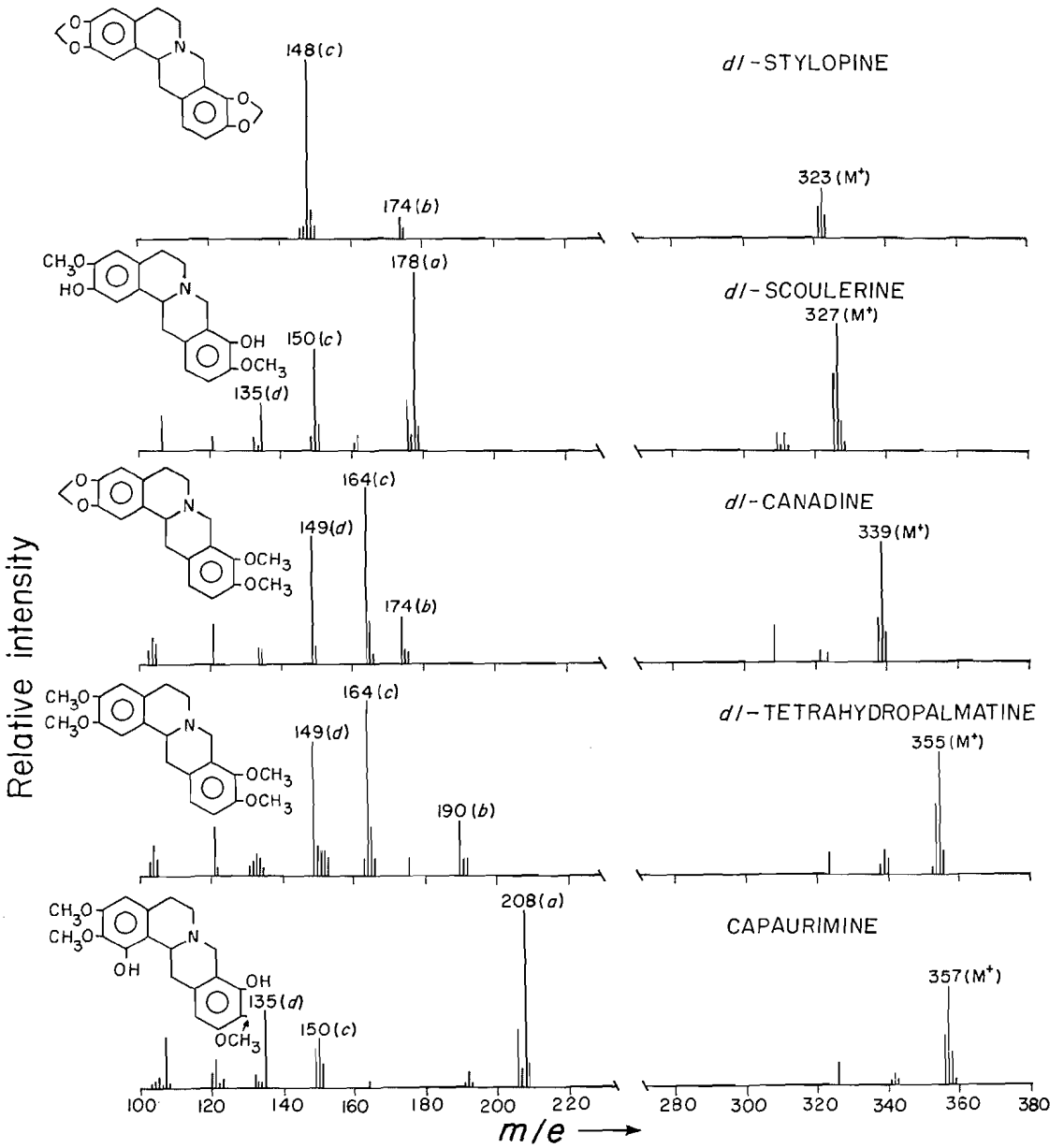

FIG. 2. The mass spectra of protoberberine alkaloids.

The alkaloids of group (*i*) are characterized by the presence of a base peak corresponding to ion *a* in their mass spectra. Moreover, the 9-hydroxy-10-methoxy compounds may be differentiated from 9-methoxy-10-hydroxy compounds. Those with the former substitution pattern preferentially expel a methyl group from ion *c* yielding an ion at *m/e* 135 whereas the latter, exemplified by tetrahydrothalifendine (4), apparently lose a hydrogen atom giving rise to an ion at *m/e* 149. It seems unlikely, however, that one could differentiate between a 10-hydroxy-11-methoxy compound and a 10-methoxy-11-hydroxy compound because ion *c* from the two systems is equivalent.

In the tetrahydroprotoberberines of group (*ii*)

Can. J. Chem. Downloaded from www.nrcresearchpress.com by 210.87.254.5 on 09/05/12
For personal use only.

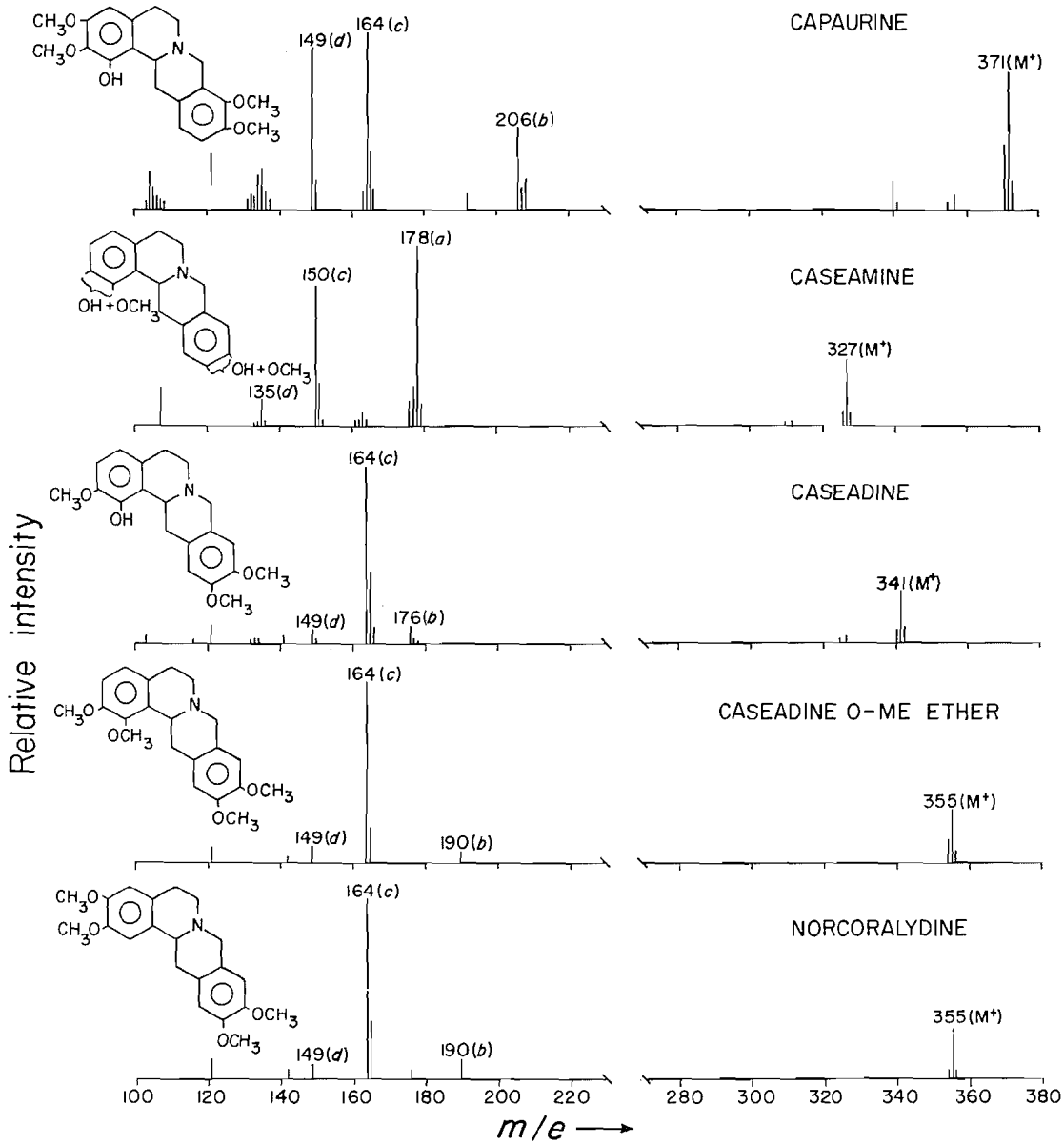

FIG. 3. The mass spectra of protoberberine alkaloids.

the molecular ion and ion *d* are more intense relative to the base peak of the spectrum than they are in group (*iii*). Thus, molecular ion peaks are of the order of 60% of the base peak in group (*ii*) vs. 30% for group (*iii*), while the ions of type *d* are in excess of 70% in the former vs. 10% in the latter. The differences in intensities of these two ions relative to the base peak allow the two groups to be differentiated from one another by mass spectrometry. The differences in intensities of ion *d* between the two groups may be rationalized in the following manner. Loss of a methyl radical from **2** would yield **3**, whereas loss of a methyl radical from **4** would result in **5** or **6**. In **5** and **6**, the charge is concentrated on oxygen where it is more easily tolerated. Ion **5** may be more favorable than **6** since in scoulerine, capaurimine, and tetrahydrothalifendine (4) the

Can. J. Chem. Downloaded from www.nrcresearchpress.com by 210.87.254.5 on 09/05/12
For personal use only.

TABLE I

Fragment ions and their intensities in the mass spectra of ten tetrahydroprotoberberine alkaloids

Alkaloid	Substitution pattern	M^+	Ion intensities (a)	(b)	(c)	(d)
dl-Stylopine	2,3 and 9,10 = —O>CH₂<O—	323(28)	—	174(12)	148(100)	—
d-Scoulerine	2,9 = OH, 3,10 = OCH_3	327(70)	178(100)	176(28)	150(58)	135(26)
dl-Canadine	2,3 = —O>CH₂<O— 9,10 = OCH_3	339(68)	176(6)	174(26)	164(100)	149(72)
dl-Tetrahydropalmatine	2,3,9,10 = OCH_3	355(69)	192(10)	190(30)	164(100)	149(76)
Capaurimine	1,9 = OH, 2,3,10 = OCH_3	357(54)	208(100)	206(33)	150(28)	149(22) 135(44)
Capaurine	1 = OH, 2,3,9,10 = OCH_3	371(78)	208(18)	206(46)	164(100)	149(92)
Caseamine	1 + 2 = 10 + 11 = OH + OCH_3	327(37)	178(100)	176(15)	150(69)	135(16)
Caseadine	1 = OH, 2,10,11 = OCH_3	341(30)	178(2)	176(10)	164(100)	149(8)
Caseadine *O*—Me ether*	1,2,10,11 = OCH_3	355(30)	—	190(6)	164(100)	149(9)
Norcoralydine	2,3,10,11 = OCH_3	355(28)	—	190(12)	164(100)	149(8)

*The complete spectrum of this alkaloid is also given in ref. 2.

methyl group or the hydrogen, as the case may be, attached to C-10 is preferentially lost.

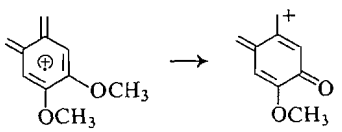

2 3

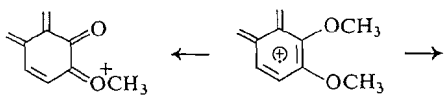

6 4

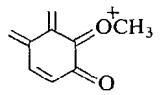

5

Proton Magnetic Resonance Spectra of Tetrahydroprotoberberine Alkaloids

During the course of this study we recorded the p.m.r. spectra of the alkaloids listed in Table I except for *d*-scoulerine and caseamine. We found that the oxygenation pattern of ring D may be deduced from an examination of the protons at C-8. These protons are separated from the rest of the alicyclic protons by the nitrogen atom and give a simple pattern. In the case of 9,10-substitution an AB quartet, or half the AB quartet when the high field half is obscured by the methoxyl signals, was invariably observed ($\tau_A \approx 5.65$; $\tau_B \approx 6.35$; $J_{AB} \approx 16$Hz). A similar pattern has been reported in the p.m.r. spectrum of tetrahydrojatrorrhizine (5). In alkaloids with 10,11-substitution the C-8 protons appear to be a broad singlet ($\tau \approx 5.95$) partially underlying the *O*-methyl signals. Typical spectra of the two classes of compounds are found in Fig. 4 where the spectra of *dl*-stylopine, *dl*-canadine, and norcoralydine are given. The spectrum of caseadine has been reported previously (2).

The tetrahydroprotoberberine alkaloids may be expected (2) to have the conformation shown in 7 or its mirror image, regardless of the substi-

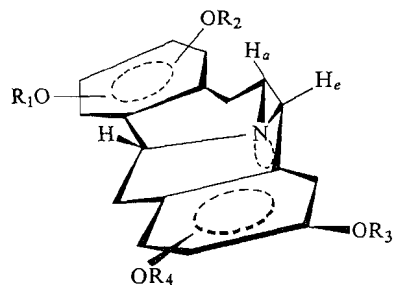

7

tution pattern of rings A and D. Since a broad singlet is observed for the protons at C-8 in the spectrum of those alkaloids which are unsubstituted at C-9, the axial and the equatorial protons at C-8 seemingly have the same chemical shift. The introduction of an oxygen substituent at C-9, however, apparently causes a downfield shift of the equatorial proton and an upfield

Can. J. Chem. Downloaded from www.nrcresearchpress.com by 210.87.254.5 on 09/05/12
For personal use only.

Can. J. Chem. Downloaded from www.nrcresearchpress.com by 210.87.254.5 on 09/05/12
For personal use only.

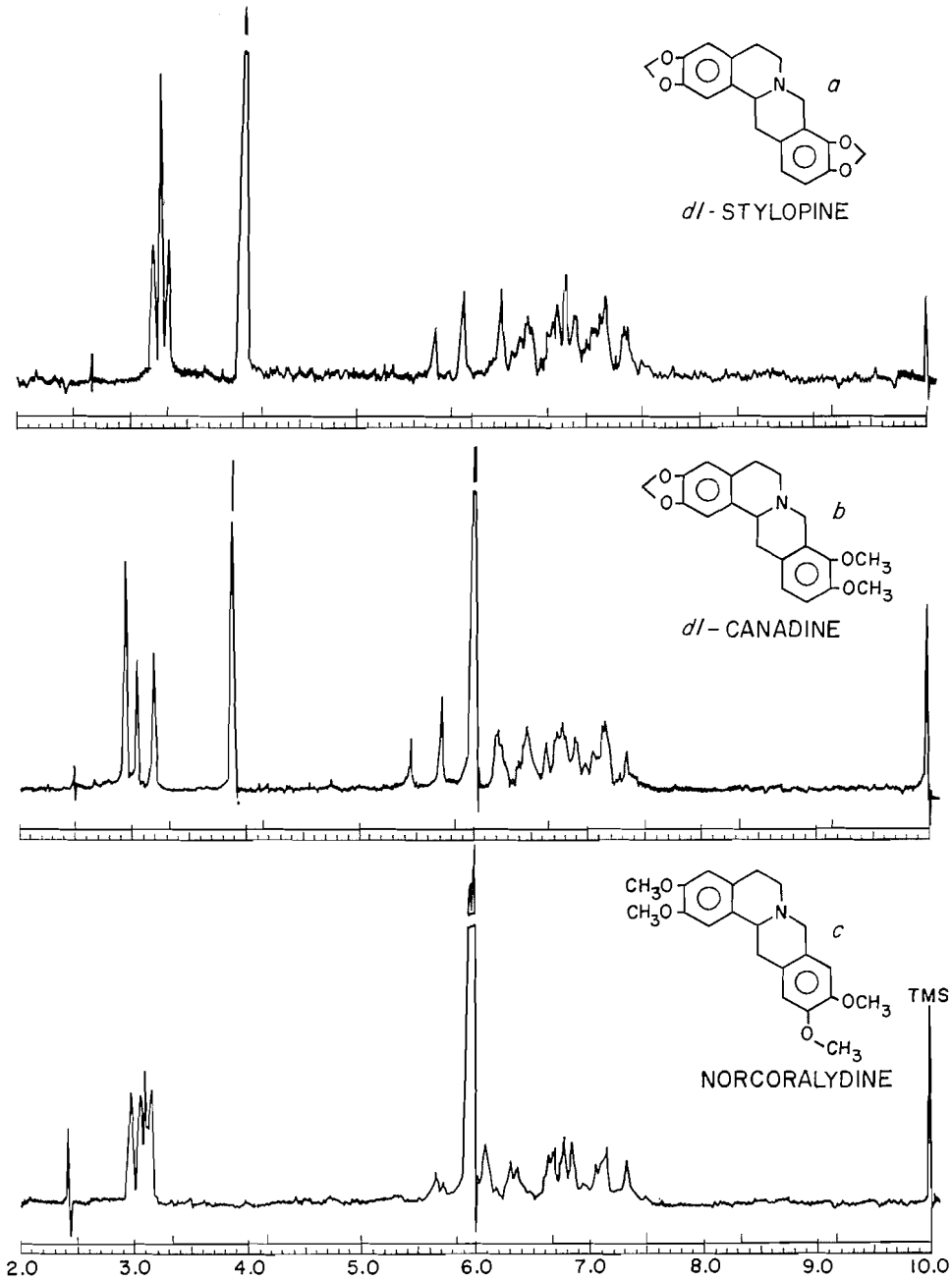

FIG. 4. The p.m.r. spectra of (*a*) *dl*-stylopine, (*b*) *dl*-canadine, and (*c*) norcoralydine.

shift of the axial proton at C-8 and an AB quartet is observed. Thus, the p.m.r. spectrum of a tetrahydroprotoberberine provides another criterion for the establishment of the substitution pattern in ring D. The p.m.r. spectra should prove particularly valuable in the study of alkaloids with a methylenedioxy function in ring D where an assignment based on mass spectrometry alone does not appear to be possible.

Experimental

Mass spectra were recorded on a Hitachi Perkin–Elmer RMU-6A instrument operating at an ionizing potential of 80 eV and an ionizing current of approximately 50 μA. Samples were introduced either through an all-glass inlet system maintained at 200 °C or through a vacuum-lock system. Both methods of introduction gave the same results. Spectra are plotted in terms of relative abundance, with the most intense peak (base peak) being taken as 100%. Only peaks equal to or greater than 2% of the base peak are recorded.

The p.m.r. spectra were recorded on a Varian A-60 spectrometer operating at 60 MHz. Deuteriochloroform was the solvent used in this study; the concentration of the alkaloid solutions was ca. 25 mg/ml.

Acknowledgments

We thank Dr. R. H. F. Manske, Research Laboratories, UniRoyal Co. Ltd., Guelph, Ontario for most of the alkaloids used in this study. We are grateful to McMaster University for the award of a University Postdoctorate Fellowship to one of us (C.-Y. C.) and to the National Research Council of Canada for financial support.

1. A. W. Sangster and K. L. Stuart. Chem. Rev. **65**, 69 (1965).
2. C.-Y. Chen, D. B. MacLean, and R. H. F. Manske. Tetrahedron Letters, 349 (1968).
3. M. Ohashi, J. M. Wilson, H. Budzikiewicz, M. Shamma, W. A. Slusarchyk, and C. Djerassi. J. Am. Chem. Soc. **85**, 2807 (1963).
4. M. Shamma, M. A. Greenberg, and B. S. Dudock. Tetrahedron Letters, 3395 (1965).
5. S. Pfeifer, I. Mann, L. Dolejš, V. Hañus, and A. D. Cross. Tetrahedron Letters, 83 (1967).

Can. J. Chem. Downloaded from www.nrcresearchpress.com by 210.87.254.5 on 09/05/12
For personal use only.

Cleavage of carbon–silicon bonds by lithium aluminium hydride in tetrahydrofuran

G. J. D. PEDDLE AND D. N. ROARK
Department of Chemistry, University of Alberta, Edmonton, Alberta

Received March 5, 1968

It was shown that many silicon–carbon bonds were readily broken by lithium aluminium hydride in refluxing tetrahydrofuran. The rate of cleavage was dependent upon the nature of the leaving group and of the other groups present on the silicon. Carbon–tin bonds were cleaved more readily than carbon–silicon bonds while carbon–germanium bonds were not cleaved.

Canadian Journal of Chemistry, 46, 2507 (1968)

Can. J. Chem. Downloaded from www.nrcresearchpress.com by 210.87.254.42 on 09/05/12
For personal use only.

In 1957 Kaesz and Stone (1) observed some carbon–silicon bond cleavage during the reduction of di- and trichloromethyltrichlorosilane.

$$Cl_2CHSiCl_3 \xrightarrow{LiAlH_4} Cl_2CHSiH_3 + SiH_4$$

More recently Gilman and Atwell observed the cleavage of carbon–silicon bonds in 1,1,2-triphenyl-1-silacyclobutane (2), (**1**), and in 2:3-benzo-1,1-diphenyl-1-silacyclobut-2-ene (3), (**2**), by lithium aluminium hydride in ether.

Gilman and Atwell also noted (2) that when the cleavage of **1** was done with lithium aluminium hydride in refluxing THF, the yield of **3** was reduced to 41%, due to unspecified secondary cleavage reactions. However, since no cleavage of 1,1,2-triphenyl-1-silacyclopentane was observed with lithium aluminium hydride in refluxing THF, they concluded that the cleavage of **1** was associated with the strain of a four-member ring (2).

Rühlmann and Heine (4) have reported the cleavage of carbon–silicon bonds in benzyltriphenylsilane, (**4**), by sodium hydride in cyclohexane at 200 °C and 100–200 atm of hydrogen.

We wish to report the facile cleavage of silicon–carbon bonds by lithium aluminium hydride in refluxing THF.

Results and Discussion

During a routine reduction of (−)-methyl-1-naphthylphenyl-(−)-menthoxysilane, (**5**), with lithium aluminium hydride, refluxing THF was substituted for the mixture of ethyl ether and *n*-butyl ether usually employed (5). The product obtained was not (+)-methyl-1-naphthylphenylsilane (**6**), but a virtually quantitative yield of naphthalene.

When racemic silane, (±)-**6**, was refluxed for 18 h with lithium aluminium hydride in THF in a system connected via the water condenser to a −80 °C trap, methylsilane was isolated in the trap. The volatile material in the pot was shown to contain in addition to THF, only phenylmethylsilane. When the nonvolatile pot residue

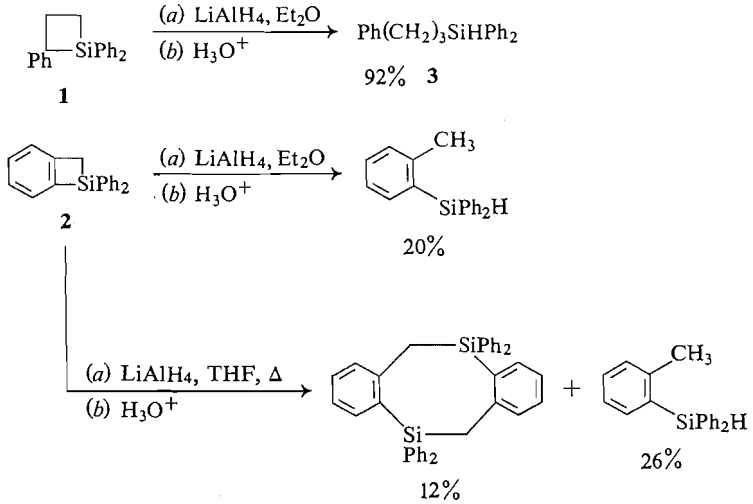

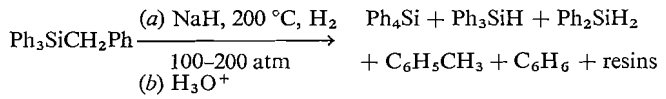

4

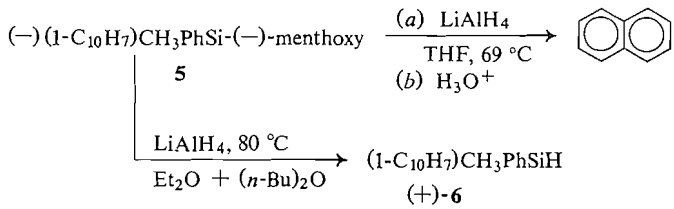

was treated with ethyl acetate followed by water, naphthalene (98%), and benzene (57%) were obtained.

The failure to isolate benzene and naphthalene among the initially volatile material at the end of the reaction, indicates that they were present as organometallic derivatives. This was confirmed during the cleavage of (±)-methyl-1-naphthylphenylmethoxysilane, when deuterium oxide was used during the workup. The mass spectrum of the naphthalene obtained indicated that it was primarily $C_{10}H_7D$.

The above results are summarized below.

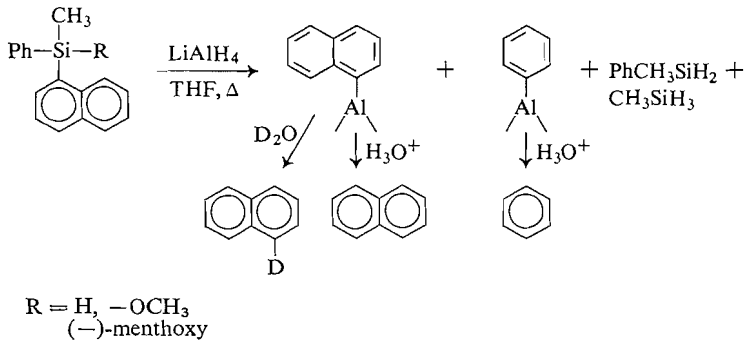

R = H, −OCH3
(−)-menthoxy

Similarly when benzyltriphenylsilane, **4**, was treated with lithium aluminium hydride in refluxing THF, the benzyl group was readily cleaved to give triphenylsilane.

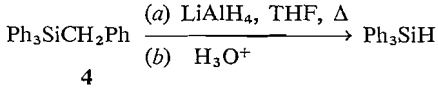

4

However, benzyltrimethylsilane was 95% recovered after refluxing for 18 h with lithium aluminium hydride in THF, and only a trace of trimethylsilane was isolated in the cold trap. No cleavage of naphthyltrimethylsilane was detected under similar conditions.

The benzyl group was rapidly cleaved from benzyltriphenyltin by lithium aluminium hydride in THF, at room temperature. Work-up gave tetraphenyltin, and an infusable mixture of tin oxides. Hexaphenylditin has been reported to give similar results when treated with lithium aluminium hydride under more vigorous conditions (6).

Benzyltriphenylgermane was not cleaved by lithium aluminium hydride in refluxing THF.

The facile cleavage of the triphenyl derivatives compared to the trimethyl compounds, the ease of cleavage $PhCH_2$ > 1-Np > Ph and the observed order of cleavage Sn > Si ≫ Ge suggest that the reaction probably involves nucleophilic attack of the hydride on the metal (7, 8).

A more detailed study of the mechanism is at present underway. Preliminary results indicate that the cleavage occurs with racemization.

Can. J. Chem. Downloaded from www.nrcresearchpress.com by 210.87.254.42 on 09/05/12
For personal use only.

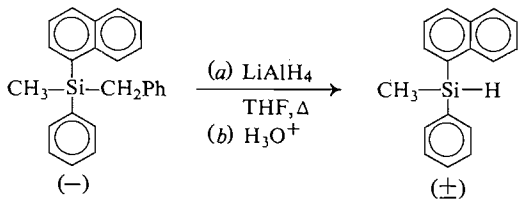

The reaction offers some possible synthetic advantages in the cleavage of silicon–carbon bonds in compounds having reactive functional groups such as silicon hydrogen bonds. A possible disadvantage to the cleavage reaction is the possibility of recombination between the more reactive organometallic derivatives and the silicon hydrides formed. Thus, in the work of Gilman and Atwell (2) the failure to observe cleavage in the case of 1,1,2-triphenyl-1-silacyclopentane probably was due to the position of equilibrium in the reaction shown below, lying far to the left.

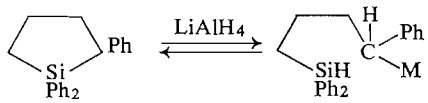

Finally, if such cleavage reactions are to be avoided during lithium aluminium hydride reduction of organosilicon compounds, THF, and presumably other polar ethers should be avoided as solvents.

Experimental

General

All reactions were carried out under an atmosphere of dry nitrogen. The THF used was freshly distilled from lithium aluminium hydride, and the *n*-butyl ether was distilled from calcium hydride before use. Lithium aluminium hydride from both Metal Hydrides Inc. and from Research Organic/Inorganic Chemical Co., was used. All melting points are uncorrected. Mass spectra, nuclear magnetic resonance (n.m.r.), and infrared (i.r.) data were determined on Metropolitan–Vickers MS-9, Varian Associates A-60, and Perkin–Elmer 421 spectrometers respectively. The n.m.r. spectra were calibrated against external TMS.

Racemic Methyl-1-naphthylphenylsilane

(±)-**6**, (+)-**6**, and (−)-**6** were readily prepared by lithium aluminium hydride reduction of (±)-methyl-1-naphthylphenylmethoxysilane and of the separated (−)-menthoxy diasteriomers respectively, following the procedures of Sommer and co-workers (5).

Reaction of (−)-Methyl-1-naphthylphenyl-(−)-menthoxysilane with Lithium Aluminium Hydride in Tetrahydrofuran

A mixture of 80 g (0.20 mole) of (−)-methyl-1-naphthylphenyl-(−)-menthoxysilane and 13 g (0.34 mole) of lithium aluminium hydride in 300 ml of THF was refluxed at 69 °C for 18 h. Following acid work-up, the resultant syrup was dissolved in ethanol and 24.5 g (97%) of naphthalene crystallized out. The naphthalene was identical in all respects to an authentic sample.

Reaction of (±)-Methyl-1-naphthylphenylsilane with Lithium Aluminium Hydride in Tetrahydrofuran

A mixture of 9.8 g (0.04 mole) of (±)-methyl-1-naphthylphenylsilane and 2.6 g (0.067 mole) of lithium aluminium hydride was refluxed for 18 h in 60 ml of THF, in a reaction vessel connected via a reflux condenser to a −80 °C cold trap.

A mass spectrum of the volatile material in the cold trap was identical to that reported for methylsilane (9). An n.m.r. spectrum (CCl_4) of the liquid in the cold trap was the same as that from a mixture of THF and methylsilane (10) and an i.r. spectrum showed a strong absorption at 2170 cm^{-1} from the Si—H of the methylsilane.

The volatile material was removed from the reaction mixture under reduced pressure. A gas–liquid chromatogram (g.l.c.) of the distillate showed only peaks for THF and for phenylmethylsilane, identified by comparison of g.l.c. retention time, n.m.r., and i.r. spectra with results from an authentic sample.

Finally the non-volatile residue was worked up with ethyl acetate followed by dilute acid. A g.l.c. of the resultant organic material showed benzene and naphthalene in a relative ratio of 0.58:1. Finally, 4.9 g (98%) of naphthalene was isolated when the other volatile materials were removed.

Reaction of (±)-Methyl-1-naphthylphenylmethoxysilane with Lithium Aluminium Hydride in Tetrahydrofuran

When (±)-methyl-1-naphthylphenylmethoxysilane and an excess of lithium aluminium hydride in THF were refluxed for 18 h and then worked up with ethyl acetate, followed by deuterium oxide, the major product obtained was [$^2H_1$]-naphthalene (73%) identified by its mass spectrum. The 27% of undeuterated naphthalene probably arose from either moisture in the ethyl acetate or proton abstraction from the acetate by some of the strong bases present.

Reaction of Triphenylbenzylsilane with Lithium Aluminum Hydride in Tetrahydrofuran

A mixture of 3.5 g (0.01 mole) of triphenylbenzylsilane and 0.57 g (0.015 mole) of lithium aluminium hydride in 50 ml THF was refluxed for 7 h and then worked up as above. Recrystallization of the product from ethanol–water gave 1.6 g (62%) of triphenylsilane, identical in all respects to an authentic sample. An n.m.r. spectrum of the oil obtained by evaporating the mother liquor showed, in addition to a multiplet at τ 2.5 p.p.m., a singlet at τ 4.54 p.p.m. from the Si—H of triphenylsilane, and a weak singlet at τ 5.14 p.p.m., probably from the Si—H of diphenylsilane.

Attempted Reaction of 1-Trimethylsilylnaphthalene with Lithium Aluminium Hydride in Tetrahydrofuran

A mixture of 8.0 g (0.04 mole) of 1-trimethylsilylnaphthalene and 2.6 g (0.068 mole) of lithium aluminium hydride in 60 ml of THF was refluxed for 18 h.

Following the usual work-up n.m.r. examination of the reaction product showed it to be 1-trimethylsilylnaphthalene. The absence of naphthalene was confirmed by g.l.c.

Can. J. Chem. Downloaded from www.nrcresearchpress.com by 210.87.254.42 on 09/05/12
For personal use only.

Reaction of Trimethylbenzylsilane with Lithium Aluminium Hydride in Tetrahydrofuran

A mixture of 2.0 g (0.012 mole) of trimethylbenzylsilane and 0.73 g (0.019 mole) of lithium aluminium hydride in 12 ml of THF was refluxed for 18 h in a reaction vessel, connected via the condenser to a −80 °C cold trap.

A mass spectrum of the material in the cold trap was identical to that of trimethylsilane (9). However, work-up as above gave 1.9 g (95%) of recovered trimethylbenzylsilane.

Reaction of Triphenylbenzylgermane with Lithium Aluminium Hydride in Tetrahydrofuran

A mixture of 0.2 g (0.00052 mole) of triphenylbenzylgermane and 0.12 g (0.0031 mole) of lithium aluminium hydride in 5 ml of THF was refluxed for 4.5 h. Following the usual work-up, recrystallization from ethanol gave 0.2 g (100%) of recovered triphenylbenzylgermane.

Reaction of Triphenylbenzyltin with Lithium Aluminium Hydride in Tetrahydrofuran

A mixture of 0.75 g (0.0017 mole) of triphenylbenzyltin and 0.09 g (0.0024 mole) of lithium aluminium hydride in THF was stirred at room temperature for 24 h. An excess of ethyl acetate was added and the mixture was then stirred for 6 h before the addition of dilute hydrochloric acid and ethyl ether. Filtration gave 0.25 g of an infusable white solid (Found: C, 28.1; H, 2.03) from which a small amount of tetraphenyltin, m.p. 226–227 °C, distilled, when the solid was heated to 320–330 °C. An additional 0.1 g of tetraphenyltin was obtained by crystallization of the ether soluble material.

Reaction of (−)-Methyl-1-naphthylphenylbenzylsilane with Lithium Aluminium Hydride in Tetrahydrofuran

A solution of 0.30 g (0.0009 mole) of (−)-methyl-1-naphthylphenylbenzylsilane (11), $[\alpha]_D^{25} = -6.45°$ (0.027 g/ml, cyclohexane) and 0.052 g (0.0013 mole) of lithium aluminium hydride in 4 ml of THF, was refluxed for 9.5 h. Work-up with ethyl acetate, followed by dilute hydrochloric acid and ethyl ether, gave 0.22 g of an oil, $[\alpha]_D^{25} = -4.7°$ (0.15 g/ml, cyclohexane). An n.m.r. spectrum of the oil indicated that it contained approximately 45% of methyl-1-naphthylphenylbenzylsilane, 45% of methyl-1-naphthylphenylsilane, and 10% of benzylmethylphenylsilane.[1] Chromatography of 0.15 g of the oil on 100 g of silica, eluted with cyclohexane–benzene, gave approximately 54 mg (36%) of (±)-methyl-1-naphthylphenylsilane, 6 mg (4%) of (±)-benzylmethylphenylsilane, and 89 mg (60%) of recovered (−)-methyl-1-naphthylphenylbenzylsilane $[\alpha]_D^{25} = -5.1°$ (0.027 g/ml, cyclohexane).

Acknowledgment

The authors wish to thank the National Research Council of Canada for their support of this work.

1. H. D. Kaesz and F. G. A. Stone. J. Chem. Soc. 1433 (1957).
2. H. Gilman and W. H. Atwell. J. Am. Chem. Soc. **86**, 2687 (1964).
3. H. Gilman and W. H. Atwell. J. Am. Chem. Soc. **86**, 5589 (1964).
4. K. Rühlmann and H. Heine. Z. Chem. **6**, 421 (1966).
5. L. H. Sommer, C. L. Frye, G. A. Parker, and K. W. Michael. J. Am. Chem. Soc. **86**, 3271 (1964).
6. G. A. Baum and W. J. Considine. J. Org. Chem. **29**, 1267 (1964).
7. C. Eaborn. Organosilicon compounds. Butterworths, London. 1960. pp. 143–159.
8. R. W. Bott, C. Eaborn, and T. W. Swaddle. J. Chem. Soc. 2342 (1963).
9. G. P. van der Kelen, O. Volders, H. van Onckelen, and Z. Eeckhart. Z. Anorg. Allgem. Chem. **338**, 106 (1965).
10. E. A. V. Ebsworth and S. G. Frankiss. Trans. Faraday Soc. **59**, 1518 (1963).
11. L. H. Sommer, K. D. Kortes, and P. G. Rodewald. J. Am. Chem. Soc. **89**, 862 (1967).

[1]The preparation and properties of this compound will be reported shortly in connection with other studies.

Can. J. Chem. Downloaded from www.nrcresearchpress.com by 210.87.254.42 on 09/05/12
For personal use only.

Can. J. Chem. Downloaded from www.nrcresearchpress.com by 210.87.254.6 on 09/05/12
For personal use only.

Reactions of nitro sugars. IX. The synthesis of branched-chain dinitro sugars by Michael addition[1,2]

HANS H. BAER AND K. S. ONG
Department of Chemistry, University of Ottawa, Ottawa, Canada

Received March 5, 1968

The reaction of methyl 2-*O*-acetyl-4,6-*O*-benzylidene-3-deoxy-3-nitro-β-D-glucopyranoside (**1**) or of methyl 4,6-*O*-benzylidene-2,3-dideoxy-3-nitro-β-D-*erythro*-hex-2-enopyranoside (**2**) with nitroalkanes led to branched-chain dinitro sugar derivatives, namely methyl 4,6-*O*-benzylidene-2,3-dideoxy-3-nitro-2-nitroalkyl-β-D-glucopyranosides (**3**). The nitroalkanes employed included nitromethane, nitroethane, 1- and 2-nitropropane, and methyl nitroacetate. The three first-mentioned nitroalkanes were added in similar fashion to methyl 4,6-*O*-benzylidene-2,3-dideoxy-3-nitro-β-D-*threo*-hex-2-enopyranoside (**5**) to give methyl 4,6-*O*-benzylidene-2,3-dideoxy-3-nitro-2-nitroalkyl-β-D-galactopyranosides (**6**). Analogous reactions of **1** and **5** with diethyl malonate produced the corresponding branched-chain glycosides **7** and **8**. The reactions appear to be highly stereoselective as far as the configurations at C-2 and C-3 in the products are concerned. However, there is evidence for the formation of side-chain epimers in three cases where the nitroalkyl side chain possesses an asymmetric carbon.

Canadian Journal of Chemistry, **46**, 2511 (1968)

Many straight-chain amino sugars, a few diamino sugars, and several nitrogen-free, branched-chain sugars are known to occur as constituents of a large variety of antibiotics (3). Nitrogenous sugars with a branched chain had not been encountered in nature until very recently when methyl garosaminide, a fragment from gentamicin C, was reported to be a 3-methylamino-3-deoxy-4-*C*-methylpentopyranoside (4). Prior to this discovery a few 3-amino-3-deoxy-3-*C*-methylhexoses (5, 6) and analogous pentoses (7) have been synthesized by cyclizations of sugar dialdehydes with nitroethane and subsequent reduction, but no branched-chain diamino sugars have thus far been described. The synthesis of such compounds would appear to command interest in view of structural relationships to known fungal and bacterial metabolites and in anticipation of their eventual detection among natural products. The present paper reports the synthesis of a number of branched-chain dinitro sugar derivatives. Although their reduction to the diamino stage has not yet been performed, this will doubtless be feasible by methods well tested in amino sugar chemistry in the recent past.

The work grew out of previous studies on nucleophilic additions and elimination–additions in suitable nitro sugar derivatives. It had been found (8–10) that methyl 4,6-*O*-benzylidene-2,3-dideoxy-3-nitro-β-D-*erythro*-hex-2-enopyranoside (**2**), which may be employed as such or generated *in situ* by dehydroacetylation of methyl 2-*O*-acetyl-4,6-*O*-benzylidene-3-deoxy-3-nitro-β-D-glucopyranoside (**1**), readily adds alcohols, ammonia, or amines to give 2-substituted 3-deoxy-3-nitro glucose derivatives.[3] In continuation, we have now applied to carbohydrates the Michael synthesis of α,γ-dinitroalkanes (11, 12). Reactions between **1** and various nitroalkanes in the presence of stoichiometric amounts of triethylamine proceeded smoothly at room temperature within 16 h and gave crystalline methyl 4,6-*O*-benzylidene-2,3-dideoxy-3-nitro-2-(α-nitroalkyl)-β-D-glucopyranosides (**3***a*–**3***d*). The yields were 60–85% with primary nitroalkanes and 45% with 2-nitropropane.

When crystalline nitroolefin **2** instead of the *O*-acetate **1** was used as the starting compound, the amine-catalyzed addition of nitroethane took place quantitatively within 30 min. However, **1** offers the practical advantage of being prepared more conveniently than **2**.

A variant in procedure was employed for the preparation of the 2-methoxycarbonylnitromethyl derivative **3***e*. This compound was obtained from **2** and methyl nitroacetate by refluxing

[1]For paper VII in this series, see ref. 1, and for paper VIII, see ref. 2.

[2]This work is taken from a Ph.D. thesis to be submitted to the University of Ottawa by K. S. O. It was reported in part at the 4th International Conference on Carbohydrates, Kingston, Ontario, July 1967.

[3]A modification of the reaction, in which the non-acetylated, parent compound of **1** is used, has also been elaborated (8).

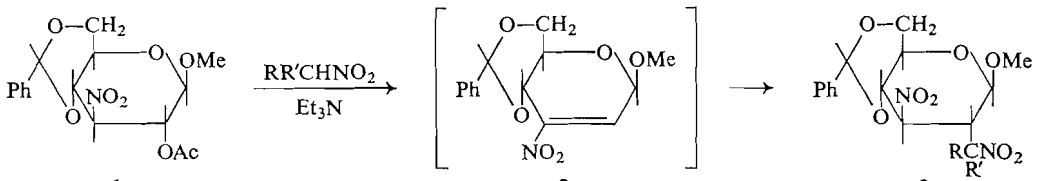

1 2 3

a, R = R′ = H
b, R = H, R′ = CH_3
c, R = H, R′ = C_2H_5
d, R = R′ = CH_3
e, R = H, R′ = CO_2CH_3

7, —$CH(CO_2C_2H_5)_2$ instead of —CRR′ NO_2

the reactants in benzene solution in the presence of a trace of potassium hydroxide.[4]

Application of the dinitro sugar synthesis to the D-*galacto* series met with inital difficulties. When methyl 2-*O*-acetyl-4,6-*O*-benzylidene-3-deoxy-3-nitro-β-D-galactopyranoside (**4**) was used, the reactions were attended with decomposition; liberation of benzaldehyde was noticed and no identifiable dinitro sugars could be isolated. Acetal bonds that are located vicinal to a primary or secondary nitro group are known to be rather easily broken by base-catalyzed elimination, and such cleavage together with certain ensuing processes (13–15) may interfere with the desired reaction path. While under the conditions of the present investigation the benzylidene group in **1** was stable enough, at least to an extent allowing the preparation of the products (**3**) in good yields, the same blocking group evidently was too labile in **4**. This difference in degree of stability between an equatorial and an axial acetal linkage activated by a neighboring nitro group is noteworthy and should be borne in mind in future planning of similar synthetic projects.

Although the 2-*O*-acetate (**4**) failed to give the desired dinitro glycosides, it was found that the nitroolefin, methyl 4,6-*O*-benzylidene-2,3-dideoxy-3-nitro-β-D-*threo*-hex-2-enopyranoside (**5**), readily added the primary nitroalkanes, namely nitromethane, nitroethane, and 1-nitropropane.[5] Also performed in the presence of triethylamine at room temperature, these Michael reactions required only 1 h and furnished crystalline methyl 4,6-*O*-benzylidene-2,3-dideoxy-3-nitro-2-(α-nitroalkyl)-β-D-galactopyranosides (**6***a*–**6***c*) in 60–85% yields. Side reactions obviously were not very serious under these conditions. By contrast, the secondary addend 2-nitropropane gave only small amounts of impure product, and prolongation of the reaction time or increase in the amount of catalyst caused extensive debenzylidenation.

As an adjunct to these studies we synthesized in like manner methyl 4,6-*O*-benzylidene-2,3-dideoxy-2-[bis(ethoxycarbonyl)methyl]-3-nitro-β-D-glucopyranoside (**7**) and -galactopyranoside (**8**) from **1** and **5**, respectively, and diethyl malonate.

In the infrared (i.r.) spectra, the asymmetric nitro stretching modes of all the dinitro glycosides appeared as double peaks. The mononitro diesters **7** and **8** exhibited single nitro and double ester carbonyl bands, and the reverse was true for the dinitro monoester **3***e* (Table I). The structures of the new compounds were confirmed by nuclear magnetic resonance (n.m.r.) spectroscopy. Table II shows the substituent resonances. In all cases the integration of the substituent and ring proton signals agreed with the molecular formulas.

Since the reactions described started from or proceeded via 2,3-unsaturated hexopyranosides and hence involved the generation of asymmetric centers at C-2 and C-3 in the products, it was necessary to ascertain the configurations at these carbons, even though it could be presumed on the basis of previous experiences with similar nucleophilic additions (8–10) that diequatorial substituent orientation is favored. Proof of configuration was provided for all compounds except **3***e* by the nature of the n.m.r. signal given by H-3, the proton on the ring carbon bearing a nitro group (see Table III). This signal appeared near

[4]We are obliged to Mr. Frank Kienzle for contributing this experiment. The technique was similar to that used in the addition to **2** of isopropyl lactate (9). The configuration of **3***e* has not been determined; its formulation as a *gluco* compound, resting upon analogy (9) and specific rotation, should be regarded as tentative.

[5]Addition of methyl nitroacetate was not attempted in this series.

Can. J. Chem. Downloaded from www.nrcresearchpress.com by 210.87.254.6 on 09/05/12
For personal use only.

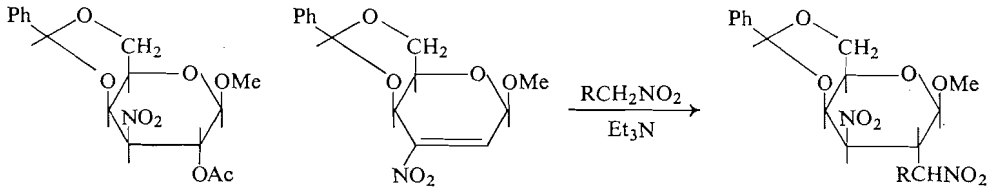

4 **5** **6**

a, R = H
b, R = CH_3
c, R = C_2H_5

8, $-CH(CO_2C_2H_5)_2$ instead of $-CHRNO_2$

TABLE I

Characteristic infrared frequencies in Nujol (cm^{-1})

Compound	Asymmetric nitro	CO	OH
3*a*	1575, 1550	—	—
3*b**	1565, 1552	—	—
3*b*+**3***b*′†	1563, 1550	—	—
3*c*	1562, 1544	—	—
3*d*	1562, 1550	—	—
3*e*	1577, 1570	1755	—
3*e*‡	1577, 1570	—	3450–3250
6*a*	1566, 1552	—	—
6*b*	1560, 1533	—	—
6*b*′	1560, 1547	—	—
6*c*	1563, 1557	—	—
7	1555	1753, 1730	—
8	1555	1755, 1735	—

*Single compound, m.p. 169–170°.
†Mixture, m.p. 134–135°.
‡After debenzylidenation; see Experimental.

τ 4.9, downfield from all other resonances excepting those due to the benzylidene group, and it was well separated from the signals adjoining upfield, or at least sufficiently so for its character to be clearly recognizable.[6] Compounds **3***a*–**3***d* and **7** gave symmetrical triplets or quartets showing large spacings of 9–11.8 c.p.s., which required H-3 to be axially oriented and coupled vicinally with two axial protons at C-2 and C-4. Thus the *gluco* configuration was established for that series. Compounds **6***a*–**6***c* and **8**, on the other hand, gave quartets with one small (4 c.p.s.) and one large (12 c.p.s.) splitting. Since H-4 was known to be equatorial in this series, $J_{3,4}$ necessarily had to be small (regardless of the disposition of H-3), and the large splitting had therefore to be attributed to the coupling of H-3 with H-2. The large splitting indicated diaxial arrangement of these protons and hence proved the *galacto* configuration.

[6]In a similar series of 3-deoxy-3-nitro glycosides, H-3 has also been found to resonate at lower field than the other ring protons (8). Only in **3***e* was the signal crowded together with others so that it was difficult to analyze.

Finally, another point of stereochemistry should be considered. Five of the ten new compounds, namely **3***b*, **3***c*, **3***e*, **6***b*, and **6***c*, possess an asymmetric carbon atom in their side chains and on account of this should be capable of existing in pairs of diastereoisomers. There is in fact evidence for the occurrence of such side-chain epimers in at least some of the cases.

The crystalline product ($[\alpha]_D$ −60 to −63°) obtained by the reaction of nitroethane with **1** (or **2**) was revealed by spectroscopy and thin-layer chromatography (t.l.c.) to be free of starting material, but it melted over a wide range above 130°. Fractional crystallization afforded **3***b* ($[\alpha]_D$ −74°, m.p. 169–170°) that appeared homogeneous on t.l.c., and in addition gave a fraction of crystals ($[\alpha]_D$ −57°, m.p. 135–136°) which on t.l.c. produced a double spot representing an epimer (**3***b*′, major component) accompanied by residual **3***b*. A complete separation of the epimers was not accomplished. Nevertheless, it could be demonstrated that both components of the mixed crystals possessed the same structure and the *gluco* configuration. The i.r. spectra of the mixture and pure **3***b* were very similar. Their n.m.r. spectra were identical as far as the benzylidene and methoxy resonances and the total proton intensity were concerned. However, in the region around τ 5, where pure **3***b* exhibited a single quartet due to H-3, the epimeric mixture gave two partially overlapping quartets (τ 4.9 and τ 5.1) with a combined intensity corresponding to one proton. The quartet at τ 4.9, which was attributed to H-3 of the epimer **3***b*′, showed the same large splittings (10 and 11.8 c.p.s.) as that at higher field which came from H-3 in **3***b*. Therefore, both components belonged to the *gluco* series. The small but significant chemical shift difference for H-3 must be caused by the configurational inequality of the nearby nitroethyl

Can. J. Chem. Downloaded from www.nrcresearchpress.com by 210.87.254.6 on 09/05/12
For personal use only.

TABLE II

Chemical shifts (τ values) and relative intensities of substituent signals (number of protons in parentheses), in deuteriochloroform, unless otherwise indicated

Compound	Phenyl	*Ph*—CH=O_2	*O*—CH_3	*C*—CH_3
3*a*	2.75 (5)	4.40 (1)	6.47 (3)	
3*b*	2.61 (5)	4.47 (1)	6.50 (3)	8.44 (3)†
3*c*	2.56 (5)	4.44 (1)	6.44 (3)	9.02 (3)‡
3*d*	2.57 (5)	4.42 (1)	6.57 (3)	8.33 (3), 8.43(3)
3*e*	2.62 (5)	4.45 (§)	6.21 (3), 6.54 (3)	
6*a**	2.58 (5)	4.27 (1)	6.58 (3)	
6*b**‖	2.58 (5)	4.27 (1)	6.63 (3)	8.52 (3)†
6*b*′¶	2.60 (5)	4.43 (1)	6.56 (3)	8.23 (3)†
6*c*	2.62 (5)	4.47 (1)	6.56 (3)	9.01 (3)‡
7	2.64 (5)	4.46 (1)	6.56 (3)	8.71 (6)‡
8	2.60 (5)	4.42 (1)	6.54 (3)	8.72 (6)‡

*In dimethyl sulfoxide-d_6.
†Doublet with spacing 7 c.p.s.
‡Triplet with spacing 7 c.p.s.
§Intensity not determined because of overlap with other signal.
‖Epimer, m.p. 222–223°.
¶Epimer, m.p. 196–197°.

groups. The methyl portions of these groups, in turn, had unequal chemical shifts indicative of environmental differences. Thus, pure **3***b* gave a sharp doublet at τ 8.44, whereas in the epimeric mixture this doublet was superimposed by a second doublet centered at τ 8.32.[7]

The addition of nitroethane to **5** gave a crystalline material ($[\alpha]_D$ +8°) shown by t.l.c. to contain two major components. These proved separable by fractional crystallization and they both possessed the composition of **6***b*. The less soluble, more slowly moving compound (**6***b*, m.p. 222–223°, $[\alpha]_D$ +2.3°) and the more soluble, faster moving compound (**6***b*′, m.p. 196–197°, $[\alpha]_D$ +23°) exhibited the same general features in their i.r. and n.m.r. spectra. In particular, the resonance of H-3 indicated for both products the *galacto* configuration as outlined above, and they must therefore represent a pair of side-chain epimers.

The crude product **6***c* (m.p. 170–174°, $[\alpha]_D$ +20°) obtained from 1-nitropropane and **5** also gave two spots on t.l.c. The slower one was of relatively weak intensity, and it persisted when the product was recrystallized to constancy of the physical data (m.p. 181°, $[\alpha]_D$ +23°). Nuclear magnetic resonance spectra of the crude and recrystallized substances were virtually identical. The triplet assignable to the methyl portion of the nitropropyl group (Table II) was accompanied by a weak satellite triplet 0.03 p.p.m. upfield, which presumably was due to the presence of some epimer. In the region of the H-3 resonance was observed only one quartet, with spacings of 4 and 12 c.p.s.

[7]Since the chemical shift difference fortuitously was of nearly the same magnitude as the coupling constant (7 c.p.s.), the two doublets combined to give the appearance of a triplet with three-proton intensity.

TABLE III

Chemical shifts (τ values) and splittings (in c.p.s.) of the H-3 signals, in deuteriochloroform solution, unless otherwise indicated

Compound	Chemical shift	Splittings
3*a*	4.9	10.0, 11.8
3*b*	5.1	10.0, 11.7
3*b*′	4.9	10.0, 11.7
3*c*	4.9	9.7, 11.3
3*d*	5.0	10.0, 10.0
6*a**	4.7	4.0, 12.0
6*b**	4.6	ca. 4, 11
6*b*′	4.8	3.7, 11.5
6*c*	4.95	4.0, 12.0
7	4.9	ca. 9, 10
8	4.85	4.0, 12.0

*In dimethyl sulfoxide-d_6.

No evidence for side-chain epimerism has as yet presented itself in connection with **3***c* and **3***e*. The subject is being examined further, and studies to determine the branch configurations are contemplated.

Experimental

Melting points were determined in capillaries in an electrically heated aluminium block equipped with a calibrated thermometer. Thin-layer chromatography (t.l.c.) was performed on silica gel G; 7.5 cm plates

Can. J. Chem. Downloaded from www.nrcresearchpress.com by 210.87.254.6 on 09/05/12
For personal use only.

Can. J. Chem. Downloaded from www.nrcresearchpress.com by 210.87.254.6 on 09/05/12
For personal use only.

(microscope slides) were adequate except for discerning the epimers **3***b* which required 20 cm plates. The solvent systems employed for irrigation were butanone – *n*-heptane, 1:2.5 (solvent *a*); butanone – *n*-heptane, 1:1 (solvent *b*), and ethyl acetate – petroleum ether (b.p. 30–60°), 1:1 (solvent *c*). The spots were made visible by spraying with ceric sulfate – sulfuric acid. Optical rotations were measured at about 23° in a Perkin–Elmer automatic polarimeter, model 141. Infrared (i.r.) spectra were recorded on a Beckman IR-8 instrument. The nuclear magnetic resonance (n.m.r.) spectra were obtained from a Varian HA-60 spectrometer and were internally standardized with tetramethylsilane.

*Reactions of Nitroalkanes with Methyl 2-O-Acetyl-4,6-O-benzylidene-3-deoxy-3-nitro-*β*-*D*-glucopyranoside (**1**)*

Compound **1** (16) was dissolved in an excess of the nitroalkane, triethylamine was added, and the reaction mixtures were allowed to stand at room temperature. The amounts of reactants used are specified below. The progress of the reactions was monitored by t.l.c. with solvent *a*. The formation of products (**3***a*–**3***d*) migrating faster than **1** was noticeable at an early stage, and complete or almost complete disappearance of **1** was observed within 16 h. Toluene (10 ml) was then added, and the mixtures were evaporated to dryness at 35° *in vacuo*. This operation was repeated twice and, if the residue was markedly yellowish, a treatment with decolorizing charcoal was included. Finally the solid residues were evaporated with ethanol and recrystallized from ethyl acetate – petroleum ether unless indicated otherwise. The materials obtained in the first recrystallization are referred to as the "crude products" in the following sections.

*Methyl 4,6-O-Benzylidene-2,3-dideoxy-3-nitro-2-nitromethyl-*β*-*D*-glucopyranoside (**3***a*)*

Compound **1** (450 mg), nitromethane (15 ml), and triethylamine (0.18 ml) gave 372 mg of crude product, m.p. 160–169°. Two further recrystallizations from the same solvents gave 302 mg (67%) of **3***a* as fine colorless needles, m.p. 168–170°, $[\alpha]_D$ −74.6° (*c*, 1.0 in chloroform).

Anal. Calcd. for $C_{15}H_{18}N_2O_8$ (354.3): C, 50.85; H, 5.12; N, 7.91. Found: C, 50.79; H, 5.21; N, 8.11.

*Methyl 4,6-O-Benzylidene-2,3-dideoxy-3-nitro-2-(1-nitroethyl)-*β*-*D*-glucopyranoside (**3***b*)*

Compound **1** (300 mg), nitroethane (5 ml), and triethylamine (0.12 ml) produced a reaction residue that exhibited two ill-separated spots on a t.l.c. plate. The first recrystallization gave two fractions of crude products (154 and 110 mg, a total of 84.5%), the second fraction being obtained by concentration of the mother liquor and addition of more petroleum ether. The first fraction, in which the faster moving component was enriched, melted over the range 155–164° and showed $[\alpha]_D$ −67.2° (*c*, 1 in chloroform). Two recrystallizations from chloroform–pentane removed the slow-moving component from this material and gave one epimer (**3***b*) in nearly pure state, m.p. 169–170°, $[\alpha]_D$ −71.2°. In a repeat experiment, several recrystallizations from ethyl acetate–petroleum ether gave a product of m.p. 170–170.5° and $[\alpha]_D$ −73.7° (*c*, 1.0 in chloroform).

Anal. Calcd. for $C_{16}H_{20}N_2O_8$ (368.4): C, 52.17; H, 5.47; N, 7.61. Found: C, 52.24; H, 5.66; N, 7.56.

The above-mentioned, second fraction (110 mg) chromatographically showed a preponderance of the slow-moving component, and it melted in the range of 130–140° and had $[\alpha]_D$ −59.2° (in chloroform). After a recrystallization from chloroform–pentane the melting point was reasonably sharp (133–134°) but t.l.c. still revealed two components (**3***b* and **3***b*′).

A number of attempts were made to achieve a complete separation of the epimers present in crystal fractions from similar experiments. One batch, for instance, was dissolved in chloroform, and pentane was added in an amount insufficient to cause immediate crystallization. In the course of 2 days the solution, which was stored at room temperature, deposited stout prisms and small aggregated crystals. By careful decantation and flotation with carbon tetrachloride it was possible to separate mechanically parts of the two kinds of crystals. The small crystals (m.p. 168–169°) gave a single, fast-moving spot; the stout prisms (m.p. 135–136°, $[\alpha]_D$ −57.4° in chloroform) showed both spots, with the slower one preponderating. A further recrystallization of these prisms from the same solvents did not change the chromatographic picture and resulted in m.p. 133–134°, $[\alpha]_D$ −59.0° (*c*, 0.7 in chloroform). The material represented a mixture of **3***b* and **3***b*′.

The i.r. spectra (Nujol) of the high-melting (*A*) and low-melting (*B*) products were very similar in their gross patterns but differed as follows (wavenumbers in cm^{-1}). *A*: 1565 weaker than 1552; 1395, sharp, medium strong; 1080, strong; 770–750, three bands, medium strong. *B*: 1563 stronger than 1550; 1377, with shoulder at 1387, strong, superimposed on Nujol peak; 1100, strong; 1003, medium strong (absent in *A*); 750, one sharp band. Both *A* and *B* had prominent peaks near 970 and 700 and very similar groups of peaks in the 1350–1130 cm^{-1} region.

Nitroolefin **2** (16) (100 mg), nitroethane (2 ml), and triethylamine (0.04 ml) were allowed to interact at room temperature for 30 min. Work-up with toluene and ethanol gave a white, crystalline material (123 mg, 98%) whose i.r. spectrum appeared as a superposition of the spectra of *A* and *B*. The rotation in chloroform was $[\alpha]_D$ −60.3° (−62.0° in a repeat experiment that had given a 95% yield), and the n.m.r. spectrum indicated a mixture of about equal amounts of epimers **3***b* and **3***b*′. Recrystallization from chloroform–pentane gave crystals (**3***b*) melting at 169° ($[\alpha]_D$ −74.4°, *c*, 1.4 in chloroform), and from the mother liquor were obtained mixed crystals that melted at 131–133°.

*Methyl 4,6-O-Benzylidene-2,3-dideoxy-3-nitro-2-(1-nitropropyl)-*β*-*D*-glucopyranoside (**3***c*)*

Compound **1** (100 mg), 1-nitropropane (5 ml), and triethylamine (0.04 ml) gave 75 mg of crude product, m.p. 165–178°. Only one spot appeared on t.l.c. plates. One additional recrystallization furnished felt-like needles (65 mg, 60%) of m.p. 184° and $[\alpha]_D$ −67.0° (*c*, 1.3 in chloroform).

Anal. Calcd. for $C_{17}H_{22}N_2O_8$ (382.4): C, 53.40; H, 5.80; N, 7.33. Found: C, 53.34; H, 5.83; N, 7.46.

*Methyl 4,6-O-Benzylidene-2,3-dideoxy-3-nitro-2-(1-methyl-1-nitroethyl)-*β*-*D*-glucopyranoside (**3***d*)*

Compound **1** (200 mg), 2-nitropropane (10 ml), and triethylamine (0.2 ml, 2.5 molar equivalents) gave 118 mg of crude product, m.p. 170–188°. Two recrystallizations furnished 92 mg (45%) of pure **3***d*, m.p. 187.5–189.5°, $[\alpha]_D$ −92.7° (*c*, 1.0 in chloroform).

Can. J. Chem. Downloaded from www.nrcresearchpress.com by 210.87.254.6 on 09/05/12
For personal use only.

Anal. Calcd. for $C_{17}H_{22}N_2O_8$ (382.4): C, 53.40; H, 5.80; N, 7.33. Found: C, 53.55; H, 5.76; N, 7.44.

Methyl 4,6-O-Benzylidene-2,3-dideoxy-2-methoxycarbonylnitromethyl-3-nitro-β-D-glucopyranoside (3e)

A solution of 650 mg of methyl 4,6-*O*-benzylidene-2,3-dideoxy-3-nitro-β-D-*erythro*-hex-2-enopyranoside (**2**) (16) in 150 ml of dry benzene containing 300 mg of methyl nitroacetate (17) was heated under reflux in the presence of a small chip of potassium hydroxide. The reaction was complete after 2 h as indicated by t.l.c. with solvent *c*. In this system, **2** gave a fast-moving and **3***e* a slow-moving spot. The cooled solution was filtered and stirred for 10 min with 3 ml of cation exchange resin, Rexyn RG 50 (H^+), together with a small amount of activated charcoal. The colorless filtrate therefrom was evaporated to give a syrup that began to crystallize on scratching. The product was triturated with a small amount of a mixture (1:2) of ethyl acetate and petroleum ether, kept in the refrigerator for a day, collected by filtration, and washed with an ice-cold mixture of the same solvents. The yield was 750 mg (86%) of **3***e*, m.p. 106–107° (unchanged upon recrystallization); $[\alpha]_D$ −56.0° (*c*, 1.0 in chloroform).

Anal. Calcd. for $C_{17}H_{20}N_2O_{10}$ (386.4): C, 49.80; H, 5.17; N, 7.26. Found: C, 49.91; H, 5.21; N, 7.15.

A sample of **3***e* (190 mg) was *debenzylidenated* by heating it for 30 min on the steam bath, in 20 ml of 75% acetic acid. The yellowish solution was evaporated with several additions of water and then of ethanol. A white solid was obtained which was recrystallized from 50% aqueous ethanol to give 76 mg (47.5%) of *methyl 2,3-dideoxy-2-methoxycarbonylnitromethyl-3-nitro-β-D-glucopyranoside* as needles, m.p. 155°, $[\alpha]_D$ −53.0° (*c*, 0.6 in ethanol).

Anal. Calcd. for $C_{10}H_{16}N_2O_{10}$ (324.3): C, 37.28; H, 4.97; N, 8.64. Found: C, 37.36; H, 5.04; N, 8.40.

Reaction of Nitroalkanes with Methyl 4,6-O-Benzylidene-2,3-dideoxy-3-nitro-β-D-threo-hex-2-enopyranoside (5)

Solutions of compound **5** (18) and triethylamine in an excess of the nitroalkane were allowed to stand at room temperature. The amounts of reactants used are specified below. The products (**6***a*–**6***c*) began to form within a few minutes, and the reactions were complete after 1 h as indicated by t.l.c. with solvent *b*. (Since **6***a* and **6***b* are sparingly soluble, trailing occurs on the plates unless smaller than usual amounts are applied.) The mixtures were then evaporated with additions of toluene (3 × 10 ml) and ethanol, to give nearly colorless to lightly-yellow residues.

Methyl 4,6-O-Benzylidene-2,3-dideoxy-3-nitro-2-nitromethyl-β-D-galactopyranoside (6a)

The crude product obtained from **5** (300 mg), nitromethane (10 ml) and triethylamine (0.12 ml) was dissolved in about 50 ml of ethyl acetate. The solution was decolorized with activated charcoal, filtered, and evaporated to a small volume. A colorless, crystalline product (256 mg, m.p. 210–221° with decomposition) separated and was collected after cooling (4°) for a few hours. Recrystallization from butanone – petroleum ether gave 243 mg (68%) of **6***a* as needles showing m.p. 227° (darkening from 210°) and $[\alpha]_D$ +8.6° (*c*, 0.6 in butanone).

Anal. Calcd. for $C_{15}H_{18}N_2O_8$ (354.3): C, 50.85; H, 5.12; N, 7.91. Found: C, 50.74; H, 5.06; N, 8.06.

Methyl 4,6-O-Benzylidene-2,3-dideoxy-3-nitro-2-(1-nitroethyl)-β-D-galactopyranosides (6b and 6b′)

The reaction mixture obtained from **5** (200 mg), nitroethane (2.5 ml), and triethylamine (0.08 ml) was evaporated with toluene (3 × 10 ml) and then with butanone to give a colorless crystalline residue decomposing at 175–185°; $[\alpha]_D$ +8.3° (*c*, 1 in butanone). Thin-layer chromatography showed two well-separated spots of comparable strength representing the epimers **6***b* and **6***b′*; traces of unidentified products were seen in addition. The material was triturated thoroughly with ethyl acetate, chilled, filtered, and washed with cold ethyl acetate containing a small amount of pentane. The filter residue (73 mg) as well as a crop of crystals (83 mg) deposited in the filtrate upon addition of pentane to incipient cloudiness consisted largely of the slow-moving epimer **6***b*; m.p. 221° and 220–221°, with decomposition. A pure product giving the slow spot only was obtained by recrystallization from a rather large amount of boiling ethyl acetate. The fine needles melted at 222–223° (decomp.) and had $[\alpha]_D$ +2.3° (*c*, 1.2 in butanone).

Anal. Calcd. for $C_{16}H_{20}N_2O_8$ (368.4): C, 52.17; H, 5.47; N, 7.61. Found: C, 52.29; H, 5.65; N, 7.43.

The mother liquors obtained above were allowed to evaporate in the air and gave crystalline residues enriched in the fast-moving epimer **6***b′*. The residues were dissolved in cold butanone or chloroform, whereby small quantities of sparingly soluble material (slow-moving epimer) could be removed by filtration. Crystallization was then induced by careful addition of pentane or petroleum ether, and the fast-moving epimer (**6***b′*) separated as beautiful prisms, m.p. 196–197° (decomp.), $[\alpha]_D$ +23.2° (*c*, 0.8 in butanone). Occasionally another recrystallization was necessary to attain these constants.

Anal. Calcd. for $C_{16}H_{20}N_2O_8$ (368.4): C, 52.17; H, 5.47; N, 7.61. Found: C, 52.30; H, 5.60; N, 7.55.

The i.r. spectra of the two epimers were rather similar but could be distinguished by the nitro group frequencies (Table I) and by differences in position and intensity of several bands in the fingerprint region.

Methyl 4,6-O-Benzylidene-2,3-dideoxy-3-nitro-2-(1-nitropropyl)-β-D-galactopyranoside (6c)

Compound **5** (200 mg), 1-nitropropane (4 ml), and triethylamine (0.08 ml) gave a slightly-yellowish crude product which was decolorized in toluene solution with activated charcoal. The material recovered (323 mg, 89%) showed m.p. 170–174° and $[\alpha]_D$ +20.1° (in butanone), and t.l.c. revealed the presence of a main product accompanied by a slightly slower by-product. Recrystallization from ethyl acetate – petroleum ether gave 200 mg (77%) of product, m.p. 175–177°. After two further recrystallizations from chloroform–pentane the fine needles had m.p. 181° and $[\alpha]_D$ +23.0° (*c*, 1.0 in butanone), and these data remained unchanged although t.l.c. indicated that the by-product was still present.

Anal. Calcd. for $C_{17}H_{22}N_2O_8$ (382.4): C, 53.40; H, 5.80; N, 7.33. Found: C, 53.65; H, 5.90; N, 7.45.

Reactions with Diethyl Malonate

Methyl 4,6-O-Benzylidene-2,3-dideoxy-2-[bis(ethoxycarbonyl)]methyl-3-nitro-β-D-glucopyranoside (7)

A solution of **1** (200 mg) in diethyl malonate (3 ml) and triethylamine (4 ml) was stirred for 16 h at room temperature. The mixture was poured into ice-water (400 ml). After stirring for 30 min a white solid was isolated and washed very thoroughly, first with water and then with petroleum ether. The product, needles of m.p. 109–111°, was dried in a vacuum desiccator. The yield was 213 mg (83%), $[\alpha]_D$ −71.5° (*c*, 0.9 in chloroform).

Anal. Calcd. for $C_{21}H_{27}NO_{10}$ (453.5): C, 55.62; H, 6.00; N, 3.09. Found: C, 55.79; H, 6.17; N, 3.25.

Methyl 4,6-O-Benzylidene-2,3-dideoxy-2-[bis(ethoxycarbonyl)]methyl-3-nitro-β-D-galactopyranoside (8)

A solution of **5** (250 mg) in diethyl malonate (2 ml) and triethylamine (4 ml) was stirred at room temperature for 12 h, during which time partial crystallization occurred. The mixture was worked up as described for **7** and yielded 240 mg (62%) of needles exhibiting m.p. 164–166° and $[\alpha]_D$ +7.8° (*c*, 0.9 in chloroform).

Anal. Calcd. for $C_{21}H_{27}NO_{10}$ (453.5): C, 55.62; H, 6.00; N, 3.09. Found: C, 55.67; H, 6.13; N, 3.22.

Acknowledgment

Financial support of this work by the National Research Council of Canada (grant A 1350) is gratefully acknowledged.

1. H. H. Baer, F. Kienzle, and F. Rajabalee. Can. J. Chem. **46**, 80 (1968).
2. H. H. Baer and F. Kienzle. J. Org. Chem. **33**, 1823 (1968).
3. J. D. Dutcher. Advan. Carbohydrate Chem. **18**, 259 (1963).
4. D. J. Cooper and M. D. Yudis. Chem. Commun. 821 (1967).
5. S. W. Gunner, W. G. Overend, and N. R. Williams. Chem. and Ind. London, 1523 (1964).
6. H. H. Baer and G. V. Rao. Ann. **686**, 210 (1965).
7. K. S. Ong. Ph.D. Thesis. University of Ottawa. 1968.
8. H. H. Baer, T. Neilson, and W. Rank. Can. J. Chem. **45**, 991 (1967).
9. H. H. Baer and F. Kienzle. J. Org. Chem. **32**, 3169 (1967).
10. H. H. Baer and T. Neilson. J. Org. Chem. **32**, 1068 (1967).
11. E. D. Bergman, D. Ginsburg, and R. Pappo. Org. Reactions, **10**, 179 (1959).
12. H. Feuer and R. Miller. J. Org. Chem. **26**, 1348 (1961).
13. H. O. L. Fischer and H. H. Baer. Ann. **619**, 53 (1958).
14. H. H. Baer and W. Rank. Can. J. Chem. **43**, 3330 (1965).
15. H. H. Baer and F. Kienzle. Ann. **695**, 192 (1966).
16. H. H. Baer and T. Neilson. Can. J. Chem. **43**, 840 (1965).
17. H. Feuer, H. B. Hass, and K. S. Warren. J. Am. Chem. Soc. **71**, 3079 (1949).
18. H. H. Baer, F. Kienzle, and T. Neilson. Can. J. Chem. **43**, 1829 (1965).

Can. J. Chem. Downloaded from www.nrcresearchpress.com by 210.87.254.6 on 09/05/12
For personal use only.

Can. J. Chem. Downloaded from www.nrcresearchpress.com by 210.87.254.6 on 09/05/12
For personal use only.

Synthesis of substituted quinazolone hydrazides: the relationship between chemical structure and monoamine oxidase inhibitory activity[1]

SURENDRA S. PARMAR AND R. C. ARORA[2]

Department of Pharmacology and Therapeutics, King George's Medical College, Lucknow University, Lucknow 3, India

Received September 19, 1967

Several substituted quinazolone hydrazides were synthesized to investigate their ability to inhibit rat liver mitochondrial monoamine oxidase. The monoamine oxidase activity was measured manometrically as oxygen uptake during oxidative deamination of tyramine. All quinazolone hydrazides, except 2-methyl-3-(3′-benzhydrazide)-4-quinazolone and 2-methyl-6,8-diiodo-3-(4′-phenylacetylhydrazide)-4-quinazolone, inhibited monoamine oxidase activity when used at a final concentration of $3 \times 10^{-4}M$. Substitution at position-6 or positions-6 and -8 of the quinazolone nucleus increased enzyme inhibitory power of quinazolone hydrazides. Monosubstituted quinazolone hydrazides exhibited maximum inhibitory effects while disubstitution resulted in a decrease in their ability to inhibit monoamine oxidase.

Canadian Journal of Chemistry, 46, 2519 (1968)

Our continuing interest in incorporating a quinazolone nucleus, capable of exhibiting anticonvulsant (1) and hypnotic (2) properties, has led to the synthesis of substituted 2-methyl-3-(4′-benzhydrazide)-4-quinazolones as monoamine oxidase inhibitors (3). Monoamine oxidase [monoamine: O_2 oxidoreductase (deaminating) E.C.1.4.3.4.], an enzyme localized chiefly in the mitochondrial fractions of cells of many tissues and species and responsible for oxidative deamination of compounds having a terminal amino group including 5-hydroxytryptamine (serotonin), epinephrine, and norepinephrine, has been suggested to be of biological importance in the activity of the central nervous system (4, 5). Inhibitors of this enzyme have been shown to possess pronounced anticonvulsant properties (6). The discovery of iproniazid, 1-isonicotinyl-2-isopropyl hydrazine, a potent inhibitor of monoamine oxidase (7), and subsequent correlation of monoamine oxidase inhibition with antidepressant effects have resulted in the synthesis of a variety of compounds possessing monoamine oxidase inhibitory properties. The possibility of high π-electron density present in heterocyclic systems (8) responsible for enzyme inhibition led us to synthesize 2-methyl-3-(3′-benzhydrazide)-4-quinazolones and 2-methyl-3-(4′-phenylacetylhydrazide)-4-quinazolones in an attempt to obtain compounds affecting the activity of the central nervous system. Furthermore, Nakamura *et al.* (9) while considering activity relationship of phenylacetylhydrazides found that *N*-benzyl-*N*′-phenylacetylhydrazide was the most effective inhibitor of rat liver monoamine oxidase in both *in vitro* and *in vivo* experiments. In the present study several substituted quinazolone hydrazides have been synthesized and tested for their ability to inhibit rat liver mitochondrial monoamine oxidase. Structure activity relationships have been investigated briefly.

The various quinazolone hydrazides have been synthesized according to Scheme 1.

Experimental

Synthesis of Anthranilic Acids (1)

The following substituted anthranilic acids used in the present study were synthesized according to the methods reported in the literature: 5-chloroanthranilic acid (10), 5-bromoanthranilic acid (11), 5-iodoanthranilic acid (12), 3,5-dichloroanthranilic acid (10), 3,5-dibromoanthranilic acid (11), and 3,5-diiodoanthranilic acid (13).

Synthesis of Acetanthranils (2)

A mixture of appropriate anthranilic acid (1 mole) and acetic anhydride (2 moles) was refluxed for 1 h for the synthesis of acetanthranils. After the excess of acetic anhydride was distilled off, the acetanthranils separated out as solid masses and were used without further purification. The acetanthranils used in the present study have been reported earlier (3, 14).

Synthesis of Quinazolones (3)

The quinazolones were synthesized by heating equimolar proportions of the appropriate acetanthranils and *m*-aminoethyl benzoate or *p*-aminophenylethyl acetate

[1]This investigation was supported by a research grant from the Council of Scientific and Industrial Research, New Delhi, India. A preliminary report of this work was presented at the Fall Meeting of the American Society for Pharmacology and Experimental Therapeutics held at Washington, D.C. in August 1967.

[2]Senior Research Fellow of the Council of Scientific and Industrial Research, New Delhi, India.

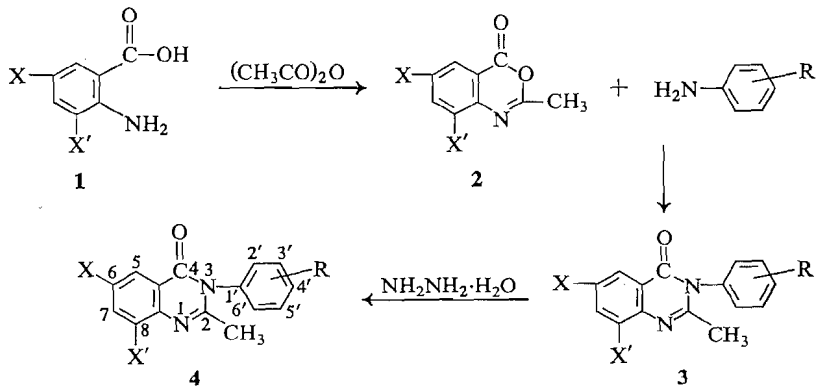

X and X′ = H, Cl, Br, or I
R = 3′-$COOC_2H_5$ or
4′-$CH_2COOC_2H_5$
R′ = 3′-$CONHNH_2$ or
4′-$CH_2CONHNH_2$

Scheme 1

TABLE I

Substituted 2-methyl-3-(3′-ethyl benzoate)-4-quinazolones*

X	X′	Melting point† °C	% yield	Formula	Nitrogen (%) Calculated	Found
H	H	125	55	$C_{18}H_{16}N_2O_3$	9.1	9.3
Cl	H	140	45	$C_{18}H_{15}ClN_2O_3$	8.1	7.9
Br	H	218	80	$C_{18}H_{15}BrN_2O_3$	7.3	7.3
I	H	195	65	$C_{18}H_{15}IN_2O_3$	6.5	6.6
Cl	Cl	188–190	40	$C_{18}H_{14}Cl_2N_2O_3$	7.4	7.4
Br	Br	145–147	42	$C_{18}H_{14}Br_2N_2O_3$	6.1	6.2
I	I	225	34	$C_{18}H_{14}I_2N_2O_3$	5.0	5.3

*Compounds of structure 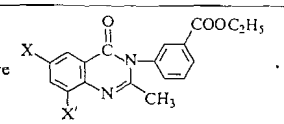

†Melting points were taken in open capillary tubes and are graphically corrected.

as reported earlier (15). The various 2-methyl-3-(3′-ethyl-benzoate)-4-quinazolones and 2-methyl-3-(4′-phenylethyl acetate)-4-quinazolones reported in Table I and Table III respectively were characterized by their sharp melting points and emperical compositions.

2-Methyl-6-chloro-3-(3′-ethyl benzoate)-4-quinazolone

A mixture of 6-chloroacetanthranil (1.95 g) and *m*-aminoethyl benzoate (1.65 g) was heated on the free flame for 10 min. On cooling the mixture 2-methyl-6-chloro-3-(3′-ethyl benzoate)-4-quinazolone separated out as a jelly-like mass. Recrystallization from ethanol yielded 1.54 g (45%) of the desired quinazolone melting at 140 °C.

Anal. Calcd. for $C_{18}H_{15}ClN_2O_3$: N, 8.1. Found: N, 7.9.

2-Methyl-6,8-dibromo-3-(4′-phenylethyl acetate)-4-quinazolone

On heating a mixture of 6,8-dibromoacetanthranil (3.18 g) and *p*-aminophenylethyl acetate (1.79 g) on a low free flame yielded 2.4 g (50%) of 2-methyl-6,8-dibromo-3-(4′-phenylethyl acetate)-4-quinazolone. On recrystallization from ethanol the quinazolone melted at 170–172 °C.

Anal. Calcd. for $C_{19}H_{16}Br_2N_2O_3$: N, 5.8. Found: N, 5.9.

Synthesis of Quinazolone Hydrazides (4)

The method of Buu-Hoi *et al.* (16) was used for the synthesis of substituted quinazolone hydrazides. A mixture of 1 mole of the appropriate quinazolone (3) was refluxed with 2 moles of hydrazine hydrate (99–100%) in absolute ethanol for 6–8 h. On distilling ethanol the quinazolone hydrazides separated out as solid masses. The physical constants of 2-methyl-3-(3′-benzhydrazide)-4-quinazolones and 2-methyl-3-(4′-phenylacetyl hydrazide)-4-quinazolones are recorded in Table II and Table IV respectively.

Can. J. Chem. Downloaded from www.nrcresearchpress.com by 210.87.254.6 on 09/05/12
For personal use only.

TABLE II

Substituted 2-methyl-3-(3′-benzhydrazide)-4-quinazolones*

X	X′	Melting point† °C	% yield	Formula	Nitrogen (%) Calculated	Found
H	H	115	60	$C_{16}H_{14}N_4O_2$	19.0	19.2
Cl	H	172	50	$C_{16}H_{13}ClN_4O_2$	17.0	17.1
Br	H	178–180	55	$C_{16}H_{13}BrN_4O_2$	15.4	15.4
I	H	180–182	45	$C_{16}H_{13}IN_4O_2$	13.4	13.7
Cl	Cl	229–230	35	$C_{16}H_{12}Cl_2N_4O_2$	15.4	15.6
Br	Br	219	37	$C_{16}H_{12}Br_2N_4O_2$	12.4	12.7
I	I	172–174	30	$C_{16}H_{12}I_2N_4O_2$	10.2	10.5

*Compounds of structure 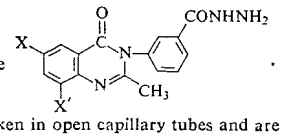

†Melting points were taken in open capillary tubes and are graphically corrected.

TABLE III

Substituted 2-methyl-3-(4′-phenylethyl acetate)-4-quinazolones*

X	X′	Melting point† °C	% yield	Formula	Nitrogen (%) Calculated	Found
H	H	110–113	50	$C_{19}H_{18}N_2O_3$	8.7	8.
Cl	H	140	60	$C_{19}H_{17}ClN_2O_3$	7.8	7.6
Br	H	142	55	$C_{19}H_{17}BrN_2O_3$	7.0	7.3
I	H	155	65	$C_{19}H_{17}IN_2O_3$	6.3	6.5
Cl	Cl	158–160	45	$C_{19}H_{16}Cl_2N_2O_3$	7.2	7.0
Br	Br	170–172	50	$C_{19}H_{16}Br_2N_2O_3$	5.8	5.9
I	I	225–228	40	$C_{19}H_{16}I_2N_2O_3$	4.8	4.7

*Compounds of structure 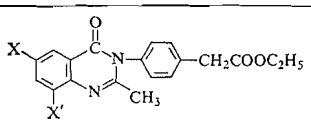

†Melting points were taken in open capillary tubes and are graphically corrected.

2-Methyl-6,8-dichloro-3-(3′-benzhydrazide)-4-quinazolone

A mixture of 2-methyl-6,8-dichloro-3-(3′-ethylbenzoate)-4-quinazolone (3.77 g) and 8 ml of hydrazine hydrate was refluxed in 50 ml of absolute ethanol for 8 h. After distilling off the ethanol 1.27 g (35%) of 2-methyl-6,8-dichloro-3-(3′-benzhydrazide)-4-quinazolone separated out as a solid mass. On recrystallization from ethanol the quinazolone melted at 229–230 °C.

Anal. Calcd. for $C_{16}H_{12}Cl_2N_4O_2$: N, 15.4. Found: N, 15.6.

2-Methyl-6-bromo-3-(4′-phenylacetylhydrazide)-4-quinazolone

On refluxing a mixture of 2-methyl-6-bromo-3-(4′-phenylethyl acetate)-4-quinazolone (4.01 g) and 10 ml of hydrazine hydrate in 50 ml of absolute ethanol for 10 h and distilling off ethanol yielded 2.7 g (70%) of 2-methyl-6-bromo-3-(4′-phenylacetylhydrazide)-4-quinazolone as a solid mass. The quinazolone on recrystallization from ethanol melted at 188 °C.

Anal. Calcd. for $C_{17}H_{15}BrN_4O_2$: N, 14.5. Found: N, 14.7.

Isolation of Rat Liver Mitochondria

Adult rats weighing 150–200 g, kept on *ad libitum* diet, were used in all experiments. Rat livers isolated from decapitated animals were immediately homogenized in ice-cold 0.25 *M* sucrose with the help of a Potter–Elvehjem homogenizer. Rat liver mitochondria were isolated by differential centrifugation of 10% (w/v) liver homogenate by the method of Hogeboom *et al.* (17) as modified by Hawkins (18). These particles were washed three times with cold 0.25 *M* sucrose (19) and suspended in the same concentration of sucrose so that 1 ml of the suspension was equivalent to 1 g of the fresh liver weight.

Determination of Monoamine Oxidase Activity

Standard Warburg manometric procedure was used for determination of rat liver mitochondrial monoamine oxidase activity. The rate of the oxygen uptake during oxidative deamination of tyramine, as the substrate, was taken as a measure of the enzyme activity (20). Rat liver mitochondria in 0.3 ml of sucrose suspension were incubated in 66 m*M* phosphate buffer, pH 7.4, at 37 °C in

Can. J. Chem. Downloaded from www.nrcresearchpress.com by 210.87.254.6 on 09/05/12
For personal use only.

TABLE IV

Substituted 2-methyl-3-(4′-phenylacetylhydrazide)-4-quinazolones*

X	X′	Melting point† °C	% yield	Formula	Nitrogen (%) Calculated	Found
H	H	98–100	60	$C_{17}H_{16}N_4O_2$	18.2	18.3
Cl	H	165–168	55	$C_{17}H_{15}ClN_4O_2$	16.4	16.6
Br	H	188	70	$C_{17}H_{15}BrN_4O_2$	14.5	14.7
I	H	175	65	$C_{17}H_{15}IN_4O_2$	12.9	12.7
Cl	Cl	194–195	50	$C_{17}H_{14}Cl_2N_4O_2$	14.8	14.5
Br	Br	208–209	55	$C_{17}H_{14}Br_2N_4O_2$	12.0	12.0
I	I	168–170	45	$C_{17}H_{14}I_2N_4O_2$	10.0	9.8

*Compounds of structure 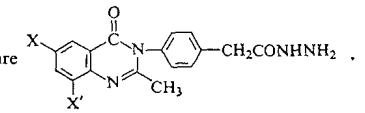 .

†Melting points were taken in open capillary tubes and are graphically corrected.

a total volume of 3 ml using tyramine at a final concentration of 10 m*M*. All the experiments were conducted in Warburg vessels using oxygen as the gas phase. The various quinazolone hydrazides were added to the main vessel, containing mitochondrial suspension, from a side arm 10 min prior to the addition of tyramine from the second side arm. The mixture was incubated for an additional hour and readings of the oxygen uptake were recorded at 10 min intervals.

Results and Discussion

The ability of various 2-methyl-3-(3′-benzhydrazide)-4-quinazolones and 2-methyl-3-(4′-phenylacetylhydrazide)-4-quinazolones to inhibit rat liver mitochondrial monoamine oxidase was investigated and the results are shown in Table V. In the present study the oxygen uptake, measured as an index of monoamine oxidase activity during oxidative deamination of tyramine, has been reported to reveal true enzyme activity in washed rat liver mitochondrial preparations (19, 21). The use of cyanide and semicarbazide suggested earlier for manometric measurements of the oxygen uptake for enzyme activity (20) was not necessary in the present experiments. The sensitization of monoamine oxidase by cyanide (22) while determining the inhibitory effects of newer quinazolone hydrazides was thus avoided in the present investigation. As is evident from Table V all quinazolone hydrazides, except 2-methyl-3-(3′-benzhydrazide)-4-quinazolone and 2-methyl-6,8-diiodo-3-(4′-phenylacetylhydrazide)-4-quinazolone, inhibited monoamine oxidase activity. All quinazolone hydrazides were used at a final concentration of $3 \times 10^{-4} M$ to determine the relative percentage of their enzyme inhibitory activities. These quinazolone hydrazides, however, exhibited lower inhibitory effects when compared to iproniazid, pheniprazine, and tranylcypromine, the well known monoamine oxidase inhibitors (19). The most active quinazolone hydrazide, 2-methyl-6-iodo-3-(4′-phenylacetylhydrazide)-4-quinazolone, was found to be approximately 10 times less active than iproniazid. Iproniazid has been reported to produce 81.9% inhibition when used at a final concentration of $3 \times 10^{-5} M$ under similar experimental conditions (19).

The degree of enzyme inhibition was found to be significantly enhanced by the introduction of a substituent at position-6 of the quinazolone nucleus where relative electronegativity of the 6-substituents presumably appears to be a factor responsible for the inhibitory power of these quinazolone hydrazides (Table V). In both series of compounds 6-iodo substituted quinazolone hydrazides i.e. 2-methyl-6-iodo-3-(3′-benzhydrazide)-4-quinazolone and 2-methyl-6-iodo-3-(4′-phenylacetylhydrazide)-4-quinazolone, exhibited maximum inhibitory effects. Amongst these hydrazides greater inhibition of monoamine oxidase was observed with 2-methyl-3-(4′-phenylacetylhydrazide)-4-quinazolones. In a similar study replacement of the amine group with the hydrazide moiety has been shown by Biel *et al.* (23) to result in the retention of the activity and an increase in their monoamine oxidase inhibitory properties. The inability of 2-methyl-3-(3′-benzhydrazide)-4-quinazolone to inhibit monoamine oxidase activity reflects its similarity to isoniazid (isonicotinic acid hydrazide) which

Can. J. Chem. Downloaded from www.nrcresearchpress.com by 210.87.254.6 on 09/05/12
For personal use only.

TABLE V

Monoamine oxidase inhibitory activity* of substituted quinazolone hydrazides†

X	X′	R′	Monoamine oxidase inhibition %
H	H	3′-$CONHNH_2$	Nil
Cl	H	3′-$CONHNH_2$	52.9 51.0(51.7) 53.7
Br	H	3′-$CONHNH_2$	56.2 55.5(55.1) 53.7
I	H	3′-$CONHNH_2$	60.5 60.6(59.1) 56.3
Cl	Cl	3′-$CONHNH_2$	24.4 24.5(24.3) 24.0
Br	Br	3′-$CONHNH_2$	28.9 29.2(29.7) 31.3
I	I	3′-$CONHNH_2$	24.0 23.5(23.8) 23.8
H	H	4′-$CH_2CONHNH_2$	26.5 26.2(26.4) 26.4
Cl	H	4′-$CH_2CONHNH_2$	75.7 70.0(72.8) 72.6
Br	H	4′-$CH_2CONHNH_2$	75.8 78.1(76.4) 75.3
I	H	4′-$CH_2CONHNH_2$	77.8 76.8(77.3) 77.4
Cl	Cl	4′-$CH_2CONHNH_2$	28.7 31.8(29.5) 28.0
Br	Br	4′-$CH_2CONHNH_2$	33.1 32.3(33.4) 34.7
I	I	4′-$CH_2CONHNH_2$	1.3 1.5(1.6) 2.0

*The vessel contents and the assay procedure are as described in the Experimental section. The percentage inhibition was calculated from the decrease in the oxygen uptake during 1 h. Washed mitochondria equivalent to 300 mg wet tissue weight were used in each Warburg vessel. The oxygen uptake in control experiments without quinazolone hydrazides ranged between 10.2–12.8 μmoles/h. The quinazolone hydrazides were used at a final concentration of 3×10^{-4} *M*. Each experiment was done in duplicate and the mean values for the oxygen uptake were recorded. The figures in parentheses are averages of three separate experiments.

†Compounds of structure 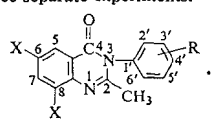 .

Can. J. Chem. Downloaded from www.nrcresearchpress.com by 210.87.254.6 on 09/05/12
For personal use only.

has also been reported to be devoid of enzyme inhibitory activity (24). These results provide further evidence towards the involvement of primary and secondary sites on the enzyme molecule which are essentially involved in the formation of an enzyme-substrate or enzyme-inhibitor complex. The greater inhibition observed with 6-substituted derivatives could presumably account for the attachment of the inhibitor to the secondary site in addition to the essential primary one by the hydrazide group. The primary site is essentially involved through the amine moiety for the formation of the enzyme-substrate complex (19). Thus greater inactivation of the enzyme activity could be achieved by the attachment of the inhibitor to two or more sites on the enzyme molecule (19, 21). The greater affinity of the iodo-substituted benzylamines as the substrates for monoamine oxidase (25) could in some way bear relationship towards greater enzyme inhibition observed with 2-methyl-6-iodo-3-(3′-benzhydrazide)-4-quinazolone and 2-methyl-6-iodo-3-(4′-phenylacetylhydrazide)-4-quinazolone. As is evident from Table V introduction of an additional substituent at position-8 of the quinazolone nucleus resulted in significant decrease in the enzyme inhibitory activity as compared to the monosubstituted quinazolone hydrazides. At present it is difficult to provide any suitable explanation for lower inhibitory effects of such 2,3,6,8-tetrasubstituted quinazolone hydrazides, which, however, exhibited slightly higher inhibitory activity as compared to 2,3-disubstituted quinazolone hydrazides. The competition between substituents at positions-6 and -8 of the quinazolone nucleus for the secondary site on the enzyme molecule could presumably account for lower inhibition observed with such 2,3,6,8-tetrasubstituted quinazolone hydrazides. Our further studies dealing with the synthesis of other related structures carrying different substituents and determination of their nature of enzyme inhibition using purified soluble enzyme preparations may prove of significant value towards elucidation of the chemical requirements of the active centers of monoamine oxidase.

Acknowledgments

The authors wish to express their thanks to Professor K. P. Bhargava and Mr. K. Kishor for their advice and encouragement. Grateful acknowledgment is made to Drs. M. L. Dhar and Nitya Anand of Central Drug Research Institute, Lucknow for providing microanalysis facilities and to the Riker Laboratories, Northridge, California for the supply of research chemicals.

1. M. L. Gujral, P. N. Saxena, and R. P. Kohli. Indian J. Med. Res. **45**, 207 (1957).
2. M. L. Gujral, R. P. Kohli, and P. N. Saxena. J. Assoc. Physicians India, **2**, 29 (1955).
3. S. S. Parmar and R. C. Arora. Can. J. Chem. **44**, 2100 (1966).
4. E. A. Zeller. Pharmacol. Rev. **11**, 387 (1959).
5. B. Belleau. *In* Adrenergic mechanisms. A CIBA Foundation symposium. *Edited by* J. R. Vane, G. E. Wolstenholme, and M. O'Cooner. Churchill, London. 1960 p. 223.
6. D. J. Prockop, P. A. Shore, and B. B. Brodie. Ann. N.Y. Acad. Sci. **80**, 643 (1959).
7. E. A. Zeller, J. Barsky, and E. R. Berman. J. Biol. Chem. **214**, 267 (1955).
8. C. J. Paget and C. S. Davis. J. Med. Chem. **7**, 626 (1964).
9. K. Nakamura, Y. Masuda, H. Tatsumi, and K. Fujimoto. Japanese J. Pharmacol. **13**, 186 (1963).
10. M. M. Endicott, B. B. Alden, and M. L. Sherrill. J. Am. Chem. Soc. **68**, 1303 (1946).
11. A. S. Wheeler and W. M. Oats. J. Am. Chem. Soc. **32**, 770 (1910).
12. C. J. Klemme and J. H. Hunter. J. Org. Chem. **5**, 227 (1940).
13. V. H. Wallingford, H. G. Decker, and M. Kruty. J. Am. Chem. Soc. **74**, 4365 (1952).
14. S. S. Parmar and R. C. Arora. J. Med. Chem. **10**, 1182 (1967).
15. K. Kishor, R. C. Arora, and S. S. Parmar. J. Med. Chem. **8**, 550 (1965).
16. Ng. Ph. Buu-Hoi, Ng. D. Xuong, Ng. H. Nam, E. Binnon, and R. Rover. J. Chem. Soc. 1358 (1953).
17. G. H. Hogeboom, W. C. Schneider, and G. E. Palade. J. Biol. Chem. **172**, 619 (1948).
18. J. Hawkins. Biochem. J. **50**, 577 (1952).
19. S. S. Parmar. Biochem. Pharmacol. **15**, 1497 (1966).
20. N. H. Creasey. Biochem. J. **64**, 178 (1956).
21. S. S. Parmar. *In* Symposium on CNS drugs. C.S.I.R. Publication. Regional Research Laboratory, Hyderabad, India. 1966. p. 198.
22. M. C. Pant, S. S. Parmar, and K. P. Bhargava. Can. J. Biochem. **42**, 1114 (1964).
23. J. H. Biel, A. E. Drukker, P. A. Shore, S. Spector, and B. B. Brodie. J. Am. Chem. Soc. **80**, 1519 (1958).
24. E. A. Zeller. *In* Metabolic inhibitors. Vol. II. *Edited by* R. M. Hochster and J. H. Quastel. Academic Press, New York. 1963. p. 53.
25. E. A. Zeller. Ann. N. Y. Acad. Sci. **107**, 811 (1963).

Can. J. Chem. Downloaded from www.nrcresearchpress.com by 210.87.254.6 on 09/05/12
For personal use only.

Can. J. Chem. Downloaded from www.nrcresearchpress.com by 210.87.254.6 on 09/05/12
For personal use only.

Isolation, structure, and synthesis of a stilbene glucoside from the bark of *Picea glauca* (Moench) Voss.

D. H. ANDREWS,[1] J. C. HOFFMAN,[2] AND C. B. PURVES[3]
Division of Industrial and Cellulose Chemistry, McGill University, Montreal, Quebec

AND

H. H. QUON[4] AND E. P. SWAN[5]
Canada Department of Forestry and Rural Development, Forest Products Laboratory, Vancouver 8, British Columbia

Received January 22, 1968

The fractionation of phlobaphenes from white spruce bark by column chromatography gave the non-crystalline stilbene glucoside *trans* 3,4′5-trihydroxy-3′-methoxystilbene-3-*O*-β-D-glucopyranoside (**1**). Purification was achieved through deacetylation of its hexaacetate (**2**). Compound **1** was cleaved with emulsin or dilute acid to the aglycone **4**, and D-glucose. The acetate, benzoate, and dihydro-derivatives of **1**, and the acetate, benzoate, methyl ether, and dihydro-derivatives of **4** were prepared. Oxidation of the benzoate derivative of **1** with chromic acid gave dibenzoyl-α-resorcylic acid. Similar oxidation of **2** gave acetylvanillic acid together with an uncharacterized acid which was hydrolyzed to D-glucose and α-resorcylic acid. The structure of **1** was therefore as shown, and its derivative **2** was synthesized. Vanillin was condensed with 3,5-dihydroxyphenylacetic acid and the product was decarboxylated and deacetylated. This compound was condensed with tetra-*O*-acetyl-α-D-glucopyranosyl bromide to yield a mixture of products which, after acetylation, were separated, using preparative thin-layer chromatography, to give the desired **2**.

Canadian Journal of Chemistry, **46**, 2525 (1968)

Introduction

At present, bark is a major waste product in the pulp and paper industry. Not only does it possess little commercial value, but it also provides a difficult disposal problem. One object of this research is to discover whether materials of potential value are present in the bark in sufficient amounts to justify their extraction on a large scale.

In particular, stilbene derivatives have been found in the bark of *Picea* species (1). One of these was piceatannol (2, 3) in *P. excelsa*. This research describes the isolation, characterization, and synthesis of a stilbene glucoside which was not derived from piceatannol. Subsequent to part of this work, this product was isolated by Manson (4).

Discussion of Results

Harwood (5) undertook an extraction, on a pilot-plant scale, of a large quantity of white spruce bark. By using various solvents and precipitants he separated the methanol-soluble extractives into fractions, one of which was material insoluble in water, ether, and ligroin, comprising 1.5% of the original bark. After considerable effort, it was shown that 16% of this material (0.24% of the bark) was compound **1**. The best method of isolation was by Magnesol column chromatography using acetone as the eluant. The removal of the last traces of phlobaphenes was extraordinarily difficult, and since **1** was not obtained crystalline, it was converted to the crystalline acetate derivative **2**, and this in turn was deacetylated. Both **1** and **2** were acid and base labile. The best method of cleaving **1** to the aglycone **4** was by heating with dilute oxalic acid, and the best method of deacetylating **2** was a modified barium methylate-catalyzed methanolysis.

The structure **1** for the product isolated from

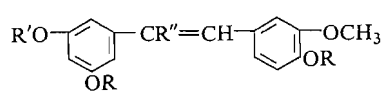

1 R = R″ = H, R′ = β-D-glucopyranosyl
2 R = $COCH_3$, R′ = β-D-glucopyranosyl tetraacetate, R″ = H
3 R = R′ = $COCH_3$, R″ = COOH
4 R = R′ = R″ = H

[1]Present address: Central Research Laboratory, Canadian Industries Ltd., McMasterville, Quebec.
[2]Present address: Department of Theology, University of Windsor, Windsor, Ontario.
[3]Deceased.
[4]Present address: Department of Chemistry, Simon Fraser University, Burnaby, British Columbia.
[5]To whom correspondence should be addressed.

Can. J. Chem. Downloaded from www.nrcresearchpress.com by 210.87.254.6 on 09/05/12
For personal use only.

the bark was supported by analytical data for it, and its acetyl derivative **2**. Similarly, the aglycone **4** and its triacetate, tribenzoate, and tri-*O*-methyl ether were analytically defensible. The ultraviolet (u.v.) spectra of these products were very similar to those from *trans* stilbenes (6). Compounds **1** and **4** each consumed a mole equivalent of hydrogen to yield the expected products, and the dihydro-derivative of **4** had the expected u.v. spectrum. Treatment of **1** with emulsin yielded D-glucose and **4**, indicating the β-glucoside configuration. Oxidation of the benzoate of **1** as well as **2** with chromic acid gave the appropriate derivatives of α-resorcylic and vanillic acids. Finally, the oxidation of **2** gave an acid which in turn could be cleaved to α-resorcylic acid and D-glucose. This placed the carbohydrate on the resorcinol moiety rather than the guaiacol moiety of **1**, which was therefore *trans* 3,4′,5-trihydroxy-3′-methoxystilbene-3-*O*-β-D-glucopyranoside.

Unfortunately, the structural diagram given for the present stilbene glucoside (**1**) in the previous publication (4) is incorrect and shows rhapontin. The two compounds are not identical, as can be seen by comparison of physical constants found here and given by Kawamura for rhapontin (7). In particular, **2** melted at 162–163 °C and rhapontin hexaacetate melted at 135–136 °C.

The synthesis of **2** was similar to the synthesis of 3,3′,4′,5-tetrahydroxystilbene by Cunningham, Haslam, and Haworth (2). 3,5-Dihydroxyphenylacetic acid was condensed with vanillin under Perkin reaction conditions to give **3** which was deacetylated and decarboxylated to the aglycone **4**. This latter reaction gave low yields, probably because of concurrent demethylation. The isolation of the product was facilitated by the use of polyamide columns (8) rather than silica gel. The aglycone (**4**) was condensed with tetra-*O*-acetyl-α-D-glucopyranosyl bromide in a Koenigs–Knorr reaction. The reaction was monitored by thin-layer chromatography (t.l.c.) and the desired product, from reaction of the glucosyl moiety with the resorcinol ring, was identified and separated by preparative t.l.c., from the other major product which resulted from similar substitution on the guaiacol ring. It was easy to differentiate the former from the latter because, for mono-substitution, there was much more of the former produced. The desired product was then acetlyated to give **2**, mixture m.p. undepressed, and with u.v. and infrared spectra, together with t.l.c. behavior, all identical with the original **2**.

Experimental

Melting points are uncorrected. Elemental analyses in the synthetic work only, were performed by Clark Microanalytical Laboratory, Urbana, Illinois. Paper chromatography was performed on Whatman No. 1 paper using the organic phase of butanol – acetic acid – water (4:1:5) as a developing solvent.

Isolation of the Stilbene Glucoside (1)

The phlobaphene obtained from Harwood (5) was dried in a vacuum desiccator over phosphorus pentoxide for several days, and then extracted exhaustively with ether. One hundred grams of the product were extracted with acetone. The extract was not concentrated, but was applied as obtained to a short column (95 × 70 mm), consisting of a sintered glass funnel of Magnesol and operated under suction. Elution with 4500 ml of acetone required approximately 1 h. The acetone extracts yielded 15.6 g of slightly colored material which showed as **1** on a paper chromatogram.

Reactions of the Stilbene Glucoside (1)

Stilbene glucoside (**1**) was a yellow-white amorphous powder. It produced a characteristic fluorescent spot on a paper chromatogram, R_f 0.40; $[\alpha]_D^{21}$ −54.1° (*c*, 2 in acetone). Found: OCH_3, 7.33, 7.34. Ultraviolet (u.v.) spectrum (methanol): λ_{max} 325, shoulder at 300 mμ (log ε 4.22 and 4.06).

Compound **1** (1.0 g) in pyridine (10 ml) was reacted with acetic anhydride (4 ml) for three days at room temperature. The reactants were poured into water to yield (crystallized from hot methanol) compound **2**, 1.35 g of white needles, m.p. 162–163 °C, $[\alpha]_D^{20}$ −22.6° (*c*, 2 in acetone). Ultraviolet spectrum (methanol): λ_{max} 300 and 315 mμ (log ε of both 4.37).

Anal. Calcd. for $C_{20}H_{15}O_8$ $(COCH_3)_6(OCH_3)$, (mol. wt., 672): C, 58.9; H, 5.36; OCH_3, 4.61; acetyl, 38.4. Found (mol. wt., 635, 654; Rast): C, 58.8, 59.1; H, 5.50, 5.54; OCH_3, 4.54, 4.60; acetyl, 38.1, 39.4.

Hydrogenation of **2** was carried out in acetic acid (3 ml) with palladium–charcoal in the Siggia (9) apparatus. Duplicate estimations showed the uptake of 1.08 and 0.97 moles of hydrogen per mole of **2**. The product was recrystallized from ethanol. The white needles, 0.105 g had m.p. 94–95.5 °C.

Anal. Calcd. for $C_{20}H_{17}O_8$ $(CH_3CO)_6(OCH_3)$: acetyl, 38.3; OCH_3, 4.60. Found: acetyl, 37.9, 37.5; OCH_3, 4.3, 4.5.

Compound **1** was methylated repeatedly with ethereal diazomethane. The product had R_f 0.66. Attempts to crystallize the product were not successful.

Hydrolyses

A sample of **2** (0.9 g) dissolved in anhydrous methanol (50 ml) was added to barium methylate in methanol (10 ml of 0.69 *N*). A yellow precipitate formed immediately. The reaction mixture was kept at about 5 °C with occasional shaking for 5 h. The precipitate was separated from

Can. J. Chem. Downloaded from www.nrcresearchpress.com by 210.87.254.6 on 09/05/12
For personal use only.

the supernatant liquid by filtration, and was washed with anhydrous methanol. The precipitate was then added to a mixture of dry ice and water, and the barium carbonate formed was separated by filtration. The filtrate was evaporated under reduced pressure to dryness, and an acetone extract of the dry residue (made at room temperature) was again evaporated to dryness. The residue was taken up in *n*-butanol and the product recovered in the usual way. The material was nearly white in color. Chromatographic analysis showed the presence of **1** with very little impurity; yield, 0.40 g. Found: acetyl, 0.7, 0.9. The product (34 mg) was re-acetylated. This product had m.p. 162–163 °C and a mixture m.p. with **2** was not depressed.

Compound **1** (2.0 g) was added to oxalic acid solution (100 ml of 1%) and the mixture was warmed. After 1 h the material was still not completely dissolved. After a further hour of heating on the steam cone, a chromatogram showed two spots of R_f 0.47 and 0.78. The hydrolysate was extracted overnight with chloroform, and chromatography of the chloroform extract showed the spot, R_f 0.79, of **4** while that of the aqueous residue retained a strong spot for compound **1** plus a faint spot for the aglycone. A brown solid which had again formed in the still for the chloroform was recovered and dried. This process was repeated five more times, the length of the heating period being increased gradually. A total of 0.563 g of crude aglycone (**4**) was obtained. The above procedure was repeated four times until 2.65 g of crude **4** had been accumulated.

The aqueous residue was treated with a slight excess of calcium hydroxide, and the calcium oxalate which precipitated was removed by filtration. The excess calcium hydroxide was removed by shaking the filtrate with IR 120. The filtrate was clarified and then it was mixed with phenylhydrazine hydrochloride and sodium acetate, in excess, and heated on a water bath. Yellow crystals of glucosazone were separated, m.p. 204–205 °C (decomposed). The product (0.2 g) was mixed with water (18 ml), sulfuric acid (1 ml of 0.5 *N*), copper sulfate pentahydrate (0.6 g), and isopropanol (12 ml). The solution was heated under reflux for 1 h, then it was concentrated to about 5 ml with the formation of brown-colored crystals. These were recrystallized from water to give white needles, m.p. 195–196 °C, mixture m.p. with the osatriazole (11) prepared from D-glucose showed no depression.

Emulsin (25 mg) was dissolved in distilled water (50 ml) containing compound **1** (300 mg). After the reaction mixture had been left at room temperature for 22 h, a determination of copper reducing power, carried out according to the Somogyi method (10) on a 0.5 ml aliquot, was equivalent to 1.07 mg of D-glucose. After 45 h this value had increased to 1.22 mg. Since the theoretical amount of D-glucose present on complete hydrolysis would be 1.28 mg for a 0.5 ml aliquot (assuming a molecular weight of 420 for **1**) the hydrolysis was considered to be complete. Chromatographic analysis of the hydrolysate showed that an appreciable amount of compound **1** (R_f 0.40) was still present. In addition, a new spot (R_f 0.79) was observed which produced the same fluorescence as compound **1**. The reaction mixture was therefore extracted continuously for several hours with chloroform, during which time material crystallized out on the flask at the surface of the chloroform. The addition of petroleum ether until the chloroform solution became slightly turbid, caused material (**4**) to separate in the form of flaky brown crystals, 150 mg.

Reactions of the Aglycone (4)

Purification was by recrystallization from ethyl acetate–petroleum ether. The recrystallized aglycone was in the form of near-white clusters, optically inactive, m.p. 182–183 °C. Ultraviolet spectrum (methanol): λ_{max} 325 and shoulder at 300 mμ (log ε 4.37 and 4.27).

Anal. Calcd. for $C_{14}H_{11}O_3(OCH_3)$, (mol. wt., 258): C, 69.7; H, 5.46; OCH_3, 12.0. Found (mol. wt., 251; Rast): C, 69.7, 69.7; H, 5.62, 5.65; OCH_3, 11.9, 12.0.

The aglycone in ethanol was hydrogenated with palladium–charcoal catalyst in the apparatus described by Siggia (9). Hydrogen consumed was equivalent to 0.93 and 0.95 moles per mole of aglycone. The reaction mixtures from these hydrogenations were filtered to remove the catalyst, and the filtrates from two runs, containing originally 72 mg of aglycone, were combined. After evaporation of the solvent, the residue was crystallized from benzene to yield white needles, m.p. 152–153.5 °C. Ultraviolet spectrum (methanol): λ_{max} 280 mμ (log ε 3.64).

Anal. Calcd. for $C_{14}H_{10}(OH)_3(OCH_3)$: C, 69.2; H, 6.20; OCH_3, 11.9. Found: C, 69.5, 69.2; H, 6.25, 6.47; OCH_3, 11.8, 11.7.

The aglycone (0.1 g) was dissolved in pyridine (3 ml) – acetic anhydride (2 ml) and the reaction mixture was left at room temperature overnight. The reaction mixture was worked up as usual and the product was recrystallized from ethanol–water to yield the triacetate of **4** as coarse needles, m.p. 103–104 °C. Ultraviolet spectrum (methanol): λ_{max} 315 with shoulder at 300 mμ (log ε 4.35 and 4.34).

Anal. Calcd. for $C_{14}H_8O_3(C_2H_3O)_3(OCH_3)$: OCH_3, 8.08; acetyl, 33.6. Found: OCH_3, 7.96, 7.91; acetyl, 33.1, 34.0.

The aglycone (0.1 g) was dissolved in anhydrous pyridine (2 ml) and benzoyl chloride (0.5 ml). The reaction mixture was warmed over a low flame for 1 min, and then poured into cold water (20 ml). The product, the tribenzoate of **4**, was worked up as above and was recrystallized from a chloroform–ethanol mixture to needles, yield 0.16 g, m.p. 108.5–110 °C.

Anal. Calcd. for $C_{14}H_8O_3(C_6H_5CO)_3(OCH_3)$: C, 75.8; H, 4.59; OCH_3, 5.44. Found: C, 75.4, 75.3; H, 5.02, 4.95; OCH_3, 5.40, 5.62.

Dimethyl sulfate (2 ml) was added to a solution of the aglycone (0.2 g) in ethanol (2 ml). A solution of sodium hydroxide (40%) was added, in drops, until the reaction mixture was alkaline. The mixture was cooled and it was diluted with water, whereupon a golden-yellow oil separated, and after several days the tri-*O*-methyl ether of **4** crystallized as pale-yellow clusters of needles, yield 0.10 g, m.p. 66.5–68 °C. Ultraviolet spectrum (methanol): λ_{max} 320 and shoulder at 305 mμ (log ε 4.31 and 4.28).

Anal. Calcd. for $C_{14}H_8(OCH_3)_4$: C, 72.0; H, 6.66; OCH_3, 41.3. Found: C, 72.1, 72.1; H, 6.73, 6.80; OCH_3, 40.3, 40.6.

Oxidations

The aglycone benzoate (1.1 g) was dissolved in acetic acid (50 ml) and maintained at 60–70 °C. Chromium trioxide (1.8 g) dissolved in acetic acid (60 ml) was slowly added to the solution over a period of 1 h. After the reaction was complete, a small volume of methanol was

Can. J. Chem. Downloaded from www.nrcresearchpress.com by 210.87.254.6 on 09/05/12
For personal use only.

added. The reaction mixture was evaporated almost to dryness under reduced pressure, then mixed with water (100 ml) and extracted four times with ether in a separatory funnel. The ether solution was washed twice with hydrochloric acid (5%), then twice with water, and finally it was dried over anhydrous sodium sulfate. Evaporation of the ether left crude, yellow crystals, which were recrystallized from acetic acid to yellow-white crystals, yield 0.185 g, m.p. 224–232 °C. α-Resorcylic acid was synthesized (12) and benzoylated. The product had m.p. 231–233 °C, mixture m.p. undepressed with the above. Their X-ray powder diffraction spectra were identical.

Compound **2** (2.65 g) was dissolved in acetic acid (100 ml) and the solution was heated in a water bath to about 63–64 °C. Chromium trioxide (3.0 g) dissolved in acetic acid (200 ml) was added with stirring over a period of 1 h. The mixture was worked up as described above to yield the ether extract which was extracted with 6% aqueous sodium bicarbonate solution. The bicarbonate extract was acidified to liberate organic acids and then re-extracted with ether; this ether extract was dried over anhydrous sodium sulfate. After being filtered, the ether extract was evaporated to dryness and the resultant oil kept *in vacuo* for three days, until partial crystallization occurred, and the uncrystallized portion was removed by washing quickly with ethanol (15 ml) and filtering. The product was recrystallized from ethanol to yield yellow-white crystals, 0.43 g, m.p. 189–191 °C. The product (0.43 g) was dissolved in water (10 ml) containing sodium hydroxide (250 mg). After standing at room temperature for 2 h, the solution was neutralized with sulfuric acid (10 ml of 5%) and it was heated under reflux for 2 h. The mixture was then cooled to room temperature, saturated with sodium chloride, and extracted with ether. The ether extract was dried and evaporated to yield 0.10 g of crude product, m.p. 221–229 °C. When recrystallized from acetic acid, the product had m.p. 237–239 °C, and showed no depression in m.p. when admixed with synthetic α-resorcylic acid. The aqueous layer was deionized and examined by paper chromatography. Only one spot with the characteristic color reactions and R_f value of D-glucose was found.

The ethanol reserved from the uncrystallized portion of the original product yielded an oil on evaporation. This oil partially dissolved in hot water, leaving a dark-brown gum which was removed on the filter. The filtrate deposited a fluffy white solid (100 mg) which after three recrystallizations from ethanol had m.p. 138–143 °C (acetylvanillic acid melted at 145–147 °C). The water-insoluble gum was dissolved in ethanol (10 ml) and water (5 ml) and barium hydroxide octahydrate (2 g) was added. The mixture was allowed to stand at room temperature overnight. The brown precipitate which formed was removed on a filter and was dissolved in dilute hydrochloric acid. The acidified solution was filtered and extracted with ether. When dried and evaporated, the ether extract yielded 0.10 g of product, m.p. 198.5–203 °C, raised to 206–208 °C by recrystallization from water, mixture m.p. with vanillic acid 207–209 °C. A sample of this product was acetylated. The acetate had m.p. 147–149 °C, mixture m.p. with acetylvanillic acid undepressed. The X-ray patterns of vanillic acid and the isolated acid, m.p. 206–208 °C, were taken and proved to be identical.

*3,4′,5-Triacetoxy-3′-methoxystilbene-α-carboxylic acid (**3**)*

Sodium 3,5-dihydroxyphenylacetate (5.9 g), vanillin (4.2 g) and acetic anhydride were heated in a sealed tube for 8 h at about 175 °C. The mixture was cooled and poured into ice water (500 g). The viscous brown oil which separated was washed with water and then dissolved in ethyl acetate (200 ml). Acidification of the sodium bicarbonate extract of the ethyl acetate yielded 0.5 g of the product, m.p. 220–221 °C, recrystallized from methanol. Ultraviolet spectrum (ethanol): λ_{max} 283 and 310 mμ (log ε 4.38 and 4.18). Infrared (i.r.) spectrum (KBr): ν_{max} 1770, 1680, 1615 cm^{-1}.

Anal. Calcd. for $C_{22}H_{20}O_9$: C, 61.7; H, 4.71. Found: C, 61.5; H, 4.82.

*3,4′,5-Trihydroxy-3′-methoxystilbene (**4**)*

The stilbene-α-carboxylic acid (3.9 g), copper powder (4 g) and freshly distilled quinoline (40 ml) were heated to about 185 °C under a nitrogen atmosphere for 3 h. Ethyl acetate (150 ml) was added to the cooled mixture and after filtration the resulting solution was washed several times with dilute hydrochloric acid. The solvent was evaporated *in vacuo* and the residue was treated with 0.2 *N* sodium hydroxide (100 ml) at about 95 °C in a nitrogen atmosphere for 2 h. The solution was cooled and extracted once with ether (25 ml) which was discarded. The aqueous solution was acidified with dilute sulfuric acid and extracted with ethyl acetate. Evaporation of the ethyl acetate left a dark-brown oil (192 mg) which was dissolved in methanol (2 ml) and placed on a column (1 × 30 cm) packed with polyamide powder (Brinkman Instruments). The column was eluted with methanol–water (1:1) to yield finally the product, 30 mg, m.p. 199 °C crystallized from methanol, which gave an orange color with diazotized sulfanilic acid when applied to a thin-layer chromatography plate. Ultraviolet spectrum (ethanol): λ_{max} 285 and 324 mμ (log ε 4.45 and 4.54). Infrared spectrum (KBr): ν_{max} 3300 and 1645 cm^{-1}. Continued elution of the column gave a small amount of a second stilbene (ultraviolet fluorescent) which, however, gave a yellow color with the diazotized sulfanilic acid reagent. The orange color from the desired product was attributed to the guaiacyl nucleus, whereas the yellow color from the second product was attributed to a catechol nucleus produced from the former by demethylation.

The triacetate of this stilbene was prepared by taking the decarboxylation mixture, before it was treated with base, and adding pyridine (5 ml) and acetic anhydride (5 ml); the reaction mixture was kept at room temperature for one day and then worked up in the usual manner. The product was purified on thick-layer plates of silica gel using methylene dichloride as the developing solvent, followed by extraction of the product from the silica gel and recrystallization from methanol, m.p. 105–106 °C. Ultraviolet spectrum (ethanol): λ_{max} 303 and 316 mμ (shoulder at 332 mμ), (log ε of both 4.44). Infrared spectrum (KBr): ν_{max} 1760 cm^{-1}.

Anal. Calcd. for $C_{21}H_{20}O_7$: C, 65.6; H, 5.24. Found: C, 65.5; H, 5.42.

3,4′,5-Trihydroxy-3′-methoxystilbene-3-O-β-D-glucopyranoside Hexaacetate

The stilbene **4** (29 mg), silver oxide (32 mg), and drierite (50 mg) in anhydrous chloroform (5 ml) was treated with

tetra-*O*-acetyl-α-D-glucopyranosyl bromide (21 mg) in anhydrous chloroform (5 ml) for two days at room temperature. Thin-layer chromatographic (t.l.c.) examination of the reaction mixture, on silica gel G, using the developing solvent benzene – ether – ethanol (16:4:1), showed the major product of the reaction (substitution of one of the resorcinol ring hydroxyls) had R_f 0.21, and the minor product (substitution of the guaiacol ring hydroxyl) had R_f 0.13. The major product was separated on a thick layer of silica gel using the above solvent and, after extraction of the product from the silica gel, the product was treated with pyridine (0.5 ml) and acetic anhydride (0.3 ml). The reaction mixture stood at room temperature overnight and was worked up by removing the volatile reagents *in vacuo*. The product was recrystallized from methanol to m.p. 164–165 °C, undepressed on mixing with the natural sample. Similarly, the u.v. and i.r. spectra and t.l.c. behavior of both samples were identical. Ultraviolet spectrum (ethanol): λ_{max} 301 and 319 mμ (shoulder at 332 mμ) (log ε 4.63 and 4.65). Infrared spectrum (KBr): ν_{max} 1740 and 1760 cm^{-1}.

Anal. Calcd. for $C_{33}H_{36}O_{15}$: C, 58.9; H, 5.40. Found: C, 58.9; H, 5.33.

Acknowledgments

We thank the National Research Council of Canada for the awards of a Studentship and a Fellowship to D.H.A., and a bursary and two studentships to J. C. H. Also, we thank F. W. Matthews and Dr. T. K. H. Ruck for the X-ray diffraction spectra and Dr. K. D. Luke for the ultraviolet spectra.

1. G. BILLEK. *In* Progress in the chemistry of organic natural products. Vol. 22. *Edited by* L. Zechmeister. Springer-Verlag, New York. 1964. p. 115.
2. J. CUNNINGHAM, E. HASLAM, and R. D. HAWORTH. J. Chem. Soc. 2875 (1963).
3. W. GRASSMAN and H. ENDRES. J. Chem. Soc. 4579 (1965).
4. D. W. MANSON. Tappi, **43**, 59 (1960).
5. V. D. HARWOOD. Ph.D. Thesis. McGill University, Montreal, Que. 1949.
6. W. E. HILLIS and N. ISHIKURA. J. Chromatog. **32**, 323 (1968).
7. S. KAWAMURA. J. Pharm. Soc. Japan, **58**, 405 (1938).
8. W. GRASSMAN, H. HORMANN, and A. HARTL. Makromol. Chem. **21**, 37 (1957).
9. S. SIGGIA. Quantitative organic analysis via functional groups. John Wiley and Sons, Inc., New York. 1949.
10. M. SOMOGYI. J. Biol. Chem. **160**, 61 (1945).
11. R. M. HANN and C. S. HUDSON. J. Am. Chem. Soc. **66**, 735 (1944).
12. A. W. WESTON and C. M. SUTER. Organic syntheses. Vol. 21. John Wiley and Sons, Inc., New York. 1941. p. 27.

Can. J. Chem. Downloaded from www.nrcresearchpress.com by 210.87.254.6 on 09/05/12
For personal use only.

Can. J. Chem. Downloaded from www.nrcresearchpress.com by 210.87.254.42 on 09/05/12
For personal use only.

Additivity of substituent effects on the proton–proton coupling constants in substituted benzenes. Investigation of some trisubstituted benzenes

T. SCHAEFER, G. KOTOWYCZ[1], H. M. HUTTON[2], AND J. W. S. LEE[3]
Chemistry Department, University of Manitoba, Winnipeg, Manitoba

Received March 7, 1968

An additivity scheme based on the changes in ortho, meta, and para proton coupling constants of benzene induced by a single substituent is applied to a number of trisubstituted benzenes. Ortho coupling constants are well reproduced (root mean square deviations = 0.05 c.p.s.) by the scheme but for meta and para couplings saturation effects are indicated. For the latter two couplings there are two substituents ortho to one of the protons involved. Measurements indicate that a temperature range of 100 °C has a negligible effect on the couplings but that polar solvents are to be avoided in obtaining data for the testing of additivity schemes.

Canadian Journal of Chemistry, 46, 2531 (1968)

Introduction

The additivity of substituent effects on the proton coupling constants in some mono- and disubstituted benzene derivatives has recently been demonstrated (1). In connection with chemical shift studies (2, 3) we have recently determined accurate proton coupling constants for numerous polysubstituted benzenes. The coupling constant data for 14 of these compounds appeared particularly relevant to a test of additivity effects in trisubstituted benzenes. These data are used in such a test in the work reported here.

Experimental

Measurements were made on samples of commercial origin as 3 mole % solutions in carbon tetrachloride or 5 mole % solutions in carbon disulfide. Internal tetramethylsilane served as a reference in determining peak positions by period averaging techniques on a DA-60-I spectrometer operated in the frequency-sweep mode. Three-spin systems were analyzed using a computer program[4] based on the algebraic approach of Castellano and Waugh (4). The coupling constants so derived are assumed to be accurate to at least 0.03 c.p.s. and are given in Table II. The methyl protons were decoupled in the toluene derivatives to facilitate accurate peak position measurements.

Discussion

A stringent test of an additivity scheme is devised as follows. In Table I, the differences ΔJ between the coupling constants in the monosubstituted benzenes (10 w/w % solutions in carbon tetrachloride (5, 6)) and benzene (7) are given. For the 1-X-2-Y-4-Z-benzenes (formula II)

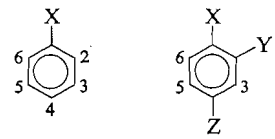

I II

in Table II, the predicted coupling constants can then be written with reference to the monosubstituted benzenes (Formula I):

$$J_o = J_{56} = \Delta J_{23}{}^{X} + \Delta J_{34}{}^{Y} + \Delta J_{23}{}^{Z} + J_o{}^{B}$$

$$J_m = J_{35} = \Delta J_{35}{}^{X} + \Delta J_{24}{}^{Y} + \Delta J_{26}{}^{Z} + J_m{}^{B}$$

$$J_p = J_{36} = \Delta J_{36}{}^{X} + \Delta J_{36}{}^{Y} + \Delta J_{36}{}^{Z} + J_p{}^{B}$$

where $J_o{}^{B}, J_m{}^{B}, J_p{}^{B}$ are the unperturbed couplings in benzene. In Table II, the predicted and observed couplings are presented. It should be noted that the ΔJ values for CH_3 are derived from our data.

Ortho Coupling Constants, J_{56}

The agreement (root mean square (r.m.s.) deviation = 0.05_5 c.p.s.) between the predicted and observed coupling constants is striking, considering that the errors in the predicted coupling constants should be cumulative. This suggests either that a cancellation of errors occurs in the sums taken in the equations above or that the original data on the monosubstituted benzenes is even more accurate than suggested (5, 6). From the values of ΔJ_{34} in Table I, it is also clear that in the trisubstituted benzenes the distant atom (Y) has little effect on $J_o = J_{56}$. On the other hand, the negative sign of ΔJ_{34} tends to confirm an

[1]Holder of an NRCC Studentship, 1966–1967.
[2]Permanent address, Brandon University, Brandon, Manitoba.
[3]Summer student, 1967.
[4]Adapted to an IBM 360/65 from a Fortran II listing by J. R. Cavanaugh.

TABLE I

Effect of substituents on the proton coupling constants in monosubstituted benzenes

X*	ΔJ_{23}†‡	ΔJ_{34}	ΔJ_{24}	ΔJ_{26}	ΔJ_{35}	ΔJ_{36}
I	0.39	−0.07	−0.23	0.51	0.38	−0.22
Br	0.51	−0.10	−0.25	0.75	0.41	−0.23
Cl	0.51	+0.02	−0.25	0.88	0.30	−0.17
F	0.82	−0.07	−0.30	1.37	0.45	−0.26
NO_2	0.82	−0.07	−0.22	1.03	0.11	−0.14
NH_2	0.48	−0.15	−0.26	1.16	0.23	−0.22
OH	0.61	−0.15	−0.28	1.34	0.37	−0.20
CH_3§	0.08	−0.09	−0.00	—	0.18	0.00

*Numbering begins with the substituent.
†Defined as $J_X - J_B$ where J_B are the couplings (±0.04 c.p.s.) in benzene: $J_o = 7.54$, $J_m = 1.37$, $J_p = 0.69$ c.p.s. (ref. 7).
‡In c.p.s. with a probable error of more than 0.05 c.p.s., derived from monosubstituted benzenes in CCl_4 (5, 6).
§Derived from data on trisubstituted benzenes in Table II and probably have an error of at least ±0.05 c.p.s.

TABLE II

Predicted and observed coupling constants in c.p.s. in some trisubstituted* benzenes†

				$J_o = J_{56}$		$J_m = J_{35}$		$J_p = J_{36}$	
Compound	X	Y	Z	Predicted	Observed‡	Predicted	Observed‡	Predicted	Observed‡
1	Cl	Cl	I	8.46	8.43	1.93	2.05	0.13	0.23
2	Cl	Cl	Br	8.58	8.55	2.17	2.37	0.12	0.26
3	Cl	Cl	Cl	8.58	8.59	2.30	2.42	0.18	0.23
4	Cl	Cl	F	8.89	8.81	2.79	2.91	0.09	0.30
5	Br	Br	Br	8.46	8.47	2.28	2.26	0.00	0.22
6	F	Br	Br	8.77	8.71	2.32	2.45	−0.03	0.30
7	Cl	Br	Cl	8.46	8.59	2.30	2.41	0.12	0.26
8	NH_2	CH_3	Cl	8.42	8.39	2.48	2.47	0.30	0.32
9	CH_3	I	NO_2	8.37	8.36	2.35	2.34	0.25	0.31
10	CH_3	Br	NO_2	8.36	8.38	2.34	2.36	0.24	0.33
11	CH_3	Cl	NO_2	8.46	8.39	2.34	2.36	0.30	0.32
12	Br	CH_3	Cl	8.48	8.45	2.66	2.56	0.29	0.31
13	CH_3	Cl	NH_2	8.12	8.08	2.46	2.43	0.30	0.32
14	CH_3	NO_2	NO_2	8.37	8.42	2.37	2.39	0.41	0.39

*Of formula 1-X-2-Y-4-Z-benzene.
†Compounds **1** to 7 measured as 3 mole % or less in carbon tetrachloride. Compounds 8 to **14** were measured as 5 mole % or less in carbon disulfide.
‡Assumed accurate to ±0.03 c.p.s.

alternating effect (8) of the electronegativity of X on coupling constants.

Meta Coupling Constants, J_{35}

The r.m.s. deviation of predicted from observed values is 0.09_5 c.p.s., the largest deviations occurring in compounds **1** to **7**. If ΔJ_{35} for CH_3 is set equal to zero the predicted values are fairly consistently low by about 0.15 c.p.s. Since the substituent effects appear to be short-range they presumably involve the σ electrons (1). It is also reasonable to suppose that the σ system becomes less susceptible to perturbation with increasing substitution. On this assumption the deviation above is of the wrong sign *unless* the magnitude of ΔJ_{24} (negative sign) is decreased by 50% or more in the trisubstituted benzenes. Such a decrease appears plausible because C-3 in these compounds (formula II) is perturbed by two ortho substituents (such is not the case for the ortho coupling constants). However, the deviation is small and its confirmation must await further work.

Para Coupling Constants, J_{36}

For compounds **1** to **7** in Table I, it is obvious that the predicted value of J_p is much too small. Because ΔJ_{36} is negative this discrepancy can be rationalized in a way similar to that for J_m above. Carbon-3 is again subjected to a perturbation by two ortho substituents and it is very definitely indicated here that Z saturates C-3, making

Can. J. Chem. Downloaded from www.nrcresearchpress.com by 210.87.254.42 on 09/05/12
For personal use only.

Can. J. Chem. Downloaded from www.nrcresearchpress.com by 210.87.254.42 on 09/05/12
For personal use only.

it much less susceptible to a perturbation by Y (formula II). This conclusion is borne out by compounds **8** to **14** where no ΔJ_{36} term has been applied for the methyl group. The agreement between predicted and observed values is now very good.

Saturated Effects in 1,3,5-Trisubstituted Benzenes

If the saturation effects are real, then a test for ΔJ_{24} can be made with 1,3,5-trisubstituted benzenes because there are two ΔJ_{24} terms in the expression for J_m. Our measurements on 1-bromo-3,5-dichloro- and 1-iodo-3,5-difluorobenzenes give three predicted J_m values which are up to 0.13 c.p.s. less than the observed values. However, this is too small a value to confirm the saturation phenomenon.

Saturation Effects in Tetrasubstituted Benzenes

Some years ago, we measured some meta coupling constants from ^{13}C sidebands in tetrasubstituted benzenes (9); while these measurements were only accurate to 0.1 c.p.s. and were done in various solvents they may give an indication of saturation effects. Thus, for 2,4,6-tri-X-phenols where X = Br, Cl, NO_2 we find, respectively -0.3 ± 0.2, -0.4 ± 0.2, -0.5 ± 0.2 for predicted minus observed values. For 2,6-dibromo-4-nitrophenol the discrepancy rises to -1.0 ± 0.2 c.p.s. While these results do indicate appreciable saturation effects, the fact that hydrogen bonding between the hydroxyl group and its ortho neighbors is highly probable unfortunately introduces another possible perturbation on the ΔJ values which should not be neglected. In fact, ring proton coupling constant data may well be used in the future to study interactions between substituents (1).

ΔJ Values Derivable from Polysubstituted Benzenes

If strict additivity is operative, irrespective of the degree of substitution, then ΔJ values can be derived very easily from highly substituted benzenes. This would be a very useful approach. For example, the determination of coupling parameters in toluene is a formidable problem even for the powerful analytical techniques used by Goldstein and co-workers (10). It was therefore hoped that the ΔJ values for CH_3 deduced from our compounds would serve as excellent starting parameters for such an analysis. This is probably so for ΔJ_{23} but because of the saturation problem the other ΔJ values for CH_3 in Table I are of doubtful accuracy.

Solvent and Temperature Effects on J

Work on *p*-nitroanisole (11) indicates a 0.1 c.p.s. dependence of $J_o + J_p$ on solvent. This is large enough to suggest the use of inert solvents whenever possible in the study of additivity schemes. A similar change in J_o and J_m for compound **12** in Table II is found in going from CS_2 to acetone. Our extensive study (3) of 3,5-dichlorosalicylaldehyde at various concentrations (1 to 10 mole %) in various solvents (100% acetone to 100% CS_2 mixtures, 100% C_6F_6 to 100% CS_2 mixtures, CCl_4, C_6H_{12}, C_6D_6, $CDCl_3$, CH_2Cl_2, CH_3CN, $(CH_3)_2SO$) over a range of temperatures (−7 to 120 °C) shows a range for J_m of from 2.49 ± 0.03 c.p.s. in CCl_4 to 2.65 ± 0.03 c.p.s. in $(CH_3)_2SO$. The high values are found in the polar solvents and if they are excluded a constant, temperature-independent value is obtained. Thus, for a saturated (less than 5 mole %) solution in CCl_4 we find $J_m = 2.49 \pm 0.03$ from 14 to 114 °C.

Conclusions

The additivity of substituent effects in mono- and disubstituted benzenes is still valid in 1,2,4-trisubstituted benzenes but small saturation effects are indicated when a proton has two ortho substituents. Small solvent effects are noticeable in polar solvents and these are comparable in magnitude to the suggested saturation effects.[5]

Acknowledgments

We are grateful to Dr. J. Cavanaugh for a listing of the 3-spin computer program and to the National Research Council of Canada for financial assistance.

1. S. CASTELLANO and R. KOSTELNIK. Tetrahedron Letters, **51**, 5211 (1967).
2. B. R. RICHARDSON and T. SCHAEFER. Can. J. Chem. **46**, 2195 (1968).
3. G. KOTOWYCZ. Ph.D. Thesis. University of Manitoba, Winnipeg, Manitoba. 1967.
4. S. CASTELLANO and J. S. WAUGH. J. Chem. Phys. **34**, 295 (1961).
5. S. CASTELLANO, R. KOSTELNIK, and C. SUN. Tetrahedron Letters, **46**, 4635 (1967).

[5]After this paper was submitted Goldstein and coworkers (12) demonstrated additivity of substituent effects in a large number of disubstituted benzenes.

6. S. CASTELLANO, C. SUN, and R. KOSTELNIK. Tetrahedron Letters, **51**, 5205 (1967).
7. J. M. READ and J. H. GOLDSTEIN. J. Mol. Spectry. **23**, 179 (1967).
8. A. D. COHEN and T. SCHAEFER. Mol. Phys. **10**, 209 (1965).
9. H. M. HUTTON, W. F. REYNOLDS, and T. SCHAEFER. Can. J. Chem. **40**, 1758 (1962).
10. J. M. READ, R. W. CRECELY, and J. H. GOLDSTEIN. J. Mol. Spectry. **25**, 107 (1968).
11. H. M. HUTTON and T. SCHAEFER. Can. J. Chem. **43**, 3116 (1965).
12. J. M. READ, JR., R. W. CRECELY, R. S. BUTLER, J. E. LOEMKER, and J. H. GOLDSTEIN. Tetrahedron Letters, **10**, 1215 (1968).

Can. J. Chem. Downloaded from www.nrcresearchpress.com by 210.87.254.42 on 09/05/12
For personal use only.

Can. J. Chem. Downloaded from www.nrcresearchpress.com by 210.87.254.42 on 09/05/12
For personal use only.

Photochemical synthesis, 22.[1] On photochemical cycloaddition: Cyclopentenone

P. DE MAYO, J-P. PETE,[2] AND M. TCHIR
Department of Chemistry, University of Western Ontario, London, Ontario

Received April 30, 1968

Cyclopentenone has been added photochemically to a wide variety of olefins and the quantum efficiency determined. Mechanistic studies indicate a rapid reaction involving a triplet state by a process which is not stereospecific, but which does not allow complete equilibration. Evidence is provided which suggests that cyclopentenone reacts photochemically from two triplet states, but that only the higher leads to cycloaddition.

Canadian Journal of Chemistry, 46, 2535 (1968)

Recent years have seen the development of the use of cyclenone photocycloaddition to olefins and related substances as a synthetic tool. This process has been used for both the generation of cyclobutanes as such (1–3) or for their subsequent modification (4–8). A desire to extend the application of this useful device prompted us to undertake a study of the cycloaddition process in more detail, and part of that study is reported here.

For practical purposes a knowledge of the probable effects of substitution on both the cyclenone and the substrate is desired, not only as regards the orientation and stereochemistry of addition, but also as regards the rate of addition. The latter would be important in syntheses where more than one olefin linkage was available for attack. A knowledge of external effects such as solvent, concentration, or temperature is also necessary. At the present time the literature offers little guidance, and the present and later studies will be an attempt to provide the data for meaningful prediction.

An important preliminary survey of the photocycloaddition reactions of cyclohexenone has been reported (9). This work will be referred to in the Discussion section, but there is reason to believe that the photochemical properties of cyclopentenone (with which the present report is exclusively concerned) differ in some important respects from those of cyclohexenone. Our own studies with cyclohexenone will be reported later.

Whilst primarily concerned here with the mechanism of photocycloaddition to olefins, the photodimerization of cyclopentenone (10–12), under some conditions a completing process (13), is obviously of relevance and our observations in this regard, though presently limited, are here recorded.[3]

Experimental

Materials

Cyclopentenone (Aldrich) was distilled under reduced pressure (nitrogen) and was greater than 99.9% pure by gas–liquid chromatography (g.l.c.). *Cyclohexene* (Phillips pure grade) was shaken with acidic ferrous sulfate, dried, distilled, refluxed with and distilled from maleic anhydride, and redistilled from sodium wire (nitrogen). It was passed through a column of alumina (layers of Woelm acid, base, and neutral) into the reaction vessel (nitrogen). *Cyclopentene* (Aldrich) was treated in a similar manner. *Cyclooctene* (Aldrich) was purified through the silver nitrate complex (14). *cis-3-Hexene* was prepared by the hydroboration of 3-hexyne (15). The product contained 3% of the *trans* isomer. *Tetramethylethylene*, *cis-dichloroethylene*, *trans-dichloroethylene*, *trans-3-hexene*, *isopropenyl acetate*, *piperylene* (mixed isomers), and *trans-piperylene* (Aldrich) were all purified by distillation and passage through alumina. No isomerization induced by the alumina was detected. *Ketene dimethylacetal* was prepared by the method of Corey and co-workers (9).

Isopropanol (Fisher reagent grade) and *t-butanol* were distilled from calcium hydride. *Benzene* (Phillips research grade) was used without further purification as were *cyclohexane*, *n-pentane* (Fisher spectranalyzed grade), *acetic acid* (Analar), and *diethyl ether* (Malinckrodt analytical reagent). *Acetonitrile* was distilled from phosphorus pentoxide and calcium carbonate.

The calibrating compounds in g.l.c. analysis, *naphthalene*, *2-methylnaphthalene*, and *acenaphthene* (Eastman) were crystallized from ethanol–water (twice) and sublimed.

Sensitizers: *Acetophenone* was fractionally distilled,

[1]For Part 21, see J. L. Charlton and P. de Mayo. Can. J. Chem. 46, 1041 (1968).

[2]On leave from the C.N.R.S. and recipient of a N.A.T.O. Fellowship. Present address: Laboratoire de Chimie Organique, Faculté des Sciences, 1 rue Grandville, 54-Nancy, France.

[3]A review covering cyclenone additions has appeared very recently (50).

Can. J. Chem. Downloaded from www.nrcresearchpress.com by 210.87.254.42 on 09/05/12
For personal use only.

benzophenone and *p-bromoacetophenone* were recrystallized from cyclohexane. *4-methylacetophenone* (Aldrich) was freed from contaminants by preparative g.l.c. and then distilled. *Pyrene* and *triphenylene* were chromatographed on alumina and recrystallized. The purity of the sensitizers was checked by g.l.c. and by emission spectra.

General Procedure

Preparative

In general the ketone (0.3–1.0 *M*) was irradiated using the olefin as solvent. Either an immersion apparatus (volume 200 ml) or smaller tubes strapped to the side of the well were used. The light source was a Hanovia 450 W medium pressure mercury arc with a cylindrical Pyrex filter. The products were isolated by fractional distillation and purified by g.l.c. (5% carbowax 20 M on Chromosorb P 5 ft × ¼ in.). All adducts showed carbonyl stretch at 1727–1735 cm^{-1} (CCl_4) and had nuclear magnetic resonance (n.m.r.) spectra (Varian A-60, CCl_4 solvent) compatible with their gross structures. The olefinic derivatives, where formed, had a carbonyl stretch at 1745–1750 cm^{-1}, and gave clear evidence of olefinic protons in their n.m.r. spectra.

Quantum Yields

Purified adducts were calibrated against one of the standards by g.l.c. using a 5% carbowax 20 M phase on Diatoport S. Temperature: 85–160°. The light source was an Osram 200 W super-pressure arc, the filter solutions being those of Kasha (16). The 334 mμ band was also isolated with a Bausch and Lomb monochromator (1200 grooves per mm). The optical bench was as previously described (17) and transmittance–reflectance ratios were determined at each wavelength. The freeze–thaw method of degassing was used to a residual pressure of less than 5×10^{-4} mm. After irradiation the calibrating compound was added and the amount of adduct determined. Irradiations were carried to about 3% conversion. Actinometry was by the ferrioxalate method (18).

Quantum Yield of Disappearance of Cyclopentenone

Irradiations in cyclopentene and cyclohexene were at 334 mμ (filter system). Naphthalene was used as the calibrating substance.

Quenching of Cycloaddition to Cyclohexene

(*a*) *Piperylene—Irradiation at 313 mμ*

A 0.05 *M* solution of cyclopentenone in benzene containing 1.5 *M* cyclohexene was used with added piperylene (0.2–0.8 *M*). The results are given in Table II.

(*b*) *Acenaphthene*—Irradiation in a merry-go-round with Pyrex filter and an additional filter of acenaphthene in cyclohexane (15 g/l) using a 450 W medium pressure arc. A 0.15 *M* solution of cyclopentenone in benzene or cyclohexane was used.

Intersystem Crossing Efficiency of Cyclopentenone

The ketone (0.3 *M*) in benzene containing varying amounts of *trans*-piperylene (contains 0.24% *cis*-piperylene) was irradiated at 313 mμ on an optical bench. The amount of *cis*-piperylene formed was determined using a 25 ft column of 25% ββ′-oxydipropionitrile on Diatoport S at 25°. It was assumed that the *cis* and *trans* isomers had the same response on the hydrogen flame detector. Conversion was kept below 4%. The quantum yield was calculated by the method of Hammond and co-workers (19). The results are given in Table V. Controls for adventitious isomerization were performed.

Dimerization of Cyclohexene and Cyclopentene

These could not be determined on the optical bench for lack of a suitable light source. The solution to be irradiated (5% benzene: 5 ml) in an 8 mm quartz tube was degassed by freeze–thaw cycles. The filter (a saturated solution of a 1:6 weight ratio of $CoSO_4 \cdot 7H_2O$ and $NiSO_4 \cdot 6H_2O$ in water) was placed in the well of a Hanovia reactor and the sample tube immersed under conditions such that its position was exactly reproducible. The well was cooled with circulating water. Independent controls with a thermopile indicated that the lamps (Rayonet RPR-100 photochemical reactor low pressure mercury lamps) had a steady output and that the warm-up time was less than 2 s. The cycloalkene solutions were irradiated for 60 min. The flux was determined using a similar tube containing ferrioxalate. The yield of dimer was determined by g.l.c. on a carbowax column. An authentic specimen of cyclohexene dimer was prepared by similar irradiation and isolation by g.l.c. A specimen of cyclopentene dimer was prepared by the method of Korte and Scharf (20).

In the case of cyclohexene the quantum yield of dimerization was 3.4×10^{-2}; that of cyclopentene was 1.1×10^{-2}. Using a value for the yield of benzene triplets of 24%[4] (21) the quantum yield of dimerization becomes 0.14 and 0.046 respectively.

Isomerization of trans-3-Hexene

A solution of cyclopentenone (0.1 *M*) and *trans*-3-hexene (0.93 *M*) in *n*-pentane was degassed and irradiated at 313 mμ. The yield of *cis*-3-hexene was determined by g.l.c. using an 8 ft column of 25% phenylacetonitrile saturated with silver nitrate on Chromosorb W. The conversion was less than 0.25%. It was assumed that the *cis* isomer had the same detector response as the *trans*. The quantum yield was 0.033. Acetophenone under the same conditions gave the *cis* olefin with a quantum yield of 0.12.

Sensitization Experiments

The cyclopentenone was ca. 0.1 *M* or 0.3 *M*. Enough sensitizer was added to absorb greater than 80% of the light. Cyclohexene was used as the solvent. Irradiations were conducted at 313 mμ. Control experiments established that cyclopentenone absorption followed Beer's Law. The results are indicated in Table VI.

Cyclopentenone–Isopropanol Irradiation

Irradiation of cyclopentenone in isopropanol gave dimer or the tertiary alcohol (**2**) first described (24, 25) by Pfau depending on concentration. With the ketone at concentrations below 0.01 *M* the alcohol was formed and identified by comparison with an authentic specimen prepared by the method of Pfau. The n.m.r. spectrum showed bands δ: 1.2 (s, 6H), 2.1 p.p.m. (m, 7H), and 2.4 p.p.m. (s, 1H) in accordance with the suggested structure. The peak at 2.4 p.p.m. disappeared on exchange with D_2O.

The quantum yield of disappearance of cyclopentenone was determined at a dilution (0.012 *M*) such that no dimer was formed. The irradiation was conducted at 313 mμ in a 5 cm path cell. A conversion of ca. 30% was observed. The disappearance of the cyclopentenone was measured, after dilution, spectrophotometrically at 217

[4]The quantum yield of benzene triplets in solution is in some doubt. In the gas phase a yield of 65% seems well established (22, 23).

Can. J. Chem. Downloaded from www.nrcresearchpress.com by 210.87.254.42 on 09/05/12
For personal use only.

mμ. The results are indicated in Table VIII together with the effect of addition of 0.011 and 0.046 *M* cyclohexene. In another experiment it was observed that in a 1:1 mixture of isopropanol–cyclohexene no tertiary alcohol was formed.

Quenching of Benzophenone Photoreduction in Isopropanol

Solutions of benzophenone (0.045 *M*) in isopropanol, containing the appropriate concentration of cyclopentenone (0.002 to 0.02 *M*) were degassed by nitrogen purge. The samples were irradiated on a merry-go-round using a 450 W mercury lamp and filters consisting of Pyrex and 2,7-dimethyl-3,6-diazacyclohepta-1,6-diene iodide (4 mg per 100 cm^3 of water, 1 cm path) (16). Upon completion of irradiation (10–15% conversion of benzophenone) the solution was transferred to a volumetric flask, diluted with ethanol, and the absorbance measured at 253 mμ (λ_{max} of benzophenone in ethanol). The values are given in Table VII and the Stern–Volmer plot in Fig. 4. (least squares plot).

TABLE I

Quantum yields of cycloaddition of cyclopentenone to olefines

Substance	Wavelength (mμ)	Φ^a	Φ^b diss
Cyclohexene	366	0.50	
	334	0.49	
	313	0.48	.57
Cyclopentene	334	0.32	.39
Cyclooctene	334	0.26	
trans-Dichloroethylene	313	0.17	
cis-Dichloroethylene	313	0.24	
cis-3-Hexene	334	0.31	
trans-3-Hexene	334	0.22	
Tetramethylethylene	334	0.12[c]	
Isopropenylacetate	334	0.16	
1,1-Dimethoxyethylene	313	0.34[d]	

[a]Olefin as solvent.
[b]Quantum yield of disappearance of cyclopentenone determined by gas–liquid chromatography. These values may be subject to a larger error (±.05) than the quantum yields of cycloaddition (±.02).
[c]Plus 25% olefinic products: see text.
[d]2.37 *M* in cyclohexane.

Results and Discussion

The photocycloaddition of cyclopentenone to cyclopentene was first reported by Eaton (13).[5] In Table I are recorded the quantum yields of cycloaddition of cyclopentenone to a number of olefins using the olefin as solvent. These values are not strictly comparable with each other (except for isomers) since the molar concentrations of the various substances are slightly different in the neat liquids. However, as will be shown below, the values obtained in neat hydrocarbon do not differ much from the value obtained (in two cases) by extrapolation to infinite concentration, and so are a tolerable measure of overall reactivity.

Since it was not possible, for various reasons connected with absorptivity, to irradiate always at the same wavelength it was first demonstrated that the quantum yield of cycloaddition was independent of wavelength over the range used. In the case of cyclohexene identity of Φ was found at 313, 334, and 366 mμ.

Whilst the range of activity is not wide perhaps one or two points emerge. In the two pairs of isomers available it appears that the *cis* isomer is more reactive than the *trans*. This may be due, conceivably, to the fact that in alignment for cycloaddition the *trans* isomer must have one group directly over the face of the cyclopentenone molecule. It would also seem that the attack on the double bond is electrophilic since the ketene acetal is more reactive than isopropenyl acetate and the dichloroethylenes are less reactive than the hexenes. Tetramethylethylene, which on this basis might be expected to be the most reactive of the aliphatic olefins is the least reactive. Conceivably the factors which render the *trans* isomers of the disubstituted alkenes less reactive than the *cis* may be operative here *a fortiori*. Even if the olefinic addition products observed in this case—which had spectroscopic properties suggesting they were of the same type found by Corey and his collaborators (9) in the addition of cyclohexenone to isobutylene—are included the quantum yield remains very low.

Constraint of a disubstituted alkene into the form of a ring does not have a unique effect. Cyclooctene is less reactive than the hexene, cyclopentene is comparable, and cyclohexene is the most reactive substrate yet encountered.

Although it may be true that some more general principle might be deduced from these results we rather doubt that, in fact, these figures are to be simply interpreted. The reasons for this will emerge in subsequent discussion. The results may, nonetheless, serve as a practical guide.

The products of the cycloaddition were, of course, the normal cyclobutane derivatives. Whilst, as was reported by Eaton, addition to cyclopentene gives a single isomer (**1**) this is not the case with the other substrates.

For these substances the products consist of a mixture of the configurational isomers. With the

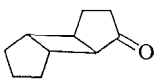

1

[5]The first photocycloaddition of a cyclenone to an olefinic linkage was that of Ciamician and Silber who reported the intramolecular formation of carvone camphor from carvone (26, see also 27).

TABLE II

Composition of adducts obtained by cycloaddition

Substance	Number of products[a]	Ratios[b]
cis-2-Butene	4	1.0/2.71/2.57/0.14
trans-2-Butene	4	1.0/1.18/2.50/0.07
cis-Dichloroethylene	3	1.0/0.19/0.36
trans-Dichloroethylene	3	1.0/1.0/3.5
trans-3-Hexene	5[c]	1.0/2.32/0.06
cis-3-Hexene	5[c]	1.0/3.57/0.05
Cyclohexene	4[d]	1.0/6.1/1.5
Cyclooctene	4	1.0/0.69/1.14/0.22
Cyclopentene	1	
Isopropenylacetate	3	Poorly separated
1,1-Dimethoxyethylene[e]	2[f]	2.65/1.0

[a]As indicated by the number of resolvable peaks, hence a minimum number.
[b]Assuming the same response on gas–liquid chromatography for each isomer.
[c]The central peak was composed of three isomers.
[d]The central peak was composed of two isomers.
[e]2.37 *M* olefin in cyclohexane.
[f]This adduct has been previously reported (9) as being homogeneous. However even the crystalline adduct gave two peaks, the ratio of which changed on repeated crystallization of the mixture. We thank Mr. A. A. Nicholson for this experiment.

acetal and acetate positional isomers were also possible. The formation of *trans*-fused ring systems involving, for instance, four-membered to six-(1, 28, 29) and even five-membered (30) rings now has precedent. From the point of view of synthetic utility as well as for possible mechanistic significance it was in principle desirable to know the stereochemical results in the present instances. However the problem of separating and identifying the constituent isomers was too massive a task. As a compromise the proportions of the unidentified isomers in the mixture were determined and serve to indicate the degree of complexity of the mixture. These results are presented in Table II. It can be seen that, as was reported for the comparable cyclohexenone addition, the reaction is not stereospecific. On the other hand the addition of cyclohexenone to *cis*- and *trans*-2-butene was reported (9) to give almost identical mixtures. Inspection of Table II shows that whilst this may be approximately, and only approximately, true of the two pairs of alkenes it is most certainly not true of the dichloroethylenes. This serves to emphasize the fact that though, as suggested previously for cyclohexenone (9) a two-step process is involved, the second step is extremely rapid and proceeds at a rate approaching bond rotation.[6] A trivial explanation involving prior isomerization of the hexenes and dichloroethylenes was excluded by appropriate controls. These results render unlikely the operation of a single, singlet mechanism for the photocycloaddition. However, the contribution of a singlet pathway, as has been suggested in photocycloadditions involving maleic ester (28), cannot, at this point be excluded.

[6]Recent results by Chapman and his colleagues (private communication) indicate that in the case of cyclohexenones different stereochemical results are associated with different excited species of the same cyclenone. We thank Professor Chapman cordially for informing us of these new results. See O. L. Chapman, T. H. Koch, F. Klein, P. J. Nelson, and E. L. Brown. J. Am. Chem. Soc. **90**, 1657 (1968).

TABLE III

Quantum yield variation with cyclopentenone and 3-hexene concentration

[Alkene]	[Cyclopentenone]	Φ
8 *M* (neat)	.3	.22
8 *M* (neat)	.026	.22
.57	.024	.17
.40	.073	.15
.13	.025	.11
.071	.018	.09

The possibility that the quantum yield of cycloaddition might depend on the concentration of the cyclopentenone itself or on the nature of the solvent was next investigated. As may be seen from Table III the quantum yield of cycloaddition to 3-hexene was unaffected by the concentration of cyclopentenone as indeed, on any simple mechanism, might have been expected. Presumably at high enough concentration dimerization would become a competitive process. Such also appears to be the case when the concentration of alkene is very low (cf. cyclohexene in Table IV).

The solvent appears, for the most part to be unimportant as far as overall quantum yield is

Can. J. Chem. Downloaded from www.nrcresearchpress.com by 210.87.254.42 on 09/05/12
For personal use only.

TABLE IV

Quantum yield variation with solvent and alkene concentration

Solvent	[Cyclopentenone]	[Cyclohexene]	Product ratios	Φ^a
Cyclohexane	0.23	2.0	1.0/5.9/1.3	0.48
Cyclohexane	0.023	0.4	—	0.47
Cyclohexane	0.018	0.16	—	0.46
Cyclohexane	0.019	0.04	—	0.32[b]
Acetonitrile	0.17	2.0	1.0/6.7/1.4	0.47
tert-butanol	0.15	2.0	1.0/7.5/1.6	0.42
tert-butanol	0.019	0.16	—	0.45
Acetic acid	0.11	2.0	—	0.44
Acetic acid	0.017	0.2	1.0/8.2/1.8	0.48
Diethyl ether	0.17	2.0	—	0.44
Diethyl ether	0.025	0.4	—	0.43
Benzene	0.6	1.5	—	0.36

[a]Reproducibility ± 0.02.
[b]The quantum yield of dimerization is approximately 0.10 under these dilution conditions.

concerned. The values for diethyl ether are slightly lower than those in cyclohexane, and the variation is beyond the limits of experimental reproducibility. However, the sole serious deviant is benzene. No compelling rationalization for the effect of this solvent is forthcoming as yet. It was thought that complexation might be involved but results to be detailed below involving quenching with acenapthene both in cyclohexane and benzene render such an interpretation more complicated. As a whole it would appear, however, that for synthetic purposes, at least with nonpolar substrates, the choice of solvent is not important.

The composition of the mixture obtained is also largely unaffected by the solvent. The variations are small though real and are to be contrasted with the important variations observed in the dimerization of cyclopentenone (11, 12) and of isophorone (31). It may be that the effect of solvent in the former case is to be interpreted in terms of an interaction between the dipoles of the substrate and the excited addend (32). This interpretation has been used with success by Schenck and his collaborators (33, 34). We have used published values (11, 12) to obtain the results in Fig. 1. Considering the high concentrations of cyclopentenone, which must necessarily affect the solvent dipole value, the agreement is probably as good as can be expected (see also 50). This being the case the subtler stereochemical variation with cyclohexene is not surprising. With more polar substrates changes should be expected and the matter is under investigation.

The partial lack of stereospecificity in the adduct formation, suggesting as it does a two-step process, led us to consider the intervention of a triplet in the photoaddition.[7] Similar considerations, together with the lack of fluorescence and an expected, rapid intersystem crossing led Corey and his collaborators (9) to favor such a species.

TABLE V

Intersystem crossing efficiency of cyclopentenone

[*trans*-Piperylene]	Φ_{ic}
Neat	~1.1
4.3	0.94
1.0	0.84
0.3	0.73
0.13	0.60

A technique which has found favor for measuring, chemically, the yield of triplets is that used by Lamola and Hammond (19). This involves measuring the extent of isomerization of *trans*- to *cis*-piperylene. The results are shown in Table V. After the completion of these experiments Ruhlen and Leermakers (12) reported a triplet yield of 0.39 at 0.10 *M* piperylene and 0.66 at 0.20 *M* piperylene values which are in accord with our own. It will be noted that a quantum yield of triplets close to unity[8] is found in neat piperylene.

[7]It is generally assumed that cycloaddition involving a triplet must proceed in two steps. If, however, in the case of a cyclenone addition, the triplet saturated carbonyl (which would result from a one-step addition) could be simultaneously demoted as formed, or if it should be energetically feasible in a particular instance to generate the saturated carbonyl triplet as an intermediate, then one-step cycloaddition may perhaps occur.

[8]The use of high concentrations of piperylene render the higher values of dubious significance. It is clear, however, that some process of decay other than dimerization is available to the cyclopentenone which is rapid since it competes well with energy transfer.

Can. J. Chem. Downloaded from www.nrcresearchpress.com by 210.87.254.42 on 09/05/12
For personal use only.

Can. J. Chem. Downloaded from www.nrcresearchpress.com by 210.87.254.42 on 09/05/12
For personal use only.

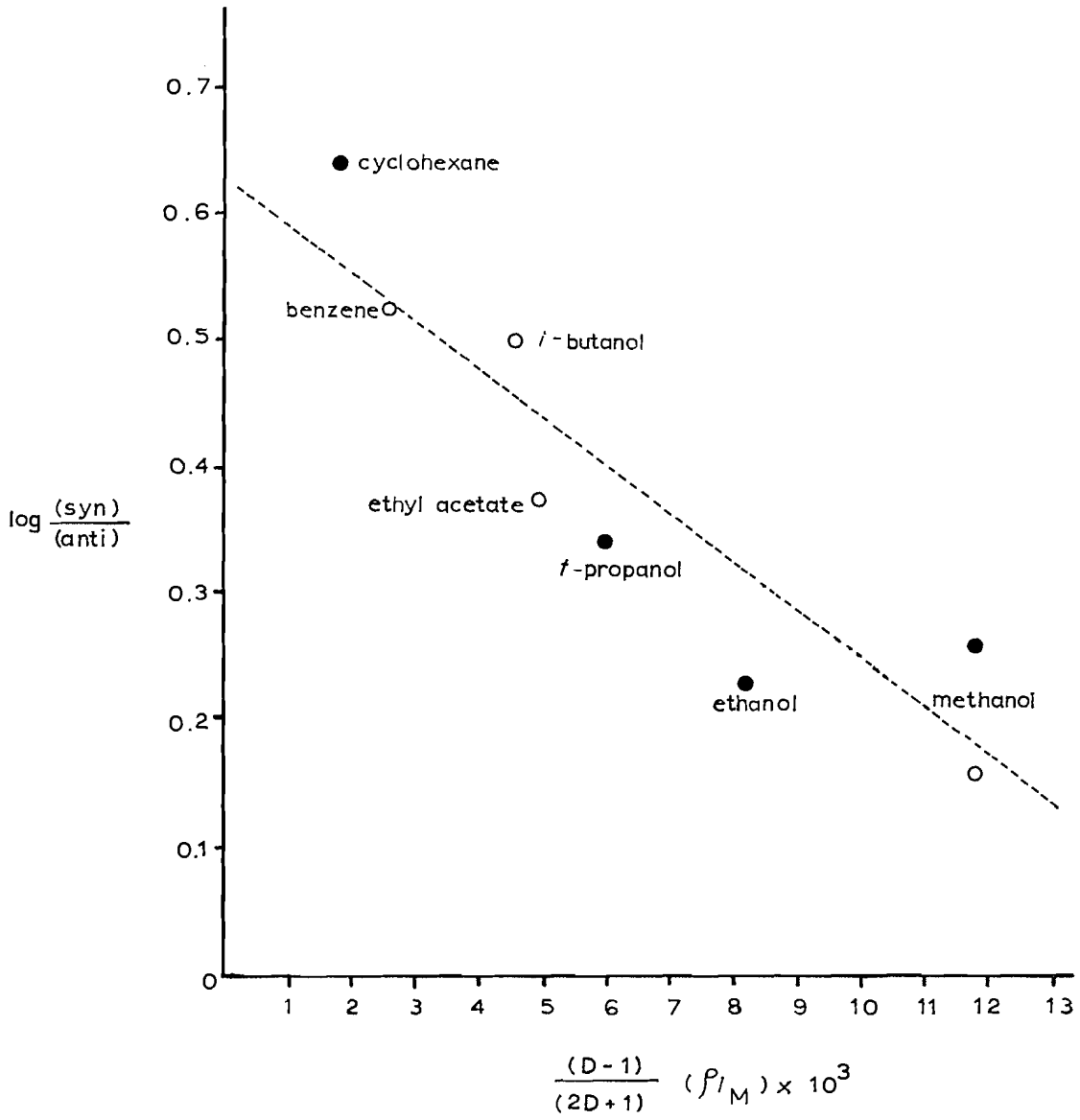

FIG. 1. Variation in dimer ratio with solvent: ● J. L. Ruhlen and P. A. Leermakers (see ref. 12); ○ P. E. Eaton and W. S. Hurt (see ref. 11).

These results, then, were in accord with the intervention of a triplet species. That the triplet species was concerned, indirectly if not directly, in the cycloaddition process was shown by a series of quenching experiments.

If the formation of adduct, in the presence of a quencher, may be represented by the following equations,

$$C \xrightarrow{h_\nu} {}^1C$$

$${}^1C \xrightarrow{k_1} {}^3C$$

$${}^3C \xrightarrow{k_2} C$$

$${}^1C \xrightarrow{k_3} C$$

$${}^3C + Q \xrightarrow{k_4} C + {}^3Q$$

$${}^3C + A \xrightarrow{k_5} CA$$

C = cyclopentenone, Q = Quencher, A = alkene, CA = adduct then the effect of added

Can. J. Chem. Downloaded from www.nrcresearchpress.com by 210.87.254.42 on 09/05/12
For personal use only.

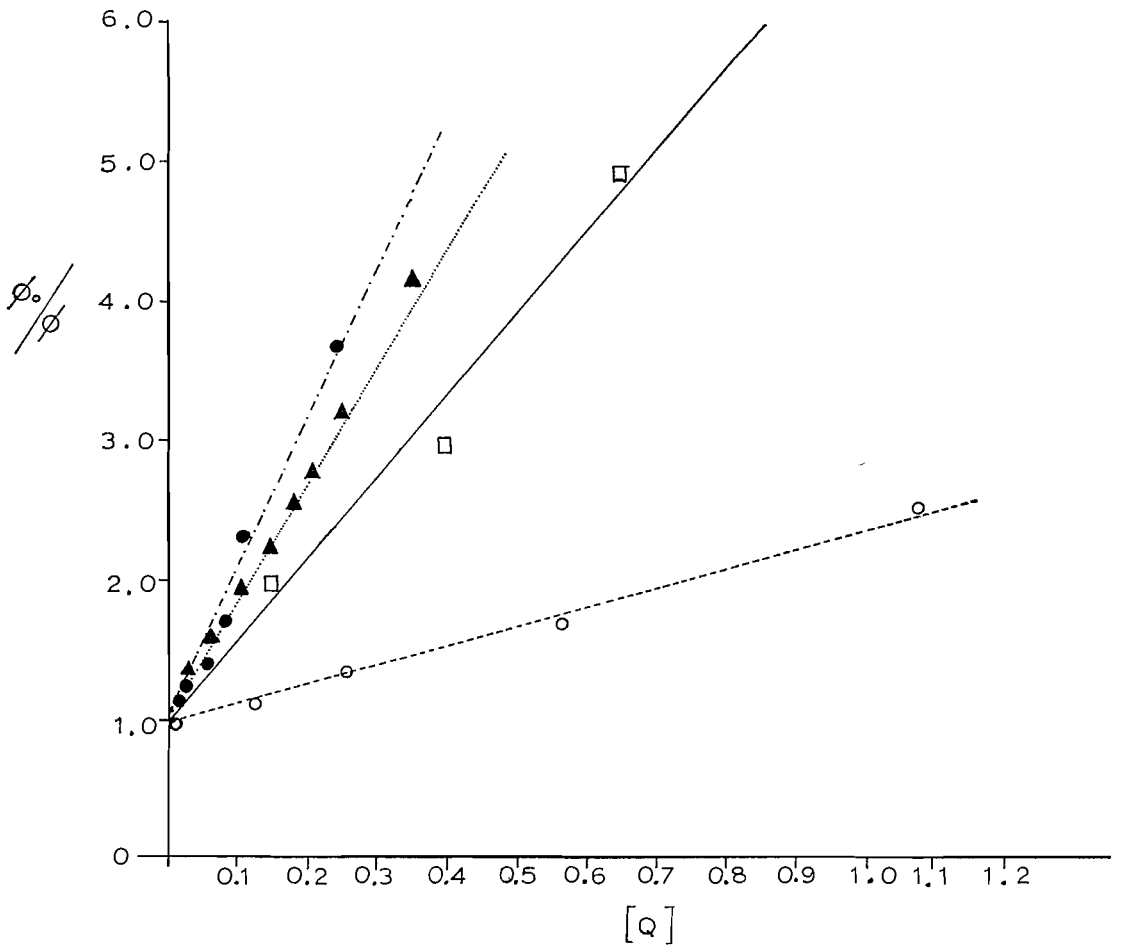

FIG. 2. Quenching of cyclopentenone–cyclohexene addition. ● Quencher: acenaphthene, solvent: cyclohexane. Cyclohexene: 2.2 *M*. ▲ Quencher: acenaphthene, solvent: benzene. Cyclohexene: 2.2 *M*. □ Quencher: piperylene, solvent: benzene. Cyclohexene: 1.5 *M*. ○ Quencher: piperylene, solvent: cyclohexene.

quencher is given by the usual Stern–Volmer expression,

$$[1] \qquad \frac{1}{\Phi} = \frac{1}{\Phi_{ic}}\left[1 + \frac{k_4[Q]}{k_5[A]} + \frac{k_2}{k_5[A]}\right]$$

where Φ_{ic} is the intersystem crossing efficiency. In Fig. 2 are shown the plots for the quenching of cycloaddition to cyclohexene by acenaphthene (E_T 59 kcal/mole) (35) in cyclohexene and benzene as solvents. The slopes $= \left[\frac{k_4}{k_2 + k_5[A]}\right]$ are very similar but not identical. Plots are given also for piperylene in benzene solvent and piperylene in neat cyclohexene. With the assumption that quenching is diffusion controlled (1×10^{10} M^{-1} s^{-1}) k_5, the rate constant for addition can be derived. It varies from 5×10^8 M^{-1} s^{-1} for piperylene in benzene solution through 4.3×10^8 (piperylene in neat cyclohexene), 3.5×10^8 (acenaphthene in cyclohexane) to 2.3×10^8 M^{-1} s^{-1} (acenaphthene in benzene solution). Values for k_2 may also be derived and, under the above set of conditions, are determined as 9.0×10^8, 46×10^8, 9.3×10^8, and 9.0×10^8 s^{-1}. Evidently in neat cyclohexene the situation is more complex, and further evidence that this is the case is presented below that in cyclohexene some additional mode of decay appears to be operative.

As has been pointed out the yield of triplets, determined by 'counting' is about unity and this appears to be general for most if not all ketonic substances.[9] However, the quantum yield of

[9]The yield of aromatic ketone triplets has long been recognized to be close to unity. That for acetone, perhaps a typical aliphatic ketone, is also close to this value (36).

Can. J. Chem. Downloaded from www.nrcresearchpress.com by 210.87.254.42 on 09/05/12
For personal use only.

cycloaddition in neat cyclohexene is only 0.48. Leaving aside, for the moment, the question of the high rate of decay (k_2) the question arose as to whether any other process in addition to cycloaddition and decay might be consuming the generated triplets.

The simplest way to measure overall chemical transformations is to measure the disappearance of the starting material. Since conversion should be carried to only a small percentage the problem is the difficult one of measuring a small difference in two large values. The quantum yields of disappearance of cyclopentenone in cyclohexene and cyclopentene shown in Table I are therefore subject to a larger error than the other quantum yields. However, it is clear that additional, unidentified, and nonreversible, chemical processes do not account for more than about 8% of the triplets.[10]

Another conceivable process by which energy could be lost could be by transfer to the alkene or cycloalkene. Although easier to measure on an alkene we first attempted for the sake of consistency to ascertain if the process was occurring with the cycloalkenes just mentioned.

If energy transfer to cyclohexene or cyclopentene occurred there could be a number of chemical consequences amongst which should be dimerization. The dimerization of cyclopentene by triplet transfer from acetone has, for instance, already been recorded (20). However, because of the complexity of the product mixture with this ketonic sensitizer we chose benzene as a sensitizer, recognizing that benzene is not chemically inert with respect to olefins. It was found that with an assumed benzene triplet yield of unity cyclohexene dimerized with a quantum yield of 3.4×10^{-2}, cyclopentene being a little lower at 1.1×10^{-2}. The actual quantum yield of intersystem crossing of benzene is not, apparently, unambiguously established in the liquid phase, but using the triplet yield determined by Lamola (21) we obtained 0.14 and 0.046 respectively as the quantum yields of dimerization of cyclohexene and cyclopentene.

Cyclohexene dimer could not be detected in the cyclopentenone cycloaddition and so, since an amount derived from a quantum yield of 10^{-3}, it is estimated, could have been detected, the consumption of cyclohexene triplets in dimerization must have been less than 0.007. Dimer could be detected ($\Phi = 7 \times 10^{-4}$) in the cyclopentene irradiation placing a maximum value on the triplet transfer from cyclopentenone to cyclopentene at 0.02.

Because of the uncertainties in the above determination, triplet transfer to 3-hexene was also investigated. Previous workers have shown (38) that acetophenone sensitizes the isomerization of 2-butene in benzene solution. Kearns has found (39) that in solution, *trans*-2-pentene is isomerized ($\Phi_{t\rightarrow c} = 0.45$) when sensitized by acetone. We have found that 3-hexene is very slowly isomerized in the cyclopentenone irradiation[11] ($\Phi = 0.033$), and assuming Kearns' value for 2-pentene as a guide, a yield of 3-hexene triplets of about 6% is obtained. The yield with acetophenone was about four times greater.

The sum of all extraneous routes for energy loss is, therefore, insufficient to account for the difference between the observed quantum yield of addition of cyclopentenone to cyclohexene and cyclopentene and unity, and so must be attributed to non-radiative decay. Yet, as has already been indicated, this process appears to have a rate constant (k_2) of the order of 10^9 s^{-1} which appears very fast indeed for a decay from a triplet to the ground state. From the Stern–Volmer expression (1), in the absence of quencher, variation of the reciprocal concentration of alkene, A, should give a linear plot against $1/\Phi$. As may be seen in Fig. 3 this is so for 3-hexene and for cyclohexene. Extrapolation to infinite concentration should give $1/\Phi_{ic}$, the quantum yield of triplets. Clearly the values obtained are different from each other, and different from the value of unity obtained by piperylene quenching where the competing processes include dimerization. The simple picture given by the set of equations presented is therefore not valid. The aberrant value of "k_{decay}" found by quenching with piperylene in neat cyclohexene reaffirms this view. The values of k_2 found cannot have, therefore, the simple interpretation originally placed on them. Since the additional decay process is operative in alkene of infinite concentration one possible interpretation is complexation, followed by both cycloaddition and radiationless decay from the same complex. In the case of neat cyclohexene, these could be processes proceeding at about

[10]Hammond and collaborators, in their study of the dimerization of cyclohexenone also observed a chemical side reaction of about the same order of magnitude (37).

[11]Conversion was kept low so that sensitization by the higher energy addition products was not an important factor.

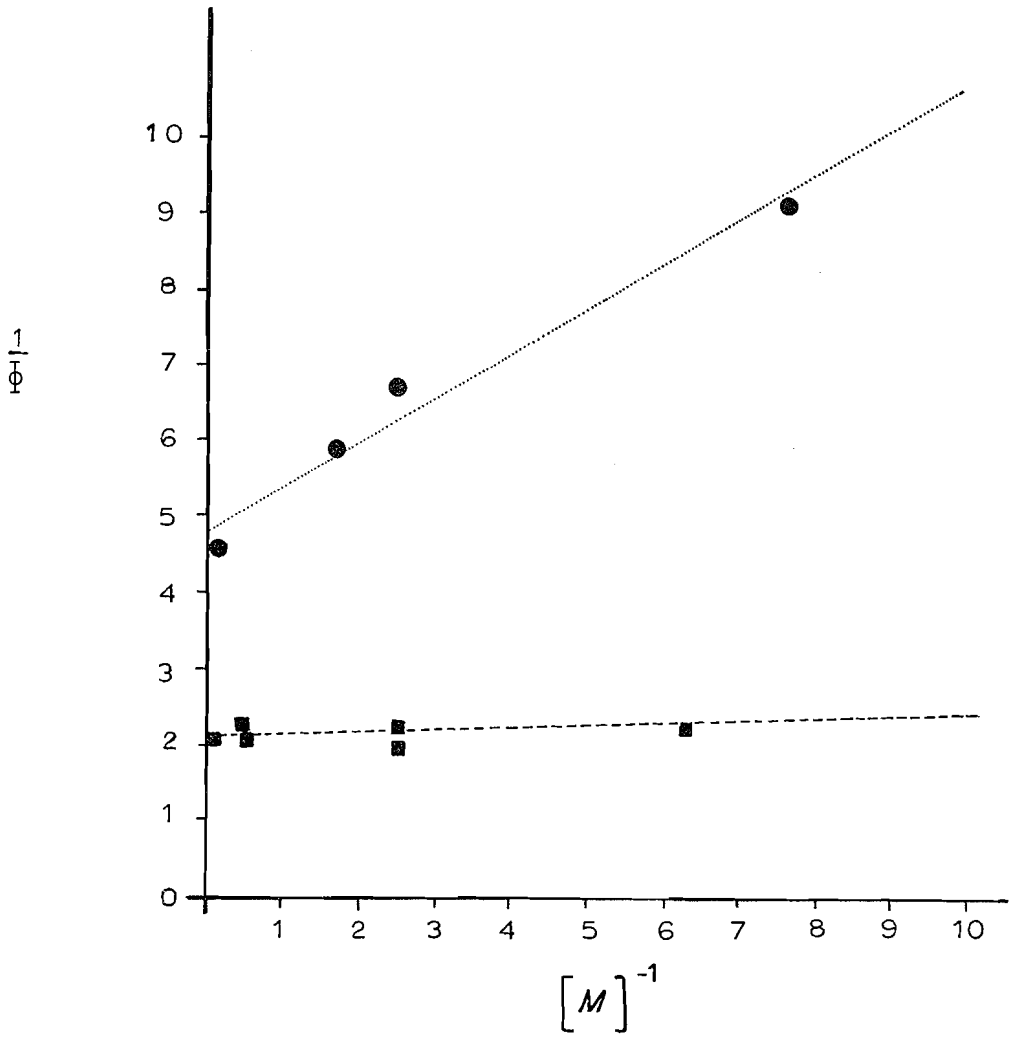

FIG. 3. Variation in quantum efficiency with olefin concentration: ● *trans*-3-hexene (A point was also obtained at 0.071 M, $^1/\Phi = 10.5$). ■ cyclohexene.

equal rates. The fact that the quantum yield of cycloaddition is significantly different only in benzene solvent may be suggestive here. Conceivably the benzene could compete with the cyclohexene for complexation with the excited cyclopentenone.

An alternative hypothesis is that at some stage in the cycloaddition process reversal is possible, but with the generation of ground state molecules. Under these circumstances cycloaddition and isomerization would have the same quenching constant. The point up to which reversal is possible might have to be early on the reaction coordinate since by this reversible addition very little, if any, isomerization of 3-hexene occurs.

It appeared in view of the above observations that whatever the details of cycloaddition might be, the reactive intermediate involved was a triplet. Similar conclusions were reached about the same time with regards the dimerization of cyclopentenone by Eaton and Hurt (11) and by Ruhlen and Leermakers (12). The former based their conclusions partly on a piperylene quenching experiment similar to that described herein for cycloaddition, and partly on a sensitization experiment using xanthone.

We have shown in our preliminary communication (40) that sensitizers having triplet above about 73 kcal/mole will sensitize cycloaddition, the highest quantum yield being 0.22 found with

Can. J. Chem. Downloaded from www.nrcresearchpress.com by 210.87.254.42 on 09/05/12
For personal use only.

TABLE VI

Sensitization of photocycloaddition

Sensitizer	E_T (kcal/mole)	[Sens.]	[Cyclopentenone]	Φ
Cyclopropylphenyl ketone	74.2	.54	.3	.21
Acetophenone	73.7	.9	.3	.16
		.9	.1	.076
4-Methyl acetophenone	72.6	.8	.3	.18
		.7	.1	.12
4-Bromo acetophenone	71.7	.9	.3	0
Benzophenone	69.2	.09	.02	−0.01
Triphenylene	67.2	.011	.019	.10
Acenaphthene	58	.03	.086	.21
Pyrene	48.7	.013	.078	.08

cyclopropylphenylketone (1 *M*) the cyclopentenone concentration being 0.3 *M*. The results are given in Table VI. No cycloaddition was observed with sensitizers having triplets energies of 71.2 kcal/mole or less. As noted (40) certain non-ketonic sensitizers, triphenylene and acenaphthene, with low triplet energies were able to induce cycloaddition, but emission studies revealed that singlet energy transfer was involved. Thus, in an E.P.A. glass at 77 °K, 0.1 *M* cyclopentenone quenched acenaphthene fluorescence by about 90%. Under these conditions triplet energy from the cyclopentenone was returned to the acenaphthene since the acenaphthene phosphorescence increased threefold.[12]

It might have been a presumption that sensitizers below 71.2 kcal/mole, e.g. benzophenone, which were incapable of inducing cycloaddition, could not transfer energy to cyclopentenone at all. However, Pfau has recorded (24, 25) that the irradiation of cyclopentenone in isopropanol with benzophenone as sensitizer gives an adduct (**2**).

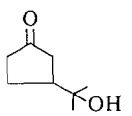

2

This could have been formed by reduction of the benzophenone triplet by the isopropanol and subsequent addition of the acetone ketyl radical to cyclopentenone. Whatever the subsequent radical processes might be, the benzophenone would, nonetheless, be consumed in the generation of (**2**). An alternative process could involve energy transfer from the benzophenone to the cyclopentenone which would itself then abstract the hydrogen atom from the isopropanol. In this sequence the benzophenone would not be consumed. A method was available to distinguish between these processes.[13]

The reduction of benzophenone by isopropanol is a well-studied triplet process (41–45) which can be quenched at a diffusion controlled rate by substances having triplet energies 3 kcal/mole lower, say, than benzophenone (69 kcal/mole). We have found that benzophenone reduction is quenched also by the addition of cyclopentenone (Table VII). A linear Stern–Volmer plot was obtained over a range of 0.002–0.02 *M* cyclopentenone. The slope (Fig. 4) was 67 M^{-1}. Using the values of hydrogen abstraction by benzophenone from isopropanol of 1.3×10^6 M^{-1} s^{-1} and a decay rate 1.5×10^7 s^{-1} (43–45)

TABLE VII

Quenching of benzophenone reduction

Absorbance[a]	Φ_0/Φ	[Cyclopentenone]
.978[b]	—	Non-irradiated
.830	1.0	0
.856	1.21	.0032
.890	1.68	.0080
.896	1.80	.013
.911	2.21	.016
.982[c]	—	Non-irradiated
.853	1.0	0
.866	1.11	.0023
.911	1.82	.0113
.921	2.11	.018
.923[d]	2.19	.023

[a]3 ml sample diluted to 250 ml and measured in 0.1 cm cell.
[b]Run I.
[c]Run II.
[d]This point not included in slope. The curve begins to flatten at greater than 0.03 *M* cyclopentenone.

[12]The dimerization of cyclohexenone, reported to be sensitized by naphthalene (37) may also perhaps be an instance of singlet energy transfer.

[13]Although benzpinacol was a product isolated in the experiments of Pfau this does not enable a conclusion to be drawn since the concentration of cyclopentenone could fall low enough so as to be incapable of quenching all the benzophenone triplets.

Can. J. Chem. Downloaded from www.nrcresearchpress.com by 210.87.254.42 on 09/05/12
For personal use only.

Can. J. Chem. Downloaded from www.nrcresearchpress.com by 210.87.254.42 on 09/05/12
For personal use only.

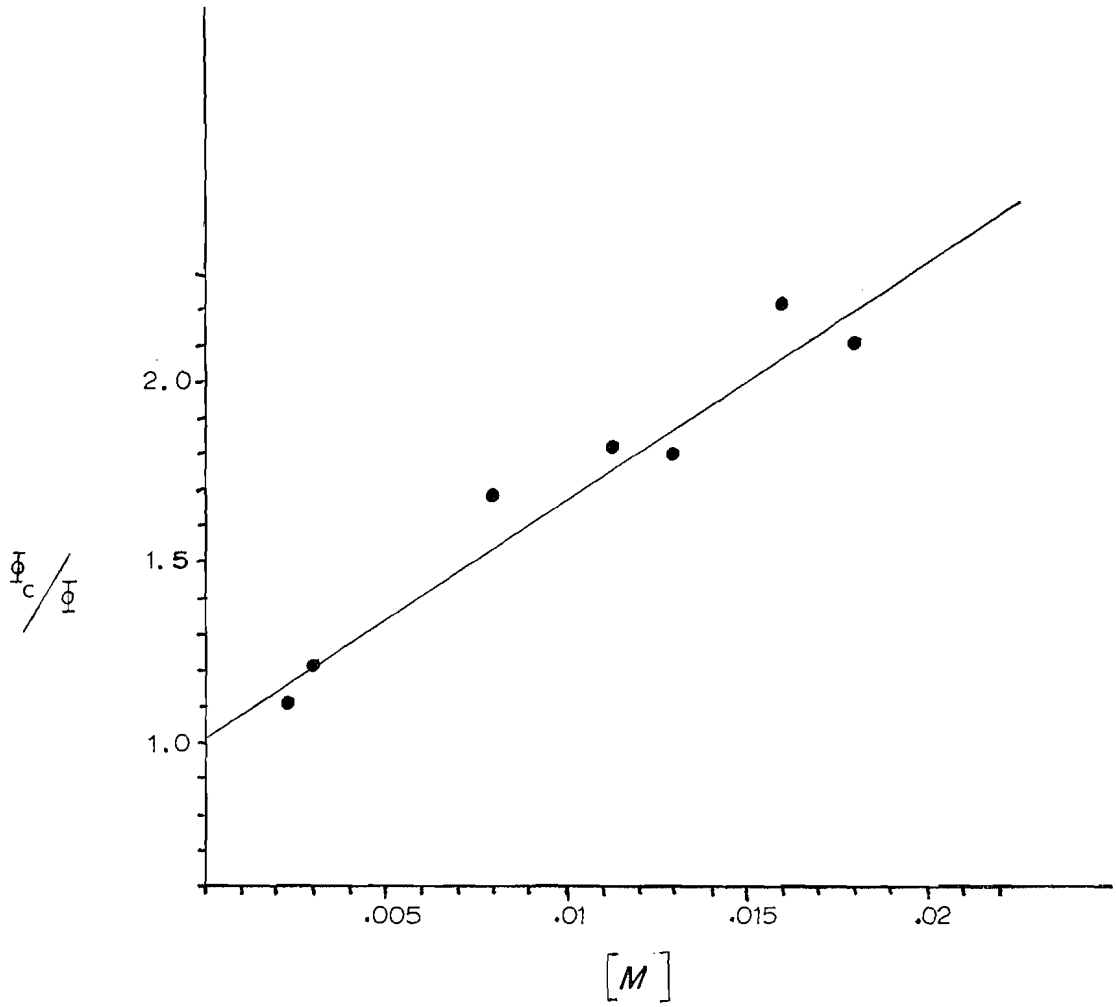

FIG. 4. Quenching of benzophenone photoreduction by cyclopentenone.

for the benzophenone triplets the quenching rate constant may be calculated as $2.1 \times 10^9\ M^{-1}\ s^{-1}$. The diffusion controlled rate is given as $3.7 \times 10^9\ M^{-1}\ s^{-1}$ (30 °C) and so clearly benzophenone energy is being transferred to cyclopentenone at close to the maximum rate.[14] Yet in the presence of cyclohexene no adduct formation takes place, despite the energy transfer. And, in contrast, direct irradiation of cyclopentenone in isopropanol leads to dimer formation and not the formation of (**2**). The conclusion seems unavoidable that two triplets of cyclopentenone exist which have different chemical reactivities, and that cycloaddition is derived from reaction of the upper triplet. If, as reported by Ruhlen and Leermakers (12) benzophenone does not sensitize the dimerization of cyclopentenone, then T_1, the lower triplet, is inactive in this cycloaddition process also.

The energy level of T_2 is not known with accuracy. A figure of near 74 kcal/mole seems reasonable and it is interesting that in a constrained cyclopentenone Herz has very recently reported emission with an O—O band estimated to be in the region indicated (46). Obviously it would be important to relate chemical properties with energy levels in a cyclopentenone which emits.

The position of the lower energy triplet is not known with certainty. Presumably it must be 66

[14]Since adduct is formed the concentration of cyclopentenone must decrease slowly. Over the range given the plot is linear but may represent, nonetheless, a lower limit for rate of energy transfer.

Can. J. Chem. Downloaded from www.nrcresearchpress.com by 210.87.254.42 on 09/05/12
For personal use only.

kcal or less because of the rate of energy transfer. By the photostationary state technique using piperylene Ruhlen and Leermakers (12) find a value of 61 kcal/mole for an unspecified triplet, but it is uncertain what this result signifies since two triplets could conceivably be involved. Although cyclopentenone quenches the phosphorescence of naphthalene this could be due to singlet quenching in agglomerates. At the moment no exact answer is available.

Reactions of excited molecules in higher and lower states of the same manifold in solution have not been observed until very recently. Kearns has reported reaction from a higher singlet of oxygen (47) and Liu from a T_2 state of anthracene (48).[15]

Since activation of cyclopentenone to the T_1 state leads, in isopropanol solution, to the alcohol (**2**) the question arises as to whether this same reaction, indicative of the state, could be induced by direct irradiation if other chemical pathways for energetic degradation of T_2 were removed. This was attempted. Using cyclopentenone in dilute solution ($< 0.02\ M$) so as to slow down the competing dimerization process the alcohol (**2**) was indeed formed. At 0.012 *M* (Table VIII) the quantum yield of disappearance of cyclopentenone[16] was 1.9. Addition of small amounts of cyclohexene quenched the reaction by giving rise to the cyclohexene adducts. The figure of 1.9 may indicate the incursion of a radical chain process. However, these experiments do appear to indicate that crossing from T_2 to T_1 will occur if the faster cycloadditive processes are suppressed.

TABLE VIII

Disappearance of cyclopentenone in isopropanol

[Cyclopentenone]	[Cyclohexene]	Φdisappearance
0.012	—	1.9
0.012	0.011	1.2
0.012	0.046	0.7

No evidence is available as to the nature of T_2 and T_1. If they are both spectroscopic species then the chemical properties of T_1 i.e. hydrogen abstraction, seem more in accord with those generally attributed to an (n, π^*) state. This would appear to require a singlet–triplet splitting of more than 12 kcal/mole for this state.

[15]See also N. C. Yang (49) for what may be a pertinent analogy in the photochemistry of 9-anthraldehyde, and also footnote 6.

[16]The quantum yield of formation of (**2**) could not be measured because of instability on g.l.c. apparatus. The only other product observed was a trace of cyclopentanone.

1. E. J. Corey, R. B. Mitra, and H. Uda. J. Am. Chem. Soc. **86**, 485 (1964).
2. J. D. White and D. N. Gupta. J. Am. Chem. Soc. **88**, 5364 (1966).
3. E. H. W. Böhme, Z. Valenta, and K. Wiesner. Tetrahedron Letters, 2441 (1965).
4. H. Hikino and P. de Mayo. J. Am. Chem. Soc. **86**, 3582 (1964).
5. E. J. Corey and S. Nozoe. J. Am. Chem. Soc. **86**, 1652 (1964).
6. B. D. Challand, G. Kornis, G. Lange, and P. de Mayo. Chem. Commun. 704 (1967).
7. G. Lange and P. de Mayo. Chem. Commun. 704 (1967).
8. R. W. Guthrie, Z. Valenta, and K. Wiesner. Tetrahedron Letters, 4645 (1966).
9. E. J. Corey, J. D. Bass, R. Le Mahieu, and R. B. Mitra. J. Am. Chem. Soc. **86**, 5570 (1964).
10. P. E. Eaton. J. Am. Chem. Soc. **84**, 2344 (1962).
11. P. E. Eaton and W. S. Hurt. J. Am. Chem. Soc. **88**, 5038 (1966).
12. J. L. Ruhlen and P. A. Leermakers. J. Am. Chem. Soc. **89**, 4944 (1967).
13. P. E. Eaton. J. Am. Chem. Soc. **84**, 2454 (1962).
14. Wm. O. Jones. J. Chem. Soc. 1808 (1954).
15. H. C. Brown and G. Zweifel. J. Am. Chem. Soc. **81**, 1512 (1959).
16. M. Kasha. J. Opt. Soc. Am. **38**, 929 (1948).
17. A. Cox, P. de Mayo, and R. W. Yip. J. Am. Chem. Soc. **88**, 1043 (1966).
18. C. G. Hatchard and C. A. Parker. Proc. Roy. Soc. London, Ser. A, **235**, 518 (1956).
19. A. A. Lamola and G. S. Hammond. J. Chem. Phys. **43**, 2129 (1965).
20. H. D. Scharf and F. Korte. Chem. Ber. **97**, 2425 (1964).
21. J. G. Calvert and J. N. Pitts Jr., Photochemistry. John Wiley and Sons, Inc., New York. 1966. p. 309.
22. W. A. Noyes, W. A. Mulac, and D. Harter. J. Chem. Phys. **44**, 2100 (1966).
23. R. B. Cundall, F. J. Fletcher, and D. G. Milne. Trans. Faraday Soc. **60**, 1146 (1964).
24. M. Pfau, R. Dulou, and M. Vilkas. Compt. Rend. 1817 (1962).
25. M. Pfau. Publications Scientifiques et Techniques du Ministère de l'Air. No. 143, Paris (1965).
26. G. Ciamician and P. Silber. Gazz. Chim. Ital. **41**, 1928 (1908).
27. G. Büchi and I. M. Goldman. J. Am. Chem. Soc. **79**, 4741 (1957).
28. P. de Mayo, S. T. Reid, and R. W. Yip. Can. J. Chem. **42**, 2828 (1964).
29. J. A. Barltrop and R. Robson. Tetrahedron Letters, 597 (1963).
30. H. D. Scharf. Tetrahedron Letters, 4231 (1967).
31. O. L. Chapman, P. J. Nelson, R. W. King, D. J. Trecker, and A. A. Griswold. Record Chem. Progr. Kresge-Hooker Sci. Lib. **28**, 167 (1967).
32. J. A. Berson, Z. Hamlet, and W. A. Mueller. J. Am. Chem. Soc. **84**, 297 (1962).
33. R. Steinmetz, W. Hartmann, and G. O. Schenk. Chem. Ber. **98**, 3854 (1965).
34. I. M. Hartmann, W. Hartmann, and G. O. Schenck. Chem. Ber. **100**, 3146 (1967).
35. A. P. Marchetti and D. R. Kearns. J. Am. Chem. Soc. **89**, 768 (1967).
36. P. J. Wagner. J. Am. Chem. Soc. **89**, 2503 (1967).
37. E. Y. Y. Lam, D. Valentine, and G. S. Hammond. J. Am. Chem. Soc. **89**, 3482 (1967).

38. C. MOUSSEBOIS and J. DALE. J. Chem. Soc. 260 (1966).
39. R. F. BORKMAN and D. R. KEARNS. J. Am. Chem. Soc. **88**, 3467 (1966).
40. P. DE MAYO, J-P. PETE, and M. TCHIR. J. Am. Chem. Soc. **89**, 5712 (1967).
41. W. M. MOORE, G. S. HAMMOND, and R. P. FOSS. J. Am. Chem. Soc. **83**, 2789 (1961).
42. G. S. HAMMOND, W. P. BAKER, and W. M. MOORE. J. Am. Chem. Soc. **83**, 2795 (1961).
43. A. BECKETT and G. PORTER. Trans. Faraday. Soc. **59**, 2039, 2051 (1963).
44. J. N. PITTS, H. W. JOHNSON, and T. KUWANA. J. Phys. Chem. **66**, 2456, 2471 (1962).
45. G. PORTER and G. WILKINSON. Trans. Faraday. Soc. **57**, 1686 (1961).
46. W. HERZ and M. G. NAIR. J. Am. Chem. Soc. **89**, 5474 (1967).
47. D. R. KEARNS, R. A. HOLLINS, A. U. KHAN, and P. RADLICK. J. Am. Chem. Soc. **89**, 5456 (1967).
48. R. S. H. LIU and J. R. EDMAN. J. Am. Chem. Soc. **90**, 213 (1968).
49. N. C. YANG, R. LOESCHEN, and D. MITCHELL. J. Am. Chem. Soc. **89**, 5465 (1967).
50. P. E. EATON. Accounts Chem. Res. **1**, 50 (1968).

Can. J. Chem. Downloaded from www.nrcresearchpress.com by 210.87.254.42 on 09/05/12
For personal use only.

Can. J. Chem. Downloaded from www.nrcresearchpress.com by 210.87.254.42 on 09/05/12
For personal use only.

Rearrangement of penicillins to anhydropenicillins[1]

SAUL WOLFE,[2] J. C. GODFREY, C. T. HOLDREGE, AND Y. G. PERRON[3]
Organic Research Division, Bristol Laboratories Division of Bristol-Myers Company, Syracuse 1, New York

Received October 25, 1967

Anhydropenicillins are derived from penicillins by the removal of a molecule of water from the nucleus with concomitant rearrangement of the thiazolidine ring to an α,β-unsaturated-γ-thiolactone. Conditions are described for the preparation of the acid chlorides of penicillins; these compounds rearrange to anhydropenicillins upon treatment with a tertiary amine. Other less effective ways of performing the rearrangement are also given. The anhydropenicillins show infrared absorption at 5.5, 5.9, 6.0, and 6.1 μ, ultraviolet absorption near 270 mμ (ε = 12 000), and they possess extraordinary chemical stability. Possible reasons for these properties are discussed.

Canadian Journal of Chemistry, 46, 2549 (1968)

The great variety of the rearrangements that have been reported for penicillins (**1**) is a feature of the chemistry of these compounds which continues to fascinate organic chemists. Until recently, however, all of the known rearrangement products were the result of thermal or acid-catalyzed intramolecular attack on the carbonyl group of the labile β-lactam (for examples see ref. 1). These products include the penicillenic acids (**2**), the penillic acids (**3**), the penillonic acids (**4**), and azlactones (**5**).

The discovery of the important therapeutic properties associated with *N*-acyl derivatives (**6**) of 7-aminocephalosporanic acid (**7**) (2, 3) has led

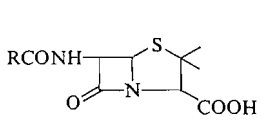

1

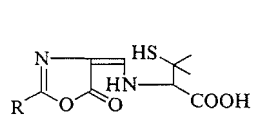

2

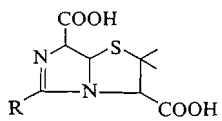

3

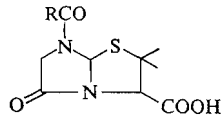

4

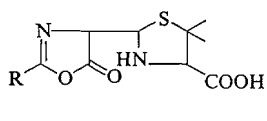

5

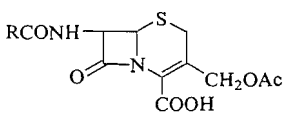

6

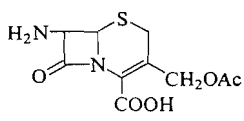

7

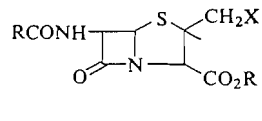

8

us as well as others to study the possibility of effecting a rearrangement of the *thiazolidine* portion of penicillin without loss of the β-lactam. One objective of this work is the partial synthesis of a cephalosporin (**6**)[4] from a penicillin. Especially valuable for such a transformation would be a compound such as **8** where a hydrogen on one of the methyl groups of penicillin has been replaced by a potential leaving group such as tosyl, halogen, or N_2^+. We expect that such a compound might be induced to rearrange to a cephalosporin derivative by a route such as that shown in Chart 1.[5]

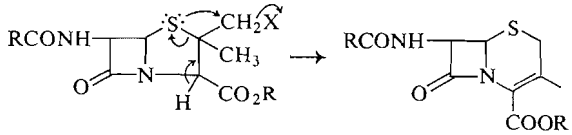

Chart 1

[1]Presented at the XIXth International Congress of Pure and Applied Chemistry, London, 1963, and as a preliminary communication in J. Am. Chem. Soc. **85**, 643 (1963). See also S. Wolfe, U.S. Patent No. 3,311,638 (1967).

[2]Department of Chemistry, Queen's University, Kingston, Ontario. Correspondence concerning this paper should be addressed to this author.

[3]Bristol Laboratories of Canada, Ltd., Candiac, Quebec.

[4]The total synthesis of the cephalosporins has been reported by R. B. Woodward, K. Heusler, J. Gosteli, P. Naegeli, W. Oppolzer, R. Ramage, S. Ranganathan, and H. Vorbrüggen, J. Am. Chem. Soc. **88**, 852 (1966).

[5]A scheme analogous to this has been achieved in a model system (4).

Can. J. Chem. Downloaded from www.nrcresearchpress.com by 210.87.254.42 on 09/05/12
For personal use only.

The synthetic problem associated with the introduction of a substituent onto an unactivated methyl group has received much attention in recent years, especially in connection with substitution at C-18 and C-19 of the steroid nucleus. Success has usually been achieved by the use of reactions in which a substituent is transferred to methyl from a reactive center generated within the same molecule (5, 6).

When penicillin is viewed in three dimensions, it can be seen (**9** (7)) that the carboxyl group, the sulfur atom, and the amide hydrogen of the side chain are potential sites from which attack on a methyl group might be initiated. Conversion of the carboxyl group into radical (anodic oxidation) or cationic (lead tetraacetate) forms does not, however, lead to intramolecular reactions. Instead, decarboxylation is the major process observed (8). Treatment of the *N*-chloro derivative of penicillin G methyl ester with triethylamine led to loss of the sulfur and formation of the oxazoline **10** (9). Morin and co-workers (10) have

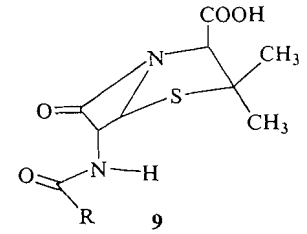

9

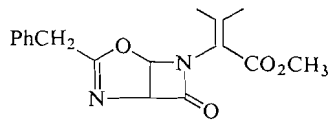

10

been successful in using the sulfur atom to initiate attack on a methyl group. Heating the methyl ester of penicillin V sulfoxide to reflux in acetic anhydride gave **11** and **12** in 40% and 20% yields, respectively (cf. ref. 11).

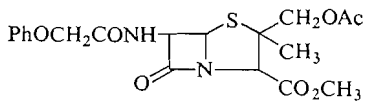

11

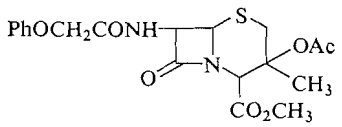

12

In this article we report a different kind of rearrangement of the thiazolidine ring from that proposed in Chart 1. Though the reaction does not involve the methyl groups directly, as a consequence of the rearrangement it appears possible to introduce substituents onto these groups and thus arrive at **8** in an indirect manner. The rearrangement was discovered in the course of experiments with penicillin acid chlorides.

Before it was shown (12, 13) that the cephalosporin nucleus contains a 6-membered ring, Abraham and Newton had suggested (14) that these compounds contained a penicillin nucleus with an additional acetoxy group α to the carboxyl function. Though this seemed incompatible with the ultraviolet (u.v.) spectrum of cephalosporins (λ_{max} ~260 mμ), we thought that access to such a compound might be had by Baeyer–Villiger oxidation of a ketene dimer potentially available from a penicillin acid chloride by treatment with a tertiary amine (e.g. **13** → **15**).

The preparation of analytically pure acid chlorides of penicillins was claimed by Villax in a British patent in 1956 (15). Because of the instability of penicillins in acid media (see above; also ref. 16), penicillin acid chlorides would not be expected to be particularly stable and our own work did not afford analytically pure compounds. However, by careful control of the stoichiometry (Chart 2) it is possible, using thionyl chloride, to observe conversion in solution of a penicillin to a penicillin acid chloride.

A $RCOOH + SOCl_2 \rightarrow RCOCl + SO_2 + HCl$

B $RCOOM + SOCl_2 \rightarrow RCOCl + SO_2 + MCl$

C $RCOOH \cdot H_2O + SOCl_2 \rightarrow RCOCl + 2\,SO_2 + 3\,HCl$

Chart 2. Stoichiometry of the conversion of acids to acid chlorides. A, Carboxylic acid to acid chloride; B, alkali metal salt to acid chloride; C, carboxylic acid hydrate to acid chloride.

Stoichiometric reaction of thionyl chloride with a carboxylic acid (A of Chart 2) leads to an acid chloride together with SO_2 and HCl. These would cause rapid destruction of a penicillin if permitted to remain in the reaction mixture. Therefore, at least 2 mole-equivalents of pyridine are added per mole of carboxylic acid. Most penicillins are available in the form of the sodium or potassium salts. As shown in B, at least 1 mole-equivalent of pyridine is then necessary. Occasionally a penicillin acid is obtained as a

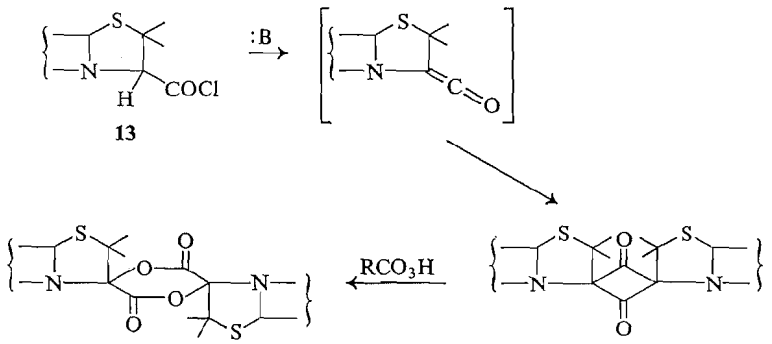

13 15 14

crystalline hydrate. As shown in C, this requires the use of 2 mole-equivalents of thionyl chloride and at least 5 mole-equivalents of pyridine. Using the quantities indicated by the appropriate equation of Chart 2, penicillins can be smoothly converted to their acid chlorides at $-20°$ in CH_2Cl_2, and the progress of the reactions followed by infrared spectroscopy.

The carbonyl region of the potassium salt of a penicillin shows absorption at 5.6 μ (β-lactam), 6.0 μ (amide I), and 6.2 μ (CO_2^-). The addition of thionyl chloride (1 mole-equivalent) to a suspension of a potassium salt (1 mole-equivalent) in methylene chloride containing pyridine (1 mole-equivalent) leads to immediate dissolution of the penicillin and the bright-yellow solution then shows absorption at 5.6, 5.8, and 6.0 μ. After 3 h at -20 °C the infrared (i.r.) spectrum shows absorption at 5.5 μ (COCl), 5.6 μ, and 6.0 μ. These spectral changes are consistent with the reaction sequence,

$$\text{PenCOOK} \xrightarrow[\text{fast}]{\text{SOCl}_2/\text{pyr}} \text{Pen-COOSOCl} \xrightarrow[\text{slow}]{\text{pyr}} \text{Pen-COCl} + \text{pyr}\cdot\text{SO}_2$$

Anhydride formation (17) was not observed so long as 1 mole-equivalent of thionyl chloride was used per mole of penicillin.

For the isolation of a penicillin acid chloride, salts were precipitated by addition of diethyl ether; after filtration and evaporation of the solvent *in vacuo* below 30°, the residue was triturated with benzene, filtered again, and the benzene solution was lyophilized. A sample of α-phenoxyethylpenicillin acid chloride prepared in this way gave a chlorine analysis of 7.5%; the theoretical value was 9.3%.

Addition of excess pyridine had no effect on penicillin acid chloride reaction mixtures. Triethylamine is a stronger base than pyridine and when this was added gradually at $-20°$ to a penicillin acid chloride reaction mixture[6] dehydrohalogenation of the acid chloride did not occur until more than *n* mole-equivalents of triethylamine had been added, where *n* was the number of mole-equivalents of pyridine used in the preparation of the acid chloride.[7]

When 2 mole-equivalents of triethylamine were gradually added to an α-phenoxyethylpenicillin acid chloride reaction mixture prepared by method B, a new spectrum appeared which now showed strong absorption at 5.5, 5.9, and 6.0 μ and medium absorption at 6.1 μ. The appearance of the spectrum indicated that treatment of the acid chloride with triethylamine under these conditions had not caused loss of the β-lactam. Evaporation of the reaction mixture and trituration of the residue with ethanol then gave a crystalline compound, m.p. 150–152°, whose i.r. spectrum (in methylene chloride) showed the same group of peaks in the carbonyl region as the reaction mixture and no peaks characteristic of either a ketene or the expected ketene dimer. The compound had an apparent molecular weight in a Signer determination of 369 and analysis indicated the molecular formula $C_{17}H_{18}N_2O_4S$. Since α-phenoxyethylpenicillin is $C_{17}H_{20}N_2O_5S$, the new compound was derived from the penicillin by loss of water and it was designated *anhydro-α-phenoxyethylpenicillin.*

Anhydro-α-phenoxyethylpenicillin was neutral and had no antibacterial activity. The compound

[6]Isolation of the acid chlorides and then treatment with triethylamine led to the formation of tars.

[7]This is a consequence, of course, of the fact that triethylamine is a stronger base than pyridine.

Can. J. Chem. Downloaded from www.nrcresearchpress.com by 210.87.254.42 on 09/05/12
For personal use only.

Can. J. Chem. Downloaded from www.nrcresearchpress.com by 210.87.254.42 on 09/05/12
For personal use only.

had ultraviolet absorption at 269 mμ (ε_{max} ($CHCl_3$) = 12 000) and this, together with the i.r. absorption at 5.9 and 6.1 μ, suggested the presence of an α,β-unsaturated carbonyl system. The i.r. absorptions at 5.5 and 6.0 μ were assigned to the β-lactam and the amide. The spectrum also showed N—H absorption at 3.0 and 6.6 μ. The nuclear magnetic resonance (n.m.r.) spectrum showed all 18 protons clearly, and comparison with the n.m.r. spectrum of α-phenoxyethylpenicillin revealed that the proton α to the carboxyl group had been lost in the formation of the anhydropenicillin; in addition, the absorption of the methyl groups of the nucleus had shifted from τ 8.50 and 8.58 to τ 7.83 and 7.92. All of these data are consistent with the structure **16** for anhydro-α-phenoxyethylpenicillin and, in agreement with this structure, acetone was obtained in 44% yield upon ozonolysis of the compound. No acetone was obtained upon ozonolysis of the parent penicillin.

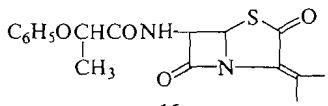

16

Because anhydropenicillins are useful intermediates for further work, a study was made of the scope of the rearrangement. It was shown that, provided the conditions described above were rigorously followed, the rearrangement is a general one for penicillins. However, the isolation of an anhydropenicillin had to be performed with care. Most anhydropenicillins were only slightly soluble in ethyl ether, ethanol, and isopropanol and these were excellent solvents for either precipitation or recrystallization of anhydropenicillins after removal of pyridine, triethylamine, and the various salts. The methylene chloride reaction mixtures were shaken with dilute HCl, water, 10% sodium bicarbonate solution, and then with water again. Evaporation of the dried methylene chloride solutions and treatment of the residue with one of the above solvents gave crystalline anhydropenicillins.

The isolated yields of anhydropenicillins were not high (ca. 20–30%). In some cases this could be attributed to the occurrence of further reactions during the isolation procedure. Thus, as noted above, the i.r. spectrum of pure anhydro-α-phenoxyethylpenicillin in methylene chloride was identical in the carbonyl region with the spectrum of the reaction mixture. Nevertheless, a second crystalline compound was also obtained when the products were isolated.[8] In addition, the isolation of **17**, the anhydro derivative of 6-*N*-tritylaminopenicillanic acid had to be performed without water treatment. Shaking the methylene chloride reaction mixture with water caused disappearance of the anhydropenicillin and formation of a new β-lactam-containing compound (18).

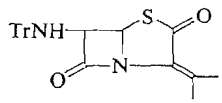

17

It is suggested that the formation of an anhydropenicillin proceeds by opening of the thiazolidine ring (**18** → **19**; X = Cl)[9] followed by recyclization at the acyl carbon (**19** → **20**).

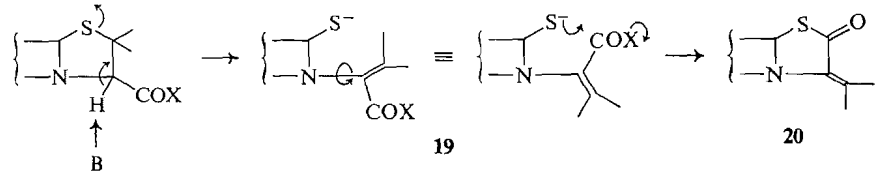

18 **19** **20**

The ring-opening depicted in **18** → **19** is an example of a reverse Michael reaction. It was thought that this step would be facilitated by the use of other carboxy derivatives in which the hydrogen α to the carboxyl group is activated towards abstraction as a proton. To test this, a number of penicillin esters and mixed anhydrides were subjected to base treatment with the results summarized in Table I. These results show that carbonic and sulfonic anhydrides are not as

[8]This compound is dimeric (see Experimental).
[9]See, for example, N. J. Leonard and R. Y. Ning, J. Org. Chem. **32**, 677 (1967).

TABLE I

The base-catalyzed rearrangement of carboxy activated penicillins to anhydropenicillins*

R_1	R_2	Conditions	% yield of anhydropenicillin
$C_6H_5OCHCONH$ (CH$_3$)	Cl	a†	22
$C_6H_5OCHCONH$ (CH$_3$)	OTs	a	12
$C_6H_5OCHCONH$ (CH$_3$)	SO_2CH_3	a	6
$C_6H_5OCHCONH$ (CH$_3$)	$OCOC_2H_5$	a	5
CH_3OCMe_2CONH	$OCOC_2H_5$	b‡	Not determined
$C_6H_4(CO)_2N$	Cl	a	28
$C_6H_4(CO)_2N$	OCH_3	c§	0
$C_6H_4(CO)_2N$	OCH_3	d‖	0

*The reaction,

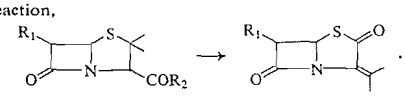

†Triethylamine in methylene chloride.
‡Sodium methoxide in methylene chloride.
§Sodium hydride in tetrahydrofuran.
‖Potassium *t*-butoxide in tetrahydrofuran – *t*-butanol.

effective substrates for the rearrangement as the acid chlorides when the base is a tertiary amine, and that methyl esters are less reactive, even towards strong base.[10]

[10]Transformations analogous to the anhydropenicillin rearrangement have been noted previously. Lur'e and Gatsenko (19) converted the acid **21** into the thiazolinone **22** by treatment with acetic anhydride, an experiment which was confirmed by Sicher and co-workers (20).

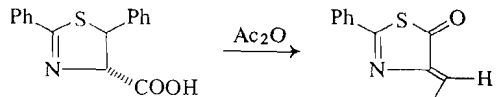

21 **22**

The action of $SOCl_2$ or PCl_5 on the acid **23** produces the thiazolinone **24** and (apparently) the acid chloride **25** (21).

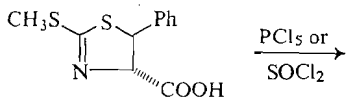

23

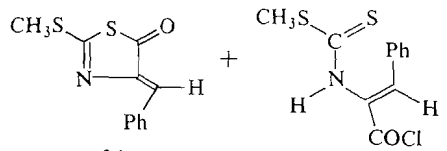

24 **25**

We turn now to a consideration of some physical and chemical properties of anhydropenicillins. The most noteworthy feature of the compounds is their chemical stability. Though the i.r. spectra seem to indicate that both carbonyl groups of the bicyclic system are under considerable strain, the anhydropenicillins are extraordinarily stable. They are recovered unchanged after prolonged refluxing in alcohol, aqueous dioxane, toluene, xylene, or after being melted.

Several groups of workers have sought relationships between the carbonyl stretching band of the β-lactam and the antibacterial activity of a penicillin (7, 22, 23). Most penicillins show i.r. absorption near 5.62 μ; monocyclic β-lactams and desthiopenicillins (**26**) absorb in the region

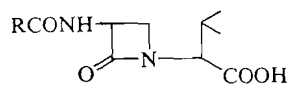

26

5.69–5.78 μ, while fused thiazolidine β-lactams absorb at 5.65 μ (24). The penicillins are considerably less stable to hydrolysis than any of the simpler β-lactam-containing compounds (22). Excluding the cephalosporins from this discussion, of those compounds containing the β-lactam

Can. J. Chem. Downloaded from www.nrcresearchpress.com by 210.87.254.42 on 09/05/12
For personal use only.

Can. J. Chem. Downloaded from www.nrcresearchpress.com by 210.87.254.42 on 09/05/12
For personal use only.

ring, the penicillins are characterized by the highest antibacterial activity, the lowest wavelength carbonyl stretching band, and the highest rate of hydrolysis. It was suggested some years ago (25) that the latter two properties are a reflection of the extent of delocalization of charge in the cyclic amide (e.g. **27**); increased participation by **27***b* would be associated with an i.r.

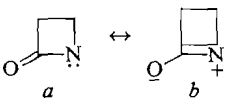

a *b*

27

shift to higher wavelengths, greater stability to hydrolysis (25), and with decreased basicity of the nitrogen atom (26).

Were the anhydropenicillins to display properties consistent with those just discussed, the fact that their i.r. absorption occurs at 5.5 μ would lead to the predictions that the anhydropenicillins should be labile and biologically active. Neither of these predictions is correct.[11] Consequently, though the position of the β-lactam band in the infrared indicates a high degree of true carbonyl character (i.e. **27***a*), there must be an additional factor which counterbalances this during the hydrolysis.

It is known that the hydrolysis of amides (29) and lactams (30) involves the formation of tetrahedral intermediates which then partition themselves between reactants and products. In a study of the concurrent alkaline hydrolysis and isotopic oxygen exchange of a series of *p*-substituted acetanilides Bender and Thomas (31) found that electron-releasing substituents cause an increase in k_3/k_2, the ratio of the rate constants for hydrolysis and exchange,

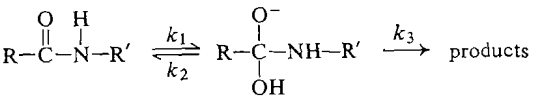

i.e., that stabilization of an anionic leaving group is not a principal factor in the breakdown of the tetrahedral intermediate. They interpreted their results to mean that a dipolar ion, e.g. **28**, is formed whose decomposition is rate limiting and whose concentration is increased as the basicity of the nitrogen atom of the anilide increases.

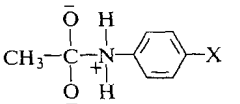

28

The same explanation, rather than a more qualitative "relief of steric strain" argument accounts nicely for the relationship already noted between the ease of hydrolysis of a β-lactam and the C=O stretching band in the i.r. spectrum. Suppression of resonance in the β-lactam ought to be associated with an increase in the basicity of the nitrogen atom and concomitant increase during hydrolysis of the concentration of a dipolar ion such as **29**. In terms of this explanation it is

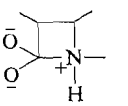

29

evident that the nitrogen atom of an anhydropenicillin is less basic than anticipated. The most reasonable explanation of this and of the i.r. absorption at 5.5 μ is that the electron pair on the nitrogen atom is delocalized *in the ground state*[12] into the adjacent α,β-unsaturated system; i.e.,

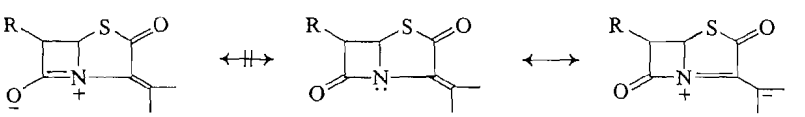

[11]Obviously it would be naive to consider that the stability of the β-lactam is the only factor affecting the antibacterial activity of a penicillin derivative. Structure-activity studies (1, 7, 27), as well as studies of the mode of action of penicillin (28) indicate that the carboxyl group is essential for activity. The absence of a carboxyl group in the anhydropenicillins is, therefore, consistent with their lack of activity.

[12]A similar proposal was made by Abraham and Newton (12) for the *excited state* of Cephalosporin C in order to account for the u.v. absorption at 260 mμ. More recent work (32, 33) indicates that this is only partly correct, the sulfur atom also participating in the chromophore of Cephalosporin C.

Can. J. Chem. Downloaded from www.nrcresearchpress.com by 210.87.254.42 on 09/05/12
For personal use only.

That the electron pair on the nitrogen atom is also delocalized *in the excited state* can be seen from the following argument. The 16-alkylidene-dehydroisoandrosterones **30***a* and **30***b* show u.v.

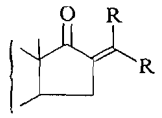

30 (*a*, R = H; *b*, R = CH_3)

absorption at 228 mμ and 250 mμ, respectively (34, 35). The replacement of the carbon α to carbonyl by oxygen leads to a decrease in both the wavelength and the intensity of the absorption. The unsaturated γ-lactone **31** showed only end absorption (ε 2400 at 230 mμ) (36). The unsaturated γ-lactone system of lactucin (**32**) was found to absorb at 208 mμ (ε 8600) (37). Replacement of the ring oxygen of an unsaturated γ-lactone by sulfur causes a small bathochromic shift. The thiolactone **33** absorbs at 220 mμ (38, 39) and the butenolide **34** has λ_{max} 214 mμ (40).

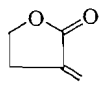

31

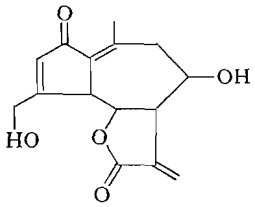

32

33

34

The introduction of substituents onto **33** results in a bathochromic shift of the low wavelength maximum (41) but there is also a substituent independent maximum at 265 mμ. The nature of this latter absorption has not been explained, but by analogy with the work already quoted (32, 33) this may be associated with an interaction between sulfur and the double bond.

If the β-lactam nitrogen does not participate in the chromophore, the u.v. maximum of an anhydropenicillin should be

$$208(\lambda_{max}\ \mathbf{32}) + 22(\lambda_{max}\ \mathbf{30}b - \lambda_{max}\ \mathbf{30}a) + 6(\lambda_{max}\ \mathbf{33} - \lambda_{max}\ \mathbf{34}) = 236\ \text{m}\mu$$

The bathochromic effect of nitrogen is thus ~34 mμ. This is a reasonable value (ref. 40, pp. 109, 243). Whether there is a second maximum near 270 mμ associated with the sulfur atom (41) cannot be stated at the present time.

Experimental

Melting points were taken on a Fisher–Johns block and are uncorrected. Infrared (i.r.) spectra were obtained on a Baird spectrometer, u.v. spectra on a Beckmann DK-2 instrument, and nuclear magnetic resonance (n.m.r.) spectra on a Varian A60 spectrometer in $CDCl_3$ with tetramethylsilane as an internal standard. Microanalyses are by R. M. Downing and his staff at Bristol Laboratories, Syracuse, New York. All solvents and chemicals were reagent grade except for the penicillins. Penicillin G and α-phenoxyethylpenicillin[13] were the commercially available materials; other penicillins were synthesized from 6-aminopenicillanic acid as described below. Thionyl chloride was purified by simple distillation; material purified by distillation from quinoline and then from linseed oil (42) did not seem more effective.

α-Phenoxyethylpenicillin Acid Chloride

(*a*) Potassium α-phenoxyethylpenicillin (12.1 g, 0.03 mole) was suspended in methylene chloride (100 ml), pyridine (2.4 ml, 0.03 mole) was added, and the mixture was cooled to −20° (internal temperature). A solution of thionyl chloride (3.6 g, 0.03 mole) in methylene chloride (50 ml) was then added in a steady stream. The internal temperature rose to −10° and the penicillin dissolved to produce a clear colorless solution. With continued external cooling the internal temperature was lowered to −20° and after 5 min the reaction mixture had begun to turn yellow. The temperature was maintained at −20° and stirring was continued for 3½ h by which time a deep yellowish-orange suspension was present. When an aliquot was removed for i.r. analysis and allowed to warm to room temperature a clear orange solution was obtained. This solution showed λ_{max} 5.5, 5.6 (sh), and 6.0 μ. The reaction mixture was then diluted with 300 ml of dry ether to precipitate salts, the cooling bath was removed, and when the internal temperature had reached 10°, the mixture was filtered and the filtrate was evaporated to dryness to produce 6.1 g (53%) of a yellow fluff. The i.r. spectrum of this fluff showed weak absorption at 5.8 μ, indicating that some hydrolysis had occurred during the work-up.

Anal. Calcd. for $C_{17}H_{19}N_2O_4ClS$: C, 53.4; H, 4.97. Found: C, 54.6; H, 5.46.

(*b*) The experiment was repeated as described in (*a*) and the substance remaining after evaporation of the ether was dissolved in benzene, the solution was filtered to remove some insoluble material, and the filtrate was then frozen and stored in a deep freeze for three days. The benzene was then removed by lyophilization to give a pale-yellow solid. The i.r. spectrum of this solid showed λ_{max} ($CHCl_3$) 5.5, 5.6 (sh), 5.8 (w), 6.0 μ.

Anal. Calcd. for $C_{17}H_{19}N_2O_4ClS$: Cl, 9.3. Found: Cl, 7.5.

[13]The trademark of Bristol Laboratories for α-phenoxyethylpenicillin is Syncillin.

Can. J. Chem. Downloaded from www.nrcresearchpress.com by 210.87.254.42 on 09/05/12
For personal use only.

The purpose of this experiment was to demonstrate that, after its preparation and isolation, the acid chloride could be stored in a convenient form until needed.

Anhydro-α-phenoxyethylpenicillin

(a) Via the Acid Chloride

Run 1—Potassium α-phenoxyethylpenicillin (365 g, 0.91 mole) was suspended in methylene chloride (3 l) containing pyridine (79 g, 1 mole). The mixture was stirred, cooled to −20°, and thionyl chloride (119 g, 1 mole) in methylene chloride (600 ml) was then added as rapidly as possible. The reaction mixture was stirred for 3 h at −20° and was then treated during 1 h with a solution of triethylamine (184 g, 1.82 moles) in methylene chloride (500 ml). Ten minutes after the addition was complete the i.r. spectrum of an aliquot showed λ_{max} 5.5, 5.9, 6.0, and 6.1 μ. The reaction mixture was then warmed to room temperature and the solvent was removed under reduced pressure. The black gum which remained solidified upon trituration with ethanol (2500 ml). Filtration, concentration of the filtrate to 1500 ml and then storage at 0° produced a crystalline compound which was collected and recrystallized thrice from acetone–water to give 20.0 g, m.p. 150–152°. The insoluble material from the ethanol trituration was extracted with acetone (2000 ml); this extract was concentrated to 500 ml and then diluted with 3000 ml of water. The precipitated solid was collected and washed with water. After drying *in vacuo* over phosphorous pentoxide, the solid weighed 56.0 g and melted at 142–145°. Three recrystallizations from acetone–water gave a tan solid; this was suspended in cold ethanol and the suspension filtered to produce 45.5 g of a white solid, m.p. 150–150.5°. The total yield of pure material was thus 65.6 g (21%).

Anal. Calcd. for $C_{17}H_{18}N_2O_4S$ (mol. wt., 346): C, 59.0; H, 5.21; N, 8.10. Found (mol. wt., 369, Signer): C, 59.16; H, 5.25; N, 8.31.

Run 2—Potassium α-phenoxyethylpenicillin (100 g, 0.25 mole) and triethylamine hydrochloride (35.0 g, 0.25 mole) were suspended in methylene chloride (1000 ml) and the mixture was stirred at 25° for 1 h to effect the conversion of the potassium salt to the triethylamine salt. The mixture was then cooled to −30° and pyridine (20 ml, 0.25 mole) was added followed with rapid stirring, by thionyl chloride (24.5 ml, 0.30 mole). The temperature was maintained at −25° to −30° for 1 h and the bright-orange suspension was then treated with 70.0 ml (0.50 mole) of triethylamine. After 10 min the mixture was warmed rapidly to room temperature and glacial acetic acid (30 ml, 0.5 mole) was added. The solution was washed with water, dried over anhydrous sodium sulfate, diluted with ether (4000 ml) and, after treatment with activated carbon, evaporated to dryness. The gum thus obtained was dissolved in hot absolute ethanol (100 ml). Cooling of this solution produced 20.4 g of yellow crystals. Recrystallization from boiling ethanol containing activated carbon gave 18.8 g (22%) of anhydro-α-phenoxyethylpenicillin, m.p. 148–150°.

(b) Via the Methanesulfonic Anhydride

Potassium α-phenoxyethylpenicillin (40.2 g, 0.10 mole) was suspended in methylene chloride (600 ml) and this suspension was treated during a 30 min period with a solution of methanesulfonyl chloride (11.5 g, 0.10 mole) in methylene chloride (50 ml). The reaction mixture was refluxed overnight and then cooled to 0° and treated dropwise over a 45 min period with a solution of triethylamine (10.1 g, 0.10 mole) in methylene chloride (50 ml). After continued stirring at 0° for 1 h and then at 30° for 2 h, water (200 ml) was added and the methylene chloride layer was separated, dried over anhydrous sodium sulfate, and then diluted with dry ether (3000 ml). After treatment with activated carbon the solution was concentrated and the residual oil was dissolved in absolute ethanol. After 48 h at 0°, the crystalline anhydro-α-phenoxyethylpenicillin, m.p. 148–150°, was collected. It weighed 2.0 g (6%).

(c) Via the Ethoxycarbonic Anhydride

Potassium α-phenoxyethylpenicillin (40.3 g, 0.10 mole) was suspended in methylene chloride (400 ml) and 13.8 g (0.10 mole) of triethylamine hydrochloride were added. The mixture was stirred for 1 h at 26°, then cooled to −3°, and ethyl chloroformate (9.52 ml, 0.10 mole) was added dropwise over a 5 min period. Stirring was continued, and after 15 min, the addition of triethylamine (14.1 ml, 0.10 mole) in methylene chloride (50 ml) was commenced. The addition required 1 h, the temperature being maintained at −3°. After an additional 2 h glacial acetic acid (11.4 ml, 0.20 mole) in methylene chloride (50 ml) was added dropwise. The temperature of the reaction mixture was then raised to 27° and maintained there for 35 min. Water (200 ml) was then added and the organic phase was separated, dried over anhydrous sodium sulfate, and evaporated under reduced pressure at 41° to an orange-brown gum. Crystallization from absolute ethanol afforded 1.77 g of anhydro-α-phenoxyethylpenicillin (5%), m.p. 146–148°. Found: C, 58.65; H, 5.47.

(d) Via the p-Toluenesulfonic Anhydride

Potassium α-phenoxyethylpenicillin (40.3 g, 0.10 mole) and *p*-toluenesulfonyl chloride (19.19 g, 0.10 mole) were stirred in methylene chloride (550 ml) for 16 h at 30–31°. Precipitation of potassium chloride during this period indicated that the mixed anhydride had formed. A solution of triethylamine (14.1 ml, 0.10 mole) in methylene chloride (50 ml) was then added during 20 min. The temperature rose to 34° and the colorless solution turned greenish-black. Stirring was continued for 7 h at 30° and the mixture was then washed with water (200 ml). The organic layer was dried over anhydrous sodium sulfate and evaporated to dryness at 40°. The residue was triturated with ethanol (100 ml) and the mixture was then kept at 5° for 24 h. There was then obtained by filtration 4.10 g (12%) of anhydro-α-phenoxyethylpenicillin, m.p. 140–144°.

Anhydropenicillin G

Potassium penicillin G (potassium benzylpenicillin) (37.2 g, 0.1 mole) was suspended in methylene chloride (250 ml) containing pyridine (8.9 ml, 0.1 mole). The mixture was cooled to −20° and thionyl chloride (8 ml, 13.3 g, 0.11 mole) was added over a 2 min period. Stirring was continued for 3 h at −20°. The temperature was then lowered to −30° and triethylamine (34 ml, 24.5 g, 0.25 mole) was added during 15 min. The temperature was allowed to rise to −20° during the next 30 min and was kept at −20° for 1.5 h and then allowed to rise to 0° during the next hour. Water (250 ml) was then added and the organic phase was separated, dried over an-

Can. J. Chem. Downloaded from www.nrcresearchpress.com by 210.87.254.42 on 09/05/12
For personal use only.

hydrous sodium sulfate, and evaporated to dryness. The black sticky mass thus obtained was dissolved in ethanol (200 ml) and this solution was kept overnight at 0°. The crystalline material which was deposited during this period was collected and recrystallized from aqueous acetone to yield 2.42 g (8%) of anhydropenicillin G, m.p. 156–158° (decomp.); λ_{max} (KBr): 5.5, 5.9, 6.0, 6.1 μ.

Anal. Calcd. for $C_{16}H_{16}N_2O_3S$: C, 60.74; N, 5.02; N, 8.86. Found: C, 60.82; H, 5.17; N, 8.85.

Anhydro-6-N-phthaloylaminopenicillin

The following procedure for the preparation of 6-*N*-phthaloylaminopenicillanic acid is adapted from one described by Nefkens and co-workers (43).

6-Aminopenicillanic acid (38.6 g, 0.18 mole) was dissolved in an aqueous solution (270 ml) containing sodium carbonate (19.1 g, 0.18 mole), and finely powdered *N*-carbethoxyphthalimide (43) (44.4 g, 0.20 mole) was added in one portion. The mixture was stirred vigorously at room temperature for 3.5 h and was then extracted twice with 100 ml portions of methylene chloride. The combined methylene chloride extracts were dried over anhydrous sodium sulfate and the solvent removed to give 17.7 g of unreacted *N*-carbethoxyphthalimide. The aqueous phase was diluted with acetone (80 ml) and was acidified to pH 3 with 2 *N* hydrochloric acid. The product crystallized immediately and was collected and washed with water. Concentration of the mother liquor produced a second crop of material which was also collected. The two crops (26.4 g) were combined and recrystallized from aqueous acetone to give 22.3 g of 6-*N*-phthaloylaminopenicillanic acid, m.p. 178–180° (decomp.). Based on the unreacted *N*-carbethoxyphthalimide the yield was 54%.

Anal. Calcd. for $C_{16}H_{14}N_2O_5S$: C, 55.49; H, 4.05. Found: C, 55.37; H, 4.15.

(a) Via the Acid Chloride

6-*N*-Phthaloylaminopenicillanic acid (20.0 g, 58 mmoles) and pyridine (10.17 ml, 0.12 mole) were dissolved in methylene chloride (230 ml). The solution was cooled to −20° and a solution of thionyl chloride (4.51 ml, 7.49 g, 63 mmoles) in methylene chloride (35 ml) was added as rapidly as possible. The reaction mixture was stirred at −15° to −20° for 3 h and was then treated during 0.5 h with a solution of triethylamine (24.3 ml, 17.5 g, 0.17 mole) in methylene chloride (70 ml). The temperature was brought to 20° and the reaction mixture was washed successively with 5% hydrochloric acid, 5% sodium bicarbonate and water, and then dried over anhydrous magnesium sulfate. Evaporation of the methylene chloride gave 16.05 g of a neutral residue. Two recrystallizations from 90% acetone gave 5.35 g (28%) of anhydro-6-*N*-phthaloylaminopenicillin, m.p. 236–237°.

Anal. Calcd. for $C_{16}H_{12}N_2O_4S$: C, 58.53; H, 3.66. Found: C, 58.84; H, 3.87.

Anhydro-α-methoxyisobutyrylpenicillin

A solution of α-methoxyisobutyric acid (11.8 g, 0.1 mole) in a mixture of acetone (20 ml) and dioxane (80 ml) was treated successively at −5° with triethylamine (15 ml, 10.8 g, 0.11 mole) and then isobutyl chloroformate (13.6 g, 0.1 mole) in dioxane (15 ml). To the mixed anhydride were added rapidly a solution of 6-aminopenicillanic acid (21.6 g, 0.1 mole) in water (100 ml) and triethylamine (15 ml, 0.11 mole), the temperature being maintained below 10°. The clear solution was stirred at 10° for 0.5 h, at 20° for 2 h, and was then diluted with 250 ml of water and extracted with ether, the ether extract being discarded. The aqueous layer was covered with fresh ether (300 ml), cooled, and acidified to pH 2 with sulfuric acid. The ether layer was separated, washed with cold water, dried over anhydrous sodium sulfate, and treated with 50 ml of a 40% solution of potassium 2-ethylhexanoate in *n*-butanol. The potassium 6-α-methoxyisobutyrylpenicillin was collected, triturated with ether and then dried *in vacuo* over phosphorous pentoxide. The yield was 24.5 g (70%), m.p. 234–236° (decomp.).

Anal. Calcd. for $C_{13}H_{20}N_2O_5SK$: C, 43.92; H, 5.67. Found: C, 43.85; H, 5.76.

The penicillin (6.33 g, 0.018 mole) was dissolved in methylene chloride (80 ml) containing triethylamine (2.67 ml, 0.019 mole) and the solution was cooled to 0°. Then ethyl chloroformate (1.90 ml, 0.02 mole) in methylene chloride (20 ml) was added dropwise during 5 min to form the mixed anhydride. Stirring was continued for 15 min at 0° and then powdered freshly prepared sodium methoxide (2.2 g, 0.04 mole) was added all at once. Stirring was continued for 2½ h at which time ice-cold pH 6 phosphate buffer (100 ml) was added. The layers were separated and the aqueous layer extracted with 50 ml of methylene chloride. The combined organic extract, after drying over anhydrous sodium sulfate, was evaporated to give a yellow gum. This gum could not be crystallized but the presence of anhydropenicillin was evident from the u.v. absorption at 269 mμ and i.r. absorption at 5.5, 5.9, and 6.1 μ.

6-(2-Hydroxy-1-naphthalamino)penicillanic Acid

To a suspension of 6-aminopenicillanic acid (4.32 g, 0.02 mole) in methanol (100 ml) was added 2-hydroxy-1-naphthaldehyde (44) (3.44 g, 0.02 mole). The mixture was stirred overnight, by which time dissolution of the 6-aminopenicillanic acid was complete, and the solvent was then removed under reduced pressure. Trituration with ether afforded the Schiff base as yellow crystals, m.p. 174–176° (decomp.); the yield was 6.6 g (90%).

Anal. Calcd. for $C_{19}H_{18}N_2O_4S$: C, 61.60; H, 4.89. Found: C, 61.40; H, 4.95.

Anhydro Derivative of 6-(2-Hydroxy-1-naphthalamino)-penicillanic Acid

The Schiff base (18.5 g, 0.05 mole) was suspended in methylene chloride (200 ml) containing pyridine (8.8 ml, 0.106 mole) and triethylamine (7 ml, 0.05 mole). The resulting solution was cooled to −20° and thionyl chloride (3.9 ml, 0.054 mole) was added as rapidly as possible. The reaction mixture was stirred for 3 h at −15 to −20° and was then treated during ½ h with triethylamine (14 ml, 0.1 mole) in methylene chloride (30 ml). Evaporation then afforded a crystalline solid which was isolated by trituration with ethanol and was recrystallized from aqueous acetone. The yield was 4.2 g (24%); m.p. 219–221° (decomp.).

Anal. Calcd. for $C_{19}H_{16}N_2O_3S$: C, 64.77; H, 4.54. Found: C, 64.47; H, 4.71.

Because the compound is a white solid and shows no i.r. absorption near 3 μ it is considered to have the cyclic structure **35**.

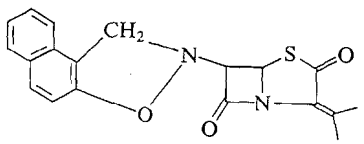

35

Isolation of Anhydro-α-phenoxyethylpenicillin "Dimer"

Run 1

Potassium α-phenoxyethylpenicillin (12.1 g, 0.03 mole) was converted to the acid chloride in the usual manner (*vide supra*) in methylene chloride (150 ml) and excess triethylamine was then added. When the i.r. spectrum of the reaction mixture showed conversion to the anhydropenicillin to be complete the mixture was warmed to room temperature, diluted with ether (800 ml), and filtered. The filtrate was evaporated to dryness, the residue triturated with tetrahydrofuran (50 ml), filtered, and re-evaporated to give 8.2 g of a brown solid (A) which smelled of pyridine.

One gram of A was dissolved in isopropyl alcohol (40 ml) and the solution was treated with decolorizing charcoal and then concentrated to 20 ml. Cooling to −10° produced a solid (B) which was collected. The filtrate from B upon dilution with water (75 ml) gave 0.2 g of a substance C. Heating B to reflux with isopropyl alcohol (40 ml) afforded an additional 0.29 g of (insoluble) C; identity of the two fractions was established by i.r. (*vide infra*).

One-half gram of A was dissolved in absolute ethanol (5 ml) and the solution was cooled to −10° to give anhydro-α-phenoxyethylpenicillin. This was collected and the filtrate was diluted with water (25 ml) to precipitate solid C (identified by its i.r. spectrum).

Run 2

Eighty grams of crude anhydro-α-phenoxyethylpenicillin prepared by the method of run 2 (*vide supra*) were recrystallized from boiling ethanol (2500 ml) and, after the purified anhydropenicillin was collected, the mother liquor was concentrated to 1000 ml and stored at 0° for two weeks. Six grams of substance C were then obtained by filtration.

A saturated solution of C (0.1 g) in methylene chloride (25 ml) was poured through a column of alumina (Woelm, activity III). Evaporation of the eluate and recrystallization from methylene chloride gave pale-yellow needles, m.p. 262–264°. The i.r. spectrum of this compound shows λ_{max} (KBr) 3.12, 3.27, 5.53, 5.93, 5.98, 6.03, 6.06, 6.10, 6.27, 6.60, 6.68 μ.

Anal. Calcd. for $C_{32}H_{32}N_4O_7S$ (mol. wt., 616.68): C, 62.32; H, 5.23; N, 9.09; S, 5.19. Found (*m/e*,[14] 616): C, 62.55, 62.20; H, 5.66, 5.48; N, 8.56, 8.84, 8.75; S, 4.98, 5.16.

Ozonolysis of Anhydro-α-phenoxyethylpenicillin

A solution of anhydro-α-phenoxyethylpenicillin (99 mg, 0.29 mmoles) in methylene chloride (10 ml) was cooled to 0° and treated for 20 min at a rate of 0.02 ft³/min with a stream of dry air containing ozone, generated at 90 V in a Welsbach ozonator. The reaction mixture, which contained a heavy precipitate, was rinsed into a distillation flask with water (12 ml), and zinc dust (100 mg) was added. All but 1 ml of the methylene chloride was removed by careful distillation and this distillate was discarded. Then the remainder of the methylene chloride and ca. 2 ml of water were distilled out and this second distillate was treated with 2.4 ml of a 2,4-dinitrophenylhydrazine reagent prepared in the usual manner (45). The mixture was warmed to distil out the remaining methylene chloride and then cooled in ice. A crystalline precipitate, 35 mg, m.p. 116–120°, was then obtained. Recrystallization from aqueous ethanol gave 30 mg (44%) of acetone 2,4-dinitrophenylhydrazone, m.p. 123.0–124.0°, identified by comparison with an authentic specimen.

[14]We are grateful to Professor D. B. MacLean for this determination.

1. H. T. Clark, J. R. Johnson, and R. Robinson (*Editors*). The chemistry of penicillin. Princeton University Press, Princeton, New Jersey. 1949.
2. G. G. F. Newton and E. P. Abraham. Biochem. J. **62**, 651 (1956).
3. B. Loder, G. G. F. Newton, and E. P. Abraham. Biochem. J. **79**, 408 (1961). R. B. Morin, B. G. Jackson, E. H. Flynn, and R. W. Roeske. J. Am. Chem. Soc. **84**, 3200 (1962). R. R. Chauvette, E. H. Flynn, B. G. Jackson, E. R. Lavagnino, R. B. Morin, R. A. Mueller, R. P. Pioch, R. W. Roeske, C. W. Ryan, J. L. Spencer, and E. V. Heyningen. J. Am. Chem. Soc. **84**, 3401 (1962).
4. G. Stork and H. T. Cheung. J. Am. Chem. Soc. **87**, 3783 (1965).
5. C. Djerassi. Steroid reactions, an outline for organic chemists. Holden-Day, Inc., San Francisco. 1963. Chap. 8.
6. J. W. ApSimon and O. E. Edwards. Can. J. Chem. **40**, 896 (1962).
7. J. F. Collins and M. H. Richmond. Nature, **195**, 142 (1962). D. Crowfoot, C. W. Bunn, B. W. Rogers-Low, and A. Turner-Jones. *In* The chemistry of penicillin. *Edited by* H. T. Clark, J. R. Johnson, and R. Robinson. Princeton University Press, Princeton, New Jersey. 1949. Chap. 11.
8. S. Wolfe and C. Ferrari. Unpublished results.
9. J. C. Sheehan. Molecular modification in drug design. Advances in Chemistry Series, No. 45, American Chemical Society, Washington, D.C. 1964. p. 15.
10. R. B. Morin, B. G. Jackson, R. A. Mueller, E. R. Lavagnino, W. B. Scanlon, and S. L. Andrews. J. Am. Chem. Soc. **85**, 1896 (1963).
11. R. Pummerer. Ber. **42**, 2282 (1909); Ber. **43**, 1401 (1910).
12. E. P. Abraham and G. G. F. Newton. Biochem. J. **79**, 377 (1961).
13. D. C. Hodgkin and E. N. Maslen. Biochem. J. **79**, 393 (1961).
14. E. P. Abraham and G. G. F. Newton. *In* Ciba Foundation Symposium, amino acids and peptides with antimetabolic activity. *Edited by* G. E. W. Wolstenholme. J. A. Churchill Ltd., London. 1958. p. 205.
15. Y. Villax. Brit. Patent No. 758,653 (1956); Chem. Abstr. **51**, 6957 (1957).
16. D. A. Johnson and C. A. Panetta. J. Org. Chem. **29**, 1826 (1964).
17. F. H. Carpenter. J. Am. Chem. Soc. **70**, 2964 (1948).
18. S. Wolfe. Unpublished results.

Can. J. Chem. Downloaded from www.nrcresearchpress.com by 210.87.254.42 on 09/05/12
For personal use only.

19. S. I. LUR'E and L. G. GATSENKO. Zh. Obshch. Khim. **22**, 262 (1952).
20. J. SICHER, M. SVOBODA, and J. FARKAS. Collection Czech. Chem. Commun. **20**, 1439 (1955).
21. D. O. HOLLAND and P. MAMALIS. J. Chem. Soc. 4596 (1958).
22. A. D. HOLLEY and R. W. HOLLEY. J. Am. Chem. Soc. **72**, 2771 (1950).
23. R. B. MORIN. 148th Nat. Meeting of the American Chemical Society. Abstr. of Papers. Chicago. Sept. 1964, p. 14P; R. B. MORIN. Personal communication.
24. L. J. BELLAMY. The infrared spectra of complex molecules. Methuen and Co., Ltd., London. 1962. pp. 214–15.
25. R. B. WOODWARD. *In* The chemistry of penicillin. *Edited by* H. T. Clark, J. R. Johnson, and R. Robinson. Princeton University Press, Princeton, New Jersey. 1949. Chap. 15.
26. R. J. GILLESPIE and T. BIRCHALL. Can. J. Chem. **41**, 148 (1963).
27. R. D. COGHILL, F. H. STODOLA, and J. L. WACHTEL. *In* The chemistry of penicillin. *Edited by* H. T. Clark, J. R. Johnson, and R. Robinson. Princeton University Press, Princeton, New Jersey. 1949. Chap. 20. Y. G. PERRON, L. B. CRAST, J. M. ESSERY, R. R. FRASER, J. C. GODFREY, C. T. HOLDREGE, W. F. MINOR, M. E. NEUBERT, R. A. PARTYKA, and L. C. CHENEY. J. Med. Chem. **7**, 483 (1964). M. CLAESEN and H. VANDERHAEGHE. Bull. Soc. Chim. Belges, **73**, 647 (1964).
28. J. L. STROMINGER, J. T. PARK, and R. E. THOMPSON. J. Biol. Chem. **234**, 3263 (1959). D. J. TIPPER and J. L. STROMINGER. Proc. Nat. Acad. Sci. U.S. **54**, 1133 (1965).
29. M. L. BENDER. Chem. Rev. **60**, 53 (1960).
30. M. I. VINNIK and Y. V. MOISEYEV. Tetrahedron, **19**, 1441 (1963).
31. M. L. BENDER and R. J. THOMAS. J. Am. Chem. Soc. **83**, 4183 (1961).
32. G. C. BARRETT, V. V. KANE, and G. LOWE. J. Chem. Soc. 783 (1964).
33. A. G. LONG and A. F. TURNER. Tetrahedron Letters, 421 (1963).
34. P. L. JULIAN, E. W. MEYER, and H. C. PRINTY. J. Am. Chem. Soc. **70**, 3872 (1948).
35. W. C. J. ROSS. J. Chem. Soc. 25 (1945).
36. C. J. CAVALLITO and T. H. HASKELL. J. Am. Chem. Soc. **68**, 2332 (1946).
37. D. H. R. BARTON and C. R. NARAYANAN. J. Chem. Soc. 963 (1958).
38. C. D. HURD and K. L. KREUZ. J. Am. Chem. Soc. **72**, 5543 (1950).
39. S. GRONOWITZ and R. A. HOFFMAN. Arkiv Kemi, **15**, 499 (1960).
40. A. I. SCOTT. Interpretation of the ultraviolet spectra of natural products. Pergamon Press. New York. 1964. p. 236.
41. A. HÖRNFELDT and S. GRONOWITZ. Arkiv Kemi, **21**, 239 (1963).
42. A. H. BLATT (*Editor*). Organic syntheses. Coll. Vol. 2. John Wiley and Sons. New York. 1943. p. 570.
43. G. H. L. NEFKENS, G. I. TESSER, and R. J. F. NIVARD. Rec. Trav. Chim. **79**, 688 (1960).
44. J. C. SHEEHAN and V. J. GRENDA. J. Am. Chem. Soc. **84**, 2417 (1962).
45. R. L. SHRINER, R. C. FUSON, and D. Y. CURTIN. The systematic identification of organic compounds. 4th ed. John Wiley and Sons. London. 1959. p. 219.

Can. J. Chem. Downloaded from www.nrcresearchpress.com by 210.87.254.42 on 09/05/12
For personal use only.

Can. J. Chem. Downloaded from www.nrcresearchpress.com by 210.87.254.40 on 09/05/12
For personal use only.

C-Aroylations of imides and *N*-aroylations of β-keto amides with aromatic esters by means of sodium hydride to form β-keto imides[1]

JAMES F. WOLFE[2] AND GEORGE B. TRIMITSIS
Department of Chemistry, Virginia Polytechnic Institute, Blacksburg, Virginia 24061

AND

CHARLES R. HAUSER
Department of Chemistry, Duke University, Durham, North Carolina 27706

Received March 15, 1968

Aroylations at the methyl groups of *N*-acetylbenzamide and *p*-benzoylaminoacetophenone, and at a methylene position of succinimide with appropriate aromatic esters were effected by means of sodium hydride in refluxing monoglyme. Benzoylation at the amide group of α-benzoylacetamide and salicylamide were accomplished similarly. The yields of β-keto imides from these *C*- and *N*-aroylations by sodium hydride, with which intermediate dianions were evidently not formed, were generally much better than those obtained through dianions produced by means of an alkali amide in liquid ammonia. The synthetic utility of the sodium hydride method is discussed.

Canadian Journal of Chemistry, 46, 2561 (1968)

N-Acetylbenzamide (**1**) has previously (1) been benzoylated at its methyl group with methyl benzoate by means of two molecular equivalents of potassium amide in liquid ammonia to form β-keto imide **2**; dianions **1**'' and **2**'' were intermediates (Scheme 1). Similarly, vinylogous imide

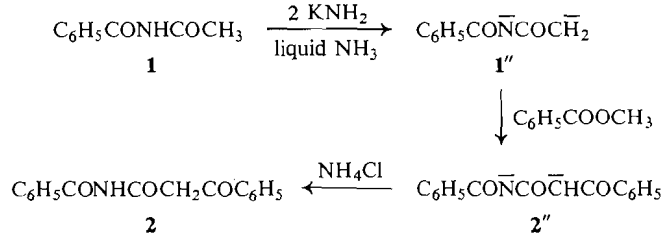

SCHEME 1

3 has been benzoylated at its methyl group to form **4** (2) and imide **5** at a methylene group to give **6** (3) through corresponding dianions.

Imides **1**, **3**, and **5** have now been benzoylated in better yields by means of sodium hydride in refluxing monoglyme, as summarized in Table I. For example, the yield of β-keto imide **2** from imide **1** with sodium hydride, eq. [1], was 85%, which is three times that (28%) obtained with potassium amide.

$$[1] \quad \mathbf{1} \xrightarrow[\text{NaH, monoglyme}]{C_6H_5COOCH_3} \mathbf{2}'' \xrightarrow{\text{acid}} \mathbf{2}$$

Whereas in the alkali amide method the imide is first converted to the dianion (see Scheme 1), in the sodium hydride method a mixture of the imide and ester is added to the reagent. When imide **1** was first treated with sodium hydride and methyl benzoate then added, the yield of **2** was only fair (36%) and much benzamide was obtained; the latter product arose through cleavage of imide **1** by the sodium hydride (see Experimental).

Similarly, imide **1** was aroylated with methyl

[1]This work was supported at Virginia Polytechnic Institute by the Petroleum Research Fund of the American Chemical Society, Grant No. 344G, and by the United States Public Health Service, Grant No. GM-14340 from the National Institute of General Medical Sciences. At Duke University, the work was supported by the National Science Foundation.

[2]Inquiries regarding this paper should be addressed to J. F. Wolfe, Virginia Polytechnic Institute.

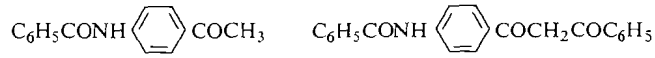

3 4

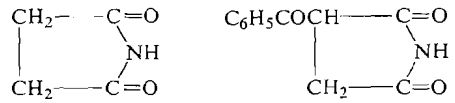

5 6

TABLE I

Yields of benzoylation products of imides by the sodium hydride and alkali amide methods

Imide	Benzoylation product	Yield (%) NaH method	Yield (%) MNH_2 method
1	**2**	85	28*
3	**4**	88	52†
5	**6**	56	44‡

*Ref. 1.
†Ref. 2.
‡Ref. 3.

anisate, methyl *p*-chlorobenzoate, and ethyl nicotinate to form the new β-keto imides **7***a–c* in yields of 79, 93, and 78%, respectively. Structural assignments for these products were supported by analyses and absorption spectra (see Experimental).

$C_6H_5CONHCOCH_2COAr$

7*a*, Ar = $C_6H_4OCH_3$-*p*

7*b*, Ar = C_6H_4Cl-*p*

7*c*, Ar = 3-Pyridyl

Next, β-keto amide **8** was benzoylated by the sodium hydride method to form the *N*-benzoyl derivative **2** in 91% yield, eq. [2]. This *N*-benzoylation represents an alternate route for the preparation of **2**, the other route involving *C*-benzoylation of imide **1**, see eq. [1].

[2] $C_6H_5COCH_2CONH_2$ (**8**) $\xrightarrow[\text{NaH method}]{C_6H_5COOCH_3}$ **2**

Similarly, salicylamide (**9**), which may be regarded as an enolized β-keto amide, was benzoylated by the sodium hydride method to give the *N*-benzoyl derivative **10** in 90% yield.

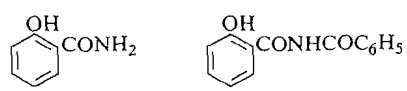

9 **10**

In contrast to sodium hydride, sodium amide was observed to effect the *N*-benzoylation of β-keto amide **8** through its dianion **8″** in only 14% yield, and none of the *N*-benzoyl derivative of **9** was obtained with sodium amide through dianion **9″**. That dianions **8″** and **9″** were formed initially was indicated by lack of stilbene formation on treatment with benzyl chloride (see Experimental).

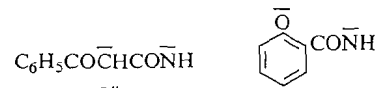

8″ **9″**

Finally, attempts were made to effect benzoylations at the methyl group of β-keto imide **11** and the phenolic imide **12** by the sodium hydride

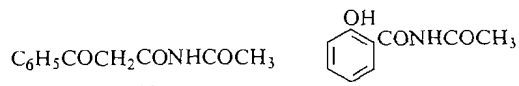

11 **12**

method. However, instead of *C*-benzoylation, cleavage of the respective acetyl groups occurred to form the β-keto amides **8** and **9** (or their anions), which underwent *N*-benzoylation to give the β-keto imides **2** and **10**, respectively.

Discussion

These results show that sodium hydride in refluxing monoglyme is preferable to an alkali amide in liquid ammonia for *C*-aroylations of imides **1**, **3**, and **5** and especially, for *N*-aroylation of β-keto amides **8** and **9**. Presumably the sodium hydride method could be extended, not only to other aromatic esters, but also to other imides and β-keto amides, thereby leading to the syntheses of many new products. In certain cases, the same product may be prepared by either *C*-aroylation of an imide or *N*-aroylation of a β-keto amide as illustrated above for **2** by eqs. [1] and [2],

Can. J. Chem. Downloaded from www.nrcresearchpress.com by 210.87.254.40 on 09/05/12
For personal use only.

$$RCONHCOCH_3 \xrightarrow[NaH]{R'COOCH_3} \underset{\mathbf{13}}{RCONHCOCH_2COR'} \xleftarrow[NaH]{RCOOCH_3} R'COCH_2CONH_2$$

SCHEME 2

respectively. These complementary courses of reaction may be generalized by Scheme 2 in which R and R′ are appropriate aroyl groups of symmetrical or unsymmetrical β-keto imides of type **13**.

Interestingly, as in previously reported aroylations of β-diketones (4) by means of sodium hydride, the present aroylations of imides and β-keto amides by this reagent evidently do not involve the intermediate formation of dianions, for example **1″**, which is the reactive intermediate in an aroylation by an alkali amide (see Scheme 1). Instead, only the imide monoanion such as **1′** (see Scheme 3), seems to be formed, at least until the ester is added. This was indicated by evolution of only about one molecular equivalent of hydrogen on addition of imide **1** or **5** to five molecular equivalents of sodium hydride in refluxing monoglyme (see Table II); yet the expected three molecular equivalents of hydrogen were evolved on addition of a mixture of the imide and methyl benzoate to the reagent in accordance with Scheme 3 (see Table III). Although somewhat more than one equivalent of hydrogen was evolved with imide **3** alone (see Table II), only the anticipated three equivalents of hydrogen were formed with a mixture of **3** and ester (see Table III).

$$\mathbf{1} \xrightarrow[(excess)]{NaH} \underset{\mathbf{1'}}{C_6H_5CO\bar{N}COCH_3} + H_2$$

$$\downarrow NaH \quad C_6H_5COOCH_3$$

$$H_2 + \mathbf{2''} \xleftarrow{NaH} C_6H_5CO\bar{N}COCH_2COC_6H_5 + H_2$$

SCHEME 3

Although a total of only three molecular equivalents of hydrogen were evolved when a mixture of β-keto amide **8** or **9** and methyl benzoate was added to the sodium hydride reagent (see Table III), prolonged treatment of **8** and **9** alone with excess reagent produced considerably more than one molecular equivalent of hydrogen (see Table II); this indicated that **8** and **9** were slowly converted to dianions **8″** and **9″**, respectively. However, formation of these dianions appears to be much too slow to account for the rate at which the benzoylations were realized in the presence of methyl benzoate (see Table III). Therefore dianions **8″** and **9″** seem not to be the reactive intermediates in these aroylations.

Several possible mechanisms for the related aroylations of β-diketones have previously been considered (4), and analogous mechanisms might also be possible for the present aroylations of imides and β-keto amides.

Experimental

Melting points were taken on a Thomas–Hoover melting point apparatus in open capillary tubes and are corrected. Analyses were performed by Galbraith Laboratories, Knoxville, Tennessee. Infrared (i.r.) spectra were taken on a Beckman IR-5A spectrophotometer using the potassium bromide pellet method. Nuclear magnetic resonance (n.m.r.) spectra were obtained on a Varian Associates A-60 spectrometer using deuteriodimethyl sulfoxide as solvent and tetramethylsilane as external standard. Chemical shifts are measured to the center of a singlet or multiplet. Thin-layer chromatograms (t.l.c.) were carried out with an Eastman Chromagram apparatus using Chromagram Sheets Type 1301R (silica gel) with fluorescent indicator and toluene–ethanol (3:1) as the developing solvent. Spots were detected with ultraviolet light. Monoglyme was distilled from sodium ribbon immediately before use. Sodium hydride was used as obtained from Metal Hydrides, Inc., Beverly, Massachusetts. Unless otherwise specified, chemicals were commercial reagent grade, and were used without further purification. All hydrogen evolution values are corrected for temperature, pressure, and water vapor pressure.

Benzoylations of Imides

In Table III are presented hydrogen evolution data accompanying these reactions. Additional details are given below.

(a) Of Imide 1

This reaction, as well as each of the subsequently described aroylations, was carried out in a 1 l three-necked flask equipped with a heating mantle, a pressure-equalizing addition funnel, and a high-efficiency reflux condenser, which was connected through a cold trap (Dry Ice–Acetone) to a Precision Scientific Co. wet-test meter filled with water. The center neck of the flask was tightly stoppered and the reaction mixture was stirred magnetically. The flask was charged with 250 ml of monoglyme and 0.25 mole of sodium hydride as an approximately 50% dispersion in mineral oil. A solution of 8.15 g (0.05 mole) of **1** (5) and 10.89 g (0.08 mole) of methyl benzoate in 100 ml of dry monoglyme was placed in the addition funnel. The system was then flushed with dry nitrogen and closed to the atmosphere. The sodium hydride – monoglyme slurry was brought to reflux, and when thermal equilibrium had been established, an initial reading was

Can. J. Chem. Downloaded from www.nrcresearchpress.com by 210.87.254.40 on 09/05/12
For personal use only.

TABLE II

Evolution of hydrogen from imides and β-keto amides with sodium hydride

Imide or β-keto amide	H_2 from addition of active hydrogen compound: Calculated for 1 mole equivalent (ml)	Found (ml)	% of theory	Reaction period (h)
1	1120	1220	109	6*
3	1120	1500	123	10.5
5	1120	1096	98	4.5*
8	560†	797	142	12
9	1120	1990	178	58

*Hydrogen evolution did not increase significantly with longer reaction periods.
†In this experiment 0.025 mole of **8** to 0.125 mole of sodium hydride was used; in all other experiments 0.05 mole of active hydrogen compound to 0.25 mole of sodium hydride was employed.

TABLE III

Evolution of hydrogen when a mixture of an imide or β-keto amide and methyl benzoate was added to excess sodium hydride

Imide or β-keto amide	H_2 from addition of active hydrogen compound and ester: Calculated for 3 mole equivalent (ml)	Found (ml)	% of theory	Reaction period (h)*
1	3360	3560	106	11
3	3360	3330	99	23
5	3360	3260	97	44
8	3360	3360	100	1
9	3360	3340	99	4

*Hydrogen evolution did not increase significantly with longer reaction periods.

taken on the test meter. The solution of imide and ester was added over a period of 25 min, the resulting reaction mixture was allowed to reflux until hydrogen evolution had ceased, and a final reading was taken on the test meter (see Table III). Most of the monoglyme was removed under reduced pressure and the remaining pasty residue was cooled to 0 °C in an ice–water bath. The residue was then treated with 150 ml of ether followed, after a few minutes, by 20 ml of cold water; initially, the water was added dropwise until the excess sodium hydride had been destroyed. The solid which separated between the layers was collected by filtration, treated with excess cold 6 *N* HCl, washed with 5% sodium bicarbonate solution, and recrystallized from 95% ethanol to afford 11.33 g (85%) of *N*,α-dibenzoylacetamide (**2**), m.p. 170–171 °C. A mixture melting point determination with an authentic sample of **2** (1) showed no depression; the i.r. spectra of the two samples were identical.

In one experiment, imide **1** (0.025 mole) was added to 0.125 mole of sodium hydride in 150 ml of monoglyme and the reaction mixture was allowed to reflux for 2 h during which time one molecular equivalent of hydrogen was evolved. Methyl benzoate (0.04 mole) was then added and refluxing was continued for 5 h; slightly less than two additional equivalents of hydrogen were evolved during this period. The reaction mixture was processed in the usual manner to afford 2.46 g (36%) of β-keto imide **2**. Thin-layer chromatography (t.l.c.) of the residues obtained by concentration of both the ethereal and aqueous layers revealed that they consisted primarily of benzamide.

In another experiment, imide **1** (0.025 mole) was treated with 0.125 mole of sodium hydride in refluxing monoglyme for 6 h but methyl benzoate was excluded. The reaction mixture was processed as usual to afford a crude semisolid which consisted predominately of benzamide as shown by t.l.c. In order to establish that **1** was not hydrolyzed to benzamide during the basic work-up of the reaction, a 1 g sample of **1** was treated with 100 ml of 5% aqueous sodium hydroxide solution for 30 min. The basic solution was acidified with cold 12 *N* hydrochloric acid and extracted with ether. The extracts were dried (Na_2SO_4) and concentrated to afford 0.8 g (80%) of recovered **1**.

(b) Of Imide 3

A mixture of 11.96 g (0.05 mole) of **3** (2) and 10.89 g (0.08 mole) of methyl benzoate in 100 ml of monoglyme, was added to 0.25 mole of sodium hydride in 250 ml of refluxing monoglyme. The reaction mixture was heated at reflux for 23 h. The solvent was removed under reduced pressure and the residue was treated as described above to yield 17.39 g of crude product. This was further purified through its copper chelate (2) to give 15.14 g (88%) of **4**, m.p. 183–185 °C, (lit. (2) m.p. 184.5–186 °C), mixture m.p. 183–185 °C.

(c) Of Imide 5

A solution of **5** (4.95 g, 0.05 mole) and methyl benzoate (10.89 g, 0.08 mole) was treated with 0.50 mole of sodium hydride in refluxing monoglyme for 44 h. The reaction mixture was processed in the usual manner to afford, after one crystallization of the crude product from absolute ethanol, 5.71 g (56%) of pure **6**, m.p. 138–140 °C, (lit. (3) m.p. 137.5–138 °C), mixture m.p. 138–140 °C. The i.r.

Can. J. Chem. Downloaded from www.nrcresearchpress.com by 210.87.254.40 on 09/05/12
For personal use only.

Can. J. Chem. Downloaded from www.nrcresearchpress.com by 210.87.254.40 on 09/05/12
For personal use only.

spectrum of this compound was identical with that of an authentic sample of **6** prepared by the potassium amide method (3).

*Aroylations of Imide **1** with other Aromatic Esters*

The general procedure for these aroylations was essentially the same as for the benzoylations described above. In all cases a mixture of 0.05 mole of **1**, 0.08 mole of the appropriate ester, and 0.25 mole of sodium hydride was refluxed in 350 ml of monoglyme, and the resulting mixture was processed in the usual manner. Additional details are given below.

(a) With Methyl Anisate

The reaction mixture was refluxed for 9 h. The crude product was recrystallized from absolute ethanol to afford 11.2 g (79%) of *N-benzoyl-α-(p-methoxybenzoyl)-acetamide* (*7a*), m.p. 177–178 °C; n.m.r. peaks at δ 7.7 (m, 9, aromatic), at 4.56 (s, 2, $COCH_2CO$), and at 3.82 p.p.m. (s, 3, CH_3O); and i.r. absorption at 3400 (NH) and 1690 cm^{-1} (C=O).

Anal. Calcd. for $C_{17}H_{15}NO_4$: C, 68.67; H, 5.08; N, 4.71. Found: C, 68.44; H, 5.12; N, 4.85.

(b) With Methyl p-Chlorobenzoate

The crude produce obtained after 6.5 h of refluxing was recrystallized from absolute ethanol to give 14.0 g (93%) of *N-benzoyl-α-(p-chlorobenzoyl)acetamide* (*7b*), m.p. 168–169 °C; n.m.r. peaks at δ 7.85 (m, 9, aromatic), and at 4.60 p.p.m. (s, 2, $COCH_2CO$); and i.r. absorption at 3400 (NH) and 1695 cm^{-1} (C=O).

Anal. Calcd. for $C_{16}H_{12}ClNO_3$: C, 63.69; H, 4.01; Cl, 11.75; N, 4.64. Found: C, 63.49; H, 3.87; Cl, 11.93; N, 4.52.

(c) With Ethyl Nicotinate

The reaction mixture was allowed to reflux for 6 h. The monoglyme was removed and the residue was treated with ether and water. The solid which separated between the layers was collected by filtration and dissolved in 300 ml of cold 3 *N* hydrochloric acid. The acidic solution was neutralized with solid sodium bicarbonate. The crude yellow solid which precipitated from the neutral solution was recrystallized from tetrahydrofuran to afford 10.47 (78%) of *N-benzoyl-α-nicotinoylacetamide* (*7c*), m.p. 166–167 °C; n.m.r. peaks at δ 7.80 (m, 9, aromatic) and at 5.76 p.p.m. (s, 2, $COCH_2CO$); and i.r. peaks at 3400 (NH) and at 1600 cm^{-1} (C=O).

Anal. Calcd. for $C_{15}H_{12}N_2O_3$: C, 67.16; H, 4.51; N, 10.44. Found: C, 67.45; H, 4.67; N, 10.26.

*Benzoylations of β-Keto Amides **8** and **9** by Means of Sodium Hydride*

Hydrogen evolution data for these reactions are presented in Table III.

*(a) Of β-Keto Amide **8***

A mixture of 8.15 g (0.05 mole) of **8** (6) and 0.08 mole of methyl benzoate was treated with 0.25 mole of sodium hydride in 350 ml of refluxing monoglyme for 1 h. The reaction mixture was processed as described above for the aroylations of imides to afford 12.5 g (91%) of the *N*-benzoyl derivative **2**, which was identical in all respects with the product obtained from the benzoylation of imide **1**.

*(b) Of Amide **9***

Treatment of 6.86 g (0.05 mole) of **9** with 0.08 mole of methyl benzoate and 0.25 mole of sodium hydride in 350 ml of refluxing monoglyme for 4 h produced 13.50 g (90%) of *N*-benzoylsalicylamide (**10**), m.p. 203–204 °C (lit. (7) m.p. 201 °C). The infrared spectrum of **10** was identical with that of an authentic sample.

*Results of Amides **8** and **9** with Sodium Amide*

To 0.10 mole of sodium amide prepared from 0.10 g-atom of sodium in 500 ml of commercial anhydrous liquid ammonia (8) was added 0.05 mole of **8**. The resulting suspension was allowed to stir for 30 min then 0.05 mole of methyl benzoate in 100 ml of anhydrous ether was added and stirring was continued for 1.5 h. The ammonia was evaporated (steam bath) as an equal volume of ether was added. The ethereal suspension was added to 300 ml of cold 3 *N* hydrochloric acid to precipitate 1.84 g (14%) of the *N*-benzoyl derivative **2**.

In a second experiment 0.025 mole of **8** was treated with 0.063 mole of sodium amide in liquid ammonia followed after 45 min by 0.05 mole of benzyl chloride[3] in 50 ml of anhydrous ether. After 3 h the reaction mixture was processed as described above. The ethereal layer was dried (Na_2SO_4) and concentrated to afford a crude solid which was shown by t.l.c. to consist primarily of unchanged **8**.

Treatment of a 0.05 mole sample of **9** with sodium amide (0.10 mole) in liquid ammonia followed by addition of methyl benzoate produced none of the desired *N*-benzoyl derivative **10**. Similarly, treatment of **9** with sodium amide and benzyl chloride gave a nearly quantitative recovery of starting material; no stilbene was detected.

*Attempted Benzoylations of Imides **11** and **12***

*(a) Of Imide **11***

To a suspension of 0.25 mole of sodium hydride in 250 ml of refluxing monoglyme was added a solution of 10.25 g (0.05 mole) of **11** (10) and 10.89 g (0.08 mole) of methyl benzoate in 350 ml of monoglyme. The reaction mixture was allowed to reflux for 18 h before being processed in the normal fashion. The solid residue which separated between the layers was collected by filtration, treated with hydrochloric acid, washed with sodium bicarbonate solution, and recrystallized from absolute ethanol to afford 12.7 g (95%) of **2**, m.p. 170–171 °C, mixture m.p. 170–171 °C. The i.r. spectrum of this material was identical with that of a sample of **2** prepared as described above.

*(b) Of Imide **12***

A mixture of 8.96 g (0.05 mole) of **12**, 0.08 mole of methyl benzoate, and 0.25 mole of sodium hydride in 250 ml of monoglyme was refluxed for 8 h. The reaction was processed in the manner described in section (*a*) above to afford, after one recrystallization of the crude product from 95% ethanol, 8.53 g (71%) of *N*-benzoylsalicylamide **10**, m.p. 201–202 °C, mixture m.p. 201–202 °C.

Measurements of Evolution of Hydrogen from Imides and Keto Amides with Sodium Hydride

In order to determine the extent of ionization of these active hydrogen compounds by sodium hydride, a 0.025–0.05 mole sample of the appropriate imide or amide in

[3]Addition of the benzyl chloride was not accompanied by the transient purple color associated with stilbene formation and no stilbene was isolated. Thus, the two molecular equivalents of sodium amide were apparently consumed in the twofold ionization of **8** to form **8″**. See ref. 9.

100 ml of monoglyme, contained in the addition funnel of the apparatus described above, was added over a 15 min period to 0.125–0.25 mole of sodium hydride in refluxing monoglyme. The resulting mixture was allowed to reflux as periodic readings were taken on the test meter. When hydrogen evolution was essentially complete, the reaction time and total volume of hydrogen were noted. These values are presented in Table II.

1. S. D. WORK, D. R. BRYANT, and C. R. HAUSER. J. Am. Chem. Soc. **85**, 872 (1964).
2. C. R. HAUSER and C. J. EBY. J. Org. Chem. **22**, 909 (1957).
3. D. R. BRYANT and C. R. HAUSER. J. Am. Chem. Soc. **83**, 3468 (1961).
4. M. L. MILES, T. M. HARRIS, and C. R. HAUSER. J. Org. Chem. **30**, 1007 (1965).
5. J. B. POLYA and T. M. SPOTSWOOD. Rec. Trav. Chim. **67**, 927 (1948).
6. C. R. HAUSER and C. J. EBY. J. Am. Chem. Soc. **79**, 725 (1957).
7. J. MCCONNAN and A. W. TITHERLEY. J. Chem. Soc. **89**, 1331 (1906).
8. C. R. HAUSER, F. W. SWAMER, and J. T. ADAMS. Org. Reactions, **8**, 122 (1954).
9. C. R. HAUSER, W. R. BRASSEN, P. S. SKELL, S. W. KANTOR, and A. E. BRODHAG. J. Am. Chem. Soc. **78**, 1653 (1956).
10. J. F. WOLFE and C. L. MAO. J. Org. Chem. **31**, 3069 (1966).

Can. J. Chem. Downloaded from www.nrcresearchpress.com by 210.87.254.40 on 09/05/12
For personal use only.

Can. J. Chem. Downloaded from www.nrcresearchpress.com by 210.87.254.105 on 09/05/12
For personal use only.

Intramolecular hydrogen bonding in cycloalkane-1,2-diol monoacetates[1]

ROBERT W. WRIGHT[2] and R. H. MARCHESSAULT

Cellulose Research Institute and Chemistry Department, State University of New York College of Forestry, Syracuse, New York

Received February 13, 1968

Intramolecular hydrogen bonding in cyclopentane- and cyclohexane-1,2-diol monoacetates was studied by high resolution infrared spectroscopy in the 3μ region. Intramolecular hydrogen bonding was exhibited by all compounds and the data are interpreted in terms of preferred conformations, assuming the acetate group to be exclusively in the "planar *trans*" form.

trans-Cyclopentane-1,2-diol monoacetate exhibited two hydroxyl absorption bands. One band was assigned to free hydroxyl stretching and the other to hydrogen bonding with the carbonyl oxygen so that an equilibrium between two ring conformations must be assumed to exist in solution. With *cis*-cyclopentane-1,2-diol monoacetate only a strong high frequency band was observed, and this was attributed to hydrogen bonding to the alkoxyl oxygen.

trans- and *cis*-cyclohexane-1,2-diol monoacetate both exhibited two hydroxyl absorption bands. With the former, the hydroxyl group was assumed to be exclusively in an equatorial position to permit hydrogen bonding to both the alkoxyl and carbonyl oxygens. Similarly, in the latter, the high frequency band was attributed to hydrogen bonding to the alkoxyl oxygen atom while the low frequency band was assigned to hydrogen bonding to the carbonyl oxygen.

Canadian Journal of Chemistry, **46**, 2567 (1968)

Introduction

Kuhn (1) and Cole and Jefferies (2) demonstrated the use of infrared spectroscopy as a tool for the conformational analysis of cycloalkane-1,2-diols. With these compounds, there exists the possibility for intramolecular hydrogen bond formation between the hydroxyl functions with one of the oxygens acting as the donor and the other as the acceptor for the hydrogen atom. When two absorption bands appear in the hydroxyl stretching region, an equilibrium between free and intramolecular hydrogen-bonded conformers is postulated. The higher frequency band always corresponds to the stretching mode of a free hydroxyl. The presence of only a single band indicates a conformation, as occurs with *trans*-cyclopentane-1,2-diol, in which hydrogen bonding is not possible. This approach has been fruitful in studying conformational equilibria for compounds where oxygen occurs in the ring, e.g., dioxane or pyran type molecules (3). For monohydroxyl derivatives, the appearance of absorption bands for both free and hydrogen-bonded hydroxyl groups was interpreted in terms of an equilibrium between two conformers. Figure 1 summarizes the generally accepted interpretation of the observed free and intramolecular hydrogen bonding in the cycloalkane-1,2-diols involved in this study.

Since the difference in rates of reaction for conformers of the cycloalkanols are usually small (factors of 2 to 5) (4), hydrogen bonding effects can be important. Depending on the reaction mechanism, the hydrogen bond may enhance or completely reverse (5–7) the "normal" behavior, based on the elementary rules of conformational analysis (8). The present study deals with a situation which is of common occurrence in polysaccharides, steroids, and other natural products, i.e., a free hydroxyl in close proximity to an esterified one. This situation allows two hydrogen bond acceptor sites: at the alkoxyl and at the carbonyl oxygens. Henbest and Lovell (5) showed that in *cis*-cycloalkane-1,3-diol monoacetates, intramolecular hydrogen bonding involved only the alkoxyl oxygen atom. This type of bonding caused a decrease in the infrared alkoxyl and an increase in the carbonyl absorption frequency. More recently, Bruice and Fife (9) reported the infrared spectra of the cyclopentane-1,2-diol monoacetates. The spectra were interpreted as indicating a hydrogen bond to the alkoxyl oxygen atom in the *cis* isomer and to the carbonyl oxygen atom in the *trans* isomer. Again these assignments were inferred from the known geometries of the molecules and from the observed shifts in the absorption bands for the two types of carbon–oxygen bonds in the acetate ester.

---

[1]Presented at 147th National American Chemical Society Meeting, Philadelphia, Pennsylvania, 1964.

[2]Present address: Owens-Illinois Technical Center, Toledo, Ohio.

Can. J. Chem. Downloaded from www.nrcresearchpress.com by 210.87.254.105 on 09/05/12
For personal use only.

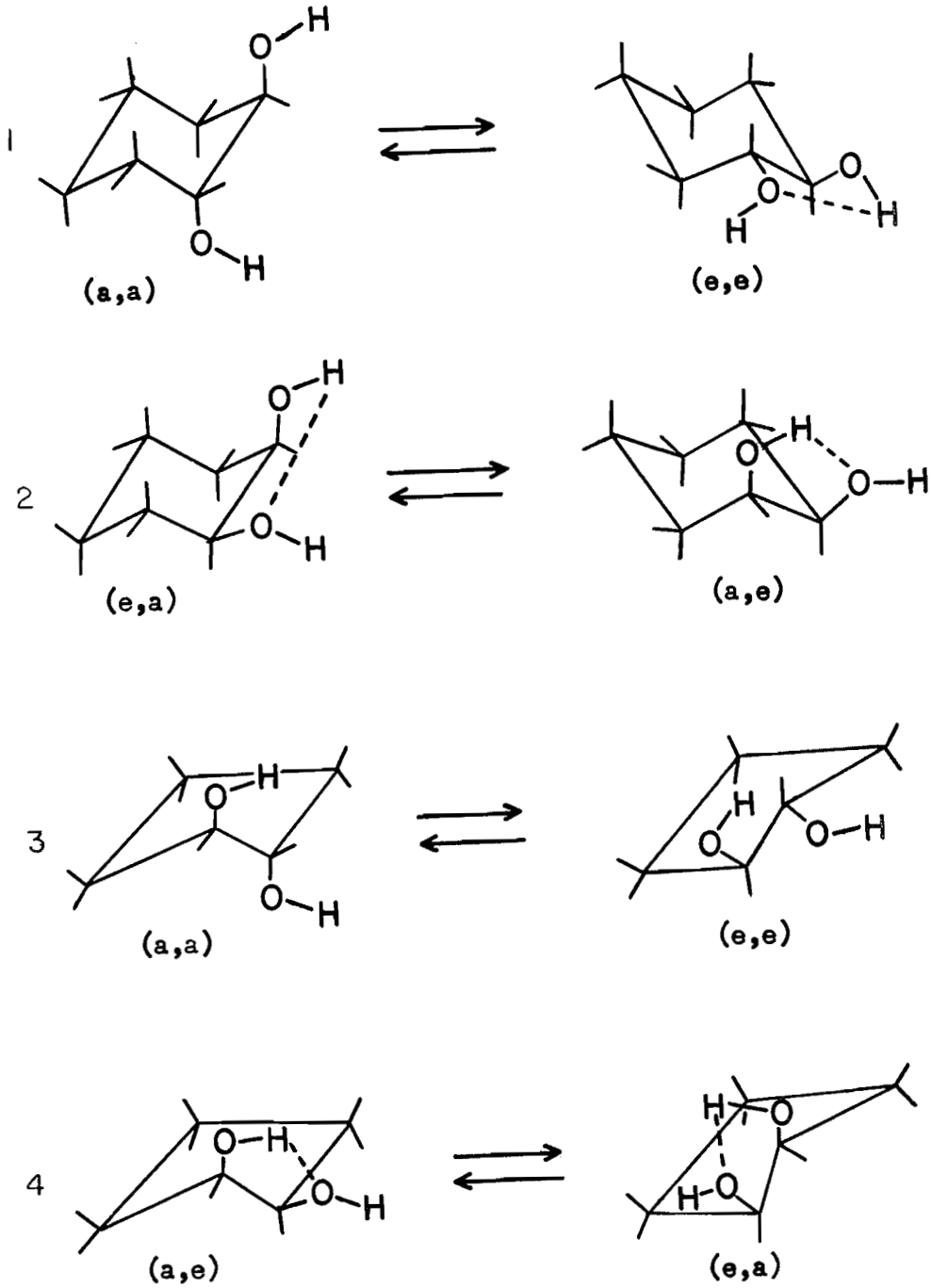

FIG. 1. Conformations of some cycloalkane-1,2-diols: **1**, *trans*-cyclohexane-1,2-diol; **2**, *cis*-cyclohexane-1,2-diol; **3**, *trans*-cyclopentane-1,2-diol; **4**, *cis*-cyclopentane-1,2-diol.

Can. J. Chem. Downloaded from www.nrcresearchpress.com by 210.87.254.105 on 09/05/12
For personal use only.

TABLE I

Cycloalkane diols and acetate derivatives

Compound	% C		% H		% Acetyl		Refractive index* at 19.8 °C	Melting point* (°C)	References
	Calcd.	Found	Calcd.	Found	Calcd.	Found			
cis-Cyclopentane-1,2-diol	58.78	58.64	9.87	9.85	—	—	—	28 (29.8)	16
cis-Cyclopentane-1,2-diol monoacetate	58.30	56.80	8.35	8.34	29.86	29.56	1.4592 (1.4576†)	—	11
trans-Cyclopentane-1,2-diol	58.78	58.93	9.87	9.81	—	—	—	53–54 (50;53.7)	11,16
trans-Cyclopentane-1,2-diol monoacetate	58.30	58.01	8.35	8.46	29.86	31.43	1.4531 (1.4553‡)	—	11
cis-Cyclohexane-1,2-diol	62.04	62.12	10.41	10.20	—	—	—	96.5–97.5 (97–98)	12
cis-Cyclohexane-1,2-diol monoacetate	60.73	60.66	8.92	8.89	27.21	26.64	1.4649 (1.4650§)	—	17
trans-Cyclohexane-1,2-diol	62.04	61.74	10.41	10.20	—	—	—	102–104 (101.5–103)	13
trans-Cyclohexane-1,2-diol monoacetate	60.73	60.56	8.92	8.78	27.21	25.96	1.4635 (1.4685§)	—	18
trans-Cyclohexane-1,2-diol diacetate	59.98	59.49	8.05	7.83	43.00	40.73	1.4483 (1.4457§)	—	19

*Literature values are in parentheses.
†Reference 17.
‡Reference 20.
§Reference 25.

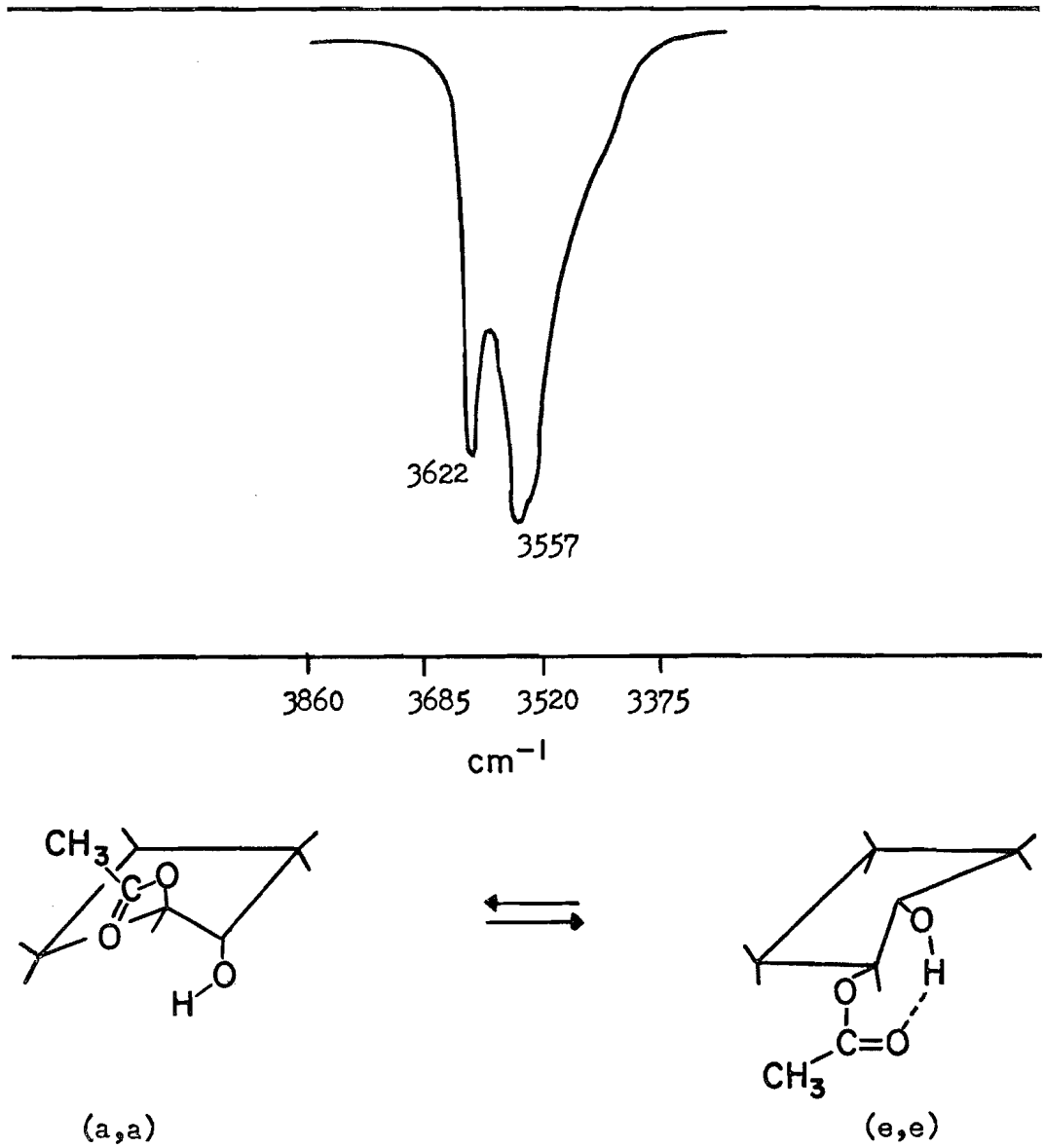

FIG. 2. The infrared spectrum of *trans*-cyclopentane-1,2-diol monoacetate.

Experimental

Compounds

The cycloalkane-1,2-diols were prepared by methods reported in the literature: *cis*-cyclopentane-1,2-diol was obtained by the procedure of Wiberg and Saegebarth (10) and the *trans* isomer by that of Owen and Smith (11). *cis*-Cyclohexane-1,2-diol was synthesized by the silver acetate, iodine, water method (12) and *trans*-cyclohexane-1,2-diol via the epoxidation of cyclohexane (13). The compounds were purified either by repeated distillation or recrystallization, and their purity was checked by analysis for carbon and hydrogen as well as analysis for the α-glycol grouping by periodate oxidation (14).

Each of the monoacetates of the above compounds was purified by vapor-phase chromatography using an Aerograph Autoprep model A700. A 20 ft column packed with 30% SE-30 silicone rubber on Chromosorb P was used. The *cis*-cyclopentane-1,2-diol monoacetate is an intermediate in the preparation of *cis*-cyclopentane-1,2-diol (10). A similar procedure was used for preparing the *cis*-cyclohexane-1,2-diol monoacetate (12). *trans*-Cyclopentane-1,2-diol monoacetate was prepared by sulfuric acid catalyzed partial acetylation of the parent diol with

Can. J. Chem. Downloaded from www.nrcresearchpress.com by 210.87.254.105 on 09/05/12
For personal use only.

TABLE II

Hydroxyl group infrared absorption frequency as a measure of hydrogen bonding in cycloalkane-1,2-diols and cycloalkane-1,2-diol monoacetates

Compound	Parent diol cm^{-1}	Monoacetate* cm^{-1}	Bonding in monoacetate	Extent
trans-Cyclopentane	3620	3622 (s)	Free	
		3557 (v,s.)	Carbonyl	Major
cis-Cyclopentane	3633	3610 (s)	Alkoxyl	Major
	3572			
trans-Cyclohexane	3634	3627 (s)	Alkoxyl	Major
	3602	3540 (b,s.)	Carbonyl	
cis-Cyclohexane	3626	3610 (s)	Alkoxyl	Major
	3587	3539 (w)	Carbonyl	

*s: strong; b: broad; w: weak; v: very.

acetic anhydride in glacial acetic acid. The crude product was extracted with ether and purified as mentioned above. The *trans*-cyclohexane-1,2-diol monoacetate was prepared by reacting cyclohexene oxide (15) with glacial acetic acid using the procedure of Owen and Smith (11). *trans*-Cyclohexane-1,2-diol diacetate was isolated during purification of the corresponding monoacetate. Each of the purified acetates was a clear viscous oil. Table I lists the analytical data and some physical constants for the parent compounds and the derived acetates.

Solvents and Solutions

Spectrograde carbon tetrachloride was distilled over P_2O_5 and stored over P_2O_5 until used. Reagent grade 1,2,4-trichlorobenzene was used for calibration.

The compounds studied were weighed into dry, stoppered volumetric flasks. After weighing, the compounds were stored for several days in a desiccator over P_2O_5. The solutions were prepared at room temperature in a dry-box equipped with a vacuum exhaust to allow rapid exchange of the nitrogen atmosphere. In order to avoid intermolecular association, all solutions were made up to 0.007 *M* or less. Spectra were always rerun on subsequent dilutions to insure that the relative intensities of the absorption bands were concentration independent.

Infrared Spectroscopy

All spectra were recorded on a Baird Associates double-beam spectrophotometer equipped with either a lithium fluoride or sodium chloride prism. The former prism was used for measurements in the 3μ region while the latter was used for exploratory purposes and to measure carbonyl frequencies in the 6μ region. The carbonyl overtones in the region of interest were assigned from spectra of dilute solutions of the diacetates.

The spectra were recorded using 1.7 cm cells (not carefully matched) with sodium chloride windows. Filling and cleaning of the cells was performed in a dry-box. All measurements were conducted at room temperature (23 °C).

For the 6μ region, polystyrene was used as a calibration standard. Initially, 1,2,4-trichlorobenzene (2.1–2.5μ) and polystyrene (3.2–3.5μ) were used to calibrate the 3μ region. The calibration gave, within experimental error, the same frequencies for the cyclohexane-1,2-diols as reported by Kuhn (1). All frequencies reported for the monoacetates were, therefore, referred to their parent diols as standards. The frequencies could be measured in this way to $\pm 3\ cm^{-1}$ although absolute frequencies were accurate only to $\pm 10\ cm^{-1}$.

Results

The relevant high resolution spectra for the 3μ region are reproduced in Figs. 2–5. Hydroxyl stretching bands are present in all the spectra indicating the presence of either free hydroxyl or hydrogen bonding to the alkoxyl oxygen and/or carbonyl oxygen. The assignments of the various bands, which are summarized in Table II, were made by comparing the observed OH stretching frequencies with the characteristic free and intramolecularly bonded stretching frequencies for the parent cycloalkane diols. The latter are listed in the second column of Table II and correspond to the values reported by Kuhn (1).

It is clear that all three of the possible hydroxyl types were observed. In *trans*-cyclopentane-1,2-diol monoacetate where bonding to the alkoxyl oxygen is sterically impossible, both free and carbonyl-bonded hydroxyl are present. This suggests that at room temperature an equilibrium exists between conformers exhibiting the two forms. Similar conclusions can be reached upon examination of the spectra for the other compounds. In all cases, the hydrogen bond to the carbonyl oxygen, on the basis of intensity, yields the strongest (largest $\Delta\nu$), but not the preponderant hydrogen bond. This clearly indicates a preference for hydrogen bonds yielding five-membered rather than seven-membered rings as recently illustrated for a series of model acyclic compounds (20). The absorption bands assigned to the hydrogen bond involving a carbonyl oxygen were also broader than those bands associated with either a free or an alkoxyl oxygen hydrogen bond. This undoubtedly is a

Can. J. Chem. Downloaded from www.nrcresearchpress.com by 210.87.254.105 on 09/05/12
For personal use only.

Can. J. Chem. Downloaded from www.nrcresearchpress.com by 210.87.254.105 on 09/05/12
For personal use only.

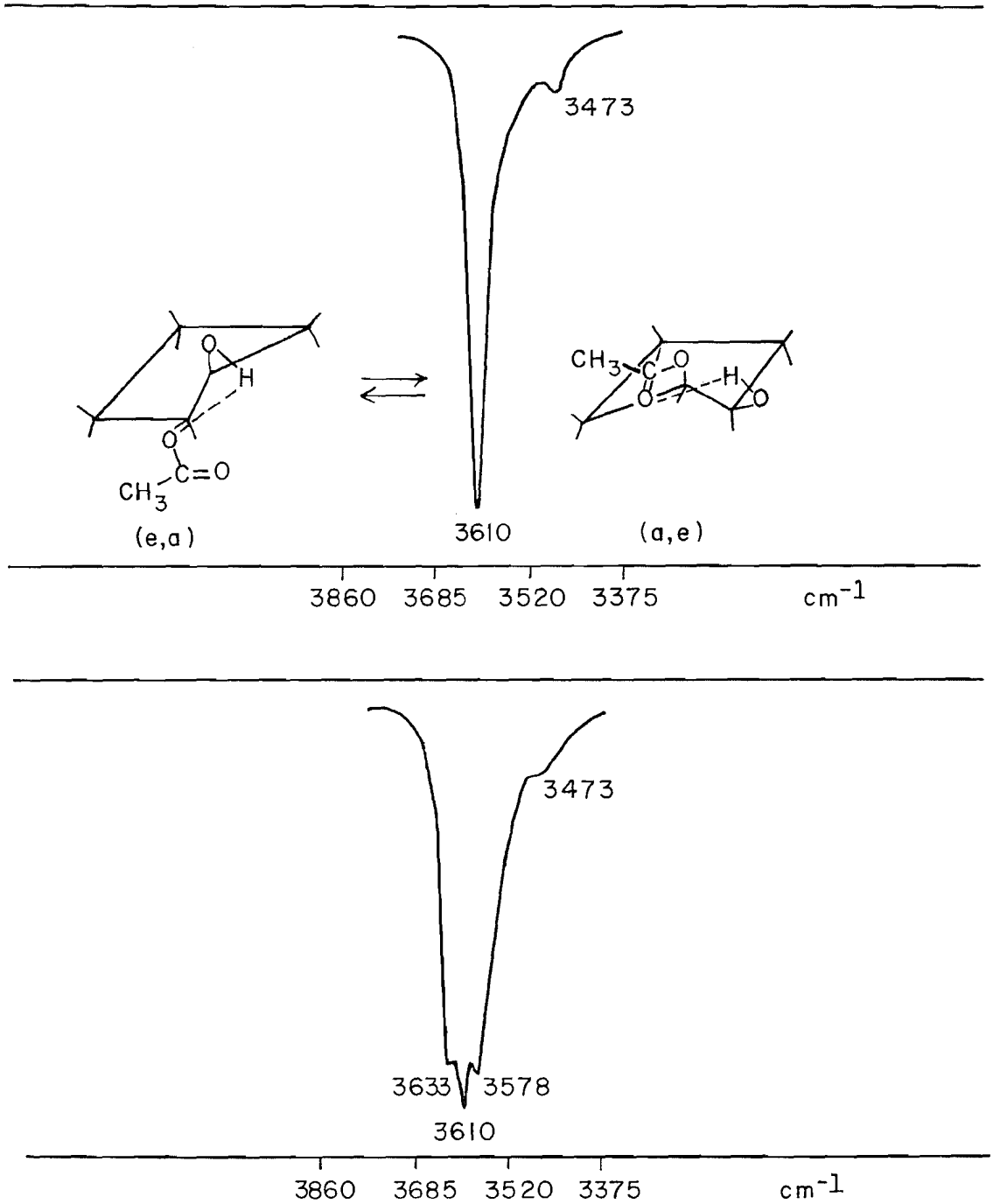

FIG. 3. The infrared spectra of: (*a*) *cis*-cyclopentane-1,2-diol monoacetate; (*b*) the same compound mixed with parent diol.

Can. J. Chem. Downloaded from www.nrcresearchpress.com by 210.87.254.105 on 09/05/12
For personal use only.

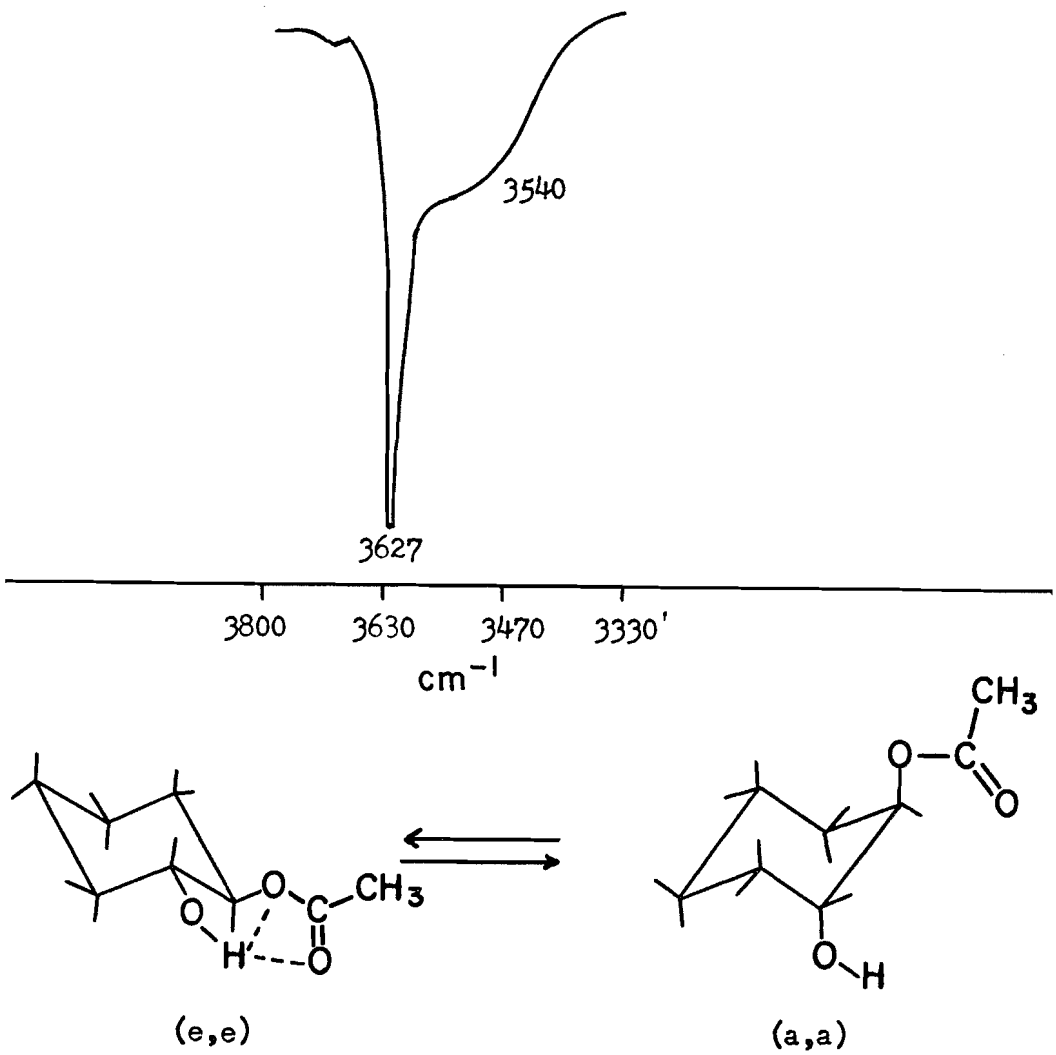

FIG. 4. The infrared spectrum of *trans*-cyclohexane-1,2-diol monoacetate.

reflection of greater numbers of steric arrangements possible in the former due to the nature of the acetoxy group.

Another general feature of the data for monoacetates, summarized in Table II, is the much smaller frequency shift compared to the parent diols for the intramolecular hydrogen bond involving the alkoxyl oxygen. This, of course, denotes a weaker hydrogen bond in the monoacetate. The effect can be accounted for by invoking the influence of the carbonyl group on the electron density at the alkoxyl oxygen.

In the *trans*-cyclohexane-1,2-diol system, the frequency of the carbonyl stretching mode for the monoacetate was compared to that of the diacetate. For the latter, a value of 1750 cm^{-1} was recorded while the monoacetate absorbed at 1730 cm^{-1}. This indicates hydrogen bonding to the carbonyl oxygen.

Discussion

In the case of the *trans*-cyclopentane-1,2-diol monoacetate there may be a conformation factor favoring the appearance of free hydroxyl. Rather than simply representing rotational isomers involving the ring-appended acetyl and hydroxyl groups, the two O—H bonds (Fig. 2)

Can. J. Chem. Downloaded from www.nrcresearchpress.com by 210.87.254.105 on 09/05/12
For personal use only.

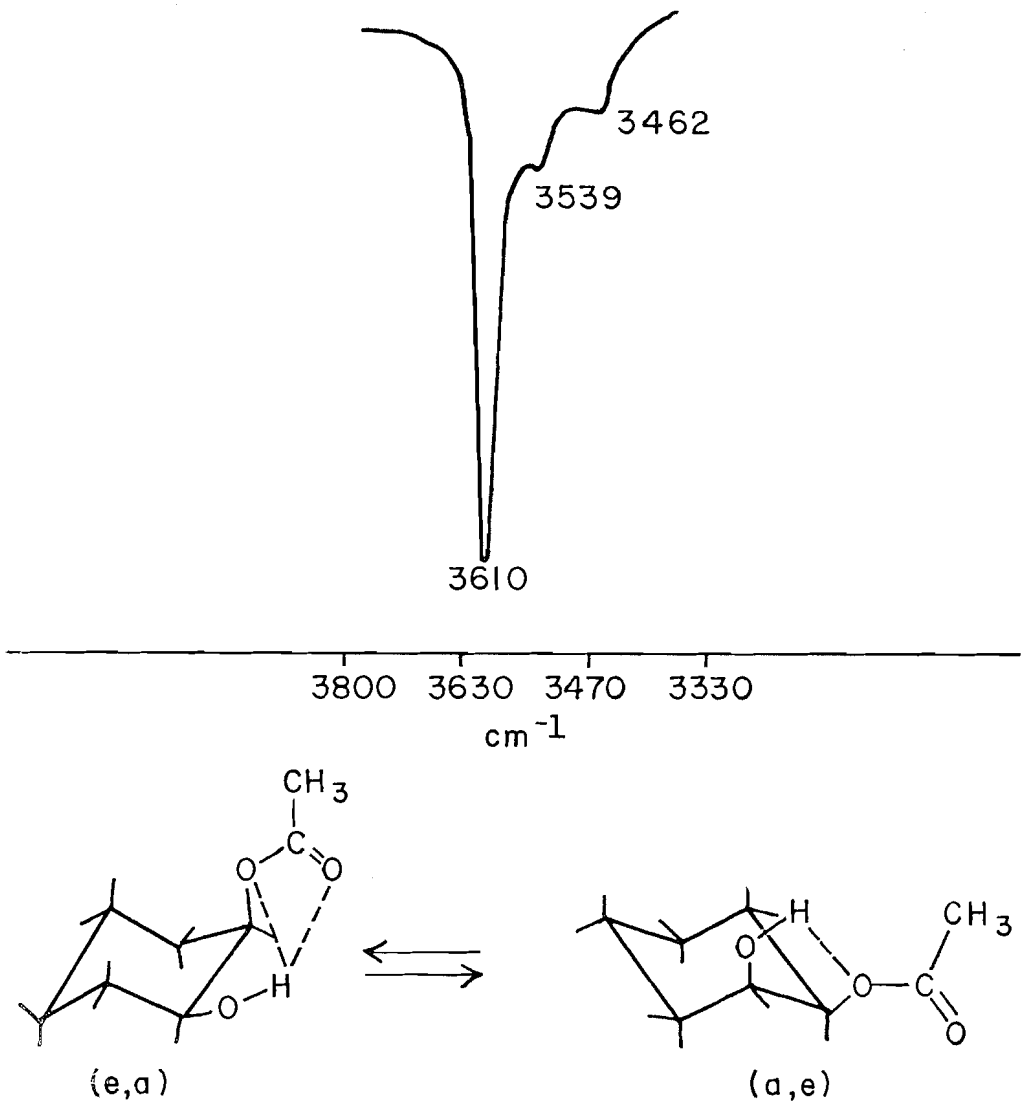

FIG. 5. The infrared spectrum of *cis*-cyclohexane-1,2-diol monoacetate.

may each be associated with a distinct ring form. Assuming that the resonance stabilized "planar *trans*" arrangement of the ester group prevails, two distinct half-chair conformers (Fig. 2) are visualized wherein the two C—O bonds occupy diequatorial and diaxial positions, respectively. Examination of molecular models shows that the former clearly allows hydrogen bonding while the latter does not. The same conclusion can be reached by considering hydrogen-bonding distances in the envelope forms of the cyclopentane ring.

By contrast with the *trans* isomer, the spectrum (Fig. 3) for *cis*-cyclopentane-1,2-diol monoacetate shows only a single hydrogen-bonded OH frequency and no free hydroxyl. The weak band at 3473 cm^{-1} is assigned to a carbonyl overtone. Bruice and Fife (9) reported a high frequency band at 3618 cm^{-1} (within experimental error, this is equivalent to the 3610 cm^{-1} band in this study) and a very weak low frequency absorption at 3542 cm^{-1}. They assigned these bands to free and to alkoxyl oxygen-bonded hydroxyls, respectively. Although we did not observe the low

Can. J. Chem. Downloaded from www.nrcresearchpress.com by 210.87.254.105 on 09/05/12
For personal use only.

frequency band, we prefer to interpret the data reported by these workers in terms of two hydrogen bonds. This is in accord with conformational considerations similar to the above which always lead to molecular forms with an axial–equatorial relation between substituents, i.e., dihedral angles in the range of 60 °C. In such cases, the hydrogen bonding pattern cannot be related to conformer equilibria.

Some support is given to our interpretation by the spectrum of a dilute carbon tetrachloride solution containing both the parent diol and *cis*-cyclopentane-1,2-diol monoacetate (Fig. 3*b*). The three distinct bands corresponding to the two diol frequencies (free and intramolecularly hydrogen bonded) and the monoacetate frequency are clearly distinguishable. The observed shift in the *cis* monoacetate hydroxyl frequency might also be attributed to the inductive effect of the neighboring acetate group, but this is not considered likely since a shift of this magnitude (23 cm^{-1}) was not observed for the *trans* monoacetate. On this basis, the above interpretation of the data in terms of two hydrogen bonds is preferred.

trans-Cyclohexane-1,2-diol monoacetate can assume the two forms shown in Fig. 4. The axial–axial conformation seems to be an unlikely one both from an energetic point of view and on the basis of experimental evidence for the diol. Furthermore, molecular models indicate that the maximum hydrogen bonding distance is exceeded in this conformer for both the carbonyl and alkoxyl oxygen. The apparent absence of free hydroxyl in the spectrum of this compound implies that the diequatorial conformer is exclusively present. An explanation for the unusually small frequency shift in the 3627 cm^{-1} band assigned to the intramolecular hydrogen bond to alkoxyl oxygen was suggested above. The relatively broad band centered at 3540 cm^{-1} is referred to hydrogen bonding with the carbonyl oxygen. However, the possibility that the 3627 cm^{-1} band may be related to the free OH stretching mode of the axial–axial conformer cannot be completely dismissed. Although less favored sterically, it has been suggested (4) that dipole–dipole interaction is more favorable in this conformer.

By contrast with the previous compound, *cis*-cyclohexane-1,2-diol monoacetate provides a more complex system since both of the ring forms shown are expected to be present. Four hydrogen bonds are possible: two for each of the alkoxyl and the carbonyl oxygens. In the spectrum shown in Fig. 5, only two hydrogen-bonded OH frequencies were observed. As indicated, the band at 3610 cm^{-1} is attributed to hydrogen bonding with the alkoxyl oxygen, and the 3539 cm^{-1} absorption to hydrogen bonds involving the carbonyl oxygen. From these data, it is not possible to arrive at any conclusions concerning the conformations responsible for the bands observed. Until appropriate model systems which permit isolation of the separate conformers have been examined, the foregoing is offered as a possible interpretation.

1. L. P. KUHN. J. Am. Chem. Soc. **76**, 4323 (1954); **74**, 2492 (1952).
2. A. R. H. COLE and P. R. JEFFERIES. J. Chem. Soc. 4391 (1956).
3. S. A. BARKER, J. S. BRIMACOMBE, A. B. FOSTER, D. H. WIFFEN, and G. ZWEIFEL. Tetrahedron, **7**, 10 (1959).
4. E. L. ELIEL. Stereochemistry of carbon compounds. McGraw-Hill Book Co., Inc., New York. 1962. pp. 235–236.
5. H. B. HENBEST and B. J. LOVELL. J. Chem. Soc. 1965 (1957).
6. S. M. KUPCHAN, W. S. JOHNSON, and S. RAJAGOPALAN. Tetrahedron, **7**, 47 (1959).
7. K. W. BUCK, A. B. FOSTER, A. R. PERRY, and J. M. WEBBER. J. Chem. Soc. 4171 (1963).
8. D. H. R. BARTON and R. C. COOKSON. Quart. Rev. London, **10**, 44 (1956).
9. T. C. BRUICE and T. H. FIFE. J. Am. Chem. Soc. **84**, 1973 (1962).
10. K. B. WIBERG and K. A. SAEGEBARTH. J. Am. Chem. Soc. **79**, 6256 (1957).
11. L. N. OWEN and P. N. SMITH. J. Chem. Soc. 4026 (1952).
12. F. V. BRUTCHER, JR. and G. EVANS III. J. Org. Chem. **23**, 618 (1958).
13. A. ROEBUCK and H. ADKINS. Organic syntheses. Coll. Vol. III. John Wiley and Sons, Inc., New York. 1955. p. 217.
14. ROBERT W. WRIGHT. Ph.D. Thesis, State University of New York, College of Forestry, Syracuse, New York. 1964.
15. A. E. Osterberg. Organic syntheses. Coll. Vol. I. John Wiley and Sons, Inc., New York. 1946. p. 185.
16. P. E. VERKADE, J. COOPS, JR., C. J. MAAN, and A. VEKADE-SANDBERGEN. Ann. Chem. **467**, 217 (1928).
17. S. WINSTEIN, H. V. HESS, and R. E. BUCKLES. J. Am. Chem. Soc. **64**, 2796 (1942).
18. M. GODCHOT. Compt. Rend. **176**, 449 (1923).
19. S. WINSTEIN and R. E. BUCKLES. J. Am. Chem. Soc. **64**, 2780 (1942).
20. A. B. FOSTER, A. H. HAINES, and M. STACEY. Tetrahedron, **16**, 177 (1961).

Proton magnetic resonance spectra of some aromatic amines and derived amides

R. F. C. BROWN
Department of Chemistry, School of General Studies, Australia National University, Canberra, Australia

AND

L. RADOM AND S. STERNHELL
School of Chemistry, University of Sydney, Sydney, Australia

AND

I. D. RAE
Department of Chemistry, Monash University, Clayton, Australia

Received February 7, 1968

The chemical shifts of ring protons in substituted anilines, *N*-methylanilines, some heterocyclic amines, and their derived acetamides and 4′-bromobenzamides are reported. The magnitude of the downfield shift accompanying acylation is related to the preferred configuration of the amide.

Canadian Journal of Chemistry, 46, 2577 (1968)

Introduction

In connection with another project (1) we have commented on the relation between the downfield shifts of ring protons accompanying acetylation of anilines and the substitution pattern in the aromatic ring. The present work represents a systematic extension of these observations and rationalization of the principal effects observed.

Experimental

(a) Preparation of Compounds

The majority of the compounds used in this investigation were available from commercial sources and were purified, when necessary, in the usual manner. Others were prepared by methods described in the literature, and had the reported physical constants. Their proton magnetic resonance (p.m.r.) spectra were in accord with their structures. New compounds, and those previously prepared whose constants differed significantly from the literature values, are listed in Table I.

(b) Recording of Spectra

All spectra were determined on Varian A-60 spectrometers, the sweep widths of which were checked with standard solutions. The data are for very dilute (approximately 2%) solutions in CCl_4 (or $CDCl_3$ for solubility reasons, where indicated), but concentration effects in the range 2–10% appeared to be negligible. Further, in spite of examples of solvent association involving $CDCl_3$ (2), no significant solvent effects could be noted in cases where measurements in both solvents were performed.

(c) Interpretation of Spectra

The spectra obtained under the conditions described above varied greatly in their complexity, but most of the pertinent resonances could be located without difficulty and were assigned as shown in Table II, principally on the basis of the general rule that $J_{ortho} \gg J_{meta} > J_{para}$. Many spectra could not be completely analyzed, because often only the principal lines were discernible in the dilute solutions used. For this reason the data in Table II are reported in Hz at 60 MHz, rather than in parts per million (p.p.m.), in accordance with the accepted convention (3).

Discussion

Since Table II is so large as to obscure significant trends in the data presented, it is convenient to proceed to analysis through a number of abstractions. Our major interest lay in the changes in aromatic proton resonances which arose from acylation of the amino group. Changes of this type have also been described by Carter (*4a*) and by Siddall and Stewart (*4b*) in papers published after the completion of this work, and we have already alluded to them in our preliminary publication (1). Other authors have approached the analysis of such systems in their own ways, (e.g. by comparing acetanilides with the corresponding toluenes (5), and by comparison of *ortho*- and *para*-substituted anilides (6)), and have arrived at similar conclusions.

Effects of N-Acylation on the Spectra of Aromatic Amines

(a) Configuration about the CO—N Bond

As the following arguments will be concerned with the long range shielding effects of the amide side chain, it is important to establish the stereochemistry of the amide group. In the first instance, the *N*-acyl derivatives have been treated as if the configuration about the nitrogen atom

TABLE I

Derivatives of 4-bromobenzanilide

Substituents		Analytical data (%) C	H	N	Melting point (°C) Observed	Literature	Reference
4′-Me					239	223	67
						233	68
4′-Cl					221	217.5	68
2′,5′-diMe	Calculated	59.2	4.6	4.6	166		
	Found	59.2	4.6	4.8			
2′,5′-diCl	Calculated	45.3	2.3	4.1	140		
	Found	45.0	2.6	4.2			
2′,5′-diMeO	Calculated	53.6	4.2	4.2	93		
	Found	53.6	4.4	4.3			
2′-Me—N—Me	Calculated	59.2	4.6	4.6	72		
	Found	59.6	4.8	—			
4′-Me—N—Me	Calculated	59.2	4.6	4.6	119		
	Found	—	—	4.1			
2′,4′-diMe—N—Me	Calculated	60.4	5.1	4.4	86		
	Found	60.1	5.0	—			
2′,5′-diMe—N—Me	Calculated	60.4	5.1	4.4	96		
	Found	60.4	5.2	—			
4′-Cl—N—Me	Calculated	51.8	3.4	4.3	81		
	Found	52.0	3.5	—			
2′,5′-diCl—N—Me	Calculated	46.8	2.8	3.9	105		
	Found	46.8	3.0	—			
2′,5′-diMeO—N—Me	Calculated	54.9	4.6	4.0	113		
	Found	55.1	4.8	3.7			

were planar. In general, of course, this configuration will be pyramidal (7–10) although the deviation from planarity is minimized when the electron density on nitrogen is reduced by electron withdrawing substituents (10–15).

X-Ray crystallographic studies (16) have shown that, in crystalline acetanilide, the carbonyl group is oriented toward the aromatic ring as in structure (**1**). The infrared spectra of a number of *N*-aryl acetamides, however, indicate the existence of up to 10% of another form (assigned the *trans* configuration (**2**)) in carbon tetrachloride solutions (17). In solutions of certain *N*-alkyl acetanilides, other workers have reported mixtures of the two forms (18, 19) although these are not generally observed (4, 20). In the present work *cis–trans* mixtures were observed for 2′-nitro-*N*-methylacetanilide and for two 2′,6′-disubstituted acetanilides.

It was observed that the relevant portions of the infrared (i.r.) and proton magnetic resonance (p.m.r.) spectra of *p*-acetotoluidide and *p*-pivalotoluidide were identical, each corresponding to a single *cis* or *trans* isomer. Since a *trans*-pivaloyl derivative (**2**, R = CMe_3) would be strongly destabilized by steric interactions, it follows that both compounds exist totally in the *cis* form (**1**) in deuteriochloroform solution. This is in accord with the proposals of other authors based on p.m.r. spectroscopy that *N*-monosubstituted amides in which the acyl group is larger than formyl exist solely (4, 21), or to a very large extent (22), in the *cis* conformation (**1**) in solution. Measurements of dipole moments have also been construed as support for the predominance of *cis* amides (23).

(b) Acylation Shifts and Hydrogen Bonding

In this section attention is focussed on the changes in the aromatic proton resonances which result when a primary aromatic amine is acylated, i.e. the "acylation shift". Either acetylation or 4-bromobenzoylation of a primary amino group causes pronounced downfield shifts of the ortho proton resonances. For acetylation (for which a better array of results is available), these fall in two ranges, viz. 45–63 Hz and 91–132 Hz, and it is apparent that the larger shifts are associated with the presence of a certain type of ortho substituent which can hydrogen bond with the amide proton.

Thus the larger shifts may be rationalized as the result of long range deshielding by the amide carbonyl group (24, 25), which is *cis* to, and *approximately* coplanar with, the aromatic ring,

a configuration (3) in which the carbonyl group would exert its maximum deshielding effect (26[1]). Independent evidence for this hypothesis is provided by the chemical shifts of the amide N—H protons (where the relevant resonances could be located) which are significantly downfield in cases where hydrogen bonding is postulated. The solvent effects described in the accompanying paper (28) and independent observations from the laboratory of the Polaroid Corporation (6) also support this proposal. Further, the conversion of an *N*-methylaniline to its amide is never associated with the larger acylation shifts of the ortho protons (cf. Table II).

Pertinent information may also be obtained from the acylation shifts of *meta* and *para* protons. *Para* proton resonances are shifted downfield by 18–32 Hz, due largely to the reduction of shielding at this position when the nitrogen lone pair of electrons is deployed in resonance with the amide carbonyl. The smaller shifts of *meta* protons may be correlated with the preferred configuration (3) because H-5′ appears to be more affected than H-3′ when hydrogen bonding substituent is present at C-2′, e.g. the 2,4-dichloroaniline case (13 vs. 9 Hz). Those meta protons which are adjacent to a 2′-nitro group suffer only very small acylation shifts, perhaps due to some unexpected changes in the shielding effects of the highly anisotropic nitro group (29–31).

The data in Table II also indicate an approximate correspondence between the known hydrogen bonding ability of the ortho substituents (32) and the acylation shifts for the 6′-protons (cf. Br, 91; Cl, 102; OR, 106–107; NO_2, 114–132; COOMe, 124–126 Hz, at 60 MHz).

(c) Configuration about the Ar—N Bond in Acetanilides

Anisotropic and electronic changes are expected to be the major contributors to the observed acylation shifts of the aromatic protons. It is most informative to attempt a separation of these contributions since by so doing the conformations of the acetanilides about the Ar—N bond may be brought under further scrutiny.

Because of their distance from the amide group, we may assume that anisotropic effects on the *para* protons will be negligible. If we then arbitrarily equate the electronic contributions to the *ortho* and *para* acylation shifts (i.e. 18–32 Hz) the difference between the two total shifts is the anisotropic contribution to the *ortho* shift. This residual shift amounts to roughly 30 Hz in the absence of intramolecular hydrogen bonding[2] and 100 Hz in the presence of a strong hydrogen bond. The geometries of the hydrogen bond and the amide group require the carbonyl group to be almost in the ring plane when hydrogen bonding operates. In the non-hydrogen-bonded cases, if the same geometry applies, we would expect the anisotropic contribution to ortho acylation shifts to be just half that of the hydrogen-bonded cases, (since the carbonyl now has *two* possible coplanar orientations) i.e. about 50 Hz. The discrepancy between the observed 30 Hz and even such a crudely calculated 50 Hz is sufficiently large to warrant the proposal that the amide and ring planes of acetanilides are not coincident in the absence of a strong intramolecular hydrogen bond. With the amide group slightly inclined to the plane of the ring, the carbonyl group exerts less than its maximum deshielding on the ortho protons (24, 25). Similar behavior has been described for the related thioacetanilides (33).

Strong support for this proposal comes from the X-ray crystallographic structure determination of acetanilide (16), and from dipole moment studies for solutions of several anilides in benzene and in dioxan (34). In both studies angles of approximately 38° between the planes containing the amide group and the aromatic ring were proposed.[3] For *N*-acetyl indoline, where coplanarity is ensured by the carbons of the indoline ring rather than a hydrogen bond, the acylation shift of H-7 is 106 Hz (35).

(d) Ring Proton Shifts Accompanying the Acetylation of N-Methylanilines

The effects of acetylation on the shifts of *ortho* and *para* protons are comparable (approximately 35 Hz), suggesting that anisotropic effects of the amide group do not play an important role. The

[1]Rationalization of our results in terms of a recently proposed (G. J. Karabatsos, G. C. Sonnichsen, N. Hsi, and D. J. Fenoglio. J. Am. Chem. Soc. **89**, 5067 (1967).) model for the anisotropy of the carbonyl group is possible with slight extension of the deshielding cone. For a comment on deshielding by the amide group as a whole, however, see reference (4*b*).

[2]Carter (4), employing a different rationale, has theorized that this difference should be about 0.3 p.p.m., i.e. 18 Hz.

[3]The X-ray result, however, (4) has recently been recalculated as 17° 42′.

TABLE II

Proton magnetic resonance data for aromatic and heterocyclic amines and their *N*-acyl derivatives

Structure	Substituent R	Proton resonances*† N—H	H–2	H–3	H–4	H–5	H–6	COMe	N—Me	Other
	NH_2	202	382	406	—	406	382	—	—	134
	NHAc	N	445(63)	425(19)	—	425	445	126	—	137
	NHMe	206	394(12)	422(18)	—	422	394	—	170	135
	NMeAc	—	425(31)	437(15)	—	437	425	113	196	144
	NHCOAr	N	449(67)	428(22)	—	428	449	—	—	139 453, 464
	NMeCOAr	—	421(27)	438(16)	—	438	421	—	209	139, 438
	$NHCOCMe_3$	N	445(63)	426(20)	—	426	445	—	—	77, 138
	NH_2	210	—	N	N	N	403	—	—	130
	NHAc	470	—	N	N	N	448(45)	124	—	131
	NHMe	210	—	N	400(?)	N	398(−5)	—	175	129
	NMeAc	—	—	(multiplet 429–443)			(31–45)	108	193	136
	NMeCOAr	—	—	(multiplet 428–439)			(30–41)	—	203	132, 436
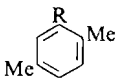	NH_2	196	—	409	383	—	380	—	—	123, 131
	NHAc	455	—	423(14)	411(28)	—	441(61)	124	—	128, 136
	NHMe	N	—	418(9)	389(6)	—	387(7)	—	173	126, 139
	NMeAc	—	—	(multiplet 415–435)			(28–48)	107	191	131, 141
	NHCOAr	475	—	427(18)	415(32)	—	454(74)	—	—	132, 138 451, 464
	NMeCOAr	—	—	(multiplet 413–420)			(26–33)	—	201	127, 134 435
	NH_2	194	—	408	—	407	386	—	—	125, 132
	NHAc	N	—	420(12)	—	416(9)	442(56)	126	—	130, 138
	NHMe	N	—	416(8)	—	419(12)	394(8)	—	173	127, 135
	NMeAc	—	—	(multiplet 420–425)			(26–31)	104	188	132, 141
	NMeCOAr	—	—	416(0)	—	416(—3)	416(22)	—	201	128, 136 435
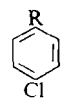	NH_2	212	396	428	—	428	396	—	—	
	NHAc	N	449(53)	437(9)	—	437	449	130	—	
	NHMe	217	389(−7)	427(−1)	—	427	389	—	166	
	NMeAc	—	428(39)	445(18)	—	445	428	113	194	
	NHCOPh	N	448(52)	434(6)	—	434	448	—	—	454
	NHCOAr	N	452(56)	436(8)	—	436	452	—	—	457
	NMeCOAr	—	418(29)	435(8)	—	435	418	—	207	439
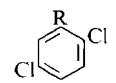	NH_2	240	—	430	398	—	405			
	NHAc	N	—	437(7)	420(22)	—	507(102)	133		
	NHMe	263	—	427(−3)	397(−1)	—	397(−8)	—	171	
	NMeAc	—	—	(multiplet 435–445)			(38–48)	110	191	
	NHCOPh	501	—	442(12)	424(26)	—	523(118)	—	—	~450, 470
	NHCOAr	507	—	443(13)	426(28)	—	520(115)	—	—	460, 471
	NMeCOAr	—	—	(multiplet 430–440)			(33–43)	—	201	437

TABLE II (*continued*)

Structure	Substituent R	Proton resonances*†								
		N—H	H-2	H-3	H-4	H-5	H-6	COMe	N—Me	Other
	NH_2	238	—	433	—	420	397			
	NHAc	N	—	442(9)	—	433(13)	499(102)	133	—	
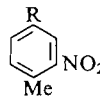	NH_2	222	425	—	—	415	396	—	—	143
	NHAc	N	473(48)	—	—	425(10)	453(57)	129	—	150
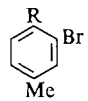	NH_2	231	—	433	—	414	397	—		132
	NHAc	450	—	441(8)	—	425(11)	488(91)	136	—	138
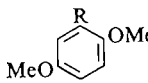	NH_2	227	—	404	375	—	381	—	—	223, 228
	NHAc	N	—	410(6)	394(19)	—	487(106)	131	—	227, 230
	NHMe	251	—	399(−5)	368(−7)	—	373(−8)	—	168	223, 226
	NMeAc	—	—	(multiplet 413–415)			406(33)	110	191	228, 229
	NHCOAr	510	—	409(5)	395(20)	—	493(112)	—	—	226, 229 452, 465
	NMeCOAr	—	—	(multiplet 402–406)			(29–33	—	201	220, 222 438
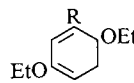	NH_2	225	—	400	373	—	377	—	—	80, 82 235, 239
	NHAc	468	—	407(7)	391(18)	—	484(107)	130	—	81, 84 239, 242
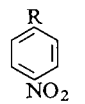	NH_2	N	398	485	—	485	398	—	—	
	NHAc	N	461(63)	493(8)	—	493	461	134	—	
	NHMe	277	394(−4)	489(4)	—	489	394	—	178	
	NMeAc	—	448(54)	500(11)	—	500	448	123	203	
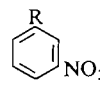	NHMe	248	443	—	451	435	411	—	173	
	NMeAc	—	485(42)	—	490(39)	453(18)	455(44)	120	200	
	NMeCOAr	—	484(41)	—	487(36)	440(5)	450(39)	—	214	444
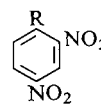	NH_2	N	—	551	—	499	418			
	NHAc	N	—	551(0)	—	512(13)	550(132)	143		
	NHMe	N	—	547(−4)	—	497(−2)	414(−4)	—	188	
	$NHCMe_3$	N	—	550(−1)	—	495(−4)	431(13)	—	—	97
	NMeAc	—	—	530(−17)	—	513(16)	457(43)	125	203	

TABLE II (*continued*)

Structure	Substituent R	Proton resonances*† N—H	H-2	H-3	H-4	H-5	H-6	COMe	N—Me	Other
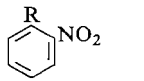	NH_2	N	—	490	412	444	403	—	—	
	NHAc	N	—	493(3)	434(22)	459(15)	529(126)	138		
	NHMe	470	—	492(2)	409(−3)	450(6)	397(−6)	—	183	
	NMeAc	—	—	479(−14)	(unresolved multiplet)			113	191	
								134	205	
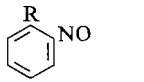	NH_2	358	—	479	—	431	403	—	—	135
	NHAc	N	—	478(−1)	—	446(15)	517(114)	136	—	136
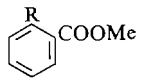	NH_2	375	—	472	396	436	399	—	—	231
	NHAc	N	—	481(9)	423(27)	452(16)	523(124)	133	—	235
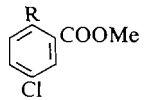	NH_2	342	—	470	—	434	396	—	—	232
	NHAc	N	—	479(9)	—	449(15)	522(126)	133	—	236
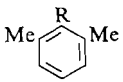	NH_2	209	—	417	396	417	—	—	—	129
	NHAc	N	—	425(8)	425(29)	425(8)	—	133	—	135
	NHMe	181	—	417(0)	417(21)	417(0)	—	—	165	137
	NMeAc	—	—	429(12)	429(12)	429(12)	—	103	188	133
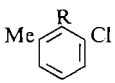	NH_2	237	—	427	394	416	—	—	—	
	NHAc	N	—	437(10)	426(34)	426(10)	—	130	—	134
	NHMe	221	—	429(2)	403(9)	419(3)	—	—	167	138
	NMeAc	—	—	435(6)	435(32)	435(16)	—	106	189	137
	NH_2	277	—	387	443	395	483	—	—	
	NHAc	569	—	495(108)	470(27)	421(26)	494(9)	131	—	
	NH_2	235	483	—	419	419	477	—	—	
	NHAc	591	526(43)	—	488(69)	436(17)	497(20)	131	—	
	NH_2	251	495	392	—	392	495			
	NHAc	550	508(13)	455(63)	—	455	508	132	—	

TABLE II (*concluded*)

Structure	Substituent R	Proton resonances*† N—H	H–2	H–3	H–4	H–5	H–6	COMe	N—Me	Other
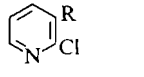	NH_2	N	—	—	422	422	467	—	—	
	NHAc	465	—	—	523(101)	437(15)	488(21)	137	—	
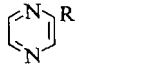	NH_2	236		476	—	487	487	—	—	
	NHAc	532		575(99)	—	502(15)	495(8)	138	—	
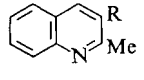	NH_2	230	—	—	430	(complex multiplet)				156
	NHAc	N	—	—	515(85)	(complex multiplet)		134	—	160
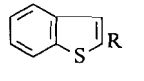	NH_2	N	—	371	(complex multiplet)‡					
	NHAc	N	—	414(43)	(complex multiplet)‡					
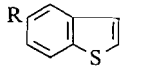	NH_2	N	(complex multiplet)		415	—	398§			
	NHAc	N	(complex multiplet)		487(72)	—	439(41)			
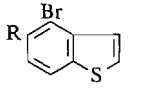	NH_2	N	(complex multiplet)		—	—	407§			
	NHAc	N	(complex multiplet)		—	—	465(58)			
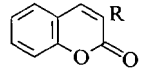	NH_2	256	—	—	403	436	436			
	NHAc	486	—	—	521(118)	(multiplet	437–48)	135		
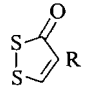	NH_2	240	—	—	—	423				‖
	NHAc	471	—	—	—	545(122)		132		
	NHMe	252	—	—	—	388(−35)		—	173	
	NHCOPh	504	—	—	—	558(135)				
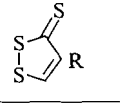	NH_2	270	—	—	—	446				‖
	NHAc	510	—	—	—	582(136)		136		
	NHMe	283	—	—	—	418(−28)		—	178	
	NHCOPh	576	—	—	—	563(117)				

*The centers of appropriate multiplets are reported in Hz at 60 MHz. Figures in parenthesis are acylation shifts for amides, and shifts with respect to primary amines in the cases of secondary amines.
†The entry "N" in the table denotes a resonance which was not assigned due to excessive broadening or overlapping (Ar = *p*-bromophenyl).
‡See ref. (69).
§M. Martin-Smith, S. T. Reid, and S. Sternhell. Unpublished data.
‖See ref. (1).

shifts would be expected to depend on the conformation about the Ar—N bond in a complex manner, but they are consistent with the amide carbonyl spending most of its time out of the ring plane. The configuration about the CO—N bond is discussed in a later section.

Heterocyclic Amines and their N-Acetyl Derivatives

The effects discussed above are also discernible in the spectra of compounds where the ring is heterocyclic. However, certain additional phenomena may also be observed. Entries 22 and 28 in Table II (3-aminopyridine, 5-aminobenzothiophene) show that the chemical shifts of the two ortho protons may not change by the same amount upon acetylation of the amino group. Of the carbocyclic examples studied, only 4-methyl-3-nitroaniline is suitable for the observation of this dissymmetry (from the point of view of orientation and polarity of substituents) and, indeed, the two ortho protons show unequal acylation shifts (48 and 57 Hz). This effect is general in polynuclear and heterocyclic systems (36), e.g. aminobenzophenanthrenes (37), and probably arises from preferential orientation of the polar amide group with respect to other polar groups in the molecule or an unequal transmission of electronic effects (e.g. due to partial bond fixation). Rotation about the Ar—N bond must be rapid enough, however, that the average chemical shifts are observed.

This effect is seen more dramatically in the behavior of 2-aminopyridines and pyrazines.[4] Acetylation of the amino group produces a large downfield shift of the 3-proton, similar in size to those associated with intramolecular hydrogen bonding of the amide proton. While weak hydrogen bonding between an amino proton and a heterocyclic nitrogen has been suggested on the basis of infrared spectroscopy (39), it seems more likely in this case that observed conformational preferences are due to dipole–dipole stabilization[5] of e.g. (**4**) with respect to (**5**). In dimethyl sulfoxide solutions, where the intramolecular hydrogen bond would not be expected to persist (41) the shielding is still large (42) as would be predicted by the dipole–dipole model.

Hydrogen bonding between the amide hydrogen and the adjacent carbonyl or thiocarbonyl group probably plays an important part in the behavior of the amino-coumarin, dithiolone, and dithiolethione systems.

Chemical Shifts of other Protons

(a) Secondary versus Primary Amines

The electronic effects of *N*-methylation are expected to be slight (43) for the chemical shifts of ring protons in aniline and *N*-methylaniline are very similar (4*a*). They are very different, however, in *N*,*N*-dimethylaniline (27). Where the *s-trans* configuration e.g. (**6**) is stabilized by intramolecular hydrogen bonding (29, 30, 44) the spectra of the secondary amines were examined for evidence of deshielding of H-6 due to the proximity of the methyl group (45–58). In fact small upfield shifts of this proton are observed and these probably arise from enhanced electron donation by the methylamino group as compared to the amino group (43). Pursuing this matter a

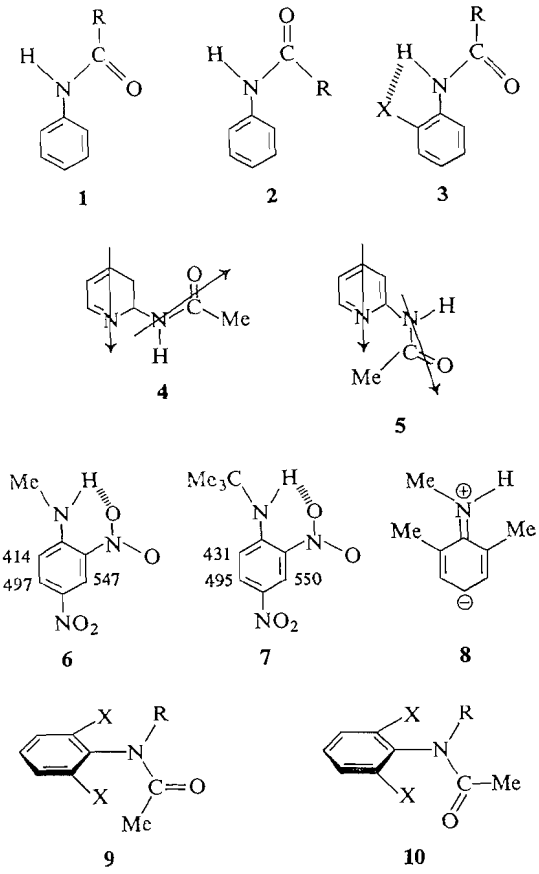

[4]Similar results (38) have been reported for 3-amino-2,6-naphthyridines.

[5]For a review of dipolar interactions in alicyclic compounds see ref. 40.

little further, the *N*-methyl derivative (**6**) was compared with its *N*-butyl analogue (**7**) where the extra bulk of the alkyl substituent brings it much closer to H-6 and is clearly responsible for the extra deshielding (17 Hz) of this proton.

The effect of *N*-methylation in inhibiting resonance between the nitrogen atom and the aromatic ring may be seen in the 2,6-disubstituted cases. Relative to that of 2,6-dimethylaniline, the resonance position of the 4-proton of *N*,2,6-trimethylaniline is moved downfield by 21 Hz. The shift may be ascribed to steric inhibition of resonance with consequent reduction in the contributions of structures like (**8**) to resonance. Steric inhibition of resonance in *N*,*N*,2,6-tetramethylanilines has been studied by means of ultraviolet spectroscopy (59), basicity measurements (60), and, most recently, by ^{19}F magnetic resonance (61). *N*-Methylation of 2-chloro-6-methylaniline produces a smaller downfield shift of the 4-proton (9 Hz), possibly because the formation of an intramolecular hydrogen bond to the chlorine atom acts to preserve planarity (62).

(b) N-Methyl Proton Resonances

The proton resonances arising from the *N*-methyl protons are shifted downfield when the nitrogen is acylated, the extent of the shift being dependent *inter alia* upon the presence or otherwise of an ortho substituent on the aromatic ring. The shifts are 25–28 Hz for acetylation of unhindered amines, and 15–23 Hz when one or more ortho substituents are present. The ranges for *p*-bromobenzoylation are respectively 39–41 and 28–33 Hz. These differences are consistent with the idea that there is substantial deviation from planarity in the *N*-methyl anilides. Ortho substitution dictates greater twisting about the Ar—N bond to relieve steric interactions and the *N*-methyl protons will thus suffer increased shielding by the ortho substituted benzene ring, thus lessening the acylation shift.

(c) Chemical Shifts of Acetyl Methyl Protons

The arguments already advanced concerning the conformations of *N*-methyl anilides are also useful in rationalizing the chemical shifts of the acetyl methyl protons. The angle between the amide and ring planes is expected to increase along the series acetanilide, *N*-methylacetanilide, ortho substituted *N*-methyl acetanilide. As it does so we might expect that the acetyl methyl protons would pass from a region (close to the plane of the aromatic ring) where they suffer a net deshielding, to one (above the ring plane) where a shielding effect might operate. Although the actual chemical shifts are influenced to some extent by the ring substituents, they do fall in the anticipated order: 124–143 Hz, 113–123 Hz, and 104–125 Hz for the three structural types. The latter two ranges provide independent evidence that the presence of an ortho substituent in an *N*-methylacetanilide requires an increased angle between the amide and ring planes, a finding which is difficult to reconcile with the proposal (19) that these planes are orthogonal in *N*-methylacetanilide itself.[6]

The sensitivity of the acetyl methyl protons to the bulk of the aromatic moiety requires that the *N*-methylacetanilides exist in a *trans* configuration about the CO—N bond (**9**) in order that the methyl group and the aromatic ring be proximate. The choice of type (**9**) over (**10**) is in accord with other findings for *N*-methylacetanilides (4*a*, 19, 63*a*,*b*).

In the case of the 2′,6′-disubstituted anilides, both *cis* and *trans* configurations are present in solution. The major isomer, for which the aromatic resonances are easily discerned, is reported in Table II (entries 19 and 20). The minor isomer, representing 20% of the molecules in solution, showed methyl proton resonances which closely resembled those of its *N*-methyl analogue (with the exception of the *N*-methyl protons, of course) thus fixing its configuration as a *trans* one (**9**). The major isomer, therefore, possesses the *cis* configuration (**10**) in which the acetyl methyl protons are little affected by the (now distant) benzene ring. The dominance of *cis* forms for secondary amides and *trans* forms for tertiary amides has also been remarked by Carter (4*a*) and by Weil *et al.* (63*b*).

(d) Proton Resonances from the p-Bromobenzoyl Moiety

In the *N*-*p*-bromobenzoyl derivatives of the primary amines the protons of the *p*-bromobenzoyl moiety give rise to the familiar symmetrical pattern with four prominent lines, characteristic of a para disubstituted benzene. In the *N*-methyl analogues, however, these resonances have collapsed to a single, although sometimes slightly broadened, line which appears at higher

[6]One possible point of reconciliation is the different solvents used. Namely, deuteriochloroform vs. pyridine (19).

field than the original multiplet. Presumably, in the *N*-methyl amides, the carbonyl group is twisted out of the *p*-bromophenyl ring plane with a consequent reduction in its electron withdrawing and anisotropic effects on the chemical shifts of the ring protons. Similar changes have been reported for other systems in which an aromatic ring is bonded to a trigonally hybridized carbon (64–66).

Acknowledgments

We are indebted to Dr. Gustav Ehrhardt, Farbwerke Hoechst AG., for a generous gift of 2,5-dimethoxy-*N*-methylaniline, and to Drs. J. R. Bartels-Keith and R. F. H. Cieciuch (Polaroid Corporation, Cambridge, Massachusetts) and Dr. Brian M. Lynch (St. Francis Xavier University, Antigonish, Nova Scotia) for prior communication of results, and cooperation in simultaneous publication. L. R. expresses his thanks to the Commonwealth Scientific and Industrial Research Organization for a postgraduate award. I. D. R. expresses his appreciation of a conversation with Dr. R. Y. Moir, Queen's University, Kingston, Ontario.

1. R. F. C. Brown, I. D. Rae, and S. Sternhell. Australian J. Chem. **18**, 1211 (1965).
2. P. Laszlo. Bull. Soc. Chim. France, 2658 (1964).
3. G. Slomp. J. Am. Chem. Soc. **84**, 673 (1962).
4. (*a*) R. E. Carter. Acta Chem. Scand. **21**, 75 (1967); (*b*) T. H. Siddall, III, and W. E. Stewart. J. Mol. Spectry. **24**, 290 (1967).
5. D. Y. Curtin and J. D. Druliner. J. Org. Chem. **32**, 1552 (1967).
6. J. R. Bartels-Keith and R. F. H. Cieciuch. Private communication.
7. W. N. Speckamp, U. K. Pandit, P. K. Korver, P. J. van der Haak, and H. O. Huisman. Tetrahedron, **22**, 2413 (1966).
8. K. Deutsch. Ann. Physik. **16**, 300 (1965).
9. D. G. Lister and J. K. Tyler. Chem. Commun. 152 (1966).
10. F. A. L. Anet and J. M. Osyany. J. Am. Chem. Soc. **89**, 352 (1967).
11. J. C. Brand, D. R. Williams, and T. J. Cook. J. Mol. Spectry. **20**, 193 (1966).
12. C. C. Constain and J. M. Dowling. J. Chem. Phys. **32**, 158 (1960).
13. E. W. Randall and J. J. Zuckerman. Chem. Commun. 732 (1966).
14. R. J. B. Marsden and L. E. Sutton. J. Chem. Soc. 599 (1936).
15. J. Karle and I. L. Karle. J. Am. Chem. Soc. **89**, 804 (1967).
16. C. J. Brown and D. E. C. Corbridge. Acta Cryst. 7, 711 (1954).
17. R. A. Russell and H. W. Thompson. Spectrochim. Acta, **8**, 138 (1956).
18. L. K. Dyall and J. E. Kemp. Spectrochim. Acta, **22**, 467 (1966).
19. B. F. Pedersen and B. Pedersen. Tetrahedron Letters, 2995 (1965).
20. T. H. Siddall, III, and C. A. Prohaska. J. Am. Chem. Soc. **88**, 1172 (1966).
21. L. A. LaPlanche and M. T. Rogers. J. Am. Chem. Soc. **86**, 337 (1964).
22. R. H. Barker and G. J. Boudreaux. Spectrochim. Acta, A, **23**, 727 (1967).
23. J. W. Smith. J. Chem. Soc. 4700 (1961); M. Gomel and H. Lumbroso. Bull. Soc. Chim. France, 1196 (1962); H. B. Thompson and K. M. Hallberg. J. Phys. Chem. **67**, 2486 (1963).
24. D. L. Hooper and R. Kaiser. Can. J. Chem. **43**, 2363 (1965).
25. H. Paulsen and K. Todt. Angew. Chem. Intern. Ed. Engl. **5**, 899 (1966).
26. L. M. Jackman. Applications of nuclear magnetic resonance spectroscopy in organic chemistry. The Pergamon Press, Ltd., Oxford. 1959. Chap. 7.
27. R. R. Fraser and R. Renaud. J. Am. Chem. Soc. **88**, 4365 (1966).
28. I. D. Rae. Can. J. Chem. This issue.
29. I. D. Rae. Australian J. Chem. **18**, 1807 (1965).
30. J. Heidberg, J. A. Weil, G. A. Janusonis, and J. K. Anderson. J. Chem. Phys. **41**, 1033 (1964).
31. R. W. Frank and M. A. Williamson. J. Org. Chem. **31**, 2420 (1966).
32. A. N. Hambly. Rev. Pure Appl. Chem. **15**, 212 (1961).
33. I. D. Rae. Can. J. Chem. **45**, 1 (1967).
34. M. J. Aroney, R. J. W. Le Fèvre, and A. N. Singh. J. Chem. Soc. B, 1183 (1966).
35. K. Nagarajan, M. D. Nair, and P. M. Pillai Tetrahedron, **23**, 1683 (1967).
36. L. M. Jackman and S. Sternhell. Applications of nuclear magnetic resonance spectroscopy in organic chemistry. Pergamon Press, Ltd., Oxford. 1968. Chap. 3 and 4.
37. R. H. Martin, N. Defay, and F. Greets-Evrard. Tetrahedron, **21**, 2421 (1965).
38. R. Tan and A. Taurina. Tetrahedron Letters 2737 (1965).
39. A. N. Hambly and B. V. O'Grady. Australian J. Chem. **17**, 860 (1964).
40. E. L. Eliel, N. L. Allinger, S. J. Angyal, and G. A. Morrison. Conformational analysis. Interscience Publishers, Inc., New York. 1965. p. 460 (substituted cyclohexanes), p. 375 (the anomeric effect in sugars).
41. I. D. Rae. Australian J. Chem. **20**, 1173 (1967).
42. W. Brugel. Z. Elektrochem. **66**, 159 (1962).
43. H. H. Jaffe. Chem. Rev. **53**, 191 (1953).
44. M. J. Kamlet, H. G. Adolphe, and J. C. Hoffsommer. J. Am. Chem. Soc. **86**, 4018 (1964).
45. A. D. Buckingham. Can. J. Chem. **38**, 300 (1960).
46. T. Schaefer, W. F. Reynolds, and T. Yonemoto. Can. J. Chem. **41**, 2969 (1963).
47. V. M. S. Gill and W. A. Gibbons. Mol. Phys. **8**, 199 (1964).
48. W. Nagata, T. Teresawa, and K. Tori. J. Am. Chem. Soc. **86**, 3746 (1964).
49. S. Winstein, P. Carter, F. A. L. Anet, and A. J. R. Bourn. J. Am. Chem. Soc. **87**, 5247 (1965).
50. F. A. Bovey, F. P. Hood, E. Piers, and H. E. Weaver. J. Am. Chem. Soc. **87**, 2060 (1965).
51. M. A. Battiste and M. E. Brennan. Tetrahedron Letters, 5857 (1966).
52. N. S. Bhacca and D. H. Williams. Applications of nuclear magnetic resonance spectroscopy in organic chemistry. Holden-Day, Inc., San Francisco. 1964. pp. 183–191.
53. K. Tori and K. Kuriyama. Chem. and Ind. London. 1525 (1963).
54. R. J. Abraham and J. S. E. Holker. J. Chem. Soc. 806 (1963).

55. K. TORI and T. KOMENO. Tetrahedron, **21**, 309 (1965).
56. C. REID. J. Mol. Spectry. **1**, 18 (1957).
57. D. R. ARNOLD, D. J. TRECKER, and E. B. WHIPPLE. J. Am. Chem. Soc. **87**, 2596 (1965).
58. N. NAKAGAWA, S. SAITO, A. SUZUKI, and M. ITOH. Tetrahedron Letters, 1003 (1967).
59. L. L. INGRAHAM. *In* Steric effects in organic chemistry. *By* M. S. Newman. John Wiley and Sons, Inc., New York. 1956. pp. 485–487.
60. H. C. BROWN and A. CAHN. J. Am. Chem. Soc. **72**, 2939 (1950).
61. M. J. S. DEWAR and Y. TAKEUCHI. J. Am. Chem. Soc. **89**, 390 (1967).
62. S. ABRAHAMSSON, M. INNES, and B. LAMM. Acta Chem. Scand. **21**, 224 (1967).
63. (*a*) J. P. CHUPP and J. F. OLIN. J. Org. Chem. **32**, 2297 (1967);
(*b*) J. A. WEIL, A. BLUM, A. H. HEISS, and J. K. KINNAIRD. J. Chem. Phys. **46**, 3132 (1967).
64. B. M. LYNCH and Y. Y. HUNG. Can. J. Chem. **42**, 1605 (1964).
65. I. CROSSLAND. Acta Chem. Scand. **20**, 258 (1966).
66. L. G. TENSMEYER and C. AINSWORTH. J. Org. Chem. **31**, 1878 (1966).
67. R. E. DUNBAR and C. C. MOORE. Microchem. J. **3**, 491 (1959).
68. L. A. TETYUEVA and P. A. PETYUNIN. Zh. Obshch. Khim. **28**, 739 (1958).
69. G. F. STACY, F. W. VILLAESCUSA, and T. E. WALLNER. J. Org. Chem. **30**, 4074 (1965).

Can. J. Chem. Downloaded from www.nrcresearchpress.com by 210.87.254.40 on 09/05/12
For personal use only.

Solvent effects on the conformations of ortho-substituted acetanilides

IAN D. RAE
Department of Chemistry, Monash University, Clayton, Victoria, Australia

Received February 7, 1968

In acetanilides bearing nitro, halogen, alkoxyl, or carboxyl substituents in the *ortho* position, the intramolecular hydrogen bond is disrupted by polar solvents and the acetamido group adopts a position out of the plane of the aromatic ring. These changes are studied by means of changes in the deshielding effect of the amide carbonyl group on the remaining *ortho* proton.

Canadian Journal of Chemistry, 46, 2589 (1968)

Introduction

The conformations of ring-substituted acetanilides in deuteriochloroform solutions have been explored in some detail (1) by means of proton magnetic resonance (p.m.r.) spectroscopy and this paper reports the changes which occur when certain of these are dissolved in more polar solvents. Since this paper forms part of a loosely connected series it is advantageous to briefly review our earlier proposals before proceeding to a discussion of the present results.

It has been proposed that, in acetanilides bearing 2′-substituents which may hydrogen bond with the amide proton, the amide carbonyl group is constrained to lie approximately in the plane of the aromatic ring from whence it exerts its maximum deshielding influence on the 6′-proton (1). That the carbonyl is, in fact, oriented towards the ring as shown in structure **1** is attested by infrared (2) and X-ray crystallographic measurements (3), by electric dispersion studies (4), and by p.m.r. spectroscopy (1). In the case of some similarly substituted formanilides (5) the chemical shift of the formyl proton in the *trans* isomer (**2**) was used to calculate the angle between the amide- and ring-planes, and it was observed that this angle increased with increasing solvent polarity.

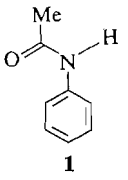

1

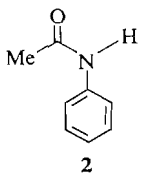

2

This device was not available to the study of acetanilides so the "acylation shift" technique was again employed to study the solvent effects. In this method the effect of the amide carbonyl on the chemical shifts of the aromatic protons, and hence the extent of coplanarity, is gauged by comparing the spectra of aromatic amines and their *N*-acetyl derivatives. The observed downfield shifts of the aromatic protons upon acylation of the amine include contributions from electronic and anisotropic effects but these may be separated. Anisotropic effects on protons *meta* and *para* to the amido function are expected to be small by comparison with those at the *ortho* position, the difference being a measure of the anisotropic effect, from which the conformation may be deduced.

In this work attention is focussed on the acylation shifts for the 6′-protons of 2′-substituted acetanilides. A number of solvents were employed with several representative amine–amide pairs, and the behavior of a wider range of compounds in a single solvent, dimethyl sulfoxide, was studied.

Experimental

The compounds employed are all well known aromatic amines and their *N*-acetyl derivatives. Proton magnetic resonance (p.m.r.) spectra were recorded on a Varian A-60 spectrometer for dilute solutions (approximately 7% w/v) at approximately 30 °C. Twofold dilution of selected solutions produced no significant changes in the p.m.r. spectra, and saturated solutions of some of the nitroamines having concentrations below 7% were used where necessary. Spectra were interpreted by first order analysis only, i.e. AB pattern treated as AX, the errors introduced being negligible compared to the effects under study. 2′-Carbomethoxyl-4′-nitroacetanilide in dimethyl sulfoxide solution showed a complex multiplet of width approximately 10 Hz for the aromatic proton signals, and the protons involved were simply assigned a chemical shift corresponding to the position of the center of gravity of the multiplet.

Discussion

(a) Influence of Solvent Polarity

The data of Table I reveal the effects of changing solvent polarity on the deshielding

TABLE I

Acylation shifts for substituted acetanilides

Solvent	Acylation shifts of aromatic protons*								
	2′,4′-Dinitro acetanilide			2′,5′-Dichloro acetanilide			2′,5′-Dimethoxy acetanilide		
	H-3	H-5	H-6	H-3	H-4	H-6	H-3	H-4	H-6
$CDCl_3$	0	13	132	7	22	102	6	18	106
MeCOOEt	3	21	110	15	30	94	11	24	108
$MeO(CH_2)_2OMe$	1	21	109	15	31	90	12	25	109
$MeNO_2$	3	19	109	12	27	85	10	23	95
MeCN	2	18	105	14	29	84	11	24	98
Me_2CO	1	20	98	15	32	87	12	35	104
$(CH_2)_4SO_2$	3	22	93	17	33	77	13	27	93
MeOH	−5	19	85	18	35	66	12	24	78
$CH_2CH_2CH_2CONMe$	−5	25	58	21	39	72	15	29	89
$MeCONMe_2$	−5	26	56	20	39	70	15	29	96
$(CH_2)_4SO$	−6	22	56	21	41	69	16	31	91
Me_2SO	−7	21	54	21	41	65	16	32	86

*Change in chemical shift of the cited proton upon acetylation of the amine (Hz at 60 MHz).

effect exerted by the amide carbonyl on the aromatic protons. Since there is little electronic interaction between the aromatic ring and the acetamide moiety in acetanilide (6) the solvent effect is chiefly noticed at the 6′-positions of the three anilides, and arises therefore chiefly from anisotropy changes. For each anilide, the acylation shift of H–6′ is least in those solvents which are best able to hydrogen bond with the amide proton, and thus disrupt the intramolecular hydrogen bond which constrains the molecule to planarity in less polar solvents. Thus, with increasing solvent polarity, the amide group spends less time in or near to the plane of the benzene ring and deshielding of the 6′-proton is consequently reduced. The acylation shifts of other aromatic ring protons are, however, *increased* in the more polar solvents, an observation not easily explained by the present model. Such changes may also be operative at the *ortho* positions where their effect might remain undiscerned because of numerically much larger changes in the opposite sense. These solvent effects may be tentatively identified as being of the more general type previously reported (7) rather than those highly specific ones under discussion here. When a 2-nitroaniline is acetylated the nitro group appears to be slightly rotated from the ring plane even in relatively nonpolar solvents (1), thus minimizing the acylation shift at H-3′ due to a compensating reduction of deshielding by the nitro group (8). In polar solvents this rotation of the nitro group is enhanced to the point where acetylation produces not a downfield but an *upfield* shift in resonance position of H-3′.

The solvent order is roughly that of dipole moments rather than of solvent basicity (9). It is interesting to note that the sulfoxide is much more effective in hydrogen bonding than is the analogous sulfone (10), and that no special role may be attributed to methanol, the only protic solvent employed.

(b) Comparison of Ortho Substituents

The proton magnetic resonance (p.m.r.) spectra of a number of amine–amide pairs in dimethyl sulfoxide, a highly polar solvent, are presented in Table II. It is instructive to compare acylation shifts for H-6′ in the various structural types, both in deuteriochloroform (1) and dimethyl sulfoxide: (Table III, Hz at 60 MHz).

While the substituent order in dimethyl sulfoxide solutions closely resembles that in deuteriochloroform, the differences are quite important. The carboxyl group, excluded from the deuteriochloroform work for solubility reasons, is seen to resemble the carbomethoxyl group as expected. The figures reflect the hydrogen bonding ability of the 2′ substituent under conditions of adverse competition with molecules of solvent, and may be rationalized in the following way.

Can. J. Chem. Downloaded from www.nrcresearchpress.com by 210.87.254.40 on 09/05/12
For personal use only.

TABLE II

Proton magnetic resonance spectra of anilines and acetanilides in dimethyl sulfoxide

Compound	R	R′	Chemical shifts of aromatic protons* H-3	H-4	H-5	H-6
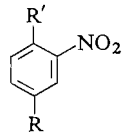	NO_2	NH_2	517	—	480	418
	NO_2	NHAc	510(−7)†	—	501(21)	472(54)
	Me	NH_2	457	—	426	408
	Me	NHAc	458(1)	—	444(18)	444(36)
	COOH	NH_2	506	—	464	415
	COOH	NHAc	497(−9)	—	485(21)	465(50)
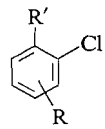	4-Cl	NH_2	428	—	417	400
	4′-Cl	NHAc	450(22)	—	435(18)	460(60)
	5-Cl	NH_2	423	384	—	402
	5′-Cl	NHAc	443(20)	424(40)	—	467(65)
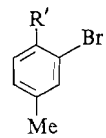	—	NH_2	422	—	407	394
	—	NHAc	441(19)	—	421(14)	440(46)
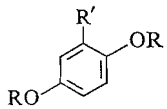	Me	NH_2	393	356	—	369
	Me	NHAc	409(16)	388(32)	—	455(86)
	Et	NH_2	392	354	—	368
	Et	NHAc	407(15)	386(32)	—	453(85)
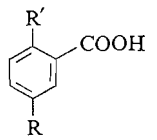	H	NH_2	469	395	438	409
	H	NHAc	483(14)	431(36)	459(21)	513(104)
	Cl	NH_2	451	—	427	401
	Cl	NHAc	465(14)	—	448(21)	502(101)
	NO_2	NH_2	515	—	470	397
	NO_2	NHAc	514(−1)	—	496(26)	516(119)
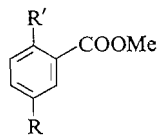	H	NH_2	457	385	429	382
	H	NHAc	468(11)	422(37)	449(20)	489(88)
	Cl	NH_2	450	—	429	401
	Cl	NHAc	463(13)	—	451(22)	486(85)
	NO_2	NH_2	507	—	475	403
	NO_2	NHAc	506(−1)	—	505(31)	506(103)
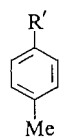	—	NH_2	403	—	403	382
	—	NHAc	417(14)	—	417(14)	441(59)
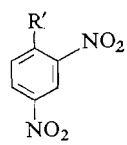	—	NHMe	522	—	489	420
	—	NMeAc	507(−15)	—	501(12)	457(37)

*Hz from tetramethylsilane at 60 MHz.
†Figures in parenthesis are acylation shifts.

Can. J. Chem. Downloaded from www.nrcresearchpress.com by 210.87.254.40 on 09/05/12
For personal use only.

TABLE III

Acylation shifts for H–6′ in deuteriochloroform and dimethyl sulfoxide

2′-Substituent	—Br	—Cl	—OR	—NO_2	—COOMe	—COOH
$CDCl_3$	91	102	106–107	114–132	124–126	—
DMSO	46	60–65	85–86	36–54	85–103	101–119

The nitro, carboxyl, and carbomethoxyl groups participate in the intramolecular hydrogen bonding to yield a six-membered ring as opposed to the five-membered ring formed when the hydrogen bond involves an atom attached directly to the ring. The extra degree of freedom involved, i.e. rotation about the bond linking the 2′-substituent and the aromatic ring, should render the intramolecular hydrogen bond much more vulnerable to the ravages of solvent molecules, and this appears to be the reason for the sharp change in the configuration-stabilizing properties of the nitro group. The carbomethoxyl group, however, is much less affected and this suggests that in deuteriochloroform both nitro and carbomethoxyl substituents exert the maximum possible effect, i.e. in maintaining the amide carbonyl as nearly as possible in the ring plane. In dimethyl sulfoxide solutions the inherently greater hydrogen bonding ability of the carbomethoxyl group is evident from the manner in which it maintains its position as a powerful stabilizer of configuration **1**, while the nitro group is one of the poorest.

Semiquantitative calculations on the system **3**–**4** have indicated that the enthalpy of formation of a hydrogen bond from an amino proton is 0.9 kcal/mole greater to COOEt than to NO_2 (11). Apart from this evidence of different hydrogen bonding abilities, there also exists definite evidence that the carboxyl group, when exposed to similar steric hindrance, is far less easily rotated from the plane than is the nitro group. Thus, an *ortho* methyl substituent produces a 34° twist of the nitro group in *ortho*-nitrotoluene (12), but virtually none of the carboxyl group in *ortho*-toluic acid (13). A particularly informative case is *ortho*-nitrobenzoic acid (14), in which the nitro group is twisted 54° from the plane of the benzene ring while the carboxyl group is twisted only 22°, in order to minimize the conflict between them.

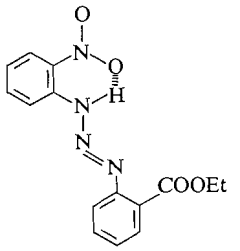

3

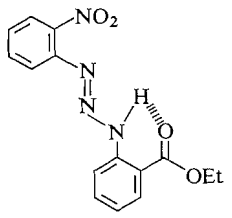

4

The final two entries in Table II are included to demonstrate that, in the absence of a hydrogen bonding interaction between the amide group and the 2′ substituent, acylation shifts are essentially independent of the solvent. The acylation shifts presented differ by only a few Hz from those derived from deuteriochloroform solutions (1).

1. R. F. C. Brown, I. D. Rae, L. Radom, and S. Sternhell. Can. J. Chem., this issue and references cited therein.
2. R. A. Russell and H. W. Thompson. Spectrochim. Acta, **8**, 138 (1956).
3. C. J. Brown and D. E. C. Corbridge. Acta Cryst. **7**, 711 (1954).
4. M. J. Aroney, R. J. W. Le Fèvre, and A. N. Singh. J. Chem. Soc. B, 1183 (1966).
5. I. D. Rae. Can. J. Chem. **44**, 1334 (1966).
6. H. Baba and S. Suzuki. J. Chem. Phys. **32**, 1706 (1960).
7. J. W. Emsley, J. Feeney, and L. H. Sutcliffe. High resolution nuclear magnetic resonance spectroscopy. Vol. 2. The Pergamon Press, Ltd., Oxford. 1966.
8. I. Yamaguchi. Mol. Phys. **6**, 105 (1963).
9. C. Reichardt. Angew. Chem. Intern. Ed. Engl. **4**, 29 (1965).
10. D. Barnard, J. M. Fabian, and H. P. Koch. J. Chem. Soc. 2442 (1949).
11. V. C. Farmer, R. L. Hardie, and R. H. Thomson. *In* Hydrogen bonding. *Edited by* D. Hadzi. The Pergamon Press, Ltd., London. 1959. p. 475.
12. B. M. Wepster. *In* Progress in stereochemistry. Vol. 2. Academic Press, Inc., New York. 1958. pp. 99–156.
13. C. Katayama, A. Furusaki, and I. Nitta. Bull. Chem. Soc. Japan, **40**, 1293 (1967).
14. M. Kurahashi, M. Fukuyo, and A. Shimada. Bull. Chem. Soc. Japan, **40**, 1296 (1967).

Can. J. Chem. Downloaded from www.nrcresearchpress.com by 210.87.254.40 on 09/05/12
For personal use only.

Can. J. Chem. Downloaded from www.nrcresearchpress.com by 210.87.254.5 on 09/05/12
For personal use only.

Selective deshielding of aromatic protons in some ortho-substituted acetanilides

JAMES R. BARTELS-KEITH AND RONALD F. W. CIECIUCH
Polaroid Corporation, Cambridge, Massachusetts 02139

Received April 22, 1968

Certain *ortho*-substituted acetanilides exhibit proton magnetic resonance signals at unusually low field for the amido proton and the aromatic proton adjacent to the acetamido group. This effect, explicable in terms of intramolecular hydrogen-bonding, has been observed for nitro, carbonyl, sulfamoyl, and sulfonyl substituents. Solvent effects are discussed.

Canadian Journal of Chemistry, 46, 2593 (1968)

Introduction

We have examined the 60 MHz proton magnetic resonance (p.m.r.) spectra of a number of nitroacetanilides and find that certain *o*-nitroacetanilides exhibit signals at unusually low field for the aromatic proton adjacent to the acetamido group and for the amido proton itself. This effect we ascribe to intramolecular hydrogen-bonding between the amido group and a nitro-oxygen, already demonstrated by infrared (i.r.) (1) and ultraviolet (u.v.) (2) spectral studies, and recently reported for 2,4-dinitroacetanilide (3). Such hydrogen-bonding would be expected to favor the conformation (**1**), in which the N—H and C=O groups have the *trans* configuration which has been deduced for acetanilide in solution from dipole moment (4–7), i.r. (5, 8), and p.m.r. (9, 10) studies. In this configuration, the 6-H proton might be expected to experience a strong deshielding effect owing to the proximity and orientation of the carbonyl group (11). Further discussion of the anisotropic effects of the carbonyl group has appeared recently (12).

We now find that similar effects occur with acetanilides containing *ortho*-substituents other than nitro, such as acyl, carbethoxy, sulfamoyl, and sulfonyl groups. Parallel studies on the p.m.r. spectra of substituted anilides have recently been reported by several other groups (13–16) whose findings and conclusions corroborate our own. Of particular interest is the observation (13, 14, 17, 18), that acetanilides bearing *ortho* halogen or methoxy substituents also exhibit a well-marked *ortho* effect which may be attributed to intramolecular hydrogen-bonding.

Results and Discussion

Results obtained for some nitroacetanilides are summarized in Table I. The splitting patterns in the p.m.r. spectra of compounds (**1***b*), (**1***c*), and (**1***d*) (19) permit unambiguous assignment of the

TABLE I

Proton magnetic resonance spectra of nitroacetanilides (chemical shifts in τ values)

Compound	Solvent	Temperature	Aromatic protons 2	3	4	5	6	NH	Other protons
1*a*	$CDCl_3$	30°	—	1.80	2.84	2.36	1.23	−0.29	7.73($COCH_3$)*
	CD_3CN	70°	—	1.82	2.72	2.28	1.51	0.18	
1*b*	$CDCl_3$	30°	—	1.95	—	2.52	1.31	−0.25	
	CD_3CN	70°	—	2.03	—	2.48	1.69	0.31	
1*c*	$CDCl_3$	30°	—	2.37	—	2.80	1.40	0.00	6.20(OCH_3)*
	CD_3CN	70°	—	2.43	—	2.78	1.82	0.74	7.79($COCH_3$)*
1*d*	$CDCl_3$	30°	—	1.83	3.37	—	1.58	−0.75	6.11(OCH_3)*
	CD_3CN	70°	—	1.75	3.23	—	1.68	−0.45	7.72($COCH_3$)*
2†	CD_3CN	70°	1.36	—	2.04‡	2.46	~2.2‡	1.19	
3*a*†	CD_3CN	70°	2.16	1.75	—	1.75	2.16	1.13	
3*b*†	CD_3CN	70°	2.37	—	—	2.19	2.91	1.50	6.10(OCH_3)§ 7.92($COCH_3$)§

*Values refer to chloroform-*d* solutions.
†Insufficient solubility in chloroform-*d*.
‡Complex multiplets.
§Values refer to acetonitrile-d_3 solutions.

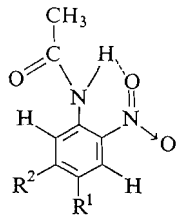

1*a*, $R^1 = H$; $R^2 = H$
1*b*, $R^1 = CH_3$; $R^2 = H$
1*c*, $R^1 = OCH_3$; $R^2 = H$
1*d*, $R^1 = H$; $R^2 = OCH_3$

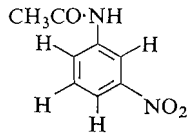

2

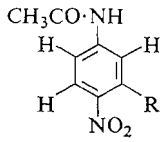

3*a*, R = H
3*b*, R = OCH_3

aromatic proton signals on the basis of the general rule that $J_{ortho} \gg J_{meta} > J_{para}$. Analysis of the p.m.r. spectrum of *o*-nitroacetanilide (**1***a*) itself was facilitated by the observation of weak coupling ($J \simeq 0.5$ Hz) between the 5-H and NH protons. The existence and nature of this type of long range coupling has been well established by Karabatsos and Vane (20). Spectra were determined in both chloroform-*d* at 30° and in acetonitrile-d_3 at 70°, the anilides (**2**), (**3***a*), and (**3***b*) being inadequately soluble in the former solvent.

The occurrence of intramolecular hydrogen-bonding in *ortho*-nitroacetanilides is confirmed by the p.m.r. spectra of compounds (**1***a–d*), which show broad NH resonances at consistently lower field by more than 1 p.p.m. than do *meta*- (**2**) and *para*-nitroacetanilides (**3***a*,*b*). Changing the solvent from chloroform-*d* at 30° to acetonitrile-d_3 at 70° results in a pronounced upfield shift of the NH by 0.30–0.75 p.p.m. This effect may be attributed to a partial breakdown of the intramolecular hydrogen bond by the more polar solvent. Even in the latter, however, intramolecular hydrogen-bonding still occurs, as indicated by comparison with *m*-nitroacetanilide (**2**), *p*-nitroacetanilide (**3***a*), and 3-methoxy-4-nitroacetanilide (**3***b*), all of which show NH resonances at τ 1.1–1.5, a range consistent with the absence of intramolecular hydrogen-bonding.

The 6-H resonance also occurs at unusually low field for the ortho-nitroacetanilides (**1***a–d*), in contrast to compounds (**2**), (**3***a*), and (**3***b*) which show aromatic proton resonances in positions that would be expected in the absence of intramolecular hydrogen-bonding. While the 3-protons in (**1***a*) and (**3***a*), both being *meta* to the acetamido group and *ortho* to the nitro group, differ by less than 0.1 p.p.m., the 6-H protons, both being *ortho* to the acetamido group and *meta* to the nitro group, differ by 0.65 p.p.m. For comparison, the *o*-proton in acetanilide itself is at τ 2.51 (chloroform-*d*) (10) and the *m*-proton in nitrobenzene at τ 2.52, compared to the τ value 1.23 for (**1***a*). That the *ortho* effect in compounds (**1***a–d*) is indeed due to intramolecular hydrogen-bonding is confirmed by the marked solvent sensitivity (0.1–0.42 p.p.m.) of the 6-H resonance, in contrast to the other aromatic proton resonances, which undergo only small shifts (< 0.15 p.p.m.) upon change of solvent. This solvent effect may be attributed, again, to a partial breakdown of the intramolecular hydrogen bond in the more polar solvent. The resulting reduction in population of molecules having the *trans* conformation (see **1**) should diminish the net deshielding effect of the carbonyl group on the 6-H.

Comparison of the four anilides (**1***a–d*) further reveals variations in solvent sensitivity of the 6-H and N—H protons. In *o*-nitroacetanilide (**1***a*), itself, the upfield shifts upon change of solvent from chloroform-*d* at 30° to acetonitrile-d_3 at 70° are 0.28 p.p.m. for the 6-proton and 0.47 p.p.m. for the NH proton. For 5-methoxy-2-nitroacetanilide (**1***d*), the upfield shifts are smaller, 0.10 and 0.30 p.p.m. respectively, while for 4-methoxy-2-nitroacetanilide (**1***c*), they are much greater, 0.42 and 0.74 p.p.m. respectively. If we assume that the magnitudes of these upfield shifts are determined by the ease with which the intramolecular hydrogen bond can be broken, we may rank these compounds according to the strength of the hydrogen bond. We then find that the strength of intramolecular hydrogen-bonding decreases in the order 5-methoxy-2-nitroacetanilide (**1***d*) > *o*-

Can. J. Chem. Downloaded from www.nrcresearchpress.com by 210.87.254.5 on 09/05/12
For personal use only.

TABLE II

Proton magnetic resonance spectra of acetanilides with carbonyl-containing substituents (in τ values)

Compound	Solvent	Temperature	Aromatic protons 2	3	4	5	6	NH	Other protons*
4*a*	$CDCl_3$	30°	—	1.98	2.96	2.48	1.31	−1.07	5.64(OCH_2)
	CD_3CN	30°	—	1.99	2.95	2.48	1.43	−0.80	7.80($COCH_3$)
	CD_3CN	70°	—	2.04	3.00	2.54	1.50	−0.50	8.60(C·CH_3)
5*a*	$CDCl_3$	30°	2.38	2.04	—	2.04	2.38	1.41	5.64(OCH_2)
	CD_3CN	30°	2.33	2.06	—	2.06	2.33	1.41	7.81($COCH_3$)
	CD_3CN	70°	2.38	2.10	—	2.10	2.38	1.60	8.60(C·CH_3)
4*b*	$CDCl_3$	30°	—	2.10	2.91	2.46	1.25	−1.67	7.40($ArCOCH_3$)
	CD_3CN	30°	—	2.01	2.88	2.45	1.38	−1.53	7.83(N·$COCH_3$)
	CD_3CN	70°	—	2.03	2.89	2.46	1.42	−1.30	
5*b*†	CD_3CN	30°	2.34	2.09	—	2.09	2.34	1.44	7.53($ArCOCH_3$)
	CD_3CN	70°	2.35	2.10	—	2.10	2.35	1.57	7.97(N·$COCH_3$)
4*c*	$CDCl_3$	30°	—	~2.5‡	2.96	~2.5‡	1.39	−0.77	7.82($COCH_3$)
6	$CDCl_3$	30°	3.06	3.06	—	—	0.94	−1.80	2.19(8-H)
									2.28(7-H)
									7.72($COCH_3$)
7	$CDCl_3$	30°	0.89	0.89	—	1.77	2.22	−2.48	7.70($COCH_3$)

*Values refer to chloroform-*d* solutions, except for (5*b*), which was run in acetonitrile-d_3 only.
†Insufficient solubility in chloroform-*d*.
‡Complex multiplets, overlapped by benzoyl proton resonances.

nitroacetanilide (**1***a*) > 4-methyl-2-nitroacetanilide (**1***b*) > 4-methoxy-2-nitroacetanilide (**1***c*). We suggest that in (**1***d*), the methoxy group, being *para* to the nitro group, results in greater electron density on the nitro-oxygen atoms than in *o*-nitroacetanilide (**1***a*) itself, and so in a stronger hydrogen bond than in (**1***a*). In (**1***c*), and to a lesser extent in (**1***b*), the substituent has the opposite effect, since it is *para* to the acetamido group and so should increase the electron density in the vicinity of the amido proton, thus resulting in a weaker hydrogen bond in (**1***c*) and (**1***b*) than in (**1***a*). The absolute position of the NH resonance itself is also well correlated with the suggested degree of intramolecular hydrogen-bonding, since the NH τ values increase in the order (**1***d*) < (**1***a*) < (**1***b*) < (**1***c*). The absolute position of the 6-H resonance, however, bears no simple relation to the strength of intramolecular hydrogen bonding, since it is determined in part by other factors such as the inductive and mesomeric effects of the ring substituents.

Our results for acetanilides with carbethoxy and keto substituents are summarized in Table II. The aromatic proton signals of *o*-acetamidoacetophenone (**4***b*) (21) were unambiguously assigned on the basis of the splitting patterns. In particular, the *meta* coupling constants $J_{3,5}$ and $J_{4,6}$ differed appreciably ($J_{3,5} = 1.8$ Hz, $J_{4,6} = 1.4$ Hz) and the 5-H – NH coupling ($J = 0.6$ Hz) was resolved (20). The latter coupling was too weak to be resolved in the spectrum of ethyl *o*-acetamidobenzoate (**4***a*) (22), but the aromatic proton spectra of the two compounds were so similar in other respects that the assignments for (**4***a*), and, from similar considerations (**4***c*) (23), may be considered unambiguous. Further support for these assignments is afforded by the position of the 3-H resonance, which is almost the same for both *ortho*- [(**4***a*) and (**4***b*)] and para-[(**5***a*) (24) and (**5***b*) (21)] substituted materials, and is typical of a proton *ortho* to a carbonyl group.

Although the 3-protons in (**4***a*), (**5***a*), (**4***b*), and (**5***b*) differ by less than 0.1 p.p.m. in the same solvent, the 6-protons in (**4***a*) and (**4***b*) are greater than 0.8 p.p.m. downfield of the 6-H protons in (**5***a*) and (**5***b*), which resonate at the expected position. The positions of the N—H as well as these 6-H resonances suggest that the anilides (**4***a*, *b*, and *c*) exhibit intramolecular hydrogen bonding at least as strong as do the *o*-nitroacetanilides, although effects due to the differing anisotropies of the carbonyl and nitro groups cannot be excluded.

The position of the NH resonances for ethyl *o*-acetamidobenzoate (**4***a*) and *o*-acetamidoacetophenone (**4***b*) indicate that intramolecular hydrogen bonding is stronger in the latter than in the former. This conclusion is further borne out by a study of solvent effects. A change of solvent

Can. J. Chem. Downloaded from www.nrcresearchpress.com by 210.87.254.5 on 09/05/12
For personal use only.

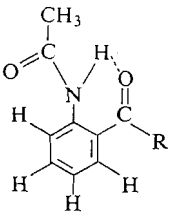

4*a* R = OC_2H_5
4*b* R = CH_3
4*c* R = C_6H_5

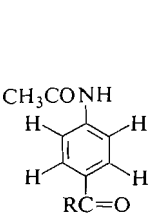

5*a* R = OC_2H_5
5*b* R = CH_3

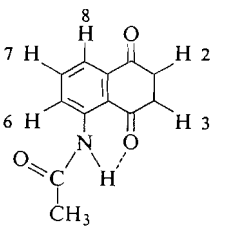

6

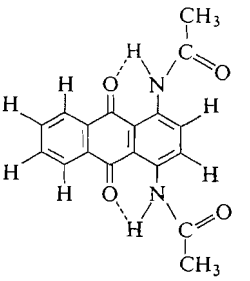

7

from chloroform-*d* to acetonitrile-d_3 results in an upfield shift of 0.27 p.p.m. for (**4***a*), but of only 0.14 p.p.m. for (**4***b*), reflecting the greater resistance of the hydrogen bond in (**4***b*) to breakdown by the more polar solvent. The intramolecular hydrogen bond should also be partially broken on raising the temperature. Measurements in acetonitrile-d_3 at 30° and at 70° show the expected further upfield shift of the NH resonance, but again, the upfield shift is less for (**4***b*) (0.23 p.p.m.) than for (**4***a*) (0.30 p.p.m.). The *para*-substituted analogues (**5***a*) and (**5***b*) show somewhat similar but smaller temperature shifts (0.19 and 0.13 p.p.m. respectively), but for (**5***a*) the NH resonance is insensitive to the change of solvent.

Turning to the 6-H resonance, we find that this resonance occurs in almost the same position in (**4***a*) (τ 1.31) and (**4***b*) (τ 1.25). This suggests that in the ester (**4***a*), intramolecular hydrogen-bonding is already strong enough to fix the acetamido group, so that the 6-proton feels the maximum deshielding effect of the acetamido-carbonyl group. Any further increase in the strength of the hydrogen bond (as in **4***b*) should then have little effect on the position of the 6-H resonance. In line with this reasoning, we find relatively small solvent and temperature effects for the 6-H resonance in both (**4***a*) and (**4***b*).

Still stronger hydrogen bonds, indicated by the lower field positions for the NH resonances, are found for 5-acetamido-1,4-naphthoquinone (**6**) (25) and, more particularly, for 1,4-bisacetamidoanthraquinone (**7**) (26). In both compounds the quinone carbonyl is ideally and rigidly placed for strong intramolecular hydrogen bonding, but in the anthraquinone derivative (**7**) an additional factor is the mesomeric interaction between benzenoid and quinonoid rings. This interaction, to which compound (**7**) owes its red color, undoubtedly contributes to the exceptionally strong hydrogen bonding in this compound. The 6-H in (**6**) and the 2-H and 3-H in (**7**) are more deshielded than the corresponding protons in any other compounds we have examined, although the deshielding no doubt includes the direct influence of the carbonyl groups. The aromatic proton spectrum (6-, 7-, and 8-H) of (**6**) was analyzed as an ABX system, and that of (**7**) by comparison with theoretical AA′BB′ spectra (27). In both compounds, the aromatic protons other than those adjacent to acetamido groups give signals close to the expected positions, confirming the spectral assignments.

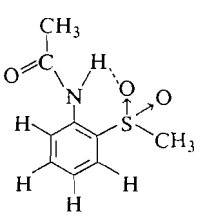

8

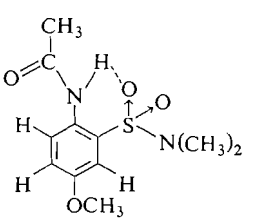

9

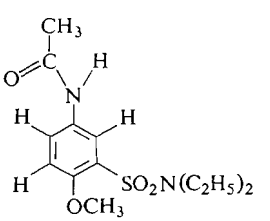

10

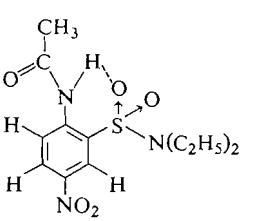

11

Can. J. Chem. Downloaded from www.nrcresearchpress.com by 210.87.254.5 on 09/05/12
For personal use only.

TABLE III

Proton magnetic resonance spectra of acetanilides with sulfur-containing substituents (in τ values)

Compound	Solvent	Temperature	Aromatic protons 2	3	4	5	6	NH	Other protons*
8	$CDCl_3$	30°	—	2.06	2.74	2.34	1.51	0.47	6.93(SO_2CH_3)
	CD_3CN	30°	—	2.07	2.70	2.31	1.57	0.62	7.77($COCH_3$)
	CD_3CN	70°	—	2.07	2.71	2.32	1.58	0.64	
9	$CDCl_3$	30°	—	2.71	—	2.87	1.68	0.76	6.15(OCH_3)
	CD_3CN	30°	—	2.72	—	2.80	1.79†	0.93	7.27(NCH_3)
	CD_3CN	70°	—	2.72	—	2.80	1.77	1.00	7.82($COCH_3$)
10	$CDCl_3$	30°	2.14	—	—	3.02	1.80	1.33	6.12(OCH_3)
	CD_3CN	30°	1.91	—	—	2.90	2.24	1.57	6.65(NCH_2)
	CD_3CN	70°	1.95	—	—	2.92	2.26	1.68	7.87($COCH_3$) 8.93($C{\cdot}CH_3$)
11	$CDCl_3$	30°	—	1.38	—	1.68	1.20	0.12	6.63(NCH_2)
	CD_3CN	30°	—	1.44	—	1.67	1.27	0.33	7.72($COCH_3$)
	CD_3CN	70°	—	1.47	—	1.70	1.31	0.42	8.83($C{\cdot}CH_3$)

*Values refer to chloroform-*d* solutions.
†Each line of the expected doublet appears as a triplet with a separation of 1.8 Hz.

We have also examined a few acetanilides in which the hydrogen-bonding entity is a sulfonyl group. Our results (see Table III) show that intramolecular hydrogen-bonding is relatively weak in both the sulfone (**8**) (28) and the sulfonamide (**9**). The further splitting of the 6-H doublet observed for (**9**) in acetonitrile-d_3 at 30°, and the equally unexpected crossover of the 2-H and 6-H resonances of (**10**) on changing from chloroform-*d* to acetonitrile-d_3 as solvent, have no ready explanation at present. It is possible that somewhat stronger intramolecular hydrogen-bonding occurs in 2-(*N*,*N*-diethylsulfamoyl)-4-nitroacetanilide (**11**), as measured by the positions of the 6-H and NH resonances, although in the absence of suitable analogues we cannot evaluate the general inductive effect of the nitro and sulfamoyl groups. Spectral assignments in this series were unequivocal, with the reservation that for the sulfone (**8**), the 6-H proton had to be assigned on the basis of a comparison of solvent shifts. Temperature shifts in this series were relatively small.

Most of the compounds used in this study were either commercial materials, appropriately purified, or known compounds prepared by routes described in the literature (see references). 2-(*N*,*N*-Dimethylsulfamoyl)-4-methoxyacetanilide (**9**) was prepared by addition of the diazonium salt of 5-methoxy-2-nitroaniline (**12**) (19) to a solution of sulfur dioxide in acetic acid in the presence of hydrochloric acid and cuprous chloride (29); the resulting sulfonyl chloride (**13**) was converted into the *N*,*N*-dimethylsulfonamide (**14**), which on hydrogenation to the aniline (**15**) followed by acetylation gave (**9**). 3-(*N*,*N*-Diethylsulfamoyl)-4-methoxyacetanilide (**10**) was prepared by chlorosulfonation of aceto-*p*-anisidide (**16**), followed by treatment of the resulting sulfonyl chloride (**17**) with diethylamine. The structure (**10**) of the product was confirmed by comparison of the p.m.r. and infrared spectra with those of the anilide (**9**), whose synthesis was unequivocal. 2-(*N*,*N*-Diethylsulfamoyl)-4-nitroacetanilide (**11**) was synthesized from sodium 2-amino-5-nitrobenzenesulfonate (**18**), which on treatment with phosphorus pentachloride gave the sulfonyl chloride (**19**). The latter, on treatment with diethylamine, gave (**20**), which on acetylation with acetic anhydride in the presence of zinc chloride gave (**11**).

Experimental

Proton magnetic resonance (p.m.r.) spectra were determined on a Varian Associates A-60 spectrometer for 10% w/v solutions. Tetramethylsilane was used as an internal standard. Infrared spectra were recorded on a Perkin–Elmer model 421 spectrophotometer, using KBr disks. Ultraviolet spectra were determined on a Cary model 11 spectrophotometer. Microanalyses were performed by Galbraith Laboratories, Knoxville, Tennessee, and by Werby Laboratories, Boston, Massachusetts.

5-Methoxy-2-nitrobenzene Sulfonyl Chloride (13)

A suspension of 2-nitro-5-methoxy aniline (19) (16.82 g; 0.1 mole) in concentrated hydrochloric acid (175 ml) was diazotized at 0° by dropwise addition of a

Can. J. Chem. Downloaded from www.nrcresearchpress.com by 210.87.254.5 on 09/05/12
For personal use only.

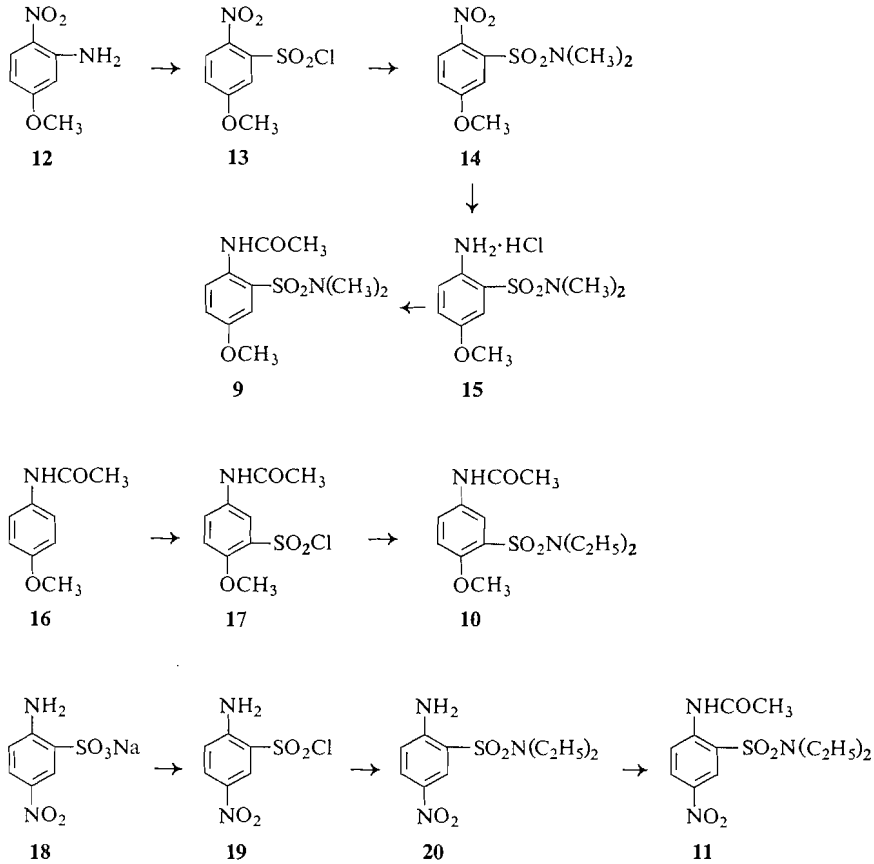

solution of sodium nitrite (7.00 g; 0.1 mole) in water (25 ml). After diazotization was complete (1 h), the mixture was stirred for a further 0.25 h, after which the excess of nitrous acid was destroyed by addition of sulfamic acid. The filtered solution was added in one portion to a solution obtained by saturating glacial acetic acid (210 ml) with sulfur dioxide at 10°, adding cupric chloride dihydrate (2.90 g; 0.017 mole), and finally warming to 15°. After the initial vigorous effervescence had subsided, the mixture was kept at 20° until evolution of nitrogen had almost ceased (20 min), and then warmed to 25° for 10 min to complete the reaction. Ice (1 kg) was then added and after 1.5 h the crystalline product was collected and washed with water. The dried product (10.63 g) after recrystallization from benzene–hexane gave pure 5-methoxy-2-nitrobenzenesulfonyl chloride, m.p. 64.5–65.5°, (7.87 g; 52%); ν_{max} 1533 and 1351 (—NO_2), and 1378, 1371, and 1173 cm^{-1} (—SO_2Cl); $\tau(CDCl_3)$ 2.01 (d, J = 9.0 Hz, 3-H), 2.30 (d, $J_{4,6}$ = 3.0 Hz, 6-H), 2.71 (q, 4-H), and 6.00 (s, 3, OCH_3).

Anal. Calcd. for $C_7H_6ClNO_5S$ (251.65): C, 33.43; H, 2.40; Cl, 14.09; N, 5.58; O, 31.81; S, 12.75. Found: C, 33.30; H, 2.43; Cl, 14.20; N, 5.68; O, 31.64; S, 12.80.

*N,N-Dimethyl-5-methoxy-2-nitrobenzenesulfonamide (**14**)*

5-Methoxy-2-nitrobenzenesulfonyl chloride was prepared as described above from 2-nitro-5-methoxy aniline (16.82 g), and the crude, wet product taken up in tetrahydrofuran (60 ml). The resulting solution was added with stirring to aqueous dimethylamine (200 ml; 25%; *ca.* 1 mole) at 0–5° during 0.5 h. The mixture was then allowed to warm slowly to room temperature, and stirring was continued overnight. The oil which appeared crystallized on addition of ice. The product was collected, washed with water, and dried, giving a yellow solid, m.p. 122–126° (18.74 g). After two recrystallizations from ethyl acetate, *N,N*-dimethyl-5-methoxy-2-nitrobenzenesulfonamide was obtained as pale-yellow rods, m.p. 127–128° (13.63 g; 52%); ν_{max} 1527 and 1351 (—NO_2), and 1321 and 1147 cm^{-1}; $\tau(CDCl_3)$ 2.29 (d, $J_{3,4}$ = 9.0 Hz, 3-H), 2.51 (d, $J_{4,6}$ = 2.8 Hz, 6-H), 2.89 (q, 4-H), 6.07 (s, 3, OCH_3), and 7.07 (s, 6, NCH_3).

Anal. Calcd. for $C_9H_{12}N_2O_5S$ (260.27):C, 41.54; H, 4.65; N, 10.77; S, 12.30. Found: C, 41.57; H, 4.71; N, 10.90; S, 12.35.

*2-(N,N-Dimethylsulfamoyl)-4-methoxyaniline Hydrochloride (**15**)*

N,N-Dimethyl-5-methoxy-2-nitrobenzenesulfonamide (13.01 g; 0.05 mole), dissolved in ethanol (150 ml), was hydrogenated at 40 lb/in.^{2} over palladium on barium sulfate catalyst (5%). Hydrogenation was complete after 0.5 h. Removal of the catalyst and evaporation of the filtrate gave a purplish oil (11.50 g) which was dissolved

Can. J. Chem. Downloaded from www.nrcresearchpress.com by 210.87.254.5 on 09/05/12
For personal use only.

Can. J. Chem. Downloaded from www.nrcresearchpress.com by 210.87.254.5 on 09/05/12
For personal use only.

in dry ether. The ethereal solution on saturation with dry hydrogen chloride at 0° gave pinkish-white needles of 2-(*N,N*-dimethylsulfamoyl)-4-methoxyaniline hydrochloride, m.p. 164–168° (12.15 g; 91%); ν_{max} 1343, 1155 cm^{-1} (—SO_2—); τ[$(CD_3)_2SO$] 1.40 (s, 3, NH_3^+), 2.75 (6-H), 2.78 (5-H), and 2.96 (3-H) (components of ABX spectrum, $J_{3,5}$ = 3.0 Hz, $J_{3,6} \simeq$ 0.5 Hz, $J_{5,6}$ = 9.0 Hz), 6.23 (s, 3, OCH_3), and 7.30 (s, 6, NCH_3).

Anal. Calcd. for $C_9H_{15}ClN_2O_3S$ (266.69): C, 40.53; H, 5.67; N, 10.51; S, 12.02. Found: C, 40.82; H, 5.80; N, 10.91; S, 12.24.

2-(N,N-Dimethylsulfamoyl)-4-methoxyacetanilide (9)

A solution of 2-(*N,N*-dimethylsulfamoyl)-4-methoxyaniline hydrochloride (1.0 g; 0.0038 mole) in water (20 ml) was adjusted to pH 12 with 50% aqueous sodium hydroxide and cooled in ice, whereupon the oil initially formed crystallized. The solid, washed with water, was added damp to a mixture of acetic anhydride (4 ml) and acetic acid (3 ml). The mixture was stirred under reflux for 0.75 h and then poured into water, and the resulting solution made alkaline (pH 11) with 10% aqueous sodium hydroxide. The crude anilide then precipitated; isolation gave material, m.p. 82–83° (0.48 g). After two recrystallizations from ethyl acetate – hexane 2-(*N,N*-dimethylsulfamoyl)-4-methoxyacetanilide was obtained as prisms, m.p. 98.5–99.5° (0.31 g); λ_{max} (EtOH) 250 (ε 11 000) and 303 mμ (ε 3900); ν_{max} 3375 (NH), 1699 (amide I), 1517 (amide II), and 1329 and 1148 cm^{-1} (—SO_2—).

Anal. Calcd. for $C_{11}H_{16}N_2O_4S$ (272.33): C, 48.52; H, 5.92; N, 10.29; S, 11.75. Found: C, 48.46; H, 5.80; N, 10.27; S, 11.71.

5-Acetamido-2-methoxybenzenesulfonyl Chloride (17)

Chlorosulfonic acid (140 ml) was cooled to 10° and stirred while aceto-*p*-anisidide (54 g; 0.33 mole) was added slowly so that the temperature of the mixture was maintained at 15–20°. The mixture was warmed with stirring for 1 h, a little below 60°, and finally cooled and cautiously poured into ice and water. The solid was collected and washed with water, giving 60 g (70%) of crude 5-acetamido-2-methoxybenzenesulfonyl chloride. A portion when recrystallized from benzene had m.p. 143–145°; λ_{max} (dioxan) 328 mμ (ε 3540); ν_{max} 3285 and 3250 (NH), 1652 (amide I), 1534 (amide II), and 1358 and 1174 cm^{-1} (—SO_2—); τ[$(CD_3)_2SO$]—0.02 (s, NH), 2.01 (d, $J_{4,6}$ = 2.5 Hz, 6-H), 2.27 (q, $J_{3,4}$ = 9.0 Hz, 4-H), 2.98 (d, 3-H), 6.23 (s, 3, OCH_3), and 7.98 (s, 3, $CO{\cdot}CH_3$).

3-(N,N-Diethylsulfamoyl)-4-methoxyacetanilide (10)

Crude 5-acetamido-2-methoxybenzenesulfonyl chloride (60.0 g; 0.23 mole) was suspended in 10% aqueous sodium hydroxide (300 ml) and diethylamine (50.0 g; 0.68 mole) added. The mixture was stirred for 3 h, after which further diethylamine (25.0 g; 0.34 mole) was added. After a further 3 h, additional diethylamine (25.0 g; 0.34 mole) was added and stirring continued overnight. The resulting solid when collected, washed with water, and dried, afforded 3-(*N,N*-diethylsulfamoyl)-4-methoxyacetanilide, m.p. 176–178° (40.3 g; 59%). A portion on recrystallization from 95% ethanol gave prisms, m.p. 178–179°; λ_{max} (EtOH) 250 (ε 16 400) and 304 mμ (ε 3340); ν_{max} 3280 (NH), 1680 (amide I), 1539 (amide II), and 1310 and 1136 cm^{-1} (—SO_2—).

Anal. Calcd. for $C_{13}H_{20}N_2O_4S$ (300.38): C, 52.01; H, 6.71; N, 9.33; S, 10.67. Found: C, 52.49; H, 6.75; N, 9.34; S, 10.60.

2-Amino-5-nitrobenzenesulfonyl Chloride (19)

A mixture of sodium 2-amino-5-nitrobenzenesulfonate monohydrate (67.0 g; 0.271 mole) and phosphorus pentachloride (75.0 g; 0.360 mole) was kept for 0.5 h with intermittent stirring, the exothermic reaction being controlled by external cooling with water. The resulting mixture was heated on the steam bath for 4 h with mechanical stirring, then cooled, and finally added to ice-water (1.2 l). After 3 h, crystallization of the gummy precipitate was complete and collection, washing with water and drying furnished 2-amino-5-nitrobenzenesulfonyl chloride as a pinkish-brown solid, m.p. 128–132° (22.1 g; 35%); ν_{max} 3470, 3350 and 1635 (NH_2), and 1360 and 1160 cm^{-1} (—SO_2—).

The product was used directly for the next step without further purification.

2-(N,N-Diethylsulfamoyl)-4-nitroaniline (20)

A suspension of 2-amino-5-nitrobenzenesulfonyl chloride (20.6 g; 0.087 mole) in dry ether (200 ml) was stirred while diethylamine (35.5 g; 0.49 mole) was added dropwise with external cooling (cold water) to moderate the reaction. The mixture was stirred for 5.5 h, and then kept overnight at 0°. The solid which appeared was collected and washed with ether. The filtrate and washings when concentrated to small bulk afforded an orange solid which when washed sparingly with ether and with hexane gave 2-(*N,N*-diethylsulfamoyl)-4-nitroaniline as a yellow solid, m.p. 165–166° (1.9 g). The ether-insoluble residue on digestion with successive portions of cold ethyl acetate until the digests were colorless, followed by evaporation of the combined digests, gave further material, m.p. 161–163° (15.1 g). The combined yield of crude product was 72%. Recrystallization from methanol furnished pale-yellow rectangular tablets, m.p. 168–169°; ν_{max} 3460, 3355, and 1628 (—NH_2), and 1326 and 1140 cm^{-1} (—SO_2—); τ[$(CD_3)_2SO$] 1.70 (d, $J_{3,5}$ = 2.7 Hz, 3-H), 1.93 (q, $J_{5,6}$ = 8.5 Hz, 5-H), 3.07 (d, 6-H), 3.8 (broad resonance, 2, NH_2), 6.72 (q, 4, J_{HH} = 7.0 Hz, $N{\cdot}CH_2{\cdot}CH_3$), and 8.95 (t, 6, J_{HH} = 7.0 Hz, $N{\cdot}CH_2{\cdot}CH_3$).

Anal. Calcd. for $C_{10}H_{15}N_3O_4S$ (273.32): C, 43.98; H, 5.50; N, 15.37; S, 11.73. Found: C, 44.23; H, 5.62; N, 15.42; S, 11.38.

2-(N,N-Diethylsulfamoyl)-4-nitroacetanilide (11)

A few crystals of anhydrous zinc chloride were added to a suspension of 2-(*N,N*-diethylsulfamoyl)-4-nitroaniline (8.2 g; 0.030 mole) in acetic anhydride (60 ml) and the mixture stirred at 70° for 15 min and then at 50–55° for 1.25 h. After removal of acetic anhydride under reduced pressure (2 mm), the residue was rubbed with water and the solid collected. The product, m.p. 120–121.5° (9.0 g), was recrystallized from the minimum volume of ethyl acetate, giving 2-(*N,N*-diethylsulfamoyl)-4-nitroacetanilide as pale-yellow needles, m.p. 121.5–122°, (7.4 g; 78%); λ_{max} ($MeOCH_2CH_2OH$) 313 mμ (ε 13 200); ν_{max} 3330 (NH), 1710 (amide I), 1515 (amide II and —NO_2), and 1340 and 1140 cm^{-1} (—SO_2—).

Anal. Calcd. for $C_{12}H_{17}N_3O_5S$ (315.36): C, 45.71; H, 5.44; N, 13.33; S, 10.15. Found: C, 45.99; H, 5.48; N, 13.25; S, 10.19.

Acknowledgments

We thank Miss Marian Jones and Mr. L. G. Gross for their assistance in the synthetic work, and Mrs. Patricia C. Morrison, Mr. M. H. Mach, and Mr. B. R. Belinky for their assistance in the determination of proton magnetic resonance spectra. We also thank Dr. R. F. C. Brown (Australian National University, Canberra, Australia), Drs. L. Radom and S. Sternhell (University of Sydney, Sydney, Australia), and Dr. I. D. Rae (Monash University, Clayton, Australia) for helpful correspondence and discussions, and for their cooperation in arranging simultaneous publication.

1. E. J. Forbes, K. J. Morgan, and J. Newton. J. Chem. Soc. 835 (1963); L. Skulski. J. Org. Chem. **28**, 3565 (1963).
2. H. E. Ungnade. J. Am. Chem. Soc. **76**, 5133 (1954); A. E. Lutskiĭ, V. N. Konel'skaya, and B. P. Kondratenko. Zh. Obshch. Khim. **30**, 3782 (1960); Chem. Abstr. **55**, 19472 (1961).
3. J. A. Weil, A. Blum, A. H. Heiss, and J. K. Kinnaird. J. Chem. Phys. **46**, 3132 (1967).
4. M. Gomel and H. Lumbroso. Bull. Soc. Chim. France, 1196 (1962).
5. T. Suzuki, M. Tsuboi, T. Shimanouchi, and S. Mizushima. Spectrochim. Acta, **16**, 471 (1960).
6. J. W. Smith. J. Chem. Soc. 4700 (1961).
7. H. B. Thompson and K. M. Hallberg. J. Phys. Chem. **67**, 2486 (1963).
8. L. K. Dyall and J. E. Kemp. Spectrochim. Acta, **22**, 483 (1966).
9. B. F. Pedersen and B. Pedersen. Tetrahedron Letters, 2995 (1965).
10. R. E. Carter. Acta Chem. Scand. **21**, 75 (1967).
11. L. M. Jackman. Applications of nuclear magnetic resonance spectroscopy in organic chemistry. The Pergamon Press, Ltd., Oxford. 1959. Chap. 7. p. 124.
12. G. J. Karabatsos, G. C. Sonnichsen, N. Hsi, and D. J. Fenoglio. J. Am. Chem. Soc. **89**, 5067 (1967).
13. R. F. C. Brown, I. D. Rae, and S. Sternhell. Australian J. Chem. **18**, 1211 (1965).
14. R. F. C. Brown, L. Radom, I. D. Rae, and S. Sternhell. Can. J. Chem. This issue.
15. I. D. Rae. Can. J. Chem. This issue.
16. B. M. Lynch, C. M. Chen, and Y-Y. Wigfield. Can. J. Chem. **46**, 1141 (1968).
17. A. Ribera and M. Rico. Tetrahedron Letters, 535 (1968).
18. T. H. Siddall and W. E. Stewart. J. Mol. Spectry. **24**, 290 (1967).
19. F. Reverdin and K. Widmer. Ber. **46**, 4066 (1913).
20. G. J. Karabatsos and F. M. Vane. J. Am. Chem. Soc. **85**, 3886 (1963).
21. N. J. Leonard and S. N. Boyd. J. Org. Chem. **11**, 405 (1946).
22. H. Mehner. J. Prakt. Chem. [2] **64**, 83 (1901).
23. A. Bischler and D. Barad. Ber. **25**, 3080 (1892).
24. A. J. Hill and M. V. Cox. J. Am. Chem. Soc. **48**, 3214 (1926).
25. J. W. MacLeod and R. H. Thomson. J. Org. Chem. **25**, 36 (1960).
26. E. Noelting and W. Wortmann. Ber. **39**, 637 (1906).
27. K. B. Wiberg and B. J. Nist. The interpretation of N.M.R. spectra. W. A. Benjamin, Inc., New York. 1962. Chap. 5. p. 318 *ff*.
28. J. Bolssens, J. A. C. Th. Brouwers, J. H. Choufoer, A. Kats, P. E. Verkade, and B. M. Wepster. Rec. Trav. Chim. **73**, 819 (1954).
29. H. Meerwein, G. Dittmar, R. Göllner, K. Hafner, F. Mensch, and O. Steinfort. Ber. **90**, 841 (1957).

Can. J. Chem. Downloaded from www.nrcresearchpress.com by 210.87.254.5 on 09/05/12
For personal use only.

Investigations on steroids. XXXIX. 14,19-Dihydroxy-14β-progesterone and related compounds[1,2]

VIRENDRA N. GUPTA[3] AND MAXIMILIAN EHRENSTEIN[4]

Division of Steroid Research, The John Herr Musser Department of Research Medicine, University of Pennsylvania, Philadelphia, Pennsylvania 19104

Received January 9, 1968

Strophanthidol (**1**) was converted into 3β,19,21-triacetoxy-5,14-dihydroxy-5β,14β-pregnan-20-one (7) which by treatment with methylmagnesium bromide gave a mixture of the two C-20 epimers of 3β,5,14,19,20,21-hexahydroxy-bisnor-5β,14β-cholane (**8**). Oxidation of **8** with sodium periodate yielded the amorphous 3β,5,14,19-tetrahydroxy-5β,14β-pregnan-20-one (**9**) which was characterized as the crystalline 3,19-diacetate (**10**). Selective oxidation of **9** with *N*-bromoacetamide, followed by dehydration of the reaction product **11** gave 14,19-dihydroxy-14β-progesterone (**12**) which was characterized as the 19-monoacetate (**13**).

Compound **12** was found to be devoid of progestational and antiprogestational activity.

Canadian Journal of Chemistry, 46, 2601 (1968)

A number of years ago, the conversion of strophanthidol (**1**) to 14,19-dihydroxy-14β-cortexone by way of 3β,5,14,19,21-pentahydroxy-5β,14β-pregnan-20-one (**6**) was described by this laboratory (1). As a continuation of this work, it appeared desirable to prepare 14,19-dihydroxy-14β-progesterone (**12**).

The reaction of a ketol ester with methylmagnesium bromide, followed by oxidation of the resulting product with sodium bismuthate (2) or sodium periodate (3) has been reported as a useful method for the conversion of a ketol side chain to the corresponding methyl ketone. Hence, 3β,19,21-triacetoxy-5,14-dihydroxy-5β,14β-pregnan-20-one (**7**) (1) was considered a suitable starting material for the synthetic work in mind. Treatment of **7** with tenfold the required amount of methylmagnesium bromide gave a small amount of crystalline material (m.p. 275–276 °C), representing one of the two C-20 epimers of 3β,5,14,19,-20,21-hexahydroxy-bisnor-5β,14β-cholane (**8**). The major part of the reaction product, consisting essentially of a mixture of the two C-20 epimers of **8**, did not crystallize. This amorphous mixture of the C-20 epimers of **8** served as starting material for the subsequent chemical reactions. Treatment of the amorphous **8** with sodium periodate gave ketonic material which did not crystallize after chromatographic purification. It was identified as 3β,5,14,19-tetrahydroxy-5β,14β-pregnan-20-one (**9**) by preparation of the crystalline diacetate, viz. 3β,19-diacetoxy-5,14-dihydroxy-5β,14β-pregnan-20-one (**10**). Oxidation of the purified amorphous **9** with *N*-bromoacetamide gave the crude 5,14,19-trihydroxy-5β,14β-pregnane-3,20-dione (**11**) in amorphous form which was subjected as such to treatment with Girard's reagent T. After chromatographic purification, 14,19-dihydroxy-14β-progesterone (**12**) was isolated in a crystalline form. In subsequent experiments it was shown that the crystalline triacetate **7** can be converted into crystalline **12** without purification of the amorphous intermediates **8**, **9**, and **11**. Compound **12** was converted into the crystalline 19-monoacetate, viz. 19-acetoxy-14-hydroxy-14β-progesterone (**13**). As expected, **13** showed the typical hypsochromic shift of the ultraviolet absorption maximum associated with the acetylation of 19-hydroxyl groups in Δ^4-3-keto steroids.[5]

In view of the successful application of a specific sequence of reactions in our studies of the 17α-strophanthidol series (4), analogous experiments were applied to strophanthidol with good

[1]This investigation was supported in whole by Public Health Service Research Grants (CY757-C7, CY757-C8, CA00757-10, and CA 00757-11) from the National Cancer Institute of the National Institutes of Health.

[2]cf. Preliminary notice: V. N. Gupta and M. Ehrenstein. New steroid hormone analogues of the 14β,19-dihydroxy series. Abstracts of papers presented at the Second International Congress on Hormonal Steroids. Milan. May 23–28, 1966. Excerpta medica. International Congress Series. No. 111. p. 126 (Abstract No. 194).

[3]Holder of a Postdoctoral Fellowship at the University of Pennsylvania, 1961–1965. Dr. Gupta came from the Department of Pharmacology, All India Institute of Medical Sciences, New Delhi, India. He was the recipient of a Fulbright Travel Only Grant. Present affiliation: International Cellulose Research Ltd., Hawkesbury, Ontario.

[4]To whom inquiries concerning this paper should be directed.

[5]Literature, cf. ref. 1. p. 512.

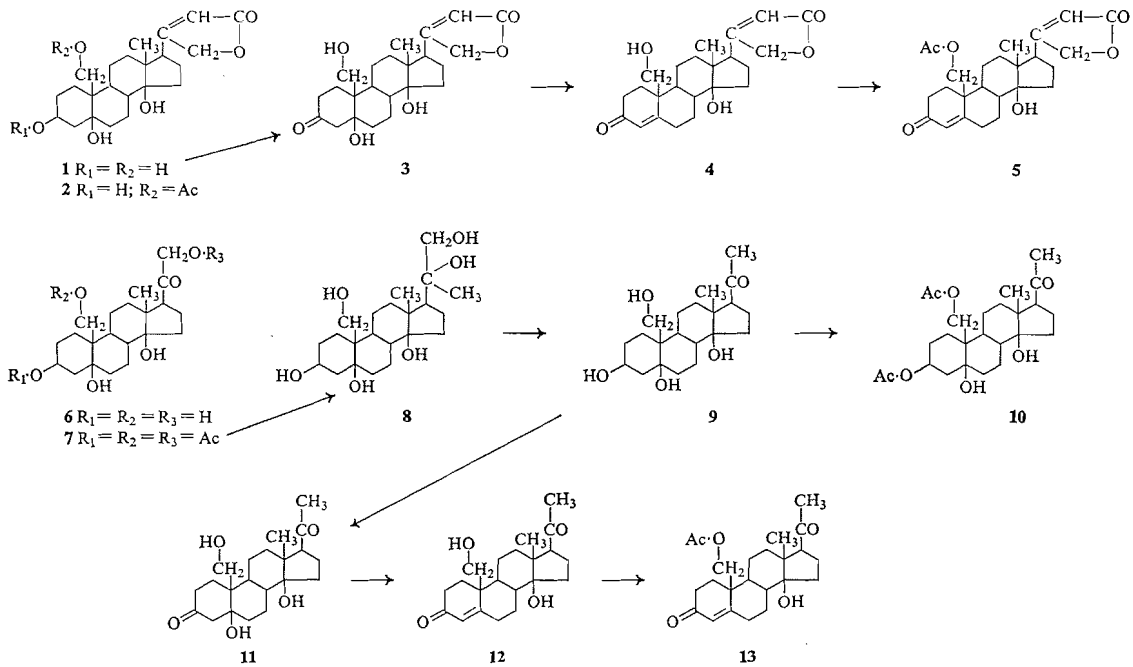

results. For the sake of convenience the findings are included in this publication. By treatment with *N*-bromoacetamide, strophanthidol (**1**) was selectively oxidized to 3-oxo-5β,14,19-trihydroxy-$\Delta^{20(22)}$-5β,14β-cardenolide (**3**). The reaction of **3** with Girard's reagent T in the usual fashion yielded 3-oxo-14,19-dihydroxy-$\Delta^{4,20(22)}$-14β-cardadienolide (19-dihydroanhydrostrophanthidone) (**4**) which was characterized as the 19-monoacetate, viz. 3-oxo-14-hydroxy-19-acetoxy-$\Delta^{4,20(22)}$-14β-cardadienolide (19-dihydroanhydrostrophanthidone 19-monoacetate) (**5**). Both, **4** (5–7) and **5** (6, 8) were previously prepared by other methods. The characteristics of the compounds obtained in this laboratory are in agreement with the earlier findings.

Biological Activity

Bioassays for progestational and antiprogestational activity were conducted by Dr. Roy Hertz, Chief of the Reproduction Research Branch, National Institute of Child Health and Human Development. 14,19-Dihydroxy-14β-progesterone (**12**) was tested in each of three Clauberg rabbits at a total dose per rabbit of 5.0 mg. No evidence of progestational activity was apparent at this dose whereas control animals showed maximum effects with a total dose of 0.5 mg of progesterone. — In another series, each of 3 Clauberg rabbits previously conditioned with estrogen were given either 0.5 mg of progesterone alone or 0.5 mg of progesterone plus 35.0 mg of **12**. All animals exhibited maximum progestational effect. Hence no antiprogestational activity was apparent.

Experimental

The melting points were determined with a Fisher–Johns melting point apparatus and are uncorrected. The true melting points are approximately 4° lower than those recorded.

The ultraviolet (u.v.) spectra were determined in 95% ethanol with a Beckman model DU spectrophotometer or a Cary model 14 recording spectrophotometer. The infrared (i.r.) spectra were measured in potassium bromide disks on the Perkin–Elmer 421 spectrophotometer.

The microanalyses were performed by Mr. Ernst Thommen, Bettingen bei Basel, Switzerland or by the Mikrolaboratorium (Director, W. Manser), Laboratorium für Organische Chemie, Eidgenössische Technische Hochschule, Zürich, Switzerland. Thanks are due to Professor V. Prelog for this courtesy.

In optical rotation determinations, no correction for crystal solvent has been made. Unless otherwise stated, the sample was dissolved in chloroform to make 2 ml of solution and the rotation was determined in a 2-dm semimicro tube.

3-Oxo-5,14,19-trihydroxy-$\Delta^{20(22)}$-5β,14β-cardenolide (3) and 3-Oxo-14,19-dihydroxy-$\Delta^{4,20(22)}$-14β-cardadienolide (19-dihydroanhydrostrophanthidone) (4) from Strophanthidol (1)

A mixture containing 800 mg of strophanthidol (**1**), 50 ml of 70% aqueous *t*-butyl alcohol and 600 mg of

N-bromoacetamide (96% purity by titration) was kept at room temperature for 20 h. It was then decolorized by adding aqueous sodium thiosulfate and diluted with 200 ml of water. After saturating with sodium chloride and extracting with chloroform–methanol (4:1), 0.8 g of an amorphous residue resulted representing crude **3** which was used for the next step without purification. Hence, it was dissolved in 50 ml of absolute ethanol and, after the addition of 1.5 g of Girard's reagent T and 2 ml of glacial acetic acid, the mixture was refluxed for 1 h. After diluting it with a solution of 2 g of sodium carbonate in 200 ml of water, it was extracted with five portions of 50 ml of chloroform, yielding 227 mg of non-ketonic material. The aqueous solution was then acidified with concentrated hydrochloric acid to pH 2 and left at room temperature for 90 min. After saturating the mixture with sodium chloride, it was extracted with six portions of 50 ml of chloroform. On drying over sodium sulfate and distilling the solvent, 543 mg of ketonic material resulted. Three recrystallizations from acetone–hexane gave 285 mg of **4**, m.p. 246–248 °C. Legal test positive. Thin-layer chromatography (t.l.c.) on Silica Gel (solvent: lower phase of chloroform – methanol – water – acetic acid, 80:20:10:0.5; reagent: *p*-toluenesulfonic acid) revealed the presence of a small amount of a faster moving impurity, which was removed by further recrystallization yielding pure **4**, m.p. 246–248 °C; $[\alpha]_D^{23}$ +90°, M_D^{23} +348° (17.0 mg in 2 ml of methanol, α +1.53°); λ_{max}(alcohol) 221 mμ, ε 19 500.[6] (Lit. (5) m.p. 232–240 °C. $[\alpha]_D^{25}$ +83° (methanol); λ_{max}(alcohol) 219 mμ, ε 17 400. Lit. (6) m.p. 247–251 °C; $[\alpha]_D^{25}$ +91° (methanol); λ_{max}(MeOH) 219 mμ, ε 22 000. Lit. (7) m.p. 240–245 °C; $[\alpha]_D^{20}$ +90° (methanol).) ν_{max}(KBr) 3495 (free OH), 3420 (broad, bonded OH), 3020 (unsaturated C—H), 1770 and 1730 (CO of lactone ring), 1640 (C-3 CO), 1610 (shoulder, C=C), 1065, and 1015 (C—O of C—OH) cm^{-1}.

Anal. Calcd. for $C_{23}H_{30}O_5$: C, 71.48; H, 7.82. Found: C, 71.07, 71.45;[8] H, 7.88,[7] 7.45.[8]

3-Oxo-14-hydroxy-19-acetoxy-$\Delta^{4,20(22)}$-14β-cardadienolide (19-dihydroanhydrostrophanthidone 19-monoacetate) (5) from 3-Oxo-14,19-dihydroxy-$\Delta^{4,20(22)}$-14β-cardadienolide (19-dihydroanhydrostrophanthidone) (4)

A mixture of 100 mg of **4**, m.p. 246–248 °C, 5 ml of pyridine, and 2 ml of acetic anhydride was kept at room temperature for 18 h. It was evaporated to dryness *in vacuo* and the residue was dissolved in ethyl acetate. The solution was washed to neutrality and evaporated to dryness yielding 106 mg of material which on crystallization from acetone–hexane gave 57 mg of **5** as long needles, m.p. 185–187 °C; $[\alpha]_D^{23}$ +103.9°, M_D^{23} +445° (13.95 mg in 2 ml of methanol, α +1.45°); λ_{max}(alcohol) 226 mμ, ε 20 500.[9] (Lit. (6) m.p. 186–187°; $[\alpha]_D$ +101° (methanol). Lit. (8) m.p. 185–187 °C. $[\alpha]_D$ +100.9° (dioxane); λ_{max}(MeOH) 226 mμ, ε 22 300); ν_{max}(KBr) 3500 (free OH), 3410 (bonded OH), 3020 (unsaturated C—H), 1772 (CO of lactone ring), 1655 (C-3 CO), 1610 (C=C), 1242 (C—O of C—OAc), 1030 and 1018 (C—O of C—OAc and C—OH) cm^{-1}.

Anal. Calcd. for $C_{25}H_{32}O_6$: C, 70.07; H, 7.53. Found:[8] C, 69.67; H, 7.24.

3β,5,14,19,20,21-Hexahydroxy-bisnor-5β,14β-cholane (8) from 3β,19,21-Triacetoxy-5,14-dihydroxy-5β,14β-pregnan-20-one (7)

Methyl bromide was passed through a suspension of 900 mg of magnesium[10] in 20 ml of ether until the metal was completely dissolved. After stirring the mixture for 30 min to remove the excess methyl bromide, a solution of 200 mg of pooled **7**, melting points 197–199 °C and 200–201 °C, in 30 ml of tetrahydrofuran was added to the Grignard reagent at room temperature. The water in the condenser was stopped and the temperature raised to 59–61 °C so that all the ether distilled off. The reaction mixture was then kept at this temperature for 6 h. After standing at room temperature overnight, it was decomposed with cold saturated aqueous ammonium chloride. After saturating with sodium chloride, the product was extracted with five 50 ml portions of ethyl acetate. The extract was washed with saturated aqueous sodium chloride and, after drying over sodium sulfate, evaporation of the solvent yielded 180 mg of material. Treatment with 5 ml of warm acetone furnished 52 mg of a crystalline product, m.p. 230–240 °C.

In five experiments carried out under the conditions stated above, a total of 2.125 g of pure **7** gave in part crystalline material which on recrystallization from acetone yielded 195 mg of prisms of constant m.p. 275–276 °C representing one of the two C-20 epimers of **8**; $[\alpha]_D^{24}$ +56.5°, M_D^{24} +225° (16.9 mg in 2 ml of 95% ethanol, α + 0.96°); ν_{max}(KBr) 3350 (broad, bonded OH), 1455 (angular and/or C-20 CH_3), 1145 (shoulder), 1132 and 1120 (shoulder) (triplet of C—O of C—OH), 1045 and 1015 (C—O of C—OH).

Anal. Calcd. for $C_{22}H_{38}O_6$: C, 66.30; H, 9.61. Found:[8] C, 66.49; H, 9.78.

The non-crystalline material resulting from these five experiments (1.6 g) was chromatographed over 50 g of Florisil. Elution with 100 ml portions of chloroform and chloroform–acetone, 19:1, 9:1, 4:1 (13 fractions) yielded 498 mg of material (*a*). Subsequent elution with chloroform–acetone, 1:1 and acetone (6 fractions) gave 883 mg of product (*b*). Finally, elution with acetone–methanol, 9:1 (6 fractions) furnished 156 mg of material (*c*). All these products were amorphous. The product (*b*) was successfully used for further conversions (*vide infra*)

[6] If the u.v. absorption curves of 3-oxo-14,19-dihydroxy-$\Delta^{4,20(22)}$-14β-cardadienolide (19-dihydroanhydrostrophanthidone) (**4**) and strophanthidol (**1**) are plotted at the respective wavelengths, and the ε values of the latter (**1**) (λ_{max}(alcohol) 217 mμ, ε 15 400) are deducted from those of the former (**4**), a curve results typical of a simple α,β-unsaturated ketone: λ_{max}(alcohol) 244 mμ, ε 15 700 (cf. ref. 9).

[7] Microanalysis by E. Thommen.

[8] Microanalysis performed at Eidgenössische Technische Hochschule, Zürich.

[9] On deducting at the respective wavelengths the ε values of strophanthidol monoacetate (**2**) (**8**) (λ_{max} (alcohol) 218 mμ, ε 15 500) from those of 3-oxo-14-hydroxy-19-acetoxy-$\Delta^{4,20(22)}$-14β-cardadienolide (**5**), a curve results typical of a simple α,β-unsaturated ketone: λ_{max}(alcohol) 240 mμ, ε 15 300. The hypsochromic shift of the maximum caused by the 19-acetoxy group is in accordance with expectations.[5]

[10] Fisher magnesium metal turnings for Grignard reaction.

indicating that it consisted largely of a mixture of the two C-20 epimers of **8**.

*3β,5,14,19-Tetrahydroxy-5β,14β-pregnan-20-one (**9**) and 3β,19-Diacetoxy-5,14-dihydroxy-5β,14β-pregnan-20-one (**10**) from 3β,5,14,19,20,21-Hexahydroxy-bisnor-5β,14β-cholane (**8**)*

Original procedure: To 883 mg of chromatographically purified amorphous **8**, (cf. preceding experiment; product (*b*)) dissolved in 60 ml of methanol, was added a solution of 1.5 g of sodium periodate in 40 ml of water. The mixture was allowed to stand at room temperature for 18 h and, after the addition of 110 ml of water and 15 ml of 10% hydrochloric acid, it was saturated with sodium chloride and extracted with five 50 ml portions of ethyl acetate. The extract was washed with two 30 ml portions of 1 *N* sodium carbonate. The carbonate phase was saturated with sodium chloride and re-extracted with four 25 ml portions of ethyl acetate. From the carbonate phase resulted, after acidification and work-up, 201 mg of acidic material. The latter on treatment with acetone–hexane yielded a crystalline product, m.p. 215–217 °C, which showed no depression of the melting point on admixture with an authentic sample of 3β,5,14,19-tetrahydroxy-5β,14β-etianic acid (10). From the ethyl acetate extracts 611 mg of neutral material resulted which was chromatographed over 20 g of Florisil. Elution with chloroform–acetone, 9:1, 4:1, 1:1, and acetone yielded 13 amorphous fractions (total 457 mg) which could not be crystallized. Subsequent experiments showed that this combined amorphous material consisted essentially of 3β,5,14,19-tetrahydroxy-5β,14β-pregnan-20-one (**9**).

A solution of 50 mg of the preceding product in 1 ml of pyridine and 0.5 ml of acetic anhydride was kept at room temperature for 20 h. Subsequently 20 ml of water and 1 ml of concentrated hydrochloric acid were added and, after 1 h standing, the mixture was extracted with four 20 ml portions of ethyl acetate, yielding 59 mg of crystalline material which was purified by chromatography over 2 g of alumina. Elution (15 fractions) with benzene and benzene–ether, 19:1, 9:1, 4:1, 1:1 gave a total of 40 mg of a product which on crystallization furnished 30.3 mg of 3β,19-diacetoxy-5,14-dihydroxy-5β,14β-pregnan-20-one (**10**), m.p. 190–192 °C. The melting point of the analytical sample (C—H determination) was 192–193 °C.

Repeat procedure: The crude product (98 mg) resulting from subjecting 7 (m.p. 197–199 °C; 120 mg) to the Grignard reaction under the stated conditions (*vide supra*) was oxidized with sodium periodate without first separating the crystalline **8**. This yielded 11 mg of acidic and 73 mg of neutral material. Treatment of the latter with 150 mg of Girard's reagent T gave 49 mg of ketonic material which was chromatographed over 4 g of Florisil. Elution with chloroform–acetone, 4:1, 1:1 gave 8 amorphous fractions which were combined (39 mg) (**9**). Subsequent acetylation yielded 37 mg of crude acetate which was chromatographed over 4 g of alumina (activity II; elution with benzene, benzene–ether combinations, ether, chloroform, and acetone). The eluate obtained with chloroform gave 27 mg of material which on treatment with acetone–hexane yielded 21 mg of **10**, m.p. 191–192 °C. Recrystallization furnished 18 mg of an analytical sample (optical rotation, i.r. curve), m.p. 193–194 °C. The mixture m.p. with the earlier analytical sample (*vide supra*) was undepressed; $[\alpha]_D^{24}$ +85.7°, M_D^{24} +386° (14.0 mg, α +1.20°); ν_{max}(KBr) 3575 (free OH), 3420 (bonded OH), 1731 (shoulder, CO of acetyl), 1728 (CO of Ac), 1688 (C-20 CO), 1450 (angular or C-21 CH_3), 1236 and 1227 (C—O of C—OAc), 1100 (C—O of C—OH), 1038 and 1017 (C—O of C—OAc) cm^{-1}.

Anal. Calcd. for $C_{25}H_{38}O_7$: C, 66.64; H, 8.50. Found:[8] C, 66.44; H, 8.51.

*5,14,19-Trihydroxy-5β,14β-pregnane-3,20-dione (**11**) and 14,19-Dihydroxy-14β-progesterone (14,19-dihydroxy-Δ⁴-14β-pregnene-3,20-dione) (**12**) from 3β,5,14,19-Tetrahydroxy-5β,14β-pregnan-20-one (**9**)*

Chromatographically purified amorphous **9**, as described in the original procedure of the preceding experiment, served as starting material. To 408 mg of **9** in 20 ml of 70% aqueous *t*-butyl alcohol 360 mg of *N*-bromoacetamide (slightly more than 2 equivalents; 97.35% purity by titration) were added. After 18 h standing at room temperature the mixture was decolorized by the addition of aqueous sodium thiosulfate and was then diluted with 50 ml of water. After saturating with sodium chloride, extraction with eight 50 ml portions of ethyl acetate yielded 420 mg of crude amorphous **11** which was used for the next stage without purification.

The crude **11** (420 mg) was dissolved in 25 ml of absolute ethanol and, after the addition of 650 mg of Girard's reagent T and 1 ml of glacial acetic acid, the mixture was refluxed for 1 h. After cooling, a solution of 400 mg of sodium carbonate in 120 ml of water was added. Subsequent extraction with ethyl acetate yielded 12 mg of non-ketonic material. The aqueous phase was then acidified to pH 2 with 1 *N* hydrochloric acid, and after standing for 90 min and subsequent saturating with sodium chloride, it was extracted with six portions of 50 ml of ethyl acetate furnishing 412 mg of crude **12**. This was chromatographed over 10 g of Florisil (18 × 62 mm). Elution was performed with 20 ml portions of: (*a*) chloroform (3 fractions, 7.1 mg); (*b*) chloroform–acetone, 19:1, 9:1 (6 fractions, 180.3 mg); (*c*) chloroform–acetone, 4:1, 1:1 (5 fractions, 134.3 mg); and (*d*) acetone (3 fractions, 21.6 mg). The product resulting from (*b*) was crystalline. Repeated recrystallization from acetone–hexane gave 71 mg of colorless plates, m.p. 213–215 °C. From the mother liquors an additional 19.3 mg of crystals, m.p. 213–215 °C, was obtained after re-chromatography. The final mother liquors were combined with the product resulting from (*c*). Re-chromatography of this material provided an additional crop of 40.4 mg of crystals, m.p. 211–213 °C. Hence the total yield of purified crystalline material resulting from this reaction was 130.7 mg. For analytical purposes it was subjected to further repeated recrystallization from acetone furnishing 40 mg of colorless plates, m.p. 215–216 °C; $[\alpha]_D^{24}$ +121.2°, M_D^{24} +419° (10.4 mg, α +1.26°). λ_{max}(alcohol) 242 mμ, ε 16 100; ν_{max}(KBr) 3415 (broad, bonded OH), 3030 (unsaturated C—H), 1687 (C-20 CO), 1665 (C-3 CO), 1638 (C=C), 1360 (CH_3 of $COCH_3$), 1025 (C—O of C—OH) cm^{-1}.

Anal. Calcd. for $C_{21}H_{30}O_4$: C, 72.80; H, 8.73. Found:[8] C, 72.70; H, 8.79.

In an abbreviated process, crystalline 14,19-dihydroxy-14β-progesterone (**12**) was prepared from the crystalline

3β,19,21-triacetoxy-5,14-dihydroxy-5β,14β-pregnan-20-one (7) without purification of the intermediates. The experimental conditions of each step were analogous to those stated in the individual experiments (*vide supra*) and the respective crude reaction products were used directly for the subsequent procedure. Hence, 875 mg of pure crystalline **7** were subjected to the Grignard reaction. By oxidizing the resulting crude amorphous carbinol **8** (647 mg) with sodium periodate, 59 mg of acidic and 545 mg of neutral material were obtained. The latter, consisting essentially of **9**, was allowed to react with *N*-bromoacetamide, yielding 545 mg of **11** which on treatment with 900 mg of Girard's reagent T yielded 76 mg of non-ketonic and 432 mg of ketonic product. The ketonic material was chromatographed over 15 g of Florisil. Elution was performed with 25 ml portions of: (*a*) chloroform (7 fractions, 7.1 mg); (*b*) chloroform–acetone, 19:1, 9:1 (12 fractions, 281.4 mg); (*c*) chloroform–acetone, 4:1, 1:1 (12 fractions, 99.2 mg). On recrystallizing the material (*b*) from acetone–hexane three times, 143.2 mg of crystalline product, m.p. 211–214 °C was obtained. On admixture with authentic **12** there was no depression of the melting point. Re-chromatography of the material contained in the mother liquors and in other fractions yielded 14.1 mg of additional, less pure **12**, m.p. 200–205 °C.

*19-Acetoxy-14-hydroxy-14β-progesterone (19-acetoxy-14-hydroxy-Δ^4-14β-pregnene-3,20-dione) (**13**) from 14,-19-Dihydroxy-14β-progesterone [14,19-dihydroxy-Δ^4-14β-pregnene-3,20-dione] (**12**)*

A solution of 5.1 mg of **12**, m.p. 215–216 °C, in 0.5 ml of pyridine and 0.25 ml of acetic anhydride was kept at room temperature for 18 h and was then worked up as usual. The reaction product, which did not crystallize spontaneously, was combined with that of a repeat experiment (total starting material: 10.3 mg of pure **12**). Chromatography over 2 g of alumina (activity II) yielded crystalline material from the eluates obtained with benzene–chloroform (4:1 and 3:1). Repeated recrystallization from ether–hexane furnished 2.6 mg of **13** as prisms, m.p. 119–121 °C; λ_{max}(alcohol) 239 mμ, ε 14 300. ν_{max}(KBr) 3400 (broad, bonded OH), 1735 (CO of —OAc), 1684 (C-20 CO), 1662 (C-3 CO), 1611 (C=C), 1360 (CH_3 of —$COCH_3$ and/or —OAc), 1223 (C—O of C—OAc), 1030 (C—O of C—OAc or C—OH) cm^{-1}.

Acknowledgment

We should like to thank Dr. David Y. Cooper, III, Harrison Department of General Surgical Research, for the determination of some of the ultraviolet spectra and Miss Maria Stojkewycz, Department of Obstetrics and Gynecology, for the determination of all infrared spectra.

1. E. J. Becker and M. Ehrenstein. J. Org. Chem. **26**, 510 (1961).
2. M. Uskoković, R. I. Dorfman, and M. Gut. J. Org. Chem. **23**, 1947 (1958).
3. P. Hegner and T. Reichstein. Helv. Chim. Acta, **24**, 828 (1941); T. Kubota and M. Ehrenstein. J. Org. Chem. **29**, 351 (1964).
4. V. N. Gupta and M. Ehrenstein. Can. J. Chem. This issue.
5. C. Tamm and A. Gubler. Helv. Chim. Acta, **42**, 239 (1959).
6. C. J. Sih, S. M. Kupchan, N. Katsui, and O. E. Tayeb. J. Org. Chem. **28**, 854 (1963).
7. M. E. Wolff and W. Ho. J. Org. Chem. **32**, 1839 (1967).
8. E. P. Oliveto, L. Weber, C. G. Finckenor, M. M. Pechet, and E. B. Hershberg. J. Am. Chem. Soc. **81**, 2831 (1959).
9. B. Fechtig, J. v.Euw, O. Schindler, and T. Reichstein. Helv. Chim. Acta, **43**, 1570 (1960).
10. M. Ehrenstein and A. R. Johnson. J. Org. Chem. **11**, 823 (1946).

Can. J. Chem. Downloaded from www.nrcresearchpress.com by 210.87.254.5 on 09/05/12
For personal use only.

Investigations on steroids. XL. 14,19-Dihydroxy-14β,17α-cortexone and other compounds derived from 17α-strophanthidol[1,2]

VIRENDRA N. GUPTA[3] AND MAXIMILIAN EHRENSTEIN[4]

Division of Steroid Research, The John Herr Musser Department of Research Medicine, University of Pennsylvania, Philadelphia, Pennsylvania 19104

Received January 9, 1968

As continuation of our early research on the synthesis of steroid hormone analogues of the 14β,17α-pregnane series (1–5,7), the conversion of 17α-strophanthidol (**5**) into 14,19-dihydroxy-14β,17α-cortexone (**19**) has been achieved.—In basic investigations the 3,19-diacetate (**6**), the 3-monoacetate (**7**), and the 19-monoacetate (**8**) of **5** were studied. Using independent routes **5** and **8** were converted into 3-oxo-14,19-dihydroxy-$\Delta^{4,20(22)}$-14β,17α-cardadienolide (**11**).—In preparing **19**, **5** was first subjected to ozonolysis yielding 3β,5,14,19,21-pentahydroxy-5β,14β,17α-pregnan-20-one (**13**) which was characterized as the 3,19,21-triacetate (**14**). Selective oxidation of **13** with *N*-bromoacetamide gave 5,14,19,21-tetrahydroxy-5β,14β,17α-pregnane-3,20-dione (**18**) which by treatment with Girard's reagent T underwent dehydration yielding **19**.—In degradation studies, oxidation of **13** with sodium periodate gave 3β,5,14,-19-tetrahydroxy-5β,14β,17α-etianic acid (**15**) which was characterized as the methyl ester (**16**) and the corresponding 3,19-diacetate (**17**). In a similar fashion, oxidation of **19** with sodium periodate gave 3-oxo-14,19-dihydroxy-Δ^4-14β,17α-etienic acid (**21**) which was characterized as the methyl ester (**22**).—Regarding compounds **13** and **14** there are discrepancies with findings reported in the literature earlier. A discussion of this matter is included in this paper.

14,19-Dihydroxy-14β,17α-cortexone (**19**) appears to exhibit sodium excreting activity in the adrenalectomized rat.

Canadian Journal of Chemistry, 46, 2607 (1968)

The transformation of the cardiac aglycone strophanthidin (**1**) into the biologically highly active 19-nor-14β,17α-progesterone and into 19-nor-14β,17α-cortexone by this laboratory (1–5) has stimulated the development of analogues of steroid hormones with unnatural configurations (cf. 6).[5] In another pertinent publication (7) we reported the synthesis of 19-hydroxy-14β,17α-progesterone and of 19-hydroxy-14β,17α-cortexone. More recently we described hormone analogues of the 14,19-dihydroxy type, viz. 14,19-dihydroxy-14β-cortexone (8) and 14,19-dihydroxy-14β-progesterone (9). As an extension of this work, it appeared desirable to synthesize the corresponding compounds of the 14β,17α-series, such as 14,19-dihydroxy-14β,17α-progesterone and 14,19-dihydroxy-14β,17α-cortexone (**19**).

Suitable starting materials appeared to be 17α-strophanthidin (**2**) and 17α-strophanthidol (**5**). Both **2** (10–13) and **5** (13), have been mentioned in the literature as products based on the enzymatic rearrangement of cymarin to 17α-cymarin. A chemical method for the rearrangement of 17β-cardenolides to the 17α-epimers was first described by Reichstein *et al.* (14, 15). It consists of heating the 17β-cardenolide in a solution of dimethylformamide in the presence of sodium *p*-toluenesulfonate and anhydrous sodium acetate. This method has recently been used for the epimerization of strophanthidin (**1**) to 17α-strophanthidin (**2**) (16). In our laboratory this procedure, slightly modified, permitted a facile conversion of **1** to **2**, as well as the conversion of strophanthidol (**4**) to 17α-strophanthidol (**5**). The latter (**5**) was also prepared by reducing **2**, either with aluminium amalgam, or with sodium borohydride. For preparative purposes it is more convenient to epimerize **4** which is easily accessible by reduction of **1** (17). It appeared indicated to characterize the 17α-compounds **2** and **5** by the preparation of a number of derivatives in which the cardenolide group is still intact.

[1]This investigation was supported in whole by Public Health Service Research Grants (CA 00757-10 and CA 00757-11) from the National Cancer Institute of the National Institutes of Health.

[2]cf. Preliminary notice: V. N. Gupta and M. Ehrenstein. New steroid hormone analogues of the 14β,19-dihydroxy series. Abstracts of papers presented at the Second International Congress on Hormonal Steroids. Milan, May 23–28, 1966. Excerpta medica. International Congress Series. No. 111. p. 126 (Abstract No. 194).

[3]Holder of a Postdoctoral Fellowship at the University of Pennsylvania, 1961–1965. Dr. Gupta came from the Department of Pharmacology, All India Institute of Medical Sciences, New Delhi, India. He was the recipient of a Fulbright Travel Only Grant. Present affiliation: International Cellulose Research Ltd., Hawkesbury, Ontario.

[4]To whom inquiries concerning this paper should be directed.

[5]In this reference there is a rather comprehensive listing of the literature pertaining to this field.

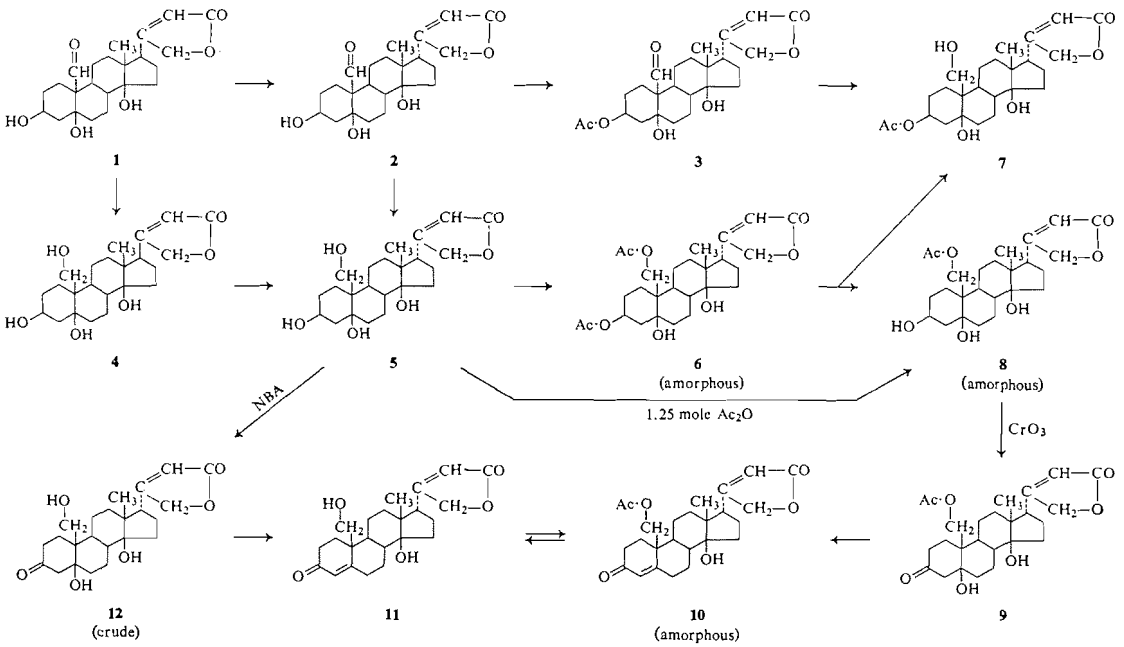

Acetylation of **5** with an excess of acetic anhydride yielded the amorphous 17α-strophanthidol 3,19-diacetate (**6**). Treatment of **6** with potassium bicarbonate in aqueous methanol furnished two different monoacetates in addition to the completely deacetylated **5**. One of these partial deacetylation products was crystalline, whereas the other one was amorphous. The crystalline product was recognized to be 17α-strophanthidol 3-monoacetate (**7**), because it could also be obtained by an unambiguous sequence of chemical reactions. Thus, the acetylation of **2** furnished the crystalline 17α-strophanthidin 3-acetate (**3**) which, by reduction with aluminium amalgam, yielded a compound which was identical with the crystalline partial deacetylation product of **6**, viz. **7**. The treatment of **5** with 1.25 moles of acetic anhydride gave, in addition to small amounts of unchanged **5** and the diacetate **6**, an amorphous product which was identical with the amorphous substance obtained by the partial deacetylation of **6**. There was no evidence of the formation of the crystalline substance **7** in this reaction. The amorphous compound accessible either by deacetylating **6** or by partially acetylating **5** was recognized to be 17α-strophanthidol 19-monoacetate (**8**) by the following sequence of chemical reactions. In analogy with experiments conducted in the 17β-series (9) **5** was selectively oxidized with *N*-bromoacetamide. This furnished 3-oxo-5,14,19-trihydroxy-$\Delta^{20(22)}$-5β,14β,17α-cardenolide(**12**)in amorphous form. Treatment of **12** with Girard's reagent T yielded a crystalline α,β-unsaturated ketone, viz. 3-oxo-14,19-dihydroxy-$\Delta^{4,20(22)}$-14β,17α-cardadienolide (**11**). This compound **11** could also be obtained by first oxidizing the amorphous **8** with chromic acid. This gave the crystalline 3-oxo-5,14-dihydroxy-19-acetoxy-$\Delta^{20(22)}$-5β,14β,17α-cardenolide (**9**) which, on treatment with Girard's reagent T, underwent dehydration furnishing the amorphous 3-oxo-14-hydroxy-19-acetoxy-$\Delta^{4,20(22)}$-14β,17α-cardadienolide (**10**). Saponification of **10** gave the crystalline compound **11** which was identical with the product prepared from **5** by way of **12** (*vide supra*). Acetylation of a sample of **11**, obtained from **12**, gave an amorphous product which was identical with compound **10** prepared from **8** by way of the crystalline **9**.

In the preparation of 14,19-dihydroxy-14β,17α-cortexone (**19**), **5** was first subjected to ozonolysis which furnished, after reductive cleavage of the ozonide and hydrolysis of the 21-glycolate, the crystalline 3β,5,14,19,21-pentahydroxy-5β,14β,17α-pregnan-20-one (**13**). Acetylation of **13** gave the amorphous 3β,19,21-triacetoxy-5,14-dihydroxy-5β,14β,17α-pregnan-20-one

Can. J. Chem. Downloaded from www.nrcresearchpress.com by 210.87.254.5 on 09/05/12
For personal use only.

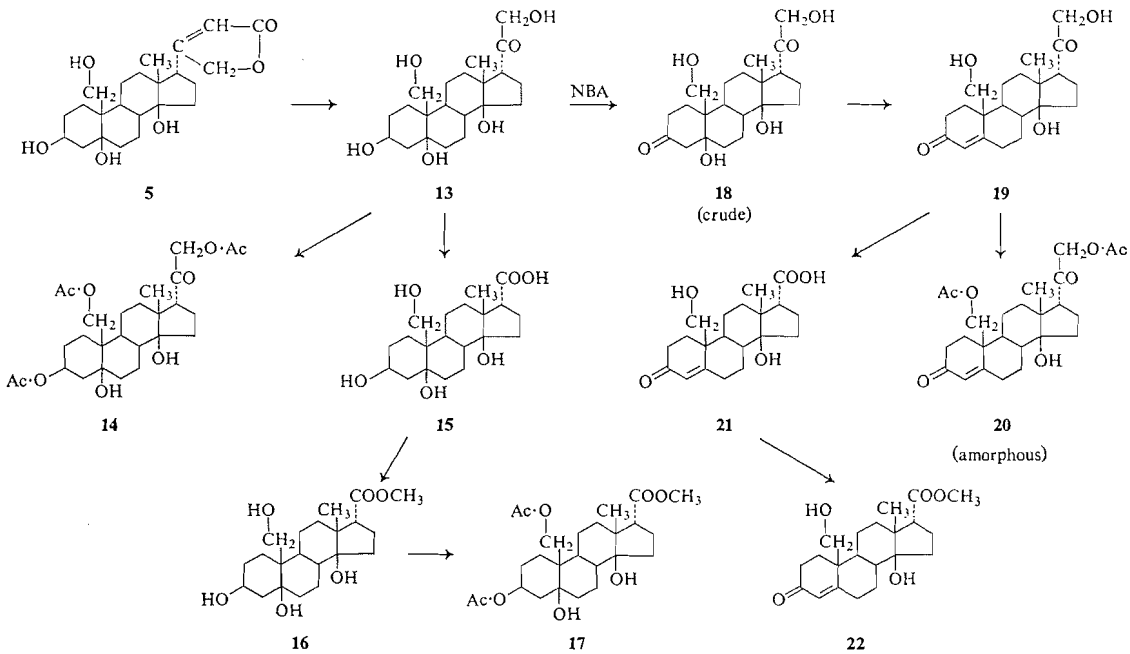

(**14**).[5a] Selective oxidation of the ketol **13** with *N*-bromoacetamide gave the crude 5,14,19,21-tetrahydroxy-5β,14β,17α-pregnane-3,20-dione (**18**) which was subjected to treatment with Girard's reagent T without previous purification. This yielded the crystalline 14,19-dihydroxy-14β,17α-cortexone (**19**). Acetylation of **19** furnished 14,19-dihydroxy-14β,17α-cortexone 19,21-diacetate (**20**) in amorphous form.

For further characterization, the ketols **13** and **19** were subjected to degradation studies. Oxidation of **13** with sodium periodate in aqueous methanol yielded predominantly an acid which was found to be identical with 3β,5,14,19-tetrahydroxy-5β,14β,17α-etianic acid (**15**) prepared previously (18) by a different approach. A small amount of neutral material was recognized as methyl 3β,5,14,19-tetrahydroxy-5β,14β,17α-etianate (**16**) which could also be obtained by treating **15** with diazomethane. The identity with an authentic sample (18) was firmly established. By acetylating **16**, methyl 3β,19-diacetoxy-5,14-dihydroxy-5β,14β,17α-etianate (17) resulted, which likewise proved identical with a product which had been prepared earlier (19) from an authentic sample (18) of **16**. The oxidation of 14,19-dihydroxy-14β,17α-cortexone (**19**) with sodium periodate gave 3-oxo-14,19-dihydroxy-Δ^4-14β,17α-etienic acid (**21**) which, by treatment with diazomethane, was converted into the methyl ester, viz. methyl 3-oxo-14,19-dihydroxy-Δ^4-14β,17α-etienate (**22**).

Discussion of Previous Work

In an earlier publication from this laboratory (19) dealing with the ozonization product of strophanthidol diacetate and its saponification, a number of by-products were described. To one of these compounds, (m.p. 243.5–244.5 °C), we assigned the structure of 3β,5,14,19,21-pentahydroxy-5β,14β,17α-pregnan-20-one, to another, (m.p. 220–222.5 °C; 221.5–223.5 °C), the structure of the corresponding 3,19,21-triacetate, viz. 3β,19,21-triacetoxy-5,14,dihydroxy-5β,14β,17α-pregnan-20-one. Hence these compounds should have proven identical with the products **13** and **14** of the present paper.

A careful reexamination of the old reference samples and comparison with the products described in the present paper, unexpectedly, did not establish identity. The melting points of the "old pentol-20-one" (m.p. 243.5–244.5 °C) and

[5a] *Note added in proof:* Meanwhile, Dr. Martin Matner in this laboratory has obtained the triacetate **14** in a crystalline form; m.p. 131–133°. The infrared spectrum is similar to that of the amorphous product. Details will be published later.

Can. J. Chem. Downloaded from www.nrcresearchpress.com by 210.87.254.5 on 09/05/12
For personal use only.

Can. J. Chem. Downloaded from www.nrcresearchpress.com by 210.87.254.5 on 09/05/12
For personal use only.

the corresponding product **13** from this work (m.p. 255–257 °C) were different and the mixture melting point was depressed (230–242 °C). Surprisingly, the sample of the "old pentol-20-one" did not show carbonyl absorption in the infrared spectrum and gave a negative reaction with blue tetrazolium. In a like fashion, the "old 3,19,21-triacetate" (m.p. 220–222.5 °C; 221.5–223.5 °C) proved to be different from the corresponding product **14** which was obtained in amorphous form.[5a] Several analytical samples of the "old 3,19,21-triacetate," melting points as quoted, gave essentially identical infrared spectra which, however, were different from that of product **14** of the present paper. Furthermore, all of the samples (altogether four) of the "old 3,19,21-triacetate" gave a negative reaction with blue tetrazolium, whereas product **14** of the present paper gave a positive reaction almost instantaneously. This shows that, despite the evidence presented at that time (including elemental analysis), the "old pentol-20-one" and the "old 3,19,21-triacetate" cannot possess the structures now assigned to **13** and **14** respectively.

The evidence in the earlier paper (19) supporting the structure of the "old pentol-20-one" included oxidation studies with periodic acid which supposedly led to 3β,5,14,19-tetrahydroxy-5β,14β,17α-etianic acid (**15**) which was claimed to be identical with authentic material (18) on the basis of the mixture melting point. Furthermore, it was claimed that both, the isolated acid (19) and the authentic acid (18), could be converted into the same ethyl ester (mixture m.p.). In view of the preceding findings the reference samples of the ethyl ester were also reexamined. Thin-layer chromatography demonstrated that the material prepared from the isolated acid represented a mixture, whereas the ethyl ester prepared from the authentic acid (18) was uniform. The infrared spectra of the two samples were not identical.

Due to the lack of sufficient material, it is not possible at this time to elucidate the actual structures of the two compounds reported earlier (19).

Biological Activity

Bioassays for mineralocorticoid activity were carried out at the Endocrine Laboratories in Madison, Wisconsin, under the direction of Dr. Elva G. Shipley. The authors are indebted to Dr. Ralph I. Dorfman, Director of the Institute of Hormone Biology, Syntex Research Center, Palo Alto, California, for having arranged these assays and for the interpretation of the observed results.

14,19-Dihydroxy-14β,17α-cortexone (**19**) appears to exhibit sodium excreting activity in the adrenalectomized rat, but under the conditions employed, it did not antagonize the sodium retaining activity of cortexone (Table I). This response will be further investigated.

Experimental

The melting points were determined with a Fisher–Johns melting point apparatus and are uncorrected. The true melting points are approximately 4 °C lower than those recorded.

The ultraviolet (u.v.) spectra were determined in 95% ethanol with a Beckman model DU spectrophotometer or a Cary model 14 recording spectrophotometer. The infrared (i.r.) spectra were measured in potassium bromide disks on the Perkin–Elmer 421 spectrophotometer.

The microanalyses were performed by Mr. Ernst Thommen, Bettingen bei Basel, Switzerland or by the Mikrolaboratorium (Director, W. Manser), Laboratorium für Organische Chemie, Eidgenössische Technische Hochschule, Zürich, Switzerland. Thanks are due to Professor V. Prelog for this courtesy.

In optical rotation determinations no correction for crystal solvent has been made. Unless otherwise stated, the sample was dissolved in chloroform to make 2 ml of solution and the optical rotation was determined in a 2-dm semimicro tube.

17α-Strophanthidin (2) from Strophanthidin (1)

A mixture consisting of 10 g of strophanthidin (**1**), 300 ml of dimethyl formamide, 5 g of anhydrous sodium acetate, and 5 g of sodium *p*-toluenesulfonate was heated at 120 °C under a stream of nitrogen for 23 h. After removing the solvent *in vacuo* the residue was suspended in 500 ml of water and extracted with two 200 ml and four 100 ml portions of ethyl acetate – methanol (9:1). The organic solution was washed with saturated aqueous sodium chloride and dried over sodium sulfate. Removal of the solvent gave a sticky residue from which yellow crystals, m.p. 242–249 °C, were obtained. Two recrystallizations from methanol gave 1.8 g of 17α-strophanthidin (**2**) as slightly pinkish needles, m.p. 252–254 °C. Legal test was positive; $[\alpha]_D^{23}$ +32°, M_D^{23} +129° (17.5 mg in 2 ml of chloroform containing 4 drops of 95% ethanol, α +0.56°). [Lit. (13) m.p. 250–254 °C, $[\alpha]_D$ +37.1° (MeOH); lit. (16) m.p. 253–255 °C, $[\alpha]_D$ +38° (MeOH)]; λ_{max}(alcohol) 219 mμ, ε 15 900; 295 mμ, ε 43. ν_{max}(KBr) 3550 (sharp, free OH), 3300 (very broad, bonded OH), 2760 (C—H stretch of CHO), 1785 and 1745 (CO of lactone ring), 1707 (CO of CHO), 1618 (C=C), 1035 (C—O of C—OH) cm^{-1}.

Anal. Calcd. for $C_{23}H_{32}O_6$: C, 68.29; H, 7.97. Found:[6] C, 68.12; H, 8.05.

[6]The microanalysis was performed at Eidgenössische Technische Hochschule, Zürich, Switzerland.

TABLE I

The influence of 14,19-dihydroxy-14β,17α-cortexone (**19**) on the sodium and potassium excretion in the male adrenalectomized rat*

Compound(s) administered	Dose (μg)	Mean body weight† (g) (range)	Na excretion‡ (mg) (range)	K excretion‡ (mg) (range)	Change in Na excretion (%)
—	—	144 (142–145)	1.17 (0.53–1.70)	2.31 (1.32–3.21)	—
Cortexone	1.5	150 (142–155)	1.10 (0.53–1.49)	4.16 (1.9–5.0)	−6
	6	150 (142–154)	0.20 (0.12–0.42)	3.64 (2.26–5.58)	−83
14,19-Dihydroxy-14β,17α-cortexone	1	144 (138–157)	1.52 (0.70–2.50)	2.54 (1.56–4.06)	+30
	25	144 (137–148)	1.57 (1.13–2.57)	2.0 (1.15–2.13)	+34
	100	144 (141–152)	2.31 (1.16–3.34)	3.31 (2.40–4.50)	+97
Cortexone 14,19-Dihydroxy-14β,17α-cortexone	6 100	148 (143–155)	0.16 (0.09–0.24)	3.15 (2.40–4.50)	−86

*Adrenalectomy was performed 48 h before the assay, and the urethras were ligated at the fourth hour. Urine was collected for 2 h from the fourth to sixth hour after treatment by subcutaneous injection.
†Five rats were used per group.
‡Urinary Na and K were determined by flame photometry.

17α-Strophanthidin 3-Acetate (3) from 17α-Strophanthidin (2)

A solution of 500 mg of **2** in 10 ml of pyridine and 10 ml of acetic anhydride was kept at room temperature for 64 h. After the addition of 100 ml of water and acidification with hydrochloric acid, the mixture was extracted with ethyl acetate and the extracts were worked up as usual, yielding 568 mg of a crude product which on two crystallizations from acetone–hexane gave 265 mg of pure **3**, m.p. 178–180 °C; $[\alpha]_D^{25}$ +43.4°, M_D^{25} +194° (17.5 mg, α +0.76°); λ_{max}(alcohol) 218 mμ, ε 15 700. ν_{max}(KBr) 3560 (free OH), 3460 (very broad, bonded OH), 2750 (C—H stretch of CHO), 1775 and 1735 (CO of lactone ring, CO of —OAc), 1715 (CO of CHO), 1615 (C=C), 1230 (C—O of C—OAc), 1030 and 1010 (C—O of C—OH and C—OAc) cm^{-1}.

Anal. Calcd. for $C_{25}H_{34}O_7$: C, 67.25; H, 7.87. Found:[6] C, 66.86; H, 8.15.

Reduction of 17α-Strophanthidin 3-Acetate (3) to 17α-Strophanthidol 3-Monoacetate (7)

Aluminium amalgam was prepared from 200 mg of aluminium foil as described previously.[7] After adding a solution of 200 mg of **3**, m.p. 178–180 °C, in 10 ml of 95% ethanol, the mixture was kept at room temperature overnight. After filtering and repeatedly extracting the aluminium hydroxide with boiling ethanol, the combined filtrates were evaporated to dryness *in vacuo*, yielding 199 mg of material. Two recrystallizations from acetone–hexane gave 119 mg of **7** as shining prisms, m.p. 231–233 °C; $[\alpha]_D^{25}$ +51.8°, M_D^{25} +232° (19.1 mg, α +0.99°). λ_{max}(alcohol) 218.5 mμ, ε 15 300. ν_{max}(KBr) 3560 (sharp, free OH), 3380 (very broad, bonded OH), 1800 and 1720 (CO of lactone ring), 1680 (CO of acetate), 1615 (C=C), 1290 (C—O of C—OAc), 1030 (C—O of C—OH and C—OAc) cm^{-1}.

Anal. Calcd. for $C_{25}H_{36}O_7$: C, 66.94; H, 8.09. Found:[6] C, 66.89; H, 8.25.

17α-Strophanthidol (5)

(A) By Epimerization of Strophanthidol (4)

A mixture containing 39.5 g of strophanthidol (**4**), m.p. 142–144 °C, 1200 ml of dimethyl formamide, 20 g of anhydrous sodium acetate, and 20 g of sodium *p*-toluenesulfonate was heated at 120 °C for 24 h under a stream of nitrogen and the solvent was then removed *in vacuo*. After the addition of 2 l of water and saturation with sodium chloride a resulting white precipitate was removed by filtration and the filtrate was extracted with six 300 ml portions of chloroform–methanol (4:1). The extracts were washed with saturated aqueous sodium chloride and dried over sodium sulfate. Removal of the solvent yielded a residue which was combined with the precipitate. Three crystallizations from methanol gave 9.88 g of **5**, m.p. 255–257 °C. The remaining material, approximately 29 g, was treated with 900 ml of dimethyl formamide, 15 g of anhydrous sodium acetate and 15 g of sodium *p*-toluenesulfonate and the reaction product was worked up as described above. This yielded 5.77 g of additional crystalline **5**, m.p. 255–257 °C. The renewed treatment of the non-crystalline material gave in analogous fashion 3.51 g of crystalline **5**, m.p. 255–257 °C. The total yield of pure **5** was: 19.16 g (48.5%). In one of the repeat experiments the total yield of **5**, m.p. 257–259 °C, obtained

[7]For method cf. ref. 17.

Can. J. Chem. Downloaded from www.nrcresearchpress.com by 210.87.254.5 on 09/05/12
For personal use only.

Can. J. Chem. Downloaded from www.nrcresearchpress.com by 210.87.254.5 on 09/05/12
For personal use only.

from 20 g of **4** was 14.24 g (71.3%). $[\alpha]_D^{22}$ +33.8°, M_D^{22} +137° (19.8 mg in 2 ml of methanol, α +0.67°); [lit. (13) m.p. 260–262 °C, $[\alpha]_D$ +41.3° (MeOH)]. λ_{max}(alcohol) 220 mμ, ε 15 000; ν_{max}(KBr) 3460 (OH), 3400 (OH), 1795 and 1730 (CO of lactone ring), 1620 (C=C), 1028 (C—O of C—OH) cm^{-1}.

Anal. Calcd. for $C_{23}H_{34}O_6$: C, 67.95; H, 8.43. Found:[6] C, 68.10; H, 8.78.

(B) By Reduction of 17α-Strophanthidin (2)

(a) With aluminium amalgam[7]—To 1.7 g of aluminium foil which had been converted into amalgam was added a solution of 1.7 g of 17α-strophanthidin (**2**) in 100 ml of 95% ethanol. After standing at room temperature overnight, 2 ml of water were added and a few hours later the mixture was worked up as usual. This yielded by direct crystallization 643 mg of pure 17α-strophanthidol (**5**), m.p. 256–258 °C, which was identical with an authentic sample (*vide supra*; mixture m.p., paper chromatogram). By further concentrating the ethanolic mother liquor, an additional 274 mg of **5**, m.p. 256–258 °C, resulted. The filtrate was then evaporated to dryness and the residue was recrystallized from acetone, furnishing 211 mg of **5**, m.p. 255–257 °C. The total yield of pure **5** was 1.13 g.

(b) With sodium borohydride[8]—To 250 mg of 17α-strophanthidin (**2**) dissolved in 15 ml of 80% aqueous dioxane was added a solution of 90 mg of sodium borohydride in 9 ml of 80% aqueous dioxane, over a period of 1 h. After stirring the mixture at room temperature for 6 h, it was acidified with sulfuric acid (Congo Red), diluted with 100 ml of water and, after saturating with sodium chloride, extracted with five 50 ml portions of chloroform–methanol (4:1). The extracts yielded an oily product which was dissolved in 15 ml of methanol and, after the addition of 1.25 g of D-mannitol and 15 ml of 0.1 *N* sulfuric acid, the mixture was refluxed for 30 min. It was then diluted with 100 ml of water and extracted with five 50 ml portions of chloroform. After drying and evaporating the solvent, the extracts yielded 212 mg of a residue which on two crystallizations from acetone gave 148.4 mg of 17α-strophanthidol (**5**), m.p. 254–256 °C, which was identical with an authentic sample (mixture m.p., paper chromatogram).

17α-Strophanthidol 3,19-Diacetate (6) from 17α-Strophanthidol (5)

A solution consisting of 1 g of **5**, 10 ml of pyridine, and 10 ml of acetic anhydride was kept at room temperature for 3 days. The mixture was worked up as usual yielding 1.4 g of a foam (not dry!) which resisted attempts at crystallization and, therefore, was chromatographed over 50 g of alumina (activity II). Elution with benzene and benzene–chloroform yielded practically no material. Six portions of 100 ml of chloroform eluted: (1) 562.0 mg, (2) 499.6 mg, (3) 159.5 mg, (4) 31.0 mg, (5) 8.4 mg, and (6) 4.0 mg of amorphous product. Subsequent elution with chloroform–methanol gave 79.0 mg of material. Paper chromatography (system: chloroform–benzene (1:1) – formamide; reagent: alkaline 3,5-dinitrobenzoic acid) indicated that fractions (1), (2), (3), and (4) were uniform. They represented the pure diacetate **6** and were combined (total yield: approximately 1.2 g). This amorphous product resisted all attempts at crystallization; ν_{max}(KBr) 3500 (very broad, bonded OH), 1775 (CO of lactone ring), 1735 (CO of lactone ring and acetate), 1620 (C=C), 1320 (CH_3 of OAc), 1230 (C—O of C—OAc), 1030 (C—O of C—OH and C—OAc) cm^{-1}.

Partial Deacetylation of 17α-Strophanthidol 3,19-Diacetate (6): 17α-Strophanthidol 3-Monoacetate (7) and 17α-Strophanthidol 19-Monoacetate (8)

To 690.8 mg of chromatographically purified amorphous **6** (*vide supra*) dissolved in 50 ml of methanol was added a solution of 700 mg of potassium bicarbonate in 25 ml of water. After standing at room temperature for 16 h, the mixture was diluted with 250 ml of water and saturated with sodium chloride. Extraction with six 80 ml portions of chloroform–methanol (4:1) and working up as usual gave a residue which was chromatographed over 100 g of alumina (activity I; 40 × 105 mm). Elution was performed with 100 ml portions of solvent. Chloroform (fractions 1–3) yielded no material. Chloroform–methanol, 199:1 (fractions 4–5) gave 249.0 mg of amorphous product (*a*). Further elution with chloroform–methanol, 199:1 (fractions 7–11) yielded 105.5 mg of crystalline material (*b*). Chloroform–methanol, 99:1 (fractions 12–13) and 49:1 (fractions 14–17) eluted a total of 218.2 mg of amorphous product (*c*). Practically nothing was obtained with chloroform–methanol, 19:1 (fractions 18–20). Chloroform–methanol, 9:1, 4:1, 1:1 (fractions 21–23) gave a total of 92 mg of crystalline material (*d*). The products (*a*), (*b*), (*c*), and (*d*) were examined by paper chromatography (system: benzene–chloroform (1:1) – formamide; reagent: alkaline 3,5-dinitrobenzoic acid). The product (*a*) was uniform; the R_f value was identical with that of the starting material **6**. The more polar crystalline material (*b*) was likewise uniform; two recrystallizations from acetone–hexane gave 88.1 mg of shining plates, m.p. 230–232 °C. This was identified as 17α-strophanthidol 3-monoacetate (**7**) by comparison with an authentic sample (*vide supra*) (mixture m.p.; identical R_f value). The amorphous product (*c*) was recognized to be 17α-strophanthidol 19-monoacetate (**8**) by comparison with an authentic sample (*vide infra*) (identical i.r. spectrum; same R_f value in t.l.c.). The crystalline material (*d*), on two recrystallizations from acetone–hexane, gave 62 mg of colorless needles, m.p. 254–257 °C, and there was no depression of the m.p. upon admixture with an authentic sample of 17α-strophanthidol (**5**).

Partial Acetylation of 17α-Strophanthidol (5): 17α-Strophanthidol 19-Monoacetate (8)

To a solution of 2 g of **5** in 10 ml of pyridine was added 0.6 ml of acetic anhydride (1.25 moles) and the mixture was kept at room temperature for 16 h. It was then diluted with 100 ml of water, acidified with 10 ml of concentrated hydrochloric acid and, after standing 30 min, extracted successively with five 40 ml portions of ether and of chloroform. The aqueous phase was then saturated with sodium chloride and extracted with five portions of 40 ml of chloroform–methanol (4:1). All these extracts represented mixtures as established by paper chromatography. They were combined and the reaction product was chromatographed over 150 g of alumina (activity I;

[8]For method cf. ref. 20.

Can. J. Chem. Downloaded from www.nrcresearchpress.com by 210.87.254.5 on 09/05/12
For personal use only.

40 × 150 mm). Elution was performed with 100 ml portions of solvent. Methylene chloride – methanol, 49:1 (fractions 1–2) eluted 0.2 g of amorphous product (*a*). Methylene chloride – methanol, 49:1 (fractions 3–7), 19:1 (fractions 8–9), 9:1 (fraction 10) gave a total of 1.9 g of amorphous material (*b*). Methylene chloride – methanol, 9:1 (fraction 11), 4:1 (fractions 12–13), 1:1 (fractions 14–15) yielded 0.2 g of crystalline product (*c*). Examination of the individual fractions by paper chromatography (system: benzene–chloroform (1:1) – formamide; reagent: alkaline 3,5-dinitrobenzoic acid) showed that (*a*) represented 17α-strophanthidol 3,19-diacetate (**6**) (comparison with authentic sample; *vide supra*). There was no evidence of the presence of 17α-strophanthidol 3-monoacetate (7). The uniform material (*b*) was recognized as 17α-strophanthidol 19-monoacetate (**8**) (cf. the subsequent reactions). ν_{max}(KBr) 3420 (very broad, bonded OH), 1775 (CO of lactone ring), 1732 (CO of lactone ring and OAc), 1617 (C=C), 1240 (C—O of C—OAc), 1030 (C—O of C—OAc and C—OH) cm^{-1}. The crystalline compound (*c*) was identified as 17α-strophanthidol (**5**).

3-Oxo-5,14-dihydroxy-19-acetoxy-$\Delta^{20(22)}$-5β,14β,17α-cardenolide (9) from 17α-Strophanthidol 19-Monoacetate (8)

To 1 g of chromatographically purified **8**, as prepared by partial acetylation of **5** (cf. the preceding experiment), dissolved in 10 ml of pyridine was added a solution of 1 g of chromium trioxide in 10 ml of pyridine. The mixture was stirred for 4 h at room temperature and was then allowed to stand for 16 h. Subsequently it was diluted with a solution of 3 g of sodium sulfite in 50 ml of water and 90 min later the mixture was extracted with two 75 ml and four 50 ml portions of chloroform. The extracts were repeatedly washed with dilute hydrochloric acid and water. After drying, evaporation of the solvent yielded 824 mg of a material which, by two crystallizations from acetone–hexane, furnished 531 mg of **9** as needles and prisms, constant m.p. 212–214 °C; uniform in t.l.c. (solvent: chloroform–methanol, 4:1; reagent: *p*-toluenesulfonic acid); $[\alpha]_D^{23}$ +30.6°, M_D^{23} +137° (14.05 mg in 2 ml of chloroform containing 3 drops of methanol, α +0.43°); λ_{max}(alcohol) 219 mμ, ε 15 300; ν_{max}(KBr) 3570 and 3500 (free and bonded OH), 3110 (unsaturated C—H stretch), 1790 (shoulder), and 1740 (CO of lactone ring and of OAc), 1705 (C-3 CO), 1615 (C=C), triplet consisting of 1290, 1250, and shoulder at 1225 (C—O of C—OAc), 1035 (C—O of C—OH and C—OAc) cm^{-1}.

Anal. Calcd. for $C_{25}H_{34}O_7$: C, 67.24; H, 7.68. Found: C, 67.14,[9] 67.09;[6] H, 7.71,[9] 7.39.[6]

3-Oxo-14-hydroxy-19-acetoxy-$\Delta^{4,20(22)}$-14β,17α-cardadienolide (10) and 3-Oxo-14,19-dihydroxy-$\Delta^{4,20(22)}$-14β,17α-cardadienolide (11) from 3-Oxo-5,14-dihydroxy-19-acetoxy-$\Delta^{20(22)}$-5β,14β,17α-cardenolide (9)

A solution of 0.45 g of **9**, m.p. 212–214 °C, in 15 ml of glacial acetic acid was refluxed for 30 min, cooled, and diluted with 100 ml of water. The aqueous solution was neutralized with sodium bicarbonate and extracted with six portions of 50 ml of chloroform. The extracts were washed with water, dried over sodium sulfate, and the solvent was distilled to yield 0.4 g of a foam. Attempts at crystallization failed. This product represented practically pure **10**. The t.l.c. and the i.r. spectra were identical with those obtained with an authentic sample (*vide infra*). Saponification of **10** was first attempted with aqueous methanolic potassium bicarbonate, at room temperature, but was found to proceed to an insignificant extent. Hence, 200 mg of **10** (preceding sample) dissolved in 10 ml of methanol was mixed with a solution of 200 mg of sodium carbonate in 5 ml of water. The mixture was kept at room temperature for 16 h and was then diluted with 100 ml of water, acidified with dilute hydrochloric acid, saturated with sodium chloride, and extracted with five 50 ml portions of chloroform to give 121 mg of reaction product which was chromatographed over 6 g of alumina (activity II; 10 × 70 mm). Elution was performed with 20 ml portions of solvent. Chloroform–methanol, 99:1 (6 fractions) eluted 50 mg of product (*a*). Chloroform–methanol, 19:1, 9:1 (6 fractions) gave 25 mg of material (*b*). On paper chromatography the product (*a*) showed a single spot with the same mobility as that of **11**. The material (*b*) gave several spots indicating the presence of a mixture. The product (*a*), on two crystallizations from acetone–hexane gave 32 mg of prisms, m.p. 258–260 °C which proved identical with authentic **11** (*vide infra*) (mixture m.p.; paper chromatogram).

3-Oxo-5,14,19-trihydroxy-$\Delta^{20(22)}$-5β,14β,17α-cardenolide (12) and 3-Oxo-14,19-dihydroxy-$\Delta^{4,20(22)}$-14β,17α-cardadienolide (11) from 17α-Strophanthidol (5)

A mixture containing 1 g of pure **5**, 50 ml of 70% aqueous *t*-butyl alcohol, and 750 mg of *N*-bromoacetamide was kept at room temperature for 20 h. It was then decolorized by adding aqueous sodium thiosulfate and diluted with 200 ml of water. Subsequently it was saturated with sodium chloride and extracted with six 80 ml portions of chloroform–methanol (4:1) yielding 1 g of crude amorphous **12** which resisted attempts at crystallization. It was used for the next step without purification. Hence, the crude **12** was dissolved in 80 ml of absolute ethanol and, after the addition of 2 g of Girard's reagent T and 3 ml of glacial acetic acid, the mixture was refluxed for 1 h. After cooling, a solution of 3 g of sodium carbonate in 320 ml of water was added. Subsequent extraction with four 50 ml portions of chloroform yielded 6 mg of non-ketonic material. The aqueous phase was then acidified with concentrated hydrochloric acid to pH 2 and, after standing for 90 min and subsequent saturating with sodium chloride, it was extracted with six portions of 50 ml of chloroform to give the ketonic material which on two crystallizations from methanol yielded 520 mg of pure **11**, m.p. 258–260 °C. The mixture m.p. with **5**, (m.p. 256–258 °C), was depressed (215–235 °C). Renewed recrystallization of **11** gave the analytical sample, m.p. 259–261 °C. It gave only one spot in a paper chromatogram (system: chloroform–formamide; reagent: alkaline *m*-dinitrobenzene.[10] $[\alpha]_D^{22}$ +102.4°, M_D^{22} +396° (21.1 mg in 2 ml of methanol,

[9]Microanalysis performed by E. Thommen.

[10]In this paper chromatogram (16 h) the relative mobility of **11** and 17α-strophanthidol (**5**) was 1:0.75. Approximately the same ratio (1:0.7) was found to exist with the corresponding compounds of the 17β-series. Individually, the 17β-compounds moved slightly faster than the 17α-epimers.

Can. J. Chem. Downloaded from www.nrcresearchpress.com by 210.87.254.5 on 09/05/12
For personal use only.

α +2.16°). λ_{max}(alcohol) 223 mμ, ε 20 800;[11] ν_{max}(KBr) 3560 (free OH), 3340 (bonded OH), 3020 (unsaturated C—H stretch), 1805 and 1720 (CO of lactone ring), 1655 (C-3 CO), 1615 (C=C), 1035 (C—O of C—OH) cm^{-1}.

Anal. Calcd. for $C_{23}H_{30}O_5$: C, 71.48; H, 7.82. Found:[6] C, 71.72; H, 7.99.

*3-Oxo-14-hydroxy-19-acetoxy-$\Delta^{4,20(22)}$-14β,17α-cardadienolide (**10**) from 3-Oxo-14,19-dihydroxy-$\Delta^{4,20(22)}$-14β,17α-cardadienolide (**11**)*

A mixture of 100 mg of **11**, m.p. 258–260 °C, 4 ml of pyridine, and 2 ml of acetic anhydride was allowed to stand at room temperature for 20 h. It was evaporated to dryness *in vacuo* and the residue was worked up as usual yielding 105.3 mg of material which did not crystallize. It was chromatographed over 5 g of alumina (activity II; 10 × 52 mm). Elution with benzene, benzene–ether combinations, ether, and ether–chloroform combinations furnished only traces of material. Elution with chloroform gave a total of 96 mg of **10** which resisted attempts at crystallization. It was uniform in paper chromatogram and t.l.c.; ν_{max}(KBr) 3450 (very broad, bonded OH), 3085 (unsaturated C—H stretch), 1775 (CO of lactone ring), 1730 (CO of lactone ring and of acetate), 1650 (C-3 CO), 1615 (C=C), 1230 and 1030 (C—O of C—OAc) cm^{-1}.

*3β,5,14,19,21-Pentahydroxy-5β,14β,17α-pregnan-20-one (**13**) from 17α-Strophanthidol (**5**)*

A total of 3 g of **5**, m.p. 253–256 °C, was dissolved in a mixture of 75 ml of methanol and 225 ml of ethyl acetate. This solution was cooled in dry ice – acetone and oxygen containing approximately 3% ozone was passed in for 20 min. The lilac colored, clear solution was allowed to remain in the cold bath for 10 min. After this time the color had practically disappeared and the ozonization was resumed for a further 15 min. The mixture was then kept in the cold for 1 h (retention of lilac color) and, after removing the excess ozone by passing oxygen through, the solvent was evaporated *in vacuo* at room temperature leaving an amorphous powder. To a solution of this residue in 60 ml of glacial acetic acid 6 g of zinc dust were gradually added with simultaneous stirring and, after slightly warming the mixture for 90 min, the potassium iodide – starch reaction was negative. The precipitate was removed by filtration and washed with acetic acid. The filtrate was evaporated to dryness *in vacuo* and the resulting residue was extracted repeatedly with ample amounts of chloroform yielding, after removal of the solvent, 1.45 g of material. By dissolving the precipitate (*vide supra*) in dilute hydrochloric acid and extracting with chloroform, 0.25 g of additional material resulted, increasing the total yield of the crude 21-glycolate of **13** to 1.69 g.

To the preceding crude glycolate (1.69 g), dissolved in 100 ml of ethanol, a solution of 1.7 g of sodium carbonate in 30 ml of water was added and the mixture was refluxed under an atmosphere of nitrogen for 45 min. It was then diluted with 250 ml of water, saturated with sodium chloride, and extracted with chloroform–methanol (9:1). The extracts yielded in the usual fashion a residue which upon crystallization from methanol–ether gave 787 mg of prisms, m.p. 252–254 °C, representing pure **13**.

Repeat experiments were carried out under similar conditions in such a fashion that, after the ozonization of two 3 g lots of starting material (**5**), the solutions were combined and worked up together. In two of these later experiments, 6 g of starting material (**5**) yielded 3.62 g (m.p. 250–252 °C) and 2.81 g (m.p. 254–256 °C) of **13** respectively. Repeated recrystallization from methanol gave the analytical sample, m.p. 255–257 °C. The mixture m.p. with the starting material (**5**) was depressed. The product gave only one spot on paper chromatography (system: chloroform–formamide; reagent: alkaline blue tetrazolium) as well as t.l.c. (solvent: chloroform–methanol, 4:1; reagent: *p*-toluenesulfonic acid); the mobility was slower than that of **5**; $[\alpha]_D^{23}$ −35.2°, M_D^{23} −135° (12.35 mg in 2 ml of methanol, α −0.44°); ν_{max}(KBr) 3470 (free OH), 3320 (very broad, bonded OH), 1692 (C-20 CO), 1045 and 1010 (C—O of C—OH) cm^{-1}.

Anal. Calcd. for $C_{21}H_{34}O_6$: C, 65.94; H, 8.96. Found: C, 65.83,[9] 65.57;[6] H, 9.02,[9] 9.14.[6]

*3β,19,21-Triacetoxy-5,14-dihydroxy-5β,14β,17α-pregnan-20-one (**14**) from 3β,5,14,19,21-Pentahydroxy-5β,14β,17α-pregnan-20-one (**13**)*

Several attempts to obtain the triacetate **14** in a crystalline form failed, even after chromatography over alumina. A uniform amorphous sample[5a] was prepared as follows. A solution of 15 mg of the free ketol **13**, m.p. 256–258 °C, in 2 ml of pyridine and 1 ml of acetic anhydride was kept at room temperature for 40 h. The excess acetic anhydride was destroyed by the addition of 25 ml of water and subsequent standing at room temperature. After acidifying the mixture with 2 ml of concentrated hydrochloric acid and extracting with ethyl acetate, the extracts were worked up as usual yielding 15 mg of the amorphous triacetate **14**. The product gave only one spot in t.l.c. (several concentrations; solvent: chloroform–methanol, 4:1 and chloroform–isopropanol, 4:1 respectively; reagent: *p*-toluenesulfonic acid). With blue tetrazolium the substance gave a pronounced blue color almost instantaneously. ν_{max}(KBr) 3540 (broad, bonded OH), 1720 (with shoulders towards higher frequency, CO), 1235 (C—O of C—OAc), 1055 (C—O of C—OH), 1030 (C—O of C—OAc) cm^{-1}.

*5,14,19,21-Tetrahydroxy-5β,14β,17α-pregnane-3,20-dione (**18**) and 14,19-Dihydroxy-14β,17α-cortexone (14,19,21-Trihydroxy-Δ^4-14β,17α-pregnene-3,20-dione) (**19**) from 3β,5,14,19,21-Pentahydroxy-5β,14β,17α-pregnan-20-one (**13**)*

A mixture consisting of 440 mg of **13**, m.p. 256–258 °C, 25 ml of 70% aqueous *t*-butyl alcohol, and 340 mg of *N*-bromoacetamide (freshly purified (22); m.p. 100–108 °C; purity 97%) was kept at room temperature for 20 h. It was subsequently decolorized by the addition of aqueous sodium thiosulfate. After saturating with sodium chloride, extraction with five 50 ml portions of chloro-

[11]If the u.v. absorption curves of the 3-oxo-14,19-dihydroxy-$\Delta^{4,20(22)}$-14β,17α-cardadienolide (**11**) and 17α-strophanthidol (**5**) are plotted, and at the respective wavelengths, the ε values of the latter (**5**) are deducted from those of the former (**11**), a curve results, typical of a simple α,β-unsaturated ketone: λ_{max}(alcohol) 244 mμ, ε 14 800 (cf. ref. 21).

Can. J. Chem. Downloaded from www.nrcresearchpress.com by 210.87.254.5 on 09/05/12
For personal use only.

form–methanol (4:1) yielded 350 mg of the crude **18** in amorphous form. Since attempts at crystallization failed, the material was used for the next step without purification. To a solution of the crude **18** in 40 ml of absolute ethanol was added 0.6 g of Girard's reagent T and 1 ml of glacial acetic acid. After refluxing the mixture for 1 h and subsequent cooling, a solution of 1 g of sodium carbonate in 160 ml of water was added and extraction with chloroform was performed yielding only a trace of non-ketonic material. The aqueous phase was acidified to pH 2 with concentrated hydrochloric acid and, after 1.5 h standing, it was saturated with sodium chloride and extracted with six 40 ml portions of chloroform yielding 250 mg of ketonic material. This was chromatographed over 15 g of Florisil (15 × 132 mm). Elution was performed with 50 ml portions of solvent. Chloroform–acetone, 4:1, 1:1 (6 fractions) eluted 183 mg of a foam. Two crystallizations from acetone–hexane gave 99.3 mg of pure 14,19-dihydroxy-14β,17α-cortexone (**19**), m.p. 205–207 °C. From the mother liquors resulted 30.2 mg of additional **19**, m.p. 202–204 °C; $[\alpha]_D^{22}$ +32.4°, M_D^{22} +117° (17.6 mg in 2 ml of chloroform containing 5 drops of methanol, α +0.57°); λ_{max}(alcohol) 243 mμ, ε 13 700; ν_{max}(KBr) 3400 (very broad, bonded OH), 3015 (unsaturated C—H stretch), 1715 (C-20 CO), 1650 (shoulder, C-3 CO), 1635 (C=C), 1040 (C—O of C—OH) cm^{-1}.

Anal. Calcd. for $C_{21}H_{30}O_5$: C, 69.59; H, 8.24. Found:[6] C, 69.82; H, 8.37.

*14,19-Dihydroxy-14β,17α-cortexone-19,21-diacetate (19,21-Diacetoxy-14-hydroxy-Δ⁴-14β,17α-pregnene-3,20-dione) (**20**) from 14,19-Dihydroxy-14β,17α-cortexone (14,19,21-Trihydroxy-Δ⁴-14β,17α-pregnene-3,20-dione) (**19**)*

To a solution of 56.3 mg of **19**, m.p. 201–204 °C, in 4 ml of pyridine was added 2 ml of acetic anhydride and the mixture was kept at room temperature for 18 h. It was brought to dryness *in vacuo* and the residue was worked up as usual yielding 77 mg of the crude diacetate **20** which did not crystallize. By chromatographing over alumina (activity II) and eluting with ether–chloroform, 1:4, a total of 50 mg of purified diacetate **20** resulted which still resisted attempts at crystallization. ν_{max}(KBr) 3450 (very broad, bonded OH), 1735 (CO of acetate), 1715 (C-20 CO), 1655 (C-3 CO), 1620 (shoulder, C=C), 1230 (C—O of C—OAc), 1030 (C—O of C—OH and C—OAc) cm^{-1}.

*3β,5,14,19-Tetrahydroxy-5β,14β,17α-etianic acid (**15**) from 3β,5,14,19,21-Pentahydroxy-5β,14β,17α-pregnan-20-one (**13**)*

To 100 mg of **13**, m.p. 256–258 °C, in 10 ml of methanol was added a solution of 170 mg of sodium metaperiodate in 1.5 ml of water. The mixture was kept at room temperature for 17 h and, after the addition of 40 ml of water, it was acidified with one drop of concentrated hydrochloric acid and saturated with sodium chloride. Extraction with ethyl acetate yielded the crude reaction product (111 mg; not dry) which by t.l.c. was found to be a mixture of the free acid and its methyl ester. Hence, it was taken up in 5 ml of methanol and, after the addition of 40 ml of water and 5 ml of 5% sodium carbonate, the mixture was saturated with sodium chloride and extracted with six 25 ml portions of ethyl acetate yielding 15 mg of neutral material. This, by recrystallization from acetone–hexane, gave 7.8 mg of needles, m.p. 215–220 °C, identified as methyl ester (*vide infra*) by t.l.c. and mixture m.p. The carbonate phase was acidified to Congo Red with hydrochloric acid. Subsequent extraction with six 25 ml portions of ethyl acetate gave 80 mg of acidic product which upon two recrystallizations from acetone–hexane yielded 62 mg of prisms, m.p. 247–249 °C, representing the acid **15**. The mixture m.p. with authentic material (18) (redetermined m.p. 252–255 °C) was 251–254 °C. Both the product and the authentic material (18), gave only one spot in a t.l.c. on Silica Gel (solvent: chloroform–methanol, 4:1; reagent: *p*-toluenesulfonic acid) with the same R_f value. The product apparently tenaciously retains crystal solvent and hence no satisfactory result was obtained upon elemental analysis. The analyses are recorded as obtained with different lots of the product (*a*, *b*) and also with an old reference sample *c* (see ref. 18).

Anal. Calcd. for $C_{20}H_{32}O_6$: C, 65.19; H, 8.75. $C_{20}H_{32}O_6 \cdot \frac{1}{2}H_2O$: C, 63.63; H, 8.81. Found: (*a*)[9] C, 63.86; H, 8.78. (*b*) C, 64.04,[9] 64.07;[6] H, 8.75,[9] 8.65.[6] (*c*)[9] C, 63.93; H, 8.96.

The i.r. absorption spectra obtained with samples of old authentic material (18), were identical, but were different from the spectra obtained with samples prepared according to the preceding procedure. The differences of the spectra can possibly be explained on the basis of differences of crystal packing.[12]

*Methyl 3β,5,14,19-Tetrahydroxy-5β,14β,17α-etianate (**16**) from 3β,5,14,19-Tetrahydroxy-5β,14β,17α-etianic Acid (**15**)*

To 21 mg of **15**, m.p. 247–248 °C, in 5 ml of methanol was added ethereal diazomethane (prepared from *N*-methyl-*N*-nitroso-*N'*-nitroguanidine) until a pale-yellow color persisted. After standing at room temperature for 45 min the excess diazomethane was destroyed by the addition of a trace of acetic acid and the solution was worked up in the usual fashion yielding 24 mg of neutral material. Recrystallization from acetone–hexane gave 17 mg of the methyl ester **16** as fine needles, m.p. 224–225 °C. From the mother liquors resulted 2.7 mg of needles, m.p. 221–223 °C. The material gave only one spot in a t.l.c. on Silica Gel (solvent: chloroform containing 0.5% acetic acid–methanol, 4:1; reagent: *p*-toluenesulfonic acid). The product gave no depression of the m.p. when mixed with an authentic sample of the methyl ester, m.p. 225–226 °C (18). Furthermore, the i.r. absorption spectra were completely identical; $[\alpha]_D^{23}$ −2.8°, M_D^{23} −11° (10.85 mg in 2 ml of chloroform containing 2 drops of methanol, α −0.03°;[13] ν_{max}(KBr) 3480, 3400, and 3300 (OH), 1708 (CO of ester), 1030 (C—O of C—OH and ester) cm^{-1}.

Anal. Calcd. for $C_{21}H_{34}O_6$: C, 65.94; H, 8.96. Found:[6] C, 66.08; H, 9.07.

---

[12]The authors are indebted to Dr. R. Norman Jones for his opinion regarding this matter.

[13]The optical rotation was not reported in the earlier paper (18). It was determined at that time by Dr. G. W. Barber on the authentic sample as follows: $[\alpha]_D^{27}$ +3.5 ±5°, M_D^{27} +13.5 ±20° (5.64 mg in 2 ml of chloroform containing 2 drops of ethanol, α +0.02 ±0.03°).

Can. J. Chem. Downloaded from www.nrcresearchpress.com by 210.87.254.5 on 09/05/12
For personal use only.

Methyl 3β,19-Diacetoxy-5,14-dihydroxy-5β,14β,17α-etianate (17) from Methyl 3β,5,14,19-Tetrahydroxy-5β,14β,17α-etianate (16)

A solution of 6.4 mg of **16**, m.p. 223–225 °C, in 1 ml of pyridine and 0.5 ml of acetic anhydride was kept at room temperature for 18 h. After the addition of 20 ml of water and 30 min standing, the mixture was worked up as usual yielding the crude product which was not quite uniform (t.l.c.). It was reacetylated with 0.5 ml of acetic anhydride in 1 ml of pyridine (20 h). The resulting product which gave only one spot on t.l.c. was chromatographed over 2 g of alumina (activity II). Elution with benzene–chloroform, 4:1 and 1:1, gave from ether–hexane 5.7 mg of needles; softening and resolidification at 73–75 °C, m.p. 184–185 °C. The m.p. of a sample which had been prepared previously (19) from authentic material (18), and which softened and resolidified at 74–76 °C, was 175–181 °C; mixture m.p.: softening and resolidification at 73–76 °C, m.p. 181–184 °C. The identity was also confirmed by t.l.c. and comparison of the i.r. absorption spectra, ν_{max}(KBr) 3575 and 3540 (OH), 1725 (CO of —OAc), 1707 (C-20 CO), 1435 (CH_3 of —$COOCH_3$), 1287, 1269 and 1237 (CO of C—OAc), 1170 (CO of —$COOCH_3$); 1035 and 1020 (C—O of C—OAc), 1000 (C—O of C—OH) cm^{-1}.

3-Oxo-14,19-dihydroxy-Δ⁴-14β,17α-etienic Acid (21) from 14,19-Dihydroxy-14β,17α-cortexone (19)

To 69.2 mg of **19**, m.p. 204–207 °C, dissolved in 7 ml of methanol was added a solution of 125 mg of sodium metaperiodate in 2 ml of water. On standing at room temperature, white crystals began to separate within 1 h. After a total period of 23 h the reaction mixture was diluted with 50 ml of water, acidified with a few drops of hydrochloric acid, and saturated with sodium chloride. Extraction with chloroform furnished, after drying over sodium sulfate and evaporation of the solvent, 40.3 mg of product. Two crystallizations from acetone–hexane gave 25.4 mg of **21** as fine needles, m.p. 246–248 °C; $[\alpha]_D^{25}$ +79.3°, M_D^{25} +276° (11.1 mg in 2 ml of chloroform containing 5 drops of 95% ethanol, α +0.88°); λ_{max}(alcohol) 244 mμ, ε 14 700; ν_{max}(KBr) 3440 (bonded OH), 3260 (OH), 3090 and 3020 (unsaturated C—H stretch), 1720 (CO of —COOH), 1635 (C-3 CO), 1610 (shoulder, C=C), 1020 (C—O of C—OH) cm^{-1}.

Anal. Calcd. for $C_{20}H_{28}O_5$: C, 68.94; H, 8.10. Found:[6] C, 68.43; H, 8.41.

Methyl-3-oxo-14,19-dihydroxy-Δ⁴-14β,17α-etienate (22) from 3-Oxo-14,19-dihydroxy-Δ⁴-17β,17α-etienic Acid (21)

To a solution of 29.8 mg of **21**, m.p. 245–248 °C, in 5 ml of ethanol was added ethereal diazomethane until a pale-yellow color persisted. After 30 min standing the solvents were evaporated *in vacuo* leaving 34.5 mg of a residue. Two crystallizations from acetone–hexane gave 16.1 mg of **22** as prisms, m.p. 211–213 °C; $[\alpha]_D^{25}$ +68.8°, M_D^{25} +249° (7.7 mg, α 0.53°); λ_{max}(alcohol) 243 mμ, ε 14 500; ν_{max}(KBr) 3470 and 3385 (bonded OH), 3020 (shoulder, unsaturated C—H stretch), 1725 (CO of $COOCH_3$), 1635 (C-3 CO), 1615 (shoulder, C=C), 1360 (CH_3 of —$COOCH_3$), 1165 (C—O of —$COOCH_3$), 1040 (C—O of C—OH) cm^{-1}.

Anal. Calcd. for $C_{21}H_{30}O_5$: C, 69.59; H, 8.34. Found:[6] C, 70.12; H, 8.80.

Acknowledgment

We should like to thank Dr. David Y. Cooper, III, Harrison Department of General Surgical Research, for the determination of some of the ultraviolet spectra and Miss Maria Stojkewycz, Department of Obstetrics and Gynecology, for the determination of all infrared spectra.

1. M. Ehrenstein. J. Org. Chem. **9**, 435 (1944).
2. W. M. Allen and M. Ehrenstein. Science, **100**, 251 (1944).
3. G. W. Barber and M. Ehrenstein. Ann. **603**, 89 (1957).
4. C. Djerassi, M. Ehrenstein, and G. W. Barber. Ann. **612**, 93 (1958).
5. M. Ehrenstein, G. W. Barber, and R. Hertz. Endocrinology, **60**, 681 (1957).
6. P. Crabbé, A. Cruz, and J. Iriarte. Can. J. Chem. **46**, 349 (1968).
7. M. Ehrenstein and M. Dünnenberger. J. Org. Chem. **21**, 783 (1956).
8. E. J. Becker and M. Ehrenstein. J. Org. Chem. **26**, 510 (1961).
9. V. N. Gupta and M. Ehrenstein. Can. J. Chem. This issue.
10. W. A. Jacobs. J. Biol. Chem. **88**, 519 (1930).
11. A. Katz and T. Reichstein. Pharm. Acta Helv. **19**, 231 (1944).
12. R. Berthold, W. Wehrli, and T. Reichstein. Helv. Chim. Acta, **48**, 1659 (1965).
13. F. Burkhardt, W. Meier, A. Fürst, and T. Reichstein. Helv. Chim. Acta, **50**, 607 (1967).
14. A. Kuritzkes, J. v.Euw, and T. Reichstein. Helv. Chim. Acta, **42**, 1502 (1959).
15. J. H. Russel, O. Schindler, and T. Reichstein. Helv. Chim. Acta, **43**, 167 (1960).
16. I. P. Kovalev, E. V. Titov, V. T. Chernobai, and N. F. Komissarenko. Ukr. Khim. Zh. **31** 5, 513 (1965); Chem. Abstr. **63**, 5727 (1965).
17. M. Ehrenstein and A. R. Johnson. J. Org. Chem. **11**, 823 (1946).
18. G. W. Barber and M. Ehrenstein. J. Org. Chem. **16**, 1615 (1951).
19. C. P. Balant and M. Ehrenstein. J. Org. Chem. **17**, 1576 (1952).
20. A. Hunger and T. Reichstein. Ber. **85**, 635 (1952).
21. B. Fechtig, J. v.Euw, O. Schindler, and T. Reichstein. Helv. Chim. Acta, **43**, 1570 (1960).
22. N. Rabjohn. Org. Syn. IV, 104 (1963).

Can. J. Chem. Downloaded from www.nrcresearchpress.com by 210.87.254.105 on 09/05/12
For personal use only.

Tetrahydropyranyl protecting group. I. Tetrahydropyran-2-yl isocyanate

D. E. HORNING AND J. M. MUCHOWSKI
Bristol Laboratories of Canada, Candiac, Quebec

Received April 10, 1968

It is shown that monoalkyl and unsymmetrical dialkyl ureas, and alkyl carbamates, are preparable *via* a two-step sequence involving tetrahydropyran-2-yl isocyanate, and a primary or secondary amine, or an alcohol, respectively.

Canadian Journal of Chemistry, 46, 2617 (1968)

The synthesis of monoalkyl and/or unsymmetrical dialkyl ureas is usually accomplished[1] by the alkylamination of isocyanic acid, the amination of alkyl isocyanates and carbamyl chlorides, and by amine exchange with urea. Each method has specific advantages, but none is generally applicable.

The decomposition of nitrourea (into nitramide and isocyanic acid) in the presence of a suitable amine is reported (3) to be an excellent route to both mono and unsymmetrical dialkyl ureas, but this attractive method has not enjoyed widespread application.

In connection with another problem, we required a method whereby medium quantities of high molecular weight ureas (of the type discussed above) could be obtained routinely and efficiently. The solution, in our estimation, was essentially one of equipping isocyanic acid with a "handle" whose removal could be easily accomplished subsequent to urea formation. The results presented below show that the tetrahydropyranyl group adequately fulfilled the stipulated requirements.

Tetrahydropyran-2-yl isocyanate, which has recently been described in the patent literature (see Experimental), is a stable liquid conveniently prepared in the laboratory from 2-chlorotetrahydropyran and silver cyanate. It reacted with primary and secondary amines to give excellent yields of 1-alkyl-3-tetrahydropyran-2-yl and 1,1-dialkyl-3-tetrahydropyran-2-yl ureas (see Table I). Their structures were substantiated by a nitrogen analysis, by infrared absorptions at 3435 ±20, 3355 ±25, 1665 ±15, and 1550 ±15 cm^{-1} for the 1,3-disubstituted members,[2] and at 3468, 1652, and 1514 cm^{-1} for the trisubstituted compound, and lastly, and most significantly, by the conversion to the known ureas (Table II) in satisfactory overall yield.

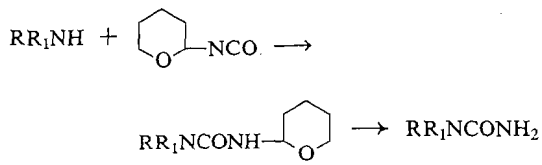

The removal of the tetrahydropyranyl group was effected with 1% hydrochloric acid (ca. 0.1 *N*) in refluxing 10% aqueous methanol (1 h).[3] For preparative purposes, the high yields obtained in the initial condensation, make the purification of the intermediate unnecessary; it is sufficient to evaporate the solvent *in vacuo*, and then to proceed directly with the cleavage of the tetrahydropyranyl group.

Tetrahydropyranyl isocyanate can also be used to synthesize alkyl carbamates, as is exemplified by the preparation of benzyl carbamate in 82% overall yield from the corresponding alcohol.

[1]For brief compilations of the methods used to synthesize these compounds see refs. 1 and 2, and the papers cited therein.

[2]A series of eight 1,3-disubstituted ureas had strong absorption bands which occurred within the four specified regions. An absorption at 1670 cm^{-1} has been tentatively assigned to the carbonyl stretching frequency of ureas (4).

[3]These conditions are somewhat more vigorous than necessary since 1-benzyl-3-tetrahydropyran-2-yl urea was completely converted to benzyl urea in 2.5 h at room temperature, or in less than 5 min at reflux temperature. (The progress of the reaction was followed by thin-layer chromatography on alumina.)

The protected urea was recovered unchanged after 1 h at reflux temperature in benzene-containing acetic acid and a trace of *p*-toluenesulfonic acid.

TABLE I

1-Substituted-3-tetrahydropyran-2-yl ureas*

R	R_1	Yield (%)†	Melting point (°C)†	% N Calculated	% N Found	Crystallization‡ solvent
n-Butyl	H	86	79–81	13.99	13.88	A
n-Propyl	*n*-propyl	100§	60–64	11.38§	11.56	A
Benzyl	H	95	118–120	11.96	12.08	B
Phenyl	H	93	181.5–183‖	12.72	12.81	C

*The preparation sequence can be represented as:

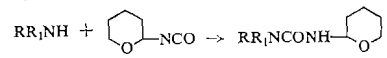

†The yields and melting points refer to once crystallized products. Unless otherwise stated, the analytical specimens had the tabulated melting points.
‡A, cyclohexane – petroleum ether (b.p. 35–60°); B, benzene–cyclohexane; C, benzene.
§100% Yield of the cyclohexane solvate, $C_{12}H_{24}N_2O_2$:1/6 C_6H_{12}. The presence of cyclohexane was corroborated by a strongly ringing peak of the correct intensity at δ 1.40 in the n.m.r. spectrum. No other solvent absorptions were detectable.
‖The analytical specimen had m.p. 185–186°.

TABLE II

1-Substituted ureas*

R	R_1	Yield (%)†	Melting point (°C)† Observed	Melting point (°C)† Reported	Crystallization solvent
n-Butyl	H	46‡§	97–98	96‖	Benzene
n-Propyl	*n*-propyl	74§¶	133–135¶**	136‖**	Ether
Benzyl	H	72§	147–149	150††	Ethyl acetate
Phenyl	H	76	147–148	147‖	Water

*The preparation sequence may be represented as:

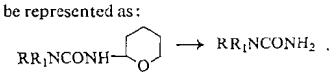

†The yields and melting points refer to once crystallized products. The yields are based on the starting amine.
‡After chromatography on silica gel and crystallization.
§Without isolation of the intermediate tetrahydropyranyl urea.
‖See ref. 3.
¶Isolated as the picrate.
**Melting point of the picrate.
††See ref. 5.

Experimental

The melting points were determined in a Gallenkamp melting point apparatus and are not corrected. The infrared (i.r.) spectra were measured in chloroform on a Perkin–Elmer 237-B grating spectrophotometer. The nuclear magnetic resonance (n.m.r.) spectrum was determined in deuteriochloroform at 60 Mc.p.s. on a Varian A-60A spectrometer, with tetramethylsilane as an internal standard.

Tetrahydropyran-2-yl Isocyanate

A 1 l, 3-necked flask, equipped with a calcium chloride tube, a thermometer, and a gas inlet tube, was charged with 800 ml of anhydrous benzene, and 35.0 g (0.29 mole) of 2-chlorotetrahydropyran (6). The magnetically stirred solution was cooled to 0°, and while the apparatus was flushed with purified dry nitrogen, 58.0 g (0.386 mole) of silver cyanate (7) was added all at once; a 6° temperature rise occurred. The cooling bath was removed and the mixture was stirred at room temperature for 2 h with protection from light. The solids were removed by filtration through Celite, the filter cake was washed with dry benzene, and the filtrate was flash distilled *in vacuo* (ca. 15 mm) below 30°. The oil which remained was fractionally distilled *in vacuo*, and the fraction, 23.2 g, b.p. 61–62°/16 mm, n_D^{20} = 1.4519, was collected. The flash distillate from above was evaporated *in vacuo* at 20° to give 2.1 g of an oily residue, which on fractionation *in vacuo* gave an additional 1.15 g of the isocyanate. The combined yield was 24.35 g (66.5%).

Tetrahydropyranyl isocyanate had a strong i.r. absorption (liquid film) at 2257 cm^{-1}. The n.m.r. spectrum consisted of a singlet with fine structure at δ 5.07, a complex multiplet between δ 3.50 and 4.15, and a broad singlet at δ 1.68, with an integral ratio of 1:2:6 respectively.

This isocyanate has recently been prepared from isocyanic acid and tetrahydropyran (8), and from 2-chlorotetrahydropyran and alkali metal cyanates in mixed solvent systems (9). It is reported to have b.p. 51–52°/7 mm (8), and 47–48°/11 mm, and n_D^{20} = 1.4500 (9).

Preparation of Ureas

(a) 1-Substituted-3-tetrahydropyran-2-yl Ureas

A solution of 1.27 g (10 mmoles) of tetrahydropyran-2-yl isocyanate in 30 ml of anhydrous benzene containing 10 mmoles of the amine, was heated at reflux temperature

Can. J. Chem. Downloaded from www.nrcresearchpress.com by 210.87.254.105 on 09/05/12
For personal use only.

for 2 h. If the urea did not crystallize on cooling, the solvent was removed *in vacuo*, and the solid residue was crystallized from the solvent system indicated in Table I.

Alternatively, the crude residue could be used directly in the next step as described below.

(b) 1-Substituted Ureas

The urea, in a solution made up of 1 part of 10% hydrochloric acid and 9 parts of methanol (10 ml/mmole), was heated at reflux temperature for 1 h on a steam bath. Most of the solvent was removed *in vacuo*, the residue was diluted with water, and the urea was extracted into ethyl acetate. The dried (sodium sulfate) extract was evaporated *in vacuo*, and the residue was crystallized from the appropriate solvent (Table II), or it was taken up in ether and added to an excess of picric acid in the same solvent.

Benzyl Carbamate

To a solution of the isocyanate (1.907 g, 15 mmoles) in 45 ml of dry benzene, was added 1.58 ml (1.65 g, 15.3 mmoles) of benzyl alcohol and 1 ml of anhydrous pyridine. After 24 h at reflux temperature (when 5 wt % of sodium hydride was utilized as a catalyst, the reaction was complete in 4 h), the solvent was removed *in vacuo*, the solid residue was taken up in hot cyclohexane (10 ml) diluted with 10 ml of petroleum ether (b.p. 30–65°), seeded, and left to cool. A beautifully crystalline solid, 3.19 g, m.p. 82–83° was obtained. Evaporation of the mother liquor and crystallization of the residue as above, gave an additional 0.06 g of the product, m.p. 81–82.5°. The combined yield was 3.25 g or 92.2% based on the isocyanate. For analysis, the solid was twice crystallized from the above solvent system, and then dried *in vacuo* over phosphorous pentoxide at room temperature for 15 h. The melting point was not raised.

Anal. Calcd. for $C_{13}H_{17}NO_3$: N, 5.95. Found: N, 6.07.

The tetrahydropyranyl group was removed in the same manner as described in the urea section. The yield of benzyl carbamate obtained upon crystallization of the crude product from 1:1 benzene–cyclohexane, was 89% or 82% based on the starting isocyanate. The product had m.p. 85–88°, undepressed on admixture with an authentic specimen of benzyl carbamate.

1. R. B. WAGNER and H. D. ZOOK. Synthetic organic chemistry. John Wiley and Sons, Inc., New York. 1961. p. 645.
2. P. A. S. SMITH. Open-chain nitrogen compounds. Vol. 1. W. A. Benjamin, Inc., New York. 1965. p. 275.
3. T. L. DAVIS and R. C. BLANCHARD. J. Am. Chem. Soc. **51**, 1790 (1929).
4. L. J. BELLAMY. The infrared spectra of complex molecules. 2nd ed. Methuen and Co. Ltd., London. 1958. p. 223.
5. W. L. GARBRECHT and R. M. HERBST. J. Org. Chem. **18**, 1014 (1953).
6. C. D. HURD and R. D. KIMBROUGH. J. Am. Chem. Soc. **83**, 236 (1961).
7. L. BIRCKENBACH and M. LINHARD. Ber. **62**, 2261 (1929).
8. J. L. HARPER. U.S. Patent No. 3, 168, 545 (1965); Chem. Abstr. **62**, 11689 (1965).
9. K. F. ZENNER, G. OERTEL, and H. HOLTSCHMIDT. Ger. Patent No. 1, 205, 087 (1965); Chem. Abstr. **64**, 19413 (1966).

Oligomerization of isoprene

KYOICHI SUGA, SHOJI WATANABE, HIDEO KIKUCHI, AND TORU WATANABE

Department of Applied Chemistry, Faculty of Engineering, Chiba University, Yayoicho, Chiba, Japan

Received March 20, 1968

The oligomerization of isoprene with lithium naphthalene and the dimerization of isoprene with alkali dispersion are described. Isoprene dimer, prepared by the action of lithium naphthalene, is a mixture of 2,6-dimethyl-2,6-octadiene and 2,7-dimethyl-2,6-octadiene, but the trimer, tetramer, and hexamer are a mixture of 3,4-adducts of isoprene to the above mentioned isoprene dimer. The authors have found that alkali dispersion in the presence of a Lewis base is able to dimerize isoprene.

Canadian Journal of Chemistry, **46**, 2619 (1968)

It is well known that alkali naphthalene and alkali dispersion are effective for the natural polymerization of conjugated dienes. The studies on the microstructure of polyisoprene and polybutadiene have been investigated by many workers (1). These studies have not, however, confirmed the production of oligomers of isoprene, such as monoterpene and sesquiterpene. The natural oligomerization of α-methylstyrene to the tetramer has recently been studied (2), but the oligomerization of isoprene has not been reported. It may be suspected that an oligomer of isoprene may be prepared from the monomer in the presence of excess lithium naphthalene. The authors prepared various isoprene oligomers by the action of lithium naphthalene and alkali dispersion in tetrahydrofuran solution.

Anionic oligomerization of isoprene, involving lithium naphthalene and proceeding in a tetrahydrofuran solution in the usual fashion (3), affords isoprene oligomers, and the typical results are presented in Table I. From these results, it can be said that the use of 1 mole of isoprene per mole of lithium gives mainly the

Can. J. Chem. Downloaded from www.nrcresearchpress.com by 210.87.254.105 on 09/05/12
For personal use only.

for 2 h. If the urea did not crystallize on cooling, the solvent was removed *in vacuo*, and the solid residue was crystallized from the solvent system indicated in Table I.

Alternatively, the crude residue could be used directly in the next step as described below.

(b) 1-Substituted Ureas

The urea, in a solution made up of 1 part of 10% hydrochloric acid and 9 parts of methanol (10 ml/mmole), was heated at reflux temperature for 1 h on a steam bath. Most of the solvent was removed *in vacuo*, the residue was diluted with water, and the urea was extracted into ethyl acetate. The dried (sodium sulfate) extract was evaporated *in vacuo*, and the residue was crystallized from the appropriate solvent (Table II), or it was taken up in ether and added to an excess of picric acid in the same solvent.

Benzyl Carbamate

To a solution of the isocyanate (1.907 g, 15 mmoles) in 45 ml of dry benzene, was added 1.58 ml (1.65 g, 15.3 mmoles) of benzyl alcohol and 1 ml of anhydrous pyridine. After 24 h at reflux temperature (when 5 wt % of sodium hydride was utilized as a catalyst, the reaction was complete in 4 h), the solvent was removed *in vacuo*, the solid residue was taken up in hot cyclohexane (10 ml) diluted with 10 ml of petroleum ether (b.p. 30–65°), seeded, and left to cool. A beautifully crystalline solid, 3.19 g, m.p. 82–83° was obtained. Evaporation of the mother liquor and crystallization of the residue as above, gave an additional 0.06 g of the product, m.p. 81–82.5°. The combined yield was 3.25 g or 92.2% based on the isocyanate. For analysis, the solid was twice crystallized from the above solvent system, and then dried *in vacuo* over phosphorous pentoxide at room temperature for 15 h. The melting point was not raised.

Anal. Calcd. for $C_{13}H_{17}NO_3$: N, 5.95. Found: N, 6.07.

The tetrahydropyranyl group was removed in the same manner as described in the urea section. The yield of benzyl carbamate obtained upon crystallization of the crude product from 1:1 benzene–cyclohexane, was 89% or 82% based on the starting isocyanate. The product had m.p. 85–88°, undepressed on admixture with an authentic specimen of benzyl carbamate.

1. R. B. WAGNER and H. D. ZOOK. Synthetic organic chemistry. John Wiley and Sons, Inc., New York. 1961. p. 645.
2. P. A. S. SMITH. Open-chain nitrogen compounds. Vol. 1. W. A. Benjamin, Inc., New York. 1965. p. 275.
3. T. L. DAVIS and R. C. BLANCHARD. J. Am. Chem. Soc. **51**, 1790 (1929).
4. L. J. BELLAMY. The infrared spectra of complex molecules. 2nd ed. Methuen and Co. Ltd., London. 1958. p. 223.
5. W. L. GARBRECHT and R. M. HERBST. J. Org. Chem. **18**, 1014 (1953).
6. C. D. HURD and R. D. KIMBROUGH. J. Am. Chem. Soc. **83**, 236 (1961).
7. L. BIRCKENBACH and M. LINHARD. Ber. **62**, 2261 (1929).
8. J. L. HARPER. U.S. Patent No. 3, 168, 545 (1965); Chem. Abstr. **62**, 11689 (1965).
9. K. F. ZENNER, G. OERTEL, and H. HOLTSCHMIDT. Ger. Patent No. 1, 205, 087 (1965); Chem. Abstr. **64**, 19413 (1966).

Oligomerization of isoprene

KYOICHI SUGA, SHOJI WATANABE, HIDEO KIKUCHI, AND TORU WATANABE

Department of Applied Chemistry, Faculty of Engineering, Chiba University, Yayoicho, Chiba, Japan

Received March 20, 1968

The oligomerization of isoprene with lithium naphthalene and the dimerization of isoprene with alkali dispersion are described. Isoprene dimer, prepared by the action of lithium naphthalene, is a mixture of 2,6-dimethyl-2,6-octadiene and 2,7-dimethyl-2,6-octadiene, but the trimer, tetramer, and hexamer are a mixture of 3,4-adducts of isoprene to the above mentioned isoprene dimer. The authors have found that alkali dispersion in the presence of a Lewis base is able to dimerize isoprene.

Canadian Journal of Chemistry, **46**, 2619 (1968)

It is well known that alkali naphthalene and alkali dispersion are effective for the natural polymerization of conjugated dienes. The studies on the microstructure of polyisoprene and polybutadiene have been investigated by many workers (1). These studies have not, however, confirmed the production of oligomers of isoprene, such as monoterpene and sesquiterpene. The natural oligomerization of α-methylstyrene to the tetramer has recently been studied (2), but the oligomerization of isoprene has not been reported. It may be suspected that an oligomer of isoprene may be prepared from the monomer in the presence of excess lithium naphthalene. The authors prepared various isoprene oligomers by the action of lithium naphthalene and alkali dispersion in tetrahydrofuran solution.

Anionic oligomerization of isoprene, involving lithium naphthalene and proceeding in a tetrahydrofuran solution in the usual fashion (3), affords isoprene oligomers, and the typical results are presented in Table I. From these results, it can be said that the use of 1 mole of isoprene per mole of lithium gives mainly the

Can. J. Chem. Downloaded from www.nrcresearchpress.com by 210.87.254.40 on 09/05/12
For personal use only.

TABLE I

Oligomerization of isoprene with lithium naphthalene

Reaction conditions (molar ratio)			Products (yield, %)				
Lithium	Isoprene	Naphthalene	Dimer	Trimer	Tetramer	High oligomer*	Residue
1	1	0.5	40	5		20	10
1	1.5	0.5	7	35	7	24	16
1	2.0	0.5	2	5	40	30	20
1	3.0	0.5	0	0	2	65	25

*It was distilled with molecular distillation, b.p. 100–210 °C at 10^{-4} Torr.

TABLE II

Nuclear magnetic resonance spectra of the saturated isoprene oligomers

	Proton numbers (δ, p.p.m.)			
Hydrocarbon	CH_3—	—CH_2—	—$\overset{\vert}{C}H$—	Total
Saturated trimer	17 (0.85)	11 (1.2)	4 (1.6)	32
Standard sesquiterpene*	15 (0.85)	14 (1.2)	3 (1.6)	32
All 3,4-adduct (trimer)‡	21	6	5	32
Saturated tetramer	22 (0.9)	15 (1.25)	5 (1.6)	42
Standard diterpene†	18 (0.9)	20 (1.25)	4 (1.6)	42
All 3,4-adduct (tetramer)‡	27	8	7	42
Saturated hexamer	36 (0.85)	26 (1.6–1.2)		62
Standard squalane	24 (0.8)	38 (1.6–1.2)		62
All 3,4-adduct (hexamer)‡	39	23		62

*2,6,10-Trimethyldodecane.
†2,6,10,14-Tetramethylhexadecane
‡These were calculated data.

dimer; the use of 1.5 moles of isoprene gives the trimer; the use of 2.0 moles of isoprene gives the tetramer; and the use of 3.0 moles of isoprene gives the hexamer, in fairly good yields, but a high oligomer was produced simultaneously in all cases.

The isoprene dimer was a mixture of 2,6-dimethyl-2,6-octadiene, head-to-tail structure (50%) and 2,7-dimethyl-2,6-octadiene, tail-to-tail structure (50%) (3). The other oligomers were a mixture of many isomers, which we have not been able to separate. The oligomers were hydrogenated completely and the existence of one double bond per one unit of isoprene was confirmed. In the saturated isoprene trimer, a small amount of a linear sesquiterpene, with head-to-tail structure, was confirmed by comparison with an authentic sample using gas–liquid chromatography.

Nuclear magnetic resonance (n.m.r.) spectral data of these saturated isoprene oligomers are shown in Table II. Proton numbers of methyl groups of saturated isoprene oligomers are larger than those of methyl groups of corresponding linear terpenic hydrocarbons. For example the proton number of methyl groups of the hexamer is 36, but that of squalane, a 1,4-adduct, is 24. It may be considered that isoprene oligomers have a high 3,4-adduct content and a low 1,4-adduct content. The structural assignment was further supported by the following spectral evidence of the original isoprene oligomers. Infrared absorption spectra of the unsaturated oligomers did not show the absorptions of a vinyl type double bond, but showed the strong absorption band of a terminal methylene group due to the presence of an isopropenyl group at 890 cm^{-1}. The ratios of the proton numbers of the terminal methylene double bond and the trisubstituted double bond are calculated from the n.m.r. spectra of oligomers, and typical results are shown in Table III. Numbers of the protons of the terminal methylene double bond due to the presence of an isopropenyl group, gradually increase in the order of trimer, tetramer, and hexamer. On the basis of the above

Can. J. Chem. Downloaded from www.nrcresearchpress.com by 210.87.254.40 on 09/05/12
For personal use only.

Can. J. Chem. Downloaded from www.nrcresearchpress.com by 210.87.254.40 on 09/05/12
For personal use only.

mentioned results, it appears that the isoprene oligomers such as trimer, tetramer, and hexamer, are a mixture of 3,4-adducts of isoprene and linear isoprene dimers.

TABLE III

Nuclear magnetic resonance spectra of olefin protons of the isoprene oligomers

Hydrocarbon	Ratio of proton numbers: $-\overset{\vert}{C}=CH_2$ (δ, p.p.m.)	$-\overset{\vert}{C}=CH-$ (δ, p.p.m.)
Trimer	1 (4.7)	1 (5.15)
Tetramer	3 (4.7)	2 (5.1)
Hexamer	2 (4.7)	1 (5.05)

Similar results were also observed during the oligomerization of butadiene. Although butadiene dimer was a mixture of 2,6-octadiene and 1,6-octadiene, as reported previously (4), the butadiene trimer was a mixture of various isomers, which were not separated. The saturated hydrocarbon from the butadiene trimer mixture contained dodecane (48%), and 3-methylundecane (52%), which were produced by 1,2-addition of butadiene to a linear dimer.

The polymerization of isoprene by means of metallic alkali dispersion produces a polyisoprene comparable to natural rubber, but the production of an isoprene dimer has not been confirmed. We have found that alkali dispersion in the presence of a Lewis base will catalyze the dimerization of isoprene. Dimerization with lithium dispersion gave a mixture of 2,6-dimethyl-2,6-octadiene (50%) and 2,7-dimethyl-2,6-octadiene (50%) in 20–30% yield, whereas sodium dispersion yielded a mixture of 2,3,5-trimethyl-1,5-heptadiene (30%), 2,3,6-trimethyl-1,5-heptadiene (10%), 2,7-dimethyl-1,6-octadiene (40%), and 2,6-dimethyl-1,6-octadiene (20%), in 20–25% yield. The effect of Lewis base on the yield of isoprene dimer was also determined. From the results in Table IV, it is clear that the use of 0.1 mole of *t*-butylamine per mole of isoprene gave the best results.

Experimental

All the experiments were carried out in a dry apparatus under nitrogen, and all the reagents were purified thoroughly.

Isoprene Dimer

This was prepared as reported previously (3).

Isoprene Trimer

To a lithium naphthalene complex which had been prepared from 0.5 mole of naphthalene and 1.0 mole of lithium turnings, 1.5 moles of isoprene were added gradually. The reaction mixture was treated in the usual fashion (3) to give a mixture of isoprene trimer in yield of 35–40%, b.p. 70–75 °C at 3 Torr, infrared (i.r.): 886 cm^{-1} ($-\overset{\vert}{C}=CH_2$), 835 cm^{-1} ($-CH=\overset{\vert}{C}-$); nuclear magnetic resonance (n.m.r.) (δ, p.p.m.): 1.65 ($CH_3-\overset{\vert}{C}=$), 2.05 ($-CH_2-\overset{\vert}{C}=$), 5.15 ($-CH=\overset{\vert}{C}-$), 4.7 ($-\overset{\vert}{C}=CH_2$).

Anal. Calcd. for $C_{15}H_{26}$: C, 87.32; H, 12.70. Found: C, 87.29; H, 12.67.

Isoprene trimer mixture (6.02 g) was hydrogenated over palladium on carbon in a methanol solution at 80 °C under an initial hydrogen pressure of 30 kg/cm^2; 1670 ml (standard temperature and pressure) of hydrogen (calcd. for $C_{15}H_{26}$, 1950 ml) were absorbed to give a saturated isoprene trimer mixture, b.p. 110 °C at 20 Torr, i.r.: 1380 and 1390 cm^{-1} (doublet). It was identified as a mixture of 2,6,10-trimethyldodecane (15%) (a linear sesquiterpene) and unidentified saturated trimer (85%) by gas–liquid chromatography (g.l.c.). The gas chromatogram with a 45 m × 0.5 mmϕ capillary column of SE-30 at a temperature of 90 °C, using helium as the carrier gas (1.0 kg/cm^2), showed ten peaks.

Isoprene Tetramer

From one mole of lithium, 0.5 mole of naphthalene, and 2.0 moles of isoprene, a mixture of tetramers was obtained in 40% yield, b.p. 125–130 °C at 3 Torr, i.r.: 885 cm^{-1} ($CH_2=\overset{\vert}{C}-$), 840 cm^{-1} ($-CH=\overset{\vert}{C}-$); n.m.r.: 1.65 ($CH_3-\overset{\vert}{C}=$), 2.05 ($-CH_2-\overset{\vert}{C}=$), 5.1 ($-CH=\overset{\vert}{C}-$), 4.7 ($-\overset{\vert}{C}=CH_2$).

Anal. Calcd. for $C_{20}H_{34}$: C, 87.50; H, 12.48. Found: C, 87.40; H, 12.43.

Isoprene tetramer mixture (5.0 g) was hydrogenated in the same way as the isoprene trimer and 1310 ml (standard temperature and pressure) of hydrogen (calcd. for $C_{20}H_{34}$, 1640 ml) were absorbed to give a saturated isoprene tetramer mixture, b.p. 100–104 °C at 3 Torr, i.r.: 1385 cm^{-1}, 1375 cm^{-1} (doublet, gem-dimethyl group). Gas chromatographic analysis showed a trace of the linear diterpene, 2,6,10,14-tetramethylhexadecane.

Isoprene Hexamer

From one mole of lithium, 0.5 mole of naphthalene, and 3.0 moles of isoprene, a mixture of isoprene oligomers was obtained in yield of 90%. After low boiling fractions were removed by vacuum distillation, the residue was distilled with a centrifugal molecular distillation still to give a mixture of isoprene oligomers in yield of 65%. It had the following properties: b.p. 80–100 °C at 5 × 10^{-3} Torr, i.r.: 895 cm^{-1} ($CH_2=\overset{\vert}{C}-$), 835 cm^{-1} ($-CH=\overset{\vert}{C}-$), n.m.r.: 1.6 ($CH_3-\overset{\vert}{C}=$), 2.0 ($-CH_2-\overset{\vert}{C}=$), 4.7 ($-\overset{\vert}{C}=CH_2$), 5.05 ($-CH=\overset{\vert}{C}-$), molecular weight,

Can. J. Chem. Downloaded from www.nrcresearchpress.com by 210.87.254.40 on 09/05/12
For personal use only.

TABLE IV

Dimerization of isoprene with alkali dispersion*

Alkali dispersion	Lewis base (mole)	Yield of isoprene dimer (%)	Gas chromatographic analysis of the dimer (%) 1†	2‡	3§
Na	None	3			
Na	*t*-Butylamine (0.01)	25	40	60	
Na	Triethylamine (0.01)	20	50	50	
Na	Ethylene diamine (0.01)	15	30	70	
Na	*N*,*N*-Dimethylbenzylamine (0.01)	15	35	65	
Na	Nicotine (0.01)	10	35	65	
Na	*p*-Toluidine (0.01)	8	30	70	
Na	α-Naphthylamine (0.01)	8	30	70	
Na	Phenothiazine (0.01)	5	30	70	
Li	None	3			
Li	*t*-Butylamine (0.001)	15	4		96
Li	*t*-Butylamine (0.01)	25	4		96
Li	*t*-Butylamine (0.05)	20	8		92
Li	*t*-Butylamine (0.1)	10	10		90
K	*t*-Butylamine (0.01)	25	30	70	

*Reaction conditions: tetrahydrofuran (100 ml), alkali dispersion (0.1 mole), isoprene (0.1 mole), reaction temperature (30 °C), reaction time (3 h). The gas chromatography column was of Polyphenylether (10%) on Celite 545 (7 m) at a temperature of 90 °C with helium as the carrier gas (40 ml/min).
†1 is a mixture of 2,3,5-trimethyl-1,5-heptadiene and 2,3,6-trimethyl-1,5-heptadiene.
‡2 is a mixture of 2,7-dimethyl-1,6-octadiene and 2,6-dimethyl-1,6-octadiene.
§3 is a mixture of 2,7-dimethyl-2,6-octadiene and 2,6-dimethyl-2,6-octadiene.

405–407 (calcd. for $C_{30}H_{50}$: 410). It did not contain squalene which has a terpenic structure.

Anal. Calcd. for $C_{30}H_{50}$: C, 87.73; H, 12.27. Found: C, 87.81; H, 12.12.

Crude isoprene hexamer (6.52 g) was hydrogenated in the same way as the isoprene trimer and 1820 ml of hydrogen (standard temperature and pressure) (calcd. for $C_{30}H_{50}$, 2064 ml) were absorbed to give a saturated oligomer. It was distilled with a centrifugal molecular still to give a saturated isoprene hexamer mixture, b.p. 82–100 °C at 5×10^{-3} Torr.

Oligomerization of Butadiene with Lithium Naphthalene

To a mixture of 27 g of naphthalene and 150 ml of tetrahydrofuran, 7.0 g (1.0 mole) of metallic lithium turnings were added. After 3 h, 81 g (1.5 moles) of butadiene were passed through gradually for 2 h, and treated in the usual way to give 15 g (b.p. 55–70 °C at 18 Torr) of a crude butadiene trimer and 24 g of a crude butadiene tetramer. The fractional redistillation of the trimer gave the trimer mixture, b.p. 64–66 °C at 20 Torr, i.r.: 960 cm^{-1} (*trans*-type double bond), 770 cm^{-1} (*cis*-type double bond), 910 and 980 cm^{-1} (a vinyl-type double bond).

Upon the hydrogenation of 2.3 g of butadiene trimer in methanol using a Pd–C catalyst, 720 ml of hydrogen (theoretical for $C_{12}H_{20}$, 927 ml) were absorbed to give a mixture of *n*-dodecane (48%) and 3-methylundecane (52%). They were shown to be identical with authentic samples by gas chromatographic analysis, using a 4 m column of Polyphenylether (10%) on Chromosorb W (60–80 mesh) at a temperature of 127 °C, with helium as the carrier gas (40 ml/min).

Dimerization of Isoprene with Sodium Dispersion

Sodium dispersion 2.3 g (0.1 mole) was suspended in purified tetrahydrofuran at room temperature under a dry nitrogen atmosphere. After addition of 0.73 g (0.01 mole) of *t*-butylamine, 7 g (0.1 mole) of isoprene was gradually added to the solution. The reaction mixture was treated in the usual manner and gave 2 g of an oily product, b.p. 50–60 °C at 25 Torr. The results of g.l.c. analysis of the oil are shown in Table IV. Fractional distillation of the oil (15 g) with spinning band column gave 2 g of hydrocarbon **1** (a mixture of 2,3,5-trimethyl-1,5-heptadiene and 2,3,6-trimethyl-1,5-heptadiene), and 3 g of hydrocarbon **2** (a mixture of 2,6-dimethyl-1,6-octadiene and 2,7-dimethyl-1,6-octadiene). The hydrocarbon **1** had the following properties: b.p. 52 °C at 24 Torr, n_D^{27} 1.4425; i.r.: 892 cm^{-1} (a terminal methylene double bond) and 832 cm^{-1} (a trisubstituted double bond); n.m.r.: 0.95 (CH_3—C(—)—, 3H), 1.65 (CH_3—C(=)—, 9H), 2.0 (—CH_2—C(=)—, 2H), 4.7 (CH_2=C(—)—, about 2H), and 5.1 (—CH=C(—)—, about 1H). The hydrocarbon **2** had the following properties: b.p. 65 °C at 24 Torr, n_D^{27} 1.4455, i.r.: 890 cm^{-1} (a terminal methylene group) and 837 cm^{-1} (a trisubstituted double bond), n.m.r.: 1.65 (CH_3—C(=)—), 2.05 (—CH_2—C(=)—), 4.75 (—C(=CH_2)—), and 5.2 (—CH=C(—)—).

The isoprene dimer mixture **1** (0.7206 g) was hydrogenated over Pd–C in a methanol solution at room temperature; 202 ml (standard temperature and pressure) of hydrogen (calcd. for $C_{10}H_{18}$, 234 ml) were absorbed to give a saturated hydrocarbon mixture. It was shown by g.l.c. to be a mixture of 2,3,5-trimethylheptane (about 70%) and 2,3,6-trimethylheptane (about 30%).

The quantitative hydrogenation of the isoprene dimer mixture **2** also required two molar equivalents of hydrogen. The hydrogenated product was shown by g.l.c. to be

a mixture of 2,6-dimethyloctane (50%) and 2,7-dimethyloctane (50%). A 9 m column of Polyphenylether (10%) on Diasolid L at a temperature of 75 °C with helium as the carrier gas (40 ml/min) was used.

Dimerization of Isoprene with Lithium Dispersion

From 0.1 mole of lithium dispersion, 0.01 mole of *t*-butylamine and 0.1 mole of isoprene, 2.5 g of isoprene dimer mixture were obtained. It was shown by g.l.c. to be a mixture of 2,6-dimethyl-2,6-octadiene and 2,7-dimethyl-2,6-octadiene.

Infrared Absorption Spectra

These were measured on a Koken IRS spectrophotometer, using liquid films.

Nuclear Magnetic Resonance Spectra

These were determined on a Japan Electron Optics Lab. instrument (60 Mc.p.s.) with carbon tetrachloride solutions and with tetramethylsilane as an internal standard.

Acknowledgment

The authors thank Dr. Sanae Tanaka of Mitsubishi Petrochemical Co., Ltd., for providing materials and for measurements of the nuclear magnetic resonance spectra.

1. L. REICH and A. SCHINDLER. Polymerization by organometallic compounds. Interscience Publishers, New York. 1966. p. 548.
2. R. L. WILLIAMS and D. H. RICHARDS. Chem. Commun. 414 (1967).
3. K. SUGA and S. WATANABE. Bull. Chem. Soc. Japan, **40**, 1257 (1967).
4. K. SUGA, S. WATANABE, and K. TAKAHASHI. Bull. Chem. Soc. Japan, **40**, 2432 (1967).

Optimum temperatures in pyrolysis gas chromatography

RUSSELL SUTTON[1] AND W. E. HARRIS
Department of Chemistry, University of Alberta, Edmonton, Alberta

Received December 29, 1967

Pyrograms were recorded for a variety of compounds pyrolyzed in the gas phase in a quartz tube. The lowest temperature at which the major pyrolytic products are first formed and the lowest temperatures causing complete pyrolysis were determined and found to differ by about 80–120 °C. The temperatures of complete pyrolysis at the described experimental conditions are 600–650 °C for the most stable compounds. At temperatures above 700 °C the compounds were degraded primarily to methane, ethane, ethylene, or carbon.

Canadian Journal of Chemistry, 46, 2623 (1968)

The temperature of pyrolysis in gas phase pyrolysis gas chromatography (p.g.c.) is of primary importance in obtaining a pyrogram that is characteristic of a reactant. A temperature causing complete pyrolysis is desirable, if the structurally significant products are not also destroyed. The reactant peak in a pyrogram would be of some value for identification, but the retention time of a reactant would usually be prohibitively longer than retention times for the lower molecular weight products. Temperatures and products of pyrolysis of a number of compounds are determined here. Comparisons are made of the results of p.g.c. obtained over a range of temperatures.

Results

The apparatus was previously described (1). Briefly, samples were passed through a gas chromatographic column at 75 °C (to remove air) and then into a heated 3 mm internal diameter 4.7 ml quartz spiral to bring about pyrolysis. The pyrolysis mixture was then sent to a Porapak Q column that was held at 100 °C for 10 min, and then programmed to about 210 °C during a period of 30 min. The helium flow through the pyrolysis tube was 8 ml/min. The sample residence time in the pyrolysis tube was calculated as described elsewhere (1) and found to be 15 s. Calculations with Rummen's (3) equations indicates that the heat transfer in the pyrolyzer was such that the sample was raised to wall temperature in about 6 s.

The products accounting for the major peaks (areas greater than 1% of the total area of all peaks in the pyrograms) were identified from retention times and mass spectra (Table I). Though methane, ethylene, and ethane are usually omitted, they are produced by nearly all compounds and only in exceptional cases are they important for identification. For example,

[1]Present address: Department of Chemistry, Knox College, Galesburg, Illinois.

Can. J. Chem. Downloaded from www.nrcresearchpress.com by 210.87.254.40 on 09/05/12
For personal use only.

a mixture of 2,6-dimethyloctane (50%) and 2,7-dimethyloctane (50%). A 9 m column of Polyphenylether (10%) on Diasolid L at a temperature of 75 °C with helium as the carrier gas (40 ml/min) was used.

Dimerization of Isoprene with Lithium Dispersion

From 0.1 mole of lithium dispersion, 0.01 mole of *t*-butylamine and 0.1 mole of isoprene, 2.5 g of isoprene dimer mixture were obtained. It was shown by g.l.c. to be a mixture of 2,6-dimethyl-2,6-octadiene and 2,7-dimethyl-2,6-octadiene.

Infrared Absorption Spectra

These were measured on a Koken IRS spectrophotometer, using liquid films.

Nuclear Magnetic Resonance Spectra

These were determined on a Japan Electron Optics Lab. instrument (60 Mc.p.s.) with carbon tetrachloride solutions and with tetramethylsilane as an internal standard.

Acknowledgment

The authors thank Dr. Sanae Tanaka of Mitsubishi Petrochemical Co., Ltd., for providing materials and for measurements of the nuclear magnetic resonance spectra.

1. L. REICH and A. SCHINDLER. Polymerization by organometallic compounds. Interscience Publishers, New York. 1966. p. 548.
2. R. L. WILLIAMS and D. H. RICHARDS. Chem. Commun. 414 (1967).
3. K. SUGA and S. WATANABE. Bull. Chem. Soc. Japan, **40**, 1257 (1967).
4. K. SUGA, S. WATANABE, and K. TAKAHASHI. Bull. Chem. Soc. Japan, **40**, 2432 (1967).

Optimum temperatures in pyrolysis gas chromatography

RUSSELL SUTTON[1] AND W. E. HARRIS

Department of Chemistry, University of Alberta, Edmonton, Alberta

Received December 29, 1967

Pyrograms were recorded for a variety of compounds pyrolyzed in the gas phase in a quartz tube. The lowest temperature at which the major pyrolytic products are first formed and the lowest temperatures causing complete pyrolysis were determined and found to differ by about 80–120 °C. The temperatures of complete pyrolysis at the described experimental conditions are 600–650 °C for the most stable compounds. At temperatures above 700 °C the compounds were degraded primarily to methane, ethane, ethylene, or carbon.

Canadian Journal of Chemistry, 46, 2623 (1968)

The temperature of pyrolysis in gas phase pyrolysis gas chromatography (p.g.c.) is of primary importance in obtaining a pyrogram that is characteristic of a reactant. A temperature causing complete pyrolysis is desirable, if the structurally significant products are not also destroyed. The reactant peak in a pyrogram would be of some value for identification, but the retention time of a reactant would usually be prohibitively longer than retention times for the lower molecular weight products. Temperatures and products of pyrolysis of a number of compounds are determined here. Comparisons are made of the results of p.g.c. obtained over a range of temperatures.

Results

The apparatus was previously described (1). Briefly, samples were passed through a gas chromatographic column at 75 °C (to remove air) and then into a heated 3 mm internal diameter 4.7 ml quartz spiral to bring about pyrolysis. The pyrolysis mixture was then sent to a Porapak Q column that was held at 100 °C for 10 min, and then programmed to about 210 °C during a period of 30 min. The helium flow through the pyrolysis tube was 8 ml/min. The sample residence time in the pyrolysis tube was calculated as described elsewhere (1) and found to be 15 s. Calculations with Rummen's (3) equations indicates that the heat transfer in the pyrolyzer was such that the sample was raised to wall temperature in about 6 s.

The products accounting for the major peaks (areas greater than 1% of the total area of all peaks in the pyrograms) were identified from retention times and mass spectra (Table I). Though methane, ethylene, and ethane are usually omitted, they are produced by nearly all compounds and only in exceptional cases are they important for identification. For example,

[1]Present address: Department of Chemistry, Knox College, Galesburg, Illinois.

Can. J. Chem. Downloaded from www.nrcresearchpress.com by 210.87.254.5 on 09/05/12
For personal use only.

TABLE I

Temperature ranges and products of pyrolysis for several substances

Substance pyrolyzed	Pyrolysis temperature range (°C)*	Major pyrolysis products	
$CH_3CO_2C(CH_3)_3$	280–340	$CH_2{=}C(CH_3)_2$	CH_3CO_2H
$(CH_2{=}CHCH_2)_2O$	340–440	$CH_3CH{=}CH_2$	$CH_2{=}CHCHO$
$CH_3CO_2CH(CH_3)CH_2CH_3$	360–460	$CH_3CH_2CH{=}CH_2$ CH_3CO_2H	$CH_3CH{=}CHCH_3$ (*cis* and *trans*)
$CH_2{=}CHCH_2OCH_2CH_3$	380–480	$CH_3CH{=}CH_2$	CH_3CHO
$HCO_2(CH_2)_3CH_3$	400–500	$CH_3CH_2CH{=}CH_2$	HCO_2H
$CH_3CO_2CH_2CH_2CH_3$	420–500	$CH_3CH{=}CH_2$	CH_3CO_2H
$CH_3CO_2CH_2CH_3$	420–520	$CH_2{=}CH_2$	CH_3CO_2H
$HCO_2CH_2CH_2CH_3$	420–520	$CH_3CH{=}CH_2$	HCO_2H
$CH_3CO_2CH(CH_3)_2$	430–530	$CH_2{=}C(CH_3)_2$	CH_3CO_2H
$HCO_2CH_2CH{=}CH_2$	460–580	$CH_3CH{=}CH_2$	CO_2
$CH_3CH_2CO_2CH_2CH{=}CH_2$	480–580	$CH_3CH{=}CH_2$	CO_2, $CH_3CH_2CO_2H$
$[(CH_3)_2CH]_2O$	540–640	$CH_3CH{=}CH_2$ $CH_3CHOHCH_3$	CH_3COCH_3
$CH_3COCH_2CH_3$	540–640	$CH_2{=}CH_2$ CO	CH_3CH_3
$CH_3CHOHCH_3$	440–640	$CH_3CH{=}CH_2$	CH_3COCH_3
$(C_2H_5)_2O$	520–660	$CH_2{=}CH_2$ CH_3CHO	CH_3CH_2OH
$(CH_3CH_2CH_2)_2O$	560–660	$CH_3CH{=}CH_2$	CH_3CH_2CHO
CH_3CH_2CHO	560–660	CH_3CH_3 $CH_2{=}CH_2$	CO

*The temperature range includes the lowest temperature at which products are detectable (corresponding to about 1% decomposition) and the temperature at which there is virtually complete pyrolysis (99% reacted).

the ethylene peak would be important to the detection of ethyl acetate pyrolyzed at 500 °C, but of lesser significance when found in the high-temperature pyrogram of *n*-butyl formate. Minor products, usually one to three in number, were not identified. Carbon is also often a product and becomes visible when it accumulates through extended use of a pyrolysis tube.

In Table I the lower temperature listed is that at which the major products were first detectable, where pyrolysis was about 1%. The upper temperature is that at which there was virtually complete pyrolysis and is the temperature at which the reactant peak area was about 1% of the total area for all peaks. The lower and upper limits are valid to about the nearest 10 °C. Note that the upper temperature limits are lower than the temperature required for pyrolysis in stainless steel tubes (2). This lower temperature may be in part due to different residence times and in part because of the use of quartz rather than stainless steel (1). It should be noted further that major products listed in Table I were still present at temperatures up to 600 °C.

The relative amounts of methane, ethane, and ethylene were slightly greater when pyrolysis occurred at the higher temperature, but became significantly greater only above 600 °C. Each of the reactants was degraded to methane, ethylene, ethane, or propylene when pyrolyzed at 700 °C. In addition, water, carbon dioxide, or carbon monoxide accompanied the hydrocarbon products from the oxygen-containing reactants pyrolyzed at 700 °C. For example, isobutyl acetate was converted to acetic acid and isobutene between 430 and 600 °C. Pyrolysis at 700 °C yielded methane, carbon dioxide, ethylene, ethane, and propylene. Acetic acid was then absent from the pyrogram, and the area of the isobutene peak was only one quarter of the area of the same peak formed at 600 °C.

Propionaldehyde and methyl ethyl ketone are a pair of compounds that yield the same major products on pyrolysis. Tertiary and isobutyl acetates are a similar pair. Identification of such materials can be achieved in several ways, such as by measuring relative peak areas or by considering the retention characteristics of the reactants with either a pre-pyrolysis or post-pyrolysis gas chromatographic column. When a chromatographic column is followed with a pyrolysis unit, which in turn is connected to a second column, a nonreactive internal standard such as benzene can aid in the interpretation of retention information. For example, if a mixture of tertiary and isobutyl acetates is injected into a column, the isobutyl acetate will reach the pyrolyzer first, and consequently the isobutene

Can. J. Chem. Downloaded from www.nrcresearchpress.com by 210.87.254.5 on 09/05/12
For personal use only.

resulting from the isobutyl acetate will slightly precede the isobutene from the *t*-butyl acetate. If benzene is also injected into the mixture, the difference in time of appearance of the two isobutene peaks can be easily fixed with reference to the benzene peak.

Discussion

The pyrolysis of a compound in p.g.c. is more extensive than the 1 to 5% decomposition occurring in many mechanistic studies of pyrolysis (e.g. ref. 4) but the products observed have not differed. Slight pyrolysis of propionaldehyde (4) and isobutane (5) yields the products observed in p.g.c. (1) (Table I). Pyrolytic conversions of ethers to olefins, alcohols, aldehydes, and ketones (6) of esters to olefins and acids, and isopropyl alcohol to acetone and propylene, are well known organic reactions that occur under a variety of conditions used for synthesis and identification. The chain rearrangements accompanying pyrolysis with a catalyst evidently do not occur in non-catalytic homogeneous pyrolysis for p.g.c. The products (pyrogram) for the compounds in Table I are, therefore, characteristic. For example, *t*-butyl acetate and *sec*-butyl acetate yield products (pyrograms) that permit an unequivocal distinction between the two compounds. Generally therefore the structures of the products are related to those of the reactants.

The temperatures (Table I) of pyrolysis in p.g.c. have been found to be comparable to those that are effective in other experimental conditions. Ritchie (7) found that simple carboxylic acid esters pyrolyze at 400–500 °C; ethers (6) have been pyrolyzed at 500–600 °C and propionaldehyde (4) at 400–600 °C.

Acknowledgment

Financial support to Russell Sutton by the National Research Council of Canada is gratefully acknowledged.

1. R. SUTTON and W. E. HARRIS. Can. J. Chem. **45**, 2913 (1967).
2. T. WOLF and D. M. ROSIE. Anal. Chem. **39**, 725 (1967).
3. F. H. T. RUMMENS. Ph.D. Thesis. Technological University of Eindhoven. The Netherlands. March, 1963.
4. ANDRE F. BOYER and M. D. M. NICLAUSE. Compt. Rend. **233**, 687 (1951).
5. J. FUSY, R. MARTIN, and M. D. M. NICLAUSE. Bull. Soc. Chim. France, 3783 (1966).
6. W. B. CONVERSE. U.S. Patent No. 2,309,576. Chem. Abstr. **37**, 3767:3(1943); P.P.T. Sah. Rec. Trav. Chim. **58**, 758 (1939).
7. P. D. RITCHIE. Soc. Chem. Ind. London, Monograph, **13**, 107 (1961).

Reactions of 1,2-dichlorohexafluorocyclopentene with secondary phosphines

RICHARD F. STOCKEL

Research and Development, Organic Chemicals Division, American Cyanamid Company, Bound Brook, New Jersey 08805

Received February 15, 1968

Dicyclohexylphosphine and diphenylphosphine react with 1,2-dichlorohexafluorocyclopentene to give almost exclusively the monoderivative via displacement of a vinylic chlorine atom. With the former phosphine a disubstituted derivative is also found. In addition to analytical values and infrared spectroscopic data, both ^{19}F and ^{31}P nuclear magnetic resonance spectra support the proposed structures.

Canadian Journal of Chemistry, **46**, 2625 (1968)

Introduction

The reaction of 1,2-dichlorohexafluorocyclopentene with various nucleophiles has been studied extensively. With amines (1) and alcohols (2) the products are either C-1 monosubstituted or C-1,3,3 trisubstituted depending on the amount of reactant and the reactivity of the nucleophile. A new reaction path was observed with phosphites, phosphonites, and phosphinite esters with displacement of both chlorine atoms to give exclusively tetraalkylperfluoro-1-cycloalken-1,2,-ylenediphosphonates (3).

The explanation why the monosubstituted derivative was not formed with these phosphorus compounds was rationalized by a reversal of the polarization of the double bond. Therefore, C-2 becomes partially positive and subsequently becomes susceptible to nucleophilic attack. This

Can. J. Chem. Downloaded from www.nrcresearchpress.com by 210.87.254.5 on 09/05/12
For personal use only.

resulting from the isobutyl acetate will slightly precede the isobutene from the *t*-butyl acetate. If benzene is also injected into the mixture, the difference in time of appearance of the two isobutene peaks can be easily fixed with reference to the benzene peak.

Discussion

The pyrolysis of a compound in p.g.c. is more extensive than the 1 to 5% decomposition occurring in many mechanistic studies of pyrolysis (e.g. ref. 4) but the products observed have not differed. Slight pyrolysis of propionaldehyde (4) and isobutane (5) yields the products observed in p.g.c. (1) (Table I). Pyrolytic conversions of ethers to olefins, alcohols, aldehydes, and ketones (6) of esters to olefins and acids, and isopropyl alcohol to acetone and propylene, are well known organic reactions that occur under a variety of conditions used for synthesis and identification. The chain rearrangements accompanying pyrolysis with a catalyst evidently do not occur in non-catalytic homogeneous pyrolysis for p.g.c. The products (pyrogram) for the compounds in Table I are, therefore, characteristic. For example, *t*-butyl acetate and *sec*-butyl acetate yield products (pyrograms) that permit an unequivocal distinction between the two compounds. Generally therefore the structures of the products are related to those of the reactants.

The temperatures (Table I) of pyrolysis in p.g.c. have been found to be comparable to those that are effective in other experimental conditions. Ritchie (7) found that simple carboxylic acid esters pyrolyze at 400–500 °C; ethers (6) have been pyrolyzed at 500–600 °C and propionaldehyde (4) at 400–600 °C.

Acknowledgment

Financial support to Russell Sutton by the National Research Council of Canada is gratefully acknowledged.

1. R. SUTTON and W. E. HARRIS. Can. J. Chem. **45**, 2913 (1967).
2. T. WOLF and D. M. ROSIE. Anal. Chem. **39**, 725 (1967).
3. F. H. T. RUMMENS. Ph.D. Thesis. Technological University of Eindhoven. The Netherlands. March, 1963.
4. ANDRE F. BOYER and M. D. M. NICLAUSE. Compt. Rend. **233**, 687 (1951).
5. J. FUSY, R. MARTIN, and M. D. M. NICLAUSE. Bull. Soc. Chim. France, 3783 (1966).
6. W. B. CONVERSE. U.S. Patent No. 2,309,576. Chem. Abstr. **37**, 3767:3(1943); P.P.T. Sah. Rec. Trav. Chim. **58**, 758 (1939).
7. P. D. RITCHIE. Soc. Chem. Ind. London, Monograph, **13**, 107 (1961).

Reactions of 1,2-dichlorohexafluorocyclopentene with secondary phosphines

RICHARD F. STOCKEL

Research and Development, Organic Chemicals Division, American Cyanamid Company, Bound Brook, New Jersey 08805

Received February 15, 1968

Dicyclohexylphosphine and diphenylphosphine react with 1,2-dichlorohexafluorocyclopentene to give almost exclusively the monoderivative via displacement of a vinylic chlorine atom. With the former phosphine a disubstituted derivative is also found. In addition to analytical values and infrared spectroscopic data, both ^{19}F and ^{31}P nuclear magnetic resonance spectra support the proposed structures.

Canadian Journal of Chemistry, **46**, 2625 (1968)

Introduction

The reaction of 1,2-dichlorohexafluorocyclopentene with various nucleophiles has been studied extensively. With amines (1) and alcohols (2) the products are either C-1 monosubstituted or C-1,3,3 trisubstituted depending on the amount of reactant and the reactivity of the nucleophile. A new reaction path was observed with phosphites, phosphonites, and phosphinite esters with displacement of both chlorine atoms to give exclusively tetraalkylperfluoro-1-cycloalken-1,2,-ylenediphosphonates (3).

The explanation why the monosubstituted derivative was not formed with these phosphorus compounds was rationalized by a reversal of the polarization of the double bond. Therefore, C-2 becomes partially positive and subsequently becomes susceptible to nucleophilic attack. This

Can. J. Chem. Downloaded from www.nrcresearchpress.com by 210.87.254.40 on 09/05/12
For personal use only.

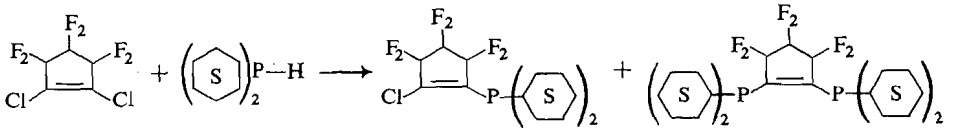

1 2

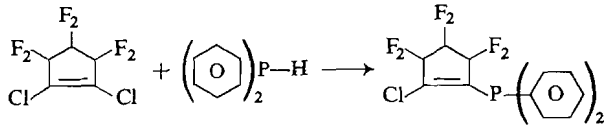

3

same type of conjugative ability has been postulated in an earlier paper involving a carboxamide group (4).

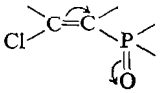

A more recent paper illustrates the subtleties found in reactions of this type. With perfluorocyclobutene, diphenylphosphine gives the disubstituted derivative, while with 1,2-dichlorotetrafluorocyclobutene only hydrogen chloride, trifluorodiphenylphosphorane, and diphenylphosphinic fluoride are found (5). It has been shown previously that cyclic perfluoroolefins behave differently than the corresponding 1,2-dichloro derivatives with various nucleophiles (6) nevertheless the monosubstituted derivative should be the first step anticipated with either olefin.

Results

In view of the 1,2-dichlorotetrafluorocyclobutene system the work done on 1,2-dichlorohexafluorocyclopentene is presented to show the intricacies involved in which so much depends on the substrate studied as well as on the reaction medium. The secondary phosphines dicyclohexylphosphine and diphenylphosphine react smoothly with 1,2-dichlorohexafluorocyclopentene to give the monoderivative in good yields. Only in the case of dicyclohexylphosphine was there obtained a disubstituted derivative in approximately 8.3%. This result can be explained by the wide difference in pK_a values found for these secondary phosphines (7). Dicyclohexylphosphine is a much stronger base than diphenylphosphine and since basicity is related to nucleophilicity this finding is not too surprising.

Another interesting aspect of this work involved the isolation of minute amounts of dicyclohexyl and diphenyl phosphinic acids, respectively, from oxidation of the starting phosphines. In contrast, the products, which are also phosphines, do not undergo any observable oxidations to the corresponding oxides under these reaction conditions. This is undoubtedly due to the decrease in basicities caused by the inductive effect of the perhalocyclopentene moiety. Thus these results with secondary phosphines are consistent with Frank's study (3) which indicate that the monosubstituted derivatives are the first formed products. When the monosubstituted products are pentavalent phosphonate materials, they can cause further reaction at C-2. When the initial products are trivalent phosphorus materials, which are reluctant to oxidize, further reaction is not encouraged by any electronic factors. If disubstituted materials are formed as with dicyclohexylphosphine the cause is probably due to the increased basicity of the phosphorus nucleophile, although ring size may also be significant.[1]

Physical Data

Nuclear Magnetic Resonance

The ^{19}F, ^{31}P, and ^{1}H nuclear magnetic resonance spectra were instrumental in elucidating the structures. The ^{19}F spectrum of **1** shows three multiplets at 106.5ϕ, 116.2ϕ, and 132.8ϕ indicating the non-equivalency of the three pair. The ^{31}P spectrum shows one broad peak at +19.1 p.p.m. This is essentially the right sign and magnitude expected for a phosphine (8). If the product were a phosphine oxide a negative

[1]Experiments are in progress dealing with 1,2-dichlorotetrafluorocyclobutene which indicate that the nucleophile, reaction medium, and ring size of the substrate are important parameters in reactions of this type.

Can. J. Chem. Downloaded from www.nrcresearchpress.com by 210.87.254.40 on 09/05/12
For personal use only.

Can. J. Chem. Downloaded from www.nrcresearchpress.com by 210.87.254.40 on 09/05/12
For personal use only.

value would be anticipated. The ^1H spectrum shows a broad aliphatic absorption between 2.5 and 1.0 δ. When benzotrifluoride was added to calculate the F:H ratio, a value of 6:22 was obtained. The ^{19}F spectrum of **2** shows two multiplets at 108.1ϕ and 134.6ϕ in the ratio of 2:1. The ^{31}P spectrum shows a broad singlet at +17.0 p.p.m. The ^1H spectrum shows broad aliphatic absorption similar to **1** between 2.1 and δ1.16. The integrated F:H ratio is 6:44.

For structure **3** the ^{31}P spectrum shows only one peak at +19.6 p.p.m., which is characteristic of a phosphine. The ^1H spectrum shows only aromatic absorption. The ^{19}F spectrum shows 3 clusters of peaks of equal intensities at 105.3, 115.4, and 131.9ϕ. The fact that the ^{19}F spectrum shows three different absorptions, points out the fact that the molecule is not symmetrical. When allyltrifluoroacetate was added to calculate the F:H ratio, a value of 6:10 was obtained.

Infrared

The final trisubstituted phosphine products are void of any absorption around 2440–2275 cm^{-1} which is the characteristic frequency of a P—H stretch (9[2]). Although not unequivocal because of interference due to C—F bands, the lack of a broad intense absorption at 1300–1140 cm^{-1} seems to indicate the absence of a P=O stretch. In case of the phenyl derivative **3** the P-ϕ moiety gives rise to peaks at 1425, 1130, and 995 cm^{-1}. Four sharp medium to large bands are observed at 1280–1120 cm^{-1}, which can be attributed to CF_2 absorption. Finally it was observed that in the mono-substituted derivatives **1** and **3**, a strong sharp peak was found at 876 cm^{-1}, but in the 1,2-disubstituted derivative **2**, no discernible peak was observed. As more of these types of compounds are synthesized, it will be interesting to see if this absorption can be used as a diagnostic test to differentiate between mono and disubstituted derivatives.

Experimental

Diphenylphosphine was prepared according to the method described by Horner and Hoffmann (10). All other reagents were purchased from commercial sources. Analytical results were obtained by our own microanalytical laboratory. Infrared spectra were run as mineral oil mulls on a Perkin–Elmer model 317 spectrophotometer. Nuclear magnetic resonance spectra were recorded with a Varian HR-60, ^1H reported as δ values using tetramethylsilane as internal standard, ^{19}F reported as ϕ values using trichlorofluoromethane as an external standard, and ^{31}P reported in p.p.m. using triethylphosphate as an external standard. For determining the H:F ratios benzotrifluoride was used for **1** and **2**, while allytrifluoroacetate was used for **3**.

Preparation of ***1****, (2-Chloro-3,3,4,4,5,5-hexafluoro-1-cyclopentan-1-yl)dicyclohexylphosphine and* ***2****, (3,3,4,4,5,5-Hexafluorocyclopent-1-en-1,2-ylene)bis(dicyclohexylphosphine)*

Dicyclohexylphosphine (18.6 g) and 1,2-dichlorohexafluorocyclopentene (24.5 g) were added to 100 ml of dimethyl formamide. The solution was stirred at room temperature for 15 h then refluxed for 5 h. The contents were then poured into 400 ml of water and the viscous organic layer isolated by decanting the water. The organic material was dried in a vacuum oven at 70 °C. Approximately 35.5 g of crude product was obtained. Acetone was added to this semi-solid and caused 2.5 g (8.3% yield) of a yellow solid to precipitate. This was identified as **2**, m.p. 194–194.5 °C.

Anal. Calcd. for **2**, $C_{29}H_{44}F_6P$: C, 61.26; H, 7.62; P, 10.91. Found: C, 60.94; H, 7.59; P, 10.90.

Removal of the acetone gave a liquid which was distilled at 114–116 °C/0.3 mm. This was identified as **1**.

Anal. Calcd. for **1**, $C_{17}H_{22}ClF_6P$: C, 50.18; H, 5.41; Cl, 8.73; P, 7.62. Found: C, 49.74; H, 5.17; Cl, 8.55; P, 7.62.

Preparation of ***3****, (2-Chloro-3,3,4,4,5,5-hexafluoro-1-cyclopentan-1-yl)diphenylphosphine*

Diphenylphosphine (18 g) and 1,2-dichlorohexafluorocyclopentene (24.5 g) were added to 100 ml of dimethyl formamide and stirred for 15 h at 75 °C. The solution was then poured into 400 ml of water and extracted with ethyl ether. After removal of ethyl ether the crude viscous oil, approximately 31.0 g (78.6% yield), was distilled at 148–149 °C/2 mm. The product **3** had a melting point of 49–50 °C.

Anal. Calcd. for **3**, $C_{17}H_{10}ClF_6P$: C, 51.71; H, 2.53; Cl, 8.99; P, 7.88. Found: C, 52.05; H, 2.98; Cl, 9.15; P, 7.47.

Acknowledgments

The author wishes to acknowledge the assistance of Dr. J. E. Lancaster and Mrs. M. Neglia of the Central Research Laboratories of American Cyanamid, for the hydrogen, fluorine, and phosphorus nuclear magnetic resonance spectra.

1. C. O. Parker. J. Am. Chem. Soc. **81**, 2183 (1959).
2. J. D. Park, L. H. Wilson, and J. R. Lacher. J. Org. Chem. **28**, 1008 (1963).
3. A. W. Frank. J. Org. Chem. **30**, 3663 (1965); **31**, 1917 (1966).
4. T. Mill, J. O. Rodin, R. M. Silverstein, and C. Woolf. J. Org. Chem. **28**, 836 (1963).
5. W. R. Cullen, D. S. Dawsen, and P. S. Dhaliwal. Can. J. Chem. **45**, 683 (1967).
6. R. F. Stockel, M. T. Beachem, and F. H. Megson. Can. J. Chem. **42**, 2880 (1964).
7. C. A. Streuli. Anal. Chem. **32**, 985 (1960).

[2]All references for the infrared spectra were taken from this source.

8. K. MOEDRITZER, L. MAIER, and L. C. D. GROENVEGH. J. Chem. Eng. Data, 7, 307 (1962).
9. N. B. COLTHUP, L. H. DALY, and S. E. WIBERLEY. Introduction to infrared and raman spectroscopy. Academic Press, Inc., New York. 1964.
10. L. HORNER and H. HOFFMANN. Newer methods of preparative organic chemistry. Vol. II. *Edited by* W. Foerst. Academic Press, Inc., New York. 1963.

3-D-Hydroxypalmitic acid: a metabolic product of the yeast NRRL Y-6954

R. F. VESONDER, L. J. WICKERHAM, AND W. K. ROHWEDDER

Northern Regional Research Laboratory, Agricultural Research Service, United States Department of Agriculture, Peoria, Illinois 61604

Received March 21, 1968

An extracellular lipid produced by the yeast NRRL Y-6954 was shown to be free 3-D-hydroxypalmitic acid. The structure of the hydroxy acid was established by the mass spectrum of its methyl ester and a direct comparison with an authentic sample of methyl 3-D-hydroxypalmitate.

Canadian Journal of Chemistry, 46, 2628 (1968)

Can. J. Chem. Downloaded from www.nrcresearchpress.com by 210.87.254.40 on 09/05/12
For personal use only.

The formation of extracellular lipids of yeasts has recently been reviewed by Stodola *et al.* (1).

In continuing work in this area, we found that free 3-D-hydroxypalmitic acid (**1**) is excreted by an unidentified yeast. In 1964, Tulloch and Spencer (2), and van Ammers *et al.* (3) reported that this acid was a component of glycolipids produced by *Rhodotorula* species.

Acid **1** was produced in a yield of 1.76 g/l by growing the yeast for 4.5 days at 25 °C in shaken flasks on a medium containing 5% malt extract and 2% Cerelose.[1] The crude acid (m.p. 70–80 °C), obtained by extraction of the culture liquor with ether, was shown by thin-layer chromatography to consist largely of one component.

Crystallization from hexane gave pure acid **1** (m.p. 79.5–80.5 °C) of formula $C_{16}H_{32}O_3$, the infrared (i.r.) spectrum of which showed hydroxyl absorption (3565 cm^{-1} (w)) and carbonyl absorption (1710 cm^{-1} (s)) in 1% chloroform. Methyl (**2**) and *p*-bromophenacyl (**3**) esters gave analytical values in accord with the $C_{16}H_{32}O_3$ formula.

The mass spectrum of methyl ester **2** was directly comparable with the mass spectrum of methyl 3-DL-hydroxyoctadecanoate observed by Ryhage and Stenhagen (4). The position of the hydroxyl group on the carbon chain is indicated by a peak at mass 103; the highest in the spectrum, this peak is due to the fragment CH_3OCCH_2CHOH obtained from cleavage of the 3,4 carbon–carbon bond. The following comparisons were also found: peaks at 194, 236 [M − 32 − 18(CH_3OH,H_2O)], and 268 [M − 18(H_2O)] for methyl ester **2**, are 28 mass numbers less than peaks 222, 264 [M − 32 − 18(CH_3OH,H_2O)], and 296 [M − 18(H_2O)] found by Ryhage and Stenhagen for methyl 3-DL-hydroxyoctadecanoate.

The mass spectrum of **2** and its direct comparison (i.r. and m.p.) with methyl 3-D-hydroxypalmitate, kindly supplied by Dr. A. P. Tulloch, established the structure of **1**.

Experimental

Melting points were determined with a Fisher–Johns apparatus and are not corrected. The infrared spectra were recorded on a Perkin–Elmer (model 137), and a Beckman (model IR8) infrared spectrophotometer. The mass spectrum was recorded on a Nuclide instrument (model 12-90 G).

Production of Crude Acid (1)

The stock culture of the yeast (NRRL Y-6954 in the ARS Culture Collection here) was maintained at 25 °C on YM agar slants (1% glucose, 0.5% peptone, 0.3% yeast extract, 0.3% malt extract, and 2% agar). A sterilized liquid medium (200 ml), consisting of 2% Cerelose and 5% malt extract contained in 500-ml Erlenmeyer flasks, was inoculated by loop with cells from 1-day-old YM slant cultures. The flasks were kept on a Gump shaker at 25 °C.

At intervals the contents of five flasks were extracted with ether. The yields of crude acid were: 2.5 days, 212

[1]Mention of firm names or trade products does not constitute endorsement by the United States Department of Agriculture over other firms or products not mentioned.

8. K. MOEDRITZER, L. MAIER, and L. C. D. GROENVEGH. J. Chem. Eng. Data, 7, 307 (1962).
9. N. B. COLTHUP, L. H. DALY, and S. E. WIBERLEY. Introduction to infrared and raman spectroscopy. Academic Press, Inc., New York. 1964.
10. L. HORNER and H. HOFFMANN. Newer methods of preparative organic chemistry. Vol. II. *Edited by* W. Foerst. Academic Press, Inc., New York. 1963.

3-D-Hydroxypalmitic acid: a metabolic product of the yeast NRRL Y-6954

R. F. VESONDER, L. J. WICKERHAM, AND W. K. ROHWEDDER

Northern Regional Research Laboratory, Agricultural Research Service, United States Department of Agriculture, Peoria, Illinois 61604

Received March 21, 1968

An extracellular lipid produced by the yeast NRRL Y-6954 was shown to be free 3-D-hydroxypalmitic acid. The structure of the hydroxy acid was established by the mass spectrum of its methyl ester and a direct comparison with an authentic sample of methyl 3-D-hydroxypalmitate.

Canadian Journal of Chemistry, 46, 2628 (1968)

Can. J. Chem. Downloaded from www.nrcresearchpress.com by 210.87.254.40 on 09/05/12
For personal use only.

The formation of extracellular lipids of yeasts has recently been reviewed by Stodola *et al.* (1).

In continuing work in this area, we found that free 3-D-hydroxypalmitic acid (**1**) is excreted by an unidentified yeast. In 1964, Tulloch and Spencer (2), and van Ammers *et al.* (3) reported that this acid was a component of glycolipids produced by *Rhodotorula* species.

Acid **1** was produced in a yield of 1.76 g/l by growing the yeast for 4.5 days at 25 °C in shaken flasks on a medium containing 5% malt extract and 2% Cerelose.[1] The crude acid (m.p. 70–80 °C), obtained by extraction of the culture liquor with ether, was shown by thin-layer chromatography to consist largely of one component.

Crystallization from hexane gave pure acid **1** (m.p. 79.5–80.5 °C) of formula $C_{16}H_{32}O_3$, the infrared (i.r.) spectrum of which showed hydroxyl absorption (3565 cm^{-1} (w)) and carbonyl absorption (1710 cm^{-1} (s)) in 1% chloroform. Methyl (**2**) and *p*-bromophenacyl (**3**) esters gave analytical values in accord with the $C_{16}H_{32}O_3$ formula.

The mass spectrum of methyl ester **2** was directly comparable with the mass spectrum of methyl 3-DL-hydroxyoctadecanoate observed by Ryhage and Stenhagen (4). The position of the hydroxyl group on the carbon chain is indicated by a peak at mass 103; the highest in the spectrum, this peak is due to the fragment CH_3OCCH_2CHOH obtained from cleavage of the 3,4 carbon–carbon bond. The following comparisons were also found: peaks at 194, 236 [M − 32 − 18(CH_3OH,H_2O)], and 268 [M − 18(H_2O)] for methyl ester **2**, are 28 mass numbers less than peaks 222, 264 [M − 32 − 18(CH_3OH,H_2O)], and 296 [M − 18(H_2O)] found by Ryhage and Stenhagen for methyl 3-DL-hydroxyoctadecanoate.

The mass spectrum of **2** and its direct comparison (i.r. and m.p.) with methyl 3-D-hydroxypalmitate, kindly supplied by Dr. A. P. Tulloch, established the structure of **1**.

Experimental

Melting points were determined with a Fisher–Johns apparatus and are not corrected. The infrared spectra were recorded on a Perkin–Elmer (model 137), and a Beckman (model IR8) infrared spectrophotometer. The mass spectrum was recorded on a Nuclide instrument (model 12-90 G).

Production of Crude Acid (1)

The stock culture of the yeast (NRRL Y-6954 in the ARS Culture Collection here) was maintained at 25 °C on YM agar slants (1% glucose, 0.5% peptone, 0.3% yeast extract, 0.3% malt extract, and 2% agar). A sterilized liquid medium (200 ml), consisting of 2% Cerelose and 5% malt extract contained in 500-ml Erlenmeyer flasks, was inoculated by loop with cells from 1-day-old YM slant cultures. The flasks were kept on a Gump shaker at 25 °C.

At intervals the contents of five flasks were extracted with ether. The yields of crude acid were: 2.5 days, 212

[1]Mention of firm names or trade products does not constitute endorsement by the United States Department of Agriculture over other firms or products not mentioned.

mg; 3.5 days, 326 mg; 4.5 days, 353 mg; 5.5 days, 331 mg; 6.5 days, 312 mg. The maximum at 4.5 days corresponded to a yield of 1.76 g/l.

3-D-Hydroxypalmitic Acid (1)

Crude acid (4.00 g, m.p. 70–80 °C) was crystallized from hexane (3.55 g, m.p. 78.8–79.8 °C). A small amount of yellow impurity (1%) was removed by charcoal. A second crystallization (200 mg) gave pure acid **1** (180 mg, m.p. 79.5–80.5 °C). $[\alpha]_D^{24}$ −13.6° (*c*, 1.3, $CHCl_3$); lit. (2), m.p. 78–79 °C, $[\alpha]_D^{25}$ −12.9° (*c*, 1.3, $CHCl_3$).

Anal. Calcd. for $C_{16}H_{32}O_3$: C, 70.54; H, 11.84. Found: C, 70.5; H, 11.9.

Methyl 3-D-Hydroxypalmitate (2)

Acid **1** (200 mg) was methylated with diazomethane. Crude ester (210 mg, m.p. 46.5–49 °C) was crystallized from hexane (160 mg, m.p. 49–49.8 °C) in fine needles. Infrared spectra of films deposited on KRS-5 plates showed hydroxyl absorption at 3390 cm^{-1} and 3300 cm^{-1} and carbonyl absorption at 1740 cm^{-1} and 1695 cm^{-1}.

Anal. Calcd. for $C_{17}H_{34}O_3$: C, 71.28; H, 11.96. Found: C, 70.9; H, 12.0.

p-Bromophenacyl 3-D-Hydroxypalmitate (3)

Acid **1** (100 mg) was converted to the *p*-bromophenacyl derivative in acetone (15 min at 70 °C) according to the DICE procedure (5). The crude product (167 mg, m.p. 108–109 °C) on crystallization from 95% ethanol gave 152 mg of *p*-bromophenacyl ester (111–111.5 °C).

Anal. Calcd. for $C_{24}H_{37}O_4Br$: C, 61.40; H, 7.94. Found: C, 61.5; H, 8.0.

1. F. H. Stodola, M. H. Deinema, and J. F. T. Spencer. Bacteriol. Rev. **31**, 194 (1967).
2. A. P. Tulloch and J. F. T. Spencer. Can. J. Chem. **42**, 830 (1964).
3. M. van Ammers, M. H. Deinema, C. A. Landheer, and M. H. Roogen. Rec. Trav. Chim. **83**, 708 (1964).
4. R. Ryhage and E. Stenhagen. Arkiv Kemi, **15**, 545 (1960).
5. F. H. Stodola. Microchem. J. **7**, 389 (1963).

Imidazo(1,2-*a*)indole and *s*-triazolo(2,3-*a*)indole derivatives by intramolecular cyclization of 1-(*o*-acetylphenyl)azoles[1]

Misbahul Ain Khan[2,3] and J. B. Polya
Department of Chemistry, University of Tasmania, Hobart, Tasmania 7001, Australia

and

Brian M. Lynch[3]
Organic Chemistry Laboratory, Saint Francis Xavier University, Antigonish, Nova Scotia

Received April 16, 1968

9-Hydroxy-9-methyl derivatives of the ring systems named in the title are formed along with the expected 1-(*o*-acetylphenyl)azoles in the Ullmann condensations of *o*-bromoacetophenone with imidazole and with 1,2,4-triazole. The structures of these compounds follow from their characteristic proton magnetic resonance spectra.

Canadian Journal of Chemistry, 46, 2629 (1968)

Common electrophilic substitution reactions with imidazole give 4(5)-substitution (1), although diazo coupling in alkaline media occurs at the 2-position (2). Reports of initial iodination at the 2-position are incorrect (3). These observations may be rationalized by assuming that 4(5)-substitution involves reaction of the conjugate acid, while 2-substitution involves the neutral molecule or the anion of imidazole (4). *N*-vinylimidazole undergoes 2-hydroxymethylation when heated with formaldehyde (5), and other *N*-substituted imidazoles undergo condensation with aldehydes to yield 2-(*N*-imidazolyl)-carbinols, while 4-alkylimidazoles give 4-alkyl-5-hydroxymethyl derivatives with formaldehyde (6).

In contrast, there is but one report classifiable as an electrophilic substitution in 1,2,4-triazoles; 4-phenyl-1,2,4-triazole is reported to undergo benzoylation in the 3-position by heating with benzoyl chloride (7). 1,2,3-Triazoles have been brominated (8) and nitrated (9) successfully.

This note reports some examples of intramolecular electrophilic substitution in imidazole and 1,2,4-triazole derivatives, leading to derivatives, of the imidazo(1,2-*a*)indole and *s*-triazolo-(2,3-*a*)indole ring systems.

[1]Abstracted in part from the Ph.D. Thesis of M.A.K., University of Tasmania, November 1967.
[2]Present address: Organic Chemistry Laboratory, Saint Francis Xavier University, Antigonish, Nova Scotia.
[3]Enquiries should be addressed to these authors.

Can. J. Chem. Downloaded from www.nrcresearchpress.com by 210.87.254.40 on 09/05/12
For personal use only.

mg; 3.5 days, 326 mg; 4.5 days, 353 mg; 5.5 days, 331 mg; 6.5 days, 312 mg. The maximum at 4.5 days corresponded to a yield of 1.76 g/l.

3-D-Hydroxypalmitic Acid (1)

Crude acid (4.00 g, m.p. 70–80 °C) was crystallized from hexane (3.55 g, m.p. 78.8–79.8 °C). A small amount of yellow impurity (1%) was removed by charcoal. A second crystallization (200 mg) gave pure acid **1** (180 mg, m.p. 79.5–80.5 °C). $[\alpha]_D^{24}$ −13.6° (*c*, 1.3, $CHCl_3$); lit. (2), m.p. 78–79 °C, $[\alpha]_D^{25}$ −12.9° (*c*, 1.3, $CHCl_3$).

Anal. Calcd. for $C_{16}H_{32}O_3$: C, 70.54; H, 11.84. Found: C, 70.5; H, 11.9.

Methyl 3-D-Hydroxypalmitate (2)

Acid **1** (200 mg) was methylated with diazomethane. Crude ester (210 mg, m.p. 46.5–49 °C) was crystallized from hexane (160 mg, m.p. 49–49.8 °C) in fine needles. Infrared spectra of films deposited on KRS-5 plates showed hydroxyl absorption at 3390 cm^{-1} and 3300 cm^{-1} and carbonyl absorption at 1740 cm^{-1} and 1695 cm^{-1}.

Anal. Calcd. for $C_{17}H_{34}O_3$: C, 71.28; H, 11.96. Found: C, 70.9; H, 12.0.

p-Bromophenacyl 3-D-Hydroxypalmitate (3)

Acid **1** (100 mg) was converted to the *p*-bromophenacyl derivative in acetone (15 min at 70 °C) according to the DICE procedure (5). The crude product (167 mg, m.p. 108–109 °C) on crystallization from 95% ethanol gave 152 mg of *p*-bromophenacyl ester (111–111.5 °C).

Anal. Calcd. for $C_{24}H_{37}O_4Br$: C, 61.40; H, 7.94. Found: C, 61.5; H, 8.0.

1. F. H. Stodola, M. H. Deinema, and J. F. T. Spencer. Bacteriol. Rev. **31**, 194 (1967).
2. A. P. Tulloch and J. F. T. Spencer. Can. J. Chem. **42**, 830 (1964).
3. M. van Ammers, M. H. Deinema, C. A. Landheer, and M. H. Roogen. Rec. Trav. Chim. **83**, 708 (1964).
4. R. Ryhage and E. Stenhagen. Arkiv Kemi, **15**, 545 (1960).
5. F. H. Stodola. Microchem. J. **7**, 389 (1963).

Imidazo(1,2-*a*)indole and *s*-triazolo(2,3-*a*)indole derivatives by intramolecular cyclization of 1-(*o*-acetylphenyl)azoles[1]

Misbahul Ain Khan[2,3] and J. B. Polya
Department of Chemistry, University of Tasmania, Hobart, Tasmania 7001, Australia

and

Brian M. Lynch[3]
Organic Chemistry Laboratory, Saint Francis Xavier University, Antigonish, Nova Scotia

Received April 16, 1968

9-Hydroxy-9-methyl derivatives of the ring systems named in the title are formed along with the expected 1-(*o*-acetylphenyl)azoles in the Ullmann condensations of *o*-bromoacetophenone with imidazole and with 1,2,4-triazole. The structures of these compounds follow from their characteristic proton magnetic resonance spectra.

Canadian Journal of Chemistry, 46, 2629 (1968)

Common electrophilic substitution reactions with imidazole give 4(5)-substitution (1), although diazo coupling in alkaline media occurs at the 2-position (2). Reports of initial iodination at the 2-position are incorrect (3). These observations may be rationalized by assuming that 4(5)-substitution involves reaction of the conjugate acid, while 2-substitution involves the neutral molecule or the anion of imidazole (4). *N*-vinylimidazole undergoes 2-hydroxymethylation when heated with formaldehyde (5), and other *N*-substituted imidazoles undergo condensation with aldehydes to yield 2-(*N*-imidazolyl)-carbinols, while 4-alkylimidazoles give 4-alkyl-5-hydroxymethyl derivatives with formaldehyde (6).

In contrast, there is but one report classifiable as an electrophilic substitution in 1,2,4-triazoles; 4-phenyl-1,2,4-triazole is reported to undergo benzoylation in the 3-position by heating with benzoyl chloride (7). 1,2,3-Triazoles have been brominated (8) and nitrated (9) successfully.

This note reports some examples of intramolecular electrophilic substitution in imidazole and 1,2,4-triazole derivatives, leading to derivatives, of the imidazo(1,2-*a*)indole and *s*-triazolo-(2,3-*a*)indole ring systems.

[1]Abstracted in part from the Ph.D. Thesis of M.A.K., University of Tasmania, November 1967.
[2]Present address: Organic Chemistry Laboratory, Saint Francis Xavier University, Antigonish, Nova Scotia.
[3]Enquiries should be addressed to these authors.

Can. J. Chem. Downloaded from www.nrcresearchpress.com by 210.87.254.6 on 09/05/12
For personal use only.

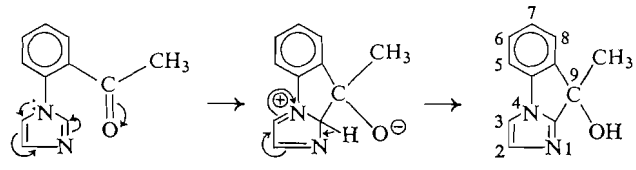

1 3

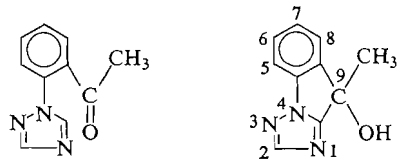

2 4

In connection with a program of synthesis of *N*-arylazoles (10), we prepared a series of 1-(*o*-acetylphenyl)diazoles and triazoles by the Ullmann condensation of the appropriate heteroaromatic compound with *o*-bromoacetophenone in pyridine solvent in the presence of copper(II) oxide and sodium carbonate. When using imidazole and 1,2,4-triazole, we isolated compounds isomeric with the expected products in addition to the azolylacetophenones **1** and **2**, and we have assigned structures **3** (9-hydroxy-9-methyl 9*H*-imidazo(1,2-*a*)indole(11)) and **4** (9-hydroxy-9-methyl-9*H*-*s*-triazolo(2,3-*a*)indole) to these compounds.

These products are formed by heating **1** and **2** under the conditions used for the Ullmann condensations, and the yield ratios **3**:**1** and **4**:**2** increase with increasing reaction times in the Ullmann reactions. The reactions almost certainly involve intramolecular electrophilic substitution, as shown for the conversion of **1** to **3**. The structures **3** and **4** are established by the following evidence: (*a*) the compounds are isomeric with the expected products **1** and **2**, yet lack any carbonyl stretching peak in the infrared spectrum, and show strong hydroxyl absorption between 3070–3160 cm^{-1}; (*b*) the proton magnetic resonance (p.m.r.) spectrum of the compound **3** in hexadeuteriodimethyl sulfoxide showed a 3-proton signal at δ 1.62 (*C*-methyl) (1-*o*-acetylphenylimidazole (**1**) showed the acetyl proton signal at δ 2.05), a broad 1-proton signal at δ 6.03 (the tertiary hydroxyl), and a 6-proton multiplet between 440 and 465 Hz (the 2-, 3-, 5-, 6-, 7-, and 8-protons). The low field signal characteristic of the 2-proton in an imidazole (cf. the 2-proton signal in 1-phenylimidazole, at δ 8.30) is absent; and (*c*) the p.m.r. spectrum of compound **4** in hexadeuteriodimethyl sulfoxide showed a 3-proton signal at δ 1.68 (C-methyl) (cf. 1-(*o*-acetylphenyl)1,2,4-triazole, acetyl protons at δ 2.20), a broad 1-proton signal at δ 6.33 (tertiary hydroxyl), a 4-proton multiplet between 435 and 462 Hz (protons 5, 6, 7, and 8 in **4**), and a 1-proton signal at δ 8.17 (proton 2 of **4**). Since the triazole ring proton signals in 1-(*o*-acetylphenyl)1,2,4-triazole fall at δ 8.20 (the 3-proton) and δ 9.00 (the 5-proton) (p.m.r. studies of various 1-aryldiazoles and -triazoles (12) confirm these assignments), it is evident that cyclization has occurred so as to occupy the position of the 5-proton of **2**.

Shirley and Alley (13) have obtained 4-oxoimidazo(1,2-*a*)indoline by dimetalation of 1-phenylimidazole followed by carbonation, so these cyclizations are not without precedent. However, these are the first examples of cyclization on to a carbon atom of a "π-electron-excessive" (14) heteroaromatic compound, and the first known examples of direct electrophilic substitution at the 5-position of 1,2,4-triazoles. Although we do not plan further work in this area, it seems likely that investigation of the thermal stability of 1-*o*-acetylphenylderivatives of other heteroaromatic compounds would be fruitful, and synthesis of fluorenol derivatives by cyclization of appropriately substituted 2-acetylbiphenyls seems promising.

Experimental

General

Analyses are by the Australian Microanalytical Service, Division of Organic Chemistry, Commonwealth Scientific and Industrial Research Organization and University of Melbourne, Parkville, Victoria, Australia.

Can. J. Chem. Downloaded from www.nrcresearchpress.com by 210.87.254.6 on 09/05/12
For personal use only.

Can. J. Chem. Downloaded from www.nrcresearchpress.com by 210.87.254.6 on 09/05/12
For personal use only.

Melting points were observed using a Gallenkamp apparatus and are uncorrected; boiling points are also uncorrected. Infrared (i.r.) spectra were recorded for the 600–3500 cm^{-1} region using a Perkin–Elmer 221 spectrophotometer. Solids were examined as mulls, and liquids as thin films. Proton magnetic resonance (p.m.r.) spectra were recorded using a Varian A-60A spectrometer fitted with a Varian V6058A Spin Decoupler, operating in the phase-lock mode. Signals are expressed in p.p.m. from tetramethylsilane, present as internal reference (for completely analyzed signals), or in Hertz (for multiplets which were not amenable to analysis). Hexadeuteriodimethyl sulfoxide was supplied by Merck, Sharp and Dohme of Canada.

Ullmann Condensations between Imidazole and o-Bromoacetophenone

(*a*) A mixture of imidazole (1.7 g), *o*-bromoacetophenone (5 g), copper(II) oxide (0.25 g), and anhydrous potassium carbonate (5 g) in pyridine (10 ml) was heated under reflux for 48 h. The reaction mixture was cooled and filtered and the residue was extracted with chloroform. Solvents were removed from the combined filtrate and extract, and the residue thus obtained was dissolved in ethanol, treated twice with charcoal, and the ethanol was removed. Crystallization of the residue from aqueous ethanol yielded 9-hydroxy-9-methyl 9*H*-imidazo(1,2-*a*)indole, 3.2 g, (65%) m.p. 182–183°.

Anal. Calcd. for $C_{11}H_{10}N_2O$: C, 71.0; H, 5.4; N, 15.1; O, 8.6. Found: C, 70.4; H, 5.5; N, 14.8; O, 9.0.

(*b*) Reaction (*a*) was repeated using a heating time of 7 h. The residue from the chloroform extract of the reaction mixture was chromatographed over alumina (Type H, Light & Co.) with benzene as eluting solvent. A small quantity of unreacted *o*-bromoacetophenone was recovered, and the eluting liquid was changed to 1:1 chloroform–benzene (v/v). Removal of solvent from the various fractions yielded 1.6 g (33%) of 1-(*o*-acetylphenyl)-imidazole as a syrupy liquid, showing ν_{CO} 1690 cm^{-1}. Found: C, 70.5; H, 5.8; N, 13.7. 1-(*o*-Acetylphenyl)imidazole formed a picrate, m.p. 185–186° (from ethanol).

Anal. Calcd. for $C_{17}H_{13}N_5O_8$: C, 49.2; H, 3.1; N, 16.9. Found: C, 49.1; H, 3.3; N, 16.6.

Further development of the chromatography column with chloroform and evaporation of the eluate yielded 2.2 g (47%), of 9-hydroxy-9-methyl 9*H*-imidazo(1,2-*a*)indole, m.p. 182–183°, identical in all respects with the product obtained in (*a*).

Thermal Cyclization of 1-(o-Acetylphenyl)imidazole

1-(*o*-Acetylphenyl)imidazole was heated for 24 h in the presence of anhydrous potassium carbonate and copper-(II) oxide in pyridine as in procedure (*a*). On working up the reaction mixture as in (*b*) above, a virtually quantitative yield of 9-hydroxy-9-methyl-9*H*-imidazo(1,2-*a*)indole, m.p. 182–183°, was obtained, identical with the product obtained in (*a*).

Ullmann Condensation Between 1,2,4-Triazole and o-Bromoacetophenone

Condensation between 1,2,4-triazole (1.73 g) and *o*-bromoacetophenone (5 g) was carried out by heating under reflux for 48 h using the general conditions described for imidazole and *o*-bromoacetophenone. The reaction mixture was cooled and filtered, and the residue was extracted with chloroform. Solvents were removed from the combined extract and filtrate and the residue thus obtained was chromatographed on alumina. Elution with benzene afforded a trace of unreacted *o*-bromoacetophenone, and elution with 1:4 chloroform–benzene (v/v), yielded 1-(*o*-acetylphenyl)1,2,4-triazole, 1.69 g (37%) m.p. 84–86°, ν_{CO} 1690 cm^{-1}. An analytical sample, m.p. 87–88°, was obtained by crystallization from chloroform–petroleum (b.p. 40–60°).

Anal. Calcd. for $C_{10}H_9N_3O$: C, 64.2; H, 4.8; N, 22.5. Found: C, 64.4; H, 4.8; N, 22.5. 1-(*o*-Acetylphenyl)1,2,4-triazole formed a picrate, m.p. 121–122° (from ethanol).

Anal. Calcd. for $C_{16}H_{12}N_6O_8$: C, 46.2; H, 2.9; N, 20.2. Found: C, 46.5; H, 3.2; N, 19.9.

Further elution with 1:1 chloroform–benzene yielded a solid, m.p. 148–151°, after removal of the eluting liquids. This material was crystallized from chloroform–petroleum (b.p. 40–60°), giving 9-hydroxy-9-methyl-9*H*-*s*-triazolo(2,3-*a*)indole, 1.07 g, (23%) m.p. 158–159°. Found: C, 63.8; H, 4.9; N, 22.7.

Acknowledgments

We wish to acknowledge the financial support given by Smith, Kline and French Laboratories (Australia) Pty. Ltd., during these investigations at the University of Tasmania, and grants in support of proton magnetic resonance facilities by the National Research Council of Canada.

1. M. Brickman, M. W. Austin, J. H. Ridd, and B. V. Smith. Chem. and Ind. London, 1057 (1962).
2. R. D. Brown, H. C. Duffin, J. C. Maynard, and J. H. Ridd. J. Chem. Soc. 3937 (1953).
3. A. Grimison and J. H. Ridd. J. Chem. Soc. 3019 (1959); M. S. R. Naidu and H. B. Bensusan. J. Org. Chem. **33**, 1307 (1968).
4. R. D. Brown. Australian J. Chem. **8**, 100 (1955).
5. British Patent No. 717,639 (1954); Chem. Abstr. **49**, 15976 (1955).
6. A. M. Roe. J. Chem. Soc. 2195 (1963); R. Grindley and F. L. Pyman. J. Chem. Soc. 3128 (1927).
7. R. Fusco, F. D'Alo, and A. Masserini. Gazz. Chim. Ital. **96**, 1084 (1966).
8. R. Huttel and A. Gebhardt. Ann. **558**, 34 (1947).
9. B. M. Lynch and T. Chan. Can. J. Chem. **41**, 274 (1963).
10. M. A. Khan. Substitution in heterocyclic nuclei. Ph.D. Thesis, University of Tasmania, November 1967; M. A. Khan and J. B. Polya. J. Chem. Soc. To be published.
11. L. T. Capell and D. F. Walker, Jr. The ring index. Suppl. I. American Chemical Society, Washington. 1963. Ring Index No. 8310.
12. W. J. Brockway, M. A. Khan, and B. M. Lynch. Can. J. Chem. To be published.
13. D. A. Shirley and P. W. Alley. J. Am. Chem. Soc. **79**, 4922 (1957).
14. A. Albert. Heterocyclic chemistry. Athlone Press (University of London). 1959. p. 133.

Hydroboration of cyclic allenes with disiamylborane

D. S. SETHI, G. C. JOSHI, AND D. DEVAPRABHAKARA
Department of Chemistry, Indian Institute of Technology, Kanpur, India

Received March 5, 1968

It has been shown that 1,2-cyclononadiene and 1,2-cyclotridecadiene undergo 78 and 100% hydroboration respectively, with disiamylborane. 1,2-Cyclononadiene gave products which represented 83% attack of boron at the central carbon atom and 17% attack at the terminal carbon atom. 1,2-Cyclotridecadiene gave 62% central carbon attack and 38% terminal carbon attack. The reactivity and selectivity may be explained mainly in terms of steric effects on a four-centered transition state.

Canadian Journal of Chemistry, 46, 2632 (1968

Can. J. Chem. Downloaded from www.nrcresearchpress.com by 210.87.254.40 on 09/05/12
For personal use only.

It has been shown that the monohydroboration of 1,2-cyclononadiene (**1**) with diborane results in the attack of diborane, primarily at the central carbon atom of the allenic linkage (1). The object of the present study was to examine the possibility of stereoselective addition of boron to the allenic linkage with disiamylborane (2), which might have revealed some useful and interesting synthetic routes. In particular we were interested to study the effect of the ring size on the reactivity and selectivity in the direction of addition. Since the monohydroboration of allenes might proceed through monoalkyl-, dialkyl-, and trialkylborane stages, the percentage of electrophilic attacks of diborane on the central and terminal carbon atoms of the allenic linkage, will be governed by the cumulative steric effect due to ring size of the allene and the intermediate organoboranes. The percentage electrophilic attacks of disiamylborane are controlled only by the steric effect of ring size of the allene. Accordingly, we undertook the hydroboration of 1,2-cyclononadiene (**1**) and 1,2-cyclotridecadiene (**2**) with disiamylborane which is known to provide greater steric control over diborane (2).

Results and Discussion

Disiamylborane was prepared by hydroboration of 2-methyl-2-butene at −5 to −10 °C under a static pressure of nitrogen (3). A solution of the appropriate allene in diglyme was added within 3 min to the above solution. This reaction mixture was left for approximately 3 h to attain room temperature. After stirring for 6 h at room temperature, the mixture was then hydrolyzed until hydrogen was no longer evolved. The product was oxidized with alkaline hydrogen peroxide in the usual manner. The percentage conversion of the allene to products was determined by gas chromatography (4). The results are summarized in Scheme 1.

The percentage electrophilic attack of boron on the central and terminal carbon atoms of the allenic linkage, as calculated from the percentage yield of the products and also the percentage conversion of the allenes to products, is shown in Table I.

These results suggest that the observed difference in the reactivity and selectivity, in the direction of addition of disiamylborane with 1,2-cyclononadiene (**1**) and 1,2-cyclotridecadiene (**2**), could be dictated solely by difference in steric requirements of the allenes in the Brown's well known postulated transition state for hydroboration (2). The electronic effect seems to be of secondary importance here, since it has been shown that monohydroboration of 1,2-cyclononadiene (**1**) with diborane, followed by oxidation, gives mainly cyclononanone (**5**) (1), while dihydroboration of propadiene yields predominantly 1,3-propanediol (5). The formation of a small quantity of cyclic monoolefins (**11**, **12**) is in complete agreement with our previous investigation (6), in which we have shown that cyclic allylic organoborane intermediates undergo slow hydrolytic cleavage at the boron–carbon bond under the experimental conditions employed. The formation of only *cis*-cyclononene (**11**) from 1,2-cyclononadiene (**1**), and a mixture of *cis*- and *trans*-cyclotridecene (**12** and **13**) containing a major quantity of *trans* isomer (**13**) from 1,2-cyclotridecadiene (**2**), may be attributed to the thermodynamic stabilities of these cyclic monoolefins (**11** and **13**) in 9- and 13-membered rings (7).

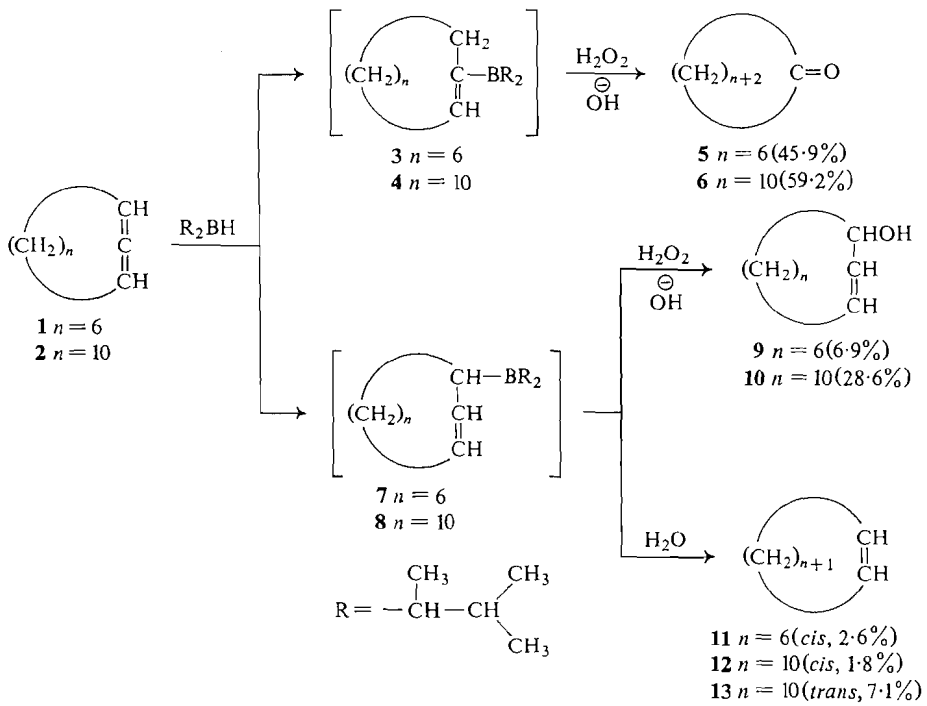

SCHEME 1

TABLE I

Percentage electrophilic attack of boron on central and terminal carbon atoms of the allenic linkage

Allene	% electrophilic attack of boron		% conversion
	Central C atom	Terminal C atom	
1,2-Cyclononadiene (**1**)	83	17	78
1,2-Cyclotridecadiene (**2**)	62	38	100

Experimental

Boiling points are uncorrected. Melting points were performed in open capillaries and are uncorrected. All infrared (i.r.) spectra were recorded on a Perkin–Elmer Infracord model 137B, as films between salt plates. Gas–liquid chromatographic (g.l.c.) analyses were made with an Aerograph model 90P instrument using 6 ft by $\frac{1}{4}$ in. columns. Nuclear magnetic resonance (n.m.r.) spectra were taken on a Varian HR-100 instrument with tetramethylsilane as the internal standard. The following liquid phases were employed (percentages by weight on 60/80 mesh chromosorb W): 15% carbowax 20M–silver nitrate; 15% ucon and 15% carbowax 20M. Samples were collected by g.l.c. for i.r. analysis. Microanalyses were carried out by Mr. A. H. Siddiqui of the Department of Chemistry, Indian Institute of Technology, Kanpur, India.

Materials

Diglyme (Ansul Co.) was first kept over calcium hydride and then distilled from lithium aluminium hydride under reduced pressure. Boron trifluoride ethyl etherate (Eastman) was treated with a small quantity of ethyl ether (to ensure an excess of this component) and distilled under reduced pressure with a few pieces of calcium hydride. Sodium borohydride from Metal Hydrides Inc. (98%) was used without purification. 2-Methyl-2-butene (Aldrich Co.) was used for the preparation of disiamylborane.

1,2-Cyclononadiene and 1,2-cyclotridecadiene were

Can. J. Chem. Downloaded from www.nrcresearchpress.com by 210.87.254.40 on 09/05/12
For personal use only.

Can. J. Chem. Downloaded from www.nrcresearchpress.com by 210.87.254.40 on 09/05/12
For personal use only.

prepared from 9,9-dibromobicyclo[6·1·0]nonane and 13,13-dibromobicyclo[10·1·0]tridecane respectively according to the procedure of Moore and Ward (8). Their properties corresponded well with those reported (8, 9).

Hydroboration of 1,2-Cyclononadiene

Pulverized sodium borohydride (3.2 g, 0.08 mole in 50 ml dry diglyme) and 2-methyl-2-butene (15.4 g, 0.22 mole) were placed in a 250 ml three-necked flask fitted with a condenser, an equilibrating dropping funnel, a thermometer, and an inlet and an outlet for nitrogen. Hydroboration was accomplished by adding boron trifluoride etherate (15.8 g, 0.11 mole) in diglyme (20 ml). The mixture was well-stirred and kept at 0 to −5 °C over a period of 0.5 h. The apparatus was flushed with nitrogen and static nitrogen pressure was maintained throughout the reaction. After allowing the mixture to stand at 0 °C for 1 h, 1,2-cyclononadiene (12.2 g, 0.10 mole) was added in 3 min. The mixture was left for approximately 3 h to attain room temperature. The mixture was then oxidized by adding 3 *N* sodium hydroxide solution, followed by 30% hydrogen peroxide. The products formed were extracted with ether. After drying over anhydrous magnesium sulfate, the samples were analyzed by g.l.c. The percentage conversion of 1,2-cyclononadiene to products as determined by g.l.c. was 78%.

Fractionation of the reaction mixture afforded *cis*-cyclononene (0.25 g, 2.6%), b.p. 60–62 °C at 16 mm, n_D^{25} 1.4748 (lit. (10), b.p. 85–86 °C at 45 mm, n_D^{27} 1.4745); cyclononanone (5 g, 45.9%), b.p. 90–91 °C at 10 mm, n_D^{25} 1.4720 (lit. (11), b.p. 94–95 °C at 13 mm, n_D^{20} 1.4729); and 3-hydroxycyclononene (0.75 g, 6.9%), b.p. 94–96 °C at 3 mm, n_D^{25} 1.4980 (lit. (12), b.p. 100 °C at 3.5 mm, n_D^{32} 1.4965). The identity of the individual products was established by comparing the g.l.c. retention times and i.r. spectra with the authentic samples.

The semicarbazone derivative of **5** had a m.p. and mixture m.p. of 184–185 °C. The m.p. and mixture m.p. of the *p*-nitrobenzoate derivative of **9** was found to be 112–114 °C.

Anal. Calcd. for C_9H_{16}: C, 87.09; H, 12.90. Found: C, 86.94; H, 12.78.

Anal. Calcd. for $C_{10}H_{19}N_3O$: C, 60.91; H, 9.64; N, 21.32. Found: C, 60.65; H, 9.71; N, 21.44.

Anal. Calcd. for $C_{16}H_{19}NO_4$: C, 66.43; H, 6.54; N, 4.84. Found: C, 66.61; H, 6.44; N, 4.94.

Hydroboration of 1,2-Cyclotridecadiene

The procedure described for 1,2-cyclononadiene was followed without any change. From 1,2-cyclotridecadiene (8.9 g, 0.05 mole), 2-methyl-2-butene (7.7 g, 0.11 mole), sodium borohydride (1.6 g, 0.04 mole), and boron trifluoride etherate (7.9 g, 0.055 mole), there was obtained a mixture of *cis*- and *trans*-cyclotridecene (0.8 g, 8.9%), b.p. 106–114 °C at 3 mm; cyclotridecanone (5.8 g, 59.2%), b.p. 116–119 °C at 3 mm, n_D^{25} 1.4828 (lit. (13), b.p. 78–83 °C at 0.4 mm, n_D^{20} 1.4822); and 3-hydroxycyclotridecene (2.8 g, 28.6%), b.p. 124–130 °C at 3 mm. The percentage conversion of 1,2-cyclotridecadiene to products as established by g.l.c. was 100%. The *cis*-cyclotridecene (20%) and *trans*-cyclotridecene (80%) were separated by g.l.c. and were identified by a comparison of their chromatographic retention times and i.r. spectra with those of authentic samples. The ketone was identified by g.l.c. and i.r. using an authentic sample for comparison, and also through its 2,4-dinitrophenylhydrazone derivative m.p. and mixture m.p. 114–115 °C (lit. (14), m.p. 113.5–114.5 °C). The g.l.c. analysis of the alcohol indicated 8% contamination of the ketone. Its 3,5-dinitrobenzoate derivative melted at 102–103 °C. The i.r. spectrum of the alcohol showed O—H band at 2.94 μ and C=C band at 6.02 μ, and the main signals in n.m.r. spectra were at $J = 4.62$ (multiplet, 2) and $J = 5.52$ (multiplet, 1).

Anal. Calcd. for $C_{13}H_{24}$: C, 86.67; H, 13.33. Found: C, 86.72; H, 13.14.

Anal. Calcd. for $C_{19}H_{28}N_4O_4$: C, 60.64; H, 7.44; N, 14.89. Found: C, 60.80; H, 7.60; N, 14.91.

Anal. Calcd. for $C_{20}H_{26}N_2O_6$: C, 61.54; H, 6.67; N, 7.18. Found: C, 61.46; H, 6.71; N, 7.03.

Acknowledgment

We thank the Council of Scientific and Industrial Research, New Delhi, India, for financial support of this work.

1. D. Devaprabhakara and P. D. Gardner. J. Am. Chem. Soc. **85**, 1458 (1963).
2. H. C. Brown. Hydroboration. W. A. Benjamin, Inc., New York. 1962.
3. H. C. Brown and G. Zweifel. J. Am. Chem. Soc. **82**, 3222 (1960).
4. S. D. Nogare and R. S. Juvet, Jr. Gas–liquid chromatography—theory and practice. John Wiley and Sons, Inc., New York. 1962. p. 259.
5. S. Corsano. Atti Accad. Naz. Lincei, Rend. Classe Sci. Fis. Mat. Nat. **34** (4), 430 (1963); Chem. Abstr. **60**, 3993 (1964).
6. D. S. Sethi and D. Devaprabhakara. Can. J. Chem. **46** 1165 (1968).
7. A. C. Cope, P. T. Moore, and W. R. Moore. J. Am. Chem. Soc. **81**, 3153 (1959).
8. W. R. Moore and H. R. Ward. J. Org. Chem. **27**, 4179 (1962).
9. H. Nozaki, T. Aratani, and R. Noyori. Tetrahedron, **23**, 3645 (1967).
10. P. D. Gardner and M. Narayana. J. Org. Chem. **26**, 3518 (1961).
11. L. Ruzicka, P. A. Pattner, and H. Wild. Helv. Chim. Acta, **26**, 1631 (1943).
12. R. K. Sharma, B. A. Shoulders, and P. D. Gardner. J. Org. Chem. **32**, 241 (1967).
13. W. Kirchhof, W. Stumpf, and W. Franke. Ann. Chem. **681**, 32 (1965).
14. L. I. Zakharkin, L. P. Vinogradova, V. V. Korneva, and S. I. Zav'yalov. Izv. Akad. Nauk SSSR, Otd. Khim. Nauk, 1309 (1962); Chem. Abstr. **58**, 7824 (1963).

Structure of hetisinone

R. T. APLIN,[1] M. H. BENN, S. W. PELLETIER,[2] J. SOLO,[3] S. A. TELANG AND H. WRIGHT[2]
Department of Chemistry, The University, Calgary, Alberta

Received March 26, 1968

The tentative structure proposed previously for a dehydrohetisine isolated from *Delphinium cardinale* Hook. has been confirmed. This alkaloid is identical with hetisinone, first obtained as a transformation product of hetisine, and subsequently isolated from *D. denudatum*.

Canadian Journal of Chemistry, 46, 2635 (1968)

Can. J. Chem. Downloaded from www.nrcresearchpress.com by 210.87.254.5 on 09/05/12
For personal use only.

Some years ago it was reported (1) that acetylation of the trihydroxy diterpenoid alkaloid hetisine (**1**, R=H) (2) gave a diacetate, which upon oxidation and saponification yielded a dehydrohetisine, named hetisinone. It was deduced that the keto function was located in ring A, hetisinone may therefore be formulated as **2**.

More recently (3), an alkaloid was isolated from *Delphinium cardinale* Hook. which also proved to be a dehydrohetisine and which was tentatively assigned the same structure as hetisinone, mainly on the basis of the failure to observe the "anomalous" ultraviolet and infrared spectral features that would have been anticipated, had the alkaloid possessed either of the alternative structures (**3**) or (**4**).[4]

We have now compared the semisynthetic and natural products and find them to be indeed identical;[5] we retain the name hetisinone for the alkaloid.

We can also now report new evidence which confirms the structure **2** for hetisinone.

Dehydration of hetisine diacetate with phosphorus oxychloride and pyridine, followed by saponification, gave a crystalline mixture of olefins, m.p. 225–227°, in excellent yield. Analysis of the proton magnetic resonance (p.m.r.) spectrum of the olefin obtained in highest purity revealed signals due to two vinylic protons at τ 4.39 (doublet, $J = 4$ c.p.s.) and τ 4.55 (multiplet), in addition to those of the exocyclic methylene function, τ 5.11 and τ 5.30. Moreover the signal for the quaternary methyl group was shifted, from τ 9.08 in hetisine, to τ 8.94.

Of the various dehydration products that may be envisaged only those represented by structures **5** or **6** accommodate these observations. Hence

[1]Dyson Perrins Laboratory, South Parks Road, Oxford, England.
[2]Department of Chemistry, University of Georgia, Athens, Georgia, U.S.A.
[3]School of Pharmacy, State University of New York at Buffalo, Buffalo, New York, U.S.A.
[4]Subsequently hetisinone was isolated from *D. denudatum* (ref. 4, footnote 7*b*).
[5]The infrared spectra (KBr) of the two alkaloids were superimposable, and the mixture m.p. was undepressed.

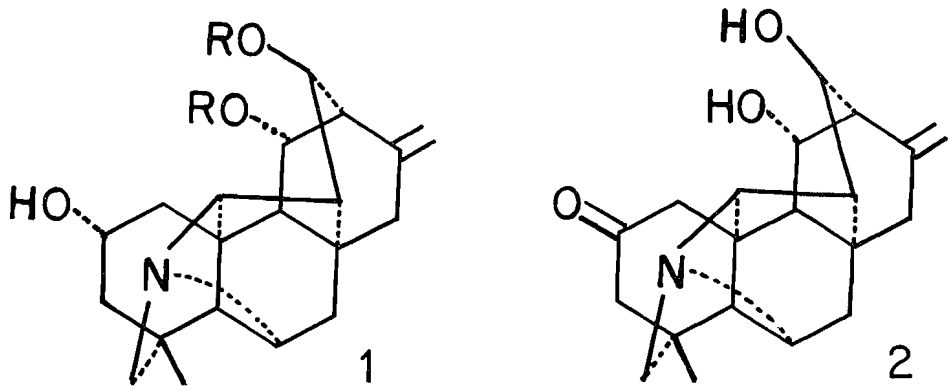

FIG. 1.

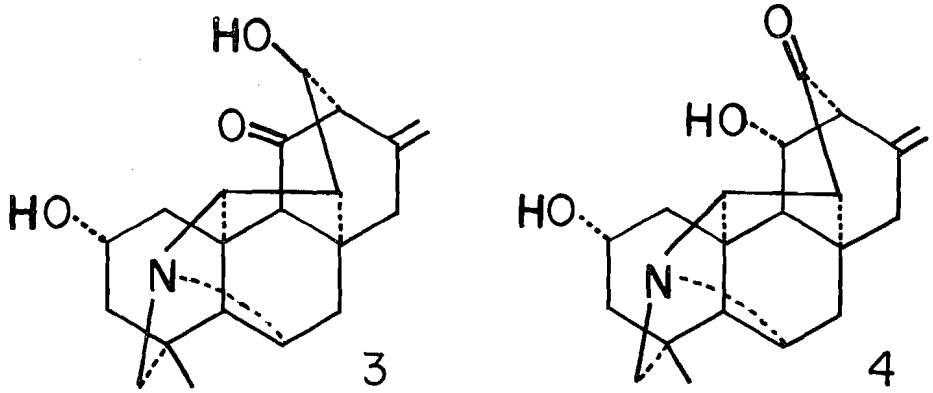

FIG. 2.

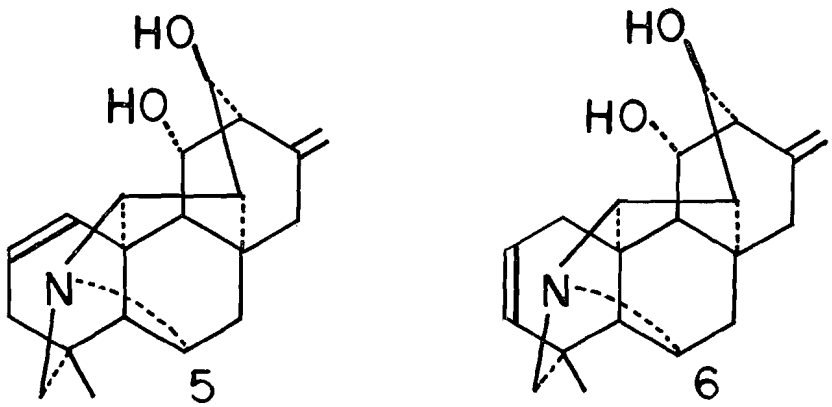

FIG. 3.

hetisine diacetate is **1** (R = Ac), and hetisinone is **2**.

Further, hetisinone is stable to bases, behavior that is consistent with structure **2**, but much less likely for either of the alternative β-ketoalcohols (**3**) or (**4**). When heated in deuterium oxide – methanol-O-*d*, containing sodium deuteroxide (5), at 80°, for 4 h, followed by reexchanging OD for OH, hetisinone gave a mixture of deuterated hetisinones which contained, by mass spectroscopic analysis,[6] 14% *d*-, 53% d_2-, 24% d_3-, and 6% d_4-species. These results also confirm[7] that hetisinone is correctly represented as **2**, not **3** or **4**.

1. S. W. PELLETIER. Tetrahedron, **14**, 76 (1961).
2. M. PRZYBYLSKA. Can. J. Chem. **40**, 566 (1962); Acta Cryst. **16**, 871 (1962).
3. M. H. BENN. Can. J. Chem. **44**, 1 (1966).
4. S. W. PELLETIER, L. H. KIETH, and P. C. PARTHASARATHY. J. Am. Chem. Soc. **89**, 4146 (1967).
5. D. H. WILLIAMS, J. M. WILSON, H. BUDZIKEWICZ, and C. DJERASSI. J. Am. Chem. Soc. **85**, 2091 (1963).

[6]These figures are corrected for M + 1 contributions. A similar distribution of deuterated species was obtained in a second experiment which was allowed to run for 48 h.

[7]Under the conditions used to effect the exchange, only **2** should incorporate up to 4 atoms of deuterium. The behavior of **3** and **4** is more hypothetical, direct exchange should result in the incorporation of only 1 atom of deuterium in **3** and no atoms of deuterium in **4**. However higher figures might result if retro-aldol ring-opening followed by exchange, and subsequent aldol recyclization were to occur.

Can. J. Chem. Downloaded from www.nrcresearchpress.com by 210.87.254.5 on 09/05/12
For personal use only.

Can. J. Chem. Downloaded from www.nrcresearchpress.com by 210.87.254.42 on 09/05/12
For personal use only.

Canadian Journal of Chemistry

Published by THE NATIONAL RESEARCH COUNCIL OF CANADA

VOLUME 46 AUGUST 15, 1968 NUMBER 16

The gold/selenium system and some gold seleno-tellurides

G. E. CRANTON[1] AND R. D. HEYDING

Department of Chemistry, Queen's University, Kingston, Ontario

Received February 13, 1968

The phase relationships in the gold/selenium system have been examined using X-ray powder diffraction techniques and differential thermal analysis. Only one stable phase, α-AuSe, is formed. A metastable modification of this compound, β-AuSe, is also formed by reaction of the elements. Both forms are monoclinic:

α-AuSe: space group *C*2, *Cm*, or *C*2/*m*; $a = 12.21 \pm 2$, $b = 3.693 \pm 4$, $c = 8.434 \pm 6$ Å, $\beta = 103.20 \pm 3°$; cell content, 8(AuSe).

β-AuSe: primitive monoclinic (space groups $P2_1$ or $P2_1/m$ are likely); $a = 6.27 \pm 1$, $b = 3.668 \pm 4$, $c = 8.35 \pm 1$ Å, $\beta = 105.95 \pm 13°$; cell content, 4(AuSe).

Both modifications decompose peritectoidally at ca. 400 °C. Gold and selenium form a monotectic at 754 °C at a composition just above 50 at. % selenium; some evidence was obtained for the presence of two liquid phases above the monotectic.

Tellurium does not substitute in the AuSe lattice to a detectable extent. However, a ternary phase which includes the composition Au_2SeTe is formed. Au_2SeTe is primitive orthorhombic with $a = 8.924 \pm 6$, $b = 7.56 \pm 1$, $c = 5.741 \pm 8$ Å. The cell contains 4 formula units. Selenium will substitute for at least 15 at. % of the tellurium atoms in the monoclinic $AuTe_2$ calaverite lattice at ca. 400 °C.

Canadian Journal of Chemistry, 46, 2637 (1968)

Introduction

While the phase relationships in the gold/tellurium system are well established (1), no systematic studies of the gold/selenium or gold/sulfur systems at temperatures below 1000 °C have been reported. Mellor (2) and Sneed *et al.* (3) report the precipitation of Au_2Se and Au_2Se_3 when hydrogen selenide is passed through potassium aurous or auric salt solutions. Friedrich (4) and Pélabon (5) attempted to add selenium to molten gold, but no compounds were observed. Recently, Vogel and Gerhardt determined the phase relationships in the gold/sulfur and gold/selenium systems above 1000 °C (6).

We have examined alloys containing 20–100 at. % selenium from room temperature to ca. 900 °C via differential thermal analysis (d.t.a.), room and high temperature X-ray powder diffraction patterns, and, to a limited extent, microscopy. A reduced phase diagram has been obtained, and crystal symmetries and cell dimensions of the intermediate phases have been determined.

Experimental

Samples were prepared by reaction of gold (A. D. MacKay, 59) and selenium and/or tellurium (Asarco, 69) in sealed, evacuated Vycor tubes. Following the initial reaction, samples were annealed at 240–800 °C for various periods of time with intermittent quenching and grinding. Quenching was accomplished either in air or in ice/water mixtures. Some samples were cooled in the annealing furnace.

One gram samples for d.t.a. were sealed *in vacuo* in Vycor tubes with reentrant thermocouple wells. Nickel sponge was used as the standard. Manually controlled heating rates were ca. 3 deg min^{-1}, and free cooling rates were ca. 5 deg min^{-1}. The apparatus was calibrated with respect to temperature at the melting points of high purity elements.

Powder diffraction patterns at room temperature were obtained in 11.46 cm Debye–Scherrer cameras. High temperature patterns were obtained in a 19 cm Unicam camera. The camera was calibrated with respect to temperature using gold and silver specimens. Guinier–de Wolff focusing camera patterns of the intermediate phases were obtained. Nickel-filtered copper radiation

[1]Present address: Department of Chemistry, York University, Toronto 12, Ontario.

($\lambda_{K\alpha_1}$ = 1.54050 Å) was used throughout. Densities were determined by a helium displacement method (7).

Several samples were annealed above 760 °C in evacuated quartz tubes in which the void volume was reduced with close-fitting quartz rods. Fragments of the product recovered on rapid quenching were polished for microscopic examination.

Results and Discussion

The Au/Se Phase Diagram

Two intermediate phases, both with 1:1 stoichiometry, were observed in the room temperature diffraction patterns of quenched specimens. The relative proportions of the two phases were not primarily a function of composition but did depend on the thermal history of the specimen during the initial reaction period. For example, the α-phase was the predominant product obtained when Au/Se mixtures were placed in a furnace at room temperature and heated slowly to 340 °C, while the β-phase predominated when elemental mixtures in the same atomic ratios were placed in a furnace preheated to 340 °C. Although the relative proportions of the two phases depended on the procedure and the reaction temperature, the results of the initial reaction were not entirely predictable. In general, lower temperatures favored the formation of the α-phase. In any group of samples of identical thermal histories, the β-phase appeared to be favored in gold-rich mixtures, and the α-phase in selenium-rich mixtures.

Once the original mixture had been allowed to react to form the intermediate phases, annealing for any length of time at temperatures below 370 °C had no effect on the relative proportions of the phases already present. Above 370 °C, however, the β-phase transformed slowly to the α-phase. In specimens containing less than 40 at. % Se or more than 60 at. % Se, this transformation was essentially complete after annealing at 370 °C for 1 month with weekly quenching and grinding. In samples containing 40 to 60 at. % Se the transformation was more sluggish. One specimen, of 1:1 stoichiometry, transformed to essentially pure α-phase only after 3 months annealing at 370–383 °C, although traces of the strongest reflections of the β-phase could still be detected in grossly overexposed diffraction patterns. In none of these studies was there any indication that this transformation is reversible.

Both phases were found to decompose on annealing above 385 °C to gold and a liquid phase.

Several specimens containing a range of proportions of α-AuSe and β-AuSe were examined in the high temperature diffraction camera from room temperature to ca. 450 °C. The decomposition of the intermediate phases with the formation of gold and a liquid occurred at 400–420 °C in the camera, i.e. 10–30° above the decomposition temperature observed in annealing studies. At 20° below the decomposition temperature, the slow transformation of β-AuSe to α-AuSe was observed; at still lower temperatures no change in the diffraction pattern with time could be detected.

The results of the annealing and high temperature diffraction studies can be rationalized by assuming that β-AuSe is a metastable modification which may form at any temperature at which the reaction between the elements occurs at an observable rate. Depending on the initial reaction conditions, either modification can be formed in excess. The instability of β-AuSe relative to α-AuSe is apparent only at temperatures just below the decomposition point.

Metastable phases are well known in the gold/tellurium system. While only one compound, $AuTe_2$, corresponding to the mineral calaverite, appears in the equilibrium phase diagram, minerals of composition $AuTe_2$ (krennerite) and Au_2Te_3 (montbrayite) are known (1, 8, 9). Luo and Clement (10) have prepared metastable cubic gold tellurides by rapid quenching techniques, and Howie and Veale (11) have synthesized a cubic gold telluride by precipitation from solution. Howie and Veale have suggested that Au_2Te_3 is an ordered modification of the cubic phase. There is no similarity in the powder patterns of α- and β-AuSe to suggest such an order–disorder relationship between the gold selenides.

The reduced phase diagram is shown in Fig. 1. The points indicate temperatures at which heat effects were observed during thermal analysis. All transformations observed during heating cycles were endothermic, and during cooling cycles all were exothermic. The peritectoid decomposition of AuSe (the d.t.a. points are for samples containing both α- and β-AuSe) occurred over a broad temperature range (20–

Can. J. Chem. Downloaded from www.nrcresearchpress.com by 210.87.254.42 on 09/05/12
For personal use only.

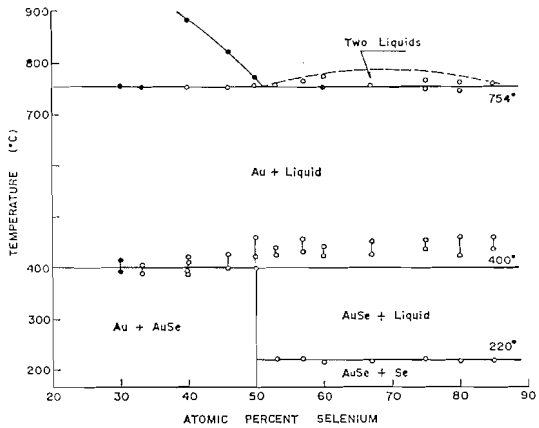

FIG. 1. Reduced phase diagram for the Au/Se system to 900 °C. Open circles, d.t.a. signal on heating cycle; closed circles, cooling cycle. Cooling cycle signals at 754 °C omitted for clarity. The dashed line indicates uncertainty.

40 °C) in these experiments. Points are shown in the diagram for the beginning and the midpoint of the broad, shallow d.t.a. peaks.

The decomposition temperature is shown as 400 °C. Gold-rich specimens decomposed during d.t.a. at 385–390 °C, and selenium-rich at 410–450 °C, regardless of the initial proportions of α- and β-AuSe in the samples. This difference is attributed to the nature of the thermal analysis, since no evidence was found for a range of stoichiometry in either modification of AuSe. During d.t.a. the decomposition reaction was irreversible.

The monotectic reaction at 754 °C was observed during heating and cooling cycles. The signals corresponding to the liquidus/solidus transformation in specimens containing less than 50 at. % Se were observed on cooling cycles only. The small signal above the monotectic observed in specimens containing more than 50 at. % Se was obtained on heating cycles only. Examination of polished sections of specimens quenched from this region of the system support the supposition that a narrow two-liquid-phase region exists. Two phase liquid regions in this composition range appear to be a feature of nearly all Group IB/VIA binary systems.

One sample containing more than 85 at. % Se was examined by d.t.a. This sample, containing 98.3 % Se, showed only the melting of Se at 220 °C and a base-line drift above 620 °C.

X-ray Diffraction Studies

The lattice parameters of gold in alloys containing 33–44 at. % Se are recorded in Table I. Apparently selenium does not dissolve in gold to an appreciable extent below 800 °C. The solubility limit at 1020 °C is 12.05 at. % Se (6).

The symmetry and unit cell dimensions of both α- and β-AuSe were determined from focusing camera data. The cell dimensions and densities are recorded in Table II. Indexed focusing camera patterns with microphotometer intensity data have been submitted to the Depository of Unpublished Data.[2]

TABLE I

Lattice dimensions of gold in the presence of selenium

Temperature of quench (°C)	Composition (at. % Se)	Lattice dimension (Å)
403	0	4.0806±5
370	40.0	4.0786±5
484	43.5	4.0788±5
786	33.3	4.0788±10
—	0	4.0786*

*See ref. 8.

Both modifications are monoclinic. In the pattern of α-AuSe the sum of h and k is even for all observed reflections, indicating an end-centered lattice. The presence of ($h0l$) reflections with l odd excludes space groups Cc and $C2/c$. The remaining possibilities are $C2$, Cm, or $C2/m$. For the primitive lattice of β-AuSe, only the space groups Pc, $P2/c$, and $P2_1/c$ can be excluded. Of the three ($0k0$) reflections within the range of the focusing camera, only the (020) is observed, and it overlaps the (301) reflection. Nevertheless, the absence of the (010) reflection may indicate that the space groups $P2_1$ and $P2_1/m$ are to be preferred.

The unit cells of the two modifications are related superficially in that $a_\alpha \simeq 2a_\beta$, $b_\alpha \simeq b_\beta$, $c_\alpha \simeq c_\beta$, and $\beta_\alpha \simeq \beta_\beta$. The molar volumes of the α- and β-forms are 46.3 and 46.2 Å^3 respectively. However, there is so little similarity in the diffraction patterns that an order–disorder relationship is very improbable. It is more likely that the two crystals contain the same structural units arranged in slightly different manners.

[2]Photocopies may be obtained free of charge upon request to: The Depository of Unpublished Data, National Science Library, National Research Council of Canada, Ottawa, Canada.

Can. J. Chem. Downloaded from www.nrcresearchpress.com by 210.87.254.42 on 09/05/12
For personal use only.

TABLE II

Crystallographic data for α- and β-AuSe, Au_2SeTe, and $AuSe_xTe_{2-x}$

Phase	Symmetry	Cell dimensions (Å)			D_x	D_m	M
		a	b	c			
α-AuSe	Monoclinic $C2$, Cm, or $C2/m$	12.21±2	3.693±4 (β=103.20±3°)	8.434±6	9.91	10.0	8
β-AuSe	Monoclinic ($P2_1$ or $P2_1/m$) (?)	6.27±1	3.668±4 (β=105.95±13°)	8.35±1	9.91	10.3	4
Au_2SeTe	Orthorhombic (primitive)	8.924±6	7.56±1	5.741±8	10.3	10.3	4
$AuTe_2$	Pseudo-orthorhombic	7.19±1	4.408±4	5.068±5	9.35	9.33	2
$AuSe_{0.1}Te_{1.9}$	,,	7.18±1	4.394±4	5.057±5	9.31	9.29	2
$AuSe_{0.2}Te_{1.8}$	,,	7.17±1	4.389±4	5.025±5	9.29	9.25	2
$AuSe_{0.3}Te_{1.7}$	,,	7.17±1	4.385±4	5.014±5	9.22	9.18	2

These structures are not isomorphous with any 1:1 compounds reported in the literature. A search for phases of slightly different atomic ratios which might be related to the gold selenides by filling of vacancies was not successful. It is not surprising that gold selenide does not form structures in keeping with general patterns in transition metal chalicides. Gold ditelluride forms structures unknown in any other binary system. In fact, the generalization to be made is that copper family chalicides and dichalicides form unique atomic arrangements to such an extent that the appearance of a common structure (e.g. the C18 structure for $CuSe_2$ (12)) is exceptional.

Substitution of Se by Te in AuSe, and Te by Se in $AuTe_2$

Tellurium will not replace selenium in either AuSe lattice to any significant extent. In attempting to effect this substitution, a new phase was obtained in a series of $AuTe_xSe_{1-x}$ samples. The range of stability of this phase was not determined, but at the composition Au_2SeTe the lattice is primitive orthorhombic with the cell dimensions recorded in Table II. Focusing camera powder diffraction data have been submitted to the Depository of Unpublished Data.[2] Au_2SeTe melts at 471 °C.

In a series of $AuSe_xTe_{2-x}$ samples annealed and quenched from 400–425 °C, substitution of Se for Te in the monoclinic (pseudo-orthorhombic) calaverite lattice was observed for $0 < x \leq 0.30$. In the interval $0.30 \leq x \leq 0.35$ a second phase appeared. The lattice parameters of the substituted calaverite structures given in Table II were obtained from relatively poor Debye–Scherrer patterns using As_2O_3 as an internal standard. If there is any variation of the monoclinic β-angle from 90° with composition, it is within ±0.5°. The melting points of $AuSe_{0.1}Te_{1.9}$, $AuSe_{0.2}Te_{1.8}$, and $AuSe_{0.3}Te_{1.7}$ are 450, 440, and 434 °C respectively. $AuTe_2$ melts at 464 °C (1).

Acknowledgments

We are indebted to Dr. L. D. Calvert of the National Research Council of Canada for the focusing camera patterns used in this study. Awards of Province of Ontario Graduate Fellowships and of Studentships by the National Research Council of Canada to G. E. Cranton are gratefully acknowledged. This study was supported by operating grants from the National Research Council of Canada.

1. M. Hansen and K. Anderko. Constitution of binary alloys. 2nd ed. McGraw-Hill Book Co., Inc., New York. 1958.
2. J. W. Mellor. A comprehensive treatise on inorganic and theoretical chemistry. Vol. X. Longmans, Green and Co., Ltd., London. 1930.
3. M. C. Sneed, J. L. Maynard, and R. C. Brasted. Comprehensive inorganic chemistry. Vol. 2. D. Van Nostrand Co., Inc., New York. 1954.
4. K. Friedrich. Metallurgie Paris, **5**, 593 (1908).
5. H. Pélabon. Ann. Chim. Phys. **17**, 566 (1909).
6. R. Vogel and R. Gerhardt. Z. Metallk. **52**, 318 (1961).
7. W. C. Schumb and E. S. Rittner. J. Am. Chem. Soc. **65**, 1692 (1943).
8. W. B. Pearson. A handbook of lattice spacings and structures of metals and alloys. The Pergamon Press, Ltd., Oxford. 1958.
9. M. A. Peacock and R. M. Thompson. Am. Mineralogist, **31**, 515 (1946).
10. H. Luo and W. Clement, Jr. J. Chem. Phys. **36**, 1870 (1962).
11. F. H. Howie and C. R. Veale. J. Inorg. Nucl. Chem. **28**, 1149 (1966).
12. G. Gattow. Z. Anorg. Allgem. Chem. **340**, 312 (1965).

Can. J. Chem. Downloaded from www.nrcresearchpress.com by 210.87.254.42 on 09/05/12
For personal use only.

Can. J. Chem. Downloaded from www.nrcresearchpress.com by 210.87.254.105 on 09/05/12
For personal use only.

Détermination des constantes de force et des amplitudes moyennes de vibration du sous-sulfure de carbone, C_3S_2

ALPHA O. DIALLO
Laboratoire d'Infrarouge, Chimie Physique, Faculté des Sciences de Paris, (91) Orsay, France

Reçu le 5 février 1968

La théorie généralisée des carrés moyens des amplitudes de vibration a été appliquée à la molécule de C_3S_2 qui possède une structure linéaire et symétrique. Les valeurs numériques des constantes de force et des carrés moyens des amplitudes parallèles et perpendiculaires, à 298 °K, pour toutes les paires d'atomes directement liés ou non ont été calculées par les méthodes de Cyvin et de Morino–Hirota. Les constantes des effets de contraction ont été déterminées au moyen des carrés moyens des amplitudes perpendiculaires.

The theory of the generalized mean amplitudes of vibration has been applied to the C_3S_2 molecule, which possesses a linear symmetrical structure. The numerical values of the force constants and the mean square parallel and perpendicular amplitudes at 298 °K of all bonded and non-bonded pairs of atoms are calculated from spectroscopic vibrational frequencies by the Cyvin and Morino–Hirota methods, utilizing the symmetry coordinates. The "shrinkage" effect constants are also evaluated by means of the perpendicular mean square amplitudes.

Canadian Journal of Chemistry, 46, 2641 (1968)

Introduction

Le sous-sulfure de carbone appartient à une série de molécules dont l'étude par les méthodes physiques a souvent révélé des anomalies de structure. Il a été observé récemment que les spectres d'absorption infrarouge de C_3O_2 (1, 2) et de C_3S_2 (3, 4), obtenus sous une résolution moyenne, sont caractérisés par la coexistence de deux types de bandes dont les unes présentent une structure fine caractéristique, cependant que les autres possèdent des formes extrêmement complexes. Le phénomène est lié à l'existence de nombreuses vibrations de basse énergie (2). Dans un cas comme dans l'autre, la fréquence fondamentale ν_7 étant très basse, les niveaux $n\nu_7$ sont suffisamment peuplés pour être associés à tous les niveaux vibrationnels permis par la symétrie moléculaire $D_{\infty h}$. Des bandes de combinaison et de différence dues au couplage entre les vibrations $n\nu_7$ et les vibrations actives en Raman apparaissent alors dans les domaines spectraux correspondant à ces dernières. Ces bandes présentent une structure fine. Par contre, les bandes issues des transitions normalement permises en absorption infrarouge qui sont perturbées par la présence de nombreuses bandes chaudes montrent en général une grande complexité.

D'autre part, les études de la diffraction électronique des molécules telles que l'allène, le butatriène, le diacétylène et le sous-oxyde de carbone font apparaître des effets de contraction qui sont interprétés en faisant intervenir les phénomènes des vibrations moléculaires (5).

De tels résultats suggèrent naturellement l'application de la théorie généralisée des amplitudes moyennes de vibration à C_3S_2. Aussi, les carrés moyens des amplitudes parallèles et perpendiculaires, ainsi que les constantes des effets de contraction ont-ils été calculés pour cette molécule à partir des fréquences fondamentales de vibration, à la température de 298 °K. De plus, la matrice des carrés moyens des amplitudes a été utilisée pour déterminer les constantes de force.

Méthode

Le modèle moléculaire considéré appartient au groupe de symétrie $D_{\infty h}$. La Fig. 1 illustre l'orientation des axes de coordonnées cartésiennes, le système de coordonnées internes, ainsi que le numérotage des atomes. R et r représentent les variations des longueurs des liaisons S—C et C—C le long de l'axe principal Z. β et η définissent les déformations angulaires des liaisons S—C—C et C—C—C dans les plans YZ et ZX.

Ainsi définie, la molécule possède sept modes de vibrations distinctes classées suivant les types de symétrie:

$$2\Sigma_g^+ + 2\Sigma_u^+ + \pi_g + 2\pi_u.$$

Les carrés moyens des amplitudes de vibration

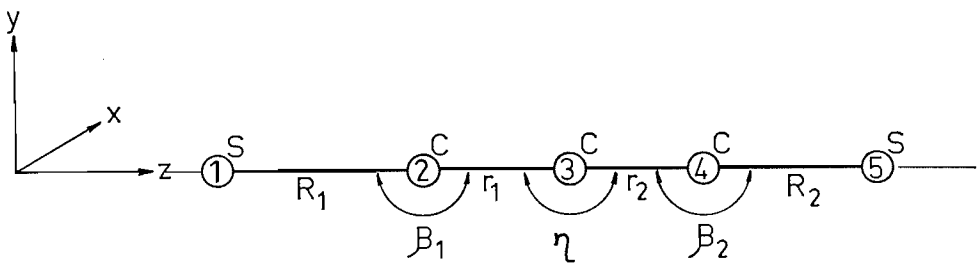

FIG. 1. Coordonnées cartésiennes de déplacement, coordinnées internes et numérotage des atomes dans la molécule de C_3S_2.

s'expriment en fonction des coordonnées cartésiennes de déplacement pour chaque paire d'atomes *i–j*. L'équation matricielle

$$[1] \qquad \zeta = AS$$

où

$$A = \mu\tilde{B}\tilde{U}G^{-1}U,$$

qui relie les coordonnées cartésiennes ζ aux coordonnées symétriques S, permet de calculer les carrés moyens des amplitudes, soit à partir des éléments Σ_{ij} d'une matrice Σ selon l'équation de Cyvin (6), soit par la méthode de Morino et Hirota (7). (Les différents symboles ont leur signification habituelle dans les notations de Wilson.) Les matrices correspondantes ont été déterminées comme dans le cas de la molécule analogue de C_3O_2 décrite ailleurs (2).

Les éléments des matrices des carrés moyens des amplitudes Σ et des constantes de force F ont été calculés par la méthode proposée par Cyvin (8) à partir des équations séculaires:

$$[2] \qquad |\Sigma G^{-1} - \Delta E| = 0$$

$$[3] \qquad |\Sigma F - \lambda\Delta E| = 0,$$

où

$$\Delta_k = \left(\frac{h}{8\pi^2 c\nu_k}\right)\coth\left(\frac{hc\nu_k}{2kT}\right)$$

$$(\lambda\Delta)_k = \tfrac{1}{2}hc\nu_k \coth\left(\frac{hc\nu_k}{2kT}\right).$$

Dans le cas des vibrations d'élongation, les carrés moyens des amplitudes parallèles définis par

$$\sigma_{ij} = \langle(\Delta z)_{ij}{}^2\rangle$$

s'expriment simplement en fonction des éléments Σ_{ij}. On obtient alors:

$$\sigma_R = \tfrac{1}{2}(\Sigma_{11} + \Sigma_{33})$$

$$\sigma_r = \tfrac{1}{2}(\Sigma_{22} + \Sigma_{44})$$

$$\sigma_{R+r} = \sigma_R + \sigma_r + \sigma_{12} + \sigma_{34}$$

$$\sigma_{2r} = 2\Sigma_{22}$$

$$\sigma_{R+2r} = \sigma_R + 2(\Sigma_{22} + \Sigma_{12})$$

$$\sigma_{2(R+r)} = 2(\Sigma_{11} + \Sigma_{22} + 2\Sigma_{12}).$$

TABLEAU I

Fréquences fondamentales et constantes de force de la molécule de C_3S_2

Fréquences observées (cm^{-1})	Type de symétrie	Valeurs des constantes de force (mdyn/Å)	
1683	Σ_g^+	f_R	7.7696
485		f_{Rr_1}	0.3627
2088.5	Σ_u^+	$f_{R_1R_2}=f_{R_1r_2}$	0
1029.8		f_r	10.238
		f_{rr}	1.0549
470	π_g	$f\beta$	0.3209
502		$f\beta\beta$	−0.0390
	π_u		
94		$f\eta$	0.0778
		$f\beta\eta$	0.0267

TABLEAU II

Eléments des matrices Σ et L de la molécule de C_3S_2

Valeurs des éléments Σ_{ij} (Å²)		Valeurs des éléments L_{ij} (u.m.a.)$^{-1/2}$	
Σ_{11}	0.001437	L_{11}	0.3249
Σ_{12}	−0.0006035	L_{12}	0.0949
Σ_{22}	0.0010377	L_{21}	−0.2786
Σ_{33}	0.0015015	L_{22}	0.0759
Σ_{34}	−0.0004775	L_{33}	0.2165
Σ_{44}	0.0020827	L_{34}	0.2602
Σ_{55}	0.0160073	L_{43}	−0.4920
Σ_{66}	0.057785	L_{44}	0.0885
Σ_{67}	−0.015147	L_{55}	0.6017
Σ_{77}	0.023225	L_{66}	0.6707
		L_{67}	0.2239
		L_{76}	−0.7502
		L_{77}	0.02843

Can. J. Chem. Downloaded from www.nrcresearchpress.com by 210.87.254.105 on 09/05/12
For personal use only.

TABLEAU III

Carrés moyens des amplitudes et constantes des effets de contraction dans la molécule de C_3S_2

Liaison	Distance (Å)	Carrés moyens des amplitudes parallèles (Å²)	Carrés moyens des amplitudes perpendiculaires (Å²)	Constantes des effets de contraction (Å)
S_1—C_2	1.56	0.001469	0.011007	—
C_2—C_3	1.28	0.0015602	0.012820	—
S_1...C_3	2.84	0.001948	0.024756	0.008354
C_2...C_4	2.56	0.0020754	0.006840	0.017359
S_1...C_4	4.12	0.002337	0.009433	0.024796
S...S	5.68	0.002534	0.0001955	0.034116

Les carrés moyens des amplitudes perpendiculaires définis par

$$\tau_{ij} = \langle(\Delta x)_{ij}^2\rangle = \langle(\Delta y)_{ij}^2\rangle$$

ont été obtenus en utilisant la méthode de Morino et Hirota (7).

Enfin, les constantes des effets de contraction ou effets de Bastiansen et Morino (5) ont été calculées à partir des carrés moyens des amplitudes perpendiculaires de vibration et des distances interatomiques selon le procédé de Morino et collaborateurs (9).

Résultats

Les distances interatomiques dans la position de l'équilibre de la molécule, obtenues par spectrométrie infrarouge et vérifiées empiriquement à partir de molécules analogues sont (4), C—S = 1.56 Å et C—C = 1.28 Å.

Les valeurs des fréquences fondamentales utilisées dans les calculs sont celles mesurées par Smith et Leroi (3) et par l'auteur (4). Elles sont indiquées dans le Tableau I, ainsi que les valeurs des constantes de force.

Le Tableau II donne les éléments des matrices Σ et L.

Enfin les valeurs des carrés moyens des amplitudes et des constantes des effets de contraction sont groupées dans le Tableau III.

Comme les constantes vibrationnelles données au Tableau III peuvent également être obtenues par les méthodes modernes de diffraction électronique, les valeurs ainsi obtenues seront certainement utiles pour l'interprétation des mesures de la diffraction. C_3S_2 en effet, comme C_3O_2, représente une molécule dans laquelle il semble difficile de distinguer entre la configuration linéaire et la forme coudée par cette seule méthode physique.

Remerciements

L'auteur exprime sa gratitude à Monsieur le Professeur Barchewitz pour son examen critique du manuscrit. Il remercie également les rapporteurs et les editeurs pour leurs suggestions concernant la présentation de l'article.

1. F. A. Miller et W. G. Fateley. Spectrochim. Acta, **20**, 253 (1964).
2. A. O. Diallo et P. Barchewitz. J. Chim. Phys. **61**, 1296 (1964).
3. W. H. Smith et G. E. Leroi. J. Chem. Phys. **45**, 1778 (1966).
4. A. O. Diallo. Thèse Doctorat d'Etat ès Sciences Physiques, Université de Paris. 1967.
5. Y. Morino. Acta Cryst. **13**, 1107 (1960).
6. S. J. Cyvin. Spectrochim. Acta, **15**, 828 (1959).
7. Y. Morino et E. Hirota. J. Chem. Phys. **23**, 737 (1955).
8. S. J. Cyvin. Acta Polytech. Scand. Chem. Met. Ser. **6**, 279 (1960).
9. Y. Morino, S. J. Cyvin, K. Kuchitsu et T. Iljima. J. Chem. Phys. **36**, 1109 (1962).

Can. J. Chem. Downloaded from www.nrcresearchpress.com by 210.87.254.105 on 09/05/12
For personal use only.

Nuclear magnetic resonance spectra of oriented 4-spin systems with C_{2v} symmetry (AA'BB'). The spectrum of thiophene

P. DIEHL, C. L. KHETRAPAL,[1] AND U. LIENHARD
Department of Physics, University of Basel, Basel, Switzerland

Received March 5, 1968

The general Hamiltonian for the nuclear magnetic resonance (n.m.r.) spectra of oriented 4-spin systems with C_{2v} symmetry of the type (AA'BB') is reported. The system can be discussed analytically, if only the direct coupling between the various nuclei is considered. The expressions for transition frequencies and intensities for such a case are given.

The proton spectrum of thiophene in the nematic phase of *p,p'*-di-*n*-hexyloxyazoxybenzene has been analyzed. The ratios of the various interproton distances are determined.

Canadian Journal of Chemistry, 46, 2645 (1968)

Can. J. Chem. Downloaded from www.nrcresearchpress.com by 210.87.254.6 on 09/05/12
For personal use only.

Introduction

Nuclear magnetic resonance (n.m.r.) spectra of oriented 4-spin systems with threefold or greater axis of symmetry and D_{2h} symmetry have been discussed by several authors (1–5). The spectra of the cases with C_{2v} symmetry do not seem to have been studied so far. Such systems have four direct couplings (D values; $D_{ij} = S_{ij} \cdot (-h\gamma^2/4\pi^2 r_{ij}^3)$, where S_{ij} is the degree of orientation along the axis joining the two protons i and j separated by the distance r_{ij}) and only two of them suffice to describe the orientation of the molecule. The remaining two direct couplings can be used to study the geometry.

The present paper deals with the general method of analysis of such spectra. The spectrum of thiophene (the structure and various notations are given in Fig. 1) has been analyzed and the geometry of the molecule discussed.

The Hamiltonian

The Hamiltonian of the system is given in Table I. Transition frequencies and intensities for a special case when the chemical shift (δ) between the two groups of protons as well as all the indirect coupling constants (J) are zero are given in Table II.

Table II indicates that the direct coupling D_A (Fig. 1) can be interchanged with D_B and D with D' without affecting the line positions. Consequently there are four possible solutions of the problem for a given set of signs of the D values from line positions only. If intensity is also considered, D and D' may still be exchanged. A unique solution can always be found from the approximate geometry of the molecule.

Experimental

The proton spectrum of a 23 mole % solution of commercially available thiophene was studied at 80 °C in the nematic phase of *p,p'*-di-*n*-hexyloxyazoxybenzene. The spectrum was recorded with a Varian spectrometer (HR 60) equipped with the Varian variable temperature assembly. Several traces were taken and the statistical error in the measurement of line position was less than ±1 Hz for each line. The average line width was 8 Hz.

Results and Discussion

Analysis of the Spectrum

The spectrum of thiophene is shown in Fig. 1. Analysis of the spectrum was first carried out without introducing δ and J and using the expressions given in Table II. Later on, known J values (6) and approximate δ values were introduced in the calculations and refined D values were obtained with an IBM 1620 computer using a modified version of Frequint IV. D and δ values were then continually changed and the spectrum calculated until a good fit with the observed spectrum was obtained. Calculations were carried out with direct and indirect couplings having the same as well as opposite signs. A good fit with the observed spectrum could not be obtained when D and J values were of the same sign. Since the indirect coupling constants in thiophene are known to be positive (6), the sign of the direct couplings must be negative. This indicates that the molecule orients preferentially with its plane along the direction of the magnetic field.

The D values reported in Table III were found to give a good fit with the spectrum. The root-mean-square deviation between the observed and

[1]Postdoctoral Fellow: on leave from Tata Institute of Fundamental Research, Bombay-5 (India).

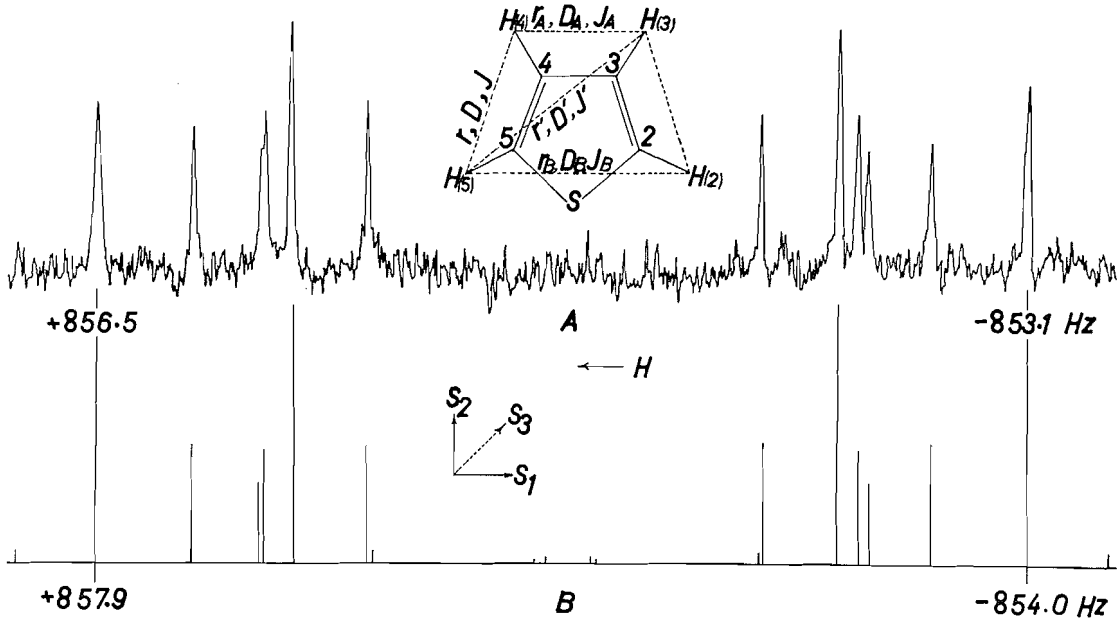

FIG. 1. Observed (A) and calculated (B) n.m.r. spectra of thiophene in *p,p'*-di-*n*-hexyloxyazoxybenzene: temperature 80 °C. Solute concentration 23 mole %.

TABLE I

Hamiltonian matrix for oriented 4-spin system with C_{2v} symmetry. $\omega_3 = \omega_4 = 0$; $\omega_2 = \omega_5 = -\delta$. $(\frac{1}{4})K$ has been subtracted from all the diagonal elements*

No.	Diagonal elements	Off-diagonal elements
1	$-\delta+(\frac{1}{2})N+(\frac{1}{2})Q+S$	
2	$-(\frac{1}{4})(Q-3R)$	
3	$-\delta-(\frac{1}{4})(Q+3R)$	$\mathcal{H}_{23} = (\frac{1}{2})(N-S)$
4	$+\delta+(\frac{1}{2})Q-(\frac{1}{2})N-S$	$\mathcal{H}_{45} = +(\frac{1}{2})(N-S)$
5	$-Q$	$\mathcal{H}_{56} = +(\frac{1}{2})(N-S)$
6	$-\delta+(\frac{1}{2})Q-(\frac{1}{2})N-S$	$\mathcal{H}_{67} = -(\frac{1}{2})(L-T)$
7	$-K$	$\mathcal{H}_{46} = 0$
		$\mathcal{H}_{57} = +(\frac{1}{2})(L+2T)$
		$\mathcal{H}_{47} = -(\frac{1}{2})(L-T)$
8	$-(\frac{1}{4})(Q-3R)$	
9	$+\delta-(\frac{1}{4})(Q+3R)$	$\mathcal{H}_{89} = +(\frac{1}{2})(N-S)$
10	$+\delta+(\frac{1}{2})N+(\frac{1}{2})Q+S$	
11	$+(\frac{1}{2})M+(\frac{1}{4})R-(\frac{1}{2})K+(\frac{1}{4})Q$	
12	$-\delta-(\frac{1}{2})M-(\frac{1}{4})R-(\frac{1}{2})K+(\frac{1}{4})Q$	$\mathcal{H}_{11\ 12} = +(\frac{1}{2})(L-T)$
13	$-(\frac{1}{2})K-(\frac{1}{2})Q+(\frac{1}{2})M-(\frac{1}{2})R$	
14	$-(\frac{1}{2})K-(\frac{1}{2})Q-(\frac{1}{2})M+(\frac{1}{2})R$	$\mathcal{H}_{13\ 14} = (\frac{1}{2})(L+2T)$
15	$+(\frac{1}{2})M-(\frac{1}{4})R-(\frac{1}{2})K+(\frac{1}{4})Q$	
16	$\delta-(\frac{1}{2})M-(\frac{1}{4})R-(\frac{1}{2})K+(\frac{1}{4})Q$	$\mathcal{H}_{15\ 16} = (\frac{1}{2})(L-T)$

*$K = J_A + J_B$. $M = J_A - J_B$. $N = J + J'$. $L = J - J'$. $J_A = J_{34}$. $J_B = J_{25}$. $J = J_{23} = J_{45}$. $J' = J_{24} = J_{35}$. $Q = D_A + D_B$; $D_A = D_{34}$. $R = D_A - D_B$; $D_B = D_{25}$. $S = D + D'$; $D = D_{23} = D_{45}$. $T = D - D'$; $D' = D_{24} = D_{35}$.

the calculated line positions was 0.7 Hz. The calculated spectrum is also shown in Fig. 1.

Structure of Thiophene

The thiophene molecule is known to be planar with C_{2v} symmetry. It has two planes of symmetry, the first being the molecular plane and the second perpendicular to it passing through the heteroatom. Therefore, only two orientation parameters (S_1 and S_2 in Fig. 1) suffice to describe the orientation of the molecule (7). In addition, there are three independent interproton distances.

Can. J. Chem. Downloaded from www.nrcresearchpress.com by 210.87.254.6 on 09/05/12
For personal use only.

Can. J. Chem. Downloaded from www.nrcresearchpress.com by 210.87.254.6 on 09/05/12
For personal use only.

TABLE II

Transition frequencies and intensities for oriented 4-spin system with C_{2v} symmetry, without chemical shift and indirect couplings. Only lines with non-zero intensity are included. The table gives only half the spectrum. The other half is symmetrical*

No.	Transition	Frequency	Intensity
1	$1s_1-s_2$	$(\frac{3}{4})(D_A+D_B)+(D+D')-(\frac{1}{2})R_1$	$2(1-Q')^2/(1+Q'^2)$
2	$2s_1-s_2$	$(\frac{3}{4})(D_A+D_B)+(D+D')+(\frac{1}{2})R_1$	$2(1+Q')^2/(1+Q'^2)$
3	$2s_0-1s_1$	$-(\frac{3}{4})(D_A+D_B)+(D+D')+(\frac{1}{2})R_1$	$(1+Q')^2/(1+Q'^2)$
4	$3s_0-1s_1$	$(\frac{1}{2})(D+D')+(\frac{1}{2})(R_1-R_2)$	I_1
5	$4s_0-1s_1$	$(\frac{1}{2})(D+D')+(\frac{1}{2})(R_1+R_2)$	I_2
6	$2s_0-2s_1$	$-(\frac{3}{4})(D_A+D_B)+(D+D')-(\frac{1}{2})R_1$	$(1-Q')^2/(1+Q'^2)$
7	$3s_0-2s_1$	$(\frac{1}{2})(D+D')-(\frac{1}{2})(R_1+R_2)$	I_3
8	$4s_0-2s_1$	$(\frac{1}{2})(D+D')+(\frac{1}{2})(R_2-R_1)$	I_4
9	$1a_0-2a_1$	$(\frac{3}{4})(D_A+D_B)-(\frac{3}{2})R_3$	2
10	$2a_0-1a_1$	$(\frac{3}{4})(D_A+D_B)+(\frac{3}{2})R_3$	2

*$R_1 = [(9/4)(D_A - D_B)^2 + (D + D')^2]^{\frac{1}{2}}$.
$R_2 = [(9/4)(D_A + D_B)^2 + 3(D + D')^2 + 6(D - D')^2 - 3(D_A + D_B) \cdot (D + D')]^{\frac{1}{2}}$.
$R_3 = [(1/4)(D_A - D_B)^2 + (D - D')^2]^{\frac{1}{2}}$.
$Q' = (D + D')/[(3/2)(D_A - D_B) + R_1]$.
The expressions for intensities I_1, I_2, I_3, and I_4 are too tedious to be given. However, they fulfill the relations: $I_1/I_3 = I_2/I_4 = [(1 - Q')/(1 + Q')]^2$.

However, there are four direct couplings. The relations between the ratios of the various interproton distances in this molecule with the direct couplings are given by eqs. [1] to [3].

$$[1] \qquad (r_B/r_A) = (D_A/D_B)^{1/3}$$

$$[2] \qquad D(r/r_A)^5 - D'\{(D_A/D_B)^{1/3} + (r/r_A)^2\}^{5/2} = -D_A(D_A/D_B)^{1/3}$$

$$[3] \qquad (r'/r_A)^2 = (D_A/D_B)^{1/3} + (r/r_A)^2$$

Equations [1] to [3] indicate that the ratios (r_B/r_A), (r/r_A), and (r'/r_A) in the thiophene molecule can be determined unambiguously independent of the orientation. The values obtained are reproduced in Table III.

The structure of thiophene has been studied earlier from electron diffraction (8) and microwave spectroscopy (9). The microwave data are much more accurate. The ratios r_B/r_A, r/r_A, and r'/r_A calculated from the microwave data are also included in Table III for comparison. The table indicates that whereas r/r_A and r'/r_A obtained by n.m.r. and the microwave techniques are equal within the limits of experimental accuracy, r_B/r_A obtained by the present method is larger (1.5 ± 0.6 %) than that obtained from the microwave data. Small differences between the geometry obtained from microwave data and the one from n.m.r. in nematic phases have been pointed out earlier also (1, 10). They may be caused by the influence of vibrational motions (10) or there may be some difference between the molecular geometry in the gas phase and the nematic medium (10).

TABLE III

The direct couplings, the ratios of various interproton distances, and the orientation parameters in thiophene (Fig. 1) (J_A = 3.3 Hz, J_B = 2.8 Hz, J = 4.7 Hz, J' = 1.0 Hz, δ = 10 Hz)

Parameter	Microwave data	Present work
D_A	—	−175.3 Hz
D_B	—	−33.0 Hz
D	—	−394.4 Hz
D'	—	−55.8 Hz
r_B/r_A	1.719	$1.745 \pm .010$
r/r_A	0.998	0.995 ± 0.005
r'/r_A	1.648	1.653 ± 0.006
S_1	—	$0.0265 \pm .0003$
S_2	—	$0.0639 \pm .0002$
S_3	—	−.0904

The orientation parameters S_1 and S_2 are related to the interproton distances in thiophene and to the various direct couplings by eqs. [4] and [5] respectively.

$$[4] \qquad S_1 = \frac{-4\pi^2}{h\gamma^2} D_A r_A^3$$

$$[5] \qquad S_2 = \frac{-4\pi^2}{h\gamma^2} r^3[D - (D_A/4)(r/r_A)^{-5} \times \{(D_A/D_B)^{1/3} - 1\}^2] \cdot [1 - \tfrac{1}{4}(r/r_A)^{-2}\{(D_A/D_B)^{1/3} - 1\}^2]^{-1}$$

It is obvious that S_1 and S_2 can be determined only if one of the proton–proton distances in thiophene is known. In order to obtain one interproton distance, the proton skeleton in thiophene obtained from the present data was compared with that obtained from the microwave data. The

r_A value which gave minimum root-mean-square deviation for the four interproton distances obtained from the n.m.r. and microwave data was selected for the calculation of S_1 and S_2. This corresponds to $r_A = 2.627$ Å. The S_1 and S_2 values thus obtained are also included in Table III.

Acknowledgment

The authors are grateful to the Swiss National Foundation for the Advancement of Science for financial support.

1. G. ENGLERT *et al.* Z. Naturforsch. **23a**, 152 (1968).
2. C S. YANNONI *et al.* J. Am. Chem. Soc. **89**, 2833 (1967).
3. H. SPIESECKE and J. B. JOURDAN. Angew. Chem. **79**, 475 (1967).
4. A. SAUPE. Mol. Cryst. **1**, 527 (1966).
5. P. DIEHL and C. L. KHETRAPAL. Mol. Phys. **14**, 327 (1968).
6. R. FREEMAN and N. S. BHACCA. J. Chem. Phys. **38**, 293 (1963).
7. L. C. SNYDER. J. Chem. Phys. **43**, 4041 (1965).
8. V. SHOMAKER and L. PAULING. J. Am. Chem. Soc. **61**, 1769 (1939).
9. B. BAK *et al.* J. Mol. Spectry. **7**, 58 (1961).
10. A. SAUPE *et al.* Advan. Chem. Ser. **63**, 51 (1967).

Can. J. Chem. Downloaded from www.nrcresearchpress.com by 210.87.254.6 on 09/05/12
For personal use only.

Can. J. Chem. Downloaded from www.nrcresearchpress.com by 210.87.254.42 on 09/05/12
For personal use only.

Studies on hydrogen–oxygen systems in the electrical discharge. II. The reactions of hydrogen atoms with liquid ozone[1]

KAZIMIERA HERMAN AND PAUL A. GIGUÈRE
Département de Chimie, Université Laval, Québec, Québec

Received February 9, 1968

We have reinvestigated in detail the infrared spectra between 4000 and 600 cm^{-1} of the solid products formed by reacting liquid ozone at −190 °C with a stream of hydrogen gas dissociated in an electrodeless discharge. Extreme care was exercised to get "clean" spectra, free from any contaminants. All the spectra thus obtained showed very clearly the characteristic absorption bands of H_2O_2 at 2840 and 1430 cm^{-1}, and the much weaker one at 880 cm^{-1}; with deuterium atoms the former bands were shifted to 2100 and 1080 cm^{-1} respectively. Thus previous contentions that hydrogen peroxide is not one of the primary products of that reaction are disproved. The other infrared bands of H_2O_2 were not conspicuous, due either to their diffuse nature in the vitreous spectra or to extensive overlapping by the strong absorption of H_2O, the other major component. Warming the material up to −110 °C caused some devitrification, but no significant change in the spectra. No new bands which could be assigned unambiguously to the hypothetical molecule H_2O_4 were observed.

On a repris en détail l'étude des spectres infrarouges du solide obtenu en faisant réagir un film d'ozone liquide condensé à −190 °C avec un courant d'hydrogène atomique produit dans la décharge électrique. Les plus grandes précautions étaient de rigueur pour éliminer toutes contaminations susceptibles de fausser les résultats. Tous les spectres ainsi obtenus montraient très nettement les bandes d'absorption caractéristiques de H_2O_2 à 2840 et 1430 cm^{-1} ainsi que celle, beaucoup plus faible, à 880 cm^{-1}; avec le deutérium atomique les deux premières se trouvait en décalées à 2100 et 1080 cm^{-1}. Ce résultat contredit les allégations antérieures à l'effet qu'il n'y a pas de peroxyde d'hydrogène dans les produits primaires de cette réaction. Les autres bandes infrarouges de H_2O_2 n'étaient pas très évidentes, soit à cause de leur contour diffus dans les spectres vitreux, soit à cause du chevauchement des fortes bandes de l'eau, l'autre constituant majeur. En laissant réchauffer le solide jusque vers −110 °C il commençait à se dévitrifier, mais son spectre d'absorption ne changeait pas. Par ailleurs on n'a pas observé de nouvelles bandes pouvant être attribuées avec certitude à une molécule hypothétique comme H_2O_4.

Canadian Journal of Chemistry, 46, 2649 (1968)

Introduction

In the long controversy (cf. ref. 2 for a review) surrounding the hypothetical polyoxides of hydrogen H_2O_3 and H_2O_4, the main evidence advanced so far has been of an indirect nature; namely, the observation that some oxygen is evolved upon warming the condensate from dissociated water vapor and other related hydrogen–oxygen systems. More particularly, in the case of the liquid ozone – atomic hydrogen reaction it has been claimed repeatedly (3–5) that the molar ratio of evolved oxygen to residual hydrogen peroxide is constant and equal to unity. However, this claim is not at all supported by the actual data which show that the ratio does vary within wide limits with the slightest experimental changes, and even within a given set of experimental conditions (6). We have suggested elsewhere (7) a more likely source for the evolved oxygen in the decomposition of some of the ordinary hydrogen peroxide, which is undoubtedly present among the primary reaction products at liquid nitrogen temperature. Effectively, the infrared spectra have confirmed that presence in the case of dissociated water (8, 9) and hydrogen peroxide vapor (9), and in the reaction of *solid* ozone with hydrogen atoms (10). However, it has been objected (11) that in the latter system the situation is different from that in *liquid* ozone where some diffusion of the primary species produced is possible. Although not too convincing, this argument has prompted us to reinvestigate again that same system very carefully by means of infrared spectroscopy, the most suitable technique for this problem.

Experimental

An apparatus was built (Fig. 1) somewhat along the lines of that used before in this laboratory for studying ammonium ozonide (12). This time, however, the ozone was produced from commercial oxygen gas (Linde, USP grade, 99.5%) in a silent discharge type of ozonizer (Precision Glass Co.), featuring a dry ice cooled discharge tube at atmospheric pressure for higher yields (about 10% by weight). The discharged stream was led into a trap, A, filled with granular silica gel. When cooled in a dry ice – acetone bath this trap condenses the ozone quantitatively. This technique (13) offered many advantages. First, it

[1]For Part I, see ref. 1.

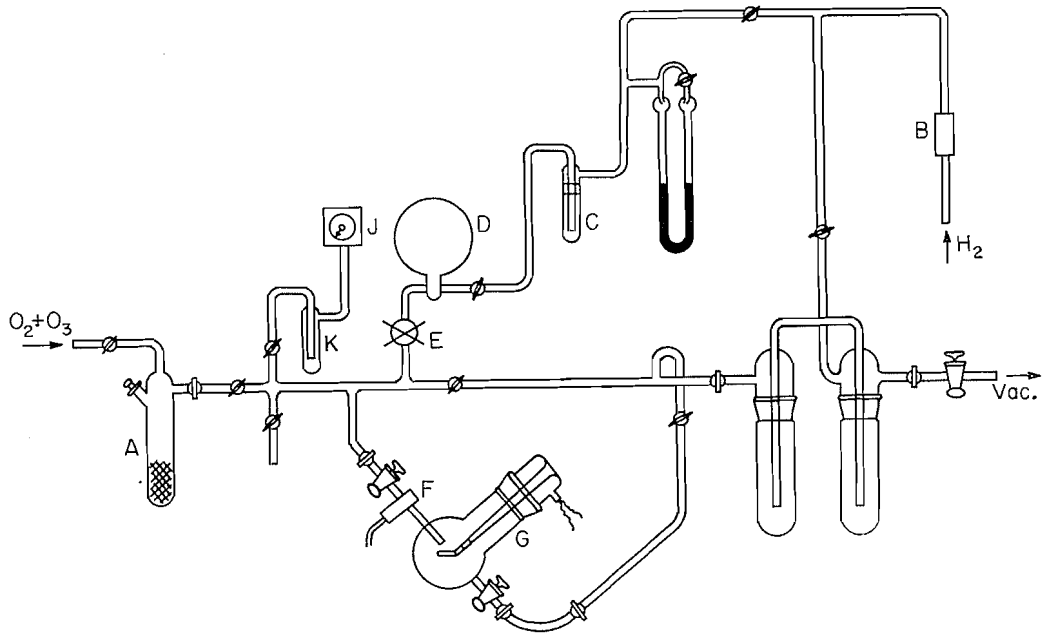

FIG. 1. Diagram of the apparatus for studying the reaction products from liquid ozone and hydrogen atoms.

allowed preparation of a very pure ozone by removal, through pumping down to about 10^{-2} Torr, of all the nitrogen oxides as well as molecular oxygen. Removing the latter made the handling of ozone much safer. Furthermore, the ozone stored in this absorbed form showed very little decomposition. When needed some of the ozone was distilled slowly, under its own vapor pressure, into the infrared absorption cell. There it formed liquid films of about 20 μ thickness upon the liquid nitrogen cooled NaCl support plate. The temperature of the latter, as measured with a copper–constantan thermocouple, never rose above −185 °C during a reaction.

The hydrogen gas, 99.95% pure (Matheson, research grade), was circulated through a "Deoxo" catalyst, B, followed by a liquid nitrogen trap, C, to reduce the residual oxygen to less than 1 p.p.m. It was then stored in a 2 l Pyrex flask, D, from which it could be withdrawn at a metered rate (20 ml/min) through a calibrated needle valve, E. The deuterium gas, 99.5% pure (Matheson C.P. grade), was similarly handled. For the dissociation a microwave discharge was used (Raytheon MD-7 "Microtherm") with an output of 80 W at 2450 Mc. The cavity, F, was of the tunable variety (Evenson, type 5 (14), Ophtos Instrument Co.). It was located on the inlet tube (8 mm diameter Pyrex) of the infrared cell, G, immediately ahead of the sample holder plate to minimize any contamination from the stopcock grease. The grease (also used on all the stopcocks and ground joints) was of the fluorocarbon type (Kel-F, N° 90). Once initiated by means of a Tesla coil the microwave discharge in hydrogen was very stable, provided the pressure remained in the neighborhood of 0.5 Torr. This could be monitored continuously with an electrical manometer, J (General Electric molecular vacuum gage), protected by a liquid nitrogen trap, K.

The infrared absorption cell was similar to that described before (12), except that in order to facilitate the preparation of a thin film of liquid ozone on the cold NaCl plate, the copper block holding the latter was set at 45° off the axis of the coolant well, and the whole cell was tilted also at 45° from the vertical. All the spectra were recorded with a Perkin-Elmer double-beam infrared spectrometer, model 621.

Discussion of Results

Before presenting the experimental results it is appropriate to record here various observations of major significance in understanding them. First is the all-important requirement of securing "clean" spectra, that is, free of all possible contaminants. The combination of a violent tool, such as the electrical discharge, with an extremely sensitive analytical device, like modern infrared spectrometers, is bound to give rise to all sorts of spurious clues, as we have experienced before (15).

Sources of Contamination

Among the more common sources of contamination are the nitrogen oxides originating either in the manufacture of ozone or from minute leaks in the vacuum system. The pub-

Can. J. Chem. Downloaded from www.nrcresearchpress.com by 210.87.254.42 on 09/05/12
For personal use only.

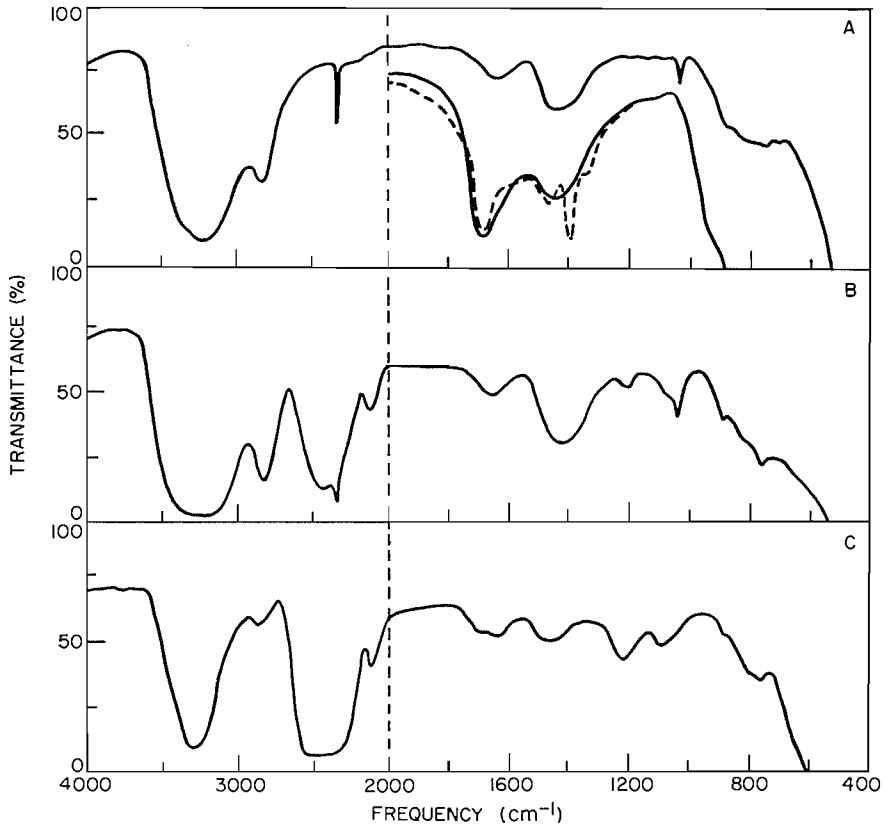

FIG. 2. Infrared spectra of the trapped products from various hydrogen–oxygen systems: A. Liquid ozone with hydrogen atoms. Also shown for a thicker sample, before (solid line) and after (broken line) melting and freezing again. B. Liquid ozone with hydrogen and deuterium atoms. C. Heavy water vapor and ordinary hydrogen, both in the electrical discharge.

lished infrared spectra of condensed ozone are a case in point. Besides the 8 absorption bands found in the solid at 4 °K in the range 700 to 350 cm^{-1} (16), and of which only 3 are fairly strong at 704, 1050, and 2110 cm^{-1}, some 16 additional bands have been detected by the same authors after a trace of air had entered the discharge apparatus. Another group of workers has published on three occasions (5, 17, 18) three almost entirely different infrared spectra of liquid ozone showing up to 20 bands. Some of these, admittedly, belong to the various nitrogen oxides. None of these were present in our spectra of liquid ozone. There was no interference either from some spurious bands which we have observed occasionally (19) at 3380 and 1090 cm^{-1} when a stream of electrically dissociated hydrogen is brought in contact with a cold rock-salt plate. Possibly these arise from some siloxane compound due to corrosion of the glass walls of the discharge tube by atomic hydrogen. They were generally too weak to be noticeable in our spectra, since the reaction time was rather short, 10 or 15 min at the most.

Stopcock grease is another source of contamination, following either from reaction with hydrogen atoms (20) or from oxidation by gaseous ozone. Even with a fluorcarbon grease the strong fundamental band of solid CO_2 at 2344 cm^{-1} was usually noticeable in our spectra. Reaction of the liquid ozone with the salt plate is also a cause of contamination. Attempts to replace NaCl plates by some other material more transparent in the far infrared were unsuccessful. Both AgCl and CsI reacted immediately, the latter turning dark purple, then milky white after

Can. J. Chem. Downloaded from www.nrcresearchpress.com by 210.87.254.42 on 09/05/12
For personal use only.

Can. J. Chem. Downloaded from www.nrcresearchpress.com by 210.87.254.42 on 09/05/12
For personal use only.

bombardment with dissociated hydrogen. Hardly any trace of the H_2O_2 bands was found in that case.

Upon reacting with hydrogen atoms the liquid ozone became covered quickly with a clear pellicle which grew in thickness as the reaction advanced. Because of this the reaction was never quite complete, as witnessed by faint streaks of blue color and the persistence of the strongest infrared band of ozone at 1030 cm^{-1}.

The "Clean" Spectra

Examination of a typical infrared spectrum of the reaction products (Fig. 2A) shows the three strong absorption regions of ice centered at 800, 1650, and 3250 cm^{-1}. Also quite conspicuous are the two characteristic bands of hydrogen peroxide at about 2840 cm^{-1} (on the low-frequency side of the broad O—H stretching bands) and near 1400 cm^{-1}. These are respectively the first overtone and the fundamental OH bending bands of the H_2O_2 molecule (21). The first overtone is the most reliable index of that molecule as it always shows the same general contour and frequency in all condensed mixtures of hydrogen peroxide and water, whether vitreous or crystalline (22). In contrast, the corresponding fundamentals were always merged into a single broad band in the vitreous condensates. Only after melting and freezing again were the two components ν_2 and ν_6 resolved at 1450 and 1385 cm^{-1}, as illustrated in Fig. 2A for a thick sample. Comparison with the spectra of various frozen mixtures recorded before in this laboratory (21) points out to a mole fraction of hydrogen peroxide of 0.2 to 0.3 in our reaction products.

Lastly, the O—O stretching mode, which is almost inactive in infrared due to the symmetry of the molecule, was barely noticeable as a weak shoulder at 880 cm^{-1} on the high-frequency slope of the strong libration bands of ice. In the deuterated systems it stood out more clearly, albeit still rather weak. All the other bands of D_2O and D_2O_2 showed the expected shifts, by a factor of about 0.75 towards the lower frequencies, save for a small band at 760 cm^{-1} reported before in the spectra of solid D_2O_2 (23), and for which there is no obvious equivalent in H_2O_2. In another set of experiments, where an equimolar mixture of H_2 and D_2 was used in the discharge, the spectra of the products (Fig. 2B) showed all the bands of the isotopic molecules H_2O, H_2O_2, D_2O, and D_2O_2, the last two being noticeably less abundant for uncertain reasons. As for the hybrid species HDO and HDO_2, extensive overlapping of their spectra by those of the parent molecules precludes definite conclusions about their relative concentrations, although from the weakness of the band at 880 cm^{-1} it is certain that very little HDO_2 was present. A similar situation was observed in the trapped products from a discharge through a mixture of D_2O and H_2 (Fig. 2C) which yielded sizable quantities of H_2O and H_2O_2.

Upon warming up to about −110 °C the glassy condensate turned opaque white due to incipient devitrification. However, this was not accompanied by any significant change in the spectra besides a drop in intensity of the sharp band, at 1030 cm^{-1}, of residual O_3 because of partial sublimation. It seems likely that the phase change, which must be very slow at that temperature, was not completed in the time allowed (about 1 h).

Conclusions

The present results prove unquestionably that hydrogen peroxide is one of the main primary products in the reduction of liquid ozone by hydrogen atoms. Previous claims to the contrary do not survive close examination. For instance, the Russian authors (5, 18) have reported infrared spectra which show quite plainly (besides many spurious features) the strong absorption bands of H_2O_2 near 1400 cm^{-1} and 2800 cm^{-1}. They assign the first band to trapped HO_2 radicals. This is untenable since it is well known that the maximum concentrations of free radicals which may be trapped, even at liquid helium temperature and in an inert matrix, never exceed a few times 0.1% (24). Besides, the 1450 cm^{-1} band in the Russian spectra (5) persists even up to −80 °C, at which temperature, of course, all free radicals would have recombined. They then assign the 2800 cm^{-1} band, one of the strongest in their spectra (17, Fig. 2), to the residual ozone in their sample. The only difficulty here is that the 2800 cm^{-1} band of solid ozone (16) is a ternary combination, about 10 times weaker than the fundamental at 1050 cm^{-1}. Yet the latter shows only medium intensity in their tracings.

As for the American authors (6), it is unfortunate that they did not publish their actual spectra

so that their conclusions could be checked. They do, however, mention that "the absorption peaks exhibited by the hydrogen atom–ozone product in the 3330 to 2780 cm^{-1} region were attributed to ice". Now, there is no appreciable absorption near 2780 cm^{-1} in thin films of ice. The strong O—H stretching band of H_2O (and also H_2O_2) is centered fairly symmetrically about 3300 cm^{-1}, as may be gathered from our Fig. 2C. Therefore, since their spectra showed absorption near 2800 cm^{-1} there is some presumption that their sample contained hydrogen peroxide.

Finally, our results show that any other species, such as H_2O_4, if at all present in our samples, could not be a major component. It may be argued that the material we studied was fundamentally different from that, obtained in a U-trap (6), which shows a 1 to 1 ratio of evolved oxygen to residual hydrogen peroxide, and hence is presumed to contain no H_2O_2. On the basis of chemical intuition alone, we are inclined to doubt that merely changing the shape of the trap is sufficient to prevent formation of any hydrogen peroxide, in favor of some hypothetical species such as H_2O_4.

Acknowledgment

This work was made possible through the financial assistance of the National Research Council of Canada.

1. N. HATA and P. A. GIGUÈRE. Can. J. Chem. **44**, 869 (1966).
2. M. VENUGOPALAN and R. A. JONES. Chem. Rev. **66**, 133 (1966).
3. N. I. KOBOZEV, L. I. NEKRASOV, and E. N. EREMIN. Zh. Fiz. Khim. **30**, 2580 (1956).
4. N. I. KOBOZEV, I. I. SKOROKHODOV, L. I. NEKRASOV, and E. I. MAKAROVA. Zh. Fiz. Khim. **31**, 1843 (1957).
5. T. V. YAGODOVSKAYA and L. I. NEKRASOV. Russ. J. Phys. Chem. **41**, 108 (1967).
6. J. A. WOJTOWICZ, F. MARTINEZ, and J. A. ZASLOWSKY. J. Phys. Chem. **67**, 849 (1963).
7. P. A. GIGUÈRE. ICSU Rev. **4**, 172 (1962).
8. P. A. GIGUÈRE and E. A. SECCO. J. Phys. Radium, **15**, 508 (1954).
9. T. V. YAGODOVSKAYA and L. I. NEKRASOV. Russ. J. Phys. Chem. **38**, 953 (1964).
10. P. A. GIGUÈRE and D. CHIN. J. Chem. Phys. **51**, 1685 (1959).
11. L. I. NEKRASOV, I. L. SKOROKHODOV, and N. I. KOBOZEV. Russ. J. Phys. Chem. **35**, 337 (1961).
12. K. HERMAN and P. A. GIGUÈRE. Can. J. Chem. **43**, 1746 (1965).
13. G. A. COOK, A. D. KIFFER, C. V. KLUMPP, A. H. MALIK, and L. A. SPENCE. Ozone chemistry and technology. Advan. Chem. Ser. **21**, Am. Chem. Soc. Washington. 1959. p. 44.
14. F. C. FEHSENFELD, K. M. EVENSON, and H. P. BROIDA. Rev. Sci. Instr. **36**, 294 (1965).
15. P. A. GIGUÈRE and K. B. HARVEY. J. Chem. Phys. **25**, 373 (1956).
16. K. B. HARVEY and A. M. BASS. J. Mol. Spectry. **2**, 405 (1958).
17. T. V. YAGODOVSKAYA and L. I. NEKRASOV. Russ. J. Phys. Chem. **37**, 1269 (1963).
18. T. V. YAGODOVSKAYA and L. I. NEKRASOV. Russ. J. Phys. Chem. **40**, 698 (1966).
19. K. HERMAN. Unpublished results.
20. A. E. ENNOS. Brit. J. Appl. Phys. **5**, 27 (1954).
21. W. C. SCHUMB, C. N. SATTERFIELD, and R. L. WENTWORTH. Hydrogen peroxide. Reinhold Publishing Corp., New York. 1955.
22. P. A. GIGUÈRE and K. B. HARVEY. J. Mol. Spectry. **3**, 36 (1959).
23. P. A. GIGUÈRE and C. CHAPADOS. Spectrochim. Acta, **22**, 1131 (1966).
24. A. M. BASS and H. P. BROIDA. Formation and trapping of free radicals. Academic Press, Inc., New York. 1960.

Can. J. Chem. Downloaded from www.nrcresearchpress.com by 210.87.254.42 on 09/05/12
For personal use only.

Can. J. Chem. Downloaded from www.nrcresearchpress.com by 210.87.254.5 on 09/05/12
For personal use only.

Absolute rate constants for hydrocarbon oxidation. XI. The reactions of tertiary peroxy radicals[1,2]

J. A. HOWARD AND K. U. INGOLD
Division of Applied Chemistry, National Research Council of Canada, Ottawa, Canada

Received February 1, 1968

Rate constants have been measured for the chain-terminating self-reactions of six tertiary peroxy radicals. The rate constants vary from $\sim 1 \times 10^3\ M^{-1}\ s^{-1}$ for *t*-butylperoxy to $\sim 6 \times 10^4\ M^{-1}\ s^{-1}$ for 1,1-diphenylethylperoxy radicals. It is suggested that the variation in the rate constants may be related to differences in the stability of the alkoxy radical products of tetroxide decomposition.

Rate constants for hydrogen atom abstraction from aralkanes by tertiary peroxy radicals do not seem to be significantly affected by the structure of the attacking radical.

In solution the triphenylmethylperoxy radical probably exists in equilibrium with the triphenylmethyl radical and oxygen. Chain termination in oxidations involving the triphenylmethylperoxy radical as the chain carrier occurs by the reaction of this radical with a triphenylmethyl radical.

Canadian Journal of Chemistry, **46**, 2655 (1968)

Introduction

The oxidation of cumene in the absence and presence of cumene hydroperoxide and the induced decomposition of *t*-butyl hydroperoxide and cumene hydroperoxide have shown that many interactions of tertiary peroxy radicals are non-terminating (2–8). The self-reaction of tertiary peroxy radicals can be represented by

$$ROO^{\cdot} + ROO^{\cdot} \rightleftarrows ROOOOR \rightarrow$$

$$\begin{array}{l} \xrightarrow{\text{terminating}} ROOR + O_2 \\ [RO^{\cdot} + O_2 + {}^{\cdot}OR]_{\text{cage}} \\ \xrightarrow{\text{non-terminating}} 2RO^{\cdot} + O_2 \end{array}$$

where $ROO^{\cdot}$ and $RO^{\cdot}$ represent tertiary peroxy and alkoxy radicals, respectively. The alkoxy radical can undergo β scission and the resulting alkyl radical will add oxygen to give what will generally be a primary or secondary peroxy radical. For example, the alkoxy radical from *sec*-butylbenzene will yield the ethylperoxy radical:

$$C_6H_5{-}\overset{\displaystyle CH_3}{\underset{\displaystyle CH_2CH_3}{\overset{|}{\underset{|}{C}}}}{-}O^{\cdot} \rightarrow C_6H_5COCH_3 + CH_3CH_2^{\cdot}$$

$$CH_3CH_2^{\cdot} \xrightarrow{O_2} CH_3CH_2OO^{\cdot}.$$

A 2-phenylbutyl-2-peroxy radical will react faster with an ethylperoxy radical than with another 2-phenylbutyl-2-peroxy radical. The measured termination rate constant, $2k_t$, for the oxidation of *sec*-butylbenzene contains a contribution from the direct terminating interaction of two 2-phenylbutyl-2-peroxy radicals (rate constant $2k_{t(d)}$) and a contribution from terminating reactions of the ethylperoxy radical. The relative importance of the two processes will be very dependent on the experimental conditions (6–8). For most tertiary hydrocarbons, chain termination probably occurs in a generally similar fashion.

We have determined $2k_{t(d)}$ for cumene by oxidizing the hydrocarbon with sufficient cumene hydroperoxide to eliminate any termination reaction involving the methylperoxy radical (7). The present work extends these measurements of the rate constants for direct termination to a wider selection of tertiary peroxy radicals. The rate constants for hydrogen atom abstraction from a number of aralkanes (k_p) have also been measured in order to determine whether the nature of R in a tertiary peroxy radical has any effect on the reactivity of the radical.

Experimental

The rate constants for the oxidation of hydrocarbons in the presence of hydroperoxides were determined from the photochemically initiated reactions[3] using the rotating sector method. The background thermal rate of oxidation was always less than 10% of the photo-rate. Oxidation rates of the α,α′-azo-bis-isobutyronitrile (AIBN) thermally initiated reactions generally gave values of $k_p/(2k_t)^{\frac{1}{2}}$ which agreed with the values found from photo-initiation.

[1]Issued as NRCC No. 10131.
[2]For Part X see ref. 1.

[3]α,α′-Azo-bis-cyclohexylnitrile (ACHN) was used as the photoinitiator.

TABLE I

Induced decomposition of tertiary hydroperoxides at 30°

Hydroperoxide	Concentration (M)	$R_i \times 10^7$ ($M\,s^{-1}$)	$(d[O_2]/dt)/R_i$*
t-Butyl	2.2	0.14–2.9	4.0
Cumene	0.5–1.6	0.14–2.5	3.4
1,1-Diphenylethyl	0.22	0.14	1.4
Triphenylmethyl	0.11	5.6	0.5
2-Phenylbutyl-2	0.1–1.5	0.4–5.0	−0.5
1,1,3,3-Tetramethylbutyl	0.5–1.6	0.2–4.0	−0.6

*Corrected for nitrogen evolved and oxygen absorbed by the initiator.

All the hydrocarbons were oxidized with sufficient hydroperoxide to ensure that only peroxy radicals from the hydroperoxide propagated and terminated the chain reactions. In order to obtain $k_p/(2k_t)^{\frac{1}{2}}$ the measured rates of oxidation were corrected for: (i) nitrogen evolved by the initiator, (ii) oxygen absorbed by the initiating radicals, (iii) oxygen evolved in the self-reactions of peroxy radicals, and (iv) oxygen absorbed by the alkyl radicals formed by β scission of the alkoxy radicals produced in the non-terminating reactions of the tertiary peroxy radicals.

Oxygen is evolved in fairly large quantities in the radical-chain-induced decomposition of *t*-butyl hydroperoxide (4, 9) and cumene hydroperoxide (10). The number of oxygen molecules evolved per chain initiated at 30° for these two hydroperoxides and for the four other hydroperoxides studied in this work are listed in Table I.[4] Increased β scission must lead to decreased oxygen evolution and the differences in these numbers should reflect differences in the stabilities of the alkoxy radicals. The stability appears to increase in the order 1,1,3,3-tetramethylbutyl ~ 2-phenylbutyl-2 < 1,1-diphenylethyl < cumyl < *t*-butyl.[5] This order of stability is consistent with previous work on alkoxy radicals (11, 12).

The background thermal rate increased during photo-oxidations in the presence of *t*-butyl hydroperoxide. The value of $2k_{t(d)}$ for *t*-butylperoxy is therefore less accurate than for the other tertiary peroxy radicals.

The rates of chain initiation were determined by the induction period method using 2,6-di-*t*-butyl-4-methoxyphenol as the inhibitor. At the end of the induction period the oxidation rate was the same as in the absence of the inhibitor. Rates of chain initiation and values of $k_p/(2k_t)^{\frac{1}{2}}$ were, therefore, frequently determined in the same experiment.

Materials

1,1,3,3-Tetramethylbutyl hydroperoxide (Lucidol) was purified via its sodium salt. 2-Phenylbutyl-2-hydroperoxide was prepared by the emulsion oxidation of *sec*-butylbenzene and was purified via its sodium salt (13). Triphenylmethyl hydroperoxide and 1,1-diphenylethyl hydroperoxide were prepared from the corresponding alcohols by the acid-catalyzed reaction with hydrogen peroxide. The purification of *t*-butyl hydroperoxide and cumene hydroperoxide, and of the hydrocarbons and initiators, have been described previously (14). The purity of the hydroperoxides was, of course, checked by conventional methods. However, these are not sufficiently sensitive to detect trace impurities and, as a result, we have previously incorrectly reported that cumene hydroperoxide slightly reduces the rate of oxidation of cumene (14, Part VI). For the present work we checked hydroperoxide purity by the procedure developed by Thomas (6) in which purification is repeated until the rate of oxidation of cumene containing the hydroperoxide reaches a constant value (under standard conditions).

[4]The hydroperoxide concentrations were the same in these experiments as in the oxidation experiments.

[5]The triphenylmethoxy radical has not been placed in this list because it is unlikely that this radical is formed in significant quantities from the hydroperoxide under the conditions of these experiments (see below).

Results

(i) *The Oxidation of sec-Butylbenzene and 1,1-Diphenylethane*

The rate constants for the oxidation of *sec*-butylbenzene and 1,1-diphenylethane at 30° are given in Tables II and III. Addition of the appropriate hydroperoxide to its parent hydrocarbon increases the rate of oxidation in both cases and the limiting rates are both about 60% higher than the rates in the absence of hydroperoxide. The addition of cumene hydroperoxide to cumene also increases the rate by about 60% under similar conditions (5–7, 14). In this last case, the increase in rate is due to a decrease in the rate of chain termination, as originally suggested by Traylor (5) and subsequently confirmed by our own direct measurements (7, 14). The data in Tables II and III show that a similar explanation applies to the rate enhancement produced in *sec*-butylbenzene and 1,1-diphenylethane by the addition of their respective hydroperoxides. That is, the termination rate constants are decreased by the addition of hydroperoxide because the more rapid termination process via alkoxy radical β scission is suppressed (cf. refs. 5–8, 14). The direct termination rate constants were measured at the limiting oxidation rates both in the parent hydrocarbon and in cumene.

Can. J. Chem. Downloaded from www.nrcresearchpress.com by 210.87.254.5 on 09/05/12
For personal use only.

TABLE II

The oxidation of *sec*-butylbenzene

Hydrocarbon [*M*]	Hydroperoxide [*M*]	$R_i \times 10^7$ ($M\ s^{-1}$)	Chain length	$k_p/(2k_t)^{\frac{1}{2}} \times 10^3$ ($M^{-\frac{1}{2}}\ s^{-\frac{1}{2}}$)	k_p ($M^{-1}s^{-1}$)	$2k_t \times 10^{-4}$ ($M^{-1}\ s^{-1}$)
		30°				
s-BuPh [6.4]	None	0.15	9	0.18	0.075	17.6
s-BuPh [6.4]	None	0.38	6	0.18	0.077	19.0
s-BuPh [6.4]*	None	0.18	9	0.18	—	—
s-BuPh [6.3]	*s*-BuPh [0.12]	1.9	5	0.30	0.06	3.5
s-BuPh [4.9]	*s*-BuPh [1.47]	5.4	2	0.25	0.05	3.5
s-BuPh [5.8]*	*s*-BuPh [0.5]	0.18	13	0.29	—	—
s-BuPh [4.9]	*i*-PrPh [1.6]	2.5	6	0.94	0.07	0.6
i-PrPh [7.0]	*s*-BuPh [0.12]	1.9	14	0.88	0.14	2.6
i-PrPh [6.6]	*s*-BuPh [0.5]	3.1	10	0.87	0.16	3.3
i-PrPh [6.6]†	*i*-PrPh [0.5]	0.1–2.0	24–40	2.0	0.18	0.6
		56°				
s-BuPh [6.4]	None	0.61	16	0.60	0.45	5.8
s-BuPh [6.4]*	None	0.52	14	0.48	—	—
s-BuPh [6.2]	*s*-BuPh [0.24]	3.4	11	1.0	0.25	6.3
s-BuPh [6.2]*	*s*-BuPh [0.24]	0.52	25	0.94	—	—
s-BuPh [5.9]*	*s*-BuPh [0.5]	0.52	20	0.93	—	—

*Thermally initiated oxidations.
†Result from ref. 7.

TABLE III

The oxidation of 1,1-diphenylethane at 30°

Hydrocarbon [*M*]	Hydroperoxide [*M*]	$R_i \times 10^7$ ($M\ s^{-1}$)	Chain length	$k_p/(2k_t)^{\frac{1}{2}} \times 10^3$ ($M^{-\frac{1}{2}}\ s^{-\frac{1}{2}}$)	k_p ($M^{-1}s^{-1}$)	$2k_t \times 10^{-4}$ ($M^{-1}\ s^{-1}$)
Ph_2Et [5.4]*	None	0.5–1.7	14–21	1.2	0.44	13.5
Ph_2Et [5.2]	Ph_2Et [0.2]	1.7	23	1.8	0.45	6.2
Ph_2Et [5.2]	*i*-PrPh [0.25]	1.7	40	6.0	0.46	0.6
i-PrPh [6.9]	Ph_2Et [0.18]	1.7	12	0.72	0.18	6.4
i-PrPh [6.6]	Ph_2Et [0.36]	1.7	12	0.71	0.18	6.4
i-PrPh [6.9]†	Ph_2Et [0.18]	0.075	53	0.80	—	—
i-PrPh [6.6]†	Ph_2Et [0.36]	0.075	53	0.51	—	—
i-PrPh [6.6]‡	*i*-PrPh [0.5]	0.1–2.0	24–40	2.3	0.18	0.6

*As a result of further work the rate constants have been increased slightly from the values given previously (14).
†Thermally initiated oxidation.
‡Result from ref. 7.

The results for the 2-phenylbutyl-2-peroxy radical at 30 and 56° give $2k_t = 2 \times 10^9 \exp(-9000/RT)\ M^{-1}\ s^{-1} = 1.8 \times 10^5\ M^{-1}\ s^{-1}$ at 30°, and $2k_{t(d)} = 3 \times 10^8 \exp(-5600/RT)\ M^{-1}\ s^{-1} = 3.0 \times 10^4\ M^{-1}\ s^{-1}$ at 30°. These activation energies are of comparable magnitude to those obtained for chain termination in the oxidation of cumene (7, 8, 15) and for the self-reaction of other tertiary peroxy radicals (15, 16). The higher activation energy of the overall termination process compared with the direct process probably reflects the greater rate of alkoxy radical β scission at higher temperatures and the greater ease of diffusion of the two alkoxy radicals out from the cage in which they are formed.

The rate constant for the overall self-reaction of 2-phenylbutyl-2-peroxy radicals has been estimated by electron spin resonance (e.s.r.) to be $2.5 \times 10^9 \exp(-5500/RT)\ M^{-1}\ s^{-1} = 2.9 \times 10^5\ M^{-1}\ s^{-1}$ at 30° (15). For *t*-butylperoxy and cumylperoxy radicals the combination of the alkoxy radicals in the cage (the direct reaction) occurs at about 1/8 to 1/10 of the rate of the overall self-reaction (9, 10 and Table I). Our present determination of $2k_{t(d)}$ suggests that a similar value exists for this ratio for 2-phenylbutyl-2-peroxy radicals, i.e. $2k_{t(d)}/2k_{e.s.r.} \sim 0.1$ at 30°.

(ii) The t-Butylperoxy and 1,1,3,3-Tetramethylbutylperoxy Radicals

The rate constants for direct termination and for hydrogen atom abstraction from cumene by *t*-butylperoxy and 1,1,3,3-tetramethylbutylperoxy radicals are given in Table IV. The data were obtained by oxidizing cumene with the two

Can. J. Chem. Downloaded from www.nrcresearchpress.com by 210.87.254.5 on 09/05/12
For personal use only.

TABLE IV

The oxidation of cumene with *t*-butyl hydroperoxide and 1,1,3,3-tetramethylbutyl hydroperoxide at 30°

Cumene (M)	Hydroperoxide [M]	$R_i \times 10^7$ ($M\ s^{-1}$)	Chain length	$k_p/(2k_t)^{\frac{1}{2}} \times 10^3$ ($M^{-\frac{1}{2}}\ s^{-\frac{1}{2}}$)	k_p ($M^{-1}\ s^{-1}$)	$2k_t \times 10^{-3}$ ($M^{-1}\ s^{-1}$)
1.6	*t*-Butyl [2.3]	3.0	20	6.1	0.22	1.3
6.6	Tetramethylbutyl [2.0]	2.5	17	1.4	0.14	10.2

hydroperoxides. The direct termination constants are both in excellent agreement with the values obtained by following the decay of the peroxy radicals produced by photolysis of solutions of the hydroperoxides in the cavity of an e.s.r. spectrometer (15), viz. $1.3 \times 10^3\ M^{-1}\ s^{-1}$ for *t*-butylperoxy radicals in benzene and $1.5 \times 10^4\ M^{-1}\ s^{-1}$ for tetramethylbutylperoxy radicals in methanol (15). The direct termination constant for *t*-butylperoxy radicals is also in excellent agreement with the value obtained by Hendry from the oxidation of cumene and *t*-butyl hydroperoxide (8), viz. $2 \times 7 \times 10^2 = 1.4 \times 10^3\ M^{-1}\ s^{-1}$ at 35° (8).

(iii) The Triphenylmethylperoxy Radical

The rates of oxidation of cumene (17, 18) and cyclohexene (18) are reduced by the addition of polyarylmethanes such as triphenylmethane. The retarded rates are decreased by a decrease in the oxygen pressure (18). Furthermore, the retarding effect of triphenylmethane is greater at 90° than at 60° (18). It was suggested that the triphenylmethyl radical had a low reactivity towards oxygen but a high reactivity towards peroxy radicals so that the triphenylmethyl radical tended to persist in the oxidation system until it reacted with a peroxy radical (and thus terminated a chain) (18). More recently, Janzen and co-workers (19, 20) have shown that the reaction of the triphenylmethyl radical with oxygen, in a solid crystal lattice permeable to oxygen, is reversible,

$$Ph_3C^{\cdot} + O_2 \rightleftarrows Ph_3COO^{\cdot}$$
$$(\Delta H = -9 \pm 1\ \text{kcal/mole}).$$

The forward reaction is very fast but the decomposition of the peroxy radical requires an activation energy of about 10 kcal/mole.

Our results on the oxidation of cumene, tetralin, and 9,10-dihydroanthracene with triphenylmethyl hydroperoxide suggest that the

TABLE V

The oxidation of cumene, tetralin, and 9,10-dihydroanthracene with triphenylmethyl hydroperoxide at 30°

Hydrocarbon [M]	[Ph_3COOH] [M]	[O_2]* (mm)	$R_i \times 10^7$ ($M\ s^{-1}$)	$d[O_2]/dt \times 10^6$ ($M\ s^{-1}$)	$Q \times 10^3$ ($s^{\frac{1}{2}}$)	$2k_t \times 10^{-8}$ ($M^{-1}\ s^{-1}$)
Cumene [7.0]	0.07	680	0.5	0	—	—
Tetralin [1.66]	0.07	670	5.2	1.05	6.7	—
Tetralin [1.66]	0.07	160	5.2	0.77	9.7	—
Tetralin [7.05]	0.14	670	6.7	4.6	5.9	2.3
Tetralin [7.2]	0.07	670	4.9	5.1	7.3	—
Tetralin [7.2]	0.07	660	4.9	4.7	7.0	—
Tetralin [7.2]	0.07	90	4.9	2.6	10	—
Tetralin [7.2]	0.07	90	4.9	2.4	9.7	—
Dihydroanthracene [0.2]	0.025	660	3.4	5.5	8.4	—
Dihydroanthracene [0.2]	0.07	680	0.8	1.7	5.1	0.75
Dihydroanthracene [0.2]	0.07	680	2.6	4.0	6.8	1.7
Dihydroanthracene [0.2]	0.07	660	0.8	2.0	6.1	0.60
Dihydroanthracene [0.2]	0.07	660	2.6	4.6	7.9	—
Dihydroanthracene [0.2]	0.07	570	0.8	2.2	7.1	—
Dihydroanthracene [0.2]	0.07	300	0.8	1.6	7.1	—
Dihydroanthracene [0.2]	0.07	210	2.6	1.9	5.7	2.0
Dihydroanthracene [0.2]	0.07	150	0.8	1.05	6.7	—
Dihydroanthracene [0.2]	0.11	660	5.6	5.0	5.9	—
Dihydroanthracene [1.0]	0.07	660	2.6	24.5	8.4	—

*The oxygen pressure in solution in mole/l was taken to be 10^{-5} × pressure [O_2] in mm (cf. ref. 21), e.g. 680 mm [O_2] ≡ $6.8 \times 10^{-3}\ M$ n solution.

Can. J. Chem. Downloaded from www.nrcresearchpress.com by 210.87.254.5 on 09/05/12
For personal use only.

TABLE VI

Rate constants (in M^{-1} s^{-1}) for hydrogen atom abstraction from aralkanes by tertiary peroxy radicals at 30°

	Aralkane					$2k_{t(d)} \times 10^4$	
Peroxy radical	Toluene	Ethyl-benzene	Cumene	Tetralin	Styrene	Measured	Calculated*
t-Butyl	0.05	0.20	0.22	2.0	1.05	0.13	0.078
Cumyl†	0.03	0.18	0.18	1.65	2.1	0.60	0.55
1,1,3,3-Tetramethylbutyl	0.04	0.32	0.14	2.0	—	1.0	1.5
2-Phenylbutyl-2	0.05	0.22	0.15	1.3	—	3.0	3.9
1,1-Diphenylethyl	—	—	0.18	—	1.7	6.3	5.6
Average	0.04	0.23	0.17	1.7	1.6		

*Calculated from the measured rates of oxidation of cumene assuming that $k_p = 0.17\ M^{-1}$ s^{-1} in all cases.
†Data from ref. 7.

triphenylmethyl radical – oxygen reaction is reversible in solution. The experimental data given in Table V can be most readily explained by the following reaction scheme[6].

[1] $I_2 \rightarrow ROO^{\cdot}$ (Rate R_i)

[2] $ROO^{\cdot} + Ph_3COOH \rightarrow ROOH + Ph_3COO^{\cdot}$

[3] $Ph_3COO^{\cdot} + RH \xrightarrow{O_2} Ph_3COOH + ROO^{\cdot}$

[4] $Ph_3C^{\cdot} + O_2 \rightleftarrows Ph_3COO^{\cdot}$

[5] $Ph_3C^{\cdot} + Ph_3COO^{\cdot} \rightarrow$ non-radical products.

Hence,

$$\frac{-d[O_2]}{dt} = k_3[RH]\left(\frac{R_i K_4[O_2]}{2k_5}\right)^{1/2}.$$

The quantity

$$Q = \frac{-d[O_2]}{dt} \Big/ k_3[RH](R_i[O_2])^{1/2} = \left(\frac{K_4}{2k_5}\right)^{1/2}$$

should be a constant independent of the nature of the hydrocarbon and independent of the hydrocarbon, hydroperoxide, and oxygen concentrations. In evaluating Q, the rate constants k_3 for tetralin and 9,10-dihydroanthracene were assumed to be the same as for the attack of cumylperoxy radicals on these two substrates, viz. 1.65 M^{-1} s^{-1} and 70 M^{-1} s^{-1} at 30° (14). This assumption is justified by the fact that all tertiary peroxy radicals appear to have very similar reactivities in abstraction (see below).

[6]The yield of 0.5 moles of O_2 evolved per chain initiated in the induced decomposition of triphenylmethyl hydroperoxide (Table I) is readily accounted for by reactions [1], [2], [4], and [5] of this scheme.

The values of Q given in Table V are reasonably constant for 9,10-dihydroanthracene, but with tetralin Q does appear to increase slightly as the oxygen pressure decreases. The average value of Q is 7.3×10^{-3} s$^{\frac{1}{2}}$ and hence $Q^2 = K_4/2k_5 = 53.3 \times 10^{-6}$ s. The termination constant in these systems ($2k_5$) was determined by rotating sector measurements (Table V). The average value was $1.5 \times 10^8\ M^{-1}$ s^{-1}. Therefore, $K_4 = 53.3 \times 10^{-6} \times 1.5 \times 10^8 = 8 \times 10^3\ M^{-1}$, or, if the equilibrium constant is calculated in terms of the oxygen pressure (in atmospheres) above the liquid phase, then $K_4 = 8 \times 10^3 \times 7.6 \times 10^{-3} = 60$ atm^{-1} at 30°. This value is in satisfactory agreement with the estimate of Janzen *et al.* (20) of approximately 25 atm^{-1} for this equilibrium constant in a crystal lattice at 27°.

Discussion

We have previously suggested that primary and secondary peroxy radicals are about 3–5 times as reactive in hydrogen atom abstraction as tertiary peroxy radicals (7, 14, 22). The lower reactivity of the tertiary radicals was attributed to a steric effect. The possibility existed that tertiary peroxy radicals, ROO$^{\cdot}$, would show a decreasing reactivity as the size of the group R increased. Rate constants for addition to styrene and for abstraction from four representative aralkanes by some tertiary peroxy radicals were determined by oxidizing the hydrocarbons with tertiary hydroperoxides. The results are summarized in Table VI. The variations in the measured propagation rate constants[7] show no systematic change with

[7]Hendry (8) gives values of 0.10 and 0.20 M^{-1} s^{-1} for abstraction from cumene by *t*-butylperoxy and cumylperoxy radicals respectively at 35 °C.

Can. J. Chem. Downloaded from www.nrcresearchpress.com by 210.87.254.5 on 09/05/12
For personal use only.

Can. J. Chem. Downloaded from www.nrcresearchpress.com by 210.87.254.5 on 09/05/12
For personal use only.

increasing size of the attacking radical and may only represent random experimental errors. The reactivity of tertiary alkyl and aralkyl peroxy radicals does not seem to be significantly affected by the structure of the radical. Presumably the steric environment varies less between the different tertiary peroxy radicals than between tertiary and secondary peroxy radicals.

In the presence of triphenylmethyl hydroperoxide, chain termination in the oxidation of tetralin and 9,10-dihydroanthracene occurs predominantly by the reaction

[5] $Ph_3COO^{\cdot} + Ph_3C^{\cdot} \rightarrow$ non-radical products

(see Results section). The rate constant for this reaction is $\sim 1.5 \times 10^8\ M^{-1}\ s^{-1}$. The equilibrium constant for the process

[4] $Ph_3C^{\cdot} + O_2 \rightleftarrows Ph_3COO^{\cdot}$

is $\sim 8 \times 10^3\ M^{-1}$, giving a ratio of $[Ph_3COO^{\cdot}]/[Ph_3C^{\cdot}] = 60$ at 760 mm O_2. For reaction [5] to predominate over the "normal" termination process, reaction [6], k_6 must be $< 1.5 \times 10^8/60$, i.e. $k_6 < 2.5 \times 10^6\ M^{-1}\ s^{-1}$.

[6] $Ph_3COO^{\cdot} + Ph_3COO^{\cdot} \rightarrow$ non-radical products

Rate constants for direct termination by the self-reactions of tertiary peroxy radicals are summarized in Table VI. These rate constants increase by a factor of 50–70 between the *t*-butylperoxy and the 1,1-diphenylethylperoxy radicals. The measured rate constants presumably represent the product of the tetroxide equilibrium constant K, the rate constant for its decay to alkoxy radicals and oxygen $2k'$, and the fraction, f, of such decompositions which lead to a radical combination in the cage, i.e. $2k_{t(d)} = K2k'f$.

$$2ROO^{\cdot} \overset{K}{\rightleftarrows} ROOOOR \xrightarrow{2k'} \begin{cases} \xrightarrow{f} ROOR + O_2 \\ [2RO^{\cdot} + O_2] \\ \xrightarrow{1-f} 2RO^{\cdot} + O_2 \end{cases}$$

The differences in $2k_{t(d)}$ are probably associated with changes in K or $2k'$, since it seems unlikely that the ratio of radical combination in the cage to radical diffusion from the cage can differ greatly from one pair of alkoxy radicals to another.[8] In theory, at least, it is possible to separate $2k_{t(d)}$ into its component parts (15, 16). We hope eventually to correlate variations in the tetroxide equilibrium constant and stability with respect to its irreversible decomposition with the structure of the tertiary alkyl group.

1. J. A. Howard and K. U. Ingold. J. Am. Chem. Soc. **90**, 1058 (1968).
2. H. S. Blanchard. J. Am. Chem. Soc. **81**, 4548 (1959).
3. P. D. Bartlett and T. G. Traylor. J. Am. Chem. Soc. **85**, 2407 (1963).
4. R. Hiatt, J. Clipsham, and T. Visser. Can. J. Chem. **42**, 2754 (1964).
5. T. G. Traylor and C. A. Russell. J. Am. Chem. Soc. **87**, 3698 (1965).
6. J. R. Thomas. J. Am. Chem. Soc. **89**, 4872 (1967).
7. J. A. Howard, W. J. Schwalm, and K. U. Ingold. Preprints of the International Oxidation Symposium. San Francisco, California. 1967. **1**, p. 3.
8. D. G. Hendry. J. Am. Chem. Soc. **89**, 5433 (1967).
9. A. Factor, C. A. Russell, and T. G. Traylor. J. Am. Chem. Soc. **87**, 3692 (1965).
10. J. R. Thomas. J. Am. Chem. Soc. **87**, 3935 (1965).
11. J. K. Kochi. J. Am. Chem. Soc. **84**, 1193 (1962).
12. C. Walling and A. Padwa. J. Am. Chem. Soc. **85**, 1593 (1963).
13. E. G. E. Hawkins. J. Chem. Soc. 2076 (1949).
14. J. A. Howard and K. U. Ingold. Can. J. Chem. This issue; and previous papers in this series.
15. J. R. Thomas and K. U. Ingold. Preprints of the International Oxidation Symposium. San Francisco, California. 1967. **1**, p. 517.
16. P. D. Bartlett and G. Guaraldi. J. Am. Chem. Soc. **89**, 4799 (1967).
17. G. A. Russell. J. Am. Chem, Soc. **78**, 1047 (1956).
18. D. G. Hendry and G. A. Russell. J. Am. Chem. Soc. **86**, 2371 (1964).
19. C. L. Ayers, E. G. Janzen, and F. J. Johnston. J. Am. Chem. Soc. **88**, 2610 (1966).
20. E. G. Janzen, F. J. Johnston, and C. L. Ayers. J. Am. Chem. Soc. **89**, 1176 (1967).
21. F. R. Mayo and A. A. Miller. J. Am. Chem. Soc. **80**, 2480 (1958).
22. B. S. Middleton and K. U. Ingold. Can. J. Chem. **45**, 191 (1967).

[8]In the solvents typically used for studies of hydrocarbon oxidation this ratio is about 1/8 to 1/10 for *t*-butylperoxy and cumylperoxy radicals (see Table I and refs. 9 and 10).

Can. J. Chem. Downloaded from www.nrcresearchpress.com by 188.143.235.115 on 09/06/12
For personal use only.

Absolute rate constants for hydrocarbon oxidation. XII. Rate constants for secondary peroxy radicals[1,2]

J. A. Howard and K. U. Ingold
Division of Applied Chemistry, National Research Council of Canada, Ottawa, Canada

Received February 1, 1968

Rate constants have been measured for hydrogen abstraction from four aralkanes and addition to two aralkenes by five secondary and one primary peroxy radical. These rate constants appear to show a slight dependence on the structure of the attacking peroxy radicals which may be due to the inductive effects of the substituents on the radical. The secondary and primary peroxy radicals are generally about 2–4 times more reactive than tertiary peroxy radicals in abstraction and 4–8 times more reactive in addition. The lower reactivity of tertiary peroxy radicals is probably due to steric factors.

Canadian Journal of Chemistry, 46, 2661 (1968)

Introduction

When hydroperoxides are added to oxidizing hydrocarbons in sufficient concentrations, the peroxy radicals involved in chain propagation and termination are derived entirely from the hydroperoxide (1–8). We have utilized this fact to measure propagation rate constants (both hydrogen abstraction and peroxy radical addition) for cumylperoxy radicals (4, 5) and for a number of other tertiary peroxy radicals (7). We have also measured the rate constants for the self-chain-terminating reaction of some tertiary peroxy radicals (5, 7). In the present paper this hydrocarbon–hydroperoxide oxidation procedure has been used to obtain propagation and termination rate constants for a number of secondary peroxy radicals and for the primary *n*-butylperoxy radical.

Experimental

Procedure

The measurement of rates of oxidation, absolute rate constants, and rates of initiation has been described in previous papers in this series (4–7). All the rate constants were measured at 30°.

Materials

Tetralin hydroperoxide and 9,10-dihydroanthracyl-9-hydroperoxide were prepared by oxidation of the appropriate hydrocarbon and purified by crystallization (9, 10). *n*-Butyl hydroperoxide and *sec*-butyl hydroperoxide were prepared from the respective alkyl methane sulfonates (11). Diphenylmethyl hydroperoxide was prepared from benzhydrol (12). We are indebted to Dr. R. C. Williamson Jr. for a generous gift of cyclohexyl hydroperoxide.

[1]Issued as NRCC No. 10132.
[2]For part XI see preceding paper.

Results

Tetralin Hydroperoxide

This compound has no significant influence on the propagation and termination rate constants for the oxidation of tetralin (see Table I). Results for the oxidation of six other hydrocarbons in the presence of tetralin hydroperoxide are also given in Table I. The cross propagation constants (i.e., attack by α-tetralylperoxy radicals on the substrate) have been calculated from the measured values of $k_p/(2k_t)^{\frac{1}{2}}$ taking $2k_t = 7.6 \times 10^6\ M^{-1}\ s^{-1}$ (4). Tetralin hydroperoxide oxidizes at about half the rate of the parent hydrocarbon.

Diphenylmethyl Hydroperoxide

The results obtained with this hydroperoxide are given in Table II. The average termination constant for oxidations involving diphenylmethylperoxy radicals is $2.8 \pm 1.0 \times 10^7\ M^{-1}\ s^{-1}$. The value obtained with neat diphenylmethane (13) is excluded from the average because the photo-initiated oxidation of diphenylmethane is strongly autocatalytic[3] and the rate of oxidation is quite low (13). Both of these factors make an accurate determination of the absolute rate constants rather difficult. Since diphenylmethyl hydroperoxide does not affect the initial value of $k_p/(2k_t)^{\frac{1}{2}}$ for diphenylmethane (see Table II), the autocatalysis is not due to the

[3]The thermally initiated oxidation at 30° is not autocatalytic. This reaction was initiated with $1.0 \times 10^{-3}\ M$ di-*t*-butylperoxyoxalate, a concentration which gave the same rate of initiation as the photo-reaction. Benzophenone is a photo-initiator for the oxidation of both diphenylmethane and tetralin. It is probably responsible for the autocatalysis of the photo-initiated oxidation of diphenylmethane.

TABLE I

Rate constants (in M^{-1} s^{-1}) for hydrocarbon oxidations in the presence of tetralin hydroperoxide

Hydrocarbon [M]	Hydroperoxide [M]	$R_i \times 10^7$* (M s^{-1})	Chain length	$k_p/(2k_t)^{\frac{1}{2}} \times 10^3$	$2k_t \times 10^{-6}$	k_p†
Tetralin‡ [1.7–7.3]	—	1–2	8–32	2.3	7.6	6.3
Tetralin [1.7]	0.11	2.3	8	2.3	7.2	6.3
Tetralin [1.6]	0.1	0.08§	44	2.4	—	6.6
Toluene [8.7]	0.43	0.25	4	0.04	—	0.1
Ethylbenzene [8.0]	0.11	2.0	3	0.18	—	0.5
Cumene [7.0]	0.11	2.4	2	0.18	—	0.5
Cumene [6.7]	0.43	1–5	2–5	0.20	—	0.55
Styrene [0.7]	0.12	2.3	4.5	3.1	—	8.5
Styrene [0.7]	0.47	1.4	6	3.2	—	8.8
α-Methylstyrene [1.7]	0.27	3.9	15	5.7	—	16
Dihydroanthracene [0.1]	0.32	3.1	15	85	—	240

*Reactions photochemically initiated unless otherwise noted.
†Calculated using $2k_t = 7.6 \times 10^6$ M^{-1} s^{-1}.
‡From ref. 4.
§Thermally initiated.

TABLE II

Rate constants (in M^{-1} s^{-1}) for hydrocarbon oxidations in the presence of diphenylmethyl hydroperoxide

Hydrocarbon [M]	Hydroperoxide [M]	$R_i \times 10^7$* (M s^{-1})	Chain length	$k_p/(2k_t)^{\frac{1}{2}} \times 10^3$	$2k_t \times 10^{-7}$	k_p†
Diphenylmethane‡,§ [6.0]	—	1.1	8	0.38	16	4.8
Diphenylmethane [6.0]	0.1	1.2	8	0.39	—	2.1
Ethylbenzene [8.0]	0.1	0.4	5	0.15	—	0.8
Cumene [6.7]	0.1	0.1	6	0.1	—	0.5
Tetralin§ [7.2]	0.1	1.5	26	1.25	2.0	6.6
Styrene [2.0]	0.1	2.6	12	3.0	2.7	16
α-Methylstyrene‖,¶ [1.8]	0.1	2.3	17	4.7	3.6	25
Dihydroanthracene‖ [0.2]	0.1	3.0	17	47	—	250

*Photochemically initiated.
†Calculated using $2k_t = 2.8 \times 10^7$ M^{-1} s^{-1}.
‡From ref. 13.
§Autocatalytic.
‖Autoretarding.
¶Reduction of pressure from 660 to 88 mm had no effect on the rate of oxidation.

accumulation of hydroperoxide. The revised termination rate constant is more consistent with the values found for other secondary benzylic peroxy radicals (14) and has been used to calculate all the cross propagation rate constants.

9,10-Dihydroanthracyl-9-hydroperoxide

The propagation and termination constants for the oxidation of 9,10-dihydroanthracene at 30° were originally reported as $k_p = 176$, $2k_t = 9.2 \times 10^6$ M^{-1} s^{-1} (14). Values about twice as large have since been obtained in a further series of experiments at various hydrocarbon concentrations and rates of initiation. All the propagation constants given in Table III have been calculated using the revised value of $2k_t = 2.0 \pm 0.4 \times 10^7$ M^{-1} s^{-1}. The hydroperoxide itself oxidizes at a relatively high rate ($k_p/(2k_t)^{\frac{1}{2}} = 21 \times 10^{-3}$ $M^{-\frac{1}{2}}$ s$^{-\frac{1}{2}}$) and this limits the determination of cross propagation constants to those hydrocarbons which are themselves fairly readily oxidized. Oxidation of the hydroperoxide at 30° gave about 5% hydrogen peroxide and 5% anthracene, based on the absorbed oxygen. The concentration of these two products increased fairly rapidly on storage of the oxidized hydroperoxide at −10 °C, which suggests that the expected 9,10-dihydroanthracyl-9,10-dihydroperoxide is quite unstable. The oxidation of 9,10-dihydroanthracene at 30° gave the mono-hydroperoxide as the sole primary product.

n-Butyl Hydroperoxide, sec-Butyl Hydroperoxide, and Cyclohexyl Hydroperoxide

The results obtained with these three hydroperoxides are given in Tables IV, V, and VI. The average termination constants (which have been reported previously (6)) are: *n*-butyl $2k_t = 4.3 \pm 2.4 \times 10^7$; *sec*-butyl $2k_t = 1.5 \pm 0.2 \times 10^6$; and cyclohexyl $2k_t = 2.0 \pm 0.9 \times 10^6$ M^{-1} s^{-1}.

Can. J. Chem. Downloaded from www.nrcresearchpress.com by 188.143.235.115 on 09/06/12
For personal use only.

TABLE III

Rate constants (in M^{-1} s^{-1}) for hydrocarbon oxidations in the presence of 9,10-dihydroanthracyl-9-hydroperoxide

Hydrocarbon [M]	Hydroperoxide [M]	$R_i \times 10^7$* (M s^{-1})	Chain length	$k_p/(2k_t)^{\frac{1}{2}} \times 10^3$	$2k_t \times 10^{-7}$	k_p†
Dihydroanthracene [0.1–0.2]	—	0.1–2.5	16–136	79	2.0	350
Dihydroanthracene [0.1]	0.1	2.9	13	70	—	310
Ethylbenzene [8.0]‡	0.1	2.1	5	0.13	2.0	0.6
Tetralin [3.3]	0.1	2.2	10	1.5	4.4	6.5
Styrene [0.7]	0.1	2.2	7	4.8	—	21
α-Methylstyrene [1.7]	0.1	2.9	24	7.5	—	33

*Photochemically initiated.
†Calculated using $2k_t = 2.0 \times 10^7$ M^{-1} s^{-1}.
‡The rate of oxidation increased from an initial value of 8.3×10^{-7} M s^{-1} to a value of 9.5×10^{-7} M s^{-1} after the absorption of 5.7×10^{-3} M O_2.

TABLE IV

Rate constants (in M^{-1} s^{-1}) for hydrocarbon oxidations in the presence of *n*-butyl hydroperoxide

Hydrocarbon [M]	Hydroperoxide [M]	$R_i \times 10^7$* (M s^{-1})	Chain length	$k_p(2k_t)^{\frac{1}{2}} \times 10^4$	$2k_t \times 10^{-7}$	k_p†
Toluene [9.3]	0.24	0.4	1.5	0.2	—	0.1
Ethylbenzene [8.0]	0.24	1.8	2.0	0.83	—	0.55
Cumene [7.1]	0.24	0.4	2.0	0.70	—	0.45
Tetralin [7.2]	0.24	1.8	16	9.8	7.0	6.4
Styrene [3.4]	0.31	3.3	13	22	—	14
α-Methylstyrene [1.8]	0.12	2.5	15	42	4.1	27
α-Methylstyrene [1.8]	0.24	3.0	13	37	1.7	24
Dihydroanthracene [0.2]	0.4	3.2	16	470	—	310

*Photochemically initiated.
†Calculated using an average $2k_t = 4.3 \times 10^7$ M^{-1} s^{-1}.

These values are smaller than the values found for peroxy radicals of generally similar structure but in which the peroxy group is adjacent to a π-electron system (14). McCarthy and MacLachlan (15) have previously obtained $2k_t = 2.8 \times 10^6$ M^{-1} s^{-1} for cyclohexylperoxy radicals by the pulse radiolysis of aerated cyclohexane.

Inhibition Experiments

The propagation rate constant for the direct oxidation of styrene, k_p^{SS}, is 41 M^{-1} s^{-1} (14). This value is significantly larger than the values found for the addition to styrene of the secondary peroxy radicals used in this work, i.e. k_p^{RS} ~ 6.0–21 M^{-1} s^{-1}. Similarly, the propagation rate constant obtained by the direct oxidation of α-methylstyrene is 10 M^{-1} s^{-1} (14), which is comparable to the values found for attack on this substrate by some of the secondary peroxy radicals rather than by the tertiary cumylperoxy radical for which k_p is only 3.9 M^{-1} s^{-1} (5). The propagation constants for the self-oxidation of β-methylstyrene and for its attack by cumylperoxy radicals exhibit a similar anomaly (5).

In an attempt to confirm some of these differences in rate constants we carried out some experiments in which the oxidation of styrene was inhibited with 2,6-di-*t*-butyl-4-methylphenol (BMP). The rate constant ratio $k_p^{SS}/k_{inh}^{S} = 5.25 \times 10^{-3}$, where k_{inh}^{S} is the rate constant for hydrogen abstraction from BMP by the styrylperoxy radical. Inhibition experiments on styrene containing tetralin hydroperoxide (0.23 M) gave $k_p^{TS}/k_{inh}^{T} = 1.3 \times 10^{-3}$. Inhibition of tetralin gave $k_p^{TT}/k_{inh}^{T} = 0.8 \times 10^{-3}$, a value which was not affected by the addition of tetralin hydroperoxide. Hence, $(k_p^{SS}/k_{inh}^{S}) \times (k_{inh}^{T}/k_p^{TT}) \approx (5.25/0.8) = 6.6$. The ratio of the directly measured propagation constants $k_p^{SS}/k_p^{TT} = 41/6.4 = 6.4$, which implies that $k_{inh}^{S} \approx k_{inh}^{T}$. Therefore, $(k_p^{SS}/k_{inh}^{S}) \times (k_{inh}^{T}/k_p^{TS}) \approx (k_p^{SS}/k_p^{TS}) \approx (5.25/1.3) \approx 4$, in good agreement with the ratio obtained from the absolute rate measurements, i.e., $k_p^{SS}/k_p^{TS} = 41/8.8 = 4.7$. The ratio $k_p^{TT}/k_p^{TS} = 6.4/8.8 = 0.73$ is in reasonable agreement with the value of 0.43 at 60° found by Mayo *et al.* (16).

Discussion

The addition of the hydroperoxides of tetralin, diphenylmethane, and 9,10-dihydroanthracene to their parent hydrocarbons has little or no

Can. J. Chem. Downloaded from www.nrcresearchpress.com by 188.143.235.115 on 09/06/12
For personal use only.

TABLE V

Rate constants (in M^{-1} s^{-1}) for hydrocarbon oxidations in the presence of *sec*-butyl hydroperoxide

Hydrocarbon [*M*]	Hydroperoxide [*M*]	$R_i \times 10^7$* (M s^{-1})	Chain length	$k_p/(2k_t)^{\frac{1}{2}} \times 10^4$	$2k_t \times 10^{-6}$	k_p†
Toluene [9.1]	0.3	2.5	4	0.65	—	0.1
Ethylbenzene [8.0]	0.15	1.4	9	4.1	2.7	0.5
Cumene [7.1]	0.15	1.5	6	3.4	1.0	0.4
Tetralin [7.3]	0.075	1.6	57	32	1.4	4.0
Tetralin [7.2]	0.15	1.6	62	34	2.2	4.2
Tetralin [7.2]	0.3	1.9	55	35	1.3	4.3
Styrene [3.4]	0.2	3.0	29	46	—	5.6
Styrene [3.2]	0.7	1.1	60	57	—	7.0
α-Methylstyrene [1.8]	0.15	2.5	34	98	0.55	12
Dihydroanthracene [0.1]	0.17	2.8	24	1300	—	160
Dihydroanthracene [0.2]	0.75	1.3	60	900	—	110

*Photochemically initiated.
†Calculated using an average $2k_t = 1.5 \times 10^6$ M^{-1} s^{-1}.

TABLE VI

Rate constants (in M^{-1} s^{-1}) for hydrocarbon oxidations in the presence of cyclohexyl hydroperoxide

Hydrocarbon [*M*]	Hydroperoxide [*M*]	$R_i \times 10^7$* (M s^{-1})	Chain length	$k_p/(2k_t)^{\frac{1}{2}} \times 10^3$	$2k_t \times 10^{-6}$	k_p†
Ethylbenzene [8.0]	0.13	1.1	8	0.35	1.7	0.5
Ethylbenzene [7.9]	0.26	1.1	8	0.35	—	0.5
Tetralin [7.2]	0.13	1.9	52	3.1	3.0	4.5
Styrene [3.4]	0.17	2.8	31	4.8	—	6.8
α-Methylstyrene [1.8]	0.13	2.4	34	9.6	—	14
Dihydroanthracene [0.2]	0.18	2.6	29	73.5	—	104
Dihydroanthracene [0.2]	0.47	4.1	28	88	—	125
Dihydroanthracene [0.2]	0.9	1.6	48	97	—	137

*Photochemically initiated.
†Calculated using $2k_t = 2.0 \times 10^6$ M^{-1} s^{-1}.

effect on the rate constants for chain termination (see Tables I, II, and III). This contrasts with the results obtained with tertiary hydroperoxides and their parent hydrocarbons (7) and implies that essentially all self-reactions of secondary peroxy radicals are chain terminating (cf. 6).

The cross propagation rate constants obtained in this work are summarized in Table VII. The general similarity in the rate constants found for the attack of secondary peroxy radicals on any particular hydrocarbon is reassuring evidence for the validity of the present experimental approach. The differences in propagation rate constants may perhaps be within the overall limits of experimental error, since it is difficult to measure termination rate constants to better than a factor of two by the rotating sector method. In certain cases, it is possible that insufficient hydroperoxide was employed to completely suppress all terminations (particularly cross terminations) involving the peroxy radical from the hydrocarbon. However, some of the major discrepancies in k_p values could not be resolved even by careful repetition of the experiments. While it is always a serious mistake to try to deduce more from experimental data than is warranted by the experimental accuracy, the propagation constants in Table VII do appear to increase along the series, *sec*-butyl ~ cyclohexyl < tetralyl < diphenylmethyl < dihydroanthracyl. This suggests that phenyl groups on the α-carbon atom increase the reactivity of the peroxy radical. The effect of the phenyl groups could perhaps be attributed to their electron-withdrawing inductive effect ($-I$ effect) which will increase the electrophilicity of the peroxy radical. Propagation reactions involving either attack of a peroxy radical on a saturated carbon–hydrogen bond or addition to a conjugated olefin are known to involve polar effects of the following type (5, 17–21).

$$\mathrm{ROO\cdot} + \mathrm{RH} \xrightarrow{k_p} [\mathrm{ROO}^{\delta-} : \mathrm{H}^{\delta+}\cdot\mathrm{R}] \rightarrow \mathrm{ROOH} + \mathrm{R\cdot}$$

$$\mathrm{ROO\cdot} + \mathrm{CH_2{=}CHR} \xrightarrow{k_p} [\mathrm{ROO}^{\delta-} : \mathrm{CH_2}^{\delta+}\text{–}\dot{\mathrm{C}}\mathrm{HR}] \rightarrow \mathrm{ROOCH_2\dot{C}HR}$$

A decrease in the electron density at the terminal

Can. J. Chem. Downloaded from www.nrcresearchpress.com by 188.143.235.115 on 09/06/12
For personal use only.

TABLE VII

Rate constants (in M^{-1} s^{-1}) for the reactions of some peroxy radicals with some hydrocarbons

Hydrocarbon	Peroxy Radical						Average tertiary*
	n-Butyl	*sec*-Butyl	Cyclohexyl	Tetralyl	Diphenylmethyl	Dihydroanthracyl	
Toluene	0.1	0.1	—	0.1	—	—	0.04
Ethylbenzene	0.5_5	0.5	0.5	0.5	0.8	0.6	0.23
Cumene	0.4_5	0.4	—	0.5	0.5	—	0.17
Tetralin	6.4	4.2	4.5	6.3	6.6	6.5	1.7
Styrene	14	6.3	6.8	8.8	16	21	1.6
α-Methylstyrene	25	12	14	16	25	33	3.9†
Dihydroanthracene	310	140	~160‡	240	250	330	70†

*From preceding paper
†Values for the cumylperoxy radical (5).
‡Obtained by extrapolation of data in Table VI.

oxygen of the peroxy radical in its ground state should facilitate the formation of dipolar structures of this type and should therefore increase the reactivity of the peroxy radical. The effect of α-phenyl groups on the reactivity of tertiary peroxy radicals is small (7), possibly because the accelerating $-I$ effect is countered by an opposing steric effect.

The importance of polar effects on peroxy radical selectivity and relative reactivity has recently been stressed by Mayo *et al.* (16). More directly, we have previously shown that the rate constant for hydrogen atom abstraction from 2,6-di-*t*-butyl-4-methylphenol (where the transition state involves a similar separation of charge (20, 22)) by ring-substituted polystyrylperoxy radicals increases as the substituents become more electron attracting (21).[4] The propagation constants for the oxidation of the styrenes containing electron-withdrawing substituents (21) could also be interpreted in terms of a greater reactivity for their peroxy radicals compared with the unsubstituted polystyrylperoxy radical. The propagation rate constants obtained by the direct oxidation of styrene, α-methylstyrene and β-methylstyrene (14) are appreciably larger than would be expected on the basis of the values obtained with non-polymeric peroxy radicals (see Results section and also ref. 5). Possibly the poly(peroxystyryl)peroxy radical ($ROOCH_2C(H,Ph)OO^{\cdot}$) has an enhanced reactivity compared with most other secondary peroxy radicals because of the $-I$ effect of the oxygen on the β carbon. If polar factors do, in fact, have a real influence on the absolute reactivities of peroxy radicals, then considerably larger effects should arise in the oxidation of ethers, esters, ketones, and alcohols.

The propagation rate constants for the *n*-butylperoxy radical are larger than the values found for *sec*-butylperoxy and cyclohexylperoxy but are, nevertheless, within the overall range of values found for the various secondary peroxy radicals.

Our previously determined average cross propagation rate constants for tertiary peroxy radicals (5, 7) are given in Table VII for comparison with the values found for secondary peroxy radicals. The secondary (and primary) peroxy radicals are generally about 2–4 times more reactive than tertiary peroxy radicals in abstraction and 4–8 times more reactive in addition. The lower reactivity of the tertiary peroxy radicals is presumably due to steric factors. However, an explanation for the difference in the relative reactivities for abstraction and addition, assuming this difference is real, is not readily apparent.

The results of the present work suggest that the absolute reactivities of peroxy radicals may be influenced both by polar and by steric effects.

[4]At 40°, k_{inh} values are 8.5, 10.8, and 14.8 × 10^3 M^{-1} s^{-1} for the peroxy radicals derived from 4-methoxystyrene, styrene, and 3-chlorostyrene, respectively (21).

1. J. R. Thomas and C. A. Tolman. J. Am. Chem. Soc. **84**, 2079 (1962).
2. T. G. Traylor and C. A. Russell. J. Am. Chem. Soc. **87**, 3698 (1965).
3. J. R. Thomas. J. Am. Chem. Soc. **89**, 4872 (1967).
4. J. A. Howard, W. J. Schwalm, and K. U. Ingold. Preprints of the International Oxidation Symposium, San Francisco, California. 1967. **1**, p. 3.
5. J. A. Howard, K. U. Ingold, and M. Symonds. Can. J. Chem. **46**, 1017 (1968).
6. J. A. Howard and K. U. Ingold. J. Am. Chem. Soc. **90**, 1058 (1968).
7. J. A. Howard and K. U. Ingold. Can. J. Chem. This issue.
8. D. G. Hendry. J. Am. Chem. Soc. **89**, 5433 (1967).
9. A. E. Woodward and R. B. Mesrobian. J. Am. Chem. Soc. **75**, 6189 (1953).

Can. J. Chem. Downloaded from www.nrcresearchpress.com by 188.143.235.115 on 09/06/12
For personal use only.

10. A. F. BICKEL and E. C. KOOYMAN. J. Chem. Soc. 2215 (1956).
11. H. R. WILLIAMS and H. S. MOSHER. J. Am. Chem. Soc. **76**, 2987 (1964).
12. A. G. DAVIES, R. V. FOSTER, and A. M. WHITE. J. Chem. Soc. 1541 (1953).
13. J. A. HOWARD and K. U. INGOLD. Can. J. Chem. **44**, 1119 (1966).
14. J. A. HOWARD and K. U. INGOLD. Can. J. Chem. **45**, 793 (1967).
15. R. L. MCCARTHY and A. MACLACHLAN. Trans. Faraday Soc. **57**, 1107 (1961).
16. F. R. MAYO, M. G. SYZ, T. MILL, and J. K. CASTLEMAN. Preprints of the International Oxidation Symposium, San Francisco, California. 1967. **1**, 777.
17. G. A. RUSSELL. J. Am. Chem. Soc. **78**, 1047 (1956).
18. G. A. RUSSELL and R. C. WILLIAMSON, JR. J. Am. Chem. Soc. **86**, 2357 (1964).
19. D. G. HENDRY and G. A. RUSSELL. J. Am. Chem. Soc. **86**. 2368 (1964).
20. J. A. HOWARD and K. U. INGOLD. Can. J. Chem. **42**, 1044 (1964).
21. J. A. HOWARD and K. U. INGOLD. Can. J. Chem. **43**, 2737 (1965).
22. J. A. HOWARD and K. U. INGOLD. Can. J. Chem. **40**, 1851 (1962); **41**, 1744, 2800 (1963); **42**, 2324 (1964).

Can. J. Chem. Downloaded from www.nrcresearchpress.com by 188.143.235.115 on 09/06/12
For personal use only.

Extended Hückel molecular orbital calculations on some titanium–oxygen systems[1]

YU-PING HSIA
Department of Chemistry, University of Bridgeport, Bridgeport, Connecticut

Received January 24, 1968

Extended Hückel molecular orbital calculations have been performed on localized TiO_6^{8-} units with the precise geometry of such a unit in solid rutile, anatase, and brookite TiO_2 and tetragonal $BaTiO_3$. The relative values of one-electron energy levels in these compounds are obtained in terms of a "self-consistent" charge and population calculation. Examination of the resulting energy levels and charge distributions has led to reasonable explanations of previously unexplained data on (1) the visible and near-ultraviolet absorption spectra of these compounds, (2) the low energy X-ray absorption edges of rutile, anatase, and brookite TiO_2, and (3) the pressure dependence of the absorption edges of rutile TiO_2 and tetragonal $BaTiO_3$.

Canadian Journal of Chemistry, 46, 2667 (1968)

Can. J. Chem. Downloaded from www.nrcresearchpress.com by 210.87.254.42 on 09/05/12
For personal use only.

Introduction

The extended Hückel molecular orbital (m.o.) theory applied to transition metal compounds has been carried out for various ions and compounds (1–12). Although the initial results are encouraging, it is clear that there is a need for a standard and consistent method of choosing the parameters in the calculation which can be transferred from one transition metal compound to another. It also seems desirable to explore whether this method can explain other phenomena besides the normal absorption spectra. Since the structures and optical data of rutile, anatase, and brookite TiO_2 and $BaTiO_3$ are available (13–26), it is of interest to examine these compounds by performing molecular orbital calculations on hypothetical localized TiO_6^{8-} units with the exact geometries of the units in the parent compounds.

Procedure

An extended Hückel m.o. computer program written in Fortran IV language has been used in carrying out the "self-consistent" charge and population calculation. The output of this program gives the molecular orbital energy values as well as the total gross electron population in the atomic orbitals. The method of obtaining the total gross electron population and the gross charge is similar to Mulliken's method of electron population analysis (27). In the calculation, we consider only the 2s and 2p atomic orbitals of each of the oxygen atoms and only the 3d, 4s, and 4p atomic orbitals of the titanium atom in constructing the molecular orbitals. Therefore, a total of 33 orbitals are involved in bonding. In the case of the compounds discussed here, 48 electrons are used in bonding. The ground state is constructed by placing these electrons in the lowest-lying molecular orbitals. The analytic 2s and 2p oxygen self-consistent field radial functions used in our calculations are those given by Ballhausen and Gray (2). The titanium 3d, 4s, and 4p atomic wave functions used are those published by Richardson and co-workers (28, 29). The needed diatomic overlap integrals between the various atomic orbitals at various distances are calculated through two overlap integral evaluation programs written in the symbolic programming language IT for the univac 1105 electronic digital computer.

The diagonal effective Hamiltonian matrix elements for the titanium orbitals are approximated as the negative of the valence state ionization energies (v.s.i.e.) of the titanium ion of appropriate charge. Curves of v.s.i.e. as a function of charge on Ti for various electronic configurations can be drawn from the data in Moore's (30) table of atomic spectra. The valence state ionization energy values for fractional charges are obtained by interpolation of these v.s.i.e. vs. degree of ionization curves. Thus if a charge and electronic population are assumed the corresponding v.s.i.e. values can be calculated. The use of the v.s.i.e.'s for fractional charges on oxygen gives unreasonable values for the m.o. energy levels, similar to the results of

[1]Partially taken from the Ph.D. Thesis of Yu-ping Hsia, Illinois Institute of Technology.

Can. J. Chem. Downloaded from www.nrcresearchpress.com by 210.87.254.42 on 09/05/12
For personal use only.

Tyree and co-workers (4) for fluoride complexes. Thus, the diagonal effective Hamiltonian matrix elements for the oxygen orbitals are estimated simply as the negative of the valence state ionization energies of neutral oxygen atom.

The off-diagonal terms are approximated in a manner similar to that used by Wolfsberg and Helmholz (1):

$$H_{ij} = K_x \frac{H_{ii} + H_{jj}}{2} S_{ij}.$$

The values of K_x employed in this calculation are chosen so that the calculated first charge transfer energy for rutile TiO_2 will exactly fit the experimental data. The final determined values of K_x are $K_\sigma = 1.59$, $K_\pi = 1.79$, $K_{L-L} = 1.69$, where K_σ, K_π, and K_{L-L} are related to the off-diagonal terms of sigma titanium–oxygen overlaps, pi titanium–oxygen overlaps, and oxygen–oxygen overlaps respectively. These values can be compared with $K = 1.75$ recommended by Hoffmann (31) for hydrocarbons, $K = 1.80$ used by Cotton and Harris (11) for copper(II) and nickel(II) complexes, and $K_\sigma = 1.6$ and $K_\pi = 1.87$, which Wolfsberg and Helmholz used in making calculations of the energy levels of homonuclear diatomic molecules of first and second row elements.

Results and Discussion

In the compound we studied, the coordination number of the titanium ion is six. However, their symmetries are not octahedral; rather, they depart from a perfectly octahedral system to a greater or lesser extent. We will construct the m.o. energy level diagram of the rutile TiO_2 system which has a relatively higher symmetry in the compounds we studied. The unit cell of crystalline rutile TiO_2 is tetragonal, and the TiO_6 unit in this compound belongs to the D_{2h} point group. The method of constructing molecular orbital energy level diagrams has been illustrated by various authors (32, 33). We will not give the detailed procedure here but will show the orbital transformation scheme of D_{2h} symmetry in Table I and the molecular orbital energy diagram of this symmetry in Fig. 1. In Fig. 1, the molecular orbitals are connected to the atomic orbitals from which they are mainly derived. However, it should not be forgotten that unconnected atomic orbitals with the same symmetries as molecular orbitals also

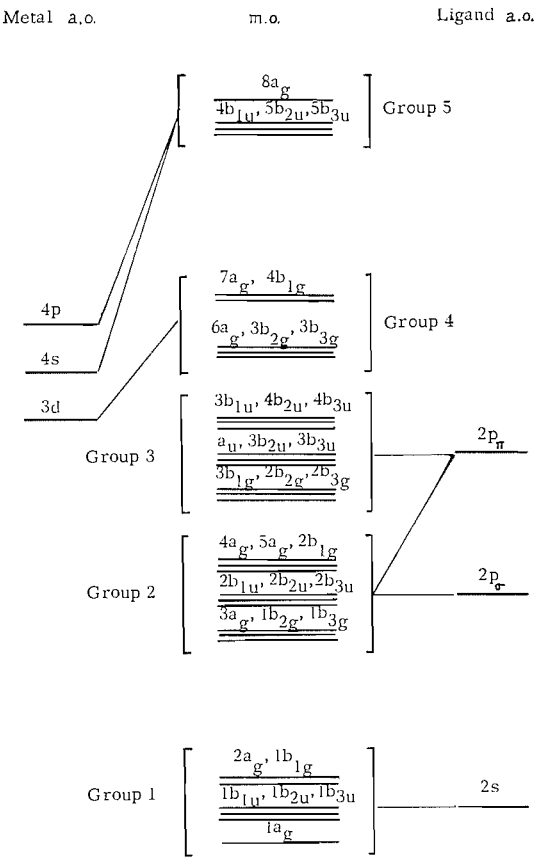

FIG. 1. Molecular orbital energy level diagram for D_{2h} complexes.

contribute some portions in forming the molecular orbitals. The brackets in the diagrams enclose m.o. levels of comparable energies derived essentially from the same atomic orbitals. By means of these brackets, we are able to divide the 33 m.o. levels into five groups, as shown in the figures for later discussions. There is a consistent ordering of the groups in the compounds we studied; however, permutations of m.o. levels occur within some groups.

Placing the 48 electrons in the lowest-lying orbitals in the D_{2h} symmetry compounds, we obtain the ground state

$$(\text{group } 1)^{12}(\text{group } 2)^{18}(\text{group } 3)^{18}$$
with symmetry A_g.

The first allowed charge transfer corresponds to the excitation of a group 3 m.o. level electron to the lowest m.o. level in group 4, provided

TABLE I

Orbital scheme in D_{2h} symmetry

Representation	Ti orbitals	Ligand orbitals (σ)	Ligand orbitals (π)
a_g	4s	$6^{-1/2}(s_1+s_2+s_3+s_4+s_5+s_6)$	$1/2(x_2+x_4+y_1-y_3)$
	$3d_{x^2-y^2}$	$6^{-1/2}(z_1+z_2+z_3+z_4+z_5+z_6)$	
	$3d_{z^2}$	$12^{-1/2}(2s_5+2s_6-s_1-s_2-s_3-s_4)$	
		$12^{-1/2}(2z_5+2z_6-z_1-z_2-z_3-z_4)$	
b_{1u}	$4p_z$	$2^{-1/2}(s_5-s_6)$	$1/2(x_1-x_3+y_2+y_4)$
		$2^{-1/2}(z_5-z_6)$	
b_{2u}	$4p_y$	$1/2(s_1+s_4-s_2-s_3)$	$12^{-1/2}(x_2-x_4-y_1-y_3+2x_5+2x_6)$
		$1/2(z_1+z_4-z_2-z_3)$	$12^{-1/2}(x_2-x_4-y_1-y_3-2x_5-2x_6)$
b_{3u}	$4p_x$	$1/2(s_1+s_2-s_3-s_4)$	$12^{-1/2}(x_2-x_4+y_1+y_3+2y_5-2y_6)$
		$1/2(z_1+z_2-z_3-z_4)$	$12^{-1/2}(x_2-x_4+y_1+y_3-2y_5+2y_6)$
b_{1g}	$3d_{xy}$	$1/2(s_1+s_3-s_2-s_4)$	$1/2(x_2+x_4-y_1+y_3)$
		$1/2(z_1+z_3-z_2-z_4)$	
b_{2g}	$3d_{xz}$		$12^{-1/2}(x_1+x_3+y_2-y_4+2y_5+2y_6)$
			$12^{-1/2}(x_1+x_3+y_2-y_4-2y_5-2y_6)$
b_{3g}	$3d_{yz}$		$12^{-1/2}(x_1+x_3-y_2+y_4+2x_5-2x_6)$
			$12^{-1/2}(x_1+x_3-y_2+y_4-2x_5+2x_6)$
a_u			$1/2(x_1-x_3-y_2-y_4)$

that it is an allowable electronic transition. According to Laporte's rule, only transitions between A_g and states of u symmetry in D_{2h} will be allowed. It should be noted that the 9 m.o. levels in group 3, and the 3 lower levels in group 4, are very close. Therefore, a total of 27 possible transitions should be considered. We found that there are 13 allowed transitions and 14 forbidden transitions. Because of the proximity of the energy levels in group 3 and the difficulty of identifying the exact symmetry for the molecular orbitals, owing to the considerably low symmetries of the compounds studied, we assumed that the difference between the highest energy level in group 3 and the lowest energy level in group 4 is the first charge transfer transition in our calculations.

Table II lists the final values of the coulomb integrals, H_{ii}, used for the Ti orbitals and the final self-consistent electron populations and gross charges on Ti for rutile, anatase, brookite, and tetragonal $BaTiO_3$. The final energy levels of the 33 molecular orbitals at the self-consistent charge and electron population for these compounds are shown graphically in Fig. 2. Table III shows the calculated first charge transfer energy and the corresponding observed energy for these compounds. As we mentioned before, the K_x parameters are so chosen that the calculated energy for rutile is exactly fitted to the experimental data. The calculated result for

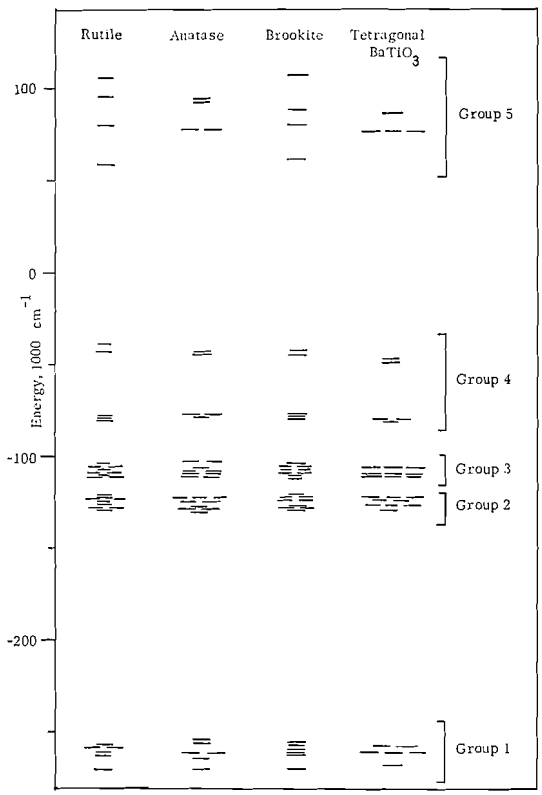

FIG. 2. Energy level diagrams for rutile, anatase, brookite, and tetragonal barium titanate.

Can. J. Chem. Downloaded from www.nrcresearchpress.com by 210.87.254.42 on 09/05/12
For personal use only.

TABLE II

The final coulomb integrals, the self-consistent electron populations, and charges on Ti for rutile, anatase, brookite, and tetragonal barium titanate

		Rutile	Anatase	Brookite	Tetragonal $BaTiO_3$
Coulomb integrals for Ti ($1000\ cm^{-1}$)	3d	−102.40	−102.50	−102.40	−102.20
	4s	−93.90	−94.30	−94.00	−93.80
	4p	−63.00	−63.30	−63.00	−62.80
Electron populations on Ti	3d	3.0547	3.0423	3.0475	3.0432
	4s	0.0651	0.0562	0.0613	0.0748
	4p	0.1071	0.1234	0.1208	0.1296
Final charges on Ti		0.7731	0.7781	0.7704	0.7524
Coulomb integrals for oxygens ($1000\ cm^{-1}$)	2s		−260.00		
	$2p_\sigma$		−120.00		
	$2p_\pi$		−110.00		
K_x used	K_σ		1.59		
	K_π		1.79		
	K_{L-L}		1.69		

anatase is somewhat smaller than the observed one, but is in agreement with the experimental data that the observed energy for anatase is larger than that for rutile. The result for brookite does not follow the experimental trend. However, there is a possibility that 3.26 eV is not the exact first charge transfer energy for brookite since the compound studied was admittedly not pure (20). The result for tetragonal $BaTiO_3$ shows excellent agreement between the observed and calculated value as shown in Table III.

After relating the calculated m.o. energy levels to the experimental data from reflectance or transmission spectra of the compounds, it may be worthwhile to compare and discuss other data and aspects with our extended Hückel m.o. calculations.

Companion and Wyatt (20) proposed that the absorptions beginning at 3.00, 3.23, and 3.26 eV for rutile, anatase, and brookite respectively correspond to electron transfer excitations from the O^{2-} 2p levels to empty levels on the Ti^{4+} ions. Our results show that all m.o. levels in group 3 are mainly derived from oxygen 2p orbitals, and all the empty m.o. levels in group 4 are mainly from titanium 3d orbitals; therefore, our assumption that the absorption refers to the transition of an electron from a group 3 m.o. level to a group 4 m.o. level agrees completely with what they proposed.

Kahn, Frederikse, and Becker (34) have shown that the overall widths of the valence and conduction band of rutile TiO_2 are each of the order of 4 eV, where the valence band is the band derived from oxygen 2p orbitals and the conduction band is considered as that from the titanium 3d orbitals. Our group 2 and group 3 m.o. levels are mainly from oxygen 2p orbitals and group 4 m.o. levels are mainly from titanium 3d orbitals; we can relate the former levels to the valence band and the latter levels to the conduction band. The overall widths of these bands for rutile, anatase, brookite, and tetragonal $BaTiO_3$ are calculated and given in Table IV.

TABLE III

The calculated and observed first charge transfer energy for rutile, anatase, brookite, and tetragonal barium titanate

	Calculated energy		Observed energy		
Compound	$1000\ cm^{-1}$	eV	$1000\ cm^{-1}$	eV	Reference
Rutile	24.24	3.00	24.24	3.00	(20)
Anatase	24.70	3.06	26.06	3.23	(20)
Brookite	24.12	2.99	26.30	3.26	(20)
Tetragonal barium titanate	25.43	3.15	25.43	3.15	(22, 23)

Can. J. Chem. Downloaded from www.nrcresearchpress.com by 210.87.254.42 on 09/05/12
For personal use only.

TABLE IV

The calculated valence band and conduction band of rutile, anatase, brookite, and tetragonal barium titanate

Compound	Valance band[a]		Conduction band[b]	
	1000 cm^{-1}	eV	1000 cm^{-1}	eV
Rutile	25.01	3.10	40.68	5.04
Anatase	26.87	3.33	34.71	4.30
Brookite	25.57	3.17	37.04	4.59
Tetragonal barium titanate	22.42	2.78	33.58	4.16

[a]The valence band refers to the difference between the highest m.o. level in group 3 and the lowest m.o. level in group 2.
[b]The conduction band refers to the difference between the highest and the lowest m.o. level in group 4.

It can be seen from Table IV that our calculated values of valence and conduction bands for rutile TiO_2 are close to what Kahn, Frederikse, and Becker suggested.

The X-ray K absorption spectra of rutile, anatase, and brookite have been reported by Vainshtein and co-workers (24–26). The two lower energy peaks (between 15–19 eV) with separation about 3–4 eV may be due to the internal transitions of K electrons to the empty 3d levels of Ti^{4+} in the compounds. This separation can be related to the difference between octahedral t_{2g} and e_g orbital on Ti^{4+}. It is assumed that further splittings due to the distortion of the octahedron were not observed. This argument may be supported by the work done by Hanson and Knight (35), who have demonstrated the presence of a weak absorption near the onset of the K edge in several transition metal oxides with incomplete d levels and identified those as K $\rightarrow$ 3d transitions. In the group 4 m.o. energy levels of our calculated results, the differences between the lower three m.o. levels (related to t_{2g} orbitals) and the upper two m.o. levels (related to e_g orbitals) are 34 930 cm^{-1} (4.33 eV), 32 860 cm^{-1} (4.07 eV), and 31 970 cm^{-1} (3.96 eV) for rutile, anatase, and brookite respectively. These results can certainly support the above argument concerning the two lower energy peaks in Vainshtein's X-ray data. Also, in Vainshtein's X-ray spectra there was a 15–17 eV separation between the two higher energy peaks in rutile, anatase, and brookite. These two higher energy peaks were usually suggested as K–4p transitions (20). This may not be a good assumption as we will see in the following discussions.

Cotton and Ballhausen (36) have shown theoretically by means of an ionic model that the splitting of the K–4p absorption for first row transition elements can be related to the splitting of the degeneracy of the 4p energy levels in the ion by the crystal field. They were able to make a prediction of the splittings, on the basis of symmetry, that for D_{4h} symmetry, the p orbitals should split into only two levels and for C_{2v} symmetry, they should split into three levels. In the C_{2v} symmetry, Cotton and Ballhausen were able to show that two of the three levels were accidentally degenerate in the crystal field approximation. However, in the case of the D_{2h} symmetry, they predicted that the p orbitals will split into three levels without any chance of accidental degeneracy. They further estimated that the magnitude of the splitting of the 4p orbitals should be around 7 eV. In their experimental data (37), X-ray K absorption edges in some cupric complexes were observed. It appeared that the separations between two peaks of 5–7 eV, averaging $\sim$ 5.5 eV, were observed and were in agreement with the prediction of the splitting of the 4p levels in the D_{4h} field. According to the prediction, the splitting of the p level into three components in the Cu(II) DL-prolinate dihydrate should, in principle, occur; however, the p level did not split experimentally. They explained that fact by adopting the argument of the spectrochemical series of Fajans and Tsuchida (for example see ref. 38) that because of the relatively poor resolution of X-ray work, the splitting large enough to be clearly discernible will only occur when the atoms on different axes are different. As we mentioned before, rutile TiO_2 has a symmetry of D_{2h}, while anatase and brookite have even lower symmetry. According to the prediction by Cotton and Ballhausen, the p orbitals in these dioxides should split into three levels, which may or may not be seen from the X-ray absorption spectra. Since in the three dioxides the atoms on different axes are the same (namely, all are oxygens), the splitting of p orbitals may not be observed. If it was observed at all, as a rule, splitting of 4 p orbitals and hence of the 1s–4p absorption band into three instead of two components should be observed in most cases, and the splitting values should not be as big as 15–17 eV, as shown in Vainshtein's spectra. In our calculations, we tried to adjust all possible parameters (K_x, H_{ii}, and H_{jj}) in reasonable ranges and could not make any two of the three p levels degenerate in rutile and brookite.

Can. J. Chem. Downloaded from www.nrcresearchpress.com by 210.87.254.42 on 09/05/12
For personal use only.

TABLE V

The final coulomb integrals, the self-consistent electron populations, and charges on Ti for pressure dependent calculations of rutile

		R[a]	PR (0.96)[b]	PR (0.94)[c]	PR (0.92)[d]
Coulomb integrals for Ti (1000 cm^{-1})	3d	−102.40	−102.30	−102.20	−102.10
	4s	−93.90	−93.90	−93.90	−93.90
	4p	−63.00	−63.00	−63.10	−63.10
Electron populations on Ti	3d	3.0547	3.0613	3.0639	3.0688
	4s	0.0651	0.0583	0.0553	0.0526
	4p	0.1071	0.0979	0.0951	0.0907
Final charges on Ti		0.7731	0.7825	0.7857	0.7879
Coulomb integrals for oxygens (1000 cm^{-1})	2s		−260.00		
	$2p_\sigma$		−120.00		
	$2p_\pi$		−110.00		
K_x	K_σ		1.59		
	K_π		1.79		
	K_{L-L}		1.69		

[a]Normal rutile calculation.
[b]Distance between Ti and O_5 and Ti and O_6 in rutile = 0.96 × distance between Ti and O_5 and Ti and O_6 in normal rutile.
[c]Distance between Ti and O_5 and Ti and O_6 in rutile = 0.94 × distance between Ti and O_5 and Ti and O_6 in normal rutile.
[d]Distance between Ti and O_5 and Ti and O_6 in rutile = 0.92 × distance between Ti and O_5 and Ti and O_6 in normal rutile.

Furthermore, from our final results, the splitting of 4p orbitals can be calculated through analysis of group 5 m.o. levels as 46 930 cm^{-1} (5.82 eV), 16 890 cm^{-1} (2.10 eV), and 45 120 cm^{-1} (5.59 eV) for rutile, anatase, and brookite respectively. Both in rutile and brookite, the calculated values are in good agreement with the prediction given by Cotton and Ballhausen. Based on the above discussions, we doubt the idea that the two higher energy peaks in the X-ray spectra of titanium oxides and other compounds are both due to K–4p transitions. Since it has been discussed (36) that for an isolated first transition series metal ion, the K absorption edge would have a first maximum corresponding to the 1s–4p transition, which is then followed by a series of maxima corresponding to 1s–np (n = 5, 6) transitions, we can probably assign the two higher energy peaks in Vainshtein's X-ray data as K–5p transitions.

The pressure dependence of the absorption edges of tetragonal barium titanate and rutile TiO_2 has been shown by Suchan, Belchan, and Drickamer (39). There is a red shift of absorption edge in $BaTiO_3$ and a blue shift of that in rutile TiO_2 as the pressure is increased. The authors did not give a very clear explanation of why these shifts occurred. They only suggested that the fact that the average Ti—O bond length is 0.05 Å greater in $BaTiO_3$ than in rutile TiO_2 was responsible for the difference in shifting. However, no quantitative explanation was given. We carried out extended Hückel m.o. calculations on this subject by assuming that the applied pressure is perpendicular to the Z axis of the compound and thus the changes in metal–ligand distance for ligands 5 and 6 (on Z axis) are much greater than those for ligands 1, 2, 3, and 4. In the calculations, the assumptions for H_{ii}, H_{jj}, H_{ij}, and K_x are the same as those used for calculations on normal rutile, anatase, brookite, and tetragonal barium titanate. The metal–ligand distances for ligands 1, 2, 3, and 4 are kept unchanged while those for ligands 5 and 6 are varied by factors of 0.96, 0.94, and 0.92 for the original compounds in order to examine the pressure effect on the energies. Tables V and VI list the final values of the coulomb integrals H_{ii}, the final self-consistent electron populations, and gross charges on Ti for such calculations. All the first charge transfer energies are calculated and are given in Table VII. Results concerning the calculations on normal rutile and tetragonal barium titanate are also included in the above tables for comparison. It is obvious from Table VII that the calculated first charge transfer energy undergoes a blue shift in rutile and a red shift in tetragonal barium titanate as ligands 5 and 6 are pressed further. This is in agreement with the observed results by Drickamer and co-workers. It can be seen from Tables V–VI that in both rutile and tetragonal barium titanate the electron population in 4s and 4p orbitals decreases, while the electron population

Can. J. Chem. Downloaded from www.nrcresearchpress.com by 210.87.254.42 on 09/05/12
For personal use only.

TABLE VI

The final coulomb integrals, the self-consistent electron populations, and charges on Ti for pressure dependent calculations of tetragonal barium titanate

		BA[a]	PBA (0.96)[b]	PBA (0.94)[c]	PBA (0.92)[d]
Coulomb Integrals for Ti (1000 cm^{-1})	3d	−102.20	−102.10	−102.00	−101.90
	4s	−93.80	−93.60	−93.60	−93.50
	4p	−62.80	−62.70	−62.70	−62.60
Electron populations on Ti	3d	3.0432	3.0557	3.0604	3.0668
	4s	0.0748	0.0674	0.0645	0.0614
	4p	0.1296	0.1188	0.1143	0.1082
Final charges on Ti		0.7524	0.7581	0.7608	0.7636
Coulomb integrals for oxygens (1000 cm^{-1})	2s		−260.00		
	$2p_\sigma$		−120.00		
	$2p_\pi$		−110.00		
K_x	K_σ		1.59		
	K_π		1.79		
	K_{L-L}		1.69		

[a]Normal barium titanate calculation.
[b]Distance between Ti and O_5 and Ti and O_6 in $BaTiO_3$ = 0.96 × distance between Ti and O_5 and Ti and O_6 in normal $BaTiO_3$.
[c]Distance between Ti and O_5 and Ti and O_6 in $BaTiO_3$ = 0.94 × distance between Ti and O_5 and Ti and O_6 in normal $BaTiO_3$.
[d]Distance between Ti and O_5 and Ti and O_6 in $BaTiO_3$ = 0.92 × distance between Ti and O_5 and Ti and O_6 in normal $BaTiO_3$.

in 3d orbitals and the total gross charge on Ti increase as the pressure is increased. In the case of rutile, the calculation shows that the highest m.o. energy level of group 3 (largely $2p_y$ character) remains unchanged while the lowest m.o. energy level of group 4 (largely $3d_{yz}$ and $3d_{xz}$ character) shifts toward less negative value as the pressure increases. Thus ΔE (first charge transfer energy), which is the difference between these two levels, increases. On the other hand, both the highest m.o. energy level of group 3 (largely $2p_x$ and $2p_y$ character) and the lowest m.o. energy level of group 4 (largely $3d_{xy}$ character) in tetragonal $BaTiO_3$ shift toward less negative values, with the former shifting more rapidly than the latter. Therefore, ΔE decreases as the pressure increases. It seems that the above explanations based on our extended Hückel m.o. calculations offer a plausible reason for the experimental data.

TABLE VII

The first charge transfer energies of pressure dependent calculations on rutile and tetragonal barium titanate

Rutile	ΔE (in 1000 cm^{-1})	$BaTiO_3$	ΔE (in 1000 cm^{-1})
R	24.24	BA	25.43
PR (0.96)	25.45	PBA (0.96)	25.15
PR (0.94)	25.50	PBA (0.94)	24.98
PR (0.92)	25.56	PBA (0.92)	24.82
	Blue shift		Red shift

Acknowledgments

The author thanks the American Chemical Society Petroleum Research Fund (ACS–PRF Grant 896 A–3 to the Illinois Institute of Technology) for major support of this work. He thanks Dr. J. Anysas in permitting the use of his computer program and Dr. A. L. Companion for her valuable discussions in this work.

1. M. Wolfsberg and L. Helmholz. J. Chem. Phys. **20**, 837 (1952).
2. C. J. Ballhausen and H. B. Gray. Inorg. Chem. **1**, 111 (1962).
3. L. L. Lohr, Jr. and W. N. Lipscomb. J. Chem. Phys. **38**, 1607 (1963).
4. H. D. Bedon, S. M. Horner, and S. Y. Tyree, Jr. Inorg. Chem. **3**, 647 (1964).
5. R. F. Fenske and C. C. Sweeney. Inorg. Chem. **3**, 1105 (1964).
6. A. Viste and H. B. Gray. Inorg. Chem. **3**, 1113 (1964).
7. F. A. Cotton and T. E. Haas. Inorg. Chem. **3**, 1004 (1964).
8. H. Basch, A. Viste, and H. B. Gray. J. Chem. Phys. **44**, 10 (1966).
9. R. L. Oakland and G. H. Duffey. J. Chem. Phys. **46**, 19 (1967).
10. H. Basch and H. B. Gray. Inorg. Chem. **6**, 639 (1967).
11. F. A. Cotton and C. B. Harris. Inorg. Chem. **6**, 924 (1967).
12. F. A. Cotton, C. B. Harris, and J. J. Wise. Inorg. Chem. **6**, 909 (1967).
13. M. L. Huggins. Phys. Rev. **27**, 638 (1926).
14. P. Ehrlich. Z. Elektrochem. **45**, 362 (1939).
15. W. H. Bauer. Acta Cryst. **9**, 515 (1956).
16. D. T. Cromer and K. Herrington. J. Am. Chem. Soc. **77**, 4708 (1955).
17. R. Weyl. Z. Krist. **111**, 401 (1959).

Can. J. Chem. Downloaded from www.nrcresearchpress.com by 210.87.254.42 on 09/05/12
For personal use only.

18. S. R. YOGANARASIMHAN and C. N. R. RAO. Anal. Chem. **33**, 155 (1961).
19. B. C. FRAZER, H. R. DANNER, and R. PEPINSKY. Phys. Rev. **100**, 745 (1955).
20. A. L. COMPANION and R. E. WYATT. Phys. Chem. Solids, **24**, 1025 (1963).
21. R. G. BRECKENRIDGE and W. R. HOSLER. Phys. Rev. **91**, 793 (1953).
22. R. C. CASELLA and S. P. KELLER. Phys. Rev. **116**, 1469 (1959).
23. M. CARDONA. Phys. Rev. **140**, A651 (1965).
24. E. E. VAINSHTEIN, I. B. STARYI, and M. N. BRIL. Dokl. Akad. Nauk SSSR, **105**, 934 (1955).
25. E. E. VAINSHTEIN and E. A. ZHURAKOVSKII. Bull. Acad. Sci. USSR Div. Chem. Sci. English Transl. 1444 (1959).
26. E. E. VAINSHTEIN, I. B. STARYI, and M. N. BRIL. Bull. Acad. Sci. USSR Phys. Ser. English Transl. **20**, 713 (1956).
27. R. S. MULLIKEN. J. Chem. Phys. **23**, 1833 (1955).
28. J. W. RICHARDSON, W. C. NIEUWPOORT, R. R. POWELL, and W. F. EDGELL. J. Chem. Phys. **36**, 1057 (1962).
29. J. W. RICHARDSON, R. R. POWELL, and W. C. NIEUWPOORT J. Chem. Phys. **38**, 796 (1963).
30. C. E. MOORE. Atomic energy levels. Natl. Bur. Std. U.S. Circ. 467. 1949 and 1952.
31. R. HOFFMANN. J. Chem. Phys. **39**, 1397 (1963).
32. C. J. BALLHAUSEN. Introduction to ligand field theory. McGraw Hill Book Co., Inc., New York. 1962. p. 152.
33. F. A. COTTON. Chemical applications of group theory. Interscience Publishers, Inc., New York. 1963. p. 117.
34. A. H. KAHN, H. P. R. FREDERIKSE, and J. H. BECKER. Transition metal compounds. Grodon and Breach Science Publishers, New York and London. 1963.
35. H. P. HANSON and J. R. KNIGHT. Phys. Rev. **102**, 632 (1956).
36. F. A. COTTON and C. J. BALLHAUSEN. J. Chem. Phys. **25**, 617 (1956).
37. F. A. COTTON and H. P. HANSON. J. Chem. Phys. **25**, 619 (1956).
38. L. E. ORGEL. J. Chem. Phys. **23**, 1004 (1955).
39. H. L. SUCHAN, A. S. BELCHAN, and H. G. DRICKAMER. J. Phys. Chem. Solids, **10**, 343 (1959).

Can. J. Chem. Downloaded from www.nrcresearchpress.com by 210.87.254.42 on 09/05/12
For personal use only.

Can. J. Chem. Downloaded from www.nrcresearchpress.com by 210.87.254.105 on 09/05/12
For personal use only.

An empirical periodic correlation of $J_{^{13}C-H}$ for the methyl group

C. P. YUE

Department of Chemistry, University of British Columbia, Vancouver 8, British Columbia

Received March 5, 1968

The carbon-13-proton coupling constant J^{13}_{C-H} for the methyl group is found to correlate linearly with the product $E_X \times \gamma_{X-C}$, where E_X is the electronegativity of the substituent X and γ_{X-C} is the X—C bond distance. Unknown values of J^{13}_{C-H} for the methyl group are predicted from the linear correlation. It is concluded that the "size effect" and the "polarization effect" are important in determining J^{13}_{C-H}.

Canadian Journal of Chemistry, **46**, 2675 (1968)

Considerable work has been done on the interpretation and correlation of carbon-13-proton coupling constants $J_{^{13}C-H}$. It is generally accepted that the s character in the C—H bond is the predominant factor (1–5). Factors other than the s character which have also been studied by various authors include: charge polarization (6), variations in the C—H bond distance (2, 7), and the electronegativity of substituents (4, 5, 8–11). More recently, Douglas (10) obtained separate straight lines for each atomic period when $J_{^{13}C-H}$ for monosubstituted methanes was plotted against Pauling's electronegativity. The present work is an attempt to obtain a more general correlation for $J_{^{13}C-H}$ for the methyl group which will fit all the experimental data and predict unknown $J_{^{13}C-H}$ values.

Literature values for the carbon-13-proton coupling constant $J_{^{13}C-H}$, X—C bond distance γ_{X-C} in Å, Pauling's electronegativity E_X, and atomic number Z_X of X for $(CH_3)_nX$ compounds are shown in Table I. Calculated values of various parameters defined by different authors are also shown in Table I. According to Juan and Gutowsky (5), α_H^2 is the s character of the carbon hybrid orbital for the C—H bond, α_X^2 is the s character for the C—X bond, and Δ_X is a measure of the affinity of X for s character. The parameter D is the deviation parameter defined by Reeves (12) and $\Delta(X)$ is the linear parameter of Douglas (13). A comparison of the calculated values of Δ_X, D, and $\Delta(X)$ shows

TABLE I

J^{13}_{C-H} coupling constants and related parameters* for $(CH_3)_nX$ compounds

Me_nX†	J^{13}_{C-H} (c.p.s.)	γ_{X-C}‡ (Å)	E_X§	Z_X	α_H^2	α_X^2	Δ_X	D	$\Delta(X)$ (c.p.s.)
Me_2Cd	126 (ref. 16)	(2.25)	1.7	48	0.252	0.244	+0.008	+0.0143	+1
Me_2Hg	130 (ref. 4)	(2.26)	1.9	80	0.260	0.220	+0.040	+0.0785	+5
Me_6Al_2	113 (ref. 4)	1.99	1.5	13	0.226	0.322	−0.096	−0.1964	−12
Me_3Ga	122 (ref. 4)	(2.02)	1.6	31	0.244	0.268	−0.024	−0.0464	−3
Me_3In	126 (ref. 4)	2.16±0.04	1.7	49	0.252	0.244	+0.008	+0.0143	+1
Me_4C	124 (ref. 2)	1.54±0.02	2.5	6	0.248	0.256	−0.008	−0.0143	−1
Me_4Si	118.2±0.4 (ref. 17)	1.88±0.02	1.8	14	0.236	0.292	−0.056	−0.1142	−6.8
Me_4Ge	124.0±0.4 (ref. 17)	1.98±0.03	1.8	32	0.248	0.256	−0.008	−0.0143	−1
Me_4Sn	127.2±0.1 (ref. 17)	2.18±0.03	1.8	50	0.254	0.238	+0.016	+0.0321	+2.2
Me_4Pb	134.0±0.2 (ref. 17)	2.29±0.05	1.8	82	0.268	0.196	+0.072	+0.1428	+9
Me_3N	131 (ref. 2)	1.47±0.02	3.0	7	0.262	0.214	+0.048	+0.0964	+6
Me_2O	140 (ref. 18)	1.42±0.03	3.5	8	0.280	0.160	+0.120	+0.2321	+15
Me_2S	138 (ref. 4)	1.82±0.03	2.5	16	0.276	0.172	+0.104	+0.2033	+13
Me_2Se	139 (ref. 19)	(1.93)	2.4	34	0.278	0.166	+0.112	+0.2178	+14
Me_2Te	139.7 (ref. 19)	(2.12)	2.1	52	0.279	0.163	+0.116	+0.2321	+14.7
MeF	149 (ref. 2)	1.38_5	4.0	9	0.298	0.106	+0.192	+0.3677	+24
MeCl	150 (ref. 2)	1.78_5	3.0	17	0.300	0.100	+0.200	+0.3820	+25
MeBr	152 (ref. 2)	1.93_8	2.8	35	0.304	0.088	+0.216	+0.4106	+27
MeI	151 (ref. 2)	2.13_9	2.5	53	0.302	0.094	+0.208	+0.3963	+26

*For definitions of these parameters, see text.
†Me stands for methyl.
‡Values for bond distance are taken from ref. 14. Values in parentheses are estimated from covalent radii; see Pauling (15).
§Pauling's electronegativity.

TABLE II

Predicted J^{13}_{C-H} coupling constants and related parameters* for some $(CH_3)_nX$ compounds

Me_nX	J^{13}_{C-H} (c.p.s.)	α_H^2	α_X^2	Δ_X	D	$\Delta(X)$ (c.p.s.)	E_X	γ_{X-C} (Å)	Z_X
Me_2Zn	119±2	0.238	0.286	−0.048	−0.0964	−6	1.6	(2.08)	30
Me_3B	117±2	0.234	0.298	−0.064	−0.1282	−8	2.0	(1.59)	5
Me_3Tl	130±2	0.260	0.220	+0.040	+0.0785	+5	1.8	(2.25)	81
Me_3P	127±2	0.254	0.238	+0.016	+0.0321	+2	2.1	(1.83)	15
Me_3As	128±2	0.256	0.232	+0.024	+0.0464	+3	2.0	(1.96)	33
Me_3Sb	130±2	0.260	0.220	+0.040	+0.0785	+5	1.9	(2.15)	51
Me_3Bi	132±2	0.264	0.208	+0.056	+0.1107	+7	1.9	(2.23)	83
Me_2Mg	107±2†	0.214	0.358	−0.144	−0.3100	−18	1.2	(2.15)	12

*For definition of these parameters, see text and Table I.
†$J_{^{13}C-H}$ experimental value for CH_3MgBr 107.7 (±1), see Fraenkel, Adams, and Williams (20).

that they are essentially the same measure of the change in $J_{^{13}C-H}$ for $(CH_3)_nX$ compounds considered as monosubstituted methanes.

A careful study of Table I reveals that the changes in $J_{^{13}C-H}$ for $(CH_3)_nX$ compounds can be correlated to both the electronegativity E_X of the substituent X and the X—C bond distance γ_{X-C}. Within a group, the relative changes in the size of X are more rapid than the relative changes in the electronegativity E_X; the reverse is true for elements within an atomic period. The "size effect" of the substituents on $J_{^{13}C-H}$ has been discussed by Muller and Pritchard (2); they attributed this to a demand for carbon p character by the substituent X due to its more diffuse electron cloud and more effective overlap, the s character in the X—C bond is thus reduced and is less than the s character in the C—H bond. The shift of electron density from the substituent X to the carbon nucleus is also much easier for elements of larger size and as a result $J_{^{13}C-H}$ increases as the size of X increases. On the other hand, if the increase in the electronegativity of X is more rapid, the "polarization effect" which is in opposite direction to the "size effect" will be dominant. For a substituent X whose electronegativity is larger than H will cause nonequivalent hybrids of carbon orbitals (5), the s character in the C—H bond will then be greater than the s character in the X—C bond and thus increase $J_{^{13}C-H}$.

A plot of $J_{^{13}C-H}$ against $E_X \times \gamma_{X-C}$ is shown in Fig. 1; a reasonably good straight line is obtained. Predicted values of $J_{^{13}C-H}$ are shown in Table II together with other parameters. It is concluded that $J_{^{13}C-H}$ in $(CH_3)_nX$ compounds can be accounted for by the "size effect" and the "polarization effect" of X.

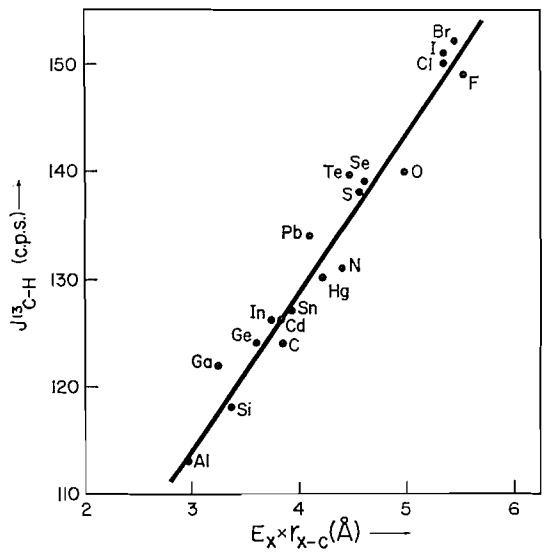

FIG. 1. Correlation between $J_{^{13}C-H}$ and $E_X \times \gamma_{X-C}$.

Acknowledgments

The author is grateful to Dr. D. P. Chong for helpful discussion and for reading the manuscript and to the referees for their valuable comments.

1. N. MULLER and D. E. PRITCHARD. J. Chem. Phys. **31**, 768 (1959).
2. N. MULLER and D. E. PRITCHARD. J. Chem. Phys. **31**, 1471 (1959).
3. J. N. SHOOLERY. J. Chem. Phys. **31**, 1427 (1959).
4. N. MULLER. J. Chem. Phys. **36**, 359 (1962).
5. C. S. JUAN and H. S. GUTOWSKY. J. Chem. Phys. **37**, 2198 (1962).
6. D. M. GRANT and W. M. LITCHMAN. J. Am. Chem. Soc. **89**, 6775 (1967).
7. D. S. BASTOW and J. W. RICHARDSON. J. Chem. Phys. **42**, 4018 (1965).
8. H. SPIESECKE and W. G. SCHNEIDER. J. Chem. Phys. **35**, 722 (1961).

Can. J. Chem. Downloaded from www.nrcresearchpress.com by 210.87.254.105 on 09/05/12
For personal use only.

9. R. M. HAMMAKER. J. Chem. Phys. **43**, 1843 (1965).
10. A. W. DOUGLAS. J. Chem. Phys. **45**, 3465 (1966).
11. R. DITCHFIELD, M. A. JENSEN, and J. N. MURRELL. J. Chem. Soc. A, 1674 (1967).
12. L. W. REEVES. J. Chem. Phys. **40**, 2128 (1964).
13. A. W. DOUGLAS. J. Chem. Phys. **40**, 2413 (1964).
14. L. E. SUTTON (*Editor*). Tables of interatomic distances and configuration in molecules and ions. Chem. Soc. London, 1958.
15. L. PAULING. Nature of the chemical bond. Cornell Univ. Press, Ithaca, New York. 1960.
16. B. KLOSE. Ann. Physik, **8**, 220 (1961).
17. G. W. SMITH. J. Chem. Phys. **39**, 2031 (1963).
18. N. MULLER and P. I. ROSE. J. Am. Chem. Soc. **84**, 3973 (1962).
19. W. MCFARLANE. Mol. Phys. **12**, 243 (1967).
20. G. FRAENKEL, D. G. ADAMS, and J. WILLIAMS. Tetrahedron Letters, 767 (1963).

Can. J. Chem. Downloaded from www.nrcresearchpress.com by 210.87.254.105 on 09/05/12
For personal use only.

Can. J. Chem. Downloaded from www.nrcresearchpress.com by 210.87.254.5 on 09/05/12
For personal use only.

A calorimetric study of periodate species in aqueous solution[1]

E. E. Mercer and D. T. Farrar[2]
Department of Chemistry, University of South Carolina, Columbia, South Carolina 29208

Received January 18, 1968

Heats of several reactions involving sodium periodate, $NaIO_4$(c), have been measured in an isothermal jacketed calorimeter. The apparent acid ionization constant of periodic acid was redetermined at an ionic strength of 0.13. From these data the following values for heats of formation at 25.00° have been calculated: $NaIO_4$(c), -105.15 ± 0.30; IO_4^-(aq), -38.8 ± 0.4; H_5IO_6(aq), -188.9 ± 1.0; $H_4IO_6^-$(aq), -186.3 ± 1.0 kcal/mole.

Canadian Journal of Chemistry, 46, 2679 (1968)

The use of sodium periodate, $NaIO_4$, as a calorimetric oxidizing agent is being investigated in this laboratory. This substance offers many advantages since it is a powerful oxidizing agent which reacts rapidly and smoothly; the solid salt is readily available in high purity and it is readily soluble in acidic and neutral solutions.

To date only a moderate amount of work has been performed on the thermodynamics of periodate species. Until recently the heat of formation of periodic acid, H_5IO_6, was based on the work of Thomsen (1), which gives $\Delta H_f^0 = -183.0$ kcal/mole for H_5IO_6(aq) and $\Delta H_f^0 = -184.4$ kcal/mole for H_5IO_6(c). In a recent paper Stern and Jasnosz (2) reported the heat of solution and reduction of periodic acid and calculated -186.5 kcal/mole for ΔH_f^0 of H_5IO_6(c).

Enthalpy data on periodates rests largely on solubility studies of slightly soluble salts, such as KIO_4 (3). This data was later interpreted by Crouthamel *et al.* (4) in the light of the hydrolysis reactions which periodate undergoes in solution. The value of ΔH_f^0 for $NaIO_4$(c) was calculated by Kaputsinsky and Yatsimirsky (5) from the heats of formation of Na^+(aq), IO_4^-(aq), and their experimentally measured heat of solution. This gives a value of -104.0 kcal/mole for the standard heat of formation of $NaIO_4$(c). Since the value of the standard heat of formation of IO_4^-(aq) is quite uncertain on the basis of previous work, we have made calorimetric measurements to establish an accurate value for the heat formation of $NaIO_4$(c). In addition, we have been able to determine the heats of formation of several aqueous periodate species from the heats of solution of $NaIO_4$(c) in acidic medium. To interpret the calorimetric results adequately, it was necessary to repeat the equilibrium constant determination made by Crouthamel *et al.* (4) at a higher ionic strength than they used.

Experimental

The Calorimeter

This was similar in design to calorimeter "D" reported by Sunner and Wadsö (6). The principal features are shown in cross section in Fig. 1. The reaction vessel (L) has a volume of 46 ml and was made from 20 mil tantalum by Fansteel Metallurgical Corporation. This is supported by a thin-walled Pyrex tube (D) inside the brass jacket (G). A three blade platinum stirrer (J) also serves as a holder for the sample ampule (K). The two cylindrical wells (E) hold a heater, for electrical calibration, and a Veco 32A11 thermistor respectively. Both

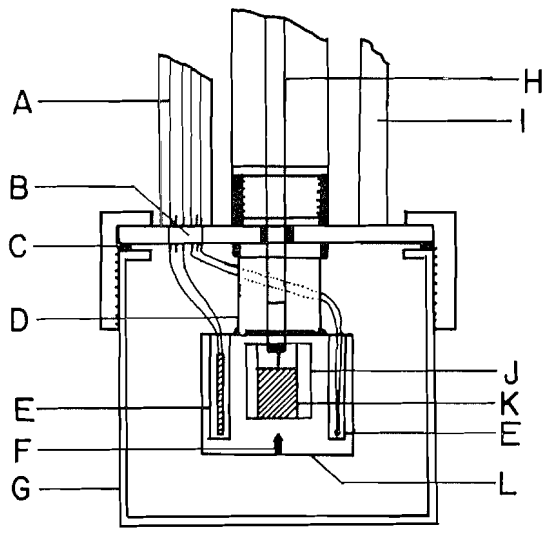

FIG. 1. Cross-sectional diagram of the calorimeter: A, leads to heater and thermistor; B, pyroceram electrical connection; C, O-ring seal; D, glass support tube; E, heater and thermistor wells; F, breaking pin; G, brass submarine; H, stirring shaft; I, to vacuum line; J, platinum stirring blades; K, ampule; L, tantalum reaction vessel.

[1]This work was supported by the U.S. Atomic Energy Commission under contract number AT-(40-1)3542.
[2]NDEA Fellow, 1964–1967.

Can. J. Chem. Downloaded from www.nrcresearchpress.com by 210.87.254.5 on 09/05/12
For personal use only.

wells were filled with oil as a heat exchange medium, prior to sealing with epoxy glue. The lower portion of the stirring shaft is made of Teflon and is attached to steel shaft. In operation the outer jacket is evacuated to $< 10^{-5}$ Torr with a mercury diffusion pump, and a stirring speed of 800 r.p.m. is used within the reaction vessel. The calorimeter assembly was immersed in a constant temperature bath, adjusted so the equilibrium temperature of the calorimeter was near 25.00°.

In a calorimetric run the sample was introduced by lowering the stirring shaft, breaking the ampule on pin (F). A sharp point of platinum was attached to the end of the stirring shaft to simultaneously break the upper end of the ampule. The ampules were blown into a mold from 3 mm glass tubing in a manner identical with that used by Sunner and Wadsö (6). Several empty sample ampules were broken under the conditions used in the experiments. The heat effect averaged zero and never exceeded 3×10^{-3} calories.

The thermistor used to sense the temperature changes in the reaction vessel is one arm of a Wheatstone bridge. The bridge imbalance is amplified with a Hewlett-Packard model 425A d.c. amplifier, the output of which is recorded on a 10 mV Honeywell Electronik 16 recorder. Calibration of the thermistor was accomplished by determining its resistance at more than 30 points, between 22.00 and 28.00 °C. These points were fitted by computer to the equation

$$[1] \qquad \ln R/R_0 = B(1/T - 1/T_0),$$

where R_0 and T_0 were the experimentally determined values at 25.00°. Using this equation the temperature may be found from the thermistor resistance to ±0.01° and small temperature differences to better than $\pm 1 \times 10^{-4}$°.

The energy equivalent was determined electrically for each calorimetric run by passing current from a model IV Sargent coulometric current source through the calorimeter heater. The potential drop across the heater was determined using a Calibrations Standards Corporation model DC-200 AR precision d.c. voltmeter. Electrical calibrations were performed after the chemical reaction had taken place. The sample ampule was broken to initiate reaction when the temperature of the calorimeter was 25.00 ±0.03°, and the maximum temperature change was 0.30°. The assigned reaction temperature under these conditions is the initial temperature of the reaction (7). Performance checks on the calorimeter showed a thermal leak modulus of 4.5×10^{-3} deg deg^{-1} min^{-1}. The calorimeter reached thermal equilibrium in less than 1 min after an electrical heating. The thermal lag observed for a fast chemical reaction was of still shorter duration.

Chemicals

Tris(hydroxymethyl)aminomethane (THAM) was obtained from Eastman Organic Chemicals with a purity of 99.94%. Before use, it was dried in vacuum overnight at 80°.

The sodium periodate was Baker and Adamson reagent grade. It was washed with dilute nitric acid and dried for 2 h at 105°. Titration with sodium thiosulfate of iodine liberated in the reduction of the sodium periodate gave an assay of 100.04%.

Reagent grade hydriodic acid was distilled to remove the hypophosphorous acid used as a preservative. The diluted acid was standardized by titration against THAM.

All other chemicals used were reagent grade and were used without further purification.

Results

The entire calorimetric system was checked using the heat of reaction of THAM with 0.1 *M* HCl (8, 9). Gunn reported a heat of reaction of −7107.1 ± 1.0 cal/mole for a THAM concentration of 6 g/l. In a private communication, Gunn suggested that a value of −7114 cal/mole indicated by further work was a more accurate value. Three runs made with our calorimeter gave values of −7113, −7116, and −7124 cal/mole, for an average of −7118 cal/mole. This agreement is well within the estimated experimental error which we anticipated for our system.

Calorimetric Measurements

It was necessary to determine several heats of reaction involving sodium periodate and the products of these reactions. The heat of reaction of $NaIO_4$(c) with 0.536 *M* HI is summarized in Table I. Under these conditions the periodate is reduced completely to triiodide ion. The experimentally measured heats of solution of NaI(c) and I_2(c) in the same medium are given in Tables II and III. These three heats,

TABLE I

The heat of reaction of $NaIO_4$(c) with 0.536 *M* HI at 25.00°

Sample weight (mg)	Heat evolved (cal)	$-\Delta H_5$ (kcal/mole)
29.085	17.825	131.06
27.780	17.017	131.02
28.025	17.088	130.39
28.500	17.387	130.49
29.170	17.822	130.68
		Av. 130.73±0.25

TABLE II

The heat of solution of NaI(c) in 0.536 *M* HI at 25.00°

Sample weight (mg)	Heat evolved (cal)	$-\Delta H_6$ (kcal/mole)
33.1	0.370	1.68
32.5	0.361	1.67
56.1	0.630	1.68
47.7	0.527	1.66
		Av. 1.67±0.01

Can. J. Chem. Downloaded from www.nrcresearchpress.com by 210.87.254.5 on 09/05/12
For personal use only.

along with standard heats of formation available in the literature, are sufficient to determine the standard heat of formation of $NaIO_4$(c).

TABLE III

The heat of solution of I_2(c) in 0.536 *M* HI at 25.00°

Sample weight (mg)	Heat absorbed (cal)	ΔH_7 (kcal/mole)
132.8	0.559	1.070
131.3	0.545	1.054
134.0	0.567	1.076
132.7	0.573	1.096
		Av. 1.074±0.012

TABLE IV

The heat of solution of $NaIO_4$(c) in 0.100 *M* $NaClO_4$ at 25.00°

Sample weight (mg)	Heat absorbed (cal)	ΔH (kcal/mole)
334.5	13.654	8.73
332.9	13.555	8.71
330.0	13.507	8.76
328.7	13.371	8.70
330.8	13.517	8.74
		Av. 8.73±0.03

In order to determine the heats of formation of the many aqueous periodate species from the heat of formation of $NaIO_4$(c), the heat of solution of sodium periodate was measured in 0.100 *M* $NaClO_4$ solution and 0.100 *M* $HClO_4$ solution. These heats are summarized in Tables IV and V. As expected, the heat of solution of sodium periodate in the acidic solution showed a marked concentration dependence. This is due to the hydration and hydrolysis reactions which take place in solution.

Determination of the Acid Ionization Constant of H_5IO_6

The nature of periodate in acid to neutral solution has been studied by Crouthamel *et al.* (4) by both spectrophotometric and potentiometric methods. They were able to interpret their results in terms of the three equilibria:

[2] $H_5IO_6(aq) \rightleftarrows H^+(aq) + H_4IO_6^-(aq)$

[3] $H_4IO_6^-(aq) \rightleftarrows IO_4^-(aq) + 2H_2O$

[4] $H_4IO_6^-(aq) \rightleftarrows H^+(aq) + H_3IO_6^{-2}(aq).$

They found for reaction [2], $K_2 = 5.1 \times 10^{-4}$, $\Delta H_2 \simeq 0$ kcal/mole; for reaction [3], $K_3 = 40$, $\Delta H_3 = 10.9$ kcal/mole; for reaction [4], $K_4 = 2.0 \times 10^{-7}$, $\Delta H_4 \simeq 0$ kcal/mole. All of these equilibrium constants were measured in solutions which were very dilute. The authors noted that there were rather large activity coefficient changes with ionic strength. Since all of our heats of solution were made at approximately $\mu = 0.13$, it was necessary to determine the apparent equilibrium constants under these conditions. Potentiometric and spectrophotometric measurements were made at 25°, identical with those made earlier (4, 10), except that sufficient sodium perchlorate was added to maintain an ionic strength of 0.13. It was assumed that the equilibrium constant for the dehydration, K_3, would be insensitive to changes in ionic strength. The results of these measurements are summarized in Table VI.

TABLE V

The heat of solution of $NaIO_4$(c) in 0.100 *M* $HClO_4$ at 25.00°

Concentration of $NaIO_4 \times 10^2$	Heat absorbed (cal)	ΔH_{obs} (kcal/mole)	$-\Delta H'$ (kcal/mole)
2.98	−0.135	−0.098	13.15
3.87	0.121	0.068	13.20
4.29	0.311	0.158	13.21
4.95	0.683	0.300	13.23
5.00	0.737	0.321	13.22
5.12	0.801	0.340	13.24
5.22	0.916	0.381	13.22
5.68	1.292	0.495	13.20
6.29	1.956	0.676	13.15
6.61	2.345	0.771	13.15
7.20	3.037	0.917	13.14
7.50	3.369	0.976	13.17
7.80	3.862	1.076	13.12
8.23	4.408	1.164	13.17
			Av. 13.18±0.04

Can. J. Chem. Downloaded from www.nrcresearchpress.com by 210.87.254.5 on 09/05/12
For personal use only.

TABLE VI

The first acid ionization constant for H_5IO_6 at an ionic strength of 0.13 at 25°

Method	Concentration of periodate (M)	$K_2 \times 10^4$
Spectrophotometric	1.74×10^{-4}	10.1
Spectrophotometric	3.48×10^{-4}	9.4
Potentiometric	3.01×10^{-2}	10.3
		Av. 9.9

Thermodynamic Calculations and Discussion

The Heat of Formation of $NaIO_4(c)$

When sodium periodate dissolves in hydriodic acid the iodine(VII) is quantitatively reduced to iodine(0). This may be expressed in the equation

[5] $NaIO_4(c) + [aHI, bH_2O] = [NaI, 4I_2, (a - 8)HI, (b + 4)H_2O],$

where brackets indicate the solution. Also,

[6] $NaI(c) + [4I_2, (a - 8)HI, (b + 4)H_2O] = [NaI, 4I_2, (a - 8)HI, (b + 4)H_2O]$

[7] $I_2(c) + \frac{1}{4}[(a - 8)HI, (b + 4)H_2O] = \frac{1}{4}[4I_2, (a - 8)HI, (b + 4)H_2O].$

The heats of reactions [5]–[7] are given in Tables I, II, and III respectively. In our experiments, typical values used were $a = 1770$, $b/a = 103$. Additional heats needed to complete the cycle for calculation of the heat of formation of $NaIO_4(c)$ are:

[8] $H_2(g) + \frac{1}{2}O_2(g) + \frac{1}{4}[(a - 8)HI, bH_2O] = \frac{1}{4}[a - 8)HI, (b + 4)H_2O]$

[9] $\frac{1}{2}H_2(g) + \frac{1}{2}I_2(c) + \frac{1}{8}[(a - 8)HI, bH_2O] = \frac{1}{8}[aHI, bH_2O]$

[10] $Na(c) + \frac{1}{2}I_2(c) = NaI(c).$

These heats were found or calculated from standard reference sources (11). Reaction [8] is the apparent heat of formation of water in HI solution and does not differ significantly from that of the pure liquid, −68.315 kcal/mole. The apparent heat of formation of HI, reaction [9], was calculated to be −12.94 kcal/mole; ΔH_{10} is −68.77 kcal/mole. The standard heat of formation of $NaIO_4(c)$ is $\Delta H_f^0(NaIO_4(c)) = -\Delta H_5 + \Delta H_6 + 4\Delta H_7 + 4\Delta H_8 - 8\Delta H_9 + \Delta H_{10} = -105.15 \pm 0.30$ kcal/mole. The uncertainty cited here and for other derived results are based upon the standard deviations of the individual numbers. In some cases it was necessary to estimate the uncertainty of numbers taken from standard sources. Generally the most pessimistic estimate was used.

The Heats of Formation of Aqueous Periodate Species

From the heats of formation of $Na^+(aq)$ and $NaIO_4(c)$, taken with the heat of solution of sodium periodate in sodium perchlorate solution, the heat of formation of $IO_4^-(aq)$ may be calculated. In unbuffered near-neutral solution, the only important periodate species present are IO_4^- and $H_4IO_6^-$. From K_3 above, approximately 2.4% of the periodate ion is hydrated. Correcting the heat of solution given in Table IV for hydration, and using $\Delta H_3 = 10.9$ kcal/mole (4), we find $\Delta H_{11} = 9.00$ kcal/mole for the reaction:

[11] $NaIO_4(c) = Na^+(aq) + IO_4^-(aq).$

The heat of formation of IO_4^- in solution of $\mu = 0.13$ is then found to be -38.8 ± 0.4 kcal/mole. While this heat of formation was not obtained under conditions approaching infinite dilution, it is expected to be within 0.2 kcal of the standard heat of formation.

It is considerably more difficult to interpret the heats of solution of $NaIO_4(c)$ in 0.100 M $HClO_4$. From examination of the equilibrium constants for reactions [2] and [3], there are significant concentrations of H_5IO_6, $H_4IO_6^-$, and IO_4^- present in all solutions. The observed heat of solution in acid can be expressed as

[12] $\Delta H_{obs} = \Delta H_{11} - f_4\Delta H_3 - f_5(\Delta H_2 + \Delta H_3),$

where ΔH_{obs} are the heats of solution measured in kcal/mole, f_4 = fraction of periodate present as $H_4IO_6^-$, f_5 = fraction of periodate present as H_5IO_6, and the subscripts on each ΔH refer to the respective equations.

The concentrations of the several ions appearing in eqs. [2] and [3] were expressed in terms of f_4, f_5, C_{HClO_4} = the formal concentration of perchloric acid, and C_{NaIO_4} = the formal concentration of sodium periodate. The equilibrium constant expression for eq. [3] was solved for f_4 in terms of f_5, which upon substitution in [12] gives

[13] $\Delta H' = Q/f_5,$

where $\Delta H' = -\Delta H_2 - K_3\Delta H_3/(K_3 + 1)$ and $Q = \Delta H_{obs} + \Delta H_3/(K_3 + 1) - \Delta H_{11}$. When the same substitution for f_4 is made in the equilibrium constant expression for reaction [2], a quadratic equation in f_5 is obtained:

Can. J. Chem. Downloaded from www.nrcresearchpress.com by 210.87.254.5 on 09/05/12
For personal use only.

[14] $C_{NaIO_4}f_5^2 - (C_{HClO_4} + C_{NaIO_4} + K_2K_3 + K_2)f_5 + C_H = 0.$

Elimination of f_5 from [13] and [14] and rearranging gives

[15] $(\Delta H')^2 + a(\Delta H') + b = 0,$

where $a = (C_{HClO_4} + C_{NaIO_4} + K_2K_3 + K_2)Q/C_{HClO_4}$ and $b = C_{NaIO_4}Q^2/C_{HClO_4}$. $\Delta H'$ was calculated from each experimental heat of solution and these values are given in Table V. The average value for this quantity is -13.18 kcal/mole with an average deviation of ± 0.04. A graphical comparison of the calculated and observed heats of solution is shown in Fig. 2. We have reinterpreted the data of Stern and Jasnosz (2) and find that the $\Delta H'$ calculated is in complete agreement with our data. However, because of the very high concentrations which were used in that study, the uncertainty in $\Delta H'$ is somewhat greater.

TABLE VII

The heats of formation of periodates at 25°

Substance	ΔH_f° (kcal/mole)
$NaIO_4$(c)	-105.15 ± 0.30
IO_4^-(aq)	-38.8 ± 0.4
H_5IO_6(aq)	-188.9 ± 1.0
$H_4IO_6^-$(aq)	-186.3 ± 1.0

From these data and Crouthamel's (4) value for ΔH_3, we find the heat of ionization of H_5IO_6 is $+2.55$ kcal/mole. While our estimated uncertainty of this heat is ± 0.7 kcal/mole, this seems to be quite a large heat of ionization. The plot of log K_2 vs. $1/T$ given by Crouthamel *et al.* (4) did exhibit considerable curvature at low temperatures so that this heat of ionization would not be inconsistent with their data. It is also possible that the heat of dehydration is somewhat more positive than that reported by previous investigators (4, 12). Kren *et al.* (13) have recently made an n.m.r. study of the dehydration equilibrium and found a considerably more positive heat for this reaction. It would appear that further investigation of the enthalpy of the dehydration reaction is necessary before conclusions can be drawn.

From the heats of solution presented, we have calculated the heats of formation of several periodate species. These are given in Table VII along with the other heats of formation calculated from our data.

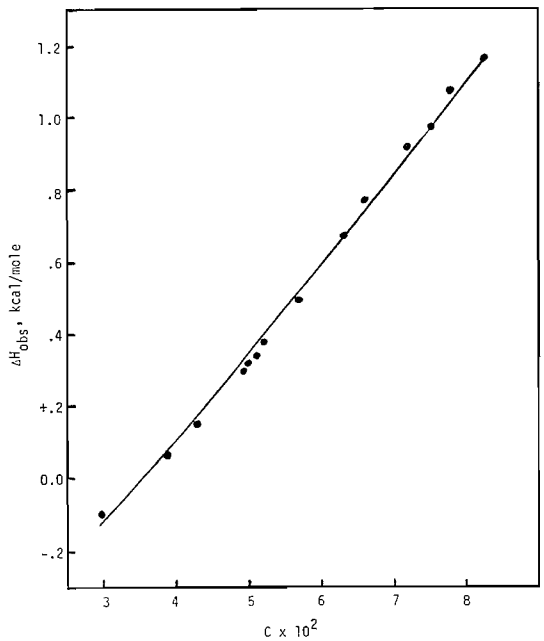

FIG. 2. Heat of solution of $NaIO_4$(c) in 0.100 M $HClO_4$ at 25.00° as a function of periodate concentration. The line was calculated using the average value of $\Delta H'$ (see text), and the points represent the experimental data.

1. J. THOMSEN. Thermochemische Untersuchungen. Vol. II. Johann Ambrosius Barth, Salomonstrasse 18B, Leipzig, Germany. 1882.
2. J. H. STERN and J. J. JASNOSZ. J. Chem. Eng. Data, **9**, 534 (1964).
3. J. H. JONES. J. Am. Chem. Soc. **69**, 536 (1947).
4. C. E. CROUTHAMEL, A. M. HAYES, and D. S. MARTIN. J. Am. Chem. Soc. **73**, 82 (1951).
5. A. F. KAPUTSINSKY and K. B. YATSIMIRSKY. Zh. Obshch. Khim. **19**, 2191 (1949).
6. S. SUNNER and I. WADSÖ. Acta Chem. Scand. **13**, 97 (1959).
7. Experimental thermochemistry. Vol 1. *Editor* F. D. Rossini. Interscience Publishers Inc., New York. 1956. p. 16–18.
8. R. J. IRVING and I. WADSÖ. Acta Chem. Scand. **18**, 195 (1964).
9. S. R. GUNN. J. Phys. Chem. **69**, 2902 (1965).
10. C. E. CROUTHAMEL, H. V. MEEK, D. S. MARTIN, and C. V. BANKS. J. Am. Chem. Soc. **71**, 3031 (1949).
11. (*a*) Selected values of thermodynamic properties. Natl. Bur. Std. (U.S.). Circ. 500, 1952. (*b*) Natl. Bur. Std. Tech. Note 270–1, 1965.
12. S. H. LAURIE, J. M. WILLIAMS, and C. J. NYMAN. J. Phys. Chem. **68**, 1311 (1964).
13. R. M. KREN, H. W. DODGEN, and C. J. NYMAN. 153rd National Meeting of the American Chemical Society, Miami Beach, Florida. April 1967. Paper No. L84.

Studies on complex compounds. V. Coordination compounds of mercury and biologically active amines[1]

C. H. MISRA, SURENDRA S. PARMAR,[2] AND S. N. SHUKLA

Department of Pharmacology and Therapeutics, King George's Medical College, Lucknow University, Lucknow, and Department of Chemistry, Lucknow University, Lucknow, India

Received August 8, 1967

Five mercury complexes were synthesized by condensation of mercuric chloride with different biologically active amines. In the present study D-amphetamine, L-amphetamine, DL-amphetamine, methylamphetamine, ephedrine, and tyramine were used where a stereoisomeric effect was observed during the formation of the mercury complexes. The complex compound synthesized from DL-amphetamine was found to be a mixture of the mercury complexes of D-amphetamine and L-amphetamine, and the difference in their solubilities was utilized for their separation. The estimation of the carbon, hydrogen, and nitrogen content, the determination of the amount of chlorine and mercury, and measurements of the infrared absorption spectra at 700–3500 cm^{-1} indicated the ratio of 2:1 for amine to mercury in these coordination compounds. Further characterization of these mercury complexes was done by ultraviolet absorption spectra and conductance measurements.

Canadian Journal of Chemistry, 46, 2685 (1968)

Can. J. Chem. Downloaded from www.nrcresearchpress.com by 210.87.254.40 on 09/05/12
For personal use only.

Interference with cellular metabolism by inhibition of certain enzyme systems has been shown to be the property of various organomercury compounds (1). Mercury has also been reported to combine with ligands of physiological importance such as phosphoryl, carboxyl, amido, and amino groups. The present study describes the synthesis of mercury complexes of biologically active amines with a view to studying the relative coordinating abilities of nitrogen and oxygen and to investigate their effects on certain enzyme systems for obtaining a better knowledge of their physiological significance (2). The involvement of a stereoisomeric effect was observed during the formation of such mercury complexes with isomeric amphetamines.

Experimental

Materials

Most of the amines and mercuric chloride (B.D.H.) used in the present study were of analytical grade and were available commercially. Stereoisomeric amphetamines (D-amphetamine and L-amphetamine), DL-amphetamine, and methylamphetamine were used as bases after separation from their respective sulfates by treating with an equivalent amount of dilute sodium hydroxide solution and subsequent extraction with ether. Tyramine base was separated from its hydrochloride with a dilute solution of liquor ammonia while ephedrine, as a base, was used without further purification. The purity of the amines was checked by their boiling or melting points. Absolute ethanol, ether dried over sodium wire, and purified anhydrous nitrobenzene (3) were used throughout these experiments.

Analyses

The mercury content of the complexes was estimated volumetrically (4) and gravimetrically (5). The chlorine content was determined gravimetrically as AgCl. The carbon, hydrogen, and nitrogen contents of these complexes were determined by well-known combustion methods.

Preparations

Mercury complexes were prepared by mixing 2.2 moles of the appropriate amine with 1 mole of mercuric chloride in absolute ethanol as described earlier (4). The analyses and melting points are summarized in Table I.

Results

Properties of Mercury Coordination Compounds

All complexes are white in color except the tyramine–mercury complex which is of slightly brownish color. Complexes of D-amphetamine, DL-amphetamine, and methylamphetamine were obtained as fine powders while those synthesized from L-amphetamine, tyramine, and ephedrine were crystalline in nature. Complexes synthesized from D-amphetamine, DL-amphetamine, ephedrine, and tyramine are insoluble in water while complexes of L-amphetamine and methylamphetamine are sparingly soluble in boiling water. All complexes are soluble in acetone except those synthesized from ephedrine and tyramine. Mercury complexes of L-amphetamine and methylamphetamine are soluble in solvents like cyclohexane, cyclohexanol, dioxane, and nitrobenzene. All complexes undergo decomposition on boiling with dilute sodium hydroxide

[1]This investigation was supported by a research grant from the Indian Council of Medical Research, New Delhi.

[2]Inquiries should be addressed to Professor S. S. Parmar.

Can. J. Chem. Downloaded from www.nrcresearchpress.com by 210.87.254.40 on 09/05/12
For personal use only.

TABLE I

Mercury coordination compounds of biologically active amines

	Melting point (°C)	Yield (%)	Calculated (%)					Found (%)					Adduct
			C	H	N	Cl	Hg^{2+}	C	H	N	Cl	Hg^{2+}	
D-$[C_6H_5-CH_2-CH(CH_3)-NH_2]_2 HgCl_2$	145[a]	80	39.9	4.7	5.1	13.1	37.0	40.0	5.4	5.1	12.9	37.1	2:1
L-$[C_6H_5-CH_2-CH(CH_3)-NH_2]_2 HgCl_2$	118–119	75	39.9	4.7	5.1	13.1	37.0	40.5	5.4	5.1	13.0	37.3	2:1
DL-$[C_6H_5-CH_2-CH(CH_3)-NH_2]_2 HgCl_2$	131.5	72	39.9	4.7	5.1	13.1	37.0	40.5	5.4	5.1	13.0	37.3	2:1
$[C_6H_5-CH_2-CH(CH_3)-NHCH_3]_2 HgCl_2$	208	70	42.1	5.2	4.9	12.4	35.2	42.3	5.1	4.8	11.8	35.4	2:1
$[C_6H_5-CH(OH)-CH(CH_3)-NHCH_3]_2 HgCl_2$	132	60	39.8	4.9	4.6	11.8	33.3	39.5	4.9	4.9	12.0	34.0	2:1
$[HO-C_6H_4-CH_2CH_2NH_2]_2 HgCl_2$	172	60	35.1	4.0	5.1	13.0	36.7	35.0	4.0	4.9	12.8	36.6	2:1

[a]Melting points were determined in open capillary tubes and are corrected.

Can. J. Chem. Downloaded from www.nrcresearchpress.com by 210.87.254.40 on 09/05/12
For personal use only.

solution, as is indicated by the appearance of a characteristic smell of the original amine. These mercury complexes, though soluble in dilute nitric acid, are oxidized with concentrated nitric acid (4) where a definite change in the color of the compounds is observed. The mercury complex obtained from DL-amphetamine could be separated into complexes of D-amphetamine and L-amphetamine by taking advantage of their solubility differences. The ethanol soluble portion contained the complex of L-amphetamine. On isolation these complexes were found to be identical with those synthesized from either D-amphetamine or L-amphetamine. Such a possibility was further confirmed by determining the specific rotation of the ethanol soluble compound obtained from the mixture of D-amphetamine and L-amphetamine complex. This complex showed a laevorotatory nature $[\alpha] = -20$.

Conductivity Measurements

The conductance measurements were made with a Mullard conductivity bridge (type E/300) at 20° with a conductivity cell having a cell constant of 1.05. All complexes were used at a final concentration of 1 μmole and were taken in nitrobenzene, except the complexes of L-amphetamine and methylamphetamine where ethanol was used as a solvent. The results of the conductance measurements are given in Table II.

TABLE II

Conductivity of mercury complexes

Complex	Solvent used	Molar conductance (mho)
Dichloro-bi(D-amphetamine)mercury(II)	Nitrobenzene	0.95
Dichloro-bi(L-amphetamine)mercury(II)	Ethanol	0.75
Dichloro-bi(DL-amphetamine)mercury(II)*	Nitrobenzene	0.58
Dichloro-bi(methylamphetamine)mercury(II)	Ethanol	1.05
Dichloro-bi(ephedrine)-mercury(II)	Nitrobenzene	0.35
Dichloro-bi(tyramine)-mercury(II)	Nitrobenzene	0.45

*Consists of a mixture of dichloro-bi(D-amphetamine)mercury(II) and dichloro-bi(L-amphetamine)mercury(II).

Absorption Spectra

The ultraviolet absorption spectra of complexes synthesized from L-amphetamine, methylamphetamine, and ephedrine were carried out in ethanol with a Beckman G-2400 spectrophotometer in the range of 200 mμ–300 mμ. These results were checked with a Hitachi Perkin–Elmer UV–VIS spectrophotometer. Such studies with complexes of D-amphetamine, DL-amphetamine, and tyramine could not be undertaken due to the lack of proper solvent. No definite peaks could be observed with complexes obtained from L-amphetamine and methylamphetamine. The characteristic wavelengths and the log of their extinction coefficients for the ephedrine–mercury complex were found to be 215 mμ and 4.71 and 265 mμ and 3.48 for the first and second maxima respectively, as compared with the absorption peak at 205 mμ for the first maxima and 258 mμ for the second maxima observed with ephedrine.

Infrared Spectra

The infrared spectra were obtained with a Perkin–Elmer Infra-cord spectrophotometer model 137 equipped with NaCl optics. The spectra of those complexes examined in KBr films in the range 700 to 3500 cm^{-1} have been

TABLE III

Frequency (cm^{-1}) assignments for D-amphetamine, L-amphetamine, and their mercury complexes

	D-Amphetamine		L-Amphetamine	
Assignment	Ligand	Hg complex	Ligand	Hg complex
NH Asymmetric stretching	3338 b	3178 sh	3325 s	3151 s
NH Symmetric stretching	3231 sh	3124 s	3231 sh	3151 s
NH_2 Degenerate deformation	—	1603 sh	1599 b	1585 s
	1599 b	1611 s	—	—
NH_2 Symmetric deformation	1468 m	1491 m	1468 m	1491 m
	1451 s	1452 s	1451 s	1468 s
NH_2 Rocking	742 s	746 s	742 s	748 s

ABBREVIATIONS: b = broad; m = medium; s = sharp; sh = shoulder.

TABLE IV

Frequency (cm^{-1}) assignments for methyl amphetamine, ephedrine, tyramine, and their mercury complexes

	Methylamphetamine		Ephedrine		Tyramine	
	Ligand	Hg complex	Ligand	Hg complex	Ligand	Hg complex
NH Asymmetric stretching	3283 w	3178 s	—	3145 b	3270 w	3124 m
NH Symmetric stretching	—	—	—	3205 w	—	—
NH_2 Degenerate deformation	1497 m	1596 m	1138 m	1596 b	1514 s	1611 sh
	1456 m	1491 s	1491 s	1483 s	1462 m	1600 s
NH_2 Symmetric deformation	1379 s	1341 s	1391 w	1387 w	1392 s	1370 w
	1341 m	1333 m	1379 m	1316 w	1263 w	1243 s
NH_2 Rocking	742 b	752 s	—	751 s	781 m	787 w

ABBREVIATIONS: b = broad; m = medium; s = sharp; sh = shoulder; w = weak.

compared with their corresponding ligands. These results are recorded in Tables III and IV. For detailed investigation, the spectra of the complexes of ephedrine and tyramine were measured with a Perkin–Elmer 337 grating infrared spectrophotometer in KBr and Nujol mull phase.

Discussion

The ratio of the ligand with $HgCl_2$, found to be 2:1 in these complexes (Table I), indicates that these complexes exist as

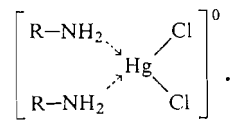

Conductance measurements have indicated the nonelectrolytic nature (6) of all the coordination compounds which presumably exist as monomers. At present, the probability for the existence of a polymeric structure due to halogen bridging (7, 8) cannot be ruled out. Furthermore, the low affinity of mercuric ion for oxygen as compared with its affinity for nitrogen, could account for the coordination through nitrogen preferentially over oxygen (9). The presence of the OH group in tyramine and ephedrine could render oxygen available to take part in the formation of the complex compound. However, the positive shift in the OH stretching vibration observed in the infrared spectrum of the ephedrine complex has indicated that coordination does not occur through the oxygen. The frequency assignments for OH stretching and NH asymmetric stretching vibrations could not be clearly established in the infrared spectrum of ephedrine. On the other hand, the OH stretching vibration was found to occur at 3373 cm^{-1} (Fig. 1) with dichloro-

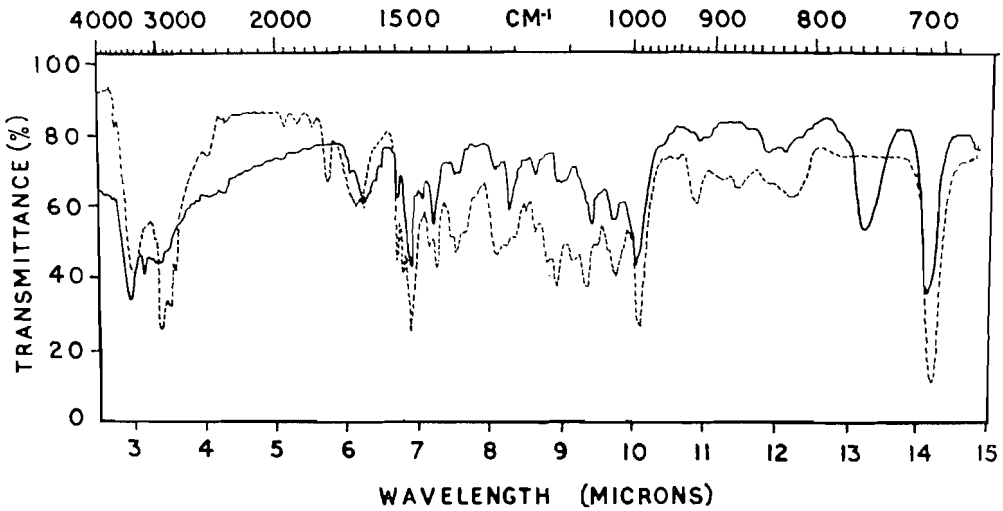

FIG. 1. Infrared spectra of dichloro-bi(ephedrine)mercury(II) in KBr (solid line), ephedrine in $CHCl_3$ (broken line).

Can. J. Chem. Downloaded from www.nrcresearchpress.com by 210.87.254.40 on 09/05/12
For personal use only.

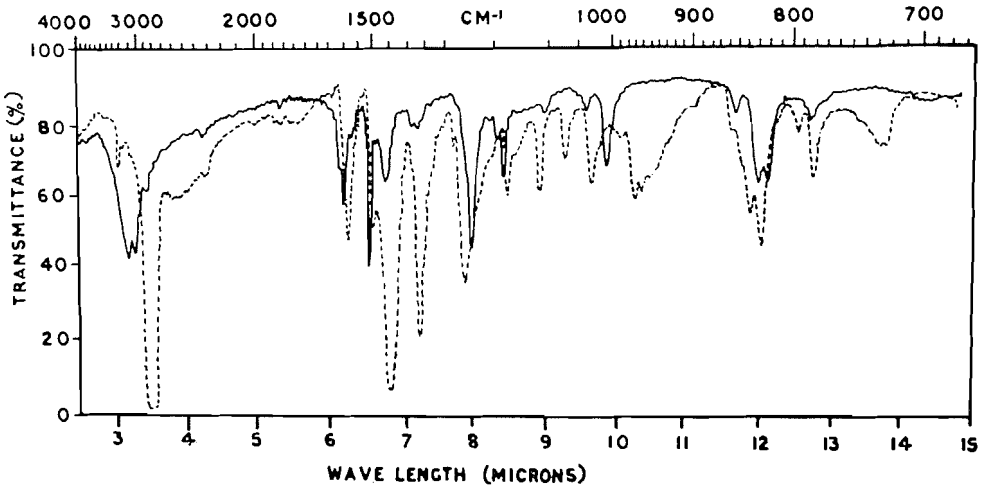

FIG. 2. Infrared spectra of dichloro-bi(tyramine)mercury(II) in KBr (solid line), tyramine in Nujol (broken line).

bi(ephedrine)mercury(II). The possibility of covalent bonding by replacement of hydrogen from the OH group is ruled out due to the inability of the alcoholic group to undergo ionization (10). Such a change in the spectrum was not observed with the tyramine–mercury complex (Fig. 2). The interaction of the free phenolic group with KBr during grinding (11) could presumably account for such a difference, since a negative shift was actually observed in the OH stretching vibration. Further support for such an explanation was provided by the positive shift in the OH stretching vibrations observed during measurement of the infrared spectra of the complex in Nujol mull phase. The OH-stretching vibration at 3309 cm^{-1} observed with tyramine was found to be at 3385 cm^{-1} for dichloro-bi(tyramine)mercury(II). The infrared spectra of the complexes obtained from D-amphetamine (Fig. 3), L-amphetamine (Fig. 4), methylamphetamine (Fig. 5), ephedrine (Fig. 1), and tyramine (Fig. 2) have indicated a negative shift in the NH stretching vibration and in the NH_2 degenerate deformation by comparison with their ligands (Tables III and IV). Donation of a pair of electrons from the primary and secondary amino groups to the metal ion may possibly account for such a negative shift. The

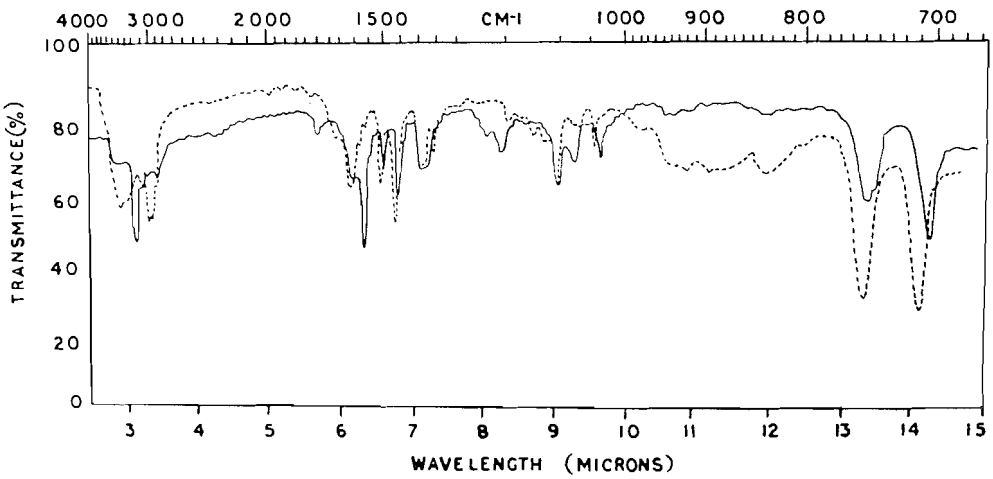

FIG. 3. Infrared spectra of dichloro-bi(D-amphetamine)mercury(II) in KBr (solid line), D-amphetamine (broken line).

Can. J. Chem. Downloaded from www.nrcresearchpress.com by 210.87.254.40 on 09/05/12
For personal use only.

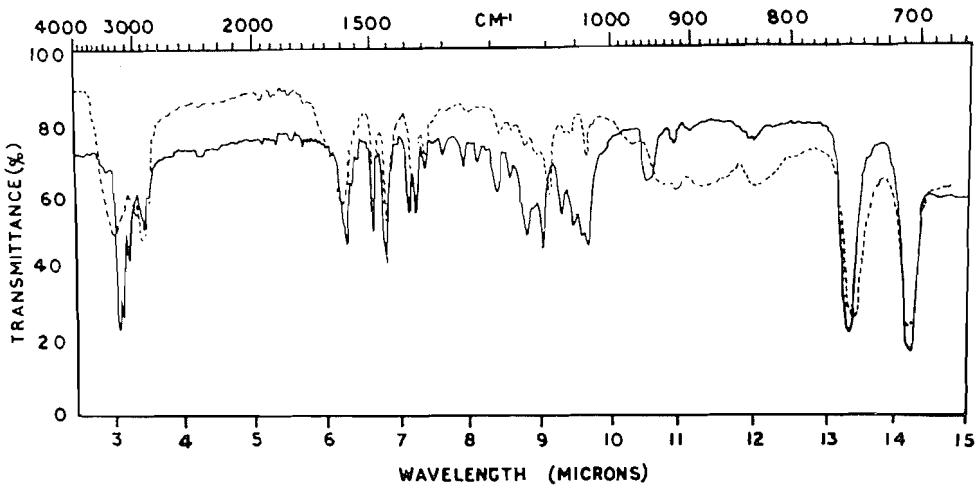

FIG. 4. Infrared spectra of dichloro-bi (L-amphetamine)mercury(II) in KBr (solid line), L-amphetamine (broken line).

observed shifts in NH_2 symmetric deformation and NH_2 rocking vibration (12, 13) have provided further support for such an explanation. The ability of D-amphetamine and L-amphetamine to form different complexes points towards the existence of stereoisomeric effects during complex formation. Solubility differences have been utilized for separation of the complexes of stereoisomeric amphetamines from dichloro-bi(DL-amphetamine)mercury(II). At present the possibility of the formation of a mixed complex presumably through the following reversible equilibrium cannot be ruled out. The reaction thus could possibly be driven to the right in a solvent in which one of the compounds is insoluble.

$$2\text{Hg(D-amphetamine)(L-amphetamine)} \rightleftharpoons \text{Hg(D-amphetamine)}_2 + \text{Hg(L-amphetamine)}_2$$

However, further experimental evidence will be required to elucidate such a mechanism where liberation of the ligands from the mixed complex is necessary before the formation of the complexes of D- and L-amphetamine separately.

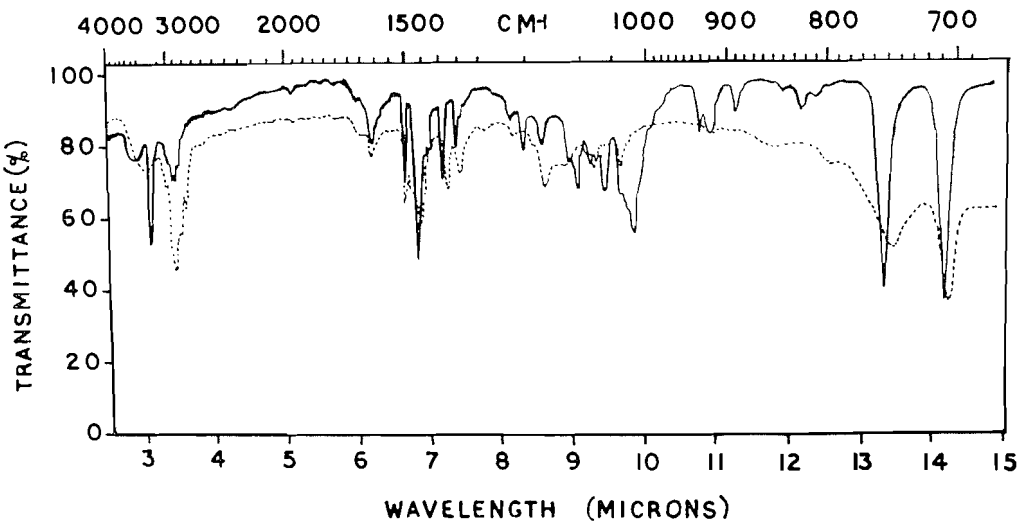

FIG. 5. Infrared spectra of dichloro-bi(methylamphetamine)mercury(II) in KBr (solid line), methylamphetamine in KBr (broken line).

Can. J. Chem. Downloaded from www.nrcresearchpress.com by 210.87.254.40 on 09/05/12
For personal use only.

Acknowledgments

The authors wish to express their thanks to Dr. M. L. Dhar, Dr. Nitya Anand, and Dr. S. C. Agarwal from the Central Drug Research Institute, Lucknow, for providing facilities for microanalysis and infrared and ultraviolet absorption measurements respectively. Grateful acknowledgment is made to Professor K. P. Bhargava and Dr. J. P. Barthwal for their advice and encouragement and to the University Grants Commission, New Delhi, for Retired Professor Scientist Award to one of us (S. N. S.). A generous gift of a Hitachi Perkin–Elmer UV–VIS spectrophotometer by the Perkin–Elmer Corporation, Norwalk, Connecticut, and of chemicals by Riker Laboratories, Northridge, California, is gratefully acknowledged.

1. S. M. A. SMOLT, C. W. KREKE, and E. S. COOK. J. Biol. Chem. **224**, 999 (1957).
2. S. S. PARMAR, C. H. MISRA, and S. N. SHUKLA. In preparation.
3. A. I. VOGEL. Practical organic chemistry. Longmans, Green and Co., Ltd., London. 1948. p. 173.
4. C. H. MISRA, S. S. PARMAR, and S. N. SHUKLA. J. Inorg. Nucl. Chem. **28**, 147 (1966).
5. C. H. MISRA, S. S. PARMAR, and S. N. SHUKLA. J. Inorg. Nucl. Chem. **29**, 2589 (1967).
6. R. BLACKHOUSE, M. E. FOSS, and R. S. NYHOLM. J. Chem. Soc. 1714 (1957).
7. G. J. SUTTON. Australian J. Chem. **15**, 563 (1962).
8. G. E. COATES and D. RIDLEY. J. Chem. Soc. 166 (1964).
9. T. W. WIRTH and N. DAVIDSON. J. Am. Chem. Soc. **86**, 4325 (1964).
10. I. C. SMITH. Dissertation, Kansas State University, Manhattan, Kansas. 1961.
11. V. C. FARMER. Spectrochim. Acta, **8**, 374 (1957).
12. C. N. R. RAO. Chemical application of infrared spectroscopy. Academic Press, Inc., London. 1963. p. 361.
13. S. MIZUSHIMA, I. NAKAGAWA, and J. V. QUAGLIANO. J. Chem. Phys. **23**, 1367 (1955).

Can. J. Chem. Downloaded from www.nrcresearchpress.com by 210.87.254.40 on 09/05/12
For personal use only.

Can. J. Chem. Downloaded from www.nrcresearchpress.com by 210.87.254.40 on 09/05/12
For personal use only.

Primary process(es) in the mercury-photosensitized decomposition of dimethyl ether at 2537 Å

R. PAYETTE, M. BERTRAND, AND Y. ROUSSEAU
Département de Chimie, Université de Montréal, Montréal, Québec

Received December 29, 1967

The mercury-photosensitized decomposition of dimethyl ether has been studied at room temperature and at pressures ranging from 10 to 200 Torr.

The formation of an excited dimethyl ether (DME) molecule has been verified by following the rates of formation of methane, ethane, and carbon monoxide with various ether pressures.

The study of the variation of the quantum yield of molecular hydrogen formation with absorbed light intensity at high ether pressures has shown that the primary process involves the dissociation of ether molecules into hydrogen atoms and methoxy methyl radicals:

$$Hg\ 6(^3P_1) + CH_3OCH_3 \rightarrow H + CH_2OCH_3 + Hg\ 6(^1S_0).$$

The results presented in this paper indicate that the excited DME molecule can originate in a radical recombination between hydrogen atoms and methoxy methyl radicals.

Canadian Journal of Chemistry, 46, 2693 (1968)

Introduction

The mercury-photosensitized decomposition of dimethyl ether[1,2] (DME) at 2537 Å has been studied by Marcus, Darwent, and Steacie (1), who found that at 25 °C and for pressures between 28 and 500 Torr, the products consisted almost entirely of hydrogen and 1,2-dimethoxyethane. According to these workers the primary process was the dissociation of the ether molecules into hydrogen atoms and methoxy methyl radicals. Using a light intensity of 4.5×10^{-7} einstein min^{-1} (measured from the rate of hydrolysis of a 0.5 *N* solution of monochloracetic acid as actinometer) a quantum yield of 0.8 was found for the hydrogen formation. No evidence was found for the occurrence of excited molecules or for the scission of the C—O bond.

Pottie, Harrison, and Lossing (2) have studied the same reaction using a fast flow system coupled to a mass spectrometer. With the system at 55 °C, they allowed a few microns of ether to be carried through a strongly illuminated tubular reactor by a stream of helium at a pressure of 8 Torr. Their results indicated two primary modes of dissociation of DME. These are (i) cleavage of C—H bonds and (ii) cleavage of C—O bonds. The probability of the occurrence of these two reactions is similar. The nonoccurrence of the mode of dissociation involving a C—O split in the 28 to 500 Torr region was interpreted by Lossing *et al.* (2) in terms of an excited ether molecule which could be completely deactivated at these pressures and hence not be able to dissociate.

Loucks and Laidler (3*a*) have recently presented a mechanism for the mercury-photosensitized decomposition of DME at temperatures from 200 to 300 °C and over a pressure range of 3 to 600 Torr. Under these conditions, the products found were CO, H_2, C_2H_6, CH_4, $CH_3OC_2H_5$, and $CH_3OCH_2CH_2OCH_3$. These authors stated that the primary process involves a C—H bond split, but they found no evidence for a primary C—O bond split.

The intention of this study was to investigate the possible occurrence of an excited DME molecule and to elucidate the primary process(es) in the mercury-photosensitized decomposition of DME. From a consideration of the quenching cross-section values of the molecules indicated in Table I, a qualitative attempt can be made to predict the primary quenching interaction between a Hg $6(^3P_1)$ atom and a DME molecule. As the ratio of quenching cross section of DME to ethane is greater than 60, a preferential attack center is indicated in the DME. This leads us to believe that a Hg $6(^3P_1)$ atom will attack the non-bonding electrons of the oxygen atom in DME. Moreover, Rousseau, Strausz, and Gunning (4) have already pointed out the electrophilic character of the Hg $6(^3P_1)$ atom.

[1]Paper presented at the "34e Congrès de l'ACFAS", Quebec, Nov. 4–6, 1966. Cf. Ann. l'ACFAS. **33**, 56 (1967).

[2]Paper presented at the 50th CIC Conference, Toronto, June 4–7, 1967.

Can. J. Chem. Downloaded from www.nrcresearchpress.com by 210.87.254.40 on 09/05/12
For personal use only.

Knight and Gunning (5) studied the mercury-photosensitized decomposition of methanol at 2537 Å. Methanol has a quenching cross-section value similar to that of DME. Their results indicated a primary quenching process which involved the rupture of the O—H bond and which had a quantum yield of approximately unity. Thus, *a priori*, if the center of attack for a Hg $6(^3P_1)$ atom is the non-bonding electrons of oxygen in DME, one can visualize a primary split at the C—O bond in DME.

Experimental

Materials

Dimethyl ether from Air Products and Chemicals Inc. was used without further purification except trap to trap distillations at −131 °C. Its purity was verified by mass spectrometry.

Apparatus and Procedure

The reaction was studied at room temperature in a static system. The diameter of the cylindrical quartz cell was 4.5 cm and its length 9.5 cm. The light source was a commercial mercury low pressure resonance lamp (Hanovia, SC 2537). In order to eliminate the 1849 Å wavelength, the cell was separated from the lamp by a distance of 11 cm in air.When the light intensity in the center of the lamp was required, a vycor cell 2 cm in diameter and 22 cm long was used.

The reaction products were analyzed using a Hitachi RMU-6D mass spectrometer.

Light intensities were measured by the nitrous oxide – *n*-butane actinometer (8); the pressure of the mixture was 200 Torr in all cases.

Results and Discussion

The products measured following the mercury-photosensitized decomposition of DME at room temperature and at pressures between 10 and 200 Torr are H_2, CO, CH_4, C_2H_6, and $CH_3OCH_2CH_2OCH_3$. Since the object of this study was to elucidate the primary process(es) involved in the decomposition of DME, all the products which may be formed as a result of secondary reactions have not been measured.

If an excited DME molecule is produced in the system, the two following modes of deactivation may be anticipated:

$$[1] \quad (CH_3OCH_3)^* + M \rightarrow CH_3OCH_3 + M$$

$$[2] \quad (CH_3OCH_3)^* \rightarrow CH_3 + OCH_3.$$

In [1] the excited DME molecule is deactivated by collision at high pressure, but in [2] its excess energy is involved in the rupture of the weakest bond. The latter process will predominate at low pressures but the two modes of deactivation will be in competition over a considerable pressure range.

TABLE I

Quenching cross-section data for Hg $6(^3P_1)$ atoms

Substrate	σ_Q^2 (Å^2)	Reference
$CH_3—CH_3$	0.11	(6)*
$CH_3—CH_2—CH_3$	1.3	(6)*
$CH_3—O—H$	8	(7)*
$CH_3—O—CH_3$	7	(7)*
$(CH_3—O—CH_3)$	3.3	Present study†
$(CH_3—O—CH_2)_2$	12.5	Present study†

*σ_Q^2 value from physical data.
†σ_Q^2 value from chemical data.

Methane and ethane, which are decomposition products, probably arise from abstraction and recombination reactions:

$$[3a] \quad CH_3O + CH_3 \rightarrow CH_4 + CH_2O$$

$$[3b] \quad CH_3 + CH_3OCH_3 \rightarrow CH_4 + CH_2OCH_3$$

$$[4] \quad 2CH_3 \rightarrow C_2H_6.$$

Carbon monoxide may arise from the mercury-photosensitized decomposition of formaldehyde as this reaction has a large relative cross section (9):

$$[5] \quad Hg\ 6(^3P_1) + CH_2O \rightarrow H_2 + CO + Hg\ 6(^1S_0).$$

Hence, a study of the variation of the rates of formation of CH_4, CO, and C_2H_6 with variation in the DME pressure will enable the production of excited DME molecules to be verified.

Using two different light intensities, 12.8 and 57.4 μeinstein min^{-1}, DME was irradiated at room temperature and pressures between 10 and 200 Torr. The results are reported in Table II. This table shows a decrease in the ratios CH_4/H_2, CO/H_2, and C_2H_6/H_2 as the ether pressure in the system is increased. At a pressure of 10 Torr, appreciable quantities of CH_4, CO, and C_2H_6 are produced especially at a light intensity of 57.4 μeinstein min^{-1}. At 200 Torr these product yields are negligible compared with that of hydrogen. These results indicate that excited DME molecules are produced in the system and it is of interest to establish the origin of these excited molecules.

Lossing *et al.* (2) did not exclude the formation of excited DME molecules in the primary process and this reaction may be included as one of the

TABLE II

Pressure effect on the mercury-photosensitized decomposition of dimethyl ether at 2537 Å

$P_{CH_3OCH_3}$ (Torr)	$(CH_4/H_2).10^2$	$(CO/H_2).10^2$	$(C_2H_6/H_2).10^2$
	A. For 12.8 μeinstein min^{-1}		
11	6.50	7.5	2.9
22	2.25	3.5	0.2
44	1.11	1.9	—
100	0.38	0.88	—
200	0.25	0.40	—
	B. For 57.4 μeinstein min^{-1}		
10	29.7	32.7	5.8
25	9.4	10.1	2.1
50	3.8	4.4	1.0
100	2.6	2.8	0.5
200	1.1	1.3	—

three primary processes that may occur. These reactions are

[6] $Hg\ 6(^3P_1) + CH_3OCH_3 \rightarrow H + CH_2OCH_3 + Hg\ 6(^1S_0)$

[7] $Hg\ 6(^3P_1) + CH_3OCH_3 \rightarrow CH_3 + OCH_3 + Hg\ 6(^1S_0)$

[8] $Hg\ 6(^3P_1) + CH_3OCH_3 \rightarrow (CH_3OCH_3)^* + Hg\ 6(^1S_0).$

However, [8] is not the only process in which excited DME molecules can be produced. They may also originate from any of the following recombinations:

[9] $H + CH_2OCH_3 \rightarrow (CH_3OCH_3)^*$

[10] $CH_3 + OCH_3 \rightarrow (CH_3OCH_3)^*$

[11] $CH_3O + CH_2OCH_3 \rightarrow (CH_3OCH_3)^* + CH_2O.$

In order to elucidate the primary quenching process(es), experiments have been carried out to determine the relative probability of reaction [6].

Steacie *et al.* (1) have suggested that molecular hydrogen can arise by hydrogen abstraction from the substrate:

[12] $H + CH_3OCH_3 \rightarrow H_2 + CH_2OCH_3.$

However, we have already seen that [9] will also remove hydrogen atoms from the system and form excited DME molecules.

As reaction [12] represents the only way in which hydrogen atoms are removed in a radical–molecule reaction, the variation in the quantum yield of hydrogen with the change in intensity of the absorbed light will provide a means of determining the probability of the primary quenching reaction which involves dissociation of the C—H bond. As the formation of products [9] are proportional to I_a^2 (I_a refers to absorbed light intensity) and molecular hydrogen formation is proportional to I_a, a decrease in the absorbed light intensity will indicate that the reaction leading to molecular hydrogen is favored.

DME, at a pressure of 200 Torr, has been irradiated at various light intensities in order to determine whether the quantum yield of hydrogen reaches a constant value, which is less than unity, as the value of I_a is gradually decreased. The results are shown in Table III and in Fig. 1. The value of the quantum yield reported by Steacie *et al.* (1), who used a different method of actinometry, is included in Fig. 1 and it is found to lie on the curve drawn through the values shown in Table III.

As the value of the quantum yield of hydrogen is not less than unity at low light intensities, it is probable that the only primary process is dissociation into hydrogen atoms and methoxy methyl radicals. Hence the interaction between an excited Hg atom, $Hg\ 6(^3P_1)$, and a DME molecule leads exclusively to a C—H bond split. If this occurs, excited ether molecules will probably arise from a radical recombination. As reactions [10] and [11] are not considered to occur to any significant extent, the excited molecule will not be produced from the interactions of methyl and methoxy radicals. Reaction [9] represents the only method of producing excited DME molecules. These excited molecules will most probably be in a vibrationally excited state

Can. J. Chem. Downloaded from www.nrcresearchpress.com by 210.87.254.40 on 09/05/12
For personal use only.

TABLE III

Light intensity effect on the mercury-photosensitized decomposition of dimethyl ether at 2537 Å*

Product	I_a (μeinstein min^{-1})	Irradiation time (min)	$\Phi_{Product}$ (mole einstein^{-1})
H_2	57.4	2	0.26
H_2	12.8	4	0.37
$(CH_3OCH_2)_2$	1.39	30	0.68
H_2	1.39	30	0.65
H_2	0.012	120	1.0
$(CH_3OCH_2)_2$	0.012	120	1.0

*$P_{CH_3OCH_3}$ = 200 Torr.

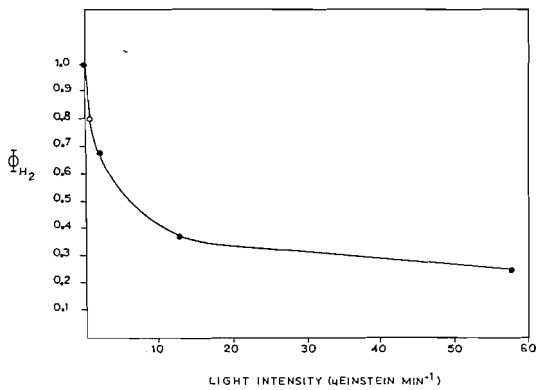

FIG. 1. Hydrogen quantum yield versus absorbed light intensity (○ represents the value found by Steacie *et al.*).

as a low-lying excited electronic state is absent in simple aliphatic ethers.

In addition to H_2, CO, CH_4, and C_2H_6 we have identified 1,2-dimethoxyethane in the products resulting from the mercury-photosensitized decomposition of DME. This heavy liquid arises from a radical recombination reaction, but the products resulting from the disproportionation of methoxy methyl radicals, i.e. ethylene oxide or 1,4-dioxane, have not been observed.

[13] $2CH_3OCH_2 \rightarrow CH_2\text{—}CH_2 + CH_3OCH_3$ (O) or

[14] $H + CH_3OCH_2 \rightarrow CH_2\text{—}CH_2 + H_2$ (O)

The results in Table III indicate that reactions [13] and/or [14] are not important under the experimental conditions. The quantum yield for the formation of 1,2-dimethoxyethane is very close to that of hydrogen and also approaches unity as the light intensity is decreased (1.2×10^{-8} einstein min^{-1}).

This result eliminates the possibility of unimolecular decomposition of methoxy methyl radical into methyl radical and formaldehyde. This observation is not unexpected from a consideration of the activation energy of 24.8 kcal reported by Loucks and Laidler (3*b*) for this reaction.

Takezaki, Mori, and Kawasaki (10) have recently reported on the mercury-photosensitized decomposition of DME at a pressure of 100 Torr and at a temperature of 25 °C. These studies were carried out in the presence and absence of nitrous oxide. With pure ether, 1,2-dimethoxyethane and trimeric products were detected and the hydrogen yield was found to be twice that of the condensable products. A possible explanation of these results may be that a large light intensity causes photolysis of the products.

We have measured the quenching cross section of DME by a chemical method using nitrous oxide and taking 3.6 for *n*-butane quenching cross section as reference. The values found were 3.3 for DME and 12.5 for 1,2-dimethoxyethane. The large quenching cross section of 1,2-dimethoxyethane may lead to the 1,2-dimethoxyethane preferentially quenching the Hg $6(^3P_1)$ atoms at high light intensities:

[15] Hg $6(^3P_1) + CH_3OCH_2CH_2OCH_3 \rightarrow CH_3OCH_2CHOCH_3 + H +$ Hg $6(^1S_0)$

[16] Hg $6(^3P_1) + CH_3OCH_2CH_2OCH_3 \rightarrow CH_3OCH_2CH_2OCH_2 + H +$ Hg $6(^1S_0)$.

This may account for the large yield of hydrogen compared with that of dimeric and trimeric products.

In some aspects the mercury-photosensitized decomposition of DME resembles that of alkanes; however, since DME has a much larger

Can. J. Chem. Downloaded from www.nrcresearchpress.com by 210.87.254.40 on 09/05/12
For personal use only.

quenching cross section than ethane, the C—H bond must be strongly activated by the presence of an oxygen atom.

The present work is further supported by the work of Filseth[3] on the mercury-photosensitized decomposition of methyl ethyl ether at 52 °C. Filseth proposed a primary decomposition pattern similar to that proposed here for DME in which excited methyl ethyl ether molecules also originate from radical recombination reactions. As for the possible disproportionation of ethoxy methyl radicals, Filseth has also failed to observe propylene and/or trimethylene oxides among reaction products in his system.

Conclusion

The present work is an attempt to clarify certain anomalies present in the literature concerning the apparent contradiction between the results of Steacie and of Lossing. In fact, they do not contradict each other but are both valid depending upon the experimental conditions involved.

The present study has shown that the choice of experimental conditions is very important in the determination of the primary processes occurring in a reaction sequence. In particular, the use of a low light intensity has been found to be essential in eliminating radical–radical reactions and photolysis of the products.

This study, using a wide pressure and light intensity range, has found evidence for excited DME molecules and a process of their formation has been proposed.

[3]Paper presented at the International Conference of Photochemistry. München. September 6–9, 1967.

Acknowledgments

We thank the National Research Council of Canada for financial support, and Mr. J. C. Regenass for the mass spectrometric analysis.

1. R. A. Marcus, B. de B. Darwent, and E. W. R. Steacie. J. Chem. Phys. **16**, 987 (1948).
2. R. F. Pottie, A. G. Harrison, and F. P. Lossing. Can. J. Chem. **39**, 102 (1961).
3. (*a*) L. F. Loucks and K. J. Laidler. Can. J. Chem. **45**, 2763 (1967). (*b*) L. F. Loucks and K. J. Laidler. Can. J. Chem. **45**, 2767 (1967).
4. Y. Rousseau, O. P. Strausz, and H. E. Gunning. J. Chem. Phys. **39**, 962 (1963).
5. A. R. Knight and H. E. Gunning. Can. J. Chem. **39**, 2251 (1961).
6. B. de B. Darwent. J. Chem. Phys. **18**, 1532 (1950).
7. B. de B. Darwent and M. K. Phibbs. J. Chem. Phys. **22**, 110 (1954).
8. Y. Rousseau and H. E. Gunning. Can J. Chem. **41**, 465 (1963).
9. A. G. Harrison and F. P. Lossing. Can. J. Chem. **38**, 544 (1960).
10. Y. Takezaki, S. Mori, and H. Kawasaki. Bull. Chem. Soc. Japan, **39**, 1643 (1966).

Can. J. Chem. Downloaded from www.nrcresearchpress.com by 210.87.254.40 on 09/05/12
For personal use only.

Can. J. Chem. Downloaded from www.nrcresearchpress.com by 210.87.254.105 on 09/05/12
For personal use only.

Some reactions of pentafluorothiophenol. Preparation of some pentafluoro-phenylthio metal derivatives

M. E. PEACH
Department of Chemistry, Acadia University, Wolfville, Nova Scotia

Received March 7, 1968

The new compounds $M(SC_6F_5)$, where M = Cs, Tl, Cu, Au, and Ph_3Pb; $M(SC_6F_5)_2$, where M = Pb, Cd, Hg, Ni, and Pt; $M(SC_6F_5)_3$, where M = As or Bi; and $Sn(SC_6F_5)_4$ have been prepared from pentafluorothiophenol and metal ions in aqueous solution. $Zn(SC_6F_5)_2$ has been prepared from zinc oxide and pentafluorothiophenol in methanol. The compounds have been characterized, and their infrared spectra and ^1H and ^{19}F nuclear magnetic resonance spectra examined.

Some of the reducing properties of pentafluorothiophenol and its polymerization have been studied.

Canadian Journal of Chemistry, **46**, 2699 (1968)

The reactions, if any, of an aqueous suspension of pentafluorothiophenol with various metal ions can be divided into three categories, (1) formation of pentafluoro-phenylthio metal derivatives, (2) reduction forming bis(pentafluoro-phenyl) disulfide, and (3) polymerization forming perfluoropoly(phenylene sulfide); one specific reaction or a combination may be observed with a particular metal ion. This paper describes the reactions of pentafluorothiophenol with aqueous solutions containing the ions, or compounds, Cs^+, Pb^{2+}, Cu^{2+}, Cd^{2+}, Al^{3+}, Tl^+, Hg^{2+}, Hg_2^{2+}, As_2O_3, AsO_4^{3-}, Sb^{3+}, Bi^{3+}, Sn^{4+}, Sn^{2+}, Fe^{3+}, Fe^{2+}, Cr^{3+}, Ni^{2+}, Co^{2+}, $AuCl_4^-$, $PtCl_6^{2-}$, Mn^{2+}, Zn^{2+}, UO_2^{2+}, VO^{2+}, Bu_4N^+, Ph_3PbCl, Ph_2PbCl_2, TeO_3^{2-}, NH_4OH, and the reactions of a methanolic or ethanolic solution of pentafluorothiophenol with the oxides ZnO, SnO_2, SnO, GeO_2, TiO_2, PbO_2, and MnO_2.

The preparation of certain metallic mercaptides from the corresponding thiol (or sodium mercaptide) and an aqueous solution of the metal ion is well known. The mercaptides of Tl(I), Fe(II), Ni(II), Co(II), Zn, Cd, Hg(II), Sn(IV), and Bi(III) were first prepared by Claeson (1); it is probable that the only well-characterized mercaptides were Tl(I), Zn, Cd, Hg(II), and Bi(III). Some metal derivatives of pentafluorothiophenol are known; transition metal derivatives and complex ions have been precipitated from aqueous solution, i.e. $M(SC_6F_5)_4^{2-}$, where M = Co(II), Pd(II), Pt(II), Zn, Cd, Hg(II) (3); $M(SC_6F_5)_2^-$, where M = Cu(I), Ag(I), Au(I) (3); $Ag(SC_6F_5)$ (3); $Pd(SC_6F_5)_2$ (3); and $K(SC_6F_5).1.5H_2O$ (4). The compound $Cu(SC_6F_5)$ has been prepared from cuprous oxide and pentafluorothiophenol in ethanol; no details of its physical properties are given, although it has been utilized to prepare bis(pentafluorophenyl) sulfide by its reaction with bromopentafluorobenzene in dimethyl formamide (5). Very recently the compounds $Ni(SC_6F_5)_2$, $Pd(SC_6F_5)_2$, and $Pt(SC_6F_5)_2$ have been prepared from the metal acetate and pentafluorothiophenol in acetone–water (Ni) and benzene (Pd, Pt) solutions; the triphenylphosphine adducts and the complex ions $Pd(SC_6F_5)_4^{2-}$ and $Pt(SC_6F_5)_4^{2-}$ have also been prepared (6).

The pentafluoro-phenylthio derivatives of Cs, Pb(II), Cd, Hg(II), Bi(III), As(III), and Tl(I) have been prepared in aqueous solutions from the corresponding metal ion and a suspension of pentafluorothiophenol: the ions Cu^{2+}, $PtCl_6^{2-}$, and $AuCl_4^-$ were reduced by pentafluorothiophenol forming Cu(I), Pt(II), and Au(I), pentafluoro-phenylthio derivatives respectively. The following type of reaction is typical for these ions with thiols (2):

$$2Cu^{2+} + 4C_6F_5SH \rightarrow 2CuSC_6F_5 + C_6F_5SSC_6F_5 + 2H^+.$$

No reaction was observed with the metal ions Co^{2+}, Cr^{3+}, Sn^{2+}, Fe^{2+}, Al^{3+}, Mn^{2+}, VO^{2+}, or UO_2^{2+}, and pentafluorothiophenol. Mercurous nitrate reacted with pentafluorothiophenol to form mercury and bis(pentafluoro-phenylthio) mercury. This reaction must be due to the insolubility of bis(pentafluoro-phenylthio) mercury forcing the equilibrium $Hg_2^{2+} \rightleftharpoons Hg + Hg^{2+}$ over to the right. Attempts to prepare $ClHgSC_6F_5$ and $O_3NHgSC_6F_5$ by the reaction of 1 mole of pentafluorothiophenol and 1 mole of mercuric chloride or nitrate resulted in the precipitation of bis(pentafluoro-phenylthio) mercury. The compound $ClHgSCF_3$, which is obtained by mixing mercuric chloride and bis(trifluoromethylthio) mercury in ether, can be

converted to $O_3NHgSCF_3$ in aqueous solution by treatment with silver nitrate (7).

It is doubtful whether Claeson succeeded in preparing pure $Sn(SEt)_4$ (1); the product has been claimed to be Cl_3SnSEt (8). Good yields of stannic mercaptides are reported from the reaction of stannic chloride in benzene with sodium mercaptide either as a suspension or in an alcoholic solution (8–11), but the products are reported as unstable in moist air (9). Stannic mercaptides can be prepared in alcoholic solution by the reaction of a thiol and stannous chloride in air (10), a disulfide and metallic tin with hydrochloric acid (10), or in benzene solution by the displacement of alkoxy groups of tetraalkoxy tin by alkylthio groups from a thiol (11): these latter authors claim that stannic mercaptides are hydrolytically stable. Water is not the ideal solvent for the preparation of stannic mercaptides: stannic chloride is only soluble in acidic solution and the presence of an excess acid decomposes stannic mercaptide. $Sn(SC_6F_5)_4$ could be obtained by vacuum sublimation of the crude product obtained in aqueous solution from the reaction of stannic chloride and pentafluorothiophenol.

The mercaptides of cobalt(II) (1, 12), iron(II) (13), and nickel(II) (1, 14, 15) can be prepared in basic, usually ammoniacal, solution. Ferrous mercaptide can be formed in ammoniacal ethanol–water by the reaction of a thiol with ferrous ions, the excess thiol present reducing any ferric ion to ferrous ion (13); the mercaptide is easily oxidized. An acidic solution of ferric chloride was reduced by an excess of pentafluorothiophenol to the ferrous state, but this did not form bis(pentafluoro-phenylthio) iron with the excess pentafluorothiophenol present. The reaction of a thiol with an ammoniacal ethanol solution of nickel or cobalt chloride forms nickel mercaptides and cobaltous (nitrogen atmosphere) or cobaltic (air atmosphere) mercaptides (16). Using a somewhat similar procedure nickel chloride formed a red-brown compound with pentafluorothiophenol, analysis of which showed it to contain impurities, and the infrared (i.r.) spectrum indicated the presence of polymeric species. With cobaltous chloride two distinct products were formed, a dark-green impure pentafluoro-phenylthio derivative of cobalt and a white polymeric compound of approximate composition $C_{24}F_{17}S_4H$. If the addition of the ethanol were omitted and the solution refluxed immediately after the addition of the pentafluorothiophenol, to expel the excess ammonia, almost pure bis(pentafluoro-phenylthio) nickel precipitated in high yield as a black product; this was ground up with Nujol to give a deep-red mull. A similar experiment with cobaltous chloride gave less than a 10% yield of an impure pentafluoro-phenylthio derivative of cobalt. The necessity of using an alkaline solution for the preparation of nickel, cobalt, and iron mercaptides makes the aqueous method unsuitable for the preparation of derivatives of pentafluorothiophenol due to its ready polymerization in alkaline solution. The preparation from metal carbonyls or related compounds and thiols or disulfides appears to be more satisfactory. A red nickel compound $[Ni(SC_6F_5)_2]_n$ has been prepared from nickel tetracarbonyl and pentafluorothiophenol (3); the compounds $[C_6F_5SFe(CO)_3]_2$, $C_6F_5SFe(CO)_2(\pi\text{-}C_5H_5)$, $[C_6F_5SNi(\pi\text{-}C_5H_5)]_n$, $[C_6F_5SRh(CO)_2]_2$, and $[C_6F_5SRh(C_2H_4)_2]_2$ have very recently been prepared from pentafluorothiophenol or bis(pentafluoro-phenyl) disulfide and $Fe_3(CO)_{12}$, $[\pi\text{-}C_5H_5Fe(CO)_2]_2$, $[\pi\text{-}C_5H_5]_2Ni$, $[ClRh(CO)_2]_2$, and $[ClRh(C_2H_4)_2]_2$ respectively (17). Hexameric nickel mercaptides can be prepared from nickel chloride and bis(alkylthio)dimethyl tin; somewhat lower yields of the hexamer were obtained from the action of the disulfide on nickel tetracarbonyl (18). An interesting preparation of nickel mercaptides from nickel and the corresponding disulfide has been developed, which is claimed to yield hexameric nickel mercaptides (19).

If an ammoniacal solution of zinc sulfate and ammonium chloride is treated with pentafluorothiophenol, a basic zinc mercaptide that appeared to contain little polymeric derivative of pentafluorothiophenol was formed. Zinc mercaptide has been prepared from an ammoniacal solution of zinc sulfate and the corresponding thiol (16).

A methanolic suspension of zinc oxide reacted quantitatively with pentafluorothiophenol to give the methanol soluble $Zn(SC_6F_5)_2$. In a similar experiment with magnesium oxide a product containing very little magnesium was isolated. When pentafluorothiophenol was mixed with a saturated aqueous solution of calcium oxide a basic pentafluoro-phenylthio derivative of uncertain composition was obtained. Evaporation of the water from an aqueous stoichiometric mixture of cesium carbonate and pentafluoro-

Can. J. Chem. Downloaded from www.nrcresearchpress.com by 210.87.254.105 on 09/05/12
For personal use only.

Can. J. Chem. Downloaded from www.nrcresearchpress.com by 210.87.254.105 on 09/05/12
For personal use only.

thiophenol, which slowly dissolved, enabled $Cs(SC_6F_5)$ to be isolated. No reaction was observed with suspensions of the less basic oxides, titanic, germanic, stannic, or stannous, and pentafluorothiophenol in methanol; the expected products would probably be soluble in methanol. Pentafluorothiophenol must therefore be weakly acidic. A solution of pentafluorothiophenol in methanol reacted with plumbic oxide to form bis(pentafluoro-phenylthio) lead and bis(pentafluoro-phenyl) disulfide.

$$PbO_2 + 4C_6F_5SH \rightarrow Pb(SC_6F_5)_2 + C_6F_5SSC_6F_5$$

This reaction may proceed via the intermediate formation of tetra(pentafluoro-phenylthio) lead. A similar reaction has been observed to occur between plumbic oxide and thiophenol in chloroform; lead tetraacetate and iodine pentoxide, but not chromium trioxide, also oxidized thiophenol (20).

Pentafluoro-phenylthio derivatives of triphenyl lead and diphenyl lead were prepared in aqueous solution from the corresponding chloride, pentafluorothiophenol, and sufficient sodium hydroxide to neutralize the hydrogen chloride formed. (Pentafluoro-phenylthio)triphenyl tin was prepared analogously (21); all these reactions probably proceed via the hydroxide. The organotin derivatives n-$Bu_3Sn(SC_6F_5)$ and n-$Bu_2Sn(SC_6F_5)_2$ have been prepared from the corresponding organotin oxide and pentafluorothiophenol (21). Bis(pentafluoro-phenylthio)diphenyl lead decomposed at room temperature according to the equation

$$3Ph_2Pb(SC_6F_5)_2 \rightarrow 2Ph_3PbSC_6F_5 + Pb(SC_6F_5)_2 + C_6F_5SSC_6F_5.$$

A similar decomposition has been observed for bis(phenylthio)diphenyl lead (22).

Pentafluorothiophenol is readily oxidized, as are most thiols (2), to bis(pentafluoro-phenyl)-disulfide; bromine has been used as an oxidant (4). Reduction of the ions Cu^{2+}, $AuCl_4^-$, and $PtCl_6^{2-}$ and the compounds PbO_2 and H_2TeO_3 has resulted in the formation of pentafluorophenylthio derivatives of Cu(I), Au(I), Pt(II), Pb(II), and metallic tellurium respectively. These reactions may depend on the stability of the mercaptides so formed; no plumbic mercaptides have been reported (23). In an oxygen-free system the reduction of ferric ion to ferrous ion and no reaction of uranyl or chromic ions were observed. Qualitative tests showed that the vanadate, tungstate, and molybdate ions were reduced by pentafluorothiophenol in aqueous solution. Pentafluorothiophenol can be classified as a weak reducing agent. The oxidizing properties of bis-(pentafluoro-phenyl) disulfide have not been studied, although various phosphorus compounds such as triphenyl phosphine can be oxidized by disulfides (24).

In alkaline solution some polymerization of pentafluorothiophenol was observed forming perfluoropoly(phenylene sulfide), which can also be prepared by the reaction of sodium hydrogen sulfide with hexafluorobenzene in pyridine or by decomposition of pentafluoro-phenylthio potassium at 300° (4). The mechanism postulated is the nucleophilic attack by the pentafluorothiophenolate ion on other C_6F_5 nuclei, probably in the ortho and meta positions (4). Any alkaline medium will be favorable for this type of reaction, causing ionization of pentafluorothiophenol. Polymerization was observed to varying extents in ammoniacal solutions. Tetra-n-butyl ammonium bromide in aqueous solution reacted with pentafluorothiophenol to give a polymeric compound: the mechanism of this reaction is obscure but the tetra-n-butylammonium ion may decompose forming tri-n-butylamine, which would be basic, and n-butyl bromide. Manganese dioxide reacted with an ethanolic solution of pentafluorothiophenol in stoichiometric ratio MnO_2:C_6F_5SH of 1:4 to form perfluoropoly (phenylene sulfide); under similar conditions no reaction occurred between manganese dioxide and thiophenol. $Mn(SC_6F_5)_4$ must be formed initially, and then this decomposes to $C_6F_5SSC_6F_5$ and $Mn(SC_6F_5)_2$; if the latter is ionic, the $C_6F_5S^-$ ion can react with the $C_6F_5SSC_6F_5$ forming $C_6F_5SC_6F_4SSC_6F_4SC_6F_5$ and manganous fluoride. The manganous fluoride would be solvolyzed forming ethyl fluoride, which is readily soluble in ethanol, and manganous oxide.

Iodine in carbon tetrachloride solution is known to react quantitatively with various organotin sulfur compounds (R_3SnSR') forming the organotin iodide and the corresponding disulfide (21). Extension of this reaction showed that it could be used titrimetrically to estimate some pentafluoro-phenylthio derivatives.

$$2Cu(SC_6F_5) + I_2 \rightarrow 2CuI + C_6F_5SSC_6F_5$$

This reaction produced a brown color characteristic of a sulfenyl iodide, which disappeared fairly

Can. J. Chem. Downloaded from www.nrcresearchpress.com by 210.87.254.105 on 09/05/12
For personal use only.

slowly. The limiting factor in the titrimetric method is the color of the product and whether it is possible to detect the color change produced on addition of a slight excess of iodine, although the metal iodide could be isolated in most cases, see Table I.

TABLE I

Titration of compounds with iodine in CCl_4

Compound	Amount taken (mmoles)	Iodine used (mmoles)	Metal iodide recovered (mmoles)
$Hg(SC_6F_5)_2$	0.443	0.452	—
$Bi(SC_6F_5)_3$	0.278	—	0.244
$Pb(SC_6F_5)_2$	0.400	0.408	0.392
$Cu(SC_6F_5)$	0.469	0.235	0.450

The infrared (i.r.) spectra of the compounds prepared have been examined in the range 4000–670 or 250 cm^{-1}. The observed bands can be assigned to the C_6F_5— group and the C—S and M—S frequencies. The spectra agree well with the data published for the C_6F_5— group (25) and the C_6F_5S— group (3, 21). The C—S stretching frequency has been assigned as 860 cm^{-1} (3), but this is rather high (21) and is observed in both covalent and ionic, e.g. cesium derivatives, pentafluoro-phenylthio derivatives. In the polymeric species there were two very strong well-defined peaks at approximately 975 and 952 cm^{-1}, whereas in the simple pentafluoro-phenylthio derivatives there is only a very strong peak at about 970 cm^{-1}; these peaks are within the region where the C—F frequencies would be expected. The metal-sulfur stretching frequencies would be expected to lie below or about 300 cm^{-1}. In the ring compounds $[R_2MS]_3$, M = Ge, Sn, or Pb, the M—S frequencies are found to lie between 370–290 cm^{-1} (Sn) and 336–290 cm^{-1} (Pb) (only recorded to 250 cm^{-1}) (26). The compounds $Cu(SC_6F_5)$, $Au(SC_6F_5)$, $Ni(SC_6F_5)_2$, and $Pt(SC_6F_5)_2$ are insoluble in common organic solvents, see Table III, and can be considered as polymeric species containing linkages of the types

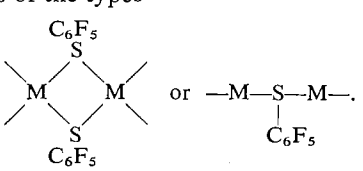

Nickel and palladium mercaptides are in general polymeric, although hexameric nickel mercaptides are known (18). In the compound $(Me_2S)_2Pt_2Cl_2$, which has a sulfur-bridged structure, and a similar compound $(Me_2S)_2Pd_2Br_4$, which has a bromine-bridged structure and terminal Me_2S—Pd bonds, the bridged sulfur metal bond is stronger than the terminal bond, hence an i.r. band at 420 cm^{-1} is assigned as the Pt—S—Pt frequency (27), whereas in the compounds $PtHal_2(SMe_2)_2$ the Pt—S frequencies are assigned as $\nu_{symmetric}$ 345 cm^{-1} and $\nu_{asymmetric}$ 312 cm^{-1} (28). In various thiocyanate complexes, $M(SCN)_n^{x-}$, it is found that the M—S stretching frequency falls between the M—Cl and M—Br frequencies, and the tentatively assigned frequencies are Pd—S, 289 m; Pt—S, 280 m; Au—S, 301 m; and Hg—S, 210 w cm^{-1} (29). Comparison of the spectra of the pentafluoro-phenylthio compounds with that of bis(pentafluorophenyl) disulfide in the region 500–250 cm^{-1} reveals that the bands which may be associated with the M—S modes, but cannot be ascribed with any degree of certainty due to the differing literature values, are: Tl, 270 w; Pb, 361 w, 285 sh, 259 s; Zn, 396 m, 370 vw, 327 m, 305 w, 284 s; Cd, 286 s; Hg, 346 s; Cu, 368 w, 326 m, 282 w; Au, 331 s, 285 m; Pt, 331 s, 270 w; Bi, 300 m, 269 s; Ph_3Pb, 282 w cm^{-1}.

The proton magnetic resonance (p.m.r.) of the (pentafluoro-phenylthio)triphenyl lead in acetone solution is a multiplet, the envelope of which occurs from −7.87 to −7.38 p.p.m. relative to tetramethylsilane as an internal standard. Details of the ^{19}F chemical shifts and some coupling constants are shown in Table II. The chemical shifts are of the same magnitude as those reported previously for the C_6F_5S— group (17, 21). The resonances of the ortho and meta fluorine are complex multiplets of doublets and triplets respectively. The para fluorine appears as a triplet, each of which is split into a triplet.

Experimental

All reagents were available commercially. Microanalyses were performed by Mikroanalytisches Laboratorium Beller, Göttingen, Western Germany. Infrared spectra were recorded in the 4000–700 cm^{-1} region on a Perkin Elmer 21 with rocksalt optics, as mulls with Nujol or Fluorolube and in the 800–250 cm^{-1} range on a grating Perkin Elmer 221 as potassium bromide discs. Nuclear magnetic resonance spectra were recorded on a Varian A 60.

The new compounds prepared are shown in Table III together with some physical properties and analyses.

Method A

A slight excess, maximum 5%, of pentafluorothiophenol was added to approximately 3 mmoles of metal

TABLE II

^{19}F chemical shifts in acetone solution relative to $CFCl_3$ as internal standard (p.p.m.) and coupling constants (c.p.s.)

Compound	δ(ortho)	δ(para)	δ(meta)	$J_{para-meta}$	$J_{para-ortho}$
$Zn(SC_6F_5)_2$	133.5	164.1	166.4	20.3	2.8
$Cd(SC_6F_5)_2$	133.0	161.4	164.5	19.8	4.0
$Hg(SC_6F_5)_2$	132.9	160.8	165.3	20.0	1.2
$Pb(SC_6F_5)_2$	133.3	163.0	165.4	21.3	—
$Ph_3Pb(SC_6F_5)$	132.3	162.3	166.1	20.3	—
$Bi(SC_6F_5)_3$	130.3	158.2	165.2	20.0	—
$(C_6F_5S)_2$	134.1	151.3	162.9	19.8	4.0

ion in 25 ml water or dilute acid. The mixture was stirred magnetically until a solid formed and no more pentafluorothiophenol appeared to be present. The product was filtered off, washed, and dried. Any bis(pentafluorophenyl) disulfide formed was removed by washing with methanol or ether and isolated after removal of the solvent; its identity was confirmed by its m.p., lit. 51° (4). For the copper, gold, and platinum reactions the starting materials were $CuSO_4.5H_2O$, $HAuCl_4.3H_2O$, and $H_2PtCl_6.6H_2O$ respectively; otherwise simple salts with the metal ion in the same oxidation state as the product were employed.

No visible reaction was observed with cobaltous chloride, chromic chloride, stannous chloride, aluminium chloride, ferrous chloride, manganous nitrate, vanadous sulfate, or uranyl nitrate. Using mercurous nitrate, mercury and bis(pentafluoro-phenylthio) mercury were formed which were separated by dissolving the bis(pentafluoro-phenylthio) mercury in methanol from which it could be obtained on removal of the solvent. When 1 mole of pentafluorothiophenol and 1 mole of mercuric chloride or nitrate were allowed to react, a 96% yield of $Hg(SC_6F_5)_2$ was obtained; the identity of $Hg(SC_6F_5)_2$ was checked by its melting point.

An acidic solution of potassium tellurate (0.97 mmoles) was reduced to black metallic Te (0.86 matoms), and the pentafluorothiophenol oxidized to bis(pentafluoro-phenyl) disulfide (1.52 mmoles, m.p. 50°, lit. 51° (4)); a transient yellow compound was formed initially.

Using antimony trichloride, an impure antimony compound, shown to contain the C_6F_5S— group from its i.r. spectrum, was obtained. This compound decomposed to $C_6F_5SSC_6F_5$, m.p. 50°, on vacuum sublimation at 250° leaving a grey residue, m.p. > 350°.

With stannic chloride dissolved in dilute HCl an impure tetra(pentafluoro-phenylthio) tin was obtained which was purified by vacuum sublimation. If 4.25 mmoles of stannic chloride were dissolved in concentrated HCl, diluted, and treated with 17.0 mmoles of pentafluoro-thiophenol, a non-crystalline yellow precipitate formed from which 0.83 mmoles of $C_6F_5SSC_6F_5$, m.p. 50°, could be extracted with ether, leaving 2.32 mmoles of stannic sulfide.

Anal. Calcd. for SnS_2: Sn, 64.9. Found: Sn, 65.3.

When pentafluorothiophenol was treated with tetra-*n*-butyl ammonium bromide a perfluoropoly(phenylene sulfide) precipitated from the solution, see Table IV.

Pentafluorothiophenol (7.86 mmoles) was added to 165 ml of a saturated aqueous solution of calcium oxide (3.54 mmoles). The product isolated after removal of the water was a basic pentafluoro-phenylthio derivative of calcium of nonstoichiometric composition.

Pentafluorothiophenol (2.36 mmoles) was added to 25 ml of an aqueous solution of cesium carbonate (1.18 mmoles) and dissolved slowly; evaporation of the water yielded pentafluoro-phenylthio cesium, see Table III.

Method B

Nickel chloride (3.68 mmoles) was dissolved in 20 ml water, and 20 ml concentrated ammonia and pentafluorothiophenol (7.86 mmoles) were added. A slight white precipitate formed, but the solution was immediately refluxed; the white precipitate dissolved and a black precipitate formed, which was filtered off, washed, and dried.

Impure Zn $(SC_6F_5)_2$ could be prepared similarly from zinc sulfate. The product probably contained some basic zinc compound: the i.r. spectrum showed little polymeric material to be present.

Similar treatment of 2.10 mmoles of manganous chloride resulted in the formation of 175.7 mg of a brown product (2.23 mmoles of manganic oxide).

Using a method somewhat similar to that of Bradley and March (16), ammonia was added to a solution of approximately 2.0 mmoles of nickel chloride in 20 ml water until the ammine formed, then 4.7 mmoles of pentafluorothiophenol and 100 ml ethanol were added. The ethanol was slowly fractionated off leaving a dark-red precipitate and a green solution. The solid was filtered off, washed, and dried, giving 1.27 mmoles of impure $Ni(SC_6F_5)_2$ (65% yield). The i.r. spectrum showed the presence of polymeric $(C_6F_4S)_n$ groups.

When 1.92 mmoles of cobaltous chloride were similarly treated, two products, a white perfluoropoly(phenylene sulfide), of approximate formula $C_{24}F_{17}S_4H$, containing four C_6F_5 nuclei (397 mg), see Table IV, and 597 mg of a dark-green impure pentafluoro-phenylthio cobalt, m.p. > 350°, were obtained.

Method C

Approximately 4 mmoles of zinc oxide were stirred magnetically with a methanol solution of a slight stoichiometric excess of pentafluoro-thiophenol until the oxide had dissolved. The methanol–water was fractionated off, and the product washed and dried.

The reaction of 1.17 mmoles of plumbic oxide and 4.73 mmoles of pentafluorothiophenol resulted in the formation of yellow bis(pentafluoro-phenylthio) lead (1.05 mmoles) and 0.45 mmoles of bis(pentafluoro-phenyl) disulfide, which were isolated and separated after removal of the methanol by fractionation.

Can. J. Chem. Downloaded from www.nrcresearchpress.com by 210.87.254.105 on 09/05/12
For personal use only.

Can. J. Chem. Downloaded from www.nrcresearchpress.com by 210.87.254.105 on 09/05/12
For personal use only.

TABLE III

Products and analyses

Product	Color	Melting point (°C)	Method	Found (%)				Calculated (%)				Solubility*	Yield (%)
				C	H	F	S	C	H	F	S		
$Tl(SC_6F_5)$	Pale yellow	300 (decomp.)	A	18.1	0	23.7	8.4	17.9	0	23.6	8.0	2	65
$Pb(SC_6F_5)_2$	Yellow	256	A	23.7	0	31.7	10.8	23.8	0	31.4	10.6	1,2	53
$Sn(SC_6F_5)_4$	Yellow	144	A	31.8	0	43.2	14.7	31.5	0	41.5	14.0	1,2	5
$Zn(SC_6F_5)_2$	White	>350	C	30.9	0	40.8	13.9	31.1	0	41.0	13.8	1,2	95
$Cd(SC_6F_5)_2$	White	>350	A	27.8	0	37.3	11.8	28.2	0	37.2	12.6	1,2	56
$Hg(SC_6F_5)_2$	White	188	A	23.9	0	31.9	10.9	24.1	0	31.7	10.7	1,2,3,5	83
$Cs(SC_6F_5)$	White	>350	A	21.7	0	—	10.1	21.7	0	—	9.7	1,2	85
$Cu(SC_6F_5)$	Yellow	280 (decomp.)	A	27.5	0	37.2	11.6	27.4	0	36.2	12.2	Nil	86
$Au(SC_6F_5)$	Gold	246	A	18.1	0	24.1	7.8	18.2	0	24.0	8.1	Nil	95
$Ni(SC_6F_5)_2$	Deep red	340 (decomp.)	B	32.4	0	42.9	14.7	31.5	0	41.6	14.1	Nil	99
$Pt(SC_6F_5)_2$	Yellow	>350	A	25.8	0	31.7	11.0	24.3	0	32.0	10.8	Nil	42
$As(SC_6F_5)_3$	White	77	A	31.6	0	42.1	14.4	32.1	0	42.4	14.3	1,2,3,4,5	47
$Bi(SC_6F_5)_3$	Yellow	290 (decomp.)	A	26.4	0	35.1	11.8	26.8	0	35.3	11.9	1,2,3,4,5	93
$Ph_3Pb(SC_6F_5)$	Yellow	93	D	44.5	2.02	15.2	5.3	45.2	2.38	14.9	5.0	1,2,3,4,5	93

*Solubilities: 1 = methanol, 2 = acetone, 3 = ethyl ether, 4 = chloroform, 5 = benzene.

TABLE IV

Analysis of perfluoropoly(phenylene sulfide) and related compounds

Origin	Melting point (°C)	Analysis			
		C	H	N	Molecular weight*
$NH_4OH + C_6F_5SH$	182	39.0	0.0	0.0	—
n-$Bu_4NBr + C_6F_5SH$	335 (decomp.)	39.7	0.6	0.2	—
$Co^{2+} + C_6F_5SH$	147	38.4	0.0	—	749
$MnO_2 + C_6F_5SH$	147	38.6	0.2	—	747
$(C_6F_5S)_2$	51 (4)	36.2	0.0	0.0	398
$(C_6F_5S)_3C_6F_2SH$	—	38.9	0.0	0.0	741
$(C_6F_5SC_6F_4S)_2$	—	38.0	0.0	0.0	759
$(C_6F_4S)_n$	—	40.0	0.0	0.0	199n

*Determined by Rast's method in camphor.

No reaction was observed between germanic, titanic, stannic, or stannous oxides and pentafluorothiophenol, or between chromic oxide and thiophenol.

Method D

Triphenyllead chloride (1.8 mmoles) in 30 ml ethanol was treated with 5.5 mmoles of pentafluorothiophenol and sufficient 0.1 *N* aqueous caustic soda added to neutralize the hydrogen chloride formed; a white precipitate which formed immediately was filtered off after stirring magnetically for 16 h. (Pentafluoro-phenylthio)-triphenyl tin has been prepared similarly (21).

The reaction of diphenyllead dichloride (1.86 mmoles) and 3.93 mmoles of pentafluorothiophenol was studied similarly; a pale-yellow suspension and a bright-yellow solid melting near room temperature formed. The pale-yellow suspension was impure $Ph_3Pb(SC_6F_5)$, m.p. 83°, 1.39 mmoles; the yellow material was separated by vacuum sublimation yielding 0.33 mmoles of $C_6F_5SSC_6F_5$, m.p. 47°, as the sublimate and 0.69 mmoles of $Pb(SC_6F_5)_2$, m.p. 252°, as yellow residue.

Method E

When the products may be easily oxidized, approximately 2 mmoles of oxidant, the requisite amount of pentafluorothiophenol in 25 ml water or dilute acid, were sealed in a flask under vacuum. The flask was shaken mechanically for about a week and opened in a nitrogen atmosphere glove box; any unreacted pentafluorothiophenol was removed using a separating funnel and any solid by filtration, and the solution allowed to drip into an excess of ferric ammonium sulfate. The amount of ferric ion reduced was estimated volumetrically using potassium permanganate. A blank using pentafluorothiophenol alone showed that it formed an approximately 0.1 *M* solution in water; the subsequent results had to be corrected by this factor. No reduction or mercaptide formation was observed with ferrous sulfate, uranyl nitrate, or chromic chloride. Ferric chloride (1.87 mmoles) was reduced quantitatively to the ferrous state. Experiments with arsenic(V) were tricky due to the formation of somewhat soluble $As(SC_6F_5)_3$, which is very difficult to separate from $C_6F_5SSC_6F_5$; the experiments showed that As(V) was reduced to As(III), but it is impossible to say whether the reduction was quantitative.

Ammonium vanadate (1.06 mmoles) and 5.34 mmoles of pentafluorothio-phenol reacted to form a brown precipitate of vanadium trisulfide (0.29 mmoles) and bis(pentafluoro-phenyl) sulfide (0.43 mmoles), m.p. 80°, lit. 84–85° (5), which could be isolated by washing the precipitate with ethanol, equivalent to the decomposition

$$2V(SC_6F_5)_3 \rightarrow V_2S_3 + 2(C_6F_5)_2S$$

Experiments with ammonium molybdate and sodium tungstate showed that reduction, as observed by the color changes green-blue (Mo) and blue (W in acidic solution), occurred with pentafluorothiophenol, although meaningful interpretation of the results was not possible.

The reaction of manganese dioxide and pentafluorothiophenol in ethanol was studied in a flask sealed under vacuum. When the ratio MnO_2:C_6F_5SH was 1:4 a slow reaction occurred resulting in the formation of perfluoropoly(phenylene sulfide), see Table IV, and a brown solid, m.p. >350°, presumably manganic oxide formed from oxidation of manganous oxide. When the ratio MnO_2:C_6F_5SH was 1:2 all the manganese dioxide did not dissolve in 2 weeks. No reaction was observed with manganese dioxide and thiophenol.

Reactions with Iodine

The procedure for the reaction of pentafluoro-phenylthio derivatives with iodine in carbon tetrachloride was similar to that described for the fracture of Sn—S bonds, except that the insoluble pentafluorophenylthio derivatives were stirred magnetically during the course of the slow titration (21). The results are shown in Table I.

Infrared Data

The infrared absorption peaks in the region 4000 to 250 cm^{-1} are as follows; * indicates peaks recorded only in the 4000–700 cm^{-1} region:

$Tl(SC_6F_5)$: 1609 m, 1506 vs, 1472 vs, 1125 m, 1078 s, 992 m, 967 vs, 856 vs, 718 m, 712 m, 620 m, 582 m, 510 m, 444 m, 392 m, 312 w, 270 w, 254 w, 250 w.

$Pb(SC_6F_5)_2$: 1634 w, 1628 w, 1513 s, 1483 sh, 1477 vs, 1340 m, 1130 w, 1086 m, 1077 m, 1010 m, 973 s, 963 vs, 865 s, 858 s, 718 m, 714 m, 628 s, 623 s, 586 w, 513 w, 489 w, 445 w, 394 w, 361 w, 319 sh, 311 m, 285 m, 269 sh, 259 s.

$Sn(SC_6F_5)_4$*: 1626 m, 1523 sh, 1508 vs, 1480 vs, 1400 w, 1346 w, 1293 w, 1286 vw, 1144 w, 1088 vs, 1016 m, 974 vs, 859 vs, 718 w.

Can. J. Chem. Downloaded from www.nrcresearchpress.com by 210.87.254.105 on 09/05/12
For personal use only.

$Zn(SC_6F_5)_2$: 1634 m, 1626 m, 1538 m, 1508 s, 1490 sh, 1478 vs, 1344 m, 1293 m, 1285 m, 1145 m, 1094 s, 1080 vs, 1014 s, 970 vs, 855 vs, 721 m, 712 sh, 629 m, 513 w, 445 w, 399 sh, 396 w, 327 w, 305 m, 284 w, 270 w, 262 w.

$Cd(SC_6F_5)_2$: 1632 m, 1621 m, 1508 vs, 1480 vs, 1340 m, 1305 w, 1290 w, 1134 m, 1090 s, 1084 s, 1020 m, 976 vs, 859 vs, 719 m, 711 vw, 693 vw, 631 s, 512 m, 496 vw, 489 vw, 393 m, 320 m, 286 m, 258 m.

$Hg(SC_6F_5)_2$: 1634 m, 1626 m, 1539 sh, 1510 vs, 1480 vs, 1400 m, 1354 m, 1338 m, 1293 w, 1284 w, 1140 m, 1104 sh, 1091 s, 1031 m, 1019 m, 974 vs, 860 vs, 722 m, 720 sh, 712 w, 636 m, 591 w, 442 w, 403 w, 395 w, 386 m, 346 m, 312 m, 256 w, 250 w.

$Cs(SC_6F_5)$*: 1615 m, 1570 w, 1500 vs, 1473 vs, 1367 m, 1340 w, 1322 w, 1263 w, 1236 w, 1113 w, 1068 s, 1007 m, 976 sh, 955 vs, 863 vs, 825 w, 719 w, 705 vw.

$Cu(SC_6F_5)$: 1630 m, 1623 m, 1526 sh, 1514 s, 1490 vs, 1482 s, 1475 s, 1445 sh, 1341 m, 1143 m, 1097 s, 1088 s, 1010 m, 977 vs, 972 vs, 860 sh, 855 vs, 718 m, 713 sh, 627 s, 511 w, 442 w, 368 w, 326 w, 310 m, 282 w, 258 w.

$Au(SC_6F_5)$: 1623 m, 1506 vs, 1478 vs, 1395 w, 1336 w, 1288 w, 1143 m, 1084 s, 978 vs, 845 vs, 718 m, 634 m, 405 w, 381 w, 358 w, 331 m, 312 m, 285 vw, 265 m.

$Ni(SC_6F_5)_2$*: 1625 m, 1511 s, 1482 vs, 1390 w, 1292 w, 1143 m, 1087 s, 979 s, 852 s, 718 m.

$Pt(SC_6F_5)_2$: 1632 w, 1626 w, 1511 vs, 1484 vs, 1340 m, 1293 w, 1145 w, 1087 s, 981 s, 849 s, 722 m, 650 w, 632 m, 512 w, 491 w, 401 w, 331 m, 312 w, 270 w, 265 w.

$As(SC_6F_5)_3$*: 1632 m, 1625 sh, 1539 m, 1522 sh, 1507 vs, 1485 vs, 1399 m, 1353 m, 1290 m, 1286 m, 1142 m, 1088 s, 1017 m, 975 vs, 856 vs, 720 m.

$Bi(SC_6F_5)_3$: 1622 m, 1505 vs, 1472 vs, 1379 m, 1339 m, 1285 w, 1140 m, 1130 w, 1096 sh, 1079 s, 1025 sh, 1010 m, 968 vs, 855 vs, 720 sh, 718 m, 627 m, 587 w, 513 w, 442 w, 395 w, 385 w, 378 m, 311 s, 300 sh, 269 w.

$Ph_3Pb(SC_6F_5)$: 3026 m, 1630 w, 1619 w, 1561 m, 1505 s, 1485 sh, 1478 s, 1474 s, 1426 s, 1395 m, 1326 m, 1079 s, 1055 m, 1026 w, 1013 m, 993 s, 972 vs, 857 s, 734 vs, 730 vs, 722 s, 715 sh, 695 s, 449 m, 441 m, 282 w, 256 w.

$C_6F_5SSC_6F_5$: 1633 m, 1511 vs, 1489 vs, 1398 m, 1283 m, 1271 w, 1250 w, 1146 w, 1100 sh, 1089 vs, 1022 m, 973 vs, 856 vs, 724 m, 728 m, 639 m, 588 w, 488 w, 443 w, 418 w, 398 m, 380 m, 319 s, 311 s, 256 w, 249 w.

Perfluoropoly(phenylene sulfide)*, from $Bu_4NBr + C_6F_5SH$: 1635 w, 1618 w, 1510 s, 1490 sh, 1474 s, 1253 m, 1245 m, 1092 s, 975 s, 955 vs, 859 m, 808 s, 718 m.

Acknowledgment

This work was supported by a grant from the National Research Council of Canada.

1. P. Claeson. J. Prakt. Chem. **15**, 193 (1877).
2. E. E. Reid. Organic chemistry of bivalent sulfur. Vol. I. The Chemical Pub. Co., Inc., New York. 1958. pp. 107–169.
3. W. Beck, K. H. Stetter, S. Trados, and K. E. Schwarzhans. Chem. Ber. **100**, 3944 (1967).
4. P. Robson, M. Stacey, R. Stephens, and J. C. Tatlow. J. Chem. Soc. 4754 (1960).
5. L. J. Belf, M. W. Buxton, and G. Fuller. J. Chem. Soc. 3372 (1965).
6. R. S. Nyholm, J. F. Skinner, and M. H. B. Stiddard. J. Chem. Soc. A, 38 (1968).
7. H. J. Emeléus and H. Pugh. J. Chem. Soc. 1108 (1960).
8. H. J. Backer and J. Kramer. Rec. Trav. Chim. **52**, 916 (1933).
9. H. J. Backer and J. Kramer. Rec. Trav. Chim. **53**, 1101 (1934).
10. H. Wuyts and A. Vangindertalen. Bull. Soc. Chim. Belges, **30**, 323 (1921).
11. R. C. Mehrota, V. D. Gupta, and D. Sukhani. J. Inorg. Nucl. Chem. **29**, 1577 (1967).
12. L. Markó and G. Bor. J. Organometal. Chem. Amsterdam, **3**, 162 (1965).
13. W. Manchot and H. Gall. Ber. **60**, 2175 (1927).
14. W. Manchot and F. Kaess. Ber. **60**, 2318 (1927).
15. K. A. Jensen. Z. Anorg. Allgem. Chem. **252**, 227 (1944).
16. D. C. Bradley and C. H. March. Chem. and Ind. London, 361 (1967).
17. J. Cooke, M. Green, and F. G. A. Stone. J. Chem. Soc. A, 110 (1968).
18. E. W. Abel and B. C. Crosse. J. Chem. Soc. A, 1377 (1966).
19. H. Dunken and O. Wallbraum. Z. Chem. **7**, 323 (1967).
20. T. Mukaiyana. Bull. Chem. Soc. Japan, **46**, 2388 (1967).
21. M. E. Peach. Can. J. Chem. **46**, 211 (1968).
22. W. E. Davidson, K. Hills, and M. C. Henry. J. Organometal. Chem. Amsterdam, **3**, 285 (1965).
23. E. W. Abel and D. A. Armitage. Advan. Organometal. Chem. **5**, 1 (1967).
24. A. Schönberg and M. Z. Barakat. J. Chem. Soc. 892 (1949); R. S. Davidson. J. Chem. Soc. C, 2131 (1967).
25. I. J. Hyam, E. R. Lippincott, and R. T. Bailey. Spectrochim. Acta, **22A**, 695 (1966).
26. H. Schumann. Z. Anorg. Allgem. Chem. **354**, 192 (1967).
27. P. L. Goggin, R. J. Goodfellow, D. L. Sales, J. Stokes, and P. Woodward. Chem. Commun. 31 (1968).
28. J. R. Adkins and P. J. Hendra. J. Chem. Soc. A, 1325 (1967).
29. D. Forster and D. M. L. Goodgame. Inorg. Chem. **4**, 715 (1965).

Can. J. Chem. Downloaded from www.nrcresearchpress.com by 210.87.254.105 on 09/05/12
For personal use only.

Phase equilibria in the system: silver tetrafluoroborate – 1-pentene[1]

H. W. QUINN AND R. L. VANGILDER
Exploratory Research Laboratory, Dow Chemical of Canada, Ltd., Sarnia, Ontario
Received February 19, 1968

A determination has been made of the phase diagram within the region 0.40 to 0.85 mole fraction of 1-pentene. Complexes with 1:2 and 1:3 stoichiometry melting congruently at 43.3 and −30.3 °C respectively have been observed. Evidence was also obtained for the existence of a 1:1 complex stable only in the solid state below about −10 °C.

Canadian Journal of Chemistry, **46**, 2707 (1968)

Can. J. Chem. Downloaded from www.nrcresearchpress.com by 210.87.254.105 on 09/05/12
For personal use only.

Introduction

Only limited phase equilibrium data have been reported for the interaction of unsaturated hydrocarbons with Ag(I). In studies of the solubility of silver perchlorate in benzene and in toluene, Hill (1, 2) noted the presence of the corresponding 1:1 complexes.

Our earlier investigations (3, 4) of the complexing of monoolefins with silver tetrafluoroborate have indicated that the most stable complex with many of these has a silver ion:olefin stoichiometry of 1:2. Some olefins form a much less stable 1:3 complex and ethylene alone also forms 1:1 and 2:3 complexes stable at ambient temperature.

The object of the present study was to establish with a greater degree of certainty the stoichiometry of the $AgBF_4$ complexes formed by a simple monoolefin. The choice of 1-pentene was based on its fairly high volatility, which facilitated transfer from one part of the apparatus to another, and on the prior knowledge[2] that it formed a complex with a moderately low melting point. The latter characteristic was desirable since elevated temperatures tend to produce some breakdown in the silver salt. The phase diagram has been developed by the conventional use of cooling curves and by differential scanning calorimetry. Some of the observed heat effects have been correlated with crystallographic phase changes indicated by the Debye–Scherrer patterns obtained over a range of temperature for certain compositions.

Experimental

Anhydrous silver tetrafluoroborate was prepared as previously described (5).

Phillips Research Grade 1-pentene of 99.99% purity was employed. Prior to use it was dried by passage in the vapor phase through phosphorus pentoxide and freeze-outgassed at liquid nitrogen temperature.

Determination of Cooling Curves

The complex was prepared in a closed system by contact of $AgBF_4$ with liquid olefin in a vacuum-jacketed freezing-point cell equipped with an axially mounted thermowell. Stirring was accomplished with an axially mounted metal spiral covered with Teflon fluorocarbon operated by a solenoid at about 90 oscillations per minute.

The composition of the system was changed by condensing a weighed quantity of olefin into the freezing-point cell immersed in a liquid nitrogen trap.

The temperature of the system was measured with a copper–constantan thermocouple previously calibrated to ±0.1 °C with a platinum resistance thermometer. The reference junction was kept at 0 °C in an ice bath.

A continuous plot of thermal electromotive force (e.m.f.) vs. time was made by a millivolt recorder (Philips PR2216A/21). Each cooling curve was recorded on the 1 mV range by applying an opposing e.m.f. of appropriate value from a Leeds and Northrup K-3 potentiometer.

For that portion of the cooling curve above 0 °C, a cooling rate of about 0.5 °C/min was used. However, for lower temperatures, the cooling rate was about 1.8 °C/min. All systems were cooled from +60 to −78 °C.

Differential Scanning Calorimetry

Using a Perkin–Elmer DSC-1 differential scanning calorimeter, an estimation was made of the heat effects in the system upon heating from −43 to +50 °C. Compositions in the range from 0.43 to 0.67 mole fraction of olefin were investigated. The differential scanning calorimeter was calibrated using the melting points of water and benzophenone (melting points determined with a platinum resistance thermometer) for the lower and upper temperature ranges respectively. Endotherm temperatures were designated by the intersection of the peak slope with the base line.

X-ray Diffraction

Debye–Scherrer powder patterns were obtained on several samples containing up to about 67 mole % olefin. The samples were loaded into a covered wedge holder or a capillary and exposed to X-irradiation while the diffracted radiation was recorded on photographic film in a Debye–Scherrer camera. The sample temperature, over the range 25 to −40 °C, was regulated by means of an MRC cryocollimator and the exposure time at each temperature was 3 h.

[1]Contribution No. 160.
[2]Determined in this laboratory.

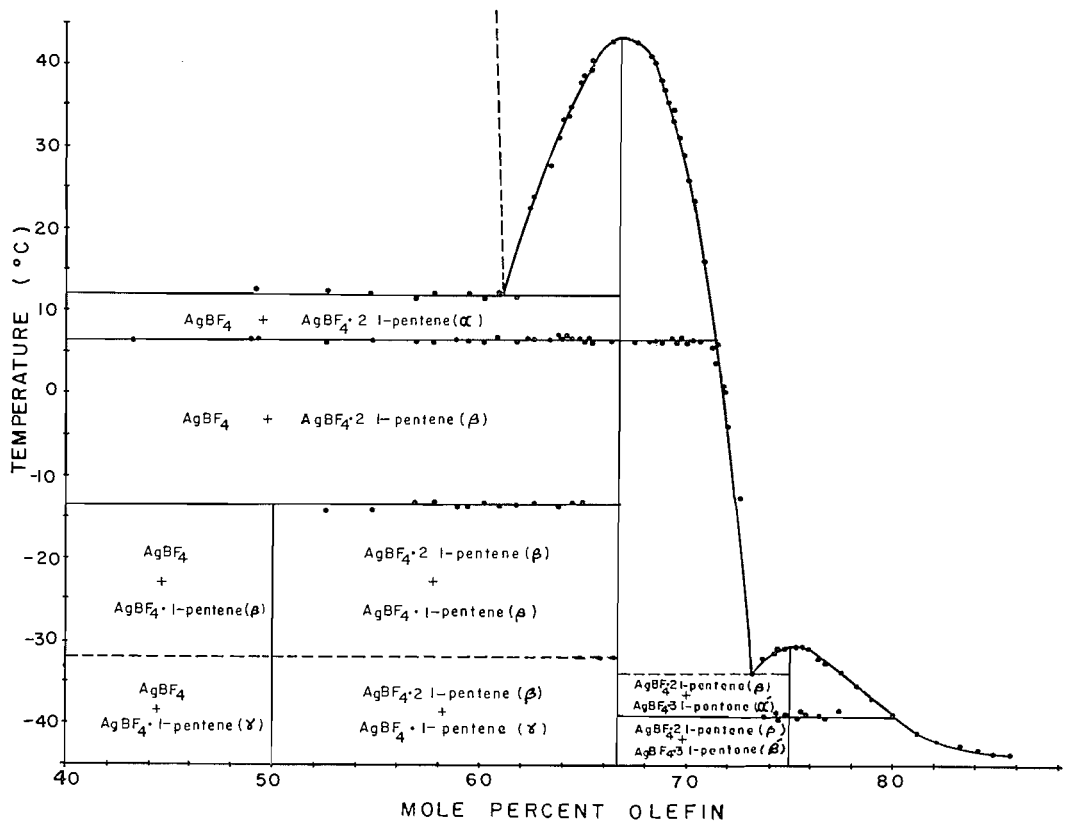

FIG. 1. Phase diagram for the system $AgBF_4$–1-pentene in the region 0.40 to 0.85 mole fraction of 1-pentene.

Results

Data from Cooling Curves

The phase diagram (Fig. 1) for $AgBF_4$–1-pentene shows the existence of compounds having congruent melting points of 43.3 and −30.3 °C at 0.67 and 0.75 mole fraction of olefin respectively.

Above 0.82 mole fraction of olefin a decrease in the depression of the freezing point was detected. In the same composition range two liquid phases were observed. Over the composition range 0.78 to 0.73 mole fraction of olefin the cooling curves showed an inflection point at about −39 °C.

All compositions below about 0.63 mole fraction of 1-pentene were found to freeze at about 12 °C. At these compositions an undissolved solid remained above 12 °C (persisting above 60 °C), the quantity of which increased with decreasing 1-pentene concentration. For the compositions in the range from less than 0.50 to greater than 0.67 mole fraction of olefin a plateau in the cooling curve was observed at 6.5 °C. Another break in the cooling curve was observed at about −13 °C for all compositions below 0.67 mole fraction of olefin.

Differential Scanning Calorimetry

Differential scanning calorimetry of systems with compositions below 0.67 mole fraction of olefin showed, upon heating, endotherms A, B, and C at +7, −8, and −32 °C respectively. The magnitude of endotherm A increased with increasing 1-pentene concentration to a value of about 150 cal/mole of olefin at about 0.67 mole fraction of olefin, while endotherm B increased with decreasing olefin concentration to a maximum value of similar magnitude at about 0.50 mole fraction of olefin. Although endotherm C was observed to be markedly smaller in magnitude than endotherm B, B and C demonstrated a similar dependence upon system composition since neither endotherm appeared at the 1:2 stoichiometry.

Since the thermal effects within the composi-

Can. J. Chem. Downloaded from www.nrcresearchpress.com by 210.87.254.105 on 09/05/12
For personal use only.

Can. J. Chem. Downloaded from www.nrcresearchpress.com by 210.87.254.105 on 09/05/12
For personal use only.

tion range from 0.43 to greater than 0.67 mole fraction of olefin have been assessed by two independent studies, the endotherms A and B are believed to correspond to the breaks in the cooling curves at 6.5 and −13 °C respectively. The temperature discrepancy between −8 and −13 °C can be rationalized by the endotherms having been obtained upon heating the system while the break in the cooling curve at −13 °C was observed with a rather rapid rate of cooling.

X-ray Diffraction

The Debye–Scherrer pattern for a sample of composition corresponding to the stoichiometric 1:2 complex showed one crystalline phase (α) at 25 and 10 °C with a second (β) appearing at 0 °C. No additional phases appeared upon cooling to −40 °C.

Upon cooling samples containing less than about 67 mole % olefin, phase α alone was observed at 25 (provided that the system had crystallized) and 10 °C; phase β also was observed at 0 °C. Although at −20 °C, still only α and β were present, at −40 °C, a new phase γ was observed. In some of these samples lines attributable to uncomplexed $AgBF_4$ also appeared.

Discussion

The evidence for a congruently melting compound at 0.67 mole fraction of 1-pentene confirms the existence of the 1:2 complex. It will be observed that the curvature of the liquidus curve is fairly sharp, indicating that the complex is not dissociated to a significant extent at its melting point (6).

There is a eutectic point at 12 °C and at 0.63 mole fraction of olefin. While it is obvious that one of the components of the eutectic composition is the 1:2 complex, it is only assumed that the other is $AgBF_4$. The presence of X-ray diffraction lines attributable to $AgBF_4$ in samples containing less than 0.63 mole fraction of olefin constitutes the basis for this assumption. The presence of undissolved solid even at 60 °C in systems containing only slightly less than 0.63 mole fraction of olefin suggests a very steep liquidus curve in this part of the $AgBF_4$ region.

The evidence for a congruently melting compound at 0.75 mole fraction of olefin establishes the existence of a 1:3 complex. The lower slope in the liquidus curve for the 1:3 than that for the 1:2 complex indicates greater dissociation of the former at its melting point. 1-Pentene behaves then quite analogously to propylene, 1-butene, and *cis*-2-butene in that it forms complexes of 1:2 and 1:3 Ag^+–olefin stoichiometry (3).

The flattening of the liquidus curve above 0.82 mole fraction of 1-pentene can be attributed to the separation of the liquid system into an olefin-rich and a complex-rich phase.

Although not observed experimentally, a eutectic point is believed to exist at about −34 °C and at approximately 0.73 mole fraction of olefin, considered to be a reasonable point of intersection of the liquidus curves for the 1:2 and 1:3 complexes. The thermal effect at −39 °C for compositions in the range from 0.73 to 0.78 mole fraction of olefin can perhaps be interpreted as a phase change in the solid 1:3 complex.

The fact that the thermal effect at 6.5 °C extends over the composition range from less than 0.50 to greater than 0.67 mole fraction of olefin suggests that it involves only the solid 1:2 complex. The observation from differential scanning calorimetry that the heat effect at +7 °C increases with increasing olefin concentration substantiates this suggestion. The conversion of phase α to phase β between 10 and 0 °C indicates that the thermal effect at 6.5 °C results from the crystallographic phase change. The fact that this thermal effect is observed for compositions below 0.50 mole fraction of olefin suggests that at 6.5 °C a 1:1 complex does not exist. This conclusion supports the earlier assumption that the undissolved solid at temperatures above the eutectic temperature is uncomplexed $AgBF_4$.

The observation that the thermal effect at −8 °C tends to a maximum at 0.50 mole fraction of 1-pentene and to approach a zero value at 0.67 mole fraction of olefin suggests the formation of a 1:1 complex at that temperature. If this is indeed the case it must result from the interaction of solid $AgBF_4 \cdot 2$ 1-pentene and uncomplexed solid $AgBF_4$. We have observed also that uncomplexed solid $AgBF_4$ added to the 1:2 complex results in the same heat effect at −8 °C.

This solid–solid reaction would be expected to be rather slow, perhaps diffusion-controlled, and would result in the rather broad endotherms observed. Since no crystallographic phase change is observed in this temperature region, it is possible that the β-lattice of the 1:2 complex is retained. The thermal effect may be attributable largely to the difference in the energy of the coordinate bond in the two complexes.

The endotherm C at −32 °C and the appearance of the new crystallographic phase γ may result from the rearrangement at lower temperature of the 1:2 β-lattice to produce the more stable 1:1 lattice.

Acknowledgments

The authors are indebted to D. R. Petersen and L. R. Ruhberg, Chemical Physics Research Laboratory, The Dow Chemical Company, Midland, Michigan, for determination of the Debye–Scherrer patterns.

1. A. E. Hill. J. Am. Chem. Soc. **44**, 1163 (1922).
2. A. E. Hill and F. W. Miller. J. Am. Chem. Soc. **47**, 2702 (1925).
3. H. W. Quinn and D. N. Glew. Can. J. Chem. **40**, 1103 (1962).
4. H. W. Quinn, J. S. McIntyre, and D. J. Peterson. Can. J. Chem. **43**, 2896 (1965).
5. H. W. Quinn. Can. J. Chem. **45**, 1329 (1967).
6. A. Findlay, A. N. Campbell, and N. O. Smith. The phase rule. 9th ed. Dover Publications, New York. 1951. p. 146.

Can. J. Chem. Downloaded from www.nrcresearchpress.com by 210.87.254.105 on 09/05/12
For personal use only.

Effect of counter-ion in the anionic polymerization of styrene in cyclohexane[1]

J. E. L. ROOVERS AND S. BYWATER
Applied Chemistry Division, National Research Council of Canada, Ottawa, Canada

Received March 21, 1968

The propagation reaction in the anionic polymerization of styrene has been studied in cyclohexane with the counter-ions: K, Rb, and Cs. Some association of the ion-pairs was found with K. Absolute propagation rate constants were determined in the three cases. Some experiments were carried out in benzene–cyclohexane mixtures to check that the results were consistent with those previously observed in benzene.

Canadian Journal of Chemistry, 46, 2711 (1968)

Can. J. Chem. Downloaded from www.nrcresearchpress.com by 210.87.254.40 on 09/05/12
For personal use only.

Introduction

The anionic polymerization of polystyryl alkali salts in benzene was found to involve ion-pairs which may be associated into inactive dimers (1). The absolute rate constants for the propagation reaction of polystyryl potassium, rubidium, and cesium in benzene were reported. The order of reactivity was found to decrease from potassium to cesium. Although benzene is not capable of the strong solvating effects known to occur with ethers in these systems, it is recognized to interact weakly with polar species. In order to assess the importance of such effects, the previously reported work has been repeated in cyclohexane, where they would be expected to be negligible.

Experimental

The purification and storage of monomers and solvents have been described previously (1, 2). Potassium was obtained from Fisher Scientific Co. and rubidium and cesium were prepared in situ by reacting the respective chlorides (Spex Industries Inc.) with calcium. All manipulations are carried out in sealed high vacuum systems utilizing fragile bulbs and break-seals for mixing reactants. Glassware was pretreated with butyl-lithium solutions and rinsed with solvent distilled from the solutions (1, 2).

Because sufficiently high concentrations of active centers (~~~~⊖ metal⊕) could not be obtained on reacting small amounts of either styrene or α-methylstyrene with a metal film in cyclohexane, polystyrene living polymers were prepared in benzene. Benzene was then replaced by cyclohexane. In order to do this, two extra side arms were attached to the apparatus described previously (1). One side arm was provided with a 100 ml flask, the other through a break-seal with an ampul of cyclohexane. The benzene solution of living polystyrene (Rb, Cs) or poly-α-methylstyrene (1) (K) was filtered and transferred to the 100 ml flask. The solution was frozen and freeze dried; benzene was condensed into the flask containing the metal film and sealed off. The resulting dry living polymer was then dissolved in cyclohexane. Gas chromatographic analysis showed that in this way less than 0.2% benzene was left in the polymerization medium.

Polystyryl- and poly-α-methylstyryl potassium are completely soluble in cyclohexane at 40 °C. However, the solubility of polystyryl rubidium and polystyryl cesium is limited to active center concentrations of about 7×10^{-4} and 1.5×10^{-4} mole/l respectively. The insoluble material, when "killed" is easily dissolved in cyclohexane. The polymer in cyclohexane at 40° is close to the solubility limit, especially for polymers of high molecular weight. Addition of polar groups must decrease the solubility further. Even when working below the above concentration limits, if the molecular weight became too high (repeated additions of monomer), sometimes at high conversions precipitation was visible and indicated by an apparent slowing of the rate.

In order to make measurements in benzene–cyclohexane mixtures (50/50 vol.), living polymers were prepared in the same way as above, with the 100 ml flask being replaced by a graduated flask. The benzene solution of living polymer was adjusted to the required volume by removing the excess benzene and adding cyclohexane. The exact composition of the solvent was determined gas chromatographically and it did not vary by more than 3% for the various experiments. Active center concentrations were determined by their ultraviolet (u.v.) absorption using either a Bausch and Lomb 505 or a Cary 14 recording spectrophotometer. The near u.v. spectra (λ_{max}: 330 ± 3 mμ) of the polystyryl salts in cyclohexane are noticeably narrower than in benzene. Especially in the case of polystyryl cesium, the shoulder at 370 mμ disappears in transferring the living polymer from benzene to cyclohexane.

The extinction coefficients were determined by measuring the decrease in optical density caused by the addition of a known amount of *t*-butanol, or by termination with an excess of the alcohol, followed by repeated extraction of the alkali-metal salts into water and subsequent analysis by X-ray fluorescence. Values found in cyclohexane were (M^{-1} cm^{-1}): 1.32×10^4 (K, 330 mμ), 1.25×10^4 (Cs, 334 mμ). In benzene, they were: 1.27×10^4 (Rb, 332 mμ), 1.16×10^4 (Cs, 334 mμ). The latter value is lower than that previously reported (1) and is the result of several determinations by both methods. The lower value can be correlated with the increased broadness of the absorption band in benzene.

The propagation reaction was measured by following

[1]Issued as NRCC No. 10139.

Can. J. Chem. Downloaded from www.nrcresearchpress.com by 210.87.254.40 on 09/05/12
For personal use only.

the decrease of absorption caused by styrene at 291.5 mμ. Rates were measured at 40° in cyclohexane and at 20° for benzene–cyclohexane mixtures.

Results

A. Cyclohexane

As was observed previously in benzene (1), the log–log plot of propagation rate for polystyryl potassium against total polystyryl potassium concentration exhibits some curvature, although this is appreciably less than in benzene at the lower temperature. The order in polystyryl potassium, which at low concentration (between 2 and 5×10^{-5} M) is virtually first order, decreases at higher concentrations because of the presence of both monomeric and dimeric (inactive) ion-pairs in equilibrium (1). Using $k_p = 30$ M^{-1} s^{-1} and a dissociation constant (K_D) for the dimer–monomer equilibrium of 3×10^{-3} M, a calculated curve is obtained which best fits the experimental results (Fig. 1).

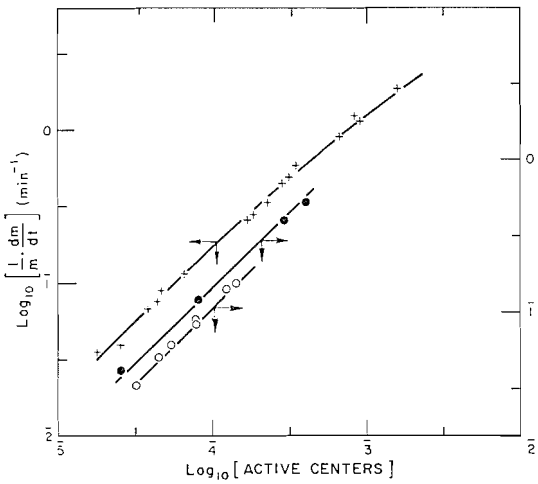

FIG. 1. Variation of propagation rate with concentration of active centers in cyclohexane at 40°. Experimental points are: (+) polystyryl potassium, (●) polystyryl rubidium, (○) polystyryl cesium. The line for potassium is that calculated for $K_D = 3 \times 10^{-3}$, $k_p = 30$.

The propagation rate of polystyryl rubidium and cesium can only be studied at quite low concentrations of active centers for reasons given above. Within the range studied, the rate appears to be directly proportional to the concentration. Presumably, as in benzene, aggregation is less important for these species. The absolute rate constants for the addition of styrene to the rubidium and cesium salts are 22.5 M^{-1} s^{-1} and 19 M^{-1} s^{-1} respectively.

B. Measurements in a Mixture of Benzene – Cyclohexane

Since the experimental difficulties are great in working in cyclohexane, it seemed advisable to check that the results were consistent with those obtained previously in benzene. For this purpose, a few reactions were carried out in 50/50 (vol.) benzene–cyclohexane at 20°. For potassium, the results again indicate a varying order with respect to the alkali-metal concentration, and a propagation constant for the ion-pair of 27 M^{-1} s^{-1}. K_D was within the limits of accuracy equal to that in benzene at the same temperature. Two experiments were carried out with both rubidium and cesium as counter-ion, from which k_p was evaluated to be 15 and 12 M^{-1} s^{-1} respectively. The experiments with rubidium were repeated in benzene at 20°, as the previously obtained rate constant depended on two points alone. The average of five points gave a rate constant of 22 M^{-1} s^{-1}, slightly higher than that obtained earlier.

Discussion

Only one previous report has been made of rate constants in cyclohexane. Dainton *et al.* (3) reported a first order rate constant of 7.7 M^{-1} s^{-1} for polystyryl potassium at 30°. Our results, over a wider range of concentrations, indicate that some association occurs in the concentration range they used ($2–7 \times 10^{-4}$ M), but that the apparent rate constant would only be about 35% too low. To obtain results consistent with the present work, a higher activation energy than is normally found in these systems would be required. There remains a possibility that at 30° the polystyryl potassium was not entirely in solution.

A comparison of the results in cyclohexane, benzene, and their mixtures is of interest in order to assess any specific effects of benzene. There appears to be little or no effect on the dimerization equilibrium for the potassium salt. The value of K_D at 40° extrapolated from previous data at 20° and 30° should be about 2×10^{-3} in benzene. This is close to the observed value in cyclohexane at 40° (3×10^{-3}). The difference is probably within the combined errors involved in the three determinations, and in any case is in the opposite direction to that expected from specific solvation of the ion-pair by benzene.

The rate constants for the propagation reaction show some changes between benzene and cyclohexane (Table I). The effect is smallest for cesium and largest for potassium. That the differences in

TABLE I

Rate constants (M^{-1} s^{-1}) for the propagation reaction of polystyryl K, Rb, Cs

	Counter-ion		
	K	Rb	Cs
Benzene 20°	38	22	13
50/50 (benzene/cyclohexane) 20°	27	15	12
Cyclohexane 40°	30	22.5	19
Benzene 40°*	83	48.5	29

*Extrapolated from results at lower temperature using observed activation energies.

rate are real is confirmed by the figures for the benzene–cyclohexane mixture. The faster rate in benzene may be, in part, due to the small difference in its dielectric constant (cyclohexane 2.01, benzene 2.27). This may well be the only effect for cesium, which shows only a small increase in rate between cyclohexane and tetrahydrofuran. For potassium, however, the difference in rate is rather large and the possibility of some stabilizing interaction with benzene in the transition state cannot be excluded.

Despite the progressive difference in rates between the two solvents, the overall order in reactivity is still K > Rb > Cs both in benzene and cyclohexane. This is opposite to the order observed by Szwarc *et al.* (4) in dioxane but more similar to that reported by Dainton *et al.* (3) in the same solvent (K ≈ Rb > Cs). In all cases the differences in rate for the three counter-ions are not large, perhaps as a result of larger opposing effects. There is no compelling reason to expect that the reactivity order will be the same in two solvents of roughly the same dielectric constant but of widely differing basicity. That the lithium ion-pairs are almost as extensively solvated by dioxane as by tetrahydrofuran has been shown by Alexander and Bywater (5). This specific solvation will decrease as the counter-ion becomes larger (6) and must influence the propagation rates in ethers. Other factors of importance in determining relative rates could be: (i) differing amounts of steric interference to the incoming monomer with different counter-ions, (ii) differing coulombic energies of charge separation (4), and (iii) different extents of polarization of the monomer molecule by the counter-ions.

It was not possible to measure an activation energy for any of the reactions because the air bath on the spectrophotometer cannot be used at temperatures much above 40°, and lower temperatures are excluded by solubility considerations. The values must be close to those obtained in benzene (7.2–7.4 kcal/mole) because reasonable agreement is obtained for estimated rate constants at 20° in cyclohexane using $E \approx 7.3$, or by linear extrapolation of the results in benzene and the 50/50 mixture.

1. J. E. L. Roovers and S. Bywater. Trans. Faraday Soc. **62**, 701 (1966).
2. D. J. Worsfold and S. Bywater. Can. J. Chem. **38**, 1891 (1960).
3. F. S. Dainton, G. C. East, G. A. Harpell, N. R. Hurworth, K. J. Ivin, R. T. LaFlair, R. H. Pallen, and K. M. Hui. Makromol. Chem. **89**, 257 (1965).
4. D. N. Bhattacharyya, C. L. Lee, J. Smid, and M. Szwarc. J. Phys. Chem. **69**, 624 (1965).
5. I. J. Alexander and S. Bywater. J. Polymer Sci. In press.
6. D. N. Bhattacharyya, C. L. Lee, J. Smid, and M. Szwarc. J. Phys. Chem. **69**, 612 (1965).

Can. J. Chem. Downloaded from www.nrcresearchpress.com by 210.87.254.40 on 09/05/12
For personal use only.

Can. J. Chem. Downloaded from www.nrcresearchpress.com by 210.87.254.6 on 09/05/12
For personal use only.

Solubility in the potassium stannate – potassium hydroxide – water system at 0 to 95.0 °C

P. ROSENBLUM[1]
M&T Products of Canada Limited, Hamilton, Ontario

Received February 21, 1968

Solubilities and phase relations have been determined in the $K_2Sn(OH)_6$–KOH–H_2O system between 0 and 95.0 °C. The isotherms consist of only one major solubility branch, that of $K_2Sn(OH)_6$, while the solubility branch of KOH is indistinguishable, since the isothermal invariant point is extremely close to the solubility of potassium hydroxide. Solid phases have been determined by Schreinemakers' method and checked with the polarizing microscope.

Canadian Journal of Chemistry, **46**, 2715 (1968)

Introduction

Information on the $K_2Sn(OH)_6$–KOH–K_2CO_3–H_2O system, and most of its ternary subsystems, except KOH–K_2CO_3–H_2O (1), is lacking in the literature. Lowenheim (2) has done some preliminary studies of the system, and solubility curves for the $K_2Sn(OH)_6$–KOH–H_2O system between 10 and 110 °C are given by Lowenheim (2), but no phase studies have been carried out.

This report is the first part of a study of the $K_2Sn(OH)_6$–KOH–K_2CO_3–H_2O quaternary system and presents data on the solubility relations in the $K_2Sn(OH)_6$–H_2O ternary system between 0 and 95.0 °C.

Experimental

The method consisted of charging stainless steel bottles with a solution of one of the solutes and an excess of the second solute and then rotating these in a thermostat at the required temperature for 24 h. The saturated solution was sampled with a special weight-pipette and the wet residue by a steel-gauze spoon, and then the samples were analyzed.

The thermostat used in these studies was a well-lagged stainless steel tank, the temperature being maintained to within 0.05 °C by means of a Sargent Thermonitor model S thermistor-type temperature regulator. The jacketted weight-pipettes were equipped with teflon or teflon-clad glass plugs, and the solution sample was drawn through a sintered-glass filter. Each concentration was done in duplicate. The potassium hydroxide used was "Baker Analyzed" reagent pellets, and the potassium stannate was used as obtained from the plant. The $K_2Sn(OH)_6$ batch used for this work analyzed as follows (dry weight basis): % Sn = 39.28 (i.e. 98.95% $K_2Sn(OH)_6$); % KOH = 1.23. Samples of the wet residue were examined with a polarizing microscope, and a drop of solution from each bottle was observed as crystallization took place under the microscope.

The Sn was determined by the standard iodate method and the KOH by titration with hydrochloric acid to the phenolphthalein end-point, after the prior precipitation of stannate and carbonate with barium chloride. Total alkali (KOH, K_2CO_3, and $K_2Sn(OH)_6$) in the solutions was found by titration with the same hydrochloric acid solution to the screened methyl-orange end-point, while the carbonate was calculated by difference. The free alkali in the wet solids was obtained by difference between the total alkali and the alkali equivalent of the Sn.

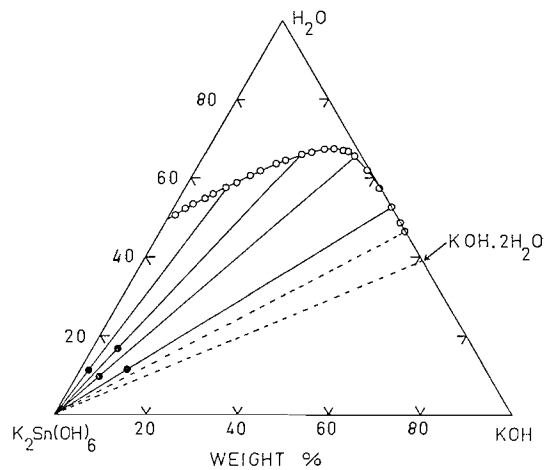

FIG. 1. The $K_2Sn(OH)_6$–KOH–H_2O system at 25.0 °C: ○, solution composition; ●, wet residue composition.

Throughout the investigation the wet residue from the solubility bottles was subjected to examination with a polarizing microscope. The solid phases present were identified by graphical plotting of tie-lines according to Schreinemakers' method and checked by microscopic examination. Since the isothermal invariant point is very close to the solubility of potassium hydroxide on the phase diagram (Fig. 1), it was not possible to use the intersection of tie-lines to locate the composition of the

[1]Present address: 86 Brighton Avenue, Downsview, Ontario.

TABLE I

The ternary system $K_2Sn(OH)_6$–KOH–H_2O at 0 °C

	Saturated solution			Wet residue		
Point	$K_2Sn(OH)_6$ (wt. %)	KOH (wt. %)	Density (g/ml)	$K_2Sn(OH)_6$ (wt. %)	KOH (wt. %)	Solid phase
1	47.67	0.43	1.582	87.93	0	$K_2Sn(OH)_6$
2	45.94	1.36	1.564	85.96	0.51	"
3	43.10	3.23	1.536	87.22	1.02	"
4	37.09	6.00	1.490	85.16	1.66	"
5	31.11	9.25	1.441	84.23	1.87	"
6	24.05	13.11	1.396	84.76	2.60	"
7	17.18	17.63	1.357	84.76	2.90	"
8	10.74	21.84	1.329	86.29	2.95	"
9	5.05	26.56	1.317	83.98	4.43	"
10	2.23	29.23	1.321	82.77	4.97	"
11	0.84	31.90	1.344	80.37	6.52	"
12	0.33	35.16	1.370	76.07	9.09	"
13	0.22	38.01	1.401	78.84	8.61	"
14	0.11	41.30	1.432	75.99	10.37	"
15	0.10	48.43	1.515	55.09	21.99	"
16	0.38	47.93	—	12.56	46.40	$K_2Sn(OH)_6$+KOH.$2H_2O$
17	0.24	47.98	—	2.52	52.05	$K_2Sn(OH)_6$+KOH.$2H_2O$
18	0	47.99	—	—	—	KOH.$2H_2O$

TABLE II

The ternary system $K_2Sn(OH)_6$–KOH–H_2O at 25.0 °C

	Saturated solution			Wet residue		
Point	$K_2Sn(OH)_6$ (wt. %)	KOH (wt. %)	Density (g/ml)	$K_2Sn(OH)_6$ (wt. %)	KOH (wt. %)	Solid phase
1	48.26	1.02	1.578	89.98	0.16	$K_2Sn(OH)_6$
2	45.14	2.49	1.551	88.72	0.38	"
3	42.93	3.56	1.532	88.11	0.69	"
4	39.40	5.78	1.503	86.95	1.18	"
5	37.10	6.86	1.485	87.98	1.42	"
6	33.44	8.86	1.455	87.17	1.59	"
7	30.72	10.34	1.439	85.13	2.24	"
8	26.66	12.54	1.412	84.88	2.59	"
9	23.86	14.19	1.394	85.69	2.45	"
10	19.52	16.54	1.371	74.43	5.76	"
11	16.95	18.25	1.357	76.62	5.14	"
12	12.80	20.99	1.339	77.68	5.41	"
13	10.16	22.96	1.329	78.79	6.02	"
14	6.91	25.57	1.320	70.18	8.82	"
15	4.96	27.61	1.319	74.21	7.79	"
16	3.20	29.65	1.322	82.84	5.04	"
17	2.25	31.06	1.328	79.04	6.54	"
18	1.30	33.04	1.340	84.71	4.67	"
19	0.40	37.49	1.374	75.64	9.20	"
20	0.10	42.22	1.424	79.14	8.43	"
21	0.03	47.37	1.483	78.46	9.88	"
22	0.03	51.26	1.530	68.79	15.97	"
23	0.05	53.50	1.558	0.29	57.18	KOH.$2H_2O$
24	0.02	53.53	1.558	0.47	56.00	"
25	0	53.36	1.557	—	—	"

Can. J. Chem. Downloaded from www.nrcresearchpress.com by 210.87.254.6 on 09/05/12
For personal use only.

TABLE III

The ternary system $K_2Sn(OH)_6$–KOH–H_2O at 40.0 °C

	Saturated solution			Wet residue		
Point	$K_2Sn(OH)_6$ (wt. %)	KOH (wt. %)	Density (g/ml)	$K_2Sn(OH)_6$ (wt. %)	KOH (wt. %)	Solid phase
1	51.46	0.28	1.608	95.16	0	$K_2Sn(OH)_6$
2	49.23	1.22	1.588	90.23	0.12	"
3	46.47	2.72	1.560	89.62	0.25	"
4	41.31	5.17	1.516	87.95	1.27	"
5	35.27	8.78	1.469	85.99	1.72	"
6	28.86	12.43	1.426	85.41	2.36	"
7	22.07	16.33	1.386	86.67	2.63	"
8	15.43	20.67	1.350	86.67	3.25	"
9	9.21	24.48	1.329	84.81	3.46	"
10	4.51	29.69	1.324	83.37	4.87	"
11	2.26	32.41	1.332	84.93	4.99	"
12	0.98	36.04	1.356	84.45	5.57	"
13	0.41	39.23	1.386	83.30	7.18	"
14	0.20	42.34	1.416	81.26	7.15	"
15	0.14	43.95	1.434	72.34	8.03	"
16	0.11	47.65	1.476	79.22	9.71	"
17	0.14	49.70	1.504	80.17	9.33	"
18	0.09	52.38	1.532	79.92	10.16	"
19	0.05	57.18	1.596	0.60	76.08	$KOH.H_2O$
20	0.04	57.46	1.595	0.34	71.52	"
21	0	57.67	1.595	—	—	"

TABLE IV

The ternary system $K_2Sn(OH)_6$–KOH–H_2O at 60.0 °C

	Saturated solution			Wet residue		
Point	$K_2Sn(OH)_6$ (wt. %)	KOH (wt. %)	Density (g/ml)	$K_2Sn(OH)_6$ (wt. %)	KOH (wt. %)	Solid phase
1	53.25	0.87	1.622	90.22	0.08	$K_2Sn(OH)_6$
2	52.12	1.13	1.605	91.08	0.00	"
3	49.86	2.45	1.584	90.19	0.92	"
4	44.86	5.11	1.544	88.05	1.24	"
5	37.38	9.01	1.481	88.46	1.41	"
6	34.60	10.21	1.461	87.58	3.22	"
7	29.24	12.76	1.425	87.07	2.40	"
8	23.18	16.38	1.386	85.08	2.74	"
9	17.97	19.72	1.367	87.58	2.68	"
10	12.62	23.49	1.343	90.14	2.39	"
11	8.57	26.84	1.331	86.39	3.80	"
12	5.07	30.60	1.330	83.50	5.71	"
13	2.50	34.15	1.343	81.58	6.14	"
14	1.73	36.13	1.353	83.82	5.87	"
15	0.73	39.66	1.381	83.90	6.44	"
16	0.35	42.96	1.421	64.71	15.76	"
17	0.18	45.58	1.447	81.94	8.31	"
18	0.14	48.80	1.479	81.43	8.89	"
19	0.14	49.81	1.494	84.28	9.02	"
20	0.12	52.95	1.530	81.68	9.91	"
21	0.15	58.14	1.604	1.17	71.96	$K_2Sn(OH)_6$+$KOH.H_2O$
22	0	59.09	1.606	—	—	$KOH.H_2O$

Can. J. Chem. Downloaded from www.nrcresearchpress.com by 210.87.254.6 on 09/05/12
For personal use only.

TABLE V

The ternary system $K_2Sn(OH)_6$–KOH–H_2O at 95.0 °C

	Saturated solution			Wet residue		
Point	$K_2Sn(OH)_6$ (wt. %)	KOH (wt. %)	Density (g/ml)	$K_2Sn(OH)_6$ (wt. %)	KOH (wt. %)	Solid phase
1	56.62	0.26	1.647	91.43	0.33	$K_2Sn(OH)_6$
2	54.92	1.03	1.631	89.97	0.20	"
3	52.19	2.52	1.605	90.60	2.30	"
4	47.54	4.91	1.561	87.85	1.16	"
5	42.14	8.18	1.518	89.79	1.53	"
6	36.64	11.31	1.478	90.01	1.22	"
7	30.13	14.67	1.430	84.63	3.66	"
8	22.89	19.31	1.397	84.03	4.32	"
9	17.58	22.71	1.367	86.67	4.69	"
10	12.07	26.81	1.345	86.14	4.39	"
11	7.88	31.21	1.335	88.16	4.05	"
12	4.19	36.48	1.343	86.85	4.67	"
13	2.36	38.40	1.363	83.87	7.47	"
14	1.34	41.40	1.381	83.55	7.17	"
15	0.87	44.29	1.402	84.91	6.32	"
16	0.69	45.33	1.415	83.77	6.97	"
17	0.37	48.54	1.458	90.32	6.77	"
18	0.33	51.76	1.489	82.26	9.68	"
19	0.46	61.94	—	7.15	73.55	$K_2Sn(OH)_6$+$KOH.H_2O$
20	0	63.11	—	—	—	$KOH.H_2O$

saturating solid when potassium hydroxide was in excess. No attempt was made to determine the composition of the solid, but the formula used was that given by Seidell (1) and by Cohen-Adad and Michaud (3), namely $KOH.2H_2O$ at 0 and 25.0 °C and $KOH.H_2O$ at 40.0 °C and above.

The crystals of potassium stannate found in the wet residue from the solubility bottles form mainly large granules of spherical shape at low and medium potassium hydroxide concentrations and are, therefore, not useful for the study of crystal form. At higher potassium hydroxide concentrations the stannate also appears as hexagonal platelets, the amount appearing as platelets increasing at the expense of the spheres as the potassium hydroxide concentration is increased. At very high potassium hydroxide concentrations, the wet residue is a mush consisting of platelets and only a few spheres.

Examination of stannate crystallizing from droplets on a microscope slide proved interesting and enabled a correlation of the various observations in the literature on the different crystal habits of $K_2Sn(OH)_6$.

Equilibration experiments were conducted at all the temperatures studied. A 24 h rotation period gave a solubility which was within 1% of the maximum value (obtained after 4 days at 0 °C, 3 days at 25 °C). This rotation period was used for all subsequent experiments, since it was considered to be sufficiently within the accuracy of the experimental measurements.

The major sources of error arose from non-equilibrium conditions with a 24 h rotation period (1% below maximum at 25.0 °C and 0.6% below maximum at 40.0 °C) and from the sampling procedure. In the latter case, crystallization around the sintered-glass filter or at the surface of the saturated solution in the solubility bottle could cause a decrease in solubility, this error tending to increase as the bath temperature was raised. Another source of error was the presence, at all times, of some carbonate in the solutions, but the amount of carbonate was never greater than 1%.

Results and Discussion

The results are given in Tables I to V. The phase diagram (Fig. 1) in which are plotted the data at 25.0 °C is typical for all other temperatures studied.

It can be seen from the data and from Fig. 1 that the solubility isotherm for the $K_2Sn(OH)_6$–KOH–H_2O system from 0 to 95.0 °C consists of only one saturation curve, that of $K_2Sn(OH)_6$, and in this respect is similar to the solubility isotherm for the analogous sodium system. The solubility branch for potassium hydroxide is one point and is virtually indistinguishable from the composition of the eutectic solution. The ternary system $K_2Sn(OH)_6$–KOH–H_2O, therefore, belongs to the simple eutectic type exhibited by such systems as NaCl–NaOH–H_2O (4), K_2SO_4–KOH–H_2O (5), and KBH_4–KOH–H_2O (6). The solubility of $K_2Sn(OH)_6$ decreases rapidly with an increase in the KOH concentration. This is similar to the behavior in the $Na_2Sn(OH)_6$–NaOH–H_2O system, but the latter decrease is less. The solubility of $K_2Sn(OH)_6$ shows the more common increase with temperature in contrast with the solubility of Na_2Sn-

Can. J. Chem. Downloaded from www.nrcresearchpress.com by 210.87.254.6 on 09/05/12
For personal use only.

$(OH)_6$ which decreases with an increase in temperature, except at high alkali concentrations.

For the most part, the Schreinemakers' lines intersect at the $K_2Sn(OH)_6$ vertex of the phase diagram and give a clear-cut indication of the compound in equilibrium with the saturated solution. These lines give no evidence for the existence of a compound analogous to the one reported by Urazov, Lipshits, and Lovchikov (7) as existing at 75.0 °C in the $Na_2Sn(OH)_6$–NaOH–H_2O system, namely $Na_3[Sn(OH)_6]H_2O$, or, more probably, $Na_2Sn(OH)_6.NaOH.H_2O$. There is also no evidence at 0 °C of the field of existence of any hydrated form of $K_2Sn(OH)_6$, although Zocher (8) was able to prepare both $K_2Sn(OH)_6.H_2O$ and $K_2Sn(OH)_6.2H_2O$ at low temperatures.

Droplets of the saturated solutions were examined under the polarizing microscope as crystallization took place. The $K_2Sn(OH)_6$, crystallizing from saturated solutions in which the KOH concentration was low, formed colorless, oblique, rhombic prisms with symmetrical extinction (9). These crystals belong to the trigonal class and have the axial ratio $a:c = 1:1.9588$ (10). As the KOH concentration increased, the acute lateral edges of the rhombohedra became truncated and loss of the two opposite corners (normal to the crystallographic c-axis) took place, i.e. the (0001) and (000$\bar{1}$) faces appeared. On still further increase in the KOH concentration, these faces became more pronounced, causing the crystals to grow lying on these faces, rather than on the rhomb faces. The crystals were then oriented with the c-axis, or optic axis, parallel to the axis of the microscope, and the uniaxial interference figure was readily observed. Birefringence was positive. As the KOH concentration increased still further, the (0001) and (000$\bar{1}$) faces grew very large, and six-sided basal pinacoid plates resulted. At extremely high KOH levels only these plates were present. The foregoing explains the varying observations in the literature on the crystal habit of potassium stannate (rhombohedron vs. platelet).

1. A. SEIDELL. Solubilities of inorganic and metal organic compounds. 3rd ed. Vol. I. D. Van Nostrand Co., Inc., New York. 1940.
2. F. A. LOWENHEIM (*Editor*). Modern electroplating. 2nd ed. John Wiley & Sons, Inc., New York. 1963. p. 350.
3. R. COHEN-ADAD and M. MICHAUD. Compt. Rend. **242**, 2569 (1956).
4. F. A. FREETH. Phil. Trans. Roy. Soc. London, Ser. A, **223**, 35 (1922).
5. V. B. TULINOVA, A. A. STATSENKO, and V. E. PLYUSHCHEV. Russ. J. Inorg. Chem. English Transl. **5**, 1224 (1960).
6. V. I. MIKHEEVA and M. S. SELIVOKHINA. Russ. J. Inorg. Chem. English Transl. **8**, 227 (1963).
7. G. G. URAZOV, B. M. LIPSHITS, and V. S. LOVCHIKOV. Russ. J. Inorg. Chem. English Transl. **4**, 1088 (1959).
8. H. ZOCHER. Z. Anorg. Allgem. Chem. **112**, 1 (1920).
9. J. W. MELLOR. A comprehensive treatise on inorganic and theoretical chemistry. Vol. VII. Longmans, Green and Co., Ltd., London. p. 415.
10. J. BELLUCCI and N. PARRAVANO. Z. Anorg. Allgem. Chem. **45**, 151 (1905).

Can. J. Chem. Downloaded from www.nrcresearchpress.com by 210.87.254.6 on 09/05/12
For personal use only.

Thermal decomposition of di-*tert*-butyl peroxide at high pressure

D. H. SHAW AND H. O. PRITCHARD
Centre for Research in Experimental Space Science, York University, Toronto, Ontario

Received February 26, 1968

The thermal decomposition of di-*tert*-butyl peroxide has been studied in the presence of carbon dioxide at total pressures from 0.05 to 15 atm and temperatures from 90–130 °C. The first-order rate constant for the decomposition is independent of total pressure in this range, with Arrhenius parameters $E = 37.8 \pm 0.3$ kcal/mole and $\log A\,(s^{-1}) = 15.8 \pm 0.2$. A reevaluation of previous data on this reaction leads us to recommend $E = 37.78 \pm 0.06$ kcal/mole and $\log A\,(s^{-1}) = 15.80 \pm 0.03$ over the temperature range 90–350 °C; extension of this range to higher temperatures using a shock tube would be worthwhile.

Canadian Journal of Chemistry, **46**, 2721 (1968)

Can. J. Chem. Downloaded from www.nrcresearchpress.com by 210.87.254.5 on 09/05/12
For personal use only.

It has been postulated by Birss (1) and by Bose and Hinshelwood (2) that in the thermal decomposition of di-*tert*-butyl peroxide (DTBP), a second channel exists between reactants and products which they called induced decomposition. The evidence upon which these arguments are based is in our view not very strong, and we believe that the postulate is unnecessary. It was found that the rate of decomposition at 160 °C increased with pressure between 50 and 600 mm. However, since the explosion limit of the peroxide decomposition is estimated (3) to be around 600 mm at 150 °C, the probable cause of the rise in rate with pressure becomes apparent. It was also found that added gases, namely SF_6, CF_4, CO_2, CCl_4, SiF_4, and N_2O caused an acceleration of the reaction, whereas acetone, *n*-hexane, and N_2 were without effect. It was recognized later by Archer and Hinshelwood (4) that in the case of CCl_4, the acceleration may have been partly a chemical effect involving chlorine atoms. More recently, Flowers, Batt, and Benson (5) showed that the peroxide decomposition was strongly catalyzed by HCl by a mechanism involving chlorine atoms, and further evidence for the existence of chlorine atoms in the peroxide/CCl_4 reaction is available (6). Also, Batt and Cruickshank (7) have shown that CH_3F is formed in the peroxide/SF_6 decomposition. We suggest that all these observed accelerations in the presence of CF_4, SiF_4, CO_2, and N_2O are due either to chemical reaction of some kind or to the presence of trace quantities of chlorinated impurities; it is reasonable to suppose that the N_2, acetone, and hexane used in the above experiments were free from chlorinated impurities. Our own experiments described below show that carefully purified CO_2 has no effect on the rate of peroxide decomposition up to a pressure of 15 atm, and we believe that the idea of induced decomposition should not be included in the current theoretical description of unimolecular reactions.

Materials and Experimental Technique

Commercial di-*tert*-butyl peroxide contains about 0.2% of minor impurities including 0.04% acetone (8); these were removed by preparative scale gas chromatography. Carbon dioxide was made from commercial dry-ice: the gas was condensed onto phosphorus pentoxide *in vacuo*, degassed, and then sublimed into a storage vessel; mass-spectrometer analysis failed to reveal any impurity.

Each experiment was carried out in a stainless steel pressure vessel equipped with a needle-valve; 10 cc and 75 cc vessels were used. Known amounts of peroxide and carbon dioxide (sufficient to give final pressures of 30–300 mm and 0–15 atm respectively) were condensed into the vessel from the vacuum system using liquid nitrogen, and the valve was then closed off. The reaction was started by placing the vessel in an oil bath held in the temperature range 90–130 °C and terminated after about 3% reaction by removing it and cooling in water. This temperature range was chosen for a number of reasons: (i) it is well removed from the explosion limit, and complications due to self-heating (3) will be absent; (ii) it takes 6 min for the temperature inside the pressure vessel to become equal to that outside, but since reaction times at these temperatures range from 3 days to 1 h, the correction is negligible; and (iii) side reactions, particularly the attack of methyl radicals on the peroxide, are unimportant at these temperatures (8–10). (One minor problem was the long-term stability of commercial thermostats: over a period of 3 days, several small excursions (±0.1 °C) in the bath temperature occurred; since the rate constant for this reaction varies by about 14% per °C, reactions were always carried out in pairs, with a pressurized and an unpressurized vessel strapped together in the bath.)

At small percentage conversions, the rate of formation of acetone can be used as a measure of the rate of decomposition of the peroxide (3, 11). Thus, since it was not in general possible to transfer the whole contents of the reaction vessel to the vapor phase chromatographic (v.p.c.) inlet, the reaction mixture was first trapped out

TABLE I

Summary of published work on the thermal decomposition of di-*tert*-butyl peroxide

Figure 1 label	Temperature range (°C)	Method*	Number of points	E (kcal/mole)	Log A (s^{-1})	Reference
a	140–160	S, P, N	7	40.88±0.53	17.43±0.80	12
b	130–170	S, P, U	5†	38.15±0.14	15.94±0.07	15
c	130–160	S, P, U	4†	37.68±0.15	15.71±0.08	3
d	115–170	S, A(M), T	33	33.07±0.59	13.16±0.31	16
e	125–175	S, A(M), K	32	35.04±1.60	14.04±0.83	17
f	130–155	S, A(M), U, K	30	38.54±0.74	16.30±0.39	9
g	101–145	S, A(M), U	14	39.30±0.44	16.63±0.24	11
h	90–130	S, A(Ac), U, C	56	37.83±0.32	15.82±0.18	This work
i	175–275	F, A(M), T	36	36.17±0.39	15.05±0.17	16
j	280–350	F, A(Pe), H	24	36.46±0.36	15.33±0.13	18
k	160–280	F, A(M), U, C	31	38.29±0.30	16.07±0.14	19
m	155	S, P, U	1†	—	—	20
$n - n'$	90–350	Excluding *m*	272	37.90±0.14	15.81±0.07	—
$n - n'$	90–350	Excluding *d*, *e*, *f*, *m*	177	37.78±0.06	15.80±0.03	—

*S, static system; F, flow system; P, k based on pressure rise; A, k based on chemical analysis; M, methyl radical balance at end of run; Ac, acetone formation at end of run; Pe, peroxide depletion, monitored continuously; U, undiluted; N, diluted with nitrogen; T, diluted with toluene; K, diluted with acetone or diethylketone; C, diluted with carbon dioxide; H, diluted with helium.
†These are composite points: the total number of determinations is not given.

in the vacuum system. The ethane and carbon dioxide were removed by carefully controlled distillation at −135 °C, after which the residue of acetone and peroxide was transferred to the v.p.c. inlet for analysis: the columns used were packed with 7% Apiezon L and 3% Carbowax 1500 on 80–100 mesh Chromosorb W. Calculation of the rate constant was based on the acetone/peroxide ratio in the final products, assuming first-order kinetics for the reaction

$$\text{DTBP} \rightarrow 2CH_3COCH_3 + 2CH_3;$$

apart from ethane ≫ methane > ethylene no other significant products were found, in agreement with earlier studies (3, 6, 8, 11).

Results and Discussion

The factor which limited the pressure range of these experiments was our ability to separate quantitatively a mixture containing about 10^{-6} mole of acetone in a large excess of CO_2; after careful calibrations, we found that 0.1 mole of CO_2 was about the upper limit using LeRoy stills. We found that within our experimental accuracy (±2% in the absence of CO_2, ±5% in the presence of 10–15 atm CO_2) there was no detectable difference in the rate constant between the pressurized and the unpressurized runs. Nor was there any detectable difference when the pressure vessel was packed with steel balls. In addition we constructed pyrex vessels the same shape as the steel ones, and either unpacked, or packed with glass beads, the decomposition rate was the same as in the steel vessels. Thus the homogeneity of the reaction (12, 13) seems to be amply confirmed.

A least-squares treatment of 56 experiments[1] carried out under all conditions gives an Arrhenius plot with $E = 37.82 \pm 0.32$ kcal/mole and $\log A\ (s^{-1}) = 15.82 \pm 0.18$, in the temperature range 90–130 °C. This reaction has been studied previously by a number of workers, both in static and in flow systems, and on the whole, the agreement is excellent, even though some rate constants have been based on the total pressure change, the CH_3 radical balance, the rate of formation of acetone, or the rate of depletion of peroxide. In all this earlier work, which is collected together in Fig. 1, the total pressure was in the range 5–500 mm. We have summarized the data in Table I and have, where possible, recalculated the least-squares lines[2]

[1]A list of these rate constants, together with all others used in Table I, can be obtained, free of charge, upon request from: The Depository of Unpublished Data, National Science Library, National Research Council of Canada, Ottawa, Canada.

[2]The normal least-squares treatment assumes that the temperature is precisely known and that all the uncertainty exists in the rate-constant measurement. In our work, the uncertainty in k due to small fluctuations in temperature is of a similar order of magnitude to the normal analytical uncertainties. We have consequently used the method of York (14) in reducing our own data. In fact, it makes little difference to the derived Arrhenius parameters, but we believe it is a logically superior procedure and one which should be adopted through the whole of kinetics in future. All the data in Table I have been recalculated in this way with (for want of a better criterion) the assumption that the errors in temperature and rate constant are ±0.1 °C and ±5% respectively. When data at higher temperatures become available, a careful reassessment of the likely errors in temperature for each determination should be made.

Can. J. Chem. Downloaded from www.nrcresearchpress.com by 210.87.254.5 on 09/05/12
For personal use only.

Can. J. Chem. Downloaded from www.nrcresearchpress.com by 210.87.254.5 on 09/05/12
For personal use only.

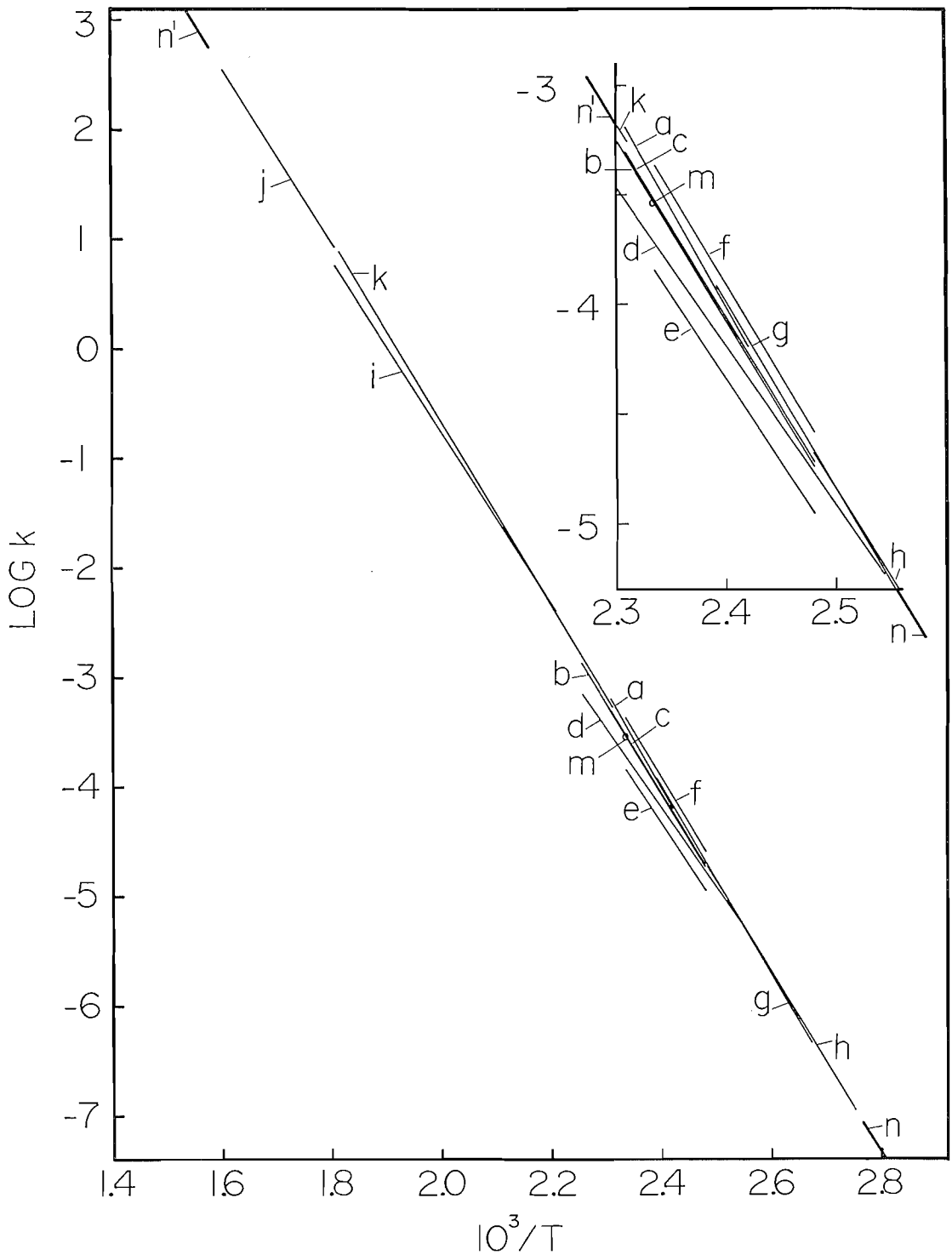

FIG. 1. Arrhenius plot of all published data on the thermal decomposition of di-*tert*-butyl peroxide. The labels on the individual determinations refer to entries in Table I. See inset for more details in the range 125–160 °C.

from the original data. There is a spread in activation energy from 33 to 41 kcal/mole among the individual determinations, but a least-squares treatment of all 272 points gives $E = 37.90 \pm 0.14$ kcal/mole and $\log A\ (s^{-1}) = 15.81 \pm 0.07$. It can be seen from Fig. 1 that with the exception of three sets of data (9, 16, 17) the remainder are remarkably confluent, and a least-squares treatment of the reduced set of 177 points gives $E = 37.78 \pm 0.06$ kcal/mole and $\log A\ (s^{-1}) = 15.80 \pm 0.03$; we recommend these as selected values for the Arrhenius parameters of this reaction in the temperature range 90–350 °C.

It would appear that (with the exception of the three cases noted) the variation in activation energy from investigation to investigation is due to small systematic errors occurring within each set of experiments, since taking all the data together, we get a remarkably good Arrhenius plot. There seems no longer any doubt (21) that the frequency factor of this reaction in its high pressure region is abnormally high. Furthermore, the Arrhenius plot appears to be linear over almost a factor of two in the temperature range (363–623 °K) and about nine orders of magnitude in k, although one cannot at this stage rule out the possibility that it is beginning to curve downwards at the highest temperatures. The linearity of Arrhenius plots is important theoretically, and this reaction seems to be a good test case, both because of its freedom from side reactions and because of its abnormal A-factor. There is little hope of extending the temperature range downward because the rate constant rapidly becomes too low, but there is scope for work at significantly higher temperatures in shock waves. However, there would be no point in undertaking such an experiment unless both the measurement of the temperature and the rate constant are of a very high precision.

1. F. W. Birss. Proc. Roy. Soc. London, Ser. A, **247**, 381 (1958).
2. A. N. Bose and C. N. Hinshelwood. Proc. Roy. Soc. London, Ser. A, **249**, 173 (1959).
3. L. Batt and S. W. Benson. J. Chem. Phys. **36**, 895 (1962); **38**, 3031 (1963).
4. G. Archer and C. N. Hinshelwood. Proc. Roy. Soc. London, Ser. A, **261**, 293 (1961).
5. M. C. Flowers, L. Batt, and S. W. Benson. J. Chem. Phys. **37**, 2662 (1962).
6. D. M. Tomkinson and H. O. Pritchard. J. Phys. Chem. **70**, 1579 (1966).
7. L. Batt and F. R. Cruickshank. J. Phys. Chem. **70**, 723 (1966).
8. D. H. Shaw and H. O. Pritchard. Can. J. Chem. **45**, 2749 (1967).
9. G. O. Pritchard, H. O. Pritchard, and A. F. Trotman-Dickenson. J. Chem. Soc. 1425 (1954). G. O. Pritchard. Ph.D. Thesis, Manchester University, Manchester, England. 1955.
10. E. R. Morris and J. C. J. Thynne. Trans. Faraday Soc. **63**, 2470 (1967).
11. A. R. Blake and K. O. Kutschke. Can. J. Chem. **37**, 1462 (1959).
12. J. H. Raley, F. F. Rust, and W. E. Vaughan. J. Am. Chem. Soc. **70**, 88 (1948).
13. M. Szwarc and J. S. Roberts. J. Chem. Phys. **18**, 561 (1950).
14. D. York. Can. J. Phys. **44**, 1079 (1966).
15. F. W. Birss, C. J. Danby, and C. N. Hinshelwood. Proc. Roy. Soc. London, Ser. A, **239**, 154 (1957).
16. J. Murawski, J. S. Roberts, and M. Szwarc. J. Chem. Phys. **19**, 698 (1951).
17. M. T. Jaquiss, J. S. Roberts, and M. Szwarc. J. Am. Chem. Soc. **74**, 6005 (1952).
18. F. P. Lossing and A. W. Tickner. J. Chem. Phys. **20**, 907 (1952).
19. M. F. R. Mulcahy and D. J. Williams. Australian J. Chem. **14**, 534 (1961).
20. A. H. Price and R. T. K. Baker. J. Chem. Educ. **42**, 614 (1965).
21. P. Molyneux. Tetrahedron, **22**, 2929 (1966).

Can. J. Chem. Downloaded from www.nrcresearchpress.com by 210.87.254.5 on 09/05/12
For personal use only.

Can. J. Chem. Downloaded from www.nrcresearchpress.com by 210.87.254.40 on 09/05/12
For personal use only.

Electronic absorption spectra and photodecomposition of some substituted ferrocenes[1]

A. M. TARR[2] AND D. M. WILES
Division of Applied Chemistry, National Research Council of Canada, Ottawa, Canada

Received February 7, 1968

The photostabilities of various ferrocene derivatives in solution have been studied as a function of solvent and, to a lesser extent, of incident wavelength. Some substituted ferrocenes, like ferrocene itself, did not decompose in methanol solution on exposure to near-ultraviolet light or sunlight; the remainder decomposed rapidly. Solutions of some derivatives in a number of other solvents also proved susceptible to photolysis. Qualitative evidence suggests that solute–solvent interaction leads to photochemically unstable species. Ferric ions do not appear to be formed in significant quantities during the degradative processes.

Of the substituted ferrocenes investigated in this work, *p*-acetophenylferrocene appears to have considerable merit as a relatively stable and therefore protective light absorber. None of the derivatives, however, is as stable as ferrocene, which is prohibitively volatile for most practical applications.

Canadian Journal of Chemistry, 46, 2725 (1968)

Introduction

Many papers have been published in recent years on the chemistry of ferrocene and its derivatives. This reflects not only the growing interest in organometallic compounds in general, but also the fact that ferrocene is susceptible to electrophilic substitution so that a multitude of ferrocene derivatives may be synthesized. The versatility of ferrocene as a reagent and its amber color suggest that it should be possible to synthesize ferrocene derivatives which would be suitable as protective absorbers of light in the near-ultraviolet region.

Benzoylferrocene and some hydroxy- and methoxy-benzoylferrocenes (as 1 to 5% additives) have been shown to be efficient inhibitors of degradation, by sunlight, of certain polymer films (1). Brief reference has been made (2) to the photodecomposition of ferrocenes in hydroxylic solvents, but no data on these systems are available. Although considerable information has been reported on the physical and chemical properties of metallocenes, very little has appeared on the photostability of these substances.

In the present work, the ultraviolet (u.v.) absorption spectra and stability of some substituted ferrocenes have been investigated in various organic solvents, especially oxygen-containing molecules. This represents part of a study to determine the efficiency of ferrocene derivatives in retarding the photochemical depolymerization of fiber-forming macromolecules.

[1]Issued as NRCC No. 10135.
[2]National Research Council of Canada Postdoctorate Fellow 1966–1967.

Experimental

Materials

Ferrocene (Matheson) was filtered and recrystallized from benzene solution and finally sublimed, m.p. 174°. The following ferrocene derivatives were prepared; the method of purification and melting point observed, using a Mettler FP1 apparatus, are given. Phenylferrocene (3), recrystallized (hexane) and vacuum sublimed, 112°. Benzylferrocene (2), recrystallized (ethanol–water) and vacuum sublimed, 76°. 1,1′-Dibenzylferrocene (2), recrystallized (ethanol–water), 103.5°. Hydroxymethylferrocene (4), recrystallized (water), 79°. Acetylferrocene (5), recrystallized (hexane) and vacuum sublimed, 85°. 1,1′-Diacetylferrocene (5), recrystallized (hexane) and vacuum sublimed, 127°. Benzoylferrocene (2), recrystallized (benzene/hexane) and vacuum sublimed, 109°. 1,1′-Dibenzoylferrocene (2), recrystallized (hexane), 105°. (2-Benzoylvinyl)ferrocene (6, 7), recrystallized (ethanol, then hexane), 136°. *p*- and *m*-Acetophenylferrocenes (8), chromatographed on silica gel, recrystallized (hexane), 175° and 74°. Diferrocenylethane (9), chromatographed on alumina, recrystallized (hexane), 196°.

Three hitherto unreported compounds were prepared as follows.

(2-p-Bromobenzoylvinyl)ferrocene—The method for (2-benzoylvinyl)ferrocene (6) was modified by replacing 3.5 g acetophenone by 3.8 g *p*-bromoacetophenone. The mixture was stirred at room temperature for 1 h, the precipitate (3.5 g) was separated, washed with cold ethanol, and recrystallized, first from ethanol, then from hexane, m.p. 165°.

Anal. Calcd. for $C_{19}H_{15}BrOFe$ (m.w., 395): C, 57.72; H, 3.80. Found: C, 58.23; H, 3.69.

A second modification of the method, replacing 3.5 g acetophenone by 2.45 g 2-octanone, gave *1-ferrocenyl-1-nonen-3-one*. The mixture was stirred at room temperature for 1 h, half the solvent was evaporated, and the red crystals which formed (3.9 g, wet) were recrystallized, first from ethanol, then from hexane, m.p. 80°.

Anal. Calcd. for $C_{19}H_{24}OFe$ (m.w., 324): C, 70.69; H, 7.37: Found: C, 70.40; H, 7.41.

N-p-biphenyl ferrocenaldimine was prepared (cf. ref. 7) by mixing concentrated solutions (in ethanol) of ferrocenecarboxaldehyde and 4-aminobiphenyl, and allowing to

Can. J. Chem. Downloaded from www.nrcresearchpress.com by 210.87.254.40 on 09/05/12
For personal use only.

TABLE I

Photodecomposition of DBZF in organic solvents (irradiated in Pyrex)

Solvent	Dielectric constant	Solution	Precipitate	Comments
Decalin		Easy	None; stable solution	
Isooctane		Slow	None; stable solution	
Methanol	32	Easy	Dark brown → Solution finally	precipitate in 4 days
1-Propanol	20	Easy	Red-brown → Solution finally	precipitate in 4 days
Ethylene glycol	37	Slow	Dark-brown → becomes colorless	3 weeks
Ethyl acetate	6	Rapid	Red-brown → becomes colorless	7 days
Diethyl ether	4.5	Rapid	Rusty appearance	3 days
Acetone	21	Rapid	Rusty appearance	18 h
Dioxane	2.2	Rapid	Sticky, red-brown	4 days (solution colorless in 10 days)
CCl_4	2.2	Easy	Powdery, dark brown	6 weeks
CS_2	2.6	Rapid	Dark brown	3 months
THF	7	Rapid	None; small color change only	Dark amber (18 h) → pale yellow (6 weeks)
Acetonitrile		Rapid	None; small color change only	Dark amber (2 days)
Dimethyl phthalate	8.5	Easy	None; small color change only	
Pyridine	12	Rapid	None; solution becomes deep purple or purple-brown	Color change in 2 h
DMF		Rapid	None; solution becomes deep purple or purple-brown	Color change in 4 days
DMSO		Rapid	None; solution becomes deep purple or purple-brown	Color change in 10 h

stand overnight at 0°. The crystalline precipitate was separated and recrystallized from hexane, m.p. 137–138°.

Anal. Calcd. for $C_{23}H_{19}NFe$ (m.w., 365): C, 75.63; H, 5.25; N, 3.84. Found: C, 75.19; H, 5.39; N, 4.02.

Procedure

Ultraviolet–visible spectra of solutions, covering a 300 mμ interval in the range 200–540 mμ, were measured using 1 cm quartz cells and a Bausch and Lomb 505 spectrophotometer. Solvent compensation in the reference beam was employed. All solvents were of reagent grade with the following exceptions: isooctane and CCl_4 were 'spectro' grade; decalin was fractionated to give 97% *cis* isomer; tetrahydrofuran (THF) was dried using CaH_2; dimethyl sulfoxide (DMSO) was vacuum distilled; acetonitrile, dimethyl phthalate, and N,N-dimethyl formamide (DMF) were practical grade.

Results

Photolysis of Ferrocenes

At the outset of this investigation we were interested in the mechanisms responsible for the effectiveness of ferrocenes as degradation preventives for polymers (1). Work in this laboratory (10) has shown that ferrocenes are similarly effective in protecting cotton cellulose. Therefore it is of interest to establish, if possible, the conditions under which ferrocene and some of its derivatives can harmlessly dissipate absorbed energy of the magnitude associated with near-ultraviolet radiation.

The stability of excited ferrocene is well illustrated by the very low G values reported for its radiolysis (11). However, it can be photolyzed in alkyl halide solutions (12) because of a charge-transfer reaction, e.g., in CCl_4 (Fc = ferrocenyl),

$$FcH + CCl_4 \xrightarrow{h\nu} FcH^+ + \cdot CCl_3 + Cl^-.$$

The cyclopentadienyl radical has been detected in the flash photolysis of ferrocene (13). We have photolyzed in an evacuated system (*a*) dry ferrocene and (*b* and *c*) solutions of ferrocene in decalin (97% *cis*) or 1-propanol, using light from a high-pressure Hg arc (200 W) and a filter cutoff at 230 mμ. Exposures were 15 h. No changes were detected in the u.v. spectrum of the ferrocene or in the isomer ratio of the decalin, nor were any volatile products found by mass spectrometry. Under these conditions a solution of ferrocene in CCl_4 was extensively decomposed. The photolysis of benzoylferrocene (BZF), as the pure solid or dissolved in decalin, also gave negative results. When 1,1′-dibenzoylferrocene (DBZF) was photolyzed alone for 40 h, the 470 and 354 mμ peaks in its u.v. spectrum were shifted by 1–2 mμ towards the blue, and a trace of benzene was detected mass spectrometrically in the volatile products. (An attempted vacuum sublimation of BDZF appeared to yield the monobenzoyl derivative slowly at 120°.) Although emission (480–685 mμ) has been reported (14) from ferrocene excited in its 324 mμ band, we were unable to detect any emission from ferrocene or BZF, either solid or dissolved in 5:1 isopentane–methylcyclohexane glass at 77 °K.[3] This is in agreement with the work of Smith (15).

Photostability of Solutions of BZF and DBZF

DBZF solutions in decalin or isooctane are unaffected by prolonged exposure to light. However, 10^{-4} *M* solutions of DBZF in methanol, made up for the measurement of its u.v. spectrum, decomposed in Pyrex on exposure to sunlight. They became cloudy in 24 h; after 2 weeks they were colorless, and a dark-brown precipitate had formed, presumably containing inorganic iron. This precipitate, after being dried at 100°, contained (%) C, 56.53; H, 4.24; Fe, 15.5; on the basis of one Fe atom, this corresponds to $C_{17}H_{15}O_5Fe$ (DBZF is $C_{24}H_{18}O_2Fe$). Analysis also indicated 11.1% benzoyl and 4.9% methoxy content, which for a pure compound would require a molecular weight of at least 945 or 630, respectively. Two decomposition products were detected in the liquid phase by gas–liquid chromatography, the second of which was identified as methyl benzoate by comparison with an authentic sample. The more volatile component might have been an acetal. Infrared examination of the products was inconclusive.

The decomposition of BZF and DBZF in methanol is a photochemical reaction, since solutions kept in the dark are stable for long periods. The ease of solubility and the photodecomposition of DBZF were tested in 17 solvents, which are divided into 4 groups depending on their behavior (see Table I). An interesting feature is that whereas ferrocene is stable in methanol but photolyzes in CCl_4, DBZF decomposes much more rapidly in methanol. This reaction is stimulated by absorption in either the 470 or the 354 mμ band, as shown by photolyses using

[3]We are indebted to Dr. F. R. Lipsett of the Radio and Electrical Engineering Division, National Research Council of Canada, for these results.

Can. J. Chem. Downloaded from www.nrcresearchpress.com by 210.87.254.40 on 09/05/12
For personal use only.

Can. J. Chem. Downloaded from www.nrcresearchpress.com by 210.87.254.40 on 09/05/12
For personal use only.

selective filters (Corning Nos. 3–73 and 7–51 respectively). Two authors have reported (2, 16) that photodecomposition of BZF in 2-propanol is very slow, and we have confirmed this. On the other hand, reaction is fairly rapid in 1-propanol. The first sign of decomposition is the gradual filling of the trough at 314 mμ in the u.v. spectrum (isooctane); this effect is rapid enough to make calculations of the extinction coefficient from spectra of DBZF in methanol somewhat inaccurate. As decomposition proceeds, a Tyndall cone appears under suitable illumination, all troughs and peaks disappear from the spectrum, and finally the precipitate settles out.

The development of absorption in the 300–350 mμ region was used to estimate the relative rates of decomposition of BZF and DBZF in a slow-reacting solvent, dimethyl phthalate, when photolyzed at 296–302 mμ (Bausch and Lomb monochomator). The difference between the spectra of irradiated and unirradiated solutions was a featureless absorption beginning about 500 mμ and increasing in intensity towards shorter wavelengths. Intensities measured at 330 mμ after various photolysis times indicated that DBZF reacted approximately 4 times faster than BZF, assuming that the reaction is the same for both compounds.

A solution of DBZF in carefully degassed methanol, after 3 h photolysis in Pyrex under vacuum, took on a color very similar to Fe^{2+} ions in water, and a grey-green precipitate formed. When air was admitted to the system weak positive tests for Fe^{2+} were obtained with *o*-phenanthroline and $K_4Fe(CN)_6$, and the usual brown 'decomposition' color rapidly developed. It appears that a slow initial reaction between DBZF and solvent is followed by oxidation under atmospheric conditions. Similar green intermediates were found in degassed glycol solutions but not in acetone.

An electron spin resonance spectrum of ferric chloride in acetone has been reported (17) and we looked for a similar signal from a solution of DBZF in LiCl-saturated acetone. The unirradiated solution had a sharp signal (ΔH = 50 G, g = 2.0115) which was replaced after irradiation by a very broad signal ($\Delta H \sim$ 1200 G) upon which a stronger signal ($\Delta H \sim$ 300 G) developed asymmetrically as irradiation progressed. Ferric chloride (g = 2.016, ΔH = 55 G (17)), does not appear to be present.

It is obvious that the nature of the solvent profoundly affects the photostability of solutions of ferrocenes. An attempt was made, therefore, to detect some evidence of solute–solvent interaction in systems where this might be most easily observed. Infrared spectra of DBZF and diacetylferrocene (DAF) in CCl_4 containing 0.1–5.0% methanol by volume showed no significant shifts in the 1650, 1290 (DBZF), and 1685, 1280 cm^{-1} (DAF) absorptions, but considerable broadening was noticeable, indicating some interaction between the keto group and methanol (Table II). Because of its infrared opacity, methanol could not be used in higher concentrations.

It has been observed (10) that some ferrocene derivatives reduce the rate of actinic degradation of cellulose fibres on which they are adsorbed. The hydroxylic nature of cellulose prompted us to test the effect of dissolved sugars on the stability of DBZF solutions. In dry THF, DBZF is stable after a small initial color change. However, in THF saturated with dextrose (whose solubility is very small) most of the DBZF was decomposed by 2 days' exposure to sunlight. A further experiment of this kind involved dihydroxyacetone (DHA), which is also an effective chelating agent for Fe^{3+} ions (18). Solutions in methanol and acetone, containing 2 moles DHA per mole DBZF, decomposed much faster than solutions containing DBZF alone. After photolysis, spectral analysis for iron showed that about 10% remained in solution, confirming that Fe^{3+} is not a product of the decomposition of DBZF and showing that DHA is very effective in promoting this decomposition. DBZF was also readily photolyzed in 1:1 methanol:water, the decomposition taking place at a rate similar to the methanol solution containing 2:1 DHA:DBZF.

Ultraviolet Spectra and Stability of other Substituted Ferrocenes

Wavelengths and molar extinction coefficients (ε) for the u.v. spectra of various substituted ferrocenes are listed in Table III. All spectra were taken in isooctane solution; six spectra were also recorded in methanol solution to illustrate the solvent shifts. All previously reported spectra of these compounds were measured in 95% ethanol; agreement with our data for methanol solution is generally good. Compounds 1 to 6, 14, and 15 (Table III) were not significantly affected by prolonged exposure to daylight in methanol; the

TABLE II
Infrared evidence for solute–solvent interaction

Solvent	DBZF		DAF	
	Frequency (cm^{-1})	Width at half-height (cm^{-1})	Frequency (cm^{-1})	Width at half-height (cm^{-1})
CCl_4	1288	12	1279	13
CCl_4/5% MeOH	1289	16	1278	29
CCl_4	1652	15	1683	12
CCl_4/5% MeOH	1648	27	1683	30

remainder faded and gave precipitates similarly to DBZF.

Table III illustrates the small effect on the ferrocene spectrum caused by hydrocarbon and hydroxymethyl substituents compared with the effect of a ketonic substituent, which bathochromically shifts the lowest-energy u.v. transition of ferrocene (440 mμ ~ 65 kcal) by 6–46 mμ (in isooctane). This shift is approximately doubled in the five examples taken in methanol. The maximum ε for this band, which is increased by a factor of 3–25 by the presence of a carbonyl group, increases further (about 50%) in methanol. Carbonyl substituents cause a less predictable shift of the 326 mμ ferrocene band, which is the important one in a useful u.v. light absorber. It is possible that C=O absorptions are interfering here. The band intensity increases by 20–50 times (isooctane), and by a further 10–20% in methanol solution. The higher-energy transitions, although relatively intense, are not well identified, and of little importance, being outside the wavelength range of sunlight in most cases.

The requirements for an ultraviolet-light absorber to protect cellulose or other polymeric materials are: (i) high ε below, say, 400 mμ; (ii) low volatility; and (iii) good photochemical stability, especially in the presence of hydroxyl groups. In Table III, compounds 14 and 15, *p*- and *m*-acetophenylferrocenes, are the only compounds to satisfy these criteria, and the spectrum of the para-compound is more suitable than the meta-compound. Its chief drawback at present is an inefficient method of preparation.

Discussion

The experiments on the photodecomposition of substituted ferrocenes (of which DBZF is a good example) in various solvents illustrate three facts. Firstly, decomposition of DBZF is initiated by both the 470 and 354 mμ bands of the spectrum. This is reasonable since the 440 mμ and 326 mμ bands of ferrocene have both been attributed to metal-ring charge transfer (19) and it appears that the shifted transitions in DBZF are of the same type. Secondly, a carbonyl group conjugated with the ferrocene ring increases the intensity of these transitions, but also introduces instability into the molecule, except when separated from the ring by a phenylene group. This may indicate that interaction between the carbonyl oxygen and the iron atom, which is possible in all cases except compounds 14 and 15 (Table III), may be involved in the breakdown mechanism. Finally, and least simply rationalized, almost any oxygen- or nitrogen-containing solvent leads to decomposition of DBZF, which in most cases gives ultimately a clear or pale-yellow solution over a fine or gelatinous precipitate of various brown shades. Three 'powerful' polar solvents (pyridine, DMF, and DMSO) developed a very deep purple-brown solution but gave no precipitate. No systematic correlation is apparent between the behavior of DBZF and the dielectric constant of the solvent. Since rapid decomposition occurs in 1:1 methanol:water, the presence of water in the solvent may be important. It is noteworthy that hydrocarbons, CCl_4, CS_2, and dimethyl phthalate, all poor solvents for water, have the least effect on DBZF. The remaining solvents all have a capacity for dissolving water. The slow reaction in CCl_4 and CS_2 may be due to polarizability effects or to solvent photolysis. However, in view of the low reactivity of DBZF in 2-propanol, reaction could be caused by impurity in some cases; dioxane is an unexpectedly" reactive" solvent and is well known to be difficult to purify.

Since the only products identified from the DBZF/methanol photolysis are methyl benzoate

Can. J. Chem. Downloaded from www.nrcresearchpress.com by 210.87.254.40 on 09/05/12
For personal use only.

Can. J. Chem. Downloaded from www.nrcresearchpress.com by 210.87.254.40 on 09/05/12
For personal use only.

TABLE III

Ultraviolet spectra of substituted ferrocenes*

	Compound	(low-energy → high-energy transitions →)							
		λ_{max}	(ε_{max})	λ_{max}	(ε_{max})	λ_{max}	(ε_{max})	λ_{max}	(ε_{max})
1	Ferrocene (=FcH)	440	(95)	326	(55)			240 sh	(~3 500)
2*a*	Phenyl-	451		~345 sh		278	(10 400)	238	(13 500)
2*b*	Phenyl- (in MeOH)	451	(280)	~345 sh		278	(10 500)	239	(19 900)
3	Benzyl-	440	(136)	325	(82)	254	(34 800)	< 240	
4	Dibenzyl-	440	(168)	324	(110)	252	(5 640)	< 240	
5	$Fc.CH_2.CH_2.Fc$	441	(220)	324	(140)			255 sh	
6	$Fc.CH_2OH$	437	(108)	323	(72)			< 240	(~4 000)
7*a*	Acetyl-	446	(335)	319	(1 140)	266	(5 600)	220	(24 000)
7*b*†	Acetyl- (in MeOH)	457	(545)	337	(1 430)	268	(7 500)	225	(16 500)
8	Diacetyl	456	(305)	320	(1 370)	258	(9 500)	224	(24 000)
9*a*	Benzoyl-	459	(610)	355	(1 220)	273	(6 950)	240	(20 400)
9*b*	Benzoyl- (in THF)	465		359		274		244	
9*c*‡	Benzoyl- (in MeOH)	479	(900)	362	(1 410)	275	(8 880)	248	(13 300)
10	Dibenzoyl-	470	(700)	354	(1 970)	276	(12 550)	247	(22 300)
11*a*	FcCH=CH.COϕ	476	(1940)	383	(2 680)	314	(17 300)	265	
11*b*	FcCH=CH.COϕ (in MeOH)	515	(2810)	~400 sh		326		265	
12*a*§	FcCH=CH.CO—C$_6$H$_4$—Br	486	(2250)	387	(2 680)	318	(19 000)	273	(16 900)
12*b*	FcCH=CH.CO—C$_6$H$_4$—Br (in MeOH)	> 520	(~3300)	~405 sh		331		276	
13§	$Fc.CH=CH.COC_6H_{13}$	462	(770)	358 sh	(1 460)	299	(10 200)	257	(7 700)
14*a*	Fc—C$_6$H$_4$—$COCH_3$	454	(850)	364	(2 760)	297	(15 000)	260	(11 300)
14*b*	Fc—C$_6$H$_4$—$COCH_3$ (in MeOH)	464	(1440)	374	(2 960)	304	(17 700)	265	(11 100)
15	Fc(C$_5$H$_4$)$COCH_3$	448	(405)	~360 sh		283			
16§	Fc—CH=N—C$_6$H$_4$—ϕ	457	(1270)	328	(18 300)	~284 sh		264	(19 300)

*Taken in isooctane against isooctane unless specified otherwise; sh = shoulder.
†See ref. 3 for spectrum in EtOH.
‡See ref. 17 for spectrum in EtOH.
§The preparation and spectrum of this compound have not been reported previously.

and an intractable iron-containing solid (possibly ferrous benzoate), any mechanism is necessarily highly speculative. Ferrocene undergoes various electron or proton transfer reactions, the products of the former being relatively unstable compared with the latter: ferricenium $C_{10}H_{10}Fe^+$ breaks down on reaction with a free radical, e.g. benzoate (20), while the $C_{10}H_{10}Fe^-$ ion gives iron and cyclopentadiene (21). It has been stated (22) that intermolecular H bonding between alcohols and ferrocene involves the ring rather than the iron atom, but in acyl ferrocenes the carbonyl group is available for H bonding. If, as seems reasonable, the lower-energy transitions in DBZF involve metal → ring charge transfer (possibly with carbonyl excitation), the charge-transfer reaction, analogous to the ferrocene–CCl_4 case (12), could occur.

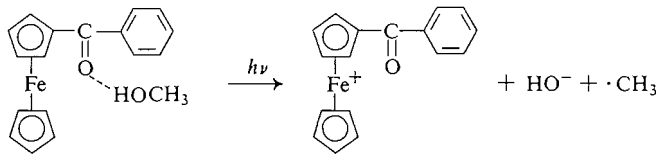

Reaction between the radical and the benzoylferricenium ion could then lead to breakdown of the molecule.

Acknowledgments

The authors are grateful to Mr. T. Suprunchuk for technical assistance, and to Mr. J. D. Cooney for helpful discussions.

1. R. G. Schmitt and R. C. Hirt. J. Appl. Polymer Sci. **7**, 1565 (1963).
2. M. Rausch, M. Vogel, and H. Rosenberg. J. Org. Chem. **22**, 903 (1957).
3. M. Rosenblum. J. Am. Chem. Soc. **81**, 4530 (1959).
4. J. K. Lindsay and C. R. Hauser. J. Org. Chem. **22**, 355 (1957).
5. M. Rosenblum and R. B. Woodward. J. Am. Chem. Soc. **80**, 5443 (1958).
6. R. E. Bozak and J. E. Lakner Can. J. Chem. **45**, 773 (1967).
7. J. Boichard, J-P. Monin, and J. Tirouflet. Bull. Soc. Chim. France, 851 (1963).
8. T. G. Traylor and J. C. Ware. J. Am. Chem. Soc. **89**, 2304 (1967).
9. P. L. Pauson and W. E. Watts. J. Chem. Soc. 3880 (1962).
10. J. D. Cooney and D. M. Wiles. Unpublished results.
11. B. K. Krotoszynski. J. Chem. Phys. **41**, 2220 (1964).
12. J. C. Brand and W. Snedden. Trans. Faraday Soc. **53**, 894 (1957).
13. B. A. Thrush. Nature, **178**, 155 (1956).
14. D. R. Scott and R. S. Becker. J. Chem. Phys. **35**, 516 (1961).
15. F. J. Smith. Ph.D. Thesis, Louisiana State University, Baton Rouge, Louisiana. 1965. p. 76.
16. N. Weliky and E. S. Gould. J. Am. Chem. Soc. **79**, 2742 (1957).
17. R. M. Golding and L. E. Orgel. J. Chem. Soc. 363 (1962).
18. P. S. Davis and D. J. Deller. Nature, **212**, 404 (1966).
19. M. Rosenblum. Chemistry of the iron group metallocenes. Interscience Publishers, Inc., New York. 1965. p. 42.
20. A. L. J. Beckwith and R. J. Leydon. Tetrahedron Letters, No. 6, 385 (1963).
21. D. S. Trifan and L. Nicholas. J. Am. Chem. Soc. **79**, 2746 (1957).
22. D. S. Trifan and R. Bacskai. J. Am. Chem. Soc. **82**, 5010 (1960).

Can. J. Chem. Downloaded from www.nrcresearchpress.com by 210.87.254.40 on 09/05/12
For personal use only.

On pseudo-rotation in $(AsCH_3)_5$ and $(AsCF_3)_5$

E. J. WELLS, R. C. FERGUSON, J. G. HALLETT, AND L. K. PETERSON
Department of Chemistry, Simon Fraser University, Burnaby 2, British Columbia

Received February 26, 1968

Two internal rearrangement processes can be deduced from the temperature dependences of the ^1H and ^{19}F nuclear magnetic resonance (n.m.r.) spectra of the asymmetric puckered five-membered ring compounds $(AsCH_3)_5$, $(AsCF_3)_5$, and $(PCF_3)_5$. The first is a fast "butterfly" motion of the ring puckering which yields a time-averaged plane of symmetry perpendicular to the ring through the puckered atom. This motion could not be stopped in any of the three compounds by cooling, even to −130 °C in the case of $(AsCF_3)_5$. The second is a slow pseudo-rotation, or a rotation of the perpendicular symmetry plane around the ring yielding a time-averaged fivefold rotation axis. There is a choice between two mechanisms for this second rearrangement, either a "clickstop" process in which the puckering progresses around the ring by one position at a time, or a "pancake" process in which the puckering drops randomly into any one of the five ring positions from a planar transition state. This choice can be resolved for this cyclic permutation process by appeal to the n.m.r. lineshapes. The present data for $(AsCH_3)_5$ favor the "clickstop" mechanism in spite of a competing intermolecular process at elevated temperatures with other components in the system which are in equilibrium with the ring compound.

Canadian Journal of Chemistry, 46, 2733 (1968)

Can. J. Chem. Downloaded from www.nrcresearchpress.com by 210.87.254.42 on 09/05/12
For personal use only.

Introduction

Pseudo-rotation in five-membered puckered ring compounds has been discussed theoretically by several authors (1, 2) with particular reference to cyclopentane. Subsequently the far-infrared absorption spectrum of tetrahydrofuran was interpreted (3) in terms of this motion, and very recently the ring puckering modes in 2,5-dihydrofuran have been investigated (4) by the same technique. We recently reported (5) a nuclear magnetic resonance (n.m.r.) study of the asymmetric puckered ring compound $(PCF_3)_5$ and ascribed the temperature dependence of the ^{19}F spectrum to pseudo-rotation within the ring. However, in that molecule, the details of the process occurring are obscured in the n.m.r. data by severe ^{31}P—^{19}F scalar spin coupling. We point out here that these details can be plucked from the related isostructural (6–8) arsenic compounds by taking advantage of the fast quadrupolar relaxation of the spin-3/2 ^{75}As nucleus under the fluctuating field gradients caused by thermal motion in the liquid. Thus, "isotopic" substitution of ^{31}P by quadrupolar ^{75}As affords automatic, inexpensive heteronuclear decoupling.

Experimental

Arsenomethane $(AsCH_3)_5$

The yellow oil was prepared (9) by the reduction of sodium methyl arsenate with hypophosphorous acid. The oil was washed with dilute NaOH and then water and purified by fractionation at 110 °C under high vacuum. In addition to the main 2:2:1 triplet in the n.m.r. spectrum, weak bands were also observed to high field with a total relative intensity at 42 °C of approximately 7%, which could not be reduced by further fractionation. Samples gradually precipitated a red solid on standing for about a week at room temperature or 0 °C (1, 8, 9). This transformation is rapidly reversible above 180 °C, and the clear yellow oil could always be regenerated by immersion of the sample tube in an oil bath at 190 °C for a few minutes. Unsuccessful attempts to fractionate the material by vapor phase chromatography (v.p.c.) using an SE30 silicone oil column at 165 and 185 °C gave a low intensity hump followed by severe tailing lasting upwards of an hour. On the basis of these experiences and the n.m.r. data obtained, we now believe that the lines to high field of the dominant triplet are due to species derived from, and in equilibrium with, the parent ring compound $(AsCH_3)_5$, and thus can never be removed from the spectrum.

Arsenoperfluoromethane $(AsCF_3)_5$

A mixture of $(CF_3As)_x$ was prepared by mercury dehalogenation of CF_3AsI_2 (10, also L. K. Peterson, unpublished work). The volatile components ($x = 4$, 5) were treated with $(CF_3)_2AsCl$ to remove mercury, the $(CF_3)_4As_2$ so formed and the excess $(CF_3)_2AsCl$ being readily separated from mercuric chloride and the less volatile cyclic polyarsines. The latter were sealed under vacuum in a 9 in. U tube (9 mm tubing) which, with the exception of the tip of one limb, was maintained at 4–5 °C above ambient temperature for several days. Large colorless crystals of more volatile tetramer (m.p. 98.5°, lit. (10) 98.2°) condensed on the walls of the cold limb, which was sealed off from the system. The less volatile dense[1] liquid remaining at the bottom of the tube was almost pure pentamer (11) (11% tetramer present, from n.m.r. integration).

Results

(a) $(AsCH_3)_5$

The temperature dependence of the 60 MHz proton spectrum of neat $(AsCH_3)_5$ is shown in Fig. 1. The predominant signal is a 2:2:1 triplet

[1] Liquid $(AsCF_3)_5$ floats pyrex glass.

TABLE I

Temperature dependence of 60 MHz ^1H spectrum of neat $(AsCH_3)_5$

	Chemical shift relative to line β (Hz)						Full width at half height (Hz)			
T (°C)	δ_α	δ_γ	δ_δ	δ_ε	δ_ζ	δ_η	Δ_α	Δ_β	Δ_γ	Δ_ζ
42	−1.51	1.05					1.15	1.20	1.20	
98	−1.35	0.95	2.25	5.4	6.6	9.5	0.65	0.65	0.55	0.40
119	−1.22	0.85	2.0	5.0	6.5		0.80	0.80	0.60	0.50
138	−1.05	0.77	1.9	4.9	6.4		0.65	0.65	0.48	0.40
158	−1.15	0.82		5.0	6.5	9.0	0.75	0.75	0.55	1.3
169	−1.12	0.78		5.0	6.5	9.2	0.78	0.82	0.80	1.5
174	−1.10							2.65		
177	−1.03							2.85		~4.0 (lines ε & 5)
179	−0.90							2.90		
182	−1.0							2.90		
183	Coalescence							2.95		
188								2.70		
192	Coalescence								2.90	
196									3.30	
202									4.30	
Solution in $CDCl_3$										
42	−1.85	0.70		5.1	6.3	10.1	0.40	0.50	0.40	

NOTE: $J^{13}_{C-H}(\alpha) = J^{13}_{C-H}(\beta) = 135.0$ Hz; $J^{13}_{C-H}(\gamma) = 134.8$ Hz. There is a barely detectable relative isotope shift of about −0.1 Hz for protons bound to the ^{13}C-methyl group giving rise to spectral line γ, compared with the ^{13}C side bands from lines α and β.

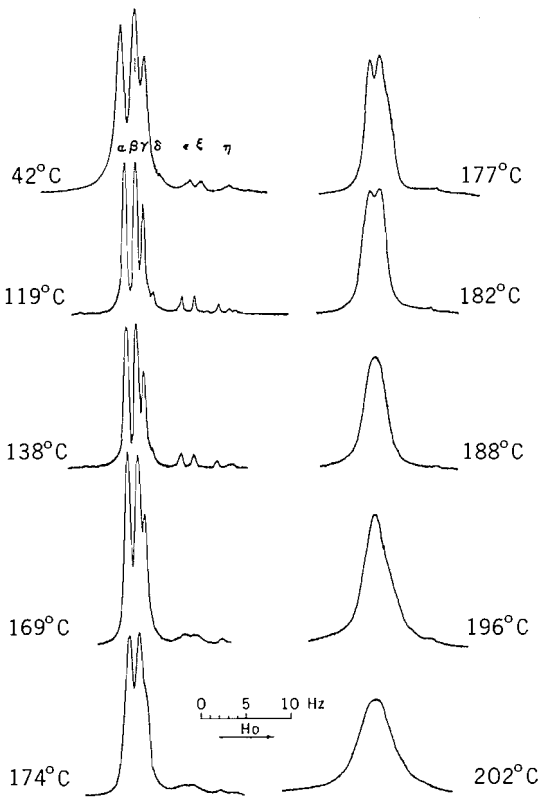

FIG. 1. Temperature dependence of 60 MHz ^1H spectrum of neat vacuum-fractionated arsenomethane.

approximately 2.3 p.p.m. downfield from external tetramethylsilane (TMS) and spanning only 2 Hz or 0.033 p.p.m. The lines are viscosity broadened at 42 °C with a full width at half height of 1.2 Hz, but sharpen to a width of 0.65 Hz on heating above 100 °C. The line width contribution in excess of the homogeneity width $(\pi)^{-1}R_2^* = 0.3$ Hz of our Varian A56/60 spectrometer is ascribed to residual ^{75}As—^1H coupling in the limit of rapid ^{75}As quadrupolar relaxation (i.e. $R_1(^{75}As) = 1/T_1 \gg 2\pi J_{As—H}$). At 160 °C the lines of the triplet begin to broaden again and coalescence is reached at 183 °C. Above 183 °C the merged line first sharpens and then begins to broaden once more. The resonance lines of the minor constituent to high field also broaden between 160 and 190 °C and have coalesced under the main peak at 192 °C. A 1:3 solution of $(AsCH_3)_5$ in $CDCl_3$ showed no change in the spectrum on cooling to −55 °C.

The main features of the spectra are given in Table I. The entries represent averages of several spectra obtained from various runs on different samples. Temperature calibration was made by ethylene glycol resonance separation, and the figures are believed to be reliable to within 3 °C.

The mass spectrum of $(AsCH_3)_5$ obtained on a Hitachi Perkin–Elmer RMU-6E instrument operating at an inlet temperature of 200 °C and an

Can. J. Chem. Downloaded from www.nrcresearchpress.com by 210.87.254.42 on 09/05/12
For personal use only.

Can. J. Chem. Downloaded from www.nrcresearchpress.com by 210.87.254.42 on 09/05/12
For personal use only.

ionizing beam energy of 80 eV shows a rich fragmentation pattern consisting of long progressions with $\Delta(m/e) = 15$. The parent ion at mass 450 is weakly visible, and there is some evidence for a polymeric ion at mass 525. The largest ionic species of high intensity falls at mass 270 $[(AsCH_3)_3^+$?] and, thereafter, at 255, 225, 165, 163, 150, 105, 103, 90, 89, 88, and finally 75.

(b) $(AsCF_3)_5$

The 56.4 MHz ^{19}F spectrum of neat $(AsCF_3)_5$ at 42 °C is shown in Fig. 2 and is also seen to be a 2:2:1 triplet (lines α, β, and γ) with lines β some 2.10 kHz (38.3 p.p.m.) to high field of external $CFCl_3$. The total range of the ^{19}F shifts in this molecule is 175 Hz, or 2 orders of magnitude larger than the proton shifts in the methyl analog. Some residual coupling on the two more intense peaks is visible with a magnitude of approximately 1.5 Hz and is presumably due to long range F—F interactions; this splitting appears to be temperature dependent. Owing to severe bumping and rapid refluxing of this material within the sample tube, we were unable to obtain spectra above 160 °C, and to that limit the main features of the spectrum are maintained. The triplet structure of the resonance is also visible down to −55 °C where viscosity broadening of the neat liquid causes a full width at half maximum of 25 Hz.

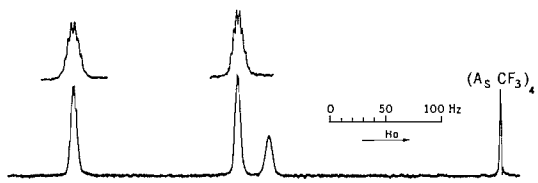

FIG. 2. 56.4 MHz ^{19}F spectrum of $(AsCF_3)_5$ liquid at 42 °C. $(AsCF_3)_4$ is present as impurity.

Slow passage spectra of $(AsCF_3)_5$ in solution in $CFCl_3$ could be obtained down to −100 °C, where the simple triplet structure of the spectrum is still visible. By immersing the sample in liquid nitrogen and allowing it to warm back to −100 °C in the probe, fast passage spectra could be obtained down to the melting point of the solution, estimated to be about −130 °C. The spectra here reproduce the triplet structure observed at higher temperatures. The n.m.r. data for $(AsCF_3)_5$ is assembled in Table II. The temperatures quoted are nominal, but are probably good to within 5 °C.

TABLE II

Temperature dependence of 56.4 MHz ^{19}F spectrum of $(AsCF_3)_5$

	Chemical shift relative to line β (Hz)		
T (°C)	δ_α	δ_γ	$\delta_{(AsCF_3)}$
(*a*) Neat $(AsCF_3)_5$			
+160	−146	+19	
130	−145	20	+238
100	−145	24	240
42	−146	28	236
0	−147	33	236
−30	−148	36	234
−50	−147	37	234
−55	−146	38	231
(*b*) $(AsCF_3)_5$ in $CFCl_3$			
+42	−142	30	
−45	−140	40	
−66	−136	42	
−86	−137	47	
−100	−133	48	

The $(AsCF_3)_4$ present as an impurity yields a single sharp line for its ^{19}F resonance, indicating at least time-average symmetry for the four CF_3 groups and thus a cyclic structure. It probably has strict D_{2d} symmetry, analogous to $(PCF_3)_4$ (6).

Discussion

1. Low Temperature Process

If the structure of these molecules in solution is similar to that found by X-ray scattering in the solid for $(PCF_3)_5$ (7) and $(AsCH_3)_5$ (8), then there is no element of symmetry at all and each substituent group should have its own unique chemical shift. The n.m.r. pattern should be five lines of equal intensity and varying shifts. The 2:2:1 pattern in $(AsCH_3)_5$, taken alone, could be reconciled as accidental degeneracy of the shift of two pairs of methyl groups, in view of the very small total chemical shift. However, the reappearance of this pattern in $(AsCF_3)_5$, where the relative chemical shifts are much larger, makes this explanation unlikely. In $(PCF_3)_5$ both the ^{19}F spectrum and the ^{31}P spectrum below 150 °C were found (5) to be broad bands of relative intensity 2:3, the breadth being caused by complex ^{31}P—^{19}F couplings. It seems very likely that this coupling in $(PCF_3)_5$ obscures the resolution of both nuclear resonances into the simple 2:2:1 structure we now observe for the analogous arsenic compounds.

The implication of this "oversimplified" spectrum then common to all three five-membered rings is that each ring has an effective plane of

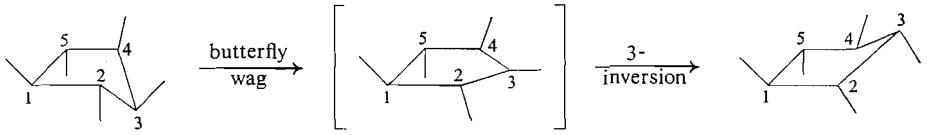

1 2 3

symmetry in the liquid phase. We propose that the mechanism by which these rings generate a time-average symmetry plane from the instaneous structure which is locked by crystal forces in the solid is a "butterfly wag" of the ring puckering atom through the approximate plane defined by the other four ring atoms, and a simultaneous inversion at the puckering atom.

Structure **3** is the equivalent to structure **1**, as may be seen by a twofold rotation of **3** about an axis perpendicular to the 1—5 bond in the plane defined by ring atoms 1, 2, 4, 5; however, in **3** the role of atoms 1, 5 and 2, 4 are interchanged with respect to that in **1**. The complete process is equivalent to holding the puckering atom and its substituent fixed and inverting each substituent at ring atoms 1, 2, 4, and 5. The effective symmetry plane is more evident in the latter description.

This process must be fast, since the expected quintet of lines does not separate in any of the compounds down to −55 °C and, in particular, in $(AsCF_3)_5$ even on cooling to −130 °C. For this molecule we can estimate a minimum puckering inversion frequency of 315 s^{-1} at 143 °K by assuming a value of 50 Hz for the chemical shift difference between F nuclei on positions 1 and 5 or positions 2 and 4 in the locked configuration **1**. If the As inversion process is via quantum-mechanical tunneling through the potential barrier in the Wentzel–Kramers–Brillouin (W.K.B.) sense[2] then this observed lower limit represents an ensemble average of inversion frequencies over the appropriate occupied levels of the normal vibrational modes of the arsenic ring. On the other hand, if the inversion process takes place by thermal excitation *over* the potential barrier with a transition state represented by some structure such as **2**, then the observed lower limit for the inversion frequency implies an upper limit for $\Delta G^{\ddagger}$ of 6.5 kcal $mole^{-1}$.

Dennison and Uhlenbeck (14) have derived an expression, based on the W.K.B. method[3], for tunneling through a potential barrier under the approximation that the variable for the tunneling motion is predominantly a single normal vibrational mode. They find that the tunneling frequency ν is given by

$$[1] \qquad \nu = (\nu_0/\pi) \exp I,$$

where ν_0 is the vibrational frequency of the active mode and

$$[2] \quad I = -\hbar^{-1} \int_{-S_0}^{S_0} \{2\mu[V(S) - \varepsilon]\}^{\frac{1}{2}} \, dS,$$

with μ the reduced mass for the vibrational coordinate, $V(S)$ the potential energy, ε the total energy, S the normal coordinate for the vibration or tunneling motion, S_0 that S for which $V(S) = \varepsilon$ with respect to the maximum of the barrier.

Thus, the tunneling frequency varies in an approximately inverse exponential fashion with the weighted area cut off the potential hill by the vibrational eigenvalue, and increases rapidly with the quantum number of the active vibration.

Now in general a process will occur by that route which maximizes its frequency. We believe that the present data allow us to choose between the tunneling and the transition state mechanisms in favor of the transition state route.

(1) The tunneling frequency of inversion for AsH_3 has been estimated from eqs. [1] and [2] by Costain and Sutherland (16) and by Berry (17) using various forms for the potential energy function $V(S)$, and these estimates are slower than our lower bound for the frequency in $(AsCF_3)_5$ by 9 and 4 orders of magnitude respectively. Moreover, the tunneling frequency in $(AsCF_3)_5$ is expected to be even slower than than that in AsH_3 because:

(*a*) the reduced mass μ is much larger,

(*b*) the As—C bond length (1.95 Å) and As—As bond length (2.43 Å) here are each much larger than the As—H bond length (1.52 Å), implying

[2]For discussions of tunneling phenomena, see Townes and Schawlow (12) and Hertzberg (13).

[3]For a discussion of the W.K.B. method, see Messiah (15).

Can. J. Chem. Downloaded from www.nrcresearchpress.com by 210.87.254.42 on 09/05/12
For personal use only.

Can. J. Chem. Downloaded from www.nrcresearchpress.com by 210.87.254.42 on 09/05/12
For personal use only.

a "wider" potential barrier against tunneling, i.e. larger S_0, and

(*c*) the relevant ring distorting vibration in $(AsCF_3)_5$ is expected to be much lower than the active ν_2 vibration in AsH_3 (974 cm^{-1}), so that in eq. [1] $\nu_0(AsCF_3)_5 < \nu_0(AsH_3)$.

(2) The possibility of d_π bonding in the five-membered As ring favors a flat transition state such as **2**, lowering the height of the potential barrier $V(S = 0)$ and thus increasing the probability of thermal promotion over the barrier. This effect works against the cumulative effects 1*a*–1*c* above with respect to tunneling, but cannot counteract the dominating reduction in tunneling frequency caused by 1*a* and 1*b*.

The overall low temperature process in these five-membered rings can then be described as an entropy-increasing one utilizing the ring flexibility. In this respect it is similar to the chair–chair process well known in cyclohexanes and related heterocyclic molecules. The As inversion at the puckering center is incidental to the ring process, and probably results from second order effects such as steric repulsion in the ring flip reaction coordinate. Tunneling inversion of the ring atoms is too slow to be observable; if each ring atom could invert randomly and rapidly by tunneling, the rings would probably be pseudo-flat and the observed 2:2:1 pattern would collapse to a single line. In this respect the temperature dependence of the ^{19}F spectrum of hypothetical $(AsF)_5$ would be interesting.

As an aside, we point out that the above analysis of inversion by tunneling vs. transition state is in principle applicable also to nitrogen in the chair–chair process of N-heterocyclic compounds. Berry's (17) estimate of the tunneling frequency in the ground vibrational state of NF_3 yields a value of 0.03 s^{-1}, and for reasons similar to those above, this value is probably larger than the N-tunneling frequency in N-heterocyclics. Then the pure tunnel process would be too slow to be observable by n.m.r. methods. Consistent with this, most organic chemists (18, 19) regard observed N-inversion in ring compounds as taking place at the transition state of the ring process. However, at least for perfluoropiperidine (20) the N-inversion is rapid down to −115 °C and is apparently independent of the ring process, indicative of tunnel inversion. The ring puckering flip motion has recently been observed through the microwave spectra of the four-membered heterocycles trimethylene oxide (21) and trimethylene sulfide (22), where the motion is fast (8.23 GHz for the latter in its ground vibrational state) and occurs by tunneling.

Finally, there is no evidence[4] in the X-ray data of Burns and Waser (8) on $(AsCH_3)_5$ in the solid for the ring puckering flip motion inferred here in the liquid. From their structural data, such a motion involves a translation of the puckering As atom by 2.5 Å through the average plane defined by the other four ring atoms, and a similar motion of the CH_3 substituent center by 0.92 Å. Therefore, ring puckering inversion would not be expected in the solid state.

2. High Temperature Process

The spectra of both $(PCF_3)_5$ and $(AsCH_3)_5$ collapse at elevated temperatures, although in neither case could the process be followed to sufficiently high temperatures on our equipment to reach the fast exchange limits, where presumably the spectra are single sharp lines. The observed collapse is completely reversible with temperature. The ^{19}F spectrum of $(AsCF_3)_5$ showed no significant broadening to 160 °C; if $(AsCF_3)_5$ has a process analogous to the other two compounds, then it must occur at somewhat higher temperatures.

For $(PCF_3)_5$ we ascribed (5) this high temperature process to intramolecular pseudo-rotation of the ring puckering around the ring. However, other possible mechanisms were also considered, among which were intermolecular CF_3 exchange and ring opening. The pentamer is known to pyrolyze slowly to the more stable tetramer (23) and the mechanism could conceivably involve intermolecular CF_3 exchange. This process was ruled out in our consideration of the $(PCF_3)_5$/$(PCF_3)_4$ spectra because the ^{19}F spectrum of the tetramer component remained sharp to 200 °C, whereas CF_3 exchange would be indiscriminate and involve both the pentamer and tetramer species. Ring opening of the pentamer at elevated temperatures would lead presumably to pyrolytic polymerization (which requires some 48 h at 250 °C to be detectable in the bulk (23)) and thus could not account for the reversible changes observed in the spectra at 200 °C. No spurious bands were detected at any temperature in the ^{19}F spectra of these P ring compounds.

[4]F. Einstein. Private communication.

Can. J. Chem. Downloaded from www.nrcresearchpress.com by 210.87.254.42 on 09/05/12
For personal use only.

With $(AsCH_3)_5$, on the other hand, the appearance of weak lines of constant intensity ratio to high field of the main pattern over the temperature range from 25 to 160 °C in the neat liquid, and the slow but reversible deposition of a red solid on standing, point to an equilibrium process which is describable as a ring opening (8).

$$(AsCH_3)_5 \overset{\text{rapid}}{\rightleftharpoons} (AsCH_3)_n \overset{\text{slow}}{\rightleftharpoons} (AsCH_3)_x$$

A	B	C
ring, yellow oil, stable > 100 °C	open chain, (yellow?)	polymer, red-brown solid, stable < 100 °C

Burns and Waser (8) find a direct solid–solid transformation A → C which is rapid (time scale of hours) at 4 °C. We infer the presence of the intermediate B from the constancy of the pattern of the weak lines, and from the fact that these lines appear in the spectrum of a freshly distilled sample showing no trace of red solid. Vapor density measurements of Waser and Schomaker (1) at high temperatures and low pressures give evidence for a range of association from 5 to 3.

Our mass spectral date is relevant here, but unfortunately inconclusive. We find no evidence in the splitting pattern of arsenomethane in the vapor for any polymeric ions larger than $[As_6(CH_3)_5]^+$, but this may merely reflect the very low vapor pressure of the parent polymers. Ionic species with 4 or 5 As atoms do not make a significant contribution to the mass spectrum, which consists predominantly of fragments with 1, 2, or 3 As atoms. But the existence of a strong peak corresponding to the vapor ion $(AsCH_3)_3^+$ cannot *per se* be taken to imply the existence of the simple trimer in the bulk liquid.

If B results from a simple ring opening of A, then it must be either a biradical or a zwitterion. The ^1H resonance of a biradical would probably not be detectable because of severe intramolecular $I{\cdot}S$ interaction, and moreover, the solvent $(AsCH_3)_5$ peaks would be broadened by a similar intermolecular interaction. Both these inferences are contrary to our observations. Thus the interesting possibility exists that B is a zwitterion on an open chain of As atoms. This state of affairs is then consistent with the previous observation (1) that the overall transformation A → C in the liquid is catalyzed by solid C and is surface dependent and with our observation of tenacious sticking to a v.p.c. column. The n.m.r. spectrum of the high field lines assigned to species B shows that B is not simple. In particular it cannot be just a single simple chain with 1 methyl group per arsenic atom. We are unable to rationalize that part of the B spectrum which is visible, or even to decide whether the spectrum represents a distribution of chain lengths or a single entity of complex structure.

On heating above 155 °C, the weak bands assigned to species B broaden and finally merge at 192 °C with the strong resonance triplet due to ring compound A. This is presumably due to the fast intermolecular equilibrium A ⇄ B. As far as we can tell, this is not a catalyzed process, since the line widths of B and the coalescence temperature are both independent of the purity and history of the sample.

In spite of this intermolecular equilibrium, we nevertheless believe that the line shapes observed for the strong A triplet over the temperature range 170–190 °C are governed primarily by another, purely intramolecular process analogous to that observed in $(PCF_3)_5$, i.e. pseudo-rotation of the ring puckering. Possibly the two processes are fundamentally linked in this As ring; when the five-membered ring gains enough flexibility to surmount the barrier to pseudo-rotation by thermal excitation of the ring torsional modes, there is almost enough torsional energy to tear apart the weak As—As bonds. Put another way, very few pseudo-rotations take place in a given molecule before bond scission occurs. The evidence that the visible collapse of the A triplet is due to an intramolecular rather than an intermolecular process follows.

(1) Line Widths

For intermolecular exchange between predominant species A, equilibrium fractional population p_A, and low abundance species B, of population p_B, the site lifetimes τ_A and τ_B, and hence the n.m.r. line widths $\Delta\nu_A$ and $\Delta\nu_B$ below coalescence, are related by

$$[3] \qquad \frac{p_A}{p_B} = \frac{\tau_A}{\tau_B} = \frac{\Delta\nu_B}{\Delta\nu_A}.$$

By peak areas we find this ratio to be about 14:1, whereas at the A triplet coalescence temperature (183 °C) the relevant line width ratio is approximately 2:1. Moreover, above the A triplet coalescence (183 → 192 °C) the line narrows slightly with increasing temperature, but broadens again on further heating to 202 °C. This behavior is indicative of a double exchange process if the mixture remains diamagnetic.

Can. J. Chem. Downloaded from www.nrcresearchpress.com by 210.87.254.42 on 09/05/12
For personal use only.

(2) Electron Diffraction Data

Waser and Schomaker (1) find evidence in the electron diffraction by the vapor at 200 °C that the non-bonded As atoms in the ring change their relative distances by an intramolecular process, accounting for a broad peak in the radial distribution function centered at 3.44 Å. The fast intramolecular butterfly wag motion discussed above cannot change the cross-ring As—As distance, whereas such an observation is consistent with pseudo-rotation.

(3) Nonrandom Memory

The most compelling evidence that the observed process is intramolecular in nature comes from a detailed consideration of the line shapes of the A triplet under the exchange process, as discussed in the next section, which shows that if the process is pseudo-rotation, then the ring puckering advances by a "clickstop" process by only one position around the ring. This built-in memory argues strongly against an intermolecular mechanism which we expect to be random. But a completely specific intermolecular mechanism wherein the ring opens to a chain which recloses to form the ring in the identical configuration would yield an opening out of the distinct chemical shifts in the fast exchange limit. The spectrum is observed to collapse.

3. Mechanism of Pseudo-Rotation in $(AsCH_3)_5$

Unlike most exchange processes, a cyclic intramolecular motion such as pseudo-rotation allows a choice to be made among the various possible mechanisms from a detailed fit of the observed lineshap with those calculated from the different possibilities. We take the A triplet collapse of $(AsCH_3)_5$ to be due to intramolecular pseudo-rotation and assign for example the 2:2:1 pattern of the low temperature spectrum with the protons of the 1, 5-methyl groups at low field, those of the 2, 4-methyl groups to the central peak, and those of the 3-methyl group at the puckering center to the high field line. Two limiting mechanisms were considered: a "clickstop" one where the puckering advances by just one position around the ring, and a "pancake" one where the primary step is a thermal excitation to a flat long-lived transition state from which the puckering drops randomly into any one of the five available sites. With respect to a frequency reference frame rotating at the time-average degenerate Larmor frequency of the central line β (so that $\omega_2 = \omega_4 = 0$), and in the basis of the total proton magnetizations of the methyl substituents, the Anderson–Weiss **A** matrices[5] for the two cases are as follows:

$$[4]\quad \mathbf{A}_{\text{clickstop}} = \begin{bmatrix} i\omega_1 - R_1 - k & k/2 & 0 & 0 & k/2 \\ k/2 & -R_2 - k & k/2 & 0 & 0 \\ 0 & k/2 & i\omega_3 - R_3 - k & k/2 & 0 \\ 0 & 0 & k/2 & -R_4 - k & k/2 \\ k/2 & 0 & 0 & k/2 & i\omega_5 - R_5 - k \end{bmatrix}$$

$$[5]\quad \mathbf{A}_{\text{pancake}} = \begin{bmatrix} i\omega_1 - R_1 - 0.8k & 0.2k & 0.2k & 0.2k & 0.2k \\ 0.2k & -R_2 - 0.8k & 0.2k & 0.2k & 0.2k \\ 0.2k & 0.2k & i\omega_3 - R_3 - 0.8k & 0.2k & 0.2k \\ 0.2k & 0.2k & 0.2k & -R_4 - 0.8k & 0.2k \\ 0.2k & 0.2k & 0.2k & 0.2k & i\omega_5 - R_5 - 0.8k \end{bmatrix}$$

ω_1, ω_3, ω_5 (rad s^{-1}) are the relative chemical shifts from the origin, R_i $(=1/T_{2i})$ are the apparent transverse relaxation rates, including inhomogeneity contribution R^*, and k (s^{-1}) is the first order rate constant for the transfer of magnetization out of a particular site under the exchange process.

These matrices represent ensemble averages for the time dependence of the site magnetizations. Thus a particular molecule will transfer 3-methyl magnetization either to site 2 *or* to site 4 under

[5]For a discussion of the general properties of the **A** matrix, see Abragam (24) or Gutowsky (25).

clickstop pseudo-rotation, but the average magnetization is sprayed equally to both sites by the exchange.

The absorption response $I(\omega)$ of the system to irradiation at an arbitrary frequency ω is then given by

$$[6] \qquad I(\omega) \propto -\mathrm{Re}[\boldsymbol{I}\cdot\mathbf{B}^{-1}\cdot\boldsymbol{M}(\mathrm{O})],$$

where $\mathbf{B} = \mathbf{A} - \omega\mathbf{U}$, $\mathbf{U}$ being the unit matrix; $\boldsymbol{I}$ is the row vector of units; $\boldsymbol{M}(\mathrm{O})$ is a column vector whose components are proportional to the thermal equilibrium values of the site magnetizations. In our basis, $\boldsymbol{M}(\mathrm{O})$ is the column vector of units.

A Fortran IV computer program was written to invert the complex 5×5 $\mathbf{B}$ matrix and plot the scaled function $I(\omega)$ point by point as a function of ω for values of the spectral parameters

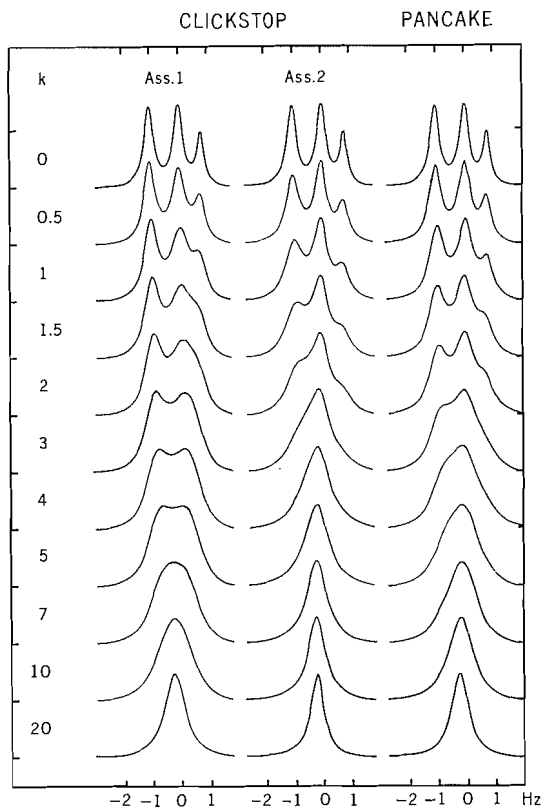

FIG. 3. Comparison of computed spectra for intramolecular exchange between lines α, β, and γ of the $(AsCH_3)_5$ triplet. Assignment 1 is α = 1,5-methyls, β = 2,4, γ = 3 and assignment 2 is α = 2,4, β = 1,5, γ = 3. The random pancake mechanism is independent of assignment. The input parameters are $\omega_\alpha = -2\pi \times 1.05\ s^{-1}$, $\omega_\beta = 0$, $\omega_\gamma = +2\pi \times 0.80\ s^{-1}$, $R_\alpha = R_\beta = 1.32\ s^{-1}$, $R_\gamma = 1.04\ s^{-1}$. (See footnote 6 in text.)

obtained from low temperature (i.e. non-exchanging) spectra[6] and for various values of the exchange parameter k. Eleven minutes of IBM system 360/40 computer time were required to calculate and output nine different k-value spectra each of 120 ω points corresponding to a single assignment and a single exchange mechanism. The computed spectra for the two possible assignments which maintain the mirror plane due to puckering inversion and for the two limiting mechanisms are presented in Fig. 3. We point out that the random mechanism yields a line shape independent of assignment. For the assignment most likely on chemical grounds (line α from 1,5-methyl groups, line β from 2,4-methyl groups) the difference in the computed line shapes for the two mechanisms are not dramatic, owing to the smallness of the chemical shift, but comparison with the observed spectra in Fig. 1 nevertheless favors the clickstop or nonrandom mechanism, mainly with respect to the rapid merging of the high field line γ with the central line β, and the development of a rather well-defined doublet. The absence of this doublet for the second assignment (line α from methyl groups 2,4 and β from 1, 5) in either mechanism argues against this unlikely possibility.

Owing to the very limited temperature range over which the spectrum broadens and collapses, no serious attempt was made to obtain experimental k's versus temperature, and thus the enthalpy of activation. However, the clickstop mechanism yields $k = 7.0\ s^{-1}$ at 456 °K from the observed spectra. Assuming then that the intramolecular pseudo-rotation proceeds by thermal activation through a transition state atop the potential barrier, the Eyring rate equation

$$[7] \qquad k = \kappa \frac{KT}{h} \exp\left(-\Delta G^{\ddagger}/RT\right)$$

[6]In practice, a satisfactory fit could not be acheived by this procedure, since the experimental line shapes of the individual members of the triplet are apparently not the Lorentzians implied by the use of the phenomenological R's in eqs. [4] and [5]. The observed line shapes are squarer than Lorentzian, and we suppose this to be due to unresolved $J_{H-C-As-As-C-H}$ coupling, although such an effect could conceivably arise from As—H coupling if such coupling were small and not in the limit of rapid ^{75}As-quadrupolar collapse. We thus attempted to fit the reference low temperature spectrum by a sum of Lorentzians to achieve a *resolution* in the computed spectrum comparable to that observed. Empirically we find that $R_{\text{theoretical}} \approx \frac{2}{3}R_{\text{exptl}}$, as obtained from the half line width.

Can. J. Chem. Downloaded from www.nrcresearchpress.com by 210.87.254.42 on 09/05/12
For personal use only.

(where k is the rate constant for the process, K is the Boltzmann constant, κ is the transmission coefficient, assumed unity, and the other symbols have their usual meaning) yields $\Delta G^{\ddagger} = 25.3$ kcal mole^{-1} for clickstop pseudo-rotation in $(AsCH_3)_5$. This compares with an estimated value (5) of 23.5 kcal mole^{-1} for the similar process in $(PCF_3)_5$. It is not possible to say from the present data whether the process occurs in $(AsCF_3)_5$. If it does, then $\Delta G^{\ddagger}$ is certainly greater than 21.5 kcal mole^{-1}.

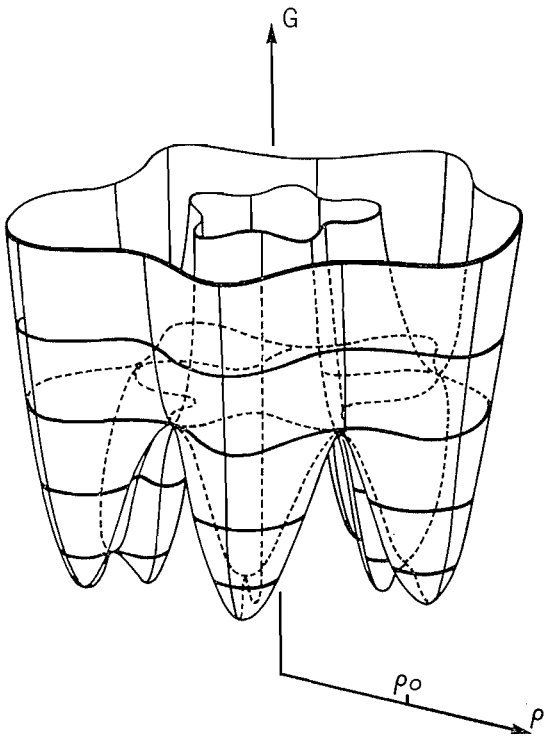

FIG. 4. Schematic diagram of free energy surface for internal ring modes in $(AsCH_3)_5$ and $(PCF_3)_5$. The phase angle of the ring puckering is taken as the cylindrical polar angle coordinate, and the surface is symmetric in the puckering coordinate ρ about ρ_0 where the ring is planar. Free pseudo-rotation can only occur above the saddle points in the annulus, here about 25 kcal above the minima.

We may wonder at the magnitude of this barrier to ring rippling in these five-membered rings. Indeed, the values we find for this group of compounds are comparable to the barriers to hindered rotation about partial double bonds (24 kcal mole^{-1} for N,N-dimethylnitrosamine, 21 kcal mole^{-1} for N,N-dimethylformamide). The similarity in the values may be more than accidental, in that the pseudo-rotation takes place through a torsional mode of the ring which involves a rotation about several of the As—As bonds in $(AsCH_3)_5$. Thus the barriers we measure are understandable qualitatively in terms of d_π bonding between some of the ring atoms, but the detailed problem of the existence of delocalized π bonds in a puckered ring is a much more complex matter. The average As—As bond distance in $(AsCH_3)_5$ from the X-ray data of the solid (8) is 2.428 Å, close to twice the covalent radius (2.42 Å) assigned to As by Pauling (26). This would appear to rule out a bond order of more than unity, but may simply imply the existence of multiple bonding in the model compounds (gaseous As_4 and crystalline arsenic) chosen to evaluate the radius.

Figure 4 is a sketch, not to scale, of the free energy surface for the two internal ring modes of puckering inversion of the C_S form and pseudo-rotation in $(AsCH_3)_5$ and $(PCF_3)_5$ and possibly also in $(AsCF_3)_5$.

Conclusion

The puckered five-membered rings of $(AsCH_3)_5$ and $(AsCF_3)_5$ have an effective plane of symmetry in the liquid phase below 160 °C on a time scale of the order of 10^{-2} s. This symmetry is attributed to a concerted butterfly wag of the ring puckering through the ring plane and simultaneous inversion at the puckering atom. Apparently the As atom inverts through a planar transition state rather than by quantum-mechanical tunneling. The collapse of the proton resonance spectrum of $(AsCH_3)_5$ above 170 °C is ascribed to intramolecular pseudo-rotation of the ring puckering with a $\Delta G^{\ddagger}$ of 25.3 kcal mole^{-1} and at still higher temperatures to an intermolecular equilibrium caused by ring opening. The mechanism of the pseudo-rotation seems to be a clickstop jump of the ring puckering from one position to the next rather than a random process.

Acknowledgments

We wish to thank H. P. K. Lee for the original preparation of arsenomethane. We are grateful to Professor B. O. West for communicating his own results on the proton spectrum of $(AsCH_3)_5$ in advance of publication. Dr. T. N. Bell kindly obtained the mass spectrum of $(AsCH_3)_5$. The

Can. J. Chem. Downloaded from www.nrcresearchpress.com by 210.87.254.42 on 09/05/12
For personal use only.

National Research Council of Canada provided financial assistance which is gratefully acknowledged.

1. J. WASER and V. SCHOMAKER. J. Am. Chem. Soc. **67**, 2014 (1945).
2. (*a*) J. E KILPARTRICK, K. S. PITZER, and R. SPITZER. J. Am. Chem. Soc. **69**, 2483 (1947); **80**, 6697 (1958). (*b*) K. S. PITZER and W. E. DONATH. J. Am. Chem. Soc. **81**, 3213 (1959). (*c*) J. B. HENDRICKSON. J. Am. Chem. Soc. **83**, 4537 (1967).
3. W. J. LAFFERTY, D. W. ROBINSON, R. V. ST. LOUIS, J. W. RUSSELL, and H. L. STRAUSS. J. Chem. Phys. **42**, 2915 (1965).
4. T. UEDA and T. SHIMANOUCHI. J. Chem. Phys. **47**, 4042 (1967).
5. E. J. WELLS, H. P. K. LEE, and L. K. PETERSON. Chem. Commun. 894 (1967).
6. J. DONOHUE. Acta Cryst. **15**, 708 (1962).
7. C. J. SPENCER and W. N. LIPSCOMB. Acta Cryst. **14**, 250 (1961); **15**, 509 (1962).
8. J. H. BURNS and J. WASER. J. Am. Chem. Soc. **79**, 859 (1957).
9. C. S. PALMER and A. B. SCOTT. J. Am. Chem. Soc. **50**, 536 (1928).
10. A. H. COWLEY, A. B. BURG, and W. R. CULLEN. J. Am. Chem. Soc. **88**, 3178 (1966).
11. R. C. DOBBIE and R. G. CAVELL. Inorg. Chem. **6**, 1450 (1967).
12. C. H. TOWNES and A. L. SCHAWLOW. Microwave spectroscopy. McGraw-Hill Book Co., Inc., New York. 1955. p. 300.
13. G. HERZBERG. Infrared and raman spectra. D. Van Nostrand Co., Inc., Princeton. 1945, pp. 220, 294.
14. D. M. DENNISON and G. E. UHLENBECK. Phys. Rev **41**, 313 (1932)
15. A. MESSIAH. Quantum mechanics. Vol. I. John Wiley and Sons, Inc., New York. 1961. p. 231.
16. C. C. COSTAIN and G. B. B. M. SUTHERLAND. J. Phys. Chem. **56**, 321 (1952).
17. R. S. BERRY. J. Chem. Phys. **32**, 933 (1960).
18. J. F. KINCAID and F. C. HENRIQUES. J. Am. Chem. Soc. **62**, 1474 (1940).
19. A. T. BOTTINI and J. D. ROBERTS. J. Am. Chem. Soc. **80**, 5203 (1958).
20. L. W. REEVES and E. J. WELLS. Discussions Faraday Soc. **34**, 177 (1962).
21. S. I. CHAN, T. R. BORGERS, J. W. RUSSELL, H. L. STRAUSS, and W. D. GWINN. J. Chem. Phys. **44**, 1103 (1966).
22. D. O. HARRIS, H. W. HARRINGTON, A. C. LUNTZ, and W. D. GWINN. J. Chem. Phys. **44**, 3467 (1966).
23. W. MAHLER and A. B. BURG. J. Am. Chem. Soc. **80**, 6161 (1958).
24. A. ABRAGAM. Principles of nuclear magnetism. Oxford University Press, London. 1961. pp. 447–451, 504.
25. H. S. GUTOWSKY, R. L. VOLD, and E. J. WELLS. J. Chem. Phys. **43**, 4107 (1965).
26. L. PAULING. The nature of the chemical bond. Cornell Univ. Press, Ithaca, New York. 1948. p. 165.

Can. J. Chem. Downloaded from www.nrcresearchpress.com by 210.87.254.42 on 09/05/12
For personal use only.

Can. J. Chem. Downloaded from www.nrcresearchpress.com by 210.87.254.105 on 09/05/12
For personal use only.

The electrochemistry and the kinetics of the formation of ruthenium(II) nitrogen complexes

I. J. Itzkovitch and John A. Page
Lash Miller Chemical Laboratories, University of Toronto, Toronto 5, Ontario

Received March 5, 1968

Electrolysis at a mercury cathode controlled at −0.50 V (vs. standard calomel electrode s.c.e.) in a H_2SO_4–K_2SO_4 electrolyte with pH of 2.6 and saturated with Ar gas has been used to prepare $Ru^{II}(NH_3)_5X$. The reaction of this species with N_2 in the aqueous base electrolyte at 26 °C has been studied and found to follow the equations:

$$Ru^{II}(NH_3)_5X + N_2 \xrightarrow{k_m} Ru(NH_3)_5N_2^{2+}$$

$$Ru^{II}(NH_3)_5X + Ru(NH_3)_5N_2^{2+} \xrightarrow{k_d} (Ru(NH_3)_5)_2N_2^{4+}.$$

In base electrolyte saturated with N_2 at 1 atm ($C_{N_2} \approx 6 \times 10^{-4}$ *M*) the value of the apparent first order constant, k'_m is 4.4×10^{-5} s^{-1} and the value of k_d is 4.2×10^{-2} l $mole^{-1}$ s^{-1}.

The electrochemistry of the various ruthenium species was also investigated in the H_2SO_4–K_2SO_4 electrolyte. At the dropping mercury electrode, $Ru^{III}(NH_3)_5Cl$ gave a well-defined one electron reduction wave with $E_{1/2} = -0.27$ V; $Ru^{II}(NH_3)_5X$ gave a well-defined one electron oxidation wave with $E_{1/2} = -0.25$ V. The nitrogen complexes gave oxidation waves at a rotating platinum microelectrode, the monomer with $E_{1/2} = +0.72$ V and the dimer with $E_{1/2} = +0.78$ V.

Canadian Journal of Chemistry, **46**, 2743 (1968)

Introduction

The spontaneous reaction of N_2 with $Ru^{II}(NH_3)_5X$ in aqueous solution has been reported by Harrison and Taube (1) and by these authors with Weissberger (2). The products were the mononuclear $Ru(NH_3)_5N_2^{2+}$ first isolated by Allen and Senoff (3), and a binuclear $(Ru(NH_3)_5)_2N_2^{4+}$ that was characterized by Job's method, elementary analysis, and infrared spectra.

In this previous work the $Ru^{II}(NH_3)_5X$ was prepared from the Ru^{III} complex by the reducing action of excess Zn in an H_2SO_4 electrolyte. In this paper, starting with $Ru^{II}(NH_3)_5X$ prepared by controlled potential electrolysis, we report on the electrochemistry and on the kinetics of the formation of both the mono- and bi-nuclear nitrogen complexes.

Experimental

Pure $Ru(NH_3)_5Cl.Cl_2$ was first prepared and pure $Ru(NH_3)_5N_2.Cl_2$ was prepared from this material using sodium azide according to the procedures of Allen *et al.* (4). The purity of the products was established by infrared spectra, by the coulometric results on the reduction of dissolved $Ru(NH_3)_5Cl.Cl_2$, and by agreement of the extinction coefficient for the dissolved $Ru(NH_3)_5N_2.Cl_2$ with published values.

The studies were carried out in a base electrolyte 0.099 *M* in K_2SO_4 and 0.01 *M* in H_2SO_4; the measured pH of the electrolyte was 2.6 at 25 °C. Oxygen was removed and excluded from the electrolyte with either nitrogen (N_2) or argon (Ar) gases. The nitrogen gas (Linde, less than 10 p.p.m. oxygen) was purified by passage over hot (500 °C) copper turnings; the argon gas (Matheson, high purity) was used directly. The gases were then saturated with water vapor before use.

Polarograms were recorded on a Sargent model XV instrument using a conventional H-cell with a saturated calomel reference electrode and either a dropping mercury or a rotating platinum microelectrode. The solutions for polarography were maintained at 25.0 °C; the mercury electrode had a flow rate, *m*, equal to 1.514 mg Hg s^{-1}. The electrolyses were carried out in a H-type double diaphragm cell using the control apparatus and current integrator as previously described (5). The working electrode was a mercury pool (56 cm^2) and the volume of the solution electrolyzed was always 180 ml. A Metrohm EA402A saturated calomel electrode was used as reference. All potentials (*V*) reported are in volts relative to a saturated potassium chloride calomel electrode.

The kinetic studies were carried out in the electrolysis cell; the temperature was maintained at 26±1 °C in these runs. Spectra were recorded on a Bausch and Lomb Spectronic 505 using a flow system connected to the electrolysis cell and matched 0.1 cm and 1.0 cm quartz cells. The flow system was essentially glass but utilized a peristaltic pump with neoprene tubing. The extinction coefficients used are given in Table I.

TABLE I

Extinction coefficients: K_2SO_4–H_2SO_4 electrolyte

	222 mμ	262 mμ
$Ru^{II}(NH_3)_5X$*	0.068×10^4	0.055×10^4
$Ru^{II}(NH_3)_5N_2$†	1.64×10^4	0.084×10^4
$(Ru^{II}(NH_3)_5)_2N_2$‡	0.30×10^4	4.8×10^4

*Controlled potential reduction of $Ru(NH_3)_5Cl.Cl_2$.
†Pure $Ru(NH_3)_5N_2.Cl_2$.
‡Pure $(Ru(NH_3)_5)_2N_2.(BF_4)_4$ synthesized by Frank Botteley.

TABLE II

Electrochemical behavior: K_2SO_4–H_2SO_4 electrolyte

	$E_{1/2}$	i_d
$Ru^{III}(NH_3)_5Cl$ $2.72\times10^{-3}M$	−0.27 V (t=4.94 s)	+9.95 μA at −0.50 V (t=4.94 s)
$Ru^{II}(NH_3)_5X$ $2.33\times10^{-3}M$	−0.25 V (t=4.91 s)	−4.67 μA at −0.05 V (t=4.80 s)
$Ru^{II}(NH_3)_5N_2$	+0.72 V r.p.e.*	Anodic wave
$(Ru^{II}(NH_3)_5)_2N_2$	+0.78 V r.p.e.*	Anodic wave

*r.p.e. = rotating platinum electrode.

Electrochemistry

Typical electrochemical behavior of the ruthenium species is summarized in Table II.

The $Ru(NH_3)_5Cl.Cl_2$ in the base electrolyte was found to give a well-defined reduction wave at the dropping mercury electrode (d.m.e.) in the presence of 0.004% Triton X-100 as a maximum suppressor. For the system in Table II, a plot of log $i/(i_d - i)$ against $E_{d.m.e.}$ was linear with a slope of 1/(65 mV) indicating some degree of irreversibility. The polarographic behavior was independent of whether Ar or N_2 gas was used to displace dissolved oxygen from the electrolyte.

Controlled potential mercury cathode electrolysis of solutions of $Ru(NH_3)_5Cl.Cl_2$ in the base electrolyte (Ar gas) were found to proceed smoothly at −0.50 V to a negligible residual current. Plots of log i against time were linear indicating a diffusion-controlled process; the slope was $-1/(2.5\times10^3$ s), corresponding to a half-life of 750 s.

The electrolyses proceeded smoothly to a negligible residual current (<100 μA), and the quantity of electricity when corrected for background effects always corresponded closely to a 1 faraday per mole reduction ($n = 1.02\pm0.02$ on 3 reductions). Spectra were recorded at intervals during these electrolyses; it was observed that concurrent with the formation of the first appreciable amount of $Ru^{II}(NH_3)_5X$, the spectrum showed a rapid shift in the wavelength of maximum absorption from 326 to 310 mμ. The new spectrum was characteristic of that of $Ru(NH_3)_5(HSO_4)^{2+}$ (6) and indicates a ruthenium(II)-catalyzed substitution in the ruthenium(III) complex; as the electrolysis proceeded from this point an isobestic point was obtained at 268 mμ suggesting a clean reduction to a single $Ru^{II}(NH_3)_5X$ species. Polarography of the reduced solutions (Ar gas) gave a well-defined oxidation wave at the dropping mercury electrode in the presence of 0.004% Triton X-100. For the system in Table II, a plot of log $(i_d - i)/i$ against $E_{d.m.e.}$ was linear with a slope of 1/(74 mV).

The polarography of the nitrogen complexes was also investigated using solutions of $Ru^{II}(NH_3)_5N_2$ and $(Ru^{II}(NH_3)_5)_2N_2$ obtained in the kinetic runs subsequently described. Both of these species were found to give oxidation waves at a rotating platinum microelectrode (Ar gas). The species were difficult to oxidize; the half-wave potential of the monomer was 1.0 V positive to that of the $Ru^{II}(NH_3)_5X$, and the dimer was even more difficult to oxidize.

Kinetics

The formation of the nitrogen complexes was considered to take place according to the equations

$$[1] \qquad A + N_2 \overset{k_m}{\rightarrow} M$$

$$[2] \qquad A + M \overset{k_d}{\rightarrow} D$$

$$[3] \qquad \frac{dC_D}{dt} = k_d \cdot C_A \cdot C_M$$

$$\frac{dC_M}{dt} = k_m \cdot C_A \cdot C_{N_2} - k_d \cdot C_A \cdot C_M,$$

so that for a solution saturated with nitrogen gas at 1 atm:

$$[4] \qquad \frac{dC_M}{dt} = k'_m \cdot C_A - k_d \cdot C_A \cdot C_M.$$

Here A is $Ru^{II}(NH_3)_5X$, M is the monomer $Ru^{II}(NH_3)_5N_2$, and D is the dimer $(Ru^{II}(NH_3)_5)_2N_2$.

Can. J. Chem. Downloaded from www.nrcresearchpress.com by 210.87.254.105 on 09/05/12
For personal use only.

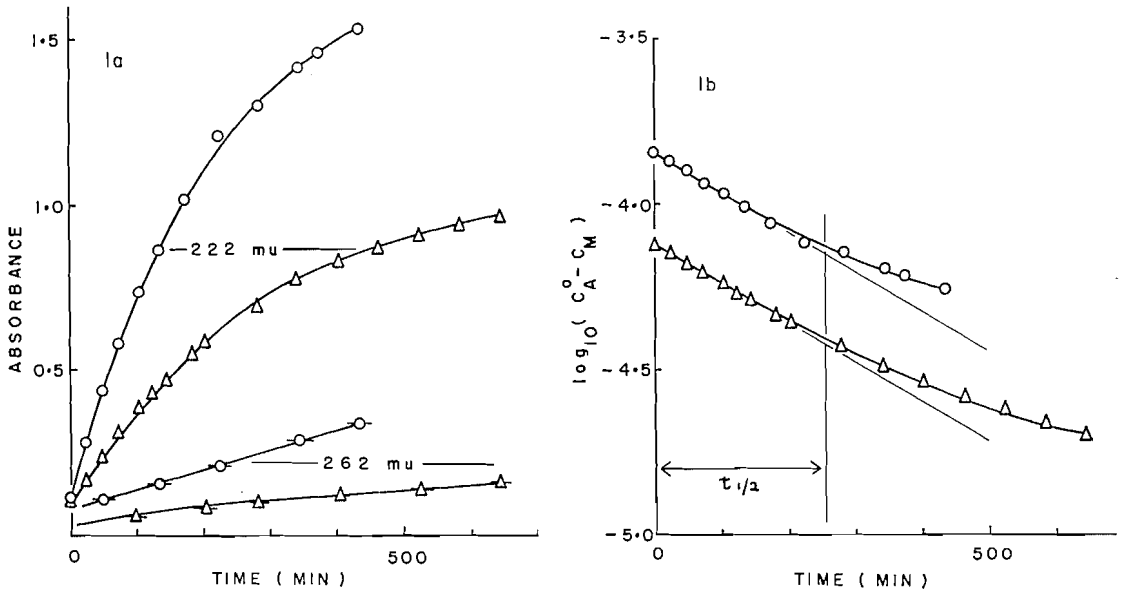

FIG. 1*a*. Formation of $Ru(NH_3)_5N_2^{2+}$: (○) $C^0_A = 1.45 \times 10^{-4}$ *M*; (△) $C^0_A = 0.75 \times 10^{-4}$ *M*; $l = 1.0$ cm.
FIG. 1*b*. Rate of formation of $Ru(NH_3)_5N_2^{2+}$, *C* in moles l^{-1}.

In each case, the solutions of known initial concentration, C^0_A, were prepared by controlled potential electrolysis (−0.50 V) of weighed amounts of $Ru(NH_3)_5Cl.Cl_2$ dissolved in the known volume of the base electrolyte (Ar gas). The electrolysis was continued till a negligible residual current was obtained (< 100 μA). The nitrogen reactions were then initiated either by switching the gas stream from Ar to N_2 (I, II) or by adding a weighed amount of $Ru(NH_3)_5N_2.Cl_2$ (III). All these reactions were carried out in the electrolysis cell and the electrodes were not removed nor the circuit interrupted. Thus the mercury cathode (−0.50 V) was always in contact with the ruthenium solution, but in every case the residual current remained negligible (and cathodic) throughout. Three types of kinetic runs were carried out:

I. Runs at relatively low initial concentrations of A to evaluate k'_m (Fig. 1*a*). The concentration of M was simply calculated from the absorbance at 222 mμ and plots of log $(C^0_A - C_M)$ against time gave a value of 4.4×10^{-5} s^{-1} for k'_m (Fig. 1*b*), corresponding to a half-life of 255 min in the N_2 saturated solution.

The plots show positive deviations at long times from the expected linear relation; this is due to the formation of significant amounts of D.

II. Runs at relatively high initial concentrations of A to evaluate $k = k_d/k'_m$ (Fig. 2*a*). Combination of eqs. [3] and [4] yields

$$\frac{kC_M}{1 - kC_M}\,dC_M = dC_D$$

and integration gives

$$-C_M - \frac{1}{k}\ln(1 - kC_M) = C_D,$$

so that C_D is a function of C_M, independent of C^0_A and time of reaction. In these runs, the concentrations of M and D at different times were calculated from the simultaneous relations:

$$A^{222} = \varepsilon_M{}^{222} \cdot l \cdot C_M + \varepsilon_D{}^{222} \cdot l \cdot C_D$$
$$A^{262} = \varepsilon_M{}^{262} \cdot l \cdot C_M + \varepsilon_M{}^{262} \cdot l \cdot C_M.$$

Kinetic runs were carried out at three different initial concentrations of A, and curves calculated for three different values of *k* are superimposed on the experimentally found concentration ratios (Fig. 2*b*). A value of *k* equal to 1.0×10^3 l $mole^{-1}$ gives a good fit to the experimental ratios.

III. One run was carried out to evaluate k_d directly (Fig. 3*a*). Reaction [2] was studied in the absence of reaction [1] in a solution saturated with Ar gas and with C^0_A equal to C^0_D. The

Can. J. Chem. Downloaded from www.nrcresearchpress.com by 210.87.254.105 on 09/05/12
For personal use only.

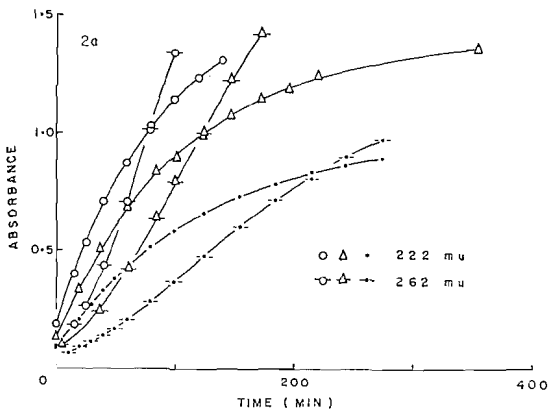

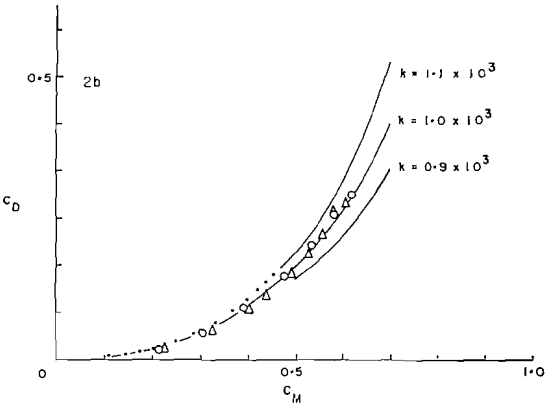

FIG. 2*a*. Formation of $Ru(NH_3)_5N_2^{2+}$ and $(Ru(NH_3)_5)_2N_2^{4+}$: (○) $C^0_A = 2.90 \times 10^{-3}$ *M*; (△) $C^0_A = 1.95 \times 10^{-3}$ *M*; (●) $C^0_A = 1.33 \times 10^{-3}$ *M*; $l = 0.1$ cm.
FIG. 2*b*. Fit of experimental results to assigned k ($k = k_d/k'_m$), C in moles $l^{-1} \times 10^3$.

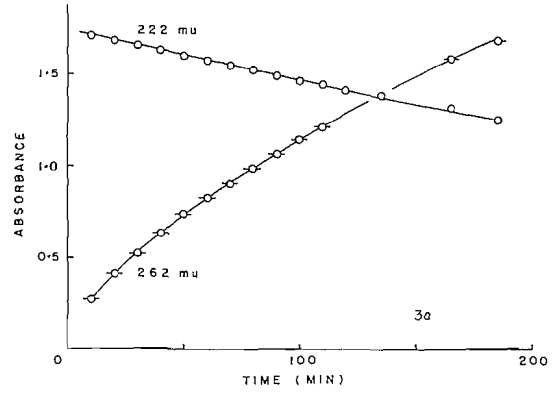

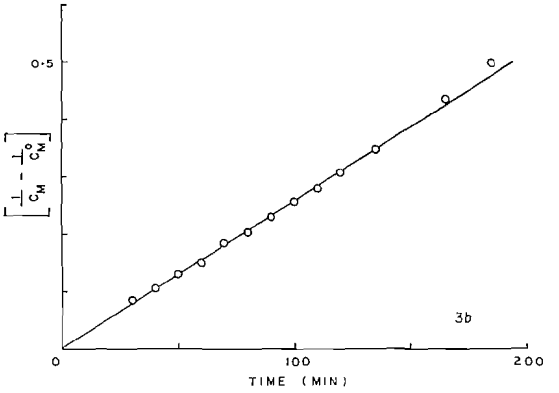

FIG. 3*a*. Decomposition of $Ru(NH_3)_5N_2^{2+}$: $C^0_A = C^0_M = 1.04 \times 10^{-3}$ *M*; $l = 0.1$ cm.
FIG. 3*b*. Rate of formation of $(Ru(NH_3)_5)_2N_2^{4+}$, C in moles $l^{-1} \times 10^3$.

concentrations of M and D were determined as in II. A plot of

$$\left[\frac{1}{C_M} - \frac{1}{C^0_M}\right]$$

against time gave a value of 4.2×10^{-2} l mole^{-1} s^{-1} for k_d (Fig. 3*b*).

The ratio of k_d/k'_m calculated from the kinetic runs in I and III is 9.5×10^2; this is in good agreement with the results of II.

Discussion

The solubility of N_2 in water at 25 °C is given as 6.2×10^{-4} *M* (7). A second order rate constant for the reaction of $Ru^{II}(NH_3)_5X$ with N_2 can be calculated from this value ($k_m = 7.1 \times 10^{-2}$ l mole^{-1} s^{-1}) and is not much different from the rate constant obtained for the reaction of $Ru^{II}(NH_3)_5X$ with $Ru(NH_3)_5N_2^{2+}$ ($k_d = 4.2 \times 10^{-2}$ l mole^{-1} s^{-1}); thus coordinated N_2 is about as reactive as dissolved N_2.

It was also noted that the reactions that produce the nitrogen complexes proceed to a position of equilibrium. The reactions can be reversed by passing Ar gas through a solution of the complexes but it was observed that the rate of decomposition was very slow compared with the rate of formation. Attempts were made to evaluate the magnitude of the equilibrium constants, but these were unsuccessful because the analytical data was not exact enough to calculate the small equilibrium concentration of $Ru^{II}(NH_3)_5X$ by difference.

Can. J. Chem. Downloaded from www.nrcresearchpress.com by 210.87.254.105 on 09/05/12
For personal use only.

The remarkable stability of the nitrogen complexes to oxidation is indicated by the very positive half-wave potentials observed; presumably this stability is associated with π bonding between the ruthenium(II) and the nitrogen ligand (4, 8).

Acknowledgments

We are indebted to Mr. Frank Bottomley for his valuable assistance and advice. We also wish to thank the National Research Council of Canada and the Province of Ontario for their financial assistance.

1. D. E. HARRISON and H. TAUBE. J. Am. Chem. Soc. **89**, 5706 (1967).
2. D. E. HARRISON, E. WEISSBERGER, and H. TAUBE. Science, **159**, 320 (1968).
3. A. D. ALLEN and C. V. SENOFF. Chem. Commun. 621 (1965).
4. A. D. ALLEN, F. BOTTOMLEY, R. O. HARRIS, V. P. REINSALU, and C. V. SENOFF. J. Am. Chem. Soc. **89**, 5595 (1967).
5. J. A. PAGE and E. J. ZINSER. Talanta, **12**, 1051 (1965).
6. R. O. HARRIS. Ph.D. Thesis, University of Toronto, Toronto, Ont. 1963.
7. H. STEPHEN and T. STEPHEN. (*Editors*). Solubilities of inorganic and organic compounds. Vol. I. The Pergamon Press, Ltd., New York. 1963. Part 1, p. 85.
8. J. CHATT. New Scientist, **15**, 350 (1968).

Can. J. Chem. Downloaded from www.nrcresearchpress.com by 210.87.254.105 on 09/05/12
For personal use only.

Can. J. Chem. Downloaded from www.nrcresearchpress.com by 210.87.254.105 on 09/05/12
For personal use only.

Electron spin resonance study of γ-irradiated tetraethylammonium iodide

L. FABES[1] AND J. K. S. WAN
Department of Chemistry, Queen's University, Kingston, Ontario

Received March 21, 1968

γ-Irradiation of polycrystalline tetraethylammonium iodide at 77 °K leads to the breaking of a C—C bond and the primary radicals $\dot{C}H_3$ and $(C_2H_5)_3\overset{+}{N}\dot{C}H_2$ were detected by electron spin resonance. The methyl radicals were found to disappear readily at 120 °K. In the range of 263–273 °K a secondary reaction between $(C_2H_5)_3\overset{+}{N}\dot{C}H_2$ and the parent ion $(C_2H_5)_4\overset{+}{N}$ was observed; the resulting secondary radical $(C_2H_5)_3\overset{+}{N}\dot{C}HCH_3$ was found to be stable up to 373 °K.

Canadian Journal of Chemistry, 46, 2749 (1968)

Introduction

It has recently been shown that radical $\dot{N}H_3^+$ trapped at low temperature in γ-irradiated NH_4PF_6 can undergo secondary reaction forming $\dot{N}_2H_4^+$ when warmed up to higher temperatures (1). Similarly, $(CH_3)_3\dot{N}^+$ trapped in irradiated $(CH_3)_4NPF_6$ produces $\dot{N}_2(CH_3)_2^+$ (2). In a detailed study of irradiated tetramethylammonium halides, Tench (3, 4) found that $\dot{C}H_3$, $(CH_3)_3\overset{+}{N}\dot{C}H_2$, and $(CH_3)_3\dot{N}^+$ were formed at 77 °K, the last radical being stable up to 100 °C. The formation of $(CH_3)_3\overset{+}{N}\dot{C}H_2$ was, however, attributed to secondary reactions involving positive holes (Cl or Br atoms) with the parent tetramethylammonium ions. Thus, the primary effect of the γ-radiation on the parent cation appears to be the breaking of an N—C bond. In another brief report, Burrell (5) showed that γ-irradiation of powdered tetrabutylammonium halides produces $(C_4H_9)_3\overset{+}{N}CH_2CH_2\dot{C}HCH_3$ and suggested the C—H split. However, since Burrell's results were based on room temperature electron spin resonance (e.s.r.) observations only, it is not certain whether the reported radical is formed at low temperature.

The present investigation on tetraalkylammonium halides was undertaken to establish the primary radiolytic processes and the reactivity of the radicals in the solid lattice at various temperatures. The results obtained with tetraethylammonium iodide will be reported here.

[1]Holder of an Ontario Graduate Fellowship 1967–68.

Results and Discussion

The white powdered tetraethylammonium iodide turned green upon irradiation at 77 °K. The color changed to yellow when the sample was warmed up to room temperature. This presumably is due to formation of I_2. It has now been established that γ-irradiation of solid ammonium halides leads to formation of V_k centers which are trapped and detected at low temperatures (6). Although the expected V_k center, I_2^-, was not observed in the present study using only polycrystalline samples, its presence cannot be excluded. Similarly, the absence of e.s.r. signals from I atoms may be due to matrix interaction, which broadens the signals beyond detection.

The e.s.r. spectrum of $(C_2H_5)_4NI$ irradiated and observed at 77 °K is shown in Fig. 1A. When the sample was warmed for a short period in the range of 77 to 120 °K, the spectrum changed to that as shown in Fig. 2A. Thus, it is assumed that the spectrum in Fig. 1A consists of more than one type of radicals. In attempting to identify the species responsible for such spectrum, several possible processes at 77 °K were considered:

[1] $(C_2H_5)_4N^+ \rightsquigarrow (C_2H_5)_3\dot{N}^+ + \dot{C}_2H_5$

[2] $\rightsquigarrow (C_2H_5)_3\overset{+}{N}\dot{C}HCH_3 + H$

[3] $\rightsquigarrow (C_2H_5)_3\overset{+}{N}\dot{C}H_2 + \dot{C}H_3$

Reaction [1] involving an N—C split is analogous to that of the tetramethylammonium halides (3, 4). Reaction [2] with a C—H bond split would be similar to the process suggested by Burrell (5). Reaction [3], however, has not been postulated.

Can. J. Chem. Downloaded from www.nrcresearchpress.com by 210.87.254.105 on 09/05/12
For personal use only.

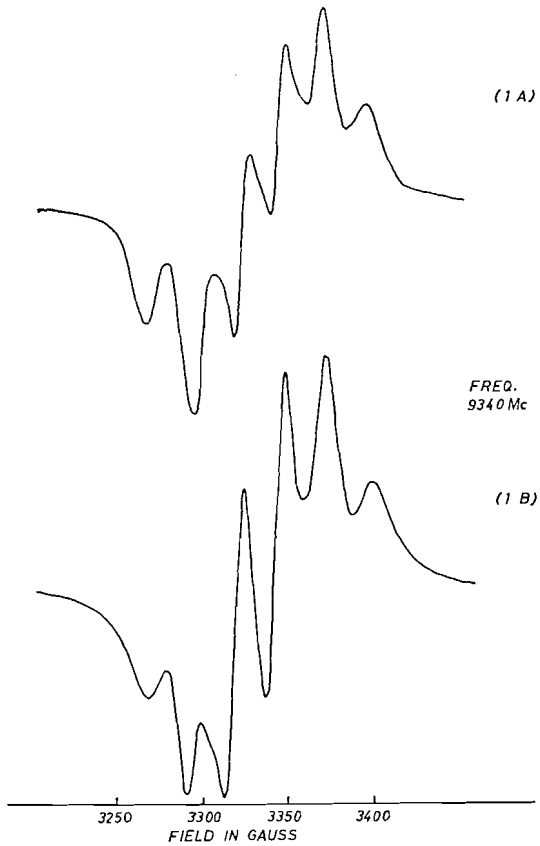

FIG. 1. The e.s.r. spectra at 77 °K of Et_4NI irradiated at 77 °K: (A) experimental spectrum, (B) calculated spectrum based on a 3 to 1 mixture of $(C_2H_5)_3\dot{N}\dot{C}H_2$ and $\dot{C}H_3$.

Since the experimental spectrum in Fig. 1A consists of an even number of lines, the presence of $(C_2H_5)_3\dot{N}^+$ is considered unlikely. While spectral parameters for $\dot{C}H_3$ are readily available (7), hyperfine splitting constants for the other nitrogen-containing radicals were taken from analysis of the experimental spectra and were used in computation of theoretical spectra. Their values are listed in Table I. Figure 1B gives the calculated spectrum of a 3 to 1 mixture of $(C_2H_5)_3\dot{N}\dot{C}H_2$ and $\dot{C}H_3$; Fig. 2B is the calculated spectrum of the single species $(C_2H_5)_3\dot{N}\dot{C}H_2$; Fig. 3B represents the theoretical spectrum of $(C_2H_5)_3\dot{N}\dot{C}HCH_3$.

By comparing Fig. 1A with 1B, it is concluded that the major process at 77 °K is reaction [3] involving a C—C bond split. This agrees with the mass spectrometric studies of amines which show the fission of the α,β C—C bond as the major process upon electron impact (8). Further confirmation of this process was provided by similar low temperature e.s.r. studies of irradiated tetra-*n*-propylammonium and tetra-*n*-butylammonium iodides (9). Thus, it must be concluded that the role of hyperconjugation, as suggested by Burrell (5), plays a very minor part in the primary radiolytic process.

When the irradiated sample was warmed to 120 °K, the spectrum rapidly changed to that shown in Fig. 2A. This change is due to disappearance of $\dot{C}H_3$, leaving behind the radicals $(C_2H_5)_3\dot{N}\dot{C}H_2$, which are stable to 120 °K. The apparently high reactivity of $\dot{C}H_3$ at low temperatures probably accounts for its low ratio observed in the experimental spectrum in Fig. 1A; particularly some of the $\dot{C}H_3$ will certainly disappear during the transfer of the irradiated sample to the cavity. Because of the apparent absence of other new radicals formed, it is sug-

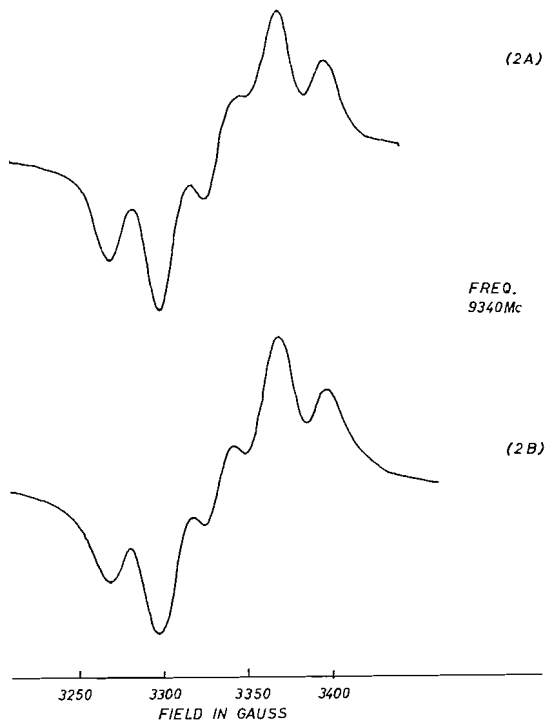

FIG. 2. The e.s.r. spectra at 120 °K of Et_4NI irradiated at 77 °K: (A) experimental spectrum, (B) calculated spectrum of $(C_2H_5)_3\dot{N}\dot{C}H_2$.

TABLE I

Spectral parameters for radicals in computed spectra

	$(C_2H_5)_3\overset{+}{N}\dot{C}H_2$	$(C_2H_5)_3\overset{+}{N}\dot{C}HCH_3$	$\dot{C}H_3$
g-factor	2.0035±0.0002	2.0040±0.0002	2.0035±0.0002
Isotropic couplings			
a_N (G)	23.1±0.5	16.3±0.5	—
a_H (G)	33.6±0.5	13.9±0.5	23.0±0.5
Maximum-slope half-width (G)	8.2	6.2	4.0

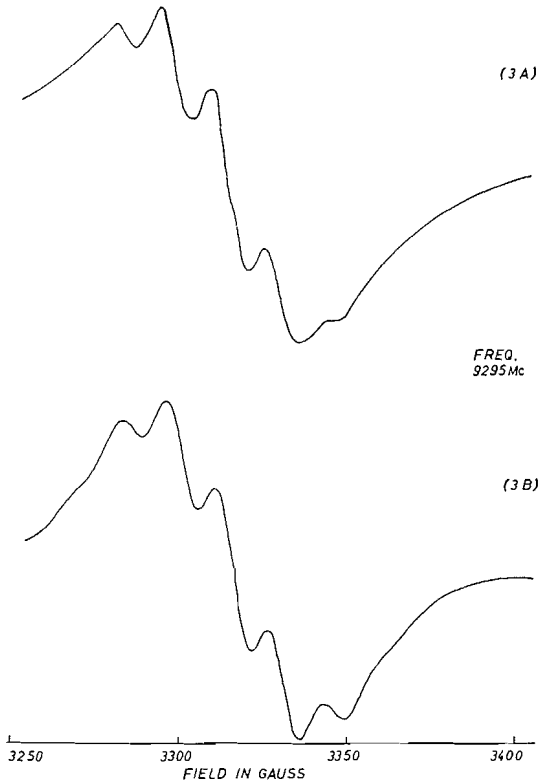

FIG. 3. The e.s.r. spectra at 373 °K of Et_4NI irradiated at 77 °K: (A) experimental spectrum, (B) calculated spectrum of $(C_2H_5)_3\overset{+}{N}\dot{C}HCH_3$.

gested that $\dot{C}H_3$ disappeared mostly via self-combination or via combination with positive holes (I atoms).

When the temperature of the irradiated sample was raised from 120 to 300 °K, the spectrum in Fig. 2A changed gradually to the one shown in Fig. 3A. This is interpreted as due to the secondary reaction

[4] $(C_2H_5)_3\overset{+}{N}\dot{C}H_2 + (C_2H_5)_4N^+ \rightarrow (C_2H_5)_3\overset{+}{N}CH_3 + (C_2H_5)_3\overset{+}{N}\dot{C}HCH_3.$

The resulting radical $(C_2H_5)_3\overset{+}{N}\dot{C}HCH_3$ was observed in Fig. 3A and its theoretical spectrum is given in Fig. 3B. This secondary radical was found to be stable up to 373 °K. The exclusive abstraction of H atom at the α-carbon in reaction [4] can be explained by the weakness of the α C—H bonds. Abstraction of H atoms from the parent ions by positive holes (I atoms) is considered less effective (4). A sample of tetraethylammonium iodide was also irradiated at room temperature and examined at room temperature by e.s.r. The spectrum observed was identical with that in Fig. 3A.

In view of the controversial question on whether a neutral quaternary ammonium radical can exist (10, 11), it is perhaps interesting to point out that one of the possible resonance structures of the radical $(C_2H_5)_3\overset{+}{N}\dot{C}H_2$ is a neutral ammonium configuration $(C_2H_5)_3\dot{N}\overset{+}{C}H_2$. However, in this case there is little doubt that the configuration of a carbonium cation will be much less stable than the ammonium cation. Furthermore, the analysis of the e.s.r. spectrum at 77 °K indicated that the configuration of $(C_2H_5)_3\dot{N}\overset{+}{C}H_2$ contributes little to the resonance.

Experimental

Tetraethylammonium iodide (Baker Co.) was recrystallized three times from alcohol. The recrystallized compound was checked by nuclear magnetic resonance. The powdered samples were placed in quartz tubes sealed off after evacuation to 10^{-4} Torr. Samples were irradiated at 77 °K in a 19 500 curies source of 1.3 MeV ^{60}Co γ-rays. The dose rate was approximately 2 Mrads/h and the total dose was 1 to 3 Mrads. Electron spin resonance spectra were obtained with a Varian V4502 spectrometer and auxiliary equipment. A Hewlett Packard frequency meter was used to measure the microwave frequency and fremy salt was employed for field calibration.

Acknowledgments

The authors are grateful to Miss Larisa Alekov for her help in setting up the computing program,

Can. J. Chem. Downloaded from www.nrcresearchpress.com by 210.87.254.105 on 09/05/12
For personal use only.

and to Miss Sylvia Esterby for some technical assistance. Financial support by the National Research Council of Canada, and the Ontario Department of University Affairs, is gratefully acknowledged.

1. J. K. S. WAN, J. R. MORTON, and H. J. BERNSTEIN. Can. J. Chem. **44**, 1957 (1966).
2. J. K. S. WAN. Ber. Bunsenges. Physik. Chem. **72**, 245 (1968).
3. A. J. TENCH. J. Chem. Phys. **38**, 593 (1963).
4. A. J. TENCH. J. Phys. Chem. **67**, 923 (1963).
5. E. J. BURRELL, JR. J. Chem. Phys. **32**, 955 (1960).
6. H. R. ZELLER, L. VANNOTTI, and W. KANZIG. Physik Kondensierten Materie, **2**, 133 (1964).
7. M. BERSOHN and J. C. BAIRD. An introduction to electron paramagnetic resonance. W. A. Benjamin, Inc., New York. 1966. p. 238.
8. J. H. BEYNON. Mass spectrometry and its applications to organic chemistry. Elsevier Publ. Co., Inc., Amsterdam. 1960. p. 388.
9. L. FABES. M. Sc. Thesis, Queen's University, Kingston, Ontario. 1968.
10. J. K. S. WAN. J. Chem. Educ. **45**, 40 (1968).
11. J. K. LITTLEHAILES and B. J. WOODHALL. Chem. Commun. 665 (1967). J. MYATT and P. F. TODD. Chem. Commun. 1033 (1967).

Hydrogen atom abstraction from substituted toluenes by *tert*-butoxy radical[1]

R. D. GILLIOM AND J. R. HOWLES
Department of Chemistry, Southwestern at Memphis, Memphis, Tennessee 38112

Received February 8, 1968

The relative rates of abstraction of benzylic hydrogen from substituted toluenes by *tert*-butoxy radicals generated from *tert*-butyl hypochlorite have been reexamined. Abstraction from *para*-methylanisole was shown to occur at the ether methyl as well as at the benzylic methyl group. For this reason the compound was excluded from an analysis of the polar effect. A slightly better Hammett correlation was obtained using *sigma* rather than *sigma-plus* values.

Canadian Journal of Chemistry, 46, 2752 (1968)

A recent report by Kennedy and Ingold (1) states that a Hammett $\rho\sigma$ relationship affords a better correlation with σ^+ constants than with σ constants for hydrogen abstraction by *tert*-butoxy radicals from substituted toluenes. This result differs from earlier observations (2, 3). Because of the interpretive significance (1, 3) of these results we have reexamined the correlation.

Experimental

Materials

Reagent grade commercial toluene and carbon tetrachloride were distilled from phosphorus pentoxide and benzene was distilled from sodium as constant-boiling heart cuts.

p-Fluorotoluene and *p*-methylanisole were obtained from Eastman; anisole was obtained from Matheson, Coleman and Bell. These materials were used as supplied, their purity being checked by gas–liquid chromatography.

p-Phenoxytoluene was prepared by the method of Russell and Williamson (4), b.p. 150° (14 mm), lit. (4) b.p. 110–112° (2 mm).

tert-Butyl hypochlorite was prepared as previously described (3) with b.p. 79.0–80.0°, lit. (3) b.p. 78.5–80.0°.

Chlorination Procedure

Relative reactivities were determined by competitive experiments using solutions of ca. 0.5 *M* in each of two hydrocarbons, ca. 0.1 *M* in hypochlorite, and containing appropriate internal standards, e.g. chlorobenzene. After placing the solution in a 40.0° oil bath and degassing for 15 min with bubbling nitrogen, it was irradiated with a 275 W sunlamp, placed externally, until all hypochlorite was consumed as shown by the KI test. Gas chromatographic analysis of the hydrocarbons was carried out on silicone grease and on Apiezon columns. Relative reactivity values were obtained as previously described (3). The results are reported in Table I.

Results and Discussion

The relative reactivities for the reaction of *tert*-butoxy radicals with substituted toluenes at 40° obtained by Kennedy and Ingold (1), Walling and Jacknow (2), and Gilliom and Ward (3) are compared with the values obtained in this work in Table II. Agreement is good between the sets of data except for *p*-phenoxytoluene. The different reactivities obtained for this compound may be due to the different analytical procedures employed. Kennedy and Ingold (1) compared *p*-phenoxytoluene with diphenylmethane by measuring hydrocarbon consumption. Gilliom and Ward (3) compared

[1]This investigation was supported in part by a grant under the Undergraduate Research Participation Program of the National Science Foundation.

Can. J. Chem. Downloaded from www.nrcresearchpress.com by 210.87.254.105 on 09/05/12
For personal use only.

and to Miss Sylvia Esterby for some technical assistance. Financial support by the National Research Council of Canada, and the Ontario Department of University Affairs, is gratefully acknowledged.

1. J. K. S. WAN, J. R. MORTON, and H. J. BERNSTEIN. Can. J. Chem. **44**, 1957 (1966).
2. J. K. S. WAN. Ber. Bunsenges. Physik. Chem. **72**, 245 (1968).
3. A. J. TENCH. J. Chem. Phys. **38**, 593 (1963).
4. A. J. TENCH. J. Phys. Chem. **67**, 923 (1963).
5. E. J. BURRELL, JR. J. Chem. Phys. **32**, 955 (1960).
6. H. R. ZELLER, L. VANNOTTI, and W. KANZIG. Physik Kondensierten Materie, **2**, 133 (1964).
7. M. BERSOHN and J. C. BAIRD. An introduction to electron paramagnetic resonance. W. A. Benjamin, Inc., New York. 1966. p. 238.
8. J. H. BEYNON. Mass spectrometry and its applications to organic chemistry. Elsevier Publ. Co., Inc., Amsterdam. 1960. p. 388.
9. L. FABES. M. Sc. Thesis, Queen's University, Kingston, Ontario. 1968.
10. J. K. S. WAN. J. Chem. Educ. **45**, 40 (1968).
11. J. K. LITTLEHAILES and B. J. WOODHALL. Chem. Commun. 665 (1967). J. MYATT and P. F. TODD. Chem. Commun. 1033 (1967).

Hydrogen atom abstraction from substituted toluenes by *tert*-butoxy radical[1]

R. D. GILLIOM AND J. R. HOWLES
Department of Chemistry, Southwestern at Memphis, Memphis, Tennessee 38112

Received February 8, 1968

The relative rates of abstraction of benzylic hydrogen from substituted toluenes by *tert*-butoxy radicals generated from *tert*-butyl hypochlorite have been reexamined. Abstraction from *para*-methylanisole was shown to occur at the ether methyl as well as at the benzylic methyl group. For this reason the compound was excluded from an analysis of the polar effect. A slightly better Hammett correlation was obtained using *sigma* rather than *sigma-plus* values.

Canadian Journal of Chemistry, 46, 2752 (1968)

A recent report by Kennedy and Ingold (1) states that a Hammett $\rho\sigma$ relationship affords a better correlation with σ^+ constants than with σ constants for hydrogen abstraction by *tert*-butoxy radicals from substituted toluenes. This result differs from earlier observations (2, 3). Because of the interpretive significance (1, 3) of these results we have reexamined the correlation.

Experimental

Materials

Reagent grade commercial toluene and carbon tetrachloride were distilled from phosphorus pentoxide and benzene was distilled from sodium as constant-boiling heart cuts.

p-Fluorotoluene and *p*-methylanisole were obtained from Eastman; anisole was obtained from Matheson, Coleman and Bell. These materials were used as supplied, their purity being checked by gas–liquid chromatography.

p-Phenoxytoluene was prepared by the method of Russell and Williamson (4), b.p. 150° (14 mm), lit. (4) b.p. 110–112° (2 mm).

tert-Butyl hypochlorite was prepared as previously described (3) with b.p. 79.0–80.0°, lit. (3) b.p. 78.5–80.0°.

Chlorination Procedure

Relative reactivities were determined by competitive experiments using solutions of ca. 0.5 *M* in each of two hydrocarbons, ca. 0.1 *M* in hypochlorite, and containing appropriate internal standards, e.g. chlorobenzene. After placing the solution in a 40.0° oil bath and degassing for 15 min with bubbling nitrogen, it was irradiated with a 275 W sunlamp, placed externally, until all hypochlorite was consumed as shown by the KI test. Gas chromatographic analysis of the hydrocarbons was carried out on silicone grease and on Apiezon columns. Relative reactivity values were obtained as previously described (3). The results are reported in Table I.

Results and Discussion

The relative reactivities for the reaction of *tert*-butoxy radicals with substituted toluenes at 40° obtained by Kennedy and Ingold (1), Walling and Jacknow (2), and Gilliom and Ward (3) are compared with the values obtained in this work in Table II. Agreement is good between the sets of data except for *p*-phenoxytoluene. The different reactivities obtained for this compound may be due to the different analytical procedures employed. Kennedy and Ingold (1) compared *p*-phenoxytoluene with diphenylmethane by measuring hydrocarbon consumption. Gilliom and Ward (3) compared

[1]This investigation was supported in part by a grant under the Undergraduate Research Participation Program of the National Science Foundation.

Can. J. Chem. Downloaded from www.nrcresearchpress.com by 210.87.254.42 on 09/05/12
For personal use only.

TABLE I

Relative reactivities of hydrocarbons toward *t*-butyl hypochlorite at 40 °C

Hydrocarbon	Solvent	No. of expts.	k/k_0*
Toluene	—	—	1.0 (assumed)
p-Phenoxytoluene	C_6H_6	5	1.43 ± .18
	CCl_4	5	1.38 ± .19
p-Fluorotoluene	C_6H_6	3	0.99 ± .03
p-Methylanisole	C_6H_6	4	3.4 ± .4
Anisole	C_6H_6	3	1.04 ± .10 (1.01)†
	CCl_4	3	1.14 ± .11

*Experimental error represents average deviation of the number of experiments shown. Each experiment represents at least triplicate analysis.
†See ref. 5.

p-phenoxytoluene with cyclohexane by selective solvolysis of the benzyl chloride and comparison of this with total chloride. Chlorination of either ring of the *p*-phenyltoluene would give an apparently high reactivity by the method of Kennedy and Ingold (2) and an apparently low value by the solvolytic technique. Both of these approaches involve two determinations, that of *p*-phenoxytoluene with a second compound and that of toluene with the same second compound. In both cases, values obtained for the relative reactivity of the second compound with toluene differ from previously reported values (1, 3). To eliminate this uncertainty we have determined the relative reactivity by direct comparison of *p*-phenoxytoluene with toluene. Also we have used the hydrocarbon consumption technique.

From Tables I and II it can be seen that values obtained in this work agree with the original value reported by Gilliom and Ward (3). Although this agreement suggests that ring substitution of the *p*-phenoxytoluene is not important, we tested this conclusion by treating diphenyl ether with *tert*-butyl hypochlorite under the same conditions used to determine relative reactivities. That no diphenyl ether was consumed was shown by comparing the gas chromatographic peak with a chlorobenzene standard before and after reaction with toluene. Because of the agreement obtained between solvolytic and hydrocarbon consumption techniques and, more important, because of the *direct* comparison of *p*-phenoxytoluene with toluene now available, the lower value seems preferable (cf. Table II).

The value for *p*-methylanisole obtained in this work agrees with that of Kennedy and Ingold (1) and appears to support the σ^+ correlation reported by those workers. This agreement must be fortuitous, however, as anisole itself disappears at nearly the same rate as toluene (Table I), suggesting abstraction of hydrogen from the

TABLE II

Relative reactivities of substituted toluenes toward *t*-butyl hypochlorite at 40 °C

Substituent	This work		Ref. 1	Ref. 2	Ref. 3
p-CH_3O	3.4*	—	3.2	—	—
p-C_6H_5O	1.43	1.38	2.13	—	1.42
p-CH_3†	—	—	1.47	1.53	1.52
m-CH_3†	—	—	1.07	1.17	1.14
H‡	1.00	1.00	1.00	1.00	1.00
p-F	0.99	—	—	—	—
p-Cl	—	—	0.89	0.71	0.67
m-Cl	—	—	0.59	0.52	0.52
p-Br	—	—	—	—	0.71
p-CN	—	—	0.36	—	0.29
m-NO_2	—	—	0.29	—	—
p-NO_2	—	—	0.25	—	—
Solvent	C_6H_6	CCl_4	CCl_4	Reactants	C_6H_6

*See text for significance.
†Experimental result divided by statistical factor of 2.
‡Assumed.

Can. J. Chem. Downloaded from www.nrcresearchpress.com by 210.87.254.42 on 09/05/12
For personal use only.

ether methyl and/or ring substitution under the reaction conditions. When the product mixture from a toluene–anisole chlorination is treated with ethanolic KOH at room temperature, one of the product peaks is completely converted to a new gas chromatographic peak of longer retention time, while a peak with the same retention time as benzyl chloride is converted to a material of the same retention time as benzyl ethyl ether at a much slower rate. Treatment of the product mixture with aqueous silver nitrate results in rapid loss of the same peak as above and the formation of material of the same retention time as phenol and the formation of material of the same retention time as formaldehyde. These qualitative results are consistent with the presence of chloromethyl phenyl ether in the product mixture (cf. ref. 5). In addition, a trace of material with the same retention time as a mixture of chloroanisoles was noted. These results strongly suggest that related reactions also occur with *p*-methylanisole. That this is so was demonstrated by mixing a product mixture with alcoholic KOH. Within 10 min after mixing, one product gas chromatographic peak had been destroyed and a new peak had appeared. A second peak was also destroyed with concomitant formation of another at a rate slower than the first. It is clear that *p*-methoxytoluene is destroyed by processes competitive with benzylic hydrogen abstraction.

Using the value obtained in this work for *p*-phenoxytoluene and the previously unknown value for *p*-fluorotoluene (Table I), along with the values reported previously by one of us (3), the following correlations[2] were obtained:

$$\log k/k_0 = -0.76\sigma - .00;\ s, 0.045;\ r, 0.983;$$

$$\log k/k_0 = -0.60\sigma^+ - .06;\ s, 0.073;\ r, 0.954.$$

Including the values for *m*- and *p*-nitrotoluene (1) does not significantly affect the conclusion that σ-substituent constants give a somewhat better correlation than σ^+ values. The correlations including the nitro results are:

$$\log k/k_0 = -0.76\sigma - .00;\ s, 0.040;\ r, 0.991;$$

$$\log k/k_0 = -0.64\sigma^+ - .07;\ s, 0.068;\ r, 0.974.$$

1. B. R. KENNEDY and K. U. INGOLD. Can. J. Chem. **44**, 2381 (1966).
2. C. WALLING and B. B. JACKNOW. J. Am. Chem. Soc. **82**, 6113 (1960).
3. R. D. GILLIOM and B. F. WARD, JR. J. Am. Chem. Soc. **87**, 3944 (1965).
4. G. A. RUSSELL and R. C. WILLIAMSON, JR. J. Am. Chem. Soc. **86**, 2357 (1964).
5. C. WALLING and M. J. MINTZ. J. Am. Chem. Soc. **89**, 1515 (1967).
6. Y. OKAMOTO and H. C. BROWN. J. Am. Chem. Soc. **80**, 4979 (1958).
7. D. H. MCDANIEL and H. C. BROWN. J. Org. Chem. **23**, 420 (1958).

[2]The values of σ^+ are from ref. 6 with the exception of the value for *p*-phenoxy which is taken from ref. 4. The values of σ are from ref. 7.

Reductions with sulfurated borohydrides. I. Preparation of sulfurated borohydrides

J. M. LALANCETTE, A. FRÊCHE, AND R. MONTEUX
Département de Chimie, Faculté des Sciences, Université de Sherbrooke, Sherbrooke, Québec

Received February 27, 1968

Sodium borohydride reacts with sulfur at room temperature in the presence of appropriate organic solvents to give a sulfurated borohydride: $NaBH_2S_3$. The formulation of this hydride has been established by infrared, nuclear magnetic resonance, and elementary analysis. Thermal decomposition and hydrolysis are reported. The reaction observed with $NaBH_4$ appears to be general between borohydrides and the lower elements of Group VIA: Se and Te. A facile preparative method of $NaBH_2S_3$ is presented.

Canadian Journal of Chemistry, **46**, 2754 (1968)

The reaction of borohydrides with elements of Group VIA has received very little attention. Except for the reactions with oxygen, the only report on the subject describes the combination of sulfur with sodium and potassium borohydrides (1). This reaction calls for direct combination of elemental sulfur with the hydride, at a temperature between 160 and 300°, and gives

Can. J. Chem. Downloaded from www.nrcresearchpress.com by 210.87.254.42 on 09/05/12
For personal use only.

ether methyl and/or ring substitution under the reaction conditions. When the product mixture from a toluene–anisole chlorination is treated with ethanolic KOH at room temperature, one of the product peaks is completely converted to a new gas chromatographic peak of longer retention time, while a peak with the same retention time as benzyl chloride is converted to a material of the same retention time as benzyl ethyl ether at a much slower rate. Treatment of the product mixture with aqueous silver nitrate results in rapid loss of the same peak as above and the formation of material of the same retention time as phenol and the formation of material of the same retention time as formaldehyde. These qualitative results are consistent with the presence of chloromethyl phenyl ether in the product mixture (cf. ref. 5). In addition, a trace of material with the same retention time as a mixture of chloroanisoles was noted. These results strongly suggest that related reactions also occur with *p*-methylanisole. That this is so was demonstrated by mixing a product mixture with alcoholic KOH. Within 10 min after mixing, one product gas chromatographic peak had been destroyed and a new peak had appeared. A second peak was also destroyed with concomitant formation of another at a rate slower than the first. It is clear that *p*-methoxytoluene is destroyed by processes competitive with benzylic hydrogen abstraction.

Using the value obtained in this work for *p*-phenoxytoluene and the previously unknown value for *p*-fluorotoluene (Table I), along with the values reported previously by one of us (3), the following correlations[2] were obtained:

$$\log k/k_0 = -0.76\sigma - .00;\ s, 0.045;\ r, 0.983;$$

$$\log k/k_0 = -0.60\sigma^+ - .06;\ s, 0.073;\ r, 0.954.$$

Including the values for *m*- and *p*-nitrotoluene (1) does not significantly affect the conclusion that σ-substituent constants give a somewhat better correlation than σ^+ values. The correlations including the nitro results are:

$$\log k/k_0 = -0.76\sigma - .00;\ s, 0.040;\ r, 0.991;$$

$$\log k/k_0 = -0.64\sigma^+ - .07;\ s, 0.068;\ r, 0.974.$$

1. B. R. KENNEDY and K. U. INGOLD. Can. J. Chem. **44**, 2381 (1966).
2. C. WALLING and B. B. JACKNOW. J. Am. Chem. Soc. **82**, 6113 (1960).
3. R. D. GILLIOM and B. F. WARD, JR. J. Am. Chem. Soc. **87**, 3944 (1965).
4. G. A. RUSSELL and R. C. WILLIAMSON, JR. J. Am. Chem. Soc. **86**, 2357 (1964).
5. C. WALLING and M. J. MINTZ. J. Am. Chem. Soc. **89**, 1515 (1967).
6. Y. OKAMOTO and H. C. BROWN. J. Am. Chem. Soc. **80**, 4979 (1958).
7. D. H. MCDANIEL and H. C. BROWN. J. Org. Chem. **23**, 420 (1958).

[2]The values of σ^+ are from ref. 6 with the exception of the value for *p*-phenoxy which is taken from ref. 4. The values of σ are from ref. 7.

Reductions with sulfurated borohydrides. I. Preparation of sulfurated borohydrides

J. M. LALANCETTE, A. FRÊCHE, AND R. MONTEUX
Département de Chimie, Faculté des Sciences, Université de Sherbrooke, Sherbrooke, Québec

Received February 27, 1968

Sodium borohydride reacts with sulfur at room temperature in the presence of appropriate organic solvents to give a sulfurated borohydride: $NaBH_2S_3$. The formulation of this hydride has been established by infrared, nuclear magnetic resonance, and elementary analysis. Thermal decomposition and hydrolysis are reported. The reaction observed with $NaBH_4$ appears to be general between borohydrides and the lower elements of Group VIA: Se and Te. A facile preparative method of $NaBH_2S_3$ is presented.

Canadian Journal of Chemistry, **46**, 2754 (1968)

The reaction of borohydrides with elements of Group VIA has received very little attention. Except for the reactions with oxygen, the only report on the subject describes the combination of sulfur with sodium and potassium borohydrides (1). This reaction calls for direct combination of elemental sulfur with the hydride, at a temperature between 160 and 300°, and gives

Can. J. Chem. Downloaded from www.nrcresearchpress.com by 210.87.254.42 on 09/05/12
For personal use only.

the corresponding thioperborate; it is accompanied by the evolution of all the hydrogen on the starting borohydride, see eq. [1].

[1] $$MBH_4 + 3S \rightarrow MBS_3 + 2H_2$$
$$M = Na, K.$$

We have found that borohydrides react with sulfur and lower elements of Group VIA under much milder conditions in the presence of many organic solvents. The reactions take place readily at room temperature, with hydrogen evolution, and stop before the thioperborate stage to give a thioborohydride retaining half of its hydrogens. In the case of $NaBH_4$, the amount of sulfur combined with the hydride has been estimated by plotting the amount (molar) of hydrogen evolved per mole of $NaBH_4$ present against the number of moles of sulfur available in the reaction mixture. It can be seen from Fig. 1 that the amount of hydrogen evolved, for 1 mole of hydride, remains constant at $1H_2$ when at least 3 moles of sulfur (3/8 S_8) are available in the reaction mixture. The amount of hydrogen remaining on the sulfurated hydride (2H) has been determined by hydrolysis and by pyrolysis. Both methods indicated that 1 mole of hydrogen remains on the hydride after the reaction with sulfur. The analysis has been completed by flame determination of boron and sodium. All these analyses are in accordance with the formulation $NaBH_2S_3$ for the sulfurated hydride. The formation of this product would then be described by eq. [2] and its hydrolysis by eq. [3].

[2] $$NaBH_4 + 3S \xrightarrow[25°]{\text{solvent}} NaBH_2S_3 + H_2$$

[3] $$NaBH_2S_3 + 3H_2O \rightarrow 2H_2 + H_3BO_3 + [NaSH + 2S]$$

The reaction appears to be general with the lower elements of Group VIA. The hydrogen evolution is brisk with sulfur (cooling may be required), rapid with selenium, and slow with tellurium.

The infrared spectrum of $NaBH_2S_3$ shows the typical absorption of the B—S bond around 930 cm^{-1} (2) and confirms that no borohydride remains in the product of the reaction; a trace of absorption remains in the 2300 cm^{-1} region, where $NaBH_4$ absorbs very strongly. There is no indication of S—H absorption.

The nuclear magnetic resonance measurements proved to be very difficult because of solubility problems. The only solvent in which it has been possible to dissolve $NaBH_2S_3$ is hexamethylphosphoric triamide. In that solvent, the quadruplet of $NaBH_4$ was absent and a new triplet (at 11.33 τ) appeared. There was no indication of S—H protons. As hydrogen remains on the compound and there are no SH groups, hydrogen must be located on the boron, although the reason why a triplet is observed is not evident.

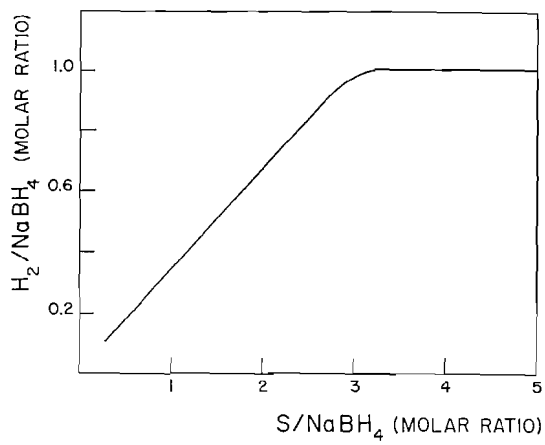

FIG. 1. Evolution of hydrogen from $NaBH_4$ in the presence of sulfur: influence of $S/NaBH_4$ ratio on $H_2/NaBH_4$ ratio.

From these analyses, it can be seen that the structure of the sulfurated hydride must include B—S and B—H bonds. The composition of the sulfurated hydride is given as "S_3". This value must be taken as an average and the existence of larger or smaller "S" fragments cannot be excluded. It was not possible to settle this point by mass spectrometry.

The role of the solvent is difficult to appreciate fully in the present state of the problem, although the capacity for dissolving both sulfur and borohydride seems to be important. We have noted that ethers, especially those which are strong donors, were very effective in promoting the reaction. An evaluation of the effect of common solvents on the reaction of sulfur with sodium borohydride is presented in Table I. It can be seen that tetrahydrofuran, diglyme, and hexamethylphosphoric triamide (three donors) are the most appropriate solvents for the reaction.

The study has been made mainly with sodium borohydride as substrate. However, hydrogen

Can. J. Chem. Downloaded from www.nrcresearchpress.com by 210.87.254.42 on 09/05/12
For personal use only.

TABLE I

Effects of solvent in the preparation of sulfurated borohydrides

Solvents	T^*	Hydrogen evolution
Ethyl ether (3)	—	None
Isopropyl ether	—	Very slow, incomplete
Tetrahydrofuran	15 min	Fast
Diglyme	2 min	Very fast
Hexamethylphosphoric triamide,	2 min	Very fast
Dioxan	10 h	Very sluggish
Diethylamine Triethylamine Carbon disulfide	—	Incomplete, act as inhibitors
Dimethylsulfoxide, alcohols, ketones	—	React with the solvent
Hydrocarbons (benzene, pet. ether)	—	None

*Time required for the evolution of 90% of the expected amount of hydrogen, according to eq. [2].

evolution measurements and reduction tests have shown that a similar reaction was obtained with lithium, potassium, and tetraethylammonium borohydrides.

The sulfurated borohydrides can be obtained as white or slightly yellow solids. They are reasonably stable at room temperature, if kept in a dry nitrogen atmosphere, but decompose rapidly in the presence of oxygen or atmospheric moisture. Precautions similar to those required for the manipulation of $LiAlH_4$ must be followed to avoid decomposition or hydrolysis, and then results are very reproducible. The sulfuration procedure is extremely simple and fast. It is best to prepare the sulfurated hydride immediately before use.

We have noted that the sulfurated borohydrides are strong reducers toward organic substrates. This will be reported in detail in later papers.

Experimental

Infrared (i.r.) measurements were made with a Perkin–Elmer, model 137 spectrometer and nuclear magnetic resonance (n.m.r.) spectra were determined with a Varian A-60 instrument.

(1) Preparation of Sulfurated Sodium Borohydride

A mixture of 7.56 g (0.20 mole) of sodium borohydride and 19.20 g (0.60 mole) of sulfur was treated with 50 ml of anhydrous tetrahydrofuran (THF), with stirring in a 500 ml flask bearing a condenser. The gas evolution was brisk and the reaction exothermic; cooling with a water bath was used to control the reflux. After the initial reaction had subsided, stirring at 25° was continued for 30 min. The solvent was then evaporated at room temperature, under vacuum, and the residual lump washed three times (vigorous shaking) with anhydrous petroleum ether. A white or slightly yellow solid was then obtained if adequate precautions were taken to exclude moisture and oxygen from the product. The sulfurated hydride was stable in a nitrogen atmosphere for several weeks, although a light-yellow coating appeared gradually on the lumps. The solid was insoluble or only very slightly soluble in common organic solvents with which it did not react except with hexamethylphosphoric triamide in which it was quite soluble. Infrared (Nujol) of $NaBH_2S_3$: bands were observed at 1055 cm^{-1} (medium), 935 cm^{-1} (strong), and 895 cm^{-1} (weak). A very weak band was observed at 2300 cm^{-1}, and no band at 1120 cm^{-1}. Infrared (Nujol) of $NaBH_4$: bands were observed at 2300 cm^{-1} (very strong) and 1120 cm^{-1} (very strong). Analyses for sodium and boron were made by flame analysis with a Beckman DU photometer. Standards were prepared with sodium borate for Na and B analysis.

Anal. Calcd. for $NaBH_2S_3$: Na, 17.4; B, 8.2. Found: Na, 16.7; B, 7.75.

Nuclear magnetic resonance measurements: $NaBH_4$ in dimethoxyethane (internal TMS): 8.37 τ; 9.72 τ; 11.07 τ; 12.42 τ. $NaBH_4$ in hexamethylphosphoric triamide (internal TMS): 8.30 τ; 9.66 τ; 11.00 τ; 12.37 τ. $NaBH_2S_3$ in hexamethylphosphoric triamide (internal TMS): 11.22 τ; 11.33 τ; 11.48 τ.

(2) Determination of the Amount of Sulfur Incorporated on Sodium Borohydride

Mixtures of sodium borohydride and sulfur were prepared with an $S/NaBH_4$ ratio varying between 0.3 and 5. The weight of the mixture was kept constant to within 2% (2.00 g sample) and treated with 10 ml of anhydrous THF, at 25°, with good stirring. Each experiment was carried out under similar conditions and the hydrogen evolved was measured with a "Wet Test" meter. Volumes were corrected. The gas collected was hydrogen containing only traces (less than 1%) of H_2S, as shown by washing with a 10% solution of lead acetate. The results are reported in Fig. 1.

Similar experiments using a 3/1 ratio for $S/NaBH_4$ were made to compare the speed of reaction with various solvents (Table I), and the reaction of lithium, potassium, and tetraethylammonium borohydride.

(3) Pyrolysis of $NaBH_2S_3$

The pyrolysis was made in an apparatus consisting of a 1 l flask bearing a barometer and a side arm in which a sample could be placed. The system was flushed with nitrogen, the sample was introduced, and the whole system evacuated. The side arm was then heated (300–400°) until no more evolution of gas was indicated by the barometer. After cooling, the pressure was noted and the amount of gas evolved determined, the volume of the system being 1215 cm^3. In a typical experiment, a 2.00 g sample gave 11.8 mm of volatile material (a mixture of H_2, 27%, and H_2S, 73%) and 2.4 mm of higher sulfanes that condensed in the flask as an oily yellow liquid.

Anal. Calcd. for $NaBH_2S_3$: H, 1.52. Found: H, 1.40.

Can. J. Chem. Downloaded from www.nrcresearchpress.com by 210.87.254.42 on 09/05/12
For personal use only.

(4) Hydrolysis of $NaBH_2S_3$

A mixture of 3.21 g (0.10 mole) of sulfur and 1.13 g of $NaBH_4$ (0.030 mole) was treated with 100 ml of hexamethylphosphoric triamide under conditions similar to those used in preparation (1). The reaction was very rapid and 685 ml of H_2 (corrected) was evolved (101% of $1H_2$). After standing overnight, the solution was treated by 200 ml (excess) of water, and 1350 ml of H_2 (corrected) was evolved (100% of $2H_2$).

The residue left after hydrolysis was a yellow viscous product containing sodium, and extraction by water yielded boric acid.

Acknowledgments

We thank the National Research Council of Canada and the Defense Research Board of Canada (grant no. 9530-30) for financial assistance.

1. F. Chopin and P. Hagenmuller. Bull. Soc. Chim. France, 3031 (1965).
2. A. Cabana, J. Brault, and J. M. Lalancette. Spectrochim. Acta, **22**, 377 (1966).
3. H. Noeth and G. Mikulashek. Z. Anorg. Allgem. Chem. **311**, 241 (1961).

Can. J. Chem. Downloaded from www.nrcresearchpress.com by 210.87.254.42 on 09/05/12
For personal use only.

Octacyanomolybdate(IV) ion, scavenger for hydroxyl radical

B. K. Sharma
Department of Chemistry, University of Delhi, Delhi, India

Received February 27, 1968

The oxidation of potassium octacyanomolybdate(IV) in 0.4 *M* sulfuric acid solutions (oxygenated) has been studied; $G[Mo(CN)_8^{3-}]$ was found to be 2.7, which is close to the $G(OH)$ value of 2.9.

Canadian Journal of Chemistry, 46, 2757 (1968)

The oxidation of acidified solutions of potassium ferrocyanide by gamma radiation has been studied by Hughes and Wills (1). Similar work on octacyanomolybdate(IV) has not been done. We prepared $K_4Mo(CN)_8.2H_2O$ by the method of Furman and Miller cited in ref. 2 and irradiated its aqueous oxygenated solutions (1.0–5.0) $\times 10^{-3}$ *M*, after acidification with 0.4 *M* sulfuric acid, with gamma radiation from a 1000 curie ^{60}Co source (Gamma-220 cell, Atomic Energy of Canada Limited). The dose rate was 7×10^{16} eV/min/ml, as determined by a Fricke dosimeter. Temperature of irradiation was 30 °C and the time of irradiation varied from 30 to 300 min. The yield of octacyanomolybdate(V) was determined colorimetrically, using a Beckman differential spectrophotometer (model DK-2) at $\lambda = 380$ mμ ($\varepsilon = 1200$)(3). At this wavelength absorption by octacyanomolybdate(IV) was negligible. In view of the photosensitive nature of octacyanomolybdates(IV and V), all operations were done in the dark.

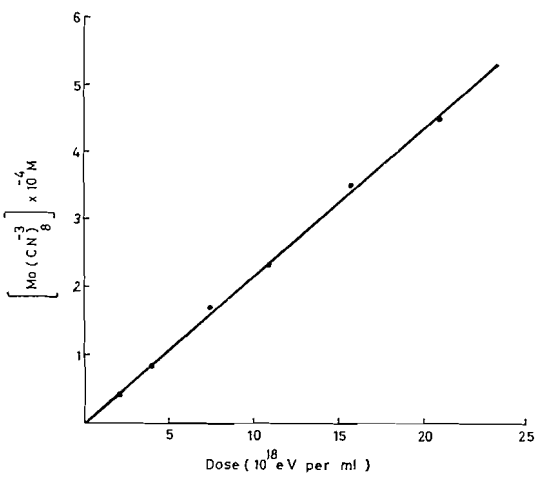

Fig. 1. Oxidation of $Mo(CN)_8^{4-}$ ion.

The production of $Mo(CN)_8^{3-}$ was found to be linear with dose (Fig. 1) and independent of $Mo(CN)_8^{4-}$ concentration in the range (1.0–5.0) $\times 10^{-3}$ *M*.

Gamma radiation is known to decompose water giving H, OH, H_2, and H_2O_2. The hydrogen atom is also known to react with dissolved oxygen to produce the HO_2 radical. Hence the following reactions could occur in the radiolysis of oxygenated and acidified solutions of octacyanomolybdate(IV).

$$Mo(CN)_8^{4-} + OH \rightarrow Mo(CN)_8^{3-} + OH^-$$
$$Mo(CN)_8^{4-} + HO_2 \rightarrow Mo(CN)_8^{3-} + HO_2^-$$
$$Mo(CN)_8^{4-} + H_2O_2 \rightarrow Mo(CN)_8^{3-} + OH + OH^-$$

The vertical scale in Fig. 1 is in error and should be multiplied by a factor of 2.

FOR ERRATA SEE 1.47E2 19 Cy p 355

(4) Hydrolysis of $NaBH_2S_3$

A mixture of 3.21 g (0.10 mole) of sulfur and 1.13 g of $NaBH_4$ (0.030 mole) was treated with 100 ml of hexamethylphosphoric triamide under conditions similar to those used in preparation (1). The reaction was very rapid and 685 ml of H_2 (corrected) was evolved (101% of $1H_2$). After standing overnight, the solution was treated by 200 ml (excess) of water, and 1350 ml of H_2 (corrected) was evolved (100% of $2H_2$).

The residue left after hydrolysis was a yellow viscous product containing sodium, and extraction by water yielded boric acid.

Acknowledgments

We thank the National Research Council of Canada and the Defense Research Board of Canada (grant no. 9530-30) for financial assistance.

1. F. Chopin and P. Hagenmuller. Bull. Soc. Chim. France, 3031 (1965).
2. A. Cabana, J. Brault, and J. M. Lalancette. Spectrochim. Acta, **22**, 377 (1966).
3. H. Noeth and G. Mikulashek. Z. Anorg. Allgem. Chem. **311**, 241 (1961).

Can. J. Chem. Downloaded from www.nrcresearchpress.com by 210.87.254.42 on 09/05/12
For personal use only.

Octacyanomolybdate(IV) ion, scavenger for hydroxyl radical

B. K. Sharma
Department of Chemistry, University of Delhi, Delhi, India

Received February 27, 1968

The oxidation of potassium octacyanomolybdate(IV) in 0.4 *M* sulfuric acid solutions (oxygenated) has been studied; $G[Mo(CN)_8^{3-}]$ was found to be 2.7, which is close to the $G(OH)$ value of 2.9.

Canadian Journal of Chemistry, 46, 2757 (1968)

The oxidation of acidified solutions of potassium ferrocyanide by gamma radiation has been studied by Hughes and Wills (1). Similar work on octacyanomolybdate(IV) has not been done. We prepared $K_4Mo(CN)_8.2H_2O$ by the method of Furman and Miller cited in ref. 2 and irradiated its aqueous oxygenated solutions (1.0–5.0) $\times 10^{-3}$ *M*, after acidification with 0.4 *M* sulfuric acid, with gamma radiation from a 1000 curie ^{60}Co source (Gamma-220 cell, Atomic Energy of Canada Limited). The dose rate was 7×10^{16} eV/min/ml, as determined by a Fricke dosimeter. Temperature of irradiation was 30 °C and the time of irradiation varied from 30 to 300 min. The yield of octacyanomolybdate(V) was determined colorimetrically, using a Beckman differential spectrophotometer (model DK-2) at $\lambda = 380$ mμ ($\varepsilon = 1200$)(3). At this wavelength absorption by octacyanomolybdate(IV) was negligible. In view of the photosensitive nature of octacyanomolybdates(IV and V), all operations were done in the dark.

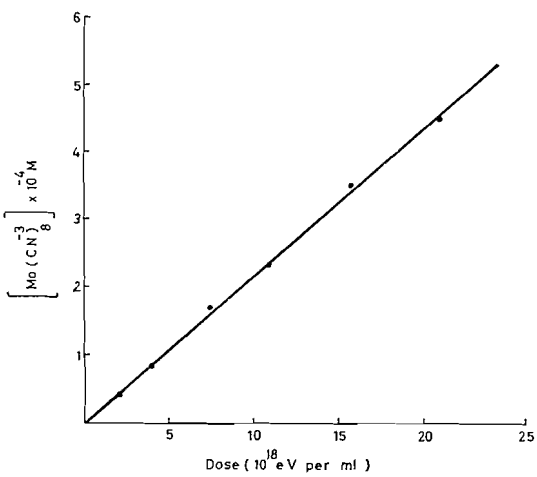

Fig. 1. Oxidation of $Mo(CN)_8^{4-}$ ion.

The production of $Mo(CN)_8^{3-}$ was found to be linear with dose (Fig. 1) and independent of $Mo(CN)_8^{4-}$ concentration in the range (1.0–5.0) $\times 10^{-3}$ *M*.

Gamma radiation is known to decompose water giving H, OH, H_2, and H_2O_2. The hydrogen atom is also known to react with dissolved oxygen to produce the HO_2 radical. Hence the following reactions could occur in the radiolysis of oxygenated and acidified solutions of octacyanomolybdate(IV).

$$Mo(CN)_8^{4-} + OH \rightarrow Mo(CN)_8^{3-} + OH^-$$
$$Mo(CN)_8^{4-} + HO_2 \rightarrow Mo(CN)_8^{3-} + HO_2^-$$
$$Mo(CN)_8^{4-} + H_2O_2 \rightarrow Mo(CN)_8^{3-} + OH + OH^-$$

The vertical scale in Fig. 1 is in error and should be multiplied by a factor of 2.

FOR ERRATA SEE 1.47E2 19 Cy p 355

According to Hughes and Wills (1), the oxidation of $Fe(CN)_6^{4-}$ by H_2O_2 produced by the radiolysis of water is a slow thermal reaction. We made a separate study of the oxidation of $Mo(CN)_8^{4-}$ by H_2O_2 in amounts likely to be present in our radiolytic experiments and we also found that oxidation was slow and negligible. Hughes and Wills thought that the radical HO_2 played no part in the oxidation of ferrocyanide. On the other hand, it was destroyed by dimerization to give H_2O_2. Since the $Mo(CN)_8^{4-}$ has a higher oxidation potential then $Fe(CN)_6^{4-}$, it would be even more unlikely that HO_2 should oxidize $Mo(CN)_8^{4-}$.

The only species which could bring about rapid oxidation of $Mo(CN)_8^{4-}$ is thus the radical OH. In agreement with this we obtained $G[Mo(CN)_8^{3-}] = 2.70$, which is close to the accepted value of $G(OH) = 2.9$ in acidic medium (4). The octacyanomolybdate(IV) ion in acidic medium thus acts as a scavenger for the OH radical.

Acknowledgment

The author's thanks are due to Dr. H. B. Mathur and Dr. M. P. Reddy of the National Chemical Laboratory, India, for making the gamma cell available to him; to Mr. H. M. Saxena for help in the preparation of $K_4Mo(CN)_8.2H_2O$; and to Professor R. P. Mitra, Head of the Department of Chemistry, University of Delhi, for helpful discussions and encouragement.

1. G. HUGHES and C. WILLS. J. Chem. Soc. 4848 (1962).
2. L. F. ANDRIETH. Inorganic synthesis. Vol. III. McGraw-Hill Book Co., Inc., New York. 1950. p. 160.
3. P. C. H. MITCHELL and R. J. P. WILLIAMS. J. Chem. Soc. 4570 (1962).
4. A. O. ALLEN. The radiation chemistry of water and aqueous solutions. D. Van. Nostrand Co., Inc., New York. 1961. Chap. 4.

Erratum: Densities and magnetic susceptibilities of thallium amalgams

W. T. FOLEY, REBECCA FAI-YING CHIU, AND JOHN R. DELOREY
Department of Chemistry, St. Francis Xavier University, Antigonish, Nova Scotia

Received May 16, 1968

(Ref.: Can. J. Chem. **46**, 1197 (1968))

Canadian Journal of Chemistry, **46**, 2758 (1968)

In the discussion of the magnetic susceptibility of the 31.53 wt. % thallium amalgam at a temperature of −79 °C, the claim was made that the alpha phase remained as an unstable phase. A better interpretation of this datum is that at −79 °C the magnetic susceptibility of the alloy of 31.53 wt. % thallium is really the magnetic susceptibility of a mixture of beta-thallium and an alloy of 30.7 wt. % thallium.

Can. J. Chem. Downloaded from www.nrcresearchpress.com by 210.87.254.42 on 09/05/12
For personal use only.

Can. J. Chem. Downloaded from www.nrcresearchpress.com by 210.87.254.42 on 09/05/12
For personal use only.

Cyanide ion complexes of some aromatic nitro compounds

E. BUNCEL, A. R. NORRIS, AND W. PROUDLOCK
Department of Chemistry, Queen's University, Kingston, Ontario

Received June 19, 1968

The results are presented of spectral studies which characterize the complexes formed in deuterochloroform solution between cyanide ion and 1,3,5-trinitrobenzene, 2,4,6-trinitrotoluene, and 2,4,6-trinitrobenzaldehyde.

Canadian Journal of Chemistry, 46, 2759 (1968)

The species formed in the interactions of aromatic nitro compounds with anionic and neutral bases have been under study since 1902 (1) but it is only in the last several years that definitive evidence on their structures has become available, chiefly through ^1H nuclear magnetic resonance (n.m.r.) studies (2–4).

The n.m.r. work has confirmed Meisenheimer's (1) formulation of the structure of the stable adduct formed from 2,4,6-trinitroanisole and methoxide ion as a σ-complex (**1**), but has also revealed that a metastable complex is first formed by addition of methoxide ion at C-3 (4). The structures of amine and acetonate adducts of various nitro compounds have similarly been elucidated (5, 6).

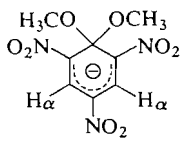

1

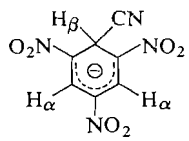

2

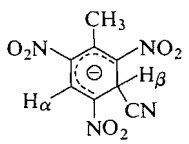

3

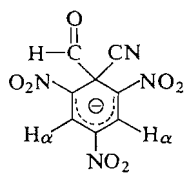

4

In contrast, corresponding clarification with cyanide ion has not yet been obtained, even though the structures of cyanide ion complexes of aromatic nitro compounds have long been speculated upon (7). The visible spectrum of the 1,3,5-trinitrobenzene – cyanide ion system showed changes with time but the initial spectrum was ascribed (8–10) to the σ-complex (**2**). Recently such spectral changes were interpreted in terms of both charge-transfer and σ-complex formation (11). A red complex formed from 1,3-dinitrobenzene and cyanide ion in dimethylformamide was formulated as a σ-complex on the basis of its electronic and infrared spectra but no detectable n.m.r. spectrum could be observed (11).

We report here results of n.m.r. studies which establish the structure of the complex formed between cyanide ion and 1,3,5-trinitrobenzene. We also present the first evidence of σ-complex formation by 2,4,6-trinitrotoluene and 2,4,6-trinitrobenzaldehyde with cyanide ion. Unexpectedly, the structures of these cyanide ion complexes are not equivalent.

The resonance absorption of 1,3,5-trinitrobenzene in deuterochloroform at $-30°$ (singlet at 9.40 p.p.m. downfield relative to tetramethylsilane as external standard) undergoes characteristic changes on the addition of cyanide ion (introduced as the deuterochloroform soluble tetraphenylarsonium salt). Thus a deuterochloroform solution of 1,3,5-trinitrobenzene (0.6 *M*) and cyanide ion (0.4 *M*) shows, in addition to the parent trinitrobenzene peak now shifted to 9.36 p.p.m. and the multiplet in the 7.80 p.p.m. region due to the tetraphenylarsonium group, two new resonances at 8.42 and 5.48 p.p.m. (singlets, relative areas 2:1). The appearance of these absorptions is consistent with the formation of σ-complex **2**. The absorption at 8.42 p.p.m. is assigned to the H_α hydrogens, upfield relative to the parent trinitrobenzene hydrogens as a result of increased shielding in the complex,

Can. J. Chem. Downloaded from www.nrcresearchpress.com by 210.87.254.42 on 09/05/12
For personal use only.

while the absorption at 5.48 p.p.m. is assigned to the H_β hydrogen. The observed chemical shifts are similar to those reported for σ-complexes of 1,3,5-trinitrobenzene with methoxide, ethoxide, and acetonate ions (4–6). Since both free and complexed trinitrobenzene are observed at the molar concentration of reagents employed, it follows that exchange of cyanide ion between the two species is a relatively slow process. The n.m.r. spectral pattern does not change appreciably over the range −30 to +30 °C. The visible spectrum of an n.m.r. sample diluted with methylene chloride (absorption maxima at 442 and 558 mμ) is characteristic of the σ-complex of 1,3,5-trinitrobenzene with cyanide ion (10, 12).

The interaction of cyanide ion with 2,4,6-trinitrotoluene in deuterochloroform has been examined similarly. At −30 °C, 2,4,6-trinitrotoluene shows resonance absorptions at 9.04 and 2.82 p.p.m. On the addition of cyanide ion new absorptions characteristic of complex formation are observed at 8.65, 5.76, and 2.74 p.p.m. (singlets, relative areas 1:1:3) in addition to those of uncomplexed 2,4,6-trinitrotoluene (singlets at 9.00 and 2.77 p.p.m.). The structure of the complex consistent with these absorptions is **3**. The spectrum due to the complex is unchanged after several hours at −30 °C but at room temperature complete decay of the complex occurs within several hours. The final product of the interaction has not yet been identified. The possibility that other interactions such as electron transfer (13) and proton transfer (14, 15) may occur has been noted.

In contrast, cyanide ion interacts with 2,4,6-trinitrobenzaldehyde by addition at C-1 to form the σ-complex **4**. The n.m.r. spectrum (in $CDCl_3$ at −30°) of the complex is characterized by two singlet absorptions, the aldehydic hydrogen at 10.14 p.p.m. and a signal at 8.55 p.p.m. due to the equivalent aromatic hydrogens (relative areas 1:2). Uncomplexed 2,4,6-trinitrobenzaldehyde shows absorptions at 10.73 and 9.37 p.p.m. (singlets, relative areas 1:2) in this medium. The complex appears to be stable for several hours at −30 °C.

The factors which determine the site of nucleophilic attack in various nitro compounds are not at present clearly understood and neither is the possibility of interconversion among such complexes. Structural and medium effects relating to these questions are under study.

Acknowledgment

Financial support by the Defense Research Board and the National Research Council of Canada is gratefully acknowledged. The authors are indebted to Dr. K. E. Russell for many helpful discussions.

1. J. Meisenheimer. Ann. **323**, 205 (1902).
2. M. R. Crampton and V. Gold. Chem. Commun. 256 (1965).
3. R. Foster and C. A. Fyfe. Tetrahedron, **21**, 3363 (1965).
4. K. L. Servis. J. Am. Chem. Soc. **89**, 1508 (1967).
5. M. R. Crampton and V. Gold. J. Chem. Soc. 4293 (1964); Chem. Commun. 549 (1965); J. Chem. Soc. B, 893 (1966); J. Chem. Soc. B, 23 (1967).
6. R. Foster and C. A. Fyfe. J. Chem. Soc. B, 53 (1966); Chem. Commun. 1219 (1967). R. Foster, C. A. Fyfe, P. H. Emslie, and M. I. Foreman. Tetrahedron, **23**, 227 (1967).
7. C. A. Lobry de Bruyn. Rec. Trav. Chim. **2**, 203 (1883). A. Hantzsch and H. Kissel. Ber. **32**, 3144 (1899).
8. R. Foster. Nature, **176**, 746 (1955).
9. F. Čůta and E. Beránek. Collection Czech. Chem. Commun. **23**, 1501 (1958).
10. A. R. Norris. Can. J. Chem. **45**, 2703 (1967).
11. B. Vickery. Chem. Ind. London, 1523 (1967).
12. E. Buncel, A. R. Norris, and K. E. Russell. Quart. Rev. London, **22**, 123 (1968).
13. G. A. Russell and E. G. Janzen. J. Am. Chem. Soc. **84**, 4153 (1962).
14. E. F. Caldin and G. Long. Proc. Roy. Soc. London, Ser. A, **226**, 263 (1955).
15. E. Buncel, K. E. Russell, and J. Wood. Chem. Commun. 252 (1968).

Vol. 46
2761-3998
1968

Canadian Journal of Chemistry

Published by THE NATIONAL RESEARCH COUNCIL OF CANADA

VOLUME 46 SEPTEMBER 1, 1968 NUMBER 17

Configuration of the ring nitrogen in *N*-oxides and the conformation of tropanes.[1] Part XVIII

NAGABHUSHANAM MANDAVA AND GABOR FODOR
Chemistry Department, Laval University, Quebec 10, Quebec

Received January 3, 1968

The configurations of ring nitrogen in the amine oxides of tropine, oscine, atropine, and scopolamine have been investigated by nuclear magnetic resonance (n.m.r.) spectroscopy. Oxygen function(s) at C-6β (and 7β) were found to deshield the low-field, equatorial *N*-methyl signal. Analysis of the n.m.r. spectra of epoxides of some tropane bases, in particular the coupling constants, clearly indicates preponderance of the (slightly distorted) chair conformation even in the tropanes with a bulky group in the 3α (*endo*) position. The protons on the epoxide carbons are magnetically non-equivalent in scopolamine (**5***b*) and its *N*-oxide while appearing as a singlet in the alkamine, i.e. scopine (**5***a*).

Canadian Journal of Chemistry, 46, 2761 (1968)

Configuration of N-Oxides

In previous papers the determination of the configurations of quaternary salts of the tropane alkaloids by both chemical and physical methods (1–4) was described.

Quaternizations with the carbethoxymethyl group of 3α,6β-tropandiol and of 3α,6α-oxido-7β-hydroxytropane (1) and furthermore, *N*-ethylation of tropine (3) took a preferred equatorial course while in simple piperidines both equatorial and axial attack occurred, with axial predominating (5, 6). It was deemed therefore of interest to study the stereochemistry of amine oxides formed from some tropane bases.

A single *N*-oxide formation in scopolamine, atropine, and tropine each (type **1** or **2**) has been described (7). Scopolamine *N*-oxide had been reported (8) to undergo a transannular reaction on the action of hydrogen bromide to give scopinium bromide (**3**) which was, in turn, reduced to pseudoscopine (**4**). Since **3** cannot be formed from the *N*-oxide **1***b*, but only from structure **2***b*, this conversion may be considered (9, 10) as chemical evidence for the axial configuration of scopolamine amine oxide. Unfortunately, however, this experiment could not be repeated so far (11, 12). Although the melting points of a sample of pseudoscopine, prepared by reduction of scopinone (13) and that of its picrate coincided with those reported for **4** previously (8) a real indentification by mixture melting points, infrared, and nuclear magnetic resonance (n.m.r.) is still lacking.

The n.m.r. spectra of scopolamine, atropine, tropine, and oscine *N*-oxides were studied in order to determine their configurations. In the amine oxide hydrobromides methyl and hydroxy groups are attached to nitrogen in sterically non-equivalent positions. However, the large solvent dependence of the hydroxyl does not permit any configurational conclusions. The alternate possibility is the assignment of the configuration of the methyl by comparison based on empirical rules. Since chemical shifts in the piperidine series can be correlated with those of cyclohexane derivatives for reasons of geometry, recent n.m.r. data (5, 14–17) are also relevant to the configurations of the *N*-methyl group in the tropanes. They all show appreciable differences (4–16 c.p.s.) between equatorial and axial *N*-methyl signals in the methiodides, the equatorial one being more deshielded.

Scopolamine *N*-oxide has the *N*-methyl signal at 199 c.p.s. while the lower field, equatorial signal of (—)scopolamine methiodide (**6***b*) is at

[1]For Part XVII, see G. Fodor and F. Soti. J. Chem. Soc. 6830 (1965).

Can. J. Chem. Downloaded from www.nrcresearchpress.com by 210.87.254.105 on 09/05/12
For personal use only.

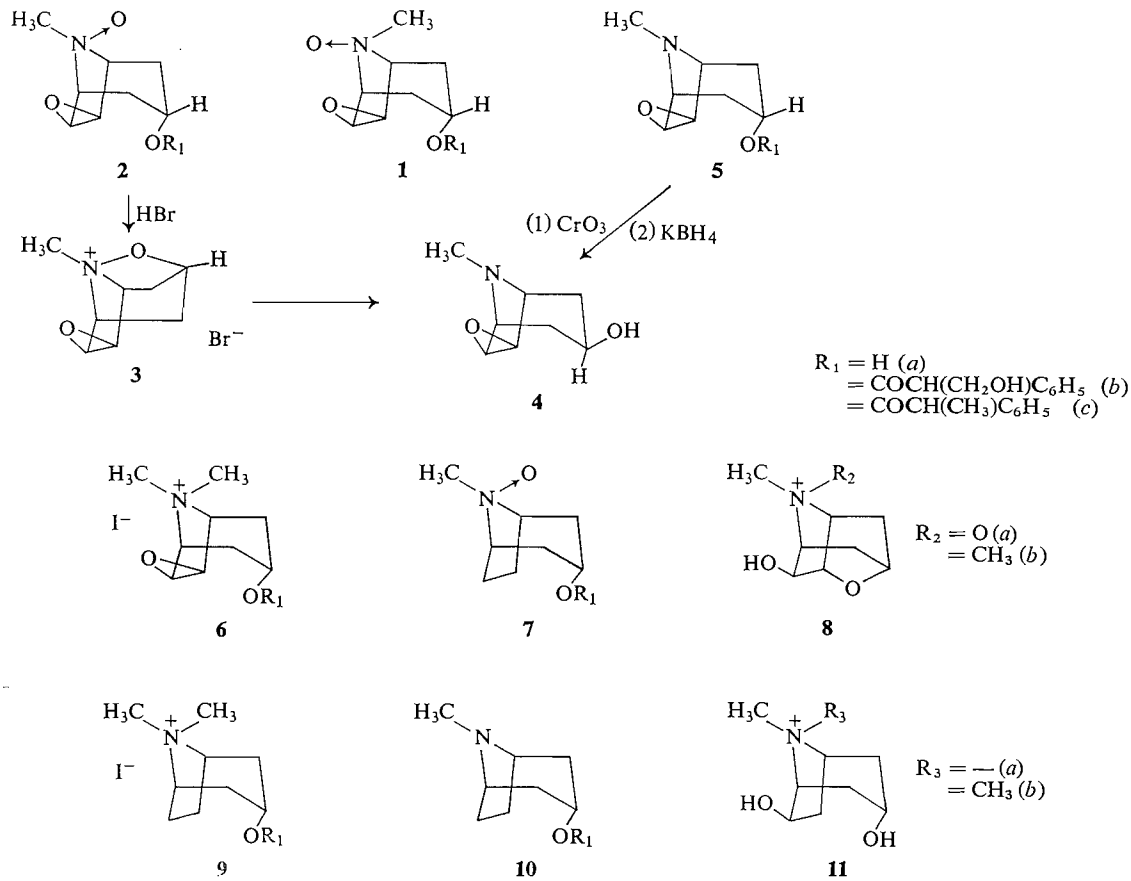

198 c.p.s. Similarly, in atropine *N*-oxide (**7***b*) the *N*-methyl group resonates very close to the same frequency (190 c.p.s.) as the low-field one (191.5 c.p.s.) in atropine methiodide (**9***b*). The same applies to the position of these signals in tropine *N*-oxide (**7***a*) and tropine methiodide (**9***a*) and also to oscine *N*-oxide and oscine methiodide (**8***a*) and (**8***b*) (Table I).

Nevertheless, an argument can be raised that the magnetic environment of the methyls on nitrogen in the amine oxide (**2***b*) and in the methiodide (**6***b*) may not be comparable, owing to the difference in polarity between methyl and semipolar oxygen. However, the position of the *N*-methyl signal of scopolamine *N*-oxide is shifted barely by 1.5 c.p.s. in its hydrobromide thus indicating that the charge on nitrogen is not a factor in deshielding the *N*-methyl group in the *N*-oxide.

Careful inspection of the chemical shifts for *N*-methyl group in a variety of tropanes reveals further interesting correlations (see Table I).

First, presence of an epoxide function at carbons 6β and 7β in scopolamine (**5***b*) results in deshielding by 15 c.p.s. of the methyl signal of atropine (**10***b*), and by 14 c.p.s. when comparing scopine (**5***a*) with tropine (**10***a*). Substitution of a hydrogen in tropine at C-6β by hydroxyl similarly shifts the same signal by 8 c.p.s. downfield in **11***a*. The chair form of the piperidine ring in tropanes and the high population of the *N*-methyl equatorial conformation have been ascertained by n.m.r. and X-ray data (3–4, 21) for the tertiary bases, so this paramagnetic shift can possibly be formulated as some effect of the neighboring oxygen on the *N*-methyl in equatorial position. Considering now the quaternary i.e. *N*,*N*-dimethyl tropanium salts, substitution by the epoxy group results in a downfield shift of the lower-field methyl signal by 13 c.p.s. from

149184

Can. J. Chem. Downloaded from www.nrcresearchpress.com by 210.87.254.105 on 09/05/12
For personal use only.

TABLE I

Comparison of *N*-methyl signals in *N*-oxides, methiodides, and bases in DMSO-d_6

Compound		*N*-Methyl resonance (c.p.s.)		
		Equatorial	$\Delta\delta_{eq}$	Axial
7*b*	Atropine *N*-oxide	190		—
2*b*	6β,7β-Epoxyatropine (scopolamine) *N*-oxide	199	9	—
7*a*	Tropine *N*-oxide	192		—
8*a*	7β-Hydroxy-3α,6α-oxidotropane (oscine) *N*-oxide	200	8	—
9*b*	Atropine methiodide	191.5		184.5
6*b*	6β,7β-Epoxyatropine (scopolamine) methiodide	198	7.5	187
9*a*	Tropine methiodide	189.5		186
6*a*	6β,7β-Epoxytropine (scopine) methiodide	202	12.5	186
11*b*	6β-Hydroxytropine methiodide	199	(**11***b*–**9***a*) 9.5	188
8*b*	7β-Hydroxy-3α,6α-oxidotropane (oscine) methiodide	203	(**8***b*–**9***a*) 13.5	199
10*a*	Tropine	140	8	—
5*a*	6β,7β-Epoxytropine (scopine)	148		—
11*a*	6β-Hydroxytropine	148	(**11***a*–**10***a*) 8	—
10*b*	Atropine	129		—
5*b*	6β,7β-Epoxyatropine (scopolamine)	144	15	—

tropine methiodide (**9***a*) to scopine methiodide (**7***a*) and by 7.5 c.p.s. between the methiodides of atropine (**9***b*) and scopolamine (**5***b*). The deshielding by epoxides of hydrogen close in space was extensively studied by Tori *et al.* (18) in bicycloalkanes. It is noteworthy to add that the higher field methyl signal remained completely unaffected in the epoxy compounds as compared with the references (see Table I), which again is consistent with its axial position.

It should be pointed out that the exchange of a proton by a hydroxyl at C-6β of tropine methiodide (**9***a* → **11***b*) is marked by a downfield shift of 9.5 c.p.s. for the equatorial while by only 2 c.p.s. for the axial *N*-methyl signals. Similar deshielding by an adjacent hydroxyl group on the methyl protons was observed by Eliel *et al.* (19), in methyl cyclohexanols, and also reviewed by Williams *et al.* (20) for C-18 methyls in steroids.

The deshielding of the *N*-methyl signal in scopolamine *N*-oxide (**2***b*) amounts to 9 c.p.s. versus atropine amine oxide (**7***b*). Similarly, oscine *N*-oxide (**8***a*) (obtained on alkaline hydrolysis of scopolamine *N*-oxide (**2***b*)) has a methyl signal shifted downfield by 8 c.p.s. when compared with tropine *N*-oxide (**7***a*).

All these data clearly demonstrate the same tendency in anisotropic shift and are considered as complementary evidence for the equatorial position of the *N*-methyl group in these amine oxides.[2] Similar correlations could be detected when comparing the positions of *N*-methyl signals in quaternary piperidinium and pyrrolidinium salts with and without a neighboring hydroxyl function.

Conformation of the Piperidine Ring in Tropane Bases

In case of 3β-cyano tropane, dipole moment measurements by Bishop *et al.* (4) showed the value calculated for the chair form unequivocally. The n.m.r. spectra of the same compound showed a coupling constant, $J = 9$ c.p.s. for the axial proton at C-3 with those at C-2 and C-4, leading to the identical conformational conclusions as the μ values. However, dipole moment data obtained with the 3α-form were inconsistent with either classical conformer. The n.m.r. spectrum of 3α-cyano tropane has C-3 proton coupled ($J = 5$ c.p.s.) with a rather complex broad proton signal comprising the C-2, C-4, C-6, and C-7 protons. In the present

[2]The final test to this configuration will be given by the X-ray study of scopolamine *N*-oxide hydrobromide, already in progress.

Can. J. Chem. Downloaded from www.nrcresearchpress.com by 210.87.254.105 on 09/05/12
For personal use only.

Can. J. Chem. Downloaded from www.nrcresearchpress.com by 210.87.254.105 on 09/05/12
For personal use only.

work, it has been shown that scopolamine, scopine, and their *N*-oxides gave a simplified pattern due to replacement of the 6β- and 7β-protons (22) by oxygen and, in consequence, to the downfield shift (23) of the α-protons[3] on these carbons. Thus protons C-2 and C-4 could now be identified, making the determination of conformations more conclusive.

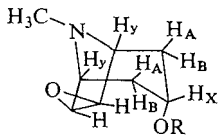

The n.m.r. spectrum of scopine (**5***a*) has been analyzed in detail in chloroform-*d* and benzene solutions. The epoxide protons gave rise to a singlet at δ 3.6. The C-1 and C-5 protons gave a pseudoquartet (J = 2 c.p.s., base-width 17 c.p.s.) at δ 3.5. The hydroxyl proton appeared as a singlet in benzene at δ 3.37 while in chloroform-*d* it coincided with the epoxide proton singlet and the *N*-methyl protons at δ 2.49.

The C-3 proton appeared as a pseudo-triplet at δ 3.9 p.p.m. (apparent J = 5.2 c.p.s.; base-width 17 c.p.s.; half-width 10 c.p.s.). This was analyzed as the X part of two ABX systems with spacing between the terminal lines equal to $2(J_{AX} + J_{BX})$ neglecting the long-range and virtual couplings. Comparison with the previously reported results (24) on the similarly situated protons in tropine (**10***a*) strongly supports our contention that the C-3 proton in scopine has an equatorial orientation.

The C-2 and C-4 methylene protons (δ 1.2–2.33) have been analyzed as the AB part of ABXY spectrum (23, 25, 26) assuming $J_{XY} = 0$. Using double resonance technique, the AB portion was simplified to 8 line-pattern as in AB part of ABX type (23, 27) by irradiating the C-3 or the C-1 and C-5 proton pair. Using the procedure of Pople *et al.* (28, 29) —J_{AB} 14.2 c.p.s. and δ_{AB} 39 c.p.s. were calculated.

The broad multiplets for C-3, and C-1 and C-5 protons were simplified to doublets upon saturation of the upfield signals and the coupling constants J_{AX} 4.1, J_{BX} 1.1, J_{AY} 4.0, and J_{BY} 2.0 c.p.s. were extracted.

In the n.m.r. spectrum of scopolamine the five aromatic protons of the tropic acid residue appeared at δ 7.3. The methylene and methine protons within the same acyl group resonated as a multiplet (δ 3.52–4.32). The C-3 proton gave a pseudotriplet (J = 5 c.p.s.; base-width 16.4 c.p.s.; half-width 10 c.p.s.) at δ 4.98 while the C-1 and C-5 protons exhibited a sextet at δ 3.98. The singlet due to the *N*-methyl group appeared at δ 2.4.

Analysis of the AB part (C-2 and C-4 protons at δ 1.1–2.3 p.p.m.) of ABXY system gives J_{AB} 14.4 c.p.s., δ_{AB} 30.8 c.p.s., J_{AX} 4.8; J_{BX} 0.4, J_{AY} 4.0, J_{BY} 1.2 c.p.s.

It is now established by spin-decoupling experiments and the calculated parameters that the six-membered ring in the tropane skeleton is in the chair form with some distortion. The J_{AB} value deviates to the extent of 10–12% from those of the ideal chair conformer of cyclohexane (J_{AB} = 12.2 c.p.s.) (27). The coupling constants J_{AX} and J_{AY} of 4–5 c.p.s. and J_{BX} and J_{BY} of 0.4–2.0 c.p.s. correspond to the dihedral angles of ca. 40° and 80°, respectively. This either means that the conformation is a distorted chair or that the Karplus curve (30) has to be considerably modified for piperidine. The former seems to be more reasonable in view of the recent X-ray crystallographic and n.m.r. study on pseudotropine (21) which indicated the deformed chair for piperidine ring. The deformation can be attributed to the ethylene bridge at C-1 and C-5 and to the steric hindrance of the atoms of this bridge with the C-3 atom.

The epoxide ring protons[4] in scopolamine appear quite unexpectedly as a pair of AB doublets (δ 2.84, 3.37; J_{AB} 2.9 c.p.s.) due to magnetic non-equivalence. The same was observed with the epoxide ring hydrogens in scopolamine *N*-oxide (δ 3.45, 3.75; J_{AB} 3.2 c.p.s.) and scopolamine hydrobromide (δ 3.22, 3.83; J_{AB} 3.5 c.p.s.), and by Johns and Lamberton (32) for acetyl scopolamine and α-methyl phenyl acetyl scopine (**5***c*) while no such doublet was found for anhydro scopolamine. Scopine was not available to these authors. They attributed magnetic non-equivalence of the C-6 and C-7 protons of the tropic acid esters (*i*) to the presence of an asymmetric center and (*ii*) an attached group of sufficient magnetic anisotropy to produce observable shielding. It has also been pointed out

[3]Concerning the α,β-convention, see ref. 22.

[4]For a table on n.m.r. data of epoxides and a compilation of references, see ref. 31.

Can. J. Chem. Downloaded from www.nrcresearchpress.com by 210.87.254.105 on 09/05/12
For personal use only.

(32) that the magnitude of diamagnetic shifts indicates inequalities in conformer populations favoring orientations with the phenyl ring close to the C-6 and C-7 protons. Our results which include the n.m.r. spectrum of scopine further support the above explanation of the magnetic non-equivalence of the epoxide ring protons in scopolamine.

There is no visible coupling between the C-6 and C-5 protons or between the C-7 and C-1 in the tropane derivatives that contain the epoxide ring at C-6 and C-7 and this, in part, is in complete agreement with the lack of observable coupling between similarly situated vicinal protons in the spectra of bicycloalkane epoxides (18).

Scopine (**5***a*), scopolamine (**5***b*), and the *N*-oxide (**2***b*) all showed an equatorial proton at C-3 of the tropane skeleton. The *J* values agree with those we have obtained with other tropanes having bulky axial groups at C-3. Consequently, present investigations are in harmony with the concept of the distorted chair form resulting from the repulsion between the bulky C-3 group and C-6 and C-7 protons.

Experimental

The nuclear magnetic resonance (n.m.r.) spectra were measured on a Varian A-60 spectrometer equipped with a Varian model V-6058 A spin decoupler. The internal reference standard was TMS except in D_2O where the previously calibrated methyl signal of sodium *p*-toluenesulfonate or acetone was taken as standard. The accuracy of ± 0.05 c.p.s. and ± 0.2 c.p.s. was obtained for coupling constants and line positions, respectively.

Scopolamine N-Oxide

This was prepared from scopolamine *N*-oxide hydrobromide by treatment with an aqueous solution of potassium carbonate followed by continuous extraction with methylene chloride. This was purified by recrystallization from methanol–acetone, m.p. 132–134°.

Atropine N-Oxide

This was prepared from 1.5 g of atropine base in 250 ml ether and 50 ml of 5.7% ethereal solution of monoperphthalic acid. The hydrogen phthalate of the amine oxide separated after 10 h and was washed with ether. This showed one *N*-methyl signal in the n.m.r. spectrum. Liberation by aqueous potassium bicarbonate and extraction of the residue with ethanol, after evaporation of water, afforded the *N*-oxide (0.8 g), m.p. 130–131° (reported (7) m.p. 127–128°).

Tropine N-Oxide

This was prepared according to Polonovski (7), and had m.p. 162°.

Oscine N-Oxide

This was prepared by hydrolysis of 2.5 g scopolamine *N*-oxide hydrobromide with a solution of 5 g barium hydroxide in 125 ml water for 35 min at 20°. The solution was then adjusted to pH 2 by cold 12% sulfuric acid and the suspension was extracted with ether. Evaporation of the ether extracts followed by recrystallization from ether – petroleum ether afforded fine needles of tropic acid, yield 1 g, m.p. 129–130°.

The aqueous suspension was treated with barium chloride and centrifuged. Evaporation of the solution under vacuum at 30° gave a solid which on extraction with methanol yielded oscine *N*-oxide hydrochloride. Recrystallization from DMSO and ether allowed further purification. The free amine oxide was obtained when the hydrochloride was stirred with silver oxide in methanol for 2 h at 20° followed by filtration and evaporation of the solvent *in vacuo*, m.p. 220–222°.

Acknowledgment

The support of the National Research Council of Canada (grant A-2839) is gratefully acknowledged.

1. G. Fodor, J. Toth, and J. W. Vincze. J. Chem. Soc. 3504 (1955).
2. G. Fodor. Bull. Soc. Chim. France, 1032 (1956); Tetrahedron, **1**, 86 (1957); Chem. and Ind. London, 1500 (1961).
3. C. H. MacGillavry and G. Fodor. J. Chem. Soc. 597 (1964).
4. R. J. Bishop, G. Fodor, A. R. Katritzky, F. Soti, L. E. Sutton, and F. J. Swinbourne. J. Chem. Soc. (C), 74 (1966).
5. H. O. House, B. A. Tefertiller, and C. G. Pitt. J. Org. Chem. **31**, 1073 (1966).
6*a*. D. R. Brown, J. McKenna, J. M. McKenna, J. M. Stuart, and B. G. Hutley. Chem. Commun. 380 (1967).
6*b*. D. R. Brown, R. Lygo, J. McKenna, J. M. McKenna, and B. G. Hutley. J. Chem. Soc. (B), 1184 (1967), and references cited therein.
7. M. and M. Polonovski. Bull. Soc. Chim. France, (IV), **39**, 1161, 1162 (1926).
8. M. and M. Polonovski. Bull. Soc. Chim. France, (IV), **43**, 79 (1928).
9. J. Meinwald. J. Chem. Soc. 712 (1953).
10. R. C. Cookson. Chem. and Ind. London, 337 (1953).
11. J. Meinwald and O. L. Chapman. J. Am. Chem. Soc. **81**, 5800 (1959).
12. G. Fodor. Acta Chim. Acad. Sci. Hung. **5**, 421 (1955).
13. A. Heusner and K. Zeile. Chem. Ber. **91**, 2399 (1958); Tetrahedron, **3**, 312 (1958).
14. A. T. Bottini and M. K. O'Rell. Tetrahedron Letters, 423, 429 (1967).
15. A. T. Bottini, B. F. Dowden, and L. Sousa. J. Am. Chem. Soc. **87**, 3249 (1965).
16. A. T. Bottini, B. F. Dowden, and R. L. van Etten. J. Am. Chem. Soc. **87**, 3250 (1965).
17. J.-L. Imbach, A. R. Katritzky, and R. A. Kolinski. J. Chem. Soc. (B), 556 (1966).
18. K. Tori, K. Kitahonoki, Y. Takano, H. Tanida, and T. Tsuji. Tetrahedron Letters, 559 (1964).

19. E. L. ELIEL, M. H. GIANNI, TH. H. WILLIAMS, and J. B. STOTHERS. Tetrahedron Letters, 741 (1962).
20. T. WILLIAMS, R. PHILION, J. IACOBELLI, and M. USOKOVIĆ. J. Org. Chem. **33**, 509 (1968).
21. H. SCHENK, C. H. MACGILLAVRY, S. SKOLNIK, and J. LAAN. Acta Cryst. **23**, 423 (1967).
22. G. FODOR and K. NADOR. J. Chem. Soc. 721 (1953).
23. J. W. EMSLEY, J. FEENEY, and L. H. SUTCLIFFE. High resolution nuclear magnetic resonance spectroscopy. Vol. 1. The Pergamon Press, Ltd., Oxford. 1965. Chap. 8; J. A. POPLE, W. G. SCHNEIDER, and H. J. BERNSTEIN. High resolution nuclear magnetic resonance. McGraw-Hill Book Co., Inc., New York. 1959. Chap. 6.
24. C-Y. CHEN and R. J. W. LE FÈVRE. J. Chem. Soc. 3473 (1965).
25. N. V. RIGGS. Australian J. Chem. **16**, 521 (1963).
26. R. J. ABRAHAM and H. J. BERNSTEIN. Can. J. Chem. **39**, 216 (1961).
27. F. A. L. ANET. J. Am. Chem. Soc. **84**, 1053 (1962); D. H. WILLIAMS and N. S. BHACCA. J. Am. Chem. Soc. **86**, 2742 (1964); A. C. HUITRIC, J. B. CARR, W. F. TRAGER, and B. J. NIST. Tetrahedron, **19**, 2145 (1963).
28. J. A. POPLE and T. SCHAEFER. Mol. Phys. **3**, 547 (1960).
29. H. J. BERNSTEIN, J. A. POPLE, and W. G. SCHNEIDER. Can. J. Chem. **35**, 65 (1957); G. W. A. MILNE and L. A. COHEN. Tetrahedron, **23**, 65 (1967).
30. M. KARPLUS. J. Chem. Phys. **30**, 11 (1959); J. Am. Chem. Soc. **85**, 2870 (1963).
31. G. G. LYLE and L. K. KEEFER. J. Org. Chem. **31**, 3921 (1966).
32. S. R. JOHNS and J. A. LAMBERTON. Chem. Commun. 458 (1965).

Can. J. Chem. Downloaded from www.nrcresearchpress.com by 210.87.254.105 on 09/05/12
For personal use only.

Can. J. Chem. Downloaded from www.nrcresearchpress.com by 210.87.254.42 on 09/05/12
For personal use only.

Reactions of ozonides. VI. Conditions for by-product ester production in the oxidative ozonolysis of oleic acid

D. G. M. DIAPER
Department of Chemistry, Royal Military College of Canada, Kingston, Ontario

AND

J. PASERO AND M. NAUDET
Laboratoire de Chimie des Corps Gras, Département de Chimie Organique et Laboratoire National des Matières Grasses (ITERG), Faculté des Sciences, Marseille, France

Received August 29, 1966[1]

Addition of water to various solvents used for oxidative ozonolysis of oleic acid increases acid product yield and diminishes ester by-product yield but the effect is non-stoichiometric. Hydrolysis of peranhydride intermediates and chain-termination mechanisms are possible explanations. Octyl nonanoate is identified as a by-product of nonanal autoxidation; its yield is diminished by adding water or ethanol. Reduced platinum oxide catalyzes oleic acid and 5-decene ozonide autoxidation but platinum on charcoal is without significant effect.

Canadian Journal of Chemistry, **46**, 2767 (1968)

Relatively little attention has been paid to the oxidation of ozonides. The majority of the work on their decomposition recorded in the literature has been reductive, leading either to aldehydes and ketones (1), or to alcohols (2, 3), or the products of condensation and reduction such as amines (4, 5). Among former studies of oxidative decomposition, that of Rieche *et al.* (6, 7) was the earliest serious attempt to explore the reaction variables. Formation of esters as by-products from long-chain ozonides was reported by Düll (8) and discussed in detail by Pasero *et al.* (9–12).

The techniques of oxidation of ozonization products hitherto reported include use of alkaline hydrogen peroxide emulsion (13) and performic acid (14–16), as well as thermal autoxidation and peroxide oxidation of preformed ozonide (9). There would appear to be some practical advantages in the first as a preparative technique, although the possibility of chemical reaction by the emulsifier obfuscates mechanism discussions. Moreover the reported yields were not as good as those found after performic acid oxidation although the systems are not strictly comparable. Thermal autoxidation is effective, but ester by-product formation is a serious disadvantage. Large-scale preparation of α,ω-aliphatic dicarboxylic acids by ozonolysis has recently become industrially important. Azelaic acid for synthetic fiber production has been prepared from oleic acid for some years (17) and there is some indication (18) of awakening interest in production of brassylic acid from erucic acid in a similar manner for a similar purpose.

Reaction by-products are here undesirable, not only because of the economics of production, but also because mechanical properties of fibers are severely affected by relatively small amounts of impurities having only a slightly shorter chain-length.

Formation of ester by-products is the major drawback of ozonization product oxidation for acid preparation or analytical work. Esters begin to form right at the start of oleic acid ozonization (11) and occur both in non-aqueous solvent systems and in aqueous and polar media (13, 14). Free alcohols corresponding to the esters are not found. The following mechanism of ester formation (9, 19) has been advanced.

$$2\,RCO_3H \rightarrow (RCO)_2O_2 + H_2O_2$$

$$(RCO)_2O_2 \rightarrow CO_2 + RCOOR$$

These products are therefore attributed to the decomposition of peracids formed in aldehyde oxidation. Procedures for acid preparation from ozonolysis products should therefore be studied in the light of aldehyde autoxidation mechanisms, since the presence of carbonyl compounds during ozonization (20) and among the products of thermal decomposition of ozonides (21) is well known.

[1]Revision received April 9, 1968.

TABLE I

Nonanal autoxidation

Experiment	Substrate	Time (h)	Relative yields from g.l.c. peak areas (%) Nonanal	Nonanoic acid	*n*-Octyl nonanoate
1	Nonanal alone	1	37.1	60.7	2.2
		3	11.1	84.2	4.7
		24	0	95.5	4.5
2	Nonanal pretreated with 1% O_3	1	21.3	74.8	3.9
		3	8.3	86.5	5.2
		24	0	94.8	5.2
3	As(2) with 1.0% H_2O	1	38.2	58.7	3.1
		3	10.1	86.2	3.7
		24	0	96.8	3.2
4	As(2) with 6.5% H_2O	1	41.4	56.8	1.8
		3	12.2	86.1	1.7
		24	0	97.8	2.2
5	As(2) with 0.5% EtOH	1	53.2	45.7	1.1
		3	12.7	85.1	2.2
		24	0	97.8	2.2
6	As(2) with 7.3% EtOH	1	56.3	42.7	1.0
		3	16.6	81.6	1.8
		24	0	97.7	2.3

We have studied the octyl nonanoate yield in the autoxidation of nonanal, one of the ozonization products from oleic acid, alone and in the presence of ethanol and water. We have also investigated oxidation catalysis by reduced platinum oxide. This catalyst was used successfully by Heyns for sugars (22) and by Sneeden and Turner for steroids (23). Acid and ester yields from isolated 5-decene ozonide and from oxidation of oleic acid mixed ozonization products have also been determined.

Experimental

Materials

Ozonized air was produced from a Welsbach Trailigaz apparatus at a flow rate of 125 l/h of dry air using 14 000 V at 50 w. Nonanal was fractionally distilled and stored under nitrogen. It was found to be 99.5% pure (gas–liquid chromatography (g.l.c.), retention time 4.3 min) and to have no impurities of retention time between 4.3 and 25 min on a neopentyl glycol sebacate column eluted with helium at 160 °C at 80 ml/min.

Two samples of oleic acid were used. Sample A, 99% pure (Nutritional Biochemicals) was converted to its methyl ester and analyzed by g.l.c. in a Varian Aerograph 1200 instrument having a 250 ft capillary Golay column coated with neopentyl glycol sebacate. Stearate and palmitate impurities were detected in 0.2 and 0.4% concentrations respectively. Sample B, m.p. 13.6° from olive oil, was examined spectroscopically and by g.l.c. and found to have negligible amounts of polyunsaturated acids, position and *trans* isomers (9). They were stored in the refrigerator under CO_2.

A reference sample of octyl nonanoate was prepared from 1-octanol and the acid chloride. A sample from nonanal oxidation was collected by preparative g.l.c. and its retention time and infrared (i.r.) spectrum were identical with those of the authentic sample. After saponification, the acid in ether was converted by diazomethane to the methyl ester which gave a single g.l.c. peak identified as methyl nonanoate. $LiAlH_4$ reduction gave a mixture of alcohols which were treated with trifluoroacetic anhydride. Peaks of approximately equal size were found in the g.l.c. trace identified by co-chromatography with authentic 1-octanol and 1-nonanol trifluoroacetates.

Attempts were made to isolate preparative quantities of the monomeric ozonides of oleic acid and of methyl elaidate by column chromatography on silica gel but pure fractions were obtained in impracticably small quantity. 5-Decene ozonide was obtained pure in 1–1.5 g quantities by this method. The i.r. spectrum had a strong peak at 9.1μ and the product was free from carbonyl and hydroxyl impurities. It was stable in the refrigerator for several weeks. The nuclear magnetic resonance (n.m.r.) peaks were found at 0.95 p.p.m. (CH_3) and 5.00 p.p.m. (CH) besides the broad CH_2 multiplet. A sample was reduced by $LiAlH_4$ and trifluoroacetylated; its g.l.c. showed a single peak, 1-pentanol trifluoroacetate.

Nonanal Autoxidation

Samples of 2–5 g of nonanal were placed in a small ground joint flask that had been carefully cleaned to avoid heavy metal ion contamination. The flask was furnished with a reflux condenser and a fused-in sintered glass gas inlet through which dry oxygen was passed at 15 ml/min while the apparatus was immersed in a boiling water bath. Samples were treated with ethereal ethanol-free diazomethane and analyzed by g.l.c. as described below.

Can. J. Chem. Downloaded from www.nrcresearchpress.com by 210.87.254.42 on 09/05/12
For personal use only.

TABLE II

Acid and ester production from oleic acid ozonide autoxidation. Effect of water in various solvents

Number	Solvent	Water concentration (vol. %)	Molar equivalent oleic acid* or 5-decene ozonide	Ester found (molar equivalent)	Acid found (molar equivalent)
101	Chloroform	0	5.67	1.62	11.3
102	Chloroform	50	3.61	0.67	8.18
104	Dioxan	0	3.58	0.838	13.0
103	Dioxan	50	2.67	0.45	9.05
105	Acetone	0	2.025	0.445	4.68
107	Acetone	0.5	4.06	0.80	10.32
108	Acetone	5	1.76	0.37	4.69
106	Acetone	10	2.27	0.148	6.30
109	Ethanol	0	4.04	6.20	4.96
111	Ethanol	0.5	3.12	4.78	3.83
110	Ethanol	20	2.54	1.99	5.32
112	Ethanol	40	2.63	2.10	5.40
119	Dimethyl formamide	0	4.41	4.41	9.12
120	Dimethyl formamide	2	4.83	4.53	9.76
121	Dimethyl formamide	10	4.79	4.56	9.39
122	Nitromethane	0	4.36	1.76	8.82
125	Nitromethane	0	2.36	0.883	6.18
126	Nitromethane	0.4	3.16	—†	8.98
123	Nitromethane	1	5.36	1.53	13.7
127	Nitromethane	2	4.31	3.02	11.3
124	Nitromethane	20	4.52	—†	13.9
128	Acetic acid	0	2.79	0.303	14.28
129	Acetic acid	7	3.57	0	14.08
130	Acetic acid	30	2.85	0.253	21.1
151	Acetone	0	2.017	0.443	4.72
152	Acetone	0.5	2.03	0.41	5.06
153	Acetone	0.5	2.04	0.38	5.00
154	Acetone	5	2.23	0.144	6.18
155	Acetone	0	3.12	0.37	5.22
156	Acetone	0	2.04	0.24	3.53
157	Chloroform	0	3.16	0.41	5.14
158	Acetone	1.0	2.08	0.11	3.57
159	Chloroform	1.0	3.15	0.19	5.17

*Sample B in runs 101–130, sample A in runs 151–154, 5-decene ozonide in runs 155–159.
†Saponification solution too dark for end point determination.

Immediately before experiments 2–6 (Table I) oxygen containing ozone was passed at 0.520 mmole of ozone per min until 0.01 mole of O_3 per mole of aldehyde had been introduced. Water and ethanol were used in experiments 3–6 in the weight percentages indicated in Table I.

A Burrell KD gas chromatograph with a 20 ft neopentyl glycol sebacate column was used for g.l.c. At 160° with helium at 75 ml/min, retention times for authentic samples of nonanal, methyl nonanoate, and ethyl 10-undecenoate were respectively 4.8, 7.2, and 24.8 min. 1-Octanol gave a tailed peak at 6.3 min and was not detected in significant amounts in the analyses. At 245° at this flow rate retention times for nonanal, methyl nonanoate, and ethyl 10-undecenoate were 2.1, 2.5, and 4.1 min, respectively, with 8.4 min for dimethyl sebacate and 11.6 min for *n*-octyl nonanoate. In analyses of autoxidized nonanal, minor peaks due to unidentified compounds were also observed at 2.6, 3.5, 4.6, 5.0, 5.2, and 10.6 min. In the 160° trace at 80 ml/min methyl heptanoate, methyl octanoate, and methyl nonanoate had retention times 4.6, 5.2, and 7.8 min respectively. Each analysis showed peaks attributable to methyl heptanoate and methyl octanoate having areas approximately 7–9% of the methyl nonanoate peak. Free nonanoic acid gave a tailed peak at 8.6 min at 245°; samples showing this were given a second treatment with diazomethane.

Internal standards were used for determination of the concentrations of nonanal, methyl nonanoate, and *n*-octyl nonanoate in the samples. Dimethyl sebacate and ethyl 10-undecenoate were selected because they were available pure, had suitable retention times, and gave peaks in a region of the analytical trace in which product peaks did not occur. *n*-Octyl nonanoate concentrations were determined by comparison of peak areas with dimethyl sebacate peak areas at 245°, and nonanal and methyl nonanoate concentrations were similarly determined relative to ethyl 10-undecenoate at 160°. Calibration curves were made for mixtures of known concentrations of these authentic substances. The reference standard solution contained 3.376 g of ethyl 10-undecenoate and 0.802 g of dimethyl sebacate in 12.938 g of solution in hexane. In a typical analysis, a weighed aliquot of ethereal solution was mixed with a known weight of this standard solution, transfers being made by hypodermic needle through serum caps. From the trace at 160°, peak areas of nonanal, methyl nonanoate, and ethyl 10-undecenoate were compared with calibration curves to give the concentrations of the first two substances.

Can. J. Chem. Downloaded from www.nrcresearchpress.com by 210.87.254.42 on 09/05/12
For personal use only.

TABLE III

Catalytic oxidation of oleic acid ozonization products at room temperature

Solvent*	Substrate (mmoles)†	O_2 uptake time‡ (h)	Volume of oxygen absorbed (% of theory)	Titration values: Acid (molar equivalent)	Titration values: Ester (molar equivalent)
Acetic acid	4.68 (B)	4.1	102	15.04	1.12
Methyl acetate	5.70 (B)	5.6	86	14.31	0.45
Dioxan	4.07 (B)	—	0	10.65	1.26
Ethanol	1.49 (B)	9	111	—	—
Ethanol	2.12 (A)	11.2	121	—	—
Acetone	3.32 (B)	4	37	8.07	0.64
Acetone (10 ml) and water (1 ml)	2.95 (B)	3.5	63	6.99	0.90
Acetone (10 ml) and water (4 ml)	2.92 (B)	—	10	6.08	0.64
Acetone	2.56 (A)	12	135	6.83	0.71
Acetone	2.19 (D)	6.3	85	3.85	0.13
Ethanol	3.14 (D)	10	128	—	—
Acetic acid	4.19 (D)	5.3	108	9.27	0.93

*Each sample contained approximately 50 mg of PtO_2 in 10–15 ml of solvent.
†Oleic acid samples indicated (A) or (B). (D) designates chromatographed 5-decene ozonide.
‡Approximate time for O_2 uptake to reach half the final value.

The early peaks were too narrow for reliable measurement at 245° but the *n*-octyl nonanoate concentration was similarly determined by comparing the peak area with that due to the known concentration of dimethyl sebacate. Figures in Table I were obtained by adding the number of millimoles of nonanal and methyl nonanoate to twice the number of millimoles of *n*-octyl nonanoate and expressing each as a percentage of the total. They are not percentage yields. Each figure was the mean of results from three injections of the same solution.

Ester Titration Study

The ozonization vessel was a 50 ml pear-shaped flask with two standard taper necks. One carried a reflux air condenser or water condenser and the other a gas inlet reaching to the bottom. Oleic acid (0.5–1.0 g, Sample B crystallized, distilled, and stored at 0° under CO_2) was accurately weighed into the flask and the solvent was introduced. Ozonized air was passed while the condenser and solution were cooled at −20° or at slightly higher temperatures if the solutions froze. Completion was assured by observation of the liberation of iodine in a potassium iodide trap by the gas effluent, and also by timing. After solvent removal under suction, a reflux air condenser was attached and oxygen was passed while the flask was immersed in a bath at 95°. When volatile solvents were used, the distillation step before heating was omitted. Effluent gas was bubbled through a trap containing ethanol. Autoxidation times were 15–20 h.

After autoxidation, the contents of the trap were placed in the flask with the sample and 10 ml of ethanol were used to rinse the condenser tube and inlet into the flask. After boiling under reflux for a few minutes to ensure that all entrained material was returned to the flask, titration of acidity was performed using standard ethanolic *N* potassium hydroxide. The saponification equivalent was determined using *N* ethanolic alkali in excess (from a 5 ml pipette) and back-titration with 0.5 *N* ethanolic HCl. Neutral water was added as necessary to dissolve precipitated KCl and the analysis was performed in a stream of CO_2-free air. Before titration, the flask was cooled to avoid fading of the phenolphthalein color. Results are given in Table II.

The samples containing the larger quantities of water were ozonized at room temperature rather than −10° because of the freezing problem. Similar experiments in tetrahydrofuran and dioxan gave apparent ester yields in the range 8.0–47.2%, but these were not considered reliable measurements of ester content since these solvents are attacked by ozone and oxygen, giving aldehydes and other products.

A chromatographically pure sample of 3.57 g of 1-octene ozonide (36) and water (1.0 g) was slowly heated to 100° while oxygen passed at 15 ml/min. After 10 h at 100° with O_2 passing the product was rinsed out with ether and dried. Heptoic acid (2.75 g, 95%) was isolated by distillation and found by titration of a weighed sample to be 94.3% pure. This was used to make the amide (m.p. 92–94°) identical with an authentic sample. The acid was free from aldehyde and peroxide.

Catalytic Oxidation (Table III)

The sample was contained in an outside taper conical flask with a side arm, and was stirred magnetically. The apparatus was attached to a gas measuring tube with taps to control the addition of oxygen and hydrogen. The catalyst was first hydrogenated (in the case of PtO_2) and the flask was then evacuated before filling with oxygen. For catalytic oxidation, the oxygen was purified by passage through chromic acid, sulfuric acid, soda lime, and silica gel. An explosion occurred when a volatile solvent was employed and the evacuation step was neglected. After gas uptake was completed, the solution was centrifuged to remove catalyst, evaporated under reduced pressure and the acid and saponification equivalents of the residual solid were determined in the usual manner.

Samples of 5-decene ozonide and oleic acid ozonization

Can. J. Chem. Downloaded from www.nrcresearchpress.com by 210.87.254.42 on 09/05/12
For personal use only.

Can. J. Chem. Downloaded from www.nrcresearchpress.com by 210.87.254.42 on 09/05/12
For personal use only.

mixture were stirred in the apparatus with oxygen but in the absence of catalyst. No significant uptake occurred in acetone. After 2 days the 5-decene sample was analyzed by thin-layer chromatography (t.l.c.) and found to be unchanged.

Platinum catalyst on charcoal was also employed by introducing it into the ozonization flask and passing at will oxygen or ozonized oxygen into the mixture. The catalyst was prepared by the method of Heyns and Paulsen (22).

Identification of Ozonization Products from Oleic Acid

The saponification solutions from oleic acid ozonization product autoxidation were treated as follows.

The solution was diluted with water, acidified, and extracted with ether. After solvent removal, methanolic boron trifluoride was used to convert acidic products to methyl esters. Two major and two minor products were found in the mixture, corresponding to methyl azelate, methyl pelargonate, octanol, and methyl 8-hydroxyoctanoate. These products were identified by g.l.c. retention times and co-chromatography with authentic samples on a polyester column (9). Further information on the identity of the products was obtained from the reduction products from the mixed acids. After lithium aluminium hydride reduction, the mixed alcohols, isolated in ether, were trifluoroacetylated and analyzed by g.l.c. as described above. The chromatograms of the products showed peaks due to the trifluoroacetates of 1-octanol, 1-nonanol, nonane-1,9-diol, and octane-1,8-diol, checked with authentic samples.

Preparative Catalytic Oxidation

5-Decene ozonide (3.2 g) in ethyl acetate (25 ml) and water (0.2 ml) was shaken with reduced PtO_2 (about 50 mg) in a Burgess–Parr apparatus containing oxygen at 50 p.s.i. for 24 h. The solution was aldehyde-free (Schiff test) and gave a negative peroxide reaction. Valeric acid (3.1 g, 87%) isolated by distillation was found to be 92% pure by titration with alkali. Its methyl ester g.l.c. trace showed a methyl butanoate peak whose area was less than 1% of that of the methyl pentanoate.

Results

n-Octyl nonanoate was obtained as a by-product of nonanal oxidation in yields of about 1–5%, the lower figure occurring in the presence of water or ethanol. During autoxidation at 100° chain degradation to heptanoic and octanoic acids occurred to about the same extent (7–9%), suggesting simultaneous α- and β-oxidation.

Little quantitative information can be derived from acid and ester titration values when mixed ozonization products were oxidized, but there was a noticeable trend to increased yields of acid and diminished yields of ester in polar solvents and in the presence of water. The theoretical yield of acid is 2 equivalents per mole from 5-decene and 3 from oleic acid. The ester by-products from oleic acid have 1 equivalent of acid per mole of ester (9). The water effect was non-stoichiometric. Ethanol and acetic acid obviously interfered with titration results, the former by esterification and the latter by incomplete solvent removal. Nitromethane, dimethyl formamide, and dioxane or their oxidation products also interfered with titration figures and it was only in chloroform and acetone that reasonable results could be obtained. Ester yields from 5-decene ozonide were less than those from oleic acid mixed ozonization products, but were also diminished in the presence of water.

Reduced platinum oxide was found to be a catalyst for oxidation of isolated ozonide and of mixed ozonization products at room temperature. The platinum–charcoal preparation of Heyns and Paulsen (22) was found to have no discernible catalytic capability. Ester by-products of the catalytic reaction were detected in quantities comparable with those in the uncatalyzed thermal autoxidation.

Discussion

Yields of ester by-products of oleic acid ozonide autoxidation have been reported to be about 30% within wide variations of conditions (9, 10) including change of the terminal functional group. In reacting solvents (14) ester by-product yields were lower, and yields of the expected acid products, nonanoic acid, and azelaic acid, were near-quantitative. Performic acid oxidation of 1-alkylcycloalkene ozonization products (15, 24), emulsion ozonization (13) of alkenes in aqueous hydrogen peroxide, and low-temperature ozonization (25) gave smaller yields of esters. We found that catalyzed room-temperature autoxidation of isolated ozonide or mixed ozonization products gave somewhat lower ester yields. We also found that addition of water or ethanol to the system partly suppresses the ester-forming degradation, both in aldehyde autoxidation and in ozonization product autoxidation.

Comparison of yields of esters and acids from oleic acid can be calculated from the "acid" and "saponification" titration figures of Tables II and III. Each original molecule of oleic acid may give 3 equivalents of acid if it is totally oxidized to pelargonic and azelaic acids, or it will give 1 equivalent of acid and 1 equivalent of ester if it reacts entirely by the alternative route. Thermal autoxidation of ozonized oleic acid in chloroform, dioxan, and acetone in the absence of water thus gave 33.4%, 17.1%, and 24.0% "ester route" decomposition. For 5-decene

Can. J. Chem. Downloaded from www.nrcresearchpress.com by 210.87.254.42 on 09/05/12
For personal use only.

ozonide autoxidation (2 moles of acid or 1 of ester per mole) the figures were a little lower, 12.4% in acetone and 13.8% in chloroform. Catalytic oxidation figures were lower in methyl acetate (8.9%) and about the same in acetone (25.8%). The high figure in dioxane (28.7%) is attributed to solvent attack. Again 5-decene ozonide gave a lower "ester route" figure (6.5%). The lower yields from nonanal autoxidation are not strictly comparable with these results because the experiments were performed under reflux rather than in an apparatus which permitted volatile by-product removal to a trap (9). Moreover gas flow rate and dispersion are doubtless factors in determining the effective concentration of volatile components. In both types of experiment, water addition and polarity of the residual solvent significantly affected ester yield, but both ratios and overall yields were widely variable and quantitative correlation was not established.

It is accepted that aldehyde autoxidation (which is very sensitive to catalysis by ozone (26)) proceeds by a chain mechanism at rates comparable to those observed (27–32) through the peracid radical as follows.

$$RCO^{\cdot} + O_2 \rightarrow RCO_3^{\cdot}$$

$$RCO_3^{\cdot} + RCHO \rightarrow RCO_3H + RCO^{\cdot}$$

Aroylperoxy radicals from aromatic aldehydes (33–35) can abstract protons from solvents and can also decompose by a chain mechanism giving esters (19). Water or ethanol may intervene by terminating the radical chains which without inhibitors may involve up to 200 000 cycles (26, 32). If diacylperoxide decarboxylation is the ester-producing step, water can intervene by diminishing diacylperoxide concentration.

Among other products of ozonolysis which have been found to give acid products by decomposition are the 1-hydroxy-hydroperoxides (37) and the dihydroxyperoxides of Rieche *et al.* (7). Hydroperoxy-ozonides (38) contain more than enough oxygen and polymeric peroxides (39) approximately the stoichiometrically correct amount for decomposition to acids; their decomposition has not yet been studied in detail.

Chain degradation during oxidation occurs not only by the ester-forming side reaction and the familiar β-oxidation, but also by α-oxidation as already reported (40). Catalytic oxidation of ozonization products over Adams catalyst appears to offer some advantage if chain degradation is to be minimized.

Acknowledgment

Support by Defence Research Board Grant 9530-17 is gratefully acknowledged by D.G.M.D.

1. P. S. Bailey. Chem. Rev. **58**, 925 (1958).
2. D. G. M. Diaper and D. L. Mitchell. Can. J. Chem. **38**, 1976 (1960).
3. J. A. Sousa and A. L. Bluhm. J. Org. Chem. **25**, 108 (1960).
4. D. G. M. Diaper and D. L. Mitchell. Can. J. Chem. **40**, 1189 (1962).
5. K. A. Pollart and R. E. Miller. J. Org. Chem. **27**, 2392 (1962).
6. A. Rieche and R. Meister. Chem. Ber. **65**, 1274 (1932).
7. A. Rieche, R. Meister, and H. Sauthoff. Ann. **553**, 187 (1942).
8. H. Düll. Doctoral Thesis, Heidelberg. 1933.
9. J. Pasero. Doctoral Thesis, Marseille. 1963.
10. J. Pasero and M. Naudet. Rev. Franc. Corps Gras, **7**, 189 (1960); **10**, 453 (1963).
11. J. Pasero, L. Comeau, and M. Naudet. Bull. Soc. Chim. France, 493 (1965).
12. J. Pasero, J. Chouteau, and M. Naudet. Bull. Soc. Chim. France, 1717 (1960).
13. M. I. Fremery and E. K. Fields. J. Org. Chem. **28**, 2537 (1963).
14. R. G. Ackman, M. E. Retson, L. R. Gallay, and F. A. Vandenheuvel. Can. J. Chem. **39**, 1956 (1961).
15. D. G. M. Diaper. Can. J. Chem. **33**, 1720 (1955).
16. Y. Kishimoto and N. S. Radin. J. Lipid Res. **4**, 437 (1963).
17. C. G. Goebel, A. C. Brown, H. F. Oehlschlaeger, and R. P. Rolfes. U. S. Patent No. 2,813,113 (1953).
18. Chem. Eng. News, **42**, (48), 31, (1964); H. J. Nieschlag *et al.* Ind. Eng. Chem. Prod. Res. Develop. **6**(2), 120 (1967); Chem. Abstr. **67**, 2719*y* (1967).
19. D. Lefort, D. Tempier, and J. Sorba. Bull. Soc. Chim. France, 442, (1960); 1385 (1959).
20. S. Fliszar, D. Gravel, and E. Cavalieri. Can. J. Chem. **44**, 1013 (1966).
21. S. D. Razumorskii and Yu. N. Yur'ev. Zh. Organ. Khim. **3**(2), 251 (1967).
22. K. Heyns and H. Paulsen. Angew. Chem. **69**, 600 (1957).
23. R. P. Sneeden and R. B. Turner. J. Am. Chem. Soc. **77**, 190 (1955).
24. D. G. M. Diaper and D. L. Mitchell. Can. J. Chem. **43**, 319 (1965).
25. O. S. Privett and C. Nickell. J. Am. Oil Chem. Soc. **39**, 414 (1962).
26. E. Briner and G. Papazian. Helv. Chim. Acta, **23**, 497 (1940).
27. H. R. Cooper and H. W. Melville. J. Chem. Soc. 1984 (1951).
28. J. R. McNesby. Diss. New York Univ. (1951).
29. H. L. J. Backstrom. J. Am. Chem. Soc. **49**, 1460 (1927).
30. D. A. Lillard and E. A. Day. J. Am. Oil Chem. Soc. **41**, 549 (1964).
31. C. Walling and E. A. McElhill. J. Am. Chem. Soc. **73**, 2927 (1951).
32. C. E. H. Bawn. Discussions Faraday Soc. **14**, 181 (1953).

33. M. M. ALEKSANKIN and I. P. GRAGEROV. Zh. Obshch. Khim. **31**, 3167 (1961); Chem. Abstr. **57**, 2125*d* (1962).
34. H. M. WHITE and P. S. BAILEY. J. Org. Chem. **30**, 3037 (1965).
35. R. E. ERICKSON, D. BAKALIK, C. RICHARDS, M. SCANLON, and G. HUDDLESTON. J. Org. Chem. **31**, 461 (1966).
36. D. G. M. DIAPER. Preprints of papers delivered to the Intern. Oxidation Symp. San Francisco. 1967. Vol. I. p. 319.
37. E. G. E. HAWKINS. Organic peroxides. E. and F. N. Spon, London. 1961. p. 145.
38. O. S. PRIVETT and C. NICKELL. J. Am. Oil Chem. Soc. **41**, 72 (1964).
39. F. L. GREENWOOD and H. RUBINSTEIN. J. Org. Chem. **32**, 3369 (1967).
40. M. LOURY. Compt. Rend. **258**, 238 (1964).

Can. J. Chem. Downloaded from www.nrcresearchpress.com by 210.87.254.42 on 09/05/12
For personal use only.

Can. J. Chem. Downloaded from www.nrcresearchpress.com by 210.87.254.105 on 09/05/12
For personal use only.

Carbon tetrachloride as solvent in proton magnetic resonance. Importance of size and charge effects of proximate substituents

T. SCHAEFER, B. RICHARDSON, AND R. SCHWENK
Chemistry Department, University of Manitoba, Winnipeg, Manitoba

Received April 10, 1968

A model (not a theory), based on steric and charge removal characteristics of the substituents, is used to rationalize the low-field shifts caused by carbon tetrachloride (compared to cyclohexane) in the proton resonance spectra of 22 polyhalosubstituted benzenes. The low-field shifts are as large as 0.16 p.p.m. and these are found for protons situated between two ortho fluorine substituents. Larger halogens present a steric hindrance to the approach of the polarizable C—Cl bonds of the solvent and lead to smaller shifts. The charge removed from the region of the C—H bonds by the substituents is estimated by means of a function of the bond dipole divided by the bond length. A shape effect, arising when two hydrogens are *ortho* to each other, also appears to be present if there are bulky distant groups.

Canadian Journal of Chemistry, 46, 2775 (1968)

Introduction

Carbon tetrachloride is commonly used as a solvent in proton magnetic resonance spectroscopy because it contains no protons, has a low dielectric constant, and because it dissolves sufficient amounts of a wide variety of organic compounds. It is a more versatile solvent than cyclohexane or tetramethylsilane. But this means that carbon tetrachloride interacts rather more strongly with a wide variety of molecules than do the latter two solvents and therefore a significant solvent effect (1, 2) on the proton shifts is probable. Furthermore, carbon tetrachloride is often used as a reference solvent in studying, for example, the large proton shifts induced by benzene (2, 3). Benzene solvent shifts[1] are then defined as 'shift in benzene minus shift in carbon tetrachloride', and have important applications in structure and conformation determination (2, 4). Now, it is here suggested that 0.1 p.p.m. or more of these benzene solvent shifts may arise from the use of carbon tetrachloride as the reference solvent and that conclusions based on small benzene solvent shifts may be of doubtful validity.[2]

Recently Williams, Ronayne, and Wilson (5) have demonstrated a steric effect in carbon tetrachloride (and other) solvent shifts. This arises because a solute C—H bond may be shielded by bulky groups from collisions with the solvent molecules while the internal reference (tetramethylsilane) is not so shielded. The net result is an *apparent* upfield shift of the C—H proton. The observed shifts in this paper are intended to demonstrate that, in addition to causing a steric effect, the substituent may change the charge distribution near the C—H bond and hence may alter the time-averaged distribution of the carbon tetrachloride molecules near the C—H bond.

The consequence is a second contribution to the observed shift and is here called the charge effect.

Experimental

The proton resonance spectra were measured and calibrated by period averaging techniques on a DA-60I spectrometer operated in the frequency-sweep mode. The compounds were prepared as degassed, 3 mole % or less (saturated) solutions in carbon tetrachloride and cyclohexane, using internal tetramethylsilane as a reference.

Spectra were treated as A, A_2, AB_2, ABX, ABC, ABXR or other cases, as the situation warranted. Second or higher order 3-spin spectra were analyzed on an IBM 360/65 computer using a program written by J. Cavanaugh in Fortran II and adapted to this computer by H. M. Hutton.

Results and Discussion

In Table I the solvent shifts Δ (shift in cyclohexane minus the shift in carbon tetrachloride) are given for 22 polyhalobenzenes.[3] In many cases the Δ values are probably accurate to better than 0.005 p.p.m. but in some cases the error may be as large as 0.01 p.p.m.[4]

[1]Sometimes called ASIS values (2), an abbreviation for 'aromatic solvent induced shifts'.

[2]This statement applies even more strongly to the use of deuterated chloroform as a reference solvent.

[3]There is a low-field shift in carbon tetrachloride in every case.

[4]The detailed shifts and coupling constants in cyclohexane, carbon tetrachloride, and benzene solutions will be reported in connection with studies of additivity effects of substituents.

TABLE I

Proton solvent shifts, Δ,* induced by carbon tetrachloride in some polyhalosubstituted benzenes†

Compound	Proton	Δ(p.p.m.)
1, Benzene	—	0.041
2, Penta F	—	0.161
3, 1,2,4,5-Tetra F	$H_{3,6}$	0.159
4, 1,3,4,5-Tetra F	$H_{2,6}$	0.137
5, 1,2,3,4-Tetra F	$H_{5,6}$	0.141
6, Penta Cl	—	0.120
7, 1,2,4,5-Tetra Cl	$H_{3,6}$	0.111
8, 1,2,3,4-Tetra Cl	$H_{5,6}$	0.121
9, 1,2,4,5-Tetra Br	$H_{3,6}$	0.073
10, 1,4-Di Br-2,5-di F	$H_{3,6}$	0.120
11, 2,4,6-Tri-Br-1-I	$H_{3,5}$	0.069
12, 1,3,5-Tri Cl	$H_{2,4,6}$	0.076
13, 1,3,5-Tri Br	$H_{2,4,6}$	0.064
14, 1-Br-3,5-di Cl	H_2	0.071
	$H_{4,6}$	0.085
15, 1-I-3,5-di F	H_2	0.061
	$H_{4,6}$	0.120
16, 1,2,3-Tri Cl	$H_{4,6}$	0.103
	H_5	0.134
17, 1,3,4-Tri Br	H_2	0.063
	H_5	0.104
	H_6	0.110
18, 1,3-Di-Br-4-F	H_2	0.065
	H_5	0.143
	H_6	0.097
19, 1,4-Di-Cl-3-Br	H_2	0.074
	H_5	0.110
	H_6	0.117
20, 1,3,4-Tri Cl	H_2	0.087
	H_5	0.114
	H_6	0.120
21, 1-I-3,4-di Cl	H_2	0.059
	H_5	0.115
	H_6	0.087
22, 1-Br-3,4-di-Cl	H_2	0.073
	H_5	0.115
	H_6	0.105
23, 1-F-3,4-di-Cl	H_2	0.114
	H_5	0.116
	H_6	0.131

*Defined as the shift in 3 mole % cyclohexane solutions minus the shift in 3 mole % carbon tetraehloride solutions, both shifts in p.p.m. being to low-field of internal tetramethylsilane. The shifts are negative and therefore Δ is positive.

†The solvent shifts are assumed to have contributions from the charge effect, the steric effect and the shape effect. The major contribution is that of the charge effect as discussed in the text. Additive steric contributions are applicable only when the proton is situated between two halogens and are

I = 0.038, Br = 0.025, Cl = 0.015, F = 0.000 p.p.m.

Shape effects are not defined quantitatively but can amount to as much as 0.03 p.p.m. depending on the substitution pattern.

Reaction Field Effects

These cannot account for the major part of the observed shifts because (*i*) the dielectric constants of carbon tetrachloride and cyclohexane differ by only 0.2 units[5] (*ii*) the group dipoles are 1.48, 1.58, 1.56, and 1.40D for C—F, C—Cl, C—Br, and C—I respectively (6) (*iii*) the reaction field model based on the dipolar effect predicts *upfield* shifts in carbon tetrachloride for, say, the 3-protons in the 1,2,4-trisubstituted benzenes (*iv*) even the quadrupolar reaction field model (1) predicts much smaller low-field shifts than observed for the 1,2,4,5-tetrasubstituted benzenes. However, there may be relatively small reaction field shifts which are mentioned again below.

Steric Effects

The presence of steric effects is demonstrated in Fig. 1 where the Δ values of the 2-protons in 1-X-3,4-dichlorobenzenes plot smoothly versus the van der waals radius of X. A similar curve, but displaying considerable curvature, is obtained for the 6-protons (not plotted). The plot of Δ values of the 5-protons in Fig. 1 (dashed line) indicates a steric effect depending mainly on the *ortho* substituent (the charge effect discussed below may counteract the steric effect of the more distant neighbors).

A steric effect alone cannot explain the Δ value of 0.042 p.p.m. for benzene itself. The C—Cl bond is four times as polarizable as a C—H bond (7). Each collision of a carbon tetrachloride molecule with a C—H bond in the benzene molecule is more effective (than a cyclohexane collision) in disrupting the diamagnetic circulation of the C—H bond electrons and leads to less screening in carbon tetrachloride than in cyclohexane solution.[6] However, the presence of internal reference molecules should cancel these effects (although packing arrangements can conceivably be present).

Alternatively, there is evidence for weak complex formation between benzene and carbon tetrachloride (9). The observed Δ value can then be attributed to the complex.

Charge Effect

There is another approach to the Δ value of benzene solute molecules which encompasses also

[5]The 10% increase in the reaction field effect in going from cyclohexane to carbon tetrachloride causes a low-field shift of about 0.01 p.p.m. We find that chloroform, with a dielectric constant of 4.8, gives Δ values only a fraction larger than carbon tetrachloride.

[6]We are specializing the usual dispersion model, in which the total polarizability of the molecule is considered, to one in which the bond polarizabilities are emphasized. The calculation of cohesive energies of a liquid may well be given by the former procedure (8). However, the mean square electric fields at a particular C—H bond due to a colliding solvent molecule depend on r^{-6}. These fields cause the deshielding and hence the nearest C—Cl bond is most effective. It may be noted that the polarizabilities of cyclohexane and carbon tetrachloride (and the boiling points) are very similar.

Can. J. Chem. Downloaded from www.nrcresearchpress.com by 210.87.254.105 on 09/05/12
For personal use only.

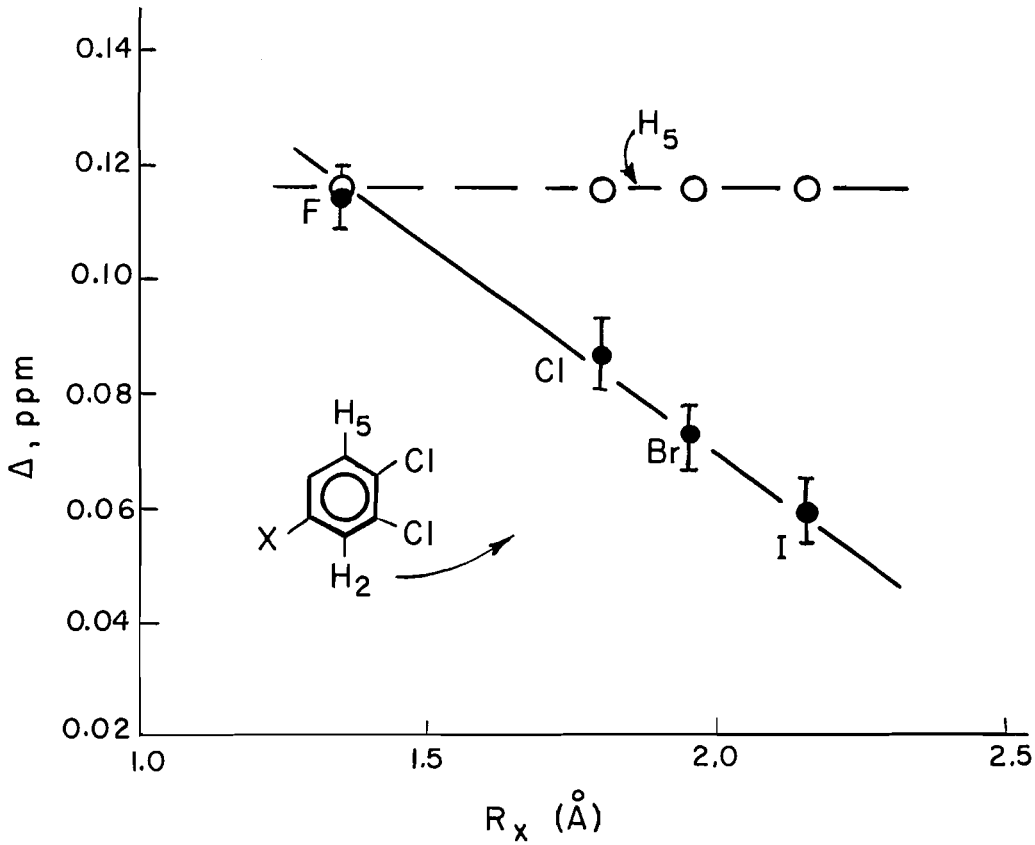

FIG. 1. The solvent shift Δ, in p.p.m., of protons-2 and -5 is plotted versus the van der waals' radius, R_x of the substituent, X in 1-X-3,4-dichlorobenzenes. Δ = shift in a 3 mole % cyclohexane solution minus the shift in a 3 mole % carbon tetrachloride solution. A positive Δ value means a low-field shift in carbon tetrachloride relative to cyclohexane.

the other Δ values in Table I. The carbon tetrachloride molecules may be thought of as regions of relatively high electron density. It follows that they will tend to concentrate near regions of relatively low electron density.[7] In benzene the C—H bonds contain trigonally hybridized carbon atoms and consequently a lower electron density near the proton than the C—H bonds in tetramethylsilane. The Δ value of benzene protons can thus arise because the highly polarizable C—Cl bonds are found more often near, and collide more often with, the C—H bonds in benzene than with the C—H bonds in tetramethylsilane.

A *charge* effect of this nature must be superimposed on the steric effect in substituted benzenes. There is no certain way of determining exactly how much the charge distribution in the immediate vicinity of the C—H bond is altered by a substituent.[8] A semiquantitative approach is devised as follows. A measure of the amount of charge removed from the ring region by a substituent X, is taken to be u/r (11). Here u is the dipole moment of the C—X bond and r is the C—X bond length.[9] The *ortho* substituent is

[7]Such appears to be the situation in benzene solutions, as suggested by one of us long ago (10).

[8]Hückel molecular orbital calculations are probably too crude for polyhalobenzenes. There is the further difficulty that three halogens have *d* orbitals available for conjugation and that only the π system is considered. Fluorine is a π donor and a strong σ acceptor. What matters, it seems, is its net electron withdrawal (π or σ) from the ring. A very strong π donor may overshadow any σ withdrawal and lead to Δ values lower than for the benzene protons (see later sections of the discussion).

[9]We use u/r values of 1.14, 0.93, 0.84, and 0.68 e.s.u. units for F, Cl, Br, and I, respectively. These are obtained from the dipole moments (12) of, and bond lengths (13) in, the phenyl halides.

Can. J. Chem. Downloaded from www.nrcresearchpress.com by 210.87.254.105 on 09/05/12
For personal use only.

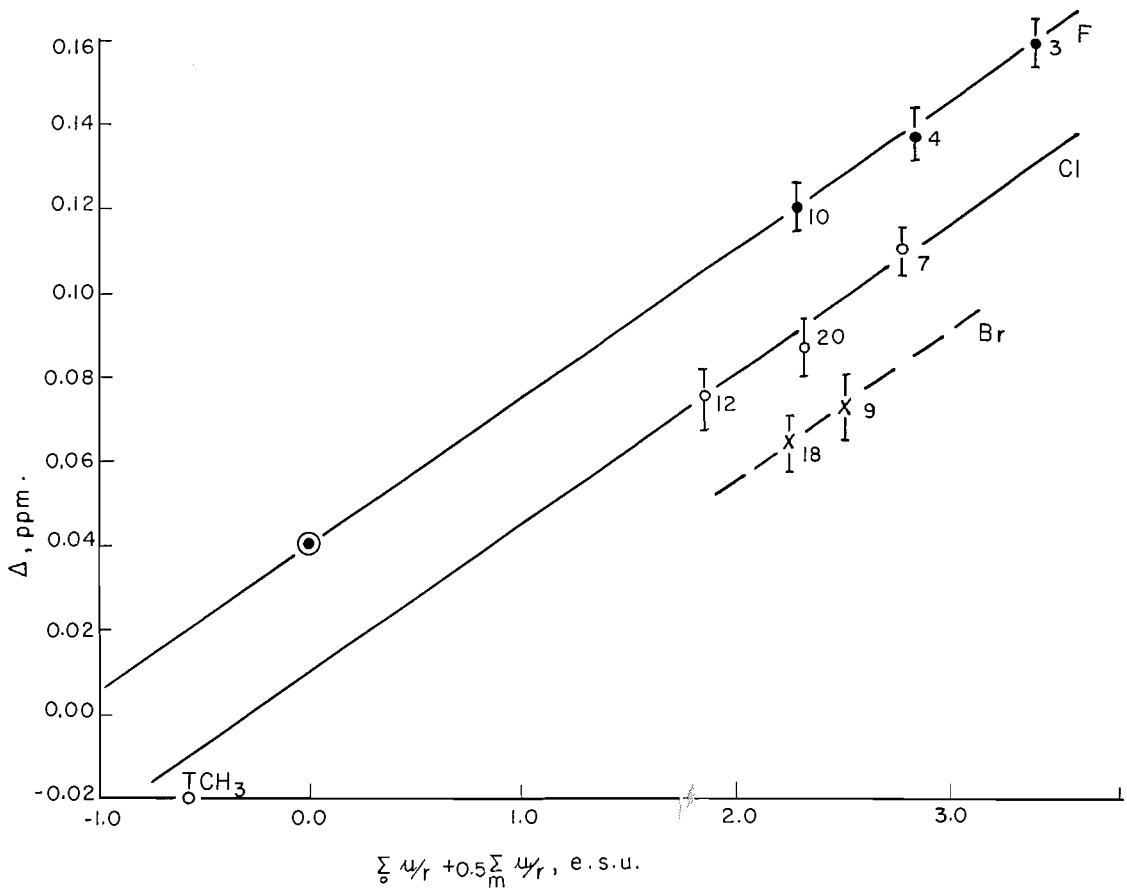

FIG. 2. The Δ values (defined in the text and in the caption of Fig. 1) of protons situated between two identical halogen substituents are plotted versus the function of u/r (defined in the text). The numbering of the points refers to Table I.

naturally most effective at removing charge from the region near the C—H bond. In this paper the expression $\Sigma_o\, u/r + 0.5\, \Sigma_m\, u/r$ is used as an approximation to the change in charge distribution induced by the substituent.[10]

In Fig. 2, Δ values from Table I are plotted versus the u/r function for some protons situated between two *identical* halogens. A straight line through the points for benzene and those for two *ortho* fluorine substituents suggests negligible steric hindrance by fluorine (van der waals' radii are H = 1.2 Å and F = 1.35 Å (15); the van der Waals' radius of the flat benzene ring is 1.70 Å suggesting that the substituent must have a radius of this value before steric effects become appreciable). The straight line through points 7, 12, and 20 for two *ortho* chlorine substituents (van der waals' radius of Cl = 1.80 Å) suggests the modification of charge effects by steric hindrance. Points 9 and 18, referring to two *ortho* bromine substituents, indicate even greater steric hindrance by bromine (less convincing Δ values for bromine can be found in Table I).

Methyl groups are net electron donors (whether by an inductive or hyperconjugative mechanism) and hence their u/r value is negative (−0.29). In Fig. 2 the Δ value of mesitylene is also given and suggests that electron donors do indeed cause negative Δ values.[11]

[10]The sums are over *ortho* (*o*) and *meta* (*m*) substituents. Benzene solvent shifts for the present and related series of compounds are as large as 1.2 p.p.m. and a very similar formula can correlate about 60 Δ values with a precision approaching 0.02 p.p.m. (14).

[11]This conclusion is confirmed by our benzene solvent effect studies (14). Negative Δ values for benzene as solvent have been observed previously in the presence of strong electron donors (16).

Can. J. Chem. Downloaded from www.nrcresearchpress.com by 210.87.254.105 on 09/05/12
For personal use only.

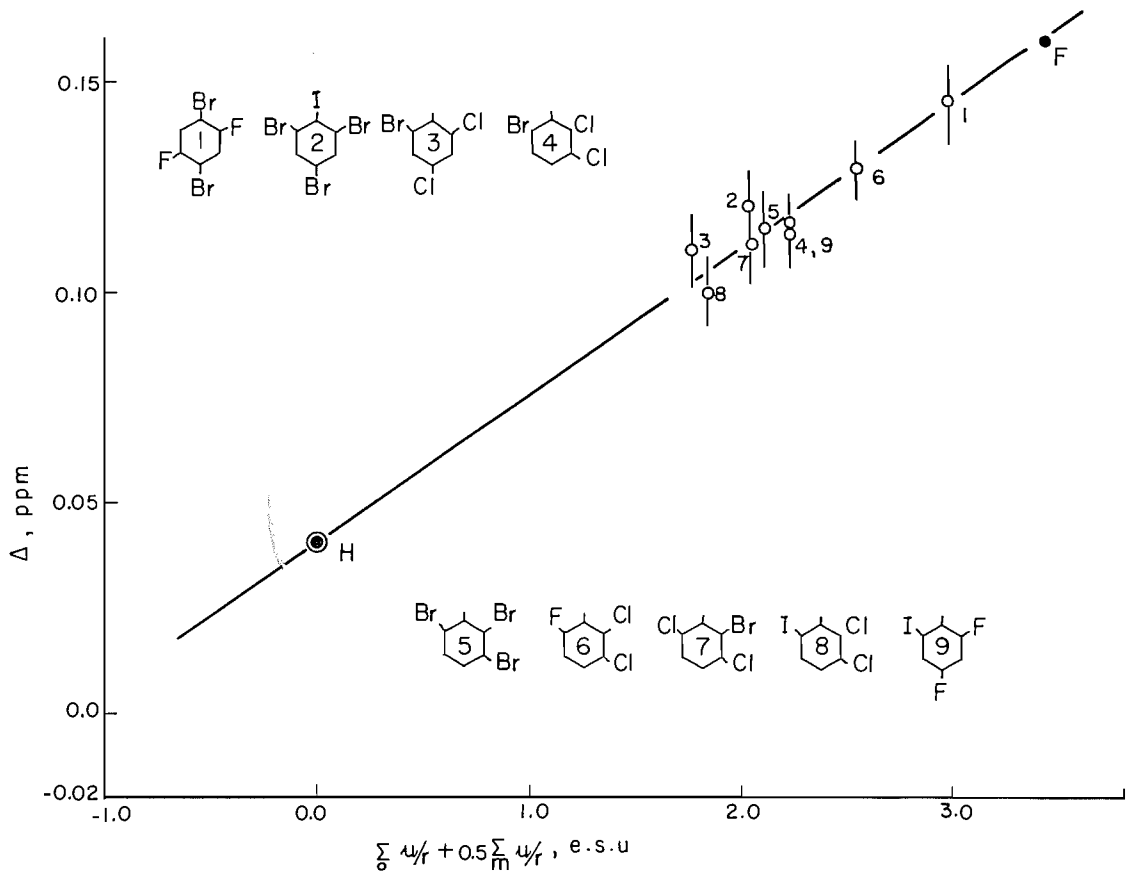

FIG. 3. The Δ values (defined in the text and in the caption of Fig. 1) of protons situated between, for the most part, unlike halogen substituents are plotted versus the function of u/r (defined in the text). The numbering refers to the formulae drawn in the figure and the Δ values have been corrected for steric effects as discussed in the text. The solid line is the top line from Fig. 2.

Assume that the lines in Fig. 2 establish the combined steric and charge effects of the substituent. Then the Δ values in Table I for *unlike ortho* substituents must lie on the top line of Fig. 2 after corrections are made for steric effects. Steric effects equalling 0.015 p.p.m. for one chlorine and 0.025 p.p.m. for one bromine are taken from Fig. 2. Thus, the steric correction for a proton situated between chlorine and bromine is 0.040 p.p.m.

In Fig. 3 the top line of Fig. 2 is redrawn. Points 1 to 7 are the corrected Δ values of the protons situated between F, Br; Br, Br; Br, Cl; and F, Cl (the Br, Br points are those not used in Fig. 2). Within experimental error they fall on the reference line. Points 8 and 9 represent protons situated between Cl, I; and I, F. A steric correction of 0.038 p.p.m. was applied for I. No shifts of protons situated between two iodines are available in Table I. Hence point 9 is consistent with point 8 or vice versa. The three steric corrections: I = 0.038, Br = 0.025, Cl = 0.015 p.p.m. plot precisely linearly against the van der waals' radii.

Shape Effect

Consider the Δ values in Table I of those protons with only one *ortho* halogen substituent. They are plotted (circles) in Fig. 4 *without* applying a steric correction. Many of the points show a significant positive deviation from the reference line implying not only the absence of a steric correction under such conditions, but also the presence of a shape effect in which bulky distant substituents force the carbon tetrachloride molecules towards the unsubstituted region of the benzene ring. For example, the largest positive

Can. J. Chem. Downloaded from www.nrcresearchpress.com by 210.87.254.105 on 09/05/12
For personal use only.

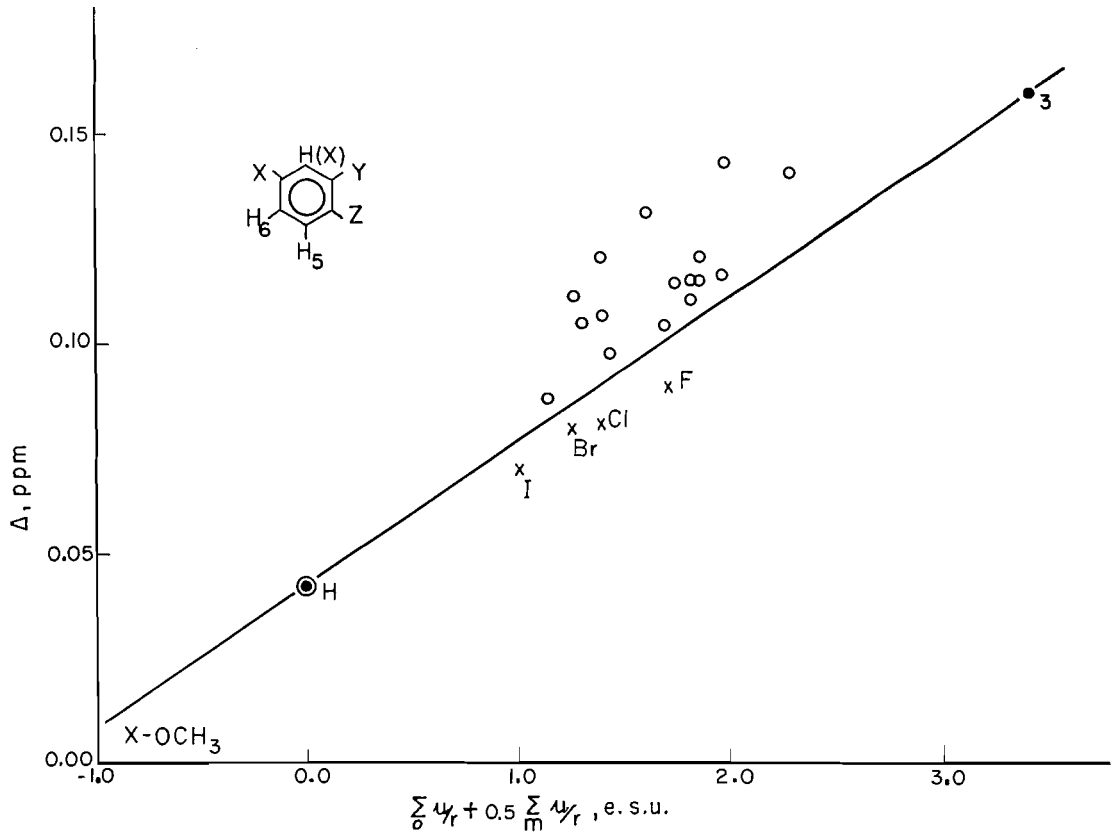

FIG. 4. The Δ values (defined in the text and in the caption of Fig. 1) of protons having only one *ortho* substituent are plotted versus the function of u/r (defined in the text). The open circles refer to protons-5 and -6 of the tri- or tetra-substituted compounds. The crosses refer to symmetrically *p*-disubstituted benzenes.

deviation is found for a proton next to a (small) fluorine while there are two distant (large) bromine atoms placed *meta* to the proton.

On the other hand, the positive deviation for proton 6 in 1,3,4-trichlorobenzene is 0.030 p.p.m. but is only 0.027 p.p.m. for the analogous bromobenzene. These deviations are equal within experimental error although that of the bromo compound is expected to be a little larger. The deviations for proton-5 in these two compounds are zero within experimental error and are expected to be smaller than those for proton 6 because proton-6 is more remote from the third substituent.

To test the idea of a shape effect we plot (crosses) the Δ values of some symmetrically *p*-disubstituted benzenes in Fig. 4 (3 mole % solutions: OCH_3 = 0.008, Cl = 0.080, Br = 0.080, I = 0.070, F = 0.089 p.p.m.).[12] The methoxy group is a strong π donor and we have taken u/r = 0.89 units (using the =C—O bond length). The oxygen atom is not appreciably larger than fluorine and the methyl group is probably too distant to present appreciable steric hindrance. All of the points show a small negative deviation from the reference line. This result is taken to mean that steric corrections are indeed almost negligible in the presence of only one *ortho* substituent.[13]

[12]Unfortunately, the low solubility of *p*-dinitrobenzene in cyclohexane prevents the measurement of its Δ value.

[13]There is the difficulty that fluorine also shows a negative deviation. Notice also that the *meta* methoxy group has been ignored in arriving at the abscissa in Fig. 4. This procedure is perhaps justified because a mesomeric donor is not expected to substantially affect the charge distribution at the *meta* position.

Can. J. Chem. Downloaded from www.nrcresearchpress.com by 210.87.254.105 on 09/05/12
For personal use only.

Some support for a shape factor comes from the Δ value of proton 5 in 1,2,3-trichlorobenzene (Table I). This Δ value of 0.134 p.p.m., however, may have a significant contribution (perhaps as large as 0.02 p.p.m.) from the reaction field because here all three C—Cl dipoles contribute a deshielding reaction field shift (in contrast to any of the other polyhalobenzenes in Table I).

Effect of Electron Donors

According to the present model, net electron-donor substituents will cause Δ values smaller than those found for unsubstituted benzene. The point for trimethylbenzene in Fig. 2 is compatible with this conclusion although a steric effect is also present. The charge-effect prediction is presently under extensive investigation in this laboratory. For example, the Δ value for *p*-dimethoxybenzene is 0.008 p.p.m., five times smaller than for benzene itself. The results of these studies will be presented in due course.

Conclusions

The low-field shifts found for protons of polyhalosubstituted benzenes in carbon tetrachloride depend on the size of the substituents as well as on the amount of charge removed from the ring by the substituents. A further (shape) effect also appears to be present. Reaction field effects cannot account for the major part of the observed shifts. The present approach presents a workable model with predictive powers and is to be tested by further work.

Acknowledgment

We are grateful to the National Research Council of Canada for financial support.

1. A. D. BUCKINGHAM, T. SCHAEFER, and W. G. SCHNEIDER. J. Chem. Phys. **32**, 1227 (1960).
2. P. LASZLO. *In* Progress in nuclear magnetic resonance spectroscopy. Vol. III. *Edited by* J. W. Emsley, J. Feeney, and L. H. Sutcliffe. The Pergamon Press, Ltd., Oxford. 1967.
3. N. S. BHACCA and D. H. WILLIAMS. Tetrahedron Letters, **42**, 3127 (1964).
4. T. LEDAAL. Tetrahedron Letters, **6**, 651 (1968).
5. D. H. WILLIAMS, J. RONAYNE, and R. G. WILSON. Chem. Commun. 1089 (1967).
6. J. W. SMITH. Electric dipole moments. Butterworths Scientific Publications, London. 1955. p. 96.
7. C. P. SMYTH. Dielectric constant and molecular structure. The Chemical Catalog Co., Inc., New York. 1931.
8. B. LINDER. J. Chem. Phys. **33**, 668 (1960).
9. R. F. WIENER and J. M. PRAUSNITZ. J. Chem. Phys. **42**, 3643 (1965).
10. T. SCHAEFER. Can. J. Chem. **39**, 1864 (1961).
11. R. E. MAYO and J. H. GOLDSTEIN. J. Mol. Spectry. **14**, 173 (1964).
12. A. L. MCCLELLAN. Tables of experimental dipole moments. W. H. Freeman and Co., San Francisco. 1963.
13. L. E. SUTTON (*Editor*). Interatomic distances. The Chemical Society. London. 1958.
14. R. SCHWENK and T. SCHAEFER. To be published.
15. L. PAULING. The nature of the chemical bond. 3rd ed. Cornell University Press, Ithaca, New York. 1960.
16. W. G. SCHNEIDER. J. Phys. Chem. **66**, 2653 (1962).

Can. J. Chem. Downloaded from www.nrcresearchpress.com by 210.87.254.105 on 09/05/12
For personal use only.

Analysis of the proton and fluorine magnetic resonance spectra of 1,3,5-trifluorobenzene dissolved in a nematic liquid crystal

C. T. YIM[1] AND D. F. R. GILSON
Department of Chemistry, McGill University, Montreal, Quebec
Received April 22, 1968

The proton and fluorine magnetic resonance spectra of 1,3,5-trifluorobenzene oriented in a nematic liquid crystal have been analyzed. The proton and fluorine chemical shift anisotropies are −2.98 p.p.m. and 104 p.p.m. respectively. The absolute signs of the indirect spin–spin coupling constants are: $J_{HH'}$, J_{FF}, and J_{HF} (*ortho*) all positive, and J'_{HF} (*para*) negative.

Canadian Journal of Chemistry, **46**, 2783 (1968)

Introduction

The analysis of nuclear magnetic resonance spectra of molecules dissolved in nematic liquid crystals affords a method of determining the anisotropies of chemical shifts and the signs of the indirect spin–spin coupling constants (1, 2). Snyder has concluded that the diamagnetic shielding of fluorine nuclei in hexafluorobenzene and monofluorobenzene is greatest when the applied magnetic field is perpendicular to the molecular plane and least when parallel to the plane and perpendicular to the carbon fluorine bond (3, 4). Molecular beam magnetic resonance experiments led to the opposite conclusion, that maximum shielding occurs when the applied field is directed along the C—F bond (5). The anisotropy of the fluorine chemical shift has also been determined in 1,2,4-trifluorobenzene from the field dependence of the second moment of the resonance line of a polycrystalline sample (6). No other studies of fluorine substituted benzenes appear to have been reported. We have analyzed the anisotropic spectrum of 1,3,5-trifluorobenzene oriented in a nematic liquid crystal. The high symmetry of this molecule simplifies the analysis and the direction of the shift of the proton resonance on changing from the nematic to isotropic phase indicates the direction of molecular alignment (7, 8). The spectrum of a solution of 1,3,5-trifluorobenzene in carbon disulfide has been previously analyzed by Jones, Hirst, and Bernstein (9).

Experimental

A sample of 1,3,5-trifluorobenzene (99.9%) was obtained from the Pierce Chemical Company and used without further purification. A mixed liquid crystal was used consisting of *p-p'* di *n*-butoxy- (3.5%), *p-p'* di *n*-pentoxy- (34.8%), and *p-p'* di *n*-hexoxyazoxybenzene, (61.7%). Proton and fluorine magnetic resonance spectra were recorded at 56.4 MHz, using a Varian DP60 nuclear magnetic resonance spectrometer, on a 30 mole % solution of 1,3,5-trifluorobenzene containing a small amount of tetramethylsilane. A field modulation technique was employed for baseline stabilization and calibration of the spectra (8, 10, 11). The modulation amplitude and phase were adjusted to minimize the first sideband, and the two second sidebands used for calibration. The appearance of the spectra of molecules dissolved in nematic liquid crystals is extremely sensitive to temperature gradients across the sample (7, 8, 12). Therefore, the sample was equilibrated in a thermostat at the desired temperature before transferring to the probe, and the sample position and the flow rate of heating gas adjusted to give minimum line width across the spectrum. Spectra were measured at 62 °C. Line widths were about 5 Hz at the center and increased to about 15 Hz at the extrema of the spectra.

Results

The observed spectra are reproduced in Fig. 1; since the spectra are symmetric about the center only one-half is shown in each case. The center of the proton spectrum in the nematic phase was 6.24 p.p.m. to low field from internal TMS. The center of the fluorine spectrum was 18.38 p.p.m. to high field from external trifluoroacetic acid. In the isotropic phase at 102 °C the shifts were −6.53 p.p.m. and +28.58 p.p.m. respectively.

Theoretical spectra were computed using the program given by Wiberg (13) but rewritten to include the direct dipole coupling constants D_{ij}. Since the proton resonance position shifts to *lower* field in the isotropic relative to the nematic phase, the solute molecules are aligned with their molecular planes parallel to the applied field and therefore the sign of the only motional constant required, $C_{3z^2-r^2}$, is negative. For the first trial

[1]Holder of University Graduate Fellowship, 1967–1968.

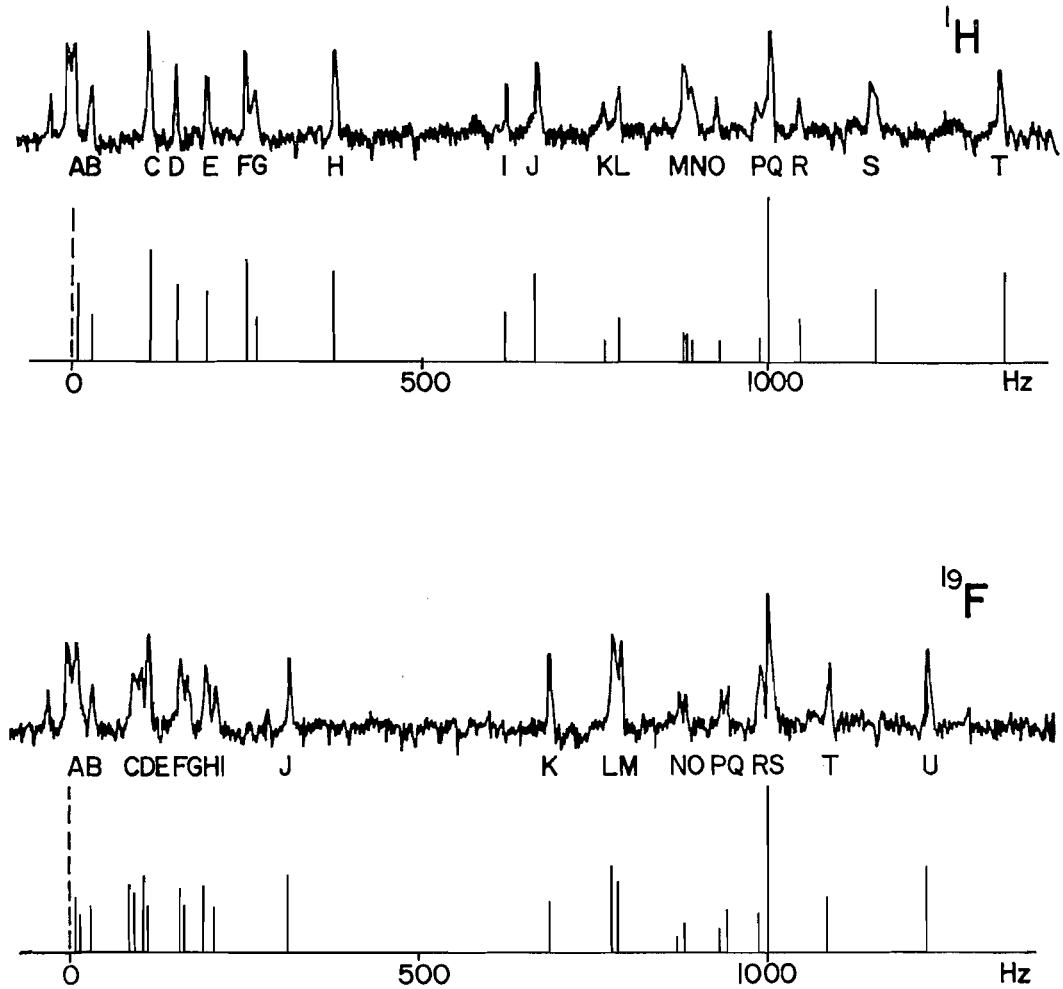

FIG. 1. Proton and fluorine magnetic resonance spectra of 1,3,5-trifluorobenzene dissolved in a nematic liquid crystal. The spectra are symmetric about the center and only one-half is shown.

calculation only the direct dipole coupling constants were included, with values based on a structure with D_{3h} symmetry and bond distances C—C = 1.39 Å, C—H = 1.08 Å, and C—F = 1.31 Å. The theoretical spectra obtained were in approximate agreement with experiment except for a scale factor. Examination of the theoretical line positions and the values of D_{ij} showed that lines J(H), Q(H), T(H), and L(F), S(F), and U(F) correspond to transitions of the a_3 subspectra of the isotropic case analyzed by Jones *et al.* (9), with the addition of the direct dipole coupling. Similarly lines M(H) and O(F) are the transitions between the A_2 symmetry levels, plus dipolar coupling.

$$\nu(\mathrm{J(H)}) = (J_{HF} + D_{HF}) + \tfrac{1}{2}(J'_{HF} + D'_{HF}) - \tfrac{3}{2}D_{HH}$$

$$\nu(\mathrm{T(H)}) = (J_{HF} + D_{HF}) + \tfrac{1}{2}(J'_{HF} + D'_{HF}) + \tfrac{3}{2}D_{HH}$$

$$\nu(\mathrm{L(F)}) = (J_{HF} + D_{HF}) + \tfrac{1}{2}(J'_{HF} + D'_{HF}) - \tfrac{3}{2}D_{FF}$$

$$\nu(\mathrm{U(F)}) = (J_{HF} + D_{HF}) + \tfrac{1}{2}(J'_{HF} + D'_{HF}) + \tfrac{3}{2}D_{FF}$$

$$\nu(\mathrm{Q(H), S(F)}) = (J_{HF} + D_{HF}) + \tfrac{1}{2}(J'_{HF} + D'_{HF})$$

$$\nu(\quad \mathrm{(H), O(F)}) = (J_{HF} + D_{HF}) - \tfrac{1}{2}(J'_{HF} + D'_{HF})$$

TABLE I

Experimental and calculated line positions, in Hz from center of resonance, at 56.4 MHz

	Proton spectrum*			Fluorine spectrum†		
Line	Experimental frequency	Calculated frequency	Calculated intensity	Experimental frequency	Calculated frequency	Calculated intensity
A	5.49±0.2	5.03	2.9	6.35±0.5	5.05	2.2
		9.98	0.4		10.0	1.4
B	30.90±0.5	31.07	1.6	31.55±1.0	31.09	1.6
C	105.9±0.5	106.8	4.0	90.53±1.5	88.3	2.4
		110.0	0.7			
D	152.4±1.5	153.4	2.5	96.45±1.5	95.6	1.9
		154.3	0.7			
E	193.7±1.5	195.3	2.4	108.5±1.5	106.8	2.6
					110.2	1.6
F	250.2±1.0	251.2	3.6	154.5±1.5	153.4	2.5
G	269.7±1.5	271.8	1.5	166.4±2.0	164.8	1.5
H	370.7±2.0	371.4	3.1	193.7±1.5	192.5	2.2
I	624.0±1.5	623.8	1.6	209.1±2.5	207.5	1.2
J	665.9±2.0	666.8	3.0	313.5±2.0	312.6	2.7
K	759.0±4.0	759.6	0.6	683.1±3.5	682.6	1.9
L	782.7±1.5	783.2	1.2	774.4±3.0	773.8	3.0
M	879.7±2.0	878.0	1.0	783.3±3.0	783.3	2.4
		880.0	1.0			
N	885.5±2.0	888.4	1.0	867.9±3.0	866.5	0.6
O	921.8±3.0	923.7	0.8	879.2±2.0	878.0	1.0
P	985.3±3.0	985.2	0.8	923.7±3.0	923.8	0.8
Q	1001.6±3.0	1000.3	6.0	935.7±3.0	935.2	1.5
R	1041.7±3.0	1042.2	1.5	986.2±3.0	985.3	1.5
S	1144.7±3.0	1144.6	2.3	1001.3±3.0	1000.3	6.0
T	1333.1±3.0	1333.7	3.0	1085.2±3.0	1085.9	2.0
U				1226.9±3.0	1226.7	3.0

*Spectrum center: −352.1±1.0 internal TMS.
†Spectrum center: +1036.4±3.0 external CF_3COOH.

For the second stage of spectrum calculation, the most reasonable fit to the positions of these eight lines was obtained with the inclusion of the indirect spin–spin coupling constants, J_{ij}, and variation of the magnitude of the motional constant. Closest agreement was found with J_{HH}, J_{FF}, and J_{FF} (*ortho*) all positive, and J'_{HF} (*para*) negative. Changes in the magnitudes of the indirect coupling constants from the values given by Jones *et al.* did not improve the agreement.

The final refinement of the theoretical spectrum included the pseudo-dipole coupling constants, D_{ij}^{pseudo}, and variation of the direct dipole coupling to give the best overall fit to both spectra. The experimental (mean of five spectra) and calculated line positions are compared in Table I. The root mean square derivation of all observed lines from their calculated frequencies was 1.2 Hz. Final parameters are listed in Table II.

TABLE II

	D_{ij}	J_{ij}	D_{ij}^{pseudo}
F—F	−152.0	5.8	1.0
H—H	−224.3	2.3	2.0
H—F *ortho*	−948.1	9.0	—
H—F *para*	−119.6	−1.7	−1.0

NOTE: $C_{3z2-r2} \equiv -0{\cdot}3269$; $\Delta\sigma_F = +104 \pm 2$ p.p.m.; $\Delta\sigma_H = -298 \pm 0.3$ p.p.m.

Discussion

For a molecule for which only one motional constant is required the chemical shift in the nematic phase is given by

$$[1] \quad \overline{\sigma_{zzi}} = \tfrac{1}{3}(\sigma_{xxi} + \sigma_{yyi} + \sigma_{zzi}) + C_{3z2-r2}\tfrac{2}{3}(5)^{-\frac{1}{2}}(\sigma_{zzi} - \tfrac{1}{2}(\sigma_{xxi} + \sigma_{yyi}))$$

where the z-axis is the molecular three-fold axis. The first term in equation [1] is given by the chemical shift in the isotropic phase, thus the anisotropies of the chemical shift can be obtained;

$$\Delta\sigma_H = (\sigma_{zz} - \tfrac{1}{2}(\sigma_{xx} + \sigma_{yy})) = -2.98 \pm 0.3 \text{ p.p.m.}$$

and

$$\Delta\sigma_F = +104 \pm 2 \text{ p.p.m.}$$

The anisotropy of the proton chemical shift is surprisingly similar to that of benzene itself, −2.88 p.p.m. (8). A value closer to that of 1,3,5-trichlorobenzene, −4.90 p.p.m. (7), might be expected due to the presence of the *ortho* halogen substituents in each case. However, too much significance should not be attached to these values at the present time since the effects of changes in solvent anisotropic susceptibility with change of phase (14, 15) have been neglected. The anisotropy of the fluorine chemical shift is to be compared with the anisotropy in hexafluorobenzene +154 p.p.m. (3). In the isotropic phase the fluorine resonance of 1,3,5-trifluorobenzene is 56 p.p.m. to low field from hexafluorobenzene (16). When this result is combined with the anisotropic data, then

$$\Delta\sigma_{zz}(C_6F_6 - C_6H_3F_3) = 90 \text{ p.p.m.}$$

$$\Delta\tfrac{1}{2}(\sigma_{xx} + \sigma_{yy})(C_6F_6 - C_6H_3F_3) = 39 \text{ p.p.m.}$$

The *ortho* fluorine substituents affect the shielding in hexafluorobenzene perpendicular to the molecular plane to a greater extent than the shielding parallel to the plane.

The optimized dipole coupling constants can be used to recalculate the relative distances between hydrogen and fluorine nuclei. Snyder observed that, for hexafluorobenzene, the ratios of the D_{ij} values obtained did not correspond to the values calculated from ideal geometry (3). The discrepancies were attributed to the anisotropy of the indirect spin–spin coupling constants and the averaging over the internal motions of the molecule (12). The introduction of the pseudo-dipole coupling constants is intended to account for these effects. For protons the anisotropy of the coupling constants will be small and it is tempting to set the pseudo-dipole coupling equal to zero. However, the amplitudes of vibration will be larger for the lighter nucleus and therefore the pseudo-dipole coupling constants have been included in the analysis of 1,3,5-trifluorobenzene. Since only *relative* distances can be obtained, it is necessary to assume a given value for one of the internuclear distances in the molecule. In the present analysis a value of 1.390 Å was assumed for the carbon–carbon bond length, and 1.080 Å for the carbon–hydrogen bond length, which led to a carbon–fluorine bond length of 1.296 Å. This distance is consistent with the electron diffraction data on metadifluorobenzene and paradifluorobenzene (17), but is shorter than the value of 1.33 Å obtained from the microwave spectrum of monofluorobenzene (18).

Acknowledgment

We are grateful to the National Research Council of Canada for financial support.

Note Added in Proof

A referee has informed us that J. Nehring and A. Saupe have examined the spectrum of 1,3,5-trifluorobenzene in a nematic liquid crystal. Their results are quoted as a private communication, Laszlo, ref. 19 and are in agreement with the present study.

1. A. D. BUCKINGHAM and K. A. MCLAUCHLAN. Progr. Nucl. Magn. Resonance Spectry., **2**, 63 (1967).
2. A. SAUPE and G. ENGLERT. Phys. Rev. Letters, **11**, 462 (1963).
3. L. C. SNYDER and E. W. ANDERSON. J. Chem. Phys. **42**, 3336 (1965).
4. L. C. SNYDER. J. Chem. Phys. **43**, 4041 (1965).
5. S. I. CHAN and A. S. DUBIN. J. Chem. Phys. **46**, 1745 (1967).
6. E. R. ANDREW and D. P. TUNSTALL. Proc. Phys. Soc. **81**, 986 (1963).
7. G. ENGLERT and A. SAUPE. Z. Naturforsch. **19*a***, 172 (1964).
8. A. SAUPE. Z. Naturforsch. **20*a***, 572 (1965).
9. R. G. JONES, R. C. HIRST, and H. J. BERNSTEIN. Can. J. Chem. **43**, 683 (1965).
10. W. A. ANDERSON. Rev. Sci. Instr. **33**, 1160 (1962).
11. L. F. JOHNSON. *In* NMR and EPR Spectroscopy. Pergamon Press, Inc., New York. 1960. p. 185.
12. L. C. SNYDER and S. MEIBOOM. J. Chem. Phys. **47**, 1480 (1967).
13. K. B. WIBERG. Computer programming for chemists. W. A. BENJAMIN, Jr., New York. 1965. p. 196.
14. A. D. BUCKINGHAM and E. E. BURNELL. J. Am. Chem. Soc. **89**, 3341 (1967).
15. R. A. BERNHEIM and T. R. KRUGH. J. Am. Chem. Soc. **89**, 6784 (1967).
16. C. T. YIM and D. F. R. GILSON. Unpublished results.
17. H. OOSAKA, A. SEKINE, and T. SAITO. Bull Chem. Soc. Japan, **27**, 182 (1954).
18. B. BAK, D. CHRISTENSEN, L. HANSEN-NYGAARD, and E. TANNENBAUM. J. Chem. Phys. **26**, 134 (1957).
19. P. LASZLO. Progr. Nucl. Magn. Resonance Spectry., 3, 321 (1967).

Can. J. Chem. Downloaded from www.nrcresearchpress.com by 210.87.254.105 on 09/05/12
For personal use only.

Effect of solvent and anion upon the proton magnetic resonance spectrum of the 1-methylpyridinium ion

W. F. Reynolds and U. R. Priller
Department of Chemistry, University of Toronto, Toronto 5, Ontario

Received January 30, 1968

The proton magnetic resonance spectra of 1-methylpyridinium bromide and iodide have been measured over a range of concentrations in different solvents. It is found that, with the exception of acetonitrile solutions, the infinite dilution chemical shifts are related to solvent dielectric constant. Extrapolated shifts for a nonpolar medium agree with previously calculated chemical shifts for the pyridinium ion. Proton chemical shifts in concentrated solutions are affected by cation–anion interactions. These interactions are interpreted in terms of ion pair formation.

Canadian Journal of Chemistry, **46**, 2787 (1968)

Introduction

The method of estimating π electron densities in aromatic molecules and ions from proton chemical shift measurements has been widely applied (1–14). It was originally assumed that there was a linear relationship between excess π electron density at a carbon atom and the chemical shift of the adjacent proton relative to internal benzene (1). More recent papers usually include consideration of effect of polar groups, anisotropic magnetic susceptibility, etc. (15).

Problems are found when this method is used to estimate π electron densities in heteroaromatic cations. It has been concluded that proton chemical shifts for the pyridinium ion are partly determined by the effect of the counter ion and by the effect of the electric field of the N—H^+ group (9, 16). Similarly cation–anion and cation–solvent interactions have a significant effect upon proton chemical shifts in 1,4-diethylpyridinium halides (17).

On the other hand, it has been claimed that proton chemical shifts for the pyridinium ion in several solvents (18) and for the 1-methylpyridinium ion in water (19) are directly related to π electron densities estimated from simple Hückel Molecular Orbital Calculations. This would suggest that the effect of the counter ion and the effect of the electric field of the N—H^+ group are unimportant.

This paper reports the results of the investigation of the effect of solvent and concentration upon the ring and 1-methyl protons of 1-methylpyridinium bromide and iodide. The primary purpose of this investigation was to obtain an estimate of the infinite dilution proton chemical shifts in a nonpolar medium for comparison with theoretical calculations of the proton chemical shifts for the pyridinium ion (16). At the same time, information was obtained about the nature of cation–anion and cation–solvent interactions in this system. The 1-methylpyridinium ion was chosen since it was felt that interaction with anions should be less than in the case of pyridinium ion.

Experimental

1-Methylpyridinium iodide was prepared by the method of Prescott (20), and had m.p. 116.5–117.5 °C.

Anal. Calcd. for C_6H_8IN: C, 32.6; H, 3.62; I, 57.4; N, 6.33. Found: C, 32.6; H, 3.76; I, 57.6; N, 6.32.

2-Methylpyridinium bromide was prepared by the method of Prescott (20). After drying under vacuum at 110° in a drying pistol for two days, the compound melted at 153–155 °C. It was hygroscopic and exposure to the atmosphere was kept at a minimum.

Anal. Calcd. for C_6H_8BrN: C, 41.4; H, 4.63; Br, 45.9; N, 8.04. Found: C, 41.0; H, 5.29; N, 7.82; Br, 45.8.

Acetone, acetonitrile, and dimethyl sulfoxide were Fisher Certified Reagents. They were freshly distilled over Linde 5A molecular sieve before use. The salts were readily soluble except in acetone. 1-Methylpyridinium bromide was not sufficiently soluble in acetone to allow accurate spectral measurements.

Proton magnetic resonance spectra were recorded on an HA-100 spectrometer operating in the frequency sweep mode. The probe temperature was 27.5 ± 1 °C. The spectrometer was locked on to the solvent peak. Methyl proton peaks in aqueous solutions were measured in D_2O with the spectrometer locked on to internal *t*-butyl alcohol. Each solution contained 0.1–0.2 volume % benzene as an internal reference. Peak positions were calibrated by measuring differences of sweep and manual oscillator frequencies. Each peak position was determined from an average of four measurements.

The spectrum of the most dilute solution of 1-methylpyridinium iodide in acetone was accumulated on a C-1024 time-averaging computer. Fifty sweeps were accumulated.

Spectral peaks were usually too broad to allow for

TABLE I

Infinite dilution chemical shifts (in p.p.m. from internal benzene) for 1-methylpyridinium bromide and iodide in different solvents

Proton	Water	Dimethyl sulfoxide	Aceto-nitrile	Acetone
1-CH_3(Br)	+3.06	+3.01	+3.04	—
1-CH_3(I)	+3.06	+3.00	+3.04	2.67
2,6-H(Br)	−1.32	−1.62	−1.30	—
2,6-H(I)	−1.32	−1.62	−1.28	−1.84
3,5-H(Br)	−0.60	−0.77	−0.64	—
3,5-H(I)	−0.60	−0.77	−0.64	−0.93
4-H(Br)	−1.09	−1.19	−1.13	—
4-H(I)	−1.09	−1.19	−1.13	−1.38

complete analysis. Chemical shifts were estimated from the centers of gravity of spectral multiplets. Estimated maximum error in chemical shift measurements is 0.02 p.p.m. Repeated peak measurements were always consistent to well within this limit.

Results

Infinite dilution proton chemical shift measurements relative to internal benzene are given in Table I. Plots of proton chemical shifts versus concentration are given in Figs. 1–4.

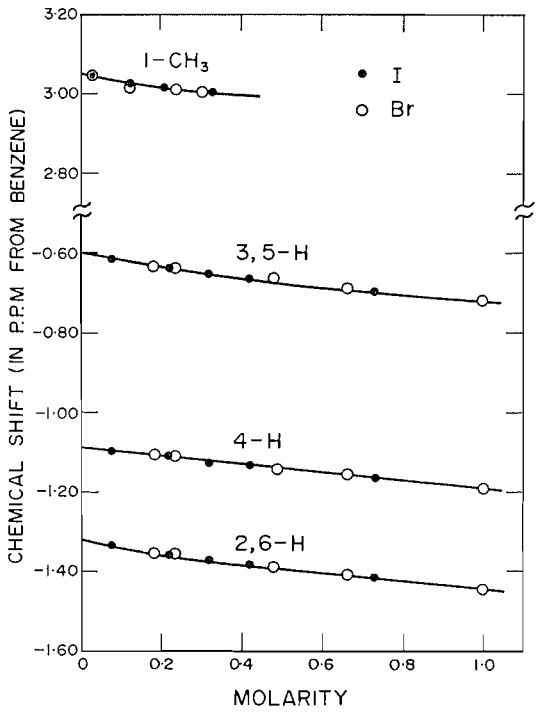

FIG. 1. Plot of proton chemical shifts for 1-methylpyridinium bromide and iodide vs. concentration in water.

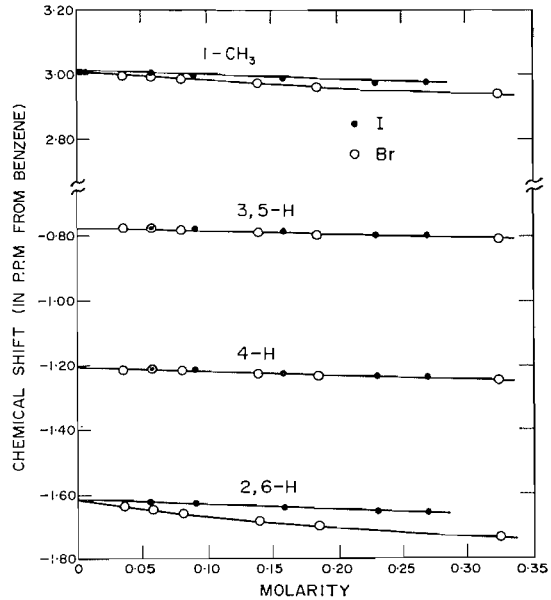

FIG. 2. Plot of proton chemical shifts for 1-methylpyridinium bromide and iodide vs. concentration in dimethyl sulfoxide.

Discussion

(a) Effect of Solvent

The solvents chosen were those for which charge transfer complex formation between iodide and 1-methylpyridinium ions should be minimized (21). It is believed that the chemical shift values reported in Table I are true infinite dilution values. Previous investigations of closely related systems provide considerable support for this assumption. The association constant for 1-methylpyridinium iodide ion pair formation in water is 2.3 (22). This would imply approximately 95% ion pair dissociation at the minimum concentration used in this investigation. Kosower (21) also found that 1-alkyl,4-carbomethoxypyridinium iodide ion pairs were largely dissociated in acetone, acetonitrile, and dimethyl sulfoxide at the minimum concentrations used in this investigation; but that ion pair formation was essentially complete in chloroform at concentrations as low as 10^{-4} *M*. Chuck and Randall (17) found that the "infinite dilution" chemical shifts for the 1-methylene and 2,6 protons of 1,4-diethylpyridinium halides in chloroform were anion dependent. In our system identical dilution shifts were obtained for both salts in water, dimethyl sulfoxide, and

Can. J. Chem. Downloaded from www.nrcresearchpress.com by 210.87.254.105 on 09/05/12
For personal use only.

Can. J. Chem. Downloaded from www.nrcresearchpress.com by 210.87.254.105 on 09/05/12
For personal use only.

acetonitrile. This strongly suggests that our results represent true infinite dilution shifts while those of Chuck and Randall obtained in chloroform do not. This would agree with the previously quoted results of Kosower in similar systems.

With the exception of acetonitrile solutions, the infinite dilution chemical shifts in the different solvents appeared to be related to the observed order of solubility. (The approximate solubilities for 1-methylpyridinium iodide in water, dimethyl sulfoxide, acetonitrile, and acetone are respectively 27 *M*, 6 *M*, 1 *M*, and 0.05 *M*.)

Infinite dilution chemical shifts should then also be related to physical measurements of the solvating ability of the solvent. Although the use of dielectric constant as a measure of solvating power has been criticized (21), it has been recently claimed that solvation energies of polar

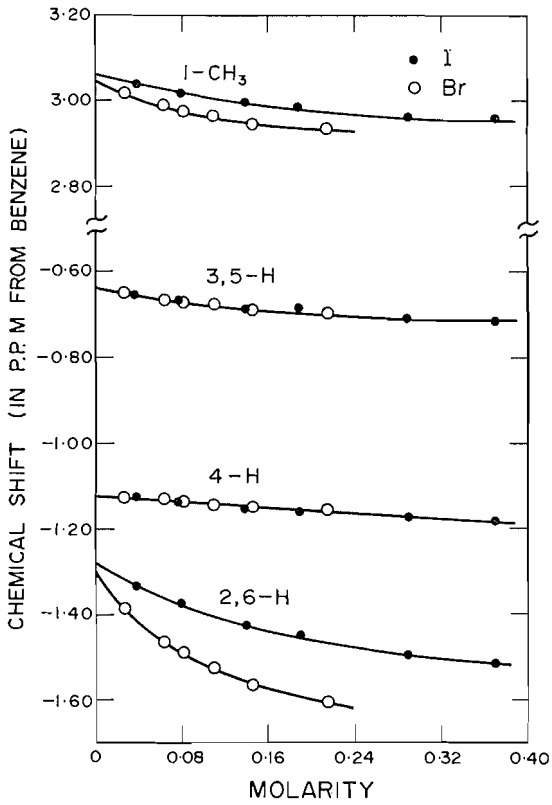

FIG. 3. Plot of proton chemical shifts for 1-methylpyridinium bromide and iodide vs. concentration in acetonitrile.

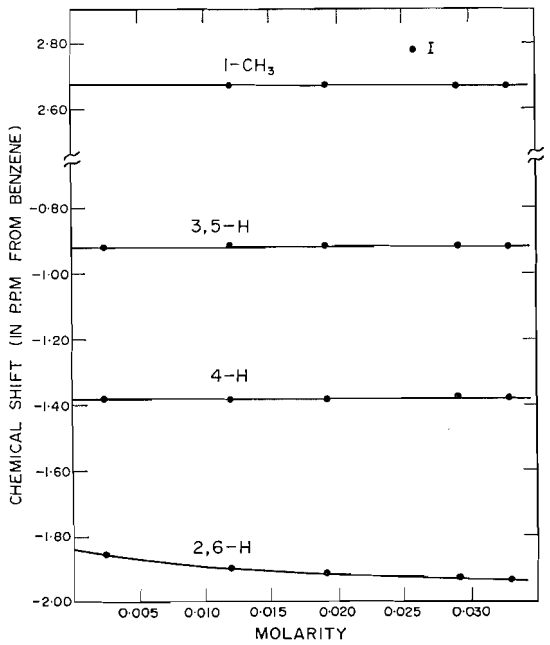

FIG. 4. Plot of proton chemical shifts for 1-methylpyridinium bromide and iodide vs. concentration in acetone.

solutes in polar solvents are quantitatively related to dielectric constant (23). Consequently, plots of infinite dilution chemical shifts versus various functions of solvent dielectric constant were prepared. Best straight lines were obtained for the empirical correlation factor $\varepsilon^{1/2}$ (24). This plot is shown in Fig. 5. It is not claimed that the extrapolated shifts represent accurate infinite dilution shifts in a nonpolar, noninteracting medium. However, they probably do represent approximate values of these desired quantities.

It is believed that the most probable mode of solvent–cation interaction is direct solvation of the positive charge center. This would decrease the effect of the positive charge and consequently cause high field shifts relative to the infinite dilution chemical shifts in nonpolar solvents.

An alternate explanation would involve hydrogen bonding between solvent and solute C—H protons (25). This explanation has been rejected since it implies that the ordering of hydrogen bond strengths is acetone > dimethyl sulfoxide >water. This is in disagreement with previously reported measurements of relative hydrogen bonding strengths for these solvents (26, 27).

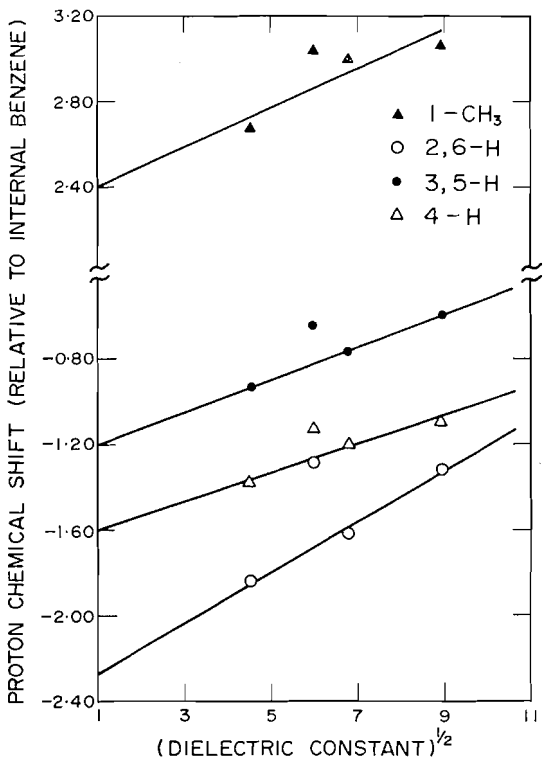

FIG. 5. Plot of infinite dilution proton chemical shifts in different solvent vs. (dielectric constant)$^{1/2}$ for the solvent at 27.5 °C.

We have been unable to find any physical measure of the solvating power of acetonitrile which would account for the apparently anomalous chemical shifts in this solvent. It is possible that the apparent high field shift is due at least partly to the anisotropic diamagnetic susceptibility of this solvent.

(b) Cation–Anion Interactions

The identical dilution curves for 1-methylpyridinium bromide and iodide in water are difficult to rationalize. The slopes of the dilution curves for the different protons are quite similar. Consequently, it was originally believed that the dilution effect might involve the reference rather than the solute. However, this must be rejected for two reasons. Firstly, the chemical shift difference between the solvent and reference is essentially constant. Secondly, the changes in chemical shift for the different ring protons upon dilution are slightly but significantly different. For example, the dilution shifts for 1-methylpyridinium iodide in water over a concentration range from 2.4 to 0.1 *M* are +0.21 p.p.m. for 2,6 protons, +0.19 p.p.m. for 3,5 protons and +0.17 p.p.m. for the 4 protons.

From the above evidence, it must be concluded that the dilution curves are due to cation–anion interactions. In contrast with interactions in other solvents, these interactions appear to be relatively non-specific in nature since the effect is the same for both anions and appears to affect all ring positions to an almost equal extent.

The interaction could be due to solvent-separated ion pairs or to highly solvated intimate ion pairs. The former suggestion would appear to account for more satisfactorily the non-specific nature of the interaction. However, the latter suggestion would appear to be more consistent with the fact that 1-methylpyridinium iodide forms a charge transfer complex. It has been claimed that this charge transfer complex is electrostatically equivalent to an intimate ion pair and that the ion pair is strongly solvated in water (21). It is difficult to distinguish between these possibilities by nuclear magnetic resonance (n.m.r.) spectroscopic measurements.

There is evidence for a specific interaction between the anion and the positive charge center of the 1-methylpyridinium ion in the other solvents. The slopes of the dilution curves are steepest for the 1-methyl and 2,6 protons and the slopes for these protons are anion-dependent in dimethyl sulfoxide and acetonitrile. This is most probably due to the formation of intimate ion pairs with minimum solvation. The dilution curves suggest that the anion is located almost directly above the nitrogen atom of the 1-methylpyridinium ion in the ion pair. The fact that the interaction is less for the iodide ion is probably due to the tendency of iodide ions to form complexes with dimethyl sulfoxide, acetonitrile, and acetone (28).

(c) Comparison with Theoretical Calculations of Proton Chemical Shifts for the Pyridinium Ion

Estimated infinite dilution shifts in a non-polar medium are given in Table II. Although these extrapolated chemical shifts are presumably only approximately correct, they are in reasonable agreement with previously calculated proton chemical shifts for the pyridinium ion in the absence of ion pairing (16). Best agreement is obtained with model 4(*b*) (see Table II) which uses scaled-down π electron densities obtained

Can. J. Chem. Downloaded from www.nrcresearchpress.com by 210.87.254.105 on 09/05/12
For personal use only.

TABLE II

Extrapolated infinite dilution chemical shifts (in p.p.m. from internal benzene) for the 1-methylpyridinium ion in a nonpolar medium compared with previously calculated chemical shifts for the pyridinium ion

Proton	$\Delta\sigma$ for 1-methyl-pyridinium ion	$\Delta\sigma$* calculated for pyridinium ion
1-CH_3	+2.4	—
2,6-H	−2.28	−2.33
3,5-H	−1.20	−1.19
4-H	−1.60	−1.37

*Taken from ref. 16, model 4(*b*)

from a V.E.S.C.F. calculation (29) and allows for the electric field effect of the N—H^+ bond.

Since the ratios of ring proton chemical shifts are not too different from those for the pyridinium ion, the possibility that these chemical shifts are determined solely by π electron densities (as estimated by simple Hückel Molecular Orbital Calculations (18)) cannot be excluded. However, evidence from other heteroaromatic systems suggests that better agreement is obtained between theoretical and calculated proton chemical shifts when effects other than π electron density effects are considered (9, 12, 15).

Acknowledgments

The financial support given by the National Research Council of Canada and the Department of University Affairs of the Province of Ontario is gratefully acknowledged.

1. G. Fraenkel, R. E. Carter, A. McLachlan, and J. H. Richards. J. Am. Chem. Soc. **82**, 5846 (1960).
2. H. Spiesecke and W. G. Schneider. Tetrahedron Letters, 468 (1961).
3. I. C. Smith and W. G. Schneider. Can. J. Chem. **39**, 1158 (1961).
4. C. MacLean and E. L. Mackor. Mol. Phys. **4**, 241 (1961).
5. J. C. Shug and J. C. Deck. J. Chem. Phys. **37**, 2618 (1962).
6. A. Zweig, J. E. Lehnsen, J. E. Lancaster, and M. T. Neglia. J. Am. Chem. Soc. **85**, 3940 (1963).
7. T. Schaefer and W. G. Schneider. Can. J. Chem. **41**, 966 (1963).
8. M. P. Schweizer, S. I. Chan, G. K. Helmkamp, and P. O. P. Ts'o. J. Am. Chem. Soc. **86**, 696 (1964).
9. V. M. S. Gil and J. N. Murrell. Trans. Faraday Soc. **60**, 248 (1964).
10. S. Forsen, B. Akermark, and T. Alm. Acta Chem. Scand. **18**, 2313 (1964).
11. W. W. Paudler and H. L. Blewitt. Tetrahedron, **21**, 353 (1965).
12. A. H. Gawer and B. P. Dailey. J. Chem. Phys. **42**, 2658 (1965).
13. L. M. Jackman, Q. N. Porter, and G. R. Underwood. Australian J. Chem. **18**, 1221 (1965).
14. W. W. Paudler and J. E. Kuder. J. Heterocyclic Chem. **3**, 33 (1966).
15. P. J. Black, R. D. Brown, and M. L. Heffernan. Australian J. Chem. **20**, 1305 (1967).
16. G. Kotowycz, T. Schaefer, and E. Bock. Can. J. Chem. **42**, 2541 (1964).
17. R. J. Chuck and E. W. Randall. Spectrochim. Acta, **22**, 221 (1966).
18. B. M. Lynch and H. J. M. Dou. Tetrahedron Letters, 2627 (1966).
19. R. J. Chuck and E. W. Randall. J. Chem. Soc. B, 261 (1967).
20. A. B. Prescott. J. Am. Chem. Soc. **18**, 91 (1896).
21. E. M. Kosower. J. Am. Chem. Soc. **80**, 3253 (1958).
22. E. M. Kosower and J. C. Burbach. J. Am. Chem. Soc. **78**, 5838 (1956).
23. R. J. Abraham, L. Cavalli, and K. G. R. Pachler. Nuclear magnetic resonance in chemistry. Academic Press, Inc., New York. 1965. p. 111.
24. G. Kotowycz and T. Schaefer. Can. J. Chem. **45**, 1093 (1967).
25. T. Schaefer and W. G. Schneider. J. Chem. Phys. **32**, 1218 (1960).
26. W. C. Drinkard and D. Kivelson. J. Phys. Chem. **62**, 1494 (1958).
27. A. L. McClellan, S. W. Nicksic, and J. C. Guffy. J. Mol. Spectry. **11**, 340 (1963).
28. E. M. Kosower. J. Am. Chem. Soc. **80**, 3261 (1958).
29. R. D. Brown and M. L. Heffernan. Australian J. Chem. **12**, 554 (1959).

Can. J. Chem. Downloaded from www.nrcresearchpress.com by 210.87.254.105 on 09/05/12
For personal use only.

Can. J. Chem. Downloaded from www.nrcresearchpress.com by 210.87.254.105 on 09/05/12
For personal use only.

Model reactions for a synthesis of streptamine based on the diamination of nitrocyclitol acetates[1]

HANS H. BAER AND MARGARET C. T. WANG
Department of Chemistry, University of Ottawa, Ottawa, Canada

Received April 25, 1968

Treatment of *trans,trans*-2-nitro-1,3-cyclohexanediol diacetate with ammonia followed by acetylation gives *trans,trans*-1,3-diacetamido-2-nitrocyclohexane (**4**). Catalytic hydrogenation of **4** and subsequent acetylation lead to *trans,trans*-2,6-diacetamidocyclohexylamine (**5**) and *trans,trans*-1,2,3-triacetamidocyclohexane (**6**), respectively. Permanganate oxidation of **4** affords *cis*-2,6-diacetamidocyclohexanone (**7**; 2,4-dinitrophenylhydrazone, **8**). Sodium borohydride reduction of **7** produces *trans,trans*-2,6-diacetamidocyclohexanol (**9**; *O*-acetate, **10**).

Canadian Journal of Chemistry, 46, 2793 (1968)

In continuation of our studies on aminations of nitro sugars (1, 2) it was decided to examine the possibility of introducing, in one operation, two amino groups in the positions β and β′ to the nitro function. Sugars and polyols that contain the structural moiety —$CHNH_2$—$CHNO_2$—$CHNH_2$— should be useful precursors for the preparation of vicinal triamino compounds, diamino ketones, diamino alcohols, and related derivatives, and it is suggested that efforts at synthesis along these lines will benefit particularly the field of carbohydrate antibiotics. The present paper reports a series of model reactions carried out on 1,2,3-trisubstituted cyclohexanes.

The point of departure was *trans,trans*-2-nitro-1,3-cyclohexanediol (**1**) which was prepared by cyclization of glutaric dialdehyde with nitromethane (3). Acetylation of the diol **1**, previously performed in 75% yield with acetic anhydride and sulfuric acid (3), was carried out with boron trifluoride as a catalyst. This catalyst has proved very effective in nitro sugar acetylations (4) and the diacetate **2** was thus conveniently obtained in 95% yield.

When a tetrahydrofuran solution of **2** was agitated with aqueous ammonia at 40° for 8 h, both acetoxy functions were replaced by amino groups. Conversions of aliphatic β-acetoxynitro compounds into vicinal nitroamines have been achieved before (1, 2, 5–11), but the present example appears to be the first one involving a diamination of a β,β′-diacetoxynitro compound. The general process is explained (7) as a β-elimination of acetic acid followed by addition of ammonia to the intermediate nitroalkene; in the special case of **2** this sequence takes place twice.

The free nitrodiamine **3** proved rather unstable and difficult to purify. However, *N*-acetylation of the reaction product gave stable *trans,trans*-1,3-diacetamido-2-nitrocyclohexane (**4**) in a yield of 70.5% (based on **2**). Platinum-catalyzed hydrogenation of **4** in acetic acid solution readily furnished *trans,trans*-2,6-diacetamidocyclohexylamine (**5**), and the latter was acetylated to *trans, trans* - 1,2,3 - triacetamidocyclohexane (**6**). The structures of **5** and **6** were confirmed, and the configuration was proved, by the nuclear magnetic resonance (n.m.r.) parameters listed in Table I. In particular, **5** exhibited a clear, one-proton triplet assignable to H-2, and its spacing of 10.5 c.p.s. indicated that the hydrogens at C-1, C-2, and C-3 must all possess axial (and the substituents therefore equatorial) orientation. Moreover, the methyl resonances of the acetamido groups in **5**, as well as in **6**, appeared as a single, sharp peak. Since the signals of axial and equatorial acetamido substituents in the cyclohexane series are known (12–19) to differ markedly in their chemical shifts, the observed magnetic equalities implied identical disposition of the substituents, a fact which is in accordance only with the *trans,trans* configuration. Although no spectrum was obtained of **4** because of its poor solubility, the configuration proved in **5** and **6** can safely be extended to it, as catalytic hydrogenation of nitro compounds in an acidic medium generally proceeds with retention (20).

It has not been investigated whether small amounts of one or both of the possible stereoisomers of **3** arise in the reaction of **2** with

[1]Presented before the 4th International Conference on Carbohydrate Chemistry at Kingston, Ontario, July, 1967, and abstracted from the M.Sc. thesis of M. C. T. Wang, University of Ottawa, 1968.

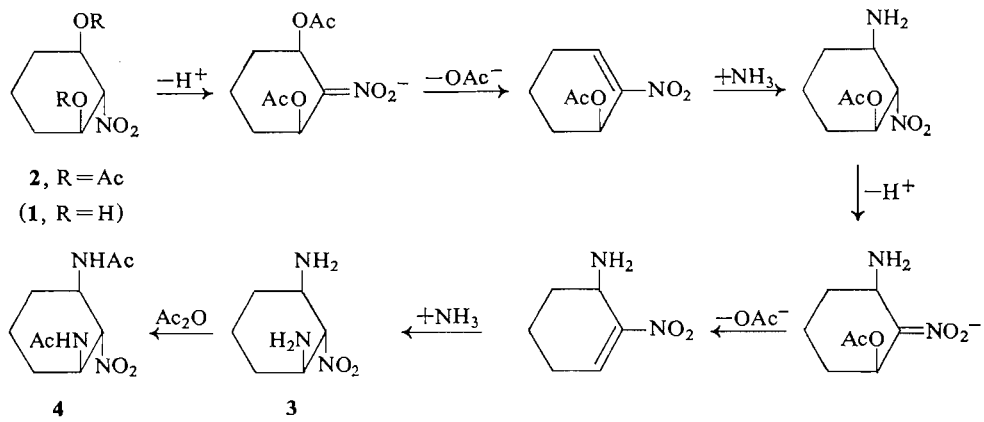

TABLE I

60-Mcycles nuclear magnetic resonance parameters*

Compound	Solvent	H-1, H-3	H-2	*O*-Ac	*N*-Ac	$(CH_2)_3$
5	D_2O	6.38(2,m)	7.53(1,t)†		8.02(6,s)	8.42(6,m)
6	$CDCl_3$‡				8.05(s)	
	D_2O	6.24(3,m)			8.05(9,s)	8.54(6,m)
7	$CDCl_3$‡				7.95(s)	
9	CH_3OH	§	§		8.03(6,s)	8.45(6,m)
10	CH_3OH	§	§	8.03(3,s)	8.11(6,s)	8.50(6,m)

*Chemical shifts of compounds measured in deuteriochloroform or methanol are given vs. internal tetramethylsilane = 10 τ, those of compounds measured in deuterium oxide are given vs. the DOH signal which was assigned a value of 5.20 τ. Number of protons by integration and character of signal are given in parentheses; s, sharp singlet; t, sharp triplet; m, broad multiplet.
†Splitting, 10.5 c.p.s.
‡Poor solubility of compound prevented evaluation of peaks other than the acetamido signal.
§Signals overlapped by solvent bands.

ammonia. At any rate the *trans,trans* product predominates strongly, which is in line with numerous observations recorded (1, 2, 21, 22) for nucleophilic elimination–additions of a similar nature. Furthermore, in a recent communication Lichtenthaler and associates (23) reported that cyclization of glutaric dialdehyde with nitromethane in the presence of four moles of benzylamine gives, in 60% yield, *trans,trans*-1,3-bis-benzylamino - 2 - nitrocyclohexane,[2] and they stated (though without specifying the conditions) that the same compound is formed with ease when the diol **1** is treated with benzylamine.

The next aim was to convert the nitro derivative **4** into *cis*-2,6-diacetamidocyclohexanone (**7**). Since the Nef reaction, which is widely used for the conversion of secondary nitro groups into keto groups has been known to fail or give poor results with sterically hindered nitro compounds (24), oxidative denitration with permanganate (25) was employed. The ketone **7** was obtained in yields of 62–70%. The structure of this product was confirmed by its infrared data, by the lack of high-intensity ultraviolet absorption near 250 mμ in alkaline solution indicating absence of a nitronate grouping, and by the preparation of a 2,4-dinitrophenylhydrazone (**8**). The n.m.r. spectrum of **7** in deuteriochloroform exhibited one sharp singlet (6H) for the two acetamido groups. The signal occurred at 7.95 τ, which might be taken to indicate a *syn*-diaxial orientation (19). Such conformation, though unfavorable on steric grounds, could be stabilized by mutual hydrogen bonding of the acetamido groups. On the other hand, the substituents of **7** could well occupy the equatorial position notwithstanding the low τ-value, for the latter might be due to a deshielding effect exerted by the adjacent ring carbonyl group. Hasegawa and Sable (19) explained thus

[2]The authors (23) also obtained **6** from this compound by catalytic reduction and debenzylation followed by acetylation.

Can. J. Chem. Downloaded from www.nrcresearchpress.com by 210.87.254.105 on 09/05/12
For personal use only.

Can. J. Chem. Downloaded from www.nrcresearchpress.com by 210.87.254.105 on 09/05/12
For personal use only.

the occurrence of a low-field, "axial" acetoxy signal in *scyllo*-inosose pentaacetate, a compound that contains no axial substituents.

Borohydride reduction of the ketone **7** furnished in 65% yield crystalline *trans,trans*-2,6-diacetamidocyclohexanol (**9**), from which the *O*-acetate **10** was prepared with acetyl chloride. The *trans,trans* configuration followed from the n.m.r. spectrum of **10** which exhibited a singlet (3H) at 8.03 τ and a singlet (6H) at 8.11 τ. The former was attributed to an equatorial acetoxy group and the latter, to two equatorial acetamido groups in accordance with abundant chemical shift data found in the literature (12–19) on substituted cyclohexanes.[3] It must be said that the spectrum of **10** was taken in methanol solution because of insufficient solubility in chloroform, the solvent to which most recorded data refer. However, Hasegawa and Sable (19) compared chemical shifts in numerous acetylated cyclitols including aminocyclitols, in pure chloroform and chloroform–methanol mixtures, and their study revealed only small solvent effects which caused no ambiguity in assignments. Similarly, we have found the acetoxy signal of **2** in methanol to be at 7.98 τ, i.e. at virtually the value (7.99 τ) recorded (3) for a chloroform solution.[4]

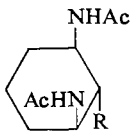

5, R = NH_2
6, R = NHAc
9, R = OH
10, R = OAc

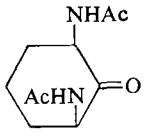

7

The reactions **2** → **3** → **4** → **7** → **9** constitute a model sequence for a synthesis of streptamine (all *trans*-2,6-diamino-1,3,4,5-cyclohexanetetrol). As a first step in utilizing this scheme for such a synthesis, penta-*O*-acetyl-deoxynitro-*scyllo*-inositol was subjected to diamination followed by *N*-acetylation and 1,3-diacetamido-2-deoxy-2-nitro-*scyllo*-inositol was obtained in a yield of 76%. The crystalline product decomposed at 295–299°, showed infrared bands in Nujol at 3420, 3300, 3280, and 3120 cm^{-1} (OH and NH) as well as at 1640 (amide I) and 1560 cm^{-1} (amide II and NO_2), and it gave an n.m.r. signal for its acetamido protons at 8.05 τ (in methanol).[5] Treatment with ammonia of tetra-*O*-acetyl-1,4-dideoxy-1,4-dinitro-*neo*-inositol led to aromatization giving 2,5-dinitroaniline.[5]

Experimental

Infrared (i.r.) spectra were recorded on a Beckman IR-8 instrument and were obtained from Nujol mulls. Only the most characteristic frequencies are listed (ν_{max} in cm^{-1}). Melting points were taken in an electric aluminium block apparatus equipped with a calibrated thermometer. All evaporations were carried out *in vacuo* at 35° (bath temperature).

trans,trans-2-Nitro-1,3-cyclohexanediol Diacetate (2)

Boron trifluoride etherate was added dropwise with swirling to a suspension of the diol **1** (10 g) in acetic anhydride (25 ml). When several drops of the catalyst had been added the diol dissolved with evolution of heat. The solution was kept at ambient temperature for 15 min and was then poured with chilling into an excess of methanol. Evaporation, with two portions of fresh methanol being eventually added, gave a light-colored crystalline residue which was recrystallized from ethanol–water to yield 14.5 g (95%) of colorless needles, m.p. 89–92° (90–91.5° after another recrystallization). Lit. (3), m.p. 89–90°. Infrared data: 1750 cm^{-1} (C=O); 1575, 1385 cm^{-1} (NO_2); 1240, 1040 cm^{-1} (C—O—C).

trans,trans-1,3-Diacetamido-2-nitrocyclohexane (4)

A mixture of concentrated aqueous ammonia (50 ml) and tetrahydrofuran (50 ml) containing the di-*O*-acetate **2** (5 g) was vigorously stirred for 8 h at 40°. The two phases were then separated, and the aqueous layer was extracted four times with 50 ml portions of tetrahydrofuran. The combined organic layer and extracts were evaporated to give a pale-yellow syrup.[6] The syrup was dissolved in methanol (25 ml) and acetylated with acetic anhydride (10 ml) which was added with initial ice cooling and then allowed to react overnight at room temperature. A first crop of **4** (3.22 g, m.p. 283–284° with decomposition) crystallized directly from the reaction mixture. A second crop (0.28 g, m.p. 279–280° with decomposition) was obtained from the filtrate by evaporation with several successive additions of methanol followed by trituration of the residue with water. The total yield of **4** was 70.5%. Recrystallization from ethanol–water gave fine needles of m.p. 285–286° (with gradual darkening

[3]Abnormal chemical shifts that may render configurational assignments unreliable have been observed in sugar derivatives (26) and nucleosides (27) containing magnetically anisotropic groupings. (See also the discussion of **7**, above.) No such complicating factors are present in **10**.

[4]Larger solvent effects have been noted in dimethyl sulfoxide (17) and in acetone and benzene (28).

[5]Details to be published elsewhere.

[6]In early experiments we tried to isolate a crystalline reaction product from this syrup. Treatment with cold water gave in a yield of 38–44% a solid showing amine and nitro bands and lacking carbonyl absorption in the infrared. It was presumably the diamine **3**, but attempts at purification were unsatisfactory and the substance darkened in the course of a day.

Can. J. Chem. Downloaded from www.nrcresearchpress.com by 210.87.254.105 on 09/05/12
For personal use only.

from 267°). Infrared data: 3300 cm^{-1} (NH); 1560, 1370 cm^{-1} (NO_2); 1660, 1560, 1315 cm^{-1} (amide).

Anal. Calcd. for $C_{10}H_{17}N_3O_4$ (mol. wt., 243.3): C, 49.37; H, 7.04; N, 17.27. Found: C, 49.61; H, 7.22; N, 17.03.

trans,trans-2,6-Diacetamidocyclohexylamine (5)

The nitro compound **4** (1.22 g) in a mixture of acetic acid (75 ml) and water (30 ml) was shaken under hydrogen at ordinary pressure and temperature in the presence of platinum catalyst (0.7 g of PtO_2, prehydrogenated). The hydrogen uptake (410 ml) was complete after 20 h. Removal of the catalyst and solvent gave a crystalline residue that was recrystallized from ethanol – ethyl acetate. The yield was 653 mg (61.2%) of white needles which after a further recrystallization from ethanol – water melted at 263–265° (with gradual darkening from 230°). Infrared data: 3370 cm^{-1} (NH_2); 3300 cm^{-1} (NH); 1640, 1560, 1315 cm^{-1} (amide); 1140 cm^{-1} (C—N).

Anal. Calcd. for $C_{10}H_{19}N_3O_2$ (mol. wt., 213.3): C, 56.30; H, 8.98; N, 19.67. Found: C, 56.14; H, 9.03; N, 19.88.

The mother liquor from which the above 653 mg of **5** had crystallized was evaporated to dryness and the residue was *acetylated* in a manner similar to that described in the next paragraph. From the yield of triacetamido compound (412 mg) thus obtained it was calculated that at least another 344 mg of **5** had been present. Hence 93.5% of the hydrogenation product was accounted for.

trans,trans-1,2,3-Triacetamidocyclohexane (6)

The total of crude amine **5** that had been obtained in a hydrogenation of **4** (1.22 g) was dissolved in methanol (20 ml) and acetic anhydride (7 ml) was added. The mixture, which immediately deposited a white precipitate, was stirred for 1 h at 25° and was then evaporated several times with additions of ethanol. The tri-*N*-acetyl derivative **6** (1.13 g, 86.5%) crystallized thereafter from a small amount of ethanol. It was recrystallized from ethanol–water to give pure **6** which sublimed above 300° but neither melted nor decomposed below 360° (sealed capillary). Infrared data: 3300 cm^{-1} (NH); 1645, 1550, 1315 cm^{-1} (amide).

Anal. Calcd. for $C_{12}H_{21}N_3O_3$ (mol. wt., 255.3): C, 56.45; H, 8.29; N, 16.46. Found: C, 56.36; H, 8.15; N, 16.27.

cis-2,6-Diacetamidocyclohexanone (7)

Compound **4** (243 mg) was finely powdered and dissolved by prolonged stirring in 0.1 *N* aqueous potassium hydroxide solution (170 ml). To the solution was added 2 *M* magnesium sulfate (24 ml) and then water to a final volume of 500 ml. The mixture (which was turbid due to precipitated magnesium hydroxide) was cooled in an ice-water bath, and potassium permanganate (136 mg) in water (9 ml) was slowly added with magnetic stirring over a period of 3½ h. Stirring was thereafter continued for 30 min at 0–5° and 1 h at 25°. The inorganic precipitate was removed by filtration through a layer of Celite, and the filtrate was acidified to pH 3 with *N* hydrochloric acid and evaporated to dryness with several additions of ethanol. The dry residue was extracted with ten 50 ml portions of boiling chloroform from which upon cooling a few milligrams of unreacted **4** crystallized out. Evaporation of the chloroform gave crude **7** which was recrystallized from ethanol – petroleum ether (30–60°) to give 144 mg (70%) of colorless needles decomposing at 215–225° (with partial sublimation at about 180°). Infrared data: 3280 cm^{-1} (NH); 1730 cm^{-1} (C=O); 1645, 1565, 1320 cm^{-1} (amide), (shoulders at 1674 and 1600 cm^{-1}).

Anal. Calcd. for $C_{10}H_{16}N_2O_3$ (mol. wt., 212.3): C, 56.59; H, 7.60; N, 13.20. Found: C, 56.49; H, 7.49; N, 13.34.

cis-2,6-Diacetamidocyclohexanone-2,4-dinitrophenylhydrazone (8)

To a solution of the ketone **7** (28 mg) in ethanol (1.5 ml) was added a solution of 2,4-dinitrophenylhydrazine (50 mg) in hot ethanol (2 ml) containing concentrated hydrochloric acid (0.1 ml). The reaction mixture was boiled for 4 min and then cooled with ice. The hydrazone **8** separated as yellow crystals that were washed with cold ethanol (36 mg, 69.5%). Their melting point of 267–269° was raised to 269–270° by recrystallization from ethanol. Infrared data: 3320, 3250 cm^{-1} (NH); 1675, 1540 cm^{-1} (amide); 1515, 1500 cm^{-1} (NO_2); 1630, 1615 cm^{-1} (phenyl).

Anal. Calcd. for $C_{16}H_{20}N_6O_6$ (mol. wt., 392.4): C, 48.98; H, 5.14; N, 21.43. Found: C, 48.88; H, 5.14; N, 21.31.

trans,trans-2,6-Diacetamidocyclohexanol (9)

The ketone **7** (119 mg) was dissolved in hot water (2.5 ml). To the cooled solution was added sodium borohydride (15 mg) in water (1 ml). The reaction mixture was allowed to stand at room temperature for 90 min and was then diluted with water and deionized with a cation exchange resin, Rexyn 101(H^+). The filtrate was evaporated and the boric acid was removed by several evaporations with methanol. The residue was crystallized from ethanol – ethyl acetate to give 78 mg (65%) of **9** as fine needles that decomposed around 260°. Upon recrystallization from ethanol **9** showed m.p. 286.5–288° with decomposition; it partially sublimed near 210°. Infrared data: 3380, 3140, 3090 cm^{-1} (OH and NH); 1630, 1550, 1320 cm^{-1} (amide).

Anal. Calcd. for $C_{10}H_{18}N_2O_3$ (mol. wt., 214.3): C, 56.04; H, 8.47. Found: C, 55.97; H, 8.37.

trans,trans-2,6-Diacetamidocyclohexanol Acetate (10)

The compound **9** (50 mg) was dissolved in hot glacial acetic acid (0.5 ml), and acetyl chloride (0.3 ml) was added dropwise after the solution had been cooled to room temperature. The reaction mixture, which separated into two phases, was magnetically stirred for 20 min at 45° whereby a clear solution resulted. The solution was evaporated to dryness with repeated additions of methanol and finally of ethanol. The crystalline residue was recrystallized from ethanol – petroleum ether (30–60°) to give 52 mg (86.5%) of **10** as needles which sintered and decomposed in the range 250–265°. Another recrystallization (from ethanol) gave a product that incurred partial sublimation at 250° and sintered from 280°. Infrared data: 3300 cm^{-1} (NH); 1730 cm^{-1} (C=O); 1650, 1560, 1315 cm^{-1} (amide); 1245, 1050 cm^{-1} (C—O—C).

Anal. Calcd. for $C_{12}H_{20}N_2O_4$ (mol. wt., 256.3): C,

56.24; H, 7.87; N, 10.93. Found: C, 56.03; H, 8.04; N, 11.08.

Acetylation of **9** with acetic anhydride and boron trifluoride etherate (4) gave an identical product.

Acknowledgment

This work was supported by Research Grant A1350 from the National Research Council of Canada.

1. H. H. BAER and T. NEILSON. J. Org. Chem. **32**, 1068 (1967).
2. H. H. BAER, T. NEILSON, and W. RANK. Can. J. Chem. **45**, 991 (1967).
3. F. W. LICHTENTHALER. Ber. **96**, 845 (1963).
4. H. H. BAER, F. KIENZLE, and F. RAJABALEE. Can. J. Chem. **46**, 80 (1968).
5. F. D. CHATTAWAY. J. Chem. Soc. 355 (1936).
6. H. IRVING. J. Chem. Soc. 797 (1936).
7. H. IRVING and H. I. FULLER. J. Chem. Soc. 1989 (1948).
8. R. L. HEATH and J. D. ROSE. J. Chem. Soc. 1486 (1947).
9. C. A. GROB and W. v. TSCHARNER. Helv. Chim. Acta, **33**, 1070 (1950).
10. C. SATOH and A. KIYOMOTO. Chem. Pharm. Bull. Tokyo, **12**, 615 (1964).
11. C. SATOH, A. KIYOMOTO, and T. OKUDA. Carbohydrate Res. **5**, 140 (1967).
12. F. W. LICHTENTHALER. Ber. **96**, 2047 (1963).
13. F. A. L. ANET, R. A. B. BANNARD, and L. D. HALL. Can. J. Chem. **41**, 2331 (1963).
14. M. NAKAJIMA, A. HASEGAWA, and F. W. LICHTENTHALER. Ann. **680**, 21 (1964).
15. M. NAKAJIMA, A. HASEGAWA, and T. KUROKAWA. Ann. **689**, 229 (1965).
16. M. NAKAJIMA, A. HASEGAWA, and N. KURIHARA. Ann. **689**, 235 (1965).
17. F. W. LICHTENTHALER and H. LEINERT. Ber. **99**, 903 (1966).
18. H. H. BAER and R. J. YU. Tetrahedron Letters, 807 (1967).
19. A. HASEGAWA and H. Z. SABLE. J. Org. Chem. **33**, 1604 (1968).
20. R. L. AUGUSTINE. Catalytic hydrogenation. Marcel Dekker, Inc., New York. 1965. p. 94.
21. H. H. BAER and F. KIENZLE. J. Org. Chem. **32**, 3169 (1967).
22. H. H. BAER and K. S. ONG. Can. J. Chem. **46**, 2511 (1968).
23. F. W. LICHTENTHALER, T. NAKAGAWA, and A. EL-SCHERBINEY. Angew. Chem. **79**, 530 (1967).
24. W. E. NOLAND. Chem. Rev. **55**, 137 (1955).
25. H. SHECHTER and F. T. WILLIAMS. J. Org. Chem. **27**, 3699 (1962).
26. D. HORTON, J. B. HUGHES, J. S. JEWELL, K. D. PHILIPS, and W. N. TURNER. J. Org. Chem. **32**, 1073 (1967).
27. R. J. CUSHLEY, K. A. WATANABE, and J. J. FOX. J. Am. Chem. Soc. **89**, 394 (1967).
28. D. HORTON, W. E. MAST, and K. D. PHILIPS. J. Org. Chem. **32**, 1471 (1967).

Can. J. Chem. Downloaded from www.nrcresearchpress.com by 210.87.254.105 on 09/05/12
For personal use only.

Can. J. Chem. Downloaded from www.nrcresearchpress.com by 210.87.254.40 on 09/05/12
For personal use only.

Synthesis of 6-*O*-α- and β-D-xylopyranosyl-D-mannopyranose. (Glycosidation of α- and β-D-xylopyranosyl chloride 2,3,4-tri(chlorosulfate))[1,2]

H. J. JENNINGS

Division of Biosciences, National Research Council of Canada, Ottawa, Canada

Received April 1, 1968

Crystalline β-D-xylopyranosyl chloride 2,3,4-tri(chlorosulfate) has been prepared by the reaction of sulfuryl chloride with D-xylose. Anomerization of β-D-xylopyranosyl chloride 2,3,4-tri(chlorosulfate) yielded crystalline α-D-xylopyranosyl chloride 2,3,4-tri(chlorosulfate). Both α- and β-D-xylopyranosyl chlorides gave high yields of their inversion products on methyl glycosidation (Königs–Knorr conditions) demonstrating the non-participating properties of the chlorosulfate group. Using modified Königs–Knorr conditions β-D-xylopyranosyl chloride 2,3,4-tri(chlorosulfate) was condensed with 1,2,3,4-tetra-*O*-acetyl-β-D-mannopyranose to give predominantly 6-*O*-α-D-xylopyranosyl-D-mannopyranose. A similar condensation using α-D-xylopyranosyl chloride 2,3,4-tri(chlorosulfate) did not yield the analogous 6-*O*-β-D-xylopyranosyl-D-mannopyranose, therefore, for comparative purposes it was synthesized by the method of Bredereck and co-workers (1).

Canadian Journal of Chemistry, **46**, 2799 (1968)

Introduction

Methylation studies on the extracellular polysaccharide of *Cryptococcus laurentii* (NRRL Y-1401) have indicated the presence of a (1,6)-linked D-xylose-D-mannose unit (2). Partial hydrolysis of the polysaccharide has failed to yield this (1,6)-linked disaccharide and therefore the configuration of its linkage is not known. In order to detect this (1,6)-linked disaccharide by chromatographic means and to determine the configuration of its linkage, both the α- and β-D-(1,6)-linked disaccharides were synthesized and their chromatographic properties were studied.

The chemical synthesis of both α- and β-1,2-*cis* glycosides from α- and β-1,2-*trans* acetohalides, using Königs–Knorr conditions has proved difficult due to the participation of the 2-acyloxy group (3, 4). One approach to this problem has been to utilize modified halogenoses, which have easily removable non-participating groups on position C-2 of the halogenose (5–7). These methods have met with some success but they usually require multi-step procedures for the synthesis of the halogenose. In order to find a more general approach to the problem it was necessary to synthesize a halogenose analogous to the acetohalides, having a 1,2-*trans* configuration; and for simplicity, easily removable non-participating groups on all the ring hydroxyls. Preliminary work on the reaction of sulfuryl chloride on reducing sugars (8) has indicated the possible utility of this approach as the reaction produced l-chlorides containing both chlorosulfate and chlorodeoxy groups. However, it has been demonstrated that chloro-substitution can be inhibited by low temperature isolation of the intermediate chlorosulfate esters (9). The ease of removal of the chlorosulfate ester group (10) and some evidence in support of its non-participating properties (11) have also been reported.

Discussion

Low temperature isolation of the products of the reaction of D-xylose with sulfuryl chloride yielded a crystalline compound, the elemental analysis of which was consistent with structure **1**. Isolation of the products of this reaction at room temperature has yielded 4-chloro-4-deoxy-L-arabinopyranosyl chloride 2,3-di(chlorosulfate) (8). The yield of **1** was improved over that reported in an earlier communication (12) by allowing the reaction mixture to warm up to −10 °C and then maintaining it between −10 and 0 °C for 30 min before isolation of the product. Previously the product had been isolated as soon as the reaction mixture had warmed up to −20 °C. This increased yield could probably be attributed to the fact that chloro-substitution of an intermediate 1-chlorosulfate ester takes place at this stage of the reaction. Methanolysis of **1** using silver carbonate gave a crystalline methyl glycoside, still containing three chlorosulfate groups. That this glycoside was a methyl α-D-pyranoside was

[1]Issued as NRCC No. 10155.
[2]For preliminary communication see ref. 12.

Can. J. Chem. Downloaded from www.nrcresearchpress.com by 210.87.254.40 on 09/05/12
For personal use only.

confirmed by dechlorosulfation and subsequent acetylation of it, to give crystalline methyl 2,3,4-tri-*O*-acetyl-α-D-xylopyranoside (13) which on deacetylation gave methyl α-D-xylopyranoside (14). The specific rotation (−91°) of **1** was consistent with its β-D-configuration,[3] and this was further substantiated by the anomerization of **1** which gave an isomeric crystalline compound designated as the α-D-chloroanomer,[3] an assignment consistent with its high positive specific rotation (+101.5 °). Methanolysis of the α-D-chloroanomer using silver carbonate yielded crystalline methyl β-D-xylopyranoside 2,3,4-tri(chlorosulfate); the synthesis of an authentic sample of this is reported in this paper.

The methanolysis products of both **1** and its α-D-anomer once again confirm the non-participating properties of the chlorosulfate group as the 1,2-*trans*-chloride (**1**) gave 92% of the inversion product (methyl α-D-glycoside) whereas the 1,2-*cis*-chloride (α-D-anomer of **1**) gave only 75% of the inversion product (methyl β-D-glycoside). If participation had occurred, then one would have expected a preponderance of inverted product from the 1,2-*cis*-chloride. The reason for the higher degree of retention (25%) in the case of the 1,2-*cis*-chloride is not readily apparent. One other factor emerging from these methanolysis reactions is that the rate of methanolysis of the α-D-chloroanomer was appreciably slower than that of the β-D-chloroanomer and this proved a dominant factor when both were applied to disaccharide syntheses.

When **1** was condensed with **2** under normal Königs–Knorr conditions the reaction was very slow; however, the introduction of a catalytic quantity of silver perchlorate (5) to the reaction mixture enabled the condensation to occur at a much faster rate. The condensation yielded a syrupy mixture which on analysis by thin-layer chromatography (t.l.c.) was found to contain **3**, together with excess **1** and a small quantity of unreacted **2**. Dechlorosulfation of the mixture and its subsequent dissolution in water enabled the unreacted tetraacetate (**2**) to be removed by chloroform extraction. Continuous chloroform extraction of the aqueous solution then yielded the disaccharide tetraacetate (**4**) leaving dechlorosulfated **1** and any of its artefacts in the aqueous solution. The specific rotation (+14 °) of chromatographically pure (t.l.c.) **4** indicated that it had an α-D-glycosidic link, but deacetylation and subsequent reduction of a small amount of **4** showed that the reduction product was in fact a mixture of 6-*O*-α- and β-D-xylopyranosyl-D-mannitol in the ratio of 19:1 respectively, (determined by gas–liquid chromatography (g.l.c.)). Deacetylation of **4** using sodium methoxide yielded a methanol insoluble complex and a further yield of this complex was obtained by the addition of more sodium methoxide to the product of the deionized mother liquors. Deionization of the combined sodium complexes gave chromatographically pure **5** in an overall yield of 42%, based on **2**. The fact that the sodium complex yielded pure **5** despite the evidence that **4** was in fact a mixture of α-D- and β-D-anomers can best be explained by the relative insolubility of the sodium complex of **5** compared to that of **6**, and the relatively small quantity (5%) of **6** in the mixture.

Because of the unreactive nature of the α-D-chloride even in the presence of silver perchlorate, the β-D-linked disaccharide (**6**) was synthesized by the condensation of tri-*O*-acetyl-α-D-xylopyranosyl bromide with 1,2,3,4-tetra-*O*-acetyl-6-*O*-trityl-α-D-mannopyranose in nitromethane solution using silver perchlorate (1). The resultant disaccharide heptaacetate could not be obtained crystalline from the mixture of syrupy reaction products (t.l.c.), therefore it was isolated by the application of the mixture to a silica gel column. Deacetylation of the resultant syrupy heptaacetate gave crystalline **6** obtained as its methanol adduct (elemental analysis and p.m.r.) in a yield of 40%. Small amounts of **5** and another unidentified disaccharide were detected by paper chromatographic analysis of the deacetylated heptaacetate.

The structural proof of **5** and **6** was obtained in the following manner. The acid hydrolysis of both **5** and **6** yielded xylose and mannose and the acid hydrolysis of their reduced products gave xylose as the only detectable reducing sugar. Methylation of **5** and **6** and subsequent hydrolysis of their methylated products yielded in both cases, equal amounts of crystalline 2,3,4-tri-*O*-methyl-D-xylopyranose and syrupy 2,3,4-tri-*O*-methyl-D-mannopyranose. Thus the D-xylose residue of both **5** and **6** was linked glycosidically

[3]These assignments have since been confirmed by proton magnetic resonance data, and will be communicated at a later date.

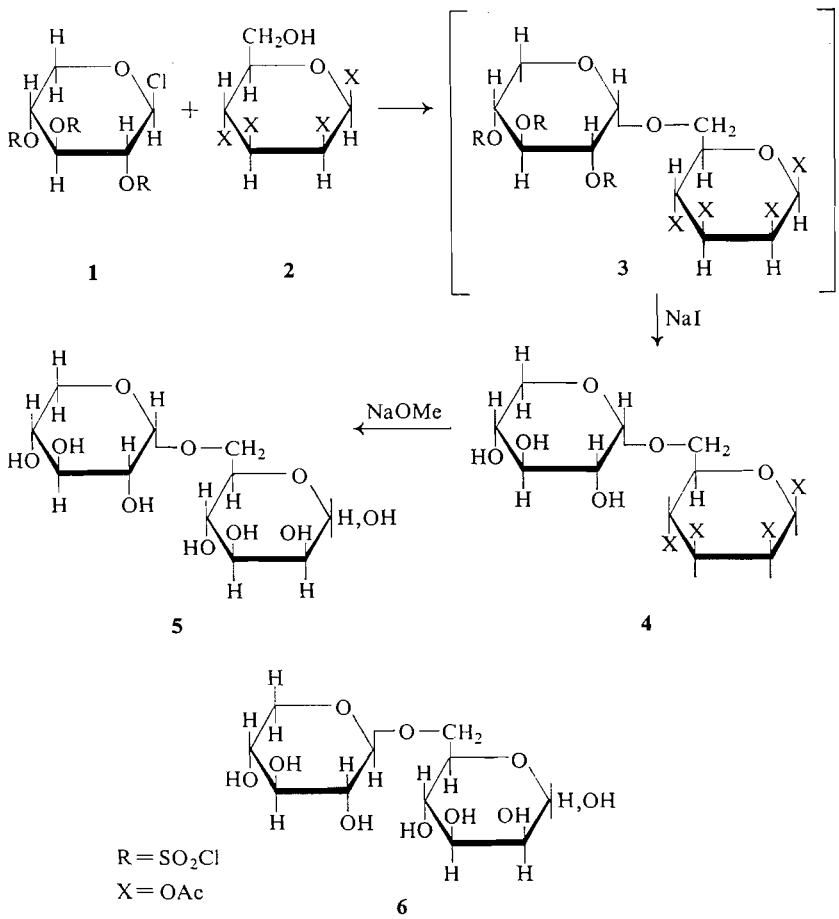

1 2 3 4 5 6

to the 6-position of the D-mannose residue. The syrupy tri-*O*-methyl mannopyranose derivative was identified as 2,3,4-tri-*O*-methyl-D-mannopyranose by comparison of the retention volumes of its methyl glycoside (15) and its trimethylsilylated methyl glycoside (16) with those of an authentic sample (g.l.c.).

Both **5** and **6** were shown to be anomerically pure as both were clearly resolved by paper chromatography and by g.l.c. analysis of the trimethylsilyl ethers of their reduced products. The specific rotations of **5** and **6** (+95.7 ° and −23.8 °) and of the octaacetates of their reduced products (+73 ° and −9 °) indicated that they were α-D- and β-D-anomers, respectively. Further evidence was obtained by p.m.r. spectroscopy (Table I). The spectrum of **6** showed three doublets at τ 4.94, τ 5.21, and τ 5.63 and in the intensity ratio of 2:1:3 respectively. The doublets at τ 4.94 and τ 5.21 had small coupling constants and were assigned to the H^{α} and H^{β} anomeric protons (16, 17) of the D-mannose residue. This was confirmed when the spectrum of α-D-mannose gave almost identical doublets in the same intensity ratio (Table I). The ratio of H^{α} and H^{β} (2:1) corresponds roughly to the equilibrium ratio of D-mannose (18) and the rapid anomerization of α-D-mannose was probably due to the presence of acetonitrile (internal reference). The doublet at τ 5.63 with a $J_{1,2}$ coupling of 7.0 c.p.s. was assigned to the glycosidic proton of the D-xylose residue and the large coupling constant is consistent with an axial–axial arrangement (19) of protons on C-1 and C-2 of the D-xylose moiety (C-1 conformation) of the β-linked disaccharide (**6**). The spectrum of **5** gave only two signals in the region of the anomeric protons, a doublet at τ 4.93 and a narrow multiplet at τ 5.20 (intensity ratio 1:2 respectively). This reversal of the

Can. J. Chem. Downloaded from www.nrcresearchpress.com by 210.87.254.40 on 09/05/12
For personal use only.

TABLE I

Chemical shifts (τ) and coupling constants (c.p.s.) of anomeric protons of 6-*O*-α- and β-D-xylopyranosyl-D-mannopyranoses

	Non-reducing		Reducing			
			α-D-anomer(H^{α})		β-D-anomer(H^{β})	
Compound	Chemical shift	Coupling constant	Chemical shift	Coupling constant	Chemical shift	Coupling constant
D-Mannose	—	—	4.95	$J_{1,2} = 1.4$	5.24	$J_{1,2} = 1.2$
5	5.20	$J_{1,2} < 3.0$	4.93	$J_{1,2} = 1.4$	5.20	$J_{1,2} < 3.0$
6	5.63	$J_{1,2} = 7.0$	4.94	$J_{1,2} = 1.4$	5.21	$J_{1,2} = 1.2$

intensity ratio in comparison with that of equilibrated mannose can be explained by the superimposition of the H^{β} anomeric proton of D-mannose and the glycosidic proton of the α-D-linked xylose residue. This downfield shift of the glycosidic proton of the α-D-anomer compared to that of the β-D-anomer is consistent with previous assignments (17). Although the signal at τ 5.20 was complex, it had a narrow overall width (less than 3.0 c.p.s.) and this would be consistent with an axial–equatorial (19) arrangement of protons of C-2 and C-1 of the D-xylose moiety (C-1 conformation) of the α-D-linked disaccharide (**5**).

Further evidence for the β-D-linkage of **6** was obtained by the isolation of its crystalline phenylosazone derivative; the physical constants of which are in fairly good agreement with those reported for the phenylosazone derivative of epimeric 6-*O*-β-D-xylopyranosyl-D-glucopyranose (20).

Experimental

Melting points were determined on a Kofler hot stage and are uncorrected, and optical rotations were measured at 21 ± 3 °. Solutions were deionized by passage through Amberlite I.R. 120 (H^+ form) ion exchange resin, and were concentrated below 50 °C under diminished pressure.

Paper chromatograms were run by the descending method using the following solvent systems (v/v): (*a*) butan-1-ol – ethanol – water (3:1:1), (*b*) butan-1-ol – pyridine – water (6:4:3). Reducing sugars were located on chromatograms by *p*-anisidine hydrochloride (21) or alkaline silver nitrate (22) and their rates of movement are quoted relative to that of maltose (R_m).

Thin-layer chromatography (t.l.c.) was performed on silica gel (Adsorbosil-1) coated plates, with the solvent mixtures (v/v); (*i*) benzene–acetone (19:1), (*ii*) benzene–acetone (9:1), (*iii*) benzene–acetone (4:1), and (*iv*) chloroform–methanol (9:1).

A Pye Argon Chromatograph was used for gas–liquid chromatography (g.l.c.) and the column packings were (*a*) 10% Carbowax 6000 on Chromosorb W, 100–120 mesh, and (*b*) 10% Neopentylglycol Sebacate on Gas Chrom. *a*, 100–120 mesh. Relative amounts of the separated components were estimated by triangulation of the peaks on the gas–liquid chromatogram.

The proton magnetic resonance (p.m.r.) spectra were obtained from a Varian A60A spectrometer, using deuterium oxide as the solvent. Chemical shifts were measured relative to tetramethylsilane using acetonitrile as internal reference. Dechlorosulfations were carried out essentially by the method used previously in the preparation of 3,4,6-trichloro-3,4,6-trideoxy-D-allose (9). Only catalytic quantities of sodium iodide were required to effect the complete removal of the chlorosulfate groups.

*β-D-Xylopyranosyl Chloride 2,3,4-Tri(chlorosulfate) (**1**)*

D-Xylose (10 g) was treated with sulfuryl chloride (26 ml) and pyridine (40 ml) in chloroform solution (8). The reaction mixture was stirred continuously for 2 h at −70 °C and then the temperature of the reaction mixture was allowed to rise to −10 °C. A further addition of cold (−10 °C) chloroform (100 ml) was made at this stage and the temperature of the reaction mixture was maintained between −10 and 0 °C for 30 min by intermittent cooling of the reaction mixture in an acetone – solid carbon dioxide bath. The reaction mixture was then partitioned by the addition of ice-cold 10% sulfuric acid[4] and the chloroform layer was then washed successively with saturated sodium bicarbonate solution and water. The final chloroform solution was dried (anhydrous sodium sulfate), filtered, and concentrated to a syrup which rapidly crystallized. The crude crystalline product (23 g, 74%) was recrystallized from chloroform – light petroleum (b.p. 30–60 °C) and gave crystals (19 g, 61%), m.p. 84 °C and $[\alpha]_D$ −91° (*c*, 1.06 in chloroform).

Anal. Calcd. for $C_5H_6Cl_4S_3O_{10}$: C, 12.95; H, 1.30; Cl, 30.55; S, 20.70. Found: C, 13.12; H, 1.27; Cl, 31.07; S, 20.50.

Methyl α-D-Xylopyranoside 2,3,4-Tri(chlorosulfate)

Crystalline **1** (2 g) was dissolved in chloroform (20 ml) and anhydrous methanol (20 ml) was added. The solution was then shaken in an aluminium foil covered flask for 16 h with silver carbonate (6 g) and drierite (2 g). The mixture was then filtered, and the filtrate was concentrated to a residue which was treated with chloroform and the

[4]Periodically an emulsion was formed at this stage. This could be run off and dispersed by shaking it with warm water (30–40 °C) without detriment to the final product.

Can. J. Chem. Downloaded from www.nrcresearchpress.com by 210.87.254.40 on 09/05/12
For personal use only.

Can. J. Chem. Downloaded from www.nrcresearchpress.com by 210.87.254.40 on 09/05/12
For personal use only.

mixture again filtered to remove silver salts. The chloroform solution was then concentrated to a syrup (1.8 g, 91%) which crystallized. Recrystallization from methanol–water gave colorless crystals (1.0 g, 51%), m.p. 96 °C and $[\alpha]_D$ + 78.5° (*c*, 1.25 in chloroform).

Anal. Calcd. for $C_6H_9Cl_3S_3O_{11}$: C, 15.70; H, 1.96; Cl, 23.15; S, 20.90. Found: C, 15.91; H, 1.89; Cl, 23.25; S, 20.63.

The crystals above (1g) were dechlorosulfated with sodium iodide in aqueous acetone solution in the presence of barium carbonate (9). The filtrate was concentrated to dryness, and the residue was acetylated using pyridine and acetic anhydride. The ionic material was removed by partitioning the acetylation mixture between chloroform and water. The chloroform solution on concentration yielded a crystalline mass which when recrystallized from ethanol gave large crystals (0.5g, 63%), m.p. 84 °C and $[\alpha]_D$ +120.1° (chloroform) for methyl 2,3,4-tri-*O*-acetyl-α-D-xylopyranoside. Deacetylation (23) of the above triacetate yielded crystalline methyl α-D-xylopyranoside (14) as confirmed by m.p. 90 °C and the undepressed mixture m.p. with the authentic compound.

The mother liquors from the recrystallization of the tri(chlorosulfate) derivative above were concentrated to a syrup (0.75 g). A small amount of the syrup (25 mg) was dissolved in aqueous methanol, and sodium methoxide solution was added until the solution remained slightly alkaline (pH 8). The solution was concentrated to dryness and the residue was trimethylsilylated (24). Injection onto column (*a*) at 135 °C gave two peaks with identical retention volumes to those of the trimethylsilyl derivatives of methyl α- and β-D-xylopyranosides. The ratio of α-D- to β-D-anomer as represented by the peak areas was 5:1.

α-D-Xylopyranosyl Chloride 2,3,4-Tri(chlorosulfate)

Crystalline **1** (2 g) was refluxed for 15 min with aluminium chloride (0.14 g) in absolute chloroform solution. The reaction mixture was partitioned by the addition of water and the resultant chloroform layer was washed with saturated sodium bicarbonate solution and water. The final chloroform solution was dried (anhydrous sodium sulfate), clarified with charcoal, filtered, and concentrated to a syrup. The syrup slowly crystallized and recrystallization from chloroform – light petroleum (b.p. 30–60 °C) gave crystals (0.75 g, 37.5%), m.p. 98 °C and $[\alpha]_D$ +101.5° (*c*, 1.42 in chloroform).

Anal. Calcd. for $C_5H_6Cl_4S_3O_{10}$: C, 12.95; H, 1.30; Cl, 30.55; S, 20.70. Found: C, 12.90; H, 1.20; Cl, 30.15; S, 20.32.

This anomerization also yielded other products which will be reported in a future publication.

Methyl β-D-Xylopyranoside 2,3,4-Tri(chlorosulfate)

The methyl glycosidation of the above chloride (1g) was achieved by the same procedure used for the methyl glycosidation of its β-D-chloroanomer (**1**), except that the reaction mixture was shaken for 4 days.[5] The product was a syrup (0.5 g) which slowly crystallized. Recrystallization (×3) from chloroform – light petroleum (b.p. 30–60 °C) gave crystals (0.05 g, 5%), m.p. 111–112 °C and $[\alpha]_D$ −33.3° (*c*, 1.52 in chloroform).

Anal. Calcd. for $C_6H_9Cl_3S_3O_{11}$: C, 15.68; H, 1.97; Cl, 23.15; S, 20.92. Found: C, 15.90; H, 2.04; Cl, 23.46; S, 20.62.

This compound had an identical melting point and specific rotation to the authentic crystalline tri(chlorosulfate), prepared by treating methyl β-D-xylopyranoside with sulfuryl chloride by the same procedure as was used in the synthesis of **1**. The mixture melting point of the authentic and derived compounds was also undepressed.

The mother liquors of the crystalline methyl glycosidation product were concentrated to a syrup (0.4 g) and the ratio of methyl α-D- to methyl β-D-anomers (1:3 respectively) was determined by g.l.c. on column (*a*), the method previously used in the methyl glycosidation of **1**.

6-O-α-D-Xylopyranosyl-1,2,3,4-tetra-O-acetyl-β-D-mannopyranose (4)

Crystalline 1,2,3,4-tetra-*O*-acetyl-β-D-mannopyranose (**2**) (25) (4.8 g, 0.014 mole) was dissolved in absolute chloroform and the solution was shaken in an aluminium foil covered flask for 1 h with silver carbonate (16 g), silver perchlorate (26) (0.5 g, 0.0024 mole), drierite (10 g) and glass beads. Crystalline **1** (11 g, 0.024 mole) was then added to the mixture and the shaking of the flask was continued. The reaction was monitored by t.l.c. in solvent (*iii*) and after 16 h[6] the reaction was almost complete as indicated by the disappearance of the spot corresponding to **2**. Excess compound **1** had $R_2 = 2.4$ (where **2** had $R_2 = 1.0$) and compound **3** (not isolated) had $R_2 = 1.9$. The reaction mixture was then filtered and the filtrate was concentrated to a syrup.

The syrupy mixture above was dissolved in aqueous methanol and dechlorosulfated with sodium iodide in the presence of excess barium carbonate (9). The mixture was filtered and the filtrate was concentrated to small volume. After the addition of water, the aqueous solution was extracted once with chloroform to remove excess **2**, and then it was continuously extracted with chloroform for 8 h. Concentration of the chloroform solution gave impure **4** as a glass (3.8 g, 55%) which had $[\alpha]_D$ + 14° (*c*, 1.0 in chloroform).

Anal. Calcd. for $C_{19}H_{28}O_{14}$: C, 47.50; H, 5.8. Found: C, 46.40; H, 5.6.

Thin-layer chromatography in solvent (*iv*) indicated one major component with a negligible quantity of an impurity which co-chromatographed with **2**. A small quantity of **4** (10 mg) was catalytically deacetylated using sodium methoxide and the deacetylated residue was reduced with sodium borohydride. The reduced product was trimethylsilylated (24) and injection onto column (*b*) at 203 °C gave two peaks which had identical retention volumes to the trimethylsilyl derivatives of the reduced derivatives of **5** and its β-D-anomer (**6**). Their relative retention times were 1.0:0.85 respectively and the amount of **6** present in the mixture, as calculated from the peak areas was 5%.

[5]When the products of this reaction were isolated after 1 day, the major product was crystalline starting material (α-D-xylopyranosyl chloride 2,3,4-tri(chlorosulfate)).

[6]The reaction proceeded at a much slower rate when the silver perchlorate was omitted.

Can. J. Chem. Downloaded from www.nrcresearchpress.com by 210.87.254.40 on 09/05/12
For personal use only.

6-O-α-D-Xylopyranosyl-D-mannopyranose (5)

The syrup above (3.8 g) was catalytically deacetylated using 0.44 *M* sodium methoxide in methanol (80 ml). The solution on standing for 16 h at 0 °C, produced a methanol insoluble sodium complex, which was filtered and washed with methanol. The sodium complex (1.7 g) had m.p. 120–122 °C (decomp.).

Anal. Calcd. for $C_{11}H_{20}O_{10}Na$: C, 37.15; H, 6.23. Found: C, 36.51; H, 6.23.

Paper chromatographic analysis of the complex in solvent (*a*) indicated one component at R_m 1.62 which co-chromatographed with pure **5**. The mother liquors and methanol washings from above were deionized and concentrated to a syrup. The syrup was further treated with 0.044 *M*, sodium methoxide solution (40 ml) and a further quantity of the chromatographically pure sodium complex (0.4 g) was obtained. The mother liquors from this last treatment were shown by paper chromatography to contain **5** (R_m 1.62), the β-D-anomer of **5** (**6**) (R_m 1.35) and a trace of mannose (R_m 2.62). Compound **5** was still the major component of the mixture by visual estimation.

The combined sodium complexes (2 g) above were dissolved in aqueous methanol and deionized. Concentration of the eluate gave a syrup which crystallized when dissolved in an ethanol–methanol solution. However, the melting point of the crystals could not be determined due to their extremely hygroscopic nature. Therefore the ethanol–methanol solution was concentrated to a glassy syrup (1.9 g, 42% based on **2**) of $[\alpha]_D$ + 95.7° (*c*, 1.44 in water).

Anal. Calcd. for $C_{11}H_{20}O_{10}$: C, 42.31; H, 6.46. Found: C, 42.48; H, 6.65.

Paper chromatographic analysis of the syrup indicated one component at R_m 1.62 in solvent (*a*). The p.m.r. spectrum of **5** showed two doublets (anomeric signals) at τ 4.93 and τ 5.20 (Table I). The signals were in the ratio of 1:2 respectively. Acid hydrolysis of **5** gave mannose and xylose as determined by paper chromatography in solvents (*a*) and (*b*).

6-O-α-D-Xylopyranosyl-D-mannitol

Crystalline **5** (0.25 g) was reduced with sodium borohydride in aqueous solution and the solution was deionized and concentrated to a non-reducing syrup (0.25 g). A small amount of the reduced product was trimethylsilylated (24) and injection onto column (*b*) at 203 °C gave one homogeneous peak of retention time 11 min. Acid hydrolysis of the syrup gave xylose as the only detectable reducing sugar (paper chromatography in solvents (*a*) and (*b*)). The reduced product gave a syrupy octaacetate which had $[\alpha]_D$ + 73° (*c*, 1.28 in chloroform).

Anal. Calcd. for $C_{27}O_{18}H_{38}$: C, 49.73; H, 5.88. Found: C, 48.75; H, 5.46.

Methylation of 5 and the Isolation of Characterization of the Subsequent Hydrolysis Products

Crystalline **5** (0.2 g) was methylated by the Haworth procedure (27) and continuously extracted with chloroform. Concentration of the chloroform solution gave a syrup which was further methylated by the method of Purdie and Irvine (28) to yield a fully methylated syrupy product (0.2 g). The syrup was then hydrolyzed and the syrupy mixture of products was isolated by the method of Bishop and co-workers (29). The syrupy mixture was shown to contain two reducing components which were separated and isolated by preparative t.l.c. using solvent (*iii*) also as described by Bishop and co-workers (29).

The faster moving component (0.07 g) crystallized spontaneously, and recrystallization from light petroleum (b.p. 30–60 °C) gave large colorless crystals, m.p. 88 °C, undepressed on admixture with an authentic sample of 2,3,4-tri-*O*-methyl-D-xylopyranose (30).

The slower component was a syrup (0.07 g) which had $[\alpha]_D$ + 1° (*c*, 1.5 in water). It was chromatographically indistinguishable from an authentic sample of 2,3,4-tri-*O*-methyl-D-mannose when the derived and authentic methyl ethers were methanolyzed (15) and injected onto column (*b*) at 155 °C and when the trimethylsilyl esters (16) of the methanolysis products were injected onto column (*b*) at 170 °C.

6-O-β-D-Xylopyranosyl-D-mannopyranose (6)

An attempt to synthesize the above β-linked disaccharide from α-D-xylopyranosyl chloride 2,3,4-tri(chlorosulfate) and **2**, by the same procedure used in the synthesis of **5** was abandoned due to the extremely slow rate of reaction. This was again determined by monitoring the reaction mixture on t.l.c. as before. Even after 8 days the spot representing **2** was still very strong and the spot having a similar mobility to **3** was very faint. Therefore, the method of Bredereck and co-workers (1) was utilized in this synthesis, using tetra-*O*-acetyl-α-D-xylopyranosyl bromide (6.8 g) and syrupy 1,2,3,4-tetra-*O*-acetyl-6-*O*-trityl-α-D-mannopyranose (25) (11.8 g) with silver perchlorate (6.2 g) in nitromethane solution. The reaction produced a syrup (39 g) which on dissolution in ethanol yielded crystalline triphenyl carbinol (melting point and mixture melting point 165–166 °C). No further crystallization could be induced. Thin-layer chromatography in solvent (*iii*) indicated the presence of one major component preceded by three minor components and followed by two other minor components. The syrup was chromatographed on silica gel (Mallinckrodt, 100 mesh) whence elution of the faster moving components was achieved using solvent (*i*). The slower moving major component was eluted with solvent (*ii*) and concentration of the eluate gave a chromatographically pure colorless syrup (7.5 g, 65%) of $[\alpha]_D$ + 14° (*c*, 2.01 in chloroform). The syrup was deacetylated using sodium methoxide (0.044 *M*) and the solution on standing for 16 h at 0 °C yielded a precipitate which was found to be methanol soluble. Therefore the whole solution was deionized and concentrated to a syrup (3.5 g, 91%). Paper chromatographic analysis of the syrup in solvent (*a*) indicated three components at R_m 1.04, R_m 1.35 (**6**, main component), and R_m 1.62 (co-chromatographed with **5**). The syrup crystallized on standing and the crude crystalline product was recrystallized from ethanol–methanol to give colorless needles (2.7 g, 40% based on the 6-trityl derivative) of m.p. 125–127° and $[\alpha]_D$ − 30° (5 min) → −23.8° (equilibrium) (*c*, 1.35 in water).

Anal. Calcd. for $C_{11}H_{20}O_{10}.CH_3OH$: C, 41.86; H, 7.03. Found: C, 41.69; H, 6.86.

The crystals gave the same analysis even after they were desiccated under vacuum for 4 h at 100 °C. The p.m.r. spectrum of the crystals showed a singlet at τ 6.76 (OMe) and doublets (anomeric signals) at τ 5.63, τ 5.21, and τ

4.94 (see Table I). The signals were in the intensity ratio of 9:3:1:2. When the spectrum of methanol was obtained in deuterium oxide with acetonitrile as internal reference, it also showed a singlet at τ 6.76. Paper chromatographic analysis of the crystals in solvent (*a*) indicated one component at R_m 1.35.

The crystals gave a crystalline phenylosazone derivative which when recrystallized from ethanol–water gave yellow needles, m.p. 212–214 °C and $[\alpha]_D$ − 104° (*c*, 1.67 in pyridine). Helferich reports (20) m.p. 220 °C and $[\alpha]_D$ − 109.7° (pyridine) for the phenylosazone derivative of 6-*O*-β-D-xylopyranosyl-D-glucose (primeverose).

Acid hydrolysis of the above crystalline disaccharide (**6**) gave mannose and xylose as determined by paper chromatography in solvents (*a*) and (*b*). Methylation of **6** (0.2 g) and the isolation and characterization of the subsequent hydrolysis products was carried out by the same procedures as used with **5**. Both 2,3,4-tri-*O*-methyl-D-xylopyranose and 2,3,4-tri-*O*-methyl-D-mannopyranose were obtained in almost identical yields.

Acknowledgments

The author wishes to thank Mrs. B. McLean for technical assistance and Mr. A. E. Castagne for determination of the microanalyses and the p.m.r. spectra.

1. H. Bredereck, A. Wagner, H. Kuhn, and H. Ott. Chem. Ber. **93**, 1201 (1960).
2. R. J. Stoodley. M.Sc. Thesis. Queen's University, Kingston, Ontario. 1959.
3. R. U. Lemieux. Advan. Carbohydrate Chem. **9**, 1 (1954).
4. L. T. Haynes and F. H. Newth. Advan. Carbohydrate Chem. **10**, 207 (1955).
5. M. L. Wolfrom, A. O. Pittet, and I. C. Gillam. Proc. Nat. Acad. Sci. **47**, 700 (1961); M. L. Wolfrom, A. Thompson, and D. R. Lineback. J. Org. Chem. **28**, 860 (1963).
6. P. A. J. Gorin and A. S. Perlin. Can. J. Chem. **39**, 2474 (1961).
7. P. W. Austin, F. E. Hardy, J. G. Buchanan, and J. Baddiley. J. Chem. Soc. 1419 (1965).
8. H. J. Jennings and J. K. N. Jones. Can. J. Chem. **40**, 1408 (1962).
9. H. J. Jennings and J. K. N. Jones. Can. J. Chem. **43**, 2372 (1965).
10. H. J. Jennings and J. K. N. Jones. Can. J. Chem. **41**, 1151 (1963).
11. B. Coxon, H. J. Jennings, and K. A. McLaughlan. Tetrahedron, **23**, 2395 (1967).
12. H. J. Jennings. Chem. Commun. 722 (1967).
13. R. L. Whistler, K. A. Kimmell, and D. F. Durso. J. Am. Chem. Soc. **73**, 3530 (1951).
14. C. S. Hudson. J. Am. Chem. Soc. **47**, 265 (1925).
15. Y. C. Lee and C. E. Ballou. J. Biol. Chem. **239**, 1316 (1964).
16. Y. C. Lee and C. E. Ballou. Biochemistry, **4**, 257 (1965).
17. J. M. Van Der Veen. J. Org. Chem. **28**, 564 (1963).
18. F. J. Bates. Polarimetry, saccharimetry, and the sugars. Nat. Bur. Std. (U.S.), Washington. 1942. p. 481.
19. R. U. Lemieux, R. K. Kullnig, H. J. Bernstein, and W. G. Schneider. J. Am. Chem. Soc. **80**, 6098 (1958).
20. B. Helferich and H. Rauch. Ann. **455**, 168 (1927).
21. L. Hough, J. K. N. Jones, and W. H. Wadman. J. Chem. Soc. 1702 (1950).
22. W. E. Trevelyan, D. P. Procter, and J. S. Harrison. Nature, **166**, 444 (1950).
23. G. Zemplén and E. Pacsu. Chem. Ber. **62**, 1613 (1929).
24. C. C. Sweeley, R. Bentley, M. Makita, and W. W. Wells. J. Am. Chem. Soc. **85**, 2497 (1963).
25. D. D. Reynolds and W. L. Evans. J. Am. Chem. Soc. **62**, 66 (1940).
26. H. Bredereck, A. Wagner, G. Faber, H. Ott, and J. Rauther. Chem. Ber. **92**, 1135 (1959).
27. W. N. Haworth. J. Chem. Soc. **107**, 8 (1915).
28. T. Purdie and J. C. Irvine. J. Chem. Soc. **83**, 1021 (1903).
29. C. T. Bishop, M. B. Perry, F. Blank, and F. P. Cooper. Can. J. Chem. **43**, 30 (1965).
30. F. P. Phelps and C. B. Purves. J. Am. Chem. Soc. **51**, 2443 (1929).

Can. J. Chem. Downloaded from www.nrcresearchpress.com by 210.87.254.40 on 09/05/12
For personal use only.

Can. J. Chem. Downloaded from www.nrcresearchpress.com by 210.87.254.5 on 09/05/12
For personal use only.

Synthesis of steroidal pyrimidine *N*-oxides[1]

J. ROMO, L. RODRÍGUEZ-HAHN, AND M. JIMÉNEZ
Instituto de Química de la Universidad Nacional Autónoma de México, México 20, D. F., México

Received March 18, 1968

Several steroidal pyrimidine *N*-oxides were synthesized by treatment of different *N*-acyl derivatives of steroidal β-amino-α,β-unsaturated ketones with hydroxylamine. This procedure has been applied to obtain steroidal pyrimidine *N*-oxides with the heterocyclic ring condensed with rings A and B of the steroidal moiety. Some chemical and spectral properties of these derivatives are discussed.

Canadian Journal of Chemistry, 46, 2807 (1968)

Recently, steroidal pyrimidines with the heterocyclic ring fused to the positions 2,3 or 16,17 have been reported by Ruggieri *et al.* (1, 2). The synthesis of pyrimidine *N*-oxides by cyclization of the adequate amidoximes has also been described (3).

We now wish to describe a procedure for the synthesis of steroidal (3,2-*d*) and (17,16-*d*) pyrimidine *N*-oxides of the androstane and estrane series and of the pyrimidines derived from them.

Treatment of 16-acetyl-17-aminoandrosta-5,16-dien-3β-ol, diacetate (**1***b*) (4) with hydroxylamine hydrochloride and pyridine in methanol solution afforded in good yield the (17,16-*d*) pyrimidine *N*-oxide **2***b*. It analyzed for $C_{25}H_{34}O_3N_2$. In the infrared (i.r.) spectrum **2***b* did not show hydroxyl bands. A carbonyl band at 1740 cm^{-1} corresponds to the 3-acetoxy group. The ultraviolet (u.v.) spectrum of **2***b* exhibited four maxima at 207, 217, 263, and 306 mμ (ε, 19 500, 21 900, 10 200, and 5500, respectively). The maxima at 217 and at 306 mμ are probably attributable to the *N*-oxide function since they disappear when the spectrum of **2***b* is determined in a strong acid medium (5). The nuclear magnetic resonance (n.m.r.) spectrum[2] of **2***b* showed two singlets at δ 2.70 and δ 2.47 corresponding to two aromatic methyl groups. A singlet at δ 2.02 is ascribed to the acetate. The position of the pyrimidine *N*-oxide function as shown in formula **2***b* results from the cyclization of the intermediary oxime.

Alkaline hydrolysis of **2***b* gave the free alcohol **2***a*. The i.r. spectrum of **2***a* showed a hydroxyl band at 3630 cm^{-1} and did not exhibit carbonyl bands. Two aromatic methyl groups are responsible for two singlets at δ 2.71 and δ 2.48 in the n.m.r. spectrum of **2***a*.

Acetylation of **2***a* with acetic anhydride – pyridine did not form **2***b*. Instead the diacetate **3***d* ($C_{27}H_{36}O_4N_2$) was obtained. This reaction is known to occur in heterocyclic rings bearing an *N*-oxide function. It has been previously reported in *N*-oxides of pyrimidine and purine (6–8). The u.v. spectrum of the diacetate **3***d* (λ_{max} 207, 217, and 257 mμ; ε, 7900, 6900, and 5300, respectively) suggested that the pyrimidine *N*-oxide has been transformed into a pyrimidine (9). This was confirmed by the presence of two strong bands in the i.r. spectrum of **3***d* at 1590 and 1570 cm^{-1} which are characteristic of a pyrimidine ring (8, 9). The i.r. spectrum of **3***d* also showed a strong carbonyl band at 1735 cm^{-1} with a shoulder at 1745 cm^{-1}, assigned to two acetoxy groups. One of them substituted at C-3, and the other one formed in the acetylation and attached to the pyrimidine moiety. The singlet corresponding to one of the aromatic methyl groups observed at δ 2.70 in the n.m.r. spectra of **2***a* and **2***b* is absent in the n.m.r. spectrum of the diacetate **3***d*. The singlets at δ 2.48 at δ 2.21 and at δ 2.07 in the n.m.r. spectrum of **3***d* are assigned to an aromatic methyl group and to two acetoxy groups. A sharp singlet (2 H) at δ 5.28 is ascribed to the methylene group bearing the acetoxy function formed in the acetylation. The alternative structure **4** was rejected since the singlet at δ 2.70 present in the n.m.r. spectra of **2***a* and **2***b* corresponds to the methyl group attached to the carbon between the nitrogen atoms of the pyrimidine ring, and this is the signal which is absent in the n.m.r. spectrum of the diacetate **3***d*.

---

[1]Contribution No. 265 from the Instituto de Química de la Universidad Nacional Autónoma de México.

[2]The n.m.r. spectra were determined by Mr. Eduardo Díaz on a Varian A-60A spectrometer in deuteriochloroform solution using TMS as the internal reference. The chemical shifts are reported in p.p.m. as δ values.

Can. J. Chem. Downloaded from www.nrcresearchpress.com by 210.87.254.5 on 09/05/12
For personal use only.

Treatment of the pyrimidine *N*-oxide **2***b* with acetic anhydride yielded two products. One of them was identified as the diacetate **3***d* already described. The second product ($C_{25}H_{34}O_3N_2$) possesses structure **3***c* since it showed a hydroxyl band at 3450 cm^{-1} in the i.r. spectrum and on acetylation produced the diacetate **3***d*.

Reduction of the pyrimidine *N*-oxide (**2***b*) with zinc in acetic acid yielded the pyrimidine **3***b* ($C_{25}H_{34}O_2N_2$) (λ_{max} 207, 215, and 260 mμ; ε, 7900, 7200, and 7100, respectively). Its i.r. spectrum showed the pyrimidine bands at 1595 and 1570 cm^{-1} (8, 9). Alkaline hydrolysis of **3***b* afforded the alcohol **3***a*.

Pyrimidine *N*-oxides of this series with different substituents can be prepared by treatment of the appropriate acyl derivative of **1***a* with hydroxylamine. When the dipropionyl derivative **1***c* was treated with hydroxylamine hydrochloride and pyridine, the pyrimidine *N*-oxide **2***c* was obtained. In the n.m.r. spectrum the latter showed two quadruplets centered at δ 3.13 and at δ 2.32 attributed to the methylene of the ethyl group substituted in the pyrimidine ring and to the methylene of the propionyl ester, respectively. The singlet at δ 2.50 is assigned to the methyl group attached to the aromatic ring. The primary methyl groups are responsible for triplets centered at δ 1.36 and δ 1.15.

Treatment of the pyrimidine *N*-oxide **2***c* with acetic anhydride gave the acetoxy derivative **3***f*. Its i.r. spectrum had a broad carbonyl band at 1735 cm^{-1} (ester groups). The n.m.r. spectrum of **3***f* indicated that the acetoxy group is linked to the methylene of the ethyl group substituted in the pyrimidine ring. It showed a singlet at δ 2.46 corresponding to the aromatic methyl group. A quadruplet (1 H, $J = 6.5$ c.p.s.) at δ 5.89, a doublet (3 H, $J = 6.5$ c.p.s.) at δ 1.63, and a singlet at δ 2.18 (3 H) were attributed to the acetoxyethyl side chain.

Zinc reduction of the pyrimidine *N*-oxide **2***c* afforded the pyrimidine **3***e*.

Acetylation of 16-acetyl-17-benzoylaminoandrosta-5,16-dien-3β-ol (**1***f*), previously described (4) afforded the acetate **1***e*. Prolonged treatment of **1***e* with hydroxylamine hydrochloride and pyridine afforded in low yield the pyrimidine *N*-oxide **2***h*.

The urethane **1***f* prepared by treatment of **1***a* with ethyl chloroformate gave the hydroxypyrimidine *N*-oxide **2***e* by reaction with hydroxylamine. The n.m.r. spectrum of **2***e* showed a complex signal at δ 7.17 which disappeared on equilibration with deuterium oxide. A singlet at δ 2.48 was assigned to the aromatic methyl group.

Saponification of the hydroxypyrimidine *N*-oxide **2***e* yielded the free alcohol **2***f*. It gave a positive ferric chloride test. Treatment of **2***e* with acetic anhydride and pyridine afforded two products **2***g* and **2***h* in which the *N*-oxide function is still present. The diacetate **2***h* had i.r. bands at 1810 cm^{-1} (acetyl group substituted in the pyrimidine ring) and at 1735 cm^{-1} (C-3 acetyl group).

The monoacetate **2***g* only had a carbonyl i.r. band at 1730 cm^{-1} corresponding to the C-3 acetate. Treatment of **2***g* with acetic anhydride formed the acetate **2***h*.

Reduction of the pyrimidine *N*-oxide gave the hydroxypyrimidine **3***g*.[3] Its i.r. spectrum showed only the C-3 acetyl band at 1730 cm^{-1}. In the n.m.r. spectrum of **3***g* the aromatic methyl group is responsible for a singlet at δ 2.35 showing a displacement to higher field due to the reduction of the *N*-oxide function. It gave a negative ferric chloride test.

Acetylation of **3***g* with acetic anhydride and pyridine gave **3***h*. It had an i.r. band at 1775 cm^{-1} corresponding to the acetoxy group substituted in the heterocyclic ring.

The facility and good yield with which the pyrimidine *N*-oxides described above are obtained, prompted us to investigate the possibility of obtaining pyrimidine *N*-oxides in which the *N*-oxide function is near the C-18 angular methyl group.

Treatment of the formyl derivatives **5***a* (11) and **9***a* (12) with ammonium hydroxide gave the corresponding ketoamines **5***b* and **9***b*. They gave positive ferric chloride tests. Both products were acetylated to the acetylamino derivatives **5***c* and **9***c*.

Treatment with hydroxylamine hydrochloride and pyridine of the β-amido-α,β-unsaturated ketones described above afforded the corresponding pyrimidine *N*-oxides directly; cyclization occurs very rapidly and the intermediary oximes could not be isolated. A similar treat-

[3]Hydroxypyrimidines have been prepared by condensation of malonic ester derivatives with substituted ureas, see ref. 10.

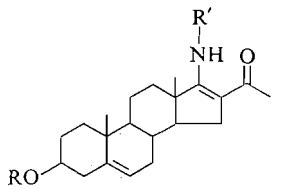

1 *a*, R = R′ = H
b, R = R′ = Ac
c, R = R′ = Et—C=O
d, R = H, R′ = Bz
e, R = Ac, R′ = Bz
f, R = R′ = Et—O—C=O

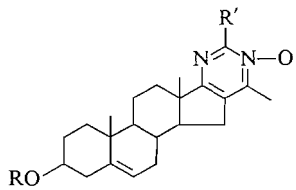

2 *a*, R = H, R′ = CH_3
b, R = Ac, R′ = CH_3
c, R = Et—C=O, R′ = Et
d, R = Ac, R′ = C_6H_5
e, R = Et—O—C = O, R′ = OH
f, R = H, R′ = OH
g, R = Ac, R′ = OH
h, R = Ac, R′ = AcO

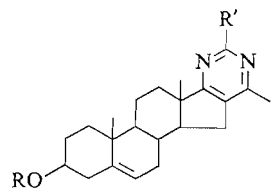

3 *a*, R = H, R′ = CH_3
b, R = Ac, R′ = CH_3
c, R = Ac, R′ = CH_2OH
d, R = Ac, R′ = CH_2OAc
e, R = Et—C=O, R′ = C_2H_5
f, R = Et—C=O, R′ = CH—CH_3
g, R = Ac, R′ = OH |
h, R = Ac, R′ = AcO OAc

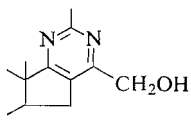

4

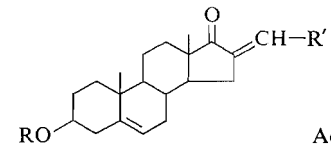

5 *a*, R = H, R′ = OH
b, R = H, R′ = NH_2
c, R = Ac, R′ = NHAc

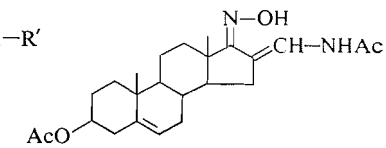

6 *a*, *b*

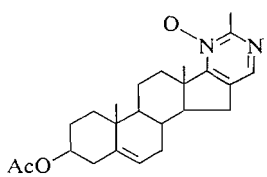

7

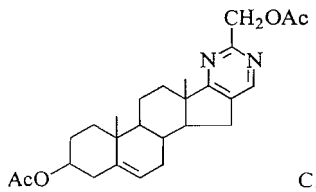

8

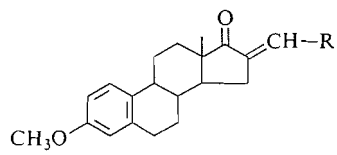

9 *a*, R = OH
b, R = NH_2
c, R = NHAc

ment of the amidoketones **5***c* and **9***c* gave the oximes **6***a* and **10***a*, respectively.

The oxime **6***a* was heated with γ-collidine in order to force the formation of the pyrimidine *N*-oxide; however, the product isolated was an isomer of **6***a*.

Exposure of the isomer **6***b* to acids caused ring closure. The resulting pyrimidine *N*-oxide **7** showed the following singlets in the n.m.r. spectrum: at δ 8.00 (1 H, aromatic proton), at δ 2.75, and at δ 2.05 (aromatic methyl group and C-3 acetyl group, respectively).

We were not able to produce ring closure by exposure of the oxime **6***a* to acids. Apparently the γ-collidine treatment of the oxime **6***a* affected the C-16 side chain, forming an isomer more prone to undergo cyclization.

Treatment of the pyrimidine *N*-oxide **7** with acetic anhydride resulted in formation of the pyrimidine derivative **8**.

Treatment of the oxime **10***a* with γ-collidine gave the isomer **10***b*. Ring closure of the latter was produced on exposure to acids. The n.m.r. spectrum of the resulting pyrimidine *N*-oxide **11** exhibited singlets at δ 8.00 (1 H) and at δ 2.72 (3 H) corresponding to the hydrogen and methyl group substituted in the heterocyclic ring.

Alkaline hydrolysis of the non-crystalline acetoxy derivative **12***a* obtained by acetic anhydride treatment of **11** gave the pyrimidine **12***b*.

A pyrimidine *N*-oxide (3,2-*d*) was prepared by a similar procedure. The 2-aminomethylene derivative **13***b* was obtained by treatment of 2-formyl-5α-androstan 17β-ol,3-one (13, 14) with ammonium hydroxide. Treatment with hydroxylamine of the acetamido derivative **13***c* prepared by acetylation of the amine **13***b* gave the oxime **14**. When this oxime was heated with γ-collidine the pyrimidine *N*-oxide **15** was obtained. In the n.m.r. spectrum it showed a

Can. J. Chem. Downloaded from www.nrcresearchpress.com by 210.87.254.5 on 09/05/12
For personal use only.

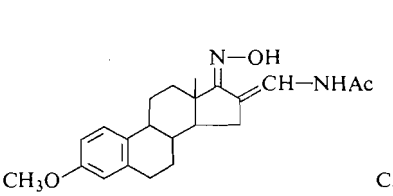

10 *a*, *b*,

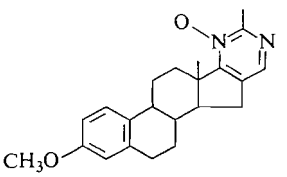

11

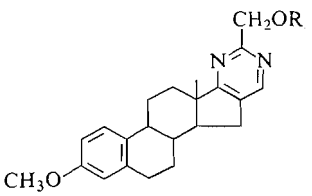

12 *a*, R = Ac
b, R = H

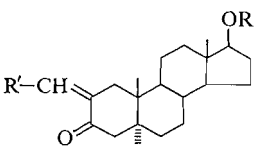

13 *a*, R = H, R′ = OH
b, R = H, R′ = NH_2
c, R = Ac, R′ = NHAc

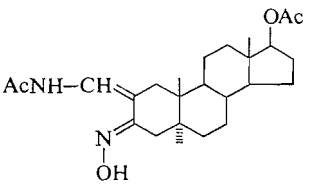

14

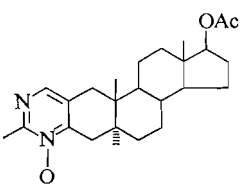

15

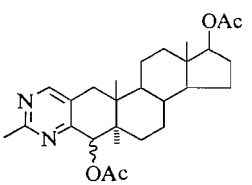

16 *a*, *b*,

singlet at δ 7.90 attributed to the pyrimidine aromatic proton. A triplet centered at δ 4.65 corresponded to the hydrogen substituted at C-17. Two singlets at δ 2.7 and δ 2.03 are assigned to the pyrimidine methyl group and the acetyl group, respectively. Treatment of the pyrimidine *N*-oxide **15** with acetic anhydride yielded two products *a* and *b* (**16**). The i.r. spectra of both products had carbonyl bands at 1735 cm^{-1} (double strength, acetyl groups). The n.m.r. spectra of both derivatives (**16**) had the same signals with very similar chemical shifts as described above for the pyrimidine *N*-oxide **15**. The presence of a singlet at δ 2.68 corresponding to the pyrimidine methyl group in *a* and *b* indicates that the latter remained untouched and that the newly formed acetoxy group is substituted at C-4 in the steroid nucleus. Comparison of the n.m.r. spectra of the products *a* and *b* indicates that these derivatives (**16**) differ in stereochemistry at C-4. The pyrimidine **16***a* exhibited in the n.m.r. spectrum a singlet at δ 2.19 assigned to the C-4 acetyl methyl group. The chemical shift and the coupling constant of a doublet (J = 10 c.p.s.) at δ 5.70, attributed to the C-4 proton, corresponds to an axial substituent, therefore the C-4 acetoxy group must be equatorial. The n.m.r. spectrum of **16***b* showed a singlet at δ 2.10 ascribed to the C-4 acetoxy group. The C-4 equatorial hydrogen is responsible for a doublet (J = 4 c.p.s.) at δ 6.05 (C-4 axial acetoxy group).

The pyrimidine *N*-oxides **7**, **11**, and **15** showed maxima at 220 and at 265 mμ, in the u.v. spectrum. When the latter was determined in strong acid medium the maximum at 220 mμ decreased in intensity.

Experimental

Melting points are uncorrected; the analyses were performed by Dr. F. Pascher, Bonn, Germany. Infrared (i.r.) spectra and rotations were run in chloroform unless otherwise stated. Ultraviolet (u.v.) spectra were run in 95% ethanol. The chromatograms were run using alumina Alcoa F-20.

Dimethylpyrimidine N-Oxide **2***b*

A solution of **1***b* (5 g) in methanol (75 ml) and pyridine (7 ml) was treated with hydroxylamine hydrochloride (5 g) and heated under reflux for 1 h. It was then concentrated to a small volume and diluted with water. The precipitate

Can. J. Chem. Downloaded from www.nrcresearchpress.com by 210.87.254.5 on 09/05/12
For personal use only.

Can. J. Chem. Downloaded from www.nrcresearchpress.com by 210.87.254.5 on 09/05/12
For personal use only.

formed was collected and washed with water. Crystallization from ethyl acetate – ether yielded the pyrimidine **2***b* (4 g) as brilliant plates, m.p. 250–252°. Further crystallizations from ethyl acetate – ether raised the m.p. to 256–258°; negative ferric chloride test; $[\alpha]_D$ −53°; λ_{max}, 207, 217, 263, 306 mμ; ε, 19 500, 21 900, 10 200, and 500; λ_{max} (pH 3)[4] 207, 266 mμ; ε, 19 300, 20 200; i.r. bands at 1740 cm^{-1} (acetyl group), at 1630 cm^{-1} (C=C double bonds), and at 1550 cm^{-1} (C=N double bonds).

Anal. Calcd. for $C_{25}H_{34}O_3N_2$: C, 73.14; H, 8.35; O, 11.69; N, 6.82. Found: C, 73.45; H, 8.47; O, 11.75; N, 6.68.

Alkaline Hydrolysis of the Dimethylpyrimidine N-Oxide 2b

A solution of **2***b* (3.2 g) in methanol (50 ml) was mixed with potassium hydroxide (3 g) in water (6 ml), heated under reflux for 1 h, concentrated to a small volume, poured in water, and the precipitate collected. Crystallization from methanol–acetone yielded **2***a* (2.6 g), m.p. 275–278°. Further crystallizations from methanol–acetone raised the m.p. to 279–281°, $[\alpha]_D$ −41°; λ_{max}, 205, 216, 262, and 304 mμ; ε, 20 000, 21 100, 10 500, 6100; i.r. bands at 3640 cm^{-1} (hydroxyl group), at 1625 cm^{-1} (C=C double bonds), and at 1550 cm^{-1} (C=N double bonds).

Anal. Calcd. for $C_{23}H_{32}O_2N_2$: C, 74.96; H, 8.75; O, 8.68; N, 7.60. Found: C, 74.92; H, 8.88; O, 8.91; N, 7.67.

Treatment of the Dimethylpyrimidine N-Oxide 2a with Acetic Anhydride and Pyridine

A solution of **2***a* (100 mg) in acetic anhydride (5 ml) and pyridine (5 ml) was heated on the steam bath for 1 h and then poured into water. The precipitate formed was extracted with ethyl acetate. The organic extract was washed with dilute hydrochloric acid, aqueous sodium bicarbonate, dried on anhydrous sodium sulfate, and evaporated. The solid residue (60 mg) was crystallized from acetone–hexane. This yielded **3***d* as needles, m.p. 144–147°; $[\alpha]_D$ −57°; λ_{max}, 207, 217 (shoulder), and 257 mμ; ε, 7900, 6900, 5300; i.r. bands at 1735 cm^{-1} with a shoulder at 1745 cm^{-1} (acetyl groups), and at 1590 and 1570 cm^{-1} (pyrimidine ring).

Anal. Calcd. for $C_{27}H_{36}O_4N_2$: C, 71.65; H, 8.02; O, 14.14; N, 6.19. Found: C, 71.94; H, 8.03; O, 13.63; N, 6.45.

Treatment of the Dimethylpyrimidine N-Oxide 2b with Acetic Anhydride

A solution of **2***b* (750 mg) in acetic anhydride (5 ml) was heated on the steam bath for 1 h, poured in water, and the precipitate extracted with ethyl acetate. The organic extract was washed with aqueous sodium bicarbonate, evaporated to dryness, and the gummy residue chromatographed on alumina. The crystalline fractions, eluted with benzene–hexane 1:1, were combined and recrystallized from acetone–hexane. This yielded the diacetate **3***d* (175 mg), m.p. 142–146°, which was identified by the standard methods with the product obtained in the above acetylation with acetic anhydride and pyridine.

The crystalline fractions eluted with benzene and increasing proportions of ethyl acetate were combined. Crystallization from ethyl acetate afforded **3***c* (150 mg) as needles, m.p. 245–248°; $[\alpha]_D$ −56° (dioxane); λ_{max}, 207, 217 (shoulder), and 258 mμ; ε, 8400, 7100, 5600; i.r. bands at 3450 cm^{-1} (hydroxyl group), at 1740 cm^{-1} (acetyl group), and at 1595 and 1570 cm^{-1} (pyrimidine ring).

Anal. Calcd. for $C_{25}H_{34}O_3N_2$: C, 73.14; H, 8.35; O, 11.69; N, 6.82. Found: C, 72.97; H, 8.30; O, 11.83; N, 6.78.

Acetylation of the derivative **3***c* with acetic anhydride–pyridine afforded the diacetate **3***d*, m.p. 142–146°.

Zinc Reduction of the Pyrimidine N-Oxide (2b)

A solution of the pyrimidine oxide **2***b* (5 g) in acetic acid (50 ml) was treated with zinc dust (10 g), heated under reflux for 1 h, filtered, evaporated to a small volume *in vacuo*, and diluted with water. The precipitate was extracted with ethyl acetate, the organic solution washed with aqueous sodium bicarbonate, dried with anhydrous sodium sulfate, concentrated, and cooled. The crystalline precipitate of **3***b* was collected and washed with ether, yield 1.3 g, m.p. 236–238°. Further crystallizations from ethyl acetate raised the m.p. to 239–241°; $[\alpha]_D$ −53°; λ_{max}, 207, 215 (shoulder), and 260 mμ; ε, 7900, 7200, 7100; i.r. bands at 1730 cm^{-1} (acetyl group), and at 1595 and 1570 cm^{-1} (pyrimidine ring).

Anal. Calcd. for $C_{25}H_{34}O_2N_2$: C, 76.10; H, 8.69; O, 8.11; N, 7.10. Found: C, 76.30; H, 8.77; O, 8.20; N, 7.09.

Alkaline Hydrolysis of the Dimethylpyrimidine 3b

A solution of **3***b* (500 mg) in methanol (20 mg) was mixed with potassium hydroxide (500 mg) in water (2 ml), heated under reflux for 1 h, concentrated, poured in water, and the precipitate collected and washed with water. Crystallization from methanol – ethyl acetate yielded **3***a* (410 mg) as prisms, m.p. 243–245°. Further crystallizations from the same solvents raised the m.p. to 248–250°; $[\alpha]_D$ −47° (dioxane); λ_{max}, 208, 215 (shoulder), and 259 mμ; ε, 7900, 7700, 7000; λ_{max} (pH 3) 208, 267 mμ; ε, 9400, 7200; i.r. bands at 3610 cm^{-1} (hydroxyl group), and at 1590 and 1570 cm^{-1} (pyrimidine ring).

Anal. Calcd. for $C_{23}H_{32}ON_2$: C, 78.36; H, 9.15; O, 4.54; N, 7.95. Found: C, 78.15; H, 9.12; O, 4.74; N, 8.03.

Acetylation of **3***a* with acetic anhydride – pyridine on the steam bath for 1 h afforded the acetate **3***b*.

16-Acetyl-17-aminoandrosta-5-16-dien-3β-ol Dipropionate (1c)

The amino derivative **1***a* (4) (1 g), in pyridine (5 ml) and propionic anhydride (5 ml), was heated on the steam bath for 1 h, poured in water, and the precipitate collected and washed with water. Crystallization from methanol yielded **1***c* (1.165 g) as brilliant plates, m.p. 181–183°; $[\alpha]_D$ −204°; λ_{max}, 207 and 313 mμ; ε, 10 000, 14 300; i.r. bands at 1740 cm^{-1} (ester group), 1640 cm^{-1} (hydrogen bonded, α,β-unsaturated ketone), and at 1580 cm^{-1} (C=C double bonds).

Anal. Calcd. for $C_{27}H_{39}O_4N$: C, 73.43; H, 8.90; O, 14.49; N, 3.17. Found: C, 73.20; H, 8.84; O, 14.68; N, 3.25.

Methylethylpyrimidine N-Oxide 2c

A solution of the dipropionate **1***c* (900 mg) in methanol (25 ml) and pyridine (3 ml) was treated with hydroxylamine hydrochloride (1 g), heated under reflux for 1 h,

[4]The ethanol solution was acidified with hydrochloric acid to pH 3 and the spectrum determined immediately.

Can. J. Chem. Downloaded from www.nrcresearchpress.com by 210.87.254.5 on 09/05/12
For personal use only.

concentrated, poured in water, and the precipitate collected and washed with water. Crystallization from ethyl acetate yielded **2***c* (670 mg) as small needles, m.p. 183–185°. Further crystallizations from the same solvents raised the m.p. to 193–195°; $[\alpha]_D$ −52°; λ_{max}, 207, 218, 265, and 306 mμ; ε, 19 300, 21 900, 10 200, 5900; λ_{max} (pH 3) 207, 268 mμ; ε, 18 600, 9800; i.r. bands at 1740 cm^{-1} (ester group), at 1620 (C=C double bonds), and at 1535 cm^{-1} (C=N double bonds).

Anal. Calcd. for $C_{27}H_{38}O_3N_2$: C, 73.94; H, 8.73; O, 10.94; N, 6.39. Found: C, 74.09; H, 8.69; O, 11.18; N, 6.27.

Treatment of the Methylethylpyrimidine N-Oxide 2c with Zinc Dust

A solution of the pyrimidine *N*-oxide **2***c* (500 mg) in acetic acid (5 ml) was treated with zinc dust (1 g) and the method used was the same as that described for the preparation of **3***b*. Chromatography of the crude product on alumina yielded the methylethylpyrimidine **3***e* (360 mg), m.p. 154–156° (needles from hexane–pentane); $[\alpha]_D$ −59°; λ_{max}, 207, 214 (shoulder), and 259 mμ; ε, 9000, 8500, 6600; i.r. bands at 1730 cm^{-1} (ester group), and at 1585 and 1560 cm^{-1} (pyrimidine ring).

Anal. Calcd. for $C_{27}H_{32}O_2N_2$: C, 76.73; H, 9.06; O, 7.57; N, 6.63. Found: C, 77.20; H, 9.16; O, 7.31; N, 6.77.

Treatment of the Methylethylpyrimidine N-Oxide 2c with Acetic Anhydride

A solution of **2***c* (500 mg) in acetic anhydride (5 ml) was treated as described before. The crude product was purified by chromatography on alumina. Crystallization from hexane–pentane furnished **3***f* as needles, (310 mg), m.p. 183–185°; $[\alpha]_D$ −8°; λ_{max}, 206, 217 (shoulder), and 257 mμ; ε, 8300, 7000, 6900; i.r. bands at 1735 cm^{-1} with a shoulder at 1745 cm^{-1} (ester groups), and at 1590 and 1570 cm^{-1} (pyrimidine ring).

Anal. Calcd. for $C_{29}H_{40}O_4N_2$: C, 72.47; H, 8.39; O, 13.32; N, 5.83. Found: C, 72.60; H, 8.67; O, 12.69; N, 5.90.

16-Acetyl-17-benzoylaminoandrosta-5,16-dien-3β-ol Acetate (1e)

Acetylation of **1***d* (4) (1.25 g) with acetic anhydride – pyridine on the steam bath for 1 h yielded the acetate **1***e* (600 mg) as pale-yellow prisms, m.p. 196–198°; $[\alpha]_D$ −68°; λ_{max}, 205, 241, and 331 mμ; ε, 16 100, 12 900, 12 500; i.r. bands at 1730 cm^{-1} (ester group), at 1700 cm^{-1} (benzamide group), 1630 cm^{-1} (hydrogen bonded, α,β-unsaturated ketone), and 1610 and 1580 cm^{-1} (C=C double bonds).

Anal. Calcd. for $C_{30}H_{37}O_4N$: C, 75.76; H, 7.84; O, 13.46; N, 2.95. Found: C, 75.29; H, 7.98; O, 14.14; N, 2.81.

Methylphenylpyrimidine N-Oxide 2d

A solution of **1***e* (600 mg) in methanol (25 ml) and pyridine (1 ml) was treated with hydroxylamine hydrochloride (600 mg), heated under reflux for 15 h, concentrated, diluted with water, and the precipitate collected and washed with water. The crude product was chromatographed on alumina. Crystallization from ethyl acetate – ether yielded **2***e* (100 mg) as pale-yellow needles, m.p. 240–242°; $[\alpha]_D$ −27°; λ_{max}, 206, 250, and 286 mμ; ε, 21 500, 26 200, 900; i.r. bands at 1740 cm^{-1} (acetyl group), at 1680 and 1630 cm^{-1} (C=C double bonds), and at 1580 cm^{-1} (C=N double bonds).

Anal. Calcd. for $C_{30}H_{36}O_3N_2$: C, 76.24; H, 7.68; O, 10.16; N, 5.93. Found: C, 76.27; H, 7.77; O, 10.25; N, 5.76.

Urethane 1f

Ethyl chloroformate (5 ml) was added slowly to a cooled solution of the amine **1***a* (900 mg) in pyridine (10 ml). After the addition was complete the reaction mixture was left at room temperature for 2 h, heated on a steam bath for 30 min, and poured into water. The solid product obtained was collected, washed with water, and crystallized from chloroform–methanol. This yielded **1***f* (1.040 g), m.p. 188–190°. Further crystallizations from the same pair of solvents gave an analytical sample, m.p. 193–195°; $[\alpha]_D$ −135°; λ_{max}, 306 mμ; ε, 23 500; i.r. bands at 1740 cm^{-1} (ester group), at 1630 cm^{-1} (hydrogen bonded α,β-unsaturated ketone), and at 1575 cm^{-1} (C=C double bond).

Anal. Calcd. for $C_{27}H_{39}O_6N$: C, 68.47; H, 8.30; O, 20.27; N, 2.96. Found: C, 68.70; H, 8.24; O, 20.08; N, 2.86.

Hydroxypyrimidine N-Oxide 2e

A solution of **1***f* (1 g) in methanol (25 ml) and pyridine (5 ml) was treated with hydroxylamine hydrochloride (1.3 g) and heated under reflux for 1 h. The solution was concentrated, diluted with water, and the solid precipitate collected and washed with water. Crystallization from chloroform–methanol gave small needles (810 mg), m.p. 284–285°; positive ferric chloride test (red color); λ_{max}, 209, 222, 318 mμ; ε, 12 600, 10 500, 7000; λ_{max} (pH 3) 210, 334 mμ; ε, 12 800, 8200; i.r. bands at 1745 cm^{-1} (ester group), 1650, 1620, and 1575 cm^{-1}.

Anal. Calcd. for $C_{25}H_{34}O_5N_2$: C, 67.85; H, 7.75; O, 18.08; N, 6.33. Found: C, 67.69; H, 7.64; O, 17.90; N, 6.16.

Saponification of the Hydroxypyrimidine N-Oxide 2e

A solution of **2***e* (800 mg) in methanol (50 ml) was mixed with potassium hydroxide (1 g) in water (2 ml) and heated under reflux for 1 h. The solution was concentrated, diluted with water, and acidified with diluted hydrochloric acid. The precipitate was collected and washed with water. Crystallization from methanol–ether gave **2***f* (530 mg), m.p. 278–280°; positive ferric chloride test (red color); $[\alpha]_D$ −59° (ethanol); λ_{max}, 222, 316 mμ; ε, 9550, 6300; i.r. bands (Nujol) at 3200 cm^{-1} (hydroxyl group), at 1650, 1625, and 1545 cm^{-1}.

Anal. Calcd. for $C_{22}H_{30}O_3N_2$: C, 71.32; H, 8.16; O, 12.96; N, 7.56. Found: C, 71.18; H, 8.11; O, 13.26; N, 7.33.

Acetylation of the Hydroxypyrimidine N-Oxide 2f

A solution of **2***f* (500 mg) in pyridine (5 ml) and acetic anhydride (5 ml) was heated on the steam bath for 1 h, poured into water, and the solid precipitate collected and washed with water. Fractional crystallization from chloroform–hexane gave the diacetate **2***h* (300 mg), m.p. 230–232°; $[\alpha]_D$ −81°; λ_{max}, 316 mμ; ε, 6300; i.r. bands at 1810 cm^{-1} (acetyl group substituted in the pyrimidine *N*-oxide ring); at 1735 cm^{-1} (C-3 acetate), at 1685, 1650, and 1550 cm^{-1}.

Anal. Calcd. for $C_{26}H_{34}O_5N_2$: C, 68.70; H, 7.54; O,

Can. J. Chem. Downloaded from www.nrcresearchpress.com by 210.87.254.5 on 09/05/12
For personal use only.

17.60; N, 6.16. Found: C, 68.91; H, 7.46; O, 17.41; N, 6.19.

From the mother liquors of the diacetate **2*h*** crystallized the monoacetate **2*g*** (50 mg). The analytical sample had m.p. 247–250° (needles from chloroform–hexane); λ_{max}, 222, 317 mμ; ε, 11 000, 7400; i.r. bands at 1730 cm^{-1} (acetate), 1650, 1615, and 1575 cm^{-1}.

Anal. Calcd. for $C_{24}H_{32}O_4N_2$: C, 69.88; H, 7.82; O, 15.51; N, 6.79. Found: C, 69.64; H, 8.06; O, 15.74; N, 6.85.

Treatment of **2*g*** (250 mg) with acetic anhydride under reflux for 15 min, gave **2*h*** (200 mg).

Zinc Reduction of the Hydroxypyrimidine N-Oxide 2h

A solution of **2*h*** (200 mg) in acetic acid (3 ml) was heated on the steam bath with zinc dust (500 mg) for 1 h. The mixture was treated as previously described. The resulting product (**3*g***) (150 mg) had m.p. 315–317° (decomposed) (needles from chloroform–methanol); negative ferric chloride test; $[\alpha]_D$ −80°; λ_{max}, 308 mμ; ε, 4600; i.r. bands at 1730 cm^{-1} (C-3 acetate), 1660, 1645, and 1570 cm^{-1}.

Anal. Calcd. for $C_{24}H_{32}O_3N_2$: C, 72.69; H, 8.13; O, 12.11; N, 7.07. Found: C, 72.40; H, 8.19; O, 12.37; N, 7.21.

Acetylation of **3*g*** (50 mg) with acetic anhydride – pyridine gave **3*h***. The analytical sample (needles from ethyl acetate) had m.p. 308° (decomposed); i.r. bands at 1775 cm^{-1} (acetate substituted in the pyrimidine ring), 1730 cm^{-1} (C-3 acetate), and 1650, 1595, 1570 (pyrimidine ring).

Anal. Calcd. for $C_{26}H_{34}O_4N_2$: C, 71.20; H, 7.82; O, 14.59; N, 6.39. Found: C, 71.03; H, 7.61; O, 14.66; N, 6.28.

16-Aminomethylene-5-androst-5-en-3β-ol-17-one (5b)

A solution of 16-formyl-androst-5-en-3β-ol-17-one (**5*a***) (11) (4.83 g) in ethanol (25 ml) and concentrated ammonium hydroxide (25 ml) was heated under reflux for 1 h. After 15 min a precipitate began to form. The mixture was diluted with water, filtered, and the precipitate washed with water and crystallized from methanol. This yielded the amine **5*b***, m.p. 269–273°. Further crystallizations from ethanol raised the m.p. to 276–278°; positive ferric chloride test (dark green color); $[\alpha]_D$ −96° (ethanol), λ_{max}, 302 mμ; ε, 18 000; i.r. bands (Nujol) at 3300 cm^{-1} (broad, hydroxyl and amino groups), at 1655 cm^{-1} (hydrogen bonded α,β-unsaturated ketone), and at 1575 cm^{-1} (C = C double bond).

Anal. Calcd. for $C_{20}H_{29}O_2N$: C, 76.15; H, 9.27; O, 10.14; N, 4.44. Found: C, 76.07; H, 9.19; O, 10.39; N, 4.24.

16-Acetylaminomethylene-androst-5-en-17-one-3β-ol Acetate (5c)

The enamine **5*b*** (1.2 g) dissolved in acetic anhydride (5 ml) and pyridine (5 ml) was heated on the steam bath for 3 h, poured into water, and the precipitate collected and washed with water. Crystallization from chloroform–ether yielded the acetylaminoketone **5*c*** (630 mg), m.p. 236–238°. Further crystallizations from the same pair of solvents raised the m.p. to 247°, $[\alpha]_D$ −101°; λ_{max}, 290 mμ; ε, 22 900; i.r. bands at 1725 cm^{-1} (acetyl groups), at 1645 cm^{-1} (hydrogen bonded α,β-unsaturated ketone).

Anal. Calcd. for $C_{24}H_{33}O_4N$: C, 72.25; H, 8.33; O, 16.02; N, 3.51. Found: C, 72.22; H, 8.16; O, 16.10; N, 3.49.

The oxime (**6*a***) had m.p. 184–185°; (needles from methanol–ether) $[\alpha]_D$ −113°; λ_{max}, 280 mμ; ε, 17 400; i.r. bands at 3450 and 3580 cm^{-1} (hydroxyl group), at 1725 and 1700 cm^{-1} (acetyl groups), and at 1650 and 1625 cm^{-1}.

Anal. Calcd. for $C_{24}H_{34}O_4N_2$: C, 69.53; H, 8.27; O, 15.44; N, 6.76. Found: C, 69.45; H, 8.18; O, 15.46; N, 6.67.

Treatment of the Oxime 6a with γ-Collidine

The oxime **6*a*** (200 mg) in γ-collidine (4 ml) was heated under reflux for 15 min. Ethyl acetate was added, and the organic solution was washed with dilute hydrochloric acid and water, dried, and evaporated. Crystallization of the residue from methanol–ether yielded the oxime **6*b*** (85 mg), m.p. 255–256°; $[\alpha]_D$ −153° (dioxane); i.r. bands (Nujol) at 3250 cm^{-1} (hydroxyl group), at 1735 cm^{-1} (acetyl group), and at 1655 cm^{-1} (broad), 1600 cm^{-1}.

Anal. Calcd. for $C_{24}H_{34}O_4N_2$: C, 69.53; H, 8.27; O, 15.44; N, 6.76. Found: C, 69.79; H, 8.33; O, 15.46; N, 6.73.

Treatment of the Oxime 6b with Trifluoroacetic Acid

A solution of the oxime **6*b*** (350 mg) in trifluoroacetic acid (2 ml) was left at room temperature for 15 min, diluted with water, and the precipitate extracted with chloroform. The organic layer was washed with water, dried, and evaporated. Crystallization of the residue from chloroform–ether gave the pyrimidine *N*-oxide **7** (200 mg) as small leaflets, m.p. 230–232°; λ_{max} 223, 265 mμ; ε, 23 400, 7760; λ_{max} (pH 3) 223, 265 mμ; ε, 10 200, 7700; i.r. bands at 1730 cm^{-1} (acetyl group), and at 1575 cm^{-1} (pyrimidine nucleus).

Anal. Calcd. for $C_{24}H_{32}O_3N_2$: C, 72.69; H, 8.13; O, 12.11; N, 7.07. Found: C, 72.47; H, 8.00; O, 12.11; N, 7.05.

A solution of **6*b*** (230 mg) in acetic acid (5 ml) was treated with concentrated hydrochloric acid (0.5 ml) at room temperature for 15 min. Crystallization from chloroform–ether yielded **7** (90 mg), m.p. 234–236° (decomposed).

Treatment of the Pyrimidine N-Oxide 7 with Acetic Anhydride

A solution of **7** (200 mg) in acetic anhydride (2 ml) was heated on the steam bath for 30 min, diluted with water, and the precipitate extracted with chloroform. The organic solution was washed with aqueous sodium bicarbonate, water, dried, and evaporated. The crude solid product obtained was dissolved in benzene and passed through alumina (2 g). Crystallization from ether–hexane yielded **8** (100 mg), m.p. 122–124°; $[\alpha]_D$ −47°; λ_{max}, 220, 260 mμ; ε, 11 000, 5750; i.r. bands at 1745 and 1735 cm^{-1} (acetyl groups), and at 1590 and 1560 cm^{-1} (pyrimidine nucleus).

Anal. Calcd. for $C_{26}H_{34}O_4N_2$: C, 71.20; H, 7.82; O, 14.59; N, 6.39. Found: C, 71.45; H, 7.91; O, 14.37; N, 6.44.

16-Aminomethylene-estrone Methyl Ether 9b

A solution of 16-formyl-estrone methyl ether **9*a*** (12) (4.64 g) in ethanol (25 ml) and concentrated ammonium hydroxide (15 ml) was heated under reflux for 1 h, diluted

Can. J. Chem. Downloaded from www.nrcresearchpress.com by 210.87.254.5 on 09/05/12
For personal use only.

with water, and the precipitate collected and washed with water. Crystallization of the amine **9***b* from methanol–ether afforded pale-yellow prisms (3.42 g), m.p. 217–219°; positive ferric chloride test (dark-green color); $[\alpha]_D$ +108°; λ_{max}, 301 mμ; ε, 20 000; i.r. bands (Nujol) at 3470 and 3360 cm^{-1} (hydroxy and amine groups), at 1680 cm^{-1} (hydrogen bonded α,β-unsaturated ketone), at 1660 cm^{-1} (C═C double bonds), and at 1600 cm^{-1} (aromatic ring).

Anal. Calcd. for $C_{20}H_{25}O_2N$: C, 77.13; H, 8.09; O, 10.28; N, 4.50. Found: C, 76.84; H, 7.99; O, 10.51; N, 4.52.

16-Acetylaminomethylene-estrone Methyl Ether 9c

The amine **9***b* was acetylated as described for previous cases. Crystallization from methanol–ether yielded **9***c* (760 mg), m.p. 205–206°. The analytical sample had m.p. 211–213° (needles from methanol – isopropyl ether); $[\alpha]_D$ +102°; λ_{max}, 288 mμ; ε, 24 000; i.r. bands at 3450 cm^{-1} (NH group), at 1715 cm^{-1} (acetyl group), and at 1640 cm^{-1} (hydrogen bonded, α,β-unsaturated ketone).

Anal. Calcd. for $C_{22}H_{27}O_3N$: C, 74.75; H, 7.70; O, 13.58; N, 3.96. Found: C, 75.07; H, 7.79; O, 13.71; N, 4.05.

The oxime **10***a* had m.p. 227–228° (needles from methanol); $[\alpha]_D$ +76°; λ_{max}, 282; ε, 21 400; i.r. bands (Nujol) at 3300 cm^{-1} (hydroxyl group), at 1690 cm^{-1} (acetyl group), at 1650, and 1615 cm^{-1}.

Anal. Calcd. for $C_{22}H_{28}O_3N_2$: C, 71.71; H, 7.66; O, 13.03; N, 7.60. Found: C, 71.87; H, 7.56; O, 13.12; N, 7.55.

Treatment of the Oxime 10a with γ-Collidine

A solution of the oxime **10***a* (1.15 mg) was treated with γ-collidine as described previously for **6***a*. Crystallization from methanol–ether yielded the oxime **10***b*, m.p. 248° (decomposed) (small needles from methanol–ether; $[\alpha]_D$ +4° (dioxane); λ_{max}, 288 mμ; ε, 17 800; i.r. bands (KBr) at 3300 cm^{-1} (hydroxyl group), at 1650 and 1610 cm^{-1}.

Anal. Calcd. for $C_{22}H_{28}O_3N_2$: C, 71.71; H, 7.66; O, 13.03; N, 7.60. Found: C, 71.75; H, 7.77; O, 13.29; N, 7.57.

Treatment of the Oxime 10b with Trifluoroacetic Acid

A solution of the oxime **10***b* (650 mg) in trifluoroacetic acid (2 ml) was treated as described previously for **6***b*. Crystallization from chloroform–acetone yielded the pyrimidine *N*-oxide **11** (530 mg), m.p. 235–237°; $[\alpha]_D$ +54°; λ_{max}, 224, 268 mμ; ε, 31 630, 8100; λ_{max} (pH 3) 224, 264 mμ: ε, 23 200, 7900; i.r. bands at 1600 cm^{-1} (aromatic C═C double bonds) and at 1570 cm^{-1} (pyrimidine nucleus).

Anal. Calcd. for $C_{22}H_{26}O_2N_2$: C, 75.40; H, 7.48; O, 9.13; N, 7.99. Found: C, 75.51; H, 7.47; O, 9.19; N, 8.13.

Treatment of an acetic acid solution of **10***b* (200 mg) with hydrochloric acid afforded **11** (60 mg), m.p. 233–235°.

Treatment of the Pyrimidine N-Oxide 11 with Acetic Anhydride

The *N*-oxide (200 mg) was treated with acetic anhydride as described above for a similar case. The gummy product did not crystallize even after chromatography on alumina. It was dissolved in methanol (25 ml), mixed with a solution of potassium bicarbonate (250 mg) in water (5 ml), heated under reflux for 1 h, concentrated, diluted with water, and the precipitate collected and washed with water. Crystallization from acetone–ether yielded plates (80 mg), m.p. 172–175°; i.r. bands at 3450 cm^{-1} (hydroxyl group), and at 1590, 1575, 1545 cm^{-1} (pyrimidine nucleus).

Anal. Calcd. for $C_{22}H_{26}O_2N_2$: C, 75.40; H, 7.48; O, 9.13; N, 7.99. Found: C, 75.62; H, 7.64; O, 9.36; N, 8.13.

Aminoketone 13b

Treatment of **13***a* (13) (9 g) with ammonium hydroxide yielded **13***b* (5.4 g), m.p. 240–242°; positive ferric chloride test (purple color); $[\alpha]_D$ +48° (ethanol); λ_{max}, 316 mμ; ε, 15 850; i.r. bands (Nujol) at 3300 cm^{-1} (hydroxyl group) and at 1660 cm^{-1} (hydrogen bonded α,β-unsaturated ketone).

Anal. Calcd. for $C_{20}H_{31}O_2N$: C, 75.67; H, 9.84; O, 10.08; N, 4.41. Found: C, 75.55; H, 9 77; O, 10.13; N, 4.54.

Acetylaminoketone 13c

Acetylation of **13***b* with acetic anhydride – pyridine gave **13***c*. It had m.p. 156–158° (prisms from ethyl acetate – isopropyl ether); $[\alpha]_D$ +81°; λ_{max}, 300 mμ; ε, 15 850; i.r. bands at 1725 cm^{-1} (double strength, acetyl groups); at 1660 cm^{-1} (hydrogen bonded α,β-unsaturated ketone), and at 1590 cm^{-1} (C═C double bond).

Anal. Calcd. for $C_{24}H_{35}O_4N$: C, 71.79; H, 8.79; O, 15.94; N, 3.49. Found: C, 71.87; H, 8.88; O, 16.04; N, 3.61.

The oxime **14** had m.p. 191–192° (prisms from chloroform–hexane) $[\alpha]_D$ +56°; λ_{max}, 290 mμ; ε, 11 750; i.r. bands at 1720 cm^{-1} (acetyl group), at 1680, 1650, and 1560 cm^{-1}.

Anal. Calcd. for $C_{24}H_{36}O_4N_2$: C, 69.20; H, 8.71; O, 15.36; N, 6.73. Found: C, 69.07; H, 8.82; O, 15.37; N, 6.81.

Treatment of the Oxime 14 with γ-Collidine

A solution of the oxime **14** (500 mg) in γ-collidine (5 ml) was heated under reflux for 3 h. The method was then as described previously. The crude material obtained was chromatographed on alumina (10 g). Elution with benzene and with benzene – ethyl acetate (9:1) gave the pyrimidine *N*-oxide **15** (200 mg), m.p. 165–170° (prisms from ether–hexane). Further crystallizations from the same pair of solvents raised the m.p. to 187–188°; $[\alpha]_D$ +46°; λ_{max}, 220, 264, 298 mμ; ε, 23 400, 7400, 3300; λ_{max} (pH 3) 220, 265 mμ; ε, 20 500, 7300; i.r. bands at 1735 cm^{-1} (acetyl group) and at 1590 and 1560 cm^{-1} (pyrimidine nucleus).

Anal. Calcd. for $C_{24}H_{34}O_3N_2$: C, 72.33; H, 8.60; O, 12.04; N, 7.03. Found: C, 72.07; H, 8.59; O, 12.18; N, 7.20.

The mother liquors of the amine **13***b* were subjected to the same process as that followed in the preparation of the crystalline amine. A yield of 1.5 g of the pyrimidine *N*-oxide **15**, m.p. 184–187° was obtained in this way.

Treatment of the Pyrimidine N-Oxide 15 with Acetic Anhydride

The *N*-oxide **15** (400 mg) in acetic anhydride (5 ml) was heated under reflux for 30 min. The solution was

worked up as previously described for similar cases. The crude gummy product obtained, was chromatographed on alumina (5 g). Elution with benzene–hexane 1:1 and benzene gave a solid product **16***a* (100 mg), m.p. 173–174°; (leaflets from ether–hexane); $[\alpha]_D$ −20°; λ_{max}, 261 mμ; ε, 4570; i.r. bands at 1735 cm^{-1} (broad, acetyl groups) and at 1580 and 1555 cm^{-1} (pyrimidine nucleus).

Anal. Calcd. for $C_{26}H_{36}O_4N_2$: C, 70.88; H, 8.24; O, 14.53; N, 6.36. Found: C, 71.22; H, 7.98; O, 14.64; N, 6.46.

Elution with benzene – ethyl acetate (9:1) gave **16***b* (75 mg), m.p. 202–203°; (plates from ether–hexane); $[\alpha]_D$ +59°; λ_{max}, 261; ε, 4570; i.r. bands at 1730 and 1720 cm^{-1} (acetyl groups) and at 1575 and 1555 cm^{-1} (pyrimidine nucleus).

Anal. Calcd. for $C_{26}H_{36}O_4N_2$: C, 70.88; H, 8.24; O, 14.53; N, 6.36. Found: C, 70.68; H, 8.29; O, 14.61; N, 6.16.

Acknowledgment

We are grateful to Syntex S. A., for the determination of the rotations.

1. P. DE RUGGIERI, C. GANDOLFI, and D. CHIARAMONTI. Gazz. Chim. Ital. **92**, 768 (1962). P. DE RUGGIERI and C. GANDOLFI. U.S. Patent No. 3,129,220.
2. P. DE RUGGIERI, C. GANDOLFI, and U. GUZZI. Gazz. Chim. Ital. **96**, 152, 179 (1966).
3. R. M. CRESSWELL, H. K. MAURER, T. STRAUSS, and G. B. BROWN. J. Org. Chem. **30**, 408 (1965).
4. J. ROMO and A. ROMO DE VIVAR. J. Am. Chem. Soc. **81**, 3446 (1959).
5. M. A. STEVENS and G. B. BROWN. J. Am. Chem. Soc. **80**, 2759 (1958).
6. M. KETADA. J. Pharm. Soc. (Japan), **67**, 51 (1947).
7. M. A. STEVENS, A. GINER-SOROLLA, H. W. SMITH, and G. B. BROWN. J. Org. Chem. **27**, 567 (1962).
8. R. R. HUNT, J. F. MCOMIE, and E. R. SAYER. J. Chem. Soc. 525, 1959.
9. D. J. BROWN. The chemistry of heterocyclic compounds. The pyrimidines. *Edited by* Arnold Weissberger. Interscience Publishers, Inc., New York. 1962.
10. W. KLÖTZER. Monatsch. Chem. **95**, 266, 1729 (1964).
11. J. C. BARDHAN. J. Chem. Soc. 1848 (1936).
12. L. RUZICKA, V. PRELOG, and J. BATTEGAY. Helv. Chim. Acta, **31**, 1296 (1948).
13. J. EDWARDS and H. J. RINGOLD. J. Am. Chem. Soc. **81**, 5262 (1959).
14. R. O. CLINTON, A. J. MANSON, F. W. STONNER, H. C. NEUMAN, R. G. CHRISTIANSEN, R. L. CLARKE, J. H. ACKERMAN, D. F. PAGE, J. W. DEAN, W. B. DICKINSON, and C. CARABATEAS. J. Am. Chem. Soc. **83**, 1478 (1961).

Can. J. Chem. Downloaded from www.nrcresearchpress.com by 210.87.254.5 on 09/05/12
For personal use only.

Syntheses of α-agarofuran and isodihydroagarofuran

A. ASSELIN,[1] M. MONGRAIN, AND P. DESLONGCHAMPS
Department of Chemistry, University of Sherbrooke, Sherbrooke, Quebec
Received June 13, 1968

A new synthesis of α-agarofuran (**1**) has been realized in four steps from ketol **3** and a stereospecific synthesis of isodihydroagarofuran (dihydro-α-agarofuran) has been achieved in four steps.

Canadian Journal of Chemistry, 46, 2817 (1968)

Can. J. Chem. Downloaded from www.nrcresearchpress.com by 210.87.254.105 on 09/05/12
For personal use only.

Bhattacharyya and co-workers (1) isolated dihydroagarofuran, α-, and β-agarofuran from agarwood oil. Their proposed stereo-structures with a 7-α-isopropyl configuration for the agarofurans has been corrected to a 7-β-isopropyl configuration. This correction was achieved by Barrett and Büchi (2) who showed that (−)epi-α-cyperone (**2**) can be used for the synthesis of α-agarofuran (**1**). Recently, a new synthesis of α-agarofuran (**1**) has been reported by Marshall and Pike (3) starting also with (−)epi-α-cyperone (**2**). Furthermore, a total synthesis of norketoagarofuran (4) has been communicated by Heathcock and Kelly (5).

These recent reports (3, 5) prompt us to disclose a very simple four-step synthesis of α-agarofuran (**1**) starting with ketol **3** (6), which is the precursor of (−)epi-α-cyperone (**2**). We wish also to describe a stereospecific synthesis of isodihydroagarofuran (**9**), an epimer of natural dihydroagarofuran (**11**). Thus, the complete stereo-structure of natural dihydroagarofuran is also clarified.

Oxymercuration of crystalline ketol **3** (7) gave a 75% yield of keto–diol **4**. This keto–diol **4** has been previously reported in 40% yield, using the same general procedure (3). By refluxing compound **4** with sodium methoxide in methanol for four days and then utilizing chromatography, an 81% yield of the crystalline enone–alcohol **5** was obtained.

Reduction of compound **5** with lithium aluminium tri-*t*-butoxy hydride in ether yielded quantitatively the crystalline diols mixture **6**. A similar diols mixture, presumably in a different ratio, has been prepared by Marshall and Pike (3) using a different method. According to the reduction of similar compounds with the same reducing agent (8), the major compound in the diols mixture **6** should possess the OH grouping in the α-quasi-equatorial orientation.

Treatment of the diols mixture **6** in benzene with a small amount of *p*-toluenesulfonic acid at room temperature for 1 h gave quantitatively α-agarofuran (**1**, 80% yield) and the new crystalline diene–alcohol **7** (20% yield) which were easily separated by chromatography.[2] The identity of compound **1** was established by comparison of its infrared and nuclear magnetic resonance spectra with the published spectra of α-agarofuran (**1**). The structure of the diene–alcohol **7** was assigned on the basis of its spectral properties.

Since the diene–alcohol **7** is a minor product, this work constitutes the shortest and the most efficient synthesis of α-agarofuran (**1**).

Treatment of the enone–alcohol **5** with benzene and *p*-toluenesulfonic acid at room temperature for 24 h and chromatography, gave the starting material **5** in 70% yield and the new crystalline keto–oxide **8** in 30% yield. This keto–oxide **8** was also isolated in a low yield (6%) during the basic dehydration of keto–diol **4** leading to the enone–alcohol **5**. Thus, the secondary methyl group in compound **8** is clearly equatorial.

Reduction of keto–oxide **8** with the tosylhydrazide – sodium borohydride method (9) gave the crystalline isodihydroagarofuran **9** as the only isolable product. Thus, this work constitutes a four-step stereospecific synthesis of isodihydroagarofuran **9**.

Natural dihydroagarofuran, although being an oil, has been claimed to be isolated in the pure form and its published spectra (1) are different

[1]Holder of an NRCC Studentship, 1966–1968.

[2]Work is now directed toward the purification of both epimeric alcohols from the diols mixture (**6**). This is done in an effort to find out if there is a stereospecific conversion of the major epimeric alcohol (α-quasi-equatorial isomer) to α-agarofuran (**1**) and the other into diene–alcohol **7**.

Can. J. Chem. Downloaded from www.nrcresearchpress.com by 210.87.254.105 on 09/05/12
For personal use only.

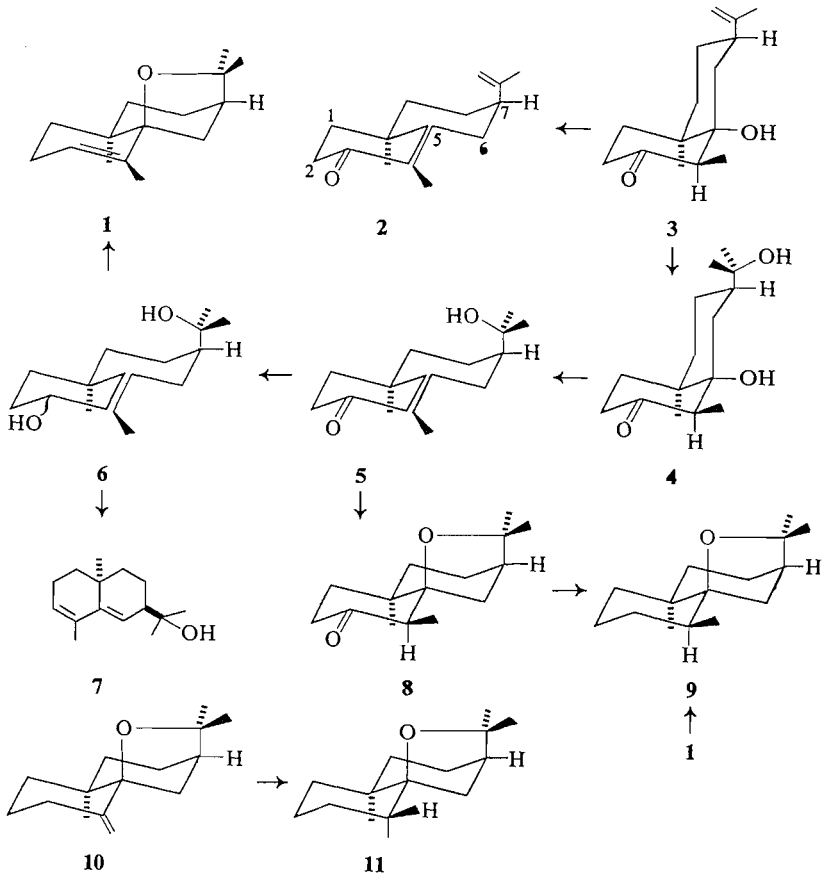

than those of compound **9**. It has also been reported (1) that catalytic reduction of β-agarofuran (**10**) gave a compound identical to natural dihydroagarofuran while catalytic reduction of α-agarofuran yielded a different oily dihydro derivative.

We have repeated the catalytic reduction with synthetic α-agarofuran (**1**) and have obtained a crystalline dihydro compound which was found to be identical to compound **9**, obtained from keto–oxide **8**.

Thus, it is clear that natural dihydroagarofuran (dihydro-β-agarofuran) possesses structure **11** with the secondary methyl group in the α-axial configuration while dihydro-α-agarofuran (iso-dihydroagarofuran) has structure **9** with the methyl group in the β-equatorial orientation.

Experimental

Melting points are not corrected. Ultraviolet (u.v.) spectra (λ_{max}) were measured on a Cary model 14 spectrophotometer and infrared (i.r.) spectra (ν_{max}) were recorded on Perkin–Elmer Infracord, model 137 spectrophotometer. Nuclear magnetic resonance spectra (n.m.r., τ values) were taken on a Varian A60 spectrometer with tetramethylsilane as an internal standard. Thin-layer chromatograms (t.l.c.) were developed with iodine. Anhydrous magnesium sulfate was used as the drying agent in working up reactions. Fisher Florisil 100–200 mesh was used for preparing all column chromatograms.

The ketol **3** was prepared according to the method of Howe and McQuillin (6) using (+)-dihydrocarvone.

Keto–Diol (4)

Ketol **3** (11.8 g, 0.05 mole) was added to a well-stirred suspension of tetrahydrofuran (100 ml), water (100 ml), and mercuric acetate (32 g, 0.1 mole) cooled with an ice-bath. After 5 min, aqueous sodium hydroxide (3 *M*, 100 ml) was added, followed by a solution of sodium borohydride (0.5 *M*, 82 ml) in aqueous sodium hydroxide (3 *M*). Acetone (15 ml) was added and the mixture was filtered through Celite. After saturation with sodium chloride, the reaction mixture was thoroughly extracted with ethyl acetate. Evaporation of the dried extract yielded a white crystalline solid (11 g) which was crystallized with ethyl acetate (9.3 g, m.p. 190–193 °C). Further recrystallization

Can. J. Chem. Downloaded from www.nrcresearchpress.com by 210.87.254.105 on 09/05/12
For personal use only.

gave an analytically pure sample, m.p. 195–197 °C (lit. m.p. 195–196 °C (3)). Infrared: ν_{max} ($CHCl_3$) 3600, 3400, and 1700 cm^{-1}; n.m.r.: τ (acetone-d_6) 8.77 (3H, singlet), 8.92 (6H, singlet), and 9.03 (3H, doublet, J = 6.5 c.p.s.).

Enone–Alcohol (5)

Keto-diol **4** (5.0 g, 19.7 mmole) was dissolved in methanol (60 ml) containing sodium methoxide (2.5 g). The mixture was refluxed for 4 days. Water (500 ml) was added and the mixture was extracted with ether. The dried organic phase was evaporated to dryness. The resulting product (4.7 g) was purified by column chromatography. The fractions were analyzed by t.l.c. (silica gel, ether–benzene (1:1)).

Elution with petroleum ether (b.p. 30–60 °C) gave a trace of material. Elution with benzene gave a mixture of compounds **5** and **8** (700 mg, R_f value: 0.7 and 0.9). Elution with ether–benzene (5%) gave pure enone–alcohol **5** (3.4 g). The mixture (700 mg) was again submitted to column chromatography yielding keto–oxide **8** (303 mg) and enone–alcohol **5** (340 mg).

Enone–alcohol **5** was recrystallized with ether–pentane to give the analytical sample, m.p. 56–56.5 °C. Infrared: ν_{max} ($CHCl_3$) 3500, 3400, 1650, and 1620 cm^{-1}; u.v.: λ_{max} (EtOH) 254 m (ε 14 800); n.m.r.: τ ($CDCl_3$) 8.18 (3H, singlet), 8.78 (6H, singlet), and 8.81 (3H, singlet).

Anal. Calcd. for $C_{15}H_{24}O_2$: C, 76.23; H, 10.23. Found: C, 76.58; H, 10.46.

Keto–oxide **8** was recrystallized with ether–pentane to give the analytical sample, m.p. 124 °C. Infrared: ν_{max} ($CHCl_3$) 1715 cm^{-1}; n.m.r.: τ ($CDCl_3$) 7.39 (1H, quadruplet, J = 6.5 c.p.s.), 8.70 (3H, singlet), 8.75 (3H, singlet), 8.85 (3H, singlet), and 8.90 (3H, doublet, J = 6.5 c.p.s.).

Anal. Calcd. for $C_{15}H_{24}O_2$: C, 76.23; H, 10.23. Found: C, 76.02; H, 10.02.

Diols Mixture (6)

An ethereal solution (10 ml) of enone–alcohol **5** (90 mg, 0.38 mmole) was slowly added to lithium aluminium tri-*t*-butoxy hydride (460 mg, 4 mmole) in ether (20 ml) at 0 °C. After stirring at room temperature for 4 h, the excess hydride was destroyed by the addition of brine and the organic phase was separated. Evaporation of the dried organic solution yielded a crystalline mixture (90 mg), m.p. 70–103 °C. Infrared: ν_{max} ($CHCl_3$) 3700 and 3500 cm^{-1}, no carbonyl absorption.

Agarofuran (1) and Diene–Alcohol (7)

The diols mixture **6** (25 mg, 0.105 mmole) was dissolved in benzene (10 ml) and treated with *p*-toluenesulfonic acid (6 mg) at room temperature for 1 h. Brine was added and the mixture extracted with ether. The dried organic phase was evaporated to dryness yielding a mixture of two compounds. This mixture was separated by column chromatography using pentane and ether–pentane mixtures. The fractions were analyzed by t.l.c. (alumina, ether–pentane (10%)). The first material obtained (21 mg, 80% yield, R_f value: 0.8) had i.r. and n.m.r. spectra identical with the published spectra (1) of α-agarofuran derived from agarwood oil.

The second fraction (5 mg, 20% yield, R_f value: 0.2) was crystalline and structure **7** was assigned on the basis of its spectral properties. This compound was recrystallized from ether–pentane but was not sent for microanalysis because of its slow decomposition at room temperature, m.p. 67.5–68 °C. Infrared: ν_{max} ($CHCl_3$) 3600, 3400 cm^{-1}; u.v.: λ_{max} (EtOH) 233, 241, and 248 mμ (ε 18 000, 20 000, and 12 800); n.m.r.: τ($CDCl_3$) 4.40(2H, multiplet), 8.12 (3H, ~quadruplet, J = 1 c.p.s.), 8.79 (6H, singlet), and 9.05 (3H, singlet).

Keto–Oxide (8)

Enone–alcohol **5** (75 mg, 0.31 mmole) was dissolved in benzene (20 ml) containing *p*-toluenesulfonic acid (32 mg). After 24 h at room temperature, the reaction mixture was mixed with brine and extracted with ether. The dried organic phase was evaporated to dryness yielding a mixture of compound **5** and keto–oxide **8** which were separated by column chromatography using ether–hexane as eluent. The fractions were analyzed by t.l.c. (alumina, ether–hexane (1:1)).

The first compound was obtained crystalline (19 mg, R_f value: 0.3) and was identical with keto–oxide **8** obtained during the basic dehydration of keto–diol **4**.

The second product (51 mg, R_f value: 0.7) was identified as the starting enone–alcohol **5**.

Isodihydroagarofuran (9)

(a) From Keto–Oxide (8)

Keto–oxide **8** (80 mg, 0.34 mmole) was dissolved in methanol (5 ml) containing *p*-toluenesulfonyl hydrazine (100 mg, 0.56 mmole), and the mixture was refluxed for 30 min. The mixture was cooled at room temperature, sodium borohydride (100 mg, 2.6 mmole) was added, and the mixture was refluxed for 1 h. Brine was added and the mixture was extracted with ether. The dried organic phase was evaporated to dryness and the product obtained was purified by column chromatography. Elution with pentane gave crystalline isodihydroagarofuran **9** (20 mg). A t.l.c. analysis was performed (alumina, pentane, R_f value: 0.6). The analytical sample was prepared by sublimation, m.p. 35.5 °C. Nuclear magnetic resonance: τ ($CDCl_3$) 8.61 (3H, singlet), 8.82 (3H, singlet), 9.00 (3H, singlet), and 9.11 (3H, doublet, J = 6 c.p.s.).

Anal. Calcd. for $C_{15}H_{26}O$: C, 81.02; H, 11.79. Found: C, 81.02; H, 11.96.

(b) From α-Agarofuran (1)

α-Agarofuran **1** (200 mg, 0.91 mmole) was hydrogenated in acetic acid (5 ml) with prereduced platinum oxide (10 mg) for 1.5 h. The catalyst was removed by filtration and the filtrate evaporated to dryness. The resulting product was purified by column chromatography. Elution with pentane yielded a crystalline material (110 mg) which had physical and spectral properties identical with those of isodihydroagarofuran **9** (obtained from procedure *a*).

Acknowledgments

Support for this work by the National Research Council of Canada, and Ayerst Laboratories, Montreal, is gratefully acknowledged.

1. M. L. Maheshwari, T. C. Jain, R. B. Bates, and S. C. Bhattacharyya. Tetrahedron, **19**, 1079 (1963).
2. H. C. Barrett and G. Büchi. J. Am. Chem. Soc. **89**, 5665 (1967).

3. J. A. MARSHALL and M. PIKE. J. Org. Chem. **33**, 435 (1968).
4. M. L. MAHESHWARI, K. R. VARMA, and S. C. BHATTACHARYYA. Tetrahedron, **19**, 1519 (1963).
5. C. H. HEATHCOCK and T. R. KELLY. Chem. Commun. 267 (1968).
6. R. HOWE and F. J. MCQUILLIN. J. Chem. Soc. 2423 (1955); 2670 (1956); 1194 (1958).
7. H. C. BROWN and P. GEOGHEGAN, JR. J. Am. Chem. Soc. **89**, 1522 (1967).
8. D. J. DAWSON and R. B. IRELAND. Tetrahedron Letters, **15**, 1899 (1968).
9. L. GAGLIOTI and M. MAGI. Tetrahedron, **19**, 1127 (1963).

Can. J. Chem. Downloaded from www.nrcresearchpress.com by 210.87.254.105 on 09/05/12
For personal use only.

Can. J. Chem. Downloaded from www.nrcresearchpress.com by 210.87.254.105 on 09/05/12
For personal use only.

$A^{(1,3)}$ interaction and conformational energy of axial–axial 1,3-dimethyl interaction

Y. L. CHOW, C. J. COLÓN, AND J. N. S. TAM
Department of Chemistry, Simon Fraser University, Burnaby 2, British Columbia

Received March 22, 1968

$A^{(1,3)}$ type strain was demonstrated *directly* from the nuclear magnetic resonance studies of the acyl and nitroso derivatives of 2-methylpiperidine (**2** series) and 2,6-*cis*-dimethylpiperidine (**1** series). In these two series, the bulky 2-methyl groups are forced to assume the axial conformation due to a severe $A^{(1,3)}$ interaction in the equatorial conformation. The free energy of activation (ΔG^*) for the internal rotation around the N—C and N—N bonds in **1***a*–**1***g* was determined. The comparison of these ΔG^* values with those of the corresponding derivatives of dimethylamine indicates the decreases are in the range of 3.6–4.7 kcal/mole which is in fair agreement with the conformational energy of 1,3-diaxial CH_3/CH_3 interaction. An argument was presented to show that this interaction energy corresponds to the decrease of ΔG^* in **1***a*–**1***g*.

Canadian Journal of Chemistry, 46, 2821 (1968)

The stereochemical consequence of reactions of 2-alkylcyclohexane derivatives (A ⇄ B) has led Johnson to conclude that there is a severe non-bonded interaction between the group X (or X′) and an equatorial alkyl group (1). This interaction was termed $A^{(1,3)}$ strain (1) and the energy was approximated with 1,3-diaxial CH_3/CH_3 interaction (3.7 kcal/mole). During our studies on the photochemical behavior of nitrosamines we became aware of some unusual reactivities (2) and nuclear magnetic resonance (n.m.r.) characteristics of *N*-nitroso-*cis*-2,6-dimethylpiperidine (**1***g*, N—NO for NCOR) that might be related to $A^{(1,3)}$ strain. The n.m.r. study on the conformational aspects of the acyl derivatives of *cis*-2,6-dimethylpiperidine (**1** series) and of 2-methylpiperidine (**2** series) was undertaken. The purpose of this communication is to demonstrate directly the presence of the $A^{(1,3)}$ interaction by n.m.r. spectroscopy in systems **1** and **2** and further to provide a method of estimating the conformational energy of 1,3-diaxial CH_3/CH_3 interaction in **1**.

The presence of the partial double bond characters in amide 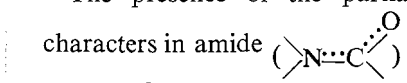 and nitrosamine 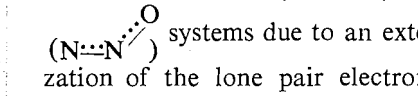 systems due to an extensive delocalization of the lone pair electrons of nitrogen with the hetero π electron system has been well documented by n.m.r. spectroscopy (3, 4). The rotational barriers due to the partial double bond character (15–21 kcal/mole for amide and 23.3 kcal/mole for dimethyl nitrosamine) apparently represent quantitatively the extent of the delocalization energy and also qualitatively the extent of the planar configuration at N=C and N=N bonds in **1** and **2** (where 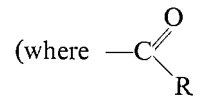 is either acyl or nitroso group). The structure of these acyl derivatives, if the $A^{(1,3)}$ interaction is ignored for a moment, must be represented by the nearly trigonal configuration at N as in **1** and **1′**. With a planar or a near planar structure at the N=C bond, it is expected, and can be shown by Dreiding Models, that $A^{(1,3)}$ interaction between O (and/or R) and α-equatorial CH_3 is severe in **1′** and that **1** is the predominant conformation. Since the delocalization energy (15 ∼ 23 kcal/mole) is several times higher than the 1,3-diaxial CH_3/CH_3 interaction, the amount of conformer **1′** will be negligibly small.

In Table I the n.m.r. chemical shifts of α-protons and α-methyl groups for the amide derivatives of 2,6-*cis*-dimethylpiperidine and 2-methylpiperidine at temperatures high enough to ensure rapid rotation about N=C bond are tabulated. Comparisons of the chemical shifts of the α-protons for **1***a*–**1***f* with the corresponding data of *N*-benzoyl-4-*t*-butylpiperidine (**3**) (5) leaves no doubt that the α-protons are equatorially oriented. The coupling pattern of the α-protons is also in good agreement with the equatorial orientation and very different from the corresponding protons (axial) of *cis*-2,6-dimethylpiperidine. It is pertinent to add

Can. J. Chem. Downloaded from www.nrcresearchpress.com by 210.87.254.105 on 09/05/12
For personal use only.

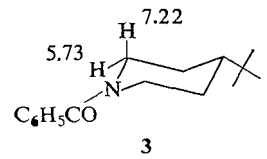

3

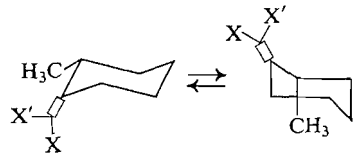

A B

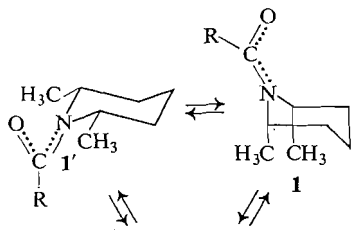

1

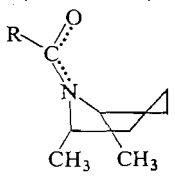

1''

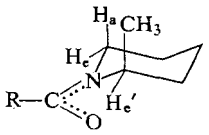

2

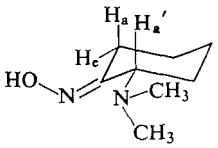

7

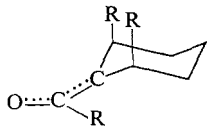

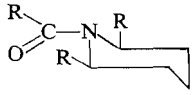

1 (R = CH_3) 4
5 (R = H) 6

that the boat conformation **1''** may contribute to a sizable extent to these amides since the β- and γ-protons in **1***a*–**1***f* exhibit time averaged narrow bands around τ 8.6 with band widths ranging between 8–15 c.p.s. In the conformation **1''**, the "bowsprit–flagpole" interaction is absent and the CH_3/CH_3 1,3-diaxial interaction in **1** is slightly relieved. With respect to **1***g* (6) an analogous situation has been observed by us as well as by others (7). On the same ground, **2***a*–**2***c* also possess α-axial methyl conformations as shown by n.m.r. data.

TABLE I

Chemical shift data*

Compound	O=C—R	Temperature (°C)	α-H†	α-CH_3†
1*a*	CHO	70	5.98	8.77
1*b*	$COCH_3$	45	5.69	8.83
1*c*	$COCH_2C_6H_5$	45	5.62	8.90
1*d*	COC_6H_5	33	5.67	8.80
1*e*	SO_2CH_3	33	5.91	8.68
1*f*	$SO_2C_6H_4CH_3$	33	5.88	8.70
1*g*	NO	33	5.03‡	8.59 8.91
2*a*	$COCH_3$	40	5.56(e) 6.17(e') 7.18(a)	8.88
2*b*	COC_6H_5	33	5.59(e) 6.09(e') 7.10(a)	8.83
2*c*	$COCH_2C_6H_5$	40	5.53(e) 6.20(e') 7.27(a)	8.95

*All spectra are taken in 10–20% (w/v) CCl_4 solution with TMS as the internal standard and the chemical shifts are expressed in τ-values.

†All α-H in the **1** series show broad quartet and all α-CH_3 show doublets ($J \cong 7$ c.p.s.) at the temperature indicated. In the **2** series, H_e shows a broad doublet, H_e' a broad quartet, and H_a a broad unsymmetrical triplet.

‡The two α-equatorial protons are accidentally isochronous.

Accepting that the compounds of the **1** series are forced to assume a conformation having a severe 1,3-diaxial CH_3/CH_3 interaction (3.7 kcal/mole) (8), such a driving force must be provided by the conjugation energy of NCO or NNO systems. Conversely, any loss in the energy barrier of the internal rotation in **1***a*–**1***g* series can be accounted for by the energy expended to force the conformation **1** (or 1,3-diaxial CH_3/CH_3 conformation of this system). Thus by comparison of the energy barriers of the internal rotation in **1** series with that of the appropriate derivatives, it is possible to determine the conformational energy of 1,3-diaxial CH_3/CH_3 interaction in these compounds. A justification of this calculation may be sought from consideration of the transition from **1** to **4** where the planar structure of is broken and the π-bond of C=O is orthogonal to *n*-electrons. Since the potential energy of the tran-

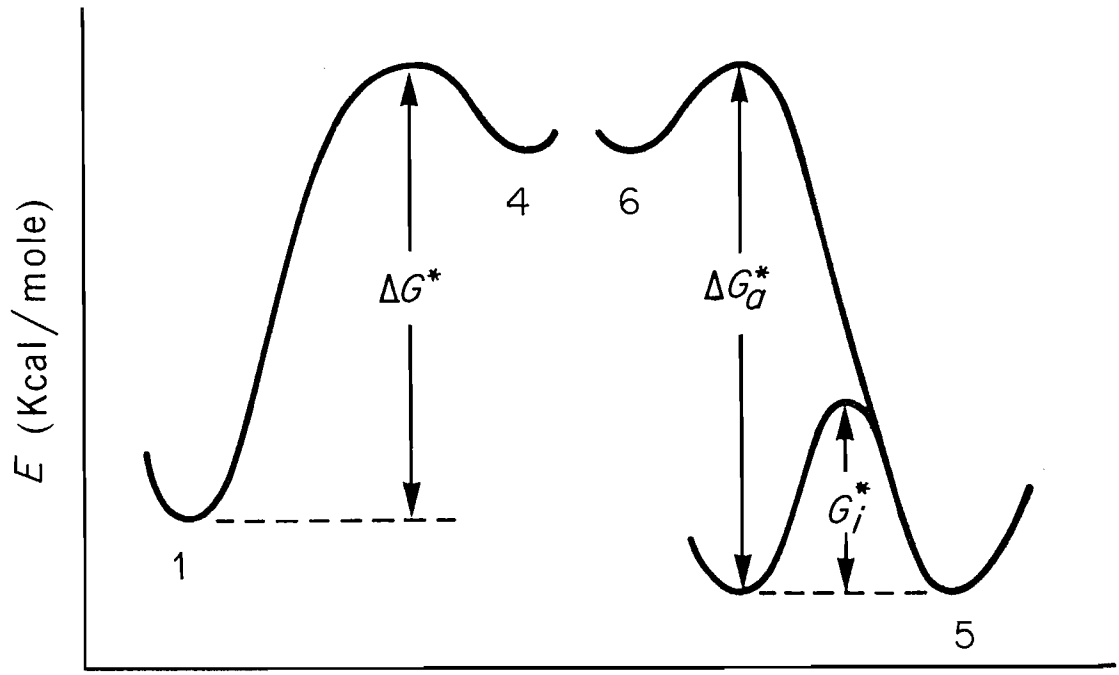

FIG. 1. Potential energy as a function of conformation.

sition state must be ΔG^* above the ground state and 5–10 kcal above the activation energy of the heterocyclic ring inversion (ca. 10 kcal/mole, ΔG^*_i), the inversion to CH_3/CH_3 diequatorial can occur freely and contemporaneously. The same can be said about the model compound, *N*-acylpiperidine, **5** ⇄ **6**. Assuming that both **6** and **4** orient themselves to avoid any possible non-bonded interaction, their potential energy is about the same. Since the transition states of both resemble **4** and **6**, it follows that the transition state energy surfaces of **4** and **6** are at nearly the same level. The difference of the energy barriers for **1** and **5** ($\Delta G^*a - \Delta G^*$) therefore, is expected to represent the 1,3-diaxial interaction[1] (see Fig. 1).

The energy barriers (ΔG^*) for the internal rotation at the corresponding coalescence temperature for **1***a*–**1***g*, are determined with respect to α-H and α-CH_3 groups (8) and are tabulated in Table II. It is seen that the coalescence of the α-CH_3 signals generally occurs at a lower temperature than that of the α-H signals due to the smaller chemical shift difference. The ΔG^* values calculated independently from both approaches are in good agreement. The ΔG^* for the internal rotation of the corresponding derivative from dimethylamine (3, 4) is given in column 7 and the energy differences over that of the cyclo derivatives ($\Delta G^*a - \Delta G^*$) are given in column 8. Implicit in this calculation is the assumption that the entropies of activation (ΔS^*) are small or comparable in both systems. The figures (3.6–4.7 kcal/mole) are in fair agreement with 1,3-diaxial CH_3/CH_3 interaction energy of *cis*-1,3-dimethylcyclohexane (5.5 kcal/mole) (9) and represents the interaction energy for the same system in these compounds.[2] The energy range is probably more accurately represented by **1***a* and **1***g* since complications from the interaction of the acyl side chain in the rigid system are at the minima in these two cases.

Furthermore, two pertinent conclusions can be derived from the data given in Table II. The rates of the internal rotation in these amides are retarded in going from carbon tetrachloride to

[1]If ΔG^* approaches the energy barrier of the ring inversion (ΔG^*_i) then the argument presented above is not justified. This may explain the low value of $\Delta G^*a - \Delta G^*$ for **1***d*.

[2]It follows that the $A^{(1,3)}$ conformational energy between O (and/or R) and an equatorial 2-methyl group in **1** and **2** series is greater than 4.7 kcal/mole but less than 12.5 kcal/mole.

Can. J. Chem. Downloaded from www.nrcresearchpress.com by 210.87.254.105 on 09/05/12
For personal use only.

TABLE II

Free energy of activation†

Compound	O=C(—R)	Solvent	Tc	Δν	ΔG*	ΔGa*‖	ΔG*a − ΔG*
1*a*	CHO	CCl_4	308	7(CH_3)	16.4	21.0	4.6
			325	33.5(H)	16.3		4.7
		MeOH	310	5.7(CH_3)	16.6		
1*b*	$COCH_3$	CCl_4	267	10(CH_3)	13.8	17.4	3.6
			274	29(H)	13.7		3.7
		MeOH	282	7(CH_3)	15.0		
1*c*	$COCH_2C_6H_5$	CCl_4	265	4(CH_3)	14.3		
			285	40(H)	14.1		
		$CDCl_3$	271	2.5(CH_3)	14.8		
			298	45(H)	14.9		
		MeOH	280	3(CH_3)	15.3		
1*d*	COC_6H_5	CCl_4‡	(242)	40(H)	(12.1)	15.3	(3.2)
		MeOH	247	10.8(CH_3)	12.5		
1*g*	NO	DCB§	373	17.2(CH_3)	19.4	23.3	3.9

†Δν is the maximum chemical shift difference of —CH_3 (or H) in c.p.s. ΔG* is the ΔG* of the internal rotation of the corresponding derivatives of dimethylamine.
‡Due to the solubility problem Tc is probably too high and Δν may not have reached the maximum and thus ΔG* should be regarded as being too high.
§DCB = *o*-dichlorobenzene.
‖These data are quoted from refs. 3 and 4.

methanol solution due to hydrogen bonding and a polar medium effect (10). Both of these effects naturally induce more electron delocalization and cause a higher energy barrier as demonstrated. The energy barrier on the other hand decreases as the electron withdrawing capacity of the substituent groups (—C(=O)R) decreases. This trend is to be expected on the basis of the same argument.

Finally in the light of the above information we should like to correct the structure of α-piperidinocyclohexanone oxime, obtained previously from the photoaddition of *N*-nitrosopiperidine to cyclohexene, as having *anti*-configuration (7) instead of *syn*-configuration (11). The assignment of *syn*-configuration was based on a probable hydrogen bonding between OH and amine-*N* centers. Such intramolecular hydrogen bonding appears to be nil from the dilution study with infrared spectroscopy. In this case a driving force from $A^{(1,3)}$ interaction should be the dominant factor leading to the more stable *anti*-configuration as shown in **7**. The reported n.m.r. parameters fit perfectly with the conformation **7**; the broad doublet at τ 7.00 corresponds to H_e and the signal at τ 8.10 to H_a (12). The assignment of τ 7.26 signal to H_a' has been proved (11).

Experimental

Nuclear Magnetic Resonance Spectra

The nuclear magnetic resonance (n.m.r.) spectra were taken in the range of 10% (w/v) solution containing 1% of tetramethylsilane with a Varian A56/60 spectrometer equipped with a variable temperature probe. Duplicate measurements were made with a sweep width of 250 c.p.s. at various temperatures. The mass spectra were taken with a Perkin–Elmer–Hitachi mass spectrometer.

Synthesis of the Compounds

The compounds were prepared by standard procedures of nitrosation and acylation as described elsewhere. The redistilled 2,6-dimethylpiperidine (Aldrich Chemical Co.) was found to be sufficiently pure *cis*-isomer (>95%) for the preparations. Each compound possessed the pertinent infrared and n.m.r. spectra and the correct mass peaks (M^+) in the mass spectrum. The physical constants of these compounds are: **1***a*, b.p. 211–212° C at 760 mm; **1***b*, b.p. 113–114 °C at 10 mm; **1***c*, m.p. 94–96 °C; **1***d*, m.p. 106–108 °C, (lit. 111 °C) (13); **1***f*, m.p. 79–80 °C; **2***a*, b.p. 111–112 °C at 10 mm; **2***b*, m.p. 42–43 °C, (lit. 44–45 °C) (13); **2***c*, b.p. 98 °C at 1 mm; **1***e* was distilled three times in a small scale apparatus at bath temperatures 110–120 °C at 10 mm. Preparation of **1***g* and **2***d* has already been described (2).

Acknowledgments

We gratefully acknowledge the financial support for this work and for the purchasing of the mass spectrometer provided by the National Research Council of Canada. We also gratefully acknowledge the technical assistance of Mr. S. Y. Lee.

Can. J. Chem. Downloaded from www.nrcresearchpress.com by 210.87.254.105 on 09/05/12
For personal use only.

1. F. JOHNSON and S. K. MALHOTRA. J. Am. Chem. Soc. **87**, 5492, 5493 (1965).
2. Y. L. CHOW and C. J. COLÓN. Can. J. Chem. **45**, 2559 (1967).
3. M. T. ROGERS and J. C. WOODBREY. J. Phys. Chem. **66**, 540 (1962).
4. C. E. LOONEY, W. D. PHILLIPS, and E. L. REILLY. J. Am. Chem. Soc. **79**, 6163 (1957).
5. H. O. HOUSE, B. A. TEFERTILLER, and C. G. PITT. J. Org. Chem. **31**, 1073 (1966).
6. Y. L. CHOW and M. M. FESER. Chem. Commun. 239 (1967).
7. R. K. HARRIS and R. A. SPRAGG. J. Mol. Spectry. **23**, 158 (1967).
8. H. S. GUTOWSKY and C. H. HOLM. J. Chem. Phys. **25**, 2228 (1956).
9. N. L. ALLINGER and M. A. MILLER. J. Am. Chem. Soc. **83**, 2145 (1961).
10. A. LOEWENSTEIN, J. F. NEWMER, and J. D. ROBERTS. J. Am. Chem. Soc. **82**, 3599 (1960).
11. Y. L. CHOW. Can. J. Chem. **43**, 2711 (1965).
12. W. F. TRAGER and A. C. HUITRIC. Tetrahedron Letters, 825 (1966).
13. I. HEILBRON. Dictionary of organic compounds. Eyre and Spottiswoode Ltd., London. 1965.

Can. J. Chem. Downloaded from www.nrcresearchpress.com by 210.87.254.105 on 09/05/12
For personal use only.

Can. J. Chem. Downloaded from www.nrcresearchpress.com by 210.87.254.6 on 09/05/12
For personal use only.

Nuclear magnetic resonance studies on the configurations and conformations of heterocyclic nitrosamines[1]

Y. L. CHOW AND C. J. COLÓN
Department of Chemistry, Simon Fraser University, Burnaby 2, British Columbia

Received May 16, 1968

The nuclear magnetic resonance spectra of various heterocyclic nitrosamines were studied in solution. A qualitative view of the long-range diamagnetic effects of a nitrosamino group is advanced and correlated with the chemical shifts of α-equatorial protons and the methyl group in those nitrosamines possessing a preferred conformation or a rigid system. The use of this correlation to decide the configuration and conformation of heterocyclic nitrosamines is discussed. A large chemical shift difference (ca. 3 p.p.m.) between a *cis* α-axial and a *cis* α-equatorial proton was noted.

Canadian Journal of Chemistry, 46, 2827 (1968)

Introduction

Recently we have reported unusual photochemical reactions of *N*-nitrosodialkylamines (1). In the course of our investigation, it was felt desirable to know the shape of a nitrosamino group in the ground state. This knowledge is no doubt an important factor in considering the mechanisms of the photochemical reactions. As a contribution to this end, a nuclear magnetic resonance (n.m.r.) study of heterocyclic nitrosamines is reported in this paper. A relevant n.m.r. study of nitrosamines has been reported recently (2).

The most unusual characteristic of a nitrosamino group is its electronic configuration in which the polar resonance form contributes extensively to the resonance hybrid. A quantum mechanical calculation (self-consistent field method) on the energy levels and the orbital coefficients reveals that the polar resonance form (**2**) can contribute up to 49% to the ground state of a nitrosamine and about the same extent to the excited state (3). The extensive resonance interaction between *n*-electrons of the amino nitrogen and π electrons of the nitroso group necessitate the representation of a nitrosamine (e.g. *N*-nitrosopiperidine) by a more realistic structure such as **3**. In this configuration the amine nitrogen is nearly trigonally hybridized to resemble a carbonyl carbon (or a carbonium ion center); e.g., the angles of C_2NN and NNO are approximately 120°. The following observations in the literature are consistent with this structural proposition: (*i*) the dipole moment, as determined on *N*-nitrosodimethylamine, shows a large value (3) of 3.98 D.U.; (*ii*) the partially localized negative charge at the nitroso oxygen makes a nitrosamine a good Lewis base; the pK_B in cyclohexane has been determined (4) to be ca. −3; (*iii*) on the same ground a cationic species (such as a carbonium ion or its progenitor) reacts at the oxygen center (5, 6) and presumably a proton[2] also reacts at this site (4); (*iv*) the nature of partial double bond character at the N—N bond is well verified by n.m.r. spectroscopic studies (of *N*-nitrosodimethylamine) in which the free activation energy (ΔG^*) of the restricted rotation around N—N bond has been shown to be 23.3 kcal/mole (at 183°) in the liquid phase (7, 8) and 21.1 kcal/mole in vapor phase (9); (*v*) the geometry of the polar form is well supported by the stereospecific collision complex formation between a nitrosamine and benzene (10, 11); and (*vi*) certain nitrosamines possess high enough activation energy barriers that the geometrical isomers are separable by low temperature operation (12).

The n.m.r. studies in acyclic series have shown the anisotropic effects of a nitrosamino group to impart remarkable long-range shielding effects on the magnetic environment of the nearby hydrogen nuclei (11, 13). In view of the slow rotation about the N—N bond, the long-range shielding effects of a nitrosamino group should render an excellent tool to look into the conformational problem of the vicinal hydrogen nuclei by n.m.r. studies. Although accurate knowledge of the anisotropy of a nitrosamino group is not

[1]A part of the results has appeared as the preliminary communication; Y. L. Chow. Angew. Chem. 51 (1967).

[2]In ref. 4 the reaction of a nitrosamine with an acid has been proposed to be "hydrogen bonded complexation" rather than an outright protonation.

TABLE I

The chemical shifts (τ values) of conformationally mobile nitrosamines

N-Nitroso-	Solvent	*cis*-CH_2	*trans*-CH_2	Δδ†
dibutylamine **4**	CCl_4	6.45	5.91	0.54
	C_6H_6	6.73 (0.28)*	6.30 (0.39)	0.43
piperidine **5**	CCl_4	6.32	5.84	0.48
	C_6H_6	6.57 (0.25)	6.23 (0.39)	0.34
	D_2O	6.15	5.82	0.33
morpholine **6**	CCl_4	6.30	5.78	0.52
	C_6H_6	6.55 (0.25)	6.27 (0.49)	0.28
	D_2O	6.03	5.68	0.35
3-azabicyclononane **7**	$CDCl_3$	6.04	5.51	0.53
pyrrolidine **8**	CCl_4	6.61	5.80	0.81
	C_6H_6	6.80 (0.19)	6.13 (0.33)	0.67
	D_2O	6.54	5.87	0.67
	$CDCl_3$	6.52	5.76	0.76
2-azaspiro[4,5]decane **9**	CCl_4	6.42	—	—
1,2,3,4-tetrahydraisoquinoline **10***a*	CCl_4	5.33	5.58	—
	C_6H_6	5.43 (0.10)	6.00 (0.42)	—
10*b*	CCl_4	6.29	4.69	—
	C_6H_6	6.50 (0.21)	5.03 (0.34)	—

*The figures in the parentheses represent the upfield shifts (in p.p.m.) of the α-methylene groups in benzene with respect to the chemical shifts in carbon tetrachloride.
†$\Delta\delta = \delta cis - \delta trans$.

available, an approximation has been proposed and has been applied successfully in correlations of the chemical shifts of protons in the vicinity and their conformations in acyclic nitrosamines (11, 13). Such approximated anisotropic effects can be observed directly, in theory, in heterocyclic systems where the conformation stability is well understood and in particular where the system is frozen or preferentially favors one form.

Results

Due to the unsymmetrical configuration along the axis of the N⋯N partial double bond, the α-protons flanking the nitrosamino group in acyclic systems are situated in different magnetic environments and give rise to two signals with different chemical shifts at temperatures lower than ca. 180° (7, 11, 13). The signal at higher field has been assigned to the *cis* α-protons[3] based on the correlation of preferential orientation of the oxygen atom about the N⋯N bond with respect to the steric hindrance at α-carbon atoms in a series of acyclic nitrosamines (11, 13).

The 60 Mc.p.s. n.m.r. spectra of various heterocyclic nitrosamines in solution were taken with tetramethylsilane as the internal standard and the chemical shifts of α-protons were estimated to within ±0.5 Hz and were expressed in τ values. These nitrosamines, listed in Table I, all possess identical configurational isomers except **10**. They are conformationally mobile and possess no preference for one conformation or the other; i.e., rapid interchange between the identical conformers. For comparison, the spectral parameters of *N*-nitrosodibutylamine (**4**) are also included. Those nitrosamines possessing either a locked conformation or a preferential conformation are grouped in Table II. The Δδ represents the chemical shift difference between the corresponding *cis* and *trans* α-protons ($\delta_{cis} - \delta_{trans}$) and Δν represents the chemical shift difference between α-axial and α-equatorial protons that are attached on the same carbon atom either on *cis* side or on *trans* side ($\delta_{ax} - \delta_{eq}$).

In Table I, all nitrosamines except *N*-nitroso-1,2,3,4-tetrahydroisoquinoline (**10**) exhibit two signals for the time averaged *cis* and *trans* α-protons; the one at a higher field is assigned to the *cis* protons and that at a lower field to the

[3]The term configuration shall be used to denote the *syn–anti* geometrical isomerism at N⋯N in order to avoid confusion with ring conformation of heterocycles. The term *cis–trans* is reserved to denote the protons on the same or opposite side of the oxygen atom. It is understood that rotation around the N—N bond is slower than the n.m.r. time scale; this causes the unsymmetrical configuration (7).

Can. J. Chem. Downloaded from www.nrcresearchpress.com by 210.87.254.6 on 09/05/12
For personal use only.

TABLE II

The chemical shifts (τ values) of nitrosamines of substituted piperidines

		cis-H			*trans*-H			Δδ*		
N-Nitroso-	Solvent	ax	eq	Δν†	ax	eq	Δν†	ax	eq	Other
4-methylpiperidine **11**	CCl_4	7.50	5.15	2.35	6.35	5.38	0.97	1.15	−0.23	9.18‡
	C_6H_6	7.83	5.18	2.65	6.80	5.57	1.23	1.03	−0.39	9.28‡
	$CHCl_3$	7.42	5.05	2.37	6.33	5.28	1.05	1.09	−0.23	9.00‡
	C_6H_{12}	7.61	5.16	2.45	6.46	5.37	1.09	1.15	−0.21	9.04‡
4-benzylpiperidine **12**	CCl_4	7.62	5.17	2.45	6.47	5.38	1.09	1.19	−0.21	7.52§
	C_6H_6	8.05	5.18	2.87	7.02	5.62	1.40	1.03	−0.44	7.83§
4-*t*-butylpiperidine **13**	CCl_4	7.67	5.05	2.62	6.45	5.27	1.18	1.22	−0.22	9.17‖
	C_6H_6	8.18	4.99	3.19	7.09	5.52	1.57	1.09	−0.53	9.42‖
3-methylpiperidine **14***a*	CCl_4	7.61	5.45	2.16	6.31	5.45	0.86	—	—	8.98¶
	C_6H_6	8.04	5.43	2.61	6.82	5.72	1.10	—	—	9.34¶
	CCl_4	7.28	5.45	1.83	6.63	5.45	1.18	—	—	9.10¶
14*b*	C_6H_6	7.75	5.43	2.32	7.14	5.72	1.42	—	—	9.40¶
trans-decahydroquinoline **15**	CCl_4	7.63	4.90	2.73	6.68	—	—	—	—	—
	C_6H_6	7.67	4.85	2.84	7.25	—	—	—	—	—

*Δδ(δ*cis* − δ*trans*) represents the chemical shift difference between the axial (or the equatorial) protons on the *cis* side and those on the *trans* side.
†Δν (δ axial − δ equatorial) represents the chemical shift difference between the axial and the equatorial protons attached to the same α-carbon either on *cis* or *trans* sides.
‡τ values for the 4-methyl group, doublet $J = 7$ Hz.
§τ values for the benzylic methylene group, doublet $J = 7$ Hz.
‖τ values for the 4-*t*-butyl group, singlet.
¶τ values for the 3-methyl group, doublet $J = 6$ Hz.

trans protons in accordance with the proposed assignment in acyclic systems (11, 13). Nitrosamine **10** shows a pair of *syn* (**10***a*) and *anti* (**10***b*) configurational isomers in a ratio of 2.5:1 in benzene solution at the probe temperature (Fig. 1) due to the unsymmetrical nature of the parent amine. The pair of singlets for benzylic protons and the triplet ($J = 6$ Hz for **10***a* and $J = 6.5$ Hz for **10***b*) for non-benzylic α-protons apparently indicate that each isomer represents rapidly equilibrating conformers. From the integration curve the triplet at τ 6.50 and the singlet at τ 5.03 possess equal weight and are assigned to *cis* and *trans* α-protons of the *anti* isomer **10***b*. The remaining set of signals (τ 5.43 and 6.00) must, therefore, belong to that of the *syn* isomer **10***a*. The calculation of Δδ must be made with respect to the benzylic (or non-benzylic) α-protons of two configurational isomers **10***a* and **10***b*. For **10** in benzene solution, Δδ for the benzylic protons is (5.43–5.03) 0.4 p.p.m. and Δδ for the non-benzylic protons (6.50–6.00) 0.5 p.p.m. Those resonated at the higher field were again assigned to the *cis* α-protons. The ratio of **10***b*/**10***a* isomers varies very little in benzene and CCl_4 and varies from 1:2.4 to 1:1.5 when the temperature is raised from 35 to 70°.

The 4-substituted nitrosopiperidines **11**, **12**, and **13** all show, in each spectrum, four one-

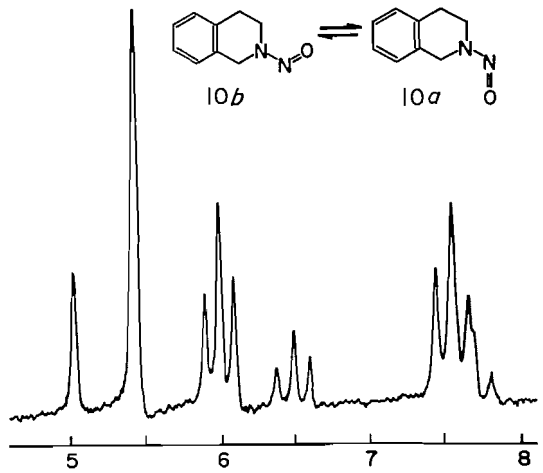

FIG. 1. The 60 Mc.p.s. nuclear magnetic resonance spectrum of **10** in benzene solution.

proton signals in the τ 5–8 region corresponding to two α-axial and two α-equatorial protons. The two signals in the lower fields (τ 5.0 region) are partially superimposed in CCl_4 or $CHCl_3$ solution and are assigned to two α-equatorial protons since both signals are split to broad doublets. The other two signals at the higher fields (τ 6.5 and 7.5 regions) are assigned to two α-axial protons in accordance with large triplet splitting ($J = 10 \sim 12$ Hz); each of the triplets is further

Can. J. Chem. Downloaded from www.nrcresearchpress.com by 210.87.254.6 on 09/05/12
For personal use only.

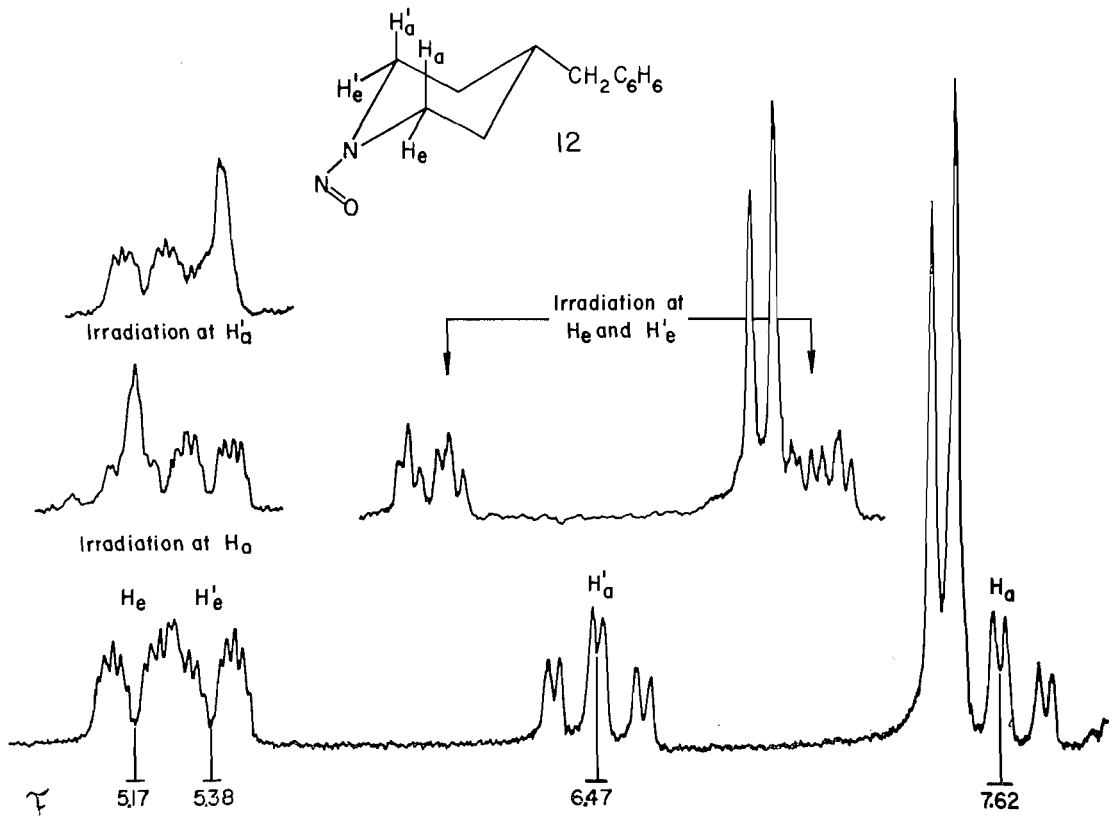

FIG. 2. The 100 Mc.p.s. nuclear magnetic resonance spectrum of **12** in benzene solution and the decoupling of the α-protons.

coupled to a proton with $J = 2 \sim 3$ c.p.s. By double resonance experiments[4] with **12** at 100 Mc.p.s. (Fig. 2) it is shown that the τ 5.38 doublet is coupled to the τ 6.47 triplet (J_{gem} = 13.5 Hz) and that the τ 5.17 doublet is coupled to the τ 7.62 triplet (J_{gem} = 13 Hz). The assignment of *cis* and *trans* orientation for these protons will be discussed in the sequel.

The much overlapped signals in the 60 Mcycle spectrum of *N*-nitroso-3-methylpiperidine (**14**) can be well separated in benzene at 100 Mc.p.s. (Fig. 3) to show that the nitrosamine is a 1:1 mixture of *syn* (**14***a*) and *anti* (**14***b*) configurational isomers. Although the signals due to α-equatorial protons are still partially superimposed to two sets of doublets, four signals (of equal weight) corresponding to four axial protons are well defined both in the chemical shifts and the splitting pattern. The assignment is shown in Fig. 3 and will be discussed below.

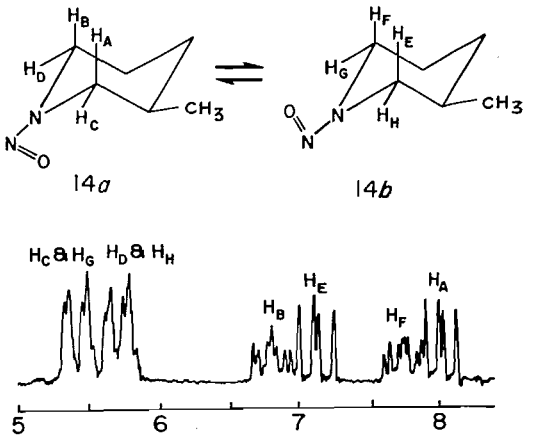

FIG. 3. The 100 Mc.p.s. nuclear magnetic resonance spectrum of **14** in benzene solution.

[4]This and other decoupling experiments were performed through the generous assistance of Dr. D. M. McGreer of the University of British Columbia and Drs. W. A. Ayer and D. Darwish of the University of Alberta, Edmonton.

Can. J. Chem. Downloaded from www.nrcresearchpress.com by 210.87.254.6 on 09/05/12
For personal use only.

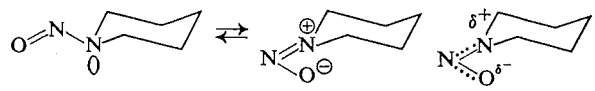

1 2 3

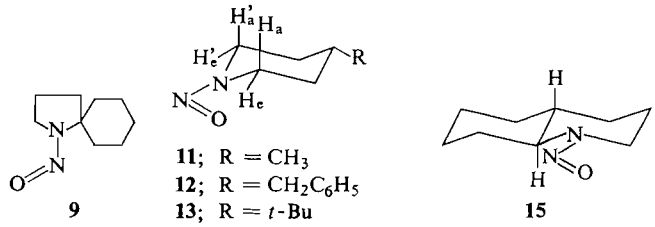

11; R = CH_3
12; R = $CH_2C_6H_5$
13; R = *t*-Bu

9 15

Finally the n.m.r. of the conformationally rigid *N*-nitrosodecahydroquinoline (**15**) exhibits only one isomer, to which the most stable *anti* configuration is assigned. The one-proton doublet, each peak of which is split further to a multiplet, at the lowest field (τ 4.90, J = 13 Hz) is readily recognized as the only α-equatorial proton. Double resonance experiments prove that this proton is coupled to the multiplet at τ 7.63 but not with the multiplet at τ 6.68.

Discussion

The wide scattering (over 3 p.p.m.) of α-proton signals in the n.m.r. spectra of **11**, **12**, and **13** indicates a propensity of anisotropic effect on the differently oriented vicinal protons. In order to understand the n.m.r. of heterocyclic nitrosamines it is, therefore, very important to consider not only the configuration at the nitrosamino group but also the ring conformation. In view of the extensive delocalization of the *N*-nitrosamine group as mentioned before, the barrier to the nitrogen inversion must be insignificant (< 1 kcal/mole) (14) in comparison to the piperidine ring inversion (ca. 10 kcal/mole). The same argument also implies that the geometry at the nitrosamine group is expected to resemble cyclohexanone oxime as shown in **3**, i.e., a trigonal hybridization at the amino nitrogen and a dihedral angle between CNN and CCHeq of ca. 15°. Thus bearing in mind that the barrier to restricted rotation about the partial N⋯N double bond is of the order of 23 kcal/mole (7, 9), the *cis* and *trans* methylene groups should give two time averaged signals at appropriate temperatures as shown in Table I.

Having defined the geometry of the nitrosamino group it is now possible to consider the anisotropic effect of the group. Using the empirical results of diamagnetic anisotropies of carbon–carbon single and double bonds (15), the previously proposed long-range shielding effects of a nitrosamino group (11) can be elaborated further and represented qualitatively by Fig. 4. The shielding cones derived from the Cα—N single bond and the N⋯N⋯O partial double bond are regarded as being fused together to form a semicircular shielding zone curved toward the *cis* side as shown in Fig. 4. The shielding zone is extended above and below and also perpendicular to the Cα—N⋯N⋯O plane. This would result in a greater shielding environment on the *cis* side than on the *trans* side; however, the deshielding zone on the Cα—N⋯N⋯O plane would probably extend nearly equally in magnitude to both sides.

With the conformation and the anisotropic effect of a nitrosamino group so defined, it is expected that 4-substituted *N*-nitroso piperidines (**11**, **12**, and **13**) should give rise to four signals corresponding to the four α-protons in different magnetic environments because of the preferred

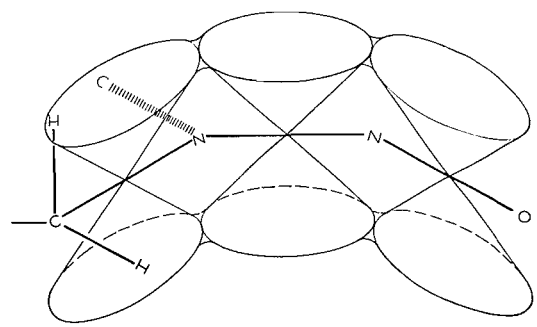

FIG. 4. The long-range diamagnetic effects of a nitrosamino group.

Can. J. Chem. Downloaded from www.nrcresearchpress.com by 210.87.254.6 on 09/05/12
For personal use only.

Can. J. Chem. Downloaded from www.nrcresearchpress.com by 210.87.254.6 on 09/05/12
For personal use only.

conformation defined by the 4-substituents. The α-equatorial protons are held nearly coplanar with the Cα—N⋯N⋯O plane, and therefore, resonate at approximately the same and at lower fields in the τ 5 region (Table II and Fig. 2). Both α-axial protons orient themselves nearly perpendicular to the Cα—N⋯N⋯O plane and into the shielding zone and therefore resonate at higher fields; the *cis* α-proton, being oriented inside the semicircular shielding zone, appears at a far higher field (τ 7.5–8.0 region). All the protons show the coupling pattern expected for an α-axial (doublets of triplets) and for an α-equatorial (multiplet of doublets) protons. The decoupling experiments have shown that the outer pair of signals represents the protons attached to the same α-carbon atom (and therefore the *cis* equatorial and *cis* axial protons). It follows that the inner pair must represent the *trans*-equatorial and *trans*-axial protons (Fig. 2). This argument is clearly illustrated by the general tendency of the positive Δδ for axial and the negative Δδ for equatorial protons as shown in Table II. The correctness of this *cis–trans* assignment is further supported by the preferential upfield shifts of *trans* protons in benzene solutions since benzene is known to shield preferentially the axial proton from the *trans*-side (10). Further support of this *cis–trans* assignment of the corresponding α-proton signals can be obtained from a consideration of **15**. The rigid framework of *trans*-decahydroquinoline makes the corresponding *syn* configuration of **15** inconceivable due to a severe $A^{(1,3)}$ interaction (16, 17). The only possible isomer, for the sole nitrosation product obtained, must possess *anti* configuration (**15**) which in turn, requires that the signals at τ 7.63 and 4.90 be assigned to the *cis*-axial and the *cis*-equatorial protons respectively since they are geminally coupled to each other ($J = 13$ Hz). The assignments indicated in Table II are consistent with each other and thus provide further support to the qualitative approach on the long-range diamagnetic effects of a nitrosamino group as proposed in Fig. 4.

For the freely mobile *N*-nitrosopiperidine (**5**) system, i.e., in the absence of the 4-substituent in **11**, **12**, and **13**, the axial and equatorial protons are rapidly interchanging and the time averaged signals for the α-protons should be the weighted mean of two chemical shifts. Taking the chemical shifts of **13** as the "pure" axial and equatorial parameters, the calculated chemical shifts for *cis* and *trans* methylene groups of **5** turns out to be τ 6.32 and 5.86, in excellent agreement with the observed values. This agreement renders support to the recently published reports that the signal at the higher field corresponds to the *cis*-methylene group and that at the lower field to *trans*-methylene (11, 13). This generalization was originally derived from steric hindrance considerations and the validity of the argument can also be seen from parameters of **8** and **9**. The only isomer of **9** should possess the configuration shown and the triplet of the *cis*-methylene group (τ 6.42) should resonate at the region corresponding to the *cis*-methylene protons of **8** (τ 6.61).

N-Nitroso-3-methylpiperidine (**14**) gives rise to a pair of *syn* (**14***a*) and *anti* (**14***b*) isomers of approximately equal energy, each of which should have the preferred conformation as shown. These rotational isomers can be detected at the n.m.r. time scale at probe temperature but cannot be isolated without resorting to an operation at very low temperature (12). The four well-separated signals corresponding to the α-axial protons are readily assigned on the basis of their splitting pattern (Fig. 3) and on the same argument applied in the case of 4-substituted nitrosopiperidines. The fact that four α-equatorial protons superimpose into two sets of signals, possibly one set for two *cis* protons and the other for the two *trans* protons, appears to indicate that the long-range shielding effect is more sensitively related to a subtle change in axial orientation. The calculation of Δδ of **14** is necessarily carried out with respect to the corresponding protons in two configurational isomers by analogy to that of **10**. For **14** in benzene, $\Delta\delta_{ax}$ are $\tau_A - \tau_E$ (0.9 p.p.m.) and $\tau_F - \tau_B$ (0.93) and $\Delta\delta_{eq}$ are $\tau_C - \tau_H$ and $\tau_G - \tau_D$ (−0.29). The reasonable agreement shown between these Δδ values and those shown in Table II apparently indicates that there is no appreciable deviation from the expected conformation in the *syn* and *anti* isomers of **10** and **14**.

The knowledge gained so far has led to the discovery of the unusual diaxial orientation of the 2,6-dimethyl group in *N*-nitroso-*cis*-2,6-dimethylpiperidine (17) as also has been found by others (2). Similarly, the complex n.m.r. spectrum of *N*-nitroso-2-methylpiperidine has been

studied by us as well as by these authors (2). Although we are able to confirm that this nitrosamine contains *syn* and *anti* isomers and that the *syn* isomer has the 2-methyl group axially oriented, we are not able to assign unambiguously the chemical shifts of the protons in the *anti* isomer even with the extensive aid of decoupling experiments at 100 Mcycles. Although the discussion so far has been based on the chair conformation, one should expect a certain degree of distortion from the perfect shape especially in the forced conformations. Unfortunately the present qualitative approach is not quite refined enough to detect the subtle distortion by the correlation shown; nor has a quantitative approach by others been successful (2).

Finally the stereospecific manner of the anisotropic effect of a nitrosamino group is even better illustrated by the unusually large chemical shift difference between the axial and equatorial protons ($\Delta\nu$ 2 $\sim$ 3 p.p.m.) of the *cis*-methylene groups. In contrast the same chemical shift difference for the *trans* side amounts only 1 $\sim$ 1.4 p.p.m. To our knowledge, a chemical shift difference of 3.19 p.p.m. between two protons attached to the same carbon atom in **13** is one of the largest ever recorded in the literature. In this connection it should be mentioned that in a conformation of piperidine derivatives where the α-axial protons are *anti*-coplanar to the lone pair electron of nitrogen atom, the chemical shift difference between the α-axial and the α-equatorial protons can be as much as ca. 0.9 p.p.m. and at the same time the Bohlman band (2700–2800 cm^{-1} in the infrared region) can be observed (18, 19). This effect is not operating in the present cases since all nitrosamines do not show, in contrast to their parent amines, the Bohlman bands. The lack of Bohlman bands coincidently lends support to the contention that the lone pair electrons of the amine nitrogen are extensively delocalized with the nitroso group and that this nitrogen does not have a pyramidal configuration.

Experimental

The n.m.r. spectra were obtained using a Varian Associates A-56/60 spectrometer with variable temperature probe and a HA-100 spectrometer with spin decoupling facilities. The infrared spectra were recorded on a Unicam SP200. All melting points were uncorrected.

The nitrosamines were prepared by nitrosation of the respective amines as described previously (1, 20). Physical constants of the new nitrosamines are; **9**, m.p. 45–46°, **12**, m.p. 54–57°.

Acknowledgment

The authors wish to thank the National Research Council of Canada for financial support of this research.

1. Y. L. Chow and C. J. Colón. Can. J. Chem. **45**, 2559 (1967), and previous papers of this series.
2. R. K. Harris and R. A. Spragg. J. Mol. Spectry. **23**, 158 (1967).
3. J. Tanaka. J. Chem. Soc. Japan, **78**, 1647 (1957).
4. W. S. Layne, H. H. Jaffé, and H. Zimmer. J. Am. Chem. Soc. **85**, 435 (1963).
5. A. Schmidpeter. Tetrahedron Letters, 1421 (1963).
6. S. Hünig, L. Geldern, and E. Lücke. Angew. Chem. **75**, 476 (1963).
7. C. E. Looney, W. D. Phillips, and E. L. Reilley. J. Am. Chem. Soc. **79**, 6136 (1957).
8. K. H. Abramson, P. T. Inglefield, E. Krakower, and L. W. Reeves. Can. J. Chem. **44**, 1685 (1966).
9. R. K. Harris and R. A. Spragg. Chem. Commun. 362 (1967).
10. Y. L. Chow and M. M. Feser. Chem. Commun. 239 (1967).
11. G. J. Karabatsos and R. A. Taller. J. Am. Chem. Soc. **86**, 4373 (1964).
12. A. Mannschreck, H. Münsch, and A. Matthews. Angew. Chem. **78**, 751 (1966).
13. H. W. Brown and D. P. Hollis. J. Mol. Spectry. **13**, 305 (1964).
14. C. C. Constain and J. M. Dowling. J. Chem. Phys. **32**, 158 (1960).
15. L. Jackman. Application of nuclear magnetic spectroscopy in organic chemistry. The Pergamon Press, Ltd., New York. 1959. Chap. 7.
16. F. Johnson and S. K. Malhotra. J. Am. Chem. Soc. **87**, 5492, 5493 (1965).
17. Y. L. Chow, C. J. Colón, and N. S. Tam. Can. J. Chem. This issue.
18. F. Bohlman, D. Schumann, and H. Schulz. Tetrahedron Letters, 173 (1965); F. Bohlman, D. Schumann, and C. Arndt. Tetrahedron Letters, 2705 (1965).
19. J. B. Lambert and R. G. Keske. J. Am. Chem. Soc. **88**, 620 (1966).
20. Y. L. Chow. Can. J. Chem. **45**, 53 (1967).

Can. J. Chem. Downloaded from www.nrcresearchpress.com by 210.87.254.6 on 09/05/12
For personal use only.

Can. J. Chem. Downloaded from www.nrcresearchpress.com by 210.87.254.42 on 09/05/12
For personal use only.

Synthesis of phenolic esters with potential long-lasting insect-repellent properties

RONALD P. QUINTANA, LORRIN R. GARSON, AND ANDREW LASSLO
Department of Medicinal Chemistry, College of Pharmacy, University of Tennessee Medical Units, Memphis, Tennessee 38103

Received January 31, 1968

The synthesis of undecanoic acid esters of resorcinol, 4-chlororesorcinol, hexachlorophene, *o*-chlorophenol, and *p*-chlorophenol is described. The compounds were designed to provide, potentially, perdurable insect-repellent activity. When the synthesis of esters of resorcinol and 4-chlororesorcinol was attempted with undecanoic acid, under acid catalysis, principally ketones and ketoesters were isolated. The originally sought esters were obtained, however, by the reaction of the phenols with undecanoyl chloride in the presence of pyridine. The infrared, nuclear magnetic resonance, and mass spectra of the compounds are discussed.

Canadian Journal of Chemistry 46, 2835 (1968)

In previous communications (1, 2), we reported on the design and synthesis of novel grisan and coumaran-3-one derivatives anticipated to exert insect-repellency following systemic administration. Since our efforts are directed toward the development of prophylactic agents effective against pathogenic (or physical) impairments inflicted through the skin, the effect of some of these compounds upon monomolecular films of representative dermal constituents has also been evaluated (2–4).

In this paper, we describe the preparation of agents (**1–9**) designed to provide long-lasting insect-repellent efficacy by means of the gradual release of an active component, undecanoic acid (5*a*), from a precursor-type molecule anchored to the epidermal surface; the release being effected by moisture, pH, esterases or other enzymes, and bacterial flora on and in the epidermal structure. In the course of the synthetic work two compounds (**10** and **11**) were obtained which, not being esters, cannot release undecanoic acid. They constitute excellent control entities (pseudo precursor-type molecules), however, for our evaluation of relative intrinsic repellencies and of relative dermophilic characteristics; in fact, they are better suited for the task than the ones originally designed for this purpose (**1**, **3**, **4**, and **5**).

The specific choice of hexachlorophene, resorcinol, and of the latter's chloro derivative, as anchoring components, has been prompted by hexachlorophene's firmly established dermal affinity (6–10) and resorcinol's reported affinity for proteins (11). While in compounds **7**, **9**, and **11**, the principal function of 4-chlororesorcinol is to provide means for anchoring the molecules to dermal tissue, in designing these molecules, we chose this moiety because it also possesses strong insect-repellent activity of its own (5*b*). Even though the primary anchoring function (i.e., phenolic hydroxyl group) is absent in compounds **1**, **3**, **4**, and **5**, we sought to determine their behavior relative to the corresponding derivatives in which the primary anchoring function was present. While it is our endeavor to develop agents most effective in terms of the projected target compounds, concurrently, we are most interested in the relative potency of our synthetic entities — with respect to each other — in terms of gradual changes in the chemical structure.

The phenolic esters of undecanoic acid were prepared by reacting undecanoyl chloride with the appropriate phenol in pyridine (12) (method *a*). When the phenol and acid chloride were reacted in 1:1 mole ratio, both mono- and diesters were obtained. Some of the phenolic esters were obtained also by the direct esterification method described by Aelony (13) (method *b*). It is interesting to note that in the reaction of hexachlorophene with undecanoic acid, no diester was isolated when the reactants were employed in a 1:1 mole ratio. The latter was obtained in 85% yield, however, when a 1:5 mole ratio was used. Hexachlorophene diundecanoate was also prepared by reacting undecanoyl chloride with hexachlorophene in pyridine (method *a*).

When resorcinol and 4-chlororesorcinol were reacted with undecanoic acid, under the acid-catalyzed conditions described by Aelony (13), ketonic materials were obtained (**8**, **10**, and **9**, **11**, respectively). Aelony reported the synthesis of resorcinol monolaurate (m.p. 82–83°, recrystallized from alcohol), but his compound has a very

Can. J. Chem. Downloaded from www.nrcresearchpress.com by 210.87.254.42 on 09/05/12
For personal use only.

different melting point from that of the resorcinol monolaurate (m.p. 49.5–50°, recrystallized from hexane) recently obtained by Van Duuren *et al.* using an acid chloride/pyridine procedure (14). In view of our findings reported in this paper, the resorcinol derivative isolated by Aelony is very probably the ketone 4-lauroylresorcinol.

In the preparation of ketones from acyl chlorides (or acid anhydrides) and aromatic components, sulfuric, perchloric, phosphoric, and other acids have been used as catalysts (15*a*). Acylation of aromatic compounds has been reported with carboxylic acids using aluminium chloride. In acylating phenols, anhydrous zinc chloride, boron trifluoride, and polyphosphoric acid have been substituted for aluminium chloride (15*b*). In fact, Snyder and Elston (16) as well as Smith and Thomson (17) have reported the synthesis of several ketoresorcinols from the respective carboxylic acids and resorcinol, using polyphosphoric acid both as a catalyst and solvent. Our observation, however, that dilute sulfuric acid (0.025 *M* in xylene) catalyzes the formation of ketoresorcinols has not been reported before.

The structures of our derivatives obtained from resorcinol and 4-chlororesorcinol were assigned, primarily, on the basis of their nuclear magnetic resonance (n.m.r.) (Table I), infrared (i.r.) (Fig. 1), and mass spectra.

It is significant (Table I) that the chemical shifts (δ) for the phenolic protons of resorcinol monoundecanoate (**6**) and 4-chlororesorcinol 1-undecanoate (**7**) are somewhat similar (6.13 and 5.60 p.p.m., respectively).[1] As expected, the δ-value for the phenolic proton of **7** is lower than that of **6**, which is consistent with the shielding effect of the *ortho*-chlorine atom. Nuclear magnetic resonance spectra of progressively less concentrated solutions of **6** and **7** showed a marked decreasing δ-value for the phenolic proton of **6**, whereas the latter compound, in which the phenolic proton is intramolecularly hydrogen bonded to the chlorine atom, demonstrated no change upon dilution. These dilution effects are consistent with the assignment of structures **6** and **7** as well as with the n.m.r. studies of Huggins *et al.* (18), and those of Allan and Reeves (19), on halophenols.

That the assignment of structure **7** is correct is further supported by the conversion of **7** to its 3,5-dinitrobenzoate derivative (**12**) under standard conditions (20). Furthermore, compound **7** gives a positive Liebermann test (21) demonstrating that the position *para* to the free phenolic group must be unsubstituted; therefore, 4-chlororesorcinol 3-undecanoate would be an unreasonable alternate structure.

The n.m.r. spectra (Table I) of 4-undecanoylresorcinol (**10**) and 4-chloro-6-undecanoylresorcinol (**11**) differ markedly from those of compounds **6** and **7**. Both compounds **10** and **11** exhibit chemical shifts (12.93 and 12.67 p.p.m., respectively) which are attributed to strong intramolecular hydrogen-bonded phenolic protons (*A'*). The assignment of these bands to the phenolic protons *ortho* to the ketonic moieties is consistent with the n.m.r. data of Van Duuren and his colleagues (14) for *o*-nitro phenolic compounds in which similar hydrogen bonding occurs. The literature provides ample evidence (15*c*, 22) that acid-catalyzed acylations of this nature, as well as others, occur exclusively in the indicated position. Compound **7** is the only non-keto ester we obtained in the acid-catalyzed reaction; one may rationalize that formation of the 1-undecanoate sterically prohibits acylation in the 6-position.

The presence of *additional* phenolic protons in compounds **10** and **11** was confirmed by the disappearance of bands at 7.00 p.p.m.[2] and 6.06 p.p.m., respectively, upon the addition of D_2O;[3] the change in integration of the samples treated with D_2O also confirms the presence of the phenolic protons. The n.m.r. spectra of progressively less concentrated solutions of **10** show no change in δ-value for the peak at 12.93 p.p.m., confirming the assignment. However, when less concentrated solutions of **11** were examined, neither of the well-defined bands at 12.67 and 6.06 p.p.m. changed, thus proving that *only* intramolecular hydrogen bonding occurs.

Additional evidence for the correct assignment

[1]The assignment of the 6.13 p.p.m. peak to the phenolic proton of **6** was further confirmed by the disappearance of this peak in the spectrum upon the addition of D_2O.

[2]The peak at 7.00 p.p.m. is combined with the aromatic protons in the spectrum of **10**. Therefore, the expected change in chemical shift for the intermolecularly hydrogen-bonded proton (*A*) of **10** could not be observed. The assignment of 7.00 p.p.m. for the phenolic proton was based upon the results of integration prior and subsequent to D_2O addition.

[3]The earlier cited phenolic proton bands at 12.93 and 12.67 p.p.m. also disappeared upon the addition of D_2O.

TABLE I

Nuclear magnetic resonance parameters for resorcinol monoundecanoate (**6**), 4-chlororesorcinol 1-undecanoate (**7**), 4-undecanoylresorcinol (**10**), and 4-chloro-6-undecanoylresorcinol (**11**)*

Compound number†	δ‡	Bands	Number of protons	Assignment§
6	6.23–7.42	Complex	4	*B*
	6.13	Broad singlet	1	*A*
	2.42, 2.53, 2.65	Triplet	2	*C*
	1.28	Singlet‖	16	*D*
	0.78–0.95	Distorted triplet	3	*E*
7	6.47–7.83	Complex	3	*B*
	5.60	Broad singlet	1	*A*
	2.40, 2.52, 2.63	Triplet	2	*C*
	1.28	Singlet‖	16	*D*
	0.80–0.95	Distorted triplet	3	*E*
10	12.93	Singlet	1	*A'*
	6.13–7.80	Complex	4	*A*+*B*
	2.75, 2.86, 3.00	Triplet	2	*C*
	1.27	Singlet‖	16	*D*
	0.80–0.95	Distorted triplet	3	*E*
11	12.67	Broad singlet	1	*A'*
	7.73	Singlet	1	*B*
	6.58	Singlet	1	*B*
	6.06	Broad singlet	1	*A*
	2.75, 2.87, 2.98	Triplet	2	*C*
	1.27	Singlet‖	16	*D*
	0.80–0.95	Distorted triplet	3	*E*

*Structures of compounds are:

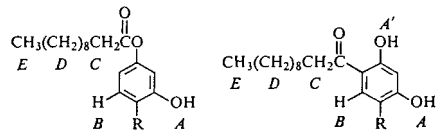

6, R = H
7, R = Cl

10, R = H
11, R = Cl

†The spectra were obtained on 10.6–10.9% solutions of the compounds in $CDCl_3$, at room temperature.
‡Chemical shift (p.p.m.) relative to tetramethylsilane (δ = 0.00).
§Assignments refer to the corresponding designations in the structures.
‖The singlet has a broad base.

of structures for **10** and **11** is provided by the fact that **10** gave a bis(3,5-dinitrobenzoate) derivative (**13**), and that **11** yielded a 2,4-dinitrophenylhydrazone (**14**). Compound **11** failed to give a positive Liebermann test (21) which indicates that the positions *para* to the phenolic groups are substituted, and therefore, the compound 4-chloro-2-undecanoylresorcinol could not be considered an alternate possibility.

The assignment of structures for compounds **6**, **7**, **10**, and **11** is also consistent with their i.r. spectra. The spectral characteristics in the 2000–4000 cm^{-1} range, for these compounds are illustrated in Figs. 1*a*, 1*b*, 1*c*, and 1*d*, respectively. In Fig. 1*a*, the absorption band at 3600 cm^{-1} is associated with the free (non-hydrogen bonded) O—H stretching of the phenolic function of **6**; the band at 3440 cm^{-1} is attributed to the O—H stretching of intermolecularly associated species (23*a*, 24). As anticipated, upon dilution, the band at 3600 cm^{-1} increased in intensity whereas the peak at 3440 cm^{-1} decreased. The spectrum (Fig. 1*b*) for 4-chlororesorcinol 1-undecanoate (**7**) indicates a different mode of hydrogen bonding than that for **6** (Fig. 1*a*). The sharp peak at 3540 cm^{-1} is due to O—H stretching of the intramolecularly hydrogen-bonded species **15** (23*b*, 24). The intensity of the band did not change upon dilution of its solutions. The shoulder-band at 3410 cm^{-1} may be due to O—H stretching of the dimeric species **16**, or to some other intermolecular association. The latter is consistent with the decrease in intensity observed for this band upon dilution.

Can. J. Chem. Downloaded from www.nrcresearchpress.com by 210.87.254.42 on 09/05/12
For personal use only.

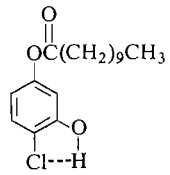

15

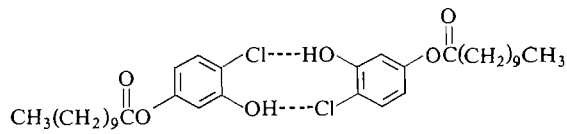

16

The spectrum (Fig. 1*c*) for 4-undecanoylresorcinol (**10**) indicates three distinct O—H stretching modes. The sharp band at 3600 cm^{-1} is associated with the free (non-hydrogen bonded) O—H stretching of the 1-hydroxyl function of **10**. The moderately broad band at 3380 cm^{-1} is attributed to the O—H stretching of intermolecularly associated species involving the 1-hydroxyl moiety. The broad absorption at 2500–3300 cm^{-1} reflects the strong intramolecular association caused by hydrogen bonding between the 3-hydroxyl group and the carbonyl function (23*c*, 24). Upon dilution of solutions of **10**, the free O—H stretching band (3600 cm^{-1}) increased in intensity, the band attributed to intermolecular bonding (3380 cm^{-1}) decreased, and the peaks associated with intramolecular association (2500–3300 cm^{-1}) remained constant.

In the spectrum of 4-chloro-6-undecanoylresorcinol (**11**) (Fig. 1*d*), the sharp peak at 3530 cm^{-1} is attributed to the O—H stretching of the relatively weak intramolecular hydrogen bond between the 3-hydroxyl function and the adjacent chloro substituent; the broad band (2500–3300 cm^{-1}) reflects, as it does in **10**, the intramolecular association of the hydroxyl group *ortho* to the carbonyl function. As expected, dilution of solutions of **11** did not cause a change in the intensities of any of the absorption bands.

Comparison of Figs. 1*a* and 1*c* with 1*b* and 1*d* shows that in the former pair, the peaks associated with free (non-hydrogen bonded) O—H stretching are 60–70 cm^{-1} higher than the bands associated with the O—H stretching of the latter pair in which a chlorine is *ortho* to the hydroxyl function. This observation is consistent with the published reports of Brown and his colleagues (25), and Ingold and Taylor (26).

It is interesting to note the effects of hydrogen bonding upon the carbonyl absorption frequencies of some of these compounds. Resorcinol monoundecanoate (**6**) shows an absorption band for the ester at 1742 cm^{-1} as compared to that of resorcinol diundecanoate at 1764 cm^{-1}, substantiating our contention of intermolecular hydrogen bonding to the carbonyl group in **6**. A comparison of hexachlorophene monoundecanoate (**2**) and hexachlorophene diundecanoate (**1**) shows a similar pattern (1767 and 1783 cm^{-1}, respectively). While in the instance of **6** we refer to intermolecular association, it should be pointed out that, in the case of **2**, *any* hydrogen bonding would have to be intramolecular; the influence of the *ortho*-chloro substituent would be expected to be the same here as in **7**.

While 10% chloroform solutions of 4-undecanoylresorcinol 1-undecanoate (**8**)[4] and 4-chloro-6-undecanoylresorcinol 3-undecanoate (**9**) did not show any identifiable O—H stretching peaks, 0.060 *M* solutions of the compounds in carbon tetrachloride exhibited weak, broad absorption bands (2500–3450 cm^{-1}). These observations are consistent with the i.r. data obtained for 4-undecanoylresorcinol (**10**) and 4-chloro-6-undecanoylresorcinol (**11**). The lack of the customarily typical O—H stretching frequencies, as observed

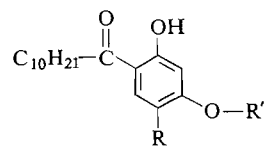

8, R = H; R′ = $C_{10}H_{21}$—CO
9, R = Cl; R′ = $C_{10}H_{21}$—CO
10, R = H; R′ = H
11, R = Cl; R′ = H

in the spectra of **8** and **9**, has been reported in the literature (23*c*). For example, in β-diketones (enolic) and phenols, in which carbonyl or nitro groups were substituted *ortho* to the hydroxyl function, the O—H absorption bands occur

[4]In the instance of compounds **8** and **10** we refer to the acyl radical in position-4, while in the case of compounds **9** and **11** we refer to it in position-6; it is apparent that the acyl substituent is located in the same position in both sets of compounds, the difference in numbering being due to the chloro substituent in **9** and **11**.

Can. J. Chem. Downloaded from www.nrcresearchpress.com by 210.87.254.42 on 09/05/12
For personal use only.

Can. J. Chem. Downloaded from www.nrcresearchpress.com by 210.87.254.42 on 09/05/12
For personal use only.

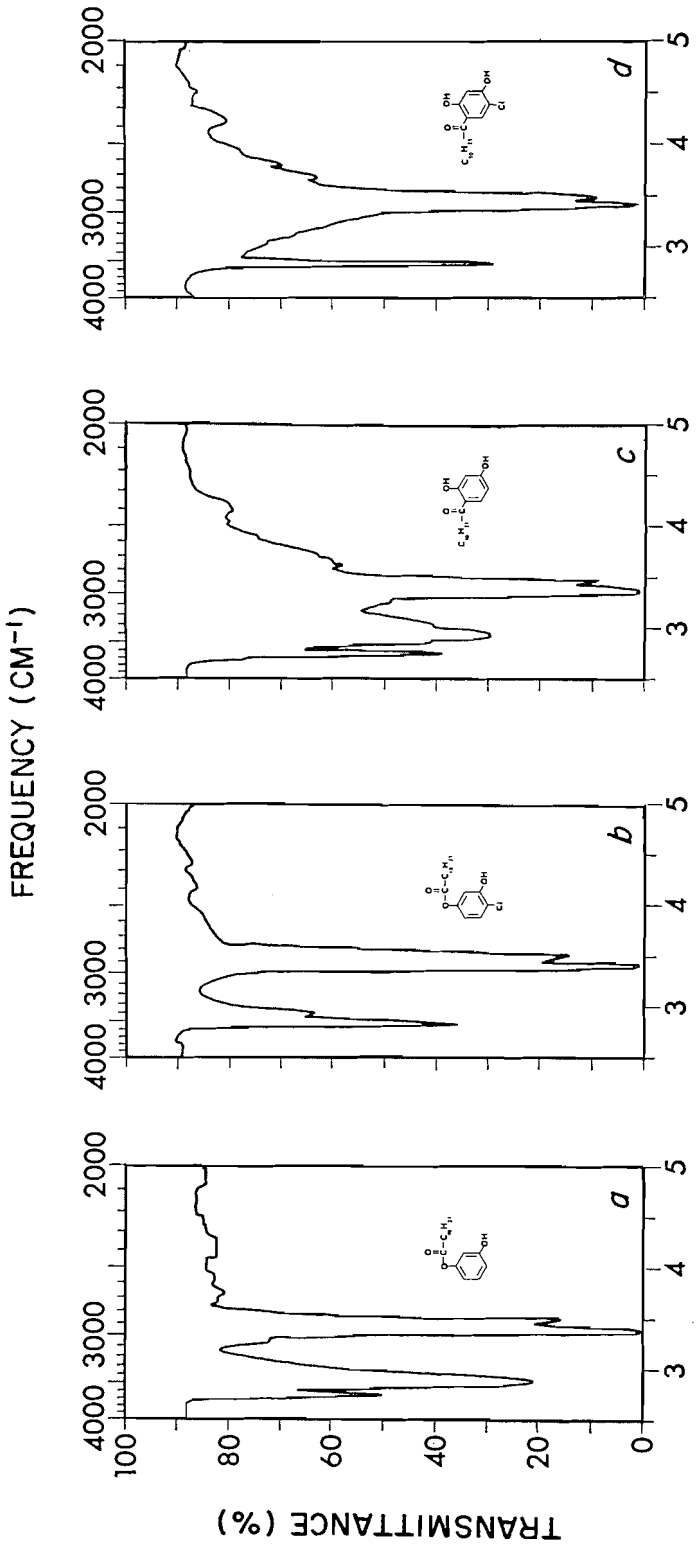

FIG. 1. Infrared spectra of 0.060 *M* solutions in carbon tetrachloride (1 mm path length): (*a*) resorcinol monoundecanoate (**6**), (*b*) 4-chlororesorcinol 1-undecanoate (**7**), (*c*) 4-undecanoylresorcinol (**10**), and (*d*) 4-chloro-6-undecanoylresorcinol (**11**).

Can. J. Chem. Downloaded from www.nrcresearchpress.com by 210.87.254.42 on 09/05/12
For personal use only.

near 2700 cm^{-1} (27). Indeed, *ortho*-hydroxyacetophenone exhibits broad, weak O—H absorption bands at 2900–3500 cm^{-1} (28).

Independently, overwhelming evidence points to the indicated structures for **8** and **9**. The mass-spectral analyses yield the calculated molecular weights of 446 and 480, respectively, and the isotope distributions about the molecular ions, and the fragmentation patterns, are in agreement for these structures. The elemental analyses coincide precisely with the theoretical values, and the ultraviolet (u.v.) and n.m.r. spectra are consistent with the respective configurations; in the n.m.r. spectra we actually observe a single phenolic proton adjacent to the carbonyl function (12.67 p.p.m.),[5] while in the u.v. spectra the absorption characteristics reflect the anticipated chromophore.

Experimental

Melting points are corrected; they were determined with a Büchi melting point apparatus. Ultraviolet (u.v.) and infrared (i.r.) spectra were obtained with the Perkin–Elmer model 202 and 137B spectrophotometers, respectively. Nuclear magnetic resonance (n.m.r.) spectra were obtained using a Varian A-60A spectrometer. Mass-spectral analyses were carried out by the Morgan–Schaffer Corporation of Montreal, Canada, employing a Hitachi Perkin–Elmer RMU-6D mass spectrometer. Combustion analyses were performed by Drs. G. Weiler and F. B. Strauss of Oxford, England.

*Hexachlorophene Diundecanoate (**1**)*

Employing the method of Migrdichian (12) (method *a*), undecanoyl chloride (60.6 g, 0.296 mole) was added dropwise to a warm solution of hexachlorophene (50.0 g, 0.123 mole) in 300 ml of pyridine. After stirring at room temperature (16 h), it was added slowly to 2.5 l of cold 6 *N* sulfuric acid. This mixture was extracted with benzene, and the benzene solution was dried over anhydrous magnesium sulfate. The oily product which remained, after removal of the solvent by distillation, was crystallized from isopropyl alcohol and recrystallized from ethanol, yielding 69 g (75.5%) of pure **1**, m.p. 49.5–50.6°, λ_{max} (cyclohexane), 210 and 321 mμ (shoulder); (ε 11 500 and 4030), ν_{max} (chloroform), 1783 cm^{-1} (ester C=O).

Anal. Calcd. for $C_{35}H_{46}Cl_6O_4$: C, 56.54; H, 6.24; Cl, 28.61. Found: C, 56.48; H, 6.29; Cl, 28.31.

*Hexachlorophene Monoundecanoate (**2**)*

This compound was prepared following the conditions described by Aelony (13) (method *b*). A reaction mixture consisting of 46.0 g (0.247 mole) of undecanoic acid, 100 g (0.246 mole) of hexachlorophene, 0.5 g of concentrated sulfuric acid, and 200 ml of xylene was refluxed (24 h) until the theoretical amount of water which resulted from esterification had been collected in a Dean–Stark trap (4.4 ml). The reaction mixture was washed with water (100 ml), dried over anhydrous magnesium sulfate, treated with Norit F.Q.P., and filtered through a bed of Celite. The solvent was removed by distillation under reduced pressure. The residual liquid product afforded 42.1 g (29.8%) of **2** following recrystallizations from hexane, aqueous ethanol, and ligroine, m.p. 87.6–88.4°, λ_{max} (ethanol), 209, 233 mμ (shoulder), 292 and 301 mμ (ε 65 000, 17 500, 3670, and 3630), ν_{max} (chloroform), 3530 (O—H stretching), and 1767 cm^{-1} (ester C=O).

Anal. Calcd. for $C_{24}H_{26}Cl_6O_3$: C, 50.11; H, 4.56; Cl, 36.98. Found: C, 50.02; H, 4.44; Cl, 37.10.

*o-Chlorophenyl Undecanoate (**3**)*

This compound was prepared by method *b* using undecanoic acid (46.5 g, 0.250 mole), *o*-chlorophenol (32.1 g, 0.250 mole), and 0.5 g of concentrated sulfuric acid. The xylene solution was washed with water, dried over anhydrous magnesium sulfate, and the solvent was removed by distillation under reduced pressure. The residual oily liquid was distilled through a 16 cm Vigreaux column, affording 43.9 g (59.2%) of **3**, b.p. 139–140° (0.12 mm), n_D^{25} 1.4876, λ_{max} (ethanol), 206 (shoulder), and 220 mμ (ε 8010 and 11 600), ν_{max} (chloroform), 1759 cm^{-1} (ester C=O).

Anal. Calcd. for $C_{17}H_{25}ClO_2$: C, 68.78; H, 8.49; Cl, 11.94. Found: C, 68.73; H, 8.51; Cl, 11.81.

*p-Chlorophenyl Undecanoate (**4**)*

This compound was prepared by method *b* using undecanoic acid (46.5 g, 0.250 mole), *p*-chlorophenol (32.1 g, 0.250 mole), and 0.5 g of concentrated sulfuric acid. The product was purified by distillation, b.p. 143–145° (0.13 mm), and solidified upon standing, yielding 43.2 g (58.2%) of **4**, m.p. 38.1–39.3°; λ_{max} (ethanol), 209 mμ (ε 25 100), ν_{max} (chloroform), 1765 cm^{-1}, (ester C=O).

Anal. Calcd. for $C_{17}H_{25}ClO_2$: C, 68.78; H, 8.49; Cl, 11.94. Found: C, 68.80; H, 8.70; Cl, 12.08.

*Resorcinol Diundecanoate (**5**) and Resorcinol Monoundecanoate (**6**)*

Employing method *a*, a mixture of 53.8 g (0.489 mole) of resorcinol in 200 ml of dry pyridine and 100 g (0.488 mole) of undecanoyl chloride yielded a solid when the reaction mixture was poured into cold 6 *N* sulfuric acid. The latter was dissolved in ether and extracted with cold 0.5 *N* NaOH. The ether phase was dried over anhydrous magnesium sulfate, and upon evaporation of the ether *in vacuo*, a solid residue was obtained. This material was recrystallized four times from 95% ethanol, affording 56.5 g (51.8%) of *resorcinol diundecanoate* (**5**), m.p. 41.3–42.0°; λ_{max} (ethanol), 204 mμ (ε 10 300), ν_{max} (chloroform), 1764 cm^{-1} (ester C=O).

Anal. Calcd. for $C_{28}H_{46}O_4$: C, 75.29; H, 10.38. Found: C, 75.30; H, 10.50.

The basic aqueous extracts were carefully acidified with cold 6 *N* sulfuric acid, and the oily liquid which separated was dissolved in ether and dried. Following evaporation of the solvent *in vacuo*, the product was recrystallized five times from hexane, yielding 14.7 g (10.8%) of

[5]The assignment of the 12.67 p.p.m. peaks to the phenolic protons of compounds **8** and **9** was further confirmed by the disappearance of these peaks in the spectra upon the addition of D_2O.

Can. J. Chem. Downloaded from www.nrcresearchpress.com by 210.87.254.42 on 09/05/12
For personal use only.

resorcinol monoundecanoate (**6**), m.p. 50.3–51.9°; λ_{max} (ethanol), 204, 220 (shoulder), and 273 mμ (ε 15 300, 8900, and 10 200), ν_{max} (chloroform), 3610, 3440 (O—H stretching), 1742 cm^{-1} (ester C=O).

Anal. Calcd. for $C_{17}H_{26}O_3$: C, 73.34; H, 9.41. Found: C, 72.99; H, 9.45.

4-Chlororesorcinol 1-Undecanoate (7), 4-Chloro-6-undecanoylresorcinol 3-Undecanoate (9), and 4-Chloro-6-undecanoylresorcinol (11)

Employing method *b*, a mixture of 46.6 g (0.250 mole) of undecanoic acid, 36.2 g (0.250 mole) of 4-chlororesorcinol, and 0.5 g of concentrated sulfuric acid, in 135 ml of xylene, was reacted to yield 88 g of crude product. When the latter was dissolved in hot ethanol, and water was added, 1.42 g (2.4%) of crude *4-chloro-6-undecanoylresorcinol 3-undecanoate* (**9**) was obtained. Recrystallization from ethanol yielded 0.72 g (1.2%) of pure **9**, m.p. 58.2–59.3°; λ_{max} (ethanol), 219, 256, and 333 mμ (ε 26 200, 9570, and 4670), ν_{max} (chloroform), 1764 (ester C=O), and 1639 cm^{-1} (ketone C=O).

Anal. Calcd. for $C_{28}H_{45}ClO_4$: C, 69.90; H, 9.43; Cl, 7.37. Found: C, 69.86; H, 9.53; Cl, 7.46.

The solvent from the aqueous ethanol solution which yielded **9** was removed by distillation under reduced pressure. Fractional crystallization of the residual oily product from hexane gave two fractions. The less soluble fraction (4.7 g, 6%), after recrystallization from hexane, yielded 3.6 g (4.6%) of pure *4-chloro-6-undecanoylresorcinol* (**11**), m.p. 98.0–98.5°; λ_{max} (ethanol), 214 (shoulder), 220, 234, 277, and 337 mμ (ε 18 100, 19 600, 10 700, 10 800, and 9620), ν_{max} (chloroform), 3500 (O—H stretching), and 1639 cm^{-1} (ketone C=O), negative Liebermann test.

Anal. Calcd. for $C_{17}H_{25}ClO_3$: C, 65.27; H, 8.06; Cl, 11.33. Found: C, 65.27; H, 7.92; Cl, 11.65.

Compound **11** afforded a *2,4-dinitrophenylhydrazone* derivative (**14**) under standard conditions (29). The derivative was recrystallized four times from 95% ethanol, m.p. 167.5–168.1°.

Anal. Calcd. for $C_{23}H_{29}ClN_4O_6$: C, 56.04; H, 5.93; Cl, 7.19; N, 11.37. Found: C, 56.17; H, 6.10; Cl, 7.06; N, 11.59.

The more soluble fraction (24.3 g, 31.1%), after recrystallization from hexane, yielded 17.5 g (22.4%) of pure *4-chlororesorcinol 1-undecanoate* (**7**), m.p. 50.8–52.6°; λ_{max} (ethanol), 207, 218 (shoulder), 279, and 338 mμ (ε 13 500, 9000, 3540, and 1270), ν_{max} (chloroform), 3500 (O—H stretching), 1757 cm^{-1} (ester C=O), positive Liebermann test.

Anal. Calcd. for $C_{17}H_{25}ClO_3$: C, 65.27; H, 8.06; Cl, 11.33. Found: C, 65.21; H, 8.18; Cl, 11.09.

Upon treatment of **7** with 3,5-dinitrobenzoyl chloride under standard conditions (20), the *3,5-dinitrobenzoate* derivative (**12**) was obtained. It was recrystallized five times from 95% ethanol, m.p. 87.4–88.7°; ν_{max} (chloroform), 1760 cm^{-1} (ester C=O).

Anal. Calcd. for $C_{24}H_{27}ClN_2O_8$: C, 56.86; H, 5.37; Cl, 6.99; N, 5.53. Found: C, 56.89; H, 5.37; Cl, 7.14; N, 5.35.

4-Undecanoylresorcinol 1-Undecanoate (8) and 4-Undecanoylresorcinol (10)

Employing method *b*, 50.0 g (0.268 mole) of undecanoic acid and 29.8 g (0.271 mole) of resorcinol yielded a crude product (76.2 g) which was dissolved in 95% ethanol. Upon cooling *4-undecanoylresorcinol 1-undecanoate* (**8**) separated (2.3 g, 3.8%). Recrystallization from 95% ethanol yielded 1.09 g (1.8%), m.p. 55.2–55.7°; λ_{max} (ethanol), 214, 258, and 322 mμ (ε 22 000, 13 300, and 5110), ν_{max} (chloroform), 1767 (ester C=O), 1642 cm^{-1} (ketone C=O).

Anal. Calcd. for $C_{28}H_{46}O_4$: C, 75.29; H, 10.38. Found: C, 75.20; H, 10.45.

Addition of water to the mother liquor yielded 22.7 g (30.4%) of *4-undecanoylresorcinol* (**10**). After recrystallization from ethanol, 13.0 g (17.4%) was obtained, m.p. 78.3–79.4°; λ_{max} (ethanol), 211, 230, 279, and 317 mμ (ε 16 600, 8480, 14 140, and 7800), ν_{max} (chloroform), 3546, 3230 (O—H stretching), 1634 cm^{-1} (ketone C=O).

Anal. Calcd. for $C_{17}H_{26}O_3$: C, 73.34; H, 9.41. Found: C, 73.39; H, 9.36.

Compound **10** afforded a *bis(3,5-dinitrobenzoate)* derivative (**13**) upon treatment with 3,5-dinitrobenzoyl chloride under standard conditions (20). The product was recrystallized six times from ethyl acetate, m.p. 94.8–96.5°; ν_{max} (chloroform), 1764 (ester C=O), and 1692 cm^{-1} (ketone C=O).

Anal. Calcd. for $C_{31}H_{30}N_4O_{13}$: C, 55.86; H, 4.54; N, 8.40. Found: C, 55.96; H, 4.79; N, 8.50.

Acknowledgments

This investigation was supported by the United States Army Medical Research and Development Command, Washington, D.C., through Research Contract No. DA-49-193-MD-2636. The authors wish to thank Mrs. R. M. Owens for the infrared and ultraviolet spectra and Mrs. P. P. Boggs for carrying out the preparative work in connection with compounds **8** and **10**. We are grateful to Dr. F. C. Chang and Mrs. M. M. Petrie for their assistance in acquiring the nuclear magnetic resonance spectra.

1. V. Dev, R. P. Quintana, and A. Lasslo. J. Med. Chem. **9**, 242 (1966).
2. R. P. Quintana, A. Lasslo, P. P. Boggs, and E. D. Yeaglin. J. Pharm. Sci. **57**, 230 (1968).
3. R. P. Quintana, A. Lasslo, and S. L. Ousley. J. Pharm. Sci. **56**, 1193 (1967).
4. R. P. Quintana, A. Lasslo, and P. P. Boggs. J. Colloid Interface Sci. **26**, 166 (1968).
5. (*a*) W. V. King. (*Compiler*). Chemicals evaluated as insecticides and repellents at Orlando, Florida. Agriculture Handbook No. 69. Entomology Research Branch, Agricultural Research Service, United States Department of Agriculture, Washington, D.C., 1954. p. 185; (*b*) p. 305.
6. W. J. Fahlberg, J. C. Swan, and C. V. Seastone. J. Bacteriol. **56**, 323 (1948).
7. I. Shemano and N. Nickerson. Federation Proc. **13**, 404 (1954).
8. G. M. Compeau. J. Pharm. Sci. **49**, 574 (1960).
9. R. B. Stoughton. Arch. Dermatol. **94**, 646 (1966).
10. M. Manowitz and V. D. Johnston. J. Soc. Cosmetic Chemists, **18**, 527 (1967).

11. H. R. CHIPALKATTI, C. H. GILES, and D. G. M. VALLANCE. J. Chem. Soc. 4375 (1954).
12. V. MIGRDICHIAN. Organic synthesis. Vol. 1. Reinhold Publishing Corp., New York. 1957. p. 321.
13. D. AELONY. J. Am. Oil Chemists' Soc. **32**, 170 (1955).
14. B. L. VAN DUUREN, M. CONKLIN, G. C. LAVERS, and A. SEGAL. J. Chem. Soc. C7, 588 (1967).
15. (*a*) G. A. OLAH. Friedel–Crafts and related reactions. Vol. 3, Part 1. Interscience Publishers, Inc., New York. 1964. p. 11; (*b*) p. 34; (*c*) pp. 174–177.
16. H. R. SNYDER and C. T. ELSTON. J. Am. Chem. Soc. **77**, 364 (1955).
17. J. SMITH and R. H. THOMSON. J. Chem. Soc. 346 (1960).
18. C. M. HUGGINS, G. C. PIMENTEL, and J. N. SHOOLERY. J. Phys. Chem. **60**, 1311 (1956).
19. E. A. ALLAN and L. W. REEVES. J. Phys. Chem. **66**, 613 (1962).
20. N. D. CHERONIS and J. B. ENTRIKIN. Semimicro qualitative organic analysis. 2nd ed. Interscience Publishers, Inc., New York. 1947. pp. 513–514.
21. F. FEIGL, V. ANGER, and R. E. OESPER. Spot tests in chemical analyses. 7th ed. Elsevier Publishing Co. New York. 1966. p. 179.
22. NG. PH. BUU-HOÏ and J. SEAILLES, JR. J. Org. Chem. **20**, 606 (1955).
23. (*a*) L. J. BELLAMY. The infrared spectra of complex molecules. 2nd ed. John Wiley and Sons, Inc., New York. 1958. pp. 95–113; (*b*) p. 96; (*c*) pp. 103–106.
24. K. NAKANISHI. Infra-red absorption spectroscopy. Holden–Day, Inc., San Francisco. 1962. p. 30.
25. I. BROWN, G. EGLINGTON, and M. MARTIN-SMITH. Spectrochim. Acta, **18**, 1593 (1962); cf. I. BROWN, G. EGLINGTON, and M. MARTIN-SMITH. Spectrochim. Acta, **19**, 463 (1963).
26. K. V. INGOLD and D. R. TAYLOR. Can. J. Chem. **39**, 471 (1961).
27. R. S. RASMUSSEN, D. D. TUNNICLIFF, and R. R. BRATTAIN. J. Am. Chem. Soc. **71**, 1068 (1949).
28. A. E. MARTIN. Nature, **166**, 474 (1950).
29. S. M. MCELVAIN. The characterization of organic compounds. 2nd ed. The Macmillan Co., New York. 1953. p. 132.

Can. J. Chem. Downloaded from www.nrcresearchpress.com by 210.87.254.42 on 09/05/12
For personal use only.

Can. J. Chem. Downloaded from www.nrcresearchpress.com by 210.87.254.5 on 09/05/12
For personal use only.

Transannular reactions in the dibenzo[*a,d*]cycloheptene series. II. Preparation of 10,11-dihydro-10,5-(epoxymethano)-5*H*-dibenzo[*a,d*]cyclohepten-13-one and derivatives

T. A. Dobson, M. A. Davis, A.-M. Hartung, and J. M. Manson
Ayerst Research Laboratories, Montreal, Quebec

Received September 7, 1967

The reaction of electrophilic reagents with the 5-substituted 5*H*-dibenzo[*a,d*]cycloheptene derivatives (**13***a–e*) and with their 10,11-dihydro analogues (**19***a–b*) occurs with transannular participation of the 5-substituent to yield derivatives of 10,11-dihydro-10,5-(epoxymethano)-5*H*-dibenzo[*a,d*]cycloheptene. The epimeric 10,11-dihydro-10-hydroxy-5*H*-dibenzo[*a,d*]cycloheptene-5-carboxamides (**22**, **23**) are described. The *syn*-hydroxy isomer **22** is readily transformed to the lactone **16***c* under neutral conditions whereas the *anti* isomer **23** requires acid catalysis for this conversion. Treatment of *anti*-11-bromo-10,11-dihydro-10,5-(epoxymethano)-5*H*-dibenzo[*a,d*]cyclohepten-13-one (**16***b*) with ammonia or primary aliphatic amines gives the epoxyamides **21***a–d* which can react with secondary aliphatic amines to give the *anti*-11-dialkylamino-10,11-dihydro-10,5-(epoxymethano)-5*H*-dibenzo[*a,d*]cyclohepten-13-ones (**25***a–d*). The epimeric *syn*-11-dialkylamino compounds **24***a–e* are obtained from the interaction of **16***b* with secondary aliphatic amines. The nuclear magnetic resonance spectra of the products are tabulated.

Canadian Journal of Chemistry, 46, 2843 (1968)

The dibenzo[*a,d*]cycloheptene ring system serves as a convenient template for the study of transannular reactions. Thus, 5-hydroxy-5*H*-dibenzo[*a,d*]cycloheptene-10,11-dione (1) exists, in part, as the hemiketal **2** and derivatives of both forms have been prepared (1). Similar behavior is exhibited by both *cis*- and *trans*-10,11-dihydroxy-10,11-dihydro-5*H*-dibenzo-[*a,d*]cyclohepten-5-ones which, in alkaline media, exist and react as the hemiketals **3***a* and **3***b* respectively (2). These early observations have recently found practical utility in the preparation of a number of pharmacologically active dibenzo[*a,d*]cycloheptene derivatives, **4** (3). A number of more complex examples have been reported. Thus, treatment of the acid chloride **5** with 1-methylpiperazine gave, as a minor by-product, the chloroketone **6** (4). The diazoketone **7** has been converted into 2,3:7,8-dibenzotricyclo[3·3·1·$0^{4,6}$]nona-2,7-dien-9-one, **8**, furnishing an example of transannular attack by an α-ketocarbene intermediate (5). Base-promoted cyclization of **9***a* and **9***b* gave **10***a* and **10***b* respectively (6). Treating the bromoacid **11** with silver nitrate caused concommitant skeletal rearrangement and formation of the lactone **12** (7). Transannular reactions in related tricyclic systems, in some cases leading to scission of the central ring, have been reported to occur with derivatives of dibenzo[*a,e*]cyclooctane (8*a*), dibenzo[*b,e*]thiocin (8*b*), and dibenz[*b,f*]azepin (8*c*). It has recently been observed that 10,11-dihydro-5*H*-dibenzo[*a,d*]cycloheptene-5-carboxamide is metabolized in animals and man to 10-hydroxy and 10,11-dihydroxy analogues which are readily transformed to derivatives of 10,11-dihydro-10,5-(epoxymethano)-5*H*-dibenzo[*a,d*]-cyclohepten-13-one (9). This observation prompted us to investigate further the transannular reactions of 5-substituted dibenzo[*a,d*]cycloheptene derivatives.

Hydroxylation of 5*H*-dibenzo[*a,d*]cycloheptene-5-carboxamide (**13***a*) with silver acetate and iodine according to the method of Woodward and Brutcher (10*a*) gave *syn*-11-acetoxy-10,11-dihydro-10,5-(epoxymethano)-5*H*-dibenzo[*a,d*]-cyclohepten-13-one (**14***a*) (for numbering, see Fig. 1). Saponification of this compound gave the *syn*-hydroxylactone **14***b* which was reconverted to **14***a* with pyridine and acetic anhydride. The *syn* orientation of the 11-substituent in **14***a*, and therefore in **14***b*, was assigned from its mode of introduction which has repeatedly been shown to result in *cis* hydroxylation (10). The *syn*-hydroxylactone **14***b* was oxidized with chromium trioxide – sulfuric acid to the ketolactone **14***c* which regenerated **14***b* upon catalytic hydrogenation.

A minor by-product from the silver acetate – iodine oxidation of **13***a* was 10,11-diacetoxy-10,11-dihydro-5*H*-dibenzo[*a,d*]cycloheptene-5-carboxamide (**15**) of uncertain geometry. Traces of anthracene derivatives were also formed but these could not be fully characterized.

Can. J. Chem. Downloaded from www.nrcresearchpress.com by 210.87.254.5 on 09/05/12
For personal use only.

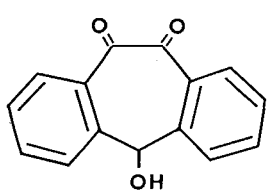

1

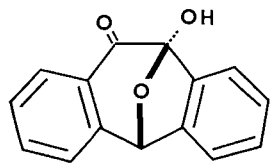

2

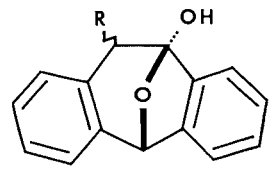

3*a*, R=cis-OH
b, R=trans-OH

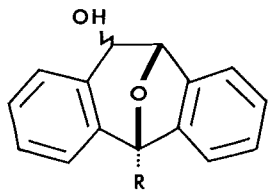

4, R=dialkylaminopropyl

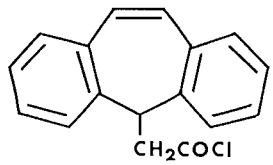

5

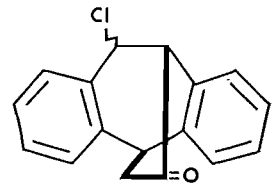

6

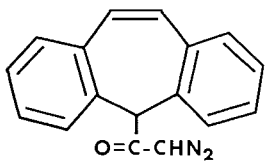

7

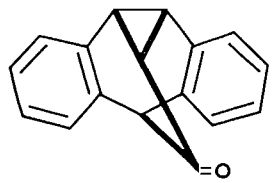

8

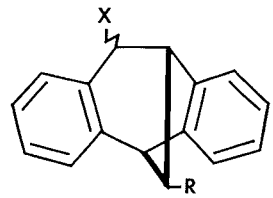

9*a*, R=anti-SO_2Ph, X=endo-Cl
b, R=anti-CO_2CH_3, X=exo-Cl

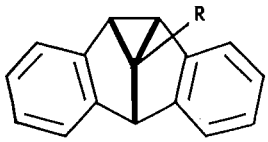

10*a*, R=SO_2Ph
b, R=CO_2H

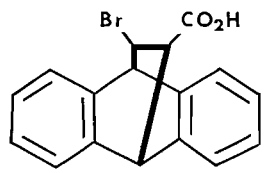

11

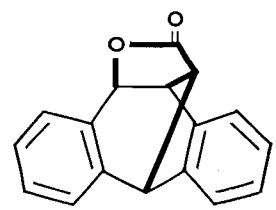

12

Attempted *trans*-hydroxylation of the same amide **13*a*** with silver acetate and iodine under the anhydrous conditions of the Prévost reaction (10*c*,11) gave only trace amounts of lactonic products. Successful *trans* hydroxylation of **13*a*** was achieved with 3-chloroperbenzoic acid to give the *anti*-11-hydroxylactone **16*a***. This compound was oxidized with chromium trioxide – sulfuric acid to the ketolactone **14*c*** thereby demonstrating the epimeric relationship of **14*b*** and **16*a***.

A number of reaction pathways are possible for the genesis of the *syn*-acetoxylactone **14*a*** as shown on p. 2847. The route **13*a*** → **A** → **B** → **14*a*** is the normal pathway of the Woodward hydroxylation reaction (10) followed by an 'OH-6' (12) anchimerically-assisted hydrolysis of the amide group. The hydroxyl-assisted hydrolysis of amides is well known (13) and inspection of a Drieding molecular model of **B** shows the hydroxyl and amide functions to be in close proximity. The alternative pathway

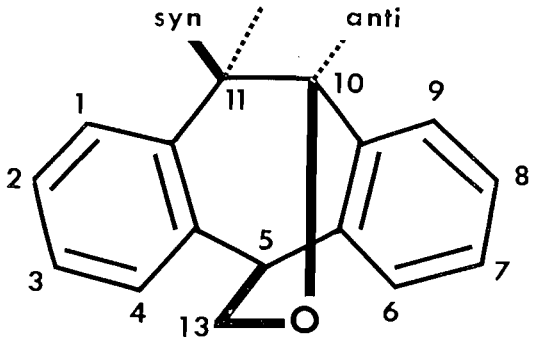

FIG. 1. The 10,11-dihydro-10,5-(epoxymethano)-5*H*-dibenzo[*a*,*d*]cycloheptene ring system.

13*a* → **A** → **C** → **14***a* is followed in the conversion of halogen-containing amides to lactones (14).

The *anti*-11-hydroxylactone **16***a* is probably derived from the transient *anti*-10,11-epoxide **D**[1] *via* the iminolactone intermediate **E** as shown on p. 2847. An alternate pathway, involving *trans*-hydration of **D** and subsequent 'OH-6' cyclization of the resulting glycol was rendered unlikely by the observation that the *syn*-10,11-epoxyamide **21***b* (see later) was unaffected by a mixture of 3-chloroperbenzoic and 3-chlorobenzoic acids in chloroform.

Addition of bromine to a solution of the amide **13***a* in chloroform gave rapidly, and in almost quantitative yield, the *anti*-11-bromo-iminolactone hydrobromide **17**. The structure of this compound is supported by its nuclear magnetic resonance (n.m.r.) spectrum which is consistent with a *trans* arrangement of the protons at C-10 and C-11, and by its very ready hydrolysis to the *anti*-11-bromolactone **16***b*. The same bromolactone was also obtained, in poor yield, from the interaction of the *syn*-11-hydroxylactone **14***b* and phosphorus tribromide and pyridine, and from displacement of the tosyl derivative of **14***b* with calcium bromide.

The geometry of **17** indicates that its formation from the amide **13***a* must involve the carboxamide function in either a concerted addition process or in an intramolecular displacement (17,18) of a bromonium ion. The intermediacy of a *trans*-10,11-dibromide would, obviously, lead to an isomeric *syn*-11-bromo-iminolactone hydrobromide.

[1]In contrast, epoxidation of 5*H*-dibenzo[*a*,*d*]cyclohepten-5-ol has been reported to give the corresponding *syn*-epoxide (15). Allylic hydroxyl groups are, however, known to promote the formation of *cis*-epoxyalcohols (16).

The propensity for transannular reaction was not confined to the amide **13***a*. Thus, addition of bromine to the diethylamide **13***d* and subsequent hydrolysis of the crude product gave the bromolactone **16***b*. Treatment of both the unsaturated acid **13***b* and its methyl ester **13***c* with bromine also gave the bromolactone. The participation of carboxyl and carboalkoxy groups in halogen and pseudohalogen additions is well known (18,19).

Addition of bromine to the unsaturated alcohol **13***e* involved participation of the hydroxyl function since the *anti*-11-bromoether **18** was produced. Bromine addition to α,α-dimethylallyl alcohol is known to proceed in a similar fashion (20).

Transannular reactions also occurred when 10,11-dihydro-5*H*-dibenzo[*a*,*d*]cycloheptene derivatives were used as substrates. Thus, irradiation and subsequent hydrolysis of a solution of the amide **19***a* and bromine in chloroform gave the unsubstituted lactone **16***c*. Treatment of the 5-hydroxyester **19***b* with either bromine or *N*-bromosuccinimide gave the 5-hydroxylactone **20**.

The *anti*-11-bromolactone **16***b* contains a potential bromohydrin system and, with this feature in view, its reactions with basic reagents were investigated. Treatment of **16***b* with aqueous sodium hydroxide solution gave the epoxyacid **21***a* whereas treatment of **16***b* with either liquid ammonia or warm ammonium hydroxide gave the *syn*-10,11-epoxyamide **21***b*. The analogous amides **21***c* and **21***d* respectively were obtained when methylamine and *t*-butylamine were employed in place of ammonia. These products undoubtedly arose by a common mechanism involving attack at the carbonyl group of **16***b* by the basic reagent, and their formation supports the geometry assigned to this compound. Both **21***a* and **21***b* reacted rapidly with hydrogen bromide to give **16***b* and with hydrogen chloride to give the *anti*-11-chlorolactone **16***d*. The *anti*-11-methoxylactone **16***e* was prepared by the acid-catalyzed reaction of methanol with both **21***a* and **21***b*.

Hydration of the epoxyamide **21***b* with dilute sulfuric acid in either dioxane or dimethyl sulfoxide gave an approximately equimolar mixture of the epimeric hydroxylactones **14***b* and **16***a*. The non-stereospecificity of the hydration performed in dimethyl sulfoxide is in contrast to the acid-catalyzed stereospecific

Can. J. Chem. Downloaded from www.nrcresearchpress.com by 210.87.254.5 on 09/05/12
For personal use only.

Can. J. Chem. Downloaded from www.nrcresearchpress.com by 210.87.254.5 on 09/05/12
For personal use only.

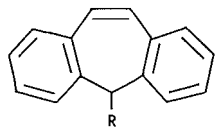

13*a*, R=$CONH_2$ *d*, R=$CON(C_2H_5)_2$
b, R=CO_2H *e*, R=CH_2OH
c, R=CO_2CH_3

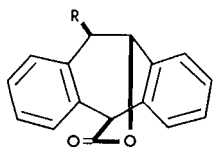

14*a*, R=OAc
b, R=OH
c, R=(=O)

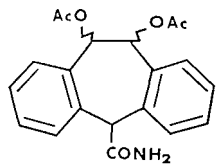

15

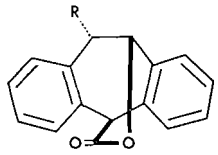

16*a*, R=OH *d*, R=Cl
b, R=Br *e*, R=OCH_3
c, R=H *f*, R=OAc

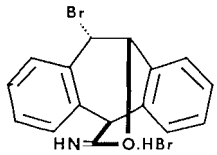

17

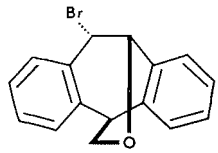

18

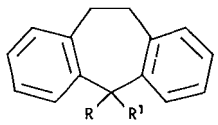

19*a*, R=H, R^1=$CONH_2$
b, R=OH, R^1=CO_2CH_3

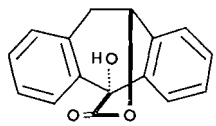

20

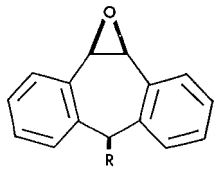

21*a*, R=CO_2H *c*, $CONHCH_3$
b, R=$CONH_2$ *d*, $CONHBu^t$

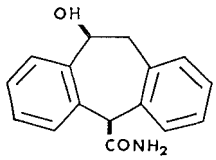

22

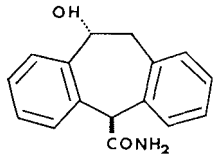

23

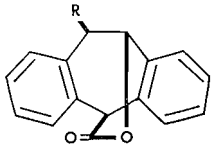

24*a*, R=dimethylamino
b, R=morpholino
c, R=piperidino
d, R=N-methylpiperazino
e, R=N-phenylpiperazino
f, R=anilino

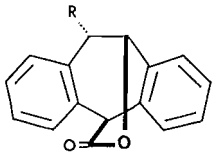

25*a*, R=morpholino
b, R=piperidino
c, R=N-methylpiperazino
d, R=N-phenylpiperazino
e, R=anilino

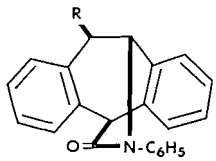

26*a*, R=OH
b, R=(=O)

hydration of both *cis* and *trans* stilbene oxides in this solvent (21). A similar hydration of the epoxyacid gave the *anti*-hydroxylactone as the predominant product.

Hydrogenation of the epoxyamide **21***b* gave the unstable *syn*-11-hydroxyamide **22**. This compound readily evolved ammonia in both the solid state and in solution to give the unsubstituted lactone **16***c* undoubtedly *via* an intramolecular attack of the hydroxyl group upon the amide function (13). It is noteworthy that the unsubstituted amide **19***a* is relatively resistant to

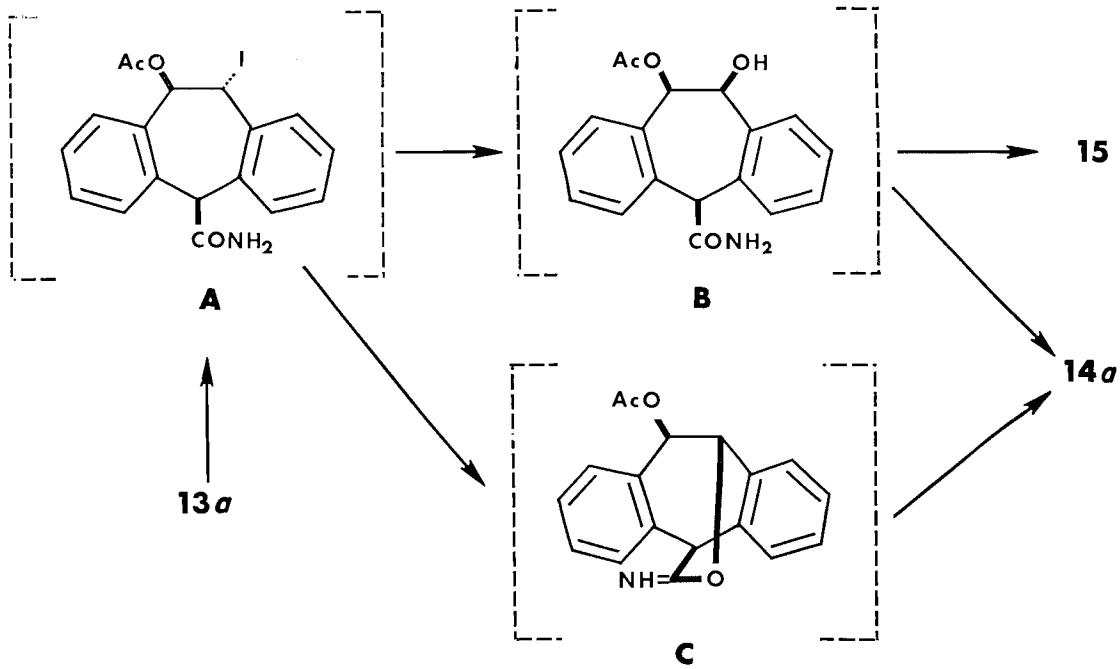

hydrolysis (22). The epimeric *anti*-11-hydroxyamide **23** was prepared in poor yield by hydroboration of the unsaturated amide **13***a*. In contrast to **22**, the *anti*-hydroxy epimer **23** was stable up to a temperature of 140°. Treatment of **23** with dilute mineral acid gave, however, the unsubstituted lactone **16***c* accompanied by a small amount of the unsaturated acid **13***b*. This cyclization may proceed *via* epimerization at either C-5 or C-10 to give **22** or it could proceed *via* a transient iminolactone.

In contrast to the behavior of the *anti*-11-bromolactone **16***b* with primary aliphatic amines, the reactions of the same substrate with secondary aliphatic amines did *not* involve the lactone ring. The products obtained were the *syn*-11-dialkylaminolactones **24**. The geometry of these products, which was inferred from their n.m.r. spectra (see Table I), is that expected to arise from direct displacement of the bromine atom of **16***b* by the secondary amine. To confirm further the structure of **24***a–e* the epoxyacid **21***a* and the *syn*-epoxyamide **21***b* were treated with several secondary amines. No reaction occurred at room temperature, even in the presence of mineral acid (23), but at elevated temperatures, the *anti*-11-dialkylaminolactones **25***a–d* were formed, as evidenced by the n.m.r. spectra of the products (see Table I).

Aniline, in its reaction with the bromolactone **16***b*, behaved as a secondary amine rather than as a primary amine since the product was the *syn*-11-anilinolactone **24***f*. The structure of this compound was demonstrated by its ready acid-catalyzed rearrangement to the *syn*-11-hydroxylactam **26***a* which is only possible with a *syn*-arrangement of anilino and lactone groups. Oxidation of **26***a* with chromium trioxide–sulfuric acid furnished the ketone **26***b* which regenerated only the parent hydroxy compound

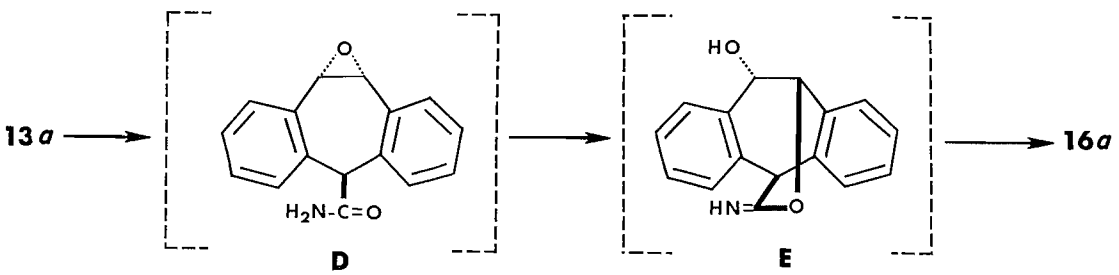

Can. J. Chem. Downloaded from www.nrcresearchpress.com by 210.87.254.5 on 09/05/12
For personal use only.

Can. J. Chem. Downloaded from www.nrcresearchpress.com by 210.87.254.5 on 09/05/12
For personal use only.

TABLE I

Proton assignments in the 11-substituted-10,11-dihydro-10,5-(epoxymethano)-5*H*-dibenzo[*a*,*d*]cyclohepten-13-one system

11-Substituent	No.	Chemical shift*, τ					$J_{10,11}$ c.p.s.
		syn-11-H	*anti*-11-H	10-H	5-H	Other	
syn-11-Acetoxy	**14***a*		4.00	4.18	5.03	7.92 (Acetate)	2.6
syn-11-Hydroxy†	**14***b*		5.21	4.30	5.11		2.5
11-Keto	**14***c*			4.16	5.07		
anti-11-Hydroxy†	**16***a*	4.54		5.01	5.40		5.0
anti-11-Bromo	**16***b*	4.37		4.23	5.37		5.2
11-Hydrogen	**16***c*	6.26	6.78	4.36	5.31		4.1, 2.6
anti-11-Chloro	**16***d*	4.36		4.36	5.32		?
anti-11-Methoxy	**16***e*	5.28		4.33	5.42	6.31 (Methyl)	4.9
anti-11-Acetoxy	**16***f*	3.63		4.37	5.37	7.89 (Acetate)	5.1
5-Hydroxy	**20**	6.24	6.80	4.28		5.76 (Hydroxy)	4.5, 2.5
syn-11-Dimethylamino	**24***a*		6.02	4.13	5.36	7.18 (Methyl)	1.8
syn-11-Morpholino	**24***b*		6.00	4.10	5.35	6.30, 7.17 (Methylene)	1.8
syn-11-Piperidino	**24***c*		6.03	4.11	5.37	7.21, 8.47 (Methylene)	1.8
syn-11-(*N'*-Methylpiperazino)	**24***d*		6.08	4.22	5.45	7.80 (Methylene and methyl)	1.8
syn-11-(*N'*-Phenylpiperazino)	**24***e*		5.92	4.11	5.35	6.90 (Methylene)	1.8
syn-11-Anilino	**24***f*		5.02	4.23	5.27	6.18 (NH)	2.0
anti-11-Morpholino	**25***a*	5.50		4.33	5.37	6.44, 7.58 (Methylene)	5.0
anti-11-Piperidino	**25***b*	5.58		4.40	5.43	7.65, 8.67 (Methylene)	4.9
anti-11-(*N'*-Methylpiperazino)	**25***c*	5.47		4.37	5.39	7.76 (Methylene and methyl)	5.0
anti-11-(*N'*-Phenylpiperazino)	**25***d*	5.42		4.34	5.37	6.87 (Methylene)	5.0
anti-11-Anilino	**25***e*	4.73		4.39	5.38	6.60 (NH)	4.8

*Spectra were determined using a Varian A-60A instrument. All spectra were obtained in deuteriochloroform solution unless otherwise noted. All compounds showed aromatic absorption at 2.5–3.0.
†Spectrum determined in dimethyl sulfoxide solution.

Can. J. Chem. Downloaded from www.nrcresearchpress.com by 210.87.254.5 on 09/05/12
For personal use only.

26*a* upon catalytic hydrogenation. The *anti*-11-anilinolactone **25***e*, isomeric with **24***f* and obtained by the interaction of the *syn*-epoxyamide **21***b* and aniline, was not rearranged by treatment with either aqueous acid or alkali.

Empirical confirmation of the geometry of many of the compounds described herein has been obtained from their n.m.r. spectra (Table I). Compounds assigned the *syn*-configuration show $J_{10,11}$ 1.8–2.6 c.p.s. whereas the compounds assigned the *anti*-configuration show $J_{10,11}$ 4.1–5.2 c.p.s. These coupling constants are similar to those reported for dibenzobicyclo[3·2·1]octadienes (24).

Experimental

*syn-11-Acetoxy-10,11-dihydro-10,5-(epoxymethano)-5H-dibenzo[a,d]cyclohepten-13-one (**14***a*)

To a well-stirred solution of the amide **13***a* (22) (50.0 g, 0.2 mole) in acetic acid (1 l) was added silver acetate (82.0 g, 0.05 mole) and then iodine (56.0 g, 0.22 mole) which was added portionwise, and then water (10 ml). The mixture was heated on the steam bath for 3 h and then solid sodium chloride was added. The mixture was cooled, filtered, and the filtrate was evaporated to dryness *in vacuo*. The residue was triturated with water and the solids were then dissolved in chloroform. This solution was washed with water, dried, and evaporated and the residue was crystallized from ethanol to give the product (30.2 g), m.p. 145–146°; ν_{max}($CHCl_3$) 1757 (lactone) and 1740 cm^{-1} (acetate).

Anal. Calcd. for $C_{18}H_{14}O_4$: C, 73.46; H, 4.80. Found: C, 73.65; H, 4.87.

From a sparingly soluble fraction of the above crude product there was obtained 1.6 g of 10,11-diacetoxy-10,11-dihydro-5*H*-dibenzo[*a*,*d*]cycloheptene-5-carboxamide (**15**), m.p. 229–230° (from ethanol or chloroform); ν_{max}(Nujol) 1770, 1750 (acetate), 1692, 1665, and 1635 cm^{-1} (amide); ν_{max}($CHCl_3$) 3480, 3370 (NH), 1760 (ester), and 1675 cm^{-1} (amide).

Anal. Calcd. for $C_{20}H_{19}NO_5$: C, 67.98; H, 5.43; N, 3.96. Found: C, 67.85; H, 5.55; N, 4.08.

Chromatography of the above crude product on silica gel gave an anthracene derivative, λ_{max}(EtOH) 263, 354, 378mμ (ε 165 700, 4670, 11 550), which gave inconsistent analytical data.

*syn-11-Hydroxy-10,11-dihydro-10,5-(epoxymethano)-5H-dibenzo[a,d]cyclohepten-13-one (**14b**)*

A solution of **14***a* (30.2 g) in methanol (600 ml) and water (300 ml) was treated with 50% sodium hydroxide solution (30 ml) and kept overnight. The methanol was removed *in vacuo*, water (200 ml) was added, and the filtered solution was acidified. The product (23.8 g), m.p. 156–157° tenaciously retained solvent of crystallization when recrystallized from ethanol or ethyl acetate – hexane. Purification was effected by dissolution in aqueous alkali or ammonium hydroxide followed by partial evaporation and acidification to give material of the above m.p. ν_{max}(Nujol) 3440 (OH) and 1725 cm^{-1} (lactone).

Anal. Calcd. for $C_{16}H_{12}O_3$: C, 75.18; H, 4.80. Found: C, 76.00; H, 4.93.

Acetylation of the hydroxylactone by acetic anhydride and pyridine gave **14***a*, m.p. 143–144°.

The *syn*-11-*p*-toluenesulfonyl derivative was prepared from **14***b* and *p*-toluenesulfonyl chloride in pyridine at 25°; m.p. 139–140° (decomp.).

Anal. Calcd. for $C_{23}H_{18}O_5S$: C, 67.97; H, 4.46; S, 7.88. Found: C, 68.06; H, 4.54; S, 7.90.

*10,5-(Epoxymethano)-5H-dibenzo[a,d]cycloheptene-11,13-(10H)-dione (**14c**)*

Jones' reagent (25) (74 ml) was added dropwise and with stirring to an ice-cold solution of a mixture of the *syn*- and *anti*-hydroxylactones **14***b* and **16***a* (61.0 g, 0.24 mole) in acetone (900 ml). The brown suspension so obtained was filtered and the filtrate was chilled, diluted with water (900 ml), and the precipitated product was recrystallized from aqueous acetone to give 48.5 g (79%), m.p. 166–167°; ν_{max}($CHCl_3$) 1758 (lactone) and 1685 cm^{-1} (ketone); λ_{max}(EtOH) 262mμ (ε 8550).

Anal. Calcd. for $C_{16}H_{10}O_3$: C, 76.79; H, 4.03. Found: C, 76.91; H, 4.09.

Hydrogenation of the ketolactone (250 mg) in dioxane (15 ml) with 10% palladium on charcoal at 25° and 1 atm gave chiefly the *syn*-hydroxylactone **14***b*, m.p. 155–156° and a little of the unsubstituted lactone **16***c*, m.p. 168–170° (from ethanol). The latter product predominated when the reduction was carried out in methanol at 50°.

*anti-11-Hydroxy-10,11-dihydro-10,5-(epoxymethano)-5H-dibenzo[a,d]cyclohepten-13-one (**16a**)*

Method (a)

A solution of the epoxyamide **21***b* (47.7 g) in dioxane (500 ml) and 1*N* H_2SO_4 (650 ml) was kept at room temperature for 2 h. The bulk of the dioxane was removed *in vacuo* and the residue was extracted with dichloromethane. This solution was extracted with water, then dried and evaporated. Crystallization of the residual oil from ethyl acetate – hexane gave a mixture (38.0 g) of the *syn* and *anti* hydroxylactones, m.p. 130–172°. Recrystallization afforded the pure *anti* isomer **16***a* (13.1 g), m.p. 187–188°; ν_{max}(Nujol) 3420 (OH), 1730 cm^{-1} (lactone).

Anal. Calcd. for $C_{16}H_{12}O_3$: C, 76.18; H, 4.80. Found: C, 76.13; H, 4.71.

The *syn* isomer **14***b* was obtained in solvated form from the above mother liquors by recrystallization from ethanol; desolvation as described above gave 8.0 g, m.p. 155–156°.

The *anti*-11-acetyl derivative **16***f*, prepared from **16***a* and acetic anhydride – pyridine, had m.p. 201–202° (from ethanol).

Anal. Calcd. for $C_{18}H_{14}O_4$: C, 73.46; H, 4.08. Found: C, 73.57; H, 5.01.

The *anti*-11-*p*-toluenesulfonyl derivative had m.p. 140–141° (decomp.).

Anal. Calcd. for $C_{23}H_{18}O_5S$: C, 67.97; H, 4.46; S, 7.88. Found: C, 68.25; H, 4.65; S, 7.81.

Method (b)

A solution of the epoxyacid **21***a* (5.6 g) in dioxane (175 ml) and 1*N* sulfuric acid (80 ml) was kept overnight at room temperature. It was processed as described above except that the crude product was extracted with dilute sodium bicarbonate solution. Recrystallization from

Can. J. Chem. Downloaded from www.nrcresearchpress.com by 210.87.254.5 on 09/05/12
For personal use only.

ethanol–hexane afforded 2.4 g of the *anti*-hydroxylactone, m.p. 188–189°; no significant amounts of the *syn* isomer were observed.

Method (c)

A solution of the amide **13***a* (10.0 g, 0.04 mole) and 85% 3-chloroperbenzoic acid (8.8 g, 0.04 mole) in dichloromethane (550 ml) was kept at room temperature until no more of the amide was consumed (14 days). A 100 ml aliquot was extracted with sodium bisulfite solution followed by sodium bicarbonate and then water. Evaporation of the solvent and recrystallization from dichloromethane–hexane gave unchanged amide, m.p. 208–210° (1.5 g). Chromatography of the mother liquors on silica gel from 75% chloroform–benzene afforded crude **16***a* as an oil (177 mg); recrystallization from ethyl acetate – pentane gave a sample m.p. 187–189°.

Treatment of another 100 ml aliquot with an additional 1.8 g of the peracid caused consumption of the remaining amide but gave no increase in yield of the hydroxylactone.

*anti-11-Bromo-10,11-dihydro-10,5-(epoxymethano)-5H-dibenzo[a,d]cyclohepten-13-imine Hydrobromide (**17**)*

A solution of bromine (16.0 g, 0.1 mole) in chloroform (50 ml) was added dropwise during 20 min to a stirred suspension of the amide **13***a* (23.5 g, 0.1 mole) in chloroform (50 ml). A red solution was obtained which soon deposited the product as pale-yellow crystals (36.0 g), m.p. 215–220° (decomp.); ν_{max}(Nujol) 1675 (C=N) and 1105 cm^{-1} (ether).

Anal. Calcd. for $C_{16}H_{13}BrNO$: Br, 40.46. Found: Br, 42.73.

The n.m.r. spectrum of this compound in dimethyl sulfoxide showed an eight-proton multiplet at 2.6 (aromatic), two one-proton doublets at 3.88 and 4.13 respectively (Ar—C(Br)(H)—C(H)(O)—Ar, $J_{10,11}$ 5.0 c.p.s.), a one-proton singlet at 5.04 (Ar—C(=)—Ar), and a broad two-proton singlet at 6.08 (O—C=NH·HBr).

*anti-11-Bromo-10,11-dihydro-10,5-(epoxymethano)-5H-dibenzo[a,d]cyclohepten-13-one (**16***b*)*

Method (a)

A mixture of **17** (300 g) and ethanol (1 l) containing water (50 ml) was heated on a steam bath for 6 h. The solvent was removed *in vacuo* and the residue was thoroughly washed with hot water. The residue was crystallized from ethanol to give the product (210 g), m.p. 160–161°; $\nu_{max}(CHCl_3)$ 1765 cm^{-1} (lactone).

Anal. Calcd. for $C_{16}H_{11}BrO_2$: C, 60.96; H, 3.72; Br, 25.35. Found: C, 60.85; H, 3.96; Br, 25.43.

Method (b)

A solution of bromine (160 mg) in chloroform (3.0 ml) was added to a stirred suspension of 5*H*-dibenzo[*a,d*]-cycloheptene-5-carboxylic acid (**13***b*) (23) (236 mg) in chloroform (10 ml). The mixture was kept at room temperature for 2 h and then evaporated to dryness. The residue was crystallized from ethanol to give **16***b* (220 mg) identified by m.p. and mixture m.p.

Method (c)

The acid **13***b* was esterified with methanol saturated with hydrogen chloride. The ester **13***c* was purified from methanol as needles, m.p. 110–111°.

Anal. Calcd. for $C_{17}H_{14}O_2$: C, 81.58; H, 5.64. Found: C, 81.30; H, 5.43.

The acid **13***b* used in the above method was replaced by **13***c* (248 mg). The same product was obtained, identified by m.p. and mixture m.p.

Method (d)

The diethylamide **13***d* was prepared from the corresponding acid chloride (22) and diethylamine in the usual manner. It was crystallized from chloroform–hexane, m.p. 141–144°.

Anal. Calcd. for $C_{20}H_{21}NO$: C, 82.44; H, 7.26; N, 4.81. Found: C, 82.20; H, 6.99; N, 4.93.

This product (1.45 g) was dissolved in chloroform (8.0 ml) and a solution of bromine (0.8 g) in chloroform (5.0 ml) was then added to it. The mixture was kept at room temperature overnight and then evaporated to dryness. The residue was repeatedly crystallized from ethanol to give **16***b* (1.0 g) identified by m.p. and mixture m.p.

Method (e)

A solution of the epoxyacid **21***a* (1.6 g) in chloroform (20 ml) was saturated with dry hydrogen bromide. The solution was kept at room temperature overnight, evaporated to dryness and the residue was crystallized from ethanol to give **16***b* (800 mg) identified by m.p. and mixture m.p.

Method (f)

The epoxyacid in the foregoing method was replaced by the epoxyamide **21***b* (1.0 g). The same product was obtained.

Method (g)

A solution of the *syn*-hydroxylactone **14***b* (1.0 g, 0.004 mole) and pyridine (0.2 ml) in dry dioxane (5 ml) was treated with phosphorus tribromide (0.5 ml) and kept overnight. Water was added and the dioxane was removed *in vacuo*. The product was extracted into benzene and the solution was washed with dilute sodium bicarbonate solution and then evaporated. Recrystallization of the residue from ethanol–hexane gave the bromolactone (150 mg), m.p. 150–151°, undepressed on admixture with an authentic specimen.

Method (h)

A solution of the *p*-toluenesulfonate ester of **14***b* (0.5 g, 0.001 mole) in dry dioxane (20 ml) was added to dry calcium bromide (0.25 g, 0.001 mole) in ethanol (2 ml). The mixture was heated under reflux for 18 h and processed as in method *g*. Recrystallization from chloroform–hexane gave **16***b* (78 mg), m.p. 153–155°.

*anti-11-Bromo-10,11-dihydro-10,5-(epoxymethano)-5H-dibenzo[a,d]cycloheptene (**18**)*

A solution of 5*H*-dibenzo[*a,d*]cycloheptene-5-methanol (**13***e*) (2.0 g, 0.01 mole; prepared from **13***c* and $LiAlH_4$) and triethylamine (1.0 g, 0.01 mole) in carbon tetrachloride (75 ml) was treated with a 10% w/v solution of bromine in the same solvent (20 ml, 0.01 mole). It was

Can. J. Chem. Downloaded from www.nrcresearchpress.com by 210.87.254.5 on 09/05/12
For personal use only.

stirred at room temperature for 3 h, then filtered and evaporated. Recrystallization of the residue from ethanol and then from carbon tetrachloride afforded **18** (0.4 g), m.p. 165–166°; ν_{max}($CHCl_3$) 1080 cm^{-1} (ether).

Anal. Calcd. for $C_{16}H_{13}BrO$: C, 63.80; H, 4.35; Br, 26.53. Found: C, 64.09; H, 4.70; Br, 26.72.

Attempted displacement of the halogen atom by heating the bromo ether with dimethylamine was unsuccessful.

*10,11-Dihydro-10,5-(epoxymethano)-5H-dibenzo[a,d]-cyclohepten-13-one (**16c**)*

Method (a)

The epoxyamide **21***b* (10 g) was hydrogenated as described above. The filtered solution was heated under reflux until ammonia evolution had ceased (6 h) and then concentrated whereupon the product crystallized as prisms (8.0 g), m.p. 169–170.5°.

Anal. Calcd. for $C_{16}H_{12}O_2$: C, 81.34; H, 5.12. Found: C, 81.27; H, 5.26.

Method (b)

The bromolactone **16***b* (4.9 g) in ethanol (550 ml) was hydrogenated with palladium–charcoal catalyst until hydrogen uptake ceased. Removal of the catalyst and evaporation of the filtrate gave an oil which was chromatographed upon silica gel. Evaporation of the chloroform eluates and crystallization of the residue gave the product (1.9 g) identified by m.p. and mixture m.p.

Method (c)

A mixture of the *anti*-hydroxyamide **23** (200 mg) and 1 *N* HCl was heated under reflux for 1 h. The solids were collected and partitioned between chloroform and 2 *N* Na_2CO_3. Evaporation of the organic phase and crystallization of the residue gave the product (170 mg) identified by m.p. and mixture m.p.

The aqueous layer was acidified and the precipitate was crystallized from methanol to give 5*H*-dibenzo[*a,d*]cycloheptene-5-carboxylic acid (10 mg), m.p. 241–242° (lit. (22) m.p. 241–242°).

Method (d)

A solution of bromine (8.0 g, 0.05 mole) and the amide **19***a* (22) (11.85 g, 0.95 mole) in chloroform (100 ml) was maintained at 45–50° and irradiated with a photoflood lamp for 8 h. The solvent was removed *in vacuo* and the residue was dissolved in a mixture of methanol (200 ml) and water (10 ml). The solution was heated under reflux for 2 h, evaporated to dryness and the residue was crystallized from methanol to give the title product (3.2 g), identified by m.p. and mixture m.p.

*Methyl 5-hydroxy-10,11-dihydro-5H-dibenzo[a,d]cycloheptene-5-carboxylate (**19b**)*

Method (a)

A solution of methyl 10,11-dihydro-5*H*-dibenzo[*a,d*]-cycloheptene-5-carboxylate (26) (3.0 g, 0.01 mole) in ether (50 ml) was added to a suspension of sodium amide (from 0.3 g, 0.01 g-atom of sodium) in liquid ammonia (125 ml). A stream of dry air was passed through the mixture for 5 h and the ammonia was allowed to evaporate overnight. Water was added and the ether layer was separated, washed with sodium bicarbonate solution, dried, and concentrated. Recrystallization of the residue from carbon tetrachloride – hexane gave 2.0 g (63% yield) of the hydroxy ester, m.p. 134–135° (lit. (27) m.p. 139–140°).

Method (b)

Following a general procedure (28), a solution of 10,11-dihydro-5*H*-dibenzo[*a,d*]cyclohepten-5-one (41.6 g, 0.2 mole) in 1,2-dimethoxyethane (150 ml) was added to sodium (11.6 g, 0.5 g-atom) suspended in the same solvent (70 ml). The mixture was stirred at room temperature for 4 h and then treated with dimethyl carbonate (20.0 g, 0.2 mole) dissolved in ether (150 ml). An additional 300 ml of ether was added and next morning the excess of sodium was destroyed by the cautious addition of water. Separation and evaporation of the organic phase gave 25 g (47%) of **19***b*, m.p. 135–137° after crystallization from carbon tetrachloride – hexane.

*5-Hydroxy-10,11-dihydro-10,5-(epoxymethano)-5H-dibenzo[a,d]cyclohepten-13-one (**20**)*

A mixture of the ester **19***b* (20.0 g, 0.075 mole), *N*-bromosuccinimide (14.2 g, 0.08 mole) and a little benzoyl peroxide in carbon tetrachloride (450 ml) was stirred under a heat lamp for 25 min and then heated under reflux for 1.5 h. It was kept overnight, filtered, and evaporated. Chromatography of the residue on silica with 25% chloroform–benzene gave the hydroxylactone (4.4 g, 23%), m.p. 130–131° (from carbon tetrachloride – hexane); ν_{max}($CHCl_3$) 3530 (OH), 1740 cm^{-1} (lactone). The compound existed in a second crystalline form, m.p. 113–114°; the solution spectra were identical.

Anal. Calcd. for $C_{16}H_{12}O_3$: C, 76.18; H, 4.80. Found: C, 76.18; H, 4.80.

The early fractions from the chromatography gave a yellow solid, m.p. 165–169° (77 mg). Recrystallization from ether–hexane gave a sample which was not analytically pure but whose spectral properties agreed with the proposed structure of 10-bromomethyl-9-anthroic acid methyl ester; ν_{max}($CHCl_3$) 1725 cm^{-1} (ester); λ_{max}(EtOH) 255, 357, 375, and 398mμ (ε 127 000; 6580; 9700 and 19 050); molecular weight by mass spectrometry: 328 (^{79}Br), 330 (^{81}Br) (in correct ratio for 1Br); calculated molecular weight, 329.

*10,11-Dihydro-10,11-epoxy-5H-dibenzo[a,d]cycloheptene-5-carboxylic Acid (**21a**)*

To a stirred suspension of the bromolactone **16***b* (19.7 g) in water (100 ml) at 90° was added 2.5 *N* NaOH solution in one portion. The mixture was kept at 90° during 35 min, rapidly cooled to 0°, and then acidified with 2 *N* HCl. The precipitate was thoroughly washed with water, dried, and then crystallized from ethyl acetate to give the product (11.6 g), m.p. 161–163° (decomp.).

Anal. Calcd. for $C_{16}H_{12}O_3$: C, 76.18; H, 4.80. Found: C, 76.33; H, 4.88.

Treating this product with ethereal diazomethane gave methyl-10,11-dihydro-10,11-epoxy-5*H*-dibenzo[*a,d*]cycloheptene-5-carboxylate, purified from methanol as needles, m.p. 179–181.5°.

Anal. Calcd. for $C_{17}H_{14}O_3$: C, 76.67; H, 5.30. Found: C, 76.60; H, 5.08.

*10,11-Dihydro-syn-10,11-epoxy-5H-dibenzo[a,d]cycloheptene-5-carboxamide (**21b**)*

Very finely-powdered bromolactone **16***b* (150 g) was added in small portions to stirred liquid ammonia (750 ml). The suspension was kept for 8 h and then the ammonia was allowed to evaporate. The residue was

Can. J. Chem. Downloaded from www.nrcresearchpress.com by 210.87.254.5 on 09/05/12
For personal use only.

thoroughly washed with hot water and the remaining solid was crystallized from ethanol to give the product (110 g), m.p. (after drying at 140°) 191–193°.

Anal. Calcd. for $C_{16}H_{13}NO_2$: C, 76.47; H, 5.22; N, 5.57. Found: C, 76.76; H, 5.27; N, 5.31.

*N-Methyl-10,11-dihydro-syn-10,11-epoxy-5H-dibenzo-[a,d]cycloheptene-5-carboxamide (**21c**)*

A mixture of the bromolactone **16***b* (20 g) and methylamine (50 g) was stirred under reflux for 12 h. The excess methylamine was evaporated and the solids were washed with water. The residue was crystallized from ethanol to give the product as needles (12.0 g), m.p. 192–194.°

Anal. Calcd. for $C_{17}H_{15}NO_2$: C, 76.96; H, 5.45; N, 5.09. Found: C, 76.84; H, 5.45; N, 5.09.

*N-tert-Butyl-10,11-dihydro-3-syn-10,11-epoxy-5H-dibenzo[a,d]cycloheptene-5-carboxamide (**21d**)*

A mixture of the bromolactone **16***b* (2.0 g) and *t*-butylamine (20 ml) was heated under reflux for 6 days. The mixture was evaporated to dryness and the solids were washed with water. The residue was crystallized from benzene–hexane to give needles (1.1 g), m.p. 172–176°; ν_{max}($CHCl_3$) 3440 (NH), 1668 cm^{-1} (C=O).

Anal. Calcd. for $C_{20}H_{21}NO_2$: C, 78.17; H, 6.88; N, 4.55. Found: C, 77.89; H, 6.88; N, 4.84.

*anti-11-Chloro-10,11-dihydro-10,5-(epoxymethano)-5H-dibenzo[a,d]cyclohepten-13-one (**16d**)*

A suspension of the epoxyacid **21***a* (1.0 g) in chloroform (20 ml) was saturated with dry hydrogen chloride. Evaporation of the solution and crystallization of the residue from ethyl acetate gave the product (809 mg), m.p. 172–173°.

Anal. Calcd. for $C_{16}H_{11}ClO_2$: C, 71.00; H, 4.07; Cl, 13.10. Found: C, 70.87; H, 4.06; Cl, 13.12.

*10,11-Dihydro-10,5-(epoxymethano)-anti-11-methoxy-5H-dibenzo[a,d]cyclohepten-13-one (**16e**)*

A solution of the epoxyacid **21***a* (1.0 g) in anhydrous methanol (25 ml) containing 3 drops of sulfuric acid was heated under reflux for 10 h. The solvent was removed *in vacuo* and the residue was partitioned between chloroform and water. Evaporation of the dried chloroform phase and crystallization of the residue gave the product (600 mg), m.p. 191–193°.

Anal. Calcd. for $C_{17}H_{14}O_2$: C, 76.67; H, 5.3. Found: C, 76.76; H, 5.08.

*10,11-Dihydro-syn-11-hydroxy-5H-dibenzo[a,d]cycloheptene-5-carboxamide (**22**)*

The epoxyamide **21***b* (500 mg) in dry methanol (30 ml) was hydrogenated at atmospheric pressure with palladium on charcoal catalyst until hydrogen uptake ceased (20 min). The filtered solution was evaporated to dryness *in vacuo* at room temperature. The residue was crystallized from cold dioxan–hexane to give the product (320 mg), m.p. 163–165° (decomp.).

Anal. Calcd. for $C_{16}H_{15}NO_2$: C, 75.87; H, 5.97; N, 5.53. Found: C, 75.78; H, 5.85; N, 5.53.

This material rapidly decomposed at room temperature with formation of **16***c*.

*10,11-Dihydro-anti-11-hydroxy-5H-dibenzo[a,d]cycloheptene-5-carboxamide (**23**)*

A solution of the amide **13***a* (22) (5.0 g) in dry tetrahydrofuran (200 ml) was added dropwise to a stirred 0.83 *M* solution of diborane in tetrahydrofuran (80 ml). The mixture was kept at room temperature for 20 h and then cautiously diluted with water. Sodium hydroxide (80 ml, 3 *N*) and hydrogen peroxide (20 ml, 30%) were then added and the mixture was kept at 50° for 1 h. The mixture was saturated with potassium carbonate and the organic layer was collected and evaporated. Repeated crystallization of the residue from ethyl acetate and then from ethanol gave the product (1.3 g), m.p. 183–185°.

Anal. Calcd. for $C_{16}H_{15}NO_2$: C, 75.87; H, 5.97; N, 5.53. Found: C, 75.86; H, 5.91; N, 5.68.

*syn-11-Dialkylamino Derivatives of 10,11-Dihydro-10,5-(epoxymethano)-5H-dibenzo[a,d]cyclohepten-13-one (**24**)*

General Procedure

The bromolactone **16***b* (0.1 mole) was added portionwise to the appropriate anhydrous secondary amine (0.3 mole). The mixture was stirred overnight, diluted with water, and the crude product which separated was recrystallized.

10,11-Dihydro-*syn*-11-dimethylamino-10,5-(epoxymethano)-5*H*-dibenzo[*a,d*]cyclohepten-13-one (**24***a*) crystallized from isopropanol as needles, m.p. 152–154°, yield 22.0 g.

Anal. Calcd. for $C_{18}H_{17}NO_2$: C, 77.39; H, 6.13; N, 5.01. Found: C, 77.64; H, 6.04; N, 5.03.

10,11-Dihydro-10,5-(epoxymethano)-*syn*-11-morpholino-5*H*-dibenzo[*a,d*]cycloheptene-13-one (**24***b*) crystallized from isopropanol as needles, m.p. 239–242°, yield 23.0 g.

Anal. Calcd. for $C_{20}H_{19}NO_3$: C, 74.74; H, 5.96; N, 4.36. Found: C, 74.78; H, 6.09; N, 4.08.

10,11-Dihydro-10,5-(epoxymethano)-*syn*-11-piperidino-5*H*-dibenzo[*a,d*]cyclohepten-13-one (**24***c*) crystallized from isopropanol as needles, m.p. 204–207°, yield 19.5 g.

Anal. Calcd. for $C_{21}H_{21}NO_2$: C, 78.97; H, 6.63; N, 4.39. Found: C, 79.21; H, 6.75; N, 4.17.

10,11-Dihydro-10,5-(epoxymethano)-*syn*-11-(*N'*-methylpiperazine)-5*H*-dibenzo[*a,d*]cyclohepten-13-one (**24***d*) crystallized from isopropanol as needles, m.p. 178–181°, yield 22.0 g.

Anal. Calcd. for $C_{21}H_{22}N_2O_2$: C, 75.42; H, 6.63; N, 8.38. Found: C, 75.70; H, 6.73; N, 8.09.

10,11-Dihydro-10,5-(epoxymethano)-*syn*-11-(*N'*-phenylpiperazino)-5*H*-dibenzo[*a,d*]cyclohepten-13-one (**24***e*) crystallized from methanol as needles, m.p. 199–202°, yield 25.0 g.

Anal. Calcd. for $C_{26}H_{24}N_2O_2$: C, 78.76; H, 6.10; N, 7.07. Found: C, 78.65; H, 5.99; N, 7.95.

*syn-11-Anilino-10,11-dihydro-10,5-(epoxymethano)-5H-dibenzo[a,d]cyclohepten-13-one (**24f**)*

A mixture of the bromolactone **16***b* (100 g) aniline (140 g) and water (500 ml) was heated in a rocking autoclave at 130° for 8 h. The reaction mixture was extracted with chloroform and the organic phase was extracted with 2 *N* HCl and then washed with water. Evaporation of the chloroform phase and crystallization of the residue from chloroform–isopropanol gave the product as needles (50 g), m.p. 203–205°; ν_{max}($CHCl_3$) 3420 (NH) and 1752 cm^{-1} (lactone).

Can. J. Chem. Downloaded from www.nrcresearchpress.com by 210.87.254.5 on 09/05/12
For personal use only.

Anal. Calcd. for $C_{22}H_{17}NO_2$: C, 80.71; H, 5.23; N, 4.28. Found: C, 80.45; H, 5.31; N, 4.02.

anti-11-Dialkylamino Derivatives of 10,11-Dihydro-10,5-(epoxymethano)-5H-dibenzo[a,d]cyclohepten-13-one (25)

General Procedure

A mixture of either the epoxyacid **21***a* (0.01 mole) or the epoxyamide **21***b* (0.01 mole), the appropriate secondary amine (0.03 mole), and either xylene or toluene (20 ml) was heated under reflux for 5–10 h. The cooled solution was diluted with ether and the precipitate was crystallized.

10,11-Dihydro-10,5-(epoxymethano)-*anti*-11-morpholino-5*H*-dibenzo[*a*,*d*]cyclohepten-13-one (**25***a*) crystallized from methanol as needles, m.p. 171–175°, yield 2.4 g.

Anal. Calcd. for $C_{20}H_{19}NO_3$: C, 74.74; H, 5.96; N, 4.36. Found: C, 74.62; H, 5.73; N, 4.10.

10,11-Dihydro-10,5-(epoxymethano)-*anti*-11-piperidino-5*H*-dibenzo[*a*,*d*]cyclohepten-13-one (**25***b*) crystallized from methanol as needles, m.p. 189–191°, yield 2.8 g.

Anal. Calcd. for $C_{20}H_{21}NO_2$: C, 78.97; H, 6.63; N, 4.39. Found: C, 78.72; H, 6.60; N, 4.35.

10,11-Dihydro-10,5-(epoxymethano)-*anti*-11-(*N'*-methylpiperazino)-5*H*-dibenzo[*a*,*d*]cyclohepten-13-one (**25***c*) crystallized from isopropanol as needles, m.p. 188–190°, yield 2.4 g.

Anal. Calcd. for $C_{21}H_{22}N_2O_2$: C, 75.42; H, 6.63; N, 8.38. Found: C, 75.11; H, 6.89; N, 8.32.

10,11-Dihydro-10,5-(epoxymethano)-*anti*-11-(*N'*-phenylpiperazino)-5*H*-dibenzo[*a*,*d*]cyclohepten-13-one (**25***d*) crystallized from isopropanol as needles, m.p. 181–183°, yield 2.8 g.

Anal. Calcd. for $C_{26}H_{24}N_2O_2$: C, 78.76; H, 6.10; N, 7.07. Found: C, 78.79; H, 5.86; N, 6.92.

anti-11-Anilino-10,11-dihydro-10,5-(epoxymethano)-5H-dibenzo[a,d]cyclohepten-13-one (25e)

A mixture of the epoxyamide **21***b* (5.0 g) and aniline (20 ml) was heated under reflux for 20 h. The reaction mixture was partitioned between 1 *N* HCl and chloroform. Evaporation of the chloroform phase and crystallization of the residue from isopropanol gave the product as needles (4.8 g), m.p. 177–179°; ν_{max}(CHCl$_3$) 1750 cm^{-1}.

Anal. Calcd. for $C_{22}H_{17}NO_2$: C, 80.71; H, 5.23; N, 4.28. Found: C, 80.85; H, 5.50; N, 4.55.

10,11-Dihydro-syn-11-hydroxy-10,5-(iminomethano)-12-phenyl-5H-dibenzo[a,d]cyclohepten-13-one (26a)

A suspension of the *syn*-anilinolactone **24***f* (10.0 g) in ethanol (150 ml) containing 2 *N* H_2SO_4 (10 ml) was heated under reflux for 6 h. Concentration of the resulting solution gave the product as needles (8.0 g), m.p. 266–267°; ν_{max}(Nujol) 1650 cm^{-1} (C=O).

Anal. Calcd. for $C_{22}H_{17}NO_2$: C, 80.71; H, 5.23; N, 4.28. Found: C, 80.41; H, 5.33; N, 4.38.

The epimeric anilinolactone **25***e* was recovered unchanged after similar treatment.

10,5-(Iminomethano)-12-phenyl-5H-dibenzo[a,d]cycloheptene-11,13-(10H)-dione (26b)

Jones' reagent was added dropwise to a cold suspension of **26***a* (5.0 g) in acetone (50 ml) until a slight excess of oxidant was present. The mixture was stirred for 30 min and then ethanol (2.0 ml) was added. The solvent was evaporated at room temperature and the residue was partitioned between water and chloroform. The organic phase was washed, dried, and evaporated and the residue was crystallized from ethanol to give needles (4.2 g), m.p. 180–182°.

Anal. Calcd. for $C_{22}H_{15}NO_2$: C, 81.21; H, 4.65; N, 4.31. Found: C, 80.91; H, 4.56; N, 4.10.

Hydrogenation of this ketone (500 mg) in methanol (20 ml) with palladium on charcoal gave the original hydroxylactam **26***a*.

Acknowledgments

We wish to thank Dr. G. S. Myers and his group for furnishing the tricyclic compounds in quantity. Spectral data were recorded by Mrs. J. Jachner and Mr. M. Boulerice, and analyses were carried out by Mr. W. J. Turnbull. The mass spectra were determined by the Morgan-Schaffer Corporation, Montreal.

1. J. RIGAUDY and L. NÉDÉLEC. Bull. Soc. Chim. France, 643, 648 (1959).
2. G. L. BUCHANAN and D. B. JHAVERI. J. Org. Chem. **26**, 4295 (1961).
3. M. E. CHRISTY, C. C. BOLAND, J. G. WILLIAMS, and E. L. ENGELHARDT. Eirean Patent No. 645/64 (1964) to Merck & Co., Inc. Presented in part at the 10th National Medicinal Chemistry Symposium, American Chemical Society, Bloomington, Indiana, June 1966.
4. C. VAN DER STELT, A. HAASJES, H. M. TERSTEEGE, and W. TH. NAUTA. Rec. Trav. Chim. **84**, 1466 (1965).
5. V. IOAN, M. POPOVICI, and C. D. NENITZESCU. Tetrahedron Letters, 3383 (1965).
6. S. J. CRISTOL and B. J. JARVIS. J. Am. Chem. Soc. **88**, 3095 (1966).
7. W. R. VAUGHAN and A. C. SCHOENTHALER. J. Am. Chem. Soc. **80**, 1956 (1958).
8. (*a*) E. CIORANESCU, A. BUCUR, M. BANCIU, and C. D. NENITZESCU. Rev. Roumaine Chim. **10**, 141 (1965); Chem. Abstr. **63**, 11456 (1965). (*b*) F. BICKELHAUPT, K. STACH, and M. THIEL. Chem. Ber. **98**, 685 (1965). (*c*) S. O. WINTHROP, M. A. DAVIS, F. HERR, J. STEWART, and R. GAUDRY. J. Med. Pharm. Chem. **5**, 1199 (1962).
9. M. KRAML, K. SESTANJ, and D. DVORNIK. Abstr. Can. Fed. Biol. Soc. **9**, 16 (1966). M. KRAML, T. A. DOBSON, K. SESTANJ, M. A. DAVIS, and D. DVORNIK. Abstracts, 152nd National Meeting of the American Chemical Society, New York, N.Y., Sept. 1966, p. 195.
10. (*a*) R. B. WOODWARD and F. V. BRUTCHER. J. Am. Chem. Soc. **80**, 209 (1958). (*b*) S. WINSTEIN, M. V. HERR, and R. E. BUCKLER. J. Am. Chem. Soc. **64**, 2787, 2796 (1942). (*c*) F. D. GUNSTONE. Advan. Org. Chem. **1**, 117 (1960). (*d*) P. S. ELLINGTON, D. H. HEY, and G. D. MEAKINS. J. Chem. Soc. C, 1327 (1966).
11. C. PRÉVOST. Compt. Rend. **196**, 1129 (1933); **197**, 1661 (1933).
12. S. WINSTEIN, R. HECK, S. LAPPORTE, and R. BAIRD. Experientia, **12**, 138 (1956).
13. L. ZURN. Ann. Chem. 56 (1960). R. B. MARTIN, R. HENDRICK, and A. PARCELL. J. Org. Chem. **29**, 158 (1964).
14. C. J. M. STIRLING. J. Chem. Soc. 181 (1960). R. C. PETTERSON and A. WAMBSGAMS. J. Am. Chem.

Soc. **86**, 1648 (1964). D. H. R. BARTON, A. L. J. BECKWITH, and A. GOOSEN. J. Chem. Soc. 181 (1965). R. S. NEALE, N. L. MARCUS, and R. G. SCHEPERS. J. Am. Chem. Soc. **88**, 3051 (1966).
15. N. L. BAULD and Y. S. RIM. J. Am. Chem. Soc. **89**, 179 (1967).
16. H. B. HENBEST and B. NICHOLLS. J. Chem. Soc. 4068 (1957). H. B. HENBEST and R. A. L. WILSON. J. Chem. Soc. 1958 (1957).
17. P. N. CRAIG. J. Am. Chem. Soc. **74**, 129 (1952).
18. L. GOODMAN and S. WINSTEIN. J. Am. Chem. Soc. **79**, 4788 (1957).
19. P. N. CRAIG and I. H. WITT. J. Am. Chem. Soc. **72**, 4925 (1950). R. T. ARNOLD and M. DE MOURA CAMPOS. J. Am. Chem. Soc. **75**, 1944 (1953). R. T. ARNOLD and K. L. LINDSAY. J. Am. Chem. Soc. **75**, 1948 (1953). G. BERTI. Tetrahedron, **4**, 393 (1958).
20. S. WINSTEIN and L. GOODMAN. J. Am. Chem. Soc. **76**, 4373 (1954).
21. G. BERTI, B. MACCHIA, and F. MACCHIA. Tetrahedron Letters, 3421 (1965).
22. M. A. DAVIS, S. O. WINTHROP, R. A. THOMAS, F. HERR, M.-P. CHAREST, and R. GAUDRY. J. Med. Chem. **7**, 88 (1964).
23. H. E. ZAUGG, R. J. MICHAELS, A. D. SCHAFFER, A. M. WENTHE, and W. H. WASHBURN. Tetrahedron, **22**, 1257 (1966).
24. S. J. CRISTOL, J. R. MOHRIG, and D. E. PLORDE. J. Org. Chem. **30**, 1956 (1965). A. R. KATRITZKY and B. WALLIS. Chem. Ind. London, 2025 (1964).
25. C. DJERASSI, R. R. ENGLE, and A. BOWERS. J. Org. Chem. **21**, 1547 (1956).
26. M. A. DAVIS, F. HERR, R. A. THOMAS, and M.-P. CHAREST. J. Med. Chem. **10**, 627 (1967).
27. M. A. DAVIS, F. A. SUNAHARA, F. HERR, and R. GAUDRY. J. Med. Chem. **6**, 513 (1963).
28. S. SELMAN and J. F. EASTHAM. J. Org. Chem. **30**, 3804 (1965).

Can. J. Chem. Downloaded from www.nrcresearchpress.com by 210.87.254.5 on 09/05/12
For personal use only.

Can. J. Chem. Downloaded from www.nrcresearchpress.com by 210.87.254.5 on 09/05/12
For personal use only.

Nuclear magnetic resonance and mass spectral properties of 5-aryltetrazoles

ROBERT R. FRASER AND K. E. HAQUE
Department of Chemistry, University of Ottawa, Ottawa, Canada

Received May 2, 1968

The nuclear magnetic resonance and mass spectral behavior of 5-phenyltetrazole, 5-*p*-nitrophenyltetrazole and the 1-methyl and 2-methyl derivatives of each have been determined. Characteristic differences between the spectra of the 1-methyl and 2-methyl isomers have been noted and found to be useful for the purpose of structural assignments. The synthesis of 1- and 2-methyl-5-phenyltetrazole containing 47.5% of ^{15}N in the 1- and 4-positions of the tetrazole ring aided interpretation of the mass spectra and also allowed measurement of a geminal and a vicinal ^{15}N—H coupling constant.

Canadian Journal of Chemistry, 46, 2855 (1968)

In connection with another problem we have prepared 5-phenyltetrazole, **1**, 5-*p*-nitrophenyltetrazole, **2**, and the two isomeric *N*-methyl derivatives of each compound, **3–6** (see Table I for the numbering of the compounds). The tetrazoles were prepared by addition of azide ion to the appropriate nitrile (1). Methylation of each tetrazole with methyl iodide (2) gave a mixture of the 1- and 2-methyl derivatives. Since both 1-methyl-5-phenyltetrazole and 1-methyl-5-*p*-nitrophenyltetrazole had been previously synthesized by the unambiguous method of von Braun and Rudolph (3), no further proof of structure is required for the methylation products. In this paper we wish to report the nuclear magnetic resonance (n.m.r.) and mass spectral properties of compounds **1–6**. Characteristic differences between the two isomeric methyl derivatives of **1** and **2** are believed to be sufficient to allow reliable structural assignments to be made to other alkylation products of 5-aryltetrazoles.

Nuclear Magnetic Resonance Spectra

Although the n.m.r. spectra of some tetrazole derivatives have been reported (4, 5) no aryltetrazoles have been previously investigated. The chemical shifts of the protons in the n.m.r. spectra of the six aryltetrazoles are reported in Table I. It can be seen that the benzene protons *ortho* to the tetrazole ring of **1** and **3** are deshielded by 0.6 to 0.7 p.p.m. relative to the *meta* and *para* protons. It can also be seen that this deshielding effect disappears entirely in **4** which possesses a methyl group in the 1-position of the tetrazole ring. This deshielding effect has been noted previously in many heterocyclic biaryls, specifically in arylpyrazoles (6, 7), 3-phenylpyridazines (8), 2,2′-bipyridyl (9), and in arylpyridines, aryltriazines, and aryltetrazines (10). Here too, it has been found that the deshielding diminishes markedly or disappears whenever a substituent is introduced into an *ortho* position of the heterocyclic ring (6–8).

The data for the *para*-nitro derivatives, **2**, **5**, and **6**, shows the same deshielding effect but to a lesser degree due to the additional effect of the nitro substituent. In nitrobenzene the nitro group deshields the protons *ortho* to it by 0.95 p.p.m. and the protons *meta* to it by 0.21 p.p.m. (11). If we add the effect of the *nitro* group to that of the tetrazole substituents in **1**, **3**, and **4**, the predicted shifts for **2**, **5**, and **6** are in qualitative agreement with the observed values but in error by between +0.15 and −0.20 p.p.m. (the predicted shifts are given in parentheses in Table I).

It is both interesting and instructive to consider the reasons for the deshielding effect on the *ortho* protons. All investigators agree that it can only occur if coplanarity of the two aromatic rings is sterically allowed. Most authors attributed it to the anisotropy of the heterocyclic ring (6–8). Castellano and co-workers have presented arguments that the effect is a composite of at least three factors (9*a*, 10). Their calculation of the effects of ring anisotropy, nitrogen anisotropy, and a Van der Waal's interaction with the nitrogen's lone pair as a function of the deviation from coplanarity accounts very well for the observed deshielding, but ring anisotropy alone

TABLE I

Chemical shifts of the aryltetrazoles*

	Compound	δH_o†	δH_m (and H_p)	δCH_3	Solvent
1	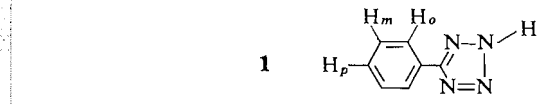	8.10	7.51		$CDCl_3$–DMSO (9:1)
2	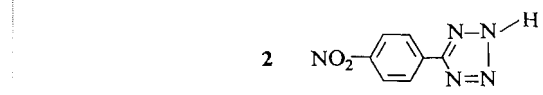	8.37 (8.31)§	8.37 (8.46)		$CDCl_3$–DMSO (9:1)
3	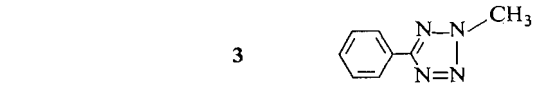	8.13	7.41	4.25	$CDCl_3$
4		7.64	7.64	4.16	$CDCl_3$
5	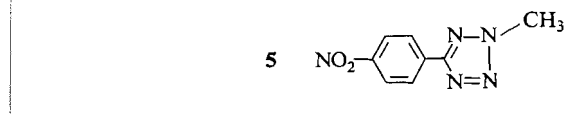	8.21 (8.34)	8.21 (8.36)	4.42	$CDCl_3$
6	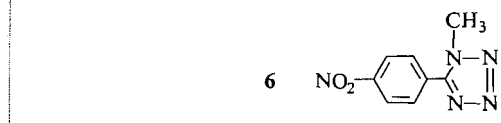	8.05‡ (7.85)	8.56‡ (8.59)	4.25	$CDCl_3$

*All chemical shifts represent the center of gravity of the multiplet and are expressed in units of p.p.m. from internal tetramethylsilane.
†H_o refers to the proton *ortho* to the tetrazole substituent.
‡Assignments for this A_2B_2 pattern were made on the assumption that substitution of a nitro group into 4 will affect H_m (to the tetrazole) more than H_o (to the tetrazole).
§Figures in parentheses represent shifts predicted on the basis of additivity of nitro and tetrazole substituent effects.

accounts for less than half of the total effect. Spotswood and Tanzer, however, present convincing evidence that the Van der Waal's term is negligible (*9b*). Experimental support for the contention that anisotropy alone cannot account for a deshielding of 0.6–0.7 p.p.m. is provided by the work of Mayo and Goldstein (12) who find the deshielding of the *ortho* protons in biphenyl to be only 0.24 p.p.m.[1]

We wish to propose, on the basis of the data in Table I that an additional factor contributes to the observed shifts. It can be seen that a change in the position of the methyl group from position-2 to -1 of the tetrazole ring causes a downfield shift in H_m as well as an upfield shift in H_o (compare **4** with **3**, and **6** with **5**). Furthermore the downfield shift is greater for **5** → **6** (0.35 p.p.m.) than for **3** → **4** (0.23 p.p.m.). We attribute the downfield shifts to an electron-donating resonance effect of the tetrazole ring in **3** and **5** that is not possible or at least greatly diminished in **4** and **6**. This effect would be expected to be greater in **5** than in **3** since the nitro group can interact directly with the electron-donating tetrazole ring. Loss of this interaction will therefore cause a larger downfield shift for **5** → **6** than for **3** → **4**. There is an observable manifestation of this effect on the *ortho* protons too. Their upfield shift is seen to be smaller for **5** → **6** (0.16 p.p.m.) than for **3** → **4** (0.49 p.p.m.). The lack of additivity in accurately predicting the shifts of **2**, **5**, and **6** is consistent with our proposal of a direct resonance interaction between the nitro and tetrazole substituents, for Diehl has

[1]It should be noted that the barriers to rotation in most of the biaryls under consideration have not been studied. Variations in conformational populations will exist and it must be assumed that they are not large enough to affect the qualitative arguments presented in this paper.

Can. J. Chem. Downloaded from www.nrcresearchpress.com by 210.87.254.5 on 09/05/12
For personal use only.

Can. J. Chem. Downloaded from www.nrcresearchpress.com by 210.87.254.5 on 09/05/12
For personal use only.

TABLE II

Mass spectral data for the methylated tetrazoles **3** and **4***

m/e	**3**	**3**-^{15}N	**4**	**4**-^{15}N
162		1.5		2.5
161	1.6	11.5	2.5	20.5
160	11.5	0.8	20.5	
134		5.2		0.5
133	10.6	49.0	1.3	3.5
132	100	65.4	5.7	8.8
131	42.2	21.2	8.5	1.4
120				1.1
119			3.1	10.5
118			21.2	11.0
117			2.5	0.6
106		3.3		0.6
105	10.0	37.5	2.5	4.1
104	73.3	47.8	12.7	11.6
103	38.9	13.6	17.2	10.0
102			2.5	1.1
92			1.6	3.3
91			9.7	6.4
90			26.2	24.7
89	13.3	8.3	11.4	11.0
88			1.6	1.2
87			2.5	
79			2.0	3.1
78	8.6	4.7	12.7	33.2
77	54.4	41.7	30.6	64.0
76	27.2	16.8	13.1	21.8
75			4.9	7.2
74			3.6	5.7
44				20.0
43	37.8	3.9	100	20.0

*Mass spectral data of 3, 4, and the same compounds labelled with 47.5% ^{15}N in each of the 1- and 4-positions of the tetrazole ring. The ion abundances are given relative to the base peak of 100 for 3 and 4. For the ^{15}N labelled compounds the parent peak *m/e* 161 is assigned the same relative abundance as in the unlabelled compound.

TABLE III

Mass spectral data for the methylated tetrazoles **5** and **6***

m/e	**5**	**6**
205	1.3	38.6
178	14.0	
177	100	5.7
176	28.8	2.9
175		4.3
163		30.0
161	3.8	
150	3.2	
149	33.9	
147		15.7
135		7.1
133		5.7
132		4.3
131	12.8	8.6
130	7.7	
119	6.4	12.9
118		20.0
117		21.4
116		7.1
103	25.6	24.3
102	12.8	18.6
91	14.1	17.3
90	7.7	65.8
89	7.0	12.9
88	7.0	28.6
87	6.4	11.4
43		100

*Ion abundances are given relative to the base peak of 100.

shown (13) that additive behavior occurs only in the absence of such interactions.

Finally we wish to report the observation of $J_{^{15}N-CH_3} = 1.85$ c.p.s. in the ^{15}N labelled 1-methyl-5-phenyltetrazole and $J_{^{15}N-N-CH_3} = 1.7$ c.p.s. in the ^{15}N labelled 2-methyl-5-phenyltetrazole. These values appear to be similar to previously recorded three-bond and four-bond ^{15}N—H coupling constants (14).

Mass Spectra

The mass spectral data for the methylated tetrazoles are presented in Tables II and III. In addition, the spectra of isotopically labelled **3** and **4** containing 47.5% ^{15}N in each of the 1- and 4-positions of the tetrazole ring were measured and are included in Table II. Certain striking differences can be noted between the fragmentation patterns of the 2-methyl and 1-methyl isomers. Since we wish to emphasize this aspect, we have summarized only the main routes of fragmentation which have been substantiated by either or both metastable peaks and a comparison of ^{15}N versus ^{14}N patterns. We have avoided the assignment of definite structures to the intermediate ions since it is not possible in most cases to determine whether they have open or cyclic structures. The fragmentation patterns are depicted in Scheme 1. The pattern for 2-methyl-5-phenyltetrazole (path A) involves loss of nitrogen from the weak molecular ion *160* to give the base peak *132* which loses a hydrogen atom forming *131* which in turn loses HCN to form *104*.

The exact same sequence is followed by **5**, the *p*-nitro analogue (i.e. *160* + 45 → *104* + 45, or *205* → *149*) which also has a base peak at P-28 or *177*. From here on the breakdown of *149* differs in that NO_2 is the next fragment lost.

In contrast, both 1-methyl isomers **4** and **6** give more complex spectra involving as the major breakdown pattern a loss of CH_2N_2 (or N_3) then N_2 (or CH_2N) producing *90* and *135* respectively. Isomers **4** and **6** also exhibit a relatively minor breakdown by the path A outlined above. The spectrum of **6** is complicated by loss of NO_2 from *163* and NO from *177* as indicated in Scheme 1.

Compound **3** – Fragmentation Path A.

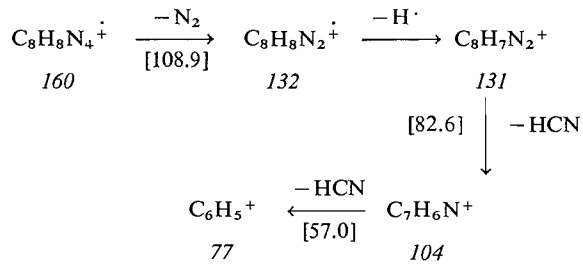

Compound **4**

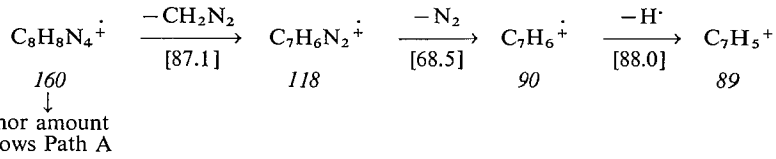

Compound **5**

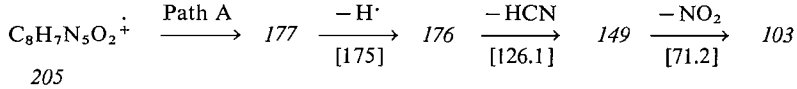

Compound **6**

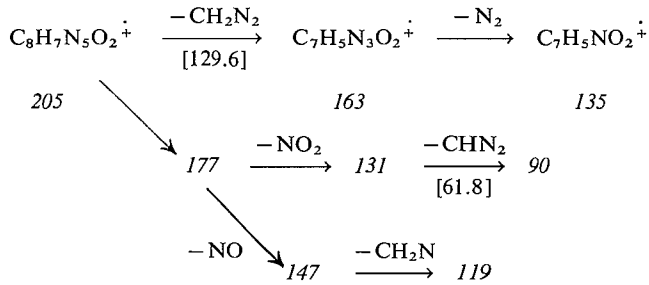

SCHEME 1

Fragmentation patterns for the mass spectral behavior of compounds **3**–**6**. The numbers in brackets represent the positions of metastable peaks.

In both of the 1-methyl isomers the base peak is *43* and the molecular ion is more intense than in the 2-methyl isomers. These differences would almost certainly provide a reliable method of structural determination of any new *N*-alkyl-5-aryltetrazoles.

In conclusion it can be stated that both n.m.r. and mass spectral analysis provide a means of distinguishing between 1- and 2-alkyl-5-aryltetrazoles. In most cases it should be possible to make a reliable structural assignment even if only one isomer is at hand.

Experimental

All n.m.r. spectra were recorded on a Varian DA-60 spectrometer. All mass spectra were obtained using an Hitachi – Perkin – Elmer RMU-6D instrument. All samples were introduced by the instrument's gas inlet system. An ionizing voltage of 50 eV was used. The boiling and melting points reported herein are uncorrected. Microanalysis was performed by A. Bernhardt, Mulheim, Germany.

5-Phenyltetrazole

The procedure of Finnegan, Henry, and Lofquist (1) was used to prepare 5-phenyltetrazole in 90% yield, m.p. 214–215°; lit. m.p. 213–215° (1).

5-p-Nitrophenyltetrazole

This compound was prepared by the same procedure in 96% yield. The product melted over the range 220–222°; lit. m.p. 218–219° (15).

Methylation of 5-Phenyltetrazole

Methylation of 5-phenyltetrazole (25 g) by the method of Henry (2) gave a mixture of products. Crystallization of the crude products from ether–benzene (10:1) gave

Can. J. Chem. Downloaded from www.nrcresearchpress.com by 210.87.254.5 on 09/05/12
For personal use only.

4.3 g (16%) of 1-methyl-5-phenyltetrazole, m.p. 101–103°; lit. m.p. 101–102° (2). Evaporation of the filtrate and recrystallization of the residue from warm petroleum ether (b.p. 30–60°) gave 15.0 g (55%) of 2-methyl-5-phenyltetrazole, m.p. 50–51°; lit. m.p. 50–51° (2).

Methylation of 5-p-Nitrophenyltetrazole

Methylation of 7.2 g of 5-*p*-nitrophenyltetrazole by the procedure of Henry (2) gave a crude mixture which was separated into ether-soluble and ether-insoluble fractions. Recrystallization of the ether-soluble fraction from 85% isopropyl alcohol gave 0.42 g (6%) of 1-methyl-5-*p*-nitrophenyltetrazole, m.p. 121–123°; lit. m.p. 123–126° (16).

Recrystallization of the ether-insoluble fraction from 85% isopropyl alcohol gave 6.5 g (88%) of 2-methyl-5-*p*-nitrophenyltetrazole, m.p. 171–172°.

Anal. Calcd. for $C_8H_7N_5O_2$: C, 46.93; H, 3.44; N, 34.12. Found: C, 47.23; H, 3.74; N, 34.30.

Preparation of ^{15}N-Labelled Tetrazoles

The procedure of Roberts and co-workers (17) was used to prepare benzonitrile-^{15}N from benzoyl chloride and NH_4Cl-^{15}N (Merck, Sharp and Dohme of Canada, 95%-^{15}N). The benzonitrile-^{15}N was then converted into the methylated tetrazoles by the same procedures used above.

Acknowledgment

The authors are indebted to the National Research Council of Canada for financial support of this research.

1. W. G. FINNEGAN, R. A. HENRY, and R. LOFTQUIST. J. Am. Chem. Soc. **80**, 3908 (1958).
2. R. A. HENRY. J. Am. Chem. Soc. **73**, 4470 (1951).
3. J. VON BRAUN and W. RUDOLPH. Chem. Ber. **74**, 264 (1941).
4. H. G. MARKGRAF, W. T. BUCHMANN, and D. P. HOLLIS. J. Org. Chem. **30**, 3472 (1965).
5. G. B. BARLIN and T. J. BATTERHAM. J. Chem. Soc. B, 516 (1967).
6. B. M. LYNCH and Y. Y. HUNG. Can. J. Chem. **42**, 1605 (1964).
7. L. G. TENSMEYER and C. AINSWORTH. J. Org. Chem. **31**, 1878 (1966).
8. I. CROSSLAND. Acta Chem. Scand. **20**, 258 (1966).
9. (*a*) S. CASTELLANO, H. GUNTHER, and S. EBERSOLE. J. Phys. Chem. **69**, 4166 (1965); (*b*) T. M. SPOTSWOOD and C. I. TANZER. Australian J. Chem. **20**, 1227 (1967).
10. H. GUNTHER and S. CASTELLANO. Ber. Bunsenges. Physik. Chem. **70**, 913 (1966).
11. H. SPIESECKE and W. G. SCHNEIDER. J. Chem. Phys. **35**, 731 (1961).
12. R. E. MAYO and J. H. GOLDSTEIN. Mol. Phys. **10**, 301 (1966).
13. P. DIEHL. Helv. Chim. Acta, **44**, 829 (1961).
14. G. BINSCH, J. B. LAMBERT, B. W. ROBERTS, and J. D. ROBERTS. J. Am. Chem. Soc. **86**, 5564 (1964).
15. R. M. HERBST and J. M. MCMANUS. J. Org. Chem. **24**, 1044 (1959).
16. E. K. HARVILL, R. M. HERBST, C. W. ROBERTS, and H. T. F. GIVENS. J. Org. Chem. **17**, 262 (1952).
17. J. B. LAMBERT, W. L. OLIVER, and J. D. ROBERTS. J. Am. Chem. Soc. **87**, 5085 (1965).

Can. J. Chem. Downloaded from www.nrcresearchpress.com by 210.87.254.5 on 09/05/12
For personal use only.

Synthesis of 2-amino-2-deoxy-D-allose, 2-amino-2-deoxy-D-altrose, and 2-deoxy-D-*ribo*-hexose from 3,4,5,6-tetraacetoxy-D-*ribo*-1-nitro-1-hexene[1]

M. B. PERRY AND JANA FURDOVÁ

Division of Biosciences, National Research Council of Canada, Ottawa, Canada

Received April 11, 1968

3,4,5,6-Tetraacetoxy-D-*ribo*-1-nitro-1-hexene with methanolic ammonia afforded a mixture of 2-acetamido-1,2-dideoxy-1-nitro-D-allitol and 2-acetamido-1,2-dideoxy-1-nitro-D-altritol, which were converted *via* the Nef reaction to 2-acetamido-2-deoxy-D-allose and 2-acetamido-2-deoxy-D-altrose. 2-Amino-2-deoxy-D-allose hydrochloride and 2-amino-2-deoxy-D-altrose hydrochloride were obtained from the 2-acetamido-2-deoxy-glycoses.

Reduction of 3,4,5,6-tetraacetoxy-D-*ribo*-1-nitro-1-hexene afforded 3,4,5,6-tetra-*O*-acetyl-1,2-dideoxy-1-nitro-D-*ribo*-hexitol which was converted *via* the Nef reaction to 2-deoxy-D-*ribo*-hexose.

Canadian Journal of Chemistry, **46**, 2859 (1968)

2-Amino-2-deoxy-D-allose and 2-amino-2-deoxy-D-altrose were prepared in 34% and 28% yield respectively from 3,4,5,6-tetraacetoxy-D-*ribo*-1-nitro-1-hexene (1) by the general procedure in which polyacetoxy-1-nitro-1-alkenes are treated with ammonia to yield epimeric 2-acetamido-1,2-dideoxy-1-nitroglycitols which may be converted *via* a modified (2) Nef (3) reaction to the corresponding 2-acetamido-2-deoxy-glycoses (4–7).

2-Amino-2-deoxy-D-allose and 2-amino-2-deoxy-D-altrose have previously been synthesized from D-ribose in 7% and 28% yield respectively by the addition of hydrogen cyanide

[1]Issued as NRCC No. 10180.

4.3 g (16%) of 1-methyl-5-phenyltetrazole, m.p. 101–103°; lit. m.p. 101–102° (2). Evaporation of the filtrate and recrystallization of the residue from warm petroleum ether (b.p. 30–60°) gave 15.0 g (55%) of 2-methyl-5-phenyltetrazole, m.p. 50–51°; lit. m.p. 50–51° (2).

Methylation of 5-p-Nitrophenyltetrazole

Methylation of 7.2 g of 5-*p*-nitrophenyltetrazole by the procedure of Henry (2) gave a crude mixture which was separated into ether-soluble and ether-insoluble fractions. Recrystallization of the ether-soluble fraction from 85% isopropyl alcohol gave 0.42 g (6%) of 1-methyl-5-*p*-nitrophenyltetrazole, m.p. 121–123°; lit. m.p. 123–126° (16).

Recrystallization of the ether-insoluble fraction from 85% isopropyl alcohol gave 6.5 g (88%) of 2-methyl-5-*p*-nitrophenyltetrazole, m.p. 171–172°.

Anal. Calcd. for $C_8H_7N_5O_2$: C, 46.93; H, 3.44; N, 34.12. Found: C, 47.23; H, 3.74; N, 34.30.

Preparation of ^{15}N-Labelled Tetrazoles

The procedure of Roberts and co-workers (17) was used to prepare benzonitrile-^{15}N from benzoyl chloride and NH_4Cl-^{15}N (Merck, Sharp and Dohme of Canada, 95%-^{15}N). The benzonitrile-^{15}N was then converted into the methylated tetrazoles by the same procedures used above.

Acknowledgment

The authors are indebted to the National Research Council of Canada for financial support of this research.

1. W. G. FINNEGAN, R. A. HENRY, and R. LOFTQUIST. J. Am. Chem. Soc. **80**, 3908 (1958).
2. R. A. HENRY. J. Am. Chem. Soc. **73**, 4470 (1951).
3. J. VON BRAUN and W. RUDOLPH. Chem. Ber. **74**, 264 (1941).
4. H. G. MARKGRAF, W. T. BUCHMANN, and D. P. HOLLIS. J. Org. Chem. **30**, 3472 (1965).
5. G. B. BARLIN and T. J. BATTERHAM. J. Chem. Soc. B, 516 (1967).
6. B. M. LYNCH and Y. Y. HUNG. Can. J. Chem. **42**, 1605 (1964).
7. L. G. TENSMEYER and C. AINSWORTH. J. Org. Chem. **31**, 1878 (1966).
8. I. CROSSLAND. Acta Chem. Scand. **20**, 258 (1966).
9. (*a*) S. CASTELLANO, H. GUNTHER, and S. EBERSOLE. J. Phys. Chem. **69**, 4166 (1965); (*b*) T. M. SPOTSWOOD and C. I. TANZER. Australian J. Chem. **20**, 1227 (1967).
10. H. GUNTHER and S. CASTELLANO. Ber. Bunsenges. Physik. Chem. **70**, 913 (1966).
11. H. SPIESECKE and W. G. SCHNEIDER. J. Chem. Phys. **35**, 731 (1961).
12. R. E. MAYO and J. H. GOLDSTEIN. Mol. Phys. **10**, 301 (1966).
13. P. DIEHL. Helv. Chim. Acta, **44**, 829 (1961).
14. G. BINSCH, J. B. LAMBERT, B. W. ROBERTS, and J. D. ROBERTS. J. Am. Chem. Soc. **86**, 5564 (1964).
15. R. M. HERBST and J. M. MCMANUS. J. Org. Chem. **24**, 1044 (1959).
16. E. K. HARVILL, R. M. HERBST, C. W. ROBERTS, and H. T. F. GIVENS. J. Org. Chem. **17**, 262 (1952).
17. J. B. LAMBERT, W. L. OLIVER, and J. D. ROBERTS. J. Am. Chem. Soc. **87**, 5085 (1965).

Can. J. Chem. Downloaded from www.nrcresearchpress.com by 210.87.254.5 on 09/05/12
For personal use only.

Synthesis of 2-amino-2-deoxy-D-allose, 2-amino-2-deoxy-D-altrose, and 2-deoxy-D-*ribo*-hexose from 3,4,5,6-tetraacetoxy-D-*ribo*-1-nitro-1-hexene[1]

M. B. PERRY AND JANA FURDOVÁ

Division of Biosciences, National Research Council of Canada, Ottawa, Canada

Received April 11, 1968

3,4,5,6-Tetraacetoxy-D-*ribo*-1-nitro-1-hexene with methanolic ammonia afforded a mixture of 2-acetamido-1,2-dideoxy-1-nitro-D-allitol and 2-acetamido-1,2-dideoxy-1-nitro-D-altritol, which were converted *via* the Nef reaction to 2-acetamido-2-deoxy-D-allose and 2-acetamido-2-deoxy-D-altrose. 2-Amino-2-deoxy-D-allose hydrochloride and 2-amino-2-deoxy-D-altrose hydrochloride were obtained from the 2-acetamido-2-deoxy-glycoses.

Reduction of 3,4,5,6-tetraacetoxy-D-*ribo*-1-nitro-1-hexene afforded 3,4,5,6-tetra-*O*-acetyl-1,2-dideoxy-1-nitro-D-*ribo*-hexitol which was converted *via* the Nef reaction to 2-deoxy-D-*ribo*-hexose.

Canadian Journal of Chemistry, **46**, 2859 (1968)

2-Amino-2-deoxy-D-allose and 2-amino-2-deoxy-D-altrose were prepared in 34% and 28% yield respectively from 3,4,5,6-tetraacetoxy-D-*ribo*-1-nitro-1-hexene (1) by the general procedure in which polyacetoxy-1-nitro-1-alkenes are treated with ammonia to yield epimeric 2-acetamido-1,2-dideoxy-1-nitroglycitols which may be converted *via* a modified (2) Nef (3) reaction to the corresponding 2-acetamido-2-deoxy-glycoses (4–7).

2-Amino-2-deoxy-D-allose and 2-amino-2-deoxy-D-altrose have previously been synthesized from D-ribose in 7% and 28% yield respectively by the addition of hydrogen cyanide

[1]Issued as NRCC No. 10180.

Can. J. Chem. Downloaded from www.nrcresearchpress.com by 210.87.254.5 on 09/05/12
For personal use only.

to a substituted D-ribosylamine, followed by hemihydrogenation and subsequent hydrolysis of the α-amino nitriles (8). 2-Amino-2-deoxy-D-allose has been synthesized from methyl 2-acetamido-4,6-*O*-benzylidene-2-deoxy-α-D-glucopyranoside by an inversion at C-3 of its 3-*O*-methylsulfonyl derivative (9, 10), from the oxazoline derived from 2-benzamido-2-deoxy-5,6-*O*-isopropylidene-D-glucofuranose (11), and by intramolecular rearrangement of D-*ribo*-hexulosylamine (12).

3,4,5,6-Tetraacetoxy-D-*ribo*-1-nitro-1-hexene with saturated methanolic ammonia solution gave a mixture of 2-acetamido-1,2-dideoxy-1-nitro-D-allitol and 2-acetamido-1,2-dideoxy-1-nitro-D-altritol which could not be separated by fractional crystallization. The mixed 2-acetamido-1,2-dideoxy-1-nitroglycitols on treatment with dilute sulfuric acid afforded a mixture of 2-acetamido-2-deoxy-D-allose and 2-acetamido-2-deoxy-D-altrose, contaminated with a small quantity of the corresponding aminoglycoses. The product after treatment with aqueous acetic anhydride, was shown by paper chromatography, to contain only the 2-acetamido-2-deoxyglycoses and pure crystalline 2-acetamido-2-deoxy-D-allose was obtained from ethanol solution of the reaction mixture. The residue remaining after the removal of the 2-acetamido-2-deoxy-D-allose was fractionated by cellulose column chromatography to yield chromatographically pure 2-acetamido-2-deoxy-D-allose and 2-acetamido-2-deoxy-D-altrose. The two 2-acetamido-2-deoxyglycoses, on hydrolysis with hot dilute hydrochloric acid, afforded chromatographically pure 2-amino-2-deoxy-D-allose hydrochloride and 2-amino-2-deoxy-D-altrose hydrochloride. The acetamidoglycoses and aminoglycoses had chemical and physical properties in close agreement with those previously recorded for these compounds. This preparative procedure gives a simple and direct route to the aminoglycoses and should be of practical value.

2-Deoxy-D-*ribo*-hexose was prepared in 88% yield from 3,4,5,6-tetraacetoxy-D-*ribo*-1-nitro-1-hexene by reduction with hydrogen to give 3,4,5,6-tetra-*O*-acetyl-1,2-dideoxy-1-nitro-D-*ribo*-hexitol which underwent the Nef reaction to yield 2-deoxy-D-*ribo*-hexose. 2-Deoxy-D-*ribo*-hexose has been prepared from methyl 2,3-anhydro-4,6-*O*-benzylidene-α-D-allopyranoside (13, 14) which with sodium thiomethoxide gave methyl 4,6-*O*-benzylidene-2-*S*-methyl-2-thio-α-D-altroside which on hydrogenation afforded methyl 2-deoxy-α-D-*ribo*-hexopyranoside. It is of interest that 2-deoxy-D-*ribo*-hexose shows inhibition of glycolysis of human leucocytes, human leukemic cells, and a number of animal tumors (15).

The method described in this note for the synthesis of 2-deoxy-D-*ribo*-hexose provides a practical route to the glycose. The physical and chemical properties of the 2-deoxy-D-*ribo*-hexose agree with those recorded by other workers and its identification was further established by its reduction with sodium borohydride to the known crystalline 2-deoxy-D-*ribo*-hexitol.

Experimental

Paper chromatography was performed by the descending method (16) on Whatman No. 1 filter paper using pyridine – ethyl acetate – water (2:5:5 v/v, top layer). The glycoses were detected with (*a*) 2% silver nitrate in acetone followed by 2% sodium hydroxide in ethanol (17), (*b*) 2% *p*-anisidine hydrochloride in ethanol (18), or (*c*) 0.02 *M* aqueous sodium metaperiodate followed by ethylene glycol – acetone – sulfuric acid (50:50:0.3 v/v) and 6% aqueous sodium 2-thiobarbiturate (19). The rates of movement of the glycoses on the chromatograms are quoted relative to D-galactose (R_{Gal}).

Gas–liquid partition chromatography was carried out using a Hewlett–Packard model 402 chromatograph with a hydrogen flame detector and fitted with glass U tubes (4 ft × 6 mm × 3 mm internal diameter) packed with 10% neopentylglycol sebacate polyester on 80–100 mesh acid washed Chromosorb W, maintained at 210°. Dry helium was used as the carrier gas and retention times of the compounds are quoted relative to 2-acetamido-2-deoxy-1,3,4,5,6-penta-*O*-(trimethylsilyl)-D-glucitol (T_{GN}).

Melting points were determined on a Fisher–Johns apparatus and are corrected. Solutions were concentrated under reduced pressure below 40°. Optical rotations were determined at 20° using a Perkin–Elmer 141 polarimeter.

*2-Amino-2-deoxy-*D*-allose and 2-Amino-2-deoxy-*D*-altrose*

A solution of 3,4,5,6-tetraacetoxy-D-*ribo*-1-nitro-1-hexene (18.5 g) in absolute methanol (160 ml) cooled to 0° was saturated with dry ammonia gas (about 1 h) and the mixture was then allowed to stand at room temperature for 18 h. The reaction mixture was concentrated to a syrup which was triturated with warm chloroform solution (3 × 100 ml) to remove acetamide. The residual syrup (12 g) was then dissolved in a solution of $Ba(OH)_2 \cdot 8H_2O$ (14.6 g) in water (220 ml) and this solution was added dropwise with vigorous stirring to a cold mixture of sulfuric acid (12.5 ml) and water (100 ml). After stirring at 10° for 2 h the mixture was left at 20° for 18 h. The solution was neutralized with barium carbonate and the filtered solution after concentration to about 100 ml was

Can. J. Chem. Downloaded from www.nrcresearchpress.com by 210.87.254.5 on 09/05/12
For personal use only.

treated with Dowex-1($CO_3^=$) ion-exchange resin (30 ml), methanol (15 ml), and acetic anhydride (0.5 ml); the mixture was then shaken at room temperature for 30 min. The filtered solution was concentrated to a syrup (10 g) and paper chromatographic examination of the product showed two spots having R_{Gal} 1.58 and 1.84 in the visual ratio of 2:1, which corresponded in rates of movement with authentic 2-acetamido-2-deoxy-D-allose and 2-acetamido-2-deoxy-D-altrose respectively.

The syrup was dissolved in hot ethanol (50 ml) and, on cooling to 5°, crystalline 2-acetamido-2-deoxy-D-allose (3.08 g) was obtained and the concentrated mother liquor, which failed to yield further crystalline material, was shown by paper chromatography to contain 2-acetamido-2-deoxyallose and 2-acetamido-2-deoxyaltrose. This mixture was fractionated on a cellulose column (4.5 × 70 cm) using butan-1-ol half-saturated with water as the mobile phase. 2-Acetamido-2-deoxy-D-altrose (3.5 g) was eluted first and was followed by the 2-acetamido-2-deoxy-D-allose (1.1 g).

2-Acetamido-2-deoxy-D-altrose

The product obtained from the cellulose column gave crystalline 2-acetamido-2-deoxy-D-altrose from its solution in ethanol and after one recrystallization from ethanol the glycose (3 g) showed a single spot on paper chromatograms (R_{Gal} 1.84) and had m.p. 99–100° and $[\alpha]_D$ −2.4° → +5° (*c*, 1 in water) (lit. m.p. 95–97° and $[\alpha]_D$ −2.7° → +4.8°(8)).

Anal. Calcd. for $C_8H_{15}O_6N$: C, 43.43; H, 6.84; N, 6.33. Found: C, 43.4; H, 6.9; N, 6.3.

The fully trimethylsilylated crystalline 2-acetamido-2-deoxy-D-altrose on gas–liquid partition chromatography gave a single peak having T_{GN} 0.76 and the glycose after equilibration in water gave trimethylsilylated derivatives having T_{GN} 0.76 (34%), 1.30 (25%), and 1.44 (41%).

2-Amino-2-deoxy-D-altrose Hydrochloride

2-Acetamido-2-deoxy-D-altrose (0.3 g) in 2 *N* hydrochloric acid (10 ml) was heated on a boiling water bath for 2 h and after treatment with charcoal, the filtered solution was concentrated to a syrup. This was then co-distilled with ethanol and benzene to yield an amorphous product (0.26 g) which was dried under vacuum over phosphorus pentoxide. The 2-amino-2-deoxy-D-altrose hydrochloride, which gave a single spot on paper chromatography, (R_{Gal} 0.47) had $[\alpha]_D$ −17.3° (*c*, 2.2 in water) (lit. $[\alpha]_D$ −14° (8)).

2-Acetamido-2-deoxy-D-allose

The 2-acetamido-2-deoxy-D-allose fraction obtained from the cellulose column gave crystalline 2-acetamido-2-deoxy-D-allose (0.9 g) from ethanol and had m.p. 200° undepressed on admixture with the 2-acetamido-2-deoxy-D-allose obtained before preparative chromatography, and the two fractions were combined (4.4 g). Two recrystallizations from ethanol afforded pure 2-acetamido-2-deoxy-D-allose (3.8 g) which gave a single spot (R_{Gal} 1.58) on paper chromatography and had m.p. 207° (lit. m.p. 197° (8), 201–203° (9), 207–208° (11)) and $[\alpha]_D$ −88° → −55° (*c*, 0.2 in water) (lit. $[\alpha]_D$ −53° (8), −48° (9), −47° (11)).

Anal. Calcd. for $C_8H_{15}O_6N$: C, 43.43; H, 6.84; N, 6.33. Found: C, 43.2; H, 6.9; N, 6.3.

The trimethylsilylated crystalline 2-acetamido-2-deoxy-D-allose on gas chromatography gave a single peak (T_{GN} 1.32) and the trimethylsilylated glycose equilibrate in water showed four peaks having T_{GN} 0.92 (9.5%), 1.32 (54%), 1.38 (30%), and 1.64 (7%).

2-Amino-2-deoxy-D-allose Hydrochloride

2-Acetamido-2-deoxy-D-allose (0.3 g) was hydrolyzed with 2 *N* hydrochloric acid in the way described for the preparation of 2-amino-2-deoxy-D-altrose hydrochloride to yield 2-amino-2-deoxy-D-allose hydrochloride (0.25 g) as an amorphous powder. This gave a single spot on paper chromatography (R_{Gal} 0.39) and had $[\alpha]_D$ +16.6° (*c*, 0.5 in water) (lit. $[\alpha]_D$ +17° (8), +29° (9), +17° (11)).

2-Deoxy-D-ribo-hexose

3,4,5,6-Tetraacetoxy-D-*ribo*-1-nitro-1-hexene (10 g) in ethanol (400 ml), was shaken with hydrogen at room temperature and pressure in the presence of palladium black (0.6 g). One mole equivalent of hydrogen was absorbed in 20 min, and the rate of reduction then became very slow. At this point the mixture was filtered and the filtrate was concentrated to a syrup (9.9 g). The 3,4,5,6-tetra-*O*-acetyl-1,2-dideoxy-1-nitro-D-*ribo*-hexitol which could not be induced to crystallize had $[\alpha]_D$ −7.2° (*c*, 7 in chloroform).

Anal. Calcd. for $C_{14}H_{21}O_{10}N$: C, 46.28; H, 5.83; N, 3.86. Found: C, 46.37; H, 5.9; N, 3.8.

3,4,5,6-Tetra-*O*-acetyl-1,2-dideoxy-1-nitro-D-*ribo*-hexitol (9 g) was dissolved at 40° in *N* sodium hydroxide solution (135 ml) and the mixture, after being kept at 20° for 1 h , was added dropwise to a cooled, stirred solution of concentrated sulfuric acid (18.9 ml) in water (27 ml). The reaction mixture was adjusted in the cold to pH 5.5 by the addition of saturated barium hydroxide solution and then finally neutralized by the addition of barium carbonate. After centrifugation and filtration the solution was treated with acetic acid (1 ml) and then passed down columns of Rexyn 101(H^+) (150 ml) and Rexyn RG6(OH^-) (30 ml) ion-exchange resins, and the eluate and washing were concentrated to a syrup (4.3 g). The syrup was dissolved in hot ethanol and on cooling the solution crystalline 2-deoxy-D-*ribo*-hexose (4.0 g) having m.p. 138° was obtained which after three recrystallizations from ethanol had m.p. 138–139° (lit. m.p. 135–136° (20)) and $[\alpha]_D$ +50° → +55.2° (*c*, 0.5 in water) (lit. $[\alpha]_D$ +58° (20)).

Anal. Calcd. for $C_6H_{12}O_5$: C, 43.90; H, 7.37. Found: C, 43.8; H, 7.4.

On paper chromatography the 2-deoxy-D-*ribo*-hexose had R_{Gal} 3.02 and gave a characteristic red spot with the periodate–thiobarbiturate spray reagents (19).

2-Deoxy-D-ribo-hexitol

2-Deoxy-D-*ribo*-hexose (120 mg) in water (5 ml) was reduced by the addition of sodium borohydride (50 mg) and after 2 h the excess borohydride was destroyed by acidification with acetic acid. The reaction mixture was passed down a column of Rexyn 101(H^+) ion-exchange resin (10 ml) and the eluate and washings after concentration to dryness were distilled with absolute methanol (5 × 20 ml) to remove boric acid and the residue was dissolved in hot ethanol (ca. 2 ml). Crystalline 2-deoxy-D-*ribo*-hexitol (95 mg) was obtained from the cooled ethanol solution and after two further recrystallizations

from ethanol it had m.p. 90° and $[\alpha]_D$ −19° (*c*, 0.8 in methanol) (lit. m.p. 90–91° and $[\alpha]_D$ −19° (*c*, 2 in methanol) (20)).

Anal. Calcd. for $C_6H_{14}O_5$: C, 43.37; H, 8.49. Found: C, 43.4; H, 8.5.

Acknowledgment

We thank Mr. A. E. Castagne for the microanalyses.

1. J. C. Sowden and H. O. L. Fischer. J. Am. Chem. Soc. **69**, 1048 (1947).
2. C. Satoh and A. Kiyomoto. Chem. Pharm. Bull. (Tokyo), **12**, 615 (1964).
3. J. U. Nef. Ann. **280**, 263 (1894).
4. A. N. O'Neill. Can. J. Chem. **37**, 1747 (1959).
5. J. C. Sowden and M. L. Oftedahl. J. Am. Chem. Soc. **82**, 2303 (1960).
6. S. D. Gero and J. Defaye. Compt. Rend. Acad. Sci. (Paris). **261**, 1555 (1965).
7. J. C. Sowden and M. L. Oftedahl. J. Org. Chem. **26**, 2153 (1961).
8. R. Kuhn and H. Fischer. Ann. **617**, 88 (1958).
9. R. W. Jeanloz. J. Am. Chem. Soc. **79**, 2591 (1957).
10. R. W. Jeanloz. Methods in carbohydrate chemistry. Vol. 1. Academic Press, New York. 1962. p. 213.
11. R. Gigg and C. D. Warren. J. Chem. Soc. 1351 (1965).
12. K. Heyns, H. Paulsen, R. Eichstedt, and M. Rolle. Chem. Ber. **90**, 2039 (1957).
13. R. W. Jeanloz, D. A. Prins, and T. Reichstein. Experientia, **1**, 336 (1945).
14. R. W. Jeanloz, D. A. Prins, and T. Reichstein. Helv. Chim. Acta, **29**, 371 (1946).
15. J. Laszlo, B. Landau, K. Wight, and D. Burk. J. Natl. Cancer Inst. **21**, 475 (1958).
16. S. M. Partridge. Biochem. J. **42**, 238 (1948).
17. W. E. Trevelyan, D. P. Procter, and J. S. Harrison. Nature, **166**, 444 (1950).
18. L. Hough, J. K. N. Jones, and W. H. Wadman. J. Chem. Soc. 1702 (1950).
19. L. Warren. Nature, **186**, 237 (1960).
20. M. Gut and D. A. Prins. Helv. Chim. Acta, **30**, 1223 (1947).

Mass-spectral rearrangements of acyloxysilanes and -germanes

A. G. Brook, A. G. Harrison, and Peter F. Jones[1]

Department of Chemistry, University of Toronto, Toronto 5, Ontario

Received March 19, 1968

The mass spectra of some acyloxytriphenylmethanes, -silanes, and -germanes have been studied. The latter two classes show unusual fragmentation–rearrangement processes.

Canadian Journal of Chemistry, **46**, 2862 (1968)

During the course of some investigations into the Baeyer–Villiger oxidation of acylsilanes it became necessary to obtain the mass spectrum of benzoyloxytriphenylsilane (triphenylsilyl benzoate), **1***a*. The major ion (*m/e* 303), formed by loss

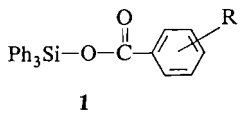

1

(*a*) R = H
(*b*) R = *m*-Cl
(*c*) R = *p*-*t*-Bu

of a phenyl group from the parent ion (*m/e* 380), further lost carbon dioxide to give the $Ph_3Si^{\oplus}$ ion (*m/e* 259) as confirmed by a metastable peak at *m/e* 221.4 for the transition 303 → 259.

$$M^{\oplus} \xrightarrow{-77} [M-Ph]^{\oplus} \xrightarrow[*]{-44} Ph_3Si^{\oplus}$$

Since this behavior differs markedly from that normally found for esters (1) we have extended our investigation to the substituted benzoyloxy compounds **1***b* and **1***c*, in order to identify the phenyl group initially lost. Neither compound showed a peak for loss of substituted-phenyl, the base peak for both being the (M−77) ion which subsequently lost CO_2. A metastable peak was observed for the loss of CO_2 in **1***c*. Thus the fragmentation path must involve loss of a phenyl group from silicon followed by migration of an aryl group to the positive silicon center, accompanied by loss of carbon dioxide.

For all these compounds the peak intensities for both the molecule-ions (<3%) and for $Ph_3Si^{\oplus}$ (<5%) were low. Major peaks for the compounds are shown in Table I. A similar rearrangement has been reported (2) for trimethylsilyl esters.

Migration to silicon is not limited to aryl groups as is shown by the mass spectrum of the acetoxy compound **2***a* for which the following pathway is the major process, (M − 77) being the

[1]Dow–Corning Fellow in Chemistry, 1967–1968.

Can. J. Chem. Downloaded from www.nrcresearchpress.com by 210.87.254.5 on 09/05/12
For personal use only.

from ethanol it had m.p. 90° and $[\alpha]_D$ −19° (*c*, 0.8 in methanol) (lit. m.p. 90–91° and $[\alpha]_D$ −19° (*c*, 2 in methanol) (20)).

Anal. Calcd. for $C_6H_{14}O_5$: C, 43.37; H, 8.49. Found: C, 43.4; H, 8.5.

Acknowledgment

We thank Mr. A. E. Castagne for the microanalyses.

1. J. C. Sowden and H. O. L. Fischer. J. Am. Chem. Soc. **69**, 1048 (1947).
2. C. Satoh and A. Kiyomoto. Chem. Pharm. Bull. (Tokyo), **12**, 615 (1964).
3. J. U. Nef. Ann. **280**, 263 (1894).
4. A. N. O'Neill. Can. J. Chem. **37**, 1747 (1959).
5. J. C. Sowden and M. L. Oftedahl. J. Am. Chem. Soc. **82**, 2303 (1960).
6. S. D. Gero and J. Defaye. Compt. Rend. Acad. Sci. (Paris). **261**, 1555 (1965).
7. J. C. Sowden and M. L. Oftedahl. J. Org. Chem. **26**, 2153 (1961).
8. R. Kuhn and H. Fischer. Ann. **617**, 88 (1958).
9. R. W. Jeanloz. J. Am. Chem. Soc. **79**, 2591 (1957).
10. R. W. Jeanloz. Methods in carbohydrate chemistry. Vol. 1. Academic Press, New York. 1962. p. 213.
11. R. Gigg and C. D. Warren. J. Chem. Soc. 1351 (1965).
12. K. Heyns, H. Paulsen, R. Eichstedt, and M. Rolle. Chem. Ber. **90**, 2039 (1957).
13. R. W. Jeanloz, D. A. Prins, and T. Reichstein. Experientia, **1**, 336 (1945).
14. R. W. Jeanloz, D. A. Prins, and T. Reichstein. Helv. Chim. Acta, **29**, 371 (1946).
15. J. Laszlo, B. Landau, K. Wight, and D. Burk. J. Natl. Cancer Inst. **21**, 475 (1958).
16. S. M. Partridge. Biochem. J. **42**, 238 (1948).
17. W. E. Trevelyan, D. P. Procter, and J. S. Harrison. Nature, **166**, 444 (1950).
18. L. Hough, J. K. N. Jones, and W. H. Wadman. J. Chem. Soc. 1702 (1950).
19. L. Warren. Nature, **186**, 237 (1960).
20. M. Gut and D. A. Prins. Helv. Chim. Acta, **30**, 1223 (1947).

Mass-spectral rearrangements of acyloxysilanes and -germanes

A. G. Brook, A. G. Harrison, and Peter F. Jones[1]

Department of Chemistry, University of Toronto, Toronto 5, Ontario

Received March 19, 1968

The mass spectra of some acyloxytriphenylmethanes, -silanes, and -germanes have been studied. The latter two classes show unusual fragmentation–rearrangement processes.

Canadian Journal of Chemistry, **46**, 2862 (1968)

During the course of some investigations into the Baeyer–Villiger oxidation of acylsilanes it became necessary to obtain the mass spectrum of benzoyloxytriphenylsilane (triphenylsilyl benzoate), **1***a*. The major ion (*m/e* 303), formed by loss

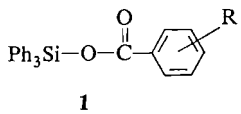

1

(*a*) R = H
(*b*) R = *m*-Cl
(*c*) R = *p*-*t*-Bu

of a phenyl group from the parent ion (*m/e* 380), further lost carbon dioxide to give the $Ph_3Si^{\oplus}$ ion (*m/e* 259) as confirmed by a metastable peak at *m/e* 221.4 for the transition 303 → 259.

$$M^{\oplus} \xrightarrow{-77} [M-Ph]^{\oplus} \xrightarrow[*]{-44} Ph_3Si^{\oplus}$$

Since this behavior differs markedly from that normally found for esters (1) we have extended our investigation to the substituted benzoyloxy compounds **1***b* and **1***c*, in order to identify the phenyl group initially lost. Neither compound showed a peak for loss of substituted-phenyl, the base peak for both being the (M−77) ion which subsequently lost CO_2. A metastable peak was observed for the loss of CO_2 in **1***c*. Thus the fragmentation path must involve loss of a phenyl group from silicon followed by migration of an aryl group to the positive silicon center, accompanied by loss of carbon dioxide.

For all these compounds the peak intensities for both the molecule-ions (<3%) and for $Ph_3Si^{\oplus}$ (<5%) were low. Major peaks for the compounds are shown in Table I. A similar rearrangement has been reported (2) for trimethylsilyl esters.

Migration to silicon is not limited to aryl groups as is shown by the mass spectrum of the acetoxy compound **2***a* for which the following pathway is the major process, (M − 77) being the

[1]Dow–Corning Fellow in Chemistry, 1967–1968.

Can. J. Chem. Downloaded from www.nrcresearchpress.com by 210.87.254.40 on 09/05/12
For personal use only.

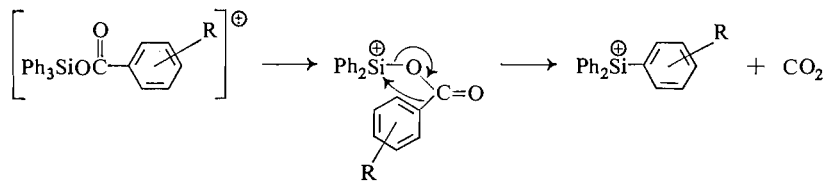

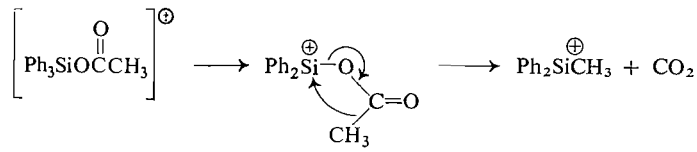

(*m/e* 318) (*m/e* 241) (*m/e* 197)

TABLE I

Relative peak intensities based on the most abundant ion (taken as 100%)

Ester	M − 77	$Ph_2\overset{\oplus}{Si}$–C$_6$H$_4$–R
1*a*	100	10.0
1*b*	100	11.8
1*c*	100	10.2

major ion. However, phenyl substitution in the

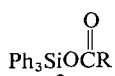

2

(*a*) R = CH_3
(*b*) R = CH_2Ph
(*c*) R = $CHPh_2$

acetoxy group markedly reduces the extent of the above process, the (M − 77) ions amounting to 30% and 0.81% respectively of the base peak in **2***b* and **2***c*, while in neither case is loss of CO_2 from the (M − 77) ion observed. Direct loss of CO_2 from the molecular ion is observed in both the latter compounds, confirmed by a metastable ion at *m/e* 311 in the case of **2***b* for the transition $Ph_3SiOCOCH_2Ph$ (394) → Ph_3SiCH_2Ph (350). Both compounds have $Ph_3Si^{\oplus}$ as the base peak, which may arise from the (M − 44) fragment, rather than directly from the parent ion, although no metastable peaks could be observed to support either pathway. Benzhydryltriphenylsilane, $Ph_3SiCHPh_2$, similarly shows $Ph_3Si^{\oplus}$ as the major ion.[2] Although loss of CO_2 from the parent ion is not limited to acyloxysilanes, the process has been reported to be most common in those esters in which an unsaturated system is in conjugation with the ester carbonyl group (3). Table II gives details of important ions.

TABLE II

Relative peak intensities based on the most abundant ion (taken as 100%)

Ester	M − 77	$Ph_2\overset{\oplus}{Si}R$	M − 44	$Ph_3\overset{\oplus}{Si}$
2*a*	100	8.35	—	2.60
2*b*	30.0	—	7.74	100
2*c*	0.81	—	3.36	100

In order to determine whether the rearrangement found in acyloxysilanes is unique to silicon, or general for the Ph_3MOCOR system, we have examined the analogous benzoyloxygermanes in addition to checking the behavior of the corresponding carbon compounds. Neither of the two representative carbon esters **3***a* or **3***b* showed any evidence for loss of phenyl nor did **3***a* show the $Ph_2\overset{\oplus}{C}CH_3$ peak expected from the rearrangement. As shown in Table III $Ph_3CO^{\oplus}$ is the base peak in both cases, with large intensities being observed for the $Ph_3C^{\oplus}$ ion.

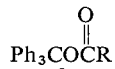

3

(*a*) R = CH_3
(*b*) R = Ph

TABLE III

Relative peak intensities based on the most abundant ion (taken as 100%)

Ester	$Ph_3CO^{\oplus}$	$Ph_3C^{\oplus}$	$RCO^{\oplus}$
3*a*	100	75.5	55
3*b*	100	61.3	95.5

[2]A. G. Brook and J. M. Duff. Unpublished studies.

Can. J. Chem. Downloaded from www.nrcresearchpress.com by 210.87.254.40 on 09/05/12
For personal use only.

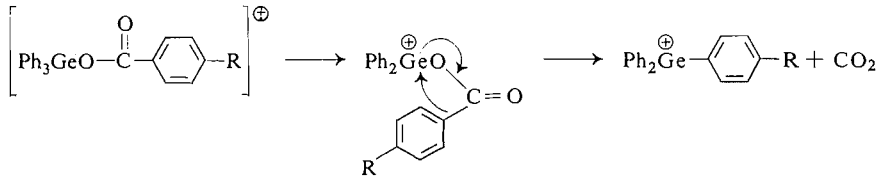

TABLE IV

Relative peak intensities based on the most abundant ion (taken as 100%)

Ester	M − 77	$Ph_2Ge^{\oplus}$–C$_6$H$_4$–R	$Ph_3Ge^{\oplus}$	$Ph_2Ge^{\oplus}$–C$_6$H$_4$–R/(M−77)
4a	100	43.0	43.0	0.43
4b	62.0	8.59	100	0.14
4c	100	31.0	32.0	0.31
4d	100	38.1	49.7	0.38

Unlike the carbon esters, benzoyloxygermanes undergo the same rearrangement as their silicon analogues. Each of the benzoates **4***a*–**4***d* shows

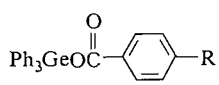

4

(*a*) R = H
(*b*) R = NO_2
(*c*) R = Br
(*d*) R = CH_3

successive loss of 77 and 44 mass units. In each case a metastable ion was obtained for the loss of CO_2.

In contrast to the triphenylsilyl compounds the triphenylgermyl compounds also show large peaks for the $Ph_3Ge^{\oplus}$ ion presumably formed by direct fission of the molecule-ion. Table IV lists the important ions. As in the benzoyloxytrimethylsilanes (2), aryl group migration is retarded by electron-withdrawing substituents, as shown by the smaller $Ph_2Ge^{\oplus}$–C$_6$H$_4$–R/(M−77) ratio found for the *p*-Br or *p*-NO_2 compounds.

Thus both the triphenylsilyl and triphenyl germyl compounds show unusual fragmentation–rearrangement processes which are unknown in carbon chemistry. Further studies on this and other organometallic systems are in progress.

Experimental

Mass spectra were run on an AEI MS-902 mass spectrometer at 70 V electron energy and a source temperature of ca. 150 °C. Samples were introduced through the direct probe system. All intensities for silicon-containing ions refer to the ^{28}Si isotope (92.3% abundance), while those containing germanium refer to the ^{74}Ge isotope (36.6% abundance). Cl- and Br-containing ions refer respectively to ^{35}Cl and ^{79}Br.

Acknowledgments

We acknowledge the assistance of Mr. David Priddle who ran the mass spectra, and the National Research Council of Canada for support of this research.

1. H. Budzikiewicz, C. Djerassi, and D. H. Williams. Interpretation of mass-spectra of organic compounds. Holden-Day. San Francisco. 1964. Chap. 1.
2. R. M. Teeter. Abstr. 10th Annual Conference on Mass Spectrometry, Am. Soc. Testing Mater., Proc., Committee E-14, New Orleans, Louisiana. 1962. p. 51; P. Brown and C. Djerassi. Angew. Chem. (Intern. Ed.) **6**, 477 (1967), ref. 74.
3. P. Brown and C. Djerassi. Angew. Chem. (Intern. Ed.) **6**, 477 (1967).

Can. J. Chem. Downloaded from www.nrcresearchpress.com by 210.87.254.40 on 09/05/12
For personal use only.

Temperature dependence of chemical shifts of protons in hydrogen bonds. Experimental evidence on an intramolecular hydrogen bond

T. SCHAEFER AND G. KOTOWYCZ[1]
Chemistry Department, University of Manitoba, Winnipeg, Manitoba

Received April 8, 1968

A temperature dependence of the chemical shift of the hydroxyl proton in the strong intramolecular hydrogen bond in 3,5-dichlorosalicylaldehyde is observed in carbon tetrachloride and benzene-d_6 solutions. Its magnitude of 0.25 to 0.30 $\times$ 10^{-2} p.p.m. per °C over a range of 100 °C is in agreement with the model described by Muller and Reiter (1).

Canadian Journal of Chemistry, 46, 2865 (1968)

Can. J. Chem. Downloaded from www.nrcresearchpress.com by 210.87.254.105 on 09/05/12
For personal use only.

Calculations by Muller and Reiter (1) predict a temperature dependence of the chemical shift of a proton in a hydrogen bond. The variation in shift arises from the anharmonicity of the low-frequency stretching vibration of X—H . . . Y. As the temperature increases the H . . . Y distance increases due to increased populations of the excited vibrational levels. Therefore the electric field exerted by Y at H decreases, leading to an upfield shift of from 0.2 to 0.8 $\times$ 10^{-2} p.p.m. per °C (1–4).

The temperature dependent shifts are observed and calculated to be linear to within about 0.04 p.p.m. over a 100 °C range. The predicted temperature dependence decreases as the dissociation energy of the hydrogen bond increases. Intermolecular hydrogen bonds commonly have heats of formation of about 6 kcal/mole (5).

The intramolecular hydrogen bond in 3,5-dichlorosalicylaldehyde is very stable. The free energy of activation for proton exchange in carbon tetrachloride solution is greater than 22 kcal/mole and lies between 19 and 20 kcal/mole at various concentrations in benzene (6).[2] The mean lifetime before exchange of the hydroxyl protons is at least 0.2 s at 100 °C in carbon tetrachloride; the lowest value is 0.02 s at 100 °C in a 10 mole % benzene solution. These lifetimes must be at least an order of magnitude greater (probably much more) than those of typical strong intermolecular hydrogen bonds. The observed temperature dependence of the hydroxyl proton shift in carbon tetrachloride and benzene is therefore assumed to be due mainly to the mechanism elaborated by Muller and Reiter (1), modified by possible solvent effects (8). The observed temperature dependence is also expected to lie near the lower limit of 0.2 $\times$ 10^{-2} p.p.m. per °C calculated by Muller and Reiter (1).

In Fig. 1, the proton resonance spectrum of 3,5-dichlorosalicylaldehyde displays the stereospecific coupling (0.6 c.p.s.) between proton 4 and

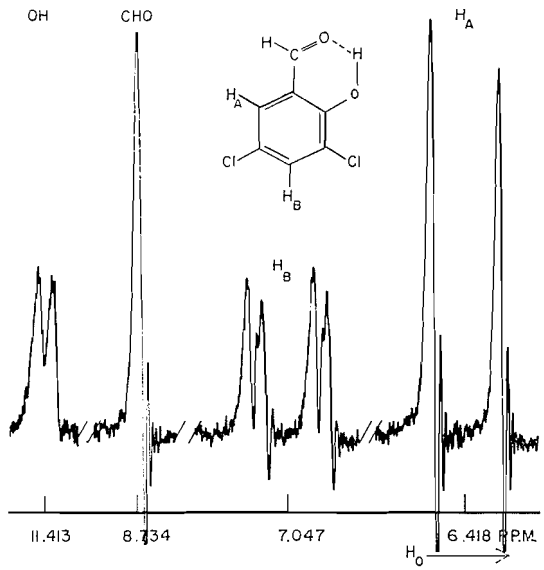

FIG. 1. The proton resonance spectrum of a degassed, 5 mole % solution of 3,5-dichlorosalicylaldehyde in benzene-d_6 at 30 °C. The shifts are in p.p.m. to low-field of internal tetramethylsilane. $J_{meta}^{H,H}$ = 2.54 ± 0.03 c.p.s., $J(OH-H_B)$ = 0.56 ± 0.02 c.p.s. (H_B = proton 4).

[1]Present address: Lawrence Radiation Laboratory, Berkeley, California.

[2]The free energy of activation was obtained by applying the method of Takeda and Stejskal (7) to the relative heights of the 4- and 6-proton resonance peaks. Proton 4 is coupled to the hydroxyl proton by 0.55 ±0.03 c.p.s. and this coupling shows an apparent decrease as the temperature increases. The mean lifetime before exchange is concentration dependent in benzene solution, implying an intermolecular proton exchange mechanism. A bimolecular rate constant of 16.8 ± 4.8 (r.m.s.) liters $mole^{-1}$ s^{-1} is found at 80 °C. Entropies of activation are −18 ±6 e.u. and heats of activation are 12 ±2 kcal/mole at 80 °C.

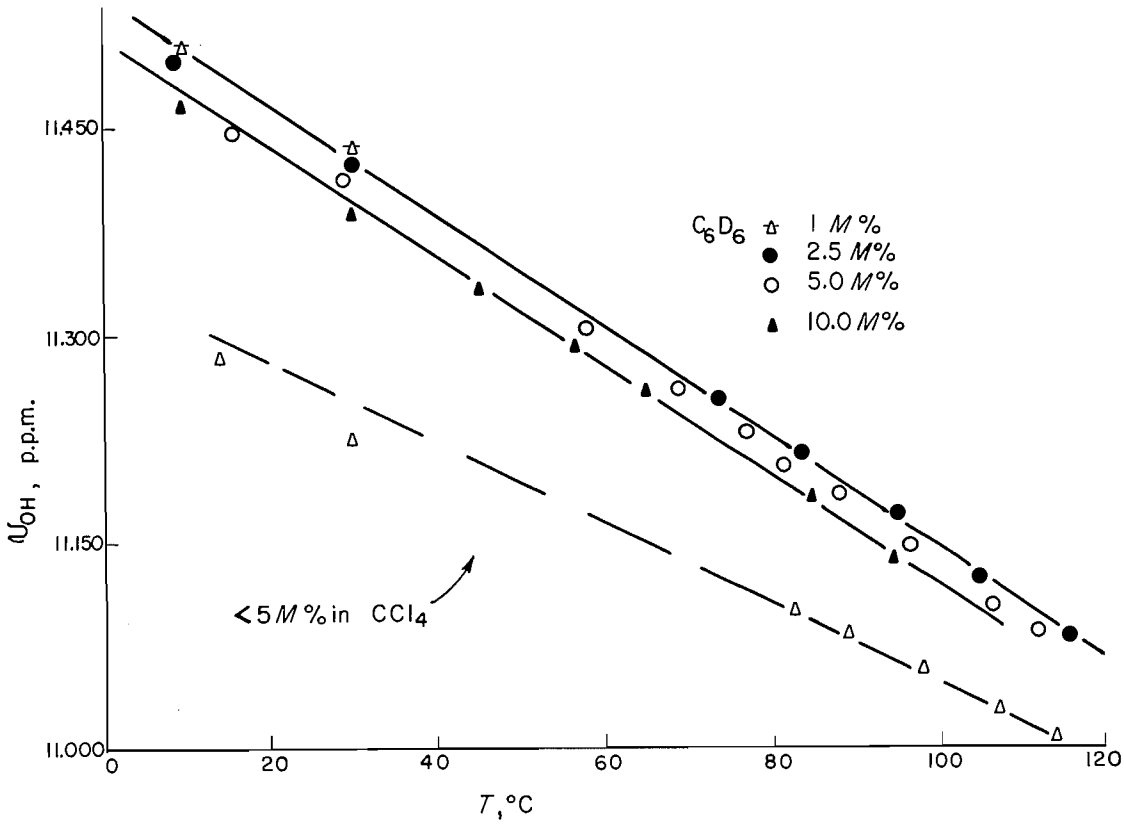

FIG. 2. The hydroxyl proton shift in p.p.m. to low-field of internal tetramethylsilane is plotted versus temperature in degrees centigrade for 3,5-dichlorosalicylaldehyde in carbon tetrachloride and benzene-d_6 solutions. The low-temperature points for the carbon tetrachloride solution are considered to be less reliable than the high-temperature points because the saturated solution, prepared at 26 °C and separated from the solid by decanting, may have changed a little in concentration at the low temperatures.

the hydroxyl proton (9, 10). In Tables I, II, and III the hydroxyl proton shift in various solvents at 30 °C and at various concentrations in benzene-d_6 is given. The temperature dependence of the hydroxyl proton shift in benzene-d_6 and carbon tetrachloride is also shown. In Fig. 2, the hydroxyl proton shift is plotted as a function of temperature over a range of 100 °C. The plots are linear to within experimental error.[3]

The temperature dependence of the shift in carbon tetrachloride is 0.27×10^{-2} p.p.m. per °C. In contrast, it is 0.015×10^{-2} p.p.m. per °C for the aldehyde proton and is 0.028×10^{-2} p.p.m. per °C for proton 4 (6). At 114 °C, the collapse of the spin multiplet is not yet complete. These results are taken as a confirmation of the model of Muller and Reiter (1). Association shifts must indeed be corrected for an intrinsic temperature dependence of the proton shielding in the hydrogen bond and the correction will increase as the strength of the bond decreases.

It may be noted that the solvent effect on the hydroxyl proton shift is much smaller than on the other protons in 3,5-dichlorosalicylaldehyde (6).[4] The largest solvent shift is observed in benzene solution and amounts to 0.15 p.p.m. (at 2.5 mole % at 30 °C). It is a *low-field shift* as predicted by the association model of Connolly and McCrindle (11, 12), confirming the presence

[3]There may be a 1–2 °C disagreement in the temperature at high and low temperatures because two different calibration procedures were used—see Experimental.

[4]Thus, in acetone the hydroxyl proton resonance shifts to low-field (relative to its position in cyclohexane) by 0.08 p.p.m. but the aldehyde proton undergoes a low-field shift of 0.32 p.p.m. This is a typical comparison (6).

Can. J. Chem. Downloaded from www.nrcresearchpress.com by 210.87.254.105 on 09/05/12
For personal use only.

Can. J. Chem. Downloaded from www.nrcresearchpress.com by 210.87.254.105 on 09/05/12
For personal use only.

TABLE I

Temperature and concentration dependence of the hydroxyl proton chemical shift of 3,5-dichlorosalicylaldehyde

Concentration in benzene-d_6*	Temperature† (°C)	Shift‡ (p.p.m.)
1	9.3	11.505
	30.0	11.436
2.5	8.5	11.495
	30.0	11.427
	74.3	11.251
	83.3	11.214
	95.0	11.171
	104.8	11.122
	116.0	11.071
5	17.8	11.448
	29.0	11.413
	58.0	11.305
	68.6	11.262
	76.8	11.227
	81.5	11.208
	88.0	11.186
	96.5	11.149
	106.3	11.106
	111.7	11.083
10	9.3	11.467
	30.0	11.389
	45.0	11.332
	56.3	11.295
	64.8	11.260
	84.7	11.184
	94.7	11.140

*In mole %.
†Relative accuracy estimated at 0.5 °C; absolute accuracy at 1–2 °C.
‡In p.p.m. to low-field of internal TMS with a precision of 0.005 p.p.m. or better in most instances.

TABLE II

Temperature dependence of the hydroxyl proton chemical shift of 3,5-dichlorosalicylaldehyde

Concentration in carbon tetrachloride	Temperature (°C)*	Shift (p.p.m.)†
Saturated, < 5 mole %	13.7	11.284
	30.0	11.249
	82.5	11.103
	89.0	11.084
	97.8	11.057
	106.8	11.027
	114.0	11.005

*Relative accuracy estimated at 0.5 °C; absolute accuracy at 1–2 °C.
†In p.p.m. to low-field of internal TMS with a precision of 0.005 p.p.m. or better in most instances.

of hydrogen bonding to the carbonyl group and not to the chlorine atom.[5] Now, the ratio of the change in shift with temperature to the association shift at 30 °C (relative to cyclohexane solution) is 0.35 ± 0.02 for each of the other protons in 5 mole % benzene-d_6 (6). Hence $0.15 \times 0.35 = 0.05$ p.p.m. is a reasonable correction to apply (for association changes) to the observed temperature dependence of the hydroxyl proton shift. Therefore the temperature dependence of the hydrogen bonded proton in benzene solution is about 0.31×10^{-2} p.p.m. per °C. A similar correction for the temperature dependence in carbon tetrachloride solution yields 0.26×10^{-2} p.p.m. per °C as the corrected value. A somewhat larger value in benzene for the intrinsic temperature dependence of the hydrogen bond proton shift[6] is conceivable because benzene affects the rate of proton exchange (6), suggesting a more strongly interacting solvent cage than in carbon tetrachloride solution. Drago (13) has shown that benzene is not an inert solvent when used as a medium for the study of heats of formation of donor–acceptor complexes. A 10% change in anharmonicity and/or bond length of the hydrogen bond due to change in solvent character from relatively inert to moderately interacting is perhaps possible.

A referee has emphasized that the model of Muller and Reiter assumes a low-frequency, asymmetric, stretching vibration of the X—H . . . Y bond. The question arises whether this holds for a strong intramolecular hydrogen bond, where X and Y are connected by a chain of bonds. Far-infrared work (14) shows that the stretching frequencies of the intramolecular hydrogen bonds in *o*-chlorophenol and *o*-nitrophenol are 84 cm^{-1} and 95 cm^{-1}, respectively. These frequencies are a little lower than those of the intermolecular hydrogen bonds in, say, *m*-chlorophenol. Furthermore they are asymmetric. The available evidence therefore is consistent with the model, even though there is no far-infrared data on 3,5-dichlorosalicylaldehyde.

[5]The aldehyde proton resonance line-width did not change at any temperature, confirming the absence of a tautomeric proton transfer to the carbonyl oxygen. The line-width of the resonance of proton 6 remained constant to within 0.02 c.p.s., showing at most a decrease with increase in temperature. This strongly indicates the absence of hydrogen bonding to chlorine. In the presence of such bonding the stereospecific coupling between proton 6 and the hydroxyl proton should have caused at least some broadening of the resonance peaks of proton 6.

[6]The upfield hydroxyl proton shift of 0.024 p.p.m. at 30 °C in going from 5 to 10 mole % in benzene is taken as a change in solvent effect and not due to a dimer-monomer equilibrium. A 40-fold increase in concentration from 0.25 to 10 mole % changed the C=O stretching frequency by less than 1 cm^{-1} from its value of 1671 cm^{-1}.

TABLE III

Solvent dependence of the hydroxyl proton chemical shift of 3,5-dichlorosalicylaldehyde*

Solvent	Concentration (mole %)	Shift (p.p.m.)†
Cyclohexane	<2.5‡	11.283
Benzene	5.0	11.410
Perfluorobenzene	<5‡	11.264
Carbondisulfide	<5‡	11.234
Chloroform-d_1	5.0	11.333
Methylene chloride	5.0	11.336
Acetone	5.0	11.363
Acetonitrile	<5‡	11.271

*Temperature: 30 °C.
†In p.p.m. to low-field of internal TMS with a precision of 0.005 p.p.m. or better in most instances.
‡Saturated solutions.

Experimental

3,5-Dichlorosalicylaldehyde from Aldrich Chemical Company was used as received and recrystallized from carbon tetrachloride, acetone, and ether. Carbon tetrachloride was redistilled and passed through Linde molecular sieve (4A). Acetone was refluxed with potassium permanganate, distilled, dried over calcium chloride, and redistilled. It was kept over alumina. Solutions in acetone were prepared on a vacuum line, in a dry box, or in air, with or without internal tetramethylsilane. The proton chemical shift did not differ by more than 0.01 p.p.m. in any of the solutions though in one, with which the least precaution had been taken, there was a coupling observable between the hydroxyl and the ring proton. Because of the small effects these precautions had on the measured hydroxyl proton shift, less stringent precautions were taken with the other solutions. They were all degassed.

The ring proton assignments were confirmed by use of mixed solvents of acetone–carbon disulfide and perfluorobenzene – carbon disulfide. This was necessary because the ring proton shifts interchange in some solvents.

Measurements were made on a DA-60-I Varian spectrometer using the frequency sweep mode and calibrations were done by period counting, using tetramethylsilane as the internal reference. The shift positions are thought to be accurate to 0.005 p.p.m. in most instances. Sample temperatures were calibrated using the Varian methanol and ethylene glycol samples. The former were used at low and the latter at high temperatures. Although the absolute temperatures may be in error by 2 °C the relative temperatures appear to be accurate to 0.5 °C.

Infrared spectra were obtained on a Perkin–Elmer 337 grating spectrophotometer. A 0.025 mm cell was used and indene line positions served to calibrate the carboxyl stretching frequencies.

Acknowledgment

We are grateful to the National Research Council of Canada for financial assistance.

1. N. Muller and R. C. Reiter. J. Chem. Phys. **42**, 3265 (1965).
2. L. W. Reeves. Trans. Faraday Soc. **55**, 1684 (1959).
3. J. C. Davis, Jr. and K. S. Pitzer. J. Phys. Chem. **64**, 886 (1960).
4. P. J. Berkeley, Jr. and M. W. Hanna. J. Phys. Chem. **67**, 846 (1963).
5. G. C. Pimentel and A. L. McClellan. The hydrogen bond. W. H. Freeman and Co., San Francisco. 1960.
6. G. Kotowycz. Ph.D. Thesis. University of Manitoba. 1967.
7. M. Takeda and E. O. Stejskal. J. Am. Chem. Soc. **82**, 25 (1960).
8. A. D. Buckingham, T. Schaefer, and W. G. Schneider. J. Chem. Phys. **32**, 1227 (1960).
9. R. Freeman. Mol. Phys. **6**, 535 (1963).
10. S. Forsén and R. A. Hoffman. J. Mol. Spectry. **20**, 168 (1966).
11. J. D. Connolly and R. McCrindle. Chem. and Ind. London, 379 (1965).
12. J. D. Connolly and R. McCrindle. Chem. and Ind. London, 2066 (1965).
13. R. S. Drago. Chem. Brit. **3**, 516 (1967).
14. W. J. Hurley, I. D. Kuntz, Jr., and G. E. Leroi. J. Am. Chem. Soc. **88**, 3199 (1966).

Synthesis of branched-chain sugars by the Wittig reaction

Alex Rosenthal and P. Catsoulacos
Department of Chemistry, University of British Columbia, Vancouver, British Columbia

Received March 25, 1968

The Wittig reaction has been extended to yield a 2,3-dideoxy branched-chain sugar from 2-deoxy-3-ketose **3**. Improvements in the procedures for the preparation of ketose (**3**) are also described.

Canadian Journal of Chemistry, 46, 2868 (1968)

Renewed interest in the chemistry of the branched-chain sugars has arisen partly because of their presence in some recently discovered antibiotics (1–3). Most synthetic work in this field has involved the condensation of Grignard reagents or diazomethane with ketoses (3, 4), or the scission of carbohydrate epoxides with organometallic reagents (5). In addition, the epoxides have been cleaved with diethyl malonate carbanion (6). Application of the oxo reaction to

Can. J. Chem. Downloaded from www.nrcresearchpress.com by 210.87.254.105 on 09/05/12
For personal use only.

TABLE III

Solvent dependence of the hydroxyl proton chemical shift of 3,5-dichlorosalicylaldehyde*

Solvent	Concentration (mole %)	Shift (p.p.m.)†
Cyclohexane	<2.5‡	11.283
Benzene	5.0	11.410
Perfluorobenzene	<5‡	11.264
Carbondisulfide	<5‡	11.234
Chloroform-d_1	5.0	11.333
Methylene chloride	5.0	11.336
Acetone	5.0	11.363
Acetonitrile	<5‡	11.271

*Temperature: 30 °C.
†In p.p.m. to low-field of internal TMS with a precision of 0.005 p.p.m. or better in most instances.
‡Saturated solutions.

Experimental

3,5-Dichlorosalicylaldehyde from Aldrich Chemical Company was used as received and recrystallized from carbon tetrachloride, acetone, and ether. Carbon tetrachloride was redistilled and passed through Linde molecular sieve (4A). Acetone was refluxed with potassium permanganate, distilled, dried over calcium chloride, and redistilled. It was kept over alumina. Solutions in acetone were prepared on a vacuum line, in a dry box, or in air, with or without internal tetramethylsilane. The proton chemical shift did not differ by more than 0.01 p.p.m. in any of the solutions though in one, with which the least precaution had been taken, there was a coupling observable between the hydroxyl and the ring proton. Because of the small effects these precautions had on the measured hydroxyl proton shift, less stringent precautions were taken with the other solutions. They were all degassed.

The ring proton assignments were confirmed by use of mixed solvents of acetone–carbon disulfide and perfluorobenzene – carbon disulfide. This was necessary because the ring proton shifts interchange in some solvents.

Measurements were made on a DA-60-I Varian spectrometer using the frequency sweep mode and calibrations were done by period counting, using tetramethylsilane as the internal reference. The shift positions are thought to be accurate to 0.005 p.p.m. in most instances. Sample temperatures were calibrated using the Varian methanol and ethylene glycol samples. The former were used at low and the latter at high temperatures. Although the absolute temperatures may be in error by 2 °C the relative temperatures appear to be accurate to 0.5 °C.

Infrared spectra were obtained on a Perkin–Elmer 337 grating spectrophotometer. A 0.025 mm cell was used and indene line positions served to calibrate the carboxyl stretching frequencies.

Acknowledgment

We are grateful to the National Research Council of Canada for financial assistance.

1. N. Muller and R. C. Reiter. J. Chem. Phys. **42**, 3265 (1965).
2. L. W. Reeves. Trans. Faraday Soc. **55**, 1684 (1959).
3. J. C. Davis, Jr. and K. S. Pitzer. J. Phys. Chem. **64**, 886 (1960).
4. P. J. Berkeley, Jr. and M. W. Hanna. J. Phys. Chem. **67**, 846 (1963).
5. G. C. Pimentel and A. L. McClellan. The hydrogen bond. W. H. Freeman and Co., San Francisco. 1960.
6. G. Kotowycz. Ph.D. Thesis. University of Manitoba. 1967.
7. M. Takeda and E. O. Stejskal. J. Am. Chem. Soc. **82**, 25 (1960).
8. A. D. Buckingham, T. Schaefer, and W. G. Schneider. J. Chem. Phys. **32**, 1227 (1960).
9. R. Freeman. Mol. Phys. **6**, 535 (1963).
10. S. Forsén and R. A. Hoffman. J. Mol. Spectry. **20**, 168 (1966).
11. J. D. Connolly and R. McCrindle. Chem. and Ind. London, 379 (1965).
12. J. D. Connolly and R. McCrindle. Chem. and Ind. London, 2066 (1965).
13. R. S. Drago. Chem. Brit. **3**, 516 (1967).
14. W. J. Hurley, I. D. Kuntz, Jr., and G. E. Leroi. J. Am. Chem. Soc. **88**, 3199 (1966).

Synthesis of branched-chain sugars by the Wittig reaction

Alex Rosenthal and P. Catsoulacos
Department of Chemistry, University of British Columbia, Vancouver, British Columbia

Received March 25, 1968

The Wittig reaction has been extended to yield a 2,3-dideoxy branched-chain sugar from 2-deoxy-3-ketose **3**. Improvements in the procedures for the preparation of ketose (**3**) are also described.

Canadian Journal of Chemistry, 46, 2868 (1968)

Renewed interest in the chemistry of the branched-chain sugars has arisen partly because of their presence in some recently discovered antibiotics (1–3). Most synthetic work in this field has involved the condensation of Grignard reagents or diazomethane with ketoses (3, 4), or the scission of carbohydrate epoxides with organometallic reagents (5). In addition, the epoxides have been cleaved with diethyl malonate carbanion (6). Application of the oxo reaction to

Can. J. Chem. Downloaded from www.nrcresearchpress.com by 210.87.254.5 on 09/05/12
For personal use only.

Can. J. Chem. Downloaded from www.nrcresearchpress.com by 210.87.254.5 on 09/05/12
For personal use only.

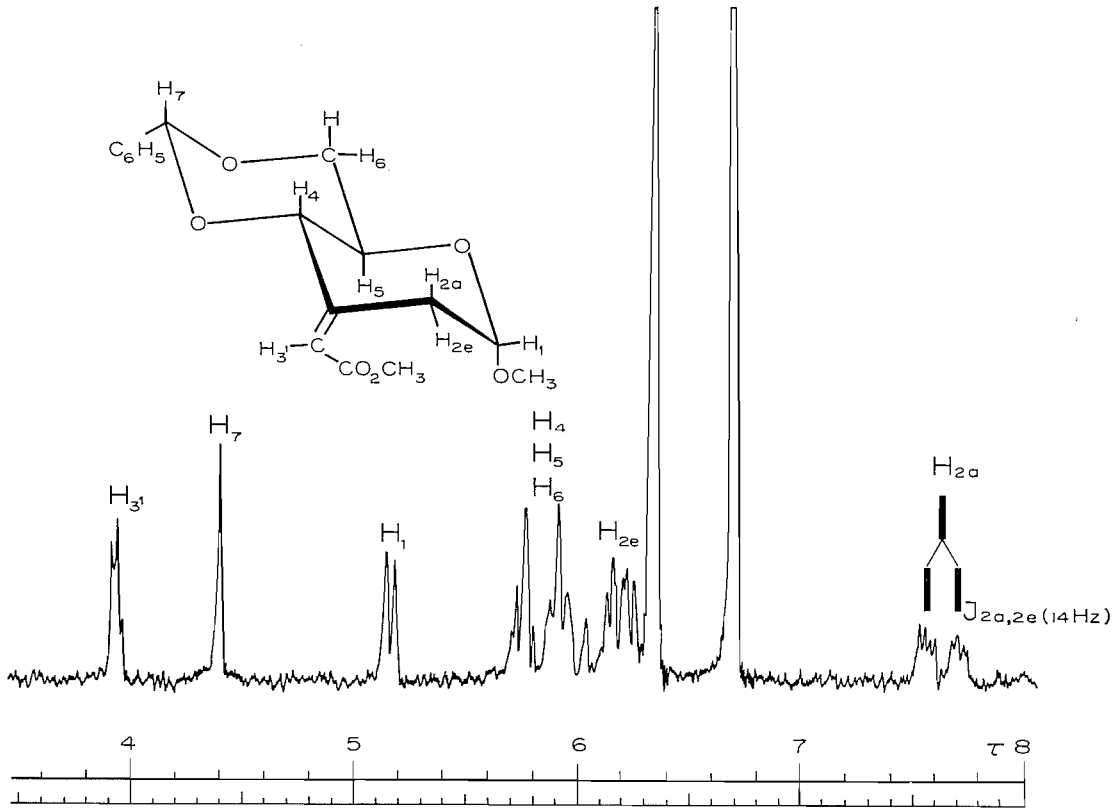

FIG. 1. Partial 100 Mc.p.s. proton magnetic resonance spectrum of methyl 4,6-*O*-benzylidene-3-*C*-(carbomethoxymethylene)-2,3-dideoxy-α-D-*erythro*-hexopyranoside in $CDCl_3$ as solvent.

unsaturated carbohydrates has given branched-chain carbohydrates (7). Condensation of Wittig reagents with ketoses has also afforded novel branched-chain sugars (8).

The extension of the Wittig reaction to a 2-deoxy-3-ketose (**3**) to yield a 2,3-dideoxy branched-chain sugar is the subject of this paper. The work described herein is also concerned with improvements in the procedures for the preparation of the ketose (**3**).

Reduction of methyl 2,3-anhydro-4,6-*O*-benzylidene-α-D-allopyranoside (**1**) with lithium aluminium hydride in tetrahydrofuran gave an 88% yield of methyl 4,6-*O*-benzylidene-2-deoxy-α-D-*ribo*-hexopyranoside (**2**). Subsequent oxidation of **2** with anhydrous methyl sulfoxide and acetic anhydride afforded methyl 4,6-*O*-benzylidene-2-deoxy-α-D-*erythro*-hexopyranosid-3-ulose (**3**) in 90% yield. The ketose (**3**) has been prepared previously in lower yields from **2** using chromium trioxide (9) and ruthenium tetroxide (10) as oxidants.

Reaction of methyl 4,6-*O*-benzylidene-2-deoxy-α-D-*erythro*-hexopyranosid-3-ulose(**3**)with phosphonoacetic acid trimethyl ester and potassium *t*-butoxide in anhydrous *N*,*N*-dimethyl formamide at room temperature for 20 h according to a procedure previously described (8, 11) resulted in a product (**4**) readily isolated in 76% yield. This product was a virtually pure substance as evidenced by thin-layer chromatography (t.l.c.) and by its proton magnetic resonance (p.m.r.) spectrum. This result was unexpected because Rosenthal and Nguyen (8) have found the condensation of phosphonoacetic acid trimethyl ester to 1,2:5,6-di-*O*-isopropylidene-α-D-*ribo*-hexofuranos-3-ulose to give both the *cis* and *trans* unsaturated branched-chain sugars.

The structure of the unsaturated sugar **4** was deduced from its p.m.r. spectrum (shown in Fig. 1). The H-1 signal at τ 5.13, which at normal sweep appears as a doublet, was resolved into a quartet at double sweep width. Irradiation of this

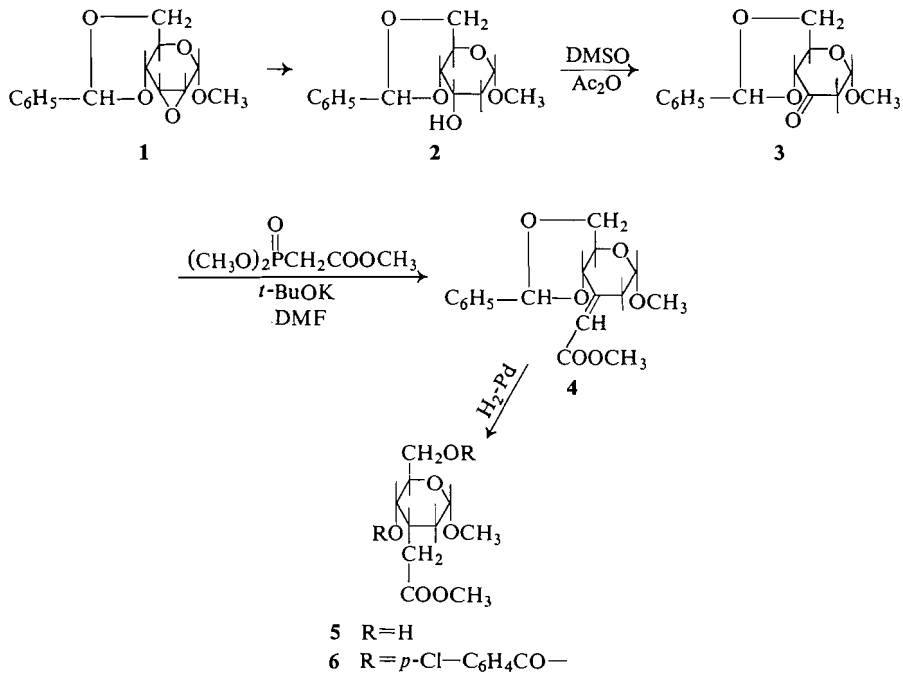

1 **2** **3** **4**

5 R=H
6 R=*p*-Cl—C_6H_4CO—

signal caused the two multiplets centered at τ 7.7 to collapse to two doublets having J = 14 Hz. Therefore, this high field group of signals is due to one H-2 proton which is coupled with the other H-2 proton and with the H-1 proton. Because there are eight peaks in the signal of the first H-2, it was assumed that this proton was coupled also with the H-3[1] proton in allylic position. Confirmation of this long-range coupling was provided by irradiation of the triplet (on magnified sweep this triplet was resolved into two doublets) at τ 3.9 which also led to a collapse of the eight lines at τ 7.7 to two doublets with the characteristic large geminal coupling (J = 14 Hz), and, in addition, resulted in an alteration of the multiplets of peaks centered at τ 6.2. Therefore, the unsymmetrical triplet at τ 3.9 must be due to H-3[1], and part of the signals at τ 6.2 must arise from the other H-2 proton (believed to be H-2e). Support for the latter assignment can be adduced from the p.m.r. spectrum of methyl 4,6-*O*-benzylidene-2,3-dideoxy-3-oximino-α-D-*erythro*-hexopyranoside and its analysis as reported by Baer and Kienzle (12). These authors also found a large downfield shift of H-2e with respect to H-2a. The large downfield shift of H-2e of **4** is attributed to the strong deshielding effect of the carbomethoxymethylene group on C-3. Therefore, compound **4** is probably *trans* methyl 4,6-*O*-benzylidene-3-*C*-(carbomethoxymethylene)-2,3-dideoxy-α-D-*erythro*-hexopyranoside.

Hydrogenation of the unsaturated product (**4**) using palladium on charcoal as catalyst gave the reduced (and debenzylidated) product (**5**) which could not be crystallized. Because of overlapping of the H-2, H-3, and H-3[1] signals (in the τ 7.0 to 8.3 region), the signals of the methine hydrogen (H-3) could not be used to deduce the structure of compound **5**. Furthermore, there was also overlapping of the H-4 and H-5 peaks. As a consequence, compound **5** was converted into its *p*-chlorobenzoate ester derivative (**6**). It is known that benzoate ester groups markedly shift the signals of secondary hydrogens downfield, often below the signal of the anomeric hydrogen (13). The p.m.r. spectrum of the benzoate derivative (**6**), shown in Fig. 2, is readily analyzed and can be used to deduce the structure of the branched-chain sugar (**6**). As expected, there is a quartet at τ 4.7 downfield from the H-1 signal (at τ 5.25). Irradiation of the multiplet of peaks at τ 7.3 resulted in the collapse of the quartet at τ 4.7 to a doublet. Because high field signals are generally attributed to hydrogen atoms attached to carbon atoms which have no

Can. J. Chem. Downloaded from www.nrcresearchpress.com by 210.87.254.5 on 09/05/12
For personal use only.

Can. J. Chem. Downloaded from www.nrcresearchpress.com by 210.87.254.5 on 09/05/12
For personal use only.

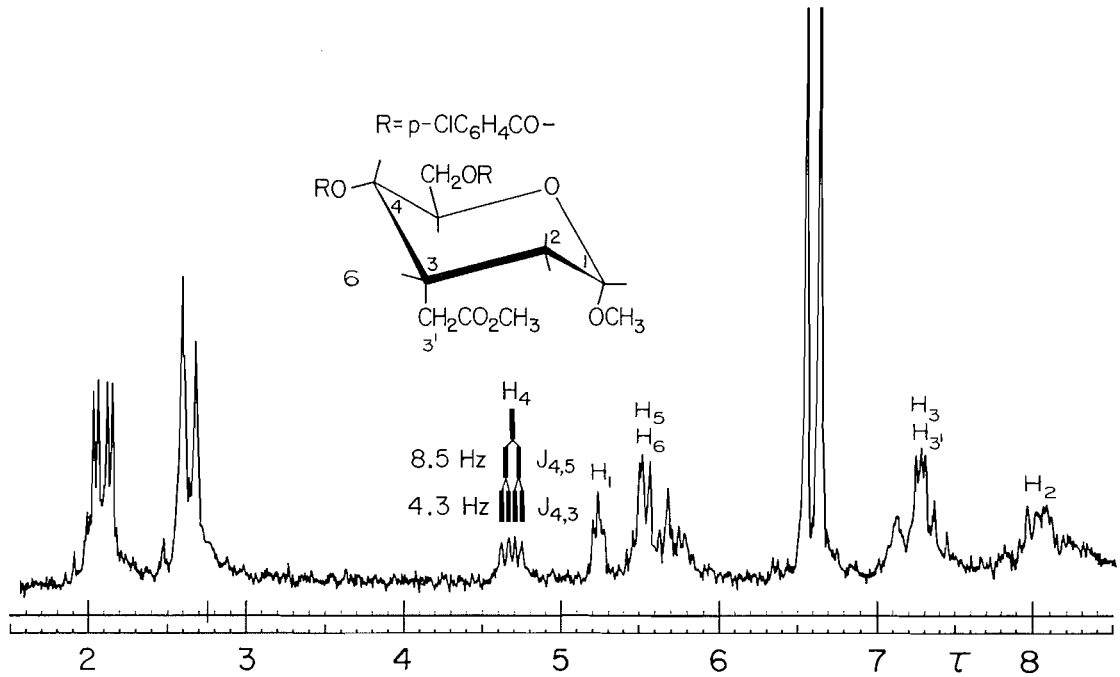

FIG. 2. The 100 Mc.p.s. proton magnetic resonance spectrum of methyl 3-*C*-(carbomethoxymethyl)-4,6-di-*O*-*p*-chlorobenzoyl-2,3-dideoxy-α-D-*ribo*-hexopyranoside in $CDCl_3$ as solvent.

oxygen atoms attached to them (13), it can be assumed that some of the peaks at τ 7.3 are due to H-3 and therefore the quartet at τ 4.7 is due to H-4. As shown in Fig. 2, the two coupling constants of the H-4 proton are 8.5 and 4.3 Hz. The larger of these must arise from the coupling of the H-4 and H-5 protons because both of these are in axial orientations. Therefore, the smaller coupling constant (J = 4.3 Hz) must be attributed to coupling between H-4 (in axial orientation) and H-3 which must be in an equatorial orientation. From this assignment it follows that the branched-chain group on C-3 must be in an axial orientation, and, therefore, compound **6** is undoubtedly methyl 3-*C*-(carbomethoxymethyl)-4,6-di-*O*-*p*-chlorobenzoyl-2,3-dideoxy-α-D-*ribo*-hexopyranoside.

Experimental

All spectra were measured with a Varian Associates 100 MHz HA spectrometer with deuteriochloroform as a solvent and tetramethylsilane as the internal standard set at τ = 10. Thin-layer chromatography was performed on silica gel G plates using benzene–methanol (97:3) as developer. The optical rotations were measured in 1 dm tubes at the D-line of sodium and room temperature (23–24°). The melting points were determined on a microstage and are uncorrected. The microanalyses were carried out by the University of British Columbia Microanalytical Laboratory.

Methyl 4,6-O-Benzylidene-2-deoxy-α-D-ribo-hexopyranoside (2)

Compound **2** was prepared using a modification of the procedure of Prins (14). To a solution of 2.5 g of methyl 2,3-anhydro-4,6-*O*-benzylidene-α-D-allopyranoside in 70 ml of anhydrous tetrahydrofuran were added 2 g of lithium aluminium hydride (in 5 portions) over a period of ten min. After the reaction mixture was refluxed for 5 h, the excess of lithium aluminium hydride was decomposed by dropwise addition of water. The solids were removed by filtration and washed with 200 ml of chloroform. The combined filtrate was washed twice with water (100 ml), dried with magnesium sulfate, and evaporated under reduced pressure to give a solid, yield 2.25 g (88%), which on recrystallization from ethyl acetate gave pure **2**; m.p. 125–127° (lit. (14), m.p. 118–120°).

Preparation of Methyl 4,6-O-Benzylidene-2-deoxy-α-D-erythro-hexopyranosid-3-ulose (3)

To a solution of methyl 4,6-*O*-benzylidene-2-deoxy-α-D-*ribo*-hexopyranoside (1.85 g) in anhydrous methyl sulfoxide (50 ml) was added anhydrous acetic anhydride (20 ml) and the resulting solution was kept at room temperature for 60 h. This solution was then mixed with a saturated aqueous solution of sodium bicarbonate. The precipitate which formed was removed by filtration, washed well with water, and air-dried, yield 1.65 g (90%).

The product was recrystallized from ethyl acetate, m.p. 174–176° (lit. (10), m.p. 176–178°). The phenylhydrazone derivative of **3** was prepared in the usual way, m.p. 177–178° (lit. (10), m.p. 176–177°).

Application of Wittig Reaction to 3 to Yield trans-Methyl 4,6-O-Benzylidene-3-C-(carbomethoxymethylene)-2,3-dideoxy-α-D-erythro-hexopyranoside (4)

An ice-cold solution of phosphonoacetic acid trimethyl ester (1.2 ml) and potassium *t*-butoxide (0.30 g) in anhydrous *N,N*-dimethyl formamide (2 ml) was added to a magnetically stirred solution (kept at 0°) of methyl 4,6-*O*-benzylidene-2-deoxy-α-D-*erythro*-hexopyranosid-3-ulose (0.5 g) in 6 ml of anhydrous *N,N*-dimethyl formamide. The mixture was stirred at room temperature for 20 h and was then poured into ice-water. The precipitate was removed by filtration, washed with water, and air-dried, yield 0.45 g, m.p. 124–126°. One recrystallization of the solid from ethyl acetate – light petroleum ether (b.p. 30–60°) afforded 0.38 g of product **4** (76%), m.p. 128–129°; $[\alpha]_D^{22}$ +213° (*c*, 2 in chloroform). Infrared spectrum: ν_{max} (Nujol) 1720 cm^{-1} (ester C=O) and 1660 (C=C). The proton magnetic resonance (p.m.r.) spectrum of **4** is shown in Fig. 1.

Anal. Calcd. for $C_{17}H_{20}O_6$: C, 63.75; H, 6.25. Found: C, 63.79; H, 6.09.

Methyl 3-C-(Carbomethoxymethyl)-2,3-dideoxy-α-D-ribo-hexopyranoside (5) and its p-Chlorobenzoate Derivative (6)

Compound **4** (0.20 g) dissolved in ethanol (40 ml), was allowed to react with hydrogen at room temperature and 1 atm pressure using 10% palladium on charcoal (0.3 g) as catalyst until the gas pressure remained constant. Work-up of the product (**5**) in the usual way gave an oil, yield 0.145 g (99%); $[\alpha]_D^{22}$ +130° (*c*, 3 in ethanol). Infrared spectrum: ν_{max} 3350 cm^{-1} (OH), 1720 (C=O). Nuclear magnetic resonance spectrum: overlapping multiplets at τ 7–8.4 equal to 5 hydrogens; multiplets centered at τ 7.32, 7.53, and 8.18, due to H-3, H-3^1, and H-2; triplet at τ 5.35 attributed to H-1; and two singlets, each equal to 3 H's at τ 6.35 and 6.70.

An amount of 0.035 g of compound **5** was allowed to react with *p*-chlorobenzoyl chloride (0.2 g) dissolved in pyridine (2 ml) at room temperature for 20 h followed by heating at about 80° for 1 h. The reaction mixture was poured into ice-water, extracted several times with chloroform, and the combined chloroform extracts washed with sodium bicarbonate and water, and then dried over magnesium sulfate. After the solvent was removed by evaporation under reduced pressure, the solid residue was recrystallized several times from ethanol (several recrystallizations or a chromatographic separation were necessary to remove the *p*-chlorobenzoic acid anhydride which accompanies the ester derivative), m.p. 104–105°, $[\alpha]_D^{22}$ +65° (*c*, 1 in chloroform). The p.m.r. spectrum of **6** is shown in Fig. 2.

Anal. Calcd. for $C_{24}H_{24}O_8Cl_2$: C, 56.36; H, 4.69. Found: C, 56.35; H, 4.70.

Acknowledgments

This work was supported in part by Public Health Service Research Grant No. CA-08382 from the United States National Cancer Institute and by the National Research Council of Canada.

1. R. U. LEMIEUX and M. L. WOLFROM. Advan. Carbohydrate Chem. **3**, 337 (1948).
2. F. SHAFIZADEH. Advan. Carbohydrate Chem. **11**, 263 (1956).
3. W. G. OVEREND. Chem. and Ind. London, 342 (1963).
4. J. S. BURTON, W. G. OVEREND, and N. R. WILLIAMS. J. Chem. Soc. 3433 (1965); 3446 (1965).
5. A. A. J. FEAST, W. G. OVEREND, and N. R. WILLIAMS. J. Chem. Soc. 7378 (1965); 303 (1966).
6. L. I. KUDRYASKOW, M. A. CHLENOV, and N. K. KOCHETKOV. Izv. Akad. Nauk. SSSR Ser. Khim. **1**, 75 (1965); Chem. Abstr. **63**, 14739 (1965).
7. A. ROSENTHAL and H. K. KOCH. J. Am. Chem. Soc. **90**, 2181 (1968).
8. A. ROSENTHAL and L. (BENZING) NGUYEN. Tetrahedron Letters, 2393 (1967).
9. B. FLAHERTY, W. G. OVEREND, and N. R. WILLIAMS. J. Chem. Soc. 398 (1966).
10. G. B. HOWARTH, W. A. SZAREK, and J. K. N. JONES. Chem. Commun. 62 (1968). P. J. BENYON, P. M. COLLINS, P. T. DOGANGES, and W. G. OVEREND. J. Chem. Soc. 1131 (1966).
11. C. SZANTY, L. TOKE, and P. KALONITS. J. Org. Chem. **31**, 1447 (1966).
12. H. H. BAER and F. KIENZLE. Can. J. Chem. **45**, 983 (1967).
13. E. J. REIST, L. V. FISHER, D. E. GUEFFROY, and L. GOODMAN. J. Org. Chem. **31**, 1506 (1966).
14. D. A. PRINS. J. Am. Chem. Soc. **70**, 3955 (1948). N. K. RICHTMYER and C. S. HUDSON. J. Am. Chem. Soc. **63**, 1727 (1941). L. F. WIGGINS. *In* Methods Carbohydrate Chem. **2**, 188 (1963).

Can. J. Chem. Downloaded from www.nrcresearchpress.com by 210.87.254.5 on 09/05/12
For personal use only.

Can. J. Chem. Downloaded from www.nrcresearchpress.com by 210.87.254.6 on 09/05/12
For personal use only.

The structures of three alkaloids from *Fumaria officinalis* L.

J. K. SAUNDERS, R. A. BELL, C.-Y. CHEN, AND D. B. MACLEAN
Department of Chemistry, McMaster University, Hamilton, Ontario

AND

R. H. F. MANSKE
Research Laboratories, UniRoyal Limited, Guelph, Ontario

Received July 9, 1968

Structures are proposed for three alkaloids isolated from *Fumaria officinalis* L. The three alkaloids, with a common ring system, are structurally related to the known ochotensimine.

Canadian Journal of Chemistry, 46, 2873 (1968)

In 1938 Manske (1) reported the isolation of alkaloid, F-37 (**1**), from *F. officinalis*. More recently two related alkaloids, **2** and **3**, have been isolated by Manske (2) from the same source. Compound **2**, a lower homologue of **1**, is converted to **1** with diazomethane. The first clue that **3** has a ring system similar to **1** and **2** came from an examination of the mass spectra of **1**, **2**, and **4** (the product obtained by reduction of **3** with lithium aluminium hydride). The fragmentation of the three compounds was similar, showing the shifts expected because of the nature of their substituents. Evidence is presented that the alkaloids have structure **A**.

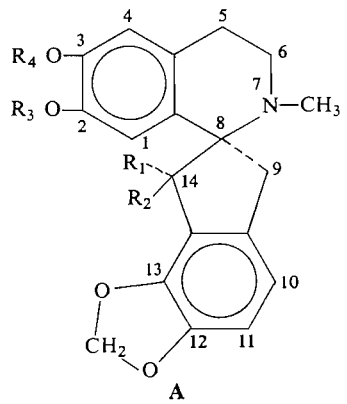

A

1 [1]$C_{21}H_{23}NO_5$; [2]$R_1 + R_2 = H + OH$; $R_3 = R_4 = CH_3$; m.p. 177°; $[\alpha]_D = -31°$ ($c = 0.97$ in $CHCl_3$).

2 $C_{20}H_{21}NO_5$; $R_1 + R_2 = H + OH$; $R_3 + R_4 = H + CH_3$; m.p. 157°.

3 $C_{20}H_{17}NO_5$; $R_1 + R_2 = O$; $R_3 + R_4 = CH_2$; m.p. 138°; $[\alpha]_D = +138°$ ($c = 1.05$ in $CHCl_3$).

4 $C_{20}H_{19}NO_5$; $R_1 + R_2 = H + OH$; $R_3 + R_4 = CH_2$; m.p. 161–166° (d).

Because of the paucity of the natural bases and their sensitivity to simple chemical reagents our structural assignment is based primarily on physical evidence. The physical properties of **3** are: λ_{max}(EtOH) 203, 237, 263, 294, and 355 mμ (log ε 4.60, 4.31, 4.05, 3.66, and 3.51) and $\nu_{max}(CHCl_3)$ 1709 cm^{-1}; of **1**: λ_{max}(EtOH) 207, 235, and 288 mμ (log ε 4.74, 3.94, and 3.74), and $\nu_{max}(CS_2)$ 3560 cm^{-1} (unchanged upon dilution). It is noteworthy that the ultraviolet (u.v.) spectrum of **4** was virtually superimposable on that of **1** and that its infrared spectrum showed a similar absorption in the hydroxyl region. The change in u.v. absorption in the transformation, **3** → **4**, is indicative of the reduction of a conjugated carbonyl group.

The proton magnetic resonance spectrum (p.m.r.) of **3** shown in Fig. 1*a*, revealed the presence of: (*i*) four aromatic protons, two ortho to each other (δ_{HA}, 7.07, δ_{HB}, 6.86; $J_{AB} = 8.0$ Hz) and two para to each other ($\delta_{HA'}$, 6.54, $\delta_{HB'}$, 6.16; $J_{A'B'} \cong 0$ Hz); (*ii*) two sets of methylenedioxy protons centered at $\delta = 6.12$ and $\delta = 5.80$; (*iii*) six aliphatic protons in the region δ 3.60–2.60 two of which are present in a benzylic AB quartet ($\delta_{HA''}$, 3.50, $\delta_{HB''} = 3.32$; $J_{A''B''} = 18.0$ Hz) while the other four are not readily analyzable;

[1]The names fumaricine and fumariline are suggested for **1** and **3**, respectively.

[2]The molecular formulas of the three natural compounds were assigned on the basis of elemental analysis and high resolution mass spectrometry; in the case of **4** the assignment is based on mass spectrometry alone.

Can. J. Chem. Downloaded from www.nrcresearchpress.com by 210.87.254.6 on 09/05/12
For personal use only.

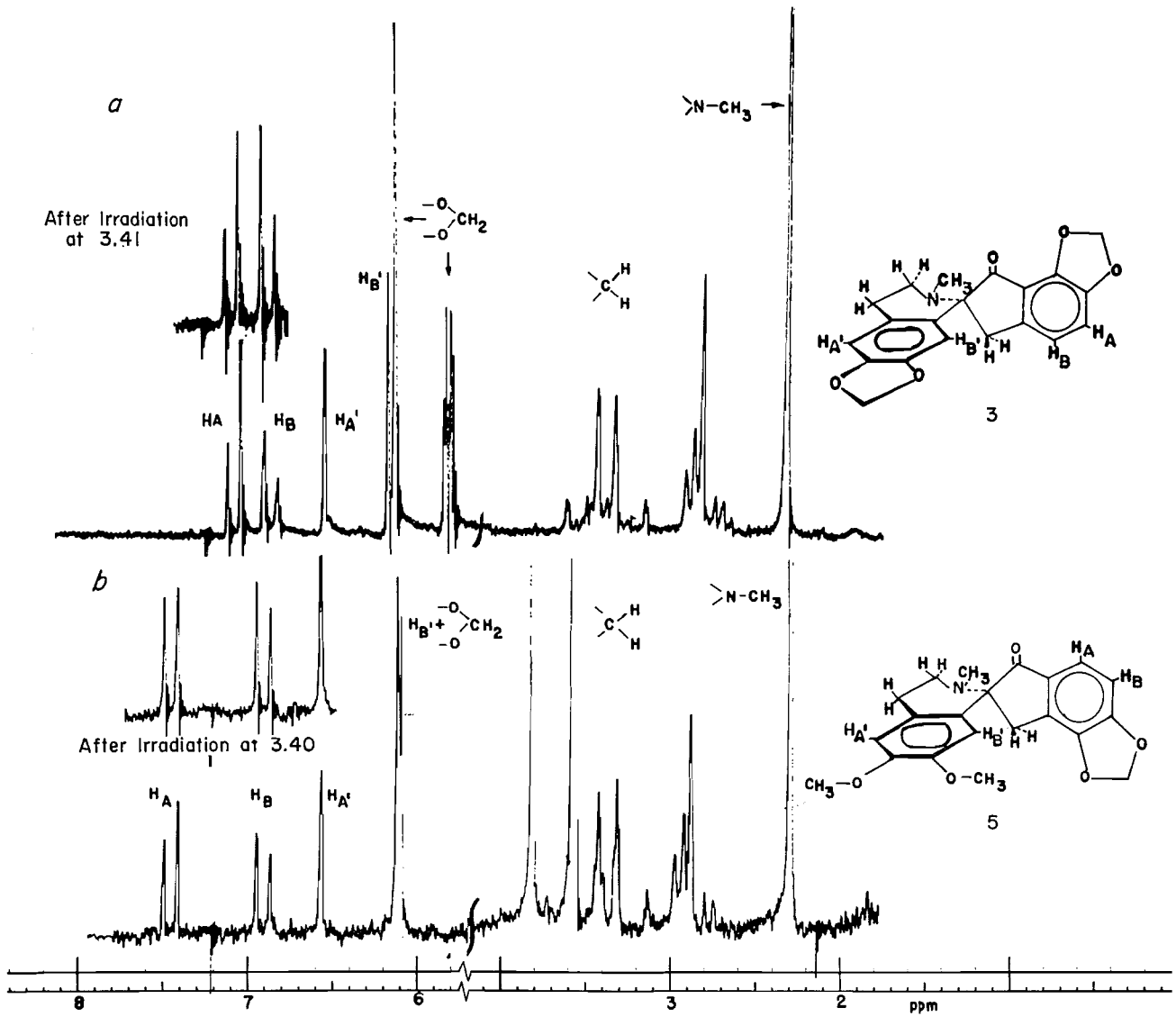

FIG. 1. The 100 MHz proton magnetic resonance spectrum of (*a*) **3** and (*b*) **5**.

Can. J. Chem. Downloaded from www.nrcresearchpress.com by 210.87.254.6 on 09/05/12
For personal use only.

and finally (*iv*) a singlet (3H) at $\delta = 2.36$ attributed to an $>N\text{-}CH_3$ group.

In the p.m.r. spectrum of **4** the hydrogen geminal to the hydroxyl group was uncoupled to neighboring aliphatic protons, an observation compatible with the fact that **3** would not exchange hydrogen for deuterium under the usual conditions of exchange of enolizable hydrogens (3). Thus it seems that the carbonyl of **3** is flanked on one side by a phenyl group and on the other by a quaternary center. These data suggest that **3** may have the gross structure **A**.

In order to substantiate gross structure **A** and to establish the orientation of the methylenedioxy groups in **3** a detailed comparison of the p.m.r. spectrum of **3** with the synthetic compound **5** (Fig. 1*b*) of established structure (4) was undertaken. Cursory examination of the spectra of **3** and **5** reveals a remarkable similarity particularly in the region of the aliphatic protons (δ 2.6–3.6). In the aromatic region, too, the two spectra exhibit a common pattern and differ appreciably only in the chemical shift of the low field protons of the AB quartet.

These observations imply that **3** and **5** have a common ring system but may differ in substitution pattern as well as in the nature of their substituents. Moreover, the product of hydride reduction of **5**, an isomer of **1**, has a mass spectrum virtually identical with the natural base **1**, lending further support to the assumption of a common ring system in **1**, **2**, **3**, and **5**.

By locating the methylenedioxy group of **3** at C-12 and C-13 instead of at C-10 and C-11 as in **5**, the properties of **3** are explicable. H_A in **5** is ortho to the carbonyl group whereas in **3** it is para. The chemical shift difference of H_A between **3** and **5** is expected of aromatic protons ortho and para to a carbonyl group (5), respectively. In each case H_B is meta to the carbonyl and absorbs at approximately the same region. H_A and H_B are long-range coupled to the AB quartet centered near 3.40 in **3** and **5** and in each the coupling is stronger to H_B. (See Fig. 1*a* and 1*b*.) H_B is ortho to the methylene group in **3** and para in **5** whereas H_A is meta in both. The coupling of the methylene to H_B in **3** ($J = 1.2$ Hz) is stronger than with H_B in **5** ($J < 1.0$ Hz). This difference is in the order expected for ortho and para benzylic coupling (6). $H_{A'}$ in **3** and **5** is broader than $H_{B'}$, because of *o*-benzylic coupling to one or both of the protons at C-5 and is, therefore, assigned to C-4. The assignment of the same substitution pattern to **1** as to **3** rests on a study of nuclear Overhauser effects discussed in an accompanying communication (7). These alkaloids have the same basic skeleton as ochotensimine (8). Whether they are precursors or oxidation products of the latter skeleton is an interesting biogenetic puzzle.

Acknowledgment

We wish to express our gratitude to Professor Stewart McLean for making available to us a generous sample of compound **5**. We thank the National Research Council of Canada for financial support of this work and McMaster University for the award of a University Fellowship to C.-Y. Chen.

1. R. H. F. MANSKE. Can. J. Research, **16B**, 438 (1938).
2. R. H. F. MANSKE. To be published.
3. H. BUDZIEKIEWICZ, C. DJERASSI, and D. H. WILLIAMS. Structure elucidation of natural products by mass spectrometry. Vol. I. Holden-Day Inc., San Francisco. 1964. p. 19.
4. S. MCLEAN, M.-S. LIN, and J. WHELAN. Tetrahedron Letters, No. 20, 2425 (1968).
5. J. W. EMSLEY, J. FEENEY, and L. H. SUTCLIFFE. High resolution nuclear resonance spectroscopy. Vol. II. Pergamon Press Ltd., Oxford. 1966. p. 750.
6. D. T. WITTIAK, D. B. PATEL, and Y. LIN. J. Am. Chem. Soc. **89**, 1908 (1967).
7. J. K. SAUNDERS, R. A. BELL, C.-Y. CHEN, D. B. MACLEAN, and R. H. MANSKE. Can. J. Chem. This issue.
8. S. MCLEAN and M.-S. LIN. Tetrahedron Letters, 3819 (1964). S. MCLEAN, M.-S. LIN, A. C. MACDONALD, and J. TROTTER. Tetrahedron Letters, 185 (1966). S. MCLEAN, M.-S. LIN, and R. H. F. MANSKE. Can. J. Chem. **44**, 2449 (1966).

Nuclear Overhauser effect studies on *Fumaria* alkaloids

J. K. SAUNDERS, R. A. BELL, C.-Y. CHEN, D. B. MACLEAN
Department of Chemistry, McMaster University, Hamilton, Ontario

AND

R. H. F. MANSKE
Research Laboratories, Uniroyal Limited, Guelph, Ontario

Received July 9, 1968

The nuclear Overhauser effect has been used to confirm the structures proposed for two alkaloids isolated from *Fumaria officinalis* L.

Canadian Journal of Chemistry, 46, 2876 (1968)

Can. J. Chem. Downloaded from www.nrcresearchpress.com by 210.87.254.42 on 09/05/12
For personal use only.

The alkaloids **2***a* and **2***b*, isolated from *F. officinalis* by Manske (1, 2) have been assigned (3) a carbon skeleton similar to that of the alkaloid ochotensimine (4). By application of the nuclear Overhauser effect (N.O.E.) (5) we have confirmed the structural assignment for **2***a* and **2***b*.

The nuclear Overhauser effects shown by the protons present in the related synthetic ketone **1** (6) were first examined. The proton magnetic resonance (p.m.r.) spectrum of **1** has signals for the protons on C-1, C-4, C-9, and C-13 as well-resolved lines, sufficiently separated from other transitions to be accurately integrated. Table I records the area increases of these signals when the transitions of neighboring protons were saturated and the internuclear distances between the observed and irradiated protons, calculated on the assumption that the ketone **1** possesses the same conformation as ochotensimine.

An N.O.E. is observed for H-4 on irradiation of the C-5 protons. The C-5 protons cannot be *independently* saturated (7) but their chemical shifts can be unequivocally assigned. The occurrence of a 21% N.O.E. between H-4 and the methoxyl group at 3.82 p.p.m. defines the chemical shift of the C-3 methoxyl. In a similar fashion the C-2 methoxyl group at 3.57 p.p.m. gives rise to a 28% N.O.E. for the aromatic proton H-1. The area increase recorded is greater than expected because of partial saturation of C-9 H_A. Thus the N.O.E. method is valuable in locating the position of methoxyl groups in aromatic rings. The *N*-methyl group in **1** can reside in a pseudo-equatorial or pseudo-axial conformation, placing the methyl group 2.5 Å and 2.3 Å, respectively, away from C-9 H_B. A 15% N.O.E. is observed. The aromatic proton at C-13 is affected by saturation at C-12 but *not* by the distant C-9 protons. The aromatic proton at C-1 shows a 25% N.O.E. on saturation of the protons at C-9. This shows the spatial proximity of H-1 and C-9 H_A, and is accounted for by the conformation shown in **1**.

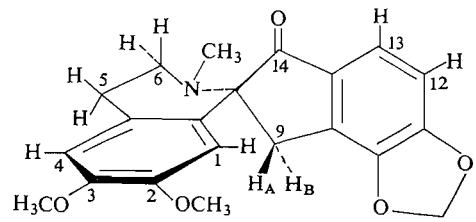

1

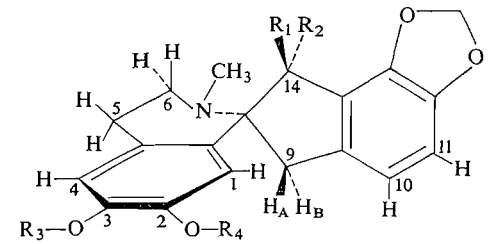

2 *a*, $R_1 + R_2 = O$; $R_3 + R_4 = CH_2$
b, $R_1 = H$; $R_2 = OH$; $R_3 = R_4 = CH_3$

Since the N.O.E. data correlate with the structure of ketone **1**, the N.O.E. data obtained for the new alkaloids **2***a* and **2***b* can be interpreted. The structure of **2***a* has been deduced from mass spectral and p.m.r. chemical shift data in an accompanying communication (3). The N.O.E. data (Table II) show similar values for **1** and **2***a* with one outstanding exception. There is a 19% N.O.E. for the C-10 proton when the C-9 protons are saturated which unequivocally places the methylenedioxy function in **2***a* at the 12,13-

TABLE I

Nuclear Overhauser effects in **1**

Observed proton	δ* (p.p.m.)	Irradiated protons	δ (p.p.m.)	% area increase	Internuclear distance (Å)†
C-1 H	6.11	C-9 H	3.40	25	1.85
C-1 H	6.11	C-2 OCH_3	3.57	28	1.80
C-4 H	6.57	C-5 H	2.87	17	2.55
C-4 H	6.57	C-5 H	2.82	17	2.80
C-4 H	6.57	C-3 OCH_3	3.82	21	1.80
C-9 H	3.40	N-CH_3	2.31	15	2.50
C-13 H	7.46	C-12 H	6.91	16	2.40

*Tetramethylsilane as internal standard.
†As measured from a Dreiding Molecular Model.

TABLE II

Nuclear Overhauser effects in **2***a* and **2***b*

Observed proton	δ (p.p.m.)		Irradiated protons	δ (p.p.m.)		% area increase	
	2*a*	**2***b*		**2***a*	**2***b*	**2***a*	**2***b*
C-1 H	6.16	6.39	C-9 H	3.41	3.29	22	19
C-1 H	6.16	6.39	C-2 OCH_3	—	3.49	—	23
C-4 H	6.54	6.57	C-5 H	2.21	2.71	25	12
C-4 H	6.54	6.57	C-3 OCH_3	—	3.81	—	21
C-9 H	3.41	3.29	N-CH_3	2.36	2.40	7	7
C-9 H	3.41	3.29	N-CH_3*	2.36	2.40		
			C-10 H*	6.86	6.73	16	16
C-10 H	6.86	6.73	C-9 H	3.41	3.29	19	20

*Triple irradiation.

position on the aromatic ring. We noted that saturation of the C-10 proton does not give an observable N.O.E. for the C-9 protons. Simultaneous saturation of *both* *N*-methyl and C-10 protons, however, results in a 16% N.O.E. for the C-9 protons. The small N.O.E. noted for the C-9 protons on saturation of the *N*-methyl group alone is a consequence of the presence of a C-10 proton. As in the case of ketone **1** an N.O.E. is observed for the C-4 proton on saturation of the C-5 protons and for the C-1 proton on saturation of the C-9 protons. Thus, not only is the gross structure of **2***a* confirmed, but its preferred conformation is defined.

The alcohol **2***b* shows in its p.m.r. spectrum two methoxyls at 3.49 and 3.81 p.p.m. and one methylenedioxy group at 5.91 p.p.m. The N.O.E.s (Table II) observed for the protons at C-1 and C-4 on saturation of the methoxyl groups indicate that they occupy the 2- and 3-positions, respectively. The methylenedioxy group must occupy the 12,13-position since saturation of the protons at C-9 shows an N.O.E. for the aromatic proton at C-10. The aromatic proton at C-1, as in the case of ketone **1** and **2***a*, again shows an N.O.E. when the protons at C-9 are saturated. Thus, the skeletal structure of the alcohol **2***b* must be identical with that of the ketone **1** and substituted as in **2***a*.

Since the proton at C-14 in **2***b* showed no N.O.E. on saturation of C-1 H, it must either be on the opposite side of the five-membered ring to C-1 H, or it must be more than 3.1–3.2 Å away from C-1 H (8). The infrared spectrum of **2***b*, $\nu_{max}(CS_2)$ 3560 cm^{-1} (unchanged on dilution) implies that the C-14 OH must be hydrogen bonded to the tertiary nitrogen (9). The coupling constant, $J_{H,OH}$ = 11.0 Hz, obtained at −10°, indicates that the dihedral angle between the C-14 H and the hydroxyl proton is 160–170° (10). Thus C-14 must possess the relative configuration as shown in **2***b*. With the nitrogen-containing ring in the half-chair conformation (as shown in **2***b*), C-14 H is 3.2 Å from C-1 H, and is too distant for an observable N.O.E. The N-CH_3 group in **2***b* would presumably occupy a pseudo-axial orientation.

In conclusion, the above examples demonstrate

Can. J. Chem. Downloaded from www.nrcresearchpress.com by 210.87.254.42 on 09/05/12
For personal use only.

the power of the nuclear Overhauser effect in the elucidation of structural, stereochemical, and conformation problems.

Acknowledgment

We wish to thank Professor Stewart McLean for making available to us a generous sample of compound **1**. We thank the National Research Council of Canada for financial support of this work and McMaster University for the award of a University Fellowship to C.-Y. Chen.

1. R. H. F. MANSKE. Can. J. Research, **16B**, 438 (1938).
2. R. H. F. MANSKE. To be published.
3. J. K. SAUNDERS, R. A. BELL, C.-Y. CHEN, D. B. MACLEAN, and R. H. F. MANSKE. Can. J. Chem. This issue.
4. S. MCLEAN, M. -S. LIN, A. C. MACDONALD, and J. TROTTER. Tetrahedron Letters, 3819 (1964). S. MCLEAN, M. -S. LIN, and R. H. F. MANSKE. Can. J. Chem. **44**, 2449 (1966).
5. F. A. L. ANET and A. J. R. BOURN. J. Am. Chem. Soc. **87**, 5250 (1965); R. H. MARTIN and J. C. NOULS. Tetrahedron Letters, 2727 (1968), and references therein.
6. S. MCLEAN, M. -S. LIN, and J. WHELAN. Tetrahedron Letters, 2425 (1968).
7. B. M. FUNG. J. Am. Chem. Soc. **90**, 219 (1968).
8. R. A. BELL and E. N. C. OSAKWE. Chem. Commun. To be published.
9. A. R. H. COLE. Technique of organic chemistry. Vol. XI. Part I. Interscience Publishers, Inc., New York. 1963 p. 148.
10. R. D. STOLOW and A. A. GALLO. Tetrahedron Letters, 3331 (1968); N. L. BOULD and Y. S. RIM. J. Org. Chem. **33**, 1303 (1968).

Can. J. Chem. Downloaded from www.nrcresearchpress.com by 210.87.254.42 on 09/05/12
For personal use only.

Reactions of hot hydrogen atoms in mercaptan–ethylene systems[1]

R. P. STEER AND A. R. KNIGHT
Department of Chemistry and Chemical Engineering, University of Saskatchewan, Saskatoon, Saskatchewan

Received July 16, 1968

Investigation of the photolysis of methanethiol and ethanethiol vapor in the presence of ethylene and inert gas has indicated the formation of energetic hydrogen atoms in the primary process. Rate constant ratios for the reactions of these species have been found to be pressure dependent.

Canadian Journal of Chemistry, **46**, 2878 (1968)

As part of a general investigation of thiyl radical reactions, we recently examined in detail the photolysis of methanethiol vapor (1). We wish to report here results of a further study of this system, and of ethanethiol,[2] in particular, the reactions of hydrogen atoms produced in the photolysis with added ethylene and inert gas.

The principal products of mercaptan photolysis, hydrogen and disulfide, can be accounted for by the established simple scheme.

[1] $$RSH + h\nu \rightarrow RS + H$$

[2] $$H + RSH \xrightarrow{k_2} H_2 + RS$$

[3] $$RS + RS \rightarrow RSSR$$

For both methanethiol (1) and ethanethiol,[2] the primary quantum yield of H_2 is unity within experimental error.

The reaction in the presence of olefins has been studied in a variety of systems, and the additional reactions involving hydrogen atoms are:

[4] $$H + C_2H_4 \xrightarrow{k_4} C_2H_5$$

[5] $$C_2H_5 + RSH \rightarrow C_2H_6 + RS$$

A simple kinetic treatment of the mechanism allows calculation of the k_2/k_4 ratio from measurements of $\Phi(H_2)$ as a function of olefin pressure. A value of 2.32 ± 0.11 was found previously (1) for the CH_3SH–C_2H_4 system, and in the present study, we find $k_2/k_4 = 2.00 \pm 0.05$ for C_2H_5SH–C_2H_4, in agreement with the value of 1.9 ± 0.1 reported by Kuntz (2).

Recent work by Gann and Dubrin (3) on the photolysis of H_2S and several other H-atom sources, however, has indicated that, in the primary process, hydrogen atoms can acquire as translational excitation almost all the energy in excess of the H–X bond strength. It was of interest therefore, to investigate the possibility that "hot" hydrogen atoms are formed in the mercaptan photolysis as well.

[1]From the Ph.D. Thesis of R. P. Steer to be submitted to the University of Saskatchewan, Saskatoon, Saskatchewan.

[2]The photolysis of pure C_2H_5SH is under investigation in this laboratory and in general exhibits the same behavior as methanethiol, but with the absence of some complicating features of that system.

the power of the nuclear Overhauser effect in the elucidation of structural, stereochemical, and conformation problems.

Acknowledgment

We wish to thank Professor Stewart McLean for making available to us a generous sample of compound **1**. We thank the National Research Council of Canada for financial support of this work and McMaster University for the award of a University Fellowship to C.-Y. Chen.

1. R. H. F. MANSKE. Can. J. Research, **16B**, 438 (1938).
2. R. H. F. MANSKE. To be published.
3. J. K. SAUNDERS, R. A. BELL, C.-Y. CHEN, D. B. MACLEAN, and R. H. F. MANSKE. Can. J. Chem. This issue.
4. S. MCLEAN, M. -S. LIN, A. C. MACDONALD, and J. TROTTER. Tetrahedron Letters, 3819 (1964). S. MCLEAN, M. -S. LIN, and R. H. F. MANSKE. Can. J. Chem. **44**, 2449 (1966).
5. F. A. L. ANET and A. J. R. BOURN. J. Am. Chem. Soc. **87**, 5250 (1965); R. H. MARTIN and J. C. NOULS. Tetrahedron Letters, 2727 (1968), and references therein.
6. S. MCLEAN, M. -S. LIN, and J. WHELAN. Tetrahedron Letters, 2425 (1968).
7. B. M. FUNG. J. Am. Chem. Soc. **90**, 219 (1968).
8. R. A. BELL and E. N. C. OSAKWE. Chem. Commun. To be published.
9. A. R. H. COLE. Technique of organic chemistry. Vol. XI. Part I. Interscience Publishers, Inc., New York. 1963 p. 148.
10. R. D. STOLOW and A. A. GALLO. Tetrahedron Letters, 3331 (1968); N. L. BOULD and Y. S. RIM. J. Org. Chem. **33**, 1303 (1968).

Can. J. Chem. Downloaded from www.nrcresearchpress.com by 210.87.254.6 on 09/05/12
For personal use only.

Reactions of hot hydrogen atoms in mercaptan–ethylene systems[1]

R. P. STEER AND A. R. KNIGHT
Department of Chemistry and Chemical Engineering, University of Saskatchewan, Saskatoon, Saskatchewan

Received July 16, 1968

Investigation of the photolysis of methanethiol and ethanethiol vapor in the presence of ethylene and inert gas has indicated the formation of energetic hydrogen atoms in the primary process. Rate constant ratios for the reactions of these species have been found to be pressure dependent.

Canadian Journal of Chemistry, **46**, 2878 (1968)

As part of a general investigation of thiyl radical reactions, we recently examined in detail the photolysis of methanethiol vapor (1). We wish to report here results of a further study of this system, and of ethanethiol,[2] in particular, the reactions of hydrogen atoms produced in the photolysis with added ethylene and inert gas.

The principal products of mercaptan photolysis, hydrogen and disulfide, can be accounted for by the established simple scheme.

[1] $$RSH + h\nu \rightarrow RS + H$$

[2] $$H + RSH \xrightarrow{k_2} H_2 + RS$$

[3] $$RS + RS \rightarrow RSSR$$

For both methanethiol (1) and ethanethiol,[2] the primary quantum yield of H_2 is unity within experimental error.

The reaction in the presence of olefins has been studied in a variety of systems, and the additional reactions involving hydrogen atoms are:

[4] $$H + C_2H_4 \xrightarrow{k_4} C_2H_5$$

[5] $$C_2H_5 + RSH \rightarrow C_2H_6 + RS$$

A simple kinetic treatment of the mechanism allows calculation of the k_2/k_4 ratio from measurements of $\Phi(H_2)$ as a function of olefin pressure. A value of 2.32 ± 0.11 was found previously (1) for the CH_3SH–C_2H_4 system, and in the present study, we find $k_2/k_4 = 2.00 \pm 0.05$ for C_2H_5SH–C_2H_4, in agreement with the value of 1.9 ± 0.1 reported by Kuntz (2).

Recent work by Gann and Dubrin (3) on the photolysis of H_2S and several other H-atom sources, however, has indicated that, in the primary process, hydrogen atoms can acquire as translational excitation almost all the energy in excess of the H–X bond strength. It was of interest therefore, to investigate the possibility that "hot" hydrogen atoms are formed in the mercaptan photolysis as well.

[1]From the Ph.D. Thesis of R. P. Steer to be submitted to the University of Saskatchewan, Saskatoon, Saskatchewan.

[2]The photolysis of pure C_2H_5SH is under investigation in this laboratory and in general exhibits the same behavior as methanethiol, but with the absence of some complicating features of that system.

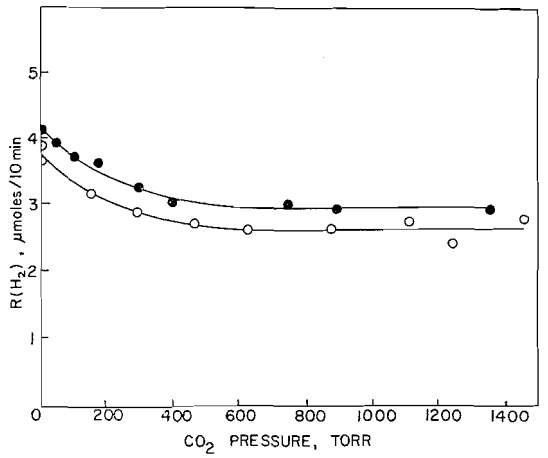

FIG. 1. Rate of hydrogen formation in the photolysis at 25 °C and 2537 Å, of 25 Torr of ethylene and 25 Torr of methanethiol, ●, or 25 Torr of ethanethiol, ○, as a function of pressure of added carbon dioxide.

Using 2537 Å light in a mercury-free system, 25 Torr each of mercaptan and ethylene were photolyzed in the presence of CO_2. The hydrogen yields[3] from both methanethiol and ethanethiol are given in Fig. 1. Although the rate of H_2 formation from both substrates is independent of inert addend pressure when olefin is absent (1), it is apparent that here the yield of this product can be reduced significantly when high pressures of CO_2 are present. It is suggested that this behavior is due to the formation of energetic hydrogen atoms in the primary process. The rate of H_2 production in the high pressure region corresponds to k_2/k_4 ratios of 1.15 ± 0.10 (CH_3SH) and 1.05 ± 0.05 (C_2H_5SH). Thus the rate constant ratios determined with RSH and C_2H_4 alone are evidently characteristic of hot hydrogen atoms, while those observed with added inert gas indicate the reactivity of thermalized hydrogen atoms.

There are two other reactions producing H_2, not usually considered for thermalized H-atoms, but which are energetically possible for H*.

$$[6] \qquad H^* + C_2H_4 \rightarrow \dot{C}_2H_3 + H_2$$

$$[7] \qquad H^* + RSH \rightarrow \dot{R}'SH + H_2$$

The kinetic plot used to obtain k_2/k_4 has zero intercept indicating that reaction [6] does not occur to an appreciable extent. With higher molecular weight olefins, abstraction from the olefin by H-atoms from H_2S is significant, and this is manifested by a non-zero intercept, corresponding to a finite value of k_6/k_4 (4). There is also evidence against the participation of [7]. In the photolysis of CH_3SD, Inaba and Darwent (5) observed D_2 but no HD. Furthermore, in both that study and the more recent investigation in this laboratory (1), $(CH_2SH)_2$ and CH_3SCH_2SH were shown to be absent from the reaction products even after prolonged irradiation when the yield of the radical–radical product C_2H_6 becomes measureable. It thus appears that the alteration in observed hydrogen yield is indicative exclusively of a change in the rate of reactions [2] and [4].

An alternative explanation of the pressure effect is the deactivation of hot ethyl radicals, formed in reaction [4], which process has been shown to be appreciably reversible. Bradley *et al.* (6), however, have demonstrated that much smaller pressures of ethylene than those used in the present study are sufficient to effect complete deactivation of C_2H_5*, and thus it is not likely that this species is important under our experimental conditions.

The methanethiol–ethylene system was also examined at 2288 Å, where a k_2/k_4 ratio for hot hydrogen atoms of 2.1 ± 0.2 was found, which is identical within experimental error to the value at 2537 Å. It is therefore probable that the primary decomposition proceeds via predissociation of the mercaptan yielding hydrogen atoms with excess energy independent of exciting wavelength. Thus, until further details of the spectroscopy of mercaptans become available, no estimate of the excess energy of the H-atoms in this system can be made.

The photolysis of mercaptans in the presence of olefins has been widely used as a method of studying the relative rates of attack of hydrogen atoms on carbon–carbon double bonds. The pressure dependence of rate constant ratios observed in the present investigation indicates that care must be exercised in comparing k values obtained by this method in different systems.

Acknowledgment

The authors are grateful to the National Research Council of Canada for financial support of this work.

[3]The yields of all other products in these systems were also determined and can be explained satisfactorily on the basis of the general mercaptan mechanism. These data will be dealt with in a subsequent publication.

Can. J. Chem. Downloaded from www.nrcresearchpress.com by 210.87.254.6 on 09/05/12
For personal use only.

1. R. P. STEER and A. R. KNIGHT. J. Phys. Chem. **72**, 2145 (1968).
2. R. R. KUNTZ. J. Phys. Chem. **71**, 3343 (1967).
3. R. G. GANN and J. DUBRIN. J. Chem. Phys. **47**, 1867 (1967).
4. B. DEB. DARWENT and R. ROBERTS. Discussions Faraday Soc. **14**, 55 (1953).
5. T. INABA and B. DEB. DARWENT. J. Phys. Chem. **64**, 1431 (1960).
6. J. N. BRADLEY, H. W. MELVILLE, and J. C. ROBB. Proc. Roy. Soc. **A236**, 318 (1956).

Can. J. Chem. Downloaded from www.nrcresearchpress.com by 210.87.254.6 on 09/05/12
For personal use only.

Can. J. Chem. Downloaded from www.nrcresearchpress.com by 210.87.254.40 on 09/05/12
For personal use only.

Canadian Journal of Chemistry

Published by THE NATIONAL RESEARCH COUNCIL OF CANADA

VOLUME 46 SEPTEMBER 15, 1968 NUMBER 18

Kinetics of hexagonal–cubic phase transformation of zinc sulfide in *vacuo*, in zinc vapor, and in sulfur vapor

TAMAS BANSAGI,[1] E. A. SECCO,[2] O. K. SRIVASTAVA,[3] AND RONALD R. MARTIN[4]

Chemistry Department, St. Francis Xavier University, Antigonish, Nova Scotia

Received March 11, 1968

The kinetics of the hexagonal–cubic phase transformation of zinc sulfide have been studied in *vacuo*, in zinc vapor, and in sulfur vapor in the temperature range 800–900 °C by a powder X-ray diffraction technique. The transformation rate is enhanced in the presence of sulfur and zinc vapor. In *vacuo* and in sulfur vapor the reaction is nucleation-controlled with activation energies of 95.0 and 98.5 ± 5 kcal, respectively. In zinc vapor the reaction is diffusion-controlled with the diffusion coefficient expressed as

$$D = 0.1 \exp(-67.0 \pm 4.0 \text{ kcal}/RT)\,\text{cm}^2\,\text{s}^{-1}$$

The modes of catalytic action by sulfur and zinc vapor on the solid phase transformation reaction are discussed.

Canadian Journal of Chemistry, 46, 2881 (1968)

Introduction

Our interest in the phase transformation of zinc sulfide stems from observations on sintering studies of ZnS powder (1) which indicated that the wurtzite–sphalerite transformation rate was enhanced by ambient vapors, viz. Zn and sulfur. This catalytic effect of a gas on a solid state reaction, while not a new one, appealed to us as a promising method for probing the nature of gas–solid interactions, especially the effect of an adsorbed species on the solid rather than the common inverse effect. Two modes of this catalytic action were visualized with their origins: (*a*) on the surface, where the most probable mode of action might be nucleation and (*b*) in the interior, where the action must involve solubility with subsequent transport or mobility steps. With regard to the latter mode, if the catalytic action is not entirely restricted to the surface, the Zn and sulfur vapor species possess a useful intrinsic parameter in their large relative difference in diameter, i.e. $r_{S_2}/r_{Zn} \sim 2$.

Experimental

The ZnS powder used in this work was from two batches of BDH laboratory reagent, I and II. In both cases, the X-ray diffractograms showed (2) peak intensities characteristic of 80% wurtzite – 20% sphalerite mixture. The particle radius of the powder is calculated to be 6.1×10^{-5} cm from nitrogen adsorption measurements (3).

The sulfide samples (ca. 200 mg) were annealed in a static system in *vacuo* or with sufficient zinc or sulfur to give the requisite pressure. The reaction chamber consisted of a quartz vessel of the design already described (4). After the anneal in the furnace at the appropriate temperature (4) and the removal of the powder from the quartz vessel, the sample was weighed, crushed in a mortar, and analyzed using a Norelco diffractometer model X-86.

The extent of reaction was determined by a method similar to that used by Edwards and Lipson (5). This method assumes that the intensity of the (111) face of the cubic structure increases at the expense of the (100) and (101) planes of the hexagonal structure. The fact that the (002) plane of the hexagonal form is common with the (111) plane of the cubic form, i.e. occurring at the same Bragg angle, allows us to define the quantity λ_t (the relative peak intensity of the (002) plane at time t).

$$\lambda_t = \frac{I_{002} + I_{111}}{I_{002} + I_{111} + I_{100}} \quad [1]$$

or

$$\lambda_t = \frac{I_{(28.53°)}}{I_{(28.53°)} + I_{(26.92°)}}$$

where $I_{(28.53°)}$ is the intensity of reflection at $2\theta = 28.53°$ for (111) and (002) faces and $I_{(26.92°)}$ is the intensity of of reflection at $2\theta = 26.92°$ for (100) face. The peak

[1]Present address: Kinetics Research Group of Hungarian Academy of Sciences, Szeged, Hungary.
[2]To whom correspondence on this paper should be addressed.
[3]Present address: Chemistry Department, Immaculata College, Immaculata, Pa.
[4]Present address: Chemistry Department, University of Western Ontario, London, Ontario.

Can. J. Chem. Downloaded from www.nrcresearchpress.com by 210.87.254.40 on 09/05/12
For personal use only.

intensity for the (100) plane was chosen over that of the (101) plane in the above definition because of its higher intensity value. Since the cubic form does not show any reflection corresponding to the Bragg angle $2\theta = 26.92°$, the cubic (sphalerite) content, defined as α_t for any time t, is given by

$$[2] \qquad \alpha_t = \frac{\lambda_t - \lambda_0}{\lambda_\infty - \lambda_0}$$

where $\lambda_\infty = 1.000$ and $\lambda_0 = 0.4624$ (calculated from intensity values reported in ASTM diffraction file (2)). The reproducibility of the λ_t values was found to be $\pm 2.3\%$. The above method of analysis was used to identify the starting material as 20% sphalerite.

Results and Discussion

For the purpose of illustrating the catalytic effect of the ambient vapors relative to *vacuo* on the wurtzite–sphalerite transition, the reaction fraction versus time curves at 840 °C are presented in Fig. 1. The α, t plots recall the α, t graphs for the thermal decomposition of solid compounds of the type (6)

$$A_{(solid)} \rightarrow B_{(solid)} + C_{(gas)}$$

in which the induction period ranges from noticeable to complete absence.

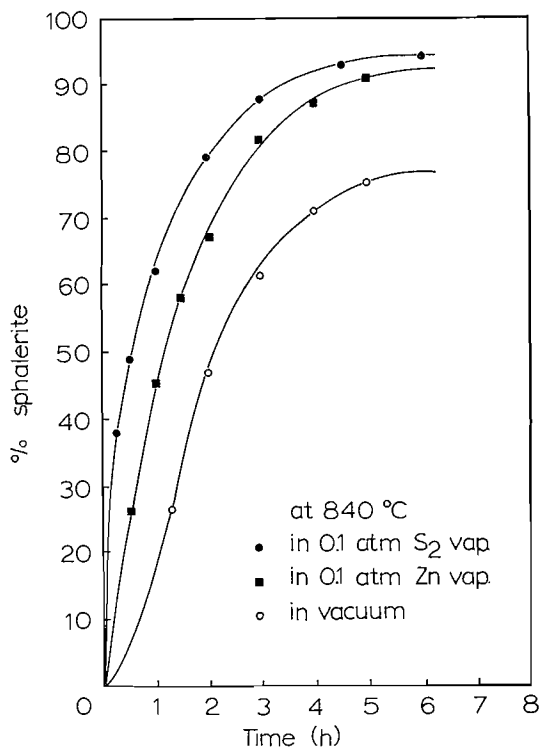

FIG. 1. Reaction fraction α, versus time plots at 840 °C in *vacuo*, in zinc vapor, and sulfur vapor.

Attempts were made to fit the data to a large number of kinetic laws and to interpret the results in terms of models based on boundary-controlled, diffusion-controlled, or nucleation-controlled processes, and also in terms of formal first-order kinetics. The best fit between the experimental results and the kinetic equations over the complete temperature range are presented here and are discussed under two categories: (i) in *vacuo* and in sulfur vapor and (ii) in zinc vapor.

(i) In Vacuo and in Sulfur Vapor

The in *vacuo* and in sulfur vapor data between 800–900 °C, for the range of reaction fraction $\alpha \geq 0.90$, were found to be compatible with a special case of the treatment given by Avrami (7) and formulated in a second-order rate expression by Honig *et al.* (8), which at sufficiently large t takes the form

$$[3] \qquad 1/(1 - \alpha) = 1 + \sigma G N_g t$$

where $(1 - \alpha)$ represents the fraction unreacted, σ is a shape factor, G is the lineal growth rate of the new phase, N_g is the initial density of germ nuclei, and t is the time. Equation [3] is recognized as the integrated form of the second-order rate law, since integration of the second-order law

$$d\alpha/dt = k(1 - \alpha)^2$$

yields

$$[3a] \qquad 1/(1 - \alpha) = 1 + kt.$$

A plot of $1/(1 - \alpha)$ versus time will yield a slope equal to the composite quantity $\sigma G N_g$ taken to be the formal rate constant k, along with an intercept of unity. Figures 2 and 3 show such plots with an intercept of unity substantiating the second-order kinetics.

The activation energy was computed for the standard Arrhenius plots of log k against $1/T$ °K shown in Fig. 4. Values for the activation energies using the least squares method were 95.0 and 98.5 $\pm$ 5.0 kcal for the reaction in *vacuo* and 0.1 atm sulfur, respectively.

With σ and N_g effectively constant, the rate constant dependence on temperature originates with the term G in the composite rate constant, i.e. $\sigma G N_g$. The observed activation energy appears, therefore, to represent the rate of growth of the new phase or, in this case, the progressive movement of the hexagonal–cubic interface.

Since the same mechanism is operative in both series of experiments, i.e. in *vacuo* and in sulfur

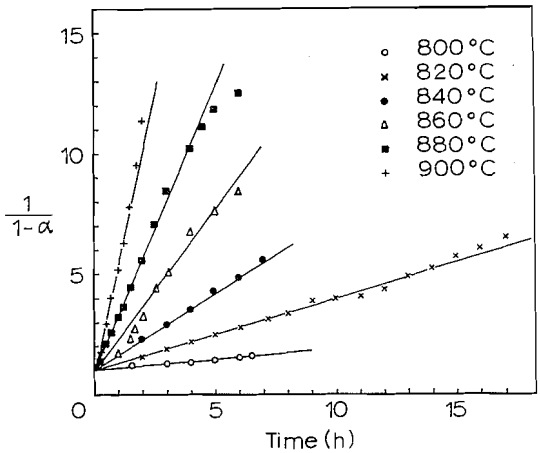

FIG. 2. Plots of $1/(1-\alpha)$ versus time at various temperatures in *vacuo*.

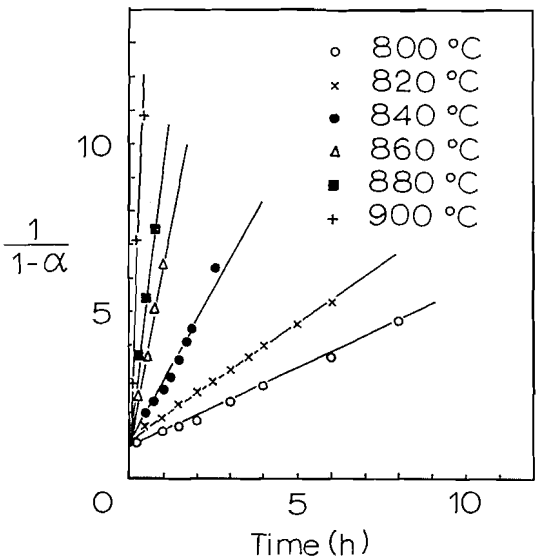

FIG. 3. Plots of $1/(1-\alpha)$ versus time at various temperatures in 0.1 atm sulfur vapor.

vapor, and, further, since σ is constant, the catalytic effect of the sulfur vapor on the reaction rate must reside in the N_g value, i.e. the density of the germ nuclei. The higher N_g value in the sulfur atmosphere must result from the adsorption of sulfur on the ZnS surface. Furthermore, we conclude from the in *vacuo* data that N_g is effectively temperature independent.

In Fig. 5(*a*) is plotted the kinetic data at different pressures of the ambient vapors. The dependence of rate on sulfur pressure is evident in Fig. 6, showing an initial rise to a maximum, followed by a virtually constant rate. The results

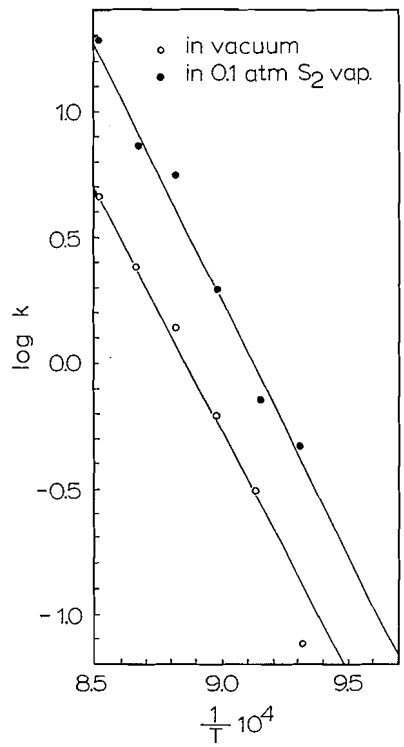

FIG. 4. Plots of log k versus $1/T$ °K for reaction in *vacuo* and in 0.1 atm sulfur vapor.

at the pressure showing the maximum rate, i.e. 0.5 atm, fit the second-order rate expression to a more extended value of α. The constant rate above 0.5 atm is consistent with a saturation effect.

The applicability of other rate laws over a limited temperature interval has been encountered: (*a*) at 900 °C, the data at 0.1 atm sulfur (where the rate is rapid, i.e. $\alpha \geq 0.80$ in 15 min) are fitted equally well to a first-order expression and the P–T (Prout–Tompkins) equation; (*b*) at 880 and 860 °C, the results fit the modified form of the P–T equation

$$\log(\alpha/1-\alpha) = k \log t + c.$$

(ii) In Zinc Vapor

The kinetic data for 0.1 atm zinc vapor are fitted equally well to a first-order rate equation and the Jander expression (9) for three-dimensional diffusion in a sphere,

$$[1-(1-\alpha)^{1/3}]^2 = (D/r^2)t$$

where D represents the diffusion constant and r the radius of the spherical particle. Figures 7 and 8 show such plots.

Can. J. Chem. Downloaded from www.nrcresearchpress.com by 210.87.254.40 on 09/05/12
For personal use only.

Can. J. Chem. Downloaded from www.nrcresearchpress.com by 210.87.254.40 on 09/05/12
For personal use only.

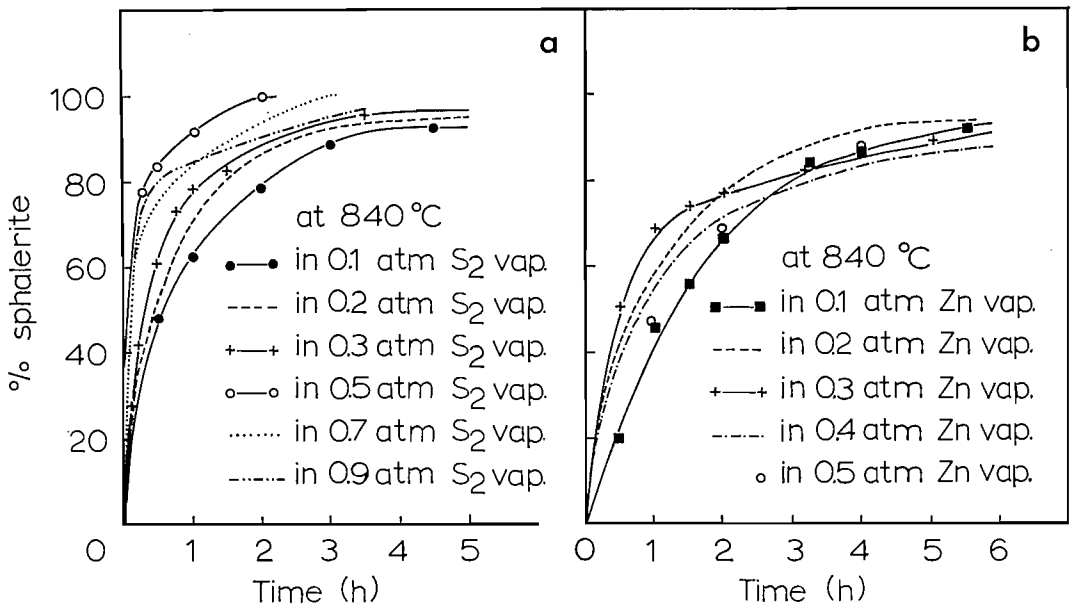

FIG. 5. (*a*) Reaction fraction α versus time plots at 840 °C at various pressures of sulfur vapor. (*b*) Reaction fraction α versus time plots at 840 °C at various pressures of zinc vapor.

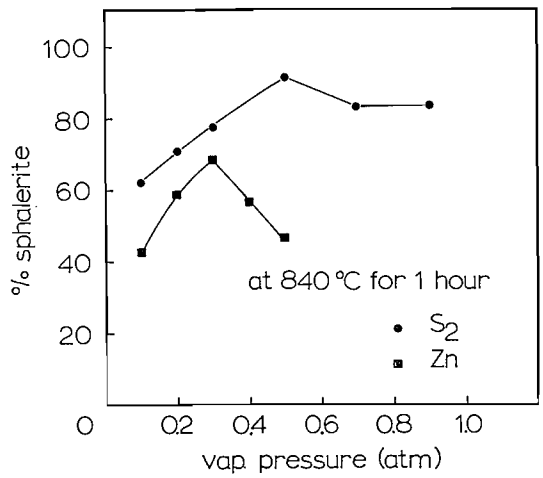

FIG. 6. Plot of dependence of reaction fraction α measured at 1 h and 840 °C on vapor pressure of zinc and sulfur.

The standard Arrhenius plots of $\log k$ versus $1/T$ °K (Fig. 9) yield straight lines with slopes corresponding to 79.6 and 67.0 kcal for the first-order and the Jander equations respectively.

Using the k values from the Jander expression to evaluate D at various temperatures, the diffusion coefficient for Zn in ZnS is calculated to be

$$D = 0.1 \exp(-67.0 \pm 4.0 \text{ kcal}/RT)\ \text{cm}^2\ \text{s}^{-1}$$

which compares with the diffusion coefficient[5]

$$D = 4.5 \exp(-61.5 \pm 4.0 \text{ kcal}/RT)\ \text{cm}^2\ \text{s}^{-1}$$

as evaluated from the exchange reaction between radiozinc vapor and polycrystalline zinc sulfide

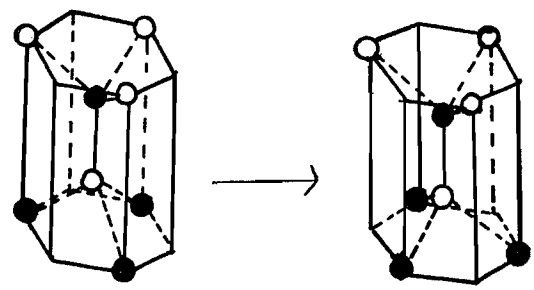

[5]The pre-exponential term D_0 value in the diffusion equation of the form $D = D_0 \exp(-\Delta E/RT)$ in the present study may be considered more reliable than the D_0 value for the exchange study, because of two uncertainties in the latter: (i) the greater facility for movement of zinc along wurtzite–sphalerite boundaries contributing to a higher exchange rate and (ii) the rapid initial exchange step rendering the initial and boundary conditions somewhat ill-defined for the standard solution in terms of a diffusion process.

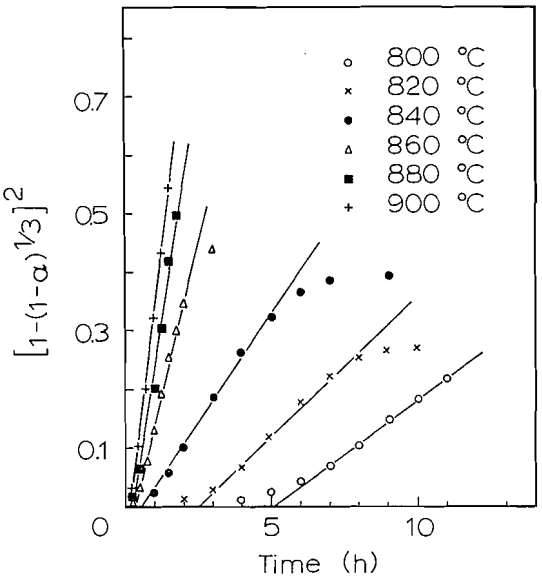

FIG. 7. The Jander expression for three dimensional diffusion in sphere plot for reaction in 0.1 atm zinc vapor at various temperatures.

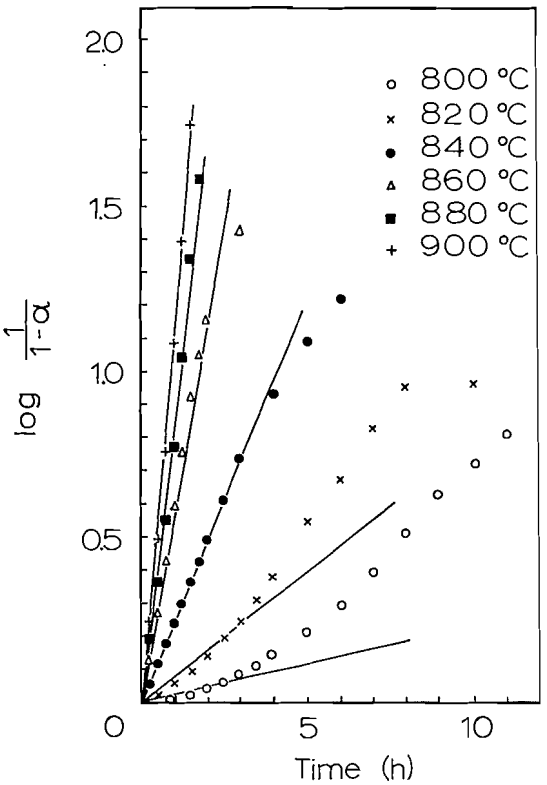

FIG. 8. Plots of $\log(1/1 - \alpha)$ versus time for reaction in 0.1 atm zinc vapor at various temperatures.

(3). The striking agreement between these two diffusion coefficients lends strong support to the interpretation that the mode of catalytic action is via zinc diffusion in the sulfide lattice, thus precluding an interpretation based on first-order kinetics.

The transformation of ZnS from the wurtzite to the blende structure may be considered as involving the fundamental step of a rotation by 60° of one tetrahedral configuration of Zn atoms relative to the tetrahedral configuration of S atoms, or vice versa, about the Zn—S bond along the *c*-axis of the unit cell as represented in the diagram above.

The enhanced conversion rate is the result of the triggering action by the mobile zinc species diffusing through the wurtzite lattice. The mode of the triggering action may be visualized to occur, assuming the structural transition to be concomitant with the mobility (and exchange) step, by a sequence or chain of events in the base of the zinc tetrahedral configuration leading to its rotation initiated by the diffusing zinc moving in to replace the zinc in the wurtzite lattice site. If this assumption is valid, then we can state that the diffusion of zinc is via a ring mechanism. Alternatively, the higher D_0 in the exchange studies may be quite genuine, signifying a diffusion rate which is more rapid than its transformation rate. In this case, we visualize the diffusing zinc species leaving in its path an intermediate configuration which is cubic oriented.

Figure 5(*b*) shows the dependence of rate on zinc pressure. Figure 6 shows an initial increase in rate, attaining a maximum at 0.3 atm and a subsequent marked decrease. The marked drop in rate is associated with saturation of the sulfide lattice with excess zinc, with the resultant effect that the "free space" required for transformation is reduced and the lattice atoms are restricted in their movement.

The applicability of a number of rate laws over a limited temperature interval (as evident especially in the Zn-catalyzed reaction data) emphasizes, to us at least, the note of caution expressed by Gill and Morrison (10) "... a common error is to assume the validity of a particular model, because it fits a portion of the kinetic results, and then make extensive conjecture about other properties of the reaction". The kinetic expression for the

Can. J. Chem. Downloaded from www.nrcresearchpress.com by 210.87.254.40 on 09/05/12
For personal use only.

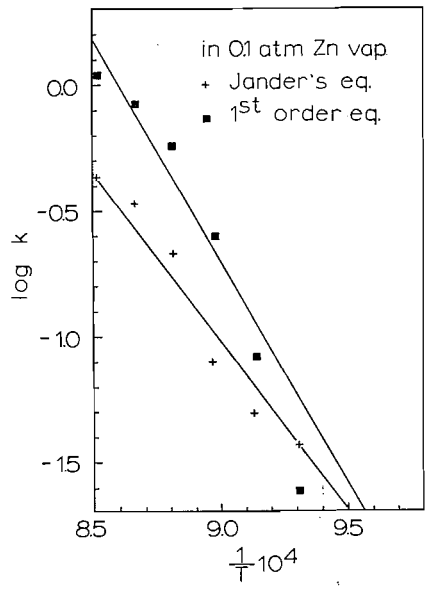

FIG. 9. Plots of $\log k$ versus $1/T$ °K for reaction in 0.1 atm zinc vapor with k obtained from the Jander expression and the first-order rate equation.

zinc sulfide exchange reaction proved very useful in support of the diffusion model.

Acknowledgment

This research work has received generous support from the National Research Council of Canada.

1. R. R. MARTIN and W. Y. SHIU. M.Sc. Thesis. St. Francis Xavier University, Antigonish, Nova Scotia. 1965.
2. A.S.T.M. File Index No. 5-0492.
3. E. A. SECCO. Can. J. Chem. **42**, 1396 (1964).
4. E. A. SECCO and W. J. MOORE. J. Chem. Phys. **26**, 942 (1957).
5. O. S. EDWARDS and H. LIPSON. J. Inst. Metals, **69**, 177 (1943).
6. P. W. M. JACOBS and F. C. TOMPKINS. Chemistry of the solid state. *Edited by* W. E. Garner. Butterworths Scientific Publications, London. 1955. Chap. 7.
7. M. AVRAMI. J. Chem. Phys. **8**, 212 (1940).
8. A. W. CZANDERNA, J. M. HONIG, and C. N. R. RAO. Trans. Faraday Soc. **54**, 1069 (1958).
9. W. JANDER. Z. Anorg. Allgem. Chem. **163**, 1 (1927).
10. E. K. GILL and J. A. MORRISON. Ann. Rev. Phys. Chem. **14**, 215 (1963).

Can. J. Chem. Downloaded from www.nrcresearchpress.com by 210.87.254.40 on 09/05/12
For personal use only.

Can. J. Chem. Downloaded from www.nrcresearchpress.com by 210.87.254.105 on 09/05/12
For personal use only.

Studies in solvolysis. Part I. The neutral hydrolysis of some alkyl trifluoroacetates in water and deuterium oxide

JUNE G. WINTER[1] AND J. M. W. SCOTT
Memorial University of Newfoundland, St. John's, Newfoundland

Received March 5, 1968

The temperature dependence of the rates of neutral hydrolysis of a series of alkyl trifluoroacetates (CF_3COOR; R = methyl, ethyl, *s*-propyl, *t*-butyl) has been determined in both light and heavy water. From these studies the thermodynamic parameters ($\Delta H^{\neq}$, $\Delta S^{\neq}$) which characterize the activation process have been calculated. Sufficient rate data have been obtained in the case of the ethyl ester to calculate the heat capacity of activation ($\Delta C_p^{\neq}$) for the hydrolysis of this compound in light water. Both the entropies and enthalpies of activation as well as the solvent isotope effects are consistent with the proposal that the primary and secondary esters react by an acyl–oxygen $B_{Ac}2$ mechanism, in contrast to the tertiary ester, which appears to react either by a carbonium ion (S_N1) process or by a route which combines both the $B_{Ac}2$ and S_N1 paths.

Canadian Journal of Chemistry, 46, 2887 (1968)

Introduction

The rate of neutral or spontaneous hydrolysis of simple alkyl esters related to the halogenoacetic acids has frequently been studied (1–11), although no systematic body of rate data is currently available concerning the reactivity of these substances in pure water and deuterium oxide. The present study surveys the temperature dependence of the rates of hydrolysis in pure water and deuterium oxide of four esters derived from trifluoroacetic acid (CF_3COOR; R = Me, Et, *s*-Pr, and *t*-Bu).

On the basis of ^{18}O tracer studies Bunton and Hadwick (8) have concluded that the spontaneous hydrolysis of methyl trifluoroacetate in pure water takes place by an acyl–oxygen fission mechanism ($B_{Ac}2$). On the other hand, Moffat and Hunt (1) consider that *t*-butyl trifluoroacetate reacts in acetone–water mixtures by a carbonium ion (S_N1) mechanism since the extent of olefin formation in this reaction is similar to that produced by the *t*-butyl halides reacting in the same media. These separate observations suggest that a change in mechanism ($B_{Ac}2 \rightarrow S_N1$) is to be anticipated in the hydrolysis reactions of the series of trifluoroacetates mentioned above. A further aim of the present study was to locate the point or region of mechanistic change using the thermodynamic parameters ($\Delta G^{\neq}$, $\Delta H^{\neq}$, $\Delta S^{\neq}$, and $\Delta C_p^{\neq}$), as well as the ratio of the rates of hydrolysis of each substrate in light and heavy water.

[1]Née Martin.

Experimental

General

Nuclear magnetic resonance (n.m.r.) spectra were recorded on a Varian A-60 spectrometer and peaks are recorded on the τ scale relative to tetramethylsilane as an internal reference. Carbon tetrachloride was used as a solvent. Infrared spectra were recorded on a Perkin–Elmer model 225 spectrometer using the liquid cell technique with solvent carbon tetrachloride.

Materials

The methyl and ethyl trifluoroacetates were Fluka A.G. purum grade and were distilled prior to use. The *s*-propyl and *t*-butyl trifluoroacetates were prepared from the corresponding alcohols and trifluoroacetic anhydride in the presence of a small amount of silver trifluoroacetate (12). The boiling points and refractive indices agreed with the literature values (1–3, 12) and saponification values indicated that the esters were better than 98% pure. The τ values and carbonyl stretching frequencies for these esters are recorded in Table I. The excellent first order plots obtained from the kinetic studies also demonstrate the kinetic homogeneity of each sample used.

Solutions

(a) Light Water

Solutions in the range 10^{-5}–10^{-4} *M* of each ester were prepared by injecting the appropriate volume of

TABLE I

Physical properties of some esters derived from trifluoroacetic acid

Ester	Nuclear magnetic resonance (τ)	Infrared ν(C=O) (cm^{-1})
—Me	6.02	1788
—Et	8.58, 5.54	1784 (1786)*
—*s*-Pr	8.64, 4.83	1787
—*t*-Bu	8.45	1782 (1777)*

*Literature values in parentheses are given in ref. 12.

Can. J. Chem. Downloaded from www.nrcresearchpress.com by 210.87.254.105 on 09/05/12
For personal use only.

ester from a micro syringe into stirred cells of a design similar to that originally described by Hyne and Robertson (13). The cells had been previously filled with backing electrolyte which was prepared by allowing a suitable amount of the appropriate substrate to react with deionized water so as to reduce the initial resistance of the solution to a convenient value. In situations where supersaturation was prevalent, a saturated solution of the appropriate ester was prepared at the required temperature. An aliquot of this solution (1 ml) was then withdrawn and injected into a suitable volume of backing electrolyte already in the cell.

(b) Heavy Water

Deuterium oxide (ca. 1 l) was obtained from Atomic Energy of Canada and was used several times with no appreciable decrease in purity. Solutions were prepared as for light water. Following each set of runs the contaminated heavy water was redistilled from a small amount of anhydrous sodium carbonate in an all glass apparatus. Subsequent analysis of the distillate using n.m.r. with purified acetonitrile as an internal standard, showed that the hydrogen content of the solvent collected from these distillations did not exceed 0.5% by weight.

Rate Measurements

The rate measurements were made using the conductance method, based on the Guggenheim treatment (14) in a form originally elaborated by Robertson (15). The equipment that was used was essentially that described in ref. 15 with minor modifications (16). Temperatures were measured by means of a Tinsley platinum resistance thermometer and bridge. The former was calibrated by the National Physical Laboratory, Teddington, England.

The excellence of the Guggenheim–Robertson Method (G.R.M.) for determining solvolytic rates in pure water is now well established in cases where the acid related to the leaving group is strong (14). Since trifluoroacetic acid is relatively weak, ($pK_a = 0.23$[2] at 25 °C (18)) the use and validity of the G.R.M. in this study requires further comment. For strong acids the reliability of the G.R.M. rests on the existence of a linear relationship between the conductance and concentration of the acid in a given reaction vessel. In the case of a weak acid (because of incomplete dissociation), this may not be correct and a quantitative assessment of the possible influence on this factor is required.

Ives (20) has suggested that the classical Ostwald Dilution Law stated in terms of conductance parameters, in a form which neglects the effect of ionic strength on both the activity and mobility of the ions of the weak electrolyte, accurately represents the variation of the equivalent conductance of the weak electrolyte as a function of concentration at high dilution ($< 10^{-4}$ *M*). For our present purpose Ives' proposal means that the variation of the equivalent conductance (Λ) of the weak electrolyte with concentration (C) is accurately represented by the equation

$$[1] \qquad 1/\Lambda = 1/\Lambda_0 + \Lambda C/K_c\Lambda_0^2$$

where Λ_0 is the limiting equivalent conductance of the weak electrolyte and K_c is the classical dissociation constant which has not been corrected for either the variation of activities or mobilities with ionic strength. The equivalent conductance Λ is related to the experimental parameters by the equation

$$[2] \qquad \Lambda = 10^3\boldsymbol{K}/RC$$

where R is the resistance, in ohms, of a solution of the electrolyte containing C moles/l in a cell of cell constant $\boldsymbol{K}$.

Combining eqs. [1] and [2] gives after some manipulation

$$[3] \qquad C = P/R + P^2/K_cR^2$$

where P is defined by the equation

$$[4] \qquad P = 10^3\boldsymbol{K}/\Lambda_0$$

This latter quantity at a fixed temperature will be a constant, for a given electrolyte and reaction vessel (cell). Equation [3] shows that the simple relationship between the concentration of the acid and the reciprocal of the resistance used by Robertson (15) for strong acids, is modified in the case of a weak acid by a further term P^2/K_cR^2.

The Guggenheim equation for the evaluation of the pseudo first order rate constant in a solvolysis experiment is

$$[5] \qquad C_{t+\tau} - C_t = C_0 \exp -kt\,[1 - \exp(-k\tau)]$$

where $C_{t+\tau}$ is the concentration of the product (acid) at time $t+\tau$ and C_t is the concentration at time t; C_0 is the initial concentration of ester, k is the pseudo first order rate constant and τ is the arbitrary time interval between the two sets of observations required in a Guggenheim first order rate constant determination. Combining eqs. [3] and [5] gives after some manipulation

$$[6] \qquad \log(1/R_{t+\tau} - 1/R_t) + \log[1 + P(1/R_{t+\tau} + 1/R_t)/K_c] = \log C_0[1 - \exp(-k\tau)]/P - kt/2.3026$$

Since the first term on the RHS of eq. [6] is a constant in any given experiment, a plot of $\log(1/R_{t+\tau} - 1/R_t)$ versus time will only be linear if the second term on the LHS of eq. [6] is negligible. If, Λ_0 and K_c for the weak acid are known it is possible to calculate the magnitude of this particular term and hence estimate the importance of the second term in eq. [6]. A typical calculation of this sort is displayed in Table II (see columns 6 and 7). The effect of the second term on the LHS of eq. [6] is clearly very small and well outside the limits of reproducibility offered by the G.R.M. (see ref. 17).

A further requirement of any precise determination of a rate constant is that this parameter should be constant over the complete reaction. Since the hydrolyses of trifluoroacetates are known to be acid catalyzed (6–8) it was important to demonstrate that no autocatalysis occurred with the present systems. The G.R.M. requires at least three half-lives for the determination of a rate constant since the parameters $R_{t+\tau}$ and R_t are each observed over the period of one half-life ($t_{1/2}$) and ideally the interval between the two sets of observations should satisfy the condition $\tau > 2t_{1/2}$. This means that the rate constants as usually determined represent at least 87.5% of a complete reaction. This period was deliberately extended in

[2] An alternative pK_a value of -0.26 has been quoted for trifluoroacetic acid by O. Redlich and G. C. Hood (19). There appears to be some uncertainty concerning the pK_a of this acid.

TABLE II

Typical calculation for the determination* of a first order rate constant using eq. [6], $T = 14.95$ °C

Time (s)	R_t	$R_{t+\tau}$	$(1/R_{t+\tau} - 1/R_t) \times 10^5 = D$	$(1/R_t + 1/R_{t+\tau})P/K_c + 1 = M$	log D	log D + log M
0	7710.0	4173.0	10.993	1.0003	$\bar{4}$.0401	$\bar{4}$.0402
41	7170.0	4137.5	10.222	1.0003	$\bar{4}$.0095	$\bar{4}$.0096
80	6760.0	4107.0	9.5558	1.0004	$\bar{5}$.9803	$\bar{5}$.9805
119	6410.0	4079.5	8.9122	1.0004	$\bar{5}$.9500	$\bar{5}$.9502
161	6100.0	4052.2	8.2845	1.0004	$\bar{5}$.9183	$\bar{5}$.9185
202	5840.0	4027.4	7.7066	1.0004	$\bar{5}$.8869	$\bar{5}$.8871
240	5630.0	4006.2	7.1993	1.0004	$\bar{5}$.8573	$\bar{5}$.8575
280	5440.0	3985.8	6.7067	1.0004	$\bar{5}$.8265	$\bar{5}$.8267
321	5270.0	3966.6	6.2352	1.0004	$\bar{5}$.7949	$\bar{5}$.7951
360	5130.0	3949.4	5.8271	1.0004	$\bar{5}$.7655	$\bar{5}$.7657
401	5000.0	3933.0	5.4259	1.0004	$\bar{5}$.7345	$\bar{5}$.7347

$P = K \times 10^3/\Lambda_0$ calculated from Λ_0 (CF_3COOH) = 332 and $K_c = 0.652$, $K = 0.1966$; cell constant obtained via a solution of known equivalent conductance. The former parameters were extrapolated to 15 °C using data from ref. 21.

TABLE III

Rates of hydrolysis of ethyl trifluoroacetate

T (°K)	$k_{obs} \times 10^4$ (n)* (s^{-1})	$k_{calcd} \times 10^4$ (s^{-1})	$k_{obs} - k_{calcd}$
273.34	6.120±0.027 (4)	6.093	+0.027
274.26	6.524±0.018 (4)	6.545	−0.021
275.54	7.193±0.010 (5)	7.230	−0.037
276.16	7.565±0.008 (4)	7.579	−0.014
277.03	8.134±0.023 (5)	8.094	+0.040
278.14	8.772±0.027 (4)	8.788	−0.016
279.14	9.489±0.044 (4)	9.463	+0.026
280.10	10.14 ±0.01 (4)	10.15	−0.01
281.14	10.90 ±0.05 (4)	10.93	−0.03
282.13	11.75 ±0.04 (4)	11.72	+0.03
283.11	12.53 ±0.03 (5)	12.56	−0.03
284.17	13.49 ±0.06 (4)	13.50	−0.01
285.15	14.54 ±0.02 (4)	14.44	+0.10
286.11	15.39 ±0.06 (4)	15.40	−0.01
287.14	16.53 ±0.05 (4)	16.49	+0.06
288.11	17.57 ±0.05 (4)	17.57	0.00
289.14	18.70 ±0.07 (4)	18.78	−0.08
290.12	20.04 ±0.07 (4)	20.00	+0.04
291.17	21.31 ±0.07 (4)	21.36	−0.05
292.16	22.80 ±0.06 (5)	22.71	+0.09
293.18	24.16 ±0.06 (4)	24.18	−0.02
294.21	25.55 ±0.05 (4)	25.73	−0.18
295.18	27.35 ±0.12 (4)	27.27	+0.08

*n = number of separate runs at given temperature.

the present study by measuring the resistances of a reacting solution over four separate half-lives and observing the resistances at identical time intervals. The separation between the individual sets of observations was small, i.e. as soon as one set of measurements was complete the next set was started. From the four sets of resistances obtained in this way, three rate constants may be obtained and one of these covers at least 93.3% of the reaction. The average rate constant from the four sets of observations was 1.762 (± 0.004) × 10^{-3} s^{-1}. This particular experiment confirms that there is no perceptible acid catalysis in these reactions and that the linear relationship between the conductance and the concentration of the product (acid) is valid over the range of substrate concentrations used.

The rate constants which have been measured in light and heavy water for the esters (R = Me, Et, *s*-Pr, and *t*-Bu) are recorded in Tables III and IV, together with the r.m.s. deviation obtained from 'n' separate large scale first order plots. For the ethyl ester the temperature dependence of the rates could be expressed within the experimental error by the equation

[7] $$\log k = -6439.0409/T - 32.7141 \log T + 100.0558$$

The numerical coefficients in eq. [7] were established by a least squares treatment (the individual rates were used; not the average experimental rates reported in Table III), and were converted to the thermodynamic quantities $\Delta H_0^{\ddagger}$, $\Delta S_0^{\ddagger}$, $\Delta C_p^{\ddagger}$, $\Delta H^{\ddagger}$, and $\Delta S^{\ddagger}$, using the procedure originally proposed by Robertson (17) (see Table VI).

The temperature dependence of the methyl, *s*-propyl, and *t*-butyl esters over a shorter temperature interval reacting in light water was adequately represented by the equation

[8] $$\log k/T = A/T + B$$

and the same equation was also used to represent the temperature dependence of each ester reacting in heavy water. Values of A and B for each ester were determined by a least squares procedure (without averaging the individual rate constants at each temperature) and converted to the thermodynamic parameters $\Delta H^{\ddagger}$ and $\Delta S^{\ddagger}$ via the relationships,

[9] $$A = -\Delta H^{\ddagger}/2.3026R$$

and

[10] $$B = \Delta S^{\ddagger}/2.3026R + \log (k/h)$$

The symbols R, k, and h in eqs. [9] and [10] have their usual significance. The enthalpies and entropies of activation calculated in this way are detailed in Table V for both light and heavy water. The $k(H_2O)/k(D_2O)$ ratios for each ester are reported in Table IV and are probably accurate to ca. ±1.0%.

Discussion

Relative Rates — Free Energies of Activation

It is generally accepted that free energies of activation provide the most useful parameters

Can. J. Chem. Downloaded from www.nrcresearchpress.com by 210.87.254.105 on 09/05/12
For personal use only.

Can. J. Chem. Downloaded from www.nrcresearchpress.com by 210.87.254.105 on 09/05/12
For personal use only.

TABLE IV

Rate constants and isotope effects for the solvolysis of trifluoroacetates in water and deuterium oxide

Ester	T (°C)	$k(H_2O) \times 10^4$ (n) (s^{-1})	$k(D_2O) \times 10^4$ (n) (s^{-1})	$k(H_2O)/k(D_2O)$*
—Me	4.98	23.09±0.10 (4)	6.486±0.008 (4)	3.54
	9.96	32.80±0.05 (4)	9.420±0.027 (4)	3.51
	14.95	46.42±0.13 (3)	13.24±0.05 (4)	3.48
—Et	4.98	8.777±0.026 (4)	2.390±0.009 (4)	3.67
	9.96	12.53±0.04 (5)	3.468±0.010 (4)	3.60
	14.95	17.57±0.05 (4)	4.956±0.017 (4)	3.54
—*s*-Pr	4.98	2.433±0.008 (4)	0.6339±0.019 (4)	3.83
	9.96	3.494±0.012 (3)	0.9194±0.028 (5)	3.79
	14.95	4.864±0.022 (4)	1.296±0.002 (4)	3.74
—*t*-Bu	4.98	0.5723±0.030 (3)	0.4623±0.030 (3)	1.24
	9.96	1.296±0.004 (4)	1.076±0.008 (4)	1.21
	14.95	2.915±0.012 (3)	2.450±0.007 (3)	1.19

*Values calculated from rate constants which have been smoothed using eq. [8].

TABLE V

Thermodynamic parameters for the solvolysis of trifluoroacetates in water and deuterium oxide (derived from the rates reported in Table IV)

Ester	$\Delta H^{\ddagger}$ (H_2O) (kcal/mole)	$\Delta H^{\ddagger}$ (D_2O) (kcal/mole)	$\Delta S^{\ddagger}$ (H_2O) (e.u.)	$\Delta S^{\ddagger}$ (D_2O) (e.u.)
—Me	10.60±0.03	10.48±0.05	−32.3±0.3	−34.0±0.4
—Et	10.53±0.03	11.08±0.03	−34.5±0.3	−35.1±0.3
—*s*-Pr	10.51±0.05	10.87±0.05	−37.1±0.6	−38.5±0.7
—*t*-Bu	25.44±0.06	26.08±0.05	13.7±0.5	15.5±0.0

TABLE VI

Thermodynamic parameters for the hydrolysis of ethyl trifluoroacetate in water at various temperatures

T (°K)	$\Delta H_T^{\ddagger}$ (kcal/mole)*	$\Delta S_T^{\ddagger}$ (e.u.)*
273.16	11.16	−32.2
298.16	9.486	−38.1
323.16	7.811	−43.5
348.16	6.137	−48.5
373.16	4.462	−53.1

*Calculated using the usual thermodynamic expressions with $\Delta C_p^{\ddagger} = -66.95$ cal mole^{-1} deg^{-1}.

for discussing the influence of structure on the reactivity of organic molecules and much has been written to substantiate this point of view (22–26). The present series of solvolytic substrates would appear to offer an interesting exception to this principle. Thus the relative rates of hydrolysis of the four esters follow the sequence Me > Et > *s*-Pr > *t*-Bu at 3.37 °C and give an acceptable Taft (27) linear free energy relationship at this temperature (see Fig. 1).

This correlation suggests that a common mechanism is operating and that the reactivities of the esters are dominated by the inductive effect of the alkyl group. Further inspection, however, reveals that these ideas are untenable.

Thus extrapolation of the rates of solvolysis to 25 °C gives a sequence of reactivity Me > Et > *t*-Bu > *s*-Pr leading to the breakdown of the Taft correlation for the tertiary ester (see Fig. 1). Moreover, the sequence of reactivity observed at 3.37 °C is typical of S_N2 processes but the range of reactivity is rather small when compared with better established S_N2 reactions (28). On the other hand, the trend in reactivities at 25 °C is typical of an S_N2–S_N1 sequence with the change in mechanism occurring in the region of the *s*-Pr ester, but again the range of reactivity is relatively small. However, these mechanistic conclusions based solely on relative rates are inconsistent with the $H_2{}^{18}O$ and olefin production studies mentioned in the introduction. These latter experiments are best interpreted in terms of acyl–oxygen fission for the methyl ester

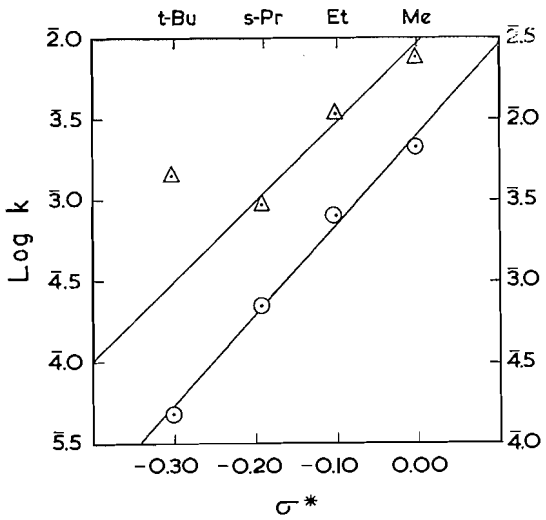

FIG. 1. Correlation of rates of hydrolysis of alkyl trifluoroacetates with the Taft σ* parameter. △ extrapolated rates at 25 °C; ⊙ extrapolated rates at 3.73 °C; the scale on right hand side is for rates at 25 °C.

and alkyl oxygen fission (S_N1 ?)[3] for the tertiary ester. The point of change in mechanism ($B_{Ac}2 \rightarrow S_N1$) for the complete series of substrates clearly remains to be established.

The observation that the rates of hydrolysis of a series of ethyl esters derived from a sequence of halogenoacetic acids decrease as the pK_a of the related acid increases (see Table VII), suggests that nucleophilic attack at the carbonyl carbon is the main driving force for the ethyl

TABLE VII

Rates of neutral hydrolysis of a series of ethyl esters related to acetic acid

Ester	pK_a*	k (s^{-1} at 25 °C)
CF_3COOEt	0.23 (−0.26)	3.29×10^{-3}†
CCl_3COOEt	0.65	2.41×10^{-4}‡
CHF_2COOEt	1.24	8.7×10^{-5}§
$CHCl_2COOEt$	1.29	7.7×10^{-6}§
CH_3COOEt	2.86	1.7×10^{-7}§

*Taken from ref. 18, value in parentheses from ref. 19.
†This work.
‡Reference 29.
§From ref. 4, with a rough correction for ionic strength effects.

[3]The possibility of a mechanistic trichotomy has not been overlooked. If mixed kinetics is a valid concept it is feasible to assume that the tertiary ester might react by three routes, i.e. $B_{Ac}2$, S_N1, and S_N2. The problem of deciding between the S_N1–S_N2 description for the tertiary ester is outside the scope of the present study but the problem is recognized. The incursion of a mixed $B_{Ac}2$–S_N1 process will, however, be discussed here below.

esters and we therefore conclude that ethyl trifluoroacetate also reacts by the $B_{Ac}2$ mechanism. This is the limit of useful information which can be gleaned from a consideration of relative rates alone, but we wish to emphasize again that without ancillary information, these quantities are mechanistically ambiguous.

Enthalpies and Entropies of Activation

If the free energies of activation prove to be mechanistically equivocal, the same cannot be said of the entropies and enthalpies of activation. These parameters fall into two distinct categories, the primary and secondary esters which have enthalpies of activation which are virtually constant at 10.5 kcal/mole, and the entropies of activation which are relatively constant in the vicinity of 35 e.u. The second category is provided by the tertiary ester which shows dramatic changes from the parameters listed above. For this ester the enthalpy of activation is ca. 15 kcal/mole higher than that observed for the primary and secondary esters and the entropy of activation is ca. 50 e.u. more positive. The above considerations are consistent with the $B_{Ac}2$ description for the primary and secondary esters and alkyl–oxygen fission (S_N1) for the tertiary ester. The actual magnitude of the enthalpies and entropies of activation are also comparable with the 'average values' of thermodynamic parameters which characterize these two mechanisms (for a detailed discussion, see refs. 30, 31, and 16).

Solvent Isotope Effect

Further substantiation of these mechanistic conclusions obtained from the response of $\Delta H^{\neq}$ and $\Delta S^{\neq}$ to structure is provided by the solvent isotope effect (s.i.e.) studies. Thus the primary and secondary esters give s.i.e. ratios in the range 3.4–3.8, which have predicted to be characteristic of spontaneous $B_{Ac}2$ processes (32). On the other hand, the tertiary ester gives a s.i.e. ratio of 1.2 which is typical of a wide range S_N1–S_N2 substrates studied by Laughton and Robertson (33–36). The s.i.e. is considered to be a rather blunt tool for distinguishing between S_N1 and S_N2 solvolytic processes (37). The data in Table V shows that the s.i.e. arises from concomitant changes in both the enthalpies and entropies of activation, but any attempt to rationalize such a dissection of the isotope effect would seem premature. These observations

Can. J. Chem. Downloaded from www.nrcresearchpress.com by 210.87.254.105 on 09/05/12
For personal use only.

Can. J. Chem. Downloaded from www.nrcresearchpress.com by 210.87.254.105 on 09/05/12
For personal use only.

do, however, suggest that the zero-point energy model used by Bunton and Shiner (32) is oversimplified. Some further points concerning the solvent isotope effects are discussed in the section (given below) dealing with heat capacities of activation.

The Heat Capacities of Activation

The heat capacity of activation for ethyl trifluoroacetate (-66.95 cal mole^{-1} deg^{-1}) approximately bisects the range of values ($-30 \rightarrow -100$ cal mole^{-1} deg^{-1}) obtained by Laughton and Robertson (33) and others (38) who have measured this parameter in water and mixed solvents for a wide range of solvolytic substrates and attempted to use it to build a more complete description of solvolytic displacement reactions. A detailed understanding of the magnitude of the heat capacity of activation for any particular substrate seems out of the question at the present time, but several qualitative points arising from the present study are worthy of mention. Since the evidence presented above indicates that the ethyl ester solvolyses by a $B_{Ac}2$ mechanism it is clear that heat capacities of activation alone will not distinguish between this path and the S_N1–S_N2 type mechanisms. However, it may be possible to distinguish between the $B_{Ac}2$ mechanism and the S_N1–S_N2 type via $\Delta C_p^{\ddagger}$ within a series of trifluoroacetates. A decision with regard to this matter must await further work in progress in the laboratory.

The strongly negative entropies and heat capacities of activation which appear to characterize the $B_{Ac}2$ process (30) suggest that activation involves the cooperation of several solvent molecules. Similar proposals with regard to the composition of the activated complex have been put forward for S_N1–S_N2 reactions although the entropies of activation for these substrates may be both positive and negative (17) contrasting with the heat capacity of activation, which is invariably negative. The latter presents some rather awkward interpretative problems. It has been cogently argued (37) that the magnitude and sign of the heat capacity of activation is primarily a consequence of the variable heat content of the initial state solvation shell which is generally expected to show a maximum stability as the interaction of the water envelope with the substrate decreases. This rather curious conclusion is a consequence of the peculiar properties of aqueous solutions of neutral molecules. Substances which contain no lyophilic groups, e.g. carbonyl or sulfoxide, induce the solvent to interact more strongly with itself and form a stronger 'iceberg'. Those substrates which contain hydrogen bonding groups such as those mentioned above, tend to reduce the stability of the 'iceberg' by providing centers of interaction between the solvent and solute, which partially 'liberates' the surrounding water molecules from the 'frozen' structure of the water in the immediate vicinity of the substrate. Arguments of this kind provide a qualitative explanation of the more positive heat capacities of activation observed for the sulfonates as compared with the halides (39). However, the heat capacity of activation for ethyl trifluoroacetate is approximately 30 cal mole^{-1} deg^{-1} more negative than the sulfonates although both series of compounds evidently contain hydrogen-bonding groups. This is presumably a consequence of an intrinsically more negative heat capacity of activation for the $B_{Ac}2$ mechanism, and this proposal is in line with the shift in the entropy of activation between the sulfonates (17) and structurally related trifluoroacetates.

For the S_N1–S_N2 solvolytic displacements Robertson and Laughton (40) have proposed that the magnitude of the s.i.e. is a manifestation of the same factors which determine the magnitude of the heat capacity of activation, i.e. the stability of the initial state solvation shell.[4] Thus the more positive heat capacities of activation of the sulfonates compared with the halides correlate with a reduced s.i.e. for the former series of compounds. The limited heat capacity data reported here do not confirm this correlation since a marked increase in the s.i.e. which characterizes the $B_{Ac}2$ mechanism is accompanied by only a moderate shift in the heat capacity of activation.

It is worth pointing out at this juncture that if solvent isotope effects are to be rationalized in terms of zero-point energies (32) the statistical theory of equilibria vitiates any fundamental correlation between the s.i.e. and $\Delta C_p^{\ddagger}$ since zero-point energies make no contribution to heat capacities.

Some Further General Comments

In the present communication we have attempted to assign the mechanism of four rate

[4]For another point of view, however, see refs. 41 and 42.

Can. J. Chem. Downloaded from www.nrcresearchpress.com by 210.87.254.105 on 09/05/12
For personal use only.

processes on the basis of the thermodynamic parameters and solvent isotope effects which characterize the thermal activation of these molecules. We are fully aware of the limitations of such a procedure and in the present section we wish to examine these limitations more closely. Although the response of $\Delta H^{\ddagger}$ and $\Delta S^{\ddagger}$ to structural changes in the present series of substrates is marked, the question arises as to just how different such parameters must be before a change in mechanism can be legitimately inferred. We are forced to the conclusion that there is no satisfactory answer to this question at the present time and it must be admitted that without the product and tracer studies mentioned earlier in this paper the present data would only be marginally convincing. Taken together, however, the two types of evidence make the case for a change in mechanism that much stronger. The possibility that the tertiary ester reacts by a mixed $B_{Ac}2/S_N1$ mechanism cannot be ruled out. Bunton and Hadwick (7) have shown that benzhydryl trifluoroacetate has an activation energy which increases with temperature and the present data for the tertiary ester also manifests an activation energy which increases with temperature, but the range of temperatures studied is too small to warrant any definite conclusion concerning this matter at the present time. If this trend is verified by future studies which are now underway, then the thermodynamic parameters reported for the tertiary ester will not be appropriate to a single process. Nevertheless, a change of mechanism in these circumstances is still evident but the change is not complete. Such a description is consistent with the sensitivity of the Taft correlation to temperature.

There are several reasons for expecting a change of mechanism in the hydrolysis reaction of the four esters studied. The most important of these is the increased stability of the trimethyl carbonium ion compared with the corresponding carbonium ions derived from the primary and secondary esters. However, other factors will tend to decrease the stability of the transition state for the $B_{Ac}2$ process as the size of the alkyl group increases. The formation of a tetrahedral intermediate (43) will involve a decrease in the CF_3—alkyl group distance and this would be expected to raise the energy of the transition state in the order t-Bu > s-Pr > Et > Me. Although the inductive effect of the alkyl groups is attenuated by the intervening oxygen atom, this effect will also follow the steric effect mentioned above and will raise the energy of the transition state by reducing the positive charge at the carbonyl carbon atom. All of the factors mentioned above will decrease the stability of the $B_{Ac}2$ transition state with increasing α-methylation and it is reasonable to deduce that alkyl–oxygen fission becomes an important reaction path for the tertiary ester.

Acknowledgments

We wish to thank the Technical Services Division at Memorial University, especially Mr. W. Gordon and Mr. R. Parsons, for their help in the construction of the apparatus. We also wish to express our gratitude to Dr. R. E. Robertson for arranging the construction of the conductance cells and to Mr. M. Jones for assisting with the least squares calculation. Finally our thanks are offered to the National Research Council of Canada for financial assistance and one of us (J. G. W.) acknowledges the award of an NRCC postgraduate bursary.

1. A. Moffat and H. Hunt. J. Am. Chem. Soc. **80**, 2985 (1958).
2. A. Moffat and H. Hunt. J. Am. Chem. Soc. **79**, 54 (1957).
3. A. Moffat and H. Hunt. J. Am. Chem. Soc. **81**, 2082 (1959).
4. W. Jencks and J. Carriuolo. J. Am. Chem. Soc. **83**, 1743 (1961).
5. F. N. Hornyak and E. S. Amis. J. Am. Chem. Soc. **79**, 2079 (1957).
6. G. Gorin, O. R. Pierce, and E. T. McBee. J. Am. Chem. Soc. **75**, 5622 (1953).
7. C. A. Bunton and T. Hadwick. J. Chem. Soc. 943 (1961).
8. C. A. Bunton and T. Hadwick. J. Chem. Soc. 3248 (1958).
9. P. M. Nair and E. S. Amis. J. Am. Chem. Soc. 77, 3452 (1955).
10. S. V. Anantakrishnan and S. Krishnamurti. Proc. Indian Acad. Sci. Sect. A, **14**, 270 (1941).
11. E. K. Euranto and N. J. Cleve. Acta Chem. Scand. **17**, 1584 (1963).
12. E. J. Bourne, M. Stacey, J. C. Tatlow, and R. Worrall. J. Chem. Soc. 3268 (1958).
13. J. B. Hyne and R. E. Robertson. Can. J. Chem. **35**, 623 (1957).
14. E. A. Guggenheim. Phil. Mag. **2**, 538 (1926).
15. R. E. Robertson. Can. J. Chem. **33**, 1536 (1955).
16. D. J. Barnes. M.Sc. Thesis. Memorial University of Newfoundland. St. John's, Newfoundland. 1966.
17. R. E. Robertson. Solvolysis in water. Progr. Phys. Org. Chem. Vol. 4. In preparation.
18. H. C. Brown, D. H. MacDaniel, and O. Hafliger. Determination of organic structures by physical methods. *Edited by* E. A. Braude and F. C. Nachod. Academic Press, Inc., New York. 1955. Chap. 14. p. 579.

19. REDLICH and G. C. HOOD. Trans. Faraday Soc. **24**, 87 (1957).
20. D. G. IVES. J. Chem. Soc. 731 (1933).
21. A. L. HENNE and C. J. FOX. J. Am. Chem. Soc. **73**, 2323 (1951).
22. R. P. BELL. The proton in chemistry. Cornell Univ. Press, Ithaca, New York. 1959. Chaps. 5 and 7.
23. ANDREW STREITWIESER, JR. Molecular orbital theory for organic chemists. John Wiley and Sons, Inc., New York. 1961. Chap. 11.
24. ANDREW STREITWIESER, JR. Solvolytic displacement reactions. McGraw-Hill Book Company, Inc., New York. 1962. Chap. 1. p. 7.
25. C. K. INGOLD. Structure and mechanism in organic chemistry. Bell and Sons, Ltd., London. 1953. Chap. 6. Sect. 19b.
26. M. G. EVANS and M. POLANYI. Trans. Faraday Soc. **32**, 1333 (1936).
27. R. W. TAFT, JR. Steric effects in organic chemistry. *Edited by* M. S. Newman. John Wiley and Sons, Inc., New York. 1956. Chap. 13.
28. C. K. INGOLD. Quart. Rev. London, **11**, 1 (1957).
29. J. KURZ. Private communication.
30. L. L. SCHALEGER and F. A. LONG. Advan. Phys. Org. Chem. Vol. 1. Academic Press, Inc., New York. 1963.
31. R. E. ROBERTSON, R. L. HEPPOLETTE, and J. M. W. SCOTT. Can. J. Chem. **37**, 803 (1959).
32. C. A. BUNTON and V. J. SHINER. J. Am. Chem. Soc. **83**, 3207 (1961).
33. P. M. LAUGHTON and R. E. ROBERTSON. Can. J. Chem. **39**, 2155 (1961).
34. P. M. LAUGHTON and R. E. ROBERTSON. Can. J. Chem. **34**, 1714 (1956).
35. R. E. ROBERTSON and P. M. LAUGHTON. Can. J. Chem. **35**, 1319 (1957).
36. P. M. LAUGHTON and R. E. ROBERTSON. Can. J. Chem. **37**, 1491 (1959).
37. R. E. ROBERTSON. Can. J. Chem. **42**, 1207 (1964).
38. G. KOHNSTAM. The transition state. Chem. Soc. Special Publication, No. 16, 1922 and references therein.
39. R. E. ROBERTSON. Can. J. Chem. **42**, 1707 (1964).
40. R. E. ROBERTSON and P. M. LAUGHTON. Can. J. Chem. **43**, 154 (1965).
41. C. G. SWAIN and E. R. THORNTON. J. Am. Chem. Soc. **84**, 817 (1962).
42. C. G. SWAIN and R. F. W. BADER. Tetrahedron, **10**, 182 (1960).
43. M. BENDER. Chem. Rev. **60**, 53 (1960).

Can. J. Chem. Downloaded from www.nrcresearchpress.com by 210.87.254.105 on 09/05/12
For personal use only.

Can. J. Chem. Downloaded from www.nrcresearchpress.com by 210.87.254.5 on 09/05/12
For personal use only.

Polarographic reduction of some Schiff bases in dimethylformamide. Part II. Some further theoretical considerations

H. G. BENSON AND J. M. W. SCOTT
Chemistry Department, Memorial University of Newfoundland, St. John's, Newfoundland

Received October 23, 1967

The ordinary Hückel molecular orbital (H.m.o.) method and the linear combination of molecular orbitals (l.c.m.o.) method in a perturbational form have been used to calculate the π-electron energy levels appropriate to a series of 24 Schiff bases (S.b.'s) of the type ArCH=NAr′, where Ar— and Ar—′ are unsubstituted aryl groups. The energy levels calculated by both the H.m.o. and l.c.m.o. treatments are shown to give a satisfactory account of the polarographic data for the S.b.'s reported in Part I of the present series. However, the l.c.m.o. method appears to offer a deeper insight into the variation of the half-wave potentials for the first electron transfer with the structure of the S.b.

Canadian Journal of Chemistry, 46, 2895 (1968)

Introduction

In Part I[1] of the present series the polarographic reduction potentials appropriate to the first reduction wave (ω_1) were presented for a series of S.b.'s derived from the amines **1–4** and the aldehydes **5–10**. In this preliminary study an approximate theoretical treatment of the variation of the half-wave potentials $E_{1/2}(\omega_1)$ with structure was presented which gave a useful account of the variation of $E_{1/2}(\omega_1)$ with the structure of the S.b.'s and also predicted certain linear free energy correlations which were observed in practice.

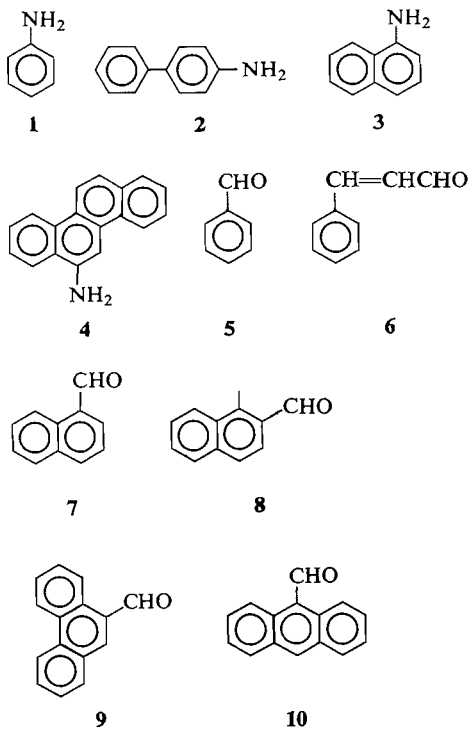

1 **2** **3** **4** **5** **6** **7** **8** **9** **10**

In the present communication we offer a more detailed theoretical treatment of the polarographic data in which the presence of the nitrogen atom in the S.b. structures is specifically included. All the Hückel molecular orbital (H.m.o.) levels for the S.b.'s have now been calculated, but for the sake of economy, only the energies corresponding to the lowest unoccupied m.o.'s will be reported here (see Table I), since these are the only theoretical quantities relevant to the empirical data reported in Part I. The crude linear combination of molecular orbitals (l.c.m.o.) treatment mentioned above will also be improved so as to include the heteroatom present in the S.b. structures.

Calculation of Energy Levels

The H.m.o. orbital energies were calculated partly on an I.B.M. 7094 II using a Jacobi matrix diagonalization procedure. In the S.b. structures the N atom was taken into account (2) with

$$[1] \quad \alpha_N = \alpha_C + h_N\beta; \quad h_N = 0.5\beta_{CC} = \beta,$$

where the notation of ref. 2 has been used. For the resonance integrals involving carbon and nitrogen atoms, $\beta_{CN} = k_{CN}\beta$ with $k_{CN} = 1$ in the l.c.m.o. calculations.

The l.c.m.o. perturbation treatment (3) is illustrated in Fig. 1. Let the pth and qth m.o.'s

[1]Reference 1 is to be considered as Part I of the present series.

TABLE I

Polarographic data and H.m.o. and l.c.m.o. energies for some Schiff bases

Number	ArCH=NAr′ Amine, $Ar'NH_2$	ArCH=NAr′ Aldehyde, ArCHO	Lowest unoccupied energy levels S.b. (ArCH=NAr′) $E_{S.b.}{}^{+}$(H.m.o.)*	$E_{S.b.}{}^{+}$(l.c.m.o.)*	$-E_{1/2}(\omega_1)$†
1	1	5	0.4129	0.4287	1.839
2	1	6	0.3007	0.3130	1.61
3	1	7	0.3377	0.3642	1.694
4	1	8	0.3799	0.4064	1.745
5	1	9	0.3348	0.3623	1.65
6	1	10	0.2360	0.2612	1.357
7	2	5	0.3891	0.4191	1.778
8	2	6	0.2893	0.3042	1.56
9	2	7	0.3240	0.3529	1.65
10	2	8	0.3604	0.3937	1.684
11	2	9	0.3215	0.3510	1.61
12	2	10	0.2298	0.2550	1.327
13	3	5	0.3915	0.4177	1.753
14	3	6	0.2914	0.3064	1.554
15	3	7	0.3262	0.3557	1.628
16	3	8	0.3642	0.3971	1.674
17	3	9	0.3236	0.3538	1.59
18	3	10	0.2311	0.2566	1.317
19	4	5	0.3384	0.3817	1.66
20	4	6	0.2629	0.2837	1.478
21	4	7	0.2921	0.3271	1.56
22	4	8	0.3208	0.3635	1.584
23	4	9	0.2902	0.3254	1.534
24	4	10	0.2147	0.2398	1.272

*All energies in units of β on a scale with $\alpha_C = 0$.
†Taken from ref. 1, eV versus standard calomel electrode.

of R and S be

$$[2] \qquad \Psi_{pR} = \sum_{r=1}^{n} a_{pr}\psi_r$$

$$[3] \qquad \Phi_{qS} = \sum_{s=1}^{m} b_{qs}\phi_s$$

If R and S are alternant radicals, the $\frac{1}{2}(n+1)$ m.o. of R and the $\frac{1}{2}(m+1)$ m.o. of S will be non-bonding molecular orbitals (n.b.m.o.) with energy α_c. These n.b.m.o.'s will be denoted by Ψ_{oR} and Φ_{oS}. In joining R to S a first order correction to the energy arises from these n.b.m.o.'s, while the other fully occupied m.o.'s of R and S remain unchanged (3). In the system RS where atom r of R is joined to atom s of S, the lowest unoccupied (+) and highest occupied (−) orbitals and their energies are respectively given by

$$[4] \qquad \xi_{RS}{}^{\pm} = \frac{1}{\sqrt{2}}\{\Psi_{oR} \mp \Phi_{oS}\}$$

and

$$[5] \qquad E_{RS}{}^{\pm} = \alpha_C \mp a_{or}a_{os}\beta,$$

where a_{or} and b_{os} are the n.b.m.o. coefficients at atom r of R and atom s of S. These n.b.m.o. coefficients are readily calculated by the method of Longuet-Higgins (4).

The functions $\xi_{RS}{}^{+}$ and $\xi_{RS}{}^{-}$ undergo a second perturbation P_{CN} corresponding to the replacement of an extracyclic methine group by nitrogen. The new Hamiltonian $H_{S.b.}$ is

$$[6] \qquad H_{S.b.} = H_{RS} + P_{CN}.$$

The perturbation P_{CN} is given in terms of its matrix elements in the $\psi_{r'}\phi_{s'}$ basis (atom r of R becomes r' in RS, etc.) to be

$$[7] \qquad \langle\phi_{os}|P_{CN}|\phi_{os}\rangle = \delta\alpha = h_N\beta,$$

$$\langle\psi_{or}|P_{CN}|\phi_{os}\rangle = \delta\beta = (k_{CN} - 1)\beta,$$

$$\langle\psi_{or}|P_{CN}|\psi_{or}\rangle = 0,$$

with all the other matrix elements in the basis $\psi_{or'}$, $\phi_{os'}$, $r' \neq r$, and $s' \neq s$ set equal to zero. Computations have been carried out for $h_N = 0.5$ and $k_{CN} = 1$. The new energy levels are given by

$$[8] \qquad E_{S.b.}{}^{\pm} = \langle\xi_{RS}{}^{\pm}|H_{RS} + P_{CN}|\xi_{RS}{}^{\pm}\rangle,$$

Can. J. Chem. Downloaded from www.nrcresearchpress.com by 210.87.254.5 on 09/05/12
For personal use only.

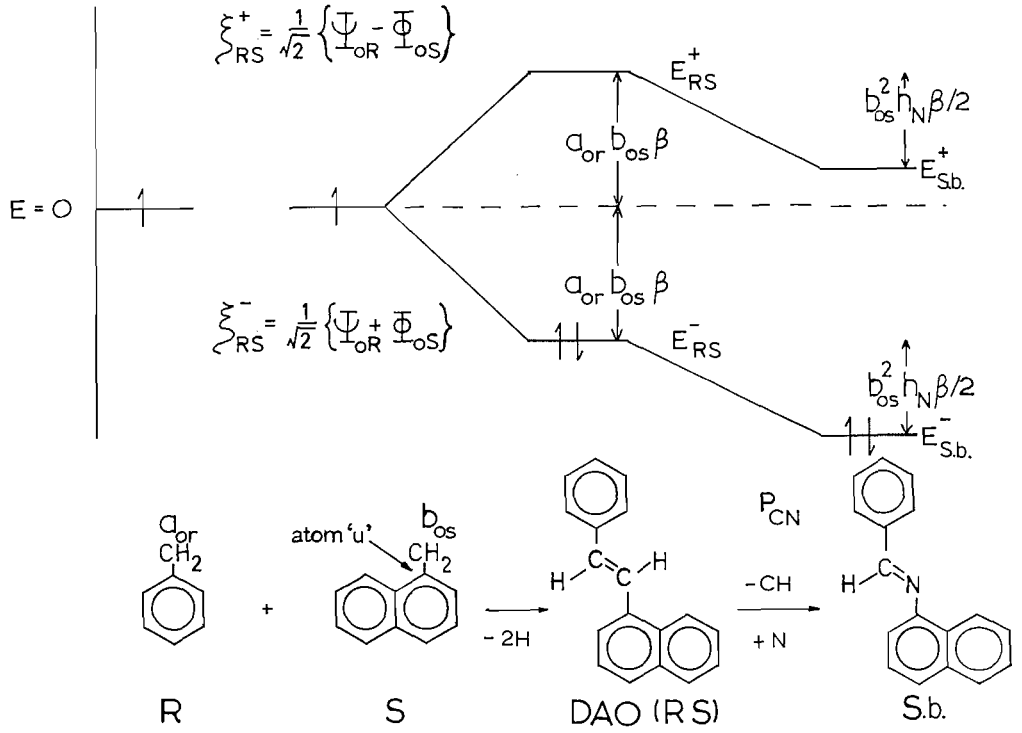

FIG. 1. A schematic diagram illustrating the l.c.m.o. perturbation calculation of the lowest unoccupied and highest occupied π-electron energy levels of R and S are not included in the figure.

from which we have

$$[9] \quad E_{S.b.}{}^{+} = \alpha_C - a_{or}b_{os}k_{CN}\beta + \tfrac{1}{2}(b_{os})^2 h_N\beta$$

for the lowest unoccupied energy of the S.b. calculated on the assumption that the changes R,S → RS → S.b. can be treated by first order perturbation theory in the π-electron approximation. The justification for the present procedure is to be found mainly in the correlation between prediction and experiment.

Discussion

In Fig. 2 we have correlated $E_{S.b.}{}^{+}$ (H.m.o.) with $E_{S.b.}{}^{+}$(l.c.m.o.). The satisfactory nature of this correlation establishes the validity of the perturbation method. In Fig. 3 the $E_{1/2}$ values reported previously (1) have been correlated with $E_{S.b.}{}^{+}$ (H.m.o.), and a least squares treatment of the data gives

$$[10] \quad E_{1/2} = 2.79 \pm 0.01 E_{S.b.}{}^{+} + 0.71 \pm 0.02,$$

leading to a value of $\beta = 2.79 \pm 0.01$ eV.

Although the above correlations are of considerable interest, the various relationships which exist within the reduction potential data (cf. Fig. 2 of Part I) merit equal theoretical attention. The latter relationships are essentially linear free energy relationships (l.f.e.r.'s) which are conveniently summarized by the equation

$$[11] \quad \partial E_{1/2}(a)/\partial E_{1/2}(b) = \text{constant}.$$

These are two distinct l.f.e.r.'s of this type which are designated respectively *a/b* and *c/d* relationships. The *a/b* correlations are those in which the amine fragments of two series of S.b.'s are held constant and where the aldehyde portions vary in the same manner. The *c/d* correlations are generated by keeping the aldehyde portions constant and varying the amine fragments in a similar fashion.

Three *a/b* correlations are illustrated in Fig. 4 using both the theoretical and empirical data in the following way. Firstly, the $E_{S.b.}{}^{+}(a)$ vs. $E_{S.b.}{}^{+}(b)$ correlations are made using the appropriate H.m.o. levels and, secondly, the $E_{1/2}$ values have been scaled (via eq. [10]) to produce

Can. J. Chem. Downloaded from www.nrcresearchpress.com by 210.87.254.5 on 09/05/12
For personal use only.

Can. J. Chem. Downloaded from www.nrcresearchpress.com by 210.87.254.5 on 09/05/12
For personal use only.

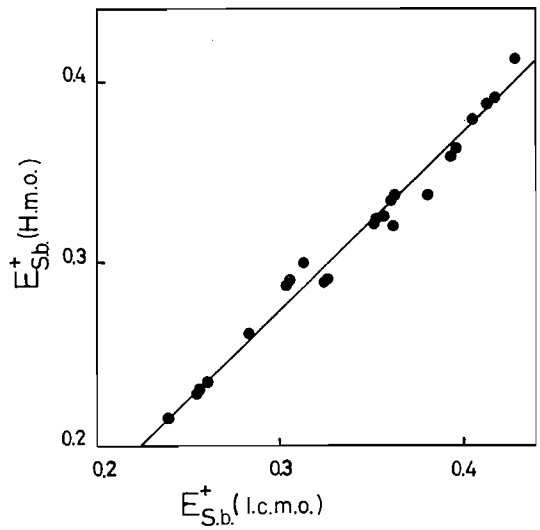

FIG. 2. A correlation between the lowest unoccupied m.o. π-electron energies calculated by the H.m.o. and l.c.m.o. methods with $h_N = 0.5$ and $k_{CN} = 1$.

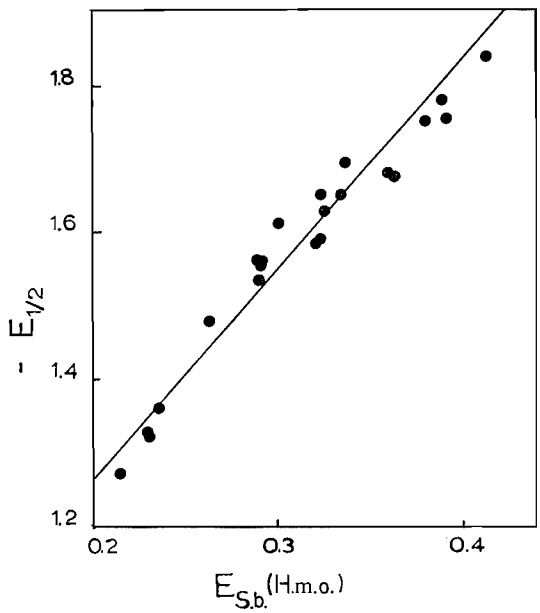

FIG. 3. A correlation of $-E_{1/2}$ (ω_1) and the lowest unoccupied m.o. π-electron energies calculated by the H.m.o. technique ($h_N = 0.5$; $k_{CN} = 1$).

'empirical' $E_{S.b.}{}^+$ values which are then correlated in the same way as the $E_{S.b.}{}^+$ (H.m.o.) levels. A completely accurate theory would give three separate lines containing coincidental empirical and theoretical points. Clearly the theory is only partly verified, for although the individual slopes of each pair of lines are reasonably similar, the theoretical and empirical points are not coincidental. The inadequacy of the theory might have been anticipated from the scatter of the points in Fig. 3. Equation [9] also offers some insight into the relationships displayed in Fig. 4.

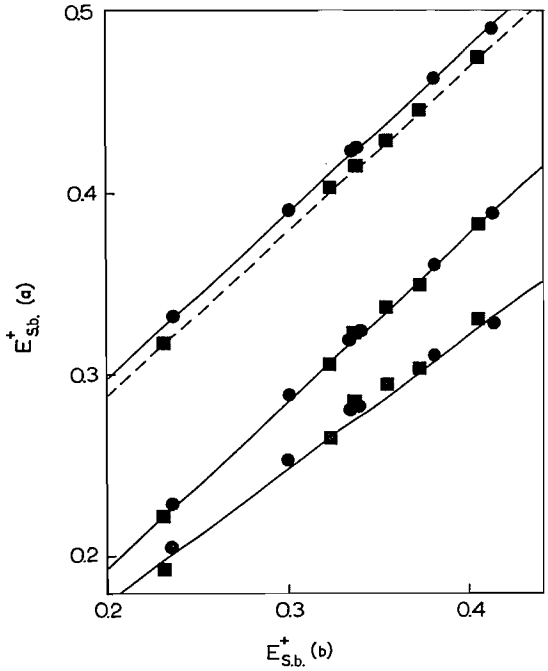

FIG. 4. A series of correlations of $E_{S.b.}{}^+(a)$ vs. $E_{S.b.}{}^+(b)$. Theoretical values (●) obtained from H.m.o. theory; empirical values (■) from $E_{1/2}$ (see text). The y axis has been adjusted for clarity of presentation. Upper curves, amine **3** (a), amine **1** (b) (y increased by 0.1 unit); middle curve, amine **2** (a) vs. amine **1** (b); bottom curve, amine **4** (a), amine **1** (b) (decreased by 0.01 unit).

Consider two series of S.b.'s denoted by $i = a$ or b and let the n.b.m.o. coefficient at atom s be $b_{os}{}^i$, then from eq. [9] we have

$$[12]\quad E_{1/2} = -a_{or}b_{os}{}^i k_{CN}\beta + \tfrac{1}{2}(b_{os}{}^i)^2 h_N\beta + C.$$

The a/b correlation is generated by differentiating with respect to a_{or} and taking the ratio of the result with $i = a$ and $i = b$, giving

$$[13]\quad \partial E_{1/2}(a)/\partial E_{1/2}(b) = b_{os}{}^a/b_{os}{}^b = \text{constant}.$$

Similarly for the c/d series, where we now have $a_{or}{}^i$ and $i = c$ or d (fixed) and b_{os} as the variable. A similar manipulation to that above gives

$$[14]\quad \partial E_{1/2}(c)/\partial E_{1/2}(d) = (b_{os}h_N - a_{or}{}^c k_{CN})/(b_{os}h_N - a_{or}{}^d k_{CN}).$$

This is only of the form of eq. [11], if $a_{or}{}^d - a_{or}{}^c = 0$, and differs from the c/d relationship predicted in Part I of the present series where the c/d relationships would also show l.f.e.r. behavior. Unfortunately no adequate experimental evidence is available at present regarding the c/d correlations.

Recently Grunwald and Leffler (5, 6) have presented a phenomenological approach to l.f.e.r.'s. In this treatment they express the standard free energy of a molecule RS in the form

$$[15]\quad G_{RS}{}^0 = G_R + G_S + I_{RS} + \text{constant},$$

where I_{RS} is the non-additive term arising from the interaction of R and S. This non-additive term can be written as

$$[16]\quad I_{RS} = C_0 + C_1\Sigma I_R{}^2 + C_2\Sigma I_R I_S + C_3\Sigma I_S{}^2 + C_4 \text{ (higher order terms)}.$$

The existence of l.f.e.r.'s demands that $C_1 = C_3 = C_4 = 0$, $C_2 \neq 0$. Grunwald (5) warns against interpreting the scalar parameters I_R and I_S in terms of definite physical interactions in view of the complexity of the interactions. On the other hand, for the relatively clear-cut problem of the half-wave potentials of the S.b.'s, we have demonstrated within the limitations of an l.c.m.o. perturbation approach that for the a/b l.f.e.r. the I_R and I_S parameters are directly related to the a_{or} and b_{os} parameters of the l.c.m.o. theory. Within the framework of the present theory, for the c/d correlations, $C_1 = C_4 = 0$ but C_2 and $C_3 \neq 0$ and hence a l.f.e.r. is not obtained, although the I_R and I_S parameters still correlate with the l.c.m.o. theory.

The effect of solvation differences between the S.b.'s and the related radical anions have not been considered here although this factor is likely to be less important than the shortcomings of the l.c.m.o. theory itself. Furthermore, it is generally believed that charge delocalization, which will be important in the radical anions, reduces the importance of solvation (7) (but see also ref. 8 for a criticism of this viewpoint).

Acknowledgments

The authors wish to express their thanks to Mr. M. Jones and the University of Toronto Computing Centre for their help in the computational work associated with this paper. We also thank the National Research Council of Canada for financial support, and one of us (H. B.) thanks the Newfoundland Provincial Government for the award of postgraduate allowance. Finally, we would like to thank one of our referees for some very helpful suggestions.

1. J. M. W. Scott and W. H. Jura. Can. J. Chem. **45**, 2375 (1967).
2. A. Streitwieser, Jr. Molecular orbital theory for organic chemists. John Wiley and Sons, Inc., New York. 1961. Chap. 4.
3. M. J. S. Dewar. J. Am. Chem. Soc. **74**, 3341, 3345, 3350, 3353, 3357 (1952).
4. H. C. Longuet-Higgins. J. Chem. Phys. **18**, 265, 275, 283 (1950).
5. E. Grunwald. Symposium on linear free energy correlations, U.S. Army Research Office, Durham, North Carolina, October 1964. p. 69.
6. E. Grunwald and J. E. Leffler. Rates and equilibria of organic reactions. John Wiley and Sons, Inc., New York. 1963.
7. S. F. Mason. J. Chem. Soc. 808 (1958).
8. A. Streitwieser, Jr. and P. M. Nair. Tetrahedron, **5**, 149 (1959).

Can. J. Chem. Downloaded from www.nrcresearchpress.com by 210.87.254.5 on 09/05/12
For personal use only.

Can. J. Chem. Downloaded from www.nrcresearchpress.com by 210.87.254.105 on 09/05/12
For personal use only.

Photolytic hydration of cyanamides

Y. L. CHOW AND K. E. HAQUE
Department of Chemistry, Simon Fraser University, Burnaby 2, British Columbia

Received March 19, 1968

N-Cyanopiperidines (**1** and **2**) have been shown to possess a n → π* transition band in the vicinity of 260 mμ and, in the presence of a dilute acid, undergo photolytic reactions leading to hydration products (**3** and **4**). The fact that the reaction can be sensitized by acetophenone demonstrates that **1** reacts through a triplet state. E_T is about 76 kcal/mole. Increasing the water content in the photolysis medium reduced the yield of the hydration product.

Canadian Journal of Chemistry, 46, 2901 (1968)

Introduction

There is some experimental evidence that the particular photolytic reactivities shown by nitrosamines are partially due to the extensive mixing of the n and π orbitals (1, 2). It has been argued that this extensive delocalization could raise the energy level of π* orbitals causing the observed difference in the electronic spectra of RNO, R_2NNO, and RONO systems (3). The observed differences in the photochemical reactions of nitrosamines and nitrites may be related to this argument.

In pursuing photochemical investigations of the related systems, we became interested in the cyanamide system. The π electrons of the carbon–nitrogen triple bond (—C≡N) differs considerably from those of the carbon–carbon triple bond in that the contribution of the polar form ($—\overset{+}{C}=N^-$) is as high as 70%, as indicated by the high dipole moment (ca. 4.0 D) of the simple nitrile (4). On the other hand the bond lengths of the carbon–carbon single bond in acetonitrile and acrylonitrile differ very slightly (1.458 Å and 1.426 Å respectively) (5) and the dipole moments of acrylonitrile and propionitrile are very close (3.8 D and 4.1 D respectively) (4). These figures strongly suggest that there is very little conjugative delocalization in acrylonitrile. In spite of this evidence it is surprising that a cyanamide shows a low intensity peak in 257 mμ region (vide infra) reminiscent of a n → π* transition band. Bearing in mind that the first transition band of acetonitrile occurs at 167 mμ (very weak) it is concluded that a sizable amount of electronic interaction may be present in the ground state of the cyanamide system. This electronic interaction apparently has shifted the first transition band to the ultraviolet region where irradiation experiments become feasible. Such considerations led us to examine the photochemical behavior of dialkylcyanamides.

Results and Discussion

The required compounds, N-cyanopiperidine (**1**) and N-cyano-4-methylpiperidine (**2**), were prepared from the parent amine via N-chloramine according to the method described by Berg (6). A dilute aqueous solution of **1** is distinctly basic and registers a value of 8–8.5 on pH paper. Thus in the 0.1 *N* hydrochloric acid solution the cyanamides are predominantly protonated and are difficult to extract into ether layers. In agreement with the required sp-hybridization of cyanamide group the geometry of N—C≡N group is linear, as is indicated from the magnetic equivalence of the α- and α′-proton chemical shifts in **1** and **2** at −40°.

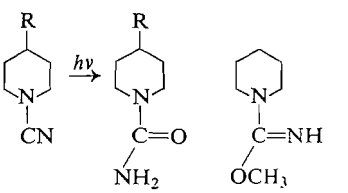

1 (R = H) **2** (R = CH_3) **3** **4** **5**

In cyclohexane solution the cyanamides showed an absorption maximum at the region 260 mμ with the extinction coefficient of ca. 200. This peak, however, hypsochromically shifts to the 245 mμ region in methanol. In analogy to the similar hypsochromic shift of nitrosamines in more polar solvent (7) this band may be assigned to n → π* transition of the cyanamide group.

The irradiation was carried out with a Hanovia medium pressure mercury lamp through a

Can. J. Chem. Downloaded from www.nrcresearchpress.com by 210.87.254.105 on 09/05/12
For personal use only.

Vycor filter and the temperature was maintained at 15–20° with cold running water. While in a methanol or methanol–water solution **1** was stable to irradiation without showing any change at 233 mμ absorption, this peak slowly tapered off in 0.1 *N* methanolic hydrochloric acid solution. The decrease of the 233 mμ absorption became progressively slower as the irradiation proceeded and finally the residual absorption submerged into the tail of the new absorption centered at a lower wavelength. After 12 h of irradiation the reaction gave about 80% of crude piperidine-N-carboxamide (**3**) and 20% of unreacted **1**. In a similar manner N-cyano-4-methylpiperidine (**2**) was photolyzed to give 4-methylpiperidine-N-carboxamide (**4**) in 53% yields.

Since stoichiometrically the reaction portrays hydration of the nitrile group, the effect of water content in the reaction media should therefore be an important factor to investigate. In the presence of 10% water, other conditions being equal, the yield of **3** was 62% and the recovery of **1** 37% after 5 h irradiation. Instead of showing any improvement, the yield of **3**, however, varied erratically in the region of 45–55% regardless of prolonged irradiation (12 h period or longer) or use of a more powerful lamp (450 W Hanovia medium pressure mercury lamp). Progressive increases in water content to 15% and 25% brought down the yield of **3** to 22% and 6% respectively. The balance of the starting material was also recovered (75% and 82%). These results suggest that a photochemical equilibrium may exist between **1** and **2** and that the equilibrium is in favor of **1** in a medium of higher water content. This conclusion was shown to be incorrect since no **1** could be detected when **3** was photolyzed either alone under the same conditions or in the presence of a small amount of **1**.

Since moisture was excluded in the photolysis in methanol containing dry hydrochloric acid, it might be assumed that an intermediate was formed which reacted further with water to give **3** on working up. Unfortunately an attempt at trapping the presumed intermediate **5** with excess diethylamine after 12 h irradiation was not successful; **3** was obtained in 81% yield again. The failure to prove the presence of an intermediate and a photochemical equilibrium does not allow one to speculate on the primary process of the photoreaction. Neither does it offer an explanation of why the yield of **3** decreases at higher water concentration.

A control experiment in which the same reaction mixture (10% water) was worked up under the same conditions after leaving at room temperature for 12 h gave nearly a quantitative recovery of **1**. It was therefore concluded that hydration of the cyanamide is a genuine photolytic reaction. Experiments to determine the multiplicity of the excited electronic state responsible for the primary photoprocess was then in order. The photosensitized conversion of **1** and **2** could not be effected with 0.1 *M* benzophenone (E_T 69.2 kcal/mole) and acetophonone (E_T 76.3 kcal/mole) (8) in the absence of hydrochloric acid (pyrex filter). That no triplet energy transfer took place could be shown by the good recovery of the respective pinacols, the expected products from a photoreduction of the ketones (9). However, in 0.1 *N* hydrochloric acid, with acetophenone as a sensitizer, the hydration of **1** to **3** took place to an extent of 35% after 4 h irradiation. Since direct photolytic hydration of **1** does not occur in pyrex apparatus where energy is cut off at 280 mμ the triplet energy transfer from acetophenone to **1** must be taking place in the acidic medium to give the hydration product. In agreement with the mechanism of the triplet energy transfer, pinacol was formed only in small quantity and the majority of acetophenone was recovered (8). In contrast, benzophenone was ineffective in sensitizing this hydration reaction under similar conditions. It can be concluded that a part, if not all, of the direct hydration of **1** proceeds through the triplet state and that the E_T of **1** lies between 69 and 76 kcal/mole. In estimating the triplet energy of **1** by sensitization experiments, it was explicitly assumed that only the Franck–Condon type of energy transfer was involved (10). It should be pointed out that the E_T of **1** would be considerably higher than 76 kcal/mole should a nonvertical energy transfer take place (10).

A mechanistic consideration of this photolytic hydration is hampered by the obvious lack of knowledge of the role played by water in the reaction. The information available at the moment allows us to propose a reasonable

Can. J. Chem. Downloaded from www.nrcresearchpress.com by 210.87.254.105 on 09/05/12
For personal use only.

mechanism for the direct photolysis as follows:

[1] $H^+ + \rangle\ddot{N}{-}C{\equiv}N \rightleftarrows \rangle\overset{\oplus}{N}{=}C{=}N{-}H$ **6**

[2] $\mathbf{6} \rightleftarrows (\rangle\overset{\oplus}{N}{=}C{=}N{-}H)_s{}^*$ **7**

[3] $\mathbf{7} \rightarrow (\rangle\overset{\oplus}{N}{=}C{=}N{-}H)_t{}^*$ **8**

[4] $\mathbf{8} \rightarrow \mathbf{6}$ + energy

[5] $\mathbf{8} \rightarrow$ product

The requirement of an acid in the photolytic hydration demonstrates that the protonated triplet state of **1** undergoes the reaction. Though the precise site of the protonation in the ground state of cyanamide is not known, the more resonance stabilized form, **6**, can be reasonably assigned to the protonated species. In the direct photolysis **6** is excited to the $n \rightarrow \pi^*$ singlet state (**7**) which crosses over to the triplet excited state (**8**). Judging from the slow conversion of the cyanamides, the intersystem crossing, [3], may be very inefficient and the singlet excited state **7** may preferentially decay to the ground state by various routes (the reverse reaction of [2]). Alternatively, the triplet excited state **8** may preferentially decay to the ground state, as shown in [4], leaving only a small fraction to react via the hydration pathway [5]. No doubt [5] represents a multistep process, the nature of which remains to be clarified.

It has been further shown that under these photolytic conditions the addition of **1** to olefins did not take place, since no other product except **3** could be isolated when the irradiation was carried out in the presence of norbornylene or 1-hexene.

Experimental

Melting points were determined on a Fisher–Johns apparatus and were uncorrected. Infrared spectra were measured in a Unicam SP 200 as Nujol dispersions or liquid film. Ultraviolet (u.v.) spectra were taken with a Cary 14 and nuclear magnetic resonance (n.m.r.) spectra with Varian A 56/60 using tetramethylsilane as the internal standard.

Preparation of the Cyanamides

The preparations followed the procedures described by Berg (6). The amine was converted to N-chloramine which, in turn, was treated with potassium cyanide in methanol–water solution. N-Cyanopiperidine has b.p. 108–110° at 15 mm, λ_{max} 257 mμ (ε, 135) in cyclohexane and 244 mμ (ε, 142) in methanol, and ν (liquid) 2220 cm^{-1}, and the n.m.r. signals (CCl_4) at τ 6.87 and 8.39 have an intensity ratio of 4:6. N-Cyano-4-methylpiperidine has b.p. 105–107° at 5 mm, λ_{max} 260 mμ (ε, 224) in methanol, ν (liquid film) 2220, 1610, and 970 cm^{-1}, and n.m.r. signals (CCl_4) at τ 7.65 (broad doublet) and 8.06 (broad triplet).

Photolysis of the Cyanamides

Into the photolysis apparatus (equipped with a quartz cold finger carrying Vycor filter) a cyanamide (0.01 mole), 2 *N* hydrochloric acid (10 ml), and the required amount of water were placed and methanol was added to make up 200 ml. The solution was irradiated with a 200 W Hanovia medium pressure mercury lamp. At intervals, aliquots were withdrawn with a pipette and suitably diluted for u.v. scans. The zero hour sample was kept in the dark to serve as the control experiment.

The reaction mixture was evaporated. The aqueous solution of the residue was neutralized and extracted with ether. The ether solution gave the unreacted cyanamide after evaporation. The aqueous solution was evaporated in a rotatory evaporator at ca. 50° to dryness. The residue was then extracted with chloroform. The dry chloroform solution was evaporated to a small volume and a small amount of ether was added to induce crystallization. The crystals were recrystallized from the same solvent mixture to give the ureas.

Piperidine-N-carboxamide obtained from photolysis has m.p. 100–101°, which is not depressed in a mixture with an authentic sample prepared according to Cahour's method (lit. 105–106°) (11). 4-Methylpiperidine-N-carboxamide has m.p. 88–90° and ν_{max} (Nujol) 3380, 3180, 1650, and 1595 cm^{-1}. The mixed melting point with a sample prepared according to Cahour's method (11) is 88–91°.

The Control Experiment

The same constituent of the photolysis solution containing 10% of water and N-cyanopiperidine was prepared. This mixture was left at room temperature overnight and was worked up by the same procedure as that for the photolysis mixture. Only N-cyanopiperidine was recovered quantitatively.

Photosensitization Experiment

A pyrex cold finger was substituted in these runs. In the photolysis apparatus, N-cyanopiperidine (1.1 g), acetophenone (2.4 g), 2 *N* aqueous hydrochloric acid (10 ml), and methanol (185 ml) were placed and irradiated in the usual manner.

After the work-up acetophenone and its pinacol were found in the neutral fraction (2.51 g), as indicated by 1675 cm^{-1} absorption and τ 8.6 and 7.45 signals. The crude product of 2,3-diphenyl-2,3-butandiol crystallized from the light petroleum solution 650 mg, m.p. 95–120°, and showed the infrared peaks at 1335, 1130, 1111, 1355, and 1145 cm^{-1} and unresolved singlets at τ 8.6. This data indicated this fraction was a mixture of the *meso* and *dl* isomers (12). The basic extract (650 mg) contains mainly

N-cyanopiperidine as shown by the infrared spectrum. The urea **3** (450 mg) was isolated and purified in the usual manner.

Acknowledgments

The authors are grateful to the National Research Council of Canada for their generous grant and to Mr. D. W. L. Chang for technical assistance.

1. Y. L. CHOW. Can. J. Chem. **45**, 54 (1967).
2. Y. L. CHOW, C. COLON, and S. C. CHEN. J. Org. Chem. **32**, 2109 (1967).
3. S. F. MASON. Quart. Rev. London, **15**, 287 (1961).
4. R. C. WEAST (*Editor-in-Chief*). Handbook of chemistry and physics. 46th ed. The Chemical Rubber Publishing Co., Cleveland, Ohio. 1966. p. E-58.
5. J. D. ROBERTS and M. C. CASERIO. Basic principles of organic chemistry. W. A. Benjamin Inc., 1965. p. 248.
6. A. BERG. Ann. Chim. Paris, 319 (1894).
7. H. H. JAFFE and M. ORCHIN. Theory and application of ultraviolet spectroscopy. John Wiley and Sons, Inc., New York, N.Y. 1962. p. 188.
8. W. G. HERKSTROETER, A. A. LAMOLA, and G. S. HAMMOND. J. Am. Chem. Soc. **86**, 4537 (1964).
9. G. S. HAMMOND and P. A. LEERMAKER. J. Am. Chem. Soc. **84**, 207 (1962).
10. G. S. HAMMOND *et al.* J. Am. Chem. Soc. **86**, 3197 (1964).
11. M. A. CAHOURS. Ann. Chim. Paris, 84 (1853).
12. D. J. CRAM and K. R. KOPECKY. J. Am. Chem. Soc. **81**, 2748 (1959).

Can. J. Chem. Downloaded from www.nrcresearchpress.com by 210.87.254.105 on 09/05/12
For personal use only.

Can. J. Chem. Downloaded from www.nrcresearchpress.com by 210.87.254.105 on 09/05/12
For personal use only.

Mechanism of decarboxylation of substituted salicylic acids. I. Kinetics in quinoline solution

G. E. DUNN, E. G. JANZEN, AND W. RODEWALD
Chemistry Department, University of Manitoba, Winnipeg 19, Manitoba

Received April 5, 1968

First-order rate constants for the decarboxylation of fourteen 4- and 5-substituted salicylic acids have been determined in quinoline solution in the temperature range 90–230 °C. Substituents have almost no effect on the rate constants, except those with large negative σ-constants: *p*-amino, *p*-hydroxy, *p*-ethoxy. The enthalpies and entropies of activation do not fit the isokinetic relationship, with the same three substituents deviating. It is suggested that the decarboxylation involves a preliminary ionization of the carboxyl group, followed by protonation of the aromatic ring of the anion so formed, and then loss of carbon dioxide. The isokinetic relationship fails because substituents affect all three steps differently, and the Hammett relationship fails because the substituent effect on the ionization is related to σ while that on the other two steps follows σ^+. The three substituents which deviate are those for which σ and σ^+ differ widely.

Canadian Journal of Chemistry, **46**, 2905 (1968)

The decarboxylation of substituted salicylic acids in aqueous solution has been thoroughly investigated. Schubert and Gardner (1) showed that the decarboxylation of 2,4,6-trihydroxybenzoic acid in aqueous perchloric acid is first order with respect to 2,4,6-trihydroxybenzoate ion and to hydrogen ion, so that the slow step could be either a unimolecular decomposition of the free acid or a bimolecular reaction between the anion and the proton. Willi (2) found that the decarboxylation of 4-substituted salicylic acids obeys the Hammett relationship using σ^+, and that the rate is increased by electron-releasing substituents. He therefore concluded that the slow step is protonation of the anion in the 1-position of the aromatic ring. Lynn and Bourns (3) demonstrated that protonation and decarboxylation are sequential rather than concerted processes by showing that the ^{13}C-carboxyl kinetic isotope effect in the decarboxylation of 2,4-dihydroxybenzoic acid varies with buffer concentration. These results make it clear that the mechanism of decarboxylation of substituted salicylic acids in aqueous solution is the following:

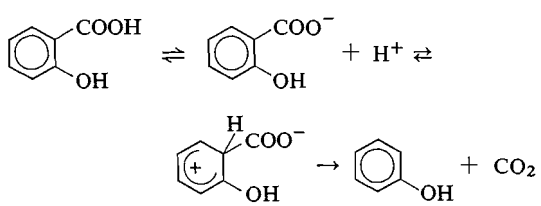

In nonaqueous solution much less information is available. Brown, Hammick, and Scholefield (4) found that in resorcinol at 110–240 °C the first-order rates of decarboxylation increased as hydroxy groups were added to the 4- and 6-positions of salicylic acid, which suggested that here, too, protonation of the aromatic ring is an important part of the rate-determining process. Clark (5) studied the decarboxylation of 4-hydroxysalicylic acid in glycols and in quinoline and concluded that these solvents were acting as nucleophiles toward the carboxyl carbon.

The present work reports the rate and activation parameters for decarboxylation of 14 substituted salicylic acids in quinoline solution.

Experimental

Synthetic quinoline distilled from and stored over barium oxide was used throughout. Salicylic acid and the 4- and 5-amino, 4- and 5-hydroxy, 4- and 5-nitro, 4-ethoxy, 5-methyl, 5-chloro, and 5-bromo substituted salicylic acids were commercial products recrystallized to constant melting point from water, aqueous ethanol, or toluene. All melting points were determined in a Hershberg apparatus (6) using calibrated Anschütz thermometers. The preparation of the 4-methyl (7) and 4-bromo (8) acids has been previously described.

5-Methoxysalicylic Acid

This acid was prepared by methylating 5-hydroxysalicylic acid. To a solution of 7.1 g of 5-hydroxysalicylic acid in 40 ml of 10% sodium hydroxide solution was added in alternate small portions 12.1 g of dimethylsulfate and 40 ml of 10% sodium hydroxide solution. The mixture was refluxed for 4 h, cooled, and acidified. The precipitated crude 5-methoxysalicylic acid was refluxed with 10% sodium hydroxide solution, then reprecipitated with mineral acid. Recrystallization from benzene and from water produced 2.8 g (37%) of product with m.p. 145.7–146.2 °C (lit. (9), m.p. 143.5 °C).

TABLE I

First-order rate constants ($k \times 10^4$ s^{-1}) for the decarboxylation of substituted salicylic acids in quinoline*

Substituent	k at temperature 93°	100°	110°	120°	126°	$\Delta H^{\ddagger}$	$\Delta S^{\ddagger}$
4-NH_2	*0.53*	*1.09*	*3.35*	*9.34*	*13.3*	28.5±0.8	−0.7±2.0

Substituent	k at temperature 130°	140°	150°	160°	170°	180°	190°	$\Delta H^{\ddagger}$	$\Delta S^{\ddagger}$
4-OH	*0.61*	*1.61*	*3.97*	*10.4*		*45.1*	*78.9*	29.5±0.5	−5.2±1.2
4-OEt	*0.13*	*0.40*	*1.02*	*2.78*	*5.81*	*14.6*	*29.7*	32.6±0.4	−0.5±0.9

Substituent	k at temperature 180°	200°	210°	220°	230°	$\Delta H^{\ddagger}$	$\Delta S^{\ddagger}$
H	*0.20*	*1.08*		4.86	*8.76*	33.4±0.4	−7.0±0.8
4-Me		3.61	6.86	12.9	*27.3*	30.7±0.8	−10.3±1.7
4-Br		3.39	6.40	11.3	*23.6*	29.3±0.9	−13.5±1.9
4-NO_2		*0.41*	0.86	2.16	4.73	38.2±0.8	+1.1±1.7
5-NO_2		*1.06*	1.99	3.93	7.89	30.7±0.8	−12.8±1.6
5-Me		1.36	3.10	5.83	*11.8*	32.9±0.8	−7.6±1.7
5-Br		1.51	3.40	6.34	*11.8*	31.1±0.9	−11.1±1.8
5-Cl		1.56	3.27	6.34	*12.1*	31.2±0.8	−10.9±1.6
5-OH		1.93	4.04	7.78	*18.2*	33.7±1.3	−5.2±2.6
5-NH_2		1.76	*3.69*	7.62	*15.9*	33.6±0.6	−5.6±1.2
5-OMe		2.23	4.53	8.43	*19.6*	32.6±1.2	−6.2±2.4

*Each rate constant is the average of two to five runs. The maximum deviation from the mean is about 3%. Numbers in italics were obtained gravimetrically; all others are manometric.

Rate Measurements

The apparatus for measuring rates of decarboxylation was similar to that previously described (10). The thermostat consisted of a 3 l round-bottom flask containing a refluxing liquid (*n*-butyl ether) into the vapors of which dipped the reaction vessel. The temperature, measured by a thermocouple in the reaction vessel, could be maintained to within ±0.05 °C by means of a manostat on the refluxing liquid. The manostat consisted of the flask containing the refluxing liquid and a ballast tank of about equal size connected to a vacuum pump through a solenoid gas valve. The gas valve was operated through a relay by a thermistor in the refluxing vapor.

The rate of carbon dioxide evolution was measured either gravimetrically as previously described (10) or manometrically. For manometric measurements the reaction vessel was modified to a bulb with a capillary neck. The reactant solution (10 ml of 0.1–0.2 *M* salicylic acid) was introduced through the capillary neck by means of a hypodermic syringe and allowed to come to thermostat temperature, then a mercury manometer was attached to the neck. Both manometric and gravimetric data were fitted by the least-squares method to the rate equation

$$\ln (x_i - x_t) = -kt + \ln (x_i - x_0)$$

where x_0, x_t, and x_i represent weight or pressure of carbon dioxide at times zero, t, and infinity respectively. The standard deviation of k within a run was about 1% and the maximum deviation of k from the mean of three to five runs was about 3%. Manometric and gravimetric rates agreed within experimental error so long as the rate constant was less than about 10^{-3} s^{-1}. At higher rates the evolution of carbon dioxide from solution was slower than the reaction.

Enthalpies and entropies of activation were calculated from a least-squares fit of the data to the equation

$$\ln \frac{k}{T} = \ln \frac{\mathbf{k}}{h} + \frac{\Delta S^{\ddagger}}{R} - \frac{\Delta H^{\ddagger}}{RT}$$

where **k** is the Boltzmann constant.

Results and Discussion

The decarboxylation of substituted salicylic acids in quinoline solution is a clean first-order reaction up to three half-lives for all 14 acids at all the temperatures investigated. Rate constants and activation parameters are shown in Table I.

Figure 1 shows a plot of the rate constants at 200 °C against σ^+. It is clear that the rates do not obey the Hammett relationship. Substituents having $\sigma^+ = -0.3$ or greater have very little effect on the rate, while 4-OH, 4-OEt, and 4-NH_2 substituents increase the rate of decarboxylation markedly. The fact that most substituents have little effect on the rate might be accounted for in one of three ways: (*a*) the substituents are insulated from the reaction site; (*b*) the substituents

Can. J. Chem. Downloaded from www.nrcresearchpress.com by 210.87.254.105 on 09/05/12
For personal use only.

Can. J. Chem. Downloaded from www.nrcresearchpress.com by 210.87.254.105 on 09/05/12
For personal use only.

influence bond making and bond breaking in opposite senses so that cancellation occurs; or (*c*) the isokinetic temperature is near 200 °C (11). Considering the structure of the reactant, (*a*) is hardly possible; (*b*) and (*c*) may be aspects of the same phenomenon, that is, cancellation may occur at the isokinetic temperature only.

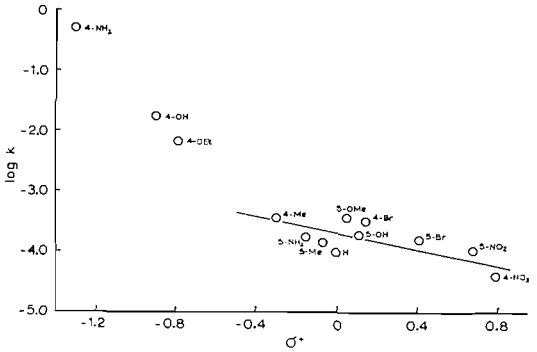

FIG. 1. Hammett plot of the rate constants for decarboxylation of salicylic acids in quinoline at 200 °C. Rate constants for the three points at upper left are calculated from the activation parameters. σ^+ values are from ref. 14.

Figure 2 is a plot of the isokinetic relationship, $\Delta H^{\ddagger}$ vs. $\Delta S^{\ddagger}$. Once again the points for 4-OH, 4-OEt, and 4-NH_2 deviate from the rest. The remaining points show a considerable scatter but, including their experimental uncertainty, they all lie on a straight line with slope = 290 ± 50 °C. The isokinetic temperature is therefore too great to account for the lack of substituent effects at 200 °C. It is also worth noting that rate constants at 100 °C calculated from the activation parameters give a Hammett plot hardly distinguishable in shape from that at 200 °C.

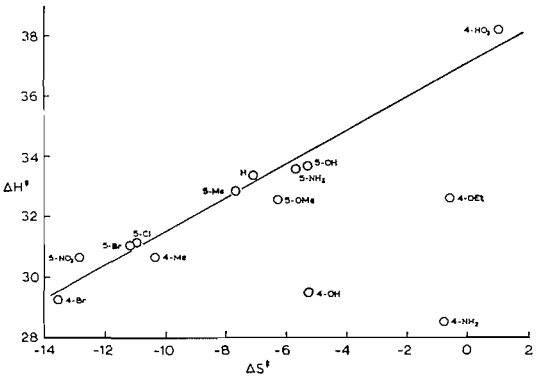

FIG. 2. Isokinetic plot for the decarboxylation of salicylic acids in quinoline.

However, even allowing for the difficulties in calculating and interpreting isokinetic temperatures (12), the 4-OH, 4-OEt, and 4-NH_2 points do not fall on the line. Deviations of this kind by a certain set of reactants from the isokinetic and Hammett relationships established by related compounds have often been taken to mean that these reactants use a different mechanism than the others (11). It can be shown that in the present case this is not necessarily so.

The first-order decarboxylation of salicylic acids in quinoline contrasts with that of substituted anthranilic acids in nitrobenzene which is second order (10). To determine whether the difference in order is a function of the acids or of the solvents, salicylic acid was decarboxylated in nitrobenzene at 200 °C. The reaction is second order with respect to salicylic acid with a rate constant of $2 \times 10^{-4}\ M^{-1}\ s^{-1}$. Conversely, a number of 4- and 5-substituted anthranilic acids have been found to decarboxylate by a first-order reaction in quinoline (13).

The bimolecular decarboxylation in neutral aprotic nitrobenzene solvent suggests that there is no convenient intramolecular route for the proton transfer from the carboxyl group to the aromatic ring which is part of the decarboxylation reaction; protonation is accomplished by transfer from one acid molecule to another. However, in the equally aprotic but basic solvent quinoline, the decarboxylation is first order. Quinoline must therefore be able to facilitate the proton transfer in a way that nitrobenzene cannot. Since quinoline is more basic than nitrobenzene it seems reasonable to suppose that it functions by accepting a proton from the carboxyl group; the quinolinium ion so formed could then serve as the protonating agent for the aromatic ring.

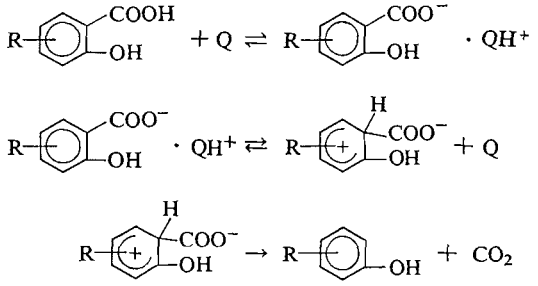

The ionization postulated for the first step has a dual function; it converts the aprotic quinoline into a protonating agent and converts the salicylic

Can. J. Chem. Downloaded from www.nrcresearchpress.com by 210.87.254.105 on 09/05/12
For personal use only.

acid to the anionic form in which it is more readily subject to protonation, as has been demonstrated by the work in aqueous solution reviewed at the beginning of this paper.

In fact, the whole mechanism proposed here for decarboxylation in quinoline bears a strong formal resemblance to the mechanism which operates in aqueous solution, with quinoline and water playing analogous roles. However, the resemblance may be more apparent than real. In a medium of such low dielectric constant as quinoline ($\varepsilon = 9$) it is extremely unlikely that the ions formed in the first step would dissociate extensively. This probability has been shown in the equations by representing the ions as pairs (dot notation) rather than as separated entities. That dissociation is small is further indicated by the fact that adding quinolinium chloride has no effect on the rate of decarboxylation (13). The association of quinolinium and salicylate ions in ion pairs would, of course, greatly facilitate the proton transfer of the second step and thus compensate for the low concentration of ions. Whether the protonation and decarboxylation of steps 2 and 3 are actually sequential, as shown, or concerted is not evident at this point.

The proposed mechanism can also account for the poor fit of the data to the Hammett relationship shown in Fig. 1. An electron-attracting substituent, say, at R would tend to increase the rate of decarboxylation by increasing the concentration of ion pairs formed in the first step. At the same time it would hinder the protonation of the aromatic ring in step 2, and facilitate the loss of CO_2 in step 3. The overall effect of a substituent could be represented by the Hammett equation modified as follows:

$$\log \frac{k}{k_0} = \rho_1\sigma + \rho_2\sigma^+ + \rho_3\sigma^+$$

where the subscripts refer to the three steps in the proposed mechanism. This formulation assumes that the third step is the slow one. If it is actually fast, or if steps 2 and 3 are concerted, the third term will disappear. Hammett's σ is appropriate for the first step since it involves the ionization of a carboxyl group, whereas σ^+ is required for the second and third steps because they involve the formation and decay of positive charge on the aromatic ring. As indicated above, a substituent will have an opposite effect on step 2 to that on steps 1 and 3; ρ_2 will be negative while ρ_1 and ρ_3 will be positive. Consequently, if ρ_2 is approximately equal in magnitude to $\rho_1 + \rho_3$, the cancellation of substituent effects postulated earlier will be accomplished. Furthermore, the cancellation will be effective only for those substituents for which σ and σ^+ are the same; that is, for all the substituents used here except 4-OH, 4-OEt, and 4-NH_2. This immediately suggests that these three apparently aberrant groups may be included in the same mechanism.

To test this possibility, the modified Hammett equation may be rearranged to

$$\frac{\log k/k_0}{\sigma} = \rho_1 + (\rho_2 + \rho_3)\frac{\sigma^+}{\sigma}$$

and Fig. 3 shows a plot of the data in this form. There is a considerable scatter of points, as might be expected from the large uncertainty that appears in the variables of the rearranged equation when σ is small, and from the fact that the acidities of substituted salicylic acids in media of low dielectric constant show considerable deviations from the simple Hammett relationship used to describe step 1 (8). Nevertheless, a linear trend is evident and the points for the "aberrant" groups 4-OH, 4-OEt, and 4-NH_2 do not deviate more than the others. The slope and intercept of the best straight line through the points give $\rho_1 = +4$ and $\rho_2 + \rho_3 = -4$. The latter value is consonant with the large negative ρ's observed in other aromatic substitutions (14) and the former value is not unreasonable for the ionization of a carboxylic acid in quinoline, when it is remembered that ρ for this reaction changes from $+1$ to $+2$ on changing the solvent from water to ethanol (15).

The three-step mechanism can also explain the failure of the activation parameters to fit the isokinetic relationship. According to Leffler and Grunwald (11), substituent effects in which resonance plays a particularly large part, such as those for which σ^+ differs sharply from σ, often do not fit the isokinetic relationship. This is because the isokinetic temperature for the resonance contribution is not the same as that for the polar contribution to the substituent effect. It may also be pointed out that a similar argument applies to multistep reactions in general. The observed enthalpies and entropies are composite quantities made up of the enthalpies and entropies

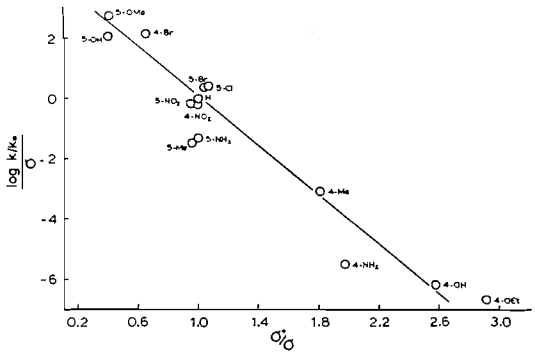

FIG. 3. Rate constants for decarboxylation of salicylic acids in quinoline at 200 °C plotted in a modified Hammett relationship. σ and σ^+ values are from ref. 14.

of the separate steps. Even though each individual step obeys the isokinetic relationship, the overall reaction will not do so unless all steps have the same isokinetic temperature.

In summary, then, it seems probable that all 14 substituted salicylic acids react by the same three-step (or two-step) mechanism. However, the data now available do not exclude the possibility that the reactive acids decarboxylate by a different mechanism than the others. Whether or not more than one mechanism applies, the fact that all the data can in principle be accommodated by a single mechanism illustrates once more (12) the danger of basing a change of mechanism on a break in the Hammett or isokinetic relationship.

Acknowledgment

The authors are grateful to the National Research Council of Canada for financial support of this project.

1. W. M. SCHUBERT and J. D. GARDNER. J. Am. Chem. Soc. **75**, 1401 (1953).
2. A. V. WILLI. Trans. Faraday Soc. **55**, 433 (1959). A. V. WILLI and J. F. STOCKER. Helv. Chim. Acta, **37**, 1113 (1954).
3. K. R. LYNN and A. N. BOURNS. Chem. and Ind. London, 782 (1963).
4. B. R. BROWN, D. L. HAMMICK, and A. J. B. SCHOLEFIELD. J. Chem. Soc. 778 (1950).
5. L. W. CLARK. J. Phys. Chem. **67**, 2831 (1963).
6. E. B. HERSHBERG. Ind. Eng. Chem. Anal. Ed. **8**, 312 (1936).
7. G. E. DUNN and F. L. KUNG. Can. J. Chem. **44**, 1261 (1965).
8. G. E. DUNN and T. L. PENNER. Can. J. Chem. **45**, 1699 (1966).
9. C. GRAEBE and E. MARTZ. Ann. **340**, 215 (1905).
10. G. E. DUNN and R. PRYSIAZNIUK. Can. J. Chem. **39**, 285 (1961).
11. J. E. LEFFLER and E. GRUNWALD. Rates and equilibria of organic reactions. John Wiley & Sons, Inc., New York. 1963. Chap. 9.
12. R. C. PETERSON. J. Org. Chem. **29**, 3133 (1964). O. EXNER. Nature, **201**, 488 (1964); Collection Czech. Chem. Commun. **29**, 1094 (1964).
13. M. A. MORELLO. Ph.D. Thesis, University of Manitoba, Winnipeg, Manitoba. 1967.
14. H. C. BROWN and Y. OKAMOTO. J. Am. Chem. Soc. **80**, 4979 (1958).
15. H. H. JAFFE. Chem. Rev. **53**, 191 (1953).

Can. J. Chem. Downloaded from www.nrcresearchpress.com by 210.87.254.105 on 09/05/12
For personal use only.

Can. J. Chem. Downloaded from www.nrcresearchpress.com by 210.87.254.5 on 09/05/12
For personal use only.

Reactor-neutron fission yields of ^{232}Th

J. W. HARVEY,[1] W. B. CLARKE, D. J. GORMAN,[2] AND R. H. TOMLINSON
Hamilton College, McMaster University, Hamilton, Ontario

Received March 7, 1967[3]

Mass spectrometric methods and a Ge(Li) γ-ray detector have been used to obtain reactor-neutron (>1 MeV) fission yields of ^{232}Th. The results have been combined with earlier mass spectrometric and radiochemical work.

Canadian Journal of Chemistry, **46**, 2911 (1968)

Introduction

Fast-neutron fission of ^{232}Th was first studied by Turkevich and Niday (1) who determined chain yields using the radiochemical technique. More recently radiochemical determinations have been given by Broom (2), Iyer *et al.* (3), Crook and Voigt (4), and Wyttenbach and Van Gunten (5). Kennett and Thode (6) have determined cumulative yields of the stable krypton and xenon isotopes, and the krypton–xenon ratio using mass spectrometry and isotope dilution. In this work we have used sensitive techniques of gas and solid source mass spectrometry to determine yields of ^{87}Kr and ^{88}Kr (relative to ^{86}Kr), ^{133}Xe (relative to ^{132}Xe), ^{133}Cs, ^{135}Cs, ^{137}Cs, ^{143}Nd, ^{145}Nd, ^{146}Nd, ^{148}Nd, and ^{150}Nd. Fission products from ^{232}Th were also examined using a Ge(Li) detector and a comparison was made with fission products from thermal neutron fission of ^{235}U. In this way ^{232}Th yields were obtained relative to an accurately known "standard".

Experimental

High purity thorium for mass spectrometer analysis of solid fission products was obtained by repeated precipitations with H_2O_2, conversion of the final precipitate to the nitrate, and then gentle ignition to convert the nitrate to the dioxide. Reagents were carefully prepurified and stored in polyethylene bottles. Reagent grade ThO_2 used for rare gas determinations was examined for the presence of uranium by α-particle counting technique and found to contain less than 100 p.p.m. U. Before irradiation, traces of atmospheric Kr and Xe were removed from ThO_2 powder by heating in vacuum to about 1400 °C. All of the samples used for mass spectrometer measurements were wrapped in at least two thicknesses of 0.015 in. cadmium metal sheet to prevent depletion of ^{135}Xe during irradiation, and to eliminate the need for a large and uncertain correction to the measured abundance of ^{135}Cs relative to ^{133}Cs and ^{137}Cs. There was also negligible effect due to the fission of trace amounts of ^{235}U in the samples. Pertinent irradiation data are shown in Table I. For the irradiation conditions used in this work it can easily be shown that there is negligible effect due to production of ^{233}U.

After irradiation the high purity ThO_2 samples were dissolved in 7 *N* HNO_3 containing a trace of HF, and the solid fission products separated from the thorium in a manner similar to that described by Danon (7). Xenon and krypton samples were obtained by heating the irradiated ThO_2 (in quartz break-seal vials) to about 1400 °C in vacuum either in the inlet system of the mass spectrometer or in a separate vacuum line. For recent accounts of the techniques used in this laboratory for analysis of gaseous and solid fission products see, for example, Farrar *et al.* (8), Clarke and Thode (9), and Pleva (10).

Several 100 mg samples of ThO_2 (U < 40 p.p.m.) were sealed in small quartz vials and irradiated for examination of the fission-product spectra with a Ge(Li) detector. In early experiments, where a cadmium wrap was used around the samples, it was found that the γ-rays from ^{233}Pa were so much more abundant than the fission-product γ-rays that reliable measurements were impossible. The ^{233}Pa peaks were reduced to tolerable levels by encasing the ThO_2 sample in a 7 g Th metal container, then in a 12 g plug of B_2O_3, followed by a cadmium wrap. Standard samples used for comparison purposes were made by mixing about 1 mg of ^{235}U oxide with 99 mg ThO_2, and were irradiated in "rabbit" positions in the reactor. The fission products so formed were almost entirely due to thermal neutron fission of ^{235}U. During the counting experiments with the standard ^{235}U samples, ThO_2 samples which were dead as far as short-lived fission products were concerned, but still contained ^{233}Pa activity, were placed near the ^{235}U samples in order to provide a correction for possible systematic error in measurements of the fission product γ-ray peaks near the ^{233}Pa γ-ray peaks. Examples of ^{232}Th fission product spectra are shown in Figs. 1 and 2. The method of fission yield measurements by comparison with the accurately known yields of ^{235}U has been described by Gordon, Harvey, and Nakahara (11) and by Gorman and Tomlinson (12). The advantage of this method is that, due to the high resolution of Ge(Li) detectors as compared with NaI(Tl) detectors, chemical separations and resulting systematic errors are avoided.

[1]Present address: Massachusetts Institute of Technology, Cambridge, Massachusetts.
[2]Present address: Lawrence Radiation Laboratory, University of California, Berkeley, California.
[3]Revision received April 24, 1968.

TABLE I
Irradiation data

Sample	Weight (g)	Approximate epithermal flux (neutrons cm^{-2} s^{-1})	t_1*	t_2*	t_3*	Elements analyzed
1	1.0	10^{12}	100 h	172.5 h	173 h	Xe
2	1.0	10^{12}	150 h	216 h	218 h	Xe
3	0.15	10^{12}	100 h	~80 m	~120 m	Kr
4	0.15	10^{12}	200 m	~90 m	~140 m	Kr
5	1.0	10^{12}	600 h		281 d	Cs, Nd
6	0.75	10^{12}	600 h		326 d	Cs, Nd
7	1.0	10^{12}	600 h		351 d	Cs, Nd
8	1.0	10^{12}	144 h		20 d	Nd
9	0.10	10^{12}	60 m			(Kr, Y, Nb, I, Te, Xe, Ba, Ce)

*t_1, time of irradiation; t_2, time from end of irradiation to fission product extraction; and t_3, time from end of irradiation to analysis. h stands for hours, m for minutes, and d for days.

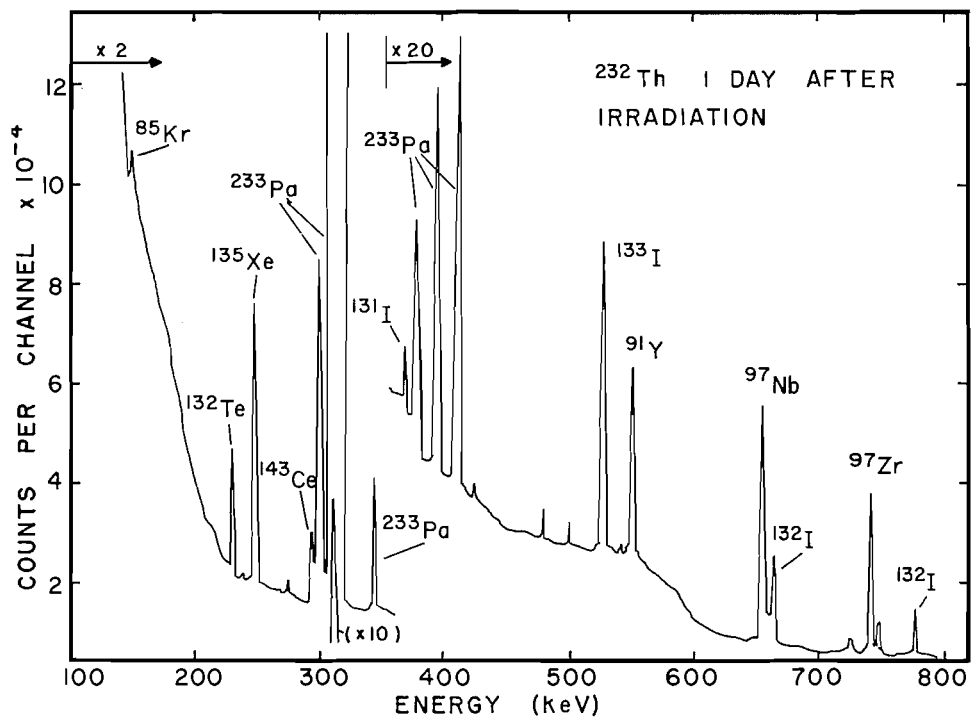

FIG. 1. γ-Spectra of fission products taken 1 day after irradiation of ^{232}Th.

Results and Discussion

A summary of the mass spectrometric determinations is given in Table II. At least two independent measurements were carried out and the quoted errors are standard deviations of mean values obtained from 10–20 double mass spectrometer scans. Relative yields obtained using a Ge(Li) detector are given in Table III. We have examined the results of radiochemical measurements reported in the literature and have made comparisons of relative yields where possible. The results of Iyer *et al.* (3) were found to agree with the more precise mass spectrometric measurements of Kennett and Thode (6) and of this work far more closely than any of the other measurements (1, 2, 4, 5). Iyer *et al.* used a

Can. J. Chem. Downloaded from www.nrcresearchpress.com by 210.87.254.5 on 09/05/12
For personal use only.

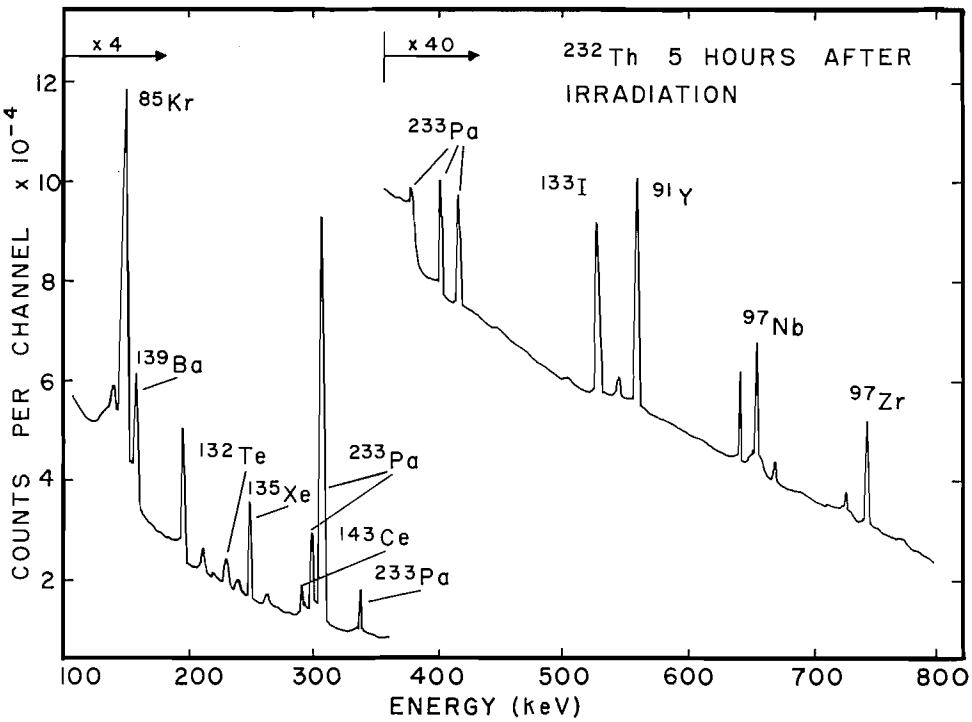

FIG. 2. γ-Spectra of fission products taken 5 h after irradiation of ^{232}Th.

TABLE II

Relative yields from mass spectrometer measurements

Mass number	Relative yield (ref. 6)		Relative yield (this work)			
	Kr	Xe	Kr	Xe	Cs	Nd
83	0.332±0.003					
84	0.608±0.003					
85	0.646±0.003					
86	1.000		1.000			
87			1.058±0.018			
88			1.115±0.011			
131		0.565±0.002				
132		1.000		1.000		
133				1.356±0.027	0.813±0.005	
134		1.876±0.010				
135					1.011±0.005	
136		1.991±0.008				
137					1.000	
143						1.000
145						0.812±0.012
146						0.696±0.020
148						0.306±0.004
150						0.153±0.012

Can. J. Chem. Downloaded from www.nrcresearchpress.com by 210.87.254.5 on 09/05/12
For personal use only.

Can. J. Chem. Downloaded from www.nrcresearchpress.com by 210.87.254.5 on 09/05/12
For personal use only.

TABLE III

Relative yields from Ge(Li) measurements

Isotope	Relative yield
^{85}Kr	1.360±0.020
^{91}Y	2.61±0.08
^{97}Nb	1.484±0.016
^{131}I	0.505±0.030
^{132}Te	1.000
^{133}I	1.409±0.025
^{135}Xe	1.835±0.020
^{139}Ba	2.53±0.05
^{143}Ce	2.46±0.05

comparison method wherein ^{232}Th targets were irradiated along with ^{235}U targets and the ^{235}U fission yields given by Katcoff (13) were used to obtain ^{232}Th relative yields. Absolute yields were then obtained by normalizing the area under a smooth curve drawn through the relative yields to 200%. Now Iyer *et al.* state that errors in Katcoff's yields (±10%) could produce a major source of uncertainty in their results. Farrar *et al.* (14) and Farrar and Tomlinson (15) have presented ^{235}U chain yields of considerably greater certainty and we have therefore used

TABLE IV

Relative and absolute yields (Reactor-neutron fission of ^{232}Th)

Mass number	Mass spectrometric relative yields	Ge(Li) relative yields	Iyer *et al.* (3) relative yields	Absolute yields (%)
77			.00167±0.00007	0.014
78–82				2.98†
83	0.332±0.003		0.332±0.027*	2.06
84	0.608±0.003			3.78
85	0.646±0.003	0.667±0.010		4.01
86	1.000			6.21
87	1.058±0.018			6.57
88	1.115±0.011			6.92
89				7.14†
90			1.192±0.047	7.40
91		1.28±0.04	1.123±0.090	7.45
92–94				19.31†
95			0.875±0.050	5.43
96				4.97†
97		0.728±0.008*	0.728±0.009	4.52
98				3.69†
99			0.461±0.008	2.86
100–102				3.97†
103			0.0235±0.0023	0.146
105–115				0.56
116–130				3.04†
131	0.339±0.001	0.303±0.017	0.366±0.016	1.56
132	0.600	0.600*		2.76
133	0.814±0.015	0.845±0.016		3.75
134	1.125±0.007			5.18
135	1.013±0.027	1.101±0.012		4.66
136	1.182±0.025			5.44
137	1.000±0.020		1.000±0.015*	4.60
138				5.79†
139		1.518±0.040	1.455±0.070	6.99
140			1.872±0.050	8.61
141			1.681±0.065	7.74
142				7.27†
143	1.476	1.476±0.040*	1.558±0.050	6.79
144			1.565±0.005	7.20
145	1.199±0.018			5.52
146	1.027±0.030			4.73
147			0.682±0.035	3.14
148	0.452±0.006			2.08
149			0.191±0.005	0.88
150	0.226±0.018			1.04
151–155				1.24†
156			0.0006±0.0001	0.003

*Normalization.
†Interpolated or extrapolated.

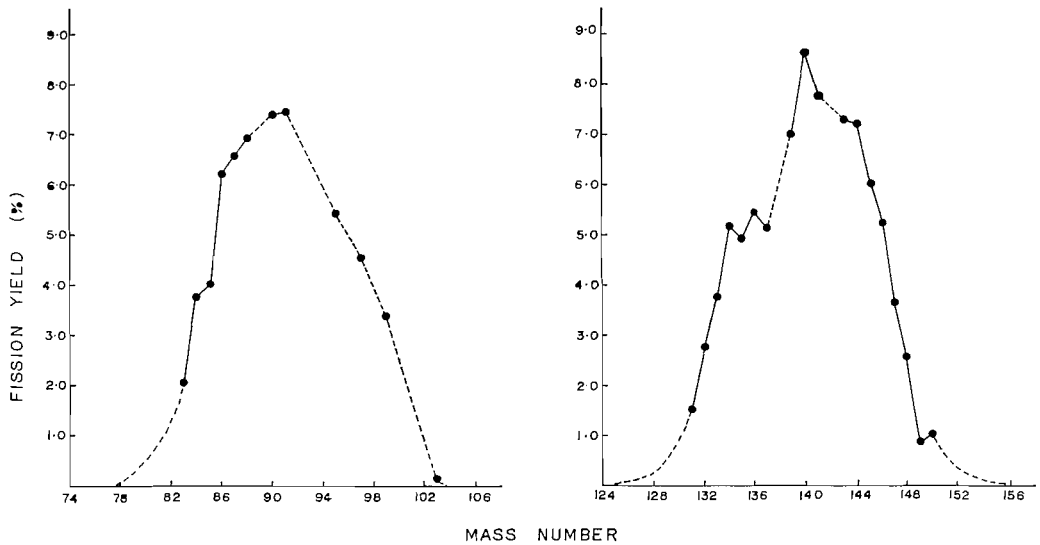

FIG. 3. Mass yield curve for reactor-neutron fission of ^{232}Th.

these yields to correct the relative ^{232}Th yields given by Iyer *et al.*

For yields in the heavy mass hump we have normalized the Xe–Cs mass spectrometric data to relative yields given by Iyer *et al.* (3) at ^{137}Cs. The Nd mass spectrometric data was normalized to the data obtained by the Ge(Li) method at mass 143, and the Ge(Li) data normalized to the Xe–Cs data at mass 132. This procedure gave relative values for all the major yields except for masses 138 and 142, which were interpolated. Relative yields in the light mass region were obtained by normalizing the data of Iyer *et al.* (3) to mass spectrometric data at mass 83, and to the Ge(Li) data at mass 97. Summation of the relative yields to 100% for both heavy and light masses allowed a determination of absolute yields (see Table IV and Fig. 3). Interpolated and extrapolated yields amounted to 17.3% for the heavy masses and 42.1% for the light masses. The general shape of the heavy mass curve as well as the detailed fine structure is, we feel, quite certain, but only the general shape of the light mass curve has been determined in this work.

Acknowledgments

We wish to thank the National Research Council of Canada for financial assistance, Dr. N. S. Oakey for his help in determining the U content of the ThO_2 samples used in this work, and also the McMaster University reactor staff for arranging the irradiations.

1. A. TURKEVICH and J. B. NIDAY. Phys. Rev. **84**, 52 (1951).
2. K. M. BROOM. Phys. Rev. **133**, B874 (1964).
3. R. H. IYER, C. K. MATHEWS, N. RAVINDRAN, K. RENGAN, D. V. SINGH, M. V. RAMANIAK, and H. D. SHARMA. J. Inorg. Nucl. Chem. **25**, 465 (1963).
4. J. M. CROOK and A. F. VOIGT. AEC-IS-558 (1962); TID-4500 (1963).
5. A. WYTTENBACH and H. R. VAN GUNTEN. Phys. Chem. Fission, Proc. Symp. Salzburg, Austria. **1**, 412 (1965).
6. T. J. KENNETT and H. G. THODE. Can. J. Phys. **35**, 969 (1957).
7. J. DANON. J. Inorg. Nucl. Chem. **5**, 237 (1952).
8. H. FARRAR, W. B. CLARKE, H. G. THODE, and R. H. TOMLINSON. Can. J. Phys. **42**, 2063 (1964).
9. W. B. CLARKE and H. G. THODE. Can. J. Phys. **42**, 213 (1964).
10. J. F. PLEVA. Ph.D. Thesis, McMaster University, Hamilton, Ontario. 1967.
11. G. E. GORDON, J. W. HARVEY, and H. NAKAHARA. Nucleonics, **24** (12), 62 (1966).
12. D. J. GORMAN and R. H. TOMLINSON. Can. J. Chem. To be published.
13. S. KATCOFF. Nucleonics, **18**, 201 (1960).
14. H. FARRAR, H. R. FICKEL, and R. H. TOMLINSON. Can. J. Phys. **40**, 1017 (1962).
15. H. FARRAR and R. H. TOMLINSON. Nucl. Phys. **34**. 367 (1962).

Can. J. Chem. Downloaded from www.nrcresearchpress.com by 210.87.254.5 on 09/05/12
For personal use only.

Can. J. Chem. Downloaded from www.nrcresearchpress.com by 210.87.254.6 on 09/05/12
For personal use only.

Infrared studies on rotational isomerism. II. 2-Fluoroethanol

PAUL BUCKLEY, PAUL A. GIGUÈRE, AND DAIJIRO YAMAMOTO[1]
Département de Chimie, Université Laval, Québec, Québec

Received March 19, 1968

The infrared spectra of CH_2FCH_2OH were measured in the vapor, liquid, and solid states from 4000 to 200 cm^{-1}. The Raman spectrum of the liquid was also measured over the same frequency range. From the results it appears that the free molecules exist almost entirely in the *gauche* configuration, which is stabilized by intramolecular hydrogen bonding. Only in the vapor at temperatures above 60 to 70 °C is there any indication of weak bands due to *trans* isomers. In the condensed phases the molecules are associated through strong hydrogen bonds (3–4 kcal/mole).

Les spectres infrarouges du 2-fluoroéthanol ont été mesurés entre 4000 et 200 cm^{-1} sous les trois états physiques. Le spectre Raman du liquide a également été enregistré pour la première fois. D'après les résultats il appert que la molécule libre existe presque exclusivement sous la configuration *gauche*; celle-ci est beaucoup plus stable que la *trans* à cause de la liaison hydrogène interne. C'est seulement dans la vapeur, et au-dessus de 60 à 70 °C que de faibles bandes dues à l'isomère *trans* apparaissent. Par ailleurs le liquide est fortement associé grâce à des liaisons hydrogène intermoléculaires de 3 à 4 kcal/mole.

Canadian Journal of Chemistry, 46, 2917 (1968)

Introduction

Contrary to the case of ethylene glycol discussed n Part I of this series (1) the question of the molecular configuration of 2-fluoroethanol (also called ethylene fluorohydrin) has attracted little attention so far. Electron diffraction data (2) have revealed the existence of only one configuration of the molecule, the *gauche*, in the vapor. From the O...F distance, and other measured or estimated bond lengths and angles, the azimuthal angle ϕ between the CCO and the CCF planes should lie between 60° and 70°. Various infrared studies (3–5) done mostly on dilute solutions in CCl_4 have led to the conclusion that in such media the 2-fluoroethanol molecules assume either the *trans* or the *gauche* configuration, with the latter largely predominant. From a careful temperature study Krueger and Mettee (5) estimated the enthalpy of isomerization to be 2 kcal/mole. As for the free molecule, only the 3 μ region has been studied (3) and the results interpreted again in terms of mixtutes of both isomers. Because of the strong electronegativity of fluorine on the one hand, and the somewhat unfavorable geometry (five-membered ring, leading to a highly bent O—H....F bond) on the other hand, the problem of intramolecular hydrogen bonding in 2-fluoroethanol is of special interest, and further spectroscopic work seemed desirable.

[1]On leave during the summer of 1967 from Meiji University, Ikuta, Kawasaki-shi, Japan.

Experimental

The sample of 2-fluoroethanol (K. & K. Laboratories, Plainfield, N.Y.), of minimum stated purity 95%, was fractionally distilled with a Vigreux column. Only the middle portion (some 40%) which distilled at 103.3 ± 0.1 °C, was used. Its refractive index at 18° was 1.3695 compared with the literature (6) value of 1.3647. The infrared spectra showed no trace of water, the most likely impurity. Attempts to prepare the OD substituted alcohol by two different methods were unsuccessful. In the first one the alcoholate was prepared by reaction with metallic sodium. While it was being purified under vacuum the alcoholate decomposed suddenly, the heat evolved turning the whole mass into a char. In the second method the borate ester was prepared for hydrolysis with heavy water. However, the reaction could not be carried out to completion.

The absorption cell for the vapor spectra was 10 cm long, with windows of NaCl, AgCl, or Mylar polyethylene, depending on the region covered. It was connected to a thermostated bulb holding the liquid alcohol under atmospheric pressure (dry nitrogen). The liquid was kept at 20 °C and the spectra were recorded with the vapor at 25, 40, 70, and 120°. The crystalline samples were obtained by cooling slowly with dry ice a film of the liquid alcohol between two salt discs in an evacuated cell. Rapid cooling with liquid nitrogen produced a glassy solid. This could be crystallized by annealing at dry-ice temperature for about 1 h. The infrared spectra were recorded with a Perkin–Elmer model 621 double beam spectrometer, and the Raman with a Cary model 81 instrument.

Results

Reproductions of some typical spectra for the three physical states are shown in Figs. 1 to 4. The assignments given in Table I appear quite straightforward except for the few following points.

TABLE I

Infrared and Raman spectra of 2-fluoroethanol (frequencies in cm^{-1})

Infrared				
Vapor (23 °C)	Liquid	Crystal (−180 °C)	Raman, liquid	Assignments
3660 s 3643 s	3560 sh 3360 vs,br	3180		O—H stretching
2983 vs 2971 vs 2958 vs	2981 s 2961 s	2991 vs 2964 vs	2962 vs	C—H stretching
2930 s	2928 s	2941 s	2904 w	C—H stretching
2897 s	2892 s	2892 m	2736 m	
1470 w				
1465 m	1458 s	1455 m	1458 s	CH_2 scissoring
1457 m		1440 m		
1383 m 1374 m	1390 br	1411 s 1394 s		OH bending and
1365 w	1355 br	1370 s		CH_2 wagging
1349 vw				
1258 vw 1250 w 1240 vw	1256 m	1270 s	1277 m	CH_2 twisting
1210 vw	1221 m	1220 w		
1157 vw				C—F stretching (t)
1111 vw	1123 m	1117 w		?
1092 vs 1075 vs	1083 vs	1078 vs	1096 m	C—O stretching
1048 vs 1038 vs 1030 vs	1031 vs	1017 vs	1036 m	C—F stretching (g)
965 w* 952 vw 926 w*	937 vw	946 w	938 w	C—C stretching
895 m		893 vs		
887 s 870 s	884 vs 871 sh	886 s 870 w	886 m 853 s	CH_2 rocking (g)
846 m	853 s	847 vs	832 w	
765 vw*				CH_2 rocking (t)
	740 m			
	660 s	683 m	663 w	OH torsion
	616 s	662 m		
524 m				
516 m	511 s	519 vs	510 w	CCO bending
506 m		511 sh		
	471 sh	483 w	470 w	CCF bending
343 vs		341 w	338 w	OH torsion
300 vs				

*Visible only at higher temperature.

OH Vibrations

The doublet at 3660, 3643 cm^{-1} must be ascribed to the O—H stretching mode of one isomer only (the *gauche* obviously) since it shows no temperature effect whatsoever over a 100° range. Kuhn *et al.* (3), who gave the frequencies as 3654, 3638 cm^{-1}, assigned them to the *trans* and the *gauche* isomers respectively. By comparison with 2-chloroethanol, and 2-bromoethanol, however, their interpretation was rather unlikely since the two components of the doublet have nearly the same relative intensities in all three halosubstituted alcohols. Normally, one would expect an appreciably lower intensity of the *trans* band in the fluoro compound. At any rate the separation of the doublet reported here is suitable for the P and R branches of the same absorption band in the free molecule. An estimate based on the calculated moments of inertia (cf. Table II) of the *gauche* molecule gives 15 cm^{-1} for the separation of the P and R maxima of a pure parallel band of the *gauche* isomer, and 12 cm^{-1} for the *trans* isomer, which is almost a symmetric top. Considering the approximations involved the agreement is reasonably good. As shown by the data in Table I a few other funda-

Can. J. Chem. Downloaded from www.nrcresearchpress.com by 210.87.254.6 on 09/05/12
For personal use only.

TABLE II

Structural parameters (2) and moments of inertia of the *gauche* CH_2FCH_2OH molecule*

C—C = 1.54 Å	C—H = 1.09 Å	$I_A = 53.34$ g cm$^2 \times 10^{-40}$
C—F = 1.36 Å	O—H = 0.97 Å	$I_B = 154.62$ g cm$^2 \times 10^{-40}$
C—O = 1.45 Å	O...F = 2.82 Å	$I_C = 184.37$ g cm$^2 \times 10^{-40}$

*All angles assumed tetrahedral, except the azimuthal, $\phi = 64°$.

mentals show the same splitting of 17–18 cm^{-1}. Close scrutiny of the high-frequency side of the O—H stretching band, especially at the higher temperatures, failed to reveal any definite sign of absorption attributable to *trans* molecules. However, this criterion alone is not conclusive because the conditions here are unfavorable. As the work on dilute solutions has shown (3–5), the separation of the *trans* and *gauche* O—H stretching fundamentals also is of the order of 12–16 cm^{-1}. Therefore, a weak *trans* component could very well escape detection under the strong R wing of the *gauche* band.

In the liquid the O—H stretching band is

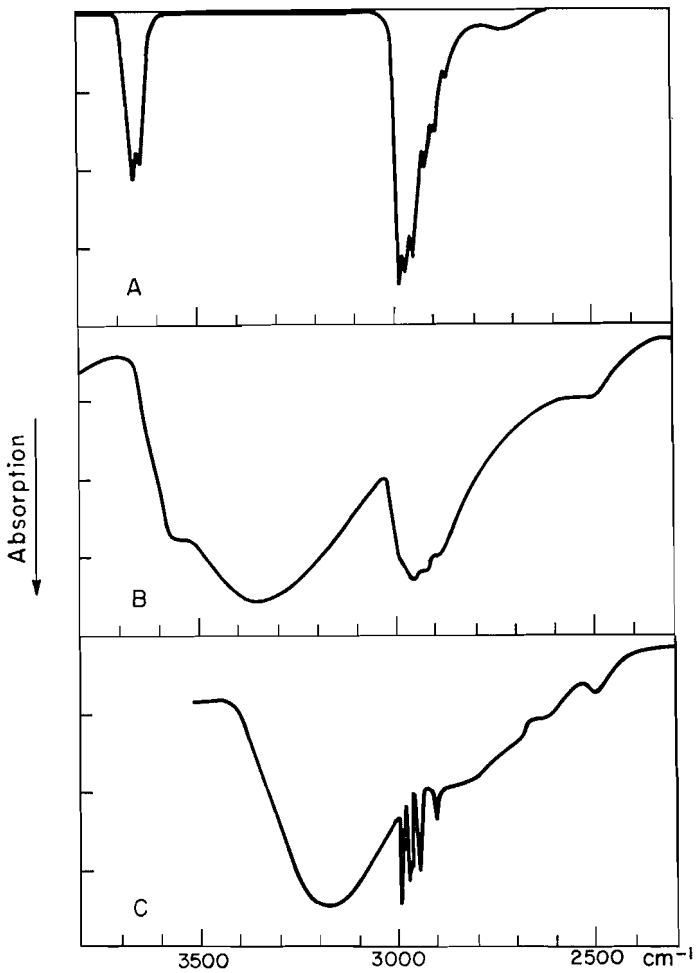

FIG. 1. Infrared absorption of CH_2FCH_2OH in the O—H and C—H stretching region. (A) Vapor at room temperature; (B) liquid; and (C) crystal at −180 °C.

Can. J. Chem. Downloaded from www.nrcresearchpress.com by 210.87.254.6 on 09/05/12
For personal use only.

Can. J. Chem. Downloaded from www.nrcresearchpress.com by 210.87.254.6 on 09/05/12
For personal use only.

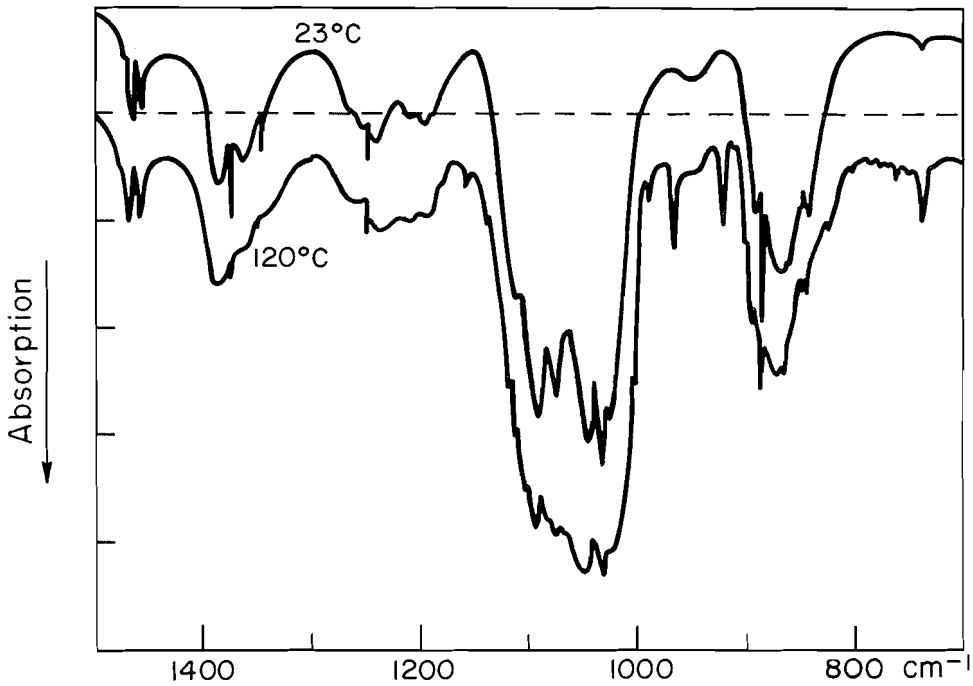

FIG. 2. Temperature effect on the infrared spectrum of 2-fluoroethanol vapor.

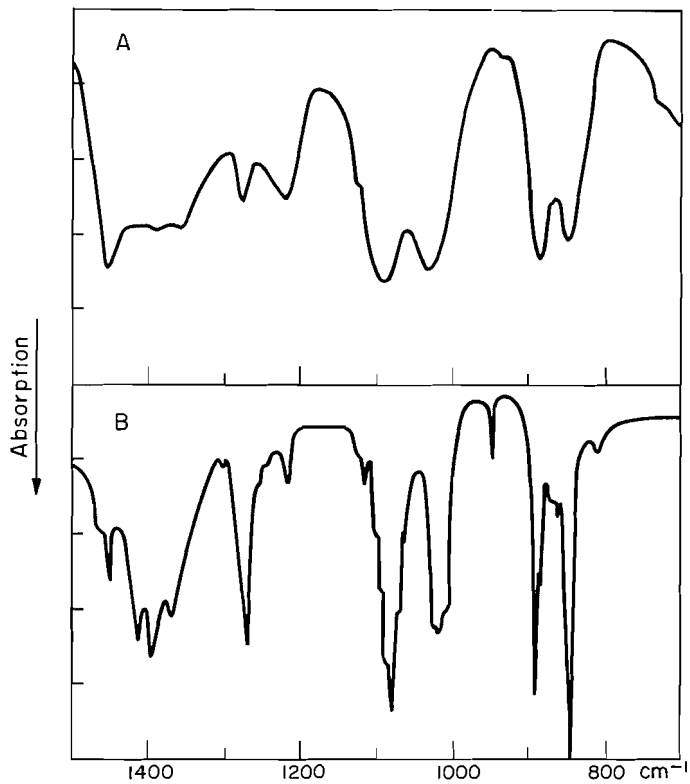

FIG. 3. Infrared spectra of (A) liquid and (B) solid 2-fluoroethanol at −180 °C.

Can. J. Chem. Downloaded from www.nrcresearchpress.com by 210.87.254.6 on 09/05/12
For personal use only.

broadened considerably and shifted some 300 cm^{-1} towards lower frequency by strong intermolecular hydrogen bonds. The shoulder near 3560 cm^{-1}, the equivalent of which appears also in the liquid 2-chloroethanol, and 2-bromoethanol (7), might belong to OH groups engaged only in internal hydrogen bonding, as there is no obvious possibility of overtones or combinations at that frequency. In the crystal (Fig. 1C) a further shift of nearly 200 cm^{-1} from the liquid O—H stretching band seems unusually large. This may arise from the high electronegativity of fluorine and/or particularly favorable packing conditions in the crystal. The usual semi-empirical correlations give values of some 3 to 4 kcal/mole for these intermolecular hydrogen bonds.

As for the OH bending band, it probably coincides with the CH_2 bending near 1400 cm^{-1} as in ethylene glycol. Lastly, the torsional mode of the "bonded" OH gives rise to a broad, jagged contour band in the 300–350 cm^{-1} region in the vapor. This frequency lies between that of a relatively free OH, around 200 cm^{-1} as in ethanol vapor, and that of a strongly hindered OH, around 650 cm^{-1} as for instance in condensed phases of ethylene glycol and the other 2-halo-substituted ethanols (8). Such a large shift is characteristic of this type of molecule, and would seem to be a better index of the intramolecular hydrogen bond strength than the small shifts of the O—H stretching frequencies. It also confirms that the isomer present in our case is the *gauche*. In contrast with the liquid, the crystal (Fig. 4C) retains some absorption near 350 cm^{-1}, which we assign tentatively to intramolecularly bonded molecules. This, coupled with the complex appearance of the vapor band, suggests for the latter a double origin. Another possibility is that the crystal band belongs to some lattice mode, although both the frequency and intensity seem too high on that account.

Skeletal Vibrations

The C—F and C—O stretching bands, although quite close together, are clearly distinguishable in all three phases. The C—C stretching vibration cannot be positively identified because it is very likely coupled with other skeletal modes, as was demonstrated in a recent force constant study of ethylene glycol (9). The two skeletal bending modes probably coincide exactly in the vapor since only one band is found around 500 cm^{-1}. In the condensed phases, however, the CCF

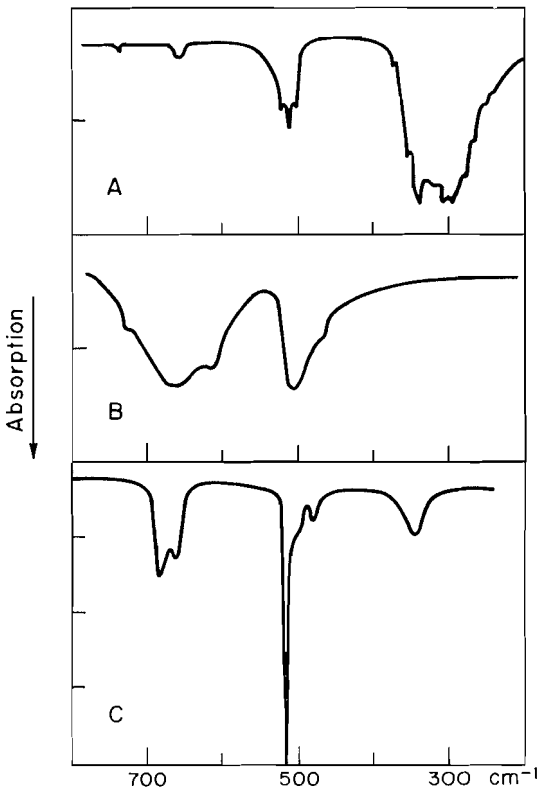

FIG. 4. Low frequency spectra of (A) gaseous, (B) liquid, and (C) solid 2-fluoroethanol.

bending frequency is slightly lower and much weaker than the CCO bending. As for the C—C torsional frequency, it must lie below the lower limit of our measurements. An unpublished microwave investigation (10) has yielded a value of 152 $\pm$ 10 cm^{-1}, i.e. of the same magnitude as in 2-chloroethanol (8).

CH_2 Vibrations

The four CH_2 stretching modes are clearly separated in the crystal; even in the liquid four distinct maxima are detectable. In the vapor partial overlap results in uneven separation of the components (Fig. 1A). As for the deformation modes, they should give rise to eight bands in the region from 800 to 1500 cm^{-1} although extensive overlap of the symmetrical and antisymmetrical components of each kind may be expected. In addition, the CH_2 wagging frequencies nearly coincide with the OH bending as was confirmed by deuteration studies in ethylene glycol (1). The "free" OH bending of *trans* molecules in the vapor should occur at an appreciably lower

Can. J. Chem. Downloaded from www.nrcresearchpress.com by 210.87.254.6 on 09/05/12
For personal use only.

frequency (around 1200 cm^{-1}). Of the various CH_2 deformations, the rocking modes are the most meaningful because of their dependence on the configuration of the molecule. In the vapor spectra they produce strong absorption with complex structure near 900 cm^{-1}, while in the crystal the two major components show weak satellites, possibly due to crystal field splitting.

High-Temperature Bands

Raising the temperature of the vapor in steps up to 120 °C caused little change in the general appearance of the original bands except for a regular decrease in intensity of the Q branches. More important, however, some new bands emerged gradually which, from their temperature behavior, could not arise from decomposition products. Therefore, we consider them as evidence for *trans* molecules and we assign them tentatively as follows: the 1157 cm^{-1} band to the C—F stretching, according to the well-known situation in the other 2-haloethanols (11); the weak pair at 765 and 740 cm^{-1} to the CH_2 rocking modes, and the stronger doublet at 965 and 930 cm^{-1} to the C—C and the C—O stretching modes, although the latter should be shifted in the opposite direction. However, strong coupling between these various skeletal modes makes somewhat delusive any specific assignment of each absorption band to a given mode.

Conclusions

The present results support the conclusion of the electron diffraction work (2) as to the only stable configuration, the *gauche*, of the 2-fluoroethanol molecule in the vapor at ordinary temperature. On the other hand existence of very low concentrations of *trans* isomers at higher temperatures seems fairly certain. These could easily escape detection by the electron diffraction method in view of the small contribution of the long O....F distance to the overall diffraction pattern. Furthermore, the temperature of the vapor at the moment of diffraction is uncertain because of the fast adiabatic expansion into vacuum.

Likewise, spectroscopic work confined to the 3 μ region is insufficient in borderline cases like this one, where the weaker component may be completely submerged under the main absorption band. The possibility of overtone and combination bands in that region complicates the situation further. Evaluation of the enthalpy of isomerization from band intensities by the usual methods does not seem warranted here as our data for the *trans* isomer are too scanty, and their assignments too uncertain. However, it seems safe to conclude that the ΔH is greater than 2 kcal/mole, the value found in dilute CCl_4 solutions (5). Stabilization of the *trans* isomer by solvent must be appreciable in the latter case; in fact it is enough to lower the O—H stretching frequency by 25–30 cm^{-1}. From the structural viewpoint it is of interest that the strong affinity of fluorine for the proton predominates over the oxygen–fluorine repulsion, even in a strongly bent hydrogen bond. Intuitively, this should tend to close the azimuthal angle ϕ to below 74°, the value reported in ethylene glycol (12). In that connection we have recently learned with interest that the azimuthal angle in 2-chloroethanol was found to be 64 ± 2° from microwave measurements (13).

In the condensed phases the situation is not so clear. Certainly the liquid is strongly associated (compare its boiling point, 103 °C, with that of the heavier 2,2,2-trifluoroethanol, 75 °C) although less strongly so than ethylene glycol (b.p. 197°) in which the two OH groups lead to a three-dimensional network of hydrogen bonds. Two mechanisms may be responsible for association in the 2-fluoro alcohol: (*a*) stabilization of *trans* isomers by intermolecular hydrogen bonds, and (*b*) bifurcated hydrogen bonds between adjacent *gauche* molecules. Against the first interpretation is the fact that in the crystal, which must contain only the most stable isomer, the spectra show no simplification with respect to those vibrations more sensitive to isomerization. On the other hand, dramatic changes occur for the OH deformation bands, indicating quite different hydrogen bond patterns in the two phases. Further studies by other techniques (nuclear magnetic resonance spectroscopy or X-ray diffraction) are suggested here.

1. P. Buckley and P. A. Giguère. Can. J. Chem. **45**, 397 (1967).
2. M. Igarashi and M. Yamaha. Bull. Chem. Soc. Japan, **29**, 871 (1956).
3. M. Kuhn, W. Lüttke, and R. Mecke. Z. Anal. Chem. **170**, 106 (1959).
4. M. Oki and H. Iwamura. Bull. Chem. Soc. Japan, **35**, 1744 (1962).
5. P. J. Krueger and H. D. Mettee. Can. J. Chem. **42**, 326 (1964).
6. Handbook of chemistry and physics. 45th ed. Chemical Rubber Publishing Co., Cleveland, Ohio. 1964.

7. M. SCHNEIDER. Unpublished results.
8. P. BUCKLEY. Ph.D. Thesis, Université Laval, Québec, Qué. 1965.
9. H. MATSUURA and T. MIYAZAWA. Bull. Chem. Soc. Japan, **40**, 85 (1967).
10. K. S. BUCKTON. Private communication.
11. S. MIZUSHIMA. Structure of molecules and internal rotation. Academic Press, Inc., New York. 1954.
12. O. BASTIANSEN. Acta Chem. Scand. 3, 415 (1949).
13. R. G. AZRAK. Private communication.

Can. J. Chem. Downloaded from www.nrcresearchpress.com by 210.87.254.6 on 09/05/12
For personal use only.

Can. J. Chem. Downloaded from www.nrcresearchpress.com by 210.87.254.6 on 09/05/12
For personal use only.

Free radicals by mass spectrometry. XXXIX. Primary steps in the mercury-photosensitized decompositions of methyl and ethyl mercaptan[1]

S. YAMASHITA[2] AND F. P. LOSSING
Division of Pure Chemistry, National Research Council of Canada, Ottawa, Ontario
Received April 2, 1968

The reaction between $Hg(^3P_1)$ atoms and methyl mercaptan at 55° is mainly H-atom removal from sulfur

$$Hg(^3P_1) + CH_3SH \rightarrow CH_3S + H + Hg(^1S_0)$$

with a minor participation (~10%) of C—S bond rupture

$$Hg(^3P_1) + CH_3SH \rightarrow CH_3 + SH + Hg(^1S_0)$$

Ethyl mercaptan dissociates by two main processes

$$Hg(^3P_1) + C_2H_5SH \rightarrow C_2H_5S + H + Hg(^1S_0)$$
$$Hg(^3P_1) + C_2H_5SH \rightarrow C_2H_5 + SH + Hg(^1S_0)$$

Some evidence was found for a small amount of dissociation by C—C bond rupture. No C—H bond rupture in either compound could be detected.

Canadian Journal of Chemistry, 46, 2925 (1968)

Introduction

The mercury ($^3P_1$) photosensitized decomposition of CH_3SCH_3 and CH_3SSCH_3 has been found to proceed by C—S and S—S bond ruptures, with no significant participation by processes involving C—H bond rupture (1). For comparison it is of interest to investigate the mode of reaction of compounds containing S—H bonds. The direct photolysis of CH_3SH has been shown by Inaba and Darwent (2) to proceed solely by S—H bond rupture with no detectable occurrence of C—H or C—S splits. Gunning and Strausz (3) have found that hot CH_3SH molecules, formed by insertion of $S(^1D)$ atoms into CH_4, dissociate mainly by S—H bond rupture, even though the CH_3—SH bond is weaker than the CH_3S—H bond by some 18 kcal/mole.

In the present work, the $Hg(^3P_1)$-photosensitized decomposition of CH_3SH has been investigated, with particular regard to the relative probability of occurrence of the three modes of decomposition:

[1] $CH_3SH + Hg(^3P_1) \rightarrow CH_3S + H + Hg(^1S_0)$

[2] $CH_3SH + Hg(^3P_1) \rightarrow H + CH_2SH + Hg(^1S_0)$

[3] $CH_3SH + Hg(^3P_1) \rightarrow CH_3 + SH + Hg(_1S_0)$

A brief investigation of the $Hg(^3P_1)$-photosensitized decomposition of ethyl mercaptan has also been made.

[1]NRCC No. 10199.
[2]Visiting Scientist from University of Osaka Prefecture, Japan.

Experimental

The reactions were studied using a fast-flow system coupled to a mass spectrometer. The techniques employed, including the method of titration of product radicals by CH_3 and CD_3 from dimethyl mercury, have been described in earlier papers of this series (4). The use of CO additions as a means of detecting the participation of electronically excited precursors has been discussed (5, 6).

The sample of methyl mercaptan was obtained from Matheson of Canada Ltd. Ethyl mercaptan was from Aldrich Chemical Co.

Results and Discussion

Methyl Mercaptan

An analysis of the stable products of the sensitized reaction at mTorr partial pressures in the presence of 8 Torr of helium at 55° is given in Table I. The yield values correspond to moles of product per mole of CH_3SH decomposed in unit time. The products CH_3SSCH_3, CH_3SCH_3, and C_2H_6 evidently arise from the radical combination steps

[4] $2CH_3S \rightarrow CH_3SSCH_3$

[5] $CH_3S + CH_3 \rightarrow CH_3SCH_3$

[6] $2CH_3 \rightarrow C_2H_6$

A fourth product, CH_3SSH, was presumably formed by the radical combination

[7] $CH_3S + SH \rightarrow CH_3SSH$

Its yield could not be measured quantitatively because of difficulties in calibration (1).

Can. J. Chem. Downloaded from www.nrcresearchpress.com by 210.87.254.6 on 09/05/12
For personal use only.

TABLE I

Products from mercury-photosensitized decomposition of CH_3SH (4.6×10^{-3} Torr) at 55° in 8 Torr of helium (decomposition 55.7%)[a]

Product	mTorr	Yield (moles formed/CH_3SH decomposed)
CH_3SSCH_3	0.216	0.131
CS_2	0.058	0.003_5
CH_3SCH_3	0.227	0.138
H_2S	0.634	0.385
C_2H_6	0.289	0.175
CH_4	0.109	0.066
H_2	0.224	0.136
CH_3SSH	Not measured	

[a]C balance 99.0%, S balance 85.5%, H balance 100.8%.

The large yield of H_2S is thought to arise mainly from the reaction of SH with substances absorbed on the walls of the reactor and ionization chamber:

[8] $$SH + H(wall) \rightarrow H_2S$$

In earlier work (7) thermal generation of SH radical in a mass spectrometer produced relatively large quantities of H_2S. Formation of H_2S by disproportionation of two SH radicals would have led to formation of a correspondingly large amount of sulfur, which was not observed. No products derived from the CH_2SH radical could be detected. From the data in Table I, one can calculate that the CH_3 yield $= (R_{CH_3SCH_3} + 2R_{C_2H_6} + R_{CH_4})/-R_{CH_3SH} = 0.55$. Similarly the CH_3S yield $= (2R_{CH_3SSCH_3} + R_{CH_3SCH_3})/-R_{CH_3SH} = 0.40$. Although the sum of these yields is satisfactorily close to unity, these yields do not necessarily represent the relative occurrence of the primary steps [3] and [1], because of the possibility of formation of CH_3 (and SH) through a recombination of CH_3S and H to give a vibrationally excited CH_3SH:

[9] $$CH_3S + H \rightarrow CH_3SH^*$$

[10] $$CH_3SH^* \rightarrow CH_3 + SH$$

This sequence is exothermic by about 18 kcal/mole, as pointed out above.

To avoid this difficulty, the CH_3S and SH radicals were "titrated" by CD_3 radicals, formed concurrently by the sensitized decomposition of $Hg(CD_3)_2$. The yields of the addition reactions

[11] $$CH_3S + CD_3 \rightarrow CH_3SCD_3$$

[12] $$SH + CD_3 \rightarrow CD_3SH$$

are shown in Fig. 1. Allowing for some disproportionation reaction (1) between the radicals in reaction [11], the limiting yields of CH_3S and SH radicals by the primary steps [1] and [3] are about 0.9 and 0.1 respectively. The yield of SH obtained in this titration is much less than the 0.55 obtained for the CH_3 yield from the products in Table I, showing that the sequence of reactions [9] and [10] does in fact produce a large number of CH_3 radicals. Under the titration conditions CH_3S radicals are removed by reaction [11] and consequently reaction [9] is suppressed. It would appear, therefore, that the primary dissociation by reaction [1] is the major one, as in the direct photolysis (2), and that reaction [3] accounts for 10%, or less, of the total. Reaction [2] is negligibly slow.

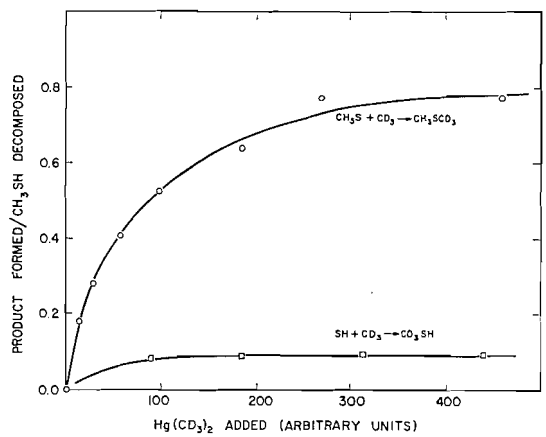

FIG. 1. Titration, by CD_3 radicals, of CH_3S and SH radicals formed in the mercury-photosensitized decomposition of CH_3SH.

The addition of CO in mTorr amounts to the reaction stream was found to increase the rate of decomposition by a factor of over two. According to our interpretation of this effect (5, 6), this is evidence for the formation of an electronically excited precursor in the primary quenching step. The corresponding oxygen analog, CH_3OH, showed no evidence for electronic excitation using the same test (6). This contrast between the behavior of —O— and —S— analogs is in agreement with that recently reported for the alkyl sulfides and disulfides (1).

Ethyl Mercaptan

A partial analysis of the products of the $Hg(^3P_1)$-sensitized decomposition of C_2H_5SH at 55° in the presence of 8 Torr of helium showed the

Can. J. Chem. Downloaded from www.nrcresearchpress.com by 210.87.254.6 on 09/05/12
For personal use only.

presence of $C_2H_5SSC_2H_5$, $C_2H_5SC_2H_5$, C_4H_{10}, H_2S, and C_2H_6. A radical combination product of parent mass $m/e = 94$ was also found, but it could not be established whether this was $(CH_2SH)_2$ or C_2H_5SSH. These radical interaction products suggest the primary dissociation steps

[13] $Hg(^3P_1) + C_2H_5SH \rightarrow C_2H_5S + H + Hg(^1S_0)$

[14] $Hg(^3P_1) + C_2H_5SH \rightarrow C_2H_5 + SH + Hg(^1S_0)$

[15] $Hg(^3P_1) + C_2H_5SH \rightarrow CH_3 + CH_2SH + Hg(^1S_0)$

It cannot be assumed, however, that all these radicals are formed in primary dissociation, because of the possibility of cracking reactions analogous to [9] and [10] occurring with CH_3SH:

[16] $C_2H_5S + H \rightarrow C_2H_5SH^*$

[17] $C_2H_5SH^* \rightarrow C_2H_5 + SH$

[18] $C_2H_5SH^* \rightarrow CH_3 + CH_2SH$

In an attempt to resolve this question, the reaction was titrated with CH_3 and CD_3 radicals by addition of $Hg(CH_3)_2$ and $Hg(CD_3)_2$ to the stream. As shown in Fig. 2, large limiting yields of $C_2H_5SCD_3$ and CD_3SH, obtained with CD_3 addition, establish C_2H_5S and SH radicals as primary products. Using CH_3 addition, the $C_2H_5SCH_3$ addition product was identified as a dialkyl sulfide rather than an isomeric thiol ($CH_3CH_2CH_2SH$ or $(CH_3)_2CHSH$ derived from $\cdot CH_2CH_2SH$ or $CH_3\dot{C}HSH$ radicals) by differences in the mass spectra. The m/e ratio of 61/76 in the $CH_3CH_2SCH_3$ spectrum is much higher than in those of the thiols. The low yield of CD_3CH_2SH in Fig. 2, obtained under titration conditions where reaction [16] is suppressed, shows that the primary step [15] is of minor importance. Although the approximate equality of the CD_3SH and $CH_3CH_2SCD_3$ yields (Fig. 2) suggest about equal rates for the primary steps [13] and [14], it should be noted that the limiting yield of C_2H_5 formation, derived from the propane yield in Fig. 2, is not in good agreement with the SH yield. The reason for this discrepancy is not known. It cannot arise from inefficiency in the titration of C_2H_5 by CH_3 since the ratio k_{disp}/k_{comb} for this radical pair is only 0.036 (8). A titration of the H-atoms from [13] by CH_3 or CD_3 radicals cannot be made quantitatively, owing to reactions of the large excess of methyl radicals in the ionization chamber to give a methane background.

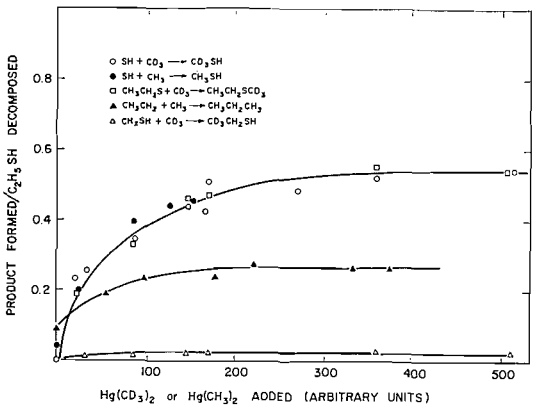

FIG. 2. Titration, by CH_3 and CD_3 radicals, of SH, CH_3CH_2S, CH_3CH_2, and CH_2SH radicals formed in the mercury-photosensitized decomposition of CH_3CH_2SH.

On account of the complex nature of the products, the ratios of the primary steps [13], [14], and [15] have not been established quantitatively. The present results indicate, however, that [13] and [14] are the main processes, with possibly a minor contribution from [15]. H-atom removal from a C-atom seems to be negligibly slow by comparison, as was found also for CH_3SH and earlier for CH_3SCH_3 and CH_3SSCH_3 (1). Addition of CO to the reaction stream gave, as for CH_3SH, an increase of over two in the rate, indicating formation of an electronically excited precursor in the primary interaction.

1. A. JONES, S. YAMASHITA, and F. P. LOSSING. Can. J. Chem. **46**, 833 (1968).
2. T. INABA and B. DE B. DARWENT. J. Phys. Chem. **64**, 1431 (1960).
3. H. E. GUNNING and O. P. STRAUSZ. Advances in photochemistry. Vol. 4. Interscience Publishers, Inc., New York. 1966. p. 143.
4. T. F. PALMER and F. P. LOSSING. Can. J. Chem. **41**, 2412 (1963).
5. J. B. HOMER and F. P. LOSSING. Can. J. Chem. **44**, 143 (1966).
6. A. JONES and F. P. LOSSING. Can. J. Chem. **45**, 1685 (1967).
7. T. F. PALMER and F. P. LOSSING. J. Am. Chem. Soc. **84**, 4661 (1962).
8. J. O. TERRY and J. H. FUTRELL. Can. J. Chem. **45**, 2327 (1967).

Can. J. Chem. Downloaded from www.nrcresearchpress.com by 210.87.254.105 on 09/05/12
For personal use only.

The transmission of polar effects. Part V.[1] The kinetics of esterification with diazodiphenylmethane and the ionization of substituted acetic and propionic acids in several solvents

KEITH BOWDEN, M. HARDY,[2] AND D. C. PARKIN
Department of Chemistry, The University of Essex, Colchester, Essex, England

Received November 20, 1967

The rate coefficients for the reaction with diazodiphenylmethane in methanol, ethanol, isopropyl alcohol, *t*-butyl alcohol, 2-methoxyethanol, 2-*n*-butoxyethanol, dimethyl sulfoxide, ethyl acetate, and toluene at 30° and the pK_a values in water, 50% ethanol–water, and 80% 2-methoxyethanol–water of 18 substituted acetic and propionic acids have been determined. A further 14 acids have been studied to a more limited extent. The effect of substitution has been estimated by linear free energy relations. The reaction constants for the ionization reaction are almost independent of the medium. This is interpreted as being due to the field effect of the proximate polar substituents passing through the molecular cavity almost alone. The occurrence of steric inhibition of solvation causing acid weakening for bulky multisubstitution is confirmed. The reaction constants for the esterification reaction are affected by the solvent. This is attributed to dependence on solvation of the transition state.

Canadian Journal of Chemistry, 46, 2929 (1968)

Introduction

As part of our examination of the mode of the transmission of polar effects, it was considered important that transmission in aliphatic systems and their dependence on the medium should be studied. Suitable reactions were considered to be the esterification of carboxylic acids with diazodiphenylmethane (DDM) and their ionization. The system chosen for this study was a series of singly substituted acetic and 3-substituted propionic acids, together with a number of more highly substituted acids. The intention was to obtain a comprehensive series of results for the esterification and ionization reactions for this model system in order to be able to discuss the influence of the substituents on reactivity in aliphatic systems.

Taft in his pioneering studies (1) made a distinct advance in understanding polar substituent effects in aliphatic systems. The aliphatic polar substituent constants, σ^*, which had been separated from the accompanying steric effects in ester hydrolysis, were found to correlate, among other reactions, the ionization of aliphatic carboxylic acids in water at 25° (1) and the esterification of the acids with DDM in ethanol at 25° (2). Hoefelmeyer and Hancock (3) and Bowden, Chapman, and Shorter (4) have extended these correlations to the esterification of aliphatic acids with DDM in toluene at 25° and in 2-*n*-butoxyethanol at 25° and toluene at 15° respectively. An obvious alternative to Taft's original approach was to base the definition on the ionization of aliphatic carboxylic acids in water at 25°. This has been completed recently by Charton (5) and constitutes a return to the original approach of Hammett for meta- and para-substituted benzoic acids. Charton chose to scale his reference system to the σ_I values of Taft and Lewis (6). These values had been obtained from two sources. These were a rescaling of the σ^* values obtained previously to "coincide" with the scale of the Hammett σ values and a separation of "inductive" and resonance effects in the Hammett σ values (6).

Hammett in his earlier studies (7) had suggested that linear free energy relations based on the ionization of aliphatic carboxylic acids would not be successful. Taft (1) showed that a separation of polar and steric effects in this system could be made using ester hydrolysis data. The polar parameter would then correlate a number of reactions of aliphatic systems, including the ionization reaction. This apparent disagreement was due to Hammett applying his treatment to ester reactions, which involve both polar and steric factors, and to ionization in other solvents, where the relationship with the ionization in water was not the same as found for the meta/para-substituted benzoic acid system. Thus it would appear that a variation on Taft's approach can be applied to suitable reaction systems where

[1]Part IV; see ref. 41.
[2]Present address: Salford Technical College, Salford, Lancashire, England.

Can. J. Chem. Downloaded from www.nrcresearchpress.com by 210.87.254.105 on 09/05/12
For personal use only.

TABLE I

pK_a values of the carboxylic acids RCO_2H at 25.0°

	R	pK_a in water	pK_a in 50% ethanol–water	pK_a in 80% 2-methoxyethanol–water
1	Me	4.75_5*	5.84*	6.84*
2	$MeCH_2$	4.87_5*	6.13*	7.18
3	$Me(CH_2)_2$	4.82*	6.15*	7.30
4	$PhCH_2$	4.31*	5.60	6.73*
5	$Ph(CH_2)_2$	4.66*	5.98	7.03*
6	$ClCH_2$	2.86_5*	3.95*	5.04*
7	$Cl(CH_2)_2$	4.08	5.35	6.31
8	$BrCH_2$	2.90*	3.84	4.97
9	$Br(CH_2)_2$	4.01	5.22	6.26*
10	$PhOCH_2$	3.17*	4.38*	5.49*
11	$PhO(CH_2)_2$	4.32	5.52	6.62
12	HO_2CCH_2	2.85_5*†	3.65*†	4.28*†
13	$HO_2C(CH_2)_2$	4.20_5*†	5.21*†	6.07*†
14	ICH_2	3.17_5*	4.36	5.50*
15	$MeOCH_2$	3.57	4.79	5.70*
16	$HOCH_2$	3.83*	4.86*	5.78*
17	$HSCH_2$	3.68*	4.76	5.88
18	$NCCH_2$	2.47*	3.39*	4.52*
19	Me_2CH	4.86*	6.22	7.39
20	Me_3C	5.03_5*	6.60	7.76*
21	Ph_2CH	3.94*	5.71	6.76
22	Ph_3C	3.96*	5.87	6.91
23	Cl_2CH	1.30	2.41	3.48*
24	Cl_3C	0.64*	1.54	2.50*
25	Br_2CH	1.48	2.53	3.60
26	Br_3C	0.72	1.64	2.60
27	$HO_2C(CH_2)_3$	4.34*†	5.66†	6.71*†
28	$HO_2C(CH_2)_4$	4.43*†	5.76†	6.71*†
29	1-$NaCH_2$‡	4.23_5*	5.70	6.67*
30	$Me(CH_2)_{16}$	5.75§	6.48	7.34
31	MeClCH	2.89_5	4.08	5.21*
32	Ph(HO)CH	3.41*	4.62	5.43*

*Literature values in water (23, 24), in 50% ethanol–water (25), and 80% 2-methoxyethanol–water (26).
†pK_a' values which are not statistically corrected.
‡1-$NaCH_2$ represents 1-naphthylacetic acid.
§Literature value at 35° (24).

polar effects control the reactivity. Steric effects must be either absent or constant for such relations to hold. A more satisfactory approach can be made by defining the aliphatic polar substituent constant in terms of the ionization reaction and using these to analyze the ionization and similar reactions controlled, alone or in the main, by polar effects.

In this report, we have studied the reactivity of a range of aliphatic carboxylic acids with DDM in 9 solvents and their ionization in 3 solvents. These results are reported here and have been analyzed by using the σ_I polar substituent constants.

Results and Discussion

The pK_a values of the carboxylic acids in water, 50% ethanol–water, and 80% 2-methoxyethanol–water are shown in Table I. The rate coefficients for the reaction of the carboxylic acids with DDM in methanol, ethanol, isopropyl alcohol, *t*-butyl alcohol, 2-methoxyethanol, 2-*n*-butoxyethanol, dimethyl sulfoxide, ethyl acetate, and toluene are shown in Table II.

Ionization Reaction

A choice of reference system must be made to analyze the results. Taft's σ^* values were obtained by averaging methods and separation of the steric effects in ester hydrolysis (1), while the σ_I values were obtained from the σ^* values and the separation of "inductive" and resonance effects (6). It therefore seemed preferable for greater reliability to return to the original Hammett-style reference. The scale chosen is the σ_I scale employed by Charton (5). In Table III are shown the σ_I values obtained from the definition, $\sigma_I = \log (K/K_0)/3.95$, where K and K_0 are the ionization constants of the substituted and the unsubstituted acetic acids in water at 25°, respectively. Thus the reaction constant, ρ_I, of this reference reaction is 3.95(5). Table IV and Figs. 1 and 2 show the application of these substituent constants in correlating the results for the ionization reaction.[3] The reaction constants for the ionization reaction show a remarkable lack of sensitivity to the medium, which changes from water (D = 78.5) to 50% ethanol–water (D = 49.1) to 80% 2-methoxyethanol–water (D = 32.0). This is quite unlike the behavior of the meta- and para-substituted benzoic acid systems where the reaction constant, ρ, changes from 1.00 (water) to 1.47 (50% ethanol–water) to 1.66 (80% 2-methoxyethanol–water) (8). The increasing susceptibility of the benzoic acid system to polar effects with a decrease in dielectric constant and polarity of the medium is usually interpreted as transmission of the polar effect via the surrounding medium sheath (9–11). The total cavity transmitting the polar effect in the meta- and para-substituted benzoic acids from the distant polar substituent contains a significant medium contribution. However, for substituents proximate to the reaction site, it would be pre-

[3]The correlations can be slightly improved by using the multiple form, $\log (K/K_0) = \rho_I\sigma_I + \delta E_s$, where E_s is the steric substituent constant (1). The improvement is not significant for the singly substituted acids, as both E_s and δ are small. Malonic acid has been excluded from these and later correlations, due to large deviations which are discussed later.

TABLE II

Esterification of the carboxylic acids RCO_2H with diazodiphenylmethane at 30.0°*

	R	k in methanol	k in ethanol	k in isopropyl alcohol	k in t-butyl alcohol	k in 2-methoxy-ethanol	k in 2-n-butoxy-ethanol	k in dimethyl sulfoxide	k in ethyl acetate	k in toluene
1	Me	1.22	0.589	0.459	0.252_5	0.257	0.163	0.00429	0.0402	0.294
2	$MeCH_2$	0.959	0.432	0.309	0.124	0.188	0.103	0.00368	0.0333	0.160
3	$Me(CH_2)_2$	1.01_5	0.445	0.306	0.132	0.189	0.111	0.00335	0.0323	0.155
4	$PhCH_2$	2.50	1.19‡	0.821	0.358	0.508	0.422	0.0118	0.126	1.37
5	$Ph(CH_2)_2$	1.49	0.740‡	0.538	0.234	0.337	0.213	0.00520	0.0678	0.491
6	$ClCH_2$	16.1	8.18	6.65_5	4.05	6.37	4.23	0.433	4.28	302
7	$Cl(CH_2)_2$	2.96	1.52	1.14	0.650	0.852	0.576	0.0237	0.321_5	7.36
8	$BrCH_2$	14.9	7.65	6.31	3.83	5.89	4.03	0.390	4.35	282
9	$Br(CH_2)_2$	4.30	2.09	1.64	1.07	1.38	0.832	0.360	0.525	8.58
10	$PhOCH_2$	12.3	6.25‡	4.94	2.57_5	3.68	2.86	0.168	1.39	93.2
11	$PhO(CH_2)_2$	2.26	1.14	0.924	0.437	0.526	0.357	0.0158	0.0972	0.991
12	HO_2CCH_2†	15.5	7.50	6.08_5	2.90	5.42	4.42	0.160	26.7	—
13	$HO_2C(CH_2)_2$†	3.47	1.58	1.10	0.472	0.721	0.449	0.0168	0.431	—
14	ICH_2	11.0	5.61	4.71	2.68	3.56	3.02	0.356	2.29_5	101
15	$MeOCH_2$	6.61	3.10	2.37_5	1.19	1.65	1.20	0.0492	0.377_5	12.1
16	$HOCH_2$	5.50	2.73	2.23_5	1.32	1.94	1.08	0.0419	1.70	—
17	$HSCH_2$	5.33	2.79	2.27_5	1.36	1.74	1.12	0.0436	0.755	—
18	$NCCH_2$	23.8_5	13.4_5	11.9	9.07	10.7_5	6.70	0.731	14.6	—
19	Me_2CH	—	0.376	—	—	0.165_5	0.0995	—	0.0327	—
20	Me_3C	—	0.242	—	—	0.110	0.0621	—	0.0224	—
21	Ph_2CH	—	1.90	—	—	0.853	0.580	—	0.183	—
22	Ph_3C	—	2.56	—	—	1.36	0.901	—	0.487	—
23	Cl_2CH	—	50.3_5	—	—	59.3_5	34.1	—	121.0	—
24	Cl_3C	—	$181._5$	—	—	252	185.0	—	—	—
25	Br_2CH	—	44.2	—	—	36.6	26.8	—	80.1	—
26	Br_3C	—	$151._5$	—	—	203	146.0	—	—	—
27	$HO_2C(CH_2)_3$†	—	1.17	—	—	0.492	0.317	—	—	—
28	$HO_2C(CH_2)_4$†	—	1.16	—	—	0.483	0.305	—	—	—
29	1-$NaCH_2$§	—	1.47	—	—	0.637	0.482	—	0.170	—
30	$Me(CH_2)_{16}$	—	0.482	—	—	0.191_5	0.115	—	0.320	—
31	MeClCH	—	8.19	—	—	5.64	3.62	—	2.76	—
32	Ph(HO)CH	—	4.46	—	—	3.91_5	1.99	—	7.47	—

*The rate coefficients, k (l mole^{-1} min^{-1}), are reproducible to ±3% or better and are the mean of at least two determinations.
†Rate coefficients are not statistically corrected.
‡Earlier studies (27) found k for phenylacetic (1.08), 3-phenylpropionic (0.735), and phenoxyacetic (6.60) acids.
§1-$NaCH_2$ represents 1-naphthylacetic acid.

dicted that the medium contribution would fall considerably or even disappear when the polar effect passes almost completely through the molecular cavity alone.[4] This appears to be so for the substituted acetic acids in this study. These have a remarkably short substituent dipole – reaction site distance (substituted acetic acids ~2.8 Å). Related studies (8) have confirmed this insensitivity for ortho-substituted benzoic acids where the reaction constant for the ionization reaction is approximately constant and always greater than that of the meta- and para-benzoic acids in the same medium. The proximate position in this case both increases the transmission and precludes medium dependence of the transmission of the polar effect.

A study of the ionization of 4-substituted bicyclo(2,2,2)octane-1-carboxylic acids in various

TABLE III

σ_I values

	R	σ_I		R	σ_I
1	Me	0.0	10	$PhOCH_2$	0.40
2	$MeCH_2$	−0.03	11	$PhO(CH_2)_2$	0.11
3	$Me(CH_2)_2$	-0.01_5	12	HO_2CCH_2*	0.40_5
4	$PhCH_2$	0.11_5	13	$HO_2C(CH_2)_2$*	0.06_5
5	$Ph(CH_2)_2$	0.02_5	14	ICH_2	0.40
6	$ClCH_2$	0.48	15	$MeOCH_2$	0.30
7	$Cl(CH_2)_2$	0.17	16	$HOCH_2$	0.23_5
8	$BrCH_2$	0.47	17	$HSCH_2$	0.27
9	$Br(CH_2)_2$	0.19	18	$NCCH_2$	0.58

*Statistically corrected.

[4]Solvent-sorting in these partially aqueous solvents (12) resulting in the proximate solvent sheath consisting almost entirely of water could have the same effect. Related studies (8), however, show a similar effect persists in pure alcohols for ortho-benzoic acids. Likewise, this also precludes a lack of sensitivity resulting from the narrowness of the medium's dielectric constant range (D between 78.5 and 32.0).

Can. J. Chem. Downloaded from www.nrcresearchpress.com by 210.87.254.105 on 09/05/12
For personal use only.

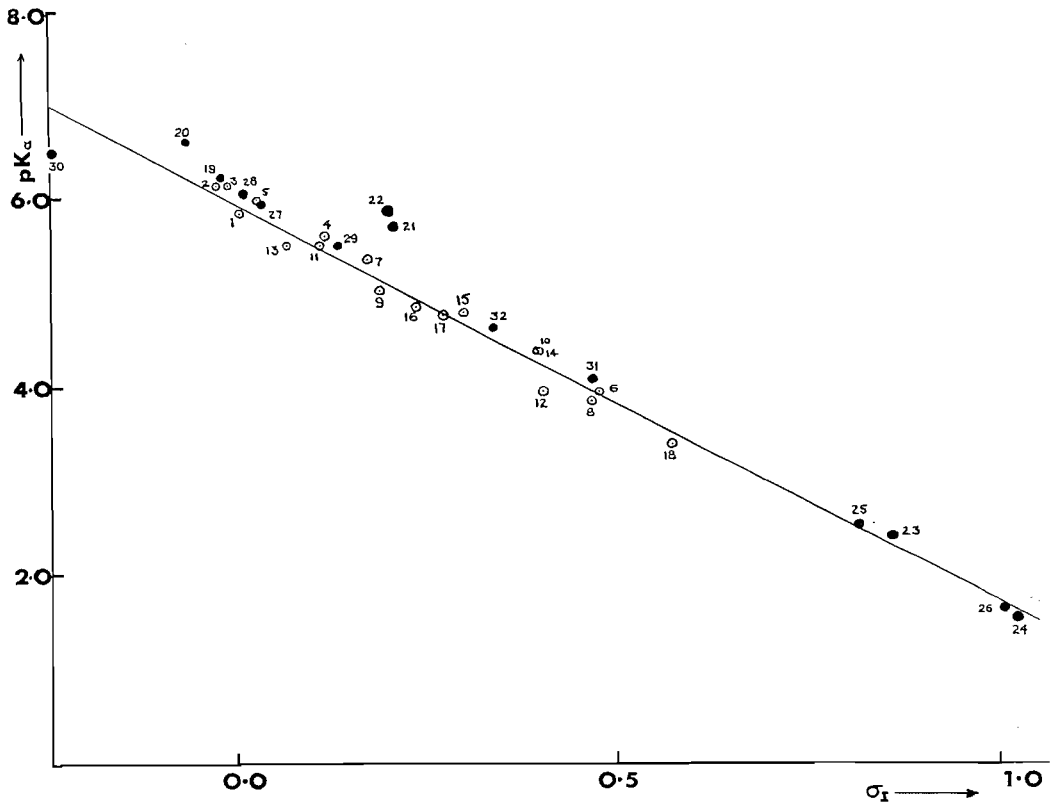

FIG. 1. The relation between the pK_a values in 50% ethanol–water and σ_I.

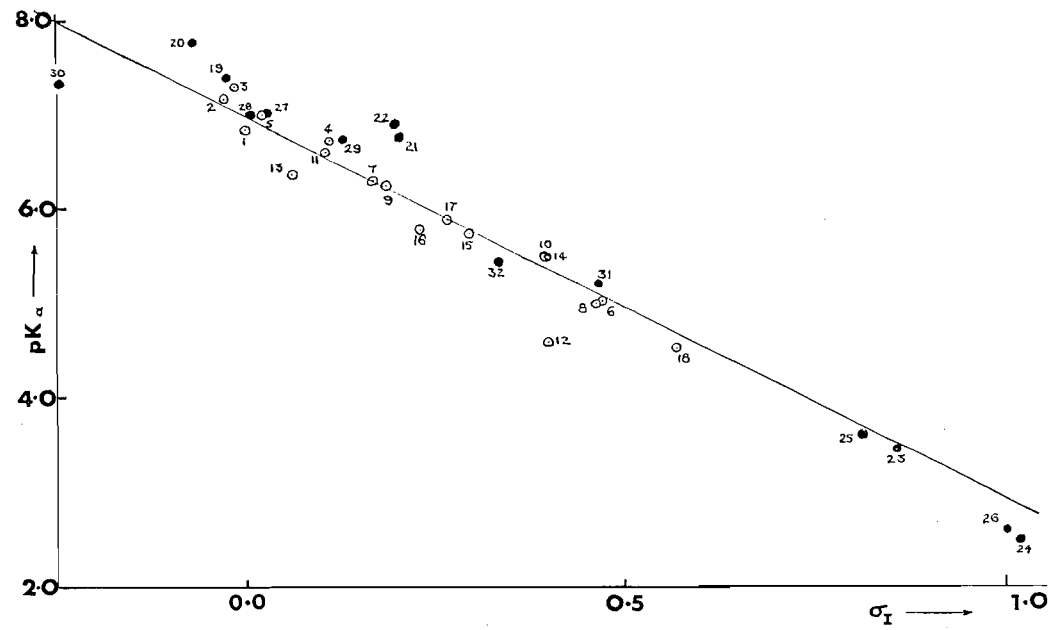

FIG. 2. The relation between the pK_a values in 80% 2-methoxyethanol–water and σ_I.

Can. J. Chem. Downloaded from www.nrcresearchpress.com by 210.87.254.105 on 09/05/12
For personal use only.

TABLE IV

Reaction constants, ρ_I, for the acids RCO_2H*

Reaction	ρ_I	log k_o	n	r
Esterification with DDM at 30.0°				
In methanol	2.338	0.102	17	0.995
In ethanol	2.441	−0.227	17	0.995
In isopropyl alcohol	2.575	−0.378	17	0.993
In *t*-butyl alcohol	2.939	−0.734	17	0.988
In 2-methoxyethanol	2.923	−0.590	17	0.990
In 2-*n*-butoxyethanol	3.010	−0.786	17	0.991
In dimethyl sulfoxide	4.132	−2.344	17	0.986
In ethyl acetate	3.756	−1.321	15	0.939
In toluene	6.355	−0.546	13	0.991
Ionization at 25.0°				
In water	3.950	−4.755	17	—
In 50% wt./wt. ethanol–water	4.179	−5.926	17	0.965
In 80% wt./wt. 2-methoxyethanol–water	4.037	−6.955	17	0.944

*n is the number of substituents studied; r is the correlation coefficient.

solvents (13) has been made, but the results are unfortunately not well correlated by linear free energy relations. Their solvent dependence appears to be complex. This can be interpreted as solvent dependence of the reaction and transmission by the medium, as for meta/para-substituted benzoic acids. The transmissive cavity for the bicyclo(2,2,2)octane acids can be expected to have a significant medium contribution.

DDM Reaction

The rate coefficients for the esterification of the carboxylic acids with DDM at 30.0° in methanol, ethanol, isopropyl alcohol, *t*-butyl alcohol, 2-methoxyethanol, 2-*n*-butoxyethanol, dimethyl sulfoxide, ethyl acetate, and toluene are shown in Table II. The reaction constants, ρ_I, are shown in Table IV and are obtained by the same method as used for the ionization reaction. The correlations are very good, as shown in Fig. 3 for ethanol, with the exception of malonic acid and the solvent ethyl acetate. It is immediately apparent that, unlike the ionization reaction, the reaction constants are dependent on the medium. Various solvent parameters are shown in Table V. There is an approximately linear relationship between the reaction constants for all the solvents, except dimethyl sulfoxide, and the reciprocal of the dielectric constant (14), as shown in Fig. 4. The related function of the dielectric constant, $(D + 1)/(2D + 1)$, correlates the results in a similar manner. The recent survey of solvent parameters by Reichardt (14) gives a number of other measures of the polarity of the medium. Data exist for the closely related solvent parameters E_T and S (14) for the solvents under study. However, these do not linearly correlate the change in the reaction constants. As shown in the Appendix, the mechanistic and kinetic implications of the reaction in aprotic solvents, particularly ethyl acetate and toluene, complicate detailed discussion of the reaction constants in these solvents. However, the following discussion seems reasonable in the light of the considerations noted (see Appendix).

It is necessary to explain the dependence of the reaction constants on the medium for the acid system in the esterification reaction with DDM, in contrast to the ionization reaction. The ionization reaction is a simple equilibrium between the acid and the conjugate anion. The medium dependence appears to be primarily caused by the portion of the substituent field effect moderated by or transmitted by the medium. The esterification reaction is a rate process and, in terms of the transition state theory, depends on the initial state – transition state equilibria. This transition state will probably be very "product-like" and resemble the ion pair that is being formed. A polar transition state, which demands solvation for stabilization, will show an increased susceptibility to polar effects, as these are increasingly required to assist and replace solvation.[5]

[5]It is probable that this effect can extend to the ionization reaction if solvation is strongly inhibited. In the ionization of 2,6-di-substituted phenols (15, 16) and benzoic acids (11), this effect is apparent in increasing the reaction constants observed from those of the parent systems.

Can. J. Chem. Downloaded from www.nrcresearchpress.com by 210.87.254.105 on 09/05/12
For personal use only.

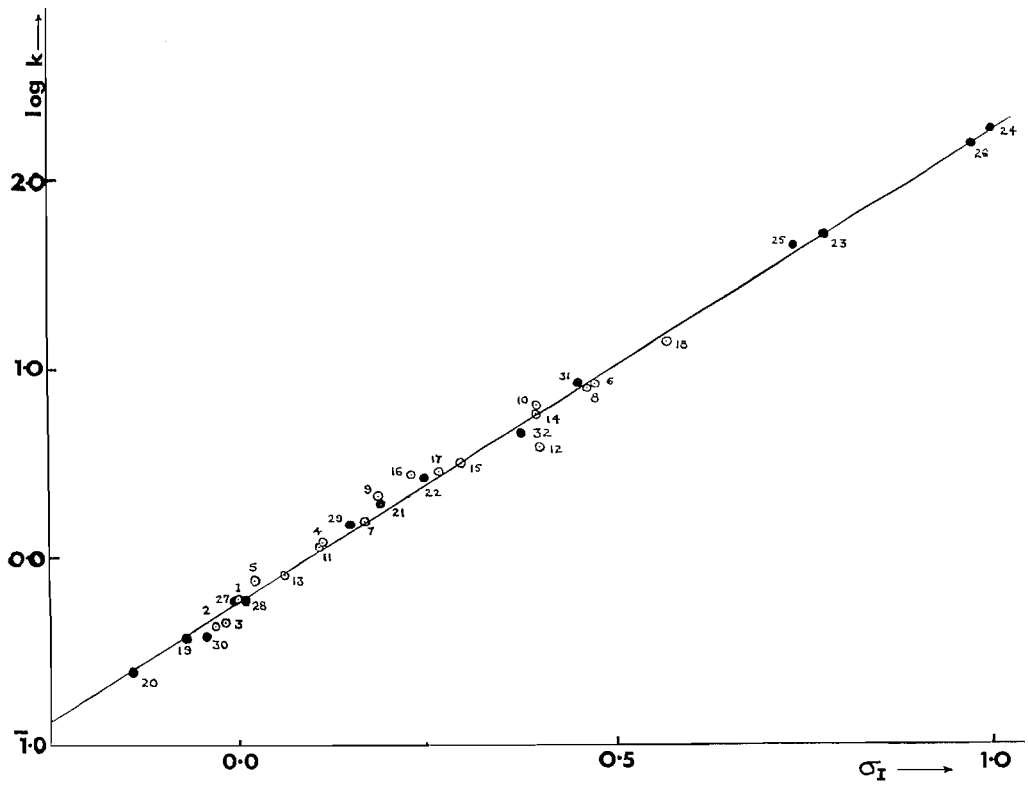

FIG. 3. The relation between log k for esterification with DDM in ethanol and σ_I.

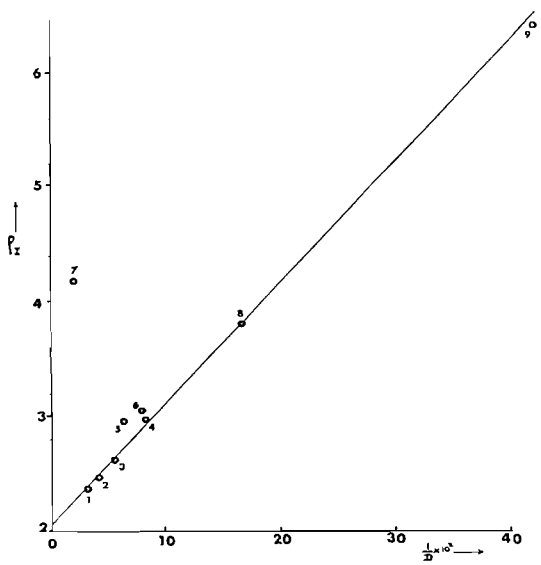

FIG. 4. The relation between ρ_I for esterification with DDM and the reciprocal of D.

The medium effect on the benzoic acid system in this reaction has been studied by Chapman, and co-workers (17) and ourselves (18). The reaction constants, ρ and ρ_I (see Tables IV and V), available for both systems show a reasonably linear relationship, except for dimethyl sulfoxide. This would thus appear to confirm that a part of the medium dependence of *the reaction constants* for the *DDM reaction* lies not in the relative effectiveness of the transmission of polar effect, but in the polarity and solvating power of the medium. The result for dimethyl sulfoxide demonstrates its comparatively poor solvating properties in spite of its high dielectric constant for this particular type of reaction. There is a reasonably linear relation between log k_0 and the reaction constants for the alcohols alone.

A common scaling of the reaction constants for the aliphatic and aromatic systems has been advocated recently and a possible derivation put forward (19, 20). That a general relation of this type is quite impossible is clearly demonstrated by

Can. J. Chem. Downloaded from www.nrcresearchpress.com by 210.87.254.105 on 09/05/12
For personal use only.

TABLE V
Solvent parameters*

Solvent†	Dielectric constant at 25°, D	E_T (kcal/mole) at 25°	ρ (DDM reaction at 30.0°)
Water	78.5	63.1	—
50% wt./wt. ethanol–water	49.1	—	—
80% wt./wt. 2-methoxyethanol–water	32.0	—	—
Methanol (1)	32.6	55.5	0.884
Ethanol (2)	24.3	51.9	0.940, 0.944
Isopropyl alcohol (3)	18.3	48.6	1.065
t-Butyl alcohol (4)	12.2‡	43.9‡	1.180, 1.278
2-Methoxyethanol (5)	15.9_5‡	52.3	1.188
2-*n*-Butoxyethanol (6)	12.7‡	—	1.330
Dimethyl sulfoxide (7)	48.9	45.0	1.206
Ethyl acetate (8)	6.0_3	38.1	2.102
Toluene (9)	2.3_8	33.9	2.670

*Literature data (14, 17, 18, 39, 40).
†Numbers in parentheses refer to Figs. 4 and 5.
‡At 30°.

the present results. The susceptibility of the reaction to polar effects will depend on at least three factors, i.e. the innate polar demand of the reaction, the reaction's dependence on solvation, and the transmission of polar effects via the medium. The relative importance of each for a particular reaction and for a particular system will vary with the reaction and system. This makes any *general* interrelations impossible.

Substituent Hydrogen-Bonding Effects

Malonic acid has been excluded from the correlations because of significant deviations for both reactions and all the solvents studied. The reference σ_I parameter is calculated from the aqueous pK_a value. It may be noted that the deviation is equivalent to an acid-strengthening effect, is almost constant in the alcoholic solvents (DDM reaction), and increases *markedly* with the decrease in water content of the partially aqueous solvents (ionization reaction). Related effects have been noted for salicylic acid (8). The occurrence of a hydrogen bond in the mono-anion of malonic acid has been recently discussed (21, 22). The deviations noted in this study are attributed to the occurrence of a hydrogen-bonded stabilization of the mono-anion or the partially ionized transition state. The importance of this stabilization increases with the decreasing availability of protic solvation. No deviations which were considered to be significant occurred for succinic acid, except in ethyl acetate (see Appendix).

The rates for glycolic and mandelic acid are also greatly increased in ethyl acetate. This can be attributed to stabilization of the partially charged transition state by the hydroxy group in an aprotic medium.

Multiple Substitution

The effect of multiple substitution has been investigated for the ionization reaction and the esterification with DDM in 4 solvents. As has been previously shown, reasonably good linear relations have been observed between the parameters calculated from the aqueous ionization and both the ionization in partially aqueous solvents and the esterification reaction. Many of the multiply substituted acids conform remarkably well to this correlation. A number of significant deviations do occur. The unexpectedly large decreases in the pK_a values of the bulky acids, i.e. pivalic, diphenylacetic, and triphenylacetic (acids 20, 21, and 22), indicate the occurrence of steric inhibition of solvation of the carboxylate anion which causes acid weakening (28–30). This effect certainly occurs in the completely aqueous system for triphenylacetic acid (acid 21), as has been previously noted (28), but appears to increase with the decreasing availability of the smaller and better protic solvating specie, water. In these cases, a better estimate of the polar substituent effect is then obtained from the esterification reaction (4). Steric effects, in general, seem to be less important in this reaction (4). Substituent constants, σ_I, obtained from the esterification reaction in alcoholic solvents are shown in Table VI for multi-substitution. These are mean

Can. J. Chem. Downloaded from www.nrcresearchpress.com by 210.87.254.105 on 09/05/12
For personal use only.

values and are obtained by using the relative rate and the reaction constant shown in Table IV. Most substituents (acids 21, 23–29, 31, 32) give values within 10% or 0.03 unit (whichever is the greater) of the value derived from the aqueous ionization reaction and the deviations are not considered significant. The deviations for the methyl substituted acids (acids 19 and 20) are rather surprising as they indicate acid-strengthening effects in aqueous ionization. This confirms the present lack of real understanding of the substituent effects of *purely* alkyl substitution on aliphatic systems on the ionization reaction. It is noteworthy that the ionization of acetic acid itself is rather less sensitive to change in medium than all other acids. It is also obvious that the aqueous pK_a value of palmitic acid (acid 30), measured at 35°, is a quite unreal estimate of the polar effect of the substituent alkyl group.

Studies (1, 31) on the additivity of polar effects in aliphatic systems have been reported. The falloff in additivity previously noted is confirmed. Two reasonable explanations of the falloff observed for di- and tri-substitution of polar groups, such as the halogeno, aryl, or hydroxy, can be put forward. The first is a saturation effect for polar influences and the second is a steric interaction. The falloff observed, for similar di- or tri-substitution, is about 1.7 and 2.2 times the effect of mono-substitution. From the present results, both appear possible. However, as the effect is observed for substituents of quite varied steric "bulk" requirements, the saturation effect appears more likely. This could result from dipole–dipole interactions in the substituent.

TABLE VI

σ_I values for multi-substitution*

	R	σ_I
19	Me_2CH	$-0.07\ (-0.02_5)$
20	Me_3C	$-0.14\ (-0.07)$
21	Ph_2CH	$0.19\ (0.20_5)$
22	Ph_3C	$0.25\ (0.20)$
23	Cl_2CH	$0.79\ (0.87_5)$
24	Cl_3C	$1.02\ (1.04)$
25	Br_2CH	$0.74_5\ (0.83)$
26	Br_3C	$0.98_5\ (1.02)$
27	$HO_2C(CH_2)_3$†	$-0.00_5\ (0.03)$
28	$HO_2C(CH_2)_4$†	$-0.01\ (0.00_5)$
29	1-Na CH_2‡	$0.15\ (0.13)$
30	$Me(CH_2)_{16}$	$-0.04_5\ (-0.25)$
31	MeClCH	$0.45_5\ (0.47)$
32	Ph(HO)CH	$0.38\ (0.34)$

*The value in parentheses is that obtained from the aqueous pK_a values.
†Statistically corrected.
‡See Table I.

Experimental

Materials

The acids were available commercially or had been previously prepared and were purified in order to give physical constants in good agreement with literature values. Neutralization equivalents were determined and were within 1% of the theoretical values, with one exception. Thiolacetic acid (97.5% pure by neutralization equivalent) could not be further purified and the experimental equivalent was used.

Diazodiphenylmethane was prepared as before (32). Solutions were stored in a refrigerator at −10° and were found to be stable at 30° in the pure solvent for periods in excess of the reaction times. Pure methanol, b.p. 64.0° (lit. 64.5° at 760 mm (33)), was prepared by Lund and Bjerrum's method (34), and pure ethanol, b.p. 78.5° (lit. 78.3° at 760 mm (33)), was prepared by Smith's method (34) using diethyl phthalate. Isopropyl alcohol, b.p. 82.5° (lit. 82.4° at 760 mm (33)), and *t*-butyl alcohol, b.p. 82.5° (lit. 82.4° at 760 mm (33)), were distilled after drying with anhydrous potassium carbonate and refluxing with sodium. Ethyl acetate, b.p. 77.0° (lit. 77.1° at 760 mm (33)), 2-methoxyethanol, b.p. 124–125° (lit. 124.4° at 760 mm (33)), and 2-*n*-butoxyethanol, b.p. 170–171° (lit. 171.2° at 760 mm (33)), were dried over freshly ignited potassium carbonate, filtered, and fractionally distilled. Dimethyl sulfoxide, m.p. 18.5° (lit. 18.45° (35)), was dried over 5 Å molecular sieves, followed by refluxing with calcium hydride, and then distilled at reduced pressure from calcium hydride under nitrogen. Toluene, b.p. 110–111° (lit. 110.1° at 760 mm (33)), was dried and distilled from sodium wire. All solvents were stored under dry nitrogen. Karl Fischer titrations on appropriate solvents gave water contents of less than 0.05%. No significant impurities (< 0.1%) were indicated by gas–liquid chromatography.

Measurements

pK_a Values

These were determined, at 25 (±0.1)°, by potentiometric titration of the acids using a Pye Dynacap pH meter. The measurements in water were made using the method previously described (36). The measurements in 50% wt./wt. ethanol–water and 80% wt./wt. 2-methoxyethanol–water were made using a method similar to that described by Simon and co-workers (26). A glass electrode (Pye Ingold No. 232), with cup-shaped membrane and fitted with a water jacket, and special calomel electrode (Pye Ingold No. 301), with nitrogen inlet for agitation, were used and calibrated with aqueous buffers as for measurements in water. The titrant, aqueous 0.1 *M* "carbon dioxide free" sodium hydroxide, was added from an Agla micrometer syringe. The pK_a values of the acids were measured using 1 ml of a 0.004 *M* solution and were calculated from the equation

$$pK_a = pH + \log([HA] - C_{H^+})/([A^-] + C_{H^+}).$$

The hydrion concentration, C_{H^+}, was taken to be antilog pH and could be neglected above pH 5.1 in comparison with [HA] and [A^-]. Correction for activity and the change in the medium over the titration could be neglected. The pK_a values obtained by this type of method using aqueous

Can. J. Chem. Downloaded from www.nrcresearchpress.com by 210.87.254.105 on 09/05/12
For personal use only.

Can. J. Chem. Downloaded from www.nrcresearchpress.com by 210.87.254.105 on 09/05/12
For personal use only.

2-methoxyethanol are stated to be accurate to ±0.07 units (26). Those obtained in this study were reproducible to ±0.02 units, relative to that of phenylacetic acid as a standard in 80% 2-methoxyethanol–water, 6.75 (lit. value 6.73 (26)), and in 50% ethanol–water, 5.60. Ionization constants were only measured for acids for which reliable literature values, at 25°, were not available, as indicated in Table I.

Two acids, palmitic and triphenylacetic, were sparingly soluble. The pK_a of the former acid in water has been obtained only at 35° (24); the pK_a of the latter acid in water at 25° has been measured by a solubility method (28). In the present work, these acids were studied at lower concentrations in 50% wt./wt. ethanol–water (0.001 *M*). These pK_a values are less certain than those of the more soluble acids. The high acidity of some acids necessitated measurements by this method to be made at higher concentrations (see (37)); i.e. in water and 50% wt./wt. ethanol–water, dichloroacetic acid (0.16 and 0.016 *M* respectively), dibromoacetic acid (0.08 and 0.008 *M* respectively), tribromoacetic acid (0.16 and 0.08 *M* respectively), and trichloroacetic acid (0.16 *M* and 0.08 *M* respectively). The aqueous pK_a values obtained by the latter method have been corrected for activity. Again, these values are not considered to be as certain as those measured by the standard method.

Rate Coefficients for DDM Reaction

These have been determined, at 30 (±0.05)°, spectrophotometrically using either a Unicam S.P. 600 or S.P. 500 spectrophotometer. The reaction was studied as a first order process using the usual sampling method (4) at 10-fold excess acid concentration (0.06 *M*), except as stated below. For fast reactions, i.e. having half-lives of less than 2½ min at 0.06 *M* acid, the original sample was retained in the cell, which was thermostatted at 30 (±0.1)°. This method was found to introduce no appreciable error when used to study acids of longer half-lives. For very fast reactions, i.e. having half-lives of less than 30 s at 0.06 *M* acid, the above method was not used. In alcoholic solvents, the reaction was then studied as a second order process by using the method previously described (41). In toluene and ethyl acetate, the dependence of the rate coefficient on the acid concentration (see Appendix) precluded the latter method being used to obtain comparable rate coefficients. These reactions were studied by mixing 1.5 ml of the acid solution, which was delivered from a syringe, with an equal volume of the DDM solution in the thermostatted cell fitted with the plastic cell cap. These solutions had been previously thermostatted at 30.0°. This enabled reactions having half-lives of down to 5 s to be studied. Even then the rate coefficients for chloroacetic and bromoacetic acids in toluene had to be measured at 0.03 *M* acid concentration and are less certain. The rate coefficients are reproducible to ±3%.

The rate coefficients in the alcoholic solvents are not corrected for the etherification which accompanies esterification, in accordance with recent mechanistic studies ((38), see Appendix).

Summary and Conclusions

The reaction constants for the ionization of substituted aliphatic acids are independent of the media used in this study.[6] This appears to be due to proximity of the substituent and the reaction site precluding transmission of the field effect by the medium. Very bulky substituents cause inhibition of solvation of the anion resulting in acid weakening. The reaction constants for the reaction of substituted aliphatic acids with DDM are dependent on the medium. This is attributed to lack of solvation of the polar transition state causing increased susceptibility of the system to polar effects.

Appendix

The Esterification of Carboxylic Acids with Diazodiphenylmethane

A number of investigations of the mechanism of the reaction of carboxylic acids with diazodiphenylmethane (DDM) have been made recently (38, 42–44). Although several details remain to be settled, the reaction in alcoholic solvents appears to involve a rate-determining proton transfer from the acid to the DDM. This is probably followed by a fast decomposition of the protonated DDM to form a benzhydryl carbonium ion pair, which is, in turn, either captured by the acid anion to form an ester or by the solvent alcohol to form an ether; i.e.

$$[1]\quad RCO_2H + Ph_2CN_2 \xrightarrow{\text{slow}} RCO_2^- Ph_2CN_2H^+$$

$$[2]\quad RCO_2^- Ph_2CN_2H^+ \xrightarrow{\text{fast}} RCO_2^- Ph_2CH^+ + N_2$$

$$[3]\quad RCO_2^- Ph_2CH^+ \begin{cases} \xrightarrow{\text{fast}} RCO_2CHPh_2 \\ \xrightarrow[+R'OH]{\text{fast}} RCO_2H + Ph_2CHOR' \end{cases}$$

In our studies (this study, refs. 18, 27, 36, 41), this reaction has been used as a probe for assessing substituent effects on carboxylic acids. In this study, the rate-determining step, in alcoholic solvents, has been confirmed as being strictly first order in DDM and in carboxylic acid as shown in Table VII for phenylacetic acid. There are no major deviations using alcohols with dielectric constants, *D*, varying from 24.2 (ethanol) to 12.2 (*t*-butyl alcohol) and acid concentrations up to

[6]A referee has drawn our attention to the data for the ionization of acetic acids in *n*-butyl alcohol saturated with lithium chloride (48). These values are correlated well by the σ_I values and give ρ_I as about 4.0. This confirms our findings.

TABLE VII

Esterification of phenylacetic acid with diazodiphenylmethane at 30.0°

Solvent	Acid (mole l^{-1})	k (l $mole^{-1}$ min^{-1})
Ethanol	0.006*	1.10
"	0.03	1.12
"	0.06	1.18
"	0.12	1.19
"	0.12	1.20
t-Butyl alcohol	0.03	0.338
"	0.06	0.362
"	0.12	0.359
2-Methoxyethanol	0.006*	0.546
"	0.03	0.494
"	0.06	0.504
"	0.12	0.511
Dimethyl sulfoxide	0.03	0.0118
"	0.06	0.0118
"	0.12	0.0118
"	0.24	0.0120
Ethyl acetate	0.006*	0.0671
"	0.03	0.0960
"	0.06	0.126
"	0.12	0.226
"	0.18	0.401
"	0.24	0.733
Toluene	0.006*	1.00
"	0.03	1.16
"	0.06	1.37
"	0.12	1.79
"	0.18	1.90
"	0.24	2.20

*Measured under second order conditions.

0.12 *M*. Previous workers (42) have found some minor deviations at higher acid concentrations than used in the present study. The interpretation of rate coefficients based on the above mechanistic pattern seems quite satisfactory.

In an aprotic solvent, the reaction products are apparently simple, since the only significant product is the ester (44). However, the kinetics of the reaction are more complex. The reaction remains strictly first order in DDM. In toluene (this study, refs. 4 and 42), ethyl acetate (this study), dioxan (45), acetonitrile (44, 45), and other aprotic solvents (45), the order in carboxylic acid is not exactly integral. The rate coefficients are usually measured under first order conditions in the presence of excess acid. The second order rate coefficients, k, are calculated by dividing the observed first order rate coefficient, k_1, by the acid concentration, [HA]. For ethyl acetate and toluene, they increase almost linearly with acid concentration, as shown in Table VII. The increase is very much more marked in ethyl acetate than in toluene. The rate coefficient, which is measured under second order conditions where

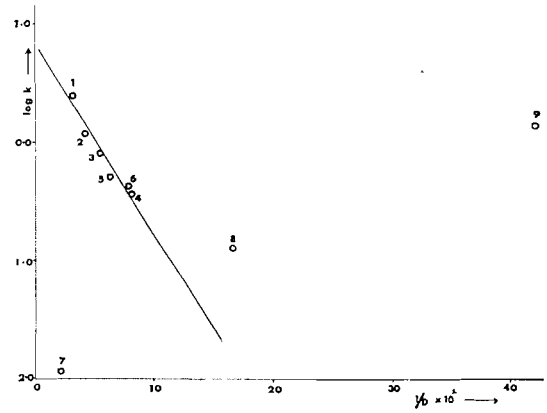

FIG. 5. The relation between log k for esterification of phenylacetic acid with DDM and the reciprocal of D.

the rate dependence closely approximates to first order in both the acid and DDM,[7] appears to fit the relation between initial acid concentration and k. Thus, the rate coefficients extrapolated to zero acid concentration from the first order measurements are close to those calculated for 0.006 *M* acid under second order conditions.

There is a discernable relation between the dielectric constant of the solvent and the rate coefficient for the reaction in alcohols. The relation between log k and the reciprocal of the dielectric constant, D, is shown in Fig. 5. For the alcohols, this is interpreted in terms of the increased difficulty in effecting the charge separation required in the transition state as the dielectric falls. Accordingly, the rate coefficients for reaction in ethyl acetate and in toluene (42) are unexpectedly high and that for dimethyl sulfoxide unexpectedly low. The previous discussion has been concerned with the transition state. The initial state stabilization will be approximately equal in the alcohols. However, the initial state will be greatly stabilized by formation of a strongly hydrogen-bonded complex in dimethyl sulfoxide and destabilized in poorly solvating toluene. These effects may account for the major part of the discrepancy in the dielectric constant – rate coefficient relation.

At the acid concentrations studied in toluene, significant association of the carboxylic acid occurs to form dimers (46, 47). This will also be true for certain other aprotic solvents, e.g. chloro-

[7]These rate coefficients are calculated using the rate equation $k = x/a(a - x)$ (41).

Can. J. Chem. Downloaded from www.nrcresearchpress.com by 210.87.254.105 on 09/05/12
For personal use only.

Can. J. Chem. Downloaded from www.nrcresearchpress.com by 210.87.254.105 on 09/05/12
For personal use only.

form (34). Whereas in others, e.g. ethyl acetate, it is expected that the likelihood of dimerization would be considerably reduced (46, 47). An explanation (42) of the increased reactivity in toluene and the variation in order with respect to acid is that the dimer is much more reactive than the monomer. Although this is possible, it does not seem likely that the hydrogen-bonded dimer is very much more reactive than the monomer. In dimethyl sulfoxide, the reaction is first order in acid, as well as the DDM. This is unlike the behavior in the other aprotic solvents referred to earlier. The carboxylic acid occurs as a monomer, strongly hydrogen bonded to the sulfoxide oxygen. This results in the abnormally low reactivity of the acid, considering the high dielectric constant of the solvent, and precludes the effect of a second acid molecule on the DDM–acid reaction.

It would appear that a second acid molecule can contribute to the reaction in most aprotic solvents. Another explanation of this role is the acid catalysis of the esterification. In solvents having no protic solvation, the assistance of a strongly hydrogen-bonding donor could assist the reaction. Reaction may occur at a faster rate between the acid and a DDM–acid complex or between DDM and an acid–acid complex than for the simple acid and DDM reaction. The second alternative has similarities to the dimer explanation, but implies a minor role for this type of reaction *not* the major reaction route. The approximately linear increase in k with [HA] seems to be more in favor of acid catalysis than of a very reactive dimer. If this is true, the extrapolated rate at zero acid concentration for toluene and ethyl acetate represents the simple acid–DDM reaction, as for alcoholic solvents.

The greatly exalted rates observed for malonic and succinic acids in ethyl acetate (this study) also indicates the possibility of an acid-catalyzed reaction. Statistical correction will not exclude two factors which could contribute in addition to the probable increased importance of intramolecular hydrogen-bonded stabilization of the polar transition state in the aprotic solvent. The factors are the increased acid groups available for an acid-catalyzed reaction and their proximity to the reacting carboxylic acid group.

These studies indicate that care must be used when comparing the reaction constants for esterification with DDM in different solvents. Direct comparison of the values obtained for alcoholic solvents is valid. Comparison with those for aprotic solvents must bear regard to the mechanistic complications present. It seems reasonable to do this unless it can be shown that a significant change in mechanism has resulted in an alteration in the previous structure–reactivity relation. This does not yet appear to be so for this reaction.

Acknowledgments

The authors would like to thank Professor N. B. Chapman and Dr. S. Shorter for their helpful correspondence and for communication of their unpublished results.

1. R. W. TAFT. *In* Steric effects in organic chemistry. *Edited by* M. S. Newman. John Wiley and Sons, Inc., New York. 1956. Chap. 13.
2. R. W. TAFT and D. J. SMITH. J. Am. Chem. Soc. **76**, 305 (1954).
3. A. B. HOEFELMEYER and C. K. HANCOCK. J. Am. Chem. Soc. **77**, 4746 (1955).
4. K. BOWDEN, N. B. CHAPMAN, and J. SHORTER. J. Chem. Soc. 5239 (1963).
5. M. CHARTON. J. Org. Chem. **29**, 1222 (1964).
6. R. W. TAFT and I. C. LEWIS. J. Am. Chem. Soc. **80**, 2436 (1958); **81**, 5343 (1959).
7. L. P. HAMMETT. Physical organic chemistry. McGraw-Hill Book Co., Inc., New York. 1940. Chap. 6.
8. K. BOWDEN and G. E. MANSER. Can. J. Chem. This issue.
9. L. P. HAMMETT. J. Am. Chem. Soc. **59**, 96 (1937).
10. W. F. SAGER and C. D. RITCHIE. J. Am. Chem. Soc. **83**, 3498 (1961).
11. K. BOWDEN. Can. J. Chem. **41**, 2781 (1963).
12. J. B. HYNE. J. Am. Chem. Soc. **82**, 5129 (1960).
13. C. D. RITCHIE and E. S. LEWIS. J. Am. Chem. Soc. **84**, 591 (1962).
14. C. REICHARDT. Angew. Chem. Intern. Ed. Engl. **4**, 29 (1965).
15. L. A. COHEN and W. M. JONES. J. Am. Chem. Soc. **85**, 3397 (1963).
16. A. FISCHER, G. J. LEARY, R. D. TOPSOM, and J. VAUGHAN. J. Chem. Soc. B, 782 (1966).
17. A. BUCKLEY, N. B. CHAPMAN, J. SHORTER, and H. M. WALL. J. Chem. Soc. B. In press. 1968.
18. K. BOWDEN and D. C. PARKIN. To be published.
19. P. R. WELLS. J. Phys. Chem. **69**, 1787 (1965).
20. C. D. RITCHIE and W. F. SAGER. *In* Progress in physical organic chemistry. Vol. II. *Edited by* S. G. Cohen, A. Streitweiser, and R. W. Taft. Interscience Publishers, Inc., New York. 1964. p. 323.
21. E. M. EYRING and J. L. HASLAM. J. Phys. Chem. **70**, 293 (1966).
22. W. E. BUDDENBAUM, W. G. KOCH, and P. E. YANKWICH. J. Phys. Chem. **70**, 673 (1966). E. S. HANRAHAN. Spectrochim. Acta, **22**, 1243 (1966).
23. G. KORTUM, W. VOGEL, and K. ANDRUSSOW. Pure Appl. Chem. **1**, 163 (1960).
24. H. C. BROWN, D. H. MCDANIEL, and O. HAFLIGER. *In* Determination of organic structures by physical methods. Vol. I. *Edited by* E. A. Braude and F. C.

Nachrod. Academic Press, Inc., New York. 1955. Chap. 14.
25. E. GRUNWALD and B. J. BERKOWITZ. J. Am. Chem. Soc. **73**, 4939 (1951).
26. W. SIMON. Angew Chem. Intern. Ed. Engl. **3**, 661 (1964). W. SIMON *et al.* Zusammenstellung von scheinbaren Dissoziationkonstanten im Losungsmittelsystem Methylcellosolve/Wasser. Juris-Verlag, Zurich. Vol. I. 1959; Vol. II. 1961; Vol. III. 1963.
27. K. BOWDEN, N. B. CHAPMAN, and J. SHORTER. Can. J. Chem. **42**, 1979 (1964).
28. M. L. KILPATRICK and E. FACKENTHAL. J. Electrochem. Soc. **100**, 185 (1953).
29. G. S. HAMMOND and D. H. HOGLE. J. Am. Chem. Soc. **77**, 338 (1955).
30. J. F. J. DIPPY, S. R. C. HUGHES, and A. ROZANSKI. J. Chem. Soc. 1441 (1959).
31. C. D. RITCHIE. J. Phys. Chem. **65**, 2091 (1961).
32. W. SCHROEDER and L. KATZ. J. Org. Chem. **19**, 718 (1954).
33. A. WEISSBERGER. Techniques of organic chemistry. Vol. VII. 2nd ed. Interscience Publishers, Inc., New York. 1955.
34. A. I. VOGEL. Practical organic chemistry. 3rd. ed. Longmans, Green & Co., Ltd., London. 1956.
35. H. C. SCHLAFER and W. SCHAFFERNICHT. Angew. Chem. **72**, 618 (1960).
36. K. BOWDEN. Can. J. Chem. **43**, 3354 (1965).
37. A. ALBERT and E. P. SERJEANT. Ionisation constants of acids and bases. Methuen & Co. Ltd., London. 1962.
38. K. BOWDEN, A. BUCKLEY, N. B. CHAPMAN, and J. SHORTER. J. Chem. Soc. 3380 (1964).
39. G. AKERLOF. J. Am. Chem. Soc. **54**, 4125 (1932).
40. W. SIMON, D. MEUCHE, and E. HEILBRONNER. Helv. Chim. Acta, **39**, 290 (1956).
41. K. BOWDEN and D. C. PARKIN. Can. J. Chem. **44**, 1493 (1966).
42. R. A. MORE O'FERRALL, W. K. KWOK, and S. I. MILLER. J. Am. Chem. Soc. **86**, 5553 (1964).
43. A. F. DIAZ and S. WINSTEIN. J. Am. Chem. Soc. **88**, 1318 (1966).
44. D. BETHELL and R. D. HOWARD. Chem. Commun. 96 (1966).
45. J. D. ROBERTS and C. M. REGAN. Anal. Chem. **24**, 360 (1952).
46. G. ALLEN and E. F. CALDIN. Quart. Rev. London, 7, 255 (1953).
47. G. C. PIMENTEL and A. MCCLELLAN. The hydrogen bond. W. H. Freeman and Co., San Francisco. 1960.
48. L. A. WOOTEN and L. P. HAMMETT. J. Am. Chem. Soc. **57**, 2289 (1935).

Can. J. Chem. Downloaded from www.nrcresearchpress.com by 210.87.254.105 on 09/05/12
For personal use only.

Can. J. Chem. Downloaded from www.nrcresearchpress.com by 210.87.254.40 on 09/05/12
For personal use only.

The transmission of polar effects. Part VI.[1] The ionization of ortho-substituted benzoic acids

KEITH BOWDEN AND G. E. MANSER
Department of Chemistry, The University of Essex, Colchester, Essex, England

Received November 20, 1967

The pK_a values of a series of ortho-substituted benzoic acids in 50% ethanol–water have been determined. The effect of ortho-substitution on the ionization of benzoic acid in this and other solvents has been correlated by a linear free energy relation. The reaction constants found are compared with those for the meta/para-substituted benzoic acids. While those for the former system are insensitive to changes in the medium, the latter vary considerably. It is suggested that this is due to transmission by the field effect passing almost entirely through the molecular cavity for ortho-substituents.

Canadian Journal of Chemistry, 46, 2941 (1968)

Introduction

The effects of ortho-substituents on reactivity has long been of great interest. Such influences have been considered to be due to proximity effects as well as to the better understood polar contributions (1). Recently it has been proposed that the effect of ortho-substituents in certain reactions is due to the efficient transmission of the polar field effect across a small distance combined with a common displacement of all substituents from the reference unsubstituted compound (2). This was considered to apply to reactions, such as the ionization of benzoic acids and their reaction with diazodiphenylmethane, and certain substituents[2] of moderate steric bulk, such as the methyl, halogeno, and methoxyl groups. A similar conclusion about the importance of the field effect was made by Hojo (3) in analyzing the ionization of di-substituted benzoic acids.

The ionization of benzoic acids has been studied in a great variety of media. Many workers (4–6) have investigated the relation between the Hammett reaction constants, ρ, for the ionization of meta- and para-substituted benzoic acids and the medium. This variation does not appear to be linearly related to the reciprocal of the dielectric constant, D, or to related functions of the dielectric constant (4, 6). A qualitative increase in ρ with a decrease in D is observed. Fair correlations exist between the reaction constants and the empirical solvent parameter, Y, defined by Grunwald and Berkowitz (5). These parameters appear to express more closely the polarity of the medium and the efficiency by which the medium moderates or "transmits" the substituent polar effects.

Early workers (7) have considered that the reactions of ortho-substituted benzoic acids could not be correlated by simple Hammett-type relations. This is undoubtedly true for many reactions where there are significant changes in the steric requirements at the reaction site which is proximate to the ortho-substituent. Attempts have been made to separate the polar and steric factors involved (8, 9), but the application of these separations has been criticized (10, 11). Other studies (12–14) have found successful correlations for systems where the ortho-substituents are no proximate to the reaction site. In this study we have attempted an extension of a more limited treatment (2) to the ionization of ortho-substituted benzoic acids in a range of solvents, using para σ values. A comparison with the ρ values found for the meta- and para-substituted benzoic acids should throw further light on the factors controlling the reaction constants.

Results and Discussion

A literature search revealed that the ionization of *both* a series of ortho- and a series of meta/para-substituted benzoic acids has been measured in water (15); 80% wt./wt. 2-methoxyethanol–water (16); methanol, ethanol, *n*-propyl alcohol, *n*-butyl alcohol, and ethylene glycol (17); 26.5%, 43.5%, and 73.5% wt./wt. dioxan–water (17); and 10% and 25% wt./wt. acetone–water (18). After the aqueous system, 50% vol./vol. ethanol–water is the medium for which the most extensive data exists for meta- and para-substituted benzoic acids (19). The absence of a set of values for

[1]Part V, see Can. J. Chem., this issue.

[2]Substituents like the ortho-*t*-butyl and ortho-hydroxy groups have specific influences. In the case of the latter substituents, these are due to significant steric and hydrogen-bonding effects respectively.

ortho-substituted benzoic acids in the latter medium prompted us to complete this deficiency. The pK_a values of the ortho-substituted benzoic acids in 50% vol./vol. ethanol–water are shown in Table I.

TABLE I

pK_a values of ortho-substituted benzoic acids at 25.0°

	Substituent	pK_a (50% vol./vol. ethanol–water)
1	H	5.76*
2	Me	5.78*
3	F	5.25
4	Cl	4.82
5	Br	4.73
6	I	4.79
7	NO_2	4.15
8	OMe	5.83
9	OH	4.12

*Literature values are 5.73 (20), 5.75 (21), 5.80 (22) (benzoic acid), and 5.76 (23) (ortho-toluic acid).

The results are analyzed by means of the Hammett equation (4, 6, 7). The data for meta- and para-substituted benzoic acids have been re-evaluated using the standard set of σ values proposed by McDaniel and Brown (19). This gives a reliable comparative set of reaction constants.

However, for ortho-substituents, the correlations are made using para σ values (19). These substituents are those of moderate steric bulk (see Table I, substituents 2–6, 8), excluding the unsubstituted acid. A value of 0.530 is used for the ortho-nitro group.[3] The ortho-hydroxy group is excluded from these correlations because of the specific hydrogen-bonding interactions (discussed later). The Hammett reaction constants, ρ, are shown in Table II.

Reaction Constants

The reaction constants for the ortho-substituents are always greater than those for meta- and para-substituents. The former reaction constants are comparatively insensitive to the medium and vary between 2.43 and 2.16 for the very well-correlated series, i.e. about 12% variation. Those for the meta- and para-substituents are markedly affected by the medium and vary between 1.00 and 1.66, i.e. about 50% variation. The relation between the reaction constant for ionization and the medium for the latter substituents has been interpreted as the transmission of the substituent polar effect via the molecular cavity and the medium (24). Conversely, this suggests that no significant part of the transmission occurs through the medium for ortho-substituents. For ortho-substituents, the substituent dipole and reaction center are close (~ 3.2 Å), unlike the para-system (~ 6.0 Å). It is both likely and reasonable that the transmissive cavity, for ortho-substitution, will be almost entirely within the molecule and is thus almost independent of the medium. The reaction constants for ortho-substitution do not show any marked variation, except for a slight fall with decreasing polarity of the medium. This could be due to the intervention of a reversed dipolar substituent effect (25, 26), the "distant" end of the substituent being increasingly effective as the polarity of the medium falls, whereas the "near" end of the substituent exerts its effect only through the molecule. For meta- and para-substituted benzoic acids, these more distant substituents have similar transmissive cavities for both ends of the dipolar substituents, both of which involve the medium to a considerable extent.

Specific Ortho-Effect

The specific acid-strengthening effect, Δ, previously noted for ortho-substitution relative to the unsubstituted acid (2, 27) is again observed and is shown in Table II. This has two likely causes, a substituent or a solvation effect. If it is a substituent effect occurring on replacement of an ortho-hydrogen, it is not a normal polar effect and would vary *markedly* with the medium. Deuterium isotope effects at the ortho-positions for benzoic acid ionization are normal in sign and size ($pK_a^D - pK_a^H$ for 2,6-dideuterobenzoic acid is 0.003) (28). A solvation effect seems more likely (2, 27). The effect decreases rapidly with decreasing water content of the partially aqueous solvents. However, a specific role of water is excluded by the observation of the almost constant and smaller effect in alcohols. It is proposed that this results from a specific displacement from the solvating sheath of a hydrogen-bonding solvating specie.

Ortho-Hydroxy Substituent

The effect of this ortho-substituent is not correlated by the para σ value. This group is

[3]The para σ value of 0.778 is reduced by interactions causing deconjugation. The value used is obtained from the ionization of ortho-nitrobenzoic acid in water and the correlation of ortho-substituents (see Table I, substituents 2–6, 8), as in this study.

Can. J. Chem. Downloaded from www.nrcresearchpress.com by 210.87.254.40 on 09/05/12
For personal use only.

TABLE II

Hammett reactions constant, ρ, for the ionization of benzoic acids at 25°

Medium	Ortho-substituents*					Meta/para-substituents*					
	ρ	$-\log K_0$	n	r	s	ρ	$-\log K_0$	n	r	s	Δ (pK_a units)
Water	2.429	3.461	7	0.988	0.045	1.000	4.203	—	—	—	0.74
50% ethanol–water	2.212	5.327	7	0.994	0.076	1.472	5.730	12	0.992	0.066	0.40
80% 2-methoxyethanol–water	2.403	6.257	7	0.983	0.134	1.661	6.611	16	0.974	0.128	0.35
Methanol	2.241	7.999	7	0.978	0.142	1.430	8.685	16	0.976	0.105	0.69
Ethanol	2.089	8.204	7	0.957	0.190	1.528	8.827	16	0.976	0.113	0.62
n-Propyl alcohol	2.100	7.951	7	0.965	0.170	1.536	8.592	16	0.978	0.108	0.64
Ethylene glycol	2.167	7.052	7	0.980	0.187	1.271	7.632	16	0.989	0.063	0.58
n-Butyl alcohol	2.048	7.981	7	0.956	0.131	1.483	8.607	16	0.977	0.106	0.63
26.5% dioxan–water	2.366	4.311	6†	0.992	0.098	1.224	4.834	13	0.993	0.054	0.52
43.5% dioxan–water	2.281	5.056	6†	0.988	0.116	1.336	5.465	16	0.987	0.072	0.41
73.5% dioxan–water	2.186	6.698	6†	0.976	0.163	1.457	7.024	16	0.986	0.080	0.33
10% acetone–water	2.420	3.892	5‡	0.999	0.037	1.129	4.471	15	0.991	0.052	0.58
25% acetone–water	2.155	4.496	5‡	0.999	0.043	1.087	5.000	15	0.990	0.053	0.50

*n is the number of substituents studied; r is the correlation coefficient; s is the standard deviation.
†Data for ortho-fluoro substituent not available.
‡Data for ortho-bromo and iodo substituents not available.

known to be acid strengthening by virtue of the stabilization of the salicyclic carboxylate anion by a strong hydrogen bond (29, and references therein). Furthermore, it appears to be increasingly effective as the polarity of the medium falls. It is suggested that there is an increase in the importance of this "internal" solvation as the external hydrogen-bonding solvation becomes less effective.

In conclusion, these studies confirm that limited relations can be applied to ortho-substituted benzoic acids. The results appear to fit satisfactorily into a field effect model for the transmission of polar effects.

Experimental

Materials

The ortho-substituted benzoic acids were available commercially. After recrystallization, they had melting points identical with or very close to those recorded in the literature. Neutralization equivalents were determined and were within 1% of the theoretical values. Pure ethanol was prepared by Smith's method (30).

Measurements

The pK_a values of the acids were measured in 50% vol./vol. ethanol–water at 25 ± 0.1° by the method previously described (31). The pK_a values are the means of at least two determinations and are considered to be accurate to ±0.02 units, relative to benzoic acid.

1. D. H. McDaniel and H. C. Brown. J. Am. Chem. Soc. **77**, 3756 (1955).
2. K. Bowden. Can. J. Chem. **43**, 3354 (1965).
3. M. Hojo. Yuki Gosei Kagaku Kjokai Shi, **23**, 341 (1965); Chem. Abstr. **63**, 6826*e* (1965).
4. H. H. Jaffé. Chem. Rev. **53**, 191 (1953).
5. E. Grunwald and B. J. Berkowitz. J. Am. Chem. Soc. **73**, 4939 (1951).
6. P. R. Wells. Chem. Rev. **63**, 171 (1963).
7. L. P. Hammett. Physical organic chemistry. McGraw-Hill Book Co., Inc., New York. 1940. Chap. 6.
8. R. W. Taft. *In* Steric effects in organic chemistry. *Edited by* M. S. Newman. John Wiley and Sons, Inc., New York. 1956. Chap. 13.
9. A. C. Farthing and B. Nam. *In* Steric effects in conjugated systems. *Edited by* G. W. Gray. Butterworths, London. 1958. p. 131.
10. N. B. Chapman, J. Shorter, and J. H. P. Utley. J. Chem. Soc. 1291 (1963).
11. K. Bowden. Can. J. Chem. **44**, 661 (1966).
12. M. Charton. Can. J. Chem. **38**, 2493 (1960).
13. I. J. Solomon and R. Filler. J. Am. Chem. Soc. **85**, 3492 (1963).
14. K. Bowden and D. C. Parkin. Can. J. Chem. **46**, in press.
15. G. Kortum, W. Vogel, and K. Andrussow. Pure Appl. Chem. **1**, 190 (1960).
16. W. Simon, A. Morikofer, and E. Heilbronner. Helv. Chim. Acta, **40**, 1918 (1957).
17. M. M. Davis and H. B. Hetzer. J. Natl. Bur. Std. (U.S.) **60**, 569 (1958). J. H. Elliott and M. Kilpatrick. J. Phys. Chem. **45**, 454, 466, 472, 485 (1941). J. H. Elliott. J. Phys. Chem. **46**, 221 (1943). M. Kilpatrick. Chem. Rev. **30**, 159 (1942). M. Kilpatrick and R. D. Eanes. J. Am. Chem. Soc. **65**, 589 (1943).

Can. J. Chem. Downloaded from www.nrcresearchpress.com by 210.87.254.40 on 09/05/12
For personal use only.

18. J. F. J. DIPPY, S. R. C. HUGHES, and B. C. KITCHINER. J. Chem. Soc. 1275 (1964).
19. D. H. MCDANIEL and H. C. BROWN. J. Org. Chem. **23**, 420 (1958).
20. F. G. BORDWELL and G. D. COOPER. J. Am. Chem. Soc. **74**, 1058 (1952).
21. J. D. ROBERTS, E. A. MCELHILL, and R. ARMSTRONG. J. Am. Chem. Soc. **71**, 2923 (1949).
22. J. D. ROBERTS and C. M. REAGAN. J. Am. Chem. Soc. **75**, 4102 (1953).
23. J. D. ROBERTS and J. A. YANCEY. J. Am. Chem. Soc. **73**, 1011 (1951).
24. L. P. HAMMETT. J. Am. Chem. Soc. **59**, 96 (1937).
25. R. GOLDEN and L. M. STOCK. J. Am. Chem. Soc. **88**, 5928 (1966).
26. K. BOWDEN and D. C. PARKIN. Chem. Commun. 75 (1968).
27. N. B. CHAPMAN, J. SHORTER, and J. H. P. UTLEY. J. Chem. Soc. 1824 (1962).
28. A. STREITWIESER and H. S. KLEIN. J. Am. Chem. Soc. **85**, 2759 (1963).
29. E. G. DUNN and T. L. PENNER. Can. J. Chem. **45**, 1699 (1967).
30. A. I. VOGEL. Practical organic chemistry. 3rd. ed. Longmans, Green and Co., Ltd., London. 1956. p. 168.
31. K. BOWDEN, H. HARDY, and D. C. PARKIN. Can. J. Chem. This issue.

Can. J. Chem. Downloaded from www.nrcresearchpress.com by 210.87.254.40 on 09/05/12
For personal use only.

Can. J. Chem. Downloaded from www.nrcresearchpress.com by 210.87.254.40 on 09/05/12
For personal use only.

Dielectric behavior of low boiling chlorides in the liquid, solid, and adsorbed states

T. McMULLEN,[1] E. D. CROZIER,[2] AND R. McINTOSH
Department of Chemistry, Queen's University, Kingston, Ontario

Received February 28, 1968

The complex dielectric constants of hydrogen, methyl, and ethyl chlorides have been measured, for the purpose of comparison with the present and future adsorption studies. The hydrogen chloride results agree with those of Cole and Swensen (22). Studies of hydrogen and ethyl chlorides adsorbed on finely divided sodium chloride show two particularly interesting phenomena. Adsorbed hydrogen chloride shows an unusually high polarizability at monolayer surface coverage, which then decreases again with increasing adsorption. Adsorbed ethyl chloride also shows a very high polarizability at a particular surface coverage, but this maximum occurs at about one-fourth of monolayer coverage, and is accompanied by loss, in contrast to the former case.

Canadian Journal of Chemistry, 46, 2945 (1968)

Introduction

Many previous investigations of the dielectric behavior of adsorbate–adsorbent systems have been undertaken, and the results have been recently reviewed by McIntosh (1). Porous adsorbents have been by far the most frequently employed because of the experimental difficulties involved in preparing a nonporous sample of high specific surface, and the precision required in the electrical measurements when the surface area is low. The interpretation of the results is difficult, however, because of the complex nature of the porous surface.

A nonporous adsorbent is consequently desirable, but studies employing this type of surface are considerably fewer in number. Other than the present sodium chloride sample, rutile is the only nonporous solid that has been used. The polar gases ammonia, sulfur dioxide, ethyl chloride, and dichlorofluoromethane gave similar results when adsorbed on rutile (2–5). The variation of the overall dielectric constant of the adsorbate–adsorbent system with the amount adsorbed was linear at low surface coverage, and as the coverage was increased there was an abrupt increase in slope, followed by a second linear section. The position of this discontinuity in terms of the amount adsorbed was found to correspond well with the Brunauer-Emmett-Teller (B.E.T.) monolayer. The temperature coefficient of the dielectric constant was negligible along the first section, but became negative in the region beyond the "kink" point.

The polar gas difluorochloroethane gave results differing from the others in one respect: there are three sections of constant slope instead of two. Furthermore, the position of the second discontinuity corresponds well with the B.E.T. monolayer, and the first with about one-half of that value. This is assumed to indicate a sudden change in apparent polarization below monolayer surface coverage, and is the only evidence of this effect with the adsorbent rutile.

In the present study, the complex dielectric constants of liquid and solid hydrogen, methyl, and ethyl chlorides were measured over the frequency and temperature range to be used in the adsorption studies, even though measurements at some of the frequencies and temperatures had been previously reported. The dielectric behavior of the adsorbed hydrogen and ethyl chlorides was then investigated, and the results are interpreted with the assumption that a dielectric constant can be assigned to an adsorbed layer. The adsorbed phase dielectric constant is determined by a modification (6) of a method (5, 7) which has been found to yield reasonable values when applied to other adsorbent–adsorbate systems.

Very briefly, the method assumes spherical particles are inserts in a medium to form a composite dielectric of constant ε. The particles, the adsorbate, and the interstices are treated as three phases. There is a further assumption that the average field of the largest phase (interstitial space) remains fixed as the quantity adsorbed is varied. The procedure is in contrast with that used

---

[1]Present address: H. H. Wills Physics Laboratory, University of Bristol, Bristol, England.
[2]Present address: Department of Physics, Simon Fraser University, Burnaby, British Columbia.

Can. J. Chem. Downloaded from www.nrcresearchpress.com by 210.87.254.40 on 09/05/12
For personal use only.

by McIntosh and his associates who assumed spherical voids in a solid dielectric, and that the field within the solid remained constant as amount of adsorbate was increased. The two procedures also differ in the use of the average macroscopic field of a phase in the new treatment, and of the average internal field of a phase in the treatment referred to in refs. 5 and 7. Both procedures lead to the same result in the case of the spherical particle model and yield the equation

$$\chi_2 = \frac{\varepsilon - 1}{4\pi} - \frac{3\varepsilon\delta_1}{2\varepsilon + 1}\cdot\frac{\varepsilon_1 - 1}{4\pi} \div \left[1 - \frac{3\varepsilon\delta_1}{2\varepsilon + 1} - \frac{\delta_3}{1 - \delta_1}\left(\frac{\varepsilon_1 - \varepsilon_0}{\varepsilon_1 - 1}\right)\right]$$

where $\chi_k \equiv (\varepsilon_k - 1)/4\pi$ and δ_k is the volume fraction of the kth phase. Subscript 1 stands for solid phase, 2 for adsorbate phase, and 3 for interstitial space phase.

The behavior of the adsorbed phase dielectric constant can then be compared with that expected for various models, one of which is the "rotational oscillator model" proposed by Kurbatov (8) and by Benson, Channen, and McIntosh (9).

Experimental

Dielectric constants and losses were measured over the frequency range 3–8000 kHz, and this necessitated two separate measuring circuits. A modified Schering bridge of design similar to that employed previously (10) covered the range 3–100 kHz. General Radio type 722 variable precision air capacitors were used as the capacitive components in three of the bridge arms, and a 200 pF mica capacitor in the fourth. Shunt resistances were required across two of the arms, and the General Radio type 602 decade resistors were employed for this purpose. Arrangement of the components, shielding, and the use of isolating transformers followed the suggestions of Hartshorn (11). The signal source was a Hewlett-Packard 205 AH audio generator, and the detector consisted of a Hewlett-Packard 450 A amplifier, and a tuned filter when necessary to reduce electrical noise, with the output fed to a Tektronix 531 A oscilloscope with type H plug-in. The reference signal to the x-plates was taken from the generator through a phase-shifting network. The residual capacitances of the bridge arms, only three of which are necessary when a substitution method is used, were determined by variation of the shunt resistances.

At higher frequencies, 480–8000 kHz, a resonant system similar to that employed by Petrie and McIntosh (12) was used. Voltage resonance was detected across a parallel network of test cell and variable measuring condenser, forming part of a series LRC circuit. The circuit was loosely coupled to a Tektronix 190A radio frequency generator by a transformer, the secondary of which provided the inductive component. Initially, a bridge-type vacuum tube voltmeter employing matched General Electric type 957 as reference and signal tubes was used, but replacement with a Hewlett-Packard 400 E voltmeter with the output displayed on a Hewlett-Packard 3439 A digital voltmeter provided increased sensitivity.

Inductance corrections were found to be important, particularly at the higher frequencies. The inductance associated with the measuring capacitor was specified by the manufacturer, and that associated with the test cell was found from a plot of the inverse of the apparent capacitance of the cell against the square of the angular frequency.

The dielectric cells used for measurements on liquid and solid methyl and ethyl chlorides, and in the adsorption studies, were made of #431 stainless steel, but in the case of liquid hydrogen chloride it was found necessary to line the cell with platinum. The liquid–solid cells were coaxial cylindrical condensers, but a multiplate cylindrical condenser was used to increase sensitivity in the adsorption studies (see ref. 1). Calibration with air, benzene, and ether distinguished the empty cell and lead capacitances.

Constant temperature was maintained to within 0.1 °C, and temperature gradients along the cell reduced to less than 0.1 °C by a thermostatting arrangement similar to that described by Shigeishi and McIntosh (13) in which cooling vanes are placed on the tube supporting the test cell, and the entire assembly is enclosed by an outer housing. Liquid nitrogen was maintained at a constant level on the outer housing by means of a modification of the level control of Fred and Rauh (14), where the thyratron tubes are replaced by silicon controlled rectifiers and thermistors are used as the temperature sensing elements. These alterations were found to increase the reliability considerably. Regulation of the current through the heating coils by a device described (15) held the temperature of the cell constant to within the desired limits.

Hydrogen, methyl, and ethyl chlorides, and butane were obtained from the Matheson Co. Hydrogen chloride was passed through columns of $CaCl_2$ and $Mg(ClO_4)_2$, and fractionally distilled several times, so that the metastable pink solid form was readily observed. Methyl chloride was passed through 10% KOH and conc. H_2SO_4. The middle fraction of a distillation was then passed through a column of fused KOH pellets, and further distilled. The purification of ethyl chloride was as described in ref. 13, and the butane sample was fractionally distilled several times. The sodium chloride powder was prepared by precipitation from the smoke (16) in an apparatus described in refs. 17 and 18. The major impurity, $NaNO_3$, should be present in amounts less than 0.05% (19).

Results and Discussion

Part I. Results for Liquid and Solid States

It was necessary to determine the density of ethyl chloride. A glass dilatometer was used to measure the volumes of a constant mass of ethyl chloride over the temperature range 0 °C to −160 °C. Assuming a value for the density of liquid ethyl chloride at 0 °C (20) the densities

Can. J. Chem. Downloaded from www.nrcresearchpress.com by 210.87.254.40 on 09/05/12
For personal use only.

shown in Table I were determined. The method of least squares was used to obtain the best straight line fitting the data in the temperature range 0 °C to −138.4 °C,

$$\rho = 0.9221 - 1.337 \times 10^{-3}T$$

The standard deviation of the experimentally determined densities from those calculated by the above equation was 1.5×10^{-3} and the probable error was 0.001.

TABLE I

Density of ethyl chloride at several temperatures

Temperature (°C)	Density (g/cc)	Temperature (°C)	Density (g/cc)
0.0	0.9214	−112.2	1.0718
−12.0	0.9380	−133.0	1.1000
−56.5	0.9985	−138.4	1.1063
−70.0	1.0160	−145.0*	1.1154
−78.4	1.0270	−150.3*	1.1219
−90.3	1.0429	−154.7*	1.1281
−98.6	1.0542	−160.1†	1.13_9

*Undercooled liquid.
†Solid state.

The complex dielectric constants of hydrogen, methyl, and ethyl chlorides were measured at 18 frequencies from 3 to 8000 kHz. In the temperature range −17.4 °C to −195 °C, measurements spaced at approximately 10 °C intervals showed that the real part, ε′, of the dielectric constant of ethyl chloride is essentially frequency independent over this range. The loss above −70 °C is small. Its increase with increasing temperature and decreasing frequency indicates that it is conductive in nature. At about −70 °C, or slightly above, Debye dispersion begins to appear at the highest frequencies, and increases with decreasing temperature until the freezing point. In the solid state ε″ again assumes a small value.

In the range between −35.9 °C and −195 °C, again covered in approximately 10 °C intervals, methyl chloride also showed no frequency dependence of ε′, although again some loss appeared at high frequencies and persisted down to freezing point. At high temperatures there was some conductive loss. Hydrogen chloride showed appreciable conduction, with the negative of the imaginary part of the dielectric constant, ε″, falling from 7.961 at 50 kHz and −87.6 °C (the highest temperature at which measurements were taken) to 6.237 at −114.2 °C and 50 kHz, and to 3.924 at −87.6 °C and 100 kHz. The corresponding values of ε′ were 11.704, 14.268, and 11.691 respectively. The dielectric constant of solid hydrogen chloride was measured at −118.7 °C and −123.7 °C, and continued to show appreciable conduction. The variations of ε′ with temperature for the three chlorides are shown in Fig. 1.

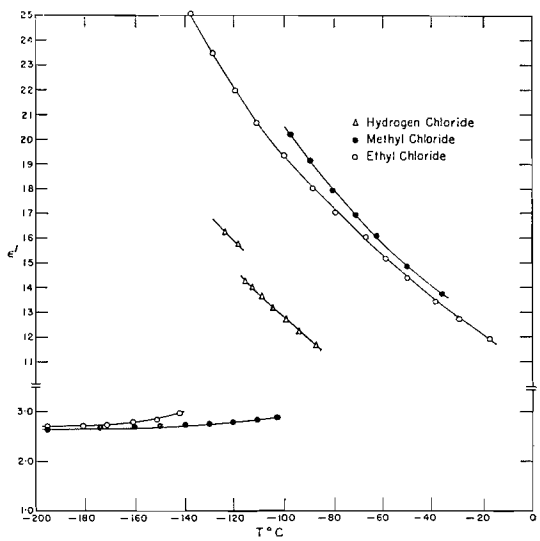

FIG. 1. Dielectric constants of low boiling chlorides in liquid and solid states.

The experimental results for the liquid state can be conveniently summarized by expressing ε′ as a polynomial function of temperature or of reciprocal temperature. The latter functional dependence is expected; it is in agreement with the dielectric theory which predicts that the static dielectric constant of a polar liquid varies as $f(\varepsilon', \rho, \mu^2/3kT)$. The unweighted averages of ε′ were determined for each temperature, and were fitted to polynomials up to the fourth degree using the IBM Fortran II program of Griffith (21). The polynomials giving the minimum unbiased standard error (defined as $(\sum_i (y_i - \bar{y})^2/D)^{\frac{1}{2}}$, where D is the number of points fitted less the number of coefficients in the polynomial) are given in Table II.

Two difficulties encountered in the measurements on liquid and solid chlorides probably lead to erroneous results. A time dependent increase in conductivity was noted, particularly in the case of hydrogen chloride. This, however, makes a negligible difference in ε′. A more serious problem is the contraction of the solid away from the

TABLE II

Dielectric constant as a function of temperature

		Standard error	Residual sum of squares
Ethyl chloride	$-17\ °C \geqslant T \geqslant -137\ °C$		
$\varepsilon' = 10.44 - 8.64 \times 10^{-2}T - 2.63_8 \times 10^{-4}T^2 - 2.96_4 \times 10^{-6}T^3$		T in °C	
		0.08	0.05_8
$\varepsilon' = -15.95 + 1.04_9 \times 10^4/T - 1.07_6 \times 10^6/T^2 + 5.52 \times 10^7/T^3$		T in °K	
		0.05_4	0.07_5
Methyl chloride	$-35\ °C \geqslant T \geqslant -98\ °C$		
$\varepsilon' = 11.78 - 3.66_2 \times 10^{-2}T + 5.07_4 \times 10^{-4}T^2$		T in °C	
		0.06_3	0.01_6
$\varepsilon' = -4.62_5 + 4.34_8 \times 10^3/T + 2.04_2 \times 10^3/T^2$		T in °K	
		0.05_9	0.01_4
Hydrogen chloride	$-87\ °C \geqslant T \geqslant -114\ °C$		
$\varepsilon' = 8.84_2 + 1.41_6 \times 10^{-2}T + 5.33_1 \times 10^{-4}T^2$		T in °C	
		0.01_9	0.001_8
$\varepsilon' = -3.17_2 + 2.75_8 \times 10^3/T$		T in °K	
		0.01_9	0.001_8

outer electrode. Unsuccessful attempts were made in eliminating the gap near the electrode by slowly solidifying the liquid keeping the dielectric cell under a temperature gradient, with the lower end cooler than the upper. A calculation of the magnitude of the error introduced in our dielectric cell by this contraction yielded the results of Table III, showing its importance for materials of high dielectric constant.

Values of the static dielectric constants of the liquids studied in this research have been reported in the literature. Cole and Swensen (22) determined ε' for hydrogen chloride in the temperature range -85 °C to -114 °C, and in the frequency range 1 kHz to 500 kHz. Their results agree with those reported above to within $\pm 1\%$. This confirmation is gratifying, because the range of reported values at or near the melting point is from 8.85 (23) to 13.1 (24) compared with our value of 14.2. Impurities, or errors in the measurement or calibration, may account for these lower values. The results of Morgan and Lowry (25) obtained for methyl chloride with frequencies between 1 kHz and 100 kHz and temperatures between -20 °C and -90 °C agree with the results reported here to within ± 0.05 for ε'. Nickerson and McIntosh (26) determined ε' for the frequency range 9 MHz to 90 MHz and in the temperature range $+20$ °C to -35 °C. Their results are about 3% lower than those obtained in this research. Presumably calibration errors should account for this discrepancy. The results of Longworth and Plesch (27) at 2 MHz for temperatures between 0 °C and -75 °C are about 10% higher than those given here, but the accuracy of their temperature control and the circuit used for the determination of ε' are questionable.

The dipole moments calculated from the liquid state values of ε' using the Onsager equation agree well with the gaseous dipole moments. Some results are shown in Table IV, along with the values of the gaseous moment suggested by McClellan (28). This agreement confirms the appropriateness of the Onsager model and implies that ethyl, methyl, and hydrogen chloride are normal polar liquids.

Representative conductivities calculated from the experimental liquid state values of ε'' are shown in Table V. Although the conductivity of

TABLE III

Effect of contraction on measured dielectric constant

Density increase	0	1.0%	2.5%	5%	10%
Gap (in cm)	0	0.003	0.006	0.012	0.023
Apparent ε	3.0	2.9_6	2.8_9	2.7_7	2.6_0
Apparent ε	15.0	13.5	11.7	9.5	7.2

Can. J. Chem. Downloaded from www.nrcresearchpress.com by 210.87.254.40 on 09/05/12
For personal use only.

TABLE IV

Dipole moments from the Onsager equation

	Ethyl chloride	Methyl chloride	Hydrogen chloride
	2.00 D at −18.7 °C 1.90 D at −137.7 °C	1.78 D at −35.9 °C 1.74 D at −97.7 °C	1.16 D at −87.6 °C 1.13 D at −112.6 °C
Suggested gaseous dipole moment (28)	2.04 D	1.94 D	1.07 D
Range of gaseous dipole moments (28)	1.74–2.09 D	1.66–2.02 D	1.03–1.95 D

hydrogen chloride is of the same order of magnitude as that found by Smyth and Hitchcock (24) and by Cole and Swensen (22), Glocker and Peck (29) using an all glass conductivity cell with platinum electrodes obtained $\sigma = 3.5 \times 10^{-9}$ mho/cm at −85 °C. The latter authors also encountered an increase in conductivity with time: the conductivity of freshly purified hydrogen chloride changed from 0.35×10^{-8} mho/cm to 2.1×10^{-8} mho/cm over a 24 h period. The conductivity of methyl chloride is a factor of 10 to 100 times larger than that reported in the literature (25). The conductivity of ethyl chloride has been reported to be less than 3×10^{-9} mho/cm (30).

TABLE V

Conductivities of the liquids

	Temperature (°C)	σ (mho/cm)
Hydrogen chloride	−87.6	2.2×10^{-7}
	−114.2	1.7×10^{-7}
Methyl chloride	−36.9	1×10^{-8}
	−97.7	6×10^{-9}
Ethyl chloride	−17.4	3×10^{-9}
	−137.7	$< 1 \times 10^{-10}$

Part II. Adsorption Studies

The System Butane/Sodium Chloride

The interpretation of the results of the dielectric behavior of adsorbent–adsorbate systems is difficult, because there is as yet no means of determining the polarizability of the adsorbed molecule. There have been several attempts at calculating this polarizability, however, and one of the most successful has been the extension of the Böttcher powder treatment (31, 32) by McIntosh and co-workers (5, 7). These authors express the polarizability in terms of the dielectric constant of the adsorbed phase. However, there is reason to believe that their model is not applicable to a powder of low packing fraction, such as the present sample of volume fraction ~ 0.1. When their formula was applied to the present results for hydrogen and ethyl chlorides, negative dielectric constants of the adsorbed phase were obtained. We intend to discuss these problems in another publication (6) and to show how an alternative formula can be derived for what may be called the "spherical particle model".

As a test of the spherical particle model for the calculation of the dielectric constant of the adsorbed phase, and for comparison with the two dipolar gases, one run, using *n*-butane as adsorbate, was carried out at −50 °C. It was expected that the nonpolar gas should yield a value equal to, or slightly less than, the dielectric constant of the liquid and that this value would remain constant or increase to the value of the dielectric constant of liquid in the higher layers. The results are shown in Table VI, along with the results of the "spherical void *F*-field method" of McIntosh *et al.* The large fluctuation in the values at low surface coverage is due to random errors because of the very small changes in the capacitance measured.

A search of the literature did not reveal a value

TABLE VI

Dielectric constant of adsorbed butane at −50 °C

Volume adsorbed (cc at S.T.P.)	11.3	100	330
ε'_2 by the spherical void *F*-field method	2.0–4.3	2.28–2.37	2.38–2.42
ε'_2 by the spherical particle model	1.8–2.9	1.89–1.94	1.94–1.96

Can. J. Chem. Downloaded from www.nrcresearchpress.com by 210.87.254.40 on 09/05/12
For personal use only.

TABLE VII

Dielectric constant of adsorbed HCl at 50 kHz

Temperature (°C)	0 cc adsorbed (extrapolated) ε'_2	Minimum value ε'_2	∞ cc adsorbed (extrapolated) ε'_2	Liquid state ε'
−70	18	10	—	10.0
−90	19	12.5	10	12.0
−110	16	15	10–15	13.8

for the dielectric constant of *n*-butane at an appropriate frequency and temperature. The square of the refractive index at −45.6 °C is 1.89 (33), and the static dielectric constant of other hydrocarbons such as *n*-pentane is not appreciably higher than the refractive index squared. It is therefore not unreasonable to assign a dielectric constant of 1.9–2.0 to liquid *n*-butane at −50 °C.

These results are not sufficiently accurate to distinguish between the two models, but they do indicate that the spherical particle model, using the liquid state density, is an adequate means of assigning a dielectric constant to an adsorbate of low dielectric constant both above and below the monolayer.

The System Hydrogen Chloride/ Sodium Chloride

Dielectric isotherms using hydrogen chloride as adsorbate were measured at three temperatures: −70 °C, −90 °C, and −110 °C. There is no appreciable dispersion of the dielectric constant at any of these temperatures. Duplicate runs at −90 °C and −110 °C showed good reproducibility, and no adsorption hysteresis or dielectric hysteresis was found. Typical plots of the overall dielectric constant of the adsorbate–adsorbent system are shown in Fig. 2.

The B.E.T. method was unsuccessful in giving the monolayer volume; the point B method indicates a monolayer volume of about 160 cc at S.T.P. Plots of the adsorbed phase dielectric constant (from the spherical particle model) versus volume adsorbed are shown in Fig. 3. Extrapolation as shown yields the values given in Table VII in which several trends are noticeable. The maximum in the curve at −110 °C corresponds well with monolayer surface coverage, and the minimum appears to occur below this value. This maximum may be considered to decrease in magnitude and to shift to higher values as temperature is increased. The temperature coefficient is positive at zero and low coverage, but becomes noticeably negative as the monolayer is approached. It appears to be small at large amounts adsorbed, but the extrapolations do not permit any quantitative determination.

In any discussion of these results, several points should be considered. The adsorption isotherms of hydrogen chloride and ethyl chloride indicate that the specific surface area of the sodium chloride sample is about 25 m^2/g. Electron photomicrographs of similar samples (34) show that the majority are cubic particles of less than 1 micron in length, and that only a small fraction have severely distorted shapes. Use of a formula given by Van Zeggeren,

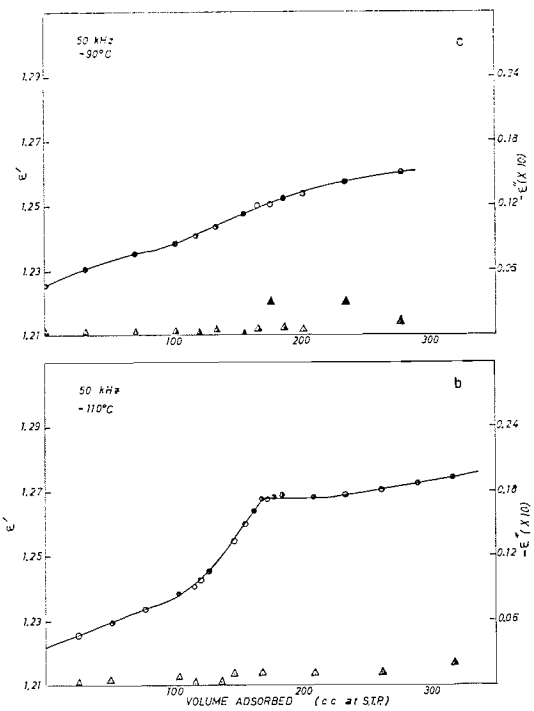

FIG. 2. Overall dielectric constants for the system NaCl–HCl. Circles are ε′, triangles −ε″.

Can. J. Chem. Downloaded from www.nrcresearchpress.com by 210.87.254.40 on 09/05/12
For personal use only.

Can. J. Chem. Downloaded from www.nrcresearchpress.com by 210.87.254.40 on 09/05/12
For personal use only.

Schreiber, and Benson (19), and an estimate assuming that the (100) face of sodium chloride is exposed, indicate that the major impurity, sodium nitrate, constitutes less than 3% of the surface area. The latter calculation also indicates that the surface is composed of approximately 0.0065 mole of sodium chloride.

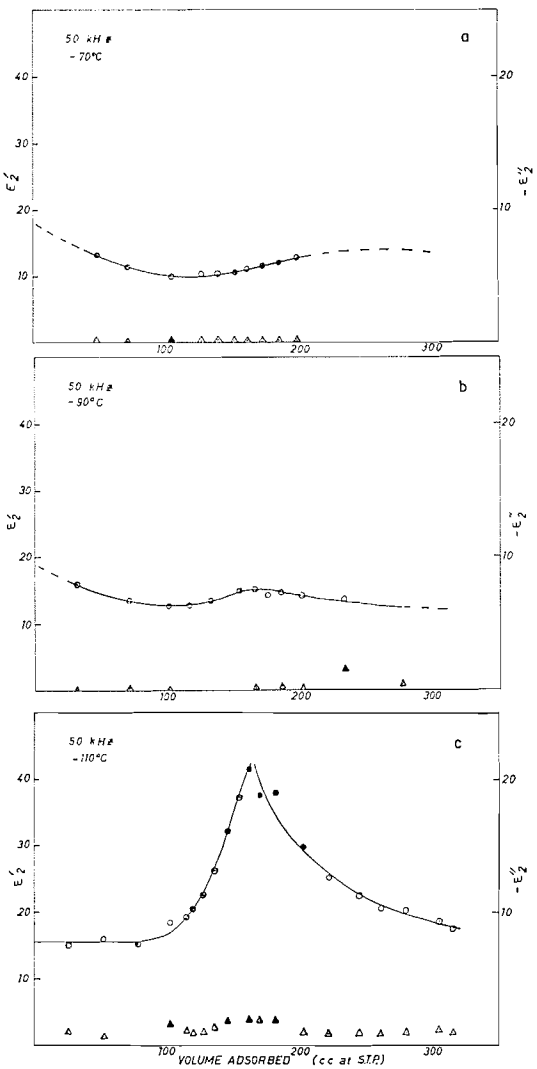

FIG. 3. Dielectric constants of the adsorbed phase for the system NaCl–HCl. Circles are ε'_2, triangles $-\varepsilon''_2$.

The reported values of the dielectric constant of sodium chloride vary between 5.3 and 6.7, in agreement with an average dielectric constant, calculated from the Böttcher formula, of 6.4. There is some fluctuation in the dielectric constant of the bare salt from run to run (as shown in Fig. 2); this is attributed to a disturbance of the bed during desorption and evacuation.

The nature of the actual adsorbed species may be questioned. There is evidence to show that hydrogen chloride dissociates on a sodium chloride surface. The reaction of hydrogen chloride gas with sodium bromide has been reported (35), and halogen exchange between sodium chloride and hydrogen chloride has been observed (36). Unfortunately, it appears impossible to determine the fraction of adsorbed molecules which exist in ionic form at any one time from the reported data. It seems reasonable to conclude, however, that the absence of low frequency Maxwell–Wagner loss in the present work, coupled with the low heats of adsorption which were observed, indicates that there is no appreciable degree of ionization in the adsorbed layer.

Consequently, we may consider an entity which is essentially molecular hydrogen chloride adsorbed on a sodium chloride surface which contains a negligible number of impurity sites, and which probably does not have an important number of severe defects and irregularities. It seems interesting, then, to search for any of the properties of the rotational oscillator mentioned previously, since Benson, Channen, and McIntosh (9) considered a fairly realistic model of hydrogen chloride adsorbed on a sodium chloride (100) face centered midway between the sodium and chloride ions, and predicted that the adsorbed molecule would perform rotational oscillations, which to a first approximation could be considered to be simple harmonic. These authors, and also Kurbatov (8), show that in addition to the expected low polarizability of the tightly bound dipole, the rotational oscillator exhibits a zero or positive temperature coefficient. It has been assumed for some time that there is a third property of this model which serves to distinguish it from the Debye-type free rotator, i.e. the property of normal dispersion or resonant absorption. It can be shown (6) that this property is to be expected of the rotational oscillator.

Turning again to the experimental results, the positive temperature coefficient at zero adsorption does indicate a rotational oscillator, and the appearance of a negative coefficient at higher coverage does not necessarily imply a departure

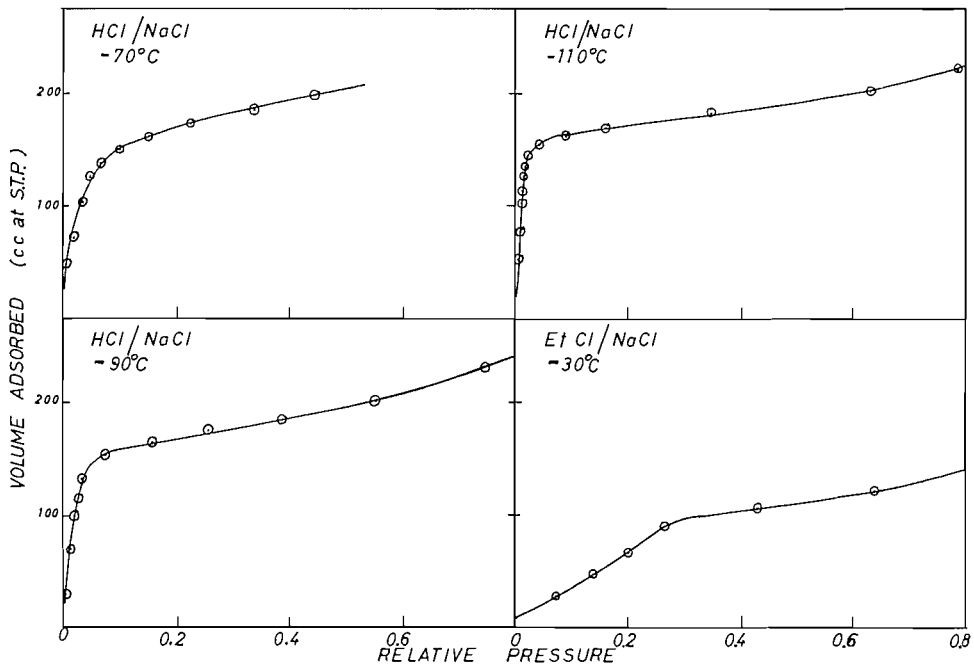

FIG. 4. Adsorption isotherms for HCl and ethyl chloride on NaCl.

from this mechanism. The convergence of the results to a value approximating the liquid state dielectric constant indicates that the polarizability is considerably greater at −110 °C and 160 cc adsorbed than in liquid hydrogen chloride, and the temperature coefficient is also much larger. The former effect can only be caused by a strong dipole–dipole correlation which enhances the susceptibility, and the latter may be attributed to a weakening of this effect with temperature. This correlation must also decrease to give a dielectric constant close to the liquid state value as surface coverage is increased beyond the monolayer.

The presence of a well-defined "knee" in the isotherms (Fig. 4) indicates that the monolayer volume is meaningful, and that the first layer is almost complete before the second layer begins to fill appreciably. Furthermore, it appears that the transition between filling of the first layer and of the second and higher layers occurs much more sharply at −110 °C than at −90 °C, and more sharply at −90 °C than at −70 °C. In conjunction with this observation it is interesting to note that the monolayer of 0.007 mole corresponds well with the 0.0065 mole of sodium chloride calculated to be in the surface, indicating a one-to-one correspondence between hydrogen chloride and sodium chloride. This correspondence would result from a two-dimensional face-centered square lattice, which leads to a correlation by electric dipole forces which enhances the polarizability, and which might give a value of the dielectric constant considerably higher than for the liquid state. Of course, if there is some occupation of the second layer, either because adsorption is carried beyond the monolayer, or because there is occupation of the second layer before the monolayer is complete, correlation is more nearly as in the liquid, and the dielectric constant assumes a lower value.

It could thus be postulated that at −110 °C the first layer is essentially complete before the second layer begins to form, giving the observed maximum, and that at higher temperatures there is some second layer formation below the monolayer volume, causing this maximum to decrease in value and to shift to greater amounts adsorbed. However, the heats of adsorption calculated for the system contradict this hypothesis to a certain extent. The usual formula for obtaining the isosteric heat of adsorption was applied to the isotherms, to yield heats of adsorption of 6.3 kcal/mole at 100 cc adsorbed, and 3.6 kcal/mole at 200 cc. These two points are approximately

Can. J. Chem. Downloaded from www.nrcresearchpress.com by 210.87.254.40 on 09/05/12
For personal use only.

Can. J. Chem. Downloaded from www.nrcresearchpress.com by 210.87.254.40 on 09/05/12
For personal use only.

equidistant from the monolayer volume of 160 cc. Use of the difference, $\Delta E = 2.7$ kcal/mole, to calculate the Boltzmann factor's $\exp(-\Delta E/RT)$ gives 0.0015, 0.0009, and 0.0001 at the three temperatures -70 °C, -90 °C, and -110 °C respectively. These values indicate that first layer completion occurs before second layer formation begins in all three cases, and that their difference is not sufficient to account for the marked change in the dielectric isotherm between -90 °C and -110 °C. The above estimation of layer occupancy is not necessarily very meaningful, however, because there are other considerations besides the Boltzmann factor.

The alternate explanation is the increase of thermal agitation as the temperature is raised from -110 °C to -90 °C causes a large fraction of the strong correlation to be destroyed. In this case, however, the temperature coefficient should not be much greater than that in the liquid, which shows an increase of 15% as the temperature is lowered from -90 °C to -110 °C, instead of the experimentally observed 175%. One is consequently led to the explanation that a strong correlation exists between dipoles at the monolayer volume, and that this correlation is destroyed as the temperature is raised partly by the filling of higher layers, and partly by thermal agitation.

There is then some evidence, namely, the positive temperature coefficient, that the adsorbed hydrogen chloride behaves as a rotational oscillator, although the fairly high value of the dielectric constant indicates that it may not be very tightly bound. No loss has been detected in the temperature range studied, so that the question of normal or anomalous dispersion cannot be answered, although we believe that we have some evidence of loss around -140 °C. The most interesting result is, however, the high value of polarizability occurring at monolayer coverage and low temperatures.

The System Ethyl Chloride/Sodium Chloride

Dielectric isotherms of ethyl chloride on sodium chloride were measured over a somewhat wider range of temperatures than for the HCl – NaCl system. The seven temperatures chosen

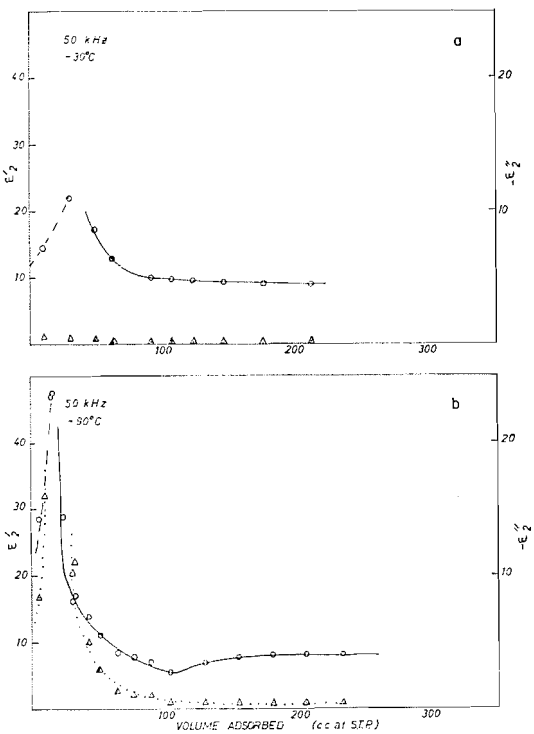

FIG. 5. Dielectric constants of the adsorbed phase for the system ethyl chloride – NaCl. Circles are ε'_2, triangles $-\varepsilon''_2$.

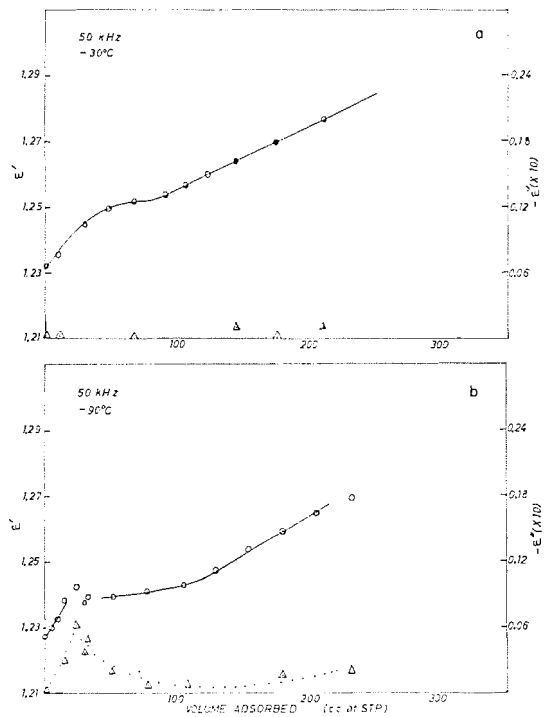

FIG. 6. Overall dielectric constants for the system ethyl chloride – NaCl. Circles are ε', triangles are $-\varepsilon''$.

TABLE VIII

Dielectric constant of adsorbed ethyl chloride at 50 kHz

Temperature (°C)	Maximum ε'_2	Recorded $-\varepsilon''_2$	Minimum	∞ cc (extrapolated)	Liquid state ε'
−10	13.6	0.4	—	8.0	11.1
−30	22.1	0.8	—	9.0	12.8
−50	34.9	4.3	—	9.0	14.4
−70	51.4	8.0	8.0	9.0	16.1
−90	47.4	34.5	6.5	8.0	18.0
−100	20.8	22.6	—	—	19.5
−110	9.3	3.3	5.5	7.5	20.7

were −10 °C, −30 °C, −50 °C, −70 °C, −90 °C, −100 °C, and −110 °C, and reproducibility was again found to be good when duplicate runs were carried out at −10 °C and −90 °C. An estimate of the monolayer volume by the point B method yielded a value of about 95 cc at S.T.P.

Typical plots of the dielectric constant of the adsorbed phase (as given by the spherical particle model) against volume adsorbed are shown in Fig. 5. The corresponding plots for the adsorbent–adsorbate system are shown in Fig. 6. The most obvious contrast with the hydrogen chloride results is the presence of a maximum in the real part of the dielectric constant at low surface coverage, accompanied by dispersion and loss. The position of this maximum appears to be about 20 cc at S.T.P. coverage, but may be as high as 30 cc at −10 °C. As can be seen from Tables VIII–XIII the maximum values of the dielectric constant and of the loss increase markedly with decreasing temperature. This eliminates the possibility of Maxwell–Wagner (or ionic conductivity) loss which is expected to increase with increasing temperature.

Because of the presence of the maximum, there are insufficient data to permit extrapolation to zero volume adsorbed, and no meaningful temperature coefficients can be obtained in the region of low surface coverage. Beyond the absorption maximum, at about 125 cc, a minimum in the dielectric constant curve appears at the lower temperature experiments. It is possible that this is the onset of the effect observed for hydrogen chloride, and it would be interesting to discover whether the minimum becomes still more pronounced at temperatures below −110 °C. In the region of high adsorption, there is little or no temperature coefficient, with the dielectric constant remaining unchanged at approximately 8–9.

The values in Table VIII reflect the shift of the absorption maximum to lower frequency as the temperature is decreased. At low temperatures and high frequencies (Tables XII, XIII) the dielectric constant is of the order of 3–5, and the loss is negligible, indicating the absence of orientational polarization. On the low frequency side of the absorption maximum, the real part

TABLE IX

The dielectric constant of adsorbed ethyl chloride at −30 °C

Frequency (kHz)	29 cc adsorbed		211 cc adsorbed		Liquid state	
	ε'_2	$-\varepsilon''_2$	ε'_2	$-\varepsilon''_2$	ε'	$-\varepsilon''$
3	23.5	0.9	9.1	0.4	12.8	1.309
5	20.1	0.3	9.1	0.3	12.8	0.795
8	23.6	—	9.1	0.2	12.8	0.497
10	23.3	—	9.2	0.2	12.8	0.406
30	22.3	0.8	9.0	0.2	12.8	0.133
50	22.1	0.5	8.9	0.2	12.8	0.077
80	22.8	1.1	8.9	0.2	12.8	0.045
100	21.7	1.1	8.9	0.2	12.8	0.037
486	20.8	0.8	8.6	—	12.8	0.009
1760	18.0	5.4	8.2	0.6	12.8	0.018
3168	17.9	3.7	8.1	0.3	12.8	0.024
8090	15.2	2.5	8.1	0.2	12.7	0.098

Can. J. Chem. Downloaded from www.nrcresearchpress.com by 210.87.254.40 on 09/05/12
For personal use only.

TABLE X

The dielectric constant of adsorbed ethyl chloride at −50 °C

Frequency (kHz)	32 cc adsorbed		246 cc adsorbed		Liquid state	
	ε'_2	$-\varepsilon''_2$	ε'_2	$-\varepsilon''_2$	ε'	$-\varepsilon''$
3	39.0	—	9.5	0.36	14.4	0.363
5	44.2	0.94	9.5	0.44	14.4	0.228
8	43.2	—	9.4	0.33	14.4	0.220
10	41.4	—	9.3	0.32	14.4	0.118
30	39.0	1.84	9.3	0.26	14.4	0.038
50	34.9	4.3	9.0	0.29	14.4	0.024
80	35.7	4.9	8.9	0.33	14.4	0.022
100	35.8	5.4	8.9	0.31	14.4	0.013
486	24.8	13.4	8.2	0.50	14.4	0.022
1760	18.2	12.2	8.1	0.62	14.4	0.020
3168	11.9	9.1	7.8	0.58	14.4	0.018
5680	8.7	6.7	8.0	0.43	14.4	0.077
8090	9.0	5.0	8.4	0.07	14.4	0.135

$\varepsilon'_2(\omega)$ assumes abnormally high values. These high values are, if there is any validity in the method of extraction of the adsorbed phase dielectric constant, completely inconsistent with the liquid state behavior.

The absence of a temperature coefficient and the low value of the dielectric constant above the monolayer indicate that the adsorbed ethyl chloride behaves as a rotational oscillator in this region. As has been mentioned previously, it is impossible to determine the behavior at low surface coverage from these two properties, but if rotational oscillation occurs at high coverage, it is certainly expected to occur at low coverage.

The discovery of a loss peak which does not appear to be of the Maxwell–Wagner type should be sufficient to distinguish the rotational oscillator model from a Debye rotator. Unfortunately, however, the present data are inadequate; there is evidence that the loss peak shows Debye dispersion, and there also exists an argument for resonant absorption. At low temperatures, where loss is the greatest, the absorption frequency is too low to permit observation of an increase in dielectric constant with frequency as ω approaches ω_{max}. However, the extremely high values of polarizability definitely suggest that this has taken place. At temperatures high enough to allow the desired part of the dispersion curve to be examined, the effect has decreased in intensity, so that the experimental error is too large for any definite conclusions to be drawn. It does appear, however, that the dispersion is of the Debye type.

Inspection of Fig. 5 suggests the possibility of a residual contribution to the abnormally high polarizability in the absence of loss. It might then be postulated that there are two effects occurring

TABLE XI

The dielectric constant of adsorbed ethyl chloride at −70 °C

Frequency (kHz)	21 cc adsorbed		244 cc adsorbed		Liquid state at −67 °C	
	ε'_2	$-\varepsilon''_2$	ε'_2	$-\varepsilon''_2$	ε'	$-\varepsilon''$
3	58.3	0.52	10.0	0.48	16.1	0.137
5	56.3	1.15	9.8	0.46	16.1	0.074
8	53.9	4.2	9.6	0.50	16.1	0.054
10	60.9	—	9.7	0.38	16.1	0.043
30	55.1	6.9	9.3	0.51	16.1	0.016
50	51.4	8.0	9.1	0.47	16.1	0.011
80	45.7	11.5	8.8	0.49	16.1	0.010
100	49.8	15.4	8.9	0.48	16.1	0.010
486	26.7	22.3	8.5	0.42	16.2	0.016
973	11.3	17.2	8.1	0.56	16.2	0.017
1760	11.5	11.2	8.1	0.46	16.2	0.023
3168	7.8	8.2	7.9	0.44	16.2	0.045

Can. J. Chem. Downloaded from www.nrcresearchpress.com by 210.87.254.40 on 09/05/12
For personal use only.

TABLE XII

The dielectric constant of adsorbed ethyl chloride at −90 °C

Frequency (kHz)	15 cc adsorbed		233 cc adsorbed		Liquid state	
	ε'_2	$-\varepsilon''_2$	ε'_2	$-\varepsilon''_2$	ε'	$-\varepsilon''$
3	171	61.1	9.1	0.5	18.0	0.207
5	110	43.4	8.7	0.6	18.0	0.130
8	153	88.6	9.0	0.4	18.0	0.081
10	102	38.2	8.6	0.4	18.0	0.068
30	55.2	42.3	8.3	0.4	18.0	0.023
50	46.9	43.3	8.1	0.4	18.0	0.015
80	31.0	35.3	8.0	0.4	18.0	0.010
100	26.1	34.6	8.0	0.3	18.0	0.009
486	8.2	8.0			18.0	0.012
973	3.7	4.7			18.1	0.019
1760	4.1	5.2			18.1	0.028
8090	6.6	9.3			18.3	0.198

in the same surface coverage region; (*i*) an unusual degree of dipole–dipole correlation, and (*ii*), dielectric absorption, now not necessarily of the resonant type, at low temperatures. The single hypothesis of resonant absorption may still be used to account for the behavior shown in Fig. 5, however, for at this temperature the absorption, although small, has shifted to higher frequencies. The unusual enhancement of the dielectric constant may be, as before, attributed to the portion of the dispersion curve where $\omega < \omega_{max}$, the resonant frequency.

It is our opinion that normal dispersion does occur, but that line broadening, which increases with temperature, causes the dispersion curve to appear Debye-like at temperatures above −90 °C. The fact that the loss peak decreases in height with increasing temperature lends additional support to this view, although there are other possible explanations of this effect. However, a careful investigation of the dielectric behavior at low surface coverage is necessary. It would also be interesting to confirm the loss peak detected in the hydrogen chloride / sodium chloride system at −140 °C and low surface coverage, and to compare this with the absorption observed in ethyl chloride.

Acknowledgment

Grateful acknowledgment is made to the National Research Council of Canada for financial support of this investigation. Computations were performed on the Queen's University IBM 360.

1. R. L. McIntosh. Dielectric behavior of physically adsorbed gases. Marcel Dekker, New York. 1966.
2. E. Petrie, R. McIntosh, and E. W. Channen. Can. J. Chem. **35**, 1534 (1957).
3. M. H. Waldman and R. McIntosh. Can. J. Chem. **33**, 268 (1955).

TABLE XIII

The dielectric constant of adsorbed ethyl chloride at −110 °C

Frequency (kHz)	30 cc adsorbed		241 cc adsorbed		Liquid state	
	ε'_2	$-\varepsilon''_2$	ε'_2	$-\varepsilon''_2$	ε'	$-\varepsilon''$
3	21.6	11.6	8.5	0.4	20.7	0.042
5	15.9	10.0	7.9	0.3	20.7	0.029
8	15.1	6.7	7.9	0.3	20.7	0.018
10	19.2	9.1	8.3	0.3	20.7	0.014
30	9.9	4.0	7.8	0.2	20.7	0.005
50	9.3	3.3	7.7	0.2	20.6	0.005
80	8.3	3.1	7.6	0.2	20.7	0.006
100	8.1	3.5	7.7	0.3	20.7	0.006
486	4.6	2.6	7.4	0.2	20.7	0.012
973	7.3	14.3	7.5	0.3	20.8	0.012
1760	5.3	0.9	7.4	0.1	20.7	0.034
5680	3.8	—	7.0	1.8	20.8	0.150

Can. J. Chem. Downloaded from www.nrcresearchpress.com by 210.87.254.40 on 09/05/12
For personal use only.

4. M. H. WALDMAN, J. A. SNELGROVE, and R. McINTOSH. Can. J. Chem. **31**, 998 (1953).
5. E. W. CHANNEN and R. McINTOSH. Can. J. Chem. **33**, 172 (1955).
6. T. McMULLEN and R. McINTOSH. Can. J. Chem. To be published.
7. R. McINTOSH, E. K. RIDEAL, and J. A. SNELGROVE. Proc. Roy. Soc. London, Ser. A **208**, 292 (1951).
8. L. N. KURBATOV. Zh. Fiz. Khim. **24**, 899 (1950).
9. G. C. BENSON, E. W. CHANNEN, and R. McINTOSH. J. Colloid Sci. **11**, 593 (1956).
10. I. D. CHAPMAN and R. McINTOSH. Can. J. Chem. **40**, 92 (1962).
11. L. HARTSHORN. Radio-frequency measurements by bridge and resonance methods. Chapman and Hall, Ltd., London. 1947.
12. S. E. PETRIE and R. McINTOSH. Can. J. Chem. **35**, 183 (1957).
13. R. SHIGEISHI and R. McINTOSH. Can. J. Chem. **44**, 1153 (1966).
14. M. S. FRED and E. G. RAUH. Rev. Sci. Instr. **21**, 258 (1950).
15. T. McMULLEN. Thesis, Queen's University, Kingston. 1968.
16. A. CRAIG and R. L. McINTOSH. Can. J. Chem. **30**, 443 (1952).
17. D. M. YOUNG and J. A. MORRISON. J. Sci. Instr. **31**, 90 (1954).
18. F. W. THOMSON, G. S. ROSE, and J. A. MORRISON. J. Sci. Instr. **32**, 325 (1955).
19. F. VAN ZEGGEREN, H. P. SCHREIBER, and G. C. BENSON. Can. J. Chem. **34**, 1501 (1956).
20. Handbook of physics and chemistry. 40th ed. Chemical Rubber Publishing Co., Cleveland, Ohio. 1958.
21. E. V. GRIFFITH. I.B.M. Madison, Wisconsin, I.B.M. Library, call no. 7.0.027C.
22. R. H. COLE and R. W. SWENSON. J. Chem. Phys. **22**, 284 (1954).
23. O. C. SCHAEFER and H. SCHLUNDT. J. Phys. Chem. **13**, 669 (1909).
24. C. P. SMYTH and C. S. HITCHCOCK. J. Am. Chem. Soc. **55**, 1830 (1931).
25. S. O. MORGAN and H. H. LOWRY. J. Phys. Chem. **34**, 2385 (1930).
26. J. D. NICKERSON and R. L. McINTOSH. Can. J. Chem. **35**, 1325 (1957).
27. W. R. LONGWORTH and P. H. PLESCH. J. Chem. Soc. 1618 (1959).
28. A. L. McCLELLAN. Tables of experimental dipole moments. W. H. Freeman and Co., San Francisco. 1963.
29. G. GLOCKER and R. PECK. J. Chem. Phys. **4**, 658 (1936).
30. A. WEISSBERGER and E. S. PROSKAUER (*Editors*). Technique of organic chemistry. Vol. VII. Interscience Publishers, Inc., New York. 1955.
31. C. J. F. BÖTTCHER. Rec. Trav. Chim. **64**, 47 (1945).
32. C. J. F. BÖTTCHER. Theory of electric polarization. Elsevier Publ. Co., Inc., Amsterdam. 1952.
33. LANDOLT-BORNSTEIN. Optische Konstanten. Vol. II. Part 8. Springer-Verlag, Berlin. 1962.
34. L. G. HARRISON, J. A. MORRISON, and G. S. ROSE. J. Phys. Chem. **61**, 1314 (1957).
35. L. G. HARRISON and R. A. SIDDIQUI. Trans. Faraday Soc. **58**, 982 (1962).
36. L. G. HARRISON, I. M. HOODLESS, and J. A. MORRISON. Discussions Faraday Soc. **28**, 103 (1959).

Can. J. Chem. Downloaded from www.nrcresearchpress.com by 210.87.254.40 on 09/05/12
For personal use only.

Can. J. Chem. Downloaded from www.nrcresearchpress.com by 210.87.254.6 on 09/05/12
For personal use only.

Ionic association and the Fuoss–Onsager conductance equation: aqueous KI

E. ANDALAFT, R. P. T. TOMKINS, AND G. J. JANZ
Department of Chemistry, Rensselaer Polytechnic Institute, Troy, New York

Received March 6, 1968

Results are reported for a reevaluation of the data for aqueous KI solutions using a modified application of the 1957 Fuoss–Onsager conductance equation in which it is reduced to a one-parameter equation with K_A as the unknown. A single value of $\mathring{a}$ is sufficient to account for the concentration dependence of conductance over the temperature range, 5–55 °C, and a small, but nevertheless finite, degree of ionic association is thus predicted for KI in aqueous solutions.

Canadian Journal of Chemistry, 46, 2959 (1968)

The data for NaI and KI solutions in 13 one-component solvents, ranging from water (D, 78) to pyridine (D, 12) have recently been reexamined (1) with the 1957 Fuoss–Onsager conductance equation (2). A modification of the conventional approach was advanced in which the Fuoss–Onsager equation reduced to a one-parameter equation with K_A as the unknown. In the present communication, the results of a reevaluation of the very precise data (3) for aqueous KI solutions, 5–55 °C, using this modified Fuoss–Onsager approach, are reported.

In the conventional application, the 1957 Fuoss–Onsager equation:

$$[1]\quad \Lambda = \Lambda_0 - Sc^{\frac{1}{2}}\gamma^{\frac{1}{2}} + Ec\gamma \log c\gamma + [J(\mathring{a}_J) - K_A\Lambda f^2]c\gamma$$

is treated as a three-parameter equation, with Λ_0, $\mathring{a}_J$ and K_A as unknowns. Substitution for J in terms of $\mathring{a}_J$ and differentiation of eq. [1] gives the result derived by Kay (4) elsewhere, i.e.

$$[2]\quad \Lambda - \Lambda_{calcd} = \Delta\Lambda_0 + c\gamma \frac{\partial J}{\partial \mathring{a}_J}\Delta\mathring{a}_J - \Delta f^2 c\gamma \Delta K_A$$

The modified approach (1) presupposes a knowledge of Λ_0 and $\mathring{a}_J$; the Fuoss–Onsager treatment then simplifies to a one-parameter expression, with K_A as the unknown, i.e.

$$[3]\quad \Lambda - \Lambda_{calcd} = -\Lambda f^2 c\gamma \Delta K_A$$

An IBM 360 computer was programmed for eq. [1] so that K_A was the only variable parameter. Λ_0 was fixed at the values in Table I, gained from a preliminary calculation cycle using eq. [1] programmed as a three-parameter equation in the conventional manner (4). The value for $\mathring{a}_J$ selected for the present work was

TABLE I

Application of the 1957 Fuoss–Onsager equation for the evaluation of the conductance of aqueous KI solutions*

Temperature (°C)	Λ_0	Three-parameter program			One-parameter program	
		$\mathring{a}_J$ (Å)	K_A	σ_Λ%†	K_A‡	σ_Λ%†
5	95.316±0.006	1.9	−1.0	0.006	0.6_3	0.03
15	121.859±0.006	1.8	−1.0	0.006	0.6_5	0.04
25	150.39±0.01	1.4	−1.4	0.01	0.6_4	0.05
35	180.67±0.01	1.7	−1.2	0.01	0.7_1	0.08
45	212.22±0.02	1.8	−1.2	0.01	0.7_2	0.08
55	244.81±0.02	1.4	−1.6	0.01	0.7_5	0.1

*Experimental data were those of Owen and Zeldes (ref. 3), using the dielectric constant values from: $D = 87.740 - 0.40008t + 9.398(10^{-4})t^2 - 1.410(10^{-6})t^3$ (see ref. 8).
†σ_Λ% is the precision for the least-squares analysis for the conductance data.
‡In the one-parameter program, $\mathring{a}_J$ is uniformly fixed at 4.5 Å.

Can. J. Chem. Downloaded from www.nrcresearchpress.com by 210.87.254.6 on 09/05/12
For personal use only.

the same as used in the reanalysis of the conductance data in various solvents (1), viz., 4.5 Å. The values for K_A found using the modified Fuoss–Onsager approach are summarized in Table I; the values for $\mathring{a}_J$ and K_A from conventional application of the 1957 Fuoss–Onsager equation to these data are also listed.

The results, in the form of log K_A vs. $1/DT$, are shown graphically in Fig. 1, together with the results for log K_A for KI in various non-aqueous solvents using this one-parameter approach (1).

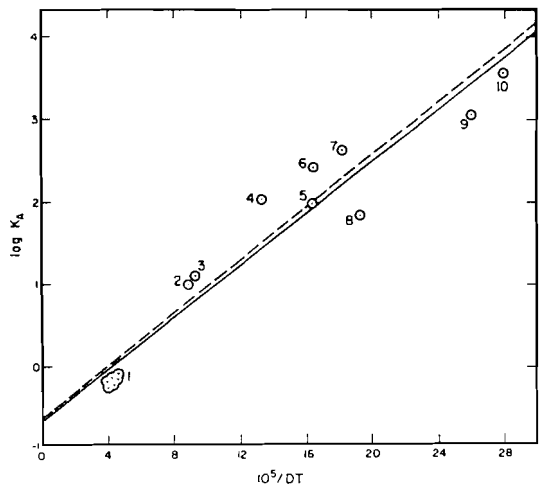

FIG. 1. Dependence of log K_A on $1/DT$. The values of log K_A for aqueous solutions (5–55 °C) are shown on the cluster of points (1); the remaining values refer to the different solvent media as follows: (2) ethanolamine, (3) acetonitrile, (4) benzonitrile, (5) acetone, (6) propanol, (7) methyl ethyl ketone, (8) acetophenone, (9) ethylene diamine, and (10) pyridine. The solid line is the least-squares fit to the results; the broken line is predicted for $\mathring{a} = 4.5$ Å.

The relationship between K_A and D, derived by statistical and thermodynamic methods (5, 6), may be written as:

$$[4] \qquad \log K_A = G_1\left(\frac{1}{DT}\right) + G_2$$

where the slope of this linear equation, G_1, is $(e^2/2.303\ \mathring{a}_K k)$ and the intercept G_2 is log $(4\pi N\mathring{a}^3/3000)$. Here $\mathring{a}_K$ is the ion pair distance (for association), and $\mathring{a}$ must be identified with $\mathring{a}_J$, the ion size parameter of the conductance equation, since it is the volume of the free ions that is important in G_2.

In Fig. 1, the least squares fit to the results is illustrated by the solid line. From the slope and intercept of this line (Fig. 1), the values found for $\mathring{a}_K$ and $\mathring{a}_J$ are 4.6 Å and 4.4 Å, respectively. The agreement is surprising, since any change in solvation on forming an ion-pair would invalidate the identification of $\mathring{a}_J$ with $\mathring{a}$ in eq. [4]. Further, these values are in close accord with the value used for $\mathring{a}_J$, i.e., 4.5 Å in the application of the Fuoss–Onsager equation as a one parameter equation for calculating K_A. A value of 4.47 Å was advanced by Latimer (7) in relating the free energies of hydration and entropies of hydration with ion size for aqueous KI solutions.

A limitation of the one-parameter approach for the application of the Fuoss–Onsager equation is that prior knowledge of Λ_0 and $\mathring{a}_J$ is necessary. The value for Λ_0 can be gained from a preliminary calculation cycle using this equation in the conventional manner. If conductance data are available in a range of solvents, the value of $\mathring{a}_J$ can be gained by additional calculations, again in the conventional manner much as in our preceding communication (1); alternatively the present results encourage the selection of the ionic distance, $\mathring{a}_J$, as equal to the sum of the crystallographic radii plus 1 Å (the ion cavity (7)). The results support the observation by Kay (4), that a single value of $\mathring{a}$ is sufficient to account for the concentration dependence of conductance over a considerable temperature range. A further result is that the value of $\mathring{a}$ also appears sufficient to describe the conductance in a wide range of solvents.

The values of the association constants, K_A, gained by this one-parameter method, appear more meaningful than those from the three-parameter approach, at least for intercomparisons from one solvent system to another; support for this view comes from the comparatively good agreement of the results and the least squares line of the linear representation, as predicted for the function of log K_A and $1/DT$, shown graphically in Fig. 1. A small, but nevertheless finite, degree of ionic association is thus predicted for KI, over the temperature range, 5–55 °C, in aqueous solutions.

Acknowledgments

Stimulating discussions in the course of this work with R. A. Robinson and R. M. Fuoss, and the continuing interest of M. J. Tait, are acknowledged with pleasure. This work was made possible, in large part, by financial

support from the United States Department of Interior, Office of Saline Water, Washington, D.C.

1. G. J. Janz and M. J. Tait. Can. J. Chem. **45**, 1101 (1967).
2. R. M. Fuoss and L. Onsager. J. Phys. Chem. **61**, 668 (1957).
3. B. B. Owen and H. Zeldes. J. Chem. Phys. **18**, 1083 (1950).
4. R. L. Kay. J. Am. Chem. Soc. **82**, 2099 (1960).
5. R. M. Fuoss. J. Am. Chem. Soc. **80**, 5059 (1958).
6. H. Y. Inami, H. K. Bodenseh, and J. B. Ramsey. J. Am. Chem. Soc. **83**, 4745 (1961).
7. W. M. Latimer. J. Chem. Phys. **23**, 90 (1955).
8. C. G. Malmberg and A. A. Margott. J. Res. Nat. Bur. Std. **56**, 1 (1956).

Can. J. Chem. Downloaded from www.nrcresearchpress.com by 210.87.254.6 on 09/05/12
For personal use only.

Electric dipole moments of ortho-, meta-, para-, and penta-fluorostyrene molecules

E. Bock and D. Iwacha
Parker Chemistry Laboratory, University of Manitoba, Winnipeg, Manitoba

Received March 4, 1968

The dipole moments of ortho-, meta-, para-, and penta-fluorostyrene were determined in dilute benzene solution at 25 °C. It was found that the magnitude of the molecular dipole moment depends on the position of the fluorine atom in the benzene ring.

Canadian Journal of Chemistry, **46**, 2961 (1968)

Introduction

The molecular electric dipole moment is a useful molecular constant in its own right. In many cases, especially in the case of simple molecules, the magnitude of the molecular dipole moment may be used to establish the molecular symmetry and in some special cases to determine the most favorable molecular conformation in the gas phase or in solution.

The dipole moments of ortho-, meta-, and para-fluorostyrene molecules are interesting also from another point of view. It has been shown that these molecules exhibit long-range H—F nuclear magnetic resonance couplings (1). It appears that the fluorine atom on the benzene ring is coupled to the terminal hydrogen atoms of the vinyl group. It was therefore interesting in this connection to determine the effect of different positions of the fluorine atom in the benzene ring on the dipole moment of the molecule.

Experimental

Fisher certified reagent benzene was used as solvent. The benzene was dried by repeated shaking with Linde molecular sieve 4A.

The solute molecules were obtained from Pierce Chemical Co. and were used without further purification.

The apparatus and experimental procedure have been described elsewhere (2, 3).

Results

The experimental results are summarized in Table I. The dipole moments derived from the experimental data are shown in Table II. As is indicated in Table II, the dipole moments were derived from the experimental data by three different methods, viz. by the Smith (4), Halverstadt–Kumler (5), and Looyenga (6) method, respectively. The reason for employing three different treatments of the experimental data was twofold: (*a*) to compare the methods of Smith and Halverstadt–Kumler, and (*b*) to correct the dipole moments for the solvent effect (method of Looyenga). In the latter two methods LeFevre's (7) bond electronic polarization was used to estimate the magnitude of the electronic polarization. From Table II it is apparent that the methods of Smith and Halverstadt–Kumler yield approximately the same dipole moments within the estimated experimental error of ± 0.1 D. The corrected dipole moment is, as expected (2), several tenths of a debye unit higher than the corresponding solution value. The following comments about the relative magnitudes of the molecular dipole moments of the ortho-, meta-, and para-fluorostyrene molecules may be in order. The smaller value of the dipole moment resulting from placing the fluorine atom in the

support from the United States Department of Interior, Office of Saline Water, Washington, D.C.

1. G. J. Janz and M. J. Tait. Can. J. Chem. **45**, 1101 (1967).
2. R. M. Fuoss and L. Onsager. J. Phys. Chem. **61**, 668 (1957).
3. B. B. Owen and H. Zeldes. J. Chem. Phys. **18**, 1083 (1950).
4. R. L. Kay. J. Am. Chem. Soc. **82**, 2099 (1960).
5. R. M. Fuoss. J. Am. Chem. Soc. **80**, 5059 (1958).
6. H. Y. Inami, H. K. Bodenseh, and J. B. Ramsey. J. Am. Chem. Soc. **83**, 4745 (1961).
7. W. M. Latimer. J. Chem. Phys. **23**, 90 (1955).
8. C. G. Malmberg and A. A. Margott. J. Res. Nat. Bur. Std. **56**, 1 (1956).

Can. J. Chem. Downloaded from www.nrcresearchpress.com by 210.87.254.6 on 09/05/12
For personal use only.

Electric dipole moments of ortho-, meta-, para-, and penta-fluorostyrene molecules

E. Bock and D. Iwacha
Parker Chemistry Laboratory, University of Manitoba, Winnipeg, Manitoba

Received March 4, 1968

The dipole moments of ortho-, meta-, para-, and penta-fluorostyrene were determined in dilute benzene solution at 25 °C. It was found that the magnitude of the molecular dipole moment depends on the position of the fluorine atom in the benzene ring.

Canadian Journal of Chemistry, **46**, 2961 (1968)

Introduction

The molecular electric dipole moment is a useful molecular constant in its own right. In many cases, especially in the case of simple molecules, the magnitude of the molecular dipole moment may be used to establish the molecular symmetry and in some special cases to determine the most favorable molecular conformation in the gas phase or in solution.

The dipole moments of ortho-, meta-, and para-fluorostyrene molecules are interesting also from another point of view. It has been shown that these molecules exhibit long-range H—F nuclear magnetic resonance couplings (1). It appears that the fluorine atom on the benzene ring is coupled to the terminal hydrogen atoms of the vinyl group. It was therefore interesting in this connection to determine the effect of different positions of the fluorine atom in the benzene ring on the dipole moment of the molecule.

Experimental

Fisher certified reagent benzene was used as solvent. The benzene was dried by repeated shaking with Linde molecular sieve 4A.

The solute molecules were obtained from Pierce Chemical Co. and were used without further purification.

The apparatus and experimental procedure have been described elsewhere (2, 3).

Results

The experimental results are summarized in Table I. The dipole moments derived from the experimental data are shown in Table II. As is indicated in Table II, the dipole moments were derived from the experimental data by three different methods, viz. by the Smith (4), Halverstadt–Kumler (5), and Looyenga (6) method, respectively. The reason for employing three different treatments of the experimental data was twofold: (*a*) to compare the methods of Smith and Halverstadt–Kumler, and (*b*) to correct the dipole moments for the solvent effect (method of Looyenga). In the latter two methods LeFevre's (7) bond electronic polarization was used to estimate the magnitude of the electronic polarization. From Table II it is apparent that the methods of Smith and Halverstadt–Kumler yield approximately the same dipole moments within the estimated experimental error of ± 0.1 D. The corrected dipole moment is, as expected (2), several tenths of a debye unit higher than the corresponding solution value. The following comments about the relative magnitudes of the molecular dipole moments of the ortho-, meta-, and para-fluorostyrene molecules may be in order. The smaller value of the dipole moment resulting from placing the fluorine atom in the

TABLE I

Physical properties of fluorostyrene in benzene solutions at 25 °C

$W \times 10^3$	ε	n	d
	Meta-fluorostyrene		
1.055	2.2749	1.4979	0.8738
3.026	2.2787	1.4979	0.8739
4.350	2.2814	1.4979	0.8742
5.759	2.2840	1.4979	0.8743
8.019	2.2893	1.4979	0.8745
	Ortho-fluorostyrene		
1.119	2.2744	1.4978	0.8738
2.505	2.2769	1.4979	0.8740
4.550	2.2806	1.4979	0.8742
5.714	2.2816	1.4980	0.8744
7.492	2.2858	1.4980	0.8746
	Para-fluorostyrene		
1.281	2.2746	1.4978	0.8739
2.379	2.2764	1.4979	0.8740
4.265	2.2795	1.4980	0.8742
6.836	2.2837	1.4980	0.8745
7.525	2.2849	1.4980	0.8746
	Penta-fluorostyrene		
1.120	2.2743	1.4977	0.8739
2.790	2.2769	1.4976	0.8745
4.251	2.2790	1.4975	0.8749
6.270	2.2822	1.4974	0.8757
7.629	2.2843	1.4973	0.8761

NOTE: W, weight fraction; ε, dielectric constant; n, refractive index; d, density.

TABLE II

Dipole moments (in debye units) derived by different methods

	Smith	Halverstadt–Kumler	Looyenga
Ortho-fluorostyrene	1.37	1.43	1.61
Meta-fluorostyrene	1.51	1.49	1.69
Para-fluorostyrene	1.31	1.36	1.57
Penta-fluorostyrene	1.80	1.78	1.93

para position in the benzene ring is somewhat surprising. For in the case of the ortho-, and para-chlorotoluenes (8) the situation is just the reverse, i.e. the dipole moment of the para isomer is larger, 1.94 D, than that of the ortho isomer, 1.43 D. The fact that the para-fluorostyrene has the smallest dipole moment would suggest that the fluorine atom is a better electron donor than the vinyl group. This conclusion is corroborated by the fact that the dipole moment of the penta-fluorostyrene molecule is significantly larger than the dipole moment of any of the three mono-fluorostyrene molecules. In terms of a simple vector model one would have expected, on account of the symmetrical positions of the two ortho and two meta fluorine atoms in the penta-fluorostyrene molecule, that its dipole moment would be of the same magnitude as that of the para-fluorostyrene molecule. The fact that the dipole moment of the penta-fluorostyrene molecule is larger suggests strongly that some electron transfer from the fluorine atoms into the benzene ring does occur.

Acknowledgments

We thank Dr. T. Schaefer for helpful discussions. We also thank Dr. H. Hutton for suggesting the present problem. The financial assistance of the National Research Council of Canada is deeply appreciated.

1. T. SCHAEFER. Private communication.
2. E. BOCK and E. F. DOJACK. Can. J. Chem. **45**, 1097 (1967).
3. E. BOCK and D. IWACHA. Can. J. Chem. In press.
4. J. W. SMITH. Trans. Faraday Soc. **46**, 394 (1950).
5. I. F. HALVERSTADT and W. D. KUMLER. J. Am. Chem. Soc. **64**, 2988 (1942).
6. H. LOOYENGA. Mol. Phys. **9**, 501 (1965).
7. R. J. W. LEFEVRE and K. D. STEEL. Chem. Ind. London, **1961**, 670.
8. L. TIGANIK. Z. Physik. Chem. Leipzig, **13**, 425 (1931).

Isomerization of nitrito- to nitro-pentakis(methylamine)cobalt(III) cation

M. PARRIS AND L. MAJID

Chemistry Department, Carleton University, Ottawa, Ontario

Received April 5, 1968

The preparations of these two linkage isomers are described. In aqueous solution the isomerization of nitrito to nitro is very similar to that for the parent pentaamine while in the solid phase it is retarded.

Canadian Journal of Chemistry, 46, 2962 (1968)

It has been concluded (1) that the isomerizations of nitrito- to nitro-pentaamminecobalt(III) and of *cis*-nitritonitro- to *cis*-dinitro-bis(ethylenediamine)cobalt(III) are intramolecular rearrangements, there being no accompanying ^{18}O exchange between free nitrite ion or solvent water

Can. J. Chem. Downloaded from www.nrcresearchpress.com by 210.87.254.6 on 09/05/12
For personal use only.

TABLE I

Physical properties of fluorostyrene in benzene solutions at 25 °C

$W \times 10^3$	ε	n	d
	Meta-fluorostyrene		
1.055	2.2749	1.4979	0.8738
3.026	2.2787	1.4979	0.8739
4.350	2.2814	1.4979	0.8742
5.759	2.2840	1.4979	0.8743
8.019	2.2893	1.4979	0.8745
	Ortho-fluorostyrene		
1.119	2.2744	1.4978	0.8738
2.505	2.2769	1.4979	0.8740
4.550	2.2806	1.4979	0.8742
5.714	2.2816	1.4980	0.8744
7.492	2.2858	1.4980	0.8746
	Para-fluorostyrene		
1.281	2.2746	1.4978	0.8739
2.379	2.2764	1.4979	0.8740
4.265	2.2795	1.4980	0.8742
6.836	2.2837	1.4980	0.8745
7.525	2.2849	1.4980	0.8746
	Penta-fluorostyrene		
1.120	2.2743	1.4977	0.8739
2.790	2.2769	1.4976	0.8745
4.251	2.2790	1.4975	0.8749
6.270	2.2822	1.4974	0.8757
7.629	2.2843	1.4973	0.8761

NOTE: W, weight fraction; ε, dielectric constant; n, refractive index; d, density.

TABLE II

Dipole moments (in debye units) derived by different methods

	Smith	Halverstadt–Kumler	Looyenga
Ortho-fluorostyrene	1.37	1.43	1.61
Meta-fluorostyrene	1.51	1.49	1.69
Para-fluorostyrene	1.31	1.36	1.57
Penta-fluorostyrene	1.80	1.78	1.93

para position in the benzene ring is somewhat surprising. For in the case of the ortho-, and para-chlorotoluenes (8) the situation is just the reverse, i.e. the dipole moment of the para isomer is larger, 1.94 D, than that of the ortho isomer, 1.43 D. The fact that the para-fluorostyrene has the smallest dipole moment would suggest that the fluorine atom is a better electron donor than the vinyl group. This conclusion is corroborated by the fact that the dipole moment of the penta-fluorostyrene molecule is significantly larger than the dipole moment of any of the three mono-fluorostyrene molecules. In terms of a simple vector model one would have expected, on account of the symmetrical positions of the two ortho and two meta fluorine atoms in the penta-fluorostyrene molecule, that its dipole moment would be of the same magnitude as that of the para-fluorostyrene molecule. The fact that the dipole moment of the penta-fluorostyrene molecule is larger suggests strongly that some electron transfer from the fluorine atoms into the benzene ring does occur.

Acknowledgments

We thank Dr. T. Schaefer for helpful discussions. We also thank Dr. H. Hutton for suggesting the present problem. The financial assistance of the National Research Council of Canada is deeply appreciated.

1. T. SCHAEFER. Private communication.
2. E. BOCK and E. F. DOJACK. Can. J. Chem. **45**, 1097 (1967).
3. E. BOCK and D. IWACHA. Can. J. Chem. In press.
4. J. W. SMITH. Trans. Faraday Soc. **46**, 394 (1950).
5. I. F. HALVERSTADT and W. D. KUMLER. J. Am. Chem. Soc. **64**, 2988 (1942).
6. H. LOOYENGA. Mol. Phys. **9**, 501 (1965).
7. R. J. W. LEFEVRE and K. D. STEEL. Chem. Ind. London, **1961**, 670.
8. L. TIGANIK. Z. Physik. Chem. Leipzig, **13**, 425 (1931).

Isomerization of nitrito- to nitro-pentakis(methylamine)cobalt(III) cation

M. PARRIS AND L. MAJID

Chemistry Department, Carleton University, Ottawa, Ontario

Received April 5, 1968

The preparations of these two linkage isomers are described. In aqueous solution the isomerization of nitrito to nitro is very similar to that for the parent pentaamine while in the solid phase it is retarded.

Canadian Journal of Chemistry, 46, 2962 (1968)

It has been concluded (1) that the isomerizations of nitrito- to nitro-pentaamminecobalt(III) and of *cis*-nitritonitro- to *cis*-dinitro-bis(ethylenediamine)cobalt(III) are intramolecular rearrangements, there being no accompanying ^{18}O exchange between free nitrite ion or solvent water

Can. J. Chem. Downloaded from www.nrcresearchpress.com by 210.87.254.40 on 09/05/12
For personal use only.

Can. J. Chem. Downloaded from www.nrcresearchpress.com by 210.87.254.40 on 09/05/12
For personal use only.

and the nitrite ligand which is coordinated. The isomerizing ligand remains at all times in the inner sphere of the complex, at least when the reaction occurs under non acid-retarded conditions. No racemization of the *cis*-nitritonitrobis(ethylenediamine)cobalt(III) occurs, but instead a mutarotation at the same rate as the isomerization does occur (2), again suggesting that no reduction of the cobalt inner coordination sphere takes place and that the intermediate is effectively heptacoordinated. Indeed, there is available a vacant antibonding π-orbital on N which, accepting d_ε electrons of Co(III), might aid such an intramolecular process in the nitrito to nitro change. Increased steric hindrance accordingly should decrease the isomerization rate and perhaps also change the equilibrium in favor of the nitrito isomer (3).

We report here the preparation of the linkage isomers nitrito- and nitro-pentakis(methylamine)cobalt(III) dichlorides and some kinetic measurements for the nitrito to nitro isomerization in the solid and in aqueous solution. The reaction appears in no way different from the corresponding pentaamminecobalt(III) isomerization.

Experimental Section

Preparation of Compounds

Methods were analogous to those used for the corresponding pentaammines (4).

$[Co(CH_3NH_2)_5NO_2]Cl_2$

A solution containing 2 g $[Co(CH_3NH_2)_5Cl]Cl_2$ (5) in 11 ml 6% aqueous methylamine was made weakly acidic (pH 4.0 $\pm$ 0.5) with HCl. Sodium nitrite (2.5 g) was added and the solution warmed to dissolve an initial red precipitate. Upon cooling, yellow crystals formed which were washed with 6 *N* HCl, then washed with alcohol, and then dried in vacuum for 10 h.

Anal. Calcd. for $C_5H_{25}Cl_2CoN_6O_2$: C, 18.1; H, 7.6; N, 25.4. Found: C, 18.3; H, 7.5; N, 25.5.

$[Co(CH_3NH_2)_5ONO]Cl_2$

The above solution of $[Co(CH_3NH_2)_5Cl]Cl_2$ in aqueous methylamine was neutralized (pH 7.0 $\pm$ 0.5) with dilute HCl, 4 g sodium nitrite dissolved therein, and then 4 ml 6 *N* HCl added. A red precipitate formed which was allowed to stand for 6 h at 5 °C, then washed with water and then alcohol, and then dried in vacuum for 10 h. Pink–red crystals were formed which slowly became orange–yellow upon standing at room temperature, but were indefinitely stable when stored at −10 °C.

Anal. Found: C, 18.1; H, 7.5; N, 25.3.

The corresponding deuterio compounds, $[Co(CH_3ND_2)_5NO_2]Cl_2$ and $[Co(CH_3ND_2)_5ONO]Cl_2$, were prepared by dissolution in D_2O followed by evaporation in vacuum. These were used only in the interpretation of infrared spectra.

Rates of Isomerization

The rearrangement of the nitrito dichloride into its nitro isomer was studied both in the solid and in the solution phase.

The Solid Phase Reaction

The changes in infrared absorption in the 1600 to 1300 cm^{-1} range, in particular the disappearance of the nitrito band at 1474 cm^{-1} and the appearance of the nitro band at 1414 cm^{-1}, were followed using Florolube mulls supported on NaCl plates held in a thermostated cell-holder (6). Infrared spectra were obtained using a Perkin–Elmer 225 grating spectrophotometer. First-order rate constants were obtained from linear plots of ln ($\pm$ ln $T_{\nu,\infty}$ $\mp$ ln $T_{\nu,t}$) versus t, where $T_{\nu,\infty}$ and $T_{\nu,t}$ are the measured transmittances for frequency ν at 'infinite' time and at time t respectively.

The Solution Reaction

The change from the pink nitrito to the yellow nitro compound was followed spectrophotometrically in the visible region. Absorption bands at 510 and 340 mμ decreased while absorption bands at 478 and 337 mμ increased, isosbestic points being discovered at 505 and 428 mμ. The spectrophotometer cell was used as reaction vessel in the thermostated cell compartment of a Cary model 14 spectrophotometer, and rate constants were obtained from a conventional Powell plot.

The Nitrito–Nitro Isomerization

Principally, evidence for this derives from the absorption spectra of the two compounds. The nitrite ion has three infrared active vibrations: ν_{as} at 1334 cm^{-1}, ν_s at 1250 cm^{-1}, and δ at 830 cm^{-1} (7). Upon N-coordination, ν_{as} rises to about 1470 cm^{-1} but ν_s falls to about 1050 cm^{-1} (8). Since the nitrito ligand is much lower in the spectrochemical series than is nitro, which is attributable to the greater π-accepting capacity of the latter (9), the dd spectra of nitro complexes occur at longer wavelengths. Table I lists pertinent spectral data for the two pentakis(methylamine)cobalt(III) and the two pentaamminecobalt(III) isomers. Assignments have been made by comparison with the deuterated and with the corresponding chloro and bromo complexes.

Their visible and infrared spectra, then, show the red isomer to be the nitrito complex and the yellow isomer to be the nitro complex. O-nitrosation of the aquo complex is indicated by the method of preparation of the red isomer, which is analogous to that proposed for the pentaammine, that is, formation *without* Co—O bond-breaking.

The reaction rates presented the same features as those observed for the pentaamine, namely a faster rate in aqueous solution than in the solid, together with some retardation by strong acids. Tables II and III contain kinetic data for the isomerizations. The rates are practically identical for

TABLE I

Some spectral data for nitrito- and nitro-pentakis(methylamine)cobalt(III) dichlorides

Compound	λ_{max} (mμ)	Log ε	ν_{as} (cm^{-1})	ν_s (cm^{-1})	δ (cm^{-1})
$Co(MeNH_2)_5ONO^{2+}$	510[a]	1.99			
	340	2.50	1474	1032	—
	229	4.56			
$Co(NH_3)_5ONO^{2+}$	491[b]	1.86	1460[c]	1065	—
	362	2.44			
$Co(MeNH_2)_5NO_2^{2+}$	478[a]	2.07	1404	1324	825
	337	3.34			
	228, 240 sh	4.30			
$Co(NH_3)_5NO_2^{2+}$	458[b]	2.00	1430[c]	1315	825
	325	3.22			
	239	4.14			

[a]0.01 *M*; 0.01 *N* in $HClO_4$.
[b]M. Linhard, H. Siebert, and M. Weigel (10).
[c]R. B. Penland, T. J. Lane, and J. V. Quagliano (11).

TABLE II

Isomerization of $[Co(CH_3NH_2)_5ONO]Cl_2$ in the solid phase (Florolube mull)[a]

Temperature (°C)	$k_1 \times 10^5$ (s^{-1})[b]
90	43 (2)
84.5	27 (2)
75.0	7.8 (0.3)
72.0	6.1 (0.3)
66.0	2.7 (0.2)

[a]$k_1 = 7.41 \times 10^{13}$ exp $[(-28500 \pm 1500)/RT]$.
[b]In-run standard deviations in parentheses.

TABLE III

Isomerization of $[Co(CH_3NH_2)_5ONO]Cl_2$ in aqueous solution (Co = 0.001 *M*, 0.01 *N* $HClO_4$)[a]

Temperature (°C)	$k_1 \times 10^4$ (s^{-1})[b]
57.0	10.7 (0.1)
52.9	7.85 (0.05)
45.4	3.25 (0.05)
40.9	2.25 (0.05)
32.8	0.90 (0.04)

[a]$k_1 = 5.75 \times 10^{10}$ exp $[(-20700 \pm 1000)/RT]$.
[b]In-run standard deviations in parentheses.

$Co(CH_3NH_2)_5ONO^{2+}$ and $Co(NH_3)_5ONO^{2+}$ solutions, although the aquation of $Co(CH_3NH_2)_5Cl^{2+}$ is faster than that of $Co(NH_3)_5Cl^{2+}$ (5).

It appears that there is little steric influence upon the isomerization in aqueous solution. Isomerization in the solid is presumably an intramolecular process but here steric factors will have more significance than in the solution. This is in accordance with the markedly higher activation enthalpy for the methylamine compound.

Partial financial support by the National Research Council of Canada is gratefully acknowledged.

1. R. K. Murmann and H. Taube. J. Am. Chem. Soc. **78**, 4886 (1956).
2. R. K. Murmann. J. Am. Chem. Soc. **77**, 5190 (1955).
3. D. M. L. Goodgame and M. A. Hitchman. Inorg. Chem. **3**, 1389 (1964).
4. R. G. Pearson, P. M. Henry, J. C. Bergmann, and F. Basolo. J. Am. Chem. Soc. **76**, 5920 (1954).
5. (*a*) M. Parris. J. Chem. Soc. A, 583 (1967). (*b*) S. C. Chan and K. Y. Hui. Australian J. Chem. **20**, 2529 (1967).
6. S. T. Zenchelsky and J. S. Showell. Anal. Chem. **29**, 167 (1957).
7. F. A. Miller and C. H. Wilkins. Anal. Chem. **24**, 1253 (1952).
8. K. Nakamoto, J. Fujita, and H. Murata. J. Am. Chem. Soc. **80**, 4817 (1958).
9. J. L. Burmeister. Coord. Chem. Rev. **1**, 205 (1966).
10. M. Linhard, H. Siebert, and M. Weigel. Z. Anorg. Allgem. Chem. **278**, 287 (1955).
11. R. B. Penland, T. J. Lane, and J. V. Quagliano. J. Am. Chem. Soc. **78**, 887 (1956).

Can. J. Chem. Downloaded from www.nrcresearchpress.com by 210.87.254.40 on 09/05/12
For personal use only.

Determination of rhenium:chlorine ratios in complexes by neutron activation

W. D. COURRIER, A. GUEST, C. J. L. LOCK, AND R. H. TOMLINSON
Department of Chemistry, McMaster University, Hamilton, Ontario

Received March 21, 1968

A method is described for the simultaneous determination of rhenium and chlorine in complex compounds. By determining atom ratios, it is unnecessary to weigh samples. The advantages of this method when applied to air-unstable compounds are described.

Canadian Journal of Chemistry, 46, 2965 (1968)

Can. J. Chem. Downloaded from www.nrcresearchpress.com by 210.87.254.5 on 09/05/12
For personal use only.

Introduction

Numerous problems have been encountered in studies of complex halides of rhenium in obtaining accurate analyses for rhenium and chlorine. Most of the compounds of interest are extremely sensitive to moisture and/or oxygen. They are difficult to handle even in a good dry-box, and it is not easy to weigh samples accurately because of decomposition. Analysis for rhenium has proved to be difficult. In our hands the standard methods for the analysis for rhenium, either spectrophotometrically using the α-furildioxime complex (1) or gravimetrically using tetraphenylarsonium perrhenate (2) or nitron perrhenate (3), have proved unreliable for these samples. This is undoubtedly because the decomposition of complexes to give chloride ion and perrhenate ion is incomplete because ions such as $ReCl_6^{2-}$ and $Re_3Cl_{12}^{3-}$ are formed (4).

Rhenium (6–8) and chlorine (9) have been determined previously by neutron activation analysis. Although neutron activation analysis is a widely used technique for determination of absolute percentages of elements, as far as we know the determination of stoichiometries or atom ratios directly has not been applied to any compound. The neutron activation analysis method described here could give absolute amounts of rhenium and chlorine, but this is not the prime purpose of the experiments. The novelty of the method lies in the determination of rhenium–chlorine atom ratios or stoichiometries by neutron activation without even weighing the sample.

Experiments

Neutron activation was carried out in the rabbit system of the McMaster University swimming pool reactor which has an available thermal neutron flux of about 10^{13} neutrons $cm^{-2}\,s^{-1}$ at a reactor power of 2 MW.

Irradiations were carried out in two-fifths dram polyethylene phials which are obtainable from Olympic Plastics, Los Angeles, California. These were heat sealed after filling to prevent leakage.

The γ-ray spectrum was obtained using a 3 in. thallium-doped sodium iodide crystal and a 400 channel analyzer (Victoreen Instrument Co., Tullamore Division, Model PIP 400). Standard solutions were prepared from rhenium metal, which was dissolved in 15% hydrogen peroxide or dilute nitric acid. Ammonium chloride was added and the solution was diluted to a known composition containing about 1 mg ml^{-1} of rhenium and 1.5 mg ml^{-1} of chloride ion.

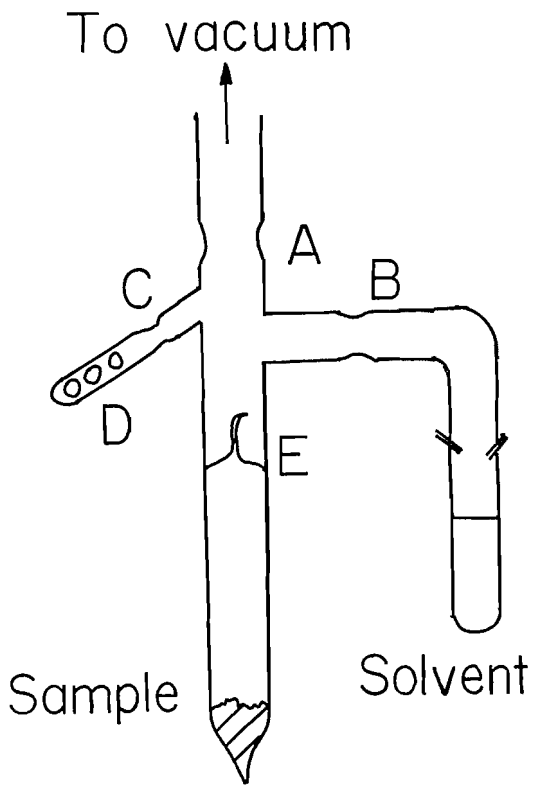

FIG. 1. Apparatus used in preparation of solutions.

Can. J. Chem. Downloaded from www.nrcresearchpress.com by 210.87.254.5 on 09/05/12
For personal use only.

Solutions of samples of air-unstable compounds were prepared in the apparatus shown in Fig. 1. A tube fitted with a break seal and containing the sample sealed under vacuum was joined to the rest of the vacuum apparatus. The rest of the apparatus was pumped down to $< 10^{-3}$ mm mercury and the solvent was frozen. The apparatus was closed under vacuum by sealing at A and both the sample and solvent were cooled in liquid nitrogen. The iron balls D in the side arm were lifted by a magnet and dropped to break the break seal E. They were then transferred back to the side arm which was sealed off at C. The solvent was poured onto the sample and the apparatus shaken and warmed, if necessary, until all the sample had dissolved and was mixed thoroughly. (Care was taken during this step if gases were evolved, such as could occur if 30% hydrogen peroxide was used as the solvent, as dangerous pressures could build up in the apparatus.) The apparatus was then refrozen in liquid nitrogen and was opened by scratching the glass at B and breaking it. The mixture was allowed to warm up and the sample poured into a flask.

A typical experiment was conducted as follows. The sample (about 10 mg) was dissolved in the minimum amount of a suitable solvent, which does not contain any easily activated nuclei such as potassium or sodium. (Suitable solvents are those which contain only carbon, nitrogen, oxygen, or hydrogen, so organic solvents are especially suitable as are water, nitric acid, and hydrogen peroxide. Hydrogen peroxide was used extensively in this work since it readily oxidized any insoluble lower oxides formed on hydrolysis to the soluble perrhenate ion.) One milliliter of the resulting solution was taken for each irradiation and transferred to a polythene capsule. The concentration was arranged so that about 1 mg of rhenium was present in the sample. A similar amount of the standard solution was taken. The sample and the standard were packed axially in a polythene rabbit container to minimize flux variation between sample and standard and irradiated for 45 s. The standard and sample were each counted for one minute as soon as possible after the irradiation, the counts being corrected for background and contamination by doing a 1 min count of capsules containing only the solvent which had been irradiated for a similar time. The counts were plotted and the Compton background subtracted and a half-life correction applied for decay during the interval between counting the sample and standard. The counts in the three channels on either side of the ^{38}Cl peak at 2.15 MeV (10) were used in the comparison of counts on sample and standard. The rhenium was determined by counting the sample about 2 h after the irradiation when the bremsstrahlung background had almost disappeared. The 0.155 MeV peak of ^{188}Re (10) was used for comparison in a manner similar to that for chlorine. The Re:Cl atom ratio was calculated using the expression,

$$\left(\frac{\text{No. of rhenium atoms}}{\text{No. of chlorine atoms}}\right)_{\text{sample}} = \frac{A_{Re}}{B_{Re}} \cdot \frac{B_{Cl}}{A_{Cl}} \cdot \frac{[Re]}{[Cl]} \cdot \frac{35.46}{186.2}$$

where A_{Re} and A_{Cl} are the counts min^{-1} of ^{188}Re and ^{38}Cl given by the sample determined as described above and B_{Re} and B_{Cl} are the counts min^{-1} of ^{188}Re and ^{38}Cl given by the standard. [Re] and [Cl] are the concentrations of rhenium and chlorine respectively in the standard, both being in the same units. It should be emphasized that unless an absolute percentage of rhenium and chlorine in the sample was required, no accurate measurements of amounts were necessary at any stage, except for the initial preparation of the standard.

Discussion

Both rhenium and chlorine have two naturally occurring isotopes which can be activated by neutron capture. The relevant nuclear data are given in Table I.

It can be seen that either rhenium isotope will give an appreciable amount of activity on short irradiation, but because of the long half-life of ^{36}Cl, of the chlorine isotopes only ^{37}Cl will give significant amounts of activity on short irradiations. Several γ-ray peaks for each of the active isotopes ^{186}Re, ^{188}Re, and ^{38}Cl appeared to be useful for counting, but the ones selected were 2.16 MeV for ^{38}Cl and 0.155 MeV for ^{188}Re as they were almost completely free from interference by the other isotopes.

TABLE I

Nuclear data for rhenium and chlorine

Natural isotope	Abundance (%) (10)	Thermal neutron capture cross section (barns) (5)	Half-life of activated species (10)
^{185}Re	37.1	~104	92.8 h
^{187}Re	62.9	66	16.9 h
^{35}Cl	75.5	30	4×10^5 year
^{37}Cl	24.5	5?	38 min

Initial irradiation experiments were done on solid samples but agreement with the expected results was very poor. Because of the high thermal neutron capture cross section of rhenium, there will be a significant number of neutrons captured and a consequent "neutron flux depression" or "self-shadowing" (12) in the sample. This would not be a problem in determining atom ratios (although it would affect absolute percentage determination) if the activation cross sections of rhenium and chlorine behaved in a similar manner as a function of neutron energy. Unfortunately, this is not so (5). Because of this, all analyses were done in solution where the presence of a non-absorbing diluent (the solvent) obviated the flux depression.

The results of this method of analysis applied to solutions are presented in Table II. The first four compounds were used to test the reliability

TABLE II

Activations analysis of rhenium halide complexes

Compound	Re (%)		Cl (%)		Re:Cl (atoms)	Error 3σ	No. of determinations
	Theor.	Found	Theor.	Found			
$(ReCl_5)_2$	51.2	51.6	48.8	49.7	1:4.98	±.06	12
$(ReCl_3)_3$	63.6	61.5	36.4	36.1	1:3.09	±.12	10
$(C_5H_5N)_2ReOCl_3$					1:3.01	±.14	5
$(NH_4)_2ReCl_6$	42.8	43.6	48.9	49.5	1:5.91	±.15	9
$ReOCl_4$*	54.1		41.4		1:3.92	±.07	18
$ReOCl_4 \cdot POCl_3$	37.5	38.7	49.9	52.2	1:7.08	±.35	6

*In the case of $ReOCl_4$, it was possible to analyze this compound for rhenium and chlorine by conventional methods after hydrolysis. Found: Re, 54.1, 54.4%; Cl, 41.3, 41.1%.

of the method. $(ReCl_3)_3$, $(NH_4)_2ReCl_6$, and $(C_5H_5N)_2$ $ReOCl_3$ are all air stable and $(ReCl_5)_2$ is an air-sensitive compound. The observed absolute percentage of rhenium and chlorine are compared with theoretical values, and the ratio of the number of atoms of rhenium to the number of atoms of chlorine is also given. The three sigma error value refers to the uncertainty in the number of atoms of chlorine, assuming that the number of rhenium atoms is exactly one. At least three independently prepared and purified samples of each compound were analyzed and each determination was done in duplicate. The total number of duplicate analyses is given in column 8. It will be seen that the method will give atom ratios with an accuracy of about 5%, and this error is low enough to enable atom ratios to be determined for stoichiometric compounds. The method is not precise enough to allow minor deviations from stoichiometry to be determined such as have been observed for $(ReCl_3)_3$ where stoichiometries can vary from $ReCl_{3.00}$ to $ReCl_{3.15}$ (11).

The two final analyses are for typical air-sensitive compounds which were analyzed by this method and whose composition has been confirmed by other physical techniques. It can be seen that excellent agreement is obtained. In the case of $ReOCl_4$ it was possible to obtain a quantitative decomposition to chloride and perrhenate ions and the analysis was confirmed by classical gravimetric methods, the perrhenate being precipitated as tetraphenylarsonium perrhenate (2) and the chloride as silver chloride (13). Air-sensitive samples were weighed on a balance in a Dri-Lab HE-43 vacuum-atmosphere dry box (Vacuum Atmospheres Corp., Los Angeles, California) which was filled with dry nitrogen.

We conclude that this is a very satisfactory method of determining the stoichiometry of rhenium–chlorine containing compounds when interfering elements are absent. Interference is only caused by elements which on neutron irradiation give appreciable amounts of γ-activity of energy close to 0.155 and 2.15 MeV. Potentially, such a method is applicable to any compounds which contain elements which can be activated. It is not even necessary to determine both elements in the same irradiation, but in this case greater care has to be taken that both sample and standard are irradiated in exactly the same neutron flux. If both elements can be determined in one irradiation as described here, even variations in neutron flux between sample and standard do not matter, since only the ratio of rhenium and chlorine activities is important, and for short irradiations this is independent of the neutron flux. Because it is unnecessary to weigh the sample it should find wide application in the analysis of very unstable compounds.

We wish to thank the National Research Council of Canada for supporting this work and granting one of us (A. G.) a Graduate Studentship. We also wish to thank the International Nickel Company for a Fellowship (W. D. C.).

1. V. W. Meloche, R. L. Martin, and W. H. Webb. Anal. Chem. **29**, 527 (1957).
2. H. H. Willard and C. C. Smith. Ind. Eng. Chem. Anal. Ed. **11**, 305 (1939).
3. W. Geilmann and A. Voigt. Z. Anorg. Allgem. Chem. **193**, 311 (1930).
4. F. A. Cotton and R. A. Walton. Inorg. Chem. **5**, 1802 (1966).
5. D. J. Hughes, B. A. Magurno, and M. K. Brussel. Neutron cross sections. U.S. Atomic Energy commission BNL-325, 2nd ed. 1958. (See suppl. BNL 325, 2nd ed. p. 102.)
6. E. D. Goldberg and H. Brown. Anal. Chem. **22**, 308 (1950).
7. D. F. C. Morris and F. W. Fifield. Talanta, **8**, 612 (1961).

Can. J. Chem. Downloaded from www.nrcresearchpress.com by 210.87.254.5 on 09/05/12
For personal use only.

8. W. HERR and E. MERZ. Z. Naturforsch. **10a**, 613 (1955).
9. W. F. LYON. Guide to activation analysis. D. Van Nostrand Co., Inc., Princeton. 1964. Appendix A, p. 143 and references therein.
10. D. STROMINGER, J. M. HOLLANDER, and G. T. SEABORG. Rev. Mod. Phys. **30**, 585 (1958).
11. F. TAHA, C. J. L. LOCK, and G. WILKINSON. Unpublished work.
12. W. F. LYON. Guide to activation analysis. D. Van Nostrand Co., Inc., Princeton. 1964. Appendix A. p. 117–121.
13. A. I. VOGEL. A text book of analytative inorganic analysis. 3rd ed. Longmans, Green & Co., Ltd., London. 1961. p. 460.

Melting points of inorganic fluorides[1]

H. KOJIMA,[2] S. G. WHITEWAY, AND C. R. MASSON
Atlantic Regional Laboratory, National Research Council of Canada, Halifax, Nova Scotia

Received March 19, 1968

An apparatus is described for purifying inorganic fluorides by passing anhydrous HF through the melts. Melting points of nine fluorides purified in this way were raised and were sometimes significantly higher than the 'best' literature values.

Canadian Journal of Chemistry, **46**, 2968 (1968)

Introduction

Melting points (m.p.) of commercial inorganic fluorides of high purity, required for cryoscopic studies, often varied significantly. Similar variations are found in the literature, see for example ref. 1. Our observations and reports in the literature suggest that these variations are caused mainly by absorbed water due to an oxide formed on heating:

$$CaF_2 + H_2O \rightarrow CaO + 2HF$$

The fluorides of the alkali metals, particularly K, Rb, and Cs, are hygroscopic. Hydrolysis is troublesome in the preparation of artificial fluorite crystals (2).

Oven-drying usually does not remove the bound water effectively and can affect the purity adversely. Thus when NaF (Fisher, C.P. grade, m.p. 983°) was heated at 140° for two days the m.p. decreased to 970°. Water is not removed quantitatively from powdered CaF_2 (2) by heating at relatively low temperature under reduced pressure.

Contaminating oxides are removed, at least partially, by heating the fluorides in the presence of a second, more volatile fluoride which acts as an oxide 'scavenger'. Thus Stockbarger (2, 3) successfully used PbF_2 to purify CaF_2:

$$CaO + PbF_2 \rightarrow PbO + CaF_2$$

The PbO and excess PbF_2 evaporate from the melt. Haven (4) used NH_4F in making single crystals of LiF and Cantor (20) purified MgF_2 and SrF_2 by treating with $NH_4F.HF$.

In our experience repeated treatment with $NH_4F.HF$ appears necessary in purifying NaF and CaF_2. Thus when NaF, m.p. 970°, was heated in dry argon with 8% of $NH_4F.HF$ its m.p. increased to 979°; further treatment of the product raised the m p. to 991°. The 'best' literature value is 995°.

Anhydrous HF was the deoxidizing agent in this work. This reagent has been used (5–10) for preparing single crystals of high purity, but melting points were of secondary interest. Anhydrous HF has also been used to prepare rare-earth fluorides from the oxides (11) and to purify molten fluorides used as solvent for UF_4 in molten-salt nuclear reactors (12). The present apparatus differs from previous designs in the use of high-frequency induction for heating and optical pyrometry for measurement of temperatures. The apparatus is simple to construct and can be built from materials readily available in a laboratory equipped for high temperature studies.

Experimental

Apparatus

Figure 1 illustrates the apparatus. All parts exposed to HF at high temperatures were of high-purity graphite (Ultra Carbon Corp.). Other parts were of Teflon.

Crucible J, the top of which fitted loosely around the bottom of the inlet tube F, held the melt. Radial grooves cut in the base of the crucible (where it touched tube G)

[1]Issued as NRCC No. 10138.
[2]NRCC Postdoctorate Fellow, 1964–1966. Present address: Faculty of Engineering, Yamanashi University, Kofu-shi, Japan.

Can. J. Chem. Downloaded from www.nrcresearchpress.com by 210.87.254.5 on 09/05/12
For personal use only.

8. W. HERR and E. MERZ. Z. Naturforsch. **10a**, 613 (1955).
9. W. F. LYON. Guide to activation analysis. D. Van Nostrand Co., Inc., Princeton. 1964. Appendix A, p. 143 and references therein.
10. D. STROMINGER, J. M. HOLLANDER, and G. T. SEABORG. Rev. Mod. Phys. **30**, 585 (1958).
11. F. TAHA, C. J. L. LOCK, and G. WILKINSON. Unpublished work.
12. W. F. LYON. Guide to activation analysis. D. Van Nostrand Co., Inc., Princeton. 1964. Appendix A. p. 117–121.
13. A. I. VOGEL. A text book of analytative inorganic analysis. 3rd ed. Longmans, Green & Co., Ltd., London. 1961. p. 460.

Melting points of inorganic fluorides[1]

H. KOJIMA,[2] S. G. WHITEWAY, AND C. R. MASSON
Atlantic Regional Laboratory, National Research Council of Canada, Halifax, Nova Scotia

Received March 19, 1968

An apparatus is described for purifying inorganic fluorides by passing anhydrous HF through the melts. Melting points of nine fluorides purified in this way were raised and were sometimes significantly higher than the 'best' literature values.

Canadian Journal of Chemistry, **46**, 2968 (1968)

Introduction

Melting points (m.p.) of commercial inorganic fluorides of high purity, required for cryoscopic studies, often varied significantly. Similar variations are found in the literature, see for example ref. 1. Our observations and reports in the literature suggest that these variations are caused mainly by absorbed water due to an oxide formed on heating:

$$CaF_2 + H_2O \rightarrow CaO + 2HF$$

The fluorides of the alkali metals, particularly K, Rb, and Cs, are hygroscopic. Hydrolysis is troublesome in the preparation of artificial fluorite crystals (2).

Oven-drying usually does not remove the bound water effectively and can affect the purity adversely. Thus when NaF (Fisher, C.P. grade, m.p. 983°) was heated at 140° for two days the m.p. decreased to 970°. Water is not removed quantitatively from powdered CaF_2 (2) by heating at relatively low temperature under reduced pressure.

Contaminating oxides are removed, at least partially, by heating the fluorides in the presence of a second, more volatile fluoride which acts as an oxide 'scavenger'. Thus Stockbarger (2, 3) successfully used PbF_2 to purify CaF_2:

$$CaO + PbF_2 \rightarrow PbO + CaF_2$$

The PbO and excess PbF_2 evaporate from the melt. Haven (4) used NH_4F in making single crystals of LiF and Cantor (20) purified MgF_2 and SrF_2 by treating with $NH_4F.HF$.

In our experience repeated treatment with $NH_4F.HF$ appears necessary in purifying NaF and CaF_2. Thus when NaF, m.p. 970°, was heated in dry argon with 8% of $NH_4F.HF$ its m.p. increased to 979°; further treatment of the product raised the m p. to 991°. The 'best' literature value is 995°.

Anhydrous HF was the deoxidizing agent in this work. This reagent has been used (5–10) for preparing single crystals of high purity, but melting points were of secondary interest. Anhydrous HF has also been used to prepare rare-earth fluorides from the oxides (11) and to purify molten fluorides used as solvent for UF_4 in molten-salt nuclear reactors (12). The present apparatus differs from previous designs in the use of high-frequency induction for heating and optical pyrometry for measurement of temperatures. The apparatus is simple to construct and can be built from materials readily available in a laboratory equipped for high temperature studies.

Experimental

Apparatus

Figure 1 illustrates the apparatus. All parts exposed to HF at high temperatures were of high-purity graphite (Ultra Carbon Corp.). Other parts were of Teflon.

Crucible J, the top of which fitted loosely around the bottom of the inlet tube F, held the melt. Radial grooves cut in the base of the crucible (where it touched tube G)

[1]Issued as NRCC No. 10138.
[2]NRCC Postdoctorate Fellow, 1964–1966. Present address: Faculty of Engineering, Yamanashi University, Kofu-shi, Japan.

Can. J. Chem. Downloaded from www.nrcresearchpress.com by 210.87.254.6 on 09/05/12
For personal use only.

Can. J. Chem. Downloaded from www.nrcresearchpress.com by 210.87.254.6 on 09/05/12
For personal use only.

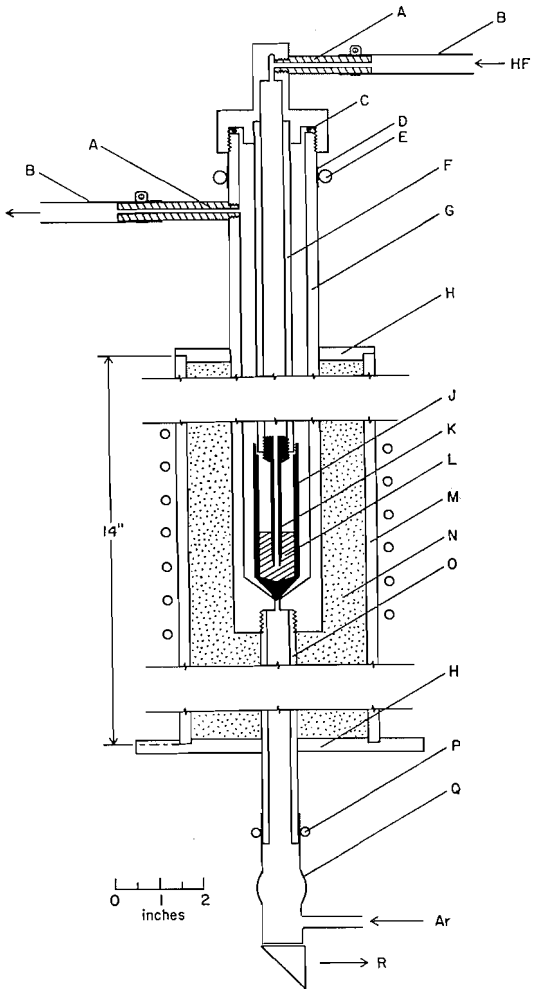

FIG. 1. Apparatus for purification of inorganic fluorides. AA, Teflon tubes; BB, Teflon tubing; C, Teflon O-ring; D, copper plating; E, copper cooling coil; F, inlet tube for HF, graphite; G, furnace tube, graphite; HH, transite; J, crucible, graphite; K, nozzle, graphite; L, molten fluoride; M, silica tube; N, lamp black insulating powder; O, inlet tube for Ar; P, copper cooling coil; Q, glass–metal seal; R, to optical pyrometer.

allowed free upward flow of argon. The top of tube F fitted tightly into the head of the assembly.

The lower end of tube O was copper-plated and soft-soldered to the metal–glass seal Q, and cooling coil P protected the seal. Hot water was passed through coil E to prevent condensation of water in the upper part of the furnace.

The central 6-in. portion of the furnace was heated by an induction generator of output 10 kVA and nominal frequency 400 kHz. Temperatures were measured by a disappearing-filament optical pyrometer focussed on the opening at the base of the crucible. The furnace was positioned below a vented hood which carried off the Ar–HF effluent.

The flow-rate of HF, controlled by a Monel valve, was monitored by bubbling it through mineral oil in a polythene trap. Hot water was circulated around the valve to prevent condensation of HF.

Materials

Commercial fluorides of high purity were used; the main impurities reported were chloride, oxide, sulfate, SiO_2, Fe, and Pb. Anhydrous HF (Matheson Co. Ltd.) was of reported purity 99.9%. Argon was dried by passage through magnesium perchlorate.

Determination of Melting Points

Melting points were determined in an atmosphere of dry argon by the method of thermal arrests with the apparatus described previously (13). Cooling rates were 1° to 10°/min, and were controlled linearly with time by a Honeywell 3-mode program controller and a saturable core reactor in series with the winding of the furnace. A graphite crucible held the fluorides, and a Pt / Pt – 13% Rh thermocouple, located in a well in the base of the crucible, measured the temperature of the melt. The electromotive force (e.m.f.) was recorded by a Westronics potentiometric recorder with a suppressed zero and a span of 2 mV. The recording unit was calibrated after each measurement with a Leeds and Northrup potentiometer. Periodic calibration of the measuring thermocouple was made against copper, m.p. 1083.3 °C, supplied by the U.S. National Bureau of Standards. We consider the melting points to be reliable to ±1°.

Results and Discussion

After the crucible (Fig. 1) had been charged with the powdered fluoride, the system was closed, the furnace flushed with dry argon at about 100 cc/s, and the temperature raised to 50–150° above the m.p. Hydrogen fluoride was passed through the melt at a rate of 1–2 cc/s. Faster rates sometimes caused ejection of fluoride from the crucible. Generally 2 to 4 h were required for complete purification. The system was then cooled to room temperature with both gases flowing. As the purified fluorides do not wet graphite, no interruption occurs in the flow of HF when the melt solidifies, and the nozzle can be removed without difficulty when the system is dismantled.

During the reaction water condenses in tubing B at the exit of the furnace, but this cannot be used to indicate the progress of purification as water appears also in the absence of fluoride at high temperatures. This may be due to a reaction of HF with CO contained in the graphite. Traces of a brownish oil with a pungent odor were detected in the exit tubing; it may be a polymer formed by the reaction

$$2n\mathrm{HF} + n\mathrm{CO} \rightarrow n\mathrm{H_2O} + \mathrm{C}_n\mathrm{F}_{2n}.$$

TABLE I

Melting points of inorganic fluorides

Fluoride	Source	Melting point (±1 °C) Before hydrofluorination	Melting point (±1 °C) After hydrofluorination	'Best' literature values	Reference
LiF	B.D.H.	843	845	845, 847	16, 17
NaF	Koch-Light	992	993	990, 995	18, 19–21
KF	B.D.H.	—	852	856, 858	22, 23
MgF_2	B.D.H.	1251	1256	1255, 1263	24, 25
MgF_2	Koch-Light	1252	1261		
CaF_2	B.D.H.	1410	1423	1418, 1419	25, 26
SrF_2	B.D.H.	1463	1473	1463	23
BaF_2	B.D.H.	1341	1355	1354	23
CdF_2	B.D.H.	1076	1078	1047, 1049, 1072	16, 27, 28

Less water appeared if the crucible was degassed before use by heating it *in vacuo* for approximately 6 h at 1400–1450° in a separate apparatus. This procedure also reduces the time required for purification.

Fluorides of high purity exhibit a crystal-like clarity when cleaved to expose a fresh surface; cloudiness or opacity generally indicates that purification is incomplete. In one experiment with CaF_2 in which the crucible was not degassed before use, the material adjacent to the graphite nozzle appeared to be of higher purity than that near the walls and this was confirmed by their m.p. Prolonged passage of HF, however, yielded a uniform product.

In determining the m.p., supercooling occurred with all purified samples and was sometimes a pronounced effect. With CaF_2 for example, supercooling by 60–70° was not uncommon. In general the higher the purity, as indicated by the m.p., the greater the degree of supercooling. The effect was used to advantage by allowing the temperature to 'line out' approximately 1° below the expected m.p. and seeding in the manner described previously (13). This ensures that temperature gradients are virtually absent when the m.p. is determined, thus allowing high precision.

Table I indicates the source of materials and their m.p. before and after purification. All results are the mean of at least three determinations.

The specimen of KF, as received, obviously contained some water and its m.p. was not determined. The m.p. after purification was 4–6° lower than the 'best' literature values. This may be due to impurities other than those removable by hydrofluorination; 0.5% Na was reported as one impurity in this material.

For all other fluorides the m.p. after purification were, within error, equal to or higher than the 'best' literature values. RbF and CsF were considered too hygroscopic to be transferred to the m.p. apparatus; it would be desirable to measure their m.p. in the apparatus used for hydrofluorination.

Of the impurities reported above, chloride and oxide would be removed as HCl and H_2O under the conditions employed, sulfate would be decomposed, and SiO_2 would be evolved as gaseous SiF_4. The fluorides of Fe and Pb are volatile at about 1300° and would distill from the higher-melting compounds.

An estimate of the purity with respect to the oxide can be obtained from the free energies of formation (14) of the fluorides from the corresponding oxides. Thus for CaF_2:

$$CaO + 2HF = CaF_2 + H_2O$$

The value of ΔG_0 for this reaction at 1450° is approximately -20 kcal so that the equilibrium constant K is of the order of 3×10^2. The mole fraction of CaO in the melt at equilibrium is

$$N_{CaO} = p_{H_2O}/K\gamma_{CaO}p_{HF}^2$$

where p_{H_2O} and p_{HF} are the partial pressures of H_2O and HF in the HF, and γ_{CaO} is the activity coefficient of CaO in liquid CaF_2. As shown elsewhere (15), γ_{CaO} is approximately 0.25 for this system; p_{HF} may be taken as 1 atm and, for 0.1% H_2O in the HF, p_{H_2O} is approximately 10^{-3} atm. Hence $N_{CaO} \approx 10^{-5}$, or 10 p.p.m. on a molar basis.

1. E. M. Levin, C. R. Robbins, and H. F. McMurdie. Phase diagrams for ceramists. American Ceramic Society, Inc., Columbus, Ohio. 1964.

Can. J. Chem. Downloaded from www.nrcresearchpress.com by 210.87.254.6 on 09/05/12
For personal use only.

2. D. C. STOCKBARGER. Discussions Faraday Soc. **5**, 294 (1949).
3. D. C. STOCKBARGER. J. Opt. Soc. Am. **39**, 731 (1949).
4. Y. HAVEN. Discussions Faraday Soc. **5**, 358 (1949).
5. H. GUGGENHEIM. J. Appl. Phys. **32**, 1820 (1961).
6. M. A. HILLER and O. M. STAFSUDD. J. Appl. Phys. **35**, 693 (1964).
7. F. WELLER and J. A. KUCZA. J. Appl. Phys. **35**, 1945 (1964).
8. S. LEGRAND and M. BINARD. Bull. Soc. Chim. France, 1900 (1964).
9. S. I. WARSHAW and R. E. JACKSON. Rev. Sci. Instr. **36**, 1774 (1965).
10. M. ROBINSON and D. M. CRIPE. J. Appl. Phys. **37**, 2072 (1966).
11. C. V. BANKS, O. N. CARLSON, A. H. DAANE, V. A. FASSEL, R. W. FISHER, E. H. OLSON, J. E. POWELL, and F. H. SPEDDING. USAEC Report IS-1. Ames Lab., Ames, Iowa. 1959.
12. A. L. MATHEWS and C. F. BAES, JR. ORNL Report TM-1129. 1965.
13. H. B. BELL and C. R. MASSON. J. Sci. Instr. **41**, 389 (1964).
14. A. GLASSNER. USAEC Report ANL-5750. U.S. Government Printing Office, Washington, D.C. 1957.
15. H. KOJIMA and C. R. MASSON. Unpublished results.
16. D. A. JONES and R. V. JONES. Proc. Phys. Soc. **79**, 351 (1962).
17. W. E. ROAKE. J. Electrochem. Soc. **104**, 662 (1957).
18. R. E. THOMA (*Editor*). ORNL Report 2548. 1959. p. 29.
19. J. F. EICHELBERGER, C. R. HUDGENS, L. V. JONES, G. PISH, T. B. RHINEHAMMER, P. A. TUCKER, and L. T. WITTENBERG. J. Am. Ceram. Soc. **46**, 279 (1963).
20. S. CANTOR. J. Phys. Chem. **65**, 2208 (1961).
21. M. A. BREDIG, J. W. JOHNSON, and W. T. SMITH, JR. J. Am. Chem. Soc. **77**, 307 (1955).
22. R. E. THOMA (*Editor*). ORNL Report 2548. 1959. p. 103.
23. B. PORTER and E. A. BROWN. J. Am. Ceram. Soc. **45**, 49 (1962).
24. A. DUNCANSON and R. W. H. STEVENSON. Proc. Phys. Soc. **72**, 1001 (1958).
25. B. F. NAYLOR. J. Am. Chem. Soc. **67**, 150 (1945).
26. J. MUKERJI. J. Am. Ceram. Soc. **48**, 210 (1965).
27. H. M. HAENDLER and W. J. BERNARD. J. Am. Chem. Soc. **63**, 5218 (1951).
28. M. RUBENSTEIN and E. BANKS. J. Electrochem. Soc. **106**, 404 (1959).

Can. J. Chem. Downloaded from www.nrcresearchpress.com by 210.87.254.6 on 09/05/12
For personal use only.

Can. J. Chem. Downloaded from www.nrcresearchpress.com by 210.87.254.40 on 09/05/12
For personal use only.

A series of stable platinum–acetylene complexes[1]

F. D. ROCHON AND T. THEOPHANIDES
Department of Chemistry, University of Montreal, Montreal 26, Quebec

Received June 6, 1968

The synthesis of a new series of platinum acetylenic complexes of the general formula $Pt(ac)_2$ are reported.

Canadian Journal of Chemistry, 46, 2973 (1968)

TABLE I

Analytical data and properties of the complexes $Pt(ac)_2$*

Compounds	Melting point (°C)	Calculated			Found		
		% C	% H	% Pt	% C	% H	% Pt
$Pt(ac^1)_2$	164–173 (decomp.)	44.85	6.78	36.46	44.65	6.85	36.24
$Pt(ac^2)_2$	186–192 (decomp.)	48.72	7.49	32.97	49.06	7.69	32.01
$Pt(ac^3)_2$	145	48.72	7.49	32.97	49.28	7.60	33.02
$Pt(ac^4)_2$	148	54.60	8.60	27.72	54.99	8.39	28.36
$Pt(ac^5)_2$	145	54.60	8.60	27.72	54.83	8.52	27.27
$Pt(ac^6)_2$	190–197 (decomp.)	52.53	6.93	30.50	52.46	6.99	31.27

*$ac^1 = C_2H_5-\underset{\underset{CH_3}{|}}{C}(OH)C\equiv C\underset{\underset{CH_3}{|}}{C}(OH)C_2H_5$, $ac^2 = (C_2H_5)_2C(OH)C\equiv CC(OH)(C_2H_5)_2$, $ac^3 = C_3H_7\underset{\underset{CH_3}{|}}{C}(OH)C\equiv C\underset{\underset{CH_3}{|}}{C}(OH)C_3H_7$,

$ac^4 = C_5H_9-\underset{\underset{CH_3}{|}}{C}(OH)C\equiv C\underset{\underset{CH_3}{|}}{C}(OH)C_5H_9$, $ac^5 = (C_3H_7)_2C(OH)C\equiv CC(OH)(C_3H_7)_2$, $ac^6 =$ 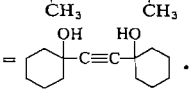 .

Complexes of unsaturated hydrocarbons with a transitional metal ion have been the subject of much study. The complexes in which an acetylene was coordinated to the platinum metal have been known for only 20 years. Gelmann and co-workers (1) have prepared the first complex of the platinum(II) ion with the acetylenic glycol $(CH_3)_2\ C(OH)C\equiv CC(OH)(CH_3)_2$. Bukhovets (2) later synthesized and characterized the analogous acetylenic complex of the Zeise's salts. Chatt and collaborators (3*a*, 3*c*) extended this series of complexes and studied them in a systematic way. Allen and Theophanides (4) later studied the hydrolysis constants and structural characteristics of some of these complexes. We now report the synthesis of a new series of platinum acetylenic complexes of the general formula $Pt(ac)_2$. The complexes are prepared by the reaction of the acetylenic derivative ($ac = R_2C(OH)C\equiv CC(OH)R_2$) in water–alcohol solution with potassium chloroplatinite. They are white and more stable in air than the well-known olefin or acetylene complexes of platinum(II). A reducing agent was not necessary for their preparation.

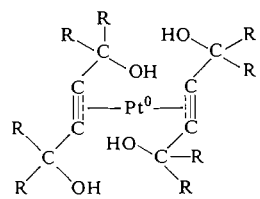

1

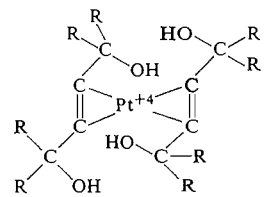

2

The complexes are best formulated as **1**, in which the two acetylenes are merely acting as donors with possible back donation from the metal to the ligand, in the same way as in the well-known olefin and other acetylene–metal complexes (3*b*).

A four-coordinated planar structure **2** is the

[1]A brief report of this work was presented at the ACFAS Conference, November 1967, in Sherbrooke, Quebec.

other extreme of representing the bonding of the acetylene to the platinum atom. The $Pt(ac)_2$ complexes must be between these two extremes. The infrared spectra of the complexes show a very strong band in the region 1880–1905 cm^{-1} which is about 250 cm^{-1} below the stretching frequency region of the disubstituted alkynes and about 200 cm^{-1} above that of the series *cis*-$Pt(PR_3)_2ac$ (3*a*, 5).

Conductivity and magnetic susceptibility measurements show that the complexes are non-ionic and diamagnetic with $\chi g = -0.2$ to -0.6×10^{-6} c.g.s. The mass spectra indicate the existence of mononuclear species with the heaviest fragment being $Pt(ac)_2$. Analytical data for the complexes are given in Table I.

The structure of the complexes is presently being studied by X-rays and complete data on the complexes will be given at a later date.

1. A. D. GELMANN and E. A. MEILAKH. Compt. Rend. Acad. Sci. USSR, **51** (3), 207 (1946); **46**, 110 (1945).
2. S. V. BUKHOVETS. Izv. Sektora Platiny i Drug. Blagorodn. Metal. Inst. Obshch. i Neorgan. Khim. Akad. Nauk USSR, **29**, 55 (1955).
3. (*a*) J. CHATT, G. A. ROWE, and A. A. WILLIAMS. Proc. Chem. Soc. 208 (1957). (*b*) J. CHATT and L. A. DUNCANSON. J. Chem. Soc. 2939 (1953). (*c*) J. CHATT, R. G. GUY, L. A. DUNCANSON, and D. T. THOMPSON. J. Chem. Soc. 5170 (1963).
4. A. D. ALLEN and T. THEOPHANIDES. Can. J. Chem. **43**, 290 (1965); (*b*) **44**, 2703 (1966).
5. C. D. COOK. Dissertation Abstr. **24**, 1384 (1963).

Can. J. Chem. Downloaded from www.nrcresearchpress.com by 210.87.254.40 on 09/05/12
For personal use only.

Can. J. Chem. Downloaded from www.nrcresearchpress.com by 210.87.254.6 on 09/05/12
For personal use only.

Canadian Journal of Chemistry

Published by THE NATIONAL RESEARCH COUNCIL OF CANADA

VOLUME 46 OCTOBER 1, 1968 NUMBER 19

Substitutions électrophiles en série naphtalénique. IV. Sur le diméthyl-2,6 naphtalène

JEAN-CLAUDE RICHER ET NICOLAS BASKEVITCH[1]

Département de Chimie, Faculté des Sciences, Université de Montréal, Montréal, Québec

Reçu le 8 janvier 1968

La chloration, la bromation et l'iodation du diméthyl-2,6 naphtalène ont été examinées. La structure des produits obtenus a été établie grâce à la résonance magnétique nucléaire.

Canadian Journal of Chemistry, 46, 2975 (1968)

Dans le cadre de nos travaux (1, 2, 3) sur les substitutions électrophiles en série naphtalénique, des réactions du diméthyl-2,6 naphtalène (**1**) ont maintenant été examinées.

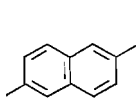

1

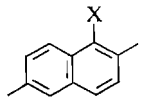

2 *a*, X = NO_2
b, X = Cl
c, X = Br
d, X = I

La réaction de nitration de cet hydrocarbure qui avait été précédemment rapportée entre autres par Mayer et Alken (4), Vesely et Medvedeva (5), Klamann et Krämer (6) ainsi que Bil et Bernstein (7) a été reprise. La mononitration du diméthyl-2,6 naphtalène (**1**) conduit au dérivé nitré en position 1 (**2***a*) déjà connu. La dinitration effectuée dans les conditions décrites par Klamann et Krämer (6) conduit à un mélange de deux produits neutres, le dinitro-1,8 (**3**) et le dinitro-1,5 diméthyl-2,6 naphtalène (**4***a*) déjà signalés dans la littérature (5, 6) ainsi qu'à un produit acide (**5**) dont la structure a déjà été prouvée (3, 8); le mélange de produits neutres contient en prépondérance le dérivé dinitré en positions 1,8 (**3**) et la proportion fraction neutre:fraction acide est de l'ordre 50:50. La nitration du nitro-1 diméthyl-2,6 naphtalène (**2***a*) conduit aux trois produits nitrés obtenus précédemment (**3**, **4***a*, **5**); dans la fraction neutre, l'isomère dinitro-1,8 (**3**) est toujours en prépondérance sur le dinitro-1,5 diméthyl-2,6 naphtalène (**4***a*) alors que la proportion fraction neutre:fraction acide est maintenant de l'ordre de 60:40. La nitration forcée (acide nitrique fumant et acide sulfurique) des dinitro-1,5 (**4***a*) et dinitro-1,8 diméthyl-2,6 naphtalène (**3**) conduit au dérivé tétranitré en positions 1,4,5,8 (**6**); les conditions semblent trop rudes pour que la réaction s'arrête au niveau des dérivés trinitrés. D'autre part la nitration forcée de l'acide mononitré (**5**) conduit à l'acide trinitro-4,5,7 méthyl-6 naphtalène carboxylique-2 (**7**).

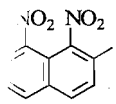

3

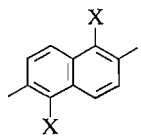

4 *a*, X = NO_2
b, X = Cl
c, X = Br
d, X = I

La chloruration de l'hydrocarbure (**1**) par le chlorure de sulfuryle donne naissance au chloro-1 (**2***b*) et au dichloro-1,5 diméthyl-2,6 naphtalène (**4***b*). Il est délicat d'arrêter la réaction au niveau de la monochloruration et le produit (**2***b*) est très difficile à isoler du fait de

[1]Les résultats rapportés dans le présent travail sont extraits du mémoire de maîtrise présenté par Monsieur Baskevitch en vue de l'obtention du grade de Maître ès Sciences en Chimie (août 1967).

Can. J. Chem. Downloaded from www.nrcresearchpress.com by 210.87.254.6 on 09/05/12
For personal use only.

son faible point de fusion. La chloruration de l'hydrocarbure (**1**) par 3 moles de chlorure de sulfuryle fournit un produit brut duquel seul le dichloro-1,5 diméthyl-2,6 naphtalène (**4***b*) a pu être isolé à la suite de nombreuses récristallisations. Tel que pourrait le laisser prévoir le travail de De la Mare et ses collaborateurs (9), la chromatographie en phase gazeuse des produits bruts de cette réaction indique toutefois la présence de plusieurs autres produits en faible proportion.

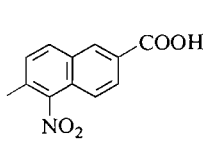

5

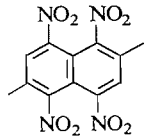

6

La bromuration du diméthyl-2,6 naphtalène (**1**) par le brome dans l'acide acétique dans les conditions décrites par Vesely et Stursa (10) conduit aux deux produits isolés par ces auteurs et pour lesquels les structures (**2***c*) et (**4***c*) ont été proposées.

Un seul produit, le diiodo-1,5 diméthyl-2,6 naphtalène (**4***d*), a pu être isolé des réactions d'iodation de l'hydrocarbure (**1**) effectuées par le chlorure d'iode. Des chromatographies sur colonnes d'alumine n'ont pu permettre d'isoler le dérivé monoiodé attendu (**2***d*).

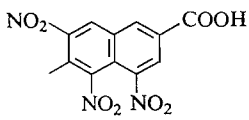

7

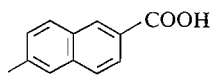

8

Discussion

(a) Sur la structure des composés obtenus

D'une manière générale, la structure de chacun des produits obtenus est attribuée en se basant sur le patron de couplage des bandes des protons aromatiques dans les spectres de résonance magnétique nucléaire (r.m.n.). Dans le cas des dérivés nitrés, la position des bandes due à ces protons a aussi été utilisée. Wells et Alcorn (11) ont en effet avancé une méthode empirique qui permet de prévoir les déplacements chimiques des différents protons aromatiques de ces molécules. Cette méthode consiste à ajouter aux déplacements chimiques des protons de la molécule non substituée des incréments déterminés expérimentalement par ces auteurs en compilant les résultats connus. Ces incréments dépendent directement de la position du proton considéré par rapport au groupe nitro. Ils représentent en quelque sorte une mesure des effets électroniques et de l'anisotropie magnétique du groupe nitro sur chaque position du cycle naphtalénique. Cette méthode a déjà été appliquée avec succès lors de l'étude des dérivés du diméthoxy-1,7 (1), du diméthoxy-2,7 (2) et du di-*t*-butyl-2,7 (3) naphtalène. Les prédictions ainsi que les valeurs expérimentales observées sont résumées dans le tableau I. La concordance entre les valeurs calculées et les valeurs expérimentales est assez bonne dans tous les cas considérés sauf en ce qui concerne le dérivé mononitré (**2***a*) en position 1. Des différences importantes surtout pour l'hydrogène en position 8 apparaissent alors entre le spectre calculé et le spectre expérimental et ce phénomène général qui a été constaté précédemment (2, 3, 11) semble se produire chaque fois qu'un groupe nitro en position α est adjacent à un substituant en position β; un encombrement stérique semble alors forcer le groupe nitro à se placer presque perpendiculaire au plan de la molécule de naphtalène (pour effets semblables voir réf. 12–16). Deux facteurs qui influencent grandement les déplacements chimiques des protons aromatiques sont affectés par le fait que le groupe nitro n'est pas dans le plan de la molécule. Ce sont d'une part l'inhibition stérique à la résonance et d'autre part l'effet de déblindage du groupe nitro, affectant surtout le proton en position 8, qui se trouverait très diminué. Il n'est pas étonnant alors de noter que le déplacement chimique de ce proton (en position 8) est plus faible que prévu.

(b) Sur le mécanisme de formation des différents composés

Il est bien connu (17) dans les substitutions électrophiles que les positions α des naphtalènes sont plus favorisées que les positions β et que les effets électroniques des substituants méthyles tendent à orienter les réactions de substitution en position ortho. Il est donc raisonnable d'attendre les dérivés monosubstitués en position 1 et disubstitués en positions 1,5 dans les réactions de substitutions électrophiles sur le diméthyl-2,6 naphtalène (**1**).

Les halogénations de cet hydrocarbure con-

TABLEAU I

Spectres de résonance magnétique nucléaire des dérivés nitrés

Produit		H-1	H-3	H-4	H-5	H-7	H-8	Méthyles
1	Trouvé	7.71	7.39	7.80	7.71	7.39	7.80	
2*a*	Calculé		7.59	8.22	7.96	7.65	8.27	
	Trouvé		7.62	8.12	7.95	7.67	7.67	2.56 et 2.61
3	Calculé		7.90	8.37	8.37	8.41		
	Trouvé		7.91	8.42	8.38	8.38		2.68 et 2.73
4*a*	Calculé		7.80	7.99		7.80	7.99	
	Trouvé		7.94	7.94		7.94	7.94	2.62
5	Trouvé	8.85	8.33	7.85		7.76	8.43	2.63
6	Calculé		8.96			8.96		
	Trouvé		8.99			8.99		2.64
7	Calculé	9.63	9.27				9.21	
	Trouvé	9.54	8.91				9.71	2.73

duisent en effet au chloro-1 (**2***b*) et au bromo-1 (**2***c*) ainsi qu'au dichloro-1,5 (**4***b*), au dibromo-1,5 (**4***c*) et au diiodo-1,5 (**4***d*) diméthyl-2,6 naphtalène. Le dérivé monoiodé (**2***d*) n'a pu être isolé. Il est à supposer que son point de fusion est inférieur à 15 °C ne permettant pas de l'isoler par cristallisations; les points de fusion des dérivés chlorés **2***b* et bromés **2***c* sont respectivement de 29–30 °C et 14–16 °C. De la Mare et ses collaborateurs (9) ont récemment mis en évidence la formation de produits d'addition lors de la chloruration du méthyl-2 naphtalène par le chlorure de sulfuryle; aucun effort spécial n'a été fait pour mettre en évidence la formation de tels produits lors de la réaction sur le diméthyl-2,6 naphtalène (**1**). Les valeurs expérimentales observées dans les spectres r.m.n. pour les dérivés halogénés sont résumées dans le tableau II. Les propriétés des produits obtenus sont résumées dans le tableau III.

Quoique le nitro-1 diméthyl-2,6 naphtalène (**2***a*) puisse être considéré comme le premier et le seul intermédiaire dans la formation de tous les produits d'oxydation ou de nitration du diméthyl-2,6 naphtalène (**1**), il est possible que l'on soit forcé de supposer la formation de l'acide méthyl-6 naphtalène carboxylique-2 (**8**) pour expliquer les quantités relatives de produits acides (**6**) versus les produits neutres formés au cours de la dinitration directe de l'hydrocarbure (**1**). La formation des dinitro-1,5 (**4***a*) et dinitro-1,8 (**3**) diméthyl-2,6 naphtalènes à partir du nitro-1 diméthyl-2,6 naphtalène (**2***a*) n'est pas étonnante puisque l'on sait (17) que le naphtalène ou le nitro-1 naphtalène conduisent aux dinitro-1,5 et dinitro-1,8 naphtalènes. La nitration poussée de l'acide mononitré (**5**) conduit à l'acide trinitro-4,5,7 méthyl-6 naphtalène carboxylique-2 (**7**); ce résultat est expliqué par les effets mésomériques combinés du groupe nitro et du groupe carboxyle dans la molécule de l'acide nitro-5 méthyl-6 naphtalène carboxylique-2 (**5**) qui orientent les substitutions suivantes vers les positions 4 et 7. Pour expliquer la formation du tétranitro-1,4,5,8 diméthyl-2,6 naphtalène (**6**) à partir du dinitro-1,8 diméthyl-2,6 naphtalène (**3**) il est nécessaire de supposer que c'est l'influence du groupe méthyle en position 6 qui oriente la nitration vers la position 5 alors que l'effet mésomérique du groupe $—NO_2$ orienterait l'attaque finale vers la position 4. Quant à la nitration du dinitro-1,5 diméthyl-2,6 naphtalène (**4***a*) les effets mésomériques de chaque groupe nitro orientant l'attaque suivante en position *péri* il n'est donc pas surprenant d'obtenir le tétranitro-1,4,5,8 diméthyl-2,6 naphtalène (**6**) lorsque les conditions de nitration sont poussées.

TABLEAU II

Spectres de résonance magnétique nucléaire des dérivés halogénés

Produit	H-3	H-4	H-5	H-7	H-8	Méthyles
2*b**	7.37	7.70	7.63	7.43	8.08	2.47 2.50
2*c**	7.28	7.63	7.56	7.33	8.07	2.30 2.50
4*b*	7.55	8.10		7.55	8.10	2.25
4*c*	7.63	8.19		7.63	8.19	2.60
4*d*	7.57	8.09		7.57	8.09	2.60

*Spectres déterminés à 60 Mc.p.s.

Partie expérimentale

Les spectres de résonance magnétique nucléaire ont été déterminés sur un spectromètre modèle JNM-4H-100

Can. J. Chem. Downloaded from www.nrcresearchpress.com by 210.87.254.6 on 09/05/12
For personal use only.

TABLEAU III

Propriétés des produits obtenus

Produit	Point de fusion (°C)		Spectres de masse	
	Ce travail	Littérature	*M/e*	Intensité relative %
2*a*	67–68 (éthanol 95%)	68 (4)	201	100
			202	13.7
			203	1.5
2*b*	29–30 (chromatographie)		190	100
			192	29.2
2*c*	14–16 (chromatographie)	33–34 (10)	234	100
			236	96.4
3	245 (éthanol 95%)	245 (6)	246	100
			247	14.1
			248	1.9
4*a*	198–199 (éthanol 95%)	179 (5)	246	100
			247	15
			248	2.4
4*b*	135–136 (méthanol)		224	100
			226	61.2
			228	10.3
4*c*	156–158 (éthanol)	160–161 (10)	312	47.3
			314	100
			316	57.6
4*d*	126–128 (méthanol)		408	100
			409	15.4
5	260–262 (AcOH)	258 (6, 8)	231	100
			232	14.4
			233	1.7
6	280 (eau)		336	100
			337	18.6
			338	4.3
7	269–270 (eau)		321	100
			322	21.5

de la Compagnie Jeolco ou dans certains cas sur un spectromètre modèle A-60 de la Compagnie Varian. Le solvant choisi est la diméthylacétamide (DMA). Les déplacements chimiques (δ) sont exprimés en p.p.m. et le tétraméthylsilane est utilisé comme référence interne. Les points de fusion ont été pris sur un "Hot Stage Apparatus" de la Compagnie "Reichert" avec un thermomètre calibré.

Les spectres infra-rouges (i.r.) ont été pris sur un spectrophotomètre "Beckman" modèle IR-8 à double réseau. Tous les spectres ont été pris en suspension dans le Nujol. Les spectres ultra-violets (u.v.) ont été mesurés dans l'éthanol 95% à l'aide d'un appareil "Bausch & Lomb" Spectronic 505. Les spectres de masse ont été mesurés sur un spectromètre de masse "Hitachi–Perkin–Elmer" modèle RMU6-D.

Les spectres de masse sous forme de graphiques, les positions des bandes dans les spectres i.r. et u.v. ainsi que les procédures expérimentales détaillées sont rapportées dans le mémoire de maîtrise de M. Nicolas Baskevitch dont une copie est déposée à la bibliothèque du Conseil National de Recherches du Canada.

Les nitrations ont été effectuées essentiellement d'après les procédures décrites par Klamann et Krämer (6) alors que les méthodes utilisées pour les halogénations correspondent à celles décrites dans un travail précédent (3).

Remerciements

Les auteurs remercient vivement le Conseil National de Recherches du Canada ainsi que le Conseil des Arts du Canada pour l'aide financière apportée sous forme d'octrois de recherches et de bourses d'études. Les auteurs remercient aussi la Compagnie Jeolco et particulièrement Monsieur Yasushi Ogawa pour la détermination de nombreux spectres de résonance magnétique nucléaire à 100 Mc.p.s. Les auteurs remercient aussi Monsieur Gilles Audet pour l'aide technique apportée.

1. J. C. Richer et C. Lamarre. Can. J. Chem. 43, 715 (1965).
2. J. C. Richer et Y. Pépin. Can. J. Chem. 43, 3443 (1965).
3. L. Erichomovitch, M. Ménard, F. L. Chubb, Y. Pépin et J. C. Richer. Can. J. Chem. 44, 2305 (1966).
4. F. Mayer et E. Alken. Ber. deut. chem. Ges. 55, 2278 (1922).
5. V. Vesely et A. Medvedeva. Collection Czech. Chem. Commun. 8, 125 (1936).

Can. J. Chem. Downloaded from www.nrcresearchpress.com by 210.87.254.6 on 09/05/12
For personal use only.

6. D. KLAMANN et U. KRÄMER. Chem. Ber. **93**, 2316 (1960).
7. M. BIL et A. BERNSTEIN. Chem. and Ind. London, 1221 (1967).
8. C. C. PRICE. J. Am. Chem. Soc. **62**, 2245 (1940).
9. G. CUM, P. B. D. DE LA MARE, J. S. LOMAS et M. D. JOHNSON. J. Chem. Soc. (B) 244, (1967).
10. V. VESELY et F. STURSA. Collection Czech. Chem. Commun. **4**, 21 (1932).
11. P. R. WELLS et P. G. E. ALCORN. Australian J. Chem. **16**, 1108 (1963).
12. J. TROTTER. Acta Cryst. **12**, 884 (1959).
13. J. TROTTER. Can. J. Chem. **37**, 1487 (1959).
14. J. TROTTER. Acta Cryst. **12**, 232, (1959).
15. J. TROTTER. Acta Cryst. **12**, 237 (1959).
16. J. TROTTER. Acta Cryst. **13**, 95 (1960).
17. P. B. D. DE LA MARE et J. H. RIDD. Aromatic substitution—nitration and halogenation. Butterworths, London. 1959.

Can. J. Chem. Downloaded from www.nrcresearchpress.com by 210.87.254.6 on 09/05/12
For personal use only.

Chemistry and pharmacology of some benzo[1,2]cyclohepta[3,4,5-*d,e*]isoquinolines

LESLIE G. HUMBER AND M. A. DAVIS
Department of Chemistry, Ayerst Research Laboratories, Montreal, Quebec

AND

G. BEAULIEU AND M.-P. CHAREST
Department of Pharmacology, Ayerst Research Laboratories, Montreal, Quebec

Received May 9, 1968

The chemistry of 1,2,3,7,8,12*b*-hexahydro-, 1,7,8,12*b*-tetrahydro-, and 7,8-dihydrobenzo[1,2]cyclohepta[3,4,5-*d,e*]isoquinolines has been investigated, leading to the synthesis of a wide variety of derivatives bearing substituents in the 2- and 3-position. Also, the reactions of 1,7,8,12*b*-tetrahydrobenzo[1,2]cyclohepta[3,4,5-*d,e*]isoquinoline with 1-buten-3-one, methyl mercaptoacetate, and 3-mercaptopropionic acid have yielded representatives of three novel pentacyclic systems; benzo[4,5]cyclohepta[1,2,3-*g,h*]benzo[*a*]quinolizine, benzo[1,2]cyclohepta[3,4,5-*d,e*]thiazolo[2,3-*a*]isoquinoline, and benzo[1,2]cyclohepta[3,4,5-*d,e*]-1,3-thiazino[2,3-*a*]isoquinoline. The central nervous system and cardiovascular pharmacology of the compounds have been investigated and the results are presented.

Canadian Journal of Chemistry, 46, 2981 (1968)

Can. J. Chem. Downloaded from www.nrcresearchpress.com by 210.87.254.42 on 09/05/12
For personal use only.

Synthetic routes to the benzo[1,2]cyclohepta-[3,4,5-*d,e*]isoquinoline ring system (e.g. **1**) have previously been developed by Humber *et al.* (1). This system contains the 5*H*-dibenzo[*a,d*]cycloheptene nucleus, which in turn is present in a number of clinically useful compounds (2) and we have therefore prepared a number of derivatives of **1** of diverse chemical types, for biological evaluation.

Chemistry

The compounds prepared are divided into 3 groups, the first consisting of 23 *N*-substituted derivatives of the 1,2,3,7,8,12*b*-hexahydro form of the ring system, **1**. The range of substituents introduced on nitrogen is shown in Table I where their physical and analytical data are collected. They were prepared from **1** by standard synthetic procedures as indicated in the Experimental section and in footnotes to Table I.

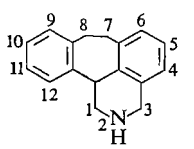

1

A second group of compounds comprises those bearing substituents at position-3 of the ring system. These were obtained by two routes, the first utilizing as starting material, 7,8-dihydrobenzo[1,2]cyclohepta[3,4,5-*d,e*]isoquinoline (**25**) (1) which was converted in good yield to the sulfonyl analogues of a Reissert compound, **26** and **27**, by the method recently described by Popp and co-workers (3), viz. the reaction with a benzene-sulfonyl chloride and potassium cyanide. They have shown that, in contrast to the behavior of classical Reissert compounds to sodium hydride which rearrange to give 1-benzoylisoquinolines (4) the "sulfonyl-Reissert compounds" yield isoquinoline-1-carbonitriles.

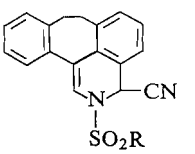

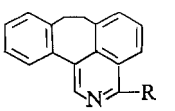

26 R = C_6H_5
27 R = 4-$CH_3C_6H_4$

25 R = H
28 R = CN
29 R = COOH
30 R = $CONH_2$
31 R = $C(=NOH)NH_2$
32 R = $C(=NOCOCH_3)NH_2$
33 R = $C(=NOCOC_6H_5)NH_2$
34 R = $C(=NOCH_2C{\equiv}CH)NH_2$
35 R =

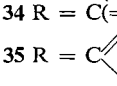

Thus, treatment of **27** with sodium hydride in xylene gave 86% of the carbonitrile **28** which was hydrolyzed to the carboxylic acid **29** with mineral acid. Alkaline hydrolysis of **28** gave the carboxamide **30**. The carbonitrile **28**, on reaction with hydroxylamine, was converted in high yield to the amidoxime **31** which, in turn, gave by acylation, the *O*-acetyl and *O*-benzoyl derivatives **32** and **33** respectively. The benzoylamidoxime **33**

Can. J. Chem. Downloaded from www.nrcresearchpress.com by 210.87.254.42 on 09/05/12
For personal use only.

TABLE I

N-substituted 1,2,3,7,8,12*b*-hexahydrobenzo[1,2]cyclohepta[3,4,5-*d*,*e*]isoquinolines

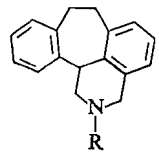

No.	R	Yield %	Melting point (°C)	Recrystallization solvent[1]	Formula	C % Calcd.	C % Found	H % Calcd.	H % Found	N % Calcd.	N % Found	Cl % Calcd.	Cl % Found
2	—CHO	67[2]	134–135	*a*	$C_{18}H_{17}NO$	82.10	82.10	6.51	6.26	5.32	5.39		
3	—$COCH_3$	92[3]	124–126	*a*	$C_{19}H_{19}NO$	82.29	81.72	6.91	6.71	5.05	5.14		
4	—$COOC_2H_5$	97[4]	98–100	*b*	$C_{20}H_{21}NO_2$	78.14	78.14	6.89	6.76	4.56	4.67		
5	—$COCHCl_2$	82[4]	132–133	*b*, *c*	$C_{19}H_{17}Cl_2NO$	65.90	65.79	4.95	5.05			20.48	20.72
6	—$COCH_2Cl$	84[4]	146–148	*d*	$C_{19}H_{18}ClNO$	73.20	72.90	5.82	5.88				
7	—$CO(CH_2)_2Cl$	86[4]	151–152	*c*, *d*	$C_{20}H_{20}ClNO$					4.30	3.96	10.88	10.94
8	—$COCH_2$(3,4-$[OCH_3]_2C_6H_3$)	76[4]	148–149	*c*	$C_{27}H_{27}NO_3$	78.42	78.52	6.58	6.40	3.39	3.37		
9	—$(CH_2)_2$(3,4-$[OCH_3]_2C_6H_3$)	68[5]	222–226	*d*, *e*	$C_{27}H_{29}NO_2 \cdot HCl$	74.38	74.22	6.94	6.95	3.21	3.02	8.13	8.31
10	—$COCH_2N(CH_3)_2$	62[6]	232–235[7]	*f*	$C_{21}H_{24}N_2O \cdot HCl$					7.85	7.51	9.93	9.70
11	—$CO(CH_2)_2N(CH_3)_2$	65[8]	90–91	*b*, *c*	$C_{22}H_{26}N_2O$					8.38	8.47		
12	—$CO(CH_2)_2NHCH_3$	68[9]	246–247	*e*, *g*	$C_{21}H_{24}N_2O \cdot HCl$					7.85	7.64		
13	—$CO(CH_2)_2N(CHO)CH_3$	55[10]	158–160	*b*, *c*	$C_{22}H_{24}N_2O_2$	75.83	75.60	6.94	6.92	8.04	7.99		
14	—$(CH_2)_2N(CH_3)_2$	58[11]	> 200	*a*, *f*	$C_{21}H_{26}N_2 \cdot 2HCl$					7.41	6.80	18.7	18.4
15	—$(CH_2)_3N(CH_3)_2$	84[12]	> 200	*e*, *g*	$C_{22}H_{28}N_2 \cdot 2HCl$					7.12	7.31	18.02	17.34
16	—NO	84[13]	140–141	*d*, *c*	$C_{17}H_{16}N_2O$	77.25	77.71	6.10	6.33				
17	—NH_2	45[13]	238–241	*g*	$C_{17}H_{18}N_2 \cdot HCl$					9.77	9.85	12.36	12.66
18	—$C(NH_2)$=NH	48[13]	> 200	*d*, *h*	$C_{18}H_{19}N_3 \cdot O \cdot 5H_2SO_4 \cdot O \cdot 5H_2O$[14]	64.50	64.28	6.31	6.42	12.53	12.16		
19	—CH_2CN	85[13]	119–121	*b*, *i*	$C_{19}H_{18}N_2$	83.17	82.92	6.61	6.52	10.21	10.25		
20	—CH_2CONH_2	70[13]	202–204	*d*	$C_{19}H_{20}N_2O$	78.05	78.52	6.90	7.16	9.58	9.60		
21	—$CONH_2$	75[13]	206–208	*d*, *e*	$C_{18}H_{18}N_2O$	77.67	77.31	6.52	6.69	10.07	9.85		
22	—SO_2NH_2	37[13]	220–222[15]	*d*	$C_{17}H_{18}N_2SO_2$	64.95	64.68	5.77	5.85	8.91	8.63		
23	—$CH_2C(NH_2)$=NOH	85[16]	187–189	*d*, *e*	$C_{19}H_{21}N_3O \cdot 2HCl$	60.01	59.80	6.10	6.25			18.65	18.34
24	—$CH_2C(NH_2)$=$NOCOCH_3$	88[17]	156–157	*j*	$C_{21}H_{23}N_3O_2$	72.18	72.02	6.63	6.43	12.03	12.10		

[1]*a*, acetone; *b*, hexane; *c*, benzene; *d*, ethanol; *e*, ether; *f*, 2-propanol; *g*, methanol; *h*, water; *i*, ethyl acetate; *j*, acetonitrile.
[2]From **1** and formic–acetic anhydride (11).
[3]By reaction of **1** with acetic anhydride in pyridine.
[4]By the reaction of **1** with the appropriate acyl chloride in ethylene dichloride and aqueous NaOH solution (e.g. see ref. 1).
[5]By reduction of **8** with $LiAlH_4$ in tetrahydrofuran.
[6]By heating **6** with an excess of dimethylamine in ethanol for 16 h in a sealed tube.
[7]The free base has m.p. 123–125° (benzene–hexane).
[8]By treating **7** as described in footnote 6.
[9]By treatment of **7** with methylamine as described in footnote 6.
[10]From **12** and formic–acetic anhydride (11).
[11]Reduction of **10** with $LiAlH_4$ in tetrahydrofuran.
[12]Reduction of **11** with $LiAlH_4$ in tetrahydrofuran.
[13]See Experimental section.
[14]Anal. Calcd.: S, 4.78; H_2O, 2.68. Found: S, 4.76; H_2O, 2.49.
[15]Anal. Calcd.: S, 10.18. Found: S, 10.07.
[16]By treatment of **19** with hydroxylamine (see preparation of **31** in Experimental section).
[17]By treatment of **23** with acetic anhydride in pyridine.

Can. J. Chem. Downloaded from www.nrcresearchpress.com by 210.87.254.42 on 09/05/12
For personal use only.

was converted to the 1,2,4-oxadiazole **35** by azeotropic removal of water from a refluxing xylene solution. The propargyl ether **34** was obtained from **31** and propargyl bromide. Reaction of the carboxylic acid **29** with lithium aluminium hydride resulted in reduction of the 2,3-double bond as well as the carboxyl group, yielding the 1,2-dihydroisoquinoline derivative **36** which was characterized as the *O*,*N*-diacetate **37**. Similar reduction of **25** gave the corresponding 1,2-dihydroisoquinoline **38** as a crystalline solid which decomposes on prolonged standing. It was characterized as the acetyl derivative **39**.

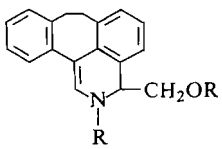

36 R = H
37 R = $COCH_3$

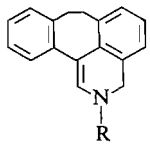

38 R = H
39 R = $COCH_3$

An alternative method of introducing substituents at the 3-position of the benzo[1,2]cyclohepta[3,4,5-*d*,*e*]isoquinoline system was available through reaction of the quaternary Schiff base methiodide **40***a* with 3-dimethylaminopropylmagnesium chloride to yield **41**, bearing a basic side chain at the desired site. Additionally, the pseudo-base **42** was obtained from **40***a* with sodium hydroxide, and reaction of **42** with cyanide ion gave the pseudonitrile **43**. Treatment of **42** with ethereal hydrogen chloride gave **40***b* as a hydrate.

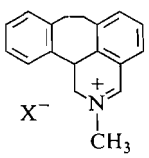

40*a* X = I
40*b* X = Cl

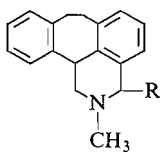

41 R = $(CH_2)_3N(CH_3)_2$
42 R = OH
43 R = CN

A third class of compounds, the novel pentacyclic systems **45**–**47**, was obtained by reaction of the Schiff base **44** (1) with various bifunctional reagents. Thus, the elegant benzoquinolizine synthesis using 1-buten-3-one (5) gave the benzo[4,5]cyclohepta[1,2,3-*g*,*h*] benzo[*a*] quinolizinone **45** as a mixture of 15*b*-α and 15*b*-β isomers (see structural formula) which were not isolated. Treatment of **44** with 2- or 3-mercapto acids or esters (6) gave the thiazolo- and thiazino-[2,3-*a*]isoquinolines **46** and **47** respectively and the latter was oxidized with *m*-chloroperbenzoic acid to the sulfoxide **48**.

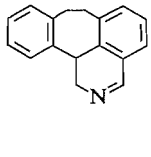

44

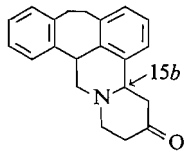

45

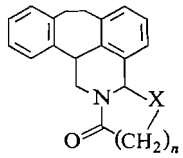

46 X = S, *n* = 1
47 X = S, *n* = 2
48 X = SO, *n* = 2

We have also been interested in obtaining the fully unsaturated form (**49**) of the benzo[1,2]cyclohepta[3,4,5-*d*,*e*]isoquinoline ring system and have indicated that this was not accessible by palladium dehydrogenation of the 1,7,8,12*b*-tetrahydro derivative **44**, which gives only the 7,8-dihydro form **25**, in high yield (1). A similar reluctance to form the fully unsaturated carbocyclic analogue **50** by attempted dehydrogenation of **51**, by a variety of methods, has recently been reported (7). We have thus attempted to obtain

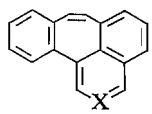

49 X = N
50 X = CH

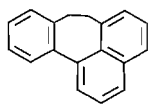

51

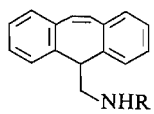

52 R = H
53 R = CHO
54 R = $COOC_2H_5$

the ring system with a 7,8-double bond by a Bischler–Napieralski reaction with the formamide **53**. Under a variety of experimental conditions (1) these attempts have not met with success, either with **53** or, with the related *N*-carbethoxy derivative **54**. The required amine (**52**)[1] for the preparation of the Bischler–Napieralski substrates was obtained by the lithium aluminium hydride – aluminium chloride reduction of 5*H*-dibenzo[*a*,*d*]cycloheptene-5-carbonitrile (9).

Pharmacology

The pharmacological properties of the compounds described in this study, as well as of some related compounds described previously, were determined. Effects on the central nervous system such as narcosis potentiation, protection against maximal electroshock seizures (MES), ataxic effect, as well as acute toxicity were studied in

[1]Compound **52** has recently been reported, without characterization, see ref. 8.

TABLE II

Effects of selected compounds on central nervous system parameters[1]

Compound	Acute toxicity LD_{50}:mg/kg	Narcosis potentiation ED_{50}:mg/kg	MES ED_{50}:mg/kg	Ataxia ED_{50}:mg/kg
55[2]	195	2.6	45	49
45	>1200	28	25.0	6.4
13	650	26	62	>160
44	260	18.6	40	36
3	475	25	72	60
56[3]	650	70	89	83
52	55	11	6.4	>10
57[4]	80	6.8	7	10.5
21	650	30	67	80
58[5]	700	27	54	120
59[6]	175	8	12.7	37
2	680	39	53	160
53	350	10	11	39
54	730	26.5	26	172
Amitriptyline HCl	94	9	11	40

[1]All compounds were injected intraperitoneally in albino mice.
[2]2-Methyl-1,2,3,7,8,12*b*-hexahydrobenzo[1,2]cyclohepta[3,4,5-*d*,*e*]isoquinoline hydrochloride. See ref. 1 for preparation.
[3]1,2,3,7,8,12*b*-Hexahydrobenzo[1,2]cyclohepta[3,4,5-*d*,*e*]isoquinolin-3-one. See ref. 1 for preparation.
[4]10,11-Dihydro-5*H*-dibenzo[*a*,*d*]cycloheptene-5-methylamine. See ref. 1 for preparation.
[5]*N*-Carbethoxy 10,11-dihydro-5*H*-dibenzo[*a*,*d*]cycloheptene-5-methylamine. See ref. 1 for preparation.
[6]*N*-Formyl 10,11-dihydro-5*H*-dibenzo[*a*,*d*]cycloheptene-5-methylamine. See ref. 1 for preparation.

mice by intraperitoneal administration (10). Virtually all of the compounds were investigated in the above tests and those which exhibited significant activity at 1/4 of the LD_{50} are collected in Table II. For comparative purposes the antidepressant drug amitriptyline (10) is also included.

Notably, significant activity is observed with tricyclic compounds **52, 53, 54, 57, 58, 59** containing the dibenzo[*a*,*d*]cycloheptene ring system of amitriptyline, with tetracyclic benzo[1,2]cyclohepta[3,4,5-*d*,*e*] isoquinolines (**2, 3, 13, 21, 44, 55, 56**) and, with the pentacyclic benzo[4,5]cyclohepta[1,2,3-*g*,*h*] benzo[*a*]quinolizine, **45**.

Several of the compounds of Table II were tested further in rats for their effects on conditioned avoidance and runway performance and on spontaneous motor activity (10). It was found in these tests that compound **55** has an activity profile similar to that of amitriptyline and the pharmacological activity and the possible therapeutic utility of this compound is under further study.

Several of the compounds were tested for their effects on blood pressure, respiration, intestinal tonus, and motility in urethane–chloralose anesthetized cats. The compounds were administered intravenously in increasing doses and those not having any effect at 20 mg/kg were considered to be inactive. The results with the other compounds are shown in Table III where the minimal doses required to cause a 20–30 mm Hg fall in blood pressure, are compared. With the exception of **1** the duration of the blood pressure fall produced by these compounds was short, the return to normal requiring less than 5 min. The magnitude of the blood pressure fall was dose-

TABLE III

Effects of selected compounds on blood pressure in cats[1]

Compound	Acute toxicity[2] LD_{50}(mg/kg)	Effect on blood pressure of cats: Dose (mg/kg) (intravenous)	Effect on blood pressure of cats: Blood pressure fall
1	120	0.5	+
8	>1200	20	0
9	>1200	20	0
10	190	0.5	+
14	140	0.5	+
15	160	0.5	+
17	125	3	+
18	—	20	0
25	325	0.5	+
31	175	20	0
40*b*	70	0.05	+
41	60	20	0
44	260	0.1	+
46	>1200	20	0

[1]Effect on blood pressure was studied by intravenous administration.
[2]LD_{50} determined intraperitoneally in the mouse.

Can. J. Chem. Downloaded from www.nrcresearchpress.com by 210.87.254.42 on 09/05/12
For personal use only.

Can. J. Chem. Downloaded from www.nrcresearchpress.com by 210.87.254.42 on 09/05/12
For personal use only.

dependent and the time course resembled that observed with parasympathomimetic agents. The most potent compound was **40***b*, the effect of which could be antagonized by atropine but not by hexamethonium. Further resemblance of **40***b* to parasympathomimetic agents was suggested by its stimulatory effect on the isolated guinea-pig ileum, an effect which was also antagonized by atropine.

The blood pressure fall caused by **1** was different from that of the other compounds, in that it was relatively long lasting; the duration of the decrease from a 1 mg/kg dose was more than 60 min.

Experimental

Melting points were taken on a Thomas–Hoover apparatus. Analyses were done by Mr. W. Turnbull and staff of our Laboratories.

*N-Nitroso-1,2,3,7,8,12b-hexahydrobenzo[1,2]cyclohepta-[3,4,5-d,e]isoquinoline (**16**)*

To a suspension of **1** (25 g) in 2-propanol (250 ml) and 2 *N* hydrochloric acid (200 ml) at 17° was added a solution of sodium nitrite (12.5 g) in water (60 ml). The mixture was heated to 75° for 3 h and another portion of sodium nitrite (12.5 g) was added and the solution kept at 75° for 12 h, diluted with water, and extracted with chloroform to yield 23.5 g of product, m.p. 140–141°.

*N-Amino-1,2,3,7,8,12b-hexahydrobenzo[1,2]cyclohepta-[3,4,5-d,e]isoquinoline (**17**)*

To a mixture of lithium aluminium hydride (1.38 g, 0.036 mole) in tetrahydrofuran (200 ml) was added **16** (9.5 g, 0.036 mole) dissolved in tetrahydrofuran. The mixture was stirred at room temperature for 3 h then worked up by conventional procedures to give the product as a gum which was converted to the hydrochloride salt.

*1,2,3,7,8,12b-Hexahydrobenzo[1,2]cyclohepta[3,4,5-d,e]-isoquinoline-2-carboxamidine Sulfate (**18**)*

A solution of *S*-methylpseudothiourea sulfate (7.24 g, 0.025 mole) in 1:1 ethanol:water (120 ml) was added over 5 min to **1** (11.9 g, 0.05 mole) in ethanol. The mixture was heated on the steam bath for 90 min. When the vigorous evolution of methyl mercaptan had subsided an additional portion of *S*-methylpseudothiourea sulfate (1.0 g) was added followed by heating for 4 h. On cooling a precipitate of **1**-sulfate was obtained. The ethanol was removed from the mother liquors *in vacuo*, the remaining aqueous solution treated with charcoal and diluted with acetone to give the product as a fluffy white solid.

*2-Cyanomethyl-1,2,3,7,8,12b-hexahydrobenzo[1,2]-cyclohepta[3,4,5-d,e]isoquinoline (**19**)*

To a solution of **1** (23.5 g, 0.1 mole) in absolute ethanol (100 ml) was added 70% aqueous glycolonitrile (16.4 g, 0.2 mole) followed by refluxing for 2 h. The cream-colored precipitate was collected and washed with cold ethanol.

*1,2,3,7,8,12b-Hexahydrobenzo[1,2]cyclohepta[3,4,5-d,e]-isoquinoline-2-acetamide (**20**)*

A mixture of **19** (5.0 g) and polyphosphoric acid (30 g) was stirred and heated at 120° for 3 h. Water was added, the mixture was made alkaline with sodium hydroxide, and extracted with chloroform to yield the product.

*1,2,3,7,8,12b-Hexahydrobenzo[1,2]cyclohepta[3,4,5-d,e]-isoquinoline-2-carboxamide (**21**)*

A refluxing solution of **1** (6.0 g) in benzene was treated with a slow stream of phosgene for 2 h. Hexane was added to obtain the *carbamoyl chloride* as a solid (5.7 g), m.p. 125–126° (petroleum ether, b.p. 80–120°). It was dissolved in liquid ammonia in a pressure bottle and allowed to stand at room temperature for 15 h. Evaporation of the ammonia gave the product as a solid.

*1,2,3,7,8,12b-Hexahydrobenzo[1,2]cyclohepta[3,4,5-d,e]-isoquinoline-2-sulfonamide (**22**)*

A solution of **1** (1.18 g, 0.005 mole) and sulfamide (0.5 g, 0.005 mole) was heated under reflux in 1,2-dimethoxyethane (20 ml) for 10 h. Evaporation of the solvent gave the product as a solid which was triturated with water, collected by filtration, and washed with hot benzene.

*2-Benzenesulfonyl-2,3,7,8-tetrahydrobenzo[1,2]-cyclohepta[3,4,5-d,e]isoquinoline-3-carbonitrile (**26**)*

Benzenesulfonyl chloride (14.66 g, 0.10 mole) was added over 2 h at 0° to a stirred mixture of **25** (11.55 g, 0.05 mole), potassium cyanide (9.75 g, 0.15 mole), water (20 ml), and methylenechloride (100 ml), and stirring was continued at 22° for 20 h. The reaction mixture was diluted with water and the organic phase washed (H_2O), dried (Na_2SO_4), treated with charcoal, and evaporated to yield the product as an amorphous solid (17.2 g, 86.5%). Two crystallizations from benzene–hexane gave analytically pure material, m.p. 186–188°.

Anal. Calcd. for $C_{24}H_{18}N_2O_2S$: C, 72.35; H, 4.55; N, 7.03; S, 8.03. Found: C, 72.46; H, 4.77; N, 6.66; S, 8.50.

By working in a similar manner but using *p*-toluenesulfonyl chloride instead of benzenesulfonyl chloride there was obtained (**27**) the *2-(p-toluenesulfonyl)* analogue of **26**, in 42% yield, m.p. 161–162° (2-propanol-methylenechloride).

Anal. Calcd. for $C_{25}H_{20}N_2O_2S$: C, 72.5; H, 4.86; S, 7.75. Found: C, 72.4; H, 4.71; S, 7.91.

*7,8-Dihydrobenzo[1,2]cyclohepta[3,4,5-d,e]isoquinoline-3-carbonitrile (**28**)*

A mixture of **27** (16.9 g, 0.041 mole), xylene (75 ml), and sodium hydride (1.03 g, 0.043 mole; as a 50% suspension in mineral oil) was refluxed for 1 h. The cooled mixture was filtered, the solvent evaporated, and the residue passed through a column of alumina (20 g) in a benzene:chloroform (1:1) solution to yield the product as an oil which solidified on trituration with hexane, (8.6 g, 86%). The analytical sample had m.p. 134–135° (2-propanol).

Anal. Calcd. for $C_{18}H_{12}N_2$: C, 84.35; H, 4.72; N, 10.93. Found: C, 84.14; H, 4.94; N, 10.51.

Can. J. Chem. Downloaded from www.nrcresearchpress.com by 210.87.254.42 on 09/05/12
For personal use only.

7,8-Dihydrobenzo[1,2]cyclohepta[3,4,5-d,e]isoquinoline-3-carboxylic Acid (29)

Concentrated hydrochloric acid (10 ml) and carbonitrile **28** (1.00 g) were heated in a sealed tube at 150° for 16 h. On cooling the product was obtained as the *hydrochloride* salt, m.p. 184–186° (methanol) (1.1 g). The analytical sample had m.p. 184–186°.

Anal. Calcd. for $C_{18}H_{14}ClNO_2$: C, 69.10; H, 4.48; Cl, 11.34. Found: C, 69.10; H, 4.46; Cl, 11.23.

The free base was obtained by treating a suspension of the salt in methylene chloride with one equivalent of triethylamine. It had m.p. 154–155° (2-propanol).

Anal. Calcd. for $C_{18}H_{13}NO_2$: C, 78.53; H, 4.76; N, 5.05. Found: C, 78.20; H, 4.91; N, 4.76.

The acid was more conveniently prepared by refluxing the carbonitrile **28** with 48% hydrobromic acid to yield the hydrobromide salt, m.p. 208–213° (methanol), converted to the free base as above.

7,8-Dihydrobenzo[1,2]cyclohepta[3,4,5-d,e]isoquinoline-3-carboxamide (30)

A solution of **28** (1.0 g) in 2-propanol (20 ml) containing potassium hydroxide (2.0 g) was refluxed for 3 h. Dilution with water, filtration, and thorough washing with water yielded the product (0.85 g), m.p. 193–194° (benzene–hexane).

Anal. Calcd. for $C_{18}H_{14}N_2O$: C, 78.81; H, 5.14; N, 10.21. Found: C, 79.09; H, 5.09; N, 10.06.

7,8-Dihydrobenzo[1,2]cyclohepta[3,4,5-d,e]isoquinolyl-3-amidoxime (31)

To a solution of hydroxylamine in methanol (prepared by treating hydroxylamine hydrochloride (2.24 g, 0.032 mole) in methanol with one equivalent of sodium methoxide and removing the sodium chloride by filtration) was added nitrile **28** (7.2 g, 0.028 mole) and the mixture was refluxed for 3 h. On cooling, the product (7.5 g, 92.5%) was obtained, m.p. 205–206°. The analytical sample had m.p. 210–211° (methanol). The *dihydrochloride* had m.p. 205–208° (methanol–ether).

Anal. Calcd. for $C_{18}H_{15}N_3O$: C, 74.72; H, 5.23; N, 14.53. Found: C, 74.69; H, 5.28; N, 14.58.

Anal. Calcd. for $C_{18}H_{17}Cl_2N_3O$: C, 59.69; H, 4.73. Found: C, 59.67; H, 5.02.

The *O-acetyl* derivative **32** was prepared with acetic anhydride in pyridine. It had m.p. 160–161° (benzene), ν_{max} ($CHCl_3$) 1758 cm^{-1}.

Anal. Calcd. for $C_{20}H_{17}N_3O_2$: C, 72.49; H, 5.17; N, 12.68. Found: C, 72.59; H, 5.20; N, 12.57.

The *O-benzoyl* derivative **33** was prepared with benzoyl chloride in pyridine. It had m.p. 186–187° (benzene–hexane), ν_{max} ($CHCl_3$) 1738 cm^{-1}.

Anal. Calcd. for $C_{25}H_{19}N_3O_2$: C, 76.32; H, 4.87; N, 10.68. Found: C, 76.54; H, 4.98; N, 10.74.

The *propargyl ether* **34** was obtained in 83% yield by treating the amidoxime **31** in toluene with sodium hydride and propargyl bromide. It had m.p. 99–100° (benzene–hexane).

Anal. Calcd. for $C_{21}H_{17}N_3O$: C, 77.05; H, 5.24; N, 12.84. Found: C, 76.76; H, 5.18; N, 12.87.

3-(7,8-Dihydrobenzo[1,2]cyclohepta[3,4,5-d,e]-isoquinolyl)-5-phenyl-1,2,4-oxadiazole (35)

A xylene solution of **33** (0.5 g) was refluxed for 20 h in an apparatus with a Dean–Starke trap. On evaporation of the solvent the product was obtained as an oil. Filtration through a column of alumina in benzene:chloroform (1:1) solution gave a solid, m.p. 137–139° (440 mg). The analytical sample had m.p. 155–156° after three crystallizations from methanol.

Anal. Calcd. for $C_{25}H_{17}N_3O$: C, 79.88; H, 4.56; N, 11.19. Found: C, 79.82; H, 4.66; N, 11.23.

3-Acetoxymethyl-2-acetyl-2,3,7,8-tetrahydrobenzo[1,2]-cyclohepta[3,4,5-d,e]isoquinoline (37)

The acid **29** (1.32 g) was refluxed for 3 h in tetrahydrofuran (25 ml) with lithium aluminium hydride (1.52 g). A conventional workup gave 0.8 g of a solid, m.p. 155–163° (benzene) which was acetylated directly by heating for 10 min on the steam bath with acetic anhydride (0.5 ml) in pyridine (1.0 ml). Dilution with water and extraction with ether gave an amorphous solid which was filtered through a column of neutral alumina with benzene to yield the product (400 mg), m.p. 138.5–139° (methanol), λ_{max} (EtOH) 240 mμ (ε, 22 800); 308 mμ (ε, 12 700); ν_{max} ($CHCl_3$) 1735 cm^{-1} (O—Ac); 1670 cm^{-1} (N—Ac). The nuclear magnetic resonance (n.m.r.) spectrum showed one vinyl proton as a doublet centered at τ 3.41 and *N*- and *O*-acetyl methyl groups as singlets at τ 7.82 and 7.98 respectively.

Anal. Calcd. for $C_{22}H_{21}NO_3$: C, 76.06; H, 6.09; N, 4.03. Found: C, 76.12; H, 6.01; N, 3.98.

2-Acetyl-2,3,7,8-tetrahydrobenzo[1,2]cyclohepta-[3,4,5-d,e]isoquinoline (39)

Compound **25** (5.6 g) was reduced with lithium aluminium hydride as described above to give the crude dihydroisoquinoline **38** as a solid (5.6 g), m.p. 111–114° on trituration with hexane, ν_{max} ($CHCl_3$) 3450 cm^{-1} (NH). It was acetylated as described above to yield the product, m.p. 173–175° (benzene–hexane), λ_{max} (EtOH) 240 mμ (ε = 23 100); 310 mμ (ε = 13 750); ν_{max} ($CHCl_3$) 1662 cm^{-1} (N—Ac); the n.m.r. showed one vinyl proton as a singlet at τ 3.32, and three acetyl methyl protons at τ 7.83 and the methylene protons adjacent to nitrogen as a singlet at τ 5.16.

Anal. Calcd. for $C_{19}H_{17}NO$: C, 82.88; H, 6.22; N, 5.09. Found: C, 82.10; H, 6.11; N, 5.07.

2-Methyl-1,7,8,12b-tetrahydrobenzo[1,2]cyclohepta-[3,4,5-d,e]isoquinolinium Iodide (40a)

Compound **44** (20 g) was dissolved in acetone and refluxed for 2 h with methyl iodide (32 ml). Cooling and filtration gave bright yellow crystals of the product, m.p. 214–217° after crystallizing from ethanol, (23.5 g), ν_{max} KBr 1666 cm^{-1}; λ_{max} EtOH 290 mμ (ε = 14 250). Good iodine analyses could not be obtained with this compound.

Anal. Calcd. for $C_{18}H_{18}NI$: I, 33.83; N, 3.73. Found: I, 35.73; N, 3.72.

The corresponding *isoquinolinium chloride* (**40b**) was prepared from the pseudo base **42** with ethereal hydrogen chloride. It was crystallized from ethanol and was obtained as a hydrate, m.p. 155–160°, ν_{max} (KBr) 1666 cm^{-1}; λ_{max} (EtOH) 292 mμ (ε = 11 600).

Anal. Calcd. for $C_{18}H_{18}ClN \cdot H_2O$: C, 71.65; H, 6.60; N, 4.64. Found: C, 72.00; H, 6.68; N, 4.59.

2-Methyl-3-(3-dimethylaminopropyl)-1,2,3,7,8,12b-hexahydrobenzo[1,2]cyclohepta[3,4,5-d,e]-isoquinoline (41)

To a solution of 3-dimethylaminopropylmagnesium

Can. J. Chem. Downloaded from www.nrcresearchpress.com by 210.87.254.42 on 09/05/12
For personal use only.

chloride in tetrahydrofuran (120 ml) prepared from magnesium (0.72 g, 0.03 g-atom) and 3-dimethylaminopropyl chloride (3.6 g, 0.03 mole) was added compound **40***a* (7.4 g, 0.02 mole) portionwise with vigorous stirring. After the initial exothermic reaction had subsided, the mixture was refluxed for 3 h, cooled, and treated with 10% aqueous ammonium chloride (20 ml). The organic phase yielded the title compound as a gum (6.0 g). The dihydrochloride salt was prepared and crystallized from a methanol–acetone mixture. It had m.p. 207–210°.

Anal. Calcd. for $C_{23}H_{32}Cl_2N_2$: N, 6.88; Cl, 17.40. Found: N, 6.10; Cl, 17.35.

*3-Cyano-2-methyl-1,2,3,7,8,12b-hexahydrobenzo[1,2]-cyclohepta[3,4,5-d,e]isoquinoline (**43**)*

Compound **40***a* (9.8 g), dissolved in 50 ml of ethanol: water (1:1), was treated dropwise with sodium hydroxide (4.18 g) in water (7 ml) over 5 min at 0°. The mixture was stirred at 22° for 1 h, extracted with ether, and the ether phase washed with water and extracted with 1 *N* hydrochloric acid. The acid solution was treated with charcoal, made alkaline with 1 *N* sodium hydroxide, and the precipitated pseudobase **42** was washed with water and dried in a desiccator over KOH pellets. It weighed 6.6 g and had m.p. 113–118°, ν_{max} ($CHCl_3$) 3600 cm^{-1}. The pseudo-base **42** (1.32 g, 0.005 mole) was dissolved in methanol (25 ml) and treated dropwise with potassium cyanide (325 mg, 0.005 mole) in water (3.0 ml). The mixture was heated on the steam bath for 10 min, cooled, and the precipitate filtered. It was recrystallized from methanol to give the product (0.85 g), m.p. 157–158°.

Anal. Calcd. for $C_{19}H_{18}N_2$: C, 83.18; H, 6.61; N, 10.21. Found: C, 82.96; H, 6.46; N, 9.94.

*2-Oxo-1,2,3,4,6,6a,11,12-octahydro-15b H-benzo[4,5]-cyclohepta[1,2,3-g,h]benzo[a]quinolizine (**45**)*

Freshly distilled 1-buten-3-one (83 ml) was added to a solution of **44**·hydrochloride (28.0 g) in absolute ethanol (300 ml) at 15°. The mixture was refluxed for 6 h and concentrated to yield 32.0 g of solid which was dissolved in 5% ethanol in water (500 ml), made alkaline with sodium carbonate, and extracted to give an oil (26.6 g). Crystallization from acetonitrile gave the product (17.8 g), m.p. 162–164°. Thin-layer chromatography on anhydrous silica gel plates with 20% methanol in benzene revealed the presence of two spots which virtually touched each other, probably 15*b*-α and 15*b*-β isomers. The presence of isomers could not be detected if the plates were not absolutely dry.

Anal. Calcd. for $C_{21}H_{21}NO$: C, 83.13; H, 6.98; N, 4.62. Found: C, 83.08; H, 7.22; N, 4.41.

*1-Oxo-1,2,7,8,12,13-hexahydro-3aH-benzo[1,2]-cyclohepta[3,4,5-d,e]thiazolo[2,3-a]isoquinoline (**46**)*

A solution of compound **44** (23.35 g, 0.1 mole) and methyl mercaptoacetate (15.9 g, 0.15 mole) in xylene (250 ml) was refluxed for 24 h. On cooling the product (15.2 g) separated. On crystallization from acetone it had m.p. 205–206°.

Anal. Calcd. for $C_{19}H_{17}NOS$: C, 74.23; H, 5.58; N, 4.56; S, 10.43. Found: C, 74.29; H, 5.73; N, 4.41; S, 10.78.

The reaction of **44** with 3-mercaptopropionic acid as described above gave *1-oxo-2,3,8,9,13b,14-hexahydro-1H-benzo[1,2]cyclohepta[3,4,5-d,e]-1,3-thiazino[2,3-a]-isoquinoline* (**47**), m.p. 201–203° (chloroform–benzene).

Anal. Calcd. for $C_{20}H_{19}NOS$: C, 74.71; H, 5.96; N, 4.36; S, 9.99. Found: C, 74.39; H, 5.85; N, 4.34; S, 10.09.

*1-Oxo-2,3,8,9,13b,14-hexahydro-1H-benzo[1,2]cyclohepta[3,4,5-d,e]-1,3-thiazino[2,3-a]isoquinoline-S-oxide (**48**)*

A solution of 85% *m*-chloroperbenzoic acid (1.07 g, 0.005 mole) in methylene chloride (20 ml) was added dropwise to a solution of **47** (1.6 g, 0.005 mole) in methylene chloride (40 ml) at such a rate that the internal temperature did not exceed 35°. The solution was washed with aqueous sodium bicarbonate and the residue from the organic phase was chromatographed on alumina (neutral, activity II). Elution with 10–25% chloroform in benzene gave the product (0.55 g), m.p. 155° (benzene–hexane).

Anal. Calcd. for $C_{20}H_{19}NO_2S$: C, 71.19; H, 5.68; N, 4.15. Found: C, 71.44; H, 5.81; N, 3.91.

*5H-Dibenzo[a,d]cycloheptene-5-methylamine (**52**) (8)*

5H-Dibenzo[*a*,*d*]cycloheptene-5-carbonitrile (9) (10.8 g, 0.05 mole), in a mixture of ether (100 ml) and tetrahydrofuran (30 ml), was added dropwise to a mixture of aluminium chloride (7.33 g, 0.05 mole) and lithium aluminium hydride (2.09 g, 0.05 mole) in ether (100 ml). The mixture was refluxed 3 h and water (9.0 ml) added. Filtration gave a precipitate which was distributed between chloroform and aqueous sodium hydroxide. The organic phase gave the product (6.1 g), m.p. 97–97.5° (hexane). The *hydrochloride* had m.p. >300° (methanol–ether). The *N-formyl* derivative **53** was prepared with formic–acetic anhydride (11) and had m.p. 118–119° (acetone).

Anal. Calcd. for $C_{16}H_{16}ClN$: C, 74.53; H, 6.26; Cl, 13.75. Found: C, 74.39; H, 6.25; Cl, 13.74.

Anal. Calcd. for $C_{17}H_{15}NO$: C, 81.90; H, 6.03; N, 5.62. Found: C, 81.94; H, 6.09; N, 5.84.

The *N-carbethoxy* derivative **54** was obtained with ethyl chloroformate in ethylene dichloride and aqueous sodium hydroxide solution (1). It had m.p. 97–99° (ethanol).

Anal. Calcd. for $C_{19}H_{19}NO_2$: C, 77.79; H, 6.53; N, 4.77. Found: C, 77.41; H, 6.30; N, 4.64.

Acknowledgments

The authors wish to thank Drs. R. Deghenghi and F. Herr for their interest and for valuable discussions. Thanks are also due to Mrs. J. Jachner for infrared, ultraviolet, and nuclear magnetic resonance spectra, and to Mr. R. Thomas for technical assistance.

1. L. G. Humber, M. A. Davis, R. A. Thomas, R. Otson, and J. R. Watson. J. Heterocyclic Chem. **3**, 247 (1966).
2. F. Hafliger and V. Burckhardt. Psychophar. macological agents. Vol. 4. Part I. *Edited by* M-Gordon. Academic Press, Inc., New York. 1964. p. 35.
3. J. M. Wefer, A. Catala, and F. D. Popp. J. Org. Chem. **30**, 3075 (1965).

4. V. BOEKELHEIDE and J. WEINSTOCK. J. Am. Chem. Soc. **74**, 660 (1952).
5. D. BEKE and C. SZANTAY. Ber. **95**, 2132 (1962).
6. A. R. SURREY. J. Am. Chem. Soc. **69**, 2911 (1947).
7. J. J. CRAIG. Australian J. Chem. **19**, 1927 (1966).
8. Neth. Pat. 65,17264, to Merck & Co. Inc. July 1, 1966.
9. M. A. DAVIS, S. O. WINTHROP, R. A. THOMAS, F. HERR, M.-P. CHAREST, and R. GAUDRY. J. Med. Chem. **7**, 88 (1964).
10. F. HERR, J. STEWART, and M.-P. CHAREST. Arch. Intern. Pharmacodyn. **134**, 328 (1961).
11. C. W. HUFFMAN. J. Org. Chem. **23**, 727 (1958).

Can. J. Chem. Downloaded from www.nrcresearchpress.com by 210.87.254.42 on 09/05/12
For personal use only.

Can. J. Chem. Downloaded from www.nrcresearchpress.com by 210.87.254.40 on 09/05/12
For personal use only.

Study of C—H··· base hydrogen bond in *N*,2,6-trichloro-*p*-benzoquinone imine with nuclear magnetic resonance and infrared spectroscopy. The assignment of *syn* and *anti* proton signals in the chloroimino group

HAZIME SAITÔ AND KENKICHI NUKADA
Basic Research Laboratories, Toyo Rayon Company, Limited, Kamakura, Japan

Received February 20, 1968

The nuclear magnetic resonance (n.m.r.) spectra of *N*,2,6-trichloro-*p*-benzoquinone imine (**1**) and the anisotropy effect of the chloroimino group are investigated. A comparison of the n.m.r. spectra of **1** with those of oximes with a similar structure shows that the extent of the anisotropy effect is the same for both the chloroimino and the hydroxyimino group. This is also confirmed by comparison of *N*-chlorocyclohexanimine with cyclohexanone oxime. A downfield shift of the C—H proton signal in solvents acting as a base is observed, which is interpreted in terms of a C—H··· base hydrogen bond. The extent of the shift is different between *syn* and *anti* sides and this gives the definite assignment for these two types of proton signals. Namely, the high-field signal, the extent of the downfield shift being larger, is assigned to *anti* protons, and the low-field one to *syn* protons. This assignment is extended to oximes owing to the equality of the anisotropy effects of the hydroxyimino and the chloroimino group. The formation of the C—H··· base hydrogen bond is confirmed by the infrared (i.r.) spectra, and the correlation between the extents of n.m.r. downfield shift and i.r. low wave number shift is discussed. Furthermore it is found that the behavior of benzene molecule as solvent is different between the chloroimino and the hydroxyimino compounds.

Canadian Journal of Chemistry, **46**, 2989 (1968)

Introduction

The assignment of *syn* and *anti* proton signals for oximes has been attempted by many workers. Phillips (1) assigned the *anti* proton to the high-field peak and *syn* to the low-field one, assuming that a large deshielding effect is caused by its proximity to the hydroxyl group. However, this notion is not confirmed on any definite experimental basis and cannot explain the phenomenon about oxime hydrochlorides (2, 3). Lustig (4) made an assignment of the *syn* and *anti* proton signals of *p*-chlorobenzaldoxime, the structure of which had been determined by the X-ray diffraction (5). Karabatsos and his co-workers (6) assigned the resonance peaks of oximes and the related compounds by comparison of nuclear magnetic resonance (n.m.r.) spectra in aliphatic and aromatic solvents. However, this method is applicable only in the case where the nature of an interaction between the solute and solvent is known with certainty.

In our previous papers, we have investigated the n.m.r. anisotropy effect[1] of the hydroxyimino group and deduced the following conclusions: (*a*) The anisotropy effect arises mainly from the lone pair electrons of the nitrogen atom (2, 3), because the separation between *syn* and *anti* proton signals disappear in oxime hydrochlorides where a proton attaches to the nitrogen atom. (*b*) Accordingly the identification of isomers concerning the orientation of two or more hydroxyimino groups is possible in dioximes (7, 8) and trioximes (9) because of the additivity of the anisotropy effect. For example, three isomers of 1,3-cyclohexanedione dioxime(7), *syn–syn*, *syn–anti*, and *anti–anti*, are identified with consideration of the above rule. (*c*) The amount of the anisotropy effect is closely relevant to the molecular conformation (3, 9). Thus the separation of *syn* and *anti* proton signals of cyclohexanone oxime, which is in a chair conformation, is larger than that of 1,4-cyclohexanedione dioxime, which is in a twisted boat conformation (8).

It is expected that in the chloroimino group there exists an anisotropy effect similar to the one in the hydroxyimino group, since both groups have the same type of an sp^2 hybridized nitrogen atom. In this paper, the effect of the chloroimino group in *N*,2,6-trichloro-*p*-benzoquinone imine (**1**) is studied by n.m.r. spectroscopy. It is found that this compound has almost the same anisotropy effect as *p*-benzoquinone dioxime (**2**) and 2,6-dimethyl-*p*-benzoquinone 4-oxime (**3**) (10), their skeletal structures being alike. A similar result is given in comparison of the n.m.r. spectra

[1]The term "anisotropy effect" is used in our series of papers for the effect, to split *syn* and *anti* n.m.r. peaks, and the difference of the chemical shifts between the *syn* and *anti* proton is used to express the extent of the effect.

TABLE I

Comparison of nuclear magnetic resonance spectra of *N*,2,6-trichloro-*p*-benzoquinone imine with those of the related compounds*

Compound	Solvent	*o*-Protons (p.p.m.)		Separation Δ (p.p.m.)	J_{HH} (c.p.s.)	Reference
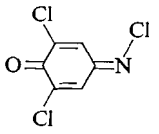 **1**	CCl_4	−7.95	−7.46	0.49	2.5	This paper
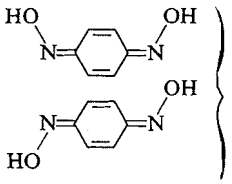 **2**	DMSO-d_6	−7.22†	−6.73†	0.49	1.5	8
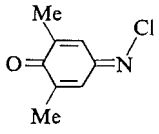 **3**	DMSO-d_6	−7.58	−7.12	0.46	1.6	10

*TMS was used as an internal standard.
†Calculated *syn* and *anti* *o*-proton signals in the absence of the long-range anisotropy effect.[3]

of *N*-chlorocyclohexanimine (**4**) and cyclohexanone oxime (**5**). Thus the equality of the anisotropy effect between the chloroimino and the hydroxyimino group is proved experimentally. Moreover, the downfield shift of *o*-protons of **1** is observed in solvents acting as a proton acceptor (base) in a hydrogen bond system. This observation prompts us to conclude that a hydrogen bond is formed between the *o*-proton of **1** and the solvent molecule. The formation of the C—H · · · base hydrogen bond is also supported by the infrared (i.r.) spectrum, in which C—H stretching frequency is shifted to a lower wave number region, though no appreciable difference is observed for C═O and C═N stretching frequency. The possibility of a C—H bond to participate in a hydrogen bond was discussed in the extensive review of Pimentel and McClellan (11). As a typical case of the C—H hydrogen bond, chloroform as a proton donor has been investigated extensively with i.r. (12–14) and n.m.r. (15–20) spectroscopy. In addition, the hydrogen bond of substituted benzenes (21), heterocyclic compounds (22) and haloalkanes (23) have been investigated. In many cases, however, only the absorption intensity becomes larger in the hydrogen bond formation, and few reports have been published in which the relatively large, low wave number shift of C—H stretching frequency is observed, (12, 13) as reported in this paper.[2] Now it is possible to assign the *syn* and *anti* proton signals of chloroimino compounds from the experimental result that the degree of the downfield shift of the C—H signal in the C—H · · · base hydrogen bond is different in the different solvent. The assignment thus obtained is one of the most definite, and can be directly extended to the hydroxyimino group because of the equality of the anisotropy effect between them.

Experimental

N,2,6-Trichloro-*p*-benzoquinone imine obtained from Merck Company was used. *N*-Chlorocyclohexanimine was prepared by the treatment of *N*,*N*-dichlorocyclohexylamine (24) with triethylamine in hexane according

[2]The increase in intensity of the C—H stretching frequency is more sensitive than the frequency shift, as an indicator of the hydrogen bond formation (ref. 11).

Can. J. Chem. Downloaded from www.nrcresearchpress.com by 210.87.254.40 on 09/05/12
For personal use only.

Can. J. Chem. Downloaded from www.nrcresearchpress.com by 210.87.254.40 on 09/05/12
For personal use only.

to the method of Reid (25). Solvents except for deuterated compounds were used after distillation. Measurements of the nuclear magnetic resonance (n.m.r.) spectra were performed on a Varian A-60 spectrometer using TMS as an internal standard. Carbon-13 satellite spectra were recorded by using a Varian C-1024 time averaging computer connected with the A-60 spectrometer. Frequency calibration was made by a usual side-band technique with an audio-frequency oscillator monitored by a frequency counter. Infrared (i.r.) spectra were taken with a Perkin–Elmer 125 spectrometer equipped with a KBr or CaF_2 cell. A variable cell was used for the compensation work.

Results and Discussion

The Anisotropy Effect of the Chloroimino Group and its Equality to that of the Hydroxyimino Group

An *o*-proton signal of *N*,2,6-trichloro-*p*-benzoquinone imine is split into two doublets, a typical pattern of the AX spin system, and this is due to the anisotropy effect of the chloroimino group. The chemical shift and coupling constant of this compound are given in Table I with those of *p*-benzoquinone dioxime (8) and 2,6-dimethyl-*p*-benzoquinone 4-oxime (10), the skeletal structures of which are similar to those of the former. In *p*-benzoquinone dioxime (**2**), there exist short- and long-range anisotropy effects, the former being relevant to the *o*-protons and the latter to *m*-protons. Because we are concerned with the anisotropy effect for *o*-protons, the value for the short range, Δ, deduced from the experiment is given in Table I.[3] In Table I are also given calculated *syn* and *anti* chemical shifts in which the long-range anisotropy effect is eliminated.

Difference in chemical shifts, Δ, between *syn* and *anti* proton signals among the three compounds are in accord with each other. *N*-Chlorocyclohexanimine (**4**) provides another example of the anisotropy effect of the chloroimino group. The separation between *syn* and *anti* α CH_2 proton signals of **4** is almost equal to that of cyclohexanone oxime as shown in Table II. These coincidences of the anisotropy effects imply that the separation of *syn* and *anti* *o*-proton signals are mainly due to the lone pair electrons of the nitrogen atom both in the hydroxyimino and the chloroimino groups but not to OH or Cl groups. This is because if the latter is the case a large variation of values should be observed between the hydroxyimino and the chloroimino compound. This result is also confirmed by the n.m.r. studies on oxime hydrochlorides (2). The separated n.m.r. signals due to *syn* and *anti* α-methylene protons in cyclohexanone oxime coalesce into an unsplit peak and new i.r. bands assigned to $\nu N^+—H$ and $\nu C{=}N^+$ appear in its monohydrochloride. Furthermore only a slight downfield shift of the unsplit n.m.r. peak is observed in its dihydrochlorides. From these observations it was concluded that a proton is attached to the nitrogen atom in the hydroxyimino group in the oxime monohydrochloride and the anisotropy effect of the hydroxyimino group is attributed to the lone pair electrons of the nitrogen atom. Unfortunately, the hydrochloride of *N*,2,6-trichloro-*p*-benzoquinone imine decomposes very rapidly and we could not obtain the i.r. and n.m.r. spectrum of this compound.

A difference of absolute proton shifts among **1**, **2**, and **3**, and between **4** and **5**, listed in Tables I and II can be interpreted in terms of the difference of the inductive effect due to the several functional groups, such as Cl, OH, and methyl groups.

Nuclear Magnetic Resonance Studies on the Solvent Effect, the C—H··· Base Hydrogen Bond and the Assignment of Syn and Anti Proton Signal

(1) General Consideration on the Solvent Effect

Chemical shifts of the *o*-proton signals in various solvents, listed in Table III, were obtained by the internal standard method using TMS. The solvent effect on TMS need not be taken into account so long as the relative values are concerned, since the extents of the interaction between TMS and the solvents are almost the same for cyclohexane, carbon tetrachloride, ethers, and ketones (26). In the fourth and fifth columns of Table III, is shown a downfield shift, except

---

[3]The short-range anisotropy effect is calculated according to the following procedure (ref. 8). Shielding constants due to the anisotropy effect of a hydroxyimino group are denoted as σ_s (*syn*) and σ_A (*anti*) for *o*-protons (short range), and as $\sigma_{s'}$ (*syn*) and $\sigma_{A'}$ (*anti*) for *m*-protons (long range), respectively. Separations between *syn* and *anti* protons for two isomers of *p*-benzoquinone dioxime are:

$$|\sigma_s + \sigma_{s'} - (\sigma_A + \sigma_{A'})| = |(\sigma_s - \sigma_A) + (\sigma_{s'} - \sigma_{A'})| = 0.593 \text{ p.p.m. for } cis \text{ isomer}$$

$$|\sigma_s + \sigma_{A'} - (\sigma_A + \sigma_{s'})| = |(\sigma_s - \sigma_A) - (\sigma_{s'} - \sigma_{A'})| = 0.400 \text{ p.p.m. for } trans \text{ isomer.}$$

The numerical values on the right hand side are obtained from the analysis of n.m.r. spectra. Combined these two equations, the short-range and long-range anisotropy effect, $|\sigma_s - \sigma_A|$ and $|\sigma_{s'} - \sigma_{A'}|$, respectively, are obtained. The former is listed in Table I.

TABLE II

Comparison of the nuclear magnetic resonance spectra of *N*-chlorocyclohexanimine (**4**) and cyclohexanone oxime (**5**)

Compound	Solvent	α CH_2 (p.p.m.)		Separation Δ (p.p.m.)	β,γ CH_2 (p.p.m.)	Reference
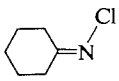 **4**	—	−2.69	−2.44	0.25	−1.70	This paper
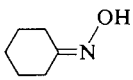 **5**	CCl_4	−2.46	−2.20	0.26	−1.60	2

benzene-d_6 solution of the last row, of the *o*-proton signal relative to the shift in cyclohexane, in which the *o*-proton signals are observed in the highest position.

The variation of chemical shift, listed in Table III, is interpreted in terms of the solvent effect. Buckingham, Schaefer, and Schneider (29) have suggested that the shielding constant due to the solvent effect σ is affected by the following five factors.

$$[1] \qquad \sigma = \sigma_b + \sigma_a + \sigma_w + \sigma_E + \sigma_H$$

σ_b is proportional to the bulk diamagnetic susceptibility of the solvent; σ_a arises from the non-vanishing anisotropy effect of the solvent; σ_w is due to the van der Waal's interaction between the solute and solvent; σ_E is the polar effect caused by the reaction field in the solvent; σ_H is due to the hydrogen bond interaction between solute and solvent molecules. It is not necessary to take the first term σ_b into account, because the present experiments were performed with the internal standard method. In Table III σ_a can be ignored except for benzene and acetonitrile because the molecules of the other solvents are not typical disk- or rod-shaped ones and therefore the non-vanishing anisotropy effect seems to be small. The anisotropy effect of benzene molecule is discussed at the end of this section. At present it is not clear why acetonitrile, the structure of which is rather rod-shaped, also behaves normally, similar to the other solvents. The contribution of van der Waal's effect, σ_w, is especially important in comparison of chemical shift between gas and condensed state because of intermolecular interaction through the van der Waal's force. This effect, however, may be neglected here, because all the data in Table III are those in solution state and therefore most of the van der Waal's contribution would be cancelled out.

A contribution from the reaction field of the solvent was shown to be a function of ε, linear or $(\varepsilon - 1)/(2\varepsilon + 2.5)$, where ε is a dielectric constant of the solvent. The downfield shift in Table III is plotted against ε or $(\varepsilon - 1)/(2\varepsilon + 2.5)$, but the smoothness of the curve is extremely poor.[4] Thus the effect of the reaction field is a minor contribution to the downfield shift. The last and the most important term is a hydrogen bond between the solute and solvent. The interaction should differ for protic and aprotic solvents.

(2) Aprotic Solvents as a Base in C—H · · · Base Hydrogen Bond

Aprotic solvents listed in Table III are bases in the usual hydrogen bond system. Generally the proton signal of a proton donor is displayed downfield by approaching to the base in the hydrogen bond formation. The most reasonable interpretation of the downfield shift shown in Table III is based on the formation of a hydrogen bond between the *o*-proton and the aprotic solvents. This type of the hydrogen bond formation is confirmed clearly by a low frequency shift

[4]The variation of chemical shift with temperature is expected to be very slight as a consequence of variation of dielectric constant, even if the reaction field effect is a predominant cause of the solvent effect. Actually the increases of the downfield shift in the high-field peak of **1** were observed as 0.1 (acetone), 0.03 (carbon tetrachloride), and 0.12 p.p.m. (tetrahydrofuran), respectively, in the range from 30 °C to −20 °C. These values are too large to be interpreted in terms of the variation of dielectric constant. Thus there should be another cause to cover the proton shift due to the temperature variation.

Can. J. Chem. Downloaded from www.nrcresearchpress.com by 210.87.254.40 on 09/05/12
For personal use only.

Can. J. Chem. Downloaded from www.nrcresearchpress.com by 210.87.254.40 on 09/05/12
For personal use only.

TABLE III

Nuclear magnetic resonance spectra of *N*,2,6-trichloro-*p*-benzoquinone imine in various solvents

Solvent*	*o*-Protons (p.p.m.)		Downfield shift (p.p.m.)†		Ratio (%)‡	Δ (p.p.m.)	Δν $CH_3OD(cm^{-1})$§	ε‖
	Low-field peak	High-field peak	Low-field peak	High-field peak				
Cyclohexane	−7.90	−7.36	—	—	—	0.54	—	2.023
Carbon tetrachloride	−7.95	−7.46	−0.05	−0.10	50	0.49	—	2.238
Chloroform	−7.97	−7.49	−0.07	−0.13	47	0.46	—	4.806
n-Butyl ether	−7.93	−7.47	−0.03	−0.11	27	0.46	101	3.08 (25 °C)
Methylene chloride	−8.00	−7.50	−0.10	−0.14	71	0.50	—	10.36
Ethyl ether	−7.97	−7.53	−0.07	−0.17	41	0.44	96	4.34
Methanol-d_4	−8.10	−7.59	−0.20	−0.23	87	0.51	—	33.58
Ethyl acetate	−8.06	−7.60	−0.16	−0.24	67	0.46	51	6.002
Tetrahydrofuran	−8.06	−7.60	−0.16	−0.24	67	0.46	117	7.58
Acetonitrile	−8.07	−7.60	−0.17	−0.24	71	0.47	87	37.5
Dioxane	−8.01	−7.61	−0.11	−0.25	44	0.40	111	2.29
Acetone-d_6	−8.11	−7.65	−0.21	−0.29	73	0.46	121	21.5
Trifluoroacetic acid	−8.14	−7.65	−0.24	−0.29	83	0.49	—	8.42
N-Methylacetamide	−8.11	−7.73	−0.21	−0 37	57	0.38	—	175.7 (30.5 °C)
Dimethyl formamide	−8.13	−7.77	−0.23	−0.41	56	0.36	147	37.6
Benzene-d_6	−7.07	−6.62	+0.83¶	+0.74¶	—	0.45	24	2.284

*From TMS, 0.05 mole fraction.
†Referred to *o*-proton signal in cyclohexane solution.
‡Ratio = $\frac{\text{Downfield shift of the low-field peak}}{\text{Downfield shift of the high-field peak}}$
§See ref. 11, p. 91.
‖The dielectric constants at 20 °C (unless otherwise noted) were taken from refs. 27 and 28.
¶Upfield shift.

Can. J. Chem. Downloaded from www.nrcresearchpress.com by 210.87.254.40 on 09/05/12
For personal use only.

of the C—H stretching band in the i.r. spectra as described in the following section. Of the solvents shown in Table III, cyclohexane is the weakest proton acceptor, and the downfield shift described above serves as a measure of the degree of the hydrogen bond formation.[5,6] The extent of the downfield shifts of the high-field signals are larger than those of the low-field signals. The ratio of the downfield shift of the low-field peak to that of the high-field one is given in the sixth column of Table III, in which the values of 27–87% are obtained. It is one of the aims of this paper to determine the assignment of these peaks definitely.

It is therefore necessary to discuss the reason of different abilities for the C—H · · · base hydrogen bond formation between the *syn* and *anti* protons. Because the hydrogen bond shift can be interpreted in terms of a rapid exchange process between the free and hydrogen-bonded proton shifts, the downfield shift is a function of the hydrogen bond shift δ_b and an equilibrium constant for hydrogen bond formation.[7] A ^{13}C—H coupling constant[8] obtained from the satellite spectrum of **1** in carbon tetrachloride (which is very weak as a base) by scanning 130 times with the aid of a time averaging computer is 173.2 c.p.s. for both the *syn* and *anti* protons. Such an invariance of ^{13}C—H coupling constant for *syn* and *anti* sides indicates that the electronic or structural natures of two kinds of the C—H bonds, such as hybridization or bond length, are almost equivalent to each other before the formation of the hydrogen bond. The hydrogen bond shift δ_b is, therefore, the same for these two kinds of *o*-protons, and the difference of the downfield shifts in the *syn* and *anti* *o*-proton signals are ascribed to that of the equilibrium constants.

This interpretation is further rationalized by the i.r. spectra as described later, in which no difference is observed between *syn* and *anti* C—H stretching frequencies. The difference of the equilibrium constants of the hydrogen bonds between *syn* and *anti* sides is interpreted in the following way. When a hydrogen bond is formed with the approach of the base to the *o*-proton, the base on the *syn* side suffers from the steric hindrance due to the chlorine atom bonded to the nitrogen atom, while there is no such effect on the *anti* side (Fig. 1). Then, the equilibrium constant in the hydrogen bond system involving the *syn* proton retains a small value compared with that of the *anti* protons. Thus it is definitely concluded that the high-field peak, the extent of the downfield shift of which being larger, is assigned to the *anti* proton, and the low-field peak to the *syn* proton. This assignment is in accordance with that of oximes 1, 4, 6, 9, in which the high-field peak has been attributed to the *anti* protons. Considering the equality of the anisotropy effects between the hydroxyimino and the chloroimino group as mentioned in the preceding section, the validity of the assignment in oximes is confirmed by the above result.

In the eighth column of Table III, Gordy's scale (30) which is considered to be a measure of base strength of the hydrogen bond system is listed. This is a shift of an O—D stretching frequency of CH_3OD to a lower wave number region (0.1 *M* solution) in various solvents. A comparison of the fourth and fifth columns with the eighth shows that there is no correlation between them. This is not so surprising since the effect of the steric hindrance in the hydrogen bond is generally different between n.m.r. and i.r. spectroscopy.

(3) Protic Solvent as a Proton Donor

In case of protic solvents[9] such as chloroform, methanol, and trifluoroacetic acid, hydrogen bonding between the nitrogen atom of the chloroimino group and the solvents would cause the neighboring proton to shift to the downfield. This was found in the anisotropic solvation of protic solvent into nitrogen atom of aziridines

[5]The downfield shift is also observed in carbon tetrachloride relative to cyclohexane solution. This result indicates that carbon tetrachloride would act as a very weak proton acceptor, and this is consistent with the results obtained by Jumper *et al.*, (ref. 16) in the analysis of self-association of chloroform.

[6]The solute is decomposed into a black substance in triethylamine and dimethyl sulfoxide.

[7]In the binary system, the proton shift is expressed according to the following equation, $\delta = K/(1+K)(\delta_b - \delta_f) + \delta_f$, where δ_f and δ_b are a proton shift in a free state and hydrogen bonded state, respectively. K is an equilibrium constant (see ref. 15).

[8]Muller and his co-workers reported that there exists a correlation between ^{13}C—H coupling constant and C—H bond length (see refs. 34 and 35).

[9]Even protic solvents such as chloroform and methanol also act as proton acceptors in C—H · · · base hydrogen bonding, because an increase of intensity and low frequency shift of the C—H stretching band is observed in these solvents as shown in the following section (see Table IV).

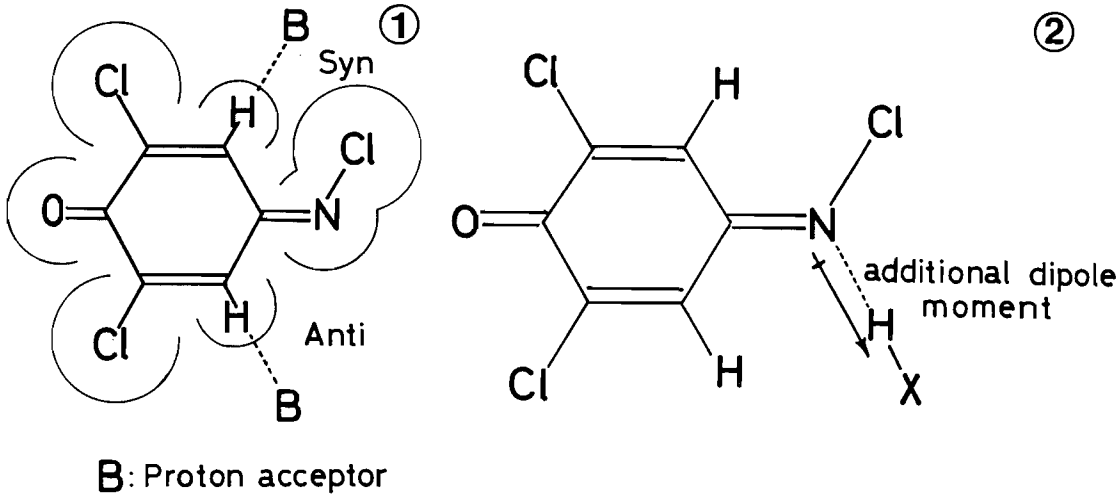

FIG. 1. C—H · · · Base hydrogen bond on *syn* and *anti* sides in *N*,2,6-trichloro-*p*-benzoquinone imine. B stands for proton acceptor. Circles around atoms indicate van der Waals' radii.

FIG. 2. Hydrogen bond between a chloroimino group and protic solvent. The arrow denotes the component of excess electric field effect caused by the hydrogen bond. X—H stands for proton donor.

(31), and was interpreted in terms of the variation of the magnetic anisotropy effect and the additional electric field effect, caused by a charge transfer effect in the hydrogen bond. The latter factor is predominant in aziridines (31) and oximes.[10] If it is assumed that the downfield shift is caused by the additional electric field effect also in chloroimines in a similar way (Fig. 2), the high-field peak, which is larger in the downfield shift, is assigned to *anti* proton. This assignment is in accord with the one for the aprotic solvent case.

(4) Solvent Effect of Benzene

The last row of Table III shows that benzene-d_6 makes the CH peak of *N*,2,6-trichloro-*p*-benzoquinone imine shift to the upfield region compared with cyclohexane solution. This upfield shift is not caused by the hydrogen bond interaction with benzene, which is rather weak as a proton acceptor as indicated in the eighth column of this Table, but by the solvent effect characteristic of aromatic compounds. The degree of upfield shift differs for *syn* and *anti* protons, as pointed out by Karabatsos and his co-workers (6) for oximes and nitrosamines. In these compounds the upfield shift of *anti* proton signal overcomes that of *syn* protons. In *N*,2,6-trichloro-*p*-benzoquinone imine, however, the larger upfield shift of the *syn* proton over the *anti* proton is observed on dilution with benzene-d_6, contrary to the results of oximes and nitrosamines. The same trend is also encountered in the dilution shift of *N*-chlorocyclohexanimine in benzene solution as illustrated in Fig. 3. The upfield shift of the *syn* proton signal extrapolated to infinite dilution relative to the undiluted state, as shown in Fig. 3, is 0.06 p.p.m. larger than that of the *anti* proton.

Karabatsos postulated that the benzene molecule solvates to *anti* position in oximes and nitrosamines. Applying this model to chloroimines, the low-field peak, which is larger for upfield shift in benzene-d_6 than the high-field peak, is assigned to *anti* proton as illustrated in Fig. 4*a*. It is important to note that the assignment for chloroimino compounds based on the Karabatsos model is reversed with ours, based on the consideration of C—H · · · base hydrogen bonding and the additional electric field model. According to the Karabatsos model, the separation between *syn* and *anti* protons should be mainly due to OH or Cl groups and the difference of chemical shift between oximes and chloroimines $\Delta = \Delta_1 - \Delta_2$ should be about 1 p.p.m., where $\Delta_1 = 0.5$ p.p.m. and $\Delta_2 = -0.5$ p.p.m. are the separation between *syn* and *anti* proton signals for the oximes and the chloroimines, respectively. It seems to us

[10]In oxime hydrochloride the major part of the downfield shift is caused by the additional electric field effect. Although we treated this effect as a point charge approximation (ref. 3), a larger downfield shift would be expected in *anti* protons adopting the dipolar model for the additional field.

Can. J. Chem. Downloaded from www.nrcresearchpress.com by 210.87.254.40 on 09/05/12
For personal use only.

Can. J. Chem. Downloaded from www.nrcresearchpress.com by 210.87.254.40 on 09/05/12
For personal use only.

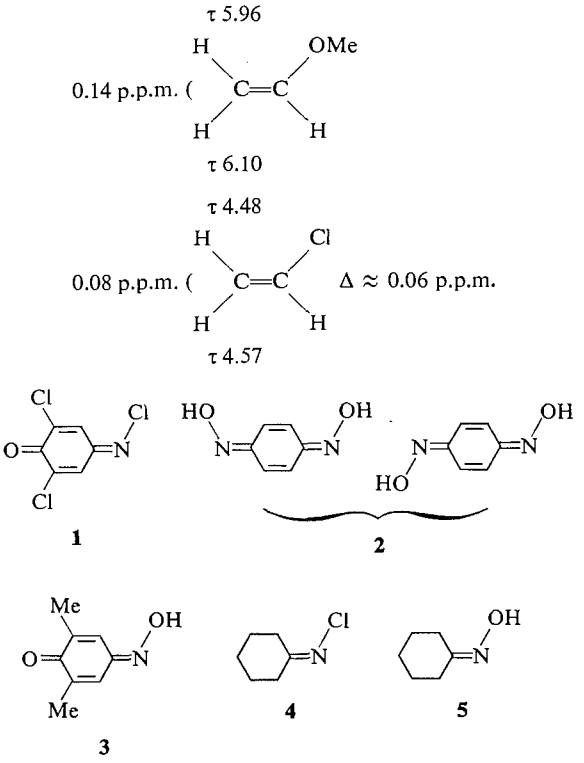

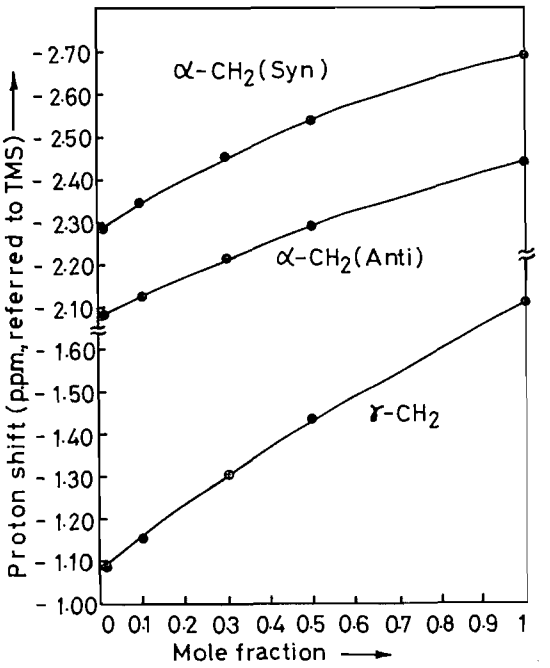

FIG. 3. A plot of methylene proton signals against mole fraction of *N*-chlorocyclohexanimine in benzene solution.

impossible to realize such a situation, considering the n.m.r. results of vinyl compounds (32). The discrepancy in assignment between our models and those of Karabatsos, is probably due to the difference of solvation sites between the hydroxyimino and the chloroimino compounds.

Confirmation of the C—H · · · Base Hydrogen Bond with Infrared Spectra

Infrared spectra were taken in the same concentration (0.05 mole fraction) as in the measurement of the n.m.r. spectra. The C—H stretching frequency is shifted to a lower wave number region in the various solvents than in cyclohexane solution but no variation in C=O and C=N stretching frequency is observed. This result indicates that the hydrogen bond is formed between the *o*-proton and the solvent molecule, and is consistent with the conclusion obtained from the n.m.r. spectra in aprotic solvents. The extent of the wave number shift of the hydrogen bonded C—H stretching vibration studied in this paper is 20–40 cm^{-1} and this is smaller than those of the bonded O—H or N—H stretching frequencies. The C—H stretching bands illustrated in Figs. 5–7 do not consist of a single peak but of a superposition of two or more peaks. By resolving[11] the C—H stretching bands into components, the frequencies and integrated intensities of the resolved peaks are obtained as given in Table IV. The integrated intensity A is calculated according to the following equation

$$[2] \qquad A = \frac{1}{cd}\ln(I_0/I)\nu_{\frac{1}{2}}$$

where c is a concentration of a solute molecule (mole/l), d is a thickness of a cell, and $\nu_{\frac{1}{2}}$ is a half-band width. The integrated intensity is proportional to the amount of the species in question for the absorption band of the same type, but this is not true when the different types of bands are compared with each other. A typical example is hydrogen bonded X—H stretching absorption, in which the integrated intensity increases abnormally. The feature of the C—H · · · base hydrogen bond depends on the types of solvent: type 1, carbon tetrachloride, cyclohexane, and chloroform; type 2, ethyl ether and *n*-butyl ether; type 3, other solvents.

[11]Resolving of the spectra was carried out by the procedure in which the spectra were folded at the center of main peak and subtracted from the original band.

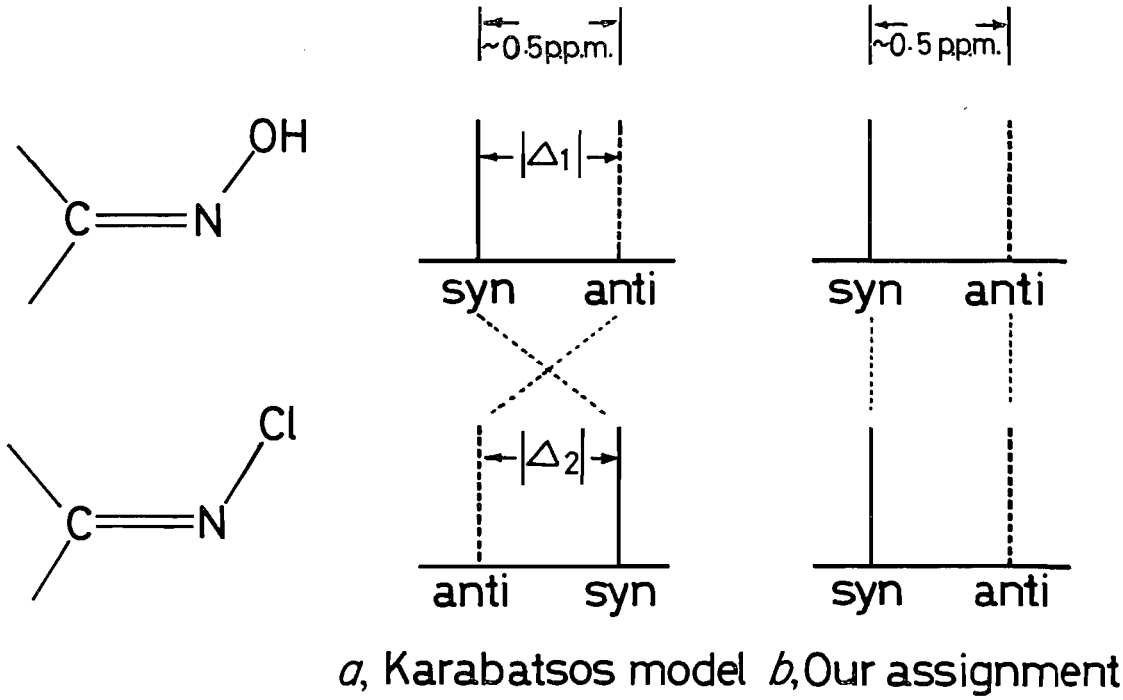

FIG. 4. Comparison of assignment between oximes and chloroimines.

TABLE IV

C—H Stretching frequencies in various solvents

Solvent*	Assignment†	ν(cm^{-1})	$\Delta\nu$(cm^{-1})‡	$\nu_{\frac{1}{2}}$(cm^{-1})§	A × 10^{-2} (mole^{-1} · l · cm^{-2})
Cyclohexane	f	3076.5	—	10	6.3
	c	3068.0	8.5	10.3	2.1
Carbon tetrachloride	f	3077.0	0.5	14	7.4
	c	3067.8	8.7	9	0.89
Chloroform	f	3076.0	−0.5	16	11
	c	3066.3	10.2	9.5	1.3
Ethyl ether	f	3078.0	1.5	16.8	5.2
	c	3067.0	9.5	11	0.52
	b	3050.0	26.5	28	14
n-Butyl ether	f	3077.5	1.0	13	6.5
	c	3068.0	8.5	10	0.91
	b	3046.0	29.7	35	14
Acetonitrile	f	3081.0	4.5	11.5	0.64
	b	3066.0	10.5	32	23
Methanol-d_4	b	3064.0	12.5	40	21
Ethyl acetate	f	3077.3	0.8	16.4	1.6
	b	3062.3	14.2	28	19
Acetone-d_6	f	3080.0	3.5	18.5	1.9
	b	3059.0	17.5	32.8	23
Dioxane	f	3074.5	−2.0	21.8	3.3
	b	3053.0	23.5	30.2	24
Tetrahydrofuran	f	3077.5	1.0	18	1.4
	b	3043.0	33.5	55	41
Dimethyl formamide	f	3076.0	−0.5	28	4.7
	b	3043.0	33.5	35	35

*0.05 mole fraction.
†f, free state; b, C—H · · · · ·solvent hydrogen bond; c, combination band.
‡Referred to 3076.5 cm^{-1} (in cyclohexane); positive sign means low wavenumber shift
§Half-band width.

Can. J. Chem. Downloaded from www.nrcresearchpress.com by 210.87.254.40 on 09/05/12
For personal use only.

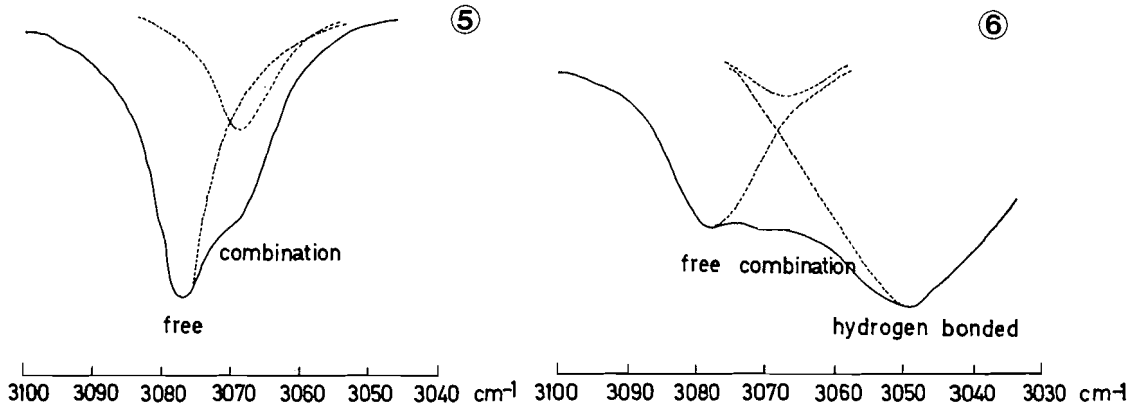

FIG. 5. C—H Stretching band of *N*,2,6-trichloro-*p*-benzoquinone imine in cyclohexane solution (0.05 mole fraction).
FIG. 6. C—H Stretching band of *N*,2,6-trichloro-*p*-benzoquinone imine in ethyl ether solution (0.05 mole fraction).

In solvents belonging to the first group (Fig. 5), a larger peak at 3076–3077 cm^{-1} and a smaller peak at 3066–3068 cm^{-1} are observed. Because cyclohexane is inactive for hydrogen bond formation, the former peak is assigned to the free C—H stretching vibration. The integrated intensity of the former increases in the order of carbon tetrachloride and chloroform solution in comparison with that of cyclohexane solution and this is consistent with the order of the downfield shift of n.m.r. spectra, as shown in Table III. Since such a downfield shift is a measure of the extent of hydrogen bond formation, this correlation suggests that in the case of carbon tetrachloride and chloroform solution, a contribution from the hydrogen bond between the solvent and *o*-proton is involved in the free C—H stretching band at 3076–3077 cm^{-1}. Similarly, for the weak hydrogen bond, the wave number shift is not observed but only the peak intensity increases. The integrated intensity of the peak at 3066–3068 cm^{-1} in carbon tetrachloride does not change by lowering the concentration of the solution to 0.0005 mole fraction. Moreover, similar peaks with almost the same intensity are also observed in ether solutions. This peak is therefore not ascribed to any kind of hydrogen bond species. A repeated recrystallization of the sample shows that this peak does not originate from any impurity. The peak at 3066–3068 cm^{-1} is then tentatively assigned to a combination or overtone of the fundamental around 1500 cm^{-1}.

The bands in solutions of the second group (ethyl and *n*-butyl ether) are resolved into three peaks (Fig. 6). The two higher frequency bands are assigned to the free C—H stretching and the combination, as described above, respectively. The lowest frequency peak is assigned to the hydrogen bonded C—H stretching frequency. The frequency shifts from the free C—H stretching are 26.5 cm^{-1} and 29.7 cm^{-1} in ethyl and *n*-butyl ether, respectively, and these values are among the largest wave number shifts studied in this paper. From this observation, it can be concluded that the basicity of the ethers is large, compared with that of acetonitrile, ethyl acetate, acetone, and dioxane (Table IV). The downfield shift of ether solutions in the n.m.r. spectra is, however, smaller than that of the latter solvents. The reason is as follows: the content of the free C—H bond in ethers is fairly large as compared with that in acetonitrile, ethyl acetate, acetone, and dioxane (Table IV), and therefore the chemical shift of the former solutions is more influenced by the free C—H site than that of the latter ones.

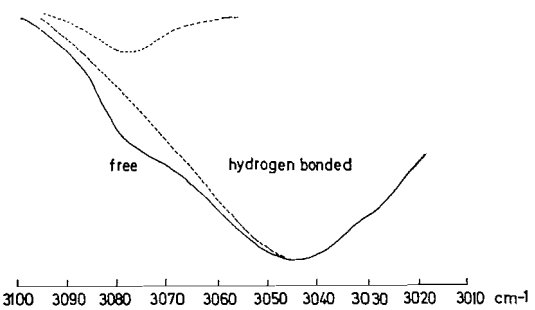

FIG. 7. C—H Stretching band of *N*,2,6-trichloro-*p*-benzoquinone imine in tetrahydrofuran (0.05 mole fraction).

Can. J. Chem. Downloaded from www.nrcresearchpress.com by 210.87.254.40 on 09/05/12
For personal use only.

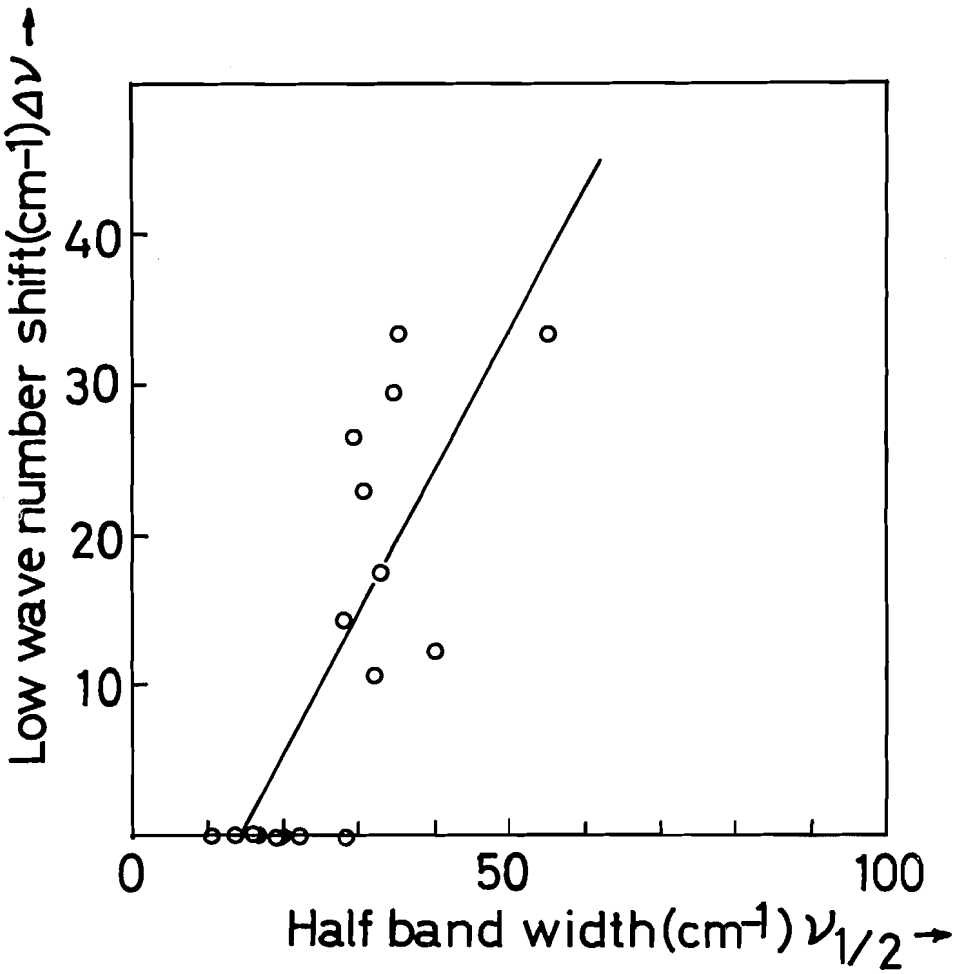

FIG. 8. A plot of the low wave number shift of C—H stretching band of *N*,2,6-trichloro-*p*-benzoquinone imine against its half-band width.

A free C—H stretching band of the third group appeared as a shoulder of the band attributed to the hydrogen bonding between C—H and the solvents (Fig. 7). The integrated intensity of the combination band is expected to be 2×10^2 cm^{-2} 1 $mole^{-1}$ as given for the cyclohexane solution and this value is negligibly small in comparison with that of the hydrogen bonded C—H stretching band ((19–40) $\times$ 10^2 cm^{-2} 1 $mole^{-1}$). The combination band, which appears in the first and second solutions, is therefore not observed in the last case.

In the preceding section the difference of the downfield shift of the n.m.r. peak between the *syn* and *anti* protons is interpreted in terms of the difference of the equilibrium constants, and this is clarified by the amount of the free CH proton. A large number of free protons are found in carbon tetrachloride, chloroform, dimethyl formamide, dioxane, *n*-butyl ether, and ethyl ether solutions (Table IV). The ratio of the downfield shift of the *syn* to *anti* protons listed in Table III is in a range of 27–56% in these solvents and this is smaller than that in other solvents (67–87%).

It was reported (33) that the following linear relation between the frequency shift $\Delta\nu$ to the lower wave number region and the half-band width of O—H stretching in hydrogen bond holds.

[3] $$\nu_{\frac{1}{2}} = 0.72\Delta\nu + 2.5\ (cm^{-1})$$

A plot of the wave number shifts of C—H stretching frequency against the half-band width

Can. J. Chem. Downloaded from www.nrcresearchpress.com by 210.87.254.40 on 09/05/12
For personal use only.

is illustrated in Fig. 8. A roughly linear correlation as expressed in the following equation is obtained with least square method and the slope of the plot in Fig. 8 is fairly in agreement with the former one.

$$[4] \qquad \nu_{\pm} = 1.07\Delta\nu + 14.3\ (\mathrm{cm}^{-1})$$

Acknowledgments

The authors are indebted to Mr. Akira Abe and Mr. Yuji Tanaka for their assistance in the experimental work.

1. W. D. PHILLIPS. Ann. N.Y. Acad. Sci. **70**, 817 (1958); J. A. POPLE, W. G. SCHNEIDER, and H. J. BERNSTEIN. High-resolution nuclear magnetic resonance. McGraw-Hill Book Co., Inc., New York. 1959. p. 374.
2. H. SAITÔ, K. NUKADA, and M. OHNO. Tetrahedron Letters, 2134 (1964).
3. H. SAITÔ and K. NUKADA. J. Mol. Spectry. **18**, 1 (1965).
4. E. LUSTIG. J. Phys. Chem. **65**, 491 (1961).
5. B. JERSLEV. Nature, **180**, 1410 (1958).
6. G. J. KARABATSOS, R. A. TALLER, and F. M. VANE. J. Am. Chem. Soc. **85**, 2326 (1958); G. J. KARABATSOS and K. L. KRUMEL. Tetrahedron, **23**, 1097 (1967).
7. H. SAITÔ and K. NUKADA. Tetrahedron Letters, 2127 (1965).
8. H. SAITÔ and K. NUKADA. J. Mol. Spectry. **18**, 355 (1965).
9. H. SAITÔ, K. NUKADA, I. TERASAWA, and M. OHNO. Abstract of 19th annual meeting of the Chemical Society of Japan. Vol. I. 1966. p. 92.
10. A. FISHER and R. M. GOLDING. J. Chem. Soc. 6032 (1965).
11. G. C. PIMENTEL and A. L. MCCLELLAN. The hydrogen bond. W. H. Freeman and Co., San Francisco. 1960. p. 197.
12. G. M. BARROW. J. Am. Chem. Soc. **76**, 5247 (1954).
13. C. M. HUGGINS and G. C. PIMENTEL. J. Chem. Phys. **23**, 896 (1955).
14. R. C. LORD, B. NOLIN, and H. D. STIDHM. J. Am. Chem. Soc. 77, 1365 (1955).
15. C. M. HUGGINS, G. C. PIMENTEL, and J. N. SHOOLERY. J. Chem. Phys. **23**, 1244 (1955).
16. C. F. JUMPER, M. T. EMERSON, and B. B. HOWARD. J. Chem. Phys. **35**, 1911 (1961).
17. B. B. HOWARD, C. F. JUMPER, and M. T. EMERSON. J. Mol. Spectry. **10**, 117 (1963).
18. P. J. BERKELEY, JR. and M. W. HANNA. J. Phys. Chem. **67**, 846 (1963).
19. A. L. MCCLELLAN, S. W. NICKSIC, and J. C. GUFFY. J. Mol. Spectry. **11**, 340 (1963).
20. P. J. BERKELEY, JR. and M. W. HANNA. J. Chem. Phys. **41**, 2530 (1964).
21. T. SCHAEFER and W. G. SCHNEIDER. J. Chem. Phys. **32**, 1218 (1960).
22. T. SCHAEFER and W. G. SCHNEIDER. J. Chem. Phys. **32**, 1224 (1960).
23. A. L. MCCLELLAN and S. W. NICKSIC. J. Phys. Chem. **69**, 446 (1965).
24. L. K. JACKSON, G. N. R. SMART, and G. F. WRIGHT. J. Am. Chem. Soc. **69**, 1539 (1947).
25. S. L. REID. U.S. Patent No. 3,137,728 (1964); Chem. Abstr. **61**, 5533*h* (1964).
26. H. SUGAWARA, H. SAITÔ, and K. NUKADA. Unpublished result.
27. N. A. LANGE. Handbook of chemistry. 10th ed. McGraw-Hill Book Co., Inc., New York. 1961. p. 1222.
28. LANDOLT–BÖRNSTEIN. Zahlenwerte und Funktionen. II Band. 6 Teil. *Edited by* K. H. Hellwege and A.M. Hellwege. Springer. 1959. p. 614.
29. A. D. BUCKINGHAM, T. SCHAEFER, and W. G. SCHNEIDER. J. Chem. Phys. **32**, 1227 (1960).
30. G. C. PIMENTEL and A. L. MCCLELLAN. The hydrogen bond. W. H. Freeman and Co., San Francisco. 1960. p. 91 and references cited therein.
31. H. SAITÔ, K. NUKADA, T. KOBAYASHI, and K. MORITA. J. Am. Chem. Soc. **89**, 6605 (1967).
32. J. W. EMSLEY, J. FEENEY, and L. H. SUTCLIFFE. High resolution nuclear magnetic resonance spectroscopy. The Pergamon Press, Ltd., London. 1966. p. 716.
33. R. MECKE. Discussions Faraday Soc. **9**, 161 (1950).
34. N. MULLER and D. E. PRITCHARD. J. Chem. Phys. **31**, 768, 1471 (1959).
35. N. MULLER. J. Chem. Phys. **36**, 3591 (1962).

Can. J. Chem. Downloaded from www.nrcresearchpress.com by 210.87.254.40 on 09/05/12
For personal use only.

Can. J. Chem. Downloaded from www.nrcresearchpress.com by 210.87.254.105 on 09/05/12
For personal use only.

Studies with halogeno sugars. II. A stable free glycosyl chloride

P. R. BRADLEY AND E. BUNCEL
Department of Chemistry, Queen's University, Kingston, Ontario

Received April 2, 1968

Dehydrochlorination of 3,4,6-tri-*O*-acetyl-2-chloro-2-deoxy-α-D-glucopyranosyl chloride with diethylamine yielded 3,4,6-tri-*O*-acetyl-2-chloro-D-glucal. The latter was further chlorinated to 3,4,6-tri-*O*-acetyl-2-deoxy-2,2-dichloro-α-D-*arabino*-hexopyranosyl chloride, which on deacetylation provided the first example of a stable, free glycopyranosyl chloride.

A 3,4,6-tri-*O*-acetyl-2-chloro-2-deoxymannopyranosyl chloride, also isolated in this work, was characterized by properties which correspond closely to the recently reassigned β anomer.

Canadian Journal of Chemistry, **46**, 3001 (1968)

Although monohalogen substitution on asymmetric carbon atoms of cyclic sugars has been achieved in numerous instances (1) and with each of the four halogens, cyclic sugars with *gem*-dihalogen substitution on ring carbons are comparatively rare. The earliest examples appear to be acetylated 2-deoxy-2,2-dichloro-D-*erythro*-pentopyranose and its glycosyl chloride, synthesized by Vargha and Kuszmann (2). More recently Brown and Jones (3) have reported a 3-deoxy-3,3-di-iodo derivative of D-*ribo*-hexofuranose. Our present work concerns the investigation of synthetic routes to 2,2-dichloro substitution of hexopyranose structures. Electronegative substitution at this position is of particular interest to us in kinetic studies of the acid hydrolysis of glycopyranosides (4).

A long-established route to 2-chlorodeoxy substitution of hexopyranoses has been via chlorination of the 1,2-glycals to 2-chlorodeoxy-D-glycosyl chlorides. In the earliest investigation of this reaction Fischer, Bergmann, and Schotte (5) passed chlorine into a cold solution of tri-*O*-acetyl-D-glucal (**1**) in carbon tetrachloride and obtained a product described as 'triacetylglucal dichloride'. Recent investigations of this substance using modern analytical techniques show that it is a mixture of *gluco* (**2**) and *manno* (**3**) epimers. Lemieux and Fraser-Reid (6), using nuclear magnetic resonance spectroscopy (n.m.r.), reported the α-D-*gluco* dichloride as the main product in greater than 80% yield, but did not detect the *manno* dichloride. Subsequently Lefar and Weill (7) subjected a crystalline sample of the dichloro-triacetyl-glycal to thin-layer chromatography (t.l.c.) and showed that it was a mixture of two major components which they identified by n.m.r. as the α-D-*gluco* and α-D-*manno* dichlorides in a ratio of roughly 4:1. The results of the present work are qualitatively similar to those of Lefar and Weill, as far as the ratio of the two components is concerned, but the minor component exhibits significantly different physical properties and n.m.r. spectrum (*vide infra*). Very recently, since the completion of our work, Igarashi, Honma, and Imagawa have reported (8) on the chlorination of D-glucal triacetate and have reassigned the configuration of the *manno* component as the β-D-mannopyranosyl chloride. Their n.m.r. and other data for this compound agree very well with those found in the present work and we concur with their reassignment. From treatment of this compound with titanium tetrachloride Igarashi *et al.* (8) isolated an isomeric dichloride which they assigned as the anomeric α-D-mannopyranosyl chloride. Igarashi *et al.* conclude that chlorination of tri-*O*-acetyl-D-glucal occurs mainly by a four-centered transition state or a concerted mechanism, which is in contrast to the two-stage oxocarbonium mechanism proposed by Lemieux and Fraser-Reid (6).

In 1963 Vargha and Kuszmann (2) reported a series of reactions leading from 3,4-di-*O*-acetyl-D-arabinal to an acetylated 2,2-dichloro-2-deoxy-D-pentose. Chlorination of di-*O*-acetyl-D-arabinal gave a mixture of 1,2-dichloro derivatives, which on treatment with sodium phenoxide followed by fractional distillation yielded a mixture of phenyl 2-chloro-2-deoxy-D-glycosides and pure syrupy 3,4-di-*O*-acetyl-2-chloro-D-arabinal. Further chlorination of the latter material and displacement of the chlorine atom at C-1 by the acetate group gave crystalline 1,3,4-tri-*O*-acetyl-2-deoxy-2,2-dichloro-D-*erythro*-pentopyranose. Our efforts to apply this

Can. J. Chem. Downloaded from www.nrcresearchpress.com by 210.87.254.105 on 09/05/12
For personal use only.

method to tri-*O*-acetyl-D-glucal in an attempt to prepare 2-deoxy-2,2-dichloro-D-*arabino*-hexopyranose did not meet with the same success. On treatment of the crystalline mixture of tri-*O*-acetyl-D-glucal dichlorides (**2** and **3**) with sodium phenoxide, using a similar technique (2), an intractable syrup was obtained, and t.l.c. indicated some eight components, which were inseparable by distillation.

A more efficient reagent for the dehydrohalogenation process was found to be diethylamine. Use of this base for the 1,2-elimination of hydrogen halides from glycosyl halides to give 2-substituted glycals originates from the work of Maurer and Mahn (9) and has provided a general method for the preparation of per-acetylated 2-hydroxyglycals (10, 11). Many of the latter compounds are readily chlorinated to fairly stable, acetylated 2-chloro-2-hydroxy-D-glycopyranosyl chlorides (9, 10). When a benzene solution of **2** and **3** was treated with diethylamine, the resulting syrup contained two major components. One was isolated in crystalline form, and from its physical characteristics and n.m.r. spectrum can be identified as the unchanged 3,4,6-tri-*O*-acetyl-2-chloro-2-deoxy-β-D-mannopyranosyl chloride, **3** (cf. 7, 8). The second component resisted crystallization and was not obtained in pure form, but fractional distillation of the residue after crystallization of **3** gave a colorless syrup containing a high proportion of 3,4,6-tri-*O*-acetyl-2-chloro-D-glucal (**4**), identified by its n.m.r. and infrared spectra. The latter compound has subsequently been reported by Lemieux and Morgan (12) in equimolar mixture with tetra-*n*-butylammonium bromide, as a product from the treatment of tri-*O*-acetyl-2-chloro-2-deoxy-α-D-glucopyranosyl bromide with pyridine in the presence of tetra-*n*-butylammonium bromide. Hurd and Jenkins (13) have recently prepared impure 3,4,6-tri-*O*-acetyl-2-bromo-D-glucal from a mixture of tri-*O*-acetyl-D-glucal dibromides, using triethylamine as the dehydrobrominating agent.

The facile dehydrochlorination of **2** in contrast to the unchanged **3** is readily explained. In the α-D-*gluco* case the C-1 chlorine and C-2 hydrogen have a *trans*-diaxial orientation, which is a prerequisite of normal E2 elimination in cyclic systems (14*a*, *b*). In the β-D-*manno* isomer (on the basis of the most recent assignment (8)) the hydrogen and chlorine are diequatorial and hence elimination would be a much slower process. The mechanism of dehydrohalogenation of pyranosyl halide structures, with particular reference to tetra-*O*-acetyl-α-D-glucopyranosyl bromide, was discussed by Lemieux and Lineback (15), who also considered reasons for the particular effectiveness of certain amines such as diethylamine in catalyzing elimination rather than leading to the formation of *N*-glycosides.

On chlorinating the syrup containing 3,4,6-tri-*O*-acetyl-2-chloro-D-glucal (**4**), one mole of chlorine was added across the double bond, yielding pure crystalline 3,4,6-tri-*O*-acetyl-2-deoxy-2,2-dichloro-α-D-*arabino*-hexopyranosyl chloride (**5**). Attempts to convert **5** to the methyl glycoside under Koenigs–Knorr conditions were

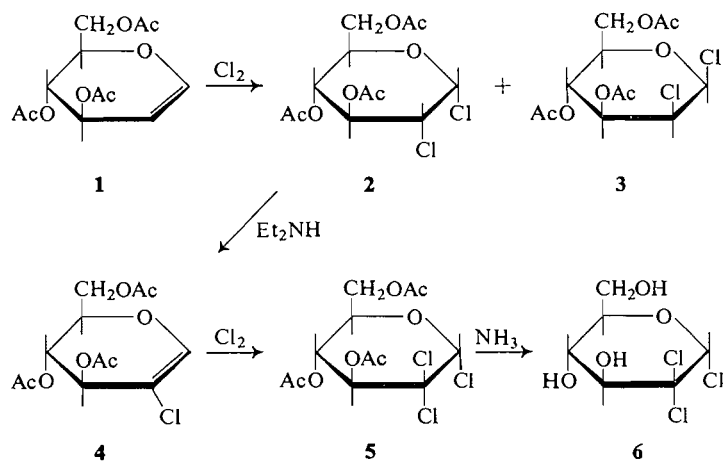

CHART 1

Can. J. Chem. Downloaded from www.nrcresearchpress.com by 210.87.254.105 on 09/05/12
For personal use only.

unsuccessful. This is perhaps not surprising when it is noted that glycosyl fluorides are also resistant to methanolysis (16), the fluorine atom being too firmly bound on C-1. Chlorine atoms at the C-2 position of a glycosyl chloride will exert an inductive (−I) effect on the C-1 position, making ionization of the 1-chlorine atom more difficult. With one chlorine atom on C-2 methanolysis takes place (although Fischer *et al.* (5) deemed it necessary to elevate the reaction temperature); with two chlorine atoms on C-2 the inductive effect appears to be too great and the reaction fails.

Deacetylation of **5** gave crystalline 2-deoxy-2,2-dichloro-α-D-*arabino*-hexopyranosyl chloride (**6**), apparently the first example of a stable, free glycosyl chloride; apart from glycosyl fluorides (17), the glycosyl halides are known generally as the acetylated (18), or benzylated (19), derivatives. Deacetylation normally results in loss of the 1-halogen atom accompanied by decomposition or the formation of anhydro sugars, but in the case of **6** this is prevented by the inductive effect described above.

The n.m.r. spectra are presented for compounds **3** and **5** since their structural assignments may still be open to question. The n.m.r. spectrum of **3** (Fig. 1) shows an absorption (doublet) at τ 4.34 assignable to the anomeric proton at C-1, which is coupled ($J_{1,2}$ = 1.2 c.p.s.) to an equatorial proton on C-2 whose resonance (quartet) appears at τ 5.43. The C-2 hydrogen is also coupled ($J_{2,3}$ = 3.2 c.p.s.) with a signal (quartet) at τ 4.90 assignable to the axial C-3 proton, which is in turn coupled ($J_{3,4}$ = 9.5 c.p.s.) to the axial C-4 proton whose signal (triplet) appears at τ 4.58. The axial proton on C-5 appears as a multiplet at τ 6.17 and the two protons on C-6 as a doublet at τ 5.80. The large signals at τ 7.9 are assignable to the nine protons of the three acetyl groups. These data do not conclusively establish the

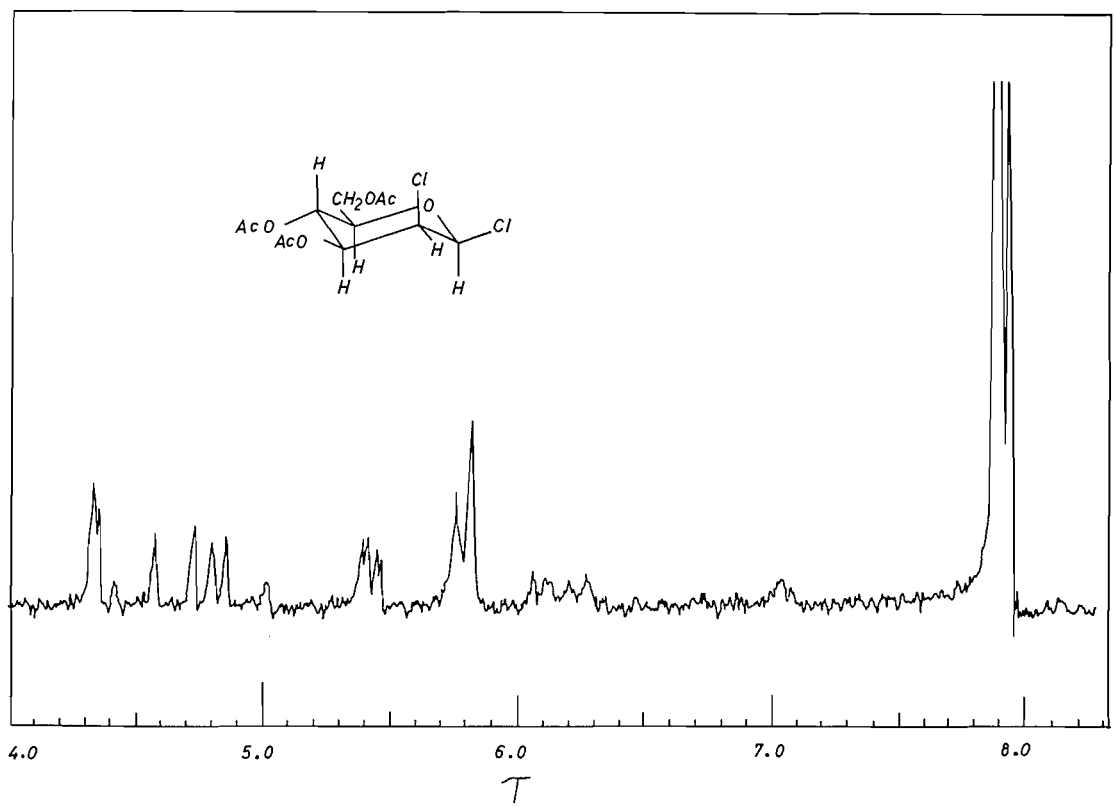

FIG. 1. The nuclear magnetic resonance spectrum of 3,4,6-tri-*O*-acetyl-2-chloro-2-deoxy-β-D-mannopyranosyl chloride (**3**) in deuteriochloroform.

orientation of the C-1 proton (7, 8), but the observed negative rotation and the chemical evidence obtained by Igarashi *et al.* (8) are in accord with the assignment as 3,4,6-tri-*O*-acetyl-2-chloro-2-deoxy-β-D-mannopyranosyl chloride.

The n.m.r. spectrum of **5** (Fig. 2) shows the anomeric proton as a sharp peak at τ 4.45. As there is no proton on C-2, no signal occurs around τ 5.4. The hydrogens on C-3 and C-4, however, are not readily identified. A spectrum taken at 100 c.p.s. sweepwidth shows the signal (shoulder) on the low-field side of the anomeric proton to be real and is probably part of the absorption due to these hydrogens. The absorption due to the C-5 hydrogen in the τ 6 region is poorly resolved but a 100 c.p.s. sweepwidth does reveal the multiplet. The n.m.r. spectrum does not prove that the anomeric proton is equatorial since there is no 1,2 spin–spin coupling. However, the anomeric effect (20), together with n.m.r. evidence on other acetylated aldopyranosyl halides (21), suggests that the more thermodynamically stable form of this halide will have the chlorine atom axially oriented.

Experimental

General Methods

Solutions were concentrated under reduced pressure using a rotary-type evaporator at temperatures not exceeding 50°. Melting points were determined on a Fisher–Johns apparatus and are uncorrected. Optical rotations were measured with a Hilger Standard Polarimeter Mk. 3. Infrared (i.r.) absorption spectra were obtained on a Perkin–Elmer model 21 spectrophotometer. The nuclear magnetic resonance (n.m.r.) spectra were determined at 60 Mc.p.s. with a Varian A-60 spectrometer, using an approximately 10% by weight solution of the compound in carbon tetrachloride or deuteriochloroform; tetramethylsilane was used as an internal standard. Thin-layer chromatography (t.l.c.) was carried out by the ascending method, using glass plates coated with silica gel 'G'. Toluene – diethyl ether, 2:1 (6) was used as eluent in all cases. The developed plates were dried in air, sprayed with either concentrated sulfuric acid or silver nitrate/sodium hydroxide reagents (22), and then heated in an oven at 150°. Rates of movement of sugars are quoted relative to the solvent front.

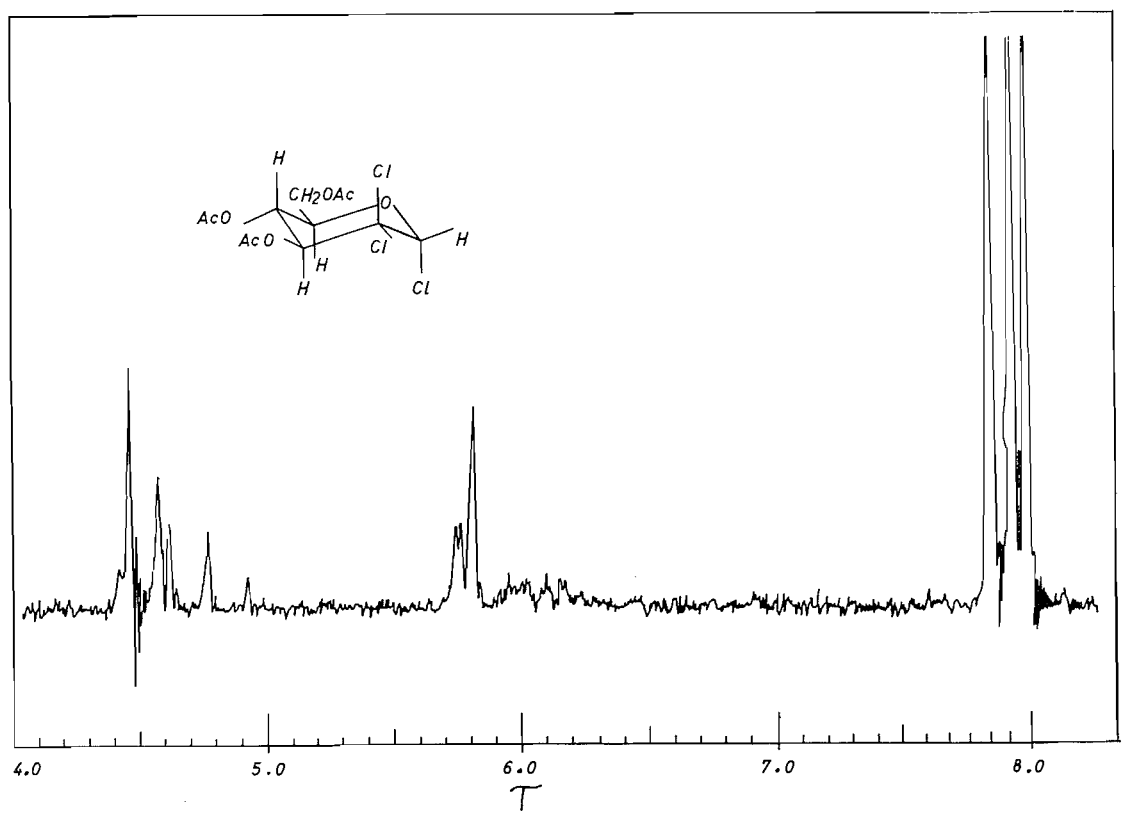

FIG. 2. The nuclear magnetic resonance spectrum of 3,4,6-tri-*O*-acetyl-2-deoxy-2,2-dichloro-α-D-*arabino*-hexopyranosyl chloride (**5**) in deuteriochloroform.

Can. J. Chem. Downloaded from www.nrcresearchpress.com by 210.87.254.105 on 09/05/12
For personal use only.

Can. J. Chem. Downloaded from www.nrcresearchpress.com by 210.87.254.105 on 09/05/12
For personal use only.

Mixture of Tri-O-acetyl-2-chloro-2-deoxy-α-D-gluco- and β-D-mannopyranosyl Chlorides (2 and 3)

3,4,6-Tri-*O*-acetyl-D-glucal (20 g), prepared by the method of Helferich *et al.* (23), was dissolved in carbon tetrachloride (100 ml) and cooled in an ice–salt mixture. Dry chlorine was passed through the colorless solution for 5–10 min, until the rapid appearance of a yellow coloration indicated that the stoichiometric intake of chlorine had been reached. After stirring for a further 15 min the slight excess of chlorine was removed by bubbling air through the solution. The solvent was then evaporated *in vacuo* at 35–40°, leaving a colorless syrup (26.0 g). The syrup was taken up in ether and crystallized by cooling in ice and seeding (the syrup resisted initial crystallization for 11 months), giving a 79% yield of solid product. After recrystallization twice from ether the white needles had m.p. 93–96°; lit. m.p. 89–93° for a 4:1 ratio of the *gluco* and *manno* dichlorides (7). A t.l.c. analysis of the product, sprayed with concentrated sulfuric acid, showed two spots in approximately 4:1 ratio. Further recrystallization of a small portion of the mixture yielded a product m.p. 98–99°, $[\alpha]_D^{25}$ +226.7° (*c*, 3.0 in chloroform); lit. for **2**, m.p. 99–100°, $[\alpha]_D^{23}$ +227.6° (8).

Treatment of 2 and 3 with Diethylamine

The crystalline mixture of **2** and **3** (9.0 g) was dissolved in dry benzene (10 ml). After the addition of diethylamine (4.3 ml) the solution was heated briefly to 60° and allowed to stand at room temperature for 40 h. The mixture slowly thickened as crystalline diethylamine hydrochloride was formed. Ether (100 ml) was added and the solution was washed with 1 *N* sulfuric acid (30 ml and 15 ml) and water (2 × 15 ml), then dried over magnesium sulfate and evaporated to a syrup. Remaining traces of benzene were removed as an azeotrope by dissolving the syrup in dry methanol (50 ml) and again evaporating to a pale-yellow syrup (8.3 g). A t.l.c. analysis of the syrup, sprayed with concentrated sulfuric acid, showed two major spots at R_f 0.57 and R_f 0.41 and a minor spot at R_f 0.25. Evidence described below identified the spot R_f 0.41 as **3** and the spot R_f 0.57 as 4.

After standing for two weeks at room temperature the syrup began to crystallize slowly, and by seeding a concentrated, ice-cold ethereal solution of the syrup two crops of a white crystalline material were obtained; total yield 0.75 g. After two recrystallizations from acetone – petroleum ether the large needle-shaped crystals of **3** had m.p. 145–147°, $[\alpha]_D^{25}$ −43.8° (*c*, 3.0 in chloroform); lit. m.p. 139–140° (7), 145.5–146° (8); $[\alpha]_D^{23}$ −44° (8).

Anal. Calcd. for $C_{12}H_{16}O_7Cl_2$: C, 42.01; H, 4.70; Cl, 20.66. Found: C, 41.88; H, 4.91; Cl, 20.71.

A t.l.c. plate, sprayed with concentrated sulfuric acid, showed a single spot of R_f 0.41, running parallel with the component present in the syrup and the previous tri-*O*-acetyl-D-glucal dichloride mixture.

A portion (3.6 g) of the residual syrup after crystallization of **3** was distilled *in vacuo* at 134°/0.3 mm, giving a colorless distillate (2.7 g). Thin-layer chromatography showed a high concentration of the component R_f 0.57, but reduced amounts of the slower moving components were still present. An i.r. spectrum of the syrup showed a characteristic peak at 1640 cm^{-1} for C=C stretching vibration, indicating the presence of a dehydrochlorination product, namely 3,4,6-tri-*O*-acetyl-2-chloro-D-glucal.

Comparison of the n.m.r. spectrum with that of **2** (cf. ref. 6) clearly indicates the nature of the C-1 hydrogen. Its absorption may be assigned to the singlet furthest down field at τ 3.37, as expected for a vinylic proton which is not coupled. The lack of a signal around τ 5.4 confirms the absence of a proton on C-2, and also indicates that the amount of **3** present as impurity was small.

3,4,6-Tri-O-acetyl-2-deoxy-2,2-dichloro-α-D-arabino-hexopyranosyl Chloride (5)

The above distilled syrup (26.5 g) containing 4 was dissolved in carbon tetrachloride (80 ml) and cooled to 0°. Dry chlorine was bubbled through the stirred solution until a persistent yellow color indicated excess. After stirring at 0° for a further 30 min a white solid began to crystallize. Partial evaporation of the solvent removed excess chlorine and concentrated the solution to a slurry, which was cooled and filtered, yielding a solid which weighed 6.0 g after one recrystallization from acetone – petroleum ether. A second recrystallization gave white needles of m.p. 168–169°; $[\alpha]_D^{25}$ −5.2° (*c*, 2.2 in chloroform). A thin-layer chromatogram, sprayed with silver nitrate/sodium hydroxide reagents and heated in an oven at 150°, showed a single brown spot of R_f 0.52 (concentrated sulfuric acid failed to char the compound on the plate).

Anal. Calcd. for $C_{12}H_{15}O_7Cl_3$: C, 38.18; H, 4.01; Cl, 28.17. Found: C, 37.99; H, 4.17; Cl, 28.15.

2-Deoxy-2,2-dichloro-α-D-arabino-hexopyranosyl Chloride (6)

A solution of **5** (0.4 g) in dry methanol (50 ml) was cooled to 0°, saturated with dry gaseous ammonia and allowed to stand for 3 h at room temperature. Examination (solvent and spray as for **5** above) of the syrup by t.l.c. revealed a single component of R_f 0.03. The syrup crystallized from ethanol–chloroform yielding 0.22 g (82%) of solid. Recrystallization from *n*-propanol–chloroform gave white needles of m.p. 176–177° (decomp.); $[\alpha]_D^{25}$ −0.8° (*c*, 1.3 in methanol).

Anal. Calcd. for $C_6H_9O_4Cl_3$: C, 28.65; H, 3.61; Cl, 42.29. Found: C, 28.54; H, 3.52; Cl, 41.98.

Attempted Koenigs–Knorr Reaction on 5

Silver carbonate (1.0 g), iodine (0.13 g), and Drierite (2.5 g) were added to a solution of **5** (0.5 g) in dry methanol (30 ml) and the mixture was stirred. Samples periodically extracted from the mixture were centrifuged and the supernatant liquor examined by t.l.c. Although traces of material of low R_f were apparent, the bulk of the starting material was unchanged after 40 h, and crystalline **5** was recoverable from the solution. Further increments of silver carbonate or elevation of the temperature failed to induce reaction.

Acknowledgments

We wish to thank Drs. G. W. Hay and J. K. N. Jones for helpful discussions. Financial support from the National Research Council of Canada and the Ontario Research Foundation is gratefully acknowledged.

1. J. E. G. BARNETT. Advan. Carbohydrate Chem. **22**, 177 (1967).
2. L. VARGHA and J. KUSZMANN. Chem. Ber. **96**, 411 (1963).
3. D. M. BROWN and G. H. JONES. Chem. Commun. 561 (1965); J. Chem. Soc. C, 252 (1967).
4. E. BUNCEL and P. R. BRADLEY. Can. J. Chem. **45**, 515 (1967).
5. E. FISCHER, M. BERGMANN, and H. SCHOTTE. Ber. **53**, 509 (1920).
6. R. U. LEMIEUX and B. FRASER-REID. Can. J. Chem. **43**, 1460 (1965).
7. M. S. LEFAR and C. E. WEILL. J. Org. Chem. **30**, 954 (1965).
8. K. IGARASHI, T. HONMA, and T. IMAGAWA. Tetrahedron Letters, **6**, 755 (1968).
9. K. MAURER and H. MAHN. Ber. **60**, 1316 (1927).
10. M. G. BLAIR. Advan. Carbohydrate Chem. **9**, 97 (1954).
11. R. J. FERRIER. Advan. Carbohydrate Chem. **20**, 67 (1965).
12. R. U. LEMIEUX and A. R. MORGAN. Can. J. Chem. **43**, 2214 (1965).
13. C. D. HURD and H. JENKINS. Carbohydrate Res. **2**, 240 (1966).
14*a*. D. V. BANTHORPE. Elimination reactions. Elsevier Publ. Co., Inc., Amsterdam. 1963.
b. G. AYREY, E. BUNCEL, and A. N. BOURNS. Proc. Chem. Soc. 458 (1961).
15. R. U. LEMIEUX and D. R. LINEBACK. Can. J. Chem. **43**, 94 (1965).
16. J. STANEK, M. CERNY, J. KOCOUREK, and J. PACAK. The monosaccharides. Academic Press, Inc., New York. 1963. p. 262.
17. F. MICHEEL and A. KLEMER. Advan. Carbohydrate Chem. **16**, 85 (1961).
18. L. J. HAYNES and F. H. NEWTH. Advan. Carbohydrate Chem. **10**, 207 (1955).
19. C. P. J. GLAUDEMANS and H. G. FLETCHER, JR. J. Org. Chem. **28**, 3004 (1963).
20. R. U. LEMIEUX. *In* Molecular rearrangements. Part II. *Edited by* P. de Mayo. Interscience Publishers, Inc., New York. 1964. p. 735.
21. D. HORTON and W. N. TURNER. J. Org. Chem. **30**, 3387 (1965).
22. W. E. TREVELYAN, D. P. PROCTOR, and J. S. HARRISON. Nature, **166**, 444 (1950).
23. B. HELFERICH, E. N. MULCAHY, and H. ZIEGLER. Chem. Ber. **87**, 233 (1954).

Can. J. Chem. Downloaded from www.nrcresearchpress.com by 210.87.254.105 on 09/05/12
For personal use only.

Can. J. Chem. Downloaded from www.nrcresearchpress.com by 210.87.254.5 on 09/05/12
For personal use only.

Synthesis of DL-*threo*- and DL-*erythro*-β-hydroxyisoleucine[1]

T. A. DOBSON[2]
Prairie Regional Laboratory, National Research Council of Canada, Saskatoon, Saskatchewan

AND

L. C. VINING
Atlantic Regional Laboratory, National Research Council of Canada, Halifax, Nova Scotia

Received May 13, 1968

DL-*threo*- and DL-*erythro*-β-Hydroxyisoleucine were prepared from *cis*- and *trans*-3-methylpent-2-enoic acids, respectively. The configuration of the *erythro* isomer was established from its synthesis by two independent routes. The diastereoisomers, and those of other β-hydroxy amino acids, can be distinguished by examination of their proton magnetic resonance spectra.

Canadian Journal of Chemistry, 46, 3007 (1968)

An investigation of the biosynthesis of aspergillic acid in cultures of *Aspergillus flavus*, which showed that this pyrazine derivative is derived from leucine and isoleucine (1), led us to conjecture that hydroxyaspergillic acid might be formed similarly from leucine and β-hydroxyisoleucine. Although subsequent work proved this to be incorrect (2), preliminary feeding trials with a mixture of the DL-*threo* and *erythro* isomers of β-hydroxyisoleucine had shown strong inhibition of aspergillic acid production without noticeable effect on the growth of *A. flavus*. In order to examine this effect further each isomeric amino acid has been prepared in a pure form. These compounds may also be of value in elucidating the biosynthesis of two other plant metabolites, cleomin (3) and linamarin (4) which contain elements of the β-hydroxyisoleucine skeleton.

Attempted synthesis of β-hydroxyisoleucine from methyl ethyl ketone and glycine using the general route for β-hydroxy α-amino acids described by Otani and Winitz (5) was unsuccessful. However the amino acid was conveniently prepared from methyl ethyl ketone and ethyl dichloroacetate via the glycidic ester. Alkaline hydrolysis (6) yielded the acid which, after reaction with benzylamine followed by hydrogenolysis as described by Liwschitz *et al.* (7) gave β-hydroxyisoleucine in an overall yield of 17% based on methyl ethyl ketone. The Darzens synthesis is known to yield a mixture of *cis* and *trans* glycidic esters (8). These were detected by gas–liquid chromatography (g.l.c.) but could not be separated on a preparative scale. Analysis by ion exchange chromatography of the β-hydroxyisoleucine obtained from this procedure showed the expected mixture of diastereoisomers, but attempts to effect the separation of milligram quantities by ion exchange chromatography with larger columns were unsatisfactory. No useful separations were obtained by paper chromatography, or by fractional crystallization.

As an alternative route to the synthesis of each of the β-hydroxyisoleucines a procedure used by West *et al.* (9) for the preparation of threonine and allothreonine was explored. 3-Methylpent-2-enoic acid, obtained as described by Kon and Linstead (10), was a liquid from which a crystalline product, m.p. 46°, was obtained by fractional distillation. This compound, previously described by several workers (11, 12), was found from g.l.c. and spectral evidence, to represent one of the isomeric α,β-unsaturated acids. The second isomer was separated in a pure form by preparative g.l.c. and obtained as a crystalline solid, m.p. 35.5°. Structures are assigned to these compounds on the basis of their nuclear magnetic resonance (n.m.r.) spectra (Table I). Jackman and Wiley (13) have observed that in *cis–trans* pairs of α,β-unsaturated esters the protons of β-methyl and methylene groups are deshielded to the extent of 0.25, and 0.5–0.9 p.p.m., respectively, by a *cis*-carbonyl function. In the lower melting acid signals for the β-methyl protons are shielded by 0.59 p.p.m. and those of the methylene protons deshielded by 0.78 p.p.m. with respect to the corresponding signals given by

[1]Issued as NRCC No. 10225.
[2]NRCC Postdoctorate Fellow, 1960–1962. Present address: Ayerst McKenna and Harrison, Montreal, Quebec.

the higher melting isomer. The acid of m.p. 35.5° is therefore assigned structure **1** in which the methylene group is *cis* to the carboxyl; the acid of m.p. 46° is assigned the *trans* structure **2**.

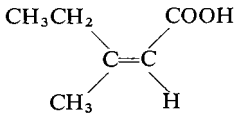

1

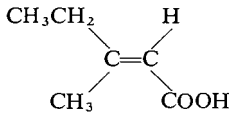

2

Addition of methyl hypobromite to **2** under the conditions described by Rüfenacht (14) yielded a 2-bromo-3-methoxy-3-methylpentanoic acid, m.p. 57–58° which, assuming *trans* addition, should have structure **3**. This, with ammonia, gave a β-methoxy-α-amino acid which was demethylated with hydrobromic acid to β-hydroxyisoleucine, m.p. 239–242° (decomp.). Pfister *et al.* (15) have shown that this series of reactions applied to *trans*-crotonic acid gives allothreonine which has the *erythro* configuration of hydroxyl and amino groups. They concluded that replacement of bromine by an amino group must proceed with retention of configuration, as found by earlier workers (16, 17) during the preparation of valine and isoleucine by this reaction, and in contrast to the inversion which occurs with other amino acids. If the stereochemistry of reactions leading to β-hydroxyisoleucine is the same as in analogous reactions used for the synthesis of allothreonine, the amino acid should have the *erythro* configuration **5**. Starting from the *cis*-unsaturated acid **1**, a similar series of reactions gave a β-hydroxyisoleucine to which the *threo* configuration, **8**, is assigned.

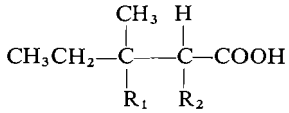

3, $R_1 = OCH_3$; $R_2 = Br$
4, $R_1 = OCH_3$; $R_2 = NH_2$
5, $R_1 = OH$; $R_2 = NH_2$
10, $R_1 = OH$; $R_2 = NHBz$

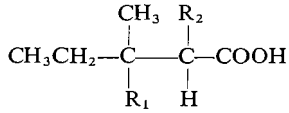

6, $R_1 = OCH_3$; $R_2 = Br$
7, $R_1 = OCH_3$; $R_2 = NH_2$
8, $R_1 = OH$; $R_2 = NH_2$

Evidence for the correctness of structure **5** is provided through an independent synthesis of *erythro* β-hydroxyisoleucine from the *trans*-unsaturated acid by the procedure of Liwschitz *et al.* (7). These workers have established that the oxirane ring formed by epoxidation of α,β-unsaturated acids is opened with benzylamine to give the 2-*N*-benzylamino-3-hydroxy acid with inversion of configuration. The α-amino-β-hydroxy acid obtained from the *trans*-unsaturated acid, should have an *erythro* configuration (viz. **2** → **9** → **10** → **5**).

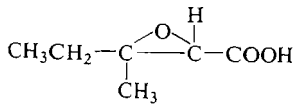

9

The n.m.r. spectra of these isomeric pairs of substituted 3-methylpentanoic acids show sufficient differences to provide a useful means of

TABLE I

Chemical shifts and coupling constants for 3-methylpent-2-enoic acids*

		cis Isomer		*trans* Isomer	
Assignments	Multiplicity	τ	Hz	τ	Hz
$CH_3-\overset{|}{C}-$	Triplet	9.09	7.4	9.25	7.5
$-CH_2-$	Quartet	7.44	7.6	8.22	7.5
$CH_3-\overset{|}{C}=$	Doublet	8.55	1.7	7.96	1.3
$=CH-$		4.36	†	4.30	1.3‡
$-COOH$	Singlet	−2.42	—	−2.82	—

*Measured in benzene-d_6 (50 mg per ml).
†Unresolved multiplet.
‡Quartet. Signals in all quartets and triplets show additional splitting with $J < 1$ Hz.

Can. J. Chem. Downloaded from www.nrcresearchpress.com by 210.87.254.5 on 09/05/12
For personal use only.

TABLE II

Chemical shifts and coupling constants of some 2,3-substituted 3-methylpentanoic acids

Compound* $CH_3CH_2C(CH_3)(R_1)CH(R_2)COOH$	$-CH_2-$		CH_3-C-	$R_1 = OCH_3$	$-CH$	
	τ	Hz§	τ	τ	τ	H‖
2-Bromo-3-methoxy-3-methylpentanoic acid(**6**)†	8.14	4.3	8.57	6.63	5.61	
2-Bromo-3-methoxy-3-methylpentanoic acid(**3**)‡	8.17	7.0	8.56	6.65	5.64	
DL-*threo*-β-Methoxyisoleucine	7.94	7.0	8.62	6.58	5.50¶	5.5
DL-*erythro*-β-Methoxyisoleucine	8.17	7.2	8.33	6.53	5.52¶	4.0
DL-*threo*-β-Hydroxyisoleucine	7.94	7.8	8.51	—	5.55¶	
DL-*erythro*-β-Hydroxyisoleucine	8.18	7.1	8.30	—	5.57¶	
N-Benzyl-DL-*threo*-β-hydroxyisoleucine	8.04	7.0	8.60	—	5.79¶	6.5
N-Benzyl-DL-*erythro*-β-hydroxyisoleucine	8.32	6.5	8.38	—	5.79¶	6.5
N-Benzoyl-DL-*threo*-β-hydroxyisoleucine‡**	8.30	7.0	8.63	—	5.23	8.8
N-Benzoyl-DL-*erythro*-β-hydroxyisoleucine‡	8.25	7.0	8.68	—	5.18	9.0

*Measured at 50 mg per ml in trifluoroacetic acid except where noted.
†50 mg per ml in chloroform-*d*.
‡50 mg per ml in acetone-d_6.
§Quartet.
‖Doublet.
¶Signal shows broad envelope.
**Deduced from spectrum of mixed isomers.

identification. Examination of Table II reveals that, in the β-hydroxy and β-methoxy-α-amino acids assigned a *threo* configuration, signals from the 4-methylene protons are invariably deshielded whereas those of the 3-methyl substituent are shielded with respect to corresponding signals given by the *erythro* isomer. The difference is very small in the α-bromo-β-methoxy acids, and the shielding effects are reversed in the β-hydroxy-α-*N*-benzoylamino acids. Thus the preferred conformation is mainly due to interaction between substituents at positions-2 and -3. Differences in the chemical shifts of β-methyl and methylene groups,

TABLE III

Chemical shift (τ values) and coupling constants (Hz) for some β-hydroxy-α-amino acids

Compound* $R_3C(R_4)CH(OH)CH(NH_2)COOH$	R_3	R_4	$-CH$	$-NH_2$
	τ	τ	τ†	τ†
DL-β-Hydroxyvaline	8.44 (CH_3)	8.14 (CH_3)	5.54	2.46
L-Threonine	8.37 doublet *J*, 6.5 (CH_3)	5.55 multiplet (H)	5.62	2.54
DL-Allothreonine	8.39 doublet *J*, 6.5 (CH_3)	5.51 multiplet (H)	5.34	2.38
DL-*threo*-β-Hydroxyaspartic acid	—	4.64† (H)	5.00	—
DL-*erythro*-β-Hydroxyaspartic acid	—	4.76† (H)	4.89	2.1
DL-*threo*-*p*-Hydroxyphenylserine	2.72‡ (phenyl)	4.28 doublet *J*, 3.7 (H)	5.35	2.7
DL-*erythro*-*p*-Hydroxyphenylserine	2.75‡ (phenyl)	4.30 doublet *J*, 4.6 (H)	5.12	2.7
DL-*threo*-*p*-Nitrophenylserine	1.85‡ (phenyl)	4.11 doublet *J*, 8.4 (H)	5.23	2.4
DL-*erythro*-*p*-Nitrophenylserine	1.87‡ (phenyl)	4.11 doublet *J*, 8.4 (H)	5.07	2.4

*Concentration, 50 mg per ml in trifluoroacetic acid.
†Signals show broad envelope.
‡Average τ values A_2B_2 systems.

Can. J. Chem. Downloaded from www.nrcresearchpress.com by 210.87.254.5 on 09/05/12
For personal use only.

attributed to the deshielding effect of a neighboring carbonyl group, suggest that **11** and **12** represent the conformations of *threo*- and *erythro*-β-hydroxyisoleucines, respectively.

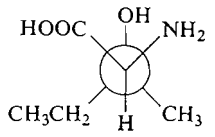

11

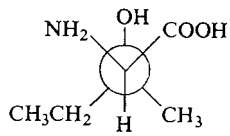

12

The proton magnetic resonance (p.m.r.) spectra of the *threo* and *erythro* forms of other α-amino-β-hydroxy acids (Table III) show similar differences which may be used to distinguish between the isomers. An estimate of the composition of isomeric mixtures can be obtained without need for the tedious and often difficult chromatographic separations which are sometimes used (18–23).

Since the *cis*-unsaturated acid **1** is less accessible than the corresponding *trans* isomer, alternate routes to *threo*-β-hydroxyisoleucine were investigated. Attempts to separate the isomeric 2-bromo-3-methoxy-3-methylpentanoic acids were not successful. Fractional crystallization of a mixture of β-methoxyisoleucines gave only the *erythro* isomer in a pure state. Benzoylation of the β-methoxyisoleucine mixture, which, in the case of *O*-methylthreonines has been shown (24) to yield a less soluble *threo* derivative, resulted in only a slight increase in the proportion of *threo* isomer after recrystallization from a variety of solvents.

Inversion of configuration at the β-position of β-hydroxy-α-amino acids can usually be accomplished via the oxazoline (25, 26). However, attempts to prepare an oxazoline by treating *N*-benzoyl-DL-*erythro*-β-hydroxyisoleucine methyl ester with thionyl chloride under the appropriate conditions gave back the starting material. More vigorous conditions did not yield the desired product. Presumably nucleophilic attack by the benzoyl oxygen is sterically hindered in this compound.

Pfister *et al.* (15) have shown that reaction between an amide of 2-bromo-3-methoxybutyric acid and ammonia gives predominantly an amino acid with opposite configuration at the α-position from that obtained when the acid itself is used. Comparable observations have been made by earlier workers (16, 17) using peptide derivatives of valine and isoleucine, and it has been suggested (15) that the configuration at the α-position is retained as the result of a neighboring group effect, the carboxyl ion participating in the transition state. Attempts to prepare DL-*threo*-β-hydroxyisoleucine taking advantage of the inversion expected when an amide or piperide derivative of DL-*erythro*-2-bromo-3-methoxy-3-methylpentanoic acid was treated with ammonia were frustrated when these compounds failed to react under the conditions described by Pfister *et al.* This lack of reactivity contrasts with the facile replacement of bromine in the α-bromo acid and is in accord with the observed effect of substitution at the β-position on the course of reactions at the α-carbon.

Experimental

Melting points were measured on a Fisher–Johns hot stage and infrared (i.r.) spectra with a Perkin–Elmer model 237 recording spectrophotometer. Proton magnetic resonance (p.m.r.) spectra were recorded on a Varian A-60A spectrometer; microanalyses were performed by Drs. F. and E. Pascher, Mikroanalytisches Laboratorium, Bonn.

Paper Chromatography

For routine paper chromatographic examination of samples the descending technique using Whatman No. 1 paper and *n*-butanol – acetic acid – water (12:3:5) was employed. Amino acids were detected with ninhydrin. R_f values of β-methoxyisoleucine and β-hydroxyisoleucine were 0.64 and 0.49 respectively. No separation of diastereoisomers was observed in this solvent system, or in those described by Drell (19), Shaw and Fox (20), Geipel *et al.* (21), or Gray *et al.* (22). A solvent mixture containing benzyl alcohol – methyl ethyl ketone – ammonia – water (20:3:1:1) gave small separations on chromatograms developed for 40 h. The relative mobilities (*erythro*-β-methoxyisoleucine, R_m 1.0) were *threo*-β-methoxyisoleucine, 1.09; *erythro*-β-hydroxyisoleucine, 1.26; *threo*-β-hydroxyisoleucine, 1.39.

Ion Exchange Chromatography

Separation of *threo*- and *erythro*-β-hydroxyisoleucine was performed with a Spinco model 120 Amino Acid Analyzer using AA-15 resin, citrate buffer of pH 3.28, and a flow rate of 70 ml per h. The *threo* isomer gave a peak at 71 min, and the *erythro* isomer at 74 min after sample application.

Gas–liquid Chromatography

Analytical separations were performed with a Varian Aerograph model 600-D instrument using a hydrogen flame ionization detector and 5 ft × 0.25 in. stainless steel columns with dimethylchlorosilane treated and acid-washed Chromosorb W (100–120 mesh size) as stationary support. Partial separation of isomeric glycidic esters was achieved on either 1% Carbowax 1540 or 1% DEGS as liquid phase at 125° (retention times 7.2, 7.6, and 7.6,

Can. J. Chem. Downloaded from www.nrcresearchpress.com by 210.87.254.5 on 09/05/12
For personal use only.

Can. J. Chem. Downloaded from www.nrcresearchpress.com by 210.87.254.5 on 09/05/12
For personal use only.

7.9 min respectively at a gas flow of 65 ml per min). For the separation of unsaturated acids 1% of either Carbowax 20 *M*, DEGS, or FFAP was a suitable liquid phase. For most routine applications a 1% FFAP column operating at 125° was used. Isomeric 3-methylpent-2-enoic acids were separated on a preparative scale with a Varian Aerograph "Autoprep" model A-700 using a 10 ft × 0.375 in. stainless steel column packed with 20% FFAP on dimethylchlorosilane treated Chromosorb W and a gas flow of 200 ml per min. The instrument was programmed to inject 0.3 ml samples automatically at 150° and a temperature gradient to 190° was applied.

β-Hydroxyisoleucine via Glycidic Ester

β-Methyl-β-ethylglycidic ester was saponified by the procedure of Johnson *et al.* (6). A saturated aqueous solution (200 ml) of the sodium salt of the acid (27.4 g) was heated under reflux with benzylamine (38.5 g) for 3 h. Excess benzylamine was removed by extraction with ether and the product applied to a column of sulfonated polystyrene cation (H^+) resin. After elution with 4 *N* aqueous ammonium hydroxide it was crystallized from water; yield 19.2 g (45%). This material, together with 5% palladium on charcoal, was suspended in glacial acetic acid (728 ml) and the mixture stirred for 12 h at 70° in an atmosphere of hydrogen. Solvent was removed *in vacuo*, the residue leached with hot water, and freed from catalyst by filtration. Addition of 2 volumes of ethanol yielded β-hydroxyisoleucine (8.25 g), m.p. 240–245° (decomp.).

Anal. Calcd. for $C_6H_{13}O_3N$: C, 48.96; H, 8.90; N, 9.52. Found: C, 49.05; H, 8.95; N, 9.41.

cis- and trans-3-Methylpent-2-enoic Acids

Ethyl 3-hydroxy-3-methylpentanoate, prepared in 57% yield by a Reformatsky reaction from methyl ethyl ketone and ethyl bromoacetate, was saponified with ethanolic potassium hydroxide. The hydroxy acid (55 g, 92% yield) was dehydrated by heating under reflux for 1.5 h with acetic anhydride (300 ml). The crude product was distilled at 1 mm Hg pressure to yield an oil (35.6 g), b.p. 65–70°. Iodimetric titration (27) gave a value of 8% for the content of β,γ-unsaturated acid.

The oil was redistilled at 1 Torr on a column (20 × 1 cm) packed with "Helipak" (Podbielniak Inc., Franklin Park, Ill.) and collected in 6 fractions over the temperature range 68–72°. Fractions 4 and 5 after cooling to 4° deposited crystals. These were recrystallized from petroleum ether (b.p. 40–60°) then aqueous methanol to give colorless prisms (5.9 g) of *trans*-3-methylpent-2-enoic acid (**2**), m.p. 46°; ν_{max}(film) at 1700, 1650, and 870 cm^{-1}.

Anal. Calcd. for $C_6H_{10}O_2$: C, 63.13; H, 8.83. Found: C, 62.93; H, 8.98.

Gas–liquid chromatographic analyses of the fractions, using an FFAP liquid phase at 125° showed that fractions 1–4 contained two products with retention times of 9.2 and 10.9 min. *trans*-3-Methylpent-2-enoic acid (**2**) isolated from fractions 4 and 5 corresponded in retention time with the slower moving component. The proportion of this acid in fractions 1 to 6 increased from 44 to 78% respectively. Fraction 6 contained approximately 6% of a third component of retention time 12.2 min. This was separated from the mixture by distribution between ether and 1% aqueous sodium bicarbonate, when it partitioned preferentially into the aqueous phase. It was purified by distillation to give an oil, $n_D^{23°}$ 1.4476, ν_{max}(film) 1715, 1655, and 900 cm^{-1}, corresponding in properties with 3-methylpent-3-enoic acid (10).

Preparative g.l.c. of fraction 1 separated the two components; the faster moving fraction was collected as an oil which crystallized on cooling, and, after recrystallization from petroleum ether (b.p. 40–60°), then water, afforded *cis*-3-methylpent-2-enoic acid (**1**) as colorless prisms, m.p. 35.5°; ν_{max}(film) at 1700, 1650, and 870 cm^{-1}.

Anal. Calcd. for $C_6H_{10}O_2$: C, 63.13; H, 8.83. Found: C, 62.77; H, 8.64.

threo- and erythro-2-Bromo-3-methoxy-3-methylpentanoic Acids

trans-3-Methylpent-2-enoic acid (1.0 g) in methanol (20 ml) containing freshly calcined heavy magnesium oxide powder (0.28 g) was treated at 0.5° with a stream of bromine vapor obtained by slow aspiration of dry air over 1.8 g bromine. After addition of bromine was complete (2 h) the reaction mixture was acidified, concentrated *in vacuo*, and diluted with water. The acidic product extracted into ether was obtained as an oil which crystallized on cooling at −10°. It was recrystallized from petroleum ether, (b.p. 60–80°) to give *erythro*-2-bromo-3-methoxy-3-methylpentanoic acid (**3**) as prisms (783 mg), m.p. 57.5–58°. ν_{max}(KBr) at 1730 cm^{-1}.

Anal. Calcd. for $C_7H_{13}O_3Br$: C, 37.36; H, 5.82; Br, 35.50. Found: C, 37.74; H, 5.91; Br, 35.56.

By a similar procedure *cis*-3-methylpent-2-enoic acid (0.5 g) yielded *threo*-2-bromo-3-methoxy-3-methylpentanoic acid (**6**) as prisms (610 mg), m.p. 53–53.5°; ν_{max}(KBr) 1735 cm^{-1}. Found: C, 37.25; H, 5.67; Br, 35.18.

Amides of DL-*erythro*-2-Bromo-3-methoxy-3-methylpentanoic Acid

The piperide of DL-*erythro*-2-bromo-3-methoxy-3-methylpentanoic acid, was prepared via the acyl chloride by the method of Pfister *et al.* (15). It was obtained in 92% yield as an oil, $n_D^{26°}$ 1.5080, ν_{max}(film) 1647 cm^{-1}. A sample was distilled at 85% at 10^{-3} Torr.

Anal. Calcd. for $C_{12}H_{22}O_2NBr$: C, 49.32; H, 7.59; N, 4.79; Br, 27.35. Found: C, 49.71; H, 7.54; N, 4.64; Br, 24.93.

By reacting the acyl chloride in benzene with dry ammonia the amide, m.p. 74.5–76°; ν_{max}(KBr) 3440, 3330, 3280, and 1677 cm^{-1} was obtained.

Anal. Calcd. for $C_7H_{14}O_2NBr$: C, 37.51; H, 6.30; N, 6.25; Br, 35.66. Found: C, 37.66; H, 6.12; N, 6.18; Br, 35.66.

threo- and erythro-β-Methoxyisoleucines

2-Bromo-3-methoxy-3-methylpentanoic acid (**3**) (6.0 g) and ammonium hydroxide (*d* 0.880, 120 ml) were heated in a sealed tube at 100° for 2.5 h. The reaction mixture was evaporated to dryness and the residue, in water, applied to a column of cation exchangeres in (H^+ form). The basic product was eluted with 4 *M* ammonium hydroxide and crystallized from aqueous ethanol to yield DL-*erythro*-β-methoxyisoleucine (**4**) as plates (3.2 g) which sublimed rapidly above 265° without melting. ν_{max}(KBr) 3070–2500, 1652, 1580, 1485, 1395, 1340, 1055, and 720 cm^{-1}.

Anal. Calcd. for $C_7H_{15}O_3N$: C, 52.15; H, 9.38; N, 8.69. Found: C, 52.53; H, 9.68; N, 8.48.

2-Bromo-3-methoxy-3-methylpentanoic acid (**6**) (450

mg) treated similarly gave DL-*threo*-β-methoxyisoleucine (**7**) as prisms (287 mg) which sublimed rapidly above 265° without melting; ν_{max}(KBr) 3050–2500, 1655, 1575, 1495, 1340, 1055, and 720 cm^{-1}. Found: C, 52.26; H, 9.17; N, 8.75.

threo- and erythro-β-Hydroxyisoleucines

DL-*erythro*-β-methoxyisoleucine (0.6 g) in 48% hydrobromic acid (18 ml) and water (12 ml) was heated under reflux for 6 h. Paper chromatographic analysis of the reaction mixture showed this to be the optimum reaction time. The solution was evaporated to dryness and the residue, in water, applied to a column of cation exchange resin (H^+ form). After elution with 4 *M* ammonium hydroxide, DL-*erythro*-β-hydroxyisoleucine (**5**) was crystallized from aqueous ethanol as plates (265 mg), m.p. 239–242° (decomp.). ν_{max}(KBr) 3400–2500, 1655, 1550, 1415, 1295, 1275, 1165, 1130, 1000, 940, and 730 cm^{-1}.

Anal. Calcd. for $C_6H_{13}O_3N$: C, 48.96; H, 8.90; N, 9.52. Found: C, 49.01; H, 8.84; N, 9.22.

Demethylation of DL-*threo*-β-methoxyisoleucine (100 mg) under similar conditions yielded DL-*threo*-β-hydroxyisoleucine (**8**) as plates (73 mg), m.p. 222–228° (decomp.); ν_{max}(KBr) 3380–2500, 1670, 1585, 1485, 1410, 1330, 1165, 1010, 920, and 715 cm^{-1}. Found: C, 49.04; H, 8.70; N, 9.77.

*N-Benzoyl-*DL-*erythro-β-Hydroxyisoleucine Methyl Ester*

N-Benzoyl-DL-*erythro*-β-hydroxyisoleucine was prepared by the procedure of West and Carter (24) in 87% yield. It crystallized from ethyl acetate as plates, m.p. 150.5–151° (decomp.); ν_{max}(KBr) 3435, 3250–2500, 1730, 1640, and 1530.

Anal. Calcd. for $C_{13}H_{17}O_3N$: C, 62.14; H, 6.82; N, 5.57. Found: C, 61.99; H, 6.45; N, 5.68.

With excess diazomethane in ether it gave *N*-benzoyl-DL-*erythro*-β-hydroxyisoleucine methyl ester, n_D^{26} 1.5288; ν_{max}(film) 3410, 1740, 1645 cm^{-1}. A sample was distilled at 110° at 10^{-3} Torr.

Anal. Calcd. for $C_{14}H_{19}O_3N$: C, 63.38; H, 7.22; N, 5.28. Found: C, 63.05; H, 7.23; N, 5.37.

DL-*erythro*-β-*Hydroxyisoleucine via* DL-*erythro-N-Benzyl*-β-*hydroxyisoleucine*

trans-3-Methylpent-2-enoic acid (3.4 g) in water (20 ml) was partially neutralized with sodium hydroxide (0.6 g) and sodium tungstate (1.0 g) added. While the mixture was stirred vigorously at 65° hydrogen peroxide (5 ml) was added drop by drop. The pH was maintained at 5.2–5.5 by adding portions of an aqueous solution of sodium hydroxide (0.6 g). Stirring was continued for 30 min after addition of hydrogen peroxide was complete, then benzylamine (6.5 g) and the balance of the sodium hydroxide solution added. This mixture was heated under reflux for 2.5 h, and excess benzylamine extracted with ether. The aqueous phase was applied to a column of cation exchange resin (H^+ form) and the basic product, eluted with 4 *M* aqueous ammonia, dried, and leached with acetone. It was crystallized from aqueous ethanol to give DL-*erythro-N*-benzyl-β-hydroxyisoleucine (**10**) as prisms (1.47 g), m.p. 209–210° (decomp.); ν_{max}(KBr) 3170–2350, 1630, 1615, 755, and 700 cm^{-1}.

Anal. Calcd. for $C_{13}H_{19}O_3N$: C, 65.80; H, 8.07; N, 5.90. Found: C, 65.53; H, 8.07; N, 5.88.

The benzylamino acid (0.51 g) in glacial acetic acid (20 ml) was stirred under hydrogen at 70° with 5% palladized charcoal (0.1 g) for 24 h. The product was crystallized from aqueous ethanol to give DL-*erythro*-β-hydroxyisoleucine (0.21 g), m.p. 238–242° (decomp.).

Acknowledgments

We thank Dr. P. Odense, Fisheries Research Laboratory, Halifax, Nova Scotia for amino acid analyses and Mr. J. van Ingen for measuring proton magnetic resonance spectra. Mr. V. E. Bell and Mr. G. Zillig provided technical assistance.

1. J. C. MacDonald. J. Biol. Chem. **236**, 512 (1961).
2. J. C. MacDonald. J. Biol. Chem. **237**, 1977 (1962).
3. B. W. Christensen and A. Kjaer. Acta Chem. Scand. **17**, 279 (1963).
4. G. W. Butler and B. G. Butler. Nature, **187**, 780 (1960).
5. T. T. Otani and M. Winitz. Arch. Biochem. Biophys. **102**, 464 (1963).
6. W. S. Johnson, J. S. Belew, L. J. Chinn, and R. H. Hunt. J. Am. Chem. Soc. **75**, 4995 (1953).
7. Y. Liwschitz, Y. Rabinsohn, and D. Perera. J. Chem. Soc. 1116 (1962).
8. V. R. Valente and J. L. Wolfhagen. J. Org. Chem. **31**, 2509 (1966).
9. H. D. West, G. S. Krummel, and H. E. Carter. J. Biol. Chem. **122**, 605 (1938).
10. G. A. R. Kon and R. P. Linstead. J. Chem. Soc. **127**, 616 (1925).
11. F. Fichter and E. Gisiger. Chem. Ber. **42**, 4707 (1908).
12. H. Bohnsack. Chem. Ber. **74**, 1575 (1941).
13. L. M. Jackman and R. H. Wiley. J. Chem. Soc. 2886 (1960).
14. K. Rüfenacht. Helv. Chim. Acta, **35**, 762 (1952).
15. K. Pfister, 3rd., E. E. Howe, C. A. Robinson, A. C. Shabica, E. W. Pietrusza, and M. Tishler. J. Am. Chem. Soc. **71**, 1096 (1949).
16. E. Fischer and H. Scheibler. Chem. Ber. **41**, 889 (1908).
17. E. Abderhalden and W. Zeisset. Z. Physiol. Chem. **200**, 179 (1931).
18. M. Y. Karpeiskii, S. V. Shlyapnikov, and V. S. Oseledchik. Dokl. Akad. Nauk SSSR, **165**, 1184 (1965).
19. W. Drell. J. Am. Chem. Soc. **77**, 5429 (1955).
20. K. N. F. Shaw and S. W. Fox. J. Am. Chem. Soc. **75**, 3421 (1953).
21. H. Geipel, J. Gloede, K-P. Hilgetag, and H. Gross. Chem. Ber. **98**, 1677 (1965).
22. D. O. Gray, J. Blake, D. H. Brown, and L. Fowden. J. Chromatog. **13**, 276 (1964).
23. M. L. Kornguth and H. J. Sallach. Arch. Biochem. Biophys. **91**, 39 (1960).
24. H. D. West and H. E. Carter. J. Biol. Chem. **119**, 109 (1937).
25. J. Attenburrow, D. F. Elliot, and G. F. Penny. J. Chem. Soc. 310 (1948).
26. K. Pfister, 3rd., C. A. Robinson, A. C. Shabica, and M. Tishler. J. Am. Chem. Soc. **71**, 1101 (1949).
27. R. P. Linstead and C. J. May. J. Chem. Soc. 2565 (1927).

Can. J. Chem. Downloaded from www.nrcresearchpress.com by 210.87.254.5 on 09/05/12
For personal use only.

Can. J. Chem. Downloaded from www.nrcresearchpress.com by 210.87.254.6 on 09/05/12
For personal use only.

Reaction of α-hydrazino carboxylic acids with ninhydrin

EDWARD RONWIN,[1] JERRY V. ROACH, AND BURRELL L. TUCKER
Department of Chemistry, Eastern New Mexico University, Portales, New Mexico

Received January 4, 1968

Several α-hydrazino carboxylic acids and their *m*-nitrobenzal hydrazones have been prepared and characterized. The latter and two of the former have not been previously reported. The α-hydrazino acids were found to react with ninhydrin to yield Ruhemann's purple, but in much lower yield than the corresponding amino acids. However, hydrazine itself yields a different colored product. Various aspects of the reaction between ninhydrin and the α-hydrazino acids were investigated and a mechanism for the formation of Ruhemann's purple is suggested.

Canadian Journal of Chemistry, 46, 3013 (1968)

Introduction

A number of α-hydrazino carboxylic acids have been prepared and characterized. Most of these acids have previously been reported (1–5), with the exception of the α-hydrazino derivatives of palmitic and stearic acids, and the *m*-nitrobenzal hydrazone derivatives (6).

As part of the characterization of the α-hydrazino acids, their reaction with ninhydrin was tested. Some reaction between the carbonyl-rich reagent, and the hydrazino group, to yield a colored complex was anticipated, but it was a complete surprise to find that the reaction gives Ruhemann's purple (7), though in much lower yields compared to the corresponding α-amino acids.

Stimulus for this work derives from the hope of the eventual synthesis of oligo- and polyhydrazino acids consisting of α-hydrazino carboxylic acid monomers bound to each other in

$$\begin{matrix} O & H & H \\ \| & | & | \end{matrix}$$

"hydrazino peptide" (—C—N—N—) bonds. This would create an entire chemistry analogous to protein chemistry, and this paper is a report of preliminary activities in this area.

As research interests expand in this field, it would be desirable for all to proceed with some common, and hopefully clear, nomenclature and symbolism. In this respect, it is suggested that the monomers, as a group, be called *hydrazino acids* and abbreviated, HA. Where the hydrazino acid has a corresponding characterized amino acid, possessing a common name, the name of the HA should be that of the amino acid, preceded by the word hydrazino. Thus the HA analogous to leucine, α-hydrazinoisocaproic acid, would be called hydrazinoleucine. If no Greek letter precedes the word, hydrazino, the group is to be understood as occupying the α-position. For shorthand notation, hydrazinoleucine would be written, HLeu.

Experimental

Materials

Most of the α-bromo carboxylic acid precursors of the HA were purchased from either Eastman Organic Chemicals or City Chemical Company, New York. The 95% hydrazine used was an Eastman Organic Chemicals product. Ninhydrin and other reagents were available here. Liquid reagents were distilled prior to use and ninhydrin was recrystallized from water.

Preparative Procedure for the Hydrazino Acids

While the exact details may vary slightly from one specific preparation to another, the general method for synthesizing HA is given below (2–5, 8–10).

Ten grams (less if the acid was in short supply or too expensive) of the corresponding α-bromo carboxylic acid were added to 50 ml of absolute ethanol at room temperature. To this mixture, an approximate 5*M* excess of 95% hydrazine was added in small portions. The solution was reduced to one-quarter its original volume over a hot plate and then placed in the deep freeze to initiate crystallization of the product. Usually crystals appeared within 1 h. After 24 h, they were filtered off, washed with absolute ethanol and dried. Recrystallization was performed by solution in ethanol–water mixtures, followed by reduction in volume, addition of absolute ethanol, and subjection to deep freeze temperatures.

In general the HA were soluble in hot and cold water, but essentially insoluble in ethanol as well as in such organic reagents as *p*-dioxane and hexane.

In all cases the racemic α-bromo acid precursors were employed, thus yielding products which were devoid of optical activity.

Preparation of m-Nitrobenzaldehyde Derivatives

Two grams of *m*-nitrobenzaldehyde were dissolved in sufficient ethanol, and 0.5 g of α-hydrazino acid was dissolved in sufficient water, to bring each into solution. The

[1]Present address: Chemistry Department, Fresno State College, Fresno, California.

Can. J. Chem. Downloaded from www.nrcresearchpress.com by 210.87.254.6 on 09/05/12
For personal use only.

TABLE I

α-Hydrazino (carboxylic) acids[a]

Chemical name	Suggested common names	Suggested abbreviation	Melting point (°C)		% yield	Appearance	Nitrogen analysis %[b]	
			Observed	Literature			Calculated	Found
α-Hydrazino-*n*-butyric	Hydrazinobutyric	HAbu	212d.	208[c]	26	White plates	23.7	23.7[d]
α-Hydrazino-3-methyl-*n*-butyric (α-Hydrazinoisovaleric)	Hydrazinovaline	HVal	250d.	230–235[e]	36	White powder	21.2	20.8
α-Hydrazinovaleric	Hydrazinonorvaline	HNval	216d.	215[f]	80	White needles	21.2	21.3[g]
α-Hydrazino-4-methylvaleric (α-Hydrazinoisocaproic)	Hydrazinoleucine	HLeu	227d.	228[h]	32	Silvery powder	19.2	19.1[i]
α-Hydrazinohexanoic (α-Hydrazinocaproic)	Hydrazinonorleucine	HNleu	220d.	221[j] 218[k] 199–201[l]	28	Silvery plates	19.2	19.2[m]
α-Hydrazinophenylacetic	Hydrazinophenylglycine	HPGly	182d.	183–184[n]	55	White powder	16.8	16.6
α-Hydrazinohexadecanoic	Hydrazinopalmitic	HPal	203		51	White powder	9.8	9.9
α-Hydrazinooctadecanoic	Hydrazinostearic	HSte	205d.		66	White powder	8.9	8.7

[a]The general procedure for α-hydrazino acid preparation is described in the Experimental section. All observed melting points are corrected.
[b]Values with footnotes were determined by the Dumas method; the others were obtained by microkjeldahl procedure.
[c]See refs. 1 and 3.
[d]Calcd: C, 40.7; H, 8.5. Found: C, 40.5; H, 8.6.
[e]See refs. 2 and 3.
[f]See refs. 1 and 3.
[g]Calcd: C, 45.4; H, 9.2. Found: C, 45.3; H, 9.1.
[h]See ref. 3.
[i]Calcd: C, 49.3; H, 9.7. Found: C, 48.9; H, 9.6.
[j]Vacirca and Ciocca, Boll. 1st sieroterap. Milanese, 23, 99 (1944).
[k]See ref. 4.
[l]See ref. 3.
[m]Calcd: C, 49.3; H, 9.7. Found: C, 49.5; H, 9.7.
[n]See ref. 5. Results are for the laevorotatory form.

TABLE II

m-Nitrobenzal hydrazones of α-hydrazino acids*

Hydrazone of	Melting point (°C)	% yield	Appearance	Nitrogen analysis %†	
				Calculated	Found
Hydrazino-*n*-butyric	112	71	Yellow powder	16.6	16.4
Hydrazinonorvaline	191–192	41	Light-yellow needles	15.8	15.6
Hydrazinovaline	162–163	27	Yellow powder	15.8	15.5
Hydrazinoleucine	82	44	Yellow needles	15.0	15.0
Hydrazinonorleucine	97–98	54	Yellow needles	15.0	14.9
Hydrazinophenylglycine	195–197	35	Yellow leaflets	14.0	13.9

*The general preparative procedure is described in the Experimental section. All melting points are corrected.
†Determined by microkjeldahl analysis in which sodium thiosulfate was added to the digestion mixture to facilitate the reduction of the nitro group.

two solutions were slowly mixed. During this process product precipitation was observed in some cases. After complete mixing, the resulting solution was reduced on a hot plate to approximately three-quarters of its original volume and cooled. The *m*-nitrobenzaldehyde derivatives were filtered off and recrystallized from 50% ethanol.

Ninhydrin Reaction Procedure for the Hydrazino Acids

Essentially, the ninhydrin reaction with HA's was carried out in a manner similar to that described for amino acids by Moore and Stein (11). In the first set of conditions, various aliquots of 0.002 *M* solutions of either α-hydrazino or α-amino acids were brought to 1 ml volumes with water in suitable test tubes. They were then treated with 1 ml of 0.2 *M* citrate buffer, pH 5, which contained 0.8 g $SnCl_2 \cdot 2H_2O$/l as reducing agent, and 20 g of ninhydrin/l. Methyl cellosolve was absent from the reagent. After mixing the HA and ninhydrin solutions, the tubes were capped and immersed in a water bath maintained at 100° for various periods of time. This set of conditions will be called the "aqueous system" in this report. The second set of conditions varied only in that methyl cellosolve was present in a 1:1 ratio with the aqueous citrate buffer, but concentrations of citrate, stannous chloride, and ninhydrin were identical to those in the aqueous system described above. However, tubes containing the reaction mixture were immersed in an oil bath maintained at 124° (the b.p. of methyl cellosolve) and kept in the bath for various times. In the 1h treatment the water would evaporate, leaving essentially a methyl cellosolve solution of reactants and products. Except for the bath temperature and reaction volumes, this system is closest to that given by Moore and Stein (11) and is referred to here as the "cellosolve–water system." A third ninhydrin reagent, which was used only in the reaction with hydrazine hydrate, consisted of a solution of ninhydrin and $SnCl_2 \cdot 2H_2O$ in methyl cellosolve (no citrate) in identical concentrations as in the above reagent solutions.

After appropriate bath immersion times, the tube contents were diluted with 5 ml (or more if required) of 1:1; *n*-propanol:H_2O, mixed well, and read in either a Bausch & Lomb Spectronic 20 or a Beckman DU recording spectrophotometer, accompanied by suitable blanks. Due to reduced atmospheric pressure indigenous to this region, salt was added to our water baths to achieve and maintain 100°.

Results and Discussion

The α-Hydrazino Acids and their m-Nitrobenzal Hydrazones

Table I presents pertinent data on the α-hydrazino acids prepared in this work including the two new ones, hydrazinopalmitic and hydrazinostearic acids. Appropriate data for the *m*-nitrobenzaldehyde derivatives are given in Table II. The *m*-nitrobenzal hydrazones of hydrazinopalmitic and hydrazinostearic acids could not be obtained due to solubility problems.

Paper Chromatography

Comparative runs were performed in duplicate for norleucine and HNleu using Whatman No. 1 paper and an eluant consisting of 60:30:10; *n*-butanol:glacial acetic acid:water, in a closed system. Approximately 26 μg of DL-norleucine were spotted and approximately 142 μg of DL-HNleu were used. The chromatograms were run for 6 h, using the ascending method. They were then dried and the color was developed with ninhydrin spray in *n*-butanol (1 g ninhydrin in 25 ml *n*-butanol). This gave the following R_f values: DL-norleucine: 0.67; DL-hydrazinonorleucine: 0.41.

Infrared Spectral Comparison of α-Hydrazino- and α-Amino-n-butyric Acids

The infrared (i.r.) spectra of α-hydrazino-*n*-butyric acid and α-amino-*n*-butyric acid were compared (Fig. 1). Four bands are germane (12). The first two are the N—H bending peaks known as amino acid I and II, which are usually seen at 6.03–6.22 μ and 6.46–6.74 μ, respectively. For aminobutyric, these are observed at 6.03–6.10 μ and 6.63 μ, respectively. Although these bands are purported to disappear on *N*-substitution in the amino acid (12), both bands are

Can. J. Chem. Downloaded from www.nrcresearchpress.com by 210.87.254.6 on 09/05/12
For personal use only.

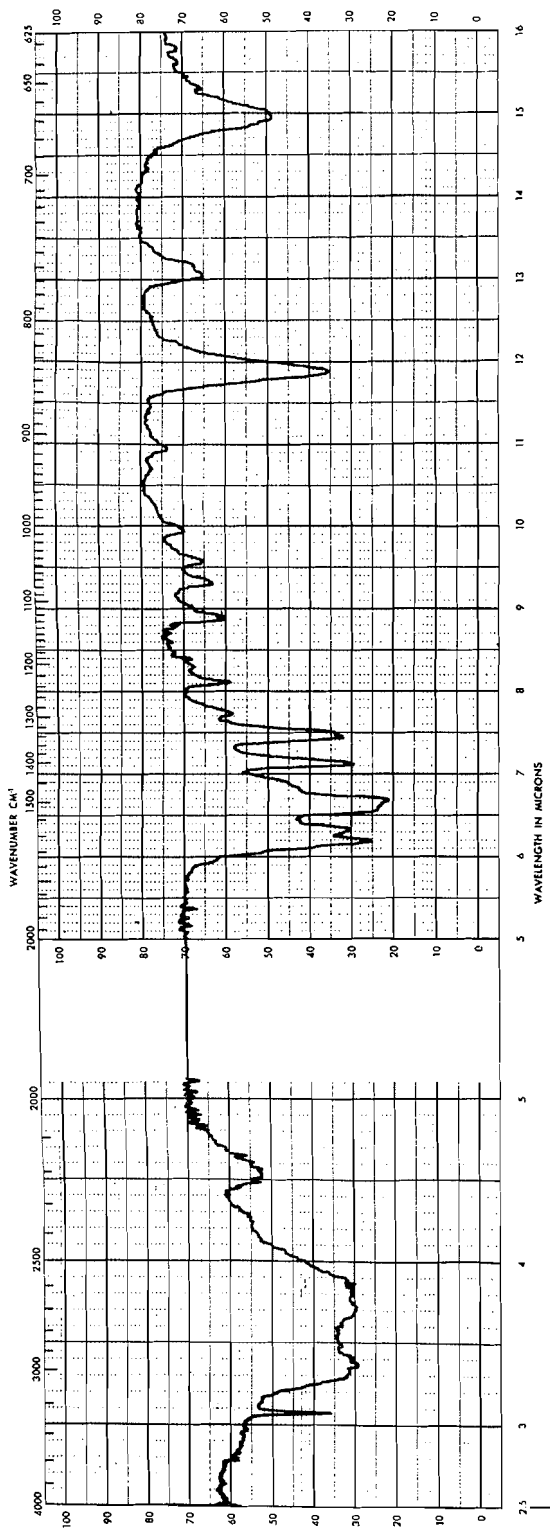

FIG. 1. Comparison of the infrared spectra of α-amino-*n*-butyric acid and α-hydrazino-*n*-butyric acid which were obtained on KBr pellets in a Beckman IR-8 recording spectrophotometer. Upper section, α-hydrazino-*n*-butyric acid; lower section, α-amino-*n*-butyric acid.

Can. J. Chem. Downloaded from www.nrcresearchpress.com by 210.87.254.6 on 09/05/12
For personal use only.

observed in similar intensity as sharper peaks at 6.19 μ and 6.68 μ for the hydrazino acid. While additional evidence will be recited below supporting a zwitterion structure for the hydrazino acid, the above observation suggests that the proton dissociated from the carboxyl group resides on the β-nitrogen atom. The amino acid I and II bands arise from N—H bending involving a nitrogen atom situate as, $(R—NH_3)^+$. Further substitution of the nitrogen atom to create, $(R—NH_2R')^+$, causes band disappearance. If the proton in the HA zwitterion resided on the α-nitrogen, this nitrogen would be situate as $(R—NH_2R')^+$ and the bands should not be observed; however, if the β-nitrogen carried the proton its structure would be, $(R—NH_3)^+$ and the bands should be seen, as is the case. (The fact that the amino acid nitrogen atom is attached to a carbon in the R group and the HA's β-nitrogen atom would be attached to a nitrogen in the R group, should influence only band position and intensity.)

The second two bands of interest are those shown by free amino acids in the zwitterion form for ionized carboxyl absorption at 6.25–6.42 μ and at approximately 7.15 μ. For aminobutyric, a strong band is seen at 6.25–6.38 μ and a somewhat weaker one is in evidence at 7.08–7.10 μ. For the HA, both peaks are distinct and sharp at 6.32 μ and 7.12 μ. These observations, considered with the complete absence of unionized carboxyl group absorption in the 5–6 μ region, and the generally similar infrared (i.r.) spectral graphs for both acids, reasonably suggest that the free α-hydrazino aliphatic acids exist as zwitterions.

Further support for this thesis is found in the relatively good water solubility and poor organic

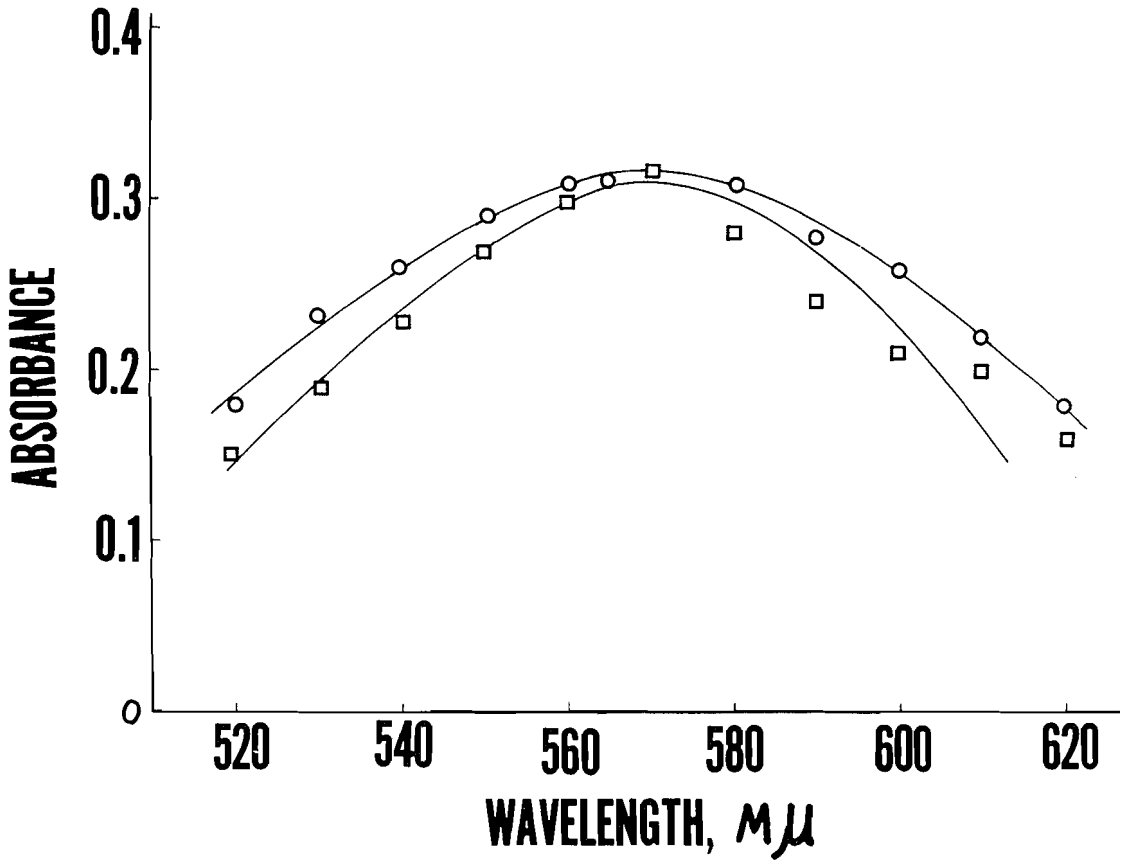

FIG. 2. Absorption spectra for hydrazinonorleucine and norleucine. Aqueous system conditions; bath time: 20 min. Acid concentration in reaction: 80γ of 0.002 *M* norleucine; 600γ of 0.002 *M* hydrazinonorleucine. ○, DL-Hydrazinonorleucine; □, DL-Norleucine.

Can. J. Chem. Downloaded from www.nrcresearchpress.com by 210.87.254.6 on 09/05/12
For personal use only.

Can. J. Chem. Downloaded from www.nrcresearchpress.com by 210.87.254.6 on 09/05/12
For personal use only.

solvent solubility displayed by the hydrazino acids; this is analogous to amino acid solubility behavior.

The infrared spectra of α-hydrazinonorleucine and norleucine were almost identical to the corresponding *n*-butyric acid analogues.

The Ninhydrin Reaction in the Aqueous System at 100°

Absorption Spectra

The complex formed in the reaction between either HA or amino acids and ninhydrin generally has a maximum absorption at 570–572 mμ; although, it is quite broad and tends to range from 560–580 mμ. This is illustrated in Fig. 2 for the ninhydrin reaction product for norleucine and the corresponding HA. Note that extraction of comparable color yields for these related acids required a 7.5 times greater molar concentration of the HA. Even higher ratios were required for other pairs.

Beer–Lambert Relationship

Figure 3 shows a graph of absorbance vs. concentration for hydrazinonorleucine, hydrazinonorvaline, hydrazinoleucine, and hydrazino-*n*-butyric acids. All were reacted with ninhydrin under aqueous system conditions. While color yields vary despite identical initial HA concentrations, it is clear that the Beer–Lambert relationship is followed. The curves give evidence that color yields among the straight chain acids increase with increasing hydrocarbon chain lengths. Further, as judged by comparison between HNleu and HLeu, branching markedly reduces color yields. (In separate data, HNval yielded roughly three times more color than HVal compared at a single concentration.)

While the results with the corresponding amino acids at 100 °C reaction temperature (11) contain no hint of either of the above phenomena, support for steric and polar effects was demonstrated by Friedman and Sigel (13), who observed a decided relationship between color yield and structure at 30°, as well as at 100°. Unfortunately, comparisons are precluded, as none of the amino acids examined in their work at 100 °C correspond to the HA in this work, and they do not correspond to those in Moore

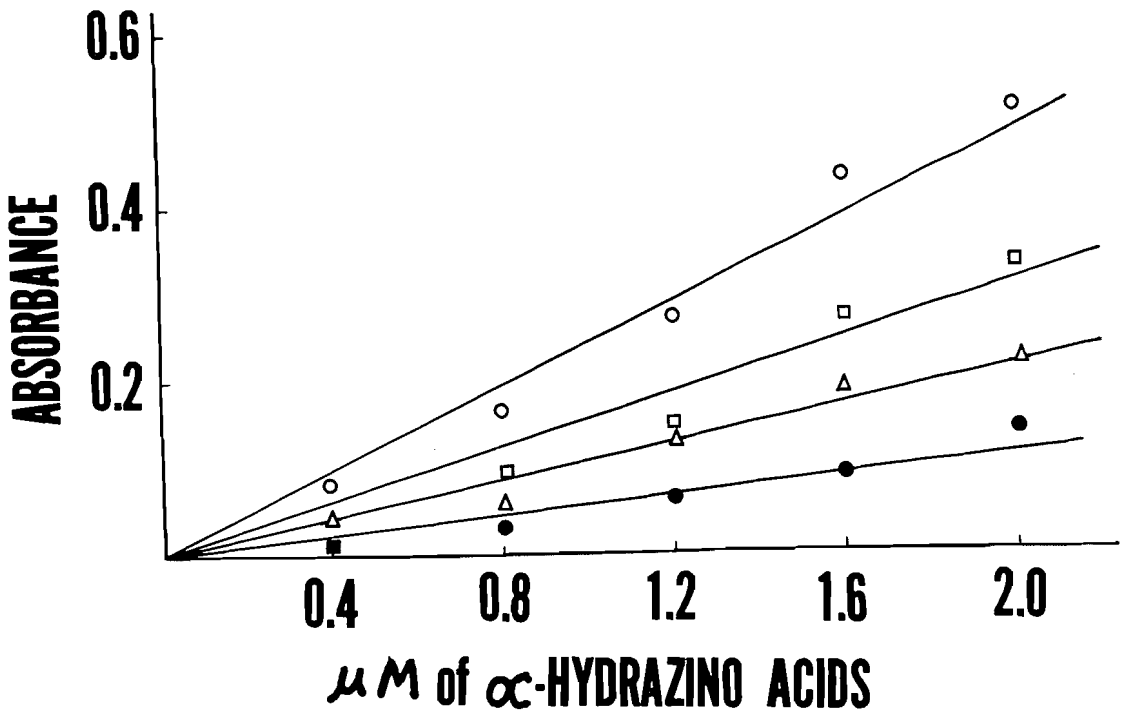

FIG. 3. Absorbance at 570 mμ vs. concentration for the hydrazino acids. Aqueous system conditions; bath time: 20 min. ○, DL-Hydrazinonorleucine; □, DL-Hydrazinonorvaline; △, DL-Hydrazino-*n*-butyric acid; ●, DL-Hydrazinoleucine.

TABLE III

Color stability of 20 min ninhydrin reaction product*

Compound	Aliquot of standard solution† (μl)	Wavelength (mμ)	Absorbance at various times after removal from bath				
			15 min	6 h	11 h	20 h	24 h
Valine	80	565	0.30	0.28	0.25	0.23	0.20
		570	0.31	0.27	0.24	0.23	0.20
Norleucine	80	565	0.30	0.28	0.27	0.23	0.20
		570	0.32	0.28	0.26	0.22	0.20
Hydrazinonorvaline	600	565	0.22	0.19	0.17	0.15	0.12
		570	0.23	0.20	0.17	0.14	0.12
Hydrazinonorleucine	600	565	0.31	0.29	0.26	0.23	0.20
		570	0.32	0.28	0.25	0.23	0.20
Hydrazinobutyric	1200	565	0.29	0.26	0.24	0.21	0.19
		570	0.30	0.26	0.23	0.21	0.20
Hydrazinovaline	1200	565	0.13	0.11	0.10	0.08	0.07
		570	0.14	0.13	0.13	0.11	0.09
Hydrazinoleucine	1200	565	0.15	0.14	0.13	0.10	0.08
		570	0.16	0.15	0.13	0.11	0.09

*Aqueous system conditions; bath temperature 100 °C.
†0.002 *M*.

and Stein's list (11), (except leucine which Friedman and Sigel used as a standard).

Color Stability as a Function of Time

Color stability as a function of time is given in Tables III and IV for the 20 min and 60 min ninhydrin reaction product, respectively. In all cases, gradual color loss is experienced with time. The exact decay rate varies with the specific acid (whether amino acid or HA) but on the whole, ranges from 30–50% over a 24 h period or approximately 1–2% per h, which corresponds with the observations of Moore and Stein for amino acids (11).

Effect of Reaction Time on Initial Color Yield

Some comparison of this relationship is possible in the data of Tables III and IV where HAbu and HVal give a slight color increase after 1 h reaction time, whereas HNleu shows a decrease, compared to the results obtained from 20 min of reaction (adjusted for concentration differentials).

In a further study, a comparison of color yield vs. reaction time was made for the ninhydrin–norleucine and ninhydrin–hydrazinonorleucine reactions (Fig. 4). Both curves have similar form, rising steeply early in the reaction and approaching maxima of color yield in the

TABLE IV

Color stability of 1 h ninhydrin reaction product*

Compound	Aliquot of standard solution† (μl)	Wavelength (mμ)	Absorbance at various times after removal from bath		
			15 min	1 h	24 h
Hydrazinobutyric	600	565	0.19	0.14	0.11
		567	0.18	0.14	0.12
		570	0.18	0.13	0.11
Hydrazinonorleucine	600	565	0.19	0.14	0.12
		567	0.17	0.15	0.11
		570	0.17	0.13	0.10
Hydrazinovaline	600	565	0.10	0.07	0.05
		567	0.09	0.08	0.04
		570	0.09	0.07	0.05

*Aqueous system conditions; bath temperature 100 °C.
†0.002 *M*.

Can. J. Chem. Downloaded from www.nrcresearchpress.com by 210.87.254.6 on 09/05/12
For personal use only.

Can. J. Chem. Downloaded from www.nrcresearchpress.com by 210.87.254.6 on 09/05/12
For personal use only.

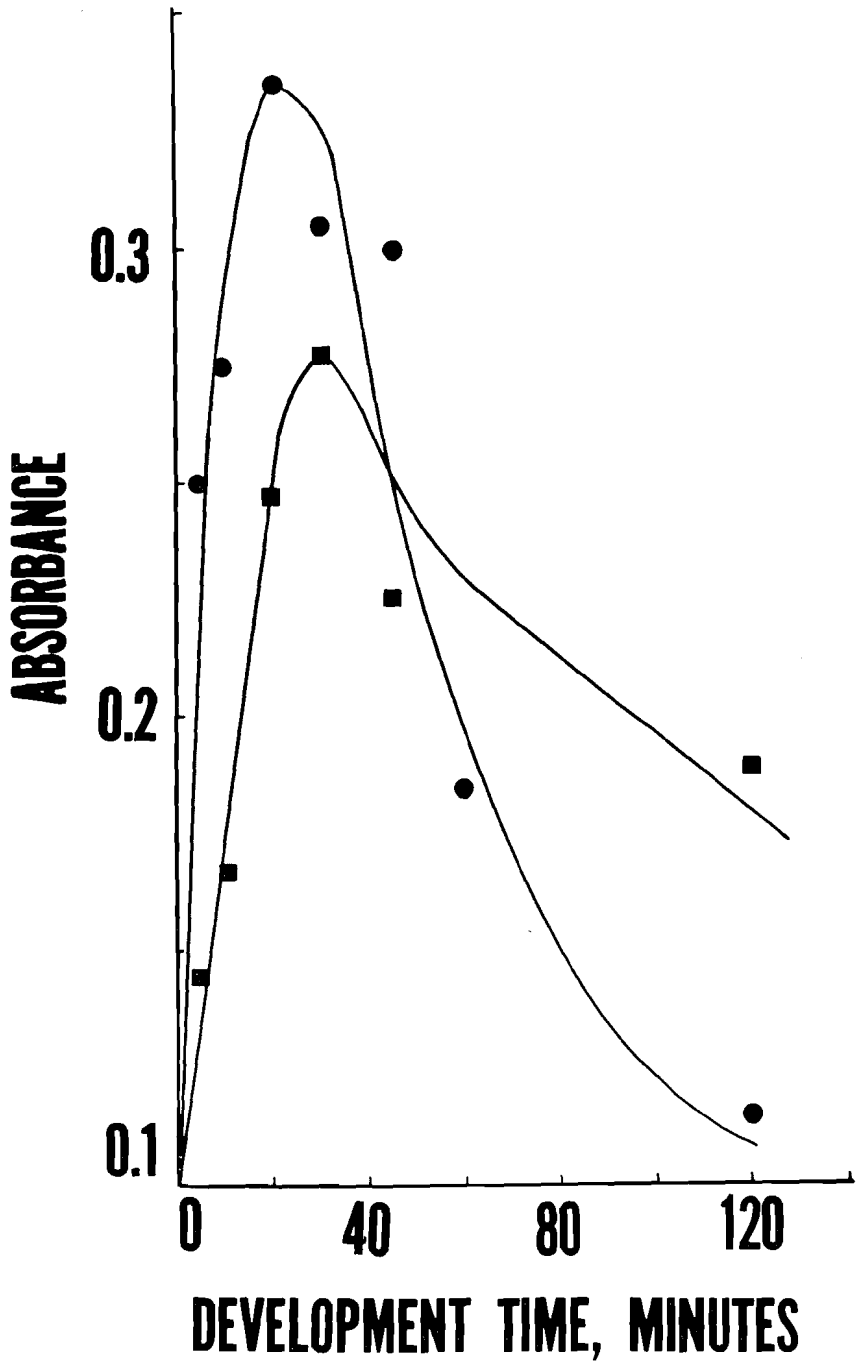

FIG. 4. Absorbance at 570 mμ vs. ninhydrin reaction time (color development time). Aqueous system conditions. Acid concentration in reaction: 80 γ of 0.002 *M* norleucine; 600 γ of 0.002 *M* hydrazinonorleucine. ●, DL-Norleucine; ■, DL-Hydrazinonorleucine.

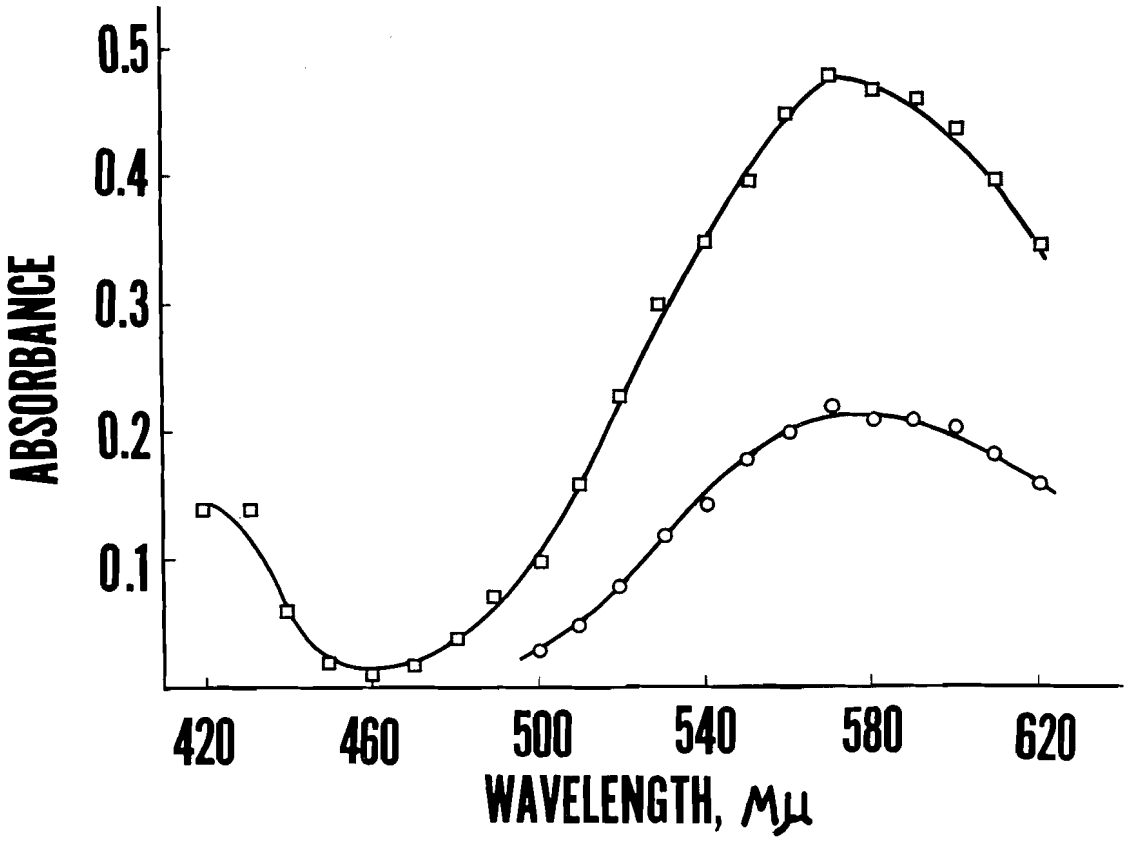

FIG. 5. Absorption spectrum of the hydrazinonorleucine and norleucine ninhydrin reaction products developed in the cellosolve–water system. Acid concentration in reaction: 80γ of 0.002 *M* norleucine and 600γ of 0.002 *M* hydrazinonorleucine. The norleucine reaction required 10 ml of 1:1; *n*-propanol:H_2O diluent rather than 5 ml as in the case of hydrazinonorleucine. Bath time: 1 h; oil bath temperature: 124 °C. ○, DL-Hydrazinonorleucine; □, DL-Norleucine.

vicinity of 22 to 30 min. Thereafter, the color yield in the HNleu case falls off rapidly, while Nleu shows a more gradual decline. The disparity in molar concentrations (7.5 times more HA) must be kept in mind for curve comparison. Also, the ordinate values tend to magnify the variances, which are minor over the first 60 min of development times.

The Ninhydrin Reaction in the Cellosolve–Water System at 124°

Absorption Spectra

The spectra of the products of the ninhydrin–hydrazinonorleucine and ninhydrin–norleucine reactions, run under cellosolve–water conditions, were compared (Fig. 5). The 570 mμ maxima in both cases is characteristic of Ruhemann's purple.

Initially, the reaction conditions are mainly aqueous, but the 1 h reaction time at 124° results in complete evaporation of the water in the reaction mixture.

Although the ratio of the initial color yield in the completely aqueous system of Nleu/HNleu was approximately 7.5, the ratio in the cellosolve–water system is more like 30. Nleu gave more than twice the color yield under these conditions compared to the aqueous system, while HNleu gave approximately one-third less color. It would appear that these conditions offer a more sensitive analytical procedure for amino acid determination than 100° bath temperatures.

Color Stability as a Function of Time

The data in Table V give the color stability for each acid as a function of time for the color developed in the methyl cellosolve–water system. These rates of color decay are comparable to

Can. J. Chem. Downloaded from www.nrcresearchpress.com by 210.87.254.6 on 09/05/12
For personal use only.

Can. J. Chem. Downloaded from www.nrcresearchpress.com by 210.87.254.6 on 09/05/12
For personal use only.

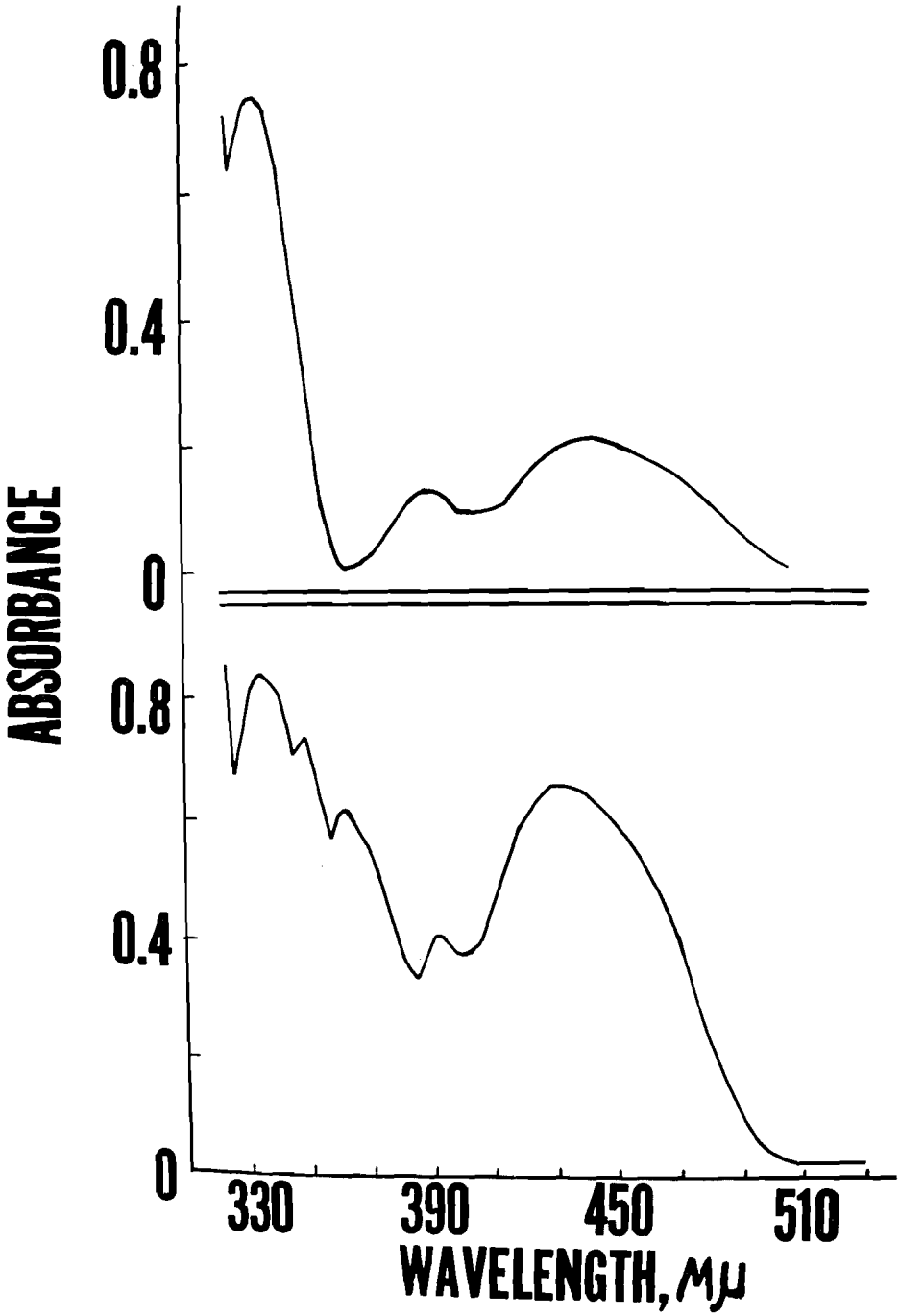

FIG. 6. Absorption spectra of the hydrazine–ninhydrin reaction product developed in two different media. Upper section: aqueous system conditions; bath time: 20 min. Lower section: anhydrous methyl cellosolve containing ninhydrin and stannous chloride, but no citrate. Product developed immediately upon mixing of the reactants at room temperature and was read as such. Concentration of hydrazine: 80 γ of the commercial preparation. The reaction mixture was diluted 1 to 25 with 1:1; *n*-propanol:H_2O, in the case of the anhydrous cellosolve system and 1:50 in the case of the aqueous system prior to reading.

TABLE V

Color stability of ninhydrin reaction product in methyl cellosolve medium*

Compound	Aliquot of standard solution† (μl)	Absorbance at various times after removal from bath				
		Initial	4 h	6 h	11 h	24 h
Norleucine	80	0.48‡	0.44	0.40	0.33	0.27
Hydrazinonorleucine	600	0.22	0.20	0.17	0.15	0.13

*1h color development time. Bath temperature, 124 °C.
†0.002 *M*.
‡10 ml of 1:1; *n*-propanol:H_2O diluent used in this case.

those observed for the reaction run in totally aqueous media.

Hydrazine Reaction with Ninhydrin

Reaction in the Aqueous System

Figure 6, upper section, presents a plot of the data for the color complex formed in the reaction between hydrazine and ninhydrin. No absorption was observed beyond 500 mμ. The first peak was seen at 440 mμ and a weaker one is observed at 385–390 mμ. In the upper ultraviolet region a pronounced peak appears at 332 mμ. Further wavelength reduction was accompanied by absorption that was too intense to be recorded. The reaction mixture was a reddish–brown in appearance. Very little fine structure was seen in the curve and then only from 335 mμ to 324 mμ.

Reaction in Anhydrous Methyl Cellosolve System

Treatment of concentrations of hydrazine and ninhydrin that were identical to those used in the aqueous system, in an anhydrous methyl cellosolve medium containing only ninhydrin and stannous chloride resulted in immediate color development at room temperature and gave the absorption spectrum shown in Fig. 6, lower section. This spectrum is essentially identical to that in Fig. 6, upper section, with major peaks appearing at 430, 390, and 334 mμ. The sharp absorptions as the wavelengths are further reduced are probably due to the keto–phenyl groupings on the ninhydrin or its reduced product or its reaction product with hydrazine. Much more fine structure was observed in this case, than in the product formed in the aqueous medium; however, no fine structure was seen for wavelengths higher than 385 mμ. In the region of the fine structure, two other broad peaks could be observed, one at 348 mμ and the other at 359 mμ and two narrow peaks appeared at 366 and 373 mμ. These additional peaks may reflect the variance in ionization states of the product in the two different solvents. The color yield in anhydrous methyl cellosolve was approximately one-half that in the water system.

The identity of the curves over much of their course point to the formation of the same color complex in both cases, which is obviously different from Ruhemann's purple.

The correspondence between the peak seen with hydrazine at 430–440 mμ and that given at the same wavelength by proline and hydroxyproline may signify some similarity of structure for the ninhydrin reaction product in each case.

Conclusions on the Ninhydrin Studies

In general, the similar absorption maxima and curve shapes of the amino acid and hydrazino acid reaction products with ninhydrin, as well as the color stability results in both the aqueous and cellosolve–water systems, reinforce with considerable confidence the notion that Ruhemann's purple (7) is formed in the reaction between hydrazino acids and ninhydrin, as is known between amino acids and the same reagent.

To account for the appearance of Ruhemann's purple in the hydrazino acid case, one could write a mechanism similar to that suggested for amino acids by Friedman and Sigel (13), which calls for an initial nucleophilic attack by the α-amino nitrogen atom of an amino acid on the C-2 of the ninhydrin molecule (with HA, the attack would be by the β-nitrogen atom of the α-hydrazino group). With the HA hydrazone, tautomerization to an azo compound followed by reduction in the stannous chloride containing medium would yield 2-amino-1,3-diketoindan.

Can. J. Chem. Downloaded from www.nrcresearchpress.com by 210.87.254.6 on 09/05/12
For personal use only.

This compound and a molecule of ninhydrin can react to give Ruhemann's purple.

One of the two anonymous referees suggested an interesting alternative mechanism, which presumably includes an initial nucleophilic attack to yield the corresponding hydrazone. A rearrangement of bonds and a splitting off of a fragment from the hydrazone would yield 2-imino-1,3-diketoindan which could then be reduced and reacted with another molecule of ninhydrin to give Ruhemann's purple.

Whatever the exact mechanism for the ninhydrin reaction with either amino acids or HA to yield Ruhemann's purple, they all appear to have two common requirements (*i*) with HA, an initial nucleophilic attack yielding a hydrazone (with amino acids, a Schiff base), and (*ii*) the formation of 2-amino-1,3-diketoindan or its corresponding anion at the 2-position carbon atom.

With hydrazine itself, a hydrazone could form which might not permit reduction to 2-amino-1,3-diketoindan or which could react with a second molecule of ninhydrin to yield the corresponding azo compound also incapable of yielding 2-amino-1,3-diketoindan.

1. W. TRAUBE and G. G. LONGINESCU. Ber. **29**, 670 (1896); **29**, 2729 (1896).
2. A. DARAPSKY. J. Prakt. Chem. **96**, 251 (1917).
3. A. DARAPSKY. J. Prakt. Chem. **146**, 219 (1936).
4. H. BERGER. J. Prakt. Chem. **152**, 267 (1939).
5. A. DARAPSKY. J. Prakt. Chem. **99**, 179 (1919).
6. A. CARMI, G. POLLACK, and H. YELLIN. J. Org. Chem. **25**, 44 (1960).
7. S. RUHEMANN. J. Chem. Soc. **99**, 1491 (1911).
8. A. DARAPSKY and M. PRABHAKAR. Ber. **45**, 1660 (1912).
9. J. BAILEY and W. T. READ. J. Am. Chem. Soc. **36**, 1758 (1914).
10. J. BAILEY and L. A. MIKESKA. J. Am. Chem. Soc. **38**, 1771 (1916).
11. S. MOORE and W. H. STEIN. J. Biol. Chem. **176**, 367 (1948).
12. R. M. SILVERSTEIN and G. C. BASSLER. Spectrometric identification of organic compounds. John Wiley and Sons, Inc., New York. (1963).
13. M. FRIEDMAN and C. W. SIGEL. Biochem. **5**, 478 (1966).

Can. J. Chem. Downloaded from www.nrcresearchpress.com by 210.87.254.6 on 09/05/12
For personal use only.

Sur la photodimérisation de l'acétate de la vitamine A

CHARLES GIANNOTTI[1]

Centre National de la Recherche Scientifique, Institut de Chimie des Substances Naturelles, Gif-sur-Yvette, Essonne, France

ET

Department of Chemistry, University of Western Ontario, London, Ontario

Reçu le 8 mars 1968

La photodimérisation de l'acétate de la vitamine A passe par l'état excité d'un triplet pour conduire à un mélange de dimères de structures cyclohexénique et cyclobutanique.

Canadian Journal of Chemistry, 46, 3025 (1968)

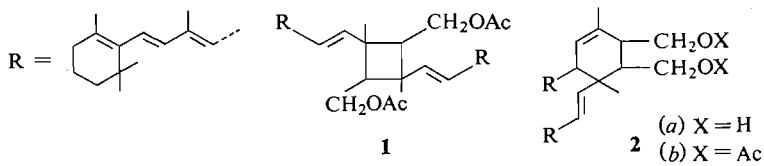

1 **2** (*a*) X = H (*b*) X = Ac

En 1962 par irradiation de la vitamine A ou de ses esters, Kaneko (1) rapporte avoir obtenu un photodimère cyclobutanique identique au kitol naturel ou aux esters correspondants. Omote (2) et Kaneko (1, 3) avaient suggéré la formule plane (**1**) pour le kitol. Plus récemment une nouvelle formule a été proposée pour ce dimère naturel (4, 5) (**2***a*) isolé à partir de l'huile de foie de baleine. Dans une nouvelle étude de l'irradiation de l'acétate de la vitamine A, il est à nouveau signalé la formation d'un seul photodimère ayant le même R_f en couche mince, des spectres ultraviolets (u.v.) et de résonance magnétique nucléaire (r.m.n.) identiques à ceux du diacétate du kitol naturel (6, 7). Il paraît curieux que l'irradiation de l'acétate de la vitamine A semble former d'une manière stéréospécifique un seul photodimère alors que le butadiène et l'isoprène donnent des mélanges complexes.

R. Srinivasan (8) montre que l'irradiation en phase liquide de dérivés butadiéniques conduit à un mélange de composés cyclobuténiques, d'isomères et de polymères. En 1963, Hammond *et al.* (9–11) prouvent que l'irradiation photosensibilisée de solutions concentrées de diènes conduit à des mélanges complexes de composés cyclobutaniques et cyclohexéniques; ainsi le butadiène donne le *trans*-divinyl-1,2 cyclobutane, le *cis*-divinyl-1,2 cyclobutane et le vinyl-4 cyclohexène tandis que l'isoprène donne naissance à un mélange dont sept produits ont été identifiés:trois dérivés dialkényl-1,2 cyclobutanes deux dérivés cyclohexéniques et deux cyclooctadiéniques.

Il est plus vraisemblable que l'irradiation de l'acétate de la vitamine A ne conduit pas à un seul composé ayant une structure du type (**1**) ou (**2***b*) mais à un mélange de produits analogues. Si le diacétate du kitol est formé, son rendement ne peut être que très faible.

Les irradiations ont été effectuées d'abord en solution hexanique puis benzénique car l'acétate de la vitamine A est plus soluble dans le benzène que dans l'hexane.

En solution hexanique, nous avons utilisé un filtre en Pyrex et une solution de naphtalène dans le cyclohexane pour isoler les bandes à 334.20, 365.02 et 366.29 mμ d'une lampe Hanovia de 85 W à vapeur de mercure. Les dimères obtenus sont d'abord séparés par une chromatographie sur colonne puis sur des couches minces commerciales, en employant la technique des passages multiples. On note que le mélange de ces dimères donne sur des couches minces une tache ayant le même R_f que le diacétate du kitol naturel (solvant hexane – acétate d'éthyle 17:3), mais en utilisant le système éther isopropylique–cyclohexane 1:1, il donne une dizaine de composés. On a isolé quatre de ces produits (A,B,C et D). Les R_f sur couche mince des composés A,B et D sont très voisins de celui du diacétate du kitol

[1]Présente adresse: Department of Chemistry, University of Western Ontario, London, Ontario.

Can. J. Chem. Downloaded from www.nrcresearchpress.com by 210.87.254.5 on 09/05/12
For personal use only.

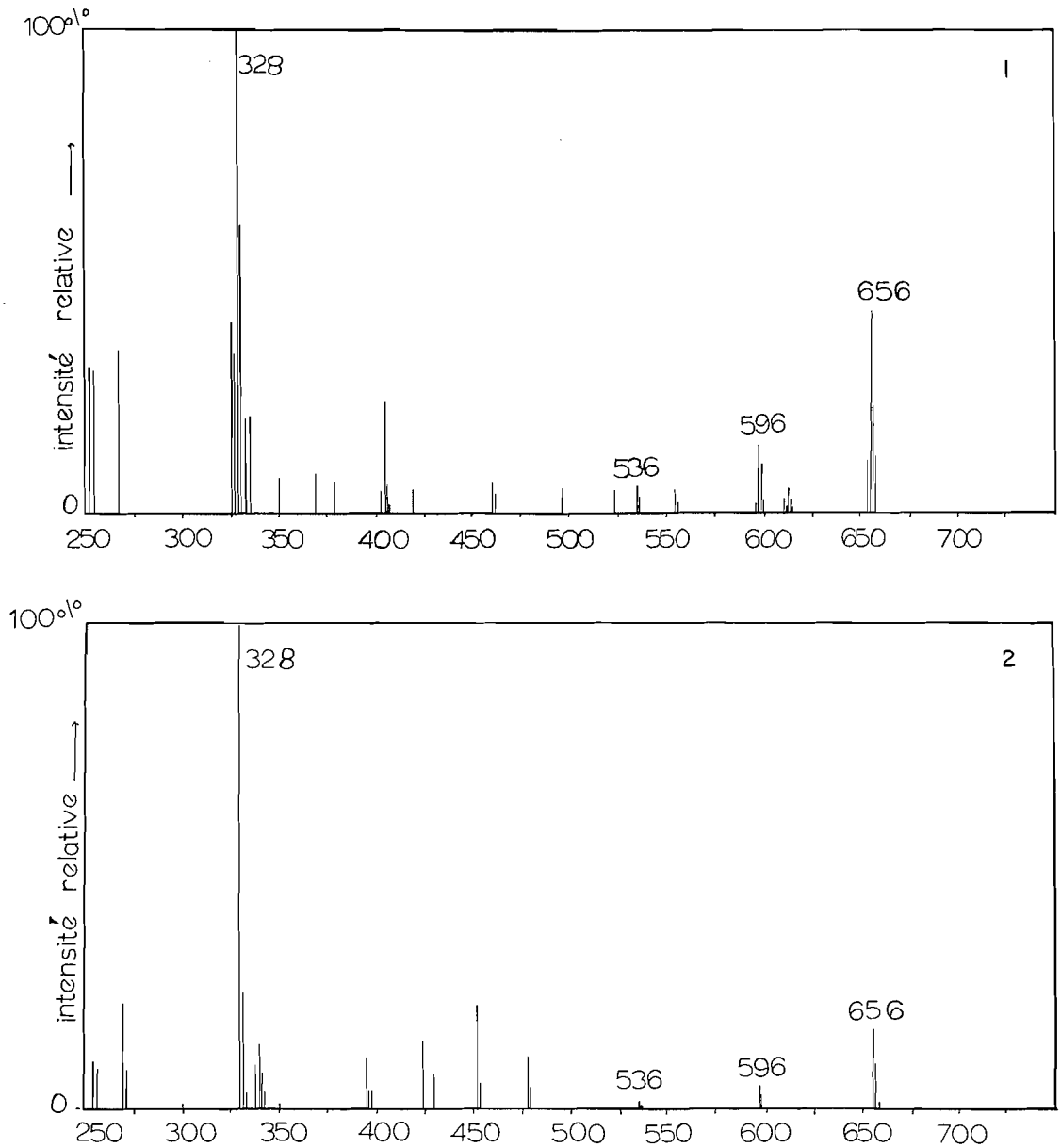

FIG. 1. Spectre de masse du diacétate de kitol.
FIG. 2. Spectre de masse du composé A.

naturel tandis que celui du produit C lui est exactement identique (dans deux systèmes de solvants différents).

Les produits A,B,C et D ont tous un poids moléculaire identique (*m/e* 656) correspondant à celui d'un dimère et des fragmentations à *m/e* 596 et 536, dues respectivement à la perte d'une ou de deux molécules d'acide acétique. Le pic de base est celui de l'ion monomère à *m/e* 328, il perd à son tour une molécule d'acide acétique pour donner un pic à *m/e* 268. Mais les spectres de masse diffèrent les uns des autres et en particulier de celui du diacétate du kitol naturel (Fig. 1) par l'intensité des pics et la présence d'autres fragmentations (Figs. 2–5).

Les spectres u.v. de ces composés dans l'alcool

Can. J. Chem. Downloaded from www.nrcresearchpress.com by 210.87.254.5 on 09/05/12
For personal use only.

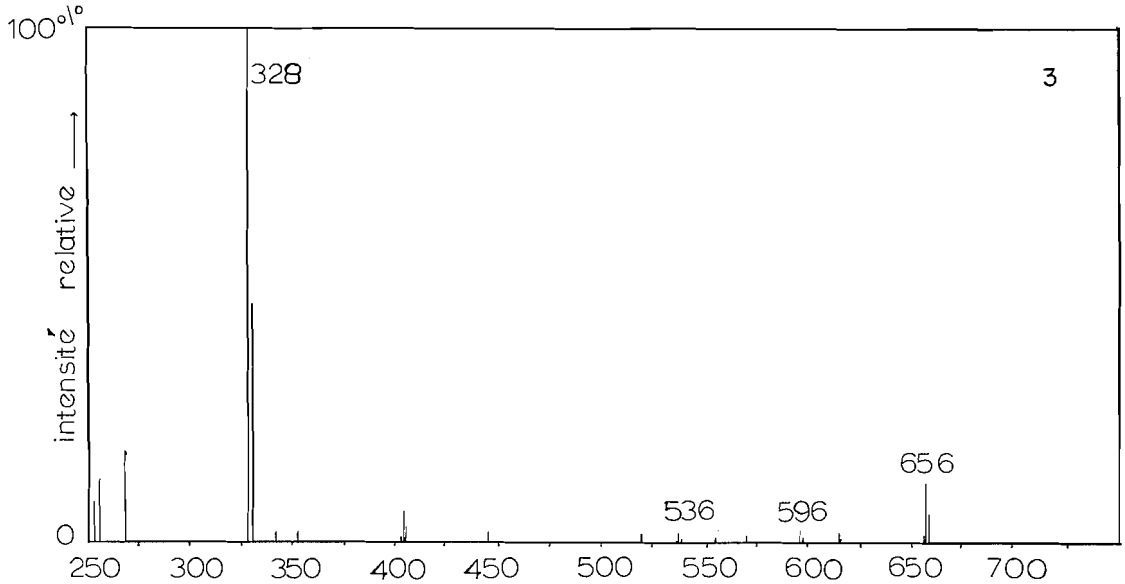

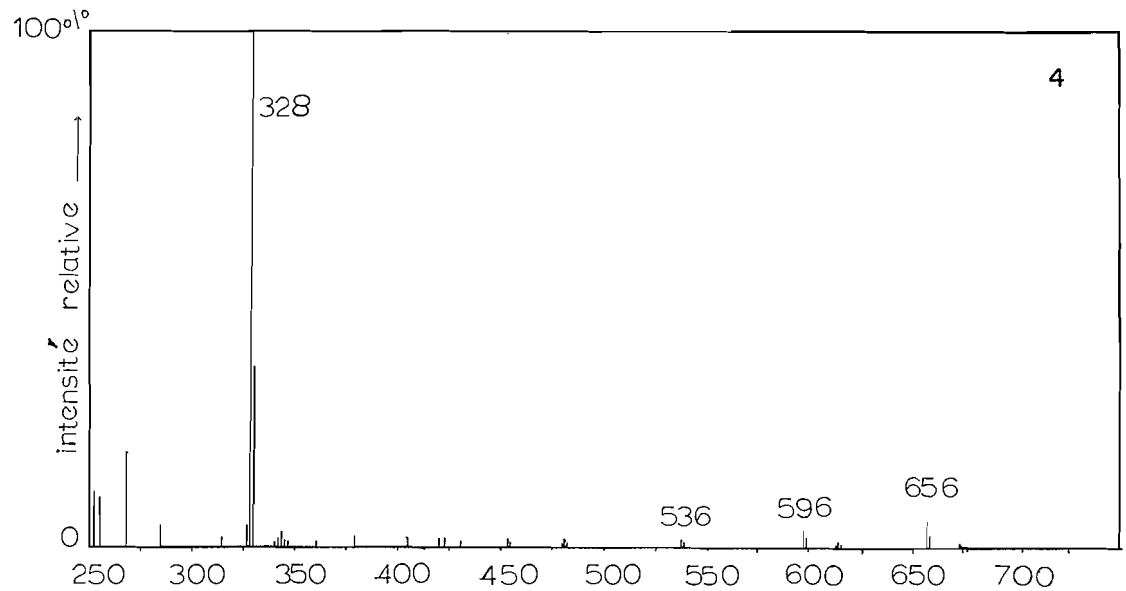

FIG. 3. Spectre de masse du composé B.
FIG. 4. Spectre de masse du composé C.

éthylique ont des maxima voisins de ceux du diacétate du kitol naturel mais non identiques.

L'hydrogénation de C et de D dans l'acide acétique, en présence d'oxyde de platine préalablement réduit donne une substance dont le spectre de masse montre en plus de l'ion moléculaire à 672 et d'autres pics à *m/e* 612 et 552, une autre fragmentation à *m/e* 458. Ce pic est en faveur d'une structure cyclohexénique du type (**2***b*) car on le retrouve dans les spectres de masse du perhydrodiacétate du kitol et de ses dérivés (5). Le reste du spectre de masse diffère de celui du perhydrodiacétate du kitol (5) par l'intensité relative des pics et par la position du pic de base à *m/e* 330 au lieu de *m/e* 329 (Figs. 6 et 7). D'autre part le photodimère C ne présente pas la même

Can. J. Chem. Downloaded from www.nrcresearchpress.com by 210.87.254.5 on 09/05/12
For personal use only.

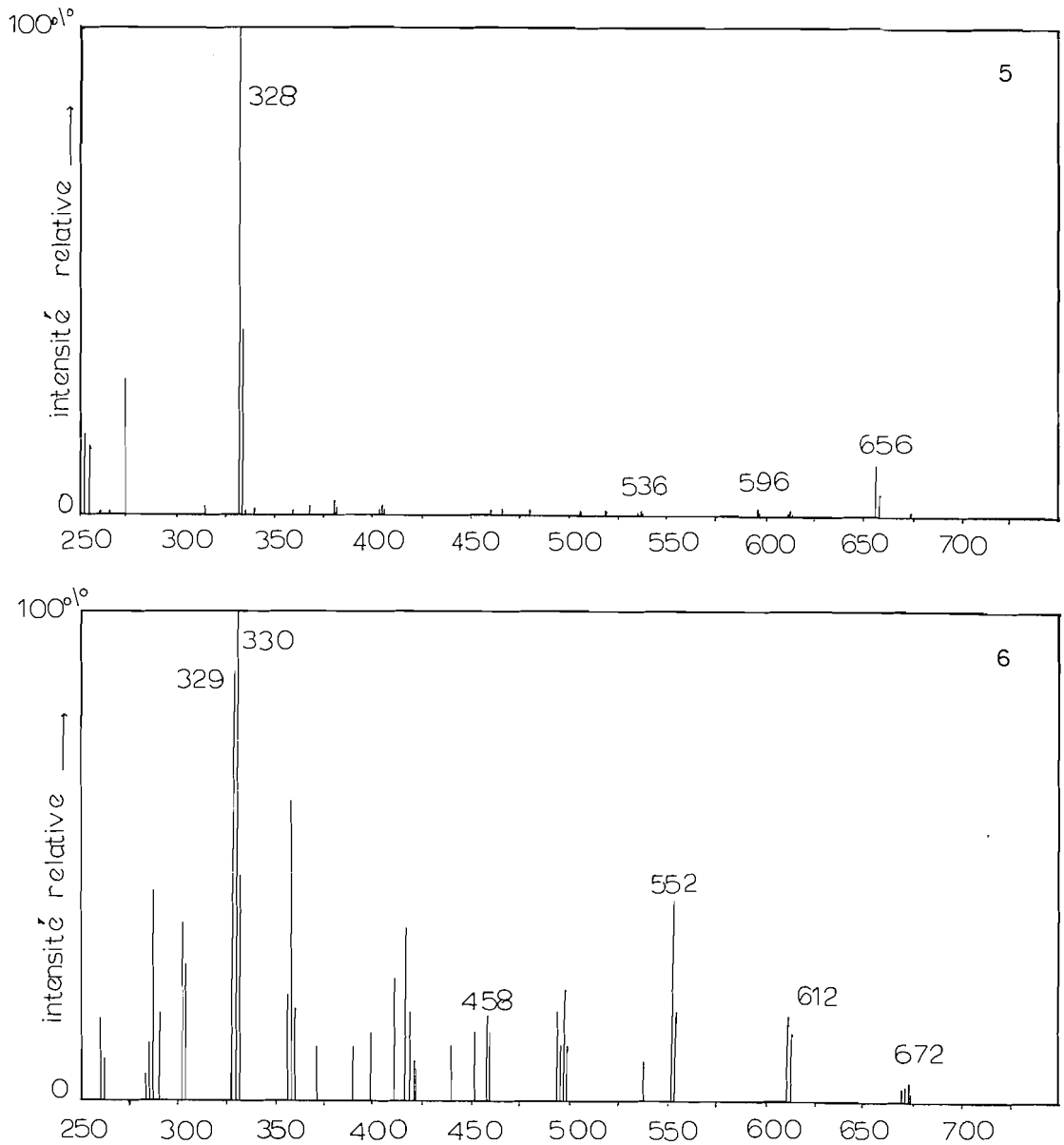

FIG. 5. Spectre de masse du composé D.
FIG. 6. Spectre de masse du composé C perhydrogéné.

coloration (bleue puis grenat après plusieurs heures lorsqu'il est révélé par une solution de trichlorure d'antimoine dans le $CHCl_3$) que le diacétate du kitol naturel, rouge brique. Il est vraisemblable que les deux systèmes de chromophores conjugués de trois et de quatre doubles liaisons *trans*, ont subi des transformations et que la stéréochimie du photodimère est différente de celle du produit naturel.

La formation des dimères en solution hexanique se fait avec un rendement faible. Pour poursuivre l'étude et rechercher la présence possible de composés à structure cyclobutanique, on a essayé des conditions donnant des dimères du même type avec un bon rendement. L'irradiation de l'acétate de la vitamine A en solution benzénique (*c* 0.1 à 0.01g/ml) en utilisant les mêmes filtres que précédemment a conduit à un mélange

Can. J. Chem. Downloaded from www.nrcresearchpress.com by 210.87.254.5 on 09/05/12
For personal use only.

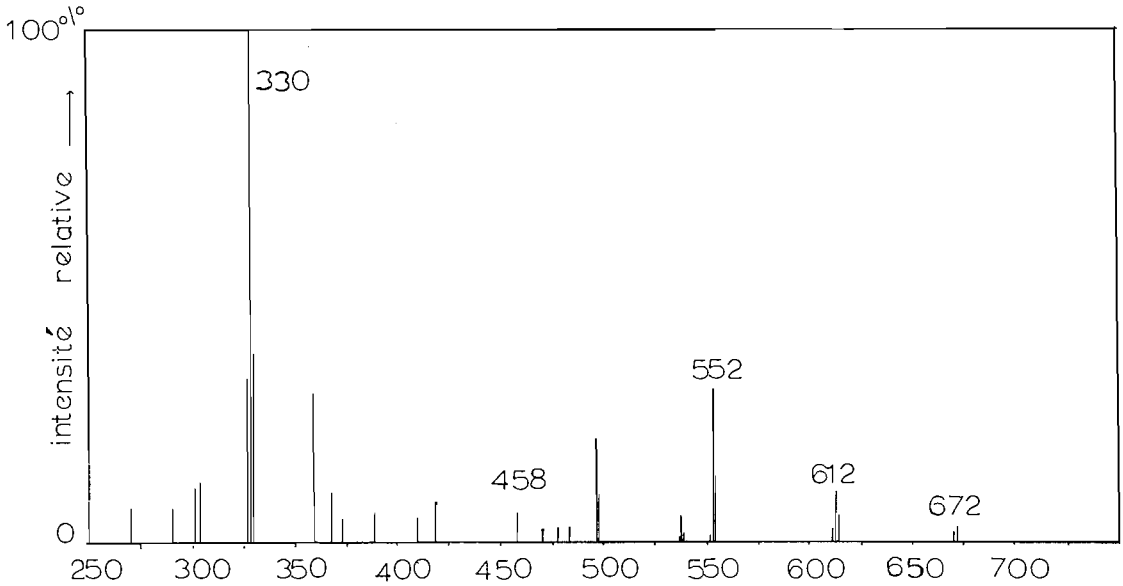

FIG. 7. Spectre de masse du composé D perhydrogéné.

de dimères (70%). Ce mélange est trouvé identique sur couche mince à celui obtenue précédemment en solution hexanique, son spectre de r.m.n. montre qu'il s'agit d'un mélange de composés de structures différentes. Des séparations multiples de ce mélange permettent de retrouver le composé C; il a des spectres de r.m.n. et u.v. très semblables à ceux déjà décrits (7) confirmant qu'il s'agit d'un produit ayant une structure du type (**2***b*). Il a un R_f et une coloration (révélée avec le trichlorure d'antimoine) identiques au photodimère C.

Les dimères ayant sur couche mince un R_f identique et très voisin au diacétate du kitol sont ozonolysés. Les produits d'ozonolyse ont été séparés en fractions acide et neutre. L'extrait acétonique de la fraction acide, après méthylation avec du diazométhane a été étudié par chromatographie en phase gazeuse.

Parmi les produits isolés, on a pu identifier un des composés cyclobutaniques; sa structure a été définitivement établie par comparaison avec le produit de synthèse (**4**). Il a été préparé de la manière suivante: on irradie pendant 2 h 1′ anhydride diméthyl-2,3 maléïque en solution dans le diacétate-1,4 butène 2; l'anhydride cyclobutanique obtenu (p.f. 108–109°) présente dans son spectre de r.m.n. deux singulets à δ 2.03 et à δ 2.08 correspondant aux méthyles tertiaires, deux singulets à δ 1.37 et à δ 1.33 attribuables aux méthyles des fonctions acétates et un multiplet à δ 4.17 provenant des protons CH_2OAc, ces signaux sont en accord avec la structure (**3**); l'anhydride (**3**) est hydrolysé puis méthylé. On obtient (**4**) avec un bon rendement.

Le produit (**4**) et celui isolé par chromatographie en phase gazeuse, après l'ozonolyse du mélange des dimères, ont les mêmes spectres infrarouges (i.r.) et de r.m.n., des temps de rétention identiques sur deux colonnes différentes. Il en résulte qu'au cours de l'irradiation de l'acétate de la vitamine A, en plus des dimères à structure cyclohexénique il se forme au moins un dimère cyclobutanique ayant la structure (**5**).

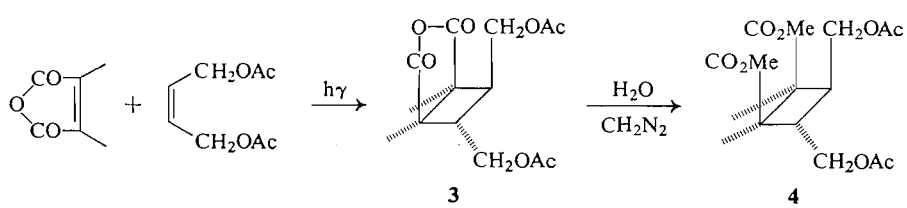

3 **4**

Can. J. Chem. Downloaded from www.nrcresearchpress.com by 210.87.254.5 on 09/05/12
For personal use only.

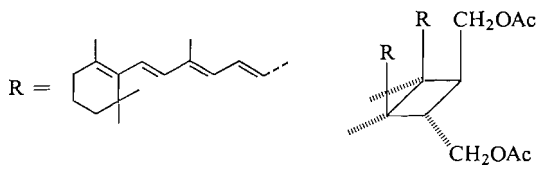

5

Les dimérisations photosensibilisées de l'isoprène et du butadiène ont été étudiées en détail (9–11). Il ressort de cette étude que la formation des dimères de l'isoprène et du butadiène passe par l'état triplet. Les triplets *cis* en présence de diènes donnent beaucoup plus de dimères cyclohexéniques que cyclobutaniques. Les triplets *trans* produisent l'effet inverse. Le mécanisme de la dimérisation de l'acétate de la vitamine A devrait aussi passer par l'état triplet pour donner à la fois des dimères cyclobutaniques et cyclohexéniques. Pour le vérifier on a effectué une réaction photosensibilisée.

On irradie une solution benzénique d'acétate de la vitamine A et de biacétyle à une longueur d'onde au-dessus de 400 mμ. On choisit une concentration de biacétyle de telle sorte qu'il absorbe toute la lumière. On filtre la lumière d'une lampe de 500 W à filament de tungstène par une solution d'acridine dans l'éthanol; cette solution présente une "fenêtre" de 275 à 305 mμ; elle est compensée par l'addition d'une gaine en Pyrex. Les dimères obtenus dans cette irradiation sont isolés comme précédemment (ils sont très semblables sur couche mince, à ceux obtenus dans les réactions non sensibilisées effectuées dans le benzène ou l'hexane) puis ozonolysés. Le mélange des produits provenant de l'ozonolyse, après séparation et méthylation présente le même diagramme en chromatographie en phase gazeuse que celui obtenu de la même manière dans la réaction non sensibilisée. Deux séparations successives sur la même colonne de silicone ont permis d'isoler un composé en tous points identique au produit de synthèse (**4**). La dimérisation de l'acétate de la vitamine A comme celle du butadiène et de l'isoprène se fait donc en passant par l'état excité d'un triplet.

Discussion

Le fait que les produits résultant de la photodimérisation de l'acétate de la vitamine A sont d'une manière prédominante des composés ayant un cycle à quatre et six chaînons suggère que le processus de la dimérisation se fait en passant par un état excité d'un triplet; ce point de vue est appuyé par la similitude des mélanges obtenus directement par irradiation ou par sensibilisation. Si c'est le cas, la vitesse de "l'intersystem crossing" doit être plus grande avec l'acétate de la vitamine A qu'avec le butadiène, une raison en serait alors une différence d'énergie faible entre singulet et triplet.

L'alternative serait que le cyclobutane soit formé à partir du premier état de singulet excité et le cyclohexène à partir d'une molécule à un niveau vibrationnel excité de l'état fondamental obtenu par conversion interne de cet état de singulet excité. Cependant il est très peu probable que ce serait alors une réaction de Diels–Alder qui se produirait d'une manière compétitive avec la désactivation vibrationnelle par collision. Bien qu'observé en phase gazeuse, aucun procédé de cette sorte ne semble avoir été obtenu en phase liquide. Par conséquent la conclusion que la dimérisation de la vitamine A acétate se fait par un processus d'un triplet non spécifique semble inévitable.

Partie expérimentale

Les spectres de résonance magnétique nucléaire (r.m.n.) ont été exécutés sur un appareil Varian A-60 en prenant la raie du tétraméthylsilane comme étalon interne, les spectres de masse sur un appareil MS9 de l'Institut de Chimie des Substances Naturelles à Gif-sur-Yvette, (France), les spectres infrarouges (i.r.) sur un appareil Beckman (IR 10), les spectres ultraviolets (u.v.), dans l'alcool éthylique, sur un appareil Cary 14 et les chromatographies en phase gazeuse sur un Aerograph A 350 B. Toutes les manipulations sur les dimères sont effectuées sous atmosphère d'azote. On a utilisé le silica gel G (Merck) pour les chromatographies sur colonne de même que pour les chromatoplaques ordinaires. On a employé les couches minces F254 commerciales (Merck) pour les séparations délicates. On révèle les produits par aspersion d'une solution saturée de trichlorure d'antimoine dans le $CHCl_3$ (*R*). Le solvant type utilisé pour les couches minces est le système; cyclohexane – éther isopropylique 1:1 (*S*).

Irradiation de l'acétate de la vitamine A dans l'hexane

Dans un réacteur de 5l on ajoute 4l d'une solution d'hexane saturée d'acétate de vitamine A (636 mg). Cette solution est désoxygénée par un courant d'azote purifié (1 h). On irradie pendant 1 h 30 min avec une lampe Hanovia pourvue d'une enveloppe de Pyrex (H8FG). Elle est refroidie par une circulation d'une solution réfrigérée de naphtalène (12.8 g dans 500 ml de cyclohexane) qu'on utilise comme filtre (12) sur une épaisseur de 0.5 cm. Après réaction on évapore l'hexane et récupère les 636 mg de produit. L'élution d'une chromato-

Can. J. Chem. Downloaded from www.nrcresearchpress.com by 210.87.254.5 on 09/05/12
For personal use only.

Can. J. Chem. Downloaded from www.nrcresearchpress.com by 210.87.254.5 on 09/05/12
For personal use only.

graphie sur colonne à l'éther isopropylique donne 57 mg de dimères. On isole en petite quantité quatre composés A,B,C et D après plusieurs séparations successives sur les couches minces commerciales en effectuant des passages multiples (*S*).

Produit A

Produit A, 1 mg, a un R_f de 0.35 (*S*); λ_{max}:237 (ε 16 400), 273 (ε 28 200), 283 (ε 27 550)mμ. Il présente une coloration bleue lorsqu'il est révélé avec (*R*).

Produit B

Produit B, 1.2 mg, a un R_f de 0.34 (*S*). Il présente une coloration rouge grenat (*R*); λ_{max}:267 (ε 16 400), 275 (ε 18 200), 285 (ε 16 300) mμ.

Produit C

Produit C, 1.5 mg, a un R_f de 0.33 (*S*) et 0.32 (hexane–acétate d'éthyle 17:3). Ces R_f sont exactement identiques à celui du diacétate du kitol naturel. La coloration de *C* est bleue (*R*) et vire au rouge grenat après plusieurs heures tandis que celle du diacétate de kitol est rouge brique (*R*).

Produit D

Produit D, 1.5 mg, R_f 0.31 (*S*) donne une coloration bleue (*R*); λ_{max}:262 (ε 20 000) mμ.

Hydrogénation de C

L'hydrogénation de 1.2 mg de C s'effectue en 12 h dans l'acide acétique, en présence de 1 mg d'oxyde de platine préalablement réduit. Le produit de la réaction est séparé sur une plaque analytique. On obtient 0.5 mg d'un composé homogène sur couche mince.

Hydrogénation de D

L'hydrogénation est conduite comme précédemment, on obtient 0.5 mg d'un composé homogène sur couche mince.

Irradiation de l'acétate de la vitamine A dans le benzène

On dissout 10.5 g d'acétate de la vitamine A dans 250 ml de benzène déthiophéné et préalablement irradié. Cette solution est traitée dans les mêmes conditions que précédemment. Après réaction on chasse le benzène sous vide. Le résidu est chromatographié, l'élution à l'éther isopropylique donne 7.32 g de dimères. La séparation de 207 mg de ceux-ci sur des couches minces préparatives conduit à 106 mg d'un produit principal se révélant en bleu sombre (*R*) et ayant un λ_{max} à 285 mμ symétrique (ε 15 350). Il est à nouveau séparé sur des plaques commerciales, on obtient un composé (39 mg) ayant un λ_{max} à 287 mμ (ε 37 500) symétrique, mais son spectre de r.m.n. montre qu'il s'agit encore d'un mélange de composés à structures différentes. Une nouvelle séparation donne un produit se révélant toujours en bleu sombre (*R*) et ayant une bande large centrée à λ_{max} 285 mμ (ε 34 000) dans son spectre u.v.; son spectre de r.m.n. est semblable à celui obtenu pour le diacétate du kitol (4, 5) et du photodimère (7). Ce composé possède exactement le même R_f et la même coloration (*R*) que le composé C obtenu dans l'irradiation effectuée dans l'hexane.

Ozonolyse des dimères

A 5 g des dimères précédents on ajoute 130 ml de chlorure de méthylène (13) et 1.2 ml de pyridine distillée sur potasse. Cette solution est ozonolysée 6 h à −70°. On laisse revenir à la température ambiante et on ajoute 20 ml d'eau distillée après avoir chassé le chlorure de méthylène, on oxyde 1 h à froid et 1/2 h au reflux avec 30 ml de péroxyde d'hydrogène à 30%. L'excès de péroxyde d'hydrogène est réduit, la phase aqueuse après extraction à l'éther et au chlorure de méthylène est portée à sec. Le solide obtenu est épuisé à l'acétone. On obtient 1.5 g de produit; après méthylation avec un excès de diazométhane et distillation dans un tube à boule $p.e._{0.1}$ 100–200° on récupère 353 mg de fraction volatile. Elle est étudiée en chromatographie en phase gazeuse sur une colonne de silicone SE 30 à 10% sur Chromosorb P. On sépare plusieurs composés ayant une bande carbonyle et acétate dans leur spectre i.r. L'un d'eux: 10.9 mg insuffisamment pur est rechromatographié sur la même colonne, on obtient 4.6 mg d'un produit (*a*) ayant les caractéristiques suivantes: i.r: ν_{max} ($CHCl_3$) 1735, 1230 cm^{-1}; r.m.n.: δ 4.15 (4H) (m), δ 3.67 (3H) (s), δ 3.65 (3H) (m), δ 2.05 (3H) (s), δ 2.00 (3H) (s), δ 1.35 (3H) (s), δ 1.25 (3H) (d).

Temps de rétention: (*i*) 7 min 45 s (colonne de silicone SE 30 sur Chromosorb P, longeur 1m débit d'hélium 2.5 cm^3/s, température 200°); (*ii*) 22 min 15 s (sur une colonne à 1.5% de Carbowax sur Chromosorb P, longeur 1.5 m débit d'hélium 2 cm^3/s, température 200°).

Synthèse de (3)

On laisse réagir pendant 12 h, 100 g de butène-2 diol-1,4 en présence de 300 g d'anhydride acétique et 400 g de pyridine; après traitement habituel on obtient 107 g de diacétate-1,4 butène-2. On dissous 2 g d'anhydride diméthyl-2,3 maléïque dans 53.5 g de diacétate butène-2. On verse le mélange dans 100 ml de cyclohexane. Cette solution est irradiée pendant 2 h avec une lampe à vapeur de mercure d'une puissance de 450 W. Après réaction on distille le cyclohexane et le diacétate-1,4 butène-2 en excès. Le résidu donne 1.5 g de cristaux brut, après plusieurs cristallisations dans le mélange chloroforme–cyclohexane on obtient 700 mg de cristaux blancs p.f. 108–109°. Le spectre i.r. montre les bandes à ν_{max} ($CHCl_3$) 1840, 1775, 1730 et 1240 cm^{-1}; r.m.n.: δ 2.03 (3H) (s), δ 2.08 (3H) (s), δ 1.37 (3H) (s) et δ 1.33 (3H) (s).

Anal. calc. pour $C_{14}H_{18}O_7$: C, 56.37; H, 6.08. Trouvé: C, 55.99; H, 6.08.

Méthyl ester (4)

On porte au reflux 157 mg d'anhydride précédent dans 5 ml d'eau distillée jusqu'à ce que la solution devienne limpide, on évapore l'eau et on méthyle avec un excès de diazométhane, après distillation au tube à boule $p.e._{0.1}$ 80–120° on obtient 150 mg d'une huile dont les spectres i.r., de r.m.n. et les temps de rétention sont absolument identiques au composé (*a*) obtenu précédemment.

Anal. calc. pour $C_{16}H_{24}O_8$: C, 55.80; H, 7.03. Trouvé: C, 55.52; H, 6.80.

Irradiation photosensibilisée de l'acétate de la vitamine A

On dissout dans 200 ml de benzène 400 mg d'acétate de vitamine A et 18.5 g de biacétyle. On irradie cette solution pendant 6 h avec une lampe à filament de tungstène d'une puissance de 500 W. Elle est refroidie par une circulation d'air et un courant d'eau. On utilise comme filtre une gaine de Pyrex et une solution de 0.5 cm d'épaisseur contenant 60 mg d'acridine pour 100 ml d'alcool éthylique à 95%. Après réaction, on chasse le solvant et on récupère le résidu. On effectue plusieurs

irradiations du même type sur 1.74 g d'acétate de vitamine A. Les produits des réactions sont rassemblés, on obtient 4.6 g de mélange. Il est chromatographié comme d'habitude, on obtient 1.2 g de dimères. Ils sont ozonolysés comme précédemment, on sépare les produits volatils, on en trouve 108 mg. Ils sont étudiés comme ci-dessus par chromatographie en phase gazeuse. On sépare 18.3 mg d'un composé qui après une deuxième purification donne 5.6 mg d'un produit ayant mêmes spectres i.r. et de r.m.n., les mêmes temps de rétention sur les deux colonnes précédentes que le produit isolé dans la réaction non sensibilisée (*a*) et celui de synthèse (**4**).

Remerciements

Je remercie M^{r}. le Professeur E. Lederer pour l'intérêt qu'il a porté à ce travail, M^{r}. le Professeur P. de Mayo pour avoir eu l'amabilité de m'avoir accueilli dans son laboratoire, M^{r}. le D^{r}. B. C. Das pour l'exécution des spectres de masse, l'OTAN et le CNRS pour des subventions ayant facilité ce travail, le D^{r}. O. Isler (Hoffmann-Laroche, Bâle) et les D^{r}. A. Brossi et L. M. Jampolsky (Hoffmann-Laroche Inc. New Jersey) pour des dons respectivement d'acétate de vitamine A et de vitamine A alcool.

1. R. KANEKO. Nippon Kagaku Zasshi, **81**, 1876 (1960).
2. Y. OMOTE. J. Chem. Soc. Japan. **80**, 191 (1959); Chem. Abstr. **55**, 3093 (1961); Bitamin, **28** 4, 267 (1963); Chem. Abstr. **60**, 5803 (1964).
3. R. KANEKO. Rept. Govt. Chem. Ind. Res. Inst. Tokyo, **57**, 194 (1962), (résumé en anglais p.22); J. Chem. Soc. Japan, **79**, 1459 (1958).
4. B. V. BURGER, C. F. GARBERS, K. PACHLER, R. BONNETT et B. C. L. WEEDON. Chem. Commun. 588 (1965).
5. C. GIANNOTTI, B. C. DAS et E. LEDERER. Chem. Commun. 28 (1966); Bull. Soc. Chim. France, 3299 (1966).
6. M. MOUSSERON-CANET, J. C. MANI, C. FAVIE et D. LERNER. Compt. rend. **262C**, 153 (1966); M. MOUSSERON-CANET. Advan. Photochem. **4**, 217 (1966).
7. M. MOUSSERON-CANET, J. C. MANI et D. LERNER. Bull. Soc. Chim. France, 3043 (1966).
8. R. SRINIVASAN. J. Am. Chem. Soc. **84**, 4141 (1962); **85**, 3048 (1963); **85**, 4045 (1963).
9. G. S. HAMMOND, N. J. TURRO, Jr. et A. FISHER. J. Am. Chem. Soc. **83**, 4674 (1961).
10. G. S. HAMMOND, N. J. TURRO et R. S. LIU. J. Org. Chem. **28**, 3297 (1963).
11. R. S. LIU, N. J. TURRO et G. S. HAMMOND. J. Am. Chem. Soc. **87**, 3406 (1965).
12. M. KASHA. J. Opt. Soc. Am. **38**, 11, 929 (1949).
13. J. KŘEPINSKY, Z. SAMEK, F. ŠORM, D. LAMPARSKY, P. OCHSNER et Y. R. NAVES. Tetrahedron Suppl. **8**, 1, 53 (1966).

Can. J. Chem. Downloaded from www.nrcresearchpress.com by 210.87.254.5 on 09/05/12
For personal use only.

Can. J. Chem. Downloaded from www.nrcresearchpress.com by 210.87.254.42 on 09/05/12
For personal use only.

Determination of —SH and —SS— groups in proteins. I. A reassessment of the use of methylmercuric iodide

W. F. FORBES
Department of Chemistry, University of Waterloo, Waterloo, Ontario

AND

C. R. HAMLIN
Department of Biochemistry, University of Rochester, Rochester, New York

Received January 9, 1968

Amperometric titration with methylmercuric iodide was found to be unsatisfactory for the quantitative determination of —SH and —SS— values in several soluble proteins. It is concluded that the "high reactivity" of the mercurial has previously been overemphasized. Consistent values can, however, be obtained by permitting protein samples to react with an excess of the mercurial, for about 100 h, followed by the polarographic estimation of the remaining reagent. Contrary to general belief, this procedure was found to be more precise than amperometric titration, and, if appropriate precautions are taken, it is applicable to considerably smaller amounts (<0.5 μmole —SH or —SS—) of either soluble or insoluble protein. The necessary experimental procedure is described and results are reported for several proteins. For the compounds studied, methylmercuric iodide did not react at non-sulfhydryl sites, and did not additionally bind to the mercaptides formed; there was no indication of disulfide bond cleavage, despite the long reaction times used.

Canadian Journal of Chemistry, **46**, 3033 (1968)

Introduction

Many procedures have been described for the determination of protein sulfhydryl and disulfide groups, without any one method or reagent having been found to be demonstrably superior. A number of review articles (1–4) catalogue the more useful methods, but a choice still has to be made from several less than ideal procedures.

Perhaps the most extensively used reagent is *p*-chloromercuribenzoate, which is used mainly in a spectrophotometric determination (5). However, the measurements must be made near 250 mμ, which is a region where proteins absorb appreciably, and where light scattering can cause serious errors. In addition, the method is unsuitable for insoluble proteins or for proteins that precipitate out during a determination.

The use of several other organic mercurials has been proposed frequently. Hughes (6) suggested that a mercurial should be monofunctional, and in order to reach inaccessible sulfhydryl groups, it should be as small as possible. He believed methylmercuric iodide to be the reagent most closely fitting these requirements, and successfully used it to obtain the sulfhydryl content of bovine serum albumin and of hemoglobin (6, 7). The importance of using a reagent of small size has been demonstrated by Fraenkel-Conrat, who found that the single sulfhydryl group of tobacco mosaic virus protein reacted with methylmercuric nitrate but not with nitroprusside, iodoacetate, or *p*-chloromercuribenzoate (8).

The technique of amperometric titration with a mercurial has been applied to the determination of protein sulfhydryl groups (9–12). Leach in this way used methylmercuric iodide on a number of proteins and simple thiols (11) and described procedures for the determination of sulfhydryl and disulfide groups in a variety of proteins. However, when his procedures were applied to soluble protein samples in these laboratories, the amperometric titrations proceeded slowly and often yielded inconsistent results. Moreover, the quantities of sample required were relatively large.

Leach also modified this titration procedure to be suitable for certain unreactive proteins, such as wool keratin (13). He termed this a "single point titration" procedure, since it involved a polarographic estimation of methylmercuric iodide, after an excess of the reagent had been allowed to react with protein over an extended period of time. A study of this method, suitably modified, showed that satisfactory disulfide and sulfhydryl determinations can thus be performed

on substantially smaller amounts of material, irrespective of the solubility of the sample.

Experimental

(i) Reagents and Samples

Mercury was washed with 10% sodium hydroxide, 10% nitric acid (14), and dried by dropping through 10% mercurous sulfate in sulfuric acid. The dried mercury was finally distilled three times in an evacuated apparatus (15) and stored in glass containers.

Methylmercuric iodide was prepared by exposing re-distilled methyl iodide and mercury to sunlight (11). Despite repeated recrystallization from methanol, methylmercuric iodide could not be obtained with a melting point greater than 140 °C, (lit. 142 °C, ref. 11). Sublimation of the dried compound (ca. 25 °C/10^{-3} mm Hg and in the dark) yielded a product, m.p. 146.2 °C (corrected). The melting point decreased for preparations exposed to light for appreciable periods of time, or which had been prepared a few days previously. Methylmercuric iodide was stored in the dark at 5 °C as a 0.1 *M* solution, in freshly distilled dimethyl formamide (DMF). Dimethyl formamide was distilled (b.p. 45 °C/24 mm) immediately before use. Water was first deionized and then glass-distilled. Hydrochloric acid was a constant-boiling solution, re-distilled from an all-glass apparatus (14). Since ammonium hydroxide is known to attack glass, solutions of ammonium hydroxide were freshly prepared by using ammonia gas from a cylinder (14).

Phosphate buffer (1 liter) was made by adding water to 2.772 g potassium dihydrogen phosphate, 4.260 g disodium hydrogen phosphate, and 1.169 g sodium chloride (analytical grade reagents). The solution was filtered and had a pH of 6.99 at 25 °C.

Other reagents used were urea ('ultra pure' reagent, Mann Research Laboratories), sodium sulfite (Fisher certified reagent), potassium chloride (Analar reagent, B.D.H.), tris(hydroxymethyl)aminomethane (Fisher primary standard), 2-octanol (Eastman), and gelatin (bacteriological grade, Fisher).

Amino acids and proteins were of the highest grade commercially available and were used without additional purification. They were obtained from General Biochemicals (G.B.), Mann Research Laboratories (Mann), Nutritional Biochemical Corp. (N.B.C.), or Sigma Chemical Company (Sigma). Most of the samples contained less than 90% protein on the basis of Kjeldahl nitrogen determinations. The moisture content and ash weight of the protein samples were therefore determined. The results of protein content, moisture content, and ash weight together accounted for virtually all the material present in the samples.

(ii) Apparatus

Polarographic measurements were made with a Sargent model XV polarograph, fitted with a micro-range extender. The dropping mercury electrode delivered drops (average weight 5.94 mg) at 3.87 s intervals, with a mercury column height of 80 cm and the capillary opening immersed in 0.05 *M* phosphate buffer at pH 7. The drop time was recorded on open circuit. Two types of sample cells were constructed (described later), and all potentials were measured at 25 ± 0.1 °C with respect to the saturated calomel electrode (S.C.E.). Sample solutions were de-gassed with oxygen-free argon (16).

(iii) Methods

(a) Amperometric Titration

A polarographic cell and reference electrode were constructed similar to the one described by Human and Leach (17), suitable for sample volumes of 2–5 ml. The titrant was delivered from a calibrated syringe microburette. The buffers, titrant, and cell additives used were similar to those used by Leach (11).

(b) Determinations Involving the Use of an Excess of Methylmercuric Iodide

The reaction between methylmercuric iodide and the sample was carried out in an all-glass container. After addition of sample and reaction solution, the contents of the reaction vessel were cooled (liquid nitrogen) and evacuated (oil pump). Finally nitrogen was introduced into the reaction vessel at slightly less than one atmosphere pressure, with a vacuum desiccator acting as reservoir.

Reaction solutions were prepared as follows.

—SH determinations (0.3 μmole MeHgI/ml; pH 7) —25.3 g urea (8 *M*), 1.9 g KCl (0.5 *M*), 2.0 ml 0.25% gelatin solution, 150 mg 0.1 *M* MeHgI in DMF, and phosphate buffer to a final volume of 50 ml.

—SH + —SS— determinations (0.35 μmole MeHgI/ml; pH 9) —25.3 g urea (8 *M*), 1.9 g KCl (0.5 *M*), 1.4 g Na_2SO_3 (0.22 *M*), 4.0 ml 2 *M* HCl, 5.0 ml 2 *M* NH_4OH, 2.0 ml 0.25% gelatin solution, 175 mg 0.1 *M* MeHgI in DMF, and distilled water to a final volume of 50 ml.

Reagents were added in the order shown, and the solutions were made up immediately before use. Gelatin solutions were prepared 2–3 h in advance, and for the disulfide determinations, the weight of sodium sulfite was kept close to 1.400 g, as the sulfite concentration affects both the position and height of the first methylmercuric iodide reduction wave. Up to 25 reaction vessels, containing the appropriate solutions, were kept in the dark with occasional swirling for the required periods of time. Polarograms of standards were run at the beginning and end of a batch of samples and three other standards were run at intervals among the samples. Each determination was repeated at least once, and no two determinations, on the same sample, were performed in a single batch of samples. Thus the duplicate determination was a true replicate, insofar as all operations, apart from the purification of reagents, were repeated in the second analysis. The difference between two such determinations was generally about 2–3% of the amount of the mean value.

The determination of the excess of methylmercuric iodide present can be carried out with any micro-polarographic cell equipped with a suitable reference electrode. The limiting factor governing the cell size is that the quantity of reducible substance, removed by reduction during the course of a determination, should be small. Approximately 1% of a reducible substance is removed from 0.5 ml of solution in 10 min, at a current flow equal to the limiting current. For this reason, a polarographic cell and reference electrode were built, suitable for about 0.5 ml of sample solution (Fig. 1).

Can. J. Chem. Downloaded from www.nrcresearchpress.com by 210.87.254.42 on 09/05/12
For personal use only.

Can. J. Chem. Downloaded from www.nrcresearchpress.com by 210.87.254.42 on 09/05/12
For personal use only.

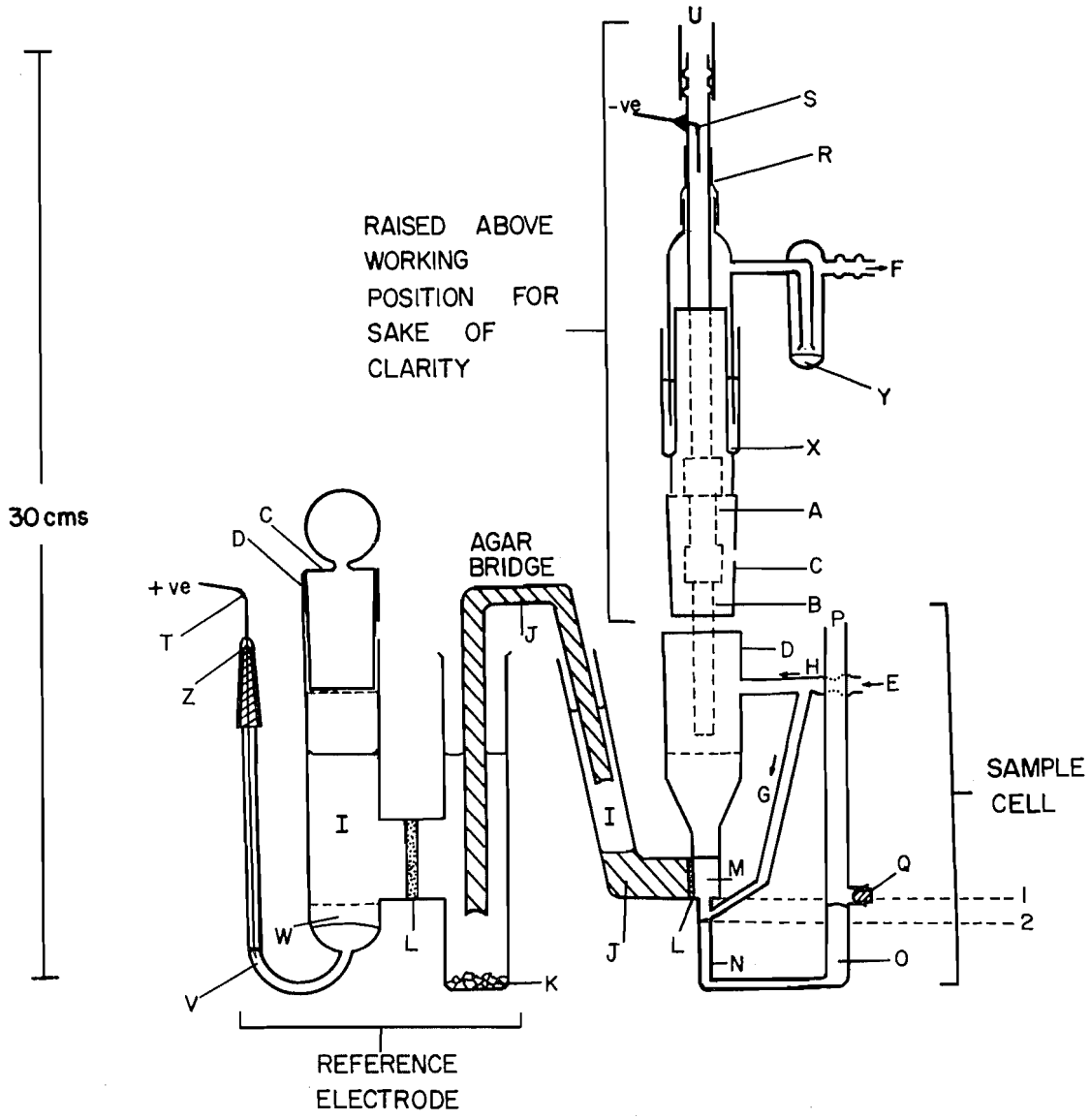

FIG. 1. Polarographic cell assembly; A, teflon tube fitting (Beckman); B, glass capillary – dropping mercury cathode; C, inner member of ground-glass joint, with vent, size 24/40; D, outer member of ground-glass joint, (with hose connector); E, inert gas flow-in; F, inert gas flow-out; G, direction of gas flow, with glass-joint valve closed; H, direction of gas flow, with glass-joint valve open; I, saturated aqueous potassium chloride; J, agar – potassium chloride plug, made by adding 40 g of potassium chloride to about 100 g agar gel, (3.5 g agar to 100 ml water) heated on a water bath; K, potassium chloride crystals; L, fritted-glass disk, extra coarse grade; M, sample compartment; N, heavy-walled glass capillary, 1 mm internal diameter; O, mercury seal; P, opening to which flexible tubing is connected; Q, small cork; R, rubber-tubing seal; S, platinum electrical contact (negative); T, platinum electrical contact (positive); U, mercury column to reservoir; V, mercury pool; W, paste of mercury and mercurous chloride; X, mercury seal; Y, mercury seal; Z, ground-glass joint, size 7/25.

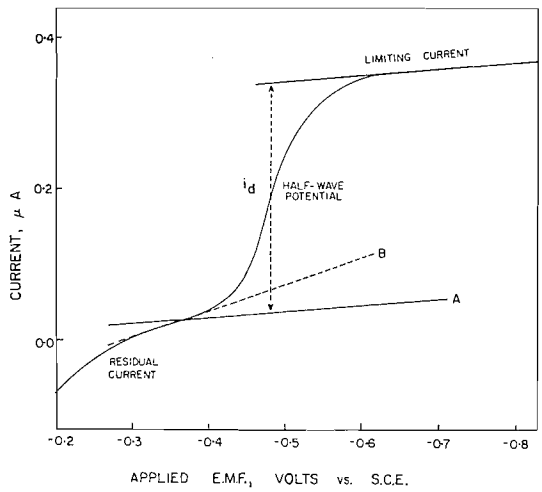

FIG. 2. First reduction wave for MeHgI in 8 *M* urea, 0.5 *M* KCl, at pH 7 and with 0.01% gelatin, (2 ml solution originally contained 0.55 μmole MeHgI and 3.3 mg protein, or approximately 0.39 μmole —SH).

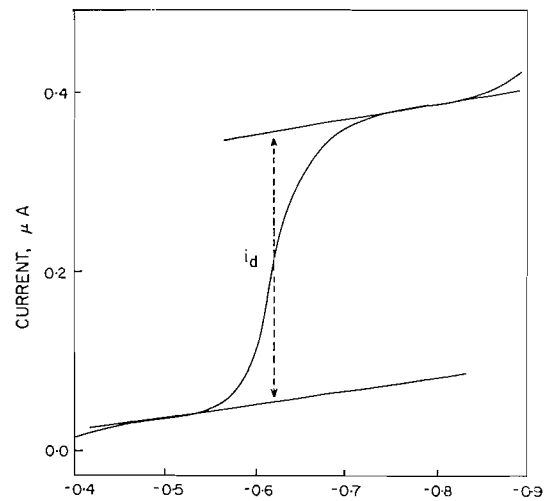

FIG. 3. First reduction wave for MeHgI in 8 *M* urea, 0.5 *M* KCl, 0.2 *M* $SO_3^=$, at pH 9 and with 0.01% gelatin. (2 ml solution originally contained 0.7 μmole MeHgI and 2.5 mg protein, or approximately 0.44 μmole —SH + —SS—).

The cell assembly and electrodes were built as five, easily-separable units. The saturated calomel reference electrode was permanently clamped. The dropping mercury electrode could be raised or lowered, without affecting the height of the mercury column above the capillary. The same capillary was used throughout. With the agar bridge removed and the dropping mercury electrode completely raised, the sample cell and the inner member of the vented-joint could be removed together. Normally only the sample cell was clamped; since the inner member of the vented-joint C was free to turn, it acted as a valve. The joint C could be removed, and thereby could give access to the sample compartment M.

(c) Measurement of Diffusion Currents

Methylmercuric iodide reacts with protein —SH groups as follows.

$$P\cdot SH + MeHgI \rightarrow P\cdot SHgMe + HI$$

The number of disulfide bonds may also be determined after reduction and sulfite ion is frequently used (18).

$$P\cdot SS\cdot P + SO_3^= \rightleftharpoons P\cdot S^- + P\cdot SSO_3^-.$$

The reaction proceeds to completion in the presence of a high concentration of sulfite and low concentration of $P\cdot S^-$. This can be achieved by the presence of a mercaptide-forming reagent, such as methylmercuric iodide. Each mole of disulfide then reacts with one mole of mercurial.

The current–voltage curves for methylmercuric iodide, and generally for mercurials of the type RHgX, show that reduction occurs in two stages (19). In the above reactions none of the reagents nor reaction products has a reduction wave at potentials more positive than that of the first methylmercuric iodide step. However, if the protein is of low molecular weight (e.g. insulin) the mercaptide formed is reduced soon after the first methylmercuric iodide wave, making the location of its limiting current plateau less distinct.

Figures 2 and 3 show typical first reduction waves for an excess of methylmercuric iodide in the presence of protein mercaptide, under the conditions used to determine —SH and —SH + —SS— contents respectively. The nonlinear, negative current (anodic current) at potentials more positive than about − 0.30 V results from the presence of certain anions (e.g. I^-) that cause variable capacitance effects at the mercury drop. In practice the capacitance current increases linearly from about −0.35 to −1.40 V. Hence the presence of a reducible species with a half-wave potential within this range should result in the formation of a wave with the slope of the residual current parallel to that of the limiting current.

Under the conditions used to determine —SH groups in proteins, the first half-wave potential of methylmercuric iodide is at about −0.45 to −0.50 V. Consequently there is virtually no region of linear increase of residual current before the commencement of the reduction wave, and it is not possible to obtain good estimates of the residual current, at the methylmercuric iodide first half-wave potential, by linear extrapolation of the current (line B). However, in the region of −0.375 V, the change of residual current should be almost linear and the reduction of mercurial should not have begun. Therefore, a line A is drawn through the region of minimum slope (ca. −0.375 V) parallel to the slope of the limiting current. This line was taken to represent the most probable values for the residual current at potentials more negative than about −0.40 V.

When determining the —SH + —SS— content, the presence of 0.2 *M* sulfite and 8 *M* urea at pH 9 displaces the wave to a more negative potential and the slope

Can. J. Chem. Downloaded from www.nrcresearchpress.com by 210.87.254.42 on 09/05/12
For personal use only.

of the residual current at about −0.50 V is parallel to the slope of the limiting current.

Once the diffusion current has been determined, it is compared to the diffusion current obtained from aliquots of the relevant reaction solution, in the absence of protein. It is assumed that there is a linear relationship between the magnitude of the diffusion currents and the concentration of free methylmercuric iodide remaining in solution. This may not be strictly valid, since the presence of some proteins could result in a small reduction of the measured diffusion currents (cf. urea, sulfite). Such an effect would explain the small apparent sulfhydryl contents of some proteins (see Table III).

Samples in solution require special consideration owing to the concentration dependence of the diffusion currents. The initial concentration of methylmercuric iodide should be the same in both the reaction and standard solutions. Either the sample is lyophilized or the standard solution should be diluted. Less preferably, a correction factor may be calculated by simple proportion.

Results

(i) Amperometric Titration

Titration of simple thiols with $2 \times 10^{-3} M$ methylmercuric iodide often produced low values, possibly because some oxidation had occurred, and it was frequently impossible to obtain sharp end-points. The use of $10^{-2} M$ mercurial improved the character of the end-points, but necessitated the use of larger samples.

Some proteins, such as serum albumin, yielded values close to those generally accepted (4), but the titration proceeded slowly, several minutes elapsing after each addition of reagent, before equilibrium was reached. With other samples (e.g. eye-lens proteins) the titration was too slow for routine use. More important, replicate determinations on the same sample afforded inconsistent values and poor end-points, and samples yielded a lower half-cystine content (—SH + 2×—SS—) by amperometric titration than by amino acid analysis. Attempts to increase the extent of reaction with mercurial by performing the titrations at higher temperatures, or to improve the sharpness of the end-points by more elaborate purification of reagents, were not uniformly successful.

(ii) Determinations Involving the Use of an Excess of Methylmercuric Iodide

(a) Control Experiments

The samples were permitted to react with an excess of methylmercuric iodide over an extended period of time (cf. 13). When this procedure was used for some of the samples that had presented difficulties using the amperometric titration, it was found that there was an additional uptake of mercurial. Experiments were therefore performed to determine the optimum concentration of mercurial and the length of time needed to allow complete reaction.

Determinations were first carried out with an initial concentration of mercurial of about $2 \times 10^{-5} M$, and sufficient sample was added to react with about one quarter of the reagent. For some proteins, it was not clear whether the reaction was complete, even after seven days. However, if larger methylmercuric iodide ($2 \times 10^{-4} M$) and protein sulfhydryl ($1 \times 10^{-4} M$) concentrations were used, and the reaction was allowed to proceed for substantially longer periods, consistent results were obtained. An additional series of determinations was performed with the concentration of methylmercuric iodide again increased ten times, but there was no significant further increase in the relative amounts of reaction.

Volatilization of mercury has been reported for various biological media as a result of bacterial action (20). However, a number of reaction solutions, containing different quantities of methylmercuric iodide, stored for 26–290 h, failed to provide any evidence that a similar loss occurs under the present experimental conditions.

Certain mercaptides, for example those of silver (21), have a strong tendency to bind additional reagent. This tendency is reduced for mercurials by the presence of sufficient chloride ion (22). However, the possibility remained that the mercaptides formed with methylmercuric iodide might bind additional reagent over long periods of time. Reaction with simple thiols showed no indication of this (see Table I). Gelatin and cytochrome *c* were also allowed to react with $3.5 \times 10^{-4} M$ methylmercuric iodide, but there was almost no uptake of reagent. These results indicate that methylmercuric iodide does not bind appreciably with thioether or other groups, under the conditions used.

Under certain circumstances, heavy metal reagents will react with disulfide groups, although the reaction is complex and not fully understood (4). An appreciable rate of reaction between methylmercuric iodide and disulfide

Can. J. Chem. Downloaded from www.nrcresearchpress.com by 210.87.254.42 on 09/05/12
For personal use only.

TABLE I

Moles of methylmercuric iodide reacting with one mole of some simple thiols in the presence of a 200% excess of mercurial

Compound	Moles MeHgI/mole thiol	Incubation time (h)
L-Cysteine hydrochloride monohydrate, (G.B. 52036)	0.99	195
L-Cysteine hydrochloride monohydrate, (Sigma C9753)	1.01	193
Glutathione, (reduced, Mann 2812)	0.96	194
Gelatin, (Pfanstiehl Labs. 5039)	0.0	54
Cytochrome *c*, (horse heart, N.B.C. 2024)	0.10	212
	0.12	156

groups would represent a serious objection to sulfhydryl and disulfide content determinations involving prolonged reaction with the mercurial. Hence a number of proteins and simple disulfide compounds, that contain no sulfhydryl groups, were reacted with methylmercuric iodide, under the conditions used to determine sulfhydryl groups (Table II).

The disulfide content of a sample is obtained by subtracting the sulfhydryl group content from the value found for the total number of moles of disulfide bonds and sulfhydryl groups. It is desirable to obtain these two values under as similar conditions of pH, sample and reagent concentration, etc., as possible. Table II shows the results obtained from an investigation to determine the feasibility of performing both analyses at the same pH.

Table II indicates that sulfhydryl determinations performed at pH 9 may be accompanied by the cleavage of disulfide bonds, which is not surprising as oxidized glutathione may be determined in the presence of cystine, owing to the more labile disulfide bond of the former at high pH (23). Unfortunately —SH + —SS— contents could not be readily determined at pH 7 because addition of 0.2 *M* sulfite raised the pH to 7.8. Moreover, the lower pH caused the first reduction wave of methylmercuric iodide to shift to a more positive potential, tending to offset the inherent advantages of a more negative potential (Fig. 3). Hence all —SH determinations were carried out at pH 7 and all —SH + —SS— determinations at pH 9.

The results in Table II again show no evidence that the mercaptides bound additional mercurial. This was also true for the products formed after disulfide bonds were split with sulfite.

(b) Application to Protein Samples

Determinations of —SH and —SH + —SS— contents were performed on a number of protein samples (Table III). Aliquots (1–2 ml) of the reaction solutions were used together with sufficient sample to react with 50–75% of the methylmercuric iodide present. Reaction times were generally from 100–200 h, which is considered to be long enough for most proteins. Since the values in Table III are expressed in moles per mole of protein, the error associated with the determination of —SH and —SS— groups is compounded with possibly inaccurate

TABLE II

Reactions of disulfides with methylmercuric iodide*

Sample	Moles —SH/mole sample (pH7)	Moles —SH/mole sample (pH9)	Moles —SH + —SS—/mole sample (pH 7.8)	Moles —SH + —SS—/mole sample (pH 9)
Cystine (G.B. 58651)	0.02	0.03	1.02‡	1.04
Oxidized Glutathione (Mann R2371)†	0.05	0.50	—	0.995
Reduced Glutathione (Mann R2812)	0.95	0.95	—	0.97
Cytochrome *c* (N.B.C. 2024)	0.11	0.11	0.17‡	0.23
Hemoglobin (Mann 6237)	1.91	1.71‡	2.05‡	1.95
Insulin (Mann R3564)†	0.16	0.28	3.23	3.24
β-Lactoglobulin (N.B.C. 7791)	2.00	2.08‡	6.16‡	5.96
Lysozyme (Mann S1428)	0.05	0.06‡	4.18‡	4.14
Ovalbumin (Mann R3827)	3.69	3.82	5.56‡	5.40
Pepsin (N.B.C. 9567)†	0.16	1.01	3.28	3.11
Ribonuclease (Mann R1249)†	0.07	0.42	3.95	3.93

*The reaction temperature was 22 °C, and reaction times were 100–500 h.
†Marked pH effect on SH determinations.
‡Single determination.

Can. J. Chem. Downloaded from www.nrcresearchpress.com by 210.87.254.42 on 09/05/12
For personal use only.

TABLE III

Analyses of sulfhydryl and disulfide contents of some proteins

Sample	Moles —SH/mole protein	Moles —SH + —SS—/mole protein	Moles —SS—/ mole protein	Moles sulfur as ½ cystine/ mole protein	Molecular weight*
Hemoglobin (bovine) (Mann 6237)	1.91	1.95	0.04	1.99	64 450 (5.95)
Insulin (bovine) (Mann R3564)	0.16	3.23	3.07	6.30	5 733 (6.30)
β-Lactoglobulin (N.B.C. 7791)	2.00	5.96	3.96	9.92	37 000 (6.41)
Lysozyme (Mann S1428)	0.05	4.14	4.09	8.23	14 300 (5.49)
Ovalbumin (Mann R3827)	3.69	5.40	1.71	7.11	46 000 (6.35)
Papain (Mann R3398)	0.64	3.87	3.23	7.10	21 000 (6.21)
Pepsin (N.B.C. 9567)	0.16	3.11	2.95	6.06	35 000 (6.71)
Phosphorylase a (N.B.C. 9532)	23.6	28.0	4.4	32.4	370 000 (6.08)
Ribonuclease (Mann R1249)	0.07	3.93	3.86	7.79	13 680 (5.71)
Ribonuclease A (N.B.C. 7699)	0.06	3.96	3.90	7.86	13 680 (5.71)

*Figures in parentheses show the nitrogen to protein conversion factors used.

values for the molecular weight. Therefore no attempt was made to assess quantitatively the accuracy of the procedure.

The results in Table III are generally close to the values expected for these proteins. Some degree of heterogeneity is expected for samples such as β-lactoglobulin (24), ovalbumin (25), and pepsin (26). Papain was delivered as a suspension, and undoubtedly had undergone some loss of activity as a result of partial oxidation. The small apparent sulfhydryl contents found for insulin and pepsin may be due to impurities, degradation products, or because certain proteins may affect the reduction of methylmercuric iodide at the dropping mercury cathode (see Experimental).

Two proteins, hemoglobin and papain, were subjected to reaction with a greatly increased excess of methylmercuric iodide (400%) for longer times than usual (600 h). There was no evidence for additional binding of mercurial or cleavage of disulfide bonds (see refs. 10 and 27).

Discussion

The determination of —SH and —SS— groups in a wide variety of protein samples may be carried out by prolonged reaction with an excess of methylmercuric iodide. The method was found to be more readily applicable to small samples than direct titration. For example, Leach (11) used 20 mg of ribonuclease to determine the —SS— content, whereas less than 1 mg was sufficient for the present procedure, and similarly reduced amounts were used for the other determinations. The long reaction times with methylmercuric iodide might have been anticipated to induce non-specific binding of the mercurial (cf. phenylmercuric hydroxide (10)), or hydrolytic cleavage of disulfide bonds (cf. *p*-chloromercuribenzoate (27)), but no such effects were observed. The reduced amounts of protein necessary thus represent one advantage of the present procedure.

Secondly, amperometric titration with methylmercuric iodide is not a suitable procedure for determining —SH and —SS— groups in some soluble proteins, such as γ-crystallin (unpublished), and it is generally unsuitable for most insoluble or partly-soluble samples. These limitations are virtually unimportant when using the preferred method.

Finally, contrary to general belief (4), the estimation of —SH and —SS— contents is more precise than amperometric titration, even for well-defined proteins such as ovalbumin or ribonuclease (cf. 11). This follows because amperometric titration assumes a greater reactivity of methylmercuric iodide with —SH groups than is believed justified.

Further work, describing the determination of —SH:—SS— ratios in a number of other proteins, is in progress.

Acknowledgments

The authors are indebted to Prof. S. J. Leach for numerous authoritative and valuable comments.

Can. J. Chem. Downloaded from www.nrcresearchpress.com by 210.87.254.42 on 09/05/12
For personal use only.

They also gratefully acknowledge the financial assistance of the Defence Research Board of Canada (Grant No. 1675-04), the National Research Council of Canada, the National Cancer Institute of Canada, and the United States Public Health Service (research grant RH00392, National Center for Radiological Health). This work was carried out during the tenure of a Canadian Commonwealth Scholarship (to C. R. H.).

1. P. D. BOYER. The enzymes. Vol. I. *Edited by* P. D. Boyer, H. Lardy, and K. Myrbäck. Academic Press, Inc., New York. 1959. Chap. 11. p. 511.
2. R. CECIL and J. R. MCPHEE. Advan. Protein Chem. **14**, 255 (1959).
3. R. BENESCH and R. E. BENESCH. Methods of biochemical analysis. Vol. 10. *Editor* D. Glick. Interscience Publishers, Inc., New York. 1962. p. 43.
4. R. CECIL. The proteins. Vol. I. *Edited by* H. Neurath. Academic Press, Inc., New York. 1963. Chap. 5. p. 379.
5. P. D. BOYER. J. Am. Chem. Soc. **76**, 4331 (1954).
6. W. L. HUGHES. Cold Spring Harbor Symp. Quant. Biol. **XIV**, 79 (1949).
7. W. L. HUGHES. J. Am. Chem. Soc. **69**, 1836 (1949).
8. H. FRAENKEL-CONRAT. Sulphur Proteins Proc. Symp. Falmouth, Mass. *Edited by* R. Benesch, R. E. Benesch, P. D. Boyer, I. Klotz, W. R. Middlebrook, A. G. Szent-Gyorgyi, and D. R. Schwarz. Academic Press, Inc., New York. 1959. p. 339.
9. W. STRICKS and I. M. KOLTHOFF. J. Am. Chem. Soc. **75**, 5673 (1953).
10. A. C. ALLISON and R. CECIL. Biochem. J. **69**, 27 (1958).
11. S. J. LEACH. Australian J. Chem. **13**, 520 (1960).
12. W. STRICKS and S. K. CHAKRAVARTI. Anal. Chem. **33**, 194 (1961).
13. S. J. LEACH. Australian J. Chem. **13**, 547 (1960).
14. W. F. HILLEBRAND, G. E. F. LUNDELL, H. A. BRIGHT, and J. I. HOFFMAN. Applied inorganic analysis. 2nd ed. John Wiley and Sons, Inc., New York. 1953.
15. W. A. CARLSON and L. F. BORCHARDT. Ind. Eng. Chem. Anal. Ed. **10**, 94 (1938).
16. L. MEITES. Polarographic techniques. 2nd ed. John Wiley and Sons, Inc., New York. 1965.
17. J. P. E. HUMAN and S. J. LEACH. Chem. and Ind. London, **9**, 149 (1956).
18. H. T. CLARKE. J. Biol. Chem. **97**, 235 (1932).
19. R. BENESCH and R. E. BENESCH. J. Am. Chem. Soc. **73**, 3391 (1951).
20. L. MAGOS, A. A. TUFFERY, and T. W. CLARKSON. Brit. J. Ind. Med. **21**, 294 (1964).
21. L. A. AE. SLUYTERMAN. Biochim. et Biophys. Acta, **25**, 402 (1957).
22. W. STRICKS, I. M. KOLTHOFF, and J. HEYNDRICKX. J. Am. Chem. Soc. **76**, 1515 (1954).
23. W. STRICKS and I. M. KOLTHOFF. Anal. Chem. **25**, 1050 (1953).
24. E. B. KALAN, R. GREENBERG, and M. WALTER. Biochemistry, **4**, 991 (1965).
25. L. G. LONGSWORTH, R. K. CANNAN, and D. A. MACINNES. J. Am. Chem. Soc. **62**, 2580 (1940).
26. T. G. RAJAGOPALAN, S. MOORE, and W. H. STEIN. J. Biol. Chem. **241**, 4940 (1966).
27. B. J. FINKLE and E. L. SMITH. J. Biol. Chem. **230**, 669 (1958).

Can. J. Chem. Downloaded from www.nrcresearchpress.com by 210.87.254.42 on 09/05/12
For personal use only.

Can. J. Chem. Downloaded from www.nrcresearchpress.com by 210.87.254.40 on 09/05/12
For personal use only.

Reaction of acetylenic hydrocarbons with α,β-unsaturated ketones in tetrahydrofuran in the presence of lithium naphthalene

KYOICHI SUGA, SHOJI WATANABE, AND TOSHIMITSU SUZUKI
Department of Applied Chemistry, Faculty of Engineering, Chiba University, Yayoicho, Chiba, Japan

Received May 7, 1968

Lithium naphthalene reacts easily with terminal acetylenic hydrocarbons, such as acetylene, methylacetylene, or phenylacetylene, to give the corresponding lithium compounds quantitatively. The reaction of these lithium compounds with α,β-unsaturated ketones gives the corresponding acetylenic carbinols in a good yield under mild conditions.

Canadian Journal of Chemistry, 46, 3041 (1968)

α,β-Unsaturated ketones have been notable for their resistance to conversion to their ethynylcarbinols. Best results have been obtained with lithium acetylide in liquid ammonia. For example, ethynyl-β-ionol, which is an important intermediate for the synthesis of vitamin A or carotene, can be prepared by the action of lithium or calcium acetylide in liquid ammonia (1). Addition reactions of alkylacetylenes, such as phenylacetylene, methylacetylene, or vinylacetylene, to α,β-unsaturated ketones can be carried out by using butyllithium or ethylmagnesium halide. Recently, the authors reported that lithium naphthalene in tetrahydrofuran solution is an excellent agent for ethylation at the α-position of naphthalene (2) and for the dimerization of conjugated dienes (3–4). In the present work the procedure using lithium naphthalene was applied to the title reaction. The reductive coupling of phenylacetylene with lithium naphthalene gave 1,4-diphenylbutane, but methylphenylacetylene, which does not have a terminal acetylenic group, could not be dimerized in the same way (5). From these results, it would be suspected that a terminal acetylenic hydrogen can be metallated easily with lithium naphthalene. This paper concerns a new convenient procedure for the reaction of acetylenic hydrocarbons with α,β-unsaturated ketones under mild conditions. The authors have now found that the reaction of acetylenic hydrocarbons with α,β-unsaturated ketones can be carried out conveniently by the action of lithium compounds of acetylenic hydrocarbons which are obtained from lithium naphthalene and acetylenic hydrocarbons in tetrahydrofuran solution.

Thus, through a solution of lithium naphthalene in tetrahydrofuran, acetylene was passed slowly to give lithium acetylide quantitatively. In a typical experiment, β-ionone (**1**) was added to this solution and ethynyl-β-ionol (**2**) was obtained in 90% yield (6). The identity of **2** was confirmed by comparison of the infrared (i.r.) absorption spectrum, nuclear magnetic resonance (n.m.r.) spectrum, and ultraviolet (u.v.) absorption spectrum with those of authentic **2** (1). With the other α,β-unsaturated ketones, high conversions to ethynylcarbinols were achieved by this new convenient method, and typical results are presented in Table I.

The reaction of α,β-unsaturated ketones with alkylacetylenes such as phenylacetylene and methylacetylene can be performed in the similar way. In a typical experiment, **1** reacted with phenylacetylene to give, predominantly, a carbinol (**3**). The composition ($C_{21}H_{26}O$) was confirmed by an elementary analysis. The i.r. absorption spectrum showed characteristic bands of the tertiary alcohol group at 3440 cm^{-1} and 1060 cm^{-1}, the ethynyl group at 2200 cm^{-1}, the phenyl group at 750 cm^{-1} and 690 cm^{-1}, and the *trans*-type double bond at 960 cm^{-1}. The u.v. absorption spectrum showed the absorption peaks at 227 mμ, 241 mμ, and 252 mμ. The n.m.r. spectrum gave a signal at 7.30 p.p.m. arising from the five protons of the aromatic nucleus. The signal at 1.04 p.p.m. was presumably due to six protons of two methyl

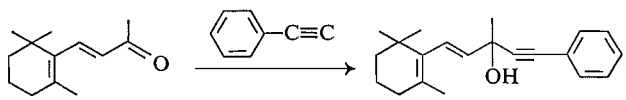

1 **3**

Can. J. Chem. Downloaded from www.nrcresearchpress.com by 210.87.254.40 on 09/05/12
For personal use only.

TABLE I

Reaction of α,β-unsaturated carbonyl compounds and saturated ketones with acetylenic hydrocarbons

Acetylenic hydrocarbon	α,β-Unsaturated ketone	Product	Yield (%)	Boiling point (°C/Torr)	n_D	Analytical data: Found (%) C	Found (%) H	Calcd. (%) C	Calcd. (%) H
Acetylene	α-Ionone	Ethynyl-α-ionol	50	96/3	n_D^{20}1.4940				
	β-Ionone	Ethynyl-β-ionol	85	107–109/3	1.5120				
	ϕ-Ionone	Ethynyl-ϕ-ionol	40	130/3	1.5251				
	Benzalacetone	1-Phenyl-1-penten-4-yn-3-ol	60	98–100/3	48–49.5*				
	Acetophenone	3-Phenyl-1-butyn-3-ol	15	90–95/11	47–49*				
	Carvone	Ethynyl-carveol	40	88–92/3	1.5235				
	Mesityloxide	3,5-Dimethyl-4-hexen-1-yn-3-ol	35	139/20	1.4616				
	Cinnamaldehyde	1-Phenyl-1-penten-4-yn-3-ol	15		67*				
	Citral	5,9-Dimethyl-4,8-decadien-1-yn-3-ol	30	90/3	1.4963				
Methylacetylene	α-Ionone	Propynyl-α-ionol	55	123/3	n_D^{15}1.5050	83.0	10.4	82.9	10.1
	β-Ionone	Propynyl-β-ionol	88	110/2	1.5393	82.3	9.7	82.9	10.1
	Carvone	Propynyl-carveol	70	96/3	1.5181	81.6	9.5	82.1	9.5
	Benzalacetone	3-Methyl-1-phenyl-1-hexen-4-yn-3-ol	40	116/3	1.5749	83.1	7.4	83.9	7.5
	Pulegone	Propynyl-pulegol	30	85/3	1.5082	82.2	9.2	82.1	9.5
	Methylethyl ketone	4-Methyl-2-hexyn-4-ol	85	53.5/20	1.4592	74.8	10.5	75.0	10.7
Phenylacetylene	β-Ionone	1-(2′,6′,6′-Trimethyl-1′-cyclohexen-1′-yl)-3-methyl-3-hydroxyl-5-phenyl-1-penten-4-yne	50	90–100/10^{-3}	n_D^{20}1.5712	85.7	8.3	85.5	8.8
	Cinnamaldehyde	1,5-Diphenyl-1-penten-4-yn-3-ol	20	186/2		87.1	5.8	87.2	6.0
	Mesityloxide	3,5-Dimethyl-1-phenyl-4-penten-1-yn-3-ol	40	118/3	1.5582	83.7	7.9	84.0	8.0
	Citral	2′-Phenylethynyl-geraniol	50	80–85/10^{-3}	1.5378	84.1	9.5	84.4	9.4
	Citronellal	2′-Phenylethynyl-rhodinol	40	166/2	1.5613	84.3	9.2	84.4	9.4
	Cyclohexanone	2′-Phenylethynyl-cyclohexanol	50	115–118/3		83.7	7.9	84.0	8.0
	Methylethyl ketone	3-Methyl-1-phenyl-1-pentyn-3-ol	50	120/4	1.5479	82.5	8.1	82.8	8.1
2-Methyl-1-buten-3-yne	β-Ionone	2,5-Dimethyl-7-(2′,2′,6′-trimethyl-6′-cyclohexen-1′-yl)-1,6-heptadiene-3-yn-5-ol	40	126–128/3	n_D^{15}1.5223	83.1	9.8	83.5	10.0
	Methylethyl ketone	2,5-Dimethyl-1-hepten-3-yn-5-ol	15	120/3		78.0	9.9	78.3	10.1
3,7.11-Trimethyl-3-dodecen-1-yne	β-Ionone	3,6,10,14-Tetramethyl-1-(2′,2′,6′-trimethyl-6′-hexen-1′-yl)-1,6-pentadecadien-4-yn-3-ol	40	100–120/10^{-3}	1.5220	83.9	11.3	84.3	11.5
	Mesityloxide	2,4,7,11,15-Penta-methyl-2,7-hexadecadien-5-yn-4-ol	30	158–160/3	1.4996	82.7	11.7	82.8	11.8
	Crotonaldehyde	7,11,15-Trimethyl-2,7-hexadecadien-5-yn-4-ol	50	155–158/3	1.4990	83.1	11.7	83.0	11.6
	Methylethyl ketone	3,6,10,14-Tetramethyl-6-pentadecen-4-yn-3-ol	50	145/3	1.4780	81.9	12.3	82.2	12.2

*Melting point.

groups, that at 1.5–1.8 p.p.m. to one allylic methyl group (1.70 p.p.m.), the other one

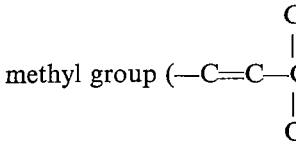

methyl group (1.65 p.p.m.)

and two cyclic methylene groups, that at 2.09 p.p.m. to one allylic methylene group, that at 2.60 p.p.m. to the one proton of a hydroxyl group, and that at 6.00 p.p.m. (quartet) to the two protons of *trans*-type double bond. These results indicated that this carbinol (**3**) was 1-(2′,6′,6′-trimethyl-1′-cyclohexen-1′-yl)-3-methyl-3-hydroxyl-5-phenyl-1-penten-4-yne. Similarly, various unsaturated acetylenic carbinols were obtained from other alkylacetylenes and various α,β-unsaturated ketones. The addition products and their properties are given in Tables I and II. The foregoing observations indicate that the α,β-unsaturated ketones react with various alkylacetylenes by using lithium naphthalene in a tetrahydrofuran solution.

Ethynylation of **1** by sodium naphthalene did not give a corresponding carbinol. Interestingly, **1** was ethynylated by using sodium naphthalene in the presence of a small amount of a Lewis base such as *t*-butylamine or by running the reaction at the lower temperature (Table III). On the difference between lithium naphthalene and sodium naphthalene, Hogen-Esch and Smid reported that lithium naphthalene, the solvent-separated ion pair, is much more reactive than sodium naphthalene, the contact ion pair (7). When a small amount of a Lewis base is added to sodium naphthalene, it would be suspected that naphthalene anion radical is activated to become solvent-separated ion pair partly by the action of a Lewis base.

Experimental

Materials

Commercial tetrahydrofuran was purified by drying it with metallic sodium and then distilling it over metallic sodium under nitrogen. Naphthalene was recrystallized from benzene several times. All carbonyl compounds were distilled before use. All the experiments were carried out in a dry apparatus under nitrogen, which had been dried by passing it through columns of calcium chloride.

Ethynylation of β-Ionone (1)

To a mixture of 0.5 mole of naphthalene and 500 ml of tetrahydrofuran, 1.0 mole of metallic lithium was added, and the mixture was agitated at room temperature in an atmosphere of dry nitrogen. After 1 h, purified dry acetylene was passed in slowly to give lithium acetylide quantitatively. One mole of **1** was gradually added to the tetrahydrofuran solution, and the mixture was stirred for an additional 3 h at room temperature. The reaction mixture was decomposed with methanol, the insoluble matter was dissolved in water, and the organic layer was isolated with isopropyl ether. The isopropyl ether extracts were washed with water, dried over anhydrous sodium sulfate, and distilled to give the following fractions: (*a*) b.p. 101–112 °C at 15 Torr, yield 40 g; (*b*) b.p. 85–95 °C at 3 Torr, yield 3 g; and (*c*) b.p. 105–115 °C at 3 Torr, yield 195 g. Gas–liquid chromatography of fraction (*a*) with a column (2 m) of Reoplex 400 on Celite 545 at a temperature of 140 °C with helium as a carrier gas (40 ml/min) showed three peaks: peak No. 1 (tetralin), retention time 15 min, peak area ratio 5%; peak No. 2 (1,4-dihydronaphthalene), retention time 23 min, peak area ratio 70%; and peak No. 3 (naphthalene), retention time 35 min, peak area ratio 25%. Naphthalene, dihydronaphthalene, and tetralin were identified by the enhancement technique employing authentic samples; their proportions were calculated from the peak area ratios. Fraction (*b*) was unchanged **1**. Fraction (*c*) was redistilled to give pure **2**, b.p. 107–109 °C at 3 Torr. The identity of **2** was confirmed by comparison of the infrared (i.r.) absorption spectra, nuclear magnetic resonance (n.m.r.) spectra, and ultraviolet (u.v.) absorption spectra with those of authentic sample. Authentic **2** was prepared by the action of lithium acetylide in liquid ammonia as reported previously (1).

Other ethynylcarbinols were prepared and identified similarly. Typical results are presented in Tables I and II.

Reaction of Acetylenic Hydrocarbons with α,β-Unsaturated Ketones

To a tetrahydrofuran solution of 0.5 mole of naphthalene and 1.0 mole of lithium, 1.0 mole of an acetylenic hydrocarbon, such as methylacetylene, phenylacetylene, or 3,7,11-trimethyl-3-dodecen-1-yne, was gradually added to give the corresponding lithium salt of the acetylenic hydrocarbon. One mole of an α,β-unsaturated ketone was gradually added, and the mixture was treated as mentioned above, and the components were separated. The typical results are presented in Tables I and II.

Reaction of Acetylenic Hydrocarbon with β-Ionone (1) Using Sodium Naphthalene

To a tetrahydrofuran solution of sodium naphthalene, which had been prepared from 0.5 mole of naphthalene and 1.0 mole of sodium cuts, 0.1 mole of a Lewis base, such as *t*-butylamine or pyridine, was added. After 1 h, 1.0 mole of an acetylenic hydrocarbon was gradually added to give the corresponding lithium salt of the acetylenic hydrocarbon. One mole of **1** was added and the reaction mixture was treated in the usual way to give the corresponding carbinol. The typical results are given in Table III.

Infrared Absorption Spectra

Spectra were measured on a Koken IRS spectrophotometer.

Nuclear Magnetic Resonance Spectra

Spectra were determined on a Japan Electron Optics Lab. instrument (60 Mc.p.s.) with carbon tetrachloride

Can. J. Chem. Downloaded from www.nrcresearchpress.com by 210.87.254.40 on 09/05/12
For personal use only.

TABLE II

Spectral data of the products

Product	Infrared absorption spectra cm^{-1}	Nuclear magnetic resonance δ, p.p.m.	Ultraviolet absorption spectra mμ	ε
Ethynyl-α-ionol	3400, 1120 (OH) 3320, 2090 (C≡CH) 970 (*trans* —CH=CH—)			
Ethynyl-β-ionol	3320, 1105 (OH) 3300, 2090 (C≡CH) 970 (*trans* —CH=CH)	5.90 (2H), 2.77 (1H) 2.52 (1H), 1.90–1.01 (9H), 1.25 (9H)	235	6 299
Ethynyl-ϕ-ionol	3400, 1105 (OH), 3320, 2100 (C≡CH)			
1-Phenyl-1-penten-4-yn-3-ol	3560, 1072 (OH) 3320, 2130 (C≡CH)	7.50 (5H), 6.30 (2H) 2.98 (1H), 2.75 (1H) 1.85 (3H)	243	21 790
3-Phenyl-1-butyn-3-ol	3400, 1090 (OH) 3320, 2120 (C≡CH)			
Ethynylcarveol	3400, 1100 (OH), 3300, 2120 (C≡CH) 890	5.35 (1H), 4.70 (2H) 3.35 (1H), 2.35 (1H) 1.74 (11H)		
3,5-Dimethyl-4-hexen-1-yn-3-ol	3400, 1075 (OH) 3320, 2121 (C≡CH)	5.30 (1H), 3.95 (1H) 2.37 (1H), 1.90 (3H) 1.75 (3H), 1.55 (3H)		
1-Phenyl-1-penten-4-yn-3-ol	3400, 1010 (OH) 3320, 2140 (C≡CH) 965, 750, 690	7.23 (5H), 6.81–5.98 (2H), 4.90 (1H) 3.44 (1H), 2.46 (1H)		
Ethynylgeraniol	3400, 1010 (OH), 3320, 2121 (C≡CH)	4.90 (1H), 5.21 (1H) 2.40 (1H), 2.91 (1H) 2.08 (4H), 1.68 (9H)		
Propynyl-α-ionol	3400, 1070 (OH) 2240 (C≡C) 970 (C=C), 830 (—C=CH)			
Propynyl-β-ionol	3400, 1070 (OH) 2240 (C≡C), 970		230 292	9 120 11 300
Propynyl-carveol	3400, 1070 (OH) 2240 (C≡C), 890, 820			
3-Methyl-1-phenyl-1-hexen-4-yn-3-ol	3400, 1075 (OH) 2240 (C≡C), 970, 750, 690		216 252	20 400 26 100
Propynyl-pulegol	3440, 1050 (OH), 2240 (C≡C)			
4-Methyl-2-hexyn-4-ol	3400, 1040 (OH), 2240 (C≡C)	3.38 (1H), 1.75 (3H) 1.35 (3H), 1.48 (2H) 0.96 (3H)		
1-(2′,6′,6′-Trimethyl-1′-cyclohexen-1′-yl)-3-methyl-3-hydroxyl-5-phenyl-1-penten-4-yne	3440, 1060 (OH) 2200 (C≡C), 970, 750, 690	7.30 (5H), 6.00 (2H) 2.60 (1H), 2.09 (2H) 1.5–1.8 (1OH) 1.04 (6H)	227 241 252	13 020 18 700 16 600
3,5-Dimethyl-1-phenyl-4-hexen-1-yn-3-ol	3400, 1080 (OH) 2240 (C≡C) 760, 690	7.25 (5H), 5.40 (1H) 1.90 (6H), 1.68 (3H)	221 242 252	9 040 16 900 16 020
1,5-Diphenyl-1-penten-4-yn-3-ol	3360, 1030 (OH) 2200 (C≡C), 1580 750, 690			
2′-Phenylethynyl-geraniol	3400, 1030 (OH) 2200 (C≡C), 1580 750, 690	7.25 (5H), 5.30 (1H) 5.10 (1H), 2.60 (1H) 2.10 (5H), 1.70–1.61 (9H)	220 243 253	6 000 8 900 9 800
2′-Phenylethynyl-rhodinol	3360, 1030 (OH) 2240 (C≡C), 1580 750, 690		220 242 252	6 000 8 900 7 800
2′-Phenylethynyl-cyclohexanol	3320, 1070 (OH) 2240 (C≡C), 1580 750, 690		220 241 252	14 150 12 400 11 200

Can. J. Chem. Downloaded from www.nrcresearchpress.com by 210.87.254.40 on 09/05/12
For personal use only.

TABLE II *(concluded)*

Product	Infrared absorption spectra	Nuclear magnetic resonance	Ultraviolet absorption spectra	
	cm^{-1}	δ, p.p.m.	mμ	ε
3-Methyl-1-phenyl-1-pentyn-3-ol	3400, 1130 (OH) 2240 (C≡C), 1580 760, 690	7.22 (5H), 2.55 (1H) 1.05 (3H), 1.54 (3H) 1.65 (2H)	221 240 251	4 850 14 350 13 060
2,5-Dimethyl-7-(2′,2′,6′-trimethyl-6′-cyclohexen-1′-yl)-1,6-heptadien-3-yn-5-ol	3440, 1065 (OH) 2200 (C≡C), 890		221 230	24 800 21 700
2,5-Dimethyl-1-hepten-3-yn-5-ol	3480, 1040 (OH) 2240 (C≡C), 910		220	20 100
3,6,10,14-Tetramethyl-1-(2′,2′,6′-trimethyl-6′-cyclohexen-1′-yl)-1,6-pentadecadien-4-yn-3-ol	3440, 1060 (OH) 2240 (C≡C), 1370 1390, 970		220 226	8 140 8 430
2,4,7,11,15-Pentamethyl-2,7-hexadecadien-5-yn-4-ol	3400, 1070 (OH) 2200 (C≡C), 1370 1390		221	21 600
7,11,15-Trimethyl-2,7-hexadecadien-5-yn-4-ol	3360, 1070 (OH) 2200 (C≡C), 1370 1380, 960		226	12 200
3,6,10,14-Tetramethyl-6-pentadecen-4-yn-3-ol	3400, 1040 (OH) 1375, 1390 2240 (C≡C)	5.40 (1H), 1.80 (3H), 1.6 (2H), 1.46 (3H), 1.27 (3H), 1.2 (10H), 0.97 (3H), 0.88 (6H)	221	6 920

TABLE III

Ethynylation of α,β-unsaturated ketones using sodium naphthalene

Acetylenic hydrocarbon	α,β-Unsaturated ketone	Product	Yield (%)	Base	Temperature (°C)
Acetylene	β-Ionone	Ethynyl-β-ionol	Trace	None	20
Acetylene	β-Ionone	Ethynyl-β-ionol	15	*t*-Butylamine	20
Acetylene	β-Ionone	Ethynyl-β-ionol	8	Pyridine	20
Acetylene	β-Ionone	Ethynyl-β-ionol	16	None	0
Acetylene	β-Ionone	Ethynyl-β-ionol	20	None	−40
Acetylene	β-Ionone	Ethynyl-β-ionol	30	*t*-Butylamine	−40
Methylacetylene	Carvone	Propynylcarveol	Trace	None	20
Phenylacetylene	Mesityloxide	3,5-Dimethyl-1-phenyl-4-penten-1-yn-3-ol	15	None	20
Phenylacetylene	Methylethyl ketone	3-Methyl-1-phenyl-1-pentyn-3-ol	16	None	20

solutions and with tetramethylsilane as an internal standard.

Acknowledgments

The authors thank Dr. Sanae Tanaka of Mitsubishi Petrochemical Co., Ltd., for his measurement of the nuclear magnetic resonance spectra, Dr. Akira Komatsu of Takasago Perfumery Co., Ltd., for materials, and Mr. Kazumasa Takahashi of Chiba University for his technical assistance.

1. W. Oroshnik and A. D. Mebane. J. Am. Chem. Soc. **71**, 2062 (1949).
2. K. Suga, S. Watanabe, and I. Torii. Chem. and Ind. London, 360 (1967).
3. K. Suga, S. Watanabe, and K. Kamma. Can. J. Chem. **45**, 933 (1967).
4. S. Watanabe, K. Suga, K. Kamma, and I. Torii. Can. J. Chem. **46**, 1154 (1968).
5. S. Watanabe, K. Suga, and K. Takahashi. Israel J. Chem. **5**, 237 (1967).
6. K. Suga, S. Watanabe, and K. Takahashi. Chem. and Ind. London, 1768 (1967).
7. T. E. Hogen-Esch and J. Smid. J. Am. Chem. Soc. **88**, 307 (1966).

Can. J. Chem. Downloaded from www.nrcresearchpress.com by 210.87.254.40 on 09/05/12
For personal use only.

Interaction between aliphatic and aromatic nitro compounds in basic media

C. A. FYFE[1]
Chemistry Department, University of British Columbia, Vancouver 8, British Columbia
Received May 14, 1968

The interaction between aromatic and aliphatic nitro compounds in basic media has been investigated. Evidence based mainly on nuclear magnetic resonance spectroscopy suggests that the brightly colored species formed are sigma complexes. The generality of the reaction is investigated and its relation to the Janovsky reaction discussed.

Canadian Journal of Chemistry, 46, 3047 (1968)

Can. J. Chem. Downloaded from www.nrcresearchpress.com by 210.87.254.42 on 09/05/12
For personal use only.

Much information as to the course of nucleophilic aromatic substitution reactions has been obtained by the investigation of stable complexes formed from highly activated substrates. The formulation **1** for these complexes with a trinitropentadienate ion as part of a six-membered ring system, was originally introduced by Meisenheimer (1) and has received strong support from subsequent investigations by visible (2, 3), infrared (i.r.) (4, 5), and nuclear magnetic resonance (n.m.r.) spectroscopy (6, 7, 8). The visible and

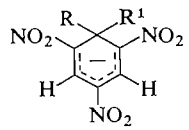

1

n.m.r. spectra of these compounds are particularly diagnostic (9). Evidence is presented in the present paper for the formation of compounds of this general type as a general reaction between aliphatic and aromatic nitro compounds in basic solutions.

Interaction of 1,3,5-trinitrobenzene with Aliphatic Nitro Compounds

When a tertiary amine is added to a solution of trinitrobenzene (TNB) in an aliphatic nitro compound, the solution becomes red, the color intensifying with time. The visible spectrum (e.g. Fig. 1) for TNB in nitromethane solution has a shape typical of structures with a trinitropentadienate ion as part of a six-membered ring with the general formula **1**.

It is thought that in the systems studied, an ion similar to **1** (where R = H, R^1 = aliphatic nitro compound residue) is formed by attack of an anion derived from the aliphatic nitro compound. In some cases, the intermediates can be isolated (see Experimental). The ultraviolet (u.v.) spectra are all similar to **1** (R = R^1 = OR) in both shape and intensity (Table I).

The i.r. spectra are very similar, showing a broad band at ~1240 cm^{-1} which is considered (4, 5) characteristic of the general structure **1**, and NO_2 bands at 1590 cm^{-1} and 1750 cm^{-1}. The n.m.r. spectra of the compounds are quite diagnostic and are discussed individually.

(a) 1,3,5-Trinitrobenzene – triethylamine – nitromethane

When triethylamine is added to a solution of TNB in nitromethane or in a 50:50 mixture of nitromethane dimethyl sulfoxide (DMSO), the solution immediately becomes bright red (λ_{max} = 456 mμ, λ_{max} = 568 mμ, Fig. 1). The absorption at $\delta = 9.2_7$ due to the TNB disappears and two new absorptions appear at $\delta = -8.4_1$ (singlet, relative intensity 2) and $\delta = -5.35$ (triplet J = 7.5 c.p.s., relative intensity 1). This new spectrum can be explained in terms of structure **2** (Y = $\overset{+}{H}NEt_3$).

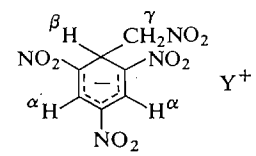

2

Several workers (6–9), have shown that the "aromatic" ring protons (Hα in **2**) in 1,3,5-trinitrocyclopentadienate cyclic systems such as **1** show absorptions at ~−8.5 p.p.m. Thus the absorption at $\sim -8.4_1$ may be assigned to Hα in **2**. Similarly the 'aliphatic' proton Hβ in **2** might be expected to occur at much higher fields. Hβ is split into a triplet by interaction with the side-chain protons Hγ (this splitting eliminates any

[1]Killam Postdoctoral Fellow.

TABLE I

Visible absorption maxima (mμ) and extinction coefficients* (mole^{-1} l cm^{-1}) of compounds of general structure 7 in dimethyl sulfoxide solution

R	λ_1†	ε_1	λ_2†	ε_2	λ_1‡	ε_1	λ_2‡	ε_2
$-CH_2NO_2$§	456	22 000	568	11 000	456	25 000	568	12 500
$CH_3\underset{\|}{C}HNO_2$‖	452	24 000	552	12 000	452	26 000	552	13 000
$CH_3CH_2\underset{\|}{C}HNO_2$‖	452	22 000	552	11 000	452	23 000	552	11 500
$CH_3-\underset{\|}{\overset{\|}{C}}(CH_3)-NO_2$‖	450	23 000	545	11 500	450	23 000	545	11 500

*Reported to nearest 500, estimated errors 10%.
†By dissolution of isolated compound in dimethyl sulfoxide.
‡By 100 × dilution of a solution of compound 3 in a mixture of dimethyl sulfoxide and the appropriate aliphatic nitro compound.
§Cation K^+.
‖Cation $\overset{+}{N}HEt_3$.

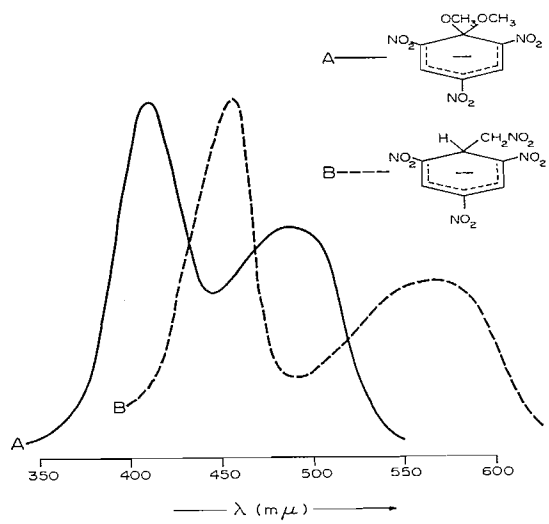

FIG. 1. (A), Compound **1**, R = R^1 = OCH_3 in methanol; (B), trinitrobenzene in CH_3NO_2 plus triethylamine (compound 2).

possibility of reaction via the nitrogen or oxygen of the NO_2 group).

An identical spectrum is formed when nitromethane is added to a solution of **3** in DMSO indicating the solvolysis [1].

The complete spectrum of compound **2** in DMSO with assignment is shown in Fig. 2.

(b) Trinitrobenzene – triethylamine – nitroethane

Addition of triethylamine to TNB in nitroethane gives a bright red coloration (λ_{max} = 452 mμ, λ_{max} = 555 mμ). In concentrated solutions,

[1]

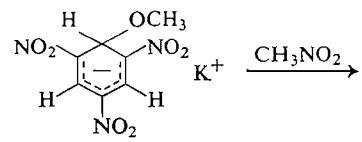

3

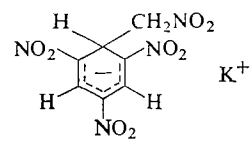

2

however, there is precipitation and n.m.r. spectra were recorded on a solution of TNB in a 50:50 mixture of nitroethane and DMSO. Addition of triethylamine to this solution causes the disappearance of the TNB resonance and the appearance of two new resonances at δ = −8.47 (relative intensity 2) and δ = −5.67 (doublet, J = 3.2 c.p.s., relative intensity 1). These can be assigned to Hα and Hβ respectively in **4**, where Hβ is split by Hγ. Spectra under conditions of

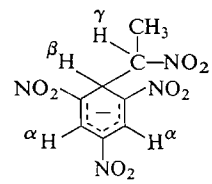

4

higher resolution reveal a small coupling within the ring $J_{H\alpha-H\beta}$ = 0.5 c.p.s., and a small nonequivalence of the two ring protons due to the

Can. J. Chem. Downloaded from www.nrcresearchpress.com by 210.87.254.42 on 09/05/12
For personal use only.

asymmetry at the carbon carrying Hγ. In no conformation of the side chain are the two ring protons equivalent, but the effect is relatively small due to the large distance involved.

Compound **4** can also be formed by the addition of nitroethane to a solution of **3** in DMSO by solvolysis similar to reaction [1].

The complete spectrum in ($^2H_6$) DMSO of the product from nitroethane solution is shown with complete assignments in Fig. 3.

(c) Trinitrobenzene – triethylamine-1-nitropropane

When triethylamine is added to TNB in 1-nitropropane/DMSO, the solution becomes very brightly colored (λ_{max} 453 mμ, λ_{max} 552 mμ) and two new resonances occur in the n.m.r. spectrum at $\delta = -8.46$ (singlet, relative intensity 2) and δ at $= -5.63$ (doublet, $J = 3.5$ c.p.s., relative intensity 1). These are consistent with protons

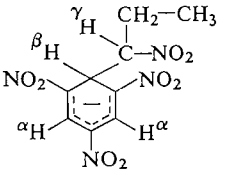

5

Hα, Hβ respectively in **5** with $J_{H\beta-H\gamma} = 3.5$ c.p.s. On higher resolution, the peak assigned to Hα splits into a doublet, and each of the peaks of the doublet resonance in Hβ into a triplet. This is thought to be due to coupling across the ring

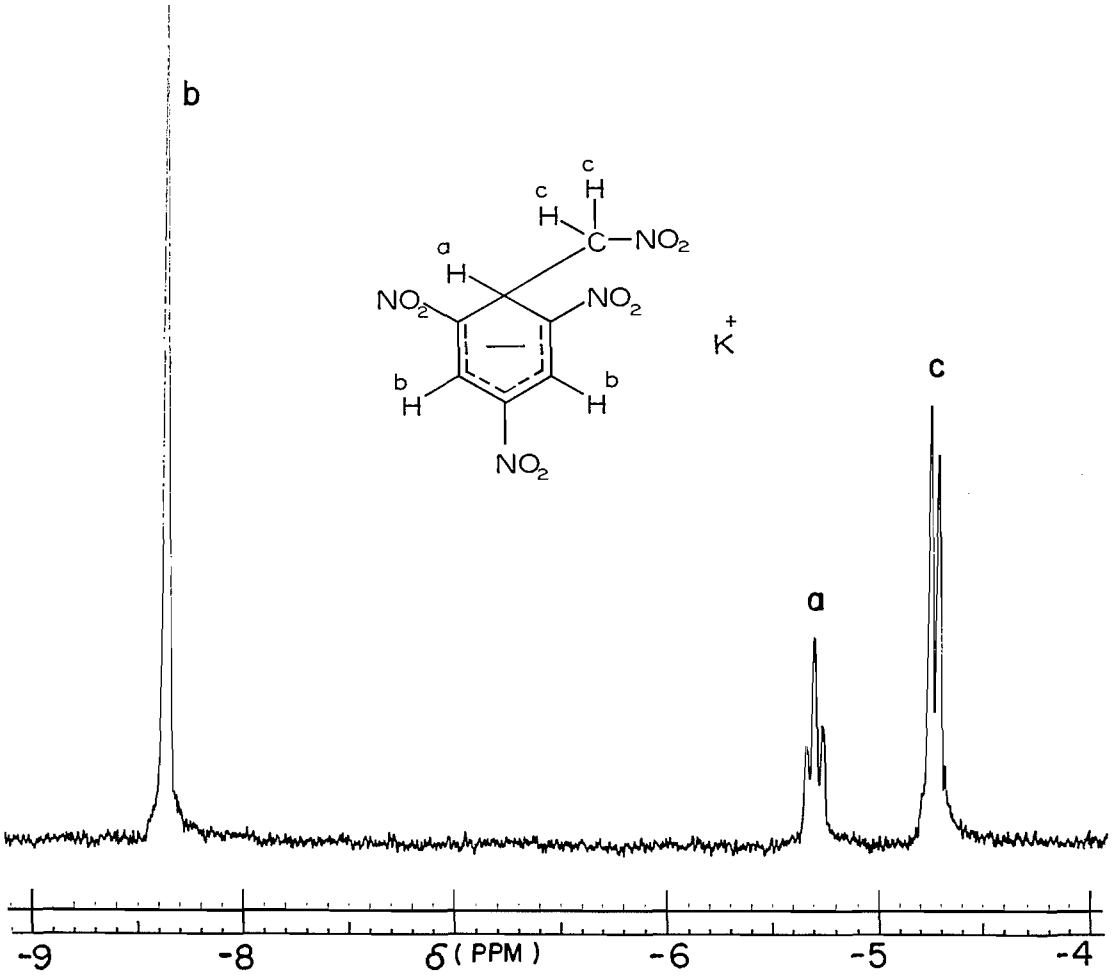

FIG. 2. 100 MHz nuclear magnetic resonance spectrum with assignments of compound **2** in DMSO.

Can. J. Chem. Downloaded from www.nrcresearchpress.com by 210.87.254.42 on 09/05/12
For personal use only.

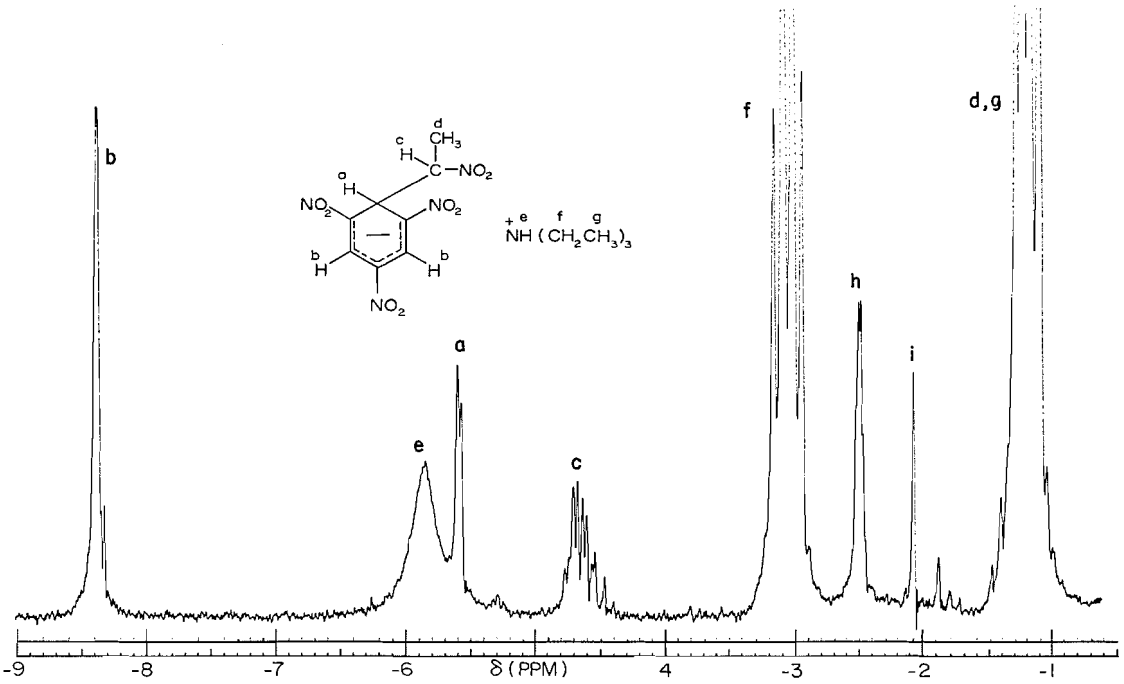

FIG. 3. 100 MHz nuclear magnetic resonance spectrum with assignments of compound **4** in [$^2H_6$] DMSO (h = [$^2H_5$] DMSO, i = impurity).

with $J_{H\alpha-H\beta} = 1$ c.p.s. There is no evidence of any asymmetry in the Hα protons as was found for the nitroethane adduct. Again the compound can be formed by the action of 1-nitropropane on compound **3** in DMSO.

(d) Trinitrobenzene – triethylamine-2-nitropropane

Addition of triethylamine to a solution of TNB in 2-nitropropane/DMSO produces an intense coloration ($\lambda_{max} = 450$ mμ, $\lambda_{max} = 545$ mμ) and new peaks in the n.m.r. spectrum at $\delta = -8.5_1$ (singlet, relative intensity 2) and at $\delta = -5.90$ (broad singlet, relative intensity 1).

These are consistent with Hα and Hβ in structure **6**. Higher resolution reveals the presence of a

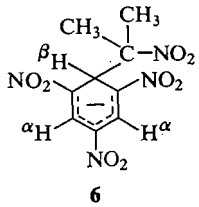

6

small coupling across the ring ($J_{H\alpha-H\beta} = 1.40$ c.p.s.) splitting Hα and Hβ into a doublet and triplet respectively. Compound **6** can also be formed by the action of 2-nitropropane on **3**.

The compounds **3**, **4**, **5**, and **6** show no exchange with either different nitro compounds or with acetone in either the presence or absence of base and are stable towards other nucleophilic reagents. They are stable in DMSO solution for several weeks. The addition of concentrated mineral acid regenerates TNB in all cases.

The chemical shifts and couplings of the Hα and Hβ protons are given in Table II.

There seems to be a correlation in the n.m.r. spectra similar to that found for the corresponding intermediates formed from ketone anions (10) in that the magnitude of the chemical shift of Hβ becomes smaller and $J_{H\beta-H\alpha}$ becomes smaller as the attached carbon atom is secondary, tertiary, and quaternary. There is a similar, but smaller, trend in the chemical shifts of the Hα resonances.

Particularly interesting is the increase in size of the small, long-range coupling $J_{H\alpha-H\beta}$ with increasing bulkiness of the attached group, which tends to suggest a change in the relative orientations of Hα and Hβ. It may be that the bulkier the

Can. J. Chem. Downloaded from www.nrcresearchpress.com by 210.87.254.42 on 09/05/12
For personal use only.

TABLE II

Chemical shifts (− δ) and couplings of Hα and Hβ protons in general structure 7* in DMSO solution

R	Type†	Hα	Hβ	$J_{H\gamma-H\beta(c.p.s.)}$	$J_{H\alpha-H\beta(c.p.s.)}$
$-\overset{\gamma}{C}H_2NO_2$	S	+8.41	+5.35	0.0	7.5
$CH_3\overset{\gamma}{C}HNO_2$	T	+8.47‡	+5.67	0.5	3.2
$CH_3CH_2\overset{\gamma}{C}HNO_2$	T	+8.46	+5.63	1.0	3.5
$CH_3-\overset{}{C}(CH_3)-NO_2$	Q	+8.51	+5.90	1.4	0

*Structure 7:

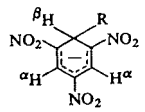

†S = secondary, T = tertiary, Q = quaternary.
‡Very close multiplet due to non-equivalence of ring protons. Shift value is for multiplet center.

attached group becomes, the closer Hβ is pushed towards being at right angles to the plane of the ring.

Other Aromatic Nitro Compounds

(a) N,N-Dimethylpicramide

The bright coloration (λ_{max} = 490 mμ) caused by the addition of triethylamine to a solution of *N,N*-dimethylpicramide in nitromethane is accompanied by the growth of two new absorptions in the n.m.r. spectrum; a doublet at δ = −8.4 (J = 1 c.p.s., relative intensity = 1), and four lines each split into a doublet J = 1 centered at δ = -5.7_7 of total intensity 1 and J^1 = 5 c.p.s., J^{11} = 8 c.p.s. These are consistent with the assignment Hα, Hβ respectively in structure **8** with $J_{H\alpha-H\beta}$ = 1 c.p.s. and Hβ split into 4 lines because of non-equivalence in the methylene induced by the asymmetry in the ring system.

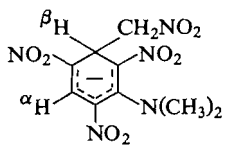

8

(b) 2,4-Dinitronaphthalene

Addition of triethylamine to a solution of 2,4-dinitronaphthalene in nitromethane gives a red coloration (λ_{max} = 538 mμ) and the appearance of an n.m.r. spectrum consistent with structure **9**, with H-1, δ = -5.1_3; H-2, δ = -6.7_8; H-3, δ = -8.6_7; H-4, H-5, H-6, multiplet center δ = −7.25. The compound can again be

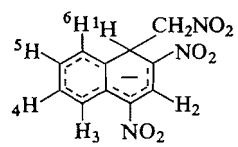

9

formed from the solvolysis of the corresponding methoxy compound.

(c) 3,5-Dinitropyridine

The red-purple color (λ_{max} = 515 mμ, shoulder ~570 mμ) produced when triethylamine is added to a solution of 3,5-dinitropyridine in nitromethane is accompanied by the appearance of two new sets of resonances in the n.m.r. spectrum. The positions and intensities of these resonances are consistent with the formation of the isomeric ions **10** and **11** with H-1, δ = −5.85; H-2, δ = −8.34; H-3, δ = −8.52, $J_{H_2-H_3}$ = 2

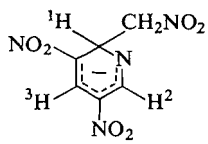

10

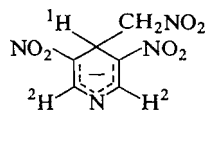

11

c.p.s. H-1 is composed of 4 lines with J^1 = 5 c.p.s.,

Can. J. Chem. Downloaded from www.nrcresearchpress.com by 210.87.254.42 on 09/05/12
For personal use only.

TABLE III

Chemical shifts ($-\delta$) and couplings (c.p.s.) for compounds **12*** and **13**

Compound	H-1	H-2	H-3	H-4	J_{12}	J_{23}	J_{34}
12	8.30	6.59	5.38	4.18	1.9	10.2	5.0
13	8.26	6.71	5.3_2	$\sim 4.5_2$	2.0	10.2	4.4

*Values from ref. 11.

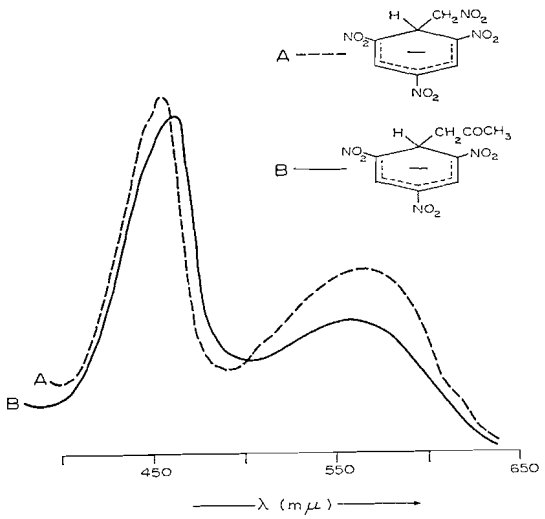

FIG. 4. Ultraviolet spectra of solutions resulting from the addition of triethylamine to solutions of TNB in (A) nitromethane and (B) acetone.

$J^{11} = 7$ c.p.s. In **11**: H-1, $\delta = -5.30$; H-2, $\delta = -8.2_2$. H-1 is a triplet, $J = 3.5$ c.p.s.

Interaction of 1,3-Dinitrobenzene with Nitromethane – Janovsky Reaction

When sodium methoxide is added to a solution of 1,3-dinitrobenzene in a solution consisting of 60% DMSO and 40% nitromethane, the solution turns pinkish-purple (λ_{max} 562 mμ). New resonances occur in the n.m.r. spectrum which are stable for several days and are consistent with the structure **12**.

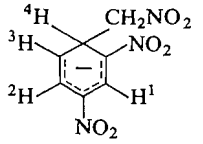

12

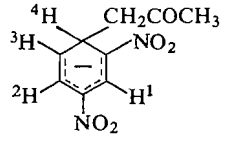

13

In Table III these are compared with the spectrum of the corresponding acetonyl adduct **13** which has recently been measured (7).

The fact that the two spectra are so similar suggests that the structure and electron distribution are very similar in the two species.

Thus the present work suggests that stable intermediates can be produced from the interaction of a variety of aromatic nitro compounds with a variety of aliphatic nitro compounds in basic solution. These are characterized as δ-complexes formed by the attack of a *carbanion* formed by proton abstraction from the aliphatic nitro compound. It might thus be expected that similar compounds could be formed by the action of base on *any* activated methylene and characterized by n.m.r.

The similarities in the u.v. spectra of the compounds characterized here and the corresponding acetonyl adducts are very striking (Figs. 4, 5). The u.v. spectra are, however, significantly different from the corresponding dialkoxy compounds although similar in general position and shape (Fig. 1). This would suggest that, perhaps, the u.v. spectra are really characteristic of (for example in the case of TNB) the basic unit **14**,

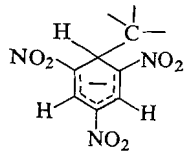

14

e.g. malononitrile gives (λ_{max} 450 mμ, λ_{max} 550 mμ).

This is important insofar as it has been suggested that aromatic nitro compounds in general and 1,3-dinitrobenzene in particular could be used as biological testing agents for the grouping —CH_2—CO (Janovsky reaction); the test being the production of a color in basic solution of the unknown compound. The present work suggests, however, that equally stable and well characterized compounds with very similar u.v. spectra are formed from aliphatic nitro compounds under these conditions and this is probably true for *any*

Can. J. Chem. Downloaded from www.nrcresearchpress.com by 210.87.254.42 on 09/05/12
For personal use only.

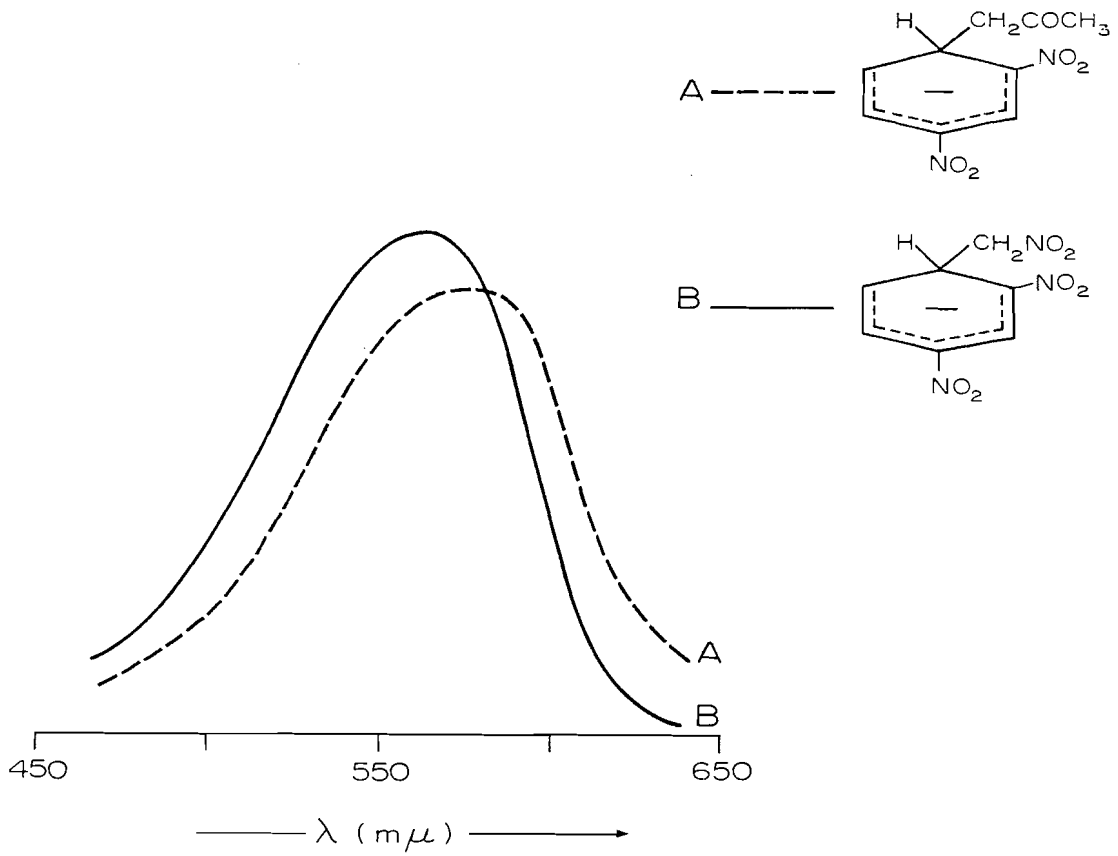

FIG. 5. Ultraviolet spectra of solutions resulting from the addition of sodium methoxide to solutions of 1,3-dinitrobenzene in (A) 50% DMSO, 50% acetone, and (B) 50% DMSO, 50% nitromethane.

active methylene. Some care would have to be exercised in any use of these reactions as chemical tests.

Experimental

Nuclear magnetic resonance spectra were recorded at 60 Mc.p.s. on a JEOL C-60H spectrometer and at 100 Mc.p.s. on a Varian HA-100 spectrometer. Chemical shifts in p.p.m. were measured from tetramethylsilane as internal reference. Ultraviolet spectra were measured on a Beckman SP 800 spectrophotometer and extinction coefficients measured on a Cary model 16 spectrophotometer. Infrared spectra of Nujol mulls were recorded using a Perkin–Elmer Infracord spectrophotometer.

With the exception of 3,5-dinitropyridine, the chemicals used were from commercial sources and on purification gave melting points and boiling points in agreement with

TABLE IV

Microanalyses of solid complexes

Compound	Formula	Calculated			Found		
		C	H	N	C	H	N
2*‡	$C_7H_5N_4O_8K$	26.92	1.60	17.94	27.18	2.01	17.80
4†	$C_{14}H_{23}N_5O_8$	43.19	5.91	17.99	43.40	6.08	17.88
5†	$C_{15}H_{25}N_5O_8$	44.67	6.20	17.37	44.62	6.31	17.33
6†	$C_{15}H_{25}N_5O_8$	44.67	6.20	17.37	44.71	6.13	17.41

*Cation K^+.
†Cation $\overset{+}{N}HEt_3$.
‡Analysis indicated the salt contained a small amount of triethylamine when the cation was $\overset{+}{N}HEt_3$.

Can. J. Chem. Downloaded from www.nrcresearchpress.com by 210.87.254.42 on 09/05/12
For personal use only.

published values. 3,5-Dinitropyridine was prepared in good yield by the method of Plažek (12), m.p. 104–105 °C (lit. 106 °C). The various solid complexes, precipitated from solution in the corresponding aliphatic nitro compound by the addition of a large amount of dry ether, gave the following microanalyses.

Acknowledgments

The author would like to acknowledge the help given by Miss P. A. Watson in the measurement of some of the n.m.r. spectra and Mr. P. P. Borda for performing the microanalyses; also the encouragement given by Professor C. A. McDowell during this work, the Department of Chemistry for the provision of facilities and the University of British Columbia for the award of a Killam Postdoctoral Fellowship.

1. J. Meisenheimer. Ann. **323**, 205 (1902).
2. R. Foster. Nature, **176**, 746 (1955).
3. J. B. Ainscough and E. F. Caldin. J. Chem. Soc. 2528 (1956).
4. R. Foster and D. L. Hammick. J. Chem. Soc. 2153 (1954).
5. L. K. Dyall. J. Chem. Soc. 5160 (1960).
6. M. R. Crampton and V. Gold. J. Chem. Soc. 4293 (1964).
7. R. Foster, C. A. Fyfe, and J. W. Morris. Rec. Trav. Chim. **84**, 516 (1965).
8. K. L. Servis. J. Am. Chem. Soc. **87**, 5495 (1965).
9. R. Foster and C. A. Fyfe. Rev. Pure Appl. Chem. **16**, 61 (1966).
10. R. Foster and C. A. Fyfe. J. Chem. Soc. B, 53 (1966).
11. R. Foster and C. A. Fyfe. Chem. Commun. 1219 (1967).
12. E. Plažek. Rec. Trav. Chim. **72**, 569 (1953).

Can. J. Chem. Downloaded from www.nrcresearchpress.com by 210.87.254.42 on 09/05/12
For personal use only.

Can. J. Chem. Downloaded from www.nrcresearchpress.com by 210.87.254.40 on 09/05/12
For personal use only.

Complexes of *N*-methylxanthines with carboxylic acids

DENYS COOK AND ZEPHYR R. REGNIER
Research Laboratories, Food and Drug Directorate, Department of National Health and Welfare, Ottawa, Canada

Received May 10, 1968

Complexes of caffeine and theobromine, with acetic and salicylic acid, have been studied by means of infrared spectroscopy. In the complexes with aromatic acids a fairly strong hydrogen bond exists between the carboxylic OH group and the nitrogen atom N-9 in the imidazole ring. The acetic acid complexes involve no strong intermolecular forces and are probably weak lattice complexes.

The complexes with aromatic acids are discussed in relation to theories of lipid solubility and gastrointestinal absorption.

Canadian Journal of Chemistry, 46, 3055 (1968)

Introduction

The formation of complexes of molecules of the xanthine series, caffeine, theobromine, and theophylline with carboxylic acids has been inferred from a variety of measurements (1–4). Although it has been suggested that the complexes with aromatic carboxylic acids are a result of interactions between the π electrons of such rings (4), their physical structure is still in doubt.

A study of the infrared (i.r.) spectra of such complexes seemed a possible way of solving this structural problem. This method has already been used to show that in salts of xanthines with strong acids protonation occurs at N-9 in the imidazole ring for caffeine (5), theobromine (6), and theophylline (7), while the spectra of the salts of the last two chemicals with strong bases has enabled the easy identification of their anions (7). This preliminary work has considerably facilitated the interpretation of the i.r. spectra of the complexes.

Results and Discussion

The principal absorption bands in the spectra of the free bases and the complexes with aromatic acids are listed in Table I.[1]

Caffeine Complexes

Caffeine – Acetic Acid Complex

Several diagnostically useful differences are observed in the spectra of caffeine and those of its salts (6). An increase in carbonyl frequency, ν_{CO}, and in ν_{CH} for the C_8—H bond, are both attributed to the effect of the positive charge. In addition new bands are present in the salt spectra due to stretching, in-plane bending, and out-of-plane bending of the protonated N_9^+—H group.

For the acetic acid complex of caffeine the i.r. spectrum shows nearly all the caffeine bands to be at the same frequency as in the free base, with additional bands due to acetic acid. Of these the strongest is at 1720 cm^{-1}. The monomer has its carbonyl frequency at $\sim$ 1790 cm^{-1} (8), and the dimer at 1715 cm^{-1} (i.r., liquid) and 1675 cm^{-1} (Raman, liquid) (9). The crytsalline solid which is composed of infinite chains of hydrogen-bonded monomers (10) has a doublet at 1659/1645 cm^{-1} (i.r., solid, 0 °C) (11).

The acetic acid in the caffeine – acetic acid complex must therefore be in the dimeric form and has little or no interaction with the caffeine molecules. This conclusion is in accord with the physical properties of the complex: it loses acetic acid readily on exposure to air reverting to caffeine. (The hydrate of caffeine also is efflorescent.) Other bands in the spectrum are at frequencies similar to those in the liquid acetic acid dimer (9) with minor shifts in some bands connected with the OH group vibrations as a result of a slightly different molecular environment. A slight weakening of the acetic acid dimer hydrogen bond strength in the complex may be inferred from the slightly higher value of ν_{OH} and lower value of γ_{OH} in the complex compared to the free base.

The alternative structure of a free caffeine molecule fitting into a lattice composed of infinite chains of hydrogen-bonded monomeric units can be dismissed as there is no new band

[1]A complete listing of the bands in the spectra has been filed with the Depository of Unpublished Data. Photocopies may be obtained free of charge from The Depository of Unpublished Data, National Science Library, National Research Council of Canada, Ottawa, Canada.

TABLE I

Principal absorption bands in the infrared spectra of the free bases and their complexes with aromatic acids

	Caffeine		Theobromine			
	Base	Salicylic acid complex	Base	Salicylic acid complex	Salicylic acid	
ν_{NH}			3150m	3158m,b		
ν_{CH}	3108m	3132m	3112m	3138m		
ν_{NH}			3030m	3045m,b		
ν_{NH}			2825m	2834m		
					3235m,b	ν_{OH}
					3005m	
		2435m		2465m,b	2858m	
					2720m	
					2592m	
ν_{CO}	1698vs	1709s	1688vs	1705s		
ν_{CO}	1656vs	1666s	1665s,sh	1665s,sh	1660vs	ν_{CO}
γ_{NH}			860m			

NOTE: Assignments on the left are for the free bases and the complexes. Those on the right are for salicylic acid.

in the i.r. spectrum of the complex at ~1650 cm^{-1} (11).

Caffeine – Salicylic Acid Complex

The complex is equimolar. In it the salicylate portion is not in the form of its anion since its i.r. spectrum would show strong bands due to vibrations of the COO^- group at ~1590 and 1390 cm^{-1}. The acid must therefore be unionized, but it is not in the same form in the complex as is found in the pure crystalline acid hydrogen-bonded centrosymmetrical dimer (12) because the prominent bands due to COOH stretching in the acid are absent from the spectrum of the complex.

This information coupled with the elevation of ν_{CH} and ν_{CO} in the caffeine part of the complex is conclusive evidence of the interaction at N-9 of a carboxylic acid COOH group, which gives similar effects but of smaller magnitude than a protonating acid. Structure **1** would be consistent with these results.

Salicylic acid deuterated at the COOH and OH was prepared and the caffeine complex of this also was made. The spectrum of the salicylic acid-d_2 : caffeine complex did not contain the distinctive bands centered near 2418/2233/2072 cm^{-1} of salicylic acid-d_2. Bands associated with the COOH and OH groups at 2440, 1310, 1238, 851, 809, and 786 cm^{-1} in the caffeine – salicylic acid complex disappear on deuteration. None of the bands associated with the caffeine molecules alter significantly on deuteration.

The spectrum of salicylic acid in dilute solution in CCl_4 shows two carbonyl bands at 1662 and 1694 cm^{-1}, the latter being due to the monomer. Differences of 30–60 cm^{-1} have been noted in ν_{CO} between monomeric and dimeric forms in benzoic acid (13), acrylic acid (14), and acetic acid (8). In the case of a solution of fatty acid in pyridine/CCl_4 the difference in carbonyl frequency between solution dimer and complexed monomer (COOH . . . N) was about 20 cm^{-1} (15). The band centered at 1666 cm^{-1} in the caffeine : salicylic acid complex is therefore probably made up of contributions from carbonyl group vibrations of both molecules.

Another possible structure was found to be untenable after a consideration of Dreiding models. This was a planar model with the phenolic OH group rotated 180° away from its intramolecular hydrogen bond with the COOH group, and forming a O—H . . . N-9 bond (about 2.7 Å long) with the caffeine molecule. Short H . . . H contacts of 1.6 Å between C_8—H (caffeine) and C_3—H (salicylic acid), and 2.5 Å between the phenolic OH and N_3CH_3 group

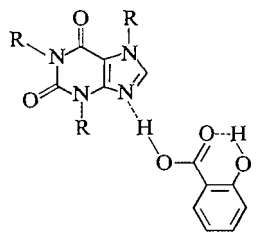

1, $R_1 = R_3 = R_7 = CH_3$

2, $R_1 = H, R_3 = R_7 = CH_3$

Can. J. Chem. Downloaded from www.nrcresearchpress.com by 210.87.254.40 on 09/05/12
For personal use only.

Can. J. Chem. Downloaded from www.nrcresearchpress.com by 210.87.254.40 on 09/05/12
For personal use only.

make this model entirely unrealistic. Rotation of the OH group out of the salicylic acid molecular plane would relieve some of these short contacts but seems unlikely in view of the great stabilization by internal hydrogen bonding. Moreover, the carboxylic acid group in this conformation would be free to form the dimer but this has been shown above to be an unlikely structural factor.

Theobromine Complexes

Theobromine – Acetic Acid Complex

The contour of the multiple NH stretching band near 3050 cm^{-1} in the complex is very similar to that in the free base, but the peaks are at slightly higher frequency. The stretching vibration of the CH group in the imidazole ring is also at higher frequency. The same hydrogen bonding that occurs in the free base therefore probably persists in the complex. It has been suggested that this takes the form of a centrosymmetrical dimer involving N_1—H . . . O=C_6 hydrogen bonds (6). The slightly higher frequencies in the complex imply a small lengthening of the hydrogen bond, also indicated by the decrease in the out-of-plane NH deformation γ_{NH} from 860 to 837 cm^{-1} in the complex.

The carbonyl frequency of the acetic acid portion can be easily identified at 1720 cm^{-1}, at the same position as in the caffeine complex. The dimeric form is indicated again with little interaction between the two components of the complex.

Theobromine – Salicylic Acid Complex

The spectrum of the theobromine – salicylic acid complex does not show the strong OH stretching bands of the free acid in the 3000 cm^{-1} region, neither does it contain bands due to the salicylate anion. There is, however, a group of bands very similar in position and in shape to those in free theobromine, and again this suggests that the hydrogen bonding that occurs in the free base also occurs in the complex. A broad band containing much structure centered near 2465 cm^{-1} is assigned to the OH stretching vibration of the COOH group in the salicylic acid and may also contain a contribution from the internally hydrogen bonded OH group attached to the ring. The same type of structure (**2**) as for the caffeine complex (**1**) is proposed, and many of the bands due to the acid portion are at similar frequencies in both complexes.

The absence of any decreased theobromine carbonyl frequency rules out interaction at a carbonyl group. Carbonyl frequencies of the base are raised slightly, as in the caffeine complex.

Deuteration studies showed similar changes taking place as in the caffeine – salicylic acid complex, with bands at 2500, 2465, 1305, 1230, 810, and 765 cm^{-1} disappearing. In addition, the N_1—H hydrogen stretching and bending vibrations at 3050, 1482, 1140, and 860 cm^{-1} due to the theobromine molecule are shifted on deuteration.

Caffeine is known to alter the gastric absorption rate of salicylic acid in the rat when the two are administered together (16, 17). The precise significance of the results is not known, however, since the two research groups used a different protocol. The summaries of their work appear to present diametrically opposed views.

It is possible to rationalize these apparently opposite views by constructing the graph in Fig. 1 showing % salicylic acid not in stomach as a function of time. With salicylic acid alone group A (17) find an increasing amount absorbed which can be extrapolated to reach the 1 h values of group B (16) thus giving a broad maximum to the curve, which is essentially an absorption or blood level curve. With the salicylic acid/caffeine mixture, a higher level is reached earlier, followed by a quicker decline, which again extrapolates to the lower levels of group B after 1 h.

These blood level characteristics, a lower flatter maximum for the slowly absorbed material, and a sharper higher peak for the faster absorption are quite consistent with our knowledge of the absorption process. Within the experimental errors and standard deviations the data of both groups fit this scheme.

The lipid solubility/percent ionized concept (18) has been highly successful in explaining many facets of drug absorption. In the present context the complex of salicylic acid and caffeine by the formation of the O—H . . . N hydrogen bond effectively removes these polar groups from the environment, and is therefore much more lipid soluble, which is one of the main criteria for more rapid and complete absorption, other things being equal.

These experimental absorption figures (16, 17) are also confirmed by a very early pharmacokinetic study (19) available to us only in abstract (20) which concluded in effect that when salicylic acid was administered with caffeine to

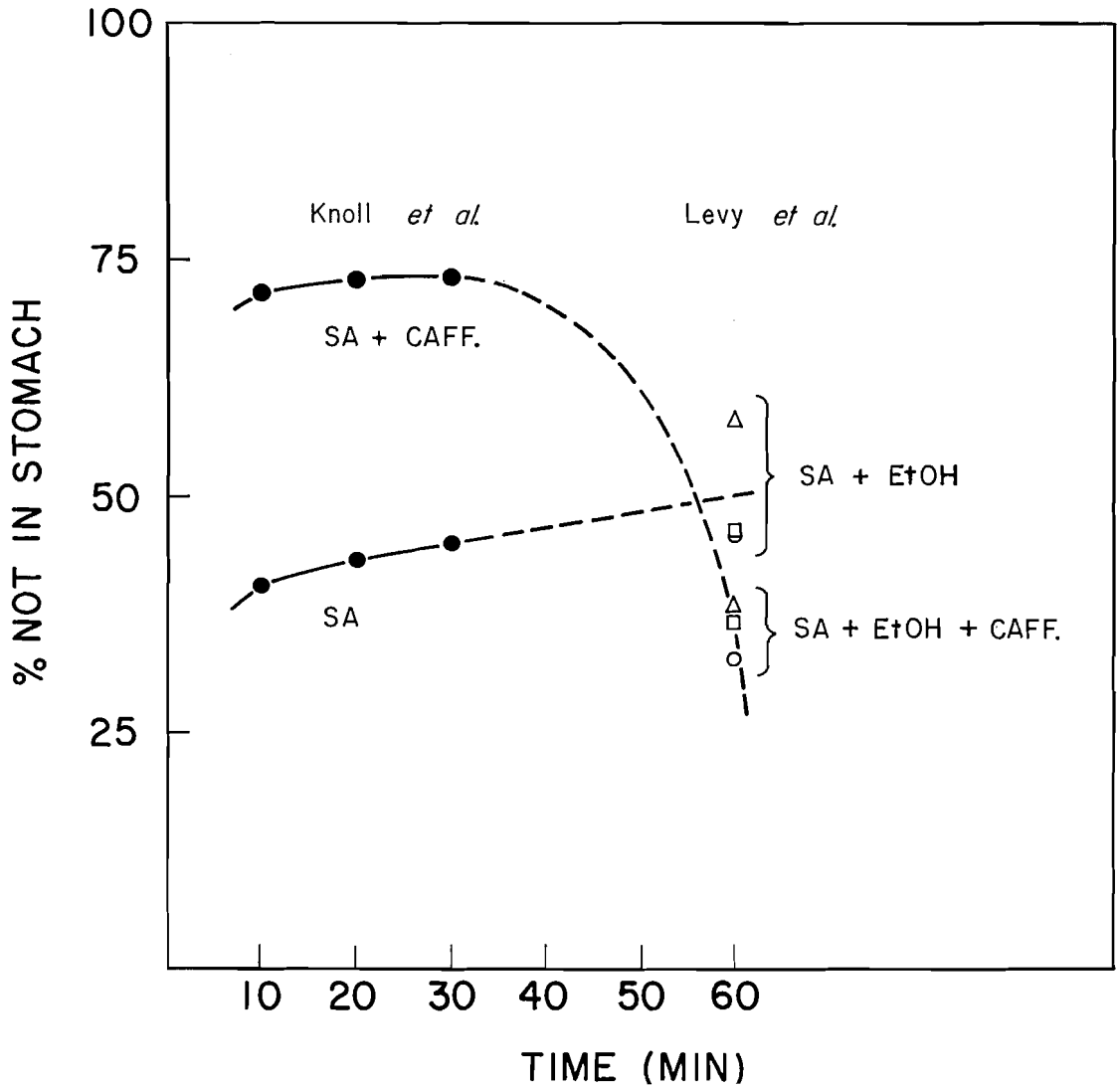

FIG. 1. Disappearance of drug from rat stomach as a function of time. ●, ref. 16; △, unstirred; □, static stirrer; ○, rotating stirrer, ref. 17.

rabbits, it gave (*i*) a maximum blood level earlier, (*ii*) a lower total quantity in blood, and (*iii*) a greater urinary excretion rate than when salicylic acid was administered alone. Allowing for the less advanced technical methodology of that day, one could only take exception to conclusion (*ii*). Species difference may account for this.

Experimental

Materials

Caffeine (anhydrous) was obtained from the Aldrich Chemical Company; theobromine from the British Drug Houses Limited; theophylline from K and K Laboratories Inc.; and salicylic acid from Anachemia Chemicals Limited.

Caffeine – Acetic Acid Complex

Caffeine was recrystallized from a small quantity of glacial acetic acid in the form of long needles, m.p. same as caffeine. The crystals lost acetic acid completely after exposure to air for 16 h.

Caffeine – Salicylic Acid Complex

Equivalent quantities of each component were dissolved in absolute ethanol. On evaporation of the solvent, the complex remained as a white solid, m.p. 138–138.5°.

Can. J. Chem. Downloaded from www.nrcresearchpress.com by 210.87.254.40 on 09/05/12
For personal use only.

The complex could also be prepared by thoroughly grinding together very small equimolar quantities of each component in an agate mortar.

Theobromine – Acetic Acid Complex

Theobromine was recrystallized from acetic acid giving a white solid, m.p. similar to that of theobromine. It lost acetic acid on exposure to air.

Theobromine – Salicylic Acid Complex

A mixture of aqueous solutions of equimolar amounts of the two components on evaporation of the solvent gave the complex as white needles, m.p. 208° (decomp.).

The stoichiometry of the complexes was checked by titrimetric methods, giving results in all cases close to equimolar values.

The spectra were recorded on a Perkin–Elmer 621 grating spectrometer, and were all of Nujol–fluorolube mulls of the solid materials.

1. T. HIGUCHI and D. ZUCK. J. Am. Pharm. Assoc. Sci. Ed. **41**, 10 (1951), and later papers.
2. R. LABES. Arch. Exp. Pathol. Pharmakol. **158**, 42 (1930).
3. G. PIROLI. Boll. Chim. Farm. **103**, 345 (1964).
4. R. S. SCHNAARE and A. N. MARTIN. J. Pharm. Sci. **54**, 1707 (1965).
5. D. COOK and Z. R. REGNIER. Can. J. Chem. **45**, 2895 (1967).
6. D. COOK and Z. R. REGNIER. Can. J. Chem. **45**, 2899 (1967).
7. D. COOK and Z. R. REGNIER. Unpublished results.
8. M. HAURIE and A. NOVAK. J. Chim. Phys. **62**, 137 (1965).
9. M. HAURIE and A. NOVAK. J. Chim. Phys. **62**, 146 (1965).
10. R. E. JONES and D. H. TEMPLETON. Acta Cryst. **11**, 484 (1958).
11. M. HAURIE and A. NOVAK. Spectrochim. Acta, **21**, 1217 (1965).
12. W. COCHRAN. Acta Cryst. **6**, 260 (1953).
13. G. ALLEN, J. G. WATKINSON, and K. H. WEBB. Spectrochim. Acta, **22**, 807 (1966).
14. W. R. FEAIRHELLER, JR. and J. E. KATON. Spectrochim. Acta, **23A**, 2225 (1967).
15. R. S. ROY. Spectrochim. Acta, **22**, 1877 (1966).
16. G. LEVY and R. H. REUNING. J. Pharm. Sci. **53**, 1471 (1964). R. H. REUNING and G. LEVY. J. Pharm. Sci. **56**, 843 (1967).
17. K. R. KNOLL, R. P. PARKE, and H. A. SWARTZ. J. Pharm. Pharmacol. **18**, 540 (1966).
18. P. A. SHORE, B. B. BRODIE, and C. A. M. HOGBEN. J. Pharm. Exp. Therap. **119**, 361 (1957).
19. C. W. MYONG. Nippon Yakurigaku Zasshi, **25**, 102 (1938), Breviaria 8–9.
20. Chem. Abstr. **32**, 3826_3 (1938).

Can. J. Chem. Downloaded from www.nrcresearchpress.com by 210.87.254.40 on 09/05/12
For personal use only.

Can. J. Chem. Downloaded from www.nrcresearchpress.com by 210.87.254.105 on 09/05/12
For personal use only.

Medium heterocyclic rings from carbohydrate precursors

J. F. STODDART AND W. A. SZAREK
Department of Chemistry, Queen's University, Kingston, Ontario

Received April 23, 1968

Chemical and physical evidence is presented to show that the structure of a dianhydride of D-ribose is di-β-D-ribofuranose 1,5′:1′,5-dianhydride. Partial acid hydrolysis of this dimer affords a ribobiose, which is shown to be 5-*O*-β-D-ribofuranosyl-D-ribose, since examination of the *O*-methyl derivative of this disaccharide yields 2,3,5-tri- and 2,3-di-*O*-methyl-D-ribose, and since quantitative measurements of the periodate consumption of the derived glycitol (4 moles of periodate per mole) are consistent with a structure corresponding to 5-*O*-β-D-ribofuranosyl-D-ribitol. In addition to confirming that both the 1 → 5′- and 1′ → 5- linkages have the β configuration, n.m.r. spectral data for the dianhydride tetraacetate leads to a conformational assignment for this derivative in chloroform at room temperature.

Periodate oxidation of the dianhydride, followed by borohydride reduction and acetylation, yields a 2,4,7,9-tetraacetoxymethyl-1,3,6,8-tetraoxacyclodecane. The conformational properties of this compound are discussed.

Canadian Journal of Chemistry, 46, 3061 (1968)

Although several investigations (1–3) have been carried out on an anhydro derivative of D-ribose, first reported by Bredereck *et al.* (4), unequivocal evidence for the structure of this compound has not been presented to date (cf. 5). An attempted (4) de-*O*-tritylation of 1,2,3-tri-*O*-acetyl-5-*O*-trityl-D-ribofuranose with hydrogen bromide in glacial acetic acid at 0° led to the isolation of a compound, which was thought to be 2,3-di-*O*-acetyl-1,5-anhydro-β-D-ribofuranose. Further investigations by Barker and Lock (1) on the product obtained from this reaction showed that it was dimeric and probably a fully acetylated derivative of di-D-ribofuranose 1,5′:1′,5-dianhydride, although some doubt remained about the assignment of this structure. Subsequently, other investigators (3, 6) and reviewers (7, 8) have supported the suggestion (1) that a 1,5′:1′,5-dianhydride structure is more likely than a 1,4′:1′,4- or a 1,5′:1′,4-dianhydride structural formulation. All these structural types are consistent (1) with the consumption of 2 moles of periodate per mole of dianhydride on oxidation, and with the isolation and characterization of 2,3-di-*O*-methyl-D-ribose from the acidic hydrolyzate of the tetra-*O*-methyl derivative of the dianhydride. In addition to reporting the preparation of some tetraoxacyclodecane derivatives from the dianhydride, we present evidence in this paper that this latter compound is di-β-D-ribofuranose 1,5′:1′,5-dianhydride (**2**).

Benzylidenation of D-ribose as described by Wood *et al.* (3) gave 2,3:2′,3′-di-*O*-benzylidene-D-ribofuranose 1,5′:1′,5-dianhydride (**1**), which

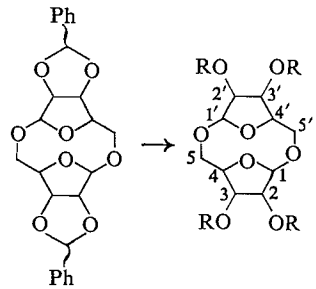

1 **2** R=H
3 R=Ac
4 R=Me

yielded the dianhydride (**2**) on catalytic de-*O*-benzylidenation. Partial hydrolysis of the dianhydride (**2**) with 0.01 *N* sulfuric acid for 2 h at 100° yielded a ribobiose (**5**) in 7% yield, as well as ribose and unchanged starting material (**2**). The disaccharide was shown to be 5-*O*-β-D-ribofuranosyl-D-ribose (**5**). Acid hydrolysis gave only ribose and methylation analysis led to the chromatographic identification of 2,3,5-tri- (**12**) and 2,3-di-*O*-methyl-D-ribose (**15**) by comparison with authentic samples. 2,3,5-Tri-*O*-methyl-D-ribose (**12**) (9) was prepared by methylating 2,3-*O*-benzylidene-D-ribofuranose (**8**) (3) using a modification (10) of a procedure reported by Falconer and Adams (11) to give the methyl 2,3-*O*-benzylidene-5-*O*-methyl-D-ribofuranosides (**9**) (3, 12), which were de-*O*-benzylidenated (3) to give **10**; methylation (10, 11) of **10** yielded **11**, which was hydrolyzed (9) to give **12**. 2,3-Di-*O*-methyl-D-ribose (**15**) (1, 13) was obtained by hydrolyzing the methyl glycosides

(**14**) obtained on methanolysis of tetra-*O*-methyl-β-D-ribofuranose 1,5′:1′,5-dianhydride (**4**). Equilibrium proportions of methyl glycosides (**13** and **14**) were examined by gas–liquid chromatography (g.l.c.) after refluxing with methanolic 2% hydrogen chloride for 16 h. On similar treatment the *O*-methyl derivative of the ribobiose (**5**) yielded a g.l.c. pattern corresponding

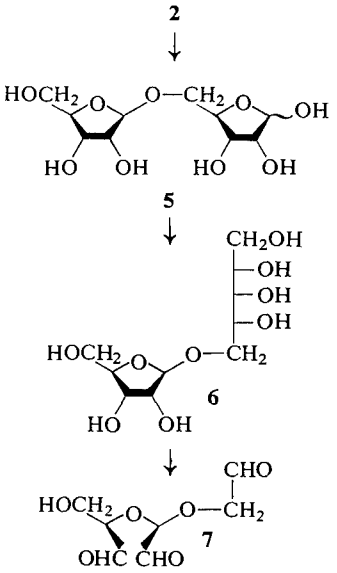

to approximately equimolar amounts of 2,3,5-tri- and 2,3-di-*O*-methyl-D-ribose as their methyl glycosides (**13** and **14**). This evidence indicated that a ribose unit was 4-*O*- or 5-*O*- substituted by a ribofuranose residue. Although the fact that the disaccharide (**5**) was released under mild conditions of acid hydrolysis would suggest that the reducing ribose unit was in the furanose form, and therefore 5-*O*-substituted, the two possibilities may be distinguished quite conveniently by reducing the ribobiose (**5**) with sodium borohydride to the glycitol (**6**) and measuring the periodate consumption of the latter. Theoretically, 4-*O*- and 5-*O*- substituted glycitols should consume 3 and 4 moles of periodate per mole, respectively. The periodate uptake of the derived glycitol (**6**) with time was measured[1] polarographically (14), and the results of this experiment are shown in Fig. 1. Although the reduced disaccharide (**6**) exhibits

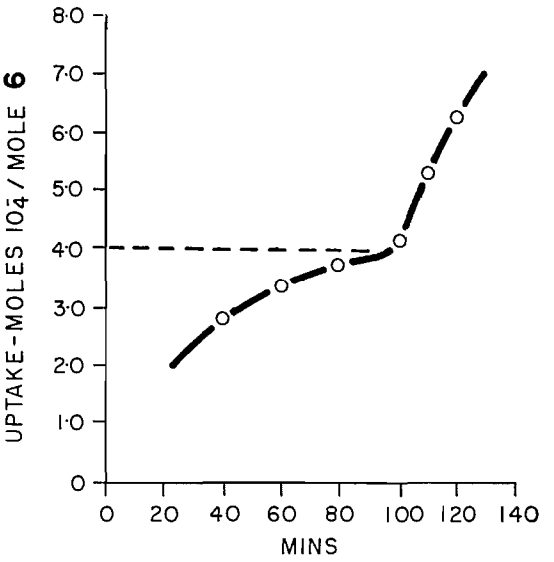

FIG. 1. Periodate oxidation of reduced disaccharide **6**.

"over-oxidation", a point of inflection[2] exists on the curve corresponding to a consumption of 4.0 moles of periodate per mole. Presumably, the reduced disaccharide (**6**) is oxidized initially to the trialdehyde (**7**) and only after this reaction is complete does "over-oxidation" of **7** ensue. It is concluded that the reduced ribobiose is 5-*O*-β-D-ribofuranosyl-D-ribitol (**6**) and hence that the reducing ribose residue in the original disaccharide (**5**) is 5-*O*-substituted and in the furanose form. The values for the specific optical rotations of the disaccharide (**5**) (+24°) and of the reduced disaccharide (**6**) (−26°) suggest that the configuration of the 1 → 5-linkage is β. This assignment is confirmed by the nuclear magnetic resonance (n.m.r.) spectrum of **6** in deuterium oxide. This shows a 1-proton broadened singlet at τ 4.95, which confirms (15, 16) a *trans* relationship between the protons on C-1 and C-2 of the ribofuranose residue and hence a β configuration for the 1 → 5 glycosidic bond. The question remained as to whether both the 1 → 5′- and 1′ → 5-linkages in the dianhydride (**2**) have the β configuration. The fact that only one ribobiose was detected after partial acid hydrolysis of **2** indicates that the

[1]The authors thank Miss Alice Wei for making these measurements.

[2]Recently, W. G. Breck, G. W. Hay, and G. Henderson (Queen's University, Kingston, Ontario) have observed a similar stepwise uptake of periodate with time for a number of disaccharides using this sensitive polarographic technique.

Can. J. Chem. Downloaded from www.nrcresearchpress.com by 210.87.254.105 on 09/05/12
For personal use only.

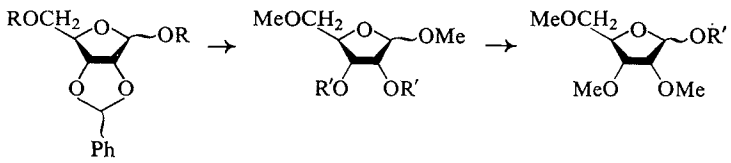

8 R=H
9 R=Me

10 R′=H
11 R′=Me

12 R′=H
13 R′=Me

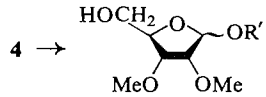

14 R′=Me
15 R′=H

presence of an α linkage as well as a β one is inherently unlikely. The n.m.r. spectral data for **2**, **3**, and **4** support this conclusion. Finally, evidence that the ribobiose (**5**) is unlikely to have arisen as a result of acid reversion follows from the identification of only ribose after prolonged acid hydrolysis (17).

Some idea of the conformation of the tetraacetate (**3**) (1, 3) and of the tetra-*O*-methyl derivative (**4**) (1) of the dimer (**2**) in chloroform-*d* was obtained from an examination of their n.m.r. spectra. The partial n.m.r. spectrum of **3** in chloroform-*d* (Fig. 2) showed a 2-proton singlet at τ 4.87, which was assigned to H-1,1′. This assignment is consistent with a β configuration at both glycosidic bonds and dihedral angles of close to 90° between H-1 and H-2 (and H-1′ and H-2′). This occurs when both ribofuranose rings assume C_2 conformations (half-chair) as shown in Fig. 3 (*a*). The remainder of the n.m.r. spectral data is consistent with this interpretation. The doublet between τ 4.45–4.60 was assigned to H-2,2′ ($J_{2,3} = J_{2',3'}$ 5.0 Hz) and the quartet between τ 4.10–4.37 to H-3,3′ ($J_{2,3} = J_{2',3'}$ 5.0 Hz, $J_{3,4} = J_{3',4'}$ 7.3 Hz). These coupling constants are consistent with dihedral angles of 30–40° between H-2 and H-3 (and H-2′ and H-3′) and 150–160° between H-3 and H-4 (and H-3′ and H-4′). The acetyl groups on C-2, C-2′, C-3, and C-3′ gave n.m.r. signals at τ values of 7.83 and 7.89. The 6-proton multiplets between τ 5.62–6.35 constitute an ABX system (18), which

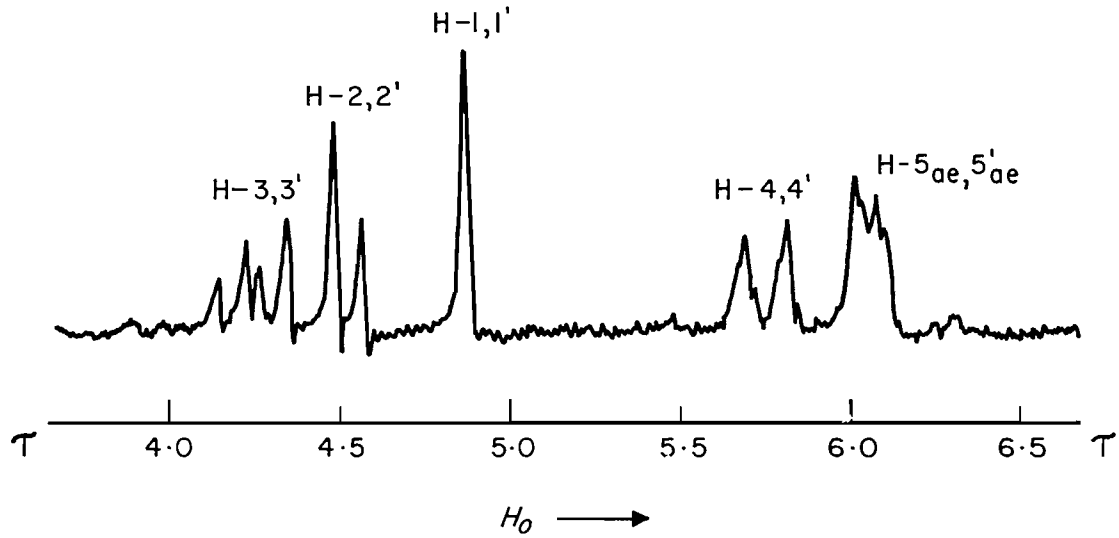

FIG. 2. Partial nuclear magnetic resonance spectrum of tetraacetate **3**.

Can. J. Chem. Downloaded from www.nrcresearchpress.com by 210.87.254.105 on 09/05/12
For personal use only.

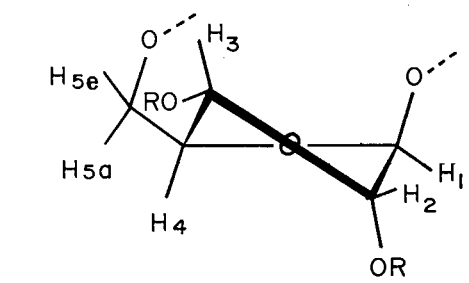

a R = Ac

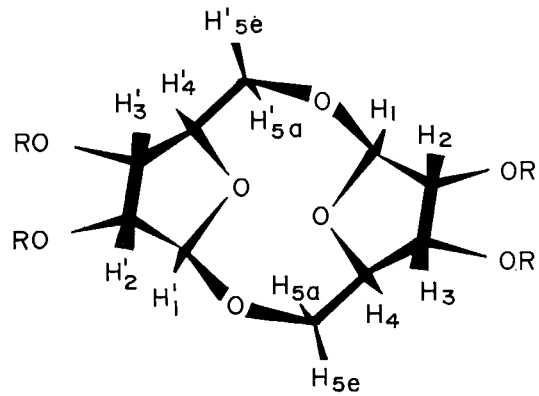

b R = Ac

FIG. 3. (*a*) Ribofuranose rings of tetraacetate **3** shown in C_2 conformation; (*b*) Conformation of tetraacetate **3** (also see Plate, acetyl groups are omitted for clarity).

is shown in more detail in Fig. 4. The X portion was assigned to the equivalent protons on C-4 and C-4′ and appeared as two triplets at lower field, because H-4,4′ is split by H-3,3′ [$J_{3,4} = J_{3',4'}$ 7.3 Hz, obtained from the splittings (9–9′), (10–10′ or 11–11′), or (12–12′) shown in Fig. 4]. The equivalent pairs of protons on C-5 and C-5′ constitute the AB portion of the spectrum. Peaks 7 and 8 of the AB pattern are presumably hidden under part of the X portion of the spectrum. The splittings (1–3) and (2–4) correspond to J_{AB} 13.5 Hz. The observation that the spacings (1–2), (3–4), and (5–6) are 1.6, 1.4, and 1.5 Hz respectively, and hence of the same order of magnitude, together with the fact that 10 and 11 (and 10′ and 11′) are coincident is evidence that J_{AX} and J_{BX} are equal. Since $J_{AX} + J_{BX}$ is given by the spacing between 9 and 12 (or 9′ and 12′), which is equal to 3.0 Hz, it follows that $J_{AX} = J_{BX} = 1.5$ Hz. This spectral interpretation is consistent with a conformation for the dimer where the projected valence angle between either of the protons on C-5 (or C-5′) and H-4 (or H-4′) is approximately 60°. This conformation, which exhibits an "up-down-up-down" arrangement of the four oxygen atoms within the 10-membered ring and which also displays a twofold (simple) axis of symmetry (19) is illustrated in Fig. 3*b*.

To date, ribose is the only pentose which has been reported to form a dimeric dianhydride. In this connection, however, it is of interest that

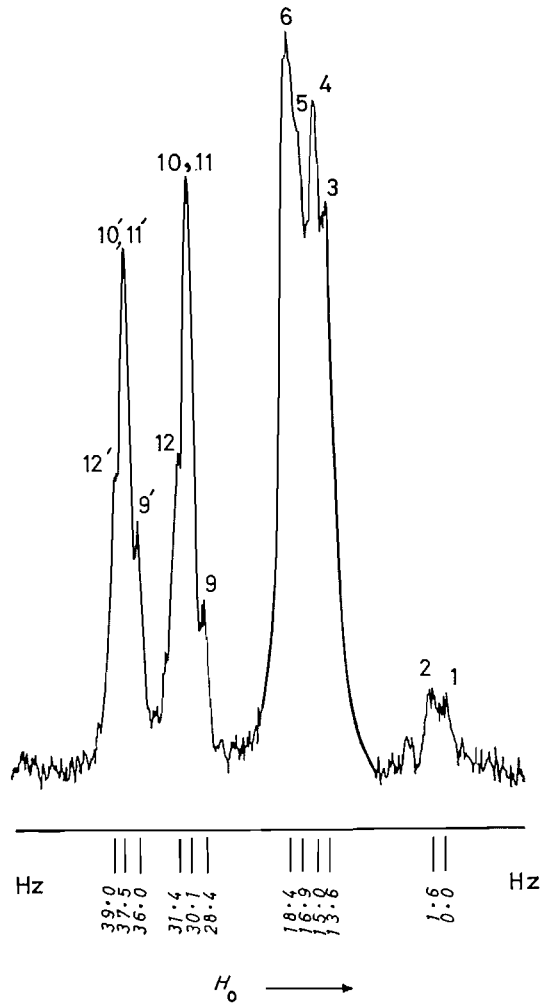

FIG. 4. Partial nuclear magnetic resonance spectrum of tetraacetate **3**, showing the ABX system for the protons on C-4 and C-5 (and C-4′ and C-5′).

Can. J. Chem. Downloaded from www.nrcresearchpress.com by 210.87.254.105 on 09/05/12
For personal use only.

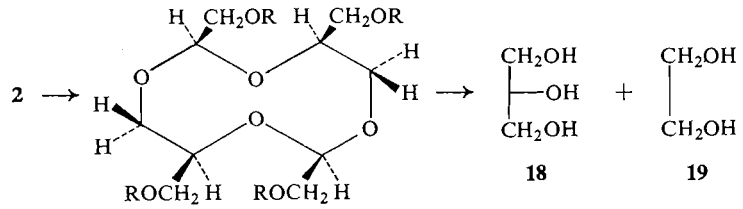

16 R = Ac
17 R = H

Schaffer and Cohen (20) have recently characterized a high-boiling substance (**20**) (21) formed during high-vacuum distillation of 2,3-*O*-isopropylidene-α-D-lyxofuranose. The configurational requirements at C-1 and C-4 are not fulfilled as they are with ribose, which readily forms (22) the dimeric anhydride, 2,3:2′,3′-di-*O*-isopropylidene-β-D-ribofuranose 1,5′:1′,5-dianhydride (**21**).

In recent years, there has been considerable interest shown in the preparation and conformational properties of homocyclic and heterocyclic 10-membered rings. Anet and Brown (23) have studied the rate of ring inversion of the nitrogen-containing 10-membered ring of protopine and Brimacombe *et al.* (24) have reported the isolation of some 4,5:9,10-biscyclohexano-1,3,6,8-tetraoxacyclodecanes from reaction of cyclohexane-*cis*- and *trans*- 1,2-diol with methylene bromide and sodium hydride in *N*,*N*-dimethyl formamide. The conformational geometries and energies of certain homocyclic 10-membered ring conformations have been computed and discussed by several authors (25–28).

When the dianhydride (**2**) was subjected to periodate oxidation followed by borohydride reduction and acetylation (29), a 2,4,7,9-tetraacetoxymethyl-1,3,6,8-tetraoxacyclodecane (**16**) was obtained. The element alanalysis, and infrared (i.r.) and n.m.r. spectra were all consistent structure proposed for this compound. with the A low-field triplet in the n.m.r. spectrum between τ 4.96–5.21 (*J* 5.4 Hz) was assigned to the acetal protons at C-2 and C-7. De-*O*-acetylation of **16** yielded 2,4,7,9-tetrahydroxymethyl-1,3,6,8-tetraoxacyclodecane (**17**), which also gave a satisfactory elemental analysis and a low-field triplet in the n.m.r. spectrum between τ 5.02–5.26 (*J* 5.5 Hz), attributable to the acetal protons on C-2 and C-7. Mild acid hydrolysis of **17** followed by borohydride reduction of the products gave glycerol (**18**) and ethylene glycol (**19**).

The fact that the n.m.r. spectrum of **16** in chloroform-*d* shows a sharp 12-proton singlet for the four acetyl groups associated with the acetoxymethyl side chains at positions 2,4,7 and 9 of the tetraoxacyclodecane ring suggests that a conformational equilibrium state exists at room temperature in this solvent. The notation introduced by Hendrickson (27) for referring to cyclodecane rings is used in Fig. 5 to show some of the possible stable conformations the substituted

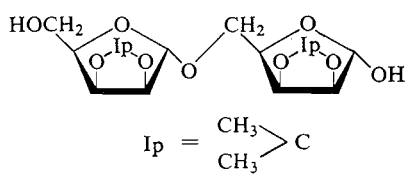

20

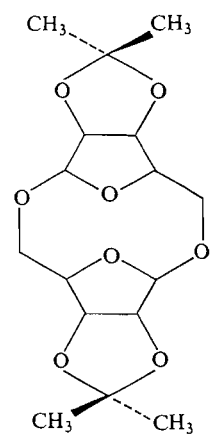

21

Can. J. Chem. Downloaded from www.nrcresearchpress.com by 210.87.254.105 on 09/05/12
For personal use only.

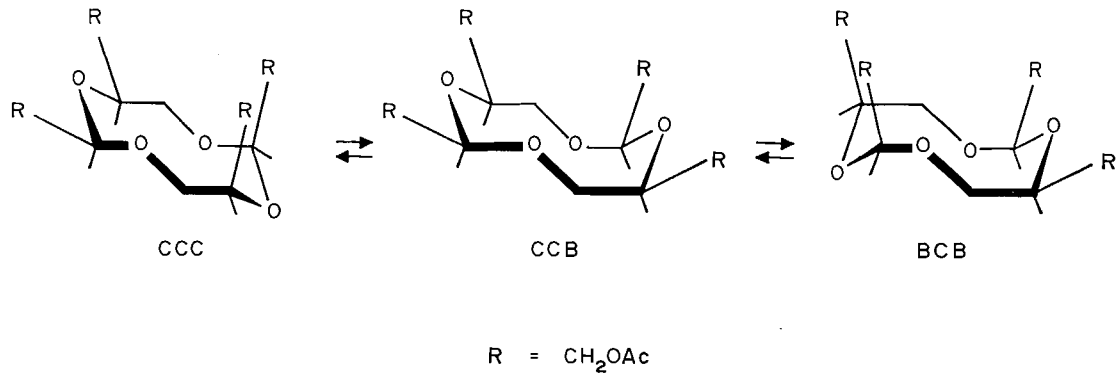

FIG. 5. Some possible conformations of substituted tetraoxacyclodecane rings (**16**).

tetraoxacyclodecane ring might assume. For the unsubstituted cyclodecane ring, the order of stability increases on going from the CCC to the CCB to the BCB conformation. When the cyclodecane ring carries one or more substituents, equatorial substituents are considered to be more stable than axial ones, and the lowest energy conformation is given by the lowest sum of ring energy and substituent energy. In the case of the tetraoxacyclodecane ring, a discussion of conformational equilibria is complicated by the presence of dipole–dipole interactions between oxygen atoms in the ring and between oxygen atoms and substituents. Figure 5 shows that there are two substituents axial and two equatorial, as well as two unfavorable 1,3 dipole–dipole interactions between oxygen atoms in the CCC conformation. In the CCB conformation, all substituents are equatorial and there is only one unfavorable 1,3 dipole–dipole interaction. The BCB conformation has no unfavorable 1,3 dipole–dipole interactions, but has two of the four substituents axial. Although qualitatively, this argument leads to the prediction that the CCB and BCB conformations will be of lower energy than the CCC one, it is hoped that low temperature n.m.r. studies will give some insight into matters relating to the rate of ring inversion and to the nature of the conformational equilibria.

Experimental

Melting points are uncorrected and were determined with a Fisher–Johns apparatus. Microdistillations were carried out on a Gallenkamp heating block. Optical rotations were measured using a Bendix ETL-NPL automatic polarimeter (type 143A) at 21 ± 2°. Paper chromatography was carried out on Whatman No. 1 and 3 MM papers using the following solvent systems (v/v): (*a* benzene – butan-1-ol – pyridine – water (1:5:3:3, upper layer); (*b*) butan-1-ol – ethanol – water (4:1:5, upper layer); (*c*) butan-1-ol – ethanol – water (3:1:1). Sugars were detected with aniline oxalate (30), alkaline silver nitrate (31), or periodate–permanganate (32) spray reagents. R_{Rib} values of sugars refer to distances moved relative to that of ribose. R_G values of *O*-methyl sugars refer to distances moved relative to that of 2,3,4,6-tetra-*O*-methyl-D-glucose. Thin-layer chromatography (t.l.c.) was carried out on glass microplates (40 × 90 mm) coated with silica gel (Camag) using the following solvent systems (v/v): (*d*) chloroform–methanol (19:1); (*e*) ethyl acetate – petroleum ether (b.p. 60–80°) (3:2); (*f*) ethyl acetate – petroleum ether (b.p. 60–80°) (1:1). The developed plates were air dried, sprayed with 5% ethanolic sulfuric acid and heated at about 150°. R_F values of sugars refer to distances moved relative to that of the solvent front. Gas–liquid partition chromatography (g.l.c.) (F and M chromatograph, type 402) of mixtures of methyl glycosides of *O*-methyl sugars (33) was carried out at nitrogen flow-rates of ca. 100 ml/min on columns of (*i*) 15% by weight of butan-1,4-diol succinate polyester on 60–80 mesh acid washed Chromosorb W (110 × 0.4 cm) at 160°, and (*ii*) 15% by weight of diethylene glycol adipate polyester on 60–80 mesh acid washed Chromosorb W (110 × 0.4 cm) at 160°. Retention times, *T*, are quoted relative to methyl 2,3,4,6-tetra-*O*-methyl-β-D-glucopyranoside as standard. Relative intensities of peaks were estimated visually: s, strong; m, medium; w, weak; vw, very weak. Infrared (i.r.) spectra were recorded on a Beckman model IR5A spectrophotometer. Nuclear magnetic resonance (n.m.r.) spectra were measured at 60 MHz in chloroform-*d* with tetramethylsilane (τ 10.00) as internal standard, and in deuterium oxide with sodium 4,4-dimethyl-4,4-silapentane-1-sulfonate (τ 10.00) as internal standard.

2,3:2′,3′-Di-O-benzylidene-D-ribofuranose 1,5′:1′,5-Dianhydride (1)

2,3:2′,3′-Di-*O*-benzylidene-D-ribofuranose 1,5′:1′,5-dianhydride (**1**) was prepared from D-ribose (10 g) according to the method of Wood *et al.* (3). Recrystallization from acetone gave the product (**1**) (5.5 g, 38%), m.p. 200–201°, $[\alpha]_D$ −41.4° (*c*, 0.66 in chloroform); λ_{max}

Can. J. Chem. Downloaded from www.nrcresearchpress.com by 210.87.254.105 on 09/05/12
For personal use only.

Can. J. Chem. Downloaded from www.nrcresearchpress.com by 210.87.254.105 on 09/05/12
For personal use only.

(Nujol) 13.1, 14.4 μm (Ph), no absorption attributable to OH. For this compound, m.p. 197–198°, $[\alpha]_D$ −36.3° (*c*, 1.1 in chloroform) have been reported (3).

Di-β-D-ribofuranose 1,5′:1′,5-Dianhydride (2)

Di-β-D-ribofuranose 1,5′:1′,5-dianhydride (**2**) was prepared by catalytic hydrogenation over 10% palladium on carbon of the di-*O*-benzylidene derivative (**1**) (5.0 g) according to the procedure of Wood *et al.* (3). Recrystallization from ethanol gave the dianhydride (**2**) (2.0 g, 67%), m.p. 224–227°, $[\alpha]_D$ +6.8° (*c*, 1.06 in water); λ_{max} (Nujol) 3.0 μm (OH); n.m.r. data in deuterium oxide: τ 5.01 (2-proton singlet, H-1,1′). Barker and Lock (1) report m.p. 229°, $[\alpha]_D^{19.5}$ +11° (*c*, 0.68 in water). Jeanloz *et al.* (2) report a corrected value of $[\alpha]_D^{20}$ +7.8° for the original value of $[\alpha]_D$ +78° reported by Bredereck *et al.* (4); the latter authors report m.p. 229–230°. Wood *et al.* (3) report m.p. 230–232°, $[\alpha]_D$ +9.5° (*c*, 1.4 in water).

Partial Acid Hydrolysis of Di-β-D-ribofuranose 1,5′:1′,5-Dianhydride (2) and Characterization of 5-O-β-D-Ribofuranosyl-D-ribose (5)

In a trial experiment, the dianhydride (**2**) (20 mg) was heated on a steam bath with 0.01 *N* sulfuric acid (6 ml). The progress of partial acid hydrolysis with time was followed paper chromatographically in solvent (*c*). After 2 h, the relative intensity of a slow moving spot with R_{Rib} 0.39 was at a maximum compared with the intensities of spots corresponding to ribose and the dianhydride (**2**) (R_{Rib} 0.97, not detectable with either aniline oxalate or alkaline silver nitrate, but developed with the periodate–permanganate spray reagent). Prolonged acid hydrolysis (16 h) yielded only ribose.

The dianhydride (**2**) (600 mg) was heated on a steam bath with 0.01 *N* sulfuric acid (180 ml) for 2 h. On cooling, the solution was neutralized with barium carbonate, filtered, treated with Amberlite resin IR-120 (H form) and concentrated to a syrup, which was chromatographed in solvent (*c*) on Whatman No. 3MM papers to separate a pure syrupy disaccharide, 5-*O*-β-D-ribofuranosyl-D-ribose (**5**) (45 mg, 7%), $[\alpha]_D$ +24° (*c*, 0.71 in water), [R_{Rib} 0.79 in solvent (*a*) and 0.43 in solvent (*b*)] from ribose and the dianhydride (**2**). Hydrolysis of the ribobiose (**5**) with 0.1 *N* sulfuric acid at 100° for 3 h gave only ribose.

A portion (10 mg) of the syrupy disaccharide was methylated (two successive treatments) with methyl iodide (1 ml) and silver oxide (1 g) in *N,N*-dimethyl formamide (1 ml). Gas–liquid chromatography of the methanolysis products revealed peaks with retention times corresponding to authentic methyl glycosides of 2,3,5-tri- (**13**) [(*i*), *T* 0.76 s, 1.25 vw; (*ii*), *T* 0.69 s, 1.18 vw] and 2,3-di-*O*-methyl-D-ribose (**14**) [(*i*), *T* 1.42 m, 1.91 s; (*ii*), *T* 1.33 m, 1.85 s]. Hydrolysis of the methyl glycosides with 0.5 *N* sulfuric acid at 100° for 4 h followed by paper chromatography in solvent (*b*) confirmed the presence of 2,3,5-tri- (**12**) [R_G 0.92, black spot (pink under ultraviolet (u.v.) light) with aniline oxalate] and 2,3-di-*O*-methyl-D-ribose (**15**) [R_G 0.77, blackish-pink spot (pink under u.v. light) with aniline oxalate].

More ribobiose (**5**) (75 mg, 14%) was obtained by partial acid hydrolysis (see above) of the dianhydride (**2**) (500 mg). The disaccharide (75 mg) was dissolved in water (20 ml) and sodium borohydride (75 mg) was added. After the reaction mixture had been allowed to stand at room temperature for 16 h, excess of borohydride was destroyed by addition of Amberlite resin IR-120 (H form) to the reaction mixture. The resin was filtered off, the solution treated with charcoal, filtered again, and the filtrate concentrated to a syrup. Paper chromatographic examination showed the presence of a reduced disaccharide, 5-*O*-β-D-ribofuranosyl-D-ribitol (**6**) [R_{Rib} 0.59 in solvent (*a*) and 0.32 in solvent (*b*)], and trace amounts of ribitol [R_{Rib} 0.80 in solvent (*a*) and 0.75 in solvent (*b*)] and ribose. The syrup was chromatographed in solvent (*b*) on Whatman No. 3MM papers to give pure 5-*O*-β-D-ribofuranosyl-D-ribitol (**6**) (23 mg, 31%), $[\alpha]_D$ −26° (*c*, 0.78 in water); n.m.r. data in deuterium oxide: τ 4.95 (1-proton broadened singlet, width at half-height 3.8 Hz, H-1). Using a polarographic technique (14), the following values for the uptake of periodate with time were obtained: 2.80 moles per mole, 40 min; 3.38 moles per mole, 60 min; 3.73 moles per mole, 80 min; 4.19 moles per mole, 100 min; 5.30 moles per mole, 110 min; 6.25 moles per mole, 120 min (see Fig. 1).

2,3,5-Tri-O-methyl-D-ribose (12)

2,3-*O*-Benzylidene-D-ribofuranose (**8**) was prepared from D-ribose (5.0 g) according to the method of Wood *et al.* (3). Recrystallization from benzene gave a product (3.8 g, 48%), m.p. 120–121°, $[\alpha]_D$ −26.6° (*c*, 1.02 in methanol), −25.6° (*c*, 0.98 in chloroform); λ_{max} (Nujol) 3.1 (OH), 13.1, 14.3 μm (Ph). For this compound, m.p. 123–124°, $[\alpha]_D$ −26.6° (*c*, 0.6 in methanol), −22.4° (*c*, 1.4 in chloroform) have been reported (3). The benzylidene compound (**8**) (500 mg) was dissolved in tetrahydrofuran (10 ml) and dimethyl sulfate (15 ml) and powdered sodium hydroxide (3 g) were added. The reaction mixture was shaken for 16 h at room temperature and then concentrated ammonia solution (5 ml) was added in stepwise fashion to the reaction mixture cooled in ice-water. Water (10 ml) was added and the mixture was stirred for 15 min before extracting the methylated product several times with chloroform. The chloroform extracts were combined, dried (anhydrous sodium sulfate), filtered, and the filtrate concentrated to dryness to give a syrup. Thin-layer chromatography of the syrupy product in solvent (*d*) showed two spots, a major fast moving one with R_F 0.83, and a minor slower moving one with R_F 0.56. The starting material (**8**) had R_F 0.30. The syrupy compound was distilled at 0.007 mm Hg and the fraction distilling between 90° and 120° was collected and shown to be a mixture of methyl 2,3-*O*-benzylidene-5-*O*-methyl-D-ribofuranosides (**9**) (345 mg, 62%), $[\alpha]_D$ −44.9° (*c*, 0.62 in chloroform); t.l.c. in solvent (*f*) showed two spots, a major one with R_F 0.61 and a minor one with R_F 0.39. The starting material (**8**) had R_F 0.21. For a similar mixture of methyl glycosides, Wood *et al.* (3) reported $[\alpha]_D$ −40.5° (*c*, 4.3 in chloroform).

The mixture of methyl ribofuranosides (**9**) (300 mg) was hydrogenated over 10% palladium on carbon as described by these authors (3) to give methyl 5-*O*-methyl-D-ribofuranosides (**10**) (175 mg, 88%), $[\alpha]_D$ −23.9° (*c*, 0.36 in methanol); R_F 0.14 in solvent (*f*). Wood *et al.* (3) have reported a similar mixture of methyl glycosides to have $[\alpha]_D$ −32.4° (*c*, 1.5 in methanol). Methyl 5-*O*-methyl-D-ribofuranosides (**10**) (148 mg) were methylated

Can. J. Chem. Downloaded from www.nrcresearchpress.com by 210.87.254.105 on 09/05/12
For personal use only.

with dimethyl sulfate (2 ml) and powdered sodium hydroxide (1 g) in tetrahydrofuran (3 ml) as described above for 2,3-*O*-benzylidene-D-ribofuranose (**8**) to give methyl 2,3,5-tri-*O*-methyl-D-ribofuranosides (**13**) (122 mg, 71%); t.l.c. in solvent (*d*) showed two spots, a major one with R_F 0.56 and a minor one with R_F 0.44. The methyl glycosides (**13**) (100 mg) were heated on a steam bath with 0.5 *N* sulfuric acid (10 ml). Thin-layer chromatography indicated complete hydrolysis of the methyl glycosides (**13**) in 4 h. The cooled solution was neutralized with barium carbonate, filtered, treated with Amberlite resin IR-120 (H form) and concentrated to a colored syrup, which was distilled at 0.02 mm Hg and the fraction distilling over between 80° and 90° collected as a colorless syrup of 2,3,5-tri-*O*-methyl-D-ribose (**12**) (60 mg, 65%), $[\alpha]_D$ +46° (*c*, 0.77 in methanol); R_F 0.28 in solvent (*d*) and R_G 0.92 in solvent (*b*) [black spot (pink under u.v. light) with aniline oxalate]. Gas–liquid chromatography of the methyl glycosides (**13**) obtained by refluxing 2,3,5-tri-*O*-methyl-D-ribose (**12**) (10 mg) with methanolic 2% hydrogen chloride (10 ml) for 16 h indicated peaks with the following retention times: (*i*), *T* 0.76 s, 1.24 vw; (*ii*), *T* 0.70 s, 1.15 vw. Barker (9) reports $[\alpha]_D$ +41.4° (*c*, 1.11 in methanol) for 2,3,5-tri-*O*-methyl-D-ribose (**12**).

Tetra-O-acetyl-β-D-ribofuranose 1,5′:1′,5-Dianhydride (3)

Di-β-D-ribofuranose 1,5′:1′,5-dianhydride (**2**) (380 mg) was acetylated (3) in the usual manner to yield a product, which was recrystallized from ethanol to give tetra-*O*-acetyl-β-D-ribofuranose 1,5′:1′,5-dianhydride (**3**) (443 mg, 86%), m.p. 165–167°, $[\alpha]_D$ +52.6° (*c*, 0.93 in chloroform); λ_{max} (Nujol) 5.72 μm (OAc), no absorption attributable to OH; n.m.r. data in chloroform-*d*: τ 4.87 (2-proton singlet, H-1,1′), τ 4.45–4.60 (2-proton doublet, $J_{2,3} = J_{2',3'}$ 5.0 Hz, H-2,2′), τ 4.10–4.37 (2-proton quartet $J_{2,3} = J_{2',3'}$ 5.0 Hz, $J_{3,4} = J_{3',4'}$ 7.3 Hz, H-3,3′) (see Fig. 2); τ 5.62–6.35 (multiplets of an ABX system, 6-protons, H-4,4′, 5a, 5a′, 5e, 5e′ with $J_{5a,5e} = J_{5a',5e'}$ 13.5 Hz, $J_{4,5a} = J_{4',5a'}$ 1.5 Hz, and $J_{4,5e} = J_{4',5e'}$ 1.5 Hz) (see Fig. 4); τ 7.83, 7.89 (12-protons, OAc groups on C-2,2′ and C-3,3′). For this compound, m.p. 169° (4), 168.5–169.5° (1), 171–172° (3) and $[\alpha]_D$ +53.5° (*c*, 1.03 in chloroform) (3) have been reported.

Tetra-O-methyl-β-D-ribofuranose 1,5′:1′,5-Dianhydride (4)

Tetra-*O*-methyl-β-D-ribofuranose 1,5′:1′,5-dianhydride (**4**) was prepared from the tetraacetate (**3**) (250 mg) according to the method of Barker and Lock (1). Recrystallization from petroleum ether (b.p. 60–80°) gave the compound **4** (26 mg, 9%), m.p. 125–126°; n.m.r. data in chloroform-*d*: τ 5.00 (2-proton singlet, H-1,1′), τ 5.63–5.88 (2-proton quartet, $J_{2,3} = J_{2',3'}$ 4.2 Hz, $J_{3,4} = J_{3',4'}$ 7.8 Hz, H-3,3′), τ 5.91–6.12 (2-proton multiplet, $J_{3,4} = J_{3',4'}$ 7.8 Hz, H-4,4′), τ 6.12–6.33 (6-proton multiplet, H-2,2′, 5a, 5e, 5a′, 5e′), τ 6.48, 6.55 (12-protons, OMe groups on C-2,2′ and C-3,3′). Barker and Lock (1) have reported m.p. 129.5–130° for this compound.

2,3-Di-O-methyl-D-ribose (15)

Tetra-*O*-methyl-D-ribofuranose 1,5′:1′,5-dianhydride (**4**) (5 mg) was heated under reflux in methanolic 2% hydrogen chloride (15 ml) for 16 h. Gas–liquid chromatography of the methanolyzate revealed peaks with retention times corresponding to the methyl glycosides (**14**) of 2,3-di-*O*-methyl-D-ribose [(*i*), *T* 1.39 m, 1.91 s; (*ii*), *T* 1.34 m, 1.85 s]. Hydrolysis of the methyl glycosides (**14**) with 0.5 *N* sulfuric acid at 100° for 4 h followed by paper chromatography in solvent (*b*) confirmed the presence of 2,3-di-*O*-methyl-D-ribose (**15**) [R_G 0.77, blackish-pink spot (pink under u.v. light) with aniline oxalate].

2,4,7,9-Tetraacetoxymethyl-1,3,6,8-tetraoxacyclodecane (16)

Di-β-D-ribofuranose 1,5′:1′,5-dianhydride (**2**) (1.3 g) was dissolved in water (30 ml) and a solution of sodium metaperiodate (2.6 g) in water (30 ml) was added. The reaction mixture was allowed to stand at 26° for 9 h. After excess of periodate and iodate had been precipitated with a 10% aqueous barium chloride solution, sodium borohydride (650 mg) was added to the filtered solution. The reaction mixture was allowed to stand at 26°. After 16 h, excess of borohydride was destroyed by addition of dry ice and the solution was concentrated to dryness. The residue was extracted several times with hot ethanol and the combined extracts were concentrated to a syrup, which was acetylated in the usual manner with acetic anhydride (25 ml) in dry pyridine (30 ml). The acetylation mixture was poured into ice-water (500 ml) and allowed to stand for 1 h before being extracted several times with chloroform. The chloroform extracts were combined, washed with saturated sodium bicarbonate solution, washed with water, dried over anhydrous sodium sulfate, filtered, and the filtrate concentrated to a syrup, which migrated as one spot on t.l.c. in solvent (*e*). This product was distilled (0.003 mm Hg) at 200–210° to give a yellow syrup, which started to crystallize after ½ h. Recrystallization from ether – petroleum ether (b.p. 60–80°) led to the isolation of needle-shaped crystals of 2,4,7,9-tetraacetoxymethyl-1,3,6,8-tetraoxacyclodecane (**16**) (1.44 g, 67%), m.p. 66–67°, $[\alpha]_D$ +15.6° (*c*, 0.82 in chloroform); R_F 0.50 in solvent (*e*); λ_{max} (Nujol) 5.78 μm (OAc), no absorption attributable to OH; n.m.r. data in chloroform-*d*: τ 4.96–5.21 (2-proton triplet, *J* 5.4 Hz, H-2,7), τ 7.93 (12-proton singlet, OAc groups on C-2,4,7,9).

Anal. Calcd. for $C_{18}H_{28}O_{12}$: C, 49.6; H, 6.55. Found: C, 49.3; H, 6.43.

2,4,7,9-Tetrahydroxymethyl-1,3,6,8-tetraoxacyclodecane (17)

The tetraacetate (**16**) (1.1 g) was dissolved in methanol (40 ml) and 2 drops of a 7% solution of sodium in methanol were added. The course of the de-*O*-acetylation was followed by t.l.c. in solvent (*e*) and the reaction appeared to be complete after 2 h. Dry ice was added to the methanolic solution after 4 h, the solution was filtered, and the filtrate was concentrated to a crystalline product. Recrystallization from ethanol yielded 2,4,7,9-tetrahydroxymethyl-1,3,6,8-tetraoxacyclodecane (**17**) (640 mg, 95%), m.p. 121–122°, $[\alpha]_D$ +24.7° (*c*, 0.53 in water); λ_{max} (Nujol) 3.08 μm (OH); n.m.r. data in deuterium oxide: τ 5.02–5.26 (2-proton triplet, *J* 5.5 Hz, H-2,7).

Anal. Calcd. for $C_{10}H_{20}O_8$: C, 44.8; H, 7.52. Found: C, 44.6; H, 7.51.

Acid Hydrolysis of 2,4,7,9-Tetrahydroxymethyl-1,3,6,8-tetraoxacyclodecane (17)

The tetraalcohol (**17**) (10 mg) was dissolved in *N*

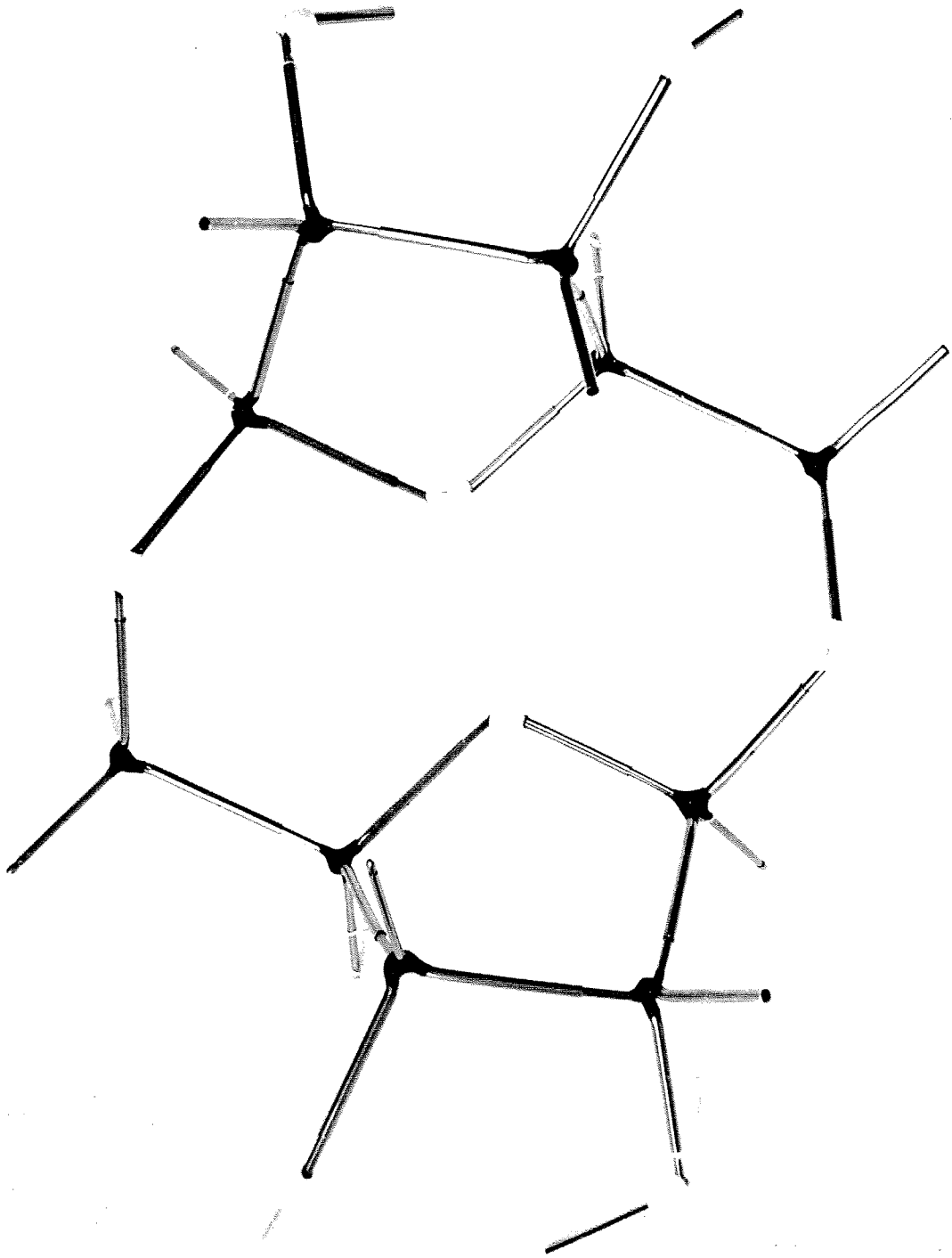

Can. J. Chem. Downloaded from www.nrcresearchpress.com by 210.87.254.105 on 09/05/12
For personal use only.

Can. J. Chem. Downloaded from www.nrcresearchpress.com by 210.87.254.105 on 09/05/12
For personal use only.

sulfuric acid (10 ml) and allowed to stand at 26°. After 2 days, the solution was neutralized with barium carbonate, filtered, and the filtrate was treated with Amberlite resin IR-120 (H form). Sodium borohydride (10 mg) was added to the solution and it was allowed to stand at 26° for 16 h. Excess of borohydride was destroyed with dry ice, and the solution was concentrated to a residue several times with methanol. Paper chromatographic examination of the residue in solvent (*b*) showed the presence of glycerol (**18**) and ethylene glycol (**19**).

Acknowledgments

The authors thank the National Research Council of Canada for a grant (A4589) in aid of this research. Some of the nuclear magnetic resonance spectra were determined at the Royal Military College, Kingston, Ontario, and we are indebted to Dr. D. G. M. Diaper for the use of the spectrometer.

1. G. R. Barker and M. V. Lock. J. Chem. Soc. 23 (1950).
2. R. W. Jeanloz, G. R. Barker, and M. V. Lock. Nature, **167**, 42 (1951).
3. H. B. Wood, Jr., H. W. Diehl, and H. G. Fletcher, Jr. J. Am. Chem. Soc. **78**, 4715 (1956).
4. H. Bredereck, M. Köthing, and E. Berger. Ber. **73**, 956 (1940).
5. J. M. Cox and L. N. Owen. J. Chem. Soc. C. 1121 (1967).
6. E. Vis and H. G. Fletcher, Jr. J. Am. Chem. Soc. **79**, 1182 (1957); N. A. Hughes and P. R. H. Speakman. Carbohydrate Res. **1**, 171 (1965).
7. R. W. Jeanloz and H. G. Fletcher, Jr. Advan. Carbohydrate Chem. **6**, 135 (1951).
8. J. Staněk, M. Černý, and J. Pacák. The oligosaccharides. Academic Press, Inc., New York. 1965. p. 360.
9. G. R. Barker. J. Chem. Soc. 2035 (1948).
10. D. G. Lance and J. K. N. Jones. Can. J. Chem. **45**, 1533 (1967).
11. E. L. Falconer and G. A. Adams. Can. J. Chem. **34**, 338 (1956).
12. G. R. Barker, T. M. Noone, D. C. C. Smith, and J. W. Spoors. J. Chem. Soc. 1327 (1955).
13. G. R. Barker and D. C. C. Smith. J. Chem. Soc. 1323 (1955).
14. W. G. Breck, R. D. Corlett, and G. W. Hay. Chem. Commun. 604 (1967).
15. M. Rudrum and D. F. Shaw. J. Chem. Soc. 52 (1965).
16. R. U. Lemieux and J. D. Stevens. Can. J. Chem. **44**, 249 (1966).
17. P. Andrews and J. K. N. Jones. J. Chem. Soc. 583 (1955).
18. J. A. Pople, W. G. Schneider, and H. J. Bernstein. High-resolution nuclear magnetic resonance. McGraw-Hill Book Co., Inc., New York. 1959.
19. E. L. Eliel. Stereochemistry of carbon compounds. McGraw-Hill Book Co., Inc., New York. 1962.
20. R. Schaffer and A. Cohen. National Bureau of Standards, Technical Note 427. Washington. 1967. p. 37.
21. P. A. Levene and R. S. Tipson. J. Biol. Chem. **115**, 731 (1936).
22. P. A. Levene and E. T. Stiller. J. Biol. Chem. **102**, 187 (1933).
23. F. A. L. Anet and M. A. Brown. Tetrahedron Letters, 4881 (1967).
24. J. S. Brimacombe, A. B. Foster, B. D. Jones, and J. J. Willard. J. Chem. Soc. C. 2404 (1967).
25. F. H. Westheimer. *In* Steric effects in organic chemistry. *Edited by* M. S. Newman. John Wiley and Sons, Inc., New York. 1956. Chap. 12.
26. (*a*) N. L. Allinger. J. Am. Chem. Soc. **81**, 5727 (1959). (*b*) N. L. Allinger, M. A. Miller, F. A. Van-Catledge, and J. A. Hirsch. J. Am. Chem. Soc. **89**, 4345 (1967). (*c*) N. L. Allinger, J. A. Hirsch, M. A. Miller, I. J. Tyminski, and F. A. Van-Catledge. J. Am. Chem. Soc. **90**, 1199 (1968).
27. J. B. Hendrickson. J. Am. Chem. Soc. **86**, 4854 (1964); **89**, 7036, 7043, 7047 (1967).
28. E. L. Eliel, N. L. Allinger, S. J. Angyal, and G. A. Morrison. Conformational analysis. John Wiley and Sons, Inc., New York. 1965.
29. J. K. Hamilton, G. W. Huffman, and F. Smith. J. Am. Chem. Soc. **81**, 2173, 2176 (1959).
30. S. M. Partridge. Partition chromatography. Biochemical Society Symposia, Vol. 3. Cambridge University Press, Cambridge. 1950. p. 52.
31. W. E. Trevelyan, D. P. Procter, and J. S. Harrison. Nature, **166**, 444 (1950).
32. R. U. Lemieux and H. F. Bauer. Anal. Chem. **26**, 920 (1954).
33. G. O. Aspinall. J. Chem. Soc. 1676 (1963).

Can. J. Chem. Downloaded from www.nrcresearchpress.com by 210.87.254.105 on 09/05/12
For personal use only.

Can. J. Chem. Downloaded from www.nrcresearchpress.com by 210.87.254.42 on 09/05/12
For personal use only.

Glycolipids of soft wheat flour. I. Isolation and characterization of 1-*O*-(6-*O*-acyl-β-D-galactopyranosyl)-2,3-di-*O*-acyl-D-glyceritols and phytosteryl 6-*O*-acyl-β-D-glucopyranosides

D. V. MYHRE

The Procter & Gamble Company, Miami Valley Laboratories, Cincinnati, Ohio 45239

Received October 17, 1967

Two groups of glycolipids were isolated from soft wheat flour. The first group, 1-*O*-(6-*O*-acyl-β-D-galactopyranosyl)-2,3-di-*O*-acyl-D-glyceritols (**1**), was saponified to yield fatty acids and 1-*O*-β-D-galactopyranosyl-D-glyceritol in the molar ratio 3:1. Methylation of **1** followed by saponification of the methylated product gave 1-*O*-(2,3,4-tri-*O*-methyl-β-D-galactosyl)-D-glyceritol which provided 2,3,4-tri-*O*-methyl-D-galactose and glyceritol upon hydrolysis. In periodate oxidation studies **1** consumed two moles of oxidant and yielded tri-*O*-acyl dialdehydes (**6**) without liberating fatty acids. Sodium borohydride reduction of **6** followed by saponification, acid hydrolysis, and another borohydride reduction gave glyceritol and ethylene glycol in the expected manner.

The second group of glycolipids, phytosteryl 6-*O*-acyl-β-D-glucopyranosides, was methylated and the products were saponified to give phytosteryl 2,3,4-tri-*O*-methyl-β-D-glucopyranosides (**12**) and fatty acids. Methanolysis of **12** gave principally β-sitosterol, campesterol, and methyl 2,3,4-tri-*O*-methyl-α- and β-D-glucosides.

Canadian Journal of Chemistry, **46**, 3071 (1968)

The lipid constituents of wheat flour have been studied extensively by many workers. Several components have been characterized including hydrocarbons, phytosteryl ester, glycerides, free fatty acids, phytosteryl β-D-glucopyranosides, cerebrosides, mono- and digalactosyl diglycerides, and several phospholipids (1, 2). Previous work in our laboratories has involved the isolation and characterization of a polysaccharide (3) and glycoproteins (4) present in soft wheat flour.

Examination of the ethanol extracted lipid components from soft wheat flour resulted in the isolation of two different groups of glycolipids. The first group proved to be a type of glycolipid which has not previously been described as a lipid component of wheat flour. Rigorous structural examination proved it to be the 1-*O*-(6-*O*-acyl-β-D-galactopyranosyl)-2,3-di-*O*-acyl-D-glyceritol group (**1**). This glycolipid group has been previously described as a component of spinach chloroplasts (*Spinacia aleracea*) and snapdragon (*Antirrhinum majus*) (5). The second group, phytosteryl 6-*O*-acyl-β-D-glucopyranoside (**9**), has been isolated previously from potatoes (6); its presence in the endosperm of wheat was indicated by chromatographic techniques (7). The present report establishes the structure of this group **9** to be the same as that occurring in the potato.

In the work reported here, unbleached commercial soft wheat flour was extracted with ethanol and the material thus obtained was fractionated by silicic acid column chromatography similar to the method used by Carter *et al.* (8). Fractions were examined by silica gel thin-layer chromatography (t.l.c.) to evaluate the resolution obtained. Such t.l.c. with a chloroform – methanol – water solvent system showed that the glycolipids of group **1** had an R_f value of 0.93 and gave a dark reddish-brown color during charring with sulfuric acid, similar to other galactosyl glyceritol lipids. Glycolipid **1** and palmitoyl glyceritol (monoglyceride) were inseparable using silicic acid column chromatography under conditions described by Hirsch and Ahrens (9).

Saponification of **1** yielded fatty acids and 1-*O*-β-D-galactopyranosyl-D-glyceritol (**2**) in the molar ratio 3:1. The latter compound (**2**) was

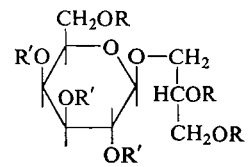

1, R = fatty acyl group; R′ = H
2, R = R′ = H
3, R = R′ = *p*-nitrobenzoyl group
4, R = fatty acyl group; R′ = CH_3
5, R = H; R′ = CH_3

nonreducing toward Fehling's solution and had a mobility identical to that of known 1-*O*-β-D-galactopyranosyl-D-glyceritol by paper chromatography with ethyl acetate – pyridine – water solvent. Acid hydrolysis of **2** gave equimolar

Can. J. Chem. Downloaded from www.nrcresearchpress.com by 210.87.254.42 on 09/05/12
For personal use only.

amounts of D-galactose and glyceritol. Compound **2** furnished the crystalline 1-*O*-(2,3,4,6-tetra-*O*-*p*-nitrobenzoyl-β-D-galactosyl)-2,3-di-*O*-*p*-nitrobenzoyl-D-glyceritol (**3**) which had an undepressed melting point upon admixture with the same derivative prepared from authentic 1-*O*-β-D-galactopyranosyl-D-glyceritol. Also, the specific optical rotation of **2** (−6° in water) indicated that this compound was identical to the 1-*O*-β-D-galactopyranosyl-D-glyceritol isolated previously (10–12).

The positions of attachment of the fatty acids in **1** were established by methylation and confirmed by periodate oxidation studies. The glycolipid group **1** was methylated according to Kuhn's procedure (13) to minimize acyl migration. The products, 1-*O*-(2,3,4-tri-*O*-methyl-6-*O*-acyl-β-D-galactosyl)-2,3-di-*O*-acyl-D-glyceritols (**4**), were saponified to give a mixture of fatty acids and 1-*O*-(2,3,4-tri-*O*-methyl-β-D-galactosyl)-D-glyceritol (**5**). Hydrolysis of **5** provided equimolar proportions of 2,3,4-tri-*O*-methyl-D-galactose and glyceritol which were identified as the *N*-phenylglycosylamine and the tri-*O*-*p*-nitrobenzoate derivatives, respectively.

In periodate oxidation studies, glycolipid **1** reduced two moles of oxidant per mole of **1** and gave the tri-*O*-acyl dialdehydes (**6**) in quantitative yield. These products had an R_f value of 0.8 in benzene–methanol solvent. Fatty acids were not detected in the periodate reaction mixture. Authentic 1-*O*-β-D-galactopyranosyl-2,3-di-*O*-acyl-D-glyceritol similarly consumed two moles of periodate. However, the dialdehyde products (**6***a*) thus obtained had an R_f value of 0.3. Since **6** was more lipophilic than **6***a*, the fatty acyl group attached to the D-galactopyranosyl residue of **1** was retained upon periodate oxidation and therefore it was attached at the C-6 position. In contrast, a glycolipid with fatty acyl substitution at the C-2 or C-4 position of the D-galactopyranosyl unit of 1-*O*-β-D-galactopyranosyl-2,3-di-*O*-acyl-D-glyceritol would be expected to yield **6***a* and fatty acids due to initial oxidation by one mole of periodate followed by spontaneous hydrolysis of the ester linkage at C-2 or C-4 and consumption of a second mole of periodate (15).

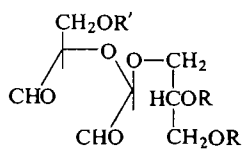

6, R = R′ = fatty acyl group
6*a*, R = fatty acyl group; R′ = H

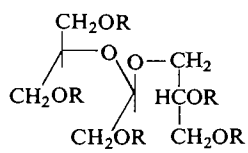

7, R = H

8, R = $CH_3C(=O)$—

Reduction of **6** with sodium borohydride and saponification yielded the pentahydric alcohol, 2-(R)-glyceritoxy-4-hydroxymethyl-(R)-diethylene glycol[1] (**7**), which was obtained free of salts by conversion to the pentaacetate (**8**) and subsequent deacetylation. Acid hydrolysis of **7** followed by reduction of the hydrolysis products with sodium borohydride yielded glyceritol and ethylene glycol which were identified as the tri-*O*-*p*-nitrobenzoate and the di-*O*-*p*-nitrobenzoate derivatives, respectively. When the dialdehydes **6***a* were carried through the same series of reactions, only glyceritol and ethylene glycol were detected. These results are in agreement with the methylation studies and also indicate the absence of acyl migration under Kuhn methylation conditions.

The fatty acids obtained from **1** by saponification were determined quantitatively by gas–liquid chromatographic analysis of the methyl esters. The mixture consisted of approximately the usual components found in the total lipid of soft wheat flour (see Table II).

The phytosteryl 6-*O*-acyl-β-D-glucopyranoside-rich mixture, obtained by fractionation of wheat flour lipids by silicic acid column chromatography, was purified further by dry column silica gel chromatography (16) using diethyl ether solvent. The phytosteryl 6-*O*-acyl-β-D-glucopyranosides thus obtained gave a typical purple color on t.l.c. development and had an R_f value of 0.83 with chloroform – methanol – water solvent.

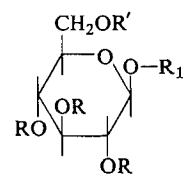

R_1 = β-sitosteryl or campesteryl residue
9, R = H; R′ = fatty acyl group
10, R = R′ = H
11, R = CH_3; R′ = fatty acyl group
12, R = CH_3; R′ = H
13, R = H; R′ = trityl
14, R = CH_3; R′ = trityl

The phytosteryl 6-*O*-acyl-β-D-glucopyranosides (**9**) yielded phytosteryl β-D-glucopyrano-

[1]Nomenclature is according to Cahn *et al.* (14).

Can. J. Chem. Downloaded from www.nrcresearchpress.com by 210.87.254.42 on 09/05/12
For personal use only.

sides (**10**) and fatty acids upon saponification according to t.l.c. analysis (7). Methanolysis of **10** gave a mixture of phytosterols and methyl α- and β-D-glucoside. Gas–liquid chromatographic analysis of the phytosterols as the trimethylsilyl derivatives indicated three components, β-sitosterol (74%), campesterol (19%), and an unknown constituent (7%). The methyl α- and β-D-glucoside mixture was hydrolyzed and crystalline D-glucose was identified by its melting point and specific optical rotation.

Further evidence for the structure of phytosteryl 6-*O*-β-D-glucopyranosides was adduced from methylation and periodate oxidation studies. Methylation of **9** by the method of Kuhn *et al.* (13) gave phytosteryl 2,3,4-tri-*O*-methyl-6-*O*-acyl-β-D-glucosides (**11**) which upon saponification yielded phytosteryl 2,3,4-tri-*O*-methyl-β-D-glucosides (**12**) with a melting point of 164–165°.

The group **12** glycolipids were prepared also by an alternate route starting with the phytosteryl β-D-glucopyranosides (**10**) isolated from soft wheat flour by silicic acid column chromatography. The glycolipid mixture (**10**) was treated with trityl chloride in pyridine to give phytosteryl 6-*O*-trityl-β-D-glucopyranosides (**13**). Methylation of **13** with dimethyl sulfate, dimethyl sulfoxide, dimethyl formamide, barium oxide, and barium hydroxide according to the method of Kuhn and Trischman (17) provided phytosteryl 2,3,4-tri-*O*-methyl-6-*O*-trityl-β-D-glucosides (**14**) which were treated with hydrogen chloride in chloroform–methanol to obtain **12**.

The phytosteryl 2,3,4-tri-*O*-methyl-β-D-glucosides derived from **9** and **10** as described above had identical melting points and mixture melting point (165°) and specific optical rotations (−28° in chloroform).

Methanolysis of **12** was accompanied by a dextrorotatory change in the specific optical rotation [−28° changing to +5° (in chloroform)]. This indicates a β-glycosidic linkage in **12**. The phytosterols and partially methylated glucosides were separated by silicic acid column chromatography. Gas–liquid chromatographic analysis of the phytosterol trimethylsilyl ethers indicated the presence of β-sitosterol and campesterol. Gas–liquid chromatographic analysis of the glycosides indicated the presence of methyl 2,3,4-tri-*O*-methyl-α- and β-D-glucosides.

The attachment of the fatty acyl group to the C-6 position of the β-D-glucopyranosyl unit in **9** was substantiated by the fact that the periodate oxidation products from **9** had a greater mobility on t.l.c. than the oxidation products from **10**. Phytosteryl 2-*O*- or 4-*O*-acyl-β-D-glucopyranosides, on the other hand, were excluded as possible isomers since both would be expected to yield periodate oxidation products indistinguishable from those obtained from **10**. The other positional isomer, phytosteryl 3-*O*-acyl-β-D-glucopyranoside, was excluded also because it would be resistant to periodate oxidation.

Experimental

Phytosterol trimethylsilyl ethers were determined with a Jarrell Ash model 700 gas chromatography unit with a hydrogen flame detector. The glass column (0.5 × 125 cm) packed with 1% XE 60 and 1% SE 52 on 100–120 mesh Gas Chrom Q was maintained at 210°. Cholestane was used as the internal standard.

Fatty acid methyl esters and the partially methylated glycosides were determined with an F and M model 500 gas chromatography unit with a thermal conductivity detector. For the fatty acid methyl esters a stainless steel column (¼ in. × 10 ft) packed with 15% cyanomethyl silicone copolymer with ethylene glycol succinate on 60–80 mesh Gas Chrom P was maintained at 190°. Peak areas were measured by triangulation. For the partially methylated glycosides a stainless steel column (¼ in. × 10 ft) packed with 15% Carbowax 20 M on 60–70 mesh Anachrom ABS was maintained at 175°.

Thin-layer chromatographic (t.l.c.) analyses were carried out by the ascending technique with silica gel G adsorbent. The following solvent systems were used: solvent *a*, chloroform – methanol – water (85:22:2); solvent *b*, diethyl ether – petroleum ether (b.p. 30–60°) (70:30); solvent *c*, benzene–methanol (90:10); solvent *d*, diethyl ether. Thin-layer plates were sprayed with 50% sulfuric acid and heated at 140° for detection of the components.

Paper chromatography was carried out by the horizontal method (18) with Whatman No. 1 filter paper and ethyl acetate – pyridine – water (40:11:6) (solvent *e*) or by the descending method with butanone–water azeotrope (solvent *f*). The components were detected on the paper with ammoniacal silver nitrate followed by heating the paper at 100–120°.

The cation exchange resin Amberlite IR-120[2] (H^+ form) and the anion exchange resin Duolite A-4[3] (OH^- form) were used throughout unless stated otherwise.

Melting points were determined with a Fisher–Johns melting point apparatus and are corrected.

All evaporations were carried out *in vacuo* with a rotary evaporator at 40° (bath temperature) unless stated otherwise.

Fractionation of the Lipids from Soft Wheat Flour

Russell–Miller American Beauty soft wheat flour (23 kg) was suspended in ethanol (46 l) and the mixture was

[2]Product of the Rohm & Haas Company, Philadelphia, Pennsylvania.

[3]Product of the Diamond Alkali Company, Redwood City, California.

TABLE I

Fractionation of the ethanol-extracted lipids of soft wheat flour

Fraction	Solvent $CHCl_3$:MeOH, v/v	Component(s)
1–50	100:0	Neutral lipid
51–70	100:0	1-*O*-(6-*O*-Acyl-β-D-galactopyranosyl)-2,3-di-*O*-acyl-D-glyceritols
120–150	98:2	Phytosteryl 6-*O*-acyl-β-D-glucopyranosides and monoglycerides
160–180	96:4	1-*O*-β-D-Galactopyranosyl-2,3-di-*O*-acyl-D-glyceritols
181–210	94:6	Phytosteryl β-D-glucopyranosides and 1-*O*-β-D-galactopyranosyl-2,3-di-*O*-acyl-D-glyceritols
301–430	92:8 90:10	Cerebrosides and 1-*O*-[6-*O*-(α-D-galactopyranosyl)-β-D-galactopyranosyl]-2,3-di-*O*-acyl-D-glyceritols

allowed to stand for several hours. The supernatant was withdrawn and filtered and the insoluble residue was extracted twice as before. The filtrates were evaporated to a syrup (215 g).

In a typical run a portion of the ethanol extracted material (20–30 g) from above was dissolved in chloroform (200 ml) and applied to a column of silicic acid (Mallinckrodt, 100 mesh) (3.6 × 88 cm) which had been washed previously, first with chloroform–methanol (50:50 v/v) and then with chloroform. The column was irrigated with chloroform followed by mixtures of chloroform and methanol as shown in Table I similar to the method of Carter *et al.* (8). Every tenth fraction (15–20 ml each) was evaporated under a stream of nitrogen and its residue was examined by t.l.c. with solvent *a*. Appropriate fractions were combined, evaporated and the residues were stored at 0° until used.

Identification of 1-O-(6-O-Acyl-β-D-galactopyranosyl)-2,3-di-O-acyl-D-glyceritols (1)

A portion of **1** (0.173 g) was dissolved in ethanol (25 ml) to which 1 *N* sodium hydroxide (3 ml) was added and the mixture was warmed to 50° for 6 h. Water (50 ml) was added to the solution and most of the ethanol was evaporated. The solution was acidified to pH 1 with 1 *N* hydrochloric acid and extracted with chloroform (2 × 25 ml) after which the combined chloroform extracts were evaporated to a thin syrup (0.133 g). The aqueous solution was passed through a column of mixed ion exchange resins and the effluent was evaporated to dryness (0.035 g). Paper chromatographic analysis of the residue with solvent *e* indicated the presence of 1-*O*-β-D-galactopyranosyl-D-glyceritol (**2**).

The syrupy **2** from above had $[\alpha]_D^{23}$ − 6° (*c*, 1 in water). This material (0.035 g) was dissolved in pyridine (5 ml) and treated with *p*-nitrobenzoyl chloride (0.3 g) at 90° for 1 h. A few drops of water were added to the reaction mixture and after 10 min the solution was poured into aqueous sodium bicarbonate (25 ml). The aqueous solution was extracted with chloroform (2 × 25 ml) and the chloroform solutions washed with water. Evaporation of the chloroform and pyridine yielded a residue which was recrystallized from acetone–ethanol to give 1-*O*-(2,3,4,6-tetra-*O*-*p*-nitrobenzoyl-β-D-galactosyl)-2,3-di-*O*-*p*-nitrobenzoyl-D-glyceritol (**3**), m.p. 164–167° and $[\alpha]_D^{22}$ +97° (*c*, 1 in chloroform).

Anal. Calcd. for $C_{51}H_{36}O_{26}N_6$: C, 53.30; H, 3.16; N, 7.32. Found: C, 53.1; H, 3.3; N, 7.18.

An authentic sample of 1-*O*-β-D-galactopyranosyl-D-glyceritol (**2**) (0.204 g) was obtained by saponification of 1-*O*-β-D-galactopyranosyl-2,3-di-*O*-acyl-D-glyceritol (tubes 160–185, Table I). The *p*-nitrobenzoyl derivative had a m.p. 163–166°, which was undepressed upon admixture with the above derivative (**3**), and $[\alpha]_D^{22}$ +97° (*c*, 1 in chloroform).

Anal. Calcd. for $C_{51}H_{36}O_{26}N_6$: C, 53.30; H, 3.16; N, 7.32. Found: C, 53.2; H, 3.1; N, 7.10.

The fatty acids extracted with chloroform after saponification of **1** were refluxed with methanol containing hydrogen chloride (2%) for 6 h after which the solution was evaporated to a small volume and diluted with chloroform (25 ml). The chloroform solution was washed with water until the washings were neutral and evaporated to dryness. The composition of the mixture of fatty acid methyl esters determined by gas–liquid chromatographic analysis is given in Table II.

Methylation of 1-O-(6-O-Acyl-β-D-galactopyranosyl)-2,3-di-O-acyl-D-glyceritols (1)

A portion of **1** (0.626 g) was dissolved in dimethyl formamide (30 ml) to which methyl iodide (6 ml) and silver oxide (6 g) were added and the mixture was stirred at room temperature for 2 days. Chloroform (60 ml) was added to the reaction mixture, the insoluble salts were removed by centrifugation and washed with chloroform (2 × 25 ml); the combined supernatant solutions were washed with 2% aqueous potassium cyanide (50 ml) and with water. The organic layer was evaporated, the dimethyl formamide being removed *in vacuo* at 0.01 mm pressure and 50–60° (bath temperature), to give a syrup (0.605 g). Two more methylations by the procedure described above yielded a light-yellow syrup (0.601 g).

Saponification of 1-O-(2,3,4-Tri-O-methyl-6-O-acyl-β-D-galactosyl)-2,3-di-O-acyl-D-glyceritols and Identification of 1-O-(2,3,4-Tri-O-methyl-β-D-galactosyl)-D-glyceritol

The thrice methylated material was dissolved in ethanol and saponified according to the method described above for **1** to give the chloroform-soluble fatty acids (0.488 g) and water-soluble 1-*O*-(2,3,4-tri-*O*-methyl-β-D-galactosyl)-D-glyceritol (**5**), the latter after deionization of the aqueous solution with mixed resins. Thin-layer chromatography of the carbohydrate material with solvent *a* indicated that **5** had an R_f value of 0.48 and that several minor impurities were also present.

Can. J. Chem. Downloaded from www.nrcresearchpress.com by 210.87.254.42 on 09/05/12
For personal use only.

TABLE II

Fatty acid composition of some components of soft wheat flour

Fatty acid	Total lipid (%)	1-*O*-(6-*O*-Acyl-β-D-galactopyranosyl)-2,3-di-*O*-acyl-D-glyceritols (%)	Phytosteryl β-D-glucopyranosides (%)
Palmitic	17.5	20.4	20.6
Stearic	1.5	1.5	2.2
Oleic	11.5	8.8	10.7
Linoleic	65.6	65.5	61.3
Linolenic	3.2	2.9	2.5
Others	0.7	0.9	2.7

The impure sample of **5** was dissolved in chloroform–methanol (97:3 v/v) (10 ml) and the solution was applied to a silicic acid column (2.2 × 25 cm, Bio Rad −325 mesh) which had been equilibrated with the same solvent. The column was irrigated with this solvent (200 ml) followed by chloroform–methanol (95:5 v/v) (300 ml) during which fractions (20 ml each) were collected. Thin-layer chromatography with solvent *a* indicated that pure **5** was present in fractions 13–20. The syrup (0.060 g) had $[\alpha]_D^{23}$ − 21.4° (*c*, 1.2 in ethanol).

Compound **5** was treated with 1 *N* sulfuric acid in a sealed tube at 100° for 10 h after which the solution was neutralized with a small column of anion exchange resin and deionized with mixed resins. The effluent was evaporated to a colorless syrup (0.052 g) which consisted of glyceritol and 2,3,4-tri-*O*-methyl-D-galactose as indicated by paper chromatographic analysis (solvent *f*). The mixture was separated by preparative paper chromatography (Whatman No. 1 filter paper) with solvent *f* to give glyceritol (0.016 g) and 2,3,4-tri-*O*-methyl-D-galactose (0.030 g). The former was converted to the tri-*O*-*p*-nitrobenzoyl derivative, m.p. and mixture m.p. 194–197° (19) and the latter was converted to *N*-phenyl-2,3,4-tri-*O*-methyl-D-galactosylamine, m.p. and mixture m.p. 168–170° and $[\alpha]_D^{23}$ −60° (5 min) changing to +41° (24 h) (*c*, 1 in methanol) (20).

*Periodate Oxidation of 1-O-(6-O-Acyl-β-D-galactopyranosyl)-2,3-di-O-acyl-D-glyceritols (**1**) and 1-O-β-D-Galactopyranosyl-2,3-di-O-acyl-D-glyceritols*

Glycolipid group **1** (0.298 g) and authentic 1-*O*-β-D-galactopyranosyl-2,3-di-*O*-acyl-D-glyceritols were each dissolved in chloroform (25 ml) and methanol (40 ml) to which 0.08 *M* sodium periodate (15 ml) was added and the reaction mixtures were allowed to stand in the dark at room temperature for 70 h during which two moles of periodate per mole of glycolipid were consumed. Periodate uptake was measured spectrophotometrically by the method of Aspinall and Ferrier (21), allowance being made for the sodium iodate which crystallized almost quantitatively from the reaction mixture. The tri-*O*-acyl dialdehydes (**6**) obtained from **1** and the di-*O*-acyl dialdehydes (**6***a*) had R_f values of 0.8 and 0.3, respectively on t.l.c. with solvent *c*. Chloroform (100 ml) and water (100 ml) were added to the reaction mixture in a separatory funnel; the chloroform layer was removed and washed with water (2 × 25 ml). Evaporation of the chloroform solution provided the dialdehydes (**6**) (0.292 g) which had $[\alpha]_D^{23}$ −15° (*c*, 1.5 in chloroform).

The dialdehydes (**6**) were dissolved in ethanol (15 ml) to which sodium borohydride (0.2 g) was added and the mixture was allowed to stand at room temperature for 20 h. Aqueous 1 *N* sodium hydroxide (5 ml) was added to the borohydride reaction mixture to complete the saponification. After several hours water (100 ml) was added, the mixture was cooled, and the pH of the solution was adjusted to 2–3 with 1 *N* hydrochloric acid. After extraction of the aqueous solution with chloroform the pH was immediately readjusted to 7 with 1 *N* sodium hydroxide and evaporated to dryness. Approximately one-tenth of the residue of **7** and salt was treated three times with 1% methanolic hydrogen chloride to remove borate ions. During the third treatment the solution was refluxed for 2 h and evaporated to dryness as before. The residue was deionized with a column of mixed cation and anion exchange resins and the effluent was evaporated to dryness. Paper chromatographic analysis of the residual syrup indicated the presence of glyceritol; 1-*O*-β-D-galactopyranosyl-D-glyceritol was not detected.

The remaining nine-tenths of **7** and salt was suspended in pyridine (100 ml) to which acetic anhydride (50 ml) was added and the mixture heated at 100° for 2 h. The cooled reaction mixture was poured into ice water (600 ml) and after standing for several hours the aqueous solution was extracted with chloroform. The residual syrup (0.058 g) obtained after evaporation of the chloroform and pyridine consisted of 2-(R)-glyceritoxy-4-hydroxymethyl-(R)-diethylene glycol pentaacetate (**8**) as the major component with R_f value of 0.6 on t.l.c. with solvent *c* in addition to some minor impurities.

Pure **8** was obtained by silicic acid column chromatography as described previously for the purification of **5**. Benzene – diethyl ether (200 ml each of 90:10 and 80:20, v/v) irrigating solvents were used instead of the chloroform–methanol mixtures.

The pentaacetate (**8**) was dissolved in methanol (5 ml), sodium methoxide (1 mg) was added and the mixture was allowed to stand at room temperature overnight (22). Thin-layer chromatography with solvent *a* indicated that deacetylation was complete; compounds **7**, **8**, and glyceritol (standard) had R_f values of 0.16, 0.96, and 0.28, respectively.

Compound **7** was treated with 0.2 *N* sulfuric acid in a sealed tube at 100° for 2 h after which the solution was neutralized, deionized, and concentrated to approximately 5 ml. Sodium borohydride (0.05 g) was added to the aqueous solution and after standing for 16 h the excess sodium borohydride was decomposed with acetic acid

Can. J. Chem. Downloaded from www.nrcresearchpress.com by 210.87.254.42 on 09/05/12
For personal use only.

Can. J. Chem. Downloaded from www.nrcresearchpress.com by 210.87.254.42 on 09/05/12
For personal use only.

and the solution evaporated to dryness. The residue was treated three times with 1% methanolic hydrogen chloride at room temperature, the solution being evaporated between each treatment. The residue was dissolved in water and deionized in the usual manner. The glyceritol and ethylene glycol were separated by preparative paper chromatography and the respective compounds were identified as the tri-*O*-*p*-nitrobenzoate (m.p. and mixture m.p. 194–197° (19) and di-*O*-*p*-nitrobenzoate (m.p. and mixture m.p. 144–145°) derivatives (23).

The dialdehydes **6***a*, obtained by periodate oxidation of 1-*O*-β-D-galactopyranosyl-2,3-di-*O*-acyl-D-glyceritols, also yielded glyceritol and ethylene glycol when carried through the same reaction sequence.

*Identification of Phytosteryl 6-O-Acyl-β-D-glucopyranosides (**9**)*

Thin-layer chromatography (solvent *d*) of the material in fractions 120–150 (see Table I) indicated two components, phytosteryl 6-*O*-acyl-β-D-glucopyranosides (**9**) and monoglycerides, with R_f values of 0.25 and 0.48, respectively. Silicic acid column chromatography with mixtures of petroleum ether (b.p. 35–60°) – diethyl ether irrigating solvent failed to resolve this mixture. Therefore "dry column" chromatography (16) was used as follows. In a typical run the mixture of **9** and monoglycerides (0.3–0.4 g) was dissolved in diethyl ether and applied to the top of a dry column of silica gel H (2.2 × 37 cm). The column was irrigated with diethyl ether, maintaining a head of solvent 1–2 cm above the adsorbent. When the solvent front reached the bottom of the column irrigation was stopped. Three segments (3.5 cm each) from the top of the column were removed and washed with chloroform–methanol (90:10 v/v) to yield **9** (0.08–0.12 g).

Phytosteryl 6-*O*-acyl-β-D-glucopyranosides (**9**) (0.110 g) were saponified by the method described previously. Thin-layer chromatography with solvent *a* indicated that **9** (R_f 0.85) gave phytosteryl β-D-glucopyranosides (**10**) (R_f 0.65) and fatty acids in the saponification treatment. An ethanolic solution of the saponification products from **9** was passed through a column of Amberlite IRA-400 anion resin (OH^- form) and the effluent was evaporated to dryness. The residue (**10**) was treated with 4% methanolic hydrogen chloride (10 ml) in a sealed tube at 100° for 10 h after which the solution was passed through a column of anion resin and the effluent evaporated to dryness. The residue of methyl α- and β-D-glucoside and phytosterols was separated into the individual components by dissolution of the mixture in water and chloroform; evaporation of the chloroform layer provided the phytosterols. A portion of this material (5 mg) was treated with hexamethyldisilazane (0.5 ml) and trimethylchlorosilane (0.05 ml) in tetrahydrofuran to give the phytosterol trimethylsilyl derivatives. Gas–liquid chromatographic analysis of the mixture indicated the presence of β-sitosterol (74%), campesterol (19%), and an unknown component (7%).

The methyl α- and β-D-glucosides obtained by methanolysis of **10** were hydrolyzed with 1 *N* sulfuric acid to give D-glucose, m.p. and mixture m.p. 146° and $[\alpha]_D^{23}$ +52° (*c*, 1 in water).

*Methylation of Phytosteryl 6-O-Acyl-β-D-glucopyranosides (**9**)*

The glycolipid mixture **9** (0.65 g) was methylated three times by the method of Kuhn *et al.* (13) as described previously for **1** to give phytosteryl 2,3,4-tri-*O*-methyl-6-*O*-acyl-β-D-glucosides (**11**). The methylated products (**11**) were saponified in alkaline aqueous ethanol after which the solution was deionized with mixed cation resin and Amberlite IRA-400 anion resin (OH^- form). The effluent was evaporated to dryness. Thin-layer chromatography of the residue with solvent *b* revealed a major component with an R_f value of 0.56. This material was purified on a silicic acid column (2.2 × 44 cm) with petroleum ether – diethyl ether (200 ml of 70:30 and 200 ml of 50:50, v/v) irrigating solvent to give a mixture of crystalline phytosteryl 2,3,4-tri-*O*-methyl-β-D-glucosides (**12**). After recrystallization from petroleum ether – diethyl ether the mixture had m.p. 164–165° and $[\alpha]_D^{23}$ −28° (*c*, 1 in chloroform).

Anal. Calcd. for $C_{38}H_{66}O_6$ (β-sitosteryl 2,3,4-tri-*O*-methyl-β-D-glucoside): C, 73.75; H, 10.75.

Anal. Calcd. for $C_{37}H_{64}O_6$ (campesteryl 2,3,4-tri-*O*-methyl-β-D-glucoside): C, 73.46; H, 10.67. Found: C, 73.89; H, 10.79.

*Methanolysis of Phytosteryl 2,3,4-Tri-O-methyl-β-D-glucosides (**12**)*

The phytosteryl glycosides (**12**) (0.032 g) were treated with 4% methanolic hydrogen chloride (10 ml) in a sealed tube at 100° for 15 h, after which the solution was passed through a small column of anion exchange resin and the effluent evaporated to dryness (0.031 g). The residual mixture of phytosterols and methyl 2,3,4-tri-*O*-methyl-α- and β-D-glucosides was resolved on a column of silicic acid (2.2 × 25 cm) using chloroform and chloroform–methanol (98:2 v/v) irrigating solvents to elute the respective materials.

The phytosterols were converted to the trimethylsilyl ether derivatives and the mixture was examined by gas–liquid chromatography which indicated the presence of β-sitosterol (73%), campesterol (23%), and an unknown constituent (4%). Gas–liquid chromatographic analysis of the methyl glycosides indicated the presence of methyl 2,3,4-tri-*O*-methyl-α- and β-D-glucosides.

*Synthesis of Phytosteryl 2,3,4-Tri-O-methyl-β-D-glucosides (**12**)*

The phytosteryl β-D-glucopyranosides (0.356 g) in fractions 181–210 of the flour lipid fractionation (Table I) were treated with trityl chloride (0.36 g) in pyridine (5 ml) at 90° for 1 h. A few drops of water were added to the cooled reaction mixture and the whole was poured into ice water (25 ml). The aqueous solution was extracted with chloroform (2 × 25 ml) and the combined chloroform extracts were evaporated to dryness to give phytosteryl 6-*O*-trityl-β-D-glucopyranosides (**13**) as a syrup. The trityl compounds (**13**) were dissolved in dimethyl sulfoxide (17 ml) and dimethyl formamide (17 ml) to which barium oxide (5.7 g) and barium hydroxide (5.7 g) were added, and the reaction flask was flushed continuously with nitrogen. Methyl sulfate (12 ml) was added dropwise during 30 min to the stirred reaction mixture at 0° after which the temperature was slowly increased to 25° and stirring continued for 18 h. Ammonium hydroxide (9 ml) was added and after stirring for 30 min the mixture was extracted with chloroform (3 × 50 ml). The combined chloroform extracts were washed with water until the

washings were neutral and evaporated to give phytosteryl 2,3,4-tri-*O*-methyl-6-*O*-trityl-β-D-glucosides (**14**) (17).

The phytosteryl 2,3,4-tri-*O*-methyl-6-*O*-trityl-β-D-glucosides were dissolved in chloroform (10 ml) and treated with 4% methanolic hydrogen chloride (5 ml) at 0° for 30 min. Aqueous sodium bicarbonate (50 ml) and chloroform (100 ml) were added to the reaction mixture after which the chloroform solution was washed with water, dried (sodium sulfate), and evaporated to dryness. The residue was dissolved in petroleum ether – diethyl ether (70:30 v/v) and the mixture was applied to a silicic acid column (2 × 24 cm). Irrigation of the column with the above solvent eluted the trityl alcohol and when the solvent was changed to petroleum ether – diethyl ether (50:50 v/v) phytosteryl 2,3,4-tri-*O*-methyl-β-D-glucosides (**12**) (0.108 g) were obtained. After recrystallization from petroleum ether, the phytosteryl 2,3,4-tri-*O*-methyl-β-D-glucosides (**12**) had m.p. 164–165° (admixture of this material with **12** obtained from **9** did not depress the m.p.) and $[\alpha]_D^{23}$ −27° (*c*, 1 in chloroform).

Anal. Calcd. for $C_{38}H_{66}O_6$ (β-sitosteryl 2,3,4-tri-*O*-methyl-β-D-glucoside): C, 73.75; H, 10.75.

Anal. Calcd. for $C_{37}H_{64}O_6$ (campesteryl 2,3,4-tri-*O*-methyl-β-D-glucoside): C, 73.46; H, 10.67. Found: C, 73.67; H, 10.76.

Acknowledgments

The helpful discussions and suggestions of Professor H. E. Carter and N. R. Artman are gratefully acknowledged. The author thanks L. R. Chapman for performing the gas–liquid chromatographic analyses and Mrs. B. Jackson and D. Etson for technical assistance.

1. C. H. Bailey. The constituents of wheat and wheat products. Reinhold Publishing Corp., New York. 1944.
2. D. K. Mecham. *In* Wheat: chemistry and technology. Vol. I. Hlynka. (*editor*). Chap. 8. American Association of Cereal Chemists, Inc., St. Paul, Minnesota. 1964.
3. D. V. Myhre. Abstracts 149th Am. Chem. Soc. Meeting, Detroit, Michigan. 1965.
4. D. V. Myhre. Unpublished results.
5. E. Heinz. Z. Naturforsch. **20***b*, 83 (1965).
6. M. Lepage. J. Lipid Res. **5**, 587 (1964).
7. M. E. McKillican. J. Am. Oil Chem. Soc. **41**, 554 (1964).
8. H. E. Carter, K. Ohno, S. Nojima, C. L. Tipton, and N. Z. Stanacev. J. Lipid Res. **2**, 215 (1961).
9. J. Hirsch and E. H. Ahrens, Jr. J. Biol. Chem. **233**, 311 (1958).
10. H. E. Carter, R. A. Hendry, and N. Z. Stanacev. J. Lipid Res. **2**, 223 (1961).
11. B. Wickberg. Acta Chem. Scand. **12**, 1183 (1958).
12. B. Wickberg. Acta Chem. Scand. **12**, 1187 (1958).
13. R. Kuhn, H. Trischmann, and I. Löw. Angew. Chem. **67**, 32 (1955).
14. R. S. Cahn, C. K. Ingold, and V. Prelog. Experientia, **12**, 81 (1956).
15. P. A. J. Gorin, L. Hough, and J. K. N. Jones. J. Chem. Soc. 2699 (1955).
16. B. Loev and K. M. Snader. Chem. and Ind. London, 15 (1965).
17. R. Kuhn and H. Trischmann. Chem. Ber. **96**, 284 (1963).
18. R. G. Strobel. Ph.D. Thesis. Maximilians University, Munich, Germany. 1957.
19. R. Jacquemain and A. Muskovits. Compt. Rend. **202**, 497 (1936).
20. J. C. Irvine and E. L. Hirst. J. Chem. Soc. **121**, 1213 (1922).
21. G. O. Aspinall and R. J. Ferrier. Chem. and Ind. London, 1216 (1957).
22. G. Zemplén. Chem. Ber. **59**, 1254 (1926).
23. I. Heilbron. Dictionary of organic compounds. Vol. II. Oxford University Press, New York. 1953.

Can. J. Chem. Downloaded from www.nrcresearchpress.com by 210.87.254.42 on 09/05/12
For personal use only.

Can. J. Chem. Downloaded from www.nrcresearchpress.com by 210.87.254.42 on 09/05/12
For personal use only.

Electrophoresis of dyed polysaccharides on cellulose acetate[1]

W. F. DUDMAN[2] AND C. T. BISHOP
Division of Biosciences, National Research Council of Canada, Ottawa, Canada

Received May 29, 1968

Polysaccharides have been shown to react with Procion dyes to give colored products. The degree of substitution varies with the dye to polysaccharide ratio used in the reaction and with the structure of the polysaccharide. The dyed polysaccharides give visible bands on gel filtration and on electrophoresis on cellulose acetate strips. Separations of mixtures of colored polysaccharides by the latter method are complete within 5 min and match the results obtained with the undyed polysaccharides by free-boundary, Tiselius electrophoresis.

Canadian Journal of Chemistry, **46**, 3079 (1968)

Studies of polysaccharide structures can only be meaningful when there is some assurance that the product examined is chemically homogeneous. There are no standard methods for the purification of polysaccharides and no generally applicable method for following a purification process. Most polysaccharides are polymolecular and methods of separation based on differences in molecular weight are therefore of limited value. The more successful techniques for resolving mixtures of polysaccharides depend upon differences in their chemical properties arising from variations in structure (1). Undoubtedly the most sensitive analytical method for assessing chemical homogeneity of polysaccharides is precipitation with specific antisera (2, 3). However, antisera specific for the particular polysaccharides being investigated may not be readily available.

Probably the most generally useful and selective method for resolving mixtures of polysaccharides is electrophoresis in borate buffer. Polysaccharides with different structures form complexes with borate to different extents thereby acquiring different charge:mass ratios that permit their separation in an electric field. Northcote (4) has described the electrophoretic separation of polysaccharides by the free-boundary (Tiselius) method and on glass columns (5); separations have also been obtained by electrophoresis on filter paper (6) and on glass-fiber sheets (7, 8). All of these techniques have some inherent disadvantages. Free-boundary electrophoresis requires complex equipment and is very time consuming. Detection of polysaccharides on filter paper is difficult because the cellulose support has the same properties as the samples. Glass-fiber paper has a loose matrix that leads to high rates of endosmotic flow in alkaline buffers; polysaccharides tend to streak and diffuse on this support.

The present paper describes a method for the electrophoresis of polysaccharides that overcomes most of the foregoing disadvantages. The use of dyed polysaccharides eliminates the problem of detection. Separations are obtained on cellulose acetate strips with simple, inexpensive equipment, and are complete in 4 min. The separations obtained match those given by the free-boundary method.

The development of reactive dyes has been described by Coffey (9). One group of these, the Procion dyes (Imperial Chemical Industries, Ltd.), have the following general structure (**1**).

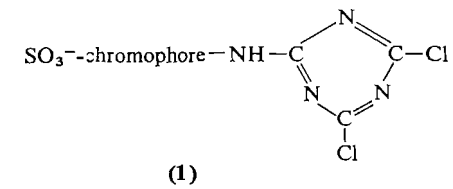

(1)

The dichlorotriazinyl group will react with hydroxyl, amino, or amide groups to form stable, covalent linkages between the dye and substrate. Although the products could be regarded as esters (of a modified cyanuric acid) they bear a closer resemblance to ethers in their stability towards acid and alkali. Procion dyes have been used as staining reagents to detect and estimate proteins on electrophoresis strips (10) but have been used with carbohydrates to only a limited extent. Cellodextrins have been dyed

---

[1]Issued as NRCC No. 10240.

[2]Visiting Scientist, 1967–1968. Permanent address: Division of Plant Industry, C.S.I.R.O., Canberra, Australia.

TABLE I

Effect of dye:polysaccharide ratio on color intensity in dyed glucan

Dye (mg)*	Dye:polysaccharide ratio	$E^{1cm}_{1\%}$†	Dye content of polysaccharide (%)‡	% of total dye bound	Number of anhydroglucose units per dye substituent
		(a) Procion blue 3GS			
2.5	1:20	1.92	2.8	59	133
5	1:10	2.55	3.7	41	100
12.5	1:4	8.38	12.2	61	27.6
25	1:2	14.39	20.9	63	14.5
50	1:1	22.90	33.4	67	7.7
		(b) Procion red 2BS			
50	1:1	44.6	27.1	54	10.6

*Used with 50 mg of glucan from *C. parapsilosis*.
†Absorption measured at 605 mμ for blue, and 530 mμ for red.
‡$E^{1cm}_{1\%}$ for Procion blue 3GS = 68.7, for Procion red 2BS = 164.2.

and the products used as substrates for cellulolytic enzymes (11). Chitin, chitosan, and xylan have also been dyed (12) and it was reported that glucose reacts with a Procion dye to give a glucoside (13). It therefore seemed clear that polysaccharides could be dyed successfully with these reactive dyes. It also seemed likely that a low degree of substitution would introduce sufficient color to make the products visible, but would not affect the chemical properties upon which separation of the polysaccharides depends.

Examination of the absorption spectra of four Procion dyes (blue 3GS, red 2BS, yellow RS, and orange GS) showed that the blue and the red would be easiest to detect on cellulose acetate strips. The extinction coefficient ($E^{1cm}_{1\%}$) for Procion blue 3GS at 605 mμ was 68.5 and that of Procion red 2BS at 530 mμ was 164.2.

As there were no differences in the visible spectra of the dyes when free or bound to polysaccharides, it was possible to determine the dye content of the colored polysaccharides by comparison of extinction coefficients at the appropriate wave lengths. From the dye content, the number of anhydrohexose units (molecular weight, 162) per dye molecule attached was given by the term $M\,(100-d)/162d$ where d is the percentage of dye in the colored polysaccharide and M is the molecular weight of the dye (641 for Procion red 2BS and 621 for Procion blue 3GS).

The dyeing procedure followed was essentially the same as that recommended for the dyeing of textiles with these dyes (14). The colored polysaccharides were readily separated from unreacted dye and inorganic salts by gel filtration through Sephadex G-15 or G-25 and were recovered from the eluates by freeze-drying.

Preliminary experiments showed that strongly colored polysaccharides were required to give bands that were sufficiently visible on cellulose acetate strips. A glucan from *C. parapsilosis* (15) was found to react well with the dyes and it was used, with Procion blue 3GS, to study the effect of dye to polysaccharide ratio on the intensity of color in the product. The results of this study are given in Table I. It was further noted that the polysaccharide reacted with only some 40–67% of the total dye available, regardless of the initial dye to polysaccharide ratio. Electrophoresis on cellulose acetate strips (0.05 *M* borate buffer) showed that mobilities of the dyed glucans increased only slightly with increasing dye content. For example, the difference in mobility was not enough to permit the separation of the most highly colored from the least highly colored sample. Since the more highly colored glucans gave bands that were readily visible on cellulose acetate strips, the effects of higher dye to polysaccharide ratios than those shown in Table I were not investigated. A dye to polysaccharide ratio of 1:1 was used as a standard procedure to provide dyed polysaccharides with strong colors for maximum sensitivity in electrophoresis.

A variety of polysaccharides were dyed with the red and the blue dyes by this procedure. The incorporation of dye into these polysaccharides is shown in Table II and was found to vary with the nature of the polysaccharide. Thus, the pectin (a pure galacturonan) was completely resistant to the dyes and the *R. trifolii* polysaccharide, which contains some 30% of uronic acid, was dyed only to a slight extent. It seems likely that this low reactivity of polyuronides

Can. J. Chem. Downloaded from www.nrcresearchpress.com by 210.87.254.42 on 09/05/12
For personal use only.

TABLE II

Extent of reaction of Procion red 2BS and Procion blue 3GS with equal weights of polysaccharides

Polysaccharide*	$E^{1cm}_{1\%}$		Dye content		Anhydrohexose units per dye substituent	
	Red	Blue	Red	Blue	Red	Blue
Sunflower pectin	0	0	0	0	—	—
R. trifolii TA1 polysaccharide	4.75	1.68	2.9	2.5	135	151
C. albicans mannan	18.4	10.1	11.3	14.7	31.0	22.3
T. sabouraudi galactomannan I	19.8	16.9	12.1	24.6	28.8	11.7
E. floccosum galactomannan I	24.3	15.6	14.8	22.7	22.9	13.1
Larch arabinogalactan	32.9	19.6	20.1	20.5	15.3	9.6
E. floccosum galactomannan II + glucan	37.5	21.1	22.9	30.6	13.4	8.7
T. sabouraudi glucan	51.5	14.7	31.5	21.4	8.6	14.2
T. sabouraudi galactomannan II	62.3	23.6	38.0	34.3	6.5	7.3
M. quinckeanum glycopeptide	68.0	27.0	41.5	39.4	5.6	5.9

*Sources of polysaccharides are given in the Experimental section.

with the dyes is due to the absence of primary hydroxyl groups. As might be expected from their structures, these dyes react more readily with primary than with secondary hydroxyl groups (14). Conversely, the more highly dyed polysaccharides, shown in Table II, have a greater proportion of primary hydroxyl groups available for substitution. Except for the pectin, all of the dyed polysaccharides listed in Table II were sufficiently colored to allow their electrophoretic behavior to be examined.

Because the samples were visible, it was a simple matter to experiment with variables to establish the most favorable conditions for electrophoresis. Variation of buffer strength showed that improved results were obtained at high molarity. The sharpest bands were obtained in a buffer (pH 9.3) that was 0.1 *M* with respect to both sodium tetraborate and sodium chloride. Using this buffer, potential gradients of 25–35 V/cm gave better separations than 10 V/cm and the resolution was not improved by increasing the voltage to 500 V/cm. Separations were complete in 3–5 min and were not improved by extending this time. Indeed, after 10 min the bands tended to diffuse and any separation already obtained became distorted. Cellulose acetate strips provided the only satisfactory support for electrophoresis. In both agar and polyacrylamide gels the dyed polysaccharides moved as broad bands and mixtures were not resolved; similar poor results were obtained on filter paper and on glass-fiber paper. The optimum conditions for electrophoresis of the dyed polysaccharides were therefore at potential gradients of 25–35 V/cm on cellulose

TABLE III

Electrophoretic mobilities of dyed polysaccharides relative to mobility of free dye*

Polysaccharide	Relative electrophoretic mobility		Number of bands	Number of components by free-boundary electrophoresis
	Red	Blue		
R. trifolii TA1 polysaccharide	0	0	1	1
C. parapsilosis glucan	0.21	0.19	1	1
C. albicans mannan	0.43	0.43	1	1
T. sabouraudi galactomannan I	0.55	0.51	1	1
E. floccosum galactomannan I	0.47	0.52	1	1
Larch arabinogalactan	0.63	0.65	1	—
E. floccosum galactomannan II	0.32	0.34	2	2
+ glucan	0.49	0.51		
T. sabouraudi glucan	0.38	0.39	1	—
T. sabouraudi galactomannan II	0.50	0.48	1	—
M. quinckeanum glycopeptide	0	0	3	3
	0.45	0.40		
	0.59	0.55		

*On cellulose acetate strips in 0.1 *M* sodium tetraborate – sodium chloride, potential gradient 25 V/cm for 4 min.

Can. J. Chem. Downloaded from www.nrcresearchpress.com by 210.87.254.42 on 09/05/12
For personal use only.

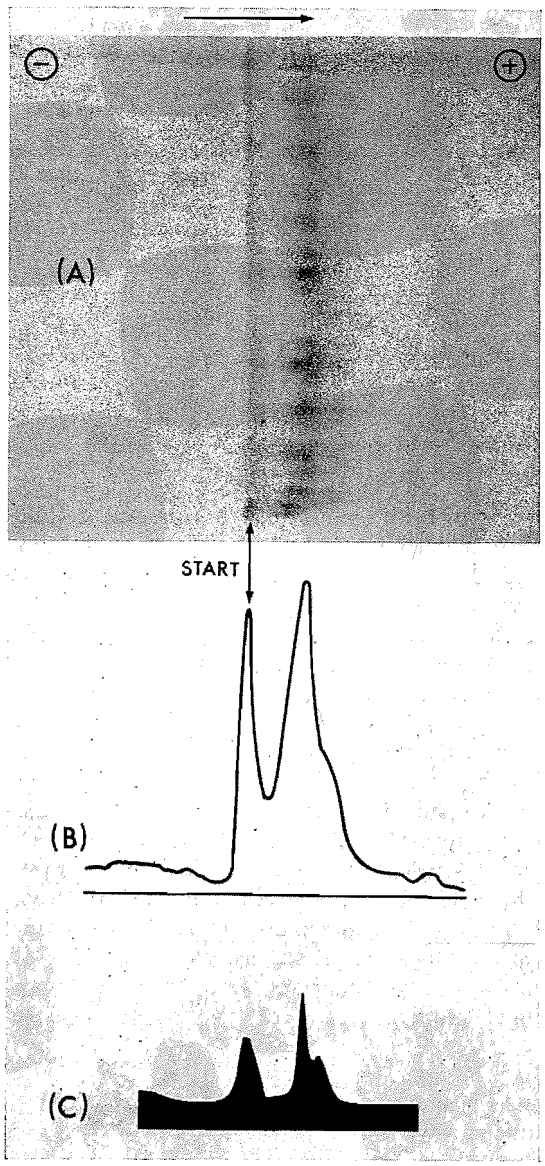

FIG. 1. Electrophoresis of *M. quinckeanum* glycopeptide. (A) Appearance of glycopeptide dyed with Procion red 2BS after 4 min electrophoresis on cellulose acetate strip in 0.1 *M* sodium tetraborate–sodium chloride, potential gradient 25 V/cm. (B) Densitometer scan of (A). (C) Schlieren pattern from free-boundaryel ectrophoresis of undyed *M. quinckeanum* glycopeptide in 0.05 *M* sodium tetraborate.

acetate strips for 3–5 min in 0.1 *M* sodium tetraborate–sodium chloride buffer. A one percent aqueous solution of the dyed polysaccharide was the most suitable concentration for samples applied as a thin streak. At concentrations of 5% the bands became distorted because of overloading.

The mobilities of the various colored polysaccharides were measured relative to that of the corresponding free dye and the results are given in Table III. Most of the colored polysaccharides were electrophoretically homogeneous and contained only one component that migrated as a single band. However, the mixture of the galactomannan II and glucan from *E. floccosum* separated into two bands and the glycopeptide preparation from *M. quinckeanum* gave three bands, one of which had no mobility. As described in the Experimental section, many of the polysaccharides listed in Tables II and III had been examined previously by free-boundary electrophoresis. The number of components detected by each method was the same. The cellulose acetate strip that held the three components separated by electrophoresis of the red-colored glycopeptide fraction was cleared in paraffin and the absorption of the bands was scanned in a densitometer. As shown in Fig. 1, the plot obtained was very similar to that given by free-boundary electrophoresis of the undyed glycopeptide fraction.

The values obtained for the relative mobilities (Table III) indicated that mixtures of some of these dyed polysaccharides should be resolvable by electrophoresis. Ten mixtures of pairs of dyed polysaccharides were made; both a red and a blue series of mixtures were prepared to see if one color was more advantageous than the other. The results of electrophoresis of these mixtures are given in Table IV. Eight of the mixtures were separated into their two components, all within 4 min. The two mixtures that were not resolved contained components whose relative mobilities differed by only 0.08–0.14. Nevertheless, one mixture with differences in mobilities in this range was effectively separated: the galactomannan II and glucan mixture from *T. sabouraudi*. The separation of one of the mixtures is shown in Fig. 2 and is typical of those in which two bands were obtained. The red and the blue mixtures gave identical results and there was no reason to prefer one color over the other.

The results presented here show that electrophoresis of dyed polysaccharides on cellulose acetate strips permits a rapid assessment of chemical homogeneity in polysaccharides with the same degree of resolution as obtained in free-

Can. J. Chem. Downloaded from www.nrcresearchpress.com by 210.87.254.42 on 09/05/12
For personal use only.

TABLE IV

Electrophoretic separation of mixtures of dyed polysaccharides*

Mixture	Difference in relative mobilities†		Result
	Red	Blue	
C. parapsilosis glucan + larch arabinogalactan	0.42	0.46	2 bands
C. parapsilosis glucan + *T. sabouraudi* galactomannan I	0.34	0.33	2 bands
C. parapsilosis glucan + *T. sabouraudi* galactomannan II	0.29	0.29	2 bands
Larch arabinogalactan + *T. sabouraudi* glucan	0.25	0.26	2 bands
C. parapsilosis glucan + *C. albicans* mannan	0.22	0.24	2 bands
C. albicans mannan + larch arabinogalactan	0.20	0.22	2 bands
T. sabouraudi galactomannan II + *T. sabouraudi* glucan	0.12	0.11	2 bands
C. parapsilosis glucan + *T. sabouraudi* glucan	0.17	0.20	2 bands (poorly separated)
Larch arabinogalactan + *T. sabouraudi* galactomannan I	0.08	0.14	1 band (not separated)
C. albicans mannan + *T. sabouraudi* galactomannan I	0.12	0.08	1 band (not separated)

*On cellulose acetate strips in 0.1 *M* sodium tetraborate – sodium chloride, potential gradient 25 V/cm for 4 min.
†From values given in Table III.

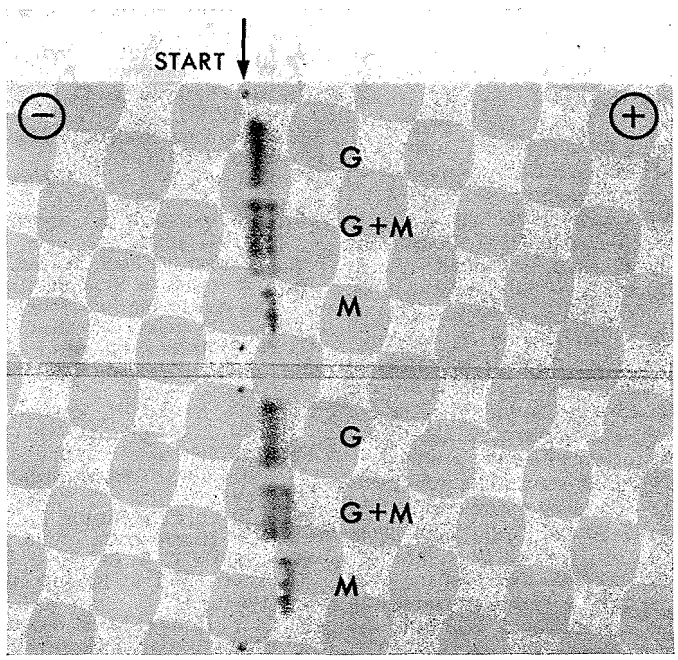

FIG. 2. Electrophoretic separation of *C. albicans* mannan (M) and *C. parapsilosis* glucan (G) on cellulose acetate strip in 0.1 *M* sodium tetraborate–sodium chloride, potential gradient 25 V/cm, for 3 min. Top strip: blue-dyed polysaccharides; bottom strip: red-dyed polysaccharides.

boundary, Tiselius electrophoresis. Such colored polysaccharides can be used also to observe or monitor the behavior of the parent polysaccharide in gel filtration or in other chromatographic systems.

Experimental

Polysaccharides

The polysaccharides used in this study were samples that were available in this laboratory. Structural investigations of the *C. parapsilosis* glucan and the *C. albicans* mannan have been published (15, 16). The

Can. J. Chem. Downloaded from www.nrcresearchpress.com by 210.87.254.42 on 09/05/12
For personal use only.

Can. J. Chem. Downloaded from www.nrcresearchpress.com by 210.87.254.42 on 09/05/12
For personal use only.

galactomannan I, galactomannan II, and glucan from *T. sabouraudi* and *E. floccosum* are under investigation now. These polysaccharides have structures that are very similar to the same series of polysaccharides from other dermatophytes (17–19), and were isolated in the same way. The *R. trifolii* polysaccharide is also under investigation at the present time and so is the glycopeptide from *M. quinckeanum*. The latter product was extracted from the cultured mycelium by ethylene glycol as described previously for isolation of the trichophytin antigen from *T. mentagrophytes* (20, 21). The results of free-boundary electrophoresis given in Table III were obtained with a Tiselius-type, Spinco model H apparatus; the buffer used was 0.05 *M* sodium tetraborate (4).

Dyeing Procedure

To a solution of the polysaccharide (50 mg) in water (5.0 ml) was added a freshly prepared solution of the dye (50 mg) in water (5 ml). After 5 min sodium chloride was added, either as a solid or as 1 ml of a concentrated solution, to give a final concentration of 2%. Thirty minutes later sodium carbonate was added to give a final concentration of 0.1%. This was essentially the procedure used for dyeing textiles (14) and the reaction is thought to be complete within an hour. However, the mixtures were set aside for 18 h (overnight) to allow most of the unreacted dye to be hydrolyzed.

Initial attempts to free the colored polysaccharides from inorganic salts and unreacted dye by dialysis were unsuccessful because the dye did not pass through the dialysis membrane. Gel filtration was a satisfactory alternate procedure. The reaction mixtures were clarified by centrifugation or diluted to reduce viscosity if neces sary and were then added directly to columns (2.5 × 30 cm) of Sephadex G-15 or G-25. Elution of the columns with water produced two widely separated colored zones. The dyed polysaccharides, excluded from the gels, were eluted in the void volume; salts and unreacted dye were retarded. To avoid contamination by inorganic salts, which were eluted more rapidly than the unreacted dye, care was taken to collect only the strongly colored portion of the polysaccharide eluate. Addition of the dye to the polysaccharides apparently increased their solubility and it was difficult to precipitate the products by ethanol or acetone. The dyed polysaccharides were therefore recovered from the eluates by freeze-drying. The amounts recovered were 45–50 mg, 90–100% of initial polysaccharide.

Visible absorption spectra of the dyes and the dyed polysaccharides were measured with a Cary model 14 recording spectrophotometer and were identical. Extinction coefficients were determined with a Beckman DU spectrophotometer.

Electrophoresis

The Gelman Sepraphore III cellulose acetate strip (2.5 × 17 cm) was soaked in the buffer solution for 5 min. The strip was then pressed between two sheets of Whatman 3 MM filter paper to remove excess buffer and the starting line was marked with a pencil. Samples (1% solutions) were applied as thin lines by using fine glass capillaries. The strip was then positioned in a Gelman Electrophoresis chamber so that the starting line was midway between the terminals which were 10 cm apart. Voltage was applied, 250–350 V, 7 mA, and migration of the bands was followed visibly. Solutions (1%) of unreacted dyes that had been kept for 24 h were used as standards to measure the relative mobilities given in Table III. The optimum time for all separations was 4 min and higher potential gradients (up to 500 V/cm) gave no improvement over the conditions cited above. Poorer results were obtained when the starting line was positioned nearer to either terminal. Broader bands were obtained in 0.01 *M* or 0.05 *M* sodium tetraborate than in the 0.1 *M* sodium tetraborate–sodium chloride buffer.

When the electrophoresis was finished the strips were removed and dried immediately in a stream of hot air. If this was not done, the bands diffused and became distorted. The dried strips could then be pressed between sheets of filter paper to flatten them prior to photography or gel-scanning.

1. H. O. Bouveng and B. Lindberg. Advan. Carbohydrate Chem. **15**, 53 (1960).
2. M. Heidelberger. Fortschr. Chem. Org. Naturstoffe, **18**, 503 (1960).
3. M. Heidelberger. Federation Proc. **23**, 627 (1964).
4. D. H. Northcote. Biochem. J. **58**, 353 (1954).
5. B. J. Hocevar and D. H. Northcote. Nature, **179**, 488 (1957).
6. I. A. Preece and R. Hobkirk. Chem. and Ind. London, 257 (1955).
7. E. J. Bourne, A. B. Foster, and P. M. Grant. J. Chem. Soc. 4311 (1956).
8. D. R. Briggs, E. F. Garner, and F. Smith. Nature, **178**, 154 (1956).
9. S. Coffey. Chem. and Ind. London, 132 (1960).
10. S. Fazekas de St. Groth, R. G. Webster, and A. Datyner. Biochim. Biophys. Acta, **71**, 377 (1963).
11. H. N. Fernley. Biochem. J. **87**, 90 (1963).
12. G. E. Krichevsku and F. I. Sadov. Izv. Vysshikh Uchebn. Zavedenii Tekhnol. Tekstil'n. Prom. **3**, 102 (1961).
13. O. A. Stamm, H. Zollinger, and E. Gaeumann. Helv. Chim. Acta, **44**, 1123 (1961).
14. E. R. Trotman. Dyeing and chemical technology of textile fibres. Charles Griffin and Co., Ltd., London. 1964.
15. R. J. Yu, C. T. Bishop, F. P. Cooper, F. Blank, and H. F. Hasenclever. Can. J. Chem. **45**, 2264 (1967).
16. R. J. Yu, C. T. Bishop, F. P. Cooper, H. F. Hasenclever, and F. Blank. Can. J. Chem. **45**, 2205 (1967).
17. C. T. Bishop, M. B. Perry, F. Blank, and F. P. Cooper. Can. J. Chem. **43**, 30 (1965).
18. C. T. Bishop, M. B. Perry, and F. Blank. Can. J. Chem. **44**, 2291 (1960).
19. C. T. Bishop, M. B. Perry, R. K. Hulyalkar, and F. Blank. Can. J. Chem. **44**, 2299 (1966).
20. R. C. Codner, C. N. D. Cruickshank, M. D. Trotter, and S. R. Wood. Sabouraudia, **1**, 116 (1961).
21. S. A. Barker, C. N. D. Cruickshank, J. H. Morris, and S. R. Wood. Immunology, **5**, 627 (1962).

Can. J. Chem. Downloaded from www.nrcresearchpress.com by 210.87.254.6 on 09/05/12
For personal use only.

Glycosidation of sugars. IV. Methanolysis of D-glucose, D-galactose, and D-mannose[1]

V. SMIRNYAGIN[2] AND C. T. BISHOP
Division of Biosciences, National Research Council of Canada, Ottawa, Canada

Received April 25, 1968

Rates of methanolysis reactions of D-glucose, D-galactose, and D-mannose have been determined. The results confirm those found earlier for pentoses that the glycosidation reaction proceeds to equilibrium through four distinguishable competing reactions: (*1*) hexose → furanosides, (*2*) anomerization of furanosides, (*3*) furanosides → pyranosides, and (*4*) anomerization of pyranosides. The glycoside compositions at equilibrium are interpreted in terms of conformational analysis for furanoid and pyranoid rings. The energy differences between the ground states also contribute to an important degree in determining the relative rates of reaction.

Canadian Journal of Chemistry, 46, 3085 (1968)

Earlier papers (1, 2) in this series described a study of the kinetics of methanolysis of the four D-pentoses and summarized the literature on this topic. The present paper reports the extension of these studies to the three hexoses, D-glucose, D-galactose, and D-mannose.

The conditions cited for the reactions were carefully controlled and products were analyzed by gas–liquid chromatography of their fully trimethylsilylated derivatives as described previously (3). Products in one of the reactions in the D-galactose series (Table VII) were analyzed colorimetrically (4) after separation by paper chromatography (5).

As with the pentoses, it was found that methanolysis proceeds to equilibrium through four distinguishable competing reactions and it was possible to establish conditions under which a single reaction predominated. Since the observations were made at constant hydrogen ion concentrations, the bimolecular reaction could be expressed in terms of first-order rate kinetics. Compositions of reaction products at different times under specific conditions are given in Tables V–VIII (see Experimental). These results show that single reactions predominated during the early periods and were characterized reasonably well by first-order rate constants. The rate constants indicated in Tables V–VIII were averaged to give the k values in Table I. As before (2), the first-order rates for reactions *3* (Table VII) and *4* (Table VIII) were reduced to 1/10 and 1/100 respectively to provide k_1 values comparable to those for reactions *1* and *2*, all relative to 0.01% of hydrogen chloride in methanol. The equilibrium constants (K) in Table I were obtained from glycoside compositions after prolonged reaction periods (Table II).

Reliable rate data for reaction *1* (Table V) could only be obtained with D-glucose; D-galactose and D-mannose were not sufficiently soluble in methanol at the concentrations used. No detailed interpretation of reaction *1* can be offered on the evidence available; the reaction was examined only to establish the identities of the initial products. Qualitative examination of the products from methanolysis of galactose confirmed the results obtained with D-glucose that furanosides were the initial products in this reaction. For D-mannose, the initial product of methanolysis was methyl β-D-mannopyranoside. This result is similar to that found earlier for the stereochemically equivalent lyxose which also gave pyranosides as initial products in methanolysis (2). Two recent reports (6, 7) have discussed the role of dimethyl acetals as intermediates in the formation of furanosides from glycoses during methanolysis. The amounts of dimethyl acetals found were small and from rate studies it was concluded that they were not intermediates in the glycosidation reaction. In the present investigation dimethyl acetals were not detected, presumably because the methods of analysis were not as sensitive as the radioactive isotope techniques used in the other studies (6, 7).

If the non-bonded interactions in the hexofuranosides are relieved in the transition states for anomerization and ring expansion, and if the energies of the transition states are near equal, then the relative orders of reactivity for the three hexoses should be the same in reactions *2*

[1]Issued as NRCC No. 10209.
[2]NRCC Postdoctorate Fellow, 1966–1968.

Can. J. Chem. Downloaded from www.nrcresearchpress.com by 210.87.254.6 on 09/05/12
For personal use only.

TABLE I

Rate constants of methanolysis reactions*

Reaction	D-Glucose				D-Galactose				D-Mannose			
	k_1	k_2	k_1+k_2	K	k_1	k_2	k_1+k_2	K	k_1	k_2	k_1+k_2	K
1. Hexose $\xrightarrow{k_1}$ furanosides	5.7	—	—	—	—	—	—	—	—	—	—	—
2. Furanoside $\underset{k_2}{\overset{k_1}{\rightleftarrows}}$ β	8.7	5.8	14.5	1.5	2.3	0.9	3.2	2.5	Very small	8.5	—	—
3. Furanosides $\underset{k_2}{\overset{k_1}{\rightleftarrows}}$ pyranosides	0.036	9×10^{-6}	—	3980	0.027—0.042	2.2×10^{-4}—3.7×10^{-4}	—	112	0.47	Very small	—	Very large
4. Pyranoside: β $\underset{k_2}{\overset{k_1}{\rightleftarrows}}$ α	0.013	0.006	0.019	2.01	0.031	0.011	0.042	2.93	0.054	0.003	0.057	17.4

*Reaction *2*: $K = [\beta]/[\alpha]$; reaction *3*: $K = [\alpha\text{-pyr}][\beta\text{-pyr}]/[\alpha\text{-fur}][\beta\text{-fur}]$; reaction *4*: $K = [\alpha]/[\beta]$. Concentrations of products for these calculations were taken from the equilibrium values given in Table II. The k_1 values for reactions *3* and *4* were normalized (reduced by 10^{-1} and 10^{-2} respectively) to make them relative to the same acid concentration that was used in reaction *2*.

Can. J. Chem. Downloaded from www.nrcresearchpress.com by 210.87.254.6 on 09/05/12
For personal use only.

and *3* (Table I) and should be as follows: mannose > glucose > galactose. Thus, the mannofuranosides with two adjacent eclipsed interactions should be the most reactive (see k_1 values, reaction *3*). The glucofuranosides, with one eclipsed interaction, should be less reactive than the mannofuranosides but more reactive than the galactofuranosides in which there are no such interactions. A reliable rate constant could not be obtained for reaction *3* in the galactose series, possibly because the reverse reaction (pyranosides → furanosides) was proceeding to a significant extent. However, the values obtained (Table VII) showed that galactofuranosides reacted at a rate that was slower or equal to that of the glucofuranosides.

In the furanoside form the three hexoses should adopt the conformations described in detail previously (2). In these conformations the anomerization of furanosides introduces or removes an eclipsed interaction and, assuming as before that ground state energies have an important influence on reaction rates, the relative reactivities of the anomeric pairs in each series should be as follows: D-mannose, $\beta \gg \alpha$; D-glucose, $\alpha \geq \beta$; D-galactose, $\alpha > \beta$. The rate constants, k_1 and k_2 (Table I) are in agreement with this prediction. In the mannofuranosides the β-anomer has all large groups eclipsed and should be much more reactive than the α-anomer. In fact, k_1 could not be determined for this reaction because the α-furanoside was stable under the conditions of reaction *2* and there was none of the β-furanoside at equilibrium. The α-anomer in the galactofuranosides has one eclipsed interaction and the β-anomer none; the former should therefore be more reactive as was indeed found. Assuming that the glucofuranosides adopt the same conformation as proposed for the xylofuranosides (2), the C_2—hydroxyl bond very nearly bisects the angle made by the bonds of the anomeric substituents, being oriented slightly more toward the α-position. This accounts for the slightly greater rate of anomerization of the α-form, a result that is the same as found for the D-xylofuranosides (2).

The relative reactivities in the hexopyranosides can also be rationalized on the assumption that the energy differences between the ground states are rate-controlling. The principles of conformational analysis of pyranoside rings are well known (8) and need not be discussed here. On this basis, the relative orders of reactivities for the three hexopyranosides should be mannose > galactose > glucose and the rate data agree ($k_1 + k_2$, reaction *4*, Table I). Similar reasoning predicts that the β-anomers will be more reactive than the α-anomers in this reaction and again the data are in agreement.

The glycoside compositions at equilibrium are shown in Table II and the free energies, calculated from the equilibrium constants are given in Table III. The latter values reflect the relative stabilities of the compounds concerned. The anomerization of glucofuranosides involves no strong interactions, only replacement of one skew interaction by another, and this reaction would be expected to have a small ΔF. Anomerization of the galactofuranosides introduces or removes an eclipsed interaction in a flexible conformation. The free energy for that reaction should therefore be greater than for the glucofuranosides but less than for the mannofuranosides where anomerization introduces a third eclipsed substituent.

TABLE II

Glycoside compositions at equilibrium*

	Furanoside		Pyranoside	
Sugar	α	β	α	β
D-Glucose	0.6	0.9	65.8	32.7
D-Galactose	6.2	16.3	57.8	19.7
D-Mannose	0.7	0.0	93.9	5.4

*Sugar (2%) in 1% methanolic hydrogen chloride at 35 °C until composition was constant; no change upon heating to 64 °C.

TABLE III

Free energies for methanolysis of hexoses

Reaction	ΔF (reaction) (cal/mole)
Glucose	
α-furanoside ⇄ β-furanoside	−248
furanoside ⇄ pyranoside	−5100
α-pyranoside ⇄ β-pyranoside	427
Galactose	
α-furanoside ⇄ β-furanoside	−592
furanoside ⇄ pyranoside	−2880
α-pyranoside ⇄ β-pyranoside	660
Mannose	
α-furanoside ⇄ β-furanoside	Very large
furanoside ⇄ pyranoside	Very large
α-pyranoside ⇄ β-pyranoside	1730

The ΔF of reactions for the furanoside → pyranoside conversions reflects the relative stabilities of the two ring forms. In galactofuranosides only the α-anomer has an eclipsed

Can. J. Chem. Downloaded from www.nrcresearchpress.com by 210.87.254.6 on 09/05/12
For personal use only.

interaction and it is easily relieved. However, the galactopyranosides have an axial hydroxyl. The free energy for ring conversion should therefore be less for galactose than for glucose, which has the most favorable pyranoside conformation, and also less than for mannose which has the least favorable furanoside conformation.

In the anomeric pyranosides the free energy differences are of the same order for glucose and galactose and very much higher for mannose. These results agree with the premise that an axial hydroxyl at C-4 has little effect on the relative stabilities of anomers and that an axial hydroxyl at C-2 has a very large effect (8, 9).

TABLE IV
Interaction energies (kcal/mole) in pyranoid hexosides

	α		β		$\Delta F\ \alpha \rightleftarrows \beta$	
	C1	1C	C1	1C	Calculated*	Found
Glucosides	2.8	7.3	3.4	8.4	−0.6	−0.43
Galactosides	3.2	6.6	3.8	7.7	−0.6	−0.66
Mannosides	2.7	5.7	4.2	7.7	−1.5	−1.73

*For the more stable chair forms.

The total interaction energies for the pyranoid hexoses are shown in Table IV and were calculated from the following values in kcal/mole: $O_1{:}O_2 = 0.50$ (skew interaction between *o*-substituents on adjacent carbon atoms); Oa:Ha = 0.40 (axial–axial interaction between a hydrogen and an *o*-substituent); Δ2 effect (9) = 0.40 (interaction of axial *o*-substituent at C-2 on equatorial anomer); anomeric effect = 1.4. These values have been established previously (8, 10–12). In the study on glycosidation of pentoses (2) it was found that a value of 1.2 kcal/mole for the anomeric effect gave the best fit with the experimental results. In the present study on hexopyranosides a value of 1.4 kcal/mole gave closer agreement. This is in accord with the results of Lemieux and Chu (12) who assigned values of 1.3 and 1.5 kcal/mole for the anomeric effect in pentoses and hexoses respectively. The larger effect in the hexopyranosides is presumably caused by the added inductive effect of the oxygen atom at C-6 (8).

The results with the three hexoses examined here fully confirm the conclusions drawn from the earlier study of the pentoses (2). The rates of reactions and equilibrium compositions can be fully rationalized by applying the same system of conformational analysis for furanoside and pyranoside rings.

Experimental

Reagents

Sugars were purified products obtained from commercial sources; no impurities were detected by paper chromatography or by gas–liquid chromatography (g.l.c.) of their fully trimethylsilylated derivatives. Methanol was reagent grade and was distilled from magnesium iodine immediately before use. Hydrogen chloride (reagent bottle) was dried by passage through calcium chloride.

Chromatography

A Pye Argon Chromatograph was used for g.l.c. The separations and conditions were described previously (3). Quantitative results were obtained by tracing the peaks from the chromatogram onto glassine paper from which they were cut out and weighed. Paper chromatograms were run by the descending method in ethyl acetate: propan-1-ol:water, 5:3:2 (v/v) which gave a complete separation of the four methyl-D-galactosides (5). Portions of the chromatograms that contained a single methyl-D-galactoside were eluted with water and the amounts present were determined spectrophotometrically after reaction with anthrone (4).

Preparation of Methyl Hexosides

Methyl hexosides were prepared by methods described in the literature. The physical properties of these compounds and the reported values were as follows.

	Found		Reported		
Methyl hexoside	Melting point	$[\alpha]_D$	Melting point	$[\alpha]_D$	Reference
Methyl α-D-glucofuranoside	62–63	+114°	63	+115°	13
Methyl β-D-glucofuranoside	Syrup	−79°	Syrup	−78°	13
Methyl α-D-glucopyranoside	166–167	+159°	165–166	+158°	14
Methyl β-D-glucopyranoside	107–110	−34°	108–110	−34°	15
Methyl α-D-galactofuranoside	92–93	+104°	91–92	+104°	5
Methyl β-D-galactofuranoside	66–67	−114°	69	−112°	5
Methyl α-D-galactopyranoside	115–117	+192°	114–116	+196°	16
Methyl β-D-galactopyranoside	176–179	+0°	178	+0°	16
Methyl α-D-mannofuranoside	120–121	+111°	118–119	+113°	17
Methyl β-D-mannofuranoside	Syrup	−110°	47	−107°	18
Methyl α-D-mannopyranoside	192–193	+80°	193–194	+79°	19
Methyl β-D-mannopyranoside	—	—	—	—	—
Isopropyl alcoholate	74–76	−60°	74–75	−53°	20

Can. J. Chem. Downloaded from www.nrcresearchpress.com by 210.87.254.6 on 09/05/12
For personal use only.

TABLE V

Reaction *1* – hexose → furanosides*

Time (h)	Unreacted hexose† D-glucose α-	Unreacted hexose† D-glucose β-	Methyl glycoside Furanoside α	Furanoside β	Pyranoside α	Pyranoside β	$k \times 10^6$ (s^{-1})†‡
0.33	32.3	67.7	0.0	0.0	0.0	0.0	
1	33.4	66.6	0.0	0.0	0.0	0.0	
2	28.2	67.4	2.0	2.4	0.0	0.0	6.4
3	28.4	65.1	3.0	3.5	0.0	0.0	6.3
5	25.7	64.5	5.5	4.3	0.0	0.0	5.8
7	26.2	61.0	6.0	6.8	0.0	0.0	5.7
9	20.7	64.0	7.6	7.7	0.0	0.0	5.2
24	18.1	44.5	20.9	15.8	0.0	0.7	5.5
30	18.3	37.3	24.3	19.3	0.0	0.8	5.4
50	10.9	29.0	34.9	23.6	0.0	1.6	5.1
75	6.2	15.2	44.2	31.7	1.2	1.5	5.6

*Conditions: 2% of initial compound in 0.01% methanolic hydrogen chloride at 35 ± 0.01 °C.
†Amounts of anomers were determined by gas–liquid chromatography of trimethylsilylated mixture.
‡Based on total D-glucose (α + β).

Reactions and Analysis of Products

Reaction vessels were screw-capped tubes fitted with rubber septums and maintained at 35 ± 0.01 °C. Samples (0.2–0.3 ml) were removed by a hypodermic syringe, neutralized by sodium methoxide and evaporated to dryness *in vacuo* at room temperature. These samples were trimethylsilylated as described previously (3, 21).

Results

Tables V–VIII show the percentage compositions at various times from which the rate constants used in the discussion were obtained.

Table V gives results for reaction *1* – hexose → furanosides. Conditions: 2% of initial compound in 0.01% methanolic hydrogen chloride at 35 ± 0.01 °C.

Table VI gives results for reaction *2* – anomerization of furanosides. Conditions: 2% of initial compound in 0.01% methanolic hydrogen chloride at 35 ± 0.01 °C.

Table VII gives results for reaction *3* – furanosides → pyranosides. Conditions: 2% of initial

TABLE VI

Reaction *2* – anomerization of furanosides*

Time (h)	Methyl glycoside Furanoside α	Furanoside β	Pyranoside α	Pyranoside β	$k \times 10^6$ (s^{-1})
a Methyl α-D-glucofuranoside					
1	96.5	3.5	0.0	0.0	9.7
3	89.6	10.4	0.0	0.0	9.8
5	85.2	14.8	0.0	0.0	8.9
10	72.6	27.4	0.0	0.0	8.6
24	51.0	49.0	0.0	0.0	7.8
30	46.7	53.3	0.0	0.0	7.1
50	39.8	60.2	0.0	0.0	5.1
b Methyl β-D-mannofuranoside					
1	3.0	97.0	0.0	0.0	8.2
4	11.8	88.2	0.0	0.0	8.7
6	17.1	82.9	0.0	0.0	8.5
10	26.2	73.8	0.0	0.0	8.5
24	52.4	47.6	0.0	0.0	8.6
32	56.2	42.4	1.4	0.0	8.5
48	69.2	28.5	2.3	0.0	7.3
72	74.5	22.7	2.8	0.0	5.7
104	79.1	18.1	2.8	0.0	4.6
c Methyl α-D-galactofuranoside					
3	97.0	3.0	0.0	0.0	2.8
5	95.7	4.3	0.0	0.0	2.4
10	92.2	7.8	0.0	0.0	2.3
24	82.3	17.7	0.0	0.0	2.2
30	79.6	20.4	0.0	0.0	2.1
50	68.9	31.1	0.0	0.0	2.1
75	55.8	44.2	0.0	0.0	2.2
120	43.9	56.1	0.0	0.0	1.9

*Conditions: 2% of initial compound in 0.01% methanolic hydrogen chloride at 35 ± 0.01 °C.

TABLE VII

Reaction *3* – furanosides → pyranosides*

Time (h)	Methyl glycoside Furanoside α	Furanoside β	Pyranoside α	Pyranoside β	$k \times 10^6$ (s^{-1})
a Methyl β-D-glucofuranoside					
2	39.6	60.4	0.0	0.0	—
5	40.3	58.7	0.0	1.0	0.55
23	38.0	58.8	1.4	1.8	0.38
30	40.3	56.4	1.5	1.8	0.32
50	33.5	61.3	2.1	3.1	0.35
120	33.8	53.9	6.2	6.1	0.36
150	32.8	51.5	7.6	8.1	0.45
200	32.3	47.5	10.2	10.0	0.31
b Methyl α-D-mannofuranoside					
0.5	93.1	6.5	0.4	0.0	—
1	89.3	9.3	1.4	0.0	4.1
2	85.0	12.1	2.9	0.0	4.1
3	81.9	13.8	4.3	0.0	4.1
22	57.2	10.5	26.8	5.5	4.8
25	52.4	9.9	31.0	6.7	5.2
67	23.5	4.5	61.0	11.0	5.1
91	15.2	2.0	71.0	11.8	5.3
119	9.8	1.5	76.1	12.6	5.1
240	2.4	0.0	84.8	12.8	4.3
c Methyl α-D-galactofuranoside					
24	32.2	63.8	3.6	0.4	0.46
50	17.5	74.9	6.3	1.3	0.44
96	16.5	70.4	10.7	2.4	0.41
125	15.4	69.2	12.6	2.8	0.37
170	13.8	69.8	14.0	2.4	0.29
260	13.5	64.5	18.1	3.9	0.27

*Conditions: 2% of initial compound in 0.1% methanolic hydrogen chloride at 35 ± 0.01 °C.

TABLE VIII

Reaction *4* – anomerization of pyranosides*

Time (h)	Methyl glycoside: Furanoside α	Furanoside β	Pyranoside α	Pyranoside β	$k \times 10^6$ (s^{-1})
a Methyl β-D-glucopyranoside					
2	0.0	0.0	0.0	100	—
4.5	0.0	0.0	2.1	97.9	1.3
22	0.0	0.0	10.0	90.0	1.3
46	0.0	0.0	19.6	80.4	1.3
70	0.0	0.0	28.4	71.6	1.3
100	0.0	0.9	36.5	62.6	1.3
170	Trace	Trace	49.4	50.6	1.2
b Methyl β-D-mannopyranoside					
0.5	0.0	0.0	0.9	99.1	5.5
1	0.0	0.0	1.9	98.1	5.5
2	0.0	0.0	3.6	96.4	5.1
3	Trace	Trace	5.6	94.4	5.4
5	Trace	Trace	9.3	90.7	5.5
8	1.9	0.0	15.4	82.7	6.6
22	1.7	0.0	41.1	57.2	7.0
50	0.0	0.0	70.1	29.9	6.7
75	0.0	0.0	81.1	18.9	6.1
144	0.0	0.0	90.8	9.2	4.7
c Methyl β-D-galactopyranoside					
2	0.0	0.0	2.4	97.6	3.4
4	0.0	0.0	4.8	95.2	3.4
6.5	0.0	0.0	6.3	93.7	2.8
24	0.0	1.7	22.3	76.0	3.2
50	0.0	2.5	38.2	59.3	2.9
98	0.0	4.9	53.0	42.1	2.5
288	0.0	8.5	66.8	24.7	1.4

*Conditions: 2% of initial compound in 1.0% methanolic hydrogen chloride at 35 ± 0.01 °C.

compound in 0.1% methanolic hydrogen chloride at 35 ± 0.01 °C.

Table VIII gives results for reaction *4* – anomerization of pyranosides. Conditions: 2% of initial compound in 1.0% methanolic hydrogen chloride at 35 ± 0.01 °C.

For each reaction the initial compound is cited as the title of the table. The k values are based on the rate of decrease of the initial compound except for reaction *3*, where they are based on decrease of total (α + β) furanoside. The rate constants marked with a dagger (†) were used to give the average values cited in the discussion (Table I).

1. C. T. Bishop and F. P. Cooper. Can. J. Chem. **40**, 224 (1962).
2. C. T. Bishop and F. P. Cooper. Can. J. Chem. **41**, 2743 (1963).
3. V. Smirnyagin, C. T. Bishop, and F. P. Cooper. Can. J. Chem. **43**, 3109 (1965).
4. I. A. Kabat and M. M. Mayer. Experimental immunochemistry. 2nd ed. Charles C. Thomas, Publisher, Springfield, Ill. 1967. p. 528.
5. I. Augestad and E. Berner. Acta Chem. Scand. **8**, 251 (1954).
6. D. D. Heard and R. Barker. J. Org. Chem. **33**, 740 (1968).
7. R. J. Ferrier and L. R. Hatton. Carbohydrate Res. **6**, 75 (1968).
8. E. L. Eliel, N. L. Allinger, S. J. Angyal, and G. A. Morrison. Conformational analysis. Interscience Publishers, Inc., New York. 1965.
9. R. E. Reeves. Advan. Carbohydrate Chem. **6**, 107 (1951).
10. S. J. Angyal and D. J. McHugh. Chem. and Ind. London, 1147 (1956).
11. S. J. Angyal, P. A. J. Gorin, and M. Pitman. Proc. Chem. Soc. 337 (1962).
12. R. U. Lemieux and P. Chu. Abstracts of Papers, 133rd Meeting of the American Chemical Society, 1958, 31N.
13. P. W. Austin, F. E. Hardy, J. G. Buchanan, and J. Baddiley. J. Chem. Soc. 5350 (1963).
14. E. Fischer. Ber. **26**, 2406 (1893).
15. W. Koenigs and E. Knorr. Ber. **34**, 957 (1901).
16. E. Bourquelot. Ann. Chim. Paris, 7, 218 (1917).
17. W. N. Haworth and C. R. Porter. J. Chem. Soc. 649 (1930).
18. E. Pacsu and A. Scattergood. J. Am. Chem. Soc. **61**, 534 (1939).
19. E. Fischer and L. Beensch. Ber. **29**, 2927 (1896).
20. H. S. Isbell and H. L. Frush. J. Res. Natl. Bur. Std. **24**, 125 (1940).
21. C. C. Sweeley, R. Bentley, M. Makita, and W. W. Wells. J. Am. Chem. Soc. **85**, 2497 (1963).

Can. J. Chem. Downloaded from www.nrcresearchpress.com by 210.87.254.6 on 09/05/12
For personal use only.

Can. J. Chem. Downloaded from www.nrcresearchpress.com by 210.87.254.5 on 09/05/12
For personal use only.

Synthesis of optically active deacetyl anisomycin

C. M. WONG, J. BUCCINI, AND J. TE RAA
Department of Chemistry, University of Manitoba, Winnipeg, Manitoba

Received June 5, 1968

Optically active (−)-deacetyl anisomycin and the enantiomer (+)-deacetyl anisomycin were synthesized starting with (+)-2R 3R tartaric acid. The asymmetric centers of the tartaric acid correspond to the C-2 and C-3 asymmetric centers of anisomycin. *N*-Benzyl tartarimide (**3**) was attacked by the Grignard reagent of anisyl chloride followed by lithium aluminium hydride reduction to give two diols (**7**) and (**8**) separated by thin-layer chromatography. The diol (**8**) was debenzylated giving the natural (−)-deacetyl anisomycin. The diol (**7**) was converted into the epoxide (**10**) by selective acetylation of the C-4 hydroxy group followed by treatments with phosphorus pentachloride and sodium ethoxide. Opening of the epoxide ring of **10** in boiling acetic acid followed by basic hydrolysis gave (+)-*N*-benzyl deacetyl anisomycin (**11**) which was debenzylated to give (+)-deacetyl anisomycin.

Canadian Journal of Chemistry, **46**, 3091 (1968)

Introduction

The structure of anisomycin was reported recently as **1** (1) and was revised to **2** (2, 3) by X-ray investigation. The absolute configuration was not reported in the X-ray result and was deduced in this laboratory (4) as 2R 3S 4S as shown in **2**. We would like to report a simple synthetic approach leading to the natural (−)-deacetyl anisomycin and the enantiomer (+)-deacetyl anisomycin not in the form of a (DL)-mixture. This synthesis also verifies our assignment of the absolute stereochemistry to anisomycin.

Results and Discussion

(+)-Tartaric acid was refluxed with benzyl amine in xylene solution to give *N*-benzyl tartarimide (**3**) (5). The Grignard reagent of anisyl chloride was then stirred with the tartarimide (**3**) in dry tetrahydrofuran in 40 °C oil bath for 1 h. After decomposition of the excess Grignard

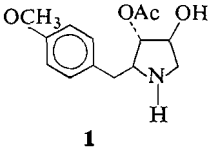

1

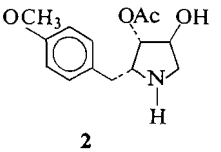

2

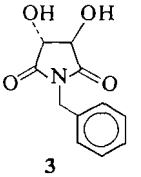

3

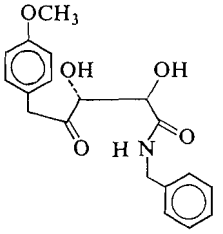

4

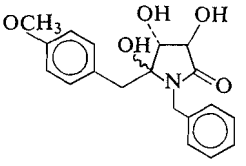

5

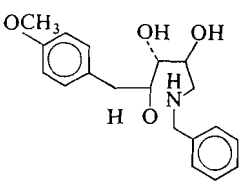

6

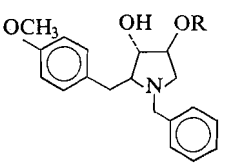

7 R = H
9 R = Ac

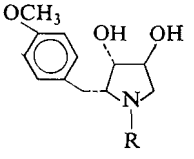

8 R = —CH_2Ph
13 R = H

Can. J. Chem. Downloaded from www.nrcresearchpress.com by 210.87.254.5 on 09/05/12
For personal use only.

reagent, the keto-amide (**4**) was isolated in 55% yield. Contrary to the usual results of the reaction of Grignard reagents with *N*-substituted maleimides (6), not even a trace of the triol (**5**) could be detected. However, if lithium aluminium hydride was added to the above reaction mixture before the excess Grignard reagent was destroyed, three compounds **6**, **7**, and **8** were isolated in 2, 12, and 3% yield respectively.

Acetylation of the diol (**7**) with acetic anhydride gave the hydroxy acetate (**9**). The assignment of the acetoxy group at C-4 was based on the smooth conversion of the acetate (**9**) to the epoxide (**10**)[1] and the conformational argument of the diol (**7**).[2] Thus, the acetate (**9**) was treated with phosphorus pentachloride in dry chloroform at room temperature followed by hydrolysis in alkaline alcoholic solution for ½ h to give the epoxide (**10**). Refluxing **10** in glacial acetic acid gave a mixture of hydroxy acetates which was hydrolyzed by aqueous sodium hydroxide solution to two glycols (**7** and **11**) in equal amounts. Total yield of the two diols from **10** was 56%. The diol (**11**) had a superimposable infrared (i.r.) spectrum but opposite specific rotation to that of *N*-benzyl deacetyl anisomycin derived from benzylation of (−)-deacetyl anisomycin in chloroform solution with benzyl bromide.

Debenzylation of the diol (**11**) in dilute ethanolic hydrochloric acid solution with 5% Pd/C under hydrogenation conditions gave deacetyl anisomycin hydrochloride quantitatively. Liberation of the free base by aqueous sodium hydroxide gave (+)-deacetyl anisomycin (**12**). The i.r. spectra of the (+)-deacetyl anisomycin and its hydrochloride were identical to those of the natural (−)-deacetyl anisomycin and its hydrochloride.

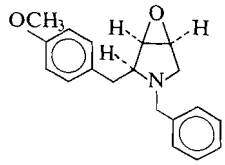

10

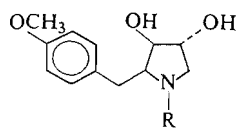

11 R = —CH_2—Ph
12 R = H

The diol (**8**) has i.r., nuclear magnetic resonance (n.m.r.), and mass spectra identical to those of **11** and those of the natural *N*-benzyl deacetyl anisomycin. Debenzylation of **8** as above gave quantitatively deacetyl anisomycin hydrochloride which by treatment with aqueous base gave (−)-deacetyl anisomycin. Both the synthetic deacetyl anisomycins and their hydrochlorides were identical in every respect to the natural products.

Experimental

All infrared (i.r.) spectra were measured on a Perkin–Elmer model 137 spectrophotometer. Melting points were measured on a Fisher–Johns apparatus and are uncorrected. Nuclear magnetic resonance (n.m.r.) spectra were measured on a Varian A 56/60 A model using TMS as internal standard. Mass spectra were measured on a Hitachi Perkin–Elmer RMU-6D mass spectrometer. All new crystalline synthetic compounds gave satisfactory analyses which were performed by Dr. C. Daessle of Montreal.

Preparation of Tartarimide (3)

Giustiniani prepared the tartarimide (**3**) by heating (+)-tartaric acid and benzylamine together (5). The yield was too low to be useful. A slightly modified method described in the following gave very good yield of the tartarimide (**3**).

2R 3R (+)-Tartaric acid (19 g) was added to *p*-xylene (500 ml) in a 2 l 3-necked flask fitted with a water separator and condenser. To the vigorously stirred and refluxing xylene solution was added benzylamine (16.5 g) in a period of ½ h and reflux was continued for 3 h. The solution was cooled in an ice bath and the crystalline product was filtered. After being washed twice with cold benzene, the crystalline product was recrystallized from water to give the tartarimide (**3**) (17 g), m.p. 196–198°, $[\alpha]_D^{25}$ + 126° (MeOH).

Reaction of Anisyl Magnesium Chloride with the Tartarimide (3)

To a 300 ml 3-necked flask containing magnesium (10 g) was added anisyl chloride (0.5 g), dissolved in

---

[1]The assignment of the epoxide ring *cis* to the anisyl ring is established by comparing the i.r. of (**10**) with the i.r. spectra of many synthetic and natural derivatives. Epoxides of the type (*i*) have strong and sharp absorption at 865 cm^{-1}. Epoxides of the type (*ii*) have strong and sharp absorption at 848 cm^{-1}.

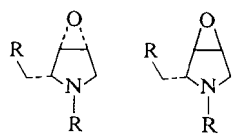

(*i*) (*ii*)

[2]For the most stable conformation of the diol (**7**), the lone pair of electrons of the basic nitrogen atom should be *cis* to the C-4 hydroxy group. Thus a base catalyzed acetylation should acetylate the C-4 hydroxy group only as shown in (*iii*).

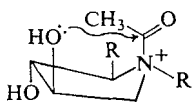

(*iii*)

Can. J. Chem. Downloaded from www.nrcresearchpress.com by 210.87.254.5 on 09/05/12
For personal use only.

anhydrous tetrahydrofuran (30 ml). After stirring for about 10 min, anhydrous tetrahydrofuran (150 ml) containing anisyl chloride (20 g) was added dropwise to the flask and the mixture was stirred vigorously for an additional 30 min. *N*-Benzyl tartarimide (**3**) (4.8 g) in anhydrous tetrahydrofuran (50 ml) was added to the Grignard reagent and the solution was stirred at room temperature overnight. Water (20 ml) was added to decompose the excess Grignard reagent. The excess magnesium was filtered and the clear solution was separated from the aqueous pasty residue which was further exhaustively extracted with ether. The combined organic extracts, dried over anhydrous magnesium sulfate, were evaporated to dryness to give a light-yellow solid residue. Recrystallization of the solid residue from nitromethane gave the white crystalline keto-amide (**4**) (5.3 g), m.p. 164–166 °C.

Infrared: ν_{max} (CH_2Cl_2) 3550, 3300, 3200, 1720, 1640, 1625, and 1590 cm^{-1}.

Mass spectra: M^+/e; 343, 325, 236, 218, 194, and 181.

Nuclear magnetic resonance: $\tau(CDCl_3)$ (diacetate of **4**); 2.84 (s, 5 H's, aromatic), 3.15 (A_2B_2, 4H's, aromatic), 4.40 (AB quartet, 2 H's, J_{AB} = 3 c.p.s., C*H*—OCOMe), 5.57–5.71 (2 quartets, 2 H's, J_{AB} = 10 c.p.s., —NH—*CH*$_2$—Ph), 6.29 (s, 2 H's, —CO—CH_2— 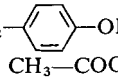 —OMe), 6.35 (s, 3 H's, —OCH_3), 8.05 (s, 3 H's, CH_3—COO—), and 8.11 (s, 3 H's, CH_3COO—).

Anal. Calcd. for $C_{19}H_{21}O_5N$: C, 66.46; H, 6.15; N, 4.08. Found: C, 66.76; H, 6.35; N, 4.09.

The first half of the above experiment was repeated and the excess magnesium was filtered from the tetrahydrofuran solution. It was then added dropwise to a refluxing tetrahydrofuran solution (300 ml) containing lithium aluminium hydride (3 g) and refluxing was continued for 6 h. After distilling off most of the solvent, ethyl acetate (500 ml) was added very slowly to the residue followed by 6 *N* hydrochloric acid (50 ml). After vigorous shaking, the ethyl acetate was separated. The aqueous fraction was made strongly basic and extracted with chloroform. Evaporation of the chloroform solution gave only a trace of residue. The ethyl acetate solution was concentrated and extracted by hydrochloric acid solution (5%). The acidic solution was made basic and the resulting precipitate was extracted into chloroform. Evaporation of the chloroform solution gave a gummy residue (2.1 g) from which the diol (**7**) (1.1 g) was obtained by crystallizing the residue from benzene and heptane, m.p. 113–114 °C, $[\alpha]_D^{25}$ +78° ($CHCl_3$).

Infrared: ν_{max} (CH_2Cl_2) 3560, 2900, 2780, 1600, and 1040 cm^{-1}.

Mass spectra: M^+/e;[3] 192, 121, and 91.

Nuclear magnetic resonance: $\tau(CDCl_3)$ 2.94 (s, 5 H's aromatic), 3.04 −3.40 (A_2B_2, 4 H's aromatic), 6.30 (s, 3 H's, —OCH_3), 6.00 and 6.72 (AB quartet, 2 H's, J_{AB} = 13 c.p.s. —N—CH_2—Ph), 6.25 (unresolved 2 H's, C_3—H and C_4—H), 7.10 (s, 2 H's, —OH), and 7.2–7.5 (unresolved 5 H's, C_2—H, C_5—H_2 and —*CH*$_2$— 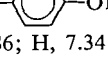 —OMe).

Anal. Calcd. for $C_{19}H_{23}O_3N$: C, 72.86; H, 7.34; N, 4.47. Found: C, 72.84; H, 7.36; N, 4.50.

The mother liquor was purified by thin-layer chromatography (t.l.c.) over silica to give the triol (**6**), m.p. 120–123 °C.

Infrared: ν_{max}(CH_2Cl_2) 3400, 1620, 1500, and 1075 cm^{-1}.

Mass spectra: M^+/e; 331, 313, 210, 121, and 91.

This triol was correlated with the lithium aluminium hydride reduction product of the keto-amide (**4**). The diol (**8**) (120 mg) was also isolated by t.l.c. from the mother liquor, m.p. 80–82 °C, $[\alpha]_D^{25}$ −51.0°.

Infrared: ν_{max}(CH_2Cl_2) 3570, 3450, 2900, 1600, and 1500 cm^{-1}.

Mass spectra: M^+/e;[3] 192, 121, and 91.

Nuclear magnetic resonance: $\tau(CDCl_3)$ 3.03 (s, 5 H's aromatic), 3.32 (A_2B_2, 4 H's aromatic), 6.16 and 6.81 (AB quartet, 2 H's, J_{AB} = 12 c.p.s. —N—*CH*$_2$—Ph), 6.42 (s, 3 H's, —OCH_3), 6.28 and 6.52 (unresolved 2 H's, C_3—H and C_4—H), 6.97 (s, 2 H's, —OH), 6.92–7.04 (unresolved 2 H's, C_5—H_2), 7.26 (broad s, 2 H's, —*CH*$_2$— 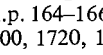 — OMe), and 7.96 (broad quartet, 1 H, C_2—H).

Conversion of the Diol (7) into the Epoxide (9)

The diol (7) (940 mg) was stirred in acetic anhydride (10 ml) for 20 min. Evaporation of the acetic anhydride to complete dryness gave a hydroxy acetate which was then dissolved in dry chloroform. To the chloroform solution was added phosphorus pentachloride (640 mg) in small portions; the mixture was stirred for 10 min and the chloroform solution was evaporated to dryness giving an orange foamy residue. To the residue was added ethanol (3 ml) followed by 20% KOH in ethanol (5 ml). After stirring for ½ h the solution was diluted with water (20 ml) and exhaustively extracted with chloroform. The chloroform solution was evaporated to dryness and the residue was separated by t.l.c. on silica to yield the epoxide (**10**) (240 mg), m.p. 113–115 °C, $[\alpha]_D^{25}$ ($CHCl_3$) +94°.

Infrared: ν_{max}(CH_2Cl_2) 1620, 1075, and 865 cm^{-1}.

Mass spectra: M^+/e; 295, 277, 174, and 91.

Nuclear magnetic resonance: $\tau(CDCl_3)$ 2.95 (s, 5 H's aromatic), 3.04 and 3.40 (A_2B_2, 4H's aromatic), 6.12 and 6.63 (AB, 2 H's, J_{AB} = 13 c.p.s. —N—CH_2—), 6.37 (s, 3 H's, —OCH_3), and 7.73 (broad doublet 1 H, C_2—H).

Anal. Calcd. for $C_{19}H_{21}O_2N$: C, 77.30; H, 7.11; N, 4.74. Found: C, 77.22; H, 7.10; N, 4.88.

Preparation of (+)-N-Benzyl Deacetyl Anisomycin

The epoxide (**10**) (240 mg) was refluxed in glacial acetic acid for 1½ h. After evaporating the glacial acetic acid to dryness, sodium hydroxide solution (1 *N*, 20 ml) was added to the residue and the solution was refluxed for 2 h. Extraction of the cold basic solution with chloroform and evaporation of the chloroform solution to

[3]All compounds with a basic nitrogen atom in the pyrrolidine ring showed no parent peak in the mass spectrum. Only fragments (*iv*) and (*v*) were observable.

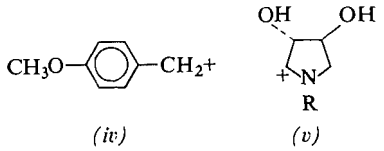

(*iv*) (*v*)

dryness gave a white foamy residue which was separated by t.l.c. on silica into two major diols (**7**) (66 mg) and (**11**) (78 mg), m.p. 79–81 °C, $[\alpha]_D^{25}$ ($CHCl_3$) +51.4°. Infrared, n.m.r., and mass spectra were identical to those of (**8**).

Debenzylation of N-Benzyl Deacetyl Anisomycin

(−)-*N*-Benzyl deacetyl anisomycin (60 mg) dissolved in ethanol (10 ml) containing 2 drops of concentrated hydrochloric acid and Pd/charcoal (5%) (20 mg) was hydrogenated for 3 h under atmospheric pressure. The catalyst was filtered off and the ethanolic solution evaporated to dryness to give the (+)-deacetyl anisomycin hydrochloride (45 mg); this was then recrystallized from methanol and ether, m.p. 224–226 °C, $[\alpha]_D^{25}$ +7°. Liberation of the free base by sodium hydroxide solution gave (−)-deacetyl anisomycin identical in every respect with the natural product. Debenzylation of (+)-*N*-benzyl deacetyl anisomycin as before gave (−)-*N*-deacetyl anisomycin hydrochloride, m.p. 219–221 °C, $[\alpha]_D^{25}$ −7°. Treatment of the hydrochloride with sodium hydroxide solution gave the free base (+)-deacetyl anisomycin, m.p. 168–170 °C, $[\alpha]_D^{25}$ ($CHCl_3$) +20°. Infrared, n.m.r., and mass spectra were identical to the natural (−)-deacetyl anisomycin except opposite sign of specific rotation.

Acknowledgments

The authors would like to express their appreciation to the National Research Council of Canada and Charles Pfizer and Co., Inc., for financial support and for the supply of anisomycin.

1. J. J. Beereboom, K. Butler, F. C. Pennington, and I. A. Solomons. J. Org. Chem. **30**, 2334 (1965).
2. J. P. Schaefer and P. F. Wheatley. Chem. Commun. **12**, 578 (1967).
3. J. P. Schaefer and P. J. Wheatley. J. Org. Chem. **33**, 166 (1968).
4. C. M. Wong. Can. J. Chem. **46**, 1101 (1968).
5. Giustiniani. Gazz. Chim. Ital. **24**, 1, 224 (1894).
6. A. Queen and A. Reipas. J. Chem. Soc. C, 245 (1967).

Can. J. Chem. Downloaded from www.nrcresearchpress.com by 210.87.254.5 on 09/05/12
For personal use only.

Can. J. Chem. Downloaded from www.nrcresearchpress.com by 210.87.254.40 on 09/05/12
For personal use only.

Reactions of ozonides. VII. Isolation and oxidation of ozonolysis products from 1-decene[1]

DENNIS G. M. DIAPER
Department of Chemistry, Royal Military College of Canada, Kingston, Ontario

Received April 26, 1968

1-Decene ozonide (**1**) was isolated by column chromatography of the mixed products of ozonation of 1-decene (**2**) in several nonpolar solvents. 1-Methoxy- (**3**) and 1-tertiary butoxynonane-1-hydroperoxide (**4**) were similarly obtained. The thin-layer chromatographic separation of these products from each other and from other ozonation products was examined. Compounds **3** and **4** were smoothly oxidized to di-(1-alkoxyalkyl)peroxides by Ce(IV). The stoichiometry of this reaction, examined by isothermal calorimetry, was 1:1. Compounds **1**, **3**, and **4** were oxidized by CF_3CO_3H and by other oxidizing agents to nonanoic acid with chain degradation loss of 2–30%.

Canadian Journal of Chemistry, 46, 3095 (1968)

Ad hoc procedures for oxidation of ozonation products without prior isolation have been used for some time, on laboratory and industrial scales (1–3). Even the most nearly quantitative method for conversion of suitable ozonation products to acids (4) allows loss of about 5% of the material by chain degradation chiefly to esters. Detailed investigations of oxidation of ozonation products, including chain degradation by-product studies, have been reported by Düll (5) and Pasero *et al.* (6–10). The role of water and catalysis in improvement of the autoxidation reaction was reported (11) but it was clear that progress in study of oxidative ozonolysis would be facilitated by use of isolated ozonation products.

In the preparation of acids from ozonides, aldehydes have been postulated to be the precursors of both acids and ester by-products. In each case an acylperoxy radical is formed and may react with aldehyde to give acid in a chain reaction (12, 13) or decarboxylate, giving ester, with (6, 14) or without intermediate diacylperoxide formation. Since most ozonide oxidation procedures so far described use oxygen or peroxides (15) as reagents, a non-peroxidic oxidant, Ce(IV), was tried. This has a high standard oxidation–reduction potential (1.6V), can be used as hexanitratoammonium cerate in many organic solvents, and attacks aldehydes only slowly (16). Its color is discharged on reduction (17). We have also examined by-product formation during oxidation of ozonation products by the powerful peroxidic agent peroxytrifluoroacetic acid.

[1]Presented in part at the Chemical Institute of Canada Annual Conference, Toronto, June 1967.

Experimental

1-Decene Ozonide (1)

This was prepared by complete ozonation of the olefin in 5% solution at 0, −20 to −30, and 25° in methylene chloride and in pentane at the same three temperatures. The crude products (10–20 g) were chromatographed on silica gel (Baker) eluted with 15–25% ether in petroleum ether (b.p., 30–60°). Yields of chromatographically pure (determined by thin-layer chromatography (t.l.c.)) decene ozonide were respectively 45, 48, 33, 59, 53, and 58%. Ozonolysis in CCl_4 and in $CHCl_3$ at room temperature gave 31 and 33% yields. Aldehyde came off the column ahead of ozonide and the fractions remaining were polymeric peroxides (18). The nuclear magnetic resonance (n.m.r.) spectrum had a multiplet, integrating for three protons, ascribed to the superimposed signals of CH_2 and CH of the ozonide ring. The CH triplet was centered at $\delta = 5.13$ p.p.m. and showed 4.4 c.p.s. splitting. The CH_2 protons were non-equivalent singlets at $\delta = 5.01$ and 5.15 p.p.m. Its infrared (i.r.) spectrum showed no OH or carbonyl peaks. There were strong absorptions at 6.82, 7.25, 9.04, and 10.30 μ. Analysis of the "active" oxygen content by iodimetry gave 98% of the theoretical titration value. Reduction by lithium aluminium hydride, followed by trifluoroacetylation (19) gave 1-nonanol trifluoroacetate identified by gas–liquid chromatography (g.l.c.) and by co-chromatography with an authentic sample.

1-Tertiary Butoxynonane-1-hydroperoxide (4)

This was prepared in tertiary butyl alcohol by ozonizing to completion at room temperature a 5% solution of the alkene. After solvent removal by rotatory evaporation, the alkoxyhydroperoxide was isolated by column chromatography as above. Recovery was 49%, based on the 1-decene used. The principal n.m.r. peak, the Bu^t singlet, was superimposed at $\delta = 1.29$ p.p.m. on the chain CH_2 signals. There was no signal in the 5–5.3 p.p.m. region, indicating freedom from ring ozonide. The i.r. spectrum showed a strong OH band, no carbonyl, two broad peroxide peaks at 11.8 and 12.3 μ, and other strong peaks at 6.85, 7.35, 8.42, and 9.19 μ. 1-Nonanol trifluoroacetate was identified after reduction and trifluoroacetylation as above; 1-octanol trifluoroacetate was a very minor impurity.

Thin-layer chromatography was extensively used in

Can. J. Chem. Downloaded from www.nrcresearchpress.com by 210.87.254.40 on 09/05/12
For personal use only.

examination of purity of ozonation products and in study of fractions from chromatographic columns. Spots were developed by 2,4-dinitrophenylhydrazine spray which revealed aldehyde, ozonide, alkoxyhydroperoxide, and polymeric ozonide. A better spray, when recognition of aldehyde was not required, was 3% KI in 1% aqueous acetic acid. Ozonide spots were light brown and alkoxyhydroperoxide spots were purple-brown. Aldehyde spots were white on a yellow background. Di-(1-alkoxynonyl) peroxide spots developed color faster than the hydroperoxide, and ozonide spots developed color quite slowly. The colors faded after a few hours (I_2 evaporation) but could be recorded permanently by Xerox copying. R_f values on silica gel G "Chromagram" sheet developed by 30% ether in petroleum ether were **1**, 0.670; **3**, 0.553; **5**, 0.592; and on another sheet **1**, 0.665; **4**, 0.562; **6**, 0.603.

Samples of ozonide, alkoxyhydroperoxide, and di-(1-alkoxyalkyl) peroxide were stable in storage alone or in inert solvents at $-10°$ for several weeks.

Di-(1-tertiary butoxynonyl) Peroxide

This was obtained from 1-tertiary butoxynonane-1-hydroperoxide (**4**, 0.81 g) in methanol (10 ml) treated at 0° with 1.2 equivalents of 0.382 *M* hexanitratoammonium cerate in methanol (20 ml). There was a vigorous effervescence and the deep orange color was instantaneously discharged to light yellow. The solution was immediately extracted with pentane in three portions and the extract was washed with sodium bicarbonate solution and dried. After column chromatography on silica eluted with pentane, 0.34 g of solid product was obtained. It was recrystallized as colorless plates from pentane at low temperature, m.p. 43–44°.

Anal. Calcd. for $C_{26}H_{54}O_4$: C, 72.50; H, 12.64. Found: C, 72.91; H, 12.88.

The equivalent weight in a peroxide iodometric titration was 226 (theory 215). The n.m.r. spectrum had a terminal methyl triplet and three peaks at $\delta = 1.25$, 1.30, and 1.41 p.p.m. where the starting material had only one at 1.29. There were no exchangeable protons but the starting material gave an HDO signal after D_2O treatment. The i.r. spectrum showed many features similar to that of the starting material, but there was no OH peak. New peaks were observed at 8.67, 8.83, and 12.64 μ. After decomposition by heat at 100° for 10 min these were lost, and new peaks at 5.78–5.85 μ (carbonyl) appeared. The spectrum of the decomposed product had no peaks in the peroxide region.

Isothermal calorimetry (20, 21) was used to examine the stoichiometry of the alkoxyhydroperoxide–Ce(IV) reaction. Methanol, (25 ml) and 5 ml of cerate solution (0.733 mmole) were mixed and precooled to 0°. A weighed sample of peroxide in methanol (10%) in a fragile glass bulb was broken inside the cerate when calorimeter fore-drift was steady. Heat evolved was measured by observing the movement of a mercury meniscus in contact with the melting ice, calibrated electrically to read 1.23 cal/cm. Twelve samples were used and the heat evolved per mole of substrate was plotted as a function of reagent ratio as previously described (21). Forty-five kcal per mole were evolved and the equivalence point was 1.06 moles of peroxide per equivalent of cerate. A similar study in 60% aqueous tertiary butyl alcohol gave 41 kcal for 1.01 moles of peroxide at equivalence. 1-Methoxynonane-1-hydroperoxide in methanol similarly evolved 45 kcal/mole at 1.08 moles/equivalent.

Di-(1-methoxynonyl) Peroxide (5)

This was similarly obtained as a viscous liquid by column chromatography of the product of oxidation of 1-methoxynonane-1-hydroperoxide (**3**) by a small excess of methanolic hexanitratoammonium cerate at 0°. The n.m.r. and i.r. spectra showed OH to be absent. A very small CO peak in the i.r. spectrum was ascribed to decomposition. The MeO singlet at $\delta = 3.32$ p.p.m. was up-field from that of the starting material ($\delta = 3.52$ p.p.m.) but the O—CH—O triplet appeared at $\delta = 4.77$ p.p.m. in both spectra. Compound **5** decomposed when boiled with excess dilute H_2SO_4 for a few minutes, giving an oily liquid whose g.l.c. showed two peaks of approximately equal area identified by co-chromatography with authentic samples as nonanal and methyl nonanoate. The peroxide decomposed completely (no KI test) when heated alone at 100° for 10 min. It lost methanol during decomposition (hot copper wire test) and the residual liquid contained nonanal (oxime, m.p., and mixture m.p. 63°).

Degradation Products

Oxidation of 1-decene ozonide (0.5–1.0 g in 10–20 ml of methanol) was performed by methanolic hexanitratoammonium cerate (4.0 equivalents, 0.135 *N*), stirred for 24 h at room temperature (Method *a*). The solution became colorless only after some hours. It was diluted with an equal volume of water and extracted with petroleum ether. The evaporated extract was examined for chain degradation products by two methods: 1-octyl trifluoroacetate in 1-nonyl trifluoroacetate and octanoic acid in nonanoic acid. For the latter, the petroleum ether extract was shaken with sodium bicarbonate solution and after acidification the dry ethereal extract of liberated mixed acids was treated with excess of alcohol-free ethereal diazomethane, evaporated, and examined by g.l.c. (column three, Table I, in which the relative methyl

TABLE I

Degradation during oxidation of 1-decene ozonation products

Substance tested	Oxidation* method	Trifluoroacetates†	Methyl octanoate
1	—	3.2	—
3	—	2.6	—
4	—	1.9	—
5	—	0.96	—
6	—	0.31	—
Product from **1**	*a*	13.2	10.7
	b	5.1	2.4
	b	5.3	2.8
	c	18.1	15.2
Product from **3**	*a*	14.1	11.2
Product from **4**	*a*	19.0	14.0

*Method *a*; 4 equivalents of methanolic Ce(IV), 24 h. Method *b*; CF_3CO_3H. Method *c*; excess $KMnO_4$ in acetone, 6 h at room temperature.

†The product was reduced by $LiAlH_4$ in ether and trifluoroacetylated by $(CF_3CO)_2O$. The figures are areas of gas–liquid chromatography peaks due to 1-octyl trifluoroacetate expressed as a percentage of the area of the 1-nonyl trifluoroacetate peak.

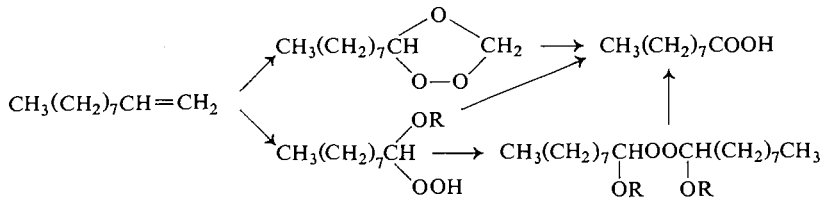

3 R = Me
4 R = *t*-Bu

5 R = Me
6 R = *t*-Bu

octanoate yield was expressed as a percentage of the methyl nonanoate yield).

A Burrell KD gas chromatograph with a 20 ft neopentyl glycol sebacate column was used for ester separation. At 160° with helium elution at 80 ml/min, retention times for authentic samples of methyl octanoate and methyl nonanoate were respectively 5.2 and 7.8 min. The trifluoroacetates of authentic 1-octanol and 1-nonanol had retention times of 5.1 and 6.9 min on a 16 ft Carbowax column eluted with helium at 67 ml/min at 140°. The second column of Table I gives the peak area attributed to octanol as a percentage of the peak area due to nonanol. The mixed alcohols were obtained and trifluoroacetylated as previously described (19).

Oxidation of 1-decene ozonide (1.32 g) by peroxytrifluoroacetic acid (22) was performed in methylene chloride (20 ml) initially at room temperature. Trifluoroacetic anhydride (5.0 ml) and 70% hydrogen peroxide (1.0 ml) were added and the solution was stirred for 2 h during which heat was evolved and the solution became homogeneous. It was washed with water, dilute ferrous sulfate solution, dried, and evaporated (Method *b*).

Nonanoic Acid from 1-Decene

The olefin (1.7 g) in 50 ml of ice-cold methanol was ozonized until mist formation ceased and a Br_2/acetic acid test was negative. Without isolation of the ozonation products, ice was added, and 31 g (4.66 equivalents) of hexanitratoammonium cerate solid and 10 ml of 2 *N* nitric acid were added in portions with stirring. After 10 h there was no more effervescence and the solution was colorless. The acid fraction, obtained by petroleum ether extraction and potassium carbonate washing, was a colorless oil (1.25 g, 65%). From it was obtained the amide, m.p. 98–99°. The neutral fraction (0.79 g) had a broad carbonyl peak in i.r., was non-peroxidic, and gave a negative fuchsin–aldehyde reaction. In a similar experiment in tertiary butyl alcohol, a 61% yield of crude acid was obtained. The methyl esters on g.l.c. gave peaks corresponding to methyl nonanoate and methyl octanoate having relative areas 6.1:1. When 1-decene (1.35 g) was ozonized in methylene chloride, the mixed products after solvent removal by rotary evaporation were similarly treated with excess hexanitratoammonium cerate in aqueous acetic acid. The yield of crude nonanoic acid was 0.625 g (41%).

Discussion

The terminal olefin, 1-decene, appears to give better yields of monomeric ozonation product than the non-terminal alkenes which may give polymeric ozonides as their main ozonation products (18).

Hexanitratoammonium cerate is a disappointing reagent for preparation of acids from an isolated ozonide or the two alkoxyhydroperoxides tried. Yields are lower than those from other techniques and there was extensive chain degradation. Peroxytrifluoroacetic acid is a much better oxidant for 1-decene ozonide and is comparable with performic acid for quantitative work (4).

It is interesting that alkoxyhydroperoxides consume one equivalent of Ce(IV) very rapidly and then three or more quite slowly. They are theoretically at the same oxidation level as acids. Shorter and Hinshelwood (23) and Shorter (24) have noted chain degradation by excess Ce(IV). The ozonide, which theoretically needs two equivalents of Ce(IV) per mole for oxidation to acid, reacted so slowly at 0° with the reagent that isothermal calorimetric study was impractical.

Tertiary-butyl hydroperoxide is susceptible to oxidation by one equivalent of Cu(II), Co(III), or Mn(III). The products are O_2, dibutyl peroxide, tertiary-butyl alcohol, and tertiary-butoxy radical formed by the following competing reactions, the former being more important than the latter by a factor of 3:1 (25).

$$2\ Bu^tOO^\cdot \rightarrow Bu^tOOBu^t + O_2$$

$$2\ BuOO^\cdot \rightarrow Bu^tOH + Bu^tO^\cdot + O_2$$

Although tertiary-alkyl peroxy radicals give dialkyl peroxides, it is generally accepted that radicals having a hydrogen atom on the oxygenated carbon disproportionate as follows (26).

$$2R_2CHOO^\cdot \rightarrow 2R_2CHO^\cdot + O_2 \rightarrow R_2C{=}O + R_2CHOH$$

From a 1-alkoxyhydroperoxide the carbonyl product of such a disproportionation is the ester. The other product is a hemiacetal and would be expected to decompose readily to the aldehyde

Can. J. Chem. Downloaded from www.nrcresearchpress.com by 210.87.254.40 on 09/05/12
For personal use only.

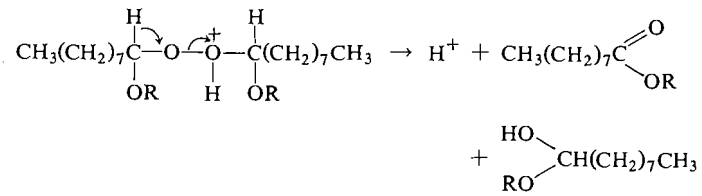

and alcohol. For 1-methoxynonane-1-hydroperoxide this decomposition route would be

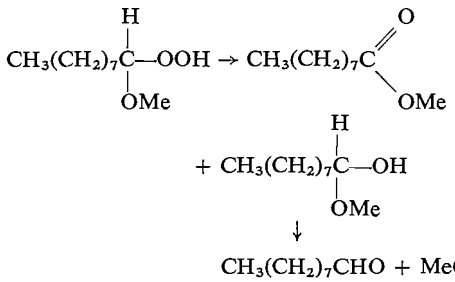

It was unexpected that the corresponding di-(1-alkoxyalkyl) peroxides should be formed and could be isolated. An aromatic peroxide of analogous structure was reported as a by-product of the ozonolysis of stilbene in methanol (27). Acid hydrolysis of the di-(1-alkoxyalkyl) peroxides proceeds as follows (28, 29). Chain reaction decomposition of these peroxides, initiated by Ce(IV), appears to be negligible since the stoichiometry observed by isothermal calorimetry is close to 1:1.

Acknowledgments

The generous assistance of S. S. Barton with isothermal calorimetry experiments is gratefully acknowledged. Support of the Defence Research Board (Grant 9530-17) is gratefully acknowledged.

1. C. G. Goebel, A. C. Brown, H. F. Oehlschlaeger, and R. P. Rolfes. U.S. Patent No. 2,813,113 (1953).
2. Chem. Eng. News, **42**, 48, 31, (1964).
3. H. J. Nieschlag, I. A. Wolff, T. C. Manley, and R. J. Holland. Ind. Eng. Chem. Prod. Res. Develop. **6**, 120 (1967). Chem. Abstr. **67**, 2719*y* (1967).
4. R. G. Ackman, M. E. Retson, L. R. Gallay, and F. A. Vandenheuvel. Can. J. Chem. **39**, 1956 (1961).
5. H. Düll. Doctoral Thesis, Heidelberg. 1933.
6. J. Pasero. Ph.D. Thesis, Marseille, France. 1963.
7. J. Pasero, J. Chouteau, and M. Naudet. Bull. Soc. Chim. France, 1717 (1960).
8. J. Pasero, L. Comeau, and M. Naudet. Bull. Soc. Chim. France, 493 (1965).
9. J. Pasero and M. Naudet. Rev. Franç. Corps Gras, **7**, 189 (1960).
10. J. Pasero and M. Naudet. **10**, 453 (1963).
11. D. G. M. Diaper. Can. J. Chem. To be published.
12. E. Briner and G. Papazian. Helv. Chim. Acta, **23**, 497 (1940).
13. D. A. Lillard and E. A. Day. J. Am. Oil Chem. Soc. **41**, 549 (1964).
14. D. Lefort, D. Tempier, and J. Sorba. Bull. Soc. Chim. France, 442 (1960); 1385 (1959).
15. M. I. Fremery and E. K. Fields. J. Org. Chem. **28**, 2537 (1963).
16. W. S. Trahanovsky and L. B. Young. J. Chem. Soc. 5777 (1965).
17. D. G. M. Diaper. Can. J. Chem. **34**, 1835 (1956).
18. F. L. Greenwood and H. Rubinstein. J. Org. Chem. **32**, 3369 (1967).
19. D. G M. Diaper. Intern. Oxidation Symp. San Francisco. Preprints of papers. 1967. Vol. I. p. 319.
20. R. E. Vallee. Rev. Sci. Instr. **33**, 856 (1963).
21. D. G. M. Diaper. Can. J. Chem. **45**, 33 (1967).
22. W. D. Emmons and A. S. Pagano. J. Am. Chem. Soc. **77**, 4557 (1955).
23. J. Shorter and C. N. Hinshelwood. J. Chem. Soc. 3276 (1950).
24. J. Shorter. J. Chem. Soc. 3425 (1950).
25. M. H. Dean and G. Skirrow. Trans. Faraday Soc. **54**, 849 (1958).
26. T. G. Traylor and C. A. Russell. J. Am. Chem. Soc. **87**, 3698 (1965).
27. W. P. Keaveney, M. G. Berger, and J. J. Pappas. J. Org. Chem. **32**, 1537 (1967).
28. A. Robertson and W. A. Waters. J. Chem. Soc. 1574 (1948).
29. M. S. Kharasch, A. Fono, and W. Nudenberg. J. Org. Chem. **15**, 748 (1950).

Can. J. Chem. Downloaded from www.nrcresearchpress.com by 210.87.254.40 on 09/05/12
For personal use only.

Can. J. Chem. Downloaded from www.nrcresearchpress.com by 210.87.254.42 on 09/05/12
For personal use only.

Bridgehead free radical stability. The decomposition of *t*-butylperoxyesters of the 1-adamantyl, 1-bicyclo[2·2·2]octyl, and 1-norbornyl systems

LEONARD B. HUMPHREY,[1] BRUCE HODGSON,[2] AND RICHARD E. PINCOCK[3]
Department of Chemistry, University of British Columbia, Vancouver 8, British Columbia
Received March 7, 1968

The *t*-butylperoxyesters of 1-adamantyl, 1-bicyclo[2·2·2]octyl, and 1-norbornyl carboxylic acids thermally undergo first order, free radical decomposition in cumene with relative rate constants at 80° of 1.0, 0.07, and 0.001 respectively. As measures of the stability of the derived bridgehead free radicals, the rates span a range much narrower than that for carbonium ion formation at these strained positions. The results are consistent with suggestions that free radicals have smaller force constants for out-of-plane bending than do the corresponding carbonium ions.

Canadian Journal of Chemistry, 46, 3099 (1968)

The best known tervalent carbon intermediate is the carbonium ion and rigorous evidence is available to indicate that this species greatly prefers a planar, sp^2 hybridized form. There is other evidence which indicates, though not as directly, that unconjugated carbanions exist in a pyramidal sp^3 form which rapidly inverts. Electronically situated between these two species is the tervalent carbon free radical, and accordingly, the pattern of possible configurations for this type of intermediate ranges from the planar sp^2 hybridized form to the pyramidal sp^3 form (1).

Considerable evidence now exists to show that the structure of the most *stable* form of unconjugated free radicals is planar, or nearly so (2). However, bond strain, as in the cyclopropyl radical, may give rise to a nonplanar, rapidly inverting structure (3, 4). In addition it has long been known that free radical intermediates at bridgehead positions (which can not invert nor become planar) can form in a number of synthetically useful reactions (1, 5). Although there is established reluctance (6) to form such nonplanar bridgehead radicals, a more quantitative and general measure of the relative ability to form a series of nonplanar free radicals is not yet available (1, 7).

Thorough studies of rates of alkyl halide solvolysis in a series of bridgehead halides has established a wide range of carbonium ion stabilities for strained bridgehead positions (8, 9), and a similar comparison of relative free radical stabilities might be obtained through an appropriate study of relative rates of free radical production. As thermal decomposition of *t*-butylperoxyesters derived from various carboxylic acids has established that the relative rates may be related to the stability of the free radical produced (for recent reviews see ref. 10) (i.e., in the reaction $R—CO_2—OC(CH_3)_3 \rightarrow R\cdot + CO_2 + \cdot OC(CH_3)_3$), we have investigated the kinetics of thermal production of the bridgehead free radicals 1-adamantyl, 1-bicyclo[2·2·2]octyl, and 1-norbornyl by decomposition of the corresponding peresters (1, 2, and 3, respectively) (some results of a similar study have recently been communicated, see ref. 11).

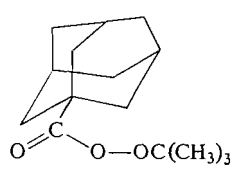

1

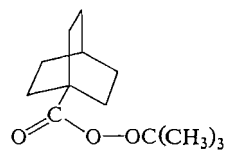

2

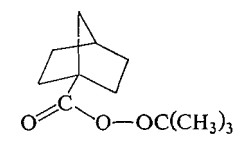

3

Results

The three peresters were prepared by reacting the acid chlorides with the sodium salt of *t*-butylhydroperoxide at 0° in ether. The initially required 1-adamantylcarboxylic acid is readily available, and 1-norbornylcarboxylic acid may

[1]Present address: Chemistry Section, University of the West Indies, St. Augustine, Trinidad, West Indies.
[2]Undergraduate Research Associate, summer 1967.
[3]Alfred P. Sloan Foundation Fellow, 1967–1969.

TABLE I

Observed first order rate constants for thermal decomposition of peresters, $R—CO_2—OC(CH_3)_3$, in cumene*

R = 1-adamantyl		R = 1-bicyclo[2·2·2]octyl		R = 1-norbornyl	
Temperature (°C)	$k_{obsd} \times 10^4 s^{-1}$	Temperature (°C)	$k_{obsd} \times 10^4 s^{-1}$	Temperature (°C)	$k_{obsd} \times 10^4 s^{-1}$
60	0.54	80	0.51	110	0.46
70	2.12	90	1.57†	120	1.56
	1.99‡		1.67		1.63‡
80	7.35	100	4.86		1.57†
	7.05		4.66‡	125	2.79
	8.50†		4.97	130	4.99

*Concentration of perester 0.02–0.05 *M* unless noted.
†Perester concentration 0.23–0.28 *M*.
‡0.09–0.1 *M* 2,6-di-*t*-butyl-4-methylphenol added.

be obtained by the procedure of Boehme (12). However, the desired 1-bicyclo[2·2·2]octylcarboxylic acid has been commonly prepared by the many step synthesis of Grob *et al.* (13). A much more convenient synthesis of this acid is by using the Koch–Haaf carbonylation reaction (see refs. 7 and 14) on (1-norbornyl)methanol (from lithium aluminium hydride reduction of methyl 1-norbornylcarboxylate) in formic acid – sulfuric acid. A 70% yield (after recrystallization) was obtained and vapor phase chromatographic analysis of an esterified portion of the crude acid products showed only ca. 5% of two other compounds.

The peresters were characterized by their infrared (i.r.) and nuclear magnetic resonance (n.m.r.) spectra, and by C—H analysis. The norbornyl perester was sufficiently stable to allow purification by slow distillation under reduced pressure; the adamantyl perester was a low melting solid (m.p. 27–28.5°) when crystallized from acetone at −75°.

The kinetics of decomposition of these bridgehead peresters in cumene were followed by loss of their carbonyl absorption at ca. 1775 cm^{-1}. The absence of significant induced chain decomposition was shown when addition of a free radical chain inhibitor (0.1 *M* 2,6-di-*t*-butyl-4-methylphenol) or variation of initial peroxide concentration (by 10-fold up to 0.23 *M*) produced no important change in observed first order rate constants. These observed constants are given in Table I.

The products of decomposition of peresters 1, 2, and 3 were not completely determined, but the adamantyl compound in degassed cumene at 70° gave 98% CO_2, 24% acetone, 75% *t*-butyl alcohol, and 51% adamantane, while the bicyclo-[2·2·2]octyl perester similarly gave high yields of CO_2 (98%). The norbornyl perester at 125° also gave high yields of carbon dioxide (92%) and of norbornane (78%). Incomplete decarboxylation was indicated with this perester, however, since 1-norbornylcarboxylic acid, ca. 10%, was also present in the nonvolatile residue of the decomposition.

Discussion

A comparison of the relative rates of these bridgehead perester decompositions with those reported for peracetate and trimethylperacetate (15) esters is given in Table II. Bartlett and Greene (6), and Sager (16) concluded from a kinetic study of diapocamphoyl peroxide that a 1-bicyclo[2·2·1]heptyl (i.e., 1-norbornyl) structure largely eliminates from tertiary radicals the considerable degree of stabilization that they otherwise normally have over primary methyl radicals. This shows up in perester decompositions in that the rate constant for the norbornyl compound is the same as that of *t*-butylperoxy acetate (15) at 110°, and only greater by a factor of six when calculated at 80° (Table II). The high yields of CO_2, and the relatively lower $\Delta H^{\ddagger}$ and $\Delta S^{\ddagger}$ from the norbornyl perester suggest that it is on the edge of a change from one bond (—O—O—) to two bond concerted decomposition ($R—CO_2—OC(CH_3)_3$) (15) but a thorough series of product studies in the presence of trapping agents would be necessary to clarify this point. The measured rate is nevertheless a lower limit to estimated relative stability of norbornyl radicals.

The faster rates, still lower $\Delta H^{\ddagger}$ and $\Delta S^{\ddagger}$'s,

Can. J. Chem. Downloaded from www.nrcresearchpress.com by 210.87.254.42 on 09/05/12
For personal use only.

TABLE II

Relative rate constants at 80° and activation parameters* for decomposition of peresters R—CO_2—$OC(CH_3)_3$

R group	$\Delta H^{\ddagger}$ kcal/mole	$\Delta S^{\ddagger}$ e.u.	k/k, R = $(CH_3)_3C$—
CH_3—†	38	17	2.2×10^{-4}
1-Norbornyl-	35.9	14.8	1.4×10^{-3}
1-Bicyclo[2·2·2]-octyl-	28.7	2.8	9.9×10^{-2}
1-Adamantyl-	29.8	11.1	1.4
$(CH_3)_3C$—‡	30.0	11.1	1.0

*It can be calculated that estimated 5% errors in observed rate constants may lead to a variation of $\Delta H^{\ddagger}$ of 3 kcal/mole. Such a variation corresponds to those experimentally observed in reference 11 and this work.
†In chlorobenzene, see ref. 15.
‡In chlorobenzene, see ref. 24.

and the essentially quantitative yields of CO_2 from the bicyclo[2·2·2]octyl and adamantyl peresters show that direct formation of the corresponding bridgehead free radicals proceeds in the transition state by a two bond mechanism, (Tabushi, Hamuro, and Oda (17) have mentioned preliminary rate data which they interpret to mean that the 1-adamantyl perester does not decompose by a concerted mechanism. This differs from our conclusions which are the same as those reported in ref. 11). The rates are therefore good relative measures of radical stability.

It has been suggested that 1-adamantyl radical is especially stable compared to simple *t*-butyl radical (18, see ref. 19 and then ref. 1 for a discussion). However, the 1-adamantyl perester decomposes at a rate only slightly greater than that of *t*-butylperoxy trimethylacetate (which gives rise directly to *t*-butyl radicals). Other studies indicate that adamantyl radical is formed no faster from concerted perester decomposition than are related 1-methylcyclohexyl or acyclic *t*-alkyl radicals which have no constraints on formation of a planar structure (20). In carbonium ion formation a rate difference of 10^3 is found between 1-adamantyl bromide and *t*-butyl bromide solvolysis (1, 8, 9); in free radical formation from perester decomposition there is little difference at all.

While some difference in ease of radical formation between the two structures might be anticipated on the basis of the carbonium ion results, and while the adamantyl radical might be weakly stabilized by suggested (18, 9) special features, it seems likely that radical formation is simply insensitive to the mild constraints of the bridged adamantyl structure. The results here show that adamantyl radical is no *more* stable than any other tertiary alkyl free radical. Only when the bonds around the radical center are pulled still farther away from planarity than is the case with the adamantyl structure is the corresponding free radical made significantly less stable. Fort and Franklin (11) have recently pointed out that, relative to *t*-butyl radical, 1-adamantyl radical is weakly destabilized by a geometrical factor. However, this is slightly overweighed by the stabilizing inductive presence of larger alkyl groups and the observed result is a near equivalence in their rates of formation.

In a study of free radical decarbonylation of bridgehead aldehydes (involving competitive decarbonylation or hydrogen abstraction by alkylcarbonyl radicals, i.e. RCO $\rightarrow$ R· + CO or RCHO), Applequist and Kaplan (18) have concluded that 1-bicyclo[2·2·2]octyl radicals are about as stable as *t*-butyl radicals. Our results show this bridgehead free radical to be significantly less stable (the difference in rate of formation is a factor of ten), and, because the radicals are formed directly and no assumptions must be made on two different competing reactions, the perester decompositions are probably better measures of radical stabilities. But, in any case, the difference between nonplanar 1-bicyclo-[2·2·2]octyl radical and unconstrained *t*-butyl radical is relatively small. (In carbonium ion formation there is a difference of six powers of ten in 1-bicyclo[2·2·2]octyl bromide and *t*-butyl bromide solvolysis rates.)

A greatly decreased rate of decomposition occurs only in the case of the norbornyl perester which is 10^3 slower than the perester giving *t*-butyl radicals. Here radical formation becomes so difficult that decarboxylation of the perester in the initial step may not even be the major reaction (see above). The factor of 10^3 represents, however, a minimum difference for relative ability to form such a nonplanar free radical. This may be compared to the factor of 10^{14} between rates of formation of carbonium ions in the 1-bicyclo[2·2·1]heptyl and *t*-butyl structures (8).

These results clarify the relative energies of 1-adamantyl and 1-bicyclo[2·2·2]octyl radicals as well as more directly confirm and expand a previous generality; free radicals may take up nonplanar configurations with relatively little expense of energy. (Assuming the difference in free energy is due only to relative radical stability

Can. J. Chem. Downloaded from www.nrcresearchpress.com by 210.87.254.42 on 09/05/12
For personal use only.

Can. J. Chem. Downloaded from www.nrcresearchpress.com by 210.87.254.42 on 09/05/12
For personal use only.

in the transition state, the free energy differences at 80° relative to *t*-butyl radical are ca. 0.2 kcal for 1-adamantyl, 1.6 kcal/mole for 1-bicyclo-[2·2·2]octyl, and 4.6 kcal/mole for 1-norbornyl.)

As has been suggested for free radicals (18), and elegantly treated in the case of carbonium ions (9), the important factor in such relative stability might be that free radicals have smaller force constants for out-of-plane bending than do the corresponding carbonium ions. Adjacent bonding electrons are less attracted to a free radical center than to a cationic center and the bonds around a radical are therefore not as subject to this shortening and tightening influence.

Another description suggests that the relative ease of deformation of radicals is a consequence of the near equality of the energy levels for sp^2 and sp^3 hybridization arising from half occupancy of an orbital. When the orbital is vacant (i.e. carbonium ions), there is a strong preference for an sp^2 planar structure; when full (i.e. carbanions), an sp^3 configuration is strongly favored. According to this, the total energy difference between hypothetical planar and pyramidal carbonium ions, carbanions, and free radicals is the smallest for free radicals. As the deviations from planarity required to accommodate radicals at strained bridgehead positions involves some fraction of this relatively smaller energy, radicals are more readily produced in a nonplanar structure than are carbonium ions. Comparison of relative rate ratios for carbonium ion formation to the corresponding ratios for radical production in the bicyclic systems reported here presents a good illustration of this point.

Experimental

t-Butyl 1-Adamantylpercarboxylate (1)

The preparative method is similar to that of Bartlett and McBride (21). A stirred suspension of 10.0 g of sodium *t*-butylperoxide in 250 ml of dry dichloromethane was cooled to −6° in an ice–salt bath. A solution of 8.6 g of 1-adamantylcarbonyl chloride in 50 ml of CH_2Cl_2 was added dropwise over ¾ h. After stirring at −6° for 4.5 h and storage at ca. −5° overnight, the white precipitate was filtered off and most of the CH_2Cl_2 was evaporated at reduced pressure. The product was taken up in 100 ml of petroleum ether (b.p. 30–60°) and washed with portions cold 8% $NaHCO_3$ solution and with water. The solution was dried ($MgSO_4$) and evaporated and the resulting oil crystallized from acetone at ca. −75°. After filtration the white solid melted at room temperature but when all the acetone was removed under vacuum the resulting solid melted at 27.0–28.5°. A yield of 5.2 g (50%) was obtained after recrystallization. The infrared (i.r.) spectrum of neat perester showed strong peaks at 2920, 1775, 1190, and 1170 cm^{-1}. Its nuclear magnetic resonance (n.m.r.) spectrum in $DCCl_3$ showed a singlet at 8.0 and a multiplet at τ 8.3.

Anal. Calcd. for $C_{15}H_{24}O_3$: C, 71.39; H, 9.59. Found: C, 71.26; H, 9.21.

t-Butyl 1-Norbornylpercarboxylate (3)

2-*exo*-Bromonorbornyl-1-carboxylic acid was prepared according to Boehme's procedure (12). Dehalogenation of this acid was best carried out by hydrogenation at 50 p.s.i. of 20 g bromoacid in 200 ml of methanol–water (3:1 by volume) containing 8 g of NaOH and 5 g of palladium (10%) on charcoal. 1-Norbornylcarbonyl chloride (b.p. 87–88.5° at 17 mm) was then prepared from the acid and thionyl chloride.

The perester was prepared at 0° from 5.0 g of acid chloride and 5.0 g of sodium *t*-butylperoxide in 70 ml of ether, by the procedure given above for the adamantyl perester. After washing with 10% $NaHCO_3$ solution and with water, the product in petroleum ether was passed through a 3 cm high Florisil column and distilled in a short path apparatus, b.p. 40° at 0.05 mm. The i.r. spectrum of this 1-norbornyl perester showed strong peaks at 3000, 1775, 1360, 1190, and 1150 cm^{-1}; the n.m.r. spectrum showed a singlet at 7.68 (bridgehead H), a multiplet centered at 8.42 and a singlet at τ 8.75.

Anal. Calcd. for $C_{12}H_{20}O_3$: C, 67.89; H, 9.50. Found: C, 68.22; H, 9.53.

Bicyclo [2·2·2]octylcarboxylic Acid

Methyl 1-norbornylcarboxylate was reduced with $LiAlH_4$ in refluxing ether for 15 h to give (1-norbornyl) methanol, m.p. 60.5–62.0° after sublimation.

To a rapidly stirred solution of 150 ml 96% H_2SO_4 and 70 ml 30% oleum at 10° were added 3 ml of formic acid. Then a solution of 10 g of (1-norbornyl)methanol in 30 ml of formic acid was added over 2.5 h, care being taken that rapid stirring kept up the frothing of the solution. The mixture was poured onto 3 l of ice and extracted with ether. After washing and extraction into 10% NaOH solution the aqueous solution was acidified and extracted with ether. After drying ($MgSO_4$), evaporation, and then recrystallization of the residue from methanol–water, 9 g (70%) of bicyclo[2·2·2]octyl acid were obtained, m.p. 139–140° (lit. 140.8–141.3°) (22). The n.m.r. spectrum, singlet at −2.8 (1 H) and τ 8.3 (13 H's), and i.r. spectrum were consistent with this structure. Vapor-phase chromatography on an esterified (with CH_2N_2) portion of the crude product showed only 5% of product other than methyl 1-bicyclo[2·2·2]octylcarboxylic acid.

t-Butyl 1-Bicyclo[2·2·2]octylpercarboxylate (2)

The acid chloride (from the above acid preparation and thionyl chloride) was treated with a 20% excess of sodium *t*-butylperoxide in ether at 5°. Workup was similar to that of the other peresters above. The product was an oil, too unstable for distillation, which showed a broad n.m.r. peak in $DCCl_3$ at 8.3 and a singlet at τ 8.7.

Anal. Calcd. for $C_{13}H_{21}O_3$: C, 68.99; H, 9.80. Found: C, 69.26; H, 9.69.

Kinetic Studies

Reaction progress was followed by disappearance of the perester carbonyl absorption at ca. 1780 cm^{-1} (15, 23).

The kinetic samples were analyzed on a Perkin–Elmer Infracord model 137. The cumene solvent used was washed with sulfuric acid, water dried with $CaCl_2$, then refluxed, and distilled from sodium.

Product Studies

Samples of 0.8 to 1.6 g of peresters were decomposed in 25 ml of degassed cumene according to a general reported procedure (23). Carbon dioxide was analyzed by pressure and by absorption on Ascarite. Volatile products in the solvent were analyzed by vapor-phase chromatography to within an estimated 10%. Products were identified by either collection (then i.r. and n.m.r. spectra) and/or by comparison of retention times with authentic samples.

Acknowledgments

We gratefully acknowledge support from the donors to the American Chemical Society Petroleum Research Fund, from the National Research Council of Canada, and from the Committee on Research of the University of British Columbia. We thank Professors R. C. Fort, Jr. and J. P. Lorand for exchanges of manuscripts prior to publication.

1. R. C. FORT, JR. and P. VON R. SCHLEYER. *In* Advances in alicyclic chemistry. *Edited by* H. Hart and G. J. Karabatsos. Academic Press, Inc., New York. p. 283.
2. R. M. NOYES, D. E. APPLEQUIST, S. W. BENSON, D. M. GOLDEN, and P. S. SKELL. J. Chem. Phys. **46**, 1221 (1967); W. A. Pryor. Free radicals. McGraw-Hill Book Co., Inc., New York. 1966; R. W. FESSENDEN. J. Phys. Chem. **71**, 74 (1967), and references therein.
3. R. S. DRAGO and H. PETERSEN, JR. J. Am. Chem. Soc. **89**, 5774 (1967).
4. H. M. WALBORSKY and C-J. CHEN. J. Am. Chem. Soc. **89**, 5499 (1967).
5. D. I. DAVIES and S. J. CRISTOL. *In* Advances in free-radical chemistry. Vol. 1. *Edited by* G. H. Williams. Logos Press Ltd., London. 1965. p. 155.
6. P. D. BARTLETT and F. D. GREENE. J. Am. Chem. Soc. **76**, 1088 (1954).
7. T. MCALLISTER, Z. DOLESEK, F. P. LOSSING, R. GLEITER, and P. VON R. SCHLEYER. J. Am. Chem. Soc. **89**, 5982 (1967).
8. R. C. FORT, JR. and P. VON R. SCHLEYER. Chem. Rev. **64**, 277 (1964).
9. G. J. GLEICHER and P. VON R. SCHLEYER. J. Am. Chem. Soc. **89**, 582 (1967).
10. W. G. BENTRUDE. Ann. Review of Phys. Chem. **18**, 283 (1967); C. RUCHARDT. Fortschr. Chem. Forsch. **6**, 251 (1966).
11. R. C. FORT, JR. and R. E. FRANKLIN. Abstracts of papers presented at the 154th Meeting, American Chemical Society, Chicago, Ill., Sept. 11–15th, 1967, p. 5–165. R. C. FORT, JR. and R. E. FRANKLIN. J. Am. Chem. Soc. **90** (1968); J. P. LORAND, S. D. CHODROFF, and R. W. WALLACE. J. Am. Chem. Soc. **90** (1968).
12. W. BOEHME. J. Am. Chem. Soc. **81**, 2762 (1959).
13. C. A. GROB, M. OHTA, E. RENK, and A. WEISS. Helv. Chim. Acta, **41**, 1191 (1958).
14. H. KOCH and W. HAAF. Ann. **618**, 251 (1958).
15. P. D. BARTLETT and R. HIATT. J. Am. Chem. Soc. **80**, 1398 (1958). R. HIATT. Ph.D. Thesis. Harvard University. Boston, Massachusetts. 1956.
16. W. F. SAGER. Ph.D. Thesis. Harvard University. Boston, Massachusetts. 1948.
17. I. TABUSHI, J. HAMURO, and R. ODA. J. Am. Chem. Soc. **89**, 7127 (1967).
18. D. E. APPLEQUIST and L. KAPLAN. J. Am. Chem. Soc. **87**, 2194 (1965); P. T. LANSBURY and J. D. SIDLER. Chem. Commun. 373 (1965).
19. F. W. BAKER, H. D. HOLTZ, and L. M. STOCK. J. Org. Chem. **28**, 514 (1963).
20. W. SCHINDEL. Unpublished results. University of British Columbia.
21. P. D. BARTLETT and J. M. MCBRIDE. J. Am. Chem. Soc. **87**, 1727 (1965).
22. J. D. ROBERTS, W. T. MORELAND, JR., and W. FRAZER. J. Am. Chem. Soc. **75**, 637 (1953).
23. P. D. BARTLETT, E. P. BENZING, and R. E. PINCOCK. J. Am. Chem. Soc. **82**, 1762 (1960).
24. P. D. BARTLETT and D. M. SIMONS. J. Am. Chem. Soc. **82**, 1753 (1960).

Can. J. Chem. Downloaded from www.nrcresearchpress.com by 210.87.254.42 on 09/05/12
For personal use only.

Can. J. Chem. Downloaded from www.nrcresearchpress.com by 210.87.254.42 on 09/05/12
For personal use only.

The dienone–imine intermediate in the Fischer indole synthesis

G. S. BAJWA AND R. K. BROWN
Department of Chemistry, University of Alberta, Edmonton, Alberta

Received February 19, 1968

Condensation of *N'*-methyl-2,6-dimethylphenylhydrazine hydrochloride with isobutyraldehyde in dry benzene gave the hydrochloride of a dienone–imine (**7**) considered to be obtained from the dienone–imine (**6**) which is believed to be an intermediate in the Fischer indole synthesis.

Canadian Journal of Chemistry, 46, 3105 (1968)

Considerable evidence (1) has accumulated to support the Robinson mechanism (2) for the Fischer indole synthesis. Some of this has dealt with attempts to isolate compounds which are thought to be intermediates, and indeed, by 1958, reports of such intermediates had appeared. One concerned the sparingly soluble hydrochloride of α-ketimino-β-(*o*-aminophenyl)-γ-butyrolactone (**1**) obtained from cyclization of α-keto-γ-butyrolactone phenylhydrazone (3, 4) in glacial acetic acid containing hydrogen chloride. The structure of the free base has been examined recently (5) with the aid of nuclear magnetic resonance spectroscopy (n.m.r.) and

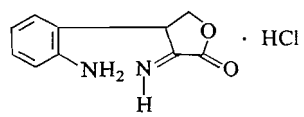

1

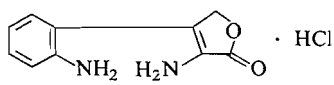

1a

found to be the enamine (**1a** free base) rather than the ketimine (**1**). Another intermediate reported (6) is 3-acetylamino-2-(*o*-aminophenyl)-butene-2 (**2**) obtained from the treatment of 2-(*N,N'*-diacetyl-β-phenylhydrazine)-butene-2 (**3**) with hot aqueous potassium hydroxide.

As yet, no report has appeared describing the isolation of the dienone–imine (e.g. **4**), although attempts have been made either to trap the dienone–imine intermediate, in the zinc chloride catalyzed reaction of ethyl pyruvate 2,6-dimethylphenylhydrazone, as the Diels–Alder adduct

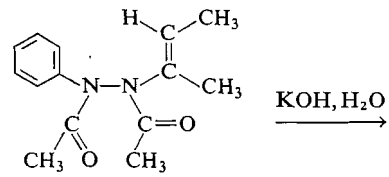

3

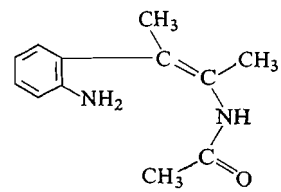

2

with maleic anhydride (7), or to arrest the reaction (8) by the use of suitably placed halogen substituents (R = Cl in **4**).

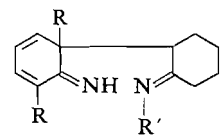

4

The present communication reports the isolation of a dienone–imine (**7**), obtained by heating a mixture of *N'*-methyl-2,6-dimethylphenylhydrazine hydrochloride and isobutyraldehyde in refluxing dry benzene (Scheme 1).

The principle in this scheme was to provide methyl substituents at locations such that (*a*) aromatization of the dienone–imine ring system, e.g. in **6**, would be difficult and (*b*) conversion of the imino system of the aldehyde or ketone moiety (cf. **6**) to the enamine would also be hindered. In this way it was hoped that there

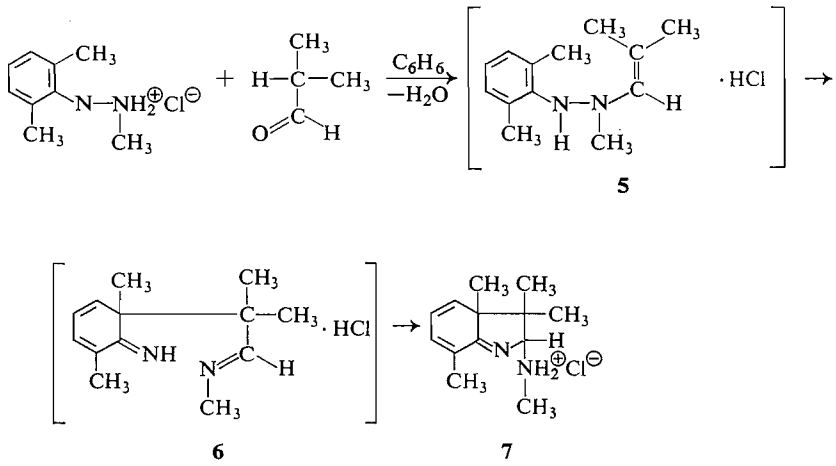

SCHEME 1

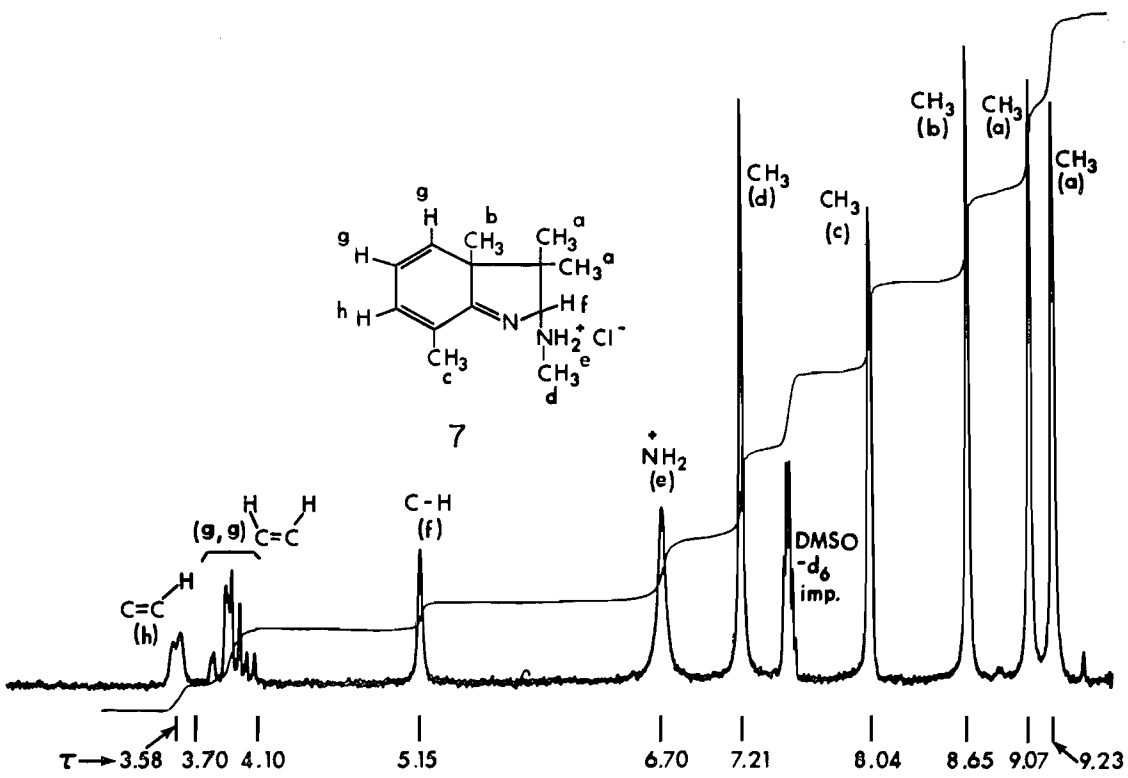

FIG. 1. 100 MHz spectrum of 7 (hydrochloride) in dimethyl sulfoxide-d_6, referred to tetramethylsilane.

Can. J. Chem. Downloaded from www.nrcresearchpress.com by 210.87.254.42 on 09/05/12
For personal use only.

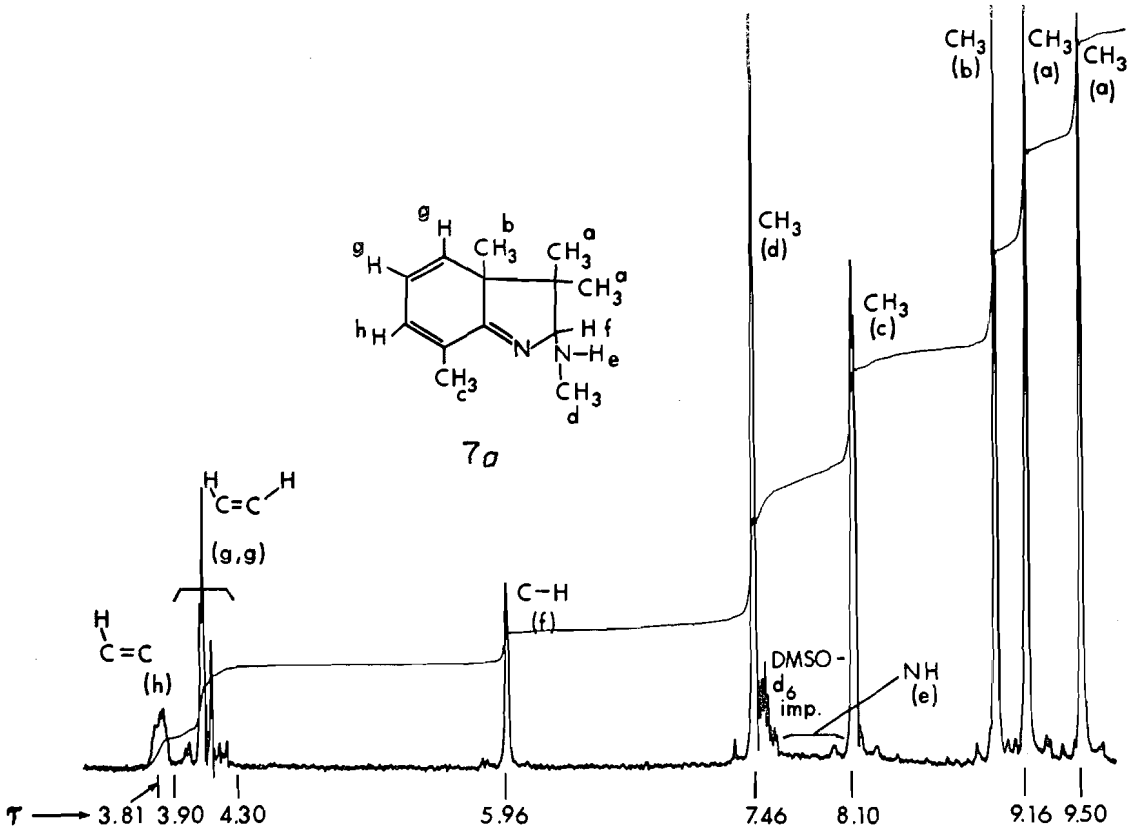

FIG. 2. 100 MHz spectrum of **7** (free amine) in dimethyl sulfoxide-d_6, referred to tetramethylsilane.

would be no 'amino' group readily available to add to an imino unit and thus bring about cyclization.

The formation of water, removed by azeotropic distillation with the benzene, provided evidence that the hydrazine had reacted with the aldehyde to form the enamine **5**. To date we have been unable to isolate this enamine or to arrest its apparently very great tendency to continue on with the next stage of the reaction (9).

The solid which was isolated, analyzed correctly for the hydrochloride of either of the dienone–imines, **6** or **7**. The ultraviolet absorption spectrum of the free base in ethanol showed a narrow band of 204 mμ and a broad band at 310 mμ, in agreement with a conjugated triene system. However, the nuclear magnetic resonance spectrum of the salt and the free base derived from it (Figs. 1 and 2) in deuterated dimethyl sulfoxide clearly showed that **7** was the correct structural assignment.

No aromatic proton signals were discernible in the region τ 2.0–3.5. The three high field singlets (τ 8.6–9.6), each representing three protons, were assigned to the three aliphatic methyl groups *a*, *a*, *b*. The protons of the two methyl groups, *a*, *a*, should have different chemical shifts, as was observed. These are time averaged because of the rotary oscillation (limited) of this *gem* dimethyl group. A sufficient decrease in the rate of this oscillation should cause a broadening of each of the signals, with eventual formation of a doublet for each. When ethanol-d_6 solutions of either the free amine or the hydrochloride were cooled to $< -40°$, the two highest field singlets (*a*,*a*) did broaden increasingly until a temperature of $-90°$ was obtained. The signal for the protons of the methyl group *b* broadened only slightly under these conditions. At this temperature precipitation of the solute occurred, thus imposing a limit to this resolution. The observed broadening, however, did support the

Can. J. Chem. Downloaded from www.nrcresearchpress.com by 210.87.254.42 on 09/05/12
For personal use only.

Can. J. Chem. Downloaded from www.nrcresearchpress.com by 210.87.254.42 on 09/05/12
For personal use only.

assignment of the two highest field signals to the methyl groups labelled *a*, *a* (Figs. 1 and 2). The remaining high field signal, *b*, must then be due to the protons of the methyl groups attached to the sp^3 hybridized carbon of what was formerly the aromatic ring.

The signal (3H) lying between τ 8.04–8.10 (Figs. 1 and 2) was assigned to the protons of the methyl group *c*, since this is the region expected for the signals of protons of a methyl group attached to C=C. The singlet, *d*, (3H) in the region τ 7.0–7.4 was assigned to the N—CH_3 group for similar reasons. The singlet (2H) at τ 6.70 (Fig. 1) was assigned to the NH proton and the proton of the hydrogen chloride since this signal disappeared when deuterium oxide was added. The coincidence of the signals for these two protons indicates that the nitrogen atom which is protonated in the hydrochloric acid salt is that which already has one proton attached (*e*). This proton in the free amine (Fig. 2) gives a broad low signal over the range τ 7.4–8.2, which is eliminated on deuteration. The spectrum of the free amine in $CDCl_3$ showed the N—H proton as a broad singlet, $w/2 \sim 3.5$ Hz at τ 8.65.

The signal (1H) at τ 5.15 (Fig. 1) and at τ 5.96 (Fig. 2) was due to the former aldehyde proton *f*. Since in structure 7 this proton is very much like the anomeric proton in the glycosides or the acetals (—O—CH—O), it is expected to produce a signal in a part of the n.m.r. spectrum where such anomeric protons absorb. This is the only reasonable signal assignment to be made for proton *f*. It is the position of the signal for *f* which is one of the two reasons why the compound under discussion must have structure **7** and not structure **6**. In structure **6**, the signal for this former aldehydic proton would appear well downfield, in the region τ 0–1.0.

The remaining three protons of structure **7** are found to absorb in the region expected for olefinic protons. The narrow multiplet (1H) centered at τ 3.58 (Fig. 1) and 3.81 (Fig. 2) was assigned to proton *h*. Support for this was obtained from the finding that irradiation at τ 3.81 (Fig. 2) caused a collapse of the narrow doublet at τ 8.10 to a singlet with loss of coupling of 1.7 Hz. In turn, irradiation at τ 8.10 clearly simplified the multiplet at τ 3.81 but had little effect on the multiplet at τ 3.95–4.3. It is expected that stronger coupling would occur between the protons of the methyl group *c* and proton *h* than between *c* and protons *g*,*g*.

All attempts to detect coupling between protons *e* and *f* have been unsuccessful. Apparently this is due to rapid exchange involving the N—H proton.

Finally, of significance is the discovery of a small, long-range coupling (0.7 Hz) between protons *f* and *h*. Such a coupling could occur only if the compound had the structure shown in **7**. No such coupling would be possible between these protons if the structure were **6**. This is the second convincing piece of evidence that structure 7 is to be preferred to structure **6**.

We had hoped that the methyl groups would prevent cyclization. However, it is clear that although structure **6** does contain two imino groups which are not easily converted to *amino* groups by proton elimination, proton catalyzed addition of the =NH unit to the *N*-methyl imino group is facilitated due to delocalization of the positive charge (Scheme 2). The loss of

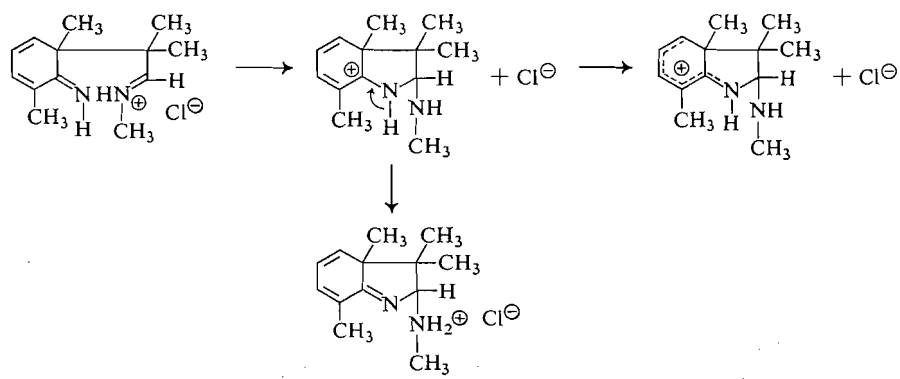

SCHEME 2

the proton on the former =N—H group would then permit the formation of the neutral molecule 7 now protonated on the methylated nitrogen atom.

The above information provides good evidence that a dienone–imine (7) has been obtained, and thus further supports the present view of the mechanism of the Fischer indole synthesis.

Experimental

Melting points are uncorrected. Elemental analyses were made by Mrs. Darlene Mahlow of the Microanalytical Laboratory in this Department. Nuclear magnetic resonance spectra were obtained by Mr. Glen Bigham with an HR 100 MHz Varian spectrometer. Ultraviolet spectra were obtained with a Perkin–Elmer 202 ultraviolet–visible spectrometer using fused silica cells. Infrared spectra were obtained with a Perkin–Elmer 421 grating spectrometer. The latter spectra were run by Mr. R. Swindlehurst and assistants.

A mixture of 1 g (0.0054 mole) of *N'*-methyl-2,6-dimethylphenylhydrazine hydrochloride (9) and 0.5 g (0.0069 mole) of isobutyraldehyde was heated for 30 min in refluxing dry benzene in an apparatus equipped with a trap to collect the azeotropically distilled water. The mixture became yellow in 10–15 min. After the 30 min reflux period, a further quantity (1 g) of isobutyraldehyde was added and refluxing was continued overnight. The cooled mixture was filtered and the solid was washed with dry ether (2 × 10 ml). Yield of crude material, 860 mg, m.p. 170–172°. This was crystallized three times by solution in 95% ethanol and addition of ether to faint turbidity. Yield of pure material (7) 520 mg (40%), m.p. 186°.

Anal. Calcd. for $C_{13}H_{21}N_2Cl$: C, 64.87; H, 8.73; N, 11.64; Cl, 14.74. Found: C, 65.00; H, 8.77; N, 11.59; Cl, 14.89.

The mother liquor was freed from benzene solvent in a rotary evaporator under vacuum giving a dark red oil (510 mg). This oil appeared to be a mixture of starting material and some dienone–imine.

The infrared spectrum of the hydrochloride (7) in Nujol showed a strong band at 1575 cm^{-1} (conjugated C=C and C=N stretching, (10)) and a weak band at 1630 cm^{-1} (nonconjugated C=N stretching (10)). A weak, though sharp band at 2440 cm^{-1} and a broad strong band at 2700–2790 cm^{-1} indicated $NH^{\oplus}$ (10, p. 260). Faint absorption in a broad band at 3400 cm^{-1} supported N—H (bonded).

The ultraviolet absorption spectrum of the hydrochloride (7) in ethanol (95%) showed a narrow band at λ_{max} 205 mμ (ε = 15 390), and a broad band at λ_{max} 320 mμ (ε = 5290).

The details of the nuclear magnetic resonance spectrum of the hydrochloride 7 in dimethyl sulfoxide-d_6 (DMSO-d_6) are shown in Fig. 1. The signal assignments are presented in the discussion.

A solution of the dienone–imine hydrochloride, 7, (0.5 g) in water (30 ml) was treated with a slight excess of 0.1% aqueous sodium bicarbonate. The ether extract (2 × 50 ml) of this solution was washed with water (3 × 30 ml) and dried ($MgSO_4$) for 30 min. The $MgSO_4$ was separated and the filtrate freed from ether in a rotary evaporator under vacuum for 6 h at room temperature. The residual yellow oil became crystalline when it stood in a refrigerator overnight. The crystals were washed with a 1:1 solution of 95% ethanol and water; yield, 304 mg of the free imine (7*a*), m.p. 37–38°.

Anal. Calcd. for $C_{13}H_{20}N_2$: C, 76.47; H, 9.80; N, 13.72. Found: C, 76.48; H, 9.67; N, 13.78.

The infrared spectrum of the free imine, 7*a*, in Nujol showed a sharp weak band at 3330 cm^{-1} (NH), a sharp medium band at 1630 cm^{-1} (C=N) and a strong band at 1585 cm^{-1} (conjugated C=C or C=N).

The nuclear magnetic resonance spectrum of the free imine, 7*a*, in DMSO-d_6, and the signal assignments are shown in Fig. 2.

The ultraviolet absorption spectrum in ethanol showed a narrow band, λ_{max} 204 mμ (ε = 6490), and a broad band, λ_{max} 310 mμ (ε = 3155).

Acknowledgments

The authors are grateful for financial assistance provided by the National Research Council of Canada during the course of this work.

1. B. Robinson. Chem. Rev. **63**, 373 (1963).
2. G. M. Robinson and R. Robinson. J. Chem. Soc. **113**, 639 (1918).
3. H. Plieninger. Ber. **83**, 273 (1950).
4. H. Plieninger and I. Nogradi. Ber. **88**, 1964 (1955).
5. R. J. Owellen, J. A. Fitzgerald, B. M. Fitzgerald, D. A. Walsh, D. M. Walker and P. L. Southwick. Tetrahedron Letters, 1741 (1967).
6. N. N. Suvorov, N. P. Sorokina, and Yu. N. Sheinker. J. Gen. Chem. USSR, Engl. Transl. **28**, 1058 (1958).
7. R. B. Carlin, W. O. Henly, Jr., and D. P. Carlson. J. Am. Chem. Soc. **79**, 5712 (1957).
8. F. R. Robinson and R. K. Brown. Can. J. Chem. **42**, 1940 (1964).
9. G. S. Bajwa and R. K. Brown. Can. J. Chem. **46**, 1927 (1968).
10. L. J. Bellamy. The infrared spectra of complex molecules. 2nd ed. 1958. John Wiley and Sons, Inc., New York. p. 268.

Can. J. Chem. Downloaded from www.nrcresearchpress.com by 210.87.254.42 on 09/05/12
For personal use only.

Temperature dependence of proton magnetic resonance solvent shifts. 3,5-Dichlorosalicylaldehyde in carbon tetrachloride and benzene

G. KOTOWYCZ[1] AND T. SCHAEFER
Chemistry Department, University of Manitoba, Winnipeg, Manitoba

Received April 29, 1968

The ring proton chemical shifts of 3,5-dichlorosalicylaldehyde as a function of temperature in carbon tetrachloride and benzene solutions indicate that if there is association with solvent molecules in benzene solution, then there is also association with carbon tetrachloride solvent molecules. The aldehydic proton shift shows a much smaller (relative) temperature dependence in the carbon tetrachloride solution.

Canadian Journal of Chemistry, 46, 3110 (1968)

TABLE I

Solvent shifts* of ring and aldehydic protons in 3,5-dichlorosalicylaldehyde†

Proton	CS_2	CCl_4	$CDCl_3$	CH_2Cl_2	C_6D_6	C_6F_6	$(CH_3)_2CO$	CH_3CN
4	−0.015	−0.076	−0.102	−0.107	0.432	0.001	−0.229	−0.167
6	−0.110	−0.127	−0.188	−0.215	0.864	−0.244	−0.525	−0.364
CHO	−0.096	−0.113	−0.131	−0.125	0.976	−0.233	−0.324	−0.149

*In p.p.m. relative to the shift in a saturated (<2.5 mole%) solution in cyclohexane. The shifts in cyclohexane, relative to internal tetramethylsilane are 7.479 (H-4), 7.282 (H-6), and 9.710 (CHO) p.p.m. Temperature of measurement was 30 ± 1 °C. Precision of measurement was ±0.002 p.p.m.
†Concentrations were 5 mole % or less (saturated) in the given solvents.

The study of aromatic solvent induced shifts (ASIS) in proton magnetic resonance has concentrated on their use for structural and conformational determinations as well as on their origin (refs. 1 and 2 give a bibliography). The notion of a 1:1 complex between the polar solute and the aromatic solvent molecules appears to be untenable (1, 2). Carbon tetrachloride is often used as the reference solvent, assumed to be inert, and at least in some instances (3) proton shifts of solute molecules show no temperature dependence in this solvent. From an extensive investigation (4) of the proton resonance of 3,5-dichlorosalicylaldehyde we here abstract the information relevant to a consideration of the origin of ASIS and the use of carbon tetrachloride as a reference solvent.

Solvent and Temperature Dependence of Ring Proton Shifts

In Table I the solvent shifts of the ring and aldehydic protons relative to a saturated solution (<2.5 mole%) in cyclohexane are given at 30 ± 1 °C. In Fig. 1, the shift of proton-6 (ortho to CHO) is plotted against temperature in the saturated (<5 mole %) carbon tetrachloride and the 5 mole % benzene-d_6 solutions. Similar plots are found for proton-4 and for 2.5, 6, 7.5, and 10 mole % solutions in benzene-d_6. The plots are definitely curved.

The curvature of the plots is presumably a concentration effect. By an extrapolation procedure in which the shift at a given temperature is plotted versus concentration, the 0 mole % solution in benzene yields a precisely linear (±0.002 p.p.m.) dependence on temperature of the ring proton shifts. The low solubility in carbon tetrachloride precluded a reliable extrapolation procedure in this solvent.

In Table II the change in shift over a range of 100 °C is divided by the solvent shift (Table I) at 30 °C for the carbon tetrachloride and benzene solutions. For the ring protons this ratio is almost the same in the two solvents. The usual procedure (1, 5) for calculating heats of formation of an assumed 1:1 complex depends on such ratios and therefore similar small values of heats of formation (0.5 to 1 kcal/mole) will be obtained for both solvents. The much greater temperature dependence of the ring proton shifts in benzene solution is a reflection of the large magnetic anisotropy of the solvent molecules and need not, of course, reflect a larger energy of interaction between solute and solvent molecules. Finally,

[1]Present address: Lawrence Radiation Laboratory, University of California, Berkeley, California.

Can. J. Chem. Downloaded from www.nrcresearchpress.com by 84.22.46.98 on 09/08/12
For personal use only.

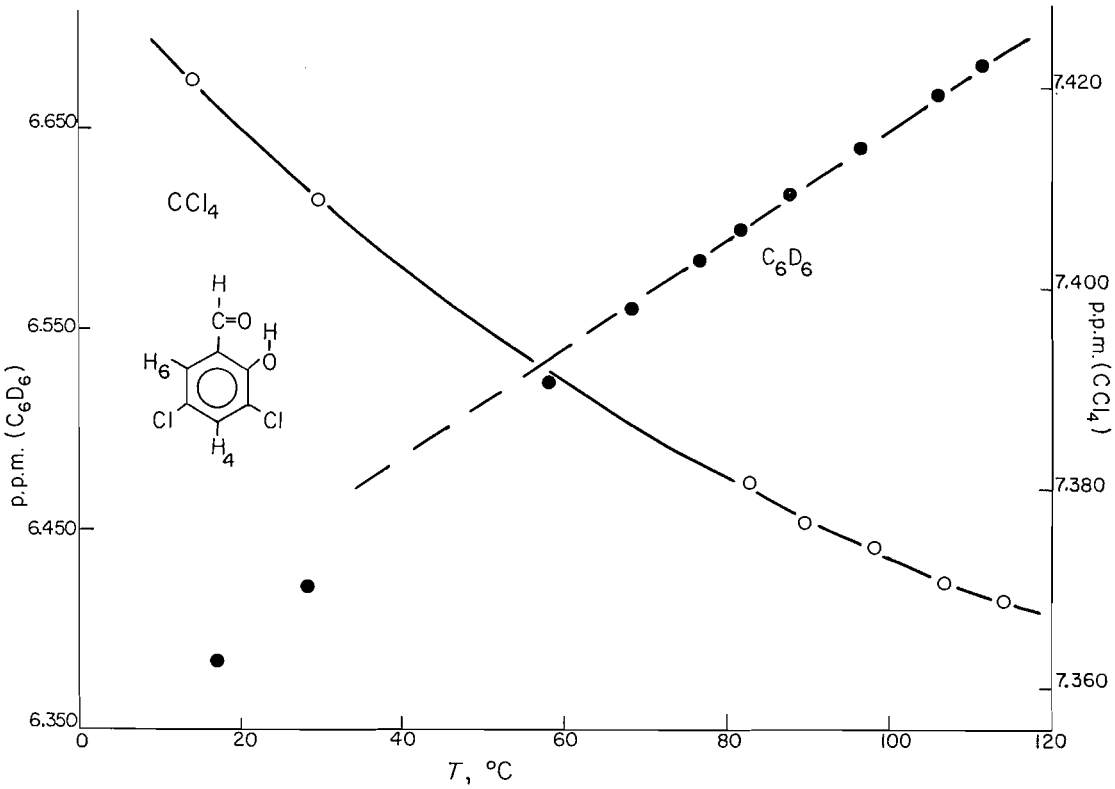

FIG. 1. The chemical shift, relative to internal tetramethylsilane, of proton-6 in 3,5-dichlorosalicylaldehyde is plotted vs. temperature for a saturated (< 5 mole %) solution in carbon tetrachloride (open circles) and for a 5 mole % solution in benzene-d_6 (closed circles). The shift scale in p.p.m. on the left refers to the benzene solution and the shift scale on the right refers to the carbon tetrachloride solution.

carbon tetrachloride should be avoided as a reference solvent in the study of aromatic proton shifts.

Aldehydic Protons

The aldehydic proton shift in the benzene solutions is a precisely linear function of the temperature over a range of 100 °C in the benzene solutions at concentrations from 2.5 to 10 mole %.

TABLE II

Ratio* of temperature shift to solvent shift at 30 °C in benzene and carbon tetrachloride solutions

Proton	CCl_4	C_6D_6
4	0.37	0.34
6	0.41	0.34
CHO	0.08	0.35

*The range of temperature is 100 °C and the change in shift over this range is divided by the solvent shift at 30 °C. The solvent shifts are taken from Table I.

We have no explanation for the contrasting behavior of the aldehydic and ring protons. Furthermore, the temperature dependence of the aldehydic proton shift in carbon tetrachloride solution amounts to only 0.008 p.p.m. between 30 and 120 °C. The ratios in Table II emphasize the exceptional behavior of the aldehydic proton in carbon tetrachloride. The intramolecular hydrogen bond holds the aldehydic proton in the position near that of proton-6 (4) and, on the basis of short-lived collisional complexes, a similar temperature dependence of the two protons might have been expected.

Such is indeed the case for the benzene solutions (Table II). Perhaps there is a short-lived complex between the aromatic solute ring (donor) and the carbon tetrachloride solvent molecule (acceptor); the existence of which is reflected in the larger temperature dependence of the ring proton shifts. There is some evidence (6) from ultraviolet data for such complexes between

Can. J. Chem. Downloaded from www.nrcresearchpress.com by 84.22.46.98 on 09/08/12
For personal use only.

benzene itself and carbon tetrachloride. In that case, the reported temperature independence of the shifts of protons in nonaromatic molecules dissolved in carbon tetrachloride (3) is consistent with the present results. It is also interesting to note that donor solvents containing oxygen have little or no effect on the Raman vibrational intensities of carbon tetrachloride (7). On the other hand, the intensity changes caused by aromatic donors have been interpreted on the basis of specific molecular interactions (7).

Other Solvents

For the present solute molecule carbon disulfide (Table I) is preferable to carbon tetrachloride as a reference solvent, contrary to one recommendation (ref. 1, p. 244). This appears to be so for other solute types as well, e.g. 1,1-difluoroethylene (8). Notice also that perfluorobenzene does not induce the high-field shifts expected from a large magnetic anisotropy. This point is under investigation,[2] especially in view of the relatively strong complexes reported to occur between aromatic donor molecules and perfluorobenzene (10). The relative solvent shifts observed in acetone and acetonitrile (dielectric constants, respectively, near 20, 35) cannot easily be explained by reaction field effects (11). Such anomalies are, of course, quite common (1, 12). In acetone and acetonitrile solutions the hydroxyl proton shifts are 11.36 and 11.27 p.p.m. to low field of internal tetramethylsilane, respectively, whereas in the cyclohexane the shift is 11.28 p.p.m. (4). The aldehyde group is therefore in the planar, hydrogen-bonded conformation and the solvent shifts are not complicated by conformational changes of the anisotropic aldehyde group.

[2]A referee suggests a small magnetic anisotropy (unknown) for perfluorobenzene. In perchlorobenzene the magnetic anisotropy is only 10% lower than in benzene (9). Susceptibility measurements on a single crystal of perfluorobenzene are needed.

Experimental

Solutions were degassed by the freeze – pump – thaw technique. Tetramethylsilane served as an internal reference. Spectra were run on a DA-60I spectrometer in the frequency sweep mode and calibration of peak positions involved period averaging techniques. Root mean square deviations of the shifts were typically 0.002 p.p.m. or less. Temperatures were measured by means of ethylene glycol or methanol samples as provided by Varian Associates. Although absolute temperatures may be in error up to 2 °C, temperature differences must be more accurate as shown by our detailed results.

Acknowledgment

We are grateful to the National Research Council of Canada for financial assistance.

1. P. LASZLO. *In* Progress in nuclear magnetic resonance spectroscopy. Vol. 3. *Edited by* J. W. Emsley, J. Feeney, and L. H. Sutcliffe. 1967. Chap. 6.
2. P. LASZLO and J. L. SOONG, JR. J. Chem. Phys. **47**, 4472 (1967).
3. R. C. FORT, JR. and T. R. LINDSTROM. Tetrahedron, **23**, 3227 (1967).
4. G. KOTOWYCZ. Ph.D. Thesis, University of Manitoba, Winnipeg, Manitoba. 1967.
5. R. J. ABRAHAM. Mol. Phys. **4**, 369 (1961).
6. R. F. WEIMER and J. M. PRAUSNITZ. J. Chem. Phys. **42**, 3643 (1965).
7. D. A. BAHNICK and W. P. PERSON. J. Chem. Phys. **48**, 1251 (1968).
8. C. J. MACDONALD and T. SCHAEFER. Can. J. Chem. **45**, 3157 (1967).
9. A. A. BOTHNER-BY and J. A. POPLE. *In* Annual review of physical chemistry. Vol. 16. *Edited by* H. Eyring. Annual Reviews, Inc. Palo Alto, California. 1965.
10. W. A. DUNCAN and F. L. SWINTON. Trans. Faraday Soc. **62**, 1082 (1966).
11. A. D. BUCKINGHAM. Can. J. Chem. **38**, 300 (1960).
12. H. M. HUTTON and T. SCHAEFER. Can. J. Chem **43**, 3116, (1965).

Reaction of iron carbonyls with amides and thionamides

HOWARD ALPER AND JOHN T. EDWARD
Department of Chemistry, McGill University, Montreal, Quebec

Received June 18, 1968

Iron pentacarbonyl in boiling butyl ether converts primary amides or thionamides to nitriles, and benzanilide or thionbenzanilide to *N*-benzylideneaniline. Diiron nonacarbonyl reacts with *p*-methoxythionbenzamide to form a complex $C_{22}H_{16}N_2S_2O_8Fe_2$; a possible structure is proposed.

Canadian Journal of Chemistry, 46, 3112 (1968)

Hieber and Spacu (1) found that thiols react with triiron dodecacarbonyl to give the mercaptides **1** (2–4), carbon monoxide, and hydrogen. Hieber and Scharfenberg later found that thionacetamide and benzthiazolin-2-thione (which they formulated as 2-mercaptobenzthiazole, now

Can. J. Chem. Downloaded from www.nrcresearchpress.com by 84.22.46.98 on 09/08/12
For personal use only.

benzene itself and carbon tetrachloride. In that case, the reported temperature independence of the shifts of protons in nonaromatic molecules dissolved in carbon tetrachloride (3) is consistent with the present results. It is also interesting to note that donor solvents containing oxygen have little or no effect on the Raman vibrational intensities of carbon tetrachloride (7). On the other hand, the intensity changes caused by aromatic donors have been interpreted on the basis of specific molecular interactions (7).

Other Solvents

For the present solute molecule carbon disulfide (Table I) is preferable to carbon tetrachloride as a reference solvent, contrary to one recommendation (ref. 1, p. 244). This appears to be so for other solute types as well, e.g. 1,1-difluoroethylene (8). Notice also that perfluorobenzene does not induce the high-field shifts expected from a large magnetic anisotropy. This point is under investigation,[2] especially in view of the relatively strong complexes reported to occur between aromatic donor molecules and perfluorobenzene (10). The relative solvent shifts observed in acetone and acetonitrile (dielectric constants, respectively, near 20, 35) cannot easily be explained by reaction field effects (11). Such anomalies are, of course, quite common (1, 12). In acetone and acetonitrile solutions the hydroxyl proton shifts are 11.36 and 11.27 p.p.m. to low field of internal tetramethylsilane, respectively, whereas in the cyclohexane the shift is 11.28 p.p.m. (4). The aldehyde group is therefore in the planar, hydrogen-bonded conformation and the solvent shifts are not complicated by conformational changes of the anisotropic aldehyde group.

[2]A referee suggests a small magnetic anisotropy (unknown) for perfluorobenzene. In perchlorobenzene the magnetic anisotropy is only 10% lower than in benzene (9). Susceptibility measurements on a single crystal of perfluorobenzene are needed.

Experimental

Solutions were degassed by the freeze – pump – thaw technique. Tetramethylsilane served as an internal reference. Spectra were run on a DA-60I spectrometer in the frequency sweep mode and calibration of peak positions involved period averaging techniques. Root mean square deviations of the shifts were typically 0.002 p.p.m. or less. Temperatures were measured by means of ethylene glycol or methanol samples as provided by Varian Associates. Although absolute temperatures may be in error up to 2 °C, temperature differences must be more accurate as shown by our detailed results.

Acknowledgment

We are grateful to the National Research Council of Canada for financial assistance.

1. P. Laszlo. *In* Progress in nuclear magnetic resonance spectroscopy. Vol. 3. *Edited by* J. W. Emsley, J. Feeney, and L. H. Sutcliffe. 1967. Chap. 6.
2. P. Laszlo and J. L. Soong, Jr. J. Chem. Phys. **47**, 4472 (1967).
3. R. C. Fort, Jr. and T. R. Lindstrom. Tetrahedron, **23**, 3227 (1967).
4. G. Kotowycz. Ph.D. Thesis, University of Manitoba, Winnipeg, Manitoba. 1967.
5. R. J. Abraham. Mol. Phys. **4**, 369 (1961).
6. R. F. Weimer and J. M. Prausnitz. J. Chem. Phys. **42**, 3643 (1965).
7. D. A. Bahnick and W. P. Person. J. Chem. Phys. **48**, 1251 (1968).
8. C. J. Macdonald and T. Schaefer. Can. J. Chem. **45**, 3157 (1967).
9. A. A. Bothner-By and J. A. Pople. *In* Annual review of physical chemistry. Vol. 16. *Edited by* H. Eyring. Annual Reviews, Inc. Palo Alto, California. 1965.
10. W. A. Duncan and F. L. Swinton. Trans. Faraday Soc. **62**, 1082 (1966).
11. A. D. Buckingham. Can. J. Chem. **38**, 300 (1960).
12. H. M. Hutton and T. Schaefer. Can. J. Chem **43**, 3116, (1965).

Reaction of iron carbonyls with amides and thionamides

Howard Alper and John T. Edward
Department of Chemistry, McGill University, Montreal, Quebec

Received June 18, 1968

Iron pentacarbonyl in boiling butyl ether converts primary amides or thionamides to nitriles, and benzanilide or thionbenzanilide to *N*-benzylideneaniline. Diiron nonacarbonyl reacts with *p*-methoxythionbenzamide to form a complex $C_{22}H_{16}N_2S_2O_8Fe_2$; a possible structure is proposed.

Canadian Journal of Chemistry, 46, 3112 (1968)

Hieber and Spacu (1) found that thiols react with triiron dodecacarbonyl to give the mercaptides **1** (2–4), carbon monoxide, and hydrogen. Hieber and Scharfenberg later found that thionacetamide and benzthiazolin-2-thione (which they formulated as 2-mercaptobenzthiazole, now

Can. J. Chem. Downloaded from www.nrcresearchpress.com by 210.87.254.105 on 09/05/12
For personal use only.

TABLE I

Nitriles obtained from reaction of amides or thionamides with iron pentacarbonyl

Reactant	Product	Yield (%)	Melting point (°C)*	Boiling point (°C)†
2-Phenylacetamide	Phenylacetonitrile	35	—	233–235 (234)
2-Phenylthionacetamide	Phenylacetonitrile	62	—	231–233 (234)
Benzamide	Benzonitrile	32	—	190–191 (191)
Thionbenzamide	Benzonitrile	64	—	188–190 (191)
p-Methoxybenzamide	*p*-Methoxybenzonitrile	28	60.0–62.0 (61–62)	—
p-Methoxythionbenzamide	*p*-Methoxybenzonitrile	61	60.0–62.0 (61–62)	—
p-Toluamide	*p*-Tolunitrile	20	26.0–28.0 (29.5)	—
m-Toluthionamide	*m*-Tolunitrile	66	—	210–212 (212)

*Values in parentheses are those given in ref. 9.
†Values in parentheses, determined at 760 mm pressure, are those given in ref. 9.

known to be the minor tautomer (5)) reacted with $Fe_3(CO)_{12}$ in ligroin at 55° to give carbon monoxide and hydrogen, again in a molar ratio of 2:1 (6). They could isolate no other product from the reaction of thionacetamide, but from the reaction of benzthiazolin-2-thione they obtained a dark-red crystalline solid, later shown (7, 8) to be $S_2Fe_3(CO)_9$ (**5**).

[1] $6\,RSH + 2\,Fe_3(CO)_{12} \rightarrow 3\,R{-}S{-}Fe_2(CO)_6{-}S{-}R + 6\,CO + 3\,H_2$

1

We have now obtained **5** in 5.5% yield from the reaction of *p*-methoxythionbenzamide (**2**; R = $CH_3OC_6H_4$) with diiron nonocarbonyl in tetrahydrofuran at room temperature for 24 h. The reaction also afforded *p*-methoxybenzonitrile (**4**; R = $CH_3OC_6H_4$) (17% yield) and a compound $C_{22}H_{16}N_2S_2O_8Fe_2$ (38% yield). This last compound we tentatively formulate as **3** (R = $CH_3OC_6H_4$), by analogy with the structure **1**. This formulation is supported by the infrared (i.r.) absorption of the compound (CCl_4 solution) at 3300 cm^{-1} (broad) (N—H); 2070, 2030, 2000, 1985, and 1945 cm^{-1} (terminal metal carbonyl); and 1605 and 1510 cm^{-1} (conjugated C=N). A possible course of the reaction is shown in eq. 2, although this must remain speculative until the gaseous products of the reaction (if any) have been determined. When **3** (R = $CH_3OC_6H_4$) was heated in butyl ether, it gave a 77% yield of the nitrile **4** (R = $CH_3OC_6H_4$).

Thionamides were not affected by the less reactive iron pentacarbonyl at room temperatures but in boiling butyl ether they were converted to nitriles. The yields of nitriles obtained from a number of thionamides, using a 1.6:1 mole ratio of metal carbonyl to thionamide, are given in Table I. Yields were not improved when the mole ratio was increased to 5.0:1; when only a catalytic amount of iron pentacarbonyl was used, no nitrile was formed.

These reactions of iron pentacarbonyl may involve as intermediates thionamide – iron carbonyl complexes similar to **3**, but none was isolated, probably because of their instability at

[2] $2\,R{-}C(=S){-}NH_2$ (**2**) + $Fe_2(CO)_9$ $\xrightarrow[-H_2]{-3CO}$ **3**; **3** $\xrightarrow[+Fe(CO)_3]{-H_2}$ **5** + 2 R—C≡N (**4**)

Can. J. Chem. Downloaded from www.nrcresearchpress.com by 210.87.254.105 on 09/05/12
For personal use only.

Can. J. Chem. Downloaded from www.nrcresearchpress.com by 210.87.254.105 on 09/05/12
For personal use only.

the temperature of boiling butyl ether. The reaction mixture also had hydrogenolytic properties, as shown by the isolation of a small amount of *N*-(*p*-methoxybenzyl)-*p*-methoxythionbenzamide from the reaction of *p*-methoxythionbenzamide.

Amides also formed nitriles, generally in lower yields (Table I); however, no systematic attempt was made to optimize yields by variation of temperature, times of reaction, or solvent.

The *N*-substituted compounds, benzanilide and thionbenzanilide, which cannot form nitriles, reacted with iron pentacarbonyl in boiling butyl ether to give *N*-benzylideneaniline. This reaction may involve hydrogenolysis of the C—S or C—O bond of an intermediate analogous to **3**. The hydrogen for this reaction cannot come from the NH group of the starting material, because *N*-deuteriothionbenzanilide gave unlabelled *N*-benzylideneaniline; solvent molecules may be involved, but a more complete study of the reaction products is required.

The *N,N*-disubstituted compound, *N*-methylacetanilide, was recovered unchanged after exposure to iron pentacarbonyl in boiling butyl ether for about 15 h.

Experimental

Melting points were measured in capillary tubes in a Gallenkamp apparatus and are corrected. Microanalyses were performed by Bernhardt Mikroanalytisches Laboratorium, Mulheim, Germany and Schwarzkopf Microanalytical Laboratory, Woodside, New York. Infrared (i.r.) spectra were obtained on Perkin–Elmer model 137, 337, or 521 spectrophotometers; the wavelength readings were calibrated with a polystyrene film. Nuclear magnetic resonance (n.m.r.) spectra were measured using a Varian Associates model A-60 spectrometer, with tetramethylsilane as a reference.

Iron pentacarbonyl (Alfa Inorganics, Inc.) was used as received; distillation of the compound did not improve results. Solvents were dried and purified by standard methods. The amides and thionbenzanilide were commercial products. The primary thionamides were kindly donated by Mr. G. D. Derdall of these laboratories.

Reaction of p-Methoxythionbenzamide with Diiron Nonacarbonyl

A mixture of *p*-methoxythionbenzamide (0.803 g, 4.80 mM) and diiron nonacarbonyl (2.794 g, 7.68 mM) in dry tetrahydrofuran (30 ml) was stirred under nitrogen at room temperature for 24 h. The solution was filtered to remove inorganic material and the filtrate evaporated at ca. 30 mm to give a crude residue showing i.r. absorption bands for an iron carbonyl complex and for a nitrile group. The residue was treated with 2–3 ml of petroleum ether, filtered, and the filtrate evaporated to give 0.110 g (17%) of *p*-methoxybenzonitrile, m.p. and mixture m.p. 60.0–62.0 °C (9). The petroleum ether-insoluble solid was dissolved in benzene and chromatographed on Florisil. Elution with benzene gave 64 mg (5.5%) of black-purple crystals of $S_2Fe_3(CO)_9$ (5), m.p. 112° (lit. m.p. 114° (8)); the compound was identified by its i.r. spectrum, which between 1200 and 4000 cm^{-1} showed only five bands (at 2090, 2070, 2050, 2020, and 2010 cm^{-1}) having a characteristic pattern (8). Further elution with benzene gave 0.558 g (38%) of the complex **3** (R = $CH_3OC_6H_4$), which decomposed above 250 °C without melting.

Anal. Calcd. for $C_{22}H_{16}N_2S_2O_8Fe_2$ (mol. wt., 612.2): C, 42.83; H, 2.63; N, 4.58; S, 10.47. Found (mol. wt., osmometry in chloroform, 606): C, 42.67; H, 2.58; N, 4.84; S, 10.77.

The complex **3** (R = $CH_3OC_6H_4$) (0.385 g) in dry butyl ether (30 ml) was refluxed with stirring under nitrogen for 15 h. The solution was cooled, filtered, and concentrated to give *p*-methoxybenzonitrile in 77% yield.

General Procedure for the Conversion of Primary Amides and Thionamides to Nitriles with Iron Pentacarbonyl

A mixture of the amide or thionamide (10–50 mmoles) and iron pentacarbonyl (1.6/1.0 mole ratio of metal carbonyl to amide or thionamide) in anhydrous butyl ether (40–50 ml) was refluxed with stirring under nitrogen for 12–18 h. The solution was cooled, filtered to remove starting material, and the solvent removed at ca. 30 mm. The nitrile was extracted from the residue with petroleum ether (b.p. 38–60 °C) and the extract evaporated to give pure nitrile (distilled if liquid). The melting points of the solid nitriles were undepressed by admixture with authentic samples. The purity of the liquid nitriles was shown by comparison of boiling points, i.r. spectra, and thin-layer chromatograms with those of authentic samples.

When the above general procedure was repeated either in the presence of a catalytic quantity of iron pentacarbonyl or with no metal carbonyl at all, no reaction was observed.

Starting with *p*-methoxythionbenzamide, a 5.4% yield of a second product, *N*-(*p*-methoxybenzyl)-*p*-methoxythionbenzamide, was obtained as a petroleum ether–insoluble solid, m.p. 85.0–87.0 °C. The i.r. spectrum of the new material (KBr disk) exhibited strong —NH absorption at 3290 cm^{-1} and thiocarbonyl stretching at 1260 cm^{-1} (—OCH_3 at 1240 cm^{-1}). The n.m.r. spectrum ($CDCl_3$) showed besides signals for the aromatic and methoxyl protons, a doublet at 4.92 p.p.m. for the methylene protons coupled to —NH—, which appears as a broad peak in the region of 7.8–8.0 p.p.m. Upon deuterium oxide exchange, the methylene doublet collapsed to a singlet and the NH absorption disappeared.

Anal. Calcd. for $C_{16}H_{17}NSO_2$: C, 66.88; H, 5.96; N, 4.89; S, 11.12. Found: C, 67.25; H, 5.85; N, 5.08; S, 11.07.

Reaction of Benzanilide and Thionbenzanilide with Iron Pentacarbonyl

When a mixture of either benzanilide or thionbenzanilide and iron pentacarbonyl in dry butyl ether reacted according to the general procedure, *N*-benzylideneaniline, m.p. 50.0–51.0 °C (5), was obtained in yields of 15% and 47% from amide and thionamide respectively. The i.r. spectrum of the product was identical to that reported by Nakanishi (10).

Reaction of N-Deuteriothionbenzanilide with Iron Pentacarbonyl

N-Deuteriothionbenzanilide was prepared by dissolving thionbenzanilide in ether and shaking with deuterium oxide for 4 h. The ether layer was separated and the ether removed to give the deuterated compound, m.p. 102.0–102.5 °C. Nuclear magnetic resonance spectra ($CDCl_3$) indicated less than 10% *N*-protiumthionbenzanilide. Reacting the deuterated compound under previously described conditions resulted in the formation of *N*-benzylideneaniline in 39% yield. The n.m.r. and i.r. spectra indicated the absence of deuterium in the product.

Acknowledgments

We are grateful to the National Research Council of Canada for financial support and for the award of a studentship (to H.A., 1965–1966 and 1966–1967).

1. W. Hieber and P. Spacu. Z. Anorg. Allgem. Chem. **233**, 353 (1937).
2. H. Reihlen, A. Gruhl, and G. V. Hessling. Ann. **472**, 268 (1929).
3. S. F. A. Kettle and L. E. Orgel. J. Chem. Soc. 3890 (1960).
4. R. B. King. J. Am. Chem. Soc. **85**, 1584 (1963).
5. A. R. Katritzky and J. M. Lagowski. *In* Advances in heterocyclic chemistry. *Edited by* A. R. Katritzky. Academic Press, Ltd., London. 1963. Vol. II. p. 62.
6. W. Hieber and C. Scharfenberg. Ber. **73**, 1012 (1946).
7. R. B. King. Inorg. Chem. **2**, 326 (1963).
8. R. Havlin and G. R. Knox. J. Organometal. Chem. Amsterdam, **4**, 247 (1965).
9. Handbook of chemistry and physics. 46th ed. *Edited by* C. D. Hodgman. The Chemical Rubber Publishing Co., Cleveland, Ohio. 1966.
10. K. Nakanishi. Infrared absorption spectroscopy. Holden-Day, San Francisco. 1964. p. 222.

Total synthesis of a curvularin isomer

Jehan F. Bagli and H. Immer
Department of Chemistry, Ayerst Research Laboratories, Montreal, Quebec

Received May 16, 1968

This paper describes a total synthesis of a biogenetically possible, hitherto unknown macrolide **4**. Starting with 3,5-dimethoxybenzaldehyde, ketone **5***a* was generated in five steps. Alkylation of this compound by bromopentene followed by decarboxylation yielded pentenyl ketone **6**. Oxymercuration–demercuration followed by dehydration gave cyclic enol ether **8**. Oxidation with *m*-chloroperbenzoic acid led to the macrolide **4**.

Canadian Journal of Chemistry, 46, 3115 (1968)

Biogenesis of macrolides fits satisfactorily in the hypothesis (1) that implicates poly-β-keto acids as precursors. In recent years, some naturally occurring mould metabolites have been reported (2–5) whose structures are characterized by the presence of an aromatic ring fused to a macrolide moiety. An obvious biogenetic pathway to these substances would appear to involve an intramolecular ring closure, to generate the aromatic ring. Such an aldol type condensation in acyclic poly-β-keto acid is known (6) to follow two pathways shown below:

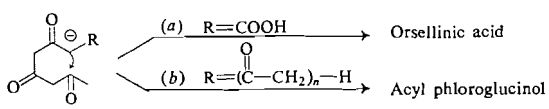

Zearalenone **1** (2) and radicicol (3) represent examples, where such an internal condensation of a precursor macrolide (derived from nine acetate units) has conceivably occurred via pathway (*a*). In contrast, curvularin **3** (4) and α,β-dehydrocurvularin (5) represent products generating from eight acetate units where the precursor macrolide has undergone a subsequent condensation of the acyl phloroglucinol type (*b*).

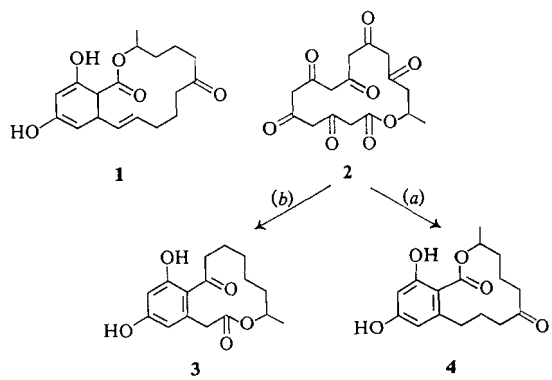

We wish to report a total synthesis of the hitherto unknown DL-isomer **4** of curvularin that is derivable from the common hypothetical

Can. J. Chem. Downloaded from www.nrcresearchpress.com by 210.87.254.105 on 09/05/12
For personal use only.

Reaction of N-Deuteriothionbenzanilide with Iron Pentacarbonyl

N-Deuteriothionbenzanilide was prepared by dissolving thionbenzanilide in ether and shaking with deuterium oxide for 4 h. The ether layer was separated and the ether removed to give the deuterated compound, m.p. 102.0–102.5 °C. Nuclear magnetic resonance spectra ($CDCl_3$) indicated less than 10% *N*-protiumthionbenzanilide. Reacting the deuterated compound under previously described conditions resulted in the formation of *N*-benzylideneaniline in 39% yield. The n.m.r. and i.r. spectra indicated the absence of deuterium in the product.

Acknowledgments

We are grateful to the National Research Council of Canada for financial support and for the award of a studentship (to H.A., 1965–1966 and 1966–1967).

1. W. Hieber and P. Spacu. Z. Anorg. Allgem. Chem. **233**, 353 (1937).
2. H. Reihlen, A. Gruhl, and G. V. Hessling. Ann. **472**, 268 (1929).
3. S. F. A. Kettle and L. E. Orgel. J. Chem. Soc. 3890 (1960).
4. R. B. King. J. Am. Chem. Soc. **85**, 1584 (1963).
5. A. R. Katritzky and J. M. Lagowski. *In* Advances in heterocyclic chemistry. *Edited by* A. R. Katritzky. Academic Press, Ltd., London. 1963. Vol. II. p. 62.
6. W. Hieber and C. Scharfenberg. Ber. **73**, 1012 (1946).
7. R. B. King. Inorg. Chem. **2**, 326 (1963).
8. R. Havlin and G. R. Knox. J. Organometal. Chem. Amsterdam, **4**, 247 (1965).
9. Handbook of chemistry and physics. 46th ed. *Edited by* C. D. Hodgman. The Chemical Rubber Publishing Co., Cleveland, Ohio. 1966.
10. K. Nakanishi. Infrared absorption spectroscopy. Holden-Day, San Francisco. 1964. p. 222.

Total synthesis of a curvularin isomer

Jehan F. Bagli and H. Immer
Department of Chemistry, Ayerst Research Laboratories, Montreal, Quebec

Received May 16, 1968

This paper describes a total synthesis of a biogenetically possible, hitherto unknown macrolide **4**. Starting with 3,5-dimethoxybenzaldehyde, ketone **5***a* was generated in five steps. Alkylation of this compound by bromopentene followed by decarboxylation yielded pentenyl ketone **6**. Oxymercuration–demercuration followed by dehydration gave cyclic enol ether **8**. Oxidation with *m*-chloroperbenzoic acid led to the macrolide **4**.

Canadian Journal of Chemistry, 46, 3115 (1968)

Biogenesis of macrolides fits satisfactorily in the hypothesis (1) that implicates poly-β-keto acids as precursors. In recent years, some naturally occurring mould metabolites have been reported (2–5) whose structures are characterized by the presence of an aromatic ring fused to a macrolide moiety. An obvious biogenetic pathway to these substances would appear to involve an intramolecular ring closure, to generate the aromatic ring. Such an aldol type condensation in acyclic poly-β-keto acid is known (6) to follow two pathways shown below:

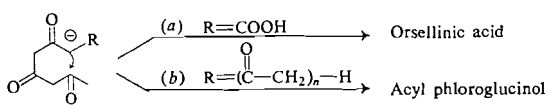

Zearalenone **1** (2) and radicicol (3) represent examples, where such an internal condensation of a precursor macrolide (derived from nine acetate units) has conceivably occurred via pathway (*a*). In contrast, curvularin **3** (4) and α,β-dehydrocurvularin (5) represent products generating from eight acetate units where the precursor macrolide has undergone a subsequent condensation of the acyl phloroglucinol type (*b*).

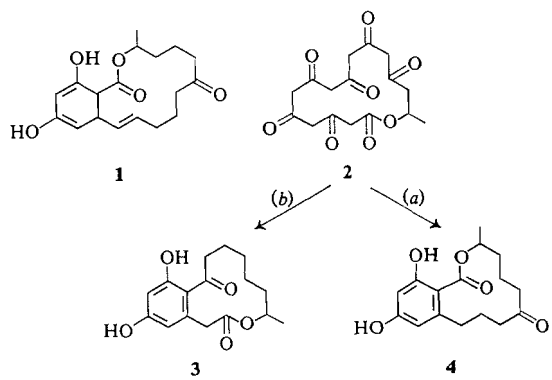

We wish to report a total synthesis of the hitherto unknown DL-isomer **4** of curvularin that is derivable from the common hypothetical

Can. J. Chem. Downloaded from www.nrcresearchpress.com by 210.87.254.40 on 09/05/12
For personal use only.

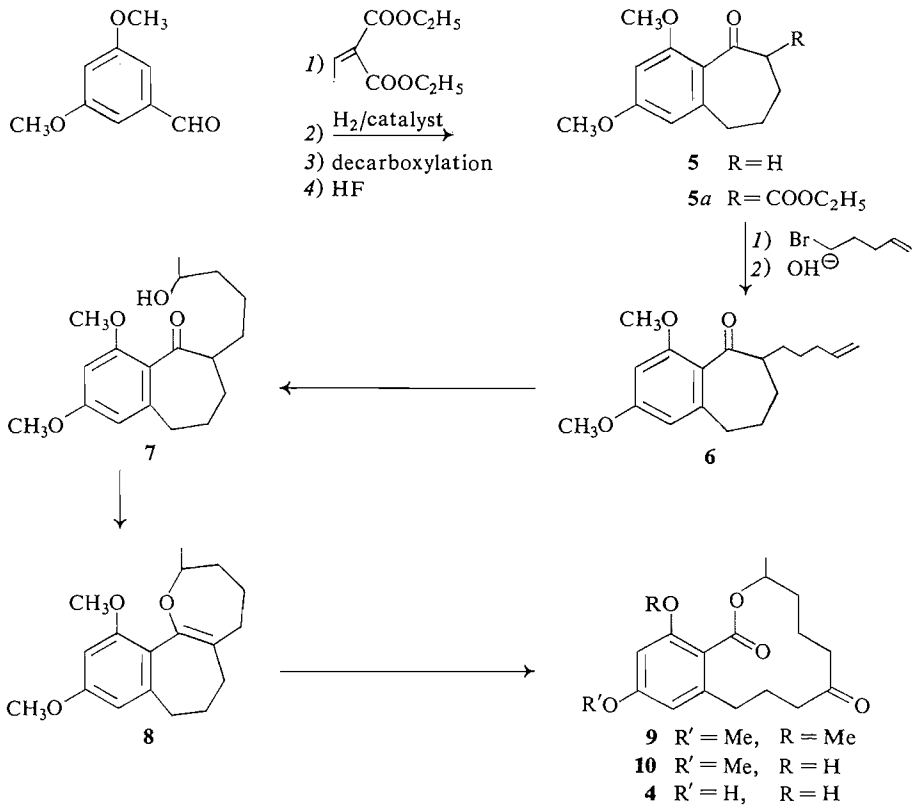

progenitor macrolide **2**, by subsequent internal cyclization via pathway (*a*). The synthetic sequence used was a modification of the general synthetic approach reported recently (7).

The known ketone **5** (8) was prepared using a modified procedure. 3,5-Dimethoxybenzaldehyde was condensed with ethylidene malonate diethyl ester (9) to yield a diene diacid. Hydrogenation of double bonds, and decarboxylation resulted in the production of the desired pentanoic acid which was cyclized with anhydrous hydrogen fluoride to ketone **5**. Carbethoxylation with diethyl carbonate and sodium hydride in dry tetrahydrofuran yielded the corresponding β-keto ester **5***a*. Alkylation of this ester with 1-bromopent-4-ene was carried out in potassium *t*-butoxide/*t*-butyl alcohol. The resulting ester was decarboxylated under basic conditions. The terminal double bond was hydrated by oxymercuration procedure of Brown and Geoghegan (10) to yield quantitatively the product **7** of Markownikoff hydration. The alcohol was dehydrated to yield the enol–ether **8**. The overall yield of enol–ether **8** from ketone **5** was 38.5%. Oxidation of enol–ether **8** with *m*-chloroperbenzoic acid resulted in generation of dimethyl ether **9**. Treatment of dimethyl ether with boron tribromide in methylene chloride at 0°, gave a mixture of phenols, from which **4** and **10** were isolated in a ratio of 6:1. The structure of phenol **10** follows from its spectral data.

Experimental[1]

7,9-Dimethoxy-2,3,4,5-tetrahydro-1H-benzocyclohepten-1-one (5)

To an ice-cold solution of dimethoxy benzaldehyde (20 g) and ethylidene malonate diethyl ester (68 g) in ethanol (120 ml) was added potassium hydroxide (40 g) and the mixture was stirred for 48 h. The mixture was then cooled, and acidified with concentrated hydrochloric acid (80 ml) and water (560 ml). The resulting acid was filtered and dried. The diene diacid (21 g) was hydrogenated in presence of platinum oxide (1.0 g, 85%) in ethanol (1.2 l) to yield, after the usual work-up, the saturated dibasic acid (23 g). The diacid was decarboxylated

[1]All experimental conditions were the same as those described in ref. 14 of our earlier communication (ref. 7), except that silica gel (0.05–0.2 mm Merck) was employed for column chromatography.

Can. J. Chem. Downloaded from www.nrcresearchpress.com by 210.87.254.40 on 09/05/12
For personal use only.

Can. J. Chem. Downloaded from www.nrcresearchpress.com by 210.87.254.40 on 09/05/12
For personal use only.

in refluxing pyridine (94 ml) over a period of 4 h. The resulting pentanoic acid (16.1 g) was cyclized during 48 h by dissolving in anhydrous hydrogen fluoride. Evaporation of hydrogen fluoride, and crystallization of the resulting residue yielded ketone **5** (10.7 g, 40%), m.p. 56–57° (reported (8), 57–58°).

2-Carbethoxy-7,9-dimethoxy-2,3,4,5-tetrahydro-1H-benzocyclohepten-1-one (5a)

Sodium hydride (4.32 g, 55% suspension) was washed free of oil and suspended in dry tetrahydrofuran (50 ml). Diethylcarbonate (13 g) was added under nitrogen atmosphere, and the mixture was heated to reflux. A solution of ketone **5** (10 g) in dry tetrahydrofuran (100 ml) was added and the mixture refluxed for 48 h. The reaction mixture was cooled, acetic acid (6.5 ml) added, and the mixture diluted with ether. The organic solution was washed several times with saturated sodium chloride solution, dried, and the solvent removed. Residue (10.63 g, 80%) was distilled, b.p. 173–175°/0.1 mm. The oil solidified and was crystallized from light petroleum to yield an analytical sample, m.p. 72.5–73.5°.

Anal. Calcd. for $C_{16}H_{20}O_5$: C, 65.74; H, 6.90. Found: C, 65.88; H, 6.89.

Infrared (i.r.): ν_{max} (Nujol) 1730, 1680, and 1600 cm^{-1}; ultraviolet (u.v.): λ_{max} 296 mμ (4655), 270 mμ (6350); nuclear magnetic resonance (n.m.r.): δ 6.4 (2H, aromatic, quartet), δ 4.3 (2H, methylene protons of ethyl ester, quartet), δ 3.73 (6H, 2 *O*-methyl), and δ 1.32 (3H, methyl group).

7,9-Dimethoxy-2-(pent-4'-enyl)-2,3,4,5-tetrahydro-1H-benzocyclohepten-1-one (6)

Potassium (2.81 g) was dissolved in *t*-butyl alcohol (200 ml). A solution of ketone **6** (10.63 g) in *t*-butyl alcohol (100 ml) was added in an atmosphere of nitrogen. 1-Bromopent-4-ene (25 ml) was added and the mixture was refluxed overnight. The mixture was cooled and neutralized with acetic acid (7 ml). *t*-Butyl alcohol was mainly evaporated under vacuum, residue was taken in ether, washed with saturated sodium chloride, dried, and the solvent was removed. The residue was distilled at 0.3 mm to remove unchanged 1-bromopent-4-ene. The crude product (12.9 g) was dissolved in ethanol, a solution of potassium hydroxide (8.45 g) in water (10 ml) was added, and the mixture refluxed for 12 h. The solvent was then removed, and the residue taken up in ether, washed, and dried. The ether was evaporated and the crude product was distilled, b.p. 155–160°/0.08 mm, m.p. 54–55° (7.6 g, 72%).

Anal. Calcd. for $C_{18}H_{24}O_3$: C, 74.97; H, 8.39. Found: C, 74.94; H, 8.38.

Infrared: ν_{max} (Nujol) 1680, 1600 cm^{-1}; u.v: λ_{max} 293 mμ (5300), 269 mμ (6500); n.m.r.: δ 6.3 (2H, aromatic, quartet), δ 5.7 and 4.95 (1H and 2H, vinylic protons, multiplet), δ 3.76 and 3.73 (6H, *O*-methyl), and δ 2.65 (3H, allylic and 1H α to ketone).

7,9-Dimethoxy-2-(4-hydroxypentyl)-2,3,4,5-tetrahydro-1H-benzocyclohepten-1-one (7)

Mercuric acetate (2.1 g) was dissolved in water (6.8 ml) and tetrahydrofuran (3.4 ml). To this was added a solution of ketone 7 (1.94 g) in tetrahydrofuran (3.4 ml), and stirred for a further 10 min. Sodium hydroxide (3*N*, 6.8 ml) was added, followed by a 0.5 molar solution (6.8 ml) of sodium borohydride in 3 *N* sodium hydroxide, and stirring was continued for 10 min. Ether (100 ml) was added and the organic solution washed with saturated sodium chloride solution, dried, and the solvent was removed to yield a crude product (2.095 g, 100%).

The compound was found to be homogeneous on thin layer plate, and *m/e* M 306, *m/e* M-18, 288; i.r.: ν_{max} (film) 3420, 1675, and 1600 cm^{-1}; u.v.: λ_{max} 291 mμ (3800), 268 mμ (4550); n.m.r.: δ 6.3 (2H, aromatic, quartet), δ 3.95 and 3.65 (7H, *O*-methyl, and a carbinolic proton), δ 2.65 (3H, 2 benzylic and 1H α to ketone), and δ 1.16 (3H, methyl doublet, $J = 6$ Hz).

10,12-Dimethoxy-2,3,4,5,7,8-hexahydro-6H-benzocyclohepten[1,2-b]oxepin (8)

A solution of ketone 7 (2.05 g) in benzene (50 ml) containing *p*-toluenesulfonic acid (50 mg) was refluxed with a water separator, for 20 h. Most of the benzene was removed, and the residue was passed through neutral alumina (60 g, activity II). Product (1.3 g, 67.5%) was eluted with petroleum ether, and recrystallized from the same solvent, m.p. 90–91°.

Anal. Calcd. for $C_{18}H_{24}O_3$: C, 74.97; H, 8.39. Found: C, 74.59; H, 8.09.

Infrared: ν_{max} (film) 1640, 1600 cm^{-1}; n.m.r.: δ 6.12 (2H, aromatic, quartet), δ 3.9 (1H, *O*-methine), δ 3.7 and 3.66 (6H, *O*-methyl, singlets), and δ 1.12 (3H, methyl, doublet $J = 6$ Hz).

12,14-Dimethoxy-3,4,5,6,9,10-hexahydro-3-methyl-8H-2-benzoxacyclododecan-1,7-dione (9)

To a suspension of *m*-chloroperbenzoic acid (6.55 g) in methylene chloride (11 ml) was added a solution of enol–ether **8** (2.64 g) in methylene chloride (11 ml), dropwise, so as to maintain boiling. The reaction mixture was allowed to stand at room temperature overnight. The solid was filtered, and the filtrate was diluted with methylene chloride. The solution was washed with potassium carbonate, and then with saturated sodium chloride solution, dried, and the solvent was removed. The residue was passed through alumina (neutral, activity II) and elution with benzene gave the desired lactone **9** (0.95 g, 35%). Crystallization from acetone–hexane gave an analytical sample, m.p. 135–138°.

Anal. Calcd. for $C_{18}H_{24}O_5$: C, 67.48; H, 7.55. Found: C, 67.20; H, 7.71.

Infrared: ν_{max} (Nujol) 1715, 1600 cm^{-1}; u.v.: λ_{max} 281 mμ (1840); n.m.r.: δ 6.27 (2H, aromatic), δ 5.08 (1H, *O*-methine), δ 3.8 and 2.76 (6H, 2 *O*-methyl singlets), and δ 1.3 (3H, methyl, doublet).

12,14-Dihydroxy-3,4,5,6,9,10-hexahydro-3-methyl-8H-2-benzoxacyclododecan-1,7-dione (4)

The lactone **9** (0.5 g) was dissolved at 0° in methylene chloride (20 ml) containing boron tribromide (4 g). The reaction mixture was stirred for 3 h at ice-cold temperature. The mixture was then diluted with chloroform and washed with sodium bicarbonate solution, followed by saturated sodium chloride solution. The crude product thus obtained was chromatographed on silica gel in acetone–hexane 3:1. The dihydroxy lactone **4** (165 mg) was eluted from the column. Crystallization from acetone–hexane gave a sample, m.p. 145°.

Anal. Calcd. for $C_{16}H_{20}O_5$: C, 65.74; H, 6.90. Found: C, 65.95; H, 7.00.

Infrared: ν_{max} (Nujol) 3450, 1700, 1650, 1620, and 1600 cm^{-1}; u.v.: λ_{max} 265 mμ (12 800), 306 mμ (5200); n.m.r.: δ 11.5 (1H, phenolic), δ 6.45 (1H, phenolic), δ 6.27 (2H, aromatic, quartet), δ 5.22 (1H, *O*-methine, multiplet), and δ 1.34 (3H, methyl, doublet $J = 7$ Hz).

A second compound (30 mg) was also eluted and was assigned the structure **10**.

*3,4,5,6,9,10-Hexahydro-14-hydroxy-12-methoxy-3-methyl-8H-2-benzoxacyclododecan-1,7-dione (**10**, m.p. 112°)*

Anal. Calcd. for $C_{17}H_{22}O_5$: C, 66.65; H, 7.24. Found: C, 66.99; H, 7.33.

Infrared: ν_{max} (Nujol) 1705, 1630, 1605, and 1585 cm^{-1}; u.v.: λ_{max} 266 mμ (16 800), 305 mμ (7250); n.m.r.: δ 11.5 (1H, phenolic), δ 6.35 (2H, aromatic, quartet), δ 5.26 (1H, *O*-methine), δ 3.84 (3H, *O*-methyl), and δ 1.38 (3H, methyl, doublet).

Acknowledgments

The authors wish to acknowledge the technical assistance of Miss M. Ebel, and thank Dr. G. Schilling and his associates for analytical data.

1. R. B. Woodward. Festschr. Arthur Stoll, 538 (1957).
2. W. H. Urry, H. L. Wehrmeister, E. B. Hodge, and P. H. Hidy. Tetrahedron Letters, 3109 (1966).
3. R. N. Mirrington, E. Ritchie, C. W. Shoppee, S. Sternhell, and W. C. Taylor. Aust. J. Chem. **19**, 1265 (1966), and references cited therein.
4. A. J. Birch, O. C. Musgrave, R. W. Rickards, and H. Smith. J. Chem. Soc. 3146 (1959).
5. H. D. Munro, O. C. Musgrave, and R. Templeton. J. Chem. Soc. (10c), 947 (1967).
6. J. H. Richards and J. B. Hendrickson. Biosynthesis of terpenes, steroids, and acetogenins. W. A. Benjamin, Inc., New York. 1964. p. 18.
7. H. Immer and J. F. Bagli. J. Org. Chem. To be published.
8. R. Huisgen, G. Siedl, and J. Wimmer. Ann. **677**, 21 (1964).
9. P. D. Gardner, W. J. Horton, G. Thompson, and R. R. Twelves. J. Am. Chem. Soc. **74**, 5527 (1952).
10. H. Brown and P. Geoghegan, Jr. J. Am. Chem. Soc. **89**, 1522 (1967).

Erratum: The structure of 5,5,5-trifluoro-4-hydroxypentenoic acid lactone

Robert Filler and Ralph M. Schure
Department of Chemistry, Illinois Institute of Technology, Chicago, Illinois 60616

Received May 31, 1968

(Ref.: Can. J. Chem. **45**, 1018 (1967))

Canadian Journal of Chemistry, 46, 3118 (1968)

On page 1020, the nuclear magnetic resonance peaks in Fig. 2 should read from left to right: (C) (B) (A) rather than (A) (B) (C).

Erratum: Ranunculin

M. H. Benn and Lois Jean Yelland
Department of Chemistry, The University of Calgary, Calgary, Alberta

Received May 6, 1968

(Ref.: Can. J. Chem. **46**, 729 (1968))

Canadian Journal of Chemistry, 46, 3118 (1968)

On page 729, line 7 of the second column should read . . . . .
"hydrogens in positions -3 and -2 of the lactone".

Can. J. Chem. Downloaded from www.nrcresearchpress.com by 210.87.254.40 on 09/05/12
For personal use only.

Can. J. Chem. Downloaded from www.nrcresearchpress.com by 210.87.254.40 on 09/05/12
For personal use only.

Canadian Journal of Chemistry

Published by THE NATIONAL RESEARCH COUNCIL OF CANADA

VOLUME 46 OCTOBER 15, 1968 NUMBER 20

Complexes of nickel(II) with substituted thioureas[1]

R. A. BAILEY

Department of Chemistry, Rensselaer Polytechnic Institute, Troy, New York, 12181

AND

TERRY ROY PETERSON

Imperial Color and Chemical Department, Hercules Incorporated, Glens Falls, New York, 12801

Received April 17, 1968

A series of Ni(II) complexes with methyl-, ethyl-, and *sym*-dimethyl-, *sym*-diethyl-, and *sym*-di-*n*-butyl-thioureas and halide, perchlorate, and thiocyanate anions have been prepared and characterized. Spectral and magnetic studies show that compounds NiL_4X_2 (L = N,N′-dimethyl and N,N′-diethylthiourea, X = halide) are tetragonally distorted octahedral species with a singlet ground state and a thermally populated triplet excited state. The remaining compounds are octahedral. Infrared evidence shows sulfur bonding of the disubstituted ligands to the metal, but suggests nitrogen coordination of the methylthiourea compounds.

Canadian Journal of Chemistry, **46**, 3119 (1968)

Introduction

In 1906 Rosenheim and Meyer (1) reported the preparation of the first examples of complexes containing Ni(II) and thiourea ligands. Characterization studies since then have shown compounds of this system to contain octahedrally coordinated nickel bonded to the sulfur atom of the thiourea (2–6). More recently, a number of compounds of Ni(II) with substituted thioureas have appeared in the literature. Holt and Carlin (7) have shown that a variety of stereochemical arrangements are possible for Ni(II) in such complexes: for example, octahedral in $[Ni(ethylenethiourea)_6](ClO_4)_2$, $[Ni(N,N'\text{-}diethylthiourea)_6](ClO_4)_2$, and $[Ni(naphthylthiourea)_4Cl_2]$; square planar in $[Ni(ethylenethiourea)_4](ClO_4)_2$, $[Ni(ethylenethiourea)_4](NO_3)_2$; and tetrahedral in $Ni(naphthylthiourea)_2I_2$. Their work consisted primarily of preparations and magnetic and spectral studies. Of particular interest was the series $Ni(N,N'\text{-}diethylthiourea)_4X_2$ ($X = Cl^-, Br^-, I^-$) where the Ni(II) ion was found to be in a tetragonal ligand field and showed anomalous magnetic behavior (8). More recently, Levitus and coworkers (9, 10) have prepared and characterized other octahedral Ni(II) complexes of substituted thioureas, using room temperature magnetic and spectral data. Infrared analysis was used to establish the mode of coordination of the thiocyanate group in some of these, but no discussion was given concerning the organic ligand. It is interesting to note that up to the present time all of the Ni(II) complexes containing thiourea ligands for which structural data are available are reported to be sulfur bonded to the organic ligand, although other metal ions such as Pt(II), Pd(II), and Cu(I) have been found to be nitrogen bonded to ligands such as N-methylthiourea (11) and N,N′-dimethylthiourea (12, 13). For the case of Fe(II) and substituted thiourea ligands, we have shown previously (14) that sulfur was the donor atom.

Pursuant to our interest in substituted thioureas as ligands we have studied Ni(II) complexes with N-ethyl-, N-methyl-, N,N′-dimethyl-, N,N′-diethyl-, and N,N′-di-*n*-butyl-thiourea and a

[1]Based on part of a thesis to be submitted by T. R. Peterson to the Graduate School of Rensselaer Polytechnic Institute in partial fulfillment of the requirements for the degree of D octor of Philosophy.

Can. J. Chem. Downloaded from www.nrcresearchpress.com by 210.87.254.40 on 09/05/12
For personal use only.

TABLE I

Analytical results (%)

Compound	Ni		C		H		N		S		Yield (%)	Color
	Calcd.	Found	Calcd.	Found	Calcd.	Found	Calcd.	Found	Calcd.	Found		
$Ni(MTU)_2Cl_2$	18.94	18.92	15.50	15.45	3.90	4.13	18.08	17.78	20.69	20.51	43	Yellow–orange
$[Ni(MTU)_6](ClO_4)_2$	7.35	7.28	18.05	18.15	4.54	4.63	21.05	21.25	24.10	24.25	73	Yellow–orange
$Ni(ETU)_2(NCS)_2$	15.32	14.96	25.07	25.34	4.21	4.46	21.93	22.05	33.47	33.61	35	Yellow–green
$[Ni(ETU)_6](ClO_4)_2$	6.65	6.84	24.49	24.38	5.48	5.43	19.04	19.15	21.79	21.85	33	Yellow
$Ni(DMTU)_4Cl_2$	10.75	10.70	26.38	26.09	5.90	5.93	20.51	20.67	23.47	23.52	35	Green
$Ni(DMTU)_4Br_2$	9.24	9.24	22.69	22.98	5.08	5.17	17.64	17.71	20.19	20.25	30	Blue–green
$Ni(DMTU)_4I_2$	8.05	7.96	19.77	19.92	4.42	4.82	15.37	15.14	17.59	17.61	50	Green
$[Ni(DMTU)_6](ClO_4)_2$	6.65	6.64	24.49	24.23	5.48	5.44	19.04	18.82	21.79	21.83	66	Orange–red
$Ni(DETU)_4Cl_2$	8.92	8.90	36.48	36.78	7.35	7.62	17.02	17.10	19.48	19.52	55	Green
$Ni(DETU)_4Br_2$	7.85	7.84	32.14	31.81	6.47	6.73	14.99	15.05	17.16	17.21	50	Blue–green
$Ni(DETU)_4I_2$	6.98	6.68	28.54	28.84	5.75	6.00	13.32	13.41	15.24	15.32	55	Green
$Ni(DETU)_4(NCS)_2$	8.34	8.42	37.55	37.67	6.87	7.09	19.90	20.15	27.34	27.34	45	Yellow–green
$[Ni(DETU)_6](ClO_4)_2$	5.59	5.55	34.28	33.98	6.91	6.88	15.99	16.15	18.31	18.15	60	Yellow–green
$[Ni(DBTU)_6](ClO_4)_2$	4.23	4.43	46.74	46.59	8.72	8.48	12.11	12.25	13.86	13.95	40	Yellow–green
$Ni(DBTU)_4(NCS)_2$	6.33	6.31	49.17	48.92	8.69	8.52	15.09	15.21	20.73	20.85	65	Yellow–green
$[Ni(DETU)_4(H_2O)_2](ClO_4)_2$	7.14	6.85	(ClO_4^-, Calcd. 28.05, Found 28.21)				13.62	13.91	15.59	15.71		Green
$[Ni(DMTU)_4(H_2O)_2](ClO_4)_2$	8.27	8.22	(ClO_4^-, Calcd. 24.25, Found 24.50)				15.78	16.02	18.06	18.02		Green

Can. J. Chem. Downloaded from www.nrcresearchpress.com by 210.87.254.40 on 09/05/12
For personal use only.

variety of anions, extending the work done on the compounds reported previously as well as including new compounds. In particular, we have considered an infrared study of the mode of bonding of the ligands.

Experimental

Chemicals

All substituted thioureas, anhydrous nickel chloride, nickel bromide, nickel iodide, and nickel perchlorate·$6H_2O$ were obtained from K and K Laboratories, Inc., and used without further purification. The remainder of the chemicals were Fisher reagent grade materials.

Analyses

Nickel was determined by ethylenediaminetetraacetic acid (EDTA) titration with murexide as indicator (15). Sulfur was determined as $BaSO_4$, after decomposition by Eschkas' mixture, and nitrogen by the Kjeldahl procedure using a copper catalyst with H_2SO_4 to effect decomposition. C, H, and some N analyses were carried out by Schwarzkopf Microanalytical Laboratory, Inc., Woodside, New York.

Physical Measurements

Magnetic data were obtained by the Gouy technique, using $Hg[Co(NCS)_4]$ as calibrant, and corrected for diamagnetism in the usual manner (16). Dewar flasks containing a liquid at the desired temperature were used to provide temperature control. Susceptibilities were constant with change in field strength (4 – 10 000 G).

Infrared spectra were taken using the KBr pellet technique on a Perkin Elmer 421 or 621 spectrophotometer. Spectra in hexachlorobutadiene mulls gave essentially identical results.

Visible spectra at room temperature were obtained by the reflectance technique from finely ground samples, using $MgCO_3$ as standard in a Beckman DU spectrophotometer.

Preparation of Complexes

All preparations were carried out by similar methods. Analytical results are given in Table I.

Dichlorotetrakis(N,N′-dimethylthiourea)nickel(II), $Ni(DMTU)_4Cl_2$, was prepared in the following way. $NiCl_2·6H_2O$ (2.4 g) was dissolved in 50 ml of absolute ethanol and the solution added to a solution of 2.1 g of N,N′-dimethylthiourea in 25 ml of absolute ethanol, refluxed for 30 min, and filtered hot. The deep-green crystals obtained by chilling the filtrate in ice were recrystallized three times from small portions of hot absolute ethanol and dried in vacuum over sulfuric acid.

Dibromotetrakis(N,N′-dimethylthiourea)nickel(II), $Ni(DMTU)_4Br_2$, and diiodotetrakis(N,N′-dimethylthiourea)nickel(II), $Ni(DMTU)_4I_2$ were prepared as above from the anhydrous nickel salts.

Hexakis(N-methylthiourea)nickel(II)perchlorate, $[Ni(MTU)_6](ClO_4)_2$; hexakis(N-ethylthiourea)nickel(II)-perchlorate, $[Ni(ETU)_6](ClO_4)_2$; hexakis(N,N′-dimethylthiourea)nickel(II)perchlorate, $[Ni(DMTU)_6](ClO_4)_2$; hexakis(N,N′-diethylthiourea)nickel(II)perchlorate, $[Ni(DETU)_6](ClO_4)_2$; and hexakis(N,N′-di-*n*-butylthiourea)-nickel(II)perchlorate, $[Ni(DBTU)_6](ClO_4)_2$, were prepared and purified as the halides noted above from $Ni(ClO_4)_2·6H_2O$. In the case of $[Ni(ETU)_6](ClO_4)_2$, final washing with small portions of cold chloroform was necessary to produce a pure product.

Diaquotetrakis(N,N′-diethylthiourea)nickel(II)perchlorate, $[Ni(DETU)_4(H_2O)_2](ClO_4)_2$, and diaquotetrakis(N,N′-dimethylthiourea)nickel(II) perchlorate, $[Ni(DMTU)_4(H_2O)_2](ClO_4)_2$, were prepared in the following way. On exposure to moist air, $[Ni(DETU)_6](ClO_4)_2$ and $[Ni(DMTU)_6](ClO_4)_2$ readily turn green and after purification by washing with chloroform give the diaquo compounds. These appear to lose water easily with decomposition. Commercial analyses for C were invariably high, approaching the expected values for loss of two water molecules, but definite compounds $[NiL_4](ClO_4)_2$ were not obtained. Analyses for Ni, S, and N made on materials stored carefully at room temperature were consistently in agreement with the hydrated formula (Table I). The presence of water was also indicated by the infrared spectra. The other perchlorates did not yield similar compounds under these conditions.

Dithiocyanatotetrakis(N, N′-diethylthiourea)nickel(II), $Ni(DETU)_4(NCS)_2$; dithiocyanatotetrakis(N,N′-di-*n*-butylthiourea)nickel(II), $Ni(DBTU)_4(NCS)_2$; and dithiocyanatobis(N-ethylthiourea)nickel(II), $Ni(ETU)_2(NCS)_2$,

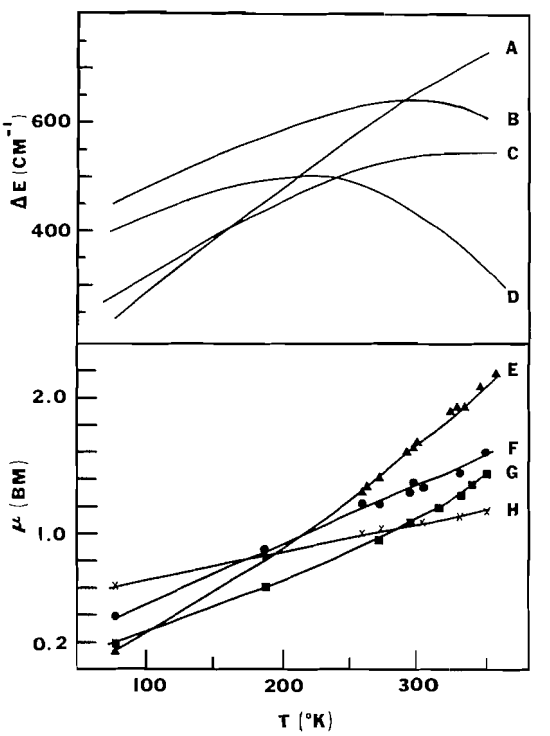

FIG. 1. Magnetic moment (lower) and energy separation ΔE between the singlet ground state and triplet excited state (upper) of tetragonal nickel(II) complexes, as a function of temperature. (A, H) $Ni(DMTU)_4Br_2$; (B, G) $Ni(DETU)_4Br_2$; (C, F) $Ni(DMTU)_4Cl_2$; (D, E) $Ni(DETU)_4Cl_2$. The iodides are very nearly coincident with the bromides.

Can. J. Chem. Downloaded from www.nrcresearchpress.com by 210.87.254.40 on 09/05/12
For personal use only.

were prepared in the following way. Nickel thiocyanate was prepared in ethanol solution from anhydrous $NiCl_2$ and NaCNS. The NaCl was filtered from the chilled solution, and the latter reacted with the ligand as in the case of the halides above.

Dichlorotetrakis(N,N′-diethylthiourea)nickel(II), $Ni(DETU)_4Cl_2$; dibromotetrakis(N,N′-diethylthiourea)-nickel(II), $Ni(DETU)_4Br_2$; and diiodotetrakis(N,N′-diethylthiourea)nickel(II), $Ni(DETU)_4I_2$, were prepared in essentially the same manner as originally reported by Holt and Carlin (7), using absolute ethanol in place of butanol and a 1:2 ratio of anhydrous metal salt to ligand. All these compounds were recrystallized three times from hot absolute ethanol and dried in vacuum over H_2SO_4. Attempts to prepare similar complexes from N,N′-di-*n*-butylthiourea were not successful due to solubility problems.

Dichlorobis(N-methylthiourea)nickel(II), $Ni(MTU)_2Cl_2$, was prepared in the following way. $NiCl_2$ (2.6 g) was dissolved in 50 ml of absolute ethanol and filtered hot. The filtrate was added to a solution of 3.6 g of N-methylthiourea dissolved in 25 ml absolute ethanol, followed by refluxing for 30 min. The deep-green solution was filtered hot and the filtrate was evaporated to 35 ml on a steam bath. Chilling the filtrate in ice yielded yellow–orange crystals which were recrystallized twice from small portions of absolute ethanol and dried in vacuum over sulfuric acid.

Results and Discussion

Dichlorotetrakis(N,N′-diethylthiourea)-nickel(II) has been discussed by Holt, Bouchard, and Carlin (8); it represents one of the few examples of a tetragonal Ni(II) complex with a spin-paired ground state and a low-lying, thermally populated triplet state giving rise to anomalous magnetic behavior. The bromo- and iodo-complexes were reported by Holt *et al.* to be diamagnetic at room temperature, but with paramagnetism appearing in the former at higher temperatures. We find that the dimethylthiourea compounds form an analogous series with these.

Our magnetic results on these compounds are shown in Fig. 1. There is some discrepancy between our results and those of Holt *et al.* for the diethylthiourea series, where we find somewhat higher moments for the chloride and a nonlinear temperature dependence. Also we observe weak paramagnetism in the bromo- and iodo-complexes even below room temperature.

This case has been considered theoretically by Ballhausen and Liehr (17) and by Maki (18). The equation which they developed for the energy separation ΔE between the singlet ground state and the first excited triplet may be written

$$\mu = \sqrt{2}g\beta(1 + 1/3 \exp \Delta E/RT)^{-1/2}$$

where temperature independent paramagnetism is neglected. The quantity $\sqrt{2}g\beta$ for a paramagnetic Ni(II) complex is generally accepted to be 3.2 B.M. (19). Values of ΔE found are in the order 300–700 cm^{-1} (Fig. 1), with a tendency to exhibit a maximum at or above room temperature. The variation of ΔE with temperature is very similar to that noted by Sacconi *et al.* (19) for a series of bis(N-alkylsalicylaldimine)nickel(II) complexes in solution and in the molten state. It may be ascribed to the effect of temperature on the molecular geometry and bond lengths. Presumably the decrease in axial component of the

TABLE II

Diffuse reflectance spectra for Ni(II) complexes

Compound	Peak positions (cm^{-1}) ν_1	ν_2	ν_3	Dq (cm^{-1})
$[Ni(MTU)_6](ClO_4)_2$	8800	13 100	19 800	880
$[Ni(ETU)_6](ClO_4)_2$	9100	14 000	—	910
$[Ni(DMTU)_6](ClO_4)_2$	8000	13 100	—	800
$[Ni(DETU)_6](ClO_4)_2$	8000	13 700	20 000	800
$[Ni(DBTU)_6](ClO_4)_2$	8700	14 000	—	870
$Ni(MTU)_2Cl_2$	7700	12 500	21 300	770
$Ni(ETU)_2(NCS)_2$	8700	14 600	—	870
$Ni(DETU)_4(NCS)_2$	9100	14 900	—	910
$Ni(DBTU)_4(NCS)_2$	9100	14 200	—	910
$[Ni(DMTU)_4(H_2O)_2](ClO_4)_2$	8300	13 900, 17 300	—	830
$[Ni(DETU)_4(H_2O)_2](ClO_4)_2$	8100	12 000, 15 000	22 200	810
$Ni(DMTU)_4Cl_2$	—	15 750	20 800	—
$Ni(DMTU)_4Br_2$	—	16 000	—	—
$Ni(DMTU)_4I_2$	—	16 100	—	—
$Ni(DETU)_4Cl_2$	8700	15 650	20 400	—
$Ni(DETU)_4Br_2$	8700	15 800	—	—
$Ni(DETU)_4I_2$	8700	15 400	—	—

Can. J. Chem. Downloaded from www.nrcresearchpress.com by 210.87.254.40 on 09/05/12
For personal use only.

field with increasing temperature causes an increase in ΔE which, at higher temperatures, may be counteracted by the overall weakening of the field with consequent stabilization of the triplet relative to the singlet ground state as discussed by Sacconi *et al.* (19). Values of ΔE are in the order $Cl^- < Br^- \sim I^-$ for both series, which is reasonable if the stronger axial field associated with Cl^- stabilizes the triplet state.

The electronic spectra, given in Table II and Fig. 2, for these complexes have also been considered for dichlorotetrakis(N,N′-diethylthiourea)nickel(II) by Holt *et al.* (8). The strong band at ca. 15 400 cm^{-1} is probably due to a singlet–singlet transition, while the band or shoulder at ca. 20 400 cm^{-1} in the chlorides arises from the ^3B state. This is missing in the bromo- and iodo-compounds because of the lower triplet population and perhaps overlap from the charge transfer band. The low energy bands in the diethyl compounds appear to be due to the ligand; the 8700 cm^{-1} band appears in the reflectance spectrum of N,N′-diethylthiourea itself, and seems to be a combination band of the vibrational frequencies.

The solid state reflectance spectra of the remainder of the Ni(II) complexes studied in this work, except for those containing water (Fig. 2, Table II), may be assigned to octahedral complexes. The bands may be assigned as follows: ν_1, 8000–9000 cm^{-1}, $^3A_2g \rightarrow {}^3T_2g$ (F), and ν_2, 13 000 – 14 000 cm^{-1}, $^3A_2g \rightarrow {}^3T_1g$ (F). The band ν_3 at ca. 20 000 – 22 000 cm^{-1} observed in some examples is probably the $^3A_2g \rightarrow {}^3T_1g$ (P) transition, although its origin as due to the spin-forbidden transition $^3A_2 \rightarrow {}^1T_2g$ (D) can not be excluded. The band positions are very similar to the spectra of octahedrally coordinated [Ni(N,N′-dicyclohexylthiourea)$_6$]$(ClO_4)_2$ previously reported by Yagupsky and Levitus (9). (The ligand band of N,N′-diethylthiourea is hidden in the stronger ligand field band in these complexes.)

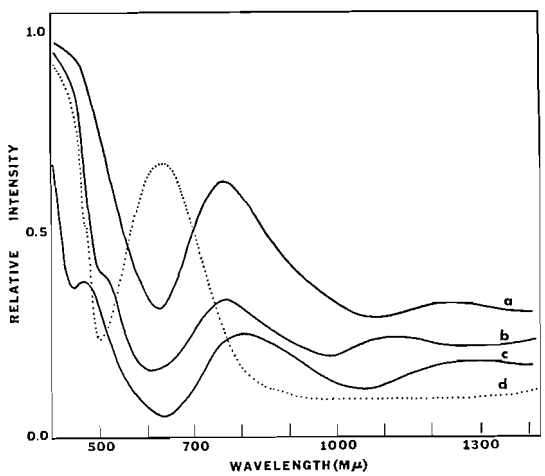

FIG. 2. Reflectance spectra of nickel(II) thiourea complexes: (*a*) [Ni(DMTU)$_6$]$(ClO_4)_2$; (*b*) [Ni(MTU)$_6$]$(ClO_4)_2$; (*c*) Ni(MTU)$_2Cl_2$; (*d*) Ni(DMTU)$_4Cl_2$.

The assignment of octahedral geometry holds for Ni(N-methylthiourea)$_2Cl_2$; application of the rule of average environments (20) using the known tetrahedral ligand field splitting energy for Cl^- rules out the possibility of a tetrahedral species. Evidently there are either two bridging chlorides or two bridging organic ligands, but the similar values of $10Dq$ prevent determining which from the ligand field spectra as was possible for the analogous Fe(II) compounds (14).

The spectra observed for [Ni(N,N′-diethylthiourea)$_6$]$(ClO_4)_2$ by Holt *et al.* (8) and for the thiocyanate complexes by Puglisi and Levitus (10) are in good agreement with our results when allowance is made for the broadness of the peaks.

The value of Dq is given by the position of the first band ν_1. The Racah parameter B may be evaluated from the equation $B = (\nu_2 + \nu_3 - 3\nu_1)/15$ for those complexes in which ν_3 can be observed (21). Values of ca. 650–700 cm^{-1} are obtained for [Ni(N,N′-diethylthiourea)$_6$]$(ClO_4)_2$ and Ni(N-methylthiourea)$_2Cl_2$ which are reasonable reductions from the free ion value of 1030 cm^{-1} (20). The only other compound for which a third band could be detected was [Ni(N-methylthiourea)$_6$]$(ClO_4)_2$, which exhibited a weak shoulder at ca. 19 800 cm^{-1}. This is most probably the aforementioned spin-forbidden transition; assignment of it to the $^3A_2g \rightarrow {}^3T_1g$ (P) transition gives a very poor fit to the energy level diagram. The latter transition in this and other complexes is probably hidden by the charge transfer band. Calculation of B in these cases from ν_1 and ν_2 only cannot be done satisfactorily, due to the uncertainty in ν_1. All the substituted thiourea ligands have Dq values around 800–900 cm^{-1} (Table II); the order being ETU > DBTU > DMTU $\sim$ DETU.

The spectra of the complexes $[NiL_4(H_2O)_2](ClO_4)_2$ fit those of other octahedral Ni(II) species of the type NiL_4X_2 (22). The structure of

Can. J. Chem. Downloaded from www.nrcresearchpress.com by 210.87.254.40 on 09/05/12
For personal use only.

TABLE III

Magnetic moments of Ni(II) thiourea complexes

Compound	$X_m \times 10^6$ (c.g.s.u.)			Diamag. corr. $\times 10^6$ (c.g.s.u.)	t.i.p. $\times 10^6$ (c.g.s.u.)	θ (°K)	μ (B.M.)		
	297 °K	188.5 °K	77 °K				297 °K	188.5 °K	77 °K
$Ni(MTU)_2Cl_2$	4580	7150	15 850	−171	272	−12	3.29	3.14	2.82
$[Ni(MTU)_6](ClO_4)_2$	3960	6000	15 270	−411	237	−5	3.14	3.03	3.01
$Ni(ETU)_2(NCS)_2$	4190	6340	16 290	−210	240	0	3.17	3.10	3.17
$[Ni(ETU)_6](ClO_4)_2$	3810	6120	14 950	−482	230	−4	3.10	3.08	2.98
$[Ni(DMTU)_6](ClO_4)_2$	4350	6510	17 000	−482	261	−2	3.24	3.13	3.10
$[Ni(DETU)_6](ClO_4)_2$	3760	6230	14 550	−625	261	−4	3.14	3.15	3.05
$Ni(DETU)_4(NCS)_2$	4010	6350	15 550	−440	230	−4	3.18	3.11	3.05
$[Ni(DBTU)_6](ClO_4)_2$	3490	5850	15 200	−909	240	−2	3.16	3.13	3.10
$Ni(DBTU)_4(NCS)_2$	3780	6260	15 380	−630	230	0	3.18	3.18	3.12
$[Ni(DMTU)_4(H_2O)_2](ClO_4)_2$	3660	5690	14 820	−371	250	+4	3.03	3.00	3.12
$[Ni(DETU)_4(H_2O)_2](ClO_4)_2$	3870	6120	15 240	−466	260	−4	3.10	3.07	3.02

X_m = uncorrected molar susceptibility.
μ = moment from $\mu = 2.84[X_m(\text{corr.})(T + \theta)]^{1/2}$ B.M., where X_m(corr.) has been corrected for diamagnetism and t.i.p. (temperature independent paramagnetism).

Can. J. Chem. Downloaded from www.nrcresearchpress.com by 210.87.254.40 on 09/05/12
For personal use only.

the ν_2 band may be due to spin orbit coupling or may be associated with the spin-forbidden $^3A_2 \rightarrow {}^1E_g$ transition. This has been discussed in detail by Ballhausen (23).

The magnetic properties of these Ni(II) thiourea complexes were measured at three temperatures: 297 °K, 188 °K, and 77 °K, respectively (Table III). The estimated experimental uncertainty amounts to less than ± 0.05 B.M., so that these limited data are useful for estimating theoretical quantities. The magnetic moments found are in the range expected for octahedral Ni(II); i.e. 2.8–3.2 B.M. (24). The resultant molar susceptibilities of these normal compounds were corrected for both diamagnetism and temperature independent paramagnetism (t.i.p.) found from the relation t.i.p. $= 8N\beta^2/10Dq$ c.g.s.u. (24). The t.i.p. values amount to approximately 250×10^{-6} c.g.s.u., about 6% of the fully corrected room temperature molar susceptibilities. Plots of $1/X_{m(\text{corr})}$ versus temperature gave straight lines for all of the complexes with values of θ between +4 and −12 °K. Except for $Ni(MTU)_2Cl_2$, the magnetic moments corrected for θ were essentially constant with temperature. (We have reported moments corrected for θ even though this is not strictly correct in the absence of definite proof of antiferromagnetic interactions.) The spin–orbit coupling constant λ' for the Ni(II) ion may be calculated from the relation $\mu = 2.83\ (1 - 4\lambda'/10Dq)$, which gives values of $-\lambda'$ of the order of 250 cm^{-1}, about 80% of the free ion value for Ni(II) of 315 cm^{-1} (23). The somewhat larger θ value and temperature dependence of the magnetic moment of Ni(N-methylthiourea)$_2Cl_2$ may suggest antiferromagnetic interactions through chloride bridges as is found with other complexes of Ni(II) containing halide bridges (25).

Gosavi *et al.* (12) have performed a normal coordinate analysis of N,N′-dimethylthiourea and have assigned the more important bands in its infrared spectrum. They have also examined the infrared spectra of some complexes containing this organic ligand with Cu(I), Pd(II), Zn(II), and Cd(II) ions (13). Based on the shifts in bands observed, the Cu(I) and Pd(II) complexes are considered to be nitrogen bonded to the ligand, whereas the Zn(II) and Cd(II) complexes are sulfur bonded.

The positions of the significant bands of free N,N′-dimethylthiourea, N,N′-diethylthiourea, and N,N′-di-*n*-butylthiourea, and their Ni(II) complexes are collected in Table IV. The free ligand peak positions are our values; they agree with those of Gosavi *et al.* except for the peak reported by them at 1287 cm^{-1} in free N,N′-dimethylthiourea. We find instead a band at 1255 cm^{-1} with shoulders at 1295 cm^{-1} and 1275 cm^{-1}. We have considered shifts with respect to the latter, as the 1295 cm^{-1} shoulder was very

TABLE IV

Significant bands in the infrared spectra of Ni(II) substituted thiourea complexes

Compound	Band position (cm^{-1})			
	ν_1, δ(NH) + ν(CS) + δ(NCN)	ν_2[a], ν(CS) + δ(NCS)	ν_3, ν(CS) + ν(CN) + ν(C′N)	ν_4, NH out-of-plane bending
(N—Bonded)[b]	+10 to 15		Increase	Decrease
(S—Bonded)[b]	+25 to 37	Increase	Decrease	Increase
DMTU	1505	1275	755	720
$Ni(DMTU)_4Cl_2$	1525	1290(I)	750	720
$Ni(DMTU)_4Br_2$	1525	1290(I)	740	720
$Ni(DMTU)_4I_2$	1535	1290(D)	750	718
$[Ni(DMTU)_6](ClO_4)_2$	1525	1290(I)	740	720
DETU	1515	1305	795	732
$Ni(DETU)_4Cl_2$	1525	1313(I)	788	738
$Ni(DETU)_4Br_2$	1520	1310(I)	790	740
$Ni(DETU)_4I_2$	1515	1310(N)	790	738
$Ni(DETU)_4(NCS)_2$	1515	1310(N)	788	745
$[Ni(DETU)_6](ClO_4)_2$	1520	1308(I)	788	735
DBTU	1510	1270	760	725
$Ni(DBTU)_4(NCS)_2$	1515	1275(I)	750	735
$[Ni(DBTU)_6](ClO_4)_2$	1515	1275(I)	755	735

[a]I = increased intensity; D = decreased intensity; N = no intensity change.
[b]Criteria of Gosavi *et al.* (12, 13).

TABLE V

Significant shifts of the infrared bands of coordinated N-methylthiourea[a]

Band (cm^{-1})	Shift of band (cm^{-1})			
	N—Bonded	S—Bonded	$[Ni(MTU)_6](ClO_4)_2$	$Ni(MTU)_2Cl_2$
1629 (NH_2 bending)	−10 to −15	0 to −5	−14	−14
1545 (amide II)	+15 to +25	+25 to +28	+10	+15
1482 (NH_2 rock, C—N sym. str., C=S str.)	0 to −15 Increased intensity	0 to +5 No intensity change	−7 Increased intensity	−12 Increased intensity
1290 (amide III)	−5 to −15	+7	0	+2

[a]Columns 2 and 3 are taken from the data of Lane *et al.* (11) and Gosavi and Rao (13).

weak. Since the infrared spectrum of both N,N′-diethylthiourea and N,N′-di-*n*-butylthiourea ligands have not been assigned we have assumed the tentative assignments made by Gosavi *et al.* (12) for the diethyl compound to be correct and have drawn the analogy for N,N′-di-*n*-butylthiourea as well. The criteria which are diagnostic of bonding mode for N,N′-dimethylthiourea according to the above workers (12, 13) are also summarized in Table IV. Other bands in the spectra of these symmetrical thiourea ligands show significant frequency changes, notably an increase for the band at about 1545 cm^{-1} and decreases for those near 1090 cm^{-1} and 655 cm^{-1}. These shifts are observed for both nitrogen and sulfur bonding and are not useful in distinguishing bond type. Examination of the band positions given in Table IV shows general agreement with the criteria proposed for metal-to-sulfur bonding. Exceptions occur for $Ni(DETU)_4I_2$ and $Ni(DETU)_4(NCS)_2$ where no shift was observed in the frequency of the band ν_1 in free N,N′-diethylthiourea. The band ν_1 in most of the N,N′-dimethylthiourea complexes is increased in frequency to a degree intermediate between that reported for N and S coordination, while the band ν_4 is essentially unchanged compared to the free ligand. A further discrepancy is noted in the band ν_2 in $Ni(DMTU)_4I_2$ where, although the frequency has increased as compared with free DMTU (1275 cm^{-1}) in accord with sulfur bonding, the intensity decreases slightly. However, this is based on a comparison of the peak height with other bands in the spectrum and is only qualitative. As an additional criterion, Gosavi and Rao (13) have reported that the NCS bending mode at 551 cm^{-1} in free N,N′-dimethylthiourea decreases in frequency in N-bonded cases, but apparently splits to higher and lower frequencies with sulfur bonding. We observe such a splitting for $Ni(DMTU)_4I_2$ (peaks at 560 cm^{-1} and 545 cm^{-1}). The other compounds containing this ligand exhibit only a band at ca. 540 cm^{-1} which can be recognized with certainty, but a possible

TABLE VI

Significant shifts in the infrared bands of coordinated N-ethylthiourea

Band (cm^{-1})	Shift of band (cm^{-1})			
	N—Bonded	S—Bonded	$Ni(ETU)_2(SCN)_2$	$[Ni(ETU)_6](ClO_4)_2$
3320, 3220, 3145 (N—H stretch)	Decrease	Unchanged	Marked increase 30–60	Marked increase 0–80
1615 (NH_2 bend)	Decrease	Unchanged	0	0
1525 (Amide II – NH def.; C—N antisym. str.)	Slight increase	Large increase	Split and shifted, +5 and +15	+10
1505, 1495, 1460 (NH_2 rock, C—N sym. str., C=S str. CH_2 deformation here also, should be unchanged)	Decrease, intensity increase	Increase, no intensity change	Bands at 1500 cm^{-1} increased intensity; 1470 cm^{-1}, decreased intensity	Bands at 1500 cm^{-1}, and 1463 cm^{-1}, both unchanged in intensity
1255 (Amide III; N—H def. and C—N str.)	Decrease	Increase	+35	Split, +15 and +35

Can. J. Chem. Downloaded from www.nrcresearchpress.com by 210.87.254.40 on 09/05/12
For personal use only.

Can. J. Chem. Downloaded from www.nrcresearchpress.com by 210.87.254.40 on 09/05/12
For personal use only.

weak band at ca. 570 cm^{-1} exists in all of them. None of these discrepancies indicates nitrogen bonding, and we believe that sulfur bonding is reasonably well confirmed for these compounds.

The infrared spectra of some N-methylthiourea complexes have been considered by Lane *et al.* (11) and later by Gosavi and Rao (13), who reported the criteria for nitrogen or sulfur bonding to the metal, which are summarized along with the data for the nickel complexes prepared in this study in Table V. The spectra of [Ni(N-methylthiourea)$_6$]$(ClO_4)_2$ and Ni(N-methylthiourea)$_2Cl_2$ more closely resemble the metal-to-nitrogen bonded case based on the observed spectral shifts of free N-methylthiourea on coordination. While the N—H stretching bands above 3000 cm^{-1} behave ambiguously, the 1629 cm^{-1} band arising from the NH_2-bending mode is shifted to a lower frequency (-14 cm^{-1}) than is generally found when metal–sulfur bonds are present. The band at ca. 1545 cm^{-1} (amide II) is shifted only +(10–15 cm^{-1}) in the nickel complexes, again in keeping with a nitrogen-bonded case, whereas metal–sulfur bonds produce higher shifts +(25–28 cm^{-1}). The band at 1482 cm^{-1} in free N-methylthiourea decreases slightly in energy but increases in intensity in these compounds, again in keeping with the presence of metal–nitrogen bonds. There is no shift in position of the band at 1290 cm^{-1} (amide III) for the case [Ni(N-methylthiourea)$_6$]$(ClO_4)_2$ and only +2 cm^{-1} for Ni(N-methylthiourea)$_2Cl_2$, and hence this is ambiguous.

In evaluating the above arguments, however, it must be noted that Lane *et al.* (11) did not consider the criteria for nitrogen bonding to be highly conclusive. Much caution must always be exercised in interpreting the infrared spectra of complexes where bands due to mixed vibrations are present and different bonding modes produce rather small variations in peak positions and intensities. Nitrogen bonding in this system is unexpected considering the similarity to the disubstituted thiourea complexes which are assigned more reliably to sulfur bonding. In particular, one would expect a significant difference in the ligand field spectra of nitrogen- and sulfur-bonded nickel, with nitrogen giving sensibly higher Dq values. This, of course, is also speculative, and the bonding mode in N-methylthiourea complexes of Ni(II) cannot be established.

The infrared spectrum of N-ethylthiourea has not been assigned. We have attempted to extend the criteria used by Lane *et al.* (11) with N-methylthiourea complexes to this system, assigning the ligand bands by analogy. The significant data are collected in Table VI. It is clear that the shifts observed are largely those expected for sulfur bonding, if the highly tentative assignments are valid.

The infrared spectra of the [$NiL_4(H_2O)_2$]-$(ClO_4)_2$ compounds are almost identical with those of the parent compounds with the exceptions that the 3300 cm^{-1} region is considerably changed, and an additional peak appears near 1600 cm^{-1}. These effects are attributable to the presence of water molecules. Evidence for coordinated water in the 600–900 cm^{-1} region (26) could not be detected, but much interference from thiourea bands occurs here. It seems probable that the waters are coordinated, however.

Nitrogen coordination of the thiocyanate group in Ni(N,N′-diethylthiourea)$_4(NCS)_2$, Ni(N,N′-di-*n*-butylthiourea)$_4(NCS)_2$, and Ni(N-ethylthiourea)$_2(NCS)_2$ was inferred by infrared

TABLE VII

Infrared bands for coordinated thiocyanate groups in Ni(II) thiourea complexes

Complex	Band (cm^{-1})[a]	Assignment
Ni(N,N′-diethylthiourea)$_4(NCS)_2$	2120 s (2100)	C—N stretching
	2070 sh —	
	789 m —	C—S stretching
	460 w —	S—C—N bending
Ni(N,N′-di-*n*-butylthiourea)$_4(NCS)_2$	2095 s (2095)	C—N stretching
	820 w (820)	C—S stretching
Ni(N-ethylthiourea)$_2(NCS)_2$	2065 s (2080)	C—N stretching
	755 w —	C—S stretching
	475 m —	S—C—N bending

[a]Band positions in parentheses as originally reported by Puglisi and Levitus (9).

analysis originally by Puglisi and Levitus (10), based mainly on the position of the C—N stretching modes. In our study of these complexes, Table VII, the positions of the C—N stretching frequencies are essentially in agreement with the earlier work. We have observed, in addition, bands attributable to the C—S stretch and the SCN bending modes which are at frequencies characteristic of coordination through the nitrogen atom of the thiocyanate group (27). This mode of bonding seems well established here.

1. A. ROSENHEIM and V. J. MEYER. Z. Anorg. Chem. **49**, 13 (1906).
2. C. R. HARE and C. J. BALLHAUSEN. J. Chem. Phys. **40**, 788 (1964).
3. R. W. OLIFF. J. Chem. Soc. 2036 (1965).
4. A. YAMAGUCHI, R. B. PENLAND, T. J. LANE, C. CURRAN, S. MIZUSHIMA, and J. V. QUAGLIANO. J. Am. Chem. Soc. **80**, 527 (1958).
5. M. NARDELLI and I. CHIERICI. Gazz. Chim. Ital. **88**, 248 (1958).
6. M. NARDELLI, L. CAVALCA, and A. BRAIBANTI. Gazz. Chim. Ital. **87**, 917 (1957).
7. S. L. HOLT, JR. and R. L. CARLIN. J. Am. Chem. Soc. **86**, 3017 (1964).
8. S. L. HOLT, JR., R. J. BOUCHARD, and R. L. CARLIN. J. Am. Chem. Soc. **86**, 519 (1964).
9. G. YAGUPSKY and R. LEVITUS. Inorg. Chem. **4**, 1589 (1965).
10. C. PUGLISI and R. LEVITUS. J. Inorg. Nucl. Chem. **29**, 1069 (1967).
11. T. J. LANE, A. YAMAGUCHI, J. V. QUAGLIANO, J. A. RYAN, and S. MIZUSHIMA. J. Am. Chem. Soc. **81**, 3824 (1959).
12. R. K. GOSAVI, U. AGARWALA, and C. N. R. RAO. J. Am. Chem. Soc. **89**, 235 (1967).
13. R. K. GOSAVI and C. N. R. RAO. J. Inorg. Nucl. Chem. **29**, 1937 (1967).
14. R. A. BAILEY and T. R. PETERSON. Can. J. Chem. **45**, 1135 (1967).
15. G. SCHWARZENBACK. Complexometric titrations. *Translated by* H. Irving. Interscience Publishers, Inc., New York. 1957. p. 79 and references therein.
16. B. N. FIGGIS and J. LEWIS. *In* Modern coordination chemistry. *Edited by* J. Lewis and R. G. Wilkins. Interscience Publishers, Inc., New York. 1960. p. 415.
17. C. J. BALLHAUSEN and A. D. LIEHR. J. Am. Chem. Soc. **81**, 538 (1959).
18. G. MAKI. J. Chem. Phys. **28**, 651 (1958); **29**, 162 (1958); **29**, 1129 (1958).
19. L. SACCONI, R. CINI, M. CIAMPOLINI, and F. MAGGIO. J. Am. Chem. Soc. **82**, 3487 (1960).
20. B. N. FIGGIS. Introduction to ligand fields. Interscience Publishers, Inc., New York. 1966. Chap. 9.
21. Y. TANABE and S. SUGANO. J. Phys. Soc. Japan, **9**, 753 (1954).
22. D. M. L. GOODGAME and M. A. HITCHMAN. Inorg. Chem. **3**, 1389 (1964).
23. C. J. BALLHAUSEN. Introduction to ligand field theory. McGraw-Hill Book Co., Inc., New York. 1962. p. 262.
24. B. N. FIGGIS and J. LEWIS. *In* Progress in inorganic chemistry. Vol. 6. *Edited by* F. A. Cotton. Interscience Publishers, Inc., New York. 1964. Chap. 2.
25. D. M. L. GOODGAME, M. GOODGAME, and M. J. WEEKS. J. Chem. Soc. 5194 (1964).
26. K. NAKAMOTO. Infrared spectra of inorganic and coordination compounds. John Wiley and Sons, Inc., New York. 1963. pp. 156–157.
27. I. BERTINI and A. SABATINI. Inorg. Chem. **5**, 1025 (1966).

Can. J. Chem. Downloaded from www.nrcresearchpress.com by 210.87.254.40 on 09/05/12
For personal use only.

Can. J. Chem. Downloaded from www.nrcresearchpress.com by 210.87.254.40 on 09/05/12
For personal use only.

Radiolysis of ortho- and meta-terphenyl[1]

A. W. BOYD
Research Chemistry Branch, Chalk River Nuclear Laboratories, Atomic Energy of Canada Limited, Chalk River, Ontario

AND

M. TOMLINSON
Materials Science Branch, Whiteshell Nuclear Research Establishment, Atomic Energy of Canada Limited, Pinawa, Manitoba

Received May 24, 1968

A summary is presented of a series of investigations of the radiolytic decomposition of ortho- and meta-terphenyl by reactor radiation with varying proportions of fast neutrons and gamma rays and of meta-terphenyl by 1.3 MeV electrons in the temperature range 100 to 450 °C with radiation intensities from 0.01 to 2 Mrads/s. The observations indicate two regions of radiolytic decomposition with a transition zone at 350 to 400 °C. In the lower temperature region, *G*(decomposition) varied little with temperature, increased with linear energy transfer (l.e.t.), was independent of intensity, and yielded mainly high boiling products. Particular attention was given to the high temperature region, where *G*(decomposition) increased rapidly with temperature, was independent of l.e.t., was greater at low intensities than at high intensities, increased with increased pulse frequency for intermittent irradiation, and yielded a greater proportion of benzene and biphenyl. Thermally initiated reaction appeared unimportant except in the absence of radiation. A reaction sequence is given which accounts for these observations in terms of reactions of radical precursors and radicals of the cyclohexadienyl type. A chain reaction occurs in the higher temperature region.

Canadian Journal of Chemistry, **46**, 3129 (1968)

Introduction

The radiolysis of the terphenyls and related aromatic compounds has been studied extensively in connection with the development of organic coolants for nuclear reactors. The results of this work and the mechanisms proposed are of interest in themselves and for their application to the radiolysis of other aromatics.

Most of the previous studies have been summarized (1) and our detailed results and procedures have been reported (2–6). The purposes of this paper are to outline our results, and to propose and discuss mechanisms to explain them.

Previous work has shown that the terphenyls are among the most radiolytically stable organic compounds with *G* values for disappearance of ~ 0.2 at temperatures up to 300 °C. The major product is the dimer which must be partially hydrogenated because the hydrogen yield is small, $G(H_2) < 0.05$. Small amounts of light hydrocarbons, benzene, biphenyl, and other polyphenyls are also formed. Above 350 °C the yields of all the products increase, with the largest increases shown by the products resulting from inter-ring cleavage. The temperature effects may be due to changes in radiation-induced reactions or to thermally initiated reactions. The relative magnitude of the radiolytic and pyrolytic contributions is uncertain. As with benzene there is an increase in gas yields and total decomposition yields with increasing l.e.t. This has been shown using the fast protons and carbon ions resulting from fast neutron scattering in reactor radiations, and helium ions. For these particles total decomposition *G* values are 3–5 times greater than for γ-rays or electrons.

To determine l.e.t. effects at high temperatures and the contribution of pyrolysis, we have done irradiations up to 450 °C with fast neutrons and γ-rays at different dose rates. We have also done both steady and intermittent irradiations with 1.3 MeV electrons at constant average dose rate.

It was found that at temperatures above 350–400 °C the l.e.t. effect is less important and that there is an increase in yields, which is not due to thermal pyrolysis, on going from high dose rates to low dose rates or from lower to higher frequency of intermittent irradiation.

An explanation is offered for the l.e.t. effects in terms of decomposition and quenching of highly excited states. The intensity dependence and other high temperature effects are explained

[1]Issued as A.E.C.L. No. 2730.

TABLE I

Comparison of integral G values for ortho- and meta-terphenyl*

Temperature (°C)	G(-terphenyl)		G(HB)†		G(biphenyl)		G(total gas)	
	Ortho	Meta	Ortho	Meta	Ortho	Meta	Ortho	Meta
100–200	0.3	0.3	0.3	0.3	0.002	0.002	0.05	0.04
300	0.4	0.35	0.35	0.35	0.02	~0.005	0.07	0.05
350	0.6	0.4	0.4	0.35	0.06	0.01	0.09	0.07
400	1.0	0.7	0.6	0.6	0.3	~0.03	0.1	0.1
425	1.8	1.0	0.9	0.65	0.4	0.1	0.15	0.11
450	4.0	1.8	1.6	1.5	0.8	0.3	0.2	0.15

*Fast neutron and γ-ray irradiations at 0.01–0.03 Mrad/s.
†HB is an abbreviation for high boilers which are the products less volatile than the terphenyls.

by a chain reaction involving multi-ring homologues of the cyclohexadienyl radical.

Experimental

Reactor Irradiations (2–4)

The objectives of the reactor irradiations were to compare the decomposition yields for fast neutrons and γ-rays and to determine the effect of varying the dose rate over a wide temperature range. To do this, four different reactor facilities were used. Three of these were annular uranium fuel rods in which the absorbed dose rates in terphenyl were 0.01, 0.03, and 0.1 Mrad/s, with about equal contributions from fast neutrons and γ-rays. The other facility contained a cadmium annulus in which the dose rate was 0.015–0.02 Mrad/s with > 95% γ-ray contribution. The samples consisted of a few grams of purified and outgassed ortho- or meta-terphenyl contained in quartz or stainless steel capsules. These were irradiated inside the uranium or cadmium annulus. Temperatures were controlled in general to within ± 2 °C. The absorbed dose and fast neutron and γ-ray contributions were determined by calorimetric and other methods (7). The total disappearance of terphenyl varied from 3–60% but in most experiments was 10–30%.

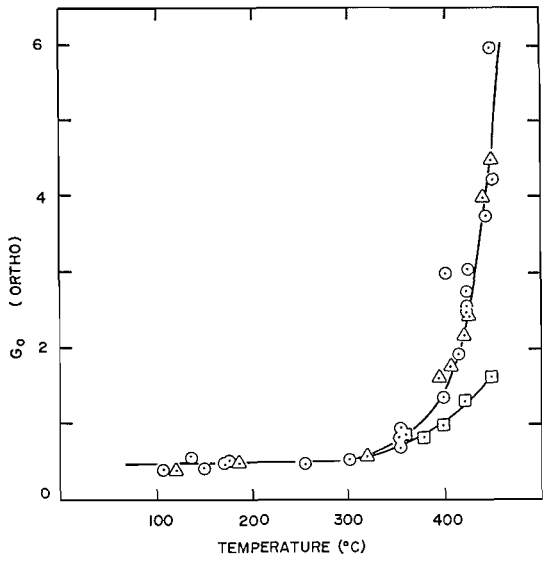

FIG. 1. Ortho-terphenyl decomposition versus temperature for reactor irradiation; ⊙, 0.01 Mrad/s; ⊡, 0.1 Mrad/s; and △, 0.03 Mrad/s.

Electron Irradiations (5)

Electron irradiations were performed in heated, preevacuated, stainless steel, irradiation cells using a beam of 1.3 MeV electrons at various currents from 3 to 104 μA. A powerful stirrer maintained temperature uniformity. Irradiation cells of 10 to 24 cm^3 liquid capacity were used. In the latter about 15 cm^3 was out of range of the electrons. The dose was determined from the charge collected and the voltage. This method agreed with calorimetric measurements to within 3%.

Analysis

After irradiation, biphenyl and terphenyl isomers were determined by gas chromatography using either glass beads coated with Apiezon L grease or KOH coated firebrick (8). There was no systematic difference between the methods. The standard deviation for replicate analysis was ± 1% wt. of total constituents for components in excess of 50% and less at lower concentrations (e.g. ± 0.3% at 5% concentration). High boilers, i.e. products less volatile than terphenyl, were determined by vacuum microsublimation (9). Total gases were determined by pressure–volume–temperature measurement and hydrogen by effusion through palladium. In some cases benzene was determined by gas chromatography.

Results

Radiolytic decomposition and high boiler production yields for these experiments are reported as initial yields calculated on the basis of second order overall kinetics[2]. No corrections were made for any pyrolysis that might have occurred during the irradiations. Mason *et al.* (10) find that the reaction order 1.7 ± 0.2 best fits their data and provides a good correlation of previous data. The reaction sequence which we

[2] $G_0 = (1/C - 1/C_0)/D$: G_0 = initial yield, in molecules/100 eV, C, C_0 = final, initial concentration of terphenyl, or material not converted to high boiler, as appropriate, in molecules/cm^3, D = dose, in 100 eV/cm^3.

Can. J. Chem. Downloaded from www.nrcresearchpress.com by 210.87.254.40 on 09/05/12
For personal use only.

TABLE II

Fast neutron and γ-ray decomposition yields for ortho- and meta-terphenyl

Temperature (°C)	Initial decomposition yields for γ-rays		Initial decomposition yields for fast neutron*		G_n/G_γ	
	Ortho	Meta	Ortho	Meta	Ortho	Meta
250	0.26	0.15	0.7	0.67	2.7	4.5
300	0.43	0.20	0.68	0.64	1.6	3.2
350	0.80	0.27	0.80	0.83	1.0	3.1
400	1.6	0.72	1.6	0.72	1.0	1.0

*Calculated from decomposition by reactor radiation assuming additivity of fast neutron and gamma ray contributions.

propose leads to a complex concentration dependence, which can be approximated closely by a kinetic order of 1.5–2.

There was a marked increase in total disappearance for temperatures above 350 °C as shown in Figs. 1 and 2. This was accompanied by increased formation of biphenyl and gas as indicated in Table I. Benzene yields were about one quarter of the biphenyl yield. Ortho-terphenyl decomposed more than meta-terphenyl and produced a greater proportion of benzene and biphenyl. The lack of material balance at the higher temperatures in Table I is due to the omission of benzene and other products that were not determined.

The effect of l.e.t. is summarized in Table II, which shows that the neutron component of reactor radiation was responsible for a decomposition yield several times greater than the yield for gamma rays at 250 °C and the effect diminished at higher temperatures, such that there was no significant l.e.t. effect at 400 °C.

Intensity dependence for ortho-terphenyl decomposition above 350 °C is evident in Fig. 1, i.e. there was less decomposition per unit dose at 0.1 Mrad/s than at 0.03 Mrad/s and 0.01 Mrad/s. The variation of the decomposition yield for meta-terphenyl at 440 °C is shown over a wide range of intensity in Fig. 3. For electron irradiation, the decomposition varied inversely as $\sqrt{I}$. The decomposition yields in reactor irradiations also varied with intensity but were less than the values extrapolated from the

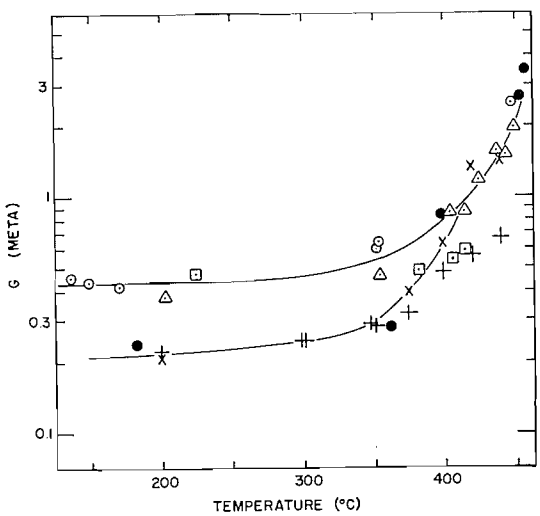

FIG. 2. Meta-terphenyl decomposition versus temperature; ⊙, 0.01 Mrad/s fast neutron and gamma; ●, 0.015 Mrad/s gamma; △, 0.03 Mrad/s fast neutron and gamma, × 5 μA electron; ⊡, 0.1 Mrad/s fast neutron and gamma, and + 50 μA electron.

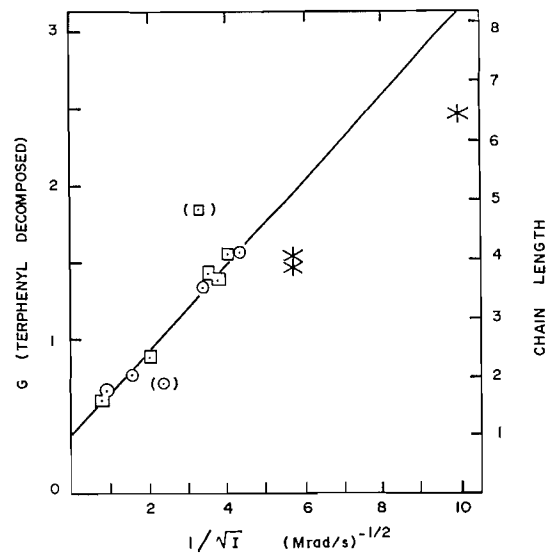

FIG. 3. Variation of meta-terphenyl decomposition at 440 °C with absorbed dose rate; ⊙, small electron irradiation cell; ⊡, large electron irradiation cell; *, reactor irradiation; (), points not included in line fit; and —, $G = (0.383 \pm 0.07) + (0.277 \pm 0.01/\sqrt{I})$ (least mean squares fit of electron irradiation data).

Can. J. Chem. Downloaded from www.nrcresearchpress.com by 210.87.254.40 on 09/05/12
For personal use only.

electron irradiation data. The yield of biphenyl increased with decreasing intensity such that the proportions of the measured products remained approximately constant.

Figure 3 includes results for electron irradiation vessels of differing capacity (10 cm^3 and 24 cm^3 liquid) the irradiation zone being the same for both. No difference in yields was detected indicating no significant contribution (e.g. from thermally initiated reactions) in the unirradiated zone.

TABLE III

Decomposition of meta-terphenyl with intermittent electron irradiation at 440 °C

Pulse frequency (cycles/s)	Residual meta-terphenyl (%)	
	Small cell	Large cell
0.00 (1 cycle)		54.8†
0.1	60.0*	51.8†
3	58.1*	46.5†
‖	48.1‡	40.6§

*Total time at 440 °C = 10 h. Irradiation time = 1 h. Heat cycle time = 9 × irradiation time. Total dose = 3240 Mrads in all cases.
†Total time at 440 °C = 24 h. Irradiation time = 2.4 h. Heat cycle time = 9 × irradiation time.
‡Irradiation and heating time = 10 h.
§Irradiation and heating time = 24 h.
‖Continuous irradiation at 0.1 × normal dose rate.

Intermittent irradiations, summarized in Table III, showed increasing decomposition with decreasing duration of the irradiation plus heat cycle. This is evidence of intermediates with lifetimes comparable with the shorter irradiation pulse time used (30 ms).

The results of various heat treatments of irradiated and unirradiated terphenyl samples are summarized in Table IV.

TABLE IV

Thermal decomposition of irradiated and unirradiated terphenyl

Treatment	Total decomposition (%)	Thermal decomposition (rate* per 10^3 h)
Ortho-terphenyl		
48 h at 424 °C	7.0	1.5
350 Mrads at 400 °C, 48 h at 424 °C	27.3	1.7
Meta-terphenyl		
48 h at 424 °C	~2.0	~0.4
560 Mrads at 400 °C, 48 h at 424 °C	18.0	1.6
3240 Mrads at 440 °C, 21.2 h at 440 °C	45.2	4.3
3420 Mrads at 440 °C, Aged at room temperature, 12.3 h at 440 °C	35.2	1.7
3420 Mrads at 440 °C, Aged at room temperature, 98 h at 440 °C	55.2	2.3

*(Total decomposition minus decomposition during irradiation) divided by heating time without radiation.

Discussion

Some comment is required on the use of high dose and extensive decomposition. The irradiation doses used were chosen to produce extensive decomposition of the starting material (typically 30%), to permit accurate determination of the loss of terphenyl and the G value for overall decomposition.

This procedure was followed, rather than the conventional examination of products at low fractional decomposition, because the principal products, which collectively constitute the high boilers, are not well defined and readily analyzable. An obvious drawback of this procedure is that the interpretation becomes complicated by the effects of the reaction products on the reactions of the starting material. This has been taken into account to some extent by taking advantage of the smooth variation of decomposition with dose to express the results in terms of initial G values. More important, however, the advantage of dealing with the partially decomposed material is that it is a real system and of practical interest.

The radiolytic behavior of ortho- and meta-terphenyl is markedly different below and above the transition temperature range of 350 to 400 °C. Below the transition, the decomposition shows little dependence on temperature and the major product is the dimer. There is no dose rate dependence but there is an increase in decomposition with an increase in l.e.t. Above 350–400 °C the decomposition and the fraction of products due to ring cleavage increase rapidly with temperature. These decomposition products show little l.e.t. dependence but the yield increased at lower dose rates and with the frequency of intermittent radiation.

A series of reactions to explain these results is given below. These reactions are divided into some speculations about the radical precursors and a series of radical reactions based chiefly on published information about the behavior of aromatic radicals.

Can. J. Chem. Downloaded from www.nrcresearchpress.com by 210.87.254.40 on 09/05/12
For personal use only.

Can. J. Chem. Downloaded from www.nrcresearchpress.com by 210.87.254.40 on 09/05/12
For personal use only.

Radical Precursors

It is assumed that the yields of primary ions and excited species (reactions [1] and [2]) are independent of temperature, l.e.t., and dose rate.

[1] $\phi_3 \rightarrow \phi_3^+ + e^-$

[2] $\phi_3 \rightarrow \phi_3^*$

The l.e.t. dependence indicates that product-forming reactions occur to a greater extent in the particle track at high l.e.t. than at low l.e.t. and that these reactions take place before dispersal of the species in the track. These processes may involve ionic species, e.g. a lower product yield from recombination of attached electrons (reactions [4] and [5]) than from unattached electrons (reaction [3]).

[3] $\phi_3^+ + e^- \rightarrow \phi_3^*$

[4] $\phi_3 + e^- \rightarrow \phi_3^-$

[5] $\phi_3^+ + \phi_3^- \rightarrow \phi_3 + \phi_3$

This mechanism requires a considerable reduction in electron attachment probability with increasing l.e.t. This seems unlikely since the ejected electrons from reaction [1] have thermalization lengths (11) in the range 80–1000 Å and therefore experience many encounters with substrate molecules prior to recombination regardless of l.e.t. Another difficulty with this mechanism is that it requires little product formation from the directly excited states of reaction [2] which is contrary to the photochemical evidence. However, the ionic mechanism cannot be entirely ruled out in the absence of further evidence. Whether ionic processes contribute directly to the l.e.t. dependence or not, they may still contribute to eventual product formation via the formation of electronically excited molecules on recombination.

It is more likely that the l.e.t. dependence may arise through competition between de-excitation of molecules in highly excited states, reaction [6], and their decomposition, which may be bimolecular as in reaction [7], or unimolecular as in reaction [8].

[6] $\phi_3^* + \phi_3 \rightarrow \phi_3 + \phi_3$

[7] $\phi_3^* + \phi_3^* \rightarrow$ products

[8] $\phi_3^* \rightarrow$ products

Since photolysis of benzene at short wavelengths (12–15) under conditions unfavorable to the second order reaction produces mainly polymer as in radiolysis, it seems likely that reaction [8] would take place rather than reaction [7]. The l.e.t. effect can arise through depletion of the substrate, thereby delaying the de-excitation reaction [6] at high l.e.t.

The decrease in the l.e.t. dependence at high temperature can be attributed to a reduction in the ratio of de-excitation to chemical reaction of the excited species. For example the efficiency of de-excitation will tend to decrease at higher temperatures because of the effect of increased molecular separation and decreased short range molecular ordering on electronic relaxation processes (16). Increase in molecular vibrational heat content ($\sim$30 kcal/mole higher at 400 °C than at 100 °C) might also be a contributing factor.

The possibility of the l.e.t. effect arising through the competition of radical reactions seems remote. It appears that recombination of the initial radicals (i.e. reverse of reaction [9] below) cannot compete with reactions leading to product formation because high l.e.t. would favor recombination, yet *G*(decomposition) is greater at high l.e.t. This lack of recombination is accounted for by the efficient scavenging of the initial radicals by the substrate as indicated below (reactions [10] and [11]).

Radical Reactions

The nature of the products at high and low temperatures, the increased yields at low dose rates and high temperatures, and the effects of intermittent irradiation can be accounted for by radical reactions.

The possible radical formation steps can be divided into those involving C—C bond breakage and those involving C—H bond breakage. Products resulting from C—C bond breakage are negligible for the low temperature region. The formation of benzene and biphenyl in the high temperature region indicates C—C rupture between the rings. Since this only occurs at high temperatures it is assumed to be a secondary decomposition reaction of a radiolysis intermediate. The principal reactions [1] to [8] of the radical precursors can therefore be summarized as reaction [9], the formation of diphenyl-phenyl radicals and hydrogen atoms.

[9] $\phi_3 \rightarrow \phi_3' + H$

e.g.

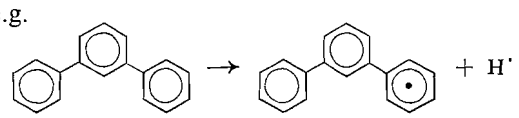

Can. J. Chem. Downloaded from www.nrcresearchpress.com by 210.87.254.40 on 09/05/12
For personal use only.

Hydrogen atoms add rapidly to the substrate as in the case of benzene (17) and biphenyl (18) to form diphenyl cyclohexadienyl radicals, as indicated in reaction [10]

[10] $$H' + \phi_3 \rightarrow \dot{\phi}_3'H$$

e.g.

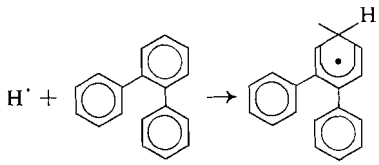

The diphenyl-phenyl radicals will also add to the substrate to form substituted cyclohexadienyl radicals with 6 rings as in reaction [11*a*]

[11*a*] $$\phi_3' + \phi_3 \rightarrow \phi_6'H$$

e.g.

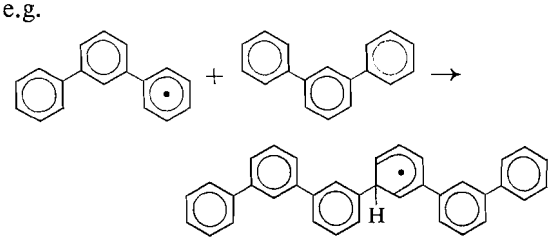

Addition to the benzene ring is favored over the endothermic H atom displacement reaction or H atom abstraction (19). For example Trosman and Bagdasar'yan (20) found that phenyl radical addition to the benzene ring occurs at least 10 times faster than H abstraction.

The 3 and 6 ring cyclohexadienyl homologues formed in reactions [10] and [11*a*] then disproportionate by reactions [12*a*] yielding a polyphenyl molecule and a cyclohexadiene homologue (dihydro-polyphenyl).

[12*a*]
$$\phi_3'H + \phi_3'H \rightarrow \phi_3 + \phi_3H_2$$
$$\phi_3'H + \phi_6'H \rightarrow \phi_3 + \phi_6H_2$$
$$\phi_3'H + \phi_6'H \rightarrow \phi_6 + \phi_3H_2$$
$$\phi_6'H + \phi_6'H \rightarrow \phi_6 + \phi_6H_2$$

The disproportionation reaction predominates over the alternative addition and abstraction reactions (21, 22) and accounts for the predominance of dimeric products at low doses (1). It is about 70 kcal/mole exothermic. Fast reactions, ($k \sim 10^9$ l/mole s corresponding to [12*a*] have been found in the pulse radiolysis of benzene derivatives with 1 and 2 rings (23).

We suggest that the reactions [9] to [12*a*] are the principal radiolytic reactions at low doses and moderate temperatures. A similar sequence of reactions will apply to other terphenyl homologues. For example, the corresponding set of reactions for 2 and 4 ring radicals are consistent with Hall and Elder's results (24) for the low dose irradiation of biphenyl near the melting point.

In general, the situation is complicated by the reactivity and thermal instability of the hydroaromatic products, both in situ and on chromatographic columns. Additional reactions occur at higher dose and higher temperatures.

We attribute the inter-ring scission occurring at higher temperatures to intramolecular decomposition of the cyclohexadienyl homologues as in reaction [13*a*]. While this reaction is approximately thermoneutral, the hydrogen migration involved can account for the activation energy which is required by the observed temperature dependence.

[13*a*]
$$\phi_3'H \rightarrow \phi_1 + \phi_2'$$
$$\phi_3'H \rightarrow \phi_2 + \phi_1'$$
$$\phi_6'H \rightarrow \phi_1 + \phi_5'$$
$$\phi_6'H \rightarrow \phi_2 + \phi_4'$$

e.g.

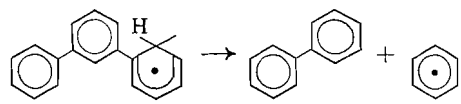

The phenyl radical homologues, ϕ_n' produced in reaction [13*a*] add to the substrate by a reaction similar to [11*a*]

[11*b*] $$\phi_n' + \phi_3 \rightarrow \phi_{n+3}H$$

These adducts may in turn undergo scission reaction [13*b*] and thereby continue a chain reaction

[13*b*] $$\phi_{x+y}H \rightarrow \phi_x + \phi_y'$$

Disproportionation reaction [12*b*] which is analogous to [12*a*] may also occur and terminate the chain

$$\phi_i'H + \phi_j'H \rightarrow \phi_i + \phi_jH_2$$

Since the propagation reactions [11] and [13] are first order with respect to the concentration of chain carriers whereas the termination reactions [12] are second order, the chain length increases as the radical concentration and the radiation intensity decreases. These reactions will therefore account for the intensity dependence as well as the formation of benzene and

Can. J. Chem. Downloaded from www.nrcresearchpress.com by 210.87.254.40 on 09/05/12
For personal use only.

biphenyl at high temperature. Also, intermittent irradiation gives a greater or lesser yield according as the time between pulses is greater or less than the average time for radical recombination (25).

The onset of scission occurs at a lower temperature for ortho-terphenyl than for meta-terphenyl, i.e. scission of the cyclohexadienyl radicals formed from ortho-terphenyl occurs more readily than for the meta intermediates. If the initial scission step, reaction [13*a*], occurs while the probability of scission of the subsequent adducts by reaction [13*b*] is low, the chain reaction does not develop. This may account for the intensity dependence occurring only over a limited range of intensity for ortho-terphenyl, i.e. more decomposition at 0.03 Mrad/s than at 0.1 Mrad/s intensity, but not significantly more at 0.01 Mrad/s than at 0.03 Mrad/s. Thermal back reactions (26) of the less stable products may also be a significant factor at low dose rates.

At the highest temperature used, some thermal decomposition was measurable in the absence of radiation. Under irradiation, the presence of radiation-generated radicals would tend to curtail the development of thermally initiated chains and suppress the thermal reaction contribution. This may account for the failure to distinguish an appreciable contribution from thermal initiation to the decomposition in the presence of radiation at the intensities used.

Some Quantitative Aspects of the Reaction Sequences

The approximate second order dependence of decomposition and polymer formation on terphenyl content may be accounted for as suggested (9) by more efficient de-excitation by the products, i.e. reaction [6] is more efficient for hexaphenyls and other higher polyphenyls than terphenyl. Kinetic analysis of this reaction scheme gives the equation:

$$[14] \qquad \ln C/C_0 - A(C - C_0) = BD$$

where C_0 is the initial concentration, C the concentration at a given dose D, and A and B are functions of the rate constants. Figure 4 shows a fit of this relation to the data of Burns *et al.* (27) which covers a wide range of dose and decomposition for biphenyl radiolysis and therefore provides a more stringent test than our own data. A curve corresponding to second order kinetics is also shown for comparison.

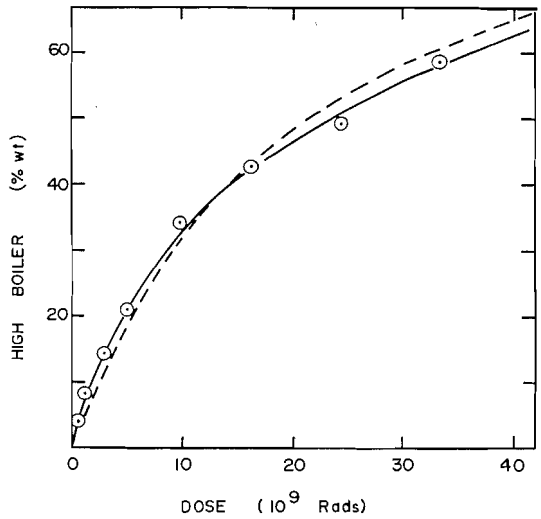

FIG. 4. Dose dependence in polyphenyl radiolysis; ⊙, observed by Burns *et al.* (27) for biphenyl; ---, empirical (second order) $1/C - 1/C_0 = 0.0471\ D$; —, theoretical $\ln (C/C_0) + 0.878(C_0 - C) = 0.01075$, $C = 1 - [HB]/100$.

As already noted, the proposed reaction sequence includes the possibility of a radical chain reaction propagated by reactions [11] and [13], and terminated by [12]. The chain length is dependent upon the initiation rate (25), i.e. the radiation intensity, in accordance with the following relation:

$$[15] \qquad \lambda = G/G_0 = 1 + k_p/\sqrt{3G_0Ik_t}$$

where λ = chain length = total reaction/initiation, G = radiolytic decomposition yield, G_0 = lower limit of G at high intensity, k_p = specific rate of propagation[3] reaction [13], k_t = specific rate of termination[3] reaction [12].

Figure 3 illustrates a test of the applicability of this relation to meta-terphenyl radiolysis at 440 °C. The description is seen to be satisfactory.

The reactor irradiation results fall slightly below the least mean square fit of the electron irradiation data. Apart from experimental

[3]Since reactions [11*a*] and [11*b*] occur also in the low temperature region, we assume the propagation rate is determined by reactions [13*a*] and [13*b*]. The parameters, k_p and k_t represent average rate constants for propagation and termination, respectively, for all chain carrying species present, weighted according to the proportions of different species present (e.g. $k_p = \Sigma_J k_{pJ} C_J / \Sigma_J C_J$ where C_J is the concentration of the Jth propagating species). For extensive decomposition, the values of k_p and k_t may change as decomposition proceeds owing to changes in the proportions of the reacting species.

uncertainties there may be more radical–radical reactions occurring due to the initial high radical concentrations resulting from the higher l.e.t. of the reactor radiation. This would be equivalent to an increase in the dose rate.

From the slope and intercept of Fig. 3, the value is obtained for the rate constant ratio $k_p^2/k_t = 4.7 \pm 0.4$ moles/l s. The intermittent irradiation results suggest a mean lifetime τ of the radical chains in the range 10 to 100 ms under the conditions used. The mean lifetime is related to k_t by $\tau = 1/k_t n$ and $k_t = 3/G_0 I \tau^2$, where n is the concentration of chain carriers. From these relations we find $k_t \approx 1 \times 10^7$ l/mole s and $k_p \approx 100\ s^{-1}$. This value of k_t for irradiated terphenyl is about 2 orders of magnitude smaller than the values found by MacLachlan and McCarthy (23) for pulse irradiated benzene and single ring derivatives and is consistent with a larger steric factor for multiring radicals in irradiated terphenyl.

It seems probable that the thermal pyrolysis contribution to decomposition over the range of dose rates 0.01–1.5 Mrads/s is small. The values for the activation energy of pyrolysis are ~ 70 kcal (1) and are thus considerably less than the energy required to break a C—H or C—C bond. This indicates pyrolysis proceeds by a chain mechanism. If the chain propagates by the same process as in electron radiolysis at dose rates of 0.05–1.5 Mrads/s, then the chain length at 440 °C (where the pyrolysis rate is $\sim 5 \times 10^{-3}$/h (1)) is greater than 30. Since the maximum chain length derived from the irradiation data in Fig. 3 is less than 8, the contribution from thermally initiated chains will be less than 1/3 of the observed pyrolysis rate in the absence of radiation and thus negligible at the dose rates and temperatures used in this work.

The reactions discussed above are thought to be the principal steps involved in the destruction of terphenyl and formation of major products. The sequence does not include reactions leading to the minor products, e.g. H_2. Nor has any attempt been made to describe the secondary radiolysis and thermal decomposition of products at high doses and high temperatures.

Conclusions

A sequence of reactions has been proposed to explain the major features of the radiolysis of the terphenyls. These account for the l.e.t. dependence and the dose dependence of the radiolysis in terms of the decomposition and deexcitation of highly excited molecules. Changes in product distribution, increased decomposition, intensity dependence, non-additivity of radiation and thermally initiated reactions, and effects of intermittent irradiation at high temperature have been accounted for in terms of radical reactions.

1. K. L. Hall. U.S. At. Energy Comm. Report IDO-11401. 1964. Chap. 3.
2. A. W. Boyd and H. W. J. Connor. Chalk River Nucl. Lab. Report, AECL-2258. 1965.
3. A. W. Boyd, H. W. J. Connor, and O. A. Miller. Chalk River Nucl. Lab. Report, AECL-2589. 1966.
4. A. W. Boyd and H. W. J. Connor. Chalk River Nucl. Lab. Report, AECL-2655. 1966.
5. Donna Wuschke and M. Tomlinson. Nucl. Sci. Eng. **31**, 521 (1968).
6. M. Tomlinson, A. W. Boyd, and S. R. Hatcher. Whiteshell Nucl. Res. Estab. Report, AECL 2641. 1966.
7. A. W. Boyd, H. W. J. Connor, and J. J. Pieroni. Chalk River Nucl. Lab. Report, AECL-2203. 1965.
8. M. Tomlinson, J. L. Smee, E. B. Winters, and M. C. Arneson. Nucl. Sci. Eng. **26**, 547 (1966).
9. T. H. Bates, W. G. Burns, B. Morris, R. Wilkinson, and T. F. Williams. At. Energy Res. Estab. G. Brit. Report, C/R 2121. 1957.
10. E. A. Mason, T. H. Timmins, D. T. Morgan, and W. N. Bley. U.S. At. Energy Comm. Report, MIT-334-70. 1966.
11. A. Mozumder and J. L. Magee. J. Chem. Phys. **47**, 939 (1967).
12. R. R. Hentz and S. J. Rzad. J. Phys. Chem. **71**, 4096 (1967).
13. L. Kaplan and K. E. Wilzback. J. Am. Chem. Soc. **89**, 1030 (1967).
14. H. R. Ward, J. S. Wishnok, and P. D. Sherman, Jr. J. Am. Chem. Soc. **89**, 162 (1967).
15. W. M. Jackson, J. L. Faris, and B. Donn. J. Phys. Chem. **71**, 3346 (1967).
16. G. W. Robinson and R. P. Frosch. J. Chem. Phys. **38**, 1187 (1963).
17. M. C. Sauer and B. Ward. J. Phys. Chem. **71**, 3971 (1967).
18. D. Campbell and D. J. Turner. Can. J. Chem. **45**, 881 (1967).
19. W. A. Pryor. Free radicals. McGraw-Hill Book Co., Inc., New York. 1966. p. 251.
20. E. A. Trosman and K. H. S. Badgasar'yan. Russ. J. Phys. Chem. English Transl. **38**, 73 (1964).
21. G. H. Williams. Homolytic aromatic substitution. The Pergamon Press Ltd., London. 1960.
22. D. H. Hey, M. J Perkins, and G. H. Williams. J. Chem. Soc. 3412 (1964).
23. A. MacLachlan and R. L. McCarthy. J. Am. Chem. Soc. **84**, 2519 (1962).
24. K. L. Hall and F. A. Elder. J. Chem. Phys. **31**, 1420 (1959).
25. F. S. Dainton. Chain reactions. 2nd ed. John Wiley and Sons, Inc., New York. 1966.
26. S. W. Benson and R. Shaw. J. Am. Chem. Soc. **89**, 5351 (1967).
27. W. G. Burns, T. H. Bates. M. East, B. Morris, R. W. Wilkinson, and T. F. Williams. At. Energy Res. Estab. G. Brit. Report, R 3743 (1962).

Can. J. Chem. Downloaded from www.nrcresearchpress.com by 210.87.254.40 on 09/05/12
For personal use only.

Can. J. Chem. Downloaded from www.nrcresearchpress.com by 210.87.254.40 on 09/05/12
For personal use only.

The nature of the coordination bond in metal complexes of substituted pyridine derivatives. III. 4-Methylpyridine complexes of some divalent transition metal ions

D. G. BREWER, P. T. T. WONG[1], AND M. C. SEARS
Department of Chemistry, University of New Brunswick, Fredericton, New Brunswick

Received April 2, 1968

Previous papers in this series investigated the nature of the coordination bond in copper(II) and zinc(II) complexes of 4-substituted pyridines by infrared spectroscopy. In this paper, the investigation has been extended to complexes of 4-methylpyridine with cobalt(II), manganese(II), and nickel(II). The geometry of the solid complexes is assigned, and the force constants associated with the metal–nitrogen bond were calculated from a normal coordinate analysis. The validity of the previously introduced R_π parameter in these systems is discussed.

Canadian Journal of Chemistry, 46, 3137 (1968)

Introduction

In previous papers (1, 2), the substituent effects upon the metal–nitrogen (ligand) and metal–chlorine stretching frequencies in the far infrared region, as well as the coordination bond strength of a series of complexes of the form $[ML_2Cl_2]$, where L is 4-methylpyridine, 4-carbinylpyridine, pyridine, 4-acetylpyridine, 4-pyridinecarboxamide, 4-carbomethoxypyridine, or 4-cyanopyridine, were studied. A new parameter, R_π, was introduced to measure the substituent effect upon the relative magnitude of π-bonding in this same series of complexes.

In the present paper, a similar investigation has been carried out on the metal complexes of 4-methylpyridine with some divalent ions Mn(II), Co(II), Ni(II), Cu(II), and Zn(II). The coordination bond strength of these complexes has been compared by means of their metal–ligand stretching frequencies, and the stretching force constants obtained by a normal coordinate calculation.

In order to compare the relative π-contribution of the divalent metal ions to the coordination bond in their 4-methylpyridine complexes, the R_π values of these complexes have also been determined. It was indicated in the previous paper (1) that this R_π parameter could only be used to compare the effects of different metal ions on the relative π-contribution to the coordination bond of the substituted pyridine complexes when the substituent is an electron-releasing group, although it was derived in order to measure any substituent effect on the π-contribution. This previous study showed that for an electron-attracting substituent, both Cu(II) and Zn(II) ions gave almost the same value for R_π in their complexes with this particular ligand, due to the delocalized nature of the π-system in these complexes under the influence of such a substituent. Therefore it seems unlikely that the π-bonding capability of metal ions in coordination with pyridines having electron-attracting substituents can be estimated from these R_π values. Since the methyl group is an electron-releasing group (17, 18), 4-methylpyridine has been chosen as a starting point for this study.

Experimental

The reagents and the preparation of the 4-methylpyridine complexes of copper(II) and zinc(II) have been described in a previous paper of this series (1).

Complexes of the form $[ML_2Cl_2]$, where M = Co(II), Mn(II), and L = 4-methylpyridine, were prepared by adding the ligand (2 moles) into the metal chloride solution (1 mole) in absolute alcohol with constant stirring. The resulting precipitates were filtered, washed several times with absolute alcohol and anhydrous ether, and dried in a vacuum desiccator over sulfuric acid.

The complex $[Ni(CH_3C_5H_4N)_4Cl_2]$ was prepared in a manner similar to the procedure for the cobalt and manganese complexes. An attempt has been made to prepare the 2:1 complex of nickel(II) according to literature procedures (4); however, this preparation also gave the 4:1 complex[2].

[1]Present address: Division of Applied Chemistry, National Research Council of Canada, Ottawa, Canada.

[2]A private communication with the author (4), disclosed that the method of preparation, using benzene, is not suitable. Use of toluene as the extraction liquid yielded 18.89 ± 0.1% nickel (calcd. 18.58%). Since toluene is not ideal, the author suggests a mixture of ~20% $CHCl_3$ and 80% toluene. However, even though a differential thermal analysis has been carried out by the author, the results of which suggest the existence of $[Ni(CH_3C_5H_4N)_2Cl_2]$, the complex does not appear to be particularly stable with reference to $[Ni(CH_3C_5H_4N)_4Cl_2]$ and $[Ni(CH_3C_5H_4N)Cl_2]$.

TABLE I

Preparation of metal complexes with 4-methylpyridine

Metal	Ratio (ligand/metal)	Calculated (%)					Found (%)				
		C	H	N	Metal	Cl	C	H	N	Metal	Cl
Ni(II)	4:1	57.41	5.62	11.16	11.69	—	57.42	5.80	10.96	11.31	—
Cu(II)	2:1	44.94	4.40	8.74	19.81	22.11	44.88	4.32	8.76	19.76	22.08
Zn(II)	2:1	44.68	4.38	8.69	—	27.36	44.50	4.29	8.49	—	26.50
Co(II)	2:1	45.59	4.46	8.86	18.65	—	45.42	4.49	8.65	18.22	—
Mn(II)	2:1	46.15	4.52	8.98	17.60	—	46.17	4.46	9.05	18.47	—

An attempt to prepare the Fe(II) complex failed, even under a reducing atmosphere (analysis always indicated that some oxidation had occurred). Further attempts are presently under way, using more highly purified initial reagents and other more stringent conditions.

Microanalysis results for the complexes are found in Table I. (The results for the copper and zinc complexes are from a previous paper (1).)

The infrared spectra of the complexes in the region between 4000–200 cm^{-1} were recorded on a Beckman IR-12 filter/grating spectrometer. In the region 4000–400 cm^{-1}, the potassium bromide disk method was used. The infrared spectra of the solid compounds in the region 400–200 cm^{-1} were recorded as Nujol mulls with polyethylene windows. The spectrometer was constantly purged with dry air and wavelength calibration of the spectrometer was checked against the rotational spectra of water vapor. The spectra were obtained using standard settings as outlined in the Beckman IR-12 instruction manual. A resolution of 2.0 cm^{-1} was determined, giving a 2.0% error in the peak absorbance. The reproducibility of the spectra was found to be ± 0.20 cm^{-1}. The infrared spectra in the region below 200 cm^{-1} were measured by means of a Perkin-Elmer model 301 spectrophotometer, which has been described elsewhere (2).

The calculations of the metal–ligand stretching force constants of the complexes were carried out by means of an IBM 1620 computer.

Results and Discussion

I. Infrared Spectra and the Metal–Nitrogen (Ligand) Stretching Force Constants

The observed metal–nitrogen stretching frequencies of 4-methylpyridine complexes of some metal chlorides are found in Table II. These bands were assigned by comparing the observed spectra of the complexes with recent studies in the literature (1, 6). The assignment of the same stretching frequency for the 4-methylpyridine complex of Mn(II) is based on the comparison of its spectra with that of a similar metal complex with bromide instead of chloride. The metal–nitrogen stretching frequency should be located in the same region in both the spectra of bromide and chloride complexes for a particular metal ion.

The data in Table II indicate that coordination between 4-methylpyridine and different metal ions gives different metal–nitrogen stretching frequencies which decrease in the following order:

$$\text{Cu(II)} > \text{Ni(II)} > \text{Zn(II)} > \text{Co(II)} > \text{Mn(II)}$$

The above order for the first row transition metal ions is identical with the prediction based on Irving's order of stability for the complexes of these metal ions (7), and it thus appears that this stretching frequency may be used as a measure of stability. Even though the stoichiometry of the Ni(II) complex is 4:1, it still falls in the correct order due to the large separation in the stretching frequencies between the Cu(II) and Zn(II) complexes. One would therefore expect the 2:1 Ni(II) complex to fall in the same order, although obviously the R_π values for the two stoichiometries would not be the same.

In order to confirm this argument, the metal–nitrogen stretching force constants for this series of divalent transition metal complexes of 4-methylpyridine were calculated by a normal coordinate treatment similar to that for the copper complex of 4-methylpyridine (2). The same modified Urey–Bradley force field was used for this calculation. Since the Urey–Bradley force constants are transferable, all the force constants of the ligand in this calculation are identical with those of the copper complex of 4-methylpyridine (2), as are most of the matrix elements. The only difference was in the recalculation of matrix elements containing the metal–ligand bond distance, r(M—N), found in Table II. The metal–ligand stretching force constants, K_7, of the complexes under study were obtained by matching the calculated frequencies with the observed ones, and are listed in Table II. The eigenvalues, λ's, of the secular equation, $|GF - E\lambda| = 0$, were obtained by the QR transformation method (19). They were further converted into wavenumbers and compare favorably with the observed frequencies, as shown in Table III.

Can. J. Chem. Downloaded from www.nrcresearchpress.com by 210.87.254.40 on 09/05/12
For personal use only.

Can. J. Chem. Downloaded from www.nrcresearchpress.com by 210.87.254.40 on 09/05/12
For personal use only.

TABLE II

Summary of relevant data for complexes studied

Complex	Stereochemistry	Absorption band (cm^{-1}) (M—N)	Interatomic distances r(M—N) (Å)	Metal–nitrogen force constants (K_7)	ν_{12} mode (cm^{-1})	R_π values	First ionization (15) potentials of metals (eV)
$[Cu(CH_3C_5H_4N)_2Cl_2]$	Distorted, polymeric, octahedral	285	2.02 (9)	1.86	1042	3.50	7.72
$[Ni(CH_3C_5H_4N)_4Cl_2]$	Polymeric, octahedral	266	2.03 (10)	1.39	1045	6.62	7.63
$[Zn(CH_3C_5H_4N)_2Cl_2]$	Tetrahedral	238	2.06 (11)	1.08	1034	−4.53	9.39
$[Co(CH_3C_5H_4N)_2Cl_2]$	Tetrahedral	235	2.14 (9)	0.93	1040	1.52	7.86
$[Mn(CH_3C_5H_4N)_2Cl_2]$	Polymeric, octahedral	230	2.27 (12)	0.80	1037	−1.98	7.43

TABLE III

Fundamental vibrational frequencies of metal complexes of 4-methylpyridine

	Cu(II)		Ni(II)		Zn(II)		Co(II)		Mn(II)	
Description	Obsd. (cm^{-1})	Calcd. (cm^{-1})	Obsd. (cm^{-1})	Calcd. (cm^{-1})	Obsd. (cm^{-1})	Calcd. (cm^{-1})	Obsd. (cm^{-1})	Calcd. (cm^{-1})	Obsd. (cm^{-1})	Calcd. (cm^{-1})
A_1 species										
ν(M—N)	285	285	266	266	238	238	235	235	230	230
ν_{6a}, ring, R-sens.	550	650	542	643	550	638	553	636	539	634
ν_1, ring, β(C—M)	1033	902	1019	908	1032	908	1032	909	1015	909
ν_{12}, ring	1042	1059	1044	1044	1034	1037	1040	1035	1037	1032
ν_{18}, ν(C—R), β(C—H)	1190	1163	1218	1161	1218	1160	1207	1160	1210	1160
ν_{9a}, β(C—H)	1231	1231	1230	1228	1230	1227	1215	1226	1226	1226
R-sens.	1432	1427	1423	1403	1432	1403	1422	1403	1427	1404
ν_{19a}, ν(C—C, C—N)	1506	1524	1505	1525	1505	1523	1505	1523	1504	1524
ν_{8a}, ν(C—C)	1621	1617	1619	1616	1617	1614	1620	1616	1619	1616
B_2 species										
M-sens.	207	251		253	207	250	207	250	207	249
ν_{15}, R-sens.	418	424	420	424	421	424	420	425	416	425
ν_{6b}, ring	669	775	669	775	669	775	669	775	673	775
ν_{18b}, β(C—H)	1101	1075	1104	1075	1103	1075	1118	1075	1098	1075
ν_3, β(C—H)	1119	1145	1123	1145	1120	1145	1123	1145	1120	1146
ν_{14}, ν(C—C, C—N)	1335	1342	1335	1342	1332	1342	1338	1342	1338	1342
ν_{19b}, ν(C—C, C—N)										
β(C—R, C—H)	1439	1398	1448	1398	1458	1398	1458	1398	1457	1399
ν_{8b}, ν(C—C)	1563	1551	1561	1550	1561	1550	1561	1550	1564	1551

Can. J. Chem. Downloaded from www.nrcresearchpress.com by 210.87.254.40 on 09/05/12
For personal use only.

Comparison of the force constants in Table II gives the same order as that obtained for the metal–nitrogen stretching frequencies, viz.

$$\text{Cu(II)} > \text{Ni(II)} > \text{Zn(II)} > \text{Co(II)} > \text{Mn(II)}$$

These results further substantiate the conclusions reached in the previous study (2); that is, the metal–nitrogen stretching frequency is directly related to the metal–nitrogen stretching force constant, and that the magnitude of the metal–nitrogen stretching frequency in the far-infrared region may be employed as a measure of the coordination bond strength for complexes of pyridine derivatives. Moreover, the coupling between the metal–nitrogen stretching vibration and the internal modes is not appreciable in these complexes.

Both the metal–nitrogen stretching frequencies and force constants show that the coordination bond strength of the Zn(II) complex is stronger than that of the Co(II) complex, which indicates that the 4-methylpyridine belongs to the first class of ligands (3). In fact the π-bonding in the complexes of 4-methylpyridine is very weak, as shown by the R_π values of its complexes in the next section.

The stereoconfigurations of the 4-methylpyridine complexes of the divalent metal ions listed in Table II were determined by a symmetry analysis of the skeletal vibrations of these complexes and by a comparison of the low frequency spectra of these complexes with those of pyridine complexes (6). The stereochemistry of the 4-methylpyridine complex of Cu(II) ion has been studied (2). There are two halogen-sensitive bands in the spectra of both Zn(II) and Co(II) complexes, which correspond to the A_1 and B_1 species of the C_{2v} point group of the tetrahedral configuration. The spectrum of the Mn(II) complex shows that there are badly resolved bands near the 200–300 cm^{-1} region, which are similar to those of the pyridine complexes of Mn(II), Fe(II), Co(II), and Ni(II) ions (6). Therefore it is suggested that Mn(II) forms a polymeric octahedral complex with 4-methylpyridine. The 4:1 Ni(II) complex only gives one halogen-sensitive band in its spectrum, which suggests that the structure of this complex is *trans*-octahedral.

II. The Relative Strength of the π-Coordination Bond in the Complexes

The vibrational frequencies of the ν_{12} mode, (pure ring deformation (1, 8)), together with the corresponding R_π values, of the transition metal complexes of 4-methylpyridine are listed in Table II. The R_π values were calculated according to the equation (given in ref. 1)

$$R_\pi = \nu_{ML} - (1.002\nu_L - 3.60)$$

where ν_{ML} and ν_L are the ν_{12} frequencies of the complex and free ligand respectively. The R_π values in Table II are very small compared with those for the pyridine complexes and the electron-attracting substituted pyridine complexes (1). It follows that the π-bond in these 4-methylpyridine complexes is quite weak. Since we are dealing with a system containing an electron-releasing substituent which inhibits back-donation of electron density from the metal to the ring, the amount of back-donation from the metal, and thus the π-bonding in these complexes, are expected to be small. The coordination bond is then primarily σ in character, resulting from the non-bonding pair of electrons on the pyridine nitrogen. Little change is therefore expected in the ν_{12} mode, as is observed experimentally (Table II).

The relative magnitude of the ν_{12} frequency, as well as the R_π values of these complexes are in the following order:

$$\text{Ni(II)} > \text{Cu(II)} > \text{Co(II)} > \text{Mn(II)} > \text{Zn(II)}$$

The above order is identical with that predicted on the basis of their first ionization potentials (16), and also from a comparison of the stability of their complexes with ligands of the first and second class (3), with the exception of manganese. For electron-releasing substituents in all of these complex systems, the electron density migrating to the pyridine ring from the substituent can enhance the donation of the non-bonding electron pair of the nitrogen atom to the metal (1, 5, 13). Any d_π back donation from all of the above metals except manganese will then be inhibited if the geometries deduced in Table II are correct. Since the d_π orbitals on the manganese are only half-filled, it is possible in this case to have electron density migrate from the ring to the metal. Since the σ- and π-bonding mechanisms are synergic (14), then less back-bonding from the metal will result, and the ν_{12} frequency and the R_π value for the manganese complex are lower than expected.

A more plausible explanation, perhaps, lies in the fact that the bridging chlorides in the manganese complex are closer to the metal than in the copper complex (which is distorted), with result-

ing better d_π–d_π overlap (2) than in the other complexes. Hence a weaker π-bond between the manganese(II) and the methylpyridine ligand should result.

In summary then, for electron-releasing substituents, the magnitude of π-bonding in these complexes can be related to the first ionization potential of the metals, provided the appropriate d_π-orbitals of the metal are filled, and the number of chlorines bound to the metal are the same. With partially filled d_π-orbitals, and different numbers of chlorines bound in the complex, the R_π parameter provides a valid indication of the relative amount of back-donation. The advantages of using R_π for all such systems is then obvious.

Acknowledgment

We are indebted to the National Research Council of Canada for the necessary funds for this investigation.

1. P. T. T. WONG and D. G. BREWER. Can. J. Chem. **46**, 131 (1968).
2. P. T. T. WONG and D. G. BREWER. Can. J. Chem. **46**, 139 (1968).
3. D. G. BREWER and P. T. T. WONG. Can. J. Chem. **44**, 1407 (1966).
4. S. M. NELSON and T. M. SHEPHERD. J. Chem. Soc. 3276 (1965).
5. S. M. NELSON and T. M. SHEPHERD. Inorg. Chem. **4**, 817 (1965).
6. R. J. H. CLARK and C. S. WILLIAMS. Inorg. Chem. **4**, 350 (1965).
7. H. IRVING and R. J. P. WILLIAMS. Nature, **162**, 746 (1948).
8. E. SPINNER. J. Chem. Soc. 3860 (1963).
9. J. D. DUNITZ. Acta Cryst. **10**, 307 (1957).
10. M. A. PORAI-KOSHITS. Kristallografiya, **2**, 378 (1957).
11. A. V. ABLOV and E. D. RUCHKIN. Zh. Strubk. Khim. **4**, 50 (1963).
12. A. FERRARI, A. BRAIBANTI, G. BIGLIARDI, and F. DALLAVALLE. Z. Krist. **119**, (3–4) (1963); **119**, 284 (1963).
13. CARL W. FRANK and L. B. RODGERS. Inorg. Chem. **5**, 615 (1966).
14. L. E. ORGEL. An introduction to transition-metal chemistry. John Wiley and Sons, Inc., New York. 1960. p. 137.
15. F. COTTON and G. WILKINSON. Advanced inorganic chemistry. John Wiley and Sons, Inc., New York. 1962. pp. 662, 470.
16. S. MATAGA and N. MATAGA. Z. Physik. Chem. Frankfurt, **33**, 374 (1962).
17. S. NAGAKURA and J. TANKA. J. Chem. Phys. **22**, 236 (1954).
18. R. J. TOMPSON and A. B. F. DUNCAN. J. Chem. Phys. **14**, 573 (1946).
19. J. G. F. FRANCIS. Computer J. **4**, 265 (1961).

Can. J. Chem. Downloaded from www.nrcresearchpress.com by 210.87.254.40 on 09/05/12
For personal use only.

Can. J. Chem. Downloaded from www.nrcresearchpress.com by 210.87.254.105 on 09/05/12
For personal use only.

Intermolecular association and dielectric relaxation in some liquid amides[1]

WALTER DANNHAUSER AND GYAN P. JOHARI
Department of Chemistry, State University of New York at Buffalo, Buffalo, New York, 14214

Received March 5, 1968

The equilibrium dielectric constants of three isomeric *N*-methylvaleramides are reported over a wide range of temperature. Analysis of the data in terms of Kirkwood's correlation factor suggests that the liquids are extensively associated into linear chains and that the extent of association is essentially independent of the size and shape of the alkyl group. Dielectric dispersion was measured (0.5–200 MHz) for these compounds as well as the isomeric *N*-butylacetamides and also *N*-ethylacetamide. The dispersion loci all follow the Debye equation and the relaxation times show a specific dependence on the size and shape of the alkyl group, but not on whether it is in the acid or the amine position. Activation energies for relaxation, viscous flow, and conduction are compared and the nature of liquid *N*-monosubstituted amides is discussed.

Canadian Journal of Chemistry, 46, 3143 (1968)

Introduction

Since Leader and Gormley's report (1) in 1951 of the exceptionally large dielectric constant of liquid *N*-monosubstituted amides, there has been a series (2–7) of investigations of the electrical properties of this interesting class of compounds. As Leader and Gormley suggested, the large dielectric constants of these liquids must be attributed to intermolecular association into essentially linear chains by CO···HN hydrogen bonds. In a previous paper (5) we reported dielectric data on a series of amides, including three isomeric *N*-butylacetamides, and analyzed the data in terms of the dipole correlation factor of Kirkwood. We concluded that the size and shape of the alkyl substituent of the amine was of secondary importance as far as steric hindrance to intermolecular association was concerned; only if the group became very large and bulky, e.g. 1-naphthyl, did there appear to be a significant effect. A study (8) of self-association of amides in solution by nuclear magnetic resonance (n.m.r.) methods led to similar conclusions.

Vaughn and Sears (2) concluded that the size of the amine alkyl group affects the magnitude of the dielectric constant to a greater extent than the size of the acid alkyl group in isomeric amides. Such variations must be due to differences in the extent and/or efficiency of near-neighbor dipole–dipole correlation and, if shown to be generally true, will be an important clue about the detailed nature of the intermolecular association in these liquids. Since the *shape* of the alkyl group is quite unimportant in determining the extent of intermolecular association of isomeric *N*-butylacetamides, we were interested to see what effects there might be in the corresponding isomeric *N*-methylvaleramides.

Vaughn and Sears (2) reported the existence of dielectric dispersion at 10 MHz for some of their compounds and even at 100 kHz we (5) found some evidence for dispersion in some of the *N*-butylacetamides. We wanted to see whether the dielectric relaxation in these extensively associated liquids would be sensitive to systematic structural modifications of the molecules. The question of whether or not dielectric relaxation in these liquids obeys the simple Debye equation was partially settled in the affirmative by Bass *et al.* (9), but they did not study isomeric species and could not assess the influence of the size and shape of the alkyl groups. Furthermore, Koizumi (10) has suggested that the dispersion loci of $RCONHCH_3$, with $R = C_3$–C_5, are skewed-arcs, which is contrary to the findings of Bass. This could be due to the effect of the size of the R group on the relaxation mechanism, and one of the goals of our work was to study this question further.

We report equilibrium dielectric constants as a function of temperature for three isomeric *N*-methylvaleramides and dielectric relaxation parameters for *N*-ethylacetamide and six isomers of $C_6H_{13}NO$.

Experimental

Samples

The source and purification of *N*-ethylacetamide (NEA) and the isomeric *N*-butylacetamides has been described before (5). *N*-Methyl-*n*-valeramide (NMnV), *N*-methylisovaleramide (NMiV), and *N*-methyl-*sec*-valeramide (NMsV) were obtained from Distillation Products

[1]Supported by the Office of Saline Water, United States Department of the Interior, via Grant 14-01-001-604 and by the Directorate of Chemical Sciences, Air Force Office of Scientific Research, via Grant AF-AFOSR-271-63.

TABLE I

Physical properties of isomeric *N*-methylvaleramides

Property	NMnV	NMiV	NMsV
b.p. (°C/mm)	89–91/2.5–3 231/760	70/0.7	70/1; 93/3.5
n_D	1.4390 at 26° 1.4401 at 25°*	1.4357 at 25°	1.4375 at 30°
ρ^{25} (g/cm^3)	0.8997 0.9033*	0.8913	0.8946†
$d\rho/dt$	-7.25×10^{-4}	-6.75×10^{-4}	-8.84×10^{-4}

*See ref. 21.
†Extrapolated value.

Corporation; NMnV was also prepared in this laboratory by reacting valeryl bromide and methyl amine. All samples were fractionally distilled at reduced pressure. The densities of the samples were determined dilatometrically as described previously (5). The physical properties of the valeramides are shown in Table I.

Bridges and Cells

The admittance bridge and cell assembly used for measurement of the equilibrium dielectric constant has been described before (5). The large conductance of the samples, especially troublesome at high temperatures, causes errors in the capacitance measurements which we estimate to be less than $\pm 2\%$ of the reported value.

Dielectric dispersion and absorption were measured over the frequency range 0.5–200 MHz by means of a Hewlett–Packard type 250A RX-meter and the coaxial plunger cell of Lovell and Cole (11). The addition of a coaxial switch between the cell and the bridge facilitates zeroing of the bridge at each test frequency and improves the overall precision, but the very large dielectric constants of the test liquids and the small capacitance range of the bridge makes these measurements rather imprecise. We estimate our data to be reliable to better than 5%. Figure 1 is typical of the results obtained for all the compounds and provides an indication of the internal consistency of the data.

Results

The equilibrium dielectric constants of the isomeric valeramides are listed in Table II. There are no literature data available for comparison. For all of the compounds studied in the very high frequency (v.h.f.) range, the dielectric dispersion is described within our experimental error by the Debye function (12)

$$[1]\quad \varepsilon^* = \varepsilon' - i\varepsilon'' = \varepsilon_\infty + (\varepsilon_0 - \varepsilon_\infty)/(1 + i\omega\tau)$$

Figure 1 is typical of the complex plane plots. Values of the equilibrium dielectric constant, ε_0, and the relaxation time, τ, obtained from analyses of the data are presented in Table III. Our data are neither precise nor extensive enough to adequately define the parameter ε_∞, the dielectric

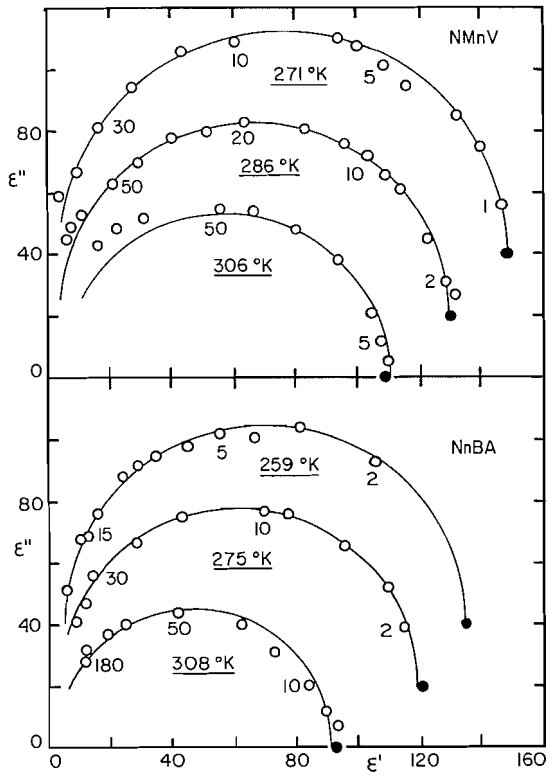

FIG. 1. Cole–Cole plots for *N*-methyl-*n*-valeramide (NMnV) and *N*-*n*-butylacetamide (NnBA). Curves have been displaced up by 20 units for clarity. Open circles denote experimental results with frequency in MHz indicated; filled circles indicate low-frequency, transformer bridge results.

constant characteristic of induced polarization. Our best estimates are $\varepsilon_\infty \approx 4$, which is significantly greater than the square of the optical index of refraction. A study of these compounds at microwave frequencies is desirable in order to examine the nature of the residual high frequency dispersion(s).

Can. J. Chem. Downloaded from www.nrcresearchpress.com by 210.87.254.105 on 09/05/12
For personal use only.

Can. J. Chem. Downloaded from www.nrcresearchpress.com by 210.87.254.105 on 09/05/12
For personal use only.

TABLE II

Equilibrium dielectric constant of isomeric *N*-methylvaleramides

Temperature (°C)	NMnV	NMiV	NMsV
−10	159	—	—
0	145	—	—
10	137	131	—
20	121	120	—
30	111	110	134
40	101	102	120
50	94.0	95.0	109
60	86.6	88.0	99.6
70	80.0	81.5	91.0
80	74.0	75.5	82.2
90	68.5	70.0	74.5
100	63.5	64.5	67.0
110	58.0	59.0	60.0
120	54.0	54.0	53.0
140	45.0	45.5	39.0
160	38.0	37.0	25.6
180	31.0	30.0	—

TABLE III

Parameters of dielectric relaxation in liquid amides

Substance	Temperature (°K)	ε_0	$\tau \times 10^9$ (s)
NEA	255	184	8.8
	261	165	6.3
	267	153	4.7
	276	143	2.8
	287	130	1.8
NnBA	259	134	41
	270	124	21
	275	118	15
	287	109	7.9
	308	94	3.2
NiBA	267	137	54
	277	127	26
	284	119	16.6
	292	112	10.4
	301	104	6.6
NsBA	276	111	47
	282	108	32
	289	104	21
	297	98.6	13.0
	307	91.8	7.4
NMnV	271	149	22.1
	279	137	14.2
	286	131	9.0
	300	114	3.9
	306	108	2.86
NMiV	286	134	13.3
	299	114	7.9
	308	102	5.3
NMsV	307	123	7.6
	323	103	3.53
	334	96	2.27
	341	87	1.77

Discussion

The equilibrium dielectric polarization of liquids is most fruitfully discussed in terms of the Kirkwood–Frohlich (13) equation:

$$[2] \quad \varepsilon_0 = \varepsilon_\infty + \left(\frac{3\varepsilon_0}{2\varepsilon_0 + \varepsilon_\infty}\right) \cdot \left(\frac{\varepsilon_\infty + 2}{3}\right)^2 \cdot \left(\frac{4\pi N \rho \mu_0^2}{3MkT}\, g\right)$$

Here ε_0 is the equilibrium dielectric constant, ε_∞ is the high frequency dielectric constant characteristic of induced polarization which we approximate by $\varepsilon_\infty = 1.1\, n_D^2$, N is Avogadro's number, M is the molecular weight, ρ is the density of the liquid, μ_0 is the dipole moment of the molecule in vacuum, and g is the dipole correlation factor. The latter (13) is a measure of the relative orientation of neighboring dipoles as influenced by specific short range forces such as intermolecular hydrogen bonding; g's greater than unity are indicative of an average parallel alignment of near-neighbor dipoles while g's less than unity indicate an average antiparallel alignment.

There are no reported values for the dipole moments of any of the compounds we studied. In the previous paper (5) we had chosen a constant value of 4.0 D for all the amides on the basis of the assumed *trans*-planar structure of the amide group and the fact that the overwhelming contribution to the dipole moment comes from the C═O and N—H groups. However, Meighan and Cole (14) have subsequently measured the dipole moments of several amides in the low pressure vapor state. They found the dipole moment of various amides to be less than 4 D and to vary from compound to compound. Pertinent values reported by Meighan and Cole are: *N*-methylformamide, 3.82 D; *N*-methylacetamide, 3.71 D; *N*-methylpropionamide, 3.59 D. These results raise doubts about the validity of our previous assumption but unfortunately they provide no basis for a more realistic assignment of the dipole moments. In contrast to the vapor-phase studies of Meighan and Cole, measurements of dipole moments of several amides in dilute dioxane solutions by Aroney, LeFevre, and Singh (15) suggest that the dipole moment is about 3.9 D, essentially independent of the nature of the amide. In lieu of definitive values for the dipole moment of the six isomers we shall continue to assume them to be all the same, and for the purpose of numerical work shall use the value $\mu_0 = 4.0$ D. The

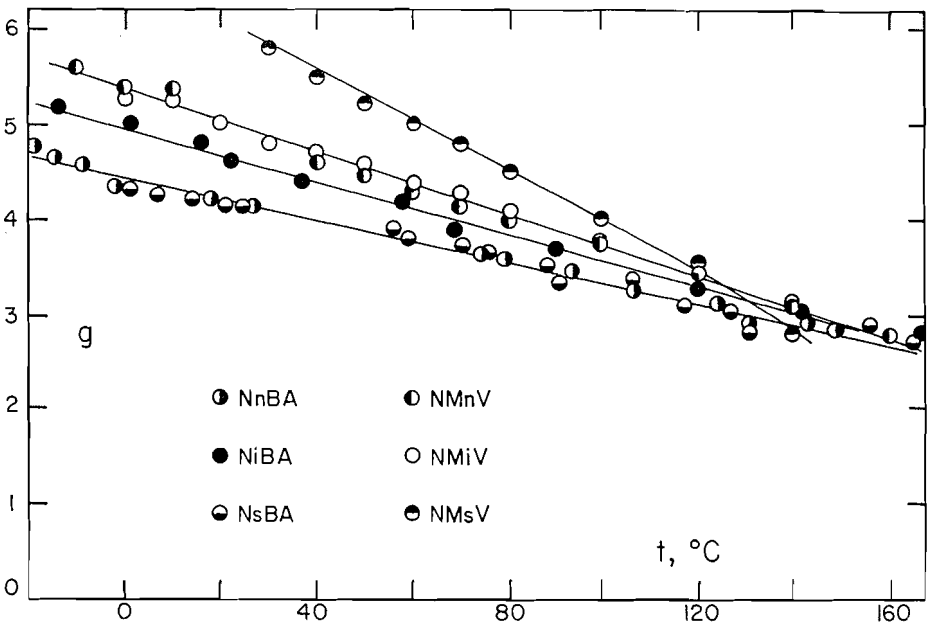

FIG. 2. Experimental correlation factor, g, as a function of temperature; $\mu_0 = 4.0$ D has been assumed for each compound.

essential part of this assumption is the equality of the dipole moments; if the value is not exactly 4 D the conclusions to be developed below still apply.

Correlation factors calculated from eq. [2] are plotted as a function of temperature in Fig. 2. The most obvious conclusions are that there is extensive parallel alignment of neighboring dipoles in these liquids even at the highest test temperatures, and that this ordering is essentially the same for the six isomers investigated and also for *N*-methylacetamide (3, 5, 9), *N*-ethylacetamide (5), *N*-*n*-propylacetamide (2), *N*-*n*-amylacetamide (2), and *N*-methylpropionamide (9). The valeramide results provide further support for our previous observation that whatever the details of the intermolecular association may be, they must be essentially the same for all these amides and are therefore insensitive to the size and shape of the acid or amine alkyl group. In this respect the amides differ greatly from the lower aliphatic alcohols, where we have recently shown (16) that the size and shape of the alkyl group can greatly influence both the extent and type of intermolecular association. Some qualitative insight into the reason for the difference comes from examinations of intermolecularly hydrogen-bonded chain models[2]. Because of the planarity of the amide group, the amide chains have an open structure and the acid or amide substituent must be very large before steric interference with near neighbors becomes important[3]. Non-linearity of the CO···H—N bond will make the intrachain packing even easier. The somewhat larger g's of NMsV and their corresponding larger temperature dependence indicates that the shape of the alkyl group may be beginning to influence the intermolecular association in this compound but it is not obvious from an inspection of models why NMsV and NsBA should differ.

We can summarize this aspect of the work by stating that pure liquid *N*-monosubstituted amides are apparently extensively associated in (transient) linear chains, both the type and extent of association being virtually independent of the particular species. The geometry of the association is such that the correlation of neighbors in a

[2]We used CPK models. See ref. 17 for a description.

[3]See ref. 5, especially the results for *N*-1-naphthylacetamide, and also ref. 9 regarding the extent of hindrance to rotation about the hydrogen bond.

Can. J. Chem. Downloaded from www.nrcresearchpress.com by 210.87.254.105 on 09/05/12
For personal use only.

TABLE IV

Parameters of the Arrhenius equation for dielectric relaxation, viscous flow, and electrical conduction

Substance	Relaxation ΔE_a (kcal/mole)	Relaxation log A	Viscosity, ΔE_a (kcal/mole)	Conductance, ΔE_a (kcal/mole)
NMA*	6.4	−14.05	—	5.0
NEA	7.4	−14.32	4.6 (4.9)†	5.6
NMP*	7.0	−14.00	—	—
NnBA	8.6	−14.61	7.4 (6.3)†	7.4
NiBA	10.4	−15.72	8.3	9.2
NsBA	10.3	−15.45	7.4	6.8
NMnV	9.6	−15.36	—	6.7
NMiV	7.4	−13.50	—	8.4
NMsV	9.2	−14.64	—	7.9

*Bass *et al.* (9).
†Vaughn and Sears (2).

chain is high[4]; consequently we estimate that the chains are short in the temperature interval studied and that both ΔH and ΔS of chain association are relatively small. Previous studies (5, 9) have come to similar conclusions.

We turn now to a discussion of dielectric dispersion in these liquids. As Cole and Cole (18) first emphasized, the dielectric absorption and dispersion of most systems does not follow the Debye function, eq. [1]. In fact, the only class of compounds which has been shown to obey the simple first order kinetics originally proposed by Debye is liquid monohydric alcohols. The molecular mechanism of the relaxation process in alcohols remains unresolved, but it is generally acknowledged *not* to be rotation of a viscous-damped spherical molecule or cluster of molecules. It is significant that alcohols associate in linear hydrogen-bonded chains, and it is generally assumed, without specifying details, that this association is a necessary condition for Debye-type relaxation. Bass *et al.* (9) have shown that pure liquid *N*-methylformamide, *N*-methylacetamide, and *N*-methylpropionamide relax according to eq. [1]. They also suggest that *N*,*N*-dimethylformamide and formamide may obey eq. [1], but in view of the limited data, the apparent much shorter relaxation times, and the demonstrated difference in the equilibrium correlation factors of the latter two compounds compared to the other three, this is unlikely and should be checked with ultra-high frequency (u.h.f.) and microwave measurements.

Figure 1 is typical of all the Cole–Cole plots generated in this investigation. The principal relaxation process is undoubtedly first order; it follows the Debye equation over the entire range of temperature. Relaxation times were determined either from an estimate of the frequency of maximum loss or from the test plot suggested by Cole (19):

$$\varepsilon' = \varepsilon_0 - \omega\varepsilon''\tau$$

In Fig. 3 we plot the logarithm of the relaxation time as a function of reciprocal absolute temperature (and also include literature data for comparison). Over the relatively short temperature intervals accessible to us the resulting curves are straight lines. The parameters of the Arrhenius equation

$$\tau = A \exp(\Delta E_a/RT)$$

are listed in Table IV.

The most striking feature of the curves of Fig. 3 is the strong dependence of the relaxation time on the "size" of the molecule as measured simply by monomeric molecular weight. For example, at room temperature the difference between the relaxation time of *N*-methylformamide (NMF) and NMnV or NnBA is a factor of 25 with *N*-methylpropionamide (NMP) falling just about half way between. The isomers NEA and

[4]See refs. 5 and 9 for attempts to estimate the degree of association. If the CO···H—N angle is close to 180°, adjacent dipoles in a chain are nearly parallel and $g \approx n$. This implies pentamers as the average degree of association at our lowest temperatures and dimers at about 200°. If the CO···H—N bond is not linear, the extent of association must be greater for the same value of the correlation factor, but only by a factor of two or three.

Can. J. Chem. Downloaded from www.nrcresearchpress.com by 210.87.254.105 on 09/05/12
For personal use only.

Can. J. Chem. Downloaded from www.nrcresearchpress.com by 210.87.254.105 on 09/05/12
For personal use only.

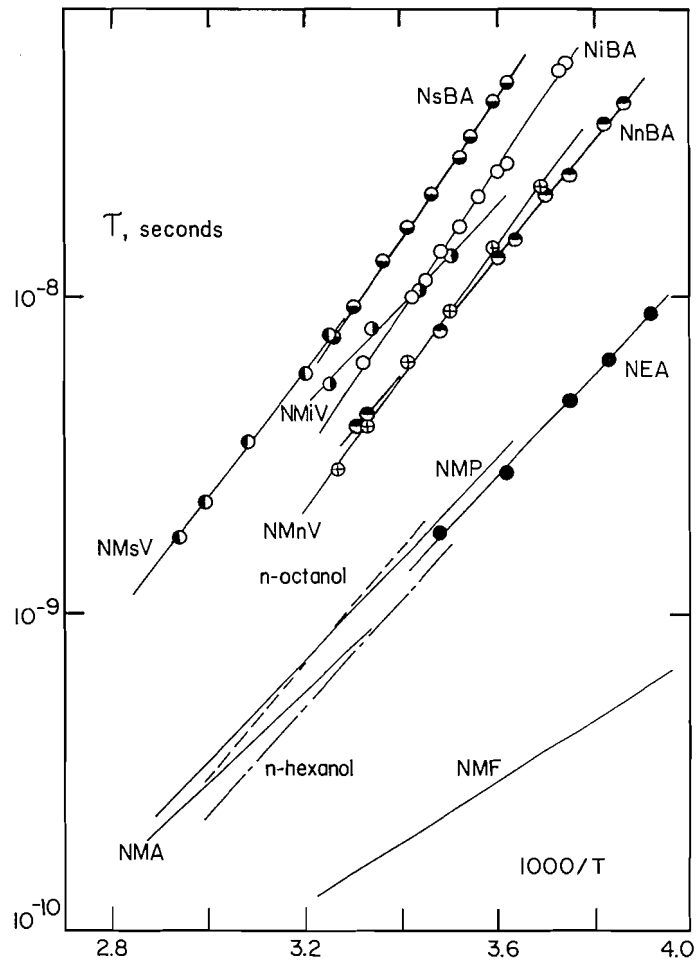

FIG. 3. Relaxation time as a function of reciprocal absolute temperature. Results for NMF, NMA, and NMP from Bass *et al.* (9). Alcohol curves obtained from data of Garg and Smyth (20).

NMP are virtually identical in their behavior and it is remarkable that the six $C_6H_{13}NO$ isomers should pair up according to the branching of the C_4 alkyl group, irrespective of whether it is the acid or the amine substituent.

The first-order relaxation kinetics and the relatively slow relaxation times found for the amides (the relaxation times of corresponding alkyl halides are some 1000 times faster) appear to be characteristic of hydrogen-bonded liquids. Despite the difference in molecular structure and the extent of intermolecular association as measured by the dipole correlation factors, the relaxation of dielectric polarization in alcohols (20) parallels both in magnitude and temperature dependence that of the amide of similar molecular weight (see Fig. 3). The conclusion that the relaxation process is not dependent on hydrogen-bond breaking as the rate-determining step is also substantiated by these results: why should the relaxation times be so different, and so characteristic of the nature of the amide, when the equilibrium polarization suggests that the intermolecular association is essentially the same for all these substances?

The viscous-damped sphere model of Debye predicts that $\tau/\eta \approx$ constant. Even though the model is inapplicable for strongly associated liquids, the proportionality of relaxation time to viscosity has often been observed. Insofar as Walden's rule is a first approximation in the sphere-in-continuum model of conduction, one

Can. J. Chem. Downloaded from www.nrcresearchpress.com by 210.87.254.105 on 09/05/12
For personal use only.

also expects that the relaxation time should be inversely proportional to conductance. We have performed a qualitative study of the viscosity–temperature relationship of NEA and the isomeric NBA's and of course we can determine the d.c. conductance from our dielectric data. Activation energies for viscous flow and conduction are listed in Table IV for comparison with the dielectric results. There is considerable uncertainty involved in ΔE_a (conductance), but it does seem that in every case except NMiV (where the dielectric data are meager and where ΔE_a (relaxation) is therefore uncertain) the activation energy for dielectric relaxation is larger than for either viscous flow or conduction. It seems unlikely that the rate-determining step for relaxation is the same as that for viscous flow, although there is apparently some similarity for the processes.

Without a detailed molecular model for relaxation as a guide, we can only conclude at this time that the relaxation process in *N*-monosubstituted amides is determined largely, but not exclusively, by the hydrogen-bond network. The sensitivity of the relaxation times to both molecular size and shape shows that attempts to consider the structured liquid as a continuum is too simplifying an approximation. Similar considerations apply to viscous flow and electrical conduction.

Acknowledgments

We thank Dr. R. Y. Lin and A. F. Flueckinger for their assistance and express our appreciation to The Office of Saline Water, the Air Force Office of Scientific Research, and The Research Foundation of State University of New York for their financial support.

1. G. R. Leader and J. F. Gormley. J. Am. Chem. Soc. **73**, 5731 (1951).
2. J. W. Vaughn and P. G. Sears. J. Phys. Chem. **62**, 183 (1958).
3. A. E. Lutskii and S. A. Mikhailenko. Zh. Strukt. Khim. **4**, 350 (1963).
4. L. R. Dawson *et al.* J. Phys. Chem. **66**, 26844 (1962); **67**, 278, 281 (1963).
5. R. Y. Lin and W. Dannhauser. J. Phys. Chem. **67**, 1805 (1963).
6. G. P. Johari and P. N. Tewari. J. Phys. Chem. **69**, 3167 (1965); **70**, 197 (1966).
7. O. D. Bonner, C. F. Jordan, and K. W. Bunzl. J. Phys. Chem. **68**, 2450 (1964).
8. L. A. LaPlanche, H. B. Thompson, and M. T. Rogers. J. Phys. Chem. **69**, 1482 (1965).
9. S. J. Bass, W. I. Nathan, R. M. Meighan, and R. H. Cole. J. Phys. Chem. **68**, 509 (1964).
10. N. Koizumi. Private communication to W. Dannhauser.
11. S. E. Lovell and R. H. Cole. Rev. Sci. Instr. **30**, 361 (1959).
12. P. Debye. Polar molecules. The Chemical Catalog Co., Inc., New York. 1929. Reprinted by Dover Publications, New York.
13. J. G. Kirkwood. J. Chem. Phys. **7**, 911 (1939); H. Frohlich. Theory of dielectrics. 1st ed. Oxford University Press, New York. 1949.
14. R. M. Meighan and R. H. Cole. J. Phys. Chem. **68**, 503 (1964).
15. M. J. Aroney, R. J. W. LeFevre, and A. N. Singh. J. Chem. Soc. 3179 (1965).
16. W. Dannhauser, L. W. Bahe, R. Y. Lin, and A. F. Flueckinger. J. Chem. Phys. **43**, 257 (1965). G. P. Johari and W. Dannhauser. J. Chem. Phys. **48**, 1911 (1968).
17. W. L. Koltun. Biopolymers, **3**, 665 (1965).
18. K. S. Cole and R. H. Cole. J. Chem. Phys. **9**, 341 (1941).
19. R. H. Cole. J. Chem. Phys. **23**, 493 (1955).
20. S. K. Garg and C. P. Smyth. J. Phys. Chem. **69**, 1294 (1965).
21. G. F. D'Alelio and E. E. Reid. J. Am. Chem. Soc. **59**, 109 (1937).

Can. J. Chem. Downloaded from www.nrcresearchpress.com by 210.87.254.40 on 09/05/12
For personal use only.

Calculation of emission–concentration and absorption–concentration relationships for spectral lines[1]

A. DEMAYO[2], L. W. HUNTER[3], AND P. KRUUS
Department of Chemistry, Carleton University, Ottawa, Canada

Received June 5, 1968

A general expression is derived for the calculation of total multiplet intensities for radiation emitted from a homogeneous source or transmitted through a homogeneous medium. The theory is then applied to the emission of radiation due to vibration–rotation transitions of HCl in an oven, and compared with experimental results. Absolute values of transition probabilities for individual vibration–rotation lines could be obtained by such a comparison. Another application of the theory is made in obtaining absorption–concentration relationships for the mercury 4358 Å line (7^3S_1–6^3P_1) with several different initial line shapes. The results are compared to absorption – 6^3P_1 concentration curves used in earlier work.

Canadian Journal of Chemistry, 46, 3151 (1968)

Introduction

Mitchell and Zemansky (1) give a discussion of the intensity distribution and total intensity of a singlet spectral line emitted in a homogeneous source, or transmitted through a homogeneous absorbing medium. Cowan and Dieke (2) give the intensity distribution and total intensity of radiation emitted from a nonhomogeneous spectral lamp, again for the case of an isolated singlet line. In both derivations, self-absorption is taken into consideration.

The intensity distribution of radiation emitted from a homogeneous source is given here in a generalized form for the case when a multiplet line of possibly overlapping components is emitted. The intensity distribution is also given for such a multiplet after transmission through a homogeneous absorbing medium.

The relationships are tested by predicting the pressure dependence of the intensities of three specific vibration–rotation lines arising from HCl vapor in an oven. In this case the overlap between the two components of each line is negligible. The calculated curves of total intensity of a line vs. gas pressure agree well with experimental curves (3). Such curves could be used to obtain absolute values of transition probabilities for individual vibration–rotation transitions without introducing any adjustable parameters.

It is also possible to determine absolute concentrations of molecules or atoms in various states from absorption measurements by making use of the relationships given here to construct appropriate absorption–concentration curves. Such cases arise when there exists an absorbing medium which has an absorption profile due to a singlet line or a multiplet line of possibly overlapping components arising due to transitions from the same lower state. If the transition probabilities for the transitions and the intensity distribution of the incident radiation is known, then it is possible to obtain the absolute concentration of the lower state by measuring the absorption of the spectral line and making use of the calculated absorption–concentration curve.

Michael and Weston (4) applied such a technique to find the concentration of hydrogen atoms in a reaction by observing the absorption of the Lyman α-line. An absorption–concentration curve was obtained by measuring hydrogen atom concentrations experimentally and not by calculation. Karl, Kruus, and Polanyi (5) determined the concentrations of Hg* 6^3P_1 and Hg* 6^3P_0 from measurements of the absorption of the 4358 and 4047 Å spectral lines. In this case, calculated absorption–concentration curves were used which were based on the work of Koedam and Kruithof (6). Some examples of absorption–concentration curves for the 4358 Å line are given here, with several different assumed incident intensity distributions. An experimentally determined incident intensity distribution (7) could also be used.

Theoretical Considerations

In this section general intensity distribution functions are derived for radiation transmitted through an absorbing medium which also emits radiation. It will be assumed that the concentrations of the various absorbing and emitting

[1]Taken in part from the thesis submitted by L. W. Hunter in partial fulfilment of the requirements for the B.Sc. (Honours) degree.

[2]Present address: Department of Energy, Mines, and Resources, Inland Waters Branch, Water Quality Division, Ottawa, Canada.

[3]Present address: Institute of Theoretical Chemistry, University of Wisconsin, Madison, Wisconsin.

Can. J. Chem. Downloaded from www.nrcresearchpress.com by 210.87.254.40 on 09/05/12
For personal use only.

molecules and the temperature are independent of both time and position. Therefore, the combined distribution function presented here does not apply rigorously to such sources as an electric arc or a flame.

The model used in the calculations is a container with a length l and plane parallel non-reflecting windows at both ends. The x-axis is chosen to pass through both windows at right angles with the origin at one window and positive sense towards the other. Radiation is taken to enter the container as a beam parallel to the x-axis through the window at the origin, and to be absorbed and emitted by molecules in the container. The radiation emitted along the x-axis through the window at $x = l$ is considered to be observed by a spectrometer.

Only the radiation travelling nearly parallel to the x-axis and in the positive sense is considered. Results derived from this model, however, are valid even though radiation is emitted isotropically in the medium under special conditions. (See next section.)

The intensity of the radiation from all sources in the energy interval ν to $\nu + d\nu$ (units cm^{-1}) and at position x (cm) inside the container is $I(\nu, x)d\nu$ (erg cm^{-2} s^{-1}). The notation $I(\nu, 0)d\nu = I_{in}(\nu)d\nu$ and $I(\nu, l)d\nu = I(\nu)d\nu$ is used.

The case of a singlet line is considered first. In this case $I(\nu, x)d\nu$ will be written as $I(\nu - \nu_0, x)d\nu$, where ν_0 denotes the center of the singlet line. Then

$$[1]\quad \frac{d}{dx}[I(\nu - \nu_0, x)]d\nu = I_{se}(\nu - \nu_0)d\nu - k(\nu - \nu_0)\cdot I(\nu - \nu_0, x)d\nu$$

The first term on the right hand side represents spontaneous emission in the medium,

$$[2]\quad I_{se}(\nu - \nu_0)d\nu = h\cdot\nu_0\cdot c\cdot n_{em}\cdot A\cdot P_{em}(\nu-\nu_0)d\nu$$

The second term represents absorption, together with a correction for stimulated emission,

$$[3]\quad k(\nu - \nu_0)d\nu = h\cdot\nu_0\cdot[n_{abs}\cdot B_{abs}\cdot P_{abs}(\nu - \nu_0)d\nu - n_{em}\cdot B_{em}\cdot P_{em}(\nu - \nu_0)d\nu]$$

Here n_{em} and n_{abs} denote the concentration of molecules in the upper and lower states respectively (molecule cm^{-3}); c, the speed of light (cm s^{-1}); h, Planck's constant (erg s^{-1}); A, the Einstein transition probability for spontaneous emission (s^{-1}); B_{abs} and B_{em}, the Einstein transition probabilities for absorption and stimulated emission (s g^{-1}) respectively. $P_{em}(\nu - \nu_0)d\nu$ is the fraction of the total intensity $\int I_{se}(\nu - \nu_0)d\nu$ in the frequency interval ν to $\nu + d\nu$ and $P_{abs}(\nu - \nu_0)d\nu$ is the corresponding function for absorption. The functions $P_{abs}(\nu - \nu_0)d\nu$ and $P_{em}(\nu - \nu_0)d\nu$ are identical (2), and will be denoted by $P(\nu - \nu_0)d\nu$.

Equation [1] can be solved for $I(\nu - \nu_0)$ using the appropriate boundary conditions to give

$$[4]\quad I(\nu - \nu_0)d\nu = I_{in}(\nu - \nu_0)\cdot\exp[-k(\nu - \nu_0)l]d\nu + \frac{c\cdot n_{em}\cdot A\cdot\{1 - \exp[-k(\nu - \nu_0)l]\}d\nu}{n_{abs}\cdot B_{abs} - n_{em}\cdot B_{em}}$$

Relationship [4] can now be generalized to the case of a multiplet line. Consider the case in which a multiplet with m possibly overlapping lines with centers at $\nu_1, \nu_2, \ldots \nu_j, \ldots \nu_m$ is emitted in the container. Then

$$[5]\quad I(\nu)d\nu = I_{in}(\nu)\cdot\exp\left[-\sum_{j=1}^{m} k_j(\nu - \nu_j)l\right]d\nu + \frac{c\left\{\sum_{j=1}^{m}\nu_j\cdot {}_jn_{em}\cdot A_j\cdot P_j(\nu - \nu_j)\right\}\left\{1 - \exp\left[-\sum_{j=1}^{m} k_j(\nu - \nu_j)l\right]\right\}d\nu}{\sum_{j=1}^{m}\nu_j\cdot({}_jn_{abs}\cdot {}_jB_{abs} - {}_jn_{em}\cdot {}_jB_{em})\cdot P_j(\nu - \nu_j)}$$

The intensity distribution $P_j(\nu - \nu_j)d\nu$ which will be considered in all cases here is the distribution due to Doppler broadening,

$$[6]\quad P_j(\nu - \nu_j)d\nu = \left(\frac{\ln 2}{\pi}\right)^{\frac{1}{2}}\cdot\frac{2}{{}_j\Delta\nu_D}\cdot\exp\left[\frac{-4(\ln 2)(\nu - \nu_j)^2}{{}_j\Delta\nu_D{}^2}\right]d\nu$$

where

$$[7]\quad {}_j\Delta\nu_D = 2(2R\ln 2)^{\frac{1}{2}}\left(\frac{\nu_j}{c}\right)\left(\frac{T}{M}\right)^{\frac{1}{2}}$$

is the Doppler half-width of the jth component of the line (cm^{-1}), M is the molecular weight of the emitting (and absorbing) molecule (g $mole^{-1}$), and R the gas constant (erg deg^{-1} $mole^{-1}$). Other

Can. J. Chem. Downloaded from www.nrcresearchpress.com by 210.87.254.40 on 09/05/12
For personal use only.

causes for broadening could easily be incorporated into the numerical calculations.

The evaluation of the total intensity,

$$I = \int_0^\infty I(\nu - \nu_0)d\nu$$

can be obtained explicitly as a series for several simple cases. For partially overlapping lines or for cases where $I_{in}(\nu)d\nu$ is a more complicated function than a Doppler or natural broadened line, it is necessary to use numerical methods for computing I. Here all computations are done numerically.

Emission of Vibration–Rotation Lines from Hot HCl Vapor

Introduction

In obtaining an absolute calibration of an infrared detection system (5), the emission of vibration–rotation lines of HCl from an oven was observed. The oven consisted essentially of a quartz cylinder of 5 cm inner diameter. The temperature along a heated section length l_1 (80 cm) was kept at 1118 ± 10 °K, and a section length l_2 (16 cm) nearer to the spectrometer was maintained at about 350 °K (3). The cone of sight of the spectrometer was narrow enough so that it did not intersect the side walls (8).

The experimental points for the $^1P_1(v' = 1, j' = 0$ to $v = 0, j = 1)$, $^2R_3(2, 4$ to $1, 3)$, and $^2R_4$ (2, 5 to 1, 4) line intensities obtained for various pressures of HCl in the oven are shown in Fig. 1. The intensities are the sum of the $H^{35}Cl$ and $H^{37}Cl$ contributions, as the slit width used in the experiment was 0.04 cm and the doublet components were thus not resolved.

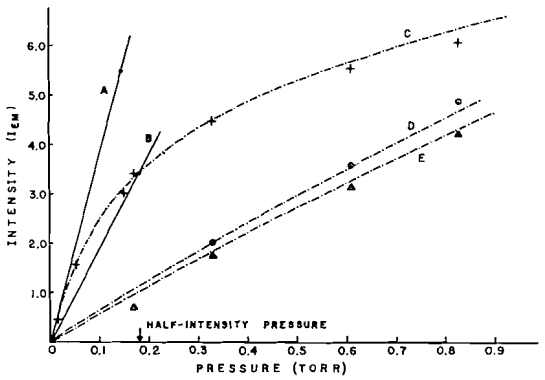

FIG. 1. Integrated emission intensity of HCl vibration–rotation lines as a function of pressure. A, linear extrapolation of calculated low-pressure values of I_{em} for $^1P_1$. B, a line with one-half the slope of A. C, calculated curve for the $^1P_1$ line; +, experimental points. D, calculated curve for the $^2R_4$ line; ⊙, experimental points. E, calculated curve for the $^2R_3$ line; △, experimental points.

It was decided to test the calculating procedure and the relationships given in the previous section by predicting the integrated intensities of the $^1P_1$, $^2R_3$, and $^2R_4$ lines as a function of the HCl pressure in the oven using a simple mathematical model.

The model assumed the HCl vapor to be in two parts. From $x = 0$ to 80 cm at a pressure p and a temperature of 1118 °K, and from $x = 80$ to 96 cm at the same pressure p and a temperature of 350 °K. The actual temperature, and hence also the actual concentrations of the emitting and absorbing molecules vary in a more complex manner in the container, of course. A more sophisticated model for calculations could be set up, but the accuracy of the experimental data does not seem to warrant it in this case.

No allowance is made in the model for thermal radiation from the end wall. It was attempted to keep this at a low level by having a cold, blackened (non-reflective) end plate present. Effects due to this type of radiation would be least at the lowest pressures, and did not seem to show up in the experimental data at pressures up to 0.5 Torr.

Radiation is emitted isotropically in the oven. The optics of the infrared detection system were such (8), however, that the increase in area subtended by the cone of sight with increase in distance from the detector is cancelled by a corresponding decrease in intensity of radiation at the detector due to the inverse square law (9). Thus no weighting function is needed for the distance coordinate and the problem can be reduced to consider radiation propagating along the x-axis only. The relationships given in the previous section can therefore be used.

Calculations

As the two components of each line do not overlap in this case, they can be treated separately and their integrated intensities then added for comparison with the experimental intensities. As $I_{in}(\nu)d\nu$ is assumed to be zero, then at $x = l_1$ for a single component, from [4], one gets

$$[8] \quad I[(\nu - \nu_0), l_1]d\nu = \frac{c \cdot n^*_{em} \cdot A}{n^*_{abs} \cdot B_{abs} - n^*_{em} \cdot B_{em}} \times \{1 - \exp[-k^*(\nu - \nu_0)l_1]\}d\nu$$

The asterisks denote quantities for the hot section.

Can. J. Chem. Downloaded from www.nrcresearchpress.com by 210.87.254.40 on 09/05/12
For personal use only.

In the second (cold) section, the amount of emission is negligible. Thus

$$[9] \quad I[(\nu - \nu_0), (l_1 + l_2)]d\nu = I(\nu)d\nu = I[(\nu - \nu_0), l_1] \cdot \exp[-k(\nu - \nu_0)l_2]d\nu$$

where $k^*(\nu - \nu_0)$ and $k(\nu - \nu_0)$ are given by [3], [6], and [7].

The concentrations n^*_{abs}, n^*_{em}, n_{abs} were calculated (9) from the ideal gas law and partition functions constructed from spectroscopic data for $H^{35}Cl$ and $H^{37}Cl$ taken from Herzberg (10). These quantities are functions of the pressure. The transition coefficients A, B_{abs}, and B_{em} were calculated (9) from the relationships given by Herman and Wallis (11) with matrix elements of the electric dipole moments of -6.70×10^{-20} e.s.u. cm for the $1 \rightarrow 0$ transitions and -9.71×10^{-20} e.s.u. cm for the $2 \rightarrow 1$ transitions (12).

Expression [9] was integrated numerically for a low value of p (10^{-4} Torr) for both (isotope) components of the three lines. The two components were then added to obtain the calculated integrated emission intensities for the three lines. This procedure was repeated at $p = 10^{-3}$ Torr. From these two points the limiting slope as $p \rightarrow 0$ was obtained. Then curves of I_{em} vs. p were calculated for pressures up to 2 Torr. These are shown in Fig. 1.

The calculated points on the I_{em} vs. p curve for the $^1P_1$ line were next fitted by a polynomial and the "half-intensity" pressure was calculated by interpolation. This is the pressure at which the emission intensity is one-half the value obtained by linear extrapolation of the two lowest pressure points. It was used to quantitatively describe the shape of the I_{em} vs. p curve. The sensitivity of this "half-intensity" pressure to changes in the assumed transition probability was examined for various l_1/l_2 ratios.

All calculations were made on a GE 415 computer.

Results

As seen in Fig. 1, the experimental points are in good agreement with the calculated curves, considering the simple model used in the calculation. The vertical (I_{em}) scale in Fig. 1 is in relative units. The calculated and experimental points were put on the same relative scale by matching the 0.33 Torr point for the $^2R_4$ line. The experiment was not initially performed for the purpose of obtaining such experimental–theoretical comparisons. The design of the apparatus used was thus not optimized for this purpose, and could be improved. This preliminary experimental data does show the feasibility of obtaining reasonably accurate emission intensity vs. pressure curves from such ovens. A more sophisticated computational model could also be set up if more accurate experimental data warrants it.

The sensitivity of the half-intensity pressure to the transition coefficients is about 1:1 for all three ratios of l_1/l_2 used (5:1; 1:1; 10:1). The sensitivity to temperature changes was not examined.

A comparison of such experimental and calculated emission–pressure curves appears to be very useful for obtaining absolute values of transition probabilities for individual vibration–rotation lines. An absolute value could be obtained by comparing the shape of an experimental I_{em} vs. p curve with calculated curves having different assumed transition probabilities by use of a half-intensity pressure or some other means. Other absolute values can be obtained from the relative slopes of emission–pressure curves at low pressures. This would thus provide a method of obtaining experimental vibration–rotation interaction factors and dipole matrix elements.

Absorption of the Mercury 4358 Å Line

Introduction

In using line absorption for obtaining absolute concentrations in stationary-state systems, it is sometimes impossible (5) or difficult to obtain the correct absorption–concentration curves by experimental means. Such curves must therefore be calculated using some mathematical model. Conversely, if correct experimental absorption–concentration curves are available, then absolute values of transition probabilities for the line considered can be obtained by comparison to calculated curves (4).

Absorption–concentration curves were calculated for the mercury 4358 Å line (7^3S_1–6^3P_1) for a homogeneous absorbing medium. The methods can, however, be generalized to other lines and to nonhomogeneous absorbing media.

Calculations

In these calculations expression [5] must be used, because several of the components overlap. Since it is assumed that $n_{em} = 0$ for all components, the second term is zero. Doppler broadening (expressions [6], [7]) was again assumed

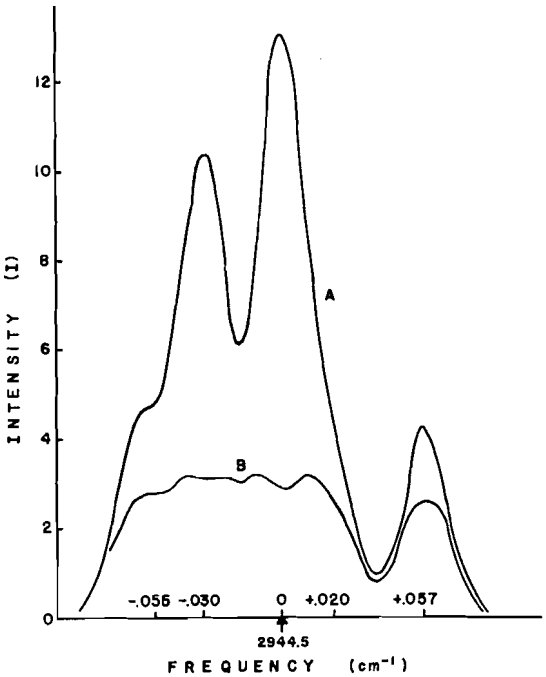

FIG. 2. Radiation intensity distribution for hyperfine components 6 to 10 inclusive of the Hg 4358 Å line. A, intensity distribution with Doppler broadening corresponding to 350 °K. B, the distribution in A after 44% absorption by an absorbing medium at 350 °K.

to be present. The Doppler broadening in the absorbing medium was taken as being caused by a temperature of 350 °K in all cases.

The hyperfine structure of the 4358 Å line shows the presence of 13 components (13). Components 6 to 10 inclusive make up 79.9% of a nonabsorbed 4358 Å line. These 5 components have considerable overlap when they are Doppler broadened at 350 °K as shown in Fig. 2, curve A. Such a curve is obtained by generalizing expression [2] to the case of a multiplet,

$$[10] \qquad I(\nu)d\nu = \sum \nu_j \cdot {}_j n_{em} \cdot A \cdot P_j(\nu - \nu_j)d\nu$$

The other components do not overlap to any great extent.

The absorption of various initial intensity distributions $I_{in}(\nu)d\nu$ was examined. The $I_{in}(\nu)d\nu$ assumed were: (*i*) natural mercury with Doppler broadening corresponding to 350 °K, and no self-absorption (shown in part in Fig. 2, curve A); (*ii*) the same as (*i*) except at 1500 °K; (*iii*) the same as (*i*) except with only the 198 isotope present; and (*iv*) the same as (*i*) except that self-absorption is assumed present.

For the first three cases, curves were obtained by numerical integration of expression [5] at various values of $Nl = \sum_j n_{abs} l$ using a GE 415 computer. The curve for the fourth case was obtained from data for the first case through the relationship

$$A = \frac{(A'' - A')}{(1 - A')}$$

where $A(Nl)$ is the absorption when self-absorption is present, $A'(N'l)$ describes the degree of self-absorption, and $A''[(N + N')l]$ is the absorption for the case with no self-absorption. This assumes that $I_{in}(\nu)$ in this case is $I(\nu)$ for the case of no self-absorption when the absorption is $A'(N'l)$. Part of $I_{in}(\nu)d\nu$ for curve F, Fig. 3, is thus shown by curve B, Fig. 2 where the shape of $I(\nu)$ in the overlapping region is shown for an absorption of 0.44.

In all calculations, B_{abs} was taken to be 6.9×10^8 s g^{-1} after Koedam and Kruithof (6), even though more recent calculations (14) give a value 20% higher.

Results

Figure 3 summarizes the results of the calculations. Curve A shows a Beer's law approximation using the value of the absorption coefficient at the middle of an assumed singlet Doppler broadened (350 °K) line to obtain the extinction coefficient. Curve B assumes the absorption of a singlet Doppler broadened line by an absorption line with the same half-width ($\Delta\nu_{em} = \Delta\nu_{abs} \equiv \alpha = 1$), and curve C with $\alpha = 3$ as calculated from data given in Mitchell and Zemansky (1). Curve D shows case (*i*), curve E case (*ii*) and case (*iv*) with $A' = 0.22$, and curve F case (*iii*) and case (*iv*) with $A' = 0.44$.

Data calculated from Koedam and Kruithof is also given, as their calculations were for a similar—but not identical—case, and as a different calculation procedure was used. The data correlates reasonably well considering the differences in initial models.

It can be seen that curves become less steep as the amount of self-absorption in the incident intensity distribution is increased. The change in the absorption–concentration curves due to self-absorption (curves D, E, F) and due to Doppler broadening of the incident radiation (curves D, E) are small, however, relative to the change produced by introducing hyperfine structure considerations (curves B, D).

Can. J. Chem. Downloaded from www.nrcresearchpress.com by 210.87.254.40 on 09/05/12
For personal use only.

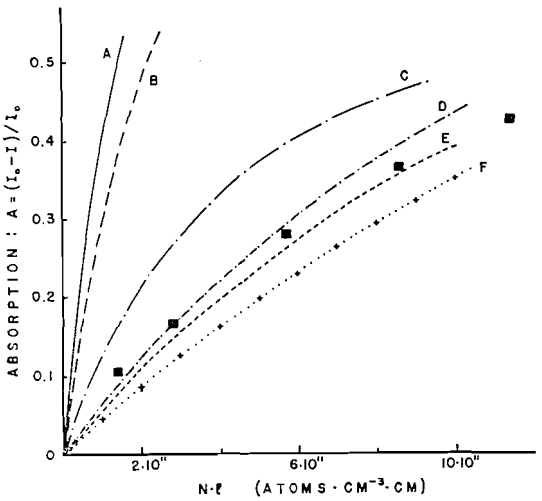

FIG. 3. Absorption–concentration curves for the Hg 4358 Å line. A, assuming Beer's law. B, singlet line absorption with $\alpha = 1$. C, singlet line absorption with $\alpha = 3$. D, Doppler broadened (350 °K) natural mercury line (no self-absorption) absorbed by natural mercury with Doppler broadening (350 °K). E, as in D, except with self-absorption ($A' = 0.22$); and as in D, except that the initial line is Doppler broadened corresponding to 1500 °K. F, as in D, except with an incident line due to the 198 isotope only; and as in D, except with self-absorption ($A' = 0.44$). ■, Data from Koedam and Kruithof (6).

Other incident intensity distributions can easily be used, including experimental distributions. It should be noted that the value of B_{abs} used in the calculations is probably only accurate to within 50%.

Conclusions

The calculation of theoretical emission–concentration and absorption–concentration curves from simple models has been shown to be feasible and potentially useful for several purposes. Copies of the computer programs used in the calculations are available on request from one of the authors (P.K.).

Acknowledgments

The authors thank Mr. G. T. Evans for help with some of the calculations, and the Computing Center of the University for computer time. This research was supported by grants from the Department of University Affairs of Ontario and the National Research Council of Canada.

1. A. C. G. MITCHELL and M. W. ZEMANSKY. Resonance radiation and excited atoms. Cambridge University Press, London. 1961.
2. R. D. COWAN and G. H. DIEKE. Rev. Mod. Phys. **20**, 418 (1948).
3. P. KRUUS. Ph.D. Thesis, University of Toronto, Toronto, Ont. 1965.
4. J. V. MICHAEL and R. E. WESTON, JR. J. Chem. Phys. **45**, 3632 (1966).
5. G. KARL, P. KRUUS, and J. C. POLANYI. J. Chem. Phys. **46**, 224 (1967).
6. M. KOEDAM and A. A. KRUITHOF. Physica, **28**, 80 (1962).
7. T. TAKO and M. OHI. Bull. Nat. Res. Lab. Metrol. Tokyo, **12**, 73 (1966).
8. P. M. MATHAI. Ph.D. Thesis, University of Toronto, Toronto, Ont. 1956.
9. L. W. HUNTER. B.Sc. Thesis, Carleton University, Ottawa, Ont. 1967.
10. G. HERZBERG. Spectra of diatomic molecules. D. Van Nostrand Co., Inc., Princeton, New Jersey. 1950.
11. R. HERMAN and R. F. WALLIS. J. Chem. Phys. **23**, 637 (1955).
12. W. S. BENEDICT, R. HERMAN, G. E. MOORE, and S. SILVERMAN. J. Chem. Phys. **26**, 1671 (1957).
13. H. SCHÜLER and E. G. JONES. Z. Physik, **74**, 631 (1932).
14. N. P. PENKIN. J. Quant. Spectry. Radiative Transfer, **4**, 74 (1964).

Can. J. Chem. Downloaded from www.nrcresearchpress.com by 210.87.254.40 on 09/05/12
For personal use only.

Can. J. Chem. Downloaded from www.nrcresearchpress.com by 210.87.254.40 on 09/05/12
For personal use only.

Average recoil ranges of ^{64}Cu and ^{196}Au produced by protons of 20–85 MeV energy in ^{65}Cu and ^{197}Au[1]

M. K. Dewanjee, G. B. Saha, and L. Yaffe

Radiochemistry Laboratory, Department of Chemistry, McGill University, Montreal, Quebec

Received February 13, 1968

Thick-target recoil experiments were performed to study (p,pn) reactions induced in ^{65}Cu and ^{197}Au in the energy range of 20–85 MeV and the average ranges projected in the forward, backward, and perpendicular directions were determined. Recoil parameters have been calculated to show approximately the amount of energy transfer and their energy dependence. The average range results have been compared with statistical theory, cascade–evaporation (85 MeV only), and inelastic scattering model calculations. The statistical calculations show reasonable agreement up to 30–40 MeV. However, the calculated projected range values, based on the cascade–evaporation and the inelastic scattering models, are consistently lower than the measured values. The analyses of the projected range values support the prevalent view that at low energies (~ 30–35 MeV), the compound nucleus mechanism is predominant and at higher energies, the direct interaction mechanism makes a major contribution.

Canadian Journal of Chemistry, 46, 3157 (1968)

Introduction

The study of simple nuclear reactions in the energy range of approximately 20–100 MeV is interesting because of the gradual transition in the reaction mechanism that occurs in this energy region. From the threshold to some intermediate energy range (30–40 MeV) the reactions seem to be governed by the formation and subsequent decay of a compound nucleus. At higher energies the available data are at present best explained by a direct interaction mechanism in which the reactions take place in a two-step cascade–evaporation process or in a one-step knock-out phase.

Recoil measurements provide a useful tool for the determination of momentum transfer and thus yield valuable information about the reaction mechanism. When a compound nucleus is formed, full transfer of incident momentum from the projectile to the struck nucleus occurs. With the direct interaction mechanism only partial momentum transfer takes place.

In the present study, we have measured the average ranges of the products formed in the ^{65}Cu(p,pn)^{64}Cu and ^{197}Au(p,pn)^{196}Au reactions, in the energy range of 20–85 MeV. The thick-target thick-catcher technique was used to measure the average ranges projected in the forward, backward, and perpendicular directions relative to the proton beam. The equations of Winsberg (1) and Sugarman *et al.* (2) have been used to derive the recoil parameters, which in turn give information regarding the deposition energy and momentum transfer in the cascade phase of the reaction.

For a quantitative comparison between the calculations and the experimental range results, statistical theory calculations at lower energies and cascade–evaporation calculations at 85 MeV have been performed for the ^{65}Cu(p,pn)^{64}Cu reaction. Also, we have performed the calculations for the (p,pn) reactions based on the mechanism of inelastic scattering of one nucleon in the diffuse surface of the nucleus followed by the evaporation of another particle from the excited residual nucleus (3–5).

Experimental

(a) Target Assembly and Irradiations

The target assembly in two orientations is shown in Fig. 1. It consists of the target (T) and activation (A) and guard foils (G). The foils to catch the recoils are labelled F (forward) and B (backward) in the forward–backward experiment and U (up) and D (down) in the perpendicular

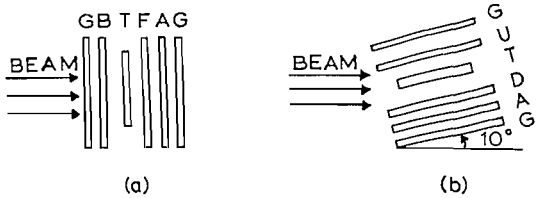

FIG. 1. Thick-target assemblies. (*a*) Forward–backward, (*b*) Perpendicular; G guard foil, B backward catcher foil, T target, F forward catcher foil, A activation foil, U upward catcher, and D downward catcher.

[1]This research received financial assistance from the National Research Council of Canada.

Can. J. Chem. Downloaded from www.nrcresearchpress.com by 210.87.254.40 on 09/05/12
For personal use only.

experiment. The copper or gold target foil of normal isotopic composition and thicknesses 8.871 and 18.911 mg/cm^2 respectively was sandwiched between the two aluminium catcher foils (9.19 mg/cm^2). The target area was about 1.5 cm^2. Before assembly all foils were washed with acetone and water to degrease them. The target superficial density was determined by weighing a known area of the target foil. The leading edge of the target was inside the catcher foils as shown in the diagram to prevent escape of recoils from the edge of the target.

An aluminium activation foil, identical with the catchers, was included to correct for impurities in the catchers which might give rise to the formation of ^{64}Cu or ^{196}Au. The guard foils prevented any separation between the different foils. The entire assembly was fixed to the target holder and irradiations carried out in the circulating beam of the McGill synchrocyclotron. The target assemblies were oriented (Fig. 1) at 90 and 10° to the beam in the forward–backward and perpendicular experiments respectively. The intensity of the proton beam was of the order of 1 μA, and the period of irradiation varied from 60–90 min.

(b) Chemical Separations

(i) Copper

The procedure used was a modification of that of Kraus and Moore (6). After irradiation the target, catchers, and activation foil were separately dissolved in a few milliliters of concentrated hydrochloric acid along with a few drops of hydrogen peroxide, 10 mg of Cu^{2+}, and 4 mg of Na^+. The solution was evaporated to dryness and redissolved in 2 ml of 4.5 *N* hydrochloric acid. This solution was passed through an ion-exchange column (Dowex 1 × 8, previously equilibrated with 4.5 *N* hydrochloric acid). The column was washed with 4.5 *N* hydrochloric acid to elute Na^+, Mn^{2+}, Co^{3+}, and Ni^{2+}. Copper was then eluted with 1.5 *N* hydrochloric acid, reduced with sodium sulfite, and precipitated as copper thiocyanate (from dilute hydrochloric acid with ammonium thiocyanate). The resulting solution was heated and centrifuged. The precipitate was then redissolved, and the solution made to volume.

Aliquots of 2 ml were usually taken for activity measurements. In several instances the thiocyanate precipitate was collected on glass fiber filter paper, dried, weighed, and after being covered with thin mylar films was used for activity measurements.

The chemical yields of the liquid sources were determined by complexometric titration (7) using disodium ethylenediamine tetraacetate with murexide indicator in the presence of NH_4Cl–NH_4OH buffer. Chemical yields were of the order of 55–75%.

(ii) Gold

The target, catchers, and activation foil were separately dissolved in aqua regia to which had been added gold, mercury, sodium, platinum, iridium, osmium, and rhenium carriers. The solution was evaporated twice to dryness with concentrated hydrochloric acid, the residue was redissolved in 5 *N* hydrochloric acid, and gold was extracted with ethyl acetate (8). The solvent layer was washed with 5 *N* hydrochloric acid and evaporated to dryness. The residue was dissolved in 2 *N* hydrochloric acid, reduced with 5% hydroquinone, washed with water and alcohol, and dissolved in aqua regia. The solution was made up to volume, and an aliquot used for activity measurements. Sometimes solid sources of gold were prepared after the hydroquinone reduction and used for activity measurements. The chemical recovery of gold was determined spectrophotometrically as the bromoaurate ion (9) at 380 mμ and the recovery was of the order of 60–80%.

(c) Activity Measurements

The characteristic γ-rays of ^{196}Au (composite peak: 0.426, 0.330, and 0.354 MeV) were measured with a NaI(Tl) crystal coupled to a 400-channel pulse-height analyzer. The annihilation radiation from ^{64}Cu was measured with a well-type NaI(Tl) crystal coupled to a single-channel analyzer gated on the 511-keV peak or with the NaI(Tl) crystal and the analyzer mentioned above. In addition, some of the samples were cross-checked by following their activities on low-background or end-window beta counters.

Results

(a) Treatment of Data

(i) At a given bombarding energy, the relative activities of different samples, at a particular time after the end of bombardment, were obtained from graphical plots or computer calculations with the CLSQ decay curve analysis program (10). Corrections for impurity activation were made for the activities in the catchers in each experiment. In general, the aluminium blank showed a production of ^{64}Cu and ^{196}Au from impurities less than 1% of the amount of total recoiling ^{64}Cu and ^{196}Au nuclei.

(ii) The edge-effect for the target foils used was negligible (11).

(iii) The formation cross section is assumed to be constant throughout the target. This is not true for reactions having steep excitation functions (12, 13). No correction was made for the beam degradation in the target assembly, the effect of which was much smaller than the uncertainty in the excitation function and the energy spread (±2 MeV) in the beam.

(b) Analysis of Data

In the parallel experiment (Fig. 1(*a*)), the fractions of the activities in the forward and backward catchers are denoted by F and B respectively. For the perpendicular experiment, the average fraction of the activity in the catchers is called P (the activities of the two catchers were approximately equal). The target thickness W is expressed in mg/cm^2 and the results are shown in Table I. The equations of Sugarman (2) are based on the vector model as shown in Fig. 2 and relate the measured FW, BW, and PW values to the recoil range parameter R ($R \propto V^N$), velocity parameters ($\eta_\parallel$, $\eta_\perp$), and anisotropy

TABLE I

Summary of recoil results from the thick-target experiments

(*a*) ^{65}Cu(p,pn)^{64}Cu reaction

E_p* (MeV)	No. of expts.	*FW* (±14%) (mg/cm²)	*BW* (±15%) (mg/cm²)	No. of expts.	*PW* (±14%) (mg/cm²)	*F/B*	*F/P*
20	1	0.131±0.018	0.0002±0.0000	1	0.047±0.007	679.30	2.77
30	3	0.180±0.025	0.0041±0.0006	1	0.039±0.006	43.89	4.61
35	2	0.292±0.041	0.0054±0.0008	1	0.044±0.006	53.90	6.64
40	2	0.275±0.039	0.0047±0.0007	2	0.048±0.007	58.56	5.76
50	2	0.168±0.024	0.0062±0.0009	1	0.063±0.009	27.15	2.69
60	3	0.148±0.021	0.0066±0.0010	1	0.061±0.009	22.46	2.43
70	1	0.125±0.018	0.0065±0.0010	1	0.059±0.008	19.20	1.92
80	1	0.141±0.020	0.0082±0.0012	1	0.091±0.013	17.16	1.55
85	1	0.104±0.015	0.0090±0.0013	2	0.058±0.008	11.66	1.81

(*b*) ^{197}Au(p,pn)^{196}Au reaction

		FW (±16%)	*BW* (±16%)		*PW* (±16%)		
20	2	0.045±0.007	0.0014±0.0002	3	0.019±0.003	31.32	2.31
25	1	0.046±0.007	0.0021±0.0003	1	0.014±0.002	21.97	3.41
30	1	0.054±0.008	0.0017±0.0003	1	0.014±0.002	30.85	3.75
40	1	0.042±0.006	0.0026±0.0004	2	0.015±0.002	16.37	2.80
50	2	0.040±0.006	0.0046±0.0007	1	0.018±0.003	8.74	2.20
60	1	0.041±0.006	0.0056±0.0009	1	0.020±0.003	7.35	2.07
70	3	0.038±0.006	0.0071±0.0011	1	0.023±0.004	5.32	1.62
80	1	0.038±0.006	0.0033±0.0005	2	0.021±0.003	11.69	1.84
85	1	0.036±0.005	0.0043±0.0007	1	0.022±0.003	8.31	1.61

*E_p, proton energy.

parameter b/a, for the angular distribution of the type $W(\theta) = (a + b \cos^2 \theta)/(a + b/3)$. The equations are valid when $\eta \ll 1$.

The effect of the variation of the velocity exponent N on the constancy of R, $\eta_{\|}$, and b/a values was studied. It was assumed that $N \simeq 1$ for fission fragments and $N \simeq 2$ for heavy atoms moving with smaller velocities. Depending on the mass and velocities of the recoiling product nuclei, intermediate values of N were also used. It was observed for higher incident energy (50 MeV on gold and 70 MeV on copper), that the variations in R, $\eta_{\|}$, and b/a were negligible for variation of N from 1.5 to 2.0. The highest acceptable values of N were picked. However, for copper irradiations below 70 MeV and for gold below 40 MeV, results of the iterations were either fluctuating or tended to give rise to absurd values for $N = 2$. In these cases, the N values were lowered till consistent results were obtained.

Since there are four unknowns ($\eta_{\|}$, $\eta_{\perp}$, R, and b/a) and only three equations, $\eta_{\perp}$ was assumed to be zero, and the equations were solved by different approximate methods. First, approximate values of the recoil parameters were calculated by the self-consistent method of analysis (2) (Sugarman's anisotropy case). The

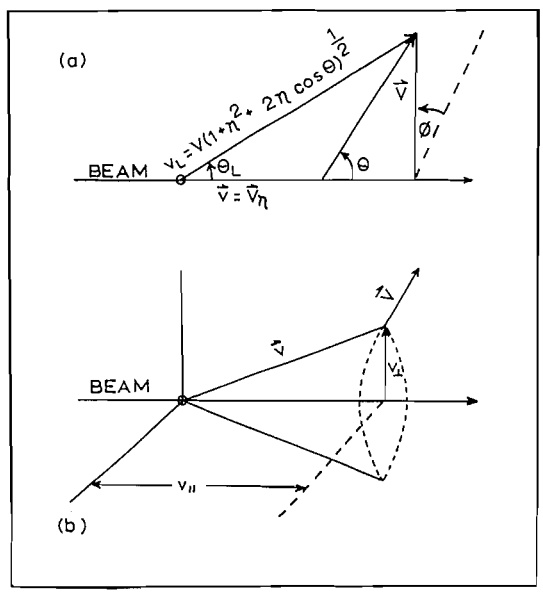

FIG. 2. Vector model representations. (*a*) Compound nucleus mechanism illustrating the forward–backward and perpendicular experiments; v impact velocity, V evaporation or reaction velocity, and $\eta = v/V$. (*b*) Direct interaction mechanism, $v_{\|}$ and $v_{\perp}$ are components of the knock-on velocity v, parallel and perpendicular to the beam direction; the vector V is the reaction velocity, and θ and θ_L are the recoil angles with respect to the beam direction in the system of the struck nucleus and laboratory system respectively.

Can. J. Chem. Downloaded from www.nrcresearchpress.com by 210.87.254.40 on 09/05/12
For personal use only.

TABLE II

Calculated *FW* values for compound nucleus formation by evaporation corrections

Proton energy (MeV)	μ^2	μ^4	FW/R_{CN}	R_{CN} (mg/cm²)	Calculated *FW* (mg/cm²)	Experimental *FW* (mg/cm²)	Approximate CN/DI
(*a*) ^{65}Cu(p,pn)^{64}Cu reaction							
20	0.159	0.025	1.089	0.062	0.068	0.131	—
30	0.460	0.212	1.166	0.091	0.106	0.180	—
40	0.611	0.373	1.159	0.112	0.129	0.275	—
50	0.702	0.492	1.140	0.140	0.159	0.168	—
60	0.762	0.581	1.121	0.172	0.193	0.148	63/37
70	0.805	0.648	1.105	0.208	0.230	0.125	52/48
80	0.837	0.701	1.091	0.248	0.271	0.141	43/57
85	0.851	0.724	1.085	0.271	0.294	0.104	35/65
(*b*) ^{197}Au(p,pn)^{196}Au reaction							
20	0.372	0.138	1.156	0.025	0.029	0.045	—
30	0.588	0.346	1.162	0.030	0.035	0.054	—
40	0.696	0.484	1.141	0.035	0.040	0.042	—
50	0.761	0.579	1.121	0.041	0.046	0.040	—
60	0.804	0.647	1.105	0.047	0.052	0.041	50/50
70	0.835	0.697	1.092	0.053	0.058	0.038	40/60
80	0.858	0.737	1.081	0.058	0.063	0.038	40/60
85	0.868	0.753	1.077	0.060	0.065	0.036	36/64

multiple iterations were performed with a computer program. In another method of analysis of the Sugarman equations R and $\eta_{||}$ were calculated for values of $b/a = 0$, $\eta_{\perp} = 0$, and $N = 2$. The equation, quadratic in $\eta_{||}$, was solved (Sugarman's isotropy case).

The corresponding equations of Winsberg (1) for $N = 2$ and $b/a = 0$ are as follows:

$$[1] \quad FW = 0.267R(1.0 + \eta)^2\left\{1.0 + 0.5\eta - \frac{(1.0 - \eta)^2[1.0 - (1.0 - \eta)^2]}{8\eta^2}\right\}$$

$$[2] \quad (F - B)W = 0.267R\eta(5.0 + \eta^2)$$

$$[3] \quad PW = 0.25R(1.0 + 0.375\eta^2)$$

The cubic equation in η was then solved numerically by Newton–Raphson's method (14) (Winsberg's isotropy case). The surprising fact is that the results of R and $\eta_{||}$ obtained in these three analyses are not significantly different. The *FW*, *BW*, and *PW* values and the corresponding recoil parameters obtained by the different methods are shown in Tables I and II, and Figs. 3, 4, and 5.

(c) Errors

The random errors in recoil studies consist of the errors associated with the resolution of decay curves, the determination of photo peak areas, counter backgrounds, chemical yields, weights of the target, nonuniformities of the target and catcher thickness, the scattering of the recoiling nuclides, dilution factors, radioactive purity, and self-absorption and back scattering of the beta radiation in the sample. The chemical procedures

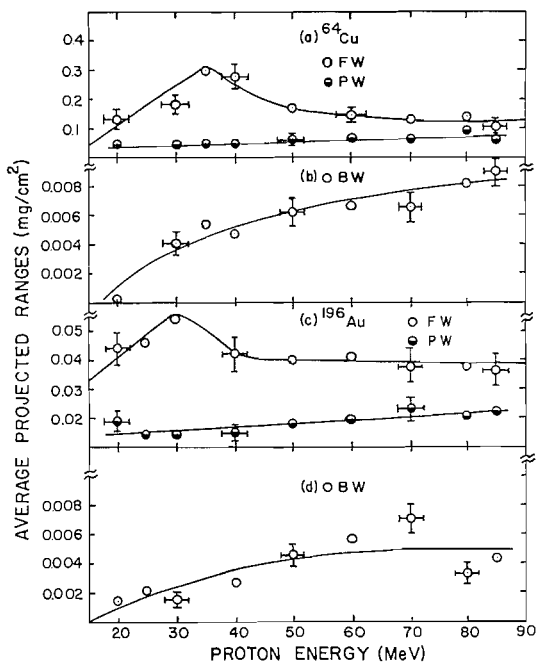

FIG. 3. Energy dependence of the *FW*, *PW*, and *BW* values: (*a*) and (*b*) refer to the ^{64}Cu data; (*c*) and (*d*) to the ^{196}Au data.

Can. J. Chem. Downloaded from www.nrcresearchpress.com by 210.87.254.40 on 09/05/12
For personal use only.

Can. J. Chem. Downloaded from www.nrcresearchpress.com by 210.87.254.40 on 09/05/12
For personal use only.

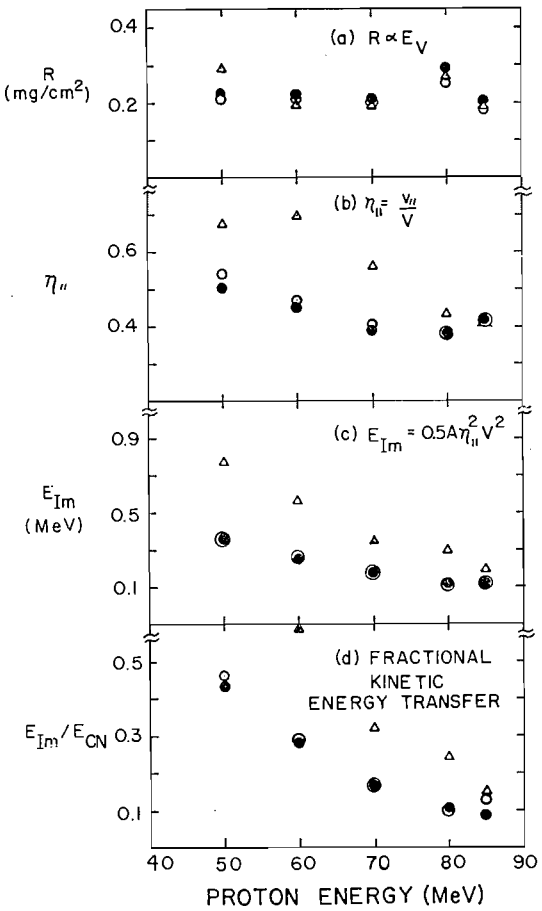

FIG. 4. Thick-target ^{64}Cu recoil parameters: (*a*) range parameter R, (*b*) velocity parameter $\eta_{\parallel}$, (*c*) impact energy E_{Im}, and (*d*) the ratio of the kinetic energy of the impact to that of the compound nucleus E_{Im}/E_{CN}; △ Sugarman's anisotropy case, ⊙ Sugarman's isotropy case, and ● Winsberg's isotropy case.

gave sufficient radiochemical purity, and radioactive decay of the samples was carefully monitored. The total error was calculated by taking the square root of the sum of the squares of the individual errors. The error amounted to ±14% for ^{64}Cu and ±16% for ^{196}Au in the determination of the *FW*, *BW*, and *PW* values. The scatter of the experimental points, determined by duplicate experiments, was found in most cases to be less than this estimated error.

Discussion

(a) Qualitative Features

Some qualitative features of the results of (p,pn) reactions studied are of interest. In Fig. 3, it is seen that the quantity *FW* increases initially, reaches a peak value at about 35 and 30 MeV for ^{64}Cu and ^{196}Au respectively, and then gradually decreases and becomes nearly constant at higher energies. The value of *BW* shows an initial rise and then levels off. The *PW* value shows a linear energy dependence and has a very small slope. The ratio *F*/*B* of the forward to the backward activity as seen from Table II becomes larger as the bombarding energy approaches the threshold of the reaction. The ratios *F*/*B* and *F*/*P* show only slight energy dependence in the high energy region. The *F*/*B* ratio at low energy involves a larger error because of the extremely low activity in the backward catcher.

The present results for ^{64}Cu and ^{196}Au may be compared with previous results obtained with medium- and heavy-mass nuclides in the energy

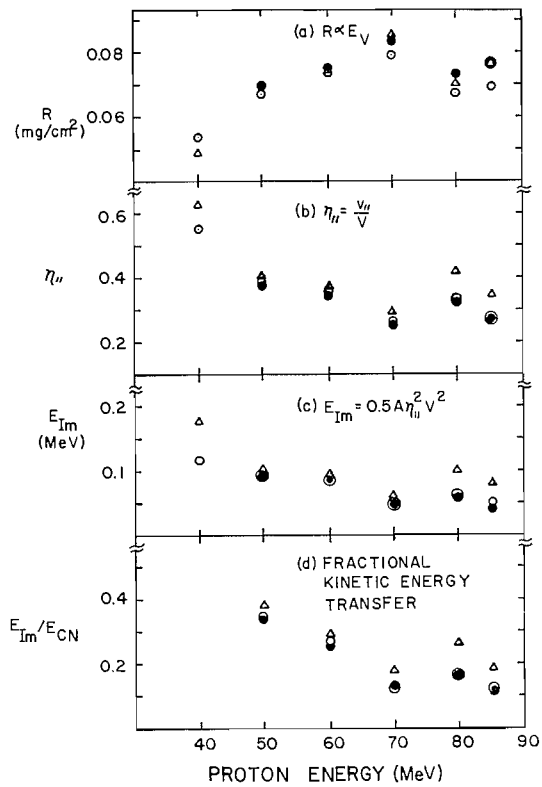

FIG. 5. Thick-target ^{196}Au recoil parameters: (*a*) range parameter R, (*b*) velocity parameter $\eta_{\parallel}$, (*c*) impact energy E_{Im}, and (*d*) the ratio of the kinetic energy of the impact to that of the compound nucleus E_{Im}/E_{CN}: △ Sugarman's anisotropy case, ⊙ Sugarman's isotropy case, and ● Winsberg's isotropy case.

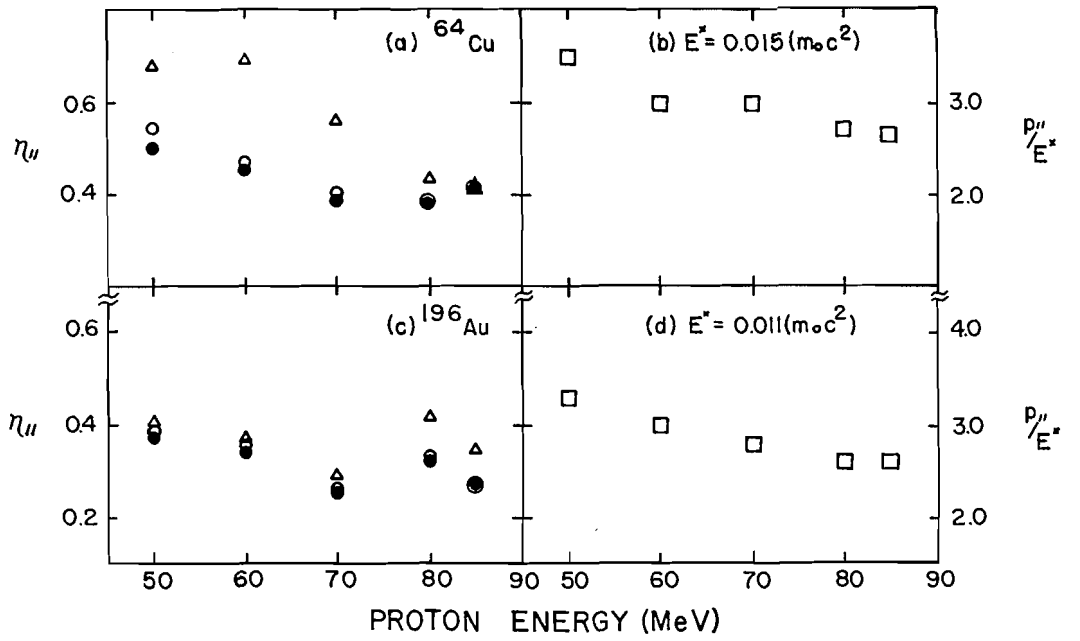

FIG. 6. Calculation of constant deposition energy by the adjustment of η_{II} with p_{II}/E^*; (*a*) and (*b*) refer to ^{64}Cu; (*c*) and (*d*) refer to ^{196}Au; △ Sugarman's anisotropy case, ○ Sugarman's isotropy case, and ● Winsberg's isotropy case.

region of interest, in terms of *FW*, *BW*, and *PW* values (mg/cm^2) and their ratios *F*/*B* and *F*/*P*. Merz and Caretto (15) reported *F*, *B*, and *P* values for the ^{65}Cu(p,pn)^{64}Cu reaction in the energy region 73–400 MeV. Their results, converted into *FW*, *BW*, and *PW* values at 73 and 85 MeV, may be compared with the present data. Our results for *FW* and *BW* values at 73 MeV (interpolated) and *PW* value at 85 MeV are larger by a factor of 2.4, 1.8, and 2.1 respectively. It is difficult to pinpoint the reason for this discrepancy.

The initial rise of the *FW* value from the threshold energy indicates a large momentum transfer for the compound nucleus type reaction. The falloff at higher energies was attributed by Fung and Perlman (16) to the onset of nuclear transparency. The simple classical expressions $P = \pm\sqrt{(2mE)}$, and hence $\Delta P/\Delta E \propto \pm E^{-1/2}$, show that, for constant deposition energy, the forward deposition momentum decreases initially as $E^{-1/2}$ and the backward momentum increases as $-E^{-1/2}$.

(b) Analytical Calculations of the Average Forward Ranges with the Effect of Evaporation

From the relations of Winsberg and Alexander (17, 18), the average forward ranges, *FW*, of ^{64}Cu and ^{196}Au were calculated from the compound nuclear range by considering the evaporation effect (19). For the normalized isotropic distribution of the emitted particles, *FW* can be written as

$$[4] \quad FW = R_{CN}\,[1.0 + 0.667\mu^2 - 0.067\mu^4]$$

where $\mu(= V/v = 1/\eta) \ll 1$, and R_{CN} is the range corresponding to the compound nuclear velocity v at a particular incident energy, and it was calculated with the Lindhard, Scharff, and Schiott (L.S.S.) range-energy relation (20). The expression (19) for the evaporation correction parameter μ^2 for the (p,pn) reactions can be written as

$$[5] \quad \mu^2 = \left(\frac{M_{CN}^2}{M_R^2 M_p E_p}\right)\sum M_e E_e = \frac{M_{CN}^2}{M_R^2 E_p}\sum E_e = \frac{M_{CN}^2}{M_R^2}\left[\frac{E_{CN}^* - S_{pr} - S_n - E_R}{E_R}\right]$$

where *M* and *E* are the mass and kinetic energy, and the subscripts CN, R, p, and e refer respectively to the compound nucleus with the excitation energy E_{CN}^*, the residual fragment,

Can. J. Chem. Downloaded from www.nrcresearchpress.com by 210.87.254.40 on 09/05/12
For personal use only.

Can. J. Chem. Downloaded from www.nrcresearchpress.com by 210.87.254.40 on 09/05/12
For personal use only.

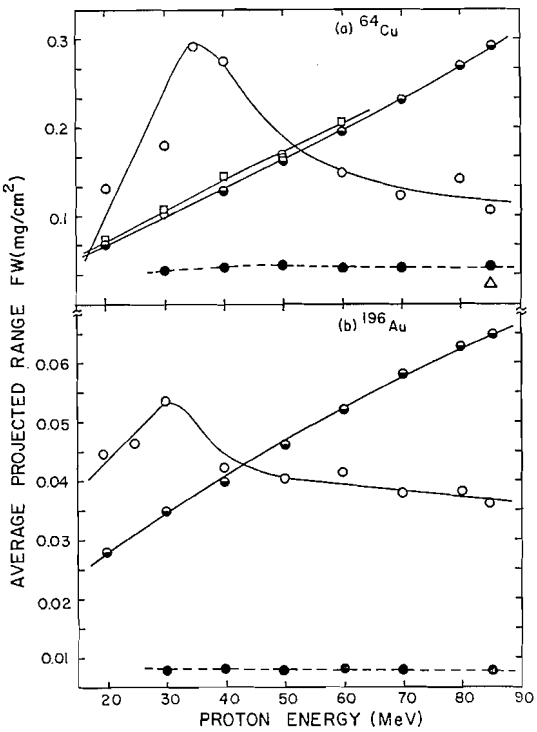

FIG. 7. Comparison of experimental and calculated *FW* values of (*a*) ^{64}Cu and (*b*) ^{196}Au; ○ experimental, ◒ compound nuclear range with evaporation effect, eq. [4], □ statistical theory, △ cascade–evaporation theory (85 MeV), ● ISE model calculations.

the bombarding particle, and the emitted particles. S_{pr} and S_n are the separation energies of the proton and the neutron respectively. The summation is carried out over all the particles and the energy of the residual nucleus was assumed to be slightly less than the difference of the Q values for the (p,p2n) and (p,pn) reactions. The residual nucleus in such a case would not have sufficient energy (7 and 5 MeV for ^{64}Cu and ^{196}Au respectively) for particle emission and the ground state of the recoiling nuclide would be reached by photon emission. The calculated results are shown in Table II and Fig. 7, along with the experimental values.

The calculated values are lower than the experimental ones at low energy, although linear energy dependence is observed. The discrepancy may be partly due (20) to the low $K_{L.S.S.}$ values calculated for the Thomas–Fermi atoms. To fit the experimental curves, $K_{L.S.S.}$ for ^{64}Cu would have to be multiplied by a factor of ~ 1.8 and that for ^{196}Au by ~ 1.3. Above 50 MeV for ^{64}Cu and 40 MeV for ^{196}Au, the experimental results fall below the calculated values. This is due to the predominance of the direct interaction mechanism above this energy range since the partial momentum transfer is not taken into account in the above calculation.

(c) Recoil Parameters

The recoil parameters calculated by the three approximate methods outlined previously are shown in Table III, and Figs. 4 and 5, where E_p = proton energy, E_V = kinetic energy due to the evaporation kick, and E_{Im} = impact energy due to momentum transfer. It is observed that the trends for the three cases are similar, with the exception that Sugarman's anisotropy case shows higher values of the recoil parameters, particularly at about 60 MeV for both ^{64}Cu and ^{196}Au. The recoil parameters at 80 MeV for ^{64}Cu and ^{196}Au show a point of inflection although the uncertainty may be higher in this case. The general nature of the variation of the recoil parameters mainly in the energy region between 50 and 85 MeV is described below.

(*i*) The range parameter $R (= KV^N)$ for ^{64}Cu at 85 MeV is about three times larger than the corresponding value for ^{196}Au, whose mass is approximately three times greater than that of ^{64}Cu. The relatively high R value for both ^{64}Cu and ^{196}Au above 50 MeV may be due to the higher excitation energy transfer to the struck nucleus in the initial phase of the reaction and hence higher evaporation velocity of the recoils.

(*ii*) The values of the velocity parameter $\eta_{||}$, for both ^{64}Cu and ^{196}Au, gradually decrease to a saturation value of ~ 0.3 around 85 MeV, at the onset of the region of constant deposition energy.

(*iii*) The variation of the impact energy (the kinetic energy transfer in the initial cascade step, $E_{Im} = 0.5A\eta_{||}{}^2V^2$) with the incident energy shows that the slope for ^{64}Cu is higher than that for ^{196}Au and at 85 MeV the E_{Im} value for ^{64}Cu (~ 0.12 MeV) is twice as large as that of ^{196}Au (0.06 MeV). However, the ratio E_{Im}/E_{CN}, which is a measure of the fractional kinetic energy transfer to the recoiling nuclide in the cascade process, approaches a value of $\sim$0.1 at 85 MeV. For full incident momentum transfer, this value should be unity.

(*iv*) The slight variation of the kinetic energy, E_V, due to the evaporation kick in the three cases for ^{64}Cu and ^{196}Au at higher energies is

Can. J. Chem. Downloaded from www.nrcresearchpress.com by 210.87.254.40 on 09/05/12
For personal use only.

TABLE III

Summary of the recoil parameters obtained from the different analyses of the thick-target results

	Winsberg's isotropy case						Sugarman's isotropy case						Sugarman's anisotropy case						
E_p* (MeV)	N	R (mg/cm^2)	η	E_V (MeV)	E_{Im} (MeV)	E_{Im}/E_{CN}	N	R (mg/cm^2)	η	E_V (MeV)	E_{Im} (MeV)	E_{Im}/E_{CN}	N	R (mg/cm^2)	η	b/a	E_V (MeV)	E_{Im} (MeV)	E_{Im}/E_{CN}
(*a*) ^{65}Cu(p,pn)^{64}Cu reaction																			
50	2	0.225	0.507	1.24	0.329	0.435	2	0.211	0.540	1.16	0.350	0.462	1.4	0.295	0.677	−10.3	1.63	0.770	0.980
60	2	0.219	0.450	1.21	0.253	0.278	2	0.207	0.471	1.14	0.261	0.288	1.4	0.194	0.696	−1.43	1.07	0.536	0.589
70	2	0.209	0.386	1.15	0.177	0.167	2	0.193	0.399	1.07	0.175	0.165	1.6	0.191	0.562	−1.13	1.05	0.343	0.323
80	2	0.292	0.278	1.61	0.129	0.106	2	0.253	0.283	1.39	0.115	0.095	2.0	0.276	0.433	−1.38	1.53	0.295	0.244
85	2	0.201	0.315	1.11	0.114	0.088	2	0.184	0.322	1.01	0.109	0.124	2.0	0.192	0.414	−0.99	1.06	0.187	0.145
(*b*) ^{197}Au(p,pn)^{196}Au reaction																			
40	—	—	—	—	—	—	2	0.054	0.548	0.465	0.133	0.658	2	0.045	0.644	−0.62	0.423	0.177	0.877
50	2	0.069	0.373	0.599	0.084	0.334	2	0.067	0.385	0.585	0.082	0.347	2	0.068	0.403	−0.24	0.587	0.096	0.381
60	2	0.075	0.343	0.655	0.078	0.256	2	0.074	0.352	0.640	0.080	0.264	2	0.074	0.368	−0.24	0.646	0.088	0.291
70	2	0.084	0.250	0.726	0.046	0.130	2	0.079	0.253	0.684	0.044	0.126	2	0.085	0.288	−0.63	0.736	0.062	0.175
80	2	0.073	0.321	0.630	0.065	0.162	2	0.067	0.328	0.579	0.063	0.156	2	0.069	0.418	−0.96	0.602	0.106	0.262
85	2	0.076	0.269	0.661	0.048	0.112	2	0.069	0.273	0.599	0.052	0.121	2	0.076	0.344	−0.96	0.661	0.079	0.184

*E_p, proton energy.

Can. J. Chem. Downloaded from www.nrcresearchpress.com by 210.87.254.40 on 09/05/12
For personal use only.

within the limits of the experimental error. This constancy of E_V reflects a constant deposition energy at the higher bombarding energies.

(*v*) The anisotropy parameter, b/a, shows high negative values for both ^{64}Cu and ^{196}Au, which are close to -1.0 at 85 MeV. The b/a values are sensitive to small variations in the measured *FW* and *BW* values which may involve higher uncertainties, though the other recoil parameters are less affected.

The analysis of Sugarman's equations (2) and the Monte Carlo calculations of Porile (21) show that the neglect of $\eta_\perp$ does not introduce a serious error into the calculation of R and $\eta_\parallel$. The calculations of $v_\parallel$ and therefore E_{lm} are approximately independent of $\eta_\perp$. Merz and Caretto (15) obtained a relatively high value of $\eta_\perp$ at higher energies for the ^{65}Cu(p,pn)^{64}Cu reaction, though no details of the calculations were given. The assumption that V and v are unique is not strictly correct, since the measured projected range values are average quantities. The rigid assumptions that $\eta_\perp = 0$ and $b/a = 0$ (in the isotropic emission cases) are not strictly valid as indicated by a sidewise peak in the angular distribution measurements (22). The assumption $b/a = 0$ is difficult to verify because the separation of the angular distribution of the evaporation kick from the net angular distribution results is difficult to achieve. The equations of Sugarman are not valid, in general, below 50 MeV, where $\eta_\parallel$ approaches unity and the neglect of higher powers of $\eta_\parallel$ is not justified. Another reason for the uncertainty in the energy calculation from the recoil parameters is the uncertainty in the electronic stopping parameter K, which in extreme cases amounts to about 50%. Because of the experimental uncertainties in the *FW*, *BW*, and *PW* values, as well as those involved in the analyses, the calculations of E_{lm} and E_V may involve large cumulative errors of the order of 20–40%.

(d) Calculation of Deposition Energy (Approximate)

Approximate values of the deposition energies for both the reactions studied were calculated by a combination of the recoil parameter $\eta_\parallel$ and the momentum component in the beam direction imparted to the struck nucleus by the incident particle. The single, fast nucleon mechanism of Fung and Perlman (16) assumes that the incident particle passes through the nucleus undeviated, but deposits an energy E^*. The component of the momentum imparted to the recoil in the direction of the beam is given by the relation

$$[6] \qquad p_\parallel = \frac{2EE^*}{p + (p^2 - 2EE^*)^{1/2}}$$

where E and p in this section refer to the total energy and momentum of the incident particle in natural units of m_0c^2 and m_0c respectively. At low bombarding energies (23), [6] reduces to the equation used by Fung and Perlman (16). The crudeness of the model lies in the assumption that the recoils move only in the forward direction, i.e. $p_\perp = 0$. Also in this mechanism, the Fermi motion of the nucleons in the nucleus was neglected. The effect of Fermi motion will cause a distribution in the recoil momentum. According to this mechanism, the deposition energy after the knock-on cascade leaves sufficient excitation energy to evaporate further particles from the residual nucleus to lead to the desired product, and this deposition energy is approximately constant in the high energy region.

Since V is approximately constant, the velocity parameter $\eta_\parallel = v_\parallel/V$ is a measure of $p_\parallel$ in the energy region of interest (60–85 MeV). In the determination of the recoil parameters, we also assumed that $\eta_\perp = 0$, i.e. $v_\perp = 0$. The ratios of $p_\parallel/E^*$ were calculated for various values of E^* (0.0 to 0.5 m_0c^2). By matching the curve of $\eta_\parallel$ vs. E_p with that of $p_\parallel/E^*$ vs. E_p, as shown in Fig. 6, a value of deposition energy E^* was found for the best fit of the two curves. The parameter $\eta_\parallel/(p_\parallel/E^*)$ was approximately found to be 0.125 for ^{196}Au with $E^* \sim 0.011$ (m_0c^2) or ~ 10.15 MeV, and 0.141 for $E^* \sim 0.015$ (m_0c^2) or ~ 14.1 MeV for ^{64}Cu. These deposition energies are just sufficient to evaporate a neutron from the excited ^{65}Cu and ^{197}Au nuclides to give rise to the (p,pn) products.

(e) Comparison with Monte Carlo Calculations

In order to make a quantitative comparison of our experimental results with the predictions of the statistical and cascade–evaporation theories, Monte Carlo calculations have been performed to obtain the recoil range values. With the evaporation formalism of Weisskopf (24) and the modified code of Dostrovsky *et al.* (25), statistical calculations (26) were carried out at 20, 30, 40, and 50 MeV with 5000 initial cascades and cascade–evaporation calculations at

Can. J. Chem. Downloaded from www.nrcresearchpress.com by 210.87.254.40 on 09/05/12
For personal use only.

85 MeV with 10 000 cascades for the ^{65}Cu(p,pn)-^{64}Cu reaction[2]. At energies above 40 MeV, the calculated cross sections for the ^{65}Cu(p,pn)^{64}Cu reaction with evaporation alone, were too low to yield a significant number of events.

The range of the recoil can be calculated from its kinetic energy by the Lindhard, Scharff, and Schiott relationship (27)

$$[7] \qquad R = KE_R$$

where the range-energy proportionality constants, K, are 0.181 and 0.115 (mg cm^{-2} keV^{-1}) respectively for ^{64}Cu and ^{196}Au in copper and gold. The average ranges projected in the forward, backward, and perpendicular directions were obtained by

$$[8] \qquad FW = R \cos \theta_R \qquad 0 < \theta_R < \pi/2$$

$$[9] \qquad BW = -R \cos \theta_R \qquad \pi/2 < \theta_R < \pi$$

$$[10] \qquad PW = \frac{R}{\pi} \sin \theta_R$$

In the evaporation calculations, the radius parameter was chosen to be 1.5 fm. A value of 0.05A was assumed for the level density parameter and pairing energy values were taken from Cameron (28).

In the cascade–evaporation calculation (29), the cascades resulting in ^{64}Cu with excitation energies below 10 MeV and in ^{65}Cu with excitation energies between 9.9 and 25 MeV were selected. These limits were based on neutron binding energies in ^{64}Cu and ^{65}Cu which are 7.9 and 9.9 MeV respectively. The lower limit of ^{64}Cu was set at 10 MeV to allow for some γ-competition in the first 2 MeV (approximately) above the threshold for neutron emission. Similarly 25 MeV was considered as the upper limit for ^{65}Cu in order to allow for neutron kinetic energy and for γ-competition.

Reflection and refraction were omitted in this calculation because recent findings by Chen *et al.* (29) show that much better agreement with experimental data was achieved at low (< 150 MeV) incident energies without refraction. We considered the formation of ^{64}Cu from ^{65}Cu only (the printed output did not include the ^{65}Zn residual nucleus). However, the evaporation calculation shows that only a small fraction ($\sim 10\%$) of ^{64}Cu at intermediate energy forms via the (P,N) cascades, followed by proton evaporation, since proton evaporation from the excited residual nucleus is suppressed by the Coulomb barrier. The ratio of ^{64}Cu formed by a knock-out mechanism to that formed by cascade–evaporation for 691 events is of the order of 0.61. The residual nucleus of the cascade step was taken as the starting nucleus for the evaporation calculation. Average values of *FW*, *BW*, and *PW* were calculated at 85 MeV, separately for the recoiling ^{64}Cu nuclide obtained as a product of the knock-out mechanism and the cascade–evaporation process. The *FW*, *BW*, and *PW* values (mg/cm^2) for ^{64}Cu formed by the knock-out mechanism are 0.0159, 0.0031, and 0.0163 and those formed by the cascade–evaporation process are 0.0278, 0.0021, and 0.0039; the averages of these two values being 0.0219, 0.0026, and 0.0101 respectively. Thus, it is apparent that the *FW* and *PW* values obtained by the cascade–evaporation process are higher than those obtained by the knock-out mechanism, since most of the kinetic energy is carried away by the promptly emitted particles in the latter process. The *BW* value obtained by the knock-out mechanism is, however, higher than that obtained by the cascade–evaporation process. This may be attributed to the forward scattering of the prompt particles in the knock-out phase.

The discrepancies between the calculations and experiments may be assigned to the neglect of: (*i*) the evaporation from the highly excited nuclei (higher than 25 MeV for excited ^{65}Cu nuclei), (*ii*) compound nucleus formation, (*iii*) proton evaporation from the excited ^{65}Zn nuclei, and (*iv*) the nucleon correlation (30) which may be sensitive to the recoil properties.

(f) Inelastic Scattering Model for Recoil Studies of Simple Reactions at Intermediate Energies

In order to interpret the recoil range results, a three-dimensional inelastic scattering model was developed (5, 31). In this semiclassical model, it is assumed that the incident proton interacts with a stationary target nucleon in the diffuse surface of the nucleus, thus resulting in the emission of either the incident or struck proton (inelastic scattering) or of the struck neutron (charge-exchange scattering). One of the collision partners is assumed to be captured, transferring its energy to the whole nucleus. The

[2]We are grateful to Dr. G. Friedlander who kindly performed the 85-MeV cascade calculations for us.

Can. J. Chem. Downloaded from www.nrcresearchpress.com by 210.87.254.40 on 09/05/12
For personal use only.

nucleus then recoils, due to the prompt emission process, and moves in a definite direction with velocity V_R. The residual nucleus with sufficient excitation energy evaporates a particle; the resulting nuclide then recoils with velocity V at a definite angle to the incident beam and has a definite range in a particular stopping medium. This idea of inelastic scattering through two-body collisions in the diffuse nuclear surface was first suggested by Eisberg and Igo (32) to interpret their (p,p′) data at 31 MeV and later confirmed by the calculation of Elton and Gomes (4). Saha and Porile (5) used a similar model for the calculation of isobaric ratios of simple reactions in the medium energy range.

The probability of emission of more than one particle in the initial cascade phase is small, since the mean free path is larger than the distance of traversal in the nuclear periphery. The probability of (P,N) and (P,P) cascades can be simply written as

$$[11] \qquad \sigma(\mathrm{P,N}) \propto \langle\sigma\rangle_{pn} N$$

$$[12] \qquad \sigma(\mathrm{P,P}) \propto \langle\sigma\rangle_{pp} Z + \langle\sigma\rangle_{pn} N$$

where N and Z are the numbers of neutrons and protons in the target nucleus; the quantities $\langle\sigma\rangle_{pn}$ and $\langle\sigma\rangle_{pp}$ are the effective nucleon–nucleon scattering cross sections (33) inside the nucleus which, in contrast to the free inter-nucleon collision cross sections σ_{pn} and σ_{pp}, take into account the momentum distribution of the bound nucleons and the operations of the exclusion principle. They are given by Winsberg and Clements (33) as:

$$[13] \qquad \langle\sigma\rangle_{pp} = \sigma_{pp}\left[1 - K_{pp}\frac{E_{Fp}}{E_p}\right]$$

and

$$[14] \qquad \langle\sigma\rangle_{pn} = \sigma_{pn}\left[1 - \frac{K_{pn}}{2E_p}(E_{Fp} + E_{Fn})\right]$$

where E_p is the incident energy inside the nucleus, E_{Fp} and E_{Fn} are the proton and neutron Fermi energies, and K_{pp} and K_{pn} are constants.

In the (P,P) or (P,N) cascade phase, enough energy is transferred to the residual nucleus to evaporate one more particle to give rise to the (p,pn) product. The evaporation probability from an excited residual nucleus left with a definite amount of excitation energy was calculated using an adaptation of the D.F.F. evaporation program (25).

The lower limit of the excitation energy of a residual nucleus for a desired product is determined by the binding energy of the evaporated particle or particles under consideration. The upper limit takes into account the binding and kinetic energies of the evaporated particle or particles under consideration along with the gamma ray energy during the de-excitation stage of the residual nucleus.

For equal mass particles, the non-relativistic formula (34) relating the energy of the incident proton E_p, captured nucleon E_C, and the center-of-mass scattering angle θ of the inelastically scattered particle, reduces to

$$[15] \qquad \cos\theta = \pm(1 - 2E_C/E_p)$$

The positive and negative signs refer to the case where either the struck nucleon or the incident proton is captured by the nucleus. The energy of the incident particle E_p inside the nuclear potential is the sum of the incident proton energy E_i, the proton separation energy S_p, and the Fermi energy E_F. Energy conservation then requires that the energy of the captured nucleon E_C inside the nucleus can be related to the excitation energy transferred to the nucleus, E^*, by $E_C = E^* + E_F'$, where E_F' is the Fermi energy of the captured nucleon.

Since a given amount of the excitation energy for a particular value of the incident energy corresponds to a definite scattering angle, the excitation energy interval required to evaporate a particular number of nucleons leads to a range of scattering angles. The fractions of the nucleon–nucleon cross sections are denoted by F_{pp} for p–p scattering, F_{pn} for p–n scattering with proton emission, and F_{np} for p–n scattering with neutron emission, and can be expressed as

$$[16] \qquad F_{pp} = 2\pi \int_{\theta_{min}}^{\theta_{max}} \left(\frac{d\sigma}{d\Omega}\right)_{pp} \cdot \sin\theta \cdot d\theta/\sigma_{pp}$$

and

$$[17] \qquad F_{pn} \text{ or } F_{np} = 2\pi \int_{\theta_{min}}^{\theta_{max}} \left(\frac{d\sigma}{d\Omega}\right)_{pn} \cdot \sin\theta \cdot d\theta/\sigma_{pn}$$

where σ corresponds to the free nucleon–nucleon scattering cross section and θ_{min} and θ_{max} are the angles corresponding to the minimum and maximum excitation energies of the residual nucleus leading to the particular product

Can. J. Chem. Downloaded from www.nrcresearchpress.com by 210.87.254.40 on 09/05/12
For personal use only.

under consideration. The scattering angle θ of the emitted particle is transformed into the laboratory angle θ_L. The recoil velocity V_R, along with the corresponding angle θ_R and hence its component V_Z in the direction of the beam, is calculated from the simple kinematic relations obtained from energy and momentum conservation as follows:

$$E_R = [E_p - E_e - 2(E_pE_e)^{1/2}\cos\theta_L]/A$$

$$V_R = (2E_R/A)^{1/2};\quad \theta_R = \sin^{-1}\left[\frac{\sin\theta_L V_e}{AV_R}\right]$$

[18]
$$V_Z = V_R\cos\theta_R$$
$$V_Y = V_R\sin\theta_R\sin\phi_R$$
$$V_X = V_R\sin\theta_R\cos\phi_R$$

where E_R and E_p are the energies of the recoil and the incident proton, E_e and V_e are the energy and velocity of the emitted particle, and A is the mass of the recoiling nucleus. θ_R and ϕ_R are the polar angles of the recoil.

The differential cross sections for p–p scattering are isotropic and σ_{pp} values were obtained from the differential cross-section values summarized by Hamada and Johnston (35). Values of σ_{pn} were derived by integrating the empirical equations of the differential cross sections for p–n scattering of Bertini (36). The Fermi energy was evaluated assuming $r_0 = 1.5$ fm. The proton binding energy was evaluated for the various target nuclei on the basis of the mass values of Myers and Swiatecki (37). Therefore, the total probability for (p,xn) and (p,pxn) reactions can be written as

[19] $$\sigma(p,xn) = \langle\sigma\rangle_{pn}F_{np}NF_{E(x-1)n}$$

[20] $$\sigma(p,pxn) = (\langle\sigma\rangle_{pp}F_{pp}Z + \langle\sigma\rangle_{pn}F_{pn}N) \times F_{Exn} + \langle\sigma\rangle_{pn}F_{np}NF_{Ep(x-1)n}$$

where $F_{E(x-1)n}$ and $F_{Ep(x-1)n}$ refer respectively to the evaporation probability of $(x-1)$ neutrons and of one proton plus $(x-1)$ neutrons following a (P,N) cascade, while F_{Exn} refers to that of x neutrons following a (P,P) cascade. The second term in [20] referring to prompt neutron emission followed by a proton evaporation from the excited nucleus was neglected, as its contribution is comparatively small.

In the actual calculation, the whole excitation energy of the excited residual nucleus (10–25 MeV for ^{65}Cu and 10–21 MeV for ^{197}Au) was divided into smaller subintervals of 2 MeV and θ_{min} and θ_{max} were calculated for each subinterval. The center-of-mass scattering angles were transformed into the corresponding laboratory angles. The average value of the angle was considered as the angle of the scattered particle for the average excitation energy for a particular subinterval. The recoil angle ϕ_R with respect to the x-axis was chosen randomly, i.e. assuming that there is no angular correlation about the axis defined by the proton beam. The only kinematic restriction comes from the incident and deposition energy. The components of the recoil velocity, along with the average energy in each subinterval, were then used for the modified D.F.F. evaporation program (25) to calculate the average range values as described previously. The average values of the ranges projected in the forward, backward, and perpendicular directions were calculated for each excitation energy subinterval and the average range values were then obtained by addition at each incident energy.

(g) Comparison with the Inelastic Scattering Model Calculations

The calculated quantities FW and PW in the energy range $\sim$ 40–85 MeV are lower than the experimental results by a factor of 5, for both the recoiling nuclides as shown in Figs. 7 and 8. The calculation did not give a statistically meaningful number of events for the backward recoils even with 2000 cascades; therefore, the calculated BW values are not shown in any figure. The following trends of the calculated average range values were observed: (*i*) the calculated FW values decrease very slightly with the incident energy, (*ii*) the PW values increase very slightly with the proton energy, (*iii*) the calculated values of the ratios as seen in Fig. 9 give reasonable agreement with experiments above 50 MeV. This is because of the cancellation of the common factors causing the discrepancies. The calculated ratio at 85 MeV for the ^{65}Cu-(p,pn)^{64}Cu reaction is in agreement with the Monte Carlo cascade evaporation calculation, and (*iv*) the calculated quantities FW_{Cu}/FW_{Au} and PW_{Cu}/PW_{Au} are nearly constant and higher than the corresponding experimental values by a factor of about 1.4.

An approximate value of the percentage contributions from the compound nucleus and the direct interaction mechanisms to the average projected range FW at a definite incident energy

Can. J. Chem. Downloaded from www.nrcresearchpress.com by 210.87.254.40 on 09/05/12
For personal use only.

was calculated from the following equation and shown in Table II

$$[21] \qquad X \cdot R_{CN} + Y \cdot R_{DI} = FW$$

where X and Y are the contributions of the compound nucleus and direct interaction mechanisms and R_{CN} and R_{DI} are the extrapolated range values calculated with the Monte Carlo evaporation program (for ^{64}Cu) or calculated FW value (for ^{196}Au) and the inelastic scattering model calculations respectively. The contribution of the direct interaction mechanism is higher at higher energies, as expected. The discrepancies between the calculations and experiments may be assigned to the same factors as discussed in detail in the previous section.

The different analyses of the average range results show that the (p,pn) reactions studied by us proceed by the compound nucleus mechanism up to 30–35 MeV and the direct interaction becomes more and more prominent at higher energies, with strong competition at the intermediate energy region. This is further confirmed by angular distribution measurements (22).

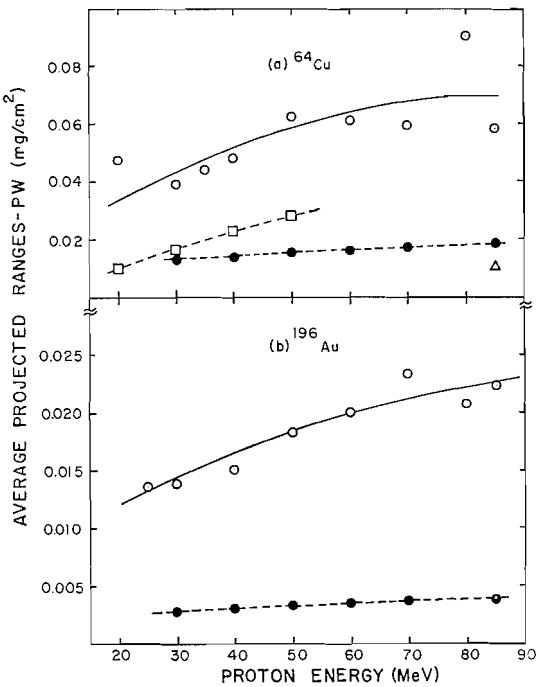

FIG. 8. Comparison of experimental and calculated PW values of (*a*) ^{64}Cu and (*b*) ^{196}Au; ⊙ experimental, □ statistical theory, △ cascade-evaporation theory (85 MeV only), and ● ISE model calculations.

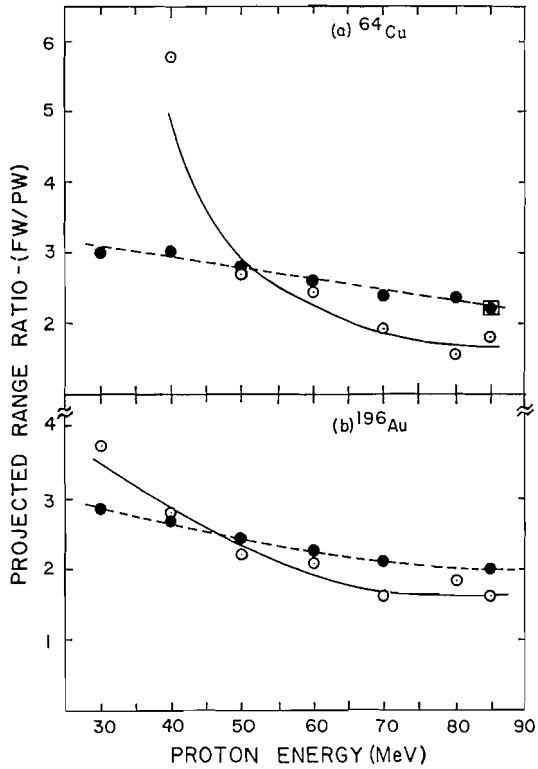

FIG. 9. Comparison of experimental and calculated FW/PW ratios of (*a*) ^{64}Cu and (*b*) ^{196}Au; ⊙ experimental value, ● ISE model calculation, and □ cascade-evaporation calculation at 85 MeV only.

Acknowledgments

The authors wish to thank Professor R. E. Bell, Director, Foster Radiation Laboratory, for his ready permission to use the McGill synchrocyclotron and Mr. R. H. Mills who cheerfully performed the irradiations. Our thanks go to Professor N. T. Porile, presently at the Department of Chemistry, Purdue University, for initially suggesting the problem during his stay at McGill University.

One of us (M. K. D.) wishes to express his gratitude to the Department of Chemistry, McGill University, for teaching assistantships from 1963–1965, and to the National Research Council of Canada for studentships from 1965–1967.

1. L. WINSBERG. University of California Radiation Laboratory Report, UCRL-8618. 1959.
2. N. SUGARMAN, H. MUNZEL, J. A. PANONTIN, K. WIELGOZ, M. V. RAMANIAH, G. LANGE, and E. L. MENCHERO. Phys. Rev. **143**, 952 (1966).

3. J. R. GROVER and A. A. CARETTO, JR. Ann. Rev. Nucl. Sci. **14**, 51 (1960).
4. L. R. B. ELTON and L. C. GOMES. Phys. Rev. **105**, 1027 (1957).
5. G. B. SAHA and N. T. PORILE. Phys. Rev. **146**, 687 (1966).
6. K. A. KRAUS and G. E. MOORE. J. Am. Chem. Soc. **75**, 1460 (1953).
7. F. J. WELCHER. The analytical uses of ethylenediamine tetraacetic acid. D. Van Nostrand Co., Inc., Princeton, New York. Reprinted 1958. p. 241.
8. J. F. EMERY and G. W. LEDDICOTTE. The radiochemistry of gold. Nucl. Sci. Ser. NAS-NS 3036. 1961.
9. E. B. SANDELL. Colorimetric determination of traces of metals. 3rd ed. (revised). Interscience Publishers Inc., New York. 1959.
10. J. B. CUMMING. Application of computers to nuclear and radiochemistry. Nat. Acad. Sci. Nat. Res. Council. Nucl. Sci. Ser., NAS-NS-3107. p. 25.
11. J. A. PANONTIN and N. SUGARMAN. J. Inorg. Nucl. Chem. **25**, 1321 (1963).
12. N. T. PORILE. Phys. Rev. **135**, A1115 (1964).
13. A. EWART, C. VALENTINE, and M. BLANN. Nucl. Phys. **69**, 625 (1965).
14. R. W. HAMMING. Numerical methods for scientists and engineers. McGraw-Hill Book Co., Inc., New York. 1962. p. 81.
15. E. R. MERZ and A. A. CARETTO, JR. Phys. Rev. **126**, 1173 (1962).
16. S. C. FUNG and I. PERLMAN. Phys. Rev. **87**, 623 (1952).
17. L. WINSBERG and J. M. ALEXANDER. Phys. Rev. **121**, 518 (1961).
18. L. WINSBERG and J. M. ALEXANDER. Phys. Rev. **121**, 529 (1961).
19. N. T. PORILE, A. M. POSKANZER, and M. RHO. Phys. Rev. **128**, 242 (1962).
20. H. E. SCHIOTT. Report Det. Fysiske Institut, Aarhus University. 1967. Unpublished.
21. N. T. PORILE. Phys. Rev. **120**, 572 (1960).
22. M. K. DEWANJEE, G. B. SAHA, and L. YAFFE. Can. J. Chem. In press.
23. A. M. POSKANZER, J. B. CUMMING, and R. WOLFGANG. Phys. Rev. **129**, 374 (1963).
24. V. F. WEISSKOPF. Phys. Rev. **52**, 295 (1937).
25. I. DOSTROVSKY, Z. FRAENKEL, and G. FRIEDLANDER. Phys. Rev. **116**, 683 (1959).
26. G. B. SAHA and N. T. PORILE. Phys. Rev. **149**, 880 (1966).
27. J. LINDHARD, M. SCHARFF, and H. E. SCHIOTT. Kgl. Danske Videnskab. Selskab Mat.-Fys. Medd. **33**, 14 (1963).
28. A. G. W. CAMERON. Can. J. Phys. **36**, 1040 (1958).
29. K. CHEN, Z. FRAENKEL, G. FRIEDLANDER, J. R. GROVER, J. M. MILLER, and Y. SHIMAMOTO. Phys. Rev. **166**, 949 (1968).
30. P. DENISOV, V. P. MILOVANOV, R. A. LATIPOVA, and P. A. CERENKOV. J. Nucl. Phys. USSR, **2**, 1042 (1965).
31. M. K. DEWANJEE. Ph.D. Thesis. McGill University, Montreal, Quebec. 1967.
32. R. M. EISBERG and G. IGO. Phys. Rev. **93**, 1039 (1954).
33. L. WINSBERG and T. P. CLEMENTS. Phys. Rev. **122**, 1623 (1961).
34. R. D. EVANS. The atomic nucleus. McGraw-Hill Book Co., Inc., New York. 1955. p. 835.
35. T. HAMADA and I. D. JOHNSTON. Nucl. Phys. **34**, 382 (1962).
36. H. W. BERTINI. Oak Ridge National Laboratory Report, ORNL-3383, 1963. Phys. Rev. **131**, 1801 (1963).
37. W. D. MYERS and W. J. SWIATECKI. University of California Radiation Laboratory Report, UCRL-11980. 1965. Unpublished.

Can. J. Chem. Downloaded from www.nrcresearchpress.com by 210.87.254.40 on 09/05/12
For personal use only.

Can. J. Chem. Downloaded from www.nrcresearchpress.com by 210.87.254.105 on 09/05/12
For personal use only.

(p,n) and (p,pxn) reactions in ^{127}I[1]

V. P. NARANG[2] AND L. YAFFE
Radiochemistry Laboratory, Department of Chemistry, McGill University, Montreal, Quebec

Received March 14, 1968

Absolute values of the cross sections of (p,n), (p,pn), (p,p2n), and (p,p3n) reactions in ^{127}I have been measured by radiochemical methods for incident proton of energies up to 80 MeV. The initial portion of the excitation function for the (p,n) reaction is characteristic of the compound nucleus mechanism, but evidence for direct interaction is present at higher energies. Above 50 MeV, cross sections are close to the predictions of Monte Carlo calculations based on the cascade-evaporation model. This is particularly true in the case of the (p,pn) and (p,p2n) reactions.

Canadian Journal of Chemistry, 46, 3171 (1968)

Introduction

Nuclear reactions, induced by medium energy protons, have been the subject of considerable investigation in recent years. Reactions of the type (p,p*x*n), in general, involve inelastic scattering of the incident proton, and are inhibited by the Coulomb barrier, in both the entrance and exit channels. It has been established (1, 2) that the compound nucleus process alone cannot explain the inelastic scattering of medium energy protons. Eisberg and Igo (1) found that, for 31-MeV protons incident on heavy nuclei, inelastic scattering accounts for about 15% of the total reaction cross section. Furthermore, the energy and the angular distribution spectra of the scattered protons have many of the characteristics of the direct interaction process. A surface interaction mechanism has also been proposed (3, 4) to interpret the results of medium energy proton interactions.

The present experiment constitutes a study of the formation cross sections of the nuclides produced when ^{127}I is bombarded with protons up to 80-MeV energy.

Ladenbauer (5), Dropesky (6), and Kuznetsova *et al.* (7) reported cross sections for these reactions at energies higher than 100 MeV. Very little information is available, however, about (p,*x*n) and (p,p*x*n) reactions of iodine below the 100-MeV range.

Values of the formation cross sections of ^{127}Xe, ^{126}I, ^{125}I, ^{124}I, and ^{123}I were determined. The results were compared with Monte Carlo calculations (8–10).

[1]This project received financial assistance from the National Research Council of Canada.

[2]Present address: International Atomic Energy Agency, Kaerntnerring 11, Vienna 1010, Austria.

Experimental Procedure

Target Assembly

A weighed amount (10–15 mg) of CuI was placed in a thin-walled aluminium tube and both ends were sealed under hydraulic pressure. Cuprous iodide was selected as a target because: (*a*) The monitor reactions employed in this work were $^{63}Cu(p,n)^{63}Zn$ and $^{65}Cu(p,pn)^{64}Cu$. Thus there is a stoichiometric distribution of the monitor inside the target. (*b*) The decomposition temperature of CuI (> 1200 °C) is high enough to ensure stability under the conditions of local heating likely to be encountered during the irradiations.

"Spec-pure" CuI (Johnson, Mathey, and Mallory) was used in this work. The level of impurities was less than 1 p.p.m. and calculations showed that none would interfere to an appreciable extent.

Irradiations

The target was mounted on the water-cooled probe of the McGill synchrocyclotron and irradiations of 10–30 min duration were made with the internal circulating beam. A calibration curve for the radial distance vs. proton beam energy, duly corrected for radial oscillations by Kirkaldy (11), was used.

Energy degradation of the proton beam by the target container, calculated on the basis of range-energy values of Sternheimer (12), was found to be less than 0.6 MeV, well within the energy spread (±2 MeV) of the proton beam.

Beam Monitoring

Cross-section values obtained by Ghoshal (13) for the reaction $^{63}Cu(p,n)^{63}Zn$ were used to monitor the beam for protons of energies below 12 MeV. Above 12 MeV cross-section values of the monitor reaction $^{65}Cu(p,pn)^{64}Cu$, as obtained by Meghir (14), were used. Cross-section values used are given in Table I.

Chemical Separations

(1) Xenon

The extraction assembly is shown in Fig. 1.

The cuprous iodide target in the aluminium tubing was introduced into a 25-ml flask (B-14) along with a few pellets of sodium hydroxide and a teflon-coated magnetic stirrer bar, and the system was evacuated to less than a micron. About 2 cc (at room temperature and pressure) of inactive xenon and 5 to 7 ml of H_2O were introduced into the flask and the stirrer turned on. The sodium

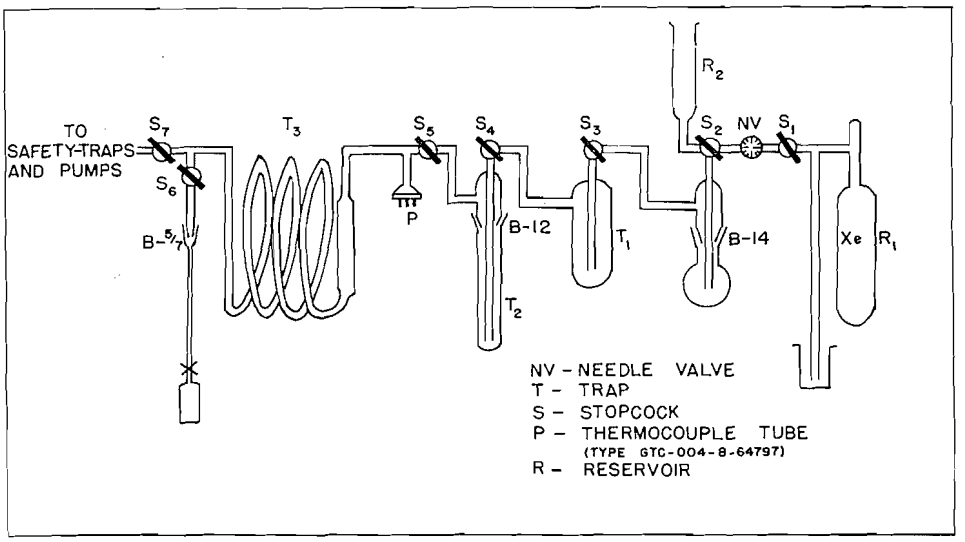

FIG. 1. Xenon purification apparatus.

hydroxide dissolved the aluminium tubing and reacted with the cuprous iodide to release the active xenon. The flask was cooled by an ice-bath during the dissolution process.

TABLE I

Cross-section values used for monitor reactions

Proton beam energy (MeV)	$^{63}Cu(p,n)^{63}Zn$* (mb)	$^{65}Cu(p,pn)^{64}Cu$† (mb)
7	200	—
11	490	—
16	—	100
21	—	360
27	—	340
35	—	290
42	—	260
49	—	230
56	—	210
63	—	190
70	—	160
80	—	140

*Reference 13.
†Reference 14.

The mixture of Xe, H_2, and water vapor was transferred into trap T_1 which contained stainless steel balls (for more effective heat transfer), and which was kept at dry ice – acetone temperature.

The mixture of Xe and H_2 was then transferred to T_3, a five-turn thin-walled trap, kept at liquid nitrogen temperature, which removed the xenon. The hydrogen was pumped out from T_3, and xenon distilled into a 2-ml pyrex glass ampul specially designed for this work.

(2) Copper

After the xenon was separated from B-14, 10 mg of Zn^{2+} carrier were added. The copper oxide was centrifuged, and was dissolved in a minimum amount of hydrochloric acid and Cu^{2+} was finally separated by ion exchange separation (15).

(3) Iodine

The filtrate from the centrifugation of copper oxide was made acidic (pH 4 to 5). The aluminium (from the target container) was precipitated as hydroxide with ammonia, and iodine was separated by solvent extraction as described by Glendenin and Metcalf (16).

(4) Zinc

After Xe, Cu, I, and Al were separated the solution contained activity attributable only to ^{63}Zn, and the activity of this was measured.

Chemical Yield Determinations

The extraction yield of xenon was taken to be 100% for the reasons: (*a*) The vapor pressure for xenon (17) at liquid nitrogen temperature is only a few microns. (*b*) The diffusion of xenon through the walls of the aluminium tubing is negligible (18, 19). (*c*) In a cross check experiment copper iodide was bombarded in a sealed quartz tube and the cross sections measured agreed within the experimental error with bombardments performed in aluminium tubing.

Standard colorimetric methods were employed for the determination of the chemical yields of Cu (20) and I (21).

The chemical yield of Zn was obtained by direct titration with ethylenediamine tetraacetic acid, using Erichrome black T indicator (22).

Radiation Detection and Measurements

Gamma radiation was measured by a 3 in. × 3 in. NaI (Tl) crystal while a thinner crystal (1 in. × 1/8 in.) was used for X-rays.

The output of the scintillation counters was fed into a 100-channel pulse-height analyzer. The energy scale was calibrated with standard γ-ray and X-ray sources. In the case of ^{126}I, the half-life was also measured with a $4\pi\beta$-proportional counter.

Can. J. Chem. Downloaded from www.nrcresearchpress.com by 210.87.254.105 on 09/05/12
For personal use only.

TABLE II

Absolute cross sections for $^{127}I(p,n)^{127}Xe$ and $^{127}I(p,pxn)$ reactions

Proton energy (MeV)	σ (mb) $^{127}I(p,n)Xe^{127}$	σ (mb) $^{127}I(p,pn)^{126}I$	σ (mb) $^{127}I(p,p2n)^{125}I$	σ (mb) $^{127}I(p,p3n)^{124}I$	σ (mb) $^{127}I(p,p4n)^{123}I$
7	17±3				
11	240±50				
16	420±80				
21	24±5	40±8			
27	6±1	42±8	8±2		
35	5±1	60±12	24±5		
42	9±2	91±18	67±13	6±1	
49	8±2	96±19	72±14	27±5	14±3*
56	10±2	83±17	97±19		180±36*
63	5±1	110±22	87±17	49±10	230±47*
70			66±13	42±8	190±38*
80		52±10	47±10	24±5	130±26*
45†	8±2				

*These are not absolute values.
†This bombardment was done with the target in a quartz tube to check possible xenon losses.

Results

(p,n) Cross Sections

The absolute disintegration rates of ^{127}Xe were determined from the total photo-peak counting rates of the 377-keV gamma ray. A branching ratio of 21% was used (23) and the conversion coefficient ($\alpha_T = 0.014$) was computed from the tables of Sliv and Band (24).

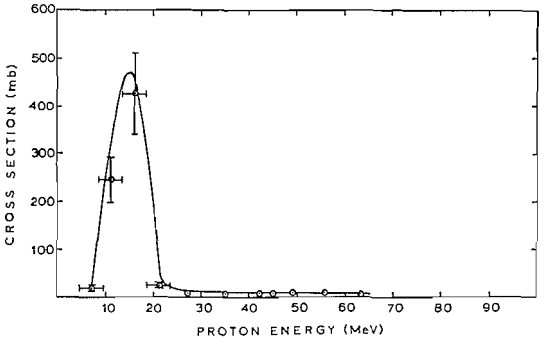

FIG. 2. Excitation function for the reaction $^{127}I(p,n)^{127}Xe$.

Decay curves were followed for about 4 months. The half-life obtained was 36.8 ± 1.4 days, which is in good agreement with that of 36.405 days obtained by Andersson *et al.* (25). The cross sections are listed in Table II and the excitation function of the reaction is shown in Fig. 2.

(p,pn) Cross Sections

The half-life as well as the cross sections of ^{126}I were determined by following the decay of the 386-keV gamma ray (branching ratio of 34% (23) and a computed conversion coefficient (24) of 0.018).

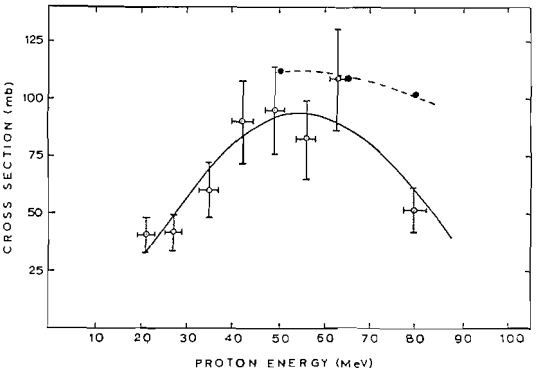

FIG. 3. Excitation function for the reaction $^{127}I(p,pn)^{126}I$; ○ experimental, ● calculated.

The cross sections are shown in Table II and the excitation function is shown in Fig. 3.

(p,p2n) and (p,p3n) Cross Sections

The product nuclei, ^{125}I, and ^{124}I both decay by orbital electron capture. The half-lives as well as cross sections were determined by following the decay of the K X-ray photo peak. In addition to ^{125}I and ^{124}I, ^{126}I and ^{123}I also give K X-rays. Fortunately, the half-lives are widely spaced and the composite decay curves were easily resolved. For disintegration rate calculations, the K-fluorescence yield of 0.88, as obtained by Broyles *et al.* (26), was used.

Can. J. Chem. Downloaded from www.nrcresearchpress.com by 210.87.254.105 on 09/05/12
For personal use only.

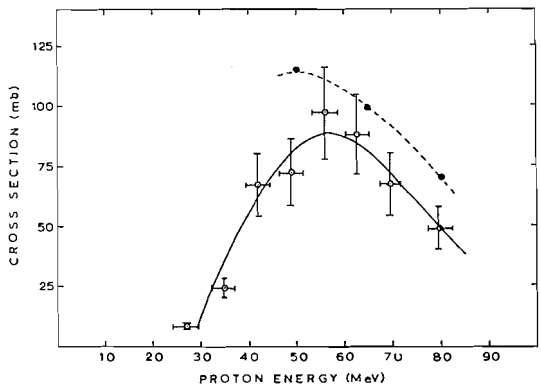

FIG. 4. Excitation function for the reaction ^{127}I-(p,p2n)^{125}I; ○ experimental, ● calculated.

The half-life of ^{125}I obtained in this work, followed over three half-lives was 59.0 ± 2.1 days, agreeing well with the value of 60.25 ± 0.06 days found by Leutz and Ziegler (27). The half-life found for ^{124}I, obtained from the composite K X-ray curves, was 4.34 ± 0.03 days and agreed well with that found by Andersson *et al.* (25), 4.15 days, but not with the value of 3.4 days found by Aagaard *et al.* (28). The excitation functions of (p,p2n) and (p,p3n) reactions are shown in Figs. 4 and 5 respectively and the cross sections are listed in Table II.

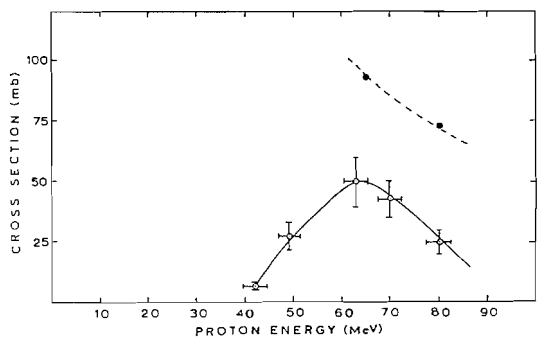

FIG. 5. Excitation function for the reaction ^{127}I-(p,p3n)^{124}I; ○ experimental, ● calculated.

The contribution due to the decay of ^{125}Xe to ^{125}I was considered insignificant, since the time for separating xenon from the reaction products was very small (~ 20 min) from the end of bombardments in comparison with the half-life of ^{125}Xe (18 h).

(p,p4n) Cross Sections

For the cross-section calculations and half-life determination of ^{123}I, the 159-keV gamma ray (branching ratio 99%) that follows the electron capture was used. The half-life, over a period of five half-lives, was 13.7 ± 0.3 h, in good agreement with that of 13.3 h obtained by Andersson *et al.* (25). The cross sections are shown in Table II and plotted in Fig. 6. These values are not absolute, since no correction was made for the contribution to the ^{123}I disintegration rate by the decay of ^{123}Xe.

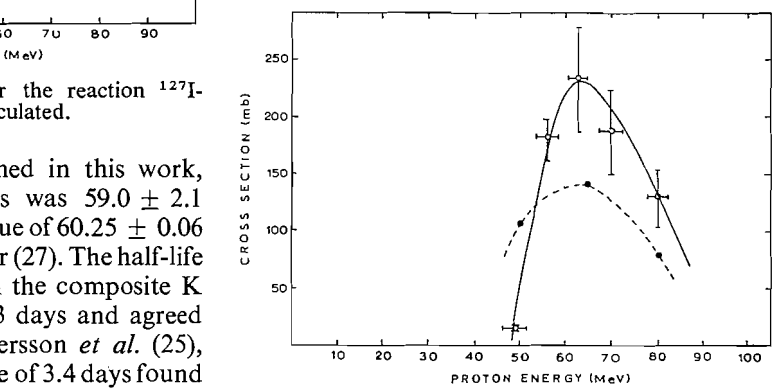

FIG. 6. Excitation function for the reaction ^{127}I-(p,p4n)^{123}I; ○ experimental, ● calculated.

Discussion

(a) (p,n) Cross Sections

The excitation function of the (p,n) reaction (Fig. 2) shows a peak at 15 ± 2 MeV and tails off at 21 MeV to almost a constant value of about 8 mb. The value of 15 ± 2 MeV is well within the range predicted by Jackson (29) on the statistical model calculations. The shape of the excitation function for this reaction at low energies is typical of those nuclear reactions proceeding through a compound nucleus reaction mechanism (30), but some evidence for direct interaction is apparent at higher energies.

(b) (p,pxn) Cross Sections

Examination of the excitation functions of (p,pxn) reactions, where x = 1 to 4 (Figs. 3–6) shows that with increasing proton bombarding energies the cross-section values decrease as x increases, with the exception of the ^{127}I(p,p4n)^{123}I reaction. In this case, the correction for the growth of ^{123}I from the decay of ^{123}Xe (1.85 h) during the interval from the end of bombardment to the time of separation of xenon fraction (~ 20 min) could not be made due to the fact

Can. J. Chem. Downloaded from www.nrcresearchpress.com by 210.87.254.105 on 09/05/12
For personal use only.

Can. J. Chem. Downloaded from www.nrcresearchpress.com by 210.87.254.105 on 09/05/12
For personal use only.

that the required data for ^{123}Xe were not available. Thus, this accounts for the apparently higher yields of ^{123}I.

Eisberg and Igo (1) observed that there are signs of the direct interaction mechanism when 31-MeV protons are incident on heavy nuclei. Monte Carlo calculations[3] were performed based on the cascade–evaporation model (31, 32). Full details of these calculations are given elsewhere (10, 33). A total of 5000 incident protons were studied in both the cascade and evaporation calculations. The geometrical cross section of ^{127}I was taken to be 1955 mb, while the maximum radius value was taken as 7.89 fm. A level density formulation was calculated from the electron-scattering data of Hofstader (34). The momentum distribution for the entire nucleus was taken as a Maxwell–Boltzmann distribution with $kT = 15$ MeV. The full curves in Figs. 3 to 6 represent the observed excitation functions and the dotted curves are those obtained by Monte Carlo calculations above 50 MeV.

The behavior of these excitation functions is in accordance with the cascade–evaporation model based on statistical theory. Since (p,p*x*n) reactions, which involve inelastic scattering of the incident protons, are inhibited by the Coulomb barrier in both the entrance and exit channels, then on the basis of statistical theory such reactions in general are expected to have much smaller cross sections than (p,*x*n) reactions. We observed that (p,n) reaction cross sections are higher than (p,pn) cross sections by a factor of about 4, while on the basis of the same theory this factor should be much larger. A similar discrepancy was noticed by Kavanagh and Bell (35) in ^{197}Au(p,p*x*n) reactions. To account for the larger values, it was argued that it is presumably due to the inelastic scattering of protons and thus can be interpreted in terms of nucleon–nucleon collision in the diffuse surface region of the target nucleus (3). Statistical calculations made by Metropolis *et al.* (8), Bernadini *et al.* (9), and Jackson (29) were on the basis of a well-defined nuclear boundary. It is surprising to note that the computations in this work, based on a non-uniform density distribution, agree with experimental observation.

In the light of surface interactions, after making corrections for the threshold, it was observed that, as the incident energy of the protons increases, the ratio between the (p,pn) and (p,p3n) cross sections also increases. Similar conclusions are evident from the data of Ladenbauer (5), Kuznetsova *et al.* (7), and Fink and Wiig (36).

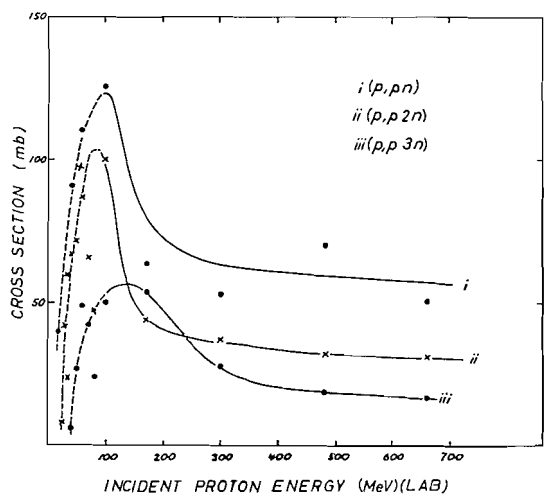

FIG. 7. Excitation functions for (p,pn), (p,p2n), and (p,p3n) reactions; dash line is from present work, solid line is from ref. 7.

In Fig. 7 the results of the (p,pn), (p,p2n), and (p,p3n) reactions are plotted along with those of Kuznetsova *et al.* (7) at higher energies. The dotted parts in the excitation functions are from the present work while the solid lines are those of Kuznetsova *et al.* Very good agreement with their results is clearly evident.

1. R. M. EISBERG and G. IGO. Phys. Rev. **93**, 1039 (1954).
2. B. L. COHEN. Phys. Rev. **105**, 1549 (1957).
3. R. J. GRIFFITHS and R. M. EISBERG. Nucl. Phys. **12**, 225 (1959).
4. R. M. EISBERG. Proceedings of the International Conference on Nuclear Structure. Kingston, Canada. *Edited by* D. A. Bromley and E. W. Vogt. Univ. of Toronto Press, Toronto. 1960.
5. I. M. LADENBAUER. UCRL-8200. Radiation Laboratory, University of California, Berkeley, California. 1958.
6. B. DROPESKY. Ph.D. Thesis. University of Rochester, Rochester, New York. 1953.
7. M. YA. KUZNETSOVA, V. N. MERKHEDOV, and V. A. KHALKIN. Soviet Physics JETP English Transl. **34** 7, 759 (1958).
8. N. METROPOLIS, S. BIVINS, M. STORM, J. M. MILLER, G. FRIEDLANDER, and A. TURKEVICH. Phys. Rev. **110**, 185, 204 (1958).
9. G. BERNADINI, E. T. BOOTH, and S. J. LINDENBAUM. Phys. Rev. **85**, 826 (1952); **88**, 1017 (1952).

[3]The authors are very grateful to Dr. H. W. Bertini of Oak Ridge National Laboratory, Oak Ridge, Tennessee, for performing these calculations for us.

10. H. W. BERTINI. ORNL-3383, ORNL-3433. Oak Ridge National Laboratory, Oak Ridge, Tennessee.
11. J. S. KIRKALDY. Ph.D. Thesis. McGill University, Montreal, Quebec. 1953.
12. R. M. STERNHEIMER. Phys. Rev. **117**, 137 (1959).
13. S. N. GHOSHAL. Phys. Rev. **80**, 939 (1950).
14. S. MEGHIR. Ph.D. Thesis. McGill University, Montreal, Quebec. 1962.
15. K. A. KRAUS and F. NELSON. Proc. Intern. Conf. Peaceful Uses Atomic Energy. Geneva, 1959. Vol. 7. pp. 113–125.
16. L. E. GLENDENIN and R. D. METCALF. Radiochemical studies: The fission products. Book II. *Editors*. C. D. Coryell and N. Sugarman. McGraw-Hill Book Co., Inc., New York. 1951. Paper 278. p. 1625.
17. D. R. STULL. Vapour pressure of pure substances. The Dow Chemical Co., Midland, Michigan. 1947.
18. Y. ADDA, G. BREBAC, and V. LEVY. Rev. Met. Paris, **58**, 743 (1961).
19. D. J. NEIL. Physics Division, Aluminum Laboratories Ltd., Kingston, Canada. Private communication.
20. C. J. RODDEN. Analytical chemistry of the Manhattan project. McGraw-Hill Book Co., Inc., New York. 1950.
21. A. G. COLLINS and J. W. WATKINS. Anal. Chem. **31**, 1182 (1959).
22. F. J. WELCHER. The analytical uses of ethylenediaminetetraacetic acid. D. Van Nostrand Co., Inc., New York. 1958.
23. Nuclear Data Sheets. National Academy of Sciences, National Research Council, Washington, D.C.
24. L. A. SLIV and I. M. BAND. Coefficients of internal conversion of gamma radiation. Part I and Part II. Academy of Sciences, USSR 1958.
25. G. ANDERSSON, G. RUDSTAM, and G. SORENSEN. Arkiv Fysik, **28**, 27 (1965).
26. C. D. BROYLES, D. A. THOMAS, and S. K. HAYNES. Phys. Rev. **89**, 715 (1953).
27. H. LEUTZ and K. ZIEGLER. Nucl. Phys. **50**, 648 (1964).
28. P. AAGAARD, G. ANDERSSON, J. O. BURGMAN, and A. C. PAPPAS. J. Inorg. Nucl. Chem. **5**, 105 (1957).
29. J. D. JACKSON. Can. J. Phys. **34**, 767 (1956).
30. N. BOHR. Nature, **137**, 344 (1936).
31. R. SERBER. Phys. Rev. **72**, 114 (1947).
32. M. L. GOLDBERGER. Phys. Rev. **74**, 1268 (1948).
33. H. W. BERTINI. Phys. Rev. **131**, 1801 (1963).
34. R. HOFSTADER. Rev. Mod. Phys. **28**, 214 (1956).
35. T. M. KAVANAGH and R. E. BELL. Can. J. Phys. **39**, 1172 (1961).
36. R. W. FINK and E. O. WIIG. Phys. Rev. **96**, 185 (1954).

Can. J. Chem. Downloaded from www.nrcresearchpress.com by 210.87.254.105 on 09/05/12
For personal use only.

Can. J. Chem. Downloaded from www.nrcresearchpress.com by 210.87.254.40 on 09/05/12
For personal use only.

Spectrofluorometric studies. III. Ortho- and para-difluorobenzene

J. L. DURHAM[1], G. P. SEMELUK, AND I. UNGER
Department of Chemistry, University of New Brunswick, Fredericton, New Brunswick

Received February 8, 1968

Spectrofluorometric techniques have been used to determine gas phase singlet and triplet yields in ortho- and para-difluorobenzene as a function of exciting wavelength and pressure. The importance of the "around the corner effect" in such measurements as the cause of large errors is briefly discussed.

In the case of ortho-difluorobenzene, maxima in fluorescent yield are produced by the exciting wavelengths 2490, 2580, and 2700 Å; minima at 2540 and 2660 Å. Triplet yields, using the sensitized biacetyl emission technique, have been determined at 2500, 2580, 2660, and 2700 Å. The sums of the singlet and triplet yields at these wavelengths are 0.34, 0.52, 0.75, and 0.97 respectively.

Para-difluorobenzene has the largest quantum yield of fluorescence of any fluorinated benzene yet examined. The fluorescent yield shows only one definite minimum at 2740 Å. Triplet yields have been determined at 2660, 2740, and 2760 Å. The sums of the singlet and triplet yields at these wavelengths are 0.5, 0.5, and 0.7 respectively.

Canadian Journal of Chemistry, 46, 3177 (1968)

Introduction

In recent years, phototransposition reactions of ring carbon atoms and photoinduced valence isomerizations in substituted benzenes have been receiving a good deal of attention. Since, in general, the yields of such reactions appear to be quite low, a systematic approach to these investigations seems justified. One such approach is implied by the suggestion (1 and references therein; 2[2]) that there might be a connection between quantum deficit—the difference between unity and the sum of the singlet and triplet yields $(1 - [\phi_S + \phi_T])$—and these photoisomerizations. Thus, such studies might well begin with an examination of the variation of fluorescent and triplet yields with wavelength, pressure, and other significant variables. Of the two quantities in the quantum deficit expression, the fluorescent (singlet) yield ϕ_S is usually the easier to determine.

There are a variety of ways of detecting triplet states and estimating quantum yields of triplet formation for molecules whose triplet states do not exhibit any phosphorescence in the gas phase (3). We have been using a combination of two techniques, the sensitized emission technique (4) and the olefin isomerization technique developed by Cundall and co-workers (5) and by Tanaka and his associates (6), to detect the triplet states of fluorinated benzenes in the gas phase. To avoid the difficulties associated with the measurement of absolute emission quantum yields (7), we have based our quantum yields on the quantum yield of a "standard" molecule, benzene, which we use to "calibrate" the measuring system. The method, whose details have been described previously (8), becomes particularly convenient when used in conjunction with commercially available spectrophotofluorometers, as we have shown in our investigation of the photochemistry of meta-difluorobenzene (2). It can, however, lead to serious errors for molecules having large extinction coefficients even for the relatively short 1 cm absorption path provided in the commercial instruments. The error due to this "around the corner effect" (9) results from the fact that as the pressure of the gas under study is increased, proportionately more absorption, and also emission, occur closer and closer to the front window of the cell, while the emission is being viewed from a relatively narrow region in the center of the cell. The occurrence of this effect in solution, and the manner of compensating for it, have been discussed by Hercules (10). In the present study we have found the "around the corner effect" to be relatively unimportant for ortho-difluorobenzene (*o*-DFB) (and in the previous study (2) on meta-difluorobenzene) but very pronounced for para-difluorobenzene (*p*-DFB). A short analysis of this technique of using benzene fluorescent yield to calibrate the spectrophotofluorometer will allow evaluation of the method.

For benzene at a concentration C_B in a cell of 1 cm path length with the emission monochromator observing the central 0.1 cm (that is, from 0.45 to 0.55 cm from the entrance window), we have for the fluorescent intensity of benzene

$$F_B = (I_{ab})_B \Phi_B K_{inst}$$

[1]Holder of an NRCC Scholarship 1967–68.
[2]Reference 2 is Part I of "Spectrofluorometric Studies."

Can. J. Chem. Downloaded from www.nrcresearchpress.com by 210.87.254.40 on 09/05/12
For personal use only.

Using the fluorescent yield of benzene, Φ_B (11, 12) from the literature, F_B measured in arbitrary units, and absorbed intensity $(I_{ab})_B$ determined experimentally, it is possible to obtain the instrument constant K_{inst}. $(I_{ab})_B$ is customarily obtained from the difference $I_0 - I$ where I_0 is the intensity incident on the front "face" of the vapor, and I the intensity leaving the back "face". This is of course non-rigorous, and should be

$$(I_{ab})_B = I_0(e^{-0.45\varepsilon_B C_B} - e^{-0.55\varepsilon_B C_B})$$

where ε_B is the extinction coefficient of benzene at the wavelength of irradiation, and 0.45 and 0.55 are the "emission coordinates" in cm. However, direct comparison of the unknown with benzene may cancel out the resulting error.

A comparison of the two methods gives:

(a) When I_{ab} is obtained by difference we get

$$K_{inst} = \frac{F_B}{\Phi_B(I_{ab})_B} = \frac{F_B}{\Phi_B(I_0 - I)} = \frac{F_B}{\Phi_B I_0(1 - e^{-\varepsilon_B C_B})}$$

For the unknown difluorobenzene we have

$$F_D = (I_{ab})_D \Phi_D K_{inst}$$

or

$$\Phi_D = \frac{F_D}{(I_{ab})_D K_{inst}}$$

Assuming that the K_{inst} are the same in both cases (they will have some dependence on polarization effects of the materials in the cell) we obtain

$$(\Phi_D)_a = \Phi_B \frac{F_D}{F_B} \frac{(I_0)_B}{(I_0)_D} \frac{(1 - e^{-\varepsilon_B C_B})}{(1 - e^{-\varepsilon_D C_D})}$$

(b) When I_{ab} is obtained from the rigorous method we obtain

$$(\Phi_D)_b = \Phi_B \frac{F_D}{F_B} \frac{(I_0)_B}{(I_0)_D} \frac{(e^{-0.45\varepsilon_B C_B} - e^{-0.55\varepsilon_B C_B})}{(e^{-0.45\varepsilon_D C_D} - e^{-0.55\varepsilon_D C_D})}$$

A direct comparison then gives

$$\frac{(\Phi_D)_a}{(\Phi_D)_b} = \frac{(1 - e^{\varepsilon_B C_B})}{(1 - e^{\varepsilon_D C_D})} \cdot \frac{(e^{-0.45\varepsilon_D C_D} - e^{-0.55\varepsilon_D C_D})}{(e^{-0.45\varepsilon_B C_B} - e^{-0.55\varepsilon_B C_B})}$$

or

$$\frac{(\Phi_D)_a}{(\Phi_D)_b} = \frac{(1 - 10^{-a_B C_B})}{(1 - 10^{-a_D C_D})} \times \frac{(10^{-0.45 a_D C_D} - 10^{-0.55 a_D C_D})}{(10^{-0.45 a_B C_B} - 10^{-0.55 a_B C_B})}$$

It is obvious that if $a_B C_B \simeq a_D C_D$, then both methods of calculation will give the same result. However, if this approximate equality is not maintained, it is possible that the values may be very different. Generally speaking, there is a greater spread of "a" values than of "C" values, so the major influence in the present experiments will be due to the extinction coefficient differences.

As examples of the magnitude of errors which could result from an undiscriminating use of $I_0 - I$ at a typical benzene concentration of 10^{-3} mole l^{-1} (approximately 18 Torr at room temperature) and $a_B = 40$ l mole^{-1} cm^{-1}, the error will be only -4% when $a_B C_B = a_D C_D/10$, but will become -91% when $a_B C_B = a_D C_D/100$.

In the case of p-DFB, $a_D \simeq 10^3$, and when $C_D = 10^{-3}$ mole l^{-1}, the error would be -21%. Thus it is clear that for p-DFB, the absorbed intensity must be calculated from

$$I_{ab} = I_0(10^{-0.45aC} - 10^{-0.55aC})$$

Finally, since it is unlikely that Beer's law would be obeyed over any appreciable pressure range, extinction coefficients must be calculated separately for each pressure used.

The calculation of biacetyl-sensitized emission yields involves the consideration of an additional complication—whether a significant proportion of biacetyl triplets diffuse out of the viewing zone of the emission monochromator before emitting. An evaluation of this factor leads to the conclusion that under our experimental conditions this "broadening" of the emitting zone does not lead to a significant error.

We present here the variation of singlet and triplet yields for ortho- and para-difluorobenzene with exciting wavelength, over a range extending from 2340 Å to 2820 Å.

Experimental

Ortho- and para-difluorobenzene were obtained from the Aldrich Chemical Company and purified by preparative vapor phase chromatography. Fluorescence studies were carried out in a mercury and grease-free system, equipped with Hoke packless diaphragm metal valves. The sensitized emission studies with *o*-DFB were done in a system containing high vacuum (lightly greased) stopcocks and a mercury manometer; mixing was accomplished by flash vaporization. In the case of *p*-DFB, the triplet measurements were made in a grease-free and mercury-free high vacuum system completely equipped with Hoke packless diaphragm metal valves, with mixing effected by an all-glass pump which circulated the vapors through a flow-through cell. Adequate mixing was indicated by constant absorption and emission. Absorption was con-

TABLE I

Fluorescent yield dependence on wavelength and pressure of *o*-difluorobenzene and biacetyl

Exciting wavelength (Å)	Pressure (Torr) BiA	Pressure (Torr) *o*-DFB	Equation
2420	0	5–47	$\Phi_f = 0.035 \pm 0.005$
2460	0	5–47	$\Phi_f = 0.111 \pm 0.008$
2500	0	5–45	$1/\Phi_f = 6.80 + 3.03 \times 10^3$[*o*-DFB]*
2500	0.15–32	30	$1/\Phi_f = 7.95 + 3.43 \times 10^3$[BiA]*
2540	0	6–48	$1/\phi_f = 8.21 + 86.7$[*o*-DFB]
2580	0	5–48	$1/\phi_f = 2.90 + 1.50 \times 10^3$[*o*-DFB]
2580	0.14–30	30	$1/\phi_f = 3.34 + 1.39 \times 10^3$[BiA]
2620	0	5–48	$1/\phi_f = 3.65 + 0.718 \times 10^3$[*o*-DFB]
2660	0	5–48	No simple relation
2660	0.09–40	30	$1/\phi_f = 16.7 + 15.7 \times 10^3$[BiA]
2700	0	6–48	$1/\phi_f = 3.40 + 1.10 \times 10^3$[*o*-DFB]
2700	0.10–30	30	$1/\phi_f = 5.40 + 4.61 \times 10^3$[BiA]
2740	0	5–48	No simple relation

*[BiA] and [*o*-DFB] represent the concentration of biacetyl and *o*-difluorobenzene respectively, in moles per liter.

tinuously monitored as a check on lamp stability, since a large part of the errors result from intensity variations which take place during a sequence of emission scanning measurements. All other apparatus, materials, and procedures have been described previously (2). The reported quantum yields are based on the singlet and triplet yields of benzene (11, 12).

Results and Discussion

The results obtained in this study are summarized as much as possible in the form of equations which appear in Tables I, II, and III. Some of the results which could not be so reduced are given in Tables IV and V. Figure 1 gives the variation of the fluorescent yield with exciting wavelength for *o*-DFB at a few of the pressures investigated. Figure 2 illustrates the fluorescent yield of *p*-DFB at a pressure of 48 Torr, as a function of exciting wavelength. This figure also indicates the magnitude of the error, both quantitative and qualitative, which can result from the "around the corner effect". An error from this same cause at high pressures is also shown at 2660 Å in Fig. 1.

Ortho-difluorobenzene

o-DFB exhibits fluorescent emission only when excited by radiation of 2420 to 2740 Å. As shown in Fig. 1, maxima occur near 2490, 2580, and 2700 Å, a shallow minimum at 2540 Å, and a pronounced minimum at 2660 Å. The fluorescent yield is pressure independent from 2420 to about 2500 Å, but strongly pressure dependent from 2500 Å upwards. The fluorescent emission is not quenched by *cis*-butene-2. However, it is self-quenched when the exciting wavelength is greater then 2500 Å, and it is strongly quenched by biacetyl (BiA). Table I summarizes these observations, except in a few cases, in the form of Stern–Volmer relations which give good representations of the data.

TABLE II

Sensitized emission yield dependence on wavelength and pressure of *o*-difluorobenzene and biacetyl

Exciting wavelength (Å)	Pressure (Torr) *o*-DFB	Pressure (Torr) BiA	Equation
2500	30	0.15–32	$1/\phi_p = 4.29 + (4.79 \times 10^{-4}/[\text{BiA}]) \pm 6.8\%$, max. 18.9%
2500	4–48	10	$\phi_p = 0.0733 + 86.9$[*o*-DFB] $\pm 4.3\%$, max. 11%
2580	30	0.15–30	$1/\phi_p = 3.03 + (4.06 \times 10^{-4}/[\text{BiA}]) \pm 7.7\%$, max. 13.8%
2580	6–48	10	$\phi_p = 0.261 + 9.54$[*o*-DFB] $\pm 5.3\%$, max. 7.3%
2660	30	0.4–40	$1/\phi_p = 4.08 + (1.89 \times 10^{-4}/[\text{BiA}]) \pm 7.7\%$, max. 18%
2660	5–48	10	No simple relation
2700	30	0.10–30	$1/\phi_p = 3.17 + (2.38 \times 10^{-4}/[\text{BiA}]) \pm 12\%$, max. 21%
2700	4.8–48	10	$\phi_p = 0.189 + 50.0$[*o*-DFB] $\pm 7.6\%$, max. 21%

Can. J. Chem. Downloaded from www.nrcresearchpress.com by 210.87.254.40 on 09/05/12
For personal use only.

TABLE III

Fluorescent yield dependence on wavelength and pressure of *p*-difluorobenzene and biacetyl

Exciting wavelength (Å)	Pressure (Torr) BiA	Pressure (Torr) *p*-DFB	Equation
2340	0	5–48	$\Phi_f = 0.09 \pm 0.01$
2380	0	5–47	$\phi_f = 0.101 + 21.2[p\text{-DFB}]$*
2420	0	5–47	$\phi_f = 0.151 + 20.0[p\text{-DFB}]$
2460	0	5–48	$\phi_f = 0.21 \pm 0.01$
2500	0	5–48	$\phi_f = 0.220 + 6.85[p\text{-DFB}]$
2540	0	5–48	$1/\phi_f = 3.34 + 0.202 \times 10^3[p\text{-DFB}]$
2580	0	5–47	$1/\phi_f = 2.02 + 0.858 \times 10^3[p\text{-DFB}]$
2620	0	5–47	$1/\phi_f = 1.88 + 0.797 \times 10^3[p\text{-DFB}]$
2660	0	5–47	$1/\phi_f = 2.28 + 0.568 \times 10^3[p\text{-DFB}]$
2660	10	4–43	$1/\phi_f = 3.51 + 1.37 \times 10^3[p\text{-DFB}]$
2700	0	5–48	$1/\phi_f = 2.04 + 0.636 \times 10^3[p\text{-DFB}]$
2740	0	5–48	$1/\phi_f = 1.84 + 1.06 \times 10^3[p\text{-DFB}]$
2740	10	3–42	$1/\phi_f = 3.52 + 1.58 \times 10^3[p\text{-DFB}]$
2760	0	5–48	$1/\phi_f = 2.03 + 0.351 \times 10^3[p\text{-DFB}]$
2760	10	5–48	$1/\phi_f = 2.87 + 0.778 \times 10^3[p\text{-DFB}]$
2780	0	5–48	$1/\phi_f = 1.96 + 0.239 \times 10^3[p\text{-DFB}]$
2820	0	5–48	$1/\phi_f = 1.20 + 0.525 \times 10^3[p\text{-DFB}]$

*[*p*-DFB] represents the concentration of *p*-difluorobenzene in moles per liter.

The excitation of *o*-DFB in the presence of BiA, at the wavelengths producing the three maxima and the deep minimum in the fluorescent yield, results in a pronounced sensitized emission from BiA which is strongly quenched by *cis*-butene-2. This observation, combined with the fact that *cis*-butene-2 does not quench fluorescent emission of *o*-DFB nor the emission of BiA excited directly, is good evidence that the sensitized emission is due to energy transfer from a triplet state of *o*-DFB to BiA (2, 8). Table II summarizes the results of these sensitized emission yields in the form of linear equations and also gives an indication of the precision with which each equation reproduces the actual observations. Of particular interest in this respect is the equation obtained at an excitation wavelength of 2700 Å and at a constant pressure of 30 Torr *o*-DFB. This equation is the result of combining two sets of data obtained on different days, and therefore reflects, in addition to the usual uncertainties, the errors due to a change in lamp intensity and those associated with reproducing the wavelength setting on the excitation monochromator. In general, the fluorescent yield measurements would be expected to be more reliable than the triplet yield determinations.

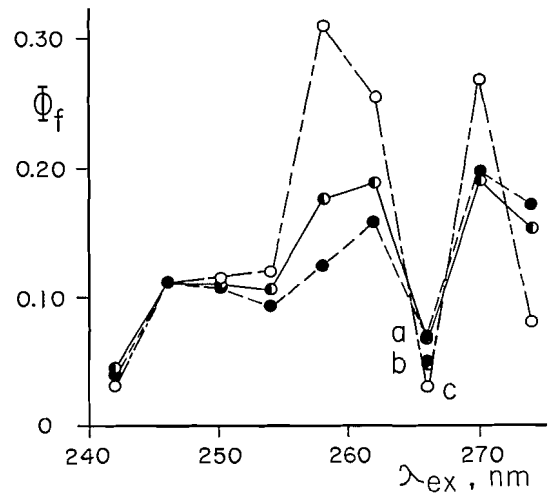

FIG. 1. Variation of fluorescent quantum yield as a function of exciting wavelength, at (○) 5 Torr, (◐) 31 Torr, and (●) 48 Torr of *o*-DFB. For these two points (*a*) Beer's law was used to calculate the absorbed intensity at the cell center. For these two points (*b*) absorbed intensity was taken as the total light absorbed. Both methods yield point (*c*).

Para-difluorobenzene

When *p*-DFB is excited by radiation between 2380 and 2780 Å it fluoresces very strongly, with a quantum yield larger than that for any fluorinated benzene yet examined. The fluorescence is quenched by BiA as well as being self-quenched. It is, however, unaffected by the presence of *cis*-butene-2. Stern–Volmer relations adequately describe most of the results as is noted in Table III. An examination of Fig. 2 shows that the variation of fluorescent yield with exciting wavelength for

Can. J. Chem. Downloaded from www.nrcresearchpress.com by 210.87.254.40 on 09/05/12
For personal use only.

TABLE IV

Comparison of sensitized emission yield obtained by consideration of total light absorbed and of light absorbed only in the center of the cell (excitation wavelength: 2660 Å)

Φ_t calculated from:				
Total absorbance	Absorbance at center of cell using Beer's law	Pressure (Torr) *p*-DFB	Pressure (Torr) BiA	Molar absorptivity (1000 cm²/mole)
0.02	0.03	30.4	0.59	1078
0.12	0.22	"	1.31	1087
0.06	0.11	"	2.84	1083
0.05	0.08	"	4.86	1086
0.03	0.06	"	7.86	1094
0.05	0.10	"	16.9	1079
0.06	0.10	"	21.5	1079
0.06	0.11	"	31.7	1000
0.15	0.16	3.7	10.0	1789
0.11	0.11	7.3	"	1534
0.02	0.02	11.3	"	1230
0.02	0.02	15.3	"	1201
0.08	0.12	25.3	"	1132
0.05	0.10	35.4	"	1028
0.03	0.08	43.4	"	985

this molecule is quite different from that for meta-difluorobenzene and ortho-difluorobenzene: only at 2740 Å is there a minimum which persists over the pressure range investigated. This behavior is contrary to the predictions of a Hückel molecular orbital calculation (2) which indicates that there are no large differences in the excited states of these molecules.

Table IV compares the triplet yields at 2660 Å in various partial pressures of *p*-DFB and BiA, calculated in the two ways discussed above. The

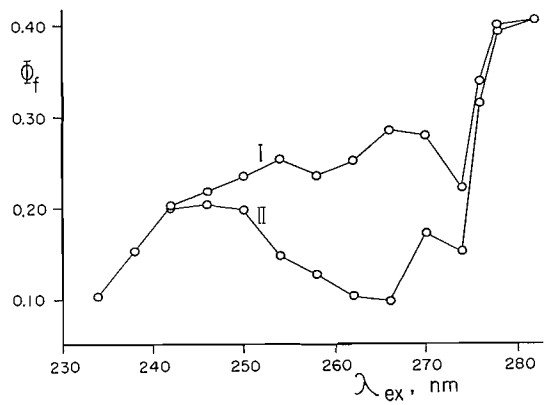

FIG. 2. Variation of fluorescent quantum yield as a function of exciting wavelength. *p*-DFB pressure = 48 Torr. Curve I: absorbance at center of cell used to calculate Φ_f. Curve II: total absorbance used to calculate Φ_f.

TABLE V

Sensitized emission yield dependence on wavelength and pressure of *p*-difluorobenzene and biacetyl

Exciting wavelength (Å)	Pressure (Torr) *p*-DFB	Pressure (Torr) BiA	Yield
	30.2	0.62	0.02
	"	1.32	0.10
	"	2.86	0.09
	"	4.87	0.11
	"	7.85	0.14
	"	16.7	0.13
2740	"	20.7	0.13
	"	30.8	0.17
	3.5	9.65	0.21
	7.3	"	0.21
	11.1	"	0.19
	15.1	"	0.19
	25.2	"	0.16
	34.7	"	0.17
	42.1	"	0.17
	29.5	1.30	0.05
	"	1.98	0.10
	"	3.41	0.08
	"	5.37	0.15
	"	8.35	0.11
	"	17.1	0.15
	"	21.1	0.16
	"	31.0	0.25
2760	5.0	9.72	0.24
	10.2	"	0.21
	15.5	"	0.20
	20.4	"	0.23
	30.0	"	0.18
	39.7	"	0.19
	47.6	"	0.18

Can. J. Chem. Downloaded from www.nrcresearchpress.com by 210.87.254.40 on 09/05/12
For personal use only.

calculations show variation from good agreement to disagreement by a factor of two. In addition this table, as well as Table V, provides a summary of the sensitized emission (triplet) yield results which were obtained in this investigation. They, too, indicate that *p*-DFB behaves differently from the other two isomers. No simple relation could be found which would adequately represent these data, in contrast to the *o*-DFB case. The fluctuations, as pressure of either *p*-DFB or BiA is increased, appear to be real, since the measurements were made with handling procedures and apparatus considerably improved over those used in the *o*-DFB study. We have no explanation for this behavior and prefer to reserve judgment until a study using much narrower bandwidth of exciting radiation is completed.

Summary

Using triplet yields which had been corrected for biacetyl quenching of the fluorescent (singlet) yields, quantum deficits were determined for both molecules at various wavelengths. These are listed in Table VI. The deficit is largest at the shorter wavelengths in both cases.

An indication of unusual behavior at 2660 Å is provided by the erratic dependence on pressure of both fluorescent yield and triplet yield for *o*-DFB, and of triplet yield in the case of *p*-DFB, suggesting that the behavior of these molecules on excitation with radiation wavelengths in this region should be subjected to closer scrutiny.

TABLE VI

Quantum yield deficits for *o*-DFB and *p*-DFB

Exciting wavelength (Å)	Molecule	Quantum deficit $1 - (\phi_S + \phi_T)$
2500	*o*-DFB	0.66
2580	"	0.48
2660	"	0.25
2660	*p*-DFB	0.5
2700	*o*-DFB	0.03
2740	*p*-DFB	0.5
2760	"	0.3

Acknowledgments

The authors gratefully acknowledge a grant from the Associated Alumni of the University of New Brunswick towards the purchase of the instrumentation used in this study, and other financial assistance from the National Research Council of Canada. We wish to thank Mrs. M. MacBeath for assisting in collecting some of the data.

1. K. E. WILZBACH, J. S. RITSCHER, and L. KAPLAN. J. Am. Chem. Soc. **89**, 1031 (1967).
2. F. W. AYER, F. GREIN, G. P. SEMELUK, and I. UNGER. Ber. Bunsenges. Physik. Chem. **72**, 283 (1968).
3. W. A. NOYES, JR. and I. UNGER. Advan. Photochem. **4**, 49 (1966).
4. H. ISHIKAWA and W. A. NOYES, JR. J. Chem. Phys. **37**, 583 (1962).
5. R. B. CUNDALL, F. J. FLETCHER, and D. G. MILNE. Trans. Faraday Soc. **60**, 1146 (1964).
6. M. TANAKA, T. TERAO, and S. SATO. Bull. Chem. Soc. Japan, **38**, 1945 (1965).
7. G. M. ALMY and B. R. GILLETTE. J. Chem. Phys. **11**, 188 (1943).
8. I. UNGER. J. Phys. Chem. **69**, 4284 (1965).
9. W. A. NOYES, JR. and C. S. BURTON. Ber. Bunsenges. Physik. Chem. **72**, 146 (1968).
10. D. M. HERCULES. Anal. Chem. **38**, 29A (1966).
11. W. A. NOYES, JR., W. A. MULAC, and D. A. HARTER. J. Chem. Phys. **44**, 2100 (1966).
12. W. A. NOYES, JR. and D. A. HARTER. J. Chem. Phys. **46**, 674 (1967).

Can. J. Chem. Downloaded from www.nrcresearchpress.com by 210.87.254.40 on 09/05/12
For personal use only.

Can. J. Chem. Downloaded from www.nrcresearchpress.com by 210.87.254.5 on 09/05/12
For personal use only.

Preferential solvation of Co^{2+} and Ni^{2+} ions in mixed solvents: n.m.r. methods[1]

L. S. FRANKEL AND T. R. STENGLE
Department of Chemistry, University of Massachusetts, Amherst, Massachusetts, 01002

AND

C. H. LANGFORD[2]
Moore Laboratory of Chemistry, Amherst College, Amherst, Massachusetts, 01002

Received April 2, 1968

A method for the study of preferential solvation in the outer coordination spheres from paramagnetic broadening of solvent proton n.m.r. signals was proposed by Frankel, Stengle, and Langford. It is now extended to determinations of the relative concentrations of water and dioxane, dimethylformamide, or dimethylsulfoxide in the inner coordination spheres of Co^{2+} and Ni^{2+} ions in the binary solvent mixtures. The assumptions of the analysis are cross-checked by a new method based on the contact shifts experienced by protons on solvent molecules in the coordination spheres of paramagnetic ions. The second method depends upon assumptions independent of the first. Three cases are presented as tests of these n.m.r. approaches. It is clear that highly precise solvation sphere populations will be difficult to obtain but that useful and significant information can be obtained in situations to which alternative methods are almost totally inapplicable.

The results indicate that dimethylsulfoxide and dimethylformamide are good competitors for coordination sites but that dioxane is excluded by water.

Canadian Journal of Chemistry, 46, 3183 (1968)

Introduction

Frankel, Stengle, and Langford (1) proposed a method for finding the *fraction* of the solvation shell of a paramagnetic solute occupied by a given solvent in a mixed solvent solution. It is based on the broadening of a nuclear magnetic resonance (n.m.r.) proton signal resulting from contact with a paramagnetic species. In the case that exchange between sites in the paramagnetic environment (solvation shell) is rapid, the observed n.m.r. line width is governed by McConnell's equation (2):

$$[1] \qquad \frac{1}{T_2} = \frac{P_A}{T_{2A}} + \frac{P_M}{T_{2M}}$$

where T_2 is the observed transverse relaxation time (equal to π times the width at half height of the n.m.r. absorption line), P_A is the probability that a proton is in the diamagnetic environment (bulk solution), P_M is the probability that a proton is in the paramagnetic environment (solvation shell), and T_{2A} and T_{2M} are the transverse relaxation times in the diamagnetic and paramagnetic environments respectively. In the case that exchange is slower, $1/T_2$, the observed relaxation time, may be controlled by the average lifetime τ_M of a solvent molecule in the solvation shell. Then, an analog of eq. [1] may apply in which T_{2M} is replaced by τ_M. (For a discussion of the range of validity of these simple equations see Stengle and Langford (3) or Swift and Connick (4).) The equation becomes:

$$[2] \qquad \frac{1}{T_2} = \frac{P_A}{T_{2A}} + \frac{P_M}{\tau_M}$$

(In other circumstances, proportionality to P_M remains (3, 4).) We define $\Delta\nu$, the excess line width of the nuclear magnetic resonance absorption band, by eq. [3].

$$[3] \qquad \pi\Delta\nu = \frac{1}{T_2} - \frac{P_A}{T_{2A}} = \frac{P_M}{T_{2M}}$$

$1/T_{2A}$ may be measured in the absence of paramagnetic ions (4), and in any dilute solution of paramagnetic ions $P_M \ll P_A$ so that P_A is approximately one. Equation [3] becomes:

$$[4] \qquad \pi\Delta\nu = \frac{1}{T_2} - \frac{1}{T_{2A}} = \frac{P_M}{T_{2M}}$$

Now, consider values of $\Delta\nu$ obtained for protons on water molecules when a paramagnetic ion, e.g. Co^{2+}, is dissolved in a mixture of water and N,N-dimethylformamide (DMF). Let $\Delta\nu_0$ be the excess broadening in pure water solutions

[1]Taken in part from the Ph.D. thesis of L. S. Frankel, University of Massachusetts, Amherst, Massachusetts, 1966.

[2]Present address: Department of Chemistry, Carleton University, Ottawa 1, Canada.

Can. J. Chem. Downloaded from www.nrcresearchpress.com by 210.87.254.5 on 09/05/12
For personal use only.

and $\Delta\nu$ be the excess broadening of water protons produced by Co^{2+} ions in water–DMF mixtures. From eq. [4],

$$[5] \qquad \frac{\Delta\nu}{\Delta\nu_0} = \frac{P_M}{P_{M_0}} \cdot \frac{T_{2M_0}}{T_{2M}}$$

where the subscript 0 designates the quantities for solution in pure water. If $T_{2M_0} = T_{2M}$, i.e. if the mixing of the solvents does not seriously affect the relaxation time in the paramagnetic environment, $\Delta\nu/\Delta\nu_0$ measures P_M/P_{M_0}, the relative probability of a water molecule occupying a site in the solvation sphere of Co^{2+}. Coupled with appropriate information about the probability of finding a water molecule in the *bulk* (diamagnetic) environment (simply the bulk composition of any solution dilute with respect to Co^{2+}), it reveals the number of water molecules in the Co^{2+} solvation shell in the mixed solvent *relative* to the number present in solution in pure water.

The crucial assumption, $T_{2M} = T_{2M_0}$, is plausible but by no means secure. It will certainly fail in some circumstances. If enough is known of relevant relaxation mechanisms, appropriate account can be taken of the variation of T_{2M}, but the method will finally remain inapplicable to some systems. Fortunately, two cross checks are available. The first is not based on truly independent assumptions; the second is so based. First we may derive values of P_M/P_{M_0} for the same system from measurements of the broadening of the proton signals from the second component of the solvent. (P_{M_0} now refers to the probability of DMF occupying a solvation sphere site on Co^{2+} in pure DMF and P_M the corresponding probability in the mixed solvent.) Since most mechanisms (3) for modification of T_{2M} would shift both solvents in the same direction, a failure of the key assumption would lead to an inconsistent value of the *total* solvation shell population. Second, we may derive values of P_M/P_{M_0} from measurements of the contact shift experienced by solvent protons upon coordination to a paramagnetic ion (5). Analysis of the n.m.r. resonance frequency proceeds on entirely fresh assumptions.

Let $\Delta\omega_P$ be the resonance frequency observed for a nucleus in a solution containing paramagnetic ions (e.g. Co^{2+}) minus the resonance frequency for the same nucleus in the absence of such ions. Then we may write the simple equation:

$$[6] \qquad \Delta\omega_P = -P_M\Delta\omega_M$$

under the particular restrictions on the values of lifetimes and relaxation times of nuclei in the paramagnetic environment similar to those on eq. [1] and discussed in ref. 3. In eq. [6], $\Delta\omega_M$ is the shift of the resonance frequency between the diamagnetic and paramagnetic environments. Using the subscript 0 as before:

$$[7] \qquad \frac{\Delta\omega_P}{\Delta\omega_{P_0}} = \frac{P_M\Delta\omega_M}{P_{M_0}\Delta\omega_{M_0}}$$

If it may be assumed that $\Delta\omega_M < \Delta\omega_{M_0}$, P_M/P_{M_0} is again determined. Two corrections must always be made. $\Delta\omega_M$ is the difference between the resonance frequency of a nucleus in a molecule coordinated in the solvent and in the same molecule free in the solvent. The second term of this difference will vary with bulk magnetic

TABLE I

Data for determination of preferential solvation of Co^{2+} in water–DMF mixtures (concentration of Co^{2+} = 0.090 *M*)

Mole fraction water	μ_{eff}	H_2O		DMF	
		$\Delta\omega_P$ (Hz)	$\Delta\nu$ (Hz)	$\Delta\omega_P$ (Hz)	$\Delta\nu$ (Hz)
1.000	4.9	40	5.0		
0.910	4.9	53	6.8	45	2.8
0.814	5.0	67	8.7	55	3.4
0.709	5.0	87	11.3	64	4.4
0.609	5.0	111	13.4	74	4.8
0.529	5.0	137	16.6	82	5.5
0.409	5.1	169	23.5	92	6.4
0.320	5.1	217	31.2	101	7.6
0.214	5.1	291	43.7	118	9.1
0.134	5.2	349	70	126	11.3
0.040	5.2			142	13.3
0.000	5.2			156	16.8

Can. J. Chem. Downloaded from www.nrcresearchpress.com by 210.87.254.5 on 09/05/12
For personal use only.

susceptibility of the solution and mixture composition (especially if there are changes in solvent–solvent interactions such as hydrogen bonding). The corrections are easily made from data on chemical shifts in the absence of paramagnetic ions and the use of an internal non-coordinating standard. The crucial assumption of this method is no more secure than the crucial assumption of the line-broadening method, but it is *independent*. If results of both approaches are in agreement, the applicability of both approaches is supported.

Experimental

Materials

The metal complexes $Ni(OH_2)_6(ClO_4)_2$ and $Co(OH_2)_6(ClO_4)_2$ were obtained from G. Frederick Smith Chemical Co. $Co(DMF)_6(ClO_4)_2$ was prepared by Babiec's method (6). Solutions were prepared from distilled water of "conductance" quality, Fisher "certified reagent" *p*-dioxane and DMF, and dimethylsulfoxide (DMSO) purified by fractional distillation under reduced pressure (7).

Preparation of Solutions

A weighed sample of an appropriate metal complex was placed in a volumetric flask and a known volume of each solvent required for the mixture was added from a buret. The low molar volume of water required a 5 ml buret which could be read to 0.002 ml.

N.M.R. Measurements

Proton relaxation times were measured by observing the width at half height of the pure absorption mode signal on a Varian A-60 or Varian DP-60 nuclear magnetic resonance spectrometer. The former instrument was operated at 60.0 MHz and the latter at 56.4 MHz. Chemical shifts were determined from the same spectra. The quantity $\Delta\omega_P$ of eq. [6] was taken to be the chemical shift of the proton signal in a solution containing the paramagnetic solute from the position of resonance in the same solvent mixture lacking paramagnetic solute. It was *corrected* for changes in the bulk magnetic susceptibility by the following procedure. A water–dioxane solution was prepared with a sufficiently small dioxane concentration to assure that water occupied all coordination sphere sites about a known concentration of paramagnetic ion. The *dioxane* chemical shift in this solution was compared with that in the same solvent mixture without paramagnetic solute. This shift was identified as the bulk susceptibility correction. Similar measurements in the other solvents revealed that this shift was a function of solvent composition only in the case of Co^{2+} in DMF–water mixtures. The bulk susceptibility corrections found were proportional to the known magnetic moments of the ions as expected (8, 9). All measurements were made at the ambient probe temperature of the spectrometer (39°).

Results

In the introduction, we illustrated the theory with the example of the Co^{2+} ion in water–DMF solvent mixtures. We shall present a fairly detailed exposition of the results for this system (in which the greatest complications arise). The other two simpler systems may then be conveniently summarized.

Table I lists values of $\Delta\omega_P$ and $\Delta\nu$ for protons of water and DMF in solutions 0.090 *M* in Co^{2+} as a function of the water mole fraction. From the values of $\Delta\omega_P$ and $\Delta\nu$, values of P_M/P_{M_0} may be calculated for both water and DMF. P_M is simply nC_M/N (where n is the number of solvation shell sites occupied by the solvent under observation, C_M is the concentration of paramagnetic ions expressed in moles contained in the final sample volume, and N is the number of moles of solvent under observation in the bulk), if $nC_M \ll N$. Values of $\Delta\nu/\Delta\nu_0$ or $\Delta\omega_P/\Delta\omega_{P_0}$ normalized to the same C_M correspond to $(n/n_0)(N_0/N)$. Figure 1 shows a plot of n/n_0 as a function of the mole fraction of water. The curve rising from left to right is based on studies of the DMF formyl proton. The curve falling from left to right is based on studies of the water protons.

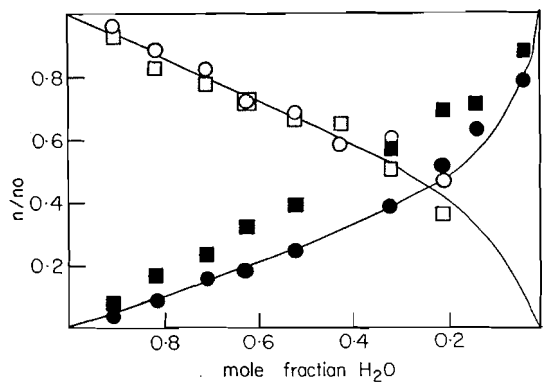

FIG. 1. The preferential solvation curve of Co^{2+} in aqueous DMF solutions. $[Co^{2+}] = 0.0896\ M$. Open circles, water relaxation time; open squares, water contact shift; solid circles, DMF formyl proton relaxation time; solid squares, DMF formyl proton contact shift.

It was found that the bulk susceptibility correction determined in chemical shift studies on $Co(OH_2)_6^{2+}$ and $Co(DMF)_6^{2+}$ differed slightly. The calculated effective magnetic moment (8) changes from 4.9 bohr magnetons in water to 5.2 bohr magnetons in DMF. Since the effective magnetic moment enters to the first power in the equation governing $\Delta\omega_P$ (5) and squared in the equation governing T_{2M} if the electron nuclear coupling is dipolar (5) (as in the Co^{2+} case, ref. 9),

TABLE II

Line width values for determination of preferential solvation

	A. 0.087 *M* Co^{2+} in water–dioxane mixtures							
Mole fraction H_2O	1.000	0.950	0.876	0.785	0.568	0.453	0.344	0.199
Line width (Hz)	4.9	6.0	7.7	11.9	24.9	33.0	49.3	90.
	B. 0.050 *M* Ni^{2+} in water–DMSO mixtures							
Mole fraction H_2O	1.000	0.903	0.799	0.786	0.765	0.735	0.710	0.682
Line width (Hz)	11.4	15.8	21.9	21.5	21.4	22.1	23.0	24.8
Mole fraction H_2O	0.632	0.585	0.546	0.502	0.379			
Line width (Hz)	25.0	25.8	24.5	24.5	24.8			

the experimental values of $\Delta\omega$ and $\Delta\nu$ were corrected for variations of magnetic moment before n/n_0 values were calculated. Here a failure of the simple assumptions has arisen in a way that can be taken into account. Of course, it is very helpful that the required corrections are small.

Table II contains values of $\Delta\nu$ for solutions of Co^{2+} in dioxane–water mixtures and for Ni^{2+} solutions in DMSO–water mixtures. The corresponding $\Delta\omega$ values are collected in Table III. Figure 3 shows plots of n/n_0 for Ni^{2+} in DMSO–water. We have chosen to show a plot of $\Delta\nu$ and $\Delta\omega$ for Co^{2+} in dioxane–water. Detailed analysis of this case reveals complete preference for water up to the solubility limit (as we have reported in a preliminary fashion with respect to Mn^{2+} in dioxane–water (10)). The curves in Fig. 2 show the characteristic feature of strong preferential solvation. $\Delta\nu$ and $\Delta\omega$ rise as the bulk concentration of water falls.

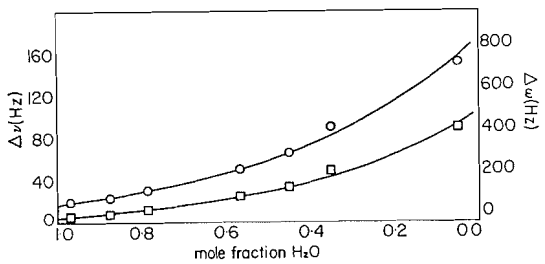

FIG. 2. The preferential solvation curve of Co^{2+} in aqueous dioxane solutions. $[Co^{2+}] = 0.087$ *M*. Circles, contact shift; squares, relaxation time.

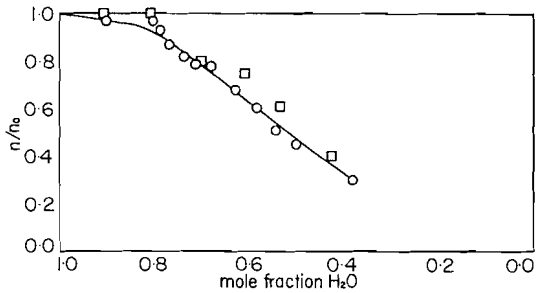

FIG. 3. The preferential solvation curve of Ni^{2+} in aqueous DMSO solutions. $[Ni^{2+}] = 0.050$ *M*. Circles, relaxation time; squares, contact shift. At the low water mole fractions the two signals overlap and analysis could not be continued.

Discussion

Figure 2 contains the results of a simple use of the methods. The case of a constant solvation shell is probably the circumstance most favorable to the assumptions. The result that $Co(OH_2)_6^{2+}$ is the species in all accessible mixtures is interesting. It bears on the understanding of the conductivity of salts in dioxane–water mixtures (see, e.g., ref. 11) and on analysis of kinetics in mixed solvents (12).

Figures 1 and 3 show the more complicated and probably more interesting results. Here the error, which amounts in many cases to 5 to 10% of the

TABLE III

Chemical shift values for determination of preferential solvation

	A. 0.087 *M* Co^{2+} in water–dioxane mixtures							
Mole fraction H_2O	1.000	0.950	0.876	0.785	0.568	0.453	0.344	0.199
$\Delta\omega_P$ (Hz)	38	46	64	103	204	272	393	710
	B. 0.050 *M* Ni^{2+} in water–DMSO mixtures							
Mole fraction H_2O	1.000	0.907	0.809	0.701	0.612	0.548	0.537	
$\Delta\omega_P$ (Hz)	17	24	34	39	46	44	46	

Can. J. Chem. Downloaded from www.nrcresearchpress.com by 210.87.254.5 on 09/05/12
For personal use only.

Can. J. Chem. Downloaded from www.nrcresearchpress.com by 210.87.254.5 on 09/05/12
For personal use only.

total solvation shell composition, is a limitation. Since all values involve ratios including the values of $\Delta\nu$ and $\Delta\omega$ in the *pure* solvent and will reflect small deviation from the assumptions, it seems unlikely that the error can be greatly reduced. When bulk solvent concentration is high (pure solvent) $\Delta\nu$ and $\Delta\omega$ are inevitably relatively small. As a consequence, it seems unlikely that data of sufficient accuracy to evaluate the successive formation constants of the seven expected complexes (ignoring geometrical isomers) can be accurately evaluated. Actually, the limitation is not more serious than that encountered by other methods. The alternative techniques, which share with the n.m.r. methods the important feature of reflecting a short range interaction, are electronic and vibrational spectroscopy. To derive solvation curves from these spectra requires knowledge of extinction coefficients for all of the intermediate species. Usually, these are accessible only by a difficult and uncertain "parameter fitting" technique. As an example, the visible absorption maximum for $Ni(DMSO)_6^{2+}$ is only about 20 mμ shifted from $Ni(OH_2)_6^{2+}$ and the extinction coefficient differs by a similarly small amount. Preliminary experiments[3] indicate that an attempt to derive even an approximate preferential solvation curve would be *hopeless*.

The "semiquantitative" determinations of preferential solvation derived via n.m.r. should be useful. They are, for example, precise enough to be used to understand the small variations encountered in ion size parameters obtained from conductivity data in mixed solvents. They are also as precise as most rate constants currently available from fast reaction studies and should make possible study of fast reactions, and catalytic behavior, of metal ions in mixed solvents. The precision is also adequate for assessment of *relative* thermodynamic coordinating tendencies for comparison with predictions based on theoretical calculations or spectroscopic correlations.

Finally, the data on Co^{2+} shown in Fig. 1 reveal the limitation of the technique. Curves derived from $\Delta\nu$ and $\Delta\omega$ for water protons, and $\Delta\nu$ for DMF protons, are in good agreement as to the composition of the solvation shell. The agreement of these three can hardly be fortuitous. But the curve based on $\Delta\omega$ for DMF protons differs by more than acceptable uncertainty. It must be that the assumption concerning $\Delta\omega_M$ fails even after correction for μ_{eff}.

The reported preferential solvation curves suggest that DMSO or DMF are good ligands for Ni^{2+} or Co^{2+} in water. Dioxane does not appear to be a successful competitor. These conclusions are consistent with available prior information (13).

[3]C. H. Langford. Unpublished results.

Acknowledgment

This investigation was supported by the Directorate of Chemical Sciences, U.S. Air Force Office of Scientific Research, Grant No. 212–65.

1. L. S. FRANKEL, T. R. STENGLE, and C. H. LANGFORD. Chem. Commun. 373 (1965).
2. H. M. MCCONNELL. J. Chem. Phys. **28**, 430 (1958).
3. T. R. STENGLE and C. H. LANGFORD. Coord. Chem. Rev. **2**, 349 (1967).
4. T. J. SWIFT and R. E. CONNICK. J. Chem. Phys. **37**, 307 (1962).
5. A. ABRAGAM. The principles of nuclear magnetism. Oxford University Press, London. 1961.
6. J. S. BABIEC, C. H. LANGFORD, and T. R. STENGLE. Inorg. Chem. **5**, 1362 (1966).
7. D. W. MEEK, R. S. DRAGO, and T. S. PIPER. Inorg. Chem. **1**, 285 (1962). D. W. MEEK, D. K. STRAUB, and R. S. DRAGO. J. Am. Chem. Soc. **82**, 6013 (1960).
8. D. F. EVANS. J. Chem. Soc. 2003 (1959).
9. N. A. MATWIYOFF. Inorg. Chem. **5**, 788 (1966).
10. L. FRANKEL, T. R. STENGLE, and C. H. LANGFORD. Abstracts of Papers, 152nd National Meeting of the American Chemical Society, New York. 1966.
11. G. ATKINSON and C. J. HALLADA. J. Am. Chem. Soc. **83**, 3759 (1961).
12. G. ATKINSON and S. K. KOR. J. Phys. Chem. **69**, 128 (1965).
13. R. S. DRAGO and K. PURCELL. Progr. Inorg. Chem **6**, 271 (1964).

Can. J. Chem. Downloaded from www.nrcresearchpress.com by 210.87.254.42 on 09/05/12
For personal use only.

Reactions of acetylenes with noble-metal halides. VI.[1] The reactions of 2-butyne with chlorodicarbonylrhodium dimer

J. W. KANG, S. MCVEY, AND P. M. MAITLIS[2]
Department of Chemistry, McMaster University, Hamilton, Ontario

Received March 19, 1968

Chlorodicarbonylrhodium dimer ($[Rh(CO)_2Cl]_2$) reacted with 2-butyne at 80° in benzene to give a mixture of compounds which contained hexamethylbenzene, duroquinone, chloro(π-duroquinone)-rhodium dimer, and chloro(π-tetramethylcyclopentadienone)rhodium. At 25° 2-butyne and $[Rh(CO)_2Cl]_2$ reacted to give a brown solid of variable composition (C), which could not be purified. Reaction of (C) with CO in methylene chloride gave a related solid (D) also of variable composition. Treatment of (C), or better (D), with an excess of triphenylphosphine gave chloro(dimethylmaleyl)bis(triphenylphosphine)-rhodium and $(Ph_3P)_2RhCOCl$. The former was identified by analysis, spectra, and its oxidation to dimethylmaleic anhydride. Reaction of (D) with *p*-toluidine gave chloro(dimethylmaleyl)carbonylbis(*p*-toluidine)rhodium, which on treatment with excess triphenylphosphine also gave chloro(dimethyl-maleyl)bis(triphenylphosphine)rhodium.

Canadian Journal of Chemistry, 46, 3189 (1968)

Introduction

The reactions of acetylenes with metal carbonyls have been studied by numbers of workers and many types of metal complexes and organic compounds have been isolated from these reactions. The reactions most intensively studied were those of various acetylenes with iron, cobalt, and molybdenum carbonyls, where very significant contributions have been made by Hübel and his collaborators (1–7) and by other workers (7–19). In many cases the X-ray structural determinations of the complexes have been carried out so that the structures of these complexes are now well understood. However, the precise nature of the reactions involved here, in which the acetylenes couple with each other and with CO to give the observed complexes and organic products, still remain obscure to a very large degree. The above-mentioned reactions, unfortunately, do not appear to lend themselves easily to detailed mechanistic investigations since such a large number and such a wide variety of products are obtained and since the conditions are in many cases rather stringent.

In 1963 Dickson and Wilkinson reported that hexafluoro-2-butyne reacted with carbon monoxide in the presence of chlorodicarbonylrhodium dimer as catalyst to give tetrakis(trifluoromethyl)cyclopentadienone (20). No intermediate complexes could be characterized from this reaction but hexafluoro-2-butyne reacted with dicarbonyl-π-cyclopentadienylrhodium to give π-tetrakis(trifluoromethyl)cyclopentadienone-π-cyclopentadienylrhodium and a complex of unusual structure, π-hexakis(trifluoromethyl)benzene-π-cyclopentadienylrhodium (21). The fact that such relatively simple reactions occurred with rhodium carbonyls tempted us to examine the former reaction in greater detail using other acetylenes.

In a preliminary note (22) on the reactions of diphenylacetylene and 3-hexyne with chlorodicarbonylrhodium dimer we noted that the former gave 47% of the RhCl complex of tetraphenylcyclopentadienone as the main product, while the latter gave the RhCl complex of tetraethylcyclopentadienone and some tetraethyl-*p*-benzoquinone. The latter reaction will be discussed fully in a later paper. Both reactions proceeded smoothly in refluxing benzene. Our success with these reactions prompted us to try the reaction of dimethylacetylene with $[Rh(CO)_2Cl]_2$; we expected that the products here would be more easily characterizable and we also hoped to isolate and characterize some intermediates in the reactions.

Results and Discussion

In refluxing benzene $[Rh(CO)_2Cl]_2$ (**1**) reacted with a large excess of 2-butyne to give a dark-purple benzene-insoluble solid (A), and a mixture (B) which was shown to contain mainly hexamethylbenzene (and a small amount of duroquinone, both isolated by chromatography) and

[1]Part V, see ref. 27.
[2]Fellow of the Alfred P. Sloan Foundation and author to whom any correspondence should be addressed.

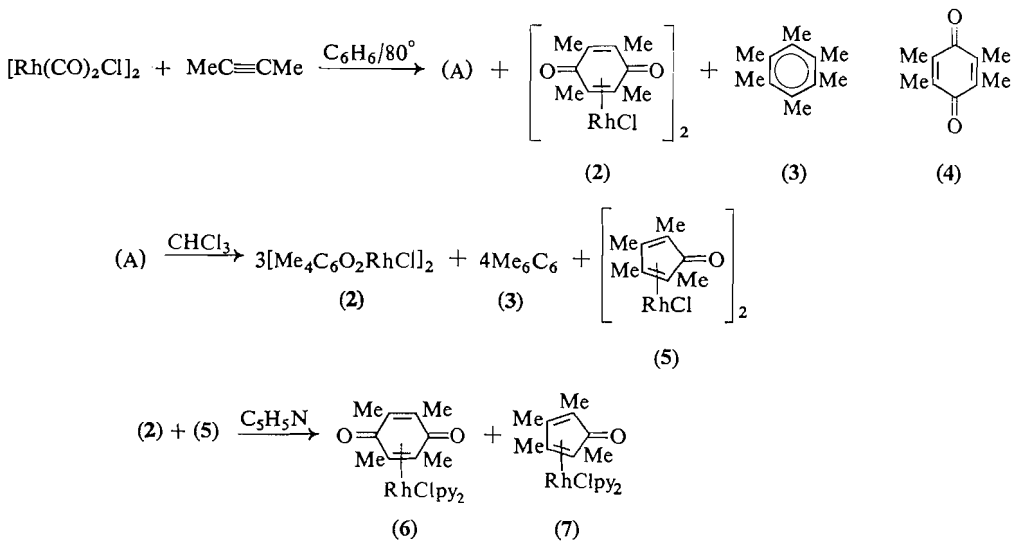

CHART 1

chloro(π-duroquinone)rhodium dimer (isolated and characterized as its bis(pyridine) adduct (**6**) (23)).

The purple solid (A) was soluble in chloroform; however, osmometric molecular weight measurements showed that the material was very unstable in solution and that it rapidly disproportionated (Chart 1). In fact proton magnetic resonance (p.m.r.) spectra in deuterochloroform only showed two singlets due to the presence of hexamethylbenzene (7.78 τ) and chloro(π-duroquinone)rhodium (8.33 τ) and another pair of singlets of equal intensity (8.12, 8.51 τ) which were assigned to the two pairs of inequivalent methyls in chloro(π-tetramethylcyclopentadienone)rhodium. On addition of a few drops of pyridine to this solution, both the latter complexes were converted into their bis(pyridine) adducts. By fractional crystallization it was possible to isolate and identify hexamethylbenzene and the bis(pyridine) adducts (**6**) and (**7**).

From the integration of the p.m.r. spectrum of (A), it appeared that for every four molecules of hexamethylbenzene, three of the duroquinone complex dimer (**2**), and two of the cyclopentadienone complex dimer (**5**), were present. This stoichiometry was quite reproducible and agreed well with the analysis which corresponded to $[(\text{hexamethylbenzene})_2(\text{duroquinone})_3(\text{tetramethylcyclopentadienone})_2Rh_5Cl_5]_n$. That (A) has a real existence in the solid state and is not just a mixture of (**2**), (**3**), and (**5**) is shown by the fact that it could be prepared reproducibly by different workers at different times and that it contained large amounts of hexamethylbenzene and yet was insoluble in benzene, in which hexamethylbenzene is normally very soluble. The structure of (A) remains, however, unknown.

Three different types of products were therefore formed in this reaction, hexamethylbenzene, duroquinone, and tetramethylcyclopentadienone, if we ignore for the moment the fact that part of the duroquinone and all the cyclopentadienone were complexed to RhCl. Although in terms of moles obtained hexamethylbenzene was by far the main product, no information can be gained from these experiments regarding the mode of its formation since we have shown that at least one of the complexes produced in the reaction, chloro(π-duroquinone)rhodium (**2**), will itself catalyze the trimerization of 2-butyne. Greatest significance must therefore be attached to the formation of the duroquinone (total 2.0 mmoles, as (**2**) and (**4**)) and the cyclopentadienone complex (**5**) (equivalent to 0.8 mmole of the cyclopentadienone) from 1.3 mmoles of chlorodicarbonylrhodium dimer. Since the materials balance accounts for 92% of the CO and the Rh originally present in (**1**), this means that in the presence of a large excess of 2-butyne about 77% of the CO available is incorporated into duroquinone and almost 15% into tetramethylcyclopentadienone.

Can. J. Chem. Downloaded from www.nrcresearchpress.com by 210.87.254.42 on 09/05/12
For personal use only.

Can. J. Chem. Downloaded from www.nrcresearchpress.com by 210.87.254.42 on 09/05/12
For personal use only.

In an effort to obtain information about the possible intermediates in this reaction we attempted the reaction of 2-butyne with chlorodicarbonylrhodium dimer in benzene at 25°. Again, a fairly rapid reaction occurred and a brown solid (C) was precipitated. Repeated attempts to purify (C) were without success, reliable analytical data were difficult to obtain, and it finally became clear that although from its appearance and its solid state infrared spectrum the composition of (C) appeared constant, it was in fact a nonstoichiometric compound of the general formula, $(C_4H_6)_m$-$(Rh(CO)_2Cl)_n(H_2O)_p$. The solid state infrared spectrum was complex and showed the presence of terminal metal carbonyl bands at 2075 (vs), 2025 (vs), possibly a bridging carbonyl at 1870 (m–w), and a broad strong band at 1680 cm^{-1} probably indicative of the presence of ketonic carbonyls. The presence of bound water was indicated by a broad band at 3500 cm^{-1} and especially by the breadth of the band at 1680 cm^{-1}; both were considerably reduced by vigorous drying of the sample.

On passing CO into a suspension of (C) in methylene chloride a new yellow solid (D) and $[Rh(CO)_2Cl]_2$ were obtained. The infrared spectrum of (D) was much simpler than that of (C) and only showed two strong sharp bands at 2070 and 1690 cm^{-1} in the carbonyl region, and a medium intensity one at 1605 cm^{-1} which we ascribed to $\nu_{C=C}$ (24). At first sight, the analytical data and the infrared spectrum of (D), combined with the production of $[Rh(CO)_2Cl]_2$ by the CO reaction, suggested that we had been able to purify (C) from the main contaminant,

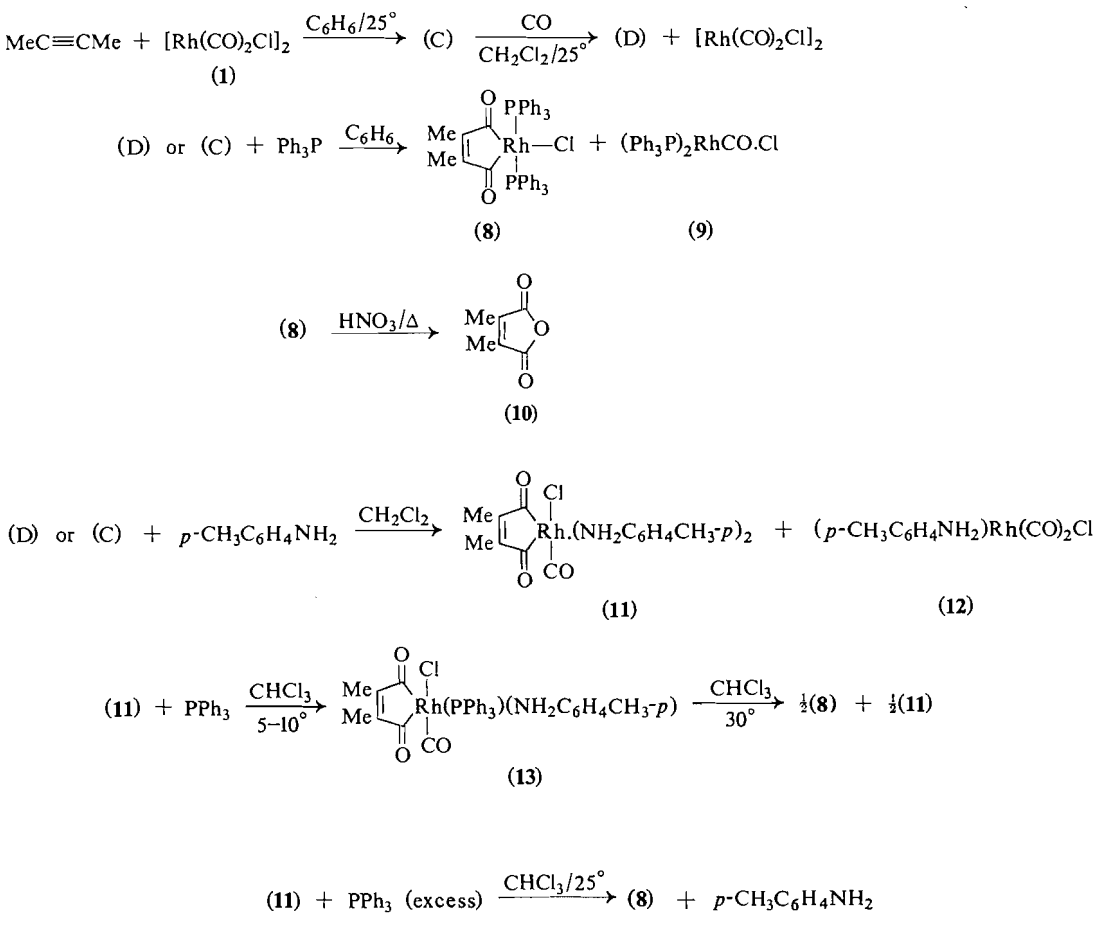

CHART 2

Can. J. Chem. Downloaded from www.nrcresearchpress.com by 210.87.254.42 on 09/05/12
For personal use only.

$[Rh(CO)_2Cl]_2$, and that (D) had a formula corresponding to $(C_4H_6CO)RhCOCl$ (25). Repeat analyses of (D) were, however, not consistent with this formulation and the results of the reactions of (D) with *p*-toluidine and triphenylphosphine described below made this view untenable. From these reactions it now appears that (D) also contains some $[Rh(CO)_2Cl]_2$ and a rhodium complex which we suggest may contain a chloro(dimethylmaleyl)carbonylrhodium moiety (14).

An excess of triphenylphosphine reacted with (D) to give a high yield of a crystalline yellow complex, (**8**), and some chlorocarbonylbis(triphenylphosphine)rhodium (**9**).

The structure for (**8**) was proposed on the following evidence: (*a*) Elemental analysis and molecular weight measurements[3]. (*b*) The p.m.r. spectrum of (**8**) only showed one single, unsplit resonance in the methyl region (8.96 τ), and a multiplet in the phenyl proton region (2.68 τ) with intensity ratio 6:30. (*c*) The infrared spectrum in the 1600–2100 cm^{-1} region showed no terminal or bridging metal carbonyl bands but only a single strong band at 1635 cm^{-1} which can be ascribed to a C=C—CO—Rh group (24). (*d*) The compound was exceedingly stable to oxidation (no reaction with boiling 7 *N* HNO_3 during 1 h) and to reduction (60% of the starting material was recovered after 4 h refluxing with zinc in acetic acid). However, after boiling with 14 *N* nitric acid, a 67% yield of dimethylmaleic anhydride was obtained from (**8**).

Treatment of (D) with *p*-toluidine in methylene chloride gave a high yield of chloro(dimethylmaleyl)carbonylbis(*p*-toluidine)rhodium (**11**), identified by its elemental analysis and the following evidence: (*a*) The infrared spectrum of (**11**) showed the presence of a terminal metal carbonyl at 2055 cm^{-1} (vs) and a ketonic carbonyl at 1650 cm^{-1} (vs). (*b*) The p.m.r. spectrum of (**11**) (which, due to the low solubility of the compound in chloroform at 25°, was measured at 60°) showed singlets at 7.80 and 7.72 τ (due to the methyl protons of the dimethylmaleyl- and the *p*-toluidine respectively), and at 5.44 τ (due to the amine protons), and a quartet at 2.92 τ (due to the *p*-disubstituted phenyl protons), with the expected intensity ratio of 6:6:4:8. (*c*) On treatment of (**11**) with an excess of triphenylphosphine in chloroform at 25°, both the *p*-toluidine and the carbonyl ligands were replaced, and a 91% yield of the bis(triphenylphosphine) complex (**8**) was obtained.

If the reaction of (D) with triphenylphosphine is assumed to proceed quantitatively, with the component of structure presumed to be (**14**) giving rise to (**8**) and the bound $[Rh(CO)_2Cl]_2$ only giving (**9**), then the formula of the sample of (D) used in this reaction is approximately $[(C_4H_6C_2O_2RhCOCl)_4(Rh(CO)_2Cl)_1]_n$. Analogously, if in the reaction of (D) with *p*-toluidine the component (**14**) gives rise only to (**11**), while the bound $[Rh(CO)_2Cl]_2$ only gives (**12**), then the formula of this sample is approximately $[(C_4H_6C_2O_2RhCOCl)_6(Rh(CO)_2Cl)_1]_n$. An overall yield of 63% of (**11**) has also been obtained from these reactions when neither (C) nor (D) was isolated.

The compound (C) also underwent these reactions with triphenylphosphine and *p*-toluidine, giving (**8**) and (**11**) respectively, though in lower yield. The substitution products of $[Rh(CO)_2Cl]_2$, namely (**9**) and (**12**), were again the only other materials which could be isolated from these reactions.

One other complex could also be prepared from the bis(*p*-toluidine) complex (**11**) with triphenylphosphine under very mild conditions. In this case only one *p*-toluidine ligand was replaced, giving a 75% yield of chloro(dimethylmaleyl)carbonyl(*p*-toluidine)triphenylphosphinerhodium (**13**). The structure of this was again confirmed by analysis, and its infrared and p.m.r. spectra. Although (**13**) appeared quite stable in the solid, in solution it disproportionated fairly rapidly with loss of CO to give a 44% yield of chloro(dimethylmaleyl)bis(triphenylphosphine)rhodium (**8**) and a 39% yield of chloro(dimethylmaleyl)carbonylbis(*p*-toluidine)-rhodium (**11**). This disproportionation was also evident from the p.m.r. spectrum of (**13**) which changed rapidly with time until it became that of a mixture of (**8**) and (**11**).

The complexes (**8**), (**11**), and (**13**) all have the common feature of a very low frequency and intense ν_{CO} at 1635, 1650, and 1650 cm^{-1} respectively. This suggests that the keto groups

[3]This implies (**8**) to contain five-coordinate Rh(III); while this is not unknown, it is somewhat unusual (24). Since (**8**) retains solvent of crystallization very tenaciously, it is also possible that (**8**) may be six-coordinate in solution with a solvent occupying one coordination site.

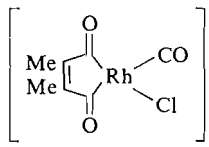

(14)

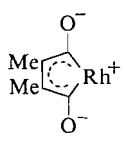

(15)

are very strongly polarized and that structure (**15**) is important in describing the ground state of the system. Baird *et al.* (24) have reported similar values for ν_{CO} and $\nu_{C=C}$ in complexes of the type $CH_2{=}CH.CO.[M]$, where [M] = $C_5H_5Fe(CO)_2$—, $C_5H_5W(CO)_3$—, and $(Ph_3P)_2RhCl_2$—.

The lack of consistent data on (C) and (D) makes it difficult to speculate on their natures and the role, if any, which they play as intermediates in the high temperature formation of the *p*-benzoquinone and the cyclopentadienone complexes.

However, when (D) was reacted with 2-butyne in the absence of solvent in a bomb at 80° a red-purple solid was obtained, with properties and spectra identical with the product (A) formed in the high temperature reaction of 2-butyne with $[Rh(CO)_2Cl]_2$.

Furthermore, when a suspension of (D) in benzene was refluxed with an excess of 3-hexyne, a mixture of products was obtained. These consisted of the rather insoluble blue $[Et_4C_4Rh(CO)Cl_2Rh]_2$[4], and chloro(π-tetraethylcyclopentadienone)rhodium trimer[4], hexaethylbenzene, and a yellow oil which were separated by chromatography on Florisil. The yellow oil was shown by thin layer chromatography to consist of two components, a major and a minor one, of very similar R_f values, in the region for tetrasubstituted *p*-benzoquinones. The infrared spectrum of the oil agreed with the conclusion that a mixture of *p*-benzoquinones was present. The p.m.r. spectrum showed the presence of only one singlet due to a methyl group and a quartet and a triplet due to ethyl groups. Although their positions agreed exactly with those for tetramethyl- and tetraethyl-*p*-benzoquinone, and the integrated intensities agreed with a 43:57 mixture of the two compounds, both the thin layer chromatogram and the mass-spectral cracking pattern of the oil were different to those of a synthetic mixture. In particular the larger spot on the thin layer chromatogram did not have the correct R_f value for duroquinone, though the minor component did have the same R_f as tetraethyl-*p*-benzoquinone. The mass-spectral cracking pattern of the oil also showed a strong peak at *m/e* 192, corresponding to $[Me_2Et_2C_6O_2]^+$, which was virtually absent in the synthetic mixture. Although we were unable to obtain the 2,3-diethyl-5,6-dimethyl-*p*-benzoquinone pure, the evidence indicates that the oil was a mixture of it and duroquinone in the approximate ratio 86:14.

The multitude of products typical of the reaction of 3-hexyne and $[Rh(CO)_2Cl]_2$[4] obtained in this reaction makes its interpretation difficult. However, it is tempting to suggest that the 2,3-diethyl-5,6-dimethyl-*p*-benzoquinone is obtained from an intermediate such as (**14**) by addition of the 3-hexyne to the dimethylmaleyl group, rather in the manner of a Diels–Alder reaction, but occurring in a metal complex.

Experimental

2-Butyne was purchased from Farchan Chemical Co. Chlorodicarbonylrhodium dimer was prepared by the method of McCleverty and Wilkinson (26). Proton magnetic resonance spectra were run on a Varian A60 spectrometer, using deuterochloroform as solvent with tetramethylsilane as internal reference. Infrared spectra, except where stated, were run as KBr discs. All reactions were carried out in an atmosphere of dry nitrogen.

The Reaction of Chlorodicarbonylrhodium Dimer with 2-Butyne at 80°

2-Butyne (2.0 ml, 25.5 mmoles) was added to a solution of 0.5 g (1.3 mmoles) of chloro(dicarbonyl)rhodium dimer (**1**) in 20 ml of benzene and the mixture refluxed for 5 h. Another 2 ml of 2-butyne were then added and the refluxing continued for a further 15 h. The solution was cooled and filtered to give 0.6 g of a dark-purple solid (A) which was washed with benzene and dried. Removal of the solvent from the filtrate left a reddish solid; this was extracted with light petroleum, leaving 0.22 g of a red petroleum-insoluble solid (B). The light petroleum extracts were chromatographed on Florisil to give 0.7 g hexamethylbenzene (**3**, eluted in light petroleum) and 0.06 g duroquinone (eluted in benzene), identified by melting points and infrared spectra.

The solids (A) and (B) were closely related as shown by their p.m.r. spectra. Both showed resonances at 7.78, 8.12, 8.33, and 8.51 τ, though of different intensities; in addition (B) showed two further weak resonances at 8.00 τ (probably duroquinone) and 8.45 τ. The peaks at 7.78 and 8.33 τ were due to hexamethylbenzene and chloro(π-duroquinone)rhodium dimer (**2**) and the peaks at 8.12 and 8.51 τ were assigned to the two different

[4]Details of the reaction of 3-hexyne with $[Rh(CO)_2Cl]_2$, and the X-ray structural determination $[Et_4C_4Rh(CO)Cl_2Rh]_2$ by L. F. Dahl and L. Bateman, will be reported shortly.

Can. J. Chem. Downloaded from www.nrcresearchpress.com by 210.87.254.42 on 09/05/12
For personal use only.

Can. J. Chem. Downloaded from www.nrcresearchpress.com by 210.87.254.42 on 09/05/12
For personal use only.

methyl resonances in chloro(π-tetramethylcyclopentadienone)rhodium (**5**, see below). By integration, the intensities of the four main resonances in (B) were estimated as 7:1:17:1 (on this scale the intensities of the resonances at 8.00 and 8.45 τ were < 0.5) and this suggested that (B) was a mixture of mainly chloro(π-duroquinone)rhodium dimer and hexamethylbenzene in a molar ratio of 1.8:1. The material (B) could not be crystallized satisfactorily; however, addition of pyridine to a solution of (B) in methylene chloride followed by addition of light petroleum gave orange crystals of chlorobis(pyridine)(π-duroquinone)rhodium (**7**) shown to be identical with an authentic sample prepared previously by its infrared spectrum and behavior on heating in a melting point capillary (23).

The solid (A) was obtained reproducibly with the same stoichiometry as shown by integration of its p.m.r. spectrum. The intensity ratio of the resonances at 7.78, 8.12, 8.33, and 8.51 τ was 3:1:3:1, and suggested a molar ratio of hexamethylbenzene:chloro(π-duroquinone)rhodium:chloro(π-tetramethylcyclopentadienone)rhodium of 2:3:2. After the addition of a few drops of pyridine to a solution of (A) in $CDCl_3$ the peaks were unchanged in intensity and now appeared at 7.79, 8.45, 8.55, and 8.88 τ (3:1:3:1). The resonance at 7.79 τ is virtually unchanged by comparison with authentic hexamethylbenzene, and that at 8.55 τ is close to that of chlorobis(pyridine)(π-duroquinone)rhodium (**6**) previously reported (10) as 8.62 τ; the small difference must be ascribed to a solvent effect. The two peaks of equal intensity 1 were therefore again presumed to be due to chlorobis(pyridine)(π-tetramethylcyclopentadienone)rhodium (**7**). By fractional crystallization of the products obtained from reaction of (A) with pyridine it was possible to isolate hexamethylbenzene and chlorobis(pyridine)(π-duroquinone)rhodium (identified by comparison with authentic samples). In addition a small amount of a new orange crystalline material was also obtained. This was identified as chlorobis(pyridine)(π-tetramethylcyclopentadienone)rhodium by its p.m.r. spectrum which only showed two resonances of equal intensity at 8.45 and 8.88 τ, its infrared spectrum which showed a strong band at 1645 cm^{-1} due to the cyclopentadienone carbonyl (9), and by a partial analysis.

Anal. Calcd. for $C_{19}H_{22}ClN_2ORh$: N, 6.47. Found: N, 6.89.

From these results it is apparent that (A) is only stable in the solid state; the analysis of a sample agreed with the formulation $[(hexamethylbenzene)_2(duroquinone)_3(tetramethylcyclopentadienone)_2Rh_5Cl_5]_n$.

Anal. Calcd. for $[C_{72}H_{96}Cl_5O_8Rh_5]_n$: C, 48.55; H, 5.43; Cl, 9.95; Rh, 28.89. Found: C, 47.62; H, 5.04; Cl, 10.55; Rh, 29.37.

The solid state infrared spectrum of (A) showed a strong broad peak at 1640 cm^{-1} in the carbonyl region. Osmometric molecular weight measurements showed that the molecular weight varied with time and came to equilibrium after about 2 h; the value then corresponded to an average molecular weight of 515.

By isolation of the organic materials and from integration of the p.m.r. spectra of (A) and (B) approximately 5.2 mmoles hexamethylbenzene, 0.4 mmole duroquinone, 0.8 mmole chloro(π-duroquinone)rhodium dimer, and 0.4 mmole chloro(π-tetramethylcyclopentadienone)rhodium dimer were obtained in this reaction. This material balance accounts for approximately 92% of the rhodium and the carbonyl content of the initial chlorodicarbonylrhodium dimer.

The Reaction of Chlorodicarbonylrhodium Dimer with 2-Butyne at 25°

2-Butyne (3 ml, 38 mmoles) was added to a solution of 0.5 g (1.3 mmoles) chlorodicarbonylrhodium dimer in 20 ml of benzene at 25°. The solution was stirred for 24 h after which the brown solid (C) which had precipitated was filtered off, washed with benzene and ether, and dried in vacuo; yield of solid, 0.62 g, melting point (m.p.) 145–160° (decomp.). From the filtrate, a small amount (~ 10 mg) of duroquinone could be isolated. The solid (C) was quite insoluble in all except strongly coordinating solvents such as pyridine, in which it decomposed. All attempts to recrystallize it were therefore abortive. The infrared spectrum in the carbonyl region was extremely complex and bands were noted at 2075 (vs), 2025 (vs), 1870 (m–w), and 1680 (s–broad) cm^{-1}. In addition the spectrum showed a broad band at 3500 cm^{-1} indicating the presence of bound water.

Analyses on the material were difficult and not reproducible; however, one sample analyzed reasonably satisfactorily for $[CH_3C_2CH_3]_{0.9}.Rh(CO)_2Cl.0.5H_2O$.

Anal. Calcd. for $C_{5.6}H_{6.4}ClO_{2.5}Rh$: C, 26.68; H, 2.56; Cl, 14.07; Rh, 40.82. Found: C, 26.38; H, 2.46; Cl, 13.91; Rh, 41.34.

In order to obtain some evidence about the nature of the organic ligand present here, a mass spectrum of the solid was run at 120°; the only higher molecular weight species identifiable was at *m/e* 54 corresponding to $C_4H_6^+$.

On passing carbon monoxide into a suspension of 500 mg of (C) in 20 ml of methylene chloride at 25° for 2 h the brown solid slowly turned yellow. Filtration followed by washing with methylene chloride and vacuum-drying afforded 0.270 g of a pale-yellow solid (D), m.p. 205–213° (decomp.). The filtrate was evaporated to dryness on a rotary evaporator, and the residue extracted with hot hexane to give 0.12 g of chlorodicarbonylrhodium dimer (**1**), identified by its infrared spectrum. The solid (D) was likewise amorphous and almost completely insoluble in solvents with which it did not react. The infrared spectrum of (D) was, however, significantly simpler and cleaner than that of (C); it was also possible to measure the spectrum of a weak methylene chloride solution of (D). Both this and a KBr disc showed only two strong and sharp bands in the carbonyl region, at 2070 and 1690 cm^{-1}. In addition a band (also present in the spectrum of (C)) which we ascribe to $\nu_{C=C}$ occurred at 1605 cm^{-1} (m). Analyses of (D) were again unreliable and also inconsistent; the best analysis is quoted below, together with that expected for the compound it largely appears to contain, $C_4H_6(CO)_2RhCOCl$, from its reactions described below.

Anal. Calcd. for $C_7H_6ClO_3Rh$: C, 30.40; H, 2.19; Cl, 12.83; O, 17.36; Rh, 37.22. Found: C, 28.96; H, 2.35; Cl, 14.32; O, 16.48; Rh, 34.70.

*Chloro(dimethylmaleyl)carbonylbis(p-toluidine)rhodium (**11**)*

p-Toluidine (1 g) was added to a suspension of 300 mg of the complex (D) in 30 ml methylene chloride. The

Can. J. Chem. Downloaded from www.nrcresearchpress.com by 210.87.254.42 on 09/05/12
For personal use only.

mixture was stirred for 3 h at 25°, and then the insoluble product was filtered off as yellow crystals of the complex (**11**), m.p. 162–166° (decomp.). From the filtrate a further small amount of (**11**) was obtained. The combined solids were recrystallized from chloroform to give 385 mg of pale-yellow crystals of (**11**), m.p. 166–168° (decomp.).

Anal. Calcd. for $C_{21}H_{24}ClN_2O_3Rh$: C, 51.39; H, 4.93; Cl, 7.22; N, 5.71; O, 9.78. Found: C, 51.68; H, 4.88; Cl, 6.56; N, 5.67; O, 9.78.

From the mother liquors of (**11**), 38 mg of ether-soluble chlorodicarbonyl-*p*-toluidinerhodium (**12**) were obtained, identified by comparison of its infrared spectrum with that of an authentic sample.

The infrared spectrum of (**11**) in $CHCl_3$ showed the presence of a terminal metal carbonyl at 2055 cm^{-1} (vs) and a ketonic carbonyl at 1650 cm^{-1} (vs). The p.m.r. spectrum of (**11**), measured at 60° in $CDCl_3$, consisted of a singlet at 7.80 τ (methyl protons of the dimethylmaleyl group), a singlet at 7.72 τ (*p*-toluidine methyl protons), a singlet at 5.44 τ (NH_2 protons), and a quartet at 2.92 τ (*p*-toluidine phenyl protons). The intensity ratio was the expected 6:6:4:8.

The *p*-toluidine complex was also obtained, in about 20% yield from the complex (C). The major product from this reaction was chlorodicarbonyl-*p*-toluidinerhodium (**12**).

Chloro(dimethylmaleyl)carbonyl-p-toluidinetriphenylphosphinerhodium (13)

A solution of 170 mg (0.64 mmole) of triphenylphosphine in 5 ml of chloroform was added to a suspension of 310 mg (0.64 mmole) of the bis-*p*-toluidine complex (**11**) and stirred for 10 min at 5–10°. The yellow solution was then quickly filtered, and the solvent removed on a rotary evaporator to leave a yellow solid. This was recrystallized from benzene–hexane and gave 310 mg (75%) of yellow crystals of pure (**13**), m.p. 161–163° (decomp.).

Anal. Calcd. for $C_{32}H_{30}ClNO_3PRh$: C, 59.50; H, 4.68; Cl, 5.48; N, 2.17; P, 4.79. Found: C, 59.00, 59.11; H, 4.74, 4.80; Cl, 5.53; N, 2.40; P, 5.11.

The infrared spectrum of (**13**) showed the presence of a terminal metal carbonyl at 2050 cm^{-1} (vs), and a ketonic carbonyl at 1650 cm^{-1} (vs).

The p.m.r. spectrum of a freshly prepared solution of (13) showed resonances at 7.84 τ (singlet, dimethylmaleyl methyl protons), 7.67 τ (singlet, *p*-toluidine methyl protons), 5.53 τ (broad, *p*-toluidine amine protons), 3.61, 3.03 τ (two doublets, *p*-toluidine phenyl protons), and 2.4 τ (multiplets, triphenylphosphine protons). After a very short time, however, the spectrum changed due to the occurrence of the disproportionation described below. As solid precipitated in the nuclear magnetic resonance tube during this disproportionation no meaningful integrations could be carried out. However, after 24 h the spectrum was that of a mixture of chloro(dimethylmaleyl)carbonylbis(*p*-toluidine)rhodium (**11**) and chloro(dimethylmaleyl)bis(triphenylphosphine)rhodium (**8**).

Chloro(dimethylmaleyl)bis(triphenylphosphine)rhodium (8)

1. From Complex (D)

A mixture of a sample of the complex (D) (500 mg) and 2.0 g of triphenylphosphine in 30 ml of benzene was stirred at 25° for 5 h. The solution was filtered and solvent removed, leaving an oily residue which was extracted with hot hexane to remove excess triphenylphosphine. The insoluble yellow solid was crystallized from methylene chloride at 5° to give 270 mg of yellow crystals of chlorocarbonylbis(triphenylphosphine)rhodium (**9**), identified by its infrared spectrum. Addition of hexane to the methylene chloride mother liquors precipitated the crude chloro(dimethylmaleyl)bis(triphenylphosphine)rhodium (**8**). This was recrystallized from methylene chloride – hexane to give 1.2 g of yellow crystals of the pure complex, m.p. 279–281° (decomp.). It was found that the solid retained methylene chloride of crystallization tenaciously. The analytical sample was therefore dried at 150°/12 mm.

Anal. Calcd. for $C_{42}H_{36}ClO_2P_2Rh$ (mol. wt. 773): C, 65.25; H, 4.69; Cl, 4.58. Found (mol. wt. 777): C, 65.50; H, 4.62; Cl, 4.45.

The infrared spectrum of (**8**) showed the presence of a very strong band at 1635 cm^{-1} (ascribed to ν_{CO}); no bands in the metal carbonyl region were present.

The p.m.r. spectrum of (**8**) consisted of a singlet at 8.96 τ (due to two equivalent methyl groups) and a multiplet at 2.68 τ (phenyl protons), with the expected intensity ratio of 1:5.

Chromatography of the hexane solution (which was used to wash out the excess triphenylphosphine) gave, apart from triphenylphosphine, a small amount (approx. 20 mg) of duroquinone.

2. From Complex (C)

Treatment of 500 mg of complex (C) with triphenylphosphine in benzene as above afforded, after an identical work-up, 550 mg of chlorocarbonylbis(triphenylphosphine)rhodium and 920 mg of pure chloro(dimethylmaleyl)bis(triphenylphosphine)rhodium, which were identified by infrared and p.m.r. spectra, and by their melting points.

3. From Chloro(dimethylmaleyl)-carbonylbis(p-toluidine)rhodium (11)

A mixture of 300 mg of (**11**) and 500 mg triphenylphosphine in 10 ml of chloroform was stirred at 25° for 3 h. Addition of hexane to the filtered solution gave a yellow solid, which after recrystallization from methylene chloride – hexane afforded a 430 mg (91%) yield of yellow crystals of (**8**), m.p. 279–281° (decomp.).

4. From Chloro(dimethylmaleyl)carbonyl-p-toluidinetriphenylphosphine rhodium (13)

A solution of 150 mg of (**13**) in 1 ml of chloroform was allowed to stand at 25° for 48 h. A pale-yellow crystalline precipitate was filtered off, washed with a small volume of cold chloroform, and air-dried. This was shown to be chloro(dimethylmaleyl)carbonylbis(*p*-toluidine)rhodium (**11**) (yield, 45 mg (39%)) by its m.p. and infrared spectrum. The combined filtrates were evaporated to dryness and the residue recrystallized from methylene chloride – hexane to give 78 mg (44%) of chloro(dimethylmaleyl)-bis(triphenylphosphine)rhodium, (**8**), again identified by its m.p. and infrared spectrum.

Oxidation of Chloro(dimethylmaleyl)bis-(triphenylphosphine)rhodium (8) to Dimethylmaleic Anhydride (10)

A suspension of 500 mg of (**8**) in 50 ml of concentrated nitric acid was refluxed, with stirring, for 1 h. The

Can. J. Chem. Downloaded from www.nrcresearchpress.com by 210.87.254.42 on 09/05/12
For personal use only.

solution was cooled and poured into ice-water, and the mixture was then extracted with chloroform. After drying the chloroform extract (sodium sulfate), and removal of solvent, an oily residue was obtained. This was sublimed at 25°/0.1 mm to give 55 mg (67%) of 2,3-dimethylmaleic anhydride (**10**) as colorless crystals, m.p. 92–94°.

Anal. Calcd. for $C_6H_6O_3$: C, 57.15; H, 4.80. Found: C, 57.10; H, 4.95.

Trimerization of 2-Butyne by Chloro(π-duroquinone)-rhodium Dimer (2)

2-Butyne (2 ml) was added to a solution of 0.2 g (0.33 mmole) chloro(π-duroquinone)rhodium dimer (**2**) in 15 ml of benzene and the solution was refluxed for 5 h. A further 2 ml of 2-butyne was then added and the solution refluxed for a further 15 h. The solution was then evaporated to dryness and the reddish residue extracted with light petroleum. This left an insoluble red solid (0.12 g, 60% recovery) which was shown to be chloro-(π-duroquinone)rhodium. The light petroleum extracts were combined and chromatographed on Florisil to give 1.03 g (6.4 mmoles) of hexamethylbenzene and 22 mg of duroquinone (eluted in benzene). Based on the amount of 2-butyne used, a 38% conversion to hexamethylbenzene was effected.

Reaction of (D) with 2-Butyne

Attempts to prepare the complex (A) from (D) and 2-butyne in the same manner as the complex (A) was obtained from $[Rh(CO)_2Cl]_2$ and 2-butyne were unsuccessful. However, by heating 2-butyne and (D) for 4 h in a bomb at 80°, a purple solid was obtained after extraction with benzene, which had identical properties, including p.m.r. spectrum, with that of (A).

Reaction of (D) with 3-Hexyne

3-Hexyne (2.0 ml, 1.46 g) was added to a suspension of 0.6 g of (D) in 20 ml of benzene, and the mixture was refluxed for 6 h. The solvent was then removed and a small amount of benzene added, which redissolved all the solid except a small amount (40 mg) of the blue $[Et_4C_4RhCO.Cl_2Rh]_2$ formed in the reaction. Chromatography of the benzene solution on Florisil gave 150 mg of hexaethylbenzene, 0.23 g of a yellow oil (eluted in benzene), and 0.25 g of a red solid which eluted in methylene chloride – ethanol. The latter was shown to consist principally of chloro(π-tetraethylcyclopentadienone)rhodium trimer. The yellow oil was not homogeneous and since the p.m.r. spectrum was identical with that of a 57:43 mixture of tetraethyl-*p*-benzoquinone and duroquinone (due to the accidental equivalence of the ethyl and the methyl protons) it was at first assumed that the oil was a mixture of the tetraethyl- and tetramethyl-*p*-benzoquinones in the above ratio. However, careful comparative thin layer chromatography showed that, while one of the two overlapping spots obtained was tetraethyl-*p*-benzoquinone, the other did *not* have the R_f value of duroquinone. Furthermore the mass-spectral cracking pattern of a 57:43 mixture of tetraethyl- and tetramethyl-*p*-benzoquinone was quite different to that of the oil above, notably in that the oil showed a strong peak at *m/e* 192, corresponding to $[Me_2Et_2C_6O_2]^+$. It was therefore concluded that the oil consisted mainly of 2,3-diethyl-5,6-dimethyl-*p*-benzoquinone and a smaller amount of tetraethyl-*p*-benzoquinone. All attempts to isolate the former in a pure state failed. The oil showed ν_{CO} at 1645 cm^{-1} (vs).

Acknowledgments

We thank the National Research Council of Canada for the award of a Postdoctorate Research Fellowship (to S. M.), and for supporting this work, and Johnson, Matthey, and Mallory for the loan of rhodium trichloride.

1. W. Hübel, E. H. Braye, A. Clauss, E. Weiss, U. Krüerke, D. A. Brown, G. S. D. King, and C. Hoogzand. J. Inorg. Nucl. Chem. **9**, 204 (1959).
2. W. Hübel and E. H. Braye. J. Inorg. Nucl. Chem. **10**, 250 (1959).
3. W. Hübel and C. Hoogzand. Chem. Ber. **94**, 2829 (1961).
4. W. Hübel and R. Merenyi. J. Organometal. Chem. Amsterdam, **2**, 213 (1964).
5. E. H. Braye and W. Hübel. J. Organometal. Chem. Amsterdam, **3**, 25, 38 (1965).
6. J. F. Blount, L. F. Dahl, C. Hoogzand, and W. Hübel. J. Am. Chem. Soc. **88**, 292 (1966).
7. L. F. Dahl, R. F. Doedens, W. Hübel, and J. Nielsen. J. Am. Chem. Soc. **88**, 446 (1966).
8. W. Reppe and H. Vetter. Ann. **582**, 133 (1953).
9. E. Weiss, R. G. Merenyi, and W. Hübel. Chem. and Ind. London, 407 (1960).
10. H. W. Sternberg, R. A. Friedel, R. Markby, and I. Wender. J. Am. Chem. Soc. **78**, 3621 (1956).
11. R. Clarkson, E. R. H. Jones, P. C. Wailes, and M. C. Whiting. J. Am. Chem. Soc. **78**, 6206 (1956).
12. A. A. Hock and O. S. Mills. Acta Cryst. **14**, 139 (1961).
13. J. R. Case, R. Clarkson, E. R. H. Jones, and M. C. Whiting. Proc. Chem. Soc. 150 (1959).
14. H. W. Sternberg, R. Markby, and I. Wender. J. Am. Chem. Soc. **80**, 1009 (1958).
15. R. Markby, H. W. Sternberg, and I. Wender. Chem. Ind. London, 1381 (1959).
16. G. N. Schrauzer. Chem. Ind. London, 1403, 1404 (1958); J. Am. Chem. Soc. **81**, 5307 (1959).
17. L. F. Dahl and D. L. Smith. J. Am. Chem. Soc. **83**, 753 (1961).
18. H. Greenfield, H. W. Sternberg, R. A. Friedel, J. H. Wotiz, R. Markby, and I. Wender. J. Am. Chem. Soc. **78**, 120 (1956).
19. H. W. Sternberg, J. G. Shukys, C. D. Donne, R. Markby, R. A. Friedel, and I. Wender. J. Am. Chem. Soc. **81**, 2339 (1959).
20. R. S. Dickson and G. Wilkinson. Chem. Ind. London, 1432 (1963); J. Chem. Soc. 2699 (1964).
21. M. R. Churchill and R. Mason. Proc. Roy. Soc. London, Ser. A, **292**, 61 (1966).
22. P. M. Maitlis and S. McVey. J. Organometal. Chem. Amsterdam, **4**, 254 (1965).
23. S. McVey and P. M. Maitlis. Can. J. Chem. **44**, 2429 (1966).
24. M. C. Baird, J. J. Mague, J. A. Osborn, and G. Wilkinson. J. Chem. Soc. A, 1347 (1967).
25. P. M. Maitlis and S. McVey. Abstracts. Autumn Meeting, Chemical Society (England). Brighton, England. September 1966. p. B27.
26. J. McCleverty and G. Wilkinson. Inorg. Syn. **8**, 211 (1966).
27. E. O. Greaves and P. M. Maitlis. J. Organometal. Chem. Amsterdam, **6**, 104 (1966).

The chlorosulfuric acid solvent system. Part II. The solutes $SeCl_4$ and $TeCl_4$; evidence for the formation of the $SeCl_3^+$ and $TeCl_3^+$ ions

E. A. Robinson and J. A. Ciruna

Lash Miller Chemical Laboratories and Erindale College, University of Toronto, Toronto 5, Ontario

Received March 18, 1968

From the results of electrical conductivity measurements on solutions in chlorosulfuric acid and the Raman spectra of solutions in chlorosulfuric acid (and fluorosulfuric acid) it is shown that $SeCl_4$ and $TeCl_4$ ionize quantitatively in these strong acid solutions to give the $SeCl_3^+$ and $TeCl_3^+$ cations.

By comparison of the spectra with the vibrational spectra of solid $SeCl_4$ and solid $TeCl_4$, reported by other workers, it is suggested that the solids contain covalent MCl_4 molecules rather than the ionic species $MCl_3^+.Cl^-$, suggested previously.

Canadian Journal of Chemistry, 46, 3197 (1968)

Can. J. Chem. Downloaded from www.nrcresearchpress.com by 210.87.254.6 on 09/05/12
For personal use only.

Introduction

In a recent paper (1) some results of electrical conductivity measurements on solutions of simple bases in chlorosulfuric acid are described. The SO_3Cl^- ion was found to have a much higher mobility than typical cations such as the alkali metal ions, so that to a good approximation most strong bases were found to give very similar specific conductance – concentration curves.

[1] $$MSO_3Cl = M^+ + SO_3Cl^-$$

In addition it was found that the alkali metal chlorides react quantitatively with chlorosulfuric acid:

[2] $$MCl + HSO_3Cl = M^+ + SO_3Cl^- + HCl$$

The resulting hydrogen chloride behaves as a very weak base of the chlorosulfuric acid solvent system

[3] $$HCl + HSO_3Cl \rightleftharpoons H_2Cl^+ + SO_3Cl^-$$

so that to a first approximation the formation of hydrogen chloride has little effect on the specific conductivities of the solutions.

In 1954 Gerding and Houtgraaf (2) claimed, on the basis of similarities between the Raman spectra of $SeCl_4$ and $AsCl_3$, and $TeCl_4$ and $SbCl_3$, respectively, that selenium tetrachloride and tellurium tetrachloride exist as $SeCl_3^+Cl^-$ and $TeCl_3^+Cl^-$ in the solid state, and the spectra of the adducts $SeCl_4.AlCl_3$ and $TeCl_4.AlCl_3$, both in the solid and molten states, were interpreted in terms of the structures $SeCl_3^+AlCl_4^-$ and $TeCl_3^+AsCl_4^-$. Gerding (3) also studied the spectra of the sulfur trioxide adducts $SeCl_4.SO_3$ and $TeCl_4.SO_3$. From similarities between their spectra and those of $SeCl_4.AlCl_3$ and $TeCl_4.AlCl_3$, respectively, he concluded that they are best formulated as the ionic chlorosulfates $SeCl_3^+SO_3Cl^-$ and $TeCl_3^+SO_3Cl^-$.

Recently there has been a renewed interest in these selenium and tellurium cations. Adams and Lock (4) have examined the far infrared and Raman spectra of $TeCl_4$ and concluded that while the structure is $TeCl_3^+Cl^-$ in the solid state, $TeCl_4$ exists as discrete irregular tetrahedral molecules in benzene solution. By comparison of the vibrational spectra of $SCl_3.AsF_6$, $SeCl_3.AsF_6$, and $TeCl_3.AsF_6$ (obtained from the reaction of the tetrachlorides with AsF_5) with those of PCl_3, $AsCl_3$, and $SbCl_3$, respectively, Sawodny and Dehnicke (5) have established their ionic character ($MCl_3^+AsF_6^-$). However, Hayward and Hendra (6) have recently drawn attention to the fact that the frequencies of some of the Raman lines in the solid tetrachlorides are lower than those in their $AlCl_3$ complexes. In addition these workers found that a frequency previously ascribed to the ν_1 stretching mode of $TeCl_3^+$ in the spectrum of solid $TeCl_4$ was resolved into two lines. This anomaly was explained as due to either a degenerate mode split by crystal forces or by assuming that solid $TeCl_4$ has a structure intermediate between C_{2v} and C_{3v} due to a charge-transfer interaction between the halide ion and the central tellurium atom. In contrast, George, Katsaros, and Wynne (7) interpreted their infrared data in terms of the presence of pyramidal MCl_3^+ cations in solid $SeCl_4$ and $TeCl_4$. These findings have been recently supported by Beattie and Chudzynska (8) from an analysis of their infrared and Raman studies on the tetrachlorides. In benzene and acetonitrile, the infrared spectra of tellurium tetrachloride was consistent

with that of a monomeric structure of C_{2v} symmetry.

In the present work evidence (from the results of electrical conductivity and Raman spectral measurements) is presented for the formation of $SeCl_3^+$ and $TeCl_3^+$ in solutions of $SeCl_4$ and $TeCl_4$ in chlorosulfuric acid, and the previous results on solid $SeCl_4$ and $TeCl_4$ are discussed.

Experimental

Chlorosulfuric acid, reagent grade (British Drug Houses), was used as described previously (1). *Fluorosulfuric acid* (Allied Chemical) was purified by distillation at atmospheric pressure and the fraction boiling at 162 °C was collected and used. *Selenium and tellurium tetrachlorides* were prepared directly from the elements. Ten grams of metal were placed in a 200 ml round bottom flask with a 7 mm inlet side arm and a guard tube containing magnesium perchlorate at the neck. A slow stream of chlorine was passed over the sample until the exothermic reaction was complete. The products were purified by sublimation at atmospheric pressure in a chlorine atmosphere and stored in sealed ampuls. Analysis of these compounds gave the following:

	Theoretical		Found	
	%M	%Cl	%M	%Cl
$SeCl_4$	35.76	64.24	35.91	64.06
$TeCl_4$	47.36	52.64	—	52.59

The apparatus and technique used in carrying out electrical conductivity measurements at 25 °C have been described earlier (1). Raman spectra were obtained on Kodak IIaO photographic plates by means of a Hilger and Watts spectrometer equipped with a Toronto mercury arc (excitation source: 4358 Å). The spectra were recorded by scanning the plates with a Joyce Loebl double beam MK IIIC microdensitometer.

Results and Discussion

a. Electrical Conductivity Measurements

Electrical conductivity measurements on solutions of $SeCl_4$ and $TeCl_4$ in chlorosulfuric acid are shown in Table I and Fig. 1, where they are compared to the conductivities of solutions of the strong base KSO_3Cl and those of potassium chloride.

$$[4] \qquad KSO_3Cl = K^+ + SO_3Cl^-$$

$$[5] \qquad KCl + HSO_3Cl = K + SO_3Cl^- + HCl$$

Because the mobility of the chlorosulfate ion in chlorosulfuric acid is much greater than those of common cations, all strong bases give approximately the same equivalent conductivities in HSO_3Cl (1). Thus it is clear that $SeCl_4$ and $TeCl_4$ both behave as strong bases according to either

TABLE I

Specific conductivities (κ) of solutions of selenium tetrachloride, tellurium tetrachloride, and hydrogen chloride in chlorosulfuric acid of concentration ω* at 25 °C

$SeCl_4$		$TeCl_4$		HCl	
ω	$10^2\kappa$	ω	$10^2\kappa$	ω	$10^3\kappa$
0	0.0330	0	0.0368	0	0.3619
0.0106	0.1753	0.0127	0.2070	0.0230	0.5425
0.0115	0.1867	0.0159	0.2509	0.0278	0.5733
0.0214	0.3266	0.0303	0.4407	0.0557	0.7256
0.0294	0.4387	0.0343	0.4925	0.0797	0.8254
0.0338	0.4959	0.0486	0.6640	0.1007	0.9155
0.0400	0.5816	0.0557	0.7485	0.1170	0.9532
0.0449	0.6431	0.0719	0.9259	0.1183	0.9696
0.0501	0.7126	0.0762	0.9739	0.1332	1.0173
0.0570	0.7968	0.0955	1.1693	0.1507	1.0491
0.0654	0.8986	0.0964	1.1760	0.1540	1.0734
0.0735	0.9965	0.1125	1.3296	0.1550	1.0607
0.0768	1.0403	0.1132	1.3318		
0.0817	1.0928	0.1374	1.5435		
0.0959	1.2649	0.1415	1.5818		
0.1049	1.3642	0.1617	1.7355		
0.1154	1.4753	0.1691	1.7973		
		0.1870	1.9187		
		0.1905	1.9500		

*Concentration expressed as moles/kg of solution.

$$[6] \qquad MCl_4 + HSO_3Cl = HMCl_4^+ + SO_3Cl^-$$

or

$$[7] \qquad MCl_4 + HSO_3Cl = MCl_3^+ + SO_3Cl^- + HCl$$

Experimentally it was found that rather concentrated solutions lost hydrogen chloride, indicating that the reaction occurs according to [7].

b. Raman Spectra

That ionization does indeed occur according to [7] was confirmed by Raman spectral measurements on solutions of $SeCl_4$ and $TeCl_4$, respectively, in chlorosulfuric and fluorosulfuric acid. The results are summarized in Table II. Solutions in fluorosulfuric acid were studied in addition to those in chlorosulfuric acid because the ν_3 and ν_1 frequencies of $SeCl_3^+$ were obscured by the intense S—Cl stretching frequency of the acid at 416 cm^{-1}.

Each spectrum contained four lines, in addition to those due to solvent, and a line close to 1050 cm^{-1} attributable to the SO_3Cl^- (or SO_3F^-) anion (9). The highest of the four frequencies was in each case polarized as expected for a MCl_3^+ species having C_{3v} symmetry. The spectra are in excellent agreement with those previously reported for the AsF_6^- salts by Sawodny

Can. J. Chem. Downloaded from www.nrcresearchpress.com by 210.87.254.6 on 09/05/12
For personal use only.

Can. J. Chem. Downloaded from www.nrcresearchpress.com by 210.87.254.6 on 09/05/12
For personal use only.

TABLE II

Comparison of spectra of $SeCl_4$ and $TeCl_4$ in the solid state with those of $SeCl_3$ and $TeCl_3^+$

$SeCl_4$						$SeCl_3^+$			
(*a*)	(*b*)	(*c*)		(*d*)	(*e*)	(*f*)	(*g*)	(*h*)	
Raman(*s*)	i.r.(*s*)	Raman(*s*)	i.r.(*s*)	Raman(*s*)	i.r.(*s*)	Raman	Raman	Raman	Assignment
[560]		590							
[515]									
474						—	430(*p*)	437	ν_1(a)
441						—	415	390	ν_3(e)
388				384					
	371	375			371				
		361	367	354					
346	348	348	351	346	348				
	275								
258		249							
206	205					207	206	200	ν_2(a)
	190					173	172	168	ν_4(e)
164	165	163							
	145								
127		132							
96									
	80								
69									

$TeCl_4$										$TeCl_3^+$			
(*a*)	(*b*)	(*c*)		(*d*)		(*e*)				(*f*)	(*g*)	(*h*)	
Raman(*s*)	i.r.	Raman(*s*)	i.r.(*s*)	i.r.(*s*)	i.r.(1)	Raman(*s*)	i.r.(*s*)	Raman(2)	i.r.(3)	Raman	Raman	Raman	Assignment
[492]													
415										404(*p*)	399(*p*)	412	ν_1(a)
374		376				376		371	377	375	385	385	ν_3(e)
	358	353	365	364	362								
342	347	343	350	353	347	347	350		354				
[290]					280			280	280				
[246]				237	240		239						
								225					
191	191			186	181		185			170	170	170	ν_2(a)
143	150	150	154	151			153	145		148	150	150	ν_4(e)
							129						
	101												
87	73												
	57												

NOTE: (*a*) Gerding and Houtgraaf (2), (*b*) George, Katsaros, and Wynne (7), (*c*) Hayward and Hendra (6), (*d*) Adams and Lock (4), (*e*) Beattie and Chudzynska (8), (*f*) present results in chlorosulfuric acid, (*g*) present results in fluorosulfuric acid, (*h*) Sawodny and Dehnicke (5), (*s*) spectra of crystalline solid; (1) in benzene solution, (2) in propionitrile solution, (3) in acetonitrile solution; (*p*) polarized line.

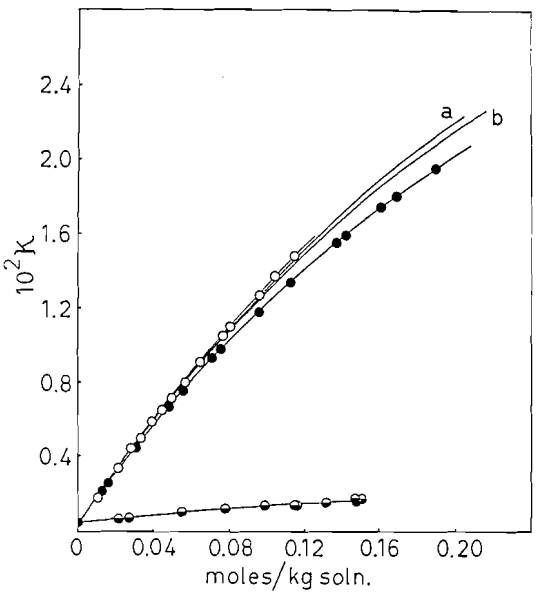

FIG. 1. Specific conductivities of selenium tetrachloride ○, tellurium tetrachloride ●, hydrogen chloride ◒, potassium chloride (*a*), and potassium chlorosulfate (*b*) in chlorosulfuric acid at 25 °C. The specific conductivity values for (*a*) and (*b*) are taken from ref. 1.

and Dehnicke (5). It is significant, however, that although these solution spectra are fully in accord with those of the hexafluoroarsenate salts, there are important discrepancies between the individual frequencies and those assumed previously to be due to the MCl_3^+ cations in solid $SeCl_4$ and solid $TeCl_4$. In particular, the ν_1 and ν_3 frequencies have significantly lower values in the solids than in those cases where the presence of trichloro-cations is definitely established (Table II). Since it is reasonable that the metal–halogen bonds in MCl_3^+ would be stronger than those in covalent MCl_4 molecules, consistent with the observed higher stretching frequencies for the MCl_3^+ ions, there is reason to believe that the formulation of $SeCl_4$ and $TeCl_4$, respectively, as $SeCl_3^+Cl^-$ and $TeCl_3^+Cl^-$ is not justified.

Spectral evidence to date has been inexplicit in showing that $SeCl_3^+$ and $TeCl_3^+$ ions do in fact exist in the crystalline state (Table II). Instead of a four band spectrum consistent with a C_{3v} structure for the MCl_3^+ ion, the infrared and Raman spectra of solid $TeCl_4$ and $SeCl_4$ consistently show complex spectra which may be more reasonably attributed to a trigonal bipyramidal structure. Nine fundamental frequencies would be expected for these tetrachlorides (C_{2v} symmetry) in which eight would be infrared active and all nine would be Raman active. Katsaros and George (7) justified their seven band infrared spectrum for $TeCl_4$ in favor of $TeCl_3^+Cl^-$ by assuming that three bands were due to impurities and a lattice vibration. Adams and Lock (4) found five bands in their infrared spectra for both solid $TeCl_4$ and $TeCl_4$ dissolved in benzene. With various assumptions, the spectra were claimed to be consistent with a $TeCl_3^+Cl^-$ structure in the solid and the existence of covalent $TeCl_4$ molecules in solution. Similarly, Beattie and Chudzynska (8) argued that a five band infrared spectrum of solid $TeCl_4$ was consistent with an ionic formulation. Some doubt also exists concerning Gerding and Houtgraaf's (2) interpretation of the Raman spectra of solid $SeCl_4$ and $TeCl_4$ in terms of $MCl_3^+Cl^-$. Although as many as ten bands were observed in the $SeCl_4$ spectrum and six for $TeCl_4$, only four of the intense bands were assumed to be significant and the rest were discounted.

It seems necessary that a critical reassessment be made for the assignments of the bands in the infrared and Raman spectra of solid $TeCl_4$ and $SeCl_4$. The metal–chlorine stretching frequencies assigned in the solid state are substantially lower than those for the MCl_3^+ ion. Moreover, the complexity of the spectra, as compared with the present spectrum of the MCl_3^+ ion, strongly suggests that both $SeCl_4$ and $TeCl_4$ exist as trigonal bipyramidal molecules in the crystalline state.

Acknowledgments

The National Research Council of Canada and the University of Toronto are thanked for generous financial assistance. One of us (J. A. Ciruna) is indebted to NRCC for the award of a scholarship.

1. E. A. ROBINSON and J. A. CIRUNA. Can. J. Chem. 1968. In press.
2. H. GERDING and H. HOUTGRAAF. Rec. Trav. Chim. **73**, 737, 739 (1954).
3. H. GERDING. Rec. Trav. Chim. **75**, 589 (1956).
4. D. M. ADAMS and P. J. LOCK. J. Chem. Soc. A, 145 (1967).
5. W. SAWODNY and K. DEHNICKE. Z. Anorg. Allgem. Chem. **349**, 169 (1967).
6. G. C. HAYWARD and P. J. HENDRA. J. Chem. Soc. A, 646 (1967).
7. J. W. GEORGE, N. KATSAROS, and K. J. WYNNE. J. Inorg. Chem. **6**, 903 (1967).
8. I. R. BEATTIE and H. CHUDZYNSKA. J. Chem. Soc. A, 984 (1967).
9. R. J. GILLESPIE and E. A. ROBINSON. Can. J. Chem. **40**, 644 (1962).

Can. J. Chem. Downloaded from www.nrcresearchpress.com by 210.87.254.6 on 09/05/12
For personal use only.

Can. J. Chem. Downloaded from www.nrcresearchpress.com by 210.87.254.42 on 09/05/12
For personal use only.

Theoretical views on Szilard Chalmers reactions in solid systems. II. Parent reformation by billiard-ball collisions

W. H. WONG[1] AND D. R. WILES
Chemistry Department, Carleton University, Ottawa, Canada

Received April 11, 1967[2]

The problem of billiard-ball replacement reactions of atoms centrally located in the molecule has been approached, using the approximation of simple two-body collisions. The reentry process has been separated into steps which can be handled by straightforward mathematical operations. Collision diameters for given energy transfer were calculated using an exponentially screened potential.

Species treated include dicyclopentadienyl metals, arene metal carbonyls, and hexacoordinated complex ions, although the method is applicable to many other types of compound. An important result is that the probability of successful billiard-ball replacement is not sensitive to the initial energy, as long as this is not too low. It is concluded that this method is, at its present stage, most useful in calculating lower limits for billiard-ball reformation by following the projectile energy down to ca. 100 eV. Below this energy it is considered that thermal decomposition of the reformed molecule is likely. Results of the calculation are compared with experimental data, and further experiments are suggested by which the contribution of billiard-ball collisions may be directly assessed.

Canadian Journal of Chemistry, 46, 3201 (1968)

Introduction

In current studies of the behavior of atoms recoiling from nuclear reactions, the main question is, of course, not how they get out of their molecules, but how they get back in — either to reform the original molecule or to give a different one. Two simple mechanisms have been commonly invoked in attempts to understand the observed phenomena: diffusion back to the original site, followed by recombination with the original partners, and the so-called "billiard-ball" collisions with nearby molecules, giving direct replacement to form the same species at another site. The first of these was dealt with in Part I of this series (1). It was concluded that the present experimental evidence does not agree with the calculated possible back-diffusion reformation, and that this back diffusion makes a very minor contribution to reformation if, indeed, any at all.

The interpretation of parent retention by a billiard-ball collision mechanism was first put forward by Libby (2) to interpret his studies of liquid organic halide systems. In his theory, the radioactive atom, recoiling with a kinetic energy above the bond-breaking energy v, collides elastically with another atom in a similar nearby molecule such that after the collision, the atom retains an amount of energy less than some critical value ε, is trapped, and forms bonds with the rest of the molecule. Considering only single-component systems, Libby obtained the expression

$$[1] \qquad R = \frac{\varepsilon}{v}$$

for the retention, R, of the radioactive atoms in the parent compounds.

This approach has been further developed by Miller, Gryder, and Dodson (3) and by Capron and Oshima (4), who obtained the corresponding expressions for multicomponent systems (e.g. CCl_4–Br_2 solution). The calculated values for the CCl_4–Br_2 system which emerged from their calculations showed fairly good agreement with the experimental results. More recently, Nesmeyanov (5) has reported fairly good agreement between calculated and experimental results for bromoethane diluted with chloromethanes.

Although many processes can be considered which may lead to the reformation of the parent compound, the similarity of the observed retention values for many of these compounds ($Fe(C_5H_5)_2$ (6), $Ru(C_5H_5)_2$ (7), $Cr(C_6H_6)_2$ (8), $C_5H_5Mn(CO)_3$ (9), $C_6H_6Cr(CO)_3$ (10), and others) suggests a process which is structure dependent, rather than one which may depend primarily on the chemical behavior of the individual metal ions. Some experiments have been reported which show the importance of radical diffusion reactions, but to date only in the case of compounds irradiated in solution: $C_5H_5Mn(CO)_3$ (11) and $CH_3C_5H_4Mn(CO)_3$

[1]Present address: Chemistry Department, University of Toronto, Toronto, Ontario.
[2]Revision received April 25, 1968.

Can. J. Chem. Downloaded from www.nrcresearchpress.com by 210.87.254.42 on 09/05/12
For personal use only.

(12). We are, however, faced with a phenomenon which does involve physical recoil and, evidently, collisions which result in the transfer of energy from one atom to another. It is thus reasonable to consider this collision process to assess the possibility of the reformation of the parent molecule by a 'hot' process, and in particular by a billiard-ball collision.

The several previous studies of this nature (3, 4, 13) have been made on alkyl halide molecules, in which the halogen atom—the collision partner—is on the 'outside' of the molecule and can be knocked out of the molecule with high efficiency. On the other hand, many organometallic compounds have the relevant atom—the metal atom—more or less buried within the molecule. The dicyclopentadienyl 'sandwich' compounds illustrate this situation. Thus, the nature of the calculation is somewhat different from that of the previous studies, although of course the phenomenon is the same, and the basic approach is quite similar.

The present work, then, attempts to examine the collision process to determine: firstly, those aspects of the collision which are peculiar to the replacement of central atoms; secondly, what parameters of the equations developed can be isolated as being critical and independently measurable; thirdly, whether any estimates of the extent of billiard-ball reformation can be made which could be compared with experimental data; and finally, what new experiments can be suggested by the calculations.

General Theory

The basic mechanism conceived in the application of the billiard-ball model involves an energetic atom moving rapidly through the solid (or liquid) and colliding with a molecule. In order to effect the billiard-ball replacement, it must collide with an atom of its own mass in a nearly 'head on' collision, so that virtually all of its energy is transferred to the collision partner. In all calculations on such interactions there are several points of considerable uncertainty (14): (*i*) The atomic interaction potential is not known, which means that the effective sizes of the atoms are not known as a function of interaction energy. In the present work, the Bohr exponentially screened potential, as described in Part I (1), is used to determine the effective collision-parameters for any given energy exchange. (*ii*) The minimum energy v required to remove the collision partner from the molecule, and the maximum energy ε below which the projectile atom will be trapped within the molecule-cage are not known, although the value of 25 eV has been suggested for each by Seitz and Koehler (15) and by Harbottle and Sutin (16). (*iii*) The assumption of hard-sphere collisions is scarcely valid (17) although it is difficult to devise a more reliable substitute. In the calculations presented here we must be aware of these uncertainties.

Since the present mechanism requires collisions with well-shielded atoms, such as the iron atom in ferrocene, it must be noted that if the parent molecule is to be reformed, neither the incoming nor the outgoing atom may suffer energetic collisions with ligand atoms. The total interaction is thus divided artificially into sections, which are assigned calculable probabilities as follows: (*a*) The probability that the recoiling atom will strike a relevant molecule is considered to be identically 1 for pure systems. (*b*) The probability is P_a that the projectile atom will be headed directly toward the central, isotopic, atom in the struck molecule. (*c*) The probability is P_{in} that the projectile will be able to strike the central atom without first displacing any ligand atom. It is assumed, for simplicity, that the trajectory is randomly oriented with respect to the molecular axes. (*d*) The probability is P_{ex} that the energy exchange with the isotopic atom will both (*i*) remove the initial target atom and (*ii*) leave the initial projectile with too little energy to escape. Following earlier work (15, 16) we assume that the target atom must be given at least 25 eV. The projectile must be left with an energy less than ε, where ε is a parameter to be examined in this work. (*e*) The probability is P_{out} that the struck target atom will escape without suffering collision with any ligand atom.

The probability, P, that any given collision with a molecule will result in a complete billiard-ball replacement is given by

$$[2] \qquad P = P_a \cdot P_{in} \cdot P_{ex} \cdot P_{out}$$

Each of these individual probabilities is expected to vary with projectile energy. They are discussed in more detail below.

Separated Probabilities

P_a

To estimate the probability of collision with the 'target' atom, we use the ratio of the pro-

Can. J. Chem. Downloaded from www.nrcresearchpress.com by 210.87.254.42 on 09/05/12
For personal use only.

jected cross section of the atom to that of the molecule. The effective size of the atom, for this purpose, is calculated from the hard-sphere radius, while the size of the molecule is calculated from the bond lengths plus the soft-sphere collision parameter, assuming a spherically symmetrical molecule. This is similar to the method used by Shaw (13) for bromine–carbon collisions. Thus, for ferrocene for example, the Fe—C bond distance is 2.05 Å. The collision parameter for Fe on C is found to be 1.03 Å by methods described by Hirschfelder, Curtiss, and Bird (18), and the hard-sphere radius for Fe on Fe is found to be typically 0.915 Å for a projectile energy of 300 eV. Hence,

$$P_a = \frac{(0.915)^2}{(2.05 + 1.03)^2} = 0.088$$

Typical values of P_a are given in Table I.

This approach consciously ignores any orientation effect which may result from 'channeling' of the recoil atom by the lattice. It is our belief that, since the projectile starts its trajectory on a lattice point, channeling is not likely to produce a predictable or detectable effect for the first few, high energy, collisions (19). Thus the term P_a, depending only on the direction of the projectile's motion, is not a function of the projectile energy.

TABLE I

Probability (P_a) that a random projectile striking a molecule or ion will aim at its central (target) atom

Molecule	P_a	Ion	P_a
$Fe(C_5H_5)_2$	.088	$ReCl_6^{2-}$	.065
$Mn(C_5H_5)_2$	.077		
$Ru(C_5H_5)_2$	.077	$Co(NH_3)_6^{2+}$	.063
$Cr(C_6H_6)_2$	.073	$Co(NH_3)_6^{3+}$	.092
$CpMn(CO)_3$	.084		

P_{in}

The projectile atom is considered to be aiming directly at the central, isotopic atom, from any random direction. Thus, the probability of its entering a molecule to engage in a billiard-ball collision, without damaging the molecule, is equal to the probability of its getting out of its own molecule at the same energy, without causing damage. This latter probability has been calculated (1) and the values may be used directly. Briefly, this probability was considered to be one minus the total fractional solid angle subtended by a group of circles, each of which defined the region within which the atom at the center of the circle would receive a momentum impulse of not less than 25 eV. Proper allowance was made for 'overlapping' of the circles representing closely spaced ligand atoms.

This term was found to vary only slowly with projectile energy down to about 100 eV, becoming smaller at lower energies.

P_{ex}

The hard-sphere collision is isotropic, and the cross section for transfer of energy in any fractional interval is independent of the value of the energy. Thus, for a particle of initial energy E, colliding with another particle of the same mass, the probability of transferring energy between E and $(E - \varepsilon)$ (that is, all of its energy except ε or less) is given by

$$[3] \qquad P_{ex} = \frac{\varepsilon}{E}$$

The validity of this term, then, depends on the assumption of a hard-sphere collision, and on the validity of the value of ε. This latter can be chosen to be 25 eV, following the lead of others in the field (15, 16), although we shall examine the effect of variation in the choice of ε.

It is useful to have an energy limit below which no collision is considered. This purely mathematical parameter, E_c, can be varied independently of the physical parameters with the objective of identifying the departure of the mathematical model from the physical reality.

P_{out}

In order for parent reformation by this mechanism to be successful, the outgoing species after the collision should not disrupt the molecule's ligands in its flight. Since the incoming recoil species, having a kinetic energy E, could retain an energy between 0 and ε, the outgoing isotopic atom may have an energy ranging from E to $(E - \varepsilon)$. Further, if we assume the collision partners to be of the same mass, the maximum angle of scattering will be

$$[4] \qquad \phi = \cos^{-1}\sqrt{\left(1 - \frac{\varepsilon}{E}\right)}$$

Thus, the outgoing atom will deviate from the incoming path by an angle ranging from zero to ϕ. However, the value of this scattering angle, averaged over the whole energy range of the incoming species, is quite small, and without

Can. J. Chem. Downloaded from www.nrcresearchpress.com by 210.87.254.42 on 09/05/12
For personal use only.

introducing serious error we may approximate the outgoing atom's path as being collinear with that of the incoming atom.

If we confine our attention to molecules with inversion centers, it turns out that the trajectories for which the outgoing atom would damage the ligands are the same as those for which the incoming atom would cause damage. Thus, a successful incoming ensures a successful outgoing. In these cases, then,

$$[5] \qquad P_{in} \cdot P_{out} \equiv P_{in\text{-}out} = P_{in}$$

In other cases, although there may be no inversion center, the effect may be the same. This would be so for manganocene, ruthenocene, cyclopentadienylmanganese tricarbonyl, and others, in which the ligands on one side of the central atom effectively obscure those on the other side. An important result of this is the prediction of equal billiard-ball probabilities for groups of similar molecules such as dibenzenechromium and benzenechromium tricarbonyl, or manganocene, cyclopentadienylmanganese tricarbonyl and, still quite accurately, methylcyclopentadienylmanganese tricarbonyl.

In still other cases, notably the tetrahedral and trigonal molecules, it is convenient to perform the reflection operation, and generate a molecule with an inversion center (turning the tetrahedron into a cube, for example). Once again eq. [5] holds.

Of all these various terms, P_{in} is seen to depend on the choice of ν and will vary with the projectile's energy, although the variation will be small at energies above about 100 eV. P_{ex} will be given by ε/E and thus is directly dependent on the value chosen for ε. At very low energies, the incoming and outgoing trajectories will be farther from collinear, and eq. [5] will not hold. P_a is somewhat uncertain, since the effective sizes of the atom and the molecule are difficult to define unambiguously, and the possible effect of directional selectivity has been ignored. This term will not, however, be strongly influenced by energy variation.

With these uncertainties recognized, then, we proceed to examine the application of the model to various cases.

Case 1. Probability of Parent Reformation in a Single Collision

For the calculation of parent reformation in a single collision of specified projectile energy, the various partial probabilities are easily determined. P_a is taken from calculations done as described above and reported in part in Table I. The value of $P_{in\text{-}out}$, as described above, is obtained for some molecules in Paper I (1). P_{ex} is calculated simply from eq. [3], using selected values for ε. The results of these calculations for a series of typical compounds are given in Fig. 1 for a range of values of ε.

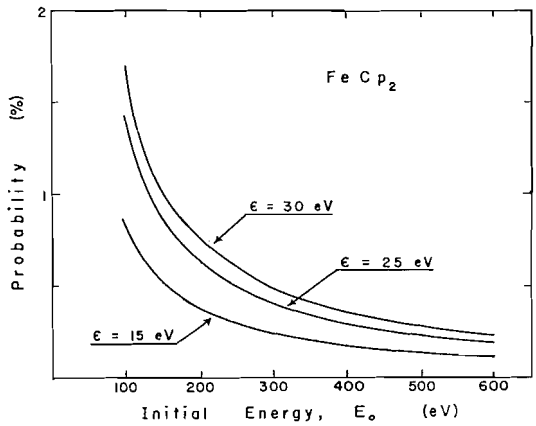

FIG. 1. Calculated probability of billiard-ball reformation in a single collision. The $FeCp_2$ curves will quite well represent a number of analogous compounds such as $MnCp_2$, $CpMn(CO)_3$, $CH_3CpMn(CO)_3$, $Cr(C_6H_6)_2$, $(C_6H_6)Cr(CO)_3$, and others.

Case 2. Probability of Parent Reformation Following a Given Number of Collisions with Carbon Atoms

This case differs from the previous one in that each successive collision reduces the energy of the projectile and thus, according to the data of Fig. 1, increases the probability of parent reformation in the next collision. Two simplifying assumptions have been made here: (*i*) these moderating collisions are considered to be only with carbon atoms (or other light atoms), (*ii*) successive collisions do not occur in the same molecule. These assumptions lead to no significant error, and greatly simplify the mathematical operations.

If the initial energy of the projectile atom is E_0, after one collision with a light atom its energy is expected to be evenly distributed in the range between E_0 and a minimum of γE_0, in which γ is given by

$$[6] \qquad \gamma = \left(\frac{M_1 - M_2}{M_1 + M_2}\right)^2$$

where M_1 is the mass of the projectile atom and

Can. J. Chem. Downloaded from www.nrcresearchpress.com by 210.87.254.42 on 09/05/12
For personal use only.

M_2 is the mass of the carbon atom. The expected average energy after one such collision will be

$$[7] \qquad \langle E_1 \rangle = \tfrac{1}{2}(1 + \gamma)E_0$$

If the projectile atom of energy E_1 undergoes a second collision with a carbon atom, it will then have an average energy of

$$\frac{E_1 + \gamma E_1}{2}$$

The energy distribution function of the projectile atom after two collisions with carbon atoms will be (4, 20)

$$\frac{dE_1}{E_0(1 - \gamma)} \cdot \frac{dE_2}{E_1(1 - \gamma)}$$

Therefore, the expected average energy of the projectile is

$$[8] \quad \langle E_2 \rangle = \int_{\gamma E_0}^{E_0} \int_{\gamma E_1}^{E_1} \frac{E_1 + \gamma E_1}{2} \cdot \frac{dE_1}{E_0(1 - \gamma)} \cdot \frac{dE_2}{E_0(1 - \gamma)}$$

$$= \tfrac{1}{4}(1 + \gamma)^2 E_0$$

Similarly, after the third collision with a carbon atom, the expected average projectile energy is

$$[9] \quad \langle E_3 \rangle = \int_{\gamma E_0}^{E_0} \int_{\gamma E_1}^{E_1} \int_{\gamma E_2}^{E_2} \frac{dE_1}{E_0(1 - \gamma)} \cdot \frac{dE_2}{E_1(1 - \gamma)} \cdot \frac{E_2(1 + \gamma)}{2} \cdot \frac{dE_3}{E_2(1 - \gamma)}$$

$$= \tfrac{1}{8}(1 + \gamma)^3 E_0$$

The partial probabilities corresponding to these expected average energies are obtained in the manner described for Case 1, and the overall probability can be considered as the sum of the probabilities for the successive collisions. These are shown for up to three moderating collisions in Fig. 2.

Case 3. General Formulation of Parent Reformation in a Steady-State System

In all cases, steady state is reached almost instantly if we consider only the 'hot' reactions—as many atoms are being reduced to an energy less than ε (or E_c) per unit time as are being added to the system at energy E_0. In such a system, a distribution function $N(E)$ is a valid, if not easily calculable, function between ε and E_0. As before, the billiard-ball collision can be successful only if the projectile atom transfers at least ν eV and is left after the collision with less than ε eV. It is thus possible to estimate the parent reformation by the following calculation:

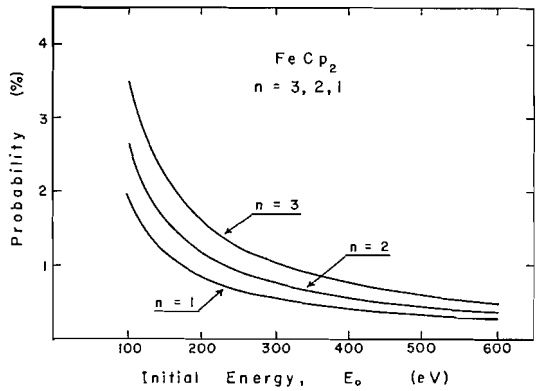

FIG. 2. Calculated probability of billiard-ball reformation after a series of n collisions with carbon atoms.

Three processes lead to the reduction of the projectile atoms energy below the critical value E_c: (*i*) direct billiard-ball collisions, (*ii*) billiard-ball collisions as result of which the ligand structure has been damaged, and (*iii*) collisions with carbon atoms. Of these, some direct collisions (*iv*) will result in retention if the energy is dropped below ε. The numbers involved, per unit time, in these processes are given by:

$$[10a] \quad N(i) = \int_{E_c}^{E_0} P_a \cdot P_{in} N(E) \frac{E_c}{E} dE$$

$$[10b] \quad N(ii) = \int_{E_c}^{E_0} P_a \cdot (1 - P_{in}) N(E) \frac{E_c}{E} dE$$

$$[10c] \quad N(iii) = \int_{E_c}^{E_0} (1 - P_a) N(E) \frac{E_c - \gamma E}{E - \gamma E} dE$$

$$[10d] \quad N(iv) = \int_{E_c}^{E_0} P_a \cdot P_{in} N(E) \frac{\varepsilon}{E} dE$$

This being the case, the extent of parent reformation is equal to $N(iv)$ and the fractional parent reformation is given by

$$[11] \qquad R = \frac{N(iv)}{N(i) + N(ii) + N(iii)}$$

In order to solve this expression, some simplification is necessary. Although P_{in} is a function of the energy, it is only slowly varying, and may be

TABLE II

Calculated billiard-ball replacement yields compared with experimental retention values

Compound	Energy (eV)	Calculated billiard-ball replacement (%)* when E_c = 50 eV	E_c = 100 eV	Experimental retention* R (%)	Reference
$Fe(C_5H_5)_2$	15	2.8	1.6	12	6
	30	5.6	3.1		
$Co(C_5H_5)_2$		†	†	65	21
$Ni(C_5H_5)_2$		†	†	25	21
$Cr(C_6H_6)_2$	15	2.8	1.4	12	8
	30	5.7	2.8		
$Ru(C_5H_5)_2$	15	4.8	2.2	7–8	7, 24
	30	9.6	4.4		
$Cr(CO)_6$	15			43–54	22
	30				
$Mo(CO)_6$	15			71–74	22
	30				
$W(CO)_6$	15			50–55	23
	30				
$C_5H_5Mn(CO)_3$	15	3.6	1.7	12–18	9, 24
	30	7.2	3.5		
$CH_3C_5H_4Mn(CO)_3$		‡	‡	6–8	12, 26
$C_6H_6Cr(CO)_3$		‡	‡	10	10

*We emphasize that the calculated values represent lower limits on billiard-ball yields only, while the retention values refer to total retention after chemical processing.
†Similar to $Fe(C_5H_5)_2$.
‡Similar to $C_5H_5Mn(CO)_3$.

regarded as effectively constant, unless the energy is too low. The value of P_{in} used is that corresponding to an average energy obtained from the relation

$$[12] \qquad \langle E \rangle = \frac{\int_{E_c}^{E_0} EN(E)\mathrm{d}E}{\int_{E_c}^{E_0} N(E)\mathrm{d}E}$$

The other partial probability, P_a, is nearly independent of energy, and is taken from Table I above. The distribution function $N(E)$ is taken according to Miller, Gryder, and Dodson (3) to be

$$[13] \quad N(E) = Q\delta(E - E_0) + \frac{Q}{[(1 - \langle P_a \rangle)(1 - \gamma) + \langle P_a \rangle]E}$$

in which Q is the rate of generation of the recoil species and $\delta(E - E_0)$ is the Dirac delta function centering at E_0.

Combining all of these (for the detailed mathematical operations, see the Appendix), we obtain for the fractional parent reformation

$$[14] \qquad R = \frac{\langle P_a \rangle \langle P_{in} \rangle}{\langle P_a \rangle E_c + (1 - \langle P_a \rangle)\Delta}$$

where

$$\Delta = \frac{1 - \frac{\gamma}{1 - \gamma} \ln \frac{1}{\gamma}}{\frac{1}{E_0}[(1 - P_a)(1 - \gamma) + P_a] + \left(\frac{1}{E_c} - \frac{1}{E_0}\right)}$$

This expression can be solved directly between E_c and E_0, where both E_c and E_0 can be selected. The results of the calculated data for ferrocene, a typical case, are shown in Fig. 3. These data and some for other systems are given in Table II.

Discussion

The results of the calculations for Case 1—for a single collision—show that above a certain energy the probability of a successful billiard-ball collision is both very low and not strongly energy dependent. This would be the case, for example, at all energies above about 200 eV for the metallocene compounds. The same qualitative result is valid for Case 2—the case of a specified small number of collisions where Fig. 2 shows only slight dependence of the total billiard-ball yield on the initial energy above about 250 eV.

When we follow the projectile atom down to

Can. J. Chem. Downloaded from www.nrcresearchpress.com by 210.87.254.42 on 09/05/12
For personal use only.

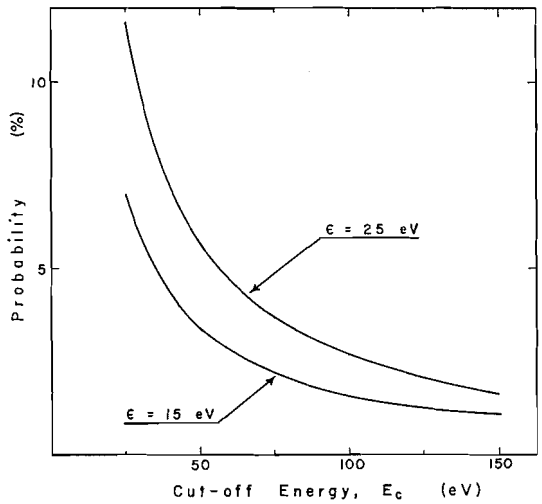

FIG. 3. Calculated total probability of billiard-ball reformation as a function of E_c, the energy below which no collision is considered. The data are for $FeCp_2$, but adequately represent a large number of similar compounds.

'epithermal' energies, that is, past its last collision, the problem becomes very sensitive to several parameters. This is the problem as stated in Case 3 which is, after all, the most important aspect of the present development. We can first compare the experimental retentions for a number of compounds with those calculated from this theory, as in Table II. The calculated values are obtained by the method of Case 3, using $\varepsilon = 15$ eV and 30 eV, and using $E_c = 50$ eV and 100 eV. We see from Table II that the agreement seems to be encouragingly good for some cases. Unfortunately, however, at least one aspect of recent work suggests that the agreement in Table II may be more apparent than real. There is good evidence (12, 25) to show that in liquid $CH_3CpMn(CO)_3$ the bulk of the 'retention' is the result of radical diffusion reactions, and is not due to hot collision processes at all. Although one cannot extrapolate these results confidently from liquids to solids, it seems likely that the same type of situation may be prevalent in molecular solid systems. For example, the very high values shown for retentions in the metal hexacarbonyls and for some of the cyclopentadienyl metal compounds clearly indicate a very great deal of purely chemical recombination. Moreover, the variation in retention with irradiation conditions also suggests the occurrence of substantial reformation by processes other than high energy collisions.

Through the use of the rather artificial parameter E_c, it is possible to stop the calculation at any energy and calculate the hot retention down to that energy. This calculation should give minimum values for the hot retention. At the lowest energies (25–50 eV) the assumption of a rectilinear trajectory during the billiard-ball collision (eqs. [4] and [5]) would be a poor approximation. The impulse approximation for the collision of the recoil atom with ligand atoms (P_{in}) will likewise be less good at low energies, although the difference is not likely to be large. Failure of these two assumptions will have the effect of leaving the reformed molecule in a high state of excitation. Coupled with this is the fact that by the time the projectile has reached low energy a good deal of energy will have been dissipated in the vicinity—in the hot zone. Thus, thermal dissociation of the reformed molecule may well follow a successful billiard-ball collision at low energies. Even though this same molecule should coalesce once again on final cooling of the hot zone the process would be susceptible to scavenging and could scarcely now be called a billiard-ball reaction. This argument would then support the use of E_c as not only a mathematically useful device but as a physically plausible limit below which reformed molecules are liable to thermal dissociation. We suggest that a reliable lower limit for billiard-ball reformation may be obtained using $E_c = 100$ eV.

Regrettably, it is not at present possible in solid state studies to separate the hot reactions from those which occur by diffusion in the hot zone or by other slower processes. It seems quite necessary to make more vigorous attempts to measure this elusive phenomenon. The most apparent barrier to the usefulness of this theory is the difficulty of independently testing the various parameters. However, this difficulty may yield to the possibility of simulating recoil reactions by ion implantation techniques. It is not an inconceivable experiment now to use a beam of radioactive ions to bombard single molecules in the vapor state, or to bombard adsorbed monolayers at selected initial energies. Although this type of experiment may not be possible with a wide range of compounds, studies of this sort should make possible the direct test of several of the parameters of the present work. Such studies are being undertaken at present in our laboratory with the hope that it may be possible to determine directly the values of ε, ν, and E_c.

Can. J. Chem. Downloaded from www.nrcresearchpress.com by 210.87.254.42 on 09/05/12
For personal use only.

A further recommended approach, whose theoretical development has been completed (27), is to bombard mixed systems so that the recoil atom must replace one of a very different mass. The experiments can easily be done by neutron irradiation (as by using a target of $RuCp_2$ in solid solution in $FeCp_2$) or by ion beam methods (as by bombarding $FeCp_2$ with ruthenium atoms).

Acknowledgments

We are grateful to Mr. W. A. Robertson for helpful discussions and to the National Research Council of Canada for financial support.

Appendix

Solution to eq. [11],

$$R = \frac{N(iv)}{N(i) + N(ii) + N(iii)}$$

If $E_0 > E_c/\gamma$

$$[i] \quad R = \frac{\int_{E_c}^{E_0} P_a P_{in} \frac{\varepsilon}{E} N(E)dE}{\int_{E_c}^{E_0} P_a P_{in} \frac{E_c}{E} N(E)dE + \int_{E_c}^{E_0} P_a(1 - P_{in}) \frac{E_c}{E} N(E)dE + \int_{E_c}^{E_c/\gamma} (1 - P_a) \frac{E_c - \gamma E}{E - \gamma E} N(E)dE}$$

Assuming P_a and P_{in} to be constant, we get

$$[ii] \quad R = \frac{\varepsilon P_a P_{in} \int_{E_c}^{E_0} N(E) \frac{dE}{E}}{E_c P_a \int_{E_c}^{E_0} N(E) \frac{dE}{E} + (1 - P_a) \int_{E_c}^{E_c/\gamma} \frac{E_c - \gamma E}{1 - \gamma} N(E) \frac{dE}{E}}$$

$$[iii] \quad \frac{1}{R} = \frac{E_c}{\varepsilon P_{in}} + \frac{(1 - P_a)}{\varepsilon P_a P_{in}} \left[\frac{\int_{E_c}^{E_c/\gamma} N(E) \frac{E_c - \gamma E}{1 - \gamma} \frac{dE}{E}}{\int_{E_c}^{E_0} N(E) \frac{dE}{E}} \right]$$

with $N(E) = Q\delta(E - E_0) + Q/GE$

where $G = [(1 - \langle P_a \rangle)(1 - \gamma) + P_a]$

The integral in the numerator of expression [*iii*] can be expressed as

$$[iv] \quad \frac{E_c}{1 - \gamma} \int_{E_c}^{E_c/\gamma} N(E) \frac{dE}{E} - \frac{\gamma}{1 - \gamma} \int_{E_c}^{E_c/\gamma} N(E)dE$$

But, substituting [13] into [*iv*] and noting that if the integration range does not include E_0, the integration including the delta function will vanish, one obtains

$$[v] \quad \frac{E_c}{1 - \gamma} \frac{Q}{G} \int_{E_c}^{E_c/\gamma} \frac{dE}{E^2} - \frac{\gamma}{1 - \gamma} \frac{Q}{G} \int_{E_c}^{E_c/\gamma} \frac{dE}{E}$$

$$= \frac{E_c Q}{(1 - \gamma)G} \left[\frac{1}{E_c} - \frac{\gamma}{E_c} \right] - \frac{\gamma}{1 - \gamma} \frac{Q}{G} \ln \frac{1}{\gamma}$$

$$= \frac{Q}{G} \left[1 - \frac{\gamma}{1 - \gamma} \ln \frac{1}{\gamma} \right]$$

The integral in the denominator of expression [*iii*] is

$$[vi] \quad \int_{E_c}^{E_0} N(E) \frac{dE}{E} = Q \int_{E_c}^{E_0} \frac{\delta(E - E_0)}{E} dE + \frac{Q}{G} \int_{E_c}^{E_0} \frac{dE}{E^2}$$

$$= \frac{Q}{E_0} + \frac{Q}{G} \left(\frac{1}{E_c} - \frac{1}{E_0} \right)$$

Then

$$[vii] \quad \Delta = \frac{[v]}{[vi]} = \frac{\frac{Q}{G} \left[1 - \frac{\gamma}{1 - \gamma} \ln \frac{1}{\gamma} \right]}{Q \left[\frac{1}{E_0} + \frac{1}{G} \left(\frac{1}{E_c} - \frac{1}{E_0} \right) \right]}$$

$$= \frac{1 - \frac{\gamma}{1 - \gamma} \ln \frac{1}{\gamma}}{\frac{G}{E_0} + \frac{1}{E_c} - \frac{1}{E_0}}$$

Can. J. Chem. Downloaded from www.nrcresearchpress.com by 210.87.254.42 on 09/05/12
For personal use only.

and [*iii*] becomes

$$\frac{1}{R} = \frac{E_c}{\varepsilon\langle P_{in}\rangle} + \frac{(1 - P_a)}{\varepsilon\langle P_{in}\rangle\langle P_a\rangle}\Delta$$

Therefore

$$[14] \qquad R = \frac{\varepsilon\langle P_{in}\rangle\langle P_a\rangle}{E_c\langle P_a\rangle + (1 - P_a)\Delta}$$

1. D. R. WILES and W. H. WONG. Can. J. Chem. **45**, 1813 (1967).
2. W. F. LIBBY. J. Am. Chem. Soc. **69**, 2523 (1947).
3. J. M. MILLER, J. W. GRYDER, and R. W. DODSON. J. Chem. Phys. **18**, 579 (1950).
4. P. C. CAPRON and Y. OSHIMA. J. Chem. Phys. **20**, 1403 (1952).
5. A. N. NESMEYANOV. *In* Chemical effects of nuclear transformations. Vol. I. I.A.E.A. Vienna. 1965. p. 438.
6. N. SUTIN and R. W. DODSON. J. Inorg. Nucl. Chem. **6**, 91 (1958).
7. G. HARBOTTLE and U. ZAHN. *In* Chemical effects of nuclear transformations. Vol. II. I.A.E.A. Vienna. 1965. p. 133.
8. F. BAUMGÄRTNER, U. ZAHN, and J. SEEHOLZER. Z. Naturforsch. **15a**, 1086 (1960).
9. T. COSTEA, I. NEGOESCU, P. VASUDEV, and D. R. WILES. Can. J. Chem. **44**, 885 (1966).
10. F. BAUMGÄRTNER and U. ZAHN. Radiochim. Acta, **1**, 51 (1963).
11. U. ZAHN. Radiochim. Acta, **7**, 170 (1967).
12. I. C. YANG and D. R. WILES. Can. J. Chem. **45**, 1357 (1967).
13. P. F. D. SHAW. Radiochim. Acta, **1**, 177 (1963).
14. J. A. BRINKMAN. J. Appl. Phys. **25**, 961 (1954).
15. F. SEITZ and J. S. KOEHLER. Solid State Phys. **2**, 307 (1956).
16. G. HARBOTTLE and N. SUTIN. J. Phys. Chem. **62**, 1344 (1958).
17. J. E. WILLARD. Ann. Rev. Nucl. Sci. **3**, 194 (1953).
18. J. O. HIRSCHFELDER, C. F. CURTISS, and R. B. BIRD. Molecular theory of gases and liquids. John Wiley and Sons, Inc., New York. 1954. p. 51.
19. J. B. GIBSON, A. N. GOLAND, M. MILGRAM, and G. H. VINEYARD. Phys. Rev. **120**, 1229 (1960).
20. L. CRABS, J. DEBAISIEUX, D. APERS, and P. C. CAPRON. Bull. Acad. Roy. Belg. Ser. 5, **XLV**, 891 (1959).
21. O. H. WHEELER and M. L. MCCLIN. Radiochim. Acta, **7**, 181 (1967).
22. G. HARBOTTLE and U. ZAHN. Radiochim. Acta, **8**, 114 (1967).
23. S. R. NARAYAN and D. R. WILES. Unpublished work.
24. U. ZAHN. Radiochim. Acta. **8**, 177 (1967).
25. S. C. SRINIVASAN, I. C. YANG, and D. R. WILES. Inorg. Nucl. Chem. Letters, **2**, 399 (1966).
26. I. G. DEJONG and D. R. WILES. Chem. Commun. 519 (1968).
27. W. A. ROBERTSON, D. R. WILES, and W. H. WONG. To be published.

Can. J. Chem. Downloaded from www.nrcresearchpress.com by 210.87.254.42 on 09/05/12
For personal use only.

Can. J. Chem. Downloaded from www.nrcresearchpress.com by 210.87.254.40 on 09/05/12
For personal use only.

Cinétique de l'adsorption compétitive

J. F. Baret et A. G. Bois
Laboratoire de Physique Industrielle, Faculté des Sciences de Marseille, Place Victor Hugo-13-Marseille (3e)

Reçu le 11 décembre 1967

A partir du modèle de Langmuir nous avons déduit une expression de la cinétique de l'adsorption compétitive

$$n = n_\infty[1 - Ne^{pt} - N'e^{p't}]$$

dont la forme simple permet une confrontation avec les résultats expérimentaux. En effet, une détermination en deux temps des constantes N, p, N' et p' permet de montrer que cette relation décrit bien la cinétique d'adsorption de l'alcool laurique en compétition avec l'ergostérol à l'interface huile-eau.

Canadian Journal of Chemistry, **46**, 3211 (1968)

Si un interface est créé à la limite d'une phase contenant deux substances susceptibles de s'adsorber, il y aura compétition entre elles à l'interface. La cinétique de ce processus d'adsorption compétitive peut être étudiée dans le cadre du modèle théorique imaginé par Langmuir. Dans ce modèle, on suppose que la couche de molécules adsorbées est *monomoléculaire*, *idéale* et *localisée*. La signification des deux premiers concepts est la même dans le cas de l'adsorption compétitive que dans le cas de l'adsorption simple. Par contre la notion de localisation mérite d'être précisée si la couche adsorbée contient deux espèces moléculaires différentes. En effet, lorsqu'il n'y a qu'un seul adsorbat la localisation de la couche adsorbée implique simplement l'existence d'un nombre bien défini de sites d'adsorption *fixes* ayant tous la même surface (celle de la molécule adsorbée au maximum de concentration interfaciale). Dans le cas de deux solutés, il faut définir une double division de l'interface en cases "potentielles", les unes correspondant aux molécules 1 occupant l'aire, σ_1, à l'interface et les autres aux molécules 2 d'aire, σ_2. Cette division de *toute* la surface de l'interface ne préjuge rien de l'occupation réelle ultérieure de l'interface. Elle implique seulement qu'à l'instant initial les molécules 1 et 2 se trouveront respectivement devant $C_{s01} = S/\sigma_1$ et $C_{s02} = S/\sigma_2$ sites *virtuellement disponibles*.

Au bout d'un temps t après la création de l'interface, une certaine aire S_1 est occupée par des molécules 1 et une autre S_2 par des molécules 2,

$$S_1(t) = n_1(t)\sigma_1 \text{ et } S_2(t) = n_2(t)\sigma_2$$

$n_1(t)$ et $n_2(t)$ sont les nombres de molécules adsorbées à l'instant t. Il reste donc une surface $S_f(t)$ qui à cet instant est innocupée. Dans l'intervalle de temps dt suivant la probabilité qu'à une certaine molécule de l'espèce 1 de s'adsorber, est d'une part proportionnelle à

$$e^{-\varepsilon_a/kT}$$

ε_a étant la hauteur de la barrière d'énergie d'adsorption (1) et d'autre part proportionnelle au nombre de façons différentes dont cette molécule peut se loger à l'interface, c'est-à-dire proportionnelle au nombre de sites qui à l'instant t, restent potentiellement disponibles aux molécules 1: $C_{s1}(t) = S_f(t)/\sigma_1$.

L'aire libre $S_f(t)$ à l'instant t étant

$$S_f(t) = S - S_1(t) - S_2(t) = S - n_1(t)\sigma_1 - n_2(t)\sigma_2$$

Autrement dit, la probabilité d'adsorption d'une molécule 1 à l'instant t, ayant à sa disposition une aire libre $S_f(t)$, est indépendante des proportions respectives de molécules 1 et 2 dans la portion d'interface $S - S_f(t)$ déjà occupée et de la façon dont les deux espèces moléculaires se partageront ultérieurement l'aire, $S_f(t)$.

Au cours de cet intervalle de temps dt un certain nombre de molécules 1 vont se désorber, la probabilité de désorption est, en appelant ε_d la hauteur de la barrière d'énergie d'adsorption, proportionnelle à $\exp(-\varepsilon_d/kT)$.

Donc la quantité résultante, dn_1, de molécules 1 qui au cours de l'intervalle dt sont passées à l'état adsorbé, est donnée par:

$$dn_1(t) = C_1 \frac{S_f(t)}{S} k_1 e^{-\varepsilon_a/kT} - n_1(t)k_1' e^{-\varepsilon_d/kT}$$

k_1 et k_1' constantes de proportionnalité ou

$$[1] \quad \frac{dn_1(t)}{dt} = C_1\left(C_{s01} - n_1(t) - n_2(t)\frac{\sigma_2}{\sigma_1}\right) \times A_1 - n_1(t)B_1$$

Can. J. Chem. Downloaded from www.nrcresearchpress.com by 210.87.254.40 on 09/05/12
For personal use only.

De même, on obtiendrait:

$$[2] \quad \frac{dn_2(t)}{dt} = C_2\left(C_{s02} - n_2(t) - n_1(t)\frac{\sigma_1}{\sigma_2}\right) \times A_2 - n_2(t)B_2$$

A_1, A_2, B_1 et B_2 sont des constantes dépendant des probabilités d'adsorption et de désorption.

Le système d'éq. [1] et [2] peut être résolu en utilisant les conditions initiales:

$$n_1(0) = 0 \text{ et } n_2(0) = 0$$

On obtient ainsi:

$$[3] \quad \begin{aligned} n_1 &= n_{1\infty}[1 - \alpha e^{pt} - \alpha' e^{p't}] \\ n_2 &= n_{2\infty}[1 - \beta e^{pt} - \beta' e^{p't}] \end{aligned}$$

avec d'une part

$$[3'] \quad \left.\begin{matrix} p \\ p' \end{matrix}\right\} = -\tfrac{1}{2}[C_1A_1 + B_1 + C_2A_2 + B_2] \pm \tfrac{1}{2}[(C_1A_1 + B_1 - C_2A_2 - B_2)^2 + 4A_1A_2C_1C_2]^{1/2}$$

$$\alpha = \frac{p' + pp'/B_2}{p' - p}$$

$$\alpha' = \frac{p + pp'/B_2}{p - p'}$$

$$\beta = \frac{p' + pp'/B_1}{p' - p}$$

$$\beta' = \frac{p + pp'/B_1}{p - p'}$$

et d'autre part

$$[4] \quad \begin{aligned} n_{1\infty} &= C_{s01}\frac{C_1A_1}{C_1A_1 + B_1 + C_2A_2B_1/B_2} \\ n_{2\infty} &= C_{s02}\frac{C_2A_2}{C_2A_2 + B_2 + C_1A_1B_2/B_1} \end{aligned}$$

Ces expressions [4] donnent les nombres de molécules adsorbées lorsque l'équilibre est atteint. Crisp (2) et Fowler (3) les ont obtenues en utilisant d'autres notations

$$C_1 = \frac{B_1}{A_1}\frac{\theta_1}{1 - \theta_1 - \theta_2}$$

$$C_2 = \frac{B_2}{A_2}\frac{\theta_2}{1 - \theta_1 - \theta_2}$$

avec $\theta_1 = \dfrac{n_{1\infty}\sigma_1}{S}$ et $\theta_2 = \dfrac{n_{2\infty}\sigma_2}{S}$

Le nombre total de molécules présentes à l'interface $n = n_1 + n_2$ s'écrit

$$[5] \quad n = n_\infty[1 - Ne^{pt} - N'e^{p't}]$$

avec alors $$n_\infty = \frac{C_1A_1B_2C_{s01} + C_2A_2B_1C_{s02}}{B_1B_2 + C_1A_1B_2 + C_2A_2B_1}$$

et $$N = \frac{n_{1\infty}\alpha + n_{2\infty}\beta}{n_\infty}, \quad N' = \frac{n_{1\infty}\alpha' + n_{2\infty}\beta'}{n_\infty}$$

Les deux termes exponentiels qui déterminent dans [5] l'allure de la cinétique d'adsorption ne sont pas caractéristiques de l'un ou l'autre corps, mais ils dépendent au contraire des propriétés interfaciales de chacun.

Cas limites

1. Cas où il n'y a qu'un seul adsorbat

$$n_1^0(t) = \frac{C_1A_1C_{s01}}{C_1A_1 + B_1}[1 - e^{-(C_1A_1 + B_1)t}]$$

cette relation est classique.

2. Cas où le nombre de molécules adsorbées de l'espèce 2 est constant

$$n_1^2(t) = \frac{C_1A_1C_{s01}(1 - n_2C_{s02})}{C_1A_1 + B_1} \times [1 - e^{-(C_1A_1 + B_1)t}]$$

3. Cas où les molécules adsorbées de l'espèce 2 sont à tout instant en équilibre avec la solution

$$n_1^{2eq}(t) = n_{1\infty}^{2eq}\left[1 - e^{-\left(B_1 + C_1A_1 - \frac{C_1A_1C_2A_2}{B_2 + C_2A_2}\right)t}\right]$$

avec $$n_{1\infty}^{2eq} = \frac{C_1A_1C_{s01}}{C_1A_1 + B_1 + \dfrac{C_2A_2B_1}{B_2}} = n_{1\infty}$$

Dans les pages suivantes nous allons essayer d'apprécier la validité de l'expression générale [5] en étudiant l'adsorption compétitive de l'ergostérol et de l'alcool laurique.

Conditions expérimentales

Nous avons fait adsorber de façon compétitive l'ergostérol et l'alcool laurique à l'interface eau–huile de paraffine. Les solutés sont dissous dans l'huile, ils sont insolubles dans l'eau.

L'huile est débarrassée de toutes traces d'im-

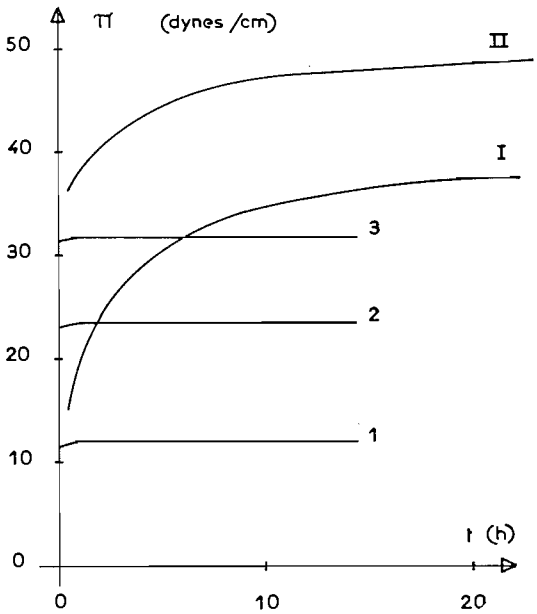

FIG. 1. Variation de la tension interfaciale eau–solution avec le temps, pour les solutions: (I) ergostérol 1/5000; (II) ergostérol 1/3000; 1, alcool laurique 1/700; 2, alcool laurique 1/200; 3, alcool laurique 1/100.

puretés tensioactives par traitement sur charbon actif (Acticarbone[1]), terre adsorbante (Clarsil[1]) et tamis moléculaire (Siliporite[1]). L'eau est tridistillée. Les solutés sont utilisés sous leur forme commerciale.

Six solutions binaires et les solutions avec un seul soluté pour ces mêmes concentrations ont été étudiées.

Ergostérol	1/5000	+	Alcool laurique	1/700
"		+	" "	1/200
"		+	" "	1/100
Ergostérol	1/3000	+	" "	1/700
"		+	" "	1/200
"		+	" "	1/100

On place ces solutions (à 20 °C) dans un tensiomètre à goutte pendante dont le principe a été décrit par ailleurs (4) et l'on suit au cours du temps l'évolution de la tension interfaciale (Figs. 1–3). Nous savons (5–7) que lorsqu'il y a adsorption on peut relier la tension régnant à un interface au nombre de molécules de soluté adsorbées à l'interface.

Nous prendrons en première approximation: $\pi = n(kT/S)$ (nous supposons la proportionnalité de la pression interfaciale au nombre de molécules) étant entendu qu'une équation moins simple serait souhaitable, elle a néanmoins le mérite de permettre un calcul assez aisé.

k et T sont définis comme constante de Boltzmann et température absolue, $\pi = \gamma_0 - \gamma$ est la

[1]Fabriqués par le Ceca, rue Murillo, Paris.

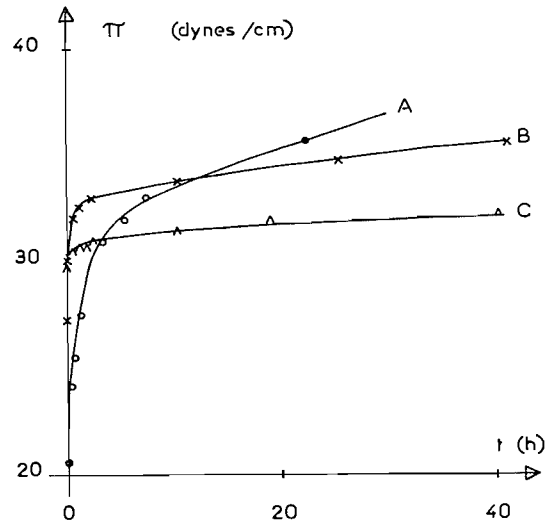

FIG. 2. Evolution au cours du temps de la tension interfaciale eau–solution binaire d'ergostérol à 1/5000 et d'alcool laurique: (A) 1/700 (○); (B) 1/200 (+); (C) 1/100 (∧). Les courbes sont tracées à partir de l'éq. [6] et du Tableau I; les points sont expérimentaux.

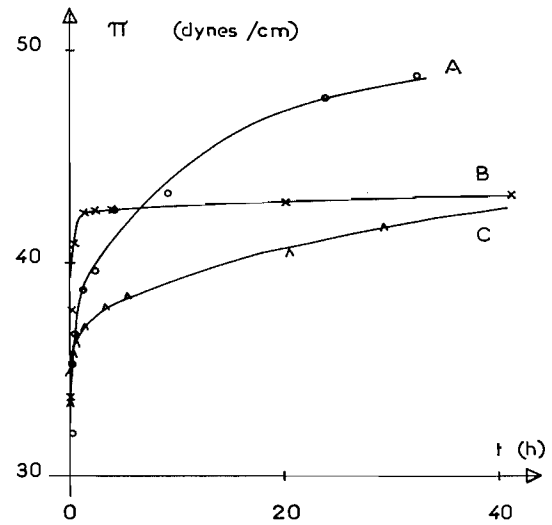

FIG. 3. Evolution au cours du temps de la tension interfaciale eau–solution binaire d'ergostérol à 1/3000 et d'alcool laurique: (A) 1/700 (○); (B) 1/200 (+); (C) 1/100 (∧). Les courbes sont tracées à partir de l'éq. [6] et du Tableau I; les points sont expérimentaux.

Can. J. Chem. Downloaded from www.nrcresearchpress.com by 210.87.254.40 on 09/05/12
For personal use only.

TABLEAU I

Concentration ergostérol	1/5000	1/5000	1/5000	1/3000	1/3000	1/3000
Concentration alcool laurique	1/700	1/200	1/100	1/700	1/200	1/100
p (h^{-1})	−0.0312	−0.0224	−0.0400	−0.0812	−0.0396	−0.0263
N	+0.235	+0.125	+0.0469	+0.232	+0.0284	+0.179
p' (h^{-1})	−0.730	−2.26	−0.890	−3.97	−6.42	−0.875
N'	+0.204	+0.0789	+0.0206	+0.206	+0.170	+0.0451

différence de tension interfaciale huile–eau et solution–eau. n est le nombre de molécules de soluté adsorbé sur l'interface.

Comme $$n = n_1 + n_2$$

L'expression de π en fonction du temps s'écrit:

[6] $$\pi = \pi_\infty[1 - Ne^{pt} - N'e^{p't}]$$

avec $$\pi_\infty = \frac{1}{S} n_\infty kT$$

Pour apprécier la validité de notre interprétation théorique il faut trouver des valeurs numériques des constantes N, p, N' et p' telles que l'éq. [6] décrivent les courbes expérimentales $\pi(t)$.

Nous effectuerons cette détermination en deux étapes. Tout d'abord nous allons utiliser les valeurs expérimentales de π correspondant aux grandes valeurs du temps. En effet puisque $p' < p < 0$ (la relation [3'] indique que p' est négatif et au cours de la résolution nous avons observé que le produit pp' est positif)

$$e^{p't} < e^{pt}$$

et il y aura toujours un moment, aussi faible que soit l'écart entre p et p', où le temps sera suffisamment grand pour que

$$e^{p't} \ll e^{pt}$$

et par conséquent pour lequel [6] peut s'écrire

[7] $$\pi \simeq \pi_\infty[1 - Ne^{pt}]$$

(Cette équation n'a aucun rapport avec le cas limite no. 3.) Evidemment plus grand sera l'écart entre p et p' plus vite $e^{p't}$ deviendra négligeable devant e^{pt}.

Pour l'alcool laurique et l'ergostérol, les points obtenus en portant $\text{Log}(1 - [\pi/\pi_\infty]) = f(t)$ pour des temps supérieurs à 5 h se placent sur des droites, à partir desquelles grâce à [7], on obtient N et p (voir Tableau I), puisque

[7'] $$\text{Log}(1 - [\pi/\pi_\infty]) = \text{Log}(N) + pt$$

Nous allons maintenant utiliser ces valeurs de N et P, dans l'éq. [6], pour déterminer N' et p'.

$$\text{Log}(N') + p't = \text{Log}(1 - [\pi/\pi_\infty] - Ne^{pt})$$

Les points se placent approximativement sur des droites dont la pente est p' et l'ordonnée a l'origine $\text{Log}(+N')$.

Une propriété de la fonction exponentielle nous a permis de déterminer les quatre constantes du processus d'adsorption compétitive, pour apprécier la validité de cette détermination nous avons tracé Figs. 2 et 3 les courbes $\pi = f(t)$ obtenues par l'éq. [6] et les valeurs numériques du Tableau I.

Les valeurs expérimentales de la pression interfaciale ont été reportées sur les mêmes graphiques π–t, elles se placent avec une bonne précision sur les courbes théoriques.

1. J. F. Baret. J. Phys. Chem. **72**, 2755 (1968).
2. D. J. Crisp. J. Colloid Sci. **11**, 356 (1956).
3. R. H. Fowler. Proc. Cambridge Phil. Soc. **31**, 262 (1935).
4. R. Merigoux et M. Taxy. Rev. Inst. Franc. Petrole Ann. Combust. Liquides, **16**, 159 (1961).
5. J. T. Davies et E. X. Rideal. Interfacial phenomena. Academic Press, Inc., New York. 1961.
6. S. Ross et E. S. Chen. Ind. Eng. Chem. **57**, 40 (1965).
7. N. D. Weiner et G. Zografi. J. Pharm. Sci. **54**, 436 (1965).

Can. J. Chem. Downloaded from www.nrcresearchpress.com by 210.87.254.40 on 09/05/12
For personal use only.

Can. J. Chem. Downloaded from www.nrcresearchpress.com by 210.87.254.42 on 09/05/12
For personal use only.

Réactions dans le sulfolane. III. Etude des interactions eau–sulfolane[1]

R. L. Benoit et G. Choux
Département de Chimie, Université de Montréal, Case Postale 6128, Montréal, Québec

Reçu le 11 avril 1968

On a mesuré les pressions de vapeur du système eau–sulfolane à 30, 40 et 50 °C et les chaleurs de mélange à 30 °C. Les fonctions thermodynamiques d'excès ΔG^E, ΔH^M et ΔS^E ont été calculées. La chaleur de dissolution $\overline{\Delta H}^{\infty}_{H_2O} = 1.6$ kcal/mole indique que le groupement sulfone est un faible accepteur de protons. La connaissance de l'activité de l'eau permet de comparer les valeurs des fonctions d'acidité H_- en milieu hydroxyde dans les systèmes eau–sulfolane et eau–diméthylsulfoxyde.

Heats of mixing at 30 °C and vapor pressures at 30, 40, and 50 °C have been measured for the system water–sulfolane. The excess thermodynamic functions ΔG^E, ΔH^M, and ΔS^E have been calculated. The value of the heat of solution $\overline{\Delta H}^{\infty}_{H_2O} = 1.6$ kcal/mole indicates that the sulfone group is a weak proton acceptor. The effects of water activity on the H_- acidity function values in hydroxide media have been compared for the systems water–sulfolane and water–dimethylsulfoxide.

Canadian Journal of Chemistry, 46, 3215 (1968)

Introduction

Dans le cadre de l'étude de réactions dans la tétraméthylènesulfone (sulfolane) (1), un solvant polaire aprotique, on a mesuré les pressions de vapeur et les chaleurs de mélange du système sulfolane–eau. Ces déterminations ont été faites d'une part pour compléter les résultats des mesures d'indice de réfraction, constante diélectrique et densité (2) qui semblent indiquer que les interactions sulfolane–eau sont minimes, d'autre part pour mieux comprendre l'influence de l'eau sur les équilibres en solution, telle la dissociation d'acides et de bases. En effet, la solvatation des anions qui est faible dans le sulfolane est modifiée en présence d'eau ou de solvants hydroxyliques (1), et la connaissance de l'activité de l'eau devrait permettre d'apprécier son rôle dans les mélanges eau–sulfolane. C'est ainsi que l'on a examiné les valeurs de la fonction d'acidité H_- de solutions d'hydroxydes dans des mélanges sulfolane–eau (3) et qu'on les a reliées aux valeurs correspondantes dans les mélanges diméthylsulfoxyde–eau (4).

Résultats

Les valeurs de la chaleur de mélange ΔH^M et des pressions totales mesurées à 30° sont données dans le Tableau I. Les pressions totales à 30, 40 et 50° pour X_w variant entre 0 et 1 de 0.10 en 0.10 sont portées dans le Tableau II et représentées dans la Fig. 1. Les pressions partielles d'eau et de sulfolane à 30° calculées selon la méthode de Boissonas (5) avec un intervalle $\Delta X = 0.05$ sont indiquées dans le Tableau II. Les valeurs des pressions de vapeur du sulfolane pur p_s ont été obtenues à partir de mesures effectuées à 60° et 70° qui complètent les valeurs de 250° à 118°, données dans la littérature (6), en extrapolant $\log p_s = f(1/T)$ pour 30, 40 et 50°. La connaissance des pressions partielles permet le calcul des coefficients d'activité γ_w et γ_s selon le système de référence symétrique. La validité des résultats a été vérifiée suivant le procédé de Redlich–Kister (7). Les surfaces mesurées au-dessus et en dessous de l'axe X_w en portant $\partial Q/\partial X_w = \mathrm{Ln}\,(\gamma_w/\gamma_s)$ vs. X_w sont égales. On a calculé les paramètres de la fonction

TABLEAU I

Chaleurs de mélange et pressions totales du système eau–sulfolane

X_w	ΔH^M (cal/mole)	X_w	$p_t^{30°}$ (mm Hg)	X_w	$p_t^{30°}$ (mm Hg)
0.057	81	0	0.02	0.275	20.06
0.076	104	0.0024	0.08	0.302	20.44
0.121	157	0.0034	0.35	0.345	22.40
0.145	185	0.0060	0.82	0.450	24.94
0.205	230	0.0073	0.86	0.480	25.57
0.294	278	0.0108	1.48	0.550	26.15
0.360	290	0.0141	1.70	0.620	27.74
0.377	293	0.0210	2.46	0.687	28.27
0.461	301	0.0270	3.26	0.735	28.84
0.521	291	0.0410	4.85	0.790	29.00
0.615	252	0.090	8.74	0.810	29.10
0.703	208	0.130	13.15	0.927	30.36
0.801	162	0.175	15.63	0.945	30.79
0.919	73	0.207	17.47	1.000	31.82

[1]Présenté en partie au Congrès de l'ACFAS, Sherbrooke, Qué., 4 novembre 1967.

TABLEAU II

Pressions à 30, 40, 50°, pressions partielles et coefficients d'activité à 30° du système eau–sulfolane*

X_w	$p_t^{30°}$	$p_t^{40°}$	$p_t^{50°}$	$p_w^{30°}$	$p_s^{30°}$	$\gamma_w^{30°}$	$\gamma_s^{30°}$
0	0.02	0.04	0.08	0	0.0200		1.000
0.10	9.80	18.70	31.07	9.78	0.0183	3.074	1.015
0.20	17.10	29.05	45.55	17.08	0.0167	2.684	1.045
0.30	20.80	35.72	57.65	20.78	0.0158	2.177	1.128
0.40	23.67	40.81	66.00	23.65	0.0148	1.858	1.234
0.50	25.80	44.65	72.48	25.75	0.0139	1.621	1.386
0.60	27.43	47.30	77.73	27.42	0.0129	1.436	1.616
0.70	28.47	49.10	81.43	28.46	0.0121	1.278	2.022
0.80	29.07	50.77	84.22	29.06	0.0114	1.141	2.850
0.90	30.00	52.42	87.46	29.99	0.0097	1.047	4.853
1.00	31.82	55.32	92.47	31.82	0.000	1.000	

*Les pressions sont exprimées en mm Hg.

Q à 30, 40 et 50° où X_w et X_s représentent les fractions molaires en eau et en sulfolane:

$$[1] \quad Q = \frac{\Delta G^E}{RT} = X_w X_s[B + C(X_s - X_w) + D(X_s - X_w)^2]$$

à 30°	$B = 1.60$	$C = 0.31$	$D = 0.30$
à 40°	$B = 1.57$	$C = 0.29$	$D = 0.28$
à 50°	$B = 1.50$	$C = 0.24$	$D = 0.28$

Les valeurs de ΔG^E, ΔH^M et $T\Delta S^E$ sont données au Tableau III et ces fonctions sont représentées Fig. 2.

Discussion

Les valeurs obtenues pour les fonctions thermodynamiques d'excès permettent de comparer le système eau–sulfolane à d'autres systèmes eau–solvant. Si l'on observe comme pour les solvants peu basiques des déviations positives à la loi de Raoult ($\Delta G^E > 0$), il est à noter que le terme $T\Delta S^E$ joue ici un rôle mineur, contrairement au cas du système eau–dioxane, par exemple. Les valeurs élevées du coefficient d'activité de l'eau γ_w dans le sulfolane, voisines de celles observées dans le phosphate de tributyle (8), sont vraisemblablement attribuables à une dépolymérisation partielle de l'eau. Dimère dans

TABLEAU III

Fonctions thermodynamiques d'excès du système eau–sulfolane*

X_w	$\Delta G_{30°}^E$	$\Delta H_{30°}^M$	$T\Delta S_{30°}^E$
0	0	0	0
0.10	104	142	38
0.20	146	230	84
0.30	192	280	88
0.40	223	300	77
0.50	240	298	58
0.60	241	270	29
0.70	224	224	0
0.80	182	168	−14
0.90	110	96	−14
1.00	0	0	0

*ΔG^E, ΔH^M et $T\Delta S^E$ sont donnés en cal/mole.

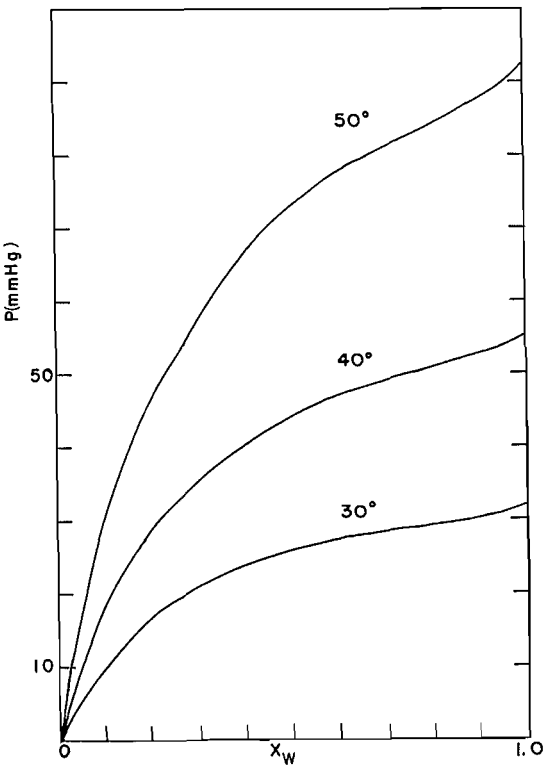

FIG. 1. Pressions totales du système sulfolane–eau, mesurées à 30, 40 et 50 °C.

Can. J. Chem. Downloaded from www.nrcresearchpress.com by 210.87.254.42 on 09/05/12
For personal use only.

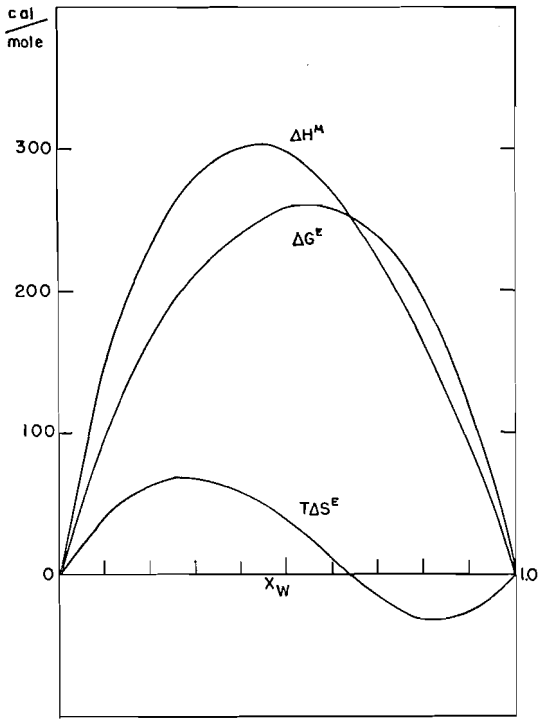

FIG. 2. Fonctions thermodynamiques d'excès du système sulfolane–eau, à 30 °C.

le tributylphosphate, l'eau, aux faibles concentrations, serait d'ailleurs présente sous la même forme dans le sulfolane (9), ce qui demanderait à être confirmé. Le volume partiel molaire d'excès de l'eau reste cependant faible dans ces mélanges eau–sulfolane (2), ce qui peut être causé par la formation d'associations eau–sulfolane, compensant la dépolymérisation de l'eau.

La valeur de la chaleur partielle de mélange de l'eau à dilution infinie $\overline{\Delta H}^{\infty}_{w}$ (kcal/mole) dans un solvant peut être utilisée pour situer la force de la fonction sulfone en tant qu'accepteur de protons parmi d'autres fonctions (10). On obtient:

$$CH_3NO_2\ (2.4) < CH_3CN\ (1.9) < (CH_2)_4SO_2\ (1.6) < (CH_3)_2CO\ (1.05) < (CH_3)_2SO\ (-1.28)$$

Les valeurs de $\overline{\Delta G}^{\infty}_{w}$ conduisent à un classement analogue. Il est donc ainsi confirmé que le groupe —SO_2 n'a que des propriétés de donneur faible comme l'a déjà montré Drago *et coll.* (11) avec le phénol et l'iode. L'ordre obtenu d'après les valeurs des enthalpies de formation des complexes entre ces deux acides de Lewis et les solvants étudiés est d'ailleurs sensiblement le même que celui donné ci-dessus. Le sulfolane apparaît ainsi comme n'ayant que de faibles propriétés solvatantes en complète opposition avec le diméthylsulfoxyde (DMSO).

La connaissance de l'activité de l'eau dans les mélanges eau–sulfolane devrait faciliter l'interprétation de son influence sur le déplacement d'équilibres dans de tels mélanges. En particulier, l'eau solvate préférentiellement certaines particules impliquées dans ces équilibres et c'est le cas entre autre des petits anions tel OH^- (12). On a ainsi examiné le rôle de l'eau sur l'équilibre

$$[2] \qquad HA + OH^-_{aq} \rightleftarrows A^- + xH_2O$$

Cet équilibre a été étudié dans les mélanges eau–sulfolane-hydroxyde de tétraméthylammonium 0.011 *M* par Stewart *et coll.* (3). Les valeurs de la fonction d'acidité $H_- = pK_{HA} + \log([A^-]/[HA])$ obtenues par ces auteurs sont portées dans la Fig. 3, en fonction du logarithme de l'activité de l'eau. Si l'on néglige l'hydratation de l'acide indicateur HA et de son gros anion A^-, et que l'on attribue à l'ion OH^- un nombre d'hydratation de *n* (13), on peut écrire:

$$[3] \quad H_- = pK_w + \log [OH^-_{aq}] - (n + 1) \log a_w + \log \frac{f_{HA} f_{OH^-_{aq}}}{f_{A^-}}$$

où K_w est le produit ionique de l'eau et f_x le coefficient d'activité de solvatation de l'espèce X (14). La pente de la courbe donnant H_- en fonction de log a_w, Fig. 3, varie rapidement quand a_w passe de 1 à 0.5. Il n'est donc pas possible d'attribuer à *n* une valeur constante en négligeant ou considérant comme constant le dernier terme de l'éq. [3] dans ce domaine de a_w. Comme d'autre part des déterminations semi-quantitatives de la solubilité d'un indicateur HA ont montré que log f_{HA} varie de 0 à −2.7 quand a_w passe de 1 à 0.5, pour rester ensuite sensiblement constant, il s'ensuit que le terme log $(f_{OH^-_{aq}}/f_{A^-})$ doit augmenter rapidement dans l'intervalle $1 > a_w > 0.5$. Cet accroissement reflète vraisemblablement surtout celui de $f_{OH^-_{aq}}$. Par contre, dans le domaine $0.5 > a_w > 0.2$, où les valeurs de H_- sont, il faut le noter, les moins certaines, la pente de la courbe H_- vs. log a_w devient constante et sensiblement égale à −5; on pourrait alors prendre pour nombre d'hydratation de OH^-, $n = 3$ (13), ce qui donnerait pour le terme log

Can. J. Chem. Downloaded from www.nrcresearchpress.com by 210.87.254.42 on 09/05/12
For personal use only.

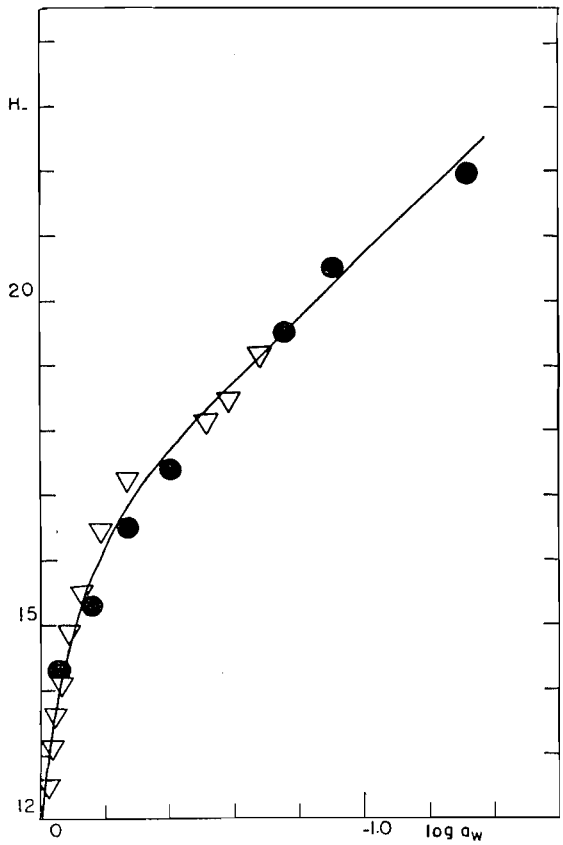

FIG. 3. Variations de la fonction d'acidité H_- avec log a_w dans le sulfolane (▽) (3) et dans le DMSO (●) (4).

($f_{OH^-_{aq}}/f_{A^-}$) une variation en fonction de log a_w égale à environ +1.

Il nous a paru intéressant de porter sur la Fig. 3, les valeurs de H_- correspondant au système eau–diméthylsulfoxyde-hydroxyde de tétraméthylammonium 0.011 M (4) en fonction de log a_w.

Les valeurs de l'activité de l'eau dans le DMSO ont été calculées à 25 °C à partir des résultats de Kenttamaa et Lindberg à 70 °C (15), en tenant compte des chaleurs molaires partielles de dissolution de H_2O (16). Les nouveaux points se placent sensiblement sur la courbe H_- vs. log a_w obtenue dans le sulfolane. H_- serait ainsi une fonction unique de l'activité de l'eau pour ces deux solvants polaires aprotiques. Si, à fractions molaires X_w égales les solutions d'hydroxyde dans le DMSO donnent des valeurs de H_- plus élevées que dans le sulfolane, cela tient à la plus faible activité de l'eau dans le premier solvant.

L'activité de l'eau semble ainsi avoir une grande influence sur les équilibres dans les solvants polaires aprotiques contenant de l'eau. Des mesures en cours de la fonction d'acidité H_0 de solutions acides devraient permettre de confirmer ce point de vue.

Partie expérimentale

(1) Purification du sulfolane

Le sulfolane gracieusement fourni par Shell Canada Ltd. est soumis à un vide de 10^{-1} mm Hg de manière à éliminer certaines impuretés volatiles (butadiène, eau), puis il est traité deux fois par le charbon actif. Une distillation simple sous 0.5 mm Hg à 70 °C permet d'obtenir un produit transparent dès 220 mμ dont l'analyse polarographique confirme la pureté. Sa température de fusion est de 28.4; il est conservé sur tamis moléculaire 4A à 35 °C.

(2) Mesures microcalorimétriques des chaleurs de mélange ΔH^M

Le sulfolane et l'eau sont introduits et pesés dans les compartiments séparés de la cellule de mesure du microcalorimètre de type Tian–Calvet (17). Une couche d'huile de paraffine non miscible à l'eau et au sulfolane évite les échanges par diffusion gazeuse. Lorsque l'équilibre thermique est atteint le calorimètre est basculé plusieurs fois jusqu'à mélange complet des deux liquides. La mesure de la surface enregistrée, comparée à un étalonnage du calorimètre par effet Joule, donne la quantité de chaleur entrant en jeu dans le mélange. Cette quantité, rapportée à la somme des nombres de moles d'eau et de sulfolane introduites est la chaleur de mélange ΔH^M. Les mesures sont faites à 30 °C.

(3) Mesures des pressions de vapeur des mélanges eau–sulfolane

Un mélange d'eau et de sulfolane est introduit dans un flacon à joint rodé pour vide, que l'on fixe au tensimètre. L'ensemble est placé dans un bain à température constante (30.00, 40.00, 50.00 ± 0.02°). Le mélange est agité magnétiquement et dégazé par vides successifs. Le tensimètre est vidé jusque 10^{-3} mm Hg, et le flacon est mis en communication avec le manomètre. La différence des niveaux dans les deux branches du manomètre est mesurée avec un cathétomètre permettant d'apprécier 0.01 mm, avec une reproductibilité de 0.05 mm. La mesure est effectuée au moins deux fois pour la même solution. On détermine ensuite le titre en eau du mélange en comparant son indice de réfraction à 30° à la courbe n_D^{30} vs. X_{H_2O} préalablement construite, dont les résultats publiés par Della Monica *et coll.* (2) confirment la validité. Comme l'analyse est effectuée après la mesure, il n'est pas nécessaire de faire de corrections de volumes morts, ni d'éviter des variations de la composition du mélange initial lors du dégazage.

Le domaine $X_w < 0.10$ a fait l'objet d'une étude particulière, à 30 °C, l'eau étant dosée par le réactif de Karl Fischer.

Can. J. Chem. Downloaded from www.nrcresearchpress.com by 210.87.254.42 on 09/05/12
For personal use only.

Remerciements

Nous remercions le Conseil National de Recherches du Canada pour une subvention et nous exprimons notre reconnaissance au professeur M. Rinfret qui nous accorda toutes facilités pour l'utilisation d'un microcalorimètre.

1. R. L. BENOIT, M. GUAY ET J. DESBARRES. Can. J. Chem. **46**, 1261 (1968).
2. O. SCIACOVELLI, L. JANELLI ET A. DELLA MONICA. Gazz. Chim. Ital. **97**, 1012 (1967).
3. R. STEWART ET J. O'DONNELL. Can. J. Chem. **42**, 1681 (1964).
4. D. DOLMAN ET R. STEWART. Can. J. Chem. **45**, 911 (1967).
5. C. G. BOISSONNAS. Helv. Chim. Acta, **22**, 541 (1939).
6. SHELL CHEMICAL COMPANY. Technical Bulletin No. I. C. 63.13R (1964).
7. O. REDLICH ET A. T. KISTER. Ind. Eng. Chem. **40**, 345 (1948).
8. J. R. JOHNSON, S. D. CHRISTIAN ET H. E. AFFSPRUNG. J. Chem. Soc. A, 1924 (1967).
9. R. L. BURWELL, JR. ET C. H. LANGFORD. J. Am. Chem. Soc. **81**, 3799 (1959).
10. J. R. HOLMES, D. KIVELSON ET W. C. DRINKARD. J. Am. Chem. Soc. **84**, 4677 (1962).
11. R. S. DRAGO, B. WAYLAND ET R. L. CARLSON. J. Am. Chem. Soc. **85**, 3125 (1963).
12. A. J. PARKER. Quart. Rev. London, **16**, 163 (1962).
13. C. H. ROCHESTER. Quart. Rev. London, **20**, 511 (1966).
14. J. VEDEL. Ann. Chim. **2**, 367 (1967).
15. J. KENTTAMAA ET J. J. LINDBERG. Suomen Kemistilehti, B, **33**, 98 (1960).
16. W. DRINKARD ET D. KIVELSON. J. Phys. Chem. **62**, 1494 (1958).
17. E. CALVET ET H. PRAT. Microcalorimétrie. Applications physico-chimiques et biologiques. Masson et Cie, Paris. 1956.

Can. J. Chem. Downloaded from www.nrcresearchpress.com by 210.87.254.42 on 09/05/12
For personal use only.

Theoretical calculations of hot-spot initiation in explosives

H. J. BRUCKMAN, JR. AND J. E. GUILLET
Department of Chemistry, University of Toronto, Toronto 5, Ontario

Received March 15, 1968

The heat balance equations for the thermal decomposition of hot spots in explosives have been solved using an iterative computer method. This yields a value of T_c, the critical temperature for hot-spot initiation, which is a function of the size and duration of the hot spot and of the physical and chemical properties of the explosive. It is demonstrated that there is a strong correlation between the ranking of explosives in terms of shock sensitivity and their ranking in terms of T_c. In general explosives having low values of T_c are more sensitive to shock and other forms of accidental initiation than those having high values.

Using the computer program, it was shown that the major factor affecting T_c was not the energy released in the explosion, but the rate of decomposition, as expressed in terms of the parameters A and E_a in the Arrhenius equation. Consideration of reagent depletion also indicated certain limits beyond which the heat production cannot be maintained for the time necessary to initiate explosion and insensitivity should result. Considerations of this type could be used to predict safe handling procedures for explosives.

Canadian Journal of Chemistry, 46, 3221 (1968)

Can. J. Chem. Downloaded from www.nrcresearchpress.com by 210.87.254.6 on 09/05/12
For personal use only.

Introduction

When a condensed explosive suffers rapid decomposition, the process can conveniently be divided into four stages of development. These are initiation, deflagration, transition from deflagration to detonation, and detonation. This paper is concerned only with the initiation phase, that is, the processes occurring during the period of time until deflagration starts.

Macek (1) terms initiation as the stage in which the chemical decomposition has not yet released sufficient energy for self-propagation and hence is dependent on an external source of energy. If this external energy source is insufficient or is removed before sufficient energy for self-propagation (deflagration) is generated, the rate of decomposition will slow down and cease.

The sensitivity of an explosive may then be related to the minimum necessary amount of external energy that must be imparted to the explosive, within limited time and space in order to accomplish initiation. It is usually assumed that this energy is ultimately delivered to the explosive in the form of heat.

Sensitivity poses a twofold problem. The first is concerned with the mechanism of degradation of the energy of the stimulus (shock, friction, impact, etc.) into heat. This aspect of the problem has not been investigated in this work. The second aspect of sensitivity is fundamentally a heat balance problem involving the kinetics of the explosive reaction.

A method of calculating the critical amount of heat energy necessary to initiate deflagration in peroxides and other detonable substances has been developed. This method has been used to predict how the critical amount of heat (or temperature) varies with the physical and kinetic properties of an explosive.

Hot-Spot Initiation

Belajev (2) in 1938 first demonstrated that deflagrations in liquid explosives could be initiated by very small hot spots in the explosive. The theoretical treatment of the factors involved in such a "thermal explosion" was first given by van't Hoff (3), expanded by Frank-Kamenetski (4), and applied by Robertson (5) to condensed phase explosions. Rideal and Robertson (6) applied this theory to obtain estimates of hot-spot sizes and temperatures necessary to accomplish initiation. Bowden and Yoffe (7) have collected a considerable amount of experimental evidence in support of this "hot-spot theory". Further verification of these results has been reported by Collins and Cook (8).

More recently Boddington (9) and Friedman (10) have extended the original theoretical treatment of Rideal and Robertson (6). Both attempted an analytical solution of the heat balance equations, using a number of assumptions, including non-depletion of the reagent. Boddington obtains an expression in terms of a parameter ϕ, whose value determines whether or not the explosive will reach a critical stage. He also reports an exact solution to the equations (including reagent depletion) by a numerical method, and uses this to calculate critical hot-spot temperatures for several explosives as a function

Can. J. Chem. Downloaded from www.nrcresearchpress.com by 210.87.254.6 on 09/05/12
For personal use only.

of time and size. The ranking of sensitivity obtained agrees quite well with that of Rideal and Robertson. Friedman's analytical solution was used to calculate theoretical drop-heights for an impact test through a correlation equation for 16 explosives. The theory predicts the experimental sensitivities to within 40%. These results seem to confirm the validity of this treatment in predicting the sensitivity of solid explosives. In the present work, a numerical solution to the heat balance equations has been developed and solved using a high-speed digital computer. The method is similar to, but not identical with, that of Boddington (9).

Theory of Hot-Spot Initiation

In the development of the theory it is assumed that a hot spot is formed in a liquid explosive by an external energy stimulus. If this hot spot is to have the possibility of surviving, its temperature must exceed a certain critical value at which the rate of heat production by decomposition in the hot spot is greater than the rate of heat dissipation to the surroundings. This is the critical temperature calculated by Rideal and Robertson (6). This heat condition is referred to as criterion I.

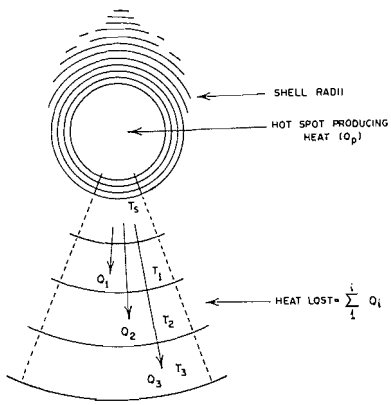

FIG. 1. Hot-spot model illustrating heat flow.

A situation meeting the conditions of criterion I insures that the hot spot will survive for a time. However, the possibility exists that the hot spot will cool and die out at some later time, due to consumption of the reactant which would reduce the heat production and temperature, thus quenching the reaction. In order to consider this possibility a new calculation procedure was developed to monitor the temperature of a thin spherical shell in the body of the explosive that encloses the original hot spot. The situation is shown schematically in Fig. 1. It is assumed that initiation is complete and propagation begins when the temperature of this layer is equal to or greater than the original hot-spot temperature. This original hot-spot temperature is defined as the critical temperature. This condition is referred to as criterion II.

Calculation of Heat Loss and Production

The heat calculation procedure employed was basically that used by Rideal and Robertson (6). In order to keep the treatment in terms of experimentally determined quantities, the following assumptions are made: (*i*) The explosive is homogeneous and isotropic. (*ii*) The hot spots are sharply defined spheres in an infinite amount of explosive. (*iii*) The hot spots are formed in zero time by an external energy source. (*iv*) The decomposition reactions are first order. (*v*) Heat loss proceeds only through the mechanism of conduction. (*vi*) The heat of reaction is the same as in the ordinary thermal decomposition.

Heat Production

The rate of a first order chemical decomposition taking place at T °K can be expressed as:

$$-\frac{dc}{dt} = kc$$

where $k = Ae^{-E/RT}$, c = concentration in moles per liter at time t, A = frequency factor, E = energy of activation, and R = gas constant.

If Q is the heat of reaction per mole, the rate of heat production per liter is:

$$[1] \qquad \frac{dq}{dt} = cQAe^{-E/RT}$$

The quantity of heat generated in a chosen time interval "Δt" in a given volume, V, of reactant is:

$$[2] \qquad \Delta q = \frac{V\rho}{M}\cdot\Delta t\cdot cQAe^{-E/RT}$$

where V = volume of reactant in liters,
ρ = density (g/l),
M = gram molecular weight of reactant.

Rideal and Robertson (6) used eq. [2] and assumed constant concentration for the short time intervals considered. In this work eq. [2] is extended to account for variation of reactant concentration as the reaction proceeds. By integration of eq. [1] we can obtain an expression

Can. J. Chem. Downloaded from www.nrcresearchpress.com by 210.87.254.6 on 09/05/12
For personal use only.

for the concentration of reagent c as a function of time t in the form

$$[3] \qquad c = c_0 \exp\left[-(t - t_0)Ae^{-E/RT}\right]$$

and the rate of heat production per liter can now be expressed as

$$[4] \qquad \frac{dq}{dt} = c_0 QA \times \exp\left[-\frac{E}{RT} - (t - t_0)Ae^{-E/RT}\right]$$

If Q' is the heat of decomposition of the pure reagent in cal/g, the total heat generated in a time interval $t - t_0$ in a hot spot of volume V will be given by

$$[5] \qquad q = V\rho Q' \frac{c_0 - c}{c_0}$$

where c_0 and c are the concentrations at times t_0 and t calculated by substitution in eq. [3].

Heat Loss

Consider a hot spot of temperature T °K formed in zero time in an explosive at T_0 °K. The variation of temperature outside the hot spot caused by heat conduction is given by the Fourier equation in spherical polar coordinates as:

$$[6] \qquad \frac{\partial\theta}{\partial t} = \frac{K}{\rho s}\left(\frac{\partial^2\theta}{\partial r^2} + 2\frac{\partial\theta}{\partial r}\right)$$

where K = thermal conductivity, ρ = density, s = specific heat, and $\theta = T - T_0$.

If the radius of the hot spot is "a", the boundary conditions are:

$$\theta = f(r) \text{ when } t = 0 \quad \text{for } r > a,$$

and

$$\theta = \phi(t) \text{ when } t = 0 \quad \text{for } 0 < r < a$$

The solution of this problem is given by Carslaw and Jaeger (11)

$$[7] \qquad \theta_r = \frac{1}{2r\sqrt{(\pi Bt)}}\int_a^\infty r' f(r') \times \left[\exp\left(\frac{-(r - r')^2}{4Bt}\right) \times \exp\left(\frac{r + r' - 2a^2}{4Bt}\right)\right] dr' + \frac{2a}{r\sqrt{\pi}}\int_{\frac{r-a}{2\sqrt{(Bt)}}}^\infty \phi\left[t - \frac{(r - a)^2}{4B\mu^2}\right] e^{-\mu^2}\, d\mu$$

where $B = K/\rho s$, μ = a constant.

The equation can be simplified if two further conditions are imposed on the system: (*i*) The ambient temperature is initially constant through the material, i.e.

$$f(r) = \text{constant} \quad \text{at } t = 0.$$

Since only the difference between ambient and hot-spot temperature is required, the constant can be set equal to 0 if the hot-spot temperature is also adjusted.

(*ii*) The hot-spot temperature is constant throughout its volume and during the time interval considered (this would be valid near the critical temperature), i.e.

$$\phi(t) = \text{constant} = \theta_0$$

where θ_0 = temperature of the hot spot in °K − ambient temperature in °K.

Using these relations, eq. [7] reduces to

$$[8] \qquad \theta_r = \frac{2a\theta_0}{r\sqrt{\pi}}\int_{\frac{(r-a)}{2\sqrt{(Bt)}}}^\infty e^{-\mu^2}\, d\mu$$

This integral can be evaluated in terms of the error function to give:

$$[9] \qquad \theta_r = \frac{a\theta_0}{r}\,\text{erfc}\left[\frac{(r - a)}{2\sqrt{(Bt)}}\right]$$

If radiation and convection contribute negligible heat loss, the heat lost by the spot is then:

$$[10] \qquad q_e = \int_a^\infty 4\pi r^2 \rho s \theta_r\, dr$$

where θ_r is given by eq. [9].

Equations [9] and [10] were used in an iterative computer program which conducts a systematic search of initial hot-spot temperatures until the critical temperature for a specified time interval and hot-spot size was found. The program used both criteria I and II in calculating critical temperatures.

Explosive Parameters

The physical and chemical parameters used in critical hot-spot temperature calculations are given in Table I. The values of density, heat capacity, and thermal conductivity were taken as 1.0 g/cm^3, 0.3 cal/g, and 3.0 × 10^{-4} cal/cm^2 s/cm °C respectively. Variation of these parameters was found (this work) to change the critical hot-spot temperature only slightly.

TABLE I

Explosive parameters

Explosive	Molecular weight (g/mole)	Heat of decomposition (kcal/mole)	Activation energy (kcal/mole)	Frequency factor (s^{-1})	Reference
Pentaerythritol tetranitrate (P.E.T.N.)	316	74	47.0	6.3×10^{19}	6
Cyclonite (R.D.X.)	207	191	47.5	3.2×10^{18}	6
Cyclotetramethylenetetra-nitramine (C.T.M.T.N.A.)	276	253	52.7	5.0×10^{19}	6
Ethylenedinitramine (E.D.N.A.)	151	86	30.5	6.3×10^{12}	6
Tetryl	287	55	38.4	2.5×10^{15}	6
Ethylenediamine dinitrate (E.D.A.D.N.)	176	129	40.5	1.3×10^{13}	6
Ammonium nitrate (A.N.)	80	13.5	40.5	6.3×10^{13}	6
Nitroglycerine (N.G.)	227	114*	48.0	3.0×10^{20}	12
Trinitrotoluene (T.N.T.)	227	114*	34.4	2.5×10^{11}	13

*Estimated value.

Calculations

The first calculations performed were those done by Rideal and Robertson (6). In this case only the hot spot itself was considered (criterion I) and no correction was made for reagent depletion. The results are shown in Table II. It is apparent that our calculations give slightly higher critical temperatures, but the order of sensitivity is the same. For these calculations the hot-spot size was 10^{-3} cm radius and the time interval 10^{-4} s.

TABLE II

Comparison of T_c values (°C)*

Explosives	This work	Rideal and Robertson
P.E.T.N.	367	350
R.D.X.	400	385
C.T.M.T.N.A.	423	405
E.D.N.A.	432	400
Tetryl	456	425
A.N.	638	590
E.D.A.D.N.	639	600

*Program I, criterion I. Time = 10^{-4} s. Hot-spot radius = 10^{-3} cm.

Table III compares the results of different methods of calculation. It is apparent that if one only considers the hot spot itself (criterion I), reactant depletion has only a slight effect on the critical hot-spot temperature, except for the less sensitive explosives like ammonium nitrate. The shell model (criterion II), however, causes a considerable increase in the calculated hot-spot temperature, and makes some changes in the ranking of sensitivity.

A comparison of the critical hot-spot temperatures (as calculated by program 2) with a variety of sensitivity tests is given in Table IV. It can be seen that the ranking of explosives in terms of critical hot-spot temperatures is completely consistent with the rankings obtained by a wide

TABLE III

Comparison of T_c values calculated by various programs

Explosive	Critical temperature (°C)		
	Criterion I, no reactant depletion (computer program 1)	Criterion I, reactant depletion (computer program 2)	Criterion II, reactant depletion (computer program 3)
N.G.	342	344	392
P.E.T.N.	368	377	422
R.D.X.	407	409	465
C.T.M.T.N.A.	428	430	493
E.D.N.A.	442	449	482
Tetryl	462	568	619
E.D.A.D.N.	652	662	729
A.N.	647	783	729
T.N.T.	710	736	775

Can. J. Chem. Downloaded from www.nrcresearchpress.com by 210.87.254.6 on 09/05/12
For personal use only.

Can. J. Chem. Downloaded from www.nrcresearchpress.com by 210.87.254.6 on 09/05/12
For personal use only.

TABLE IV

Critical hot-spot temperatures (T_c) compared with experimental sensitivity tests*

Explosive	T_c (°C) (Program 2, this work)	Impact sensitivity (cm) (ref. 14)	Impact sensitivity (cm) (ref. 10)	T_c (°C) [250 s] (ref. 14)	Figure of insensitivity (ref. 6)	Impact time lag (ref. 6)	U.S. Naval Ordinance impact test (ref. 1)	U.S. Naval Ordinance gap test (ref. 1)	Figure of insensitivity (ref. 15)	T_c (°C) [3 mg sample] (ref. 16)
N.G.	344	4–8	6	390						210
P.E.T.N.	377	13	12	430	40	230	13		38	215
R.D.X.	409		24		50–60	260	24	8.20	64	
C.T.M.T.N.A.	430				50					
E.D.N.A.	449				51		34			150
Tetryl	468	36	36	880	70	350	38	6.63	72	265
E.D.A.D.N.	662				120			6.65		
T.N.T.	736	160	50	1040			200	3.50	120	
A.N.	783				120		7320	0		300

*Time = 10^{-4} s, hot-spot radius = 10^{-3} cm.

Can. J. Chem. Downloaded from www.nrcresearchpress.com by 210.87.254.6 on 09/05/12
For personal use only.

range of experimental tests. This correlation is very striking, especially in view of the experimental difficulty and known variability in tests of this kind. This leads one to the conclusion that the calculations may indeed have some real significance in terms of the mechanism of shock initiation in explosives.

Presumably one may also estimate the sensitivity of an unknown explosive by calculations of this type. In view of this it became of considerable interest to determine which of the chemical and physical properties of an explosive contribute most to its sensitivity. With the computer program this can be determined by selecting a particular set of properties and determining the variation in T_c as one of these is varied over the range of interest. A hypothetical explosive is considered with the properties given in Table V. The results of the calculations are shown in Figs. 2–7.

TABLE V

Properties of hypothetical explosive

Explosive parameter	Symbol	Value
Density	ρ	1.0 g/cm^3
Specific heat	s	0.5 cal/g
Thermal conductivity	K	4.0×10^{-4} cal/cm^2 deg cm
Molecular weight	M	200 g/mole
Heat of decomposition	ΔH	80.0 kcal/mole
Activation energy	E	31.52 kcal/mole
Frequency factor	A	2.7×10^{15} s^{-1}

(a) Density

Figure 2, line *a*, shows that the critical temperature increases slowly as density decreases, then more rapidly until a "critical density" is reached, e.g. between 0.4 and 0.5 g/cm^3 for the hypothetical explosive. At or below this density the heat produced in the hot spot can never be greater than the heat lost due to conduction. Below this density the explosive becomes insensitive to hot-spot initiation.

(b) Specific Heat

Figure 2, line *b*, shows that the critical temperature increases very slightly with specific heat. At very low values of specific heat, the critical temperatures begin to drop rapidly indicating a rapid increase in sensitivity. However, over the usual ranges, T_c is nearly independent of specific heat.

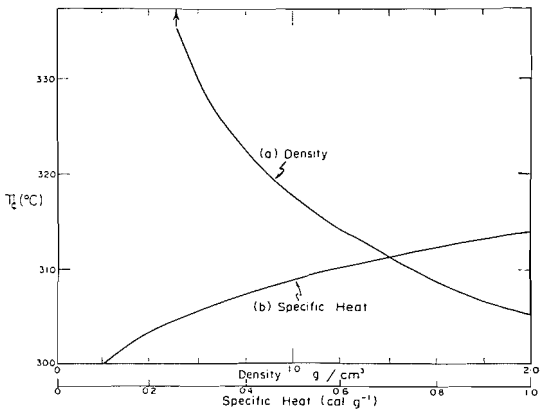

FIG. 2. Variation of T_c with (*a*) density, and (*b*) specific heat of a hypothetical explosive.

(c) Thermal Conductivity

Figure 3, line *a*, shows that the critical temperature rises rapidly at low values of thermal conductivity and becomes almost linear variation for the higher values. Near a "critical conductivity" the temperature rises sharply and past this critical value the explosive becomes insensitive. In this condition heat is always conducted away from the hot spot faster than it can be produced. This could explain the desensitizing effects of aluminium powder, for example, with certain explosives.

(d) Molecular Weight and Heat of Decomposition

Figure 3, line *b*, and Fig. 4 show that changes in molecular weight and heat of decomposition are equivalent to changes in the heat of decomposition per gram of explosive. This quantity has a critical value which is reflected in critical molecular weight and molar heat of decomposition.

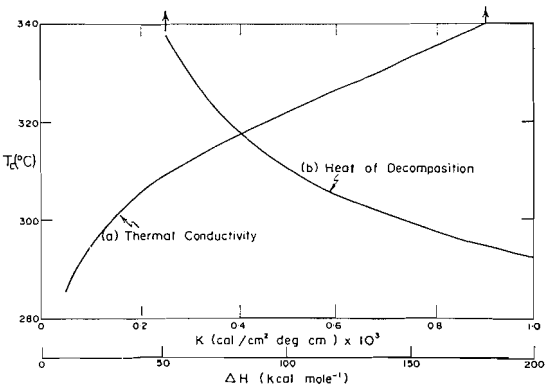

FIG. 3. Variation of T_c with (*a*) thermal conductivity and (*b*) molar heat of decomposition.

For molecular weights greater than about 340 or molar heats of decomposition less than 50 kcal/mole^{-1} the amount of heat generated is no longer sufficient to maintain the temperature of the hot spot and decomposition will cease. The occurrence of such a critical point allows one to calculate the dilution necessary to render an explosive insensitive to hot-spot initiation.

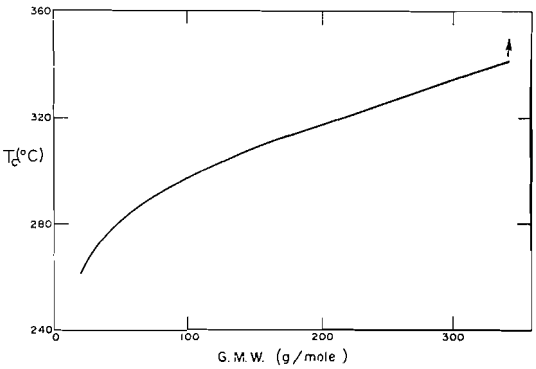

FIG. 4. Variation of T_c with gram molecular weight (G.M.W.).

The value of T_c is surprisingly insensitive to relatively large variations in ΔH outside this critical region, indicating that the probability of initiation is nearly independent of the energy released during explosion.

(e) Arrhenius Parameters

Inspection of Fig. 5 indicates that by far the greatest variation in T_c is caused by changes in the Arrhenius parameters, and is therefore related to the rate of decomposition of the explosive at a particular temperature. The critical temperature

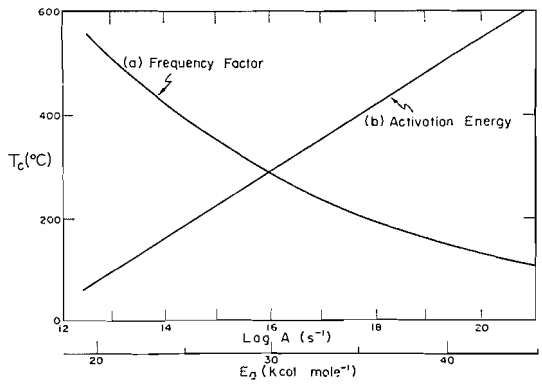

FIG. 5. Variation of T_c with Arrhenius parameters: (*a*) frequency factor, log A, (*b*) activation energy, E_a.

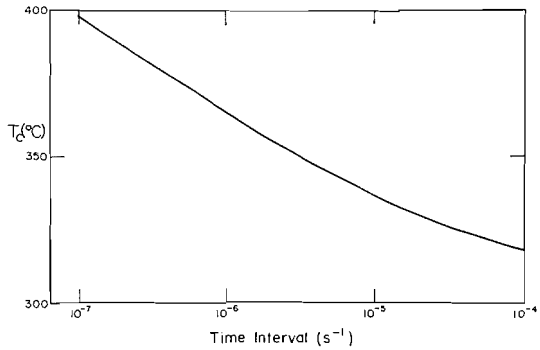

FIG. 6. Variation of T_c with hot-spot duration.

is lower than room temperature for activation energies lower than 18 kcal/mole (Fig. 5, line *a*), and increases almost linearly with activation energy until a critical value of the activation energy is reached, above which the hot spot cannot produce more heat than is conducted away over the time interval considered, i.e. the explosive becomes insensitive.

The value of T_c decreases rapidly as log A increases (Fig. 5, line *b*), and there exists a lower critical value below which the explosive becomes insensitive.

(f) Time Interval

Figure 6 shows that the critical temperature is a decreasing function of time until the time interval considered exceeds 10^{-4} s. Then, the heat produced can no longer balance the heat lost from the spot over the interval. This would suggest that the shorter the duration of a thermal shock, the less sensitive the explosive will be.

(g) Hot-Spot Radius

Figure 7 shows that the value of T_c decreases as the size of the hot spot increases although the

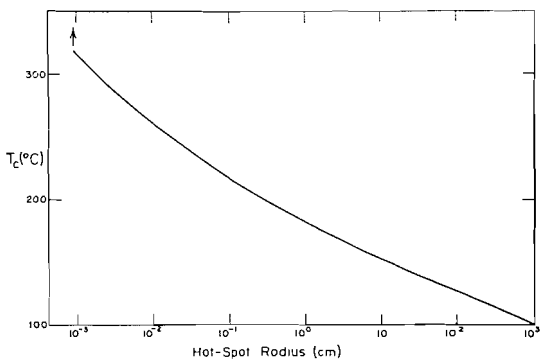

FIG. 7. Variation of T_c with hot-spot radius.

Can. J. Chem. Downloaded from www.nrcresearchpress.com by 210.87.254.6 on 09/05/12
For personal use only.

effect is not as large as might have been expected. Changing the radius from 1 mm to 10 m causes only a 100 °C decrease in T_c. The change is more rapid at smaller radii and reaches a lower limit between 10^{-3}–10^{-4} cm beyond which the heat flow cannot be balanced, and the explosive becomes insensitive. This suggests that hot spots must exceed a radius of 10^{-4} cm to be effective in initiating explosion.

Conclusions

Several important conclusions may be drawn from the results of these studies. First it is obvious that the inclusion of the depletion of material in the hot spot has an important bearing on the calculation, and represents a considerable improvement over the theory of Rideal and Robertson. Although the effect on the calculation of critical hot-spot temperatures, T_c, is not large, the inclusion of depletion allows the prediction of a number of critical points above or below which explosion cannot be initiated regardless of the strength of the stimulus. In principle this should permit the calculation of the amount of diluent, for example, necessary to make an explosive insensitive under all conditions of initiation.

The other important conclusion is that the sensitivity of an explosive to hot-spot initiation is almost entirely dependent on its rate of decomposition as a function of temperature, as expressed by the Arrhenius parameters. This effect far outweighs all others. Explosives with a low activation energy and a high frequency factor will tend to be highly sensitive to hot-spot initiation. This effect is much more important than the energy produced per gram ($\Delta H/M$), the thermal conductivity or density, as long as certain critical limits are exceeded. The application of this to other types of explosives will be considered in a further communication.

Acknowledgment

This work was made possible by a grant from the Defence Research Board of Canada (Grant No: DRB 9530-50) whose support is gratefully acknowledged.

1. A. MAČEK. Chem. Rev. **62**, 41 (1962).
2. A. F. BELAJEV. Compt. rend. acad. sci. U.R.S.S. **18**, 267 (1938).
3. J. H. VAN'T HOFF. Etudes de dynamique chimique. F. Muller, Amsterdam. 1884.
4. D. A. FRANK-KAMENETSKI. Acta Physicochim. U.R.S.S. **10**, 365 (1939).
5. A. J. B. ROBERTSON. Ph.D. Thesis, Cambridge University, Cambridge. 1947.
6. E. K. RIDEAL and A. J. B. ROBERTSON. Proc. Roy. Soc. London, Ser. A, **195** (1948).
7. F. P. BOWDEN and A. D. YOFFE. Initiation and growth of explosion. Cambridge University Press, London. 1952.
8. T. K. COLLINS and M. A. COOK. The measurement of sensitivity time lag and burning velocity of explosives by drop test. T.R. No. 48, Contract N7-ONR-45107, Proj. No. 357239, E. R. G., Univ. of Utah. December 15, 1955.
9. T. BODDINGTON. Proc. 9th Int. Symp. Combustion. Academic Press Inc., New York. 1963. p. 287.
10. M. H. FRIEDMAN. Proc. 9th Int. Symp. Combustion. Academic Press Inc., New York. 1963. p. 294.
11. H. S. CARSLAW and J. C. JAEGER. Conduction of heat in solids. 2nd ed. Oxford University Press, London. 1959.
12. S. ROGINSKY. Physik. Z. Sowjetunion, **1**, 640 (1932).
13. A. J. B. ROBERTSON. Trans. Faraday Soc. **44**, 977 (1948).
14. J. WENOGRAD. Trans. Faraday Soc. **57**, 1612 (1961).
15. J. L. COPP, S. E. NAPIER, T. NASH, W. J. POWELL, H. SKELLY, A. R. UBBELOHDE, and P. WOODWARD. Trans. Roy. Soc. London, Ser. A, **241**, 197 (1949).
16. H. HENKIN and R. MCGILL. Ind. Eng. Chem. **44**, 6 (1952).

Can. J. Chem. Downloaded from www.nrcresearchpress.com by 210.87.254.6 on 09/05/12
For personal use only.

Can. J. Chem. Downloaded from www.nrcresearchpress.com by 210.87.254.5 on 09/05/12
For personal use only.

Thermal effects in flash photolysis with special reference to Br atom recombination[1]

GEORGE BURNS
Department of Chemistry, University of Toronto, Toronto 5, Ontario

Received August 17, 1967

Thermal effects, which accompany flash photolyses, are known to interfere with the determination of reaction rate constants. There are two approximate models currently being used in literature to estimate the magnitude of these effects (1, 8). The first model (1) is the more widely accepted. It is based on the assumption that thermal effects are due to the cooling of reacting gas at the walls of the reaction vessel. The second model (8) is based on the assumption that thermal effects are due to nonuniformity in the concentrations of free radicals produced in flash photolysis; it neglects the heat exchange at the wall of the reaction vessel.

It is shown that the second model can be used to calculate the magnitude of thermal effects in reaction vessels of reasonable length. The model was applied to calculate k_{Br_2}, the rate constant for the reaction $2Br + Br_2 \rightarrow 2Br_2$. The value of k_{Br_2} is found to be very sensitive to the choice of model for thermal effects. At room temperature the most reasonable value of k_{Br_2}, using the second model, is $(4.3 \pm 1.3) \times 10^{10}$ l^2 mole^{-2} s^{-1}. This value agrees very well with independent determinations of k_{Br_2} using a stationary photochemical technique. The first model for treatment of thermal effects (1) was used previously to show that such effects do not influence the measured rates of chemical reactions, and calculations of rate constants using this model have not usually been attempted. In one case (5), however, the first model (1) for thermal effects was employed to calculate a value for k_{Br_2} which was found to be six times larger than our value. Consequently, the second model (8) appears to be a better approximation for quantitative evaluation of thermal effects.

Using the raw data (8) and $k_{Br} = 43 \times 10^9$ l^2 mole^{-2} s^{-1}, the value of k_{Ar}, the recombination rate constant of Br atoms in excess of argon, was found to be $(3.0 \pm 0.2) \times 10^9$ l^2 mole^{-2} s^{-1}, which agrees well with data available in the literature.

Canadian Journal of Chemistry, 46, 3229 (1968)

Introduction

In flash photolysis, a large portion of the absorbed light is converted to heat and, thus, such reactions are accompanied by a rise in temperature. In the gas phase, such "thermal effects" create temperature and pressure gradients which complicate, or make impossible, the measurement of rate constants. It is common, therefore, to study flash photolytic reactions in very dilute gaseous solutions. Since the concentration of light absorbing molecules in such solutions is small, the temperature rise may be negligible. However, in such solutions it is not possible to study reactions over a wide range of concentrations, and thus many reactions escape quantitative evaluation. A better understanding of thermal effects is therefore desirable.

Two approximate models for treatment of thermal effects have been proposed in the past. The first model, suggested by Christie *et al.* (1) uses the physical picture previously employed in static photolysis by Rabinowitch and Wood (2). Christie *et al.* suggested that temperature and pressure gradients are created by the cooling of the photolyzed gas near the wall of the reaction vessel. Such cooling would result in an increase of gas density near the walls and in a decrease of gas density in the center of the cylindrical reaction vessel. In conventional flash photolysis, observations are made longitudinally along the central portion of the reaction vessel. Thus, the reacting molecules escape detection as the central portion of the gas in the vessel expands. This model was considered by Bunker and Davidson (3), and by Strong, Chien, Graf, and Willard (4), who showed that under their experimental conditions such thermal effects may be neglected. Givens and Willard (5) used their model to calculate the rate constants in the presence of thermal effects. However, when Burns (6) studied flash photolytic reactions under nonisothermal conditions, he detected no appreciable heat exchange between the wall of the reaction vessel and the reacting gas mixture during the course of the reaction. Consequently, in his experiments, the reaction vessel behaved as an effective calorimeter even though the temperature rise was of the order of 100 °C.

[1]This work was supported in part by the Directorate of Chemical Sciences, Air Force Office of Scientific Research, Grant Number AF AFOSR 506-66.

Can. J. Chem. Downloaded from www.nrcresearchpress.com by 210.87.254.5 on 09/05/12
For personal use only.

More recently, Blake and Burns (7) obtained direct experimental evidence that the heat exchange between the walls of the reaction vessel and the flash irradiated gas is considerably slower than the rate of flash photolytic reaction. For this purpose, they flash photolyzed a dilute solution of I_2 in argon at 1000 °K. At this temperature I_2 is appreciably dissociated; the concentration and the recombination rates of iodine atoms are relatively high, so that the recombination reaction is essentially completed within a few tenths of a millisecond. Blake and Burns found that the heat liberated during recombination raises the gas temperature which, in turn, affects the equilibrium constant of the $I_2 \rightleftharpoons 2I$ reaction. As a result, the equilibrium concentration of atoms, after the flash photolytic recombination is essentially completed, is higher than [I] before flash photolysis. The return to thermal equilibrium was observed by Blake and Burns, but this process was found to be considerably slower than the recombination reaction.

Another model, proposed by Burns and Hornig (8), takes an opposite point of view and assumes that flash photolytic reactions are so fast that cooling at the walls can be neglected. The authors used a flash photolysis apparatus in which the analyzing beam is perpendicular to the reaction vessel and to the flash lamps. In an apparatus of such geometry, the cooling at the walls, even if it were present, could be in the first approximation averaged out. They ascribe thermal effects in their apparatus to nonuniformity in the concentration of free radicals produced in flash photolysis. These nonuniformities created sound waves which were directly observed on the oscilloscope screen.

Both approaches (1) and (8) are admittedly approximate, and a complete treatment of thermal effects should include both models. The object of this communication is to investigate which model provides a leading term in the quantitative expression for thermal effects corrections, and to determine whether a reaction rate constant may be calculated from data obtained in the presence of thermal effects.

Burns and Hornig (8) calculated corrections due to thermal effects for a case of an infinitely long reaction vessel in contact with a short length flash lamp. This is not a common geometry, and a more general treatment of thermal effects using Burns and Hornig's model is desirable. Below, a more general equation for evaluation of thermal effects is derived. The requirement that the reaction vessel be infinitely long compared with the flash lamp is eliminated.

This communication deals with a special case of Br atom recombination reactions but the method may be extended to studies of other gas phase reactions initiated by flash photolysis. Use of a Br atom recombination reaction affords a convenient means for comparing the two models (refs. 1 and 8) which treat thermal effects in flash photolysis quantitatively.

Corrections for Thermal Effects Associated with the Recombination of Bromine Atoms

In order to calculate the recombination rate constant of Br atoms, it is necessary to relate the constant to $[Br_2]$ which is determined experimentally. For any homogeneous media

$$[1] \quad \dot{[Br_2]} = \left(\frac{\partial[Br_2]}{\partial\alpha}\right)_{P,T}\dot{\alpha} + \left(\frac{\partial[Br_2]}{\partial P}\right)_{T,\alpha}\dot{P} + \left(\frac{\partial[Br_2]}{\partial T}\right)_{P,\alpha}\dot{T}$$

where α is the degree of dissociation of bromine, T is the temperature, and P is the pressure. Only the first term of this equation is associated with changes in $[Br_2]$ due to recombination, while the second and third terms are associated with temperature and pressure changes. [1] can be simplified as follows:

$$[2] \quad \left(\frac{\partial[Br_2]}{\partial T}\right)_{\alpha,P} = \frac{-[Br_2]}{T}$$

$$[3] \quad \left(\frac{\partial[Br_2]}{\partial P}\right)_{T,\alpha} = \frac{[Br_2]}{RT[M]}$$

Further,

$$[4] \quad \dot{H} = \dot{E} + P\dot{V} + \dot{P}V \text{ and } \dot{E} = \dot{Q}^1 - P\dot{V}$$

where H is the enthalpy, E is the energy, and Q^1 is the heat evolved. Under conditions of high dilution, $[M] \gg [Br_2]$, [4] can be rewritten as

$$[5] \quad [M]C_{P_M}\dot{T} = \dot{q} + \dot{P}$$

where q is the heat evolved per unit volume. Generally, the relationship between $\dot{P}$ and $\dot{T}$ is somewhat involved because at any given moment $\dot{P}$ and $\dot{T}$ have different values along the reaction vessel. However, if it is possible to assume that $\dot{P}$ is the same in every part of the vessel, the dependence between $\dot{P}$ and $\dot{T}$ is simple. Such an

Can. J. Chem. Downloaded from www.nrcresearchpress.com by 210.87.254.5 on 09/05/12
For personal use only.

assumption may be justified. For example, in an infinitely long vessel (8), pressure gradients are dissipated in a free expansion. If the expansion is much faster than the recombination time, there is no increase in pressure ($\dot{P} \approx 0$). In a vessel of finite length, the compression waves dissipate the pressure gradients. These waves, as they are reflected back and forth through the cell (8), give rise to oscillations in the record. It takes several oscillations before pressure gradients are dissipated. If the oscillations are fast compared with the recombination time, the local pressure fluctuations can be averaged out by using the midpoints of the waves. Therefore, for an infinitely long vessel and for a reasonably short vessel, $\dot{P}$ can be assumed to be the same in every part of the vessel.

In the experiments of Burns and Hornig (8), the reaction vessel was 27 cm long. The compression waves generated in the center of the vessel were propagated with the velocity of sound and reached the end walls in about 0.4 ms. Thus the pressure gradients disappeared in about 1 ms which is faster than the recombination time, 2–5 ms.

Generally, not all the chemical energy is converted to heat during the reaction; part of the energy reappears as kinetic energy of outgoing waves. However, if the nonuniformity in vessel illumination is not too pronounced, most of the energy will be converted into heat. In the present discussion, we assumed that this is the case.

From the ideal gas law

$$[6] \qquad \dot{P} = [\mathrm{M}]R\dot{T}_\mathrm{a}$$

where 'a' refers to the average value of T throughout the vessel. From [5] and [6]

$$[7] \qquad \dot{P} = R\dot{q}_\mathrm{a}/C_{V_\mathrm{M}}$$

For the central region 'c', where the bromine concentration was measured by an analyzing beam, combining [5] and [7] gives

$$[8] \qquad \dot{T}_\mathrm{c} = \frac{\dot{q}_\mathrm{c}}{[\mathrm{M}]C_{P_\mathrm{M}}} + \frac{R\dot{q}_\mathrm{a}}{C_{V_\mathrm{M}}[\mathrm{M}]C_{P_\mathrm{M}}}$$

Substitution of [2], [3], [7], and [8] into [1] yields

$$[9] \qquad [\dot{\mathrm{Br}}_2] = \left(\frac{\partial[\mathrm{Br}_2]}{\partial\alpha}\right)_{T,P}\dot{\alpha} - \frac{[\mathrm{Br}_2]}{C_{P_\mathrm{M}}[\mathrm{M}]T}(\dot{q}_\mathrm{c} - \dot{q}_\mathrm{a})$$

Equation [9] is general and can be applied to the calculation of thermal effects, provided the assumptions discussed are valid.

During recombination of Br atoms, two types of thermal effects are important: the initial and the recombination heating. When the flash dissociates the bromine molecules, the atoms are released with kinetic energy equal to the difference between the photon energy and the energy necessary to produce two bromine atoms. The excess kinetic energy is degraded to heat in a very few collisions. This process is referred to here as the *initial heating effect* and is completed within the duration of the flash (15 μs). Subsequently, atoms recombine, evolving heat. This process is referred to here as the *recombination heating effect* and lasts milliseconds.

For each type of thermal effect, [9] can be simplified further. For the recombination heating effects

$$[10] \qquad \left(\frac{\partial[\mathrm{Br}_2]}{\partial\alpha_\mathrm{c}}\right)_{T,P}\dot{\alpha}_\mathrm{c} = k_\mathrm{r}[\mathrm{Br}]^2[\mathrm{M}]$$

The values of $\dot{q}_\mathrm{c}$ and $\dot{q}_\mathrm{a}$ may be related in the following way. Let us define S via

$$[11] \qquad [\mathrm{Br}]_\mathrm{av} = S[\mathrm{Br}]_\mathrm{c}$$

Here $[\mathrm{Br}]_\mathrm{c}$ is the atom concentration in the central region of the vessel where the measurements of the reaction rate constant were made and $[\mathrm{Br}]_\mathrm{av}$ is the average bromine atom concentration in the reaction vessel. Then, assuming that during recombination no radiative processes are operative,

$$[12] \qquad \dot{q}_\mathrm{c} = Dk_\mathrm{r}[\mathrm{Br}]_\mathrm{c}^2[\mathrm{M}]$$

and

$$[13] \qquad \dot{q}_\mathrm{a} = Dk_\mathrm{r}S^2[\mathrm{Br}]_\mathrm{c}^2[\mathrm{M}]$$

where D is the dissociation energy of bromine. [12] and [13] together give

$$[14] \qquad \dot{q}_\mathrm{c} - \dot{q}_\mathrm{a} = \dot{q}_\mathrm{c}(1 - S^2)$$

Substitution of [14], [10], [12], and [13] into [9] then yields

$$[15] \qquad [\dot{\mathrm{Br}}_2] = k_\mathrm{r}[\mathrm{Br}]^2[\mathrm{M}] \times \left(1 - \frac{D(1 - S^2)[\mathrm{Br}_2]}{[\mathrm{M}]C_{P_\mathrm{M}}T}\right)$$

For the particular case of an infinitely long

Can. J. Chem. Downloaded from www.nrcresearchpress.com by 210.87.254.5 on 09/05/12
For personal use only.

reaction vessel, $\dot{P}$ and S are zero. For this case, [15] simplifies further to

$$[16] \quad [Br_2] = k_r[Br]^2[M]\left(1 - \frac{D[Br_2]}{C_{P_M}[M]T}\right)$$

This equation is equivalent to equation [16] of ref. 8. [15] can be easily integrated for small degrees of dissociation of bromine, and assuming that

$$[17] \qquad T = T_c = T_a \quad \text{and } \dot{S} = 0$$

the integration yields

$$[18] \quad \frac{1}{[Br]} - \frac{1}{[Br]_0} = 2k_r[M]t \times \left(1 - \frac{D(1 - S^2)[Br_2]}{[M]C_{P_M}T}\right)$$

Similarly the integration of [16] yields

$$[18a] \quad \frac{1}{[Br]} - \frac{1}{[Br]_0} = 2k_r[M]t \times \left(1 - \frac{D[Br_2]}{[M]C_{P_M}T}\right)$$

The initial heating effect can also be calculated from [9]. These effects proceed independently of recombination. Therefore $\dot{\alpha} = 0$, and since the heat evolved is proportional to the concentration of atoms produced,

$$[19] \qquad \dot{q} = Q[\dot{Br}]$$

where Q is the proportionality constant. In this case

$$[19a] \qquad \dot{q}_c - \dot{q}_a = \dot{q}_c(1 - S)$$

Then [9] integrates for small heating effects to

$$[20] \quad \Delta[Br_2] = -\frac{[Br_2](1 - S)Q[Br]_{c \text{ at } t=0}}{C_{P_M}[M]T}$$

For an infinitely long reaction vessel, this equation simplifies further to

$$[20a] \quad \Delta[Br_2] = -\frac{[Br_2]Q[Br]_{c \text{ at } t=0}}{C_{P_M}[M]T}$$

It is interesting to note here that the magnitude of thermal effects correction depends largely upon the *uniformity* of illumination in the reaction vessel, and is thus affected by the temperature *gradient* in the photolyzed gas. As can be seen from [18] and [20], if the reaction vessel is uniformly illuminated, both initial and recombination heating effects reduce to zero, because in that case, $S = 1$, even though there may be an appreciable change in the temperature of the photolyzed gas.

Since both an inert gas (argon in ref. 8) and Br_2 act as third bodies, the apparent (measured) rate constant is given (8) by

$$[21] \qquad k_{app} = k_{Ar} + \frac{[Br_2]}{[Ar]}k_{Br_2}$$

The value of k_{app} depends upon the assumptions used to calculate thermal effects. As $[Br_2]/[Ar]$ ratio increases, thermal effects also increase, as in [18], and k_{Br_2} and k_{Ar} decrease. Moreover, heat exchange at the walls of the reaction vessel becomes more pronounced as the temperature of the gas increases. All these effects would decrease the value of k_{app}. Therefore, the plot of k_{app} vs. $[Br_2]/[Ar]$ ratio would yield a straight line in a limiting case of small thermal effects where [18] is valid. At a higher $[Br_2]/[Ar]$ ratio, the plot would have a negative second derivative.

Twelve values of k_{app} over a 15-fold $[Br_2]/[Ar]$ ratio are known (8). These data were obtained by plotting $[Br]^{-1}$ versus time over a time interval of several milliseconds, which were the typical intervals used by previous workers (5). From this data, we have calculated the values of k_{Br_2} using [18] (Table I). The value of S in [18] was measured in a separate experiment (9) and was found to be equal to 0.9. The magnitude of k_{Br_2}, as well as the probable error in Table I, were calculated using the principle of least squares.

TABLE I

Recombination rate constants of Br atoms in $Br_2(k_{Br_2}) \times 10^{-9}$ in l^2 mole^{-2} s^{-1} calculated from data given in ref. 8

Thermal effects neglected	6±7*
Thermal effects included	43±13
Givens and Willard (5)	260
Christie, Roy, and Thrush (10)	49
Basila and Strong (11)	48

*The uncertainty is given as standard deviation.

When all 12 determinations of k_{app} are included in determination of k_{Br_2} using [21], $k_{Br_2} = 24 \times 10^9$ l^2 mole^{-2} s^{-1}; if the k_{app} measured at highest $[Br_2]/[Ar]$ is not included in the calculations, $k_{Br_2} = 43 \times 10^9$ l^2 mole^{-2} s^{-1}; if the k_{app} measured at the two highest $[Br_2]/[Ar]$ are not included in the calculations,

Can. J. Chem. Downloaded from www.nrcresearchpress.com by 210.87.254.5 on 09/05/12
For personal use only.

$k_{Br_2} = 58 \times 10^9$ l^2 mole^{-2} s^{-1}; if three points at highest [Br_2]/[Ar] are not included, $k_{Br_2} = 52 \times 10^9$ l^2 mole^{-2} s^{-1}. Thus, as the k_{app} values at highest [Br_2]/[Ar] ratio are discarded one by one, the value of k_{Br_2} first increases, as would be expected if the plot of k_{app} displays a negative second derivative. However, if this process is continued, the value of k_{Br_2} begins to fluctuate and the correlation coefficient passes through a maximum. Thus, when all 12 points are used to calculate k_{Br_2}, the correlation coefficient is 0.63. When 11 points at lowest [Br_2]/[Ar] are used, the correlation coefficient is 0.78; with 10, the correlation coefficient is 0.73; with 9, 0.60; with 8, 0.18. The most probable value of k_{Br_2} is obtained using the maximum number of experimental points consistent with a minimum per cent error in k_{Br_2} and thus the maximum correlation coefficient. This value of k_{Br_2} is $(43 \pm 13) \times 10^9$ l^2 mole^{-2} s^{-1}, which is about the average of three k_{Br_2} values, reported above (58×10^9, 43×110^9, and 24×10^9 l^2 mole^{-2} s^{-1}). This result agrees well with that of Christie, Roy, and Thrush (10), who used a static photolysis method for k_{Br_2} determination. The agreement suggests that the assumptions used in the derivation of [18] are reasonable, provided the [Br_2]/[Ar] ratio is smaller than 2.5×10^{-3}, the highest [Br_2]/[Ar] used in calculating k_{Br_2}. The value of k_{Br_2} obtained by Basila and Strong (11) also agrees well with our results. These authors extrapolated the [Br]$^{-1}$ versus time plot to $t = 0$ in their flash photolysis experiments and used the initial slope of their plots to calculate k_{app}. It can be seen from [1], [18], and [20] that the extrapolation yields correct values of k_{app} provided that the value of $\dot{P}$ term plus $\dot{T}$ term in [1] is small, or the value of S in [18] and [20] is nearly unity, i.e. if the reaction vessel is irradiated uniformly by the flash lamp. It thus appears that this condition was obtained by Basila and Strong. They were, therefore, able to obtain k_{app} without using either one of the models ((1) or (8)) to correct for thermal effects.

The value of k_{Br_2} obtained by Givens and Willard (5) is much higher than ours. The discrepancy is probably due to the assumptions used by these authors in their calculations of thermal effects. The present results suggest that the high value of k_{Br_2} obtained by the authors (5) might be due to the nonuniformity of illumination of their reaction vessel by the flash. However, since detailed information of intensity distribution in their vessel is not available, it would be futile to speculate what rate they would have obtained, had they used a different model. It is apparent, however, that these authors studied recombination in the presence of large thermal effects because in some of their experiments, the measured concentration of molecular bromine *decreased* with time as the recombination proceeded. This implies that in these experiments, the sum of the second and third terms of [1] was larger than the first.

Their high value of k_{Br_2} was cited by them as evidence of the relative stability of a Br_3 molecule. Our value of k_{Br_2} is about 17 times larger than k_{Ar} which implies that Br_3 is extremely unstable relative to I_3.

Using the raw data (8) and $k_{Br_2} = 43 \times 10^9$ l^2 mole^{-2} s^{-1}, the value of k_{Ar}, the recombination rate constant of Br atoms in excess of argon, was found to be $(3.0 \pm 0.2) \times 10^9$ l^2 mole^{-2} s^{-1}. This value of k_{Ar} agrees well with the literature values, tabulated elsewhere (12).

In order to make our model more general, further improvements can be made. In particular, it should be possible to set up a computer program for arbitrary vessel illumination, which would take into account the propagation of pressure waves in the vessel; in this case, S in [11] would become a function of space and time. Our other assumptions may also be treated with greater rigor. In particular, cooling at the wall must be included at some stage, especially if slow reactions at low pressures would be studied.

It is interesting to note, however, that despite the simplicity of our model, meaningful values of k_{Br_2} have been obtained. To the author's best knowledge, it is the first meaningful rate constant calculated from raw data, which was obtained in the presence of appreciable thermal effects in flash photolysis. In fact, the comparison of first three values of k_{Br_2} (Table I) indicates that the model for thermal effects corrections essentially determines the value of k_{Br_2}.

Conclusions

Although flash photolysis proved to be an extremely powerful technique to study fast photochemical reactions, it had not been possible to obtain quantitative data, if the thermal effects in flash photolyzed gas were appreciable. Thus,

the k_{Br_2} calculated from flash photolysis data ranges from 6×10^9 to 260×10^9 l^2 $mole^{-2}$ s^{-1}, depending upon the model used in evaluation of thermal effects corrections.

It appears that thermal effects are due primarily to the nonuniformity in irradiation of reacting gas. Using this model (8) for treatment of thermal effects, a value of k_{Br_2} was obtained which agrees well with k_{Br_2} obtained by independent methods, not affected by thermal effects. In principle, it may be possible to construct a flash photolysis apparatus in which extremely high uniformity of illumination is achieved. In such an apparatus thermal effects will be due to the temperature gradients created by the heat exchange at the walls of the reaction vessel, which is a model suggested previously (1–5).

Acknowledgments

This work was conducted in part at Princeton University. The author wishes to express his appreciation to Dr. Donald F. Hornig, for the inspiration he has always provided. The author is indebted to the General Electric Company and to the Gulf Research and Development Company for fellowships. The work was supported in part by the Office of Naval Research, by the National Research Council of Canada, and by the Defence Research Board of Canada, grant number 9530-54. Acknowledgment is also made to donors of the Petroleum Research Fund, administered by the American Chemical Society, for partial support of this research. Calculations of k_{Br_2} were performed, in part, by Dr. R. K. Boyd and Mr. J. Morriss. The author also wishes to thank the referees for helpful comments.

1. M. I. Christie, A. J. Harrison, R. G. W. Norrish, and G. Porter. Proc. Roy. Soc. London, Ser. A, **231**, 446 (1955).
2. E. Rabinowitch and W. C. Wood. J. Chem. Phys. **4**, 497 (1936).
3. D. L. Bunker and N. Davidson. J. Am. Chem. Soc. **80**, 5085 (1958).
4. R. L. Strong, J. C. W. Chien, P. E. Graf, and J. E. Willard. J. Chem. Phys. **26**, 1287 (1957).
5. W. G. Givens, Jr. and J. E. Willard. J. Am. Chem. Soc. **81**, 4773 (1959).
6. G. Burns. Can. J. Chem. **45**, 2369 (1967).
7. J. A. Blake and G. Burns. To be published.
8. G. Burns and D. F. Hornig. Can. J. Chem. **38**, 1702 (1960).
9. G. Burns. Ph.D. Dissertation, Princeton University, Princeton, New Jersey. 1960.
10. M. I. Christie, R. S. Roy, and B. A. Thrush. Trans. Faraday Soc. **55**, 1139 (1959).
11. M. R. Basila and R. L. Strong. J. Phys. Chem. **67**, 521 (1963).
12. J. K. K. Ip and George Burns. Discussions Faraday Soc. **44**, 241 (1967).

Can. J. Chem. Downloaded from www.nrcresearchpress.com by 210.87.254.5 on 09/05/12
For personal use only.

Can. J. Chem. Downloaded from www.nrcresearchpress.com by 210.87.254.6 on 09/05/12
For personal use only.

Radiolysis of methylcyclopentane. III. Liquid phase mechanism and comparison of cycloalkanes

GORDON R. FREEMAN AND E. DIANE STOVER
Chemistry Department, University of Alberta, Edmonton, Alberta

Received March 21, 1968

The initial yields of the major products of the gamma radiolysis of liquid methylcyclopentane (MCP) at 25° are: $G(H_2) = 4.2$, G(1-methylcyclopentene plus methylenecyclopentane) = 2.7, G(3- plus 4-methylcyclopentene) = 1.0, G(open chain hexene) = 1.0, and G(bimethylcyclopentyl) = 0.9. The effects of scavengers on the product yields are reported and the mechanism is discussed.

The liquid phase radiolytic decompositions of cyclohexane (CH), methylcyclohexane (MCH), cyclopentane (CP), and MCP are compared. The net amount of C—C bond cleavage is much greater in the five-membered than in the six-membered rings. Methyl substitution on the ring reduces $G(H_2)$ by about one unit, mainly because of the formation of a type of ion (QH^+) that does not yield hydrogen when neutralized by an electron. The QH^+ type ions are formed in MCH and MCP, but not in CH and CP. In all the systems, another type of ion (N^+) that does not yield hydrogen when neutralized by an electron is formed with a G value of about unity. The type of ion (PH^+) that does yield hydrogen when neutralized by an electron has a G value of 3.4 in CH and CP, but only 2.0 in MCP. It is concluded that G(total ionization) is in the vicinity of 4.4 in the liquid compounds, virtually the same as the gas phase values.

Canadian Journal of Chemistry, 46, 3235 (1968)

Introduction

The study of the radiolysis of liquid methylcyclopentane (MCP) was divided into three parts. In part I (1), MCP was mixed with known proton and electron scavengers to test a nonhomogeneous kinetics model of charge scavenging (2). In part II (3), the idea that unsaturated compounds reduce the hydrogen yield from the radiolysis of saturated hydrocarbons by scavenging thermal hydrogen atoms was challenged by showing that the results fit the nonhomogeneous kinetics charge scavenging mechanism. The present article represents the termination of a general study of the radiolysis of cycloalkanes. At the end of the Discussion section, results from the radiolyses of several cycloalkanes are summarized and new conclusions are drawn.

The radiolysis of MCP has previously received a small amount of attention in general investigations of the yields of *readily scavengable* and *not readily scavengable* products (4) and of radicals (4, 5) in the gamma radiolysis of hydrocarbons.

Experimental

Most of the materials and experimental techniques used have been described elsewhere (1).

Carbon dioxide (99.9% minimum purity) from Air Reduction Co. and hydrogen chloride (99%) from Matheson were used as supplied. 1-Methylcyclopentene (1-MC), obtained from Aldrich Chemical Co., and hexene-1 from Phillips Petroleum Co. were vacuum distilled before use. 3-Methylcyclopentene (3-MC) was prepared by reducing 2-methylcyclopentanone to the alcohol, converting this to the acetate, and heating the acetate to 450° in a sealed tube. The mixture of 1-MC and 3-MC so obtained was separated by gas chromatography. Bimethylcyclopentyl (BMCP) was prepared by heating MCP with di-*tert*-butyl peroxide at 145° in a sealed tube for 24 h, followed by vacuum distillation (6).

The dose given to the binary solutions was 2.0×10^{20} eV/g, at a dose rate of 3.6×10^{19} eV/g h. The irradiation temperature was 25°.

The liquid products were measured by gas chromatography. The chromatograph was calibrated by injecting standard solutions of the radiolysis products in MCP solvent.

Results

Effect of Dose

The yields of products from pure MCP were measured at doses over the range from 1×10^{19} to 4×10^{20} eV/g. The yields of hydrogen, 1-MC, 3-MC, and hexene decreased with increasing dose up to about 1×10^{20} eV/g, then remained constant as the dose was further increased (Fig. 1). The yield of the product tentatively identified as methylcyclopentyl-methylcyclopentene (MCMC) increased with increasing dose (Fig. 1). The other product yields were, within experimental error, independent of dose over the entire range.

The initial yields G_i were obtained by extrapolation to zero dose and are listed in Table I. Hydrogen was measured at doses down to 3×10^{18} eV/g and the curve in Fig. 1 indicates that $G_i(H_2) = 4.5 \pm 0.4$. However, the value 4.2 was estimated during the scavenging studies (1, 3). The latter value is thought to be the more reliable, so it is included in Table I.

Can. J. Chem. Downloaded from www.nrcresearchpress.com by 210.87.254.6 on 09/05/12
For personal use only.

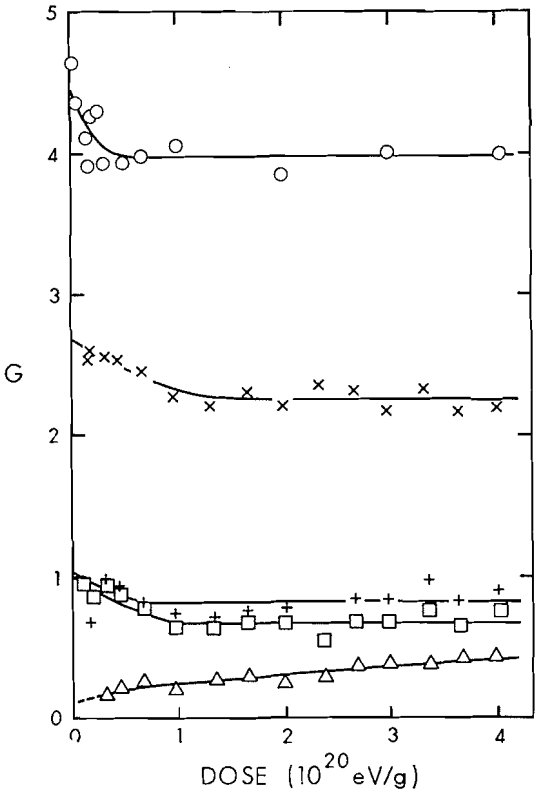

FIG. 1. Effect of dose on product yields: ○, hydrogen; ×, 1-methylcyclopentene; +, 3-methylcyclopentene; □, hexene; △, methylcyclopentylmethylcyclopentene.

TABLE I

Initial product yields and hydrogen balance

Product	G_i	H_2 equivalent
CH_4	0.12±0.03	−0.12±0.03
C_2–C_5	[a]	−0.24[b]
1-MC	2.7±0.1	+2.7±0.1
3-MC	1.0±0.2	+1.0±0.2
Hexene	1.0±0.1	0.0
BMCP	0.9±0.1	+0.9±0.1
MCMC	0.1±0.1	+0.2±0.2
Total H_2 equivalent		+4.4±0.6
H_2	4.5±0.4	
	4.2[c]	

[a]Not measured.
[b]Estimated by analogy with the results for cyclopentane in ref. 12.
[c]References 1 and 3.

By analogy with the results of the methylcyclohexane investigation (7), methylenecyclopentane was probably a product of MCP radiolysis, but would have isomerized rapidly to 1-MC on the gas chromatographic column. The product referred to as 1-MC therefore probably includes methylenecyclopentane. Furthermore, the product referred to as 3-MC probably includes 4-MC, as these two compounds would not have separated on the chromatographic column used (silica gel).

Effects of Additives

To study the effects of charge scavengers on the product yields, ND_3 was added as a positive ion scavenger and CO_2 was added to scavenge the electrons. The yields from the binary solutions were calculated from the energy absorbed in

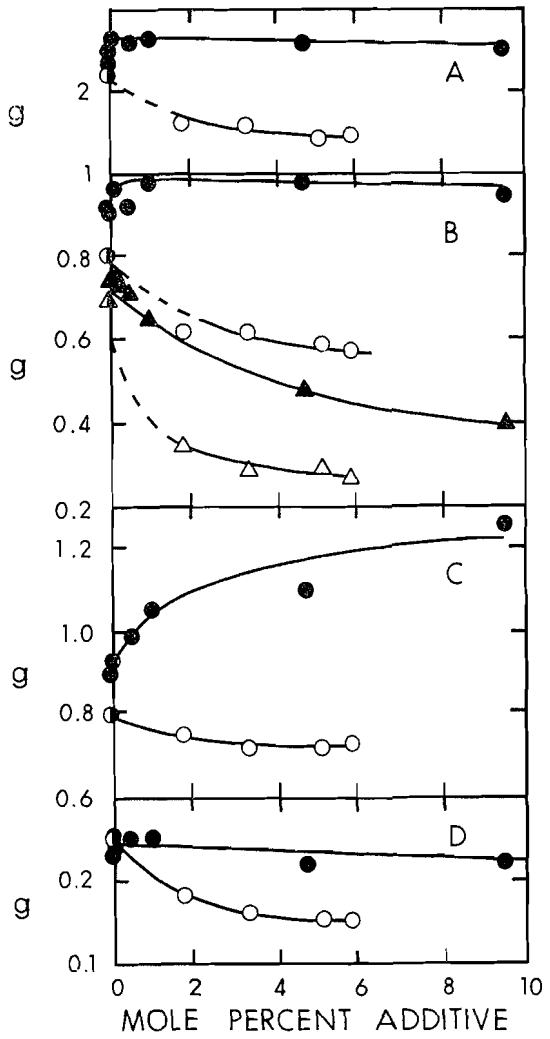

FIG. 2. Product yields in MCP—additive solutions. Additives: open points, CO_2; filled points, ND_3. A: 1-methylcyclopentene. B: circles, 3-methylcyclopentene; triangles, hexene. C: bimethylcyclopentyl. D: methylcyclopentylmethylcyclopentene.

Can. J. Chem. Downloaded from www.nrcresearchpress.com by 210.87.254.6 on 09/05/12
For personal use only.

MCP only (based on electron fraction) and are given the symbol g(prod.).

The methane yield was unaffected by the presence of either ND_3 or CO_2.

The addition of CO_2 to MCP decreased the yields of all the C_6 and C_{12} hydrocarbon products (Fig. 2). By contrast, the addition of ND_3 increased the yields of 1-MC, 3-MC, and BMCP, although it decreased the yield of hexene and had a negligible effect on the yield of MCMC. The yields of 1-MC and 3-MC in solutions that contained 0.1 mole % or more ND_3 were nearly the same as the zero dose yields, G_i, in pure MCP (cf. Figs. 1 and 2).

During the radiolysis of the MCP–CO_2 solutions a carboxylic acid was formed (identified by infrared absorption spectroscopy) but it was not measured quantitatively.

The addition of 0.84 and 1.65 mole % of HCl to MCP increased $G(H_2)$ to 6.16 and 6.35 respectively. The effects of the other additives on the hydrogen yields are reported elsewhere (1, 3).

Discussion

Hydrogen Balance

Since MCP has the empirical formula C_6H_{12}, the "H_2 equivalent" of a product C_mH_n can be defined as $(m - \frac{1}{2}n) \times G(C_mH_n)$. If the product analysis were complete, then the total H_2 equivalent of all the hydrocarbon products should equal $G(H_2)$. This is shown in Table I to be true for the present system, within the rather large experimental error.

Mechanism

A. Methane

The methane yield, $G_i(CH_4) = 0.12$, was unaffected by the presence of 5 mole % of CO_2 or ND_3, but it was decreased to 0.06 by the presence of 1% of 1,3-cyclohexadiene (3). These results are consistent with the suggestion that about half of the methane is formed by methyl radical abstraction reactions. The other half of the methane is formed by *not readily scavengable* reactions, such as the disproportionation of radicals in liquid cages or the direct decomposition of excited species.

B. 1-MC, 3-MC, and BMCP

About half of the 1-MC and 3-MC and about 80% of the BMCP were *readily scavengable* by 1,3-cyclohexadiene (3). Carbon dioxide reduced the yields of these compounds by only about 30% (Fig. 2). ND_3 increased the yields of 1-MC and 3-MC from the values characteristic of the dose used (2×10^{20} eV/g) in pure MCP to the zero-dose values for pure MCP, and it increased the yield of BMCP to somewhat beyond the zero-dose value (Fig. 2). These facts are consistent with the following mechanism. The *readily scavengable* portion of the products is formed mainly by the disproportionation and combination of methylcyclopentyl radicals in the bulk medium.

[1] $2C_6H_{11} \rightarrow$ (1-MC, 3-MC) + MCP

[2] $\rightarrow$ BMCP

The most abundant isomer of the C_6H_{11} radical in the solution is probably **1**, because the tertiary C—H bond is weaker than the secondary C—H bonds, which must be broken to form the isomers

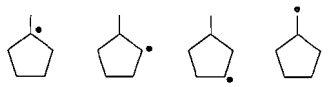

1 **2** **3** **4**

2 and **3**. The least abundant isomer is probably the cyclopentylmethyl radical **4**, because a relatively strong primary C—H bond must be broken to form it. Much of the earlier discussion of the disproportionation/combination ratios, k_d/k_c, of the analogous methylcyclohexyl radicals (7) applies here and will not be repeated. However, it may be assumed that the values of k_d/k_c for the various isomers are in the order **1** > **2** ≈ **3** > **4**. The relative abundances of the isomeric radicals and the relative values of k_d/k_c can explain why, for the *readily scavengable* portion G_{rs} of the products (3), G_{rs}(1-MC) = 2.5G_{rs}(3-MC) and G_{rs}(1-MC + 3-MC)/G_{rs}(BMCP) = 3.0.

1,3-Cyclohexadiene inhibits the formation of these products somewhat more readily than does CO_2 because the former can scavenge C_6H_{11} radicals

[3] $C_6H_{11} + C_6H_8 \rightarrow C_6H_{11}—C_6H_8\cdot$

as well as electrons or hydrogen atoms, which are precursors of the radicals, whereas CO_2 probably only scavenges electrons.

[4] $CO_2 + e^-_{solv} \rightarrow CO_2^-{}_{solv}$

[5] $CO_2^-{}_{solv} + C_6H_{12}^+ \rightarrow$ products

ND_3 apparently inhibits secondary reactions that cause the yields of 1-MC, 3-MC, and BMCP to decrease with increasing dose in "pure"

Can. J. Chem. Downloaded from www.nrcresearchpress.com by 210.87.254.6 on 09/05/12
For personal use only.

MCP. Since ND_3 reacts only with the positive ions, the latter must be responsible for most of the secondary reactions that destroy the C_6 and C_{12} products.

The *not readily scavengable* portions of 1-MC, 3 MC, and BMCP are presumably formed by ionic and radical reactions in spurs and by

[6] $$C_6H_{12}^* \rightarrow H_2 + C_6H_{10}$$

C. Hexene

About 70% of the hexene was *readily scavengable* by CO_2 (Fig. 2B) and by 1,3-cyclohexadiene (3). ND_3 also reduced the yield of hexene, but it was an order of magnitude less efficient than was CO_2 as an inhibitor (Fig. 2B). Thus the *readily scavengable* hexene has an ionic precursor.

[7] $$C_6H_{12}^+ + e^-_{solv} \rightarrow \text{hexene (open chain)}$$

Inhibition can occur by reaction [8] or [10],

[8] $$e^-_{solv} + S \rightarrow S^-$$

[9] $$S^- + C_6H_{12}^+ \rightarrow \text{no hexene}$$

[10] $$C_6H_{12}^+ + NH_3 \rightarrow C_6H_{11} + NH_4^+$$

where S is an electron scavenger such as CO_2 or 1,3-cyclohexadiene (3). Good positive ion scavengers are an order of magnitude less efficient than good electron scavengers at the same concentration (1). This explains the difference between the effects of ND_3 and CO_2 (Fig. 2B). The *not readily scavengable* portion of the hexene ($G \approx 0.3$) may be formed by the isomerization of excited molecules.

[11] $$C_6H_{12}^* \rightarrow \text{hexene (open chain)}$$

D. MCMC

The yield of MCMC increased with increasing dose, which indicates that the product was formed at least in part by secondary reactions such as

[12] $$H + C_6H_{10} \rightarrow H_2 + C_6H_9$$

[13] $$C_6H_{11} + C_6H_9 \rightarrow C_6H_{11}C_6H_9$$

The formation of MCMC was negligibly affected by ND_3, but it was inhibited by CO_2 (Fig. 2D). This is because ND_3 does not reduce the yields of hydrogen atoms, methylcyclopentenes, or methylcyclopentyl radicals, whereas CO_2 inhibits the formation of all of them by scavenging electrons.

E. Hydrogen

The only new hydrogen result reported in this article is that the addition of hydrogen chloride increases the hydrogen yield from 4.2 to 6.4. To interpret this result quantitatively, it is necessary to recapitulate the hydrogen-forming mechanism that was elucidated in an earlier article (1). This recapitulation will also facilitate the comparison of cycloalkanes in the next section.

It was shown (1) that the following reactions take place during gamma radiolysis of pure MCP, with the indicated yields.

		G
[14]	$C_6H_{12} \rightsquigarrow e^-_{solv} + PH^+ + ?$	2.0
[15]	$\rightsquigarrow e^-_{solv} + QH^+ + ?$	~ 1.2
[16]	$PH^+ + e^-_{solv} \rightarrow H, H_2 + \text{products}$	2.0
[17]	$QH^+ + e^-_{solv} \rightarrow \text{no H or } H_2$	~ 1.2

The ions PH^+ and QH^+ include $C_6H_{12}^+$ and $C_6H_{11}^+$ and may partly result from ion-decomposition and fast ion–molecule reactions[1]. Both PH^+ and QH^+ can donate a proton to ammonia (1).

[18] $$PH^+ + NH_3 \rightarrow P + NH_4^+$$

[19] $$QH^+ + NH_3 \rightarrow Q + NH_4^+$$

[20] $$NH_4^+ + e^-_{solv} \rightarrow NH_3 + H$$

[21] $$H + C_6H_{12} \rightarrow H_2 + C_6H_{11}$$

The replacement of reaction [17] by [19] followed by [20] and [21] causes the hydrogen yield to increase, in the presence of ammonia, by a maximum of about 1.2 units (1). Other hydrogen-forming reactions in MCP are (3):

		G
[22]	$C_6H_{12} \rightsquigarrow C_6H_{12}^*$	2.2
[23]	$C_6H_{12}^* \rightarrow H + C_6H_{11}$	1.6
[6]	$\rightarrow H_2 + C_6H_{10}$	0.6

Part of the H and H_2 that have been assigned to reactions [23] and [6] might actually be formed by the rapid decomposition of excited ions, i.e., some of the question marks in reactions [14], [15], and [24] (see later) might represent H or H_2. If this is so, the estimated yields of reactions [23] and [6] are smaller than those indicated by a corresponding amount.

The addition of hydrogen chloride to MCP increased the hydrogen yield from 4.2 to 6.4, which is one unit more than the increase caused by the addition of ammonia (1). This indicates that in pure MCP reactions [24] and [25] occur in addition to [14]–[17], [21]–[23], and [6].

[1] PH^+ and QH^+ might be empirically different, or they might be empirically the same but able to react in two different ways upon neutralization by an electron.

TABLE II

Product yields from liquid cycloalkanes[a]

Product	G values for cycloalkane, C_nH_{2n}			
	c-C_6H_{12}[b] (n = 6)	c-C_5H_{10}[c] (n = 5)	c-$C_6H_{11}CH_3$[d] (n = 7)	c-$C_5H_9CH_3$[e] (n = 6)
H_2	5.6	5.4	4.8	4.2
CH_4	0.006	0.03	0.08	0.12
C_2	0.1[f]	0.6	0.1	[g]
C_3	0.02[f]	0.6	0.02	[g]
C_nH_{2n-2}	3.2	3.0	3.5	3.7
Open chain C_nH_{2n}	0.40	0.74	0.64	1.0
Open chain C_nH_{2n+2}	0.08	0.14		
$C_{2n}H_{4n-2}$	1.8	1.3	0.75	0.9
Total C_{2n}	2.0	1.5	0.9	1.0
Polymer (C_n units)	[g]	0.7	[g]	[g]
—C_nH_{2n}	≥7.7	8.3	≥5.9	>6.7

[a]Gamma radiolysis yields extrapolated to zero dose; temperature ~25°.
[b]Reference 16.
[c]Reference 12.
[d]Reference 7.
[e]Present work.
[f]Reference 17.
[g]Not measured.

$$C_6H_{12} \rightsquigarrow e^-_{solv} + N^+ + ? \qquad G \sim 1.0 \tag{24}$$

$$N^+ + e^-_{solv} \rightarrow \text{no H or } H_2 \qquad \sim 1.0 \tag{25}$$

In the presence of ammonia, N^+ does not react to form an ammonium ion.

$$N^+ + NH_3 \rightarrow \text{no } NH_4^+ \tag{26}$$

In the presence of HCl, reaction [27] occurs and is followed by either [28] or [29].

$$e^-_{solv} + HCl \rightarrow HCl^-_{solv} \tag{27}$$

$$HCl^-_{solv} \rightarrow H + Cl^-_{solv} \tag{28}$$

$$HCl^-_{solv} + (PH^+, QH^+, N^+) \rightarrow H \text{ or } H_2 + \text{products} \tag{29}$$

where all the ions are probably selectively solvated by HCl molecules.

Thus it appears that G(total ionization) ≈ 4.2 in pure liquid MCP, similar to the values in liquid cyclohexane (8) and alcohols (9, 10).

Comparison of Cycloalkanes

This article marks the termination of our extended comparative investigation of the radiolysis of cycloalkanes, so it is useful to give a brief summary at this point. Several new conclusions can be drawn.

The yields of products from the liquid phase gamma radiolyses of cyclohexane (CH), cyclopentane (CP), methylcyclohexane (MCH), and MCP are given in Table II.

The hydrogen yield is reduced somewhat by changing from a six-membered to a five-membered ring, but it is reduced more markedly by methyl substitution on the ring.

The methane yields are slightly higher from the methyl substituted compounds, but in no case is methane a major product. A major increase in the amount of C—C bond cleavage is observed upon going from six-membered to five-membered rings. The yield of C_2 products from CP is sixfold that from CH, and the amount of ring-opening to form open chain C_n compounds in CP or MCP is nearly double that in CH or MCH. This reflects the greater stability of the six-membered rings.

The value of the ratio $G(C_nH_{2n-2})/G(C_{2n}H_{4n-2})$ is 1.8 for CH, 2.3 for CP, 4.7 for MCH, and 4.1 for MCP. Thus, the greatest change in this ratio occurs upon methyl substitution on the ring and reflects, at least in part, the fact that k_d/k_c is larger for tertiary alkyl radicals such as **1** than for secondary alkyl radicals such as cyclopentyl.

The addition of ammonia to CH (11, 12) or CP [up to 10 mole % ND_3 added (12)] had no effect on the hydrogen yields from the hydrocarbons, in contrast to the behavior of the MCP system. This means that in CH and CP, ions of type QH^+ (cf. reactions [17] and [19]) are not produced. However, the yield of PH^+ type ions (cf. reactions [16] and [18]) is 3.4 in CH (13) and in CP (12). Thus the yield of PH^+ in CH or CP roughly equals $G(PH^+ + QH^+) = 3.2$ in MCP. The formation of type QH^+ ions is associated with methyl substitution on the ring

Can. J. Chem. Downloaded from www.nrcresearchpress.com by 210.87.254.6 on 09/05/12
For personal use only.

TABLE III

Yields of types of ions that undergo neutralization

System	G(ion type)			
	PH^{+a}	QH^{+b}	N^{+c}	Total ions
c-C_5H_{10} (liquid, 25°)	3.4	0.0	~1	~4.4
c-C_6H_{12} (liquid, 25°)	3.4	0.0	1.2	4.6
c-$C_5H_9CH_3$ (liquid, 25°)	2.0	~1.2	~1.0	~4.2
c-$C_6H_{11}CH_3$ (vapor, 110°)	2.1	1.3	1.0	4.4

[a]PH^+ yields hydrogen when neutralized by an electron and it reacts with ammonia by proton donation.
[b]QH^+ does not yield hydrogen when neutralized by an electron, but it does react with ammonia by proton donation.
[c]N^+ neither yields hydrogen when neutralized by an electron nor donates a proton to ammonia.

and is the major cause of the lower values of $G(H_2)$ from the methyl-substituted compounds (Table II).

The addition of hydrogen chloride to CH increased $G(H_2)$ from 5.6 to 6.8 (14). This means that the yield of N^+ type ions in CH is 1.2.

A similar study of the vapor phase MCH system has been reported (15). A summary of the results for all these systems is given in Table III. It is surprising that the yields of the different types of ions should be so similar in liquid MCP at 25° and in MCH vapor at 0.5 atm and 110°. Similar yields doubtlessly occur in liquid MCH.

The total yield of scavengable ions in the liquid phase hydrocarbons is about 4.4 units (Table III), which means that the W values (23 eV) are virtually the same in the gas phase and in the liquid phase.

Acknowledgment

The authors wish to thank J. van Dyke for the preparation of 3-methylcyclopentene.

1. E. D. Stover and G. R. Freeman. J. Chem. Phys. **48**, 3902 (1968).
2. G. R. Freeman. J. Chem. Phys. **46**, 2822 (1967).
3. E. D. Stover and G. R. Freeman. Can. J. Chem. **46**, 2109 (1968).
4. T. J. Hardwick. J. Phys. Chem. **66**, 1611 (1962).
5. R. H. Schuler and R. R. Kuntz. J. Phys. Chem. **67**, 1004 (1963).
6. E. H. Farmer and C. G. Moore. J. Chem. Soc. 131 (1961).
7. G. R. Freeman. J. Chem. Phys. **36**, 1534 (1962).
8. N. H. Sagert and A. S. Blair. Can. J. Chem. **45**, 1351 (1967).
9. J. C. Russell and G. R. Freeman. J. Phys. Chem. **72**, 808, 816 (1968).
10. K. N. Jha and G. R. Freeman. J. Chem. Phys. **48**, 5480 (1968).
11. F. Williams. J. Am. Chem. Soc. **86**, 3954 (1964).
12. L. G. Walker. Ph.D. Thesis, University of Alberta, Edmonton, Alberta. 1967.
13. M. G. Robinson and G. R. Freeman. J. Chem. Phys. **48**, 983 (1968).
14. J. W. Fletcher. Ph.D. Thesis, University of Alberta, Edmonton, Alberta. 1966.
15. W. J. Holtslander and G. R. Freeman. Can. J. Chem. **45**, 1649 (1967).
16. S. K. Ho and G. R. Freeman. J. Phys. Chem. **68**, 2189 (1964).
17. G. R. Freeman. J. Chem. Phys. **33**, 71 (1960).

Can. J. Chem. Downloaded from www.nrcresearchpress.com by 210.87.254.6 on 09/05/12
For personal use only.

Can. J. Chem. Downloaded from www.nrcresearchpress.com by 210.87.254.105 on 09/05/12
For personal use only.

Square planar metal complexes of thiosemicarbazide

ROLAND A. HAINES AND KENNETH K. W. SUN
Department of Chemistry, University of Western Ontario, London, Ontario

Received March 15, 1968

Square planar complexes of nickel(II), palladium(II), and platinum(II) containing the ligand thiosemicarbazide (Htsc) have been studied. Both the *cis* and *trans* geometric isomers have been obtained for the complexes with the general formula $[M(Htsc)_2]^{2+}$ while only the *trans* isomer was obtained for the neutral species $[M(tsc)_2]$. Infrared and diffuse reflectance spectra are presented and discussed with reference to the stereochemistry of the complexes.

Canadian Journal of Chemistry, 46, 3241 (1968)

Introduction

For many years thiosemicarbazide, $H_2N—CS—NH—NH_2$ (Htsc), has been known to form complexes with certain transition metal ions and most of this work has been reported by Jensen (1–3). It was found that two types of metal complexes could be formed with a square planar configuration. These were referred to as the "ionic" and "neutral" complexes with the general formulae $[M(Htsc)_2]^{2+}$ and $[M(tsc)_2]$ respectively. In the latter complexes a hydrogen atom has been lost from thiosemicarbazide, thus allowing it to act as a uninegative ligand. In this early work the metal complexes were prepared and analyzed but no information regarding their basic physical properties was determined.

In recent years an X-ray structure determination (4) of the green compound $[Ni(Htsc)_2]SO_4 \cdot 3H_2O$ has shown it to have a square planar *trans* configuration with coordination occurring between the sulfur atom and the terminal "hydrazine" or N^3 nitrogen atom.

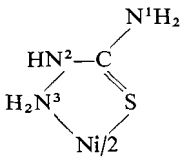

Other studies (5) have indicated that in solution thiosemicarbazide can act as either a bidentate or monodentate ligand. Coordination in the latter case would be expected to occur through the sulfur atom as is observed in analogous complexes of thiourea and related ligands (6–9).

A variety of colored compounds containing thiosemicarbazide can be obtained depending on the method of preparation and also on the anion used. Since no attempt had been made previously to explain adequately these striking features, it was considered desirable to undertake such an investigation. In this paper ionic and neutral complexes containing nickel(II), palladium(II), and platinum(II) are described.

Experimental

Preparation of Complexes

Thiosemicarbazide was obtained from Eastman Organic Chemicals while the common metal salts used as starting materials were obtained from either Fisher Scientific Co. or Alfa Inorganics Inc.

Bis(thiosemicarbazide)nickel(II) Nitrate Dihydrate

A blue solid separated out on standing when a 3 *M* $Ni(NO_3)_2$ solution was mixed with a 0.1 *M* aqueous solution of thiosemicarbazide in the molar ratio of $Ni(NO_3)_2$: $SCN_3H_5 = 1:2$.

Anal. Calcd. for $[Ni(SCN_3H_5)_2](NO_3)_2 \cdot 2H_2O$: Ni, 16.08; C, 6.58; H, 2.76; N, 30.70; S, 17.57; H_2O, 8.99. Found: Ni, 16.45; C, 6.45; H, 2.61; N, 30.59; S, 17.61. Loss in weight by drying at 70 °C in vacuum, 9.10%.

Bis(thiosemicarbazide)nickel(II) Nitrate

This was precipitated as a red solid when a 0.1 *M* alcoholic (95%) solution of $Ni(NO_3)_2$ was mixed with a 0.2 *M* alcoholic (90%) solution of thiosemicarbazide at ~ 70 °C, in the molar ratio of 1:2.

Anal. Calcd. for $[Ni(SCN_3H_5)_2](NO_3)_2$: Ni, 16.08; C, 6.58; H, 2.76; N, 30.70; S, 17.57. Found: Ni, 16.00; C, 6.73; H, 2.78; N, 30.66; S, 17.42.

Trans-bis(thiosemicarbazide)nickel(II) Sulfate Trihydrate

It was prepared by the method of Jensen (3). A green solid crystallized out when a 0.5 *M* $NiSO_4$ solution was mixed with a 0.1 *M* thiosemicarbazide solution in the molar ratio of 1:2. From 0.1 *M* solutions with molar ratio $NiSO_4$:$SCN_3H_5 = 1:4$ the compound was precipitated as dark-brown hexagonal crystals which gave a green powder on grinding.

Anal. Calcd. for $[Ni(SCN_3H_5)_2]SO_4 \cdot 3H_2O$: Ni, 17.42; C, 7.13; H, 2.99; N, 24.93; S, 28.54; H_2O, 13.82. Found: Ni, 16.90; C, 7.19; H, 3.08; N, 24.78; S, 28.40. Loss in weight by drying at 70 °C in vacuum, 13.74.

Cis-bis(thiosemicarbazide)nickel(II) Sulfate

This too was prepared by the method of Jensen (3). A brown solid crystallized out when a boiling 0.5 *M*

Can. J. Chem. Downloaded from www.nrcresearchpress.com by 210.87.254.105 on 09/05/12
For personal use only.

$NiSO_4$ solution was mixed with a 0.5 *M* thiosemicarbazide solution in the molar ratio of 1:2. The precipitate and mother liquor were boiled for about 5 min before filtering. The compound could also be prepared by boiling the green *trans*-isomer in its mother liquor for 20 min.

Anal. Calcd. for $[Ni(SCN_3H_5)_2]SO_4$: C, 7.13; H, 2.99; N, 24.93; S, 28.54. Found: C, 7.11; H, 3.05; N, 24.76; S, 28.42.

Bis(thiosemicarbazide)nickel(II) Chloride

A green solid was prepared in a manner similar to that for $[Ni(SCN_3H_5)_2](NO_3)_2$ using $NiCl_2$.

Anal. Calcd. for $[Ni(SCN_3H_5)_2]Cl_2$: Ni, 18.82; C, 7.70; H, 3.23; N, 26.94; S, 20.56. Found: Ni, 18.77; C, 8.01; H, 3.33; N, 26.84; S, 20.52.

Bis(thiosemicarbazido)nickel(II)

A solid nickel salt ($Ni(NO_3)_2.6H_2O$ or $NiCl_2.6H_2O$ only; $NiSO_4.6H_2O$ produces the ionic form $[Ni(SCN_3H_5)_2]SO_4$) was slowly dissolved in a 0.1 *M* thiosemicarbazide solution in the molar ratio of 1:2. NH_4OH (1.0 *N*) was added dropwise until the solution was weakly alkaline and a brownish green solid was precipitated. The precipitate was washed several times with hot 95% alcohol.

Anal. Calcd. for $[Ni(SCN_3H_4)_2]$: Ni, 24.57; C, 10.05; H, 3.37; N, 35.17; S, 26.84. Found: Ni, 24.27; C, 10.07; H, 4.03; N, 35.11; S, 26.55.

Bis(thiosemicarbazide)palladium(II) Nitrate

This was precipitated as an orange-yellow solid when a 0.1 *M* solution of $Pd(NO_3)_2$ was added to a 0.1 *M* solution of thiosemicarbazide in the molar ratio of 1:2.

Anal. Calcd. for $[Pd(SCN_3H_5)_2](NO_3)_2$: C, 5.82; H, 2.44; N, 27.15; S, 15.54. Found: C, 6.01; H, 2.36; N, 27.03; S, 15.69.

Cis-bis(thiosemicarbazide)palladium(II) Sulfate

A 0.02 *M* hot solution of K_2PdCl_4 was added to a 0.02 *M* hot solution of thiosemicarbazide in the molar ratio of 1:2. The solution mixture was boiled for 5 min before 1:1 H_2SO_4 was added slowly to precipitate the orange-yellow solid.

Anal. Calcd. for $[Pd(SCN_3H_5)_2]SO_4$: C, 6.24; H, 2.62; N, 21.84; S, 25.00. Found: C, 6.38; H, 2.48; N, 21.74; S, 24.84.

Bis(thiosemicarbazide)palladium(II) Chloride

A 0.05 *M* solution of K_2PdCl_4 was added to a 0.05 *M* solution of thiosemicarbazide in the molar ratio of 1:2. An orange-yellow solid crystallized out on standing.

Anal. Calcd. for $[Pd(SCN_3H_5)_2]Cl_2$: C, 6.68; H, 2.80; N, 23.37; S, 17.81. Found: C, 6.79; H, 2.96; N, 23.22; S, 17.73.

Bis(thiosemicarbazido)palladium(II)

A 0.02 *M* solution of K_2PdCl_4 was added to a 0.02 *M* solution of thiosemicarbazide in the molar ratio of 1:2. NH_4OH (1.0 *N*) was added dropwise until the solution was weakly alkaline and a greenish yellow solid was precipitated.

Anal. Calcd. for $[Pd(SCN_3H_4)_2]$: C, 8.38; H, 2.81; N, 29.32; S, 22.34. Found: C, 8.57; H, 2.65; N, 29.43; S, 22.31.

Trans-bis(thiosemicarbazide)platinum(II) Sulfate

A 0.02 *M* solution of K_2PtCl_4 was added to a 0.02 *M* solution of thiosemicarbazide in the molar ratio of 1:2. H_2SO_4 (1:1) was added dropwise until a yellow solid was precipitated.

Anal. Calcd. for $[Pt(SCN_3H_5)_2]SO_4$: C, 5.07; H, 2.13; N, 17.75; S, 20.32. Found: C, 4.99; H, 2.10; N, 17.94; S, 20.41.

Bis(thiosemicarbazide)platinum(II) Chloride

It was prepared by the method of Jensen (2). A yellow solid crystallized out when a 0.1 *M* K_2PtCl_4 solution was added to a 0.1 *M* solution of thiosemicarbazide in the molar ratio of 1:2.

Anal. Calcd. for $[Pt(SCN_3H_5)_2]Cl_2$: C, 5.36; H, 2.25; N, 18.75; S, 14.31; Cl, 15.82. Found: C, 5.38; H, 2.18; N, 18.61; S, 14.25; Cl, 15.62.

Bis(thiosemicarbazido)platinum(II)

A 0.02 *M* solution of K_2PtCl_4 was added to a 0.02 *M* solution of thiosemicarbazide in the molar ratio of 1:2. NH_4OH (1.0 *N*) was added dropwise until the solution was weakly alkaline and a silky blue solid was precipitated.

Anal. Calcd. for $[Pt(SCN_3H_4)_2]$: C, 6.40; H, 2.15; N, 22.39; S, 17.09. Found: C, 6.53; H, 2.07; N, 22.36; S, 16.88.

General Comments

All nickel analyses were carried out in this laboratory by standard methods and all microanalyses by Alfred Bernhardt, West Germany.

Infrared spectra were obtained using a Beckman IR-10 spectrophotometer using potassium bromide disks and Nujol mulls. Visible reflectance spectra were recorded on a Unicam SP 500 spectrophotometer with a standard reflectance attachment. Solution spectra were recorded on a Beckman DK-1 spectrophotometer using 1 cm quartz cells. Magnetic moments were measured on a Gouy balance and tubes were calibrated with $HgCo(SCN)_4$. Powder patterns were obtained with a Philips Debye–Scherrer camera model PW 1024/10 using copper K_α radiation.

Results and Discussion

Nickel(II) Complexes

Ionic complexes with the general formula $[Ni(Htsc)_2]^{2+}$ were prepared as the Cl^-, NO_3^-, or SO_4^{2-} salts and certain differences were observed.

When SO_4^{2-} is the anion, two solid diamagnetic compounds can be prepared, a green species with the formula $[Ni(Htsc)_2]SO_4.3H_2O$ and a brown compound with the formula $[Ni(Htsc)_2]SO_4$. Previously these two compounds have been referred to as α and β respectively and an X-ray study has shown that the α isomer has the *trans* arrangement of ligands (4). The brown β compound is not simply an anhydrous form of the green species, however. We have taken X-ray powder patterns of the anhydrous green compound and the β compound and these confirm that the compounds are different. The infrared

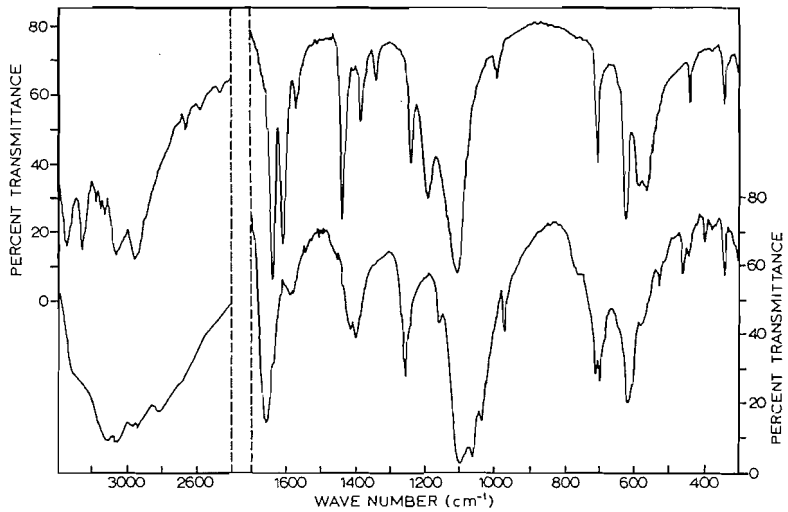

FIG. 1. Infrared spectra of *trans*-$[Ni(Htsc)_2]SO_4 . 3H_2O$ (top) and *cis*-$[Ni(Htsc)_2]SO_4$ (bottom).

spectra of the two complexes also show marked differences in certain regions of the spectrum and a comparison of the regions of interest is shown in Fig. 1. Our investigations indicate that the β compound is the *cis* isomer of the complex. This possibility had been suggested by earlier workers (1–3) but solely on the basis of color differences.

When NO_3^- is the anion, two colored forms can also be isolated, a paramagnetic blue compound with the formula $[Ni(Htsc)_2](NO_3)_2 . 2H_2O$ and a diamagnetic red compound with the formula $[Ni(Htsc)_2](NO_3)_2$. On heating, the two water molecules are lost from the blue compound and the red species is obtained. The latter may also be prepared independently from ethanol solutions of starting materials. These two compounds have usually been regarded as the hydrated and the anhydrous forms of the same complex (1). However, the blue compound has an infrared spectrum similar to that of the α or *trans* isomer while the red compound has a spectrum which resembles that of the *cis* isomer. X-Ray powder patterns confirm that the red compound obtained by heating the blue species is similar to the red compound prepared independently from ethanol solutions. Hence the blue compound is a hydrated form of the *trans* isomer and on heating is converted into the anhydrous *cis* isomer. Attempts to prepare the anhydrous *trans* isomer by heating under vacuum proved unsuccessful.

When Cl^- is the anion, only the *trans* form of the complex is obtained, regardless of the method of preparation. The green product is diamagnetic and is readily soluble in water. At higher temperatures the *cis* isomer may possibly be produced but all attempts to convert the *trans* into the *cis* isomer by heating have proved unsuccessful.

Palladium(II) Complexes

Evidence for *cis–trans* isomerism was also found in the $[Pd(Htsc)_2]^{2+}$ complexes. When SO_4^{2-} is the anion, the *trans* form is obtained from solutions at room temperature and the *cis* from hot solutions. In each case the infrared spectra showed the same features as the corresponding nickel species. Although the *cis* isomer could be prepared in a pure state, the *trans* isomer was contaminated by small amounts of the *cis* form.

When NO_3^- is the anion, the *cis* isomer is obtained both from room temperature solutions and boiling solutions. From preparations at ~0 °C a small amount of the *trans* form was produced as shown by the infrared spectra. However, the *cis* isomer was still predominant.

The use of Cl^- as the anion produced only the *trans* isomer. Attempts to prepare the *cis* isomer were unsuccessful as for the corresponding nickel(II) complex.

Platinum(II) Complexes

When SO_4^{2-} is the anion, only the *trans* isomer can be obtained from solutions at room temperature. From hot solutions, the *cis* isomer

Can. J. Chem. Downloaded from www.nrcresearchpress.com by 210.87.254.105 on 09/05/12
For personal use only.

TABLE I

Infrared spectra

Frequencies (cm^{-1})				
Htsc	*trans*-$[Ni(Htsc)_2]SO_4 \cdot 3H_2O$[a,b]	*cis*-$[Ni(Htsc)_2]SO_4$[a,b]	*trans*-$[Ni(tsc)_2]$[a,b]	Assignment
3370 (s)	3350 (s)	3300 (sh)	3455 (s)	NH and NH_2 stretch
3260 (s)	3255 (s)	3120 (s)	3285 (m)	
3180 (s)	3180 (m)	3060 (s)	3235 (sh)	
3090 (sh)	3150 (m)	2970 (s)	3195 (s)	
2980 (m)	3125 (m)	2935 (s)	3185 (sh)	
	3060 (s)	2820 (m)	3120 (sh)	
	2955 (s)		3095 (s)	
1642 (s)	1632 (s)	1656 (s)	1638 (s)	NH_2 bend
1618 (s)	1603 (s)	1635 (sh)	1597 (s)	
1530 (m)	1563 (w)	1590 (w)		NH wag and CN stretch[c]
1483 (m)	1434 (m)	1417 (w)	1525 (w)	Amide II and CN stretch
1317 (m)	1382 (w)	1397 (w)	1364 (w)	Amide III
1287 (m)	1340 (vw)		1323 (m)	
			1286 (w)	
1165 (m)	1237 (m)	1257 (m)	1229 (m)	NH_2 rock
			1139 (w)	
1000 (s)	990 (vw)	1001 (sh)	1022 (vw)	NH_2 deformation
			960 (m)	NN stretch[d]
802 (m)	703 (m)	713 (m)	704 (m)	CS stretch
		703 (m)	683 (m)	

[a]Only stretching frequencies associated with the ligand are reported; bands due to the anion are not included. Relative band intensities are denoted by s, m, w, vw, and sh, meaning strong, medium, weak, very weak, and shoulder, respectively.
[b]The Pt(II) and Pd(II) complexes show extremely similar spectra to their Ni(II) analogue.
[c]In agreement with ref. 16.
[d]This work, see text.

is produced, but there is evidence of some decomposition. For both isomers the infrared spectra match the corresponding nickel species.

With Cl^- as the anion, the complex was obtained only in the *trans* configuration. Compounds containing NO_3^- were not prepared.

General

The features noted for all these complexes may be summarized in a simple manner. From solutions at room temperature or lower, complexes containing SO_4^{2-} or NO_3^- are produced in the *trans* configuration while higher temperatures are required to prepare the *cis* isomer. However, only the *trans* form is obtained when Cl^- is the anion.

The infrared spectra for the various nickel(II) complexes are tabulated in Table I, together with assignments for most of the major peaks. These assignments were based on corresponding assignments in thiosemicarbazide (10) and in some copper(II) complexes (11). Our bands bear strong similarities in most cases and a repetition of the arguments used in the assignment is not needed.

For comparison of the *cis–trans* isomers of the complexes, certain regions of the infrared spectrum are quite distinctive. For the region around 3400–3000 cm^{-1}, where NH_2 stretching frequencies are observed, the *trans* isomers show two sharp strong bands in the high frequency region. The corresponding *cis* isomers show only broad bands throughout this range of frequencies. In the region around 1600 cm^{-1}, corresponding to NH_2 bending modes, two sharp bands are observed for the *trans* isomer, while a single broad band is observed for the *cis* compounds.

The region around 500 cm^{-1} and lower is also useful in distinguishing the isomers. The *trans* isomer is characterized by two very distinct peaks at $\sim$ 435 and 330 cm^{-1}. For the *cis* isomer many more peaks are found in this region and the 330 cm^{-1} peak is shifted to slightly higher energies. This latter band is probably a ring deformation mode similar to that observed in glycine complexes (12). This band appears to be rather low in energy for an M—N band (12) and an M—S band is usually found at lower energies. (A single spectrum of one of the nickel compounds was taken on a Beckman IR-11 spectrophotometer and revealed a band at 292 cm^{-1} which is

Can. J. Chem. Downloaded from www.nrcresearchpress.com by 210.87.254.105 on 09/05/12
For personal use only.

TABLE II

Absorption spectra

Complex	Reflectance spectra (mμ)
$[Ni(tsc)_2]$	356; 460 (sh); 580
trans-$[Ni(Htsc)_2]Cl_2$	354 (sh); 438; 495 (sh); 596
trans-$[Ni(Htsc)_2]SO_4 . 3H_2O$	428; 480 (sh); 586
cis-$[Ni(Htsc)_2]SO_4$	446; 490; 586 (sh)
cis-$[Ni(Htsc)_2](NO_3)_2$	340 (sh); 448; 532; 606 (sh)
trans-$[Ni(Htsc)_2](NO_3)_2 . 2H_2O$	363; 392 (sh); 571; 611 (sh); 784; 818
$[Pd(tsc)_2]$	356 (sh); 412
trans-$[Pd(Htsc)_2]Cl_2$	362; 434 (sh)
trans-$[Pd(Htsc)_2]SO_4$	344; 362; 430
cis-$[Pd(Htsc)_2]SO_4$	344; 426 (sh)
cis-$[Pd(Htsc)_2](NO_3)_2$	368 (sh); 378; 397 (sh); 414 (sh)
$[Pt(tsc)_2]$	342; 360 (sh); 530 (sh); 624 (sh); 632
trans-$[Pt(Htsc)_2]Cl_2$	362; 415 (sh)
trans-$[Pt(Htsc)_2]SO_4$	353; 425 (sh)
cis-$[Pt(Htsc)_2]SO_4$	354; 530 (sh); 640 (sh)

Complex	Solution spectra (mμ)[a]
trans-$[Ni(Htsc)_2]Cl_2$	235; 374; 597; 936 (sh); 990; 1050 (sh)
trans-$[Pd(Htsc)_2]Cl_2$	230; 267; 338 (sh); 426
cis-$[Pd(Htsc)_2](NO_3)_2$	233; 344; 425

[a]Not all of the ionic species are readily soluble in water. Representative samples are shown here.

typical of an M—S band.) The larger number of bands observed for the *cis* compounds both in glycine complexes (12) and in our own series is no doubt due to the fact that no center of symmetry is present in these molecules.

An interesting feature regarding the infrared spectra should be mentioned here. All of our conclusions based on infrared arguments arose from spectra taken both as a mull and in potassium bromide pellets. The spectra were identical for both techniques. However, in all cases where the pellets contained the *cis* isomer, spectral changes occurred on standing for long periods of time, corresponding to slow conversion to the *trans* isomer. Preparations of the pure *cis* isomers, however, have been kept for months without any apparent changes. The conversion to the *trans* form in the pellet may be linked to the fact that complexes containing Cl^- could only be obtained in the *trans* configuration. In both cases there may be interaction of the halide ion in the axial positions, causing a preference for the *trans* arrangement.

In our studies the marked color changes observed for some of the nickel(II) complexes have been particularly striking. It might be thought that a situation similar to that found in the Lifschitz salts is present. For those complexes the different colors arose from a square planar – octahedral interconversion and recent studies (13, 14) have shown that the different colors arise from mixtures of the two geometric arrangements. It does not appear that a similar mechanism is at work here, however. For palladium(II) and platinum(II) which are almost exclusively found in a square planar arrangement, magnetic measurements carried out in our laboratory support the diamagnetism which would be predicted. All the nickel(II) compounds exhibit diamagnetism also with the single exception of the blue nitrate species. It is paramagnetic to the extent of two unpaired electrons and has an effective magnetic moment of 3.19 bohr magnetons. The paramagnetism of this compound is not too surprising since the complex very likely has an octahedral arrangement with the two water molecules in axial positions. With one exception the other complexes are anhydrous and hence would not have the possibility of water coordination[1].

Another possible explanation for the various color changes involves square planar – tetrahedral interconversion. However, our magnetic measurements do not support this possibility since the tetrahedral form would be paramagnetic. The reflectance spectra (see below) also tend to rule out the presence of a tetrahedral structure.

[1]The only exception is the *trans* nickel(II) compound containing SO_4^{2-}. X-Ray studies (4) show that the water molecules are too distant from the nickel atom to partake in coordination.

Can. J. Chem. Downloaded from www.nrcresearchpress.com by 210.87.254.105 on 09/05/12
For personal use only.

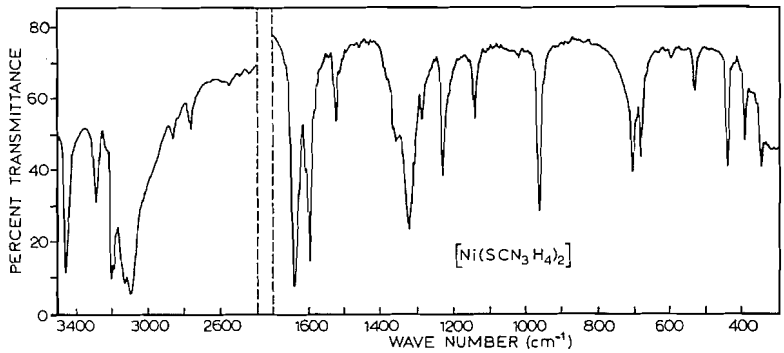

FIG. 2. Infrared spectra of *trans*-[Ni(tsc)$_2$].

The reflectance spectra maxima for these compounds are tabulated in Table II and give support to the above conclusions regarding the structures of the complexes. The spectra for the nickel(II) compounds show that the blue species containing NO_3^- is indeed octahedral with tetragonal distortion. This is shown by the splitting observed for the lowest energy spin-allowed band ($^3A_{2g} \rightarrow {}^3T_{2g}$) for this compound only. Such splitting is absent for all the other complexes. From a comparison of relative shapes of the absorption curves and peak positions it can be seen that those nickel(II) compounds assigned the *trans* configuration on the basis of infrared spectra are quite similar. In the same manner, it can be seen that the spectra of those assigned the *cis* configurations resemble each other and are significantly different from the *trans* isomers.

All of the soluble nickel(II) complexes form a blue aqueous solution and give the same absorption spectrum. This spectrum is not characteristic of either isomer, nor is it the same as that of the octahedral blue compound containing NO_3^-. There may be an equilibrium set up in solution involving thiosemicarbazide as a monodentate ligand (5).

The reflectance spectra for the palladium(II) and platinum(II) complexes are more complicated due to the shift of all d–d absorption bands to higher energies. For palladium(II) those compounds assigned the *trans* configuration show similar reflectance spectra. The two *cis* compounds, however, do not appear to have such close agreement at first glance. However, on closer examination it appears that this is due to severe overlap of some bands in the *cis* compound containing NO_3^-. Some of the bands in this compound are shifted to lower energies relative to those of the SO_4^{2-} analogue, producing a different appearance. Such a shift is observed in the corresponding nickel(II) compound but no serious interference occurs.

The reflectance spectra of the platinum(II) compounds show very little fine structure since the d–d bands are now overlapping with charge transfer bands. The *trans* isomers give similar spectra and the *cis* compound shows an overall shift to lower energies. However, for both cases the bands are not very distinct.

Thus the reflectance spectra also support a square planar arrangement throughout the series. In no cases is a spectrum which is typical of a tetrahedral complex obtained.

Neutral Complexes

Compounds with the general formula [M(tsc)$_2$] are all diamagnetic and have quite similar infrared spectra, regardless of the metal. The spectrum for [Ni(tsc)$_2$] is shown in Fig. 2 and the structure of this compound has been previously determined by X-ray methods (15). A *trans* arrangement of the ligands was shown to be present and the loss of a proton from the middle nitrogen was indicated. The two colored forms of the nickel complex which are known, grey-green and reddish brown, had been suspected to be merely different crystal modifications of the same compound. We have studied the infrared spectra of both species and found identical spectra, regardless of color, so that they are indeed the same compound. On the basis of infrared comparisons, the *trans* configuration can be assigned to the neutral complexes of nickel(II), palladium(II), and platinum(II) since similar spectra are observed in all cases.

The infrared spectra of the neutral complexes

Can. J. Chem. Downloaded from www.nrcresearchpress.com by 210.87.254.105 on 09/05/12
For personal use only.

show the two high frequency NH_2 bands characteristic of the *trans* ionic compounds. They occur at slightly higher frequencies in the neutral species and this is not unexpected since the loss of a hydrogen atom from the ligand could cause the nitrogens to be more negative and hence a stronger bond is produced.

The most striking feature, however, is the appearance of a strong band at 960 cm^{-1} in all cases. This cannot be the NH_2 deformation mode of the ligand, since that band becomes very weak when coordination takes place. One possibility corresponds to an N—N stretching vibration. Calculations in the ligand thiocarbohydrazide (16), which is quite similar to our ligand, predicted a band at 1049 cm^{-1} in the free ligand while a value of 1027 cm^{-1} for this mode is assigned from Raman spectra of hydrazine hydrochloride (17).

For thiosemicarbazide, the band due to NH_2 deformation prevails in this region. However, in the ionic and neutral compounds this band becomes very weak and for the neutral species a new strong band at 960 cm^{-1} also appears. Such features can be explained if the band is indeed a N—N vibration. Strictly speaking, in a symmetrical molecule the N—N vibration is infrared forbidden by symmetry arguments. In the ligand and ionic complexes it should be allowed but is probably very weak. For the neutral compounds, however, the vibration becomes more intense and this may be explained by the X-ray study (15) which shows that the C=N double bond is almost completely localized in the C—N^2 region. Hence the N^2 and N^3 atoms are very much different. The position of the band at lower energy is also consistent with the observed lengthening of the N^2—N^3 bond (15).

Acknowledgment

We are grateful to the National Research Council of Canada for financial support of this work.

1. K. A. Jensen and E. Rancke-Madsen. Z. Anorg. Allgem. Chem. **219**, 243 (1934).
2. K. A. Jensen. Z. Anorg. Allgem. Chem. **221**, 6 (1934).
3. K. A. Jensen. Z. Anorg. Allgem. Chem. **229**, 265 (1936).
4. R. Gronbaek and S. E. Rasmussen. Acta Chem. Scand. **16**, 2325 (1962).
5. M. K. Akhmedli and L. F. Zhirova. Russ. J. Inorg. Chem. **5**, 1323 (1960).
6. A. Yamaguchi, R. B. Penland, S. Mizushima, T. J. Lane, C. Curran, and J. V. Quagliano. J. Am. Chem. Soc. **80**, 527 (1958).
7. A. Lopez-Castro and M. R. Truter. J. Chem. Soc. 1309 (1963).
8. G. Fava Gasparri, A. Musattim, and M. Nardelli. Chem. Commun. 602 (1966).
9. W. T. Robinson, S. L. Holt, and G. B. Carpenter. Inorg. Chem. **6**, 605 (1967).
10. M. Mashima. Bull. Chem. Soc. Japan, **37**, 974 (1964).
11. M. J. Campbell and R. Grzeskowiak. J. Chem. Soc. A, 396 (1967).
12. R. A. Condrate and K. Nakamoto. J. Chem. Phys. **42**, 2590 (1965).
13. W. C. E. Higginson, S. C. Nyburg, and J. S. Wood. Inorg. Chem. **3**, 463 (1964).
14. S. C. Nyburg and J. S. Wood. Inorg. Chem. **3**, 468 (1964).
15. L. Cavalca, M. Nardelli, and G. Fava. Acta Cryst. **15**, 1139 (1962).
16. G. R. Burns. Inorg. Chem. **7**, 277 (1968).
17. R. G. Snyder and J. C. Decius. Spectrochim. Acta, **13**, 280 (1959).

Can. J. Chem. Downloaded from www.nrcresearchpress.com by 210.87.254.105 on 09/05/12
For personal use only.

Can. J. Chem. Downloaded from www.nrcresearchpress.com by 210.87.254.40 on 09/05/12
For personal use only.

The hydrogenation of allene. II. The reaction of allene with hydrogen catalyzed by nickel, cobalt, and iron

R. S. MANN AND D. E. TIU[1]

Department of Chemical Engineering, University of Ottawa, Ottawa 2, Canada

Received May 17, 1968

The reaction between allene and hydrogen over unsupported nickel, iron, and cobalt catalysts has been studied in a static constant volume system for a wide range of temperature and reactant ratios. The reaction over metals is largely simple hydrogenation, the early stages being principally a selective formation of propylene with small yields of reduced polymers of allene. The orders of the hydrogenation were 1 and 0 with respect to hydrogen and allene respectively, and were temperature independent. The overall apparent activation energies for nickel, iron, and cobalt were 6.5, 7.6, and 6.9 kcal/mole respectively. Selectivity was highest with nickel, and least with cobalt.

Canadian Journal of Chemistry, 46, 3249 (1968)

Introduction

Very little work has been reported about the kinetics of the hydrogenation of allene over metal catalysts. Bond *et al.* (1) have reported about the selectivities observed in the first stage of the reaction for alumina supported ruthenium, rhodium, osmium, iridium, and platinum catalysts. Recently Mann and To (2) have reported the kinetics of allene hydrogenation over pumice-supported nickel catalysts. They found that the orders with respect to hydrogen and allene were 1 and 0 respectively.

This paper describes a detailed study of the kinetics of allene hydrogenation over unsupported nickel, cobalt, and iron, and the effect of various experimental variables upon the selectivity of the reaction in presence of these metals.

Experimental

The apparatus, materials, and experimental techniques were the same as reported in an earlier paper by Mann and Naik (3) for methylacetylene hydrogenation. All catalysts were prepared by methods similar to those described earlier (4) except that a 4.4 *M* ammonium bicarbonate solution was used to completely precipitate iron as a bicarbonate. Pressure changes were observed with a mercury manometer, and the reaction products analyzed by a Fisher gas partitioner (model 25) mounted on the top of a Fisher thermal stabilizer (model 27) maintained at 30 °C. The two columns employed were a 14 ft long 30% hexamethylphosphoramide on Fisher Columpak, and an 8 ft long activated 13 x molecular sieve.

Results and Discussion

(a) Pressure–Time Curves

According to Bond (4), who studied the hydrogenation of acetylene over nickel–pumice catalyst, the kinetic form of the pressure–time curves depends upon: (*i*) initial hydrogen/hydrocarbon ratios, (*ii*) the order of admission of reactants if admitted into the reaction vessel separately, and (*iii*) the pretreatment of the catalyst if both the reactants are added together. The pressure–time curves for allene hydrogenation over nickel, iron, and cobalt catalysts were of the type of curve AFG in Fig. 1 for all hydrogen/allene ratios up to 2. When the initial hydrogen/allene ratio was more than 2, a different form of pressure–time curve (Fig. 1, curve ADE) was

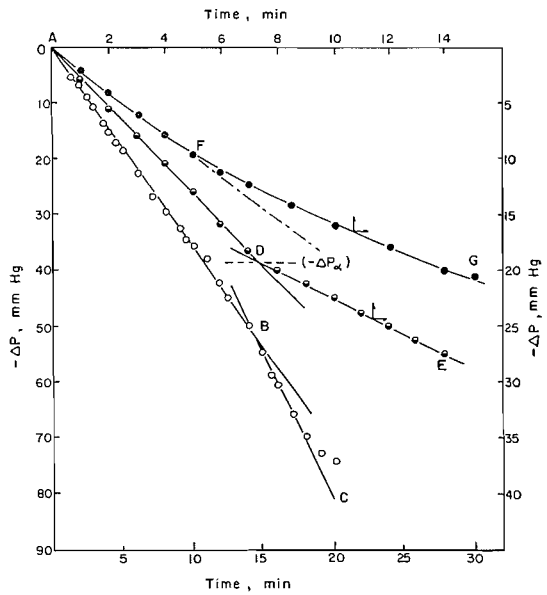

FIG. 1. Pressure–time curve. Curve ABC, (cobalt powder) P_{H_2} = 125 mm, $P_{methylacetylene}$ = 50 mm, at 48 °C (8). Curve ADE, (iron powder) P_{H_2} = 104 mm, P_{allene} = 40 mm, at 75 °C. Curve AFG, (iron powder) P_H = 60 mm, P_{allene} = 40 mm, at 90 °C.

[1]Present address: Commission Scolaire, Regionale de L'Outaouais, Hull, Quebec.

TABLE I

Order of reaction and activation energies for nickel, iron, and cobalt

Catalyst	Weight of catalyst	Temperature range (°C)	Average order*		Activation energy (kcal/mole)
			m	n	
Nickel	0.3	60–130	0.00 ± 0.00	0.98 ± 0.02	6.46 ± 0.05
Cobalt	0.3	26–130	-0.02 ± 0.02	0.99 ± 0.02	7.55 ± 0.05
Iron	0.1923	42–130	0.00 ± 0.02	1.00 ± 0.02	6.88 ± 0.05

*m and n are orders of reaction with respect to allene and hydrogen, $r = kP_{C_3H_4}{}^m P_{H_2}{}^n$.

observed. In the present study the shape of the pressure–time curve was not affected by: (*i*) the order of admission of reactants, (*ii*) the temperature of the reaction vessel, or (*iii*) the nature of the catalyst. It depended only on the initial hydrogen/allene ratio ($\bar{R}$). The point of intersection of the two slopes, $(-\Delta P_\alpha)$, depended on hydrogen/allene ratios, it increased with increased values of $\bar{R}$.

(b) Orders of Reaction by the Initial Rate Method

Using a fixed allene pressure (40 mm) and a wide range of hydrogen pressures (30–240 mm) the order of reaction with respect to hydrogen was determined at several temperatures. The order of reaction with respect to hydrogen was always 1 and independent of temperature for all catalysts (Table I). The reaction order with respect to allene (m) over the catalyst was determined for a constant hydrogen pressure of 60 mm and wide range of allene pressures (30–150 mm). The order of reaction with respect to allene (n) for nickel, iron, and cobalt was mostly 0, and became slightly negative with increased temperatures.

(c) Temperature Dependence of Rate Constants

Plots of log to the base 10 of specific rate against the reciprocal of absolute temperature were good straight lines over a wide range of temperature for iron, nickel, and cobalt satisfying the Arrhenius equation. The derived apparent activation energy for each catalyst is given in Table I.

(d) The Effect of Experimental Variables upon Selectivity of Catalysts

Selectivity (S) is defined as the ratio of propylene to propylene plus propane.

$$S = P_{\text{propylene}}/(P_{\text{propylene}} + P_{\text{propane}})$$

Propylene, propane, and some polymers were observed as initial products of the reaction under conditions studied, propylene being the major product.

(i) Dependence of Selectivity upon Pressure Fall, and Course of Reaction

The dependence of selectivity upon the pressure fall and the course of reaction were investigated for various hydrogen/allene ratios over nickel, cobalt, and iron catalysts at several temperatures. The course of the reaction was followed by means of an analysis of the reaction products for various reactant ratios ($\bar{R}$ = 0.5–4) at different pressure falls. With an initial hydrogen/allene ratio of 2 (H_2 = 80 mm, C_3H_4 = 40 mm) over nickel, cobalt, and iron, at 105, 40, and 42 °C, respectively the main initial reaction is the selective formation of propylene with relatively little propane.

The selectivity was dependent on the pressure fall. While it dropped slowly with the pressure fall (progress of reaction) for nickel and cobalt catalysts, it increased steadily with the pressure fall for iron catalyst (Fig. 2). The increase in the selectivity with increased pressure fall was due to the fact that while the rate of formation of propylene increased, the rate of formation of propane virtually did not change.

Polymerization is maximum for cobalt and least for nickel. While the amount of polymerization was nearly independent of pressure fall for cobalt and iron, it was dependent on pressure fall and decreased rapidly after about 50% reaction had taken place.

(ii) Dependence of Selectivity upon Initial Pressures of Hydrogen and Allene

Measurements were made of the selectivity of nickel, cobalt, and iron at several temperatures, as a function of initial hydrogen pressure by using a fixed allene pressure (40 mm) and varying the hydrogen pressures between 40 and 240 mm. Products were analyzed when the total pressure fall was equal to 20 mm of total pressure.

Can. J. Chem. Downloaded from www.nrcresearchpress.com by 210.87.254.40 on 09/05/12
For personal use only.

Can. J. Chem. Downloaded from www.nrcresearchpress.com by 210.87.254.40 on 09/05/12
For personal use only.

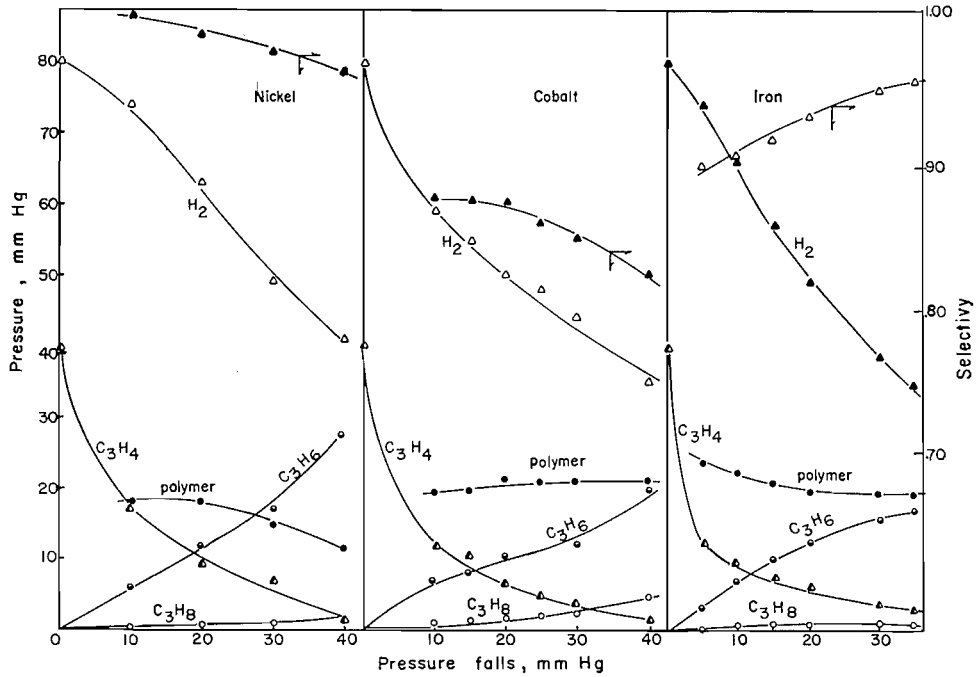

FIG. 2. Course of reaction over nickel, cobalt, and iron, $P_{\text{allene}} = 40$ mm, $P_{H_2} = 80$ mm, Ni at 105 °C, Co at 40 °C, Fe at 42 °C.

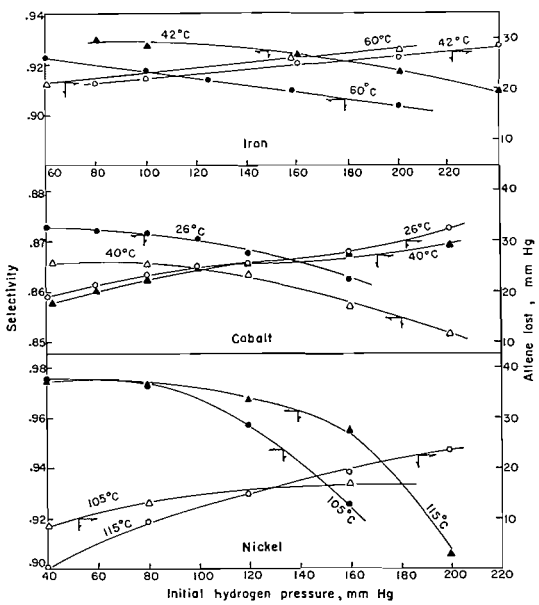

FIG. 3. Dependence of selectivity upon initial pressure of hydrogen, $P_{\text{allene}} = 40$ mm, $\Delta P = 20$ mm.

The results are shown in Fig. 3. The selectivities were dependent on the initial hydrogen pressures, and decreased with increased initial pressures of hydrogen. For a hydrogen/allene ratio of 2, the selectivities were 0.97, 0.87, and 0.93 for nickel, cobalt, and iron respectively.

Though no significant variation of selectivity with initial allene pressures (40–240 mm) for a fixed initial hydrogen pressure (80 mm) was observed for nickel ($S = 0.963$–0.978), and cobalt (0.861–0.851), it varied with initial allene pressures for iron. While the selectivity increased with increased pressures of allene for nickel, it decreased for cobalt and iron. The selectivities were 0.972, 0.861, and 0.935 for nickel, cobalt, and iron for a hydrogen/allene ratio of 2. The effect of allene pressures on polymer formation is shown in Fig. 4. The amounts of polymers increased with allene pressures, giving a nonlinear relationship.

(iii) Dependence of Selectivity upon Temperature

The effect of temperature on the selectivity was studied for several reactant ratios. The products

Can. J. Chem. Downloaded from www.nrcresearchpress.com by 210.87.254.40 on 09/05/12
For personal use only.

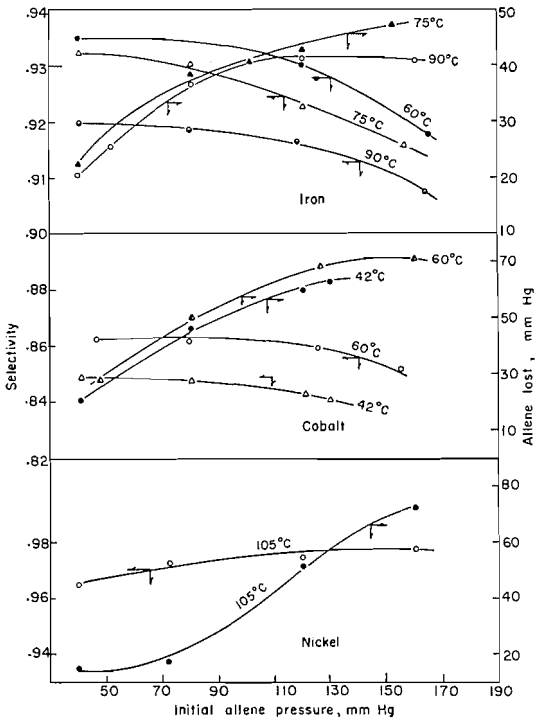

FIG. 4. Dependence of selectivity upon initial pressure of allene, $P_{hydrogen}$ = 80 mm, ΔP = 20 mm.

were analyzed at several temperatures for a total pressure fall of 20 mm. The temperature dependence of the selectivity for a reactant ratio of 2 (P_{H_2} = 80 mm, $P_{C_3H_4}$ = 40 mm) is shown in Fig. 5.

With increased temperature, the propylene/propane ratios and the selectivity increased. At 100 °C, the selectivities were nearly the same for all the three catalysts, though cobalt was comparatively more active at lower temperatures than iron or nickel.

Polymerization is maximum for cobalt and least for nickel. The percentage of polymerization decreased with temperature for all the catalysts.

(e) Comparison with the Results of Previous Investigators and General Discussions

Unlike the findings of Bond and Mann (5) for acetylene hydrogenation over nickel, cobalt, and iron powders, none of the catalysts studied did get poisoned when allene was admitted first into the reaction vessel. This is probably due to the fact that allene was not as strongly adsorbed on the surface as acetylene. The catalytic activity of the catalyst remained fairly constant for several days. However, the use of higher partial pressures of hydrogen tended to slightly enhance the activity of the catalyst reversibly, while higher partial pressures of allene often poisoned the catalyst reversibly, thus suppressing its activity.

The kinetic study of Bond and Sheridan (6, 7) for allene hydrogenation was limited to pumice-supported nickel, platinum, and palladium, and the study of Mann and To (2) was limited to supported nickel catalyst. Though Bond (4) has studied the shape of the pressure–time curve in detail for acetylene hydrogenation over nickel catalyst, no such studies are reported for allene hydrogenation. Hence no direct comparison could be made of the results obtained for unsupported nickel, cobalt, and iron catalysts in this investigation with any published work.

The pressure–time curves obtained in allene hydrogenation over nickel, iron, and cobalt were of Type I (curve ADE, Fig. 1) for hydrogen/allene ratios greater than 2, and of Type III (curve AFG, Fig. 1) for ratios less than 2. These curves are similar to those observed by Mann and To (2) for allene hydrogenation over supported nickel, and also to that observed by Mann and Khulbe

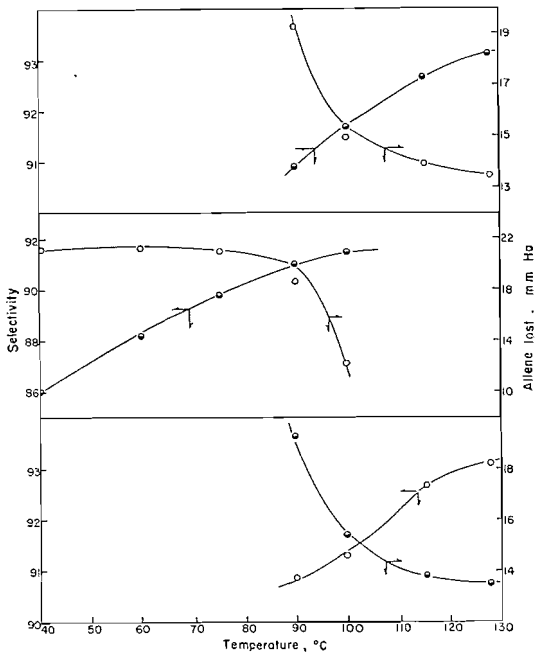

FIG. 5. Dependence of selectivity and polymerization upon temperature, $P_{hydrogen}$ = 80 mm, P_{allene} = 40 mm, ΔP = 20 mm.

Can. J. Chem. Downloaded from www.nrcresearchpress.com by 210.87.254.40 on 09/05/12
For personal use only.

(8) for methylacetylene hydrogenation over unsupported nickel and iron. In the case of methylacetylene hydrogenation over unsupported cobalt Mann and Khulbe (8) obtained a different pressure–time curve (Curve ABC, Fig. 1) exhibiting two stages of reaction, with an acceleration point ($-\Delta P_\alpha$), corresponding to the start of second stage of reaction, indicating further hydrogenation of propylene to propane. No such curves were observed for allene hydrogenation over unsupported cobalt.

The kinetic form of the pressure–time curve depends on the nature and especially on the concentration of species in the reactive layer at the moment massive reaction begins. The catalysts were reduced and activated in a stream for about 24 h. The species of reactive layer were richer in hydrogen and admission of hydrogen and allene was not enough to nullify the effect of pretreatment of the catalyst. Allene was strongly adsorbed on the surface, and was able to maintain high coverage of the surface, thereby making the competition from propylene for readsorption unimportant.

The order of reaction with respect to initial hydrogen pressure was 1 for nickel, cobalt, and iron and was independent of temperature. This was similar to the findings of Mann and Khulbe (8) for methylacetylene hydrogenation over these catalysts. While the order of reaction with respect to methylacetylene was found to be 0 and temperature dependent for nickel and cobalt, it is 0 order with respect to initial allene pressure and nearly temperature independent.

The activation energies for the unsupported nickel, cobalt, and iron are 6.5, 7.6, and 6.9 kcal/mole respectively for allene hydrogenation and are lower than those observed for pumice-supported catalysts (Ni = 7.8, Co = 10.8, Fe = 9.4). The lower activation energies for unsupported metals as compared with those of supported metals agree well with previous findings.

The general characteristics and product analysis of allene hydrogenation on nickel, cobalt, and iron were found to be similar to those obtained on supported nickel catalyst by us earlier (2) and by Bond and Sheridan (6, 7).

For a hydrogen/allene ratio of 2, the ratio of the rates of formation of propylene/propane were much higher over nickel catalyst than over cobalt or iron. The formation of propylene/propane over nickel was more than two to three times higher than reported by Bond and Sheridan (6, 7) for hydrogenation of allene over nickel–pumice catalyst.

Unlike the results obtained in methylacetylene hydrogenation over nickel and cobalt, selectivity of these were dependent on pressure fall, and generally decreased with increased pressure fall. It was found that the selectivity for iron increased with pressure fall, while for nickel and cobalt it increased.

Selectivity increased with increased temperature for nickel, cobalt, and iron. Similar results have been reported earlier by Bond and Turkevitch (9), who noted that the rate of propylene exchange on platinum increased relative to the rate of deuteration as the temperature is raised, and by Mann and Khulbe (8) for methylacetylene hydrogenation on nickel, cobalt, and iron. The increase in the selectivity with temperature in allene hydrogenation is possibly due to a decrease in the surface coverage of hydrogen as the temperature is raised or to a genuinely higher activation energy for propylene desorption relative to hydrogen.

In agreement with the findings of Mann and Khulbe (8) for methylacetylene hydrogenation and Sheridan (10, 11) for acetylene hydrogenation, it has been found that the reaction between allene and hydrogen over unsupported nickel, iron, and cobalt shows a close general similarity and that nickel was considerably more active than iron, which in turn was more active than cobalt. The hydrogenation of allene on nickel is highly selective ($S = 0.96$) in the sense that very little propane appears as long as any allene remained unreacted. This is in accordance with previous experience. The extent of polymerization was less than that with acetylene, but higher than that with methylacetylene. This difference is attributed to differing steric hindrances by the methyl groups of the hydrocarbons adsorbed on the surface of the catalyst.

The results largely confirm the expected similarity between the hydrogenation of methylacetylene, allene, and acetylene. Therefore it may be presumed that the reaction mechanism for these reactions is the same.

Acknowledgments

The authors are grateful to National Research Council of Canada for financial assistance

through a grant A-1125 (to R. S. M.) and a bursary (to D. E. T.).

1. G. C. BOND, G. WEBB, P. B. WELLS, J. M. WINTERBOTTOM. J. Catalysis, **1**, 74 (1964).
2. R. S. MANN and E. To. Can. J. Chem. **46**, 161 (1968).
3. R. S. MANN and S. C. NAIK. Can. J. Chem. **45**, 1023 (1967).
4. G. C. BOND. J. Chem. Soc. 2075 (1958).
5. G. C. BOND and R. S. MANN. J. Chem. Soc. 3566 (1959).
6. G. C. BOND and J. SHERIDAN. Trans. Faraday Soc. **48**, 658 (1952).
7. G. C. BOND and J. SHERIDAN. Trans. Faraday Soc. **48**, 664 (1952).
8. R. S. MANN and K. C. KHULBE. Can. J. Chem. **45**, 2755 (1967).
9. G. C. BOND and J. TURKEVITCH. Trans. Faraday Soc. **49**, 281 (1953).
10. J. SHERIDAN. J. Chem. Soc. 133 (1945).
11. J. SHERIDAN. J. Chem. Soc. 470 (1945).

Can. J. Chem. Downloaded from www.nrcresearchpress.com by 210.87.254.40 on 09/05/12
For personal use only.

Can. J. Chem. Downloaded from www.nrcresearchpress.com by 210.87.254.40 on 09/05/12
For personal use only.

Infrared spectra of pyridine sorbed on porous glass

M. J. D. Low and V. V. Subba Rao
Department of Chemistry, New York University, New York, N.Y., 10453

Received March 7, 1968

Infrared spectra were recorded of pyridine (PY) sorbed on highly dehydroxylated, deuterated, and fluoridated porous glass, as well as on pure silica and boria-impregnated silica. The hydrogen atoms of sorbed PY exchange with surface OD groups. Physical adsorption occurs by hydrogen bonding of PY to SiOH and B—OH groups via the PY nitrogen atom; there is some interaction of the ring π system with OH groups. Surface B:PY complexes form by coordination of PY to boron; the B:PY may be hydrogen bonded to B—OH groups. Some PY dissociates, and OH groups are generated.

Canadian Journal of Chemistry, 46, 3255 (1968)

Recent work has shown that much of the surface activity of porous glass could be attributed to the presence of minority components (1–6). The sorption of nitrogenous materials was of particular interest, and it was found that boria or alumina contaminants influenced the nature and extent of the interactions between siliceous surfaces and adsorbates such as NH_3 (4), HCN (7), aniline (8), substituted anilines, or trimethylamine (9). We have now studied the sorption of pyridine (PY) in order to provide some information about the behavior of a heterocyclic compound.

The adsorption of PY on porous glass was studied by Yaroslavskii (10) and Yaroslavskii and Terenin (11), who noted hydrogen bonding of PY to surface hydroxyls. However, their spectra were recorded in the overtone region and consequently are of limited utility (12). In a brief study, Nikitin (13) found that adsorption of PY on dehyrated as well as on deuterated porous glass produced broad bands centered near 2900 and 2200 cm^{-1}, which were attributed to surface OH and OD groups, respectively, perturbed by hydrogen bonding to PY via the ring nitrogen; smaller bands near 3650 and 2702 cm^{-1} were similarly attributed to perturbed surface OH and OD groups; and the C—H bands of adsorbed PY were shifted slightly to higher wave numbers with respect to the band positions of PY in CCl_4 solution. Sidorov, using Nikitin's procedure, observed bands at 1596 and 1620 cm^{-1} when PY was adsorbed on 0.1 mm thick deuterated porous glass (19). Such previous work was brief and apparently carried out under conditions of low resolution and with relatively poorly degassed adsorbents. We now report the results observed when PY was sorbed on highly dehydroxylated, deuterated, and fluoridated porous glass as well as on pure and impregnated silicas.

Experimental

Most of the experimental procedures have been described elsewhere (1–6). Corning Code 7930 porous glass was purchased from Corning Glass Works in the form of 1 mm thick sheets. Samples approximately 10 mm × 25 mm were used. Some samples were reduced in thickness to approximately 0.1 mm by grinding with carborundum powder. However, the 3703 cm^{-1} B—OH band (1, 2) of spectra of such thin specimens was diminished with respect to the 3748 cm^{-1} SiOH band, suggesting that some boria had been leached out during the grinding and subsequent washing procedures. As we were interested in observing effects attributable to surface boria, most of the work was carried out with 1 mm thick samples even though this meant that the useful 1700–1400 cm^{-1} region of the "ring" vibrations (13) could not be studied. Some experiments were carried out with pure Cab-O-Sil silica[1] and with Cab-O-Sil impregnated with boria by means of the incipient wetness method. Spectral grade PY was degassed by alternate freezing and thawing in vacuo. Adsorption occurred at room temperature (approximately 30°).

Spectra were recorded with Perkin–Elmer Models 521 or 621 spectrophotometers fitted with Reeder thermocouples, using normal operating procedures. A second cell in the "reference" beam was used to compensate atmospheric and PY vapor absorption. The ordinates of spectra, except those of Fig. 3, are displaced to avoid overlapping of traces. The spectra of Figs. 1–4 were obtained with 1 mm thick specimens of porous glass.

Results

The spectra of Figs. 1 and 2 are typical of those observed when PY was sorbed on highly degassed porous glass. A group of bands were observed at 3166, 3135, 3101, 3078, 3045, and 3025 cm^{-1}; there were shoulders near 3090 and 3070 cm^{-1}. These bands grew in intensity with increasing

[1]Obtained from G. Cabot Co., Boston, Mass.

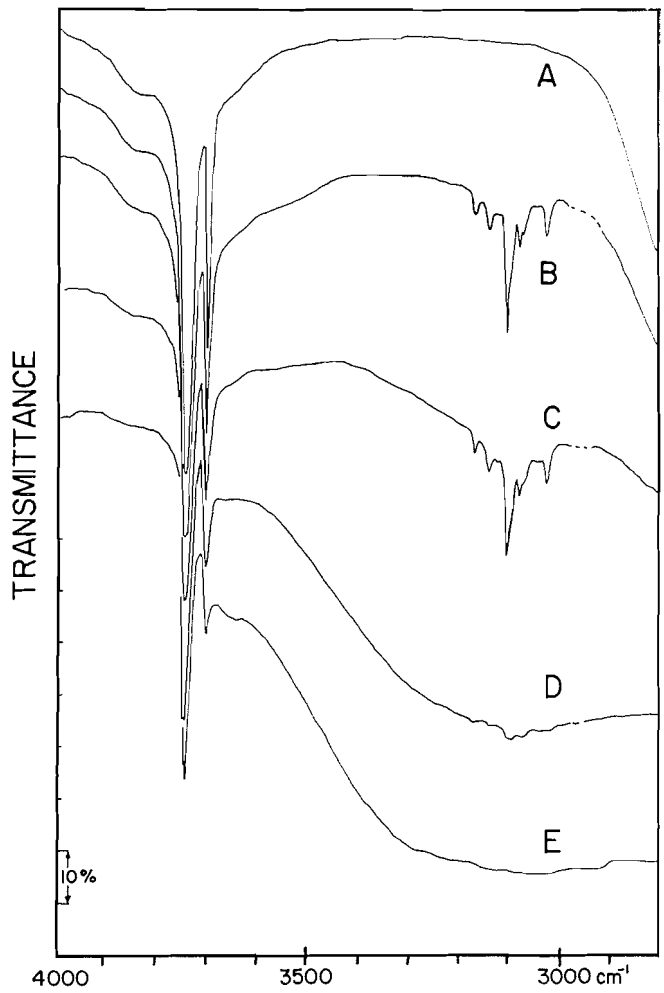

FIG. 1. Adsorption—porous glass. A, Porous glass degassed at 750° for 15 h. The sample was then exposed to PY at 30° at the following pressures in microns: B, 10; C, 25; D, 100; E, 200. The transmittance was 90% at 4000 cm^{-1} for each spectrum.

PY pressure but did not change significantly in frequency. At the highest pressures the bands became indistinct, e.g. spectra D, E, Fig. 1, but reappeared when the adsorbent was degassed. Pumping at 200° removed the bands entirely.

The bands in the C—H region were superimposed on a broad absorption reaching from about 3700 to 2000 cm^{-1}, hereafter termed the 3000 cm^{-1} band. At low PY pressures a second broad absorption could be observed from about 3650 to 3450 cm^{-1}, e.g. spectrum B, Fig. 1, like that observed by Nikitin (13). That absorption, hereafter termed the 3500 cm^{-1} band, merged with the broader 3000 cm^{-1} band but became distinct again when the sorbed PY was pumped off, e.g. spectrum G, Fig. 2.

The OH bands were also affected by PY sorption. The band generally ascribed to isolated surface silanols shifted to 3744 cm^{-1}, broadened, and declined in intensity with increasing PY pressure, and then resumed its original position at 3747 cm^{-1} when the sorbed PY was pumped off. The band attributed to surface B—OH groups (1, 2) exhibited similar behavior in shifting by 2–3 cm^{-1}. Subsequent to an adsorption–desorption cycle, the SiOH and B—OH bands were broadened slightly and a shoulder formed on the low wavenumber side of both OH bands.

Can. J. Chem. Downloaded from www.nrcresearchpress.com by 210.87.254.40 on 09/05/12
For personal use only.

Can. J. Chem. Downloaded from www.nrcresearchpress.com by 210.87.254.40 on 09/05/12
For personal use only.

Spectra of PY sorbed by a "thin" glass specimen, in addition to features such as those described above, showed weak and indistinct bands near 1621 and 1590 cm^{-1}.

Figure 3 shows some results obtained when PY was sorbed on deuterated porous glass. Spectrum A of the deuterated specimen has small bands at 3746 and 3700 cm^{-1} due to residual OH groups and prominent bands at 2762 and 2731 cm^{-1} due to OD groups (2). (The band near 2900 cm^{-1} was caused by contamination of the cell windows during the fluoridation procedure.) When PY was sorbed there was a considerable increase in the intensities of the OH bands and a decrease in those of the OD bands. The latter, shown recorded with ordinate expansion in the insert of Fig. 3, shifted to 2760 and 2729 cm^{-1}. A broad band formed near 2500 cm^{-1}. Bands in the C—H region were like those described previously. Some very weak and indistinct bands near 2300 cm^{-1} were attributed to deuteropyridine.

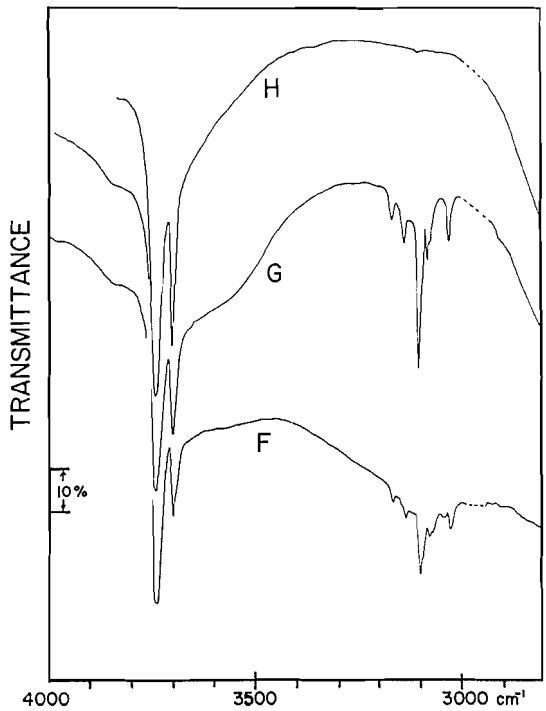

FIG. 2. Desorption—porous glass. Continuation of the sequence of Fig. 1. After spectrum F had been recorded, the sample was degassed at the following temperatures in °C and times in h: F, 30°, 15; G, 100°, 6; H, 200°, 15. The transmittance was 90% at 4000 cm^{-1} for each spectrum.

Spectra recorded during an adsorption–desorption cycle with fluoridated porous glass are shown in Fig. 4. The absence of bands in the OH region of spectra A shows that all surface OH groups had been removed. The group of bands formed in the C—H region after the sample was exposed to PY were like those described previously. They were removed by pumping at 200°. However, small bands near 3740 and 3700 cm^{-1} formed when the sample was degassed.

Some experiments were also carried out with silicas. The 1700–1300 cm^{-1} region was slightly transparent, so that the bands due to the ring vibrations of adsorbed PY could be observed. Some results are shown in Fig. 5. When PY was sorbed on pure Cab-O-Sil, small bands were formed at 3091, 3066, 3045, and 3020 cm^{-1} in the C—H region. These are shown superimposed

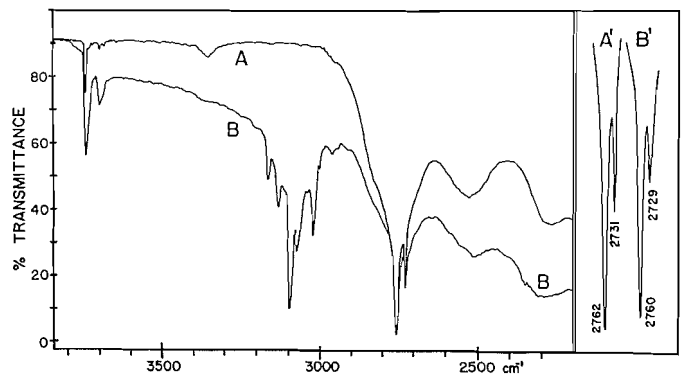

FIG. 3. Adsorption—deuterated porous glass. A,A′: "background" of porous glass after deuteration and degassing. B,B′: after 15 h exposure to 30 microns PY at 30° followed by degassing at 30° for 30 min. A′,B′ were recorded with 5 times ordinate expansion.

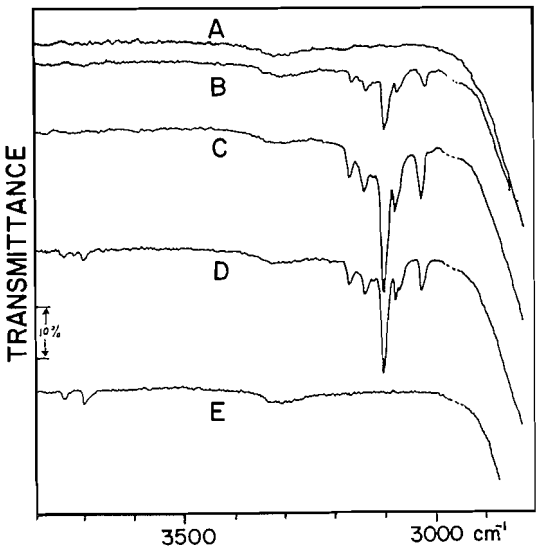

FIG. 4. Fluoridated porous glass. A, "background" spectrum of fluoridated and degassed porous glass specimen. B, after exposure to 200 microns PY at 30° and degassing for 15 h at 30°. C, after exposure to 1000 microns PY at 30° and degassing after 10 h at 30°. D, after degassing for 1 h at 100°. E, after further degassing for 3 h at 200°. The transmittance was 92% at 3800 cm^{-1} for each spectrum.

on the 3000 cm^{-1} band in spectrum A′, and expanded in spectrum A. Also, bands at 1593 and 1443 cm^{-1} and a shoulder near 1580 cm^{-1} were observed. All these bands could be removed by pumping at room temperature. PY sorption diminished and shifted the silanol band from 3746 to 3745 cm^{-1}.

Spectra B to E of Fig. 5 show the effects of PY sorption on boria-impregnated Cab-O-Sil. The groups of bands formed in the C—H region and their behavior as well as the changes observed in the O—H region, were like those found with porous glass. Also, bands were observed at 1624, 1593, 1580, and 1493 cm^{-1}. Degassing at 200° removed the bands in the C—H and the 1700–1400 cm^{-1} regions.

Discussion

The various spectra indicate that at least 3 processes occurred when PY was sorbed by porous glass. For convenience, these are discussed individually below. It is difficult to distinguish between the different surfaces the PY species experienced by considering only spectra recorded with porous glass, because there were no discernible differences in the rates of appearance, or removal by pumping, of the various bands of sorbed PY. However, comparison of porous glass spectra with those of silicas is useful. Spectra of porous glass show 4 absorptions in the C—H region (column 1, Table I) at wavenumbers close to those of 4 bands found in spectra of Cab-O-Sil. Although the positions of the 3090 and 3070 cm^{-1} shoulders in porous glass spectra are uncertain because of

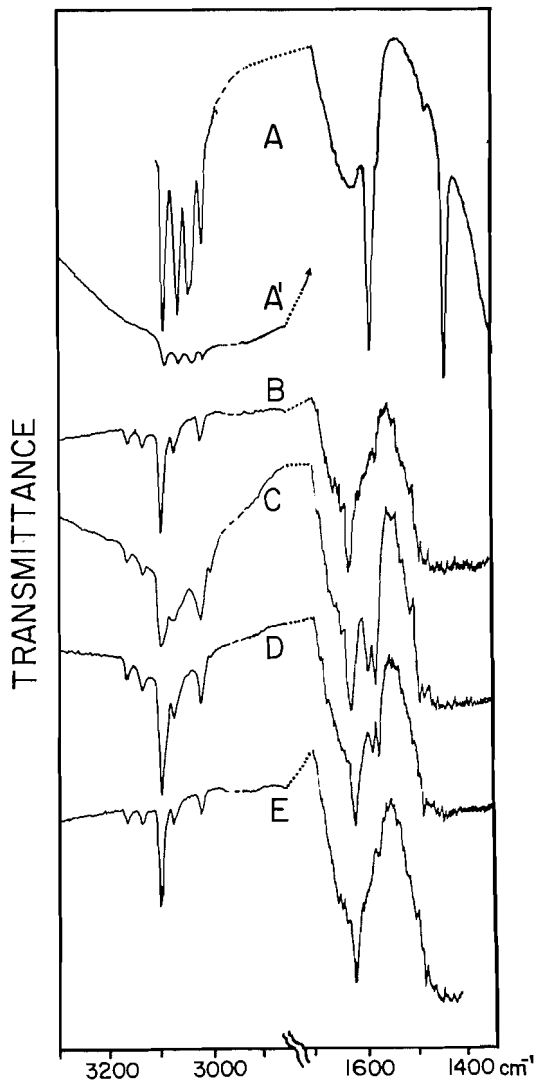

FIG. 5. Adsorption on silicas. A, A′: pure silica, after exposure to 120 microns PY at 30°. Spectra B–E were obtained with 3% B_2O_3–SiO_2. After degassing at 800° for 4 h the latter was exposed at 30° to 10 microns (B), and 100 microns of PY (C), and was then degassed at 30° for 30 min (D), and at 100° for 3 h (E).

Can. J. Chem. Downloaded from www.nrcresearchpress.com by 210.87.254.40 on 09/05/12
For personal use only.

TABLE I

PY bands in the C—H region

Cab-O-Sil, physical adsorption	Porous glass and $B_2O_3.SiO_2$				
	Physical adsorption	B:PY chemisorption	SiO_2/Al_2O_3, chemisorption[a]	Porous glass[b]	PY in CCl_4[c]
3091	3090 sh[d]	3166	3147	3088	3079
3066	3070 sh[d]	3135	3114	3063	3058
3045	3045	3101	3087	3036	3028
3020	3025	3078		3021	3002
				2999	

[a]The same 3 bands were reported for PY chemisorbed on Brønsted or Lewis acid sites (16).
[b]Data of Nikitin (13).
[c]Data of Sidorov (14).
[d]sh means shoulder.

strong overlapping with bands at 3101 and 3078 cm^{-1}, this similarity suggests that the larger group of bands found with porous glass is composed of two overlapping groups. The bands of these are listed in columns 2 and 3 of Table I. The strong overlapping of bands centered near 3090 and 3101 cm^{-1} would account for the relatively high intensity of the 3101 cm^{-1} band found with porous glass and boria-impregnated silica. The division of the bands found with porous glass and with boria-impregnated silica is used in the discussion below to distinguish between physical adsorption and chemisorption effects.

Physical Adsorption

Some of the effects observed are common to Cab-O-Sil, porous glass, and boria-impregnated silica. They are: the diminution of the hydroxyl bands, the shift of the hydroxyl bands, the formation of the 3000 cm^{-1} band, the relative ease of removing sorbed PY, and the relatively small shift of bands of sorbed PY (columns 1 and 2, Table I) from the band positions of unadsorbed PY (column 6, Table I). Also, the 1593, 1580, and 1443 cm^{-1} bands found with PY sorption on Cab-O-Sil were like those reported by Parry (15), who recorded spectra over the 1700–1400 cm^{-1} region of PY adsorbed on Cab-O-Sil. In general, the effects observed were like those reported for porous glass by Nikitin (13). Column 5 of Table I lists the bands of sorbed PY observed by Nikitin; the band positions, as well as the band shifts with respect to the PY bands in CCl_4 solution, are close to those found with Cab-O-Sil.

The various effects point to a relatively weak and reversible interaction of PY with surface OH groups and, in view of the similarities outlined above, the earlier mechanisms (10, 11, 13, 15) are adopted for PY sorption on Cab-O-Sil and also on highly degassed porous glass and boria-impregnated silica. A significant fraction of the sorbed PY is taken to be hydrogen-bonded to SiOH and B—OH groups via the ring nitrogen atom (13), resulting in the shifts of PY bands in the C—H region and in the formation of the 3000 cm^{-1} band due to the hydrogen bonding. Further support for this comes from the experiments with fluoridated porous glass. In the absence of OH groups rather high PY pressures were needed to produce detectable bands in the spectra, indicating that the adsorption was low, and the broad 3000 cm^{-1} band attributed to hydrogen bonding to OH groups was not detected. The 3500 cm^{-1} band was also not found.

The 3500 cm^{-1} band, e.g. spectrum G, Fig. 2, is also ascribed to hydrogen bonding. It is attributed to an interaction between the π system of the aromatic ring of sorbed PY and surface hydroxyls, like that found with the sorption of aniline on siliceous surfaces (8). Such π–OH interactions have been studied by Galkin, Kiselev, and Lygin (17) with a variety of aromatic adsorbates and are discussed by Kiselev and Lygin (18).

Chemisorption

The bands listed in column 3 of Table I are ascribed to chemisorbed PY, in analogy to similar bands reported for PY sorption on silica–alumina (16) by Basila, Kantner, and Rhee (16). The same set of 3 bands were ascribed to coordinately-bonded PY and to the pyridinium ion. However, additional information comes from spectra of sorbed PY in the 1700–1400 cm^{-1} region. The results of Parry (15), later repeated by Basila,

Can. J. Chem. Downloaded from www.nrcresearchpress.com by 210.87.254.40 on 09/05/12
For personal use only.

Can. J. Chem. Downloaded from www.nrcresearchpress.com by 210.87.254.40 on 09/05/12
For personal use only.

Kantner, and Rhee (16), showed that it was possible to distinguish between hydrogen bonded PY, coordinately bonded PY, and the pyridinium ion. Spectra of PY on boria-impregnated silica gave rise to bands at 1624, 1593, 1580, and 1493 cm^{-1}, while bands at 1593, 1580, and 1443 cm^{-1} were found with Cab-O-Sil. Comparison of the spectra of Fig. 5 with Parry's data indicates that hydrogen-bonded PY occurred on Cab-O-Sil, but that coordinately-bonded PY as well as hydrogen-bonded PY formed on boria-impregnated Cab-O-Sil. The results thus indicate that a portion of the PY sorbed on boria-impregnated Cab-O-Sil formed a B:PY complex which gave rise to the bands in the C—H region listed in Column 3 of Table I. The formation of identical bands with PY sorption on porous-glass is strong evidence for the occurrence of the same B:PY complex on the porous glass surface.

The absence in all spectra of bands at 3260 and 3188 due to N—H stretching vibrations (16) and of a band at 1540 cm^{-1} due to N—H deformation (15), all characteristic of the pyridinium ion, would imply the absence of significant numbers of Brønsted sites on the various adsorbents studied. However, Farmer and Mortland found in their study of the PY–PYH^+ complex in montmorillonite that a characteristic 1550 cm^{-1} band could be completely suppressed when the pyridinium ion was involved in strong hydrogen bonding (19). Also, N—H stretching bands might not be detectable because of broadening due to hydrogen bonding. Some doubt is therefore raised about the total absence of Brønsted sites on the various adsorbents studied and, as the same bands apparently exist for PY chemisorbed on Brønsted and Lewis sites (16) (column 4, Table I), this cannot be resolved by examining the PY bands in the C—H region. However, the various additional bands found with PY sorption on boron-impregnated Cab-O-Sil can be attributed to the presence of boria, so that the suggestion that the B:PY complex formed on porous glass and on boria impregnated silica is reasonable.

The similarity of Nikitin's spectra of PY sorbed on porous glass to those of PY sorbed on Cab-O-Sil shows that the predominant reaction observed then was physical adsorption. Nikitin's sample of porous glass may have had a low boria content *per se* or have been degassed at relatively low temperature, so that no appreciable amount of boron diffusion to the glass surface occurred (2), and therefore no appreciable quantities of a B:PY complex was formed.

By combining gravimetric and infrared data dealing with PY sorption on silica–alumina, Basila, Kantner, and Rhee found that the removal of a portion of the chemisorbed PY was accompanied by an increase in the number of free, non-hydrogen bonded surface OH groups, indicating that a hydrogen bonding interaction existed between these two surface species. Their experiments indicated that, on the average, each chemisorbed PY molecule was bonded to a single surface OH group (16). With the present data it is interesting to note in spectra of sorption–desorption cycles such as in Figs. 1 and 2, that the intensity changes of the B—OH band were greater than those of the SiOH band, and that the 3500 cm^{-1} band ascribed to π-OH interaction appeared before the 3000 cm^{-1} band had reached significant proportions (spectrum B, Fig. 1) and remained after much of the physically adsorbed PY had been removed (spectrum G, Fig. 2). The effects cannot be quantitative because of strong overlapping of bands. However, taken together the effects suggest a larger involvement in hydrogen bonding for the B—OH than the SiOH groups and, in view of the hydrogen bonding of chemisorbed PY to surface OH groups, hydrogen bonding of the B:PY complex to neighboring B—OH groups.

Dissociation

It has been mentioned earlier that the surface OH group concentration was greater after PY sorption and desorption than that on the original surface, shown especially by the increase of the B—OH band. A similar effect was described for PY sorption on silica–alumina by Basila, Kantner, and Rhee, who attributed the increase in OH groups subsequent to evacuation of a PY-containing sample at 500° to the decomposition of chemisorbed PY with consequent generation of surface OH groups (17). The present data suggest the same effect.

Spectra of fluoridated porous glass (Fig. 4) show that small bands due to SiOH and B—OH groups were formed when sorbed PY was pumped off. As fluoridated glass is quite reactive (5, 9) to H_2O, the small build up of OH bands removes the suspicion that an H_2O contaminant was responsible and points to a dissociation of sorbed

PY. Significantly, the B—OH band formed was larger than the SiOH band (spectrum E, Fig. 4) and, along with the generally larger changes in B—OH bands than in SiOH bands, suggests that surface boron was to some extent involved in the dissociation process. Similarly, the spectra of PY on deuterated porous glass suggest the generation of OH groups, but the data are complicated by some exchange of the PY ring hydrogens. Contrary to Basila, Kantner, and Rhee's observation that only OD and ND vibrations occurred when PY was sorbed on deuterated silica–alumina (17), some very weak and indistinct bands near 2300 cm^{-1} attributed to the C—D stretchings of deuteropyridine were found with porous glass. However, the intensity decrease of the OD bands (spectra A′, B′, Fig. 3) was not solely caused by exchange with C—H, because the shift of the OD bands and the formation of the broad 2500 cm^{-1} band indicated hydrogen bonding of PY to OD groups. Although a part of the OH groups formed on the deuterated glass (spectrum B, Fig. 3) can be ascribed to the OD—CH exchange, a part can be attributed to the PY dissociation. The dissociation mechanism is not known.

Acknowledgment

Support by grants from the Communicable Disease Center, N.I.H., and N.S.F. grant GP1434, is gratefully acknowledged.

1. M. J. D. Low and N. Ramasubramanian. Chem. Commun. **20**, 1965.
2. M. J. D. Low and N. Ramasubramanian. J. Phys. Chem. **70**, 2740 (1966).
3. M. J. D. Low and N. Ramasubramanian. J. Phys. Chem. **71**, 7309 (1967).
4. M. J. D. Low, N. Ramasubramanian, and V. V. Subba Rao. J. Phys. Chem. **71**, 1726 (1967).
5. M. J. D. Low and N. Ramasubramanian. J. Phys. Chem. **71**, 3077 (1967).
6. M. J. D. Low, N. Ramasubramanian, and P. Ramamurthy. J. Vac. Sci. Technol. **4**, 111 (1967).
7. M. J. D. Low, N. Ramasubramanian, P. Ramamurthy, and A. V. Deo. J. Phys. Chem. **72**, 2371 (1968).
8. M. J. D. Low and V. V. Subba Rao. Submitted for publication.
9. M. J. D. Low and V. V. Subba Rao. Unpublished results.
10. N. G. Yaroslavskii. Metody Issled. Strukt. Visokodispers. i Poristykh Tel, Akad. Nauk SSSR, Trudy Soveshchaniya, 1951, 153 (1953).
11. N. G. Yaroslavskii and A. N. Terenin. Dokl. Akad. Nauk SSSR, **66**, 885 (1949).
12. A. V. Kiselev and V. I. Lygin. *In* Infrared spectra of adsorbed species. *By* L. H. Little. Academic Press, Inc., New York. 1966. p. 226.
13. V. A. Nikitin. Opt. i Spectroskopiya **1**, 593 (1956).
14. A. N. Sidorov. Opt. i Spectroskopiya **8**, 51 (1960).
15. E. P. Parry. J. Catalysis, **2**, 371 (1963).
16. M. R. Basila, T. R. Kantner, and K. H. Rhee. J. Phys. Chem. **68**, 3197 (1964).
17. G. A. Galkin, A. V. Kiselev, and V. I. Lygin. Trans. Faraday Soc. **60**, 431 (1964).
18. A. V. Kiselev and V. I. Lygin. *In* Infrared spectra of adsorbed species. *By* L. H. Little. Academic Press, Inc., New York. 1966.
19. V. C. Farmer and M. M. Mortland. J. Chem. Soc. A, 344 (1966).

Can. J. Chem. Downloaded from www.nrcresearchpress.com by 210.87.254.40 on 09/05/12
For personal use only.

Can. J. Chem. Downloaded from www.nrcresearchpress.com by 210.87.254.105 on 09/05/12
For personal use only.

Anion-molecule complexes in solution. II. The complexing of halide ions with acetylated β-D-glucopyranosyl derivatives

J. S. MARTIN, JUN-ICHI HAYAMI[1], AND R. U. LEMIEUX
Department of Chemistry, University of Alberta, Edmonton, Alberta

Received February 13, 1968

Tetra-*O*-acetyl-β-D-glucopyranosyl halides and phenoxides in solution in acetonitrile showed a specific deshielding of H-1, H-3, and H-5 on addition of tetraethylammonium halides. The shifts and equilibrium constants increased as the anion radius decreased. The ortho hydrogens of the phenoxide aglucons were also significantly deshielded. The strong dependence of the equilibrium constants of the phenoxide compounds on *p*-substituents indicated considerable involvement of the phenyl groups in a specific conformation. A simple electrostatic model was successful in correlating the energies and predicting the structures of the complexes. It was not necessary to postulate specific hydrogen bonding to account for association of the anion with an electrophilic *region* of the molecule. The calculations required specific orientations of acetoxy groups with respect to the pyranose ring which are consistent with those of related studies. In favorable circumstances, the method may be used as a probe for electrophilic regions in molecules.

Canadian Journal of Chemistry, 46, 3263 (1968)

Introduction

In the course of an investigation of the reactions of the anomeric tetra-*O*-acetyl-D-glucopyranosyl chlorides (TGP chlorides) (1), it was found that the nuclear magnetic resonance (n.m.r.) signals assigned to the hydrogens at the 1, 3, and 5 positions of certain β-anomers (see Fig. 1) were specifically shifted to lower shielding when tetraethylammonium halide salts were added to their solutions in thoroughly dry acetonitrile. A typical instance is shown in Fig. 2. The spectrum of a TGP derivative shows signals, identified in Fig. 2, in the range τ 4 to 6 which are characteristic of the hydrogens on the pyranose ring. Note how, on addition of tetraethylammonium chloride, the signals assigned to H-1, H-3, and H-5, and certain of the ring hydrogen signals of β-TGP *p*-nitrophenoxide move to lower shielding (τ) values, the magnitude of the deshielding increasing as the salt concentration increases.

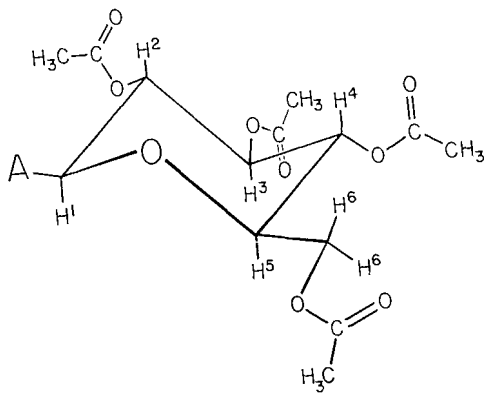

FIG. 1. Tetra-*O*-acetyl-β-D-glucopyranosyl derivatives (A = halide or phenoxide) to show the approximate orientations of the acetoxy groups.

Since our first report of this phenomenon (2), Green and Martin (3), in Paper I of this series, interpreted the similar shifts of the hydrogen signals of haloforms in terms of simple 1:1 association of the halide ion with the hydrogen-bearing molecule. The association is usually directed toward the hydrogen site, and may be regarded as a form of hydrogen bonding to the nucleophilic halide ion.

The deshielding effect was *not* observed when halide salts were added to solutions of the same hydrogen-bonding substrates in a strongly solvating medium, such as deuteriochloroform. The substrate is therefore in competition with the solvent for the halide ion. Acetonitrile is known to solvate anions relatively weakly (4, 5); a manifestation of this is the powerful nucleophilicity of halide ions in this solvent (6). Thus the β-TGP derivatives are displaced from halide ions by deuteriochloroform, but not by acetonitrile.

Experimental

The derivatives of glucose, all previously well known compounds, were prepared by following the standard procedures (7, 8) and they possessed the expected physical constants. The acetonitrile and the quaternary ammonium halides were purified as previously described (1). Solutions

[1]Postdoctorate Fellow, 1963–1964. Present address: Institute for Chemical Research, Kyoto University, Kyoto, Japan.

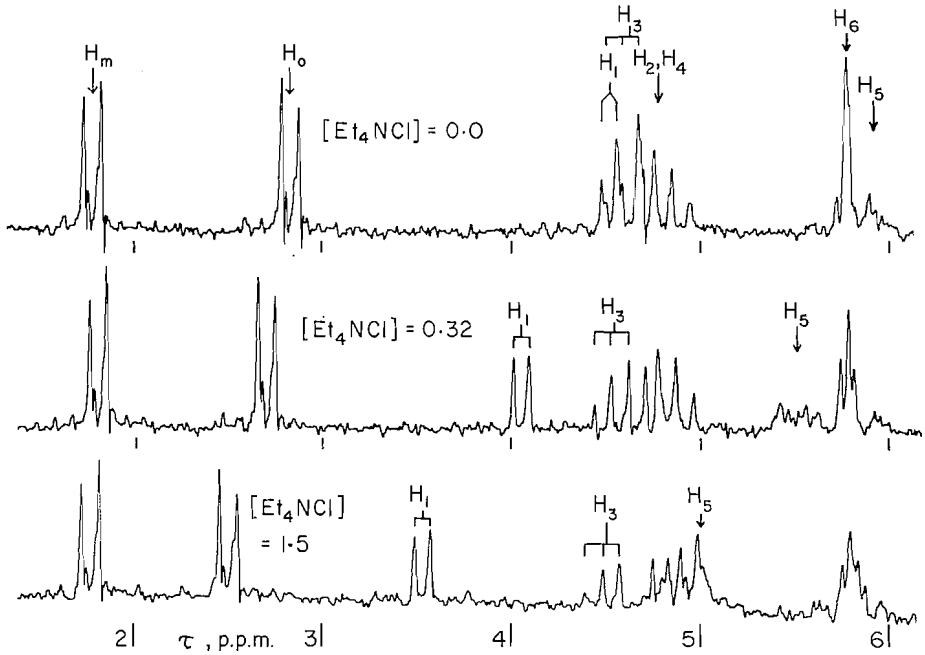

FIG. 2. Changes of 100 MHz spectrum of tetra-*O*-acetyl-β-D-glucopyranosyl *p*-nitrophenoxide in acetonitrile on addition of tetraethylammonium chloride.

were prepared under dry nitrogen, and sample tubes were carefully sealed to exclude oxygen and water.

H-1 n.m.r. spectra were obtained at 100 MHz, at ambient probe temperature (35 ± 1 °C). Line positions were measured to 0.1 Hz by standard sideband methods, referred to 3% internal tetramethylsilane. The use of a spherical, inert internal reference effectively compensates for most general solvent effects (9).

Chemical shifts were approximated as the first moments of multiplets associated with the nuclei in question. Rigorous moment analysis (10) permits the shifts to be derived from the *second* moment of the multiplet relative to the first moment of the total spectrum. The error arising from our approximate method of analysis can be shown to be of the order of $\Sigma_j J_{ij}^2/4(\nu_j - \nu_i)$, where ν_i is the shift sought, in Hz, and ν_j and J_{ij} are the appropriate shifts of, and couplings to, other strongly interacting nuclei.

Typically, the chemical shift of H-1 could be derived by this method with an accuracy of 0.005 p.p.m. at all concentrations. Inspection of Fig. 2 indicates that at certain concentrations the shifts of H-3 and H-5 will be inaccessible. Consequently only the variation of the H-1 shift with concentration was used for analysis.

The AA′BB′ benzene-ring spectra of para-substituted TGP phenoxides were analyzed for the chemical shifts by regarding the four strongest lines as an AB spectrum. This is known to yield very accurate values of the shifts in these systems (11).

Equilibrium Analysis

All solutions were made up with a substrate (TGP compound, S) concentration of about 0.1 *M*. The shieldings of substrate hydrogens were then observed as a function of salt (I) concentrations over the range 0 to 1.4 *M*, the value of which is primarily limited by the salt solubility in acetonitrile. These conditions favor 1:1 complex formation. At the concentrations used, the substrate was usually the minority constituent, so S_nI complexes were unlikely; in all cases, multiple-ion complexes SI_n are energetically unfavorable.

Subject to the assumption of 1:1 complexes, the substrate-ion association equilibrium with the complex, C, may be represented by

$$[1] \qquad \frac{[C]}{[S][I]} = K$$

Since only a single sharp spectrum is observed at any concentration, the transfer of substrate molecules between the free and complexed forms must be very rapid. The observed chemical shift, ν, of a nucleus is then the concentration-weighted average of its values, ν_s in the free form and ν_c in the complex. Thus,

$$[2] \qquad \frac{[C]}{[S] + [C]} = \frac{\nu - \nu_s}{\nu_c - \nu_s} = \frac{\Delta}{\Delta_c}$$

Can. J. Chem. Downloaded from www.nrcresearchpress.com by 210.87.254.105 on 09/05/12
For personal use only.

Can. J. Chem. Downloaded from www.nrcresearchpress.com by 210.87.254.105 on 09/05/12
For personal use only.

The equilibrium constant, K, and the limiting shift of the complex, Δ_c, cannot be observed directly. Equations [1] and [2] may be combined to yield Scott's modification (12) of the Benesi–Hildebrand equation (13):

$$[3] \qquad [I]/\Delta = 1/K\Delta_c + [I]/\Delta_c$$

If a set of observed values of Δ versus [I] is converted to $y = [I]/\Delta$ and $x = [I]$, and these fitted to a best straight line,

$$[4] \qquad y = b_1 + b_2x$$

then,

$$[5] \qquad \Delta_c = 1/b_2$$

and,

$$[6] \qquad K = b_2/b_1$$

The free ion concentration, [I], differs from the total ion concentration, $[I]_0$, by the complex concentration:

$$[7] \qquad [I] = [I]_0 - [C]$$

An initial estimate was made of K and Δ_c using the total ion concentration, $[I]_0$, as an approximation to [I]. A better value of [I] at each concentration could then be computed using the relation,

$$[8] \qquad [I] = [I]_0 - [S]_0(\Delta/\Delta_c)$$

The equilibrium analysis was then repeated, with better estimates of the values of [I], until a self-consistent set of values was obtained. This usually occurred within 5 to 10 iterations. The analysis was carried out by means of a Fortran program, SHEBA, on the IBM 360 – 65/67 computer. SHEBA is described in more detail in Paper I (3).

The error estimates of K and Δ_c are derived from standard errors of the linear regression coefficients by the usual methods (14), with the modification that error estimates on the observed quantities (chemical shifts and concentrations) are included in the derived standard errors. The error estimates of the shieldings included the probable error, described above, resulting from the approximations used in the spectral analysis.

In all cases the variation of the H-1 shift with concentration was used to deduce the equilibrium constant and the complex shift, Δ_1, of H-1. The complex shifts of other nuclei were determined from the slopes of least-squares fits of these shifts versus the H-1 shifts. The points were weighted inversely as their probable errors. In a few cases, sufficient precise shifts of a nucleus other than H-1 were available to allow an independent determination of the equilibrium constant. In all cases, this second determination agreed to within its (somewhat larger) error range with the equilibrium constant derived from the H-1 shifts.

Experimental Results

The equilibrium constants and significant complex shifts of the complexes analyzed are shown in Table I. In all cases but one, these are in agreement with the preliminary results, obtained by the original Benesi–Hildebrand method, reported previously (2). The values originally reported for the chloride ion complex with β-TGP fluoride appear to have been significantly in error. This is discussed in the Appendix.

No evidence of significant complex formation of chloride ion was found for any of the following substrates: penta-*O*-acetyl-β-D-glucopyranose, tetra-*O*-acetyl-α-D-glucopyranosyl chloride, and tetra-*O*-acetyl-α-D-glucopyranosyl *p*-nitrophenoxide.

The following features of the data in Table I are considered significant:

1. In every case, the complex shifts of H-1 and H-5 are of comparable magnitude, and considerably greater than that of H-3. No significant shifts of any other hydrogens on the pyranose system were observed.
2. For the complexes of β-TGP phenoxides there is significant shifting of the benzene-ring hydrogens which are ortho to the aglucon oxygen.
3. The equilibrium constant increases as the radius of the halide ion decreases for the complexing of the three halide ions, Cl^-, Br^-, and I^-, with β-TGP *p*-nitrophenoxide. This is consistent with the behavior of haloform complexes (3) and indicates that the binding energy of the complex is primarily electrostatic.
4. The equilibrium constants, and to a lesser extent the complex shifts, of the complexes of β-TGP phenoxide derivatives are strongly influenced by the nature of substitution at the physically remote *p*-position of the benzene ring.
5. The relative shifts of H-1, H-3, and H-5 in the chloride complexes of the β-TGP chloride are essentially the same as those in the fluoride.

Discussion

It has been shown (15, 16) that the shielding change, $\delta\sigma$, of a hydrogen bonded to carbon,

TABLE I

Results of equilibrium analyses of β-TGP complexes

Substrate β-TGP derivative	Salt	Equilibrium constant (l mole^{-1})	Shift ratios	Complex shifts, (p.p.m.)
Chloride	Et_4NCl	1.07 ± 0.06	$\Delta_3/\Delta_1 = 0.227 \pm .041$ $\Delta_5/\Delta_1 = 0.799 \pm .073$	$\Delta_1 = -1.52 \pm 0.06$ $\Delta_3 = -0.35 \pm 0.07$ $\Delta_5 = -1.21 \pm 0.12$
Fluoride	Et_4NCl	0.67 ± 0.15	$\Delta_3/\Delta_1 = 0.226 \pm .051$ $\Delta_5/\Delta_1 = 0.871 \pm .073$	$\Delta_1 = -1.14 \pm 0.22$ $\Delta_3 = -0.26 \pm 0.08$ $\Delta_5 = -0.99 \pm 0.21$
Phenoxide	Et_4NCl	0.64 ± 0.05	$\Delta_3/\Delta_1 = 0.168 \pm .042$ $\Delta_5/\Delta_1 = 0.803 \pm .08$ $\Delta_o/\Delta_1 = 0.39 \pm .08$ $\Delta_m/\Delta_1 = 0.00 \pm .02$	$\Delta_1 = -1.29 \pm 0.10$ $\Delta_3 = -0.22 \pm 0.06$ $\Delta_5 = -1.04 \pm 0.13$ $\Delta_o = -0.50 \pm 0.11$ $\Delta_m = 0.00 \pm 0.03$
p-Methoxyphenoxide	Et_4NCl	0.13 ± 0.06	$\Delta_3/\Delta_1 = 0.17 \pm .16$ $\Delta_5/\Delta_1 = 1.14 \pm .3$ $\Delta_o/\Delta_1 = 0.23 \pm .02$ $\Delta_m/\Delta_1 = 0.08 \pm .02$	$\Delta_1 = -2.8 \pm 1.4$ $\Delta_3 = -0.5 \pm 0.5$ $\Delta_5 = -3.2 \pm 1.8$ $\Delta_o = -0.6 \pm 0.3$ $\Delta_m = -0.2 \pm 0.1$
p-Nitrophenoxide	Et_4NCl	2.03 ± 0.11	$\Delta_3/\Delta_1 = 0.116 \pm .008$ $\Delta_5/\Delta_1 = 0.859 \pm .059$ $\Delta_o/\Delta_1 = 0.28 \pm .03$	$\Delta_1 = -1.31 \pm 0.04$ $\Delta_3 = -0.15 \pm 0.01$ $\Delta_5 = -1.13 \pm 0.08$ $\Delta_o = -0.37 \pm 0.04$
p-Nitrophenoxide	Et_4NBr	1.38 ± 0.12	$\Delta_3/\Delta_1 = 0.065 \pm .034$ $\Delta_5/\Delta_1 = 0.985 \pm .16$	$\Delta_1 = -1.23 \pm 0.06$ $\Delta_3 = -0.08 \pm 0.04$ $\Delta_5 = -1.22 \pm 0.21$
p-Nitrophenoxide	Et_4NI	1.05 ± 0.14	$\Delta_3/\Delta_1 = 0.00 \pm .07$ $\Delta_5/\Delta_1 = 1.37 \pm .3$	$\Delta_1 = -0.78 \pm 0.08$ $\Delta_3 = 0.00 \pm 0.05$ $\Delta_5 = -1.07 \pm 0.27$

produced by an electrostatic field $\boldsymbol{E}$ (e.s.u.) may be represented by the equation,

$$[9] \quad \delta\sigma = 3.0 \times 10^{-12} E_z - 0.74 \times 10^{-18} E^2$$

where E_z is the component of the field along the bond in the direction H → C. This equation predicts, for example, that a chloride ion collinear with and in van der Waals contact with a C—H hydrogen will produce a shielding change of −1.8 p.p.m. If the ion is farther away, or off-axis, the shielding change will be smaller. Thus, the complex shift provides an indication of the position of the ion relative to the C—H bond.

This model gave reasonable estimates of the haloform complex shieldings (3) provided that the following reservations were kept in mind.

The ion–molecule contact may be at distances somewhat shorter than those defined by the appropriate sums of atomic and ionic radii. In hydrogen bonding, this shortening is commonly of the order of 0.5 Å. At this distance, the predicted shift of a C—H hydrogen by a collinear chloride ion is −2.7 p.p.m.

Tetraethylammonium halides are primarily in the form of ion pairs in acetonitrile solution (17). There is evidence (18) that the opposed net field of the counter-ion reduces the effective field of the anion at the shielded hydrogen by a factor of about one-third.

The absolute values of complex shifts are subject to all systematic errors in the equilibrium analysis resulting, for example, from non-ideal solution behavior, failure to account for solvent participation in the complex (19), and errors in the estimate of the uncomplexed H-1 shielding.

Since the shifts of H-3, H-5, etc. are derived experimentally from their linear variation with the H-1 shielding, the *ratios* of the complex shifts are less sensitive to errors affecting their *absolute* values. In the following computations, only shift ratios are used to determine the ionic position relative to the affected hydrogens, assuming that

Can. J. Chem. Downloaded from www.nrcresearchpress.com by 210.87.254.105 on 09/05/12
For personal use only.

Can. J. Chem. Downloaded from www.nrcresearchpress.com by 210.87.254.105 on 09/05/12
For personal use only.

the ion is at some point in van der Waals contact with the molecule[2].

It is not possible to establish, by n.m.r. alone, whether a substrate forms one unique complex with an ion, or several complexes of different geometry in rapid equilibrium. Kuntz and Johnston (20) have shown that in the latter case the observed shift/concentration behavior is indistinguishable from that of a system exhibiting a single complex, of equilibrium constant equal to the sum of individual constants, and with limiting shifts equal to the weighted means of the values in the various complexes. It is possible, therefore, that we have observed not a single complex, in which the ion has a position close to several nearby hydrogens, but a series of rapidly-equilibrating complexes, in each of which the ion interacts specifically with a single hydrogen. This postulate has the virtue of permitting all interactions of ions with hydrogens to be collinear with the C—H bonds (21).

We conclude, however, that the ion–molecule interaction we have observed involves association of the anion with a single, electrophilic region of the molecule, and that it is purely electrostatic. We base this conclusion primarily on the excellent agreement between the observations of relative shifts and stabilities of these complexes with predictions based on a semiclassical electrostatic model of the interaction, which is presented in the following section.

Ion–Molecule Association Energies

We shall assume, for simplicity, that the overall process of complex formation is displacement of one or more solvent molecules from the ion. Significant complex formation will be observed if the process is to some extent exothermic. This will be true if the energy *decrease* on binding a substrate molecule to the ion exceeds the energy *increase* on removing from the ion the solvent molecules which are displaced by the substrate.

[2]The actual values of complex shifts predicted for these structures by eq. [9] are in reasonable agreement with the observed values presented in Table I. For example, the predicted shifts of H-1 are all in the range −0.7 to −1.6 p.p.m., as are the observed shifts. The agreement with experiment is within experimental error for the β-chloride and β-fluoride complexes; less close for the phenoxy-substituted compounds. The electrostatic model and experiment agree that the complex shifts in complexes of β-*p*-nitrophenoxide should decrease in the order $Cl^- > Br^- > I^-$.

The solubility of the salts indicates that they interact strongly with the solvent; it can be estimated (3) that the solvation energy of a chloride ion in acetonitrile is −60 to −70 kcal. Thus stable complex formation indicates that the ion–substrate interaction energy falls below a certain critical value, whose magnitude should be approximately the binding energy of a single solvent molecule, that is, about −10 kcal (3).

The Electrostatic Model

A model which will account for stereospecific association of an ion with certain regions of a molecule must take into account properties of local structures. The simplest such model which uses input parameters which may be obtained independently is one which computes the interaction of the ionic field with each bond. In Paper I (3), a model was developed which sums the energies of interaction of the ion with the permanent and induced dipoles of the bonds as follows:

$$[10] \quad U_e = -\sum_{i<j}\eta_{ij}(\boldsymbol{\mu}_{ij}\boldsymbol{E}_{ij} + \tfrac{1}{2}\boldsymbol{E}_{ij}\boldsymbol{\alpha}_{ij}\boldsymbol{E}_{ij})$$

$\eta_{ij} = 1$ if atoms i and j are bonded; otherwise $\eta_{ij} = 0$. $\boldsymbol{\mu}_{ij}$ is the permanent bond dipole moment. $\boldsymbol{\alpha}_{ij}$ is the bond polarizability tensor. This is assumed to be axially symmetric, with components $\alpha_{\parallel ij}$ along the bond and $\alpha_{\perp ij}$ perpendicular to it. $\boldsymbol{E}_{ij}$ is the electrostatic field due to the ion at bond ij.

The evaluation of ion–molecule interaction energies using this equation was previously described in more detail (3).

A computer program, IONPOT, was written to carry out the calculations, which tend to be extensive and repetitive. IONPOT is given the atomic coordinates relative to a suitably chosen set of axes, and brings the ion down from the positive z direction. When the ion is just touching the van der Waals surface of the molecule, the energy is computed using eq. [10], and all appropriate hydrogen shieldings are computed using eq. [9]. These operations are performed over a specified grid of uniform intervals in the x and y coordinates of the ion, yielding a potential map of the molecular surface, projected on the x–y plane.

Coordinates of the atoms in the rigid part of the β-D-glucopyranose structure were taken from Ferrier's X-ray analysis of the β-D-glucose

Can. J. Chem. Downloaded from www.nrcresearchpress.com by 210.87.254.105 on 09/05/12
For personal use only.

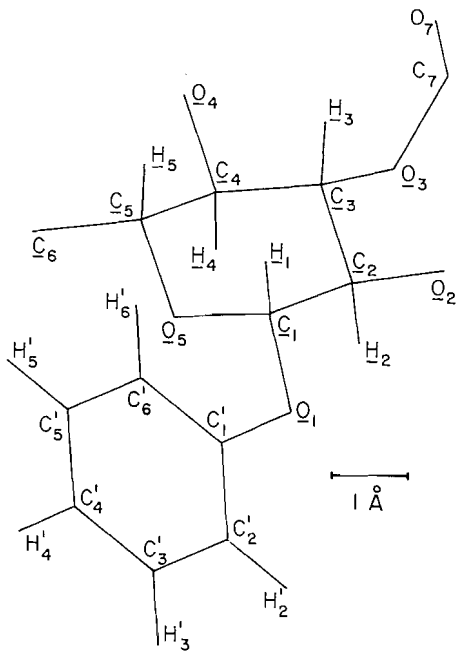

FIG. 3. Isometric projection of part of the tetra-*O*-acetyl-β-D-glucopyranosyl phenoxide molecule, according to Ferrier's analysis of the crystal structure of β-D-glucopyranose (22). Atoms C-7 and O-7 are part of the 3-acetoxy group in its most probable orientation.

crystal structure (22). The symbols for these atoms are underlined in Fig. 3. The hydrogen positions were recomputed from Ferrier's data, to give C—H bond lengths of 1.10 Å. The bond dipoles and polarizabilities, atomic polarizabilities, and van der Waals radii used were taken from

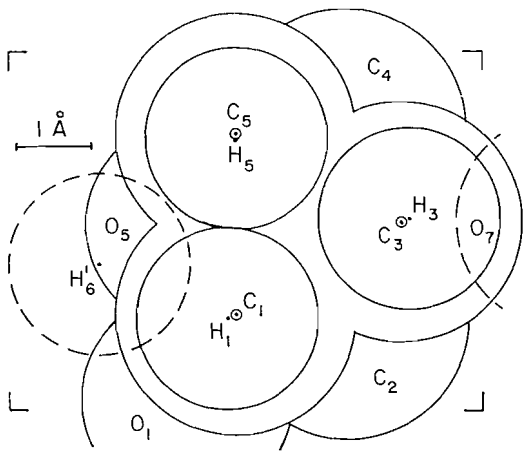

FIG. 4. Projection of part of the structure of Fig. 3, from above the plane defined by C-1, C-3, and C-5.

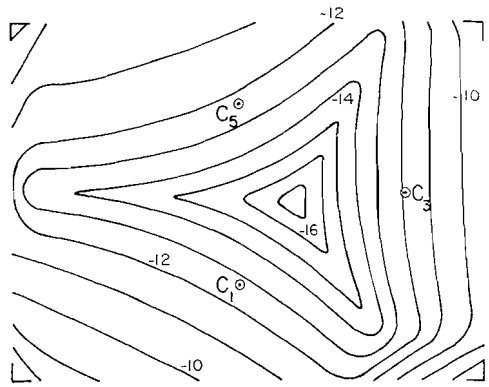

FIG. 5. Ion–molecule interaction equipotentials for chloride ion and tetra-*O*-acetyl-β-D-glucopyranosyl chloride, without the acetyl groups.

standard sources (23–28). The values used in the computations are listed in Table II.

The molecular surface of interest is obviously the side of the pyranose ring bearing atoms H-1, H-3, and H-5. Ferrier's atomic coordinates were accordingly transformed to put C-1, C-3, and C-5 in the *x*–*y* plane, as shown in Fig. 4, with the attached hydrogens facing upwards in the positive *z* direction. Note that these three hydrogens in the

TABLE II

Parameters used in the electrostatic computations

(*a*) Atomic and ionic properties

Atom/ion	Radius (Å)	Polarizability × 10^{24} (cm^3)
H	1.20	0.4
C	1.60	1.0
O	1.40	0.8*
F	1.35	0.7*
Cl	1.80	2.8*
Cl^-	1.81	—

(*b*) Bond properties

Bond	Bond dipole (*D*)	Bond polarizability × 10^{24} (cm^3) $\alpha_{\parallel}$	$\alpha_{\perp}$
C—C	0.00	1.88	0.02
C⋯C (Av.)	0.00	2.25	0.48
C—H	0.00	0.79	0.58
C—O	1.15	1.47†	0.84†
C=O	2.80	1.99	0.75
C—F	1.80	0.96†	0.55†
C—Cl	1.90	3.67	2.08

*Estimated from bond polarizabilities.
†Estimated from mean polarizability, assuming $\alpha_{\perp}/\alpha_{\parallel} = 0.57$ (see ref. 27).

Can. J. Chem. Downloaded from www.nrcresearchpress.com by 210.87.254.105 on 09/05/12
For personal use only.

β-pyranose system form a compact cluster, with the three C—H bonds essentially parallel. An examination of the local bonding suggests that this region of the molecule should be attractive to a negative ion, since C-1, C-3, and C-5 are all positively charged by reason of their bonding to various oxygen atoms.

Figure 5, which is drawn to the same scale as Fig. 4, is a contour map of the potential energy of interaction of a chloride ion with the region of β-TGP chloride shown in Fig. 4. Only those atoms which are conformationally rigid were used in the computation, those atoms with underlined symbols in Fig. 3. O-1 was replaced by a chlorine atom, at a suitable bond distance from C-1. The most striking feature of Fig. 5 is the potential well, more than 17 kcal deep, near the center of the H-1/H-3/H-5 triangle. A computation of this type reveals no such feature on the other side of the ring; nor is there any point on the corresponding surface of the α-anomer where the energy is computed to be less than −7 kcal.

It is not feasible to include in the computation interaction all of the atoms in the β-TGP chloride molecule, since the acetoxy groups and the groups bonded to C-6 are conformationally mobile. However, it is possible to assess the approximate magnitude of some of the more important contributions from these groups.

Mathieson (29) has surveyed X-ray crystal structure analyses of ester groups in equatorial orientation, and concludes that the carbonyl oxygen is preferentially in the region of the methine hydrogen geminal to the acetoxy group.

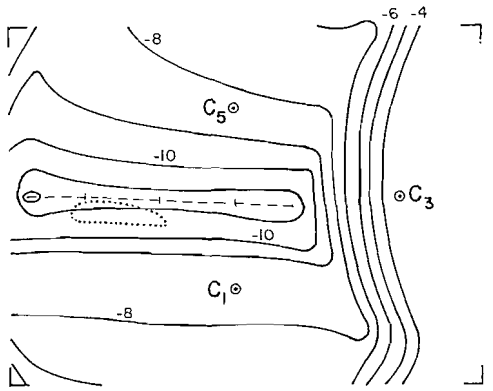

FIG. 6. As in Fig. 5, including the carbonyl of the 3-acetyl group (C-7 and O-7, of Fig. 3). The dotted curve encloses the ionic positions indicated by the complex shifts.

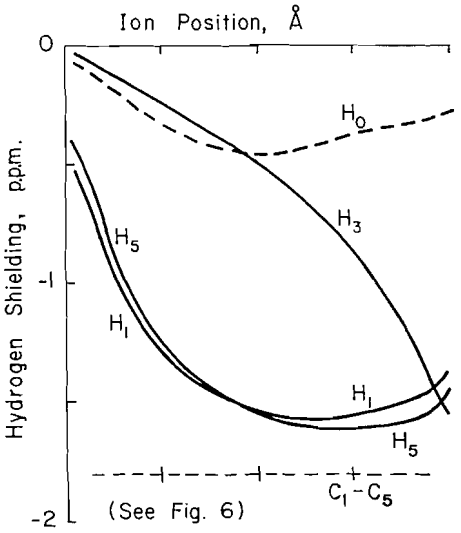

FIG. 7. Chemical shift changes of β-TGP hydrogens vs. position of chloride ion on molecular van der Waals surface. The dashed line at the bottom corresponds to the dashed line along the potential trough in Fig. 6.

The strong deshielding on acetylation of an alcohol confirms that this is also the preferred conformation in the liquid phase.

At ring positions 2 and 4, the very polar C=O bonds will therefore be directed away from the H-1/H-3/H-5 side of the ring, and should not impede an anion approaching the ring from this side. In fact, since they are aligned with their positive ends directed toward the ion, their effect, if any, will be attractive. The presence of two negatively charged oxygens in the vicinity of H-2 and H-4 will make that region even less attractive to a negative ion.

The carbonyl group of the acetoxy at position 3 is obviously in a position to exert a strong influence on the complex energies in the neighborhood of H-3. Atomic coordinates for its atoms (C-7 and O-7 in Fig. 3) were estimated using typical bond lengths and angles, and assuming that H-3, C-3, O-3, C-7, and O-7 are coplanar. This puts O-7 in its position of closest approach to H-3, at a distance about 0.1 Å less than the 2.2 Å commonly observed (29), and will probably result in a slight overestimate of its effect on the complex energy.

The potential map of the model of β-TGP chloride including the 3-acetoxy group is shown in Fig. 6. There is no question that the acetoxy group influences the energies profoundly,

Can. J. Chem. Downloaded from www.nrcresearchpress.com by 210.87.254.105 on 09/05/12
For personal use only.

especially in the vicinity of H-3. The presence of a second acetoxy-oxygen near H-1 in the penta-acetate ought to raise the ion–molecule energy over this entire region of the molecule. The observed failure of penta-*O*-acetyl-β-D-glucopyranose to complex chloride ion presumably reflects this destabilization by two acetoxy groups on the same side of the molecule.

When the 3-acetoxy interaction is included, the potential well of Fig. 5 becomes a long, level potential trough running out of the H-1/H-3/H-5 triangle beyond H-1 and H-5. The displacement of the minimum toward H-1 and H-5 is consistent with the observation that H-1 and H-5 have the largest complex shifts. Since the energy at the bottom of the trough (defined by the dashed line in Fig. 6) varies by less than 1 kcal, it is not reasonable to expect this rather crude model to specify with any accuracy the location of the potential minimum along the trough, and thus the location of the ion in the β-TGP chloride complex.

It seems reasonable, however, to make the following predictions, based on the form of the potential map (Fig. 6) of the β-chloride.

1. The ion should be found somewhere near the bottom of the trough.
2. Since the model we have used for the β-chloride is common to all β-TGP derivatives, the long, level trough predicted by the model indicates that the position of minimum potential energy, and thus the location of the ion in a particular complex, should be profoundly influenced by substituents in this region: in particular, by substituents on C-1.

It should be possible to locate the ion along the potential trough by examining the variation of the complex shifts of H-1, H-3, and H-5. Figure 7 shows the variation of these shifts, computed using eq. [9], as a function of position of a chloride ion along the potential minimum line, indicated by the dashed line in Fig. 6. It is apparent that the model will account for most of the shifts reported in Table I if the ion is located between 1 and 2 Å to the left (outside) of the line joining C-1 and C-5.

In the next three sections, the chloride ion complexes of specific molecules are discussed, and their equilibrium constants and complex shifts interpreted with respect to the models defined above.

Complexes of β-TGP Chloride and Fluoride with Chloride Ion

These compounds differ only in that both the bond moment and polarizability of the C-1—Cl bond are greater than those of the C-1—F bond; the somewhat larger equilibrium constant of the β-TGP chloride thus reflects a somewhat more negative energy of interaction of this compound with the ion. The actual energy difference is small; using the parameters in Table II, we computed a potential energy diagram with a potential trough which, though about 1 kcal less deep than that of the β-TGP chloride shown in Fig. 6, was nevertheless in essentially the same place.

The complex shifts are in the same proportions in the two molecules, to within their error ranges. The dotted curve in Fig. 6 encloses the region in which eq. [9] predicts shift ratios within experimental error of those observed. This region is entirely within 0.5 Å of the potential trough, and the energies computed within it are within 2 kcal of the minimum computed values. Considering the approximations inherent in the model, and the sensitivity of the computed energies to small changes in the positions of conformationally mobile groups, this agreement is satisfactory.

Complexes of β-TGP Phenoxide with Chloride Ion

The deshielding of the benzene-ring hydrogens H-2′ and H-6′ in Fig. 3, which are ortho to the point of attachment to O-1′, indicates that these hydrogens must be close to the ion in the complex. Strong interaction of the corresponding hydrogens with the ion in complexes of benzyl alcohol with bromide ion has been reported (30).

The fact that the symmetry of the AA′BB′ spectrum of a *p*-substituted phenoxy derivative is unchanged on formation of the complex reflects the fact that the benzene ring is free to rotate: on the average, H-2′ and H-6′ interact equally with the ion.

Study of molecular models suggests that the orientation of C-1′ relative to the pyranose ring is restricted to that shown in Fig. 3. The benzene ring has somewhat more freedom to rotate about the O-1—C-1′ bond. Each of its conformers will, of course, have a symmetrically equivalent twin, in which the positions of H-2′ and H-6′ are exchanged.

One possible orientation of the benzene ring is shown in Fig. 3; one ortho-hydrogen (H-6′), is

Can. J. Chem. Downloaded from www.nrcresearchpress.com by 210.87.254.105 on 09/05/12
For personal use only.

located in a position between O-5 and H-1 where it may interact strongly with an ion in the vicinity of H-1 and H-5. In this conformer, H-6′ is shown in dashed outline in Fig. 4. The second allowed conformer is related to the first by a rotation of about 90°.

The energy of the complex will be a weighted average over all conformers accessible to the benzene ring. Figure 8 is the potential energy contour map of the conformer depicted in Fig. 3. The region of minimum potential is very broad, and includes the region, enclosed by the dotted curve, which defines positions of the ion consistent with the observed shift ratios.

The observed complex shift of ortho-hydrogens will be an average over all conformations. If only the conformation shown in Fig. 3 and its symmetrically equivalent twin are appreciably populated, the observed ortho shift will be $(\delta\sigma_{2'} + \delta\sigma_{6'})/2$. Computed values of this quantity are shown by the dashed curve in Fig. 7.

If the ion is within the dotted curve in Fig. 8, the computed ortho shift is about 0.25 of the H-1 shift. The observed value[3] of Δ_o/Δ_1 is 0.4.

The other possible conformation of the benzene ring would remove both H-2′ and H-6′ from the vicinity of the ion, contribute very little to their complex shifts, and thus make worse the discrepancy between the observed and predicted values. The large complex shift of the ortho-hydrogens thus indicates that the conformation of the benzene ring shown in Fig. 3 is the predominant one in the complex.

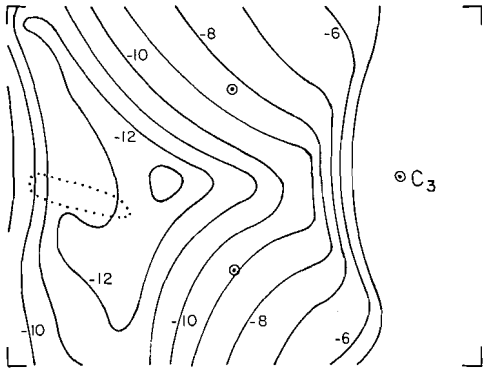

FIG. 8. Ion–molecule interaction equipotentials for chloride ion and tetra-*O*-acetyl-β-D-glucopyranosyl phenoxide. The dotted curve encloses the ionic positions indicated by the complex shifts.

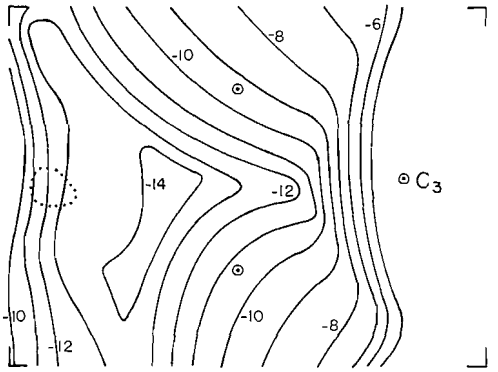

FIG. 9. Ion–molecule interaction equipotentials for chloride ion and tetra-*O*-acetyl-β-D-glucopyranosyl *p*-nitrophenoxide. The dotted curve encloses the ionic positions indicated by the complex shifts.

Complexes of Para-Substituted β-*TGP Phenoxides with Chloride Ion*

The complex equilibrium constants and shifts of these compounds are extremely sensitive to the nature of a substituent on the para-position of the benzene ring. Since the electron-withdrawing nitro group stabilizes the anion complex and the electron-donating methoxy group destabilizes it, it appears that the mechanism involved is

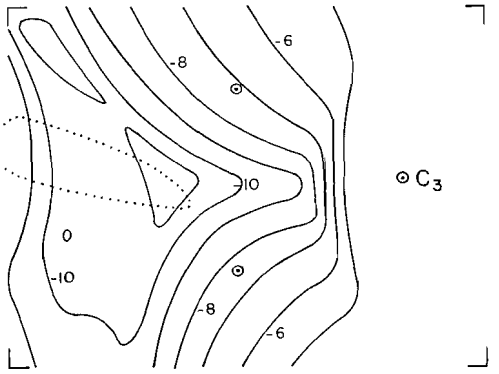

FIG. 10. Ion–molecule interaction equipotentials for chloride ion and tetra-*O*-acetyl-β-D-glucopyranosyl *p*-methoxyphenoxide. The dotted curve encloses the ionic positions indicated by the complex shifts.

[3]The computed value of Δ_o, −0.3 p.p.m., is the average of $\delta\sigma_{6'} = -0.9$ p.p.m. and $\delta\sigma_{2'} = +0.3$ p.p.m. Better agreement with the experimental value would be obtained if the value of $\delta\sigma_{2'}$ were nearly zero. Dielectric polarization of the benzene ring could shield the nucleus of H-2′ from the ionic field: such a mechanism has been postulated (3) to explain a surprisingly small electrostatic shift of the hydrogen in iodoform by an ion on the far side of the highly polarizable C—I bonds.

Can. J. Chem. Downloaded from www.nrcresearchpress.com by 210.87.254.105 on 09/05/12
For personal use only.

transfer of charge out of or into the benzene pi-electron system.

These substituents are known to interact with the benzene ring primarily by a mesomeric mechanism, which typically produces roughly equal charge density changes at the positions ortho and para to the substituent, and little or no change at the meta position (31). The magnitude of the charge density changes may be estimated from the hydrogen shielding changes characteristic of these substituents. The nitro group produces a deshielding of about -0.4 p.p.m. at the para position; the methoxy group a shielding of about $+0.4$ p.p.m. (32). Using the constant of proportionality of 10 p.p.m./electron (33), one deduces that the nitro group is reasonably represented as producing a net positive charge of 0.04 electron or $+2 \times 10^{-11}$ e.s.u. at C-1′, C-3′, and C-5′; the methoxy group produces charges of the same magnitude and opposite sign.

Using the benzene ring conformation of the previous calculation, and representing the substituent perturbations by the charges deduced above, potential energy maps representative of β-TGP *p*-nitrophenoxide (Fig. 9) and β-TGP *p*-methoxyphenoxide (Fig. 10) complexes were computed. As expected, the minimum energy decreases on nitro substitution and increases on methoxy substitution. Both changes, relative to the unsubstituted compound, are of the order of 1.5 kcal. Since the computations are performed for the most favorable conformer only, these computed changes probably overestimate the actual changes.

The actual energy changes on substitution may be estimated as follows. Since $d(\ln K)/d(\Delta H) = -1/RT$, at 308 °K the threefold increase of the equilibrium constant on nitro substitution corresponds to a decrease in ΔH of ca. 0.6 kcal; the fivefold decrease on methoxy substitution corresponds to an increase of ca. 1 kcal. These magnitudes are quite consistent with the predictions of the electrostatic model.

The ionic positions consistent with the complex shift ratios are contained within the dotted curves in Figs. 9 and 10. The positions of the ion, well outside the H-1/H-3/H-5 triangle in the unsubstituted and nitrophenoxy derivatives, suggest that the benzene ring is sufficiently attractive to the ion that it is capable of pulling it away from the pyranose ring, presumably in conformations where the benzene ring is relatively remote from the pyranose ring. In the methoxy-substituted compound, the negative charge on the benzene ring repels the ion back towards the H-1/H-3/H-5 triangle. Precise correlation of the ionic positions with the computed potential minima is not to be expected, since the exact position of the benzene ring is not known.

Conclusions

A conceptually simple electrostatic model is successful in correlating the energies, and predicting the structures, of complexes of anions to tetra-*O*-acetyl-D-glucopyranosyl derivatives. This model contains no adjustable parameters, and ascribes no special hydrogen bonding properties to hydrogens bonded to electrophilic carbons. The complexes may therefore be regarded as involving the ion in an interaction with the molecule as a whole, rather than with any atom or functional group.

The computed energies correlate with the observed stability constants if it is postulated that complex formation involves competition with the solvent for the ion; in acetonitrile, the ion–molecule interaction energy must therefore be below about -10 kcal for complex formation to be observed. Using the model and this criterion, one predicts that the pentaacetate and the α-tetraacetates will not form stable complexes: this is confirmed by experiment.

Semiquantitative prediction of relative complex energies appears feasible for structurally similar β-TGP derivatives.

Acknowledgments

The research was supported by National Research Council of Canada Grants T-172 (R. U. L.) and A-2051 (J. S. M.). The assistance of Mrs. S. Fraga and G. Bigam is gratefully acknowledged.

Appendix

The Scott and Benesi–Hildebrand Equilibrium Analyses of the β-TGP Fluoride Complex

Our experimental data, the observed shifts of H-1 of tetra-*O*-acetyl-β-D-glucopyranosyl fluoride, 0.1 *M*, as a function of tetraethylammonium chloride concentration, are given in Table III. The error ranges given are reasonable assessments of the reliability of the measurements, based on our experience. Error ranges in plotted quantities

Can. J. Chem. Downloaded from www.nrcresearchpress.com by 210.87.254.105 on 09/05/12
For personal use only.

TABLE III

Shift (Δ) of H-1 of β-TGP fluoride as a function of tetraethylammonium chloride concentration [I]

[I] (*M*)	Δ (p.p.m.)
0.100 ± .005	−0.090 ± .007
0.400 ± .005	−0.217 ± .007
0.600 ± .005	−0.309 ± .007
0.800 ± .005	−0.382 ± .007
1.000 ± .005	−0.421 ± .007
1.200 ± .005	−0.491 ± .007
1.400 ± .005	−0.574 ± .007

are derived solely from them, by standard methods (14).

Figure 11 is a plot of the Scott line (12), defined by eq. [3], whose slope and intercept yielded the equilibrium constant, $K = 0.63\ M^{-1}$ and complex shift, $\Delta_1 = -1.14$ p.p.m., reported in Table I. In the least-squares analysis, the points were weighted inversely as the error ranges shown; consequently the point at lowest ion concentration was given the least weight.

Figure 12 is the Benesi–Hildebrand (13) plot of the same data, which yielded the values $K = 1.55\ M^{-1}$ and $\Delta_1 = -0.66$ p.p.m. reported previously (2). These were deduced from the slope and intercept of the best straight line, which is represented as

$$[11] \qquad 1/\Delta = 1/\Delta_c + (1/K\Delta_c)(1/[I])$$

Note that in Fig. 12 the point at lowest concentration, which is known to be the least reliable,

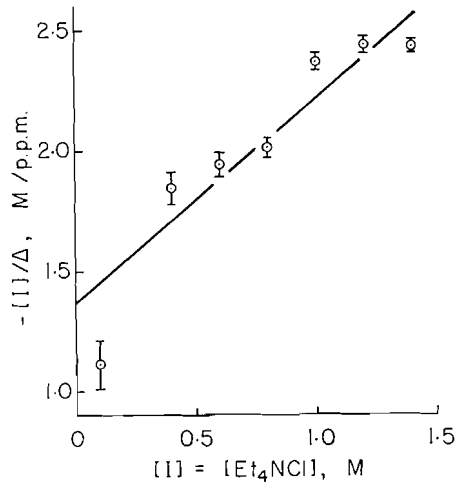

FIG. 11. Scott–Benesi–Hildebrand analysis of the tetra-*O*-acetyl-β-D-glucopyranosyl fluoride complex with chloride ion.

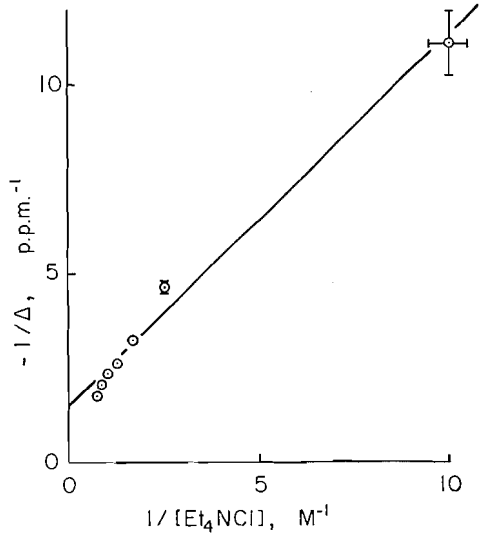

FIG. 12. Benesi–Hildebrand analysis of the tetra-*O*-acetyl-β-D-glucopyranosyl fluoride complex with chloride ion.

assumes extraordinary importance. It is apparent that it alone has an effect on the slope and intercept of the best straight line greater than that of all the other points combined. Since, consistent with its lower reliability, this point appears to deviate markedly from the others, it therefore leads to misleading results in the Benesi–Hildebrand analysis.

Omitting the point at lowest concentration, the Scott analysis yields $K = 0.43$, $\Delta_1 = -1.49$; the Benesi–Hildebrand analysis yields $K = 0.41$, $\Delta_1 = -1.54$. These shifts are comparable to those in the β-TGP chloride complex, as would be expected; these values are therefore probably more representative of the actual complex.

We have chosen to report in Table I results which are representative of *all* of our data points. It should be pointed out that, as the error ranges reported would suggest, the data set for this complex was one of the two least reliable sets in the study.

The following conclusions may be drawn from this experience.

1. Care must be exercised to ensure that no experimental point assumes importance out of proportion to its reliability. In our present (Scott) method of analysis, we guarantee this by evaluating error ranges as described above, and weighting the points inversely.
2. The points used in a linear regression analysis

should be spaced as evenly as possible. Since the Scott analysis involves concentration linearly, the points are conveniently taken at uniform intervals of donor concentration. If the Benesi–Hildebrand analysis is to be used, the points should be taken in a donor concentration series given by $[I] = I_0/n$, $(n = 1, 2, 3 \ldots)$. This will, of course, yield an inordinate number of points at low concentrations, where the relatively small shifts will have errors that are large in proportion to their magnitudes.

3. The extrapolation to "infinite concentration" in the Benesi–Hildebrand method is usually over a span which is long compared to the variance of the experimental points. As Scott has pointed out (12), this is over a region where deviations from ideality are pronounced. The intercept so obtained, $1/\Delta_c$, is usually very small relative to the variance of $1/\Delta$, and thus yields a value of Δ_c of dubious reliability.

We conclude that our adaptation of the Scott analysis yields values of K and Δ_c which are more reliable than those obtained by the Benesi–Hildebrand method. It is apparent that the values originally reported (2) for the chloride ion complex of β-TGP fluoride, which were obtained by the Benesi–Hildebrand method, are in error.

1. R. U. LEMIEUX and JUN-ICHI HAYAMI. Can. J. Chem. **43**, 2162 (1965).
2. R. U. LEMIEUX, J. S. MARTIN, and JUN-ICHI HAYAMI. Preliminary report, Inter. symp. on n.m.r., Tokyo. September, 1965. No. M-2-17.
3. R. D. GREEN and JOHN S. MARTIN. J. Am. Chem. Soc. **90**, 3659 (1968).
4. R. ALEXANDER and A. J. PARKER. J. Am. Chem. Soc. **89**, 5549 (1967).
5. J. F. COETZEE and J. J. CAMPION. J. Am. Chem. Soc. **89**, 2517 (1967).
6. S. WINSTEIN, L. G. SAVEDOFF, S. SMITH, I. D. R. STEVENS, and J. S. GALL. Tetrahedron Letters, **9**, 24 (1960).
7. R. L. WHISTLER and M. L. WOLFROM (*Editors*). Methods in carbohydrate chemistry. Vol. 2. Academic Press, Inc., New York. 1963.
8. E. M. MONTGOMERY, N. K. RICHTMYER, and C. S. HUDSON. J. Am. Chem. Soc. **64**, 690 (1942).
9. W. G. SCHNEIDER. J. Phys. Chem. **66**, 2653 (1962).
10. W. A. ANDERSON and H. M. MCCONNELL. J. Chem. Phys. **26**, 1496 (1957).
11. J. S. MARTIN and B. P. DAILEY. J. Chem. Phys. **37**, 2594 (1962).
12. R. L. SCOTT. Rec. Trav. Chim. **75**, 787 (1956).
13. H. A. BENESI and J. H. HILDEBRAND. J. Am. Chem. Soc. **71**, 2703 (1949).
14. A. G. WORTHING and J. GEFFNER. Treatment of experimental data. John Wiley and Sons, Inc., New York. 1943.
15. A. D. BUCKINGHAM. Can. J. Chem. **38**, 300 (1960).
16. P. J. BERKELY and M. W. HANNA. J. Am. Chem. Soc. **86**, 2990 (1964).
17. D. F. EVANS, C. ZAWOYSKI, and R. L. KAY. J. Phys. Chem. **69**, 3878 (1965).
18. T. E. FENTON, R. D. GREEN, and J. S. MARTIN. Unpublished work.
19. P. J. TROTTER and M. W. HANNA. J. Am. Chem. Soc. **88**, 3724 (1966).
20. I. D. KUNTZ and M. D. JOHNSTON. J. Am. Chem. Soc. **89**, 6008 (1967).
21. G. C. PIMENTEL and A. L. MCCLELLAN. The hydrogen bond. W. H. Freeman and Co., San Francisco. 1960. pp. 263–265.
22. W. G. FERRIER. Acta Cryst. **16**, 1023 (1963).
23. A. L. MCCLELLAN. Tables of experimental dipole moments. W. H. Freeman and Co., San Francisco. 1963.
24. LANDOLT-BORNSTEIN. Zahlenwerten und Funktionen. Vol. I. Part 3. Springer-Verlag, Berlin. 1951.
25. L. G. GROVES and S. SUGDEN. J. Chem. Soc. 1992 (1937).
26. K. G. DENBIGH. Trans. Faraday Soc. **36**, 936 (1940).
27. R. P. SMITH, T. REE, J. L. MAGEE, and H. EYRING. J. Am. Chem. Soc. **73**, 2263 (1951).
28. Handbook of chemistry and physics. 44th ed. Chemical Rubber Co., Cleveland. 1963.
29. A. M. MATHIESON. Tetrahedron Letters, **46**, 4137 (1965).
30. J. B. HYNE and W. B. MCG. CASSIE. 49th Conference of the Chemical Institute of Canada, Saskatoon, June 1966.
31. G. W. WHELAND and L. PAULING. J. Am. Chem. Soc. **57**, 2086 (1935).
32. H. SPIESECKE and W. G. SCHNEIDER. J. Chem. Phys. **35**, 731 (1961).
33. T. P. SCHAEFER and W. G. SCHNEIDER. Can. J. Chem. **41**, 966 (1963).

Can. J. Chem. Downloaded from www.nrcresearchpress.com by 210.87.254.105 on 09/05/12
For personal use only.

The mercury (6^3P_1) photosensitized hydrogenation of ethylene. Kinetics of the reaction $C_2H_5 + H_2 = C_2H_6 + H$

L. E. REID[1] AND D. J. LE ROY

Lash Miller Chemical Laboratories, University of Toronto, Toronto 5, Ontario

Received March 19, 1968

A quantitative study has been made of the reaction of ethyl radicals with molecular hydrogen in the gas phase in the temperature range 240 to 320 °C. The mercury (6^3P_1) photosensitized decomposition of hydrogen in the presence of ethylene was used to generate ethyl radicals. Extinction coefficients for the absorption of 2537 Å by mercury vapor were measured and Beer's law was shown to be obeyed under the experimental conditions used. The corrections required to allow for the nonuniformity of radical concentrations in the cell were small. After delineating the experimental conditions necessary to minimize secondary reactions, the rate constant (cm^3 $mole^{-1}$ s^{-1}) for the reaction $C_2H_5 + H_2 = C_2H_6 + H$ was found to be given by $\log_{10} k = 12.5_7 - 13.7/\theta$. Experiments in the presence of added carbon dioxide showed the absence of hot radical effects at the working pressure of 92 Torr of hydrogen.

Canadian Journal of Chemistry, 46, 3275 (1968)

Can. J. Chem. Downloaded from www.nrcresearchpress.com by 210.87.254.6 on 09/05/12
For personal use only.

Relatively few atom transfer reactions of the type $R + X_2 = RX + X$, where X = H or D, have been studied (1–3), and in the even fewer cases where the reaction of a given radical with both H_2 and D_2 has been investigated there is some doubt about the magnitude of the isotope effect on the activation energy. For n-C_3F_7 radicals, values of 14.0 (4) and 13.8 (5) kcal $mole^{-1}$ have been found for the reaction with D_2, 1.9 (4) and 1.5 (5) kcal $mole^{-1}$ greater than for the reaction with H_2. For the reaction of C_2F_5 with D_2 and H_2 (4) the activation energies were almost the same: 12.6 and 12.4 kcal $mole^{-1}$, respectively. An intermediate isotope effect was found in the case of CF_3; values of 9.5 (6) and 10.2 (7) kcal $mole^{-1}$ were found for the reaction with D_2, 0.9 (6) and 0.7 (7) kcal $mole^{-1}$ greater than for the reaction with H_2, although the probable errors quoted by the authors in these cases were such that a negligible isotope effect would also be compatible with their results. In the case of C_2H_5 radicals the value found for the reaction with D_2 was 13.3 kcal $mole^{-1}$ (8) while the value for the reaction with H_2 (9), as subsequently corrected (10), was only 11.3 kcal $mole^{-1}$.

The apparent isotope effect for C_2H_5 radicals (8, 10), 2.0 kcal $mole^{-1}$, is very close to the difference between the zero point energies of H_2 and D_2. However, there is no theoretical justification for equivalence with zero point energy differences, and recent measurements in this laboratory (11) show no such correlation in the case of the three-center exchange reactions of atomic and molecular hydrogen and deuterium.

If we accept a value of 6.8 kcal $mole^{-1}$ (12) or greater (13) for the activation energy of the reaction

$$H + C_2H_6 = C_2H_5 + H_2$$

and a value of about 6.2 kcal $mole^{-1}$ (14, 15) for $-\Delta H$, then the activation energy for the reaction

$$C_2H_5 + H_2 = C_2H_6 + H$$

should be $\geqslant$13.0 kcal $mole^{-1}$. In view of the uncertainty in this value we felt it necessary to reinvestigate the reaction.

Aside from possible errors in the interpretation of the earlier results (9), our present knowledge of quantitative photosensitization suggests that the conditions used in the earlier investigation were far from being ideal. Another factor which cannot be neglected in producing ethyl radicals by the mercury-photosensitized hydrogenation of ethylene is the exothermicity of the reaction

$$H + C_2H_4 = C_2H_5$$

which amounts to about 40 kcal $mole^{-1}$ (16). Although there is some question about the efficacy of vibrational energy in bringing about a bimolecular reaction (17, 18), the presence of vibrationally hot ethyl radicals could, conceivably, cause an apparent lowering of the activation energy of the abstraction reaction.

In the present study of the abstraction of hydrogen atoms from H_2 by ethyl radicals we again chose the method of mercury photosensitization to produce the ethyl radicals. This avoided problems arising from the abstraction

[1]Present address: Research Department, Imperial Oil Enterprises Ltd., Sarnia, Ontario.

of hydrogen from photolytic sources of ethyl radicals, such as diethyl ketone, and at the same time it permitted us to gain some insight into possible hot radical effects. It also enabled us to further the development of mercury photosensitization as a quantitative tool.

Experimental

Chemicals

All gases were supplied by Matheson, with the exception of ethylene, which was Phillips research grade. Hydrogen was purified by passage through Deoxo units and silica gel traps cooled with liquid nitrogen. Gas chromatographic analysis did not reveal any measurable amounts of impurities.

Apparatus

The reaction vessel was a quartz cylinder 5 cm in diameter and 6 cm long; it was connected to a circulating system which included a glass–Teflon magnetically operated circulating pump which had a capacity of approximately 900 cm^3 min^{-1}. The cell was contained in a close-fitting aluminium block furnace with quartz windows on each end.

A considerable amount of emphasis was placed on the accurate control of the mercury vapor concentration in the cell and on the measurement of light intensities. The former was obtained by including in the circulating system a pre-saturator containing dispersed mercury and kept at a temperature of 6° to 10° above the ultimate saturating temperature, and then a final saturator consisting of four traps immersed in a single accurately controlled thermostat. The mercury lamp was of the low pressure rare gas type with water-cooled electrode chambers (19); these were maintained at 30 ± 0.03 °C. The lamp was housed in an aluminium box with an aperture in front of the entrance window of the cell furnace. The incident and transmitted light was monitored by a double-beam system which included two Westinghouse WL-775 diode photocells, associated bridge circuits, and a dynamic capacitor electrometer; these particular photocells are insensitive to light from the lamp at wavelengths greater than 2537 Å.

Analysis of Products

At the end of a run, liquid nitrogen was placed on a trap adjacent to the cell and circulation was maintained until all condensables were frozen out. The trap was then isolated and warmed to room temperature. The contents were then swept into the first of two gas chromatographic columns using hydrogen as the carrier gas. Column A was a 23-ft length of ¼-in. copper tubing containing 20% by weight of bis-2-(2-methoxyethoxy)ethyl ether on 60/80 mesh Chromasorb-P. Column B was a 6-ft length of ¼-in. copper tubing containing 60-mesh activated silica gel. By means of a two-column switching device, only ethane and ethylene were allowed to enter column B.

Known amounts of acetylene (shown not to be one of the products) were swept from a calibrated chamber by the carrier gas and used as a reference. Ethane and ethylene were eluted from column B at 30 °C using a flow rate of 40 cm^3 min^{-1}; *n*-butane, butene-1, and acetylene were eluted at 0 °C with a flow rate of 47 cm^3 min^{-1}; *n*-hexane was eluted at 50 °C with a flow rate of 61 cm^3 min^{-1}. The quantitative analysis of every product was based on its calibrated relative molar response, i.e. its peak area relative to that for the known amounts of acetylene. The calibration was done using standard samples containing the pertinent compounds in concentrations approximating those in the reaction products. When large amounts of carbon dioxide were present this was irreversibly absorbed in a trap containing 20-mesh Ascarite, placed ahead of column A.

Results and Discussion

Under proper experimental conditions the most important reactions occurring will be the following:

$$[1] \quad Hg(6^3P_1) + H_2 = Hg(6^1S_0) + 2H$$

$$[2] \quad H + C_2H_4 = C_2H_5$$

$$[3] \quad 2C_2H_5 = C_4H_{10}$$

$$[4] \quad 2C_2H_5 = C_2H_6 + C_2H_4$$

$$[5] \quad C_2H_5 + H_2 = C_2H_6 + H$$

At the lowest pressures of hydrogen used (92 Torr) the quenching of $Hg(6^3P_1)$ atoms is essentially complete. Even at the largest pressures of ethylene used (ca. 4 Torr) only a small amount of quenching will be done by ethylene; a negligible amount by the products. The rate of reaction [1] can then be equated to ϕI_a, where ϕ is slightly less than unity and I_a is the *local* rate of absorption of the resonance radiation. A steady-state treatment of reactions [1] to [5], inclusive, which we will refer to as the *basic mechanism*, gives the result:

$$[i] \quad d(C_2H_6)/dt = \phi I_a k_4/(k_3 + k_4) + (\phi I_a)^{\frac{1}{2}}(H_2)k_5/(k_3 + k_4)^{\frac{1}{2}}$$

$$[ii] \quad d(C_4H_{10})/dt = \phi I_a k_3/(k_3 + k_4)$$

Assuming, for the moment, the validity of the *basic mechanism*, information about k_5 could be obtained by varying (H_2) at constant I_a, or by varying I_a at constant (H_2). The former method was used by Le Roy and Kahn (9), but it involves problems relating to the constancy of I_a and ϕ with pressure broadening of the absorption line and changes in the composition of the reaction mixture. Since knowledge of I_a is required in any event, we have used the second method in the present work. By keeping both (C_2H_4) and (H_2) constant in a given series of experiments both ϕ and I_a can more easily be kept under quantitative control, the latter by controlling the

Can. J. Chem. Downloaded from www.nrcresearchpress.com by 210.87.254.6 on 09/05/12
For personal use only.

Can. J. Chem. Downloaded from www.nrcresearchpress.com by 210.87.254.6 on 09/05/12
For personal use only.

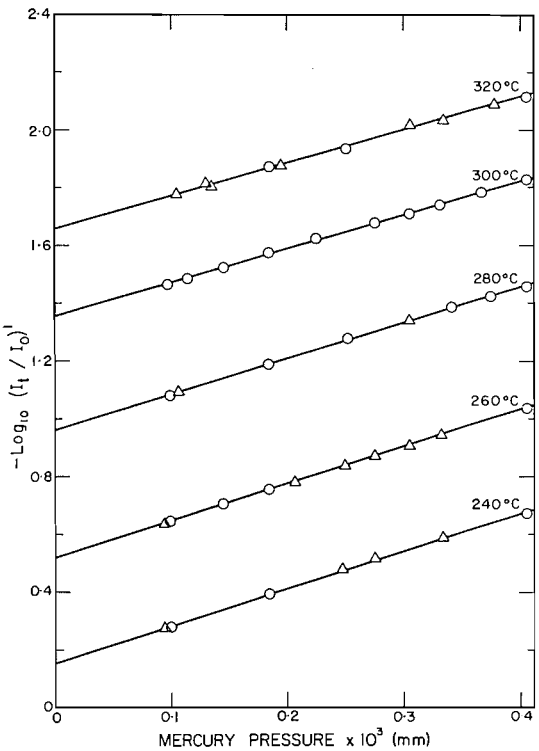

FIG. 1. Beer's law plots for the absorption of 2537 Å. $(I_t/I_0)'$ is the ratio of the photocurrent originating from the transmitted beam to that from the reference beam. ○, Hydrogen pressure 93.0 Torr; △, hydrogen pressure 92.0 Torr; ethylene pressure 0.80 Torr. Ordinates increased by 0.35, 0.80, 1.20, and 1.50 for 260, 280, 300, and 320 °C, respectively.

incident light intensity and/or the mercury concentration.

By varying the experimental conditions, we have been able to find those for which the *basic mechanism* is valid to a high degree of accuracy. This preliminary work will be described first.

Rate of Light Absorption

It is not generally recognized that Beer's law is obeyed for the absorption of 2537 Å radiation for the lamps, and some of the mercury vapor concentrations, frequently used in mercury photosensitization. Some years ago Pinder and Le Roy (20) found that ε in the expression

$$[iii] \qquad I_t/I_0 = e^{-\varepsilon(\text{Hg})L}$$

was essentially constant for values of (Hg)L less than 2×10^{-3} Torr cm, having a value of 1.5×10^{-14} cm^2 atom^{-1} in the presence of 300 Torr of propane. McAlduff and Le Roy (21) found that ε had a constant value of 0.56×10^{-14} cm^2 atom^{-1} for $L = 28$ cm, (Hg) in the range 0.6×10^{-4} Torr to 1.8×10^{-4} Torr, and in the presence of 8 Torr or less of nitrogen. Beer's law was still obeyed but pressure broadening raised the value of ε to 1.6×10^{-14} cm^2 atom^{-1} in the presence of 80 Torr of nitrogen. The values of ε obtained are applicable to the kind of lamp used, and are generally smaller than those *calculated* by the method of Mitchell and Zemansky (22).

In order to calculate the *local* and *average* rates of light absorption in the present experiments, we investigated the validity of Beer's law for a series of temperatures, mercury concentrations, and substrate compositions. As shown in Fig. 1, Beer's law is obeyed for mercury pressures in the range up to 4×10^{-4} Torr with an optical path length of 6 cm and in the presence of 92 Torr of hydrogen. The value of ε is unaffected by the addition of 0.8 Torr of ethylene. It is also independent of temperature in the range 240 to 320 °C. Its average value was $2.6_9 \times 10^{-14}$ cm^2 atom^{-1} with a mean deviation over the range of 0.03×10^{-14} cm^2 atom^{-1}.

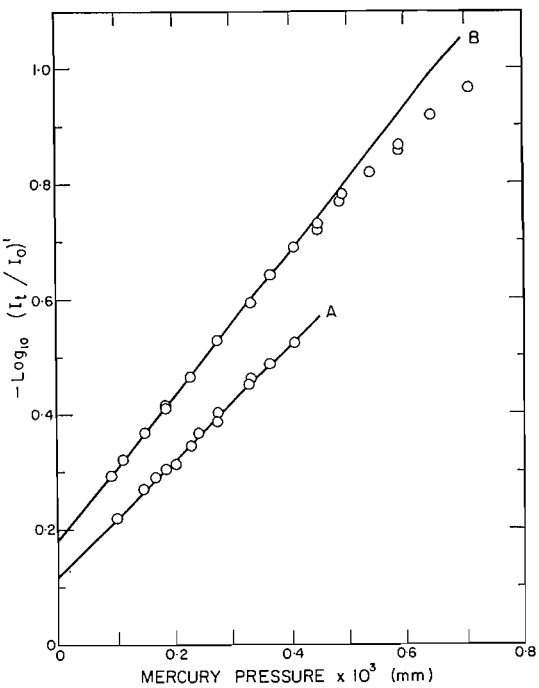

FIG. 2. Beer's law plots at 240 °C. A, 94.2 Torr hydrogen plus 301 Torr carbon dioxide. B, 92.3 Torr hydrogen; ordinate increased by 0.075.

Can. J. Chem. Downloaded from www.nrcresearchpress.com by 210.87.254.6 on 09/05/12
For personal use only.

The addition of 301 Torr of carbon dioxide *lowers* the value of ε (to $2.0_6 \times 10^{-14}$ cm^2 atom^{-1}) as shown in curve *A* of Fig. 2. Curve *B* of Fig. 2 shows that the upper limit for the validity of Beer's law is reached for a mercury pressure of about 4×10^{-4} Torr, for a path length of 6 cm. For this reason all definitive experiments in the present research were done with mercury pressures less than or equal to this value.

Reactions Likely to Affect the Validity of the Basic Mechanism

Evidence for the occurrence of reaction [6]

[6] $$H + C_2H_5 = C_2H_6$$

in systems similar to the present one has been given previously (23, 17). Since the basic requirement is that (H) become comparable with (C_2H_5) in order that [6] compete with [3] or [4] it would be favored by low ethylene concentrations which would permit (H) to increase relative to (C_2H_5). It would also be favored by reasonably high total pressures because the exothermicity is greater than the C—C bond dissociation energy and without deactivation we would expect atomic cracking leading to CH_3, rather than C_2H_6, formation. The lowest total pressures used were of the order of 92 Torr, and no evidence was found for odd-numbered hydrocarbons. There is, therefore, no evidence for atomic cracking. However, as shown in Fig. 3, ethane formation increases sharply at low ethylene pressures, which we attribute to reaction [6]. Since the *basic mechanism* predicts that the rate of ethane formation is independent of ethylene concentration, it will not be valid if the ethylene concentration is too low.

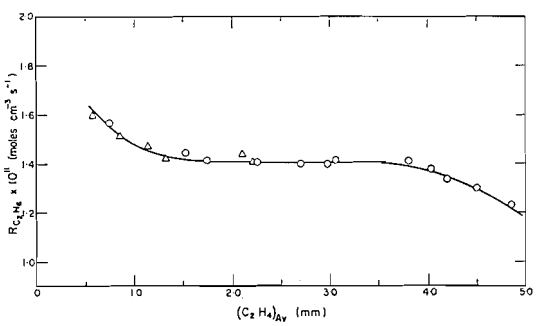

FIG. 3. Rate of ethane formation as a function of average ethylene pressure at 240 °C. ○, 93.0 Torr hydrogen; △, 93.0 Torr hydrogen and 308 Torr carbon dioxide. Corrected to constant average light absorption.

Some years ago, Pinder and Le Roy (20) made a detailed study of reaction [7] using a system similar to the present one,

[7] $$C_2H_5 + C_2H_4 = C_4H_9$$

but at temperatures ($\leqslant$123 °C) at which reaction [5] was of no importance and with ethylene pressures (20–50 Torr) considerably higher than those used in the present work. Since [7] is a chain-stopping step it would deplete the ethyl radical concentration and lead to low values of (C_2H_6). It was therefore important to ascertain the upper limits for the ethylene concentrations that would minimize the importance of [7] as well as the reactions which would follow from it. That such upper limits exist is illustrated by the decrease in the rate of ethane production at high ethylene pressures shown in Fig. 3.

One of the reactions sequential to [7] is [8]:

[8] $$C_4H_9 + H_2 = n\text{-}C_4H_{10} + H$$

This will be favored at high concentrations of hydrogen and at the high concentrations of ethylene required for the formation of butyl radicals by [7]. Since its kinetic parameters will be similar to those of reaction [5] it will be considerably more important at high temperatures than at low temperatures. The important influence of hydrogen pressure and ethylene pressure at 320 °C is shown in Fig. 4. To minimize the effect of reaction [8] at this temperature requires ethylene pressures less than 1 Torr and hydrogen pressures less than 100 Torr. Higher ethylene pressures could be used at lower temperatures.

Other reactions sequential to [7] are:

[9] $$C_4H_9 + C_2H_5 = n\text{-}C_6H_{14}$$

and

[10] $$C_4H_9 + C_2H_5 = C_4H_8 + C_2H_6$$

As would be expected, small amounts of *n*-hexane were found under conditions favoring reaction [7]; butene-1 was also found under similar conditions but in considerably smaller quantities. Reaction [10] is a negligible source of ethane even at high ethylene pressures, but the rate of formation of butene-1 correlates nicely with the ethylene pressure, as shown in Fig. 5.

Evaluation of $k_5/k_3^{\frac{1}{2}}$

It will be evident from the foregoing that by careful adherence to the proper experimental conditions, values of $k_5/k_3^{\frac{1}{2}}$ can be obtained by using the *basic mechanism*.

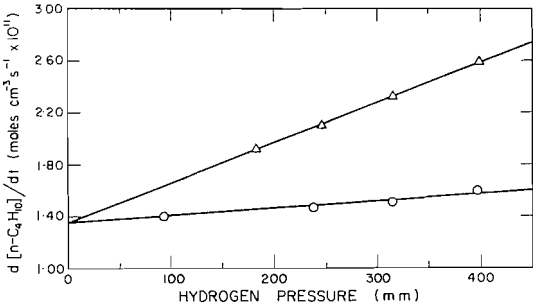

FIG. 4. Effect of ethylene and hydrogen pressures on the rate of formation of *n*-butane at 320 °C. Rate of light absorption 1.78×10^{-11} einstein cm^{-3} s^{-1}. ○, Average ethylene pressure 0.69 Torr; △, average ethylene pressure 4.62 Torr.

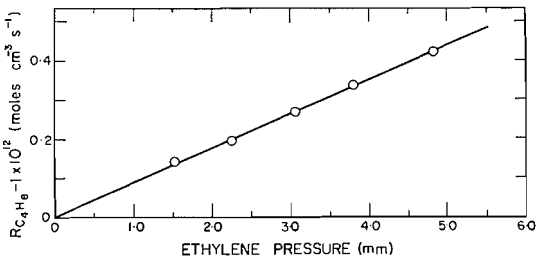

FIG. 5. Rate of formation of butene-1 as a function of the average ethylene pressure at 240 °C. Hydrogen pressure 93.4 Torr; rate of light absorption 1.16×10^{-11} einstein cm^{-3} s^{-1}.

To obtain expressions for the *observed* rates of formation of ethane and butane in the cell, it is necessary to integrate the *local* rates given in eqs. [*i*] and [*ii*]. The rate of light absorption per unit volume from a homogeneous parallel beam at a distance x cm from the entrance window is given by

$$[iv] \qquad I_a = I_0\varepsilon(\mathrm{Hg})e^{-\varepsilon(\mathrm{Hg})x}$$

where I_0 is the incident light intensity per unit area. By performing the necessary integrations it can be seen that the *basic mechanism* predicts that the ratio of the observed rates of formation of ethane and butane will be given by the expression

$$[v] \qquad \frac{R_{C_2H_6}}{R_{C_4H_{10}}} = \frac{k_4}{k_3} + \frac{k_5(H_2)}{k_3^{\frac{1}{2}}(R_{C_4H_{10}})^{\frac{1}{2}}}\delta$$

where

$$[vi] \qquad \delta = \frac{2(1 - e^{-\varepsilon(\mathrm{Hg})L/2})}{[\varepsilon(\mathrm{Hg})L(1 - e^{-\varepsilon(\mathrm{Hg})L})]^{\frac{1}{2}}}$$

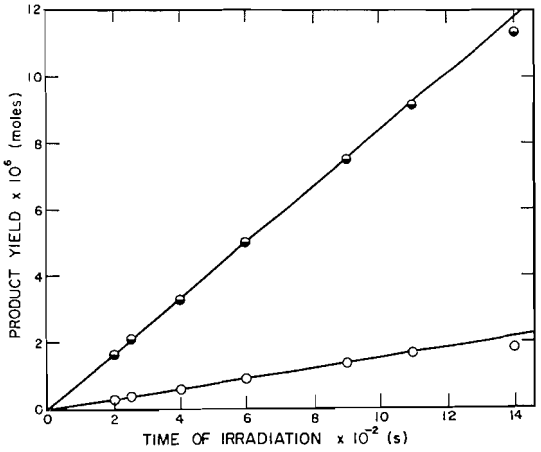

FIG. 6. Formation of ethane, ◒, and *n*-butane, ○, as functions of irradiation time at 320 °C. Initial ethylene pressure 0.77 Torr; hydrogen pressure 93.3 Torr; average rate of light absorption 1.78×10^{-11} einstein cm^{-3} s^{-1}.

By restricting (Hg) to $\leqslant 4 \times 10^{-4}$ Torr, all values of δ were only slightly less than unity. Although the maximum deviation from unity was only 1.5%, corrections were made in every case.

In all of the runs used to evaluate $k_5/k_3^{\frac{1}{2}}$, the hydrogen pressure was kept constant at 92 Torr. The average ethylene pressure for a given experiment ranged from 0.68 Torr to 2.26 Torr, depending on the conditions required. The average rate of light absorption in the cell was varied[2] from about 1.4×10^{-12} to 16×10^{-12} einstein cm^{-3} s^{-1}. The rates of formation of ethane and butane were constant with time up to quite large conversions; for the experiment illustrated in Fig. 6 the amount of ethylene consumed was 31.4%. The consumption of ethylene was usually limited to the range 4 to 15%, except at 320 °C where up to 24% was required for analytical purposes.

Plots of $R_{C_2H_6}/R_{C_4H_{10}}$ against $(H_2)\delta/(R_{C_4H_{10}})^{\frac{1}{2}}$ are shown in Fig. 7 for five temperatures in the range 240 °C to 320 °C. An Arrhenius plot of the slopes of these curves is given in Fig. 8. The derived parameters, together with their standard deviations, are:

$$A_5/A_3^{\frac{1}{2}} = 9.1_2 \pm 1.2 \times 10^5 \text{ cm}^{3/2} \text{ mole}^{-1/2} \text{ s}^{-1/2}$$

$$E_5 - E_3/2 = 13.7_3 \pm 0.2_6 \text{ kcal mole}^{-1}$$

[2]Based on the rate of formation of products at room temperature, where there is no chain reaction.

Can. J. Chem. Downloaded from www.nrcresearchpress.com by 210.87.254.6 on 09/05/12
For personal use only.

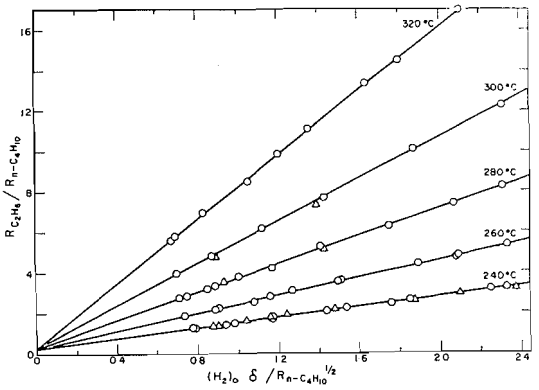

FIG. 7. Ratio of the rates of formation of ethane to butane in terms of eq. [v]. ○, 92 Torr hydrogen; △, 92 Torr hydrogen, 300 Torr carbon dioxide.

Taking $\log_{10} A_3 = 13.3_4(1)$ and $E_3 = 0$,

$$\log_{10} k_5 = 12.5_7 - 13.7_3/\theta$$

where $\theta = 2.303 \times 1.987 \times 10^{-3}T$, and k_5 is in $cm^3\ mole^{-1}\ s^{-1}$.

The A factors for reactions [5] and [11] are related by the expression

$$[vii] \qquad A_5/A_{11} = e^{\Delta S^0/R}$$

in which ΔS^0 is the standard entropy change for reaction [5].

$$[11] \qquad H + C_2H_6 = C_2H_5 + H_2$$

Using the known values of S^0_{298} for H_2 (31.21 e.u.), C_2H_6 (54.85 e.u.), and H (27.39 e.u.) (24), and the estimated value of 59.11 e.u. for C_2H_5 (25, 26), $\Delta S^0_{298} = -8.08$ e.u. Combining this with the value of A_5 obtained in the present investigation, we calculate that A_{11} should be $2.1 \times 10^{14}\ cm^3\ mole^{-1}\ s^{-1}$. This is much nearer the value estimated by Baldwin and Melvin (13) (1.5×10^{14}) than that given by Berlie and Le Roy (12) (3.4×10^{12}). It is also in line with the A factors found for H atom abstraction from other hydrocarbons (2).

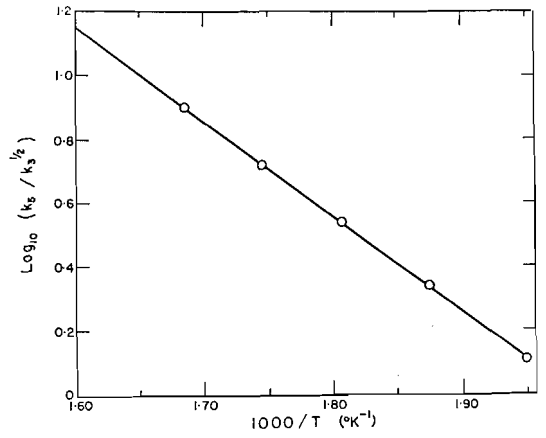

FIG. 8. Arrhenius plot for $k_5/k_3^{\frac{1}{2}}$.

The value of E_{11} obtained by Berlie and Le Roy (12) (6.8 kcal $mole^{-1}$) would also appear to be low. Thus, if we accept the value of 6.2 kcal $mole^{-1}$ for ΔH^0_{298} for reaction [5] (14, 15) and the value of E_5 obtained in the present investigation, E_{11} would be 7.5 kcal $mole^{-1}$. This is appreciably less than the value of 9.7 kcal $mole^{-1}$ given by Baldwin and Melvin (13). Whether, in view of the uncertainty in ΔH^0_{298} and its temperature coefficient, the discrepancy of 0.7 kcal $mole^{-1}$ relative to the value of Berlie and Le Roy (12) is significant or not is doubtful. However, they did not correct their results for diffusion effects (27) and we believe that this would lead to a value of E_{11} that would be slightly too low.

Disproportionation and Combination of Ethyl Radicals

It is evident from eq. [v] that the intercepts of Fig. 7 should give values of k_4/k_3. Because of the extrapolations involved these are rather uncertain. Values ranged from 0.256 ± 0.074 at 532 °K to 0.284 ± 0.055 at 593 °K. A number of experiments done at room temperature gave a value of 0.132 ± 0.017, in good agreement with generally accepted values (1, 2).

We are inclined to believe that the present results give some support for a positive temperature coefficient for k_4/k_3. If we treat the average values for each temperature as if they were single measurements and apply least squares, the value of $E_4 - E_3$ is found to be 0.906 ± 0.030 kcal $mole^{-1}$ and $\log_{10} A_4/A_3$ is -0.213 ± 0.014. The standard deviations given present, of course, a rather too favorable view of the precision, since the standard deviations at each temperature are quite large.

Possible Hot Radical Effects

To study the effect of excess vibrational energy on the *unimolecular* decomposition of free radicals (16) it is usually necessary to use lower pressures than those used in the present research. However, in the present system the molecules most likely to deactivate the hot radicals formed in reaction [2] are the same ones which undergo

Can. J. Chem. Downloaded from www.nrcresearchpress.com by 210.87.254.6 on 09/05/12
For personal use only.

Can. J. Chem. Downloaded from www.nrcresearchpress.com by 210.87.254.6 on 09/05/12
For personal use only.

reaction [5]. Even at a hydrogen pressure of 92 Torr it was therefore necessary to use an inert third body to ascertain whether the rate of [5] was being enhanced because some of the ethyl radicals were vibrationally hot.

Carbon dioxide was used for this purpose and the effect of its presence on ϕ and ε taken into account. As shown in Fig. 7, the presence of 300 Torr of carbon dioxide had no effect on the value of k_5.

The conclusions to be drawn from this are not clear cut. We knew already, before doing experiments with carbon dioxide, that every collision of a hot ethyl radical with a hydrogen molecule did not lead to reaction; otherwise k_5 would be independent of temperature. This would be a reasonable prediction in any event because of the large number of vibrational degrees of freedom in the radical. It would seem reasonable to assume that if excess vibrational energy can be effective in supplying some or all of the critical energy for a bimolecular reaction such as [5] it would have to be localized in some way. For an ethyl radical the probability of such localization would likely be appreciably less than unity, so that the probability of deactivation, rather than reaction, on collision with an H_2 molecule would be large. The fact that 300 Torr of carbon dioxide caused no decrease in the rate of [5] from that obtained in the presence of 92 Torr of hydrogen is in keeping with such a model, as well as with the alternative assumption that vibrational energy is completely ineffective.

As shown in Fig. 3, the addition of carbon dioxide is also ineffective in changing the rate of formation of ethane at low ethylene concentrations, where the evidence suggests that reaction [6] is coming into play. It is not surprising that an *increase* in the rate of formation of ethane was not observed under these conditions, because this would have implied that in the absence of carbon dioxide, excited ethane molecules formed in [6] were decomposing by [12].

[12] $$C_2H_6\dagger = 2CH_3$$

The absence of odd-numbered hydrocarbons showed that this was not the case.

Acknowledgments

The authors are grateful to the National Research Council of Canada for continued financial support, and for the award of scholarships to one of us (L.E.R.). We also wish to thank the Senate of the University of Toronto and Canadian Industries Limited for the award of a C.I.L. Fellowship (to L.E.R.).

1. J. A. Kerr and A. F. Trotman-Dickenson. Progr. Reaction Kinetics, **1**, 105 (1961).
2. S. W. Benson and W. B. De More. Ann. Rev. Phys. Chem. **16**, 397 (1965).
3. J. M. Tedder and J. C. Walton. Progr. Reaction Kinetics, **4**, 37 (1967).
4. G. O. Pritchard and J. K. Foote. J. Phys. Chem. **68**, 1016 (1964).
5. G. H. Miller and E. W. R. Steacie. J. Am. Chem. Soc. **80**, 6486 (1958).
6. G. O. Pritchard, H. O. Pritchard, H. I. Schiff, and A. F. Trotman-Dickenson. Trans. Faraday Soc. **52**, 849 (1956).
7. P. B. Ayscough and J. C. Polanyi. Trans. Faraday Soc. **52**, 960 (1956).
8. M. J. Wijnan and E. W. R. Steacie. J. Chem. Phys. **20**, 205 (1952).
9. D. J. Le Roy and A. Kahn. J. Chem. Phys. **15**, 816 (1947).
10. G. R. Hoey and D. J. Le Roy. Can. J. Chem. **33**, 580 (1955).
11. D. J. Le Roy, B. A. Ridley, and K. A. Quickert. Discussions Faraday Soc. In press. 1967.
12. M. R. Berlie and D. J. Le Roy. Discussions Faraday Soc. **14**, 50 (1953).
13. R. R. Baldwin and A. Melvin. J. Chem. Soc. 1785 (1964).
14. S. W. Benson. J. Chem. Educ. **42**, 502 (1965).
15. J. A. Kerr. Chem. Rev. **66**, 465 (1966).
16. B. S. Rabinovitch and D. W. Setser. Advan. Photochem. **3**, 1 (1964).
17. R. J. Cvetanović. Advan. Photochem. **1**, 115 (1963).
18. R. R. Baldwin, R. F. Simmons, and R. W. Walker. Trans. Faraday Soc. **62**, 2486 (1966).
19. H. W. Melville. Trans. Faraday Soc. **32**, 1525 (1936).
20. J. A. Pinder and D. J. Le Roy. Can. J. Chem. **35**, 588 (1957).
21. J. E. McAlduff and D. J. Le Roy. Can. J. Chem. **43**, 2279 (1965).
22. A. C. G. Mitchell and M. W. Zemansky. Resonance radiation and excited atoms. Cambridge University Press, London. 1934.
23. M. J. Smith, P. A. Beatty, J. A. Pinder, and D. J. Le Roy. Can. J. Chem. **33**, 821 (1955).
24. F. D. Rossini, K. S. Pitzer, R. L. Arnett, R. M. Braun, and G. C. Pimentel (*Editors*). Selected values of physical and thermodynamic properties of hydrocarbons. American Petroleum Institute Research Project 44. Carnegie Press, Pittsburgh. 1953.
25. W. M. D. Bryant. J. Polymer Sci. **6**, 359 (1951).
26. J. C. Calvert and J. N. Pitts, Jr. Photochemistry. John Wiley and Sons, Inc., New York. 1966.
27. W. R. Schulz and D. J. Le Roy. Can. J. Chem. **40**, 2413 (1962).

Can. J. Chem. Downloaded from www.nrcresearchpress.com by 210.87.254.40 on 09/05/12
For personal use only.

Thermal reactions of propylene oxide[1]

ARTHUR T. BLADES
Research Council of Alberta, Edmonton, Alberta

Received January 17, 1967[2]

Heterogeneous reactions have been shown to contribute to the formation of propionaldehyde, acetone, and allylol in the pyrolysis of propylene oxide. Methyl vinyl ether, however, is formed entirely homogeneously and may be an intermediate in the oxygen atom – propylene system.

Canadian Journal of Chemistry, 46, 3283 (1968)

Recent data on the pyrolysis of ethylene oxide (1, 2) have been explained on the basis of the primary formation of "hot" acetaldehyde followed either by its unimolecular decomposition or collisional deactivation. A similar scheme has been proposed for propylene oxide (2) for which the expected products would be acetone and propionaldehyde. While these rearrangement products were observed in preliminary pyrolyses in a static system, two additional isomers were also identified, allylol and methyl vinyl ether. Carbon monoxide, methane, ethane, and ethylene were also formed, and their rates of formation appeared to increase with reaction time, suggestive of a free radical decomposition of the primary products. In order to minimize these secondary processes, all further studies were carried out with a 1:1 mixture of propylene oxide and propylene and at conversions not exceeding 10%. Under these conditions, the fragmentation products were essentially eliminated.

In the study of the rearrangement reactions, difficulty was experienced in obtaining reproducibly conditioned reactor surfaces. Doubling the surface of a pyrex reactor by the insertion of an open ended tube greatly enhanced the rate of propionaldehyde, acetone, and allylol formation, while coating with silver chloride reduced the rates of these reactions. On the other hand, the rate of formation of methyl vinyl ether was virtually unaffected by these surface conditions. Studies of the rates of formation of propionaldehyde, allylol, and methyl vinyl ether in the seasoned pyrex and silver chloride coated reactors

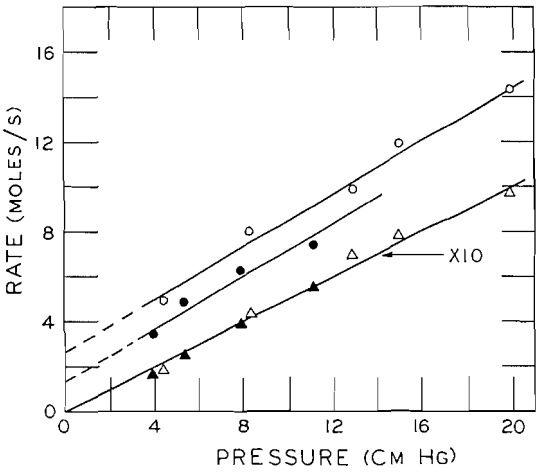

FIG. 1. Initial rates of formation of propionaldehyde (circles) and methyl vinyl ether (triangles) × 10 vs. total pressure at 413°: (○, △) seasoned pyrex reactor; (●, ▲) silver chloride coated reactor.

as a function of pressure at 413° are shown in Figs. 1 and 2. The propionaldehyde data give a constant slope and variable intercept which would imply a zero order, surface dependent process, and a first order, surface independent process. The allylol data is less definite and, in view of the drastic dependence on surface, may be totally heterogeneous in origin. Only the production of methyl vinyl ether gives a zero intercept and surface independence, and is therefore almost certainly an exclusively homogeneous rearrangement product.

Methyl vinyl ether has not been observed in the oxygen atom addition to propylene where excited propylene oxide is the primary product and propionaldehyde and acetone arise from its

[1]Contribution No. 418 from the Research Council of Alberta, Edmonton, Alberta.
[2]Revision received May 24, 1968.

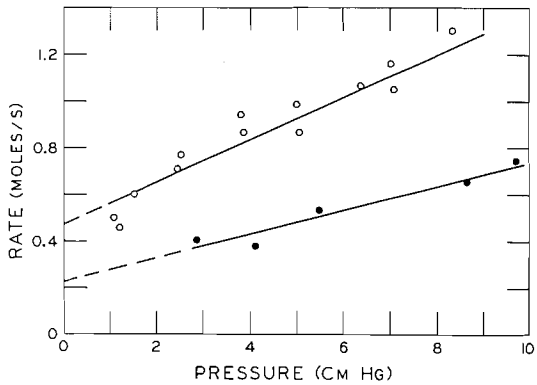

FIG. 2. Initial rates of formation of allyl alcohol vs. total pressure at 413°: (○) seasoned pyrex reactor; (●) silver chloride coated reactor.

rearrangement (3). If methyl vinyl ether is also a secondary product in this reaction, it would have about 90 kcal/mole of excess energy, and this is much greater than the 50 kcal/mole[3] activation energy for its rearrangement to propionaldehyde. Under these circumstances it would not survive long enough to be collisionally stabilized and thus does not appear as a product in the oxygen atom – propylene system.

Thus, while persistent heterogeneous reactions have frustrated the original purpose of this study of the thermal reactions of propylene oxide, a new process has been observed which may be of interest in other systems where it is not directly observable.

1. M. L. NEUFELD and A. T. BLADES. Can. J. Chem. **41**, 2956 (1963).
2. S. W. BENSON. J. Chem. Phys. **40**, 105 (1964).
3. R. J. CVETANOVIĆ. Can. J. Chem. **36**, 623 (1958).

[3]A. T. Blades. Unpublished results.

The γ-radiolysis of cyclohexane with electron scavengers. V. C_6F_{12} as an electron scavenger in the vapor phase[1]

N. H. SAGERT AND A. S. BLAIR[2]
Research Chemistry Branch, Chalk River Nuclear Laboratories, Chalk River, Ontario

Received April 1, 1968

The radiolysis of cyclohexane in the vapor phase has been examined in the presence of up to 3 mole % perfluorocyclohexane. The results indicate that perfluorocyclohexyl radicals are produced with a yield of 2.0 *G* units at 3% perfluorocyclohexane. It is concluded that these radicals are formed when the perfluorocyclohexyl anions are neutralized. The relevance of this neutralization to the liquid phase radiolysis of cyclohexane is discussed.

Canadian Journal of Chemistry, 46, 3284 (1968)

Introduction

The radiolysis of liquid cyclohexane using perfluorocyclohexane (PCH) as an electron scavenger has been examined previously (1–3) and evidence has been presented that about one carbon–fluorine bond is broken for each electron scavenged (1). Two possible mechanisms by which this bond breaking could occur were discussed. Dissociation of the PCH anion formed by electron capture could occur;

[1] $$e^- + C_6F_{12} \rightarrow C_6F_{12}^-$$

[2] $$C_6F_{12}^- \rightarrow C_6F_{11} + F^-$$

or bond breaking could occur on neutralization.

[3] $$C_6F_{12}^- + C_6H_{12}^+ \rightarrow C_6F_{11} + C_6H_{11} + HF$$

Although reaction [2] is 1.8 eV endothermic in the gas phase (4), it could conceivably take place in the liquid because of solvation effects. We have, therefore, studied the radiolysis of cyclohexane vapor with PCH in an attempt to decide between these alternatives, since reaction [2] can be ruled out in the gas phase.

A considerable yield of C_6F_{11} radicals was indicated (~ 2.0 *G* units) thus showing that bond breaking can take place in the neutralization step. However, the low efficiency observed suggests

[1]Issued as A.E.C.L. No. 2729.
[2]A.E.C.L. Summer Student, 1967. Present address: Department of Chemistry, University of Toronto, Toronto, Ontario.

Can. J. Chem. Downloaded from www.nrcresearchpress.com by 210.87.254.40 on 09/05/12
For personal use only.

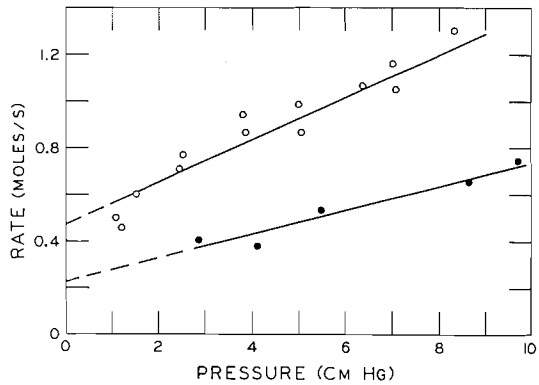

FIG. 2. Initial rates of formation of allyl alcohol vs. total pressure at 413°: (○) seasoned pyrex reactor; (●) silver chloride coated reactor.

rearrangement (3). If methyl vinyl ether is also a secondary product in this reaction, it would have about 90 kcal/mole of excess energy, and this is much greater than the 50 kcal/mole[3] activation energy for its rearrangement to propionaldehyde. Under these circumstances it would not survive long enough to be collisionally stabilized and thus does not appear as a product in the oxygen atom – propylene system.

Thus, while persistent heterogeneous reactions have frustrated the original purpose of this study of the thermal reactions of propylene oxide, a new process has been observed which may be of interest in other systems where it is not directly observable.

1. M. L. NEUFELD and A. T. BLADES. Can. J. Chem. **41**, 2956 (1963).
2. S. W. BENSON. J. Chem. Phys. **40**, 105 (1964).
3. R. J. CVETANOVIĆ. Can. J. Chem. **36**, 623 (1958).

[3]A. T. Blades. Unpublished results.

The γ-radiolysis of cyclohexane with electron scavengers. V. C_6F_{12} as an electron scavenger in the vapor phase[1]

N. H. SAGERT AND A. S. BLAIR[2]
Research Chemistry Branch, Chalk River Nuclear Laboratories, Chalk River, Ontario

Received April 1, 1968

The radiolysis of cyclohexane in the vapor phase has been examined in the presence of up to 3 mole % perfluorocyclohexane. The results indicate that perfluorocyclohexyl radicals are produced with a yield of 2.0 *G* units at 3% perfluorocyclohexane. It is concluded that these radicals are formed when the perfluorocyclohexyl anions are neutralized. The relevance of this neutralization to the liquid phase radiolysis of cyclohexane is discussed.

Canadian Journal of Chemistry, 46, 3284 (1968)

Introduction

The radiolysis of liquid cyclohexane using perfluorocyclohexane (PCH) as an electron scavenger has been examined previously (1–3) and evidence has been presented that about one carbon–fluorine bond is broken for each electron scavenged (1). Two possible mechanisms by which this bond breaking could occur were discussed. Dissociation of the PCH anion formed by electron capture could occur;

[1] $$e^- + C_6F_{12} \rightarrow C_6F_{12}^-$$

[2] $$C_6F_{12}^- \rightarrow C_6F_{11} + F^-$$

or bond breaking could occur on neutralization.

[3] $$C_6F_{12}^- + C_6H_{12}^+ \rightarrow C_6F_{11} + C_6H_{11} + HF$$

Although reaction [2] is 1.8 eV endothermic in the gas phase (4), it could conceivably take place in the liquid because of solvation effects. We have, therefore, studied the radiolysis of cyclohexane vapor with PCH in an attempt to decide between these alternatives, since reaction [2] can be ruled out in the gas phase.

A considerable yield of C_6F_{11} radicals was indicated (~ 2.0 *G* units) thus showing that bond breaking can take place in the neutralization step. However, the low efficiency observed suggests

[1]Issued as A.E.C.L. No. 2729.
[2]A.E.C.L. Summer Student, 1967. Present address: Department of Chemistry, University of Toronto, Toronto, Ontario.

Can. J. Chem. Downloaded from www.nrcresearchpress.com by 210.87.254.6 on 09/05/12
For personal use only.

TABLE I

G values of selected products from the radiolysis of pure cyclohexane vapor

Product	*G* values			
	This work		Ref. 8	Ref. 9
	"0" dose (T = 133 °C)	2.3×10^{19} eV/g (T = 133 °C)	3×10^{19} eV/g (T = 100 °C)	3×10^{19} eV/g (T = 125 °C)
H_2	4.6	4.3	4.7	5.3
CH_4	0.5_5	0.4_1	0.36	0.6
C_6H_{10}	2.4_0	2.0	1.0	2.2
$(C_6H_{11})_2$	0.75	0.7	0.8	1.0

that neutralization may not be the only source of C_6F_{11} radicals in the radiolysis of the liquid.

Experimental

The sources of cyclohexane and PCH have been described (1). The ethylene was Phillips research grade (99.96 mole %).

The irradiation cells were Pyrex cylinders of 350 ml volume, 5.5 cm diameter, fitted with a breaking device (5). The cells were cleaned by heating in air to just below the softening point of Pyrex for 8 h, followed by heating at 350 °C for 18 h while being pumped to 10^{-6} Torr.

The cyclohexane was degassed on a mercury-free, grease-free vacuum line and stored over a sodium mirror. Samples of about 1.1 ml liquid volume were accurately measured out in a calibrated tube and transferred to the irradiation cell. PCH was weighed out roughly, degassed, and transferred to the irradiation cell. Its exact concentration was measured by gas chromatography after the irradiation (1).

Samples were irradiated at 133 °C ± 3 °C in a ^{60}Co γ-source at dose rates of 5.02×10^{17} eV/g min as determined by ethylene dosimetry using $G(H_2) = 1.31$ (6). The total dose given the cyclohexane was 2.26×10^{19} eV/g unless otherwise noted. Analytical procedures have been described previously (1). Mixed dimer was identified by mass spectrometry using a Consolidated 21–130 mass spectrometer. No authentic standards could be obtained to aid in identification, but only peaks characteristic of C_6H_{11} and C_6F_{11} groups were observed.

Results and Discussion

The radiolysis of liquid cyclohexane produces largely hydrogen, cyclohexene, and bicyclohexyl (7) but the radiolysis of cyclohexane vapor produces a wider variety of products (8, 9). Since we were primarily concerned with the neutralization processes, as outlined in the Introduction, we were interested mainly in those products derived directly from cyclohexyl radicals. Since there seems to be some uncertainty about the product yields from the radiolysis of pure cyclohexane vapor, yields of the products studied are given in Table I. The results of Theard (8) and of Blachford and Dyne (9) are included for comparison. In general, our results are in better agreement with those of Theard than of Blachford and Dyne, allowing for the increased cyclohexene yields at higher temperatures found by the latter workers.

When PCH is added to the cyclohexane vapor, increases are noted in the cyclohexene and bicyclohexyl yields and $C_6F_{11}H$ is produced. The yields of these products, along with those of hydrogen and methane, are shown in Fig. 1 as a function of PCH concentration for a dose of 2.26×10^{19} eV/g. A small yield of mixed dimer, $C_6F_{11}.C_6H_{11}$, was noted, but its gas chromatographic peak area was only about 10% that of bicyclohexyl at 10^{20} eV/g and was less at lower doses. As mentioned previously, no authentic standards were available to determine the detector sensitivity for this product, but its yield as a function of dose indicated that it could be a secondary product.

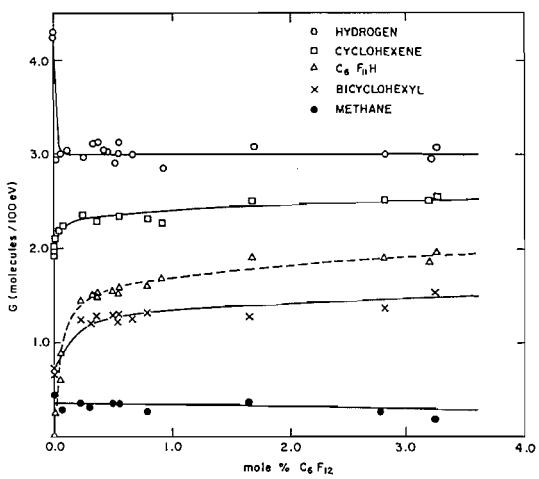

FIG. 1. Product yields from the cyclohexane–PCH system. Dose = $2.6_6 \times 10^{19}$ eV/g, T = 133 °C.

Can. J. Chem. Downloaded from www.nrcresearchpress.com by 210.87.254.6 on 09/05/12
For personal use only.

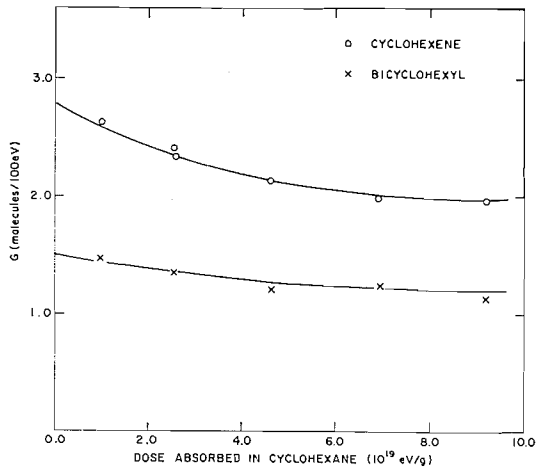

FIG. 2. Dose dependence of product yields from the cyclohexane–PCH system. PCH = 0.5 mole %, T = 133 °C.

Hydrogen and $C_6F_{11}H$ yields were independent of dose up to 10^{20} eV/g, but the cyclohexene and, to a lesser extent, the bicyclohexyl yields were dose dependent. These yields are shown in Fig. 2 as a function of dose for 0.5 mole % of PCH. For this discussion, initial yields of cyclohexene and bicyclohexyl at 3% PCH are taken as 2.9 and 1.7 G units respectively. The marked dependence on dose is similar to that observed in the liquid cyclohexane – PCH system (1).

Arguments favoring the assumption that PCH acts mainly as an electron scavenger in hydrocarbon systems have been summarized by one of us (1) and by Rajbenbach (2). The hydrogen yield is decreased to 3.0 G units, and the difference between this and the initial yield in the absence of scavenger is the yield of hydrogen having free electrons as precursors (1.6 G units). The residual yield of 3.0 G units presumably comes from excited states formed directly (reaction [5]). Since the W values for many hydrocarbons are around 24 eV/ion pair (6), we may follow Theard (8) in taking the electron yield in cyclohexane to be 4.2 G units.

[4] $C_6H_{12} \rightsquigarrow (RH^+, M_1^+ \ldots M_N^+) + e^-$ $G = 4.2$

[5] $C_6H_{12} \rightsquigarrow C_6H_{12}^* \rightarrow \rightarrow H_2 + \text{products}$ $G = 3.0$

[6a] $(RH^+, M_1^+ \ldots M_N^+) + e^- \rightarrow \rightarrow H_2 + \text{products}$ $G = 1.6$

[6b] $\rightarrow \text{no } H_2$ $G = 2.6$

Thus, about 1.6 G units of hydrogen are produced by ion neutralization. This number is very close to the estimate made by Theard (8) from the increase in the hydrogen yield on adding HI to cyclohexane vapor. The direct yield of hydrogen (reaction [3]) is also very close to that measured in methylcyclohexane vapor by Holtslander and Freeman (10).

If all the electrons are scavenged by PCH, then about 4.2 PCH anions are formed for every 100 eV absorbed (reaction [1]). Although in the liquid phase the PCH anion may be able to decompose by reaction [2], this dissociation is 1.8 eV endothermic in the gas phase and therefore must be excluded. The evidence for this endothermicity is good and is based on appearance potential measurements for F^- made by Bibby and Carter (4). It is possible that the appearance potential is somewhat larger than the true endothermicity and that products are formed with some excess energy. However, Bibby and Carter presented evidence that, in their system, products were not formed with excess kinetic energy and the bond dissociation energies they derived were in reasonable agreement with those determined thermochemically, with the exception of D(C—F) from CF_4.

The PCH anion will eventually be neutralized by a molecular or radical ion, and the process may yield C_6F_{11}.

[7] $C_6F_{12}^- + (RH^+, M_1^+ \ldots M_N^+) \rightarrow C_6F_{11} + \text{products}$

[8] $C_6F_{11} + C_6H_{12} \rightarrow C_6F_{11}H + C_6H_{11}$

The yield of $C_6F_{11}H$ and of mixed dimer imply a C_6F_{11} yield of about 2.0. Thus neutralization to give C_6F_{11} (reaction [7]) occurs for about half of the neutralizations.

Turning to the radiolysis of liquid cyclohexane with PCH, it is clear that neutralization could produce some of the C_6F_{11} formed. However, in liquid cyclohexane up to 3.3 G units of $C_6F_{11}H$ are produced (1). Since the total yield of electrons in liquid cyclohexane is between 3 and 4 (11), the production of C_6F_{11} is quite efficient in the liquid. Thus, if neutralization takes place with the same efficiency for the production of C_6F_{11} in the gas and liquid phases, then the large yields in the liquid phase mean that dissociation is likely an important fate of the PCH anion in the liquid. On the other hand, neutralization may produce fewer C_6F_{11} radicals in the gas phase than it does in the liquid phase. Therefore this work does not

Can. J. Chem. Downloaded from www.nrcresearchpress.com by 210.87.254.6 on 09/05/12
For personal use only.

lead to a firm conclusion about the source of the C_6F_{11} formed in the liquid phase radiolysis, but it does indicate that some could be formed by the neutralization reaction.

The increase in the bicyclohexyl yield can be largely accounted for by the cyclohexyl radicals produced in reaction [8]. The increase is about 0.95 *G* units and if the ratio of disproportion to combination of cyclohexyl radicals is 0.455 (12), then about 2.8 *G* units of cyclohexyl are required, although only about 2.0 are produced in reaction [8]. Cyclohexyl radicals may be produced as products in the neutralization (reaction [7]). Although the molecular ions decompose quickly to form smaller ions and radicals, at the pressures used an appreciable fraction of the ions will be cyclohexane ions or cyclohexyl ions. In the liquid state, of course, most of the ions remain as cyclohexane ions, and a larger yield of cyclohexyl radicals is expected from the neutralization (reaction [3]). Neutralizations involving PCH anions may produce more free radicals capable of abstracting hydrogen atoms from cyclohexane to form cyclohexyl radicals than do electron neutralizations; however, this has been shown not to be so for SF_6 anions (10).

1. N. H. SAGERT. Can. J. Chem. **46**, 95 (1968).
2. L. A. RAJBENBACH. J. Am. Chem. Soc. **88**, 4275 (1966).
3. M. B. FALLGATTER and R. J. HANRAHAN. Abstr. papers, 154th Meeting, American Chemical Society, Chicago, Ill., 1967. V 75.
4. M. M. BIBBY and G. CARTER. Trans. Faraday Soc. **62**, 2637 (1966).
5. FARHATAZIZ and P. J. DYNE. An anthology of experimental techniques in radiation chemistry. At. Energy Can. Ltd. Rept. AECL-2113. 1964. p. 7.
6. G. G. MEISELS. J. Chem. Phys. **41**, 51 (1964).
7. P. J. DYNE and J. A. STONE. Can. J. Chem. **39**, 2381 (1961).
8. L. M. THEARD. J. Phys. Chem. **69**, 3292 (1965).
9. J. BLACHFORD and P. J. DYNE. Can. J. Chem. **42**, 1165 (1964).
10. W. J. HOLTSLANDER and G. R. FREEMAN. Can. J. Chem. **45**, 1649 (1967).
11. N. H. SAGERT and A. S. BLAIR. Can. J. Chem. **45**, 1351 (1967).
12. P. W. BECK, D. V. KNIEBES, and H. E. GUNNING. J. Chem. Phys. **22**, 672 (1964).

Solvent effects on the electronic spectrum of *trans*-dichlorobis(diphenyl sulfide)platinum(II)

C. V. SENOFF[1]

Lash Miller Chemical Laboratories, University of Toronto, Toronto, Ontario

Received April 18, 1968

The electronic spectrum of *trans*-$PtCl_2(Ph_2S)_2$ has been measured in a variety of organic solvents and the effect of the solvent on the observed absorption bands is discussed.

Canadian Journal of Chemistry, 46, 3287 (1968)

Introduction

The effect of solvent on the electronic spectrum of square planar complexes has been studied by several workers (1–3). During the course of investigating the coordinating properties of diphenyl sulfide towards platinum(II), it was discovered that the electronic spectrum of *trans*-dichlorobis(diphenyl sulfide)platinum-(II) exhibited a marked dependence on the solvent used. A more detailed study of this solvent dependency was undertaken and the results of this study are now reported.

Experimental

Trans-dichlorobis(diphenyl sulfide)platinum(II)

A hot, filtered solution of 1.0 g of potassium chloroplatinate(II) in 10 ml of water was mixed with 0.89 g of diphenyl sulfide (Eastman Chemicals) in 20 ml of warm 1,4-dioxane (or ethanol). The resulting clear, red solution was then shaken for 3 h. The amber-colored precipitate that formed was filtered under reduced pressure and washed successively with hot water, ethanol, and ether. The crude complex was recrystallized from the minimum amount of acetone (or benzene). The amber-colored needle-like crystals were collected, washed as before, and dried in vacuo over boiling ethanol. Yield 0.60 g; m.p. 194–196° (decomp.) (lit. (4) m.p. 195°).

Anal. Calcd. for $C_{24}H_{20}Cl_2S_2Pt$: C, 45.14; H, 3.13. Found: C, 45.90; H, 3.42.

Trans-dibromobis(diphenyl sulfide)platinum(II)

This compound was prepared in the same way as the

[1]Present address: Department of Chemistry, University of Guelph, Guelph, Ontario.

Can. J. Chem. Downloaded from www.nrcresearchpress.com by 210.87.254.6 on 09/05/12
For personal use only.

lead to a firm conclusion about the source of the C_6F_{11} formed in the liquid phase radiolysis, but it does indicate that some could be formed by the neutralization reaction.

The increase in the bicyclohexyl yield can be largely accounted for by the cyclohexyl radicals produced in reaction [8]. The increase is about 0.95 *G* units and if the ratio of disproportion to combination of cyclohexyl radicals is 0.455 (12), then about 2.8 *G* units of cyclohexyl are required, although only about 2.0 are produced in reaction [8]. Cyclohexyl radicals may be produced as products in the neutralization (reaction [7]). Although the molecular ions decompose quickly to form smaller ions and radicals, at the pressures used an appreciable fraction of the ions will be cyclohexane ions or cyclohexyl ions. In the liquid state, of course, most of the ions remain as cyclohexane ions, and a larger yield of cyclohexyl radicals is expected from the neutralization (reaction [3]). Neutralizations involving PCH anions may produce more free radicals capable of abstracting hydrogen atoms from cyclohexane to form cyclohexyl radicals than do electron neutralizations; however, this has been shown not to be so for SF_6 anions (10).

1. N. H. SAGERT. Can. J. Chem. **46**, 95 (1968).
2. L. A. RAJBENBACH. J. Am. Chem. Soc. **88**, 4275 (1966).
3. M. B. FALLGATTER and R. J. HANRAHAN. Abstr. papers, 154th Meeting, American Chemical Society, Chicago, Ill., 1967. V 75.
4. M. M. BIBBY and G. CARTER. Trans. Faraday Soc. **62**, 2637 (1966).
5. FARHATAZIZ and P. J. DYNE. An anthology of experimental techniques in radiation chemistry. At. Energy Can. Ltd. Rept. AECL-2113. 1964. p. 7.
6. G. G. MEISELS. J. Chem. Phys. **41**, 51 (1964).
7. P. J. DYNE and J. A. STONE. Can. J. Chem. **39**, 2381 (1961).
8. L. M. THEARD. J. Phys. Chem. **69**, 3292 (1965).
9. J. BLACHFORD and P. J. DYNE. Can. J. Chem. **42**, 1165 (1964).
10. W. J. HOLTSLANDER and G. R. FREEMAN. Can. J. Chem. **45**, 1649 (1967).
11. N. H. SAGERT and A. S. BLAIR. Can. J. Chem. **45**, 1351 (1967).
12. P. W. BECK, D. V. KNIEBES, and H. E. GUNNING. J. Chem. Phys. **22**, 672 (1964).

Solvent effects on the electronic spectrum of *trans*-dichlorobis(diphenyl sulfide)platinum(II)

C. V. SENOFF[1]

Lash Miller Chemical Laboratories, University of Toronto, Toronto, Ontario

Received April 18, 1968

The electronic spectrum of *trans*-$PtCl_2(Ph_2S)_2$ has been measured in a variety of organic solvents and the effect of the solvent on the observed absorption bands is discussed.

Canadian Journal of Chemistry, 46, 3287 (1968)

Introduction

The effect of solvent on the electronic spectrum of square planar complexes has been studied by several workers (1–3). During the course of investigating the coordinating properties of diphenyl sulfide towards platinum(II), it was discovered that the electronic spectrum of *trans*-dichlorobis(diphenyl sulfide)platinum-(II) exhibited a marked dependence on the solvent used. A more detailed study of this solvent dependency was undertaken and the results of this study are now reported.

Experimental

Trans-dichlorobis(diphenyl sulfide)platinum(II)

A hot, filtered solution of 1.0 g of potassium chloroplatinate(II) in 10 ml of water was mixed with 0.89 g of diphenyl sulfide (Eastman Chemicals) in 20 ml of warm 1,4-dioxane (or ethanol). The resulting clear, red solution was then shaken for 3 h. The amber-colored precipitate that formed was filtered under reduced pressure and washed successively with hot water, ethanol, and ether. The crude complex was recrystallized from the minimum amount of acetone (or benzene). The amber-colored needle-like crystals were collected, washed as before, and dried in vacuo over boiling ethanol. Yield 0.60 g; m.p. 194–196° (decomp.) (lit. (4) m.p. 195°).

Anal. Calcd. for $C_{24}H_{20}Cl_2S_2Pt$: C, 45.14; H, 3.13. Found: C, 45.90; H, 3.42.

Trans-dibromobis(diphenyl sulfide)platinum(II)

This compound was prepared in the same way as the

[1]Present address: Department of Chemistry, University of Guelph, Guelph, Ontario.

Can. J. Chem. Downloaded from www.nrcresearchpress.com by 210.87.254.6 on 09/05/12
For personal use only.

dichloro-derivative except that potassium bromoplatinate-(II) was used in place of potassium chloroplatinate(II). The compound crystallized from acetone as reddish-brown needles; m.p. 200–203°.

Anal. Calcd. for $C_{24}H_{20}Br_2S_2Pt$: C, 39.61; H, 2.75. Found: C, 39.63; H, 2.21.

Infrared Spectra

The infrared spectra were recorded on either a Perkin–Elmer 521 or a Beckman IR-11 spectrophotometer as Nujol mulls between CsBr or CsI plates.

Electronic Spectra

The electronic spectra were recorded on a Bausch and Lomb Spectronic 505 spectrophotometer using matched ground glass stoppered 1.0 cm quartz cells. Solution concentrations were in the range 10^{-3}–10^{-5} *M*. The spectrum of at least three different solutions of the complex were determined in a given solvent. Some spectra were not stable and changed significantly on prolonged standing at room temperature. In these instances, the spectra were recorded as soon as possible (usually within a few minutes) and the molar extinction coefficient at a given maximum was evaluated from a plot of absorbance versus time which was extrapolated to "zero" time.

Solvents

(i) Chloroform

Fisher "Spectranalyzed" reagent was used.

(ii) Dichloromethane

Fisher "Spectranalyzed" reagent was used.

(iii) Benzene

Thiophene-free reagent grade benzene was dried over sodium ribbon, distilled from freshly cut sodium, and used immediately.

(iv) Tetrahydrofuran

Reagent grade tetrahydrofuran was first dried over sodium ribbon and then refluxed over sodium in the presence of a small amount of $LiAlH_4$. The solvent was then distilled and used immediately.

(v) 1,4-Dioxane

This solvent was purified by the method outlined by Vogel (5).

(vi) Dimethyl Sulfoxide

This solvent was obtained from a freshly opened bottle of Baker "Analyzed" reagent.

(vii) Acetonitrile

Reagent grade acetonitrile was refluxed over phosphorus pentoxide until the P_4O_{10} remained unchanged. It was then distilled twice and used immediately.

Results and Discussion

The far infrared spectra (400–200 cm^{-1}) of $PtX_2(Ph_2S)_2$ (X = Cl, Br) indicate that these compounds have the *trans*- rather than the *cis*-configuration as reported previously (4, 6). The strong band at 345 cm^{-1} exhibited by *trans*-$PtCl_2(Ph_2S)_2$ and absent in the spectrum of *trans*-$PtBr_2(Ph_2S)_2$ has been assigned to the vPtCl vibration. The corresponding vPtBr mode was observed at 255 cm^{-1}. Theory predicts one infrared active vPtX mode for the *trans*-isomer (C_{2h} symmetry) and two such modes for the *cis*-isomer (C_{2v} symmetry). No other bands were observed between 400–200 cm^{-1} for these compounds. Attempts so far to isolate the corresponding *cis*-isomers have been unsuccessful.

Examination of the spectral data presented in Table I indicates that the spectrum of *trans*-$PtCl_2(Ph_2S)_2$ in chloroform, dichloromethane, and benzene is significantly different from the spectrum observed in tetrahydrofuran, 1,4-dioxane, acetonitrile, and dimethyl sulfoxide. The intense bands between 33.0 and 43.3 kK may be readily associated with one or more of the following types of charge transfer processes—an internal ligand to ligand, a ligand to metal, or a metal to ligand electronic transition. The less intense bands occurring between ca. 25.0 and 30.0 kK may be associated with d–d electronic transitions (7).

In coordinating solvents such as tetrahydrofuran, 1,4-dioxane, acetonitrile, and dimethyl sulfoxide, the d–d bands are better resolved. The highest energy d–d band has been assigned to the transition, $d_{z^2} \rightarrow d_{x^2-y^2}$, by taking into account the proposed d-level ordering in square planar complexes of platinum(II) (8, and references cited therein). The remaining d–d band has accordingly been assigned to the $d_{xz,yz} \rightarrow d_{x^2-y^2}$ transition. In poorly coordinating solvents such as chloroform, dichloromethane, and benzene, the d–d bands are not well resolved because of their proximity to the intense charge transfer band at about 33.0 kK. Consequently, no attempt has been made to assign these absorptions to specific d–d transitions. The solvents may now be arranged in the following order of increasing solvent interaction by noting the change in position of the *highest* energy d–d band from solvent to solvent, viz. acetonitrile $\sim$ dimethyl sulfoxide < 1,4-dioxane $\sim$ tetrahydrofuran. This particular order is derived from the fact that increasing solvent interaction at the vacant octahedral sites will increase the energy of the d_{z^2} orbital of platinum relative to the vacant $d_{x^2-y^2}$ orbital and the $d_{z^2} \rightarrow d_{z^2-y^2}$ transition will occur at lower energy.

The spectra in poorly coordinating solvents are characterized by the presence of an intense band at ca. 33.0 kK which is not observed in

Can. J. Chem. Downloaded from www.nrcresearchpress.com by 210.87.254.6 on 09/05/12
For personal use only.

TABLE I

Electronic spectral data for *trans*-$PtCl_2(Ph_2S)_2$ in various polar solvents

Solvent	ν (kK)	ε	Transition
Chloroform	(40.0) sh	~16 700	Charge
	37.3 sh	12 300	Charge
	36.1	12 100	Charge
	33.2	14 800	Charge
	(28.2)	~600	d–d
	(24.7)	~200	d–d
Dichloromethane	(40.0) sh	~19 200	Charge
	37.5 sh	12 900	Charge
	36.4	12 800	Charge
	33.3	15 200	Charge
	(28.2)	~800	d–d
	(24.7)	~300	d–d
Benzene	33.4	18 500[a]	Charge
	(28.2)	~600	d–d
Tetrahydrofuran	43.3	24 600	Charge
	40.0	20 800[a]	Charge
	36.6 sh	10 800[a]	Charge
	28.4	460	d–d
	(24.7)	~300	d–d
1,4-Dioxane	43.3	22 940[a]	Charge
	39.8	18 800[a]	Charge
	36.5 sh	9 100[a]	Charge
	(28.6)	~500	d–d
	(24.7)	~200	d–d
Acetonitrile	43.5 sh	23 800	Charge
	40.3	23 600	Charge
	(36.6) sh	10 400	Charge
	29.9	250	d–d
	26.9	140	d–d
Dimethyl sulfoxide	[b]	—	—
	(36.8) sh	13 000	Charge
	29.8 sh	340	d–d

NOTE: Parentheses denote uncertainty in band position.
[a]Extrapolated value.
[b]Solvent absorbs.

the spectra recorded in better coordinating solvents (Table I). The following qualitative explanation is offered to account for the absence of this particular band in the latter group of solvents. This is based on the assumption that the band at 33.0 kK is due to an electron transfer from an orbital localized on one of the ligands to the $6p_z$ orbital of platinum. It then follows that potential coordinating solvents such as tetrahydrofuran, 1,4-dioxane, acetonitrile, and dimethyl sulfoxide will be capable of interacting with the $6p_z$ orbital and will raise its energy relative to the energy of the ligand orbitals. The net effect will be to shift this particular band to higher energy. Unfortunately, this band shift cannot be clearly resolved from the spectra and is probably obscured by the other intense bands occurring at higher energy or by strong solvent absorption (see Table I).

Acknowledgment

The author wishes to thank Professor A. D. Allen for helpful discussions throughout the course of this work.

1. J. CHATT, L. E. ORGEL, and G. A. GAMLEN. J. Chem. Soc. 486 (1958).
2. C. M. HARRIS, S. E. LIVINGSTONE, and J. H. REECE. J. Chem. Soc. 1505 (1959).
3. A. K. SUNDARAM and E. B. SANDELL. J. Am. Chem. Soc. **77**, 855 (1955).
4. K. A. JENSEN. Z. Anorg. Allgem. Chem. **231**, 365 (1937).
5. A. I. VOGEL. Textbook of practical organic chemistry. Longmans, Green and Co., Ltd., London. 1956. p. 177.
6. H. A. TAYIM and J. C. BAILAR, JR. J. Am. Chem. Soc. **89**, 4430 (1967).
7. T. DUNN. *In* Modern coordination chemistry. *Edited by* J. Lewis and R. G. Wilkins. Interscience Publishers, Inc., New York. 1960.
8. H. BASCH and H. B. GRAY. Inorg. Chem. **6**, 365 (1967).

Can. J. Chem. Downloaded from www.nrcresearchpress.com by 210.87.254.6 on 09/05/12
For personal use only.

Can. J. Chem. Downloaded from www.nrcresearchpress.com by 210.87.254.42 on 09/05/12
For personal use only.

Canadian Journal of Chemistry

Published by THE NATIONAL RESEARCH COUNCIL OF CANADA

VOLUME 46 NOVEMBER 1, 1968 NUMBER 21

Reductive *C*-alkylation[1]

B. V. GREGOROVICH,[2] K. S. Y. LIANG,[3] D. M. CLUGSTON,[4] AND S. F. MACDONALD

Division of Pure Chemistry, National Research Council of Canada, Ottawa, Canada

Received April 19, 1968

At 95–115°, paraformaldehyde and hydriodic acid completely *C*-methylate aromatics such as benzene and phenol. Pyrroles are *C*-methylated similarly, carbethoxy and acetyl groups being lost. In hydriodic acid at 15–45°, typical pyrroles retain these groups and all free positions are *C*-alkylated, methylated by paraformaldehyde, or otherwise alkylated by the appropriate carbonyl compound. The alkylation of a 2-free- by a 2-formylpyrrole led to a dipyrrylmethane. With pyrroles, hydriodic acid may be replaced by another strong acid and a reducing agent. This was necessary when a β-free pyrrole gave the iodo–alkyl derivative rather than the expected product.

Canadian Journal of Chemistry, 46, 3291 (1968)

Introduction

Not infrequently, two or more general reactions of organic chemistry are carried out under similar conditions; the reagents involved would be compatible and the product of one reaction would be the substrate for another. New or improved methods have been developed by combining such reactions in one-step procedures, but only sporadically. For example, it is frequently possible to avoid the isolation of intermediates, a real advantage if these are unstable or are mixtures, or one reagent may be continuously regenerated; both are illustrated by the oxidation of olefins with permanganate and periodate (1).

An approach so clearly defined was ripe for more systematic treatment. In the first instance, it had suggested to us that acids would be quite generally reduced to methyl derivatives by a combination of the McFadyen–Stevens and Wolff–Kishner reductions, if the limitations on the former method were due to the lability of aldehydes in alkali. However, although the benzenesulfonylhydrazides of 2,4-dimethyl-5-carboxypyrrole and (contrary to the report (2) from this laboratory) of benzoic acid were reduced to 2,4,5-trimethylpyrrole and toluene respectively, using the Huang modification in the latter case, the generality of the method was limited.

In a second and more fruitful application, we have regarded reductive *C*-alkylation as possible whenever the substrate would condense with a carbonyl compound to an intermediate known to be reducible in a compatible medium.[5] Although less developed than analogous reductive *N*-alkylations (3–6), some of the possibilities here had already been exploited. Others, however, were readily derived.

Ethyl cyanoacetate, for example, had been alkylated by catalytic hydrogenation in acetic acid – piperidine with aldehydes or ketones (8). The reduction of isoquinoline and benzaldehyde to 4-benzyltetrahydroisoquinoline was interpreted as the reductive *C*-alkylation of an enamine (9). More frequently, *C*-alkylations had been carried out like *N*-alkylations, by alcohols, alkali alcoholate, and/or Raney nickel at about 200°, and similarly interpreted. 2-Naphthol was thus monoalkylated at the 1-position (10), fluorene at the 9-position (11), oxindole (12), and indoles at the 3-position, and indoles also gave indole-3-acetic acids with α-hydroxy acids (13). Pyrroles

[1]Issued as NRCC No. 10224.

[2]NRCC Postdoctorate Fellow 1966-1967.

[3]NRCC Postdoctorate Fellow 1966–1967; present address, 50 MacDonald Road, 7th Floor, Hong Kong.

[4]NRCC Postdoctorate Fellow 1966–1967; present address, Department of Chemistry, McMaster University, Hamilton, Ontario.

[5]The term "reductive *C*-alkylation" has also been applied to a quite unrelated method wherein sodium adducts of aromatic compounds are alkylated with methyl iodide (7).

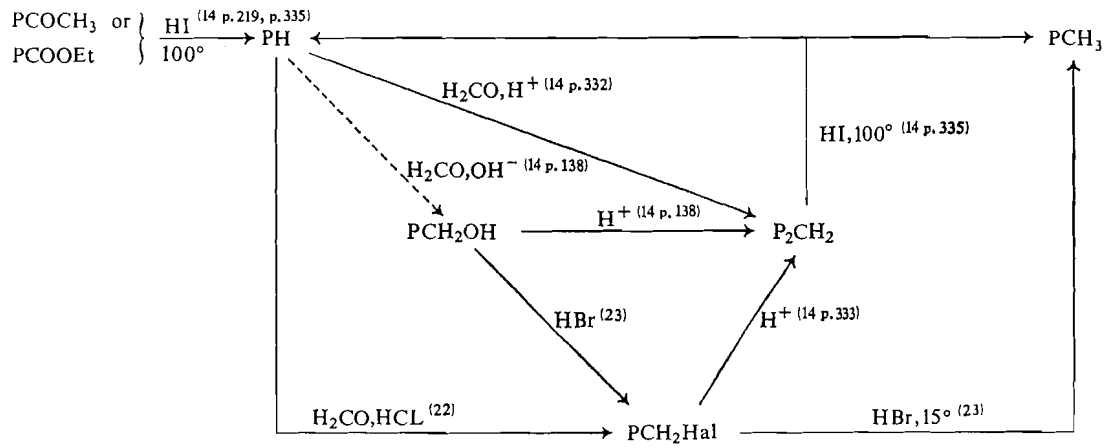

SCHEME 1
P = α- or β-pyrryl

were *C*-alkylated by this method, carbethoxy and acyl groups being lost (see ref. 14, p. 33, 55, 58). The self-alkylation of alcohols under similar conditions (Guerbet reaction) has been assumed to involve dehydrogenation, the reductive *C*-alkylation of an aldehyde by an aldehyde, and further reduction (15). The scope of these reactions is largely determined by the requirement for basic conditions. We have found complementary methods employing acid catalysts. These had been most nearly represented by the Friedel–Craft alkylation of benzene with dichloroalkanes in the presence of a hydrogen donor—a saturated hydrocarbon with a tertiary carbon atom (16).

The iodomethylation of aromatic compounds to benzyl iodides with formaldehyde and hydrogen iodide, although seldom employed (17), is presumably as effective as their chloromethylation. Benzyl iodide, however, is evidently reduced to toluene by hydriodic acid at 140° (18). These two reactions suggest the reductive methylation of benzene by formaldehyde and hydriodic acid at the higher temperature. The result would be the same if diphenylmethanes were formed and then reduced to a mixture of methylated and unmethylated products, and this is not improbable in view of the reduction of triphenylmethane (19) and of 4,4′-dihydroxydiphenylmethanes (20). In either case the concurrent condensation and reduction would recycle incompletely methylated products. As methyl groups unlike chloromethyl groups (17) favor further substitution hexamethylbenzene should result, unless demethylation intervened, for 1,2,3,5-tetramethyl benzene is demethylated to 1,3,5-trimethylbenzene by hydriodic acid at 160° (21).

We found that *p*-xylene, tetralin, and phenol were converted into hexamethylbenzene (82%), 5,6,7,8-tetramethyl-1,2,3,4-tetrahydronaphthalene (73%), and pentamethylphenol (25%) respectively by paraformaldehyde, hydriodic acid (*d* 1.95), acetic acid or acetic anhydride, and hypophosphorous acid at 90–115°. Hexamethylbenzene was also obtained from benzene (35%) under conditions which minimized losses by volatilization, and from *o*-dichlorobenzene under conditions chosen to illustrate the use of immiscible solvents. As the chloromethylation of phenols usually leads to tars (17), the behavior of phenol here suggests that reductive *C*-alkylations are not necessarily limited by the stability of the unreduced intermediates.

Scheme 1 is a composite of pyrrole condensations and reductions, which had been carried out only on derivatives bearing carbethoxy or acyl groups. Where not directly involved as indicated, these groups are essential to stabilize the carbinols, halomethylpyrroles, and dipyrrylmethanes. In all these reactions, except one leading to an acid-labile product, only formaldehyde and a halogen acid are required, and the only terminal product is the methyl derivative. Formaldehyde and hydriodic acid should then replace all α- or β-hydrogen, carbethoxy, or acyl groups by methyl,

Can. J. Chem. Downloaded from www.nrcresearchpress.com by 210.87.254.42 on 09/05/12
For personal use only.

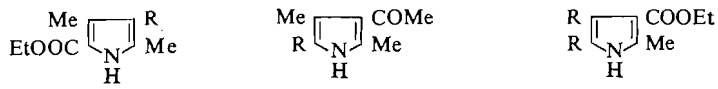

1 **2** **3**

a) R = H
b) R = Me
c) R = Et
d) R = CH_2Et
e) R = CH_2CMe_3
f) R = $CHMe_2$

g) R = $CHEt_2$
h) R = $CHMe \cdot CH_2CHMe_2$
i) R = $CH_2C_6H_5$
j) R = $CHMeC_6H_5$
k) R = $CH < (CH_2)_5$

l) R = CH_2COOH
m) R = $CHMe \cdot COOH$
n) R = $CHMe \cdot CH_2CH_2COOH$
o) R = CH_2CHMe_2
p) R = $CHI \cdot CHMe_2$

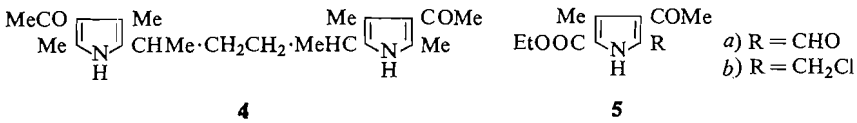

4 **5**

a) R = CHO
b) R = CH_2Cl

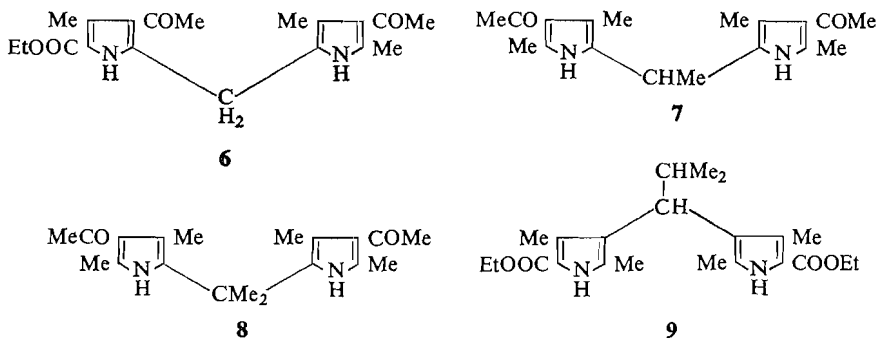

6 **7**

8 **9**

if the unstabilized intermediates did not suffer their usual degradation to unrecognizable products.

We did obtain 2,3,4,5-tetramethylpyrrole from 2,4-dimethylpyrrole and from its 5-carbethoxy-, 3,5-dicarbethoxy-, and 3-acetyl derivatives (37, 50, 35, and 68%), using paraformaldehyde with hydriodic, acetic, and hypophosphorous acids at about 100°. Presumably the intermediates are stabilized here by their complete protonation in the strong acid or, if oxidation initiates the side-reactions, by the reducing conditions.

Tetramethylpyrrole had previously been obtained from 2,4-dimethyl-3,5-dicarbethoxypyrrole with sodium in methanol at about 220° (24), a general method referred to above. Its further development was not promising. The yields were variable, carbethoxy and acetyl groups were first lost (25*a*), the subsequent alkylation of the α-position preceded that of the β (25*b*), and ethyl (25*a*) or propionic acid (25*c*) groups might be replaced. Some α,α′- and β,β′-dipyrrylmethanes were converted to tetramethylpyrrole but the bridges, at least when substituted, were lost (25*c*).

We found, however, that the paraformaldehyde – hydriodic acid reagent was effective at room temperature, *C*-methylating the free positions of pyrroles while leaving carbethoxy and acetyl groups intact. Thus **1***a*, **2***a*, and **3***a* were converted to **1***b* (64%), **2***b* (73%), and **3***b* (75%).

To determine the range of alkyl groups which might be introduced by carbonyl compounds and hydriodic acid in favorable cases, we used 2,4-dimethyl-3-acetylpyrrole, **2***a*, for which an improved preparation is given. This was stirred magnetically at about 35° with the carbonyl compound, hydriodic acid, hypophosphorous acid, and (usually) acetic anhydride. In general, the reaction and its end were indicated by the iodine color and its disappearance. An intermediate sometimes separated then, although only under modified conditions when benzaldehyde was used, redissolved. Most of the crude products could be precipitated by water and were then substantially pure and free of halogen. The

Can. J. Chem. Downloaded from www.nrcresearchpress.com by 210.87.254.42 on 09/05/12
For personal use only.

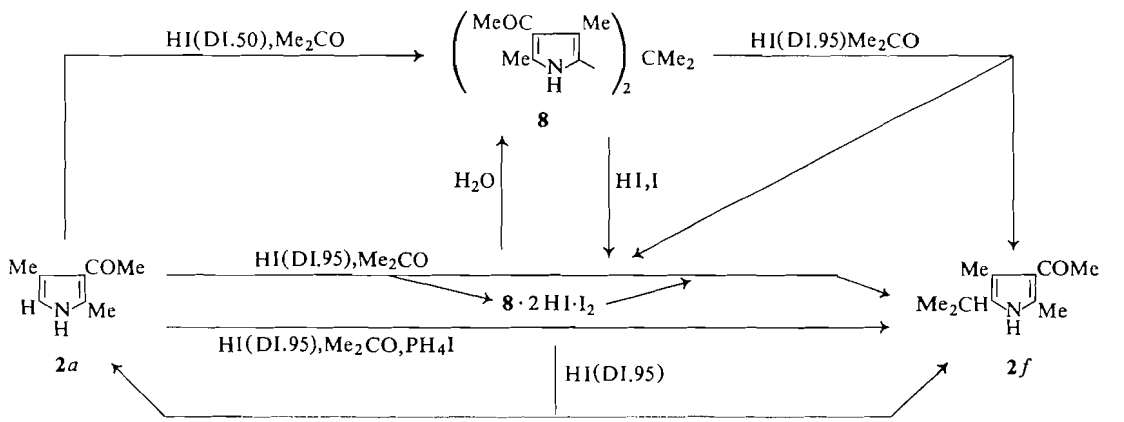

SCHEME 2

5-alkyl derivatives **2***c*–**2***o* resulted, as did **4** when 2,5-hexandione was used (60–90%). Chloroacetone, like acetone, gave **2***f*. The alkylation of **2***a* with the pyrrole aldehyde **5***a* required more definite conditions but at 45° **6** resulted (73%). The same product had been obtained conventionally from **2***a* and **5***b* in 21% yield (32). Another pyrrole, **3***a*, was ethylated to **3***c* (54%).

As might be expected, hydriodic acid could be replaced by another strong acid and a reducing agent. This proved necessary for the alkylation of **1***a* with isobutyraldehyde for, when hydriodic acid was used, the intermediate 3-(1-iodoisobutyl) derivative **1***p* (see below) was not reduced. However, **1***a* was alkylated to **1***o* (82%) by isobutyraldehyde, hydrogen chloride in acetic acid, and amalgamated zinc at 20°. The pyrrole **2***f* was obtained from **2***a* and acetone using hydriodic acid as above (92%), using hydrogen bromide in acetic acid and stannous bromide (77%), or using sulfuric acid in acetic acid and zinc amalgam (<24% crude). Formic acid, so useful in the reductive alkylation of amines, has not proved useful here although, with sodium formate, it will reduce crystal violet to dimethylaniline and bis-(*p*-dimethylamino-phenyl)methane (26).

We were interested in the intermediates which sometimes separated then redissolved when hydiodic acid was used in the alkylations, particularly after isobutyraldehyde failed to alkylate **1***a*. The behavior of 3-(1-iodoalkyl)-pyrroles was unknown but 3,3′-dipyrrylmethanes could not be intermediates for, with hydriodic acid at 100°, their bridges were incompletely reduced if methylene or split off if substituted (25*c*). Either 2-(1-iodoalkyl)pyrroles or 2,2′-dipyrrylmethanes might be intermediates. The former should be easily reduced (Scheme 1). The latter, whether or not their bridges were substituted, had been reduced to 2-free and 2-alkyl pyrroles at 100° (25*d*) and their reduction at lower temperatures had not been attempted.[6]

The methylation of **1***a* with paraformaldehyde and hydriodic acid in acetic acid at 20° suggested then that the 3-iodomethyl derivative was the intermediate, particularly as the chloromethyl derivative had been prepared by chloromethylation (22). There is now no doubt that 3-iodoalkyl derivatives can be formed, but they may not be easily reduced. When **1***a* was stirred with isobutyraldehyde, hydriodic acid, hypophosphorous acid, and acetic anhydride at about 35°, **1***p* crystallized out. More vigorous conditions resulted in unidentified products, and there was no evidence that the dipyrrylmethane 9, which was prepared for comparison, was involved.

When **2***a* was alkylated with acetone and

[6]*Note added in proof*:—As will be reported later with R. A. Chapman, we have reduced porphyrins (e.g. 1,3,5,7-tetramethyl-2,6-diethyl-4,8-di-*n*-propyl-porphin) with hydriodic and acetic acids at 100° as usual, then added paraformaldehyde and continued the heating. Instead of mixtures of homologous pyrroles ill-suited to g.l.p.c. (cf. 35), the products were then easily separated and identified tetra-substituted pyrroles. Porphyrins are converted into these tetra-substituted pyrroles equally directly by potassium methylate at 220° (36). However, the behavior of meso-substituted α, α′-dipyrrylmethanes with hydriodic acid (see above) and with potassium methylate (p. 3293) suggests that *meso-substituents on porphyrins will be retained on the pyrroles* when hydriodic acid, but not when potassium methylate is used.

Can. J. Chem. Downloaded from www.nrcresearchpress.com by 210.87.254.42 on 09/05/12
For personal use only.

Can. J. Chem. Downloaded from www.nrcresearchpress.com by 210.87.254.42 on 09/05/12
For personal use only.

hydriodic acid in the same way, a complex of the dipyrrylmethane **8**, presumably $\mathbf{8}\cdot 2HI\cdot I_2$ (see Experimental), separated then redissolved more slowly. Further experiments, summarized in Scheme 2, showed that **8** was indeed the intermediate or, when weaker hydriodic acid was used, the final product. When strong hydriodic acid was used, the dipyrrylmethane initially formed was reduced to a mixture of **2***a* and **2***f*, the former being recycled in the presence of acetone. However, unless the iodine liberated in the reduction was rapidly removed by phosphonium iodide, it combined with the dipyrrylmethane to form the less soluble complex.

We did not attempt to isolate the dipyrrylmethane **7** as an intermediate in the alkylation of **2***a* by paraldehyde and hydriodic acid. However, **7** was converted into **2***c* by the same mixture. In the absence of the aldehyde, **7** had been reduced by hydriodic acid at 100° to 2,4-dimethylpyrrole and its 5-ethyl derivative (25*d*). It is thus reasonable to assume that in the alkylation of **2***a*, the critical intermediates are easily reduced dipyrrylmethanes.

Experimental

The hypophosphorous acid used was 50%. The hydriodic acid was of density about 1.94 or 1.95–1.96 and was stored at 0° over phosphonium iodide (for which a convenient preparation is given).

The hydriodic acid – acetic anhydride mixture was best made by adding the acetic anhydride slowly to the hydriodic acid, cooled with water and stirred magnetically, then adding the hypophosphorous acid; otherwise, a yellow solid might form. When the reaction temperatures are not specified, there was a rise to 35–45° due to magnetic stirring.

Melting points were determined on a hot-stage and are corrected. The products gave negative Beilstein tests for halogen, their assigned structures were consistent with their nuclear magnetic resonance (n.m.r.) spectra, and the pyrroles gave positive Ehrlich's reactions hot.

Phosphonium Iodide (cf. ref. 34)

Hydriodic acid (d = 1.95, 115 ml) and red phosphorus (50 g) were stirred magnetically in a 250 ml flask, surmounted by a 6 in. air condenser under a reflux condenser and heated by an oil bath. The bath temperature was slowly raised to 80° (frothing!), held at that temperature for 1½ h, then slowly raised to 105°. The phosphonium iodide was periodically removed from the air condenser and stored at 0° under hydriodic acid (d 1.95); yield 74 g.

2,4-Dimethyl-3-acetyl-pyrrole (2a)

2,4-Dimethyl-3-acetyl-5-carbethoxypyrrole (8 g) and 40 ml of 10% aqueous sodium hydroxide were heated for 4 h at 175° in a Teflon lined brass tube. The contents of the tube were ground up and filtered. The solid was washed with water and distilled (125°, 1 × 10^{-3} mm) to give a colorless product (4.72 g, 90%), m.p. 140–140.5° (lit. (14, p. 185) 137°).

Anal. Calcd. for $C_8H_{11}O$: C, 70.04; H, 8.08; N, 10.21. Found: C, 70.22; H, 8.21; N, 9.99.

Hexamethylbenzene

(a) From Benzene

Hydrogen iodide in acetic acid (20 ml, density 1.6, about 50%), 3 g of paraformaldehyde and 1 ml of benzene were stirred at 20° for 18 h in a stoppered flask (an oil separated, presumably diiodomethyl ether (27)), then heated for 18 h at 90° under a reflux condenser. The mixture was cooled, 5 ml of hypophosphorous acid and 20 ml of acetic anhydride were added, and heating continued for 4 h at 110°. It was again cooled, 5 ml of hypophosphorous acid added, and again heated for 18 h at 115°. The mixture was cooled somewhat, decolorized with hypophosphorous acid, and poured into water. The solid which separated was dried, boiled with 10 ml of pyridine, recovered by pouring the mixture into water (this removed any halogen), ground and washed with 20 ml of methanol, dried, sublimed (about 100°, 0.1 mm), and crystallized from 25 ml of methanol as colorless plates (589 mg), m.p. 165–166.5° (lit. (28) 166.6°) after changing to needles or prisms at ca. 105° and to plates at ca. 145°. A further 45 mg were obtained from the methanolic mother liquor (total 635 mg, 35%). No aromatic protons were apparent in the n.m.r. spectrum when the intensity was increased 100 times.

Anal. Calcd. for $C_{12}H_{18}$: C, 88.82; H, 11.18. Found: C, 88.63; H, 11.10.

(b) From p-Xylene

Hexamethylbenzene, m.p. 165.5–166.5° was obtained similarly but more conveniently and in 82% yield, from *p*-xylene (1 ml), 10 ml of hydriodic acid (d = 1.95), 40 ml of acetic anhydride, and 2 g of paraformaldehyde, at 90 °C then at a gentle reflux (116°), using hypophosphorous acid.

Anal. Found: C, 88.74; H, 11.04.

(c) From o-Dichlorobenzene

A mixture of *o*-dichlorobenzene (1.47 g), hydriodic acid (20 ml), paraformaldehyde (2.4 g), and *n*-heptane (20 ml) was stirred (Vibromischer) at 95° (bath temperature) under reflux for 10 h, decolorizing it periodically with phosphonium iodide. The heptane layer was separated and washed with 20% aqueous pyridine (2 × 25 ml), with 10% hydrochloric acid, and with water. It was then dried and the heptane was evaporated. The residue was recrystallized from pentane as colorless crystals (621 mg, 38%). For analysis, it was sublimed (65°, 1 × 10^{-2} mm), m.p. 164–165°.

Anal. Found: C, 88.64; H, 11.31.

5,6,7,8-Tetramethyl-1,2,3,4-tetrahydronaphthalene

1,2,3,4-Tetrahydronaphthalene (1 ml) was added to a mixture of paraformaldehyde (2 g), hydriodic acid (10 ml), and acetic anhydride (40 ml). The mixture was then stirred and heated under reflux for 4½ h at 90–100° then at ca. 116° for 5 h. During the heating, the solution was periodically cooled to 60° and decolorized with hypophosphorous acid (total 7 ml). The warm solution was added to 125 ml of

Can. J. Chem. Downloaded from www.nrcresearchpress.com by 210.87.254.42 on 09/05/12
For personal use only.

water, the resulting mixture was cooled, and the crystalline crude product was separated. This was boiled for 5 min with pyridine and the hot solution poured into boiling water (125 ml) containing 10 ml of acetic acid. The mixture was cooled and the product was separated, dried, sublimed (75°, 1×10^{-4} mm), and extracted into 20 ml of methanol. When the solution was concentrated then allowed to cool, 925 mg of the product separated and a further 94 mg (total 74%) were obtained by concentrating the mother liquors. The product formed large colorless plates, m.p. 81.5–82° (lit. (29)79–79.5°).

Anal. Calcd. for $C_{14}H_{20}$: C, 89.29, H, 10.71. Found: C, 89.43; H, 10.49.

Pentamethylphenol

To phenol (4.06 g) in acetic acid (40 ml) was added hydriodic acid (43 ml) and paraformaldehyde (6.47 g). The mixture was kept at 95° under nitrogen and stirred for 6 h, adding hypophosphorus acid periodically to decolorize it. Ammonium hydroxide was then added dropwise to the cooled (0°) and stirred solution until it was basic (pH ~8). The product was extracted with ether (3 × 30 ml), which was dried over anhydrous magnesium sulfate, filtered, and then removed *in vacuo* to leave the crude product (2.1 g). Several recrystallizations from *n*-hexane gave the product, 1.64 g (25%), m.p. 127–129°. (lit. (30) 125°). The infrared spectrum had the hydroxy absorption at 3625 cm^{-1}.

Anal. Calcd. for $C_{11}H_{16}O$ (mol. wt., 164): C, 80.44; H, 9.83. Found (mol. wt., 160 (vapor pressure), 164 (mass spectroscopy)): C, 80.12; H, 9.91.

2,3,4,5-Tetramethylpyrrole

*(a) From 2,4-Dimethyl-5-carbethoxypyrrole (**1a**)*

2,4-Dimethyl-5-carbethoxypyrrole (1.64 g), acetic acid (25 ml), hydriodic acid (25 ml), and paraformaldehyde (0.589 g) were heated at 95–100° for 3 h under nitrogen with stirring. The solution was decolorized with hypophosphorous acid, made alkaline with ammonia at 0°, and extracted with ether (2 × 75 ml). The ether was removed from the dried extract ($MgSO_4$) at 20° in a rotary evaporator to leave the crude product, avoiding its exposure to air. The product was purified by distillation (10 mm, 60°) to give 0.628 g (52%), m.p. 106–108° (lit. (14, p. 44) 110°).

Anal. Calcd. for $C_8H_{13}N$: C, 77.99; H, 10.64; N, 11.37. Found: C, 77.88; H, 10.51; N, 11.22.

(b) From 2,4-Dimethyl-3,5-dicarbethoxypyrrole

2,4-Dimethyl-3,5-dicarbethoxypyrrole (2.4 g), acetic acid (35 ml), hydriodic acid (35 ml), and paraformaldehyde (1.2 g) were heated at 100° for 4 h under a stream of nitrogen. The crude product was obtained as in (*a*) above, then distilled (15 mm, 65°) to yield 0.44 g (36%), m.p. 107–109°.

*(c) From 2,4-Dimethyl-3-acetylpyrrole (**2a**)*

2,4-Dimethyl-3-acetylpyrrole (1.58 g) in 25 ml of acetic acid was added in five portions during 1 h to a stirred mixture of paraformaldehyde (2.07 g), hydriodic acid (25 ml), and hypophosphorous acid (3 ml) maintained at 115° under nitrogen. The mixture was heated at 115° for a further 3 h, and the crude product then isolated as in (*a*) above. Distillation (65°, 10 mm) gave 996 mg (68%) of colorless crystals, m.p. 108–110°.

Anal. Found: C, 77.74; H, 10.59; N, 11.19.

(d) From 2,4-Dimethylpyrrole

2,4-Dimethylpyrrole (2.06 g) in acetic acid (50 ml) was added over 2 h to a stirred solution of paraformaldehyde (5.21 g) in hydriodic acid (75 ml), acetic acid (25 ml), and hypophosphorous acid (6 ml) at 105° under nitrogen. The solution was heated 4 h longer, then brought to pH 9 with ammonium hydroxide at 0°. Isolated as in (*a*) above and washed with a little pentane, the colorless product (0.996 g. 37%) melted at 107–109°. The analytical sample, m.p, 109–111°, had been redistilled (60°, 8 mm).

Anal. Found: C, 77.94; H, 10.56; N, 11.29.

*2,3,4-Trimethyl-5-carbethoxypyrrole (**1b**)*

2,4-Dimethyl-5-carbethoxypyrrole (**1a**) (0.83 g), acetic acid (10 ml), hydriodic acid (10 ml), and paraformaldehyde (0.60 g) were stirred for 3 h at 25° under nitrogen. Hypophosphorous acid (about 1 ml) was added dropwise to decolorize the solution. The cooled solution (0°) was made basic with ammonium hydroxide and the product was extracted with ether (2 × 20 ml). The extract was dried over magnesium sulfate, filtered, and the ether removed in a rotary evaporator at 20°. Recrystallization from benzene gave the product, 0.58 g (64%), m.p. 125–126° (lit. (14, p. 239) 128°).

Anal. Calcd. for $C_{10}H_{15}O_2N$: C, 66.27; H, 8.34; N, 7.73. Found: C, 66.35; H, 8.18; N, 7.90.

*2,3,5-Trimethyl-3-acetylpyrrole (**2b**)*

2,4-Dimethyl-3-acetylpyrrole (**2a**), (0.68 g), acetic acid (15 ml), hydriodic acid (15 ml), and paraformaldehyde (0.6 g) were stirred for 3 h under nitrogen at 25°. The solution was decolorized with hypophosphorous acid, made alkaline with ammonium hydroxide at 0°, and extracted with ether. The ether was evaporated from the dried extract ($MgSO_4$) leaving the crude product which was crystallized from benzene as colorless elongated prisms (0.55 g, 73%), m.p. 204–207° (lit. (14, p. 188) 207–209°).

Anal. Calcd. for $C_9H_{13}NO$: C, 71.49; H, 8.67; N, 9.26. Found: C, 71.29; H, 8.68; N, 9.38.

*2,4,5-Trimethyl-3-carbethoxypyrrole (**3b**)*

2-Methyl-3-carbethoxypyrrole (**3a** (33), 0.99 g), acetic acid (15 ml), hydriodic acid (20 ml), and paraformaldehyde (0.78 g) were stirred for 3 h at 25°. The crude product was isolated as was that of the 3-acetyl derivative (above) and sublimed (82°, 4×10^{-3} mm) as fine colorless needles (75%), m.p. 103–103.5° (lit. (14, p. 248) 104–105°).

Anal. Calcd. for $C_{10}H_{15}NO_2$: C, 66.27; H, 8.34; N, 7.73. Found: C, 66.35; H, 8.17; N, 7.88.

*2,4-Dimethyl-3-isobutyl-5-carbethoxypyrrole (**1o**)*

Acetic anhydride (20 ml) was slowly added to 5 ml of concentrated hydrochloric acid with stirring and cooling, and 668 mg of 2,4-dimethyl-5-carbethoxypyrrole (**1a**) were dissolved in the resulting solution. Amalgamated zinc (10 g, 20 mesh) and 0.75 ml of isobutyraldehyde were then added at 20°, and the mixture was stirred for 15 min at 20–25°. The zinc was separated, washed with acetic acid, and the liquids were poured into water to precipitate the crude product. It was dried and extracted into pentane (thimble), the pentane was evaporated, and the residue was recrystallized from aqueous ethanol (13 ml of 55%) as colorless needles (681 mg), m.p. 115–117° (lit. (31), 116–117°) after changing to fine needles at about 112°, and to plates at about 115°. A further 51 mg were obtained from the mother liquors (total 732 mg, 82%). The n.m.r. spectrum and the X-ray powder photograph were identical

Can. J. Chem. Downloaded from www.nrcresearchpress.com by 210.87.254.42 on 09/05/12
For personal use only.

with those of authentic material, and the mixed m.p. was 115–117°.

Anal. Calcd. for $C_{13}H_{21}NO_2$: C, 69.92; H, 9.48; N, 6.27. Found: C, 70.08; H, 9.67; N, 6.25.

2,4-Dimethyl-3-acetyl-5-ethylpyrrole (2c)

A solution of 2,4-dimethyl-3-acetylpyrrole (**2a**, 548 mg) in 10 ml of hydriodic acid containing a little solid phosphonium iodide was cooled in an ice–salt bath. Paraldehyde (0.35 ml) was added and the solution was stirred for 4½ h without further cooling. The solution was then added to 100 ml of ice water to precipitate the light-brown product (385 mg, 58%), m.p. 153–160°. For analysis, it was sublimed *in vacuo* then recrystallized from ether (thimble) as grey needles, m.p. 163° after changing to plates at 140°.

Anal. Calcd. for $C_{10}H_{15}O$: C, 72.69; H, 9.15; N, 8.48. Found: C, 72.67; H, 8.88; N, 8.69.

2,4-Dimethyl-3-acetyl-5-n-propylpyrrole (2d)

2,4-Dimethyl-3-acetylpyrrole (**2a**, 1.02 g), acetic acid (15 ml), hydriodic acid (25 ml), and propionaldehyde (1.74 g), were stirred at 25° for 3 h under nitrogen. The crude product was isolated as was that of the 2,4,5-trimethyl derivative, **2b**, except that 2 × 50 ml ether were used. Recrystallization from benzene gave the product 0.786 g (59%), m.p. 157–158°.

Anal. Calcd. for $C_{11}H_{17}ON$: C, 73.70; H, 9.56; N, 7.81. Found: C, 73.73; H, 9.39; N, 7.79.

2,4-Dimethyl-3-acetyl-5-isobutylpyrrole (2o)

(*a*) 2,4-Dimethyl-3-acetylpyrrole (**2a**, 548 mg) was dissolved in hydriodic acid (10 ml), acetic anhydride (10 ml), and hypophosphorous acid (2 ml). Isobutyraldehyde (0.75 ml) was added and the solution was stirred for 35 min. No precipitate formed. Water precipitated a yellow iodine complex (864 mg), m.p. unsharp from 90°, Beilstein test for halogen positive. This was converted into the desired product by dissolving it in ethanol and adding ammonium hydroxide. For analysis it was recrystallized from aqueous ethanol, m.p. 152° after changing to smaller crystals at 125°.

Anal. Calcd. for $C_{12}H_{19}NO$: C, 74.57; H, 9.91; N, 7.25. Found: C, 74.40; H, 9.73; N, 7.43.

(*b*) When the above reaction was run in the presence of a little added phosphonium iodide, the color faded within 1 min and after 5 min water precipitated the colorless product (0.7 g, 91%). It melted at 150–152° (phase change at 125°) after being recrystallized from ethanol.

2,4-Dimethyl-3-acetyl-5-neopentylpyrrole (2e)

2,4-Dimethyl-3-acetylpyrrole (**2a**, 548 mg) was warmed to solution in a mixture of 10 ml of hydriodic acid, 10 ml of acetic anhydride, and 2 ml of hypophosphorous acid. The solution was cooled to 35° and 0.85 ml of pivalaldehyde (Columbia Organic Chemicals Co.) was added. The solution was stirred for 10 min, by which time the initially dark brown color had changed to yellow, and then it was poured into 125 ml of water. The product separated as a colorless powder (769 mg, 93%), m.p. 156–163°. For analysis, it was recrystallized from ether–pentane, sublimed at 115° (10^{-4} mm), and again recrystallized by extraction into hexane (thimble) as long colorless plates, m.p. 166–167° after changing to prisms below 130°.

Anal. Calcd. for $C_{13}H_{21}NO$: C, 75.31; H, 10.21; N, 6.76. Found: C, 75.13; H, 10.30; N, 6.58.

2,4-Dimethyl-3-acetyl-5-isopropylpyrrole (2f)

(a) Using Hydriodic Acid

Hydriodic acid (10 ml) and 2 ml of hypophosphorous acid were cooled and stirred while 10 ml of acetic anhydride was slowly added. 2,4-Dimethyl-3-acetylpyrrole (**2a**, 548 mg) was dissolved in the solution, 0.6 ml of acetone added, and the mixture was stirred for ½ h by which time a yellow precipitate had formed and redissolved and the solution had turned yellow; the final temperature was 37°. The solution was poured into 100 ml of water and 30 ml of ammonium hydroxide kept at 20°. The nearly colorless product separated as plates (662 mg, 92%). At 138° these changed to cubes which either melted at 165° or turned to irregular needles, m.p. 171–173°. For analysis, it was recrystallized from aqueous ethanol as colorless plates, m.p. 165.5° or 171.5–173°.

Anal. Calcd. for $C_{11}H_{17}NO$: C, 73.70; H, 9.56; N, 7.81. Found: C, 73.59; H, 9.48; N, 7.76.

(b) Using Hydrogen Bromide and Stannous Bromide

Anhydrous stannous bromide (5 g) was stirred to solution in 20 ml of hydrogen bromide in acetic acid (30–32%). 2,4-Dimethyl-3-acetylpyrrole (**2a**, 548 mg) was added and the mixture was warmed to dissolve this, then cooled to 30°. Acetone (0.6 ml) was added and the solution was stirred at 35° for 2½ h. then poured into water at 10°. The product was separated and washed with dilute hydrochloric acid then with water. It formed colorless micro-prisms (549 mg, 77%), m.p. 166–167° or 173–174.5° after changing to cubes at about 136°. For analysis it was recrystallized from aqueous ethanol as prismatic rods, m.p. 172°, 172–173° when mixed with the product of (*a*) above.

Anal. Found: C, 73.92; H, 9.23; N, 7.88.

(c) Using Sulfuric Acid and Zinc

2,4-Dimethyl-3-acetyl-pyrrole (**2a**, 548 mg), 1 ml of acetone, and 10 g of amalgamated zinc (20 mesh) were added to a solution of 1 ml of concentrated sulfuric acid in 20 ml of acetic acid. The mixture was stirred for 1 h at 45°. The liquid was decanted from the zinc into 100 ml of water forming a solution from which the crude product separated at 15° (174 mg, m.p. 164–169°, after the usual solid phase changes). For analysis, it was extracted into ether (thimble) then recrystallized from 3 ml of aqueous ethanol as nearly colorless elongated prisms, m.p. 170–172° (171–173° when mixed with the product of (*a*) above) after a solid phase change at 142°.

Anal. Found: C, 73.60; H, 9.40; N, 7.92.

2,4-Dimethyl-3-acetyl-5-(3-pentyl)pyrrole (2g)

3-Pentanone (0.85 ml) was added to a solution of 548 mg of 2,4-dimethyl-3-acetylpyrrole (**2a**), in 10 ml of hydriodic acid, 10 ml of acetic anhydride, and 2 ml of hypophosphorous acid. The solution was stirred for 1¾ h then poured into 200 ml of water to precipitate the product as tiny nearly colorless prisms (651 mg, 79%), m.p. about 186–189°. For analysis it was recrystallized from ethanol as colorless plates, m.p. 188.5° after a solid phase change at 135°.

Anal. Calcd. for $C_{13}H_{21}NO$: C, 75.31; H, 10.21; N, 6.76. Found: C, 75.13; H, 10.04; N, 6.78.

2,4-Dimethyl-3-acetyl-5-(4-methyl-2-pentyl)pyrrole (2h)

Methyl isobutylketone (1.1 ml) was added to a solution of 548 mg of 2,4-dimethyl-3-acetyl-pyrrole, **2a**, in hydriodic

Can. J. Chem. Downloaded from www.nrcresearchpress.com by 210.87.254.42 on 09/05/12
For personal use only.

acid (10 ml), acetic anhydride (10 ml), and hypophosphorous acid (2 ml). The solution was stirred for 4 h then poured into a mixture of 150 ml of water and 30 ml of ammonium hydroxide. The product separated as tiny colorless prisms (709 mg, 80%), m.p. 140–141.5°. For analysis, it was recrystallized from aqueous ethanol (charcoal) as tiny colorless prisms, m.p. 142–143°, some changing to plates at 120°.

Anal. Calcd. for $C_{14}H_{23}NO$: C, 75.97; H, 10.47; N, 6.33. Found: C, 75.81, H, 10.37; N, 6.38.

2,4-Dimethyl-3-acetyl-5-benzylpyrrole (2i)

A solution of 10 ml of hydriodic acid, 10 ml of acetic anhydride, and 2 ml of hypophosphorous acid containing 548 mg of 2,4-dimethyl-3-acetylpyrrole, **2***a*, was stirred magnetically while a solution of 0.6 ml of benzaldehyde in 5 ml of acetic anhydride was slowly added over 20 min. The solution was stirred for 10 min then poured into water. The crude product which separated was recrystallized from acetone (thimble) as nearly colorless irregular plates (85%), m.p. 165.5–167° after a partial change to prismatic rods above 165°.

Anal. Calcd. for $C_{13}H_{17}NO$: C, 79.26; H, 7.54; N, 6.16. Found: C, 79.22; H, 7.50; N, 6.18.

2,4-Dimethyl-3-acetyl-5-(1-phenyl-ethyl)pyrrole (2j)

A solution of 0.6 ml of acetophenone in 5 ml of acetic anhydride was slowly added to a stirred mixture of 10 ml of hydriodic acid, 10 ml of acetic anhydride, and 2 ml of hypophosphorous acid containing 548 mg of 2,4-dimethyl-3-acetylpyrrole, **2***a*. The mixture was allowed to stand for two days at room temperature then poured into water. The crude product which separated was recrystallized from acetone (thimble) as nearly colorless rhombic plates (75%), m.p. 146–148.5°.

Anal. Calcd. for $C_{16}H_{19}NO$: C, 79.63; H, 7.94; N, 5.80. Found: C, 79.47; H, 7.78; N, 5.79.

2,4-Dimethyl-3-acetyl-5-cyclohexylpyrrole (2k)

A solution of 10 ml of hydriodic acid, 10 ml of acetic anhydride, and 2 ml of hypophosphorous acid was stirred magnetically at 40° while 548 mg of 2,4-dimethyl-3-acetylpyrrole, **2***a*, were dissolved in it; 0.5 ml of cyclohexanone was then added, and an additional 0.5 ml of cyclohexanone was added after a few minutes. The solution was stirred at 40° for 1½ h then poured into water. The crude product which separated, m.p. 186–188° was recrystallized from ethanol as colorless rhombic prisms (82%), m.p. 188.5–189° after changing to flat prisms above 153°.

Anal. Calcd. for $C_{14}H_{21}NO$: C, 76.66; H, 9.65; N, 6.39. Found: C, 76.49; H, 9.50; N, 6.30.

2,4-Dimethyl-3-acetyl-pyrrole-5-acetic Acid (2l)

Glyoxylic acid monohydrate (500 mg) was added to a solution of 548 mg of 2,4-dimethyl-3-acetylpyrrole **2***a*, in 10 ml of hydriodic acid and 2 ml of hypophosphorous acid. The solution was stirred for 1 h at 15°. A yellow crystalline solid containing iodine was removed by filtration, washed with ether, dried, then slurried with 5 ml of water. The solid (Beilstein test for halogen now very weak) was again separated, washed with 5 ml of water, dried, and extracted into 40 ml of ether (thimble). When the ether solution was concentrated the product separated as yellow prisms (550 mg, 70%), m.p. 195–205°. For analysis, it was recrystallized by dissolving it in 40 parts of cold 50% aqueous acetone, boiling off the acetone, and cooling. It separated as nearly colorless prismatic rods, m.p. 206–210°, after changing to prisms at 155° and evolving gas at 175°. Before melting, it evidently decarboxylated to the 5-methyl derivative (see above), the m.p. of which was not depressed by the resolidified melt.

Anal. Calcd. for $C_{10}H_{13}NO_3$ (eq. wt., 195): C, 61.52; H, 6.71; N, 7.18. Found (eq. wt., 197): C, 61.35; H, 6.90; N, 7.10.

2,4-Dimethyl-3-acetyl-5-(1-carboxyethyl)pyrrole (2m)

A solution of 548 mg of 2,4-dimethyl-3-acetylpyrrole **2***a*, in 10 ml of hydriodic acid and 2 ml of hypophosphorous acid was treated with 0.4 ml of pyruvic acid and stirred for 10 min at 40° when yellow crystals containing iodine formed. After 2 days at 0° the crystals were separated, dried, and slurried with 5 ml of water. They dissolved and a colorless product then separated which gave a very weak Beilstein test for halogen. This was washed with water, dried, and recrystallized from ether (thimble) as tiny colorless rods (493 mg, 59%), m.p. 156–158° (decomp.).

Anal. Calcd. for $C_{11}H_{15}NO_3$ (eq. wt., 209): C, 63.14; H, 7.23; N, 6.69. Found (eq. wt., 207): C, 63.11; H, 6.98; N, 6.80.

2,4-Dimethyl-3-acetyl-pyrrole-5-(4-pentanoic) Acid (2n)

A solution of levulinic acid (0.6 ml) in 5 ml of acetic anhydride was slowly added to a solution of 548 mg of 2,4-dimethyl-3-acetylpyrrole, **2***a*, in hydriodic acid (10 ml), acetic anhydride, and hypophosphorous acid (2 ml). The solution was stirred for 12 h then the volatile solvents were removed in a vacuum desiccator over potassium hydroxide. Water (10 ml) was added to the residue to yield the product as an oil which soon solidified to salmon colored prisms which were washed with water to yield 742 mg (78%), m.p. 175–177°. For analysis, it was recrystallized from acetone (thimble) as nearly colorless prisms, m.p. 175–180°.

Anal. Calcd. for $C_{13}H_{19}NO_3$ (eq. wt., 237): C, 65.80; H, 8.07; N, 5.90. Found (eq. wt., 234): C, 66.03; H, 8.20; N, 5.91.

2,5-Bis-(3,5-dimethyl-4-acetyl-2-pyrryl)hexane (4)

2,5-Hexandione (1 ml) was added to a solution of 548 mg of 2,4-dimethyl-3-acetylpyrrole **2***a* in 10 ml of hydriodic acid, 10 ml of acetic anhydride, and 2 ml of hypophosphorous acid. The solution was stirred for 1½ h then poured into 150 ml of water to precipitate the nearly colorless product (442 mg, 62%), m.p. 263–268°. For analysis it was twice recrystallized from acetone (thimble) as a colorless crystalline powder, m.p. 275–279° after changing to needles at 271°.

Anal. Calcd. for $C_{22}H_{32}N_2O_2$: C, 74.12; H, 9.05; N, 7.86. Found: C, 74.01; H, 9.04; N, 7.94.

3,5,4′-Trimethyl-4,3′-diacetyl-5′-carbethoxydipyrrylmethane (6)

Hydriodic acid (10 ml) was stirred and cooled while 10 ml of acetic anhydride were added slowly. Hypophosphorous acid (2 ml) and 548 mg of 2,4-dimethyl-3-acetylpyrrole, **2***a*, were added and the mixture was stirred at room temperature until the latter dissolved. 2-Formyl-3-acetyl-4-methyl-5-carbethoxypyrrole (**5***a*, 892 mg) was

Can. J. Chem. Downloaded from www.nrcresearchpress.com by 210.87.254.42 on 09/05/12
For personal use only.

added and the mixture was stirred at 40–45° for 2 h, then poured into 150 ml of water. The precipitate was separated, dried, slurried with 15 ml of ethanol, and then filtered, dried, and extracted into 40 ml of acetone (thimble). The product (781 mg) crystallized from the acetone as colorless plates, m.p. 209–212° and concentrating the acetone gave a further 219 mg (total, 73%). The X-ray powder photograph and the n.m.r. spectrum were identical with those of authentic material (32) for which we found the m.p. to be 210–213°; the mixed m.p. was 209–213°.

Anal. Calcd. for $C_{19}H_{24}O_4N_2$: C, 66.26; H, 7.02; N, 8.13; OEt, 13.08. Found: C, 66.11; H, 7.23; N, 8.18; OEt, 12.97.

2-Methyl-4,5-diethyl-3-carbethoxypyrrole (3c)

A solution of 612 mg of 2-methyl-3-carbethoxypyrrole **3***a* (33) in 10 ml of hydriodic acid, 10 ml of acetic anhydride, and 2 ml of hypophosphorous acid was stirred while 0.35 ml of paraldehyde was dropped in. Stirring was continued for ½ h and the solution was then poured into water. For analysis, the pale-yellow micro-crystals which separated (0.45 g 53%, m.p. 104–106°) were recrystallized from aqueous ethanol.

Anal. Calcd. for $C_{12}H_{19}NO_2$: C, 68.86; H, 9.15; N, 6.67. Found: C, 68.73; H, 9.09; N, 6.85.

Experiments Relating to the Intermediates

2,4-Dimethyl-3-(1-iodo-isobutyl)-5-carbethoxypyrrole (1p)

2,4-Dimethyl-5-carbethoxypyrrole (**1***a*, 668 mg) in hydriodic acid (10 ml), acetic anhydride (10 ml), and hypophosphorous acid (2 ml) was treated with 0.75 ml isobutyraldehyde. The solution was stirred for 15 min while the solution turned dark then lightened as a precipitate formed. This was separated and washed well with water, leaving the product as colorless crystals (1 g), m.p. 119–121°. For analysis it was recrystallized from heptane.

Anal. Calcd. for $C_{13}H_{20}NO_2I$: C, 44.71; H, 5.77; N, 4.01; I, 36.33. Found: C, 44.55; H, 6.15; N, 4.13; I, 36.29.

meso-Isopropyl-2,2′,4,4′-tetramethyl-5,5′-dicarbethoxydipyrrylmethane (9)

2,4-Dimethyl-5-carbethoxypyrrole (**1***a*, 668 mg) and isobutyraldehyde (0.75 ml) were refluxed for 15 min in ethanol containing two drops of hydrochloric acid. Water was added to the cooled solution to precipitate colorless crystals, m.p. 120–125° after being recrystallized from heptane.

Anal. Calcd. for $C_{22}H_{32}N_2O_4$: C, 68.01; H, 8.30; N, 7.21. Found: C, 67.99; H, 8.37; N, 7.35.

The Complex of meso-Dimethyl-3,3′,5,5′-tetramethyl-4,4′-diacetylpyrromethane (8) with HI and Iodine

(*a*) The pyrrole **2***a* (548 mg) was stirred with hydriodic acid, acetic anhydride, hypophosphorous acid, and acetone as in the preparation of **2***f* (above). After 5 min the precipitated complex (723 mg, 45%) was separated and well washed with acetic acid, m.p. 167° (decomp.), KI–starch test positive.

Anal. Calcd. for $C_{19}H_{26}O_2N_2.2HI.I_2$: C, 27.70; H, 3.40; N, 3.42; I, 61.60. Found: C, 28.18; H, 3.46; N, 3.48; I, 61.56.

(*b*) The above experiment was repeated giving 470 mg of the complex, m.p. 157–159° (decomp.), further identified by its n.m.r. spectrum. The acid mother liquors were poured into water (100 ml) and ammonium hydroxide (30 ml) to precipitate 370 mg of **2***f*, identified by m.p., mixed m.p., and n.m.r. spectrum.

(*c*) The experiment was again repeated in the presence of a little added phosphonium iodide. The color appeared more slowly, disappeared more rapidly, and no precipitate formed. After 15 min the pale solution was poured into water and ammonium hydroxide to precipite **2***f* (604 mg, 85%) identified by m.p., mixed m.p., and n.m.r. spectrum.

(*d*) The complex prepared as in (*a*) was treated with water or ethanol to give **8** (see below).

(*e*) The complex (548 mg) prepared as under (*a*) was stirred in 10 ml of hydriodic acid, 10 ml of acetic anhydride, and 2 ml of hypophosphorous acid. No acetone was added. When the solution became clear, water precipitated 310 mg of a product, m.p. 152–160°, a 1:1 mixture of **2***a* and **2***f* as indicated by the n.m.r. spectrum.

(*f*) No precipitate was obtained by adding either iodine or hydriodic acid to **8** (see below) in acetic acid. However, the complex separated when both were added, m.p. 145–150° (decomp.), mixed m.p. with the complex obtained as above 153–155° (decomp.). Found: C, 28.48; H, 3.61; N, 3.26; I, 62.10.

meso-Dimethyl-3,3′,5,5′-tetramethyl-4,4′-diacetylpyrromethane, 8

(*a*) The pyrrole **2***a*, hydriodic acid, acetic anhydride, hypophosporous acid, and acetone were stirred together as in the preparation of **2***f* but hydriodic acid (d = 1.50) was used. After 5 min the yellow precipitate of **8** was separated from the pale-yellow solution (no iodine color). The product (75%), m.p. 225–227°, melted at 235–237° alone or mixed with authentic material (32) after it was recrystallized from ethanol.

Anal. Calcd. for $C_{19}H_{26}O_2N_2$: C, 72.58; H, 8.34; N, 8.91. Found: C, 72.67; H, 8.44; N, 8.78.

(*b*) The pyrromethane **8** was stirred with hydriodic acid (d = 1.50), acetic anhydride, hypophosphorous acid, and acetone. Warming was necessary to bring it into solution. Water precipitated nearly pure **8**, m.p. 215–217°, identified by its n.m.r. spectrum.

(*c*) The pyrromethane **8** (548 mg) was stirred in hydriodic acid (10 ml, d = 1.95), 10 ml of acetic anhydride, 2 ml of hypophosphorous acid, and 0.3 ml of acetone. The solution darkened, a yellow precipitate appeared, then the solution lightened and the precipitate redissolved. After ½ h water and ammonium hydroxide precipitated 535 mg (86%) of *2f*, identified by its m.p., mixed m.p., and n.m.r. spectrum.

2,4-Dimethyl-3-acetyl-5-ethyl-pyrrole (2c) from meso-Methyl-3,3′-5,5′-tetramethyl-4,4′-diacetylpyrromethane (7)

meso-Methyl-3,3′,-5,5′-tetramethyl-4,4′-diacetylpyrromethane (**7** (14, p. 351), 548 mg) in 10 ml of hydriodic acid, 10 ml of acetic anhydride, 2 ml of hypophosphorous acid, and 0.34 ml of acetaldehyde was stirred for 15 min. The solution was then poured into water to precipitate the product as pale-yellow crystals (400 mg 66%), m.p. 161–162°.

1. R. U. Lemieux and E. von Rudolff. Can. J. Chem. **33**, 1701 (1955).
2. E. Baltazzi. Compt. Rend. **254**, 702 (1962).

3. W. S. EMERSON. Organic reactions. Vol. IV. John Wiley and Sons, Inc., New York. pp. 174–196. 1948.
4. M. L. MOORE. Organic reactions. Vol. V. John Wiley and Sons, Inc., New York. pp. 301–316. 1949.
5. HOUBEN-WEYL. Methoden der organischen chemie. Vol. XI. Part I. 4th ed. *Edited by* Eugen Müller. Georg Thiem, Verlag, Stuttgart. pp. 602–671.
6. F. K. SIGNAIGO and H. ADKINS. J. Am. Chem. Soc. **58**, 709 (1936); C. AINSWORTH. J. Am. Chem. Soc. **78**, 1035 (1956).
7. W. HÜCKEL and R. CRAMER. Ann. Chem. **630**, 89 (1960).
8. E. R ALEXANDER and A. C. COPE. J. Am. Chem. Soc. **66**, 886 (1944).
9. R. GREWE, W. KRÜGER, and E. VANGERMAIN. Chem. Ber. **97**, 119 (1964).
10. J. W. CORNFORTH, R. H. CORNFORTH, and R. ROBINSON. J. Chem. Soc. 682 (1942).
11. K. L. SCHOEN and E. I. BECKER. J. Am. Chem. Soc. **77**, 6030 (1955).
12. E. WENKERT and N. V. BRINGI. J. Am. Chem. Soc. **80**, 5575 (1958).
13. H. E. JOHNSON and D. G. CROSBY. J. Org. Chem. **28**, 1246 (1963).
14. H. FISCHER and H. ORTH. Die chemie des pyrrols. Vol. I. Akadem. Verlag. Leipzig. 1934.
15. E. F. PRATT and D. G. KUBLER. J. Am. Chem. Soc. **76**, 52 (1954).
16. L. SCHMERLING, R. W. WELCH, and J. P. LUVISI. J. Am. Chem. Soc. **79**, 2636 (1957).
17. R. C. FUSON and C. H. MCKEEVER. Organic reactions. Vol. I. John Wiley and Sons, Inc., New York. pp. 63–74. 1942.
18. C. GRAEBE. Chem. Ber. **8**, 1055 (1875).
19. W. MARKOWNIKOFF. Chem. Ber. **30**, 1218 (1897).
20. J. VON BRAUN. Ann. Chem. **472**, 1 (1929).
21. A. KLAGES and C. STAMM. Chem. Ber. **37**, 1715 (1904).
22. T. H. CURRY. Ph.D Thesis. Ohio State University. Columbus, Ohio. 1953.
23. H. FISCHER, E. STURM, and A. FRIEDRICH. Ann. Chem. **461**, 244 (1928).
24. U. COLACICCHI and C. BERTONI. Atti reale accad. Lincei, **5**, 653 (1912).
25. H. FISCHER and E. BARTHOLOMÄUS. Z. Physiol. Chem. (*a*) **80**, 6 (1912); (*b*) **77**, 185 (1912); (*c*) **83**, 50 (1913); (*d*) **87**, 255 (1913).
26. A. KOVACHE. Ann. Chim. Paris, **10**, 184 (1918).
27. V. E. TISHCHENKO. J Russ. Phys. Chem. Soc. (St. Petersburg), 464 (1887); Chem. Ber. **20**, ref. 701 (1887).
28. H. A. SMITH and E. F. H. PENNEKAMP. J. Am. Chem. Soc. **67**, 279 (1945).
29. M. C. KLOETZEL, R. P. DAYTON, and H. L. HERZOG. J. Am. Chem. Soc. **72**, 273 (1950).
30. A. W. HOFMANN. Chem. Ber. **18**, 1826 (1885).
31. J. L. ARCHIBALD, D. M. WALKER, K. B. SHAW, A. MARKOVAC, and S. F. MACDONALD. Can. J. Chem. **44**, 345 (1966).
32. W. SCHLESINGER, A. H. CORWIN, and L. J. SARGENT. J. Am. Chem. Soc. **72**, 2871 (1950). A. F. MIRONOV, R. P. EVSTIGNEEVA, A. V. CHUMACHENKO, and N. A. PREOBRAZHENSKII. J. Gen. Chem. USSR (Engl. Transl.), **34**, 1493 (1964).
33. A. TREIBS and W. OTT. Ann. Chem. **615**, 156 (1958).
34. E. FISCHER and H. LEUCHS. Chem. Ber. **35**, 3793 (1902).
35. H. V. MORLEY and A. S. HOLT. Can. J. Chem. **39**, 755 (1961).
36. H. FISCHER and H. RÖSE. Z. Physiol. Chem. **87**, 38 (1913).

Can. J. Chem. Downloaded from www.nrcresearchpress.com by 210.87.254.42 on 09/05/12
For personal use only.

Can. J. Chem. Downloaded from www.nrcresearchpress.com by 210.87.254.105 on 09/05/12
For personal use only.

Secondary deuterium kinetic isotope effects on the thermolysis of 1-pyrazolines

BASIL H. AL-SADER AND ROBERT J. CRAWFORD
Department of Chemistry, University of Alberta, Edmonton, Alberta

Received June 13, 1968

Secondary kinetic isotope effects on four deuterated 1-pyrazolines support the formation of a trimethylene intermediate during gas phase thermolysis. Calculation of cyclization relative rate constants for the trimethylene intermediates reveals that substitution of hydrogen by deuterium has no effect when the terminal methylenes are substituted, but the rate constants are decreased when the central methylene's hydrogens are substituted. Explanations are advanced for all of the observed effects.

Canadian Journal of Chemistry, **46**, 3301 (1968)

Introduction

Secondary deuterium kinetic isotope effects offer a useful method of characterizing the bond cleavages occurring in the rate-determining transition state of thermolysis reactions. Seltzer and co-workers (1) have established that the substitution of hydrogen by deuterium on the nitrogen bearing carbon of an azoalkane increases $\Delta G^{\ddagger}$ by 80 to 110 cal per deuterium (i.e. 12 to 15% per deuterium at 105°) when that carbon–nitrogen bond is breaking. A similar effect has been observed in solvolytic processes (2). Wolfsberg and Stern (3) suggest that the α-isotope effect arises from the difference in the initial and transition states of the force constants of the HCX bond, the major contribution arising from the bending force constant.

In earlier work it has been suggested that both carbon–nitrogen bonds are being cleaved in the rate-determining step of 1-pyrazoline thermolysis, and that a nitrogen free intermediate is produced (4). This interpretation arose from a progressive decrease in activation energy on going from 1-pyrazoline (**1**) to 3,3,5,5-tetramethyl-1-pyrazoline (**2**). The decrease per methyl group, approximately one kcal mole^{-1}, was that expected by analogy with azoalkane thermolysis (4). However one kcal mole^{-1} per methyl group is comparable to some conformational factors encountered in cyclic compounds, thus the increase in rate could arise from an increase in ground state energies. The replacement of hydrogen by deuterium leads to a predictable value for the kinetic isotope effect (1) and at the same time removes any conformational complications, or serious changes in non-bonded interactions.

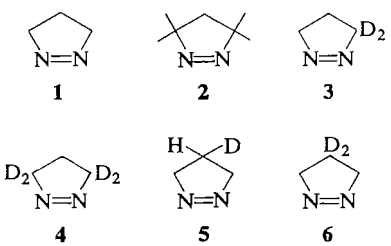

1 **2** **3** **4** **5** **6**

Experimental

All samples of deuterated 1-pyrazolines were purified by gas–liquid chromatography (g.l.c.) using a Wilkens Aerograph Autoprep model A-700 with a 20 ft 10% Ucon-insoluble or Fluoropak column. Deuterium analyses were carried out on a Metropolitan–Vickers MS-2, single focussing mass spectrometer. The nuclear magnetic resonance (n.m.r.) spectra were measured using a Varian A-60 and an HR-100 spectrometer.

1,3-Dibromopropane-1,1,3,3-d_4

A solution of freshly distilled diethyl malonate (24.5 g, 0.15 mole) in dry ether (160 ml) was added dropwise to a well stirred solution of lithium aluminium deuteride (6.75 g, 0.16 mole) in dry ether (350 ml) at such a rate as to maintain steady reflux. After completion of addition, the refluxing was continued for an additional 3h, cooled to 0°, and water added slowly to decompose the excess deuteride. The solution was then acidified with dilute hydrobromic acid, the ether layer removed by distillation, and the crude product in the aqueous layer converted, without isolation, to the dibromide by the addition of 48% hydrobromic acid (116 g) and concentrated sulfuric acid (50 ml). The mixture was then refluxed for 7 h, and 10 to 15 ml of 48% hydrobromic acid were added at the end of each hour. The 1,3-dibromopropane was then distilled out of the solution, the organic layer was washed several times with a potassium carbonate solution, and dried over anhydrous sodium sulfate. Distillation gave 12.7 g (40% yield based on malonate), b.p. 165°.

1,3-Dibromopropane-1,1-d_2

A solution of freshly distilled β-propiolactone (14.4 g, 0.2 mole) in 160 ml dry ether was added, with stirring, to a solution of lithium aluminium deuteride (4.2 g) in 300 ml dry ether. The work-up and conversion to the dibromide was carried out in the same manner as for the aforementioned tetradeuterio sample.

TABLE I

Rate constants and secondary kinetic isotope effects for α-deuterated 1-pyrazolines at 229.40±0.05°

Compound		10^4k (s^{-1})	k_H/k_D Observed	k_H/k_D Corrected to 105°	$\Delta\Delta G^{\neq}$ per deuterium cal $mole^{-1}$
1		23.82			
		23.98			
		23.77			
	Avg.	23.86±0.11			
3*		20.06			
		19.87			
	Avg.	19.96±0.13	1.19±0.01	1.26±0.01	86±6
4*		16.94			
		17.20			
	Avg.	17.07±0.18	1.40±0.02	1.55±0.02	84±6

*Mass spectral and nuclear magnetic resonance analyses indicate samples to have greater than 98% deuteration in the positions indicated.

1,3-Dibromopropane-2,2-d_2

Diethyl malonate-2,2-d_2 prepared by exchanging diethyl malonate with sodium ethoxide in ethanol-*O*-*d*, (four exchanges) was reduced as above using lithium aluminium hydride and converted to the dibromide without isolation of the glycol.

1,3-Dibromopropane-2-d_1

Deuterium bromide, prepared by the addition of phosphorus tribromide to deuterium oxide, was added to allyl bromide using the photochemical method of Kharasch and Mayo (5).

1-Pyrazolines

The deuterated 1-pyrazolines were prepared from the corresponding pyrazolidines which in turn were synthesized from the deuterated 1,3-dibromopropanes by the previously described method (6).

Kinetic Method

The apparatus used is essentially that described by Smith and Bagley (7). The thermocouple used for temperature measurements was a four-junction model, and was calibrated against roll sulfur, tin (analytical), and lead (analytical).

Product Analysis

The exact product compositions were obtained by sealing degassed samples (2 μl) in small Pyrex bulbs (0.5 ml) and heating to 241 °C for greater than nine half-lives. The bulbs were placed in a bulb crusher and the products carried directly onto a 20 ft column of mineral oil on fire brick in tandem with a 20 ft column of 10% di-*n*-butyl malonate on Diatoport. Integrations were carried out using a planimeter.

Results and Discussion

The rate constants measured for each of the α-deuterated pyrazolines are recorded in Table I. The β-deuterated pyrazolines run at a different temperature are given in Table II. The results confirm that both carbon–nitrogen bonds are breaking in the rate-determining transition state.

The β-deuterium isotope effects are somewhat larger than those normally found (8). However, comparisons with other systems are difficult in that in the trimethylene species produced the hydrogens attached to the central methylene are β to both newly formed sp^2 centers. Hoffmann (9) has recently dealt with the singlet trimethylene species and hyperconjugative interactions play an important role in the stabilization of the species. It may be in fact just this hyperconjugative interaction that is giving rise to the enhanced β-deuterium isotope effects. Hodnett (10) has observed a value for the secondary β-tritium isotope effect on the isobutyl radical. This would tend to suggest 18 cal $mole^{-1}$ for the β-deuterium effect. A considerably smaller effect has been observed by Seltzer and Hamilton (11) for the 1-phenylethyl-2,2,2-d_3 radical; however, delocalization of the radical may account for the suppression of hyperconjugation in this case.

The proportion of cyclopropane and propylene produced on thermolysis of each of the pyrazolines is indicated in Table III. These proportions are controlled by the product-determining steps (Scheme 1) (4).

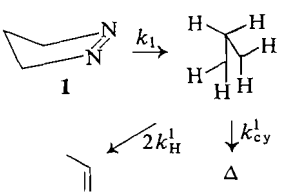

SCHEME 1

Can. J. Chem. Downloaded from www.nrcresearchpress.com by 210.87.254.105 on 09/05/12
For personal use only.

Can. J. Chem. Downloaded from www.nrcresearchpress.com by 210.87.254.105 on 09/05/12
For personal use only.

TABLE II

Rate constants and secondary kinetic isotope effects for β-deuterated 1-pyrazolines

Compound	Temperature		10^4k (s^{-1})	k_H/k_D Observed	k_H/k_D Corrected to 105°	$\Delta\Delta G^{\ddagger}$ per deuterium (cal $mole^{-1}$)
1	224.0		15.3			
	226.9		19.3			
5	224.0		14.76*			
			14.24			
		Avg.	14.50	1.05±0.01	1.06±0.01	52±10
6	226.9		17.00†			
			17.30			
		Avg.	17.15	1.12±0.01	1.14±0.01	56±10

*Corrected for 4.9% $C_3H_6N_2$ (mass spectral analysis).
†Corrected for 11.3% $C_3H_5DN_2$ and 0.1% $C_3H_6N_2$ (mass spectral analysis).

TABLE III

Cyclopropane and propylene yields on thermolysis of pyrazolines at 241°

Compound		Cyclopropane	Propylene
1		88.45	11.55
		88.34	11.66
		88.51	11.49
		88.40	11.60
	Avg.	88.43±0.07	11.57±0.07
3		87.98	12.02
		87.99	12.01
		87.99	12.01
	Avg.	87.99±0.01	12.01±0.01
4		87.29	12.71
		87.51	12.49
		87.49	12.51
	Avg.	87.43±0.17	12.57±0.17
5		89.23	10.77
		89.32	10.68
		89.07	10.93
	Avg.	89.21±0.13	10.79±0.13
6		90.43	9.57
		90.17	9.83
		90.29	9.71
		90.17	9.83
	Avg.	90.27±0.12	9.73±0.12

Integration of the n.m.r. spectrum of the propylene produced from **3** indicates a 52:48 ratio of CD_2H—CH=CH_2 to CD_2=CH—CH_3, thus an inverse intramolecular kinetic isotope effect for k_H^3/k_D^3 of 0.92. This is consistent with the observed increase in propylene formed from **3** relative to **1**. Inverse isotope effects of this magnitude have been observed earlier in the change of hybridization of a deuterated carbon from sp^2 to sp^3 (12).

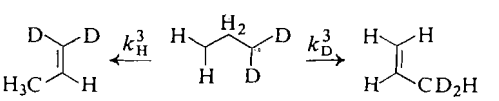

The further increase in propylene yield on going from **3** to **4** is consistent with an isotope effect of 0.92 in the product-determining step. Using the isotope effect data from the n.m.r. observations we can effectively calculate the isotope effect on the cyclization reactions. Assuming[1] that $k_H^1 = k_H^3$ on the basis that the changes in

$$\text{e.g. } \frac{k^1_{cy}}{2k^1_H} = \frac{88.43}{11.57}$$

and

$$\frac{k^3_{cy}}{k_H^3 + k_D^3} = \frac{k^3_{cy}}{2.09k_H^3} = \frac{87.99}{12.01}$$

hybridization occurring are the same in each case then we find that $k^1_{cy} = 1.00k^3_{cy}$. Similarly by assuming that $k_D^3 = k_D^4$ we find that $k^3_{cy} = 1.01k^4_{cy}$. This would suggest that there is little or no change in the CH force constants of the terminal methylene groups of the trimethylene intermediate on going to cyclopropane; a fact borne out by the very similar frequencies of the C—H stretching vibrations of cyclopropane (3075 and 3009 cm^{-1}) (13) and the terminal methylene stretching frequencies of propylene (3089 and 2991 cm^{-1}) (14). The CH_2 bending, wagging, and rocking modes for cyclopropane (1475, 975, and 854 cm^{-1}) (13) and the terminal CH_2 of propylene (1420, 963, and 912 cm^{-1}) (14) similarly have a compensatory effect such that the total change in force constant on going from sp^2 in the trimethylene species to cyclopropane is negligible.

[1]This assumption seems justified on the basis that any secondary β-isotope effect would be expected to be smaller than the secondary α-isotope effect which is itself very small (see next paragraph).

The n.m.r. spectrum of propylene derived from **5** indicates that it is a 60:40 mixture of $CH_2{=}CD{-}CH_3$ to $CH_2{=}CH{-}CH_2D$, i.e. an isotope effect $k^5_H/k^5_D = 1.50 \pm 0.08$. There may be a small secondary isotope effect upon k^5_H, however, this is not expected to be greater than 1 to 2% since, using the Hammond hypothesis (15), one would expect the transition state to resemble strongly the intermediate rather than the propylene. Wiberg has shown that isotope effects of this

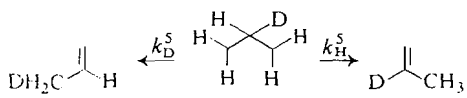

type are in the order of 1% (16). Assuming $k^1_H = 1.01\ k^5_H$ we can compare the cyclization rate constants k^1_{cy} and k^5_{cy}. The analytical data in Table III indicate that:

$$\frac{k^1_{cy}}{2k^1_H} = \frac{88.43}{11.57} \quad \text{and} \quad \frac{k^5_{cy}}{k^5_H + k^5_D} = \frac{89.21}{10.79}$$

Using the aforementioned n.m.r. data we find that $k^1_{cy} = 1.13\ k^5_{cy}$. Similarly if we go through some type of calculations assuming that $k^5_D = 1.01\ k^6_D$ then we find that $k^5_{cy} = 1.13\ k^6_{cy}$. Thus deuterium substitution at the 4-position of the pyrazolines slows down the rate at which the intermediate cyclizes to cyclopropane. The quantity is exactly that observed for sp^3 carbons going to sp^2, in keeping with the previously mentioned characteristics of the cyclopropane structure.

It is evident that this study of secondary kinetic isotope effects is consistent with the proposed formation of the trimethylene intermediate in the thermolysis of 1-pyrazoline, and provides a strong case for the cleavage of both carbon–nitrogen bonds in the rate-determining transition state.

Acknowledgments

We wish to thank Dr. S. Seltzer for fruitful discussions, and Dr. A. Hogg for his help with the mass spectrometry. Acknowledgment is also made to the donors of the Petroleum Research Fund, administered by the American Chemical Society, for support of this research.

1. S. Seltzer and S. G. Mylonakis. J. Am. Chem. Soc. **89**, 6584 (1967); S. Seltzer and F. T. Dunne. J. Am. Chem. Soc. **87**, 2628 (1965); S. Seltzer. J. Am. Chem. Soc. **85**, 14 (1963).
2. V. J. Shiner, Jr., W. E. Buddenbaum, B. L. Murr, and G. Lamaty. J. Am. Chem. Soc. **90**, 418 (1968).
3. M. Wolfsberg and M. J. Stern. Pure Appl. Chem. **8**, 225, 325 (1964).
4. R. J. Crawford and A. Mishra. J. Am. Chem. Soc. **88**, 3963 (1966); R. J. Crawford and D. M. Cameron. Can. J. Chem. **45**, 691 (1967).
5. M. S. Kharasch and F. R. Mayo. J. Am. Chem. Soc. **55**, 2468 (1933).
6. R. J. Crawford, A. Mishra, and R. J. Dummel. J. Am. Chem. Soc. **88**, 3859 (1966).
7. G. G. Smith and F. D. Bagley. Rev. Sci. Instr. **32**, 703 (1961).
8. E. A. Halevi. Progr. Phys. Org. Chem. **1**, 180 (1963).
9. R. Hoffmann. J. Am. Chem. Soc. **90**, 1475 (1968).
10. E. M. Hodnett and P. S. Juneja. J. Org. Chem. **33**, 1233 (1968).
11. S. Seltzer and E. J. Hamilton, Jr. J. Am. Chem. Soc. **88**, 3775 (1966).
12. E. A. Halevi. Progr. Phys. Org. Chem. **1**, 168 (1963).
13. A. W. Baker and R. C. Lord. J. Chem. Phys. **23**, 1636 (1955).
14. R. C. Lord and P. Venkateswarlu. J. Opt. Soc. Am. **43**, 1079 (1958).
15. G. S. Hammond. J. Am. Chem. Soc. **77**, 334 (1955).
16. K. B. Wiberg. Physical organic chemistry. J. Wiley and Sons, Inc., New York. 1964. p. 360.

Can. J. Chem. Downloaded from www.nrcresearchpress.com by 210.87.254.105 on 09/05/12
For personal use only.

Can. J. Chem. Downloaded from www.nrcresearchpress.com by 210.87.254.6 on 09/05/12
For personal use only.

Photolysis of some alkyl-1-pyrazolines[1]

RALPH MOORE, ANUPAMA MISHRA, AND ROBERT J. CRAWFORD
Department of Chemistry, University of Alberta, Edmonton, Alberta

Received June 17, 1968

The direct and photosensitized photolysis of six methylated-1-pyrazolines is described. Examination of the products suggests that direct photolysis leads to an excited singlet trimethylene, whereas a triplet is produced on benzophenone photosensitization. The trimethylene produced from **4** and **5** is related to the intermediates produced on addition of triplet methylenes to *cis*- and *trans*-2-butene. Evidence is presented to support the claim that no intermediate is involved in the addition of singlet methylene to *cis*- and *trans*-2-butene.

Canadian Journal of Chemistry, 46, 3305 (1968)

A considerable amount of discussion has been generated about trimethylene since its proposal, in 1934 (1), as a possible intermediate in the thermal isomerization of cyclopropane. The thermolysis of 1-pyrazolines has been interpreted to proceed through a trimethylene intermediate of defined stereochemistry (2) and representing a distinct energy minimum on the potential surface (3). The extended Hückel molecular orbital calculations of Hoffmann (3) reveal that the antisymmetric trimethylene (**1**) is the lowest singlet state for that particular configuration, and that there exists an excited singlet which is "floppy" with no barriers to internal rotation. Simmons (4) has carried out a Pariser – Parr – Pople calculation which places the triplet state of trimethylene some 0.5 eV below the lowest singlet (**1**). The singlet trimethylene intermediate $(A)^2$ implicated in cyclopropane isomerizations (5), and pyrazoline thermolysis does not however play a role in the addition of singlet methylene to olefins (3, 6) as previously implied (7). It seems reasonable to assume however that the triplet trimethylene implicated in the addition of triplet methylene to olefins (see Gaspar and Hammond (8) and refs. 3, 7, and 9) may be produced by the triplet photosensitized decomposition of 1-pyrazolines.

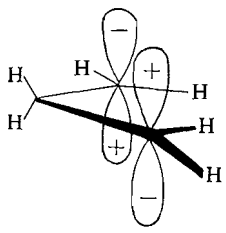

1

We have undertaken a study of the photochemical decomposition of 1-pyrazolines, by direct photolysis in an attempt to gain insight into the chemistry of the "floppy" excited singlet $(A)^1$ $(S)^1$ trimethylene intermediate (3), and by triplet benzophenone photosensitization in an attempt to obtain the triplet trimethylene. The latter is particularly desirable since so much of the chemistry of triplet trimethylene has been extracted from the reactions of triplet methylene wherein complicating side reactions do not allow a clear choice (10) except by careful scavenging experiments (10*c*).

Results and Discussion

In order to assess the possible role of "hot cyclopropanes" we first examined the direct photolysis of 3-methyl-1-pyrazoline (**2**) and 4-methyl-1-pyrazoline (**3**) (Table I). The results from the thermolysis experiments reported earlier are included for comparison (2). The isobutylene

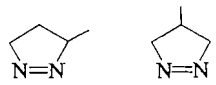

2 **3**

produced from **2** and the linear butenes from **3** are products which are pressure sensitive and arise from the re-opening of the initially formed "hot methylcyclopropane". The addition of 600 Torr of nitrogen does not completely quench this reaction, but decreases it by a factor of 5 and adds to the amount of methylcyclopropane.

[1]This research was presented, in part, in a thesis by Ralph Moore in partial fulfilment of the requirements for the Ph.D. degree, August, 1967. Presented at the Symposium International sur la Chimie des Petits Cycles et ses Applications, Louvain, Belgium, September, 12–15, 1967.

TABLE I

Photolysis of 3-methyl (**2**) and 4-methyl-1-pyrazoline (**3**)

No.	Photolysis method	Pressure (Torr)	Product, mole %						
			C_2H_4					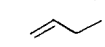	
	2								
1	Direct	7–8	2.8	7.1	69.4	2.50	~9	~10	0.91
2	Direct	7–8	2.6	7.4	71.3	1.93	~8	~9.5	0.66
3	Direct	600 (N_2)	2.2	7.5	78.7	0.4	~6.5	~7	Trace*
4	Direct	600 (N_2)	2.2	7.1	79.4	0.6	5.5–6	6–6.5	Trace
	Thermal	100–200	0	0	93.3	1.16	1.9	3.7	0
	3								
1	Direct	7–8	—	11.4	55.2	2.9	~4	6	20.6
2	Direct	7–8	—	11.4	55.6	2.5	~3.5	~5.5	21.5
3	Direct	600 (N_2)	—	9.8	66.6	0.18	~0.8	~1	21.6
4	Direct	600 (N_2)	—	9.6	67.5	0.11	~0.8	~1	21.0
	Thermal	100–200	—	0	52.3	0	0	0	47.7

*"Trace" may be taken as less than 0.1%.

It is obvious too that some fragmentation to produce ethylene and propene occurs, but that this reaction is not notably pressure sensitive. The results in Table I were obtained using an Osram 200W super pressure mercury arc with a Corex filter. The 1-pyrazolines all undergo $n \rightarrow \pi^*$ absorption at approximately 320 mμ and it is this absorption band that is affecting reaction (11).

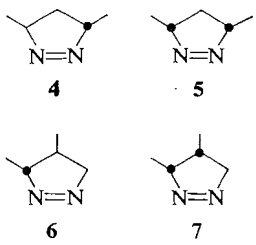

4 **5**

6 7

Table II lists the products produced under a variety of photolytic conditions for *trans*-3,5-dimethyl-1-pyrazoline (**4**). Table III similarly lists the products of photolysis of *cis*-3,5-dimethyl-1-pyrazoline under various photolytic conditions. A control run demonstrated (by nuclear magnetic resonance (n.m.r.)) that **4** and **5** were not interconverted during the photolysis experiments. It is obvious that the fragmentation process occurs only on direct photolysis and does not appear to be dependent upon pressure or phase. The generally accepted mechanism for

TABLE II

Photolysis products of *trans*-3,5-dimethyl-1-pyrazoline (**4**)

No.	Time (min)	Pressure (Torr)	Product, mole %							
					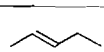		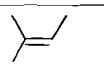	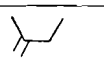	C_2H_4	
1*	60	5–6	26.7	59.5	2.2	3.0	Trace	~0.2	6.1	7.9‡
2*	120	5–6	26.2	60.0	2.2	3.1	Trace	0.1–0.2	8.3	8.5
3	60	60 (N_2)	26.1	60.5	1.9	2.7	Trace	0	6.9	8.8
4	60	600 (N_2)	24.7	61.9	2.1	3.3	0	0	6.1	8.0
5	120	600 (N_2)	24.9	61.1	2.2	3.2	0	0	7.0	8.6
6†	Thermal	100–200	25.4	72.6	1.1	0.9	0	0	0	0
7	60	Neat liquid	43.9	42.3	3.0	4.2	0	0	Trace	6.6
8	270	Neat liquid	44.6	41.5	2.8	4.4	0	0	1.6	6.7
9	120	95% EtOH	45.6	44.5	2.8	3.9	0	0	Trace	2.8§
10*	180	ϕ_2CO‖	61.2	38.8	Trace	Trace	0	0	Trace	Trace

*Average of three or more runs.
†Ref. 2.
‡Mole % calculated on the basis of the amount of nitrogen produced, because of fragmentation may exceed 100.
§1% of diethyl ether produced via the fragmentation reaction.
‖Benzophenone used as photosensitizer.

Can. J. Chem. Downloaded from www.nrcresearchpress.com by 210.87.254.6 on 09/05/12
For personal use only.

TABLE III

Photolysis products of *cis*-3,5-dimethyl-1-pyrazoline (**5**)*

No.	Time (min)	Pressure Torr	Product, mole %							
									C_2H_4	
1	15	5.6	42.5	47.1	1.1	1.0	Trace	0.2	7.3	8.1
	30	5.6	42.1	47.7	1.0	0.9	Trace	0.2	7.6	8.2
3†	60	5.6	41.7	47.0	1.1	1.0	Trace	0.2	7.3	8.2
4	195	5.6	41.3	48.0	1.2	0.9	Trace	0.2	7.1	8.5
5	60	600 (N_2)	41.1	48.9	0.3	0.3	0	0	6.3	9.6
6	Thermal	(3)	66.1	33.2	0.68	0	0	0	0	0
7	60	EtOH sol'n	61.7	33.9	1.0	0.5	—	—	Trace	2.7‡
8	600	EtOH sol'n	61.8	34.0	1.5	0.8	—	—	~0.2	2.2‡
9	60	ϕ_2CO§	60.1	38.9	<0.2	Trace	0	0	0	0.8
10	120	ϕ_2CO§	60.4	39.3	<0.2	Trace	0	0	0	0.3

*All runs corrected for the presence of 15% of **4**.
†Average of three runs.
‡2.5% Diethyl ether also produced.
§Benzophenone used on a photosensitizer.

photolysis of azo compounds involves the loss of nitrogen to produce hydrocarbons (12) generally believed to form via radical intermediates (13). Benzophenone is a good triplet sensitizer even with more constrained bicyclic azo compounds (13*b*). Our results for direct photolysis are consistent with the scheme.

[1] $Py + h\nu \rightarrow Py^*$

[2] $Py^* \rightarrow Int^* + N_2$

[3] $Py^* \rightarrow$ cleavage olefins + N_2

[4] $Py^* \rightarrow Py + h\nu$ (fluorescence)

[5] $Int^* \rightarrow$ cyclopropanes + olefins

The reaction [4] has been observed by Strausz (11) to be analogous to that reported by Solomon, Thomas, and Steel (13). Similarly Strausz has not observed any evidence for conversion of the pyrazoline singlet (Py*) to a triplet.

The absence of branched C-5 olefins as photolysis products of [4] and [5] at 600 Torr of added nitrogen is taken to indicate that the initially produced "hot dimethylcyclopropane (DMCP)" is collisionally quenched. Both ethylene and propylene are produced upon direct photolysis, the decreased yields in ethanol solution are believed to be due to analytical difficulties in assessing all of the cleavage products (e.g. ethylene, propylene, diethyl ether, methyl ethyl ether) rather than having any mechanistic significance.

Tables IV and V present the proportions of the products observed from photolysis of *trans*-3,4-dimethyl-1-pyrazoline (**6**) and *cis*-3,4-dimethyl-1-pyrazoline (**7**) respectively.

Cyclopropane Forming Reactions

A curious feature arises from the photolysis of *trans*-(**4**) and *cis*-3,5-dimethyl-1-pyrazoline (**5**). In the gas phase the *trans* compound exhibits stereoselectivity in a manner similar to the thermal decomposition while the *cis* exhibits the opposite behavior. In liquid phase the *trans* now exhibits behavior different from the thermal results while the *cis* shows stereoselectivity similar to the thermal decomposition. In general the stereoselectivity observed in the thermal process seems to be decreased in the photolytic process and conrotation ring closure does not appear to be the predominating path for the intermediate as it is in the thermal process. This is not unreasonable since the thermal process would be expected to produce the ground state singlet of the intermediate while photolysis may produce an excited singlet. Hoffmann (3) only predicts conrotatory ring closure for the ground state singlet $(A)^2$ whereas the excited state (A^1) (S^1) is not expected to show any distinct preference.

It is also tempting to suggest that since the true ground state of the trimethylene intermediate has been predicted (4) to be a triplet, then in solution, some intersystem crossing may occur to give a triplet diradical which is expected to result in an increase in the amount of *trans*-DMCP. However, this is not supported by the results from the liquid phase photolysis of **6** and **7** (Tables IV and V).

In the direct photolysis results for *trans*-(**6**) and *cis*-3,4-dimethyl-1-pyrazoline (**7**) the cyclopropanes from both pyrazolines tend to retain the stereochemistry of the starting material. On

Can. J. Chem. Downloaded from www.nrcresearchpress.com by 210.87.254.6 on 09/05/12
For personal use only.

TABLE IV

Photolysis products of *trans*-3,4-dimethyl-1-pyrazoline (**6**)

No.	Time (min)	Conditions	Product,* mole%					
							2-Pentene	
1	60	5–6 Torr†	37.2	24.4	16.4	14.5	0.5	5.7
2	60	5.6 Torr + 55 Torr N_2	39.3	24.7	14.7	14.3	Trace	5.7
3	60	5–6 Torr + 600 Torr N_2	41.3	24.8	14.1	13.2	—	5.5
4	Thermal	100–200 Torr	21.8	46.0	16.3	15.8	—	0‡
5	120	EtOH sol'n	50.7	13.0	18.3	14.1	—	3.1§
6	240	EtOH sol'n	48.1	13.2	19.5	15.0	—	3.1
7	120	ϕ_2CO, EtOH	72.7	27.8	1.5	1.1	—	1.9
8	240	ϕ_2CO, EtOH	72.4	22.4	1.8	1.5	—	2.0
9	1100	ϕ_2CO, C_6H_6‖	72.0	26.2	0.8	0.3	0.7¶	—

*In all direct photolysis runs a trace of ethylene and propylene was detected.
†The vapor pressure of **6** at 25 °C.
‡Ref. 2.
§Approximately 0.5% of methyl ethyl ether also detected.
‖Benzophenone to pyrazoline ratio 40:1.
¶Tentatively identified as 3-methyl-1-butene.

increasing the pressure the cyclopropanes become even more stereoselective. Again, in this case, we have one compound **7** which roughly parallels the thermal results, while the other, **6**, exhibits the opposite behavior. This again may be due to the differences between the ground state singlet and the excited singlet of the trimethylene intermediate. The cyclopropane ratios in this case tell even less than those from **4** and **5** because even if one could predict which rotation (*con-* or *dis-*) should predominate in ring closure, both rotations may give rise to either *cis-* or *trans-*DMCP.

The cyclopropanes formed do, however, follow the stereochemical pattern found by Rinehart and VanAuken (14). They found that in the photolysis of *cis-* and *trans*-3,4-dimethyl-3-carbomethoxy-1-pyrazoline the resulting cyclopropanes tended to favor the stereochemistry of the substrate while the stereoselectivity was much less pronounced in the thermal results. This parallels fairly well the results for **6** and **7**.

One of the most interesting features of Tables II to V, is the ratio of *trans/cis* DMCP produced from the isomeric pairs. The pyrazolines **4** and **5** on photosensitization would be expected to produce the secondary–secondary triplet diradical **8**, whereas the pyrazolines **6** and **7** would produce the secondary–primary triplet diradical **9**. If in these species rotation is fast, then the same ratio of *trans/cis* DMCP is expected from **4** as from **5**, and from **6** as from **7**. Table VI presents a summary of these ratios. We feel that the values 2.77 and 2.63 obtained for **6** and **7** are in good agreement with the 2.9 value obtained by Mc-

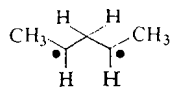

8

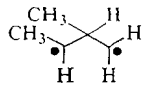

9

TABLE V

Photolysis products of *cis*-3,4-dimethyl-1-pyrazoline (**7**)

No.	Time (min)	Conditions	Product,* mole%					
							2-Pentene	
1	60	5–6 Torr†	37.6	43.0	4.7	4.8	1.6	7.2
2	60	5 + 600 Torr N_2	35.4	50.6	3.4	2.8	—	6.9
3	Thermal	100–200 Torr	35.2	43.7	14.4	7.1	—	—
4	180	EtOH sol'n	26.4	60.4	5.0	3.7	—	4.0
5	240	ϕ_2CO, EtOH sol'n	66.2	32.1	0.5	tr.	—	1.3
6	1100	ϕ_2CO, C_6H_6‡	70.6	26.8	1.5	0.1	0.8§	—

*In all direct photolysis runs a trace of ethylene and propylene was detected.
†The vapor pressure of **7** at 25°.
‡Benzophenone to pyrazoline ratio 40:1.
§Tentatively identified as 3-methyl-1-butene.

Can. J. Chem. Downloaded from www.nrcresearchpress.com by 210.87.254.6 on 09/05/12
For personal use only.

Can. J. Chem. Downloaded from www.nrcresearchpress.com by 210.87.254.6 on 09/05/12
For personal use only.

TABLE VI

Ratio of *trans* to *cis*-1,2-dimethylcyclopropane

Source	Ratio	Reference
4	1.58	This work
5	1.55	This work
6	2.77	This work
7	2.63	This work
Methylene addition	2.9	Ref. 10*c*
Equilibrium value*	6.0	Ref. 15

*Extrapolated from higher temperatures.

Knight, Lee, and Rowland using methyl iodide as a scavenger and triplet CHT by photolysis of CHTCO in the presence of *cis*- and *trans*-2-butene to generate **9**. The two diradicals **8** and **9** do not close to an equilibrium mixture of *cis*- and *trans*-DMCP but to a ratio which reflects their various transition state energies for the ring closure processes.

Olefin Forming Reactions

The photosensitized decomposition of both **4** and **5** decreases the olefin yield to near zero and it may be that the small amounts seen are due to some direct photolysis taking place. Alternatively, it is hardly conceivable that the triplet diradical could produce olefins directly, so after spin inversion occurs, the resulting intermediate is probably completely collisionally stabilized and may close almost exclusively to the cyclopropanes. It has been shown in the thermal isomerization of dimethylcyclopropanes that *cis–trans* isomerization occurs 100 times faster than olefin formation (15), so the collisionally deactivated intermediate would be expected to give no more than a total of one percent olefin.

The photosensitized results for **4** and **5** show no trace of 1-pentene. This product would be expected to arise if the triplet diradical underwent a 1,4-hydrogen migration (Scheme 1) similar to that proposed (10*d*) for the formation of 3-methyl-1-butene in the addition of triplet methylene to 2-butene.

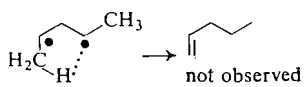

SCHEME 1

The olefin, 2-methyl-1-butene, is a particularly interesting product arising from **6** and **7** (Tables IV and V). In the case of singlet methylene addition to 2-butene, there is no way for 2-methyl-1-butene to be formed by direct insertion into a C—H bond, whereas for **6** and **7** both the thermolysis (6) and the direct photolysis give rise to substantial amounts of this product. In the addition of singlet methylene to 2-butene, the olefin 2-methyl-1-butene is seen *only* at low pressures where the isomerization of the initially formed cyclopropanes is not completely quenched. However, the trimethylene intermediate produced from **6** and **7** always yields this product. This then appears to eliminate the possibility of singlet methylene initially giving rise to a trimethylene intermediate when it adds to olefins, no matter how short lived that intermediate is. This is in direct opposition to the suggestion of DeMore and Benson (7) and is in accord with the predictions of Hoffmann (3), the experimental observations of Crawford and Ali (6), and the idea of Skell and Woodworth put forward in 1956 (16).

The data from the photosensitized decomposition of **6** and **7** also show a large decrease in the olefin yield. This, coupled with the results from **4** and **5**, leads to the conclusion that the triplet diradical probably produces only trace amounts of olefin, if any at all. The results of Bader and Generosa (10*d*) support this idea since at high pressures of inert gas (where supposedly the concentration of triplet methylene is high) when methylene is added to *cis*-2-butene, the yield of 2-methyl-1-butene is zero and the 2-methyl-2-butene is tending to zero. The small amount of 2-methyl-2-butene present may result from singlet insertion or from some abstraction recombination mechanism involving triplet methylene. (See ref. 10*a*, reactions [2] and [13].)

Cleavage Reactions

Carbon–carbon bond cleavage products have been observed in the photolysis of 1-pyrazolines before (14, 17). One instance of cleavage has also been observed by Crawford and Mishra (2), in the thermolysis of 4,4-dimethyl-1-pyrazoline. In all direct photolysis of the pyrazolines investigated in this work cleavage products were observed.

Two routes are possible for the formation of cleavage products:

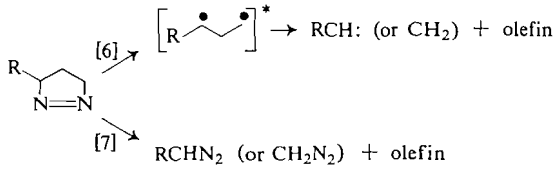

Can. J. Chem. Downloaded from www.nrcresearchpress.com by 210.87.254.6 on 09/05/12
For personal use only.

Both paths [6] and [7] would eventually lead to the production of either methylene, for pyrazolines unsubstituted in the 3-position, or ethylidene, for pyrazolines with a methyl group in the 3-position.

That methylene is produced from the photolysis of 1-pyrazoline (**1**) is strongly implicated by the presence of 1,1,2,2-tetramethylcyclopropane resulting from the photolysis of **1** in 2,3-dimethyl-2-butene solvent. In addition, all direct photolyses of pyrazolines carried out in ethanol produced small amounts of either methyl ethyl or diethyl ether. The ether products quite probably arise from the reaction of methylene or ethylidene with the O—H bond of the alcohol solvent.

The photolysis of 3-methyl-1-pyrazoline (**2**) results in two different cleavage products. These arise from the cleavage of two different carbon–carbon bonds. The route resulting in propylene

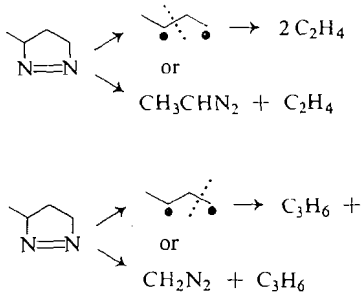

formation appears to be preferred, and is essentially pressure independent. The other mode of cleavage also is likely pressure independent.

No matter how the cleavage occurs, both *trans*- (4) and *cis*-3,5-dimethyl-1-pyrazoline (5) can only produce two olefins, ethylene and propylene. These olefins were observed in 6–9% yield in the direct photolysis runs.

So far, the cleavage products tell nothing regarding the mechanism of their formation. However, the cleavage products from *trans*-(**6**) and *cis*-3,4-dimethyl-1-pyrazoline (**7**) impart somewhat more information than the previous ones. The pyrazoline **6** yielded ethylene, propylene, and only *trans*-2-butene. Not a trace of *cis*-2-butene could be detected. The opposite is true for **7**, only *cis*-2-butene (other than ethylene and propylene) was found and not a trace of *trans*-2-butene. This means that the cleavage reaction is entirely stereospecific. This is identical with the result obtained by Rinehart and VanAuken (14) in the photolysis of *cis*- and *trans*-3,4-dimethyl-3-carbomethoxy-1-pyrazoline. However, because of the stereospecificity, the favored route is eq. [7] which supports the mechanism of Rinehart and VanAuken (14). If eq. [7] is operative, then this is just the reverse of the 1,3-dipolar addition of diazomethane to olefins. However, the addition is a thermal process while the reverse is only observed photochemically. It is possible that the cleavage process is a direct dissociation to nitrogen, olefin, and methylene. This would circumvent the problem of a thermally allowed process being observed in a photochemical reaction. The reason for this is not clear at present.

Experimental

All ultraviolet (u.v.) spectra were obtained on a Perkin–Elmer model 202 spectrophotometer. Nuclear magnetic resonance (n.m.r.) spectra were obtained on Varian Associates A-60 and HR-100 spectrometers. Mass spectra were measured on an A.E.I. MS-9 mass spectrometer.

Materials

(a) The 1-Pyrazolines

Pyrazolines **1**, **2**, **3**, **4**, and **5** were prepared in the manner described previously from the corresponding 1,3-dibromides (2). All were purified by preparative gas–liquid chromatography (g.l.c.) using an Aerograph Autoprep model A-700. Each pyrazoline was checked for purity by n.m.r. Pyrazoline **5** was found to contain 15% **4** by a 100 Mc.p.s. n.m.r. spectrometer. Ultraviolet spectra of all pyrazolines were determined to ensure the absence of any appreciable amounts of 2-pyrazoline. Pyrazolines **6** and **7** were prepared following the procedure of Crawford and Ali (6) from the appropriate 2-butene and diazomethane. These were also purified by preparative g.l.c., and checked for purity by n.m.r. and u.v. spectra. All of the pyrazolines were stored in break seals at −78 °C for indefinite periods with no detectable deterioration.

(b) Hydrocarbon Standards for Gas–liquid Chromatography

All reference hydrocarbons, with the exception of 2,3-dimethyl-2-butene (TME), were commercially available. The TME was prepared by standard literature procedures and purified by preparative g.l.c.

Apparatus

(a) Vacuum Rack

A conventional high vacuum apparatus with a Welch Duo Seal vacuum pump and a mercury diffusion pump was used (Fig. 1). The system consisted of a 250 ml quartz cell, A, for gas phase photolysis; three standard U-traps, 1, 2, 3, along with a small U-trap, 4; a spiral trap, F; a 5/20 ground glass joint, B; mercury float valves, G and H; and a system for the introduction of samples into the g.l.c., E. Section E consisted of two, three-way Hoke valves bolted on the ends of a piece of wood, and a two-way Hoke valve bolted in the middle as shown. Point J represents where the effluent gas from the

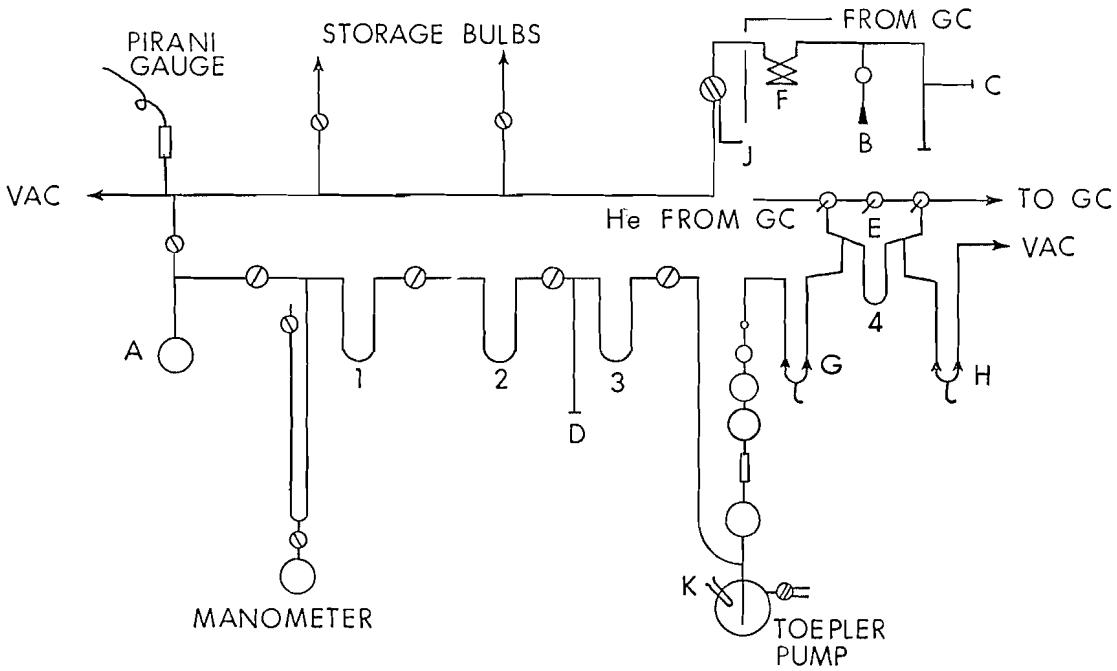

FIG. 1. Conventional high vacuum apparatus with a Welch Duo Seal vacuum pump and mercury diffusion pump.

g.l.c. could be diverted into the apparatus for the collection of any desired peak in trap F. Point C was used for break seals in which material trapped in F could be stored. Point D was used for break seals containing product from liquid photolysis in order to analyze the product in the g.l.c.

The light source used was an Osram 200 W super pressure mercury arc with a Corex glass filter.

(b) Gas–Liquid Chromatography

An F and M model 500 programmed temperature gas–liquid chromatograph was used for product analysis of the photolysis of 1-pyrazoline (**1**) in TME.

All other product analyses were done on a g.l.c. consisting of a Gow–Mac model TR-11-B,w thermal conductivity cell with a Gow–Mac model 40-05C power supply in conjunction with a Sargent model SR recorder. The helium used with this system was purified by passing through ascarite followed by a column of molecular sieves 4A at 77 °K.

Product Analysis

(a) 1,1,2,2-Tetramethylcyclopropane

For the photolysis of **1** in TME a 20 ft column of saturated silver nitrate in propylene glycol on Diatoport was used in tandem with 20 ft of 10% 1,2,3-tris (2-cyanoethoxy)-propane (TCP) on firebrick. The columns were used at room temperature with a helium flow rate of 50 ml/min.

(b) Products of All Photolyses Except Above

The products from the photolysis of all pyrazolines in gas phase or ethanol were determined using a 20 ft column of saturated silver nitrate/propylene glycol on firebrick in tandem with a 9 ft column of 20% dimethylsulfolane (DMS) on Chromosorb W. The columns were used at room temperature with a flow rate of 60 ml/min helium. In some cases where serious overlapping of peaks occurred in this system, it was necessary to run the product mixture through either the silver nitrate or the DMS column separately in order to isolate a certain peak and determine its area relative to another peak (or peaks). Peak areas were measured by using a planimeter and all were corrected for relative responses (18).

Photolyses Procedure

The photolyses and product analyses of all compounds were performed in the same manner (except **1** in TME and neat **4**), only typical representative cases will be given.

*(a) Photolysis of **1** in TME*

To a 10 ml quartz cell, 1 cm thick, was added a solution of 0.245 g of 1-pyrazoline in 9.0 ml of TME. The solution was degassed, and the cell attached to a mercury filled gas burette. After 15 h irradiation, the solution was frozen using liquid nitrogen and was kept frozen for 2 h. This would presumably freeze down most of the cyclopropane and propylene which had left the solution. Following this it was found that 70% of the theoretical amount of nitrogen had been evolved. The solution was then allowed to come to room temperature and a sample was taken into a syringe for injection into the g.l.c. The percentages of products found were; cyclopropane, 77%; propylene, 14%; and tetramethylcyclopropane, 8–9%. These values have little quantitative significance due to the almost certain loss of the low boiling products, propylene and cyclopropane. The purpose of the experiment was to indicate the presence of methylene in the reaction as evidenced by the presence of tetramethylcyclopropane.

Can. J. Chem. Downloaded from www.nrcresearchpress.com by 210.87.254.6 on 09/05/12
For personal use only.

Can. J. Chem. Downloaded from www.nrcresearchpress.com by 210.87.254.6 on 09/05/12
For personal use only.

(b) Photolysis of **5** *— Gas Phase with No Nitrogen Added*

The pyrazoline **5**, which was stored on the vacuum rack at −78 °C, was allowed to come to room temperature. The pyrazoline vapor was then allowed to flow into the reaction cell, A, and the cell isolated from the rest of the system. The residual pyrazoline vapor was then pumped off. The light source was allowed to warm up for approximately 15 min, then placed about 15 cm from the reaction cell and the sample irradiated for 60 min, after which time anywhere from 40–50 μmoles of pyrazoline were found to have decomposed.

After the lamp was turned off, traps 1 and 2 were cooled to 77 °K, and the nitrogen pumped through them into the Toepler pump where it was measured. It was found necessary to use 30–35 cycles of the Toepler to remove the nitrogen. The nitrogen was then removed through float valves G and H. Following this, traps 1 and 2 were warmed to −78 °C using dry ice – acetone baths and the hydrocarbon products distilled into the Toepler pump by means of the cold finger, K, at 77 °K. This method was found to distil over almost quantitatively the hydrocarbons while the unreacted pyrazoline remained in traps 1 and 2. The hydrocarbons were measured in the Toepler pump and then frozen over into trap 4. The nitrogen and hydrocarbon yield checked to within ±6% of one another.

After isolating trap 4 with float valves G and H, the helium carrier gas was diverted through the trap, after the trap had been allowed to warm to room temperature. The hydrocarbons were thus swept into the g.l.c. where they were analyzed. Any material which required further identification was collected by connecting the line from the g.l.c. to the vacuum system at point J and allowing the helium to flow through the spiral trap F, cooled to 77 °K, and out through joint B. After removing the helium, the product could be transferred into a break seal at point C.

(c) Direct Photolysis of **5** *in Ethanol*

A solution of 0.213 g of **5** in 5.00 ml of 95% ethanol was prepared. For photolysis, 0.40 ml of this solution was diluted with 1.60 ml of 95% ethanol and the resulting solution used to fill several small Pyrex glass bulbs (~0.3 ml). The bulbs were then thoroughly degassed (3–5 freeze–thaw cycles) on the vacuum line at point B (Fig. 1) and sealed. A bulb containing the degassed solution was then irradiated for 1 h at a distance of about 15 cm from the light source.

After irradiation, the bulb was placed in the bulb crusher which was connected to the g.l.c., heated to 110°, and crushed. The hydrocarbon products were separated from the ethanol and unreacted pyrazoline by using a 20 ft column of 20% Carbowax 1500 on Chromosorb W used at room temperature with a flow rate of 40–50 ml/min. The hydrocarbon product was collected in trap F. After the helium was pumped off, the product was frozen into a break seal at C, sealed, and transferred to D. The break seal was broken, the products frozen into the Toepler pump and measured. They were then transferred to U-trap 4, and passed into the g.l.c. using the silver nitrate–DMS column. The amounts of product typically found for 2 h irradiation ranged from 15–25 μmoles.

(d) Benzophenone Photosensitized Photolysis of **5**

A solution of 1.59 *M* benzophenone (B.D.H. reagent grade, twice recrystallized) in 95% ethanol was prepared. This solution (1.60 ml) was then used to dilute 0.40 ml of the previously described solution of **5**. This gave a solution which was 0.087 *M* in **5** and 1.27 *M* in benzophenone, a molar ratio of benzophenone to **5** of 14.6:1. Since benzophenone and **5** have approximately the same molar extinction coefficient at 3200 Å, and benzophenone has a much broader absorption band, most of the incident light should be absorbed by the benzophenone. The solution was then put into bulbs, degassed, irradiated, and analyzed as described previously. Typical amounts of product for 2 h irradiation were 8–13 μmoles.

(e) Benzophenone Photosensitized Photolysis of **6** *and* **7**

A solution of benzophenone and **6** (or **7**) of 40:1 molar ratio in benzene was placed in a small Pyrex bulb of approximately 0.5 ml capacity, degassed, and sealed. The solution was irradiated using a Hanovia medium pressure lamp for 18 to 24 h. The samples were analyzed as described above.

(f) Photolysis of **4** *(Neat Liquid)*

To a quartz epr tube fitted with an inner 5/20 joint was added liquid **5** to a height of about ½ in. The tube was attached at point D (Fig. 1) through a stopcock by means of an outer 5/20 joint, degassed, and irradiated for 2 h. After irradiation, the product was transferred to the U-trap 1. The nitrogen was pumped into the Toepler and measured as previously described; found, nitrogen, 23.2 μmoles. Traps 2 and 3 were then placed in dry ice–acetone baths (−78 °C) and trap 1 allowed to warm to room temperature. The hydrocarbons were frozen into the Toepler pump, measured, and found to equal 23.3 μmoles. The hydrocarbons were then passed into the g.l.c. and analyzed in the usual manner.

(g) Correction for **4** *in* **5**

The sample of **5** used contained 15% **4** (n.m.r.). The product yields given for **5** are corrected for the presence of **4**, no interconversion of **4** to **5** could be detected either in the gas phase or liquid phase photolysis.

In order to make a simple correction for **4** in **5**, they must decompose at comparable rates. Three runs of each compound were performed; the total amount of product for equivalent times was determined by use of the Toepler pump. The rates of decomposition were found to be comparable. Runs of **5** to various percentages completion also showed no change.

Control Experiments

(a) Product Lost on Trapping from Gas–Liquid Chromatography

A gas phase photolysis experiment was done on **5**. The products were trapped and re-run through the g.l.c. as previously described. It was found that most of the ethylene was lost, about one-half of the propylene was lost, and the percent of other products remained almost unchanged. Actual results are given in Table VII, along with the results of a similar experiment using **7**.

(b) Interconversion of DMCP under the Reaction Conditions

cis-1,2-Dimethylcyclopropane (56 Torr) was placed in the reaction cell along with ~0.5 Torr of **4**, and irradiated for 2 h. After irradiation, nitrogen found, 1.96 μmoles. Product analysis showed that the *trans*-DMCP peak was only 0.055% of the *cis*-DMCP peak and that the ratio of

TABLE VII

Product loss on trapping from gas–liquid chromatography (mole %)

	From **5**		From **7**	
	No. of times trapped		No. of times trapped	
Product	0	1	0	1
cis-DMCP	47.7	49.4	43.2	43.4
trans-DMCP	42.1	44.3	37.8	38.2
trans-2-Pentene	1.0	1.0	0.87	0.83
cis-2-Pentene	0.9	0.9	0.57	0.60
2-Methyl-2-butene	—	—	4.37	4.32
2-Methyl-1-butene	0.15	0.14	4.72	4.76
cis-2-Butene	—	—	7.15	7.16
Propene	8.2	3.7	1.28	0.67
Ethylene	7.6	1.5	0.92	0.11

trans-DMCP to propylene equalled 3.04:1. In regular gas phase runs with 60 Torr nitrogen present, the same ratio was 3.20:1 and 2.79:1. Since all the *trans*-DMCP may be accounted for by the decomposed pyrazoline and since the ratio of *trans*-DMCP to propylene is similar to that in regular gas phase runs, then it may be assumed that *cis*-DMCP is not converted to *trans*-DMCP under the reaction conditions. A similar result was obtained using *trans*-DMCP.

A small sample (37.7 μmoles) of *cis*-DMCP was added to a 1.27 *M* benzophenone solution in ethanol in a small bulb, degassed, and sealed. The solution was irradiated for 3 h. The only detectable hydrocarbon after irradiation was *cis*-DMCP which measured 33.1 μmoles. Hence, *cis*-DMCP is not consumed or isomerized under reaction conditions. A small sample of *cis*-DMCP was added to a concentrated solution of benzophenone in benzene and exposed to a Hanovia medium pressure lamp for 72 h. Subsequent g.l.c. analysis indicated less than 1% decomposition of which 3-methyl-1-butene was the principal product with only a trace of *trans*-DMCP.

(c) Additional Products in Solution Photolysis

A small Pyrex glass bulb filled with the previously described solution of **5** in ethanol was attached at point D through a stopcock. After degassing, the stopcock was closed, and the solution irradiated for 3 h. Following this, the stopcock was opened and the solution frozen over into U-trap 2. The nitrogen was pumped into the Toepler. The solution was then transferred into trap 1 and again the Toepler was used to remove any nitrogen. The nitrogen was measured and pumped off.

After the nitrogen was removed, the solution was frozen into the Pyrex bulb at D, and the bulb sealed off. It was then placed in the bulb crusher, run through the Carbowax column, and the products trapped in F as before, (flow rate used in this case 30–35 ml/min to minimize loss in trapping). The products were then transferred back to D and into the Toepler as before and measured.

Two similar experiments were carried out for the photosensitized decomposition of **5**, except that now the DMS column was used in order to separate the acetaldehyde from the hydrocarbons. In each case the trapping efficiency was 90% or greater.

Acknowledgments

We wish to thank Professor O. P. Strausz for helpful discussions. Acknowledgment is also made to the National Research Council of Canada for financial support of this work.

1. T. C. Chambers and G. B. Kistiakowsky. J. Am. Chem. Soc. **56**, 399 (1934).
2. R. J. Crawford and A. Mishra. J. Am. Chem. Soc. **88**, 3963 (1966).
3. R. Hoffmann. J. Am. Chem. Soc. **90**, 1475 (1968).
4. H. E. Simmons. Private communication.
5. R. J. Crawford and T. R. Lynch. Can. J. Chem. **46**, 1457 (1968).
6. R. J. Crawford and L. Ali. J. Am. Chem. Soc. **89**, 3909 (1967).
7. W. B. DeMore and S. W. Benson. Advan. Photochem. **2**, 219 (1964).
8. P. P. Gaspar and G. S. Hammond. *In* Carbene chemistry. *Edited by* W. Kirmse. Academic Press Inc., New York. 1964. p. 235.
9. R. J. Cvetanovic, H. E. Avery, and R. S. Irwin. J. Chem. Phys. **46**, 1993 (1967).
10. (*a*) D. F. Ring and B. S. Rabinovitch. J. Phys. Chem. **72**, 191 (1968). (*b*) R. W. Carr and G. B. Kistiakowsky. J. Phys. Chem. **70**, 118 (1966). (*c*) C. McKnight, P. S. T. Lee, and F. S. Rowland. J. Am. Chem. Soc. **89**, 6802 (1967). (*d*) R. F. W. Bader and J. I. Generosa. Can. J. Chem. **43**, 1631 (1965).
11. O. P. Strausz. Private communication.
12. C. Worsham and O. K. Rice. J. Chem. Phys. **46**, 2021 (1967).
13. (*a*) B. S. Solomon, T. F. Thomas, and C. Steel. J. Am. Chem. Soc. **90**, 2249 (1968). (*b*) P. D. Bartlett and P. S. Engel. J. Am. Chem. Soc. **90**, 2960 (1968); S. D. Andrews and A. C. Day. Chem. Commun. 667 (1966); A. C. Day. Private communication.
14. K. L. Rinehart, Jr. and T. V. VanAuken. J. Am. Chem. Soc. **82**, 5251 (1960); **84**, 3136 (1962).
15. M. C. Flowers and H. M. Frey. Proc. Roy. Soc. London, Ser. A, **257**, 122 (1960).
16. P. S. Skell and R. C. Woodworth. J. Am. Chem. Soc. **78**, 4496 (1956).
17. D. E. McGreer, R. S. McDaniel, and M. G. Vinje. Can. J. Chem. **43**, 1389 (1965). D. E. McGreer, N. Chiu, M. G. Vinje, and K. C. Wong. Can. J. Chem. **43**, 1407 (1965). D. E. McGreer, N. Chiu, and M. G. Vinje. Can. J. Chem. **43**, 1398 (1965).
18. A. E. Messner, D. M. Rosie, and P. A. Argabright. Anal. Chem. **31**, 230 (1959). W. A. Dietz. J. Gas Chromatog. **5**, 68 (1967).

Can. J. Chem. Downloaded from www.nrcresearchpress.com by 210.87.254.6 on 09/05/12
For personal use only.

Can. J. Chem. Downloaded from www.nrcresearchpress.com by 210.87.254.105 on 09/05/12
For personal use only.

Friedel–Crafts rearrangements. III. Deuterium tracer studies of the mechanism of cyclialkylation of phenylalkyl chlorides[1]

L. R. C. Barclay and E. C. Sanford
Department of Chemistry, Mount Allison University, Sackville, New Brunswick

Received April 2, 1968

A series of dideuterated primary phenylalkyl chlorides 1-chloro-3-phenylpropane-2,2-d_2 (**4**), 1-chloro-3-phenylpropane-1,1-d_2 (**9**), 1-chloro-4-phenylbutane-2,2-d_2 (**8**), 1-chloro-5-phenylpentane-4,4-d_2 (**5**), 1-chloro-5-phenylpentane-3,3-d_2 (**6**), and 1-chloro-5-phenylpentane-2,2-d_2 (**7**) were synthesized by alkylations of malonic ester with phenylalkyl chlorides. Deuterium was introduced by exchange of the sodium salt of the alkylated malonic ester with D_2O, followed by hydrolysis and decarboxylation. The resulting acids were reduced by hydride to primary alcohols and these were converted to the dideuterated primary chlorides by decomposition of the intermediate chlorosulfite esters. Nuclear magnetic resonance (n.m.r.) spectra confirmed the position of the deuterium in the chlorides. Friedel–Crafts cyclialkylation of the deuterated phenylpentyl chlorides yielded labelled 1-methyltetralins in which the label was located by n.m.r. and mass spectroscopy. The results demonstrated that rearrangement precedes cyclialkylation of 1-chloro-5-phenylpentane. Extensive deuterium scrambling between C-1, C-2, and C-3 accompanied the cyclialkylation of **5** but not that of **8**. Reaction mechanisms are suggested to account for these results.

Canadian Journal of Chemistry, 46, 3315 (1968)

Introduction

Intramolecular alkylation of aryl-substituted halides (cyclialkylation) is the simplest intramolecular counterpart of the classical Friedel–Crafts alkylation. Nevertheless, certain generalizations that have been made on the lack of isomerizations during cyclialkylations (1, 2) have recently been shown to be incorrect. For example, we found that cyclialkylation of 1-chloro-5-phenylpentane yielded 1-methyltetralin (3) and not benzsuberane as was previously reported (1). Results reported by Khalaf and Roberts (4) on the cyclialkylation products from related phenylalkyl chlorides corroborate our view.

Deuterium labelling of phenylalkyl chlorides is a very useful method of providing information on the mechanism of rearrangements and hydride exchange accompanying Friedel–Crafts cyclialkylations. For example, the case for using deuterium labelling in the side-chain of a 5-phenylpentyl chloride is given in Scheme 1.

Two distinct possibilities can be considered for the pathway of the cyclialkylation–rearrangement of a 5-phenylpentyl chloride (**5**) leading to 1-methyltetralin. In one mechanism (path 2) benzsuberane could form as an intermediate, followed by a 1,2-aryl shift analogous to the Schmerling–Roberts (5, 6) phenonium ion mechanism for rearrangements of alkylbenzenes. With the deuterium label, two routes (*a*) and (*b*) exist for this rearrangement which is thus expected to give two differently labelled methyltetralins (*a*) and (*b*), one of which has deuterium in the methyl group.

On the other hand, rearrangement in the side-chain prior to cyclization (path 1) by the equilibration of carbonium ions or through a hydrogen bridged ion, would yield methyltetralin (*b*) without deuterium in the methyl group. It is expected that one could discriminate between the two pathways by nuclear magnetic resonance (n.m.r.) and mass spectral analyses of the product.

Discussion of Results

(a) Syntheses of Deuterium Labelled Compounds

The classical malonic ester synthesis was adapted to the synthesis of most of the deuterium labelled compounds. The typical synthetic scheme is outlined in Scheme 2 for the synthesis of 1-chloro-3-phenylpropane-2,2-d_2 (**4**) and 1-chloro-5-phenylpentane-4,4-d_2 (**5**). In these cases, the deuterium was introduced by exchange on the salt (**1**) of diethyl benzylmalonate followed by decarboxylation. Variations of this scheme were used for the synthesis of 1-chloro-5-phenylpentane-2,2-d_2 (**7**) and of 1-chloro-4-phenylbutane-2,2-d_2 (**8**). The deuterium label in **7** was introduced by exchange on diethyl 3-phenylpropylmalonate and in **8** by exchange on diethyl 2-phenylethylmalonate. 1-Chloro-5-phenylpentane-3,3-d_2 (**6**) was synthesized by extending the

[1]Taken in part from the M.Sc. Thesis of E. C. Sanford, Mount Allison University, 1966.

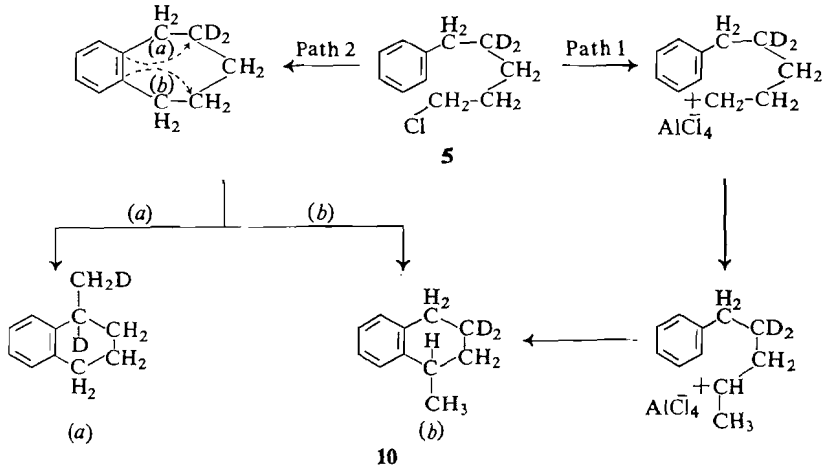

SCHEME 1

chain of **8** through the Grignard reagent. For the synthesis of 1-chloro-3-phenylpropane-1,1-d_2 (**9**), deuterium was introduced by lithium aluminium deuteride reduction of methyl 3-phenylpropionate. The remainder of the multi-step conversions involved classical steps as outlined in the typical scheme.

Decomposition of chlorosulfite esters by the method of Boozer and Lewis (7) proved to be a very convenient method for the preparation of the labelled phenylalkyl chlorides from the alcohols. The chlorosulfite ester of 4-phenyl-1-butanol-2,2-d_2 yielded some tetralin-2,2-d_2 (25%) as well as **8**. The n.m.r. spectrum of this tetralin was similar to that from cyclialkylation of **8**.

The data on integrations and assignments for the n.m.r. spectra of the phenylalkyl chlorides are outlined in Table I. Compounds **4**, **7**, and **8**, containing a $-CD_2-$ group at position-2, were clearly distinguished by the broad singlet in the

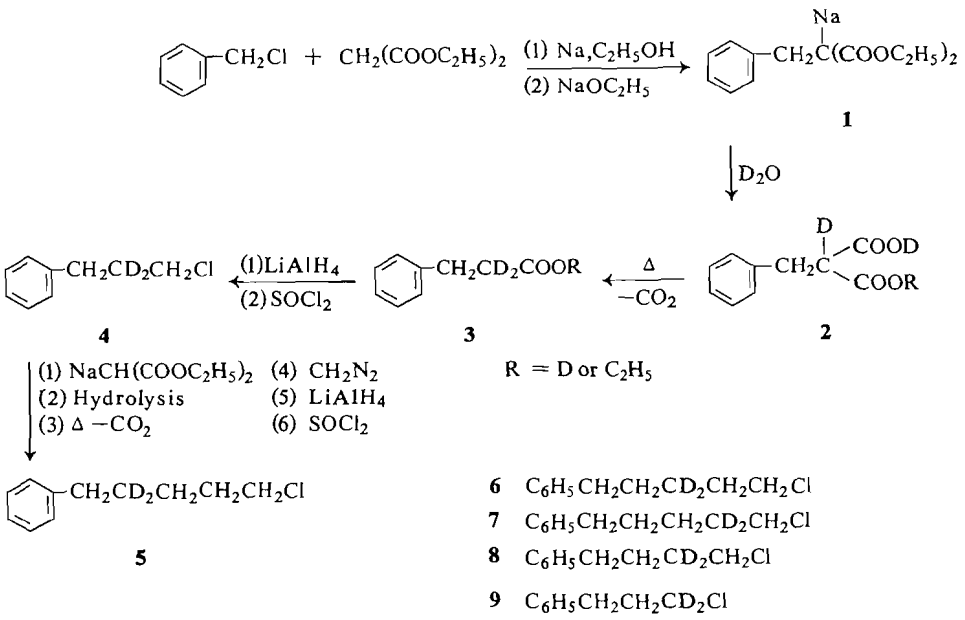

SCHEME 2. Synthesis of deuterated phenylalkyl chlorides.

Can. J. Chem. Downloaded from www.nrcresearchpress.com by 210.87.254.105 on 09/05/12
For personal use only.

Can. J. Chem. Downloaded from www.nrcresearchpress.com by 210.87.254.105 on 09/05/12
For personal use only.

TABLE I

Nuclear magnetic resonance spectral data on methylene protons

Compound	Chemical shift*	Multiplicity	Relative area†	Assignment
$C_6H_5CH_2CH_2CH_2Cl$	6.55	Triplet	1.90	$-CH_2Cl$
	7.23	Triplet	2.00	$Ph-CH_2-$
	7.90	Quintet	1.90	$2-CH_2$
$C_6H_5CH_2CD_2CH_2Cl$ (**4**)	6.57	Singlet	1.92	$-CH_2Cl$
	7.26	Singlet	1.92	$Ph-CH_2$
$C_6H_5CH_2CH_2CD_2Cl$ (**9**)	7.33	Triplet	2.00	$Ph-CH_2-$
	8.10	Triplet	1.94	$2-CH_2-$
$C_6H_5CH_2CH_2CD_2CH_2Cl$ (**8**)	6.61	Singlet	2.00	$-CH_2Cl$
+ Tetralin	7.41	Triplet	—‡	$Ph-CH_2-$
	8.30	Triplet	—‡	$3-CH_2-$
$C_6H_5CH_2CH_2CH_2CH_2CH_2Cl$	6.57	Triplet	1.90	$-CH_2Cl$
	7.40	Triplet	2.00	$Ph-CH_2-$
	8.41	Complex multiplet	6.00	$2,3,4-(CH_2)_3-$
$C_6H_5CH_2CH_2CH_2CD_2CH_2Cl$ (**7**)	6.60	Singlet	1.90	$-CH_2Cl$
	7.42	Triplet	1.97	$Ph-CH_2-$
	8.53	Complex multiplet	4.22	$3,4-(CH_2)_2-$
$C_6H_5CH_2CH_2CD_2CH_2CH_2Cl$ (**6**)	6.54	Triplet	1.91	$-CH_2Cl$
	7.38	Triplet	1.90	$Ph-CH_2-$
	8.30	Multiplet	3.83	$-CH_2CD_2CH_2$
$C_6H_5CH_2CD_2CH_2CH_2CH_2Cl$ (**5**)	6.58	Triplet	1.97	$-CH_2Cl$
	7.43	Singlet	1.97	$Ph-CH_2-$
	8.48	Complex multiplet	3.88	$2,3-(CH_2)_2-$

*τ values determined in CCl_4 containing TMS.
†Integrations are based on the aromatic protons which absorbed near τ 2.9, set equal to 5.
‡Tetralin absorbs in this region.

region near 6.6 p.p.m. These results indicate essentially complete deuterium substitution at position-2. The line broadening is attributed to weak spin–spin coupling of the $-CH_2Cl$ protons with vicinal deuterium nuclei. Compounds **4** and **5** containing the $C_6H_5CH_2CD_2-$ group showed the broad singlet in the 7.3–7.4 region expected from the benzylic protons in these compounds. Compound **9** gave the expected n.m.r. spectrum. The absence of absorption in the 6.6 p.p.m. region indicates the presence of the $-CD_2Cl$ group and the two triplets, at 7.33 and 8.10 p.p.m. (broad), confirms the structure given to **9**. The assignment of the structure to compound **6** is not quite so obvious. The two triplets at low field, 6.54 and 7.38 p.p.m., are assigned to the $-CH_2-Cl$ and benzylic protons respectively. From the integration and the simplification of the absorption at higher field (compared to the spectrum of unlabelled compound), the absorption in the 8.30 p.p.m. region is assigned to the methylenes at positions-2 and -4.

(b) Cyclialkylations of Deuterated Phenylalkyl Chlorides

The conditions and cyclization products from cyclialkylations of the phenylalkyl chlorides are summarized in Table II.

TABLE II

Cyclialkylations of dideuterated phenylalkyl chlorides*

Labelled chloride (mmole)	Catalyst (mmole)	Temperature (°C)	Time (h)	Cyclialkylation† products
$C_6H_5CH_2CD_2CH_2CH_2CH_2Cl$(6)	$AlCl_3$(6)	25	2.5	1-Methyltetralin-3,3-d_2 (**10**)
$C_6H_5CH_2CH_2CD_2CH_2CH_2Cl$(9)	$AlCl_3$(9)	25	3.0	1-Methyltetralin-2,2-d_2(**11**)
$C_6H_5CH_2CH_2CH_2CD_2CH_2Cl$(6.5)	$AlCl_3$(6.5)	25	3.0	1-Methyl(*d*)-tetralin-1-*d*(**12**) and 1-Methyl(*d*)tetralin(**13**)
$C_6H_5CH_2CH_2CD_2CH_2Cl$(4.5)	$AlCl_3$(4.5)	25	1.5	Tetralin-2,2-d_2(**14**)

*Petroleum ether (b.p. 60–80°) was used as the solvent.
†Various byproducts due to hydride ion exchange and dehydrogenation also formed and are discussed in a separate publication (8).

TABLE III

Nuclear magnetic resonance spectral data on cyclialkylation products

Labelled tetralin	Chemical shift*	Multiplicity	Relative area†	Assignment
1-Methyltetralin-3,3-d_2 (**10**)	8.83–8.71	Doublet	3.07	$-CH_3$
	8.35	Multiplet(AB of ABX)‡	2.08	$-CH_2-$(C-2)
	7.32 and 7.15	Singlet and Multiplet	2.92	Benzylic $-CH_2-$ and $-CH-$
1-Methyltetralin-2,2-d_2 (**11**)	8.80–8.70	Doublet	2.83	$-CH_3$
	8.23	Multiplet	2.33	$-CH_2-$(C-3)
	7.29	Triplet and Multiplet	2.72	Benzylic $-CH_2$ and $-CH-$
1-Methyl(*d*)-tetralin-1-*d* (**12**)	8.83–8.72	Doublet and Singlet	2.40	$-CH_2D$
and	8.26	Multiplet	3.38	$-CH_2CH_2-$(C-2,3)
1-methyl(*d*)-tetralin (**13**)	7.32		2.45	Benzylic $-CH_2-$ and $-CH-$
Tetralin-2,2-d_2 (**14**)	8.30	Triplet	2.05	$-CH_2-$(C-3)
	7.33	Singlet and Triplet	3.80	2-Benzylic $-CH_2-$

*τ values were determined in CCl_4 containing TMS..

†The integrations are averaged from two separate cyclialkylations in each case, and are relative to the aromatic hydrogens at τ 3.0, set equal to 4.

‡This multiplet collapsed to a doublet on irradiation in the region of the methine proton absorption.

The n.m.r. and mass spectroscopic data for determining the position of the label in the cyclic products are summarized in Tables III and IV. The product from cyclialkylation of 1-chloro-5-phenylpentane-4,4-d_2 (**5**) was 1-methyltetralin-3,3-d_2 (**10**). This is clear from the integrations and the spin–spin splitting in the n.m.r. spectrum of **10**. The mass spectrum of this product (Table IV) gave supporting evidence for this structure in the expected parent mass and simple fragmentations comparable to that of 1-methyltetralin.

The assignment of structure **10** as the only labelled methyltetralin from cyclialkylation of **5** proves that benzsuberane cannot form even as an intermediate in the cyclialkylation–rearrangement. This clearly demonstrates that the rearrangement must take place in the side-chain prior to cyclization (Scheme 1, path 1).

It was hoped that additional information on the mechanism of the cyclialkylation–rearrangement would be obtained by cyclialkylation of phenylalkyl chlorides with the deuterium label closer to the reaction site. Furthermore, it was very desirable to have comparative n.m.r. and mass spectral evidence on other deuterium labelled 1-methyltetralins, especially one with deuterium in the methyl group. With these objectives in mind, cyclialkylations of 1-chloro-5-phenylpentane-3,3-d_2 (**6**) and 1-chloro-5-phenylpentane-2,2-d_2 (**7**) were carried out.

The product from cyclialkylation of **6** was found to be mainly 1-methyltetralin-2,2-d_2 (**11**) from n.m.r. and mass spectra (Tables III and IV). The n.m.r. spectrum of **11** was clearly distinguished from that of **10** because spin–spin coupling between the methylene protons (C-3 and C-4) was still present in **11** but absent in **10**. The mass spectral peaks at 120 and 104 also distinguished **11** from **10**. There was evidence of some deuterium scrambling. The slightly low integration for the $-CH_3$ group and a peak in the mass spectrum at 132 is indicative of some deuterium in the methyl group. The low integration for the three benzylic hydrogens is probably due to deuterium scrambling into the methine position-1.

Cyclialkylation of 1-chloro-5-phenylpentane-2,2-d_2 (**7**) yielded a 1-methyltetralin showing complex n.m.r. and mass spectra. The spectral results are attributed to a mixture of labelled compounds such as 1-methyl(*d*)-tetralin-1-*d* (**12**) and 1-methyl(*d*)-tetralin (**13**). In particular, this mixture would account for the appearance of both a doublet (**13**) and a singlet (**12**) for methyl absorption in the n.m.r. spectrum as well as for the fractional integrations observed. The appearance of two parent masses (148 and 147) and two sets of related fragmentations in the mass spectrum confirmed this interpretation. The appearance of a peak at $m/e = 133$, probably due to loss of CH_3 from mass 148, is indicative of the presence of some 1-methyltetralin-1,2-d_2 in the mixture.

A reaction mechanism is required which accounts for the rearrangement prior to cyclialkylation as well as the hydrogen scrambling observed between C-1, C-2, and (to a lesser extent) C-3 during the cyclialkylation. One possibility involves hydrogen-bridged ion intermediates as outlined in Scheme 3. Such an

Can. J. Chem. Downloaded from www.nrcresearchpress.com by 210.87.254.105 on 09/05/12
For personal use only.

TABLE IV

Mass spectroscopic data on cyclialkylation products

Hydrocarbon	Peak*	Relative intensity	Fragmentation
1-Methyltetralin	146	31	Parent mass
	131	100	Less $-CH_3$
	118	19	Less $-C_2H_4-$
	104	10	Less 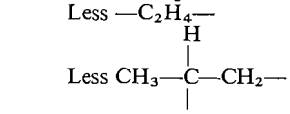
1-Methyltetralin-3,3-d_2 (**10**) 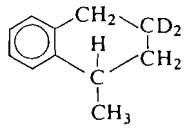	148	28	Parent mass
	133	100	Less $-CH_3$
	118	25	Less $-CH_2CD_2-$(2,3)
	106	9	Less 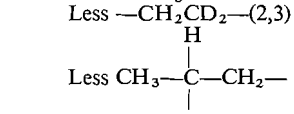
1-Methyltetralin-2,2-d_2 (**11**) 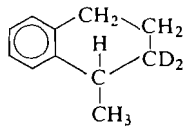	148	35	Parent mass
	133	100	Less $-CH_3$
	132	54	Less $-CH_2D$
	120	16	Less $-CH_2CH_2-$(3,4)
	118	22	Less $-CD_2CH_2-$(2,3)
	104	21	Less 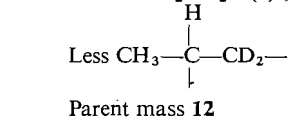
1-Methyl(*d*)-tetralin-1-*d* (**12**) and 1-Methyl(*d*)-tetralin (**13**) 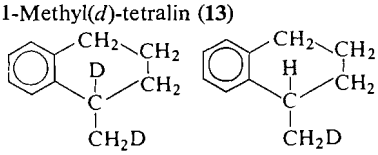	148	34	Parent mass **12**
	147	31	Parent mass **13**
	133	55	Less CH_3
	132	100	**12** less $-CH_2D$
	131	64	**13** less $-CH_2D$
	120	17	**12** less $-C_2H_4-$
	119	25	**13** less $-C_2H_4-$
	104	20	
Tetralin-2,2-d_2 (**14**)	134	49	Parent mass
	133	29	M-1 and monodeuterocompound
	106	35	Parent less $-CH_2CH_2-$(3,4)
	105	39	133 less $-CH_2CH_2-$(3,4) and tetralin-1,2-d_2 less $-CHD-CH_2-$(2,3)
Tetralin	132	48	Parent mass
	131	13	M-1
	105	10	
	104	100	Less $-CH_2CH_2-$(2,3)

*Partial mass spectra only are shown for comparison of peaks in the higher mass range.

intermediate (**15**) accounts for the formation of 1-methyltetralin. Obviously deuterium at position-4 of **15** would appear entirely at position-3 in the 1-methyltetralin. The minor amount of deuterium scrambling from C-3 to C-2 and C-1 observed in cyclialkylation of 1-chloro-5-phenylpentane-3,3-d_2 (**6**) can be accounted for by some equilibration between **15** and the hydrogen-bridged ion **15***a* prior to cyclization.

1-Chloro-5-phenylpentane-2,2-d_2 (**7**) underwent extensive scrambling of deuterium between C-1, C-2, and C-3 during the cyclialkylation. Rearrangements through intermediates **15** and **15***a* account for the appearance of deuterium in the methyl group as well as positions-1 and -2 in the 1-methyltetralin formed.

The results can also be accounted for in an analogous manner by writing a series of hydride shifts with the cyclization occurring through a carbonium ion (compare Scheme 1). Intermolecular hydride transfer at the labile tertiary position-1 of 1-methyltetralin also occurred to account for the appearance of the monodeuterated compound (**13**) and other side reactions (8).

Can. J. Chem. Downloaded from www.nrcresearchpress.com by 210.87.254.105 on 09/05/12
For personal use only.

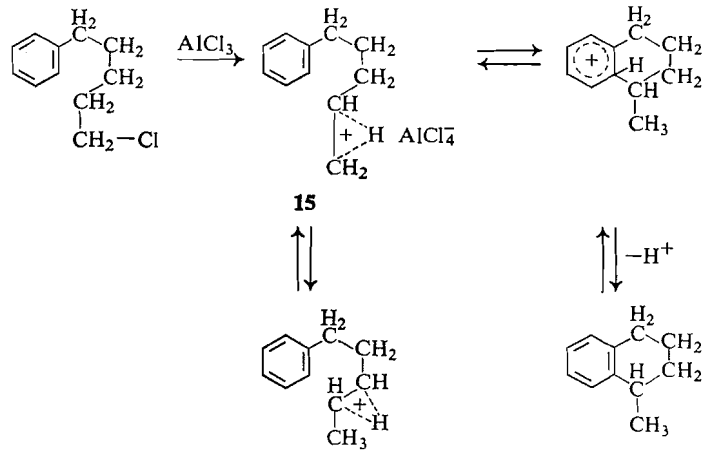

SCHEME 3

It was found [Part (*a*)] that phenylbutyl chlorosulfite ester underwent direct cyclization to tetralin (25%). This result is analogous to the aryl participation forming tetralin observed during solvolyses on arylalkyl benzenesulfonates (9, 10). There was no significant aryl participation in the 5-aryl-1-pentyl series (10). The question of a possible concerted process versus a carbonium ion process in the cyclialkylation of a primary phenylbutyl chloride was raised by Khalaf and Roberts (4). Their observation that 1-chloro-2-methyl-4-phenylbutane underwent partial rearrangement of both hydride and methide was indicative of a carbonium ion type of reaction. It was thought that cyclialkylation of 1-chloro-4-phenylbutane-2,2-d_2 (**8**), with deuterium label next to the reaction center, would provide a better test of these mechanisms. The major product from cyclialkylation of **8** was tetralin-2,2-d_2 (**14**) according to the n.m.r. results (Table III). However, there is also evidence for some scrambling and loss of deuterium which complicates the results. The consistently low integration for the two benzylic methylenes indicates some deuterium rearrangement (at least 10%) into position-1. This could also account at least in part for the increased intensity of the 105 peak in the mass spectrum of the product (Table IV) compared to that of tetralin. The intensity of the M-1 peak in the product is indicative of the presence of some monodeutero compound. Despite these complications, the relatively low proportion of deuterium rearrangement can be accounted for by a concerted mechanism (Scheme 4). The results are not sufficiently unequivocal to rule out the alternative carbonium ion process in which the favored six-membered ring forms faster than a 1,2-hydride shift can occur.

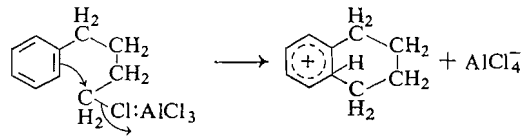

SCHEME 4

Experimental

Infrared (i.r.) spectra were recorded on a Perkin–Elmer model 137 Infracord. Nuclear magnetic resonance (n.m.r.) spectra were measured on a Varian A-60 spectrometer equipped with a spin decoupler. Reaction products were analyzed on an F & M model 500 programmed temperature gas chromatograph equipped with a dual column attachment. The column packings contained 30% Apiezon grease on Chromosorb W. Melting points were determined on a Thomas Hoover capillary melting point apparatus and are uncorrected. The deuterium oxide (99.7%) used was obtained from Merck, Sharp and Dohme of Canada Limited. Literature values for the refractive indices and boiling points reported are for the corresponding non-deuterated samples.

(a) Syntheses of Deuterium Labelled Compounds

Ethyl 3-Phenylpropanoate-2,2-d_2 (3)

To a solution of sodium ethoxide in ethanol, prepared from 4.30 g (0.186 mole) of sodium and 100 ml of absolute alcohol, were added 40 g (0.186 mole) of diethyl benzylmalonate, prepared according to the procedure given by Gatterman (11). The solution was heated under

Can. J. Chem. Downloaded from www.nrcresearchpress.com by 210.87.254.105 on 09/05/12
For personal use only.

Can. J. Chem. Downloaded from www.nrcresearchpress.com by 210.87.254.105 on 09/05/12
For personal use only.

reflux for 2 h with stirring and the excess alcohol distilled *in vacuo*. Ten grams of deuterium oxide were added and the mixture stirred until the sodium salt dissolved. It was then heated under reflux for 30 min. The solution was acidified with D_2SO_4, prepared by hydrating sulfur trioxide with deuterium oxide (12). The mixture was extracted with anhydrous ether and the extract dried with anhydrous sodium sulfate. The ether was distilled and the residue was heated in an oil bath at 170° until evolution of carbon dioxide ceased. The residue was distilled *in vacuo*. The fraction distilling at 162–170°/4.5 mm gave 22 g (70%) of the dideuterated ester, n_D^{20} 1.4934 (lit. (13), 1.4954). The i.r. spectrum showed ester carbonyl absorption at 1730 cm^{-1}. The n.m.r. spectrum showed aromatic absorption at τ 2.82, a symmetrical quartet centered at τ 5.95, a singlet at τ 7.11 and a triplet centered at τ 8.85, with intensity ratios of 5:2:2:3, consistent with the proposed structure.

3-Phenyl-1-propanol-2,2-d_2

To a solution of 10 g (0.27 mole) of lithium aluminium hydride in 500 ml of anhydrous ether were added slowly with stirring 32 g (0.18 mole) ethyl 3-phenylpropanoate-2,2-d_2. The mixture was heated under reflux with stirring for 9 h and allowed to set overnight at room temperature. The mixture was poured onto ice and treated with dilute sulfuric acid. The organic material was extracted with ether. Evaporation of the ethereal extract left 24.5 g (100%) of alcohol which showed hydroxyl absorption in the i.r. at 3400 cm^{-1}. Carbonyl absorption was absent. The n.m.r. spectrum showed aromatic absorption at τ 2.81 with singlets at τ 5.81, 6.50, and 7.41. The intensity ratios were 5:1:2:2, consistent with the proposed structure.

1-Chloro-3-phenylpropane-2,2-d_2 (4)

To 20 g (0.145 mole) of 3-phenyl-1-propanol-2,2-d_2, cooled in an ice bath, were added slowly with swirling 17.25 g (0.145 mole) of thionyl chloride. After the addition was complete, excess thionyl chloride was removed *in vacuo*. The resulting chlorosulfite ester was decomposed in an oil bath at 120°, until sulfur dioxide ceased to be evolved. The residue was then vacuum distilled. The fraction which distilled at 130°/2.5 mm weighed 14 g (62%); n_D^{20} 1.5227 (lit. (14), n_D^{25} 1.5160).

Diethyl 3-Phenylpropyl-2,2-d_2-malonate

To a solution of sodium ethoxide, prepared from 2.14 g (0.093 mole) of sodium cuttings in 30 ml of absolute alcohol, were added 14.9 g (0.093 mole) of diethyl malonate. After heating under reflux for 30 min, 14 g (0.093 mole) of 1-chloro-3-phenylpropane-2,2-d_2 were added in one portion and the resulting mixture was heated under reflux for 2.5 h. The ethanol was distilled *in vacuo*, then water was added and the mixture extracted with ether. The ethereal solution was dried over anhydrous sodium sulfate and the ether distilled. The residue was distilled under reduced pressure. The fraction which distilled at 194° gave 13.7 g (53%) of the ester (lit. (15), 189–198°/13 mm).

5-Phenyl-1-pentanol-4,4-d_2

A mixture of 13.7 g (0.043 mole) of diethyl 3-phenylpropyl-2,2-d_2 malonate and 12 g of 50% aqueous potassium hydroxide solution was heated on a steam cone until homogeneous. The alkaline solution was acidified with dilute hydrochloric acid and the oil which separated extracted with ether. The residue from evaporation of the dried ethereal extracts crystallized. Recrystallization from petroleum ether yielded crystals, m.p. 92–93° (lit. (16), 92–95°). The acid was heated at 180° in an oil bath until carbon dioxide was no longer evolved. Eight grams of acid were obtained (92% yield). Recrystallization from petroleum ether gave crystals, m.p. 57–58°. The mixture melting point of this sample with an authentic sample of 5-phenylpentanoic acid (Aldrich Chemical Co. Inc.) was 57–58° (lit. (17), 58–59°). The acid was esterified by distilling an ethereal solution of diazomethane, prepared according to the procedure of Arndt (18), into an ethereal solution of the acid until the yellow color remained. The ethereal solution of ester was concentrated and reduced directly with 3.4 g of lithium aluminium hydride dissolved in ethyl ether. After heating under reflux overnight, the solution was poured onto ice, decomposed with 10% sulfuric acid, and extracted with ether. The ethereal extract was dried over anhydrous sodium sulfate and the ether distilled. This gave 6.3 g (80%) of neutral material, n_D^{25} 1.5148 (lit. (19), 1.5122) which showed hydroxyl absorption in the i.r. at 3400 cm^{-1}. The n.m.r. spectrum showed aromatic absorption at τ 2.88, a triplet centered at τ 6.50, a singlet at τ 7.45, and a multiplet centered at τ 8.58 with intensity ratios of 5:2:2:4 consistent with the proposed structure.

1-Chloro-5-phenylpentane-4,4-d_2 (5)

To 2 g (0.012 mole) of 5-phenyl-1-pentanol-4,4-d_2 was added dropwise at room temperature 1.23 g (0.012 mole) of thionyl chloride. The excess thionyl chloride was distilled *in vacuo* and the chlorosulfite ester was decomposed at 130° until evolution of sulfur dioxide ceased. The residue was distilled *in vacuo*. The fraction distilling at 114°/1.7 mm amounted to 1.5 g (70%) (lit. (20), 111–112°/5–6 mm).

1-Chloro-5-phenylpentane-2,2-d_2 (7)

Diethyl 3-phenylpropylmalonate was prepared from 1-chloro-3-phenylpropane, diethyl malonate and sodium ethoxide, according to the procedure used in the synthesis of diethyl 3-phenylpropyl-2,2-d_2 malonate (above). Diethyl 3-phenylpropylmalonate 20 g (0.027 mole) was treated with an alcoholic solution of sodium ethoxide and the alcohol removed *in vacuo*. The solid residue was refluxed with deuterium oxide and acidified with D_2SO_4 according to the procedure previously described for the preparation of **3**. Decarboxylation of the residue at 170° in an oil bath gave 12.46 g, (94%) of 5-phenylpentanoic acid-2,2-d_2. The n.m.r. spectrum showed aromatic absorption at τ 2.86 and two multiplets centered at τ 7.39 and 8.35 with intensity ratios of 5:2:4 consistent with the proposed structure.

5-Phenylpentanoic acid-2,2-d_2 (12.4 g, 0.072 mole) was converted to the methyl ester with an ethereal solution of diazomethane. The ethereal solution of the ester was concentrated and added slowly to a solution of lithium aluminium hydride (5.4 g, 0.144 mole) in ether. After refluxing for 2 h, the solution was poured onto ice, decomposed with 10% sulfuric acid, and extracted with ether. The ether extract was dried over anhydrous sodium sulfate and the ether was distilled. An i.r. spectrum on the residue showed hydroxyl absorption at 3400 cm^{-1}. The alcohol obtained was treated directly with a slight excess

Can. J. Chem. Downloaded from www.nrcresearchpress.com by 210.87.254.105 on 09/05/12
For personal use only.

of thionyl chloride. After 5 min, the excess thionyl chloride was distilled *in vacuo*, and the chlorosulfite ester decomposed in an oil bath at 120° for approximately 1 h. The residue was distilled *in vacuo*. The fraction boiling at 115°/3 mm yielded 3.5 g (30%) 1-chloro-5-phenylpentane-2,2-d_2; n_D^{20} 1.5145 (lit. (3), n_D^{23} 1.5149).

4-Phenyl-1-butanol-2,2-d_2

Diethyl 2-phenylethylmalonate was prepared from 1-chloro-2-phenylethane, diethylmalonate, and sodium ethoxide according to the usual procedure; b.p. 162°/1.3 mm (lit. (21), 182–187°/17 mm). Diethyl 2-phenylethylmalonate (20 g, 0.076 mole) was treated with an alcoholic solution of sodium ethoxide and the alcohol removed *in vacuo*. The solid residue was refluxed with deuterium oxide and acidified with D_2SO_4 according to the previously described procedure. Decarboxylation of the residue at 170° in an oil bath gave a mixture of acid and ester. The mixture of acid and ester was added to an ethereal solution of diazomethane. The ethereal solution was concentrated and added slowly to a solution of lithium aluminium hydride (3.5 g) in ether. After refluxing overnight, the solution was poured onto ice, decomposed with 10% sulfuric acid, and extracted with ether. The ether extract was dried over anhydrous sodium sulfate, and the ether distilled. This gave 9.6 g (84%) of 4-phenyl-1-butanol-2,2-d_2. The i.r. spectrum showed hydroxyl absorption at 3400 cm^{-1}. Carbonyl absorption was absent. The n.m.r. spectrum showed aromatic absorption at τ 2.92, two singlets at τ 6.52 and 6.75, a triplet centered at τ 7.42 and a multiplet centered at τ 8.40 with intensity ratios of 5:2:1:2:2 consistent with the proposed structure.

1-Chloro-4-phenylbutane-2,2-d_2

To 7.0 g (0.097 mole) of 4-phenyl-1-butanol-2,2-d_2 at room temperature were added dropwise 5.8 g (0.047 mole) of thionyl chloride. The reaction was instantaneous and excess thionyl chloride was removed *in vacuo*. The residue was decomposed at 130°, until evolution of sulfur dioxide ceased. The residue was distilled *in vacuo* and the fraction distilling at 126°/1.2 mm pressure amounted to 4 g (50%). Vapor-phase chromatographic analysis of the product showed two components in the ratio 3:1.

Using authentic samples of non-deuterated compounds as internal standards, these were found to be 1-chloro-4-phenylbutane-2,2-d_2 (75%) and 2,2-d_2-tetralin (25%).

1-Chloro-5-phenylpentane-3,3-d_2 (6)

To a solution of 4 g of the above mixture of 1-chloro-4-phenylbutane-2,2-d_2 and tetralin in anhydrous ether was added 0.55 g of magnesium turnings. This was heated under reflux with stirring for 20 h, then poured onto crushed dry ice. Water was added and the solution acidified with dilute hydrochloric acid. The oil which separated was extracted with ether. The ether extracts were extracted with dilute alkali, the alkali portion acidified with dilute hydrochloric acid, and again extracted with ether. The ether extracts were dried with anhydrous sodium sulfate. Distillation of the solvent gave 3 g of 5-phenylpentanoic acid-3,3-d_2 (approximately 70%). The acid was added directly to an ethereal solution of diazomethane. The ethereal solution was concentrated and added slowly to a solution of lithium aluminium hydride (1 g) in ether. After refluxing for 2 h, the solution was poured onto ice, decomposed with 10% sulfuric acid, and extracted with ether. The ether extract was dried over anhydrous sodium sulfate. Distillation of the ether gave 2.5 g (90%) of the desired alcohol. The i.r. spectrum showed hydroxyl absorption at 3400 cm^{-1}. Carbonyl absorption was absent. The n.m.r. spectrum of the 5-phenyl-1-pentanol-3,3-d_2 obtained showed aromatic absorption at τ 2.82, a singlet at τ 6.02, a triplet centered at τ 6.49, a triplet centered at τ 7.44, and a multiplet centered at τ 8.48 with intensity ratios of 5:1:2:2:4 consistent with the proposed structure.

Thionyl chloride 1 g (0.0084 mole) was added to 1.4 g (0.0084 mole) of 5-phenyl-1-pentanol-3,3-d_2 at room temperature. Excess thionyl chloride was immediately removed *in vacuo* and the chlorosulfite ester decomposed at 130° in an oil bath for 15 min. The residue was vacuum distilled, b.p. 130°/1 mm. One gram (70%) of 1-chloro-5-phenylpentane-3,3-d_2 (**6**) was obtained.

3-Phenyl-1-propanol-1,1-d_2

To a solution of 0.5 g (0.009 mole) of lithium aluminium deuteride in 50 ml of anhydrous ether was added slowly with stirring 3 g (0.018 mole) of methyl 3-phenylpropionate. The mixture was refluxed for 2 days, poured into ammonium chloride solution, and extracted with ether. Evaporation of the dried ethereal extracts gave 2.4 g (quantitative yield) of alcohol. The i.r. spectrum showed hydroxyl absorption at 3400 cm^{-1}. The n.m.r. spectrum showed aromatic absorption at τ 2.80, a singlet at τ 6.09, and two triplets centered at τ 7.34 and 8.22 with intensity ratios of 5:1:2:2, consistent with the proposed structure.

1-Chloro-3-phenylpropane-1,1-d_2 (9)

To 1.8 g (0.012 mole) of 3-phenyl-1-propanol-1,1-d_2, cooled in an ice bath, were added 1.43 g (0.012 mole) of thionyl chloride. After ½ h heating at 130° in an oil bath, the product was vacuum distilled. The fraction collected at 106°/2.35 mm weighed 1.25 g (70%).

(b) Cyclialkylations of Phenylalkyl Chlorides

The cyclialkylations were carried out in a flask containing a magnetic stirrer and fitted by a flexible rubber tube to a small flask containing the catalyst. The hydrogen chloride gas was released through an attached drying tube. The organic chloride was dissolved in petroleum ether and the aluminium chloride added at room temperature. The progress of the cyclialkylations was followed by vapor-phase chromatography (v.p.c.) analysis of small aliquots. These were worked up by pouring into ice, and extracting with ether. The ether extracts were washed free of acid, dried with anhydrous sodium sulfate, the ether distilled, and the residue analyzed by v.p.c. The reactions were terminated when the starting chloride had disappeared. Preliminary reactions was carried out on unlabelled phenylpentyl chloride using various solvents and amounts of aluminium chloride and ferric chloride. Optimum conditions were found using an equimolar amount of phenylalkyl chloride and aluminium chloride in petroleum ether using contact times of 2–3 h. Under these conditions the relative amount (v.p.c.) of 1-methyltetralin was approximately 90%. Under other conditions side reactions due to hydride ion exchange and dealkylation predominated (8).

Cyclialkylations of deuterium labelled phenylalkyl chlorides were carried out under conditions outlined above and are summarized in Table II. The components were analyzed in a preliminary manner by comparison of

their v.p.c. retention times with 1-methyltetralin. The labelled cyclialkylated products were collected from the v.p.c. by repeated injections and analyzed by n.m.r. and mass spectroscopy.

Acknowledgments

The financial support provided by the National Research Council of Canada is gratefully acknowledged. Funds provided by Imperial Oil Limited assisted with the purchase of a n.m.r. spin–spin decoupler. We thank Dr. D. B. MacLean, McMaster University, Hamilton, Ontario, for providing the mass spectroscopic evidence.

1. G. Baddeley and R. Williamson. J. Chem. Soc. 4647 (1956).
2. L. R. C. Barclay. Friedel-Crafts and related reactions. Vol. II. *Editor* G. A. Olah. Interscience Publishers, Inc., New York. 1964. p. 786.
3. L. R. C. Barclay, B A. Ginn, and C. E. Milligan. Can. J. Chem. **42**, 579 (1964).
4. A. A. Khalaf and R. M. Roberts. J. Org. Chem. **31**, 89 (1966).
5. L. Schmerling, R. W. Welch, and J. P. Luvisi. J. Am. Chem. Soc. **79**, 2636 (1957).
6. R. M. Roberts and Y. W. Han. J. Am. Chem. Soc. **85**, 1168 (1963).
7. C. E. Boozer and E. S. Lewis. J. Am. Chem. Soc. **75**, 3182 (1953).
8. L. R. C. Barclay and E. C. Sanford. Can. J. Chem. This issue.
9. R. Heck and S. Winstein. J. Am. Chem. Soc. **79**, 3105, 3114 (1957).
10. E. J. Corey and C. K. Savers. J. Am. Chem. Soc. **79**, 248 (1957).
11. L. Gattermann. Laboratory methods of organic chemistry. MacMillan and Co. Ltd., London. 1952. p. 255.
12. J. O. Halford and L. C. Anderson. J. Am. Chem. Soc. **58**, 736 (1936).
13. W. Steinkopf and A. Wolfram. Ann. **430**, 113 (1922).
14. S. S. Rossander and C. S. Marvel. J. Am. Chem. Soc. **50**, 1491 (1928).
15. J. V. Braun and O. Kruber. Ber. **45**, 384 (1912).
16. A. G. Anderson and H. Greef. J. Am. Chem. Soc. **74**, 5124 (1952).
17. J. V. Braun. Ber. **43**, 2837 (1910).
18. F. Arndt. Organic syntheses. Coll. Vol. II. John Wiley and Sons, Inc., New York. p. 165.
19. M. Gouge. Compt. Rend. **225**, 637 (1949).
20. J. B. Conant and W. R. Kirner. J. Am. Chem. Soc. **46**, 232 (1924).
21. G. Schroeter, L. Lichtenstadt, and D. Irineau. Ber. **51**, 1587 (1918).

Can. J. Chem. Downloaded from www.nrcresearchpress.com by 210.87.254.105 on 09/05/12
For personal use only.

Can. J. Chem. Downloaded from www.nrcresearchpress.com by 210.87.254.40 on 09/05/12
For personal use only.

Friedel–Crafts rearrangements. IV. Cyclialkylations and hydride transfers on phenylalkyl chlorides

L. R. C. BARCLAY AND E. C. SANFORD
Department of Chemistry, Mount Allison University, Sackville, New Brunswick

Received April 2, 1968

A number of phenylalkyl chlorides were synthesized for a comparative study of Friedel–Crafts cyclialkylations and competing reactions involving hydride exchange. The synthetic work showed that phenylbutyl alcohols, especially a tertiary alcohol, may cyclize directly with chlorinating agents to yield tetralins. Cyclialkylation products from phenylpentyl chloride include 1-methyltetralin (**4**), *n*-pentylbenzene, 1-methyl-3,4-dihydronaphthalene, and methylnaphthalene. A reaction sequence is given involving dealkylation of **4** and hydride transfers. Phenylbutyl chloride yielded tetralin, *n*-butylbenzene, and naphthalene. 1-Chloro-4-methyl-4-phenylpentane yielded 1,1-dimethyltetralin (**10**), 2-methyl-5-phenylpentane (**11**), and a small amount of 2-methyl-2-phenylpentane (**12**). Hydrocarbon **11** formed from **10** after cyclialkylation, while **12** formed by hydride transfer preceding cyclization. Phenylpropyl chloride yielded mainly a hydride transfer product (propylbenzene) and not indane. Treatment of this chloride containing deuterium labels at C-1 and C-2 showed that the hydride ion rearranges from the carbon adjacent to the halogen. 1-Chloro-3-methyl-3-phenylbutane yielded a complex mixture including *t*-pentylbenzene, 2-phenyl-3-methylbutane, and products of higher molecular weight.

Canadian Journal of Chemistry, 46, 3325 (1968)

Introduction

It has been shown (1) that Friedel–Crafts cyclialkylation of phenylpentyl chloride yielded 1-methyltetralin by rearrangement in the side chain prior to cyclization. Hydride exchanges leading to alkylbenzenes and other products also take place as competing reactions to cyclialkylation. The results of modern methods of product identification have changed previous views on these reactions so that Khalaf and Roberts have reclassified the field as "new Friedel–Crafts chemistry" (2).

The present investigation was undertaken to determine the extent of hydride exchange and related competing reactions in cyclialkylation of various phenylalkyl chlorides. It was desirable to study the effect of varying the substrate (phenylalkyl chloride) and reaction conditions on the ratio of cyclialkylation to competing reactions. In particular, for synthetic applications it is important to determine whether hydride transfers take place prior or after the cyclization reaction.

Discussion of Results

The phenylalkyl chlorides required were prepared by decomposition of the chlorosulfite esters of the alcohols or by the action of zinc chloride – hydrochloric acid on the alcohols. Because of the previous observation (1) that the chlorosulfite ester of 4-phenyl-1-butanol underwent partial conversion directly to tetralin, the reaction products were analyzed for hydrocarbons

TABLE I

The action of chlorinating agents on phenylalkyl alcohols*

Number	Alcohol	Reagent	Temperature (°C)	Time (h)	Products (%)†
1	$C_6H_5(CH_2)_3OH$	$SOCl_2$	120	1	$C_6H_5(CH_2)_3Cl$(85)
2	$C_6H_5C(CH_3)_2CH_2CH_2OH$	$SOCl_2$	150	0.5	$C_6H_5C(CH_3)_2CH_2CH_2Cl$(68)
3	$C_6H_5(CH_2)_4OH$	$SOCl_2$	130	1	$C_6H_5(CH_2)_4Cl$(63), tetralin(37)
4	$C_6H_5C(CH_3)_2(CH_2)_3OH$	$SOCl_2$	145	1	$C_6H_5C(CH_3)_2(CH_2)_3Cl$(86), 1,1-dimethyltetralin(14)
5	$C_6H_5(CH_2)_3CH(CH_3)OH$	$HCl–ZnCl_2$	25	17	$C_6H_5(CH_2)_3CH(CH_3)Cl$(44) n-$C_5H_{11}C_6H_5$(5), 1-methyltetralin(49)
6	$C_6H_5(CH_2)_3C(CH_3)_2OH$	$HCl–ZnCl_2$	25	20	1,1-Dimethyltetralin(93)

*In the $SOCl_2$ reactions, equimolar amounts of alcohol and reagent were used. The reactants were mixed at room temperature and the temperature given is for the decomposition of the chlorosulfite ester. The $HCl–ZnCl_2$ was prepared as the Lucas reagent and saturated with HCl gas after mixing with the alcohol.

†In numbers 3–6 the percentages are relative amounts by vapor-phase chromatographic analysis rather than yields.

TABLE II

Friedel–Crafts cyclialkylations of phenylalkyl chlorides*

Number	Chloride	Solvent	Temperature (°C)	Time (h)	Products (%)§
1	$C_6H_5(CH_2)_5Cl$(**1**)	PE†	Reflux	0.6	1-Methyltetralin(**4**)(42), *n*-C_5H_{11}-C_6H_5(**3**)(23), 1-methyl-3,4-dihydronaphthalene(**6**)(5), residue(27)
2	(**1**)	CS_2	25	50	4(43), 3(34), 6(3), residue(20)
3	(**1**)	CH_2Cl_2	0	1	4(17), 3(3.3), methylnaphthalene (26), residue(54)
4	(**1**)	CH_3NO_2‡	25	72	Ratio 4:3 = 1.8:1, mainly unreacted **1**
5	$C_6H_5(CH_2)_4Cl$	PE†	25	1	Tetralin(56), *n*-$C_4H_9C_6H_5$(12), naphthalene(17), residue(17)
6	$C_6H_5C(CH_3)_2(CH_2)_3Cl$	PE†	25	2	1,1-Dimethyltetralin(34), C_6H_5C-$(CH_3)_2CH_2CH_2CH_3$(3.5), *iso*-$C_6H_{13}C_6H_5$(32)
7	$C_6H_5(CH_2)_3Cl$	PE†	Reflux	1.2	*n*-$C_3H_7C_6H_5$(48), indane (trace), residue(52)
8	$C_6H_5CH_2CH_2CD_2Cl$	PE†	Reflux	1	$C_6H_5CH_2CH_2CD_2H$ H,D
9	$C_6H_5CH_2CD_2CH_2Cl$	PE†	Reflux	1	$C_6H_5CHCHCH_2D$
10	$C_6H_5C(CH_3)_2CH_2CH_2Cl$	PE(30–60°)	Reflux	0.2	2-Methyl-3-phenylbutane (mainly) + *t*-$C_5H_{11}C_6H_5$(22), compounds mass 158(58), residue(21)

*An equimolar ratio of aluminium chloride and phenylalkyl chloride was used unless otherwise specified.
†Petroleum ether (b.p. 60–80°).
‡Ferric chloride (0.50 molar ratio) was used.
§Percentages are relative amounts by vapor-phase chromatographic analyses. Products were identified by vapor-phase chromatographic internal standards and nuclear magnetic resonance analyses. The "residues" refer to long retention time components on the vapor-phase chromatograph which were not identified.

as well as chlorides (Table I). The thionyl chloride method gave a significant amount of cyclic compound from primary alcohols when the aromatic ring and hydroxyl were situated so as to produce a six-membered ring directly (Nos. 3 and 4 in Table I). The corresponding secondary and tertiary alcohols cyclized readily with zinc chloride–hydrochloric acid (Nos. 5 and 6 in Table I), and this is a very convenient synthesis for 1,1-dimethyltetralin. There was some evidence, such as the detection of pentylbenzene in No. 5, that hydride ion exchange can occur in these reactions.

The conditions and products of cyclialkylation of various phenylalkyl chlorides are outlined in Table II. The main cyclization product from phenylpentyl chloride, under varying conditions of catalyst, solvent and temperature, was 1-methyltetralin (**4**) (No. 1–4 in Table II). The hydride exchange product *n*-pentylbenzene was formed in each case, even with the milder catalyst ferric chloride–nitromethane (No. 4). A small yield of 1-methyl-3,4-dihydronaphthalene (**6**) was formed in petroleum ether or carbon disulfide solvents. When the reaction mixture was homogeneous (No. 3), a significant amount of methylnaphthalenes formed.

In order to obtain information on the nature of the hydride exchange process yielding *n*-pentylbenzene, a cyclialkylation was set up from which aliquots were analyzed at various intervals, (see Table III). The results indicated that a very good yield of 1-methyltetralin can be obtained after 75 min when the phenylpentyl chloride had all reacted. Then the relative amount of 1-methyltetralin decreased concomitant with an increase in pentylbenzene. This result shows that, for this reaction, most or all of the pentylbenzene is formed by dealkylation and hydride exchange on 1-methyltetralin rather than by hydride exchange

TABLE III

The action of aluminium chloride on phenylpentyl chloride*

Time (min)	Relative %†		
	Chloride	1-Methyltetralin	Pentylbenzene
20	73.6	24.4	Trace
30	59.6	40.2	0.31
75	0	92.0	7.9
1350	0	58.4	41.6

*An equimolar ratio of phenylpentyl chloride and aluminium chloride in petroleum ether at room temperature.
†Determined by vapor-phase chromatographic analysis.

Can. J. Chem. Downloaded from www.nrcresearchpress.com by 210.87.254.40 on 09/05/12
For personal use only.

TABLE IV

The action of aluminium chloride on hydrocarbons*

Hydrocarbon	Temperature (°C)	Time (h)	Products (%)†
1-Methyltetralin (**4**)	25	4.5	**4**(69), *n*-$C_5H_{11}C_6H_5$(10), 1-methylnaphthalene(6), residue(10)
Benzsuberane	60–80	15	No reaction
1,1-Dimethyltetralin (**10**)	25	9	2-Methyl-5-phenylpentane(30), **10**(15)
Indane	60–80	1	No reaction

*An equimolar ratio of hydrocarbon and aluminium chloride was used in petroleum ether.
†Determined by vapor-phase chromatographic analyses.

prior to cyclialkylation. As expected, treatment of 1-methyltetralin with aluminium chloride under conditions similar to cyclialkylation (Table IV) yielded the hydride exchange products pentylbenzene and 1-methylnaphthalene.

The pathway which shows the interrelationships between the various compounds in the cyclialkylation of phenylpentyl chloride (**1**) is given in Scheme 1. As discussed previously (1, 3), 1-methyltetralin (**4**) forms by rearrangement in the side chain (**2**). The labile tertiary hydrogen at C-1 of **4** is probably the source of hydride ion which forms *n*-pentylbenzene (**3**) from **2**. A resonance stabilized tertiary carbonium ion (**5**) would form in this hydride transfer process. The latter could form 1-methyl-3,4-dihydronaphthalene (**6**). Hydride and proton transfers from **6** also account for methylnaphthalene (**8**). This scheme accounts for the results in Table III and for the products from the action of aluminium chloride on **4** (Table IV).

Cyclialkylation of phenylbutyl chloride also yielded hydride exchange products along with tetralin (Table II, No. 5) and ref. 2. The formation of naphthalene is indicative of a hydride transfer mechanism similar to that for cyclialkylation of **1** (Scheme 1). It was desirable to determine whether the hydride transfer process producing alkylbenzenes occurs entirely after cyclization or whether some occurs prior to this. For the phenylbutyl

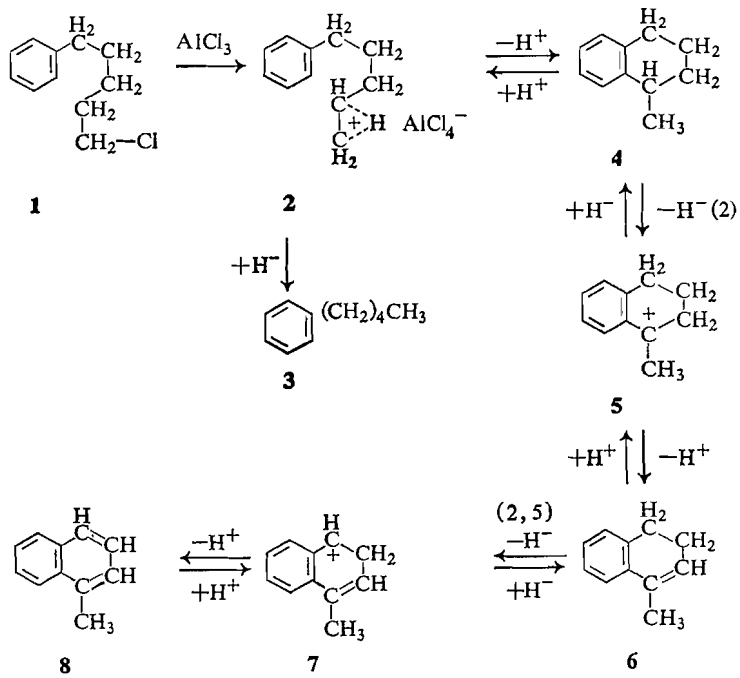

SCHEME 1

Can. J. Chem. Downloaded from www.nrcresearchpress.com by 210.87.254.40 on 09/05/12
For personal use only.

Can. J. Chem. Downloaded from www.nrcresearchpress.com by 210.87.254.40 on 09/05/12
For personal use only.

systems, this was determined by cyclialkylation of a phenylalkyl chloride that would form one alkylbenzene by hydride exchange prior to cyclization but, after a cyclic product was formed, would dealkylate and exchange in a different manner to produce another alkylbenzene. The experiment on cyclialkylation of 1-chloro-4-methyl-4-phenylpentane (**9**) was chosen for this purpose (Table II, No. 6). There was obtained a similar amount of cyclic product, 1,1-dimethyltetralin (**10**) and 2-methyl-5-phenylpentane (**11**), but only a small amount (3.5%) of 2-methyl-2-phenylpentane (**12**). Compound **11** forms after cyclization from 1,1-dimethyltetralin but **12** does not (Table IV and ref. 2). Thus a certain amount (i.e. 3.5%) of alkylbenzene forms by hydride ion transfer prior to cyclization of a phenylbutyl chloride. This may occur through a complex (**9**), (Scheme 2) or a bridged ion similar to **2** (Scheme 1). Once formed, the 1,1-dimethyltetralin (**10**) dealkylates preferentially at the quaternary carbon with formation of a tertiary carbonium ion which later would form 2-methyl-5-phenylpentane (**11**) by hydride transfer.

Reinvestigations of the action of aluminium chloride on phenylpropyl chloride have shown that the products are *n*-propylbenzene (2, 4), di-*n*-propylbenzene, and polymers. This refutes the report that indane was formed as the main product (5), (see also Table II, No. 7). The fact that indane itself is stable to the action of aluminium chloride (Table IV and ref. 2) indicates that the hydride transfer cannot take place on indane. Phenylpropyl chlorides containing deuteriums at C-1 (**13**) and C-2 (**14**) have recently been synthesized (1) and these provide interesting substrates for studying the origin of the hydride ion transfer forming *n*-propylbenzene. Aluminium chloride treatment of 1-chloro-3-phenylpropane-1,1-d_2 (**13**) yielded an *n*-propylbenzene, 1-phenylpropane-3,3-d_2 (**15**), without significant deuterium rearrangement according to the nuclear magnetic resonance (n.m.r.) spectrum (Table V),

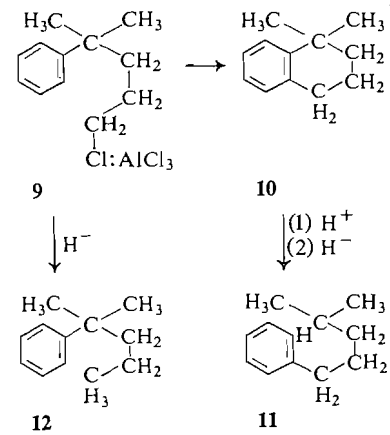

SCHEME 2

TABLE V

Nuclear magnetic resonance spectral data

Hydrocarbon	Chemical* shift	Multiplicity	Relative† areas	Assignment
$C_6H_5CH_2CH_2CHD_2$ (**15**)	9.08	Triplet plus fine structure	0.97	$-CHD_2$
	8.36	Quartet	1.93	β-CH_2—
	7.40	Triplet	1.91	α-CH_2—
C_6H_5 CHCH CH_2D	9.10	Multiplet	2.00	$-CH_2D$
DH	8.38	Multiplet	1.20	β-CHD—+—CH_2—
	7.44	Multiplet	1.80	α-CH_2—+—CHD—
C_6H_5—$CH(CH_3)CH(CH_3)_2$ (**19**)	9.27 and 9.08	Two doublets	6.0	$CH(CH_3)_2$(**19**)
	8.70	Doublet plus	3.6	—$CH(CH_3)$—(**19**)+
+		Singlet		—$C(CH_3)_2$—(**18**)
$C_6H_5C(CH_3)_2CH_2CH_3$ (**18**)‡	7.97	Complex multiplets	—	—CH—CH (**19**)
	2.93	Singlet	Main peak	C_6H_5—(**19**)
	2.83	Singlet		C_6H_5— (**18**)

*τvalues determined in CCl_4 containing TMS.
†Integrations are relative to aromatic hydrogens set equal to five.
‡Compound 18 was identified by comparison with the nuclear magnetic resonance spectrum of an authentic sample.

Can. J. Chem. Downloaded from www.nrcresearchpress.com by 210.87.254.40 on 09/05/12
For personal use only.

and mass spectrum (Table VI) of the product. This result is consistent with the non-involvement of the methyl group in the rearrangement of α- or β-^{14}C-labelled *n*-propylbenzene (6).

The absence of deuterium scrambling in (**15**) shows that indane cannot be the intermediate in the formation of *n*-propylbenzene. If it were, the indane ring would contain deuterium at position-1 and it should then dealkylate in two ways to scramble the deuterium in the side chain. Both benzsuberane and indane failed to form under Friedel–Crafts conditions but were stable under the conditions used (Table IV). Such behavior is understandable because the transition states for dealkylation of seven- and five-membered rings are expected to resemble those for their formation. Both cyclialkylation and dealkylation processes involving seven- and five-membered rings are unfavorable.

The product from aluminium chloride treatment of 1-chloro-3-phenylpropane-2,2-d_2 (**14**) showed evidence of deuterium scrambling by the complexity and integration of the n.m.r. spectrum (Table V), and by the appearance of a peak due to loss of $-CH_2D$ in the mass spectrum (Table VI). The results show that one of the two deuterium atoms has rearranged from the β-position to replace the chlorine and this is clearly the origin of the hydride exchange. Some deuterium apparently also rearranged into the benzylic position. This could occur by a second sequence of 1,2-hydride (and deuteride) shifts on the initially formed carbonium ion $C_6H_5-\overset{(+)}{C}H_2-CD-CH_2D$. It is possible that a phenonium ion (**16**) may be involved in this reaction. This intermediate is analogous to that proposed by Douglass and Roberts (6) to explain the equilibration of ^{14}C between the α and β positions of propylbenzene.

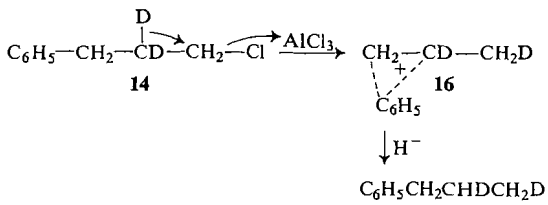

The results from the labelled phenylpropyl chloride experiments assisted in explaining the complex mixture resulting from the action of aluminium chloride on 1-chloro-3-methyl-3-phenylbutane (**17**) (Table II, No. 10). The main part (79.4%) of the mixture was separated into three fractions by vapor-phase chromatography (v.p.c.). The first fraction was shown by n.m.r. and mass spectroscopy (Tables V and VI) to be a mixture containing mostly 2-phenyl-3-methylbutane (**19**) with a smaller amount of *t*-pentylbenzene (**18**). The base peak at 105 in the mass spectrum of **19** is consistent with the reported fragmentation (7).

The interrelationships between the compounds from 1-chloro-3-methyl-3-phenylbutane (**17**) are illustrated in Scheme 3. The *t*-pentylbenzene (**18**) could form by hydride ion transfer on **17***a* or **20**. 2-Phenyl-3-methylbutane (**19**) results from a 1,2-methyl shift as illustrated here or alternately via a phenyl shift involving a phenonium ion as suggested by Schmerling and co-workers (8) to account for the rearrangement of *t*-pentylbenzene.

Two other components were separated from the reaction on **17** by their longer retention times

TABLE VI

Mass spectroscopic data*

Hydrocarbon	Peak	Relative intensity	Fragmentation
$C_6H_5CH_2CH_2CHD_2$ (**15**)	122	20	Parent mass
	105	3	Less $-CHD_2$
	91	100	Less $-CH_2CHD_2$
C_6H_5 CHCH CH_2D (DH)	122	30	Parent mass
	106	4	Less $-CH_2D$
	91	100	Less $-CHDCH_2D$
$C_6H_5-CH(CH_3)CH(CH_3)_2$ (**19**) +	148	17	Parent masses
	119	11	Less $-CH_2CH_3$ from **18**
$C_6H_5-C(CH_3)_2CH_2CH_3$ (**18**)	105	100	Less $CH(CH_3)_2$ from **19**

*Partial mass spectra are shown for comparison of peaks in the higher mass range.

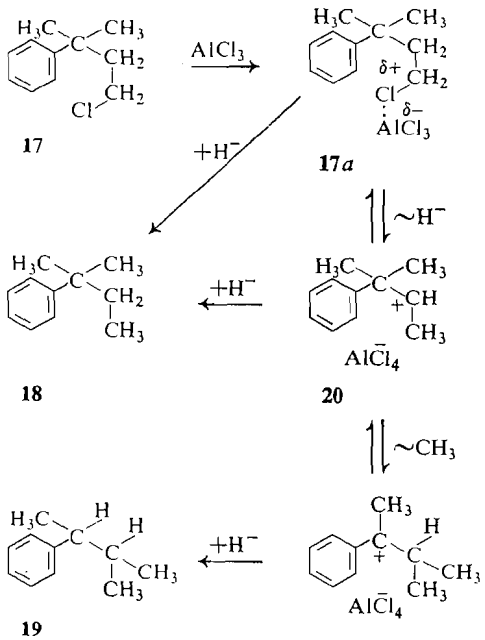

SCHEME 3

(v.p.c.). They both proved to be higher molecular weight products, showing parent masses of 158. The structures of these compounds are under investigation. Our preliminary results on cyclialkylation of **17** is in contrast with the report of Bogert and Davidson (9) that 1,1-dimethylindane formed by sulfuric acid cyclization of the corresponding alcohol 3-phenyl-3-methyl-1-butanol.

Experimental

The spectroscopic and vapor-phase chromatographic (v.p.c.) equipment used was as given previously (1).

(a) Syntheses of Phenylalkyl Chlorides

The phenylpentyl chloride, phenylbutyl chloride, and phenylpropyl chlorides were synthesized as previously described (1). The other phenylalkyl chlorides were synthesized by the action of thionyl chloride or zinc chloride – hydrochloric acid on the corresponding alcohols as outlined in Table I.

1-Chloro-3-methyl-3-phenylbutane (17)

3-Methyl-3-phenylbutanoic acid was prepared by the method of Dippy and Young (10), m.p. 58–60°, (lit. 58–59°). It was converted to 3-methyl-3-phenyl-1-butanol with lithium aluminium hydride. The alcohol was distilled under reduced pressure; $n_D^{25} = 1.5205$, (lit. (11), $n_D^{20} = 1.5227$). Treatment of the alcohol with thionyl chloride (Table I, No. 2) yielded the chloride (**17**) which was purified by vacuum distillation; $n_D^{25} = 1.5175$, (lit. (11), $n_D^{20} = 1.5191$). The identities of the alcohol and chloride (**17**) were confirmed by nuclear magnetic resonance (n.m.r.) spectra. In the n.m.r. spectrum of the chloride, the five aromatic hydrogens absorbed at 2.83 τ, the $-CH_2Cl$ group as a multiplet at 6.82τ, the β-CH_2—at 7.94τ and the two methyls as a singlet at 8.72τ. The two methylenes showed second order spin–spin splitting and absorbed as an A_2B_2-type of system.

1-Chloro-4-methyl-4-phenylpentane (9)

A Grignard reagent was prepared from 1-chloro-3-methyl-3-phenylbutane (**17** above) by refluxing, and stirring with magnesium in ether overnight. The reaction mixture was poured onto solid carbon dioxide, acidified with dilute hydrochloric acid, and the organic acid isolated by extraction with dilute sodium hydroxide. The alkaline extracts were acidified and the acid extracted with ether. Distillation of the ether yielded a liquid residue of the acid which was a solid only below room temperature. It showed carbonyl absorption (film) at 1700 cm^{-1}, and the expected n.m.r. spectrum in which the aromatic protons absorbed at 2.82 τ, the two methylenes at 8.02 τ, the methyls at 8.62 τ and the carboxylic proton at −1.78 τ. The acid was directly reduced with lithium aluminium hydride by refluxing overnight in ethyl ether solution. After working up in the usual way, the alcohol was obtained in 51% yield. It showed hydroxyl absorption (film) at 3400 cm^{-1}. The alcohol was converted to the chloride (**9**) in 86% yield (Table I, No. 4) without further purification. The chloride was purified by vacuum distillation at 130°/2 mm, n_D^{20} 1.5199 and its identity confirmed by the n.m.r. spectrum. The aromatic hydrogens absorbed at 2.84 τ, the $-CH_2Cl$ as a triplet at 6.75 τ, the two methylenes at C-2 and C-3 showed a multiplet centered near 8.38 τ, and the two methyls absorbed at 8.74 τ.

The Action of Hydrochloric Acid on 5-Phenyl-2-pentanol

5-Phenyl-2-pentanol was synthesized by reacting the Grignard reagent from 1-chloro-3-phenylpropane with acetaldehyde according to the method of Roblin and co-workers (12). The product (film) showed strong hydroxyl absorption at 3300 cm^{-1}. It was found (by v.p.c. analysis) to be at least 91% of the desired alcohol. An attempt to prepare the corresponding chloride by the action of hydrochloric acid – zinc chloride yielded a mixture containing *n*-pentylbenzene, 1-methyltetralin and the chloride, 2-chloro-5-phenylpentane (Table I, No. 5).

The Action of Hydrochloric Acid on 5-Phenyl-2-methyl-2-pentanol

5-Phenyl-2-methyl-2-pentanol was prepared by the method of Bogert and co-workers (13). The crude product was found, by v.p.c. analysis, to be at least 90% pure. It showed hydroxyl absorption at 3300 cm^{-1} (film). The alcohol was treated with hydrochloric acid – zinc chloride (Table I, No. 6). The reaction mixture was neutralized with sodium carbonate, extracted with ether, and the ether extracts dried over sodium sulfate. The crude product was found, by v.p.c. analysis, to be 93% one component. Its ultraviolet spectrum was very similar to that of the hydrocarbon tetralin. The product was determined to be 1,1-dimethyltetralin by its n.m.r. spectrum. This showed a singlet at 8.72 τ (six protons), a complex multiplet in the region 8.0–8.5 τ (four protons), a triplet for the benzylic hydrogens centered at 7.20 τ (two protons), and a multiplet in the aromatic region centered at 2.73 τ (four protons). The compound showed $n_D^{25} = 1.5280$, (lit. (13), $n_D^{25} = 1.5274$).

Can. J. Chem. Downloaded from www.nrcresearchpress.com by 210.87.254.40 on 09/05/12
For personal use only.

Can. J. Chem. Downloaded from www.nrcresearchpress.com by 210.87.254.40 on 09/05/12
For personal use only.

(b) Cyclialkylations of Phenylalkyl Chlorides

The procedures given in the previous publication (1) were followed for the cyclialkylations. Details on the experimental conditions and product compositions, determined by v.p.c., are outlined in Table II.

The products were identified initially by using authentic samples of hydrocarbons (see syntheses below) as internal standards during the v.p.c. analyses. The identifications were confirmed by collecting the main peaks from v.p.c. separations and subjecting these samples to n.m.r. and, in some cases, mass spectroscopic analyses.

(c) Syntheses of Hydrocarbons

Benzsuberane

The synthesis of benzsuberane was described previously (3).

Indane

Indane was prepared by catalytic hydrogenation of indene (Matheson Co.). The indane (n_D^{20} = 1.5381, (lit. (14), n_D^{20} = 1.5381)) showed the expected n.m.r. spectrum. The four aromatic hydrogens absorbed at 2.98 τ as a singlet, the four benzylic hydrogens gave a triplet centered at 7.20 τ, and the methylene hydrogens on C-2 absorbed as a quintet at 8.02 τ.

1-Methyl-3,4-dihydronaphthalene (6)

1-Tetralone (Aldrich Chemical Co.) (10 g, 0.07 mole) was reacted with an equimolar amount of methylmagnesium iodide in refluxing ether and a nitrogen atmosphere for 3 h. The crude reaction product was freed of some unreacted 1-tetralone by chromatography from petroleum ether on alumina. The purified product n_D^{25} = 1.5782 (6 g, 60%) was evidently the unsaturated hydrocarbon from the lack of hydroxyl absorption in its infrared (i.r.) spectrum and the strong absorption in the ultraviolet (u.v.) spectrum at 261 mμ. The structure of **6** was confirmed by its n.m.r. spectrum. The four aromatic hydrogens showed a multiplet at 3.08 τ, the vinyl hydrogen a multiplet at 4.39 τ, the benzylic methylene a triplet at 7.46 τ, the methylene hydrogens on C-3, a complex multiplet at 7.93 τ, and the methyl group gave a quartet (~1.5 c.p.s.) due to allylic interaction with the vinyl hydrogen and homoallylic coupling with the two hydrogens on C-3.

1-Methyltetralin

1-Methyltetralin was obtained by hydrogenation of 1-methyl-3,4-dihydronaphthalene over a palladium catalyst in methanol at 50 p.s.i. The product (n_D^{25} = 1.5350) showed the expected parent mass of 146 in the mass spectrum with a base peak at 131 for loss of CH_3.

1,1-Dimethyltetralin

1,1-Dimethyltetralin was prepared by the action of hydrochloric acid–zinc chloride on 5-phenyl-2-methyl-2-pentanol as described under part (*a*) above.

1-Methylnaphthalene and 2-Methylnaphthalene

The methylnaphthalenes were prepared by the action of methyl sulfate on the Grignard reagents prepared from commercial (Fisher Scientific) 1-bromonaphthalene and 2-bromonaphthalene according to the procedure described in ref. 15. The compounds were characterized by their n.m.r. spectra. The 1-methylnaphthalene showed a complex multiplet in the region 2.9–2.1 τ for the aromatic hydrogens and a singlet at 7.51 τ for the methyl group. 2-Methylnaphthalene showed a complex multiplet at 2.85–7.2 τ for the aromatic hydrogens and a singlet at 7.56 τ for the methyl group.

Alkylbenzenes

Samples of propylbenzene (n_D^{20} = 1.4924; lit. (16) n_D^{20} = 1.4924), pentylbenzene (n_D^{20} = 1.4885; lit. (17) n_D^{20} = 1.4885), and 2-methyl-2-phenylpentane (n_D^{25} = 1.4910; lit. (18) n_D^{25} = 1.4908) for v.p.c. and n.m.r. standards were prepared by lithium aluminium hydride reduction of the chlorides 1-chloro-3-phenylpropane, 1-chloro-5-phenylpentane and 1-chloro-4-methyl-4-phenylpentane.

Acknowledgments

The financial support provided by the National Research Council of Canada is gratefully acknowledged. We wish to thank Dr. D. B. MacLean of McMaster University, Hamilton, Ontario, for providing the mass spectroscopic analysis.

1. L. R. C. Barclay and E. C. Sanford. Can. J. Chem. This issue.
2. A. A. Khalaf and R. M. Roberts. J. Org. Chem. **31**, 89 (1966).
3. L. R. C. Barclay, B. A. Ginn, and C. E. Milligan. Can. J. Chem. **42**, 579 (1964).
4. L. R. C. Barclay and E. C. Sanford. Paper presented at the 48th Annual Meeting, Chemical Institute of Canada, Montreal, June, 1965.
5. G. Baddeley and R. Williamson. J. Chem. Soc. 4647 (1956).
6. J. E. Douglass and R. M. Roberts. J. Org. Chem. **28**, 1225, 1229 (1963).
7. F. W. McLafferty. Mass spectrometry of organic ions. Academic Press, Inc., New York. 1963. p. 458.
8. L. Schmerling, R. W. Welch, and J. P. Luvisi. J. Am. Chem. Soc. **79**, 2636 (1957).
9. M. T. Bogert and D. Davidson. J. Am. Chem. Soc. **56**, 185 (1934).
10. J. F. J. Dippy and J. T. Young. J. Chem. Soc. 3919 (1955).
11. H. Pines and L. Schaap. J. Am. Chem. Soc. **80**, 4378 (1958).
12. R. O. Roblin, D. Davidson, and M. T. Bogert. J. Am. Chem. Soc. **57**, 151 (1935).
13. M. T. Bogert, D. Davidson, and P. M. Apfelbaum. J. Am. Chem. Soc. **56**, 959 (1934).
14. W. Bojsche and M. Pommer. Ber. **54**, 102 (1921).
15. L. I. Smith. Organic syntheses. Collective Vol. II. John Wiley and Sons, Inc., New York. 1957. p. 360.
16. K. V. Auwers and H. Kolligs. Ber. **55**, 21 (1922).
17. A. I. Vogel. J. Chem. Soc. 607 (1948).
18. J. Colonge and P. Garnier. Bull. Soc. Chim. France, 436 (1948).

Can. J. Chem. Downloaded from www.nrcresearchpress.com by 210.87.254.5 on 09/05/12
For personal use only.

Addition of carbethoxynitrene to *trans*- and *cis*-propenylbenzene and the ring-opening of the resulting aziridines

H. NOZAKI, Y. OKUYAMA, AND S. FUJITA
Department of Industrial Chemistry, Kyôto University, Kyôto, Japan

Received June 4, 1968

Carbethoxynitrene (**1**) generated thermally from ethyl azidoformate adds stereospecifically to *trans*- and *cis*-propenylbenzene. Ring-opening of the aziridines thus produced, proceeds with inversion at the phenyl-substituted carbon in dry acetic acid, while the reaction in aqueous acetic acid occurs with no stereospecificity.

Canadian Journal of Chemistry, 46, 3333 (1968)

Stereospecific addition of carbethoxynitrene (**1**) to certain olefins has been recorded recently (1–3). The nitrene **1** generated by photolysis of ethyl azidoformate adds stereospecifically to *trans*- and *cis*-2-butene (1), while the addition of thermally generated **1** to *cis*-4-methyl-2-pentene occurs also in a stereospecific manner (3). The latter paper has prompted us to report similar observations made independently by using the title phenyl-substituted olefins as substrates. We also report the ring-opening reactions of the resulting aziridines.

Addition of 1 to trans- and cis-Propenylbenzene

Ethyl azidoformate was decomposed thermally using *trans*- or *cis*-propenylbenzene as a solvent at 150–160°. A quantitative volume of nitrogen was evolved within 5 h. The resulting mixtures of ethyl *trans*- and *cis*-2-methyl-3-phenylaziridine-1-carboxylate (**2***a* and **2***b*) were analyzed by means of gas–liquid chromatography (g.l.c.). The **2***a*/**2***b* ratio of the mixture from *trans*-propenylbenzene was 94:6, while the **2***a*/**2***b* ratio from *cis*-propenylbenzene was 18:82. Thus the addition of **1** to *trans*- and *cis*-propenylbenzene proceeds with fairly rigorous stereospecificity. Applying Skell's criterion (4) in carbene chemistry to this case, we may conclude that the singlet nitrene is involved. Since the *trans* to *cis* ratios are almost the same as those previously recorded for simple alkenes (1–3), the phenyl substitution in the olefinic substrate seems not to affect the reaction course. This behavior of carbethoxynitrene is in sharp contrast to that recorded for the reaction with α-methylstyrene (5). Furthermore, attack on benzene ring (6) was not found in the present case.

The cycloadducts **2***a* and **2***b* were identified by chemical transformations and alternative syntheses illustrated as shown on p. 3334. The spin coupling constants of vicinal protons on the aziridine rings of **2***a* and **2***b* were 3 and 6 Hz, corresponding to the assigned configuration.[1] Alkaline hydrolysis of **2***a* gave *trans*-2-methyl-3-phenylaziridine (**3***a*) which was in turn prepared from ethyl *erythro*-*N*-(1-phenyl-2-iodopropane)carbamate (**4***a*). Similarly, **2***b* was converted to *cis*-2-methyl-3-phenylaziridine (**3***b*) which was identified by comparison with an authentic sample (8). Aziridines **2***a* and **2***b* were obtained by treatment of **4***a* and **4***b* with sodium hydride.

Ring-opening Reactions of 2a and 2b

Participation of neighboring acylamido groups in solvolytic reactions (9) and isomerization of 1-acylaziridines into 2-oxazolines (10) are well known. To examine the possibility of the carbethoxy group participating in the ring-opening reaction of aziridine-1-carboxylates, **2***a* and **2***b* were subjected to solvolysis.

Aziridines **2***a* and **2***b* were heated at reflux in a mixture of acetic acid and acetic anhydride to give *N*-carbethoxy-*O*-acetylnorephedrine (**5***a*) and -norpseudoephedrine (**5***b*), respectively, as well as a small amount of their diastereomers (Table I). The reaction of **2***a* and **2***b* in 92% aqueous acetic acid gave a mixture of *N*-carbethoxynorephedrine (**6***a*) and -norpseudoephedrine (**6***b*) together with **5***a* and **5***b* (Table I). Configurations of **6***a* and **6***b* were established by lithium aluminium hydride reduction by which they were converted to *dl*-ephedrine and *dl*-pseudoephedrine, respectively. *O*-Acetyl products **5***a* and **5***b* were shown to have the *erythro* and *threo* configurations, as both were obtained by acetylation of **6***a* and **6***b*, respectively.

[1]The values of vicinal coupling constants of several aziridines have been reported (see ref. 7).

Can. J. Chem. Downloaded from www.nrcresearchpress.com by 210.87.254.5 on 09/05/12
For personal use only.

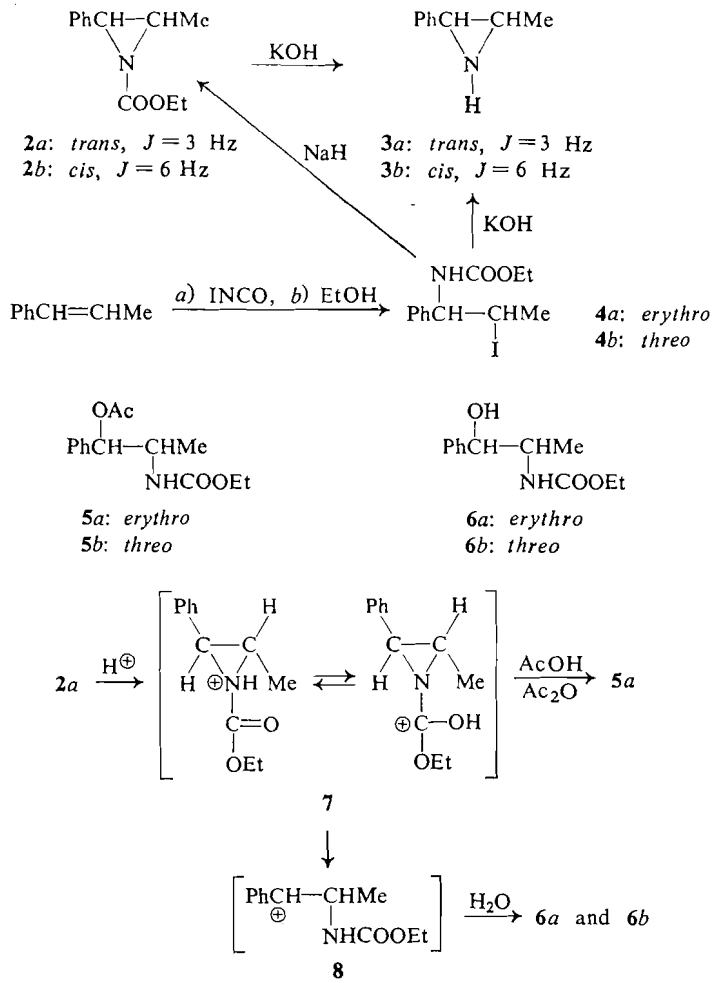

TABLE I

Ring-opening of **2***a* and **2***b*

Aziridine	Condition	OAc Products* Yield, %	5a %	5b %	OH Products† Yield, %	6a %	6b %
2*a*	$AcOH–Ac_2O$	42	89	11	—		
2*b*	$AcOH–Ac_2O$	48	25	75	—		
2*a*	aq. AcOH	43	90	10	51	30	70
2*b*	aq. AcOH	45	15	85	35	39	61

*The *erythro/threo* ratios were determined by means of the n.m.r. spectra.
†The ratios were estimated by means of the n.m.r. spectra after acetylation of the hydroxyl group.

Can. J. Chem. Downloaded from www.nrcresearchpress.com by 210.87.254.5 on 09/05/12
For personal use only.

The formation of OAc products (**5***a* and **5***b*) proceeds in a *trans* fashion, while the ring-opening to OH products (**6***a* and **6***b*) is non-stereospecific. This implies that two independent types of nucleophilic substitution have been involved.[2] Formation of the OAc products **5** is well explained by the S_N2-like attack of nucleophilic solvent to the protonated aziridine (**7**). On the other hand, non-stereospecificity in the ring-opening to **6** may be accounted for by intervention of carbonium ion **8**.

Experimental

All melting points are corrected. Nuclear magnetic resonance (n.m.r.) spectra were obtained in $CDCl_3$ or CCl_4 solution on a 60 Mc.p.s. instrument (JEOL C-60-H spectrometer) at 24°. The multiplicity of signals was indicated in abbreviated form: s, for singlet; d, for doublet; t, for triplet; q, for quartet; and m, for multiplet.

Thermolysis of Ethyl Azidoformate in trans- and cis-Propenylbenzene

A mixture of ethyl azidoformate (27.0 g, 0.23 mole) and *trans*-propenylbenzene (29 g) was added dropwise to *trans*-propenylbenzene (110 g) at 150–160°. Heating and stirring were continued (5 h) until nitrogen evolution ceased. Distillation *in vacuo* gave a mixture of **2***a* and **2***b*, b.p. 91–100°/0.3 mm in a 74% yield. Several fractional distillations afforded almost pure **2***a* which was identified by comparison of infrared and n.m.r. spectra and gas–liquid chromotography (g.l.c.) retention time with those of an authentic sample described below.

Similar decomposition of ethyl azidoformate in *cis*-propenylbenzene yielded a *cis*-rich mixture of **2**, b.p. 95–105°/0.3 mm in a 68% yield. The ratios of **2***a*/**2***b* were estimated by g.l.c. (Apiezon L, 30% on Neosorb NC, 0.3 mm × 2 m, 180°, H_2 as carrier gas).

Alkaline Hydrolysis of 2a and 2b

Aziridines **2***a* and **2***b* were treated with alcoholic potassium hydroxide as described below in the preparation of **3***a*. Distillation and preparative g.l.c. gave **2***a* and **2***b* as main products, respectively. Identification was made by comparison with authentic samples.

Ethyl erythro- and threo-N-(1-Phenyl-2-iodopropane)carbamate (4a and 4b)

A solution of silver isocyanate (20 g, 0.13 mole) (12), *trans*-propenylbenzene (11.8 g, 0.10 mole), and iodine (25.4 g, 0.10 mole) in ether (200 ml) was stirred at 0° during 1 h and then at 25° during 4.5 h. After filtration of the precipitate, ethanol (200 ml) containing a small amount of sodium ethoxide was added to the filtrate and the solution was allowed to stand for 7 days. After concentration, the residue was dissolved in ether and treated with ice water containing sodium sulfite. Evaporation of ether extract gave a crystalline residue (30.4 g, 91% yield). One recrystallization from methanol gave pure **4***a*, m.p. 78–79°; ν_{max} (Nujol) 3275, 1680, 1535 cm^{-1}; n.m.r. (in $CDCl_3$) δ 1.23 (t, OCH_2CH_3), 1.76 (d, CH_3), 4.07 (q, OCH_2CH_3), 4.3–4.7 (m, methines), 5.2–5.5 (broad, NH), and 7.27 p.p.m. (s, phenyl).

Anal. Calcd. for $C_{12}H_{16}INO_2$: C, 43.3; H, 4.8; I, 38.1; N, 4.1. Found: C, 43.4; H, 4.7; I, 38.2; N, 4.1.

Similar reaction of *cis*-propenylbenzene gave the *threo* isomer **4***b*, m.p. 58–59°; ν_{max} (Nujol) 3300, 1680, 1545 cm^{-1}; n.m.r. (in $CDCl_3$) δ 1.24 (t, OCH_2CH_3), 1.96 (d, CH_3), 4.13 (q, OCH_2CH_3), 4.3–4.6 (m, methines), 5.3–5.7 (broad, NH), and 7.25 (s, phenyl).

Anal. Calcd. for $C_{12}H_{16}INO$: C, 43.3; H, 4.8; I, 38.1; N, 4.1. Found: C, 43.5; H, 5.1; I, 37.8; N, 4.2.

trans-2-Methyl-3-phenylaziridine (3a)

Iodocarbamate **4***a* (5.95 g, 0.018 mole) was treated with ethanolic potassium hydroxide (KOH 5.0 g, water 10 ml, and ethanol 150 ml) at a refluxing temperature. After evaporation *in vacuo*, the residue was subjected to steam distillation and the distillate was extracted with ether. Distillation of the ethereal extracts gave **3***a* (1.43 g, 60%), b.p. 114–115°/26 mm. Preparative g.l.c. gave analytically pure **3***a*: ν_{max} (neat) 3300, 846 cm^{-1}; n.m.r. (in $CDCl_3$) δ 1.32 (d, CH_3), 2.10 (m, CH_3CH), 2.62 (d, $PhCH$, J = 3 Hz) 7.17 (s, phenyl).

Anal. Calcd. for $C_9H_{11}N$: C, 81.2; H, 8.3; N, 10.5. Found: C, 80.9; H, 8.4; N, 10.3.

Ethyl trans- and cis-2-Methyl-3-phenylaziridine-1-carboxylate (2a and 2b)

An oil suspension of sodium hydride (47%, 0.60 g) was rinsed with benzene twice and the mineral oil was replaced by benzene. To the resulting suspension of NaH in benzene, (20 ml) a solution of **4***a* (2.89 g, 0.0087 mole) in benzene (15 ml) was added dropwise at 50–53°. The separating solid was removed and the filtrate was subjected to fractional distillation *in vacuo* to give **2***a* as a colorless oil, b.p. 92–94°/0.15 mm in a 40% yield; ν_{max} (neat) 1720 cm^{-1}; n.m.r. (in CCl_4) δ 1.22 (t, OCH_2CH_3), 1.40 (d, CH_3), 2.47 (m, CH_3CH), 3.09 (d, $PhCH$, J = 3 Hz), 4.08 (q, OCH_2CH_3), 7.20 (s, phenyl).

Anal. Calcd. for $C_{12}H_{15}NO_2$: C, 70.2; H, 7.4; N, 6.8. Found: C, 70.5; H, 7.4; N, 6.7.

Similar treatment of **4***b* produced *cis* isomer **2***b*, b.p. 82–85°/0.09 mm in a 50% yield; ν_{max} (neat) 1720 cm^{-1}; n.m.r. (in CCl_4) δ 0.96 (d, CH_3), 1.25 (t, OCH_2CH_3), 2.70 (m, CH_3CH), 3.52 (d, $PhCH$, J = 6 Hz), 4.09 (q, OCH_2CH_3), and 7.23 (s, phenyl).

Anal. Calcd. for $C_{12}H_{15}NO_2$: C, 70.2; H, 7.4; N, 6.8. Found: C, 70.3; H, 7.5; N, 6.3.

Ring-cleavage of 2a and 2b in Acetic Acid – Acetic Anhydride

After heating a mixture of acetic acid (25 ml), acetic anhydride (6 ml), and potassium acetate (2.0 g) at reflux for 30 min, **2***a* (1.97 g, 0.0096 mole) was added in one portion. The reaction mixture was heated at reflux for an additional 3 h with stirring, poured onto ice water (100 ml), neutralized with solid Na_2CO_3, and extracted with ether. The combined extracts were dried (Na_2SO_4) and concentrated *in vacuo*. The residue was chromatographed on a Silica Gel column. Elution with 500 ml benzene–ether (9:1) gave a mixture (1.05 g, 42%) of **5***a*

[2]Similar competition of S_N1 and S_N2 mechanisms has been reported for the acid hydrolysis of aziridines (11). At this point, the authors are grateful to one of the referees for helpful suggestions.

Can. J. Chem. Downloaded from www.nrcresearchpress.com by 210.87.254.5 on 09/05/12
For personal use only.

and a small amount of **5***b*. Recrystallization from *n*-hexane–ether gave **5***a*, m.p. 74–75°, which was identical with the authentic sample described below (mixture m.p., infrared, and n.m.r. spectra).

Similar treatment of **2***b* gave chiefly **5***b* and a small amount of **5***a*. Recrystallization from *n*-hexane–ether yielded **5***b*, m.p. 68–69°, which was identical with the authentic sample described below (mixture m.p., infrared, and n.m.r. spectra).

The *erythro*/*threo* ratios were determined by n.m.r. and summarized in Table I.

Ring-cleavage of 2a and 2b in Aqueous Acetic Acid

A mixture of **2***a* (2.00 g, 0.0098 mole), acetic acid (23.0 ml), and water (2.0 ml) was heated at 48–50° for 3 h. Workup gave **5** (1.10 g, 43%) and **6** (1.11 g, 51%) as a mixture of diastereomers, both of which were separated by chromatography on a Silica Gel column. The *erythro*/*threo* ratios of **5** and **6** (after acetylation of OH group) were estimated by n.m.r. spectra and recorded in Table I, together with the results of similar treatment of **2***b*. Fractional recrystallization of the mixture of **6** (0.88 g) from *n*-hexane–ether afforded pure **6***b* (0.40 g) as less soluble colorless crystals, m.p. 95–95.5°; ν_{max} (Nujol) 3400, 3295, 1683, 1557 cm^{-1}; n.m.r. (in $CDCl_3$) δ 1.0–1.4 (t and d, OCH_2CH_3 and CH_3), 2.92 (s, OH), 3.8–4.3 (q and m, OCH_2CH_3 and CH_3CH), 4.55 (d, PhC*H*), 4.7–5.2 (broad, NH), 7.29 (s, phenyl).

Anal. Calcd. for $C_{12}H_{17}NO_3$: C, 64.6; H, 7.7; N, 6.3. Found: C, 64.5; H, 7.9; N, 6.0.

The *erythro* isomer **6***a* (0.20 g) was obtained as more soluble needles, m.p. 69–70°; ν_{max} (Nujol) 3370, 3295, 1675, 1557 cm^{-1}; n.m.r. (in $CDCl_3$) δ 0.99 (d, CH_3), 1.24 (t, OCH_2CH_3), 3.25 (s, OH), 3.9–4.3 (q and m, OCH_2CH_3 and CH_3CH), 4.85 (d, PhC*H*), 4.9–5.2 (broad, NH), 7.30 (s, phenyl).

Anal. Calcd. for $C_{12}H_{17}NO_3$: C, 64.6; H, 7.7; N, 6.3. Found: C, 64.3; H, 7.8; N, 6.1.

Lithium Aluminium Hydride Reduction of 6a and 6b

To a suspension of lithium aluminium hydride (0.4 g) in ether (10 ml) was added **6***a* (0.44 g, 0.0020 mole) in ether (10 ml) at room temperature. The reaction mixture was heated at reflux overnight. After decomposition of excess lithium aluminium hydride with wet ether and then with water, the ether layer was separated. The residual aqueous gel was treated with concentrated sodium hydroxide and filtered. The filtrate was extracted with ether. The combined extracts were dried (Na_2SO_4) and evaporated *in vacuo*. Treatment of the residue with alcoholic HCl and recrystallization from ethanol gave colorless crystals (0.32 g, 80%), m.p. 189°, which was identified by comparison with authentic *dl*-ephedrine hydrochloride.

Anal. Calcd. for $C_{10}H_{16}ClNO$: C, 59.5; H, 8.0; N, 7.0. Found: C, 59.2; H, 8.1; N, 6.7.

Lithium aluminium hydride reduction of **6***b* (0.88 g, 0.0042 mole) afforded *dl*-pscudoephedrine (free base, 0.66 g, 88%), m.p. 116–117° (*n*-hexane), which was identified by comparison with authentic sample.

N-Carbethoxy-O-acetylnorephedrine (5a) and -Norpseudoephedrine (5b)

A mixture of **6***a* (0.52 g, 0.0023 mole), acetic anhydride (2.5 g, 0.024 mole), sodium acetate (2.5 g, 0.032 mole), and benzene (15 g) was heated at reflux for 4 h. The reaction mixture was poured onto ice water and extracted with ether. The combined extracts were washed with aqueous Na_2CO_3 and dried (Na_2SO_4). Concentration and recrystallization (*n*-hexane–ether) gave **5***a* (0.57 g, 93%), m.p. 74–75°; ν_{max} (Nujol) 3320, 1763, 1690, 1548 cm^{-1}; n.m.r. (in $CDCl_3$) δ 1.0–1.4 (t and d, OCH_2CH_3 and CH_3), 2.16 (s, acetyl), 3.9–4.4 (q and m, OCH_2CH_3 and CH_3CH), 4.6–4.8 (broad, NH), 5.87 (d, PhC*H*), 7.37 (s, phenyl).

Anal. Calcd. for $C_{14}H_{19}NO_4$: C, 63.4; H, 7.2; N, 5.3. Found: C, 63.6; H, 7.5; N, 5.3.

Acetylation of **6***b* (1.00 g, 0.0045 mole) afforded the *threo* isomer **5***b* (1.15 g, 97%), m.p. 68–69° (*n*-hexane–ether); ν_{max} (Nujol) 3300, 1742, 1690, 1548 cm^{-1}; n.m.r. (in $CDCl_3$) δ 1.0–1.4 (t and d, OCH_2CH_3 and CH_3), 2.12 (s, acetyl), 3.9–4.4 (q and m, OCH_2CH_3 and CH_3CH), 4.6–5.0 (broad, NH), 5.73 (d, PhC*H*), 7.37 (s, phenyl).

Anal. Calcd. for $C_{14}H_{19}NO_4$: C, 63.4; H, 7.2; N, 5.3. Found: C, 63.6; H, 7.5; N, 5.3.

Acknowledgments

The authors are indebted to Prof. K. Sisido for help and encouragement, to Dr. R. Noyori for valuable suggestions and stimulating discussions, and to Mrs. K. Huzimoto for elemental analyses.

1. K. Hafner, W. Kaiser, and R. Puttner. Tetrahedron Letters, 3953 (1964).
2. W. Lwowski and J. S. McConaghy, Jr. J. Am. Chem. Soc. **87**, 5490 (1965).
3. J. S. McConaghy, Jr. and W. Lwowski. J. Am. Chem. Soc. **89**, 4450 (1967).
4. P. S. Skell and R. C. Woodworth. J. Am. Chem. Soc. **78**, 4496 (1956).
5. J. S. McConaghy, Jr. and W. Lwowski. J. Am. Chem. Soc. **89**, 2357 (1967).
6. K. Hafner, D. Zinser, and K. L. Moritz. Tetrahedron Letters, 1733 (1964); R. J. Cotter and W. F. Beach. J. Org. Chem. **29**, 751 (1964).
7. S. J. Brois and G. P. Beardsley. Tetrahedron Letters, 5113 (1966).
8. K. Kitahonoki, K. Kotera, Y. Matsukawa, and S. Miyazaki. Tetrahedron Letters, 1059 (1965).
9. G. E. McCasland, R. K. Clard, Jr., and H. E. Carter. J. Am. Chem. Soc. **71**, 637 (1949); S. Winstein and R. Boschan. J. Am. Chem. Soc. **72**, 4669 (1950); L. H. Welsh. J. Org. Chem. **32**, 119 (1967).
10. H. W. Heine and M. S. Kaplan. J. Org. Chem. **32**, 3069 (1967) and references cited therein.
11. V. B. Schatz and L. B. Clapp. J. Am. Chem. Soc. **77**, 5113 (1955).
12. A. Hassner, M. E. Lorber, and C. Heathcock. J. Org. Chem. **32**, 540 (1967).

Structure and reactions of lactonic and acidic sophorosides of 17-hydroxyoctadecanoic acid[1,2]

A. P. TULLOCH, A. HILL,[3] AND J. F. T. SPENCER
Prairie Regional Laboratory, National Research Council of Canada, Saskatoon, Saskatchewan

Received May 31, 1968

The complete structures of the major components of the mixture of lactonic and acidic sophorosides of 17-L-hydroxyoctadecanoic acid, which is produced by a yeast of the genus *Torulopsis*, have been determined. The principal lactonic component (**1**) (41%) has acetate groups at the 6′- and 6″-positions and the fatty acid carboxyl group is linked to the 4″-position to form a macrocyclic lactone ring. The other lactonic component (**2**) (8%) differs from the first only in the absence of the acetate group at the 6′-position. The principal acidic component (**5**) (31%) also has acetate groups at the 6′- and 6″-positions but the fatty acid carboxyl group is free. The structures were deduced by a combination of glycol cleavage and nuclear magnetic resonance studies and by examination of the products of acetobrominolysis of the acetylated lactones and acid.

The 2″,3″-glycol group of the lactones is resistant to oxidation by periodate and by lead tetraacetate in acetic acid. Studies of the rate of glycol cleavage of methyl 4,6-di-*O*-acyl-β-D-glucopyranosides showed that though an acyl group at C-4 retarded the oxidation of the 2,3-diol it did not stop it completely. The conformation of the lactone ring is probably responsible for the unreactivity of the 2″,3″-glycol group. The lactone ring, however, considerably increases the rate of acetobrominolysis of the fully acetylated lactone compared to that of the acetylated sophorosyl acid methyl ester.

Canadian Journal of Chemistry, 46, 3337 (1968)

In an earlier publication it was reported that a yeast of the genus *Torulopsis* produced extracellular glycosides which were composed of partially acetylated sophorosides of 17-hydroxyoleic and 17-hydroxystearic acids (1). Later long-chain compounds such as ethyl stearate and octadecane were found to be converted by the yeast to the fatty acid portion of the sophoroside in yields of 50–80% (2).

We observed that the crude glycoside contained about 1.8 acetate groups and also that the neutralization equivalent was usually in the range 1200–1500. However, the value expected for a diacetyl sophoroside of a hydroxy acid is about 700 suggesting that in part of the product the carboxyl group had formed an ester with one of the sugar hydroxyl groups. Then (1962) we found that samples of the sophoroside crystallized on keeping in ethanol, giving a neutral material which had a molecular weight of about 690 and contained 2 acetate groups and a macrocyclic lactone ring (3).

A preliminary report concerning the positions of the acyl groups has been made (4). In this paper we provide evidence to show that the principal lactonic component of the mixture of sophorosides, obtained by fermenting octadecane, is 17-L-[(2′-*O*-β-D-glucopyranosyl-β-D-glucopyranosyl)-oxy] octadecanoic acid 1,4″-lactone 6′,6″-diacetate (**1**), that a second lactone 17-L-[(2′-*O*-β-D-glucopyranosyl-β-D-glucopyranosyl)oxy] octadecanoic acid 1,4″-lactone 6″-acetate (**2**), is present as a minor component, and that the principal acidic component is 17-L-[(2-*O*-β-D-glucopyranosyl-β-D-glucopyranosyl)oxy] octadecanoic acid 6′,6″-diacetate (**5**).

When this work was almost complete Jones (5) (using a strain of *Torulopsis* obtained from us) isolated a lactone and proposed that it had structure (**9**), which differs from our structure (**1**) in the attachment of the ester linkages to ring B. In **9**, hydroxyl-4 of ring B is not esterified but an acetate is present at OH-3 and the fatty acid carboxyl is linked to OH-6. The two products have been compared and were indistinguishable (4). Because of the proposal of structure (**9**) we have emphasized those parts of our work which show that OH-4 is, in fact, acylated.

Structure of Lactone (1)

The major component of the hydroxy acid portion of a typical fermentation product was 17-L-hydroxyoctadecanoic acid (2) but 10–15% of 17-L-hydroxy-9-octadecenoic acid, probably produced by direct introduction of a double bond (6), was also present. Crude lactone was obtained by crystallization and, after hydrogenation to

[1]NRCC No. 10288.
[2]Part V of the series: Fermentation of long-chain compounds by *Torulopsis apicola*.
[3]NRCC Postdoctorate Fellow, 1965–1967.

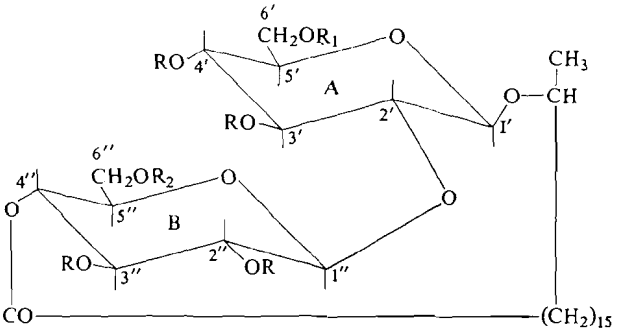

1 $R_1 = R_2 = Ac$, $R = H$
2 $R_2 = Ac$, $R_1 = R = H$
3 $R = R_1 = R_2 = Ac$
4 $R_1 = R_2 = Ac$, $R = PhNCO$

remove unsaturated components, lactones (**1**) and (**2**) were isolated by chromatography on silicic acid. Further quantities of lactone (**1**) were obtained during isolation of acid (**5**). The approximate composition of the fermentation product was lactone (**1**) (41%), lactone (**2**) (8%), and acid (**5**) (31%); the remainder consisted of possibly isomeric lactones (14%), which were not investigated further, and monoacetylsophorosyl hydroxy acid (6%). Lactones (**1**) and (**2**) are probably true fermentation products and not artefacts; lactonization of acid (**5**) during recovery of the product would be unlikely to produce a major proportion of one lactone since five secondary hydroxyl groups are available. Also acid (**5**) does not appear to lactonize readily as the neutralization equivalent was not changed by heating, in water, at 100° for several hours. Deacetylated

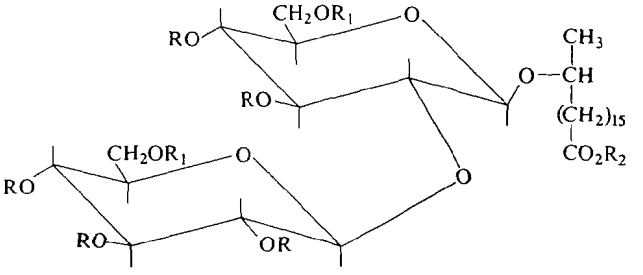

5 $R_1 = Ac$, $R = R_2 = H$
6 $R_1 = Ac$, $R = H_1$, $R_2 = CH_3$
7 $R_1 = R = H$, $R_2 = CH_3$
8 $R_1 = R = Ac$, $R_2 = CH_3$

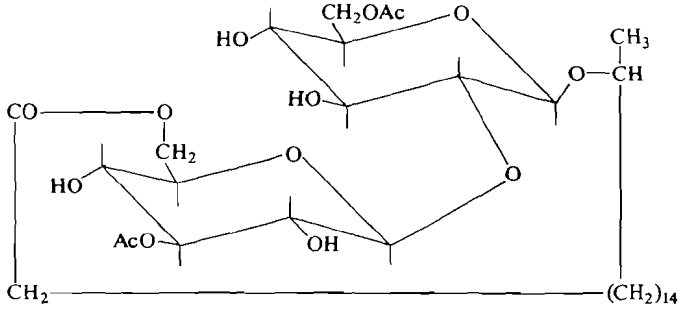

9

TABLE I

Rate of oxidation of **1**, **2**, and some diols by sodium periodate in aqueous *t*-butanol (moles/mole)

Time (h)	Compound				
	1	**2**	Methyl 4,6,di-*O*-acetyl β-D-glucopyranoside	Methyl 6-*O*-acetyl 4-*O*-stearoyl β-D-glucopyranoside*	Methyl 4,6-*O*-benzylidene β-D-glucopyranoside
0.5	0.18	0.56	—	—	—
1	0.35	0.81	—	—	—
4	0.76	0.97	0.06	—	—
8	0.92	1.02	0.09	0.1	0.48
24	0.92	1.06	0.13	0.18	0.78
48	—	—	0.46	0.20	1.11
72	1.01	1.10	0.62	0.30	1.31
168	1.23	—	1.15	0.41	1.31

*Oxidation in 47% *t*-butanol.

acid was previously observed to lactonize to some extent on keeping in the presence of formic acid (1), but this may have been due to reaction with the free primary 6-OH groups.

Saponification of **1** showed that three ester linkages were present; since 2 moles of acetic acid per mole of **1** were obtained the third linkage must involve the fatty acid carboxyl group. Compound (**1**) should contain four free hydroxyl groups, and as expected gave a hexaacetate **3** and a tetraphenylurethane **4**. Deacylation of lactone (**1**) with methanolic sodium methoxide gave methyl ester (**7**) which on acetylation yielded the heptaacetate ester (**8**).

Oxidation of Lactone (1)

Lactone (**1**) contains one readily cleavable glycol group since, on oxidation with lead tetraacetate in acetic acid in the presence of potassium acetate (7), or with sodium periodate, one mole of oxidant is used per mole of **1** (Tables I and II). The glycol group must be a 3,4 diol as reduction (8) and acid methanolysis of the oxidation product gave glycerol, D-glyceraldehyde dimethyl acetal, methyl α,β-glucosides, and fatty acid ester as shown in Table III. The fragments were analyzed by gas–liquid chromatography (g.l.c.) and also isolated by cellulose column chromatography. The recovery of the fragments was not quantitative but was adequate to determine the course of the oxidation.

The reduced oxidation product was methylated and the fragments obtained by acid methanolysis analyzed by g.l.c. Almost the entire glucosidic product was methyl α,β 2,3,4,6-tetra-*O*-methyl-glucosides with only a trace of methyl 3,4,6-tri-*O*-methyl-glucosides, showing that the 3′,4′-diol of ring A had been attacked. This conclusion was confirmed when we found that mild hydrolysis of the reduced periodate oxidation product followed by a second borohydride reduction yielded 2-*O*-β-D-glucopyranosyl-glycerol and glycerol. A little

TABLE II

Rate of oxidation of **1**, **2**, and some diols by lead tetraacetate in acetic acid (moles/mole)

Time (h)	Compound			
	1	**2**	Methyl 4,6-di-*O*-acetyl β-D-glucopyranoside	Methyl 6-*O*-acetyl 4-*O*-stearoyl β-D-glucopyranoside
1	0.16	0.22	—	—
2	0.23	0.33	—	—
4	0.40	0.55	0.1	—
8	0.58	0.74	0.15	0.13
24	0.93	1.10	0.25	0.29
48	1.09	1.22	0.42	0.52
72	1.14	1.24	0.69	0.72
168	1.38	1.61	1.12	1.50

TABLE III

Oxidation fragments obtained by oxidation of **1** with lead tetraacetate

Solvent	Products (moles)				
	Glyceraldehyde dimethyl acetal	Glycerol	Tetritols	Methyl glucosides	17-Acetoxy stearate
Acetic acid	0.34	0.53	—	1.1	1.0
Pyridine	0.35	0.98	0.64	0.05	1.0

sorbitol, also isolated, probably resulted from hydrolysis of the glucosyl-glycerol. The hydroxy fatty acid fraction was treated with methanolic hydrogen chloride to convert any glycosides to methyl esters but only a very small amount of impure methyl α,β-glucosides was isolated. The latter would have been obtained from glucosyl-hydroxyoctadecanoic acid resulting from hypothetical oxidation of the 3″,4″-diol group.

At this stage the nuclear magnetic resonance (n.m.r.) evidence (see below) suggested strongly that a 4,6-di-*O*-acyl grouping was present which is, from the oxidation results, in ring B. Ring B must therefore contain a 2,3-diol group which is not readily oxidized (we are indebted to Dr. A. S. Perlin for this suggestion). On oxidation with lead tetraacetate in pyridine, a reagent which is known to cleave "resistant diols" (9), lactone (**1**) rapidly consumed 2 moles of oxidant (Table IV). The oxidation fragments were glyceraldehyde dimethyl acetal, glycerol, tetritols, and only a trace of methyl glucosides (Table III). Glycollic aldehyde dimethyl acetal could not be detected, but the results confirmed the presence of a 2,3-diol grouping in ring B.

TABLE IV

Rate of oxidation of **1** by lead tetraacetate in pyridine (moles/mole)

Time (min)	Compound	
	1	Methyl 6-*O*-acetyl-4-*O*-stearoyl β-D-glucopyranoside
5	1.73	—
10	1.78	1.12
30	1.89	1.29
60	2.01	1.47
180	2.17	2.20

The tetritol fraction was a mixture of erythritol and D-threitol. The latter compound is probably formed by enolization of the aldehydic oxidation product or by hydrolysis and isomerization to a 2-ketose (10) which is reduced to the two tetritols.

The oxidation results provide an example of a diol made resistant to oxidation by the presence of an aliphatic ester group at the neighboring carbon atom. Honeyman and Shaw (11) examined the periodate cleavage of a large number of glycosides and found that adjacent substituents had a retarding effect on the rate of cleavage. Methyl 4-*O*-*p*-toluenesulfonyl-α-D-glucopyranoside, the only compound they examined with an ester group at C-4, was oxidized relatively slowly (about $\frac{1}{3}$ the rate of methyl 4,6-*O*-benzylidene-β-D-glucopyranoside).

We wished to determine whether the resistance of the 2,3-diol in ring B of **1** was peculiar to **1** or whether any 4,6-di-*O*-acylglucoside would behave in the same way. We accordingly investigated the oxidation of methyl 4,6-di-*O*-acetyl-β-D-glucopyranoside and methyl 6-*O*-acetyl-4-*O*-stearoyl-β-D-glucopyranoside (12). The rates of oxidation by periodate in 33% *t*-butanol and by lead tetraacetate in acetic acid are compared in Tables I and II, respectively. The oxidations were quite slow but were apparently complete after 168 h, except in the case of the oxidation of the 4-stearate by periodate. However, this compound had to be oxidized in 47% *t*-butanol owing to its low solubility and this may account for the incomplete reaction. The 6-acetate-4-stearate was oxidized very rapidly by lead tetraacetate in pyridine but extensive over-oxidation occurred (Table IV). Thus the resistance of the 2″,3″-diol of (**1**) to oxidation is only partly explained by the presence of the ester group at C-4″, steric hindrance due to the conformation of the lactone ring probably accounts for the complete resistance of the diol to periodate and to lead tetraacetate in acetic acid.

Jones (5) reported that his lactone consumed only one molar equivalent of lead tetraacetate in pyridine. This result may have been due to the presence of traces of water in the solvent since we found, on one occasion, that when undried pyridine was used only 0.92 mole of oxidant per mole of **1** was consumed.

Nuclear Magnetic Resonance Spectra

Spectra of lactones (**1**) and (**2**) were examined using a number of solvents. Those in acetone-d_6 and in pyridine were the most useful and the low field portions are shown in Fig. 1. The high field portions of the spectra of **1** contained the expected signals; in particular two acetoxyl singlets were visible. Figure 1A (lactone **1** in acetone-d_6) shows signals (in p.p.m.) attributable to H-6 centered in 4.11 and 4.27, to H-1 at 4.45 and 4.61 and a triplet, due to the carbinolic proton of a secondary acyl grouping, at 4.88. Similar signals are seen in Fig. 1C (lactone (**1**) in pyridine) but one H-6 and one of the H-1 signals are overlapping.

The H-1 signals can be assigned after consideration of the spectra of the hexaacetate (**3**) in the different solvents. In these spectra and also those of **8** one anomeric proton signal is visible at about 4.5–4.7 but is absent from the spectra of β-sophorose octaacetate and of compounds having the α-configuration at C-1′ (**10**, **19**, **20**). This signal can therefore be assigned to H-1′ and decoupling experiments (in acetone-d_6) show that it is coupled to the quartet at 3.65 which can be positively assigned to H-2′.

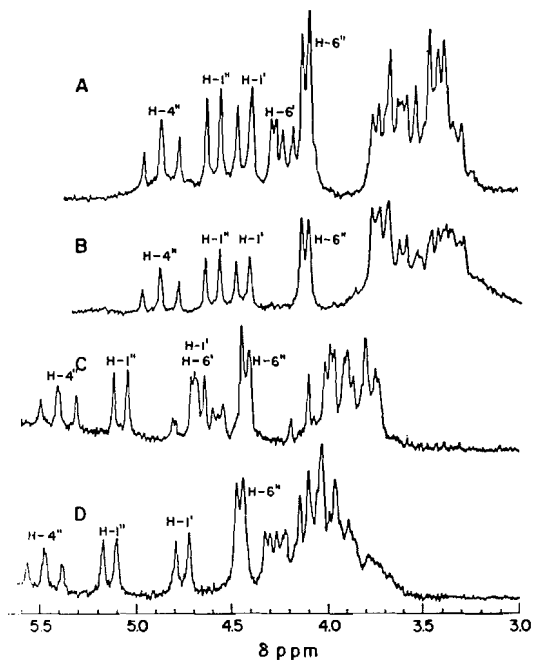

FIG. 1. Nuclear magnetic resonance spectra of: A) lactone (**1**) in acetone-d_6; B) lactone (**2**) in acetone-d_6; C) lactone (**1**) in pyridine; D) lactone (**2**) in pyridine; (3.0–5.7 p.p.m. regions).

On acetylation of **1** the H-1′ signal should be deshielded to a much smaller extent than the H-1″ signal. Table V compares the H-1 signals of **1** and **3** in three solvents and assigns them on this basis. In the case of spectra in acetone-d_6, H-1′ is apparently displaced to lower field by 0.13 p.p.m. on acetylation, however, we have found that acetylation of methyl 2,3-di-*O*-benzyl-β-D-glucopyranoside causes a similar displacement (12). Using these solvents, and also dimethyl sulfoxide-d_6, we conclude that the higher field H-1 signal is due to H-1′.

TABLE V

Assignments of H-1 signals* of lactone (**1**) and hexaacetate (**3**)

	H-1′		H-1″	
Solvent	**1**	**3**	**1**	**3**
Acetone-d_6	4.45	4.58	4.61	>4.75
Pyridine	4.68	4.66	5.08	?
Chloroform-*d*	4.46	4.45	4.56	>4.75

*In p.p.m.

Further information about the structure of **1** can be obtained by assigning the H-6 signals. From a study of the n.m.r. spectra of a number of partially acylated β-D-glucopyranosides (12) we have found that when OH-4 and OH-6 are both acylated the H-6 signals are at higher field (by 0.1–0.3 p.p.m.) than when only OH-6 is acylated, but the effect is not observed when OH-3 and OH-6 are acylated. Therefore the high field H-6 signals are those of H-6 of a glucose ring in which OH-4 is also acylated. Taking the oxidation results into account these H-6 signals are due to H-6″ and the low field H-6 signals are due to H-6′. The splittings of the low field H-6 signal which show that $J_{BX} > J_{AX}$ (where B is the H-6 proton at higher field and X is H-5) support this conclusion. We found that in the case of spectra in acetone-d_6 and in pyridine, when OH-6 alone was acylated, $J_{BX} > J_{AX}$ (12).

The low field triplet was assigned to H-4″, and the assignment was confirmed by spin-decoupling experiments in acetone-d_6. Irradiation at 4.90 did not affect the H-1 doublets but produced a change at 3.75; irradiation at 3.75 had no effect on H-1 signals but collapsed the triplet and reduced the spacing of H-6″ at 4.11 suggesting that H-5″ and probably also H-3″ are at 3.75. We have previously found that when OH-4 and OH-6 are both

acylated H-5 is at 3.75–3.90, but when only H-6 is acylated H-5 is at 3.4–3.5 (12). This was confirmed by irradiation at 4.12 which affected the 3.70 region. Irradiation at 4.61 (H-1″) affected the spectrum of 3.36 suggesting the presence of H-2″ and irradiation at 4.45 (H-1′) affected the spectrum at 3.44 suggesting the presence of H-2′. Irradiation at 3.36 and at 3.44 caused the doublets at 4.61 and 4.45 respectively to narrow and tend towards singlets. However, when these H-2 positions were irradiated there was no effect at all on the triplet at 4.90 showing that it cannot be due to H-3. Irradiation at 3.44 also affected H-6′ at 4.27 and irradiation at 4.27 affected the 3.44 region showing that, as expected, H-5′ is in this region of the spectrum.

Some additional information was also obtained from the spectrum of **1** in dimethyl sulfoxide-d_6. This was similar to the spectrum in acetone but the signals in the 4–5 p.p.m. region were closer together, H-6″ was at 4.00, H-6′ at 4.25, H-1′ at 4.40, H-1″ at 4.55, and H-4″ at 4.70. A doublet due to 2 hydroxyl protons was present at 5.23 and one-proton doublets at 5.50 and 5.60, the fact that the hydroxyl proton signals are all doublets confirms that the free hydroxyl groups of **1** are all secondary hydroxyls (13). Decoupling experiments gave the same results as those already carried out in acetone solution but also made possible a definite assignment of the H-1 signals. Irradiation at 3.20 (H-2′) affected H-1′ at 4.40 but none of the hydroxyl doublets, but irradiation at 3.05 (H-2″) caused the collapse of H-1″ at 4.55 and also the OH doublet at 5.50.

These results disagree with those that Jones (5) obtained from the spectrum of **1** in deuteriochloroform. He apparently assumed that H-2′, which is clearly at 3.70 in the spectrum of **3**, would also have the same chemical shift in the spectrum of **1** (the assumption is incorrect since acetylation of OH-3 and OH-4 will have some deshielding effect on H-2 (12)) and concluded that when irradiation of **1** at 3.70 affected the low field triplet, the triplet must be due to H-3″. However, it is most likely that H-3″ and H-5″ are at 3.70 since we found that irradiation at 3.45 (the true chemical shift of the H-2′s) causes the H-1 signals to collapse but had no effect on the low field triplet.

Thus we have established that the acyl groups are attached at the 6′-, 6″-, and 4″-positions but the point of attachment of the lactone ring has still to be determined.

Structure of Lactone (2)

By consideration of the structure of lactone (**2**) one of the possible points of attachment of the lactone ring can be eliminated. Saponification showed that **2** contained 2 ester linkages but only 1 acetate group. The n.m.r. spectra confirmed that only one acetoxyl group was present. Comparison of the low field portions of the spectra of **2** in acetone-d_6 and in pyridine (Fig. 1, B and D) with those of **1** (Fig. 1, A and C) shows that the low field H-6 signal is missing from the spectra of **2**, suggesting that only OH-6″ and OH-4″ are acylated. The spectrum in dimethyl sulfoxide-d_6 also showed a triplet due to a free primary hydroxyl group at 4.25 (spectrum measured at 70°) (13). Complete acetylation of **2** gave a hexaacetate identical with **3** obtained from **1** showing that the lactone ring is at the same position in both **2** and **1**, and must be attached to either C-4″ or C-6″.

The rate of oxidation of **2** by periodate compared to that of **1** (Table I) agreed with the conclusion that OH-6′ of ring A was not acetylated. Lactone **2** was oxidized approximately twice as rapidly as **1**, similar to the difference between the rates of oxidation of methyl-β-D-glucopyranoside and methyl 6-*O*-acetyl-β-D-glucopyranoside (Table VII).

Position of Lactone Ring of 1 and 2

Vis and Fletcher (14) found that some acetylated sophorosides undergo partial acetobrominolysis fairly readily. When the hexaacetate **3** was treated with 3% hydrogen bromide in acetic acid the α-bromosophorose hexaacetate derivative **10** was obtained in 50% yield. The low field portion of the spectrum (in deuteriochloroform) was very similar to that of α-acetobromosophorose, H-1′ appeared at 6.44 and had a spacing of 4 c.p.s., H-3′ was at 5.46 (this proton is deshielded by the axial oxygen at C-1′ (15)). Treatment of **10** with silver acetate gave the β-sophorose heptaacetate derivative **11**, which also had an n.m.r. spectrum in agreement with the proposed structure.

The isolation of **10** made it possible to confirm further that the compounds under investigation were in fact sophorosides. (The preparation of sophorose derivatives from the crude mixed glysides (1) indicated that the lactones were very probably sophorosides.) Compound (**10**) was converted to the methyl β-sophoroside derivative (**12**) by reaction with methanol. Deacylation of **12**

gave methyl β-sophoroside (**15**), which has been synthesized by Finan and Warren (16). Methyl β-sophoroside and its heptaacetate (**14**) were also prepared from β-sophorose octaacetate. The heptaacetate (**14**) was also prepared by the Koenigs–Knorr reaction using methyl 3,4,6-tri-*O*-acetyl-β-D-glucopyranoside and α-acetobromoglucose.

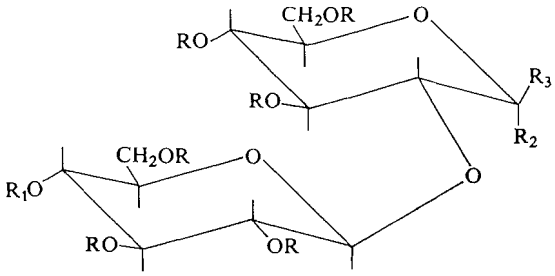

10 R = Ac, $R_1 = CH_3CH(OAc)(CH_2)_{15}CO$, R_2 = Br, R_3 = H
11 R = R_3 = Ac, $R_1 = CH_3CH(OAc)(CH_2)_{15}CO$, R_2 = H
12 R = Ac, $R_1 = CH_3CH(OAc)(CH_2)_{15}CO$, R_2 = H, $R_3 = OCH_3$
13 R = R_1 = Ac, R_2 = Br, R_3 = H
14 R = R_1 = Ac, R_2 = H, $R_3 = OCH_3$
15 R = R_1 = R_2 = H, $R_3 = OCH_3$

In addition to cleavage of the linkage between ring A and the fatty acid, cleavage between the glucose rings also took place. The material remaining after isolation of **10** was treated with silver acetate and chromatographed on silicic acid giving the β-glucose tetraacetate derivative (**16**) in a yield of about 5%. This compound was indistinguishable from **16** synthesized from β-glucose 1,2,3,6-tetraacetate and the acid chloride of 17-L-acetoxyoctadecanoic acid. The isomers with the fatty acid group at C-6 (**17**) and at C-3 (**18**) were also synthesized from the corresponding glucose tetraacetates and clearly differed from **16** in physical properties, n.m.r. spectra, and X-ray powder photographs.

The n.m.r. spectra of **16**, **17**, and **18** differ mainly in the chemical shifts of the acetoxyl signals which are assigned as shown in Table VI. The signal at 2.09 is due to the equatorial acetate at C-1′ (17), that at 2.06 is due to acetate at C-6′ (12), and the others are in the 1.98–2.02 region. These signals readily distinguish between **16** and **17**; therefore, the spectra of the materials eluted immediately before and after the fraction containing **16** were examined, but no evidence was found for the presence of compounds such as **17**, lacking acetoxyl at C-6′.

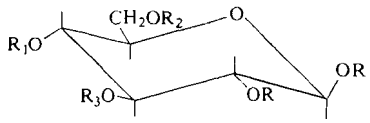

16 R = R_2 = R_3 = Ac, $R_1 = CH_3CH(OAc)(CH_2)_{15}CO$
17 R = R_1 = R_3 = Ac, $R_2 = CH_3CH(OAc)(CH_2)_{15}CO$
18 R = R_1 = R_2 = Ac, $R_3 = CH_3CH(OAc)(CH_2)_{15}CO$

TABLE VI

Assignment of acetoxyl signals* in nuclear magnetic resonance spectra of compounds (**16**), (**17**), and (**18**) in deuteriochloroform

Compound	1′-Acetoxyl	6′-Acetoxyl	2′-, 3′-, 4′-, and 17-Acetoxyls
16	2.09	2.06	1.98, 2.00, 2.01
17	2.09	—	2.01(2), 2.02(2)
18	2.09	2.06	2.01(3)

*In p.p.m.

Bonner (18) has shown that when 1,2,3,4,6-penta-*O*-acetyl-β-D-glucopyranose, which contained labelled acetate groups at C-4 or C-6, was treated with a mixture of acetic acid and acetic anhydride and sulfuric acid there was no exchange of the labelled groups with solvent acetate. Lemieux *et al.* (19) also obtained similar results. Thus it seems reasonable to assume that specific interchange of acetate and fatty acid residues will not occur during acetobrominolysis of **3**. We therefore conclude that the lactone ring is attached to C-4′′ and not to C-6′′.

Structure of Acid (5)

The n.m.r. spectrum of (**5**) (in pyridine) showed that 2 acetoxyl groups were present (singlets at 1.94 and 1.96) and that these were probably at C-6′ and C-6′′ (4 H-6 protons in the region 4.45–4.90 and no low field triplet). The methyl ester (**6**) was prepared by treating **5** with diazomethane. The spectrum of **6** in dimethyl sulfoxide-d_6 showed five low field doublets for the five secondary hydroxyl groups and also H-6 signals at 3.90–4.30 confirming that the acetate groups were at the C-6 positions. Hydroxyl doublets were not seen in the spectrum of **5** in dimethyl sulfoxide due to exchange catalyzed by the fatty acid carboxyl group (13).

Deacetylation of **6** with sodium methoxide gave the ester (**7**) identical with that obtained from lactone (**1**); **7** was also obtained by treatment of **5** with 1% methanolic hydrogen chloride at room

temperature. Periodate oxidation of **6** and **7** helped to confirm structure (**6**). Both compounds consumed 3 moles of oxidant but **7** was oxidized more rapidly than **6**, the difference in rates being comparable to the difference in the rates of oxidation of β-methyl glucoside and its 6-acetate (Table VII).

TABLE VII

Rates of oxidation of esters (**6**) and (7) and some methyl glucosides by sodium periodate in aqueous *t*-butanol (moles/mole)

	Compound			
Time (h)	**6**	**7**	6-*O*-Acetyl-β-D-glucopyranoside	β-D-Glucopyranoside
1	1.44	1.72	0.56	1.13
3	1.92	2.30	1.21	1.71
6	2.19	2.53	1.60	1.83
12	2.30	—	1.89	—
24	2.76	3.09	2.04	1.88
48	3.08	—	2.07	—

The same diacetate ester (**6**) was also obtained in 30% yield by partial deacylation of lactone (**1**) with very weak methanolic sodium methoxide. This reaction helps to relate the structure of lactone (**1**) to that of acid (**5**) and also to confirm that the lactone ring is attached at C-4″.

The structure of acid (**5**) is thus firmly established and is similar to that of lactone (**1**) except that in **5** the carboxyl group is free whereas in **1** it is combined with OH-4″ to form the large lactone ring. Acid (**5**) is also similar in structure to the 6′,6″-di-*O*-acetyl-β-sophoroside of 13-hydroxydocosanoic acid which is produced by another yeast, *Candida bogoriensis* (20). We can speculate that **5** is probably produced first and that part is then converted to lactone (**1**).

Comparison of Acetobrominolysis Reactions of 3 and 8

When the heptaacetate ester (**8**) was subjected to acetobrominolysis, α-acetobromosophorose was obtained confirming that acid (**5**) was a sophoroside. However, the reaction proceeded much more slowly than it did with lactone hexaacetate (**3**). We attempted to follow the reaction by measuring the change in rotation as the laevorotatory β-sophoroside was converted to the more dextrorotatory α-bromo derivative. As shown in Table VIII a fairly rapid rise in rotation occurred but the rotation of **8** changed much more rapidly than that of **3**.

TABLE VIII

Changes in specific rotation during acetobrominolysis of lactone hexaacetate (**3**) and methyl ester heptaacetate (**8**)

	Specific rotations*	
	Compound	
Time (h)	**3**	**8**
0	−11.4	−9.2
0.25	−8.4	+8.3
0.5	−5.4	+16.7
1.0	+1.1	+29.1
3	+13.7	+43.7
5	+23.2	+47.8
24	+43.9	+53.2
48	+55.90	—

*$[\alpha]_D^{25}$.

Lindberg (21) has shown that β-glucosides of secondary alcohols are rapidly converted to α anomers in acetic anhydride–acetic acid mixtures containing sulfuric acid. We were able to show that α anomers were produced from **3** and **8**, under acetobrominolysis conditions by following

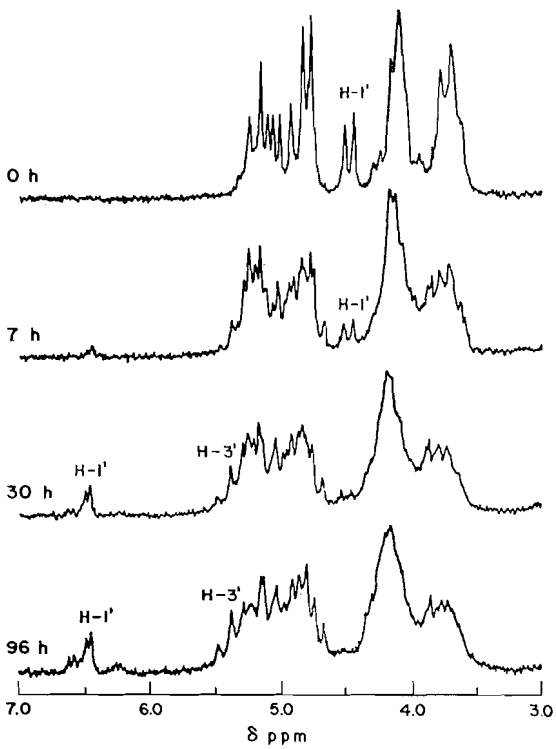

FIG. 2. Changes in the nuclear magnetic resonance spectrum of **3** during acetobrominolysis.

the reaction with the n.m.r. spectrometer. Figure 2 shows the spectral changes occurring during the reaction of **3**. The prominent doublet at 4.48, due to H-1′, disappears slowly, and after 7 h is about one quarter of the original size. However, the low field doublet at 6.47, due to H-1′ of **10**, is scarcely visible at this stage. After 30 h this signal is fairly prominent and after 96 h a small doublet at 6.62, probably due to H-1′ of **16**, has also appeared.

The spectrum obtained during acetobrominolysis of **8** showed that inversion also occurred but more rapidly than with **3**, in agreement with the results of Table VIII. The H-1′ doublet disappeared in 2 h, but the signal due to H-1′ of **13** was not visible until 3 days later. Even at 7 days the size of this signal indicated the conversion of no more than 25% of **20** to **13**. The yield of **13** actually isolated from such an experiment was 20%. The slow formation of **13** is similar to the results obtained on acetobrominolysis of the sophoroside from *C. bogoriensis* (20).

When **3** was treated with 3% hydrogen bromide in acetic acid for 7 h, the n.m.r. spectrum of the isolated product indicated that about 70% of **3** had been inverted to **19**. Compound **19** was much less soluble than **3** and could be isolated by crystallization (about 40% yield from **3**). The structure of **19** followed from the relatively high positive specific rotation and the n.m.r. spectrum. The splitting of the H-2′ signal ($J_{1',2'}$ 3.5 c.p.s.) suggested that H-1′ was equatorial (15). The H-1′ signal was obscured by the signals of H-2″, etc., but as expected for an equatorial proton (17) it was clearly at lower field than the axial H-1′ of **3** (4.45). Also the signal of H-3′ appeared at low field due to deshielding by the axial oxygen at C-1′ (15). A 2–4% yield of **19** was also obtained from the 4 day acetobrominolysis reaction of **3** during the preparation of **10**.

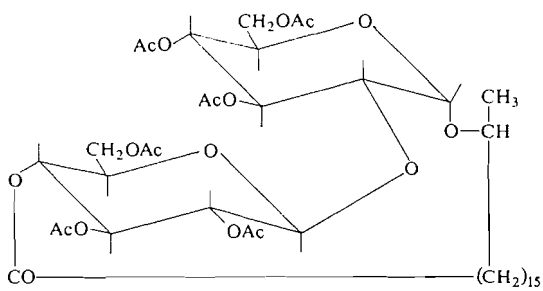

19

The heptaacetate methyl ester was completely inverted to **20** after 2 h. This product also had a large positive rotation. The n.m.r. spectrum of **20** was also in agreement with the proposed structure though the H-2′ signal was obscured by the methoxyl signal. Deacylation gave the α-sophorosyl methyl ester (**21**). The n.m.r. spectrum of (**21**) (pyridine) had a signal for equatorial H-1′ at 5.53 ($J_{1',2'}$ 4 c.p.s.).

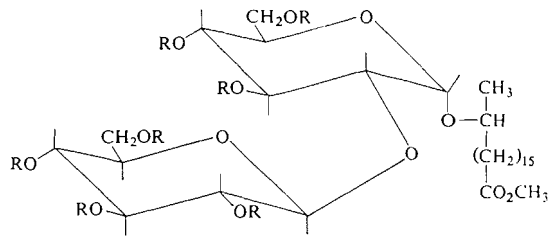

20 R = Ac
21 R = H

Thus both **3** and **8** undergo anomerization before acetobrominolysis though **8** is inverted more rapidly than **3**. However, acetobrominolysis of **3** is much faster than acetobrominolysis of **8**. We assume that the attachment of the fatty acid carboxyl to C-4″, forming the large lactone ring, in some way favors cleavage at C-1′. Acetobrominolysis at C-1″ also occurs slowly with both compounds. The spectrum of the reaction of **8**, after 7 days, suggested that acetobromoglucose was being formed at half the rate of acetobromosophorose. The mechanisms of the anomerization and acetobrominolysis reactions are being investigated.

Experimental

Nuclear magnetic resonance (n.m.r.) spectra were measured at 100 Mc.p.s. using a Varian HA-100 spectrometer. Chemical shifts are in parts per million (p.p.m.) from tetramethylsilane (internal standard). Unless otherwise stated specific rotations were measured at 25° in a 1 dm cell using a Perkin–Elmer model 141 polarimeter.

Silicic acid (Bio-Sil A from Bio-Rad Laboratories, Richmond, California) was used for silicic acid column chromatography. Silica gel G was used for thin-layer chromatography (t.l.c.). Thin-layer chromatography was used to examine fractions from column chromatography and from crystallizations. Chloroform containing 10–20% of methanol was the solvent for separations of **1**, **2**, **6**, **7**, **15**, and **21**; 1% acetic acid was added when **5** was examined. Diethyl ether was used as solvent in separations of the other compounds.

Standard grade Whatman cellulose powder was used for cellulose column chromatography. The following solvents were used as mobile phase:

Solvent *a*: benzene – ethanol – water (10:1:trace, v/v).
Solvent *b*: benzene – ethanol – water (7:1:trace, v/v).
Solvent *c*: benzene – ethanol – water (5:1:trace, v/v).
Solvent *d*: benzene – ethanol – water (3:1:trace, v/v).
Solvent *e*: *n*-butanol $\frac{1}{8}$ saturated with water.
Solvent *f*: *n*-butanol $\frac{1}{4}$ saturated with water.

Paper chromatograms were developed using Whatman No. 1 paper, *n*-butanol – ethanol – water (40:11:19, v/v/v) as solvent, and *p*-anisidine hydrochloride or silver nitrate – ammonia as spray reagents where appropriate.

Gas–liquid chromatography (g.l.c.) was carried out using an apparatus of conventional design with thermal conductivity detectors. The ethylene glycol succinate column described previously (22) was used in the analysis of the methylated methyl glucosides. Oxidation fragments (after acetylation) were analyzed using a 6 ft × $\frac{1}{4}$ in. copper column packed with silicone SE-30 on 60–80 mesh acid washed Celite (1:9 w/w). The temperature was programmed from 150–250° at 8° per min, the flow rate was 50 ml helium per min. Tests with mixtures of pure components showed that the detector response was on a weight basis (22). A short silicone column (22) was also used in preliminary analysis of fragments.

Glycolipid Production

In a typical fermentation, strain 325-66 of *Torulopsis apicola* was used. The medium was glucose (10%), yeast extract (1%), and urea (0.1%). Medium (3 l in 5 l fermentors) was inoculated and one day later addition of octadecane was begun (35 g on each of 3 subsequent days). The medium was agitated at 400 r.p.m. at 22° with an air flow of 1 l/min/fermentor. The fermentation time was 4 days after the first addition of octadecane. Six fermentors were used and the total weight of octadecane added was 630 g. The contents of the fermentors were extracted with ethyl acetate and worked up as described previously (2), the yield of crude glycolipid was 712 g.

*Isolation of Lactones (**1**) and (**2**)*

The above product was taken up in ethanol (3.5 l) and kept at 23° for 4 days and then at 12° for 2 days after which the crystalline lactone (307 g) was filtered off. Crude lactone (10 g) was hydrogenated in ethanol (200 ml) over palladium charcoal (5%, 0.5 g) for 1 h and hydrogen (51 ml corresponding to about 15% of mono-unsaturated material) was taken up. The product was chromatographed on a column of silicic acid (250 g); lactone (**1**) (7.4 g) was eluted with chloroform–methanol (98:2) (4 l) and lactone (**2**) (1.5 g) was eluted with chloroform–methanol (96:4) (2 l). The remainder of the material on the column (1.4 g), which was slowly eluted with the same solvent, appeared (t.l.c.) to be acid (**5**). Lactone (**1**) was crystallized from ethanol and had m.p. 104–106° and $[\alpha]_D^{25}$ −8.2° (*c*, 5.6 in chloroform).

Anal. Calcd. for $C_{34}H_{58}O_{14}$: C, 59.11; H, 8.46. Found: C, 58.84; H, 8.35.

The saponification equivalent was 230.3 (calcd. 230.27); 1.96 moles of acetic acid were obtained per mole of **1**. The molecular weight (osometric in acetone) was 690 (calcd. 690.8).

Nuclear magnetic resonance (acetone-d_6): terminal CH_3 1.2 (doublet); methylene chain, 1.34; acetoxyl, 2.00, 2.03; α-CH_2, 2.33; glucose ring protons, 3.15–3.85; H-6″, 4.11; H-6′, 4.24; H-1′, 4.45; H-1″, 4.61; H-4″, 4.88.

Nuclear magnetic resonance (pyridine): methylene chain and terminal CH_3, 1.37; acetoxyl, 1.92, 1.99; α-CH_2, 2.32; glucose ring protons, 3.65–4.25; H-6″, 4.42; H-6′ and H-1′, 4.60–4.86; H-1″, 5.08; H-4″, 5.43.

Lactone (**2**) was crystallized from acetonitrile and had m.p. 89–91° and $[\alpha]_D^{25}$ −13.6° (*c*, 2.0 in chloroform).

Anal. Calcd. for $C_{32}H_{56}O_{13}$: C, 59.24; H, 8.70. Found: C, 58.98; H, 8.44.

The saponification equivalent was 322.36 (calcd. 324.38); 1.03 moles of acetic acid were obtained per mole of (**2**).

Nuclear magnetic resonance (acetone-d_6): similar to that of (**1**) but only one acetoxyl at 2.03; H-6″, 4.14; H-1′, 4.48; H-1″, 4.66; H-4″, 4.90.

Nuclear magnetic resonance (pyridine): acetoxyl at 2.00; H-6″, 4.43; H-1′, 4.73; H-1″, 5.10; H-4″, 5.45.

*Preparation of Hexaacetate (**3**)*

Lactone (**1**) (2 g) was dissolved in acetic anhydride (5 ml) and pyridine (5 ml) and kept overnight. The reagents were taken off at 40° and the residue was crystallized from ethanol to give (**3**) (2.1 g) with m.p. 108–109° and $[\alpha]_D^{29}$ −7.6° (*c*, 2.2 in chloroform).

Anal. Calcd. for $C_{42}H_{66}O_{18}$: C, 58.73; H, 7.74. Found: C, 58.90; H, 7.71.

Nuclear magnetic resonance (acetone-d_6) (fatty acid protons omitted): acetoxyl, 1.93, 1.95, 1.98 (6 protons), 2.04, 2.08; H-2′, 3.65 (quartet, $J_{1',2'}$ = 7.5 c.p.s., $J_{2',3'}$ = 9.0 c.p.s.); H-5′, H-5″ 3.65–3.97; H-6′, H-6″, 3.97–4.35; H-1′, 4.58 ($J_{1',2'}$ = 7.5 c.p.s.); H-1″, H-2″, H-3″, H-3′, H-4″, H-4′, 4.74–5.34.

Lactone (**2**) was acetylated in the same way and gave the same hexaacetate (**3**) with m.p. 108° which did not depress the melting point of the above compound. The n.m.r. spectra and the X-ray powder photographs of the two compounds were indistinguishable.

*Preparation of Tetraphenylurethane (**4**)*

Lactone (**1**) (1.0 g) was refluxed in pyridine (6 ml) with phenyl isocyanate (0.8 ml) for 24 h. After removal of the pyridine the residue was extracted with ether, the ether was taken off, and the product crystallized from aqueous ethanol to give **4** (1.0 g). The melting point was 232° and $[\alpha]_D^{25}$ was +2.6° (*c*, 1.9 in chloroform).

Anal. Calcd. for $C_{62}H_{78}O_{18}N_4$: C, 63.79; H, 6.74. Found: C, 63.92; H, 6.76.

*Preparation of Methyl Ester (**7**)*

Lactone (**1**) (2.0 g) was refluxed with methanolic sodium methoxide solution (25 ml, 0.022 *N*) for 1 h, the solution was neutralized with acetic acid, and the methanol taken off. The residue was crystallized from methanol and then from methanol–water (1:3) to give 7 (1.6 g) as fine needles with m.p. 148.5–149.5° and $[\alpha]_D^{25}$ −17.6° (*c*, 4.0 in pyridine).

Anal. Calcd. for $C_{31}H_{58}O_{13}$: C, 58.28; H, 9.15. Found: C, 58.24; H, 9.19.

Nuclear magnetic resonance (pyridine): H-1′, 4.84; H-1″, 5.14.

Methyl ester (**7**) (1.0 g) was acetylated with acetic anhydride and pyridine. The reagents were removed and the product crystallized from ethanol at −15° to give the methyl ester heptaacetate (**8**) (1.1 g). The m.p. was 52.5–53.5° and $[\alpha]_D^{25}$ was −8.2° (*c*, 2.0 in chloroform).

Anal. Calcd. for $C_{45}H_{72}O_{20}$: C, 57.92; H, 7.78. Found: C, 57.70; H, 7.64.

Nuclear magnetic resonance: H-1′, 4.71 (pyridine), 4.61 (acetone-d_6), 4.46 (deuteriochloroform).

*Glycol Cleavage Reactions of Lactone (**1**)*

Conditions for Determination of Reaction Rates

Oxidations with sodium periodate were carried out in *t*-butanol–water (1:2) because **1** is insoluble in water. Aqueous *t*-butanol was used in periodate oxidation of glycolipids by Smith *et al.* (23) and in permanganate–periodate oxidations of lipids by von Rudloff (24). A fivefold excess of periodate was used and the rate was followed by the method of Neumüller and Vasseur (25).

Oxidations with lead tetraacetate in acetic acid in the presence of potassium acetate were carried out by the method of Perlin (7), and with lead tetraacetate in pyridine by the method of Goldschmid and Perlin (9). A threefold to fivefold excess of oxidant was used.

*Products of Oxidation of Lactone (**1**) with Lead Tetraacetate in Acetic Acid*

Lactone (**1**) (1.0 g) was added to a solution of lead tetraacetate (2.0 g) and potassium acetate (2.0 g) in acetic acid (200 ml) and the solution kept at room temperature for 24 h when 0.92 moles of oxidant per mole of **1** had been consumed. A solution of oxalic acid (1.0 g) in acetic acid (30 ml) was added and the mixture stirred for 30 min, the precipitate was filtered, the solvent removed, and the residual gum extracted with chloroform. After removal of the chloroform the product was reduced with sodium borohydride in methanol; after 2 h the mixture was acidified with acetic acid and the solvent taken off. Water was added and the reduction product extracted with ethyl acetate. After removal of the solvent the residue (0.8 g) was refluxed overnight with methanolic hydrogen chloride (5%). Acid was neutralized with silver carbonate, the methanol taken off, and methyl 17-hydroxystearate (0.25 g) was extracted with hexane.

The mixture of polyols (0.5 g) was chromatographed on a cellulose column; elution with solvent *a* (5 l) gave D-glyceraldehyde dimethyl acetal (identified by paper chromatography). Elution with solvent *b* (3.5 l) gave glycerol (0.13 g) which was converted to the tris-*p*-nitrobenzoate with m.p. and mixed m.p. 199–200° (26). Elution with solvent *d* (3 l) gave methyl α-D-glucopyranoside (0.27 g) which crystallized from ethanol with m.p. and mixed m.p. 172–173°.

The borohydride reduction product obtained from another oxidation was methylated twice with methyl iodide and silver oxide and the product refluxed with methanolic hydrogen chloride for 18 h. Analysis of the methylated methyl glucosides, so obtained, by g.l.c. (27) showed only methyl 2,3,4,6-tetra-*O*-methyl-α,β-D-glucopyranosides.

*Isolation of 2-O-β-D-Glucopyranosyl-glycerol from the Products of Periodate Oxidation of Lactone (**1**)*

Lactone (**1**) (1.52 g) was dissolved in 0.04 *M* sodium periodate in 33% *t*-butanol–water (70 ml), after 6 h 0.79 moles of oxidant per mole of **1** had been consumed and after 22 h 0.94 moles had been consumed. Water (200 ml) was added and the mixture extracted four times with ethyl acetate. Removal of the ethyl acetate gave the brittle resinous oxidation product, which was reduced with sodium borohydride and worked up as before. The reduction product was dissolved in dioxan (25 ml) and 0.01 *N* sulfuric acid (85 ml) added to give a pH of 2.0. After heating on a steam bath for 1 h, the mixture was extracted with ethyl acetate to give crude 17-hydroxystearic acid (0.60 g), which was refluxed overnight with 4% methanolic hydrogen chloride. The mixture was poured into water and extracted with hexane. The aqueous layer was neutralized with silver carbonate and the water taken off. The residue (0.06 g) which appeared to be a mixture of α,β-methyl glucosides, glycerol, and at least two unidentified components (from paper chromatography), was probably derived from unoxidized **1** and unhydrolyzed oxidation product. The hexane extract was a mixture of methyl 17-hydroxyoctadecanoate (m.p. and mixed m.p. 53–55°) and octadecane-1, 17-L-diol (resulting from sodium borohydride reduction of the fatty acid ester linkage). The diol was separated by crystallization from carbon tetrachloride and had m.p. 77–78° which was not depressed by admixture with authentic diol obtained by lithium aluminium hydride reduction of methyl 17-L-hydroxyoctadecanoate.

The aqueous portion, left after ethyl acetate extraction was neutralized with barium carbonate, water and dioxan taken off, and the residue dissolved in water and reduced with sodium borohydride. Acetic acid was added, the solution shaken with Amberlite IR-120 and filtered, water was removed, and methanol added and removed three times. The clear syrupy residue (0.68 g) was chromatographed on a cellulose column. Elution with solvent *b* (2 l) gave glycerol (0.12 g) which gave a tris-*p*-nitrobenzoate with m.p. and mixed m.p. 196–199°. Elution with solvent *e* gave a tetritol fraction (0.009 g) (according to paper chromatography). Elution with solvent *f* (1.2 l) gave a mixture of 2-*O*-β-D-glucopyranosyl-glycerol and sorbitol (0.24 g) from which insoluble glucosyl-glycerol (0.15 g) was obtained by treatment with hot ethanol. The mother liquors (0.09 g) were acetylated and analyzed by g.l.c., using the short silicone column. Sorbitol hexaacetate and glucosyl-glycerol hexaacetate were present and had relative retention times of 1.0 and 4.7, respectively. The analysis indicated that the mother liquors contained glucosyl-glycerol (0.04 g), giving a total of (0.19 g), and sorbitol (0.05 g). After crystallization from methanol the glucosyl-glycerol had m.p. 167–169° and $[\alpha]_D^{25}$ −29.9° (*c*, 0.9 in water), the mixed m.p. with an authentic sample (28) of m.p. 168–170° was 167–169° (lit. (29) gives m.p. 165° and $[\alpha]_D^{20}$ −30.1°).

*Products of Oxidation of (**1**) with Lead Tetraacetate in Pyridine*

Lactone (**1**) (2.0 g) was dissolved in pyridine (450 ml), which contained 34.6 μmoles of lead tetraacetate per ml, and the solution kept at 0° for 45 min. The consumption of oxidant was 2.1 moles per mole of **1**. A solution of oxalic acid in pyridine was added, the mixture allowed to stand for 1 h and then filtered. Pyridine was removed and the residue reduced with sodium borohydride and worked up as before to yield a viscous gum (1.75 g). The product obtained after acid methanolysis, neutralization with silver carbonate, and removal of methanol was extracted with hexane to give methyl 17-hydroxystearate (0.6 g). Hexane insoluble material (1.2 g) was chromatographed on a cellulose column. D-Glyceraldehyde dimethyl acetal (0.18 g) was eluted with solvent *a* (1.6 l), the bis-*p*-nitrobenzoate had m.p. 108–109° and $[\alpha]_D^{25}$ +52.0° (*c*, 0.7 in

chloroform), the mixed m.p. with authentic D-glyceraldehyde dimethyl acetal bis-*p*-nitrobenzoate was 108.5–109.5°. The authentic compound had m.p. 109–110° and $[\alpha]_D^{25}$ +55.8° (*c*, 1.0 in chloroform), (lit. (30) gives m.p. 107–108° and $[\alpha]_D^{18}$ +71.7°).

Glycerol (0.21 g) was eluted with solvent *b* (5 l), and gave a tris-*p*-nitrobenzoate with m.p. and mixed m.p. 199–200°. A mixture of tetritols and α, β-D-glucopyranosides (*c*, 3:1 by g.l.c. of acetates) (0.27 g) was eluted with solvent *c*. This fraction was acetylated and the tetritol acetates separated from those of the methyl glucosides by preparative g.l.c. (short silicone column). Analysis by g.l.c. with an ethylene glycol succinate column (22) showed that erythritol tetraacetate (relative emergence time 1.00) and threitol tetraacetate (relative emergence time 1.22) were present in equal amounts. The mixture of acetates had $[\alpha]_D^{25}$ + 15° (*c*, 1.1 in ethanol) (lit. (31) gives $[\alpha]_D^{25}$ − 32° for L-threitol tetraacetate (*c*, 4.0 in ethanol)).

Erythritol tetraacetate crystallized from a solution of the mixture in ethanol and had m.p. and mixed m.p. 85°.

*Preparation of 2′-O-(4″-O-(17-L-Acetoxyoctadecanoyl)-2″,3″,6″-tri-O-acetyl-β-D-glucopyranosyl)-3′,4′-6′-tri-O-acetyl-α-D-glucopyranosyl Bromide (**10**)*

Compound (**3**) (10 g) was dissolved in acetic acid (180 ml) and 30% hydrogen bromide in acetic acid (20 ml) was added; after 4 days at 23° the mixture was poured into ice water and extracted with methylene chloride. The extract was washed with water and dried over sodium sulfate. The solvent was removed, the residue taken up in ether (100 ml), hexane (100 ml) added, and the mixture kept at 0° when the acetobromosophorose derivative (**10**) (5.5 g) crystallized. After recrystallization from ethyl acetate it had m.p. 127–128° and $[\alpha]_D^{25}$ +65.6° (*c*, 2.2 in chloroform). Nuclear magnetic resonance (deuteriochloroform) (assigned signals only): terminal CH_3, 1.19; CH_2, 1.26; acetoxyl, 1.93–2.10 (7 singlets); H-2′, 3.78 (quartet, $J_{1',2'}$ 4 c.p.s., $J_{2',3'}$ 9.5 c.p.s.); H-6′, H-6″, 4.0–4.44; H-1″, 4.69 ($J_{1'',2''}$ 7.5 c.p.s.); H-3′, 5.46 (triplet $J_{2',3'}$ 9.5 c.p.s.); H-1′, 6.44 ($J_{1',2''}$ 4 c.p.s.).

Anal. Calcd. for $C_{44}H_{69}O_{19}Br$: C, 53.82; H, 7.08. Found: C, 53.42; H, 6.94.

*Preparation of 2′-O-(4″-O-(17-L-Acetoxyoctadecanoyl)-2″,3″,6″-tri-O-acetyl-β-D-glucopyranosyl)-1′,3′,4′,6′-tetra-O-acetyl-β-D-glucopyranose (**11**)*

Compound (**10**) (1.0 g) was dissolved in acetic acid (20 ml), silver acetate (1.0 g) added, and the mixture shaken for 2 days. After addition of methylene chloride, silver salts were filtered and the solvents removed. When the crude product (0.9 g) was chromatographed on a silicic acid column elution with chloroform–hexane (1:1) gave **11** (0.37 g). After crystallization from ether–hexane (1:2) the m.p. was 79–80° and $[\alpha]_D^{25}$ −3.3° (*c*, 1.2 in chloroform).

Nuclear magnetic resonance (deuteriochloroform): H-2′, 3.8 (quartet $J_{1',2'}$ 7.75 c.p.s.); H-1″, 4.62 ($J_{1'',2''}$ 7.75 c.p.s.); H-1′, 5.66 ($J_{1',2'}$ 7.75 c.p.s.).

Anal. Calcd. for $C_{46}H_{72}O_{21}$: C, 57.49; H, 7.55. Found: C, 57.15; H, 7.45.

*Preparation of Methyl 2′-O-(4″-O-(17-L-Acetoxyoctadecanoyl)-2″,3″,6″-tri-O-acetyl-β-D-glucopyranosyl)-3′,4′,6′-tri-O-acetyl-β-D-glucopyranoside (**12**)*

Compound (**10**) (1.3 g) was dissolved in methylene chloride (10 ml), and methanol (25 ml) and silver carbonate (1.3 g) were added and the mixture shaken for 2 days. Methylene chloride was added and silver salts removed by filtration. The solvent was taken off, leaving crude (**12**) (0.9 g) which was chromatographed on silicic acid. Elution with chloroform–hexane (1:1) gave **12** (0.63 g). After crystallization from ether–hexane (1:4) the m.p. was 65.5–66.5° and $[\alpha]_D^{25}$ was −4.0° (*c*, 1.0 in chloroform).

Nuclear magnetic resonance (deuteriochloroform): terminal CH_3, 1.19; CH_2, 1.28; acetoxyl 1.96–2.09; α-CH_2, 2.24; OCH_3, 3.52; H-2′, 3.65 ($J_{1',2'}$ 7.75 c.p.s.); H-6′ and H-6″, 3.98–4.32; H-1′, 4.39 ($J_{1',2'}$ 7.75 c.p.s.); H-3′, H-4′, H-1″, H-2″, H-3″, H-4″, H-17, 4.68–5.26.

Anal. Calcd. for $C_{45}H_{72}O_{20}$: C, 57.92; H, 7.78. Found: C, 57.84; H, 7.84.

*Methyl β-Sophoroside (**15**) from **12***

Compound (**12**) (0.43 g) was refluxed with methanolic sodium methoxide (0.022 *N*; 40 ml) for 4 h and the solution acidified with acetic acid. After removal of the methanol the residue was distributed between hexane and water. The hexane extract yielded methyl 17-L-hydroxyoctadecanoate (0.15 g). Crystallization from hexane gave the ester (0.1 g) with m.p. 52–54°; the m.p. after admixture with authentic ester was 53–55° (2).

The aqueous extract was shaken with Amberlite IR-120 and the water removed. Crystallization of the residue (0.14 g) from ethanol–water gave (**15**) (0.08 g) which had m.p. 198–200° and $[\alpha]_D^{25}$ −30.4° (*c*, 1.1 in water). The m.p. was not depressed by admixture with **15**, prepared as described below. The mother liquors from the above crystallization were acetylated giving heptaacetate **14**. The m.p. and mixed m.p. was 126–128°.

*Synthesis of 2-O-(2′,3′,4′,6′-Tetra-O-acetyl-β-D-glucopyranosyl)-3,4,6-tri-O-acetyl-α-D-glucopyranosyl Bromide (**13**)*

β-Sophorose octaacetate (1.0 g) (1) was dissolved in acetic acid containing 3% hydrogen bromide (20 ml) and allowed to stand for 24 h. Large crystals of **13** (0.65 g) which had separated were filtered off. The filtrate was poured into water, extracted with methylene chloride, and worked up as in the preparation of **10**, giving a further quantity of **13** (0.2 g). The m.p. was 191–194° (lit. (14) 195–197°).

Nuclear magnetic resonance (deuteriochloroform): acetoxyl, 1.98–2.12 (7 singlets); H-2, 3.78 ($J_{1,2}$ 4 c.p.s., $J_{2,3}$ 9 c.p.s.); H-1′, 4.70 ($J_{1',2'}$ 7.75 c.p.s.); H-3, 5.48 ($J_{2,3}$ 9 c.p.s.); H-1, 6.45 ($J_{1,2}$ 4 c.p.s.).

*Synthesis of Methyl 2-O-(β-D-glucopyranosyl)-β-D-glucopyranoside (**15**)*

α-Acetobromosophorose (**13**) (0.8 g) was dissolved in methylene chloride and allowed to react with methanol in the presence of silver carbonate as described in the preparation of **12**. The heptaacetate (**14**) (0.46 g) so obtained was crystallized from ethanol giving methyl 2-*O*-(2′,3′,4′,6′-tetra-*O*-acetyl-β-D-glucopyranosyl)-3,4,6-tri-*O*-acetyl-β-D-glucopyranoside (**14**). The m.p. was 127–128° and $[\alpha]_D^{25}$ +0.3° (*c*, 6.6 in chloroform).

Nuclear magnetic resonance (deuteriochloroform): acetoxyl, 1.97–2.08; OCH_3, 3.54; H-2, 3.65 ($J_{1,2}$ 7.75 c.p.s.); H-1, 4.38 ($J_{1,2}$ 7.75 c.p.s.)

Anal Calcd. for $C_{27}H_{38}O_{18}$: C, 49.84; H, 5.89. Found: C, 49.94; H, 5.93.

Compound (**14**) (0.35 g) was deacylated as before giving **15** (0.20 g). The product was crystallized from ethanol–water (10:1); m.p. 200–202°, $[\alpha]_D^{25}$ −29.4° (*c*, 1.1 in water); (lit. (16) 189–190°, and $[\alpha]_D$ −28° (*c*, 0.2 in water)).

Nuclear magnetic resonance (pyridine): OCH_3, 3.50; H-1, 4.66; H-1′, 5.26.

*Preparation of **14** by Köenigs–Knorr Reaction*

Methyl 3,4,6-tri-*O*-acetyl-β-D-glucopyranoside (0.22 g) (32) was dissolved in nitromethane (0.9 ml), mercuric cyanide (0.17 g) and α-acetobromoglucose (0.28 g) were added, and the mixture was shaken for 24 h. Benzene (2 ml) was added and insoluble salts filtered off. Solvents were evaporated and the residue chromatographed on silicic acid. Elution with chloroform gave an unidentified gum, and elution with chloroform–ether (4:1) gave **14** (0.11 g). After crystallization from ethanol the m.p. was 128° and was not depressed by admixture with previously prepared **14**. The n.m.r. spectrum was indistinguishable from that of **14** prepared from β-sophorose octaacetate.

*Isolation of **16** from Acetobrominolysis of **3***

After separation of bromo-derivative (**10**) solvent was removed from the mother liquors and the residue dissolved in acetic acid (60 ml) and shaken with silver acetate (2.0 g) for 18 h. Methylene chloride was added, and silver salts filtered off to yield a viscous gum (4.84 g) which was chromatographed on silicic acid (100 g). Elution with hexane–chloroform (3:1) yielded first unidentified material (0.24 g) (the n.m.r. spectrum showed that it was not **17**), followed by a fraction (0.71 g) which after rechromatography and crystallization from ether–hexane (3:1) gave compound (**16**) (0.41 g). The melting point was 63–64° and was not depressed by admixture with synthetic material; $[\alpha]_D^{25}$ −0.24° (*c*, 8.2 in chloroform). The n.m.r. spectrum and X-ray powder photograph were indistinguishable from those of the synthetic sample. The n.m.r. spectrum of material recovered from the mother liquors of the above 0.41 g showed them to consist of impure **16**.

*Isolation of α-Lactone Hexaacetate (**19**) from Acetobrominolysis of **3***

Column chromatography of the products from the mother liquors was continued. Elution with hexane–chloroform (1:1) gave a semisolid fraction (0.69) which on crystallization from ethanol gave α-lactone hexaacetate (**19**) (0.22 g), m.p. 153.5–154.5°, $[\alpha]_D^{25}$ +42.0° (*c*, 2.1 in chloroform).

Nuclear magnetic resonance (deuteriochloroform): terminal CH_3, 1.22; CH_2, 1.28; acetoxyl, 1.98, 2.00 (6 protons), 2.02, 2.05, 2.08; αCH_2, 2.30; H-2′, 3.68 (quartet $J_{1',2''}$ 3.5 c.p.s., $J_{2',3'}$ 9 c.p.s.); H-5′, H-5″, 3.60–3.95; H-6′, H-6″, 3.96–4.34; H-1″, 4.68 ($J_{1'',2''}$ 7.75 c.p.s.); H-1′, H-4′, H-2″, H-3″, H-4″, 4.80–5.24; H-3′, 5.38 (triplet).

Anal. Calcd. for $C_{42}H_{66}O_{18}$: C, 58.73; H, 7.75. Found: C, 58.95; H, 7.70.

Finally elution with chloroform gave a fraction (1.62 g) which appeared from its n.m.r. spectrum to be impure **11**.

Preparation of 17-L-Acetoxyoctadecanoyl Chloride

17-L-Hydroxyoctadecanoic acid (16 g) was acetylated at room temperature for 18 h with acetic anhydride (50 ml) and pyridine (50 ml). The reagents were removed and the resulting 17-acetoxyoctadecanoic anhydride (the i.r. spectrum (film) showed anhydride C=O bands at 1805 and 1730 cm^{-1} (overlaps acetoxyl carbonyl at 1725 cm^{-1}) but no acid carbonyl at 1700 cm^{-1}) was dissolved in thionyl chloride (32 ml) and kept overnight. Excess reagent was taken off and the product was distilled giving the desired acid chloride (14.0 g), b.p./0.05 mm 132°, $[\alpha]_D^{25}$ +0.93° (*c*, 5.0 in chloroform).

Anal. Calcd. for $C_{20}H_{37}O_3Cl$: C, 66.54; H, 10.33. Found: C, 66.49; H, 10.19.

*Synthesis of 4′-O-(17-L-Acetoxyoctadecanoyl)-1′,2′,3′,6′-tetra-O-acetyl-β-D-glucopyranose (**16**)*

The above acid chloride (4.12 g) in methylene chloride (40 ml) was added to a solution of 1,2,3,6-tetra-*O*-acetyl-β-D-glucopyranose (4.00 g) (18) in methylene chloride (100 ml) and pyridine (2 ml). The mixture was kept overnight at room temperature and then refluxed for 2 h. The solution was washed with water, dried, solvent taken off, and the product chromatographed on a silicic acid column. Elution with hexane–ether (9:1) gave compound (**16**) (4.9 g), which was crystallized from hexane–ether. The m.p. was 63–64° and $[\alpha]_D^{25}$ was −0.32° (*c*, 10.0 in chloroform).

Nuclear magnetic resonance (deuteriochloroform): terminal CH_3, 1.18; CH_2, 1.26; acetoxyl in Table VII; α-CH_2, 2.26; H-5′, 3.7–3.9; H-6′, center 4.16; H-17, 4.84 (multiplet); H-2′, H-3′, H-4′, 4.98–5.36; H-1′, 5.72.

Anal. Calcd. for $C_{34}H_{56}O_{13}$: C, 60.69; H, 8.39. Found: C, 60.50; H, 8.20.

*Synthesis of 6′-O-(17-L-Acetoxyoctadecanoyl)-1′,-2′,3′,4′-tetra-O-acetyl-β-D-glucopyranose (**17**)*

Reaction of 1,2,3,4-tetra-*O*-acetyl-β-D-glucopyranose (18) with the acid chloride as described above gave compound (**17**). The m.p. was 70° and $[\alpha]_D^{25}$ +6.8° (*c*, 1.0 in chloroform).

Anal. Calcd. for $C_{34}H_{56}O_{13}$: C, 60.69; H, 8.39. Found: C, 60.55; H, 8.49.

*Synthesis of 3′-O-(17-L-Acetoxyoctadecanoyl)-1′,2′,4′,6′-tetra-O-acetyl-β-D-glucopyranose (**18**)*

Reaction of 1,2,4,6-tetra-*O*-acetyl-β-D-glucopyranose (33) with the acid chloride by the method used to prepare **16** gave compound (**18**). The m.p. was 62° (the mixed m.p. with **16** was depressed to 58°) and $[\alpha]_D^{25}$ +2.4° (*c*, 2.0 in chloroform).

Anal. Calcd. for $C_{34}H_{56}O_{13}$: C, 60.69; H, 8.39. Found: C, 60.44; H, 8.30.

*Isolation of Acid (**5**) from Fermentation Product*

A portion of the mother liquors in ethanol, left after crystallization of lactones (**1**) and (**2**), was hydrogenated over 5% palladium charcoal. The solvent was taken off and crude product (10 g) was chromatographed on silicic acid (200 g). Elution with chloroform–methanol (98:2) gave crude lactone (**1**) (3.8 g) which was crystallized from ethanol to give **1** (1.5 g); the material in the mother liquors appeared to consist of a mixture of isomeric lactones (from the n.m.r. spectrum). Elution with chloroform–methanol (96:4) gave first a mixture of lactones (**1**) and (**2**) and acid (**5**) (1.1 g) and next acid (**5**) (4.0 g). Finally a viscous gummy material (0.6 g) was eluted which, when examined

by t.l.c. had the R_f expected of a sophorosyl hydroxystearic acid with only one acetate group. Acid (**5**) could not be induced to crystallize but it separated from acetone solution at 0° in amorphous lumps with m.p. 107–113° and $[\alpha]_D^{25}$ −15.2° (*c*, 1.7 in chloroform). The neutralization equivalent was 712.9 (calcd. 708.82).

Nuclear magnetic resonance (pyridine): CH_2, 1.27; terminal CH_3, 1.36 (doublet); acetoxyl 1.94, 1.96 (2 singlets); α-CH_2, 2.45; glucose ring protons 3.7–4.2; H-1′, H-6′, H-6″, 4.45–4.90; H-1″, 5.06.

Anal. Calcd. for $C_{34}H_{60}O_{15}$: C, 57.61; H, 8.53. Found: C, 57.71; H, 8.37.

Preparation of Methyl Ester (6)

Acid (**5**) (1 g) was dissolved in dry acetone (25 ml) and a solution of diazomethane in methylene chloride was added until the yellow color persisted, just sufficient acetic acid to neutralize the excess diazomethane was then added and the solvents were removed at room temperature. Product (1 g) was chromatographed on silicic acid and crystallized from ethanol to give **6** (0.4 g). Like the sophoroside of methyl 13-hydroxydocosanoate (20), ester (**6**) was difficult to recrystallize in good yield. The melting point was 105–106° and $[\alpha]_D^{25}$ −20.5° (*c*, 1.4 in chloroform).

Nuclear magnetic resonance (pyridine): CH_2, 1.26; terminal CH_3, 1.36; acetoxyl, 1.94, 1.96; α-CH_2, 2.28; OCH_3, 3.58; glucose ring protons, 3.60–4.20; H-1′, H-6′, H-6″, 4.40–4.90; H-1″, 5.06.

Nuclear magnetic resonance (dimethyl sulfoxide-d_6): terminal CH_3, 1.08; CH_2, 1.26; acetoxyl, 1.99 (6 protons); α-CH_2, 2.28; glucose ring protons, 2.9–3.6; OCH_3, 3.56; H-6′, H-6″, 3.9–4.3; H-1′, H-1″, 4.32, 4.40; OH protons, 5.00, 5.08, 5.22, 5.34, 5.52.

Anal. Calcd. for $C_{35}H_{62}O_{15}$: C, 58.15; H, 8.65. Found: C, 58.31; H, 8.49.

Deacylated Ester (7) from Acid (5)

(1) Alkaline Methanolysis

Crude acid (containing small amounts of lactone and monoacetate) (25 g) was dissolved in methanol (50 ml) and treated with diazomethane in ether. Solvents were removed and the residual methyl esters dissolved in 0.022 *N* sodium methoxide in methanol (200 ml) and refluxed for 2 h. Acetic acid was added until the solution was neutral. The solution was then added to boiling water (600 ml) and the product (**7**) allowed to crystallize. The yield was 14.5 g and the m.p. and mixed m.p. with **7** obtained from lactone (**1**) was 146–148°.

(2) Acid Methanolysis

Crude acid (25 g) was dissolved in methanol (200 ml) and methanolic hydrogen chloride (4%, 60 ml) added. The solution was kept at room temperature for 18 h and the acid neutralized with silver carbonate and the product crystallized as before. Compound (**7**) (18.0 g) with m.p. 146–148° was obtained.

Preparation of Ester (6) from Lactone (1)

Lactone (**1**) (0.53 g) was dissolved in chloroform (50 ml), cooled to 0° and mixed with a solution of 0.0022 *N* sodium methoxide (25 ml) also at 0°. After exactly 8 min at 0° the solution was neutralized with acetic acid and the solvent removed at room temperature. The product was chromatographed on silicic acid; elution with chloroform–methanol (98:2) gave first starting material and then a fraction (0.15 g) which was shown by t.l.c. in chloroform–methanol (90:10) to be pure ester (**6**). Crystallization from ethanol gave **6** with m.p. 105–106°, the mixed m.p. with **6** prepared from acid (**5**) was 105–106°. The n.m.r. spectra of the two samples of (**6**) in dimethyl sulfoxide-d_6 were indistinguishable.

Optical Rotatory Measurements During Acetobrominolysis of Compounds (3) and (8)

The reading at zero time was calculated from the specific rotations of **3** and **8** in acetic acid.

Compound (**3**) had $[\alpha]_D^{25}$ −11.4° (*c*, 5.0 in acetic acid) and compound (**8**) had $[\alpha]_D^{25}$ −9.2° (*c*, 5.0 in acetic acid). The compound (0.11 g) was dissolved in acetic acid (2 ml) and 30% hydrogen bromide in acetic acid (0.2 ml) was added, the mixture was then placed in a 0.5 cm polarimeter tube at 25° and the rotation measured at intervals.

Inversion of Lactone Hexaacetate (3)

Compound (**3**) (1.0 g) was dissolved in acetic acid containing 3% hydrogen bromide (20 ml) and kept at 25° for 7 h. The reaction was worked up as described for the preparation of **10**. The n.m.r. spectrum of the recovered material (0.88 g) was measured in deuteriochloroform and the ratio of the H-1″ signal of **19** to the H-1′ signal of **3** indicated that about 70% of **3** had been converted to **19**. The product was crystallized from ethanol at room temperature and crude **19** (0.38 g), with m.p. 145–155°, was isolated. Recrystallization gave pure α-lactone hexaacetate (**19**) (0.27 g) with m.p. 154–155°.

Inversion of Heptaacetate (8)

Compound (**8**) (1.0 g) was dissolved in acetic acid containing 3% hydrogen bromide (20 ml). The solution was kept at 25° for 2 h and then worked up as above. Removal of the solvent gave **20** as a gum (0.81 g), which had the same R_f on t.l.c. as **8**, but it could not be induced to crystallize.

Nuclear magnetic resonance (deuteriochloroform) showed H-3′ at 5.38 (triplet) and H-1″ at 4.61; $[\alpha]_D^{25}$ +37.6° (*c*, 0.5 in chloroform).

Anal. Calcd. for $C_{45}H_{72}O_{20}$: C, 57.92; H, 7.78. Found: C, 58.17; H, 7.72.

Deacylation of **20** (0.75 g) with sodium methoxide and crystallization from methanol gave the α-sophoroside (**21**) (0.41 g); the m.p. was 175–176° and $[\alpha]_D^{25}$ +59.2° (*c*, 4.0 in pyridine).

Nuclear magnetic resonance (pyridine): H-1″, 5.06 ($J_{1'',2''}$ 7.75 c.p.s.) and H-1′, 5.53 ($J_{1',2'}$ 4.0 c.p.s.).

Anal. Calcd. for $C_{31}H_{58}O_{13}$: C, 58.28; H, 9.15. Found: C, 58.24; H, 8.87.

α-Acetobromosphorose (13) from 8

Compound (**8**) (1.0 g) was treated with 3% hydrogen bromide in acetic acid (22 ml), and the solution kept for 7 days at room temperature and then worked up as before. The gummy product (0.89 g) was dissolved in methylene chloride (3 ml) and hexane (1 ml) added. α-Acetobromosphorose (**13**) (0.15 g, 20%) crystallized and had m.p. 191–193° (lit. (**14**), 195–197°). The n.m.r. spectrum (deuteriochloroform) was indistinguishable from that of authentic **13**.

Nuclear Magnetic Resonance Spectra of Acetobrominolysis Reactions

The acetobrominolysis reactions of compounds (**3**) and (**8**) at 25° in 3% hydrogen bromide – acetic acid were followed by n.m.r. spectroscopy. The chemical shift of the chloroform proton in acetic acid-d_4 was 7.53 p.p.m. relative to tetramethylsilane (internal standard). A trace of chloroform was added to the reaction mixture and the chemical shifts were measured relative to the chloroform signal (the acetic acid CH_3 being used as lock signal). The chemical shifts were then calculated relative to tetramethylsilane and were as follows: H-1′ of **3**, 4.48; H-1′ of **8**, 4.49 ($J_{1',2'}$ 7.75 c.p.s. for both signals); H-3′ of **10**, 5.38; H-3′ of **20**, 5.30; H-1′ of **10** and **13**, 6.47 ($J_{1',2'}$ 4 c.p.s.); H-1′ of **16** and H-1 of α-acetobromoglucose 6.62 ($J_{1,2}$ 4 c.p.s.).

Acknowledgments

The authors are indebted to Dr. A. S. Perlin and Dr. P. A. J. Gorin for a number of helpful suggestions. They also wish to thank Professor M. L. Wolfrom for the nomenclature of the lactones, Mr. L. L. Hoffman and Mr. N. R. Gardner for experimental assistance, Mr. M. Mazurek for nuclear magnetic resonance measurements, and Mr. W. C. Haid for microanalyses and infrared measurements.

1. P. A. J. Gorin, J. F. T. Spencer, and A. P. Tulloch. Can. J. Chem. **39**, 846 (1961).
2. A. P. Tulloch, J. F. T. Spencer, and P. A. J. Gorin. Can. J. Chem. **40**, 1326 (1962).
3. J. F. T. Spencer, A. P. Tulloch, and P. A. J. Gorin. U.S. Pat. No. 3,312,684 to National Research Council of Canada (March 1965).
4. A. P. Tulloch, A. Hill, and J. F. T. Spencer. Chem. Commun. 584 (1967).
5. D. F. Jones. J. Chem. Soc. C, 479 (1967).
6. A. P. Tulloch and J. F. T. Spencer. Can. J. Chem. **46**, 1523 (1968).
7. A. S. Perlin. J. Am. Chem. Soc. **76**, 5505 (1954).
8. F. Smith and J. W. Van Cleve. J. Am. Chem. Soc. **77**, 3091 (1955).
9. H. R. Goldschmid and A. S. Perlin. Can. J. Chem. **38**, 2280 (1960).
10. R. U. Lemieux. *In* Molecular rearrangements. *Edited by* P. de Mayo. Interscience Publishers, Inc., New York. 1964. p. 743.
11. J. Honeyman and C. J. G. Shaw. J. Chem. Soc. 2454 (1959).
12. A. P. Tulloch and A. Hill. Can. J. Chem. **46**, 2485 (1968).
13. O. L. Chapman and R. W. King. J. Am. Chem. Soc. **86**, 1256 (1964).
14. E. Vis and H. G. Fletcher. J. Am. Chem. Soc. **78**, 4709 (1956).
15. R. U. Lemieux and J. D. Stevens. Can. J. Chem. **43**, 2059 (1965).
16. P. A. Finan and C. D. Warren. J. Chem. Soc. 5229 (1963).
17. R. U. Lemieux, R. K. Kullnig, H. J. Bernstein, and W. G. Schneider. J. Am. Chem. Soc. **80**, 6098 (1958).
18. W. A. Bonner. J. Am. Chem. Soc. **80**, 3697 (1958).
19. R. U. Lemieux, C. Brice, and G. Huber. Can. J. Chem. **33**, 134 (1955).
20. A. P. Tulloch, J. F. T. Spencer, and M. H. Deinema. Can. J. Chem. **46**, 345 (1968).
21. B. Lindberg. Acta Chem. Scand. **3**, 1153 (1949).
22. A. P. Tulloch and J. F. T. Spencer. J. Am. Oil Chem. Soc. **43**, 153 (1966).
23. C. R. Smith, L. H. Niece, H. F. Zobel, and I. A. Wolff. Phytochemistry, **3**, 289 (1964).
24. E. von Rudloff. Can. J. Chem. **34**, 1413 (1956).
25. G. Neumüller and E. Vasseur. Arkiv Kemi, **5**, 235 (1953).
26. E. F. Garner, I. J. Goldstein, R. Montgomery, and F. Smith. J. Am. Chem. Soc. **80**, 1206 (1958).
27. C. T. Bishop. *In* Advances in carbohydrate chemistry. Vol. 19. *Edited by* M. L. Wolform. Academic Press, Inc., New York. 1964. p. 95.
28. A. J. Charlson and A. S. Perlin. Can. J. Chem. **34**, 1200 (1956).
29. N. M. Carter. Ber. **63**, 1684 (1930).
30. W. H. Evans, A. McGookin, L. Jurd, A. Robertson, and W. R. N. Williamson. J. Chem. Soc. 3510 (1957).
31. H. Klosterman and F. Smith. J. Am. Chem. Soc. **74**, 5336 (1952).
32. E. K. Gladding and C. B. Purves. J. Am. Chem. Soc. **66**, 153 (1944).
33. K. Freudenberg and E. Plankenhorn. Ann. **536**, 257 (1938).

Can. J. Chem. Downloaded from www.nrcresearchpress.com by 210.87.254.105 on 09/05/12
For personal use only.

Structure of the extracellular bacterial polysaccharide from *Arthrobacter viscosus* NRRL B-1973[1]

J. H. Sloneker, Danute G. Orentas, C. A. Knutson, P. R. Watson, and Allene Jeanes

Northern Regional Research Laboratory, Northern Utilization Research and Development Division, Agricultural Research Service, United States Department of Agriculture, Peoria, Illinois 61604

Received July 31, 1967[2]

D-Glucose, D-galactose, and D-mannuronic acid in equimolar proportions constitute 75% of the weight of the polysaccharide elaborated by *Arthrobacter viscosus* NRRL B-1973. *O*-Acetyl groups account for the remaining 25% of the weight; 50% of the hydroxyl groups are acetylated. Acid hydrolysis of the polysaccharide revealed that the D-mannopyranosyluronic acid bonds hydrolyzed with unexpected ease. Controlled acid hydrolysis afforded three oligosaccharides identified as 4-*O*-β-D-glucopyranosyl-D-galactose; 4-*O*-β-D-mannopyranosyluronic acid-D-glucose; and *O*-β-D-mannopyranosyluronic acid-(1 → 4)-*O*-β-D-glucopyranosyl-(1 → 4)-D-galactose. The native polysaccharide was oxidized slowly by sodium metaperiodate and consumed 0.42 mole per sugar residue in 340 h at 4°. The deacetylated polysaccharide consumed 0.67 mole of periodate per sugar residue and produced 1 mole of acid per 160 to 165 sugar residues in 170 h at 4°. At 20° the deacetylated polysaccharide was oxidized excessively by periodate, 1.5 moles of oxidant was consumed, and 0.4 mole of acid was produced per sugar residue in 340 h. However, only 20% of the C_4-substituted D-glucose residues in the polysaccharide was cleaved by periodate in spite of the excessive oxidation at 20°.

The polysaccharide has a linear structure and consists predominantly of repeating trisaccharide units, *O*-β-D-mannopyranosyluronic acid-(1 → 4)-*O*-β-D-glucopyranosyl-(1 → 4)-D-galactose.

Canadian Journal of Chemistry, 46, 3353 (1968)

A new species of bacteria, *Arthrobacter viscosus* NRRL B-1973 (1), produces a viscous extracellular polysaccharide in 45% yield from glucose (2). Freshly prepared solutions of the polysaccharide show inconsistent optical rotation values that stabilize at $[\alpha]_D^{25}$ −50° to −55° in water, 35% ethanol, or 1% potassium chloride when the solutions are allowed to remain undisturbed in a polarimeter tube for several days (3). Upon acid hydrolysis the polysaccharide gives rise to D-glucose, D-galactose, and D-mannuronic acid in equal molar proportions. These three sugar residues constitute 75% of the dry weight of the polysaccharide. The remaining 25% is in the form of *O*-acetyl groups, equivalent to 50% of the theoretical value for total *O*-acetylation.

Such a degree of acetylation influences the solubility of the native polysaccharide and makes it more compatible with aqueous–organic solutions than the deacetylated form. The deacetylated polysaccharide precipitates from aqueous solutions (containing 1% potassium chloride) in about one-half the concentration of alcohol required by the native polysaccharide (3).

The native polysaccharide was partially hydrolyzed with acid under controlled conditions and the hydrolyzate was fractionated on a Dowex[3] 1 ion-exchange resin. A neutral fraction and three acidic fractions were isolated. D-Glucose, D-galactose, D-mannuronolactone, and a neutral disaccharide were recovered from the neutral fraction by preparative paper chromatography. The three acidic fractions were purified further by paper chromatography and identified as an aldotriouronic acid, an aldobiouronic acid, and D-mannuronic acid.

The neutral disaccharide, which has been identified as 4-*O*-β-D-glucopyranosyl-D-galactose, had $[\alpha]_D^{25}$ +33.4°. Reduction with sodium borohydride converted the D-galactose moiety of the disaccharide to galactitol and changed the sign of rotation from plus to minus, $[\alpha]_D^{25}$ −7.9°. Isolation of D-threitol from the deacetylated polysaccharide after periodate oxidation, borohydride reduction, and acid hydrolysis established the glucoside linkage at C-4 of the D-galactose moiety in the disaccharide. Assignment of the β-configuration was made because 4-*O*-α-D-glucopyranosyl-D-galactose has $[\alpha]_D^{25}$ +140° (4).

Only one other biological source of 4-*O*-β-D-

[1]Presented before the Division of Carbohydrate Chemistry at the 145th meeting of the American Chemical Society, New York. September, 1963.

[2]Revision received July 16, 1968.

[3]Mention of trade names should not be construed as a recommendation or endorsement by the United States Department of Agriculture over those not mentioned.

Can. J. Chem. Downloaded from www.nrcresearchpress.com by 210.87.254.105 on 09/05/12
For personal use only.

glucopyranosyl-D-galactose has been reported: A small quantity of the methylated disaccharide was isolated from the fully methylated derivative of ceramide dihexoside, recovered from human erythrocyte stroma (5).

The aldotriouronic acid has the structure, *O*-β-D-mannopyranosyluronic acid-(1 → 4)-*O*-β-D-glucopyranosyl-(1 → 4)-D-galactose. As the potassium salt, the aldotriouronic acid had $[\alpha]_D^{25}$ −7.3°. Periodate oxidation of the aldotriouronic acid followed by borohydride reduction and analysis of the acid-hydrolyzed fragments by gas–liquid chromatography (g.l.c.) (6) showed that in 3 h D-galactose was converted quantitatively to D-threitol and that 31% of the D-glucose was converted to erythritol. By 24 h, the D-threitol had completely disappeared. After 168 h, 92% of the D-glucose was recovered as erythritol; the rest was recovered as free D-glucose, some of which was still present after 263 h of oxidation. Transient formation of D-threitol can occur only if D-galactose is in the reducing end position of the aldotriouronic acid and is substituted at C-4 by D-glucose. Disappearance of D-threitol probably occurs through hydrolysis of an *O*-formyl ester which allows further oxidation of the D-galactose reducing end moiety. The relatively slow conversion of D-glucose to erythritol and the stability of erythritol to further periodate attack indicate that D-glucose is substituted at C-4 by D-mannuronic acid which occupies the nonreducing end position. Isolation of 2,3,6-tri-*O*-methyl-D-glucose from an acid hydrolyzate of the aldotriouronic acid which had been (*a*) treated with sodium borohydride to reduce the D-galactose end group, (*b*) methylated, and (*c*) treated with lithium aluminium hydride to reduce the carboxyl group of the D-mannuronosyl moiety, provides further evidence that D-glucose is substituted at C-4. Under these same conditions the D-mannuronosyl moiety was converted to 2,3,4-tri-*O*-methyl-D-mannose which shows unequivocally that the uronic acid moiety in the polysaccharide is in the pyranoside form.

The aldobiouronic acid is 4-*O*-β-D-mannopyranosyluronic acid-D-glucose. As the potassium salt, this compound had a specific optical rotation of $[\alpha]_D^{25}$ −9.9°. Periodate oxidation of the disaccharide was quite complex as evidenced by g.l.c. of the fragments after reduction and hydrolysis. In 3 h, oxidation of the D-glucose reducing end moiety provided a complete spectrum of products consisting of glycerol, 4%; erythritol, 10%; D-threitol, 2%; D-arabitol, 37%; and D-glucitol, 17%; the total accounts for 70% of the D-glucose. D-Threitol can originate from oxidation of the open chain form of D-glucose by cleavage of the C_1—C_2 and C_5—C_6 bonds to give a dialdehyde which, upon reduction with sodium borohydride, produces the 4-carbon alditol. Considerable D-glucose, isolated as D-glucitol, remains unoxidized after 3 h. After oxidation for 24 h, 57% of the original D-glucose was accounted for as glycerol, 12%, and erythritol, 45%. None of the other products were detected. The high yield and relative stability of erythritol indicate that the D-glucose is substituted at C-4 by the mannuronosyl glycoside.

The β-linked mannopyranosyluronic acid bonds do not show the acid stability generally considered characteristic of uronosyl bonds in polysaccharides. More than 95% of the D-mannuronosyl residues in the polysaccharide from *A. viscosus* is liberated in 2.5 h with 2 *N* hydrochloric acid at 100°. By comparison, in a polysaccharide from *Xanthomonas campestris* hydrolyzed under identical conditions, 90 to 95% of the D-glucuronosyl residues is recovered in an aldobiouronic acid, 2-*O*-β-D-glucopyranosyluronic acid-D-mannose (7). Anomalous acid sensitivity of β-glycosides of D-mannuronic acid has been observed previously during the synthesis of methyl β-D-mannopyranosyluronic acid (8). This acid lability may be related to the conformational instability factor (Δ2 arrangement) in the β-D-mannopyranosides (9).

The native polysaccharide reduced only 0.42 mole of sodium metaperiodate per sugar residue in 340 h at 4°. The deacetylated material is oxidized more rapidly, and oxidation is essentially complete in 48 h at 4°. After 170 h of oxidation at 4°, the deacetylated polysaccharide had consumed 0.67 mole of periodate per sugar residue but had produced only 1 mole of acid for every 160 to 165 sugar residues. Essentially, no further oxidation occurred up to 340 h. Overoxidation of the deacetylated polysaccharide occurs when the temperature of the reaction is raised to 20°. In 340 h, 1.5 moles of periodate are consumed and 0.4 mole of acid is produced per sugar residue. The amount of periodate consumed at 20° is 0.8 mole greater than at 4°. During overoxidation at 20° the molecular ratio of excess periodate consumed to acid produced is 2:1. This ratio suggests that overoxidation involves either hexose or, more probably, hexuronic acid res-

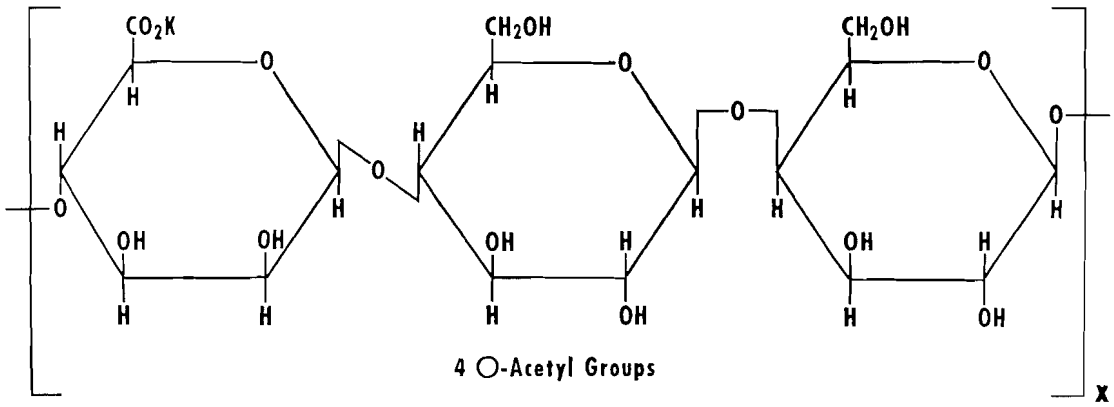

FIG. 1. Repeating trisaccharide unit in the polysaccharide produced by *Arthrobacter viscosus* NRRL B-1973.

idues within the polysaccharide chain and not erosion of the reducing end residue, which would consume periodate and produce acid in a ratio of approximately 1:1.

Samples of the deacetylated polysaccharide that had been oxidized at 4° and at 20° were reduced with sodium borohydride and examined by paper chromatography after acid hydrolysis. Approximately 80% of the original D-glucose and 20% of the D-mannuronic acid were recovered unoxidized in the hydrolyzates of both samples. D-Galactose was not detected in either sample. D-Threitol and L-erythronic acid were isolated from the hydrolyzate of the reduced product which had been oxidized at 4°. These two compounds originate from C_4-substituted D-galactose and D-mannuronic acid residues, respectively.

Our observations showed that approximately 80% of the D-glucosyl residues in the deacetylated polysaccharide is not oxidized by sodium metaperiodate either at 4° or 20° and, therefore, appeared to be substituted at C-3. However, methylation analysis of the polymer (10) as well as of the aldotriouronic acid provides unequivocal evidence that these resistant D-glucose residues are substituted at C-4 by the D-mannuronosyl residues. Although glucosides substituted at C-4 are known to be oxidized by periodate at a slow rate (7) because of steric interference (11), this alone cannot explain the unreactivity of the D-glucosyl residues in the deacetylated polysaccharide to periodate oxidation because the oxidation conditions had proved adequate for identical residues in another polysaccharide (7). However, the slower rate at which these glucosyl residues oxidize may contribute to their stability. The D-mannuronosyl and D-galactosyl residues on either side of the D-glucosyl residue have less-hindered glycols and would oxidize rapidly. The resultant carbonyl groups at C-2 and C-3 of the oxidized D-mannuronosyl and D-galactosyl residues, respectively, are in an excellent position to form 6-membered-ring hemiacetals with hydroxyl groups at C-3 and C-4 of the unoxidized D-glucosyl residues. Thus cyclic hemiacetals, which commonly occur in periodate oxidized polysaccharides and monosaccharides (12, 13) and which have been observed to block periodate oxidation (14), could account for the anomalous oxidation behavior of the deacetylated polysaccharide, as well as for the small amount of D-glucose (10–12%) remaining in samples of the aldotriouronic acid after oxidation with periodate. These findings emphasize the general need for caution when interpreting periodate oxidation data.

A structure (Fig. 1) consisting of a repeating trisaccharide unit is proposed for the extracellular polysaccharide elaborated by *A. viscosus* NRRL B-1973. Of the eight hydroxyl groups in this repeating trisaccharide unit, four are *O*-acetylated. Periodate analysis of the deacetylated polysaccharide and of the aldotriouronic acid indicates that possibly 10–12% of the D-glucose may be glycosidically substituted at C-3 and that 20% of the D-mannuronic acid may be glycosidically substituted at C-3 or exists as a 3,6-lactone. Methylation analysis of the polysaccharide confirms the structure as proposed in Fig. 1 (10).

A high degree of structural regularity in the polysaccharide is shown by the quantity of aldotriouronic acid, which amounted to 20% of the

Can. J. Chem. Downloaded from www.nrcresearchpress.com by 210.87.254.105 on 09/05/12
For personal use only.

Can. J. Chem. Downloaded from www.nrcresearchpress.com by 210.87.254.105 on 09/05/12
For personal use only.

sugar residues, obtained by partial acid hydrolysis. However, some degree of irregularity does occur since a small quantity of disaccharide containing only D-mannuronic acid was observed in hydrolyzates of fully methylated polysaccharide (10). Therefore, at least a small portion of the D-mannuronosyl residues are linked to each other.

The polysaccharide chains are essentially linear. Acid production during periodate oxidation of the deacetylated material at 4° points to a possible nonreducing end residue for every 160 or 165 sugar residues. However, the actual number of sugar residues per nonreducing end residue may be considerably higher than the values indicate because the polysaccharide overoxidizes readily to produce formic acid. Other evidence for chain linearity (15) is the formation of water-soluble films, which have high tensile strength and flexibility, from the deacetylated polysaccharide as well as from heated solutions of the native polysaccharide (16).

Experimental

Methods

Analyses by gas–liquid chromatography (g.l.c.) were made with an F and M, model 810 gas chromatograph (Hewlett Packard, F and M Scientific Division, Avondale, Pennsylvania) containing a 10 ft × 0.25 in. column of 3% ECNSS-M coated 100–120 mesh Gas Chrom Q (Applied Science Laboratories, State College, Pennsylvania). Oven temperature was programmed from 170–200° at a rate of 2° per min. Carrier gas flow was maintained at 75 ml per min at 60 p.s.i. (6). Nuclear magnetic resonance (n.m.r.) spectra were obtained with Varian HA 100 Research System (Varian Associates, Palo Alto, California) operating at 100 mHz for proton resonance. Sodium 2,2-dimethyl-2-silapentane-5-sulfonate was used as an internal standard.

Paper chromatographic methods were as follows: solvents for free sugars (*a*) ethyl acetate – acetic acid – water (3:1:3) (17) and (*b*) *n*-butyl alcohol – pyridine – water (6:4:3) (18); for hydroxamic acids (*c*) *n*-amyl alcohol – formic acid – water (4:1:5) and (*d*) *n*-butyl alcohol – acetic acid – water (4:1:5) (19); and for polyalcohols (*e*) butan-2-one – acetic acid – water saturated with boric acid (9:1:1) (20) (all v/v). Sugars on developed chromatograms were detected with ammoniacal silver nitrate. Paper used for qualitative and quantitative chromatography was Whatman No. 1, and for separation and isolation of larger quantities it was Whatman No. 3 mm.

Analytical and preparative thin-layer chromatography (t.l.c.) of the methylated sugars were carried out on glass plates coated with Silica Gel G (Merck and Co., Darmstadt, Germany) using a solvent composed of chloroform and *n*-propyl alcohol (4:1) saturated with concentrated ammonium hydroxide (21). The methyl sugars were detected by charring after the plates were sprayed with 50% ethanolic sulfuric acid.

All steps involving reduction of solution volume were carried out on a vacuum rotary evaporator at a bath temperature of 40°, unless otherwise stated.

Materials

The bacterial cultures were grown as described previously (2), and the viscous extracellular polysaccharide was isolated as follows: A laboratory preparation of polysaccharide was recovered by diluting the culture broth with water to a viscosity of 50 centipoises or less and removing the cells in a Sharples continuous centrifuge. The polysaccharide was then purified by a series of alcohol precipitations from solutions of 1% aqueous potassium chloride. Potassium chloride was removed from the purified polysaccharide by dialysis against distilled water. The retentate (22) was adjusted to about pH 6.5 and reduced in volume; the polysaccharide was recovered by lyophilization.

An experimental pilot-plant preparation of polysaccharide was purified by supercentrifugation and by precipitation with alcohol as described above. The precipitated product was recovered by dehydration with methanol and vacuum drying (23).

Deacetylated polysaccharide was obtained by hydrolyzing a 0.25% solution of the laboratory-purified product in 0.03 *N* potassium hydroxide and 1% potassium chloride (w/v) for 2.5 h at 20° under an atmosphere of nitrogen. The alkali was neutralized with 0.3 *N* hydrochloric acid and the polysaccharide was precipitated with alcohol, redissolved in water, and dialyzed against distilled water until free of salt. The pH of the solution was adjusted to about 6.5, and the polysaccharide was recovered by lyophilization.

Laboratory-purified polysaccharide was used for compositional and periodate oxidation studies. Pilot-plant-purified polysaccharide was the source of the oligosaccharides.

Reference compounds for the sugar analyses and periodate studies were as follows: Erythritol, glycerol, ribitol, D-glucitol, and D-galactose were obtained from commercial sources and were used without further purification, except D-galactose which was recrystallized from 95% ethanol. D-Glucose was obtained from the United States National Bureau of Standards.

D-Threitol was prepared in our Laboratory from methyl 4,6-benzylidene-α-D-galactopyranoside by periodate oxidation, sodium borohydride reduction, and acid hydrolysis. Details of the procedure will be published elsewhere.

Potassium (methyl-α-D-mannopyranoside) uronate was prepared by selective oxidation of a commercial grade of methyl-α-D-mannopyranoside with oxygen in the presence of platinum catalyst (8). Isolated crystalline in 44% yield, the potassium salt had $[\alpha]_D^{25}$ +48° (*c*, 0.111 water) [lit. (8) $[\alpha]_D^{17}$ +48°].

Quantitative Determination of Sugars in Polysaccharide B-1973

A sample of polysaccharide (125 mg) was dissolved in 20 ml of 2 *N* hydrochloric acid and heated for 2.5 h at 100°. The hydrolyzate was cooled in an ice bath, neutralized with silver carbonate, and filtered through Celite to remove silver chloride. Excess silver ions were precipitated with hydrogen sulfide. The solution was reduced in volume and filtered through Celite into a 5-ml volumetric flask. The hydrolyzate was chromatographed in solvent *a* for 36 h.

TABLE I

Periodate oxidation of native and deacetylated polysaccharides

Time (h)	Periodate consumption			Acid production deacetylated*	
	Native*	Deacetylated*			
	4°	4°	20°	4°	20°
8	0.11	0.46	0.54	0.00	—
24	0.15	0.55	0.66	0.00029	0.01
48	0.15	0.62	0.71	0.0019	—
96	0.17	0.66	0.76	0.0064	0.06
170	0.30	0.67	0.87	0.0061	0.11
240	0.36	—	1.02	—	0.19
340	0.42	0.68	1.51	—	0.41

*Moles per sugar residue.

D-Glucose, D-galactose, and a small amount of aldobiouronic acid (approximately 5% by weight of the unhydrolyzed polysaccharide sample) were eluted from the chromatograms and determined quantitatively by the phenol – sulfuric acid method (24).

The D-mannuronic acid content was determined on the intact polysaccharide by a modification of the borate–carbazole method (25).

The laboratory-prepared polysaccharide is composed of D-glucose, D-galactose, and D-mannuronic acid in the ratio of 1.03:1.00:1.14.

Identification and Determination of the Acyl Group

Native polysaccharide (40 mg) was deacetylated as described previously and the supernatant solution was evaporated to dryness, redissolved in 10 ml of water, and acidified with 4 *N* sulfuric acid. The acidified solution was extracted with 3 volumes of ethyl ether. The ether layer was removed, evaporated to near dryness, and neutralized with *N* sodium hydroxide. After the neutral solution was evaporated to dryness, the hydroxamic acid derivative was prepared (26). Only the hydroxamic acid derivative of acetic acid appeared on chromatograms irrigated with solvents *c* and *d* when developed with acidic ferric chloride.

The *O*-acetyl content of the polysaccharide was determined by the colorimetric porcedure based on the color complex formation of an acyl hydroxamic acid and ferric ions (27). The *O*-acetyl content of the laboratory preparation of polysaccharide was 25.2% and of the pilot-plant preparation 24.0%.

Periodate Oxidation of Native and Deacetylated Polysaccharides

A portion of a suitably concentrated solution of sodium metaperiodate was added to homogeneous aqueous dispersions of native and deacetylated polysaccharides. Polysaccharide concentration was adjusted to 0.1% by adding a minimum amount of water. The final periodate concentration was 0.02 *M*. A periodate blank was prepared accordingly. The oxidation reaction was carried out in the dark at either 4° or 20°. Periodate consumption was measured by the arsenite method (28). The acid produced during oxidation with periodate was measured by potentiometric titration with 0.005 *N* sodium hydroxide. Any error due to possible acidity in the polysaccharide was eliminated by an appropriate polysaccharide blank.

The native polysaccharide containing the *O*-acetyl groups consumed periodate relatively slowly over a period of 340 h and produced no titratable acid (Table I). However, periodate consumption by the deacetylated polysaccharide was rapid at both 4° and 20° and excessive at 20° (Table I). Acid production during oxidation at 4° was slight.

Reduction of Periodate-oxidized Deacetylated Polysaccharide and Determination of Residual Products

Ethylene glycol was added to the samples of deacetylated polysaccharide that were oxidized at 4° and at 20° (Table I) to destroy excess periodate. Iodate ions were removed from the polysaccharide solution by dialysis against distilled water. The retentates were transferred to beakers, and the polysaccharide in the retentate was reduced with sodium borohydride (20% by weight of the polysaccharide) overnight at room temperature. Excess borohydride was destroyed by acidifying the solution to pH 5 with acetic acid. The solution was readjusted to pH 6.5 with sodium bicarbonate and dialyzed against distilled water (6 days) to remove borate ions. During the long dialysis the pH of the retentate dropped to 5.4. The retentate was evaporated to dryness and the recovered polysaccharide residue was treated with small amounts of dry methyl alcohol that were removed by distillation after each addition.

A portion (100 mg) of each reduced sample was hydrolyzed for 1 h at 100° with *N* hydrochloric acid. The solutions were cooled and neutralized as described previously. Each hydrolyzate was chromatographed quantitatively on paper with solvent *b*. Eighty percent of the D-glucose originally present in the deacetylated polysaccharide appeared in the hydrolyzate of the sample oxidized at 4° with periodate; 77% in the sample oxidized at 20°. D-Galactose was not detected in either hydrolyzate.

D-Mannuronic acid was measured directly in the hydrolyzates of the two samples by a modified carbazole method (25). Approximately 20% of the original D-mannuronic acid was recovered unoxidized in both samples.

Isolation of L-Erythronic Acid and D-Threitol

A sample (340 mg) of the deacetylated polysaccharide, which had been oxidized at 4° with sodium metaperiodate

Can. J. Chem. Downloaded from www.nrcresearchpress.com by 210.87.254.105 on 09/05/12
For personal use only.

TABLE II

Ion-exchange fractionation of acid-hydrolyzed native polysaccharide

Tube No.	Fraction	Weight (mg)	Equivalent weight	Contents after hydrolysis*
10–30	*a*	719	—	D-Glucose, D-galactose, neutral disaccharide, D-mannuronolactone
280–325	*b*	453	532	D-Glucose, D-galactose, D-mannuronic acid
380–440	*c*	206	356	D-Glucose, D-mannuronic acid
505–560	*d*	135	194	D-Mannuronic acid

*Fraction *a* was not hydrolyzed.

and reduced with sodium borohydride, was hydrolyzed for 2 h at 100° in 34 ml of *N* hydrochloric acid. The solution was cooled and neutralized as described previously. Nine components in the hydrolyzate were separated by prepara tive paper chromatography on six strips of Whatman 3 mm paper (9 × 22.5 in.) irrigated with solvent *a*. The areas on the papers corresponding to L-erythronic acid and D-threitol ($R_{erythritol}$ 0.95 in solvent *b*) were excised and eluted with water. When the eluates were evaporated to dryness, 66 mg of crude L-erythronic acid and 44 mg of crude D-threitol were recovered.

After the crude L-erythronic acid was dissolved in 2 ml of water and decationized with Dowex 50 × 2 resin (H^+ form), the deionized solution was reduced in volume, decolorized with activated charcoal, and evaporated to dryness. The dry residue was extracted 10 times with 2 ml volumes of boiling ethyl acetate. Long, waxy, needlelike crystals formed upon concentration of the ethyl acetate extract. These crystals had a m.p. and a mixture m.p. with authentic L-erythronolactone of 100–101° (29).

The crude D-threitol was purified by a second chromatographic separation on Whatman 3 mm paper. The product was isolated and the dibenzylidine derivative was prepared (30). Recrystallized three times from toluene, the dibenzylidine D-threitol derivative had a m.p. of 220–221° [lit. (31), 221–224°].

Controlled Acid Hydrolysis and Fractionation by Ion-Exchange Chromatography

A 3.0 g sample of polysaccharide from the pilot-plant preparation was dissolved in 400 ml of water and warmed to 60°. Hydrochloric acid (100 ml of a 5 *N* solution) was added and the polysaccharide precipitated in a gel-like mass from the acidic solution. The precipitate was dispersed after heating the acidic mixture at 100° in an oil bath for 1.25 h. The hydrolyzate was cooled to room temperature and filtered through a sintered-glass funnel. Presumably the residue (152 mg) collected was unhydrolyzed cell debris. The filtered hydrolyzate was neutralized with silver carbonate and filtered through Celite to remove silver chloride. Excess silver ions were precipitated with hydrogen sulfide. The hydrolyzate was reduced in volume, filtered through Celite, and neutralized to pH 7 with *N* potassium hydroxide. The neutral concentrate was poured onto a column (2.5 × 74 cm) of Dowex 1 × 4 (200 to 400 mesh) resin (acetate form). After the concentrate had percolated into the resin bed, the column was washed with 100 ml of water. The neutral and acidic fractions were separated by gradient elution, which was obtained by passing *N* acetic acid into a mixing flask containing 1500 ml of water. Ten milliliter fractions were collected at a flow rate of 1 ml per min.

The carbohydrate products were detected by removing 0.5 ml portions of eluate from every fifth fraction and assaying the portions qualitatively with phenol – sulfuric acid reagent (24). The four carbohydrate-containing fractions from the pooled 10 ml fractions were recovered by lyophilization (Table II). The three acidic fractions (Table II: *b*, *c*, and *d*) were dissolved in water (10 ml) and titrated with 0.1 *N* sodium hydroxide. The equivalent weights for fractions *b*, *c*, and *d* are in good agreement for those of an aldotriouronic acid, aldobiouronic acid, and hexuronic acid, respectively. The three neutralized fractions were isolated from solution by reducing the volume of the solution, precipitating the carbohydrate material with ethyl alcohol, and recovering the precipitates by centrifugation. When dried, the precipitated products were white amorphous powders. Hydrolysis of fractions *b*, *c*, and *d* with *N* hydrochloric acid for 2 h at 100° and qualitative paper chromatography of the neutralized hydrolyzate revealed their composition (Table II).

Identification of Components in the Column Fractions

Fraction a: the Neutral Sugars

Fraction *a* (Table II) was separated into three components by preparative paper chromatography in solvent *b*. Each component was detected, excised, and eluted from the paper sections with water.

The glucose component (86 mg) was crystallized from absolute ethyl alcohol and showed $[\alpha]_D^{25}$ +53° (*c*, 0.86 water). Treatment of the glucose component with *p*-nitroaniline afforded a *p*-nitroaniline derivative of D-glucose with m.p. 182–183° (32).

The galactose component (102 mg) crystallized from absolute ethyl alcohol and showed $[\alpha]_D^{20}$ +85° (*c*, 1.02 water). Treatment with *p*-nitroaniline afforded a *p*-nitroaniline derivative of D-galactose with m.p. and mixture m.p. 216–218° (32).

The neutral disaccharide component (173 mg) was crystallized from aqueous ethyl alcohol and showed $[\alpha]_D^{20}$ +33° (*c*, 1.73 water) and m.p. 175–177°. D-Glucose and D-galactose were produced upon acid hydrolysis of the disaccharide. Oxidation behavior of the disaccharide with 0.02 *M* sodium metaperiodate (24 h at 4° in the dark) was similar to that of maltose. The disaccharide consumed 3.8 moles of periodate and produced 1.7 moles of acid; maltose, 3.9 and 1.7 moles, respectively.

The disaccharide (121 mg) was dissolved in 10 ml of

Can. J. Chem. Downloaded from www.nrcresearchpress.com by 210.87.254.105 on 09/05/12
For personal use only.

TABLE III

Periodate oxidation of the aldotriouronic acid and gas–liquid chromatographic analysis of cleavage products after borohydride reduction

Oxidation time (h)	Periodate consumption (mole)	Acid production (mole)	Hydrolysis products (yield, mole)		
			D-Threitol	Erythritol	D-Glucose
3	3.84	1.65	1.03	0.31	—
24	5.45	2.52	0	0.86	0.11
48	7.04	3.86	0	0.88	0.13
72	8.56	4.81	0	0.92	—
168	8.77	5.94	0	0.78	—
263	9.50	6.63	0	0.66	0.10–0.12

water and was reduced with sodium borohydride (30 mg) for 3 h at 25°. Excess borohydride was destroyed with acetic acid and the solution was decationized on a Dowex 50 × 2 resin column (H^+ form). Borate ions were removed as trimethylborate. A crystalline-reduced product (84 mg) was precipitated from absolute ethyl alcohol upon addition of acetone. Recrystallization three times gave a product (69 mg) with a sharp m.p., 196–196.5° and a negative specific optical rotation, $[\alpha]_D^{20}$ −7.9° (*c*, 0.69 water). The reduced disaccharide consumed 5.6 moles of periodate and produced 2.3 moles of formic acid and 1.9 moles of formaldehyde in 24 h (33).

Acid hydrolysis of the reduced disaccharide and chromatography of the hydrolyzate in solvent *e* indicated that the D-galactose moiety was converted to galactitol. After isolation by paper chromatography and acetylation with pyridine and acetic anhydride, the hexitol had a m.p. and mixture m.p. with authentic galactitol hexaacetate of 167–169° [lit. (34), 168–169°]. Therefore, the reducing end residue in the neutral dissacharide is D-galactose.

The structure, 4-*O*-β-D-glucopyranosyl-D-galactose, was assigned to the neutral disaccharide on the evidence that the periodate oxidation behavior of both the disaccharide and its reduced derivative is compatible with a 1 → 4 linkage and that the D-galactose residues in the deacetylated polysaccharide are converted to D-threitol by periodate oxidation and borohydride reduction. The neutral disaccharide has a β-configuration because the α-anomer, 4-*O*-α-D-glucopyranosyl-D-galactose, has been isolated previously and has $[\alpha]_D^{25}$ +140° (4).

Fraction b: the Aldotriouronic acid

Fraction *b*, which had a neutral equivalent of an aldotriouronic acid (Table II), was further purified by paper chromatography (solvent *a*) and was converted to the potassium salt by passing the acid over a small column of Dowex 50 × 4 (200–400 mesh) resin (potassium form). As the potassium salt, the trisaccharide had $[\alpha]_D^{25}$ −7.3° (*c*, 0.082 water) that indicated all β linkages. The potassium salt of the aldotriouronic acid (0.003 *M*) was oxidized in 25 ml of 0.03 *M* sodium metaperiodate in the dark at 4°. The results are shown in Table III.

Aliquot samples of the oxidation mixture (2 ml containing 3.2 mg trisaccharide) were taken at each time interval and treated with 100 μl of ethylene glycol to destroy excess periodate. One milliliter of 0.03 *M* barium acetate was added to precipitate the iodate ions. Ribitol (0.5 mg) was added as an internal standard for g.l.c. analysis. Precipitates of barium iodate were removed by filtration and each oxidized sample was reduced with 4.2 mg of sodium borohydride for 7 h. The samples were acidified with 1 ml of 5 *M* hydrochloric acid and hydrolyzed for 3 h at 100°. Chloride ions were removed as the silver salt. The hydrolyzates were transferred to a test tube (13 × 100 mm) and were taken to dryness. To each sample was added 40 mg of anhydrous sodium acetate and 0.5 ml of acetic anhydride. The tubes were sealed and heated in an oil bath at 100° overnight. After the acetylation tubes were broken open, acetic anhydride, and excess ethylene glycol diacetate were removed under reduced pressure. The residue was dissolved in 0.2 ml of chloroform and 2 μl portions were analyzed by g.l.c. The results are given in Table III.

A sample of aldotriouronic acid (130 mg) was reduced with sodium borohydride (50 mg) in water (10 ml) for 3 h. The solution was neutralized with acetic acid and decationized on a small column of Dowex 50 × 4 (200–400 mesh) resin (H^+ form). After drying the column eluate, borate ions were removed as trimethylborate. The reduced trisaccharide was dissolved in dry dimethyl sulfoxide (35 ml) and methylated with methylsulfinyl anion and methyl iodide (35, 36). Four volumes of water was added to the methylation reaction mixture and the methylated sugar was recovered by a threefold extraction with one-half volume of chloroform. The combined chloroform extracts were back extracted with water to remove excess dimethyl sulfoxide, and taken to dryness. The methylated trisaccharide was dissolved in dry tetrahydrofuran (10 ml) and the carboxyl group of the mannuronosyl moiety was reduced to an alcohol with lithium aluminium hydride (152 mg) in 3 h. Methanol (2 ml) was added to destroy excess hydride and metal ions were precipitated by the addition of water (10 ml). The precipitate was extracted three times with chloroform which was combined with the tetrahydrofuran–water solution. Evaporation of the pooled solutions afforded the methylated reduced trisaccharide as a viscous syrup (132 mg).

Complete hydrolysis of the methylated trisaccharide was achieved with aqueous 0.03 *M* hydrochloric acid in a sealed tube at 115° for 72 h and the liberated methyl sugars were separated by preparative t.l.c. on two 20 × 20 cm plates after two developments. Fractions corresponding to penta-*O*-methyl-D-galactitol, 2,3,6-tri-*O*-methyl-D-glucose, and 2,3,4-tri-*O*-methyl-D-mannose were detected under ultraviolet light. The latter two were recovered from

Can. J. Chem. Downloaded from www.nrcresearchpress.com by 210.87.254.105 on 09/05/12
For personal use only.

TABLE IV

Periodate oxidation of the aldobiouronic acid and gas–liquid chromatographic analysis of cleavage products after borohydride reduction

Oxidation time (h)	Periodate consumption (mole)	Acid production (mole)	Hydrolysis products (yield, mole)				
			Glycerol	Erythritol	D-Threitol	Arabitol	Glucitol
3	2.68	0.88	0.04	0.10	0.02	0.37	0.17
24	5.00	2.75	0.12	0.45	0	0	0
48	6.87	5.12	0.25	0.27	0	0	0
72	7.42	5.35	0.12	0.12	0	0	0

the silicic acid by extraction with chloroform. Removal of the chloroform from the glucose fraction afforded crystalline 2,3,6-tri-*O*-methyl-D-glucose which after recrystallization had a m.p. of 122° [lit. (37), 121–123°].

2,3,4-Tri-*O*-methyl-D-mannose, a syrup, was oxidized with bromine and lactonized to 2,3,4-tri-*O*-methyl-δ-mannonolactone which crystallized from ether (38). The n.m.r. spectrum of the crystalline lactone was identical to that of an authentic sample of 2,3,4-tri-*O*-methyl-δ-mannonolactone [m.p. 73–74°; lit. (38), 74°] which was prepared from potassium (methyl-α-D-mannopyranoside) uronate by methylation, reduction, and hydrolysis as described for the aldotriouronic acid, followed by bromine oxidation and lactonization (38). A resonance peak at 5.93 τ with a coupling constant of 3 c.p.s. was observed in both spectra and was assigned to the proton at C-2. Protons on the methoxyl groups produced peaks at 6.42, 6.52, and 6.55 τ, respectively.

On the basis of these data the structure, *O*-β-D-mannopyranosyluronic acid - (1 → 4) - *O* - β - D -glucopyranosyl-(1 → 4)-D-galactose, is proposed for the aldotriouronic acid.

Fraction c: the Aldobiouronic Acid

Fraction *c*, which had a neutral equivalent value of an aldobiouronic acid (Table II), was purified by paper chromatography (solvent *a*) and converted to the potassium salt by the method described for the aldotriouronic acid. As the potassium salt, the disaccharide had $[\alpha]_D^{25}$ −9.9° (*c*, 0.0852 water). A negative rotation indicated that the D-mannuronosyl glycoside had a β-configuration.

The potassium aldobiouronate was oxidized by periodate and the resultant products were analyzed by g.l.c. as described for the aldotriouronic acid. The results are shown in Table IV.

The structure, 4-*O*-β-D-mannopyranosyluronic acid-D-glucose, was assigned to the aldobiouronic acid.

Fraction d: D-*Mannuronic Acid*

Fraction *d* (17 mg) was dissolved in 2% methanolic hydrogen chloride (10 ml) and left overnight at room temperature. The solution was neutralized with silver carbonate, filtered, and evaporated to dryness. The dry residue was dissolved in water (5 ml) containing 10 mg of sodium borohydrate. After reduction for 3 h at room temperature, the excess borohydride was destroyed with acetic acid. Cations were removed by passing the reduction mixture over a column of Dowex 50 resin (H^+ form). Borate ions were removed as trimethylborate and the borate-free residue was hydrolyzed 2 h at 100° with *N* hydrochloric acid to remove the methyl glycoside. Chloride ions were removed in the usual way. The chloride-free solution was reduced in volume and a portion of the concentrate was analyzed by paper chromatography in solvents *a*, *b*, and *e*.

D-Mannose was identified as the major component. Small quantities of mannuronic acid and mannuronolactone were also detected. The remaining portion of the chloride-free concentrate was evaporated to dryness. The dry residue was dissolved in 0.5 ml methanol, and 20 μl of concentrated hydrochloric acid and 20 mg of *p*-nitroaniline were added. Crystals that appeared after the solution was heated for 10 min at 65° and cooled, were collected by centrifugation, redissolved in methanol, and chromatographed on paper in solvent *b*. A colored band corresponding to the D-mannose derivative was excised from the paper, eluted with 80% ethanol, and recrystallized twice from methanol. This material had a m.p. and mixture m.p. with the known *p*-nitroaniline derivative of D-mannose of 222–224° (32). The methyl glycoside methyl ester of the uronic acid from the polysaccharide produced by *A. viscosus* is converted by reduction and hydrolysis to D-mannose and, therefore, must be D-mannuronic acid.

Acknowledgments

We are indebted to S. P. Rogovin for the experimental pilot-plant polysaccharide and to W. A. Boyd for the n.m.r. spectra of 2,3,4-tri-*O*-methyl-δ-mannonolactone.

1. H. Gasdorf, R. G. Benedict, M. C. Cadmus, R. F. Anderson, and R. W. Jackson. J. Bacteriol. **90**, 147 (1965).
2. M. C. Cadmus, H. Gasdorf, A. A. Lagoda, R. F. Anderson, and R. W. Jackson. Appl. Microbiol. **11**, 488 (1963).
3. A. Jeanes, C. A. Knutson, J. E. Pittsley, and P. R. Watson. J. Appl. Polymer Sci. **9**, 627 (1965).
4. J. K. N. Jones and M. B. Perry. J. Am. Chem. Soc. **79**, 2787 (1957).
5. T. Yamakawa, N. Kiso, S. Handa, A. Makita, and S. Yokoyama. J. Biochem. Tokyo, **52**, 226 (1962).
6. J. S. Sawardeker, J. H. Sloneker, and A. Jeanes. Anal. Chem. **37**, 1602 (1965).
7. J. H. Sloneker and A. Jeanes. Can. J. Chem. **40**, 2066 (1962).
8. C. A. Marsh. J. Chem. Soc. 1578 (1952).
9. R. E. Reeves. J. Am. Chem. Soc. **72**, 1499 (1950).
10. I. R. Siddiqui. Carbohydrate Res. **4**, 277 (1967).
11. E. F. Garner, I. J. Goldstein, R. Montgomery, and F. Smith. J. Am. Chem. Soc. **80**, 1206 (1958).

Can. J. Chem. Downloaded from www.nrcresearchpress.com by 210.87.254.105 on 09/05/12
For personal use only.

12. C. D. HURD, P. J. BAKER, JR., R. P. HOLYSZ, AND W. H. SAUNDERS, JR. J. Org. Chem. **18**, 186 (1953).
13. J. E. CADOTTE, G. G. S. DUTTON, I. J. GOLDSTEIN, B. A. LEWIS, F. SMITH, AND J. W. VAN CLEVE. J. Am. Chem. Soc. **79**, 691 (1957).
14. M. L. WOLFROM AND B. O. JULIANO. J. Am. Chem. Soc. **82**, 1673 (1960).
15. R. L. WHISTLER AND G. E. HILBERT. Ind. Eng. Chem. **36**, 796 (1944).
16. P. R. WATSON, C. A. KNUTSON, J. E. PITTSLEY, AND A. JEANES. 144th Meeting, American Chemical Society, Los Angeles, California. March 31, 1963. Abstracts. p. 15*c*.
17. M. A. JERMYN and F. A. ISHERWOOD. Biochem. J. **44**, 402 (1949).
18. E. CHARGAFF, C. LEVINE, AND C. GREEN. J. Biol. Chem. **175**, 67 (1948).
19. A. R. THOMPSON. Australian J. Sci. Res. Ser. B, **4**, 180 (1951).
20. W. R. REES and T. REYNOLDS. Nature, **181**, 767 (1958).
21. P. A. SANDFORD. Unpublished data.
22. E. G. TURNER AND J. G. FEINBERG. Nature, **184**, 1139 (1959).
23. S. P. ROGOVIN. Unpublished data.
24. M. DUBOIS, K. A. GILLES, J. K. HAMILTON, P. A. REBERS, AND F. SMITH. Anal. Chem. **28**, 350 (1956).
25. C. A. KNUTSON AND A. JEANES. Anal. Biochem. **24**, 470, 482 (1968).
26. R. J. BLOCK, E. L. DURRUM, AND G. ZWEIG. A manual of paper chromatography and paper electrophoresis. 2nd ed. Academic Press, Inc., New York. 1958. p. 220.
27. E. A. MCCOMB AND R. M. MCCREADY. Anal. Chem. **29**, 819 (1957).
28. J. C. RANKIN AND A. JEANES. J. Am. Chem. Soc. **76**, 4435 (1954).
29. O. RUFF. Ber. **34**, 1368 (1901).
30. H. KLOSTERMAN AND F. SMITH. J. Am. Chem. Soc. **74**, 5336 (1952).
31. L. J. RUBIN, H. A. LARDY, AND H. O. L. FISHER. J. Am. Chem. Soc. **74**, 425 (1952).
32. F. WEYGAND, W. PERKOW, AND P. KUHNER. Ber. **84**, 594 (1951).
33. M. LAMBERT AND A. C. NEISH. Can. J. Res. Ser. B, **28**, 83 (1950).
34. P. BLADON, W. G. OVEREND, L. N. OWEN, AND L. F. WIGGINS. J. Chem. Soc. 3000 (1950).
35. P. A. SANDFORD AND H. E. CONRAD. Biochemistry, **5**, 1508 (1966).
36. L. C. GAHAN, P. A. SANDFORD, AND H. E. CONRAD. Biochemistry, **6**, 2755 (1967).
37. J. C. IRVINE AND E. L. HIRST. J. Chem. Soc. **121**, 1213 (1922).
38. F. SMITH, M. STACEY, AND P. I. WILSON. J. Chem. Soc. 131 (1944).

Can. J. Chem. Downloaded from www.nrcresearchpress.com by 210.87.254.105 on 09/05/12
For personal use only.

Can. J. Chem. Downloaded from www.nrcresearchpress.com by 210.87.254.6 on 09/05/12
For personal use only.

Substitutions électrophiles en série naphtalénique. V. Sur le di-*t*-butyl-2,6 naphtalène[1]

JEAN-CLAUDE RICHER ET NICOLAS BASKEVITCH
Département de chimie, Université de Montréal, Montréal, Québec

ET

LUCIEN ERICHOMOVITCH ET FRANCIS L. CHUBB
Frank W. Horner Ltée, Montréal, Québec

Reçu le 7 mai 1968

Les réactions de nitration et de bromuration du di-*t*-butyl-2,6 naphtalène ont été étudiées. La nature des produits obtenus a été établie grâce à la résonance magnétique nucléaire.

Canadian Journal of Chemistry, 46, 3363 (1968)

Introduction

Dans le cadre des travaux que nous avons entrepris (1) sur les réactions de substitution électrophile des naphtalènes disubstitués en positions-2 et -6 et à la suite des observations qui ont été faites précédemment (2) sur l'influence stérique qui s'exerce lors des substitutions électrophiles sur le di-*t*-butyl-2,7 naphtalène (**1**), il nous apparaissait intéressant d'établir la nature des produits de réactions du di-*t*-butyl-2,6 naphtalène (**2**). Les résultats obtenus au cours de ces études font l'objet de la présente communication.

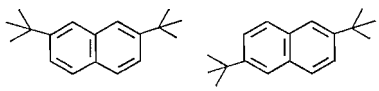

1 **2**

Résultats

La mononitration de l'hydrocarbure **2** conduit à deux produits isomères, l'un nitré en position-1 (**3***a*) et l'autre nitré en position-4 (**4***a*); ces deux produits peuvent être obtenus à l'état pur après chromatographie sur couche mince préparative (3). Les proportions relatives de chacun, tel que déterminé par la résonance magnétique nucléaire (r.m.n.) sur le mélange réactionnel brut, seraient de 40% de nitro-1 (**3***a*) et de 60% de nitro-4 (**4***a*) di-*t*-butyl-2,6 naphtalène. La réduction par l'acide chlorhydrique et l'étain en poudre de ce mélange de dérivés mononitrés permet d'isoler le chlorhydrate de l'amino-4 di-*t*-butyl-2,6 naphtalène (**4***b*). Le résidu des cristallisations de ce chlorhydrate est une huile noire de laquelle l'amino-1 di-*t*-butyl-2,6 naphtalène (**3***b*) n'a pu être isolé.

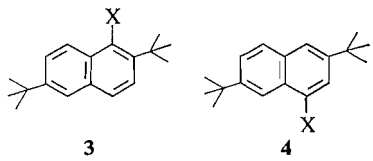

3 **4**

a) X = NO_2
b) X = NH_2

a) X = NO_2
b) X = NH_2
c) X = Br

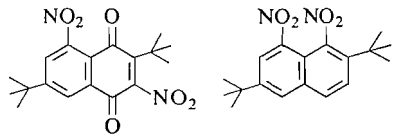

5 **6**

La nitration plus poussée de l'hydrocarbure **2** conduit à un mélange de produits duquel la dinitro-3,8 di-*t*-butyl-2,6 naphtoquinone-1,4 (**5**) est isolée par cristallisation. La chromatographie sur couche mince préparative permet d'isoler trois autres produits à l'état pur: le dinitro-1,8 (**6**), le dinitro-1,5 (**7**) et le dinitro-4,8 (**8***a*) di-*t*-butyl-2,6 naphtalène; un autre produit dont la structure n'a pas été déterminée a aussi été isolé en quantités mineures. La nitration du nitro-1 di-*t*-butyl-2,6 naphtalène (**3***a*) conduit aux dérivés dinitrés **6** et **7**. La même réaction effectuée sur le dérivé mononitré en position-4 (**4***a*) conduit aux

[1]Les résultats rapportés dans cette communication sont extraits en partie du mémoire soumis par Nicolas Baskevitch à la Faculté des Sciences de l'Université de Montréal, Montréal, Québec en vue de l'obtention du grade de Maître es Sciences, août, 1967.

TABLEAU I

Spectres de résonance magnétique nucléaire des produits obtenus*

Hydrocarbure	H-1	H-3	H-4	H-5	H-7	H-8	Divers
2	7.78	7.56	7.82	7.78	7.56	7.82	*t*-Bu 1.38
3		7.80	8.13	8.01	7.85	7.42	*t*-Bu 1.42 et 1.52
Calculé		7.76	8.24	8.03	7.82	8.29	
4*a*	8.32	8.39		8.32	7.84	8.14	*t*-Bu 1.42 et 1.47
Calculé	8.20	8.30		8.25	7.84	8.07	
4*b*	8.26	7.85		8.34	7.65	7.94	*t*-Bu 1.38 et 1.41
4*c*	7.93	7.88		8.09	7.68	7.84	*t*-Bu 1.40
5				8.21	8.42		*t*-Bu 1.40 et 1.45
6		8.10	8.46	8.38	8.46		*t*-Bu 1.47 et 1.51
Calculé		8.08	8.38	8.43	8.59		
7		8.12	7.65		8.12	7.65	*t*-Bu 1.48
Calculé		8.09	7.73		8.09	7.73	
8*a*	8.59	8.51		8.59	8.51		*t*-Bu 1.47
Calculé	8.67	8.58		8.67	8.58		
8*b*	8.15	8.09		8.15	8.09		*t*-Bu 1.48
8*c*	8.55	8.31		8.55	8.31		*t*-Bu 1.45
8*d*	8.52	7.78		8.52	7.78		
8*e*	9.38	8.41		9.38	8.41		*t*-Bu 1.44
8*f*	9.13	8.34		9.13	8.34		*t*-Bu 1.39

*Mesures effectuées à l'aide d'un appareil 100 Mc.p.s. de la Compagnie Jeolco pour des solutions dans la diméthylacétamide utilisant le tétraméthylsilane comme référence interne. Les déplacements chimiques (δ) sont en p.p.m. et peuvent être mesurés à ±0.005 p.p.m.

dinitro-1,8 (**6**) et dinitro-4,8 (**8***a*) di-*t*-butyl-2,6 naphtalènes et à la quinone nitrée (**5**).

La bromuration de l'hydrocarbure **2** conduit aux bromo-1 (**4***c*) et dibromo-1,5 (**8***b*) di-*t*-butyl-3,7 naphtalènes. Aucun dérivé tribromé ne semble se former si des conditions plus poussées sont appliquées. La réaction du dérivé dibromé (**8***b*) avec le cyanure cuivreux dans la diméthylformamide selon la méthode de Friedman et Schecter (4) conduit au dicyano-1,5 di-*t*-butyl-3,7 naphtalène (**8***c*) qui peut être transformé dans la diamide correspondante (**8***d*) par traitement avec de la potasse en présence d'alcool amylique. L'hydrolyse par l'acide sulfurique du dérivé dicyané (**8***c*) conduit à l'acide di-*t*-butyl-3,7 naphtalène dicarboxylique-1,5 (**8***e*) qui par traitement avec le diazométhane est transformé en di-*t*-butyl-3,7 naphtalène dicarboxylate-1,5 de méthyle (**8***f*).

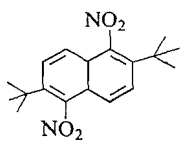

7

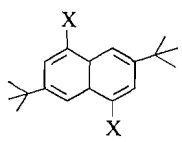

8

a) X = NO_2
b) X = Br
c) X = CN
d) X = $CONH_2$
e) X = COOH
f) X = $COOCH_3$

Discussion

La structure de chacun des produits est établie d'une manière générale en se basant sur le couplage des bandes des hydrogènes aromatiques dans le spectre r.m.n. Les positions des bandes dues à ces hydrogènes sont résumées dans le Tableau I. Dans le cas des dérivés nitrés, la méthode empirique proposée par Wells et Alcorn (5) a aussi été utilisée. Les positions des bandes prédites par application de cette méthode sont mises en regard des valeurs observées dans le Tableau I; la concordance entre les valeurs calculées et les valeurs expérimentales est étonnante dans tous les cas considérés sauf en ce qui concerne les dérivés mononitrés en position-1. Ce phénomène semble général (1, 2, 5, 6) et il se produit à chaque fois qu'un groupe nitro en position-α est adjacent à un substituant (méthyle, méthoxyle, *t*-butyle) en position-β. Le Tableau II où sont résumés les déplacements chimiques du proton en position-8 de nitro-1 naphtalènes par rapport au même proton dans le naphtalène correspondant, permet d'observer que plus le substituant placé en position-2 devient encombrant (l'effet stérique du groupe méthoxyle serait ici plus prononcé que celui du groupe méthyle) plus le proton en position-8 est déplacé vers les hauts champs; cette observation nous permet de suggérer que plus le substituant placé en position-2 est volumineux plus l'angle de

Can. J. Chem. Downloaded from www.nrcresearchpress.com by 210.87.254.6 on 09/05/12
For personal use only.

Can. J. Chem. Downloaded from www.nrcresearchpress.com by 210.87.254.6 on 09/05/12
For personal use only.

torsion du groupe nitro autour de la liaison —C—N augmente pour rendre celui-ci de plus en plus perpendiculaire au plan de la molécule du naphtalène. Cette torsion qui provoque une inhibition stérique à la résonance et un changement dans l'anisotropie du groupe nitro influencerait (1) principalement le proton en position-8 (*péri*).

TABLEAU II

Influence des substituants en position-2 sur le déplacement chimique de H-8 de nitro-1 naphtalènes

Nitro-1 naphtalènes	Δp.p.m.*
Non substitué	0.47†
Diméthyl-2,6	−0.13‡
Diméthyl-2,7	−0.12†
Diméthyl-2,3	−0.10†
Dimethoxy-2,7	−0.32§
Di-*t*-butyl-2,6	−0.40
Di-*t*-butyl-2,7	−0.45‖

*Δ = |δ dérivé nitré| − |δ naphtalène correspondant|.
†Evalué dans la référence 5.
‡Evalué d'après la référence 1.
§Evalué d'après la référence 6.
‖Evalué d'après la référence 2.

Les résultats obtenus lors de la nitration du di-*t*-butyl-2,6 naphtalène (**2**) diffèrent de ceux obtenus pour la même réaction effectuée sur le diméthyl-2,6 naphtalène (1), mais ils sont en parfait accord avec ceux obtenus lors de la réaction similaire sur le di-*t*-butyl-2,7 naphtalène (**1**). En se basant sur le fait que la dinitro-3,8 di-*t*-butyl-2,6 naphtoquinone-1,4 (**5**) ne se forme que lors de la nitration du nitro-4 di-*t*-butyl-2,6 naphtalène (**4***a*) l'on doit présumer que ce dérivé mononitré est l'unique précurseur de la quinone dinitrée. Ce résultat qui peut être rapproché de celui obtenu précédemment (2) lors de la formation de la dinitro-3,8 di-*t*-butyl-2,7 naphtoquinone-1,4 (**9**) par nitration du nitro-1 di-*t*-butyl-2,7 naphtalène (**10***a*) permet de corroborer la suggestion faite à cette occasion et selon laquelle

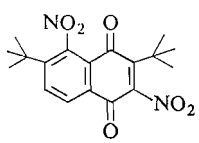

9

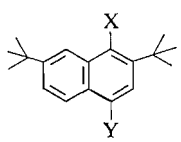

10

a) Y = H X = NO_2
b) X = H Y = Br
c) X = Y = Br

la formation de quinones (**5** ou **9**) proviendrait d'un empêchement stérique qui gène l'entrée d'un second groupe nitro entre un groupe *t*-butyle et un groupe nitro déjà en place (voir **4***a* et **10***a*). Il est intéressant de noter que le dinitro-1,8 di-*t*-butyl-2,6 naphtalène (**6**) se forme à l'exclusion de la quinone nitrée (**5**) lors de la nitration du nitro-1 di-*t*-butyl-2,6 naphtalène (**3***a*); dans ce cas–par opposition au résultat qui vient d'être discuté–le groupe qui est introduit n'est pas géné par les substituants qui sont déjà en place.

Le fait que la bromuration du di-*t*-butyl-2,6 naphtalène conduise au dérivé monobromé en position-4 (**4***c*) doit être rapproché du résultat obtenu lors de la bromuration du di-*t*-butyl-2,7 naphtalène (**1**) qui conduit aussi au bromo-4 di-*t*-butyl-2,7 naphtalène (**10***b*). Toutefois la formation du dibromo-4,8 di-*t*-butyl-2,6 naphtalène (**8***b*) est en opposition avec les résultats obtenus précédemment alors que le dibromo-1,4 di-*t*-butyl-2,7 naphtalène (**10***c*) avait été isolé. La monobromuration en position-4 (**4***c* et **10***b*) tant en série di-*t*-butyl-2,6 que di-*t*-butyl-2,7 naphtalène peut être expliquée par le fait que l'approche du brome vers la position-1 est rendue difficile à cause du groupe *t*-butyle en position adjacente. Le fait que le deuxième atome de brome s'introduise en position-1 (**10***c*) en série di-*t*-butyl-2,7 naphtalène et en position-8 (**8***b*) en série di-*t*-butyl-2,6 naphtalène s'expliquerait en se basant sur l'hypothèse que la position-8 du di-*t*-butyl-2,6 naphtalène est une position non encombrée alors que dans le cas des di-*t*-butyl-2,7 naphtalènes les positions-1 et -8 sont aussi encombrées l'une que l'autre; il apparait d'après les résultats expérimentaux obtenus que dans de telles conditions l'effet mésomérique du brome déjà présent en position-4 est suffisant pour orienter l'introduction du deuxième atome de brome vers la position-1.

Partie expérimentale

Les techniques expérimentales générales ont été décrites dans une publication précédente (1). Les spectres de masse sous forme de graphiques et la description des spectres ultraviolets et infrarouges des produits décrits dans cette publication sont rapportés en détail dans le mémoire de maîtrise de M. Nicolas Baskevitch dont une copie a été déposée à la bibliothèque du Conseil National de Recherches du Canada.

Les techniques de nitration et de bromuration sont essentiellement celles qui ont déjà été rapportées (2). Les caractéristiques des produits obtenus au cours du présent travail sont résumées dans le Tableau III.

TABLEAU III

Caractéristiques des produits obtenus

Hydrocarbure	Point de fusion	c.p.g.‡	R_i§
2	147–148*		
3*a*	80–82	5.25	0.433‖
4*a*	64–65	5.00	0.348‖
4*b*	208–210†		
4*c*	53–54		
5	236–237	14.5	0.0¶
6	170–172	20.5	0.125¶
7	234–236	9.5	0.50¶
8*a*	202–204	8.75	0.375¶
8*b*	208		
8*c*	265–267		
8*d*	362–364		
8*e*	388–390		
8*f*	167		

*Litt. (7), 147–148°.
†Pour le chlorhydrate.
‡t_R En minutes pour analyses faites à l'aide d'un chromatographe à ionisation de flamme Microtek utilisant une colonne de 4 pieds × 0.25 pouce remplie de SE-30 déposé à 5% sur du Chromoport XXX 80/90; analyses effectuées à 200 °C utilisant l'hélium comme gaz vecteur (débit 100 ml/min).
§À 26 °C sur couches minces (250 μ) de silica gel GF-254.
‖Solvant développeur: éther de pétrole p.e. 30–60°.
¶Solvant développeur: tétrachlorure de carbone.

Remerciements

Les auteurs remercient vivement le Conseil National de Recherches du Canada et le Conseil des Arts du Canada pour l'aide financière apportée sous forme d'octrois et de bourse de recherches.

Les auteurs remercient aussi la Compagnie Jeolco et particulièrement M. Yasushi Ogawa pour la détermination de nombreux spectres de résonance magnétique nucléaire à 100 Mc.p.s.

1. J. C. RICHER et N. BASKEVITCH. Can. J. Chem. Sous presse.
2. L. ERICHOMOVITCH, M. MÉNARD, F. L. CHUBB, Y. PÉPIN et J. C. RICHER. Can. J. Chem. **44**, 2305 (1966).
3. E. STAHL. Angew. Chem. **73**, 646 (1961).
4. L. FRIEDMAN et H. SCHECTER. J. Org. Chem. **26**, 2522 (1961).
5. P. R. WELLS et P. G. E. ALCORN. Australian J. Chem. **16**, 1108 (1963).
6. J. C. RICHER et Y. PÉPIN. Can. J. Chem. **43**, 3443 (1965).
7. C. C. PRICE, H. M. SHAPER, M. F. HUBER et C. BERNSTEIN. J. Org. Chem. **7**, 517 (1942).

Can. J. Chem. Downloaded from www.nrcresearchpress.com by 210.87.254.6 on 09/05/12
For personal use only.

Can. J. Chem. Downloaded from www.nrcresearchpress.com by 210.87.254.5 on 09/05/12
For personal use only.

Schmidt rearrangement of chromanones

U. T. Bhalerao and G. Thyagarajan
Regional Research Laboratory, Hyderabad-9, India

Received April 8, 1968

The mechanism of the Schmidt rearrangement has been examined in the conversion of chromanones to 1,4- and 1,5-benzoxazepinones. With substituents in the 6-, 7-, or 8-position, only electronic effects prevail resulting in the exclusive formation of 1,4-benzoxazepinones. Steric effects come into play with increasing bulk of substituents in the 5-position of the chromanone. Results now presented favor more than one pathway for the products to arise. Nuclear magnetic resonance spectra have been used to distinguish between the isomeric 1,4- and 1,5-benzoxazepinones.

Several new chromanones have been synthesized.

Canadian Journal of Chemistry, 46, 3367 (1968)

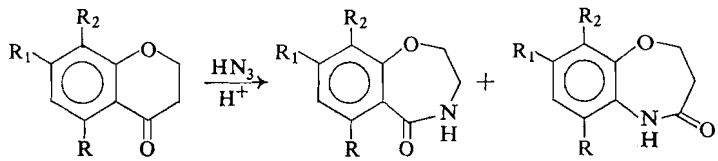

Scheme 1

1*a*: R = R_1 = CH_3; R_2 = H
b: R = R_2 = CH_3; R_1 = H
c: R = ETHYL; R_1 = R_2 = H
d: R = R_2 = H; R_1 = ETHYL
e: R = R_2 = H; R_1 = *tert*-BUTYL

2*a*: R = R_1 = CH_3; R_2 = H
b: R = R_2 = CH_3; R_1 = H
c: R = ETHYL; R_1 = R_2 = H
d: R = R_2 = H; R_1 = ETHYL
e: R = R_2 = H; R_1 = *tert*-BUTYL

3*a*: R = R_1 = CH_3; R_2 = H
b: R = R_2 = CH_3; R_1 = H
c: R = ETHYL; R_1 = R_2 = H

The mechanism of Schmidt rearrangement has been a subject of considerable attention during recent years. Smith (1, 2) suggested the iminodiazonium ion as an intermediate in this rearrangement but the universality of involvement of this intermediate has recently been questioned by Lansbury and Mancuso (3) who favor the iminium cation, because of the nonstereospecificity observed in their experiments. We have been interested in the synthesis of benzoxazepines by the Schmidt rearrangement of chromanones (4) and in this paper we present the results of our experiments in the context of the mechanism of this rearrangement.

Results

5,7-Dimethyl Chromanone[1]

Schmidt rearrangement of 5,7-dimethyl chromanone (**1***a*) gave a 60% yield of a solid (m.p. 119–124°) which was shown by nuclear magnetic resonance (n.m.r.) spectra to be a mixture of 6,8-dimethyl-2,3-dihydro-1,4-benzoxazepin-5-(4*H*)-one (**2***a*) and 6,8-dimethyl-2,3-dihydro-1,5-benzoxazepin-4(5*H*)-one (**3***a*) in a ratio of 46:54, (Scheme 1).

In the n.m.r. spectrum (Fig. 1) of the crude reaction product, peaks from the two isomers are distinctly discernible. The triplets at δ 4.5 and δ 2.75 are assignable respectively to the C-2 and C-3 methylenes of **3***a* while the triplet at δ 4.3 and the quartet[2] at δ 3.35 represent the C-2 and C-3 methylenes of **2***a*. Of the two sharp singlets, the one integrating to 9 protons is assignable to the methyls at C-6 and C-8 positions of **3***a* and at C-8 of **2***a*. The C-6 methyl of **2***a* appears as a singlet at δ 2.45 being deshielded by the amide carbonyl.

These isomeric lactams were separated by column chromatography to give **2***a*, m.p. 155°, and **3***a*, m.p. 141°, in a ratio of 46:54 respectively and were also identified individually by n.m.r. The spectrum of **3***a* showed two triplets at δ 4.5

[1]Lockhart and Evans (5) reported that in three trials, Schmidt reaction of **1***a* gave only 6,8-dimethyl-2,3-dihydro-1,5-benzoxazepin-5(4*H*)one, m.p. 123–125°, in 5% yield.

[2]A sextet (or a multiplet) would be expected from additional NH participation in spin–spin coupling of the C-3 methylene protons. However, in all these cases it appears as a quartet only.

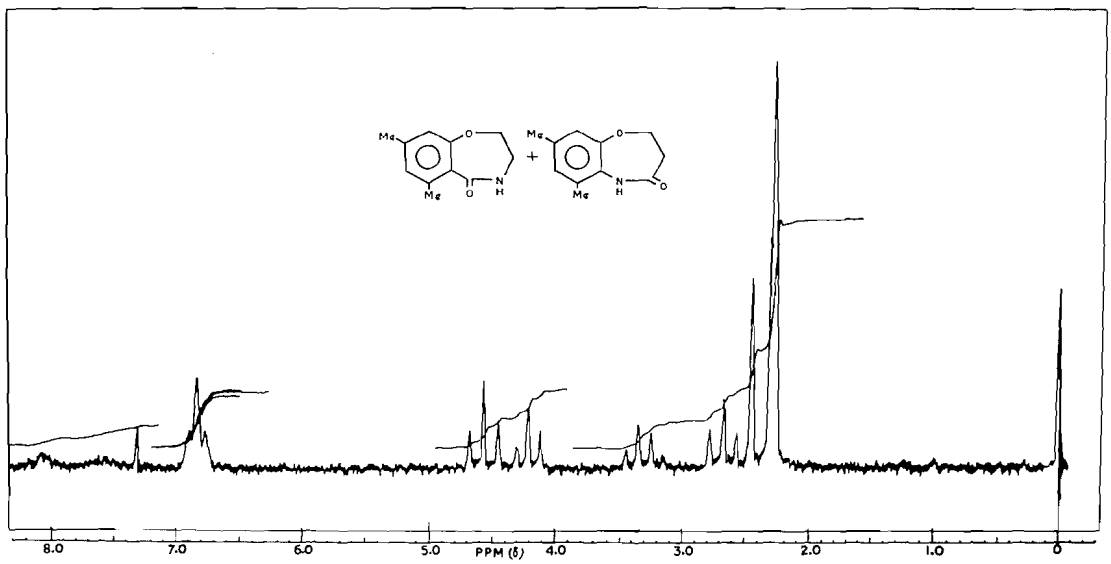

FIG. 1. Nuclear magnetic resonance spectrum of crude product from Schmidt reaction on 5,7-dimethyl chromanone (**1***a*).

(—O—CH_2) and δ 2.75 (—CH_2—CO—) and a sharp singlet (6H) at δ 2.3 for the two methyl groups besides the broad NH absorption at δ 8.5. In contradistinction, the spectrum of **2***a* showed a quartet at δ 3.35 assignable to —NH—CH_2— arising from the participation of the adjacent NH proton in spin–spin coupling. The triplet centered at δ 4.3 represents the C-2 methylene proton while the singlets at δ 2.45 and δ 2.3 arise from the C-6 and C-8 methyls respectively.

5,8-Dimethyl Chromanone

To obtain additional evidence that the bulk of the methyl group in the 5-position only affects the course of the Schmidt reaction, 5,8-dimethyl chromanone was rearranged. The product (57% yield) was a mixture of two isomeric lactams separated and identified as 6,9-dimethyl-2,3-dihydro-1,4-benzoxazepin-5(4*H*)-one, m.p. 150° (**2***b*) and 6,9-dimethyl-2,3-dihydro-1,5-benzoxazepin-4(5*H*)-one, m.p. 135–136° (**3***b*) in a ratio of 45:55 respectively. The n.m.r. spectra (see Experimental) of the individual isomers fully corroborate the structure assigned.

2,3-Dihydronaphth(2,1-b)pyran-1-one (4)

Schmidt reaction afforded a solid, m.p. 116°, shown by n.m.r. to consist of 1,4- and 1,5-isomeric products in a ratio of 40:60 respectively. Column chromatography enabled separation into 3,4-dihydronaphth(1,2-*f*)(1,4)oxazepin-1-(2*H*)-one (**5**), m.p. 143–144°, and 3,4-dihydronaphth(2,1-*b*)(1,4)oxazepin-2(1*H*)-one (**6**), m.p. 156° (Scheme 2). The structures were confirmed by n.m.r. spectra, the basis of distinction again being the NH participation in spin–spin coupling of the C-3 methylene protons. The spectrum of **6** (Fig. 2) consists of two triplets at δ 2.75

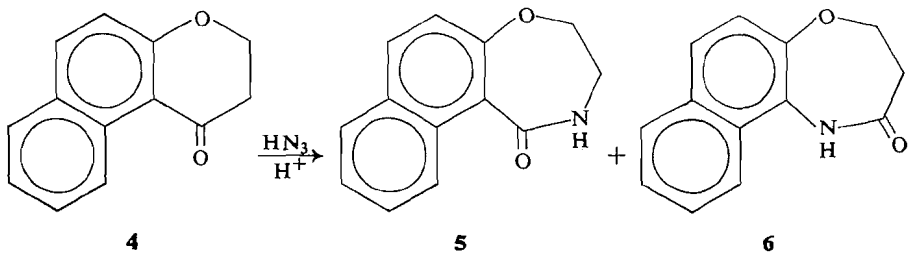

4 **5** **6**

SCHEME 2

Can. J. Chem. Downloaded from www.nrcresearchpress.com by 210.87.254.5 on 09/05/12
For personal use only.

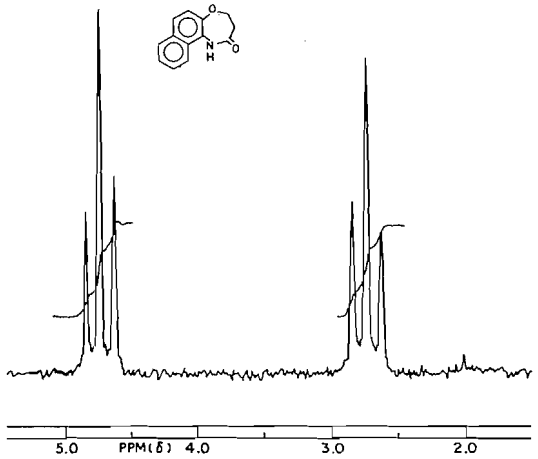

FIG. 2. Nuclear magnetic resonance spectrum (part) of 3,4-dihydronaphth(2,1-*b*)(1,4)oxazepin-2(1*H*)-one (**6**).

(—CO—CH_2—) and δ 4.75 (—O—CH_2—) the aromatic multiplet (6H) in the region δ 7.2–8.2 and a broad absorption (—NH—CO—) at δ 8.85 while that of **5** (Fig. 3) shows a quartet at δ 3.35 (—N—CH_2—) and a triplet at δ 4.35 (—O—CH_2—) assignable respectively to the C-3 and C-4 methylenes, the other features being similar.

The availability of 1-nitro-2-naphthol made possible an independent synthesis of **6**. 1-Nitro-2-naphthol on treatment with β-chloropropionic acid gave β-(1-nitro-2-naphthoxy)-propionic acid. Catalytic reduction to the amino derivative followed by cyclization under pressure at elevated temperature afforded 3,4-dihydronaphth-(2,1-*b*)(1,4)oxazepin-2(1*H*)-one (m.p. 156°) identical with the Schmidt reaction product in all respects.

5-Ethyl Chromanone

The synthesis of this chromanone was achieved as follows. Cyanoethylation of *m*-ethylphenol gave β-(*m*-ethylphenoxy)-propionitrile which upon hydrolysis followed by cyclization with phosphorus pentoxide in refluxing benzene resulted in the formation of both 5-ethyl chromanone and 7-ethyl chromanone in a ratio of 4:6 determined by gas–liquid chromatography (g.l.c.). This mixture was efficiently fractionated in a Piros–Glover M8480 spinning band micro still into 5-ethyl chromanone (**1***c*), b.p. 97.5°/1 mm and 7-ethyl chromanone (**1***d*), b.p. 113°/1 mm, identified on the basis of the respective n.m.r. spectrum. These new chromanones were converted into the corresponding oximes, the n.m.r. spectra (see Experimental) of which confirm the structures assigned to **1***c* and **1***d*.

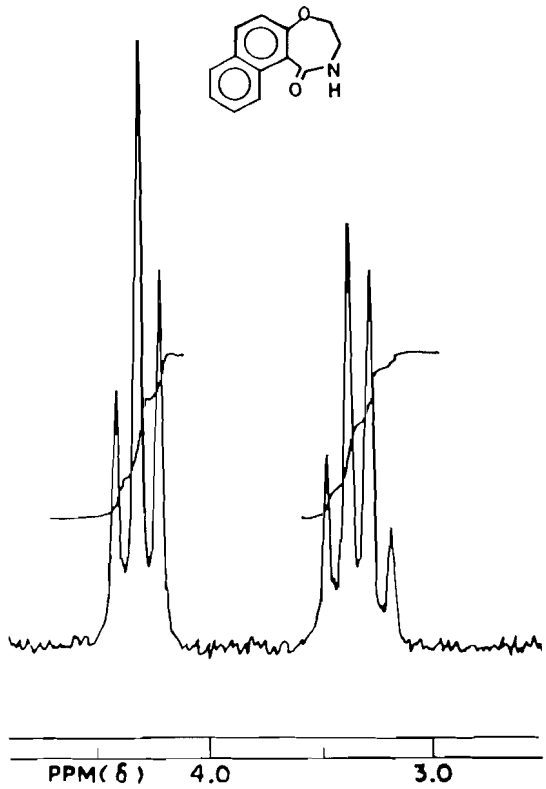

FIG. 3. Nuclear magnetic resonance spectrum (part) of 3,4-dihydronaphth(1,2-*f*)(1,4)oxazepin-1(2*H*)-one (**5**).

Schmidt rearrangement of 5-ethyl chromanone (**1***c*) gave a mixture of 6-ethyl-2,3-dihydro-1,4-benzoxazepin-5(4*H*)-one (**2***c*) and 6-ethyl-2,3-dihydro-1,5-benzoxazepin-4(5*H*)-one (**3***c*) in a ratio of 22:78 respectively (Scheme 1).

7-Ethyl Chromanone

Nuclear magnetic resonance spectra (Fig. 4) of the crude product from Schmidt rearrangement of this compound (**1***d*) indicated the exclusive presence of 8-ethyl-2,3-dihydro-1,4-benzoxazepin-5(4*H*)-one (**2***d*), m.p. 89°. The quartet (2H) at δ 2.7 and the triplet (3H) at δ 1.2 arise from the C-8 ethyl group while the quartet (2H) at δ 3.5 and the triplet (2H) at δ 4.4 are assignable to the C-3 and C-2 methylenes respectively. The deshielded C-6 aromatic proton appears as an AB type doublet at δ 7.95 ($J_{6,7}$ = 8 c.p.s.) while the C-7 proton is the doublet at δ 7.0 one limb

Can. J. Chem. Downloaded from www.nrcresearchpress.com by 210.87.254.5 on 09/05/12
For personal use only.

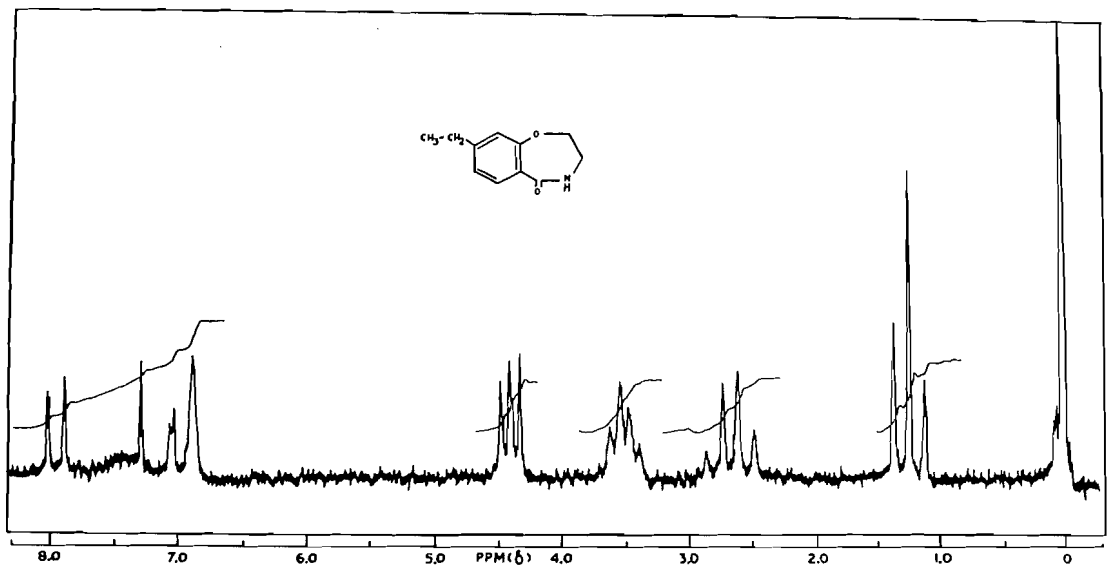

FIG. 4. Nuclear magnetic resonance spectrum of crude product from Schmidt reaction on 7-ethyl chromanone (**1***d*).

of which is merged with that of the C-9 proton. The broad absorption at δ 7.4 represents the NH.

5,7-Di-t-butyl Chromanone

Cyanoethylation of 3,5-di-*t*-butyl phenol gave β-(3,5-di-*t*-butyl phenoxy)-propionitrile, which on acid-catalyzed hydrolysis and cyclization with phosphorus pentoxide in benzene gave 5,7-di-*t*-butyl chromanone. In two trials, Schmidt rearrangement did not occur and the starting material was recovered unchanged as confirmed by g.l.c., infrared, and n.m.r.

However, when cyclization of β-(3,5-di-*t*-butyl phenoxy)-propionitrile was earlier attempted by using polyphosphoric acid at 180°, an interesting product was encountered in which one *t*-butyl group had been lost.[3] The structure of this new product was assigned as 7-*t*-butyl chromanone (**1***e*) on the basis of its n.m.r. spectrum. Schmidt rearrangement of this chromanone gave only one product identified as 8-*t*-butyl-2,3-dihydro-1,4-benzoxazepin-5(4*H*)-one (**2***e*), m.p. 162°. The n.m.r. spectrum showed one *t*-butyl group at δ 1.35 and a 2-proton signal at δ 3.55 and δ 4.4, assignable to C-3 (NH—CH_2) and C-2 (O—CH_2) methylenes respectively. In the aromatic region, the deshielded C-6 proton appeared as an AB-type doublet at δ 8.0 ($J_{6,7}$ = 8 c.p.s.), the C-9 proton *meta* coupled ($J_{7,9}$ = 2 c.p.s.) at δ 7.05 while the C-7 proton *ortho* coupled to C-6 ($J_{6,7}$ = 8 c.p.s.) and *meta* coupled to C-9 ($J_{7,9}$ = 2 c.p.s.) appeared at δ 7.15, the NH proton being a broad signal in the region δ 7.4–7.9.

The results obtained in these experiments are summarized in Table I.

Discussion

In an earlier publication (4) we had reported the Schmidt reaction on various derivatives of chromanones carrying alkyl, alkyloxy, and halogen substituents in 6- and 8-positions, the product in every case being a derivative of 1,4-benzoxazepin-5-one. Results now presented[4] show that an alkyl group in the 7-position of chromanone does not also alter the course of the reaction, the product being again a derivative of 1,4-benzoxazepin-5-one (Scheme 1). The bulk of the substituents in the 5-position, however, does

[3]Lansbury and Mancuso (3) reported an instance of de-*t*-butylation during the Beckmann rearrangement of 8-*t*-butyl,5-bromo-1-tetralone oxime in polyphosphoric acid at 110–120°.

[4]All experiments described here were carried out using concentrated sulfuric acid and sodium azide. An experiment using sodium azide and polyphosphoric acid at 60° also gave one product, 2,3-dihydro-1,4-benzoxazepin-5(4*H*)-one (as seen by n.m.r.), resulting from exclusive alkyl bond migration.

Can. J. Chem. Downloaded from www.nrcresearchpress.com by 210.87.254.5 on 09/05/12
For personal use only.

TABLE I

Migratory aptitudes in Schmidt rearrangement of chromanones*

No.	Chromanone R_3	R_2	R_1	R	Yield %	Isomer ratio % aryl migration	% alkyl migration
1	H	H	H	H	78	0	100
2	H	CH_2—CH_3	H	H	55	0	100
3	H	C—$(CH_3)_3$	H	H	51	0	100
4	H	CH_3	H	CH_3	60	54	46
5	CH_3	H	H	CH_3	57	55	45
6	2,3-Dihydronaphtho (2,1-*b*)pyran-1-one				50	60	40
7	H	H	H	CH_2—CH_3	45	78	22
8	H	C—$(CH_3)_3$	H	C—$(CH_3)_3$	—	No reaction	

*Compounds of structure 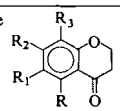

influence the course of reaction since the major product in these cases arises by aryl bond migration, namely, the derivatives of 1,5-benzoxazepin-4-one (Table I).

In chromanones unsubstituted in the 5-position only electronic effect (4, 5) prevails. Conjugation arising out of the lone pair of electrons on ethereal oxygen atom would stabilize the aryl bond[5] by imparting a partial double bond character. Since the benzenoid character of the benzene ring is lost, a phenonium type of intermediate which would favor aryl bond migration is not possible. Alkyl bond migration therefore results. The involvement of iminodiazonium ion **9** (Scheme 3, R = H) as the intermediate is consistent with conjugation with the benzene ring while the azidohydrin **7** (carbonyl carbon being of sp^3 nature) would remove conjugation with the benzene ring and thereby with ethereal oxygen.

It is seen from Table I that as the bulk of the 5-position increases there is a corresponding increase in the quantity of the product arising from aryl bond migration, namely, derivatives of 1,5-benzoxazepin-4-one. A scrutiny of the models of 2,3-dihydronaphth(2,1-*b*)pyran-1-one (**4**) and 5-ethyl chromanone (**1***c*) shows that if iminodiazonium ion were to be considered, due to enhanced steric repulsion the relative population in the equilibrium of the iminodiazonium ion **9** (Scheme 3) would be extremely low. Then 40 and 20% of sterically non-favored alkyl bond migration may arise by direct rearrangement of the azidohydrin **7**. It is conceivable that when R = H the dehydration step of the azidohydrin **7** to the iminodiazonium ions **8** or **9** is favored, whereas this dehydration will not be sterically favored, when R = CH_3 etc., since in the iminodiazonium ion the C = N is coplanar with the benzene ring and the 5-alkyl substituent, whereas in the azidohydrin the hydroxyl and the azido groups would be above and below the plane of the ring. Steric resistance to iminodiazonium ion formation may thus allow rearrangement of the azidohydrin to become dominant. The increase in aryl bond migration with increase in the bulk of the substituent in the 5-position of chromanone may be attributed to a preference by the diazo nitrogens of the azido group (due to non-bonded interaction with the substituent in the 5-position of chromanones) for a conformation which is *trans* to the aryl bond. The dissimilarity in our results (7) (when R = CH_3,C_2H_5) from Beckmann rearrangement on corresponding chromanone oximes[6] under similar conditions, and nonformation of tetrazoles[7] also indicates that an intermediate of the type of azidohydrin and not iminodiazonium ion is involved.

Steric and electronic effects thus influence the course of Schmidt rearrangement. Our evidence

[5]If such a stabilization were not to exist, then by virtue of the phenyl participation, the aryl bond should migrate as observed in the case of tetralones (1, 3).

[6]Beckmann rearrangement of chromanone oximes shows that a methyl or bulkier group in 5-position leads to exclusive aryl bond migration.

[7]We were unable to isolate any tetrazole using the conditions reported by Dimaio and Permutti (6).

Can. J. Chem. Downloaded from www.nrcresearchpress.com by 210.87.254.5 on 09/05/12
For personal use only.

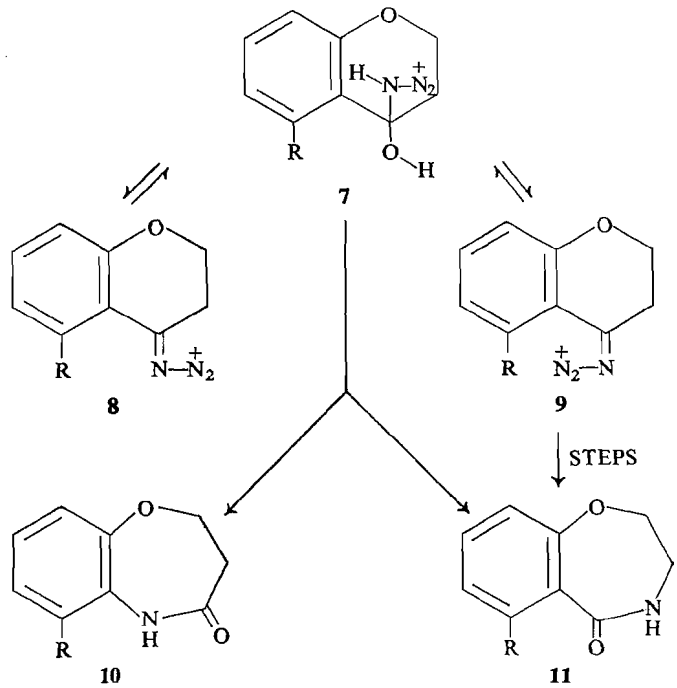

SCHEME 3

leads us to the conclusion that the products can be derived either through the iminodiazonium ion or when the latter is not sterically favored through the azidohydrin. In other words, more than one pathway, different but consistent, are possible. A similar conclusion was arrived at by Dimaio and Permutti (6) from their work on Schmidt rearrangement of *cis*-8-methyl-hydrindan-1-one.

Experimental

All melting points were determined by the capillary method and are uncorrected. Petroleum ether refers to the fraction of boiling range 40–60°. Infrared spectra were recorded on a Perkin–Elmer model F221 spectrometer equipped with sodium chloride optics and n.m.r. spectra were recorded on a Varian A-60 instrument in $CDCl_3$ solutions with TMS as the internal standard.

Synthesis of Chromanones

5,7-Dimethyl chromanone (5) and 2,3-dihydronaphth-(2,1-*b*)pyran-1-one[8] were prepared as reported in the literature.

Only typical procedures are reported here; all experiments were carried out using essentially these procedures.

Cyanoethylation of Phenols

The phenol (0.1 mole) was added to acrylonitrile (0.12 mole) containing sodium (1.5% on the weight of the phenol). The mixture was heated in an autoclave for 4–6 h at 125–135°, cooled, extracted in chloroform, and washed with 5% sodium hydroxide solution till free from the phenol. Drying over sodium sulfate and removal of solvent gave the desired nitrile. The following were prepared by this method.

β-*(3,6-Dimethyl phenoxy)-propionitrile*, yield 74%, b.p. 154°/11 mm; $\nu_{C\equiv N}$(Nujol) 2250 cm^{-1}.

Anal. Calcd. for $C_{11}H_{13}ON$: C, 75.4; H, 7.5; N, 8.0. Found: C, 75.3; H, 7.1; N, 7.9.

β-*(m-Ethylphenoxy)-propionitrile*, yield 63%, b.p. 128°/9 mm; $\nu_{C\equiv N}$ (film) 2245 cm^{-1}.

Anal. Calcd. for $C_{11}H_{13}ON$: C, 75.4; H, 7.5; N, 8 0. Found: C, 75.1; H, 7.4; N, 7.7.

β-*(3,5-Di-t-butyl phenoxy)-propionitrile*, yield 58%, m.p. 81°; $\nu_{C\equiv N}$(film) 2220 cm^{-1}.

Anal. Calcd. for $C_{17}H_{25}ON$: C, 78.7; H, 9.7; N, 5.4. Found: C, 78.6; H, 9.6; N, 5.2.

Hydrolysis of β-*Phenoxy Propionitrile*

A mixture of the nitrile (0.22 mole) and concentrated hydrochloric acid (0.2 mole) was stirred and refluxed for 5–8 h. As the reaction mixture became hot the solid dissolved, but as hydrolysis proceeded a precipitate appeared. The reaction mixture was cooled and diluted with water. The solid β-phenoxy propionic acid thus obtained was filtered and purified by dissolving in sodium bicarbonate solution, reprecipitation with hydrochloric acid, and crystallization from a suitable solvent.

The following acids were thus synthesized starting with appropriate β-phenoxy propionitriles.

β-*(3,6-Dimethylphenoxy)propionic acid*, yield 90%, m.p. 97°.

Anal. Calcd. for $C_{11}H_{14}O_3$: C, 68.0; H, 7.3; Found: C, 67.7; H, 7.0.

[8]Chakravarti and Dutta (8) refer to this compound as 1-benzo-(*f*)-chromanone.

Can. J. Chem. Downloaded from www.nrcresearchpress.com by 210.87.254.5 on 09/05/12
For personal use only.

Can. J. Chem. Downloaded from www.nrcresearchpress.com by 210.87.254.5 on 09/05/12
For personal use only.

β-*(m-Ethyl phenoxy)propionic acid*, yield 85%, m.p. 112°.

Anal. Calcd. for $C_{11}H_{14}O_3$: C, 68.0; H, 7.3. Found: C, 67.8; H, 7.0.

β-*(3,5-Di-t-butylphenoxy)propionic Acid*

Hydrolysis of β-(3,5-di-*t*-butyl phenoxy)-propionitrile with concentrated hydrochloric acid at reflux temperature for 30 h gave back the starting nitrile. However, hydrolysis occurred under pressure.

The nitrile (12 g) was heated in an autoclave with concentrated hydrochloric acid (150 ml) for 10 h, cooled, and taken up in chloroform. Drying and removal of solvent gave 10 g (83%) of β-(3,5-*t*-butyl phenoxy)propionic acid, m.p. 97° (from petroleum ether); $\nu_{C=O}$ (KBr) 1705 cm^{-1}.

Anal. Calcd. for $C_{17}H_{26}O_3$: C, 73.3; H, 9.4. Found: C, 73.1; H, 9.1.

Cyclization of β-phenoxy propionic acids to the chromanones was carried out as reported by Chakravarti and Dutta (8). New chromanones thus prepared were the following.

6,8-Dimethyl chromanone, yield 56%, b.p. 118°/4 mm; $\nu_{C=O}$ (film) 1675 cm^{-1}.

Anal. Calcd. for $C_{11}H_{12}O_2$: C, 75.0; H, 6.9. Found: C, 75.1; H, 6.8.

5- and 7-Ethyl chromanones, the mixture (4:5) of 5- and 7-ethyl chromanones was separated in an M-8480 Piros–Glover spinning band micro still, the take-off rate being 1 ml/h and at a reduced pressure of 1 mm. Two fractions were collected at 97.5 and 113°.

5-Ethyl chromanone, b.p. 97.5°/1 mm; $\nu_{C=O}$ (film) 1680 cm^{-1}.

Anal. Calcd. for $C_{11}H_{12}O_2$: C, 75.1; H, 6.8. Found: C, 74.9; H, 6.6.

5-Ethyl chromanone oxime, m.p. 70°; δ ($CDCl_3$) 7.3 (b, 1H, hydroxy), 6.7–7.2 (m, 3H, aromatic), 4.2 (t, 2H, O—CH_2), 3.1 (m, 4H, C-3 methylene and methylene of C-5 ethyl group), 1.2 (t, 3H, methyl of C-5 ethyl group) p.p.m.

Anal. Calcd. for $C_{11}H_{13}O_2N$: C, 69.1; H, 6.9; N, 7.3. Found: C, 69.0; H, 6.7; N, 7.1.

7-Ethyl chromanone, b.p. 113°/1 mm; $\nu_{C=O}$ (film) 1683 cm^{-1}.

Anal. Calcd. for $C_{11}H_{12}O_2$: C, 75.1; H, 6.8. Found: C, 74.7; H, 6.5.

7-Ethyl chromanone oxime, m.p. 111°; δ ($CDCl_3$) 8.2 (b, 1H, hydroxy), 7.9 (d, 1H, deshielded C-5 proton), 7.0 (d, 1H, C-6 proton), 6.85 (b, 1H, C-8 proton), 4.4 (t, 2H, C-2 methylene); 2.9 (t, 2H, C-3 methylene), 2.7 (q, 2H, methylene of C-7 ethyl group), 1.25 (t, 3H, methyl of C-7 ethyl group) p.p.m.

Anal. Calcd. for $C_{11}H_{13}O_2N$: C, 69.1; H, 6.9; N, 7.3. Found: C, 68.8; H, 6.7; N, 7.0.

5-7-Di-t-butyl chromanone, yield 35%, b.p. 180–182°/5 mm; $\nu_{C=O}$ (film) 1670 cm^{-1}; δ ($CDCl_3$) 1.3 (s, 9H, C-7 *t*-butyl group), 1.5 (s, 9H, C-5 *t*-butyl group), 2.8 (t, 2H, C-3 methylene), 4.4 (t, 2H, C-2 methylene), 6.9–7.1 (b, 2H, aromatic) p.p.m.

Anal. Calcd. for $C_{17}H_{24}O_2$: C, 78.4; H, 9.3. Found: C, 78.3; H, 9.1.

7-t-Butyl Chromanone

β-(3,5-Di-*t*-butylphenoxy)propionitrile (15 g) was heated with polyphosphoric acid (220 g) at 180–185° for 2.5 h. Pouring the reaction mixture into crushed ice and extraction with chloroform gave 7.5 g (50%) of 7-*t*-butyl chromanone, b.p. 140°/11 mm; $\nu_{C=O}$ (film) 1675 cm^{-1}; δ ($CDCl_3$) 7–8 (m, 3H, aromatic); 4.4 (t, 2H, C-2 methylene), 2.95 (t, 2H, C-3 methylene), 1.3 (s, 9H, protons of C-7 *t*-butyl group) p.p.m.

Anal. Calcd. for $C_{13}H_{16}O_2$: C, 76.4; H, 7.9. Found: C, 76.3; H, 7.8.

Schmidt Rearrangement[9]

Reactions were carried out under the same conditions as reported by us earlier (4).

5,7-Dimethyl chromanone (**1***a*) gave 60% yield of a crude product, m.p. 119–124°. Thin-layer chromatography using chloroform – petroleum ether (1:9) solvent system showed two spots. This crude mixture (2 g) was separated on a silica gel column. Elution first with chloroform – petroleum ether (1:9) gave 1 g of a white compound (**3***a*), m.p. 141°; elution next with chloroform gave 0.91 g of a compound (**2***a*), m.p. 155°. Similar proportions of **3***a* (2.04 g) and **2***a* (1.9 g) were obtained on separation of 4 g of the crude reaction mixture from another experiment.

Compound **3***a* was identified as *6,8-dimethyl-2,3-dihydro-1,5-benzoxazepin-4(5H)-one*, m.p. 141°; $\nu_{C=O}$ (KBr) 1650 cm^{-1}.

Anal. Calcd. for $C_{11}H_{13}O_2N$: C, 69.1; H, 6.9; N, 7.1. Found: C, 68.7; H, 6.6; N, 7.1.

Compound **2***a* was identified as *6,8-dimethyl-2,3-dihydro-1,4-benzoxazepin-5(4H)-one*, m.p. 155°; $\nu_{C=O}$ (KBr) 1660 cm^{-1}.

Anal. Calcd. for $C_{11}H_{13}O_2N$: C, 69.1; H, 6.9; N, 7.1. Found: C, 68.9; H, 6.7; N, 6.9.

5,8-Dimethyl chromanone (**1***b*) gave 57% yield of a crude mixture, m.p. 114–117°. The reaction product (2 g) was separated on a silica gel column. Elution, first with chloroform – petroleum ether (2:8) gave 1 g of a white compound (**3***b*), m.p. 135–136°; elution then by chloroform gave 0.89 g of a compound (**2***b*), m.p. 150°.

Compound **3***b* was identified as *6,9-dimethyl-2,3-dihydro-1,5-benzoxazepin-4(5H)-one*, m.p. 135–136°; $\nu_{C=O}$ (KBr) 1670 cm^{-1}; δ ($CDCl_3$) 8.4 (b, 1H, NH), 6.9 (s, 2H, C-7 and C-8 protons), 4.55 (t, 2H, C-2 methylene); 2.65 (t, 2H, C-3 methylene), and 2.25 (s, 6H, for C-6 and C-9 methyl groups) p.p.m.

Anal. Calcd. for $C_{11}H_{13}O_2N$: C, 69.1; H, 6.9; N, 7.3. Found: C, 68.9; H, 6.6; N, 7.2.

Compound **2***b* was identified as *6,9-dimethyl-2,3-dihydro-1,4-benzoxazepin-5(4H)-one*, m.p. 150°; $\nu_{C=O}$ (KBr) 1650 cm^{-1}.

Anal. Calcd. for $C_{11}H_{13}O_2N$: C, 69.1; H, 6.9; N, 7.3. Found: C, 69.0; H, 6.7; N, 7.3.

2,3-Dihydronaphth(2,1-b)pyran-1-one (**4**) gave a 50% yield of a mixture of isomeric amides (2 g) m.p. 116°, which was separated over a silica gel column. Elution with chloroform – petroleum ether (3:7) gave 1.1 g of compound **6**, m.p. 156°; elution next by chloroform gave 0.8 g of compound **5**, m.p. 143–144°.

Compound **6** was identified as *3,4-dihydronaphth(2,1-b)-(1,4)-oxazepin-2(1H)-one*, m.p. 156°; $\nu_{C=O}$ (KBr) 1675 cm^{-1}.

[9]The acidic layer was examined in each case for possible presence of hydrolytic cleavage products of the benzoxazepinones formed but none were found. In only one case a small quantity of aniline was present which may have arisen from decomposition of hydrazoic acid or as suggested by us earlier (9).

Anal. Calcd. for $C_{13}H_{11}O_2N$: C, 73.2; H, 5.2; N, 6.6. Found: C, 73.1; H, 5.2; N, 6.5.

Compound **5** was identified as *3,4-dihydronaphth-(1,2-f)(1,4)-oxazepin-1(2H)-one*, m.p. 143–144°; $\nu_{C=O}$ (KBr) 1655 cm^{-1}.

Anal. Calcd. for $C_{13}H_{11}O_2N$: C, 73.2; H, 5.2; N, 6.6. Found: 73.1; H, 5.0; N, 6.4.

7-Ethyl chromanone (**1***d*) gave *8-ethyl-2,3-dihydro-1,4-benzoxazepin-5(4H)-one* (**2***d*), m.p. 89° in 55% yield.

Anal. Calcd. for $C_{11}H_{13}O_2N$: C, 69.1; H, 6.9; H, 7.3. Found: C, 68.7; H, 6.7; N, 7.1.

5-Ethyl chromanone (**1***c*) gave a 45% yield of a mixture of isomeric amides, m.p. 120° which consisted of *6-ethyl-2,3-dihydro-1,4-benzoxazepin-5(4H)-one* (**2***c*) and *6-ethyl-2,3-dihydro-1,5-benzoxazepin-4(5H)-one* (**3***c*) in a ratio (22:78).

7-t-butyl chromanone (**1***e*) gave 50% yield of 8-*t*-butyl-1,4-benzoxazepin-5(4*H*)-one (**2***e*), m.p. 162°; $\nu_{C=O}$ (KBr) 1645 cm^{-1}.

Anal. Calcd. for $C_{13}H_{17}O_2N$: C, 71.2; H, 7.8; N, 6.4. Found: C, 70.9; H, 7.8; N, 6.5.

5,7-Di-t-butyl chromanone was recovered unchanged in two experiments as borne out by g.l.c., infrared, and n.m.r.

Synthesis of 3,4-Dihydronaphth(2,1-b)(1,4)oxazepin-2(1H)-one

β-*(1-Nitro naphthoxy)propionic Acid*

1-Nitro-2-naphthol (38 g) was dissolved in aqueous potassium hydroxide (30%, 60 ml) and heated on a water bath. To this was added in small portions, during 2 h, a solution of β-chloropropionic acid (26 g) neutralized with sodium bicarbonate. The reaction mixture was further heated for 3 h, cooled, acidified with hydrochloric acid, and extracted with ether. The ether solution was extracted with aqueous sodium bicarbonate. Neutralization of the alkaline layer with hydrochloric acid gave 13 g (25%) of β-(1-nitro naphthoxy)propionic acid, m.p. 101°; $\nu_{C=O}$ (KBr) 1700 cm^{-1}.

Anal. Calcd. for $C_{13}H_{11}O_5N$: C, 59.8; H, 4.3; N, 5.4. Found: C, 59.7; H, 4.1; N, 5.1.

β-*(1-Amino naphthoxy)propionic Acid*

β-(1-Nitro naphthoxy)propionic acid (6.5 g) was mixed with 10% palladium-on-charcoal (350 mg) in absolute ethanol (150 ml) and hydrogenated at room temperature for 3 h. Filtration of the catalyst and removal of solvent gave 5 g (87%) of β-(1-amino naphthoxy)propionic acid, m.p. 88°.

Anal. Calcd. for $C_{13}H_{13}O_3$: C, 67.5; H, 5.7; N, 6.1. Found: C, 67.4; H, 5.6; N, 6.0.

3,4-Dihydronaphth(2,1-b)(1,4)oxazepin-2(1H)-one (**6**)

β-(1-Amino naphthoxy)propionic acid (4.6 g) on heating *in vacuo* (5 ml) at 150° for 3 h gave 2 g (48%) of 3,4-dihydronaphth(2,1-*b*)(1,4)oxazepin-2(1*H*)-one, m.p. 156°; $\nu_{C=O}$ (KBr) 1675 cm^{-1}. This was identical in every respect with the Schmidt rearrangement product (mixture melting point, 156°; t.l.c., same R_f value, infrared spectra were superimposable).

Acknowledgment

We thank Dr. G. S. Sidhu for his interest in this work and for valuable discussions.

1. P. A. S. Smith. *In* Molecular rearrangements. Part I. *Edited by* P. de Mayo. Interscience Publishers, Inc., New York. 1963. p. 512.
2. P. A. S. Smith and E. P. Antoniades. Tetrahedron, **9**, 210 (1960).
3. P. T. Lansbury and N. R. Mancuso. Tetrahedron Letters, **29**, 2445 (1965).
4. G. S. Sidhu, G. Thyagarajan, and U. T. Bhalerao. J. Chem. Soc. C, 969 (1966).
5. I. M. Lockhart and D. Evans. J. Chem. Soc. 4806 (1965).
6. G. Dimaio and V. Permutti. Tetrahedron, **22**, 2059 (1966).
7. U. T. Bhalerao and G. Thyagarajan. To be published.
8. D. Chakravarti and J. Dutta. J. Indian Chem. Soc. **16**, 639 (1939).
9. G. S. Sidhu, G. Thyagarajan, and U. T. Bhalerao. Chem. and Ind. London, **9**, 1301 (1966).

Can. J. Chem. Downloaded from www.nrcresearchpress.com by 210.87.254.5 on 09/05/12
For personal use only.

Can. J. Chem. Downloaded from www.nrcresearchpress.com by 210.87.254.105 on 09/05/12
For personal use only.

Synthesis of 6-deoxy-3-*C*-methyl-2-*O*-methyl-D-allose

G. B. HOWARTH, W. A. SZAREK, AND J. K. N. JONES
Department of Chemistry, Queen's University, Kingston, Ontario

Received May 28, 1968

The preparation of 6-deoxy-3-*C*-methyl-2-*O*-methyl-D-allose is described. The compound was compared with L-vinelose, a new branched-chain sugar with the same constitution recently isolated, bound to cytidine 5′-pyrophosphate, from *Azotobacter vinelandii* strain O; the two sugars were shown to differ in configuration.

Canadian Journal of Chemistry, 46, 3375 (1968)

Introduction

Recently a new branched-chain sugar has been reported (1) to occur in a sugar nucleotide isolated from *Azotobacter vinelandii* strain O. This derivative, which has been shown to be cytidine 5′-(6-deoxy-3-*C*-methyl-2-*O*-methyl-L-aldohexopyranosyl dihydrogen pyrophosphate) (**1**), is the first sugar nucleotide isolated from living cells in which the sugar moiety is a branched-chain sugar. The trivial name vinelose has been suggested for this sugar.

It has been shown (2) that, in the biosynthesis of L-mycarose (2,6-dideoxy-3-*C*-methyl-L-*ribo*-hexose), L-cladinose(2,6-dideoxy-3-*C*-methyl-3-*O*-methyl-L-*ribo*-hexose), and L-noviose (6-deoxy-5-*C*-methyl-4-*O*-methyl-L-*lyxo*-hexose),D-glucose is utilized without intermediate breakdown and that the methyl branch is introduced into an unbranched hexose chain from methionine. Moreover, the *O*-methyl group of cladinose and noviose is supplied by methionine. The isolation of **1** from a natural source suggests that nucleotide-bound sugars probably are the actual intermediates which undergo the *C*- and *O*-methylation reactions (1). In continuation of our syntheses of branched-chain sugars we have now prepared 6-deoxy-3-*C*-methyl-2-*O*-methyl-D-allose (**15**)and compared it with an authentic sample of vinelose.[1] The two compounds are clearly distinguishable by gas–liquid chromatography of their 1,4-di-*O*-acetyl derivatives.

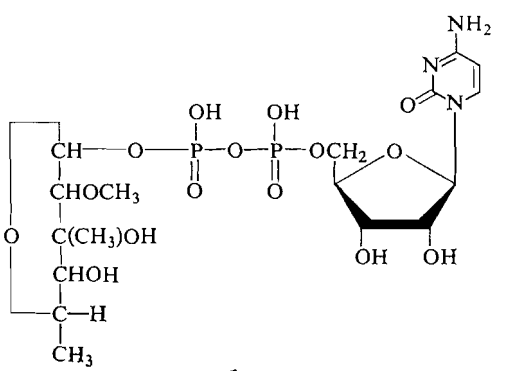

1

Results and Discussion

The preparation of methyl 4,6-*O*-benzylidene-3-*C*-methyl-2-*O*-*p*-tolylsulfonyl-α-D-allopyranoside (**4**) was readily achieved by the addition of methylmagnesium iodide to methyl 4,6-*O*-benzylidene-2-*O*-*p*-tolylsulfonyl-α-D-*ribo*-hexopyranosid-3-ulose (**3**). A small amount of methyl 4,6-*O*-benzylidene-3-*C*-methyl-α-D-allopyranoside (**5**) was formed also in the Grignard reaction. Compound **3** was obtained in high yield by oxidation of methyl 4,6-*O*-benzylidene-2-*O*-*p*-tolylsulfonyl-α-D-glucopyranoside (**2**) (3) with either the Pfitzner–Moffatt reagent (4) or ruthenium tetroxide (5). The addition product **4** was converted into the key intermediate, methyl 3-*C*-methyl-2-*O*-methyl-α-D-allopyranoside (**11**), by two routes. Treatment of **4** with sodium methoxide in dimethyl sulfoxide (6) gave in low yield the 2-*O*-methyl derivative **10**, amongst other products.[2] Catalytic de-*O*-benzylidenation of **10** then gave compound **11**. A higher overall yield of **11** was obtained by an alternative synthesis. Treatment of **4** with benzyl bromide and sodium hydroxide in tetrahydrofuran afforded methyl 3-*O*-benzyl-4,6-*O*-benzylidene-3-*C*-methyl-2-*O*-*p*-tolylsulfonyl-α-D-allopyranoside (**7**). This derivative was heated with sodium methoxide (7) to give methyl 3-*O*-benzyl-4,6-*O*-benzylidene-3-*C*-methyl-α-D-allopyranoside (**8**). Methylation of **8** with dimethyl sulfate and sodium hydroxide in tetrahydrofuran gave the crystalline 2-*O*-methyl ether **9**. Hydrogenation of compound **9** over palladium

[1]We thank Professor S. Suzuki for a gift of vinelose.

[2]A discussion of this reaction will be reported separately.

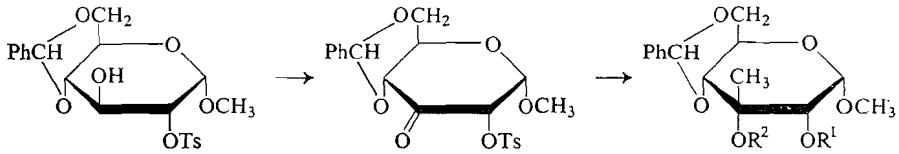

2 **3**

4 R^1 = Ts, R^2 = H
5 R^1 = R^2 = H
6 R^1 = Ts, R^2 = Ac
7 R^1 = Ts, R^2 = $PhCH_2$
8 R^1 = H, R^2 = $PhCH_2$
9 R^1 = CH_3, R^2 = $PhCH_2$
10 R^1 = CH_3, R^2 = H

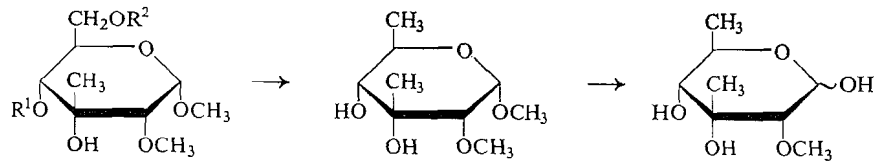

11 R^1 = R^2 = H
12 R^1 = H, R^2 = Ts
13 R^1 = R^2 = Ts

14 **15**

on carbon removed the benzyl and benzylidene groups to produce **11**.

Attempts to open the benzylidene ring in compound **9** by treatment with *N*-bromosuccinimide in boiling carbon tetrachloride to obtain the corresponding 6-bromo-4-benzoate were unsuccessful. This reaction was reported originally by Hanessian (8) and employed recently by us (5) in the synthesis of D-arcanose (2,6-dideoxy-3-*C*-methyl-3-*O*-methyl-D-*xylo*-hexose). Although **9** reacted rapidly with *N*-bromosuccinimide, several, as yet unidentified, products were formed, presumably due to the benzyl ether group.

Treatment of compound **11** with 1.1 moles of *p*-toluenesulfonyl chloride gave predominantly the 6-*O*-*p*-tolylsulfonyl derivative **12** and a small amount of the 4,6-di-*O*-*p*-tolylsulfonyl derivative **13**. Desulfonyloxylation of **12** with lithium aluminium hydride in tetrahydrofuran afforded methyl 6-deoxy-3-*C*-methyl-2-*O*-methyl-α-D-allopyranoside (**14**), which was converted to the free sugar (**15**) by acid-catalyzed hydrolysis. The nuclear magnetic resonance (n.m.r.) spectrum of **15** in deuterium oxide showed the presence of α and β anomers in the ratio 1:3, respectively. In chloroform-*d* an approximately 1:1 mixture was present. Gas–liquid chromatographic analysis of acetylation mixtures of **15** and authentic L-vinelose showed a major and a minor peak in each case (see Table I). In a preparative acetylation experiment, the compound giving rise to the major peak with **15** was isolated in crystalline form and assigned the 1,4-di-*O*-acetyl-6-deoxy-3-*C*-methyl-2-*O*-methyl-β-D-allopyranose structure on the basis of infrared and n.m.r. data. The data in Table I establish that vinelose does not possess the *allo* configuration.

TABLE I

Retention times of sugar components in acetylation mixture*

Sugar	Retention time: Major peak	Retention time: Minor peak
L-Vinelose	1.20	0.94
6-Deoxy-3-*C*-methyl-2-*O*-methyl-D-allose (**15**)	1.63	1.18

*See Experimental section for details. Retention times given here are relative to erythritol tetraacetate (1.00).

We (5, 9) have shown previously that addition of methylmagnesium iodide to methyl 4,6-*O*-benzylidene-2-deoxy-α-D-hexopyranosid-3-uloses is highly stereoselective giving predominantly in each case the axially-oriented tertiary alcohol. In these compounds attack by the Grignard reagent from the side resulting in the formation of the axial alcohol is sterically more favorable than attack from the side resulting in the formation

Can. J. Chem. Downloaded from www.nrcresearchpress.com by 210.87.254.105 on 09/05/12
For personal use only.

Can. J. Chem. Downloaded from www.nrcresearchpress.com by 210.87.254.105 on 09/05/12
For personal use only.

of the equatorial alcohol. Although it is reasonable to expect the same considerations to obtain in compound **3**, we have assigned the configuration at the branching point by other methods. Lichtenthaler and Emig (10) have shown recently, from an n.m.r. study of *C*-methyl branched cyclanol acetates, that the configuration at the branching point can be deduced from the chemical shift of the *C*-methyl acetoxy group. The tertiary hydroxyl group in compound **4** failed to acetylate with acetic anhydride/pyridine, but acid-catalyzed acetylation (acetic anhydride/-*p*-toluenesulfonic acid) rapidly gave crystalline methyl 3-*O*-acetyl-4,6-*O*-benzylidene-3-*C*-methyl-2-*O*-*p*-tolylsulfonyl-α-D-allopyranoside (**6**) in high yield. The n.m.r. spectrum of **6** showed an acetyl signal at τ 8.03, a value in the range (τ 7.93–8.04) reported (10) for tertiary acetoxy groups possessing the axial orientation. With **4** in the C1 (D) conformation, these n.m.r. data support the assigned *allo* configuration.

Experimental

Solutions were concentrated below 50° under reduced pressure. Melting points were determined on a Fisher–Johns melting point apparatus and are uncorrected. Optical rotations were measured with a Bendix ETL-NPL Automatic Polarimeter, type 143A, at 20 ± 2°. Infrared spectra were measured on a Beckman-IR5A spectrophotometer. Nuclear magnetic resonance (n.m.r.) spectra were determined at 60 MHz in chloroform-*d* and tetramethylsilane as internal standard. Thin-layer chromatography (t.l.c.) was performed, unless otherwise stated, with Silica Gel G as the absorbent, and 2:3 ethyl acetate – petroleum ether (b.p. 60–80°) as the developing solvent. The developed plates were air dried, sprayed with 5% ethanolic sulfuric acid, and heated at about 150°. Paper chromatography was carried out by the descending method on Whatman No. 1 filter paper in the following solvent systems: 6:4:3 (v/v) butan-1-ol – pyridine – water (*a*); butan-1-ol saturated with water (*b*). The sugars were detected by spraying the chromatograms with a 1:1 mixture of vanillin (1% in ethanol) and perchloric acid (3% in water) and heating (11). Gas–liquid chromatography (g.l.c.) was performed on an F and M, model 402, high-efficiency gas chromatograph employing a flame-ionization detector. The liquid phase was supplied by Chromatographic Specialities, Brockville, Ontario, and was supported on acid-washed Chromosorb W (100–120 mesh). The conditions were as follows: 5% (w/w) LAC-4R-886 polyester wax (purged for 5 days at 200°), operated at 190° with a flow-rate setting of 3.0 at 30 p.s.i. of helium (50 ml/min).

Methyl 4,6-O-Benzylidene-2-O-p-tolylsulfonyl-α-D-ribo-hexopyranosid-3-ulose (3)

This compound was prepared from methyl 4,6-*O*-benzylidene-2-*O*-*p*-tolylsulfonyl-α-D-glucopyranoside (**2**) (7.6 g) by the method of Baker and Buss (4). The crystalline product was recrystallized from ethanol to give white needles, (6 g, 80%), m.p. 163–164°, $[\alpha]_D$ +45° (*c*, 0.8 in chloroform). Baker and Buss report m.p. 165–167° and $[\alpha]_D^{25}$ +44.9 ± 0.9° (*N*,*N*-dimethyl formamide).

Methyl 4,6-O-Benzylidene-3-C-methyl-2-O-p-tolylsulfonyl-α-D-allopyranoside (4)

A solution of **3** (4.4 g) in dry benzene (250 ml) was added dropwise to a stirred solution of methylmagnesium iodide (prepared from magnesium (5 g) and methyl iodide (17 ml)) in ether (250 ml) at 0°. After standing at room temperature overnight, the reaction mixture was poured into ammonium chloride solution, and the aqueous layer was extracted with chloroform. Concentration of the dried extracts yielded a syrup which crystallized from chloroform–petroleum ether (b.p. 60–80°). Recrystallization from this solvent mixture gave **4** as white plates (3.6 g, 80%), m.p. 138–139°, $[\alpha]_D$ +45° (*c*, 2.0 in chloroform); λ_{max} (KBr) 2.84 (OH), 6.24, 7.48, 8.49 (sulfonate), 13.2, 14.3 μm (Ph); n.m.r. data: τ 2.0–2.8 (9-proton multiplet, aromatic H's), τ 4.48 (1-proton singlet, benzylidene-methine H), τ 5.2 (1-proton doublet, $J_{1,2}$ = 4Hz, H-1), τ 6.67 (3-proton singlet, OMe), τ 7.58 (3-proton singlet, aromatic Me), τ 8.8 (3-proton singlet, C-3 Me).

Anal. Calcd. for $C_{22}H_{26}O_8S$: C, 58.7; H, 5.8; S, 7.1. Found: C, 58.7; H, 5.8; S, 7.3.

Investigation of the mother liquors by t.l.c. showed the presence of **4** and a slower moving component. Fractionation on silica gel with ethyl acetate as eluent afforded the latter compound, which crystallized from chloroform–petroleum ether (b.p. 60–80°) as needles, m.p. 210–212°, $[\alpha]_D$ +95° (*c*, 0.3 in chloroform). The compound was identified as methyl 4,6-*O*-benzylidene-3-*C*-methyl-α-D-allopyranoside (**5**); λ_{max} (Nujol) 2.9, 2.98 (OH), 13.2, 14.2 μm (Ph), no absorption attributable to sulfonate; n.m.r. data: τ 2.5–2.8 (5-proton multiplet, Ph), τ 4.42 (1-proton singlet, benzylidene-methine H), τ 5.24 (1-proton doublet, $J_{1,2}$ = 4Hz, H-1), τ 6.5 (3-proton singlet, OMe), τ 8.6 (3-proton singlet, C-3 Me).

Anal. Calcd. for $C_{15}H_{20}O_6$: C, 60.8; H, 6.8. Found: C, 60.7; H, 6.7.

Methyl 3-O-Acetyl-4,6-O-benzylidene-3-C-methyl-2-O-p-tolylsulfonyl-α-D-allopyranoside (6)

A mixture of **4** (50 mg), *p*-toluenesulfonic acid (22 mg), and acetic anhydride (1.5 ml) was stirred at ambient temperature for 1h, and then poured into sodium bicarbonate solution. After effervescence had ceased, the mixture was extracted with chloroform (4 × 10 ml) and the combined extracts were washed with sodium bicarbonate solution and water. Concentration of the dried extracts afforded a clear syrup which crystallized spontaneously. Recrystallization from ether – petroleum ether (b.p. 60–80°) gave the acetate **6** as prisms (40 mg, 73%), m.p. 133–134°; λ_{max} (KBr) 5.68 (OAc), 6.24, 7.3, 8.45 μm (sulfonate), no absorption attributable to OH; n.m.r. data: τ 2.0–2.8 (9-proton multiplet, aromatic H's), τ 4.51 (1-proton singlet, benzylidene-methine H), τ 5.27 (1-proton doublet, $J_{1,2}$ = 4Hz, H-1), τ 6.7 (3-proton singlet, OMe), τ 7.6 (3-proton singlet, aromatic Me), τ 03 (3-8. proton singlet, OAc), τ 8.34 (3-proton singlet, C-3 Me).

Can. J. Chem. Downloaded from www.nrcresearchpress.com by 210.87.254.105 on 09/05/12
For personal use only.

Anal. Calcd. for $C_{24}H_{28}O_9S$: C, 53.6; H, 5.7. Found: C, 53.5; H, 5.6.

Methyl 3-O-Benzyl-4,6-O-benzylidene-3-C-methyl-2-O-p-tolylsulfonyl-α-D-allopyranoside (7)

A mixture of **4** (2.6 g), benzyl bromide (6 ml), and sodium hydroxide (12.5 g) was stirred in tetrahydrofuran at room temperature for 24 h. Thin-layer chromatography showed the presence of a compound with R_f 0.64 and the absence of starting material, R_f 0.48. The reaction mixture was freed from solid material by centrifugation and the clear liquid was concentrated to a mobile oil, which was purified by column chromatography on silica gel. Elution with benzene and then 2:3 ethyl acetate – petroleum ether (b.p. 60–80°) gave the 3-*O*-benzyl ether **7** as a syrup (3.04 g, 97%) which crystallized on standing, m.p. 49–50°, $[\alpha]_D$ +54° (*c*, 0.6 in methanol); λ_{max} (Film) 6.24, 7.3, 8.45 μm (sulfonate), no absorption attributable to OH; n.m.r. data: τ 2.1–3.0 (14-proton multiplet, aromatic H's), τ 4.65 (1-proton singlet, benzylidene-methine H), τ 6.8 (3-proton singlet, OMe), τ 7.64 (3-proton singlet, aromatic Me), τ 8.65 (3-proton singlet, C-3 Me). The region for the signals of the aromatic and benzyl–methylene protons was complex, but significantly no 2-proton singlet was evident.

Anal. Calcd. for $C_{29}H_{32}O_8S$: C, 64.4; H, 5.9; S, 5.9. Found: C, 64.8; H, 5.9; S, 5.8.

Methyl 3-O-Benzyl-4,6-O-benzylidene-3-C-methyl-α-D-allopyranoside (8)

A solution of the sulfonate **7** (3.1 g) in methanol (100 ml) containing sodium (2.6 g) was heated at reflux temperature for 3 h. Thin-layer chromatography showed that the starting material had all reacted. The product was isolated in the usual manner as a syrup (2.20 g, 99%), $[\alpha]_D$ +119° (*c*, 1.2 in tetrahydrofuran); R_f 0.52 (t.l.c.); λ_{max} (Film) 2.85 μm (OH), no absorption attributable to sulfonate; n.m.r. data: τ 2.5–2.8 (10-proton multiplet, aromatic H's), τ 4.56 (1-proton singlet, benzylidene-methine H), τ 6.55 (3-proton singlet, OMe), τ 8.42 (3-proton singlet, C-3 Me).

Anal. Calcd. for $C_{22}H_{26}O_6$: C, 68.4; H, 6.8. Found: C, 67.8; H, 6.8.

Methyl 3-O-Benzyl-4,6-O-benzylidene-3-C-methyl-2-O-methyl-α-D-allopyranoside (9)

Dimethyl sulfate (22 ml) was added dropwise with stirring to a slurry of **8** (2.2 g) and finely powdered sodium hydroxide (13 g) in tetrahydrofuran (50 ml). After the mixture was stirred at ambient temperature for 12 h, aqueous ammonia was added and the aqueous layer was extracted with chloroform. Concentration of the dried extracts yielded a crystalline product which was recrystallized from petroleum ether (b.p. 60–80°) to give white needles (1.835 g, 81%), m.p. 113–114°, $[\alpha]_D$ +108° (*c*, 0.7 in chloroform); R_f 0.65 (t.l.c.); n.m.r. data: τ 2.3–3.0 (10-proton multiplet, aromatic H's), τ 4.58 (1-proton singlet, benzylidene-methine H), τ 5.16 (3-proton broad signal, H-1 and benzyl-methylene), τ 6.54, 6.58 (3-proton singlets, C-1 OMe and C-2 OMe), τ 8.50 (3-proton singlet, C-3 Me).

Anal. Calcd. for $C_{23}H_{28}O_6$: C, 69.0; H, 7.0. Found: C, 69.3; H, 7.2.

Methyl 3-C-Methyl-2-O-methyl-α-D-allopyranoside (11)

A solution of **9** (1.27 g) in ethanol (25 ml) was hydrogenated over 10% palladium on carbon at atmospheric pressure for 12 h. Thin-layer chromatography showed complete conversion to a compound with R_f 0.07 (ether). The catalyst was removed by filtration, and the solution concentrated to give the triol **11** as a clear viscous syrup (710 mg, 97%), $[\alpha]_D$ +107° (*c*, 0.3 in chloroform); λ_{max} (Film) 2.9 (broad) μm (OH), no aromatic absorption; n.m.r. data: τ 5.02 (1-proton doublet, $J_{1,2}$ = 3.5 Hz, H-1), τ 6.48, 6.52 (3-proton singlets, C-1 OMe and C-2 OMe), τ 8.67 (3-proton singlet, C-3 Me).

Anal. Calcd. for $C_9H_{18}O_6$: C, 48.6; H, 8.1. Found: C, 48.2; H, 7.8.

Mono- and Di-O-p-tolylsulfonyl Derivatives of Methyl 3-C-methyl-2-O-methyl-α-D-allopyranoside

Syrupy methyl 3-*C*-methyl-2-*O*-methyl-α-D-allopyranoside (710 mg) in dry pyridine (10 ml) was treated with *p*-toluenesulfonyl chloride (670 mg, 1.1 moles) in pyridine (3 ml) below 0°. After the mixture was left at 5° for 24 h, t.l.c. showed the presence of the mono-*O*-*p*-tolylsulfonyl derivative (**12**), R_f 0.52 (ethyl acetate) and small amounts of the di-*O*-*p*-tolylsulfonyl derivative (**13**), R_f 0.73, and unchanged starting material. The solution was poured into water (50 ml) and the products were extracted with chloroform. Concentration of the extracts after they had been washed successively with sulfuric acid (3*N*), sodium bicarbonate solution, and water yielded a viscous syrup, which was chromatographed on silica gel, with 4:1 ethyl acetate – petroleum ether (b.p. 60–80°) as eluent. The 4,6-di-*O*-*p*-tolylsulfonyl derivative (**13**) was obtained as fine needles after recrystallization from chloroform – petroleum ether (240 mg, 14%), m.p. 129–130; λ_{max} (Film) 2.85 (OH), 6.25, 7.4, 8.45 μm (sulfonate); n.m.r. data: τ 2.0–2.8 (8-proton multiplet, aromatic H's), τ 5.1 (2-proton doublet, $J_{1,2}$ = 4 Hz, H-1), τ 6.52, 6.60 (3-proton singlets, C-1 OMe and C-2 OMe), τ 7.55 (6-proton singlet, aromatic Me's), τ 8.78 (3-proton singlet, C-3 Me).

Anal. Calcd. for $C_{23}H_{30}O_{10}S_2$: C, 52.0; H, 6.0; S, 12.0. Found: C, 51.9; H, 5.8; S, 11.7.

The mono-*O*-*p*-tolylsulfonyl derivative (**12**), was isolated as a syrup which crystallized as large prisms from chloroform – petroleum ether (870 mg, 72%), m.p. 116–118°, $[\alpha]_D$ +85° (*c*, 0.3 in chloroform); λ_{max} (KBr) 2.9 (OH), 6.25, 7.4, 8.4 μm (sulfonate); n.m.r. data: τ 2.0–2.8 (4-proton multiplet, aromatic H's), τ 5.12 (1-proton doublet, $J_{1,2}$ = 4Hz, H-1), τ 6.53, 6.61 (3-proton singlets, C-1 OMe, and C-2 OMe), τ 7.58 (3-proton singlet, aromatic Me), τ 8.73 (3-proton singlet, C-3 Me).

Anal. Calcd. for $C_{16}H_{24}O_8S$: C, 51.0; H, 6.4; S, 8.5. Found: C, 50.4; H, 6.3; S, 8.4.

Methyl 6-Deoxy-3-C-methyl-2-O-methyl-α-D-allopyranoside (14)

The 6-*O*-*p*-tolylsulfonyl derivative **12** (870 mg) was heated under reflux with lithium aluminium hydride (1 g) in tetrahydrofuran (25 ml) for 2 h. The reduced product was isolated in the usual manner as a colorless mobile liquid (445 mg, 94%), $[\alpha]_D$ +118° (*c*, 0.6 in chloroform); R_f 0.35 (ethyl acetate); n.m.r. data: τ 5.13 (1-proton doublet, $J_{1,2}$ = 4Hz, H-1), τ 6.5, 6.55 (3-proton singlets, C-1 OMe, and C-2 OMe), τ 6.93 (1-proton doublet,

$J_{2,1}$ = 4Hz, H-2), τ 8.7 (3-proton doublet, J = 6Hz, C-5 Me), τ 8.67 (3-proton singlet, C-3 Me).

*6-Deoxy-3-C-methyl-2-O-methyl-*D*-allose (15)*

A solution of the glycoside **14** (80 mg) in 2 *N* hydrochloric acid (4 ml) was heated at 90° for 2 h. The cooled solution was neutralized with Duolite A-4 (OH^-) ion-exchange resin and concentrated to a gummy residue which was extracted with hot chloroform. The extracts were concentrated to give the free sugar **15** as a clear viscous syrup (55 mg, 75%), $[\alpha]_{546}$ +5° (5 min), −5° (final) (*c*, 1.2 in water); n.m.r. data: τ 4.56 (doublet, $J_{1,2}$ = 4Hz, H-1 of α anomer), τ 4.97 (doublet, $J_{1,2}$ = 8Hz, H-1 of β anomer), τ 6.21 (singlet, C-2 OMe of β anomer), τ 6.35 (singlet, C-2 OMe of α anomer), τ 8.5–8.75 (C-3 Me and C-5 Me). For L-vinelose $[\alpha]_{546}$ +12° (*c*, 1.1 in water) has been reported (1). Paper chromatographic analysis of the syrupy product revealed only one component with R_{Rh} 1.68 in solvent *a* and 2.49 in solvent *b* (pink spot which changed to grayish blue within 24 h with vanillin–perchloric acid spray). Authentic L-vinelose had R_{Rh} 1.73 in solvent *a* and 2.50 in solvent *b*, and showed the same color change.

Gas–liquid Chromatographic Comparison of L*-Vinelose and 6-Deoxy-3-C-methyl-2-O-methyl-*D*-allose*

Acetylation of the two sugars was carried out by heating a small sample of each (< 1 mg) with 2 drops of 60% acetic anhydride in pyridine at 90° for 15 min. The solutions were examined by g.l.c. and the results are shown in Table I.

*1,4-Di-O-acetyl-6-deoxy-3-C-methyl-2-O-methyl-*β*-*D*-allopyranose*

A solution of **15** (50 mg) in 2:3 acetic anhydride and pyridine (2 ml) was heated at 90° for 1 h. The reaction mixture was poured into water (30 ml) and extracted with chloroform. Concentration of the extracts after they had been washed with sulfuric acid, sodium bicarbonate solution, and water gave a syrup which crystallized after several days. Recrystallization from chloroform–petroleum ether (b.p. 60–80°) gave prisms (40 mg, 55%), m.p. 108–110°; λ_{max} (KBr) 2.85 (OH), 5.75 μm (OAc); n.m.r. data: τ 4.13 (1-proton doublet, $J_{1,2}$ 8 Hz, H-1), τ 5.37 (1-proton doublet, $J_{4,5}$ = 9.5 Hz, H-4), τ 5.9 (1-proton multiplet, H-5), τ 6.4 (3-proton singlet, C-2 OMe), τ 6.95 (1-proton doublet, $J_{2,1}$ = 8 Hz, H-2), τ 7.83 (6-proton singlet, C-1 and C-4 OAc's), τ 8.33 (3-proton doublet, J = 9 Hz, C-5 Me), τ 8.82 (3-proton singlet, C-3 Me).

Anal. Calcd. for $C_{12}H_{20}O_7$: C, 52.2; H, 7.20. Found: C, 52.0; H, 7.1.

Acknowledgments

The authors thank the National Research Council of Canada for financial support of this research. Some of the n.m.r. spectra were determined at the Royal Military College, Kingston, Ontario, and we are indebted to Dr. D. G. M. Diaper for the use of the spectrometer.

1. S. Okuda, N. Suzuki, and S. Suzuki. J. Biol. Chem. **242**, 958 (1967).
2. H. Grisebach. Biosynthetic patterns in microorganisms and higher plants. John Wiley and Sons, Inc., New York. 1967.
3. G. J. Robertson and C. F. Griffith. J. Chem. Soc. 1193 (1935).
4. B. R. Baker and D. H. Buss. J. Org. Chem. **30**, 2304 (1965).
5. G. B. Howarth, W. A. Szarek, and J. K. N. Jones. Chem. Commun. 62 (1968); Carbohydrate Res. **7**, 284 (1968).
6. E. D. M. Eades, D. H. Ball, and L. Long, Jr. J. Org. Chem. **31**, 1159 (1966).
7. R. S. Tipson. Advan. Carbohydrate Chem. **8**, 107 (1953).
8. S. Hanessian. Carbohydrate Res. **2**, 86 (1966); Advan. Carbohydrate Chem. **21**, 143 (1966).
9. G. B. Howarth and J. K. N. Jones. Can. J. Chem. **45**, 2253 (1967).
10. F. W. Lichtenthaler and P. Emig. Tetrahedron Letters, **7**, 577 (1967).
11. A. P. Maclennan, H. M. Randall, and D. W. Smith. Anal. Chem. **31**, 2020 (1959).

Can. J. Chem. Downloaded from www.nrcresearchpress.com by 210.87.254.105 on 09/05/12
For personal use only.

Can. J. Chem. Downloaded from www.nrcresearchpress.com by 210.87.254.105 on 09/05/12
For personal use only.

Photochemistry of oximes. II. On the photo-induced formation of cycloalkanones and alkanoic acid amides from cycloalkanone oximes[1]

G. JUST AND L. S. NG[2]
Department of Chemistry, McGill University, Montreal, Quebec

Received May 29, 1968

Cycloalkanone oximes were shown to give the corresponding alkanoic acid amides when irradiated in *iso*-propanol. α-Alkylated cyclohexanone oximes gave products corresponding to preferential cleavage on the side of the more substituted carbon atom. *iso*-Propanol was shown to transfer two hydrogen atoms specifically to the excited oxime molecule, acetone being formed in the process. In 1% aqueous solution, irradiation of oximes gave the corresponding ketones, ammonia, and oxygen.

Canadian Journal of Chemistry, 46, 3381 (1968)

Introduction

Recently, we reported that irradiation of a 0.1% methanolic solution of cyclohexanone oxime gave caprolactam. The analogous reactions, using *iso*-propanol as solvent, gave (the) caproamide (1). In both reactions, a minor amount of cyclohexanone was formed.

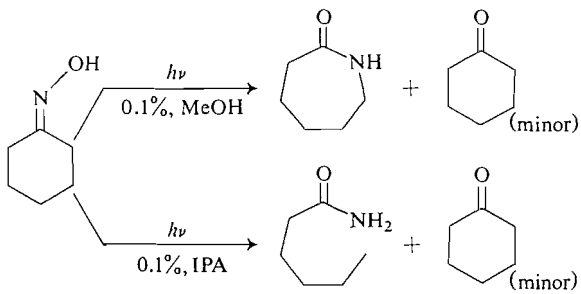

In this paper, we should like to report in detail on the latter reaction, and describe a system in which cyclohexanone formation is the major pathway. The reactions will be discussed in terms of an oxazirane intermediate, for which there is ample analogy in related systems (2–9). There is, however, at the present time no proof for such an intermediate.

Results and Discussion

The preparation of starting oximes and of amides for identification purposes is described in the Experimental section. The amides obtained were all isolated, and their spectral properties were compared with those of authentic samples.

[1]For a preliminary report, see ref. 1.
[2]Holder of a NRCC Studentship, 1967–1968. Abstracted from part of the Ph.D. Thesis of L. S. Ng, McGill University, 1968.

(a) Irradiation of Cyclic Oximes in iso-Propanol

The results of the irradiation of cyclic oximes in *iso*-propanol are summarized in Tables I and II. The main products isolated in this reaction are the corresponding amides, ketones, lactams, and unreacted starting material as shown below.

In the case of four- and five-membered ring ketoximes, the yields of the corresponding amides were improved by lengthening the time of irradiation. The results are shown in Table III.

(b) Photolysis of Unsymmetrical Cyclic Ketoximes

We next turn our attention to α-methylated

TABLE I

Irradiation of 0.1% 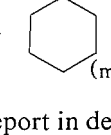 /2 h/*iso*-propanol/He[3]

n	Lactam (%)	Amide (%)	Oxime (%)	Ketone (%)
1	<1	3	87	<1
2	<1	15	75	1
3	<1	44	20	1
4	<1	50	5	6
5	<1	45	2	2
9	<1	42	30	4

[3]Yields of lactams, amides, oximes, and ketones were determined by quantitative gas–liquid chromatography, using standards prepared synthetically. The low total recoveries in certain instances, in part, are due to the photolability of the parent ketone formed. The yields indicated are average of 2 or 3 runs, and are reproducible within approximately ±3%. Results incorporated in one table were performed under conditions which were kept constant as nearly as possible. Direct comparisons of results recorded in different tables should be done with caution, especially since the intensity of the light source was not constant and rather large differences were noticed in some instances where other light sources were used.

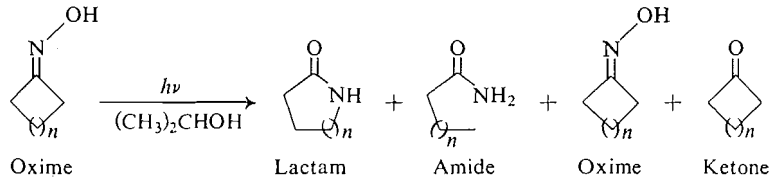

TABLE II

Irradiation of 1% 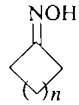 /4 h/*iso*-propanol/He[3]

n	Lactam (%)	Amide (%)	Oxime (%)	Ketone (%)
1	<1	<1	97	3
2	<1	6	94	<1
3	<1	24	75	2
4	<1	31	65	3
5	<1	28	50	6
9	1	30	66	4

unsymmetrical cyclic oximes in order to see if the formation of one isomer would be favored over the other. The oximes investigated were 2-methyl (**1**), 2,2-dimethyl (**4**), 2,2,6-trimethyl (**7**) cyclohexanone oximes, and menthone oxime (**10**). The expected products and the ratios obtained are those shown in Scheme 1. As can be seen, the cleavage occurred mainly on the side of the more substituted carbon atom.

(c) Photolysis of Oximes, Asymmetric at the α-Carbon

In the photolysis of aldehydes and ketones, the fission α to the carbonyl group prior to decarbonylation is reversible (10). Thus, 17-ketosteroids undergo facile photoepimerization. It was of interest to see if an analogous Norrish type I cleavage occurred in oximes. The photolysis of oximes having asymmetric α-carbon atoms was therefore studied, attention being focussed on "unreacted" oxime.

TABLE III

Irradiation of 0.1% 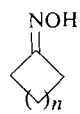 in *iso*-propanol/4h/He[3]

n	Lactam (%)	Amide (%)	Oxime (%)	Ketone (%)
1	<1	14	40	<1
2	<1	33	21	<1

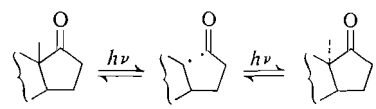

(i) 2,6-Dimethylcyclohexanone Oxime

2,6-Dimethylcyclohexanone oxime was prepared by treatment of the corresponding commercially available ketone (*cis* and *trans* mixture) with hydroxylamine in methanol. The resulting oxime was a mixture of two components. These two oximes must be *trans*- and *cis*-oximes **13** and **14**, and not *syn*- and *anti*-isomers.

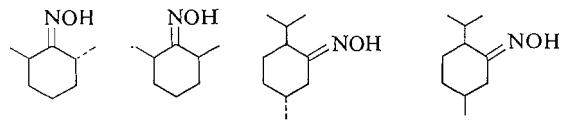

13 **14** **15** **16**

Photolyses of either **13** or **14** were conducted in both methanol and *iso*-propanol. Gas–liquid chromatographic (g.l.c.) detection of the starting material, recovered from runs that were allowed to go only to partial completion, showed no corresponding isomeric oxime.

*(ii) Menthone (**15**) and iso-Menthone Oximes (**16**)*

Both oximes were irradiated separately in *iso*-propanol for 1 h under a nitrogen atmosphere. The starting oximes recovered in each case were found by g.l.c. to contain no corresponding oxime resulting from epimerization of the α-carbon.

(d) Source of Hydrogen and Specificity of Hydrogen Abstraction in the Formation of Amides

The molecular formula of the cyclic oximes differs from that of the photoproducts obtained by reductive cleavage, by two hydrogen atoms.

$$C_nH_{2n-1}NO + 2H \rightarrow C_nH_{2n+1}NO$$

Can. J. Chem. Downloaded from www.nrcresearchpress.com by 210.87.254.105 on 09/05/12
For personal use only.

Irradiation of a 0.1% solution of oximes in *iso*-propanol in a helium atmosphere

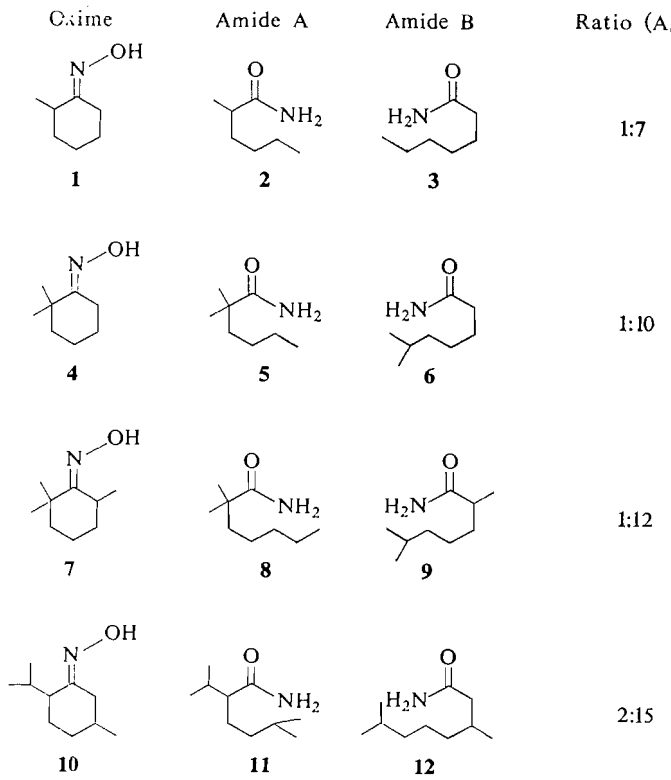

Scheme 1

These two extra hydrogen atoms are derived most probably from the solvent (*iso*-propanol) used. One way of confirming this, was to try to isolate the acetone from the photolysis mixture.

To accomplish this, the photolysis of 1% cyclohexanone oxime in *iso*-propanol[4] was carried out for 44 h. The resulting solvent was distilled with caution. Quantitative g.l.c. determination using a 6 ft Porapak R column showed that a 54% yield of acetone, with respect to the amide, was formed in this photolysis. This acetone was converted to its dinitrophenylhydrazone which was identical in infrared (i.r.) spectrum, m.p., and R_f with an authentic sample.

In order to study the specificity of hydrogen abstraction, a 0.4% solution of *O*-deuteriocyclododecanone oxime was irradiated in *O*-deuterio-*iso*-propanol. After exchange with water, the

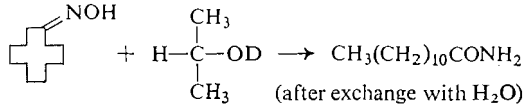

product, dodecanamide, contained less than 5% deuterium, as shown by mass spectrometric analysis. Its i.r. spectrum showed no C—D stretching band. This experiment establishes that hydrogen transfer from *iso*-propanol involves first the hydrogen attached to carbon (11) as indicated below. It is therefore evident that H_a is transferred to the terminal position of dodecanamide.

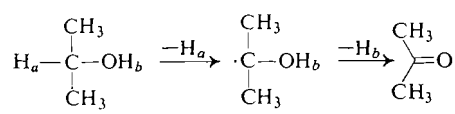

[4]*iso*-Propanol was treated with 2,4-dinitrophenylhydrazine in the presence of a drop of acid, to remove any acetone present, and distilled. Gas–liquid chromatographic analysis of the resulting *iso*-propanol indicated the absence of acetone.

Can. J. Chem. Downloaded from www.nrcresearchpress.com by 210.87.254.105 on 09/05/12
For personal use only.

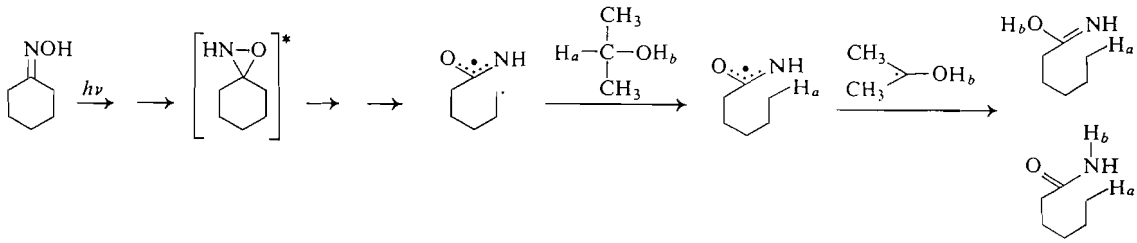

Assuming that the reaction intermediate (triplet?) has biradical character, and is derived from an oxazirane, the following scheme may be postulated.

(e) Irradiation of Cyclic Oximes in Water

Irradiation of a 0.1% aqueous solution of cyclohexanone oxime gave as major product caprolactam. This reaction will be reported elsewhere. When a 1% aqueous solution of cycloalkanone oxime was irradiated, the major product was the cycloalkanone. The results are summarized in Table IV.

TABLE IV

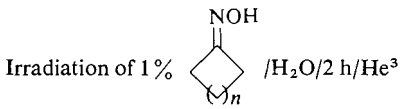

n	Lactam (%)	Amide (%)	Oxime (%)	Ketone (%)
1	3	<1	86	9
2	12	<1	70	21
3	1	<1	48	42
4	1	<1	25	56

The photolysis of a 1% aqueous cyclohexanone oxime solution was not affected by the presence of a small amount of hydrochloric acid.

(f) Fate of the Nitrogen in the Oxime

In order to investigate the fate of the nitrogen atom in the oxime, the photolysis of a 1% aqueous solution of cyclohexanone oxime was investigated in more detail. Irradiation of the initially neutral solution gave a solution with pH 9. A gas which was identified as oxygen was evolved. This gas decolorized a benzene solution of triphenylmethyl immediately and caused the precipitation of brownish-yellow ferric salts from ferrous ammonium sulfate solution. The aqueous alkaline solution was neutralized with *p*-toluenesulfonic acid and then extracted with methylene chloride for 24 h. The aqueous solution gave a salt which was identified as the ammonium salt of *p*-toluenesulfonic acid.

The photolysis of free hydroxylamine under the same condition as that in ketone formation was performed for 3 h as a control. No detectable amounts of ammonia or oxygen were formed.

From the above, it must be concluded that the O—N of the oxime or intermediate oxazirane is broken, when the ketone is formed. A scheme for explaining the reaction is shown below. The reaction intermediate might be a vibrationally excited ground state, or the ground state of the oxazirane. Oxaziranes are known to decompose in hydroxylic solvents (12) to give ketone and ammonia.

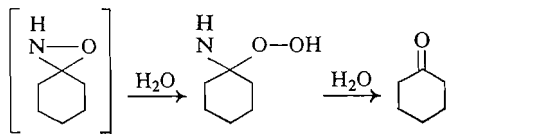

$$+ NH_3 + H_2O_2$$

$$2H_2O_2 + h\nu \rightarrow O_2 + 2H_2O \quad (13)$$

This explanation is also consistent with the fact that addition of water (10%) to the *iso*-propanol solution of cyclohexanone oxime increases the yield of ketone formation from 4% to 23% (14).

Experimental

Spectroquality *iso*-propanol was purchased from Matheson, Coleman, and Bell. All of the irradiation experiments were carried out in a quartz cell in a Rayonet Photochemical Reactor model 1061 using lamps with peak energy at 2537 Å. The melting points were determined on a Gallenkamp melting point apparatus in open capillaries, and are not corrected. The analyses were carried out by Dr. C. Daesslé of Organic Microanalysis, 5757 Decelles Ave., Montreal; Beller, Mikroanalytisches Laboratorium, 34 Gottingen, Theaterstrasse 23, Germany; and Alfred Bernhardt, Mikroanalytisches Laboratorium im Max-Planck-Institut für Kohlenforschung. The infrared (i.r.) spectra were determined on the Perkin–Elmer 337 and 257 grating spectrophotometers using 1 mm sodium chloride cells or 1 mm Amalgam FT cells

Can. J. Chem. Downloaded from www.nrcresearchpress.com by 210.87.254.105 on 09/05/12
For personal use only.

Can. J. Chem. Downloaded from www.nrcresearchpress.com by 210.87.254.105 on 09/05/12
For personal use only.

(IRT-2) from Barnes Engineering Co. Nuclear magnetic resonance (n.m.r.) spectra were recorded on a Varian A-60 instrument at 60 megacycles (tetramethylsilane = 0 p.p.m.). Merck analar grade silica gel was used for thin-layer chromatography (t.l.c.). The mass spectra were taken on a Hitachi Perkin–Elmer RMU60 mass spectrometer by Morgan and Schaffer Corporation, Montreal. The ionization potential was 70 eV and the inlet temperature for indirect introduction of a sample was 250°. Quantitative vapor-phase chromatography (v.p.c.) was made on an F and M model 700 gas chromatograph. Six feet × 6 mm diameter glass tubes were used for both reference and sample columns. Preparative gas–liquid chromatography (g.l.c.) was made on an F and M Prep-Master model 775 gas chromatograph.

Preparation of Oximes

All the oximes were prepared by treatment of the corresponding ketones with hydroxylamine in the usual manner. All ketones except the 2,2-dimethylcyclohexanone were commercially available. 2,2-Dimethylcyclohexanone was synthesized according to Johnson and Posvic (15) starting from 2-methylcyclohexanone. The ketone was converted to the corresponding oxime, m.p. 92–93 °C. The n.m.r. spectrum of this oxime in $CDCl_3$ showed a six-proton singlet at 1.15 p.p.m. and a two-proton triplet at 2.60 p.p.m. A multiplet at 1.55 p.p.m. corresponded to the remaining methylene protons of the oxime. A singlet at 9.82 p.p.m., exchangeable with D_2O was assigned to the hydroxyl proton of the oxime. The i.r. spectrum was consistent with the structure.

Anal. Calcd. for $C_8H_{15}NO$: C, 68.04; H, 10.71; N, 9.92. Found: C, 67.95; H, 10.76; N, 9.86.

Irradiation of Cycloalkanone Oximes in iso-Propanol

A 100 ml of solution containing 0.1% or 1% cycloalkanone oxime in *iso*-propanol was irradiated. The solution was purged with helium for 5 min before subjecting it to irradiation.

After the required time of irradiation, the *iso*-propanol solution was reduced to 5 ml (in the case of the 0.1% solution) or 25 ml (in the case of the 1% solution) by subjecting to fractional distillation through a Vigreux column attached to a distilling head (cat. 9214, ACE glass incorporated).

The determination of the amount of each component was performed on a 6 mm × 6 ft column packed with 5% DC 710 on Chromosorb W. The yields were determined by comparison of the area of integration with the appropriate standards. Retention time of each photoproduct in 6 mm × 6 ft 5% DC 710 on Chromosorb W column is shown in Table V.

Irradiation of Unsymmetrically Substituted Oximes in iso-Propanol and Preparation of Amide Standards for Quantitative Determination

Heptanamide (3) and 2-Methylcaproamide (2)

Five 100 mg samples of oxime **1**, each dissolved in 100 ml of *iso*-propanol were irradiated separately, with stirring, under nitrogen for 2 h. The combined solutions were concentrated to 1 ml by distilling through a 10 cm Vigreux column. The concentrated solution was then separated into its components by preparative g.l.c. at 145° oven temperature. A 6 mm × 8 ft stainless steel column packed with 5% DC 710 on Chromosorb W was used. Compounds **2**, m.p. 68–69° and **3**, m.p. 96° having retention times of 2.5 and 3.6 min were obtained in white crystalline form in yields of 10 and 81 mg respectively. Compound **3** was identical (n.m.r., i.r., mixture m.p.) to the heptanamide prepared synthetically.

TABLE V

Retention times of photoproducts in 6 mm × 6 ft 5% DC 710 on Chromosorb W column

	n	Oven temperature (°C)	Flow rate (ml/min)	Retention time (min)
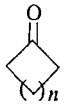	1	65	30	2.10
	2	118	40	1.30
	3	148	10	1.35
	4	148	25	1.20
	5	185	40	0.68
	8	215	40	0.95
	1	120	25	1.50
	2	120	40	1.25
	3	148	35	1.20
	4	190	36	0.95
	5	212	24	1.10
	8	215	40	1.45
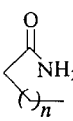	1	135	40	1.35
	2	135	40	2.65
	3	182	36	1.08
	4	190	10	2.20
	5	212	24	1.75
	8	215	40	2.30
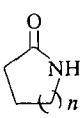	1	135	40	2.00
	2	180	40	1.60
	3	182	35	2.60
	4	190	40	1.55
	5	212	24	2.22
	8	192	40	4.90

Anal. Calcd. for $C_7H_{15}NO$ (**3**): C, 68.07; H, 11.70; N, 10.84. Found: C, 67.78; H, 11.66; N, 11.03.

The n.m.r. spectrum of **2** in CCl_4 showed two multiplets at 2.20 and 1.30 p.p.m. in a ratio of 1:6. These were assigned respectively to proton α to an amido group and three methylene groups with no functional carbon adjacent to it. A doublet at 1.15 p.p.m. with $J = 8$ c.p.s. was assigned to α-methyl group coupled to its adjacent proton. An unsymmetrical triplet at 1.20 p.p.m. ($J = 4$ c.p.s.) was assigned to the terminal methyl group in the carbon chain. A broad band in the 5.3 to 6.2 p.p.m. region was assigned to two exchangeable protons on the nitrogen of the amido group. $\nu_{max}(CHCl_3)$ 3520, 3495, 3405, 1680, and 1590 cm^{-1}.

Anal. Calcd. for $C_7H_{15}NO$ (mol. wt., 129.20): C, 68.07; H, 11.70; N, 10.84. Found (mol. wt., mass spectrum, 129): C, 67.87; H, 11.39; N, 11.20.

The fragmentation pattern in the mass spectrum was consistent with the structure. On the basis of the i.r. and n.m.r. spectra and in agreement with the analysis, the unknown compound was identified as 2-methylcaproamide (**2**).

3,7-Dimethyloctanamide (12) and 2-Isopropyl-5-methylhexanamide (11)

Menthone oxime (**10**) (1 g) was dissolved in 90 ml of *iso*-propanol. The resulting solution was irradiated in an

Can. J. Chem. Downloaded from www.nrcresearchpress.com by 210.87.254.105 on 09/05/12
For personal use only.

atmosphere of nitrogen for 24 h. After concentrating the solution to 1 ml, the components were separated by preparative g.l.c. at 170°. A 6 mm × 8 ft stainless steel column packed with 10% DC 710 on Chromosorb W was used. Compounds **12**, m.p. 104–105° and **11**, m.p. 125–126°, having retention times of 12.5 and 11.3 min were obtained as white crystals in yields of 130 and 50 mg, respectively.

Compound **11** showed characteristic amido absorption (16) at 3540, 3508, 3420, 1690, and 1610 cm^{-1}. The n.m.r. spectrum in $CDCl_3$ showed two overlapping doublets centered at 0.95 p.p.m. (J = 4 c.p.s. and 6 c.p.s. 9H), a doublet at 2.15 p.p.m. (J = 6 c.p.s. 2H), a singlet at 1.28 p.p.m. (8H), and a broad band in the region 5.5 to 6.8 p.p.m. (2H).

Anal. Calcd. for $C_{10}H_{21}NO$ (mol. wt., 171.28): C, 70.12; H, 12.36; N, 8.18. Found (mol. wt., mass spectrum, 171): C, 70.31; H, 12.06; N, 8.14.

Compound **12** exhibited absorption at 3540, 3505, 3420, 1690, and 1610 cm^{-1} characteristic of an amide in its i.r. spectrum. The n.m.r. spectrum in $CDCl_3$ showed a twelve-proton triplet (composed of two overlapping doublets) centered at 0.95 p.p.m. (J = 5 c.p.s. and 6 c.p.s.). These were assigned to the two pairs of *gem*-dimethyl groups of the two isopropyl groups. A broad band centered at 1.8 p.p.m., was interpreted as being due to the proton α to the amido group. A broad band in the 5.3 to 6.3 p.p.m. region was assigned to the two exchangeable protons on the nitrogen of the amido group. The rest of the protons of this compound appeared as a singlet at 1.28 p.p.m.

Anal. Calcd. for $C_{10}H_{21}NO$ (mol. wt., 171.28): C, 70.12; H, 12.36; N, 8.18. Found (mol. wt., mass spectrum, 171): C, 70.09; H, 12.20; N, 8.38.

The fragmentation patterns of the mass spectra of compounds **11** and **12** were consistent with the structure proposed.

6-Methylheptanamide (6) and 2,2-Dimethylcaproamide (5)

Three 100 mg samples of oxime **4**, each dissolved in 100 ml of *iso*-propanol, were irradiated separately, under an atmosphere of helium for 2 h. The combined solutions were concentrated to 0.5 ml by using a 10 cm Vigreux column. The concentrated solution was then separated into its components by t.l.c.; 100 mg of the photomixture were applied each on preheated (110° for 10 min) plates (8 in. × 8 in.) coated with 0.75 mm of silica gel. Two bands of R_f 0.3 and 0.5 were detected when ether was used as developing solvent. The separated bands were extracted with chloroform to give 50 mg and < 1 mg of compounds **6** and **5** respectively.

Compound **6**, m.p. 111–112° had ($\nu_{max}CHCl_3$), 3525, 3410, 3495, 1680, and 1590 cm^{-1} characteristic of amido group. Its n.m.r. spectrum in $CDCl_3$ showed a six-proton doublet at 0.87 p.p.m. (J = 6 c.p.s.). This was assigned to the terminal *gem*-dimethyl groups of the carbon chain. A two-proton triplet at 2.25 p.p.m. (J = 7 c.p.s.) was assigned to the methylene group α to the amido group. A broad band in the 5.7 to 6.5 p.p.m. region was assigned to the two exchangeable protons on the nitrogen of the amido group. The rest of the protons of this compound appeared as a broad band centered at 1.25 p.p.m.

Anal. Calcd. for $C_8H_{17}NO$: C, 67.09; H, 11.96; N, 9.78. Found: C, 67.09; H, 11.10; N, 9.97.

Compound **5** was isolated in too small a quantity to be fully characterized. The i.r. spectrum showed in dilute CCl_4 solution, bands at 3545, 3520, 3420, 1610, and 1680 cm^{-1} characteristic of primary amides. Its structure was established by comparison with an authentic sample, which was synthesized via the following scheme.

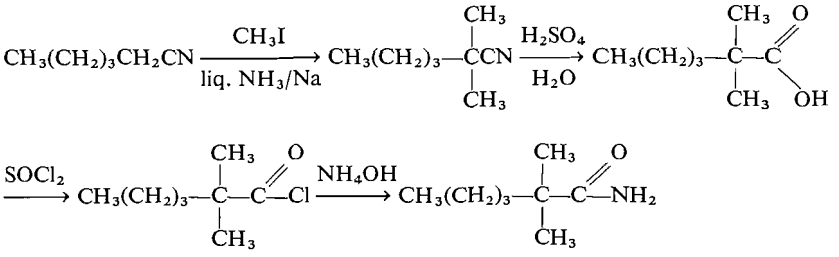

Sodium amide (4 g) was placed in a dried 3-necked flask fitted with a condenser (Dewar) and two pressure regulated dropping funnels. In one dropping funnel were placed 4 g of capronitrile and to the other were added 12 g of methyl iodide. Dried nitrogen was circulating through the containers, while filling up the Dewar condenser with dry ice; 50 ml of dried liquid ammonia (over Na) were then introduced into the system. The nitrile was added, followed by 5 min of stirring to ensure that the formation of anion was completed. Methyl iodide was then introduced, and the mixture was stirred for ½ h. Excess of ammonia was evaporated by allowing the temperature of the reaction vessel to reach room temperature. Dilute hydrochloric acid was added. The nitrile was extracted five times with ether. The combined ether extracts were washed with water, dried over magnesium sulfate, and subjected to vacuum distillation. The n.m.r. spectrum of the product indicated the total disappearance of the two α-protons accompanied by the presence of a singlet corresponding to the *gem*-dimethyl groups α to the amido group.

Anal. Calcd. for $C_8H_{15}NO$: C, 76.74; H, 12.08; N, 11.19. Found: C, 76.31; H, 12.27; N, 10.98.

The nitrile (1 g) prepared in the preceding procedure was boiled with 7 g of 20% aqueous sulfuric acid. Since no reactions seemed to occur after 12 h of refluxing, 3 ml of concentrated sulfuric acid were added, and the mixture was refluxed for 12 h, giving 900 mg of 2,2-dimethylhexanoic acid. The acid (600 mg) was converted to the acid chloride by treatment with thionyl chloride in ether

Can. J. Chem. Downloaded from www.nrcresearchpress.com by 210.87.254.105 on 09/05/12
For personal use only.

(20 ml). The acid chloride was added to an ammonium hydroxide solution and 400 mg of amide, m.p. 94–95°, were obtained. The spectral data of the amide **5** were: $\nu_{max}(CCl_4)$ 3545, 3520, 3420, 1680, and 1610 cm^{-1}, characteristic of amido group; δ ($CDCl_3$) 0.90 (triplet, J = 6 c.p.s. 3H), 1.20 (singlet, 6H), and a broad band in the region 5.8 to 6.5 p.p.m. (2H).

Anal. Calcd. for $C_8H_{17}NO$: C, 69.09; H, 11.96; N, 9.78. Found: C, 68.89; H, 12.18; N, 9.68.

2,2-Dimethylcaproamide, prepared by photolysis, was identical to this sample (i.r., R_f and retention time in g.l.c.).

2,6-Dimethylheptanamide (8) and 2,2-Dimethylheptanamide (9)

Four 100 mg samples of oxime **7**, each dissolved in 100 ml of *iso*-propanol, were irradiated separately, under an atmosphere of helium for 2 h. After concentrating the solution, the components were separated by preparative t.l.c. Benzene–ether (1:1) was used as developing solvent. The separated bands (R_f 0.2 and 0.4) were extracted with chloroform to give 60 mg and 1 mg of compounds **9**, m.p. 93–94° and **8** respectively. The spectral data of **9** were: $\nu_{max}(CHCl_3)$ 3495, 3500, 1675, and 1585 cm^{-1}; δ($CDCl_3$) 0.90 (doublets, J = 6 c.p.s. 6H), 1.20 (doublet, J = 2 c.p.s. 3H), 2.25 (multiplet), and a broad band in the region 5.8 to 6.5 p.p.m.

Anal. Calcd. for $C_9H_{19}NO$: C, 68.74; H, 12.18; N, 8.91. Found: C, 68.42; H, 12.00; N, 8.70.

Preparation of 2,2-Dimethylheptanamide (9)

Amide **9** was prepared by a method similar to that used for amide **5**. Heptanonitrile was converted to the corresponding α,α-dimethyl nitrile in liquid ammonia with methyl iodide. The resulting nitrile boiled at 58–60°/2 mm. A comparison of the n.m.r. spectra of α,α-dimethylhexanonitrile and hexanonitrile both in pure liquid form is shown below.

Heptanonitrile; δ 0.85 (t, J = 4 c.p.s., 3H), 1.30 (8H), 2.20 (t, J = 5 c.p.s., 2H) p.p.m.

α,α-Dimethylheptanonitrile; 0.80 (t, J = 4 c.p.s., 3H), 1.30 (8H), 1.05 (s, 6H) p.p.m.

Anal. Calcd. for $C_9H_{17}N$: C, 77.63; H, 12.31; N, 10.06. Found: C, 77.76; H, 12.54; N, 10.12.

α,α-Dimethylhexanonitrile (1 g) was hydrolyzed by treatment with sulfuric acid to obtain 900 mg of the corresponding acid as described in the previous section. The spectral data of this compound indicated the presence of the carboxylic acid; $\nu_{max}(CHCl_3)$ 3500 cm^{-1} and 1700 cm^{-1}; δ(neat) 12.70 p.p.m. (sharp, exchangeable proton, 1H). The remainder of the spectrum was similar to that of the corresponding nitrile.

Anal. Calcd. for $C_9H_{17}O_2$: C, 68.31; H, 11.47; O, 20.22. Found: C, 68.33; H, 11.26; O, 20.20.

Conversion of this acid to its acid chloride followed by treatment with ammonium hydroxide solution (as described above) gave the amide **9**, m.p. 104–105.5°; $\nu_{max}(CHCl_3)$ 3540, 3420, 3505, 1670, and 1580 cm^{-1}; δ ($CDCl_3$) 0.90 (triplet, 3H, J = 6 c.p.s.), 0.18 (singlet, 6H), and a broad band in the region 5.5 to 6.5 p.p.m.

Anal. Calcd. for $C_9H_{17}NO$: C, 68.74; H, 12.18; N, 8.91. Found: C, 68.65; H, 11.99; N, 9.14.

2,2-Dimethylheptanamide from photolysis was identical to this sample (R_f, g.l.c. retention time, and i.r.).

Quantitative Determination of the Ratio of Isomeric Amides

A 0.1% solution of each oxime **1**, **4**, **7**, and **10** was irradiated for 2 h under an atmosphere of nitrogen in *iso*-propanol. The resulting solutions were concentrated to 5 ml by distilling off the solvent through a 10 cm Vigreux column. The determination of the amount of each component was then performed on a 6 mm × 6 ft column packed with 10% DC 710 on Chromosorb W column. Yield of each amide was determined by using standards isolated from photolysis mixture or prepared synthetically. The g.l.c. properties of each amide are shown in Table VI. The ratio of the amides in the photolyses of the oximes are shown in Scheme 1.

TABLE VI

Retention time of amides in 6 mm × 6 ft 10% DC 710 on Chromosorb W column

Amides	Oven temperature (°C)	Flow rate (ml/min)	Retention time (min)
2	158	20	3.6
3	158	20	4.7
5	155	60	1.8
6	155	60	2.8
8	155	20	5.1
9	155	20	6.0
11	158	40	3.3
12	158	40	5.0

Photolyses of Oximes, Asymmetric at α-Carbon

2,6-Dimethylcyclohexanone Oximes

Preparation of the oxime mixture—A *cis* and *trans* mixture of 2,6-dimethylcyclohexanone (40 g) (Aldrich Chemical) was added to a cloudy solution of 50 g of sodium acetate and 40 g of hydroxylamine hydrochloride in 500 ml of methanol. The mixture was kept refluxing in a water bath overnight. Part of the methanol was distilled off and the remaining solution was poured into ice-cold water with stirring. The precipitate was filtered off and washed with water to give 37 g of crude oxime mixture.

Separation of the mixture into its pure cis and trans form—The oxime mixture (100 mg each time) was applied on plates (8 in. × 8 in.) coated with 0.75 mm silica gel. The plates were preheated in an oven at 110° for 10 min before use. Benzene–ether (9:1) was used to develop the plates. The separated bands were extracted with boiling methanol using a Soxhlet extractor to give 800 mg and 900 mg of oximes **13**, m.p. 120–121° (lit. (17) 119°) and **14**, m.p. 77–78° (lit. (17) 79°); R_f 0.7 and 0.5, respectively, from 2 g of starting oxime mixture. Oximes **13** and **14** were identified respectively as *trans*- and *cis*-isomers by analysis of their n.m.r. spectra. *trans*-Isomer **13**: δ 2.45 and 3.75 p.p.m. (methine); methylene protons are relatively sharp (rapid ring inversion). *cis*-Isomer **14**: δ 2.70 and 3.50 p.p.m. (methine); methylene protons are broad and undifferentiated.

Anal. Calcd. for $C_8H_{15}NO$: C, 68.04; H, 10.71; N, 9.92. Found, oxime **14**: C, 67.87; H, 10.53; N, 9.80. Found, oxime **13**: C, 68.18; H, 10.55; N, 10.04.

Can. J. Chem. Downloaded from www.nrcresearchpress.com by 210.87.254.105 on 09/05/12
For personal use only.

Photolyses of the cis- (14) and trans- (13) Oximes:—The photolysis of a 0.1% solution of either cis- (**14**) or trans- (**13**) isomer in its pure form was conducted in both methanol and *iso*-propanol for an appropriate length of time under an atmosphere of helium. Gas–liquid chromatographic detection (Table VI) (using 20% Hyprose SP-80 on silicon treated Chromosorb W column), of the starting oxime recovered from runs that were allowed to go only to partial completion showed no corresponding isomeric oxime. The retention time of oximes **13** (*trans-*) and **14** (*cis-*) was 6.3 min and 8.1 min, respectively, when the oven temperature was 138° and the carrier gas flow rate was 40 ml/min.

Menthone and Isomenthone Oximes

Preparation of menthone oxime—Menthone oxime, m.p. 55–56° (reported 58°) was prepared according to Beckmann (18) by treatment of menthone (oxidized from menthol according to Sandborn (19)) with hydroxylamine hydrochloride and sodium acetate in 90% ethanol.

Anal. Calcd. for $C_{10}H_{19}NO$: C, 70.96; H, 11.32; N, 8.28. Found: C, 71.05; H, 11.35; N, 8.13.

Preparation of isomenthone oxime—Isomenthone was isolated from a mixture of menthone and isomenthone (Aldrich Chem. Co.) by treatment with Girard reagent following the method described by Nigam and Levi (20). Gas–liquid chromatographic detection of the isolated isomenthone showed one peak which was different in retention time from that of menthone.

Isomenthone (0.31 g) was added to a solution of 0.31 g of hydroxylamine hydrochloride in 10 ml of water which was neutralized by sodium carbonate. After standing overnight with stirring, a white solid was formed. Usual work-up gave 0.3 g of isomenthone oxime. After recrystallization from petroleum ether (60–90°) g.l.c. detection of this isomenthone oxime showed one peak at 51 min, (menthone oxime, 47 min), using 20% Hyprose SP-80 on silicon treated Chromosorb W column at 140° oven temperature and 30 ml/min flow rate of carrier gas.

Anal. Calcd. for $C_{10}H_{19}NO$: C, 71.05; H, 11.35; N, 8.13. Found: C, 70.85; H, 11.46; N, 8.18.

Photolyses of menthone and isomenthone oximes—The photolyses of a 0.1% solution of both *cis-* and *trans-*isomers in their pure forms were conducted in *iso*-propanol under an atmosphere of nitrogen for 1 h. Detection by g.l.c., using 6 mm × 6 ft glass column of Hyprose SP-80 on silicon treated Chromosorb W of the starting oxime recovered from runs that were allowed to go only to partial completion, showed no corresponding isomeric oxime.

Source of Hydrogen in the Formation of Amides

A 1% solution of cyclohexanone oxime in *iso*-propanol[4] was irradiated under a nitrogen atmosphere for 44 h. The resulting solution was then subjected to careful distillation through a 10 cm Vigreux column. The solvent collected was identified and determined quantitatively by g.l.c. using 6 mm × 6 ft Porapak R as column. The retention time of acetone was 6 min compared with 9.4 min for *iso*-propanol at 142 °C oven temperature with a flow rate of carrier gas at 40 ml/min; 54% of acetone with respect to the amide formed in this photolysis was detected. The presence of acetone was further confirmed by converting it to its 2,4-dinitrophenylhydrazone. This hydrazone was identical (i.r., m.p., and R_f) with an authentic sample.

Anal. Calcd. for $C_9H_{10}N_4O_4$: C, 45.38; N, 23.52; H, 4.23. Found: C, 45.36; N, 23.68; H, 4.27.

Specificity of Hydrogen Abstraction in Amide Formation[5]

Preparation of O-Deuterated Cyclododecanone Oxime

Cyclododecanone oxime (3 g) was dissolved in 75 ml of boiling anhydrous hexane (freshly distilled over Na) and 640 mg of sodium hydride (52%) was added. The whole mixture was kept refluxing for 4 h. The sodium salt (2.5 g) was filtered off. This sodium salt of the oxime was converted to the *O*-deuterated oxime by stirring in 20 ml of deuterium oxide overnight. The resulting oxime showed the absence of signal corresponding to the hydroxyl group in n.m.r.

Preparation of O-Deuterated iso-Propanol

Aluminium isopropoxide (200 g) was stirred under anhydrous conditions with 1500 ml of dried ether (freshly distilled over NaH). Deuterium oxide (70 ml) was added. The whole mixture was stirred for 6 h. The gelatineous aluminium hydroxide was filtered off. The filtrate was then subjected to fractional distillation to give 80 ml of deuterated *iso*-propanol.

Photolysis of O-Deuterated Cyclododecanone Oxime in O-Deuterated iso-Propanol

O-Deuterated cyclododecanone oxime (400 mg) in 80 ml of the above *O*-deuterated *iso*-propanol was irradiated under an atmosphere of helium for 15 h. Thin-layer chromatographic separation of the resulting photoproducts gave 200 mg of dodecanamide. This amide, m.p. 88–90°, was subjected to H_2O exchange to get rid of any deuterium attached to the nitrogen of the amido group.

Anal. Calcd. for $C_{12}H_{25}NO$: C, 72.30; H, 12.64; N, 7.03. Found: C, 72.17; H, 12.68; N, 7.14.

The i.r. spectrum showed no corresponding C—D stretching. The mass spectrometric analysis indicated more than 95% of undeuterated amide.

Irradiation of Cycloalkanone Oximes in Water

Exactly the same procedure for irradiation of *iso*-propanol was applied to this system except that the resulting photolytic solution was saturated with sodium chloride, and the solution was extracted in a liquid–liquid extractor with methylene chloride for one day. The organic layer was then reduced to 25 ml for quantitative determination.

Effect of Acid

Parallel runs with and without acid were carried out using exactly the same procedure as that described for irradiation of cycloalkanone oximes in water.

Fate of the Nitrogen in the Oxime

A 1% solution of cyclohexanone oxime in distilled water was thoroughly purged with helium. The whole solution was then subjected to irradiation for 2 h. During the photolysis, a gas was generated which was trapped by passing it into a benzene solution of triphenyl radicals.

[5]All these experiments were conducted in a dry box, which had been evacuated and filled with dried nitrogen several times to ensure the complete removal of moisture.

An immediate decolorization followed by precipitate formation was observed. This gas also caused a precipitation of brownish ferric salt when passed into an aqueous ferrous ammonium sulfate solution. These free radical and oxidizing properties were attributed to the presence of oxygen gas in the photolysis system.

The aqueous photolysis solution was slightly alkaline (pH 9) (test by universal indicator). It was neutralized by cautious addition of *p*-toluenesulfonic acid. The resulting solution was subjected to liquid–liquid extraction with boiling methylene chloride for 24 h. The aqueous layer was then evaporated to dryness and gave a *p*-toluenesulfonate salt. The *p*-toluenesulfonate salts of ammonia, hydroxylamine, and hydrazine were prepared synthetically. A comparison of these (i.r.) with the one obtained from photolysis revealed that this salt was ammonium *p*-toluenesulfonate.

Anal. Calcd. for $C_7H_{11}NO_3S$: H, 5.79; C, 44.21; N, 7.37; S, 16.84. Found: H, 6.17; C, 44.09; N, 7.13; S, 17.13.

Photolysis of Hydroxylamine

The photolysis of free hydroxylamine under the same condition as that in ketone formation was performed for 3 h. No detectable ammonia or oxygen was formed.

Acknowledgments

We would like to thank Dr. K. Valentin and Miss I. Valentin for recording the n.m.r. spectra. We wish to thank the National Research Council of Canada for financial support for this work.

1. R. T. Taylor, M. Douek, and G. Just. Tetrahedron Letters, 4143 (1966).
2. J. K. Landquist. J. Chem. Soc. 2830 (1953).
3. L. Chardonnens and P. Heinrich. Helv. Chim. Acta, **32**, 656 (1949).
4. C. J. Pederson. J. Am. Chem. Soc. **79**, 5014 (1957).
5. M. J. Kamlet and L. A. Kaplan. J. Org. Chem. **22**, 576 (1957).
6. R. Bonnett, V. M. Clark, and A. Todd. J. Chem. Soc. 2102 (1959).
7. F. Kröhnke. Ann. **604**, 203 (1957).
8. L. Kaminsky and M. Lamchen. Chem. Commun. 130 (1965).
9. J. S. Splitter and M. Calven. Tetrahedron Letters, 1445 (1968).
10. H. Wehrli and K. Schaffner. Helv. Chim. Acta, **45**, 385 (1962).
11. G. S. Gould. Mechanism and structure in organic chemistry. Henry Holt and Co., New York. 1967. p. 176 and references cited therein.
12. W. D. Emmons. J. Am. Chem. Soc. **79**, 5739 (1957).
13. M. C. R. Symons. Photolysis of hydrogen peroxide in fluid and rigid media. *In* Peroxide reaction mechanisms. *Edited by* J. O. Edwards. p. 139. Interscience Publishers, Inc., New York. 1962.
14. M. Douek. Ph.D. Thesis. McGill University, 1966.
15. W. S. Johnson and Harvey Posvic. J. Am. Chem. Soc. **69**, 1361 (1947).
16. L. J. Bellamy. The infra-red spectra of complex molecules. John Wiley and Sons, Inc., New York. 1960.
17. A. Haller. Compt. Rend. **157**, 179 (1913). L. Ruzicka, D. R. Koolhaas, and A. H. Wind. Helv. Chim. Acta, **14**, 1164 (1931). R. Cornubert, C. Borrel, and H. Le Bihan. Bull. Soc. Chim. France, **49**, 1387 (1931). R. Cornubert and P. Anziani. Compt. Rend. **217**, 197 (1943).
18. E. Beckmann. Ann. Chem. **250**, 322 (1889).
19. L. T. Sandborn. *In* Organic synthesis. Vol. I. *Edited by* Gilman and Blatt. John Wiley and Sons, Inc., New York. 1956. p. 340.
20. I. C. Nigam and L. Levi. Anal. Chem. **35**, 1087 (1963).

Can. J. Chem. Downloaded from www.nrcresearchpress.com by 210.87.254.105 on 09/05/12
For personal use only.

Can. J. Chem. Downloaded from www.nrcresearchpress.com by 210.87.254.105 on 09/05/12
For personal use only.

Transannular reactions in the dibenzo[*a*,*d*]cycloheptene series. III. Preparation of 11-substituted-10,11-dihydro-10,5-(iminomethano)-5*H*-dibenzo[*a*,*d*]cycloheptenes

T. A. Dobson, M. A. Davis, and A. M. Hartung
Ayerst Laboratories, Ayerst, McKenna, and Harrison Limited, Montreal, Quebec

Received March 21, 1968

Treatment of the *syn*-epoxyamide **3** with either ammonium hydroxide or sodium hydride gives 10,11-dihydro-*anti*-11-hydroxy-10,5-(iminomethano)-5*H*-dibenzo[*a*,*d*]cyclohepten-13-one (**1***a*). This compound is readily converted to the *syn*-epimer **1***c* by oxidation to **1***b* and subsequent hydrogenation. The ketone **1***b* reacts with Grignard reagents to give the tertiary alcohols **1***k*,*l* which undergo hydrogenolysis to give the 11-substituted lactams **1***q*,*r*. Reduction of the lactams with lithium aluminium hydride gives the corresponding amines.

Canadian Journal of Chemistry, **46**, 3391 (1968)

We have recently described the preparation of a number of 10,11-dihydro-10,5-(epoxymethano)-5*H*-dibenzo[*a*,*d*]cyclohepten-13-ones (1, 2). The present paper outlines a general route to 11-substituted-10,11-dihydro-10,5-(iminomethano)-5*H*-dibenzo[*a*,*d*]cycloheptene derivatives **1** and **2**. A different approach has been used by other workers (3–6) to prepare other derivatives and the ring system has been shown to occur naturally in the alkaloids amurensine, amurensinine, and roemfrine (7, 8).

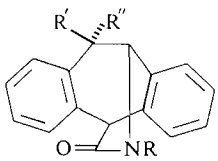

1

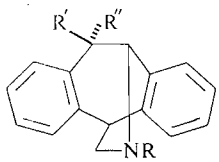

2

	R	R′(*syn*)	R″(*anti*)
1*a*,**2***a*	H	H	OH
1*b*,**2***b*	H	=O	
1*c*,**2***c*	H	OH	H
1*d*,**2***d*	CH_3	H	OH
1*e*	$CH_2C_6H_5$	H	OH
1*f*	$(CH_2)_3OCH_3$	H	OH
1*g*,**2***g*	CH_3	H	OCH_3
1*h*,**2***h*	$CH_2C_6H_5$	H	OCH_3
1*i*,**2***i*	CH_3	OH	H
1*j*,**2***j*	CH_3	OCH_3	H
1*k*,**2***k*	H	OH	CH_3
1*l*,**2***l*	H	OH	C_6H_5
1*m*	CH_3	=O	
1*n*	CH_3	OH	CH_3
1*o*	CH_3	OH	C_6H_5
1*p*	H	H	H
1*q*	H	H	CH_3
1*r*	H	H	C_6H_5

We have previously found that the *syn*-epoxyamide **3** reacts with secondary amines to give *anti*-11-dialkylaminolactones. In attempts to prepare the unsubstituted *anti*-11-aminolactone **4***a* both the *syn*-epoxyamide **3** and the bromolactone **4***b* were treated with ammonium hydroxide at 140°. The product, obtained in 70% yield in both cases, was not the expected lactone but the *anti*-11-hydroxylactam **1***a*. Oxidation of **1***a* gave the ketolactam **1***b* which regenerated **1***a* upon reduction with sodium borohydride. In contrast, catalytic hydrogenation of **1***b* gave a mixture of 20% **1***a* and 80% of the *syn*-hydroxylactam **1***c*. This hydrogenation parallels that of the ketolactone **4***c* which gives the *syn*-hydroxylactone **4***d* as the major product (2). Reduction of the two epimers **1***a* and **1***c* with lithium aluminium hydride in dimethoxyethane gave the epimeric aminoalcohols **2***a* and **2***c* respectively. Other solvents (see Experimental) were markedly inferior for these reductions in accordance with experience in the preparation of 8-hydroxy-5-phenylbenzomorphan derivatives (9). The infrared (i.r.) hydroxyl absorptions of **2***a* and **2***c* were concentration-dependent, and concentration-independent respectively, indicating that **2***a* was the *anti*-epimer and that **2***c* was the *syn*-epimer (10). These assignments were confirmed by the reaction of the *syn*-aminoalcohol **2***c* with phosgene. The product was the cyclic carbamate **5**, the structure of which was fully supported by its analytical and spectral properties. The geometry of **2***a* and **2***c*, as shown by inspection of molecular models, indicates that only **2***c* can form **5**. Cristol and Bly (11) have cited an analogous cyclic carbonate formation as a structure proof of dibenzobicyclo[3·2·1]octadiene-*exo*-4-*syn*-8-diol. In accord with these assignments only intractable mixtures were obtained when **2***a* was treated with either phosgene or diethyl oxalate (12).

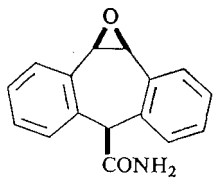

3

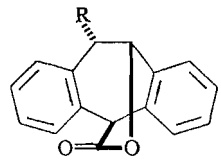

4*a*, R = NH_2; *e*, R = H
b, R = Br; *f*, R = $NHCH_2C_6H_5$
c, R = (=O); *g*, R = NHC_6H_5
d, R = *syn*—OH

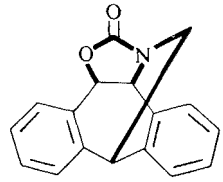

5

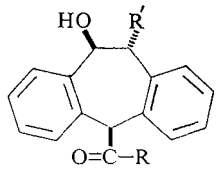

6*a*, R = R′ = $NH(CH_2)_3OCH_3$
b, R = R′ = NH_2
c, R = NH_2, R′ = H

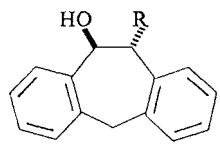

7*a*, R = NHC_6H_5
b, R = $N(CH_3)_2$

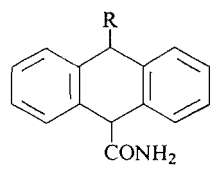

8*a*, R = H
b, R = CHO

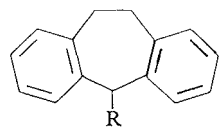

9*a*, R = CON_3
b, R = NCO

Treatment of the *syn*-epoxyamide **3** with a variety of primary amines at 140° gave the *N*-substituted-*anti*-hydroxylactams **1***d–f*. The same compounds were prepared by monoalkylating **1***a* with sodium hydride and the appropriate alkyl halide confirming that **1***a*, *d–f* belonged to the same epimeric series. Subsequent methylation of **1***d*,*e* gave the ethers **1***g*,*h*. The alkylated derivatives **1***i*,*j* of the *syn*-hydroxylactam were prepared in the same manner. Reduction of **1***d*,*g*,*h* and **1***i*,*j* with lithium aluminium hydride gave the two epimeric series of amines **2***d*,*g*,*h* and **2***i*,*j* respectively. Unlike the nuclear magnetic resonance (n.m.r.) spectra of the previously described lactones (2), the n.m.r. spectra of the lactams and amines described herein cannot be used to distinguish between *syn*- and *anti*-substitution.

Under milder conditions two exceptions to the generality of the amine–epoxyamide reaction were observed. First, treatment of **3** with benzylamine at 100° gave the *anti*-11-benzylaminolactone **4***f*. The geometry of this compound was confirmed by its n.m.r. spectrum (2). Subsequent treatment of **4***f* with either benzylamine or ammonium hydroxide at 140° gave the *N*-benzyl-*anti*-hydroxylactam **1***e*. Second, treatment of **3** with 3-methoxypropylamine at 80° gave a small yield of the secondary amide **6***a*.

These observations suggest that **1***a* arises by normal *trans*-opening of the epoxide function (13) with, most probably, simultaneous lactonization to give the initially expected aminolactone **4***a*. Epimerization of **4***a* at the benzhydrilic carbon atom (C-5) *via* an equilibrium concentration of the amide **6***b* followed by lactam formation would give **1***a*. It is improbable that **6***b* epimerizes without prior lactonization. For example, the *syn*-hydroxyamide **6***c* lactonizes at room temperature (2). The ready lactam formation of the epimerized form of **6***b* is unremarkable in view of the classical methods for forming lactam bridges (14).

It was not possible to convert the *anti*-anilinolactone **4***g* to the corresponding lactam by treatment with ammonium hydroxide since starting material or the aminoalcohol **7***a* were obtained. Presumably the anilino residue was insufficiently basic to undergo lactam formation. Decarboxylation also occurred when the *syn*-epoxyamide **3** was heated with aqueous dimethylamine at 140° since the product was the aminoalcohol **7***b*.

The present studies bear a formal similarity to the preparation of isoquinuclidones recently

Can. J. Chem. Downloaded from www.nrcresearchpress.com by 210.87.254.105 on 09/05/12
For personal use only.

Can. J. Chem. Downloaded from www.nrcresearchpress.com by 210.87.254.105 on 09/05/12
For personal use only.

reported by Huffman and co-workers (15). Their procedure requires, however, a *trans*-epoxyester as starting material and subsequent pyrolysis of the intermediate aminoester.

Treatment of the *syn*-epoxyamide **3** with sodium hydride in dry dioxane also gave **1***a*. Presumably this reaction proceeds *via* epimerization at C-5 and subsequent 'N-6' participation (16). Many examples are known of nucleophilic participation by amide nitrogen under basic conditions (17). A by-product from this reaction was 9,10-dihydroanthracene-9-carboxamide **8***a*. This side reaction was undoubtedly a base-promoted conversion of **3** since it was unaffected by both boiling dioxane and boiling water, and the *anti*-hydroxylactam **1***a* was unaffected by sodium hydride in boiling dioxane. Possibly **8***a* arose by initial rearrangement[1] of **3** to the carboxaldehyde **8***b* with subsequent base-catalyzed elimination of the formyl group (11, 19).

Attempts to ammonolyze the lactones **4***d,e* to the corresponding lactams were abortive since starting materials or decarboxylated products were obtained. In contrast, the closely related isochroman-3-one and its 4-phenyl derivative have been successfully ammonolyzed to the corresponding lactams (20, 21).

The ketolactam **1***b* showed normal ketonic properties. Enolization, which sometimes masks the ketonic character of 10,11-dihydro-5*H*-dibenzo[*a,d*]cyclohepten-10-ones (22), is precluded by the presence of the 10,5 bridge system. Thus, **1***b* formed an oxime and a ketal and readily underwent Grignard reactions to give the carbinols **1***k,l*.[2] In these Grignard reactions the lactam function was presumably protected from attack by complex formation (23, p. 876). Grignard reactions with the *N*-methyl-ketolactam **1***m* gave very poor yields of the carbinols **1***n,o* and these compounds were better prepared by methylating **1***k,l*. Lithium aluminium hydride reduction of **1***k,l* gave the aminoalcohols **2***k,l*. The i.r. hydroxyl absorptions of these compounds were concentration-independent indicating that they were *syn*-aminoalcohols. This geometry would be expected assuming that Grignard reagents, like hydrogen, tend to attack the less hindered side of **1***b*.

Hydrogenolysis of the epimeric hydroxylactams **1***a* and **1***c* with sodium in liquid ammonia gave the unsubstituted lactam **1***p* in good yield. Similar hydrogenolyses of the carbinols **1***k,l* gave **1***q,r*. Catalytic hydrogenolyses of **1***a* and **1***k* were unsuccessful, as is the case with similarly substituted benzylic alcohols (9).

The unsubstituted lactam **1***p* was also obtained, in very poor yield, by photolysis of the acyl azide **9***a*. The major product was the isocyanate **9***b* in accord with experience in the photolysis of carbocylic acyl azides (24, 25).

The more important pharmacological properties of some of the compounds described in this paper, particularly those of the amines **2***a–m*, will be described elsewhere.

Experimental

10,11-Dihydro-anti-11-hydroxy-10,5-(iminomethano)-5H-dibenzo[a,d]cyclohepten-13-one (1a)

Method a

A mixture of the *syn*-epoxyamide **3** (50 g) (2) and ammonium hydroxide (200 ml) was kept at 140° for 6 h. The solid product was collected and washed with water, chloroform and ether, and then crystallized from ethanol to give the title product (35 g) as needles, m.p. 260–262° (decomp.); ν_{max} (Nujol) 1670 cm^{-1}.

Anal. Calcd. for $C_{16}H_{13}NO_2$: C, 76.47; H, 5.22; N, 5.57. Found: C, 76.50; H, 5.08; N, 5.57.

Method b

Following the procedure of method *a*, the bromolactone **4***b* (315 g) (2) and ammonium hydroxide (2 l) gave **1***a* (178 g).

Method c

A mixture of the *syn*-epoxyamide **3** (2.51 g), sodium hydride (460 mg of a 52% suspension in mineral oil), and dioxane (50 ml) was heated under reflux for 1 h. The reaction mixture was diluted with water and then concentrated *in vacuo*. The residue was washed with water, and then with hexane, and the residue was crystallized from ethanol to give **1***a* (1.5 g), m.p. 260–262° (decomp.). The infrared (i.r.) spectrum of this material was identical with that of the product from method *a*.

The mother liquors from the above crystallization yielded 9,10-dihydroanthracene-9-carboxamide (**8***a*), m.p. and mixture m.p. with an authentic sample 151–152° (lit. (26), m.p. 151–152°).

10,11-Dihydro-10,5-(iminomethano)-5H-dibenzo[a,d]-cyclohepten-11,13-dione (1b)

Jones reagent (20 ml) (27) was added dropwise to an ice-cold stirred suspension of **1***a* (10.0 g) in acetone (150

---

[1]The influence of the 5-proton is manifest in this rearrangement. Thus, 10,11-epoxy-10,11-dihydro-5*H*-dibenzo[*a,d*]cyclohepten-5-one gave the corresponding 5,10-dione on base treatment, and gave 10-hydroxy-9-anthraldehyde on either pyrolysis or acid-treatment (18).

[2]The physical properties and chemical behavior of **1***k,l* confirmed that they were single epimers. The reaction of **1***b* with allyl magnesium bromide appeared to give a mixture of epimers which is being investigated further. Ethyl magnesium bromide reduced **1***b* to the *anti*-hydroxylactam (23, p. 147–158).

Can. J. Chem. Downloaded from www.nrcresearchpress.com by 210.87.254.105 on 09/05/12
For personal use only.

ml). The mixture was kept at 0° for 0.5 h and then diluted with isopropanol (5.0 ml). The mixture was concentrated *in vacuo*, diluted with water, and then extracted with chloroform. The combined extracts were washed with water, dried, evaporated, and the residue was crystallized from ethanol to give **1***b* (9.0 g), m.p. 197–199°; ν_{max} ($CHCl_3$) 3425, 3200, and 1685 cm^{-1}.

Anal. Calcd. for $C_{16}H_{11}NO_2$: C, 77.09; H, 4.45; N, 5.62. Found: C, 77.34; H, 4.36; N, 5.78.

The oxime derivative of **1***b* was prepared in the usual manner and recrystallized from ethanol, m.p. 290–295° (decomp.).

Anal. Calcd. for $C_{16}H_{12}N_2O_2$: C, 72.71; H, 4.58; N, 10.60. Found: C, 72.40; H, 4.69; N, 10.75.

Treatment of **1***b* (1.0 g) with sodium borohydride (0.5 g) in ethanol (30 ml) at room temperature gave **1***a* (0.93 g) identical in all respects with **1***a* prepared by method *a* above.

*10,11-Dihydro-syn-11-hydroxy-10,5-(iminomethano)-5H-dibenzo[a,d]cyclohepten-13-one (**1***c*)

A solution of the ketolactam **1***b* (100 g) in ethanol (3.0 l) was hydrogenated at 50° and 7 atm in the presence of 10% palladium-on-charcoal catalyst (0.5 g) until hydrogen uptake ceased. The catalyst was removed and the solution was concentrated to half-volume whereupon **1***c* (60 g) crystallized as fine needles, m.p. 260–263° (decomp.); ν_{max} (Nujol) 1665 cm^{-1}.

Anal. Calcd. for $C_{16}H_{13}NO_2$: C, 76.47; H, 5.22; N, 5.57. Found: C, 76.35; H, 5.13; N, 5.21.

Fractional crystallization of the residue from the mother liquors gave a further 19.0 g of **1***c* and 17.0 g of **1***a*.

*10,11-Dihydro-10,5-(iminomethano)-5H-dibenzo[a,d]cyclohepten-anti-11-ol (**2***a*)

Lithium aluminium hydride (7.25 g) was added portionwise to a stirred suspension of **1***a* (25.1 g) in 1,2-dimethoxyethane (150 ml). The mixture was stirred and heated under reflux for 10 h. The excess hydride was destroyed with water and the basic material was isolated in the usual manner. This material was recrystallized from benzene–hexane to give **2***a* (19.0 g), m.p. 130–134°; ν_{max} ($CHCl_3$) 3570, 3325, and 1020 cm^{-1}.

Anal. Calcd. for $C_{16}H_{15}NO$: C, 80.98; H, 6.37; N, 5.90. Found: C, 80.97; H, 6.65; N, 5.71.

The hydrochloride salt of **2***a* was recrystallized from ethanol, m.p. 220–225° (decomp.).

Anal. Calcd. for $C_{16}H_{16}ClNO$: C, 70.30; H, 5.85; Cl, 12.99; N, 5.12. Found: C, 70.52; H, 6.04; Cl, 12.70; N, 4.81.

Reduction of **1***a* with lithium aluminium hydride in ether gave mainly starting material; similar reductions of **1***a* in tetrahydrofuran and in dioxane gave 40% and 22% yields respectively of **2***a*.

*10,11-Dihydro-10,5-(iminomethano)-5H-dibenzo[a,d]cyclohepten-syn-11-ol (**2***c*)

The *syn*-hydroxylactam **1***c* (30 g) was treated with lithium aluminium hydride (6.0 g) in dimethoxyethane (200 ml) and then processed as described above. The crude basic material was recrystallized from methanol to give **2***c* (24.1 g), m.p. 191–193°; ν_{max} ($CHCl_3$) 3300, 1488, and 1308 cm^{-1}.

Anal. Calcd. for $C_{16}H_{15}NO$: C, 80.98; H, 6.37; N, 5.90. Found: C, 80.78; H, 6.42; N, 5.69.

*3a,12b-Dihydro-3,8-methano-2H,8H-dibenzo[3,4:6,7]cyclohepta[1,2-d]oxazol-2-one (**5**)*

A 4% solution of phosgene in benzene (30 ml) was added dropwise during 3 h to a solution of **2***c* (2.63 g) in dioxane (100 ml) and pyridine (4 drops). The mixture was kept at room temperature for 1 h and then evaporated to dryness. The residue was partitioned between chloroform and water and the organic phase was evaporated to leave the crude product. This material was recrystallized from methanol to give **5** (1.0 g), m.p. 226–228° (decomp.); ν_{max} ($CHCl_3$) 1758 cm^{-1}.

Anal. Calcd. for $C_{17}H_{13}NO_2$: C, 77.55; H, 4.98; N, 5.32. Found: C, 77.59; H, 5.00; N, 5.17.

Similar treatment of the *anti*-aminoalcohol **2***a* with phosgene gave a solid product, ν_{max} ($CHCl_3$) 1700 cm^{-1}. This material was shown to be inhomogeneous by thin-layer chromatography and it could not be purified.

*Preparation of the anti-Hydroxylactams **1**d–f*

Method a

Under the conditions described for the preparation of **1***a* (method *a*) the following compounds were obtained.

10,11-Dihydro-*anti*-11-hydroxy-12-methyl-10,5-(iminomethano)-5*H*-dibenzo[*a*,*d*]cyclohepten-13-one (**1***d*) (66.0 g), m.p. 267–270° (from ethanol); ν_{max} (Nujol) 3415, 3260, and 1650 cm^{-1} was obtained from **3** (100 g) and aqueous methylamine (600 ml of a 30% solution).

Anal. Calcd. for $C_{17}H_{15}NO_2$: C, 76.96; H, 5.70; N, 5.28. Found: C, 76.96; H, 5.53; N, 4.99.

12-Benzyl-10,11-dihydro-*anti*-11-hydroxy-10,5-(iminomethano)-5*H*-dibenzo[*a*,*d*]cyclohepten-13-one (**1***e*) (10.0 g), m.p. 224–226° (from ethanol); ν_{max} ($CHCl_3$) 3570, and 1660 cm^{-1} was obtained from **3** (30 g), benzylamine (30 g) and water (80 ml).

Anal. Calcd. for $C_{23}H_{19}NO_2$: C, 80.91; H, 5.61; N, 4.10. Found: C, 80.99; H, 5.48; N, 4.25.

10,11-Dihydro-*anti*-11-hydroxy-12-(3′-methoxypropyl)-10,5-(iminomethano)-5*H*-dibenzo[*a*,*d*]cyclohepten-13-one (**1***f*) (3.0 g), m.p. 150–152° (from ethyl acetate); ν_{max} ($CHCl_3$) 3570, 1660, and 1100 cm^{-1} was obtained from **3** (5.0 g), 3-methoxypropylamine (9.0 g), and water (40 ml).

Anal. Calcd. for $C_{20}H_{21}NO_3$: C, 74.28; H, 6.55; N, 4.33. Found: C, 74.30; H, 6.48; N, 4.39.

Method b

A mixture of the *anti*-hydroxylactam **1***a* (5.02 g, 0.02 mole), sodium hydride (920 mg of a 52% suspension in mineral oil, 0.02 mole), methyl iodide (3.12 g), and dioxane (60 ml) was stirred and heated under reflux for 4 h. The mixture was evaporated and the residue was washed with hexane and then with water and then recrystallized from ethanol to give **1***d* (4.8 g), m.p. 265–269°. The i.r. spectrum of this material was identical with that of **1***d* prepared by method *a*.

*anti-11-Benzylamino-10,11-dihydro-10,5-(epoxymethano)-5H-dibenzo[a,d]cyclohepten-13-one (**4***f*)

A mixture of the *syn*-epoxyamide **3** (25.0 g), benzylamine (30.0 g), and water (50 ml) was stirred and heated under reflux for 12 h. The reaction mixture was extracted

Can. J. Chem. Downloaded from www.nrcresearchpress.com by 210.87.254.105 on 09/05/12
For personal use only.

with chloroform and the extracts were washed with 2 *N* HCl and then with water, and then dried. The extracts were evaporated and the residue was recrystallized from ethanol to give **4***f* (8.0 g), m.p. 141–143°; ν_{max} ($CHCl_3$) 1745 cm^{-1}.

Anal. Calcd. for $C_{23}H_{19}NO_2$: C, 80.91; H, 5.61; N, 4.10. Found: C, 81.16; H, 5.83; N, 3.98.

From the mother liquors of the above crystallization there was obtained **1***e* (11.0 g), m.p. and mixture m.p. 224–226°.

10,11-Dihydro-10-hydroxy-N-(3-methoxypropyl)-11-[N-(3-methoxypropylamino)]-5H-dibenzo[a,d]cyclohepten-5-carboxamide (6a)

A solution of the *syn*-epoxyamide **3** (10.0 g) and 3-methoxypropylamine (10.0 g) in benzene (100 ml) was stirred and heated under reflux for 18 h. The resulting solution was concentrated and the concentrate was chromatographed upon alumina. The first material eluted was the lactam **1***f* (3.0 g). The second material eluted was the title product **6***a* (2.5 g) which was recrystallized from isopropanol to m.p. 123–125°; ν_{max} ($CHCl_3$) 3420, 3370, 1655, and 1110 cm^{-1}.

Anal. Calcd. for $C_{24}H_{32}N_2O_4$: C, 69.88; H, 7.82; N, 6.79. Found: C, 69.98; H, 8.02; N, 6.67.

10,11-Dihydro-anti-11-methoxy-12-methyl-10,5-(iminomethano)-5H-dibenzo[a,d]cyclohepten-13-one (1g)

A suspension of **1***d* (5.30 g, 0.02 mole), sodium hydride (1.38 g of a 52% suspension in mineral oil), methyl iodide (4.26 g, 0.03 mole), and dioxane (50 ml) was stirred and heated under reflux for 18 h. The mixture was evaporated and the residue was washed with water and then with hexane and then recrystallized from methanol to give **1***g* (5.0 g), m.p. 212–215°; ν_{max} ($CHCl_3$) 1660 cm^{-1}.

Anal. Calcd. for $C_{18}H_{17}NO_2$: C, 77.39; H, 6.13; N, 5.01. Found: C, 77.29; H, 6.05; N, 5.12.

12-Benzyl-10,11-dihydro-anti-11-methoxy-10,5-(iminomethano)-5H-dibenzo[a,d]cyclohepten-13-one (1h)

This compound was obtained from **1***e* and methyl iodide following the procedure described above. The product crystallized from methanol, m.p. 152–154°; ν_{max} ($CHCl_3$) 1652 cm^{-1}.

Anal. Calcd. for $C_{24}H_{21}NO_2$: C, 81.10; H, 5.96; N, 3.94. Found: C, 80.99; H, 6.34; N, 4.24.

10,11-Dihydro-syn-11-hydroxy-12-methyl-10,5-(iminomethano)-5H-dibenzo[a,d]cyclohepten-13-one (1i)

This compound was obtained from the *syn*-hydroxylactam **1***c* (5.02 g) and methyl iodide (3.12 g) under the conditions described for the preparation of **1***d* (method *b*). It was purified from methanol as needles (4.0 g), m.p. 218–220°; ν_{max} (Nujol) 1668 cm^{-1}.

Anal. Calcd. for $C_{17}H_{15}NO_2$: C, 76.96; H, 5.70; N, 5.28. Found: C, 76.76; H, 5.76; N, 5.20.

10,11-Dihydro-syn-11-methoxy-12-methyl-10,5-(iminomethano)-5H-dibenzo[a,d]cyclohepten-13-one (1j)

This compound was obtained from **1***i* under the conditions described for the preparation of **1***g*. It was recrystallized from benzene as needles, m.p. 189–191°; ν_{max} ($CHCl_3$) 1666 cm^{-1}.

Anal. Calcd. for $C_{18}H_{17}NO_2$: C, 77.39; H, 6.13; N, 5.01. Found: C, 77.13; H, 6.03; N, 4.99.

10,11-Dihydro-syn-11-hydroxy-anti-11-methyl-10,5-(iminomethano)-5H-dibenzo[a,d]cyclohepten-13-one (1k)

A 3 *M* ethereal solution of methyl magnesium bromide (80 ml) was added dropwise to a solution of the ketolactam **1***b* (24.9 g, 0.1 mole) in anhydrous tetrahydrofuran (200 ml). The reaction mixture was stirred and heated under reflux for 6 h and then treated with saturated ammonium chloride solution (300 ml). The organic phase was collected, dried, and evaporated. The residue was recrystallized from methanol to give **1***k* (21.2 g), m.p. 278–280°; ν_{max} (Nujol) 3590, 3210, and 1690 cm^{-1}.

Anal. Calcd. for $C_{17}H_{15}NO_2$: C, 76.97; H, 5.70; N, 5.28. Found: C, 76.88; H, 5.64; N, 5.29.

10,11-Dihydro-syn-11-hydroxy-anti-11-phenyl-10,5-(iminomethano)-5H-dibenzo[a,d]cyclohepten-13-one (1l)

This compound was obtained from **1***b* (10 g) and phenyl magnesium bromide (0.16 mole) under the conditions used for the preparation of **1***k*. The crude product was recrystallized from ethanol to give **1***l* (8.0 g), m.p. 280–285° (decomp.); ν_{max} (Nujol) 1652 cm^{-1}.

Anal. Calcd. for $C_{22}H_{17}NO_2$: C, 80.71; H, 5.23; N, 4.28. Found: C, 80.72; H, 5.30; N, 4.11.

10,11-Dihydro-12-methyl-10,5-(iminomethano)-5H-dibenzo[a,d]cycloheptene-11,13-dione (1m)

Oxidation of **1***d* (10 g) with Jones reagent (20 ml) (27) gave the above product. It was purified from methanol, m.p. 153–155°.

Anal. Calcd. for $C_{17}H_{13}NO_2$: C, 77.55; H, 4.98; N, 5.32. Found: C, 77.78; H, 4.82; N, 5.30.

*Preparation of the Lactams **1n** and **1o***

Method a

Under the conditions described for the preparation of **1***k* the following compounds were obtained.

10,11-Dihydro-*syn*-11-hydroxy-*anti*-11-methyl-12-methyl-10,5-(iminomethano)-5*H*-dibenzo[*a*,*d*]cyclohepten-13-one (**1***n*) (1.3 g), m.p. 224–227° (from methanol); ν_{max} ($CHCl_3$) 3600, 3430, and 1667 cm^{-1} from the *N*-methyl-ketolactam **1***m* (10.0 g) and methyl magnesium bromide (0.1 mole).

Anal. Calcd. for $C_{18}H_{17}NO_2$: C, 77.39; H, 6.13; N, 5.01. Found: C, 77.25; H, 6.08; N, 5.18.

10,11-Dihydro-*syn*-11-hydroxy-12-methyl-*anti*-11-phenyl-10,5-(iminomethano)-5*H*-dibenzo[*a*,*d*]cyclohepten-13-one (**1***o*) (0.3 g), m.p. 197–199° (from benzene–hexane); ν_{max} (Nujol) 1650 cm^{-1} from **1***m* (5.0 g) and phenyl magnesium bromide (0.05 mole).

Anal. Calcd. for $C_{23}H_{19}NO_2$: C, 80.91; H, 5.61; N, 4.10. Found: C, 80.83; H, 5.54; N, 3.80.

Method b

Methylation of **1***k* (5.3 g, 0.02 mole) with sodium hydride (920 mg of a 52% suspension in mineral oil, 0.02 mole) and methyl iodide (3.32 g, 0.22 mole) in anhydrous dioxane gave **1***n* (5.0 g), m.p. and mixture m.p. 224–227°.

A similar methylation of **1***l* (3.27 g, 0.01 mole) gave **1***o* (3.0 g), m.p. and mixture m.p. 197–199°.

Can. J. Chem. Downloaded from www.nrcresearchpress.com by 210.87.254.105 on 09/05/12
For personal use only.

10,11-Dihydro-10,5-(iminomethano)-5H-dibenzo[a,d]-cyclohepten-13-one (1p)

Method a

Small pieces of sodium were added to a mechanically stirred suspension of the *anti*-hydroxylactam **1a** (50.0 g) in freshly distilled liquid ammonia (500 ml) until the mixture remained blue for 5 min. An excess of ammonium chloride was then added and the ammonia was allowed to evaporate. The residue was extracted with hot water and the insoluble material was recrystallized from ethanol to give **1p** (45.0 g), m.p. 242–245°; ν_{max} (Nujol) 1675 cm^{-1}.

Anal. Calcd. for $C_{16}H_{13}NO$: C, 81.68; H, 5.57; N, 5.95. Found: C, 81.67; H, 5.62; N, 5.91.

The same product was obtained when the *syn*-hydroxylactam **1c** was used as starting material.

Method b

A solution of sodium azide (0.7 g) in water (5 ml) was added to a solution of 10,11-dihydro-5*H*-dibenzo[*a,d*]-cycloheptene-5-carbonyl chloride (2.56 g) (26) in dioxane (10 ml) at 0°. The mixture was stirred at 0° for 45 min, diluted with iced water, and extracted with hexane (3 × 20 ml portion). The combined extracts were washed with cold water and then dried at 0° with molecular sieves. The solution of the acid azide **9a** so obtained was photolyzed at 0° until an aliquot no longer absorbed energy at 2140 cm^{-1}. The precipitate which had formed was crystallized from benzene–hexane and then from ethanol to give **1p** (200 mg). Concentration of the hexane filtrate gave the isocyanate **9b** (1.5 g), m.p. 60–62° (lit. (26), m.p. 62–63°).

Preparation of the Lactams 1q and 1r

Under the conditions used for the preparation of **1p** (method *a*) the following compounds were obtained.

10,11-Dihydro-*anti*-11-methyl-10,5-(iminomethano)-5*H*-dibenzo[*a,d*]cyclohepten-13-one (**1q**) (10.7 g), m.p. 243–246° (from methanol); ν_{max} ($CHCl_3$) 3410, 3200, and 1675 cm^{-1} was obtained from **1k** (12.0 g).

Anal. Calcd. for $C_{17}H_{15}NO$: C, 81.90; H, 6.06; N, 5.62. Found: C, 81.87; H, 5.94; N, 5.70.

10,11-Dihydro-*anti*-11-phenyl-10,5-(iminomethano)-5*H*-dibenzo[*a,d*]cyclohepten-13-one (**1r**) (2.8 g), m.p. 250–252° (from methanol); ν_{max} ($CHCl_3$) 1670 cm^{-1} was obtained from **1l** (3.3 g).

Anal. Calcd. for $C_{22}H_{17}NO$: C, 84.86; H, 5.50; N, 4.50. Found: C, 84.68; H, 5.71; N, 4.36.

Treatment of the Lactones 4d, 4e, and 4g with Ammonium Hydroxide

(*a*) A solution of the *syn*-hydroxylactone **4d** (300 mg) in ammonium hydroxide (10 ml) was heated at 120° for 5 h in an autoclave. The i.r. spectrum of the solid product was devoid of carbonyl absorption. A small amount of the starting material was recovered from the ammoniacal solution.

(*b*) A solution of the unsubstituted lactone **4e** (10 g) in ammonium hydroxide (200 ml) was kept at 160° for 5 h. The reaction mixture was extracted with ether. Evaporation of the washed and dried extracts and recrystallization of the residue from hexane gave 10,11-dihydro-5*H*-dibenzo[*a,d*]cyclohepten-10-ol (7.0 g), m.p. 63–65° (lit. (28), m.p. 64–66°).

Treatment of **4e** with liquid ammonia at 200° gave an intractable resin.

(*c*) A suspension of the *anti*-anilinolactone **4g** (4.0 g) in ammonium hydroxide (80 ml) was heated at 170° for 6 h. The mixture was processed as described above to give 11-anilino-10,11-dihydro-5*H*-dibenzo[*a,d*]cyclohepten-10-ol (**7a**) (2.4 g), m.p. 177–179° (from ethanol).

Anal. Calcd. for $C_{21}H_{19}NO$: C, 83.69; H, 6.35; N, 4.65. Found: C, 83.99; H, 6.20; N, 4.86.

Similar treatment of the *syn*-epoxyamide **3** (10 g) with dimethylamine (10 g) in water (70 ml) gave 10,11-dihydro-11-dimethylamino-5*H*-dibenzo[*a,d*]cyclohepten-10-ol (**7b**) (7.0 g), m.p. 114–116° (lit. (29), m.p. 117–118°).

Preparations of the Amines 2d,g–l

Under the conditions described for the preparation of **2a**, the following compounds were prepared.

10,11-Dihydro-*anti*-11-hydroxy-12-methyl-10,5-(iminomethano)-5*H*-dibenzo[*a,d*]cycloheptene (**2d**) hydrochloride (3.8 g), m.p. 220° (decomp.) (from isopropanol–ether); ν_{max} (Nujol) 3460 and 3300 cm^{-1} was obtained from **1d** (5.0 g).

Anal. Calcd. for $C_{17}H_{18}ClNO$: C, 70.94; H, 6.30; Cl, 12.35; N, 4.87. Found: C, 70.64; H, 6.58; Cl, 12.69; N, 4.73.

10,11-Dihydro-*anti*-11-methoxy-12-methyl-10,5-(iminomethano)-5*H*-dibenzo[*a,d*]cycloheptene (**2g**) (9.7 g), m.p. 122–125° (from benzene–hexane) was obtained from **1g** (12.0 g).

Anal. Calcd. for $C_{18}H_{19}NO$: C, 81.47; H, 7.22; N, 5.28. Found: C, 81.28; H, 7.25; N, 5.14.

12-Benzyl-10,11-dihydro-*anti*-11-methoxy-10,5-(iminomethano)-5*H*-dibenzo[*a,d*]cycloheptene (**2h**) hydrochloride (3.0 g), m.p. 167–170° (decomp.) (from isopropanol) was obtained from **1h** (5.0 g).

Anal. Calcd. for $C_{24}H_{24}ClNO$: C, 76.30; H, 6.40; Cl, 9.38; N, 3.70. Found: C, 76.33; H, 6.06; Cl, 9.32; N, 3.90.

10,11-Dihydro-*syn*-11-hydroxy-12-methyl-10,5-(iminomethano)-5*H*-dibenzo[*a,d*]cycloheptene (**2i**) oxalate (6.4 g), m.p. 183–185° (decomp.) (from isopropanol–ether) was obtained from **1i** (8.0 g).

Anal. Calcd. for $C_{19}H_{19}NO_5$: C, 66.85; H, 5.61; N, 4.10. Found: C, 67.61; H, 5.63; N, 4.24.

10,11-Dihydro-*syn*-11-methoxy-12-methyl-10,5-(iminomethano)-5*H*-dibenzo[*a,d*]cycloheptene (**2j**) oxalate (3.2 g), m.p. 183–186° (decomp.) (from acetonitrile–ether) was obtained from **1j** (5.4 g).

Anal. Calcd. for $C_{20}H_{21}NO_5$: C, 67.59; H, 5.96; N, 3.94. Found: C, 67.29; H, 6.20; N, 3.83.

10,11-Dihydro-*syn*-11-hydroxy-*anti*-11-methyl-10,5-(iminomethano)-5*H*-dibenzo[*a,d*]cycloheptene (**2k**) hydrochloride (4.7 g), m.p. 233–235° (from ethanol) was obtained from **1k** (7.0 g).

Anal. Calcd. for $C_{17}H_{19}ClNO$: Cl, 12.27; N, 4.11. Found: Cl, 11.99; N, 4.60.

10,11-Dihydro-*syn*-11-hydroxy-*anti*-11-phenyl-10,5-(iminomethano)-5*H*-dibenzo[*a,d*]cycloheptene (**2l**) hydrochloride (4.1 g), m.p. 219–224° (decomp.) (from ethanol) was obtained from **1l** (6.0 g).

Anal. Calcd. for $C_{22}H_{20}ClNO$: C, 75.53; H, 5.76; Cl, 10.13; N, 4.00. Found: C, 75.68; H, 5.73; Cl, 10.21; N, 3.88.

10,11-Dihydro-10,5-(iminomethano)-5H-dibenzo[a,d]-cyclohepten-11-one (2b)

A mixture of the ketolactam **1a** (25.0 g), ethylene glycol

(20 ml), *p*-toluenesulfonic acid (250 mg) and benzene was stirred and heated under reflux (Dean–Stark) for 24 h. The resulting suspension was washed with 2*N* NaOH and the solids were collected, washed with water, and dried to give the ethylene ketal of **1***a* (27.0 g), m.p. 265–269° (decomp.). A mixture of the ketal (26.5 g) and lithium aluminium hydride (4.5 g) in tetrahydrofuran was heated under reflux for 18 h. The mixture was treated with water, filtered, and the filtrate was evaporated. The residue was dissolved in 2*N* HCl (200 ml) and kept overnight. The resulting precipitate was collected and recrystallized from ethanol to give **2***b* hydrochloride (17.0 g), m.p. 285° (decomp.); ν_{max} (Nujol) 1685 cm^{-1}.

Anal. Calcd. for $C_{16}H_{14}ClNO$: C, 70.76; H, 5.16; Cl, 13.08; N, 5.16. Found: C, 70.85; H, 5.08; Cl, 13.23; N, 5.22.

Treatment of **2***b* (3.0 g) with a mixture of formic acid (10 ml) and formaldehyde (10 ml) at room temperature overnight gave, after processing in the usual manner, 10,11-dihydro-12-methyl-10,5-(iminomethano)-5*H*-dibenzo[*a*,*d*]cyclohepten-11-one (**2***m*), m.p. 149–151° (from ethanol); ν_{max} ($CHCl_3$) 2800, and 1665 cm^{-1}.

Anal. Calcd. for $C_{17}H_{15}NO$: C, 81.90; H, 6.06; N, 5.62. Found: C, 81.80; H, 6.09; N, 5.56.

Acknowledgments

We wish to thank Dr. G. S. Myers and his group for furnishing the tricyclic compounds in quantity. Spectral data were recorded by Mrs. J. Jachner and Mr. M. Boulerice, and analyses were carried out by Mr. W. J. Turnbull. The mass spectra were determined by the Morgan–Schaffer Corporation, Montreal.

1. (*a*) T. A. Dobson, M. A. Davis, and A. M. Hartung. First Intern. Congr. Heterocyclic Chem. Albuquerque, N.M. June 12th, 1967. Abstr. No. 32. (*b*) T. A. Dobson, M. A. Davis, A. M. Hartung, and J. Manson. Tetrahedron Letters, 4139 (1967).
2. T. A. Dobson, M. A. Davis, A. M. Hartung, and J. Manson. Can. J. Chem. **46**, 2843 (1968).
3. D. A. Guthrie, A. W. Frank, and C. B. Purves. Can. J. Chem. **33**, 729 (1955).
4. Von E Waldmann and C. Chwala. Ann. Chem. **609**, 125 (1957).
5. A. R. Battersby and D. A. Yoewell. J. Chem. Soc. 1988 (1965).
6. South African Patent No. 67/2148; Derwent Farmdoc Abstracts, **30**, No. 29,127.
7. F. Sǎntavý, M. Maturová, and L. Hruban. Chem. Commun. **36**, 144 (1966). F. Sǎntavý, L. Hruban, and M. Maturová. Collection Czech. Chem. Commun. **31**, 4286 (1966).
8. M. S. Yunusov, S. T. Skramov, and S. Yu. Yunusov. Khim. Prirodn. Soedin. Akad Nauk Uz. SSR. **3**, 68 (1967); Chem. Abstr. **67**, 11625*s* (1967).
9. G. N. Walker and D. Alkalay. J. Org. Chem. **31**, 905 (1966).
10. L. J. Bellamy. The infrared spectra of complex molecules. 2nd ed. Methuen and Co., Ltd., London. 1958. p. 95ff.
11. S. J. Cristol and R. K. Bly. J. Am. Chem. Soc. **82**, 6155 (1960).
12. G. Drefahl, M. Hartmann, and A. Skurk. Ber. **99**, 1168 (1966).
13. E. L. Eliel. Stereochemistry of carbon compounds. McGraw-Hill Book Co., Inc., New York. 1962. p. 230ff.
14. W. Schneider and R. Dillman. Ber. **96**, 2377 (1963). L. H. Werner and S. Ricca. J. Am. Chem. Soc. **80**, 2733 (1958).
15. J. W. Huffman, C. B. S. Rao, and T. Kamiya. J. Am. Chem. Soc. **87**, 2288 (1965); J. Org. Chem. **32**, 697, 700 (1967).
16. S. Winstein, R. Heck, S. Lapporte, and R. Baird. Experientia, **12**, 138 (1956).
17. B. Capon. Quart. Rev. London, **18**, 71 (1964), and references therein.
18. J. Rigaudy and L. Nédélec. Bull. Soc. Chim. France, 400 (1960).
19. M. Shemyakin and L. A. Shchukina. Quart. Rev. London, **10**, 261 (1956).
20. E. Hoeft and H. Schultze. J. Prakt. Chem. **32**, 12 (1966).
21. J. Gardent and M. Hamon. Bull. Soc. Chim. France, 556 (1966).
22. J. O. Jilek, V. Seidlová, E. Svátek, and M. Protiva. Monatsh. Chem. **96**, 182 (1965). M. Protiva. Il Farmaco; Edizione Scientifica (Pavia) **21**, 76 (1966).
23. M. Kharasch and O. Reinmuth. Grignard reaction of non-metallic substances. Prentice-Hall, Inc., New York. 1954.
24. J. W. ApSimon and O. E. Edwards. Can. J. Chem. **40**, 896 (1962).
25. W. L. Meyer and A. S. Levinson. J. Org. Chem. **28**, 2859 (1963).
26. M. A. Davis, S. O. Winthrop, R. A. Thomas, F. Herr, M-P. Charest, and R. Gaudry. J. Med. Chem. **7**, 88 (1964).
27. C. Djerassi, R. R. Engle, and A. Bowers. J. Org. Chem. **21**, 1547 (1956).
28. F. J. Villani, C. A. Ellis, C. Teichman, and C. Bigos. J. Med. Pharm. Chem. **5**, 381 (1962).
29. S. Kimoto and S. Ohta. Yakugaku Zasshi, **87**, 861 (1967).

Can. J. Chem. Downloaded from www.nrcresearchpress.com by 210.87.254.105 on 09/05/12
For personal use only.

Can. J. Chem. Downloaded from www.nrcresearchpress.com by 210.87.254.40 on 09/05/12
For personal use only.

NOTES

Preparation and rearrangement of β-chloroalkyl aziridinylformates

B. M. CULBERTSON AND S. DIETZ
Research Center, Ashland Chemical Company, Minneapolis, Minnesota 55420

Received February 28, 1968

Several β-chloroalkyl chloroformates have been treated with aziridines (ethylenimine or propylenimine) to obtain excellent yields of β-chloroalkyl aziridinylformates. In each case, it was found that the aziridinylformates rearranged upon thermloysis to give good yields of *N*-(β-chloroalkyl)-2-oxazolidones.

Canadian Journal of Chemistry, 46, 3399 (1968)

In recent years, the chemistry associated with aziridines (1) and 2-oxazolidones (2) has had accelerated study. This interest, combined with a disclosure describing the rearrangement of aziridinylformate esters to *N*-alkyl-2-oxazolidones (3), prompts us to report on the discovery that β-chloroalkyl aziridinylformates rearrange with heat to give *N*-(β-chloroalkyl)-2-oxazolidones in excellent yields. This versatile and facile series of reactions may be illustrated as follows.

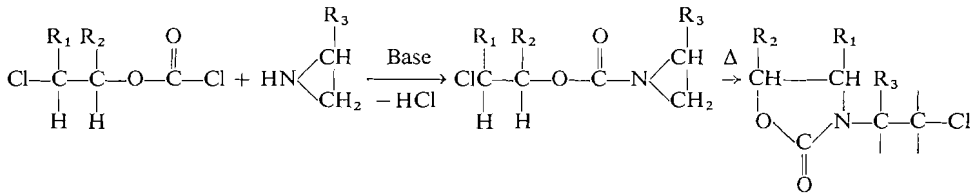

1 **2** **3** **4**

a $R_1 = R_2 = R_3 = H$
b $R_2 = CH_3(CH_2)_9$; $R_1 = R_3 = H$
c $R_1 = R_3 = H$; $R_2 = C_6H_5$
d $R_1 = C_6H_5$; $R_2 = R_3 = H$
e $R_1 = R_2 = H$; $R_3 = CH_3$

The reactions are not seriously limited by the availability of either the β-chloroalkyl chloroformates (**1**) or aziridines (**2**). Procedures for the preparation of both the β-chloroalkyl chloroformates (4) and aziridines (1) are known to the literature.

Aziridines such as **2** react exothermically with chloroformates. Therefore, the reaction is best run in an organic solvent using a slight excess of a trialkylamine base. The amine salt precipitates and is removed by filtration. Concentration of the filtrate affords nearly a quantitative yield of the aziridinylformates. In some cases, the infrared (i.r.) spectra exhibit a very small band at 1760 cm^{-1} which indicates the presence of a trace amount of the oxazolidone. Attempts to purify by distillation result in a significant conversion to the oxazolidone.

The aziridinylformates may also be prepared in a two-phase reaction using an aqueous base as the acid acceptor. The aziridines and base are dissolved in water and the aqueous mixture is added to a solution of the β-chloroalkyl chloroformate in an organic solvent such as benzene or chloroform. The organic layer is separated, washed with water, dried, and concentrated to isolate the product. Yields are usually lower using the interfacial condensation procedure.

Rearrangement to the oxazolidone occurs by heating during distillation, by direct heating (neat), or by refluxing the aziridinylformate in a suitable solvent. The preferred method for rearrangement employs the latter procedure. The reaction can be conveniently followed by i.r. analysis of the carbonyl region (1700–1800 cm^{-1}).

The carbonyl absorptions of aziridines of type **3** are reported to absorb at 1725 ± 5 cm^{-1} (5). We also found this to be the case in the formate

Can. J. Chem. Downloaded from www.nrcresearchpress.com by 210.87.254.40 on 09/05/12
For personal use only.

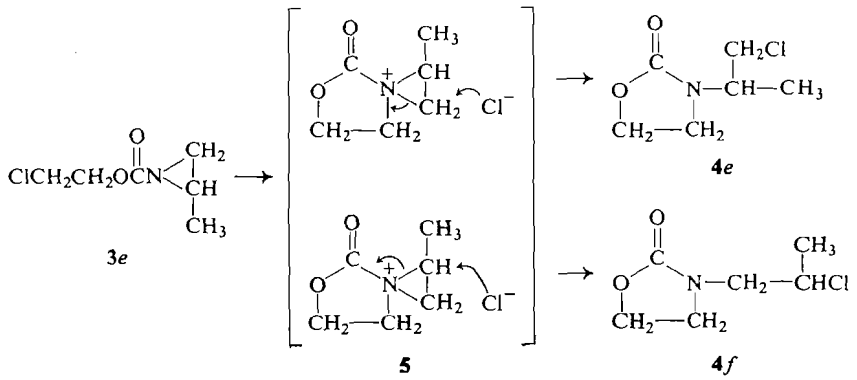

esters we prepared. The i.r. absorption of the carbonyl group of 2-oxazolidones is characteristically in the 1740–1810 cm^{-1} region and very often at or above 1760 cm^{-1} (2). However, the carbonyl of 2-oxazolidone itself is reported to absorb at 1724 (6) and 1730 cm^{-1} (7). We found that the chloroalkyl oxazolidones have a characteristic absorption at 1760 $\pm$ 5 cm^{-1}. In addition, the characteristic aziridine ring band in the 1315–1360 cm^{-1} region (5) gives way to a band at 1250–1270 cm^{-1} characteristic of the oxazolidone ring (6).

The mechanism (illustrated with **3***e* to give **4***e* and **4***f*) of the reaction probably involves an aziridinium salt (**5**) of the type proposed by Dick (8) in the preparation of piperazine followed by S_N2 attack by the strongly nucleophilic halogen anion. Further, Heine (9) also suggests the same type of mechanism for the formation of *N*-2-chlorophthalimides from 1-(*O*-chloromethylbenzoyl) aziridine. By this mechanism, one would expect that, in the case of an unsymmetrical aziridine, the ring would be opened by nucleophilic attack at the least hindered carbon atom. This was supported by experimental evidence in the case of the β-chloroethylformate derivative of propylenimine **3***e* which gave 93% **4***e* and only 7% **4***f*.

Alternatively, a carbonium ion intermediate is not likely in view of the experimental evidence. If the mechanism involves ring opening to the most stable carbonium ion, **4***f* would be expected to be the major product.

Experimental

The infrared (i.r.) spectra were obtained as liquid smears on a Perkin–Elmer model 337 spectrophotometer and the nuclear magnetic resonance (n.m.r.) spectra on a Varian A-60 instrument with tetramethylsilane as interna reference and a probe temperature of 39 °C. The purity and yield of the products were estimated by gas–liquid phase chromatography (g.l.p.c.) using a Hewlett–Packard F and M scientific model 720 equipped with a 6 ft × ¼ in. silicone gum rubber (10% on Chromosorb W) column. The chromatograph was run at a helium flow rate of 60 ml per min through the column, which was maintained at 150 or 180 °C.

Reactions of 2-Chloroethyl Chloroformate with Ethylenimine

(a) Interfacial Condensation Procedure

Ethylenimine (8.6 g, 0.2 mole) and potassium hydroxide (11.3 g, 0.2 mole) were dissolved in 100 ml water. A solution of 28.4 g (0.2 mole) of 2-chloroethyl chloroformate in 100 ml of chloroform was added slowly, with stirring, to the cold aqueous solution. Ice chips were added as needed to keep the temperature below 20 °C. The chloroform solution was separated, washed with water, and dried over anhydrous magnesium sulfate. Filtration and evaporation of the solvent afforded a 20.0 g yield of water white liquid (**3***a*). The i.r. spectrum, ν_{max} 3075 (aziridine ring CH_2 stretching), 1725 (C=O stretching), 1330 (sym ring breathing), 1190–1205 (strong, broad band, $\diagdown N-\overset{O}{\overset{\|}{C}}O-\diagup$ stretching mode), 1155 (CH_2 wagging vibration), 830 (CH_2 rocking and ring deformation), and 668 cm^{-1} (C—Cl) supported (5) the proposed structure of **3***a*. Distillation *in vacuo* (0.3 mm of Hg) afforded 8.0 g of a low boiling fraction, b.p. 58–60 °C, n_D^{25} 1.4647, and 10.0 g of a higher boiling fraction (61–120 °C) suspected to be predominately *N*-(2-chloroethyl)-2-oxazolidone (**4***a*). The i.r. spectrum of the low boiling fraction exhibited the same characteristic absorption bands as reported for **3***a*. Further, the n.m.r. spectrum (CCl_4), with a singlet at τ7.82 (N—CH_2) and an A_2B_2 multiplet region centered about τ6.0 (O—CH_2) integrated for the correct number of protons for **3***a*. Singlets, rather than doublets, have been reported before for aziridinyl ring protons (12–16).

Anal. Calcd. for $C_5H_8ClNO_2$ (**3***a*): C, 40.11; H, 5.39; N, 9.36. Found: C, 39.91; H, 5.46; N, 9.41.

The high boiling fraction was redistilled to yield 8.0 g

Can. J. Chem. Downloaded from www.nrcresearchpress.com by 210.87.254.40 on 09/05/12
For personal use only.

of **4***a*, b.p. 117–120 °C/0.3 mm of Hg, n_D^{25} 1.4875, reported for **4***a*, b.p. 110 °C/0.1 mm of Hg, n_D^{25} 1.4900 (10) and 114 °C/0.3 mm of Hg, n_D^{25} 1.4875 (11). The i.r. spectrum of **4***a* also agreed with the reported (10) i.r. spectrum of 3-chloroethyl-2-oxazolidone.

The reaction was repeated, using molar quantities of β-chloroethyl chloroformate and ethylenimine, to obtain a 101 g (68%) yield of crude **3***a*, n_D^{25} 1.4648.

(b) Solution Condensation Procedure

Benzene (70 ml) and 2-chloroethyl chloroformate (14.2 g, 0.1 mole) were combined and cooled to 5 °C. A mixture of ethylenimine (4.3 g, 0.1 mole) and triethylamine (12 g, 0.12 mole) in 30 ml benzene was added slowly with stirring and cooling. The mixture was allowed to warm to room temperature (ca. 1 h) and filtered. Evaporation of the solvent afforded a 13.5 g (91%) yield of slightly yellow colored liquid with an i.r. spectrum identical to that previously reported for **3***a*. Distillation *in vacuo* (0.3 mm of Hg) afforded 5.0 g of **3***a*, b.p. 59–61 °C, and a 7.0 g yield of **4***a*, b.p. 118–120 °C. The i.r. and n.m.r. spectrum of **3***a* and **4***a* by this procedure agreed with spectra of **3***a* and **4***a* prepared by the other procedure.

1-Chloromethylundecyl Aziridinylformate (3b)

Ethylenimine (2.15 g, 0.05 mole) and triethylamine (7.5 g, 0.075 mole) were dissolved in 25 ml of benzene and cooled to 10 °C. Crude 1-chloromethylundecyl chloroformate (14.15 g, 0.05 mole), prepared by the Jones (4) procedure, in 25 ml of benzene was added slowly with stirring and cooling to keep the reaction temperature below 20 °C. After the addition was complete, the mixture was allowed to warm to room temperature and stirred for 30 min. Triethylamine hydrochloride was removed by filtration and the solvent benzene was removed on a rotary evaporator at room temperature leaving an 11.9 g (88%) yield of crude **3***b*, ν_{max} (neat) 2920, 2850, 1730 (C=O), 1320 (—N<), 1200, and 680 (C—Cl) cm^{-1}. The g.l.p.c. data indicated crude **3***b* was ca. 85% pure.

3-(2-Chloroethyl)-5-decyl-2-oxazolidone (4b)

Distillation of crude **3***b* *in vacuo* afforded two fractions. Fraction 1, b.p. 88–89 °C/0.13 mm of Hg, with no carbonyl absorption in the i.r. spectrum, was not identified but thought to be 1,2-dichlorododecane. Fraction 2, b.p. 165–166 °C/0.07 mm of Hg, n_D^{28} 1.4698, ν_{max} (neat) 2920, 2850, 1755, 1265, 765, and 670 cm^{-1} which was collected in a 5.0 g (45%) yield, exhibited i.r. absorption bands characteristic of only the oxazolidone ring system.

Anal. Calcd. for $C_{15}H_{28}ClNO_2$: C, 62.18; H, 9.67; N, 4.84. Found: C, 62.13; H, 9.76; N, 4.56.

The n.m.r. spectrum (CCl_4), with a triplet at τ 9.12 (—CH_3), a multiplet centered at τ 8.71, and an A_2B_2 pattern centered at τ 6.38, indicated the 5-decyl isomer exclusively and integrated for the correct number of protons for **4***b*.

2-Chloro-1-phenylethyl Aziridinylformate (3c) and 2-Chloro-2-phenylethyl Aziridinylformate (3d)

Crude 2-chloro-1-phenylethyl chloroformate (4), with some isomeric 2-chloro-2-phenylethyl chloroformate (25 g, 0.1 mole), was dissolved in 25 ml benzene and cooled to ca. 5 °C. Triethylamine (15 g, 0.15 mole) and ethylenimine (4.9 g, 0.11 mole) in 25 ml benzene were added slowly with stirring and cooling. The mixture was warmed to room temperature and stirred for 1 h. After filtration to remove the amine hydrochloride, and solvent removal, a 21.0 g (82%) yield of a mixture of 2-chloro-1-phenylethyl aziridinylformate (**3***c*) and 2-chloro-2-phenylethyl aziridinylformate (**3***d*) isomers was obtained. The i.r. spectrum, ν_{max} (neat) 3025, 3000, 1735, 1335, 1190, and 700 cm^{-1} supported structures **3***c* and **3***d*. The g.l.p.c. data indicated ca. 75–80% purity with the main peak slightly split.

3-(2-Chloroethyl)-5-phenyl-2-oxazolidone (4c) and 3-(2-Chloroethyl-4-phenyl-2-oxazolidone (4d)

Heating (neat) the isomeric mixture of **3***c* and **3***d* on the steam bath for 6 h at 100 °C caused quantitative rearrangement to the oxazolidones (**4***c* and **4***d*). The rearrangement reaction was readily followed by i.r., i.e. formate C=O band at 1730 cm^{-1} diminished and vanished and the oxazolidone C=O band at 1760 cm^{-1} increased to maximum intensity. The product was twice distilled *in vacuo* (0.3 mm of Hg) to give a viscous yellow liquid, b.p. 148–149 °C, n_D^{28} 1.5473, ν_{max} (neat) 3025, 2950, 2900, 1760, 1230, 1155, 1090, 765, and 705 cm^{-1}.

Anal. Calcd. for $C_{11}H_{12}ClNO_2$: C, 58.54; H, 5.32; N, 6.22. Found: C, 58.36; H, 5.43; N, 6.01.

The n.m.r. spectrum (CCl_4), with an A_2B_2 pattern centered about τ 6.5, two AX type patterns centered at τ 5.0 and τ 5.97, a triplet centered at τ 5.41, and a singlet at τ 2.63, integrated for the correct number of protons. The complex splitting pattern indicates a mixture of isomers. From the starting materials, the 5-substituted phenyl isomer (**4***c*) should predominate. Without the n.m.r. spectra of the known 4- and 5-substituted 2-oxazolidones for comparison, no direct assignments were made.

2-Chloroethyl Methylaziridinylformate (3e)

According to the procedure used for the preparation of **3***a* (solution method), 2-chloroethyl chloroformate (28.6 g, 0.2 mole) was treated with propylenimine to give a 30.0 g (92%) yield of water white liquid (**3***e*). The g.l.p.c. curve indicated ca. 81% aziridine and 19% oxazolidone. The major portion, if not all, of the oxazolidone probably occurs due to rearrangement of the aziridine on the column. Distillation *in vacuo* (0.2 mm of Hg) gave a water white fraction, b.p. 50–53 °C, ν_{max} (neat) 3000, 2970, 2930, 1735, 1325, 1220, 1090, and 670 cm^{-1}, indicating the desired compound (**3***e*). The n.m.r. spectrum ($CDCl_3$), with doublets at τ 8.69 (CH—CH_3) and τ 8.03 (N—CH_2), multiplet at τ 7.50 (N—CH), and A_2B_2 pattern centered at τ 5.95, integrated for the correct number of protons for **3***e*.

Anal. Calcd. for $C_6H_{10}ClNO_2$: C, 44.04; H, 6.12; N, 8.56. Found: C, 43.82; H, 6.01; N, 8.35.

3-(1-Methyl-2-chloroethyl)-2-oxazolidone (4e)

The aziridinylformate prepared above (**3***e*) was heated (neat) at 100 °C for 6 h to effect rearrangement. The liquid became orange-red, ν_{max} (neat) 2985, 2925, 1755, 1430, 1260, 1055, and 760 cm^{-1} indicating transformation of **3***e* to the oxazolidone or oxazolidone mixture (**4***e* and **4***f*). Distillation yielded a pale-yellow liquid, b.p. 108–110 °C/0.2 mm of Hg, which was ca. 96% pure by g.l.p.c.

Direct distillation of the aziridinylformate (*3e*) yielded a water white liquid, b.p. 110–112 °C/0.2 mm of Hg, n_D^{25} 1.4838, which was 100% oxazolidone by g.l.p.c. The oxazolidone peak (g.l.p.c. curve) exhibited a shoulder of approximately 8% which was believed to be isomer *4f*. The i.r. spectra of the two oxazolidone mixtures, prepared by the two procedures, were identical. The n.m.r. spectrum ($CDCl_3$), with doublets at τ 8.70 and τ 8.48 and a complex pattern from τ 6.58 to τ 5.42, integrated for the correct number of protons and indicated ca. 93% isomer *4e* and 7% isomer *4f*. The relative amounts of the two isomers were estimated from integration of the methyl protons. Isomer *4f* has been reported by Arnold and Beckel (11), b.p. 107–108/0.5 mm of Hg, n_D^{25} 1.4795.

Anal. Calcd. for $C_6H_{10}ClNO_2$: C, 44.04; H, 6.12; N, 8.56. Found: C, 43.92; H, 6.05; N, 8.33.

Acknowledgments

We wish to thank C. R. Glowacki for the elemental analyses and P. J. Menardi for obtaining the n.m.r. spectra and assisting in their interpretation.

1. T. A. Foglia and D. Swern. J. Org. Chem. **32**, 75 (1967).
2. M. E. Dyen and D. Swern. Chem. Rev. **67**, 197 (1967).
3. G. E. Ham. U.S. Patent No. 3,247,220 (April 19, 1966).
4. J. I. Jones. J. Chem. Soc. 2735 (1957).
5. L. Spell. Anal. Chem. **39**, 185 (1967).
6. R. Mecke and A. Luttringhaus. Chem. Ber. **90**, 975 (1957).
7. H. K. Hall, Jr. and R. Zbinden. J. Am. Chem. Soc. **80**, 6428 (1958).
8. C. R. Dick. J. Org. Chem. **32**, 72 (1967).
9. H. W. Heine. J. Am. Chem. Soc. **85**, 2743–2745 (1963).
10. E. K. Drechsel. J. Org. Chem. **22**, 849 (1957).
11. H. Arnold and H. Bekel. French Patent No. 1,345,001; Chem. Abstr. **61**, 7020 (1964).
12. T. J. Bardos, C. Szantay, and C. K. Navada. J. Am. Chem. Soc. **87**, 5796 (1965).
13. A. B. Turner, H. W. Heine, J. Irving, and J. B. Bush, Jr. J. Am. Chem. Soc. **87**, 1050 (1965).
14. S. J. Brois. J. Am. Chem. Soc. **89**, 4242 (1967).
15. A. T. Bottini and J. D. Roberts. J. Am. Chem. Soc. **80**, 5203 (1958).
16. D. A. Tomalia and J. N. Paige. J. Heterocyclic Chem. **4**, 178 (1967).

Convenient synthesis of *t*-butyl alcohol-*d*

Saul Wolfe, Wha Suk Lee, and John R. Campbell
Department of Chemistry, Queen's University, Kingston, Ontario

Received July 13, 1967[1]

The title compound is prepared by alkaline hydrolysis (NaOD–D_2O) of a *t*-butyl ester. With *t*-butyl acetate the alcohol salts out of the reaction mixture and is easily separated and dried; however, slow concurrent exchange of the sodium acetate reduces the deuterium content of the alcohol to 95%. With *t*-butyl benzoate pure *t*-butyl alcohol-*d* is isolated by distillation of the alcohol–water azeotrope and drying.

Canadian Journal of Chemistry, 46, 3402 (1968)

t-Butyl alcohol-*d* is an important solvent for hydrogen exchange studies and several methods have been described for its synthesis. These include direct exchange with D_2O (1–3) as well as deuterolysis of magnesium (4), aluminium (4, 5), or lithium aluminium *t*-butoxide (6). Since on a molar basis the price quoted for *t*-buOD is about 20 times that of D_2O it must be assumed that the above procedures are either wasteful of D_2O or do not adapt readily to large scale preparations.

We wish to describe a simple laboratory synthesis of *t*-buOD which involves only a moderate experimental effort and ought to be adaptable to large scale preparations. The method involves the hydrolysis of a *t*-butyl ester in NaOD–D_2O and separation of the wet alcohol from the reaction mixture by salting out or by distillation of the alcohol–water azeotrope.

The alcohol is salted out of alkaline *t*-butyl acetate reaction mixtures provided that the concentration of NaOD is greater than 10%. The water content of the *t*-butanol layer is 12.15, 6.74, and 0.87% for base concentrations of 15, 30, and 50%, respectively and is reduced to about 0.3% by one distillation from a slight excess of calcium hydride. However since sodium acetate, the second product of the hydrolysis, itself exchanges in refluxing basic D_2O (7), the *t*-buOD obtained by the above procedure contains varying amounts of *t*-buOH. When the hydrolysis is performed at room temperature exchange of the acetate is largely but not completely overcome and samples

[1]Revision received June 25, 1968.

Can. J. Chem. Downloaded from www.nrcresearchpress.com by 210.87.254.40 on 09/05/12
For personal use only.

Direct distillation of the aziridinylformate (*3e*) yielded a water white liquid, b.p. 110–112 °C/0.2 mm of Hg, n_D^{25} 1.4838, which was 100% oxazolidone by g.l.p.c. The oxazolidone peak (g.l.p.c. curve) exhibited a shoulder of approximately 8% which was believed to be isomer *4f*. The i.r. spectra of the two oxazolidone mixtures, prepared by the two procedures, were identical. The n.m.r. spectrum ($CDCl_3$), with doublets at τ 8.70 and τ 8.48 and a complex pattern from τ 6.58 to τ 5.42, integrated for the correct number of protons and indicated ca. 93% isomer *4e* and 7% isomer *4f*. The relative amounts of the two isomers were estimated from integration of the methyl protons. Isomer *4f* has been reported by Arnold and Beckel (11), b.p. 107–108/0.5 mm of Hg, n_D^{25} 1.4795.

Anal. Calcd. for $C_6H_{10}ClNO_2$: C, 44.04; H, 6.12; N, 8.56. Found: C, 43.92; H, 6.05; N, 8.33.

Acknowledgments

We wish to thank C. R. Glowacki for the elemental analyses and P. J. Menardi for obtaining the n.m.r. spectra and assisting in their interpretation.

1. T. A. Foglia and D. Swern. J. Org. Chem. **32**, 75 (1967).
2. M. E. Dyen and D. Swern. Chem. Rev. **67**, 197 (1967).
3. G. E. Ham. U.S. Patent No. 3,247,220 (April 19, 1966).
4. J. I. Jones. J. Chem. Soc. 2735 (1957).
5. L. Spell. Anal. Chem. **39**, 185 (1967).
6. R. Mecke and A. Luttringhaus. Chem. Ber. **90**, 975 (1957).
7. H. K. Hall, Jr. and R. Zbinden. J. Am. Chem. Soc. **80**, 6428 (1958).
8. C. R. Dick. J. Org. Chem. **32**, 72 (1967).
9. H. W. Heine. J. Am. Chem. Soc. **85**, 2743–2745 (1963).
10. E. K. Drechsel. J. Org. Chem. **22**, 849 (1957).
11. H. Arnold and H. Bekel. French Patent No. 1,345,001; Chem. Abstr. **61**, 7020 (1964).
12. T. J. Bardos, C. Szantay, and C. K. Navada. J. Am. Chem. Soc. **87**, 5796 (1965).
13. A. B. Turner, H. W. Heine, J. Irving, and J. B. Bush, Jr. J. Am. Chem. Soc. **87**, 1050 (1965).
14. S. J. Brois. J. Am. Chem. Soc. **89**, 4242 (1967).
15. A. T. Bottini and J. D. Roberts. J. Am. Chem. Soc. **80**, 5203 (1958).
16. D. A. Tomalia and J. N. Paige. J. Heterocyclic Chem. **4**, 178 (1967).

Convenient synthesis of *t*-butyl alcohol-*d*

Saul Wolfe, Wha Suk Lee, and John R. Campbell
Department of Chemistry, Queen's University, Kingston, Ontario

Received July 13, 1967[1]

The title compound is prepared by alkaline hydrolysis (NaOD–D_2O) of a *t*-butyl ester. With *t*-butyl acetate the alcohol salts out of the reaction mixture and is easily separated and dried; however, slow concurrent exchange of the sodium acetate reduces the deuterium content of the alcohol to 95%. With *t*-butyl benzoate pure *t*-butyl alcohol-*d* is isolated by distillation of the alcohol–water azeotrope and drying.

Canadian Journal of Chemistry, 46, 3402 (1968)

t-Butyl alcohol-*d* is an important solvent for hydrogen exchange studies and several methods have been described for its synthesis. These include direct exchange with D_2O (1–3) as well as deuterolysis of magnesium (4), aluminium (4, 5), or lithium aluminium *t*-butoxide (6). Since on a molar basis the price quoted for *t*-buOD is about 20 times that of D_2O it must be assumed that the above procedures are either wasteful of D_2O or do not adapt readily to large scale preparations.

We wish to describe a simple laboratory synthesis of *t*-buOD which involves only a moderate experimental effort and ought to be adaptable to large scale preparations. The method involves the hydrolysis of a *t*-butyl ester in NaOD–D_2O and separation of the wet alcohol from the reaction mixture by salting out or by distillation of the alcohol–water azeotrope.

The alcohol is salted out of alkaline *t*-butyl acetate reaction mixtures provided that the concentration of NaOD is greater than 10%. The water content of the *t*-butanol layer is 12.15, 6.74, and 0.87% for base concentrations of 15, 30, and 50%, respectively and is reduced to about 0.3% by one distillation from a slight excess of calcium hydride. However since sodium acetate, the second product of the hydrolysis, itself exchanges in refluxing basic D_2O (7), the *t*-buOD obtained by the above procedure contains varying amounts of *t*-buOH. When the hydrolysis is performed at room temperature exchange of the acetate is largely but not completely overcome and samples

[1]Revision received June 25, 1968.

Can. J. Chem. Downloaded from www.nrcresearchpress.com by 210.87.254.5 on 09/05/12
For personal use only.

TABLE I

Preparation of *t*-butyl benzoate

Benzoic acid g (moles)	Solvent (ml)	Sulfuric acid (ml)	Isobutylene g (moles)	Yield of *t*-butyl benzoate (%)
41.0 (0.336)	CH_2Cl_2 (60)*†	2.0	15.3 (0.274)	22.8‡
30.0 (0.246)	CH_2Cl_2 (40)*†	2.0	15.6 (0.278)	33.8§
20.0 (0.164)	CH_2Cl_2 (40)*†	2.0	25.0 (0.447)	35.0§
40.0 (0.328)	Acetone (50)‖	2.0	17.1 (0.305)	44.3‡
40.0 (0.328)	Dioxane (50)¶	2.0	17.1 (0.305)	64.0‡

*Only a partial solution formed.
†Some diisobutylene was formed.
‡Based on isobutylene.
§Based on benzoic acid.
‖The reaction mixture turned black and some mesityl oxide was formed.
¶The reaction mixture was light brown; no by-products were formed.

of the alcohol containing 95% of *t*-buOD can be obtained.

When *t*-butyl benzoate is used as the substrate, sodium benzoate rather than the alcohol salts out of the reaction mixture and the wet alcohol is therefore isolated by distillation. Drying of the azeotrope over calcium hydride affords *t*-buOD containing 0.3% of D_2O and no detectable *t*-buOH.

Experimental

t-Butyl Acetate

A mixture of glacial acetic acid (52.45 g, 50 ml, 0.87 mole) and concentrated sulfuric acid (2 ml) was frozen in a 200 ml pressure bottle, and liquid isobutylene (25.9 g, 40 ml, 0.46 mole) was added. The bottle was sealed, shaken at room temperature for 24 h, and the contents then poured slowly onto excess 10% sodium bicarbonate solution. The organic layer was washed with water and dried over molecular sieve to give *t*-butyl acetate (48 ml, 80%), b.p. 97–98°; λ_{max} ($CHCl_3$) 5.75μ; τ 8.05 (3H), 8.55 (9H). The yield was not improved by the use of a longer reaction time (48 h) or an increase in the amount of catalyst (4 ml). No attempt was made to avoid a small loss of isobutylene during the transfer.

Hydrolysis of t-Butyl Acetate

A mixture of *t*-butyl acetate (15.0 g, 0.129 mole) and NaOD–D_2O (39 g, 15% w/w, 0.143 mole) was shaken vigorously at room temperature for 90 h. Hydrolysis was followed by disappearance of the peak in the upper layer at τ 8.55 and appearance of a peak at τ 8.75. The alcohol layer was then separated. It weighed 8.8 g and contained 1.06 g (12%) of D_2O as determined by Karl Fischer titration. The material was refluxed for 3 h with calcium hydride (1.25 g) and then distilled to give 7.1 g (73.5%) of *t*-butyl alcohol-*d*, b.p. 80–82°, which contained 0.34% of water, and 5% of undeuterated *t*-butyl alcohol as determined by infrared (i.r.) analysis. No attempt was made to recover unreacted D_2O or to improve the efficiency of the drying procedure.

t-Butyl Benzoate

A mixture of benzoic acid, solvent, and concentrated sulfuric acid was frozen in a 200 ml pressure bottle and the appropriate amount of liquid isobutylene was added. The bottle was sealed, shaken at room temperature for 24 h, and the contents then diluted with methylene chloride (75 ml). The methylene chloride solution was washed with 20% potassium carbonate, water, and dried over anhydrous magnesium sulfate. Removal of the solvent and distillation gave *t*-butyl benzoate, b.p. 86–87°/6 mm (lit. (8) 94°/10 mm; (9) 67–68°/1 mm), λ_{max} (CCl_4) 5.81μ, in the amounts shown in Table I. No attempt was made to recover the benzoic acid.

Hydrolysis of t-Butyl Benzoate

A mixture of *t*-butyl benzoate (30.0 g, 0.169 mole) and NaOD–D_2O (41.6 g, 20% w/w, 0.203 mole) was refluxed with stirring for 48 h by which time a clear solution had resulted and none of the ester could be detected by gas–liquid chromatography. Distillation afforded 13.6 g of the *t*-buOD–D_2O azeotrope, b.p. 81–83°. This was dried by adding in portions a total of 2.75 g of calcium hydride; after 3 h refluxing, distillation afforded 9.2 g (72.3%) of *t*-buOD, b.p. 80–82°, m.p. 24–25°, which contained 0.3% of D_2O and no detectable *t*-buOH (determined by i.r.).

Acknowledgment

We thank Mrs. H. H. Pieniak for the Karl Fischer determinations.

1. M. S. Kharasch, J. L. Rowe, and W. H. Urry. J. Org. Chem. **16**, 905 (1951).
2. K. B. Wiberg, R. K. Barnes, and J. Albin. J. Am. Chem. Soc. **79**, 4994 (1957).
3. D. J. Cram and B. Rickborn. J. Am. Chem. Soc. **83**, 2178 (1961).
4. G. Jakli, G. Jancso, and J. Illy. Chem. Abstr. **63**, 17874*h* (1965).
5. M. Morton, J. A. Cala, and I. Piirma. J. Am. Chem. Soc. **78**, 5394 (1956).
6. J. G. Pritchard and H. M. Nelson. J. Phys. Chem. **64**, 795 (1960).
7. J. G. Atkinson, J. J. Csakvary, G. T. Herbert, and R. S. Stuart. J. Am. Chem. Soc. **90**, 498 (1968).
8. M. Pfannel. Monatsh. Chem. **32**, 509 (1911).
9. M. L. Bender. J. Am. Chem. Soc. **73**, 1626 (1951).

Can. J. Chem. Downloaded from www.nrcresearchpress.com by 210.87.254.5 on 09/05/12
For personal use only.

Synthesis of abnormal peptides: cyclization of N^{α}-formyltryptophyl residue to 3,4-dihydro-β-carboline-3-carboxylic acid residue in acidic media[1]

ALDO PREVIERO, MARIA-ANTONIA COLETTI-PREVIERO, AND LÉO-G. BARRY

Département de Biochimie Macromoléculaire (CNRS) et Groupe de Recherches U-67 (INSERM), B.P. 1018, 34-Montpellier, France

Received April 30, 1968

The intramolecular reaction of N^{α}-formyltryptophan to 3,4-dihydro-β-carboline-3-carboxylic acid is realized with high yield either in trifluoroacetic acid or in formic acid – concentrated hydrochloric acid solutions. Optically active products are obtained when formylated L- or D-tryptophan are used as starting compounds. The experimental conditions employed are highly specific and the cyclization of N^{α}-formyltryptophyl residue is realized also in peptides without secondary lytic reactions. The general behavior of N^{α}-formyltryptophan in formic acid solutions is discussed.

Canadian Journal of Chemistry, 46, 3404 (1968)

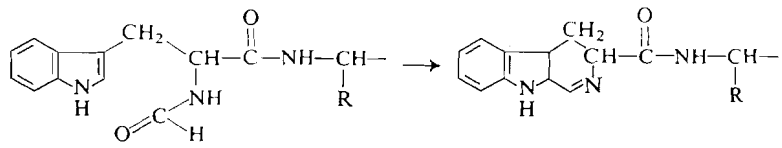

Scheme 1

The compounds containing the β-carboline nucleus are of great interest in connection with their occurrence in some alkaloids. A synthetic procedure available to obtain the members of this class consists in a condensation of tryptophan, or its simple substituted derivatives, with aldehydes to yield a 1,2,3,4-tetrahydro-β-carboline (1). These products can be converted to the fully aromatic compounds by dehydrogenation. Some difficulties arise when the 3,4-dihydro-β-carboline nucleus is desired. The partial dehydrogenation is generally difficult to realize since the dihydro derivatives are completely aromatized at a rate that does not permit their accumulation in the reaction medium. An alternative procedure to synthesize the 3,4-dihydro-β-carboline nucleus has been pointed out by Späth and Lederer (2) who directly converted the amides of tryptamine to the corresponding 3,4-dihydro-β-carboline.

The attempts to effect an analogous cyclization on N^{α}-acyltryptophan to obtain 3,4-dihydro-β-carboline-3-carboxylic acids showed that secondary reactions such as decarboxylation and dehydrogenation occurred and in the case of N^{α}-formyltryptophan no product was obtained (3, 4).

The present report is concerned with the preparation of optically active 3,4-dihydro-β-carboline-3-carboxylic acid by cyclization of N^{α}-formyltryptophan. The reaction conditions are also used to cyclize some N^{α}-formyltryptophyl peptides to obtain the corresponding 3,4-dihydro-β-carboline derivatives in good yields as depicted in Scheme 1.

Experimental

Ultraviolet (u.v.) spectra were recorded with a Cary model 15 (1 cm cells) spectrophotometer. Amino acid analyses were performed with a Beckman amino acid analyzer model 120 B using microcells with a 6.6 mm light path. Paper chromatography was carried out on Whatman No. 1 paper. The two solvents employed were aqueous solutions of ammonia 5% (v/v) and ammonium chloride 3% (w/v). 3,4-Dihydro-β-carboline derivatives were easily detected as yellow fluorescent spots in u.v. light (4).

N^{α}-formyltryptophan was obtained by treatment of the amino acid with one equivalent of acetic anhydride in formic acid (5). N^{α}-formyl-L-tryptophyl-L-phenylalanine methyl ester, N^{α}-formyl-L-tryptophyl-L-tyrosine methyl ester, and N^{α}-formyl-L-tryptophyl-L-leucine methyl ester were synthesized from N^{α}-formyl-L-tryptophan, and the corresponding amino acid esters by the carbodiimide method in dimethyl formamide. The formylated peptides were obtained as free acids by saponification of the corresponding ester derivatives.

3,4-Dihydro-β-carboline-3-carboxylic Acid (Cyclization of N^{α}-Formyltryptophan)

In a typical experiment, 50 μmoles of N^{α}-formyltryptophan were dissolved in 5 ml of anhydrous trifluoroacetic

[1]Contribution No. 15 from the Département de Biochimie Macromoléculaire et Groupe de Recherches.

Can. J. Chem. Downloaded from www.nrcresearchpress.com by 210.87.254.105 on 09/05/12
For personal use only.

TABLE I

Properties of optically active and racemic 3,4-dihydro-β-carboline-3-carboxylic acid hydrochloride

Product obtained from:	Analysis						Melting point (°C)	α_D^{20}†	R_f‡	Yield (%)	ε (362mμ)
	Calculated*			Found							
	C	N	HCl	C	N	HCl					
N^{α}-formyl-L-Try	57.49	11.17	14.54	56.92	11.15	14.62	232	+473	0.45	75	22200
N^{α}-formyl-DL-Try	57.49	11.17	14.54	57.05	11.16	14.60	240	—	0.45	72	22200
N^{α}-formyl-D-Try	57.49	11.17	14.54	57.13	11.13	14.62	232	−475	0.45	72	22200

*Analysis calculated for $C_{12}H_{11}N_2O_2Cl$.
†c = 1 in CH_3OH.
‡Paper chromatography in 3% NH_4Cl.

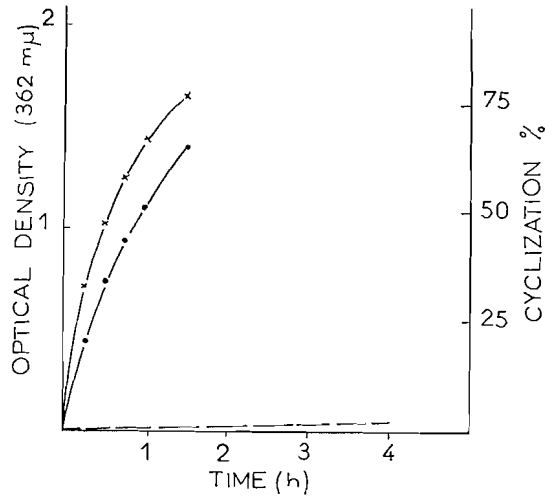

FIG. 1. Cyclization rates of N^{α}-formyltryptophan to 3,4-dihydro-β-carboline-3-carboxylic acid in trifluoroacetic acid (×—×—×) and formic acid:concentrated hydrochloric acid, 9:1 (•—•—•—•) at 50 °C. The dotted line represents the analogous reaction of N^{α}-acetyltryptophan under the same conditions.

acid and the solution was allowed to stand at 50 °C in a sealed tube. At suitable intervals of time, 0.1 ml samples of the reaction mixture were diluted with 10 ml of methanol and spectrophotometrically recorded from 250–400 mμ. A new absorption peak at 362 mμ appeared during the reaction (Fig. 1) while the characteristic absorption of tryptophan gradually disappeared (Fig. 2).

Paper chromatography in 3% NH_4Cl at the end point of the reaction showed only one product detected by its yellow fluorescence in u.v. light.

An identical reaction product was obtained when N^{α}-formyltryptophan was allowed to stand at 50 °C in a solution of formic acid containing 10% (v/v) concentrated HCl. For preparative purposes, a solution of N^{α}-formyl-L-tryptophan (0.5 g) in HCOOH (9 ml) and concentrated HCl (1 ml) was heated at 50 °C for 3 h in a sealed tube. The solution was then concentrated under reduced pressure; 3,4-dihydro-β-carboline-3-carboxylic acid hydrochloride rapidly separated as a crystalline pale-yellow product upon addition of acetic acid. The same procedure was employed for the cyclization of N^{α}-formyl-DL-tryptophan and N^{α}-formyl-D-tryptophan. The yield and the properties of the products obtained are listed in Table I.

3,4-Dihydro-β-carboline Containing Peptides

(a) Cyclization of N^{α}-Formyltryptophyl Peptide Free Acids

A solution of N^{α}-formyl-L-tryptophyl-L-phenylalanine (0.5 g) in 10 ml of anhydrous trifluoroacetic acid was

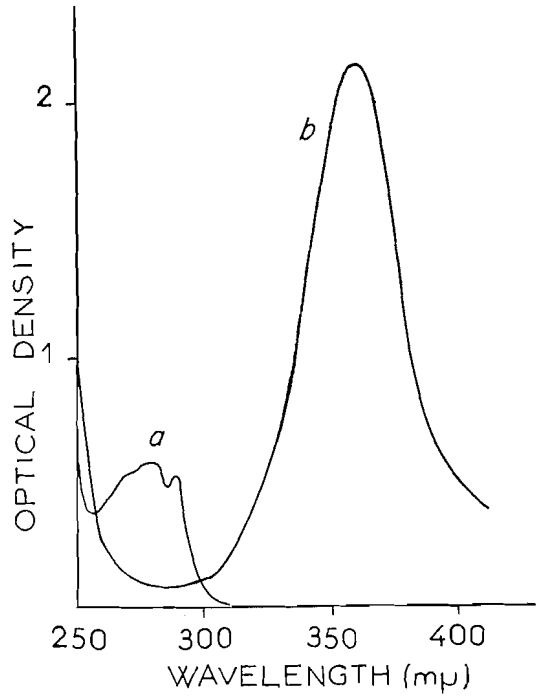

FIG. 2. Spectral changes of N^{α}-formyltryptophan (*a*) after its conversion into 3,4-dihydro-β-carboline-3-carboxylic acid (*b*) (1×10^{-7} *M* solution in methanol).

Can. J. Chem. Downloaded from www.nrcresearchpress.com by 210.87.254.105 on 09/05/12
For personal use only.

TABLE II

Properties of 3,4-dihydro-β-carboline containing peptides

3,4-Dihydro-β-carboline containing peptides from:	Amino acid recovered after acid hydrolysis (%)	Melting point (°C)	ε (362mμ)	R_f NH_3 5%	R_f NH_4Cl 3%	Yield (%)
N^{α}-formyl-L-Try-L-Phe	Phe 98	170	20 600	0.65	0.46	77
N^{α}-formyl-L-Try-L-Tyr	Tyr 100	166	20 900	0.74	0.44	73
N^{α}-formyl-L-Try-L-Leu	Leu 98	160	21 200	0.71	0.57	70
N^{α}-formyl-L-Try-L-Phe O Me	Phe 97	138	21 400	—	0.54	64
N^{α}-formyl-L-Try-L-Tyr OEt	Tyr 99	145	21 300	—	0.50	52
N^{α}-formyl-L-Try-L-Leu O Me	Leu 97	125	21 400	—	0.63	46

heated at 50 °C for 3 h in a sealed tube. The solvent was then completely removed under reduced pressure and the residue dissolved by $NaHCO_3$ 5% in water. The 3,4-dihydro-β-carboline derivative was then precipitated by acidification at pH4, collected by filtration, washed with water, and dried over P_2O_5.

N^{α}-formyl-L-tryptophyl-L-tyrosine and N^{α}-formyl-L-tryptophyl-L-leucine were submitted to the same procedure. The yields and the properties of the products obtained are listed in Table II.

(b) Cyclization of the N^{α}-Formyl Peptide Esters

A solution of N^{α}-formyl-L-tryptophyl-L-phenylalanine methyl ester (0.5 g) in anhydrous trifluoroacetic acid (5 ml) was heated at 50 °C for 3 h in a sealed tube. Thereafter, the trifluoroacetic acid solution was diluted with 50 ml of petroleum ether and the reaction product rapidly separated as an oily residue. The petroleum ether layer was removed by decantation and the residue, dissolved in ethyl acetate, was washed with 5% $NaHCO_3$, in water. The ethyl acetate layer was then dried over anhydrous Na_2SO_4 and evaporated under reduced pressure. The residue was crystallized in ethyl ether.

N^{α}-Formyl-L-tryptophyl-L-tyrosine ethyl ester and N^{α}-formyl-L-tryptophyl-L-leucine methyl ester were submitted to the same procedure and the corresponding 3,4-dihydro-β-carboline derivatives crystallized by ethyl ether and ethyl ether – petroleum ether respectively. The yields and the properties of the products obtained are listed in Table II.

Results and Discussion

Figures 1 and 2 show the spectral changes observed during the reaction of N^{α}-formyltryptophan in the described acidic media. The product obtained has an absorption spectrum similar to that of 1-methyl-3-carboxy-3,4-dihydro-β-carboline (6) and its solution is optically active when the starting compound of the synthesis is N^{α}-formylated L- or D-tryptophan. This and the analytical data reported in Table I support the conclusion that N^{α}-formyltryptophan intramolecularly reacts in acidic media to yield 3,4-dihydro-β-carboline-3-carboxylic acid.

In Fig. 1 the rate of cyclization of N^{α}-formyltryptophan to 3,4-dihydro-β-carboline-3-carboxylic acid is reported and compared with the analogous formation of dihydro harman-3-carboxylic acid from N^{α}-acetyltryptophan (6) as observed in a separate experiment. It is evident that N^{α}-formyltryptophan reacts much more rapidly than N^{α}-acetyltryptophan. This suggests that the factors affecting the cyclization reaction are not only the electron density at the point of ring closure in the aromatic nucleus, but also the reactivity of the acyl group of N^{α}-acyltryptophan. The cyclization of N^{α}-formyltryptophan can be realized either in anhydrous trifluoroacetic acid or in formic acid containing 10% of aqueous concentrated hydrochloric acid.

It seems interesting to report on the behavior of N^{α}-formyltryptophan in anhydrous solution of formic acid – gaseous hydrochloric acid. Under such conditions the tryptophan residue reacts to yield quantitatively the 1-formyltryptophan derivatives (7). Only N^{α}-formyltryptophan (**1**) fails to give quantitatively N^{α}-N'-diformyltryptophan (**2**) because the competitive reaction leading to 3,4-dihydro-β-carboline (**3**) takes place as illustrated in Scheme 2. The yield of product **2** is 48%, the yield of product **3** is 52% in HCOOH – anhydrous HCl.

The cyclization reaction of diformyltryptophan (**2**) does not occur, probably because the

Can. J. Chem. Downloaded from www.nrcresearchpress.com by 210.87.254.105 on 09/05/12
For personal use only.

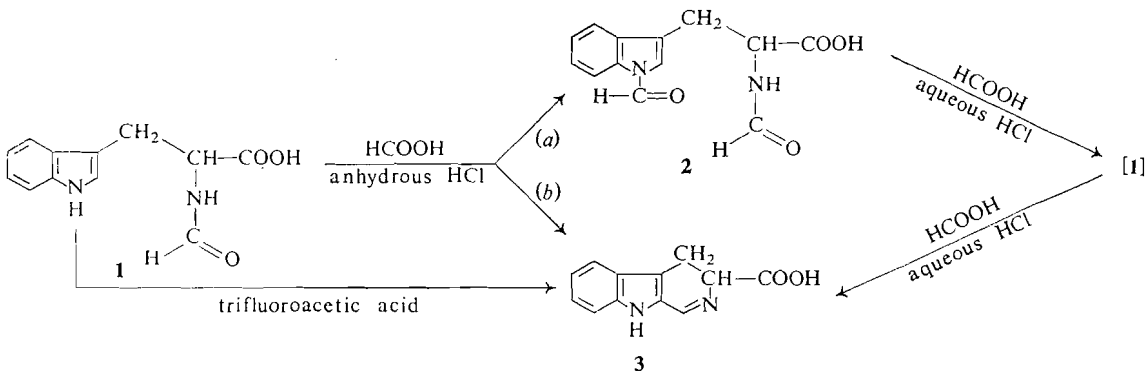

Scheme 2

electron density at the 2-position in the indole ring is reduced by the inactivating 1-formyl group. The two pathways (*a*, *b*) of the reaction are irreversible under anhydrous conditions, but, in the presence of a suitable concentration of water, reaction (*a*) becomes reversible and only product **3** is obtained.

The cyclization of N^{α}-formyltryptophyl peptide free acids and N^{α}-formyltryptophyl-peptide esters can be performed in formic acid – aqueous hydrochloric acid solution, but trifluoroacetic acid has been preferred to avoid the secondary reaction of formolysis or of hydrolysis which can occur to some extent under the conditions used.

The proposed synthetic procedures allow the easy preparation of 3,4-dihydro-β-carboline-3-carboxylic acid in optically active forms, which can be used for physiological studies concerning alkaloids. The reaction described can also be applied to selective modification of peptide substrates containing tryptophan as the *N*-terminal residue for comparative studies in the field of enzyme specificity.

1. S. Akabori and K. Sato. Chem. Ber. **63**, 2245 (1930).
2. E. Späth and E. Lederer. Chem. Ber. **63**, 2102 (1930).
3. H. R. Snyder, H. Ansch, L. Katz, S. M. Parmenter, and E. C. Späth. J. Am. Chem. Soc. **70**, 219 (1948).
4. R. Tschesche and H. Jenssen. Chem. Ber. **93**, 271 (1960).
5. C. E. Dalgliesh. J. Chem. Soc. 137 (1952).
6. R. A. Uphaus, L. I. Grossweiner, and J. J. Katz. Science, **129**, 641 (1959).
7. A. Previero, M-A. Previero, and J. C. Cavadore. Biochim. Biophys. Acta, **147**, 453 (1967).

Some structural features of the heteropolysaccharides of *Candida bogoriensis*[1]

P. A. J. Gorin and J. F. T. Spencer
Prairie Regional Laboratory, National Research Council of Canada, Saskatoon, Saskatchewan

Received June 17, 1968

The two exocellular polysaccharides of *Candida bogoriensis* contain D-mannose, D-fucose, L-rhamnose, D-glucuronic acid, and D-galactose residues. The main heteropolymer (> 80%) has an α-D-(1→3)-linked mannan main-chain as shown by successive Smith degradations. Partial hydrolysis of the heteropolymers provided several methylpentose-containing oligosaccharide fragments corresponding to possible side-chain components.

Canadian Journal of Chemistry, 46, 3407 (1968)

Information on the nature of extracellular and intracellular polysaccharides of yeasts has often been useful as an aid in classification of the parent organisms (1–8). These investigations have now been extended to include other yeasts of the genus *Candida*, which are listed in Table I. The poly-

[1]Issued as NRCC No. 10293.

Can. J. Chem. Downloaded from www.nrcresearchpress.com by 210.87.254.105 on 09/05/12
For personal use only.

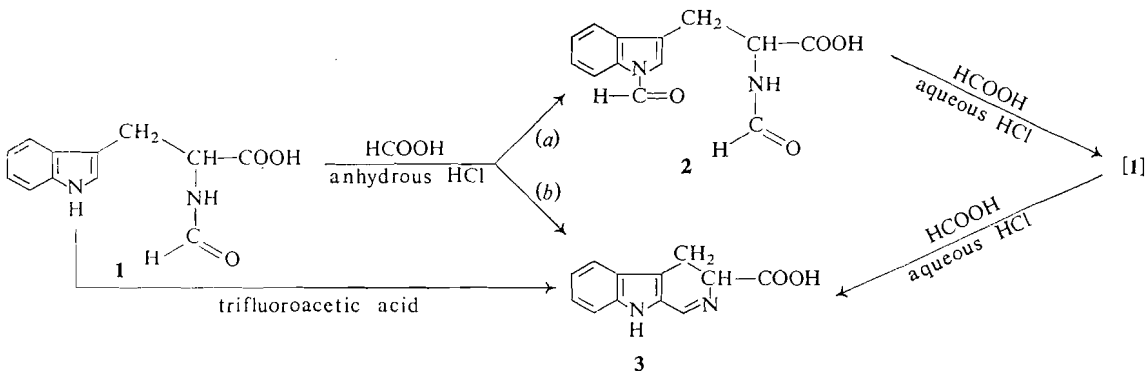

Scheme 2

electron density at the 2-position in the indole ring is reduced by the inactivating 1-formyl group. The two pathways (*a*, *b*) of the reaction are irreversible under anhydrous conditions, but, in the presence of a suitable concentration of water, reaction (*a*) becomes reversible and only product **3** is obtained.

The cyclization of N^{α}-formyltryptophyl peptide free acids and N^{α}-formyltryptophyl-peptide esters can be performed in formic acid – aqueous hydrochloric acid solution, but trifluoroacetic acid has been preferred to avoid the secondary reaction of formolysis or of hydrolysis which can occur to some extent under the conditions used.

The proposed synthetic procedures allow the easy preparation of 3,4-dihydro-β-carboline-3-carboxylic acid in optically active forms, which can be used for physiological studies concerning alkaloids. The reaction described can also be applied to selective modification of peptide substrates containing tryptophan as the *N*-terminal residue for comparative studies in the field of enzyme specificity.

1. S. AKABORI and K. SATO. Chem. Ber. **63**, 2245 (1930).
2. E. SPÄTH and E. LEDERER. Chem. Ber. **63**, 2102 (1930).
3. H. R. SNYDER, H. ANSCH, L. KATZ, S. M. PARMENTER, and E. C. SPÄTH. J. Am. Chem. Soc. **70**, 219 (1948).
4. R. TSCHESCHE and H. JENSSEN. Chem. Ber. **93**, 271 (1960).
5. C. E. DALGLIESH. J. Chem. Soc. 137 (1952).
6. R. A. UPHAUS, L. I. GROSSWEINER, and J. J. KATZ. Science, **129**, 641 (1959).
7. A. PREVIERO, M-A. PREVIERO, and J. C. CAVADORE. Biochim. Biophys. Acta, **147**, 453 (1967).

Some structural features of the heteropolysaccharides of *Candida bogoriensis*[1]

P. A. J. GORIN AND J. F. T. SPENCER
Prairie Regional Laboratory, National Research Council of Canada, Saskatoon, Saskatchewan

Received June 17, 1968

The two exocellular polysaccharides of *Candida bogoriensis* contain D-mannose, D-fucose, L-rhamnose, D-glucuronic acid, and D-galactose residues. The main heteropolymer (> 80%) has an α-D-(1→3)-linked mannan main-chain as shown by successive Smith degradations. Partial hydrolysis of the heteropolymers provided several methylpentose-containing oligosaccharide fragments corresponding to possible side-chain components.

Canadian Journal of Chemistry, 46, 3407 (1968)

Information on the nature of extracellular and intracellular polysaccharides of yeasts has often been useful as an aid in classification of the parent organisms (1–8). These investigations have now been extended to include other yeasts of the genus *Candida*, which are listed in Table I. The poly-

[1]Issued as NRCC No. 10293.

Can. J. Chem. Downloaded from www.nrcresearchpress.com by 210.87.254.6 on 09/05/12
For personal use only.

Can. J. Chem. Downloaded from www.nrcresearchpress.com by 210.87.254.6 on 09/05/12
For personal use only.

TABLE I

Polysaccharides of *Candida* spp.

Mannan-producing *Candida*		Heteropolymer-producing *Candida*	
		Organism	Monosaccharide components
C. utilis NRRL Y900	*C. zeylanoides* CBS 619	*C. bogoriensis* CBS 4101	Gal, man, fuc, rha, gA, tr. g
C. tropicalis NRRL Y1410 (see ref. 17)	*C. stellatoidea* (see ref. 17)	*C. foliarum* CBS 5234	G, man, rha, tr. gal, fuc
C. guillermondii PRL RS3	*C. reukaufii* PRL S5B2	*C. diffluens* CBS 5233	Gal, man, rha, tr. g, fuc
C. silvicola PRL 63–205	*C. natalensis* JPV 184	*C. scottii* CBS 614	Gal, man, fuc, tr. g
C. albicans serotype A } (see refs. 16–19)	*Candida* spp. CBS 2214	*C. pelliculosa* NCYC 471	Man, gal
C. albicans serotype B }	*C. obtusa* UC 60-17	*C. tepae* CBS 5115	Man, gal
C. mycoderma NYCY 327	*C. catenulata* PRL 1S20	*C. lipolytica* CBS-599	Man, gal
C. rugosa CBS 613	*C. brumptii* PRL RS18	*C. mesenterica* NCYC 390	G. man, xyl, uronic acid
C. kusei PRL RS7	*C. melinii* FJY 888b	*C. humicola* IGC 3391	G, man, xyl, uronic acid
C. lusitaneae CBS 4413	*C. oregonensis* UC 60-73	**C. nivalis* 3AH2	G, man, xyl, fuc
C. pseudotropicalis PRL 705-67	*C. macedonensis* CBS 600	**C. frigida* 5A1	G, man, xyl, fuc
C. mogii IGC *3688*	*Candida* spp. FJY 888c	**C. gelida* 2AH10	G, man, xyl, fuc
	C. parapsilosis PRL BMC-1 (see ref. 17)		

TABLE II

Physical and chemical properties of *C. bogoriensis* polysaccharides and polysaccharides formed on successive Smith degradations

Polysaccharide	Yield of polysaccharide, based on A	Component sugars	Specific rotation in H_2O	Fragments obtained on methylation–fragmentation analysis	Periodate oxidation uptake (64 h oxidation)	
					Periodate molar equivalent	Acid molar equivalent
1 *Candida bogoriensis* polysaccharide (A)	—	Gal, man, fuc, rha, gA	−136°	—	—	—
2 A, Smith × 1	38%	Man, fuc, gal, tr. ara	−90°	—	280	700
3 A, Smith × 2	28%	Man, fuc, tr. ara	−50°	2,4,6-Tri-*O*-methylmannose (5.1 pts) 2,3,4-Tri-*O*-methylfucose (1 pt) 2,4-Di-*O*-methylfucose (0.9 pt) Di-*O*-methylmannose	350	780
4 A, Smith × 3	14%	Man, fuc	+29°	2,4,6-Tri-*O*-methylmannose (4.6 pts) 2,3,4-Tri-*O*-methylfucose (1 pt) Di-*O*-methylmannose	220	580
5 A, Smith × 4	6%	Man	+63°	2,4,6-Tri-*O*-methylmannose	—	—

Can. J. Chem. Downloaded from www.nrcresearchpress.com by 210.87.254.6 on 09/05/12
For personal use only.

saccharides were isolated from yeast cells by extraction with hot aqueous alkali and hydrolyzed by acid to their component sugars. In addition to glucans, some of the extracts contained mannans and galactomannans (Table I), which were purified and compared by their proton magnetic resonance (p.m.r.) spectra (9). The H-1 portions of the spectra are useful in establishing structural differences and possible similarities between polysaccharides of different species. In contrast, other *Candida* spp. contain glucans (*Candida javanica* CBS 5236 contains glucan only) and complex heteropolymers, and the latter give viscous solutions in D_2O so that p.m.r. spectra could not be obtained. However, many of the polymers can be distinguished by their sugar composition as shown in Table I. In order to determine whether the main-chain structure of a representative of this heteropolymer group is similar to that of polysaccharides of other yeast genera, some of the structural features of *Candida bogoriensis* polysaccharides have now been elucidated.

Candida bogoriensis forms relatively large quantities of extracellular polysaccharide, which contains the same components, glucuronic acid, fucose, rhamnose, mannose, and galactose, as the aqueous alkali cell extract. The extracellular polysaccharide was isolated in a virtually nitrogen-free state by ethanol precipitation. On ultracentrifugation in 0.1 *M* aqueous NaCl, a major peak with s^0_{22} 60S and a minor peak (<20%) with s^0_{22} 9S were detected. Attempts to fractionate the components by column chromatography on Biogel A-15m, Sephadex G-200, or by gradient elution on *O*-[(2-diethylamino)ethyl]-cellulose in the borate form, were unsuccessful. Treatment of the heteropolymer solutions with cetyltrimethylammonium bromide or with Fehling's solution gave water-insoluble fractions. Each fraction gave, on hydrolysis, the same sugars as obtained from the original polysaccharide mixture. Since the extracellular polysaccharides could not be readily resolved, structural studies were carried out on the mixture.

C. bogoriensis polysaccharide has a neutral equivalent of 1580 due to uronic acid residues. Acid hydrolysis gave L-fucose (1.84 parts), L-rhamnose (1.36 parts), D-mannose (1 part), D-galactose (0.80 part), and uronic acid. The neutral sugars were isolated by cellulose column chromatography and characterized. A methylation–fragmentation analysis on the heteropolymers was only partly successful since fully methylated material was not obtained. However, paper chromatographic analysis of the fragments formed from partially methylated polysaccharide indicated that fucopyranosyl, rhamnopyranosyl, and galactofuranosyl non-reducing end-units are present. The presence of galactofuranoside residues was also indicated by the release of arabinose on complete hydrolysis of the polyalcohol obtained by reduction of the periodate-oxidized polysaccharide. This hydrolyzate also contained mannose, fucose, galactose, and a non-reducing fragment which gave a single spot on a paper chromatogram and contained fucosyl and rhamnosyl units. The polyalcohol also contained erythronic acid residues arising from 4-*O*-linked glucopyranosyluronic acid residues and these were identified by conversion to erythritol.

The polysaccharide obtained by the Smith degradation was successively degraded three more times by the same procedure. The second degradation provided a fucosylmannan containing 3-*O*-L-fucopyranosyl-L-fucopyranosyl side-chains. These were shortened to a single-unit fucopyranosyl side-chain by a further Smith degradation. Finally the fourth degradation provided a mannan which represents the main-chain of the original predominating heteropolymer. The mannan gave a single p.m.r. signal at τ 4.35, due to the presence of one linkage type and was shown by the methylation–fragmentation technique and by its specific rotation to contain α-(1→3)-linked D-mannopyranosyl units similar in structure to the main-chain present in the heteropolymers from *Cryptococcus laurentii* NRRL Y-1401 (10) and *Trichosporon cutaneum* (6). The physical and chemical characteristics of each of the five polysaccharides formed in the successive Smith degradations are given in Table II.

Further structural information on *C. bogoriensis* heteropolymers was obtained by examination of partial hydrolysis of fragments arising from side chains. These were 3-*O*-α-L-rhamnopyranosyl-L-rhamnose, 2-*O*-α-L-rhamnopyranosyl-L-fucose, 3-*O*-α-L-fucopyranosyl-L-fucose, and 4-*O*-β-D-(glucopyranosyluronic acid)-L-fucose. Other larger acidic fragments were converted to the methyl esters and reduced with sodium borohydride to mixed neutral oligosaccharides. Degradation by a Smith procedure incorporating mild hydrolytic conditions gave 2-*O*-α-L-rhamnopyranosyl-D-erythritol, thus indicating an α-L-Rhap-(1→4)-β-D-GpA-(1→4)-L-Fucp sequence.

Can. J. Chem. Downloaded from www.nrcresearchpress.com by 210.87.254.6 on 09/05/12
For personal use only.

Experimental

Paper chromatography was carried out using *n*-butanol – ethanol – water (40:11:19 v/v/v) (solvent *a*) and ethyl acetate – acetic acid – water (9:2:2 v/v/v) (solvent *b*).

Production of C. bogoriensis Heteropolysaccharide

Candida bogoriensis was grown in shaken cultures or in stirred fermentors, in a medium containing 8% glucose, 0.4% dialyzed yeast extract (with high molecular weight components removed by dialysis), 0.1% KH_2PO_4, and 0.02% $MgSO_4 \cdot 7H_2O$. New Brunswick 5 l fermentors were operated at 400 r.p.m., with an air flow rate of 0.33 vol/vol/min, at 25°. Other cultures were grown in 500 ml Erlenmeyer flasks containing 100 ml medium shaken at 230 r.p.m. on a rotary shaker having an eccentricity of 1 in. at 25°. Incubation time was 3–4 days. The cells were then removed by centrifugation and the polysaccharide was recovered from the supernatant liquid, by ethanol precipitation. The heteropolysaccharide mixture had a neutral equivalent of 1580, $[\alpha]_D$ −136° (*c*, 0.7 H_2O) and N, 0.25%. Ultracentrifugation was carried out at 59 000 r.p.m.

Methylation–Fragmentation Analysis of C. bogoriensis Heteropolysaccharides

The polysaccharides (7.0 g) were methylated by the Haworth procedure (11) and a partially methylated product (0.77 g), insoluble in aqueous alkali, isolated (—OCH_3 26.4%). A further methylation gave a product with —OCH_3, 32.7%. The two partially methylated polysaccharides were insoluble in solvents suitable for complete methylation such as *N*-*N*′-dimethyl formamide, dimethyl sulfoxide, or iodomethane. A sample was hydrolyzed in 90% formic acid at 100° for 18 h. The hydrolyzate was freed of formate esters and gave spots on paper chromatograms (solvent *a*; spray: *p*-anisidine hydrochloride) corresponding to 2,3,4-tri-*O*-methylfucose, 2,3,4-tri-*O*-methylrhamnose, and 2,3,5,6-tetra-*O*-methylgalactose.

Hydrolysis Products from C. bogoriensis Heteropolysaccharides

The heteropolymers (1.92 g) were hydrolyzed in *N* H_2SO_4 (20 ml) at 100° for 17 h, the solution neutralized ($BaCO_3$), filtered, and evaporated to a syrup. Fractionation on a cellulose column using *n*-butanol–water (16:1 v/v) as eluant gave α-L-rhamnose (0.34 g) which from EtOH–EtOAc, had m.p. and mixture m.p. 90–93° and $[\alpha]_D$ −7° → +6° (*c*, 0.6 H_2O; constant value). α-L-Fucose (0.46 g) was eluted next and was crystallized from EtOH; it had m.p. and mixture m.p. 143–145° and $[\alpha]_D$ −127° → −74° (*c*, 1.0 H_2O; constant value). Also obtained were D-mannose (0.25 g), which was converted to D-mannitol hexaacetate m.p. 121–122° and $[\alpha]_D$ +18° (*c*, 1.0 AcOH), and α-D-galactose (0.20 g), crystallized from EtOH, with m.p. and mixture m.p. 166° and $[\alpha]_D$ +128° → +76° (*c*, 0.3 H_2O; constant value).

Partial Hydrolysis Products from C. bogoriensis Polysaccharides

The heteropolymers (25 g) were partially hydrolyzed with *N* H_2SO_4 (750 ml) at 75° for 3 h. The products were fractionated on a charcoal column. Monosaccharides were eluted with water and 20% ethanol eluted a fraction (1.07 g) which gave two spots running at the speed of fucose and arabinose on a paper chromatogram in solvent *a*. Fractionation of this fraction on a cellulose column (eluant *n*-butanol–water 32:1 v/v) gave the faster running material (0.84 g), which crystallized from EtOH and had m.p. 140–143° and $[\alpha]_D$ −30° → −38° (*c*, 0.8 H_2O). It gave rhamnose on hydrolysis and it consumed 1.02, 1.03, and 1.03 moles/mole of lead tetraacetate (12) after 2, 5, and 15 min, respectively, consistent with a 3-*O*-α-L-rhamnopyranosyl-α-L-rhamnose structure.

Anal. Calcd. for $C_{12}H_{22}O_9$: C, 46.45; H, 7.15. Found: C, 46.6; H, 7.2.

The material with R_f = arabinose (0.22 g) consumed 0.47, 0.56, and 0.64 mole/mole of lead tetraacetate, based on a methylpentose-containing disaccharide, after 2, 5, and 15 min, respectively. A sample (71 mg) was oxidized with lead tetraacetate to give products with R_f = arabinose and R_f = rhamnose. Fractionation on a cellulose column (solvent: *n*-butanol–water (8:1 v/v)) gave the faster running component (15 mg) which was reduced with sodium borohydride to an alditol, $[\alpha]_D$ −104° (*c*, 0.7 H_2O). Hydrolysis gave fucose and a 5-deoxypentitol (paper chromatogram). Examination of the acetylated mixture by gas–liquid chromatography (g.l.c.) (10 ft × ¼ in. O.D. copper tube containing 2% nitrile silicone gum, X-E-60 on Chromosorb W at 180°), showed a peak with a retention time (4.2 min) identical with that of 5-deoxylyxitol acetate, but differing from that of 5-deoxyarabitol acetate (4.5 min). The parent disaccharide is therefore 3-*O*-α-L-fucopyranosyl-L-fucose. Further elution of the cellulose column gave the slower moving component (35 mg), $[\alpha]_D$ −92° which was inert to lead tetraacetate oxidation. Hydrolysis gave rhamnose and fucose and hydrolysis of the sodium borohydride reduced disaccharide gave rhamnose and alditol. A 2-*O*-α-L-rhamnopyranosyl-L-fucose structure is thus indicated.

A number of acidic oligosaccharides were obtained from the large-scale partial hydrolysis of the heteropolysaccharides by elution of the charcoal column with 20% ethanol. They had speeds relative to lactose (R_{lact}) of 1.43, 1.27, 1.10, and 1.0 on paper chromatography in solvent *b*. The material with R_{lact} 1.43 (1.3 g) gave uronic acid and fucose on hydrolysis and its acetate had m.p. 114–115° (from EtOH) and $[\alpha]_D$ +14° (*c*, 0.9 $CHCl_3$).

Anal. Calcd. for $C_{24}H_{32}O_{17}$. EtOH: C, 49.1; H, 6.0. Found: C, 49. 35; H, 5.75.

The mole of ethanol present was shown by proton magnetic resonance (p.m.r.) spectroscopy in chloroform solution. Oxidation of the unacetylated disaccharide with lead tetraacetate results in consumption of 1.45, 1.93, and 2.04 moles/mole after 2, 5, and 15 min, respectively, consistent with a (1→4)-linkage (12). This was confirmed by reduction of the methyl ester of the aldobiouronic acid with sodium borohydride in methanol. The resulting 4-*O*-β-D-glucopyranosyl-L-fucitol was characterized as its heptaacetate (13), which, from EtOH, had m.p. and mixture m.p. 125–126° and $[\alpha]_D$ −27° (*c*, 0.9 $CHCl_3$).

Anal. Calcd. for $C_{28}H_{40}O_{18}$: C, 50.6; H, 6.1. Found: C, 50.6; H, 6.1.

A portion (1.0 g) of mixed acidic oligosaccharides (3.8 g) with R_{lact} 1.00, 1.10, and 1.27 was converted to the methyl esters which were reduced with sodium borohydride in methanol to a mixture of neutral oligosaccharides (0.83 g). A portion (0.14 g) was degraded by the Smith procedure (14) which is described below. A product with R_f = arabinose on a paper chromatogram in solvent *a* was isolated by cellulose column chromatography using *n*-butanol–water (8:1 v/v) as eluant. The resulting 2-*O*-α-L-rhamno-

pyranosyl-D-erythritol (20 mg) was crystallized from EtOH and had m.p. 178–179° and $[\alpha]_D$ −52° (*c*, 0.6 H_2O).

Anal. Calcd. for $C_{10}H_{20}O_8$: C, 44.77; H, 7.52. Found: C, 44.9; H, 7.45.

Hydrolysis gave rhamnose and erythritol and periodate oxidation resulted in consumption of 2.8 moles/mole of oxidant with formation of 0.98 mole/mole of acid after 21 h.

Smith Degradations on C. bogoriensis Heteropolymers

The heteropolymers (4.0 g) were oxidized in aqueous solution (100 ml) containing sodium periodate (10 g). After 3 days the solution was evaporated to 30 ml, to which acetic acid (250 ml) was added. The precipitate was collected, dried, and shaken with sodium borohydride (1.0 g) in water (100 ml). The solution was evaporated to 20 ml, adjusted to pH 7, and ethanol added. The precipitated polyalcohols (3.14 g) were isolated by filtration, and dissolved in water (100 ml), which was acidified to pH 2 with dilute sulfuric acid. After partial hydrolysis for 1.5 h at 100° the solution was evaporated to 50 ml and excess acetone (500 ml) added. The precipitate (1.52 g) was collected and washed with ethanol. It had $[\alpha]_D$ −90° (*c*, 1.0 H_2O) and gave mannose, fucose, galactose, and a trace of arabinose on hydrolysis. The acetone-soluble portion (R_{lac} 1.0 in solvent *a*; spray: ammoniacal silver nitrate) gave rhamnose and fucose on hydrolysis.

Successive Smith degradations on the resulting polysaccharide were carried out using similar conditions. The properties and composition of the degraded polysaccharides are present in Table II. Methylation–fragmentation procedures are similar to those described in an earlier publication (6). Analysis of the methylated fragments was carried out as follows: methyl 2,4,6-tri-*O*-methylmannoside was characterized by its characteristic retention time (15) on g.l.c. 2,4-Di-*O*- and 2,3,4-tri-*O*-methylfucose structures appeared likely, from their paper chromatographic properties, the g.l.c. retention times of derived methyl fucosides and the method of preparation of the parent polysaccharides. The mannan formed by 4 Smith degradations gave a p.m.r. spectrum in D_2O with a single H-1 peak at τ 4.35. The measurement was carried out at 70° using tetramethylsilane as external standard.

Acknowledgments

The following cultures of *Candida* were kindly supplied: *C. nivalis*, *C. frigida*, and *C. gelida* by Dr. M. di Menna, New Zealand, and *C. tepae* by Dr. J. Grinbergs, Universidad Austral di Chile, Valdivia. The authors also thank Dr. C. T. Bishop for the mannans of the *C. albicans* serotypes A and B. Thanks are also due to Mr. R. J. Magus and Mr. N. R. Gardner for technical assistance. The culture of *C. bogoriensis* was supplied by Dr. M. H. Deinema, The Agricultural University, Wageningen, The Netherlands.

1. P. A. J. Gorin, K. Horitsu, and J. F. T. Spencer. Can. J. Chem. **43**, 950 (1965).
2. T. Miyazaki. Chem. Pharm. Bull. Tokyo, **9**, 715 (1961).
3. T. Miyazaki. Chem. Pharm. Bull. Tokyo, **9**, 826 (1961).
4. T. Miyazaki. Chem. Pharm. Bull. Tokyo, **9**, 829 (1961).
5. M. J. Abercrombie, J. K. N. Jones, M. V. Lock, M. B. Perry, and R. J. Stoodley. Can. J. Chem. **38**, 1617 (1960).
6. P. A. J. Gorin and J. F. T. Spencer. Can. J. Chem. **45**, 1543 (1967).
7. M. E. Slodki and L. J. Wickerham. Can. J. Microbiol. **42**, 381 (1966).
8. M. E. Slodki, L. J. Wickerham, and R. J. Bandoni. Can. J. Microbiol. **12**, 489 (1966).
9. P. A. J. Gorin, M. Mazurek, and J. F. T. Spencer. Can. J. Chem. **46**, 2305 (1968).
10. J. K. N. Jones, M. B. Perry, and R. J. Stoodley. Unpublished results.
11. W. N. Haworth. J. Chem. Soc. **8**, (1915).
12. A. J. Charlson and A. S. Perlin. Can. J. Chem. **34**, 1200 (1956).
13. P. A. J. Gorin and J. F. T. Spencer. Can. J. Chem. **39**, 2274 (1961).
14. I. J. Goldstein, G. W. Hay, B. A. Lewis, and F. Smith. Abstracts Papers Am. Chem. Soc. Meeting **135**, 30 (1959).
15. Y-C. Lee and C. E. Ballou. Biochemistry, **4**, 257 (1965).
16. C. T. Bishop, F. Blank, and P. E. Gardner. Can. J. Chem. **38**, 869 (1960).
17. R. J. Yu, C. T. Bishop, F. P. Cooper, H. F. Hasenclever, and F. Blank. Can. J. Chem. **45**, 2205 (1967).
18. T. Miyazaki. Yakugaku Zasshi, **82**, 1678 (1962).
19. D. Sikl, L. Masler, and S. Bauer. Chem. Zvesti, **19**, 21 (1965).

7-(1-Isoquinolinylmethyl)-theophyllines

D. S. Bariana

Research Department, Abbott Laboratories Limited, Montreal, Quebec

Received May 13, 1968

A number of 7-(1-isoquinolinylmethyl)-theophyllines were synthesized. The route of synthesis and the pharmacology results of these compounds are described.

Canadian Journal of Chemistry, 46, 3411 (1968)

The coronary vasodilating activity of theophylline has been enhanced by introducing a basic amino group in the theophylline molecule as in drugs Xanturil [7-(4-morpholinylmethyl)-theophylline] (**1**), and Trentadil [8-benzyl-7-(*N*-ethyl-*N*-{β-hydroxyethyl}-2-aminoethyl)-theophylline] (**2**) (1). 8-Pyridyltheophylline derivatives (3) seem to show a similar effect (2). In a

Can. J. Chem. Downloaded from www.nrcresearchpress.com by 210.87.254.6 on 09/05/12
For personal use only.

pyranosyl-D-erythritol (20 mg) was crystallized from EtOH and had m.p. 178–179° and $[\alpha]_D$ −52° (*c*, 0.6 H_2O).

Anal. Calcd. for $C_{10}H_{20}O_8$: C, 44.77; H, 7.52. Found: C, 44.9; H, 7.45.

Hydrolysis gave rhamnose and erythritol and periodate oxidation resulted in consumption of 2.8 moles/mole of oxidant with formation of 0.98 mole/mole of acid after 21 h.

Smith Degradations on C. bogoriensis Heteropolymers

The heteropolymers (4.0 g) were oxidized in aqueous solution (100 ml) containing sodium periodate (10 g). After 3 days the solution was evaporated to 30 ml, to which acetic acid (250 ml) was added. The precipitate was collected, dried, and shaken with sodium borohydride (1.0 g) in water (100 ml). The solution was evaporated to 20 ml, adjusted to pH 7, and ethanol added. The precipitated polyalcohols (3.14 g) were isolated by filtration, and dissolved in water (100 ml), which was acidified to pH 2 with dilute sulfuric acid. After partial hydrolysis for 1.5 h at 100° the solution was evaporated to 50 ml and excess acetone (500 ml) added. The precipitate (1.52 g) was collected and washed with ethanol. It had $[\alpha]_D$ −90° (*c*, 1.0 H_2O) and gave mannose, fucose, galactose, and a trace of arabinose on hydrolysis. The acetone-soluble portion (R_{lac} 1.0 in solvent *a*; spray: ammoniacal silver nitrate) gave rhamnose and fucose on hydrolysis.

Successive Smith degradations on the resulting polysaccharide were carried out using similar conditions. The properties and composition of the degraded polysaccharides are present in Table II. Methylation–fragmentation procedures are similar to those described in an earlier publication (6). Analysis of the methylated fragments was carried out as follows: methyl 2,4,6-tri-*O*-methylmannoside was characterized by its characteristic retention time (15) on g.l.c. 2,4-Di-*O*- and 2,3,4-tri-*O*-methylfucose structures appeared likely, from their paper chromatographic properties, the g.l.c. retention times of derived methyl fucosides and the method of preparation of the parent polysaccharides. The mannan formed by 4 Smith degradations gave a p.m.r. spectrum in D_2O with a single H-1 peak at τ 4.35. The measurement was carried out at 70° using tetramethylsilane as external standard.

Acknowledgments

The following cultures of *Candida* were kindly supplied: *C. nivalis*, *C. frigida*, and *C. gelida* by Dr. M. di Menna, New Zealand, and *C. tepae* by Dr. J. Grinbergs, Universidad Austral di Chile, Valdivia. The authors also thank Dr. C. T. Bishop for the mannans of the *C. albicans* serotypes A and B. Thanks are also due to Mr. R. J. Magus and Mr. N. R. Gardner for technical assistance. The culture of *C. bogoriensis* was supplied by Dr. M. H. Deinema, The Agricultural University, Wageningen, The Netherlands.

1. P. A. J. Gorin, K. Horitsu, and J. F. T. Spencer. Can. J. Chem. **43**, 950 (1965).
2. T. Miyazaki. Chem. Pharm. Bull. Tokyo, **9**, 715 (1961).
3. T. Miyazaki. Chem. Pharm. Bull. Tokyo, **9**, 826 (1961).
4. T. Miyazaki. Chem. Pharm. Bull. Tokyo, **9**, 829 (1961).
5. M. J. Abercrombie, J. K. N. Jones, M. V. Lock, M. B. Perry, and R. J. Stoodley. Can. J. Chem. **38**, 1617 (1960).
6. P. A. J. Gorin and J. F. T. Spencer. Can. J. Chem. **45**, 1543 (1967).
7. M. E. Slodki and L. J. Wickerham. Can. J. Microbiol. **42**, 381 (1966).
8. M. E. Slodki, L. J. Wickerham, and R. J. Bandoni. Can. J. Microbiol. **12**, 489 (1966).
9. P. A. J. Gorin, M. Mazurek, and J. F. T. Spencer. Can. J. Chem. **46**, 2305 (1968).
10. J. K. N. Jones, M. B. Perry, and R. J. Stoodley. Unpublished results.
11. W. N. Haworth. J. Chem. Soc. **8**, (1915).
12. A. J. Charlson and A. S. Perlin. Can. J. Chem. **34**, 1200 (1956).
13. P. A. J. Gorin and J. F. T. Spencer. Can. J. Chem. **39**, 2274 (1961).
14. I. J. Goldstein, G. W. Hay, B. A. Lewis, and F. Smith. Abstracts Papers Am. Chem. Soc. Meeting **135**, 30 (1959).
15. Y-C. Lee and C. E. Ballou. Biochemistry, **4**, 257 (1965).
16. C. T. Bishop, F. Blank, and P. E. Gardner. Can. J. Chem. **38**, 869 (1960).
17. R. J. Yu, C. T. Bishop, F. P. Cooper, H. F. Hasenclever, and F. Blank. Can. J. Chem. **45**, 2205 (1967).
18. T. Miyazaki. Yakugaku Zasshi, **82**, 1678 (1962).
19. D. Sikl, L. Masler, and S. Bauer. Chem. Zvesti, **19**, 21 (1965).

7-(1-Isoquinolinylmethyl)-theophyllines

D. S. Bariana

Research Department, Abbott Laboratories Limited, Montreal, Quebec

Received May 13, 1968

A number of 7-(1-isoquinolinylmethyl)-theophyllines were synthesized. The route of synthesis and the pharmacology results of these compounds are described.

Canadian Journal of Chemistry, 46, 3411 (1968)

The coronary vasodilating activity of theophylline has been enhanced by introducing a basic amino group in the theophylline molecule as in drugs Xanturil [7-(4-morpholinylmethyl)-theophylline] (**1**), and Trentadil [8-benzyl-7-(*N*-ethyl-*N*-{β-hydroxyethyl}-2-aminoethyl)-theophylline] (**2**) (1). 8-Pyridyltheophylline derivatives (3) seem to show a similar effect (2). In a

Can. J. Chem. Downloaded from www.nrcresearchpress.com by 210.87.254.105 on 09/05/12
For personal use only.

search for active vasodilating agents, it was undertaken in this laboratory to substitute an isoquinoline nucleus in the theophylline molecule to obtain compounds **4**, **13**, and **14**.

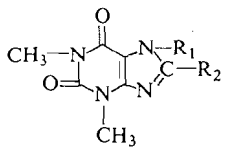

1-4

1 $R_1 = -CH_2-$(morpholine), $R_2 = H$

2 $R_1 = -CH_2-CH_2-N(C_2H_5)-CH_2-CH_2OH$, $R_2 = -CH_2-$(phenyl)

3 $R_1 = H$, $R_2 =$ 3-pyridyl

4 $R_1 = -CH_2-$(1-isoquinolyl), $R_2 = H$

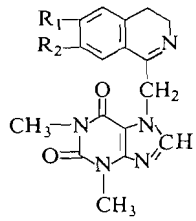

13-14

13 $R_1 = H$, $R_2 = H$

14 $R_1 = OCH_3$, $R_2 = OCH_3$

The following set of reactions was employed for the synthesis of the required intermediates for the desired product.

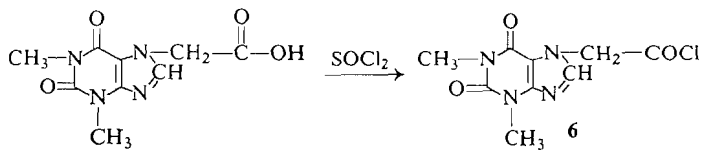

6

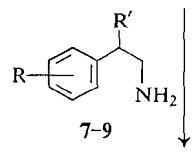

7-9

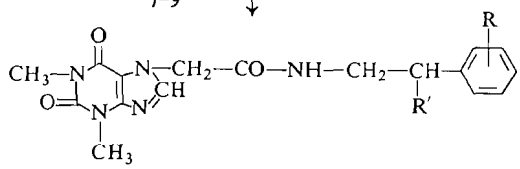

10-12

7	R = H	R′ = OH	**10**	R = H	R′ = OH
8	R = H	R′ = H	**11**	R = H	R′ = H
9	R = 3,4-dimethoxy	R′ = H	**12**	R = 3,4-dimethoxy	R′ = H

Theophylline-7-acetic acid (**5**) was treated with thionyl chloride to get the acid chloride **6** by the method of Klosa (3). The compound **6** on treatment with β-phenylethylamine (**8**) and its analogues **7** and **9** gave the amides **11**, **10**, and **12**. The amide **10** could not be isolated as a pure compound so it was used as such for further reactions. The amides **10**, **11**, and **12** on treatment with phosphorus oxychloride and phosphorus pentoxide by Bischler–Napieralski reaction gave the desired isoquinoline compound **4** and its analogues **13** and **14**.

Pharmacology

Compounds **4**, **11**, **12**, and **14** were injected into the coronary sinus of anesthetized dogs at doses of 2–10 mg/kg. Changes in the oxygen content of

Can. J. Chem. Downloaded from www.nrcresearchpress.com by 210.87.254.105 on 09/05/12
For personal use only.

coronary sinus blood, heart rate, and blood pressure were then measured. None of the compounds showed significant activity.

Experimental

Melting points were determined with the Thomas Hoover Capillary melting point apparatus. Infrared spectra were recorded on a Beckman IR-8 infrared spectrophotometer. Microanalyses were performed at the Microanalytical Laboratories of Abbott Laboratories, North Chicago, Illinois.

*N-(Phenylethyl)-1,2,3,6-tetrahydro-1,3-dimethyl-2,6-dioxo-purine-7-acetamide (**11**)*

To 12.0 g (0.05 mole) of theophylline-7-acetic acid were added dropwise 25 ml of thionyl chloride in the cold. The mixture was brought to room temperature and then refluxed on a water bath for 3 h. The thionyl chloride was removed by distillation under vacuum at low temperature. The residue was repeatedly washed with benzene to remove the last traces of thionyl chloride. A solution of 6.0 g (0.05 mole) β-phenylethylamine in 50 ml of benzene was added dropwise to the syrupy acid chloride in about 20 min. The mixture was stirred at room temperature for 48 h. The benzene was removed by distillation under vacuum and the residue was washed with acetone and filtered to give 7.0 g (40%) of a white crystalline compound. Two crystallizations from absolute ethanol afforded the analytically pure compound, m.p. 195°.

Anal. Calcd. for $C_{17}H_{19}N_5O_3$: C, 59.81; H, 5.60; N, 20.51; O, 14.06. Found: C, 59.73; H, 5.80; N, 20.32; O, 14.49.

*N-(3,4-Dimethoxyphenylethyl)-1,2,3,6-tetrahydro-1,3-dimethyl-2,6-dioxo-purine-7-acetamide (**12**)*

This compound was prepared in 36% yield from the amine (**9**) by a similar method to that used to prepare **11**, m.p. 203°.

Anal. Calcd. for $C_{19}H_{23}N_5O_5$: C, 56.84; H, 5.77; N, 17.44; O, 19.92. Found: C, 56.86; H, 5.56; N, 17.50; O, 19.73.

*7-(1-Isoquinolylmethyl)-theophylline (**4**)*

A mixture of 8.5 g (0.025 mole) of amide (**10**) (not recrystallized), 25.0 g phosphorus pentoxide, and 50.0 g of phosphorus oxychloride was refluxed with stirring for 3.5 h. The reaction mixture was cooled and added to ice. The water layer was separated and was washed with benzene twice. The aqueous solution was neutralized with 25% sodium hydroxide solution and left at room temperature for 24 h. The solution was filtered to give 2.40 g (30%) of a brownish crystalline product, m.p. 195–197°. Two recrystallizations from methanol afforded the analytically pure product, m.p. 198–200°.

Anal. Calcd. for $C_{17}H_{15}N_5O_2$: C, 63.51; H, 4.70; N, 21.79; O, 9.95. Found: C, 63.81; H, 4.77; N, 21.69; O, 9.65.

*7-(3,4-Dihydro-1-isoquinolylmethyl)-theophylline (**13**)*

This compound was prepared in 35% yield from the amide (**11**) by a similar method, m.p. 215°.

Anal. Calcd. for $C_{17}H_{17}N_5O_2$: C, 63.14; H, 5.30; N, 21.66; O, 9.89. Found: C, 62.87; H, 5.49; N, 21.51; O, 9.89.

*7-(3,4-Dihydro-6,7-dimethoxy-1-isoquinolylmethyl)-theophylline (**14**)*

This compound was prepared in 70% yield from the amide (**12**) by a similar method. The compound was recrystallized from dimethyl formamide, m.p. 220–222°.

Anal. Calcd. for $C_{19}H_{21}N_5O_4$: C, 59.51; H, 5.52; N, 18.26; O, 16.69. Found: C, 59.39; H, 5.37; N, 18.36; O, 16.89.

A hydrochloride salt of **14** was prepared by passing dry HCl gas in dimethyl formamide solution of **14**. The salt was recrystallized from aqueous methanol.

Anal. Calcd. for $C_{19}H_{21}N_5O_4 \cdot HCl$: C, 54.34; H, 5.28; N, 16.68; Cl, 8.44; O, 15.24. Found: C, 54.27; H, 5.44; N, 16.55; Cl, 8.59; O, 15.30.

Acknowledgments

The author wishes to express his appreciation to Dr. Thomas Darby, Mr. Leo Wiemeler, and Mr. Charles Shannon of the Pharmacology Department of Abbott Laboratories, North Chicago, Illinois, for pharmacological investigations and for permission to use their data.

1. W. KUNZ. *In* Progress in drug research. 6th. ed. *Edited by* Ernst Jucker. Birkhauser Verlag, Basel. 1963. p. 347–406.
2. M. PESSON, C. BATHELLIER, H. KORNOWSKI, and M. AUROUSSEAU. Ann. Pharm. Franc. **22**, No. 4, 265 (1964).
3. J. KLOSA. Arch. Pharm. **288**, 144 (1955).

8-Aryltheophyllines

D. S. BARIANA
Research Department, Abbott Laboratories Limited, Montreal, Quebec

Received May 13, 1968

The synthesis of a number of 8-aryltheophyllines is described. These compounds were tested as coronary vasodilators.

Canadian Journal of Chemistry, 46, 3413 (1968)

Theophylline and its 8-alkyl derivatives have been shown to possess coronary dilating effects (1). Prior to this investigation of 8-aryltheophyllines, the preparation of only a few compounds

Can. J. Chem. Downloaded from www.nrcresearchpress.com by 210.87.254.105 on 09/05/12
For personal use only.

coronary sinus blood, heart rate, and blood pressure were then measured. None of the compounds showed significant activity.

Experimental

Melting points were determined with the Thomas Hoover Capillary melting point apparatus. Infrared spectra were recorded on a Beckman IR-8 infrared spectrophotometer. Microanalyses were performed at the Microanalytical Laboratories of Abbott Laboratories, North Chicago, Illinois.

*N-(Phenylethyl)-1,2,3,6-tetrahydro-1,3-dimethyl-2,6-dioxo-purine-7-acetamide (**11**)*

To 12.0 g (0.05 mole) of theophylline-7-acetic acid were added dropwise 25 ml of thionyl chloride in the cold. The mixture was brought to room temperature and then refluxed on a water bath for 3 h. The thionyl chloride was removed by distillation under vacuum at low temperature. The residue was repeatedly washed with benzene to remove the last traces of thionyl chloride. A solution of 6.0 g (0.05 mole) β-phenylethylamine in 50 ml of benzene was added dropwise to the syrupy acid chloride in about 20 min. The mixture was stirred at room temperature for 48 h. The benzene was removed by distillation under vacuum and the residue was washed with acetone and filtered to give 7.0 g (40%) of a white crystalline compound. Two crystallizations from absolute ethanol afforded the analytically pure compound, m.p. 195°.

Anal. Calcd. for $C_{17}H_{19}N_5O_3$: C, 59.81; H, 5.60; N, 20.51; O, 14.06. Found: C, 59.73; H, 5.80; N, 20.32; O, 14.49.

*N-(3,4-Dimethoxyphenylethyl)-1,2,3,6-tetrahydro-1,3-dimethyl-2,6-dioxo-purine-7-acetamide (**12**)*

This compound was prepared in 36% yield from the amine (**9**) by a similar method to that used to prepare **11**, m.p. 203°.

Anal. Calcd. for $C_{19}H_{23}N_5O_5$: C, 56.84; H, 5.77; N, 17.44; O, 19.92. Found: C, 56.86; H, 5.56; N, 17.50; O, 19.73.

*7-(1-Isoquinolylmethyl)-theophylline (**4**)*

A mixture of 8.5 g (0.025 mole) of amide (**10**) (not recrystallized), 25.0 g phosphorus pentoxide, and 50.0 g of phosphorus oxychloride was refluxed with stirring for 3.5 h. The reaction mixture was cooled and added to ice. The water layer was separated and was washed with benzene twice. The aqueous solution was neutralized with 25% sodium hydroxide solution and left at room temperature for 24 h. The solution was filtered to give 2.40 g (30%) of a brownish crystalline product, m.p. 195–197°. Two recrystallizations from methanol afforded the analytically pure product, m.p. 198–200°.

Anal. Calcd. for $C_{17}H_{15}N_5O_2$: C, 63.51; H, 4.70; N, 21.79; O, 9.95. Found: C, 63.81; H, 4.77; N, 21.69; O, 9.65.

*7-(3,4-Dihydro-1-isoquinolylmethyl)-theophylline (**13**)*

This compound was prepared in 35% yield from the amide (**11**) by a similar method, m.p. 215°.

Anal. Calcd. for $C_{17}H_{17}N_5O_2$: C, 63.14; H, 5.30; N, 21.66; O, 9.89. Found: C, 62.87; H, 5.49; N, 21.51; O, 9.89.

*7-(3,4-Dihydro-6,7-dimethoxy-1-isoquinolylmethyl)-theophylline (**14**)*

This compound was prepared in 70% yield from the amide (**12**) by a similar method. The compound was recrystallized from dimethyl formamide, m.p. 220–222°.

Anal. Calcd. for $C_{19}H_{21}N_5O_4$: C, 59.51; H, 5.52; N, 18.26; O, 16.69. Found: C, 59.39; H, 5.37; N, 18.36; O, 16.89.

A hydrochloride salt of **14** was prepared by passing dry HCl gas in dimethyl formamide solution of **14**. The salt was recrystallized from aqueous methanol.

Anal. Calcd. for $C_{19}H_{21}N_5O_4 \cdot HCl$: C, 54.34; H, 5.28; N, 16.68; Cl, 8.44; O, 15.24. Found: C, 54.27; H, 5.44; N, 16.55; Cl, 8.59; O, 15.30.

Acknowledgments

The author wishes to express his appreciation to Dr. Thomas Darby, Mr. Leo Wiemeler, and Mr. Charles Shannon of the Pharmacology Department of Abbott Laboratories, North Chicago, Illinois, for pharmacological investigations and for permission to use their data.

1. W. KUNZ. *In* Progress in drug research. 6th. ed. *Edited by* Ernst Jucker. Birkhauser Verlag, Basel. 1963. p. 347–406.
2. M. PESSON, C. BATHELLIER, H. KORNOWSKI, and M. AUROUSSEAU. Ann. Pharm. Franc. **22**, No. 4, 265 (1964).
3. J. KLOSA. Arch. Pharm. **288**, 144 (1955).

8-Aryltheophyllines

D. S. BARIANA
Research Department, Abbott Laboratories Limited, Montreal, Quebec

Received May 13, 1968

The synthesis of a number of 8-aryltheophyllines is described. These compounds were tested as coronary vasodilators.

Canadian Journal of Chemistry, 46, 3413 (1968)

Theophylline and its 8-alkyl derivatives have been shown to possess coronary dilating effects (1). Prior to this investigation of 8-aryltheophyllines, the preparation of only a few compounds

Can. J. Chem. Downloaded from www.nrcresearchpress.com by 210.87.254.5 on 09/05/12
For personal use only.

Can. J. Chem. Downloaded from www.nrcresearchpress.com by 210.87.254.5 on 09/05/12
For personal use only.

TABLE I

6-Amino-5[(substituted-benzylidene)-amino]-1,3-dimethyluracils*

Compound number	R	Yield %	Recrystallization† solvent	Melting point (°C)	Carbon (%)		Hydrogen (%)		Nitrogen (%)	
					Calculated	Found	Calculated	Found	Calculated	Found
4	2,4-Dimethoxy	87	*a*	200–203	56.59	56.86	5.69	5.47	17.60	17.71
5	4-Diethylamino	80	*b*	235	61.98	61.87	7.03	6.92	21.26	21.09
6	2,3-Dimethoxy	80	*a*	258	56.59	56.33	5.69	5.69	17.60	17.79
7	3,4-Methylenedioxy	95	*b*	287	55.62	55.72	4.66	4.88	18.53	18.57
8	4-Isopropyl	57	*a*	210–211	63.97	63.79	6.71	6.87	18.65	18.57
9	3,4-Diethoxy	95	*b*	220	58.94	59.16	6.40	6.44	16.17	16.22
10	2,4-Dihydroxy	85	*b*	298–300	53.78	53.67	4.86	5.35	19.30	19.35
11	4-Dimethylamino	85	*b*	278	59.78	59.74	6.35	6.42	23.24	23.20
12	2,4-Dichloro	75	*b*	260–262	47.70	47.69	3.69	3.81	17.21	17.12
13	2,5-Dimethoxy	75	*a*	223	56.59	56.82	5.69	5.66	17.60	17.86
14	3-Methoxy-4-hydroxy	75	*a*	230	55.25	55.33	5.30	5.52	18.41	18.54
15	3,4-Dimethoxy	70	*a*	233	56.59	56.76	5.69	5.60	17.60	17.71
16	4-Methyl	90	*b*	270	61.74	61.86	5.92	6.21	20.57	20.56

*General formula: 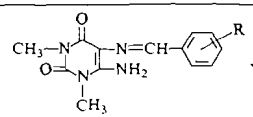

†*a* = Dimethyl formamide; *b* = mixture of dimethyl formamide and methanol.

TABLE II

8-Aryltheophyllines

Compound number	R	Yield (%)	Recrystallization† solvent	Melting point (°C)	Carbon (%)		Hydrogen (%)		Nitrogen (%)	
					Calculated	Found	Calculated	Found	Calculated	Found
17	4-Diethylamino	40	*b*	290	62.36	62.44	6.46	6.44	21.39	21.51
18	2,3-Dimethoxy	60	*a*	229	56.95	57.08	5.09	5.16	17.71	17.65
19	3,4-Methylenedioxy	35	*a*	> 360	56.04	56.11	4.02	4.30	18.65	18.82
20	4-Isopropoxy	30		340	64.41	64.56	6.08	6.15	18.77	18.64
21	3,4-Diethoxy	35	*a*	313	59.28	59.15	5.85	5.82	16.26	16.20
22	2,4-Dichloro	40	*a*	315	48.01	48.13	3.10	3.22	17.23	17.44

*General formula: 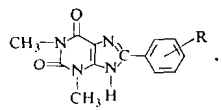

†*a* = Dimethyl formamide; *b* = mixture of dimethyl formamide and methanol.

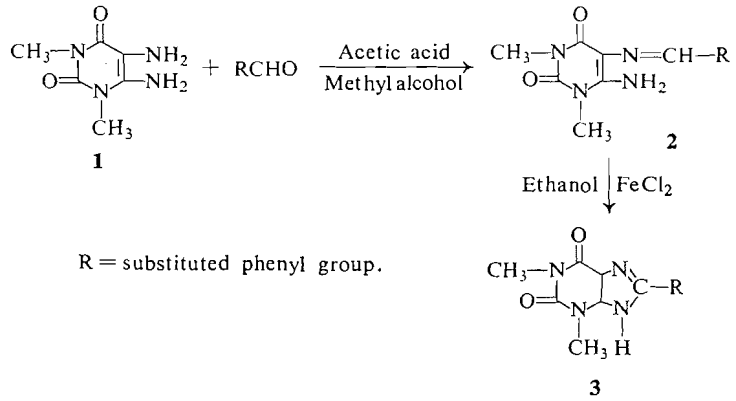

1 2 3

All the compounds were found to be inactive as vasodilators.

(2–4) had been recorded in the literature, and nothing had been published on their pharmacological activity. In order to permit a systematic evaluation of 8-aryltheophyllines as vasodilators, the present work was undertaken.

The synthesis of these compounds was carried out in two stages by known methods (2). Substituted aromatic aldehydes were condensed with 5,6-diamino-1,3-dimethyluracil (**1**) in methanolic acetic acid solution to obtain substituted benzylidinopyrimidines of the general structure **2** (Table I). The benzylidinopyrimidine intermediates on oxidation with anhydrous ferric chloride in alcohol solution gave the corresponding 8-aryltheophyllines (**3**) (Table II).

Experimental

6-Amino-1,3-dimethyl-5-benzylidinouracils

General Procedure

A solution of 5,6-diamino-1,3-dimethyluracil in methanolic acetic acid mixture (1 ml acetic acid per 5 ml methanol) was added to an equimolecular solution of an aromatic aldehyde in methanol. The mixture was allowed to stand at room temperature for 4 h. The product was filtered and recrystallized (see Table I).

8-Aryltheophyllines

General Procedure

To an alcoholic solution of 5-benzylidinopyrimidine was added a calculated amount of anhydrous ferric chloride (the ferric chloride was used mole per mole to the aromatic aldehydes used for the synthesis of respective benzylidinopyrimidines) in alcohol. A deep blue color developed. The reaction mixture was refluxed on a water bath for 4 h and allowed to stand at room temperature for 48 h. The product was filtered and recrystallized (see Table II).

1. R. CHARLIER. Coronary vasodilators. The Pergamon Press, Ltd., New York. 1961. P. 79
2. W. TRAUBE and W. NITBACK. Ber. **39**, 227 (1906).
3. GEO. P. HAGER, J. C. KRANTZ, Jr., J. B. HARMON, and R. M. BURGISON. J. Am. Pharm. Assoc. **43**, 152 (1954).
4. H. GOLDNER, G. DIETZ, and E. CARSTENS. Ann. Chem. **691**, 142 (1966).

Determination of *erythro* and *threo* configurations by nuclear magnetic resonance spectroscopy

GEORGE H. SCHMID

Department of Chemistry, University of Toronto, Toronto 5, Ontario

Received June 11, 1968

An examination of the nuclear magnetic resonance spectra of ten pairs of racemic *erythro* and *threo* isomers of 1,2-disubstituted-1-arylpropanes shows that the signals of the methyl protons of the *erythro* isomer always appear at lower field than the *threo* isomer. The vicinal coupling constant (J_{ab}) of the *erythro* isomer is found to be smaller than that of the *threo* isomer in six of the isomeric pairs indicating that the magnitude of J_{ab} is a poor criterion of configuration of the 1,2-disubstituted-1-arylpropanes.

Canadian Journal of Chemistry, 46, 3415 (1968)

It has been shown (1, 2) that the chemical shift of a methyl group β to a phenyl ring in substituted styrene systems such as **1** depends upon the relative geometry of the two groups. Thus when the

Can. J. Chem. Downloaded from www.nrcresearchpress.com by 210.87.254.5 on 09/05/12
For personal use only.

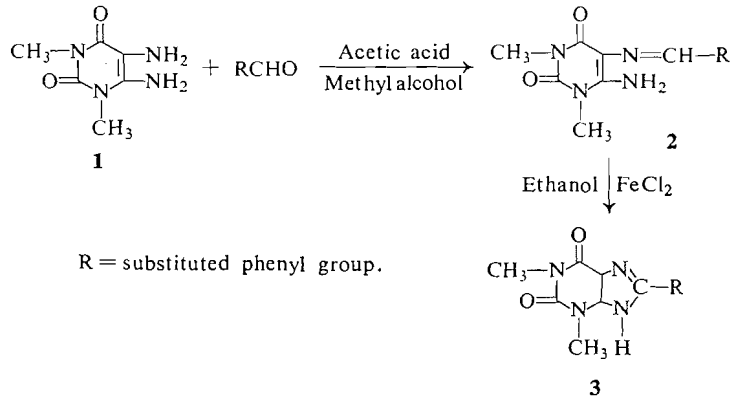

1 2 3

All the compounds were found to be inactive as vasodilators.

(2–4) had been recorded in the literature, and nothing had been published on their pharmacological activity. In order to permit a systematic evaluation of 8-aryltheophyllines as vasodilators, the present work was undertaken.

The synthesis of these compounds was carried out in two stages by known methods (2). Substituted aromatic aldehydes were condensed with 5,6-diamino-1,3-dimethyluracil (**1**) in methanolic acetic acid solution to obtain substituted benzylidinopyrimidines of the general structure **2** (Table I). The benzylidinopyrimidine intermediates on oxidation with anhydrous ferric chloride in alcohol solution gave the corresponding 8-aryltheophyllines (**3**) (Table II).

Experimental

6-Amino-1,3-dimethyl-5-benzylidinouracils

General Procedure

A solution of 5,6-diamino-1,3-dimethyluracil in methanolic acetic acid mixture (1 ml acetic acid per 5 ml methanol) was added to an equimolecular solution of an aromatic aldehyde in methanol. The mixture was allowed to stand at room temperature for 4 h. The product was filtered and recrystallized (see Table I).

8-Aryltheophyllines

General Procedure

To an alcoholic solution of 5-benzylidinopyrimidine was added a calculated amount of anhydrous ferric chloride (the ferric chloride was used mole per mole to the aromatic aldehydes used for the synthesis of respective benzylidinopyrimidines) in alcohol. A deep blue color developed. The reaction mixture was refluxed on a water bath for 4 h and allowed to stand at room temperature for 48 h. The product was filtered and recrystallized (see Table II).

1. R. CHARLIER. Coronary vasodilators. The Pergamon Press, Ltd., New York. 1961. P. 79
2. W. TRAUBE and W. NITBACK. Ber. **39**, 227 (1906).
3. GEO. P. HAGER, J. C. KRANTZ, Jr., J. B. HARMON, and R. M. BURGISON. J. Am. Pharm. Assoc. **43**, 152 (1954).
4. H. GOLDNER, G. DIETZ, and E. CARSTENS. Ann. Chem. **691**, 142 (1966).

Determination of *erythro* and *threo* configurations by nuclear magnetic resonance spectroscopy

GEORGE H. SCHMID

Department of Chemistry, University of Toronto, Toronto 5, Ontario

Received June 11, 1968

An examination of the nuclear magnetic resonance spectra of ten pairs of racemic *erythro* and *threo* isomers of 1,2-disubstituted-1-arylpropanes shows that the signals of the methyl protons of the *erythro* isomer always appear at lower field than the *threo* isomer. The vicinal coupling constant (J_{ab}) of the *erythro* isomer is found to be smaller than that of the *threo* isomer in six of the isomeric pairs indicating that the magnitude of J_{ab} is a poor criterion of configuration of the 1,2-disubstituted-1-arylpropanes.

Canadian Journal of Chemistry, 46, 3415 (1968)

It has been shown (1, 2) that the chemical shift of a methyl group β to a phenyl ring in substituted styrene systems such as **1** depends upon the relative geometry of the two groups. Thus when the

Can. J. Chem. Downloaded from www.nrcresearchpress.com by 210.87.254.5 on 09/05/12
For personal use only.

TABLE I

Selected nuclear magnetic resonance data of *erythro* and *threo* isomers of 1,2-disubstituted-1-arylpropanes*

Number	X	Y	R	Isomer	Solvent	J_{ab} (Hz)	J_{bc} (Hz)	H^c δ(p.p.m.)	Δ	Reference
2	Cl	Cl	H	*erythro*	CCl_4	8.0	6.4	1.58	.25	5
	Cl	Cl	H	*threo*		5.7	6.6	1.33		
3	OAc†	Cl	H	*erythro*	CCl_4	5.4	6.5	1.43	.13	5
	OAc†	Cl	H	*threo*		7.3	6.6	1.30		
4	OCH_3	Cl	H	*erythro*	CCl_4	—	6.5	1.45	.23	5
	OCH_3	Cl	H	*threo*		—	6.5	1.22		
5	Br	Br	H	*erythro*	CCl_4	10.3	6.0	2.00	.33	8, 9
	Br	Br	H	*threo*		5.3	7.0	1.67		
6	HO	Br	H	*erythro*	CCl_4	3.0	7.0	1.47	.11	§
	HO	Br	H	*threo*		7.5	6.5	1.36		
7	OAc†	Br	H	*erythro*	CCl_4	5.5	7.0	1.55	.10	9
	OAc†	Br	H	*threo*		8.0	7.0	1.45		
8	OH	OH	H	*erythro*	Acetone-d_6	4.0	6.5	1.02	.09	§
	OH	OH	H	*threo*		7.0	6.5	0.93		
9	OAc†	OAc†	H	*erythro*	CCl_4	4.0	6.5	1.13	.08	§
	OAc†	OAc†	H	*threo*		7.5	6.0	1.05		
10	OBz‡	OBz‡	H	*erythro*	$CDCl_3$	4.0	7.0	1.41	.09	§
	OBz‡	OBz‡	H	*threo*		7.5	6.0	1.32		
11	Br	Br	CH_3O	*erythro*	CCl_4	10.0	6.1	2.00	.34	8
	Br	Br	CH_3O	*threo*		5.4	6.6	1.66		

*Structure: 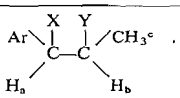

†Ac = CH_3CO.
‡Bz = C_6H_5CO.
§This work.

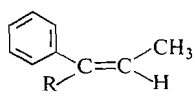

1

phenyl and the β-methyl are *cis* the chemical shift of the methyl protons appear at higher field than they do when the two groups are *trans*. The extension of this shielding effect of a phenyl ring to determine the configurations of aliphatic compounds has rarely been attempted. Barbieux and Martin (3) have shown that such a determination is possible in a series of four ethyl α,β-dialkyl-*p*-methoxydihydrocinnamates while Hyne (4) has interpreted the chemical shifts and coupling constants of two α,β-aminoalcohols on the basis of their configuration.

In Table I are listed the chemical shifts of the methyl protons of ten pairs of racemic *erythro* and *threo* isomers of 1,2-disubstituted-1-arylpropanes. These pairs of isomers are all known compounds previously reported in the literature. However, the nuclear magnetic resonance (n.m.r.) spectra of only six pairs of these compounds were reported. The remaining four pairs were prepared according to the literature references and their n.m.r. spectra recorded. The stereochemistry of compounds **2**, **3**, and **4** was assigned on the basis of the products formed upon treatment with base under conditions for *trans* elimination (5). The stereospecific ring opening of *cis*- and *trans*-1-phenyl-1,2-epoxypropane was used to establish the stereochemistry of compound **8** (6, 7, 9) from which the stereochemistry of the remaining compounds was assigned on the basis of reactions of established stereochemistry.

The data in Table I show that the chemical shift of the methyl protons of the *erythro* isomer of 1,2-disubstituted-1-arylpropanes always appears at lower field than the *threo* isomer. The difference between the chemical shift of the *erythro* and *threo* isomer Δ, varies from a maximum value of 0.34 p.p.m. for **11**, to a minimum value of 0.08 p.p.m. for **9**. The latter value is several times greater than mean deviation (±0.02 p.p.m.) for several determinations of the chemical shift.

The observed vicinal coupling constants J_{ab} for the *threo* and *erythro* isomers are also listed in Table I. It has been claimed (10) that it is a common phenomenon for the *erythro* isomer to have a larger vicinal coupling constant than does the *threo* isomer. From the data in Table I, it is clear

Can. J. Chem. Downloaded from www.nrcresearchpress.com by 210.87.254.5 on 09/05/12
For personal use only.

Can. J. Chem. Downloaded from www.nrcresearchpress.com by 210.87.254.5 on 09/05/12
For personal use only.

that in the 1,2-disubstituted-1-arylpropane series, this relationship does not hold. Only in three of the nine pairs of isomers, where values of J_{ab} are available, is the value of J_{ab} larger for the *erythro* than for the *threo* isomer. Clearly the use of J_{ab} as the sole criterion to assign configuration of acyclic molecules is undesirable.

An interesting relationship exists between the vicinal coupling constant (J_{ab}) and Δ. When the value of Δ is greater than 0.20 p.p.m., the *erythro* vicinal coupling constant is greater than the *threo* while when Δ is around 0.10 p.p.m. the reverse is true. This relationship is a reflection of the conformational preferences of the *threo* and *erythro* isomers and can be illustrated by means of the Newman projections of the *erythro* and *threo* isomers.

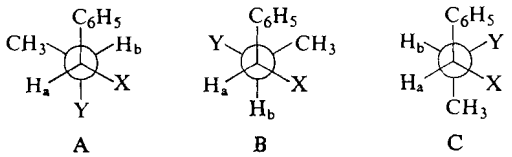

threo Isomers

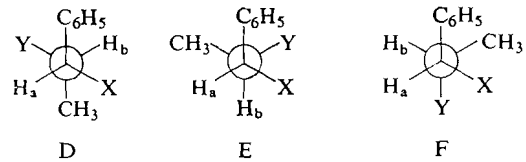

erythro Isomers

The fact that the chemical shift of the methyl protons of the *threo* isomer appears at higher field indicates that the methyl group is more shielded by the aromatic ring than is the methyl group of the *erythro* isomer. This clearly implies that for the *erythro* isomers conformation D, where the methyl group is as far away as possible from the phenyl ring, is the preferred conformation. In the case of compounds **2**, **5**, and **11** the value of J_{ab} clearly substantiates the selection of D as the most stable conformation for the *erythro* isomers. For the *threo* isomers of compounds **2**, **5**, and **11**, both A and B have the methyl group *gauche* to the phenyl ring which is the correct conformation for shielding by the phenyl ring. On the basis of the small value of J_{ab}, B seems the choice of the most stable conformation. These results indicate that the most stable conformation is that one in which the two highly electronegative atoms (Br or Cl) are *trans* to each other. On the basis of the value of Δ, it would be expected that compound **4** would show identical conformational preferences as **2**, **5**, and **11**.

In the remaining compounds a clear choice of conformational preference does not seem to exist. In the case of the *erythro* isomers as Δ decreases to about 0.10 p.p.m., J_{ab} also decreases to about 4.0 Hz making it difficult to determine the preferred conformation. The *threo* isomers seem to exist as a mixture of conformations A and B. Conformation A probably gains stability relative to B as the polarity of the groups X, Y decrease, which decreases the dipolar interaction of the two groups in A.

On the basis of the results presented here, it appears that the difference between the chemical shift of the methyl protons of *erythro* and *threo*

TABLE II

Nuclear magnetic resonance data

Compound	Chemical shift δ	Multiplicity	Relative area
6 *erythro*	1.47	Doublet	3
	4.90	Quintet	1
	5.36	Doublet	1
	6.68	Singlet	5
6 *threo*	1.36	Doublet	3
	4.81	Quintet	1
	5.15	Doublet	1
	6.66	Singlet	5
8 *erythro*	1.02	Doublet	3
	ca. 3.92		*
	4.67	Doublet	1
	6.68	Multiplet	5
8 *threo*	0.93	Doublet	3
	3.83	Quintet	*
	4.39	Doublet	1
	6.66	Singlet	5
9 *erythro*	1.13	Doublet	3
	5.16	Octet	1
	5.92	Doublet	1
	6.70	Singlet	5
9 *threo*	1.05	Doublet	3
	5.25	Sextet	1
	5.71	Doublet	1
	6.68	Singlet	5
10 *erythro*	1.41	Doublet	3
	5.68	Octet	1
	6.37	Doublet	1
	7.2–8.3	Multiplet	15
10 *threo*	1.32	Doublet	3
	5.75	Quintet	1
	6.23	Doublet	1
	7.1–8.3	Multiplet	15

*Overlap with OH.

isomers of 1,2-disubstituted-1-arylpropanes is a better criterion of their configuration than is the value of the vicinal coupling constant J_{ab}.

Experimental

All melting points and boiling points are uncorrected. Nuclear magnetic resonance (n.m.r.) spectra were measured on a Varian Associates A-60 spectrometer. Samples were measured as 10% w/v solutions in the solvent indicated in Table I and chemical shifts are reported in p.p.m. downfield from TMS as internal standard.

*erythro and threo-1-Phenyl-1,2-propanediol (**8**)*

These were prepared by the procedure of Foltz and Witkop (7); *threo* isomer, m.p. 53–54° (lit. m.p. 55–57°); *erythro* isomer, m.p. 91–92° (lit. m.p. 92–93°). The n.m.r. spectra are summarized in Table II.

*erythro and threo-1-Phenyl-1,2-propanediol Dibenzoate (**10**)*

These were prepared by the procedure of Foltz and Witkop (7); *threo* isomer, m.p. 75–78° (lit. m.p. 75.0–77.5°); *erythro* isomer, m.p. 102–103° (lit. m.p. 103–104°). The n.m.r. spectra are summarized in Table II.

*erythro and threo-1-Phenyl-1,2-propanediol Diacetate (**9**)*

These were prepared by the procedure of Fischer (6); *threo* isomer, b.p. 128–130°/1mm Hg (lit. b.p. 112–113°/0.4mm Hg); *erythro* isomer, b.p. 123–125°/1mm Hg (lit. b.p. 109°/0.4mm Hg). The n.m.r. spectra are summarized in Table II.

*erythro and threo-1-Bromo-1-phenylpropanol-2 (**6**)*

These were prepared by the procedure of Fischer (6). *threo* Isomer, b.p. 109–111°/1 mm Hg (lit. b.p. 91–92°/0.4 mm Hg); *erythro* isomer, b.p. 114–115°/1 mm Hg (lit. b.p. 88°/0.2 mm Hg). The n.m.r. data are summarized in Table II.

Acknowledgment

Financial support from the National Research Council of Canada is gratefully acknowledged.

1. M. Barbieux, W. Defay, J. Pecher, and R. H. Martin. Bull. Soc. Chim. Belges. **73**, 716 (1964).
2. G. H. Schmid and M. Heinola. J. Am. Chem. Soc. **90**, 3466 (1968).
3. M. Barbieux and R. H. Martin. Tetrahedron Letters, 2919 (1965).
4. J. Hyne. Can. J. Chem. **39**, 2536 (1961).
5. R. C. Fahey and C. Schubert. J. Am. Chem. Soc. **87**, 5172 (1965).
6. F. Fischer. Chem. Ber. **90**, 357 (1957).
7. C. M. Foltz and B. Witkop. J. Am. Chem. Soc. **79**, 201 (1957).
8. R. C. Fahey and H. J. Schneider. J. Am. Chem. Soc. To be published.
9. J. H. Rolston. Ph.D. Thesis. University of Toronto. 1967.
10. C. A. Kingsbury and D. C. Best. J. Org. Chem. **32**, 6 (1967).

Can. J. Chem. Downloaded from www.nrcresearchpress.com by 210.87.254.5 on 09/05/12
For personal use only.

Erratum: Essential oils and their constituents. XLII. Isomerization of epoxides on active alumina

ISHWAR C. NIGAM AND LEO LEVI
Research Laboratories, Food and Drug Directorate, Department of National Health and Welfare, Ottawa, Canada

Received May 25, 1967

(Ref.: Can. J. Chem. **46**, 1944 (1968))

Canadian Journal of Chemistry, **46**, 3419 (1968)

On page 1944, the insertion below the abstract reads: Canadian Journal of Chemistry, **46**, 1942 (1968).

This should be changed to read: Canadian Journal of Chemistry, **46**, 1944 (1968).

Addendum: Fischer indole synthesis. The reaction of *N'*-alkyl-2,6-dialkylphenylhydrazines with cyclohexanone

G. S. BAJWA AND R. K. BROWN
Department of Chemistry, University of Alberta, Edmonton, Alberta

Received June 20, 1968

(Ref.: Can. J. Chem. **46**, 1927 (1968))

Canadian Journal of Chemistry, **46**, 3419 (1968

On page 1933, the second column lines 11 and 10 from the bottom of the page read: ". . . gave 510 mg (53%) of *N'-formyl-N'-methyl-2,6-dimethylphenylhydrazine*."

To this should be added, ", m.p. 60°". Lines 11 and 10 shall therefore read: ". . . gave 510 mg (53%) of *N'-formyl-N'-methyl-2,6-dimethylphenylhydrazine*, m.p. 60°."

Erratum: The preparation of methyl 4-deoxy-3-*O*-methyl-α,β-DL-*threo*-pentopyranoside

F. SWEET AND R. K. BROWN
Department of Chemistry, University of Alberta, Edmonton, Alberta

Received January 22, 1967

(Ref.: Can. J. Chem. **46**, 1592 (1968))

Canadian Journal of Chemistry, **46**, 3419 (1968)

The date of receipt should read "Received January 22, 1968".

Can. J. Chem. Downloaded from www.nrcresearchpress.com by 210.87.254.42 on 09/05/12
For personal use only.

Can. J. Chem. Downloaded from www.nrcresearchpress.com by 210.87.254.42 on 09/05/12
For personal use only.

Positive and negative intramolecular nuclear Overhauser effects in an all-proton system

R. A. BELL AND J. K. SAUNDERS
Department of Chemistry, McMaster University, Hamilton, Ontario

Received September 16, 1968

The Overhauser effects recorded for the alkaloid ochotensimine (**1**) show positive effects (area increases) for adjacent protons but negative effects (area decreases) for two protons separated by an intervening proton. A qualitative explanation based on the dominance of a dipole–dipole relaxation mechanism is advanced. The Overhauser effect between geminal protons on an sp^2-carbon has been measured.

Canadian Journal of Chemistry, **46**, 3421 (1968)

In an investigation of the Overhauser effect in *Fumaria* and *Corydalis* alkaloids, we have examined the alkaloid ochotensimine (**1**) (1). We report here the results obtained for this alkaloid since it has furnished the first definite example of positive and negative[1] intramolecular nuclear Overhauser effects in an all-proton system and the first measurement of the Overhauser effect between geminal protons.

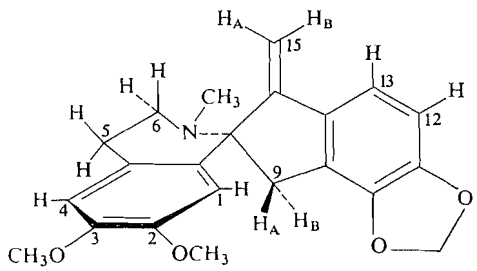

1

The structure and stereochemistry of ochotensimine have been unequivocally established by chemical (2) and X-ray methods (3). The proton magnetic resonance (p.m.r.) spectrum of the alkaloid shows signals for the protons at C-1, C-4, C-9, C-12, C-13, and C-15 as well-resolved lines, sufficiently separated from other transitions to be accurately integrated. Table I records the steady-state nuclear Overhauser effect (N.O.E.) (4*a*, 4*b*) data and the internuclear distances between the observed and irradiated protons. The area changes recorded are expressed as a percentage of the total area of each proton. The measurements were obtained on a 0.17 *M* solution of **1** in carefully degassed $CDCl_3$.

When the proton H_A-15 is saturated, the area of the signal for the proton H_B-15 increases by 40% (positive effect) but the area for the proton H-13 *decreases* by 8% (negative effect). In addition, there is a small, but nonetheless reproducible, area increase of 3% for the proton H-12. Similarly, when the proton H_B-15 is saturated, the area for the adjacent proton H-13 increases by 24% and the area for the proton H-12 decreases by 7%. The observed area decreases were not the result of spurious instrumental[2] effects nor overloading of the audio phase-sensitive detector, since any arbitrary displacement of the saturating field from the transitions of H_A-15 of H_B-15 resulted in a return to normal areas for all protons. The observed negative effects are thus an inherent property of the molecule. An inspection of a molecular model of **1** shows that the four protons H_A-15, H_B-15, H-13, and H-12 are contiguous and it is this factor which is the genesis of the positive and negative Overhauser effect behavior.

Qualitatively, the occurrence of a negative effect can be accounted for by a consideration of the Bloch phenomenological equations for interacting spins as derived by Solomon (5) and Abragam (6). For simplicity we shall consider here a system of only three neighboring

[1]Anet and Bourn (4*a*) have recorded a small negative effect in an examination of β,β-dimethylacrylic acid but have made no comment on this observation.

[2]A Varian Associates HA-100 in internal lock mode was used.

TABLE I

Nuclear overhauser effects in ochotensimine

Observed proton	δ* (p.p.m.)	Irradiated protons	δ (p.p.m.)	% area increase	Internuclear distance Å†
C-1 H	6.29	C-9 H_A	2.93	14	1.8
C-1 H	6.29	C-2 OCH_3	3.62	25	1.8
C-4 H	6.52	C-5 H	2.78	9	2.8
C-4 H	6.52	C-5 H	2.87	16	2.6
C-4 H	6.52	C-3 OCH_3	3.84	25	1.8
C-9 H_B	3.43	N-CH_3	2.22	8	2.4
C-12 H	6.78	C-15 H_A	4.89	3	6.2
C-12 H	6.78	C-15 H_B	5.62	−7	4.8
C-13 H	7.10	C-15 H_A	4.89	−8	4.0
C-13 H	7.10	C-15 H_B	5.62	24	2.4
C-15 H_A	4.89	C-15 H_B	5.62	40	1.8
C-15 H_A	4.89	N-CH_3	2.22	2	3.1
C-15 H_A	4.89	C-15 H_B‡	5.62		1.8
		N-CH_3‡	2.22	42	2.3
C-15 H_B	5.62	C-15 H_A	4.89	40	1.8
C-15 H_B	5.62	C-13 H	7.10	8	2.4
C-15 H_B	5.62	C-15 H_A‡	4.89		1.8
		C-13 H‡	7.10	47	2.4

*Tetramethylsilane as internal standard.
†As measured from a Dreiding Molecular Model.
‡Triple irradiation.

spins, but the same arguments can be applied to a four-spin system with identical results. If we label the protons H_A-15, H_B-15, and H-13 as A, B, and C respectively, then the rates of change of the longitudinal magnetizations of the three nuclei are:

$$[1]\qquad \frac{dM_z^A}{dt} = -\frac{1}{T_{AA}}(M_z^A - M_o^A) - \frac{1}{T_{BA}}(M_z^B - M_o^B) - \frac{1}{T_{CA}}(M_z^c - M_o^c)$$

$$[2]\qquad \frac{dM_z^B}{dt} = -\frac{1}{T_{BB}}(M_z^B - M_o^B) - \frac{1}{T_{AB}}(M_z^A - M_o^A) - \frac{1}{T_{CB}}(M_z^c - M_o^c)$$

$$[3]\qquad \frac{dM_z^c}{dt} = -\frac{1}{T_{CC}}(M_z^c - M_o^c) - \frac{1}{T_{BC}}(M_z^B - M_o^B) - \frac{1}{T_{AC}}(M_z^A - M_o^A)$$

The time constants T_{AA}, T_{BA}, etc. can be interpreted in terms of transition probabilities (5, 7) between the eigenstates of the three-spin system. The transition probabilities in turn will be dependent on the various relaxation mechanisms available to the system such as dipole–dipole interactions, scalar spin–spin interactions, spin–rotation interactions, and random fluctuating stationary fields. If a saturating radiofrequency field is applied to the nucleus A, then $M_z^A = 0$, and, after a sufficient time has elapsed for M_z^B and M_z^c to reach a steady state, [2] and [3] can be written as:

$$[4]\qquad 0 = -\frac{1}{T_{BB}}(M_z^B - M_o^B) - \frac{1}{T_{AB}}(-M_o^A) - \frac{1}{T_{CB}}(M_z^c - M_o^c)$$

$$[5]\qquad 0 = -\frac{1}{T_{CC}}(M_z^c - M_o^c) - \frac{1}{T_{AC}}(-M_o^A) - \frac{1}{T_{BC}}(M_z^B - M_o^B)$$

Can. J. Chem. Downloaded from www.nrcresearchpress.com by 210.87.254.42 on 09/05/12
For personal use only.

Or, rewriting [4] and [5] as explicit expressions for M_z^B and M_z^C we have:

$$[6] \qquad M_z^B = M_o^B + M_o^A\left(\frac{T_{BC}T_{BB}}{T_{AC}T_{AB}}\right) \times \left(\frac{T_{CB}T_{AC} - T_{CC}T_{AB}}{T_{CB}T_{BC} - T_{CC}T_{BB}}\right)$$

$$[7] \qquad M_z^C = M_o^C + M_o^A\left(\frac{T_{CC}T_{CB}}{T_{AC}T_{AB}}\right) \times \left(\frac{T_{AC}T_{BB} - T_{AB}T_{BC}}{T_{CC}T_{BB} - T_{BC}T_{CB}}\right)$$

If we make the assumption that the dominant relaxation mechanism is a dipole–dipole interaction (8) then $T_{AA} < T_{AB}, T_{BA}$, etc., $T_{BB} < T_{BA}, T_{AB}$, etc., and $T_{CC} < T_{CA}, T_{AC}$, etc. Now, the steady-state magnitude of M_z^B will depend on the sign of the second term of eq. [6]. That is, on the sign of $(T_{CB}T_{AC} - T_{CC}T_{AB})/(T_{CB}T_{BC} - T_{CC}T_{BB})$. From the above inequalities, the denominator is clearly positive. The numerator contains the term $T_{CB}T_{AC}$ and if we assume that a dipole–dipole interaction between the A and C protons is relatively weak since they are 4.9 Å apart, then the time constant T_{AC} will be large and the product $T_{CB}T_{AC}$ large. Thus $T_{CB}T_{AC} \gg T_{CC}T_{AB}$ and the numerator is therefore positive. The sign of the coefficient of M_o^A in [6] is thus positive and we can expect an increase in the observed value of M_z^B. For the steady-state magnitude of M_z^C, it is clear that the denominator of $(T_{AC}T_{BB} - T_{AB}T_{BC})/(T_{CC}T_{BB} - T_{BC}T_{CB})$ in [7] is negative, but the sign of the numerator will depend on the value of T_{AC}. If $T_{AC} > T_{AB}T_{BC}/T_{BB}$ then the denominator will be positive and therefore the coefficient of M_o^A will be negative. Consequently, under the above conditions there will be a decrease in the observed value of M_z^C.

The experimental results support the above assumptions and further confirm the dominance of dipole–dipole relaxation in proton systems. Indeed, for the three protons H_B-15, H-13, and H-12, where H-13 and H-12 are strongly coupled (J = 8.0 Hz), saturation of H_B-15 results in an area decrease of H-12. This implies that changes in magnetization which result from scalar spin–spin interactions (9) are weaker effects than dipole–dipole relaxation interactions. The N.O.E. observed between the protons H_A-15 and H_B-15 is the first recorded value for geminal protons and its magnitude (40%) is probably a consequence of the very small scalar coupling between these protons.

The remaining N.O.E.s recorded for ochotensimine may be satisfactorily interpreted in terms of the conformation depicted in **1** and will be discussed in the full publication.

Acknowledgments

We thank Professor Stewart McLean for making available to us a generous sample of ochotensimine. We thank the National Research Council of Canada for financial support of this work and for a Fellowship to J. K. Saunders.

1. J. K. Saunders, R. A. Bell, C. -Y. Chen, D. B. MacLean, and R. H. F. Manske. Can. J. Chem. **46**, 2876 (1968).
2. S. McLean, M.-S. Lin, and R. H. F. Manske. Can. J. Chem. **44**, 2449 (1966).
3. S. McLean, M.-S. Lin, A. C. MacDonald, and J. Trotter. Tetrahedron Letters, 3819 (1964).
4. (*a*) F. A. L. Anet and A. J. R. Bourn. J. Am. Chem. Soc. **87**, 5250 (1965); (*b*) R. H. Martin and J. C. Nouls. Tetrahedron Letters, 2727 (1968) and references therein.
5. I. Solomon. Phys. Rev. **99**, 559 (1955).
6. A. Abragam. The principles of nuclear magnetism. Oxford University Press, New York. 1961. p. 294.
7. R. A. Hoffman and S. Forsen. J. Chem. Phys. **45**, 2049 (1966); E. L. Mackor and C. MacLean. J. Chem. Phys. **42**, 4254 (1965).
8. N. Bloembergen, E. M. Purcell, and R. V. Pound. Phys. Rev. **73**, 679 (1948); I. Solomon and N. Bloembergen. J. Chem. Phys. **25**, 261 (1956); R. Kaiser. J. Chem. Phys. **42**. 1838 (1965).
9. B. M. Fung. J. Am. Chem. Soc. **90**, 219 (1968).

Can. J. Chem. Downloaded from www.nrcresearchpress.com by 210.87.254.42 on 09/05/12
For personal use only.

Can. J. Chem. Downloaded from www.nrcresearchpress.com by 210.87.254.40 on 09/05/12
For personal use only.

Canadian Journal of Chemistry

Published by THE NATIONAL RESEARCH COUNCIL OF CANADA

VOLUME 46 NOVEMBER 15, 1968 NUMBER 22

Solvation of sodium ions studied by ^{23}Na nuclear magnetic resonance

E. G. BLOOR[1] AND R. G. KIDD

Chemistry Department, University of Western Ontario, London, Ontario

Received May 31, 1968

The ^{23}Na chemical shifts, extrapolated to infinite dilution, of solutions containing sodium iodide dissolved in 14 different oxygen or nitrogen donor organic solvents have been determined. The observed range of chemical shifts can be successfully related to changes in the paramagnetic term of the general nuclear screening equation. A fair correlation between the magnitude of the paramagnetic term and the Lewis basicity of the solvent has been drawn. Those solvents showing anomalous behavior are the ones for which large magnetic anisotropies are to be expected. The ^{23}Na chemical shifts for two mixed solvent systems containing sodium iodide have been obtained, and these support the conclusion that preferential solvation of the sodium ion occurs.

Canadian Journal of Chemistry, 46, 3425 (1968)

Introduction

In recent years, the nuclear magnetic resonance (n.m.r.) technique has yielded a great deal of information about concentrated solutions of electrolytes. Most of these results have been obtained from studies of the proton magnetic resonance of the solvent water (1–5). Comparatively few results have been obtained by observing the resonance of a nucleus within the electrolyte (6). The purpose of this investigation was to obtain a detailed description of the ion–solvent interactions in nonaqueous solutions of sodium iodide using the ^{23}Na nucleus as a probe.

In spite of the rather favorable characteristics possessed by the ^{23}Na nucleus for the observance of its magnetic resonance, very little has been achieved from measurements on this nucleus. Previous studies on aqueous (2, 7, 8) and nonaqueous (8) solutions of various sodium salts failed to show any dependence of the position of the ^{23}Na resonance on the salt concentration. However, in 1966, Deverell and Richards (6) reported a linear dependence of the chemical shift on the concentrations of the sodium halides and sodium nitrate in water. The chemical shifts covered a total range of 5 p.p.m. They also found that the shielding of the sodium ion depended on the anion present, the order of increasing shielding being $I^- < Br^- < Cl^- < F^- < H_2O < NO_3^-$.

Maciel *et al.* (9) have studied the ^{7}Li resonances of lithium perchlorate and lithium bromide in various organic solvents and found that the chemical shifts of these resonances cover a range of 6 p.p.m. depending on the solvent. Since Jameson and Gutowsky (10) have noted that the chemical shifts in different compounds increase with increasing atomic number for a particular group, it is thus expected that a larger range of chemical shifts will be found for ^{23}Na salts than for ^{7}Li salts in various solvents, thus allowing any trends to be more readily discernible.

Experimental

Materials

The sodium iodide was B.D.H. laboratory reagent grade. This powder was recrystallized from water, washed with ether, and dried under reduced pressure. The resulting powder was then recrystallized from ethanol, washed with ether, and dried at 150–200 °C for 3 days at a pressure of 0.02 mm. The acetic anhydride, acetone, ethyl acetoacetate, benzaldehyde, ethyl acetate, pyridine, and anhydrous ethylenediamine were Fisher certified reagent grade. The acetonitrile, acetyl-acetone, N,N-dimethylformamide, and dimethyl sulfoxide (DMSO) were B.D.H. laboratory reagent grade. The

[1]Holder of National Research Council of Canada Studentships during 1966–68.

Can. J. Chem. Downloaded from www.nrcresearchpress.com by 210.87.254.40 on 09/05/12
For personal use only.

tetrahydrofuran and pyrrolidine were from Eastman Organic Chemicals and the glacial acetic acid was C.I.L. C.P. reagent grade. All of these solvents, except pyridine, were dried over molecular sieves (Linde 4A). The pyridine was dried over KOH pellets. All preparation and transfer operations were carried out under the dry nitrogen atmosphere of a glove box.

^{23}Na Magnetic Resonance Measurements

The ^{23}Na n.m.r. spectra were obtained from a standard Varian HR-60 spectrometer operating at a frequency of 15.083 MHz. A spherical sample container fitted with a concentric spherical insert for the reference solution was used. The sample tube had a maximum inner diameter of 14 mm and that of the insert was 3 mm. Corrections due to differences in bulk susceptibilities between samples were not applied to the chemical shifts. These would arise from any imperfections in the geometry of the cell and would be expected to be small. Each spectrum was calibrated by means of side bands generated by a General Radio variable frequency oscillator, type 1310A. The audio frequencies employed were in the range 150 Hz (for smallest chemical shifts) to 350 Hz (for largest chemical shifts) and were measured by a Hewlett–Packard 5245L electronic counter. A sweep rate of about 5 Hz/s was used and each sample was swept at least four times in both increasing and decreasing field directions. A positive δ corresponds to an upfield chemical shift and represents increased screening of the ^{23}Na nucleus.

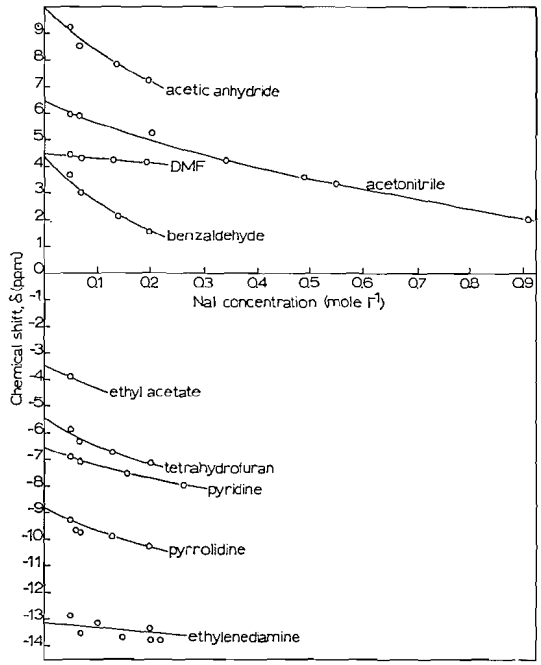

FIG. 1. ^{23}Na chemical shifts of sodium iodide in various solvents as a function of concentration.

Results

The chemical shifts with respect to an aqueous solution of sodium iodide (22.8% NaI) were determined for a minimum of four concentrations of sodium iodide in each of the solvents except DMSO and ethyl acetate (see below). The shift of the 22.8% aqueous sodium iodide reference solution from infinitely dilute aqueous sodium iodide ($\delta_{22.8\%} = -0.41$ p.p.m.) was determined from Fig. 1 of ref. 6. The chemical shifts of the nonaqueous solutions of sodium iodide relative to an infinitely dilute aqueous sodium iodide solution are given by

$$[1] \qquad \delta = \delta_{obs} + \delta_{22.8\%}$$

where δ_{obs} is the observed shift relative to the 22.8% aqueous sodium iodide external reference. The chemical shifts for each solvent were extrapolated to infinite dilution as in Fig. 1. The chemical shifts at infinite dilution, δ_0, for all the solvents studied are listed in Table I.

TABLE I

^{23}Na chemical shifts of sodium iodide at infinite dilution in various solvents

Solvent	δ_0 (p.p.m.)*	pK_a†
Acetic anhydride	9.9	
Acetonitrile	6.4	−10.13
Acetone	5.8	−7.2
Acetic acid	5.4	−6.1
Ethyl acetoacetate	5.2	
Acetyl-acetone	4.8	
Acetyl-acetone (diketone)		−6.2
Acetyl-acetone (enol)		−5.1
N,N-Dimethylformamide	4.5	−0.01
Benzaldehyde	4.3	−7.1
Water	0.0	
Dimethyl sulfoxide	~0	0
Ethyl acetate	−3.5	−6.5
Tetrahydrofuran	−5.5	−2.08
Pyridine	−6.6	5.29
Pyrrolidine	−8.9	11.27
Ethylenediamine	−13.1	

*Chemical shifts relative to infinitely dilute aqueous NaI.
†Values obtained from ref. 16.

The plots of the chemical shifts versus molar concentration of NaI in acetone, ethyl acetoacetate, and acetyl-acetone all had similar slopes to that for the NaI–benzaldehyde solutions. No concentration dependence of the ^{23}Na resonance was detectable for the solutions of sodium iodide in acetic acid in the concentration range studied for this solvent (up to 0.41 *M*). The chemical shift for only one concentration of sodium iodide in ethyl acetate was obtained because of the low solubility of NaI in this solvent. Its chemical

Can. J. Chem. Downloaded from www.nrcresearchpress.com by 210.87.254.40 on 09/05/12
For personal use only.

shift at infinite dilution was obtained by analogy with the other curves. Owing to the overlapping of the ^{23}Na resonance in the DMSO solution with the external reference signal, no direct chemical shift measurement was possible. However, the peak due to ^{23}Na in DMSO was 0.68 p.p.m. wide at half-height, thus the chemical shift would be in the range ± 0.34 p.p.m. The standard deviations of all the other chemical shifts recorded were not in excess of $\pm 2\%$ of the value of the shift.

The influence of water on the ^{23}Na chemical shifts of NaI in acetonitrile and ethylenediamine is shown in Fig. 2. The molar concentration of sodium iodide was approximately constant in each of these solutions, while the mole ratio of water in the solvent was varied. Figure 3 represents the results of a similar study of different sodium iodide concentrations in ethylenediamine–water solvent mixtures. The curves in Figs. 2 and 3 have been extrapolated to the chemical shift values expected (6) for aqueous solutions of sodium iodide of these concentrations (i.e. approximately zero).

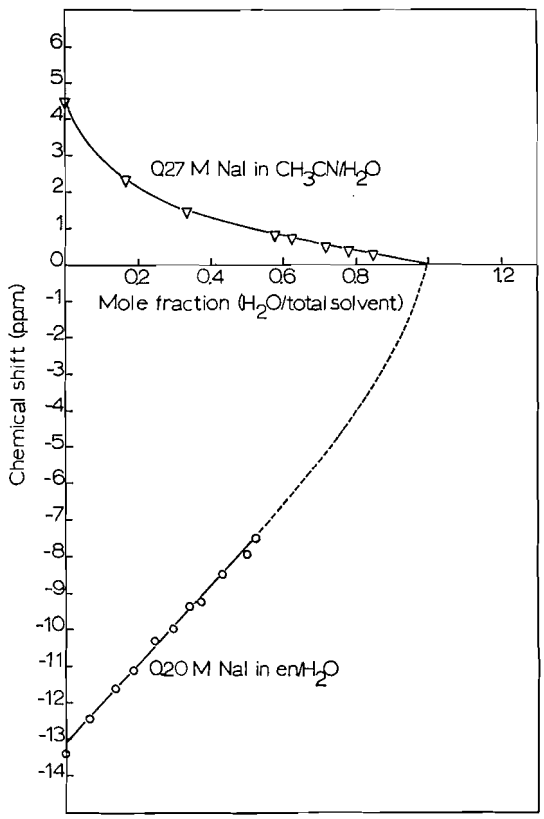

FIG. 2. Influence of water on the ^{23}Na chemical shifts of sodium iodide in acetonitrile and ethylenediamine.

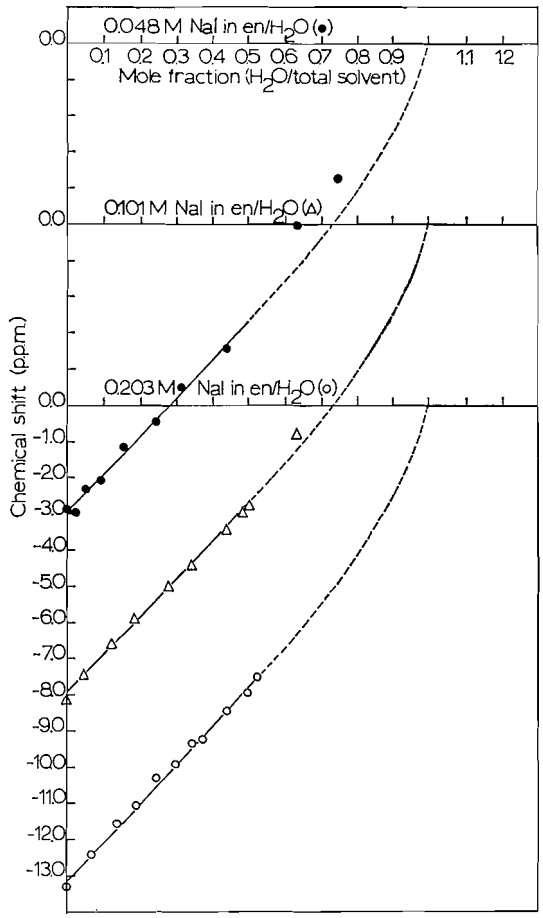

FIG. 3. Influence of water on ^{23}Na chemical shifts of sodium iodide in ethylenediamine.

Interpretation of Chemical Shifts

The position of a nuclear magnetic resonance signal is determined by the total shielding that the nucleus under investigation receives from various sources. This shielding is expressed by the screening constant, σ. A general formula for σ has been developed by Ramsey (11) but its applicability to all but the simplest systems is limited. Saika and Slichter (12) have put the calculation of screening constants on a practical basis by dividing the screening constant into three independent contributions represented by

$$[2] \qquad \sigma = \sigma_d + \sigma_p + \sigma_o$$

Can. J. Chem. Downloaded from www.nrcresearchpress.com by 210.87.254.40 on 09/05/12
For personal use only.

The σ_d term arises from the local diamagnetic currents in the molecule and is expressed by the Lamb formula,

$$[3] \qquad \sigma_d = \frac{e}{3mc^2} \sum_i \left\langle \Psi_0 \left| \frac{1}{r_i} \right| \Psi_0 \right\rangle$$

Contributions from other atoms to the shielding of the resonant nucleus are contained in σ_o. These contributions are due to anisotropies in the magnetic susceptibilities of the distant atoms and vary as the inverse cube of their distance from the resonant nucleus. These effects are generally minor on nuclei other than protons. σ_p is the paramagnetic term and is usually the dominant shielding term. It represents the contribution due to the net orbital angular momentum of electrons in the valence orbitals of the nucleus under investigation and it makes a negative contribution to the screening. Thus only electrons in p, d, f, . . . orbitals make a first-order contribution to σ_p. Electrons in s-orbitals contribute to σ_p only to the extent that they influence the effective nuclear charge of the atom and thus the inverse cube radius of the other electrons, $\langle 1/r^3 \rangle_{n,l}$, which affects σ_p.

The addition of an electron to any orbital of Na^+ will increase the diamagnetic shielding. This change in σ_d can be approximated by the following expression (13):

$$[4] \quad \sigma_d = \frac{e^2}{3mc^2} \cdot \frac{Z_{eff}}{\alpha_0 n^2} = 17.8 \times 10^{-6} \frac{Z_{eff}}{n^2}$$

where α_0 is the Bohr radius, n is the principle quantum number of the orbital to which the electron is added, and Z_{eff} is the "effective nuclear charge". The effective nuclear charge which determines the radial portion of Slater-type atomic orbitals is given by $Z_0 = Z - S$, where Z is the real nuclear charge and S is a screening constant evaluated using Slater's rules (14). It is generally recognized that for all but the lightest atoms, Slater atomic orbitals give values for the average orbital radius $\langle r \rangle$ which are too large, indicating that the strict application of Slater's rules gives a value of Z_0 which is too low. In estimating the magnitude of σ in their "atom in a molecule" model, Schneider and Buckingham have used $(Z_0 Z)^{1/2}$ for the effective nuclear charge, presumably to allow for this factor. For sodium, $Z = 11$, $Z_0 = 2.20$, and $\sigma_d = 9.7$ p.p.m. for the addition of one electron to any orbital with $n = 3$. Thus, on progressing from purely ionic sodium to atomic sodium, the changes in the diamagnetic shielding of the nuclei would result in a total chemical shift of approximately 10 p.p.m. Since neither of these two extreme cases would be expected to be encountered in a solution of sodium iodide, the actual range of chemical shifts caused by variations in the diamagnetic shielding would be much less than 10 p.p.m.

The range of chemical shifts possible from changes in the paramagnetic shielding can be approximated by the following expression for σ_p using Schneider and Buckingham's "atom in a molecule" model (13):

$$[5] \quad \sigma_p = -\frac{e^2 \hbar^2 L(L+1)}{3m^2 c^2 \Delta E} \left\langle \frac{1}{r^3} \right\rangle_{n,l}$$

$$= -7.67 \times 10^{-16} \frac{(Z_0 Z)^{3/2} L(L+1)}{n^3 l(l+1)(l+\frac{1}{2}) \Delta E}$$

where $\hbar^2 L(L+1)$ is the square of the total orbital angular momenta of the valence electrons and ΔE is taken as the first ionization potential of the sodium atom, i.e. $\Delta E = 8.22 \times 10^{-12}$ ergs (15). For Na^+ with an electron donated by the solvent to a 3p orbital, $L = l = 1$. Thus $\sigma_p = -270$ p.p.m.

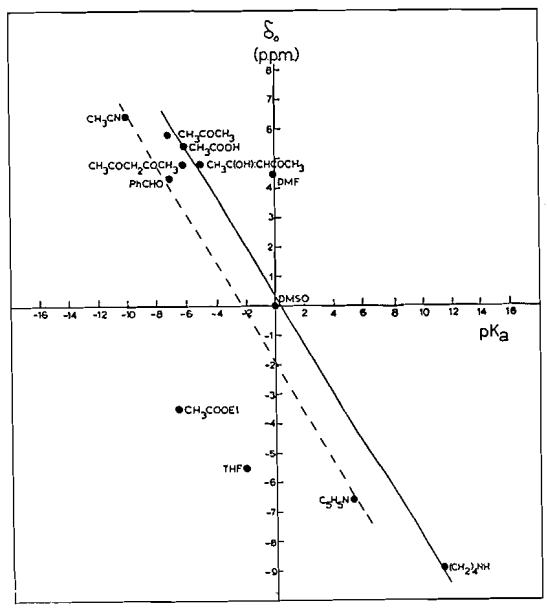

FIG. 4. Correlation of the chemical shifts at infinite dilution with the pK_a values of the solvent.

Can. J. Chem. Downloaded from www.nrcresearchpress.com by 210.87.254.40 on 09/05/12
For personal use only.

These calculations and the observed range of chemical shifts of the ^{23}Na resonances, viz. 23 p.p.m., indicate that the most important factor affecting these chemical shifts is the orbital angular momentum of electrons occupying the $n = 3$ shell of sodium and its effect upon σ_p. This arises from the overlapping of the outer p orbitals of the central sodium ion with the outer s and p orbitals of the neighboring solvent molecules or ions. Thus it would be expected that the ^{23}Na resonance would be at a lower field when sodium iodide is dissolved in a solvent of appreciable electron-donating ability than when it is dissolved in a less basic solvent. That this is indeed the case is illustrated in Table I and Fig. 4. The pK_a values were obtained (16) in aqueous solutions (except that for ethyl acetate, which was obtained in acetic acid) but these values should also be applicable to sodium iodide solutions since the behavior of these solvents toward the sodium ion would be expected to be similar to their behavior toward the hydrogen ion. Fratiello *et al.* (17) have also found a linear correlation of pK_a values with the abilities of certain solvents to solvate $AlCl_3$, $TiCl_4$, and $CoCl_2$ in aqueous solution mixtures.

The dashed line in Fig. 4 through the points due to the acetonitrile, benzaldehyde, and pyridine solutions is shifted farther downfield (by about 2 p.p.m.) than the solid line through the points due to the other solvents. This could arise from a contribution to the chemical shifts due to the magnetic anisotropies of the triply bonded nitrogen in acetonitrile and pyridine and of the ring system in benzaldehyde (18).

A grouping of all oxygen-coordinating solvents at high fields and of all nitrogen-coordinating solvents at lower fields is observed. The oxygen-coordinating solvents are further divided with those donating electrons through $\rangle C{=}O$ being at higher field strengths than those that coordinate via —O—. These divisions would seem to indicate that the sodium ion is coordinated to the $\rangle C{=}O$ of N,N-dimethylformamide and to the —O—Et group of ethyl acetate. The occurrence of the sodium resonance in acetonitrile at a markedly higher field strength than other nitrogen-containing solvents may indicate that the main solvating influence of this solvent is via interaction of the π-electrons of —C≡N with the solute ions rather than via the exposed sp lobe of the nitrogen atom.

Preferential Solvation of Na^+

The correlation of sodium ion chemical shift with solvent basicity has, in the preceding discussion, been attributed to increased strength of interaction between cation and solvent as solvent basicity is increased. The fact that the ^{23}Na paramagnetic shift increases as the solvent is changed from acetonitrile to water to ethylenediamine is a reflection of this effect. Evidence to support the contention that strength of cation–solvent interaction varies in the manner postulated above for the case of the Na^+ is presented in Fig. 2. For a 0.27 *M* solution of sodium iodide, the shielding of the Na^+ in acetonitrile is 4.5 p.p.m. greater than that of the Na^+ in water. If the strength of interaction between cation and solvent were the same for both acetonitrile and water, then in a mixed acetonitrile–water solvent system, the average environment of a Na^+ as represented by the ratio of acetonitrile/water molecules present in the first coordination sphere of Na^+ would be identical with the solvent composition as represented by the mole fraction of the acetonitrile–water system. Under these circumstances, a plot of ^{23}Na chemical shift versus mole fraction of water in solvent should be linear from 100% acetonitrile to 100% water. Figure 2 shows that this is not the case. Addition of 0.1 mole fraction water to an acetonitrile solution of sodium iodide results in a proportionately larger decrease in the chemical shift towards its value in an aqueous solution. This indicates that the Na^+–water interaction is stronger than the Na^+–acetonitrile interaction. The opposite effect is observed on adding water to an ethylenediamine solution of sodium iodide. Here the addition of 0.1 mole fraction water causes a proportionately smaller increase of the chemical shift towards its value in an aqueous solution. This increase in chemical shift is linear with a slope of −10.6 p.p.m. until the solvent is approximately equimolar in water and ethylenediamine, at which point the chemical shift increases more rapidly to zero ($\delta \simeq 0$ at 0.20 *M* NaI in H_2O). This preference of the sodium ion to be solvated by ethylenediamine rather than by water is shown by Fig. 3 to be the same at concentrations of sodium iodide equal to 0.05 *M*, 0.10 *M*, and 0.20 *M*.

Acknowledgments

We wish to thank the National Research Council of Canada for financial support of this study in the form of Studentships to E.G.B. and Operating Grants to R.G.K.

1. J. N. SHOOLERY and B. J. ALDER. J. Chem. Phys. **23**, 805 (1955).
2. J. C. HINDMAN. J. Chem. Phys. **36**, 1000 (1962).
3. B. P. FABRICAND and S. GOLDBERG. J. Chem. Phys. **34**, 1624 (1961).
4. B. P. FABRICAND, S. S. GOLDBERG, R. LIEFER, and S. G. UNGAR. Mol. Phys. **7**, 425 (1963).
5. D. W. MCCALL and D. C. DOUGLASS. J. Phys. Chem. **69**, 2001 (1965).
6. C. DEVERELL and R. E. RICHARDS. Mol. Phys. **10**, 551 (1966).
7. J. E. WERTZ and O. JARDETZKY. J. Chem. Phys. **25**, 357 (1956).
8. R. E. RICHARDS and B. A. YORKE. Mol. Phys. **6**, 289 (1963).
9. G. E. MACIEL, J. K. HANCOCK, L. F. LAFFERTY, P. A. MUELLER, and W. K. MUSKER. Inorg. Chem. **5**, 554 (1966).
10. C. J. JAMESON and H. S. GUTOWSKY. J. Chem. Phys. **40**, 1714 (1964).
11. N. F. RAMSEY. Phys. Rev. **78**, 699 (1950).
12. A. SAIKA and C. P. SLICHTER. J. Chem. Phys. **22**, 26 (1954).
13. W. G. SCHNEIDER and A. D. BUCKINGHAM. Discussions Faraday Soc. **34**, 147 (1962).
14. H. EYRING, J. WALTER, and G. E. KIMBALL. Quantum chemistry. John Wiley and Sons, Inc., New York. 1944. p. 163.
15. C. E. MOORE. Natl. Bur. Std. (U.S.), Circ. 467. Atomic energy levels. Vol. 1. 1958.
16. E. M. ARNETT. Progress in physical organic chemistry. Vol. I. *Edited by* S. G. Cohen, A. Streitwieser, Jr., and R. W. Taft. Interscience Publishers, Inc., New York. 1963. p. 223.
17. A. FRATIELLO, R. E. LEE, D. P. MILLER, and V. M. NISHIDA. Mol. Phys. **13**, 349 (1967).
18. J. A. POPLE, W. G. SCHNEIDER, and H. J. BERNSTEIN. High resolution nuclear magnetic resonance. McGraw-Hill Book Co., Inc., New York. 1959. Chap. 7.

Can. J. Chem. Downloaded from www.nrcresearchpress.com by 210.87.254.40 on 09/05/12
For personal use only.

Can. J. Chem. Downloaded from www.nrcresearchpress.com by 210.87.254.40 on 09/05/12
For personal use only.

Kinetic studies of metalloporphyrin formation. Part I. Mn(II) with hematoporphyrin

DOREEN A. BRISBIN AND ROBERT J. BALAHURA
Department of Chemistry, University of Waterloo, Waterloo, Ontario
Received December 8, 1967

The kinetics of the formation of Mn(III) hematoporphyrin in glacial acetic acid has been studied spectrophotometrically.

On addition of Mn(II) to porphyrin in glacial acetic acid a species which appears to be the monocation immediately is formed and is then converted to Mn(III) hematoporphyrin at a rate suitable for kinetic studies.

The rates of reaction were measured at 45, 50, and 55 °C and the activation energies were calculated.

Canadian Journal of Chemistry, **46**, 3431 (1968)

Introduction

Manganese is of considerable importance biologically not only in plant photosynthesis but as a recently detected component in blood (1).

Pertinent to the understanding of its biological role is the knowledge of various properties exhibited by manganese when complexed with such ligands as the porphyrins.

Previous studies on porphyrins in glacial acetic acid (2, 3) indicated the suitability of this medium for kinetic studies.

The present work was concerned with obtaining rate constants for the reaction of Mn(II) and hematoporphyrin in glacial acetic acid as well as determining the possible mechanism of the reaction.

Experimental

Materials

All chemicals used were of reagent grade. Spectrophotometric measurements were made with a Beckman DBG recording spectrophotometer and quartz cells of 1 cm path length. Kinetic experiments were carried out in a thermostated water bath and a constant temperature cell compartment, both maintained at the same temperature (±0.2 °C).

Recrystallized hematoporphyrin dihydrochloride from Mann Research Laboratory (98% spectro assay) was used to prepare stock solutions of the dication in anhydrous glacial acetic acid. The spectra of these stock solutions were checked prior to each experimental run. There appeared to be no diminution of the hematoporphyrin absorption bands, or increase of absorption in the region where a monovinyl or divinyl group would absorb if dehydration to protoporphyrin had occurred. The porphyrin cation appeared to be monomerically dispersed as demonstrated by the lack of dependence of the molar absorptivity upon concentration. Aggregation would probably affect the absorption spectrum.

Manganese(II) acetate solutions were prepared in anhydrous glacial acetic acid prior to each experimental run. The hydrated metal acetate was used but the amount of water incorporated into the solvent for the range of metal concentrations studied would be less than .01%.

Method

Kinetic measurements were carried out at 45, 50, and 55 °C (all within ±0.1 °C) in both anhydrous glacial acetic acid and anhydrous glacial acetic acid to which 1% deionized water had been added.

Separate samples of hematoporphyrin and manganese were preequilibrated at these temperatures. The two solutions were then mixed (manganous ion concentration always in large excess over porphyrin dication concentration) and the rate of incorporation of manganese into hematoporphyrin was followed by measuring the change of optical density at 462 mμ. The metal ion did not contribute to the absorption and at this wavelength the differences in the extinction coefficients of the absorbing species are large. The extinction coefficients at 462 mμ, as determined here, were 4.25×10^4 for manganese hematoporphyrin, 7.60×10^2 for the porphyrin dication, and 2.20×10^3 for the monocation reaction intermediate.

The rate constants were obtained from plots of $-\log [D_\infty - D_t]$ versus time, where D_t = absorbance at any time t, and D_∞ = absorbance at the completion of the reaction.

Results and Discussion

Immediately upon mixing porphyrin dication with manganous ion in glacial acetic acid, a very distinct spectrum is produced which is not that of the porphyrin dication or the metalloporphyrin, but appears to be that of the monocation PH_3^+. This reaction occurs at room temperature as well as the temperature range used for the kinetic studies. The spectrum which consists of peaks at 530, 555, and 600 mμ in the visible region, with a shoulder at 495 mμ and a peak at 395 mμ in the Soret region, (Fig. 1) is the same as that observed for the monocation in anionic detergent solutions (4). We observed the same spectrum for hematoporphyrin free base dissolved in glacial acetic acid.

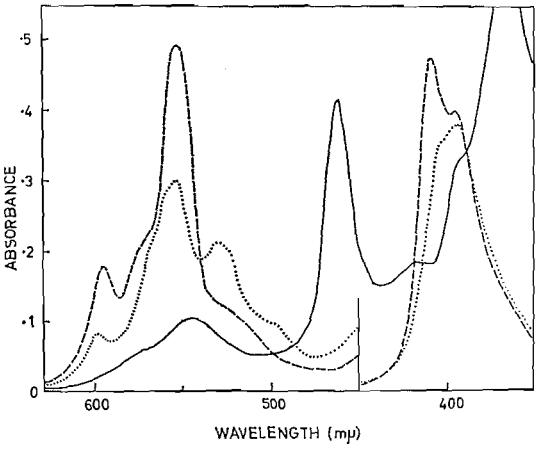

FIG. 1. Absorption spectra in glacial acetic acid: spectra of hematoporphyrin dication species (PH_4^{2+}) of concentration 3.5×10^{-5} *M* in the visible region and 2.5×10^{-6} *M* in the Soret region are given by dashed lines, that of intermediary species of concentration 2.75×10^{-5} *M* in the visible region and 2.5×10^{-6} *M* in the Soret region are given by dotted lines, and that of manganese(III) hematoporphyrin of concentration 1×10^{-5} *M* in both the visible and the Soret region are given by solid lines.

By determining a set of spectra of this species at constant manganous ion concentration, and varying the concentrations of porphyrin dication (the manganese in excess over any porphyrin concentration) it could be shown that Beer's Law is obeyed in the range of concentrations studied.

When the solutions are allowed to stand for a period of time the spectrum of this monocation species gradually changes to that of the metalloporphyrin. At room temperature this conversion is slow, but at higher temperatures, above 40 °C, it proceeds at rates convenient for kinetic studies.

The metalloporphyrin formed is the manganese(III) not manganese(II) hematoporphyrin[1]. This agrees with the findings of Calvin (5) who was able to prepare only the Mn(III) hematoporphyrin on the addition of manganous acetate to porphyrin in glacial acetic acid. The Mn(III) hematoporphyrin spectrum in glacial acetic acid has peaks at 368, 462, and 546 mμ (Fig. 1), very similar but slightly shifted from those positions noted by Calvin (5) in aqueous alkali and alcohol solutions. Addition of reducing agents or oxidizing agents to solutions of the Mn(III) porphyrin in glacial acetic acid produces spectral changes indicative of reduction of Mn(III) to Mn(II) or oxidation of Mn(III) to Mn(IV).

The species formed immediately upon mixing appears to be essentially the monocation, rather than the type of sitting-atop-complex intermediate proposed by Fleischer and Wang (6). Addition of water to solutions containing the intermediate caused the spectrum to revert to that of the dication PH_4^{2+}, a two-band spectrum in the visible region with absorption peaks at 553 and 595 mμ (Fig. 1).

We were not successful in obtaining the value for the formation constant of this starting material by a spectral method previously employed (2). Formation was complete and rapid with all concentrations which gave adequate absorbances at the suitable wavelengths, indicating a very large constant. Comparison of the spectrum of PH_3^+ with that of the starting material shows only a very slight difference in the intensities of the 495 mμ shoulder and the 530 mμ peak. The extinction coefficients at the 555 mμ peak are the same and would seem to indicate complete conversion of the PH_4^{2+} species to the PH_3^+ species.

The observation of isosbestic points in the spectra of the manganese porphyrin solutions indicates only two independent absorbing species present. Figure 2 shows the typical spectra produced when Mn(II) and porphyrin solutions were mixed ($Mn^{2+} \gg PH_4^{2+}$) and overlapping spectra taken over increasing time intervals. At least six isosbestic points were noted. The spectrum of porphyrin dication of the same concentration as above does not intersect at any of the isosbestic points. Presumably the two species present are the starting material PH_3^+ and the Mn(III) hematoporphyrin.

The reaction of Mn(II) and hematoporphyrin then appears to occur in two steps: a very rapid first step in which PH_3^+ is formed by the abstraction of a proton by manganese and a second rate-determining step whereby the intermediate further reacts with manganese to form Mn(III) hematoporphyrin probably by the displacement of the remaining protons from the nitrogen atoms by the metal. Previous work on the mechanism of metal incorporation into the porphyrin

[1]Reacting the metal and porphyrin under nitrogen or on a vacuum line also results in production of only Mn(III) hematoporphyrin.

Can. J. Chem. Downloaded from www.nrcresearchpress.com by 210.87.254.40 on 09/05/12
For personal use only.

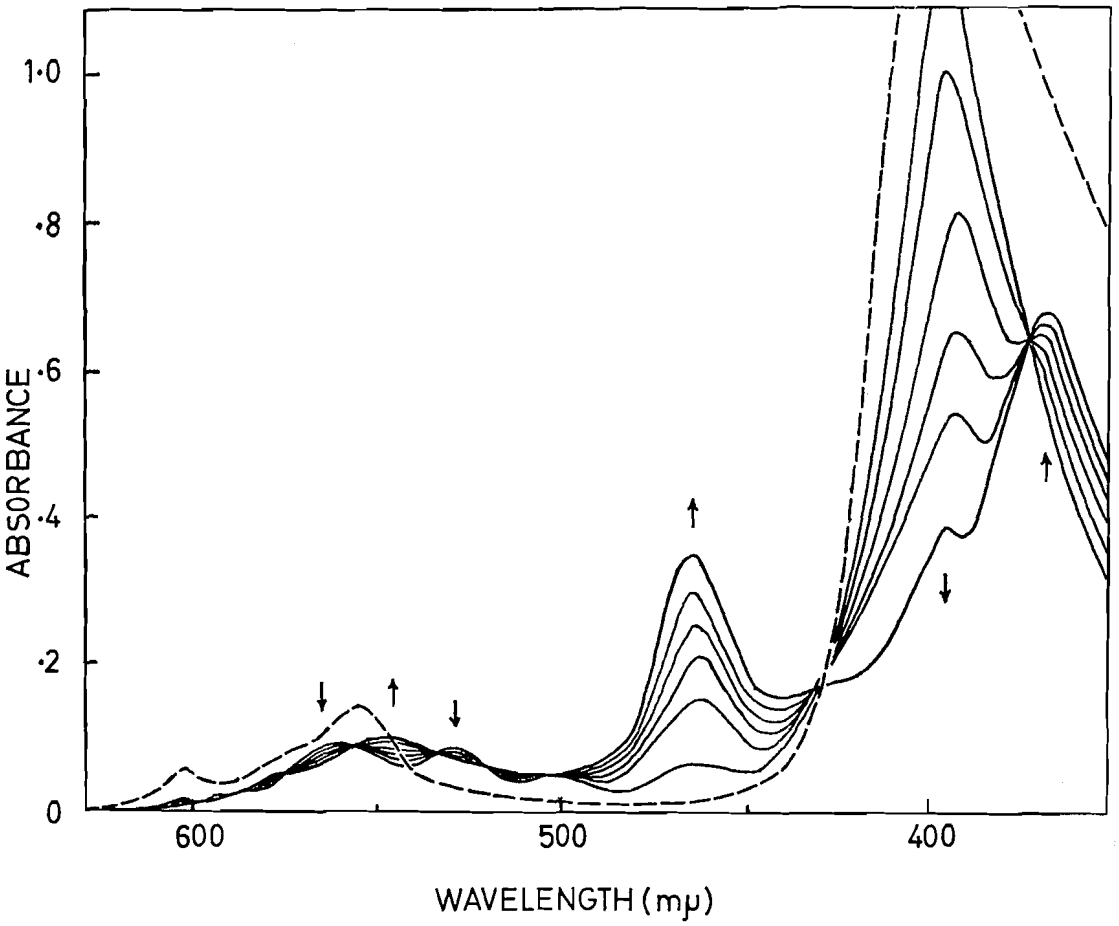

FIG. 2. Overlapping absorption spectra of manganese 5×10^{-3} *M* mixed with hematoporphyrin 1×10^{-5} *M* taken over increasing time intervals given by solid line, that of hematoporphyrin monocation (PH_3^+), 1×10^{-3} *M* given by dashed line.

ring has favored a displacement rather than a dissociation mechanism (7). One reason for favoring the former mechanism is the fact that electron-withdrawing porphyrin substituents have been shown to slow down the reaction rate, whereas they would be expected to increase the rate if a dissociation mechanism was involved in which the dianion is formed.

Preliminary experiments show that Fe(III) and Co(II) acetates are able to produce a similar PH_3^+ species in glacial acetic acid to that produced with manganese. Ni(II), however, produces what appears to be a mixture of PH_3^+ and PH_2 species, and Zn(II) and Cu(II) do not form detectable intermediates but proceed directly to the metalloporphyrin. If one assumes that the first step is a very rapid equilibrium with a very large formation constant for the PH_3^+ species, then the reaction could be written as follows:

$$PH_3^+ + Mn^{2+}{}_{solv} \xrightarrow{k} Mn(III)P + 3H^+ + e$$

Since trial runs had shown that successive evacuations of the system did not prevent the formation of the manganese(III) porphyrin, oxygen may not be the oxidant. The reaction could possibly involve the reduction of +I hydrogen and be rewritten as follows:

$$PH_3^+ + Mn^{2+} \rightarrow Mn(III)P + 2H^+ + \tfrac{1}{2}H_2$$

Dorough *et al.* (8) had postulated a similar reaction for the conversion of silver from the +I to

Can. J. Chem. Downloaded from www.nrcresearchpress.com by 210.87.254.40 on 09/05/12
For personal use only.

TABLE I

Rates of reaction of hematoporphyrin with manganese(II) in glacial acetic acid

Temp. (°C)	Hematoporphyrin (M)	Manganese (M)	Slope, k_{obsd}	Rate constant, k* (l mole^{-1} min^{-1})
55	5×10^{-6}	5×10^{-3}	−0.0475	21.9
	5×10^{-6}	3×10^{-3}	−0.0272	20.8
	1×10^{-5}	4×10^{-3}	−0.0380	21.9
	1×10^{-5}	5×10^{-3}	−0.0516	23.8
	1×10^{-5}	3×10^{-3}	−0.0301	23.1
	1×10^{-5}	2×10^{-3}	−0.0199	22.9
	1×10^{-5}	1×10^{-3}	−0.0090	20.6
			Average	22.1±0.9
50	5×10^{-6}	5×10^{-3}	−0.0327	15.1
	1×10^{-5}	4×10^{-3}	−0.0265	15.3
	5×10^{-6}	3×10^{-3}	−0.0195	15.0
	1×10^{-5}	3×10^{-3}	−0.0203	15.6
	5×10^{-6}	5×10^{-3}	−0.0315	14.5
			Average	15.1±0.3
45	5×10^{-6}	5×10^{-3}	−0.0222	10.2
	1×10^{-5}	5×10^{-3}	−0.0223	10.3
	1×10^{-5}	4×10^{-3}	−0.0173	10.0
	7×10^{-6}	5×10^{-3}	−0.0216	10.0
	7×10^{-6}	4×10^{-3}	−0.0163	9.4
	1.2×10^{-5}	5×10^{-3}	−0.0191	8.8
	1.2×10^{-5}	4×10^{-3}	−0.0184	10.6
	5×10^{-6}	5×10^{-3}	−0.0222	10.2
	5×10^{-6}	4×10^{-3}	−0.0170	9.8
	5×10^{-6}	3×10^{-3}	−0.0129	9.8
			Average	9.9±0.4

*Each k value was determined from duplicate or triplicate runs.

+II state when reacted with tetraphenylporphyrin in acetic acid.

An expression for k_{obsd} can be written for the above mechanism:

$$k_{obsd} = k\,[Mn^{2+}]$$

The experimental data fit this expression very well.

Data from all experimental runs yielded excellent straight line plots of $-\log [D_\infty - D_t]$ versus time, of slope $k_{obsd}/2.303$, where k_{obsd} = pseudo-first-order rate constant with respect to the intermediate species. Figure 3 shows two typical rate measurements, one in anhydrous glacial acetic acid, and one in anhydrous glacial acetic acid and 1% H_2O solutions.

Table I summarizes the kinetic results for the formation of manganese hematoporphyrin in anhydrous glacial acetic acid and 1% H_2O solutions.

The second-order rate constant k has been obtained by multiplying k_{obsd} (the pseudo-first-order rate constant) by $2.303/[Mn^{2+}]_t$, since the original manganese ion concentration ($[Mn^{2+}]$ ion concentration) in the rate-determining step will be approximately equal to $[Mn^{2+}]$.

The reaction on the basis of the proposed

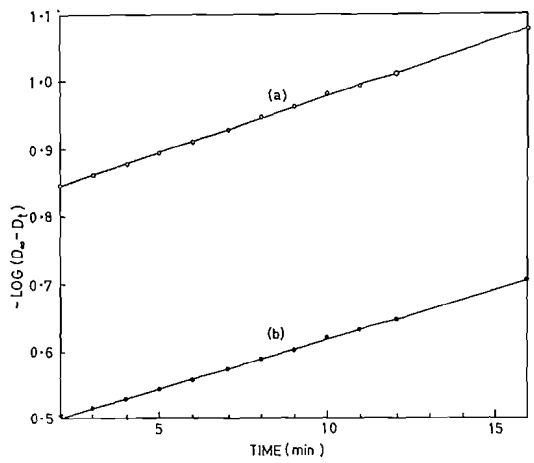

FIG. 3. Two typical rate plots of $-\log [D_\infty - D_t]$ versus time: (*a*) in anhydrous glacial acetic acid at 45 °C. Initial concentrations: hematoporphyrin, 5×10^{-6} M, manganese, 4×10^{-3} M; (*b*) in anhydrous glacial acetic acid and 1% H_2O at 45 °C. Initial concentrations: hematoporphyrin, 1×10^{-5} M, manganese, 5×10^{-3} M.

Can. J. Chem. Downloaded from www.nrcresearchpress.com by 210.87.254.40 on 09/05/12
For personal use only.

TABLE II

Rates of reaction of hematoporphyrin with manganese(II) in glacial acetic acid and 1% H_2O

Temp. (°C)	Hematoporphyrin (M)	Manganese (M)	Slope, k_{obsd}	Rate constant, k* (l mole^{-1} min^{-1})
55	5×10^{-6}	5×10^{-3}	−0.0305	14.1
	7×10^{-6}	5×10^{-3}	−0.0296	13.6
	7×10^{-6}	4×10^{-3}	−0.0250	14.4
	1×10^{-5}	5×10^{-3}	−0.0321	14.8
	1×10^{-5}	4×10^{-3}	−0.0253	14.6
			Average	14.4±0.4
50	5×10^{-6}	4×10^{-3}	−0.0165	9.5
	1×10^{-5}	4×10^{-3}	−0.0170	9.8
	1×10^{-5}	5×10^{-3}	−0.0216	9.9
	5×10^{-6}	5×10^{-3}	−0.0213	9.8
			Average	9.8±0.2
45	5×10^{-6}	5×10^{-3}	−0.0149	6.8
	5×10^{-6}	4×10^{-3}	−0.0117	6.7
	7×10^{-6}	5×10^{-3}	−0.0139	6.4
	1.2×10^{-5}	5×10^{-3}	−0.0144	6.6
	1×10^{-5}	5×10^{-3}	−0.0146	6.7
	5×10^{-6}	3×10^{-3}	−0.0090	6.9
			Average	6.7±0.1

*Each k value obtained from either duplicate or triplicate runs.

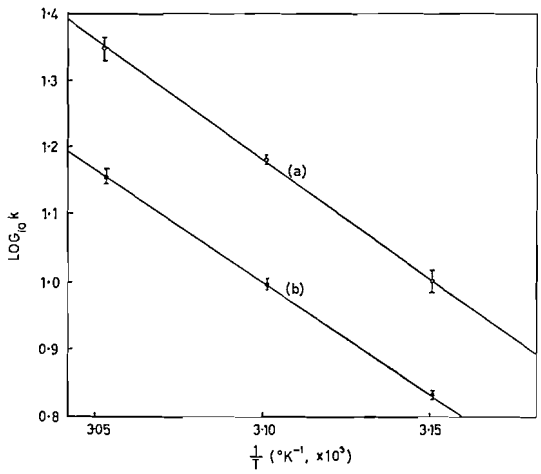

FIG. 4. Plots of $\log_{10} k$ versus $1/T$: (*a*) in anhydrous glacial acetic acid; (*b*) in anhydrous glacial acetic acid and 1% H_2O.

equation is shown to be first-order with respect to both PH_3^+ and the manganese ion.

The reaction rate at each temperature decreased with the addition of the 1% H_2O to the glacial acetic acid. This effect might be due to the triple and quadruple ion formation which Kolthoff (9) suggests occurs in glacial acetic acid containing small amounts of water, or it may be related to both hydrogen ion concentration and a mixed coordination sphere as suggested by Choi and Fleischer (3) for Cu(II) and tetrapyridylporphyrin.

Figure 4 is a plot of $\log_{10} k$ versus time used for determining the activation energies.

The activation energy for manganese(III) hematoporphyrin formation in anhydrous glacial acetic acid is 16.4 kcal/mole and $\log_{10} A = 10.5$. These results are similar to those reported for tetrapyridylporphyrin in glacial acetic acid (3) with values of 18.7 kcal/mole for the activation energy and 13.3 for $\log_{10} A$. The fact that the value of .97 l mole^{-1} min^{-1} for the second-order rate constant is considerably lower than those reported here could be due to the lower temperature used in the tetrapyridylporphyrin work and to the electron-withdrawing substituents on the porphyrin ring retarding the rate of metal incorporation.

The activation energy for manganese(III) hematoporphyrin formation in anhydrous glacial acetic acid and 1% H_2O solutions is 15.7 kcal/mole and $\log_{10} A = 9.8$.

The entropies of activation, $\Delta S^{\ddagger}$, were calculated using the equation $2.303 \log_{10} A = 2.303 \log_{10} (ekT/h) + \Delta S^{\ddagger}/R$. The values at 50 °C, for anhydrous glacial acetic acid and the glacial acetic acid and 1% H_2O solutions, were −12 and −16 cal deg^{-1} mole^{-1} respectively.

Can. J. Chem. Downloaded from www.nrcresearchpress.com by 210.87.254.40 on 09/05/12
For personal use only.

All data were fitted to a straight line with a general polynomial least-squares-curve-fitting computer program.

Factors used for calculating confidence limits were taken from standard statistical data tables using a 95% probability.

Acknowledgment

Financial support from the National Research Council of Canada is gratefully acknowledged.

1. D. C. Borg and G. C. Cotzias. Nature, **182**, 1677 (1958).
2. D. A. Brisbin and R. J. Balahura. Can. J. Chem. **44**, 2157 (1966).
3. E. I. Choi and E. B. Fleischer. Inorg. Chem. **2**, 94 (1963).
4. B. Dempsey, M. B. Lowe, and J. N. Phillips. *In* Haematin enzymes. *Edited by* J. E. Falk, R. Lemberg, and R. K. Morton. The Pergamon Press Ltd., London. 1961. p. 31.
5. M. Calvin. Rev. Pure Appl. Chem. **15**, 1 (1965).
6. E. B. Fleischer and J. H. Wang. J. Am. Chem. Soc. **82**, 3498 (1960).
7. J. N. Phillips. *In* Comprehensive biochemistry. Vol. 9. *Edited by* Marcel Florkin and Elmer H. Stotz. Elsevier Press, Inc., New York. 1963. p. 34.
8. G. D. Dorough, J. R. Miller, and Frank M. Huennekens. J. Am. Chem. Soc. **73**, 4315 (1951).
9. J. M. Kolthoff. J. Am. Chem. Soc. **78**, 1 (1956).

Can. J. Chem. Downloaded from www.nrcresearchpress.com by 210.87.254.40 on 09/05/12
For personal use only.

Can. J. Chem. Downloaded from www.nrcresearchpress.com by 210.87.254.40 on 09/05/12
For personal use only.

Oxidations involving silver. I. Kinetics of the anodic oxidation of silver in alkaline electrolytes

T. G. Clarke, N. A. Hampson, J. B. Lee, J. R. Morley, and B. Scanlon
Department of Chemistry, University of Technology, Loughborough, Leicestershire, England

Received March 5, 1968

The kinetics of the electrochemical oxidation of silver to Ag_2O in NaOH have been studied at different temperatures and hydroxyl ion concentrations. The enthalpy of activation was found to be ~ 5 kcal/mole. The kinetics of oxidation of Ag_2O to AgO are discussed.

Canadian Journal of Chemistry, 46, 3437 (1968)

Introduction

Investigations in organic electrosynthesis have, in general (see e.g. ref. 1), paid little attention to the behavior of the electrode; in contrast, progress in physico-chemical studies of electrodes has depended upon scrupulous cleanliness of electrolyte, cell, and electrode materials, to a degree not readily achievable or economically feasible for industrial organic reactions. As a consequence organic and physico-chemical studies have been largely divorced.

Interest has grown rapidly, in industrial and academic laboratories, in the applications of controlled electrosynthesis (2). We have undertaken a conjoint organo- and physico-chemical study of the behavior of solid electrode systems applied to organic oxidations of laboratory and industrial interest.

A prerequisite of a valid extrapolation of results to a new situation, is a clear understanding of all the contributing factors. The first papers in this series will analyze the factors affecting oxidations occurring at a solid silver electrode. Results for other systems will be discussed separately.

Silver in the Ag(I) state has long been used (see e.g. ref. 3), for the oxidation of organic compounds, and higher valency states appear to be the cause of the catalytic effect of silver in persulfate oxidations (see e.g. ref. 4).

A silver anode is not inert (as is platinum) but participates in the electrode reaction. In acidic solutions Ag^+ ions are in equilibrium with the electrode ($E^0 = 0.799$ V normal hydrogen electrode) and therefore it is not feasible to carry out oxidations in acid electrolytes. In alkaline solutions two electrochemically well-defined oxides are formed: Ag(I) oxide, Ag_2O ($E^0 = 0.338$ V) (15), and a higher oxide with the stoichiometric formula AgO ($E^0 = 0.599$ V) (16). The formation of these oxides may have an effect on the oxidation of organic compounds; an understanding of this effect requires a knowledge of the kinetics of oxidation of the silver electrode itself.

Studies of the differential capacitance of silver in neutral electrolytes (5) have indicated that the electrode–electrolyte interphase is uncomplicated by the intrusion of films, provided that the electrode has been pretreated under carefully controlled conditions. Further, over a considerable range of potential, electrode capacitance measurements appear to be characteristic of an uncomplicated metal–electrolyte interphase at which adsorption is absent. (The p.z.c. was readily identified by a capacitance minimum at -0.7 V). These measurements have recently been extended to electrolyte of high pH (6). The properties of the electrode–electrolyte interphase are generally similar in neutral and alkaline electrolytes; although there is some evidence for weak OH^- adsorption at potentials on the anodic side of the p.z.c. in electrolytes of high pH. A carefully prepared silver electrode provides a metal–electrolyte interphase essentially uncomplicated by surface films over a considerable range of potentials.

Subjecting the electrode to positive potentials in alkaline electrolytes results in the formation of Ag_2O

[1] $$Ag + OH^- \rightarrow \tfrac{1}{2}Ag_2O + \tfrac{1}{2}H_2O + e$$

Dirkse *et al.* (7) have examined this reaction in 35% KOH and concluded that for the low overpotential region ($\eta_D < 40$ mV) the exchange current i_0 (measured by the linear slope of current density (i)–overpotential (η_D) plots

$$i_0 = \frac{RT}{F}\left(-\frac{\partial i}{\partial \eta_D}\right)_{\eta_D \rightarrow 0}$$

Can. J. Chem. Downloaded from www.nrcresearchpress.com by 210.87.254.40 on 09/05/12
For personal use only.

where R, T, and F have their usual significance), is approximately 2×10^{-3} A cm^{-2}. No value of α, the charge transfer coefficient, has been reported (see also ref. 14).

Barradas and Fraser (8) have investigated the reaction

[2] $\frac{1}{2}Ag_2O + OH^- \rightarrow AgO + \frac{1}{2}H_2O + e$

in the high overpotential region using both current-step and potential-step techniques. The charge transfer coefficient was found to be 0.5 but a value for the exchange current could not be obtained from their results.

Organic oxidations at electrodes, when used as a preparative technique, are usually carried out at high current density and therefore at high overpotentials. Information is required on the kinetic parameters in this potential region.

This paper records the results of galvanostatic and potential sweep measurements made with solid silver electrodes in aqueous sodium hydroxide.

Experimental

Electrolytes were continuously purified by circulation through activated charcoal (9). The purification chamber was incorporated in a side limb of the electrolytic cell (Pyrex glass) and circulation of the electrolyte effected by means of a nitrogen lift pump (10). Electrolytes were maintained under an atmosphere of purified nitrogen (11) presaturated to the necessary relative humidity by passage through a bubbler containing cell electrolyte.

The construction of the silver microelectrodes ($\sim 2.5 \times 10^{-2}$ cm^2) used has been described elsewhere (5). The counter electrode was either platinum gauze or a silver rod (for experiments using a pulse generator).

The electrical circuits for galvanostatic polarization experiments and switching techniques have been described previously (10). Potentiostatic measurements were made using a fast response potentiostat coupled with a linear sweep generator (Chemical Electronics Ltd.).

Potential measurements were made against an Ag_2O/Ag NaOH (1 M) reference electrode in conjunction with a Luggin capillary.

The potential–time response under galvanostatic conditions was recorded on an oscilloscope (Hewlett Packard 130 C, and camera 196 B). The current–potential response during potentiostatic experiments was recorded either from an oscilloscope or by means of a chart recorder.

All chemicals were of analytical reagent quality; water was twice distilled in quartz from deionized stock. Experiments were made under conditions of controlled temperature (± 0.5 °C).

Electrode Pretreatment

The electrode was polished on roughened glass under conductivity water and chemically etched in 15% aqueous nitric acid (5). The electrode was thoroughly washed and inserted into the cell. (Taking ~ 17 μF cm^{-2} for the double layer capacitance of a smooth Hg electrode, values for the electrode capacitance of silver in neutral (pH ~ 7) electrolytes (5) indicate that the ratio of true area: superficial area is ~ 2.5.)

Polarization Procedure

Electrodes were polarized only once; thus each point on the current density – overpotential plots (Figs. 3 and 5) corresponds to a new electrode.

Current density – overpotential data corresponding to the formation of Ag_2O [1], was obtained by the application of a single galvanostatic current pulse (duration ~ 30 ms, rise-time < 1 μs) to a clean Ag electrode.

For the study of the formation of AgO [2], the electrode was first electrolytically oxidized, in the cell, at a current density of 2.5 mA cm^{-2} until the electrode potential began to rise to that of AgO formation. The application of a single galvanostatic current pulse to this electrode provided the required overpotential data.

Results

Potential Sweep

The application of a potentiostatically controlled potential ramp to a silver anode resulted in a current–potential curve of the form shown in Fig. 1. The curves contained three peaks. Two peaks were very pronounced and were independent of electrode–electrolyte contact time. Their positions in the potential range indicated that these peaks correspond to faradaic current flow due to reactions [1] and [2].

The third peak appeared on the cathodic side of the other two and was strongly dependent on electrode–electrolyte contact time and electrode pretreatment. The peak was absent from the

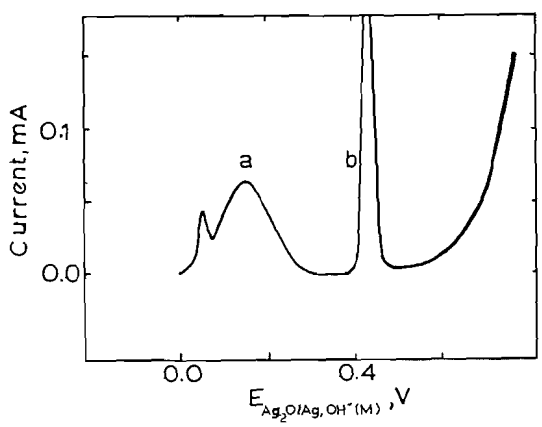

FIG. 1. Potentiostatic current–potential curve for silver in M NaOH at 23 °C. Electrode area = 2.25×10^{-2} cm^{-2}. Potential sweep rate = 0.070 V min^{-1}. Peak a is the formation of Ag_2O and peak b, the formation of AgO.

TABLE 1
Variation of kinetic parameters with temperature for the formation of Ag_2O in M NaOH

Temperature (°K)	Tafel slope $\partial\eta/\partial \log i = b$ (mV)	b/T (mV °K^{-1})	i_0 (mA cm^{-2})	$Z(1-\alpha)$ or $\lambda(1-\alpha)$	α If $\lambda = 1$	α If $\lambda = 2$	Upper limit of Tafel region (mV)
273	73	2.8×10^{-1}	1.0	0.74	0.26	0.63	>180
296	65	2.2×10^{-1}	2.8	0.90	0.10	0.55	~120
313	51	1.6×10^{-1}	3.0	1.2	0.20	0.40	~110
333	~55	~1.6×10^{-1}	~6.5	~1.2	~0.2	~0.4	~90

current response curve if the electrode was held in solution for approximately 10 min before the start of the potential sweep. The peak was greatly enhanced if an already completely oxidized electrode (AgO formation complete) was electrochemically reduced. The magnitude of the peak appeared to be independent of whether the electrode was just mechanically polished or polished and etched before insertion into the cell.

Galvanostatic Experiments

The Formation of Ag_2O

A typical overpotential–time transient is shown in Fig. 2. The trace rises from a potential value more negative than the Ag_2O/Ag equilibrium potential (line A–B). (After polarization the electrode potential falls back to line A–B.) Extrapolation of the linear portion of the curve to zero time (the intersection of the trace and line A–B), when adjusted for the pseudo-ohmic overpotential yields η_D.

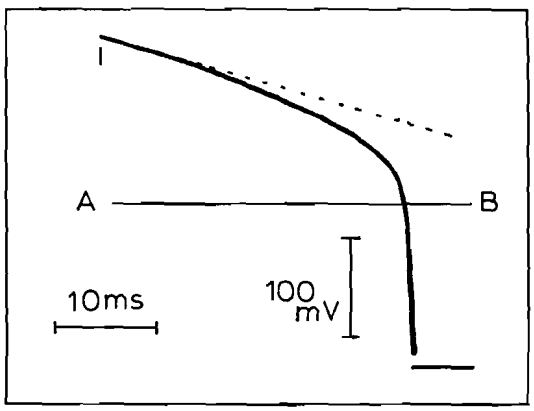

FIG. 2. Typical overpotential–time curve for the galvanostatic polarization of silver in M NaOH at 23 °C. Applied current density = 46 mA cm^{-2}.

In the low overpotential region ($\eta_D < 10$ mV) attempts to use this technique introduced a large uncertainty in the value of η_D. Attempts to make measurements on an electrode containing sufficient Ag_2O to be satisfactorily defined against a standard gave results complicated by uncertainty concerning the electrode area.

The activation overpotential, η_D, was plotted against $\log_{10} i$, a Tafel plot. A typical Tafel plot is shown in Fig. 3. The exchange current, i_0, is obtained as the intercept of the extrapolated linear region of the curve at $\eta_D = 0$. The product

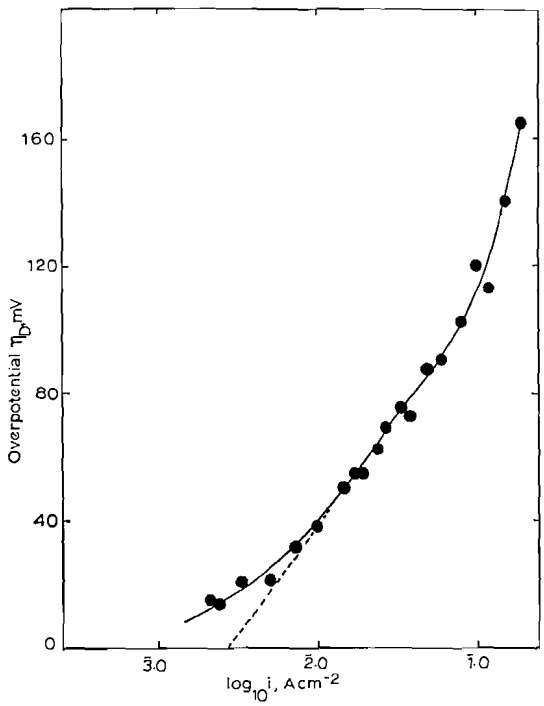

FIG. 3. Typical Tafel plot for the formation of Ag_2O in M NaOH at 23 °C.

Can. J. Chem. Downloaded from www.nrcresearchpress.com by 210.87.254.40 on 09/05/12
For personal use only.

Can. J. Chem. Downloaded from www.nrcresearchpress.com by 210.87.254.40 on 09/05/12
For personal use only.

$Z(1 - \alpha)$ was calculated from the slope of the linear region using

$$[3] \qquad \frac{\partial \eta_D}{\partial \log_{10} i} = \frac{2.303RT}{ZF(1 - \alpha)}$$

$(1 - \alpha)Z$ increased at the higher temperatures as shown in Table I. At 23 °C the value of the exchange current increased with increasing OH^- concentration (Table II).

TABLE II

Variation of exchange current, i_0, with OH^- concentration for Ag_2O formation at 23 °C

OH^- concentration (M)	Exchange current, i_0 (mA cm^{-2})
0.28	1.4
1.00	2.8
4.86	7.2

Figure 4 shows a plot of $\log_{10} i_0$ against $1/T$. Assuming that the Arrhenius equation holds over the temperature range, the value for ΔH^*, the enthalpy of activation, is 5.5 ± 2 kcal/mole. The value for i_0 at the highest temperature studied (60 °C) was only approximate as there was a greater than normal scatter of points on the Tafel plot; probably due to variations of temperature within the cell.

The Formation of AgO

Short time (~30 ms) potential–time transients were very complex, irreproducible, and difficult to interpret unambiguously. This could be ascribed to the highly resistive properties of the Ag_2O surface and to variation in this surface immediately before the perturbing pulse was applied. The requirement that the whole of the electroactive surface should be Ag_2O at zero time was uncertain.

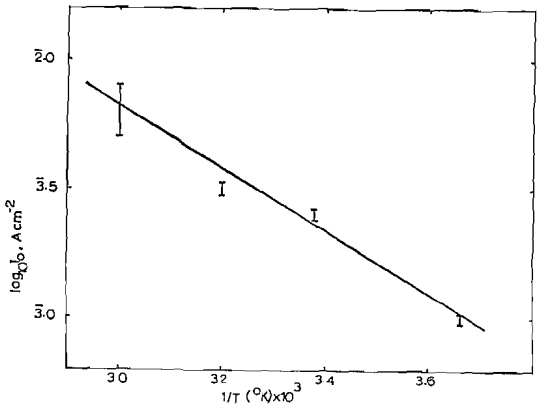

FIG. 4. Temperature dependence of Ag_2O exchange current in M NaOH.

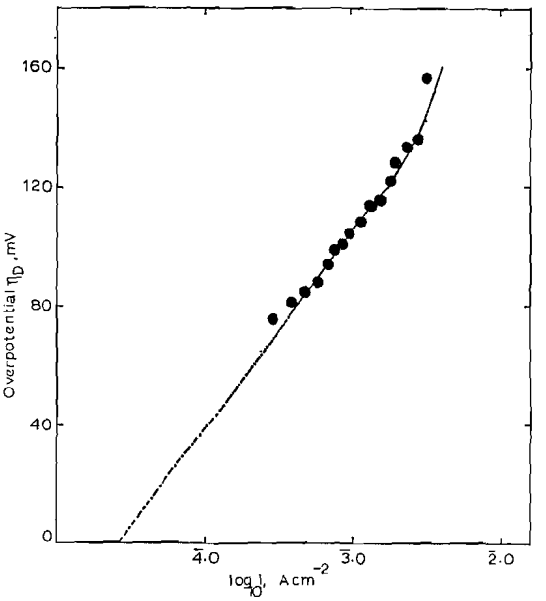

FIG. 5. Tafel plot for the formation of AgO in M NaOH at 23 °C.

Examination of the charging characteristics during the time of transition from reaction [1] to reaction [2] indicated that the transition is relatively slow (~ 2–5 s) at low rates.

Consequently, experiments made by applying long time pulses (~ 10 s) to an Ag_2O electrode on the point of rising to the overpotential characteristic of the AgO/Ag_2O system should give potentials, in the later stages, pertaining only to this system in the absence of effects due to reaction [1].

The final 'steady-state' overpotential plotted as a function of $\log_{10}$ current density for the reaction in M NaOH at 23 °C is shown in Fig. 5. The value of the exchange current is found to be 0.02 mA cm^{-2} and the charge transfer coefficient ~0.6 assuming that 2 electrons are involved in the process (8).

Discussion

Potential Sweep Experiments

Dirkse and De Vries (12) ascribed the first anodic peak on the current–potential curve to the formation of AgOH. The experimental results reported here suggest that whatever is concerned in the oxidation process is readily removed by contact with the electrolyte. Differ-

Can. J. Chem. Downloaded from www.nrcresearchpress.com by 210.87.254.40 on 09/05/12
For personal use only.

ential capacitance measurements (6) indicate that, in alkaline solutions, strong interaction of negative ions with the silver surface does not take place until $\sim +0.2$ V (n.h.e.). It seems likely, therefore, that the peak is due to removal of hydrogen (adsorbed in the electrode pretreatment) by the process

$$OH^- + H_{ads} \rightarrow H_2O + e$$

The observation that electrodes only mechanically polished under conductivity water exhibit a similar extra peak during the early stages of electrode–electrolyte contact does not necessarily vitiate the argument. Even in pure water the establishment of a double layer might involve sufficient transfer of electrons to form hydrogen atoms at the electrode surface (17).

Galvanostatic Experiments

The Formation of Ag_2O

The form of the potential–time transient (Fig. 2) is as expected for double layer charging followed by charge transfer. The initial "jump", a pseudo-ohmic overpotential, caused by the electrolyte resistance between the test electrode and the tip of the Luggin capillary is insignificant compared with the activation overpotential. After the "jump", the potential rises very rapidly with a rate, at zero time, determined by the double layer capacitance, C_L, and the current density applied to the electrode

$$-\left(\frac{\partial E}{\partial t}\right)_{t\rightarrow 0} = \frac{i}{C_L}$$

The value of C_L found from overpotential–time transients (85 ± 20 μF cm^{-2}) agreed reasonably with the value found by differential capacitance measurements at this potential (70 ± 20 μF cm^{-2}) (5, 6).

The absence of a significant concentration of potential determining species on the silver electrode means that, in our experiments, the potential of the silver electrode is initially undefined in the polarizable region. This unduly complicates measurements at low overpotential. At high overpotential (~ 100 mV at 23 °C) the log–linear relationship breaks down (Fig. 3). This might be due to a change in the charge transfer mechanism, alternatively it might indicate the limit of the experimental technique. The former explanation seems to be indicated by the observation that the upper limit of the Tafel region is extended to ~ 200 mV at low temperatures (Table I).

The general shape of the Tafel curves at higher overpotentials suggests there is no specific adsorption of the anion in this potential region.

The slope of the linear portion of the Tafel plot yields a value of $(1 - \alpha)Z \sim 0.9$ at 23 °C (Fig. 3). At higher temperatures this rises to values >1 (Table I) which indicates that Z (the number of unit charges transferred in the rate determining step) is greater than unity.

(In this connection potentiometric studies of the $Ag_2O/Ag.\ OH^-$ electrode show a dependence of electrode potential (E) on OH^- concentration (C_{OH^-}) corresponding to $Z = 2, (\partial E/\partial \log_{10} C_{OH^-} = 29$ mV), although the change in oxidation state of the silver is only $+1$.)

An interpretation for this difference can be given in terms of the transmission coefficient (13). This concept is useful in reactions of this type in which both the reactant and product sides of the electrode equation involve species which are not discrete ionic entities.

For a simple charge transfer reaction involving one ion of charge difference Z between oxidized and reduced forms the charge transfer equation, connecting faradaic current density, i, and activation overpotential, η_D, is

$$[4] \quad i = i_0 \exp\left(-\frac{\alpha ZF}{RT}\right)\eta_D - i_0 \exp\left(\frac{\beta ZF}{RT}\right)\eta_D$$

where α and β are respectively the cathodic and anodic charge transfer coefficients ($\alpha + \beta = 1$ for the same reaction), i_0 is the exchange current, and F, R, and T have their usual significance.

In this reaction the reactant is the metal lattice and the overall product, the Ag_2O crystal. The transmission coefficient, λ, is defined as the number of unit charges conveyed through the double layer each time the rate-determining step occurs once (13). Equation [4] then becomes

$$[5] \quad i = i_0 \exp\left(-\frac{\alpha\lambda F}{RT}\right)\eta_D - i_0 \exp\left(\frac{\beta\lambda F}{RT}\right)\eta_D$$

If λ has the value 2 the results are self-consistent. The value of $\lambda/Z = 2$, is commonly observed (13) and interpreted in terms of two metal ions involved, at once, in the activated state.

For a general reaction, $O + Ze = R$, the exchange current, i_0, is given by $i_0 = ZFk^0 C_R^{\alpha} C_O^{1-\alpha}$. For eq. [1] using λ we have

$$[6] \quad i_0 = \lambda Fk^0 C_{Ag}^{\lambda\alpha} C_{OH^-}^{\lambda\alpha} C_{Ag_2O}^{\lambda\beta/2}$$

Since we can consider the activities of solid Ag

Can. J. Chem. Downloaded from www.nrcresearchpress.com by 210.87.254.40 on 09/05/12
For personal use only.

and Ag_2O as unity and taking $\lambda = 2$, eq. [6] becomes

$$[7] \qquad i_0 = 2Fk^0 C_{OH^-}{}^{\alpha}$$

Correlation of i_0 and OH^- concentration data (Table II) yields an OH^- dependence of i_0 consistent with a value of $\alpha \sim 0.3$ (at 23 °C) using eq. [7]. From Table I, α obtained from the Tafel slope at 23 °C has a value 0.55.

This difference in values for α can be interpreted in terms of simple adsorption of OH^- ions at the electrode (18). If the adsorption obeys a simple Freundlich isotherm (it should be noted that there is no theoretical justification for using this isotherm, however, it appears to hold in similar cases) eq. [7] becomes

$$[8] \qquad i_0 = k' C_{OH^-}{}^{2\alpha/n}$$

where n is the Freundlich exponent and k' a constant involving λ and k^0. A value for $n = 2$, at 23 °C, would give a self-consistent α. This value for n indicates only weak adsorption of OH^-.

The variation of Tafel slope function (b/T) with temperature (Fig. 6) is probably a reflection of changes in adsorption with temperature.

The value of ΔH^* (~ 5 kcal mole^{-1}) is lower than that generally found for simple charge transfer reactions (~ 10 kcal mole^{-1}). This low value might be explained by the adsorption of electroactive species. The occurrence of a charge transfer reaction in the adsorbed state is often associated with a low enthalpy of activation (19).

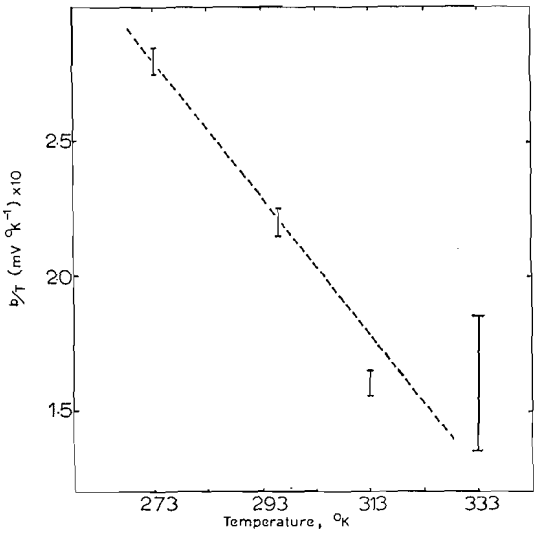

FIG. 6. Temperature dependence of the Tafel slope parameter (b/T) for the formation of Ag_2O in M NaOH.

The Formation of AgO

The Tafel plot obtained for the formation of AgO (Fig. 5) confirms the results of Barradas and Fraser (8) that $\lambda\beta$ is ~ 1. Taking λ as 2, β becomes 0.5 (i.e. $\alpha = 0.5$).

The value of the exchange current obtained in this investigation is only very approximate in view of the difficulties involved in the production of a homogeneous electrode surface. The value is ~ 2 decades smaller than for the i_0 involving the formation of Ag_2O. The large difference in these values confirms that the method of electrolytically producing Ag_2O containing only minimum amounts of AgO is feasible.

Acknowledgments

T.G.C. acknowledges financial assistance from Boots Pure Drug Co. Ltd., J.R.M. from Loughborough University of Technology, and B.S. from the Science Research Council. We thank Professor R. F. Phillips for his continued interest and encouragement.

1. M. J. ALLEN. Organic electrode processes. Chapman and Hall Ltd., London, England. 1958. p. 3.
2. S. WAWZONEK. Science, **155**, 39 (1967).
3. M. DELÉPINE and P. BONNET. Compt. Rend. **149**, 39 (1909). J. C. SHEEHAN and C. A. ROBINSON. J. Am. Chem. Soc. **73**, 1209 (1951).
4. R. G. R. BACON and D. STEWART. J. Chem. Soc. C, 1384 (1966).
5. N. A. HAMPSON, D. LARKIN, and J. R. MORLEY. J. Electrochem. Soc. **114**, 817 (1967).
6. J. R. MORLEY. Unpublished data.
7. T. P. DIRKSE, D. DE WIT, and R. SHOEMAKER. J. Electrochem. Soc. **114**, 1196 (1967).
8. R. BARRADAS and G. FRASER. Can. J. Chem. **42**, 2488 (1964).
9. G. BARKER. Modern electrochemical methods. *Edited by* G. Charlot. Elsevier Press Ltd., Amsterdam, Holland. 1958. p. 192.
10. N. A. HAMPSON, P. C. JONES, and R. F. PHILLIPS. Can. J. Chem. **45**, 2039 (1967).
11. J. P. G. FARR and N. A. HAMPSON. Trans. Faraday Soc. **62**, 3493 (1966).
12. T. P. DIRKSE and D. DE VRIES. J. Phys. Chem. **63**, 107 (1959).
13. J. WEST. Electrodeposition and corrosion processes. D. Van Nostrand Co., Inc., New York. 1965. p. 30.
14. L. G. AUSTIN and G. H. LERNER. Report No. 1, U.S. Navy Contract No. DA 49-186-AMC-197 (D). 1965.
15. T. P. DIRKSE. J. Chem. Eng. Data, **6**, 538 (1961).
16. T. P. DIRKSE. J. Electrochem. Soc. **109**, 173 (1962).
17. V. R. LOODMAA, V. É. PAST, and M. É. KHAGA. Elektrokhimiya, **2**, 927 (1966).
18. J. E. B. RANDLES. Trans. Symp. Electrode Processes, Philadelphia, Pa., 1959, 209 (1961).
19. J. P. G. FARR and N. A. HAMPSON. J. Electroanal. Chem. **13**, 433 (1967).

Can. J. Chem. Downloaded from www.nrcresearchpress.com by 210.87.254.40 on 09/05/12
For personal use only.

Transition metal acetates

D. A. EDWARDS AND R. N. HAYWARD
School of Chemistry and Chemical Engineering, Bath University of Technology, Bath, Somerset, England

Received May 3, 1968

Some anhydrous transition metal acetates (Mn(II), Co(II), Cu(II), Ni(II), Zn(II), Ag(I), Mo(II), Ce(III), La(III)) have been prepared and their infrared spectra measured in the solid state. The infrared spectra have been related to established modes of bonding of the acetate group to metals. Thermal decompositions of the anhydrous acetates have been investigated by thermogravimetric analysis; magnetic moments and visible spectra have been measured.

Canadian Journal of Chemistry, 46, 3443 (1968)

Introduction

Rao and co-workers (1) have recently reported infrared and thermal decomposition data on anhydrous acetates of the lanthanides, lead(II and IV) and copper(II). We have also obtained results upon some of these compounds together with data on several other transition metal anhydrous acetates. Our infrared results point to the unreliability of using the $\nu_{asym}(COO)$–$\nu_{sym}(COO)$ frequency separation to determine the mode of coordination of the acetate group to the metal, although such a method has been used frequently in the past (2). Visible reflectance spectroscopy and magnetic measurements have been used, where appropriate, to show the coordination number of the metal in the anhydrous acetates and to place the acetate group in the spectrochemical and nephelauxetic series.

Experimental

The anhydrous acetates of Mn(II), Co(II), Ni(II), Cu(II), Zn(II), La(III), and Ce(III) were prepared by refluxing the commercially available hydrates with a large excess of a 3:2 (vol./vol.) acetic acid – acetic anhydride mixture. After cooling, the insoluble products were filtered, washed with the solvent mixture followed by sodium-dried ether, and finally pumped under vacuum for 2 h at room temperature. Nickel acetate was found to have ½ mole of associated acetic acid after this preparation and pumping, this acid being removed by heating at 200° under vacuum. The other acetates were not similarly solvated. Molybdenum(II) acetate was prepared from the carbonyl (3) and silver(I) acetate was commercially available. Analytical results are given in Table I.

Infrared spectra were recorded as Nujol, hexachlorobutadiene, and fluorlube mulls using a Perkin–Elmer 237 grating spectrophotometer.

Visible spectra were recorded using a Unicam SP 500 spectrophotometer, the diffuse reflectance spectra being obtained using the standard attachment.

Magnetic measurements were determined by the Gouy method at room temperature.

TABLE I

Analytical results

Compound	% Metal		% Acetate	
	Found	Calcd.	Found	Calcd.
$Mn(CH_3COO)_2$	31.6	31.8	67.7	68.2
$Co(CH_3COO)_2$	32.9	33.3	66.6	66.7
$Ni(CH_3COO)_2.$ 0.5 CH_3COOH	28.0	28.4	71.2	71.6
$Zn(CH_3COO)_2$	35.2	35.6	64.3	64.4
$Cu(CH_3COO)_2$	34.8	35.0	64.7	65.0
$Ag(CH_3COO)$	64.3	64.7	35.1	35.3
$Mo(CH_3COO)_2$	44.5	44.8	—	—
$La(CH_3COO)_3$	43.9	44.0	55.6	56.0
$Ce(CH_3COO)_3$	43.4	44.2	54.3	55.8

TABLE II

Infrared frequencies (cm^{-1})

Acetate	$\nu_{sym}(COO)$	$\nu_{asym}(COO)$	$\Delta\nu$
Na	1413	1556	143
Mn(II)	1410	1585	175
Co(II)	1405	1590	185
Ni(II)	1415	1600	185
Cu(II)	1420	1595	175
Zn(II)	1410	1550	140
La(III)	1410	1540	130
Ce(III)	1410	1550	140
Mo(II)	1415	1585	170
Ag(I)	1405	1520	115
$Mn(II).4H_2O$	1400	1570	170
$Co(II).4H_2O$	1395	1550	155
$Ni(II).4H_2O$	1425	1550	125
$Cu(II).H_2O$	1410	1610	200
$Zn(II).2H_2O$	1405	1550	145
$La(III).1.5H_2O$	1420	1560	140
$Ce(III).1.5H_2O$	1415	1565	150

Thermogravimetric studies were carried out using a Stanton TR 1 thermogravimetric balance heating at 4° per minute over the range room temperature to 1000°. Products remaining at the end of such decompositions were analyzed for metal content and shown to be the oxides mentioned in Table IV.

Can. J. Chem. Downloaded from www.nrcresearchpress.com by 210.87.254.40 on 09/05/12
For personal use only.

Results and Discussion

Infrared Spectra

The free acetate ion, symmetry C_{2v}, has 15 infrared active fundamentals, all of which, except the ν_6 torsional mode, have been observed (4, 5). Four modes of coordination to metals (**1**–**4**) are possible (*2b*), but since the symmetry of the free ion is low no great differences in the infrared spectrum would be expected for each type. The ν_3 (ν_{sym}(COO)) and ν_8 (ν_{asym}(COO)) frequencies, and their difference, $\Delta\nu$, for the acetates studied here, are shown in Table II.

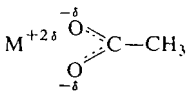

(**1**)

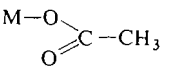

(**2**)

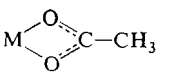

(**3**)

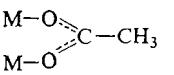

(**4**)

It has been suggested (2) that where the acetate is a unidentate ligand (**2**) a divergence of ν_{asym}(COO) and ν_{sym}(COO), compared with the free ion, is expected due to a decrease in the equivalence of the C—O bonds. Thus the ν_{asym}(COO)–ν_{sym}(COO) separation for $[Co(NH_3)_5OCOCH_3]^{2+}$ is 223 cm^{-1} (*2a*) compared with 153 cm^{-1} for sodium acetate of type (**1**). Of the compounds studied here, the tetrahydrated nickel and cobalt acetates are known to be octahedral and the corresponding manganese compound is expected to be the same, the metals being coordinated with four oxygens from the water molecules and two oxygen atoms from unidentate acetate groups (6). A large ν_{asym}(COO)–ν_{sym}(COO) separation is, however, not observed in the infrared spectrum; the small separation found could be due to hydrogen bonding with the water molecules making the C—O bonds more equivalent than expected for unidentate acetate coordination. In the corresponding anhydrous acetates the mode of coordination of the acetate group to the metal must change since the visible spectra and magnetic measurements show the acetates to be still octahedral and hence polymeric. Since overall there are only two acetates per metal atom both oxygens of the acetate group are expected to be involved in the coordination and the acetates must bond to more than one metal atom by bridging. The ν_{asym}(COO)–ν_{sym}(COO) separation, however, is unexpectedly greater than in the hydrated unidentate acetate cases. We are unable to state if all the acetate groups in the octahedral polymers are bridging (**4**) or whether some are chelating (**3**), since in the two cases we have studied where all the acetate groups are known to be bridging, copper(II) (7) and molybdenum(II) (8), a very similar degree of ν_{asym}(COO)–ν_{sym}(COO) separation is found. For bridging or chelating symmetrical acetate structures both COO stretching frequencies are shifted in the same direction on changing the metal, so the separation will not be greatly different from that of the free ion.

The structure of dihydrated zinc acetate is known (9) to be octahedral, the coordination to the metal consisting of two oxygen atoms from the two water molecules and four oxygens from two chelating acetate groups. We find, again, the infrared spectrum cannot be regarded as diagnostic of such an acetate coordination. Anhydrous zinc acetate shows an almost identical ν_{asym}(COO)–ν_{sym}(COO) separation, so the acetate could be tetrahedral with just two chelating acetate groups, but an octahedral coordination achieved by bridging and shared acetates cannot be ruled out.

Our results for anhydrous lanthanum(III) acetate are similar to those published by Rao *et al.* (1) except we find a lower ν_{sym}(COO) frequency. We have also recorded the infrared spectrum of cerium(III) acetate (10) which Rao and co-workers did not include in their study. Rao and co-workers (1) suggested that the acetate groups in lanthanum(III) acetate were unidentate, but the results, in our opinion, do not require this, and indeed, in view of the high formal positive charge on the metal and the favoring of high coordination numbers by the lanthanide elements, chelation or bridging acetate groups would seem more likely.

Thus we are of the opinion that the use of the infrared ν_{asym}(COO)–ν_{sym}(COO) separation as a means of assessing the mode of coordination of acetate groups to metals must only be used with extreme caution and cannot be regarded as universally valid.

Visible Spectra

Diffuse reflectance visible spectra have been measured for anhydrous cobalt(II), nickel(II), and copper(II) acetates, the results and assignments being given in Table III. The spectra of the cobalt and nickel salts are typical of octahedral

TABLE III

Visible spectra and magnetic moments

Acetate	μ (B.M.) at room temp.	Method	Visible spectra	
			Peak (cm^{-1})	Assignment
Mn(II)	5.90			
Co(II)	4.93	D.R.[a]	17 400 (sh)	$^4T_{1g}(F) \rightarrow {}^4A_{2g}$
			18 900	$^4T_{1g}(F) \rightarrow {}^4T_{1g}(P)$
			20 400 (sh)	
		Sol.[b]	17 400 (sh)	$^4T_{1g}(F) \rightarrow {}^4A_{2g}$
			18 900	$^4T_{1g}(F) \rightarrow {}^4T_{1g}(P)$
			20 200 (sh)	
Ni(II)	3.30	D.R.	13 500	$^3A_{2g} \rightarrow {}^1E_g(D)$
			14 600	$^3A_{2g} \rightarrow {}^3T_{1g}(F)$
			25 000	$^3A_{2g} \rightarrow {}^3T_{1g}(P)$
		Sol.	13 700	$^3A_{2g} \rightarrow {}^1E_g(D)$
			14 800	$^3A_{2g} \rightarrow {}^3T_{1g}(F)$
			25 000	$^3A_{2g} \rightarrow {}^3T_{1g}(P)$
Cu(II)	1.39	D.R.	14 800 (br)	$^2E_g \rightarrow {}^2T_{2g}$
		Sol.	14 300 (br)	$^2E_g \rightarrow {}^2T_{2g}$
Zn(II)	Diamagnetic			
La(III)	Diamagnetic			
Ce(III)	2.30			
Mo(II)	0.25			

[a]D.R. diffuse reflectance.
[b]Sol. solution in acetic acid – acetic anhydride mixture.

coordination of these metals. The splitting of the band centered at 18 900 cm^{-1} for cobalt(II) acetate has been noticed for many other octahedral cobalt(II) systems and attributed (11) to various sources. In the present example, the shoulder could be tentatively assigned (11) to the $^2T_{1g}(H) \leftarrow {}^4T_{1g}(F)$ transition, this having gained intensity by mixing with the spin-allowed transition. From these assignments for cobalt(II) acetate 10 *Dq*, the Racah parameter *B* and the nephelauxetic ratio β_{35} have been calculated using the method of Underhill and Billing (12). 10 *Dq* has been found to be 9250 cm^{-1} and *B* 790 cm^{-1}. Using the free gaseous ion *B* value of 972 cm^{-1}, β_{35} is found to be 0.81.

Calculations (12) of 10 *Dq*, *B*, and β_{35} for nickel(II) acetate give the values 8420 cm^{-1}, 916 cm^{-1}, and 0.89 respectively, using the free ion *B* value of 1030 cm^{-1}. These results place the acetate group close to water in both the spectrochemical and nephelauxetic series (for water 10 $Dq = 8600$ cm^{-1}; $B = 925$ cm^{-1}; and $\beta_{35} = 0.88$).

Manganese(II) acetate has only low intensity spin-forbidden bands in the visible region typical of high-spin octahedral manganese(II).

Magnetic Measurements

The room temperature magnetic moments are given in Table III and are typical of octahedral coordination for high-spin manganese(II), high-spin cobalt(II), and nickel(II). Manganese(II) acetate has a moment virtually identical with the 'spin-only' moment, there being no orbital contribution, but cobalt(II) and nickel(II) acetates have moments above the 'spin-only' values due to orbital contributions, from the $^4T_{1g}(F)$ ground state and ^4T excited states for cobalt, and only from the ^3T excited state and not from the $^3A_{2g}$ ground state for nickel.

The magnetic moment of copper(II) acetate agrees with previous results (13) but the magnetic moment of dimeric molybdenum(II) acetate (d^4) is grossly reduced to 0.25 B.M., indicating a much greater metal–metal interaction than in the isostructural copper acetate. This is in agreement with X-ray results (8) which show a very short Mo—Mo bond length of 2.11 Å indicating multiple bonding, whereas the Cu—Cu bond length in the dihydrate (7) is 2.6 Å in length, probably indicating weak δ copper–copper bonding. The magnetic moment of cerium(III) acetate is in the range expected for cerium(III) compounds, ground state $^2F_{5/2}$, whose magnetic results can be treated to a good approximation by L–S coupling and are essentially independent of surrounding ligands and stereochemistry.

Thermal Decompositions (14)

Thermogravimetric analysis (t.g.a.) results are shown in Table IV, the heating being carried out under normal atmospheric conditions.

Can. J. Chem. Downloaded from www.nrcresearchpress.com by 210.87.254.40 on 09/05/12
For personal use only.

TABLE IV

Thermogravimetric results

	1st decomposition stage			2nd decomposition stage			3rd decomposition stage		
		% weight change			% weight change			% weight change	
Acetate	Compound	Obsd.	Calcd.	Compound	Obsd.	Calcd.	Compound	Obsd.	Calcd.
Mn(II)	MnO	56.8	59.1	Mn_2O_3	52.8	54.4	Mn_3O_4	54.6	55.9
Co(II)	CoO	54.8	57.7	Co_2O_3	50.5	53.1	Co_3O_4	51.9	54.6
Ni(II).0.5CH_3COOH	$Ni(CH_3COO)_2$	14.2	14.5	NiO	62.4	63.9			
Cu(II)	Cu_2O + Cu	61.8	62.1	CuO	56.0	56.2			
Zn(II)	ZnO	55.1	55.6						
Mo(II)	MoO_3	31.2	32.7	[a]					
La(III)	$La_2O_2CO_3$	41.5	41.5	La_2O_3	48.4	48.4			
Ce(III)	CeO_2	45.4	45.7						
Ag(I)	Ag	35.8	35.4						

[a]No solid remains: MoO_3 volatile.

The t.g.a. of anhydrous lanthanum(III) acetate agrees well with the results of Rao *et al.* (1), the oxycarbonate, $La_2O_2CO_3$, being completely formed at 480° and decomposing to La_2O_3 at 875°. No evidence for the previously reported (15) oxyacetate was found. An oxycarbonate stage was not found in the t.g.a. of cerium(III) acetate, the only product being the formation of cerium(IV) oxide at 500°. Both manganese(II) and cobalt(II) acetates decompose to the monoxides at ca. 350°, which are then oxidized completely to M_2O_3 stages by 600° followed by M_3O_4 stages at 950°, although minor weight change discrepancies for the individual stages indicate that the decomposition stages overlap to some degree, probably due to the heating rate of the apparatus. The hemi-solvate of nickel(II) acetate loses the attached acetic acid completely in air by 280° with the formation of the anhydrous acetate, but from the subsequent weight change the acetate appears to decompose to a mixture of the metal and nickel(II) oxide, the metal present being finally oxidized to the oxide completely by 600°.

Copper(II) acetate starts to decompose at 230° to a mixture of copper metal and copper(I) oxide, both being completely oxidized to copper(II) oxide by 535°. No evidence for the formation of copper(I) acetate was found by this method, but a careful decomposition of copper(II) acetate in vacuo at 220° leads to the formation of a very hygroscopic colorless sublimate of copper(I) acetate. Since little is known of the chemistry of this compound (16) it is, at present, being fully studied.

Decompositions of zinc(II) and molybdenum(II) acetates lead to the formation of ZnO and MoO_3 at 350 and 280° respectively as sole products, whereas from silver(I) acetate only the metal is produced by 280°, there being no evidence of oxide formation at lower temperatures.

1. K. C. Patil, G. V. Chandrashekhar, M. V. George, and C. N. R. Rao. Can. J. Chem. **46**, 257 (1968).
2. (*a*) K. Nakamoto, F. Fujita, S. Tanaka, and M. Kobayashi. J. Am. Chem. Soc. **79**, 4904 (1957). (*b*) K. Nakamoto. Infrared spectra of inorganic and co-ordination compounds. John Wiley and Sons, Inc., New York. 1963.
3. T. A. Stephenson, E. Bannister, and G. Wilkinson. J. Chem. Soc. 2538 (1964).
4. K. Itoh and H. J. Bernstein. Can. J. Chem. **34**, 170 (1956).
5. K. J. Wilmshurst. J. Chem. Phys. **23**, 2463 (1955).
6. J. N. van Niekerk and F. R. L. Schoening. Acta Cryst. **6**, 609 (1953).
7. J. N. van Niekerk and F. R. L. Schoening. Acta Cryst. **6**, 227 (1953).
8. D. Lawton and R. Mason. J. Am. Chem. Soc. **87**, 921 (1965).
9. J. N. van Niekerk, F. R. L. Schoening, and J. H. Talbot. Acta Cryst. **6**, 720 (1953).
10. T. Moeller, V. Galasyn, and J. Xavier. J. Inorg. Nucl. Chem. **15**, 259 (1960).
11. A. B. P. Lever and D. Ogden. J. Chem. Soc. A, 2041 (1967).
12. A. E. Underhill and D. E. Billing. Nature, **210**, 834 (1966).
13. M. Kato, H. B. Jonassen, and J. C. Fanning. Chem. Rev. **64**, 99 (1964).
14. C. Duval. Inorganic thermogravimetric analysis. 2nd ed. Elsevier Publ. Co., Inc., Amsterdam. 1963.
15. V. N. Maskimov and K. N. Semenenko. Zh. Neorg. Khim. **3**, 1468 (1958).
16. A. Angel and A. V. Harcourt. J. Chem. Soc. 1385 (1902).

Can. J. Chem. Downloaded from www.nrcresearchpress.com by 210.87.254.40 on 09/05/12
For personal use only.

Can. J. Chem. Downloaded from www.nrcresearchpress.com by 210.87.254.105 on 09/05/12
For personal use only.

Enthalpy of formation of some alkaline earth halides

ARTHUR FINCH, P. J. GARDNER, AND C. J. STEADMAN
Moore Laboratory, Department of Chemistry, Royal Holloway College, Englefield Green, Surrey, U.K.

Received May 24, 1967[1]

The enthalpies of reaction of crystalline magnesium oxide in aqueous hydrogen bromide and iodide solutions have been determined. The enthalpies of precipitation of magnesium, calcium, and strontium fluorides and the enthalpies of solution of magnesium iodide and bromide have also been determined and the following data are derived: ΔH_f^0 (298 °K) of $MgBr_2(c)$, $MgI_2(c)$, $CaF_2(c)$, $NaMgF_3(c)$, $SrF_2(c)$ are -125.3 ± 0.4, -88.1 ± 0.35, -291.9 ± 0.2, -406.7 ± 0.3, -291.2 ± 0.3 kcal mole^{-1} respectively. $NaMgF_3$ is an ideal mixed crystal.

Canadian Journal of Chemistry, 46, 3447 (1968)

Introduction

As part of our program on solvation studies of main Group II salts, we have measured the enthalpies of reaction of magnesium oxide in aqueous hydrogen bromide and iodide, and the enthalpies of precipitation of the fluorides of magnesium, calcium, and strontium. Combination of these latter data with the identity

$$[1] \quad -\Delta H_s^0(MX_2) = \Delta H_f^0 MX_2(c) - \Delta H_f^0 M^{2+}aq - 2\Delta H_f^0 X^-aq$$

yields the standard enthalpy of formation of the crystal. Although the final data reported here are, to varying degrees of accuracy, already available in the literature, much of the experimental work was performed in the 19th century (1).

Notation and Conventions

All thermodynamic data are reported at 25.0 ± 0.1 °C or quoted at 25 °C, except where otherwise indicated. The superscript ^{0} is retained for formation of compounds in their standard state from elements in their standard state, for salts in infinitely dilute solution when $a_\pm = 1$ (this corresponds to a solute standard state of the hypothetical ideal state of unit molality), and for individual hydrated ions infinitely separated from other ions (magnitude based on $\Delta H_f^0[H^+aq] = 0$). All solutions are aqueous and the designation aq is sometimes omitted.

$\Delta H_f[MX, m_1; m_2, m_3, m_4 \ldots m_n]$ means the enthalpy of formation of MX of molality m_1 in the presence of $(n-1)$ other salts of molalities $m_2, m_3, m_4 \ldots m_n$.

Hence $\Delta H_f^0[MX, 0; 0, 0] \equiv \Delta H_f^0[M^+aq] + \Delta H_f^0[X^-aq]$.

$\Delta H_d[MX, m_1 \rightarrow 0]$ means the enthalpy of dilution of MX from molality m_1 to infinitely dilute solution.

All results were expressed in terms of the defined thermochemical calorie, 1 calorie $\equiv$ 4.1840 absolute joules.

Experimental

The calorimeter was conventional in design and of the constant-temperature-environment type. Full details are given elsewhere (2). The calorimeter contained 125 ml of solution, except where otherwise indicated. The magnitude of the thermal leakage was estimated by the "equal areas" method, which is satisfactory (3) for an overall precision of $\pm 0.3\%$. The accuracy and precision of the system were assessed by two standard reactions, one endothermic and the other exothermic. For the enthalpy of solution of potassium chloride in water the mean of 8 observations was ΔH_s (25 °C: $N = 200$) = 4.22 ± 0.01 kcal mole^{-1} (lit. (4) 4.201 ± 0.001 at $N = 200$, $T = 25$ °C), and for the neutralization of tris(hydroxymethyl)aminomethane (THAM) in excess 0.1 N hydrochloric acid the mean of 12 observations was ΔH (25 °C: $N = 600$) = -7.15 ± 0.05 kcal mole^{-1} (lit. (4) -7.107 ± 0.004 at 25 °C and $N = 1350$). The enthalpy of dilution of THAM is negligible (5). N is the mole ratio of water to solute. The uncertainty interval in the experimental data is expressed as $\pm\bar{s}$, where $\bar{s}$ is the standard deviation of the mean.

Materials

(i) Magnesium Bromide

Equimolar proportions of hydrated magnesium bromide (B.D.H.) and ammonium bromide (B.D.H.) were mixed with a little aqueous hydrogen bromide. The mixture was evaporated to dryness and then dried in vacuum (12 mm of Hg) at 200 °C overnight. The ammonium bromide was sublimed off at 400 °C and the residue was transferred to a silica tube which was evacuated and sealed. The end of the tube containing the residue was maintained at about 800°, and over a period of several days crystals of magnesium bromide condensed on to the cooler parts of the tube. Bromine analysis by a conventional procedure showed 99.9% of the theoretical amount.

[1]Revision received April 25, 1968.

Can. J. Chem. Downloaded from www.nrcresearchpress.com by 210.87.254.105 on 09/05/12
For personal use only.

(ii) Magnesium Iodide

The iodide was prepared by reaction between the elements and purified by sublimation according to the method of Biltz and Hüttig (6). The material obtained contained 100.0% of the theoretical amount of iodine.

(iii) Magnesium Oxide

Heating the AnalaR salt for a few hours at about 1000 °C gave a material which analyzed as 100.1% MgO (acidimetric).

(iv) Calcium Chloride

A sample of 99.8% purity was prepared by dehydrating the AnalaR hydrate in a stream of hydrogen chloride, gradually increasing the temperature to 500° over a period of several days.

(v) Sodium Fluoride

A saturated solution of AnalaR sodium fluoride was treated with a few percent of potassium chloride. After filtration, the sodium fluoride was precipitated by the addition of isopropanol. The material was dried for several days at 200° and fluoride analysis showed 100.4% of the theoretical amount.

Except for magnesium oxide and sodium fluoride, all the above were stored away from light in sealed vessels contained in a desiccator over phosphorus pentoxide. They were handled prior to calorimetry in a glove bag filled with dried nitrogen.

Results and Discussion

(i) Magnesium Bromide and Magnesium Iodide

In the case of these two salts, the reaction studied was $MgO(c) + 2HX(aq\ m_1) = [MgX_2\ (aq\ m_2; m_1 - \delta) + H_2O]$. The molality of the aqueous hydrogen halide ($m_1 = 0.5$ molal) and the weights of MgO taken were such that approximately 0.006 moles of HX were consumed in reaction. Hence the approximation $\delta = 0$ was made and the thermochemical equation used was

$$\Delta H_{obs} = \Delta H_f^0[H_2O, liq] + \Delta H_f[MgX_2, m_2; m_1] - 2\Delta H_f[HX, m_1] - \Delta H_f^0[MgO, c]$$

The experimental results are tabulated below (τ = the approximate duration of the main period).

$$\Delta H_f[MgBr_2, 0.027\ m; m_1] = -168.3 \pm 0.35\ \text{kcal mole}^{-1}$$

$$\Delta H_f[MgI_2, 0.025\ m; m_1] = -137.7 \pm 0.3\ \text{kcal mole}^{-1}$$

The ancillary data used for the above calculation were as follows: $\Delta H_f^0 H_2O(liq) = -68.315$ (7), $\Delta H_f^0[HBr3000H_2O] = -29.05 \pm 0.09$ (8), $\Delta H_f^0[MgO, c] = -143.7 \pm 0.3$ (9), $\Delta H_f^0[HI\text{-}50H_2O] = -13.56 \pm 0.03$ (10) kcal mole^{-1}. Enthalpies of dilution were taken from ref. 7.

TABLE I

Weight MgO (g)	m_2	$-\Delta H_{obs}$ (kcal mole^{-1} MgO)
Solution of MgO in aqueous HBr: $m_1 = 0.5$: $\tau = 2$ min		
0.1429	0.0284	35.1_5
0.1568	0.0311	35.3
0.1478	0.0293	35.1_5
0.1668*	0.0276	35.1
0.1509*	0.0250	35.4
0.1406*	0.0232	35.1
0.1469*	0.0243	35.4
Solution of MgO in aqueous HI: $m_1 = 0.5$: $\tau = 2$ min		
0.1424	0.0235	35.0
0.1546*	0.0256	34.9
0.1510*	0.0250	35.3
0.1587*	0.0262	35.2

*Experiment performed with 150 ml aqueous acid.

Data for the heat of solution of crystalline magnesium bromide and iodide in 0.5 molal aqueous hydrogen halide are given in Table II.

TABLE II

Data for heat of solution of crystalline magnesium bromide and iodide in 0.5 molal aqueous hydrogen halide

Weight $MgBr_2$ (g)	m_3	$-\Delta H_{obs}$ (kcal mole^{-1} $MgBr_2$)
Solution of $MgBr_2$(c) in 0.5 molal HBr: τ (instant)		
0.1022	0.00444	43.4
0.1670	0.00726	43.4
0.1612	0.00700	42.9
0.1359	0.00590	42.8_5
Solution of MgI_2(c) in 0.5 molal HI: τ (instant)		
0.0949*	0.00341	49.5
0.2153*	0.00774	50.1
0.1227*	0.00441	49.6
0.2490*	0.00895	49.9

*Experiment performed in 100 ml of aqueous acid.

For these experiments,

$$\Delta H_{obs} = \Delta H_f[MgX_2, m_3; m_1] - \Delta H_f^0 MgX_2(c)$$

Using the data from Table I for the first term on the right hand side of this equation (enthalpies of dilution to m_3 were taken from ref. 1 for $MgBr_2$ and assumed the same for MgI_2 [this term amounts to 0.1 kcal mole^{-1}]), we derive

$$\Delta H_f^0 MgBr_2(c) = -125.3 \pm 0.4\ \text{kcal mole}^{-1}$$

$$\Delta H_f^0 MgI_2(c) = -88.1 \pm 0.35\ \text{kcal mole}^{-1}$$

TABLE III

Precipitation of CaF_2 from aqueous NaF and $CaCl_2$(c): τ = 1 min

Weight $CaCl_2$ (g)	m_4	m_7	$-\Delta H_{obs}$ (kcal mole^{-1} $CaCl_2$)	ΔH_s^0 (CaF_2)
0.1887	0.6805	0.0272	21.1_5	1.71
0.2679	0.6323	0.0378	21.0	1.55
0.2763	0.6138	0.0398	21.2	1.72
0.3350	0.8736	0.0484	21.1	1.69
0.3420	0.8521	0.0494	21.0_5	1.66
0.3879	0.4038	0.0560	21.2	1.71
0.4195	0.5062	0.0606	21.2	1.78
				Mean 1.69±0 03

These data diverge considerably from the only available literature data (in both cases, before the year 1900) of −123.7 (11) and −86.0 (11, 12) kcal mole^{-1}.

(ii) Calcium Fluoride

The reaction studied was the dissolution of calcium chloride crystal in excess aqueous sodium fluoride (molality, m_4) saturated with calcium fluoride (molality, m_5). In addition, we define the molality of the remaining (i.e. excess) NaF as m_6 and the NaCl molality as m_7. These molalities are not all independent but are defined so for notational convenience. Hence

$$\Delta H_{obs} = 2\Delta H_f[\mathrm{NaCl}, m_7; m_5, m_6] + \Delta H_f^0\mathrm{CaF_2(c)} - 2\Delta H_f[\mathrm{NaF}, m_4; m_5] - \Delta H_f^0\mathrm{CaCl_2(c)}$$

Substituting the following approximations,

$$\Delta H_f[\mathrm{NaCl}, m_7; m_5, m_6] \doteqdot \Delta H_f[\mathrm{NaCl}, m_7; 0, 0] = \Delta H_f^0[\mathrm{NaCl}, 0; 0, 0] - \Delta H_d[\mathrm{NaCl}, m_7 \rightarrow 0]$$

$$\Delta H_f[\mathrm{NaF}, m_4; m_5] \doteqdot \Delta H_f[\mathrm{NaF}, m_4; 0] = \Delta H_f^0[\mathrm{NaF}, 0; 0] - \Delta H_d[\mathrm{NaF}, m_4 \rightarrow 0]$$

and the identity

$$\Delta H_f^0\mathrm{CaCl_2(c)} = \Delta H_f^0[\mathrm{CaCl_2}, 0] - \Delta H_s^0(\mathrm{CaCl_2})$$

we have

$$\Delta H_{obs} = -\Delta H_s^0(\mathrm{CaF_2}) + \Delta H_s^0(\mathrm{CaCl_2}) - 2\Delta H_d[\mathrm{NaCl}, m_7 \rightarrow 0] + 2\Delta H_d[\mathrm{NaF}, m_4 \rightarrow 0]$$

Also, by definition $\Delta H_s^0(\mathrm{CaF_2}) = -\Delta H_p^0(\mathrm{CaF_2})$ where p = precipitation. The content of the approximations is that the molar enthalpies of the NaCl(aq) and NaF(aq) are unaffected by small concentrations of both foreign and common ions. The difference between the molar enthalpy of a salt at a finite concentration and the same salt at the same concentration in the presence of foreign ions is a first temperature derivative of the logarithm of the ratio of the appropriate activity coefficients in the two states. Such derivatives are usually small and may be justifiably ignored. It is further assumed that the change in the nature of the ionic environment (from predominantly fluoride to chloride) thus affecting the solubility of CaF_2 is not significant thermally. In addition, it is assumed that this solubility does not change over the temperature range of the experiment (usually of the order of 0.5 °C). Some calcium fluoride, precipitated under the same conditions as the calorimetric experiment, was collected, washed, dried at 50 °C and an X-ray powder photograph obtained. This revealed that the precipitate was crystalline and belonged to the expected cubic system. Furthermore no impurities were observed. Hence the precipitated calcium fluoride is in its standard state.

The dilution enthalpies of NaF and NaCl were those of Parker (13) and the $\Delta H_s^0(\mathrm{CaCl_2})$ was derived from a datum of Ehrlich *et al.* (14) ($\Delta H_s[\mathrm{CaCl_2 2500H_2O}] = -19.04$, hence $\Delta H_s^0[\mathrm{CaCl_2}] = -19.36$ kcal mole^{-1}). This differs markedly from the Circular 500 (1) figure for $\Delta H_s^0[\mathrm{CaCl_2}]$ (i.e. −19.8). Using eq. [1] and appropriate molar enthalpies for the aqueous ions we derive $\Delta H_f^0\mathrm{CaF_2(c)}$. The choice of ancillary data for this calculation is of interest. The molar enthalpies of the alkaline earth cations do not appear to have been updated since the Circular 500 values and hence these are used. The reported values for the molar enthalpies of HF solutions diverge widely. For $\Delta H_f[\mathrm{HF20H_2O}]$, Cox and Harrop (15) report −77.40, Circular 500

Can. J. Chem. Downloaded from www.nrcresearchpress.com by 210.87.254.105 on 09/05/12
For personal use only.

TABLE IV

Data for the precipitation of $NaMgF_3$ and SrF_2

Precipitation of $NaMgF_3$ from aqueous $MgCl_2$ and NaF(c): τ = 2 min

Weight NaF (g)	Molality $MgCl_2$	Molality NaCl	ΔH_{obs} (kcal mole^{-1} NaF)
1.1608	0.114	0.147	2.11
1.1505	0.111	0.146	2.11
1.3195	0.128	0.168	2.10
1.1070	0.113	0.141	2.13

Precipitation of SrF_2 from aqueous $SrCl_2$ and NaF(c): τ = 12 min

Weight NaF (g)	Molality $SrCl_2$	Molality NaCl	ΔH_{obs} (kcal mole^{-1} NaF)
1.9073	0.197	0.363	-0.2_5
1.4820	0.145	0.283	−0.4
2.0674	0.215	0.394	−0.2

(1) quotes −75.63, the updated Circular 500 (7) quotes −76.28 kcal mole^{-1}. We have chosen a "concensus value" of $\Delta H_f[HF20H_2O]$ = −76.95 ± 0.2 (16) kcal mole^{-1} and hence $\Delta H_f^0[F^-aq]$ = −80.2 ± 0.2 kcal mole^{-1}. The error in this datum may be larger than indicated as the dilution enthalpy (7) of HF from $20H_2O$ to ∞H_2O (i.e. 3.2 kcal mole^{-1}) seems rather large. Hence

$$\Delta H_f^0 CaF_2(c) = -291.9 \pm 0.2 \text{ kcal mole}^{-1}$$

The divergence from the Circular 500 figure (−290.3) is due mainly to the choice of $\Delta H_f^0[F^-aq]$.

(iii) Magnesium Fluoride, Strontium Fluoride, and Barium Fluoride

These fluorides are all more soluble (17) than CaF_2 (MgF_2, 0.130; CaF_2, 0.016; SrF_2, 0.119; BaF_2, 1.614 g/l at 25 °C) and attempts to treat them in the manner of CaF_2 gave rise to marked precipitation from the saturated calorimetric liquids with consequent thermal effects that could not be estimated with accuracy. Thus, in these cases the reaction studied was the solution of crystalline sodium fluoride in aqueous MCl_2, where M is Mg, Sr, or Ba, and making a correction, where appropriate, for the dissolved MF_2.

$$2NaF(c) + MCl_2(aq) = xMF_2(c) + (1 - x)MF_2(aq) + 2NaCl(aq)$$

X-ray powder photographs were obtained for samples of the fluorides precipitated under the same conditions as the experiment. Examination of the powder patterns revealed:

(*a*) The "magnesium fluoride" was, in fact, a crystalline double salt of stoichiometry $NaMgF_3$.

(*b*) Strontium fluoride was crystalline and belonged to the expected cubic system.

(*c*) The "barium fluoride" was a crystalline mixture of BaClF, Ba_2ClF_3, and BaF_2 (the mixture probably contains 10% or less BaF_2).

Hence, the experimental data for the barium salt were rejected.

In the above experiments, the precipitant was present in only small excess (5 to 10%) so that the effect of the common ion (M^{2+}) on the solubility of MF_2 could be ignored. The effect of the foreign ions (Na^+, Cl^-) was also ignored. It was assumed that the solubility of strontium fluoride was equal to its aqueous solubility and that $NaMgF_3$ was insoluble.

The treatment of the data was similar to that described in detail for the other salts. Enthalpies of dilution for NaF and NaCl were from Parker (13) and for MCl_2 were from ref. 1. Using eq. [1], $\Delta H_f^0[F^-aq]$ = −80.2 ± 0.2 kcal mole^{-1}, and $\Delta H_f^0[M^{2+}aq]$ from ref. 1, we derive

$$\Delta H_f^0[NaMgF_3, c] = -406.7 \pm 0.3 \text{ kcal mole}^{-1}$$

$$\Delta H_f^0[SrF_2, c] = -291.2 \pm 0.3 \text{ kcal mole}^{-1} \quad (-290.3)$$

giving the Circular 500 value in parentheses. The most reliable value for $\Delta H_f^0[MgF_2, c]$ is −268.7

Can. J. Chem. Downloaded from www.nrcresearchpress.com by 210.87.254.105 on 09/05/12
For personal use only.

$\pm$ 0.3 (18). Using this figure and ΔH_f^0[NaF, c] $= -137.9 \pm 0.3$ kcal mole^{-1} [from eq. [1], Parker's heat of solution, $\Delta H_f^0[F^-aq] = -80.2 \pm 0.2$, and $\Delta H_f^0[Na^+aq] = -57.47$ kcal mole^{-1} (19)], the enthalpy change for the reaction

$$NaF(c) + MgF_2(c) = NaMgF_3(c) \text{ at } 298.15\ ^\circ K$$

is -0.1 ± 0.5 kcal mole^{-1}. Hence the mixed crystal is ideal.

The limits of error assigned to our final data are optimistic in the sense that they do not include an error contribution for $\Delta H_f^0[M^{2+}aq]$. These latter data are, of course, accumulated from enthalpies of solution and formation of MY_2 (in the solution experiment the crystal is assumed ionic or a hydrolysis correction is made) and similar data for HY, and then applying the reverse procedure to that used in this work. The reference point for such a tabulation is $\Delta H_f^0[H^+aq] = 0$. The accepted values are the result of averaging a very large quantity of solution and formation enthalpies of varying precision and hence it is not possible to assign a meaningful error. However, some recent collated data (20) indicate that this error could be as large as 2 kcal for calcium salts and 12 kcal for strontium salts.

Acknowledgments

We are indebted to the Science Research Council for a maintenance grant (to C. J. S.), to Miss Osborne and Dr. A. Skapski of Imperial College (London) for the X-ray results, and to the Central Research Fund of the University of London for a grant to purchase a recorder.

1. F. D. Rossini *et al.* Selected values of chemical thermodynamic properties. Natl. Bur. Std. U.S. Circ. 500. 1952.
2. A. Finch and P. J. Gardner. J. Chem. Soc. 2985 (1964).
3. A. C. Macleod. Trans. Faraday Soc. **63**, 289 (1967).
4. S. R. Gunn. J. Phys. Chem. **69**, 2902 (1965).
5. R. J. Irving and I. Wadsö. Acta Chem. Scand. **18**, 195 (1964).
6. W. Biltz and G. F. Hüttig. Z. Anorg. Allgem. Chem. **119**, 116 (1921).
7. D. D. Wagman *et al.* Selected values of chemical thermodynamic properties. Natl. Bur. Std. U.S. Tech. Notes, 270–1 and 270–2. 1965, 1966.
8. S. Sunner and S. Thorén. Acta Chem. Scand. **18**, 1528 (1964).
9. JANAF thermochemical tables, First Addendum, Natl. Bur. Std. U.S. PB 168 370–1. 1966.
10. P. B. Howard and H. A. Skinner. J. Chem. Soc. 1536 (1966).
11. N. Beketoff. Bull. Acad. Sci. URSS, **34**, 291 (1892).
12. R. Varet. Ann. Chim. Phys. **8**, 240 (1896).
13. V. B. Parker. Thermal properties of aqueous uni-univalent electrolytes. Natl. Bur. Std. NSRDS-NBS 2. 1965.
14. P. Ehrlich, K. Peik, and E. Koch. Z. Anorg. Allgem. Chem. **324**, 113 (1963).
15. J. D. Cox and D. Harrop. Trans. Faraday Soc. **61**, 1328 (1965).
16. J. D. Cox. Private communication.
17. H. Stephen and T. Stephen. Solubilities of inorganic and organic compounds. Vol. I. The Pergamon Press, Ltd., London. 1963.
18. E. Rudzitis, H. M. Feder, and W. N. Hubbard. J. Phys. Chem. **68**, 2978 (1964).
19. S. R. Gunn. J. Phys. Chem. **71**, 1386 (1967).
20. H. F. Halliwell and S. C. Nyburg. Trans. Faraday Soc. **54**, 1126 (1963).

Can. J. Chem. Downloaded from www.nrcresearchpress.com by 210.87.254.105 on 09/05/12
For personal use only.

Can. J. Chem. Downloaded from www.nrcresearchpress.com by 210.87.254.105 on 09/05/12
For personal use only.

Studies in ferrocene derivatives. V[1]. Synthesis and nuclear magnetic resonance spectra of some ferrocenyl ethylenes

W. M. HORSPOOL
Department of Chemistry, The University, Dundee, Scotland

AND

R. G. SUTHERLAND
Department of Chemistry, University of Saskatchewan, Saskatoon, Saskatchewan

Received May 13, 1968

Ferrocenylethylenes are readily synthesized from acylferrocenes and the appropriate triphenylphosphorane in dimethylsulfoxide. Details of the nuclear magnetic resonance spectra of 12 ethylenes have been recorded.

Canadian Journal of Chemistry, 46, 3453 (1968)

As part of a study on the reactions of metallocenes with electron deficient species (2) we required a number of ferrocenylethylenes. A survey (3) of the literature showed that a number of olefins were known. However, in general the method of synthesis involved several steps and most often required a wasteful dehydration step. The Wittig olefin synthesis had apparently been overlooked as a ready means for synthesis except for a few isolated cases where formyl ferrocene (4, 5) had been used as the carbonyl component. Thus a systematic study of the utility of this facile method was carried out in the ferrocene series.

We have found that, in general, the addition of a ferrocenylcarbonyl compound (**1**) to a phosphorane solution in dimethylsulfoxide, generated from a phosphonium salt by the action of dimethylsulfinyl anion (6), proceeds smoothly and in high yield. The products (**2**) are readily separated from starting material by chromatography on alumina. Table I records the olefins successfully prepared by this method.

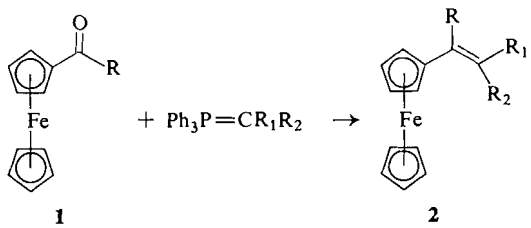

1 **2**

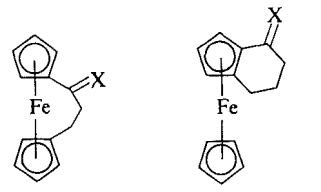

3a X = O
b X = CH_2

4a X = O
b X = CH_2

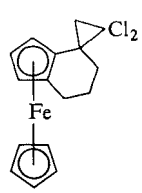

5

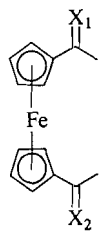

6a X = O
b X_1 = O, X_2 = CH_2
c X = CH_2

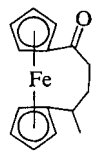

7

Apart from the use of formyl- and acetylferrocene the method was also found to be applicable to ferrocenyl cyclic ketones (**3** and **4**) giving good yields of the olefins (**3***b* and **4***b*). While **3***b* was found to be sufficiently stable for further purification and normal identification procedures, **4***b* was remarkably unstable and was reacted further and trapped as its dichlorocarbene adduct (**5**)[2]. Of particular interest was the incompleteness of the reaction of

[1]See ref. 1 for part IV in this series.

Can. J. Chem. Downloaded from www.nrcresearchpress.com by 210.87.254.105 on 09/05/12
For personal use only.

TABLE I

Wittig olefin synthesis in the ferrocene series

Reaction no.	Reactants	Product	Yield (%)
	1(R=H)+Ph_3P=CR_1R_2 (1→5)	**2**	
1	$R_1=R_2=H$	$R=R_1=R_2=H$	81
2	$R_1=H$, $R_2=CH_3$	$R=R_1=H$, $R_2=CH_3$	50
3	$R_1=R_2=CH_3$	$R=H$, $R_1=R_2=CH_3$	70
4	$R_1=H$, $R_2=C_6H_5$	$R=R_1=H$, $R_2=C_6H_5$	70
5	$R_1=H$, $R_2=COOC_2H_5$	$R=R_1=H$, $R_2=COOC_2H_5$	68
	1($R=CH_3$)+Ph_3P=CR_1R_2 (6→8)		
6	$R_1=R_2=H$	$R=CH_3$, $R_1=R_2=H$	87
7	$R_1=CH_3$, $R_2=H$	$R=R_1=CH_3$, $R_2=H$	63
8	$R_1=R_2=CH_3$	$R=R_1=R_2=CH_3$	57
9	**3***a*(X=O)+Ph_3P=CH_2	**3***b*($X=CH_2$)	64
10	**4***a*(X=O)+Ph_3P=CH_2	**4***b*($X=CH_2$)	63
11	**6***a*($X_1=X_2=O$)+Ph_3P=CH_2	**6***b*($X_1=O$, $X_2=CH_2$)	34
12	,,	**6***c*($X_1=X_2=CH_2$)	54

TABLE II

Nuclear magnetic resonance spectra of ferrocene derivatives*

Ferrocene	Vinyl protons	Substituent	Ring protons	
			Sub.	Unsub.
1. Vinyl	AXY pattern (3) A 3.40 dd (1) J_{AX}=17.1 c/s X 4.81 dd (1) J_{AY}=10.9 c/s Y 5.10 dd (1) J_{XY}=1.5 c/s	—	5.78 m 4.94 m (4)	6.03 s (5)
2. 1-Ferrocenyl-prop-1-ene	ABX pattern 3.92 d, J_{AB}=12 c/s (1) 4.41 dq, J_{BX}=7.7 c/s (1)	8.22 dd J_{AX}=1.7 c/s	5.78 m 5.90 m (4)	6.00 s (5)
3. 1-Ferrocenyl-2-methylprop-1-ene	4.16 s (1)	8.20 s (6)	5.87 m 5.96 m (4)	6.00 s (5)
4. 1-Ferrocenyl-2-phenylethylene	AB pattern (2) 3.34, J_{AB}=17.5 c/s ν_{AB}=9.0 c/s	2.75 m (5)	5.66 m 5.85 m (4)	5.97 s (5)
5. Ethyl-3-ferrocenylacrylate	AB pattern (2) 3.25, J_{AB}=15.4 c/s ν_{AB}=91.7 c/s	8.71 t (3)	5.49 m 5.72 m † (6)	5.87 s (5)
6. Isopropenyl	4.95 bs, 5.2 bs (2)	7.96 s (3)	5.72 m 5.89 m (4)	6.01 s (5)
7. 2-Ferrocenylbut-2-ene	4.26 q, J=7 c/s (1)	8.13 s (3) 8.38 d, J=7 c/s (3)	5.85 m 6.00 m (4)	6.06 s (5)
8. 2-Ferrocenyl-3-methylbut-2-ene	—	7.95 s (3) 8.26 s (6)	5.90 m (4)	5.93 s (5)
9. 2,4-(1,1′-Ferrocenylene)-but-1-ene	4.85 s (2)	7.33 m (2) 7.73 m (2)	5.86 m (8)	—
10. **4***b*	4.64 s (2)	7.69 m 8.16 m (6)	6.00 m (8)	
11. 1-Acetyl-1′-isopropenylferrocene	4.91 s 5.10 s (2)	7.71 s (3) 8.01 s (3)	5.36 m 5.65 m 5.78 m (8)	—
12. 1,1′-Di-isopropenylferrocene	4.94 s 5.13 s (4)	7.99 s (6)	5.64 m 5.85 m (8)	

*Spectra are reported in τ. All spectra were measured in CCl_4 solution apart from spectra 5, 11, and 12, which were recorded in $CDCl_3$. bs = broad singlet, s = singlet, d = doublet, dd = double doublet, t = triplet, q = quartet, dq = double quartet, and m = multiplet. Integrals are reported in brackets after the absorption to which they refer.

†Substituted ring absorption complicated by the methylene of the ester group occurring at the same place.

Can. J. Chem. Downloaded from www.nrcresearchpress.com by 210.87.254.105 on 09/05/12
For personal use only.

methylenetriphenylphosphorane with 1,1′-diacetylferrocene (**6***a*, $X_1 = X_2 = O$) when used in the correct molar proportions. (Optimum conditions for **6** are reported.) This provided a convenient synthesis of both the mono- (**6***b*, $X_1 = O$, $X_2 = CH_2$) and the di-olefin (**6***c*, $X_1 = X_2 = CH_2$). The mono-olefin was particularly useful in its reactions with base when cyclization to **7** took place (7). With the more stable phosphoranes reaction could not, as anticipated, be effected at ambient temperatures with acetylferrocene and thus the reaction with phenylmethylenetriphenylphosphorane failed to yield the methylstilbene derivative. However, ethoxycarbonylmethylenetriphenylphosphorane reacted readily with formylferrocene to give ethyl-3-ferrocenylacrylate (5).

The nuclear magnetic resonance (n.m.r.) spectra require little comment and give spectra typical of ferrocene derivatives. The protons of the unsubstituted ring, in the mono-substituted derivatives, all show up as a singlet at about 6.0 τ and the substituents on the olefinic side chain appear to have little effect. The protons of the substituted ring show up as two multiplets presumably a poorly resolved A_2B_2 system due to the difference in the shielding of the vinyl substituent. The observed spectra are recorded in Table II.

Experimental

The acylferrocenes used were synthesized by the standard methods (3). Nuclear magnetic resonance spectra were recorded on a Perkin–Elmer R 10 (60 Mc/s) spectrometer in CCl_4 or $CDCl_3$ solution.

Dimethyl Sulfinyl Anion

The reaction of sodium hydride with dimethylsulfoxide was carried out as described by Corey and Chaykovsky (6) except for the fact that it was unnecessary to remove the mineral oil from the sodium hydride suspension. This was because all the products could be separated by chromatography on alumina and none of them moved with the solvent front, thus allowing ready separation and purification.

General Procedure for Ferrocenyl Olefin Synthesis

Triphenylalkylphosphoniumhalide (34 mmole) in dimethylsulfoxide (20 ml) was added to a cool solution of dimsyl sodium (prepared from 1.63 g sodium hydride suspension and 15 ml dimethylsulfoxide) under an atmosphere of nitrogen. Stirring was continued for 10 min and a solution of the acylferrocene (32 mmole) in dimethylsulfoxide (20 ml) was added. After a further 15 min the reaction was terminated by pouring the mixture into water (200 ml). This was extracted with ether (5 × 50 ml). The organic layer was washed with water (3 × 50 ml), saturated brine solution, then dried over Na_2SO_4, and evaporated to dryness. The resulting semi-crystalline mass was chromatographed on alumina (Spence Grade H). Petroleum ether (40–60°) eluted the desired ferrocenylethylene as a yellow band. By the application of this general procedure the olefins of reactions 1–4 and 6–10, in Table I, were prepared. Table III lists the physical constants and molar scale of reaction.

TABLE III

Molar scale of reactions and physical constants of products for Table I

Phosphonium salt	Product (ref. Table I)	Molar scale m.p./b.p. (mmole)	(°C)
A*	1	25	52–53.5
B	2 (oil)	10	
C	3†	10	178/10 mm
D	4	10	121–122
A	6	32	66–69
B	7 (oil)	10	
C	8‡	10	46–48
A	9§	4	66–69
A	10‖(oil)	9	

*A stands for triphenylmethylphosphoniumbromide, B for triphenylethylphosphoniumbromide, C for triphenylisopropylphosphoniumbromide, and D for triphenylbenzylphosphoniumbromide

†A red oil. Found C, 70.47, H, 6.76%. $C_{14}H_{16}Fe$ requires C, 70.0, H, 6.67%.

‡Golden plates from aqueous alcohol. Found C, 71.38, H, 7.26%. $C_{15}H_{18}Fe$ requires C, 70.86, H, 7.09%.

§Crystallized from aqueous alcohol. Found C, 71.42, H, 6.16%. $C_{14}H_{14}Fe$ requires C, 70.81, H, 5.95%.

‖Trapped as the dichlorocarbene adduct. A fuller account of this and similar reactions will appear separately.

Ethyl-3-ferrocenylacrylate

Ethoxycarbonylmethylenetriphenylphosphorane (see ref. 8 and relevant references cited therein) (1.8 g, 5.3 mmoles) and formylferrocene (1.2 g, 5.3 mmoles) were dissolved in anhydrous ethyl acetate (85 ml) and the mixture was stirred for 4 days. The solvent was removed by distillation and the product chromatographed on alumina. Benzene eluted the product ethyl-3-ferrocenylacrylate (5) (1.02 g, 68%) as dark-red crystals m.p. 58–60.5°.

1-Acetyl-1′-isopropenylferrocene and 1,1′-Di-isopropenylferrocene

Dimsyl sodium was prepared as originally described (30 mmoles in 15 ml dimethyl sulfoxide). To this solution was added methyltriphenylphosphoniumbromide (10.71 g, 30 mmoles) in dimethylsulfoxide (55 ml) and the mixture stirredf or 10 min. 1,1′-Diacetylferrocene (5.2 g, 20 mmoles) in dimethyl sulfoxide (35 ml) was added and after a further 10 min stirring, the reaction was terminated by pouring it into water (200 ml). Conventional workup gave a semi-crystalline material which was chromatographed on alumina. Petroleum ether (40–60°)/benzene (1:1) eluted 1,1′-diisopropenylferrocene (1.17 g, 22.5%) and petroleum ether/ether (1:3) eluted 1-acetyl-1′-isopropenylferrocene (2.78 g, 53.5%) as dark-red crystals (unstable), m.p. 35–38.5° (Found C, 66.42, H, 6.07%. $C_{15}H_{16}FeO$ requires C, 67.25, H, 5.97%.)

Acknowledgment

We thank the University of St. Andrews,

Scotland, for the award of an Imperial Chemical Industries Research Fellowship (to R.G.S.).

1. W. M. HORSPOOL and R. G. SUTHERLAND. Chem. Commun. 787 (1967).
2. W. M. HORSPOOL and R. G. SUTHERLAND. Chem. Commun. 456 (1966).
3. M. ROSENBLUM. *In* Chemistry of the iron group metallocenes. Part I. John Wiley and Sons, Inc., New York. 1965.
4. J. M. OSGERBY and P. L. PAUSON. J. Chem. Soc. 4604 (1961). G. DREFAHL, G. PLOTNER, and I. WINNEFELD. Chem. Ber. **95**, 2788 (1962).
5. P. DARE and E. SIANESI. Experientia, **21**, (11), 648 (1965).
6. E. J. COREY and M. CHAYKOVSKY. J. Am. Chem. Soc. **84**, 866 (1962).
7. W. M. HORSPOOL and R. G. SUTHERLAND. Chem. Commun. 240 (1967).
8. A. MAERCKER. *In* Organic reactions. Vol. 14. 1965. p. 270.

Can. J. Chem. Downloaded from www.nrcresearchpress.com by 210.87.254.105 on 09/05/12
For personal use only.

Can. J. Chem. Downloaded from www.nrcresearchpress.com by 210.87.254.42 on 09/05/12
For personal use only.

Solvent LiCl–KCl in the nephelauxetic series for trivalent rare earths

K. E. JOHNSON[1] AND J. N. SANDOE[2]

Department of Chemistry, Sir John Cass College, London, England

Received May 28, 1968

The spectra of trivalent Ce, Pr, Nd, Sm, Eu, Tb, Dy, Tm, and Yb ions in molten LiCl–KCl at 450 °C are reported over the range 0.28 to 2.8 μ and the baricenters of terms are tabulated for a wide variety of crystal and liquid hosts. These hosts can be arranged in a nephelauxetic series and for Pr^{3+} actual nephelauxetic parameters, β, can be calculated by comparing average multiplet energies.

Canadian Journal of Chemistry, **46**, 3457 (1968)

The region of optical transparency for fused salt media can extend quite far into the infrared. For instance, the limiting wavelengths are 2.6 μ for $LiNO_3$–KNO_3 eutectic at 150 °C (1), 2.8 μ for LiCl–KCl eutectic at 450 °C (2), and 2.7 μ for a ternary sulfate at 550 °C compared with 1.4 μ for water at 25 °C. This is useful for the study of lanthanide ions since their 4f″ bands in this region are less subject to the complications of overlapping multiplets.

Banks *et al.* (3) have investigated the complete series of lanthanide ions except La^{3+}, Ce^{3+}, and Pm^{3+} in LiCl–KCl eutectic at 400 °C through the visible and near infrared regions to 1 μ. Sm^{3+} and Pr^{3+} ions have been investigated in LiCl–KCl eutectic with high resolution in the near infrared (2), while several ions were studied in LiCl–KCl–NaCl eutectic at 400 °C (4). Carnall and co-workers (5–7) discussed the spectra of all the trivalent lanthanides except La^{3+} and Ce^{3+} in $LiNO_3$–KNO_3 eutectic in terms of the transitions between LS multiplets of 4f″. Certain ions were studied from an analytical viewpoint in fluoride melts by Young and White (8, 9) and the spectrum of Nd^{3+} in LiCl–KCl and LiF was used to illustrate the use of the Unicam S.P. 700 spectrophotometer (10).

The characteristic narrow bands of these ions appeared in all melts but some fine structure was lost. Bands obtained only in nitrate melts in the 1.7 μ region were ascribed to water contamination (4). A temperature increase of 400 °C caused a bathochromic shift of the Ho^{3+} bands (4) but a 200 °C increase showed no effect on the Nd^{3+} bands (10).

This paper reports the spectra of several trivalent lanthanides in LiCl–KCl eutectic at 450 °C over the range 0.28 to 2.8 μ. Comparisons are made with the spectra in other solvents and crystals and actual or relative nephelauxetic parameters are evaluated for the 4f electrons. A discussion of the nephelauxetic effect in rare earths appears in Sinha's book (11) together with other tables of spectra.

Experimental

Preparation of Lanthanide Ion Solutions in LiCl–KCl Eutectic

Pure anhydrous eutectic was prepared by a procedure essentially following Laitinen, Tischer, and Roe (12). $SmCl_3$ was prepared by passing HCl over hydrated chloride (Johnson Matthey Ltd., London) in a silica boat while raising the temperature to 550 °C over a period of 30 h. $YbCl_3$ was purified by sublimation of so-called anhydrous material (Koch Light Laboratories) at 600 °C, 5×10^{-3} τ on to a water-cooled finger; the raw material was 3% deficient in chlorine and gave turbid solutions in the melt. These two salts could be added directly to the solvent. The hydrated chloride or oxides of the other ions (Johnson Matthey Ltd., Koch Light) were added to the solvent to produce cloudy solutions which were cleared by the addition of solid ammonium chloride. The HCl formed by dissociation of NH_4Cl reacted violently with the oxide and the H_2O, and excess reagents could be pumped off after 30 min (cf. Carnall *et al.* (5)). Solutions of Pr^{3+} could also be made from finely divided metal and a solution of NH_4Cl in LiCl–KCl.

Instrumentation

Spectra were obtained by means of three instruments, specially adapted for fused salt systems, a Beckman D.K. 2 recording spectrophotometer and both "large quartz" and "medium quartz" spectrographs of Adam Hilger Ltd. Quartz cells were employed. Full details of these operations will appear elsewhere (13).

Spectra

Figures 1–3 depict the spectra of the trivalent lanthanide ions in LiCl–KCl at 450 °C.

---

[1]Present address: Division of Natural Sciences, University of Saskatchewan, Regina, Saskatchewan.

[2]Present address: William Ramsay and Ralph Forster Laboratories, University College, London.

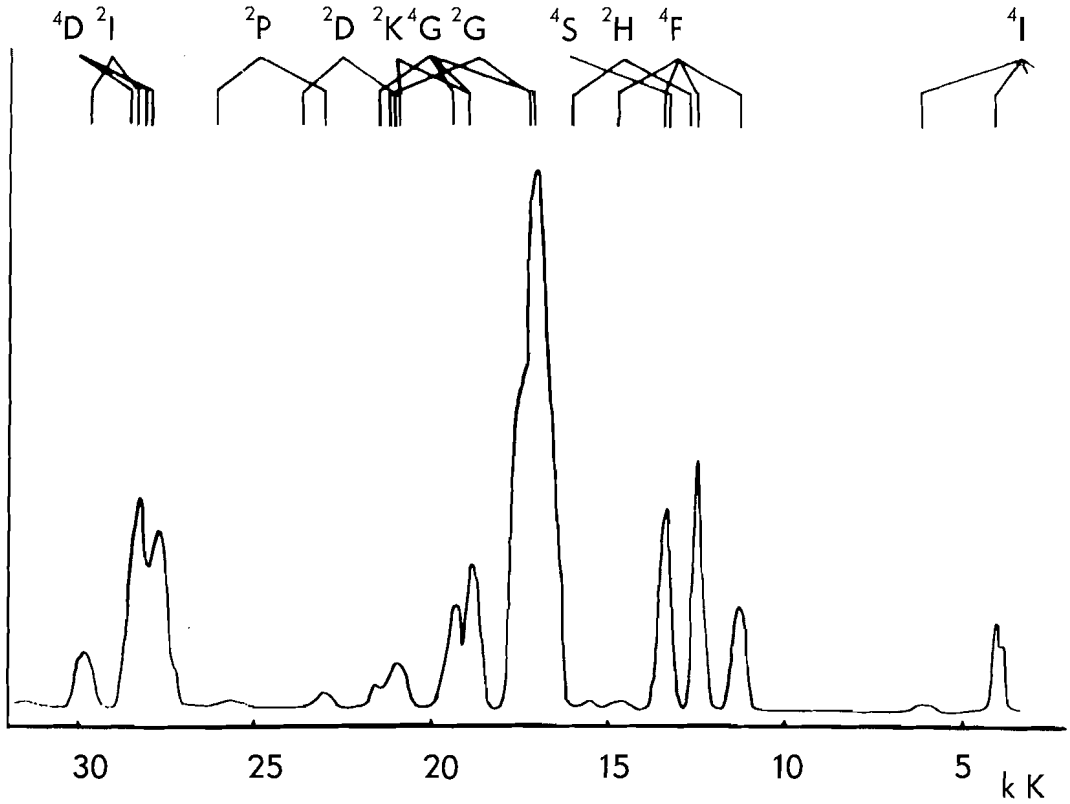

FIG. 1. Spectrum of Nd^{3+} in LiCl–KCl at 450 °C.

Discussion of Individual Ions

Cerium

The only band observed was a broad one centered at 31.1 kK, which may be ascribed to a transition from the $^2F_{5/2}$ ground state to a level of the electronic configuration $(Xe)(5d)^1$ split by the ligand field. Similar bands in this region have been observed for other environments (14–19).

Praseodymium

The spectrum resembles previous measurements at 400 °C except for the absence of two bands given by Banks *et al.* (3). Table 1D[3] summarizes the band positions and assignments for several hosts. The hosts have been arranged in order of increasing energy for a given transition. With a few exceptions, all bands move similarly for a change of host. Since the ^3P transitions are identifiable for all hosts, the ^3P energies have been compared with those for the free gaseous ion and β, the nephelauxetic parameter ($=\Sigma\ ^3P_{host}/\Sigma\ ^3P_{free\ ion}$), evaluated in each case. These quantities are listed in Table I. The values compare well with those of Jorgensen (20), based on his estimate of $\beta = 0.97$ for H_2O and with those of Wong *et al.* (21).

Neodymium

Bands not previously observed for chloride melts were found at 4 and 6 kK. The spectra in LiCl–KCl at 450 and 650 °C and in KCl at 800 °C were the same except for some loss of fine structure and changes in relative intensity with increase in temperature. The solutions changed from pale pink just above the melting point to blue at higher temperatures.

The calculated multiplet positions are included with the LiCl–KCl spectrum (Fig. 1) and the lower energy bands compared for several hosts

[3]Tables 1D through 8D together with references 32 through 80 are in the Depository of Unpublished Data. Photocopies may be obtained free of charge, upon request, from: The Depository of Unpublished Data, National Science Library, National Research Council of Canada, Ottawa, Canada.

Can. J. Chem. Downloaded from www.nrcresearchpress.com by 210.87.254.42 on 09/05/12
For personal use only.

TABLE I

Term summations (in cm^{-1}) for Pr^{3+}, Nd^{3+}, Sm^{3+}, and Dy^{3+}

		Term summation values in host						
M	Term	M_2O_3	M_2S_3	M_2O_2Te	BaM_2S_4	MI_3	$LaBr_3$	MBr_3
Pr	Σ^3P	60 680	62 140	62 450	62 670	62 940	63 220	63 330
	β	0.91	0.93	0.94	0.94	0.95	0.95	0.95
Nd	Σ^4I		12 080					
	Σ^4F	50 510					51 280	
Sm	$^{11/2}_{J=3/2}\Sigma^6F$	41 470	40 630					
Dy	$^{9/2}_{J=3/2}\Sigma^6F$	46 800	45 600		46 400			

		Term summation values in host						
M	Term	$LaCl_3$	$PbMoO_4$	MCl_3	LiCl/KCl at 450 °C	$LiNO_3/KNO_3$ at 150 °C	LaF_3	H_2O
Pr	^3P	63 510	63 770	63 780	64 080	64 400	64 600	64 700
	β	0.95	0.96	0.96	0.96	0.97	0.97	0.97
Nd	Σ^4I	12 010	12 160					
	Σ^4F	51 390					51 850	52 110
Sm	Σ^6H			18 700			18 370	
	$^{11/2}_{J=3/2}\Sigma^6F$	40 800		41 100	41 150	41 310	41 470	
Dy	$^{9/2}_{J=3/2}\Sigma^6F$	45 400				45 600		

		Term summation values in host						
M	Term	LiF at 900 °C	LiF/NaF/KF at 550 °C	MF_3	Y_2O_3	$LaCl_3.9H_2O$	YAlG	YGaG
Pr	Σ^3P	64 770	64 810	64 870				
	β	0.97	0.97	0.98				
Nd	Σ^4I				11 630		12 630	12 640
	Σ^4F				50 480		52 130	52 180
Sm	Σ^6H					18 500		
	$^{11/2}_{J=3/2}\Sigma^6F$					41 600		

in Table 2D. Only the lower bands may be assigned and then not to transitions between defined crystal field states. The $^4I_{9/2} \rightarrow {}^4I_{13/2}$ transition was split into components centered at 4.06 and 3.76 kK, a splitting (0.3 kK) comparable to that (0.28 kK) observed with a nitrate melt (5). Table 2D is arranged in order of decreasing nephelauxetic effect as indicated by summing several band energies for each host. The summations are recorded in Table I. This series is not exhaustive and, in fact, tends to complement that given by Sinha (11)[4].

Samarium

Again only the lower energy bands are capable of being assigned to transitions between multiplets. Rather than assume the $^6H_{5/2} \rightarrow {}^6F_{1/2}$ transition to be very weak (5), one can explain the spectra for several hosts if the $^6F_{1/2}$ and $^6F_{3/2}$ levels are sufficiently close to produce only one rather low energy band. The assignment of transitions to $^6F_{1/2}$, $^6F_{3/2}$, and $^6H_{15/2}$ levels in $LaCl_3$ is unique (22, 23). Table 3D summarizes the band positions for several hosts and includes a nephelauxetic order based on the sums of energies of some ^6H and ^6F terms listed therein (cf. Table I).

Europium

The spectrum in Fig. 3 shows strong absorption at high energy, characteristic of Eu^{2+} (13) and two doublets in the near infrared, not observed for solutions of $EuCl_3$ in LiCl–KCl–NaCl (4). These doublets are assigned to Eu^{3+}, $^7F_0$ transitions to crystal field split $^7F_5$ and $^7F_6$ levels. Table 4D summarizes some data on ^7F transitions. It should be noted that all Eu-doped crystals grown under normal conditions contain some Eu^{2+}.

[4]Sinha's book indicates the spectroscopic terms of interest for all the ions.

Can. J. Chem. Downloaded from www.nrcresearchpress.com by 210.87.254.42 on 09/05/12
For personal use only.

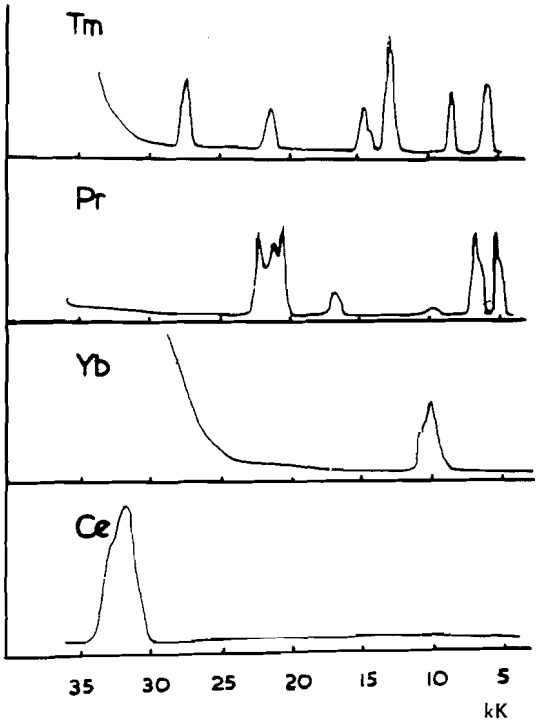

FIG. 2. Spectra of Ce^{3+}, Yb^{3+}, Pr^{3+}, and Tm^{3+} in LiCl–KCl at 450 °C.

Terbium

The bands in the 5 kK region have not been observed previously for this solvent. The assignments for the low energy bands ($^7F_6 \rightarrow {}^7F_3$, $^7F_6 \rightarrow {}^7F_{2,1,0}$) are given, in comparison with other hosts, in Table 5D. The excited states $^7F_2$, $^7F_1$, and $^7F_0$ were predicted to be 0.3 kK apart (24) so that the merging of the transitions to them is reasonable for the temperature of 450 °C. The transition to $^5D_4$ (at 20.35 kK in LiCl–KCl) was identified through Zeeman work on terbium ethylsulfate (25) but the band at 26.5 kK is open to several interpretations (24). Table 5D shows only a limited correlation between the movements of all bands with a change of host.

The broad band at 35.3 kK was a few times more intense than any f–f transitions and might be tentatively assigned to a transition to a level belonging to the electronic configuration $(Xe)(4f)^7(5d)^1$. Similar bands were reported for $TbCl_6^{3-}$ at 3.60 kK (17).

Dysprosium

The low energy bands of Dy^{3+} are compared for several hosts in Table 6D. Some ^6F term summations appear in Table I. The band at 5.88 kK showed fine structure for both LiCl–KCl and LiCl–KCl–NaCl (4) eutectics but not for $LiNO_3$–KNO_3 or $DClO_4$ (6). Generally the spectra shift as a whole with change of host.

Thulium

New bands for a chloride melt were observed at 5.62 and 8.13 kK. The breakdown of LS coupling for ions with almost full 4f″ shells has raised doubts concerning the earlier assignments of Tm^{3+} spectra. We have used the recent scheme of Carnall *et al.* (26) to assign the bands for several hosts, including LiCl–KCl eutectic (Table 7D). Again, most bands move similarly with change of host.

Ytterbium

Using solutions of 25 mg $YbCl_3$/ml, very weak peaks were obtained, particularly at 17 kK, in addition to the narrow band at ~10.5 kK and the cutoff at ~27 kK shown in Fig. 2.

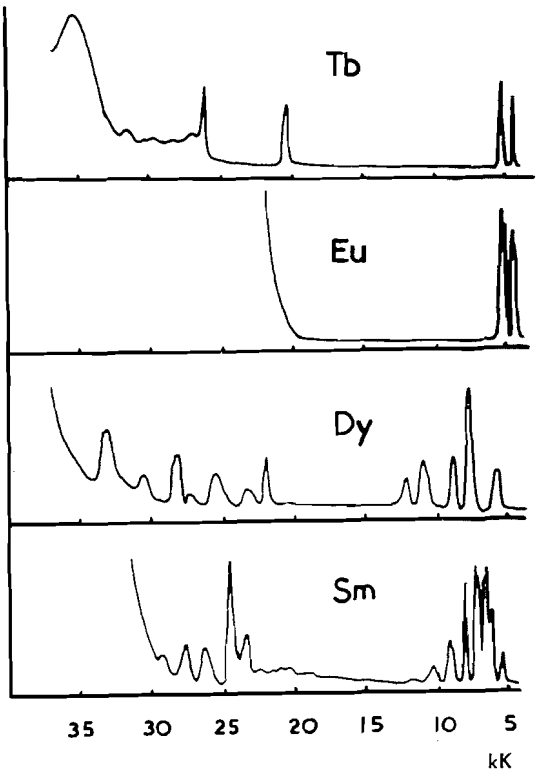

FIG. 3. Spectra of Sm^{3+}, Dy^{3+}, Eu^{3+}, and Tb^{3+} in LiCl–KCl at 450 °C.

Can. J. Chem. Downloaded from www.nrcresearchpress.com by 210.87.254.42 on 09/05/12
For personal use only.

Can. J. Chem. Downloaded from www.nrcresearchpress.com by 210.87.254.42 on 09/05/12
For personal use only.

The 10.5 kK band was resolved into three peaks and its position and structure are compared for several hosts in Table 8D. The band may be assigned as transitions between the crystal field split levels $^2F_{7/2}$ and $^2F_{5/2}$ and gives an approximate value of ζ_{4f}, the spin orbit coupling parameter, of 2970 cm^{-1}. A free ion separation has been given (27) but this is less than the values found for the crystals so that only a nephelauxetic order can be derived. Different site symmetries may account for the different sets of results for CaF_2.

Conclusions

The nephelauxetic series for Pr^{3+} and Nd^{3+} are probably the most reliable because of the relative simplicity of the configurations. A shortened list (in order of increasing $(1 - \beta)$) may be written for crystal hosts:

$$YGaG < LaCl_3.9H_2O < LaF_3 < LaCl_3 < BaM_2S_4 < M_2S_3 < M_2O_3 < Y_2O_3$$

where M is the metal under study. Sm^{3+} data agree with this order for $LaCl_3.9H_2O$, $LaCl_3$ and Sm_2S_3, and Tm^{3+} results agree for $LaCl_3.9H_2O$ vs. Y_2O_3. The results for Dy^{3+} differ from these, particularly in the case of Dy_2O_3. For other ions quantitative comparisons are not possible.

For nearly all ions the nephelauxetic effect for LiCl/KCl melt at 450° slightly exceeds that for $LiNO_3/KNO_3$ melt at 150°. When series are compared for several ions, it is seen that the liquid and crystal phases have to be treated separately.

Two steps in the evaluation of the series need justification. Firstly, is a comparison between sums of energies meaningful? We suggest that provided the terms concerned belong to the same multiplet, this procedure gives an average β with an averaged error. Terms of different multiplicity definitely have different β values (28). The second point concerns comparing ligands for different ions—an extension of the original concept of the effect. This is permissible provided series and not a specific β values are compared.

The series obtained resemble those accepted for "d" transition metal ions with such subseries as $F^- < Cl^- < Br^- < I^-$. Thus the lower β values can be associated with greater covalency.

A correlation between β and interionic distance was also noted for Pr^{3+} in praseodymium and lanthanum halide hosts as shown in Fig. 4, a linear dependence of $(1 - \beta)$ on interionic distance (29, 30). This plot obscures the direct proportionality between central ion size and β shown for Pr^{3+} substituted in a series of rare-earth chlorides (31), and may demonstrate merely a gross relation between halide ion size and halogen electronegativity.

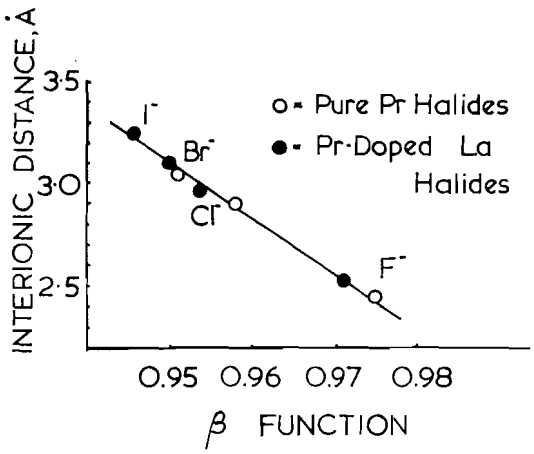

FIG. 4. Interionic distance vs. β for Pr^{3+} in halides.

Acknowledgment

This work was supported by the Ministry of Technology.

1. W. T. CARNALL. Anal. Chem. **34**, 786 (1962).
2. M. MAMIYA. J. Chem. Soc. Japan, **66**, 1625 (1963).
3. C. V. BANKS, M. R. HEUSINKVELD, and J. W. O'LAUGHLIN. Anal. Chem. **33**, 1235 (1961).
4. M. MAMIYA. Bull. Chem. Soc. Japan, **38**, 178 (1965).
5. W. T. CARNALL, D. M. GRUEN, and R. L. MCBETH. J. Phys. Chem. **66**, 2159 (1962).
6. W. T. CARNALL. J. Phys. Chem. **67**, 1206 (1963).
7. W. T. CARNALL, P. R. FIELDS, and G. E. TOOGOOD. J. Phys. Chem. **68**, 2351 (1964).
8. J. P. YOUNG and J. C. WHITE. Anal. Chem. **32**, 1658 (1960).
9. J. P. YOUNG and J. C. WHITE. Anal. Chem. **32**, 799 (1960).
10. R. A. BAILEY and J. A. MCINTYRE. Rev. Sci. Instr. **36**, 968 (1965).
11. S. P. SINHA. Complexes of the rare earths. The Pergamon Press, Ltd., London. 1966.
12. H. A. LAITINEN, R. P. TISCHER, and D. K. ROE. J. Electrochem. Soc. **107**, 546 (1960).
13. K. E. JOHNSON, J. R. MACKENZIE, and J. N. SANDOE. To be published.
14. A. A. KAPLYANSKII, V. N. MEDVEDEV, and P. P. FEOFILOV. Opt. i Spektroskopiya, **14**, 664 (1963).
15. P. P. FEOFILOV. Opt. i Spektroskopiya, **6**, 234 (1959).
16. S. FREED. Phys. Rev. **38**, 2122 (1931).
17. J. L. RYAN and C. K. JORGENSEN. J. Phys. Chem. **70**, 2845 (1966).

18. C. K. JORGENSEN and J. S. BRINEN. Mol. Phys. **6**, 629 (1963).
19. R. J. LANG. Can. J. Research, **14A**, 127 (1936).
20. C. K. JORGENSEN. Absorption spectra and chemical bonding in complexes. The Pergamon Press, Ltd., London. 1964.
21. E. Y. WONG, O. M. STAFSUDD, and D. R. JOHNSON. J. Chem. Phys. **39**, 786 (1963).
22. C. K. JORGENSEN. Orbitals in atoms and molecules. Academic Press, Inc., London and New York. 1962.
23. M. S. MAGNO and G. H. DIEKE. J. Chem. Phys. **37**, 2354 (1962).
24. G. S. OFELT. J. Chem. Phys. **38**, 2171 (1963).
25. H. G. KAHLE and H. KALSLEISH. Z. Physik. **166**, 184 (1962).
26. W. T. CARNALL, P. R. FIELDS, and B. G. WYBOURNE. J. Chem. Phys. **41**, 3797 (1965).
27. B. W. BRYANT. J. Opt. Soc. Am. **55**, 771 (1965).
28. C. E. JORGENSEN, R. PAPPALARDO, and H. H. SCHMIDTKE. J. Phys. Chem. **39**, 1422 (1963).
29. F. A. COTTON and G. WILKINSON. Advanced inorganic chemistry. Interscience Publishers, Inc., New York. 1962.
30. D. H. TEMPLETON and C. H. DAUBEN. J. Am. Chem. Soc. **76**, 5237 (1954).
31. R. D. MCLAUGHLIN and J. D. CONWAY. J. Chem. Phys. **38**, 1037 (1963).

Can. J. Chem. Downloaded from www.nrcresearchpress.com by 210.87.254.42 on 09/05/12
For personal use only.

Can. J. Chem. Downloaded from www.nrcresearchpress.com by 210.87.254.40 on 09/05/12
For personal use only.

Chalkogenides of the transition elements. VI.[1] X-Ray, neutron, and magnetic investigation of the spinels Co_3O_4, $NiCo_2O_4$, Co_3S_4, and $NiCo_2S_4$

OSVALD KNOP AND K. I. G. REID
Department of Chemistry, Dalhousie University, Halifax, Nova Scotia

AND

SUTARNO[2]
Department of Chemical Engineering, Nova Scotia Technical College, Halifax, Nova Scotia

AND

YASUAKI NAKAGAWA[3]
Department of Physics, Gakushuin University, Mejiro, Tokyo

Received February 13, 1968

The crystal structures of the spinels Co_3O_4, $NiCo_2O_4$, Co_3S_4, and $NiCo_2S_4$ were refined from X-ray and neutron powder data. Their lattice parameters at room temperature and the positional parameters of the oxygen and sulfur atoms were: Co_3O_4, 8.0835 ± 6 Å, 0.2640 ± 8; $NiCo_2O_4$, 8.114 ± 14 Å, 0.2583 ± 34; Co_3S_4, 9.4055 ± 12 Å, 0.2591 ± 5; $NiCo_2S_4$, 9.3872 ± 7 Å, 0.2591 ± 3. The thermal stabilities of the two oxides in air and in oxygen at 1 atm were investigated by thermogravimetric analysis and differential thermal analysis, and the magnetization of $NiCo_2O_4$ was measured down to 4.2 °K in fields up to 11.70 kOe. From neutron diffraction $NiCo_2O_4$ was found to be inverse, while $NiCo_2S_4$ was shown to be normal. The results of the magnetization measurements and the neutron-diffraction patterns at 111 and 393 °K were found to be equally consistent with the magnetic structure proposed for $NiCo_2O_4$ by Blasse, $Co^{2+}[Ni^{3+}Co^{3+}]O_4$ (Co^{2+} in a high-spin and Ni^{3+} and Co^{3+} in low-spin states), and with Co^{3+}-$[Ni^{2+}Co^{3+}]O_4$ (Co^{3+} in 8(*a*) in a high-spin and Co^{3+} in 16(*d*) in a low-spin state). The sublattice magnetizations were not completely aligned even at 4.2 °K; the net magnetic moment derived from the magnetization measurements was only 1.25 μ_B, which is lower than the value of 2μ_B expected from either model. At 111 °K the moments of the ions in the tetrahedral and octahedral sites were estimated to be 1.9 ± 0.2 and −0.5 ± 0.1 bohr magnetons respectively.

Canadian Journal of Chemistry, 46, 3463 (1968)

Nickel in the cubic π phase Co_8NiS_8 shows no noticeable preference for octahedral coordination (1). It is of interest to know how common this lack of preference is in other sulfide structures based on a f.c.c. framework of sulfur atoms. The structure of the sulfospinel $NiCo_2S_4$ is of this type. It contains tetrahedrally and octahedrally coordinated metal atoms, but the distribution of Co and Ni in this compound has not been previously studied. An investigation of this sulfocobaltite was therefore undertaken. For comparison a similar investigation was carried out on the corresponding oxide, $NiCo_2O_4$, which is magnetic at room temperature (2–4), and on the binary compounds Co_3S_4 and Co_3O_4. All four compounds have been described before, and some of them have been known for a long time (cf. Table I), but except for Co_3O_4 the positional parameters of the nonmetal atoms have never been determined.

Experimental

Preparation and Thermal Stability of the Oxides

Co_3O_4 was prepared by calcining reagent-grade cobalt carbonate at 700 °C in air and allowing the product to cool slowly. The composition of cobalt carbonate is always uncertain, but thermogravimetric analysis (t.g.a.) showed that the carbonate was completely decomposed into Co_3O_4 between 550 and 600 °C (Fig. 1). There was no further loss of weight until Co_3O_4 began to lose oxygen and decompose into CoO at about 950 °C.

The diffraction pattern of the product, which was a very fine jet black powder, was well defined and contained no foreign lines. However, differential thermal analysis (d.t.a.) runs in stagnant air indicated onset of an endothermic process at about 660 °C. The process was characterized by a composite peak terminating at about 1030 °C (Fig. 1). Consequently the decomposition of Co_3O_4 into CoO cannot be simple, and Co_3O_4 may undergo some transformation below the calcining temperature, 700 °C. At first glance the peak seems to consist of a small broad peak centering at about 900 °C and a much narrower

[1]For part V see ref. 21. A preliminary account of this work was read at the Chemical Institute of Canada Symposium on Structural Inorganic Chemistry in Halifax, N.S., September 1–3, 1965.

[2]Present address: Mineral Sciences Division, Mines Branch, Department of Energy, Mines and Resources, Ottawa, Canada.

[3]NRCC Postdoctorate Fellow in the Neutron Physics Branch, Atomic Energy of Canada Limited, Chalk River, Ont., 1962–63.

Can. J. Chem. Downloaded from www.nrcresearchpress.com by 210.87.254.40 on 09/05/12
For personal use only.

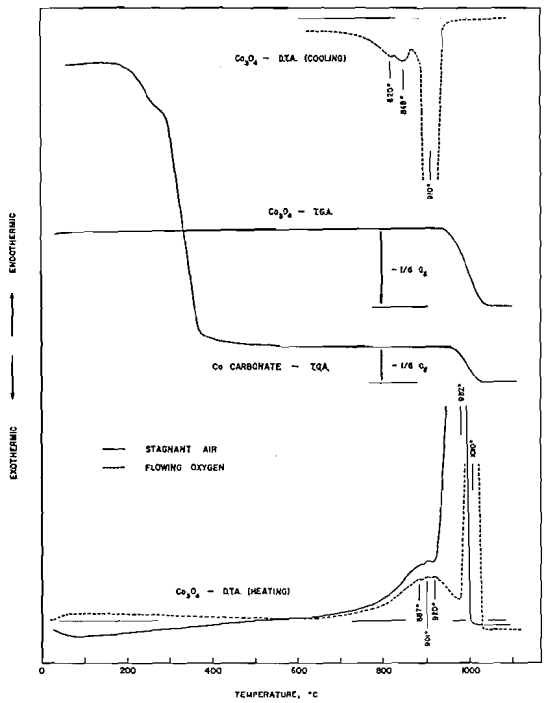

FIG. 1. T.g.a. and d.t.a. curves of cobalt carbonate and Co_3O_4 in stagnant air and in flowing oxygen. The t.g.a. curves are not on the same scale. D.t.a. peaks are cut off at half-widths. Weight changes in the t.g.a. curves refer to 1 CoO (final state on heating). Rate of heating, 6 °C/min; rate of cooling, 6 °C/min, then natural cooling.

main peak positioned at about 982 °C. However, the profile of the composite peak is less symmetric than would correspond to an overlap of the two component peaks. In this the composite peak resembles somewhat the corresponding peak for $NiCo_2O_4$ (Fig. 2), the asymmetry of which is much more pronounced. A d.t.a. run in flowing oxygen gave a similar result, but the main peak was shifted to about 1010 °C, while the broad peak remained essentially unchanged. The indications of fine structure of the broad peak are probably real, since they reappeared on cooling. The increased separation of the component peaks in oxygen showed that the main peak was symmetric.

There was no change in weight (within about ± 1 mg on a 0.5 g sample in stagnant air) that would correspond to the endothermic d.t.a. peak in the 660–920 °C range, even when the usual uncertainties in correlating t.g.a. and d.t.a. curves are taken into account.

Even though the thermal hysteresis of the main d.t.a. peak in oxygen amounted to about 100 °C, reoxidation of the CoO ultimately formed appeared to be fast and proceed through essentially the same stages as the decomposition of Co_3O_4. This must also be the case on heating in air, as the final product obtained by the decomposition of the carbonate was single-phase Co_3O_4. The calcining temperature employed in the preparation, 700 °C, may perhaps have been too high, but the product reoxidized completely during the slow cooling, and calcining at 700 °C may have improved the crystallinity of the resulting oxide.

$NiCo_2O_4$ was prepared by dissolving the requisite amount of dried Co_3O_4 and NiO (reagent grade) in nitric acid, evaporating to dryness, and decomposing the residue on a hot plate till no more nitric fumes were given off. The resulting magnetic powder was ground and thoroughly mixed by repeated screening through a 325-mesh screen. To establish a maximum safe firing temperature the mixed oxide was investigated by t.g.a. in stagnant air and in flowing oxygen (Fig. 2). In air the loose powder (not dried) began to lose weight almost as soon as the heating started. A poorly defined plateau was reached at about 200 °C; at about 350 °C a steady loss of weight set in. From there on there was a continuous and significant loss of oxygen till about 940 °C. In oxygen the weight loss became appreciable at ca. 400 °C, the shape of the t.g.a. curve being similar to that obtained in air but shifted by approximately 50 °C towards higher temperatures. The composition of the final product above 950 °C in air corresponded to $NiCo_2O_3$, i.e. $(Ni_{1/3}Co_{2/3})O$.

When the t.g.a. residue was allowed to cool in the thermobalance from 1100 °C in air, perceptible reoxidation began at ca. 830 °C. The amount of oxygen absorbed in the reoxidation was less then $\frac{1}{4}O_2$ per formula unit of $NiCo_2O_3$. Powder photographs of the cooled product contained strong but diffuse lines of a *B*1 pattern and reasonably sharp lines corresponding to the Co_3O_4 pattern. This would point to reoxidation of a homoge-

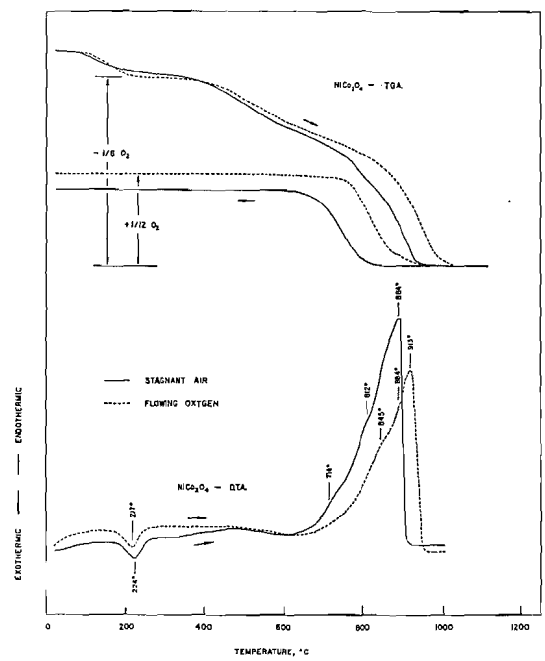

FIG. 2. T.g.a. and d.t.a. curves of $NiCo_2O_4$ (not dried) in stagnant air and in flowing oxygen. Weight changes in the t.g.a. curves refer to 1 $(Ni_{1/3}Co_{2/3})O$ (final state on heating). Rate of heating, 6 °C/min; rate of cooling, 6 °C/min to about 500 °C, then natural cooling.

Can. J. Chem. Downloaded from www.nrcresearchpress.com by 210.87.254.40 on 09/05/12
For personal use only.

neous solid-solution $NiCo_2O_3$ phase of the rock-salt type to a mixture of NiO, CoO, and Co_3O_4, the lower oxides forming at least a limited solid solution.

From these results it was concluded that 300 °C in oxygen at atmospheric pressure would be a reasonable preparation temperature. Pressed disks of the nitrate calcine were fired for 7 days at 300 °C in flowing oxygen followed by slow cooling in the furnace. They crumbled readily to a very fine jet-black, strongly magnetic powder which gave a diffuse spinel pattern that could not be measured with satisfactory accuracy. The firing was repeated but the resulting patterns were still of poor quality. Both Co_3O_4 and $NiCo_2O_4$ were so fine that there was no need of grinding the powders to pass 400 mesh.

These results were in general agreement with the findings of Holgersson and Karlsson (2) who obtained, by firing the mixed nitrate at 850 °C in air, a homogeneous solid solution of CoO and NiO, while gentle heating over a Bunsen flame produced a spinel phase. However, Lotgering (4), who fired the nitrates at 300 °C in oxygen, remarks that though $NiCo_2O_4$ is unstable above about 400 °C, he was able to determine a reversible $1/\chi$ vs. temperature curve up to about 800 °C. Gocan (20) reported that he obtained magnetic spinel phases by calcining the mixed nitrates at 400, 500, 600, and 700 °C for 4 h, while at 800 °C a mixture of NiO, CoO (two separate phases), and Co_3O_4 resulted[4].

To see if reversible reoxidation does take place on *slow* cooling, a specimen of $NiCo_2O_4$ was heated as loose powder at 700 °C for 2 days in flowing oxygen and then cooled to room temperature over 10 days without stopping the oxygen flow. The powder pattern of the product showed strong lines of a *B*1 phase as well as a weaker line pattern that appeared to correspond to that of Co_3O_4. Considering that at 700 °C the main loss of oxygen in our t.g.a. experiments had not yet taken place, our results are at variance with the findings of both Gocan and Lotgering.

Differential thermal analysis curves, in stagnant air and in flowing oxygen, of a $NiCo_2O_4$ specimen used for neutron diffraction showed similarities with the curves for Co_3O_4, but the composite endothermic peaks were much more asymmetric, and even in oxygen there was no separation of the component peaks (Fig. 2). A puzzling feature, not present in the d.t.a. curves of Co_3O_4, was a weak exothermic peak in the vicinity of 220 °C which appeared in air, oxygen, and purified argon, but only when virgin material was used. It was not observed on recycling. With the aid of infrared spectra of the oxide dispersed in KBr pellets it was eventually traced to small amounts of residual nitrate which was present even after the prolonged calcination. It seems that the initial loss of weight in the t.g.a. experiments (below say 300 or 350 °C) had its origin in the undecomposed nitrate and moisture.

Preparation of the Sulfides

Co_3S_4 and $NiCo_2S_4$ were prepared from Co_9S_8 or Co_8NiS_8, which were available in sufficient quantities from previous neutron-diffraction work (1), by adjusting the compositions with requisite amounts of sulfur and nickel and reacting the mixtures in evacuated silica ampuls. The reacted sulfides were ground to pass 100 mesh, mixed thoroughly by repeated screening, and resealed for homogenization (cf. ref. 1). This procedure was repeated when necessary. The resulting moderately sintered compacts were crushed to pass 100 mesh, except for the small amounts that were used for X-ray diffraction. These were ground carefully to pass 325 mesh.

X-Ray and Neutron Diffraction

X-Ray powder photography and measurement of integrated X-ray diffractometer intensities were carried out in a manner described elsewhere (18). Smear mounts were prepared by mixing the powders with silicone grease to a thick paste, pressing the paste into a shallow counterbore (0.4–0.6 mm deep) in a lucite slug, facing the paste with dry powder, and smoothing the resulting surface by gentle pressing against a microscope slide. Comparison with a pressed disk of $NiCo_2O_4$ showed that there was no gain in intensity on pressing, and smear mounts were used throughout. There was no evidence of preferred orientation. The wavelengths used were $FeK\alpha_1$, 1.93597 Å; $FeK\bar{\alpha}$, 1.93728 Å; $CoK\alpha_1$, 1.78892 Å; and $CoK\bar{\alpha}$, 1.79021 Å.

The neutron-diffraction experiments were performed at the NRX reactor of Atomic Energy of Canada Limited at Chalk River, Ont. As the investigation extended over 4 years, the diffraction patterns were obtained under a variety of conditions, not always strictly comparable. The neutron beam was monochromatized by Bragg reflection through 40° from the (111) plane of either an Al (λ = 1.60 Å) or a Ge crystal (λ = 2.234 Å). A single-crystal quartz filter 6 in. thick reduced the second-order (Al) and third-order (Ge) contents of the incident beam to less than 2%. A double-wall aluminium cryostat permitted measurements to be made at liquid-nitrogen and higher temperatures. Absorption corrections were determined from transmission measurements. In the more recent runs (Fig. 4) higher angular collimation was used. Other details are given in refs. 18 and 19.

The raw neutron-diffraction patterns were reduced to pF^2 patterns (19, 28). Overlapping peaks were resolved and Gaussian profiles fitted to all the peaks by a least-squares program written for the IBM 1620 (40K).

Least-Squares Refinement

The origin of the unit cell of the spinel structure (space group *Fd3m*) was taken at the center of symmetry. For a normal AB_2X_4 spinel there are 8 A atoms in 8(*a*): $\pm$(1/8, 1/8, 1/8) etc.; 16 B in 16(*d*); and 32 X in 32(*e*): $\pm(xxx)$ etc., with x in the vicinity of $\frac{1}{4}$.

An ad hoc full-matrix program written for IBM 360/50 and weighting scheme W3 of ref. 21 were used in the refinements. A three-function interpolation scheme (22) was employed to compute the X-ray scattering factors from the equidistant values listed in refs. 23 (self-consistent field) and 24 (O^{2-}) after they had been corrected for dispersion (both parts) (25)[5]. Ionic scattering factors

[4]The lattice parameters of these spinels are given as 8.292, 8.316, 8.258, and 8.280 Å for the four temperatures employed, and that of Co_3O_4 is quoted as 8.180 Å. All these values are higher than any reported by other authors. They will be even higher when the wavelength used by Gocan, $\lambda(CuK\alpha)$ = 1.537 Å, is converted to $\lambda(CuK\bar{\alpha})$ = 1.542 Å

[5]The dispersion correction for oxygen was taken from ref. 23 ($CrK\alpha$).

TABLE I

Lattice parameters of the spinel cobaltites

Compound	a_0, Å	Preparation	Reference
Co_3O_4	8.05*		5
	8.07*	From nitrate; 700 °C	6
	8.124*	From nitrate by gentle heating; one diffuse doublet not indexed	2
	8.126*		7
	8.09		8
	8.070		3
	8.092	From nitrate; 750 °C/5 h in oxygen	4
	8.084 (24 °C)	From fluoride; 850 °C/24 h, $\lambda(CoK\alpha_1) = 1.7889$ Å	9
	8.083†		10
	8.0855 ± 5	From nitrate; calcined at 500 °C, ignited at 900 °C/240 h	11
	8.065	From CoO at 860 °C in oxygen; $\lambda(CoK\alpha) = 1.790$ Å	12
	8.0835 ± 6		This work
Co_3S_4	9.38*		13
	9.401*		14
	9.416	From Co + S; 600 °C/24 h, 500 °C/60 h	4
	9.399 ± 2	From Co + S; 600 °C/24 h, 700 °C/70 h	15
	9.4055 ± 12	550 °C/4 days, 620 °C/3 days, slow cooling in furnace	This work
$NiCo_2O_4$	8.128*	From nitrates (see footnote in text)	2
	8.098		3
	8.121	From nitrates; 300 °C/5 h in oxygen. Pattern not sharp, traces of a second phase (NiO ?)	4
	8.114 ± 14		This work
$NiCo_2S_4$	9.392	From Ni + Co + S; 500 °C/10 h, 1000 °C/4 h, 1000 °C/4 h, (+S) 500 °C/48 h	4
	9.384 ± 2	From Ni + Co + S; 500°/24 h, 1000 °C/4 h, 500 °C/48 h	15
	9.3872 ± 7	500 °C/7 days, cooled to room temperature over 5 days (final heat treatment)	This work

*Adjusted to wavelengths used in this work. In refs. 2 and 7 it is not clear whether the units were Å or kX.
†Co oxalate dihydrate calcined in air at 500–750 °C/5 h. The product gave reproducible results, although gravimetric analysis and determination of the oxidizing power indicated a slight oxygen deficiency of the order of 1% (16).

were normally applied to the oxides and neutral to the sulfides. The neutron scattering amplitudes were taken from ref. 26 (for b(Co), however, see under Co_3O_4).

The same abbreviations are used in this paper as in ref. 21. The X-ray powder intensities of all four compounds have been submitted to the ASTM X-ray powder data file.

Magnetic Measurements

Intensities of magnetization of $NiCo_2O_4$ were measured, in the temperature range 4.2–533 °K, by the Faraday method using a magnetic balance. The balance was similar to that described by Hirone *et al.* (27) except that the deflection was detected by a mirror-photocell instead of a parallel-plate condenser system. At liquid-helium temperature the maximum magnetic field was limited to 8.60 kOe because of the larger pole gap required to accommodate the cryostat. At higher temperatures fields up to 11.70 kOe were used. The temperature of the powder specimen, which weighed about 10 mg, was measured with a calibrated AuCo–Cu thermocouple, ensuring good contact of the thermocouple with the powder. The balance was calibrated by measuring the magnetization of pure nickel powder.

Results and Discussion

Co_3O_4

The lattice parameter of our preparation agreed well with most of the recent determinations (Table I). The possibility that a_0 depends somewhat on the method of preparation cannot be excluded (cf. ref. 3), so that the slight differences, within the range 8.08–8.09 Å, may be real.

A refinement from X-ray data based on the normal distribution, $Co^{2+}[Co_2{}^{3+}]O_4{}^{2-}$, and using individual isotropic temperature factors gave a physically reasonable result, though the temperature factors of both Co atoms were higher than one might expect (Table II). However, the same results were obtained when the refinement was started from widely different sets of initial parameter values or when a linear combination of B(O) and x(O) was introduced as an independent parameter to counteract the B(O)–x(O) correlation, which had the largest correlation coefficient, −0.65.

No significant difference resulted when the structure was refined for an overall temperature factor (Table II) or when the inverse structure, $Co^{3+}[Co^{2+}Co^{3+}]O_4{}^{2-}$, was assumed. The x(O) value, 0.2637 ± 13, compared favorably with

Can. J. Chem. Downloaded from www.nrcresearchpress.com by 210.87.254.40 on 09/05/12
For personal use only.

TABLE II

Results of the least-squares refinements from X-ray data (FeKα)*

After cycle	B(overall), Å^2	B(A), Å^2	B(B), Å^2	B(X), Å^2	x(X)	K	R, %	e.s.d. (w)
			$Co^{2+}[Co_2^{3+}]O_4^{2-}$ (n = 15)					
0		0.20	0.20	0.60	0.2600	1.000	10.47	7.42
10		1.02±13	0.84±10	1.16±29	0.2637±13	1.004±13	2.01	1.17
0	1.00				0.2600	1.000	3.89	1.92
10	1.02±6				0.2642±10	0.995±6	2.37	1.16
			$Co^{3+}[Ni^{2+}Co^{3+}]O_4^{2-}$ (n = 11)					
0		0.20	0.20	0.60	0.2600	1.000	12.69	10.87
10		1.62±63	1.00±61	1.99±127	0.2570±45	0.987±38	5.37	4.40
0	1.20				0.2600	1.000	6.20	4.22
3	1.16±23				0.2593±38	1.002±25	6.25	4.19
			$Co[Co_2]S_4$ (n = 15)					
0		0.45	0.20	0.45	0.2600	1.000	3.19	3.32
10		0.11±18	0.27±27	0.39±27	0.2587±6	0.987±12	1.89	1.76
0	0.45				0.2600	1.000	3.94	3.91
8	0.25±9				0.2594±6	0.991±9	2.31	1.83
			$Ni[Co_2]S_4$ (n = 16)					
0		0.20	0.20	0.60	0.2600	1.000	2.83	2.64
10		0.50±14	0.14±17	0.57±17	0.2589±3	0.990±7	1.55	1.20
0	0.30				0.2600	1.000	2.82	2.26
10	0.33±7				0.2592±3	0.993±7	1.65	1.28

*Only results for the best models are listed here. For other models tried see text. First line, initial parameter values; second line, final parameter values.

that obtained by Roth (12) from CoKα intensities, 0.263[6].

Only 9 single $|F_o|$ could be extracted from the neutron-diffraction pattern of Co_3O_4 (Fig. 3) by Gaussian analysis. Correction for second-order contamination was obtained from 400/2, which is a wholly second-order peak. It amounted to about 0.8% of the first-order reduced intensity. Refinement from these limited data was rendered even less favorable by the uncertainty in the value of b(Co). Shull and Wollan's value, 0.28 (29), had been revised from CoO to 0.25 (30), from Co metal and Co_3O_4 to 0.250 ± 10 (31), and from Co_3O_4 to 0.232 ± 25 (12) (all values in 10^{-12} cm). Both 0.235 (also quoted in ref. 12) and 0.250 were tried in our refinement. An attempt was also made to include b(Co) as a parameter of refinement.

The results of a number of refinements can be summarized as follows. Refining for K and x(O) only, and putting B(overall) = 1.00, b(Co) = 0.250, gave an overall agreement which was better than for b(Co) = 0.235 at a significance level close to 10% (33), but x(O) was the same in both cases, 0.2621 ± 6. The same was true when

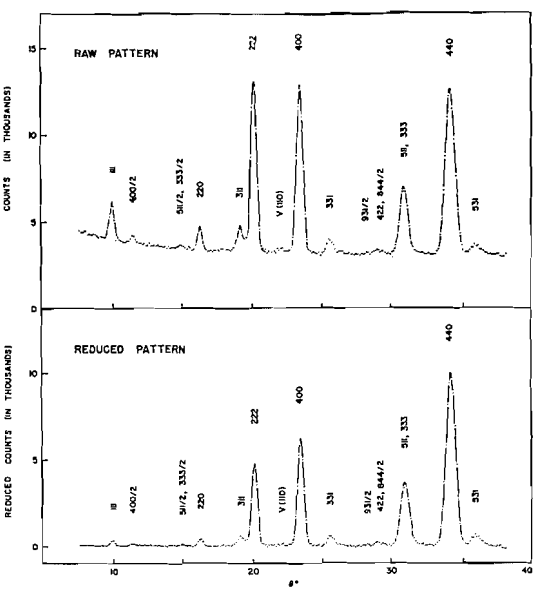

FIG. 3. Raw and reduced neutron-diffraction patterns of Co_3O_4 at room temperature (monochromator, Al(111); λ = 1.60 Å; average counting time per point, 20 min).

[6]There is a misprint in Roth's Table 1: the I_c and I_o of 622 (X-rays) cannot be 105 and 112 respectively. The values should probably be 10.5 and 11.2.

Can. J. Chem. Downloaded from www.nrcresearchpress.com by 210.87.254.40 on 09/05/12
For personal use only.

Can. J. Chem. Downloaded from www.nrcresearchpress.com by 210.87.254.40 on 09/05/12
For personal use only.

refining for K, x(O), and B(overall): $x(O) = 0.2624 \pm 6$, B(overall) $= 0.89 \pm 8$, $R = 1.84\%$, e.s.d.$(w) = 0.062$.

Attempting to refine b(Co) and K using best x(O) and B(overall) from the X-ray data gave $b(Co) = 0.257 \pm 11$, while with best x(O) and B(overall) from the neutron data, and starting from $b(Co) = 0.235$, gave 0.248 ± 5.

Even though the present data are insufficient to establish a reliable value of b(Co), they tend to confirm Moon's value of 0.250 ± 10. The strong parameter correlations in Co_3O_4 render b(Co) values derived from this compound unsatisfactory (ref. 12 and this work); Moon's results obtained with Co metal are not discussed in ref. 31 in sufficient detail to judge their reliability. Thus the value of b(Co) cannot be considered as settled even within the accuracy expected from such determinations.

Our best x(O) from neutron data, 0.2624 ± 6, does not significantly differ from Roth's value, 0.2632 ± 4 (12), and its 2σ range overlaps with that of x(O) from our X-ray data.

$NiCo_2O_4$

The high-angle lines of the $NiCo_2O_4$ powder photograph were not sharp enough for a Nelson–Riley extrapolation. A 3:2 mixture by weight of $NiCo_2O_4$ and NiO ($a_0 = 4.1765 \pm 5$ Å) was therefore used to provide internal calibration. The resulting lattice parameter was within the range of values reported in the literature (Table I).

Refinement of the structure from X-ray data was less satisfactory than for Co_3O_4. The powder pattern yielded only 11 sufficiently well-defined single reflections. Refinements based on the models $Co^{3+}[Ni^{2+}Co^{3+}]O_4^{2-}$ ($s = 0$), $Co^{2+}[Ni^{3+}Co^{3+}]O_4^{2-}$, and $Ni^{2+}[Co_2^{3+}]O_4^{2-}$ ($s = 1$), with individual isotropic temperature factors as well as with an overall temperature factor, gave results that did not significantly differ among themselves[7]. An exception was the refinement for $s = 1$ and B(overall). This was found rejectable, on Hamilton's $\mathcal{R}$ criterion (33), at the 5% significance level when compared with the refinement for $s = 0$ and B(overall).

[7]The inversion parameter s is defined by $f(M_{tetrahedral}) = sf(Ni) + (1 - s)f(Co)$ and $2f(M_{octahedral}) = (1 - s)f(Ni) + (1 + s)f(Co)$, and similarly for neutron diffraction. That is, $s = 1$ corresponds to the normal; $s = 0$, to the inverse; and $s = 1/3$, to the random (i.e. $8(a) + 16(d)$) distribution. For Co_3O_4, read Co^{2+} for Ni and Co^{3+} for Co.

The unexpectedly close similarity of the exploratory neutron-diffraction patterns of the oxide obtained at room and liquid-nitrogen temperatures and at 120 °C made it evident that the magnetic contribution to the total diffracted intensity was rather small and that unless an effort was made to ensure adequate counting statistics, attempts to interpret the magnetic structure would fail. Diffraction patterns were therefore obtained at −162 and 120 °C using counting times of about 25 min per point (Fig. 4). These were judged reasonably satisfactory for Gaussian analysis, by which 10 $|F_o|$ were extracted.

The R factors calculated from the high-temperature $|F_o|$ and a reasonable set of unrefined parameter values were 12% for $s = 0$, 22% for $s = 1/3$, and 51% for $s = 1$. The best refinement of the inverse model (using b(Co) = 0.250) resulted in $x(O) = 0.2594 \pm 30$, B(overall) $= 0.83 \pm 42$, $R = 9.08\%$, e.s.d.$(w) = 0.279$. When B(overall) was fixed to 1.00, the same x(O) and R values were obtained. The values of x(O) and B(overall) agree well with the corresponding values for $s = 0$ from the X-ray data (Table II).

Attempts to refine for K and s only did not give meaningful results.

Co_3S_4

The x(S) for $Co[Co_2]S_4$, 0.2587 ± 6, was very close to Lundqvist and Westgren's trial-and-error value, 0.260 (converted from −0.135 for a different choice of origin) (14). There was no significant difference between the refinement for the neutral model and for $Co^{1+}[Co^{1+}Co^{2+}]S_4^{1-}$ regardless of whether individual isotropic temperature factors or B(overall) were used, except that B(Co) of both Co atoms were positive indefinite.

To test the effect of the dispersion corrections the structure was also refined employing uncorrected neutral and singly ionic scattering factors. The results could be rejected at the 0.5% significance level when compared with those of the preceding paragraph. Thus the assumed degree of ionicity appears to affect the refinement much less than omission of the dispersion corrections.

$NiCo_2S_4$

Three models were used in the refinement from X-ray data: $Ni[Co_2]S_4$ ($s = 1$), $Co[NiCo]S_4$ ($s = 0$), and $(NiCo_2)S_4$ ($s = 1/3$). Since the ionicity did not appear to produce a significant difference in the refinement of Co_3S_4, only neutral atoms were used for $NiCo_2S_4$.

Can. J. Chem. Downloaded from www.nrcresearchpress.com by 210.87.254.40 on 09/05/12
For personal use only.

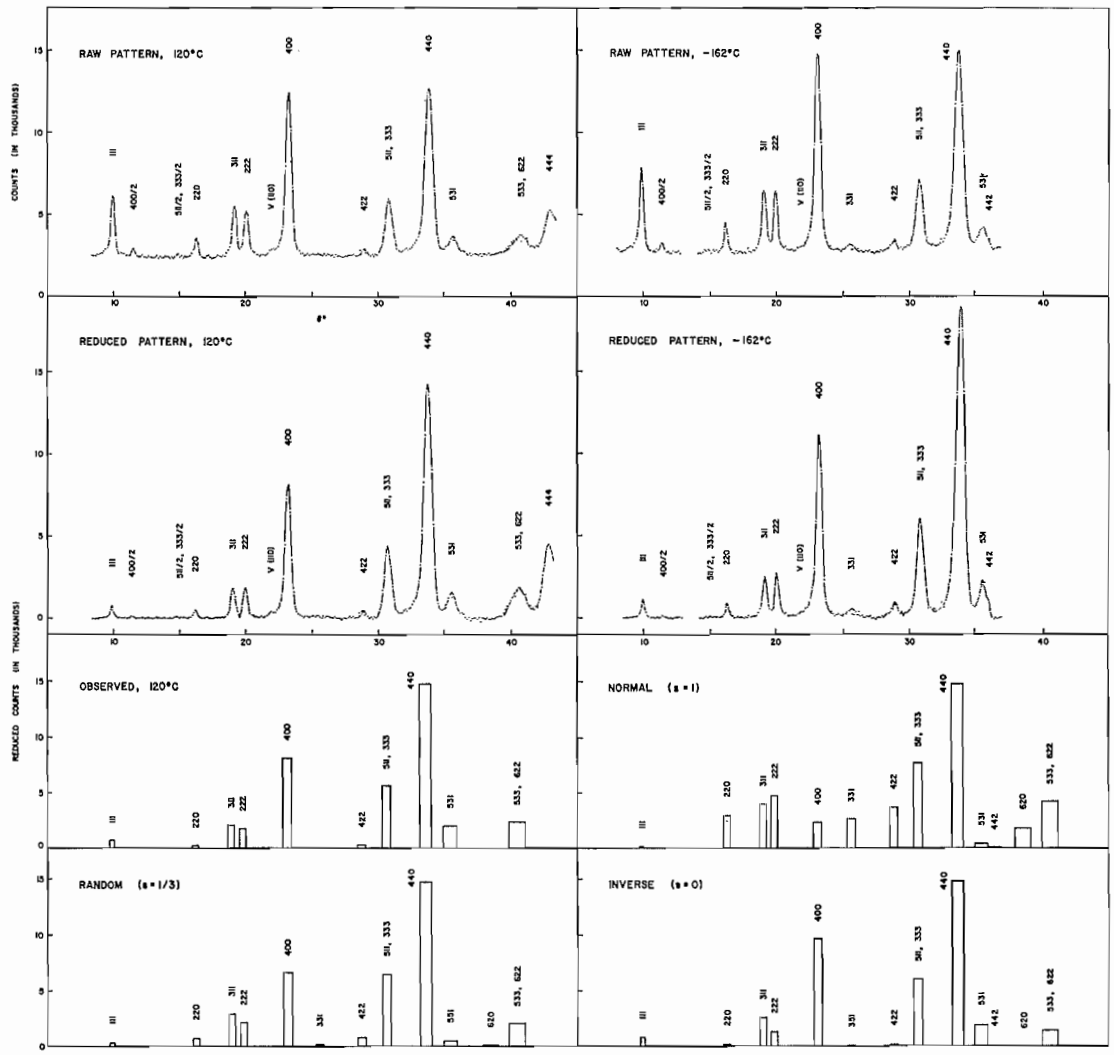

FIG. 4. Neutron-diffraction patterns of $NiCo_2O_4$ at 120 and −162 °C (monochromator, Al(111); $\lambda = 1.60$ Å; average counting time per point, 25 min). The two patterns have been matched in θ by correcting for thermal expansion. The histograms represent pF_o^2 (second-order contribution removed) and pF_c^2 patterns, the latter for three different cation distributions.

Assuming $s = 1$ to be the best model, the random structure ($s = 1/3$) could be rejected, on the $\mathcal{R}$ criterion, at a significance level between 10 and 25% and the inverse structure ($s = 0$), at the 5% level. The corresponding figures for the B(overall) refinements were 2.5% and <2.5%. There was no significant difference between the B(individual) and B(overall) refinements for $s = 1$.

In refining the structure from neutron data (12 $|F_o|$; Fig. 5) both 0.235 and 0.250 were used for b(Co), and beside the usually quoted b(S) of 0.31 (26) the value proposed by Menyuk *et al.* (32), 0.28 ± 1, was also tried (all values in 10^{-12} cm). R computed from a reasonable set of initial parameter values was between 12 and 15% for $s = 1$, while for $s = 1/3$ and 0 it amounted to 40% or more and could not be reduced by refining below 24%. Different combinations of b(Co) and b(S) values and B(overall) = 0.4 did not lead to x,K-refinements significantly different at the 25% level, although the lowest R and e.s.d.(w) values, 10.04% and 0.279 respectively, were obtained with b(Co) = 0.25 and b(S) = 0.31; the resulting x(S) was 0.2548 ± 44. A three-parameter refine-

Can. J. Chem. Downloaded from www.nrcresearchpress.com by 210.87.254.40 on 09/05/12
For personal use only.

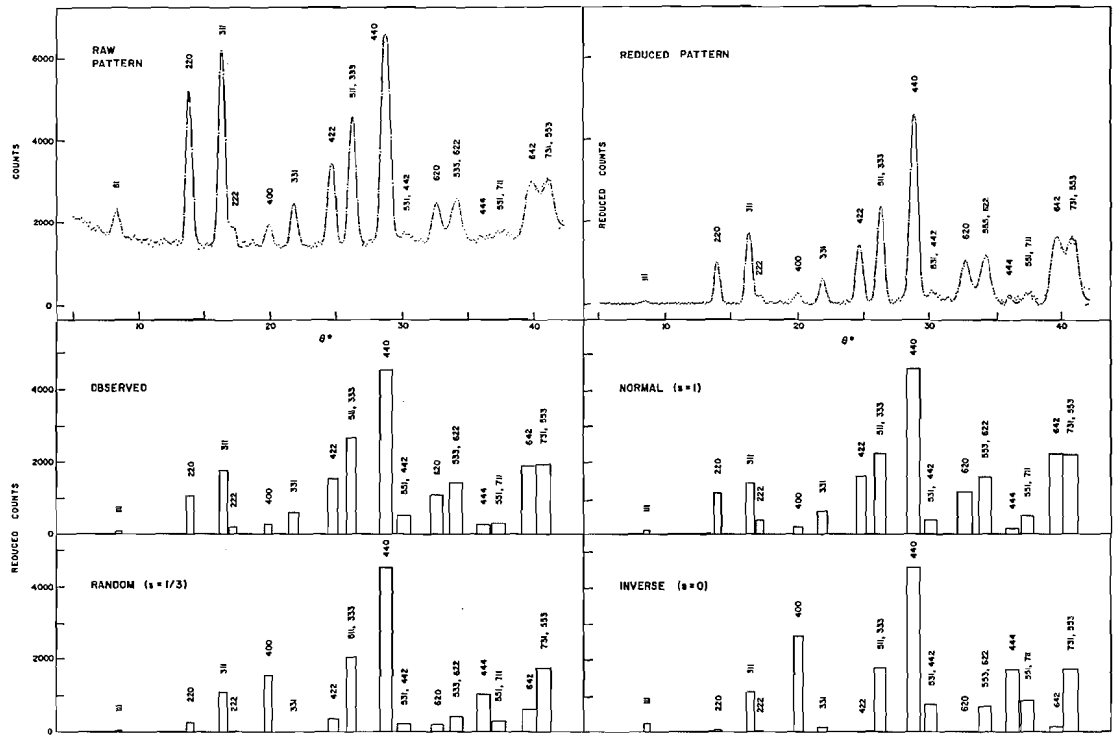

FIG. 5. Neutron-diffraction pattern of $NiCo_2S_4$ at room temperature (monochromator, Al(111); $\lambda = 1.60$ Å; average counting time per point, 7 min). The second-order contribution has been removed from the pF_o^2 histogram.

ment gave $x(S) = 0.2561 \pm 47$, $B(\text{overall}) = -0.39 \pm 55$, $R = 10.69\%$, and e.s.d.$(w) = 0.288$.

Attempts to refine the normal structure for K and s were inconclusive. If anything they seemed to indicate that s might be somewhat smaller than unity. Further treatment did not appear justified because of the uncertainties in the neutron-diffraction patterns, the smaller number of usable reflections, and the relatively low scattering amplitude of S.

Magnetic Measurements

Magnetization curves of $NiCo_2O_4$ were measured with decreasing magnetic field at different temperatures (Fig. 6A). Hysteresis was found at low fields, i.e. the magnetizations measured with increasing fields were somewhat smaller. The temperature dependence of magnetization at 11.70 and 7.88 kOe is shown in Fig. 6B. The values of magnetization were lower than those obtained by Lotgering (4).

The magnetization was not completely saturated even in a field of 11.70 kOe, and the magnetization vs. T curve was of unusual shape. Since both Lotgering's and our preparations were contaminated with small amounts of foreign phases of uncertain identity[8], it is rather difficult to estimate the "true" saturation magnetization and the Curie point. When the magnetization vs. T curve at 7.88 kOe is extrapolated to 0 °K, the magnetization reaches 29.0 e.m.u./g, which corresponds to $1.25\mu_B$ per $NiCo_2O_4$ formula unit. Blasse (34) obtained, from Lotgering's data, the value of $1.5\mu_B$ and also estimated, by extrapolating a linear portion of the magnetization vs. T curve to zero magnetization, the Curie point as 350 °K. This value seems, however, incorrect because the magnetizations at 460 °K are not yet proportional to magnetic fields (Fig.

[8]Lotgering suggests that the foreign phase in his specimen may have been NiO. If so, Co_3O_4 would also have been present, and possibly CoO as well; the lower oxide may in fact have been a solid solution (Ni,Co)O. Quite apart from the presence of foreign phases the magnetic properties of $NiCo_2O_4$ itself may depend on its exact stoichiometry and on the details of preparation. Lotgering's report that the $1/\chi$ vs. T curve was reversible up to 800 °C further complicates the situation.

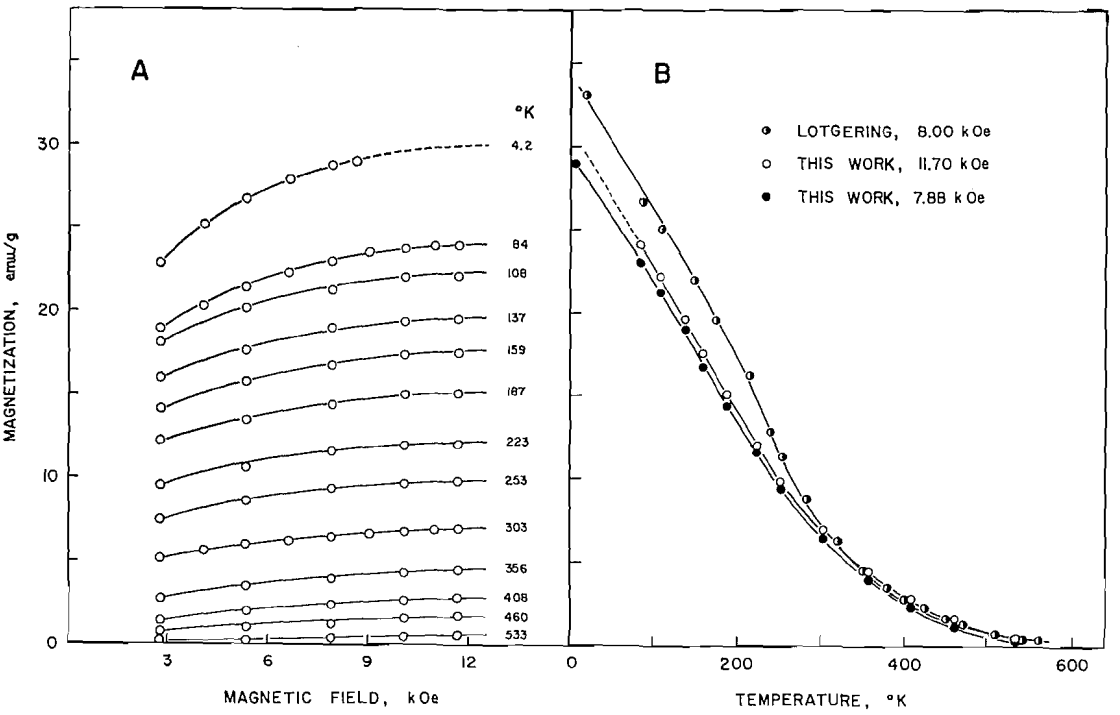

FIG. 6. (A) Field dependence of the magnetization of $NiCo_2O_4$ at different temperatures (measured with decreasing magnetic field). (B) Temperature dependence of the magnetization of $NiCo_2O_4$ at 7.88 and 11.70 kOe. Lotgering's data are reproduced from Fig. 4 of ref. 4.

6A). The true Curie point would be expected to lie in the vicinity of 500 °K.

There is little doubt that $NiCo_2O_4$ is not simply ferromagnetic but ferrimagnetic. The anomalous magnetization vs. T curve suggests the occurrence of Néel's R-type of ferrimagnetism (35), in which one of the two sublattice magnetizations is not completely aligned[9].

Magnetic Contribution to the Neutron-Diffraction Pattern of $NiCo_2O_4$

Compared with the corresponding $NiCo_2O_4$ pattern at 120 °C the reduced (pF_o^2) pattern at −162 °C showed the expected overall increase in intensity, and the 331 and 422 maxima were sharper, but no separate magnetic peaks were observed (Fig. 4). The magnetic unit cell at −162 °C thus appears to coincide with the chemical unit cell.

To determine the magnetic contribution to the total diffraction intensity at −162 °C, the integrated reduced intensities at the two temperatures of 5 reflections at low Bragg angles were evaluated by Gaussian analysis and the second-order contributions were removed. The values of the ratio $r = F_o^2(111\ °K)/F_o^2(393\ °K)$ are shown in Table IV.

Since the two patterns were not obtained under the same conditions, the two sets of pF_o^2 were normalized to 440, in which the magnetic contribution to the observed intensity should be negligibly small: $r_0 = (r/t)(t_{440}/r_{440}) = F_o^{*2}(\text{total})/F_o^{*2}(\text{nuclear})$, where F^* are temperature-independent structure factors and $t = \exp[-(B_{111} - B_{393})\sin^2\theta/\lambda^2]$. The temperature factors were estimated by assuming the oxide to behave like an isotropic Debye solid with a characteristic temperature Θ of 400 °K. This value would correspond to a B_{293} of approximately 0.6 Å^2; t

[9]Strictly speaking Néel's theory of R-type ferrimagnetism is incomplete. Either the triangular spin configuration proposed by Yafet and Kittel (36) or the ferrimagnetic spiral configuration similar to that of $MnCr_2O_4$ (37) may be realized in the present case. The results of neutron-diffraction experiments, however, are insufficient to establish these nonlinear spin arrangements. Néel's R-type arrangement may be regarded as the first approximation of such arrangements.

Can. J. Chem. Downloaded from www.nrcresearchpress.com by 210.87.254.40 on 09/05/12
For personal use only.

TABLE III

Observed and calculated structure factors (X-ray and neutron data)

	$Co^{2+}[Co_2^{3+}]O_4^{2-}$		$Co^{3+}[Ni^{2+}Co^{3+}]O_4^{2-}$		$Co[Co_2]S_4$		$Ni[Co_2]S_4$	
hkl	$10\|F_o\|$	$10\ F_c$	$10\|F_o\|$	$10\ F_c$	$10\|F_o\|$	$10\ F_c$	$10\|F_o\|$	$10\ F_c$
				X-Rays (individual temperature factors)				
111	793	799	754	761	918	939	856	879
220	1599	−1631	1420	−1516	1746	−1740	1879	−1831
311	2426	−2415	2388	−2470	2600	−2640	2669	−2703
222	1186	1136	1371	1252	433	−566	505	−524
400	2739	2793	3023	2956	4983	4935	4865	4839
331	—	−84	—	−318	—	37	—	81
422	1105	1133	1026	1089	1296	1340	1420	1403
440	4044	3992	4171	3972	6563	6523	6508	6544
531	397	−357	403	−440	597	−566	479	−547
442	—	103	—	25	—	132	—	135
620	818	836	*	813	1074	1077	1101	1114
533	1537	−1496	†	−1460	1781	−1874	1902	−1916
622	1068	1103	†	1145	—	−262	—	−164
444	1489	1475	1472	1581	3402	3455	3510	3390
551‡	559	550	*	468	1012	1022	990	1014
642	782	−781	616	−659	1060	−1110	1129	−1132
800	2427	2489	2224	2419	5076	4998	4999	4969
733					*	−550	*	−521
644					—	106	—	106
662					—	−318	—	−183
840					2758	2776	2671	2728
911§							883	855
				Neutrons (K, x, B(overall))				
111	29	27	47	53			27	−33
220	22	−24	23	−21			86	−84
311	24	−26	51	−56			82	−77
222	133	−133	86	−77			47	−59
400	185	186	239	249			64	57
331	24	26					50	49
422	12	15	18	15			81	84
440	205	204	273	266			220	227
531	23	−23	55	−48			37	34
620							108	84
533			75	−53				
622			50	−61				
444							68	56
642							72	−90

*Observed but not counted.
†533 and 622 could not be resolved.
‡Actually 551 + 711, but I_o(711) negligible.
§Actually 911 + 753, but I_o(753) negligible.

is relatively insensitive to variations in Θ. The experimental value of F_o*(magnetic) can then be obtained from $q^{-2}(r_0 - 1)\ F_o{}^{*2}$(nuclear), where $q^2 = 2/3$. Instead of $F_o{}^{*2}$(nuclear) the corresponding calculated values were employed (Table IV).

The magnetic scattering amplitudes used in the calculation of the theoretical values of F*(magnetic) were $p_A = 0.269\ f_A\ M_A$ for the cations in the 8(a) sites and $p_B = 0.269 f_B\ M_B$ for the cations in the 16(d) sites. The magnetic form factors, f_A and f_B, were tentatively chosen to be the mean values of $f(Ni^{2+})$ and $f(Co^{2+})$ given by Scatturin *et al.* (38), so that $f_A = f_B = f$. Little difference resulted when Watson and Freeman's theoretical ($\langle j_0 \rangle$ only) form factors (39) were employed.

The saturation magnetization at 111 °K was found from the magnetic-balance measurements to be approximately 0.9 μ_B per formula unit (Fig. 6). The effective magnetic moments must thus satisfy the relation $M_A + 2M_B = 0.9\ \mu_B$. In order to obtain reasonable results they must be assumed to have opposite signs ($M_A > 0$, $M_B < 0$), i.e. $NiCo_2O_4$ is ferrimagnetic.

The theoretical values of F^{*2}(magnetic) for three combinations of M_A and M_B values are

Can. J. Chem. Downloaded from www.nrcresearchpress.com by 210.87.254.40 on 09/05/12
For personal use only.

TABLE IV

Comparison of theoretical and experimental magnetic structure factors for $NiCo_2O_4$ at 111 °K*

					F^{*2}(magnetic)/16			
						Theoretical		
hkl	*f*	*r*	r_0	F_c^{*2}(nuclear)/16	Exptl.	$M_A = 1.5$ $M_B = -0.3$	1.7 −0.4	1.9 −0.5
111	0.91	1.51±0.02	1.22	1.86	0.61±0.06	0.44	0.61	0.81
220	0.80	3.66±1.30	2.90	0.29	0.83±0.57	0.42	0.53	0.67
311	0.74	1.40±0.01	1.10	2.10	0.30±0.03	0.09	0.10	0.11
222	0.73	1.36±0.01	1.06	3.92	0.35±0.06	0.06	0.10	0.15
400	0.68	1.34±0.01	1.03	42.6	1.91±0.64	0.59	0.83	1.12
440	0.52	1.36±0.01	1.00	53.7	0.0 ±0.8	0.06	0.06	0.06

*The uncertainty limits of *r* are based on the assumption that the estimate of the second-order contamination of the diffracted beam was in error by 12%.

shown in Table IV. The uncertainty limits of the corresponding experimental values were estimated from an assumed error of 12% in the estimate of the second-order contamination, but there are other sources of uncertainty. The magnetic form factor is approximate; *x*(O) may vary with temperature; the exact degree of inversion is not known; and as the discrepancy in Lotgering's and our magnetization curves shows, the value of the saturation magnetization at 111 °K must be viewed with caution. The poor crystallinity of the oxide and the presence of small amounts of impurity phases in both investigations must have affected all the measurements to a varying degree.

Taking all these factors into account, the agreement of the F^{*2}(magnetic) at 111 °K (Table IV) is not unreasonable. The best values of M_A and M_B would appear to be 1.9 ± 0.2 and -0.5 ± 0.1 bohr magnetons. They would be larger at lower temperatures.

Blasse (34) suggested that the ionic structure of $NiCo_2O_4$ might be $Co^{2+}[Ni^{3+}Co^{3+}]O_4$, with Co^{2+} in a high-spin state ($M_A = 3\ \mu_B$) and Ni^{3+} and Co^{3+} both in low-spin states ($M_B = 0.5\ \mu_B$). Assuming the spin moments at 0 °K to be antiparallel and completely collinear, the net magnetization would be 2 μ_B. The values found by experiment, however, were only 1.5 μ_B (4, 34) and 1.25 μ_B (this work) respectively. Even if the estimates of the saturation magnetization at 0 °K are in error by as much as 20%, the alignment of the spin moments cannot be complete.

Another possible structure is $Co^{3+}[Ni^{2+}Co^{3+}]O_4$, with the Co^{3+} ions in 8(*a*) and 16(*d*) in high (4 μ_B) and low (0 μ_B) spin states respectively. The Ni^{2+} ion has a moment of 2 μ_B regardless of the strength of the crystal field. The net magnetization would be the same as that of the arrangement proposed by Blasse.

The results of the neutron-diffraction study are not inconsistent with either model. The numerous unfavorable factors inherent in an investigation of $NiCo_2O_4$ preclude other models of the magnetic structure to be meaningfully tested. But the applicability of such models (e.g. Yafet–Kittel triangular arrangement or screw-type ferrimagnetism) might be investigated on an improved set of experimental data. It should be possible to increase the crystallinity of the oxide by high-pressure annealing in oxygen above 300 °C. The magnetic contribution could be increased and evaluated with more certainty from neutron-diffraction experiments at 4.2 and 500 °K on reducing the second-order component of the beam to a negligible value, and it could be separated, at liquid-helium temperatures, from the nuclear contribution by applying an external magnetic field.

Interatomic Distances

The apparent M—O and M—S distances in the cobaltites are compared with similar distances in simple oxides and sulfides of Co and Ni in Table V. The effective size of the 3*d* atom (or ion) depends not only on its oxygen or sulfur coordination but, as would be expected, also on its spin configuration (cf. ref. 48). The distances cannot be meaningfully compared unless the spin states are known with certainty and the respective spin sublattices are clearly defined. Unfortunately the compounds for which this information is available and which are otherwise

Can. J. Chem. Downloaded from www.nrcresearchpress.com by 210.87.254.40 on 09/05/12
For personal use only.

TABLE V

Interatomic distances, in Å, in the cobaltites and other compounds*

Distance	Tetrahedral coordination	Octahedral coordination
Co^{2+}—O	$Co^{2+}[Co_2^{3+}]O_4$ (h.s.): 1.946 ± 34 (this work)	CoO (*B*1, h.s.): 2.1290 ± 5 (40) 2.1301 ± 5 (41)
Co^{3+}—O		$Co^{2+}[Co_2^{3+}]O_4$ (l.s.): 1.915 ± 18 (this work)
Ni^{2+}—O		NiO (*B*1, h.s.): 2.0973 ± 5 (275 °C) (42) 2.0894(± 6) (300 °K) (43)
Co—S	$Co[Co_2]S_4$: 2.184 ± 23 (this work)	$Co[Co_2]S_4$(l.s.? Cf. refs. 15 and 49): 2.268 ± 13 (this work $Ni[Co_2]S_4$: 2.265 ± 7 (this work)
	Co_9S_8 (1 S+3 S): 2.13 ± 5; 2.21 ± 2 (44) 2.119; 2.212 (45)	Co_9S_8: 2.39 ± 3 (44) 2.392 (45)
		CoS_2 (*C*2, l.s. ? Cf. ref. 51): 2.317(± 7) (46)
Ni—S	$Ni[Co_2]S_4$: 2.179 ± 12 (this work) Ni_3S_2: 2.28 (kX ?) (47)	NiS_2 (*C*2): 2.396(± 15) (46)

*h.s., high spin; l.s., low spin. Values quoted as "this work" have not been corrected for thermal motion. They are based on weighted averages of x(X) from X-ray refinements for B(individual) and B(overall) and their uncertainty limits refer to $3\sigma(x)$ and $2\sigma(a_0)$.

suitable for comparisons are few, but some observations can still be made (Table V):

(1) The Co^{2+}—O distance (Co^{2+} in a high-spin state, $d_\varepsilon^5 d_\gamma^2$) for octahedral coordination (in CoO) is about 0.185 ± 55 Å, i.e. ca. 9%, greater than for tetrahedral coordination (in Co_3O_4).

(2) The difference in the lattice parameters of Co_3S_4 and $Ni[Co_2]S_4$ is only 0.019 ± 4 Å, and the x(S) values are identical. The M—S distances in the two spinels thus cannot be significantly different, and the spin states of the Co(VI) atom will be the same.

(3) Co_3O_4 at room temperature is known to have the ionic arrangement (h.s., high spin; l.s., low spin) $Co_{h.s.}^{2+}[Co_{l.s.}^{3+}]_2O_4$ (12). If the distribution $Co_{h.s.}^{2+}[Ni_{l.s.}^{3+}Co_{l.s.}^{3+}]O_4$ proposed by Blasse is correct, the M(IV)—O distances in Co_3O_4 and $NiCo_2O_4$ should be closely similar, but the M(VI)—O distance in $NiCo_2O_4$ should be greater than the corresponding distance in Co_3O_4, the low-spin Ni^{3+} ion being larger than low-spin Co^{3+} (48). If on the other hand the distribution is $Co_{h.s.}^{3+}[Ni_{h.s.}^{2+}Co_{l.s.}^{3+}]O_4$, the M(IV)—O distance in $NiCo_2O_4$ should be shorter than the corresponding distance in Co_3O_4, and the M(VI)—O distance in $NiCo_2O_4$ should be longer than in Co_3O_4, $Ni_{h.s.}^{2+}$ being larger than $Co_{l.s.}^{3+}$. The observed distances in $NiCo_2O_4$ were 1.874 ± 127 Å for M(IV)—O and 1.963 ± 81 Å for M(VI)—O, but because of the large uncertainty limits neither value can be invoked in support of a particular distribution.

(4) The Co(IV)—S distance in Co_3S_4, 2.184 Å, is the same as the average of the four Co(IV)—S distances in Co_9S_8, while the Co(VI)—S distance in the spinel, 2.268 Å, is more than 5% shorter than the corresponding distance in Co_9S_8, but only about 2% shorter than the Co(VI)—S distance in the pyrite-type CoS_2.

Conclusions

The combined results of the X-ray and neutron-diffraction investigation of the two ternary spinels show that $NiCo_2O_4$ is inverse, while $NiCo_2S_4$ is normal. It was surprising to see that refinements of $NiCo_2S_4$ from the rather limited volume of data provided by X-ray powder diffractometry were capable of distinguishing between models based on normal and inverse distributions.

The best values of the positional parameters of the oxygen or sulfur atoms obtained from the present X-ray data were: Co_3O_4, 0.2640 ± 8; $NiCo_2O_4$, 0.2583 ± 34; Co_3S_4, 0.2591 ± 5; $NiCo_2S_4$, 0.2591 ± 3 (weighted averages from B(individual) and B(overall) refinements).

The volume of diffraction data was too small for a reliable determination of the degree of inversion in $NiCo_2O_4$ and $NiCo_2S_4$. When $NiCo_2O_4$ and $NiCo_2S_4$ were refined for assumed values of the inversion parameter s, the x(O) and B(X) tended to vary with s but they moved in the opposite directions. The importance of this behavior is obscured by the large e.s.d.'s of the final parameter values of $NiCo_2O_4$, but in future refinements from more accurate intensity data the interdependence of the positional and thermal parameters and the degree of inversion will have to be recognized. A related problem has been

Can. J. Chem. Downloaded from www.nrcresearchpress.com by 210.87.254.40 on 09/05/12
For personal use only.

considered by Anishchenko *et al.* (50), who investigated the effect of the shape of the *f*-curves (as dependent on the effective crystal radii) on the determination of x(O) and the degree of inversion in $MgFe_2O_4$. They have pointed out that in order to determine these two quantities the experimental intensities must be accurate to 0.1%, and the location of all the ions must be known (i.e. occupancy of sites other than the classical spinel equipoints 8(*a*) and 16(*d*) must be investigated).

The segregation of the Ni atoms in the tetrahedral sites of the $NiCo_2S_4$ structure contrasts with the indifference of the Ni and Co atoms in the cubic π phase Co_8NiS_8 to a particular type of coordination. It may be just as much the result of a strong preference of Ni in the sulfospinel for tetrahedral coordination as a manifestation of a tendency of Co to occupy octahedral sites.

As regards the choice between the alternative cation distributions in $NiCo_2O_4$ that have been considered in this work, the present evidence is inconclusive. The results of magnetization measurements and the magnetic contribution to Bragg scattering at 111 °K are compatible with both models. Additional work is needed to clarify this point.

Acknowledgments

We wish to express our gratitude to the staff of the Neutron Physics Branch, Atomic Energy of Canada Limited, for placing at our disposal their neutron diffraction facilities; to Dr. F. Brisse, Mrs. E. J. Payne, and Mr. H. Nieman for assistance with the experimental work; to Mr. H. Suzuki, Institute for Solid State Physics, Tokyo, for the measurements at liquid-helium temperatures; and to Dr. N. F. H. Bright and Mr. R. H. Lake, Mineral Sciences Division, Mines Branch, Department of Energy, Mines and Resources, Ottawa, Canada, for obtaining the d.t.a. curves of the oxides.

This investigation was supported by grants in aid of research from the National Research Council of Canada and the Geological Survey of Canada to the first-named author.

1. O. KNOP and M. A. IBRAHIM. Can. J. Chem. **39**, 297 (1961).
2. S. HOLGERSSON and A. KARLSSON. Z. Anorg. Allgem. Chem. **183**, 384 (1929).
3. J. ROBIN and C. BÉNARD. Compt. Rend. **232**, 1830 (1951); **234**, 734, 956 (1952).
4. F. K. LOTGERING. Philips Res. Rept. **11**, 190, 337 (1956).
5. S. B. HENDRICKS and W. H. ALBRECHT. Ber. **61B**, 2153 (1928).
6. G. NATTA and M. STRADA. Gazz. Chim. Ital. **58**, 419 (1928).
7. S. HOLGERSSON. Lunds Univ. Arsskr. Avd. 2. **23**, 9 (1929); Kgl. Fysiograf. Sallskap. Lund Handl. **38**, 1 (1929).
8. O. KRAUSE and W. THIEL. Ber. Deut. Keram. Ges. **15**, 101 (1934).
9. H. E. SWANSON, M. I. COOK, T. ISAACS, and E. H. EVANS. Natl. Bur. Std. U.S. Circ. No. 539, **9**, 29 (1960).
10. P. COSSEE. Ph.D. Thesis, Leiden. 1956 (quoted from ref. 17).
11. R. J. MAKKONEN. Suomen Kemistilehti, B, **35**, 230 (1962).
12. W. L. ROTH. Phys. Chem. Solids, **25**, 1 (1964).
13. W. F. DE JONG and H. W. V. WILLEMS. Z. Anorg. Allgem. Chem. **161**, 311 (1927).
14. D. LUNDQVIST and A. WESTGREN. Z. Anorg. Allgem. Chem. **239**, 85 (1938).
15. R. J. BOUCHARD, P. A. RUSSO, and A. WOLD. Inorg. Chem. **4**, 685 (1965).
16. P. COSSEE. Private communication.
17. G. BLASSE. Philips Res. Rept. Suppl. **3**, (1964).
18. O. KNOP, F. BRISSE, L. CASTELLIZ, and SUTARNO. Can. J. Chem. **43**, 2812 (1965).
19. F. BRISSE and O. KNOP. Can. J. Chem. **45**, 609 (1967).
20. S. GOCAN. Acad. Rep. Populare Romine, Filiala Iasi, Studii Cercetari Stiint. Fiz. Stiinte Tehn. **14**(2), 393 (1963).
21. SUTARNO, O. KNOP, and K. I. G. REID. Can. J. Chem. **45**, 1391 (1967).
22. F. R. AHMED, E. J. GABE, G. A. MAIR, and M. E. PIPPY. A unified set of crystallographic programs for the IBM 1620 computer. September 1963. Unpublished.
23. International tables for X-ray crystallography. Vol. III. Kynoch Press, Birmingham. 1962.
24. M. TOKONAMI. Acta Cryst. **19**, 486 (1965).
25. D. T. CROMER. Acta Cryst. **18**, 17 (1965).
26. G. E. BACON. Neutron diffraction. 2nd ed. Oxford University Press, Oxford. 1962.
27. T. HIRONE, S. MAEDA, and N. TSUYA. Rev. Sci. Instr. **25**, 516 (1954).
28. F. BRISSE and O. KNOP. Can. J. Chem. **46**, 859 (1968).
29. C. G. SHULL and E. O. WOLLAN. Phys. Rev. **81** 527 (1951).
30. W. L. ROTH. Phys. Rev. **110**, 1333 (1958).
31. R. M. MOON. Phys. Rev. **136**, A195 (1964).
32. N. MENYUK, K. DWIGHT, and A. WOLD. J. Appl. Phys. **36**, 1088 (1965).
33. W. C. HAMILTON. Acta Cryst. **18**, 502 (1965).
34. G. BLASSE. Philips Res. Rept. **18**, 383 (1963).
35. L. NÉEL. Ann. Phys. [12] **3**, 137 (1948).
36. Y. YAFET and C. KITTEL. Phys. Rev. **87**, 290 (1952).
37. L. M. CORLISS and J. M. HASTINGS. Phys. Rev **126**, 556 (1962).
38. V. SCATTURIN, L. M. CORLISS, N. ELLIOTT, and J. M. HASTINGS. Acta Cryst. **14**, 19 (1961).
39. R. E. WATSON and A. J. FREEMAN. Acta Cryst. **14**, 27 (1961).
40. N. C. TOMBS and H. P. ROOKSBY. Nature, **165**, 442 (1950).
41. R. E. CARTER and F. D. RICHARDSON. J. Metals, **7**, 336 (1955).
42. H. P. ROOKSBY. Acta Cryst. **1**, 226 (1948).
43. V. S. KOGAN and T. G. OMAROV. Zh. Eksperim. Teor. Fiz. **47**, 789 (1964).

Can. J. Chem. Downloaded from www.nrcresearchpress.com by 210.87.254.40 on 09/05/12
For personal use only.

44. S. GELLER. Acta Cryst. **15**, 1195 (1962).
45. SUTARNO. Ph.D. Thesis, Nova Scotia Technical College, Halifax, N.S. 1965.
46. N. ELLIOTT. J. Chem. Phys. **33**, 903 (1960).
47. A. WESTGREN. Z. Anorg. Allgem. Chem. **239**, 82 (1938).
48. G. BLASSE. J. Inorg. Nucl. Chem. **27**, 748 (1965).
49. G. BLASSE. Phys. Letters, **19**, 110 (1965).
50. R. I. ANISHCHENKO, E. G. BOGACHEVA, and A. N. MEN'. Dokl. Akad. Nauk SSSR, **171**, 573 (1966).
51. A. F. ANDRESEN, S. FURUSETH, and A. KJEKSHUS. Acta Chem. Scand. **21**, 833 (1967).

Can. J. Chem. Downloaded from www.nrcresearchpress.com by 210.87.254.40 on 09/05/12
For personal use only.

Can. J. Chem. Downloaded from www.nrcresearchpress.com by 210.87.254.5 on 09/05/12
For personal use only.

Velocity of sound isotherms in liquid krypton and xenon

C. C. LIM, D. H. BOWMAN, AND RONALD A. AZIZ
Department of Physics, University of Waterloo, Waterloo, Ontario

Received May 2, 1968

The velocity of sound was measured with a precision of 0.1 % in liquid krypton and xenon at pressures between the vapor pressure and about 65 atm, from near their triple points to near their critical points.

A corresponding states treatment of these measurements and previous results in argon showed that, with a suitable choice of relative molecular parameters (σ,ε), the $W^*(P^*,T^*)$ surfaces were coincident to within the experimental error, except for argon near the critical temperature.

The relative values of the effective atomic radii σ obtained from this analysis were somewhat lower than those obtained from other thermodynamic properties.

Canadian Journal of Chemistry, 46, 3477 (1968)

Introduction

Previous measurements (1, 2) of the velocity of sound under saturated vapor pressure in argon, krypton, and xenon have indicated that the principle of corresponding states is obeyed extremely well in these substances. It is of interest to examine whether such similarities exist with respect to the pressure dependence of sound velocity in the region above the vapor pressure curve.

Experimental Method

The velocity of sound was measured by the resonance technique of Guptill *et al.* (3), employing a cylindrical barium titanate transducer. Measurements were made at frequencies in the range 0.5 to 2.1 MHz. The apparatus and method of measurement have been described elsewhere (1, 2, 4). The velocity of sound was measured at several pressures along each of a series of isotherms for both liquids. The temperature of the liquid was measured by means of a platinum resistance thermometer calibrated by the National Physical Laboratories. The accuracy of temperature measurements was limited to ± 0.005 °K with respect to the International Practical Temperature Scale by the accuracy of the standard resistor used for comparison. During measurements along any one isotherm, the temperature was held constant to ± 0.001 °K.

A Texas Instruments pressure gauge model 141 was used to measure the pressure. The uncertainty in pressure measurements was due to the gauge (accuracy ± 0.04 atm) and the unknown hydrostatic pressure head ($+0.04$ atm maximum).

The velocity of sound was measured to a precision of better than 0.1 % over the entire range of temperature and pressure. Uncertainties in temperature and pressure produced a comparatively small uncertainty in the velocity of sound except along the steeper portions of the isotherms near the critical temperatures.

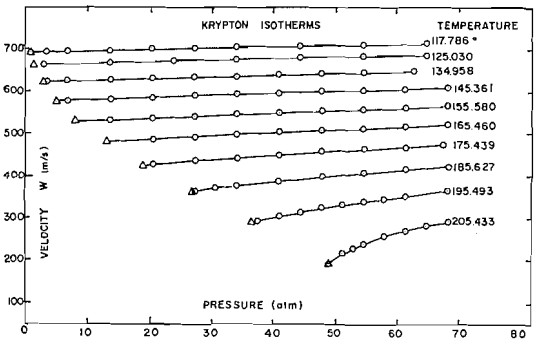

FIG. 1. Liquid krypton velocity of sound isotherms W (m/s) versus P (atm). ⊙, data points; △, values interpolated from W_σ results in ref. (2).

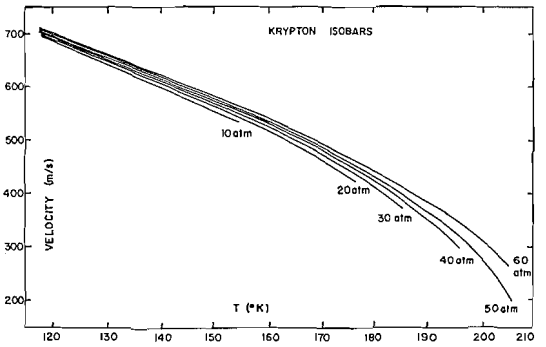

FIG. 2. Liquid krypton velocity of sound isobars W (m/s) versus T (°K).

Results

Ninety-three velocity of sound measurements were made along 11 isotherms in liquid krypton. The results are presented in Table I and plotted in Fig. 1, together with values obtained by interpolation from previous measurements (2) under saturated vapor pressure. The velocity isotherms appear similar in shape to those presented earlier for argon (4), being almost linear at the low temperatures, and steeper and more curved at the

Can. J. Chem. Downloaded from www.nrcresearchpress.com by 210.87.254.5 on 09/05/12
For personal use only.

TABLE I

The velocity of sound in liquid krypton

117.786 °K		118.099 °K		125.030 °K		134.958 °K	
P (atm)	W (m/s)	P (atm)	W (m/s)	P (atm)	W (m/s)	P (atm)	W (m/s)
3.40	693.65	0.875	691.51	2.99	663.57	3.40	622.02
6.80	694.84	3.40	692.36	13.61	667.66	6.80	623.62
13.61	697.18	13.61	695.87	23.82	671.52	13.61	626.70
20.41	699.52	23.82	699.42	34.02	675.38	20.41	629.79
27.22	701.74	34.02	702.96	44.23	679.04	27.22	632.70
34.02	704.00	44.23	706.33	54.44	682.67	34.02	635.75
44.23	707.33	54.44	709.60	64.64	686.26	40.83	638.69
54.44	710.69	64.64	712.90			47.63	641.56
64.64	713.93					54.44	644.40
						62.61	647.80

145.361 °K		155.580 °K		165.460 °K		175.499 °K	
P (atm)	W (m/s)	P (atm)	W (m/s)	P (atm)	W (m/s)	P (atm)	W (m/s)
6.80	576.92	13.61	531.80	20.41	485.47	20.41	425.82
13.61	580.72	20.41	536.49	27.22	491.56	27.22	434.11
20.41	584.46	27.22	541.05	34.02	497.08	34.02	441.90
27.22	588.11	34.02	545.50	40.83	502.54	40.83	449.25
34.02	591.69	40.83	549.82	47.63	507.83	47.63	456.25
40.83	595.22	47.63	554.08	54.44	512.92	54.44	462.89
47.63	598.68	54.44	558.19	61.24	517.86	61.24	469.26
54.44	602.08	61.24	562.24	68.05	522.71	67.27	474.66
61.24	605.39	68.05	566.18				
68.05	608.69						

185.627 °K		195.493 °K		205.433 °K	
P (atm)	W (m/s)	P (atm)	W (m/s)	P (atm)	W (m/s)
27.22	362.89	37.43	294.29	51.03	217.03
30.62	369.31	40.83	305.45	52.74	229.82
34.02	375.35	44.23	315.14	54.44	239.91
40.83	386.51	47.63	323.89	57.84	257.00
47.63	396.68	51.03	331.86	61.24	270.69
54.44	406.07	54.44	339.39	64.64	282.22
61.24	414.79	57.84	346.28	68.05	292.48
68.05	422.95	61.24	352.79		
		68.05	364.69		

higher temperatures. Interpolated values of the velocity of sound at 10, 20, 30, 40, 50, and 60 atm are plotted as functions of temperature in Fig. 2. These velocity isobars are also similar in shape to those for argon.

In xenon, 150 velocity measurements were made along 13 isotherms. The results are presented in Table II and plotted in Fig. 3, together with values obtained by interpolation from previous results (2). The velocity of sound isobars are plotted in Fig. 4. The curves are similar in shape to those for krypton and argon.

Polynomials of degree four or less were sufficient to describe the isotherms. The coefficients of the equations

$$W = A_0 + A_1P + A_2P^2 + A_3P^3 + A_4P^4$$

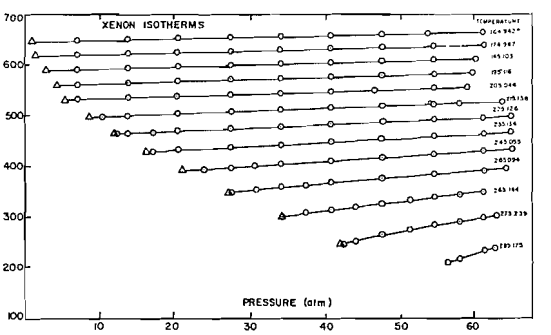

FIG. 3. Liquid xenon velocity of sound isotherms W (m/s) versus P (atm). ⊙, data points; △, values interpolated from W_σ results in ref. (2).

TABLE II

The velocity of sound in liquid xenon

164.942 °K		174.987 °K		185.103 °K		195.116 °K	
P (atm)	W (m/s)	P (atm)	W (m/s)	P (atm)	W (m/s)	P (atm)	W (m/s)
6.80	646.90	6.80	619.18	6.80	590.30	6.80	560.29
20.41	651.01	13.61	621.52	13.61	592.98	13.61	563.39
27.20	653.06	20.41	623.83	20.41	595.60	13.61	563.37
34.02	655.08	27.22	626.10	20.41	595.52	20.41	566.38
40.83	657.06	34.02	628.43	27.22	598.09	27.22	569.30
47.63	659.04	40.83	630.64	34.02	600.63	34.02	572.21
53.64	660.81	47.63	632.88	40.83	603.13	40.83	576.03
61.24	662.97	54.44	635.00	47.63	605.65	47.63	577.83
		61.24	637.14	54.44	608.08	54.44	580.64
				60.22	610.14	59.59	582.68
205.044 °K		215.138 °K		225.126 °K		235.134 °K	
P (atm)	W (m/s)	P (atm)	W (m/s)	P (atm)	W (m/s)	P (atm)	W (m/s)
9.09	530.13	10.21	497.20	11.95	462.84	17.01	427.89
13.61	532.49	13.61	499.26	13.61	463.94	20.41	431.04
20.41	536.02	20.41	503.43	17.01	466.47	27.22	437.05
27.22	539.40	27.22	507.42	20.41	468.92	34.02	442.77
34.02	542.74	34.02	511.33	27.27	473.79	40.83	448.24
40.83	545.97	40.83	515.13	34.02	478.41	47.63	453.55
46.80	548.83	47.63	518.86	40.83	482.92	54.44	458.63
54.44	552.44	54.44	522.50	47.63	487.31	61.24	463.51
58.97	554.42	57.84	524.28	54.44	491.55	64.86	466.05
		63.93	527.42	61.24	495.66		
				65.07	497.94		
245.055 °K		255.094 °K		265.144 °K		275.239 °K	
P (atm)	W (m/s)	P (atm)	W (m/s)	P (atm)	W (m/s)	P (atm)	W (m/s)
23.82	392.22	27.10	347.53	34.02	300.63	42.64	245.97
27.22	396.10	27.22	347.74	37.43	308.46	44.23	252.53
30.62	399.85	30.62	353.09	40.83	315.66	47.63	264.68
34.02	403.51	34.02	358.18	44.23	322.36	51.03	275.11
40.83	410.48	37.43	363.01	47.63	328.51	54.44	284.28
47.63	417.07	40.83	367.68	51.03	334.32	57.84	292.48
54.44	423.31	47.63	376.30	54.44	339.80	61.24	300.00
61.24	429.25	54.44	384.41	57.84	345.03	62.99	303.60
65.18	432.65	61.24	391.86	61.24	349.98		
		64.32	395.12				

285.175 °K	
P (atm)	W (m/s)
56.14	208.01
57.84	217.85
61.24	234.06
62.80	240.31

are given for each isotherm of krypton and xenon in Table III, together with the standard error of estimate in m/s. No equation is given for the highest temperature isotherm of each liquid because of the small pressure ranges obtainable.

Apart from the data under saturated vapor pressure (1, 2), no velocity of sound measurements could be found for krypton or xenon (in the region studied) with which to compare our data. Due to lack of density data in this region, we did not determine any other thermodynamic quantities from the velocity data.

Corresponding States Treatment

For reasons discussed in previous papers (1, 2),

Can. J. Chem. Downloaded from www.nrcresearchpress.com by 210.87.254.5 on 09/05/12
For personal use only.

TABLE III

Coefficients in the equation $W = A_0 + A_1P + A_2P^2 + A_3P^3 + A_4P^4$, and standard error of estimate, σ, for krypton and xenon (W is in m/s and P is in atm)

T (°K)	A_0	A_1	A_2 ($\times 10^{-4}$)	A_3 ($\times 10^{-6}$)	A_4 ($\times 10^{-8}$)	σ
			Krypton			
117.786	692.49596	0.34625273	−2.2792362			0.025
118.099	691.18907	0.34590756	0.83877825	−3.7914524		0.036
125.031	662.45855	0.38608703	−1.7407381	−1.6282384		0.025
134.958	620.42983	0.47115386	−6.8725472	2.2993145		0.011
145.361	573.03088	0.57695546	−8.8405555	1.5412190		0.009
155.580	522.05683	0.73576234	−14.668356	2.7048790		0.006
165.460	465.69110	1.0543945	−44.765677	19.061480		0.049
175.499	397.67503	1.5152133	−71.692578	24.663792		0.008
185.627	297.87769	2.9313247	−224.49534	93.850049		0.028
195.493	−64.788662	20.096566	−4249.5122	4577.0966	−1924.0122	0.041
			Xenon			
164.942	644.80654	0.30933690	−2.7871998	2.0155215	−1.3997409	0.009
174.987	616.86969	0.33946257	1.9746858	−7.0253812	2.4961259	0.019
185.103	587.48012	0.42824569	−23.577601	43.698014	−31.396868	0.021
195.116	557.06393	0.48598381	−19.211239	26.317444	−16.525592	0.011
205.044	524.94667	0.59911247	−39.536961	65.350963	−45.390191	0.524
215.138	490.62420	0.66063479	−19.311767	14.250186	−7.5872549	0.014
225.126	454.04992	0.72656183	9.3538733	−46.936923	31.159031	0.029
235.134	410.36427	1.1426070	−78.263374	79.727063	−41.055140	0.008
245.055	362.75956	1.2942674	−8.5222028	−79.475966	61.811168	0.007
255.094	290.43415	2.7359224	−292.07145	247.74997	−95.740937	0.021
265.144	156.92927	6.8820351	−1072.2958	978.00778	−361.72010	0.017
275.239	−657.20515	54.020938	−12492.175	13694.175	−5767.4570	0.023

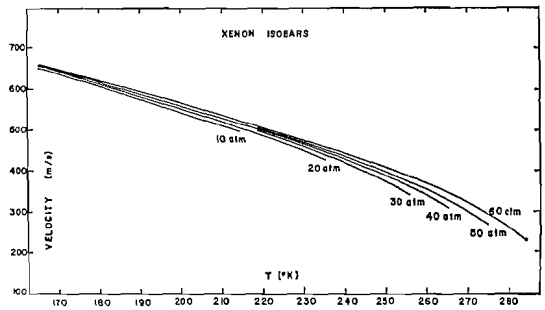

FIG. 4. Liquid xenon velocity of sound isobars W (m/s) versus T (°K).

one would expect the corresponding states principle to be valid to a good approximation in the heavier inert gas liquids: argon, krypton, and xenon. According to the quantum molecular formulation of this principle (5), the reduced velocity of sound W^* is a universal function of the reduced pressure P^*, the reduced temperature T^*, and the de Boer quantum parameter Λ^*. That is,

$$W^* = W^*(P^*,T^*,\Lambda^*)$$

where $W^* = W/(N\varepsilon/M)^{1/2}$; $P^* = P/(\varepsilon/\sigma^3)$; $T^* = T/(\varepsilon/k)$; and $\Lambda^* = h/[\sigma(m\varepsilon)^{1/2}]$. N is Avogadro's number, M is the molecular or atomic mass, k is Boltzmann's constant, h is Planck's constant, and ε and σ are the energy and length parameters in the interatomic potential function which, as a condition for the validity of the corresponding states principle, must be of the form $\Psi = \varepsilon\phi(r/\sigma)$, where ϕ is a universal function.

In a previous analysis, we compared the velocity of sound W_σ under saturated vapor pressure in liquid argon, krypton, and xenon. There, we chose as a reference, the value 119.50 °K for ε/k in argon, as found by Whalley and Schneider (6) from second virial coefficient data, assuming a Lennard–Jones (6–12) interatomic potential. We then obtained coincidence of the $W^*(T^*)$ curves by adjusting ε/k to the values 165.4_9 and 228.7_8 °K for krypton and xenon respectively. These values are close to those obtained from an analysis of vapor pressure data by Boato and Casanova (7).

The data presented here allow us to extend the comparison of the three liquids over a region of the equation of state surface not studied to any great extent. In addition, the introduction of the

Can. J. Chem. Downloaded from www.nrcresearchpress.com by 210.87.254.5 on 09/05/12
For personal use only.

TABLE IV

W^* values for Ar, Kr, and Xe for various T^* at constant P^*

	W^*		
T^*	Ar (ε/k (°K), 119.50; σ (Å), 3.41)	Kr (ε/k (°K), 165.49; σ (Å), 3.61_3)	Xe (ε/k (°K), 228.7_8; σ (Å), 3.94_4)
	At $P^* = 0.071$		
0.7216	5.44_4	5.44_4	5.44_4
0.8117	4.97_8	4.98_0	4.98_2
0.9053	4.45_8	4.45_8	4.46_5
0.9799	4.00_0	4.00_8	4.01_1
1.0632	3.41_1	3.42_7	3.43_2
1.1382	2.72_5	2.76_3	2.76_8
	At $P^* = 0.132$		
0.7216	5.51_8	5.51_8	5.51_8
0.8117	5.07_2	5.07_4	5.07_5
0.9053	4.58_0	4.58_7	4.58_8
0.9799	4.15_8	4.16_5	4.16_9
1.0632	3.64_0	3.65_4	3.65_8
1.1382	3.10_0	3.12_8	3.13_2
1.2270	2.26_0	2.31_7	(2.35_5)

pressure as an independent variable allows us to compare, using the corresponding states principle, the length parameter σ as well as the energy parameter ε.

The procedure involved in comparing the present data can be visualized by considering a surface in a three dimensional rectangular coordinate system whose coordinates are pressure P, temperature T, and the velocity of sound W. The task is then to choose appropriate reduction factors for P, T, and W so that the reduced $W^*(P^*,T^*)$ surfaces for the three liquids are coincident. It is noted here that the above procedure is a first approximation only, since it neglects possible differences due to quantum effects and many-body effects. When the reduction factors are expressed as above in terms of the molecular parameters ε and σ, then a single choice of relative ε values determines the reduction of both T and W, assuming the molecular mass is known. If one assumes the relative ε values given above are valid in this region, then one should need to adjust only the σ ratios in order to obtain coincidence. If coincidence cannot be obtained over the whole surface in this manner, the reason may be an improper choice of effective relative ε values, quantum effects, or actual lack of correspondence among the liquids.

TABLE V

Comparison of condensed state Lennard-Jones (6–12) length parameter ratios

	Kr/Ar	Xe/Ar
Boato and Casanova (7)	1.07	1.16
Horton and Leech (8)	1.07	1.16
Levelt (9)		1.16
Leadbetter and Thomas (10)		1.17
This paper	1.06_0	1.15_7

Using the above ε/k values, we adjusted σ ratios until the portions of the $W^*(P^*,T^*)$ surfaces at low T^* ($T^* = 0.7216$ was chosen because it represented the lowest temperature isotherm in argon) were coincident. The adjusted σ ratios so found were $\sigma(\text{Kr})/\sigma(\text{Ar}) = 1.06_0$ and $\sigma(\text{Xe})/\sigma(\text{Ar}) = 1.15_7$. The coincidence was well within experimental error over the whole pressure range studied at this value of T^*. Our value for $\sigma(\text{Kr})/\sigma(\text{Ar}) = 1.06_0$ compares favorably with those derived by Boato and Casanova (7) and Horton and Leech (8) (see Table V). In the case of $\sigma(\text{Xe})/\sigma(\text{Ar})$, our value of 1.15_7 again agrees quite well with those derived by Boato and Casanova and by Horton and Leech. It also agrees quite well with the value derived by Levelt (9) (see Table V). However, it should be noted that Levelt's value was derived by requiring accurate correspondence of experimental compressibility data at high densities much in the same way as ours was derived by requiring correspondence of the velocity. Leadbetter and Thomas (10) have, on the basis of their density and surface tension data, suggested a slightly higher value for $\sigma(\text{Xe})/$

Can. J. Chem. Downloaded from www.nrcresearchpress.com by 210.87.254.5 on 09/05/12
For personal use only.

Can. J. Chem. Downloaded from www.nrcresearchpress.com by 210.87.254.5 on 09/05/12
For personal use only.

σ(Ar). Choosing as a reference the value of 3.41 Å for σ(Ar) as determined from second virial coefficient data by Whalley and Schneider (6), we therefore obtained σ values of 3.41, 3.61_3, and 3.94_4 Å for argon, krypton, and xenon respectively. Using these values of σ, we determined W^* for the other higher values of T^* at two values of P^* corresponding to the 30 and 60 atm regions. The values are given in Table IV. As T^* increases, the W^* values for the three liquids deviate somewhat from each other. The differences between krypton and xenon are small, being less than 0.2% for all but the highest temperature. The W^* values for argon, however, are lower by as much as 1.4% at $T^* = 1.138$ and 2.5% at $T^* = 1.227$.

The uncertainty in W^* due to experimental error in the velocity data is 0.1%. Interpolation of W along the isotherms and isobars may have resulted in as much as 0.2% error. For the temperatures considered in Table IV, pressure measurement error could account for an uncertainty in W^* of only 0.04%. Error in temperature, due mainly to possible inaccuracy of the International Temperature Scale used (see ref. 11 for a discussion of this) resulted in an uncertainty in W and W^* of 0.06% or less.

Thus uncertainty in W^* could account for the relatively small differences between krypton and xenon in Table IV, but not between these two and argon. The lower W^* values for argon at higher T^* are similar in sign and magnitude to those observed under saturated vapor pressure near the critical point (2). Quantum effects were suggested in ref. 2 as a possible reason for these differences. More recently, it has been suggested that the observed differences may be due in part to three-body forces[1].

The possible error in σ due to uncertainty in the pressure and the W^* values, and to the estimated uncertainty of 0.04 °K in the adjusted ε/k values, is 0.01 Å. Thus, from this analysis, the relative σ values are 3.41, $3.61_3 \pm 0.01$, and $3.94_4 \pm 0.01$ Å for argon, krypton, and xenon respectively. These are smaller than those obtained by Boato and Casanova (7): 3.41, 3.66, and 3.97 Å. The reason for this is not clear at present. No definite statement can be made regarding the direction of adjustment of the σ ratios necessary to take into account quantum differences among the three liquids. It is possible that part of the discrepancy is due to quantum effects which were not considered here but were considered by Boato and Casanova.

Theoretical calculations of W^* as a function of T^* and P^* have been carried out by David and Hamann (12), using the cell model for a classical Lennard–Jones–Devonshire liquid. Their values are much higher than those presented here. They do show, however, a similar decrease of W^* with increasing T^* at constant P^*, and an increase in $(\partial W^*/\partial P^*)_{T^*}$ with T^*.

[1]J. A. Barker. Private communication.

Acknowledgment

The research was supported by a grant from the National Research Council of Canada.

1. C. C. Lim and R. A. Aziz. Can. J. Phys. **45**, 1275 (1967).
2. R. A. Aziz, D. H. Bowman, and C. C. Lim. Can. J. Chem. **45**, 2079 (1967).
3. E. W. Guptill, C. K. Hoyt, and D. K. Robinson. Can. J. Phys. **33**, 397 (1955).
4. D. H. Bowman, C. C. Lim, and R. A. Aziz. Can. J. Chem. **46**, 1175 (1968).
5. J. de Boer. Physica, **14**, 139 (1948).
6. E. Whalley and W. G. Schneider. J. Chem. Phys. **23**, 1644 (1955).
7. G. Boato and G. Casanova. Physica, **27**, 571 (1961).
8. G. K. Horton and J. W. Leech. Proc. Phys. Soc. London, **82**, 816 (1963).
9. J. M. H. Levelt. Physica, **26**, 361 (1960).
10. A. J. Leadbetter and H. E. Thomas. Trans. Faraday Soc. **61**, 10 (1965).
11. C. R. Barber and A. Horsford. Metrologia, **1**, 12 (1965).
12. H. G. David and S. D. Hamann. Australian J. Chem. **14**, 1 (1961).

Can. J. Chem. Downloaded from www.nrcresearchpress.com by 210.87.254.42 on 09/05/12
For personal use only.

Reaction of active nitrogen with perfluorinated olefins[1]

N. MADHAVAN[2] AND W. E. JONES
Department of Chemistry, Dalhousie University, Halifax, Nova Scotia

Received April 26, 1968

The reactions of the fluorocarbon olefins, C_2F_4, C_3F_6, and C_4F_8-2, with active nitrogen were studied in a flow system. The active nitrogen was produced by a microwave discharge at a concentration of 2.1×10^{-6} mole/s. The major gaseous products of the reactions are fluorocarbons and their production was studied quantitatively at the temperatures 25, 250, and 400 °C and at a large number of reactant flow rates to a maximum of approximately 3×10^{-6} mole/s.

Three nitrogen-containing compounds, FCN, N_2O, and a polymer of composition $(C_3F_5N)_n$ were detected as products in all three reactions; FCN and N_2O are found only in very small amounts.

Mechanisms for each of the reactions are discussed.

Canadian Journal of Chemistry, 46, 3483 (1968)

Introduction

The reactions of active nitrogen with most of the hydrocarbons and their derivatives have been studied by many workers. However, no studies of the products or mechanisms of the reaction of active nitrogen with perfluorinated hydrocarbons have been published. It was noted some time ago (1) that the compound perfluorobutene-2 reacted readily with active nitrogen, giving a bright-red flame similar to that produced when hydrocarbons react with active nitrogen. It was noted also at that time that very small amounts of fluorocarbon would quench completely the active nitrogen afterglow.

The kinetics of this reaction have been studied by the diffusion flame technique (2) and the values reported for the rate constants are of the same order of magnitude as those reported for the reactions of active nitrogen with similar hydrocarbons. A small spherical reaction flame was formed near the inlet jet when 0.17×10^{-6} mole/s of C_4F_8 was mixed with 2.1×10^{-6} mole/s of active nitrogen and no yellow glow was visible beyond the edge of the flame.

The reaction was further investigated to determine whether it indeed resembled the reaction of active nitrogen with the hydrocarbons in both reaction products and mechanism. It was also of interest to see whether other fluorocarbons would react in a similar manner with active nitrogen.

[1]Presented in part at the 50th Annual Conference of the Chemical Institute of Canada, Toronto, Ontario, June 1967.

[2]Holder of C.I.L. Fellowship 1965–1966, Dalhousie Centennial Scholarship 1966–1967, and an Izaak Walton Killam Memorial Scholarship 1967–1968.

Experimental

General

A conventional fast-flow system was used in the study of these reactions. The perfluoro-olefin reactant was admitted to a stream of active nitrogen produced by a microwave discharge, generated by a Burdick model MW/200 microwave unit operating at 2450 MHz and rated at 125 W. This unit was operated at 90% of its power output. With the normal flow of molecular nitrogen (187×10^{-6} mole/s), a pressure of 1.75 mm, and a concentration of nitrogen atoms of 2.1×10^{-6} mole/s, as measured by nitric oxide titration (3–5), was maintained.

The products of the reaction were trapped in a liquid nitrogen trap, separated by gas chromatography, and identified by mass and infrared spectroscopy. Quantitative determinations of product yields were made by gas chromatography by comparison of peak heights with peak height calibration curves obtained from known amounts of pure gases.

Materials

Prepurified nitrogen was obtained from the Canadian Liquid Air Co. It was further purified by passage through copper turnings heated to 400 °C and through a liquid nitrogen trap. Nitric oxide, obtained from the Matheson of Canada Co. Ltd., was purified by condensation with liquid nitrogen in a trap filled with caroxite. After noncondensable gases had been removed, the liquid nitrogen was replaced by a dry ice – acetone bath. The portion which distilled was colorless and was used for all determinations of the nitrogen atom concentration (6).

Perfluorobutene-2 was obtained from Matheson of Canada. The compound was better than 99.5 mole% C_4F_8, and was a mixture of 98% *trans*- and 2% *cis*-isomers. The gas was purified in the vacuum system by three bulb-to-bulb distillations; the first and last fifth of the gas was discarded in each distillation. The gas chromatogram of the purified gas did not show any impurities.

Hexafluoropropene and tetrafluoroethene were supplied by the Pierce Chemical Co. Hexafluoropropene was purified in the same manner as perfluorobutene-2. The cylinder of tetrafluoroethene contained about 1% of a high-boiling inhibitor. No indication of this was found after removing the tetrafluoroethene from the cylinder

Can. J. Chem. Downloaded from www.nrcresearchpress.com by 210.87.254.42 on 09/05/12
For personal use only.

and it was assumed that the inhibitor remained in the tank. A gas chromatogram of the gas used in the present study showed about 1.3% hexafluoroethane as the only impurity.

Tetrafluoromethane, hexafluoroethane, and perfluoropropane obtained from Matheson of Canada and decafluorobutane obtained from Pierce Chemicals were used for calibration of the gas chromatograph after condensation and prolonged pumping. Helium, used as the carrier gas in the gas chromatograph, was obtained from Canadian Liquid Air Co. It was purified by passage through a Matheson model 450 gas purifier.

Apparatus

The reaction system was similar to that used for previous studies of active nitrogen reactions. Three separate introduction systems were provided; one each for admitting nitrogen, reactant, and nitric oxide to the reaction vessel.

The remainder of the reaction system is shown in Fig. 1. The reaction vessel V was made of pyrex tubing 55 mm i.d. and 40 cm in length. A B55 ground joint was situated just below the exit tube to facilitate cleaning the reaction vessel. Nitrogen passing through S_N was activated before entering the top of the reaction vessel. The reactants were introduced through S_R attached to a nozzle, 1.5 mm in diameter, centered in the reaction vessel. For most reactions, the reaction flame was contained within the reaction vessel V and only for very low flow rates of fluorocarbon did it extend into the exit tube.

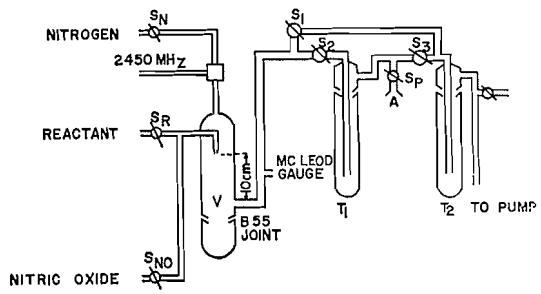

FIG. 1. Reaction system.

The reaction products were trapped in T_1 and distilled into a transfer tube at A for gas chromatographic analysis. For these measurements, it was convenient to admit all of the products collected to the gas chromatograph in one addition and this necessitated short reaction times. In order to overcome the inaccuracies caused by the relatively large amounts of reactant trapped between the capillary flow meter and S_R, it was necessary to add the bypass around trap T_1. This allowed the reaction to be initiated while the flow was through the bypass. As soon as trap T_1 had been cooled with liquid nitrogen and steady conditions obtained within the reaction vessel, the flow was directed through T_1 and the products trapped. The additional trap T_2 was kept under liquid nitrogen at all times as a protection for the pump.

The gas chromatographic analyses were made on a column maintained at 90 ± 0.5 °C. The column was prepared from 1.5 m of 0.25 in. copper tubing, packed with 40–60 mesh silica gel which had been coated with 3% squalane (7).

Results and Discussion

If the reactions of active nitrogen with the fluorocarbons did resemble closely the reactions of active nitrogen with the hydrocarbons, FCN might be expected to be the major product, paralleling the formation of HCN found in the hydrocarbon-active nitrogen reactions (8–10). From accurate mass measurement of a small peak 45 present in mass spectra of samples of total reaction products (before any separation), it is concluded that FCN does form in the reactions. The amount detected, however, was extremely small and no quantitative determination was attempted.

The major nitrogen-containing product was a polymer which formed on the reactant jet and on the walls of the reaction vessel near the reactant jet. After considerable reaction, samples of polymer were scraped from the walls of the vessel and analyzed for C, F, and N. When the microwave discharge was employed, the polymer was allowed to collect for a considerable number of experiments at different flow rates and temperatures. The results of these analyses are given in Table I.

It should be noted that there is no significant difference in composition of the polymers produced from the various compounds or when different sources of active nitrogen are used. One sample of polymer was treated with active nitrogen for 24 h and was found to produce a small amount of fluorocarbon products. It was also heated under vacuum at 250 °C for 3 h with the evolution of a noncondensable gas, probably nitrogen, as well as relatively large amounts of fluorocarbons as shown in Table II. Despite this treatment, the composition of the polymer did not vary appreciably. The polymer composition corresponds very closely to the formula $(C_3F_5N)_n$. The theoretical composition of this formula is 24.84% C, 65.50% F, and 9.66% N. Table I indicates for the polymer a percentage of nitrogen which is somewhat lower than the theoretical value. This may be due to the inclusion of small amounts of the fluorocarbon reagent or some of the reaction products in the polymer. Consideration of the actual structure of the polymer is complicated since it is not soluble in any of the

TABLE I

Elemental analysis* of the polymer from the reaction of active nitrogen with C_4F_8-2, C_3F_6, and C_2F_4

Fluorocarbon	Mode of excitation of N_2	%C	%F	%N	Total
C_4F_8-2	Condensed† discharge	25.99	65.17	8.61	99.77
C_4F_8-2‡	Microwave discharge	25.99	65.70	8.05	99.74
C_4F_8-2	Microwave discharge	26.03	65.30	8.88	100.21
C_4F_8-2	Condensed discharge	26.75	62.18	9.30	98.23
C_3F_6	Condensed discharge	25.68	63.64	9.20	98.52
C_2F_4	Condensed discharge	26.71	63.51	9.25	99.51

*Analysis performed by Alfred Bernhardt, Max Planck Institute Fuer Kohenforschung, West Germany.
†Condensed discharge polymers prepared in a system separate from that described in this work.
‡Polymer was treated with active nitrogen for 24 h and heated to 250 °C for about 3 h before analysis.

common solvents including those which are normal solvents for the teflon polymer.

In addition to FCN and polymer, an extremely small amount of a third nitrogen-containing gas, N_2O, was detected and is believed to be a by-product of the reaction. N_2O was identified by accurate mass measurement of peaks at *m/e* 44 and 30 in mass spectra of samples of unseparated products collected after reaction.

N_2O probably results from the reaction of NF or N_2F_2 with the glass walls:

[1] $$2N_2F_2 + SiO_2 \rightarrow SiF_4 + 2N_2O$$

NF or N_2F_2, the result of combination of 2NF radicals, is thus the nitrogen-containing product which directly results from the reaction of active nitrogen with the fluorocarbons. The reaction of N_2F_2 with glass is well known (11) and it is not unreasonable to expect that NF, if formed, would also attack glass. The slow surface reaction and slow desorption of N_2O to the gas phase made its quantitative estimation impractical.

Two sources of NF are possible. It may result from direct attack of N atoms on reactant fluorocarbon or fluorocarbon radicals:

[2] $$R_fF \text{ (or } R_f) + N \rightarrow R_f + NF$$

where R_f represents a fluorinated hydrocarbon.

TABLE II

Products from the decomposition of polymer under vacuum at 250 °C

Product	Yield (moles × 10^7)
C_2F_4	39.2
C_3F_6	15.5
CF_4	8.3
C_4F_8	8.2
C_4F_{10}	3.2
C_2F_6	3.1
N_2	Undetermined

NF may also result by reaction of N with F or F_2, which may form in other reactions in the overall mechanism:

[3] $$N + F \text{ (or } F_2) \rightarrow NF$$

Reaction [2] is endothermic by at least 40 kcal/mole and therefore probably not of much importance. Reaction [3] is important only if a large amount of free fluorine is formed in the reaction. Direct evidence of NF or N_2F_2 as products of the reaction has not been obtained and it is difficult to speculate further on their importance.

Silicon tetrafluoride has been identified as a second by-product of the reaction. No quantitative analysis of SiF_4 has been made because of its tendency to be adsorbed by the glass walls of the vacuum system. In addition to formation by reaction [1], SiF_4 could be formed by the attack of free fluorine atoms or fluorine on the glass.

In addition to the above products which relate directly to nitrogen content, a relatively large amount of fluorocarbons were obtained from each reaction. These fluorocarbons were separated by gas chromatography and identified. The production of each of these gases was studied quantitatively for a wide range of reactant flow rates and at the temperatures of 25, 250, and 400 °C. The reaction of active nitrogen with C_4F_8-2 gave C_2F_6, C_2F_4, C_3F_8, C_3F_6, and C_4F_{10} as fluorocarbon products and the variation of the amounts produced with flow rate and temperature is shown in Fig. 2.

In order to show the amount of reactant destroyed and the amounts of all products formed on the same graph, it was necessary to make a change of scale in the vertical axis. This is indicated at the dashed horizontal line. The dashed vertical line indicates a change of scale for the

Can. J. Chem. Downloaded from www.nrcresearchpress.com by 210.87.254.42 on 09/05/12
For personal use only.

Can. J. Chem. Downloaded from www.nrcresearchpress.com by 210.87.254.42 on 09/05/12
For personal use only.

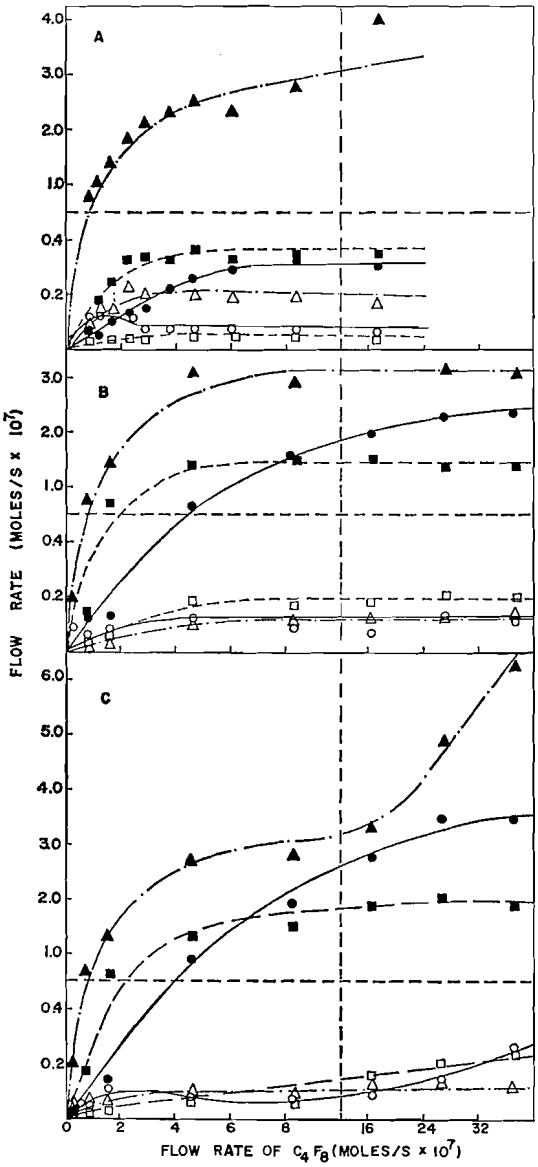

FIG. 2. Reaction of active nitrogen with perfluorobutene-2. (A) 25 ± 5 °C; (B) 250 ± 5 °C; (C) 400 ± 5 °C. Symbols in each are as follows: (▲) C_4F_8-2 reacted; product flow rates (■) C_2F_4; (●) C_3F_6; (△) C_4F_{10}; (○) C_3F_8; (□) C_2F_6. Scale changes on vertical and horizontal axes are indicated by dashed lines.

axis representing the flow rate of reactant. This was necessary in order to show that in most cases the reactants destroyed and products formed reach limiting or plateau values with the flow rate of reactant. One exception is the destruction of perfluorobutene-2 at 400 °C (Fig. 2C), where thermal decomposition of the reactant occurs at

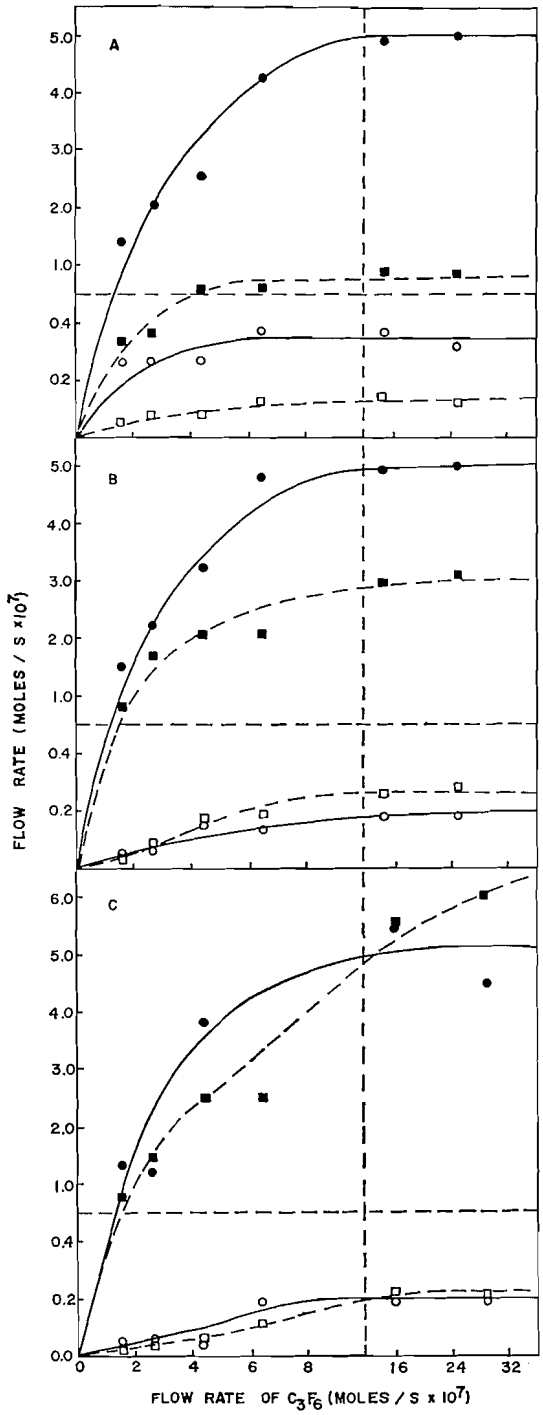

FIG. 3. Reaction of active nitrogen with perfluoropropene. (A) 25 ± 5 °C; (B) 250 ± 5 °C; (C) 400 ± 5 °C. Symbols in each are as follows: (●) C_3F_6 reacted; product flow rates (■) C_2F_4; (○) C_3F_8; (□) C_2F_6. Scale changes on vertical and horizontal axes are indicated by dashed lines.

Can. J. Chem. Downloaded from www.nrcresearchpress.com by 210.87.254.42 on 09/05/12
For personal use only.

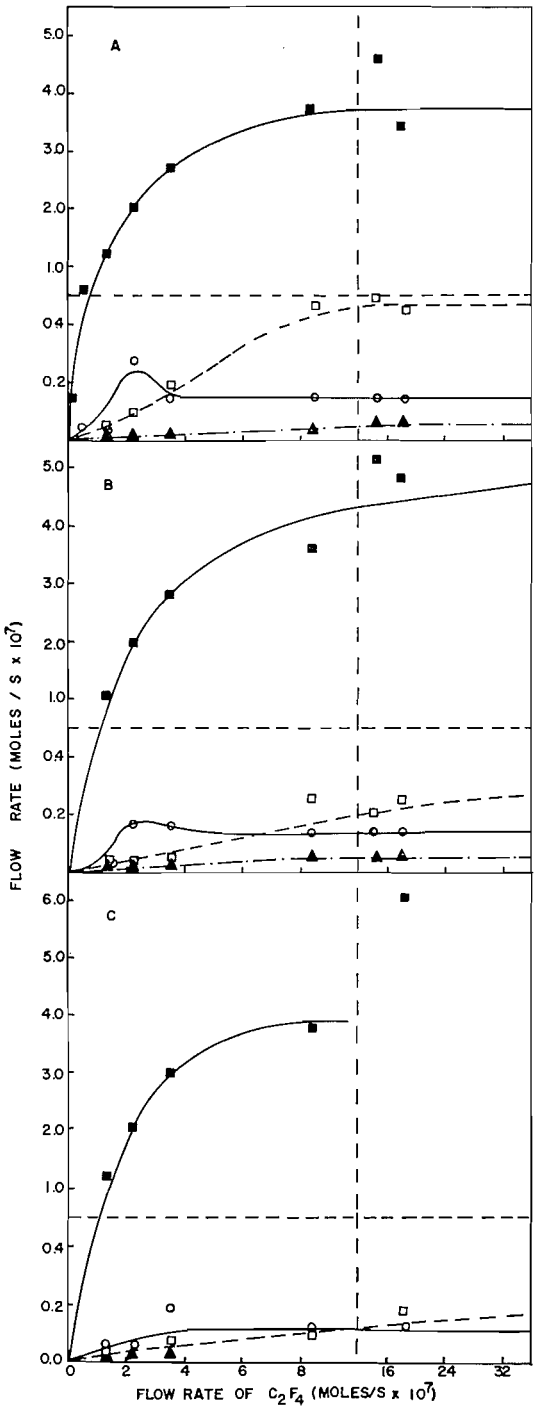

FIG. 4. Reaction of active nitrogen with perfluoroethene. (A) 25 ± 5 °C; (B) 250 ± 5 °C; (C) 400 ± 5 °C. Symbols in each are as follows: (■) C_2F_4 reacted; product flow rates (□) C_2F_6; (○) C_3F_8; (▲) CF_4. Scale changes on vertical and horizontal axes are indicated by dashed lines.

high flow rates. At each temperature, the amount of unsaturated products produced is much larger than the amount of saturated products. This is especially true at the higher temperatures where the production of unsaturates exceeds that of saturates by at least a factor of ten. The product C_3F_8 appears to go through a slight maximum at each temperature, although at 250 °C the maximum is not much larger than the scatter of the points.

Figure 3 illustrates the production of C_2F_6, C_2F_4, and C_3F_8 in the reaction with C_3F_6. The scale changes are also necessary here. The amount of unsaturated C_2F_4 produced is again much greater than the amount of saturated products produced.

The reaction with C_2F_4 produced the saturated fluorocarbons, CF_4, C_2F_6, and C_3F_8, as shown in Fig. 4. As in the other reactions, the amount of saturated products is very low compared with the amount of C_2F_4 reacted. The maxima in the C_3F_8 curves are quite evident in this reaction.

Each point on the curves represents the average of at least two separate experiments. A carbon balance was attempted at each flow rate, but because of the formation of polymer the results were very poor. For the C_4F_8-2 and C_3F_6 reactions, values of approximately 60% recovery were obtained, while for the reaction with C_2F_4, a carbon recovery of less than 20% was usual.

It appears that the reactions of active nitrogen with these three unsaturated fluorocarbons, C_2F_4, C_3F_6, and C_4F_8-2, are very closely related. It now remains to suggest a possible mechanism for these reactions. If it is assumed that nitrogen atoms are the major attacking species, it may be suggested that these atoms form a complex with the unsaturated fluorocarbon. The complex so formed would then break down to form products or intermediate radicals:

$$R_fF + N \rightarrow (R_fFN)_{\text{complex}} \begin{cases} \xrightarrow{[4]} R_f'CN + R_f'' \\ \xrightarrow{[5]} R_f''' + FCN \end{cases}$$

It would appear from the products identified that reaction [5] is not important. However, it is possible that the FCN formed in this reaction or in reactions such as:

$$[6] \qquad CF_3 + N \rightarrow FCN + 2F$$

$$[7] \qquad CF_2 + N \rightarrow FCN + F$$

might be instrumental in the formation of poly-

Can. J. Chem. Downloaded from www.nrcresearchpress.com by 210.87.254.42 on 09/05/12
For personal use only.

mer by reaction with fluorocarbon radicals or with C_2F_4; for example,

[8] $C_2F_4 + FCN \rightarrow (C_3F_5N)$ polymer

The unsaturated compounds must result from the recombination or rearrangement of radicals while the saturated fluorocarbons may result from recombination of radicals or by fluorination of unsaturated fluorocarbons.

From the preceding discussion, it is suggested that the reaction with C_2F_4 may occur as follows:

[9] $C_2F_4 + N \rightarrow (C_2F_4N)_{\text{complex}} \rightarrow CF_2N + CF_2$

[10] $(C_2F_4N)_{\text{complex}} \rightarrow FCN + CF_3$

[11] $CF_2N \rightarrow FCN + F$

[12] $CF_2 + N \rightarrow FCN + F$

[13] $CF_3 + N \rightarrow FCN + 2F$

[14] $FCN + C_2F_4 \rightarrow (C_3F_5N)$ polymer

[15] $CF_3 + F \rightarrow CF_4$

[16] $CF_3 + CF_3 \rightarrow C_2F_6$

[17] $CF_3 + CF_2 \rightarrow C_2F_5$

[18] $C_2F_5 + CF_3 \rightarrow C_3F_8$

[19] $N + F + M \rightarrow NF + M$

[20] $NF + N \rightarrow N_2 + F$

[21] $NF + NF \rightarrow N_2F_2$

From the attempted carbon balance already mentioned, it is evident that a large amount of polymer is formed in the reaction. If, as is shown in the mechanism, FCN is actually formed in several reactions but is not present in large amounts as product, it is probable that it plays a significant role in the formation of polymer.

Although the amounts of fluorocarbons found are extremely small, their consideration may give some indication of the relative importance of two initial reactions, [9] and [10]. C_2F_6 may be formed by recombination of CF_3 radicals as in reaction [16] or by fluorination of C_2F_4. As the temperature increases, the amount of C_2F_6 formed decreases (Fig. 4). This suggests that the concentration of CF_3 radicals decreases with temperature and therefore reaction [10] becomes less important. This is based on the assumption that the concentration of fluorine will not change appreciably regardless of whether [9] or [10] is predominant, since [9] is followed by formation of 2F in [11] and [12], and [10] is also followed by formation of 2F in [13].

If reaction [9] is more important at higher temperatures, the concentration of C_3F_8 would be expected to increase as the increased number of CF_2 radicals reacted, as in reactions [17] and [18]. This was not found to be the case. Rather, the amount of C_3F_8 found decreases slightly with temperature. It is probable, however, that most of the radicals recombine to form C_2F_4 (12).

The reactions [19] to [21] followed by reaction [1] account for the formation of SiF_4 and N_2O, found as minor reaction products. It was found that very small flow rates of fluorocarbons will quench the nitrogen afterglow. This could be explained by reactions [19] and [20].

The mechanism for the reaction of C_3F_6 with active nitrogen would be expected to be similar to that already discussed for C_2F_4. Several ways may be suggested for the breakdown of the complex formed with nitrogen atoms.

[22] $C_3F_6 + N \rightarrow (C_3F_6N)_{\text{complex}} \rightarrow F_2CN + C_2F_4$

[23] $(C_3F_6N)_{\text{complex}} \rightarrow C_2F_3N + CF_3$

[24] $(C_3F_6N)_{\text{complex}} \rightarrow (C_3F_5N) + F$ polymer

In this reaction, the major product is C_2F_4 (Fig. 3), which can best be accounted for by reaction [22]. The two products formed would be expected to react as has been shown in the C_2F_4 mechanism. It is difficult to explain the large production of C_2F_4 as a product if reaction [23] is important. Reaction [24] leads directly to polymer. However, with the exception of C_3F_8 which might form by fluorination of C_3F_6, it is impossible to account for the other products if reaction [24] is considered the only reaction.

The major product of the reaction of C_4F_8 with active nitrogen was C_3F_6 with slightly smaller amounts of C_2F_4 and very small amounts of saturated fluorocarbons (Fig. 2). Possible initiation steps for this reaction are:

[25] $C_4F_8 + N \rightarrow (C_4F_8N)_{\text{complex}} \rightarrow F_2CN + C_3F_6$

[26] $(C_4F_8N)_{\text{complex}} \rightarrow (C_3F_5N) + CF_3$ polymer

Reaction [25] would explain the major product C_3F_6, while C_2F_4 could form as in reaction [22]. The minor saturated fluorocarbons are easily explained as before. The polymer may form as in reaction [26] but again it is difficult to account

for all the products. It is probable that polymer forms in much the same way as in the reaction of active nitrogen with C_2F_4.

In each of the reactions, it may be noted that the saturated products, particularly C_3F_8, tend to go through maxima as the flow rate of fluorocarbon is increased. These compounds may form to a small extent by fluorination as explained earlier. If this is so, the fluorine atom concentration would be expected to be larger at low fluorocarbon flow rates because of reactions such as [11], [12], and [13], which would occur more readily when a larger number of N atoms are available.

The reactions of active nitrogen with hydrocarbons have been extensively studied and interpreted on the basis that atomic nitrogen is the major reactive species. All of the hydrocarbons have been found to produce HCN as the major product with additional formation of small amounts of hydrocarbons and occasionally NH_3. In the original study (13) of the reaction of ethylene and active nitrogen considerable polymer was obtained. With improved techniques the formation of polymer was reduced and eventually eliminated almost entirely.

In the present study on the reaction of active nitrogen with the fluorocarbon olefins the major product has been found to be a polymer. The presence of FCN has been detected but only in very small amounts. It may be possible that FCN plays a large role in the formation of polymer and this would account for the small amount found as a gaseous product.

Acknowledgments

We wish to thank Dr. W. D. Jamieson of the Atlantic Regional Laboratory, National Research Council of Canada, for the mass spectral determinations and to acknowledge financial assistance for this project from the National Research Council of Canada. We also wish to thank Canadian Industries Limited, Dalhousie University, and the Trustees of the Killam Foundation for providing scholarships to N. Madhavan during his studies at Dalhousie.

1. W. E. JONES. Ph.D. Thesis, Department of Chemistry, McGill University, Montreal, Quebec. 1962. p. 169.
2. N. MADHAVAN and W. E. JONES. J. Phys. Chem. **72**, 1812 (1968).
3. A. A. WESTENBERG and N. DEHAAS. J. Chem. Phys. **40**, 3087 (1964).
4. H. VON WEYSSENHOF and M. PATAPOFF. J. Phys. Chem. **69**, 1756 (1965).
5. J. T. HERRON, J. L. FRANKLIN, P. BRADT, and V. H. DIBELER. J. Chem. Phys. **30**, 879 (1959).
6. E. M. LEVY and C. A. WINKLER. Can. J. Chem. **40**, 686 (1962).
7. G. O. PRITCHARD, J. R. DACEY, W. C. KENT, and C. R. SIMONDS. Can. J. Chem. **44**, 171 (1966).
8. J. VERSTEEG and C. A. WINKLER. Can. J. Chem. **31**, 1 (1953).
9. G. PARASKEVOPOULOS and C. A. WINKLER. J. Phys. Chem. **71**, 947 (1967).
10. H. GESSER, C. LUNER, and C. A. WINKLER. Can. J. Chem. **31**, 346 (1953).
11. C. B. COLBURN, F. A. JOHNSON, A. KENNEDY, K. MCCALLUM, L. C. METZGER, and C. O. PARKER. J. Am. Chem. Soc. **81**, 6397 (1959).
12. F. W. DALBY. J. Chem. Phys. **41**, 2297 (1964).
13. J. H. GREENBLATT and C. A. WINKLER. Can. J. Res. B, **27**, 721 (1949).

Can. J. Chem. Downloaded from www.nrcresearchpress.com by 210.87.254.42 on 09/05/12
For personal use only.

Can. J. Chem. Downloaded from www.nrcresearchpress.com by 210.87.254.42 on 09/05/12
For personal use only.

Refinement of the crystal structure of zirconyl chloride octahydrate

THOMAS C. W. MAK
Department of Chemistry, University of Western Ontario, London, Ontario

Received December 8, 1967

The crystal structure of zirconyl chloride octahydrate, $ZrOCl_2.8H_2O$, has been refined by the least-squares method with new three-dimensional data. Existence of the $[Zr_4(OH)_8(H_2O)_{16}]^{8+}$ tetranuclear complex has been confirmed. However, the coordination polyhedron about each zirconium atom differs considerably from the D_{4d} antiprismatic geometry reported previously. It is, in fact, more closely related to the D_{2d} dodecahedron, and has twofold axial symmetry within the limits of experimental error. Mean bond lengths in the $[Zr_4(OH)_8(H_2O)_{16}]^{8+}$ complex, which approximates closely to D_{2d} point-group symmetry, are: Zr—OH (bridging) = 2.142 ± 0.019 Å and Zr—OH_2 (terminal) = 2.272 ± 0.032 Å.

Canadian Journal of Chemistry, 46, 3491 (1968)

Introduction

The crystal structure of zirconyl chloride octahydrate, $ZrOCl_2.8H_2O$, was first determined by Clearfield and Vaughan (1) using two-dimensional X-ray diffraction data. The existence of a polymeric species involving hydroxo bridges, $[Zr_4(OH)_8(H_2O)_{16}]^{8+}$, was established. The configuration about each zirconium atom was described as a distorted D_{4d} square antiprism, and a model of the tetranuclear complex with idealized D_{4h} symmetry was later used in the interpretation of X-ray diffraction data of aqueous zirconyl and hafnyl halide solutions (2). Since only the zirconium atoms were located with any degree of accuracy in the crystal-structure analysis, a precise description of the coordination polyhedron in terms of idealized geometries is unrealistic and subject to speculation. In view of the current interest in the field of higher-coordination molecular polyhedra (3), the present three-dimensional refinement was undertaken to establish the crystal structure conclusively and to provide an unambiguous description of the geometry of the complex cation.

Experimental

Single crystals of zirconyl chloride octahydrate (Fisher certified grade in powder form) from dilute hydrochloric acid are colorless needles elongated along *c*. They effloresce rapidly on exposure to air, and the following technique was developed in handling the crystals.

A needle-shaped crystal of suitable cross section was removed from the mother liquor, quickly dried with absorbent filter paper, and immediately placed on top of a slab of dry ice. A roughly equidimensional segment is cut off the needle with a dissecting knife and rolled gently on the slab to remove any decomposed powder on its surface. The crystal was then quickly transferred into a glass capillary of 0.01 mm wall thickness and sealed with epoxy glue.

The density of the crystal was measured by the flotation method in a hexane/carbon tetrachloride mixture. Unit cell dimensions were determined from high-angle reflections on a *h*0*l* Weissenberg film calibrated with superimposed sodium chloride powder lines and refined by a least-squares procedure.

Crystal Data

Zirconyl chloride octahydrate, $ZrOCl_2.8H_2O$, molecular weight = 322.26.

Tetragonal, $a = 17.11 \pm 0.02$ Å, $c = 7.71 \pm 0.01$ Å.

Volume of the unit cell: 2257 Å^3.

Density: calculated (with $Z = 8$) = 1.896, measured = 1.91 ± 0.02 g cm^{-3}.

Absorption coefficient for X-rays: $\lambda = 1.5418$ Å, $\mu = 170$ cm^{-1}.

Total number of electrons per unit cell: $F(000) = 1296$.

Absent spectra: *hhl* when *l* is odd, *h*00 when *h* is odd.

Space group is $P\bar{4}2_1c$ (D^4_{2d}).

Roughly spherical crystals of mean diameter 0.2 mm were used in the collection of intensity data. They were mounted along *b* and *c*, and multiple-film Weissenberg photographs of the *h*0*l*–*h*12*l* and *hk*0–*hk*6 zones were taken with CuK_α radiation. Deterioration of crystals sealed in glass capillaries was rather slow at the beginning, but became noticeable after about 4 days, as judged from the appearance of streaks associated with the spots on the photographs and the general increase in background. For this reason a different crystal was used for each layer of data. All Weissenberg films showed slight streaks due to some surface decomposition, but were otherwise quite acceptable. The intensities of the individual reflections were estimated visually by comparison with a calibrated strip. These data were then corrected as usual for Lorentz and polarization factors and for spot-shape variations by the empirical method of Owston (given in ref. 4). Finally a set of scaled structure amplitudes were derived using the least-squares procedure of Hamilton, Rollett, and Sparks (5) for interlayer correlation. No correction for absorption or extinction was applied. The data after reduction consisted of 1096 independent reflections of measurable intensity and 313 unobserved reflections.

Can. J. Chem. Downloaded from www.nrcresearchpress.com by 210.87.254.42 on 09/05/12
For personal use only.

TABLE I

Measured and calculated structure factors. Reading from left to right, the columns contain values of h, k, l, $10F_o$, $10F_c$, $10A_c$, and $10B_c$. Reflections with structure amplitudes marked with asterisks were unobserved and were given intensity values equal to one-third of the observable minimum

Can. J. Chem. Downloaded from www.nrcresearchpress.com by 210.87.254.42 on 09/05/12
For personal use only.

TABLE II

Final positional parameters and, in parentheses, their estimated standard deviations

Atom	x	y	z
Zr	0.0293 (1)	0.1441 (1)	−0.0044 (4)
Cl(1)	0.0147 (12)	0.3646 (12)	0.3969 (32)
Cl(2)	0.1899 (6)	0.1330 (7)	0.4691 (12)
O(1)	0.0762 (14)	0.0512 (13)	0.1469 (28)
O(2)	0.0292 (15)	0.1971 (17)	0.7161 (32)
O(3)	0.1329 (14)	0.2211 (14)	0.9873 (43)
O(4)	0.2550 (11)	0.0384 (14)	−0.0016 (38)
O(5)	0.2706 (16)	0.1741 (19)	0.8245 (35)
O(6)	0.1446 (22)	0.3395 (22)	0.6588 (61)
O(7)	0.3809 (23)	0.0372 (24)	0.2089 (69)
O(8)	0.1125 (14)	0.0703 (13)	0.8533 (30)
O(9)	0.0476 (16)	0.1957 (14)	0.2700 (32)

Refinement of the Structure

All calculations were carried out on an IBM 7040 computer using a full-matrix least-squares program kindly supplied by Professor K. N. Trueblood. The function minimized was $\Sigma w(F_o - F_c)^2$, the weighting scheme used being that of Cruickshank *et al.* (6) with $w = (2F_{min} + F_o + 2F_o^2/F_{max})^{-1}$, where $F_{min} = 10$ and $F_{max} = 250$. Atomic scattering factors for Zr^{4+}, Cl^-, and O were taken from the tabulations of Cromer and Waber (7). The refinement was commenced with Clearfield and Vaughan's published atomic coordinates (1) and reasonable estimates of the isotropic temperature factors. Four cycles of isotropic least-squares refinement were carried out and this resulted in a drop in R from 0.285 to 0.165. It was noticed that the greatest shifts were in the z direction, and that atoms Cl(1), O(6), and O(7) have unusually high temperature factors. A difference Fourier map was then computed, and the residual peaks showed that the thermal vibrations of some of the atoms were strongly anisotropic. There was, however, no indication of any other atoms still to be found in the structure. The next four cycles were carried out using anisotropic temperature factors, reducing R to 0.146. The final parameter shifts were very small, and the refinement was therefore concluded. Observed and calculated structure factors are compared in Table I. The final fractional atomic coordinates and their estimated standard deviations (calculated from the residuals and the inverse matrix in the least-squares refinement) are given in Table II, and the temperature parameters in Table III. Interatomic distances and angles are listed in Table IV.

Discussion

A projection of the structure along the c axis is illustrated in Fig. 1. It consists of a *pseudo* body-centered arrangement of Zr_4O_{24} (hydrogen atoms excluded) tetramers connected together by a network composed of Cl(1), Cl(2), O(5), O(6), and O(7). The zirconium atoms are in a slightly puckered square configuration and are bridged across each edge of the square by oxygen atoms O(1) and O(8), one above and the other below the mean plane of zirconium atoms. The coordination polyhedron about each zirconium atom is completed by the terminal oxygen atoms O(2), O(3), O(4), and O(9).

The most common geometries for discrete eight coordination are the Archimedian square antiprism of D_{4d} symmetry and the D_{2d} dodecahedron with triangular faces (Fig. 2*a*) first found in $[Mo(CN)_8]^{4-}$ (10). The coordination polyhedron found in zirconyl chloride octahydrate (Fig. 2*b*) has, within the experimental accuracy,

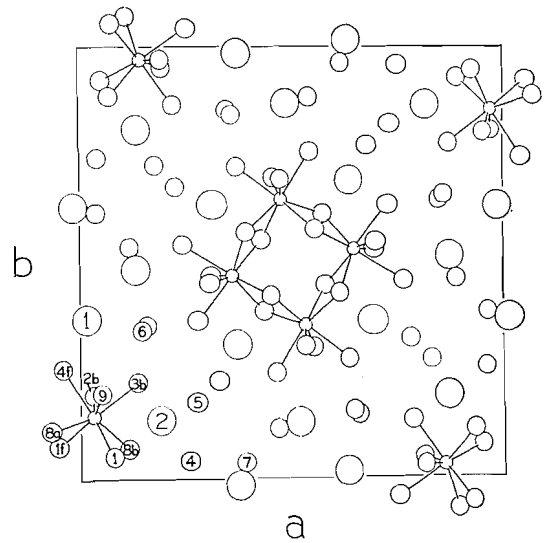

FIG. 1. Projection of the structure on (001). Zirconium, oxygen, and chlorine atoms are represented by increasingly larger circles. The atoms are numbered according to the symmetry relationship given in Table IV.

Can. J. Chem. Downloaded from www.nrcresearchpress.com by 210.87.254.42 on 09/05/12
For personal use only.

TABLE III

Anisotropic temperature coefficients ($\times 10^5$) in the expression $T = \exp[-(\beta_{11}h^2 + \beta_{22}k^2 + \beta_{33}l^2 + 2\beta_{12}hk + 2\beta_{13}hl + 2\beta_{23}kl)]$ and the equivalent isotropic thermal parameters as evaluated from Hamilton's formula (8): $B = \frac{4}{3}\sum_i\sum_j \beta_{ij}(a_i \cdot a_j)$

Atom	β_{11}	β_{22}	β_{33}	β_{12}	β_{13}	β_{23}	B (Å^2)
Zr	238	221	767	3	60	24	2.40
Cl(1)	806	791	5979	299	177	363	10.97
Cl(2)	385	488	1352	168	264	14	4.48
O(1)	285	263	607	6	38	11	2.62
O(2)	281	391	1149	47	303	293	3.53
O(3)	386	305	2179	65	468	394	4.42
O(4)	216	458	1384	20	148	392	3.72
O(5)	383	621	1239	90	90	238	4.90
O(6)	569	571	4125	170	859	420	7.72
O(7)	573	867	5562	240	45	1203	10.03
O(8)	262	257	759	25	137	53	2.63
O(9)	345	190	1205	6	401	30	3.04

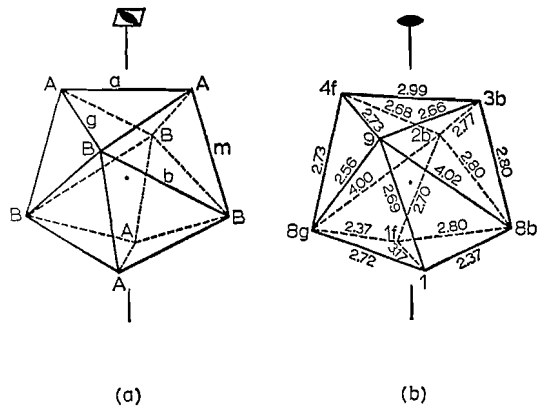

FIG. 2. (*a*) D_{2d} ($\bar{4}2m$) dodecahedron. Labelling of vertices and edges of the polyhedron follows the convention of Hoard and Silverton (9). Its shape is specified by three parameters: the angles θ_A, θ_B which the bonds M—A, M—B made with the unique axis, and the ratio of the bond lengths. (*b*) Coordination polyhedron found in zirconyl chloride octahydrate with edge lengths given in Å. The oxygen atoms are numbered according to the symmetry code of Table IV.

twofold axial symmetry. To a good approximation (i.e. assuming a planar configuration of zirconium atoms) the point-group symmetry of the discrete Zr_4O_{24} complex ($\bar{4}$ required) may be described as D_{2d} ($\bar{4}2m$).

Departing considerably from the square antiprismatic geometry as described by Clearfield and Vaughan, the C_2 coordination polyhedron found in the present structure actually more closely resembles the dodecahedron. This may be seen from a comparison of the three types of polyhedra projected along their unique axes (Fig. 3). In fact, the top halves of the C_2 polyhedron (consisting of oxygen atoms 9, 2*b*, 3*b*, and 4*f* in Fig. 2*b*) and the D_{2d} dodecahedron (Fig. 2*a*) are very similar. The O(3*b*)—Zr—O(4*f*) and O(9)—Zr—O(2*b*) angles are 84.8° and 134.0° respectively, which may be compared with the corresponding angles $2\theta_A = 70.4°$ and $2\theta_B = 147.0°$ in the dodecahedron found in $Na_4Zr(C_2O_4)_4.3H_2O$ (12). To a lesser extent, the lower half of the C_2 coordination polyhedron (atoms 1, 1*f*, 8*b*, and 8*g* in Fig. 2*b*) may also be matched with half of a dodecahedron. Referring to Fig. 2*b*, the angles O(1)—Zr—O(1*f*) = 96.9° and O(8*b*)—Zr—O(8*g*) = 130.2° should be compared, respectively, with $2\theta_A$ values in the range 70.4–86° and $2\theta_B$ values in the range 131–147° found in zirconium compounds with dodecahedral octacoordinate structures (3). As a first approximation, then, both

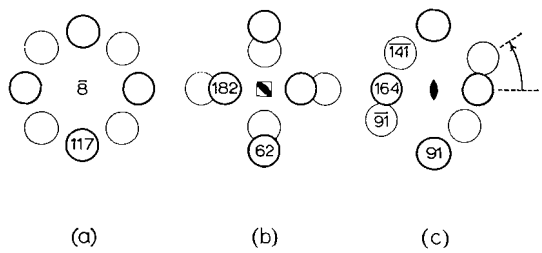

FIG. 3. Comparison of coordination polyhedra projected along their unique axes. Oxygen atoms above and below the central zirconium atoms are represented, respectively, by heavily and lightly ringed circles. Vertical distances are given in 10^{-2} Å. (*a*) D_{4d} ($\bar{8}2m$) square antiprism in $Zr(IO_3)_4$ (11). (*b*) D_{2d} ($\bar{4}2m$) dodecahedron in $Na_4Zr(C_2O_4)_4.3H_2O$ (12). (*c*) C_2 (2) coordination polyhedron in $ZrOCl_2.8H_2O$.

Can. J. Chem. Downloaded from www.nrcresearchpress.com by 210.87.254.42 on 09/05/12
For personal use only.

TABLE IV

Interatomic distances (in Å) and angles (in degrees)*

Symmetry code			
.	x	y	z
b	x	y	$-1+z$
c	x	y	$1+z$
d	y	$-x$	$-z$
e	y	$-x$	$1-z$
f	$-y$	x	$-z$
g	$-y$	x	$1-z$
h	$-\frac{1}{2}+x$	$\frac{1}{2}-y$	z
i	$\frac{1}{2}-y$	$\frac{1}{2}-x$	$-\frac{1}{2}+z$
j	$\frac{1}{2}-y$	$\frac{1}{2}-x$	$\frac{1}{2}+z$
k	$\frac{1}{2}+x$	$\frac{1}{2}-y$	$\frac{1}{2}-z$

In tetranuclear complex			
Zr—O(1)	2.129	O(1)—Zr—O(8*b*)	66.4
Zr—O(1*f*)	2.110	O(1*f*)—Zr—O(8*g*)	67.9
Zr—O(8*b*)	2.197	O(1)—Zr—O(8*g*)	79.2
Zr—O(8*g*)	2.133	O(1*f*)—Zr—O(8*b*)	81.2
Zr—O(9)	2.314	O(9)—Zr—O(3*b*)	72.0
Zr—O(2*b*)	2.338	O(2*b*)—Zr—O(4*f*)	71.8
Zr—O(3*b*)	2.210	O(9)—Zr—O(4*f*)	74.1
Zr—O(4*f*)	2.224	O(2*b*)—Zr—O(3*b*)	75.1
Zr...Zr(*d*)	3.558	O(1)—Zr—O(1*f*)	96.9
		O(3*b*)—Zr—O(4*f*)	84.8
		O(8*b*)—Zr—O(8*g*)	130.2
		O(9)—Zr—O(2*b*)	134.0
		Zr—O(1)—Zr(*d*)	114.2
		Zr—O(8*b*)—Zr(*d*)	110.5
Coordination about Cl(1)			
Cl(1)...O(6)	3.03	O(6)...Cl(1)...O(6*i*)	78.3
Cl(1)...O(6*i*)	3.10	O(6)...Cl(1)...O(7*g*)	65.2
Cl(1)...O(7*g*)	3.18	O(6)...Cl(1)...O(7*b*)	146.3
Cl(1)...O(7*h*)	2.95	O(6)...Cl(1)...O(9)	86.8
Cl(1)...O(9)	3.10	O(6*i*)...Cl(1)...O(7*g*)	142.7
		O(6*i*)...C'(1)...O(7*h*)	119.3
		O(6*i*)...Cl(1)...O(9)	67.7
		O(7*g*)...Cl(1)...O(7*h*)	89.9
		O(7*g*)...Cl(1)...O(9)	115.7
		O(7*h*)...Cl(1)...O(9)	125.7
Coordination about Cl(2)			
Cl(2)...O(2*e*)	3.12	O(2*e*)...Cl(2)...O(5)	125.4
Cl(2)...O(5*a*)	3.15	O(2*e*)...Cl(2)...O(5*i*)	106.4
Cl(2)...O(5*i*)	3.06	O(2*e*)...Cl(2)...O(9)	96.5
Cl(2)...O(9)	3.07	O(5)...Cl(2)...O(5*i*)	82.1
		O(5)...Cl(2)...O(9)	134.8
		O(5*i*)...Cl(2)...O(9)	103.5
Coordination about O(5)			
O(5)...Cl(2)	3.15	Cl(2)...O(5)...Cl(2*j*)	136.3
O(5)...Cl(2*j*)	3.06	Cl(2)...O(5)...O(3)	94.9
O(5)...O(3)	2.79	Cl(2)...O(5)...O(4*b*)	101.4
O(5)...O(4*b*)	2.69	Cl(2*j*)...O(5)...O(3)	94.1
		Cl(2*j*)...O(5)...O(4*b*)	121.8
		O(3)...O(5)...O(4*b*)	86.6
Coordination about O(6)			
O(6)...Cl(1)	3.03	Cl(1)...O(6)...Cl(1*j*)	104.0
O(6)...Cl(1*j*)	3.10	Cl(1)...O(6)...O(3*i*)	105.9
O(6)...O(3*i*)	2.69	Cl(1*j*)...O(6)...O(3*i*)	101.1
Coordination about O(7)			
O(7)...Cl(1*e*)	3.18	Cl(1*e*)...O(7)...Cl(1*k*)	119.4
O(7)...Cl(1*k*)	2.95	Cl(1*e*)...O(7)...O(4)	120.5
O(7)...O(4)	2.70	Cl(1*k*)...O(7)...O(4)	116.6

*Estimated standard deviations are: 0.022 Å for individual Zr—O bonds, 0.03 Å for Cl...O distances, 0.04 Å for O...O distances, and 0.9° for all angles.

Can. J. Chem. Downloaded from www.nrcresearchpress.com by 210.87.254.42 on 09/05/12
For personal use only.

Can. J. Chem. Downloaded from www.nrcresearchpress.com by 210.87.254.42 on 09/05/12
For personal use only.

halves of the C_2 polyhedron may be fitted individually to the dodecahedron, and the main distortion from ideal D_{2d} geometry is a rotational twist of about 30° of the lower half relative to the upper half (Fig. 3*c*). Presumably this is the steric requirement involved in the formation of the tetranuclear complex through edge-sharing of four C_2 polyhedra (Fig. 1).

Since the positions of the hydrogen atoms are unknown, the present X-ray analysis does not distinguish between hydroxyl and water groups. There is little doubt, however, that the terminal oxygen atoms O(2), O(3), O(4), and O(9), which are chemically equivalent, indeed belong to water molecules. In their two-dimensional analysis Clearfield and Vaughan identified the bridging atoms O(1) and O(8) as OH groups, citing as evidence the fact that both linking oxygen atoms have Cl(2) as their only nearest neighbor. In the light of the present analysis this argument is no longer valid since the interatomic distances concerned, O(1)...Cl(2) and O(8)...Cl(2), have increased from 3.18 to 3.45 Å and from 3.02 to 3.42 Å respectively, and are now much longer than other O...Cl contacts which lie in the range 3.0–3.2 Å (Table IV). We choose, therefore, to emphasize the important role of bridging hydroxyl groups in complex formation (13), the common occurrence of double hydroxo bridges as the dominant structural unit in all basic zirconium salts studied to date (14), and the relative stability of $[Zr_4(OH)_8(H_2O)_{16}]^{8+}$ compared with the more highly-charged $[Zr_4(H_2O)_{24}]^{16+}$ containing bridging water molecules. The very short O(1)...O(8) distance of 2.37 Å in the double bridge is in good agreement with similar distances in the range 2.34–2.44 Å found in several other basic zirconium salts (14, 15). The Zr—OH (bridging) bonds average 2.142 ± 0.019 Å, which is significantly shorter than the mean Zr—OH_2 (terminal) distance of 2.272 ± 0.032 Å. In $Zr_2(OH)_2(SO_4)_3(H_2O)_4$ (14), which contains $[Zr_2(OH)_2]^{6+}$ dimers, the Zr—OH bonds (mean length 2.123 ± 0.020 Å) are also stronger than other Zr—O bonds which average 2.217 ± 0.013 Å. The non-bonded Zr...Zr distance of 3.558 Å in $[Zr_4(OH)_8(H_2O)_{16}]^{8+}$ also agrees well with the corresponding distance of 3.545 Å in $[Zr(OH)_2]^{6+}$.

A careful examination of the environment about individual chloride ions and water molecules not bonded to the zirconium complex (Table IV) reveals that Cl(2) and O(5) are both tetrahedrally coordinated. On the other hand, Cl(1), O(6), and O(7) are respectively in five, three, and three coordination. The coordination figures are notably irregular, but all pertinent O...O hydrogen bonds and O...Cl contacts are normal. As one might expect, these chloride ions and water molecules which form a matrix holding together the zirconium complexes in the crystal lattice exhibit much more pronounced thermal motions. Indeed, the abnormally high temperature parameters obtained for Cl(1), O(6), and O(7) may be indicative of positional disorder in the structure. Any deviation from ideal stoichiometry, however, is slight since the measured and calculated densities are in good agreement.

Acknowledgments

The author gratefully acknowledges financial support for this work from the National Research Council of Canada and the Ontario Department of University Affairs. Thanks are also due to Professor K. N. Trueblood for supplying a copy of his least-squares refinement program, and to Professor J. L. Hoard for a critical reading of the manuscript.

1. A. Clearfield and P. A. Vaughan. Acta Cryst. **9**, 555 (1956).
2. G. M. Muha and P. A. Vaughan. J. Chem. Phys. **33**, 194 (1960).
3. E. L. Muetterties and C. M. Wright. Quart. Rev. London, **21**, 109 (1967). S. J. Lippard. *In* Progress in inorganic chemistry. Vol. 8. *Edited by* F. A. Cotton. Interscience Publishers, Inc., New York. 1967. p. 109.
4. J. S. Rollett (*Editor*). Computing methods in crystallography. The Pergamon Press, Ltd., New York. 1965. p. 93.
5. W. C. Hamilton, J. S. Rollett, and R. A. Sparks. Acta Cryst. **18**, 129 (1965).
6. D. W. J. Cruickshank *et al.* Computing methods and the phase problem in X-ray crystal analysis. The Pergamon Press, Ltd., New York. 1961. p. 45.
7. D. T. Cromer and J. T. Waber. Acta Cryst. **18**, 104 (1965).
8. W. C. Hamilton. Acta Cryst. **12**, 609 (1959).
9. J. L. Hoard and J. V. Silverton. Inorg. Chem. **2**, 235 (1963).
10. J. L. Hoard and H. H. Nordsieck. J. Am. Chem. Soc. **61**, 2853 (1939).
11. A. C. Larson and D. T. Cromer. Acta Cryst. **14**, 128 (1961).
12. J. V. Silverton and J. L. Hoard. Inorg. Chem. **2**, 243 (1963).
13. F. G. R. Gimblett. Inorganic polymer chemistry. Butterworths, London. 1963. Chap. 3.
14. D. B. McWhan and G. Lundgren. Inorg. Chem. **5**, 284 (1966).
15. A. Clearfield. Rev. Pure Appl. Chem. **14**, 91 (1964).

3d orbitals and bonds of second row atoms. 2. π bonding in phosphoryl compounds

K. A. R. MITCHELL
Department of Chemistry, University of British Columbia, Vancouver, British Columbia
Received March 20, 1968

The concept of $3d_\pi$ orbital bonding in molecules of second row atoms is tested by making some model calculations on phosphoryl molecules, X_3PO. Values of exponents for 3s, 3p, and 3d orbitals of phosphorus have been calculated in an electrostatic calculation where X is F, Cl, C, and H. For F_3PO, estimates have also been made on the effect of interatomic exchange. The main conclusion for F_3PO is that the molecular environment strongly contracts the 3d orbitals at phosphorus with π symmetry with respect to the P—O bond, thereby indicating the feasibility of double bond interactions with oxygen $2p_\pi$ orbitals.

Canadian Journal of Chemistry, 46, 3499 (1968)

Can. J. Chem. Downloaded from www.nrcresearchpress.com by 210.87.254.40 on 09/05/12
For personal use only.

Introduction

For some time it has been recognized that the energies and radial sizes of 3d orbitals of second row atoms are not suitable for substantial participation in bond formation (1). To make important contributions to bonding, the 3d orbitals should be sufficiently compact to allow good overlap with orbitals of the neighboring atoms, and also the 3d orbitals should have binding-energies similar to those of other participating orbitals. Recent work confirms that 3d orbitals in d^1 configurations are diffuse for both phosphorus (2) and sulfur (3), and therefore the ability of 3d orbitals to contribute to bonding, in, for example, Cl_3PO, $(F_2PN)_4$, and $(CH_3)_2SO$, depends on these orbitals being stabilized during the process of bond formation.

Recently, much experimental work has been directed at elucidating the nature of the P—O bond in phosphoryl molecules, and in particular whether this is best considered as a double bond with d_π–p_π interactions or as an ionic bond superimposed on the σ bond (4). The ionic formulation was invoked by analogy with first row examples like amine oxides, in part because d orbitals were assumed unavailable in second row bonding on account of free atom properties. The basic geometries of phosphoryl molecules may be described by either the ionic or the double bond models, and attempts at distinguishing these formulations by making measurements related to polarity (5, 6) have been inconclusive, especially because the d_π–p_π formulation is polar in the same direction as the ionic bond (1). Nevertheless, a considerable amount of experimental evidence does point to the advantages of the double bond formulation, and this includes nuclear quadrupole resonance measurements of phosphoryl molecules (7), electron spin resonance spectra of Ph_3PO^- and related anions (8), and the influence of neighboring PO groups on reaction rates of vinyl compounds (9). The ultraviolet absorption of phosphoryl compounds indicates moderately strong d_π–p_π interactions with pyrrole groups (10), although these interactions are weak with vinyl (9) or phenyl (11) groups.

In other molecular systems involving bonds between first and second row atoms, such as in the phosphates, the sulfoxides, the phosphonitrilics, and the siloxanes, a number of authors consider the model emphasizing p_π–d_π interactions to provide a valuable framework for interpreting experimental observations (1, 12–17). So far, however, the concept of $3d_\pi$ orbital bonding has not been completely justified theoretically. Various semi-empirical methods have been applied to problems of this sort, and often they allow correlations which appear to be useful; a case in point being the correlations made by Wagner (18) of PO stretching frequencies with calculated bond orders in molecules of the type X_3PO. These approaches are most convincing if the particular values of parameters for 3d orbitals that give agreement with experiment, can, at least qualitatively, be justified by some independent approach. Nonempirical methods are required for this purpose, and this is especially because the modification of the radial sizes and orbital energies of 3d orbitals in molecular environments may be sufficiently large to invalidate the use of parameters derived for 3d orbitals in free atoms

Can. J. Chem. Downloaded from www.nrcresearchpress.com by 210.87.254.40 on 09/05/12
For personal use only.

(19). It was the realization of this that encouraged Craig and Zauli to develop an electrostatic model for investigating the properties of 3d orbitals in molecules, and by this approach they showed that diffuse 3d orbitals can be strongly contracted (20). More recent developments (21), on the other hand, suggest that the influence of interatomic exchange may be important in particular cases. Consequently, there is a need for investigating $3d_\pi$ orbitals with models including exchange, and this is the main aim of the present paper.

Methods of Calculation

The calculations to test the availability of $3d_\pi$ orbitals in phosphoryl molecules, X_3PO, are based on the valence bond (v.b.) method assuming perfect pairing. The σ orbitals at phosphorus are assumed to be $3s3p^3$ hybrids, and 3d bonding is only considered in the P—O π bond. The latter assumption simplifies the investigation of the feasibility of d_π-type bonding, but, once the concept is established, d orbital contributions must additionally be anticipated in the P—X bonds. This approach to the calculation is suggested by structural data, and in particular by the observation that measured XPX angles are less than the tetrahedral value. For example, in Cl_3PO the ClPCl bond angle is 103.5° (22), and in F_3PO the FPF bond angle is 102.5° (23). Insofar as these distortions from 109.5° may be correlated with multiple bonding (24), we conclude that d orbital contributions are greater in the PO bonds than in the PX bonds.

The molecules X_3PO have C_{3v} symmetry, and it is most convenient to treat the d_π atomic orbitals at phosphorus and the p_π atomic orbitals at oxygen in the complex forms:

$$[1] \qquad \begin{aligned} d_+ &= (d_{xz} + id_{yz})/\sqrt{2} \\ p_+ &= (p_x + ip_y)/\sqrt{2} \\ d_- &= (d_{xz} - id_{yz})/\sqrt{2} \\ p_- &= (p_x - ip_y)/\sqrt{2} \end{aligned}$$

In eq. [1] local axes at both phosphorus and oxygen are defined such that the z axes lie along the internuclear directions. The v.b. wave function for the P—O π bonds is expressed by a linear combination of bond eigenfunctions, and in a basis set restricted to the orbitals of the valence shells this is

$$[2] \quad \Psi = a[\Psi(p_+^1 d_+^1, p_-^2) + \Psi(p_-^1 d_-^1, p_+^2] + b\Psi(p_+^2, p_-^2)$$

In eq. [2], $\Psi(p_+^1 d_+^1, p_-^2)$ refers to the bond eigenfunction with pairing between electrons in p_+ of oxygen and d_+ of phosphorus and two non-bonding electrons paired in the oxygen orbital p_-. The coefficients a and b in eq. [2] depend on the properties of the 3d orbitals of phosphorus in the molecular environment. If these orbitals do not participate, then $\Psi(p_+^2, p_-^2)$ is the sole contributor, corresponding to the ionic formulation. An indication of the feasibility of participation by 3d orbitals may be obtained by estimating the 3d radial functions in the twin bond eigenfunctions $\Psi(p_+^1 d_+^1, p_-^2)$ and $\Psi(p_-^1 d_-^1, p_+^2)$. These are likely to make important contributions to the v.b. wave function expressed in eq. [2] provided the 3d orbitals overlap strongly with the neighboring 2p orbitals. The bond eigenfunction $\Psi(p_+^1 d_+^1, p_-^2)$ was investigated both with the electrostatic model developed by Craig and Zauli (20), and with the model including exchange described in the first paper of this series (21).

These methods are briefly outlined. The electronic Hamiltonian for X_3PO may be written

$$[3] \qquad H = H_P + H_O + \Sigma H_X + H_{int}$$

where H_P, H_O, and H_X represent Hamiltonian operators for the isolated atoms, and the interaction operator, H_{int}, includes the interactions between the central phosphorus and the surrounding atoms; the interactions between the outer atoms are dropped in eq. [3] since their effect on the valence shell orbitals of phosphorus can be neglected in a first approximation. At phosphorus, it is convenient to write

$$[4] \qquad H_P = H_{core} + H_{val}$$

where H_{core} is the contribution of the nucleus and the inner-shell electrons, and H_{val} is the contribution of the valence shell electrons, including their interactions with the core. In the electrostatic calculation (based on the v.b. model) the molecular wave function is a single product of all occupied one-electron atomic orbitals, and the electrostatic energy is given by

$$[5] \qquad Q = (\Psi_{prod} |H| \Psi_{prod}),$$

where Ψ_{prod} is the molecular wave function. It is convenient to express energies relative to a zero defined for infinite separation of X and O atoms and the P^{5+} core, in which case we have

$$[6] \qquad Q = (\Psi_{prod} |H_{val} + H_{int}| \Psi_{prod})$$

Can. J. Chem. Downloaded from www.nrcresearchpress.com by 210.87.254.40 on 09/05/12
For personal use only.

For X_3PO, based on the $3s3p^33d$ configuration of phosphorus, the expansion of eq. [6] gives

$$[7]\quad Q = (3s\,|-1/2\nabla^2 + U|\,3s) + 3(3p\,|-1/2\nabla^2 + U|\,3p) + (3d\,|-1/2\nabla^2 + U|\,3d) + 3J(3p_x,3p_y) + 3J(3s,3p) + J(3s,3d) + 3J(3p,3d)$$

In eq. [7], the first term contains contributions for the kinetic energy of a 3s electron, and also for the energy of the 3s electron in the potential field, U, originating from the phosphorus core and the atoms surrounding phosphorus. The terms designated by J are single-center Coulomb electron repulsion integrals.

The neglect of exchange terms is the most important deficiency of the energy in eq. [6], and this derives from using a simple product molecular wave function rather than one that is properly antisymmetrized, for example, Ψ_{AS}. In general, the minimization of $(\Psi_{AS}\,|H|\,\Psi_{AS})$ by variation of atomic orbital functions for atoms of the second row is too complex to be convenient, and therefore a more tractable approach is necessary. With the assumption of perfect pairing and with the neglect of overlap integrals, the energy expression simplifies (25) and may be written

$$[8]\quad E = E^0 + Q + \Sigma K(m,n) - 1/2\Sigma K(p,q)$$

In eq. [8], E^0 is the sum of the contributions which are independent of the valence shell orbitals of phosphorus; Q is the electrostatic contribution given by eq. [6]; the first summation is over exchange integrals for all pairs of orbitals, m and n, which form localized two-electron bonds; the second summation is over exchanges for all pairs of orbitals, p and q, for which spins are random.

Although it is well-known that the energy equation [8] is not sufficiently accurate for calculating total molecular energies, it is, nevertheless, likely to be useful for estimating the radial forms of 3d orbitals in molecular environments. The evaluation of the 2-center exchange integrals was simplified, as previously (21), according to

$$[9]\quad K(s,t) = (\Psi_{st}\,|H_{int}|\,\Psi_{ts})$$

where Ψ_{st} and Ψ_{ts} are product wave functions which differ only in interchange of electrons in orbitals s and t. Strictly, this evaluation should be over $H_{val} + H_{int}$, but it was found that the use of eq. [9] resulted in no significant change in the final 3d exponents. This seems reasonable as the feature of special interest is the form of the 3d orbitals in molecular environments, and the environmental influences are included in H_{int}.

Representation of atomic orbitals is based on the Slater-type radial functions

$$[10]\quad R(r) = Nr^{n-1}e^{-\alpha r},$$

where N is a normalization constant, n the principal quantum number, and α the orbital exponent. The latter provides a measure of the inverse of orbital size since the distance of maximum radial probability, measured in atomic units (1 a.u. = 0.529 Å), is given by

$$[11]\quad r_{max} = n/\alpha$$

The simple radial function in eq. [10] seems to be useful for representing 3d orbitals in d^1 configurations of free atoms (17), but the nodeless form makes it less useful for 3s and 3p orbitals. In this work, the nodes were effectively reinstated for the 3s and 3p orbitals of phosphorus by orthogonalizing to the core orbitals. Throughout, the inner shell orbitals of phosphorus and all ligand orbitals have exponents fixed at the values given by Clementi and Raimondi (26) from a self-consistent-field variation of orbital exponents in single-term radial functions.

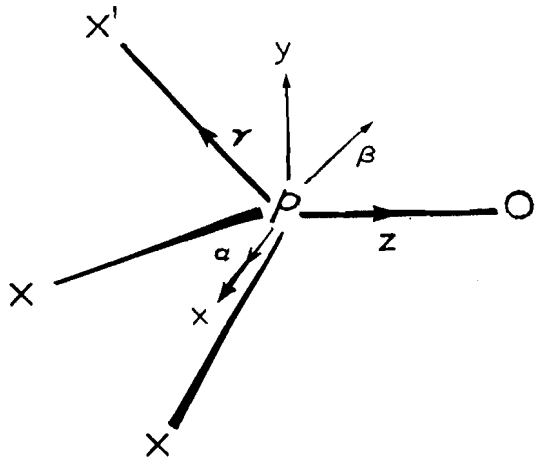

FIG. 1. Molecular and local axes in X_3PO.

Molecular axes in X_3PO are conveniently defined (Fig. 1) in relation to one of the planes XPO; the particular X group in this plane is distinguished in the following by X′. With the origin at P, z is fixed by the PO direction, x is

TABLE I

Electrostatic energy-minimized exponents and energies for phosphoryl molecules

Molecule	3d orbital at phosphorus*	Q	Phosphorus orbital exponents 3s	3p	3d
F_3PO	σ	−6.47	1.67	1.48	1.15
	π	−6.35	1.68	1.49	1.06
	δ	−6.34	1.68	1.49	1.04
Cl_3PO	σ	−6.55	1.68	1.37	1.15
	π	−6.48	1.70	1.40	0.94
	δ	−6.49	1.70	1.40	0.92
C_3PO	σ	−6.19	1.69	1.42	1.12
	π	−6.06	1.71	1.45	0.89
	δ	−6.06	1.71	1.46	0.87
H_3PO	σ	−6.09	1.75	1.53	1.11
	π	−5.91	1.78	1.58	0.41
	δ	−5.91	1.78	1.58	0.39

*3d Orbitals designated by σ, π, and δ, respectively, correspond to z^2, the degenerate pair (xz, yz), and the degenerate pair ($x^2 - y^2$, xy).

perpendicular to the X′PO plane, and y makes an acute angle with the PX′ direction. For the evaluation of 2-center integrals involving orbitals at P and X′, it is necessary to resolve the orbitals at phosphorus defined with the molecular axes in terms of orbitals defined with local axes. The latter are conveniently labelled α, β, γ, where γ is fixed by the PX′ direction, α coincides with x, and β makes an acute angle with the PO direction. For 3d orbitals the expressions needed for integral evaluation are

$$[12]\quad d_{z^2} = (\cos^2\lambda - 1/2\sin^2\lambda)d_{\gamma^2} + \sqrt{3}\sin\lambda\cos\lambda\, d_{\beta\gamma} - \frac{\sqrt{3}}{2}\sin^2\lambda\, d_{\alpha^2-\beta^2}$$

$$d_{xz} = \cos\lambda\, d_{\alpha\gamma} + \sin\lambda\, d_{\alpha\beta}$$

$$d_{x^2-y^2} = -\frac{\sqrt{3}}{2}\sin^2\lambda\, d_{\gamma^2} + \sin\lambda\cos\lambda\, d_{\beta\gamma} + (\cos^2\lambda + 1/2\sin^2\lambda)d_{\alpha^2-\beta^2}$$

where λ is the angle XPO. An extra transformation is necessary for the X atoms which lie in front of and behind the yz plane. This is readily accomplished by using additional axes obtained from x and y by rotations through $\pm\pi/3$ about the z-axis.

As well as investigating the 3d orbitals with π symmetry with respect to the P—O bond, we consider also, in parallel calculations, the 3d orbitals with σ and δ symmetries. These latter orbitals are not included in bonding schemes, and therefore the spin of an electron occupying one of these orbitals is uncorrelated with the spins of electrons in bonding orbitals on neighboring atoms. This assumption is likely to be unrealistic in detail, but nevertheless the results are reported here both to emphasize the differing effects of the molecular environment on the symmetrically inequivalent 3d orbitals, and also to point to situations where the simpler electrostatic calculations (20) may be less reliable.

Results and Discussion

The Electrostatic Model

The electrostatic energy given by eq. [7] was minimized by varying the 3s, 3p, and 3d exponents of the phosphorus orbitals. Optimized exponent values are reported in Table I for molecules X_3PO, where X is F, Cl, C, and H. Bond lengths used in atomic units are: P—O = 2.8, P—F = 2.9, P—Cl = 3.75, P—C = 3.5, and P—H = 2.6. The XPO angle is fixed at 116°, the value measured in F_3PO (23), but is useful also for Cl_3PO (22) and $(CH_3)_3PO$ (27). Fluorine and chlorine were treated in the $p_\pi^4 p_\sigma^1$ configurations, carbon in the $2s2p^3$ configuration (which should be useful for alkyls), and hydrogen in the 1s configuration.

In the $3s3p^33d$ configuration of isolated phosphorus, minimization of eq. [7] yields the following exponent values for the orbitals of the valence

Can. J. Chem. Downloaded from www.nrcresearchpress.com by 210.87.254.40 on 09/05/12
For personal use only.

Can. J. Chem. Downloaded from www.nrcresearchpress.com by 210.87.254.40 on 09/05/12
For personal use only.

shell(21): $\alpha_{3s} = 1.84$, $\alpha_{3p} = 1.61$, and $\alpha_{3d} = 0.35$. The results reported in Table I indicate, therefore, that in X_3PO molecules the electrostatic field expands slightly the 3s and 3p orbitals and contracts the 3d orbitals. In some cases the latter is very strong, with exponents being increased to over three times the free atom value. These trends are consistent with the simple qualitative pictures of bond formation; orbitals which are tightly bound in the free atoms have to be expanded to get their electron density nearer to the ligand atoms, and orbitals which are diffuse have to be contracted to achieve the same more favorable electron distribution.

The Model including Exchange

Previous work on 3d orbitals has indicated that results with the simple electrostatic model may not be reliable in particular circumstances (21). For example, if the contracted 3d orbitals strongly overlap inner shell regions of ligand atoms appreciable repulsive exchange terms come into play, and if there are no large bonding exchanges to compensate, the exchange repulsions may overcome the stabilizing effect of the electrostatic field, with the result that the orbitals remain diffuse.

Results for the minimization of eq. [8] for F_3PO are shown in Table II. In this calculation, the 3s and 3p exponents were fixed at the values that minimize the electrostatic energy. The $3d_\pi$ orbital is now more compact than that predicted by the electrostatic calculation, and the exponent is increased about four times over that for the orbital in a free phosphorus atom. By contrast, for $3d_\sigma$ and $3d_\delta$ the exchange repulsions are sufficiently large to overcome the influence of the electrostatic field, with the result that these orbitals are diffuse and have exponents similar to those appropriate to 3d orbitals in the free phosphorus atom. This comparison indicates that the ligand field splitting of 3d orbitals in molecular environments may be large. This has application to various problems of 3d orbital bonding, some of which are to be considered in further papers of this series, but it should be noted here that the differences between the 3d exponent values reported in Table II are probably slightly exaggerated, especially because 3d involvement has been neglected in the P—O and P—F σ bonds. However, as far as the present paper is concerned, the most important point is that the minimization of eq. [8] for the bond eigenfunction $\Psi(p_+^1\, d_+^1, p_-^2)$ of F_3PO shows that the $3d_\pi$ orbital is sufficiently compact to contribute significantly to the formation of the P—O π bond.

TABLE II

Energy-minimized 3d exponents for F_3PO including exchange

3d orbital at phosphorus	$E - E^{0*}$	3d exponent
σ	−6.25	0.31
π	−6.38	1.32
δ	−6.25	0.33

*Defined by eq [8].

Exchange has not been included for the other phosphoryl molecules considered in the electrostatic approximation, but expected trends can be followed to some extent. In the molecules F_3PO, Cl_3PO, C_3PO, and H_3PO, the bonding exchange term for $3d_\pi$ orbitals is primarily determined by the P—O bond, and for this reason the differences in properties of $3d_\pi$ orbitals in the various molecular environments are especially dependent on the different electrostatic fields and on the different exchange repulsions caused by the ligand atoms. The results in Table I show that the electrostatic field contracts the $3d_\pi$ orbitals in the order H < C < Cl < F, hydrogen being by far the least efficient. The differences for $3d_\pi$ orbitals in X_3PO are greater than those for the 3d orbitals of e_g symmetry in octahedral SX_6 molecules (21), although the ordering with different X is similar. Superimposed on the electrostatic field is the influence of repulsive exchanges between $3d_\pi$ and the ligand atoms. These repulsions are likely to be ordered H < C < F < Cl, with chlorine having a larger effect than fluorine on account of its greater number of electrons. Although hydrogen should be most favorable in this respect, it does seem that the weakness of the electrostatic field ensures $3d_\pi$ orbitals are less favorable for bond formation in H_3PO than in the other phosphoryl compounds, and this is consistent with the known instability of H_3PO. The electrostatic field in C_3PO is more favorable, and it seems likely that inclusion of exchange, according to eq. [8], would indicate compact $3d_\pi$ orbitals in alkyl derivatives.

The values of some two-center exchange integrals occurring in the calculation for F_3PO are reported in Table III. Exchange integrals for

TABLE III

Values of some exchange integrals* in F_3PO

Atomic orbitals		Exchange integrals with 3d exponent equal to 0.7	1.0	1.3
$3d_\pi$(P)	$2p_\pi$(O)	−0.041	−0.083	−0.096
$3d_\pi$(P)	1s(F)	−0.012	−0.026	−0.028
$3d_\pi$(P)	2s(F)	−0.041	−0.080	−0.087
$3d_\delta$(P)	1s(F)	−0.013	−0.027	—
$3d_\delta$(P)	2s(F)	−0.042	−0.082	—
$3d_\sigma$(P)	1s(O)	−0.057	−0.129	—
$3d_\sigma$(P)	2s(O)	−0.176	−0.353	—

*Evaluated according to eq. [9]. The fluorine exchanges are summed over all 3 atoms.

$3d_\pi$ bonding interactions are smaller than bonding exchanges involving $3d_\sigma$ orbitals (see Table 4 of ref. 21), and this difference arises in part because regions of overlap of π orbitals are in lower effective nuclear fields than is the case for σ orbital overlap. It is worth noting for the exponents suggested by these calculations that the total exchange repulsion experienced by a $3d_\pi$ orbital in F_3PO, from overlap with 1s and 2s orbitals at fluorine, is comparable to, and possibly slightly larger than, the magnitude of the bonding exchange with the oxygen $2p_\pi$ orbital. This being so, it is pertinent to consider whether the result reported here is likely to remain when the calculation is refined. We believe, however, that the stability of the result is ensured, in part because a small degree of angular polarization is likely. This refinement may be made by combining some $4p_\pi$ orbital at phosphorus with $3d_\pi$ to form the new orbital $3d_\pi'$

$$[13] \qquad 3d_\pi' = \cos\varepsilon\, 3d_\pi + \sin\varepsilon\, 4p_\pi,$$

where ε is a mixing parameter, and 4p is orthogonalized to the other phosphorus orbitals. This is indicated schematically in Fig. 2. Previous work (21) suggests that the electrostatic field of SF_6 may contract 4s orbitals from the free atom

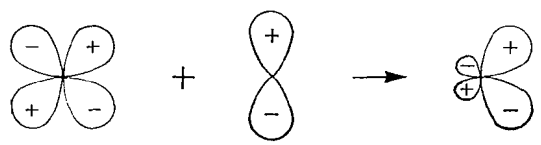

FIG. 2. Schematic representation of the mixing of $3d_\pi$ and $4p_\pi$ atomic orbitals.

size, but that contributions to σ bonds are likely to be small, both because of the lack of directional properties, and because of the constraints introduced by ensuring orthogonality to 3s. The latter problem appears less critical for π bonds since larger distances for the radial maxima should be acceptable, but, in any event, the optimized contribution of $4p_\pi$ in eq. [13] is likely to be smaller than that of $3d_\pi$.

For small mixing coefficients ε, an increase in ε would tend to increase the numerical values of the $3d_\pi'(P) - 2p_\pi(O)$ exchange, this following an increase in the corresponding overlap integral. At the same time the repulsive exchanges between $3d_\pi'$ and the ligand orbitals reduce. A repeat calculation on F_3PO, including the possibility of angular polarization, should, therefore, indicate that $3d_\pi$ orbital availability is increased compared with the prediction from the calculation reported in this paper. It should be noted, however, that at most angular polarization represents a refinement, which, unlike radial polarization, is not essential for the $3d_\pi$ bonding model to be acceptable.

The calculation of F_3PO reported in this paper represents a preliminary estimate of suitable radial functions of the phosphorus valence orbitals for use in a basis set. Since the optimized radial functions for the $3d_\pi$ orbitals turn out to have their probability maxima within internuclear regions of bonds to phosphorus, it seems likely that the $3d_\pi$ contribution to the electronic structure should be substantial. This conclusion has recently received further support from some self-consistent-field calculations made by Boyd and Lipscomb (28) on the diatomic species PO and PO^-, in which the exponents of the 3d orbitals at phosphorus were varied for minimum energy; the optimized values being 1.4 in PO and 1.1 in PO^-. We believe, therefore, that the

Can. J. Chem. Downloaded from www.nrcresearchpress.com by 210.87.254.40 on 09/05/12
For personal use only.

current theoretical evidence indicates that the concept of $3d_\pi$ bonding in phosphoryl compounds is valid, and that $3d_\pi$–$2p_\pi$ interactions are sufficiently large to influence the various features of chemical interest noted in the Introduction. In extension, it may be anticipated that d_π–p_π interactions are appreciable in other systems containing groups related to PO, such as the SO group in sulfones and sulfoxides, the SN group in thiazyl halides, and the PN group in the phosphonitrilic derivatives.

Acknowledgment

The author is grateful for support by the National Research Council of Canada.

1. D. P. Craig, A. Maccoll, R. S. Nyholm, L. E. Orgel, and L. E. Sutton. J. Chem. Soc. 332 (1954).
2. G. S. Chandler and T. Thirunamachandran. J. Chem. Phys. **47**, 1192 (1967).
3. D. W. J. Cruickshank, B. C. Webster, and D. F. Mayers. J. Chem. Phys. **40**, 3733 (1964).
4. R. F. Hudson. Advan. Inorg. Chem. Radiochem. **5**, 347 (1963).
5. R. G. Gillis, J. F. Horwood, and G. L. White. J. Am. Chem. Soc. **80**, 2999 (1958).
6. P. Haake, W. B. Miller, and D. A. Tyssee. J. Am. Chem. Soc. **86**, 3577 (1964).
7. E. A. C. Lucken and M. A. Whitehead. J. Chem. Soc. 2459 (1961).
8. M. I. Kabachnik, V. V. Voevodskii, T. A. Mastryukova, S. P. Solodovnikov, and T. A. Melenteva. J. Gen. Chem. USSR, Engl. Transl. **34**, 3277 (1964).
9. M. I. Kabachnik. Tetrahedron, **20**, 655 (1964).
10. C. E. Griffin, R. P. Peller, K. R. Martin, and J. A. Peters. J. Org. Chem. **30**, 97 (1965).
11. H. H. Jaffé. J. Chem. Phys. **22**, 1430 (1954).
12. K. Hedberg. J. Am. Chem. Soc. **77**, 6491 (1955).
13. D. W. J. Cruickshank. J. Chem. Soc. 5486 (1961).
14. R. West, L. S. Whatley, and K. J. Lake. J. Am. Chem. Soc. **83**, 761 (1961).
15. D. P. Craig and N. L. Paddock. J. Chem. Soc. 4118 (1962).
16. N. L. Paddock. Quart. Rev. London, **18**, 168 (1964).
17. K. A. R. Mitchell. Chem. Rev. To be published.
18. E. L. Wagner. J. Am. Chem. Soc. **85**, 161 (1963).
19. D. W. J. Cruickshank, B. C. Webster, and M. A. Spinnler. Int. J. Quantum Chem. **1S**, 225 (1967).
20. D. P. Craig and C. Zauli. J. Chem. Phys. **37**, 601, 609 (1962).
21. K. A. R. Mitchell. J. Chem. Soc. To be published.
22. G. R. Badgley and R. L. Livingston. J. Am. Chem. Soc. **76**, 261 (1954).
23. Q. Williams, J. Sheridan, and W. Gordy. J. Chem. Phys. **20**, 164 (1952).
24. R. J. Gillespie and R. S. Nyholm. Quart. Rev. London, **11**, 339 (1957).
25. P. A. M. Dirac. Proc. Roy. Soc. Ser. A, **123**, 714 (1929).
26. E. Clementi and D. L. Raimondi. J. Chem. Phys. **38**, 2686 (1963).
27. H. K. Wang. Acta Chem. Scand. **19**, 879 (1965).
28. D. B. Boyd and W. N. Lipscomb. J. Chem. Phys. **46**, 910 (1967).

Can. J. Chem. Downloaded from www.nrcresearchpress.com by 210.87.254.40 on 09/05/12
For personal use only.

Can. J. Chem. Downloaded from www.nrcresearchpress.com by 210.87.254.105 on 09/05/12
For personal use only.

Cinétique de l'oxydation de l'alcool benzylique par l'ion cérique[1]

D. PAQUETTE ET M. ZADOR
Département de Chimie, Université de Montréal, Montréal, Québec

Reçu le 26 avril 1968

L'oxydation de l'alcool benzylique par l'ion cérique suit un mécanisme analogue à celui proposé par Duke pour l'oxydation du butandiol-2,3, soit formation rapide d'un complexe entre l'ion cérique et l'alcool suivie de l'étape d'oxydation proprement dite. L'influence du produit s'est avérée importante dans certaines conditions expérimentales. La variation de la vitesse avec l'acidité du milieu est en accord avec la valeur de 0.4 de la constante d'hydrolyse de l'ion cérique à 25 °C. L'influence de la température a été étudiée.

Canadian Journal of Chemistry, **46**, 3507 (1968)

Introduction

Le mécanisme de l'oxydation d'alcools et de glycols par l'ion cérique a été étudié dans diverses conditions (1). Duke et Florist ont montré, pour la première fois en milieu nitrique, que la réaction procède par l'intermédiaire d'un complexe de stoechiométrie 1:1 entre l'ion cérique et l'alcool (2). D'autres études effectuées en milieu perchlorique ont conduit à des conclusions analogues (3–7).

L'étude des solutions d'ion cérique en milieu perchlorique a montré qu'il existe sous forme partiellement hydrolysée (8–10) d'après l'éq. [1]:

$$[1] \qquad Ce^{4+} + H_2O \overset{K_H}{\rightleftharpoons} CeOH^{3+} + H^+$$

A faible acidité, on a de plus constaté la tendance à former des espèces polynucléaires du type: $(Ce—O—Ce)^{6+}$ (8).

Dans le présent travail, nous nous sommes proposés d'étudier l'oxydation de l'alcool benzylique par l'ion cérique, en étudiant particulièrement l'importance de l'influence des produits et celui de l'acidité.

Méthodes expérimentales

Réactifs

Le solvant utilisé est l'eau distillée; l'alcool benzylique et la benzaldéhyde ont été purifiés par distillation sous azote. L'ion cérique a été obtenu, en solution 0.5 *M* dans l'acide perchlorique 6 *M*, de la compagnie G. F. Smith, Ohio, U.S.A. Le titre des solutions cériques a été déterminé par iodométrie (11). Les autres réactifs sont de pureté analytique.

Méthodes cinétiques

Les réactions ont été suivies par spectrophotométrie, à l'aide d'un spectrophotomètre à compartiment thermostaté à ± 0.1 °C, à des longueurs d'onde de 350 à 460 mμ.

L'étude de l'influence de la force ionique a montré qu'elle ne dépasse pas l'erreur expérimentale dans le domaine étudié ($I = 0.2$ à 1.5); ceci est en accord avec les études faites dans le cas d'autres alcools (4) et dans l'étude de l'hydrolyse de l'ion cérique (8). Elle fut néanmoins maintenue constante dans l'étude de l'influence de l'acidité. Dans le domaine de concentration utilisé, la stoechiométrie de la réaction montre qu'il y a disparition de deux ions cériques par molécule d'alcool benzylique consommée.

Le produit de la réaction, la benzaldéhyde, a été isolée par extraction et identifiée par son dérivé dinitro-2,4 phényl hydrazone et par des méthodes spectroscopiques. A haute concentration en ion cérique on est parvenu à l'isoler à raison de 85%.

Résultats et discussion

Etude du complexe Ce(IV)-$C_6H_5CH_2OH$

Par une étude spectrophotométrique, analogue à celle de Ardon (4), nous avons pu mettre en évidence la formation d'un complexe entre les deux réactifs et nous avons déterminé sa constante apparente de formation $K' = 0.8 \pm 0.2$ M^{-1} à une concentration de 0.525 *M* en $HClO_4$ à 25 °C. A cause de l'éq. [1] la constante apparente dépend de l'acidité de la solution.

Ces conclusions sont contraires à celles de Rangaswamy et Santappa (12), qui n'ont pas pu observer la formation de complexe avec l'alcool benzylique d'une part à cause de la méthode expérimentale et d'autre part, à cause des basses concentrations utilisées.

Etude cinétique

Le mécanisme de l'oxydation de l'alcool benzylique suit un schéma analogue à celui proposé par Duke pour l'oxydation du butanediol-2,3 (1):

$$[2] \quad Ce(IV) + C_6H_5CH_2OH \underset{\text{rapide}}{\overset{K'}{\rightleftharpoons}} [\text{COMPLEXE}]$$

[1]Présenté au 35ème Congrès annuel de l'Association Canadienne-Française pour l'Avancement des Sciences, Sherbrooke, Québec, novembre 1967.

Can. J. Chem. Downloaded from www.nrcresearchpress.com by 210.87.254.105 on 09/05/12
For personal use only.

$$[3]\quad [\text{COMPLEXE}] \xrightarrow[\text{lente}]{k} \text{Ce(III)} + \text{H}^+ + [\text{INTERMEDIAIRE}]$$

$$[4]\quad [\text{INTERMEDIAIRE}] + \text{Ce(IV)} \xrightarrow[\text{rapide}]{} \text{Ce(III)} + \text{H}^+ + \text{C}_6\text{H}_5\text{CHO}$$

En tenant compte des étapes [2] et [3] et de la disparition rapide d'un ion cérique supplémentaire dans l'étape [4] et en faisant les approximations habituelles, on obtient l'équation de vitesse générale:

$$[5]\qquad V = \frac{-\text{d}[\text{Ce(IV)}]}{\text{d}t} = \frac{2kK'[\text{Ce(IV)}][\text{A}]}{1 + K'([\text{Ce(IV)}] + [\text{A}])}$$

L'équation [5] est vérifiée, et en stoechiométrie et en dégénérescence par rapport à l'alcool, avec les valeurs suivantes des paramètres: $k = 2.0$ min^{-1}, $K = 0.95$ à 25 °C et à 0.525 M en HClO_4 obtenus à partir des résultats du Tableau I.

Influence de la benzaldéhyde

Nous avons étudié la réaction de l'ion cérique avec la benzaldéhyde en vue de déterminer l'intervention de celle-ci dans la vitesse de disparition de l'ion cérique lors de l'oxydation de l'alcool benzylique. Les données de vitesses initiales, présentées au Tableau II indiquent qu'il s'agit d'une réaction complexe. L'étude de l'influence de l'oxygène montre qu'il s'agit d'autoxydation; la vitesse de disparition de l'ion cérique devient très petite en absence d'oxygène.

La comparaison de vitesses initiales à haute et à basse concentration en ion cérique permet de conclure qu'à une concentration de 2.75×10^{-2} M en ion cérique, l'interférence de la benzaldéhyde est négligeable. Il apparaît qu'à basse concentration d'ion cérique l'erreur due aux produits devient très importante; le calcul à l'aide de la relation publiée par Rangaswamy et Santappa (12) donne une valeur plus de deux fois plus forte que notre constante de vitesse expérimentale pour l'oxydation de l'alcool benzylique.

TABLEAU I

Constantes de vitesse expérimentales*

A (mole l^{-1})	k'' ($\text{mole}^{-1}\,\text{l}\,\text{min}^{-1}$)	k' (min^{-1})
0.0138	1.41	
0.0250	1.51	
0.0500	1.64	
0.100		0.171
0.150		0.255
0.200		0.320
0.274		0.410

*$[\text{Ce(IV)}] = 0.0275\,M$; $[\text{HClO}_4] = 0.525\ M$; $T = 25$ °C.

TABLEAU II

Vitesse initiale de la réaction avec la benzaldéhyde*

$[\text{Ce(IV)}]$ (mole l^{-1})	$V_i = k'[\text{Ce(IV)}]$ (mole l^{-1} min^{-1})
27.5×10^{-3}	3.4×10^{-6}
6.0×10^{-3}	1.60×10^{-4}
4.0×10^{-3}	9.6×10^{-4}
2.5×10^{-3}	14.1×10^{-4}
1.0×10^{-3}	15.8×10^{-4}

*$[\text{C}_6\text{H}_5\text{CHO}] = 1.1 \times 10^{-2}\,M$; $[\text{HClO}_4] = 0.525\ M$; $T = 25$ °C.

L'influence de l'acidité a été étudiée dans le cas de l'oxydation de plusieurs alcools et l'interprétation des résultats a été faite en considérant la variation de la constante de complexation, obtenue à partir de mesures cinétiques, avec l'acidité du milieu (4–6). Pour notre part, nous avons préféré utiliser directement la variation de la vitesse avec l'acidité pour deux raisons. D'abord, ceci élimine l'erreur sur la détermination de la constante de complexation; de plus l'influence éventuelle du produit a toujours la même importance étant donné que l'on travaille à une même concentration en alcool ce qui n'est pas le cas dans les travaux mentionnés.

En considérant comme forme réactive le Ce^{4+} et en tenant compte de l'éq. [1], on obtient l'équation de vitesse suivante:

$$[6]\quad \frac{-\text{d}[\text{Ce(IV)}]}{\text{d}t} = 2k'[\text{Ce(IV)}] = \frac{2kK[\text{Ce(IV)}][\text{A}]}{1 + K[\text{A}] + K_{\text{H}}/[\text{H}^+]}$$

où $K = [\text{COMPLEXE}]/([\text{Ce}^{4+}][\text{A}])$, constante vraie de complexation.

L'équation [6] peut être transformée en une relation linéaire:

$$[7]\quad \frac{1}{k'} = \frac{1 + K[\text{A}]}{kK[\text{A}]} + \frac{K_{\text{H}}}{kK[\text{A}]} \cdot \frac{1}{[\text{H}^+]}$$

L'interprétation graphique des résultats du Tableau III par l'éq. [7] donnée dans la Fig. 1 permet de déduire la valeur de la constante

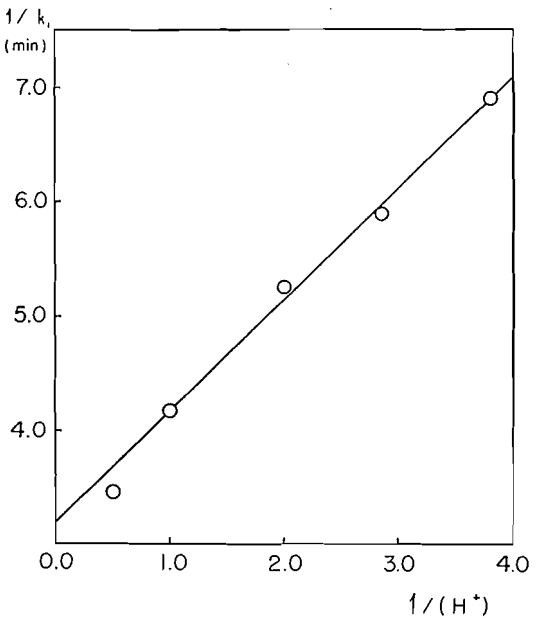

FIG. 1. Influence de l'acidité: [Ce(IV)] = 0.0275 *M*, [A] = 0.100 *M*, *T* = 25 °C. La concentration en acide est exprimée en moles par litre.

d'hydrolyse K_H et celle de la constante vraie de complexation, *K*. On obtient les valeurs suivantes:

$$K = 1.9 \pm 0.3\ M^{-1} \text{ et } K_H = 0.4 \pm 0.1\ M^{-1}$$

En interprétant directement la variation de densité optique initiale avec l'acidité nous avons obtenu la valeur de 0.5 ± 0.2 pour K_H.

TABLEAU III

Influence de l'acidité*

$[H^+]$ (mole l^{-1})	$1/[H^+]$ (mole^{-1} l)	k' (min^{-1})	$1/k'$ (min)
0.263	3.802	0.145	6.897
0.350	2.857	0.170	5.882
0.500	2.000	0.190	5.263
1.00	1.000	0.240	4.167
2.00	0.500	0.290	3.448

*[Ce(IV)] = 0.0275 *M*; [A] = 0.10 *M*; *T* = 25 °C.

Ces valeurs sont en bon accord avec celle de 0.6 obtenue par potentiométrie (10) et celle de 0.2 obtenue par l'étude spectrophotométrique dans des conditions expérimentales favorables (9).

Nos résultats ne sont par contre pas compatibles avec d'autres valeurs obtenues dans l'étude directe de l'hydrolyse dans des conditions expérimentales peu favorables (8) ou tirées de l'oxydation d'alcools (4–6). L'interférence des produits d'oxydation a été mentionnée dans certains cas (4, 7, 12) mais l'erreur produite n'a pas été estimée. Elle peut être très importante si l'on considère l'écart de plus de 100% dû à la benzaldéhyde dans certain cas. Dans le cas de l'oxydation du méthanol par exemple la formaldéhyde peut interférer sérieusement à basse concentration en méthanol d'après les résultats d'un travail indépendant (13). La valeur de K_H de 3.75, obtenue à partir de la variation de la constante de complexation (5), est environ cinq fois supérieure à la valeur de 0.7 ± 0.4 que l'on obtient en interprétant directement les données cinétiques publiées, à concentration de méthanol constante, à l'aide de l'éq. [7].

Il est à noter que nous n'avons pas tenu compte de la possibilité de formation de dimères; Offner et Skoog (9) ont démontré qu'à une concentration de 0.01 *M* en ion cérique, elle est pratiquement inexistante. Comme une légère erreur, due à la possibilité de formation d'une faible quantité de dimère, ne peut pas être exclue, la valeur obtenue représente la limite inférieure de K_H, comme on peut le montrer aisément.

Paramètres d'activation

Dans les conditions expérimentales il est difficile de séparer tous les paramètres dont dépend la vitesse de réaction; ainsi nous nous sommes bornés à déterminer les paramètres d'activation apparents. A cause de l'intervention du produit à faible concentration en ion cérique les constantes apparentes sont plus fortes dans ces conditions (Tableau IV) néanmoins, l'énergie d'activation reste la même (Fig. 2). Ce qui confirme l'identité de l'étape déterminante.

TABLEAU IV

Influence de la température*

[Ce(IV)] (mole l^{-1})	[A] (mole l^{-1})	*T* (°C)	k' (min^{-1})
0.0275	0.100	43.0	1.16
0.0275	0.100	34.0	0.430
0.0275	0.100	25.0	0.150
0.0275	0.100	18.9	0.0625
0.0275	0.100	3.6	0.0063
1.0×10^{-3}	1.0×10^{-2}	41.0	0.146
1.0×10^{-3}	1.0×10^{-2}	34.8	0.0830
1.0×10^{-3}	1.0×10^{-2}	25.0	0.0235
1.0×10^{-3}	1.0×10^{-2}	18.9	0.0102
1.0×10^{-3}	1.0×10^{-2}	3.6	0.0016

*[$HClO_4$] = 0.525 *M*.

Can. J. Chem. Downloaded from www.nrcresearchpress.com by 210.87.254.105 on 09/05/12
For personal use only.

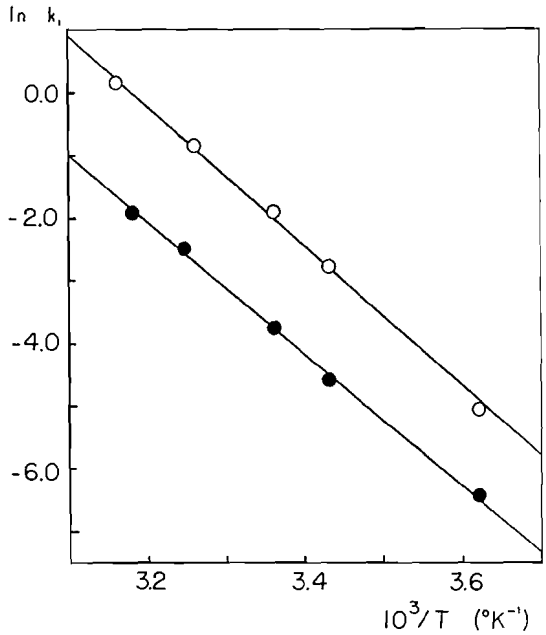

FIG. 2. Détermination de l'énergie d'activation: ○, [Ce(IV)] = 0.0275 *M*, [A] = 0.10 *M*; [$HClO_4$] = 0.525 *M*, *T* = 25 °C. ●, [Ce(IV)] = 1.0×10^{-3} *M*, [A] = 1.0×10^{-2} *M*; [$HClO_4$] = 0.525 *M*, *T* = 25 °C.

Les paramètres d'activation ont les valeurs suivantes:

$\Delta H^{\ddagger} = 21 \pm 1$ kcal mole^{-1}, $\Delta S^{\ddagger} = 6 \pm 3$ u.e.

En conclusion, l'oxydation de l'alcool benzylique par l'ion cérique suit un mécanisme identique à celui proposé par Duke (1) pour l'oxydation du butanediol-2,3. A faible concentration en ion cérique, l'interférence due aux réactions avec la benzaldéhyde est importante. La variation de la vitesse de réaction avec l'acidité du milieu due à l'intervention de l'ion cérique non hydrolysé nous a permis de déduire la constante d'hydrolyse.

Remerciements

Les auteurs remercient le Conseil National de Recherches du Canada pour l'octroi grâce auquel ce travail a pu être réalisé ainsi qu'un des arbitres pour avoir suggéré des références.

1. K. B. WIBERG. Oxidation in organic chemistry. Vol. 5A. Academic Press, Inc., New York. 1965. p. 243.
2. F. R. DUKE et A. A. FLORIST. J. Am. Chem. Soc. **71**, 2790 (1949).
3. F. R. DUKE et R. F. BREMER. J. Am. Chem. Soc. **73**, 5179 (1951). H. L. LINTZ et D. C. JOHNSON. J. Org. Chem. **32**, 556 (1967).
4. M. ARDON. J. Chem. Soc. 1811 (1957).
5. S. S. MUHAMMAD et K. V. RAO. Bull. Chem. Soc. Japan, **36**, 943 (1963).
6. B. SETHURAM et S. S. MUHAMMAD. Acta Chim. Acad. Sci. Hung. **46**, 125 (1965).
7. M. RANGASWAMY et M. SANTAPPA. Current Sci. India, **34**, 282 (1965).
8. T. S. HARDWICK et E. ROBERTSON. Can. J. Chem. **29**, 818 (1951).
9. H. G. OFFNER et D. A. SKOOG. Anal. Chem. **38**, 1520 (1966).
10. M. S. SHERRILL, C. G. KING et R. C. SPOONER. J. Am. Chem. Soc. **65**, 170 (1943).
11. H. WILLARD *et al.* Elements of quantitative analysis. D. Van Nostrand Co., Inc., New York. 1956. p. 262.
12. M. RANGASWAMY et M. SANTAPPA. Current Sci. India, **35**, 332 (1966).
13. G. HARGREAVES et L. H. SUTCLIFFE. Trans. Faraday Soc. **51**, 1105 (1955).

Can. J. Chem. Downloaded from www.nrcresearchpress.com by 210.87.254.105 on 09/05/12
For personal use only.

Can. J. Chem. Downloaded from www.nrcresearchpress.com by 210.87.254.6 on 09/05/12
For personal use only.

γ-Radiolysis of cyclohexane with electron scavengers. VI. N_2O and SF_6 as electron scavengers in the vapor phase[1]

N. H. SAGERT, R. W. ROBINSON, AND A. S. BLAIR[2]
Research Chemistry Branch, Chalk River Nuclear Laboratories, Chalk River, Ontario

Received June 17, 1968

The γ-radiolysis of cyclohexane has been examined in the vapor phase using N_2O and SF_6 as electron scavengers. Both N_2O and SF_6 reduce the hydrogen yield from 4.6 to 3.0 G units, indicating that 3.0 G units of hydrogen have neutral species as precursors, while 1.6 G units have electrons as precursors.

Radiolysis of cyclohexane vapor with more than 2% N_2O produces 10.4 G units of cyclohexene and 11.5 of nitrogen. Carbon dioxide reduces both these yields; the extrapolated value of $G(N_2)$ is equal to G(electrons) at infinite CO_2 concentration. Thus O^- is likely a precursor of that part of the nitrogen yield in excess of G(electrons), and of the cyclohexene yield associated with this nitrogen yield.

The first order molecular detachment of hydrogen is unaffected by electron scavengers, showing that most of this first order yield has neutral precursors. The implications for Dyne's general mechanism of hydrocarbon radiolysis are discussed.

Canadian Journal of Chemistry, 46, 3511 (1968)

Introduction

The electron scavengers N_2O (1, 2) and SF_6 (3) have been widely used to determine the role of electrons in the radiolysis of hydrocarbon systems. In this laboratory we have examined secondary reactions in the liquid (4) and solid phase (5) radiolysis of cyclohexane with these electron scavengers by measuring yields of the major liquid products, cyclohexene and bicyclohexyl, as well as yields of gaseous products. The work reported here extends these studies to the vapor phase.

Recently Holtslander and Freeman (6) reported about 20 G units of nitrogen and methylcyclohexene from the vapor phase radiolysis of the methylcyclohexane–N_2O system. They proposed a chain reaction to explain their results. Somewhat smaller nitrogen and phenol yields have been observed by Hentz and Rzad (7) from the radiolysis of the vapor phase benzene–N_2O system. On the other hand Johnson and Warman (8) and Warman (9, 10) have obtained 7 to 8 G units of nitrogen from the radiolysis of the propane–N_2O and *n*-butane–N_2O systems. Hence it was of interest to examine the cyclohexane–N_2O system to see if large nitrogen yields were produced, to see if these large nitrogen yields were accompanied by a corresponding increase in olefin yields, and to determine the precursors of any large nitrogen and olefin yields.

Blachford and Dyne (11) applied Dyne's isotopic technique (12) to the vapor phase radiolysis of cyclohexane using benzene as a scavenger. We applied this same technique to the cyclohexane radiolysis, using N_2O and SF_6 as specific electron scavengers, to see if electron scavengers had any effect on the first order hydrogen yield.

Experimental

The sources and purification of cyclohexane, N_2O, SF_6, and CO_2 have been described in refs. 13, 4, and 14 respectively. Perdeuterocyclohexane was obtained from Merck (Canada). It was shaken with concentrated sulfuric acid, then distilled. The distillate was first washed with dilute sodium carbonate solution, then with water, and redistilled. Irradiation and dosimetry techniques have also been described previously (13). The total dose given the cyclohexane was $2.2_2 \times 10^{19}$ eV/g unless otherwise noted, and this dose was given at a mean dose rate of 4.9×10^{17} eV/g min. All G values quoted in this article are molecules produced for each 100 eV absorbed in the entire system. Relative electron stopping powers per molecule for ethylene, N_2O, and CO_2 were taken from Meisels (15). The relative electron stopping power per molecule for cyclohexane was taken as three times that of ethylene, and that for SF_6 was taken from Davidow and Armstrong (16) and Meisels (15).

Analytical procedures have been described (4).

Results

The radiolysis of cyclohexane vapor produces a wide variety of products (11, 17). For this study,

[1]Issued as A.E.C.L. No. 2739.

[2]A.E.C.L. Summer Student, 1967. Present address: Department of Chemistry, University of Toronto, Toronto, Ontario.

TABLE I

G values of selected products from the radiolysis of pure cyclohexane vapor

Product	*G* value: This work, zero dose $T = 133$ °C	This work, dose $= 2.3 \times 10^{19}$ eV/g $T = 133$ °C	Ref. 17, dose $= 3 \times 10^{19}$ eV/g $T = 100$ °C	Ref. 11, dose $= 3 \times 10^{19}$ eV/g $T = 125$ °C
H_2	4.6	4.3	4.7	5.3
CH_4	0.5_5	0.4_1	0.36	0.6
C_6H_{10}	2.4_0	2.0	1.0	2.2
$(C_6H_{11})_2$	0.75	0.7	0.8	1.0

we measured yields of hydrogen, methane, cyclohexene, and bicyclohexyl, and yields of these products from pure cyclohexane vapor under our conditions are given in Table I.

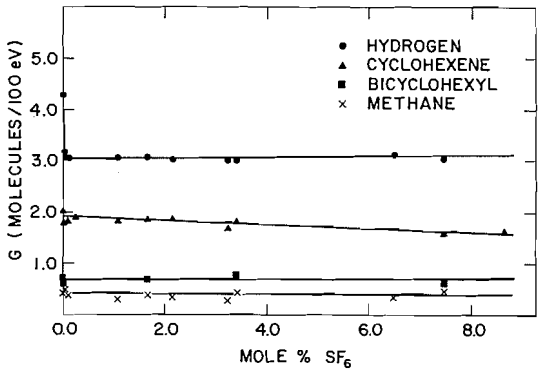

FIG. 1. Yields from the cyclohexane–SF_6 system. $T = 135$ °C. Cyclohexane pressure = 740 Torr.

Yields of hydrogen, methane, cyclohexene, and bicyclohexyl in the presence of SF_6 are shown in Fig. 1. Hydrogen is reduced to 3.0_5 G units by the smallest amount of SF_6 which could be added. This result is similar to that obtained with the SF_6–methylcyclohexane system (18). The yields of the other products studied are affected much less by SF_6. These yields are independent of dose up to doses of 5×10^{19} eV/g. Yields of hydrogen, nitrogen, cyclohexene, and bicyclohexyl in the presence of N_2O are shown in Fig. 2. Although hydrogen is reduced to 3.0_4 G units and bicyclohexyl is not greatly affected, nitrogen and cyclohexene yields are increased enormously to 11.5 and 10.4 G units respectively. These large yields are similar to the olefin and nitrogen yields obtained from the vapor phase methylcyclohexane–N_2O system (6), and to the phenol and nitrogen yields from the vapor phase benzene–N_2O system (7). Cyclohexanone and cyclohexanol were sought, but were found to be minor products ($G < 0.2$). Water was not determined. All yields in the presence of scavenger are independent of dose, within experimental error, from 0.5×10^{19} to 7.0×10^{19} eV/g. Within experimental error they are also independent of temperature from 90 to 170 °C. There is a trend toward lower yields of nitrogen and cyclohexene at the lowest pressures (Fig. 3) with a corresponding increase in bicyclohexyl.

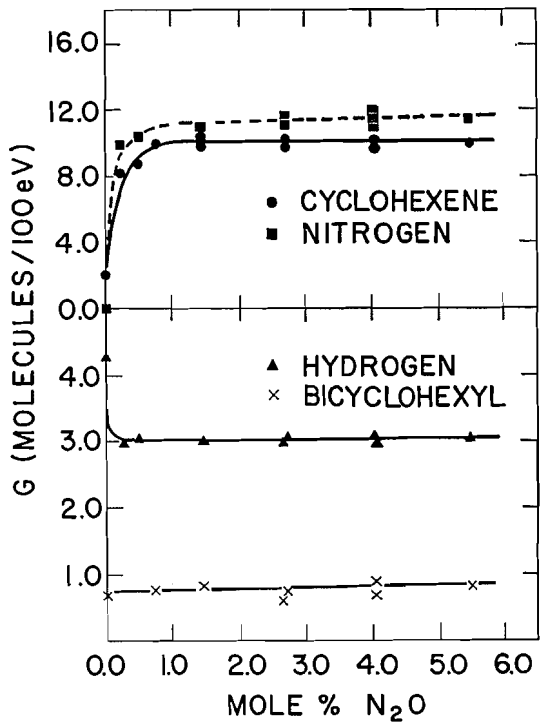

FIG. 2. Yields from the cyclohexane–N_2O system. $T = 133$ °C. Cyclohexane pressure = 740 Torr.

Can. J. Chem. Downloaded from www.nrcresearchpress.com by 210.87.254.6 on 09/05/12
For personal use only.

Can. J. Chem. Downloaded from www.nrcresearchpress.com by 210.87.254.6 on 09/05/12
For personal use only.

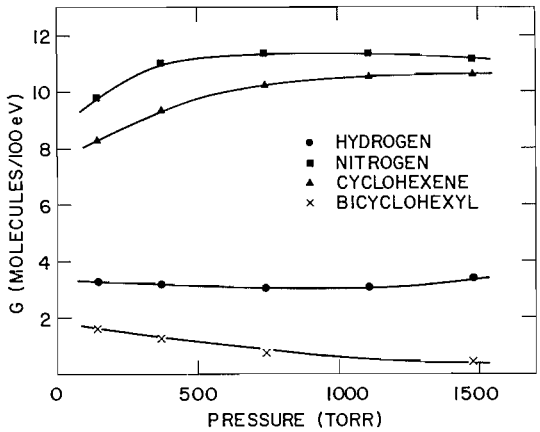

FIG. 3. Yields from the cyclohexane–N_2O system as a function of pressure at 4.0$_5$% N_2O. T = 133 °C.

Figure 4 gives yields of HD and D_2 from 4.0 electron % C_6D_{12} in C_6H_{12}. These yields are calculated on the basis of energy absorbed in the C_6D_{12}, as described by Dyne and Jenkinson (12). In dilute solutions of deuterated hydrocarbon, the D_2 yield, or G_1(D), is a measure of the first order yield of hydrogen, as second order processes producing D_2 are small. G_1(D) is not affected by electron scavengers such as N_2O, just as it is not affected by benzene (11). Similarly g(HD) is a measure of second order reactions leading to hydrogen, and it is little affected by N_2O. These yields are, within experimental error, constant over the ranges of dose, pressure, and temperature studied; that is, from 0.5 to 7.0 eV/g, from 150 to 1500 Torr, and from 90 to 170 °C.

Holtslander and Freeman (6) have argued convincingly that the large increases in olefin and

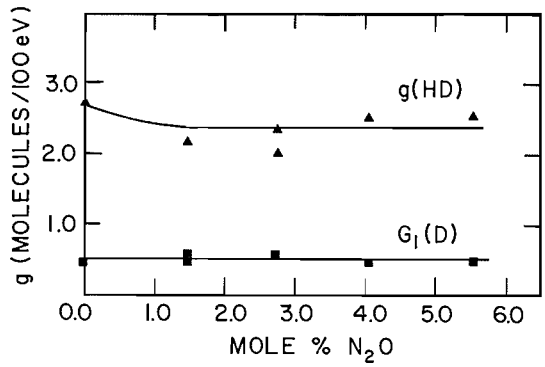

FIG. 4. Yields of HD and D_2 from 4.0% C_6D_{12} in C_6H_{12} with N_2O. T = 133 °C. Total cyclohexane pressure = 740 Torr.

nitrogen seen in the methylcyclohexane–N_2O system result from a chain reaction involving O^-. Since Warman (9, 10) has shown that CO_2 acts as an O^- scavenger, in the vapor phase at least, we added CO_2 to the cyclohexane–N_2O system to see if CO_2 could affect the large cyclohexene and nitrogen yields. The results are given in Fig. 5 and show that CO_2 does decrease these yields without affecting the hydrogen yield. The addition of 1/2 mole % SF_6 to the cyclohexane–N_2O system eliminates the nitrogen yield and reduces the cyclohexene yield to 2.6 G units.

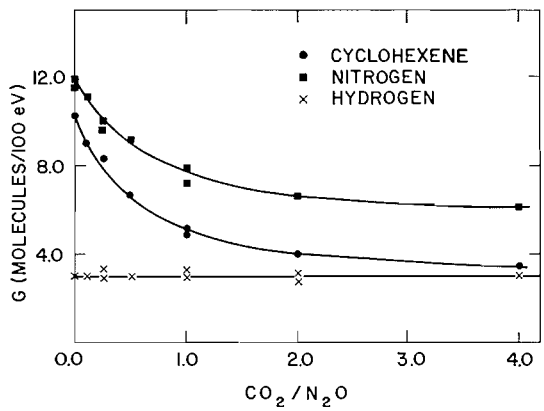

FIG. 5. Yields from the cyclohexane–N_2O–CO_2 system. 4.05% N_2O. T = 133 °C. Cyclohexane pressure = 740 Torr.

Discussion

Both SF_6 and N_2O reduce the hydrogen yield by 1.6 to 3.0 G units. This effect may be considered a result of electron capture by the additives since both N_2O and SF_6 react slowly with atoms and radicals (19, 20), but have large cross sections for the capture of thermal electrons (21, 22). In addition, both have larger ionization potentials than cyclohexane (23), so that positive charge transfer from cyclohexane to the additive is impossible. These additives have also been used as electron scavengers in the gas phase radiolysis of methylcyclohexane (18) and propane (8).

Like Theard (17), we shall take the electron yield in cyclohexane to be 4.2 G units, since the W values for many hydrocarbons are close to 24 eV/ion pair (15). Hydrogen production from pure cyclohexane vapor may then be represented by the following mechanisms:

[1a] $C_6H_{12} \sim\!\!\sim\!\!\sim\!\!\rightarrow (M_1^+ - - - + M_n^+) + e$

[1b] $C_6H_{12} \rightsquigarrow C_6H_{12}^*$

[2a] $C_6H_{12}^* \rightarrow H_2 + C_6H_{10}$

[2b] $\rightarrow H + \text{products}$

[3a] $H + \text{products}$

[3b] $(M_1^+ - - - + M_n^+) + e \rightarrow H_2 + \text{products}$

[3c] $\text{no } H_2 \text{ or } H_2 \text{ precursors}$

[4] $H + C_6H_{12} \rightarrow H_2 + C_6H_{11}$

Individual yields of these reactions, along with the methods used to obtain them are given in Table II. The significance of the deuterium

TABLE II

Yields of individual reactions in the vapor phase radiolysis of cyclohexane

Reaction	G	Source of G	Reference
[1a]	4.2	G(e)	15, 17
[1b]	3.0	Limiting yield with N_2O and SF_6	
[2a]	0.5	G_1(D)	
[2b]	2.5	G[1b]–G[2a]	
[3a]	1.6	$G(H_2)$–G[1b]	
[3b]	<0.15	Effect of N_2O on G_1(D)	
[3c]	2.6	G(e)−G[3a]−G[3b]	
[4]	4.1	G[2b]+G[3a]	
[5a]	0.7$_5$	G(bicyclohexyl)	
[5b]	0.3$_4$	$\frac{k_d}{k_c}$ G(bicyclohexyl)	24

labelling techniques in determining yields of reactions [2a] and [3b] will be described later. Bicyclohexyl will be assumed to be produced by reaction [5a].

[5a] $2C_6H_{11} \rightarrow (C_6H_{11})_2$

[5b] $\rightarrow C_6H_{10} + C_6H_{12}$

Using the G values for reactions [1] through [5] given in Table II the total cyclohexyl radical yield, as given by reaction [2b] plus reaction [4] and part of reaction [3a], is much larger than twice reaction [5a] plus [5b]. This is not surprising as much fragmentation occurs in reactions [1a], [3a], and [3c] so that the predominant fate of cyclohexyl radicals will not be combination with each other. The largest share of the cyclohexene yield is not accounted for by reactions [1] through [5] and probably arises by disproportionation of cyclohexyl radicals with other radicals, and by ion–molecule reactions.

The first order deuterium yield, G_1(D) from a 4% mixture of C_6D_{12} in C_6H_{12} is 0.5 G units. This is somewhat less than the 0.8 G units reported by Dyne, Denhartog, and Smith (25), and by Blachford and Dyne (11). Dosimetry probably accounts for some of this discrepancy as different methods of measuring the dose rate were used. This is especially likely since Blachford and Dyne reported high yields for all the products measured. The G_1(D) yield is related to reactions [2a] and [3b]. Since the electron scavengers do not effect G_1(D), apparently the entire deuterium yield arises from reaction [2a]. It should be noted, however, that any effect of scavenger on this yield must be multiplied by about 3 as described below. As any effect of scavenger is less than 0.05 G units, the yield from reaction [3b] is less than 0.15 G units.

Like the D_2 yield, the HD yield is little affected by electron scavengers. A large portion of this yield comes by way of reaction [2b] which would not be affected by electron scavengers in any case. However, it might be expected that the 1.6 G units from reaction [3a] would be affected. An answer to this problem is given by work of Ausloos and Lias (26) who showed that charge exchange

[6] $C_6D_{12}^+ + C_6H_{12} \rightleftarrows C_6H_{12}^+ + C_6D_{12}$

occurs rapidly in the vapor phase and that, under their conditions at least, the equilibrium constant for reaction [6] is 2.6. Similar equilibria will apply for all the possible combinations of charged species involved in the radiolysis, and the result will be a transfer of charge away from deuterated species to protiated species. Hence relatively more protiated species will be neutralized than would be expected on an electron fraction basis, and the yield of D atoms from reaction [3a] will be much less than the 1.5 g units estimated on such a basis. Any deuterium from reaction [3b] will also be less than that calculated on an electron fraction basis by a factor of 2.6, as mentioned above.

Dyne (27) has proposed a mechanism for the radiolysis of saturated hydrocarbons to explain his results with deuterium labelled tracers. In particular, it explains why G_1(D) is reduced by adding electron scavengers to the C_6H_{12} – 4% C_6D_{12} system, and why G_1(D) is reduced by a larger fraction than the total hydrogen yieldl This mechanism depends mainly on the proposa. that excited states formed in reaction [1b] are identical, in their kinetic behavior at least, to those formed as intermediates in reaction [3].

Can. J. Chem. Downloaded from www.nrcresearchpress.com by 210.87.254.6 on 09/05/12
For personal use only.

Can. J. Chem. Downloaded from www.nrcresearchpress.com by 210.87.254.6 on 09/05/12
For personal use only.

Although this mechanism explained their liquid phase results well, some difficulty was encountered in applying it to the vapor phase observations, where the addition of benzene did not decrease $G_1(D)$. The suggestion was made that the vapor phase results could be explained if charge transfer was a slow process in the vapor (27). However, Ausloos and Lias (26) have recently shown that reactions such as [6] occur very rapidly in the vapor phase when there is at least 0.1 eV difference in the ionization potentials of the molecules involved. Another suggestion, made earlier by Blachford and Dyne (11), is that excited states formed in reaction [1*b*] are quite different from those formed as intermediates in reaction [3]. This view is supported by our interpretation of the effect of electron scavengers, which shows that the ratio of first order hydrogen to second order hydrogen precursors is quite different for excited states formed directly (k_{2a}/k_{2b}) than for those formed by ion–electron combination (k_{3b}/k_{3a}). It appears reasonable that the excited species existing in the vapor state should be discrete excited states corresponding to the lowest level of a set of transitions. Hence different methods of population of higher levels such as neutralization or direct excitation will result in different ratios of final states. In the liquid, however, the excited states may be more analogous to excitons (28) with some charge separation (29) and with wider bands of permissible energies, so that the method of formation is less important.

The proposal that charge exchange occurs but that excited states formed in reaction [1*b*] and [3] are different also explains why Dyne, Denhartog, and Smith (25) saw that $G_1(D)$ was constant from C_6D_{12} in a number of hydrocarbons, but that the hydrogen yield from mixtures of *n*-hexane and 2-methyl pentane was not linear with electron fraction. Since the D_2 yield comes largely from reaction [1*b*] in the vapor, it is constant regardless of the other components of the mixture. However, charge exchange processes will affect the total hydrogen yield, which will tend to be more like that from the hydrocarbon of lower ionization potential (23). Dyne, Denhartog, and Smith (25) noted that the hydrogen yield from an equimolar mixture of 2-methyl pentane in *n*-hexane was more like that from 2-methyl pentane.

The large nitrogen yield for the cyclohexane–N_2O system cannot be entirely explained by the reactions proposed by Johnson and Warman (8) and Warman (9, 10) for the propane–N_2O systems

$$[7] \quad e + N_2O \rightarrow N_2O^-$$

$$[8] \quad N_2O^- \rightarrow N_2 + O^-$$

$$[9a] \quad O^- + N_2O \rightarrow N_2 + O_2^-$$

$$[9b] \quad \rightarrow NO + NO^-$$

These reactions could only account for a nitrogen yield of 2 G(e) or 8.4 G units, even if reaction [9*b*] is negligible compared to [9*a*]. In fact, Warman (10) has shown that $k_{9a}/k_{9b} = 1.2 \pm 0.1_5$. Thus in the cyclohexane–N_2O system an additional source of nitrogen must be sought. The high cyclohexene yields and the approximate equality of $G(N_2)$ and G(cyclohexene) plus G(bicyclohexyl) suggests that a chain reaction of the type proposed by Holtslander and Freeman (6) for the methylcyclohexane–N_2O system is involved. They proposed a chain which for our system would be written:

$$[10] \quad O^- + C_6H_{12} \rightarrow OH^- + C_6H_{11}$$

$$[11] \quad OH^- + C_6H_{12} \rightarrow H_2O + C_6H_{11}^-$$

$$[12] \quad C_6H_{11}^- + N_2O \rightarrow N_2O^- + C_6H_{11}$$

$$[8] \quad N_2O^- \rightarrow N_2 + O^-$$

In our system, however, this proposal is not consistent with the constant yield of dimer on adding N_2O, as an increase in cyclohexyl radicals should produce at least a small increase in dimer. A large ratio of rate constants for disproportionation to combination would result in a small increase which might escape detection. However, this ratio is, in fact, quite small (24). There are, of course, large yields of other radicals in the system which could disproportionate with cyclohexyl radicals to give cyclohexene. Another complication exists, in that in the radiolysis of pure cyclohexane vapor, several G units of cyclohexene may be destroyed by secondary reactions (11). Hence any consideration of the details of the mechanism by which the extra cyclohexene is produced will be highly speculative.

In an attempt to show that O^- was a precursor of the extra nitrogen and cyclohexene, CO_2 was added to the cyclohexane–N_2O system. Warman (9, 10) has shown that reaction [13]:

$$[13] \quad O^- + CO_2 \rightarrow CO_3^-$$

is fast compared to reaction [9]. Nitrogen and

cyclohexene were reduced by CO_2, although hydrogen was unaffected. If the competition

$$[14] \qquad O^- + C_6H_{12} \xrightarrow{(N_2O)} nN_2 + \text{products}$$

$$[13] \qquad O^- + CO_2 \rightarrow CO_3^-$$

is considered, then

$$[15] \qquad \frac{1}{G(N_2)_0 - G(N_2)} = \frac{1}{nG(e)}\left\{1 + \frac{k_{14}[C_6H_{12}]}{k_{13}[CO_2]}\right\}$$

where $G(N_2)_0$ is $G(N_2)$ in the absence of CO_2.

A plot of $\{G(N_2)_0 - G(N_2)\}^{-1}$ against $[N_2O]/[CO_2]$ for a constant ratio of $[C_6H_{12}]/[N_2O]$ is shown in Fig. 6. From this figure, $nG(e) = 6.9$,

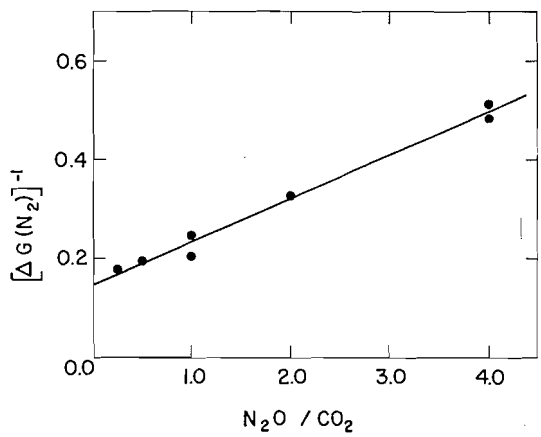

FIG. 6. Competition plot of the nitrogen yields from Fig. 5.

which gives an n of 1.6 assuming $G(e) = 4.2$. $G(N_2)_0 - nG(e)$, which should equal $G(e)$, is 4.9. Considering the approximations involved, this is in reasonable agreement with the value of 4.2 used above. The ratio k_{13}/k_{14} is given from the slope of the line in Fig. 6 as 39.2. Equation [15] is, however, a gross simplification. It assumes that nitrogen is not produced by reaction [9]. Furthermore it does not represent the chain reaction of Holtslander and Freeman (6) except for unit chain length. Since we have no direct evidence as to whether a true chain reaction of the type envisaged by Holtslander and Freeman is operating here, or whether nitrogen plus cyclohexene are produced in a number of sequential steps, more rigorous treatments are probably not justified. We have shown, however, that CO_2 can successfully compete for precursors of the extra nitrogen and cyclohexene, and thus that O^- is probably a precursor of these products.

Acknowledgments

It is a pleasure to acknowledge useful discussions with our colleagues and with Dr. J. M. Warman. Dr. W. J. Holtslander is thanked for comments on an earlier draft.

1. G. SCHOLES and M. SIMIC. Nature, **202**, 895 (1964).
2. S. SATO, R. YUGETA, K. SHINSAKA, and T. TERAO. Bull. Chem. Soc. Japan, **39**, 156 (1966).
3. S. SATO, T. TERAO, M. KONO, and S. SHIDA. Bull. Chem. Soc. Japan, **40**, 1818 (1967).
4. N. H. SAGERT and A. S. BLAIR. Can. J. Chem. **45**, 1351 (1967).
5. N. H. SAGERT. Can. J. Chem. **46**, 89 (1968).
6. W. J. HOLTSLANDER and G. R. FREEMAN. Can. J. Chem. **45**, 1661 (1967).
7. R. R. HENTZ and S. J. RZAD. J. Phys. Chem. **72**, 1027 (1968).
8. G. R. A. JOHNSON and J. M. WARMAN. Trans. Faraday Soc. **61**, 1709 (1965).
9. J. M. WARMAN. J. Phys. Chem. **71**, 4066 (1967).
10. J. M. WARMAN. Nature, **213**, 381 (1967).
11. J. BLACHFORD and P. J. DYNE. Can. J. Chem. **42**, 1165 (1964).
12. P. J. DYNE and W. M. JENKINSON. Can. J. Chem. **38**, 539 (1960).
13. N. H. SAGERT and A. S. BLAIR. Can. J. Chem. **46**, 3284 (1968).
14. N. H. SAGERT. Can. J. Chem. **46**, 336 (1968).
15. G. G. MEISELS. J. Chem. Phys. **41**, 51 (1964).
16. R. S. DAVIDOW and D. A. ARMSTRONG. Radiation Res. **28**, 143 (1966).
17. L. M. THEARD. J. Phys. Chem. **69**, 3292 (1965).
18. W. J. HOLTSLANDER and G. R. FREEMAN. Can. J. Chem. **45**, 1649 (1967).
19. T. N. BELL and K. O. KUTSCHKE. Can. J. Chem. **42**, 2713 (1964).
20. L. BATT and F. R. CRUICKSHANK. J. Phys. Chem. **70**, 723 (1966).
21. D. RAPP and D. D. BRIGLIA. J. Chem. Phys. **43**, 1480 (1965).
22. R. K. ASUNDI and J. D. CRAGGS. Proc. Phys. Soc. London, **83**, 611 (1964).
23. V. I. VEDENEYEV, L. V. GURVICH, V. N. KONDRAT'YEV, V. A. MEDVEDEV, and YE. L. FRANKEVICH. Bond energies, ionization potentials, and electron affinities. Edward Arnold and Co., London. 1966.
24. P. W. BECK, D. V. KNIEBES, and H. E. GUNNING. J. Chem. Phys. **22**, 272 (1964).
25. P. J. DYNE, J. DENHARTOG, and D. R. SMITH. Discussions Faraday Soc. **36**, 135 (1963).
26. P. AUSLOOS and S. G. LIAS. The chemistry of ionization and excitation. *Edited by* G. R. A. Johnson and G. Scholes. Taylor and Francis, London. 1967. pp. 77–89.
27. P. J. DYNE. Can. J. Chem. **43**, 1080 (1965).
28. D. L. DEXTER and R. S. KNOX. Excitons. Interscience Publishers, Inc., New York. 1965. p. 112.
29. M. BURTON. J. Phys. Chem. In press.

Can. J. Chem. Downloaded from www.nrcresearchpress.com by 210.87.254.6 on 09/05/12
For personal use only.

Can. J. Chem. Downloaded from www.nrcresearchpress.com by 210.87.254.105 on 09/05/12
For personal use only.

Infrared study of the adsorption, desorption, and degassing processes of trimethyl-borate on a porous high-silica glass system

MICHIE SHIMIZU AND H. D. GESSER
Department of Chemistry, University of Manitoba, Winnipeg, Manitoba

Received March 7, 1968

Infrared absorption has been applied to the process of adsorption, desorption, and degassing of trimethyl-borate on porous high-silica glass. The adsorbate was shown to react with the silanol and siloxane surface groups at room temperature to form ≡Si—OCH_3 and =B—OCH_3 as well as CH_3OH which after high temperature degassing left ≡SiOH and =BOH on the surface.

Canadian Journal of Chemistry, **46**, 3517 (1968)

Introduction

Many workers (1, and references cited therein) have studied the problem of methanol adsorption on silica gel, aerogel, porous high-silica glass, and silica–alumina gels, probably all with borosilicate-like "Pyrex" glass apparatus. It was brought to our attention (2) during a report on the infrared (i.r.) and electron spin resonance (e.s.r.) studies of methanol (3) on porous high-silica glass that methanol, during storage, is known to dissolve boron from borosilicate glass and form trimethyl-borate (4). We, therefore, undertook a study of the trimethyl-borate glass system to determine its possible effect on our methanol study.

Experimental

A standard vacuum line constructed of "Pyrex" glass and fitted with a mercury diffusion pump was used. Infrared spectra were recorded on a Perkin–Elmer model 337 spectrophotometer with external recorder at room temperature. The assignment of wave numbers is estimated to be within $\pm 3\,cm^{-1}$. Electron spin resonance spectra were performed on a Varian E-3 spectrometer at 77 °K. The sample cells for i.r. were made of OH-free quartz glass ("Infrasil") of 2 × 5 × 30 mm inner dimensions and 1 mm thickness. Sample tubes for e.s.r. were 3 mm i.d. and 4 mm o.d. These were fitted with a quartz to borosilicate glass seal and a stopcock as shown in Fig. 1. The stopcock which was used to introduce the adsorbate was so located as to prevent grease from contaminating the sample accidentally. The hollow corner H could hold the adsorbent (a piece of glass) as shown by the dotted line in the figure and thus empty the cell for a blank test[1].

Adsorbents

The porous high-silica glass, "VYCOR®" of Corning, code #7930, was washed with hot benzene, isopropanol,

[1]For the blank test, the baseline (as shown in curve *b*, Fig. 2) was checked for each experiment and the transmittance of *b* at 4000 cm^{-1} was chosen as 100% for the sample.

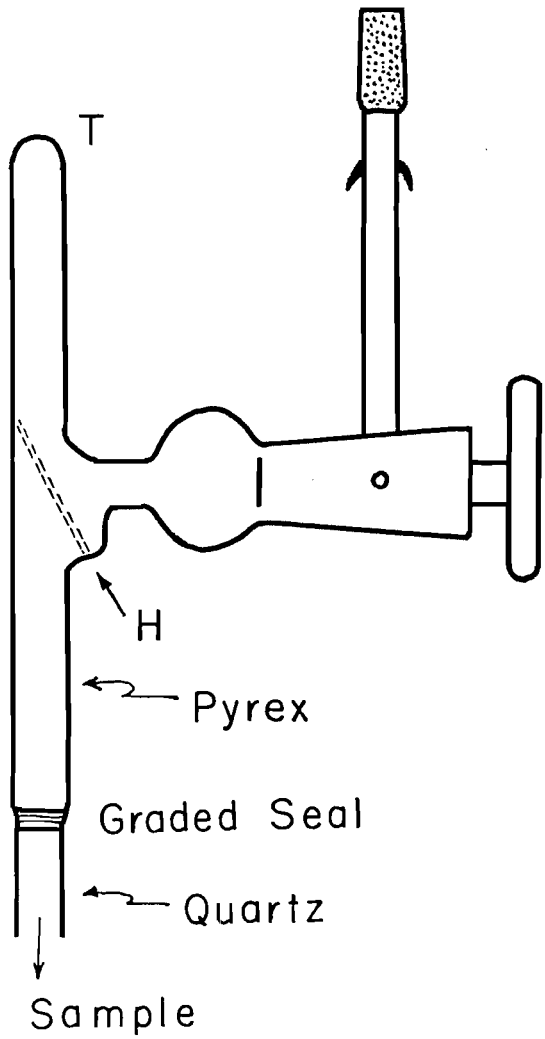

FIG. 1. The sample cell.

TABLE I

Adsorption and desorption of $B(OCH_3)_3$ on porous high-silica glass

Expt. I, adsorption		Expt. II, desorption			Expt. III, degassing after thermoleaching at 500 °C	
Expt. #	Coverage (%)	Expt. #	Desorption T (°C)	Coverage (%)‡	Expt. #	Degassing at (°C)
0	0	1′	0	50–60	1″	25
1	13	2′	25	”	2″	120
2	27	3′	120	30–40	3″	350
3*	40	4′	450–480	~20	4″	450
3†	40				5″	650
4	60	5′	650	10–15	6″	800
5	80	6′	800	0		
6	140					
7	185					
8	250					
9	350					

*Five hours after the desorption, not at equilibrium.
†Two days after the adsorption, at equilibrium.
‡Estimated by i.r. spectra.

water, 18 M HNO_3, and again with water; it was then dried at 110 °C, thermoleached in air at 480–550 °C for about 20 h until it was clear, and weighed in air. It was then degassed at 800 °C for more than 4 h in vacuo, or fluorinated (5, 6). A sample of 1 mm thickness plate and 2 mm diameter rod was used for i.r. and e.s.r. studies, respectively.

Adsorbates

The purification method for trimethyl-borate by Schlesinger *et al.* (7) was modified as follows: the trimethyl-borate (Aldrich Chemical Co., Milwaukee, Wis.) was refluxed with Drierite for several hours. Freshly activated Drierite was again added and the material was distilled at 67.8–68.2 °C under dried air. A vacuum distillation was then conducted and the middle one-third portion collected. The i.r. spectra of the vapor showed the OH stretching vibration around 3700 cm^{-1} to have completely disappeared. This is shown in Fig. 2, curve *a*. This spectrum also showed sharp strong absorptions at 1495, 1365, and 1034 cm^{-1} due to B—O and C—O respectively, and no metaborate absorption at 720 and 735 cm^{-1} (8–10). The vapor pressure of the $B(OCH_3)_3$ at 0 °C, 35.0 mm Hg, was used as p_0 during this adsorption work. After conditioning the vacuum line with vapor two or three times, the trimethyl-borate stored in the vacuum line was checked for p_0 at 0 °C, introduced into the cell for the adsorption, and also checked occasionally by i.r. The same spectra and p_0 were obtained throughout the study.

The i.r. spectra of gases were all observed in a 10 cm long Pyrex glass cell with NaCl windows. The cell showed no change in i.r. spectra when samples of trimethyl-borate or methanol were stored in it for periods of 15 min to several days.

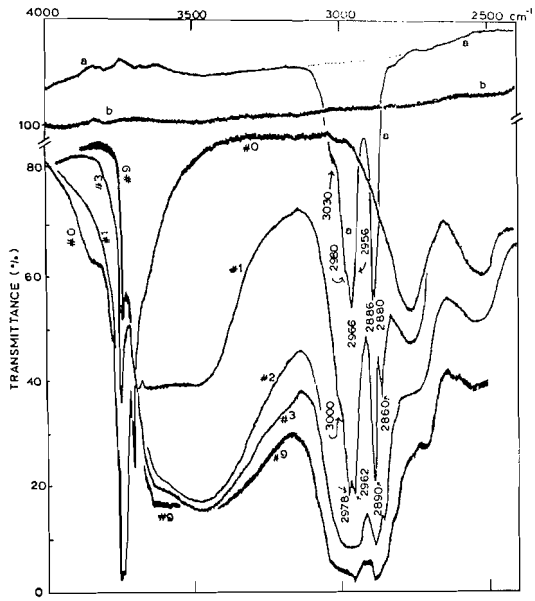

FIG. 2. Infrared spectra of the $B(OCH_3)_3$ – porous high-silica glass system for the adsorption process (expt. I). *a* is for pure $B(CH_3)_3$ gas (5 Torr, 20 °C): the dotted line is the baseline for the empty cell; *b*, the baseline for the empty adsorption cell. The transmittance axis for *a* is displaced arbitrarily.

Experimental Results

As summarized in Table I, a series of i.r. spectra were taken during the successive experiments of adsorption (expts. #1–9), desorption (expts. #1′–6′), and then degassing processes (expts. #1″–6″) of the $B(OCH_3)_3$ porous glass system. These expt. # will be referred to in the i.r. spectra and discussion.

Adsorption Isotherm

The adsorption isotherm of $B(OCH_3)_3$ on porous glass at 0 °C, was determined to be Brunauer, Emmett, and Teller (BET) type IV, and gave the value of a BET monolayer (11) as

Can. J. Chem. Downloaded from www.nrcresearchpress.com by 210.87.254.105 on 09/05/12
For personal use only.

Can. J. Chem. Downloaded from www.nrcresearchpress.com by 210.87.254.105 on 09/05/12
For personal use only.

230 μmoles/g of glass. Using this value as 100%, the surface coverage, θ, took the place of amount adsorbed for convenience. The surface area of this glass could be estimated as 48.4 m^2/g by the BET method (11) from the density of the liquid (0.9547 g/cm^3 at 0 °C, ref. 12) and using 34.9 $Å^2$ for the effective area of $B(OCH_3)_3$.

Electron Spin Resonance Measurements

The e.s.r. measurements of ultraviolet-irradiated $B(OCH_3)_3$ at coverages of θ = 0.3, 30, 60, and 90% on glass, and θ = 35% on partially fluorinated glass, gave no signal. Comparable photolysis of methanol gave measurable e.s.r. spectra on partially fluorinated glass (3). The glass pieces used in these experiments were about 0.100 g in all cases.

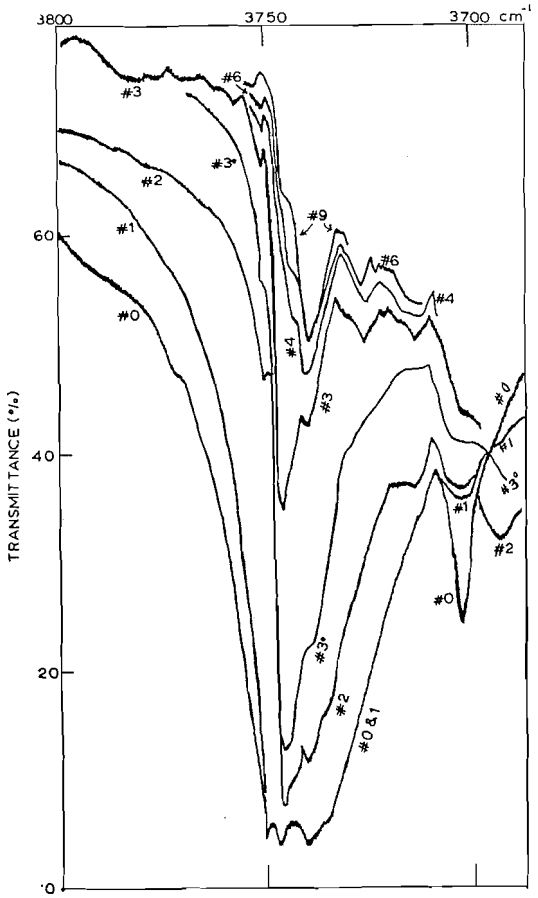

FIG. 3. Infrared spectra of the OH stretching vibration of $B(CH_3)_3$ – porous high-silica glass system during the adsorption process.

Infrared Spectra

The i.r. spectra of adsorption, desorption, and degassing processes observed successively at room temperature on one piece of glass of 0.1000 g are shown in Figs. 2–5. In these figures, the curve # corresponds to the expt. # in Table I, and some of the experiments were omitted to simplify the figures. These spectra were taken after equilibrium was reached, and where no change in the i.r. spectra was noted. The time required to reach equilibrium was generally 3 h after adsorption except in the case of expt. #3, Fig. 2, where the i.r. spectra changed gradually from #3° to #3 during 2 days. The region around 3750 cm^{-1}, where a notable change occurred, was amplified with the external recorder and is shown in Fig. 3.

In the desorption process, the gases desorbed were collected in a liquid nitrogen trap while keeping the sample at some constant temperature for 4 h. The i.r. spectra of the condensable gases were then recorded and the amount measured. No gas which was not condensable at 77 °K was obtained except from the sample degassed at 800° (expt. #6′). In this case, the desorbed gas gave no i.r. absorption spectra. It was, therefore, analyzed by combustion in a CuO furnace at

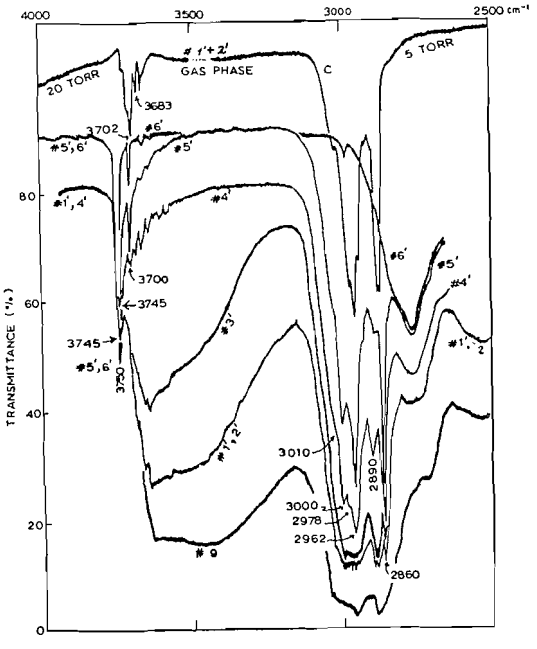

FIG. 4. Infrared spectra of the $B(CH_3)_3$ – porous high-silica glass system for the desorption process (expt. II). The transmittance axis for curves #5′ and 6′ is displaced 10% upward and *c* is arbitrarily displaced.

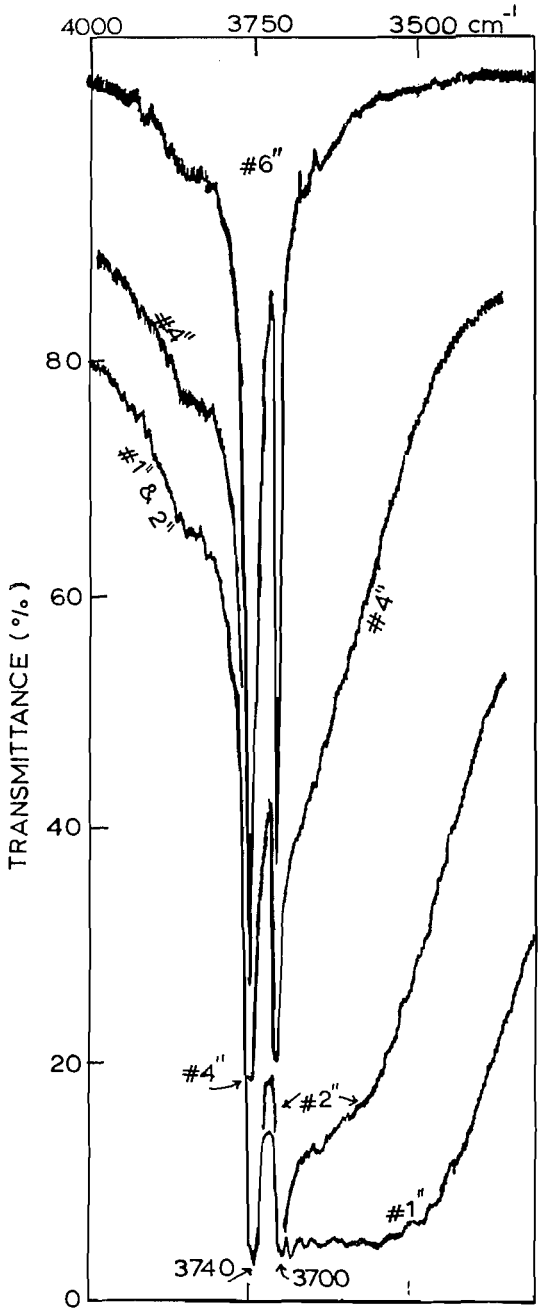

FIG. 5. Infrared spectra of the $B(CH_3)_3$ – porous high-silica glass system for the degassing process after thermoleaching at 500 °C in air (expt. III). The transmittance axes for curves #4″ and 6″ are displaced 10% and 20% upward, respectively.

215 °C, and shown to consist of CO and H_2 in a ratio of about 4:1. The coverage of glass in the desorption process was estimated roughly by a comparison of the i.r. spectra over 3000–2750 cm^{-1} with those on the adsorption process. Since the glass, after degassing at 800 °C, was colored light amber and seemed to have carbon in it, it was thermoleached in air at 500 °C for 30 h until colorless, then degassed again in vacuum, as shown in Table I, expt. III and Fig. 5. The results show that —OH is easily lost and that some of the surface metaborate was hydrolyzed to ≡B—OH.

Consideration of Experimental Results

BET Surface Area

The value of about 50 m^2/g for $B(OCH_3)_3$ is very small when compared with the values of ~ 110 m^2/g determined by methanol (3) and ~ 120 m^2/g by N_2 gas (3). Possible reasons for this are (*i*) the effective size of molecules was larger than in the bulk state because of the planar structure of the molecule, and (*ii*) the decomposition of $B(OCH_3)_3$ to give $3CH_3O$— can make the coverage larger or the area effectively smaller. This latter explanation is most probable because of the changes observed in #3° and #3 which indicated some reaction with the surface.

Infrared Spectra

The main features of the i.r. spectra of $B(OCH_3)_3$ during the adsorption process might be divided into three parts:

A. the region 3100 to 2700 cm^{-1} due to carbon–hydrogen bonding,

B. the region 3600 to 3200 cm^{-1} due to hydrogen bonding,

C. the region in the vicinity of 3700 cm^{-1} due to the —OH vibration.

A

In this region, the notable features were (*i*) the new peak at 2860 cm^{-1} and (*ii*) a broad shoulder around 3010 cm^{-1}. Considering the methoxy compounds which could be formed on the surface, these absorption spectra can be divided into two groups, A and B. Group A, at ~3000, 2962, and 2860 cm^{-1} would be considered as the methoxy bound to the surface silicons (identified by McDonald (13) and many others (14, 15)). Group B, at ~3020, 2978, and 2890 cm^{-1} can be considered as the methoxy bound to boron on the surface, since the small shifts of absorption in the adsorbed state, relative to the vapor state as shown in Fig. 2, could be reasonable in this case.

Can. J. Chem. Downloaded from www.nrcresearchpress.com by 210.87.254.105 on 09/05/12
For personal use only.

Can. J. Chem. Downloaded from www.nrcresearchpress.com by 210.87.254.105 on 09/05/12
For personal use only.

This broad band could be due to methanol on the glass, as will be described further, where the methanol is formed by hydrolysis of $B(OCH_3)_3$ (9, 10). In contrast to the methanol system (3), this system showed no "unaccountable" absorption within the region of 3100 through 3000 cm^{-1} indicating that there was no serious rearrangement in carbon–hydrogen bonding. This probably accounts for the absence of a photochemical effect in this system as compared with the methanol systems.

B

In this region, the absorptions at 3750, 3740, and 3703 cm^{-1} are well established as due, respectively, to ≡Si—OH isolated, ≡Si—OH hydrogen-bonded weakly with surroundings, and =B—OH isolated (13–15). The tail of the 3750 cm^{-1} peak towards the lower frequency side is due to neighboring —OH and will be discussed later. The tail to the higher frequency side, which has not been assigned with certainty (15), decreased noticeably at the early stage of adsorption as shown in Fig. 3, curve #1, while the absorption around 3400–3500 cm^{-1} increased. The high frequency tail might be considered as due to the water or some —OH perturbed to higher energy.

C

The absorption from 3650 to 3200 cm^{-1} is well known and due to the hydrogen-bonded hydroxyl stretching vibration (13–18). The broad absorption bands around 3450 and 3640 cm^{-1} in Fig. 2, and around 3640 cm^{-1} in Fig. 4, #1, were quite similar to those obtained for methanol and water adsorption respectively on porous glass in our work (3). This further substantiates the proposal that methanol is formed on the surface by hydrolysis of $B(OCH_3)_3$. Using the i.r. spectra to assign the functional groups as described above, the experimental results were summarized briefly in Table II.

Discussion

The reactions of $B(OCH_3)_3$ with porous high-silica glass consistent with their known properties are most probably as follows.

The Adsorption Process at Room Temperature

Reaction [1] is between siloxane and the electrophilic part of $B(OCH_3)_3$

[1] 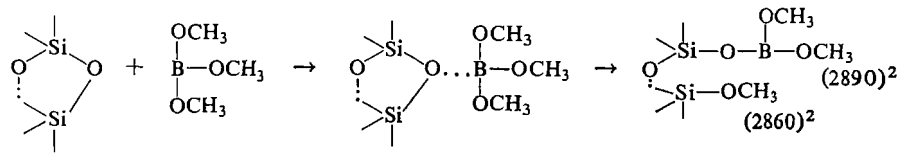

Reaction [2] is between the neighboring —OH and the hydrophilic parts of $B(OCH_3)_3$.

[2] 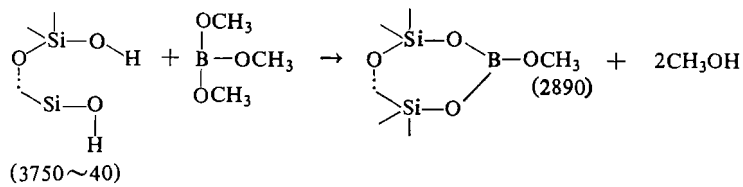

Reaction [3], between isolated =B—OH and the adsorbates, may be postulated to explain the disappearance of isolated =B—OH in curve #1, Fig. 3,

[3] 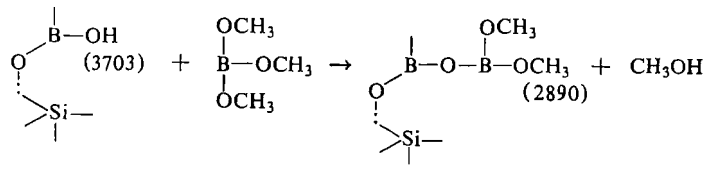

[2]Numbers in parentheses are the wave numbers (in cm^{-1}) assigned to the functional groups or bonding indicated.

The methanol which is formed in [2] and [3] could be adsorbed on the vacant surface sites making the H-bonded CH_3OH (at ~3450 cm^{-1}

Can. J. Chem. Downloaded from www.nrcresearchpress.com by 210.87.254.105 on 09/05/12
For personal use only.

TABLE II

Summary of i.r. spectra of $B(OCH_3)_3$ – porous high-silica glass system

	On glass							In gas phase			
Characteristic bonds	≡SiOH	$(\equiv SiOH)_N$	=BOH	H_2O	CH_3OH	$\equiv SiOCH_3$	$=BOCH_3$	$B(OCH_3)_3$	CH_3OH	Others	Amount
Assigned frequencies (cm^{-1})	3750 to 3740	Tail of ≡SiOH	3700 to 3703	A broad band around ~3640	A broad band around ~3450	2860 to 2863	2890	—CH_3, 1495 and 1365	—CH_3, 3683 and 1034		μ moles
Adsorbent only, expt. #0	Very strong	Strong	Sharp	None					None		
Adsorption process, expt. #1–9	Decreased up to a monolayer and remained constant beyond it at 3740		Disappeared in early stage	Increased up to a monolayer, and remained constant beyond it		Increased up to a monolayer, and became broader beyond it		Almost 100%	Trace	None	33
Desorption process											
Expt. 1′ and 2′	Remained constant, but shifted to 3745		None	Decreased but still strong	Decreased notably	Decreased to approx. a half layer		~65%	~35%	(3702)	146
Expt. 3′	Remained constant at 3745		~ None	Decreased	~ None	Remained constant	Decreased	Trace	~100%	None	9.6
Expt. 4′	Sharper and increased at 3745		Appeared at ~3700	Weak	None	Remained constant	Decreased	~ None	~100%	X† (C—H (1179) (1102))	14
Expt. 5′	Increased and shifted to 3750	Increased	Sharp	~None	None	Remained constant	~None	None	Trace	X† (C—H (1179) (1102))	3.5
Expt. 6′	Strong	None	Sharp, shifted to 3703	None	None	None	None	None	None	H_2, 20%; CO, 80%	14

*$(\equiv SiOH)_N$ denotes the "neighboring silanols".

†X = some undetermined substance(s) with the distinctive absorptions at the wave number (cm^{-1}) shown in the brackets and with some carbon–hydrogen bonding indicated by absorption in the 3050–2700 cm^{-1} region.

Can. J. Chem. Downloaded from www.nrcresearchpress.com by 210.87.254.105 on 09/05/12
For personal use only.

in Fig. 2) and ultimately forming water or a water-like structure (at ~ 3640 cm^{-1} in Fig. 2). Consider, for example, reaction [4] which may occur in a two consecutive step process

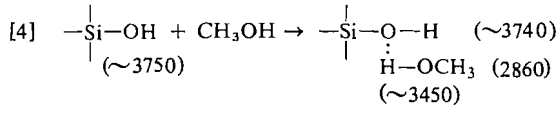

and reaction [5] where water, or a water-like structure, is formed

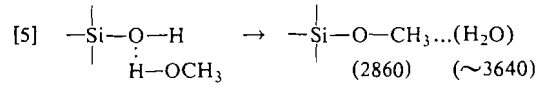

The reactions mentioned above seem to be completed by $\theta \simeq 80\%$ (expt. #5), because the i.r. spectra in the successive adsorption showed only an increase and broadening of the carbon–hydrogen absorption. Therefore, it is reasonable to assume that physical adsorption of trimethylborate occurred after expt. #6.

However, some of the silanols still remained (3740 cm^{-1}) even at $\theta \simeq 350\%$, expt. #9, as shown in Fig. 3. By removing the adsorbates at 650 to 800 °C (#5′ and 6′, Fig. 4) these silanols are shifted to 3750 cm^{-1}, which is assigned to isolated —OH. Therefore, it can be assumed that they are located on the surface of the solid and were not removed by $B(OCH_3)_3$ hydrolysis because of their inaccessibility.

The Desorption Process

After the degassing at room temperature, the adsorbates remaining on the surface could be considered as chemisorbed.

(1) This chemisorbed portion, in which θ is estimated as $\simeq 50$–60% by the i.r. spectra of carbon–hydrogen bondings, corresponds to 75–90 m^2/g of surface area as methoxy covered—a value close to that estimated by methanol in the same manner, i.e. 95 m^2/g.

(2) The change in spectra from #9 to 2′ shows a loss in methanol absorption characteristics around 3450 cm^{-1}, and an increase in sharpness in absorption at 2860 cm^{-1}, showing that reactions [4] and [5] may occur as described above.

(3) The spectrum of the vapors initially degassed from the solid in expt. #1′ + expt. #2′ is given in curve *c* in Fig. 4 and is similar to the spectrum of a 2:1 mixture of $B(OCH_3)_3$–CH_3OH in the region of 4000 to 500 cm^{-1}. The amount desorbed indicates that reaction has occurred and that methanol has been formed.

(4) The amount of methanol which was found in the desorbed gas can be regarded as a measure of the —OH liberated from the surface. As the effective surface area of the glass is 120 m^2/g, the packing number of OH per 100 Å^2 of surface, N_{OH}, was ~ 2.5 (which was removed at room temperature) plus an additional 0.5 due to CH_3OH formed at 120 °C, and an additional 0.8 at higher temperatures. Considering the remainder of hydroxyl on the solid after expt. #6′ to be less than 10%, the total packing number of hydroxyl on the original glass (#0) can be estimated as about 4. On the basis of the studies on silica gel by DeBoer *et al.* (19), $N_{OH} = 4.6$ was obtained, corresponding to a surface where each surface silicon atom is bonded to one hydroxyl group. Therefore, our value of $N_{OH} \simeq 4$ probably means that some siloxane groups exist on the surface (20). However, $N_{OH} \simeq 4$ is too large in comparison with $N_{OH} \simeq 1.5$ which was estimated by Low *et al.* (16). This discrepancy is probably accounted for by the difference in the degassing treatment. The surface —OH can be considered as neighboring but still isolated from each other, and in a continuum of energy states, making the tail of 3750 cm^{-1} as denoted by Borello *et al.* (1). For convenience, we named them the neighboring-OH in reaction [2].

With degassing at higher temperatures (up to 480 °C), the desorbed gas was almost completely methanol, the $\equiv B—OCH_3$ on the solid surface decreased, and $\equiv B—OH$ appeared. Therefore, it is proposed that the following reactions occur between $\equiv B—OCH_3$ and water produced in reaction [5]

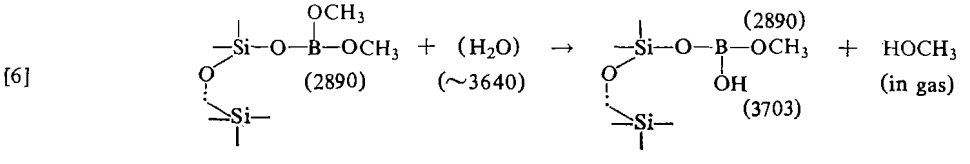

[7] 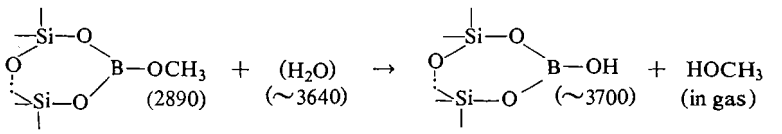

The absorption bands between 3700 and 3600 cm^{-1} (#4′ and #5′ in Fig. 4) are probably due to a combination of ═B—OH, ≡Si—OH, and even ≡C—OH since the glass at this stage was slightly amber colored. During this step, the absorption due to ≡Si—OCH_3 was still quite sharp, showing that these groups are thermally more stable than ═B—OCH_3 on the surface.

The degassing at still higher temperature in #5′ results in the complete elimination of ═B—OCH_3 and the decrease in the hydroxyls mentioned above with the increase in the isolated ═B—OH and ≡Si—OH. Because methanol was the only desorbed gas, one of the possible reactions might be

[8] 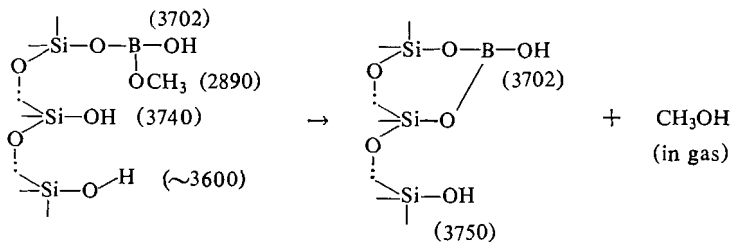

Above 650 °C, the complete elimination of ≡Si—OCH_3 gave only CO and H_2 in the gas phase, and an amber-colored solid with isolated ≡Si—OH and ═B—OH groups. This amber-colored glass was thermoleached in air at 500 °C for 30 h till colorless, then degassed again in vacuum as shown in Table I, expt. III. The results, as illustrated in Fig. 5, show that —OH is easily lost and that some of the surface metaborates have been hydrolyzed to ═B—OH. The results clearly indicate that trimethyl-borate hydrolyzes on the porous glass by reaction with the surface silanol groups to form methoxy groups which are photochemically inactive at $\lambda > 2300$ Å.

This reaction can be used to dehydrate or dehydroxylate a surface at relatively low temperatures.

Acknowledgments

This work was supported by the Directorate of Chemical Sciences, U.S. Air Force Office of Scientific Research, Grant No. AF-AFOSR 642-66 and by the National Research Council of Canada.

1. E. Borello, A. Zecchina, and C. Morterra. J. Phys. Chem. **71**, 2938 (1967).
2. A. R. Knight. Private communication.
3. M. Shimizu, H. D. Gesser, and M. Fujimoto. Unpublished results.
4. Raymond P. Porter. J. Phys. Chem. **61**, 1260 (1957).
5. T. H. Elmer, I. D. Chapman, and M. E. Nordberg. J. Phys. Chem. **67**, 2219 (1963).
6. I. D. Chapman and M. L. Hair. J. Catalysis, **2**, 145 (1963).
7. H. I. Schlesinger, H. C. Brown, D. L. Mayfield, and J. R. Gilbreath. J. Am. Chem. Soc. **75**, 213 (1953).
8. L. J. Bellamy, W. Gerrard, M. F. Lappert, and R. L. Williams. J. Chem. Soc. 112 (1958).
9. W. Gerrard. The organic chemistry of boron. Academic Press, Inc., New York. 1961.
10. H. Steinberg. Organoboron chemistry. Vol. 1. Interscience Publishers, Inc., New York. 1963.
11. S. Brunauer. The adsorption of gases and vapors. Vol. I. Princeton Univ. Press, Princeton, New Jersey. 1942.
12. J. J. Etridge and S. Sugden. J. Chem. Soc. 989 (1928).
13. R. C. McDonald. J. Phys. Chem. **62**, 1168 (1958).
14. L. H. Little. Infrared spectra of adsorbed species. Academic Press, Inc., New York. 1966.
15. M. L. Hair. Infrared spectroscopy in surface chemistry. Marcel Dekker Inc., New York. 1967.
16. M. J. D. Low and N. Ramasubramanian. J. Phys. Chem. **70**, 2740 (1966); **71**, 730 (1967).
17. K. Nakanishi. Infrared absorption spectroscopy. Holden-Day Inc., San Francisco. 1962.
18. K. Nakamoto. Infrared spectra of inorganic and coordination compounds. John Wiley and Sons, Inc., New York. 1963.
19. J. H. DeBoer, M. E. A. Hermans, and J. M. Vleeskens. Koninkl Ned. Akad. Wetenschap. Proc. Ser. B, **60**, 45, 54, 237 (1957); **61**, 2 (1958).
20. H. P. Boehm. Angew. Chem. Intern. Ed. Engl. **5**, 533 (1966).

Can. J. Chem. Downloaded from www.nrcresearchpress.com by 210.87.254.105 on 09/05/12
For personal use only.

Can. J. Chem. Downloaded from www.nrcresearchpress.com by 210.87.254.42 on 09/05/12
For personal use only.

Ion–solvent interaction of tetraalkylammonium ions in solvents of high dielectric constant. Part I. Conductance and Walden product of tetraalkylammonium ions in N-methylacetamide at different temperatures

RAJ DEO SINGH[1], PUSHTI PRAKASH RASTOGI, AND RAM GOPAL
Department of Chemistry, Lucknow University, Lucknow, India

Received January 22, 1968

Ion–solvent interaction of the tetraalkylammonium ions (R_4N^+) in N-methylacetamide has been studied from the point of view of electrical conductance and the derived Walden product. The results indicate R_4N^+ ions to be structure breakers in this solvent, quite opposite to their general behavior in aqueous solutions. The effect is conspicuous in the smaller Me_4N^+ and Et_4N^+ ions, but is less marked in the larger ions.

Canadian Journal of Chemistry, 46, 3525 (1968)

Introduction

The study of the properties of the tetraalkylammonium ions (R_4N^+) in aqueous and some nonaqueous solvents has been a subject of considerable interest during the past few years (1–9) and, at times, contradictory results have been reported regarding their behavior. For example, in place of the complete absence of solvation (10–12) of these ions in aqueous solution, to which most of the studies are confined, the opinion is gaining that these ions are also solvated (3*b*, 3*c*, 13, 14), in the sense that they cause an enhancement of the structure of water around them (15), the exception being the Me_4N^+ ion (and Et_4N^+ ion to some extent) which is solvated mainly by electrostatic ion–solvent interaction (3*b*, 3*c*, 14). It appears interesting to enquire how the R_4N^+ ions would behave in a nonaqueous solvent like N-methylacetamide (NMA) which is similar to water in many respects, e.g. both have high dielectric constant, extensive hydrogen bonding, and molecular association. NMA is also similar to R_4N^+ ions in having alkyl groups present in its molecule, so it may be expected that NMA and R_4N^+ ions would interact in a manner different from the R_4N^+–water interaction. As is now generally acknowledged, it is the presence of the alkyl groups in R_4N^+ ions which makes them 'hydrophobic' in aqueous solutions and is the cause of the abnormal properties of these ions (15).

A survey of the literature reveals that no detailed and systematic study of these ions in NMA appears to have been made with a view to investigate the effect of these ions on the structure of the solvent; some electrical conductance measurements of the salts containing the smaller R_4N^+ ions and some common classical ions have been reported by Dawson and his associates (16) and also by French and Glover (17). However, these studies are rather sketchy as far as R_4N^+ ions, in general, are concerned and a detailed investigation is very much desirable. As the temperature dependence of the electrical conductance or of the Walden product, derived therefrom, can be used to throw light on the solute–solvent interaction, it is proposed to investigate the R_4N^+–NMA interaction from this point of view in the present paper.

Experimental

NMA, obtained from M/s Distillation Products Industries, U.S.A., was left overnight on some freshly ignited quicklime and was then distilled under reduced pressure. The middle fraction of the distillate was collected and was fractionally recrystallized twice. The crystals were melted and the resulting liquid, after treatment with quicklime, was vacuum-distilled. The process of purification was continued until the electrical conductance of the middle fraction of the distillate was reduced to less than 10^{-6} mho. The sample melted at about 29.7°. It was collected in dark amber-colored bottles which were kept in a dry box. It was used, as far as possible, soon after distillation (next day). The samples gave reproducible electrical conductance at various temperatures in the 35–55° interval for at least 5 to 6 h.

Tetraalkylammonium iodides, supplied by M/s Distillation Products Industries, U.S.A., were recrystallized from suitable solvents or their mixtures. Me_4NI and Et_4NI were dissolved in absolute alcohol and precipitated from solution with ether. These were dried in a vacuum desiccator.

Pr_4NI, Bu_4NI, and Pen_4NI were dissolved in methanol and precipitated with ether. The precipitated salts were

[1]Junior Research Fellow, U.P.C.S.I.R.

TABLE I

Equivalent conductance of R_4NI in NMA at different temperatures and concentrations

Concentration, $C \times 10^2$	Equivalent conductance, Λ, at 35°	40°	45°	50°	55°
		Me_4NI			
0.05	24.35	26.36	29.16	31.61	34.45
0.10	24.22	26.22	29.00	31.44	34.26
0.25	23.95	25.91	28.66	31.05	33.86
0.50	23.65	25.57	28.28	30.65	33.37
1.00	23.20	25.08	27.74	30.05	32.70
		Et_4NI			
0.05	23.76	25.88	28.73	30.99	33.85
0.10	23.66	25.78	28.56	30.80	33.65
0.25	23.34	25.44	28.23	30.44	33.24
0.50	23.04	25.11	27.86	30.03	32.78
1.00	22.60	24.63	27.34	29.45	32.15
1.43	22.30	24.31	27.00	29.07	31.50
2.00	22.00	23.96	26.60	28.64	31.20
		Pr_4NI			
0.05	21.60	23.41	26.20	28.40	31.01
0.10	21.45	23.28	26.04	28.25	30.84
0.25	21.13	23.00	25.73	27.90	30.42
0.50	20.78	22.70	25.38	27.50	30.00
1.00	20.26	22.25	24.90	26.95	29.36
1.43	19.93	21.95	24.56	26.58	28.95
2.00	19.56	21.63	24.20	26.17	28.48
		Bu_4NI			
0.05	20.20	22.13	24.78	26.90	29.28
0.10	20.10	22.00	24.62	26.70	29.07
0.25	19.82	21.70	24.30	26.36	28.75
0.50	19.55	21.38	23.95	25.96	28.25
1.00	19.15	20.94	23.45	25.40	27.63
1.43	18.86	20.65	23.12	25.00	27.20
2.00	18.58	20.30	22.73	24.60	26.75
		Pen_4NI			
0.05	19.78	21.64	24.18	26.15	28.50
0.10	19.65	21.48	24.00	26.00	28.32
0.25	19.38	21.20	23.70	25.60	27.91
0.50	19.10	20.88	23.34	25.20	27.45
1.00	18.70	20.41	22.85	24.65	26.80
1.43	18.43	20.12	22.50	24.25	26.40
2.00	18.13	19.77	22.12	23.83	25.92
		Hex_4NI			
0.05	19.57	21.44	23.97	25.90	28.18
0.10	19.45	21.28	23.80	25.70	27.98
0.25	19.18	20.98	23.47	25.32	27.57
0.50	18.88	20.65	23.10	24.90	27.10
1.00	18.46	20.18	22.57	24.32	26.46
1.43	18.18	19.85	22.23	23.94	26.00
2.00	17.88	19.50	21.84	23.50	25.53
		Hep_4NI			
0.05	19.25	21.10	23.55	25.48	27.47
0.10	19.13	20.95	23.38	25.30	27.25
0.25	18.86	20.66	23.05	24.92	26.85
0.50	18.55	20.35	22.65	24.50	26.38
1.00	18.15	19.90	22.13	23.90	25.70
1.43	17.85	19.57	21.76	23.50	25.26
2.00	17.55	19.25	21.38	23.07	24.77

Can. J. Chem. Downloaded from www.nrcresearchpress.com by 210.87.254.42 on 09/05/12
For personal use only.

TABLE II

Limiting equivalent conductances of R_4NI salts and R_4N^+ ions at different temperatures

R_4NI and R_4N^+ ion	Limiting equivalent conductance at				
	35°	40°	45°	50°	55°
Me_4NI	24.70	26.75	29.59	32.10	35.00
Me_4N^+	11.28	12.08	13.00	14.36	15.80
Et_4NI	24.10	26.25	29.15	31.45	34.35
Et_4N^+	10.68	11.58	12.56	13.71	15.15
Pr_4NI	21.65	23.80	26.60	28.85	31.50
Pr_4N^+	8.23	9.13	10.01	11.11	12.30
Bu_4NI	20.53	22.50	25.20	27.35	29.80
Bu_4N^+	7.11	7.83	8.61	9.62	10.60
Pn_4NI	20.10	22.00	24.60	26.61	29.02
Pn_4N^+	6.68	7.33	8.01	8.87	9.82
Hex_4NI	19.90	21.80	24.41	26.34	28.72
Hex_4N^+	6.50	7.13	7.81	8.60	9.50
Hep_4NI	19.62	21.47	24.00	25.95	28.00
Hep_4N^+	6.20	6.80	7.41	8.21	9.00

dried in a vacuum desiccator. Hex_4NI and Hep_4NI were recrystallized from acetone and dried in a vacuum desiccator.

Solutions were prepared at 35° in a thermostat and corrected for the changes in volume at other temperatures from the corresponding densities which were also determined. Contact of the solvent and of the solution with the open air was reduced to a minimum. The electrical conductance was determined with a suitably grounded Kohlrausch's bridge assembly and precautions were taken to eliminate, or compensate for, the capacity and induction effects. The temperature of the oil bath was regulated within $\pm 0.01°$ in the lower temperature range and $\pm 0.02°$ in the higher temperature range. The concentrations varied from 0.0005 *M* to 0.02 *M* in general. The accuracy of the measurements was checked by determining the conductance of some electrolytes in NMA. The values of the electrical conductance were found to agree very closely (within 0.03%) with those obtained by other workers (16, 17). The electrical conductances, Λ, for different R_4NI salts, at different temperatures and concentrations, are given in Table I.

Within the concentration range studied here, the plots of Λ vs. $\sqrt{c}$ were found to be straight lines for all the R_4NI salts at all temperatures in the 35–55° range. It appears, therefore, that these salts are completely dissociated in NMA, as has been reported by Dawson *et al.* (16) and by French and Glover (17). Extrapolation of Λ vs. $\sqrt{c}$ curves to infinite dilution leads to Λ_0 values, given in Table II for various R_4NI at different temperatures.

From the Λ_0 values given in Table II, the ionic conductances, λ_0^+, of R_4N^+ ions at different temperatures were obtained, using the cationic transport number data of KBr in NMA, as reported by Gopal and Bhatnagar (18). λ_0^+ values, thus obtained, are also given in Table II.

The cationic Walden products, $\lambda_0^+\eta_0$, for different R_4N^+ ions were calculated, using the viscosity (η_0) of NMA obtained in this laboratory at different temperatures as:

	35°	40°	45°	50°	55°
η_0(in poise) =	0.03403	0.03020	0.02693	0.02413	0.02175

These values of η_0 at 40 and 50° agree very closely with those given by Dawson *et al.* (16*a*). The Walden product, $\lambda_0^+\eta_0$, for different ions has been plotted against temperature ($t°$). The $\lambda_0^+\eta_0$ vs. $t°$ curves for different ions are given in Fig. 1.

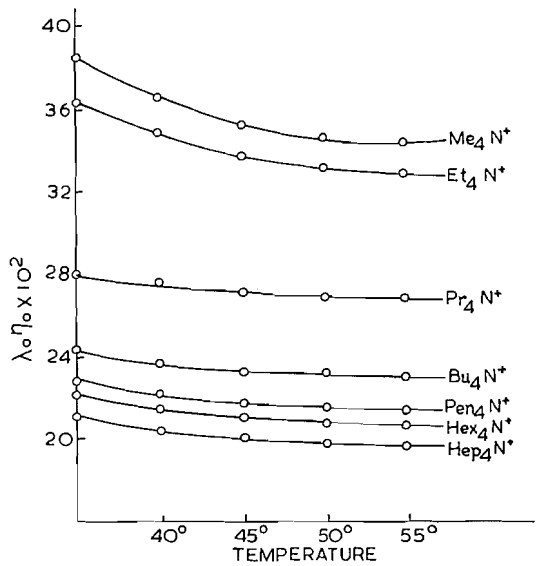

FIG. 1. Plot of $\lambda_0\eta_0$ vs. $t°$.

Discussion

It may be noted from Table II that the values of λ_0^+ and Λ_0 are very low as compared with those in water. This is expected on account of the highly viscous nature of NMA and also due

Can. J. Chem. Downloaded from www.nrcresearchpress.com by 210.87.254.42 on 09/05/12
For personal use only.

Can. J. Chem. Downloaded from www.nrcresearchpress.com by 210.87.254.42 on 09/05/12
For personal use only.

to a possible stronger ion–solvent interaction[2] because of the large dipole moment ($\approx$ 3.8 D). It is interesting to note that $\lambda_0^+ - 5$ of R_4N^+ ions are comparable to those of the much smaller alkali metal ions. In fact, λ_0^+ values of R_4N^+ ions are, in many cases, larger, e.g. at 35°, $\lambda_0(Me_4N^+) = 11.98$, $\lambda_0(Et_4N^+) = 11.63$, $\lambda_0(Pr_4N^+) = 9.03$, $\lambda_0(Bu_4N^+) = 7.80$, whereas $\lambda_0(Li^+) = 6.63$, $\lambda_0(Na^+) = 8.13$, $\lambda_0(K^+) = 8.23$, in spite of the much larger radii (10) of the R_4N^+ ions. This obviously indicates a much stronger ion–dipole interaction between the alkali metal ions and NMA molecules as compared with the R_4N^+–NMA interaction. One should expect this because of the high electrical charge density on the smaller alkali metal ions and a small surface charge density on the larger R_4N^+ ions. The inverse variation of λ_0^+ with radius in the case of R_4N^+ ions suggests, at first sight, that the ions are not solvated in NMA. However, the evidence to be brought forward in the following pages, appears to indicate some electrostatic ion–solvent interaction although it may be weak, specially in the case of the larger R_4N^+ ions.

From Fig. 1 it may be seen that the Walden product, $\lambda_0^+\eta_0$, decreases slowly with rise in temperature (about 8–10% in 20°). The fall is a little rapid in the beginning but it levels off as the temperature rises. At first, one feels tempted to overlook the decrease and to consider $\lambda_0^+\eta_0$ to be approximately constant. However, the decrease is regular and has already been reported for some R_4N^+–salts (17) and for several classical electrolytes (16). Besides, the decrease is quite comparable to that for the aqueous solutions of some common ions (ref. 10, p. 128) and should, therefore, be considered as significant. It appears to be the result of the ion–solvent interaction in NMA.

Before examining solutions in NMA in more detail, it would be instructive to refer to aqueous solutions in which $\lambda_0^+\eta_0$ of R_4N^+ ions, in general, increases with rise in temperature, the exception being, as usual, the Me_4N^+ ion for which $\lambda_0^+\eta_0$ decreases with a rise in temperature (3*b*). The general behavior of the R_4N^+ ions has been explained on the more or less universally accepted hypothesis of Frank *et al.* (15) according to which R_4N^+ ions enhance the structure of water around them. However, Me_4N^+ ion appears to be a net structure breaker in water and is also solvated due to ion–dipole interaction (3*b*, 3*c*, 14, 19). For the smaller classical ions with electrostatic solvation, $\lambda_0^+\eta_0$ also decreases with rise in temperature (10); their behavior is similar to Me_4N^+ ion and hence should be explained on similar grounds, viz. the electrostatic ion–solvent interaction gives rise to a loosening or disruption of the water structure around the solvated ionic sphere; this results in a rearrangement of the water molecules beyond the region in which the structure is broken (20). On the other hand, the larger R_4N^+ ions produce 'hydrophobic' solvation and there is no region of loosened water structure (the 'B' region of Frank). The enhanced or the 'hydrophobic' structure breaks up at higher temperatures and makes the larger R_4N^+ ions more mobile; so $\lambda_0^+\eta_0$ increases with rise in temperature for these ions. The concept of the increase of solvation[3] of ions, in general, at higher temperatures (11, 20–25), as a possible cause of the decrease of $\lambda_0^+\eta_0$ at higher temperatures (invoked by Dawson and his associates (16) to account for the similar results in NMA), does not appear convincing and need not be discussed in this communication any further.

Reverting back to solutions in NMA, the decrease in $\lambda_0^+\eta_0$ with rise in temperature, found for all the ions, both the R_4N^+ and the classical, investigated so far in this communication or elsewhere (16, 17), could be best explained by assuming their electrostatic solvation and the resultant breaking-up of the structure of the solvent medium around them. The similarity of the behavior of all the ions (both the R_4N^+ and the classical) in NMA is understandable since the special structure promotion features ('hydrophobic' solvation in aqueous solutions) of the larger R_4N^+ ions in water would be missing in NMA because of the similarity of the constituents (26) of the R_4N^+ ions and the NMA molecule (e.g. the presence of the alkyl groups). There appears to be a net structure breaking (27) in their presence as the electrostatic ion–solvent

[2]J. M. Notley and M. Spiro (33) expect similar behavior in formamide on account of its high dipole moment.

[3]An alternate suggestion, not involving a larger number of solvent molecules in solvation at the higher temperatures and yet giving an apparent impression of a larger solvation, was made by one of the present authors (R. G.). See ref. 34.

Can. J. Chem. Downloaded from www.nrcresearchpress.com by 210.87.254.42 on 09/05/12
For personal use only.

interaction appears to be stronger than the interaction between the solvent molecules. The electrostatic interaction between the smaller classical ions and the molecules of NMA is expected to be quite appreciable ($\approx$ 20–25kT) because of the high charge density on the ions and the large dipole moment of the NMA molecule (see footnote 2); even for the large R_4N^+ ions, it would be quite significant, specially in the case of the smaller members of the group. The van der Waals radius of the molecule of NMA has been estimated to be about 2.8 Å (28, 29). Assuming the centers of the dipole and of the molecule of NMA to coincide, the ion–dipole interaction energy for a R_4N^+ ion of radius 4.2 Å (say) would be about 8–10kT. This is larger than the thermal energy $3kT/2$ at ordinary temperatures and is about twice as large as the hydrogen-bonding energy ($\approx 4kT$) in either

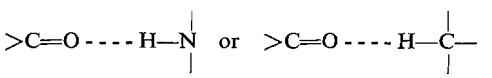

or the dipolar energy ($\approx$ 3–4kT) among the solvent molecules themselves. Thus the ion–dipole interaction energy, for at least the smaller R_4N^+ ions, appears to be sufficient to disrupt the hydrogen-bonded association in NMA. This situation should lead to a partial breakdown of the associated structure of NMA and to some electrostatic solvation of the R_4N^+ ions. Of course, the larger the ion, the smaller the interaction and for a radius of 5.2 Å, the interaction energy will be about 5–7kT and for a radius of 6.2 Å, it will be only 4–5kT, which is comparable to the energy of the hydrogen-bonded association in NMA. In other words, the structure breaking effect of the larger R_4N^+ ions may be very weak. This is, perhaps, indicated by the flatter nature of the ${\lambda_0}^+\eta_0$–t° curves for the larger R_4N^+ ions and by the steeper nature of the smaller ones, as is clear from Fig. 1. The structure breaking of the solvent around R_4N^+ ions (20) explains the negative temperature coefficient of ${\lambda_0}^+\eta_0$ because the decrease in the viscosity, η_0, of the pure solvent is much faster than the corresponding increase in ${\lambda_0}^+$ with the rise in temperature, on account of the already broken down structure of NMA (in their presence) at the lower temperatures; so the rate of the decrease of the intrinsic or local viscosity around the ion is smaller. Hence ${\lambda_0}^+\eta_0$ will decrease with the rise in temperature. Of course, for the larger R_4N^+ ions, this effect will be less marked as has already been pointed out.

The structure breaking effect of R_4N^+ ions in NMA and the existence of some electrostatic solvation are supported by the yet unpublished studies on the viscosity of R_4NI salts in NMA in this laboratory. The results indicate that the coefficient B of the Jones and Dole viscosity equation (30) namely

$$\eta = \eta_0(1 + AC^{1/2} + BC)$$

is positive and it increases with the rise in temperature. A positive B coefficient indicates ion–solvent interaction and a positive dB/dt° implies structure breaking (8, 31, 32) of the solvent in solution so that the local or intrinsic viscosity does not decrease as rapidly as η_0 when the temperature rises. A positive dB/dt° does not imply, necessarily, a higher solvation at the higher temperatures (16, 21–25). This only denotes an increase in $(\eta - \eta_0)/\eta_0$ with the rise in temperature, the coefficient A being almost independent of temperature as it denotes ion–ion interaction. It may be recalled here that in aqueous solutions, the coefficient B decreases with the rise in temperature (3c) for the 'hydrophobic' structure promoting larger R_4N^+ ions and also for the highly hydrated classical ions like Li^+, Mg^{2+}, and Ce^{3+} (23), which is quite opposite to the behavior of the net structure breaking ions like K^+, Rb^+, Cs^+, Cl^-, Br^-, and I^- ions for which dB/dt° is positive even though these ions are also solvated to some extent and their B coefficients are negative. Unfortunately, it has not been possible to assign the ionic contributions of the R_4N^+ and I^- ions to the B coefficient as yet; however, if the conductance data are any guide, it appears fairly certain that the individual ionic B values would lead to the same conclusions as have been obtained from the combined total B coefficient.

Acknowledgments

The financial assistance given by the Society of Sigma Xi and RESA of America is gratefully acknowledged. The assistance given by C.S.I.R., India, has also been very valuable.

1. B. E. Conway, R. E. Verrall, and J. E. Desnoyers. Z. Physik. Chem. Leipzig, **230**, 157 (1965).
2. B. E. Conway. Ann. Rev. Phys. Chem. **17**, 481 (1966).

3. (*a*) D. F. EVANS and R. L. KAY. J. Phys. Chem. **70**, 366 (1966). (*b*) R. L. KAY and D. F. EVANS. J. Phys. Chem. **70**, 2325 (1966). (*c*) R. L. KAY, T. VITUCCIO, C. ZAWOYSKI, and D. F. EVANS. J. Phys. Chem. **70**, 2336 (1966). (*d*) D. F. EVANS, G. P. CUNNINGHAM, and R. L. KAY. J. Phys. Chem. **70**, 2974 (1966).
4. (*a*) S. LINDENBAUM. J. Phys. Chem. **70**, 814 (1966). (*b*) G. E. BOYD, A. SCHWARZ, and S. LINDENBAUM. J. Phys. Chem. **70**, 821 (1966).
5. W. Y. WEN, S. SAITO, and CHUN-MEEI LEE. J. Phys. Chem. **70**, 1244 (1966).
6. R. GOPAL and A. K. RASTOGI. J. Indian Chem. Soc. **43**, 269 (1966).
7. G. E. BOYD, J. W. CHASE, and F. VASLOW. J. Phys. Chem. **71**, 573 (1967).
8. J. PADOVA and I. ABRAHAMER. J. Phys. Chem. **71**, 2112 (1967).
9. (*a*) R. H. WOOD, H. L. ANDERSON, J. D. BECK, J. R. FRANCE, W. E. DE VRY, and L. J. SOLTZBERG. J. Phys. Chem. **71**, 2149 (1967). (*b*) R. H. WOOD and H. L. ANDERSON. J. Phys. Chem. **71**, 1869 (1967).
10. R. A. ROBINSON and R. H. STOKES. Electrolyte solutions. Butterworths Scientific Publications, London. 1959. pp. 124–126.
11. E. R. NIGHTINGALE, JR. J. Phys. Chem. **63**, 1384 (1959).
12. R. GOPAL and M. M. HUSAIN. J. Indian Chem. Soc. **40**, 981 (1963).
13. D. S. ALLAM and W. H. LEE. J. Chem. Soc. A, 426 (1966).
14. E. R. NIGHTINGALE, JR. J. Phys. Chem. **66**, 894 (1962).
15. (*a*) H. S. FRANK and M. W. EVANS. J. Chem. Phys. **13**, 507 (1945). (*b*) H. S. FRANK and W. Y. WEN. Discussions Faraday Soc. **24**, 133 (1957). (*c*) H. S. FRANK. Z. Physik. Chem. Leipzig, **228**, 367 (1965). (*d*) W. Y. WEN and S. SAITO. J. Phys. Chem. **68**, 2639 (1964). (*e*) R. M. DIAMOND. J. Phys. Chem. **67**, 2513 (1963).
16. (*a*) L. R. DAWSON, P. G. SEARS, and R. H. GRAVES. J. Am. Chem. Soc. **77**, 1986 (1955). (*b*) L. R. DAWSON, E. D. WILHOIT, and P. G. SEARS. J. Am. Chem. Soc. **78**, 1569 (1956). (*c*) L. R. DAWSON, E. D. WILHOIT, R. R. HOLMES, and P. G. SEARS. J. Am. Chem. Soc. **79**, 3004 (1957). (*d*) L. R. DAWSON, G. R. LESTER, and P. G. SEARS. J. Am. Chem. Soc. **80**, 4233 (1958). (*e*) L. R. DAWSON, J. W. VAUGHN, M. E. PRUITT, and H. C. ECKSTROM. J. Phys. Chem. **66**, 2684 (1962).
17. C. M. FRENCH and K. H. GLOVER. Trans. Faraday Soc. **51**, 1427 (1955).
18. R. GOPAL and O. N. BHATNAGAR. J. Phys. Chem. **69**, 2382 (1965).
19. F. G. HIGGIS, J. B. HASTED, and T. J. BUCHANAN. J. Chem. Phys. **20**, 1452 (1952).
20. D. FEAKINS and K. G. LAWRENCE. J. Chem. Soc. A, 217 (1966).
21. F. S. FEATES and D. J. G. IVES. J. Chem. Soc. A, 2809 (1956).
22. S. R. GUPTA, G. J. HILLS, and D. J. G. IVES. Discussions Faraday Soc. **24**, 147 (1957).
23. M. KAMINSKY. Discussions Faraday Soc. **24**, 177 (1957).
24. M. EIGEN and E. WICKE. Z. Elektrochem. **55**, 354 (1951).
25. E. WICKE. Z. Physik. Chem. Frankfurt, **1**, 340 (1954).
26. R. GOPAL and O. N. BHATNAGAR. J. Indian Chem. Soc. **44**, 1082 (1967).
27. O. D. BONNER, C. F. JORDAN, and K. W. BUNZL. J. Phys. Chem. **68**, 2450 (1964).
28. J. R. LUMLEY. J. Mol. Spectry. **2**, 581 (1959).
29. J. KATZ and B. POST. Acta Cryst. **13**, 624 (1960).
30. G. JONES and M. DOLE. J. Am. Chem. Soc. **51**, 2950 (1929).
31. W. M. Cox and J. H. WOLFENDEN. Proc. Roy. Soc. London, Ser. A, **145**, 486 (1934).
32. R. W. GURNEY. Ionic processes in solution. McGraw-Hill Book Co., Inc., New York. 1953. p. 159.
33. J. M. NOTLEY and M. SPIRO. J. Phys. Chem. **70**, 1502 (1966).
34. R. GOPAL. J. Indian Chem. Soc. **43**, 104 (1966).

Can. J. Chem. Downloaded from www.nrcresearchpress.com by 210.87.254.42 on 09/05/12
For personal use only.

Effect of proton acceptors on the condensed phase radiolysis of cyclohexane-d_{12} in cyclopentane

J. A. STONE
Department of Chemistry, Queen's University, Kingston, Ontario
Received June 7, 1968

C_2H_5OH decreases the HD and D_2 yields from small concentrations of c-C_6D_{12} in c-C_5H_{10}. The results are consistent with a previous suggestion that the enhanced yields in this system are due to exothermic charge transfer. Charge transfer to c-C_6D_{12} is only $\sim$ 10% as efficient as proton transfer to C_2H_5OH at 4.1 mole % c-C_6D_{12} or C_2H_5OH. Experiments at 196 and 77 °K suggest that resonance charge transfer in the cyclopentane matrix may occur to some extent.

Canadian Journal of Chemistry, 46, 3531 (1968)

Introduction

When a perdeuterated hydrocarbon is irradiated at low concentration ($\sim$ 5 mole %) in a hydrocarbon solvent the yields of HD and D_2 obtained depend upon the relative ionization potentials of solute and solvent (1). Larger yields are obtained when the solvent has the higher ionization potential. Electron scavengers such as SF_6, N_2O, or CCl_4, while reducing the total amount of hydrogen obtained from the system, also eliminate the differences in yields obtained with different solvents (2, 3). Charge transfer involving molecular ions and solvent or solute molecules has been offered as an explanation for the phenomenon (4, 1).

If such ions are involved then they should be susceptible to reaction with a suitable scavenger. Both ammonia (5) and ethanol (6) have been shown to accept protons from ions in irradiated liquid cyclohexane. The purpose of the present work was to study the effect of a proton scavenger on the yields of HD and D_2 from a perdeuterated solute in a hydrocarbon solvent and to see whether the postulated charge transfer mechanism is consistent with the results obtained.

Cyclohexane-d_{12} was the chosen solute and cyclopentane the solvent. The yields of HD and D_2 from cyclohexane-d_{12} (ionization potential of c-C_6H_{12} = 9.88 eV (7)) irradiated in cyclopentane (10.53 eV (8)) are larger than would be expected from the composition of the solution (2). Ethanol, which is completely miscible in the cyclohexane-d_{12}/cyclopentane solution was chosen as proton scavenger since comparison with the work of Buchanan and Williams (6) would then be possible. Although the ionization potential of ethanol, 10.50 eV (7), is slightly lower than that of cyclopentane, charge transfer between the two is not a complication since (*a*) charge transfer appears to be much less efficient than proton transfer and (*b*) methanol with an ionization potential of 10.85 eV (7) has, within experimental error, the same effect on HD and D_2 yields as does ethanol.

Experimental

Cyclopentane (Phillips research grade) was shaken with concentrated sulfuric acid to remove cyclopentene and was then fractionally distilled, the middle 80% of the distillate being retained. Cyclohexane-d_{12} (Merck, Sharp and Dohme of Canada Ltd.) was used as received. Absolute ethanol was passed through an alumina column to both dry it and remove a trace of benzene. Anhydrous ammonia (Matheson, minimum purity 99.99%) was used as received.

Samples were made up by volume and were degassed by the pump–freeze–thaw technique. All liquid samples contained 2 ml of cyclopentane and in most cases 0.1 ml of cyclohexane-d_{12} plus an appropriate volume of ethanol. These samples were irradiated at 298 and 196 °K in cylindrical Pyrex tubes of volume $\sim$ 8 ml. Samples containing ammonia as proton acceptor were irradiated in tubes of volume $\sim$ 2.6 ml. Homogeneous solid samples were prepared by deposition from the gas phase onto the inner surface of a Pyrex vessel immersed in liquid nitrogen.

Samples were irradiated with γ-rays at a dose rate of $\sim 8 \times 10^{17}$ eV/ml min in cyclopentane to a total dose of 2.4×10^{19} eV/ml. Ferrous sulfate dosimetry was used for liquid samples. For solid phase irradiations the hydrogen yield from solid cyclohexane samples prepared by deposition from the gas phase was measured and the absorbed dose was calculated using the previously measured $G(H_2)$ of 4.65 (9).

Results

The yields of HD and D_2 from solutions of cyclohexane-d_{12} in cyclopentane were, within

experimental error, linear with c-C_6D_{12} concentration from 1 to 7 mole %. The yields were also linear with dose over the range 1–3 × 10^{19} eV/ml.

The addition of ethanol or ammonia decreased the % of HD and D_2 in the radiolytic hydrogen even though G(total hydrogen) remained essentially constant. Figure 1 shows the changes in % HD and % D_2 for a 3.5 mole % cyclohexane-d_{12} solution with added ethanol. The points are not corrected for the contribution from the direct radiolysis of ethanol to the hydrogen yield.

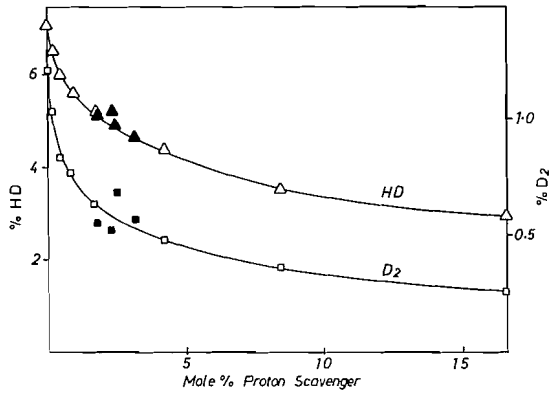

FIG. 1. The % of HD and D_2 from 3.5 mole % c-C_6D_{12} in c-C_5H_{10} with added proton scavengers. □ and △, C_2H_5OH; ■ and ▲, NH_3.

A few experiments were performed with ammonia as a proton scavenger. The results were not as reproducible as those with ethanol probably because there was some variation from sample to sample of the gas volume above the liquid. Figure 1 shows, however, that, within experimental error, ammonia has the same effect on the system as does ethanol.

For the remainder of the experiments a fixed volume, 0.1 ml, of cyclohexane-d_{12} was used together with 2 ml of cyclopentane and varying amounts of ethanol. Samples (2.1 ml) of the alkane mixture were irradiated, in the absence of ethanol, at 298, 196, and 77 °K. For doses of 2.4 × 10^{19} eV/ml the results shown in Table I were obtained.

TABLE I

Yields of HD and D_2 from 0.1 ml c-C_6D_{12} in 2 ml c-C_5H_{10}

Temperature (°K)	G(HD)	$G(D_2)$
298	0.46	0.085
196	0.52	0.044
77	0.37	0.068

Ethanol decreases these yields. In Fig. 2 the sum of the decreases in G(HD) and $G(D_2)$ as a function of ethanol concentration is plotted for each temperature. Also shown are the decreases in G(HD + D_2) for 0.1 ml of cyclohexane-d_{12} in 2 ml of cyclohexane together with various amounts of ethanol at 298 °K. In the absence of ethanol G(HD) is 0.22 and $G(D_2)$ is 0.019 for this system.

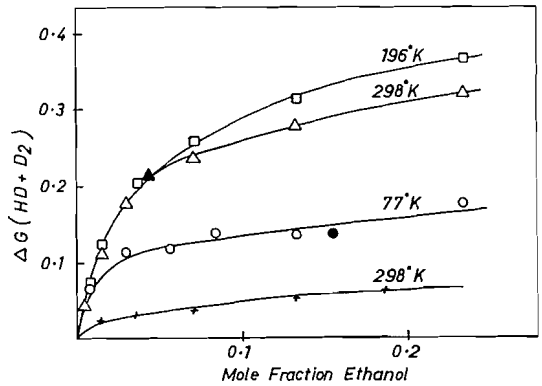

FIG. 2. The decrease in G(HD) + $G(D_2)$ from 4.1 mole % c-C_6D_{12} in c-C_5H_{10} with added ethanol. ▲ and ●, methanol substituted for ethanol; +, 4.8 mole % c-C_6D_{12} in c-C_6H_{12}.

Discussion

The results for the liquid phase at 298 °K are consistent with the proposed charge transfer mechanism formulated in eqs. [1] to [3]

[1] $c\text{-}C_5H_{10} \rightsquigarrow c\text{-}C_5H_{10}^+ + e$

[2] $c\text{-}C_6D_{12} \rightsquigarrow c\text{-}C_6D_{12}^+ + e$

[3] $c\text{-}C_5H_{10}^+ + c\text{-}C_6D_{12} \rightarrow c\text{-}C_5H_{10} + c\text{-}C_6D_{12}^+$

In the absence of ethanol, charge neutralization leads eventually to H_2, HD, and D_2 formation.

[4] $c\text{-}C_5H_{10}^+ + e \rightarrow H_2$

[5] $c\text{-}C_6D_{12}^+ + e \rightarrow$ HD or D_2

The neutralization reaction [4] will also lead to a small amount of HD via an intermediate such as a hydrogen atom. However, the isotope effect in abstraction will favor the formation of H_2 rather than HD (10). The formation of HD via reaction [4] will therefore be neglected during the rest of this discussion.

In the presence of ethanol, proton or deuteron transfer can occur in competition with [4] and [5].

[6] $c\text{-}C_5H_{10}^+ + C_2H_5OH \rightarrow c\text{-}C_5H_9 + C_2H_5OH_2^+$

[7] $c\text{-}C_6D_{12}^+ + C_2H_5OH \rightarrow c\text{-}C_6D_{11} + C_2H_5OHD^+$

Neutralization then leads to H_2 or HD formation

[8] $C_2H_5OH^+ + e \rightarrow C_2H_5OH + H$

[9a] $C_2H_5OHD^+ + e \rightarrow C_2H_5OH + D$

[9b] $\rightarrow C_2H_5OD + H$

[10a] $H + c\text{-}C_5H_{10} \rightarrow H_2 + c\text{-}C_5H_9$

[10b] $D + c\text{-}C_5H_{10} \rightarrow HD + c\text{-}C_5H_9$

In previous work (2, 3) it has been shown that electron scavengers such as SF_6, N_2O, or CCl_4 reduce the yields of HD and D_2 formed in the charge transfer process by changing the neutralization reactions [4] and [5] to those involving the positive ions and an anion, e.g. Cl^- or CCl_4^- from CCl_4. These latter processes do not lead to hydrogen formation and hence the total hydrogen yield is reduced. The effect of electron scavengers simply shows that processes dependent upon charge neutralization are involved. The mechanism summarized by reactions [6]–[10] predicts a constant hydrogen yield regardless of proton scavenger concentration. We find that $G(H_2)_{total}$ remains between 4.95 and 5.30 while the mole fraction of ethanol varies from 0 to 0.25. The highest values are found at the highest ethanol concentration.

We will assume that (*a*) the results of Buchanan and Williams (6) for the ethanol-*d*/cyclohexane system will also be applicable to the ethanol/cyclopentane system. A single experiment with 0.426 mole of ethanol-*d* per liter of cyclopentane gave $G(HD) = 1.04$. This is the same as the uncorrected value obtained when the same concentration of ethanol-*d* is irradiated in cyclohexane (6). (*b*) The total yield of ions scavengeable by ethanol is 3 G units. (*c*) At $\sim$ 0.25 mole fraction of ethanol all these ions have been scavenged.

Buchanan and Williams (6) have shown for ethanol-*d* in cyclohexane that $G(HD)$ is equivalent to one half the yield of ions scavenged at any ethanol-*d* concentration. $G(HD)$ therefore increases with increasing concentration. In the present work the increase of ion scavenging shows up as a decreasing yield of $HD + D_2$. The two sets of results, both obtained at ambient temperature, are compared in Fig. 3. The G value scales have been adjusted by multiplying $\Delta G(HD + D_2)$ by a factor of ~ 5 so that the almost linear parts of the curves coincide. Except at low solute concentrations the two show the same concentration dependence. At low ethanol concentrations the present results are expected to be lower since, if reaction [9] occurs without an isotope effect (6), then even though reaction [5] is suppressed when reaction [7] occurs there is a contribution to HD formation from [9*a*]. At higher ethanol concentrations reaction [6] will be competing effectively with reaction [3] so that the importance of the contribution of reaction [9*a*] will decrease. At these higher concentrations the exchange reaction [11] will also decrease the contribution of reaction [9*a*] to HD formation.

[11] $C_2H_5OHD^+ + C_2H_5OH \rightarrow C_2H_5OD + C_2H_5OH_2^+$

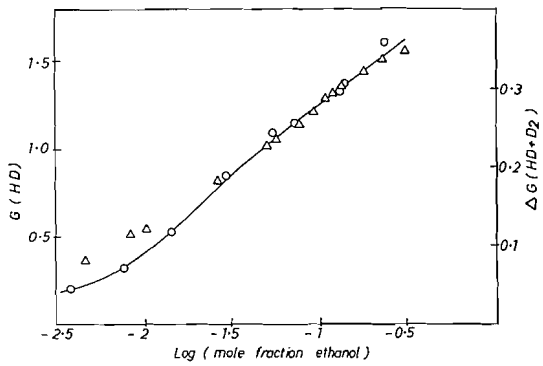

FIG. 3. $\Delta G(HD + D_2)$ from 4.1 mole % $c\text{-}C_6D_{12}$ in $c\text{-}C_5H_{10}$, ○, right scale; and $G(HD)$ from C_2H_5OD in $c\text{-}C_6H_{12}$, △, Buchanan and Williams (6), left scale.

From Fig. 3 it is possible to obtain an estimate of the relative effectiveness of charge transfer from $c\text{-}C_5H_{10}^+$ to $c\text{-}C_6D_{12}$ compared with proton transfer from $c\text{-}C_5H_{10}^+$ to C_2H_5OH. At 0.25 mole fraction of ethanol, the highest concentration used, $\Delta G(HD + D_2) = 0.36$ which will be the yield of scavengeable $c\text{-}C_6D_{12}^+$ ions, or, more correctly, the yield of ions from reactions [1] and [2] which would lead to HD or D_2 formation in the absence of ethanol. The solution is 4.9 electron % in $c\text{-}C_6D_{12}$ so that $G(HD + D_2)$ from ions formed by the direct radiolysis of $c\text{-}C_6D_{12}$ is 0.15 since for 100 electron % the value is 3. The yield of the charge exchange reaction [3] at 4.1 mole % $c\text{-}C_6D_{12}$ is given by $\Delta G(HD + D_2) - \Delta G(HD + D_2$ formed by direct radiolysis) $= 0.36 - 0.15 = 0.21$. This is an upper limit since there will be a small contribution to HD formation via reactions with protiated ions as precursors. For 4.1 mole %

ethanol-*d* in cyclohexane $G(HD) = 0.93$, i.e. the yield of scavenged ions is 1.86. Assuming that the value will hold in cyclopentane as solvent the relative efficiency of proton transfer to charge transfer is $\sim 9:1$. This will be a minimum ratio and bears out earlier suggestions of the low efficiency of charge transfer (1, 5). It is also in accord with the findings of Scala, Lias, and Ausloos in the isopentane-d_{12}/*n*-hexane system (11).

There are two possible explanations for this difference in efficiency between proton transfer and charge transfer in this system; (*a*) The efficiency per encounter of reactants for charge transfer is a factor of nine less than that for proton transfer: Freeman (12) suggests that proton transfer to ethanol occurs at every encounter. On this basis only one in nine encounters lead to charge transfer. (*b*) Only a certain fraction of the solvent molecules are eligible to engage in charge transfer reactions. Such might be the case if rapid protonation by the solvent occurs. A choice between these two alternatives cannot be made on the basis of the present results. The use of higher concentrations of perdeuterated solute to find the maximum number of ions eligible for charge transfer is not feasible since the problem of apportioning HD and D_2 yields to the various precursors cannot be solved. It is to be noted, however, that Fig. 3 shows that the spatial distribution of $c\text{-}C_6D_{12}^+$ ions in the system is the same as that for all other ions.

At 196 °K charge transfer occurs to a slightly greater extent that it does at 298 °K. The curves for these two temperatures in Fig. 2 are indistinguishable up to ~ 0.05 mole fraction of ethanol. At higher concentrations there is a greater reduction of $G(HD + D_2)$ at the lower temperature which is in keeping with the slightly larger scavengeable yield of $HD + D_2$ shown in Table I. It is not immediately apparent why charge transfer to cyclohexane-d_{12} and proton transfer to ethanol should be equally efficient at the two temperatures if both processes are dependent upon diffusion of molecules and ions. The results for irradiations in the solid phase at 77 °K are interesting since the efficiency with which ethanol reacts is comparable to that in the liquid phase, this being specially true at the lowest concentrations. At higher concentrations there is a smaller decrease in $G(HD + D_2)$ which probably reflects in large part the much lower efficiency of the charge neutralization reaction [5] in producing HD and D_2. Table I shows that $G(HD)$ and $G(D_2)$ are somewhat lower in the solid phase than in the liquid phase which would be in keeping with Sagert's study of electron scavenging (13). Since 77 °K is less than one half the melting point of cyclopentane it may be presumed that molecular diffusion is negligible during the ionic lifetime. The results show that both charge transfer and proton transfer occur under these conditions which would suggest that positive charge migration occurs in the solid phase by a process not involving molecular diffusion. Gallivan and Hamill (14) and Shida and Hamill (15) have shown that such a process probably occurs in 2-methyl-pentane glasses at 77 °K although in these cases the ionic lifetime is prolonged due to electron trapping. All the curves in Fig. 2 have similar shapes. In particular they show a very steep gradient at the lowest ethanol concentrations and in fact $\Delta G(HD + D_2)$ is the same for the $c\text{-}C_5H_{10}/c\text{-}C_6D_{12}$ system for all three temperatures at $\sim$ 0.01 mole fraction ethanol. If resonance charge transfer is responsible for all or part of the mobility of the cations which lead to HD and D_2 production at 77 °K it may also contribute to some extent to such charge migration in the liquid phase.

When ethanol is added to cyclohexane containing 4.8 mole % cyclohexane-d_{12} the yields of HD and D_2 are decreased. At 25 mole % ethanol $\Delta G(HD + D_2)$ is estimated to be 0.09, i.e. for 100 mole % $c\text{-}C_6D_{12}$ the decrease would be 2.2 instead of the expected 3. Charge exchange apparently occurs in this symmetrical system but exchange to give exclusively $c\text{-}C_6H_{12}^+$ is not complete. Previous work has shown that although a deuterated solute irradiated in the corresponding protiated solvent does produce lower yields of HD and D_2 than would be expected simply on a composition basis, these yields can be further lowered by use of a solvent of lower ionization potential (1). Abramson and Futrell (16) have found in a mass spectrometric study of ion–molecule reactions that charge exchange between $c\text{-}C_6D_{12}^+$ and $c\text{-}C_6H_{12}$ occurs in the gas phase to yield a maximum ratio of $c\text{-}C_6H_{12}^+/c\text{-}C_6D_{12}^+$ of 1.39 at the highest pressures and lowest ion repeller fields employed. The above results give the higher ratio of 1.7 in the liquid phase at 298 °K.

Acknowledgments

The author expresses his appreciation of financial support from the National Research Council of Canada and Atomic Energy of Canada Ltd., Commercial Products.

1. J. A. STONE, A. R. QUIRT, and O. A. MILLER. Can. J. Chem. **44**, 1175 (1966).
2. J. A. STONE. Can. J. Chem. **42**, 2872 (1964).
3. P. J. DYNE. Can. J. Chem. **43**, 1080 (1965).
4. T. J. HARDWICK. J. Phys. Chem. **66**, 2132 (1962).
5. F. WILLIAMS. J. Am. Chem. Soc. **86**, 3954 (1964).
6. J. W. BUCHANAN and F. WILLIAMS. J. Chem. Phys. **44**, 4377 (1966).
7. K. WATANABE. J. Chem. Phys. **26**, 542 (1957).
8. K. WATANABE, T. NAKAYAMA, and J. MOTTL. U.S. Dept. Comm. Office Tech. Serv. Rept. **158**, 319 (1959).
9. J. A. STONE. Can. J. Chem. **43**, 809 (1965).
10. R. R. HENTZ, J. Y. CHANG, and M. BURTON. J. Phys. Chem. **69**, 2027 (1965).
11. A. A. SCALA, S. G. LIAS, and P. AUSLOOS. J. Am. Chem. Soc. **88**, 5701 (1966).
12. G. R. FREEMAN. J. Chem. Phys. **46**, 2822 (1967).
13. N. H. SAGERT. Can. J. Chem. **46**, 89 (1968).
14. J. B. GALLIVAN and W. H. HAMILL. J. Chem. Phys. **44**, 1279 (1966).
15. T. SHIDA and W. H. HAMILL. J. Chem. Phys. **44**, 4373 (1966).
16. F. P. ABRAMSON and J. H. FUTRELL. J. Phys. Chem. **71**, 3791 (1967).

Can. J. Chem. Downloaded from www.nrcresearchpress.com by 210.87.254.40 on 09/05/12
For personal use only.

On the chemistry of iodonyl radicals. The oxidation of iodobenzene by *t*-butyl hypochlorite

DENNIS D. TANNER AND GEOFFREY C. GIDLEY[1]
Department of Chemistry, University of Alberta, Edmonton, Alberta

Received April 18, 1968

The reaction of iodobenzene with *t*-butyl hypochlorite proceeds by a free radical chain mechanism, forming as the sole product iodobenzene *t*-butoxy chloride (IBBC). The photoinduced or thermally induced reactions of IBBC with hydrocarbon substrates yield chlorinated hydrocarbons by a radical chain halogenation sequence involving *t*-butoxyiodonyl benzene as the principal chain-carrying species. The photolysis or thermolysis of IBBC in the absence of molecular oxygen yields products resulting from a variety of free radical chain reactions, while thermolysis in the presence of oxygen yields only iodobenzene and *t*-butyl hypochlorite.

Canadian Journal of Chemistry, 46, 3537 (1968)

Introduction

The ability of organic compounds of elements of the third period to expand their valence shell to accommodate nine electrons forming a reactive radical intermediate has been proposed in the cases of phosphorus (1–4) and sulfur (5–9). The formation of radical intermediates of compounds of elements of higher atomic number having energetically low-lying d orbitals would also be predicted favorable. Compounds of the Group VII element iodine would seem ideally suited to undergo this type of reaction.

The iodonyl radical has been suggested as an intermediate in the chlorination reactions of molecular chlorine in solvent iodobenzene (10), in the photo-initiated chlorination reactions of iodobenzene dichloride (11–13), during the iodination reactions of the *t*-butyl hypoiodite reagent (14), in the intramolecular hypoiodite reactions (15), and in the decompositions of certain iodinated peroxides (16).

To illustrate further the intermediacy of the iodonyl radical we have undertaken a study of the oxidation of iodobenzene by *t*-butyl hypochlorite.

Results

The Formation of Iodobenzene t-Butoxy Chloride

Mixtures of iodobenzene (2.9 *M*) and *t*-butyl hypochlorite (5.7 *M*) reacted slowly at room temperature or above, or more rapidly when photochemically initiated, to yield iodobenzene *t*-butoxy chloride (IBBC) (85–95%).

When the reaction was carried out in the absence of light, but in the presence of added cyclohexane, detectable amounts of cyclohexyl chloride were formed. The dark reaction of iodobenzene and *t*-butyl hypochlorite at 26° was inhibited by added *p*-cresol (2 mole %) and galvinoxyl (1%), but not by atmospheric amounts of molecular oxygen. Oxygen, however, did inhibit the induced chlorination of added cyclohexane.

$$PhI + (CH_3)_3COCl \rightarrow PhI(Cl)(OC(CH_3)_3)$$
(IBBC)

The photo-initiated reaction could be conveniently followed in its initial stages by nuclear magnetic resonance (n.m.r.) spectroscopy. Carbon tetrachloride solutions of iodobenzene (2.45 *M*) and *t*-butyl hypochlorite (2.08 *M*) showed no reaction (>3 days) at −20° in sealed degassed Pyrex n.m.r. tubes. Irradiation of the reaction mixtures at −20° allowed us to observe the progress of the photo-initiated radical formation of IBBC. The 100 Mc n.m.r. spectrum showed the gradual disappearance of the *t*-butyl hypochlorite resonance (τ 8.71) and the concurrent appearance of a new resonance attributable to the methyl protons of the IBBC (τ 8.83). Since the product was only slightly soluble (1.29 ± 0.01 g/l at 26 °C) in carbon tetrachloride the reaction could only be followed in this manner in its initial stages.

Oxygen-free carbon tetrachloride solutions of iodobenzene (1.00–2.50 *M*) and *t*-butyl hypochlorite (0.94–2.45 *M*) did not react at −20° in the dark (>3 days), while degassed and non-degassed solutions at −20° both showed a reaction after 15 min when subjected to irradiation

[1]University of Alberta Postdoctoral Fellow (1966–1968).

Can. J. Chem. Downloaded from www.nrcresearchpress.com by 210.87.254.40 on 09/05/12
For personal use only.

under a 400 W incandescent light. Inhibition of the photo-initiated formation reaction was observed (> 300 min) with added *p*-cresol (2%) and with added galvinoxyl (1%, >450 min).

The structure of IBBC was determined from its microanalysis, $C_{10}H_{14}ClIO$, and its molecular weight, 306 ± 8. The molecular weight was determined by iodometric titration. Examination by gas–liquid phase chromatography (g.l.p.c.) of the organic products from these titrations showed only the presence of iodobenzene and *t*-butyl alcohol. The identity of these products was confirmed by the isolation of each component, followed by the comparison of their infrared (i.r.) and n.m.r. spectra with those of an authentic sample.

It was observed that a very rapid quantitative reaction takes place between excess anhydrous hydrogen chloride and a suspension of IBBC in carbon tetrachloride to yield *t*-butyl alcohol and iodobenzene dichloride.

The Chlorination Reaction of IBBC

Oxygen-free methylene chloride solutions of IBBC (0.47–0.49 mmole/ml) and cyclohexane (3.3–4.5 *M*) yielded cyclohexyl chloride, *t*-butyl alcohol, and iodobenzene in 1:1:1 mole ratios, at room temperature both in the dark and under irradiation. The light-induced halogenation was greatly accelerated over that of the dark reaction, while the dark reaction could be stopped at lower temperatures. The photo-initiated chlorination was inhibited by the presence of atmospheric amounts of oxygen, traces of hydroquinone, or *sym*-trinitrobenzene (see Table I).

TABLE I

The reaction of IBBC (0.47–0.49 mmole/ml) with cyclohexane (3.3–4.5 *M*) in methylene chloride[a]

Conditions	Maximum reaction time (min)[b]	% Reaction[c]
Dark, degassed, 25°	900	2 ± 1.0
Dark, degassed, 0°	900	< 0.1
Irradiation, degassed, 25°	15	100
Irradiation, oxygen, 25°	430	65 ± 5.0
Irradiation, degassed, hydroquinone 3%, 25°	250	100
Irradiation, degassed, *sym*-trinitrobenzene, 3%, 25°	130	100

[a]Sole products were cyclohexyl chloride, *t*-butanol, and iodobenzene in ratio 1:1:1 mole per mole of IBBC. Less than 0.1% chloroform was produced.
[b]Maximum time for duplicate runs.
[c]Values reported are for duplicate experiments.

The chlorination reactions of IBBC could be conveniently carried out in heterogeneous mixtures of chlorinating reagent and carbon tetrachloride solutions of the desired substrate. Under these conditions degassed mixtures of IBBC (0.21 mmole/ml), cyclohexane (4.5 *M*), and carbon tetrachloride remained unreacted indefinitely (> 36 h) in the absence of light at 25 °C with continuous agitation, while upon irradiation a smooth conversion of the reactants to *t*-butyl alcohol, cyclohexyl chloride, and the iodobenzene was accomplished in 3–5 h.

The chlorinations of *n*-butane and 2,3-dimethylbutane were carried out in the above manner. The ratio of primary to secondary chloride in the chlorination of *n*-butane and the ratio of primary to tertiary chloride in the halogenation of 2,3-dimethylbutane were obtained by g.l.p.c. analysis of the product mixtures from these chlorinations. Values for the primary: secondary:tertiary reactivities of 1:13:144 per hydrogen in IBBC halogenations at 40 °C were calculated from these analyses in the usual manner (12).

The halogenation of 1-chlorobutane (1.62 *M*) in carbon tetrachloride at 40° with IBBC (0.155 mmole/ml) produced a >80% yield of dichlorinated butanes and a ≤0.4% yield of ortho- and para-chloroiodobenzenes.

The photo-initiated or thermally initiated reaction of IBBC (0.108 mmole/ml) with cyclohexane (1.6 *M*) in oxygen-free solutions of carbon tetrachloride at 70° yielded cyclohexyl chloride (102%), acetone (26%), and *t*-butyl alcohol (75%). Under the same conditions a carbon tetrachloride solution of *t*-butyl hypochlorite (0.109 *M*), iodobenzene (0.120 *M*), and cyclohexane (1.64 *M*) yielded cyclohexyl chloride (92%), acetone (~ 1.0%), and *t*-butyl alcohol (109%), while the halogenation of cyclohexane (1.60 *M*) with *t*-butyl hypochlorite (0.109 *M*) under these conditions yielded cyclohexyl chloride (86%), acetone (~ 1.0%), and *t*-butyl alcohol (101%).

The Photo- and Thermal-Initiated Decomposition of IBBC

Photo-Decomposition

Irradiation of continuously shaken degassed Pyrex ampuls containing heterogeneous mixtures of carbon tetrachloride and IBBC (0.45–0.60 mmole/ml) at 40° afforded a means of studying the light-initiated decomposition–re-

Can. J. Chem. Downloaded from www.nrcresearchpress.com by 210.87.254.40 on 09/05/12
For personal use only.

arrangement of the addition product, since it could be shown that under these conditions in the absence of light the IBBC could be recovered unchanged. The irradiation of the reaction mixture yields a homogeneous carbon tetrachloride solution of products after 3 h of irradiation. The qualitative and quantitative compositions of the reaction products as determined by g.l.p.c. and n.m.r. analysis are tabulated in Table II.

In addition to the products tabulated in Table II small amounts of iodosobenzene or iodoso- and iodoxy-benzene were isolated. The amounts of these products were variable between different reactions. It was found that mixtures of iodosobenzene and carbon tetrachloride upon photolysis at 40° underwent disproportionation to form iodobenzene and iodoxybenzene. It was further

$$\text{PhIO} \xrightarrow{h\nu} \text{PhIO}_2 + \text{PhI}$$

demonstrated that equimolar mixtures of iodosobenzene with IBBC yielded qualitatively the same products found in the IBBC decompositions and that the aromatic fragments from both reactants were accounted for as iodobenzene (76%) and chlorobenzene (10%).

Thermal Decomposition

The thermal decomposition of IBBC was observed when a mixture of the reagent and carbon tetrachloride was sealed in degassed and non-degassed Pyrex ampuls and thermostated at 76° in the absence of light.

TABLE II

The photo and thermal decomposition of IBBC (0.4–0.7 mmole/ml) in carbon tetrachloride

	Yield (mole/mole of IBBC)		
Products	40° with irradiation[a] (3–4 h)	76°, dark, with oxygen[a] (> 96 h)	76°, dark[a] (2–3 h)
PhI	0.87	1.00	0.88
$(CH_3)_3COCl$[b]	—	0.94	—
PhCl	0.17	—	0.17
I_2[b]	0.03	—	—
CH_3Cl	0.37	—	0.40
CH_3COCH_3	0.46	—	0.49
$(CH_3)_3CCl$	0.15	—	0.06
$(CH_3)_3COH$	0.10	—	0.24
HCl	0.04	—	0.14
$(CH_3)_2C(OH)CH_2Cl$	0.05	—	0.01
$ClCH_2COCH_3$	0.07	—	0.09

[a]The above values are representative for a specific experiment. Duplicated experiments gave similar results. The values in parenthesis are average reaction times for repeated experiments.
[b]Analyzed by iodometric titration. The identity of the *t*-butyl hypochlorite was confirmed by its n.m.r. spectrum.

When ampuls containing atmospheric amounts of oxygen reacted under the above conditions for 4 days, a pale-yellow solution resulted which contained 10% of the precipitated unreacted starting material. The residual starting material was separated from the solution by vacuum transfer and was identified by its melting point (m.p.) behavior, its mixture m.p., and its positive reaction with potassium iodide. The n.m.r. spectrum of the solution showed the presence only of *t*-butyl hypochlorite and iodobenzene. Iodometric titration of the solution showed it to contain 94% of the active halogen. The g.l.p.c. analysis of the organic layer after titration showed it to contain 101% of the theoretical amount of iodobenzene.

Decomposition in the absence of light at 76° of a degassed mixture of IBBC and carbon tetrachloride yielded the products listed in Table II. Vacuum transfer of the reaction mixture left a residual white solid (3%) whose m.p. (236–240°), mixture m.p., and i.r. spectrum identified it as iodoxybenzene. Under the reaction conditions it was shown that iodosobenzene in carbon tetrachloride was quantitatively converted to iodoxybenzene and iodobenzene. It was further shown that an equimolar mixture of iodosobenzene and IBBC under the above reaction conditions was converted to qualitatively the same products as found in IBBC decompositions and that the aromatic fragments from both reagents could be accounted for as iodobenzene and chlorobenzene.

Discussion

An attractive proposal for the mechanism of the light-initiated formation of IBBC at low temperatures is a radical chain process involving *t*-butoxy radical addition to iodobenzene followed by chain transfer from *t*-butyl hypochlorite.

$$(CH_3)_3COCl \xrightarrow{h\nu} (CH_3)_3CO^{\cdot} + Cl^{\cdot}$$

$$\text{PhI} + (CH_3)_3CO^{\cdot} \rightarrow \text{PhIOC}(CH_3)_3 \qquad (1)$$

$$\text{PhIOC}(CH_3)_3 + (CH_3)_3COCl \rightarrow \text{PhI(Cl)OC}(CH_3)_3 + (CH_3)_3CO^{\cdot}$$

The radical chain nature of the photo-initiated formation reaction was substantiated by its initiation by light, the inhibition of the reaction by small amounts of added *p*-cresol and galvinoxyl, and by the induced halogenation of added cyclohexane. The intermediacy of (**1**) was postulated

Can. J. Chem. Downloaded from www.nrcresearchpress.com by 210.87.254.40 on 09/05/12
For personal use only.

by analogy to the radical addition intermediates proposed for phosphorus (1–4) and sulfur (1, 6–8) compounds with *t*-butoxy radicals and because of the precedented involvement of iodonyl radicals in the halogenation reactions of IBBC (see discussion on chlorination reactions), iodobenzene dichloride (12, 13), and the polymeric *t*-butyl hypoiodite reagent (14).

The mechanism of the thermal formation of IBBC at 25° in the dark was shown to be a radical chain process similar to the photo-induced formation reaction, since it was inhibited by added galvinoxyl or *p*-cresol and since added cyclohexane yielded cyclohexyl chloride by induced halogenation.

The Chlorination Reaction of IBBC

The inhibition and initiation experiments (Table I) established the radical chain nature of the photo-halogenation reactions of IBBC with hydrocarbon substrates. Several possible chain mechanisms can be proposed for the light-initiated production of alkyl chlorides with IBBC.

$$\text{IBBC} + \text{RH} \xrightarrow{h\nu} \text{RCl} + \text{PhI} + (\text{CH}_3)_3\text{COH}$$

The possible chain sequence for these halogenation reactions can be constructed from combinations of the following radical and non-radical reactions.

[1] $\text{PhI(Cl)OC(CH}_3)_3 \xrightarrow{h\nu} \text{PhİOC(CH}_3)_3 + \text{Cl}^{\cdot}$

[2] $\text{Cl}^{\cdot} + \text{RH} \rightarrow \text{HCl} + \text{R}^{\cdot}$

[3] $\text{PhI(Cl)OC(CH}_3)_3 + \text{HCl} \rightarrow \text{PhI} + \text{Cl}_2 + (\text{CH}_3)_3\text{COH}$

[4] $\text{R}^{\cdot} + \text{Cl}_2 \rightarrow \text{RCl} + \text{Cl}^{\cdot}$

[5] $\text{PhI} + \text{Cl}_2 \rightarrow \text{PhICl}_2$

[6] $\text{PhICl}_2 + \text{R}^{\cdot} \rightarrow \text{PhİCl} + \text{RCl}$

[7] $\text{PhİCl} + \text{RH} \rightarrow \text{PhIHCl} + \text{R}^{\cdot}$

[8] $\text{PhIHCl} \rightarrow \text{PhI} + \text{HCl}$

[9] $(\text{CH}_3)_3\text{CO}^{\cdot} + \text{RH} \rightarrow (\text{CH}_3)_3\text{COH} + \text{R}^{\cdot}$

[10] $\text{R}^{\cdot} + \text{PhI(Cl)OC(CH}_3)_3 \rightarrow \text{RCl} + \text{PhİOC(CH}_3)_3$

[11] $\text{PhİOC(CH}_3)_3 \rightarrow \text{PhI} + (\text{CH}_3)_3\text{CO}^{\cdot}$

[12] $\text{PhİOC(CH}_3)_3 + \text{RH} \rightarrow \text{PhI(H)OC(CH}_3)_3 + \text{R}^{\cdot}$

[13] $\text{PhI(H)OC(CH}_3)_3 \rightarrow \text{PhI} + (\text{CH}_3)_3\text{COH}$

Reactions [2], [7], [9], and [12] involve abstraction by chlorine atoms, phenyl iodonyl chloride radicals, *t*-butoxy radicals, and phenyl *t*-butoxy iodonyl radicals respectively, and are therefore the product-determining steps in the radical halogenations.

The analysis of the products from the halogenations of *n*-butane and 2,3-dimethylbutane yielded calculated primary:secondary:tertiary ratios for hydrogen abstraction of 1:13:144. Reaction schemes involving a sequence of reactions [1], [2], [3], [4], or [1], [12], [10], [11], and [9] or a mixture of the two chains cannot be operative in the chlorination reactions of IBBC since chlorine atom abstraction or *t*-butoxy radical abstraction show the lower selectivity values of 1:3.9:5.1 (17) and 1:8:44 (18) respectively.

The rapid reaction of IBBC with hydrogen chloride yielded iodobenzene dichloride and *t*-butyl alcohol (reactions [3] and [5]). Since iodobenzene dichloride has been shown to undergo photo-initiated radical chain halogenation where phenyl iodonyl chloride is the abstracting species (11) the sequence of reactions [1], [2], [3], [5], [6], [7], and [8] must be considered in any evaluation of the halogenation reactions of IBBC. The primary:secondary:tertiary selectivities for hydrogen abstraction by PhİCl radicals has been reported as 1:21:368 (12). The selectivity values for IBBC are clearly lower than the values reported for iodobenzene dichloride and infer that if PhİCl radicals were operative as an abstracting species in the chain halogenation reactions of IBBC they could not be the sole chain-carrying radicals and must by necessity be involved in a mixed chain with radicals of lower selectivity, i.e. chlorine or *t*-butoxy radicals, or both. The absence of the intermediacy of iodobenzene dichloride in the reactions of IBBC was definitely established in the following manner. The chlorination of *n*-butyl chloride with iodobenzene dichloride has been reported to produce very low yields of chlorinated substrate and showed a 35% yield of the rearrangement products of iodobenzene dichloride itself (12), while under identical conditions the halogenation of 1-chlorobutane with IBBC yielded only traces (<0.4%) of these rearrangement products.

The chain sequence for halogenation by IBBC must involve, by the process of elimination, abstraction by $\text{PhİOC(CH}_3)_3$ radicals (reaction scheme [1], [12], [10], and [13]). However, the possibility that some abstraction also occurs by the less selective *t*-butoxy radical produced in reaction [11] could not be ruled out.

Can. J. Chem. Downloaded from www.nrcresearchpress.com by 210.87.254.40 on 09/05/12
For personal use only.

The Thermal- and Photo-Induced Decomposition of IBBC

The thermal decomposition of IBBC in the presence of atmospheric amounts of oxygen yielded, after 96 h, iodobenzene and *t*-butyl hypochlorite.

$$PhI(Cl)OC(CH_3)_3 \rightleftarrows PhI + (CH_3)_3COCl$$

Both the thermal decomposition in the absence of oxygen and the photoinduced decomposition appear to be qualitatively the same series of reactions although the rates of the individual competing reactions would be temperature variable (see Table II). In oxygen-free systems in the absence of light at 75° the occurrence of the radical chain halogenation of cyclohexane clearly established the presence of free radicals under the conditions of decomposition.

The products produced from the thermal- or photo-initiated reactions of IBBC (see Table II) can be rationalized on the basis of the following series of chain reactions. Phenyl *t*-butoxy iodonyl radicals produced on initiation can undergo β-scission to produce iodosobenzene and *t*-butyl radicals followed by chain transfer with IBBC to yield, by a chain sequence, *t*-butyl chloride (reactions [14] and [15]).

[14] $$Ph\dot{I}OC(CH_3)_3 \rightarrow PhIO + (CH_3)_3C^{\cdot}$$

[15] $$(CH_3)_3C^{\cdot} + IBBC \rightarrow (CH_3)_3CCl + Ph\dot{I}OC(CH_3)_3$$

An alternative path for the β-scission process is the elimination of a *t*-butoxy fragment from the iodonyl radical (reaction [16]) and subsequent radical abstraction by *t*-butoxy from a hydrocarbon source (reaction [17]) followed by transfer from IBBC (reaction [18]) to yield *t*-butyl alcohol, iodobenzene, and the observed chlorinated acetone or *t*-butyl alcohol.

[16] $$Ph\dot{I}OC(CH_3)_3 \rightarrow PhI + (CH_3)_3CO^{\cdot}$$

[17] $$(CH_3)_3CO^{\cdot} + RH \rightarrow (CH_3)_3COH + R^{\cdot}$$

[18] $$R^{\cdot} + IBBC \rightarrow RCl + Ph\dot{I}OC(CH_3)_3$$

The well-known β-scission reaction of the *t*-butoxy radicals (reaction [19]) (19, 20) followed by transfer with IBBC (reaction [20]) could account for the production of methyl chloride and acetone.

[19] $$(CH_3)_3CO^{\cdot} \rightarrow CH_3^{\cdot} + CH_3{-}\overset{\overset{O}{\|}}{C}{-}CH_3$$

[20] $$CH_3^{\cdot} + IBBC \rightarrow CH_3Cl + Ph\dot{I}OC(CH_3)_3$$

However, the observation of a noticeably low alcohol to acetone ratio (2.9) for the thermal (70°) or photochemical (70°) chlorination of cyclohexane with IBBC, compared with the high ratio obtained during chlorination of cyclohexane under similar conditions with *t*-butyl hypochlorite or mixtures of *t*-butyl hypochlorite and iodobenzene (alcohol/acetone 99/1), suggests the possibility that methyl radicals and acetone can be produced directly from the decomposition of the iodonyl radical by a three bond fragmentation. These observations coupled with the high alcohol to acetone ratios reported for the photo-decomposition of *t*-butyl hypochlorite in carbon tetrachloride support the hypothesis that the acetone and methyl chloride do not arise solely from reaction sequence [19] and [20].

The nature of the experimentally observed transformation of iodosobenzene to iodoxybenzene and its subsequent reduction to iodobenzene (reactions [21], [22]) under the conditions of the decomposition has not as yet been elucidated.

[21] $$2PhIO \rightarrow PhIO_2 + PhI$$

[22] $$PhIO_2 + \text{oxidizable substrate} \rightarrow PhI + R(O)$$

The formation of hydrogen chloride during the radical decompositions infers that the halogenation of acetone and *t*-butyl alcohol must in part at least be due to the previously reported (12) radical chain chlorination reactions of iodobenzene dichloride (reaction sequence [3], [5], [6], [7], and [8]) or via a chain halogenation by molecular chlorine (reaction sequence [3], [4], and [2]).

The production of chlorobenzene during the decompositions can be readily explained by the precedented displacement of iodine from iodobenzene by chlorine atoms, which was also observed in the halogenation reactions of iodobenzene dichloride (12).

Experimental

Materials

t-Butyl hypochlorite was prepared by the method of Teeter and Bell (21) and its purity found by iodometric titration (22).

Commercial iodobenzene, stabilized with mercury (Aldrich Chemical Co.), was distilled and traces of free iodine removed by passing it through a column of absorption alumina (Fisher Scientific Co.) immediately prior to use. Carbon tetrachloride (Fisher spectral grade) and methylene chloride (Fisher reagent grade), 2,3-dimethylbutane, and *n*-butane (Phillips Petroleum Co., research grade) were used without further purification.

Can. J. Chem. Downloaded from www.nrcresearchpress.com by 210.87.254.40 on 09/05/12
For personal use only.

Freon 112 (Matheson), cyclohexane (Fisher reagent grade), and 1-chlorobutane (British Drug Houses Ltd.) were distilled and used without further purification.

Reaction between Iodobenzene and t-Butyl Hypochlorite at Room Temperature, with Irradiation

A mixture of iodobenzene (12.2 g, 0.060 mole, 2.9 *M*) and *t*-butyl hypochlorite (12.8 g, 0.118 mole, 5.7 *M*) in a lightly stoppered Erlenmeyer flask was irradiated at room temperature by two 200 W incandescent lamps for 2½ h. The flask was then left at 0° in the dark for 9 h. The pale-yellow solid product and mother liquor were transferred to a round-bottom flask and unchanged reactants removed by distillation (25° at 0.1 mm) leaving 17.69 g (94%) of a pale-yellow solid (IBBC).

A similar solution left in the dark for 5 h and kept at 0° overnight gave the same product, but the yield was only 3%.

The yellow solid decomposed in the region 130–140 °C, leaving a white solid, m.p. 235–240°, and an oil.

Anal. Calcd. for $C_{10}H_{14}ClIO$: C, 38.45; H, 4.48. Found: C, 38.39; H, 4.37.

The equivalent weight, as determined by titration of the iodine liberated on addition of acidified aqueous potassium iodide against standard aqueous sodium thiosulfate, was found to be 153 ± 4. Examination of the organic products from these titrations by g.l.p.c. (10 ft × 1/4 in. SS column packed with 15% SF 96 on 60/80 mesh firebrick) showed the presence of iodobenzene and *t*-butyl alcohol only. These were confirmed by isolation of each component followed by comparison of their i.r. and n.m.r. spectra with those of authentic samples.

The solubility of IBBC in carbon tetrachloride was determined by titrating 5 ml aliquots of saturated solution against 0.1 *M* aqueous sodium thiosulfate. Based on these titrations, IBBC was found to have a solubility of 1.29 g/l at 26 °C.

The Reaction in the Absence of Light between Iodobenzene and t-Butyl Hypochlorite at Room Temperature (26°)

The reaction mixture consisted of iodobenzene (4.47 *M*) and *t*-butyl hypochlorite (4.19 *M*). Aliquots were transferred to Pyrex ampuls containing *p*-cresol (0.08 *M*), galvinoxyl (0.08 *M*), oxygen (atmospheric amounts), or no additives, and left at 26° in the dark for 19 h. The reaction conditions and results are tabulated in Table III.

Reaction between Iodobenzene and t-Butyl Hypochlorite at −20° in Carbon Tetrachloride

Aliquots of a carbon tetrachloride solution of iodobenzene (2.45 *M*) and *t*-butyl hypochlorite (2.08–2.45 *M*) were transferred to n.m.r. tubes, degassed by the freeze–thaw method, and stored at 77 °K until used. The change in the n.m.r. spectrum of these reaction mixtures was followed using a Varian HA-100 spectrometer with a variable temperature probe at −20 °C. In addition to the original resonance for the methyl hydrogens in *t*-butyl hypochlorite another resonance appeared about 10 c.p.s. to high field after irradiation for 1½ h. This was accompanied by precipitation of a pale-yellow solid (IBBC). The IBBC was isolated and shown to be identical with the previously characterized material in the absence of light.

Identical samples in the absence of light at the same temperature showed no reactions after 3 days.

This experiment was repeated by irradiating degassed Pyrex ampuls containing added *p*-cresol (2.0 mole %), galvinoxyl (1.0 mole %), and oxygen (atmospheric amounts). By comparison with a similar degassed solution containing no additives, the time for the reaction to begin could be assessed visually. The start of the reaction was taken to be when the solution first changed from a bright yellow to a pale opalescent yellow. The results are recorded below in Table IV.

TABLE III

Reaction between iodobenzene and *t*-butyl hypochlorite at room temperature (26°) in the dark

Conditions	Weight of IBBC (g)	Yield of IBBC (%)
Dark	0.194	14.5
Dark, oxygen	0.114	8.7
Dark, *p*-cresol	0.078	6.0
Dark, galvinoxyl	≤0.005	≤0.4

TABLE IV

Reaction between iodobenzene and *t*-butyl hypochlorite at −20° in carbon tetrachloride

Conditions	Inhibition time (min)[a]
*h*ν, degassed	9
*h*ν, not degassed	10
*h*ν, degassed, *p*-cresol	>300
*h*ν, degassed, galvinoxyl	>450

[a]The times are average values for duplicate experiments.

Reaction of IBBC with Hydrogen Chloride

To a suspension of IBBC (7.6×10^{-5} mole) in carbon tetrachloride (1.0 ml) was added dry hydrogen chloride (7.68×10^{-5} mole) dissolved in carbon tetrachloride (2.5 ml). The reaction mixture was stirred and after 5 min a yellow solid product (18.8 mg, 86%) was isolated by filtration, m.p. 112–115°. The m.p. and mixture m.p. identified the product as iodobenzene dichloride. The filtrate was treated with aqueous potassium iodide and the free iodine reduced with aqueous sodium thiosulfate. Analysis of the carbon tetrachloride phase by g.l.p.c. after reduction showed the presence of *t*-butyl alcohol (6.5×10^{-5} mole) and a small amount of iodobenzene. Both products were identified by the comparison of their g.l.p.c. retention time with those of authentic *t*-butyl alcohol and iodobenzene.

Chlorination of Cyclohexane in Methylene Chloride

Mixtures of Freon 112 (0.45 *M*) and cyclohexane (3.3–4.5 *M*) in methylene chloride containing IBBC (0.47–0.49 mmole/ml) were sealed in Pyrex ampuls, placed in a 0° or 25° bath with continuous agitation, and run under the conditions indicated in Table I. Each tube was analyzed for the disappearance of IBBC by iodo-

Can. J. Chem. Downloaded from www.nrcresearchpress.com by 210.87.254.40 on 09/05/12
For personal use only.

metric titration (21). The reaction mixtures were subjected to g.l.p.c. analysis (10 ft × 1/4 in. SS column packed with 15% SF 96 on firebrick). The g.l.p.c. traces showed a 1:1 mixture of cyclohexyl chloride to iodobenzene in those reactions which went to completion. The relative amounts of iodobenzene and cyclohexyl chloride were calculated from calibration curves of the authentic materials with Freon 112.

Chlorination of Cyclohexane in Carbon Tetrachloride

The chlorination reactions in carbon tetrachloride at 40° were carried out in the manner described for the halogenation of cyclohexane in methylene chloride. The reaction mixtures, after irradiation (approx. 3 h), were examined by n.m.r. spectroscopy and g.l.p.c. By a comparison of the integration of the n.m.r. absorption intensities and the integrated g.l.p.c. traces (corrected to mole ratios) a material balance was obtained accounting for 93% of the products; *t*-butyl alcohol, cyclohexyl chloride, and iodobenzene in a 1:1:1 mole ratio. Corresponding mixtures maintained in the absence of light under the same conditions also contained cyclohexyl chloride, but only 3% of the amount obtained from the irradiated samples. Triplicate experiments were carried out.

Reaction of t-Butyl Hypochlorite, t-Butyl Hypochlorite plus Iodobenzene, and IBBC with Cyclohexane in Carbon Tetrachloride at 70°

Carbon tetrachloride solutions of *t*-butyl hypochlorite and cyclohexane; *t*-butyl hypochlorite, iodobenzene, and cyclohexane; and IBBC and cyclohexane, each containing Freon 112 as an internal standard, were transferred to Pyrex ampuls and degassed. The reaction mixtures were irradiated at 70° until colorless and analyzed by g.l.p.c. Two different columns were used for the analyses. A 10 ft × 1/4 in. SS column packed with 10% diethylene glycol succinate (DEGS) on 60/80 mesh, acid-washed Chromosorb W was used initially to analyze the product mixtures. Freon 112 was not completely resolved from carbon tetrachloride on the DEGS column and the mixture was analyzed for cyclohexyl chloride and iodobenzene using a 10 ft × 1/4 in. SS column packed with 15% SF-96 on 60/80 mesh firebrick. An area ratio was determined for Freon 112 versus iodobenzene, and knowing this ratio it was possible to calculate a corrected area for Freon 112 using the DEGS column.

The concentration of reactants and yields of products are given in Table V.

Chlorination of 1-Chlorobutane in Carbon Tetrachloride

Mixtures of Freon 112 (0.05 *M*) and 1-chlorobutane (1.62 *M*) in carbon tetrachloride containing IBBC (0.155 mmole/ml) were sealed in Pyrex ampuls, placed in a 40° bath with continuous agitation, and irradiated with four 200 W incandescent lamps. The analyses and calculations were carried out in the manner previously reported (12). The yield of chlorinated chlorobutanes was 81% while the yield of *o*- and *p*-dichloroiodobenzene was less than 0.3%.

The Photo-Initiated Decomposition of IBBC in Carbon Tetrachloride

Mixtures of Freon 112 (0.3 *M*) and IBBC (0.4–0.7 mmole/ml) in carbon tetrachloride were degassed, sealed in Pyrex ampuls, and irradiated at 40 or 76° with continuous shaking until a colorless or iodine-colored solution was obtained. The contents of the tubes were examined by n.m.r. spectroscopy and g.l.p.c. The aromatic products were analyzed using a 10 ft × 1/4 in. column packed with 15% SF96 on 60/80 mesh, acid-washed firebrick; all of the other products analyzed by g.l.p.c. were determined using a 25 ft × 1/8 in. column packed with 5% Ucon 50 HB 2000 on 80/100 mesh Chromosorb W. The analyses gave the distribution of products listed in Table II. The identity of the products was determined by the addition of authentic materials to the reaction mixtures and noting changes in the n.m.r. spectrum and g.l.p.c. traces. The insoluble iodoso- and/or iodoxy-benzene was isolated from the reaction mixtures either by filtration or by vacuum transfer of the volatile components. The molar percentages of the products were estimated from the integrated n.m.r. spectrum, using a known amount of added methylene chloride as external standard, and from the integrated g.l.p.c. trace by conversion of peak areas to molar percentages using Freon 112 in the usual way (12). Iodoso- or iodoxy-benzene were characterized by their m.p. 190–230°. Synthetic iodosobenzene decomposed on the hot-stage of the m.p. apparatus to give iodoxybenzene. Usually a mixture of the two was obtained, giving a positive test with potassium iodide, and its infrared spectrum (Nujol mull) was consistent with the assigned structures by comparison with the i.r. spectra of the synthetic compounds (23). The duality of products was explained when it was found that at 40° in degassed Pyrex ampuls in carbon tetrachloride, irradiated suspensions of iodosobenzene (pale yellow) were shown to be converted to iodoxybenzene (white) and iodobenzene.

TABLE V

Reaction of *t*-butyl hypochlorite, *t*-butyl hypochlorite plus iodobenzene, and IBBC and cyclohexane in carbon tetrachloride at 70°

Reagents (concentration)	Products (%)			
	t-BuOH	CH_3COCH_3	$C_6H_{11}Cl$	PhI
t-Butyl hypochlorite (0.109 *M*) and cyclohexane (0.16 *M*)	101	<1.0	86	—
t-Butyl hypochlorite (0.109 *M*), iodobenzene (0.120 *M*), and cyclohexane (1.64 *M*)	109	<1.0	92	103
IBBC (0.10 mmole/ml) and cyclohexane (1.60 *M*)	75	26	102	88

Reaction of IBBC and Iodosobenzene in Carbon Tetrachloride at 40°

Mixtures of Freon 112 (0.093 *M*), IBBC (0.27 mmole/ml), and iodosobenzene (0.25 mmole/ml) in carbon tetrachloride were degassed, sealed in Pyrex ampuls, and irradiated at 40° with continuous agitation. After 7 h all the solid had disappeared, leaving a colorless solution. These were analyzed by g.l.p.c. using a 10 ft × 1/4 in. SS column packed with 15% SF96 on 60/80 mesh firebrick and the amount of chlorobenzene (0.51×10^{-4} mole) and iodobenzene (3.92×10^{-4} mole) quantitated in the manner previously described.

Reaction of t-Butyl Hypochlorite, and t-Butyl Hypochlorite plus Iodobenzene in Carbon Tetrachloride with Cyclohexane at 26°

Two reaction mixtures were prepared at room temperature in the dark. Freon 112 (0.75 *M*), *t*-butyl hypochlorite (0.86 *M*), and cyclohexane (1.80 *M*) in carbon tetrachloride (2.5 ml); and Freon 112 (0.63 *M*), *t*-butyl hypochlorite (0.86 *M*), iodobenzene (0.86 *M*), and cyclohexane (1.80 *M*) in carbon tetrachloride (2.5 ml). Degassed and non-degassed duplicate samples of each reaction mixture were left at 26° in the dark for 17 h. Aliquots of each reaction mixture were then transferred to solutions of potassium iodide (approx. 1 g) in acidified (acetic acid) water, and the liberated iodine reduced with aqueous sodium thiosulfate. The carbon tetrachloride phases were analyzed by g.l.p.c. for cyclohexyl chloride using a 10 ft × 1/4 in. stainless steel column packed with 15% SF 96 on 60/80 mesh firebrick. The results are given in Table VI.

TABLE VI

Analyses of carbon tetrachloride phases for cyclohexyl chloride by g.l.p.c.

Reagents and conditions	Yield of cyclohexyl chloride (%)
t-Butyl hypochlorite and cyclohexane	
Degassed	48 ± 2
Non-degassed	No trace (< 0.01)
t-Butyl hypochlorite, iodobenzene, and cyclohexane	
Degassed	30 ± 5
Non-degassed	No trace (< 0.01)

Acknowledgments

The authors wish to thank the National Research Council of Canada and the University of Alberta for their generous support of this work.

1. C. WALLING and R. RABINOWITZ. J. Am. Chem. Soc. **79**, 5326 (1957); **81**, 1243 (1959).
2. C. WALLING, O. H. BASEDOW, and E. S. SAVAS. J. Am. Chem. Soc. **82**, 2181 (1960).
3. F. RAMIREZ and N. MCKELVIE. J. Am. Chem. Soc. **79**, 5829 (1957).
4. C. WALLING and M. S. PEARSON. J. Am. Chem. Soc. **86**, 2262 (1964).
5. C. C. PRICE and J. ZOMLEFER. J. Am. Chem. Soc. **72**, 14 (1950).
6. W. G. BENTRUDE and J. C. MARTIN. J. Am. Chem. Soc. **84**, 1561 (1962).
7. R. J. GRITTER and D. J. CAREY. J. Org. Chem. **29**, 1160 (1964).
8. J. W. KNAPCZYK, G. H. WIEGAND, and W. E. MCEWEN. Tetrahedron Letters, 2971 (1965).
9. T. H. FISHER and J. C. MARTIN. J. Am. Chem. Soc. **88**, 3382 (1966).
10. G. A. RUSSELL. J. Am. Chem. Soc. **80**, 4987 (1958).
11. D. F. BANKS, E. S. HUYSER, and J. KLEINBURG. J. Org. Chem. **29**, 3692 (1964).
12. D. D. TANNER and P. B. VAN BOSTELEN. J. Org. Chem. **32**, 1517 (1967).
13. D. D. TANNER and G. C. GIDLEY. J. Org. Chem. **33**, 38 (1968).
14. D. D. TANNER and G. C. GIDLEY. J. Am. Chem. Soc. **90**, 808 (1968).
15. K. HEUSLER and J. KALVODA. Angew. Chem. Intern. Ed. Engl. **3**, 525 (1964).
16. J. E. LEFFLER and J. S. WEST. J. Org. Chem. **27**, 4191 (1962). J. E. LEFFLER, R. D. FAULKNER, and C. C. PETROPOULOS. J. Am. Chem. Soc. **80**, 5435 (1958). W. HONSBERG and J. E. LEFFLER. J. Org. Chem. **26**, 733 (1961).
17. P. C. ANSON, P. S. FREDRICKS, and J. M. TEDDER. J. Chem. Soc. 918 (1959).
18. C. WALLING and B. B. JACKNOW. J. Am. Chem. Soc. **82**, 6108 (1960).
19. C. WALLING and A. PADWA. J. Am. Chem. Soc. **85**, 1593 (1963).
20. C. WALLING and P. J. WAGNER. J. Am. Chem. Soc. **86**, 3368 (1964).
21. H. M. TEETER and E. W. BELL. Org. Syn. **32**, 20 (1952).
22. I. M. KOLTHOFF and E. S. SANDELL. Textbook of quantitative inorganic analysis. 3rd ed. The MacMillan Co., New York. 1952. Chap. 39.
23. R. BELL and K. J. MORGAN. J. Chem. Soc. 1209 (1960).

Can. J. Chem. Downloaded from www.nrcresearchpress.com by 210.87.254.40 on 09/05/12
For personal use only.

Apparent activation energies for electrical conduction of solid and liquid germanium(II) sulfide

M. D'Amboise, G. Handfield, and M. Bourgon
Department of Chemistry, University of Montreal, Montreal, Quebec
Received November 24, 1967

The specific conductivity of germanium(II) sulfide has been measured, under an inert atmosphere, from room temperature to the boiling point (750 °C). Interpretation of the results indicates that the intrinsic conductivity is observed in the solid in the upper temperature range: the calculated energy gap is 1.58 eV which coincides with the value of the optical gap for indirect transition. The calculated energy gap of liquid GeS is 2.3 eV and it is shown that the increase in the gap occurs on melting and is not due to a transformation in the solid.

Canadian Journal of Chemistry, 46, 3545 (1968)

Can. J. Chem. Downloaded from www.nrcresearchpress.com by 210.87.254.105 on 09/05/12
For personal use only.

Introduction

Germanium(II) sulfide, GeS, is known to be a semiconductor in the solid state. The optical and electrical properties of single crystals, films, and polycrystalline samples of this compound have been studied by Betz (1)[1], Yabumoto (2), and Lider and Solov'ev (3) at temperatures not exceeding 350 °C. The forbidden energy gap for intrinsic conduction lies between 1.5–1.8 eV and the crystals are invariably p-type (2).

In a previous publication, D'Amboise, Handfield, and Bourgon (4) reported on the electrical conductivity of liquid GeS in the temperature range 664–705 °C. From the experimental data, it was concluded that GeS remains a semiconductor in the liquid state with a forbidden energy gap E_g of 2.5 eV; this energy was calculated on the assumption that a hole-electron equilibrium prevails in the melt, i.e. that the conductivity observed is the intrinsic conductivity which varies with temperature according to the law

$$[1] \qquad \sigma = A \exp(-E_g/2RT)$$

It seemed interesting to study the variation of the electrical conductivity of solid GeS as a function of temperature, in order to determine if the increase in the energy gap i.e. from 1.5 to 2.5 eV occurs on melting or if the increase takes place in the solid at high temperatures.

Ross and Bourgon (5) investigated the thermal properties of GeS by the technique of differential thermal analysis (d.t.a.) and showed that germanium(II) sulfide disproportionates partially in the liquid state according to

$$[2] \qquad 2GeS(l) \rightleftarrows Ge(solution) + GeS_2(solution)$$

Also, the experimental facts point rather strongly, contrary to the reported phase diagram (6), to incongruent melting of GeS at approximately 650 °C because of the peritectic disproportionation

$$[3] \qquad GeS(s) \rightarrow xGe(s) + Ge_{1-x}S(l)$$

where the phase $Ge_{1-x}S$ can be considered as a solution of GeS_2 in GeS; the system becomes homogeneous at approximately 665 °C (liquidus temperature).

It was shown also that a thermal effect at 590 °C, observed by other investigators (6) and interpreted by them to be a solid-state transition, appears on d.t.a. traces of all solid samples which have undergone melting at one stage or another but is never observed on thermograms of samples which are freshly sublimed. It was concluded that this thermal effect does not correspond to a solid-state transition but is most probably due to melting of the GeS–GeS_2 eutectic: some germanium(IV) sulfide is retained in the solid phase on cooling from the liquid state.

This paper thus reports on the variation of the electrical conductivity of solid GeS as a function of temperature. Additional data on the conductivity of liquid GeS are also reported; the temperature range of study of the latter has been extended to the boiling point which has been determined to be 750 °C (5).

Experimental

Investigation of the electrical properties of solid

[1] Copies may be obtained from: University Microfilms Inc., Ann Arbor, Michigan.

Can. J. Chem. Downloaded from www.nrcresearchpress.com by 210.87.254.105 on 09/05/12
For personal use only.

semiconductors is usually performed on small single crystals. In the present work, however, emphasis was placed more on the determination of the slope (activation energy) of the conductivity curve than on the absolute value of the conductivity. A survey of the literature shows that reliable values of activation energies can be obtained from polycrystalline material. Also, because of the high temperatures involved and the resultant high vapor pressures, it seemed impossible to use small crystals which would evaporate quickly. For these reasons, all measurements reported in this paper were performed on fairly large polycrystalline samples.

Germanium Sulfide

The germanium(II) sulfide used in this study was prepared and purified in the same way as described in a previous paper (5).

Conductivity Cells

The cells (capillary-type, cell constant 300 cm^{-1}) and technique used for measuring the conductivity of liquid GeS are essentially the same as described elsewhere (4).

The cell for solid-state studies could be used as a two- or four-terminal cell and is shown in Fig. 1. Because of the high vapor pressure of GeS, a closed cell must be used. It is made of 7 mm heavy wall quartz tubing. Contacts to the sample are made by means of machined spectrographic graphite plugs fitted into 5/20 female quartz standard joints. Graphite was selected as electrode material since it is the only readily available and conducting material which is not attacked by GeS; furthermore, graphite makes excellent contact to GeS.

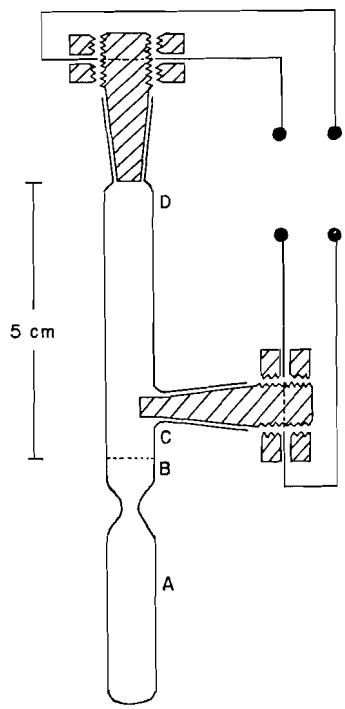

FIG. 1. Cell used for measuring the electrical conductivity of solid GeS.

The cell was enclosed in a steel casing to prevent excessive thermal gradients. Temperature measurements were made with uncalibrated chromel–alumel thermocouples situated at points B, C, and D; the maximum temperature difference between points C and D was approximately 2 °C. The temperature at point B was purposely kept a few degrees above the temperature of the sample, by means of a small heating element, to prevent sublimation of the sample to the top of the cell during the measurements. The whole assembly was enclosed in a 2.5 in. Vycor tube heated by a controlled Globar furnace.

The cells (solid-state and liquid-state) were calibrated at 25 °C with mercury, by direct current (d.c.) methods. These calibrations were checked with H_2SO_4 (30%) and KCl (1 *M*) solutions, by alternating current (a.c.) methods. In the case of the capillary-type cells, agreement between the different calibrations was very good; in the case of the cells used for solid-state studies, however, less precision was obtained because of the much lower cell constants (30 cm^{-1}); nevertheless the calibrations agreed to better than 5%. A high precision potentiometer (Honeywell 2781) and an a.c. bridge (Wayne Kerr, Model B221) operated at 1592 cycles/s were used for the calibrations. The resistance of the leads and electrodes was determined and was accounted for during the measurements.

Resistance Measurements

The resistance of the GeS samples was determined by a.c. methods, with the same bridge as was used for calibration purposes. It was verified that the contacts were ohmic. The cells were usually used as two-terminal cells; in a few cases, however, when the resistance of the samples became too low, a special adaptor was used in conjunction with the a.c. bridge which permits measurements of resistance with a four-wire system.

The a.c. results were checked by d.c. measurements (four-wire system) at several temperatures; in this case, thermoelectric effects were duly accounted for. Since no difference was found between the a.c. and the d.c. measurements, the latter were discontinued after some time and the results reported in this paper are those obtained from a.c. measurements.

Preparation of Samples

Since the thermal analysis work had indicated that sublimed samples and samples cooled from the melt had different properties it was thought wise to make runs on samples which were sublimed directly into the cell and others which were compacted by melting. In the first case, powdered GeS was introduced into reservoir A at the bottom of the cell (Fig. 1) and sublimed at 400 °C, under vacuum, over a period of a few days, until the sample reached point B; the cell was then cooled, removed from the furnace and sealed under vacuum with a hydrogen flame, at the constriction indicated in the drawing. In the second case, the cell and reservoir A, now at the top of the cell, were filled with powdered GeS; the sample was melted and kept a few hours at a temperature never above 700 °C under vacuum, then cooled to room temperature in the furnace. During melting,

Can. J. Chem. Downloaded from www.nrcresearchpress.com by 210.87.254.105 on 09/05/12
For personal use only.

the sample was contracted to point B. After cooling, the reservoir was removed and the cell sealed. The samples prepared by sublimation or melting showed no signs of voids on visual examination: the samples were very compact and had a bright, metallic appearance. As explained in a previous paper (5), the samples should have a composition very near to stoichiometric; samples cooled from the melt should contain a small amount of GeS_2 and Ge.

The measurements were made under a purified helium atmosphere. Some measurements were made under vacuum in order to determine if the helium atmosphere had any effect on the conductivity: no difference between the two sets of measurements could be observed. The presence of a helium atmosphere prevented excessive diffusion of gaseous GeS through the graphite electrodes and was adopted as standard procedure.

It was found impossible to prevent entirely the diffusion of GeS through the graphite electrodes although, at atmospheric pressure, diffusion was very slow. As a rule, measurements on a given sample were terminated when it appeared that vaporization of the sample had caused a decrease in the surface area of the electrode at the top of the cell (point B). It took a few weeks for this to happen.

Results

Solid Samples

The results are shown graphically in Fig. 2, where the log of the specific conductivity is plotted against the inverse of the absolute temperature. Samples 1, 2, and 3 are sublimed samples while sample 4 was compacted by melting. For reasons of clarity, only part of the experimental points are shown. The following experimental details are pertinent.

(*a*) The conductivity curve of sample 1 was established very slowly. The general procedure adopted was to anneal the sample at given temperatures for many hours and to measure the conductivity as a function of time until steady values indicated that equilibrium had been reached. After an increase in temperature, thermal equilibrium was established quite rapidly, in approximately 10–20 min, and the conductivity attained a value slightly lower than the equilibrium value: it took several hours, however, to obtain a final, steady value. The increase in conductivity as a function of time, after thermal equilibrium had been established, is shown in Fig. 3 at several temperatures. Since the samples were very compact, it is doubtful that this slow increase with time was due to sintering of the charge. A better explanation, perhaps, is that this increase is related to the changing stoichiometry of GeS on heating (5). This increase in conductivity with time became noticeable at approximately 430 °C; the final value of the conductivity differs from the thermal equilibrium value by approximately

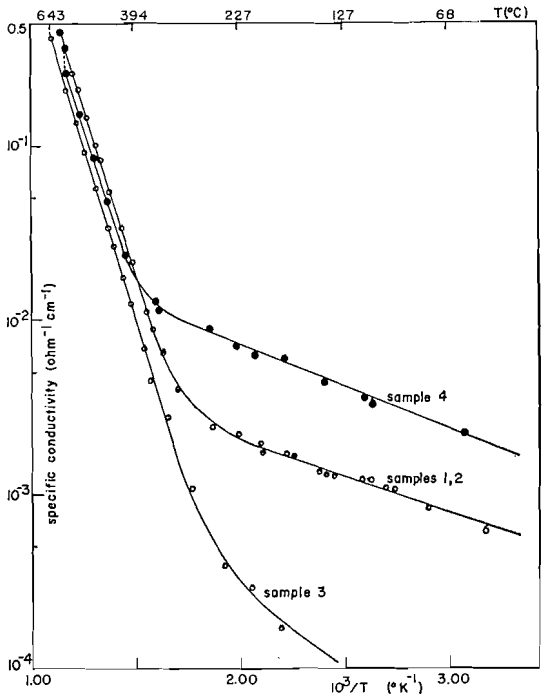

FIG. 2. Specific conductivity of solid GeS as a function of temperature. The data are for samples 1, 3, and 4; the conductivity curve of sample 2 is identical to that of sample 1.

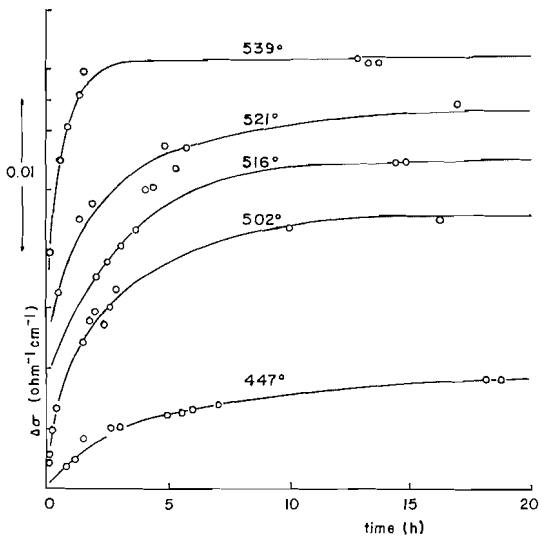

FIG. 3. Variation of conductivity σ with time at different temperatures for solid GeS (sample 1).

Can. J. Chem. Downloaded from www.nrcresearchpress.com by 210.87.254.105 on 09/05/12
For personal use only.

5%. Sample 1 was studied to a temperature of 580 °C.

(*b*) Samples 3 and 4 were studied somewhat more rapidly to temperatures of 640 and 610 °C respectively. The conductivity curve of sample 2 in the solid state was established still more rapidly and the solid–liquid transition was investigated: the results are shown in Fig. 4.

(*c*) Samples 2 and 4 showed a small discontinuity in the conductivity curves at 600 and 580 °C respectively while sample 3 showed no such discontinuity. It is to be noted that samples 2 and 4 have higher conductivities in the lower temperature region than sample 3. The fact that the slopes of the curves are identical before and after the break (see Fig. 4) is a further indication that the latter does not correspond to a change in crystal structure.

(*d*) Points B and C in Fig. 4 correspond to the temperatures of the peritectic reaction (652 °C) and the liquidus (668 °C) respectively. On cooling slowly from a temperature of approximately 700 °C the conductivity follows the path DCJF. If, however, the sample is cooled from a higher temperature there is substantial supercooling and the slope of the conductivity curve of the solid varies from one experiment to the other.

Liquid Samples

The results are shown in Fig. 5. The conductivity of samples 6 and 7 was measured in capillary-type cells as described in a previous paper (4). Other samples, studied in capillary-type cells or in cells similar to that used for solid samples gave conductivity values identical to those of samples 6 and 7. It is to be noted, however, that sample 2 in the liquid state (Figs. 4 and 5) gave higher values of the conductivity although the slope of the curve is essentially the same as that of samples 6 and 7. We have no definite explanation for the behavior of this particular sample although it can be observed, from Fig. 4, that the ratio of the conductivity values on line DC to those on line AE (the capillary-cell values) is identical to the ratio of the values on line JF to those on line BG: this is perhaps an indication that something happened in region BC which introduced a systematic error. In any event, the behavior of sample 2 in the liquid state is an isolated case and the conductivity of liquid GeS should be taken to be that represented by samples 6 and 7. It was verified in all cases that the conductivity curves of liquid samples were reproducible on repeated heating and cooling.

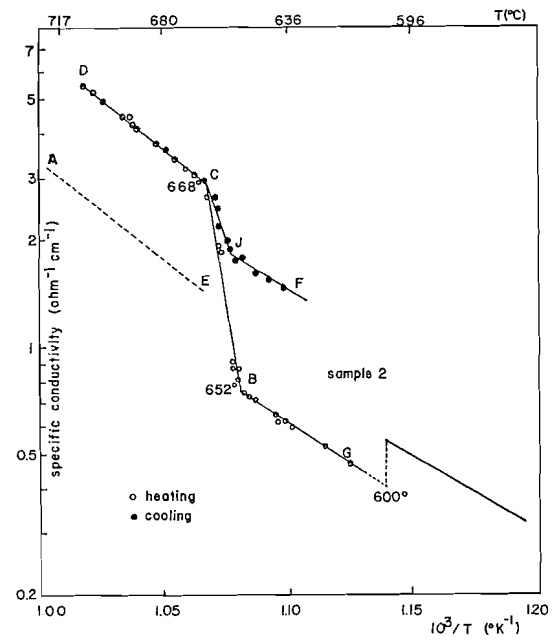

FIG. 4. Specific conductivity of GeS at high temperatures; line AE is the conductivity curve of liquid GeS as obtained in capillary-type cells.

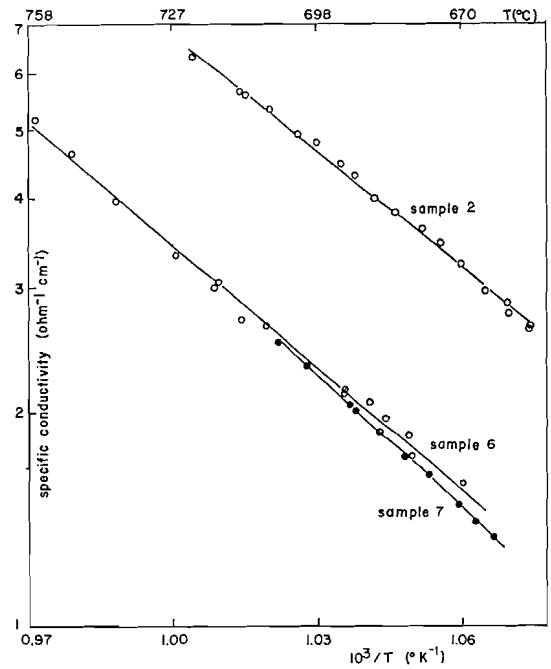

FIG. 5. Specific conductivity of liquid GeS as a function of temperature. The data for sample 7 were reported in a previous publication (4).

Can. J. Chem. Downloaded from www.nrcresearchpress.com by 210.87.254.105 on 09/05/12
For personal use only.

Discussion

For the sake of clarity, some aspects of the present work should be emphasized.

(*a*) From the results presented in Fig. 2 it appears clearly that the different solid samples have conductivity curves of identical slope in the higher temperature range in spite of different heating rates, of the different methods of compacting the samples, and in spite of small differences in composition since no special precautions i.e. controlled atmospheres, were taken to insure exact stoichiometry. No change in slope could be detected before melting.

No particular attention should be paid to the absolute value of the conductivity because of the polycrystallinity of the samples and also perhaps, because of small differences, from sample to sample, in the degree of compactness; the best that can be said about the conductivity is that it is probably of the right order of magnitude.

(*b*) Essentially the same remarks apply to the results presented in Fig. 4. Sample 2 is the only sample that could be examined from room temperature to the liquid state without interruption because of cell breakage or other causes. It is unfortunate that, for reasons unknown, the liquid gave conductivity values different from that of all the other samples although the slope of the conductivity curve is identical to that of the other samples; this has the effect of obscuring somewhat the nature of the change at the melting point. The results in Fig. 4 should be regarded as showing the different changes that GeS undergoes on passing from the solid to the liquid state as indicated by the different changes in the slope of the conductivity curve. Again, no particular attention should be paid to the absolute value of the conductivity.

(*c*) As stated before, all the liquid samples studied gave conductivity curves of identical slope (above the liquidus temperature). The absolute values of the conductivity, as exemplified by samples 6 and 7 (Fig. 5), can be regarded with confidence for reasons given in the Results section.

In brief, it can be concluded that the measured slopes are correct and that the increase in the apparent activation energy occurs upon melting and is not due to a transformation in the solid.

Low-Temperature Conductivity

At the lower temperatures, the electrical properties of GeS show a strong resemblance to the properties of SnS (7–9).

(*a*) For all samples, the conductivity increases with temperature: this is an indication that carriers are being produced. If the conductivity in this region were governed by changes in the mobility of the carriers (extrinsic conductivity) the conductivity would be expected to decrease as the temperature increases because of thermal scattering of the carriers.

(*b*) It has been shown by Albers *et al.* (8) and also by Rau (9) that SnS samples equilibrated under various sulfur atmospheres are always p-type which indicates that the existence region of SnS lies completely on the sulfur-rich side; Rau further concluded that tin vacancies constitute the main defect in SnS. There are indications that the same situation prevails in GeS (5), and other IV–VI compounds (11, 12), thus leading to p-type conductivity and to non-stoichiometry (excess sulfur). That our samples were p-type was verified by thermal probe tests. It is probable, therefore, that the variation of the low-temperature conductivity of GeS, from sample to sample, is due to small differences in the sulfur content; this interpretation is consistent with the following facts:

The highest conductivity is exhibited by sample 4 which was compacted by melting. This sample showed a small increase in the value of the conductivity at a temperature close to the GeS–GeS_2 eutectic, indicating that this sample was still two phase in spite of the quite long annealing time. Sample 2 which was sublimed directly into the cell showed a small decrease in the value of the conductivity at a somewhat higher temperature (600 °C, see Fig. 4) which could be due to the crossing of a solidus or a solvus line from a region of GeS–GeS_2 solid solution. Sample 3 which has the lowest conductivity shows no such discontinuity and should be the closest to stoichiometric composition.

(*c*) There is a decrease in the slope of the conductivity curve as the conductivity of the sample increases (compare samples 3 and 4). This behavior is similar to that of SnS (7) and other semiconductors and should be expected if the increase in conductivity is due to an increase in the amount of sulfur.

High-Temperature Conductivity (Solid)

A constant slope in the conductivity curves at high temperature does not necessarily indicate

Can. J. Chem. Downloaded from www.nrcresearchpress.com by 210.87.254.105 on 09/05/12
For personal use only.

that the intrinsic conductivity is being observed. The value of the slope could be related to the energy of formation of defects (vacancies or interstitials). We believe, however, that the high-temperature conductivity of solid GeS is the intrinsic conductivity for the reason following. The values of E_g calculated from the slopes of the different curves, using eq. [1], are respectively 1.52 (sample 1), 1.63 (sample 2), 1.60 (sample 3), and 1.53 eV (sample 4); thus giving an average value of 1.58 eV. This same value was obtained by Betz (1) from conductivity measurements on single crystals at somewhat lower temperatures, although this investigator expressed some doubts on the validity of his results.

Values of the energy gap of GeS were obtained from optical measurements by Betz (1), Lider and Solov'ev (3), and Yabumoto (2). The first found two absorption edges at 1.52 and 1.78 eV (300 °K) which were interpreted to correspond to the energy gaps for indirect and direct transitions respectively. Essentially the same results were obtained by Lider and Solov'ev who found two absorption edges at 1.61 and 1.70 eV while Yabumoto found an absorption edge at 1.80 eV.

If the energy gap is a linear function of the absolute temperature, then, the value of the gap as derived from the slope of the conductivity curve is the value at 0 °K (10). Therefore, in order to compare the thermal gap with the energy gap for indirect transition, this last one should be corrected to obtain a value at 0 °K. The variation of the energy gap as a function of temperature has been reported in the literature from the shift of the absorption edge with temperature. The energy gap decreases as the temperature increases and from the reported data it would seem that the variation of the gap with temperature is linear down to the temperature of liquid nitrogen. A decrease with increasing temperature of 4.8×10^{-4} eV/°K is representative: this is an average of the data reported by different investigators (1, 3) and it is identical with the value of the shift reported for SnS (9). The corrected value of the average gap for indirect transition is thus 1.70 eV at 0 °K which compares quite well with the value 1.58 eV obtained in the present work.

High-Temperature Conductivity (Liquid)

From the slopes of the conductivity curves of liquid GeS (samples 2, 6, and 7, Fig. 5) the average value of the activation energy for conduction is calculated to be 1.15 eV which leads, using eq. [1], to a calculated "band gap" of 2.3 $\pm$ 0.1 eV. Whether or not this apparent increase in the band gap i.e. from 1.58 to 2.3 eV, on passing from the solid to the liquid state is a reflection of the change in the structure of GeS on melting is of course open to question. It appears, however, as discussed in a previous paper (4) and in the light of results obtained on the conductivity in the liquid state of compounds which are isostructural with GeS i.e. GeSe and SnSe, that the trend in the variation of the calculated values of the different band gaps is similar to that found in the corresponding solids. Further discussion on this point will be delayed until these results have been reported; this will be done in the near future (13).

Acknowledgments

The financial support of the National Research Council of Canada is gratefully acknowledged. One of us (G.H.) wishes to thank the Ministère de l'Education de la Province de Québec for assistance in the form of a bursary.

1. C. R. Betz. Ph.D. Thesis, Northwestern University, Evanston, Illinois. 1958.
2. T. Yabumoto. J. Phys. Soc. Japan, **13**, 559 (1958).
3. K. F. Lider and L. E. Solov'ev. Soviet Phys.-Solid State, English Transl. **4**, 1102 (1962).
4. M. D'Amboise, G. Handfield, and M. Bourgon. Can. J. Chem. **44**, 853 (1966).
5. L. Ross and M. Bourgon. Can. J. Chem. **46**, 2464 (1968).
6. Liu Ch'un-Hua and A. S. Pashinkin. Dokl. Akad. Nauk SSSR, **151**, 1335 (1963).
7. J. S. Anderson and M. C. Morton. Proc. Roy. Soc. London, Ser. A, **184**, 83 (1945).
8. W. Albers, C. Haas, H. J. Vink, and J. D. Wasscher. J. Appl. Phys. **32**, 2220 (1961).
9. H. Rau. J. Phys. Chem. Solids, **27**, 761 (1966).
10. R. A. Smith. Semiconductors. Cambridge University Press, London. 1959.
11. R. F. Brebrick. J. Phys. Chem. Solids, **24**, 27 (1963).
12. D. H. Damon, M. S. Lubell, and R. Mazelsky. J. Phys. Chem. Solids, **28**, 520 (1967).
13. G. Handfield and M. Bourgon. Can. J. Chem. To be published.

Can. J. Chem. Downloaded from www.nrcresearchpress.com by 210.87.254.105 on 09/05/12
For personal use only.

Angular distributions of recoil products from some reactions induced in ^{65}Cu and ^{197}Au by protons of energy 30–85 MeV[1]

M. K. DEWANJEE, G. B. SAHA, AND L. YAFFE
Radiochemistry Laboratory, Department of Chemistry, McGill University, Montreal, Quebec

Received May 6, 1968

Angular distributions of products formed in the reactions $^{65}Cu(p,pn)^{64}Cu$, $^{197}Au(p,pn)^{196}Au$, and $^{197}Au(p,p3n)^{194}Au$ in the range of proton energy 30–85 MeV were studied. The angular distribution results of ^{64}Cu and ^{196}Au show forward peaking at low energy and sidewise peaking at higher energies. Approximate symmetry about 90° was observed for the angular distribution of ^{194}Au in the center-of-mass system. The experimental results have been compared with (*a*) Monte Carlo evaporation calculations, (*b*) cascade–evaporation calculations at 85 MeV for ^{64}Cu, and (*c*) inelastic scattering plus evaporation calculations.

Good agreement was obtained with statistical theory calculations at low energy and inelastic scattering model calculations at higher energies. The comparisons indicate that the reactions proceed by the compound nucleus mechanism at lower energies and the direct interaction mechanism predominates at higher energies.

Canadian Journal of Chemistry, 46, 3551 (1968)

Introduction

In an earlier publication (1), results of the average projected recoil ranges of the products formed in the $^{65}Cu(p,pn)^{64}Cu$ and $^{197}Au(p,pn)^{196}Au$ reactions in the energy range of 20–85 MeV were presented. This study provided information about the average momentum transfer in the initial phase of the reaction. The results were compatible with the compound-nucleus mechanism at lower energies and the direct interaction mechanism at higher energies. Recoil ranges are sensitive to the angular distribution of the recoils, particularly at higher energy. In the low energy region, the compound nucleus mechanism predominates and thus the angular distribution peaks in the forward direction. On the other hand at higher energies, the direct interaction mechanism becomes more important and therefore a sidewise peaking in the angular distribution is observed.

The angular distribution of spallation reactions at higher energies (above 350 MeV) have been studied by Reuland *et al.* (2), Poskanzer *et al.* (3), Panontin *et al.* (4), and Remsberg (5). No work has so far been reported on angular distribution in the energy range of 30–85 MeV. We have measured the angular distribution of the (p,pn) reactions in ^{65}Cu and ^{197}Au and the (p,p3n) reaction in ^{197}Au at 30–85 MeV by the technique developed by Poskanzer *et al.* (3). The results have been compared with different theoretical calculations.

Experimental

(a) Target and Irradiations

The apparatus used in the angular distribution measurements as shown in Fig. 1 is a simple adaptation of that used by Poskanzer *et al.* (3) to fit to the requirements of the McGill synchrocyclotron. Two experiments were performed at each energy: one covering the angular interval 0–90° and the other 90–108° relative to the beam. The thin target was prepared by evaporating enriched ^{65}Cu (99.7%)[2] and ^{197}Au on to aluminium backing material. To avoid any difference in the target thickness in the forward and backward experiments at the same energy, two sections of the same target prepared were used for both experiments. The target facing the catcher foil was suspended from two stainless steel attachments and oriented 45° to the beam to prevent recoil scattering in the thin target. Three identical aluminium foils were used on the collector mount, the first for recoil collection, the second for activation correction, and the third to compensate for the recoils from the aluminium mount to the blank foil. In the later experiments, the piece of the collector making an angle of 15° to the beam was removed from the mount to check whether any effect due to proton scattering was occurring. No such effect was observed. The aluminium catcher and blank foils were marked for the definite angular intervals desired and the whole assembly was checked with a template for proper centering and 45° angular orientation of the target to the proton beam. The target thicknesses for gold and copper were 3–7 and 4–8 μg/cm² respectively and the target dimensions were 0.8 cm × 1.2 cm. The collection radius and collector height were 9.53 and 5.08 cm respectively. The period of irradiation

[1]This research received financial assistance from the National Research Council of Canada.

[2]Obtained from Oak Ridge National Laboratory, Oak Ridge, Tennessee, U.S.A.

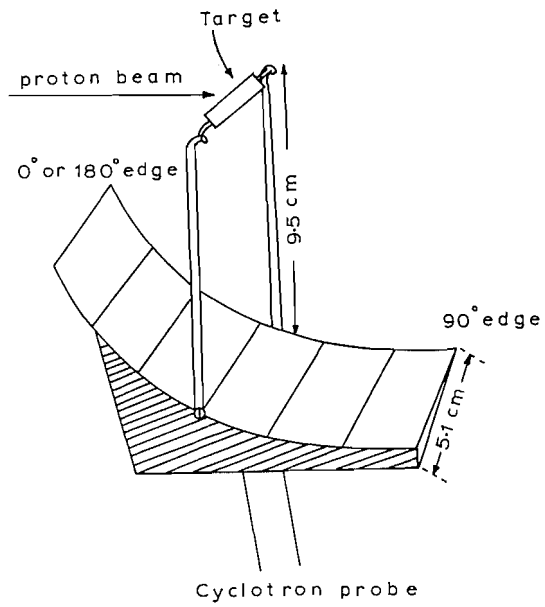

FIG. 1. Apparatus used for measurements of the angular distribution of the recoils.

was about 120 min. The target assembly was fixed to the end of the water-cooled cyclotron probe and the target was set at a definite radial distance corresponding to the desired bombarding energy.

(b) Chemical Separations and Activity Measurements

The chemical separation and activity measurements for the copper and gold samples in the angular distribution experiments were identical to those described previously (1). Solid sources (elemental gold and copper thiocyanate for gold and copper samples, respectively) were prepared and the activities measured in a low-background (< 1 count per minute) counter. The activity of ^{194}Au was determined by detecting the conversion electrons and the composite decay curve was resolved with the CLSQ decay curve analysis program (6).

TABLE I

Scattering effect of the recoils due to the orientation of the targets (90°) to the incident proton beam

	Relative activity in the angular intervals		
$\langle\theta_L\rangle_i$ (degrees)	^{197}Au (30 MeV*)	^{197}Au (85 MeV*)	^{65}Cu (85 MeV*)
7.5	2940±412	2330±326	2340±210
22.5	2190±307	2090±293	1520±137
37.5	1740±244	1650±231	1240±112
52.5	1320±185	1310±183	1010± 91
67.5	530± 74	1030±144	690± 62
82.5	240± 34	180± 25	440± 40
97.5	240± 34	180± 25	430± 39
112.5	220± 30	240± 34	370± 33
127.5	110± 15	290± 41	330± 30
142.5	120± 17	120± 17	180± 16
157.5	90± 13	140± 20	190± 17
172.5	260± 37	440± 62	1260±113

*Energy of the incident proton beam.

(c) Correction Factors

Preliminary experiments were conducted for the purpose of ascertaining the extent of scattering of low energy recoils and impurity activation in the backing and catcher materials. The scattering effect is mainly due to

(i) Angular Orientation of the Target with respect to the Proton Beam. Because of the low energy, recoils grazing the target surface will be deflected from the original direction of motion and collected mainly in the forward direction as is observed from the results shown in Table I and Figs. 2*f*, 3*a*, 3*e*. To avoid this scattering effect, the target on the aluminium backing material was oriented 45° to the beam.

(ii) Target Thickness. Targets of different thicknesses (3–25 μg/cm^2) were irradiated to observe the scattering effect. The full-width at half-maximum of the peak of the angular distribution and hence the average angle increases with the target thickness. When the target thickness is about 25 to 30% of the average recoil range observed in a thick-target experiment, no peak was observed and so target thicknesses 3 to 7% of the recoil range values were used.

(iii) The Effect of the Backing Material. This effect, specially in the backward 90° experiment, was found to be negligible by Poskanzer *et al.* (3).

It is difficult to avoid the oscillating effect (horizontal and vertical) inherent in the internal beam. The target size was made as small as possible (limited by the low-activity problem) to have indirect recoil collimation from the target.

Approximate calculations for the deflection of the ^{64}Cu and ^{196}Au nuclides, (assuming doubly-charged species), in the cyclotron magnetic field (16.5 kG) gave a value of ~1° which was far below the angular resolution (10 or 15°) that was attained in our experiment.

An activation experiment was performed in which the angular distribution of products from any copper impurity in the aluminium backing material was determined. A correction of 2–3%, resulting from the impurity activation in the aluminium catcher foil, had to be made in the first 10 or 15° angular region in each experiment. At larger angles the activation correction was negligible. No detectable gold activity due to impurity activation was found in the collector foil.

(d) Treatment of Data

The data corrected for dilution, chemical yield, self-absorption and back-scattering of electrons were treated as follows:

(*i*) Extrapolation to angular regions for which collection was not made directly.

(*ii*) Interpolation at 90° and matching of the data from the forward–backward experiments to get a continuous curve.

(*iii*) Normalization of the total activity to the same value (10 000 c.p.m.).

(*iv*) Calculation of an average angle for each distribution at a definite energy.

The mean angle $\langle\theta_L\rangle_i$ expressed in the laboratory system in degrees corresponding to each angular inter-

Can. J. Chem. Downloaded from www.nrcresearchpress.com by 210.87.254.105 on 09/05/12
For personal use only.

Can. J. Chem. Downloaded from www.nrcresearchpress.com by 210.87.254.105 on 09/05/12
For personal use only.

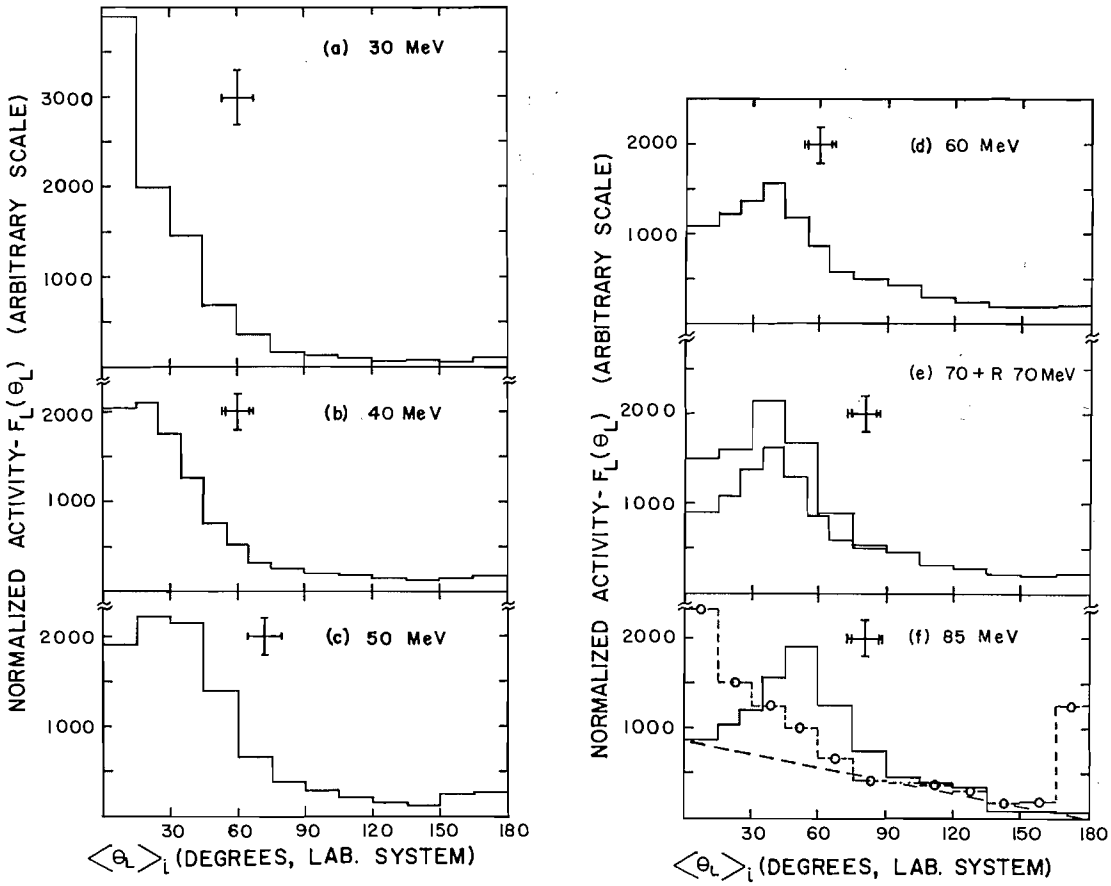

FIG. 2. Experimental angular distributions for the $^{65}Cu(p,pn)^{64}Cu$ reaction at (*a*) 30, (*b*) 40, (*c*) 50, (*d*) 60, (*e*) 70 + repeat 70, and (*f*) 85 MeV.

The ordinate represents the normalized activity in the particular angular interval. The horizontal bar indicates the spread in the angular resolution, and the vertical one represents the uncertainty in the relative activity in each angular interval. All the curves are normalized relative to each other.

In 2(*f*) the dashed line (— — —) represents the featureless distribution; and the open circle - dashed line (—○—) shows the 90 degree orientation effect of the thin-target with respect to the proton beam.

val, is given by the average of θ_{min} and θ_{max} (for that interval) provided the angular distribution is independent of angle within that interval. The relative activity of each section shows a pronounced variation with angle. The actual value of $\langle\theta_L\rangle_i$ is defined as follows:

$$[1] \qquad \langle\theta_L\rangle_{i\ \text{actual}} = \frac{\int_{\theta_{min}}^{\theta_{max}} P(\theta)\,\theta\,\sin\theta\,d\theta}{\int_{\theta_{min}}^{\theta_{max}} P(\theta)\,\sin\theta\,d\theta}$$

If one assumes a linear form of the angular distribution in a small interval $d\theta$,

$$[2] \qquad P(\theta) = a + b\theta,$$

where a is the intercept and b is the slope of an angular distribution curve of interest, then the deviation from the corresponding $\langle\theta_L\rangle_i = 0.5(\theta_{max} + \theta_{min})$ amounts to 1–3%, which is negligible compared with the experimental angular resolution. On account of the spherical symmetry the activity of each section of equal area, $(d\sigma/d\theta)$, is proportional to the differential cross section per unit solid angle, $(d\sigma/d\Omega)$. The normalized values of the activities in the angular intervals $\Delta\theta_i$, for the angular distributions of ^{64}Cu, ^{196}Au, and ^{194}Au are shown in Tables II, III, IV, and in Figs. 2 and 3.

The average laboratory recoil angle $\langle\theta_L\rangle$ may be defined as follows:

$$[3] \qquad \langle\theta_L\rangle = \frac{\sum_i \left(\frac{d\sigma}{d\theta}\right)_i \Delta\theta_i \langle\theta_L\rangle_i}{\sum_i \left(\frac{d\sigma}{d\theta}\right)_i \Delta\theta_i}$$

where $(d\sigma/d\theta)_i$ is the activity observed in the i-th section, $\Delta\theta_i$ is the angular interval subtended by the i-th

Can. J. Chem. Downloaded from www.nrcresearchpress.com by 210.87.254.105 on 09/05/12
For personal use only.

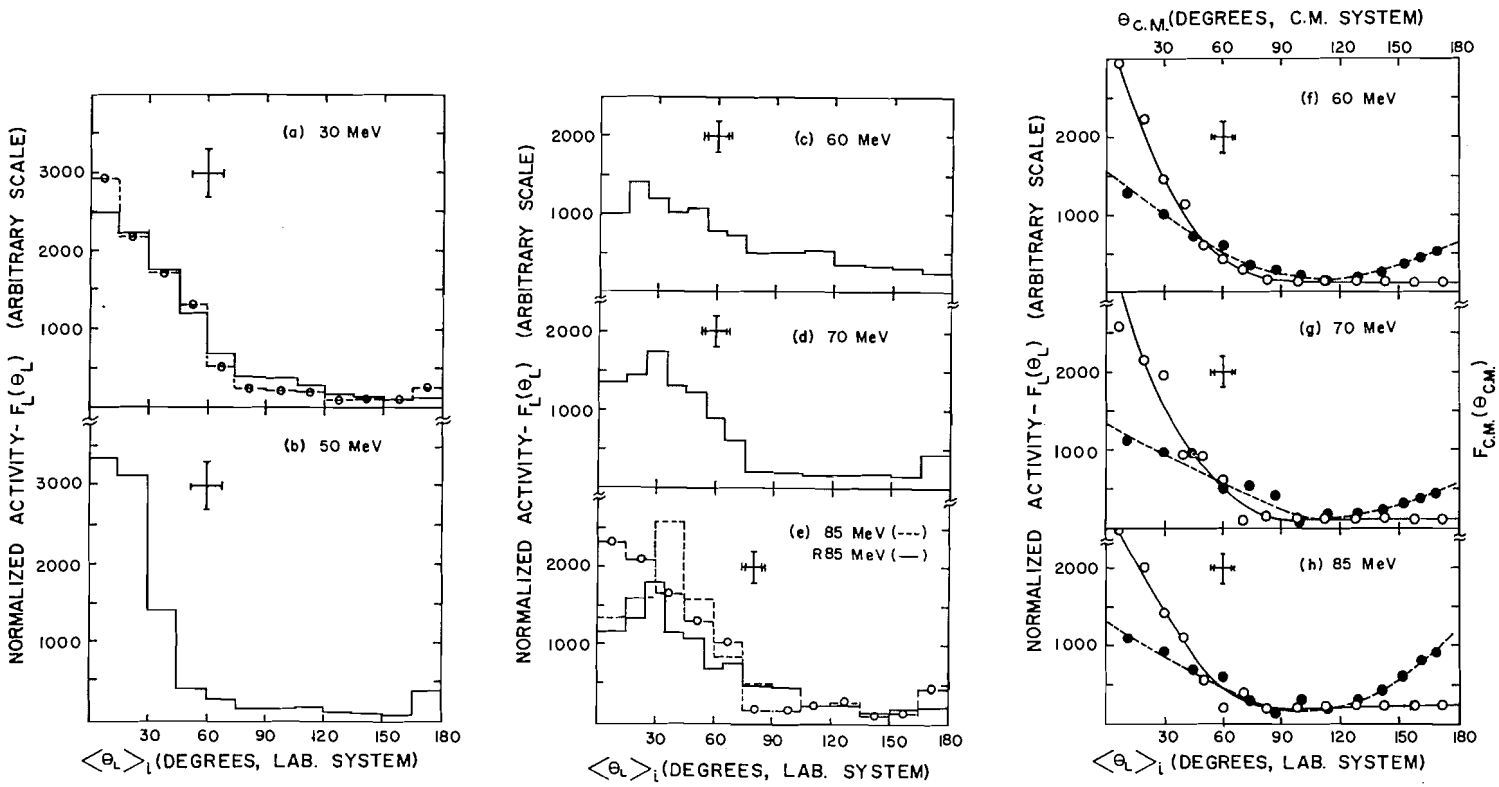

FIG. 3. Experimental angular distributions for the ^{197}Au(p,pn)^{196}Au reaction at (*a*) 30, (*b*) 50, (*c*) 60, (*d*) 70, and (*e*) 85 + repeat 85 MeV, and for the ^{197}Au(p,p3n)^{194}Au reaction at (*f*) 60, (*g*) 70, and (*h*) 85 MeV.

All the curves are normalized relative to each other. The horizontal bar shows the spread in the angular resolution, and the vertical one indicates the uncertainties in the relative activities.

In 3(*f*), 3(*g*), and 3(*h*) the solid circle – dashed lines (—●—) refer to the angular distribution for ^{194}Au in the center-of-mass system. The open circles show the experimental results.

In 3(*a*) and 3(*e*) at 30 and 85 MeV the open circle – dashed lines (—○—) represent the recoil scattering due to the orientation (90° of the thin-target with respect to the proton beam.

TABLE II

Normalized activity of ^{64}Cu in the laboratory system, $F_L(\theta_L)$ vs. laboratory angle at the midpoint of the collection interval

$\langle\theta_L\rangle_i$ (degrees)	$F_L(\theta_L)$ at energy (MeV) 30	50	70	$\langle\theta_L\rangle_i$ (degrees)	$F_L(\theta_L)$ at energy (MeV) 40	60	*R70	85
7.5	4220±380	1910±172	1490±134	7.5	2040±184	1090± 98	900± 81	870± 78
22.5	2196±198	2220±200	1610±144	20.0	2090±188	1230±111	1100± 99	1040± 94
37.5	1572±142	2140±193	2140±193	30.0	1760±158	1380±124	1370±123	1200±108
52.5	777± 70	1410±127	1680±151	40.0	1270±114	1580±142	1620±146	1550±140
67.5	390± 35	660± 59	890± 80	50.0	760± 68	1190±107	1300±117	1900±171†
82.5	197± 18	390± 35	500± 45	60.0	520± 47	880± 79	860± 77	—
97.5	168± 15	290± 26	460± 41	70.0	320± 29	560± 50	600± 54	1260±113‡
112.5	127± 11	210± 19	310± 28	82.5	250± 23	500± 45	540± 49	750± 68
127.5	89± 8	150± 14	270± 24	97.5	200± 18	430± 39	470± 42	450± 41
142.5	91± 8	120± 11	220± 20	112.5	180± 16	300± 27	320± 29	400± 36
157.5	71± 6	240± 22	210± 19	127.5	160± 14	250± 23	290± 26	340± 31
172.5	102± 9	260± 23	220± 20	142.5	140± 13	200± 18	220± 20	80± 7
				157.5	140± 13	200± 18	210± 19	90± 8
				172.5	170± 15	210± 19	200± 18	70± 6

*R = repeated irradiation.
†Midpoint of the interval 52.5°.
‡Midpoint of the interval 67.5°.

section, and $\langle\theta_L\rangle_i$ is the corresponding mean angle. The values of $\langle\theta_L\rangle$ thus calculated from the measured angular distribution are shown in Tables V and VI.

The errors in the angular distribution measurements involve the errors associated with the resolution of the decay curves, the counter backgrounds, chemical yields, weights of the target and nonuniformities of the target and catcher thickness, the scattering of the low-energy recoiling nuclides, dilution factors, radiochemical purity, self-absorption and back-scattering of the beta radiation in the sample. The estimated error amounted to ±9% for copper and ±14% for gold isotopes respectively.

Discussion

(a) Qualitative Features and the Transformation of the Results into the Center-of-Mass System

No angular distribution results of proton-induced reactions have been previously reported in the energy region of our interest. The angular distribution results of Poskanzer *et al.* (3) for the $^{27}Al(p,3pn)^{24}Na$ reaction at 0.38 and 2.2 GeV are mainly forward peaking in the laboratory system. Remsberg's (5) results of the angular distribution of ^{64}Cu formed in the (p,pn) reaction have maxima appearing at 75, 80, and 86° at 0.37, 1.0, and 2.8 GeV energies respectively. The positions of the peaks do not change greatly with the large variation of the incident energy. On the other hand the peak shift is very prominent in the energy region of our interest. The recoil angular distributions obtained from alpha (7) and other heavy-ion induced reactions

TABLE III

Normalized activity of ^{196}Au in the laboratory system $F_L(\theta_L)$ vs. laboratory angle at the midpoint of the collection interval

$\langle\theta_L\rangle_i$ (degrees)	$F_L(\theta_L)$ at energy (MeV) 30	50	85	$\langle\theta_L\rangle_i$ (degrees)	$F_L(\theta_L)$ at energy (MeV) 60	70	*R85
7.5	2500±350	3340±468	1340±188	7.5	1010±141	1350±189	1160±162
22.5	2220±311	3220±451	1580±221	20.0	1430±200	1450±203	1340±188
37.5	1760±246	1420±199	2580±361	30.0	1210±169	1750±245	1800±252
52.5	1210±169	410± 57	1590±223	40.0	1020±143	1300±182	1140±160
67.5	700± 98	280± 39	840±118	50.0	1070±150	1220±171	1070±150
82.5	390± 55	190± 27	490± 69	60.0	780±109	890±125	680± 95
97.5	390± 55	190± 27	500± 70	70.0	730±102	610± 85	750±105
112.5	290± 41	190± 27	190± 27	82.5	500± 70	200± 28	470± 66
127.5	170± 24	130± 18	290± 41	97.5	500± 70	190± 27	480± 67
142.5	140± 20	130± 18	160± 22	112.5	520± 73	150± 21	260± 36
157.5	110± 15	110± 15	210± 29	127.5	350± 49	160± 22	280± 39
172.5	120± 17	390± 55	230± 32	142.5	330± 46	160± 22	150± 21
				157.5	310± 43	140± 20	200± 28
				172.5	240± 34	430± 60	220± 31

*R = repeated irradiation.

Can. J. Chem. Downloaded from www.nrcresearchpress.com by 210.87.254.105 on 09/05/12
For personal use only.

Can. J. Chem. Downloaded from www.nrcresearchpress.com by 210.87.254.105 on 09/05/12
For personal use only.

TABLE IV

Normalized activity of ^{194}Au in the laboratory system $F_L(\theta_L)$ vs. laboratory angle at the midpoint of the collection interval

$\langle\theta_L\rangle_i$ (degrees)	$F_L(\theta_L)$ at energy (MeV)		
	60	70	85
7.5	2950±413	2550±357	2550±357
20.0	2230±312	2140±300	2100±294
30.0	1470±206	1940±272	1510±211
40.0	1130±158	930±130	1110±155
50.0	620± 87	920±129	530± 74
60.0	420± 59	590± 83	210± 29
70.0	290± 40	80± 11	400± 56
82.5	150± 21	160± 23	190± 27
97.5	110± 15	130± 18	210± 29
112.5	130± 18	120± 17	230± 32
127.5	140± 20	120± 17	240± 34
142.5	130± 18	110± 15	240± 34
157.5	120± 17	110± 15	230± 32
172.5	110± 15	100± 14	250± 35

(8) are mainly forward-peaking in the laboratory system. The peak shift with increase in incident energy is not very prominent in these cases.

The results of the angular distribution measurements of recoiling ^{64}Cu and ^{196}Au nuclides as shown in Figs. 2 and 3, indicate a clear energy dependence. At lower energies (~ 30 MeV), the angular distributions are mainly forward-peaking in the laboratory system. The differential cross sections at higher angles gradually decrease and become nearly independent of angle. At energies greater than 30 MeV notable sidewise peaks are observed at angles larger than 0°, which may be explained in terms of a direct interaction mechanism.

The positions of the peaks depend on the incident energy and the target mass. However, they are probably more affected by the incident

TABLE V

Comparison of experimental and calculated angular distributions for the ^{65}Cu(p,pn)^{64}Cu reaction

Proton energy (MeV)	Experimental peak angle θ_P (degrees)	Calcd. θ_P (degrees)		Average angle $\langle\theta_L\rangle$ (experimental) (degrees)	Calcd. $\langle\theta_L\rangle$ (degrees)		Experimental FWHM§ (histogram) (degrees)	Calcd. FWHM (degrees)
		i.s.e.	M.C.†		i.s.e.	M.C.†		
30	~5	50	~4.5	30.8	38.2	22.6	—	—
40	20	55	~13.5	32.5	47.8	~14.4	20	35
50	30	55	~13.5	31.2	53.6	—	30	20
60	40	~60	—	57.0	57.1	—	30	30
70	37.5	65	—	35.6	59.6	—	30	~30
R 70*	40	65	—	59.9	59.6	—	30	20
85	~52.5	65	—	57.6	62.4	—	40	20
85‡	~52.5	—	65	57.6	—	58.2	40	30

*R = repeated irradiation.
†Obtained by Monte Carlo evaporation program.
‡Obtained by cascade-evaporation program. At 20 MeV, calculated $\langle\theta_L\rangle \simeq 18.8°$.
§Full width at half maximum.

TABLE VI

Comparison of experimental and calculated angular distributions for the ^{197}Au(p,pn)^{196}Au reaction

Proton energy (MeV)	Experimental peak angle, θ_P (degrees)	Calcd. θ_P (degrees)	Average angle $\langle\theta_L\rangle$ (experimental) (degrees)	Calcd. $\langle\theta_L\rangle$ (degrees)	Experimental FWHM† (histogram) (degrees)	Calcd. FWHM (degrees)
30	~5	45	28.54	45.48	—	20
40	~12 (extrapolated)	55	—	52.33	—	20
50	15	55	36.73	56.60	—	20
60	20	~60	64.31	59.56	30	20
70	30	65	43.34	62.05	30	20
85	30	65	35.06	64.53	30	20
R 85*	37.5	65	56.01	64.53	30	~10

*R = repeated irradiation.
†Full width at half maximum.

Can. J. Chem. Downloaded from www.nrcresearchpress.com by 210.87.254.105 on 09/05/12
For personal use only.

energy than the target mass, e.g. at 30 MeV the peak of the ^{64}Cu angular distribution occurs at 5° whereas it is at about 53° at 85 MeV. On the other hand, the angular distribution of ^{196}Au recoils has maxima at 5° at 30 MeV while it appears at 38° at 85 MeV. However, because of the angular resolutions obtained in these experiments, recoil peaks at a given energy had an angular uncertainty of $\pm 5°$ or $\pm 7.5°$.

The angular distributions of ^{194}Au studied at 60, 70, and 85 MeV as shown in Table IV and Fig. 3 (*f, g, h*) are always forward peaking in the laboratory system. This may be attributed to the compound nucleus mechanism involving a multiparticle evaporation process.

The following characteristics of the angular distributions of ^{64}Cu and ^{196}Au were calculated (Tables V and VI) and discussed.

(1) The average angles $\langle\theta_L\rangle$ of the recoil angular distributions of ^{64}Cu and ^{196}Au are sensitive to the target thickness and the angular resolution. The $\langle\theta_L\rangle$ value for the angular distribution of ^{64}Cu, is in general smaller at lower energy than that for the angular distribution of ^{196}Au.

(2) The shape of the recoil angular distribution of simple reactions varies with the incident energy. Attempts had been made by Reuland *et al.* (2) and Remsberg (5) to draw tentative conclusions from the analysis of the area under the angular distribution curve at higher energies where the inelastic scattering and the knock-out mechanisms are competitive. The peaks of the angular distributions of some simple reactions at intermediate and higher energies appear to be superimposed on a featureless distribution [area under the arbitrary line as shown in Fig. 2(*f*)]. In fact, the initial calculation of Benioff and Person (9) based on a clean knock-out model, gives a broad featureless angular distribution. Remsberg (5) assigned the peak of the angular distribution for the ^{65}Cu(p,pn)^{64}Cu reaction to the inelastic scattering mechanism at higher energy. Similarly, the area under the curve in Fig. 2(*f*) will be an approximate measure of the contribution of the compound-nucleus mechanism, since this mechanism leads to a forward peaking of the angular distribution. The contribution of the direct mechanism at intermediate and higher energies complicates this situation. Hence the area above the featureless distribution may approximate to the contribution of the direct interaction mechanism. The peak shift is prominent in this intermediate energy region where the gradual transition from the compound nucleus to the direct interaction mechanism takes place.

(3) The full-width at half-maximum of each angular distribution curve determined after the subtraction of the featureless distribution from the net angular distribution curve amounts to approximately 30°. This is a rough measure of the peak-broadening, which in turn, is sensitive to target thickness and angular resolution.

(4) The angular distribution results are most significant when presented in the center-of-mass system wherever possible. We have transformed the laboratory angular distribution into a center-of-mass distribution by the methods prescribed by Marion *et al.* (10) and Hanson *et al.* (11). For simplicity in the transformation, the emission of a composite particle [deuteron of mass two for (p + n) emission and a particle of mass four for (p + 3n) emission] was assumed. At all energies, the angular distributions for ^{194}Au (center-of-mass system) are more or less symmetric about 90° (see Fig. 3). The anisotropy parameter b/a of the angular distribution of the form $W(\theta) = (a + b\cos^2\theta)/(a + b/3)$ is given by

$$[4] \qquad \frac{b}{a} = \frac{d\sigma(0°) - d\sigma(90°)}{d\sigma(0°)}$$

The experimental b/a values for ^{194}Au at 60, 70, and 85 MeV are 0.86, 0.87, and 0.83 respectively. At all energies, the angular distributions (center-of-mass system) for ^{64}Cu and ^{196}Au were found to be asymmetric in shape, and are not shown in the figure. This asymmetry may be attributed to (*i*) emission of a proton and a neutron instead of a deuteron (the probability of deuteron evaporation at these energies will be very small), (*ii*) unknown distribution of the effective reaction Q-values as a function of center-of-mass scattering, and (*iii*) predominance of direct interaction. On the other hand, the symmetry of the angular distribution for ^{194}Au may be due to the averaging effect of emission of 4 nucleons from the compound nucleus ^{198}Hg. Therefore, the assumption of emission of a single particle of mass 4 instead of 4 nucleons may be valid in the ^{194}Au case.

(b) Comparison with Monte Carlo Calculations

In order to make a quantitative comparison

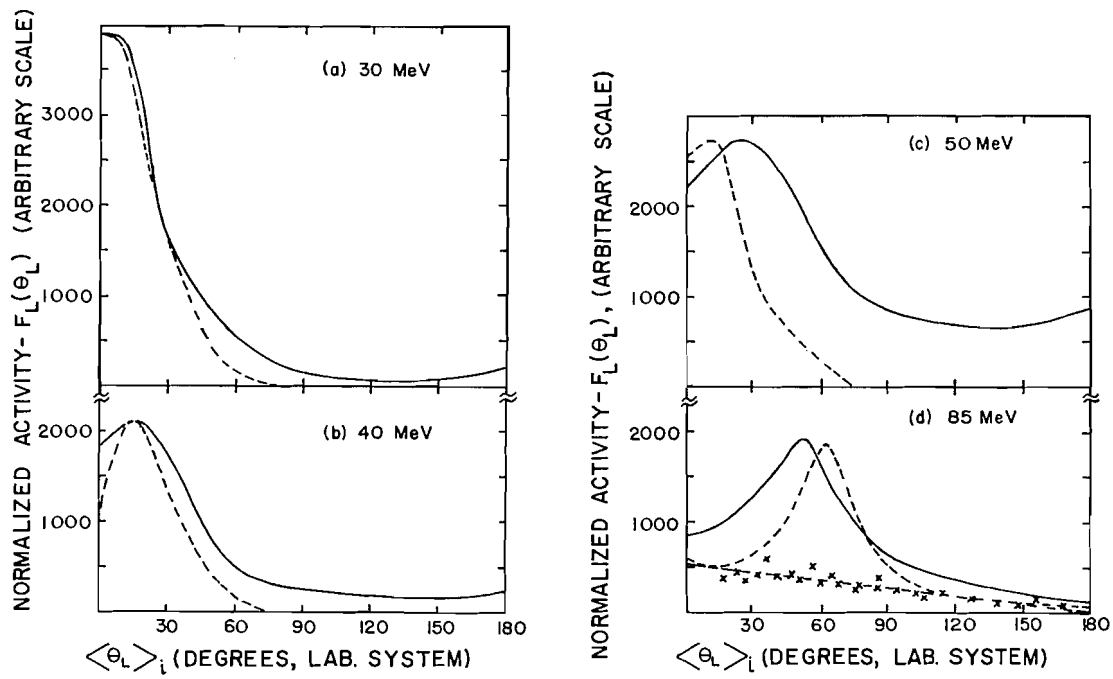

FIG. 4. Comparison of experimental and calculated angular distributions for the $^{65}Cu(p,pn)^{64}Cu$ reaction at (*a*) 30, (*b*) 40, (*c*) 50 MeV, ——— experimental, — — — statistical theory; (*d*) 85 MeV, ——— experimental, — — — cascade-evaporation at 85 MeV, —×—×— knock-out contribution at 85 MeV.
The smooth solid curve is drawn from the experimental results, with the mid-angle of each interval as the average angle.
All curves at a given energy are normalized relative to each other.

between the theoretical calculations and experimental results, several types of calculations have been performed. For ^{64}Cu, Monte Carlo statistical theory calculations were made at 30, 40, and 50 MeV according to the computer code of Dostrovsky *et al.* (12) modified by Porile (13).

In the calculations, the angular distributions of the emitted particles were assumed to be isotropic. However, the calculation was found to be insensitive to the different values of the anisotropy parameter. Variation of the b/a values from -1 to $+1$ for the formation of ^{64}Cu from ^{66}Zn (compound nucleus) at 30 MeV changes the average recoil angle by only 0.26°. An anisotropic angular distribution is to some extent related to the orbital angular momentum of the evaporated particles and the angular momentum distribution of the compound nucleus. A more detailed understanding of the level density of the residual nucleus and the anisotropy of the emission process awaits a calculation in which angular momentum effects are taken into account. No significant change in the recoil angle was observed with level density parameter 'a' equal to $A/10$ or $A/20$ in the evaporation calculation. The widely-accepted value of $a = A/20$ in the medium-mass region was chosen in all calculations.

The comparison of the calculated angular distributions and experiments is shown in Fig. 4. At 30 MeV the angular distribution of ^{64}Cu is forward peaking. An extrapolated value of $\sim 5°$ was assigned from the peak angle, θ_p, vs. proton energy curve as shown in Fig. 5. The calculated peak angle at 40 MeV appears at 13.5°, whereas the experimental value is about 20°. As the energy increases the discrepancy between the calculation and experimental peak angle becomes more prominent. The shape of the angular distribution of ^{64}Cu is not well reproduced at higher energies. The calculated yields for the differential cross section at higher angles are negligible.

The variation with energy of the calculated average angle $\langle\theta_L\rangle$ is shown in Fig. 6. The experimental $\langle\theta_L\rangle$ values are comparatively

Can. J. Chem. Downloaded from www.nrcresearchpress.com by 210.87.254.105 on 09/05/12
For personal use only.

Can. J. Chem. Downloaded from www.nrcresearchpress.com by 210.87.254.105 on 09/05/12
For personal use only.

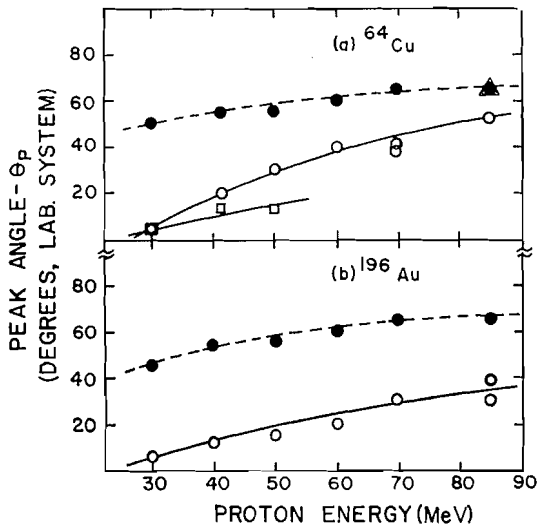

FIG. 5. Comparison of the experimental peak angles of (*a*) ^{64}Cu with the statistical theory, cascade–evaporation at 85 MeV, and the i.s.e. model calculations; (*b*) ^{196}Au with the i.s.e. model calculations; ○, experimental; □, statistical theory; △, cascade–evaporation at 85 MeV; and ●, i.s.e. model.

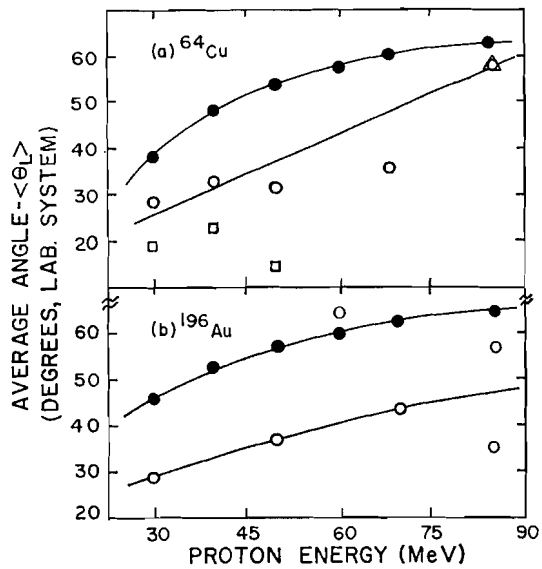

FIG. 6. Comparison of the experimental average recoil angle $\langle\theta_L\rangle$ of (*a*) ^{64}Cu with the statistical theory, cascade–evaporation and the i.s.e. model calculations; (*b*) ^{196}Au with the i.s.e. model calculations; ○, experimental; □, statistical theory; △, cascade–evaporation at 85 MeV; and ●, i.s.e. model.

high, which may be partly due to the contribution from the direct interaction mechanism and partly due to the experimental uncertainty. The change in $\langle\theta_L\rangle$ or θ_p, due to the larger evaporation kick relative to that obtained in compound nucleus formation, cannot account for the larger peak shifts at higher energies where the direct interaction mechanism plays the predominant role.

Evaporation calculations carried out for the formation of ^{196}Au from the compound nucleus ^{198}Hg at low energy, gave no meaningful results. Proton emission from the heavy nuclei is suppressed by the Coulomb barrier and the calculated cross section is nearly zero even at the incident energy of 20 MeV although different values of the coefficients of the Coulomb barrier were used. Probably the statistical theory calculation is limited in its application in the heavy mass region. However, the experimental angular distributions at 30 and 50 MeV are mainly forward-peaking, as expected on account of the predominance of the compound-nucleus contribution in this heavy mass region. This idea is further corroborated by the average range calculations (1).

A cascade–evaporation calculation for the angular distribution of ^{64}Cu at 85 MeV was also performed[3] and the results are shown in Fig. 7(*f*). The Monte Carlo code of Chen *et al.* (14) was used for the cascade phase and that of Dostrovsky *et al.* (12) for the evaporation phase. The angular distribution of ^{64}Cu formed by the knock-out mechanism is flat which may be partly attributed to the direct interaction mechanism (9); but the angular distribution calculated by the cascade–evaporation mechanism shows a sidewise peak at 65°. One would not expect the results of the (p,pn) reaction to be well-predicted by a cascade–evaporation calculation at these energies and thus the peak angle is not well reproduced by the calculation. However it nevertheless is of interest to see how the calculations check with theory at these energies.

(c) Comparison with Inelastic Scattering Model Calculations

As we have seen in the previous section, the cascade–evaporation calculation at 85 MeV is in reasonable agreement with the experimental results for the ^{65}Cu(p,pn)^{64}Cu reaction. In the absence of these calculations at other energies,

[3]We are grateful to Dr. G. Friedlander who very kindly carried out the cascade-phase calculations for us.

Can. J. Chem. Downloaded from www.nrcresearchpress.com by 210.87.254.105 on 09/05/12
For personal use only.

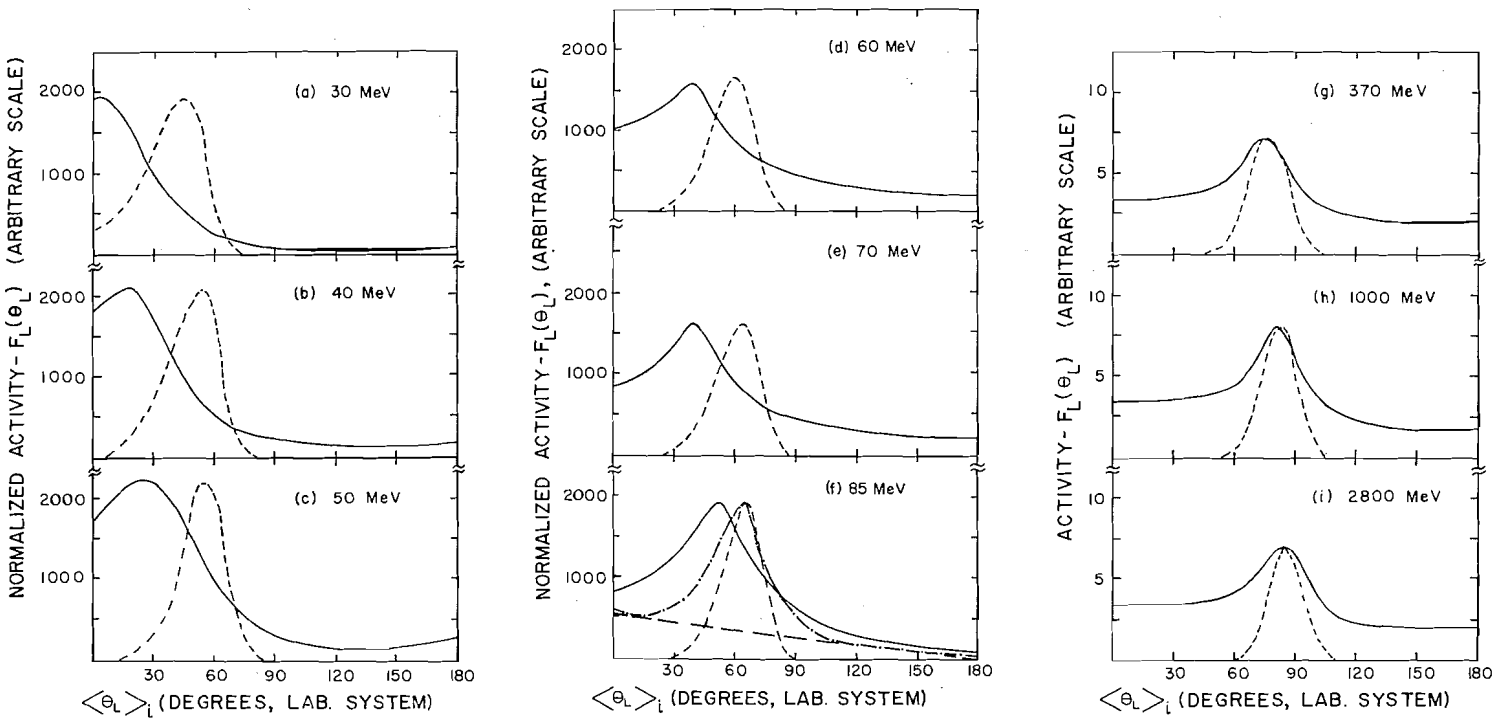

FIG. 7. Comparison of experimental and calculated angular distributions for the $^{65}Cu(p,pn)^{64}Cu$ reaction at (*a*) 30, (*b*) 40, (*c*) 50, (*d*) 60, (*e*) 70, (*f*) 85, (*g*) 370, (*h*) 1000, and (*i*) 2800 MeV; ——— experimental results taking the mid-angle as the average angle of each angular interval; — — — i.s.e. model calculations.

For the high energy results at 370, 1000, and 2800 MeV calculated results are adjusted to the experimental values.

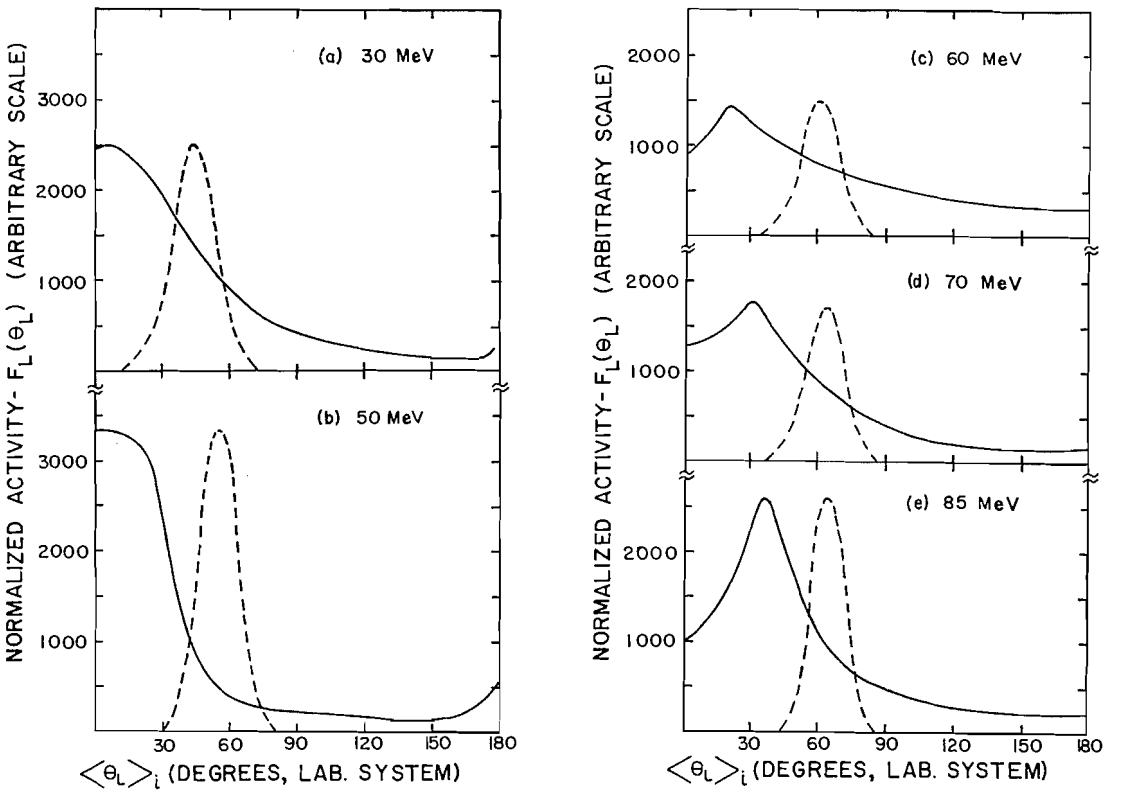

FIG. 8. Comparison of experimental and calculated angular distributions for the ^{197}Au(p,pn)^{196}Au reaction at (*a*) 30, (*b*) 50, (*c*) 60, (*d*) 70, and (*e*) 85 MeV; ——— experimental; — — — i.s.e. model calculations.

we have performed calculations based on a mechanism described by the inelastic scattering of a particle in the initial phase of the reaction followed by the evaporation of another particle (frequently referred to as the i.s.e. mechanism). The details of the calculation have been described elsewhere (1). The probability of a particular reaction being known, the recoil differential cross section $\left(\frac{d\sigma}{d\Omega}\right)_R$ can be written as

$$[5]\quad \left(\frac{d\sigma}{d\Omega}\right)_R = \sigma(p,xn)F(\theta) \qquad \text{for (p,}x\text{n) reactions}$$

$$[6]\quad = \sigma(p,pxn)F(\theta) \qquad \text{for (p,p}x\text{n) reactions}$$

where $F(\theta)$ corresponds to the probability of recoil collection per unit solid angle at an angle θ with respect to the proton beam, σ(p,*x*n) and σ(p,p*x*n) refer respectively to (p,*x*n) and (p,p*x*n) reaction cross sections calculated by the inelastic scattering model calculations. For the (p,pn) reaction, the incident proton is assumed to be scattered initially and transfers sufficient energy to the struck nucleus to evaporate another neutron. The whole energy interval for neutron evaporation was divided into subintervals. For each subinterval, the recoil angle was calculated from the kinematics of the overall reaction and then the angular distribution was obtained. Finally, the resultant angular distribution was calculated by weighting over those corresponding to each energy subinterval.

Comparisons of the calculated recoil angular distributions with the experimental results of both the ^{64}Cu and ^{196}Au nuclides are made in Figs. 7 and 8. Also included in the figures are the results of Remsberg (5). The following characteristics are observed:

(1) The peaks of the calculated angular distributions always occur at higher angles than the

Can. J. Chem. Downloaded from www.nrcresearchpress.com by 210.87.254.105 on 09/05/12
For personal use only.

Can. J. Chem. Downloaded from www.nrcresearchpress.com by 210.87.254.105 on 09/05/12
For personal use only.

experimentally observed peak angles. Better agreement is obtained at higher energies. (See also Fig. 5.)

(2) The calculated average angle $\langle\theta_L\rangle$ (Fig. 6) shows a gradual increase with energy. The experimental $\langle\theta_L\rangle$ values are in better agreement with calculations than that in the case of the peak angles.

(3) The calculated angular distributions are always sharper than the experimental values for both ^{64}Cu and ^{196}Au. The full-width at half-maximum values of the observed distributions obtained after the subtraction of the featureless distributions are in general higher (Tables V and VI) than those obtained by calculations.

(4) The calculated angular distribution does not show the prominent peak shift with the incident energy.

(5) Monte Carlo cascade–evaporation and i.s.e. model calculations at 85 MeV give the same peak angle at 65° and average angles of 59.2° and 62.4° respectively for ^{64}Cu.

The discrepancies between calculations and experiments have been attributed to the following assumptions:

(*i*) Compound nucleus formation was totally neglected. This may be one of the main reasons for the overestimation of the calculated peak angle values.

(*ii*) The case of proton evaporation from the excited residual nucleus [after neutron scattering in the (P,N) cascade] was omitted, e.g. ^{65}Zn formation from the (P,N) cascade step which may lead to ^{64}Cu by proton evaporation, was assumed negligible (correct only for heavy nuclides at low energy, where the proton emission is suppressed by the Coulomb barrier).

(*iii*) The chosen excitation energy interval of the residual nucleus for a particular value of the incident energy (10–25 MeV for excited ^{65}Cu and 10–23 MeV for excited ^{197}Au) may not be correct. The calculation shows that, within a given excitation energy interval, the recoil peak angle from the highly excited nuclei appears at the lower angle. Thus the peak of the net angular distribution at a definite incident energy may decrease to a certain extent, if we consider the emission from the higher excited states of ^{65}Cu (higher than 25 MeV for ^{65}Cu and 23 MeV for ^{197}Au as assumed in our present calculation). However, the present evaporation calculation cannot take into account evaporation from such highly excited states on account of the very low cross sections of the desired nuclides.

(*iv*) Only head-on collisions were considered in our calculation. If we also consider the overtaking collisions, better agreement with the experiments may be obtained.

(*v*) Nucleon correlation (15) which may be sensitive to recoil properties has been neglected.

Grover and Caretto (16) analyzed the inelastic scattering data of Azhgirei *et al.* (17) at 660 MeV and found that all the recoiling copper nuclei excited to about 15 MeV go into angles between 76 and 80° with respect to the beam. The kinetic energy spectrum of this recoil group shows an average recoil energy of $\sim$ 1 MeV. Such peaks should occur for other targets and other incident energies too and reflect a rather general property of the inelastic scattering of a light particle by a massive one. The required conditions for the occurrence of a peak are: (*i*) small kinetic energy transfer, i.e. low excitation energy of the residual nucleus and (*ii*) forward peaking nature of the angular distribution of the scattered particles. The critical peak angle should be less than 90°. When the excitation energy is small with respect to the incident energy, even for a small scattering angle the recoil peak angle reaches a critical value.

The overall comparison between the experiment and the calculation shows that a compound nucleus mechanism is valid at low energies. As the bombarding energy increases the direct interaction mechanism begins to compete. In the energy region of 40–85 MeV the (p,pn) reaction proceeds via a combination of compound nucleus formation and a direct interaction mechanism.

Acknowledgments

The authors wish to thank Professor R. E. Bell, Director, Foster Radiation Laboratory, for ready permission to use the McGill synchrocyclotron and Mr. R. H. Mills who cheerfully performed the irradiations. Our thanks go to Professor N. T. Porile, presently at the Department of Chemistry, Purdue University, for suggesting the problem during his stay at McGill and to Dr. L. P. Remsberg who kindly made available to us his high energy results. Thanks are gratefully offered to Professor D. Thorpe and his colleagues in the McGill Computing

Centre for assistance and guidance during the lengthy calculations.

One of us (M. K. D.) wishes to express his gratitude to the Department of Chemistry, McGill University, for a teaching assistantship from 1963–65 and to the National Research Council of Canada for Studentships from 1965–67.

1. M. K. DEWANJEE, G. B. SAHA, and L. YAFFE. Can. J. Chem. **46**, 3157 (1968).
2. D. J. REULAND, N. K. GANGULY, and A. A. CARETTO, JR. Phys. Rev. **133**, B1171 (1964).
3. A. M. POSKANZER, J. B. CUMMING, and R. WOLFGANG. Phys. Rev. **129**, 374 (1963).
4. J. A. PANONTIN, L. L. SCHWARTZ, A. F. STEHNEY, E. P. STEINBERG, and L. WINSBERG. Phys. Rev. **145**, 754 (1966).
5. L. P. REMSBERG. Private communication.
6. J. B. CUMMING. Application of computers to nuclear and radiochemistry. Natl. Acad. Sci. Natl. Res. Council, Nucl. Sci. Ser. NAS-NS-3107. 1962. p. 25.
7. G. B. SAHA and N. T. PORILE. Phys. Rev. **158**, 1027 (1967).
8. J. M. ALEXANDER. Nuclear chemistry. Vol. 1. *Edited by* L. Yaffe. Academic Press, Inc., New York. 1968. p. 273.
9. P. A. BENIOFF and L. W. PERSON. Phys. Rev. **140**, B844 (1965).
10. J. B. MARION, T. I. ARNETTE, and H. C. OWENS. Oak Ridge National Laboratory Report, ORNL-2574. 1959. Unpublished.
11. A. O. HANSON, R. F. TASCHEK, and J. H. WILLIAMS. Rev. Mod. Phys. **21**, 635 (1949).
12. I. DOSTROVSKY, Z. FRAENKEL, and G. FRIEDLANDER. Phys. Rev. **116**, 683 (1959).
13. N. T. PORILE. Phys. Rev. **135**, B371 (1964).
14. K. CHEN, Z. FRAENKEL, G. FRIEDLANDER, J. R. GROVER, J. M. MILLER, and Y. SHIMAMOTO. Phys. Rev. **166**, 949 (1968).
15. F. P. DENISOV, V. P. MILOVANOV, R. A. LATYPOVA, and P. A. CERENKOV. Soviet J. Nucl. Phys. English Transl. **2**, No. 6, 742 (1966).
16. J. R. GROVER and A. A. CARETTO, JR. Ann. Rev. Nucl. Sci. **14**, 51 (1960).
17. L. S. AZHGIREI, I. K. VZOROV, V. P. ZRELOV, M. G. MESCHERYAKOV, B. S. NEGANOV, R. M. RYNDIN, and A. F. SHABUDIN. Soviet Phys. JETP English Transl. **9**, 1163 (1959).

Can. J. Chem. Downloaded from www.nrcresearchpress.com by 210.87.254.105 on 09/05/12
For personal use only.

Yields of some light-mass nuclides produced in the proton-induced fission of ^{238}U[1]

A. H. KHAN, G. B. SAHA, AND L. YAFFE
Radiochemistry Laboratory, Department of Chemistry, McGill University, Montreal, Quebec

Received May 29, 1968

The formation cross sections of cumulatively formed ^{66}Ni, ^{67}Cu, ^{72}Zn, and ^{73}Ga, and of independently formed ^{68}Ga, ^{70}Ga, and ^{72}Ga produced in fission of ^{238}U, induced by protons of energy 20–85 MeV, have been determined. The measured yields correlate well with the data obtained by others at higher energies. From the ratios of the independent and cumulative formation cross sections of ^{72}Ga and ^{72}Zn respectively, a value of Z_p, the most probable nuclear charge, for $A = 72$ was determined for different widths of the charge dispersion curves.

Canadian Journal of Chemistry, 46, 3565 (1968)

Can. J. Chem. Downloaded from www.nrcresearchpress.com by 210.87.254.6 on 09/05/12
For personal use only.

Introduction

A voluminous amount of data on thermal neutron fission now exists and there is now a somewhat better understanding of the fission mechanism at these energies. Our theoretical understanding of the process still leaves much to be desired. Data on fission induced by charged particles at higher bombarding energies are still somewhat sparse, especially in the light-mass region. The data that do exist do not yield unambiguous information regarding the fission mechanism. In particular much more information is needed to elucidate more explicitly the nuclear charge and mass distribution in nuclear fission induced by charged particles as a function of bombarding energy.

The present work involves the measurement of the yields of ^{66}Ni, ^{67}Cu, ^{72}Zn, ^{73}Ga, ^{68}Ga, ^{70}Ga, and ^{72}Ga in the fission of ^{238}U induced by protons of energies 20–85 MeV. ^{70}Ga is 'shielded' from formation by β-decay since its neighboring isobars are stable. ^{68}Ga and ^{72}Ga are 'semi-shielded' by long-lived neighboring isobars so that the independent yields of these three can be determined. In the case of the other nuclides mentioned above only cumulative or chain yields were determined.

Lindner and Osborne (1) and Hicks and Gilbert (2) determined formation cross sections of ^{66}Ni and ^{67}Cu respectively in the fission of ^{238}U by protons of energies 61–340 MeV. Other workers have reported results at higher energies, e.g. at 170 (3), 340 (4), and 480 MeV (5).

Forster *et al.* (6) have recently described a method to determine empirically Z_p, the most probable charge, on the assumption of a Gaussian charge distribution, provided the yield ratio of an isobaric pair is known. We have measured the formation cross sections of ^{72}Ga and ^{72}Zn and their yield ratios have been used to obtain Z_p values at different energies. From these Z_p values we have further attempted to obtain information about the width of the charge dispersion curves for the low-mass region at these bombarding energies.

Experimental Procedure

(a) Targets and Irradiations

The targets used in the present work consisted of uranium foils of normal isotopic distribution having a superficial density of about 140 mg/cm^2. Prior to irradiation the uranium target foil was cleaned with nitric acid to remove the oxide layer. The foil was then sandwiched between two similarly treated foils to compensate for recoil losses. A copper monitor foil (21.44 mg/cm^2), similarly guarded with two other copper foils, was properly aligned with the target stack. The $^{65}Cu(p,pn)^{64}Cu$ reaction was used to monitor the proton beam throughout the entire energy region. The assembly of the target and monitor foils was wrapped with an aluminium foil (0.0008 in. thick) and then fixed to a target holder which in turn was attached to the cyclotron probe.

Irradiations were performed in the internal proton beam of the McGill synchrocyclotron. The duration of irradiations varied between 2 and 60 min, depending on the activity and bombarding energy desired. The beam current was of the order of 1 μA. Irradiations were performed in the energy range of 20–85 MeV at intervals of about 10 MeV, the beam energy being selected by placing the target at the appropriate radius corresponding to a desired energy. In view of the energy spread in the beam (±2 MeV) the energy degradation in the target stack was calculated to be negligible.

(b) Chemical Procedures

After irradiation, the target and monitor foils were separated from the stack and dissolved in suitable acids. The target foil was dissolved in 2 ml of conc. hydrochloric acid and a few drops of conc. nitric acid in the presence of 10 mg each of Ni, Zn, and Cu carriers and 15 mg of Ga

[1]This project received financial assistance from the National Research Council of Canada.

Can. J. Chem. Downloaded from www.nrcresearchpress.com by 210.87.254.6 on 09/05/12
For personal use only.

carrier. The copper monitor foil was dissolved in conc. hydrochloric acid plus a few drops of hydrogen peroxide.

The chemical procedures for the separation of nickel (7), copper (8), zinc (9), and gallium (10) were adopted from procedures in the literature and slightly modified to suit to the present study. They are outlined in the Appendix.

(c) Activity Measurements

The beta activities were measured by a low-background β^- proportional counter with a background of less than 1 count per minute. A ^{36}Cl standard source was used to check the characteristic behavior of the counter.

Both ^{66}Ni and ^{72}Zn decay by emitting low-energy β^--rays (0.200 and 0.300 MeV betas respectively) which undergo high self-absorption in the solid sample. However, 55-h ^{66}Ni remains in secular equilibrium with its daughter 5.1-min ^{66}Cu which emits higher energy β^- rays (2.63 and 1.59 MeV respectively). Similarly 46.5-h ^{72}Zn maintains a transient equilibrium with its daughter 14.1-h ^{72}Ga which emits β^- rays of 0.96, 0.66, and 3.16 MeV energy. The activity of these two nuclides was, therefore, measured with a 200 mg/cm^2 thick aluminium absorber so that all low-energy beta radiations were stopped and thus self-absorption correction could be avoided. ^{73}Ga decays (100%) to the isomeric state of ^{73}Ge. This isomeric transition is highly internally converted ($\sim$ 100%) and these conversion electrons would also be detected along with the activities of the Ga isotopes to a varying degree depending on the thickness of the sources. In order to stop all conversion electrons uniformly for all sources, the same 200 mg/cm^2 thick aluminium absorber was used while the activities of gallium isotopes were measured.

The activities of all nuclides were followed for several half-lives to ensure that no contaminating activities were present. The activities due to ^{72}Zn, ^{66}Ni, and ^{67}Cu at end of bombardment were obtained by graphical analysis, whereas those of the gallium isotopes were resolved by computer analysis (11). Half-lives agreed very well with the literature values (12).

The efficiency of the β^- counter was obtained for all nuclides (except for ^{68}Ga and ^{70}Ga) by calibration against a $4\pi\beta$ counter. The efficiency for ^{68}Ga and ^{70}Ga was taken to be the same as that for ^{73}Ga. A small self-absorption correction was applied to the ^{67}Cu and ^{64}Cu activities. The activities of ^{72}Zn, ^{66}Ni, and ^{73}Ga were obtained by correcting for the growth of their daughters by the well-known equations.

Results and Discussion

The counting rates at the end of bombardment were converted to disintegration rates by applying corrections for chemical yields, aliquots, branching ratios, and counting efficiencies. The disintegration rates were then used to calculate the cross sections of the respective nuclides. The monitor cross sections used were taken from Meghir and Yaffe (13) and are given in Table I. The measured cross sections are given in Table II and shown in Figs. 1–5. Also included in the figures are cross sections previously reported in the literature. The limits shown in the cross-section values determined in the present work were compounded from the uncertainties in the decay curve analysis, determination of chemical yields, target thicknesses, and counter efficiencies, and were estimated to be 20% for ^{66}Ni, ^{67}Cu, ^{72}Zn, ^{72}Ga, and ^{73}Ga. Because of the large uncertainty in the determination of the activities of ^{68}Ga, and ^{70}Ga, no limits have been quoted for these nuclides. Cross sections for ^{68}Ga and ^{70}Ga appear to be relatively high. Because of the short half-lives these have been obtained by quick chemical separation of gallium samples, probably without sufficient purification and these discrepancies are undoubtedly due to the presence of interfering nuclides. The cross sections should be regarded as upper limits only.

TABLE I

Cross sections for the $^{65}Cu(p,pn)^{64}Cu$ reaction (13)

Energy (MeV)	σ_m (mb)
20	260
30	390
40	260
50	210
60	180
70	160
77	150
85	140

The fractional cumulative yields of the chains with A = 66, 67, 72, and 73 are found to be low, as expected from the fact that, at these energies, these nuclides lie far down on the low-mass wing of the mass–yield curve.

The trends observed in our results correlate well with those of previous workers, as seen in Figs. 1–5. We have not included the results above 500 MeV since they may involve in part a fragmentation mechanism. Our results for ^{66}Ni are in line with those of Lindner and Osborne (1) and Hagebo *et al.* (3). In the case of ^{67}Cu, while our data agree reasonably well with those of Hagebo *et al.* (3) at 170 MeV and of Folger *et al.* (4) at 340 MeV, the results of Hicks and Gilbert (2) at 75–340 MeV are consistently lower than those of ours by a factor of 3–4. Such a discrepancy is difficult to explain and is not due to different values for the monitor reactions, since these correlate well. The cross sections of ^{72}Ga and

^{73}Ga reported by Hagebo *et al.* (3) at 170 MeV and by Vinogradov *et al.* (5) at 480 MeV follow reasonably well the trend observed in our results. Similar good agreement is observed for ^{72}Zn between our results and that of Folger *et al.* (4).

The excitation functions of all nuclides rise sharply with proton bombarding energy, reflecting the broadening of the charge distribution curve with energy. The formation cross sections of the individual members of a chain should increase with increasing excitation energy, pass through a maximum, and then decrease. In the mass region of our interest the maximum of the excitation function for any member of a chain in question is expected to occur at energies higher than the energy range of our interest. Thus, the increase in the cumulative yields of ^{66}Ni, ^{67}Cu, ^{72}Zn, and ^{73}Ga indicates an increasing contribution from the individual members of the respective chains. The increase in the independent yield of ^{72}Ga follows from the above. In contrast to those of ^{66}Ni, ^{67}Cu, and ^{72}Zn, the excitation function of ^{73}Ga, though cumulative, shows a sharp drop above 170 MeV. This is probably due to the net effect of its early membership in the chain, the broadening of the charge distribution, and, at the same time, the shifting of the most probable charge, Z_p, of the chain towards maximum beta stability, as has been demonstrated by Pate, Foster, and Yaffe (14). In addition, the sharp rise in the excitation functions of

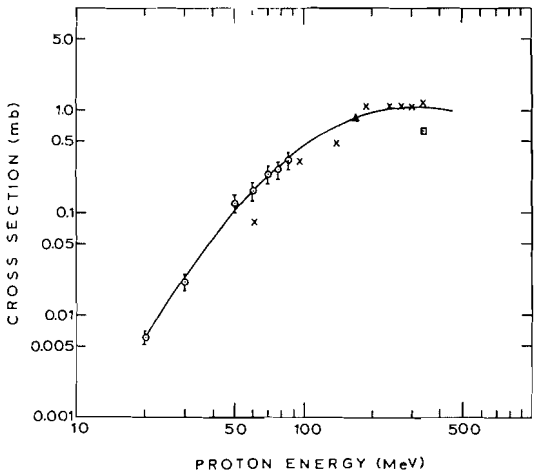

FIG. 1. Excitation function of ^{66}Ni (cumulative): ○, present work; ×, ref. 1; △, ref. 3; □, ref. 4.

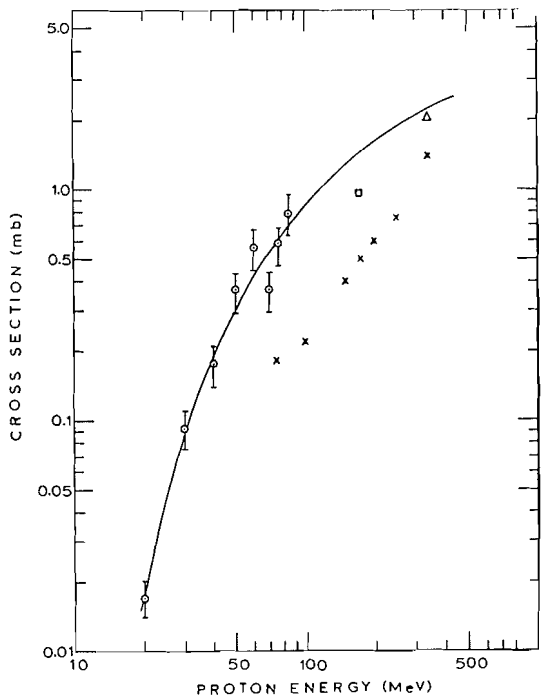

FIG. 2. Excitation function of ^{67}Cu (cumulative): ○, present work; ×, ref. 2; □, ref. 3; △, ref. 4.

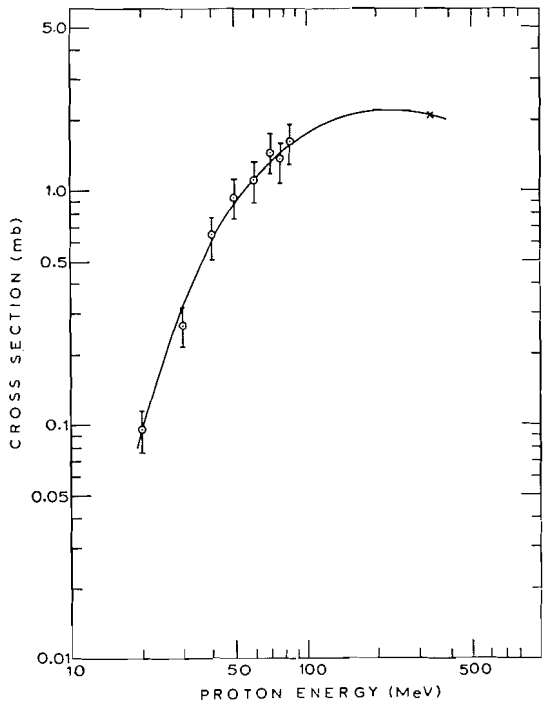

FIG. 3. Excitation function of ^{72}Zn (cumulative): ○, present work; ×, ref. 4.

Can. J. Chem. Downloaded from www.nrcresearchpress.com by 210.87.254.6 on 09/05/12
For personal use only.

Can. J. Chem. Downloaded from www.nrcresearchpress.com by 210.87.254.6 on 09/05/12
For personal use only.

TABLE II

Formation cross sections (mb) of nuclides studied

Energy (MeV)	^{66}Ni(c)*	^{67}Cu(c)	^{72}Zn(c)	^{68}Ga(i)*	^{70}Ga(i)	^{72}Ga(i)	^{73}Ga(c)	$R^{A}_{c/i}=\frac{\sigma_{72Zn}}{\sigma_{72Ga}}$
20	0.006±0.001	0.017±0.003	0.09±0.02	—	—	0.005±0.001	0.081±0.016	19.0
30	0.021±0.004	0.092±0.018	0.27±0.05	—	—	0.007±0.001	0.22±0.04	38.0
40	—	0.17±0.03	0.64±0.13	—	—	0.025±0.005	0.57±0.12	25.6
50	0.12±0.02	0.36±0.07	0.93±0.19	—	—	0.067±0.013	0.45±0.09	14.0
60	0.16±0.03	0.56±0.11	1.10±0.22	—	—	0.12±0.02	0.88±0.18	9.2
70	0.24±0.05	0.37±0.07	1.47±0.29	<0.05	<0.37	0.17±0.03	1.23±0.25	8.6
77	0.25±0.05	0.58±0.12	1.34±0.27	<0.24	<0.52	0.17±0.03	1.24±0.25	7.9
85	0.32±0.06	0.79±0.16	1.61±0.32	—	<0.82	0.34±0.07	1.44±0.29	4.8

*c and i refer to cumulative and independent yields respectively.

Can. J. Chem. Downloaded from www.nrcresearchpress.com by 210.87.254.6 on 09/05/12
For personal use only.

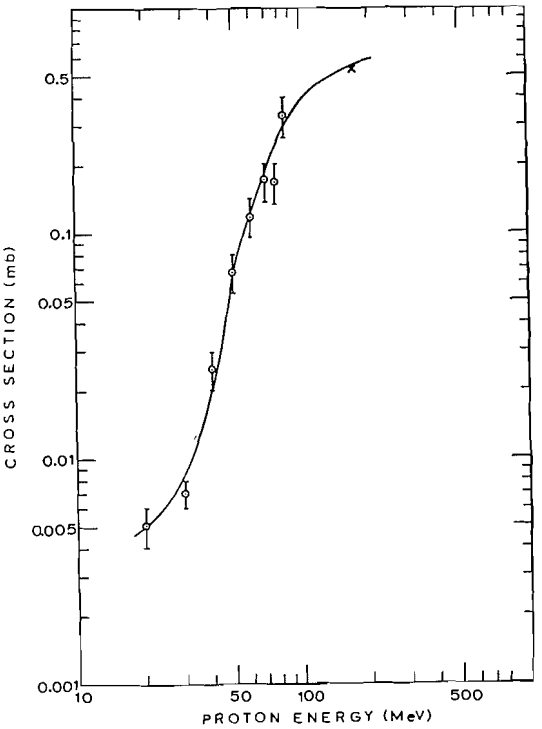

FIG. 4. Excitation function of ^{72}Ga (independent): ○, present work; ×, ref. 3.

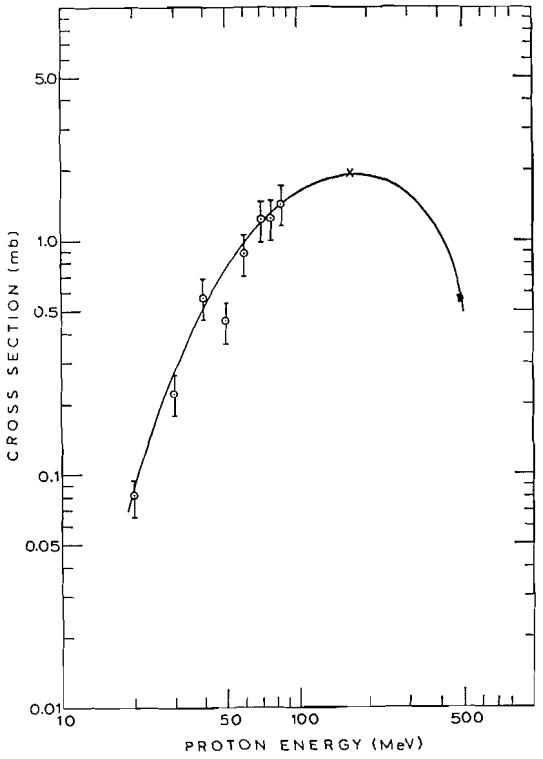

FIG. 5. Excitation function of ^{73}Ga (cumulative): ○, present work; ×, ref. 3; ●, ref. 5.

these low mass products indicate that in the energy region of our interest, they are formed from highly excited nuclei, probably compound nuclei, formed in the initial interaction between the proton and the uranium nuclei. This has been further confirmed by the recoil studies of some of these nuclides (15).

Charge distribution curves cannot be drawn readily in this mass region without the availability of many more data in each specific mass chain since one cannot make the assumption of a flat mass distribution in this mass region. Forster *et al.* (6) recently devised a method of determining empirically Z_p values for a given chain with mass A, provided the ratio $R^A_{c/i}$, of the yields of the cumulatively formed parent and the independently formed daughter, is known. The basis of this method is the assumption of a Gaussian charge distribution of the form:

$$[1] \quad P(Z) = \frac{1}{\sqrt{(\pi C)}} \exp\left[-(Z - Z_p)^2/C\right]$$

where $P(Z)$ is the fractional chain yield of an isobar of charge Z, Z_p is the most probable charge, and C is a constant defining the width of the charge distribution. Then the yield ratio, $R^A_{c/i}$, can be given as

$$[2] \quad R^A_{c/i} = \frac{\sum_{Z_i = Z'-1}^{Z_i = Z'-6} \exp\left[-(Z_i - Z_p)^2/C\right]}{\exp\left[-(Z' - Z_p)^2/C\right]}$$

where Z' is the nuclear charge of a daughter isobar and Z_i is the charge of its precursors. For a given value of C, one can calculate $R^A_{c/i}$ as a function of $(Z' - Z_p)$ values using eq. [2].

We have determined the formation cross sections for cumulatively formed ^{72}Zn and the independent yield of ^{72}Ga and thus the yield ratios $R^A_{c/i}$ are known (Table II). Following the method of Forster *et al.* (6), a family of plots of $R^A_{c/i}$ versus $(Z' - Z_p)$ for different values of C varying from 0.7 to 2.5 were obtained. The Z_p values at different proton energies were determined from these plots using the experimental $R^A_{c/i}$ values for different values of C and they are

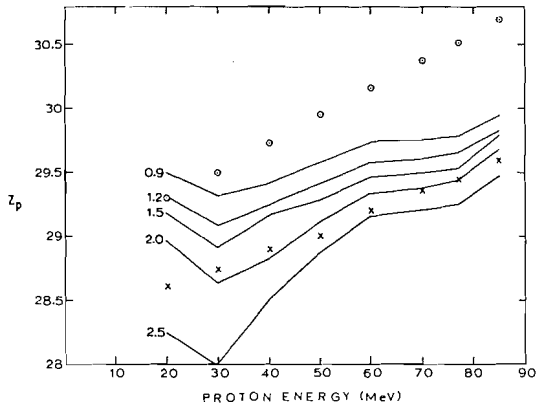

FIG. 6. Variation of Z_p with proton energy. Z_p values were obtained by the method of Forster *et al.* (6) for different C values (solid lines): ×, predicted by u.c.d.; ○, predicted by e.c.d.

shown in Fig. 6. The uncertainty in these values may amount to about 0.1–0.2 charge units. Although the rate of change of Z_p with energy is of the expected order above 30 MeV, the sudden rise in Z_p below 30 MeV is probably due to the experimental uncertainty in the determination of the cross sections of these nuclides. The increase in Z_p with energy for a given C indicates the displacement towards maximum stability with increasing energy. The effect of the C values upon Z_p is more pronounced at lower energies than at higher energies. For example, by changing C from 0.9 to 2.0, Z_p changes by 0.7 charge units at 30 MeV whereas it changes by only 0.3 units at 85 MeV.

It is obvious that unless the charge width factor C is precisely known, it is difficult to obtain unambiguous information regarding Z_p values from this analysis alone. However, one can get information about C if a value of Z_p is known. We have calculated Z_p assuming the unchanged charge division (u.c.d.) and equal charge displacement (e.c.d.) postulates (16). The formulation of these postulates requires a knowledge of the number of neutrons emitted in the pre- and post-fission processes, and information is scanty in this energy region. However, the data can be obtained approximately

[3] for e.c.d.

$$Z_p = \tfrac{1}{2}[Z_A - Z_{(A_C - A - \bar{\nu}_T)} + Z_C]$$

[4] for u.c.d. $$Z_p = \frac{Z_C A}{A_C - \bar{\nu}_T}$$

where $\bar{\nu}_T$ is the average total number of neutrons emitted in fission leading to fission products of mass A. Z_C and A_C are the charge and mass numbers of the fissioning nucleus. $\bar{\nu}_T$ was calculated from the relationship given by Unik and Huizenga (17)

[5] $$\bar{\nu}_T = 0.12E^* + 1.90$$

where E^* is the excitation energy of the fissioning nucleus. The Z_p values calculated by eqs. [3] and [4] at different energies are shown in Fig. 6. It is seen that the Z_p values obtained from the u.c.d. postulate indicate a constant C value of about 2 at all energies with a slight discrepancy at 20 MeV. On the other hand, the Z_p values obtained from the e.c.d. postulate are much larger than any of the experimental values at all energies except at 20 MeV where a value of 1.2 is observed. A constant value of C of about 2, as obtained from the u.c.d. postulate, leads to the idea that the width of the charge distribution remains constant at these energies. This seems to contradict previous work by Davies and Yaffe (18) and Pate *et al.* (14) in the mass region of 130–140 in the same energy range. The contradiction may be more apparent than real, since the mass ranges studied are so different, and is of course based on the u.c.d. postulate alone. Hagebo *et al.* (3) and Pappas and Hagebo (19) found that the light-mass fragments from the 170 MeV proton fission of uranium originate from high-deposition energy events and that the latter tend to follow the u.c.d. rule more closely than the e.c.d. rule. This conclusion, based on data obtained at 170 MeV, may be valid to some extent in our energy range.

Choppin and Meyer (20) in a study of the low-energy (7–12 MeV) fission of ^{238}U found that the independent yields determined by them could best be correlated by a Gaussian distribution with a value of C between 2 and 2.5, not too different from that determined in the present work. On the other hand McHugh (21) made a mass spectrometric study of charge distribution in ^{235}U fission for the chain of mass 135. He obtained a value of 0.9–1.0 for C at bombarding energies of 18–40 MeV, not far removed from the value of 0.86 ± 0.04 obtained by Wahl and his coworkers (22, 23) for thermal neutron fission.

Acknowledgments

One of us (A. H. K.) wishes to thank the Atomic

Can. J. Chem. Downloaded from www.nrcresearchpress.com by 210.87.254.6 on 09/05/12
For personal use only.

Energy Commission of Pakistan for granting him leave-of-absence and acknowledges with gratitude financial assistance from the Government of Canada under the Colombo Plan.

Appendix

Chemical Separation

Nickel, copper, and zinc were separated from the same targets at a given bombardment energy, whereas separate bombardments were performed for gallium. An initial separation of each of these elements was made by ion-exchange techniques. The solution from the dissolved target was passed through Dowex 1 × 8 (mesh 100–200) resin columns. Nickel was eluted with conc. hydrochloric acid and kept for further purification. The resin column was washed with 4 *N* hydrochloric acid and copper and gallium were eluted with 1.5 *N* hydrochloric acid and purified at a later time. The column was washed with 0.5 *N* hydrochloric acid and zinc was eluted with distilled water and processed for further purification.

Nickel

The concentrated hydrochloric acid solution containing nickel was made only slightly acidic by adding ammonia. The solution was scavenged with Mo, Cu, and Cd sulfides in slightly acidic medium, with ferric hydroxide, and with barium and strontium carbonates in excess ammonia, and then nickel sulfide was precipitated. The precipitate was dissolved in a small amount of acid, the solution neutralized with ammonia, and the dimethylglyoxime was precipitated from the solution and centrifuged. After the dissolution of the dimethylglyoxime in acid, the entire cycle of sulfide and hydroxide scavenging was repeated twice more. Finally the nickel dimethylglyoxime precipitate was filtered, weighed for chemical yield determination, and prepared for activity measurement.

Copper

Copper sulfide was precipitated from the 1.5 *N* hydrochloric acid solution. The sulfide was dissolved in acid, the copper reduced with sodium bisulfite, and the thiocyanate precipitated. The precipitate was dissolved, scavenged with cadmium and arsenic sulfides in the presence of potassium cyanide, and copper sulfide was again precipitated and dissolved in acid. The resulting solution was scavenged with silver chloride. The solution was made ammoniacal and scavenged with ferric hydroxide and barium and strontium carbonate precipitations. The supernatant solution was then made slightly acidic, the thiocyanate again precipitated, and two more cycles of sulfide and hydroxide scavengings were performed. Finally the copper thiocyanate was filtered, weighed, and prepared for activity measurement.

Zinc

Zinc was separated as $ZnHg(SCN)_4$ on adding $HgCl_2$–NH_4SCN mixture to the zinc fraction of the ion-exchange separation. This precipitation was repeated twice from 1 *N* nitric acid solution and the precipitate was dissolved and diluted. The sulfide was precipitated, and 12 *N* sodium hydroxide was added dropwise until the white precipitate of zinc sulfide was obtained. The sulfide was dissolved in acid and the solution made alkaline with excess of 12 *N* sodium hydroxide and scavenged with hydroxide and carbonate precipitations. The solution was made to 1 *N* in nitric acid and $ZnHg(SCN)_4$ was precipitated. The sulfide and hydroxide scavengings were repeated twice more. $ZnHg(SCN)_4$ was finally precipitated, filtered, weighed, and prepared for activity measurements.

Gallium

After the ion-exchange step, the 1.5 *N* solution containing gallium was made 6 *N* in hydrochloric acid. Gallium was extracted into isopropyl ether and back-extracted with water. The aqueous solution was scavenged with Cu, Cd, and Mo sulfides in slightly acidic condition and then with hydroxide and carbonate precipitations. Ammonia was added dropwise to the supernatant until $Ga(OH)_3$ appeared. The hydroxide was dissolved and the sulfide and hydroxide scavengings were repeated. A final ether extraction was made and gallium oxinate was precipitated with 8-hydroxyquinoline at a pH of 6. The precipitate was filtered, weighed, and prepared for activity measurement.

Because of the short half-life of the 21-min ^{70}Ga, separate bombardments were made for this nuclide. A quick separation by an ion-exchange method was performed as mentioned above. The eluate containing gallium was scavenged with Cu, Cd, and Mo sulfides. An ether-extraction step was made and finally gallium oxinate was precipitated.

Can. J. Chem. Downloaded from www.nrcresearchpress.com by 210.87.254.6 on 09/05/12
For personal use only.

1. M. LINDNER and R. M. OSBORNE. Phys. Rev. **94**, 1323 (1954).
2. H. G. HICKS and R. S. GILBERT. Phys. Rev. **100**, 1286 (1955).
3. E. HAGEBO, A. C. PAPPAS, and P. AAGAARD. J. Inorg. Nucl. Chem. **26**, 1639 (1964).
4. R. L. FOLGER, P. C. STEVENSON, and G. T. SEABORG. Phys. Rev. **98**, 107 (1955).
5. A. P. VINOGRADOV, I. P. ALIMARIN, V. I. BARANOV, A. K. LAVRUKHINA, T. V. BARANOVA, F. I. PAVLOTSKAYA, A. A. BRAGINA, and Y. YAKOVLEV. Conference on the Peaceful Uses of Atomic Energy. Moscow. 1955. U.S. At. Energy Comm. transl. 2435. 1955. p. 65. (Taken from E. Bruninx. CERN 62–69. 1962.)
6. J. H. FORSTER, N. T. PORILE, and L. YAFFE. Can. J. Chem. **44**, 2951 (1966).
7. R. L. FOLGER and H. HICKS. U.S. At. Energy Comm. Rept. AECD-2738. *Edited by* W. W. Meinke. 1949.
8. W. W. MEINKE. U.S. At. Energy Comm. Rept. UCRL-432. 1949.
9. J. M. SIEGEL and L. E. GLENDENIN. Radiochemical studies. The fission products. Book 3. *Edited by* C. D. Coryell and N. Sugarman. McGraw-Hill Book Co., Inc., New York. 1951.
10. J. A. MARINSKY and E. EICHLER. J. Inorg. Nucl. Chem. **12**, 223 (1960).
11. J. B. CUMMING. Natl. Acad. Sci. Natl. Res. Council, Nucl. Sci. Ser. NAS-NS-3107. 1962. p. 25.
12. C. M. LEDERER, J. M. HOLLANDER, and I. PERLMAN. Table of isotopes. 6th ed. John Wiley and Sons, Inc., New York. 1967.
13. S. MEGHIR and L. YAFFE. To be published.
14. B. D. PATE, J. S. FOSTER, and L. YAFFE. Can. J. Chem. **36**, 1691 (1958).
15. G. B. SAHA and L. YAFFE. To be published.
16. C. D. CORYELL, M. KAPLAN, and R. D. FINK. Can. J. Chem. **39**, 646 (1961).
17. J. P. UNIK and J. R. HUIZENGA. Phys. Rev. **134**, B90 (1960). J. R. Huizenga and R. Vandenbosch. Nuclear reactions. *Edited by* P. M. Endt and P. B. Smith. North-Holland Publishing Company, Amsterdam. 1962.
18. J. H. DAVIES and L. YAFFE. Can. J. Phys. 47, 762 (1963).
19. A. C. PAPPAS and E. HAGEBO. J. Inorg. Nucl. Chem. **28**, 1769 (1966).
20. G. R. CHOPPIN and E. F. MEYER, JR. J. Inorg. Nucl. Chem. **28**, 1509 (1966).
21. J. A. MCHUGH, JR. Univ. Calif. Radiation Lab. Rept. UCRL-10673. 1963.
22. A. C. WAHL. J. Inorg. Nucl. Chem. **6**, 263 (1958).
23. A. C. WAHL, R. L. FERGUSON, D. R. NETHAWAY, D. E. TROUTNER, and K. WOLFSBERG. Phys. Rev. **126**, 1112 (1962).

Can. J. Chem. Downloaded from www.nrcresearchpress.com by 210.87.254.6 on 09/05/12
For personal use only.

Can. J. Chem. Downloaded from www.nrcresearchpress.com by 210.87.254.42 on 09/05/12
For personal use only.

Cleavage of the carbon–phosphorus bond in chloromethyl–phosphorus compounds by phosphorus pentachloride

ARLEN W. FRANK[1]
Research Center, Hooker Chemical Corporation, Niagara Falls, New York 14302
Received May 8, 1968

A novel carbon–phosphorus bond cleavage is described. Chloromethylphosphonic dichloride (**2**) and bis(chloromethyl)phosphinic chloride (**1**) both react smoothly and quantitatively with phosphorus pentachloride at 95–100°, giving carbon tetrachloride and a P(III) fragment containing one less carbon–phosphorus bond: phosphorus trichloride from **2** and trichloromethylphosphonous dichloride from **1**. Under the same conditions, tris(chloromethyl)phosphine oxide (**3**) forms a complex (**4**) which subsequently breaks down to trichlorobis(trichloromethyl)phosphorane (**5**), diphenyl chloromethylphosphonate (**7**) suffers chlorination without cleavage, and tetrakis(chloromethyl)phosphonium chloride (**6**) is neither chlorinated nor cleaved. A concerted mechanism is proposed which accounts for all of these results.

Canadian Journal of Chemistry, 46, 3573 (1968)

Introduction

The haloform reaction has its counterpart in organophosphorus chemistry. Esters of trichloromethylphosphonic acid, for example, yield chloroform when subjected to alkaline hydrolysis (1). Under neutral or acidic conditions, however, the carbon–phosphorus bond is stable (2, 3). In the present paper, a novel type of cleavage is reported which takes place under acidic conditions, and which yields carbon tetrachloride rather than chloroform.

Results

In the course of experiments on the preparation of phosphorus compounds containing chloromethyl groups (4), it was discovered that the use of phosphorus pentachloride as the chlorinating agent in the preparation of bis(chloromethyl)-phosphinic chloride (**1**) from bis(hydroxymethyl)-phosphinic acid gave unexpectedly low yields (26–36%) of **1**, compared with the 93–94% yields attainable with thionyl chloride (4, 5). The major portion of the reaction mixture was lower boiling than **1**, suggesting that some type of fragmentation was involved.

Further investigation revealed that **1** undergoes an extensive reaction with phosphorus pentachloride at 95–100°, a temperature only slightly above that used in its synthesis. Reaction takes place smoothly according to the stoichiometry of eq. [1].

[1] $(ClCH_2)_2P(O)Cl + 5PCl_5 \rightarrow CCl_3PCl_2 + CCl_4 + POCl_3 + 4PCl_3 + 4HCl$
1

The carbon-containing fragments, trichloromethylphosphonous dichloride and carbon tetrachloride, were isolated in 87% yield and 48% yield, respectively. The trichloromethylphosphonous dichloride was further identified by the formation of a sulfur adduct, $CCl_3P(S)Cl_2$, on treatment with sulfur in the presence of aluminium chloride at 155–160°.

Chloromethylphosphonic dichloride (**2**) also reacts smoothly and quantitatively with phosphorus pentachloride at 95–100°. In this case the P(III) fragment is less easily identified, as it is 1 of the 3 moles of phosphorus trichloride produced in the reaction (eq. [2]).

[2] $ClCH_2P(O)Cl_2 + 3PCl_5 \rightarrow CCl_4 + POCl_3 + 3PCl_3 + 2HCl$
2

If less than 3 moles of phosphorus pentachloride are used, the excess **2** is recovered unchanged.

Tris(chloromethyl)phosphine oxide (**3**) also reacts smoothly with phosphorus pentachloride at 95–100°, but the product is not the expected bis(trichloromethyl)phosphinous chloride (eq. [3]). Neither $(CCl_3)_2PCl$ nor $(CCl_3)_3P$ is known.

[3] $(ClCH_2)_3PO + 7PCl_5 \not\rightarrow (CCl_3)_2PCl + CCl_4 + POCl_3 + 6PCl_3 + 6HCl$
3

A cleavage takes place, as evidenced by the formation of carbon tetrachloride and phosphorus oxychloride as cleavage fragments, but the principal product is a yellow crystalline complex (**4**), m.p. 119–122° decomp., of unidentified

[1]Present address: Southern Regional Research Laboratory, United States Department of Agriculture, New Orleans, Louisiana 70119.

Can. J. Chem. Downloaded from www.nrcresearchpress.com by 210.87.254.42 on 09/05/12
For personal use only.

structure, which breaks down when recrystallized from chloroform, with a slight exotherm and a substantial weight loss, giving trichlorobis(trichloromethyl)phosphorane (**5**) in 35% yield. The same unidentified complex (**4**) is obtained when an excess of phosphorus pentachloride is employed and the excess is subsequently removed by vacuum sublimation or destroyed by treatment with sulfur dioxide. If the phosphinous chloride is formed, as seems likely, it could give **5** either by disproportionation or by reaction with phosphorus pentachloride.

The phosphorane (**5**) is a white, crystalline solid, m.p. 193–194° decomp. (sealed tube), which has some remarkable properties. It is stable to air and moisture, and is not hydrolyzed even by boiling water, although aqueous ethanolic sodium hydroxide converts it to bis(trichloromethyl)phosphinic acid, m.p. 141–142° decomp. Its resistance to hydrolysis, unusual for a halophosphorane, is attributed partly to its extreme insolubility and partly to the inductive effect of the two trichloromethyl groups. At its decomposition point, **5** breaks down largely, but not entirely, to hexachloroethane and phosphorus trichloride (eq. [4]).

[4] $$\underset{\mathbf{5}}{(CCl_3)_2PCl_3} \rightarrow CCl_3CCl_3 + PCl_3$$

Tetrakis(chloromethyl)phosphonium chloride (**6**), $(ClCH_2)_4PCl$, does not react with phosphorus pentachloride under any conditions: in phosphorus oxychloride solution at reflux, with or without ultraviolet irradiation, or in the absence of a solvent up to 150°. It is also resistant to chlorination by elemental chlorine in C-58® octachlorocyclopentene under bright light illumination up to 130°, to sulfuryl chloride at 48°, and to benzenesulfonyl chloride at 210–220°.

Several aliphatic esters of chloromethylphosphonic acid were tested and found to be cleaved by phosphorus pentachloride, but the results were difficult to analyze because of the presence of the alkyl chlorides in the reaction mixtures. Phosphorus pentachloride is often used for the preparation of phosphonic dichlorides from the esters (6). It is obvious that some products, such as **2**, will not survive the 150° temperature required for cleavage of the second ester radical. The diphenyl ester (**7**), however, gives the product of chlorination without cleavage (eq. [5]).

[5] $$ClCH_2P(O)(OC_6H_5)_2 + 2PCl_5 \rightarrow \underset{\mathbf{7}}{CCl_3P(O)(OC_6H_5)_2} + 2PCl_3 + 2HCl$$

The cleavage of a carbon–phosphorus bond in a fluorine-containing ester, tetraethyl 3,3,4,4,5,5-hexafluoro-1-cyclopenten-1,2-ylenediphosphonate, was reported elsewhere (7). Another fluorine-containing ester, dibutyl difluoromethylphosphonate, was also cleaved by phosphorus pentachloride (8), but the products, butyl phosphorodichloridate and chlorodifluoromethane, were not those to be expected on the basis of the present work.

Discussion

A consideration of the various pathways which these reactions might follow suggests three possible mechanisms: (*a*) attack by PCl_5 on C—H, (*b*) attack by PCl_5 on P=O, and (*c*) a concerted attack on both (Chart 1).

An attack on C—H (path *a*) has considerable precedent in the literature, for it has been shown that substitutive chlorination without cleavage takes place when compounds such as $ClCH_2P(O)Cl_2$ (9), $CH_3(CCl_3)P(O)OH$ (10), or $(ClCH_2)_3PO$[2] (11–13) are treated with phosphorus pentachloride at 74–78°, i.e. below the cleavage temperature. Bannard *et al.* (9) identified phosphorus trichloride, hydrogen chloride, a trace of phosphorus oxychloride, and an unidentified crystalline substance, m.p. 175–177° decomp., as products of the reaction of **2** with phosphorus pentachloride at 74–78°. Reinhardt *et al.* (10) obtained **5** from methyl(trichloromethyl)phosphinic acid and phosphorus pentachloride, but gave no experimental details. Yakubovich and Ginsburg (11–13) reported that the reaction of **3**[2] with phosphorus pentachloride in phosphorus trichloride at gentle reflux gave, after hydrolysis, a 36% yield of chlorohydroxytris(trichloromethyl)phosphorane (**8**), m.p. 200–202° decomp., which was also obtained by the hydrolysis of dichlorotris(trichloromethyl)phosphorane (**9**), m.p. 190° decomp. (13). Two attempts were made to duplicate this experiment in the present work without success.

[6] $$\underset{\mathbf{3}}{(ClCH_2)_3PO} \xrightarrow{PCl_5} \underset{\mathbf{9}}{(CCl_3)_3PCl_2} \xrightarrow{H_2O} \underset{\mathbf{8}}{(CCl_3)_3P(OH)Cl}$$

Chlorination without cleavage is apparently possible at even higher temperatures if the

[2]Not tris(trichloromethyl)phosphine oxide, as given in the abstracts of refs. 12 and 13.

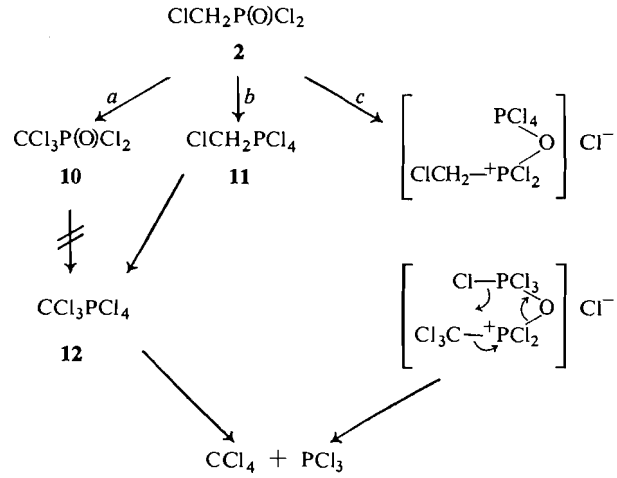

CHART 1

chlorinating agent is chlorine itself. The photochemical chlorination of **2** with chlorine gas gave trichloromethylphosphonic dichloride (**10**- as the end product, even in the presence of cata) lytic amounts of phosphorus pentachloride and reaction temperatures above 100° (14). Attempts to stop the chlorination at the dichloromethylphosphonic dichloride stage were unsuccessful (15). The photochemical chlorination of tetramethyldiphosphine disulfide, $(CH_3)_2P(S)P(S)(CH_3)_2$, in carbon tetrachloride at reflux gave **5** in 11% yield (10).

Trichloromethylphosphonic dichloride (**10**), once formed, is stable to further attack by phosphorus pentachloride. Its resistance was verified experimentally, thus eliminating path *a* from further consideration.

Path *b* calls for an exchange of phosphoryl oxygen for chlorine as the first step. An exchange in **2** would give tetrachloro(chloromethyl)phosphorane (**11**), which is known to be easily chlorinated to tetrachloro(trichloromethyl)phosphorane (**12**) (11, 12, 16, 17). This compound has a fairly low decomposition point, 125° decomp. (12, 16), and the products of its decomposition are known to be phosphorus trichloride and carbon tetrachloride (18). Trichlorobis(trichloromethyl)phosphorane (**5**), however, has a very high melting point, m.p. 193–194° decomp., and decomposes to a large extent in a different manner (eq. [4]). Path *b* is therefore unlikely, for **1** if not for **2**.

The most likely path appears to be *c*: an attack by PCl_4^+ on the phosphoryl oxygen, followed by rapid chlorination of the chloromethyl groups and expulsion of the oxygen as phosphorus oxychloride, perhaps via the intramolecular mechanism shown in the chart. Reaction does not occur with **6** because it has no phosphoryl oxygen, nor with **7** or **10** because the basicity of the phosphoryl oxygen is too low. The first step in this mechanism is patterned after Newman's mechanism for the reaction of phosphorus pentachloride with ketones (19, 20).

Experimental

Melting points were taken on a Fisher–Johns apparatus and are corrected. Infrared spectra were obtained with a Beckman IR-4 instrument, liquids neat and solids in Nujol. A careful examination of the infrared spectra of the compounds containing the CCl_3—P group failed to reveal any correlation to match the $ClCH_2$—P correlation (4). The C,H microanalyses were performed by Galbraith Laboratories, Inc., Knoxville, Tennessee.

Bis(chloromethyl)phosphinic Chloride(1)

Phosphorus pentachloride (62.4 g, 0.3 mole) was added in small portions to 12.6 g (0.1 mole) of bis(hydroxymethyl)phosphinic acid at 40°, allowing the exotherm and hydrogen chloride evolution to subside between additions. The reaction mixture was then heated at 80° for 3 h, cooled, filtered, and distilled, giving 6.5 g (36%) of **1**, b.p. 120–122° at 6 mm, n_D^{24} 1.5196, identical with the product of the thionyl chloride reaction (4).

Anal. Calcd. for $C_2H_4Cl_3OP$: Cl, 58.64; P, 17.08. Found: Cl, 58.2; P, 16.8.

The balance of the reaction products were lower boiling than **1**. The residue was negligible: 1.7 g.

On a 10-fold scale the lack of homogeneity led to difficulties. The reaction mixture was viscous and difficult

Can. J. Chem. Downloaded from www.nrcresearchpress.com by 210.87.254.42 on 09/05/12
For personal use only.

Can. J. Chem. Downloaded from www.nrcresearchpress.com by 210.87.254.42 on 09/05/12
For personal use only.

to stir, and local superheating was unavoidable. The yield of **1** dropped to 26%, and P(III) species were detected in the low-boiling fractions.

Cleavage of Bis(chloromethyl)phosphinic Chloride (1)

A mixture of 36.3 g (0.2 mole) of **1** and 208.5 g (1.0 mole) of phosphorus pentachloride was heated in an oil bath to 95–100°, whereupon an exothermic reaction set in, the phosphorus pentachloride dissolved, and copious amounts of hydrogen chloride were evolved. The reaction mixture was maintained at 95–100° for 1.5 h and then distilled, first at atmospheric pressure and then under vacuum, giving 38.2 g (87%) of trichloromethylphosphonous dichloride as a waxy solid, b.p. 60° at 15 mm, m.p. 41° (lit. (17) b.p. 69–70° at 23 mm, f.p. 47°).

Anal. Calcd. for CCl_5P: Cl, 80.5; P, 14.1. Found: Cl, 80.0; P, 13.8.

The other fragment, carbon tetrachloride, was isolated from the forerun by aqueous hydrolysis. The organic layer, separated and dried over anhydrous calcium sulfate, amounted to 15.1 g (48%), n_D^{20} 1.4634. Its identity as carbon tetrachloride was confirmed by infrared spectra.

In a separate experiment, **1** was recovered unchanged after being heated for 2 h at reflux with an excess of thionyl chloride.

Trichloromethylphosphonothioic Dichloride

The trichloromethylphosphonous dichloride (17.7 g, 0.08 mole) was heated in an oil bath with sulfur (2.5 g, 0.08 mole) and 0.1 g of anhydrous aluminium chloride (21) at 155–160° until the sulfur dissolved (30 min). The mixture solidified on cooling. The solid was washed with water, taken up in ethyl acetate, filtered to remove unreacted sulfur (1.0 g), and stripped of solvent, giving 8.8 g (35%) of crude trichloromethylphosphonothioic dichloride. Recrystallization from hexane gave the pure compound as a white, crystalline solid, m.p. 166–169° (lit. (22) orange solid, no m.p. given).

Anal. Calcd. for CCl_5PS: Cl, 70.26 (total), 28.10 (hydrolyzable); P, 12.28; S, 12.70. Found: Cl, 69.6 (total), 15.75 (hydrolyzable); P, 11.4; S, 13.28.

The principal infrared bands (in Nujol) were at 491 s (P—Cl), 546 s (P—Cl), 740 vs (C—Cl), 778 s (P=S), 798 m, 830 w, and 1267 w cm^{-1}. Only one of the two chlorines bound to phosphorus was hydrolyzable by the analytical technique used, i.e. by treatment with 0.1 *N* sodium hydroxide followed by titration with 0.1 *N* silver nitrate.

Cleavage of Chloromethylphosphonic Dichloride (2)

The reaction of 33.5 g (0.2 mole) of redistilled **2** with 83.2 g (0.4 mole) of phosphorus pentachloride, carried out exactly as described for **1**, gave only two distillate fractions: a low-boiling fraction, 86.0 g, b.p. 76–92°, n_D^{26} 1.4878, and a high-boiling fraction, 8.7 g, b.p. 78–79° at 8 mm, n_D^{26} 1.4962. The residue, n_D^{26} 1.4955, amounted to only 2.7 g. Another 6.2 g of liquid, n_D^{26} 1.4620, was collected in the trap.

The high-boiling distillate and the residue were recovered **2** (lit. (23) b.p. 78–79° at 10 mm, n_D^{20} 1.4978), amounting to 34%, i.e. one-third of the **2** used in the reaction. The low-boiling distillate and trap contents were combined and hydrolyzed by dropwise addition to water at 10–15°. The organic lower layer was separated, dried over anhydrous calcium sulfate, and distilled, giving 8.8 g (0.057 mole) of carbon tetrachloride, b.p. 76°, n_D^{20} 1.4612 (lit. (24) b.p. 76.5°, n_D^{20} 1.4602). Its identity was confirmed by infrared spectra. The aqueous layer was evaporated under reduced pressure and the residue taken up in water and stripped again. A titration showed that it contained phosphorous acid and phosphoric acid in 2.75:1 ratio. Calcd. PCl_3:$POCl_3$ ratio in eq. [2], 3:1.

A similar reaction between 0.2 mole each of **2** and phosphorus pentachloride resulted in a 69% recovery of **2**, the balance being lower-boiling products.

Cleavage of Tris(chloromethyl)phosphine Oxide (3)

A mixture of 19.6 g (0.1 mole) of **3** (25) and 167.0 g (0.8 mole) of phosphorus pentachloride was heated at 100–120° until the hydrogen chloride evolution subsided (3 h). The mixture, which contained suspended solids, was distilled until the liquid was removed, first at atmospheric pressure and then under vacuum. The distillate was worked up as in the preceding experiment, and was shown to contain carbon tetrachloride, 2.3 g (15%), b.p. 78–80°, n_D^{20} 1.4603, and a mixture of phosphorus trichloride and phosphorus oxychloride in 7.2:1 ratio. The residue was a crystalline solid containing some phosphorus pentachloride. A vacuum sublimation at 60° at 1 mm removed the excess (0.055 mole), leaving 38.9 g of **4** as a yellow, crystalline solid of unidentified structure.

Anal. Found: C, 6.93; H, 0.26; Cl, 81.4, 80.2 (total), 46.3, 45.8 (hydrolyzable); P, 10.93.

The principal bands in its infrared spectrum (in Nujol) were at 724 m, 780 vs (C—Cl), 817 w, 845 w, 970 w, 1078 s, and 1248 s cm^{-1}.

The product of another experiment in which the excess of phosphorus pentachloride was removed by treatment with sulfur dioxide analyzed as follows:

Anal. Found: Cl, 81.4 (total), 45.8 (hydrolyzable); P, 11.0.

The identity of the two products was confirmed by infrared spectra.

One recrystallization of **4** from chloroform, accompanied by a slight exotherm, gave 11.3 g (32%) of trichlorobis(trichloromethyl)phosphorane (**5**) as a white, crystalline solid, m.p. (sealed tube) 193–194° decomp. (lit. (10) m.p. (sealed tube) 187–188°).

Anal. Calcd. for C_2Cl_9P: C, 6.42; H, nil; Cl, 85.30 (total), 28.43 (hydrolyzable); P, 8.28. Found: C, 6.55; H, 0.17; Cl, 85.9 (total), 28.15 (hydrolyzable); P, 7.9.

The principal infrared bands in **5** (Nujol or Fluorolube®) were at 444 s (P—Cl), 555 s (P—Cl), 583 m, 709 w, 725 m, 735 w, and 780 vs (C—Cl) cm^{-1}. The spectrum was featureless above 780 cm^{-1}.

Bis(trichloromethyl)phosphinic Acid

Boiling water had no effect on the phosphorane (**5**); its melting point and hydrolyzable chlorine content were unchanged.

The phosphorane (1.50 g, 0.004 mole) was heated for 1 h at reflux with 100 ml of 1% sodium hydroxide solution and 100 ml of ethanol, cooled, extracted with ether, acidified with sulfuric acid, extracted again with ether, and the extract concentrated, giving 1.30 g of crude bis(trichloromethyl)phosphinic acid. Two recrystalliza-

Can. J. Chem. Downloaded from www.nrcresearchpress.com by 210.87.254.42 on 09/05/12
For personal use only.

tions from carbon tetrachloride gave the pure acid as a white, crystalline solid, m.p. 141–142° decomp.

Anal. Calcd. for $C_2HCl_6O_2P$ (molecular weight, 300.8): Cl, 70.7; P, 10.3. Found: Cl, 68.2; P, 10.5; neutralization equivalent, 296.7.

The principal infrared bands in the acid (Nujol or Fluorolube®) were at 752 m, 792 s (C—Cl), 843 m, 882 w, 1070 vs (P=O, H-bonded), 1120 s, 1273 w cm^{-1}, and two broad bands at 1700 w and 2300 w (P—OH) cm^{-1}.

Thermal Decomposition of Trichlorobis(trichloromethyl) phosphorane (5)

The phosphorane (3.75 g, 0.01 mole) was heated under nitrogen in an oil bath to 200°; it decomposed gently, starting at 184°, giving a distillate, 0.83 g, b.p. 69–70°, n_D^{20} 1.4921, which fumed and became warm on exposure to the air; lit. (24), b.p. 75°, n_D^{20} 1.5147 for phosphorus trichloride. The residue (2.22 g), which solidified on cooling, was distilled rapidly over a free flame, giving 1.32 g of a waxy solid, m.p. 161–166°, which also warmed on exposure to the air. After washing with water, there remained 0.92 g (39%) of crystalline solid, m.p. 180–181° (sealed tube), identified by infrared as hexachloroethane (lit. (26), m.p. 187° subl.).

Reaction with Diphenyl Chloromethylphosphonate (7)

A mixture of 12.9 g (0.05 mole) of 7 (27) and 10.4 g (0.05 mole) of phosphorus pentachloride began to evolve hydrogen chloride when heated to 100°. After 5 min the phosphorus pentachloride was all dissolved. The solution was cooled to 70°, treated with another 0.05 mole of phosphorus pentachloride, held at 100° for 1 h, and then distilled, giving 13.3 g (97%) of phosphorus trichloride, b.p. 74–76°, n_D^{25} 1.4965.

*Reaction with Trichloromethylphosphonic Dichloride (**10**)*

Phosphorus pentachloride (41.6 g, 0.2 mole) was mixed with 44.9 g (0.2 mole) of **10** (28) and heated at 120° for 1 h. The mixture began to fuse at 70° and was completely molten at 120°, but no volatile products were formed. The melt solidified on cooling to a hard mass of crystals.

Acknowledgments

I am grateful to Mr. Leon A. Zengierski for technical assistance and to Dr. Charles F. Baranauckas for his interest and encouragement.

1. I. S. Bengelsdorf. J. Am. Chem. Soc. **77**, 6611 (1955).
2. I. S. Bengelsdorf and L. B. Barron. J. Am. Chem. Soc. **77**, 2869 (1955).
3. A. W. Frank. J. Org. Chem. **29**, 3706 (1964).
4. A. W. Frank and I. Gordon. Can. J. Chem. **44** 2593 (1966).
5. L. H. Chance, E. K. Leonard, and G. L. Drake, Jr. Ind. Eng. Chem. Prod. Res. Develop. **5**, 252 (1966).
6. M. I. Kabachnik and P. A. Rossiiskaya. Izv. Akad. Nauk SSSR Otd. Khim. Nauk, 515 (1946); Chem. Abstr. **42**, 7242 (1948).
7. A. W. Frank. J. Org. Chem. **31**, 1521 (1966).
8. L. Z. Soborovskii and N. F. Baina. Zh. Obshch. Khim. **29**, 1144 (1959).
9. R. A. B. Bannard, J. R. Gilpin, G. R. Vavasour, and A. F. McKay. Can. J. Chem. **31**, 976 (1953).
10. H. Reinhardt, D. Bianchi, and D. Mölle. Ber. **90**, 1656 (1957).
11. A. Ya. Yakubovich, V. A. Ginsburg, and S. P. Makarov. Dokl. Akad. Nauk SSSR, **71**, 303 (1950).
12. A. Ya. Yakubovich and V. A. Ginsburg. Dokl. Akad. Nauk SSSR, **82**, 273 (1952); Chem. Abstr. **47**, 2685 (1953).
13. V. A. Ginsburg and A. Ya. Yakubovich. Zh. Obshch. Khim. **28**, 728 (1958); Chem. Abstr. **52**, 17091 (1958).
14. T. P. Traise and E. N. Walsh. U.S. Patent No. 2,924,560 (Feb. 9, 1960).
15. P. C. Crofts and G. M. Kosolapoff. J. Am. Chem. Soc. **75**, 5738 (1953).
16. A. Ya. Yakubovich and V. A. Ginsburg. Zh. Obshch. Khim. **24**, 1465 (1954).
17. L. D. Quin and C. H. Rolston. J. Org. Chem. **23**, 1693 (1958).
18. J. F. Nixon. J. Inorg. Nucl. Chem. **27**, 1281 (1965).
19. M. S. Newman and L. L. Wood, Jr. J. Am. Chem. Soc. **81**, 4300 (1959).
20. B. S. Farah and E. E. Gilbert. J. Org. Chem. **30**, 1241 (1965).
21. B. A. Arbuzov and N. I. Rizpolozhenskii. Izv. Akad. Nauk SSSR Otd. Khim. Nauk, 854 (1952); Chem. Abstr. **47**, 9903 (1953).
22. K. H. Rattenbury. U.S. Patent No. 2,993,929 (July 25, 1961).
23. M. I. Kabachnik and E. S. Shepeleva. Dokl. Akad. Nauk SSSR, **75**, 219 (1950).
24. A. I. Vogel. J. Chem. Soc. 1833 (1948).
25. D. M. Jones and T. M. Noone. J. Appl. Chem. London, **12**, 397 (1962).
26. F. K. Beilstein. Handbuch der organischen Chemie. Vol. I. 4th ed. F. Richter (*Editor*). Springer-Verlag, Berlin. 1958. p. 169.
27. M. A. McCall and R. L. McConnell. U.S. Patent No. 2,900,405 (Aug. 18, 1959).
28. K. C. Kennard and C. S. Hamilton. Org. Syn. Coll. Vol. IV, 950 (1963).

Can. J. Chem. Downloaded from www.nrcresearchpress.com by 210.87.254.42 on 09/05/12
For personal use only.

Hydrogen bonding in water and ice[1]

T. A. FORD[2] AND MICHAEL FALK[3]
Chemistry Department, Dalhousie University, Halifax, Nova Scotia
and
Atlantic Regional Laboratory, National Research Council of Canada, Halifax, Nova Scotia
Received April 23, 1968

The absorption bands due to the OH and OD stretching vibrations of HDO in ice were measured between 0 and −182° and compared with the corresponding bands in liquid water. Their frequencies were correlated with the intermolecular potential energies of H_2O and D_2O. The distributions of the intermolecular energies in ice and in water at different temperatures were derived from the profiles of the bands.

Canadian Journal of Chemistry, 46, 3579 (1968)

Introduction

Average intermolecular energies in water and ice may be calculated from thermodynamic measurements. These energies, however, are broadly distributed in liquid water, and to some extent also in ice (1); most hydrogen bonds being either weaker or stronger than the average.

In our previous paper (1), we showed how qualitative information about the broad distribution of hydrogen bonds in liquid water can be derived from the profiles of the OH and OD stretching bands (ν_3 and ν_1) of dilute HDO solutions in D_2O and in H_2O. In the present paper, we have extended the work by recording these bands in ice as a function of temperature and have compared them with the corresponding bands in water. We have correlated the intermolecular potential energies of H_2O and D_2O with the infrared absorption frequencies of HDO and have derived the distribution of energies from the spectroscopic data.

The relative contributions of hydrogen-bonding and van der Waals forces to the total intermolecular energy cannot be calculated accurately. For example, Pauling (2, 3) has made two different estimates of these contributions. We therefore use the term "hydrogen bond" qualitatively and have not attempted to separate the hydrogen bond energy from the total energy of interaction between water molecules.

Experimental

Spectra were recorded on a Perkin–Elmer model 521 grating spectrophotometer equipped with an automatic frequency marker. A low-temperature cell similar to that described by Wagner and Hornig (4) was used, the sample being held between silver chloride windows. An attenuator placed in the reference beam was adjusted to block off about 60% of the incident radiation to give a convenient base line position.

Ice films were prepared by freezing a capillary film of water, rather than by depositing the vapor on a cold surface, the method used in most previous studies of HDO in ice (5–7). Our technique ensured that the samples crystallized as hexagonal ice I (8, 9). The spectra showed that the samples crystallized completely between −10 and −25°. In no case was vitreous ice obtained, in contrast to the experience of Giguère and Harvey (10), probably because we cooled our films at the relatively slow rate of about 1° per minute.

A solution of approximately 0.3 mole % HDO in D_2O was used for studying the ν_3 band and 0.5 mole % HDO in H_2O for the ν_1 band. These concentrations led to convenient absorbances of about 0.3 for the two HDO bands in the ice spectra, at the commonly used thickness of 0.005 mm.

The thicknesses of the capillary films before freezing were estimated by comparing the absorbances with those recorded with a 0.050 mm cell. Thicknesses changed during freezing, causing uncertainty in the optical path. Use of unsealed films also introduced uncertainty in the HDO concentrations due to hydrogen–deuterium exchange with the atmosphere. This was particularly noticeable for the ν_3 band, the absorbance of which increased appreciably with time when the film was liquid. This exchange ceased once the films were frozen.

The temperature was measured with a copper–constantan thermocouple in contact with one of the silver chloride windows. The temperature scale was calibrated by observing the melting points of films of ice, anisole, ethyl acetate, methanol, and *n*-butyl ethyl ether. The accuracy of the temperature scale was about ±1°.

The spectra were recorded in several series of measurements at ascending and descending temperatures.

---

[1]Issued as NRCC No. 10 303.
[2]This work was carried out by T.A.F. at the Atlantic Regional Laboratory in partial fulfillment of the requirements for the Ph.D. degree at Dalhousie University.
[3]To whom requests for reprints should be addressed.

Can. J. Chem. Downloaded from www.nrcresearchpress.com by 210.87.254.42 on 09/05/12
For personal use only.

Results

Spectra

Spectra of a film of D_2O that contained about 0.3 mole % HDO, in the liquid at room temperature and in the solid at two temperatures, in the OH stretching region, are shown in Fig. 1. Corresponding spectra of a film of H_2O that contained about 0.5 mole % HDO, in the OD stretching region, are also shown. Thicknesses of these films were approximately 0.015 mm.

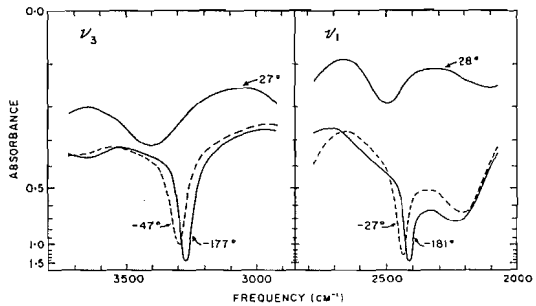

FIG. 1. Typical spectra of films of HDO, in D_2O in the OH stretching region (ν_3) (HDO concentration ~0.3 mole %), and in H_2O in the OD stretching region (ν_1) (HDO concentration ~0.5 mole %). Thickness of films ~0.015 mm.

Figure 1 shows that the ν_3 and ν_1 stretching fundamentals absorb near some of the bands of H_2O and D_2O (5, 6, 9, 10). We traced the base lines of the HDO bands by the tangent-to-tangent method (11). The choice of base line does not greatly affect the positions of the band maxima, but introduces an uncertainty in the absolute values of the half-widths and absorbances.

Frequencies

The frequencies of the band maxima are plotted in Fig. 2 along with those in liquid water from ref. 1. Owing to the sharpness of the bands in the ice spectra, the frequencies are reproducible to about ± 1 cm^{-1} and accurate to about ± 2 cm^{-1}. Our frequencies agree within experimental error with those reported in most previous infrared (6, 9, 12) and Raman (13) studies. The frequencies reported by Hornig *et al.* (5) are considerably higher than ours at comparable temperatures, probably because their samples contained some vitreous ice.

Half-widths

Figure 3 shows the half-widths. The standard deviation from a least-squares straight line is 5

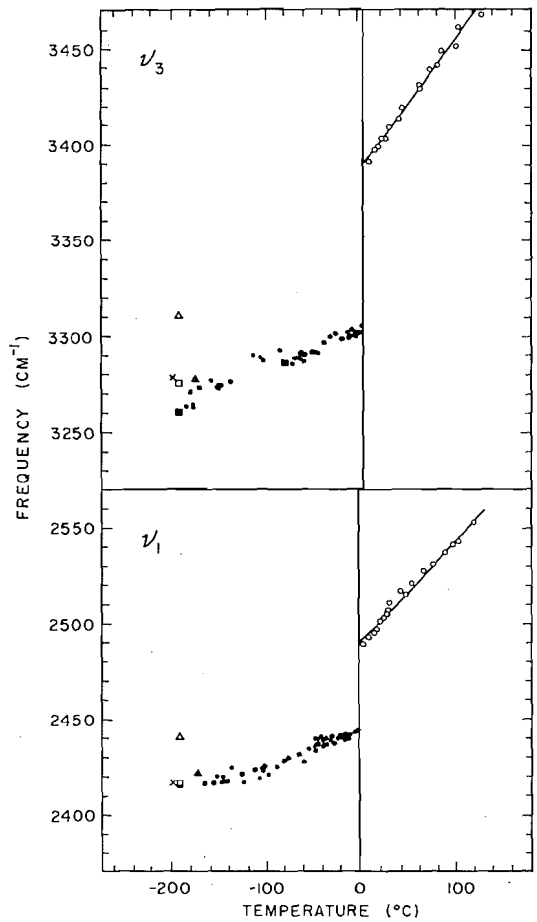

FIG. 2. Frequencies of the maxima of the ν_3 and ν_1 bands of dilute HDO in liquid water and in ice: (●) this work; (○) ref. 1; (△) ref. 5; (□) ref. 6; (▲) ref. 9; (■) ref. 12; (×) ref. 13.

cm^{-1} for ν_3 and 2 cm^{-1} for ν_1. The higher scatter for the ν_3 data is probably caused by the condensation of traces of water vapor on the silver chloride windows. Condensed H_2O would lead to apparent broadening of the ν_3 band but would not affect the ν_1 band. Frequencies of band maxima are not affected by traces of H_2O.

The half-widths appear to decrease linearly with decreasing temperature over the range investigated. The values of Haas and Hornig (6) and of Bertie and Whalley (9) are higher than ours, probably because the HDO concentrations of 5 to 10% used by them led to appreciable contributions to the half-widths from coupled vibrations of OH····OH and OD····OD pairs. The effect of increasing concentration on the

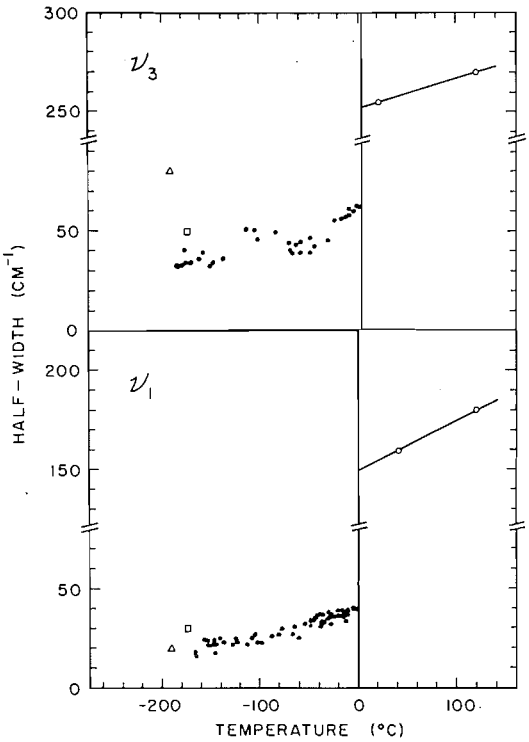

FIG. 3. Half-widths of the ν_3 and ν_1 bands of dilute HDO in liquid water and in ice: (●) this work; (○) ref. 1; (△) ref. 6; (□) ref. 9.

half-width of the ν_1 band is clearly shown in Fig. 3 of ref. 6.

Absorbances

The maximum absorbances increase by a factor of about two upon freezing. Further cooling of ice from 0 to −182° causes additional increase in the absorbances. Because the ice bands are narrower, their areas are similar to those of the corresponding bands in water. The uncertainty in the ratio of absorbances of ice and water is due largely to the $H \rightleftharpoons D$ exchange in the liquid film and the changes in film thickness upon freezing already mentioned.

Discussion

Origin of Band Widths in Water and Ice

The most striking difference in the spectra of ice and water is the far smaller half-width of ice. For example, the ν_1 band of HDO at 0° has a half-width of 149 cm^{-1} in water (1) but only 40 cm^{-1} in ice (see Fig. 3). It is interesting also to compare the half-width of the ν_1 band of ice I at −173°, found here to be 18 cm^{-1}, with that of ice II at this temperature, estimated by Bertie and Whalley (14) to be *less than* 5 cm^{-1}.

Ice II is reported to have a fully ordered structure (15), and its band width is probably due to overtone bands, sum and difference bands, and hot bands involving low-lying frequencies. Difference bands and hot bands would disappear at absolute zero, while overtones and sum bands would remain independent of temperature. Data for temperatures below −182° are lacking, and the detailed contributions to band width are still largely unknown (14).

That the half-width of the ν_1 band of ice I at −173° is *at least* 13 cm^{-1} greater than that of ice II is probably due to the permanent orientational disorder of the hydrogen positions in ice I (9, 16). This leads necessarily to a small disorder of the oxygen positions (9) and hence to broadening of the distribution of intermolecular energies, which would be expected to persist down to absolute zero[4].

The immense band width of HDO in liquid water appears to be due largely to the broad distribution of molecular interactions characteristic of the liquid state (1, 17). In our discussion we assume that the *whole* band width arises from this distribution and thus neglect contributions from the overtone, combination, and hot bands, as well as contributions from lifetime broadening. The sum of these is probably only a small fraction of the band width in the liquid (1, 17).

Correlation of HDO Frequencies with the Potential Energies of Molecular Interactions

It is now generally accepted (18) that the frequency shift $\Delta\nu$, of an OH stretching vibration upon hydrogen bonding, or upon molecular interaction in general, is a measure of the energy of the interaction. A linear relationship between $\Delta\nu$ and hydrogen bond strength was first observed by Badger and Bauer (19), who plotted the heat of vaporization of various compounds against the frequency shift for the fundamentals and second overtones. Recently, Drago and his co-workers (20–23) found a linear relationship between enthalpies of formation and OH stretching frequency shifts for hydrogen-bonded complexes of phenols with several bases, and

[4]We have attempted unsuccessfully to record the spectra of HDO in ice at liquid helium temperatures, but hope to obtain such spectra in the future.

Can. J. Chem. Downloaded from www.nrcresearchpress.com by 210.87.254.42 on 09/05/12
For personal use only.

Can. J. Chem. Downloaded from www.nrcresearchpress.com by 210.87.254.42 on 09/05/12
For personal use only.

justified this theoretically (21). Lippincott and Schroeder (24) also correlated $\Delta\nu$ with the hydrogen bond energy as calculated by using a one-dimensional potential function for the hydrogen bond. Other empirical relationships between hydrogen bond energy and $\Delta\nu$ are quoted by Pimentel and McClellan (25).

It seems reasonable to expect a correlation between the vibrational frequencies of HDO in the condensed phases at different temperatures, and some thermodynamic measure of the energy of molecular interaction. The most commonly used thermodynamic measures of the average interaction energies of ice and water are the enthalpy of sublimation, ΔH_{sub}, and of vaporization, ΔH_{vap} (25). Alternative measures would be the corresponding internal energies ΔU_{sub}, or ΔU_{vap}, which are easily obtained from the enthalpies (see Appendix I). ΔH_{sub} and ΔU_{sub} for ice are unsatisfactory, however, because both exhibit a maximum, near -60 and $-125°$ respectively (26), whereas the hydrogen bond strength would be expected to *decrease* regularly with increasing temperature for ice and water, with a discontinuity at the melting point.

The reason for this discrepancy is that ΔU_{sub}, or ΔU_{vap}, is not simply the energy used in overcoming the intermolecular forces in the crystal or liquid. Because of the differences in molecular motion in the vapor (vibrations, rotations, and translations) and condensed phases (intramolecular and intermolecular vibrations), there is a difference in average kinetic energy of the molecules in these phases at the same temperature. ΔU_{sub} or ΔU_{vap} is therefore the algebraic sum of the changes in potential energy, ΔU_{pot}, and kinetic energy, ΔU_{kin}, upon sublimation or vaporization, i.e.

$$\Delta U_{total} = \Delta U_{pot} + \Delta U_{kin}$$

ΔU_{pot} corresponds to the energy expended in transferring a molecule from the condensed phase to the vapor at the same temperature, with all the vibrational, rotational, and translational motions (including zero-point vibrations) stopped in the initial and final states. ΔU_{kin} is the kinetic contribution of the vapor less that of the crystal or liquid at the same temperature. In Appendix I, ΔU_{total} is derived from thermodynamic data. The kinetic contributions to the internal energy of vapor, liquid, and crystal, used to calculate ΔU_{kin}, are computed in Appendix II.

TABLE I

Kinetic and potential contributions to the total internal energy of vaporization of water and of sublimation of ice (kcal mole^{-1})

	ΔU_{total}*	ΔU_{kin}†	ΔU_{pot}
	H_2O		
Water, 130°	8.578	−2.094	10.672
Water, 100°	8.980	−1.885	10.865
Water, 50°	9.612	−1.647	11.259
Water, 0°	10.221	−1.485	11.706
Ice, 0°	11.656	−1.646	13.302
Ice, −100°	11.775	−1.581	13.356
Ice, −173°	11.740	−1.682	13.422
	D_2O		
Water, 300°	5.593	−3.991	9.584
Water, 200°	7.738	−2.690	10.428
Water, 120°	8.865	−2.079	10.944
Water, 100°	9.132	−1.932	11.064
Water, 50°	9.784	−1.635	11.419
Water, 4°	10.362	−1.338	11.700
Ice, 4°	11.866	−1.531	13.397
Ice, −100°	12.175	−1.340	13.515
Ice, −173°	12.130	−1.420	13.550

*See Appendix I.
†See Appendix II.

The values of ΔU_{total}, ΔU_{kin}, and ΔU_{pot} for H_2O and D_2O are collected in Table I.

Apart from the expected discontinuity at the melting point, ΔU_{pot} decreases smoothly with increasing temperature. ΔU_{kin} and ΔU_{total}, in contrast, both reach a maximum near $-125°$ (26). We therefore chose to base our energy–frequency correlation on ΔU_{pot}.

Due to the uncertainty in the estimated intramolecular and intermolecular frequencies of H_2O and D_2O (see Appendix II), the absolute values of ΔU_{pot} are probably only correct to ± 1 kcal mole^{-1}. This is satisfactory for our purpose.

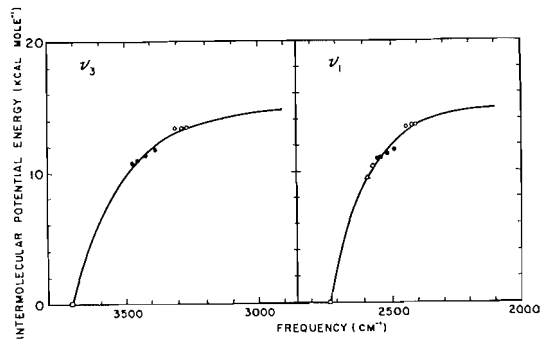

FIG. 4. Correlation of intermolecular potential energy of H_2O with ν_3 frequency of HDO, and D_2O with ν_1 frequency of HDO: (○) this work; (●) ref. 1; (□) ref. 27; (△) ref. 28.

Can. J. Chem. Downloaded from www.nrcresearchpress.com by 210.87.254.42 on 09/05/12
For personal use only.

The values of ΔU_{pot} for H_2O and D_2O are plotted against the ν_3 and ν_1 frequencies of HDO[5] in Fig. 4. A correlation curve was sought which fitted the experimental points as closely as possible, and was constrained to pass through the zero of intermolecular potential energy at the frequency, ν_0, of the ν_3 (or ν_1) vibration of HDO vapor (27). A straight line would not be satisfactory, and of several curves tested, the best fit was obtained with an empirical function of the form

$$\Delta U_{pot} = a[1 - \exp(-b\Delta\nu)]$$

where a and b are adjustable parameters and $\Delta\nu = \nu_0 - \nu$. A least-squares procedure led to the optimal values of $a = 15.089$, $b = 5.00 \times 10^{-3}$ for ν_3; and $a = 15.080$, $b = 7.19 \times 10^{-3}$ for ν_1.

A lengthy and somewhat uncertain interpolation spans the ΔU_{pot}–$\Delta\nu$ data for the liquid and the point for the vapor. This interpolation is somewhat shorter and hence less uncertain for the ν_1 correlation because of the additional frequency data of Franck and Roth (28).

Distribution of Hydrogen Bond Strengths in Water and Ice

The profiles of the ν_3 and ν_1 bands of HDO in ice and water (1) were normalized to unit peak absorbance and converted to the intermolecular potential energy scale using the correlation curves of Fig. 4. Figure 5 shows typical energy profiles for ice and water.

Most assumptions made in deriving Fig. 5 have been discussed above. An additional assumption is that the absorbance profiles of the ν_3 (or ν_1) bands represent directly the number of OH (or OD) groups vibrating at a given frequency. This neglects the variation of relative absorptivity of the OH (or OD) groups with frequency, discussed by Wyss and Falk (17).

The above assumptions are not strictly valid and their use leads to some uncertainties in the calculated distributions. In addition, there are experimental errors in the profiles of the absorption bands (for example, the crossing of the two liquid curves at 13.5 kcal mole^{-1} for D_2O is certainly an error), an error of up to 1 kcal mole^{-1} in the calculated values of ΔU_{pot} in Table I, and an uncertainty in plotting the correlation curves. These uncertainties are not serious, however, and the form of the distribution curves in Fig. 5 is certainly correct. The positions of the maxima and the half-widths of the distributions are probably correct to about $\pm 10\%$ and the total range of the distributions to about $\pm 20\%$. The curves are probably least accurate at their extremes, because of uncertainty in the choice of base lines.

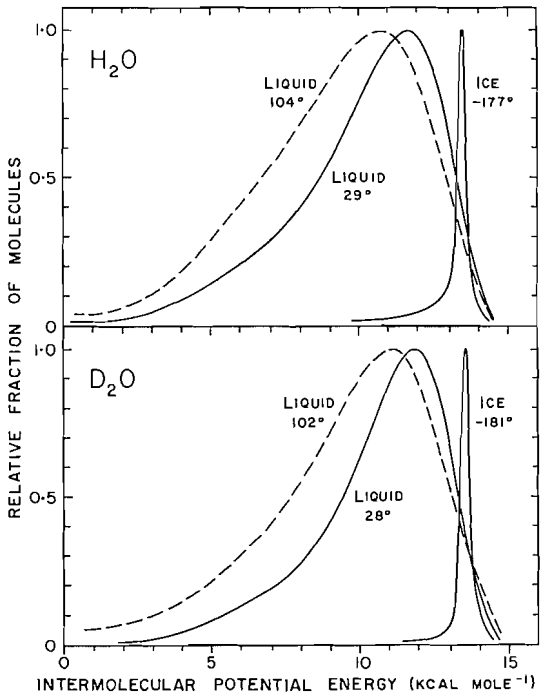

FIG. 5. Distribution of intermolecular potential energies in water and ice for H_2O and D_2O.

Comparison of the energy distribution profiles of liquid H_2O and D_2O at room temperature shows that the peak energies are essentially the same (11.75 kcal mole^{-1} for H_2O at 29° and 11.90 kcal mole^{-1} for D_2O at 28°), as are the profiles on the high energy side of the curves. On the low energy side the profiles of the D_2O curves are considerably narrower than those of H_2O. Part of this difference is caused by the shapes of the correlation curves of Fig. 4. Their nonlinearity distorts the spectral profile and tends to exaggerate any differences between the ν_3 and ν_1 bands. A difference between the two distributions

[5]It appears reasonable to expect that OH groups of HDO molecules in dilute solution in D_2O have the same distribution of molecular interactions as OH groups of H_2O molecules in pure H_2O at the same temperature, and that the same should be true of OD groups of HDO in dilute solution in H_2O and those of D_2O in pure D_2O.

Can. J. Chem. Downloaded from www.nrcresearchpress.com by 210.87.254.42 on 09/05/12
For personal use only.

would be expected, however, as the average intermolecular energy of D_2O is slightly higher than that of H_2O (29). Likewise, the maxima of the distribution curves for the ices are nearly equal (13.40 kcal mole^{-1} for H_2O at $-177°$ and 13.55 kcal mole^{-1} for D_2O at $-181°$), and the D_2O profile is narrower than that of H_2O, leading to a higher average intermolecular potential energy of D_2O ice, consistent with the findings of Whalley (30).

The distribution curves in Fig. 5 reveal some of the major differences between the liquid and the crystal:

(*i*) The peak of the intermolecular potential energy in water is lower than in ice. Part of the difference corresponds to the heat of fusion, 1.436 kcal mole^{-1} for H_2O (31) and 1.501 kcal mole^{-1} for D_2O (32), and part corresponds to the vibrational frequency shifts between water and ice (see Appendix II).

(*ii*) The distribution of intermolecular energies about their peak is many times wider in the liquid than in ice. Over 90% of energies in ice lie within 1 kcal mole^{-1} of the peak value, compared with only 10 to 20% in the liquid.

(*iii*) Some very weak molecular interactions, with energies lower than, say, 6 kcal mole^{-1}, occur in water. The enhanced motion of molecules at the sites of these interactions is responsible for the characteristic transport properties of the liquid. Such interactions occur too infrequently in ice to be spectroscopically detectable.

Acknowledgments

We wish to thank Dr. A. Cabana of the Department of Chemistry, University of Sherbrooke, for the use of the liquid helium facilities at his laboratory, Mr. P. F. Seto for assistance in the computations, Dr. C. R. Masson for helpful comments on the manuscript, and the Faculty of Graduate Studies, Dalhousie University, for providing financial assistance to one of us (T.A.F.).

Appendix I

Derivation of Total Internal Energies of Sublimation and Vaporization of Ice and Water

Internal energies of sublimation, ΔU_{sub}, and vaporization, ΔU_{vap}, of ice and water can be obtained from the corresponding enthalpies, ΔH_{sub}, and ΔH_{vap}, as follows:

$$[1]\quad \Delta U_{sub} = \Delta H_{sub} - P\Delta V_{sub} = \Delta H(\text{vapor}) - \Delta H(\text{crystal}) - P[V(\text{vapor}) - V(\text{crystal})]$$

$$[2]\quad \Delta U_{vap} = \Delta H_{vap} - P\Delta V_{vap} = \Delta H(\text{vapor}) - \Delta H(\text{liquid}) - P[V(\text{vapor}) - V(\text{liquid})]$$

The enthalpy of ice as a function of temperature was obtained by graphical integration of the heat capacity data for H_2O (33) and for D_2O (32). Internal energies of ice were assumed identical with the enthalpies at each temperature. From the enthalpies of H_2O liquid and vapor above 0° (34), the internal energies were obtained by subtracting the pressure–volume product for the liquid from that for the vapor at each temperature. Enthalpies and internal energies of D_2O liquid and vapor above 4° were obtained directly from the tables of Elliott (35). Enthalpies of vapor between the melting points and $-223°$ (36) were extrapolated linearly to $-273°$. The internal energies of vapor were assumed equal to the enthalpies at $-273°$ and to vary linearly with temperature. Heats of fusion and vaporization of H_2O were taken from ref. 31 and of D_2O from refs. 32 and 37.

From these data, graphs of enthalpy and internal energy against temperature for all three phases, crystal, liquid, and vapor, were constructed for H_2O and D_2O (26) taking zero enthalpy and internal energy to be those of H_2O and D_2O ice at $-273°$. From these graphs, internal energies of sublimation and vaporization, defined by relations [1] and [2], were obtained at several temperatures.

Appendix II

Derivation of Kinetic Contributions to the Total Internal Energies of Sublimation and Vaporization of Ice and Water

The vibrational contribution to the internal energy (or enthalpy) is the sum of the zero-point and non-zero-point energies given by:

$$[3]\qquad \Delta U_{z.p.} = \frac{1}{2} hc \sum_i \nu_i$$

and

$$[4]\quad \Delta U_{vib} = RT\sum_i (hc\nu_i/kT)/[\exp(hc\nu_i/kT) - 1]$$

where h is Planck's constant, c is the velocity of light, R is the gas constant, k is Boltzmann's constant, T is the absolute temperature, and ν_i are the fundamental frequencies.

TABLE II

Vibrational frequencies (cm^{-1}) of H_2O and D_2O used in the calculations

	ν_3	ν_1	ν_2	ν_R	ν_T
		H_2O			
No. of degrees of freedom	1	1	1	3	3
Vapor, all temps.	3755.8*	3651.7*	1595.0*	—	—
Liquid, 130°	3530†	3420†	1630‡	330§	85§
Liquid, 100°	3510†	3405†	1635‡	350§	90§
Liquid, 50°	3480†	3385†	1640‡	400§	105§
Liquid, 0°	3445†	3345†	1645‡	450§	115§
Ice, 0°	3370†	3270†	1655‡	560§	145§
Ice, −100°	3345†	3245†	1660‡	590§	155§
Ice, −173°	3330†	3230†	1665‡	615§	160§
Ice, −273°	3310†	3210†	1670‡	650‖	171‖
		D_2O			
No. of degrees of freedom	1	1	1	3	3
Vapor, all temps.	2789*	2666*	1178.7*	—	—
Liquid, 300°	2645†	2530†	1200‡	215§	65§
Liquid, 200°	2630†	2515†	1205‡	245§	75§
Liquid, 120°	2615†	2500†	1205‡	270§	80§
Liquid, 100°	2600†	2485†	1205‡	285§	85§
Liquid, 50°	2575†	2460†	1210‡	325§	100§
Liquid, 4°	2550†	2440†	1215‡	360§	110§
Ice, 4°	2505†	2395†	1220‡	435§	135§
Ice, −100°	2480†	2375†	1225‡	470§	145§
Ice, −173°	2470†	2370†	1225‡	490§	150§
Ice, −273°	2445†	2345†	1230‡	520‖	165‖

*Ref. 38.
†Estimated from ref. 39.
‡Estimated from ref. 9.
§Estimated from ref. 40.
‖Reference 40.

The frequencies used are collected in Table II. The intramolecular frequencies ν_1, ν_2, and ν_3 for the vapor were taken directly from Herzberg (38). In the condensed phases, however, intermolecular coupling of the motion of neighboring molecules causes the OH (or OD) stretching bands to become so broad that distinct features due to ν_3 and ν_1 can no longer be observed. We therefore used the ν_3 and ν_1 frequencies estimated by Whalley (39) for H_2O and D_2O, based on an assumed splitting between ν_3 and ν_1 of 100 cm^{-1}, as in the vapor. These frequencies are 3330 cm^{-1} and 3230 cm^{-1} for H_2O; and 2470 cm^{-1} and 2370 cm^{-1} for D_2O, at −173°. To obtain these frequencies for ice at temperatures other than −173°, and for water at any temperature, a linear relationship was assumed between the frequencies of the two stretching bands of H_2O (or D_2O) and the ν_3 (or ν_1) frequency of HDO for all three phases at all temperatures. These linear relationships gave the ν_3 and ν_1 frequencies of H_2O and D_2O in ice and in water over the wide range of temperatures studied (see Fig. 2).

The effect of intermolecular coupling is much smaller for the ν_2 vibration in ice, and this frequency is known at −173° with reasonable accuracy (9). The ν_2 frequency of ice and water at any temperature was calculated by assuming a linear variation of the ν_2 frequency of H_2O (or D_2O) with the ν_3 (or ν_1) frequency of HDO.

The intermolecular vibrations, ν_R and ν_T, in ice give absorptions centered at 840 cm^{-1} and 229 cm^{-1} in H_2O, and at 640 cm^{-1} and 222 cm^{-1} in D_2O (10, 41). Heat capacity calculations (40), however, show that the density of states near ν_R, at −273°, is approximately symmetrical about 650 cm^{-1} for H_2O, and 520 cm^{-1} for D_2O. Whalley (39) attributes the difference between these frequencies, and those of the maxima in the spectra, to distortions caused by variation of absorptivity with frequency. As the band maxima in this region do not represent the maxima in vibrational activity of the molecules, we chose Leadbetter's (40) frequencies for ν_R and ν_T of H_2O and D_2O ice at −273° and calculated them at other temperatures by assuming that they

Can. J. Chem. Downloaded from www.nrcresearchpress.com by 210.87.254.42 on 09/05/12
For personal use only.

varied linearly with the ν_3 (or ν_1) frequency of HDO, and were zero in the vapor phase.

The zero-point and non-zero-point energy contributions (calculated using eqs. [3] and [4] and the tables of Pitzer (42)) computed from the frequencies in Table II are recorded in Table III.[6] This table also gives the translational and rotational contributions.

1. M. FALK and T. A. FORD. Can. J. Chem. **44**, 1699 (1966).
2. L. PAULING. The nature of the chemical bond. 2nd ed. Cornell Univ. Press, Ithaca, New York. 1948. p. 304.
3. L. PAULING. The nature of the chemical bond. 3rd ed. Cornell Univ. Press, Ithaca, New York. 1960. p. 468.
4. E. L. WAGNER and D. F. HORNIG. J. Chem. Phys. **18**, 296 (1950).
5. D. F. HORNIG, H. L. WHITE, and F. P. REDING. Spectrochim. Acta, **12**, 338 (1958).
6. C. HAAS and D. F. HORNIG. J. Chem. Phys. **32**, 1763 (1960).
7. R. ZIMMERMANN and G. C. PIMENTEL. Proc. Intern. Meeting Mol. Spectry. 4th. Bologna, 1959. Vol. 2, 726 (1962).
8. K. LONSDALE. Proc. Roy. Soc. London, Ser. A, **247**, 424 (1958).
9. J. E. BERTIE and E. WHALLEY. J. Chem. Phys. **40**, 1637 (1964).
10. P. A. GIGUÈRE and K. B. HARVEY. Can. J. Chem. **34**, 798 (1956).
11. N. B. COLTHUP, L. H. DALY, and S. E. WIBERLEY. Introduction to infrared and Raman spectroscopy. Academic Press, Inc., New York. 1964. p. 75.
12. W. MAISCH. Ph.D. Thesis, Brown University, Providence, Rhode Island. 1956. Dissertation Abstr. **16**, 2323 (1956). *Quoted by* N. OCKMAN. Advan. Phys. **7**, 199 (1958).
13. M. J. TAYLOR and E. WHALLEY. J. Chem. Phys. **40**, 1660 (1964).
14. J. E. BERTIE and E. WHALLEY. J. Chem. Phys. **40**, 1646 (1964).
15. B. KAMB. Acta Cryst. **17**, 1437 (1964).
16. L. PAULING. J. Am. Chem. Soc. **57**, 2680 (1935).
17. H. R. WYSS and M. FALK. In preparation.
18. R. LUMLEY JONES. Spectrochim. Acta, **22**, 1555 (1966).
19. R. M. BADGER and S. H. BAUER. J. Chem. Phys. **5**, 839 (1937).
20. M. D. JOESTEN and R. S. DRAGO. J. Am. Chem. Soc. **84**, 3817 (1962).
21. K. F. PURCELL and R. S. DRAGO. J. Am. Chem. Soc. **89**, 2874 (1967).
22. T. D. EPLEY and R. S. DRAGO. J. Am. Chem. Soc. **89**, 5770 (1967).
23. R. S. DRAGO. Chem. Brit. **3**, 516 (1967).
24. E. R. LIPPINCOTT and R. SCHROEDER. J. Chem. Phys. **23**, 1099 (1955).
25. G. C. PIMENTEL and A. L. MCCLELLAN. The hydrogen bond. W. H. Freeman and Co., San Francisco. 1960. pp. 82–85.
26. T. A. FORD. Ph.D. Thesis. Dalhousie University, Halifax, Nova Scotia. 1968.
27. W. S. BENEDICT, N. GAILAR, and E. K. PLYLER. J. Chem. Phys. **24**, 1139 (1956).
28. E. U. FRANCK and K. ROTH. Discussions Faraday Soc. **43**, 108 (1967).
29. C. G. SWAIN and R. F. W. BADER. Tetrahedron, **10**, 182 (1960).
30. E. WHALLEY. Trans. Faraday Soc. **53**, 1578 (1957).
31. N. S. OSBORNE, H. F. STIMSON, and D. C. GINNINGS. J. Res. Natl. Bur. Std. A, **23**, 261 (1939).
32. E. A. LONG and J. D. KEMP. J. Am. Chem. Soc. **58**, 1829 (1936).
33. W. F. GIAUQUE and J. W. STOUT. J. Am. Chem. Soc. **58**, 1144 (1936).
34. R. W. BAIN. National Engineering Laboratory steam tables 1964. H.M. Stationery Office, Edinburgh. 1964.
35. J. N. ELLIOTT. At. Energy Can. Ltd. No. AECL-1673. 1963.
36. A. S. FRIEDMAN and L. HAAR. J. Chem. Phys. **22**, 2051 (1954).
37. F. D. ROSSINI, J. W. KNOWLTON, and H. L. JOHNSTON. J. Res. Natl. Bur. Std. A, **24**, 369 (1940).
38. G. HERZBERG. Infrared and Raman spectra of polyatomic molecules. D. Van Nostrand Co., Inc., Princeton, New Jersey. 1945. p. 207.
39. E. WHALLEY. Paper presented to 18th mid-America symposium on spectroscopy. Chicago, May 15–18, 1967.
40. A. J. LEADBETTER. Proc. Roy. Soc. London, Ser. A, **287**, 403 (1965).
41. J. E. BERTIE and E. WHALLEY. J. Chem. Phys. **46**, 1271 (1967).
42. K. S. PITZER. Quantum chemistry. Prentice-Hall, Inc., Englewood Cliffs, New Jersey. 1953. pp. 457–467.

[6]Table III has been placed in Depository of Unpublished Data. Photocopies may be obtained free of charge, upon request, from: Depository of Unpublished Data, National Science Library, National Research Council of Canada, Ottawa, Canada.

Can. J. Chem. Downloaded from www.nrcresearchpress.com by 210.87.254.42 on 09/05/12
For personal use only.

Can. J. Chem. Downloaded from www.nrcresearchpress.com by 210.87.254.5 on 09/05/12
For personal use only.

Hydrogen bonding in sulfanes

E. MULLER AND J. B. HYNE
Fundamental Sulphur Research Group, Alberta Sulphur Research Ltd., Department of Chemistry, University of Calgary, Calgary, Alberta

Received June 3, 1968

The position of the proton signals in the nuclear magnetic resonance spectrum of sulfanes (H_2S_x) is dependent on the sulfur chain length, the sulfane concentration, and the temperature. These proton chemical shifts are interpreted in terms of sulfane–sulfane interactions and intramolecular hydrogen bonding in sulfanes. Supporting evidence is provided by the position and appearance of the SH-absorption bands of the sulfanes in the infrared, which also establishes the existence of sulfane–solvent interactions.

It is concluded that sulfanes participate in hydrogen bonding interactions and it is suggested that there may be a special type of intramolecular hydrogen bonding operative in H_2S_3.

Canadian Journal of Chemistry, 46, 3587 (1968)

Introduction

While the phenomenon of hydrogen bonding has been well established as having a profound influence on the physical and chemical properties of water and hydrogen peroxide (1), little has been reported on the similar influence, if any, of hydrogen bonding in the analogous hydrogen polysulfide (sulfane) series of compounds. Although it is generally accepted that S—H···B type hydrogen bonds are weaker than O—H···B bonds (2), hydrogen bonding involving thiol groups and sulfur as a base has been observed in some systems (3). Furthermore, in the sulfane sequence it is possible to study the specific effects of hydrogen bonding across a much larger range of the homologous series since specific sulfanes up to H_2S_6 are accessible for study compared with the much shorter sequence of H_2O and H_2O_2 in the analogous oxygen series.

The fact that the various terminal protons in a sequence of low molecular weight sulfanes ($H_2S \rightarrow H_2S_6$) are characterized by discrete and identifiable nuclear magnetic resonance (n.m.r.) signals (4, 5) (because of the slow rate of exchange of the terminal protons) establishes the n.m.r. method as a powerful tool for the study of hydrogen bonding effects in sulfanes. This experimental technique has been fully exploited in the study reported here and has been complemented by parallel infrared investigations.

The effects of variation of solvent, concentration, temperature, and S-chain length of the substrate sulfanes have been examined with a view to elucidating the role of hydrogen bonding in sulfanes.

Results

Effect of Chain Length

In Table I, the position of the n.m.r. signals for the various lower homologues of the sulfane series in both CCl_4 and CS_2 solution are presented. The availability of high resolution n.m.r. spectrometers has permitted assignment of signals up to H_2S_9 compared with the previous limit of H_2S_6 (4, 5). As previously reported (4), the signal for H_2S_3 is anomalous in that it falls on the low field side of the smooth curve described by plotting the signals for other sulfanes against sulfur chain length. Schmidbaur *et al.* (4) suggested that this observation might reflect some special form of intramolecular hydrogen bonding in H_2S_3. The anomalous H_2S_3 proton signal position is observed in both CS_2 and CCl_4 solutions.

TABLE I

Position of sulfane n.m.r. signals in different solvents

	τ (p.p.m.)[a]	
Sulfane	CCl_4[b]	CS_2[b]
H_2S	9.33	9.23
H_2S_2	7.37	7.32
H_2S_3	6.02	5.97
H_2S_4	6.00	5.94
H_2S_5	5.86	5.81
H_2S_6	5.76	5.72[c]
H_2S_7	5.75	
H_2S_8	5.74	
H_2S_9	5.73	

[a]TMS internal reference.
[b]Total sulfane concentration: 1.0 mole l^{-1}.
[c]Average signal position for $H_2S_{\geq 6}$.

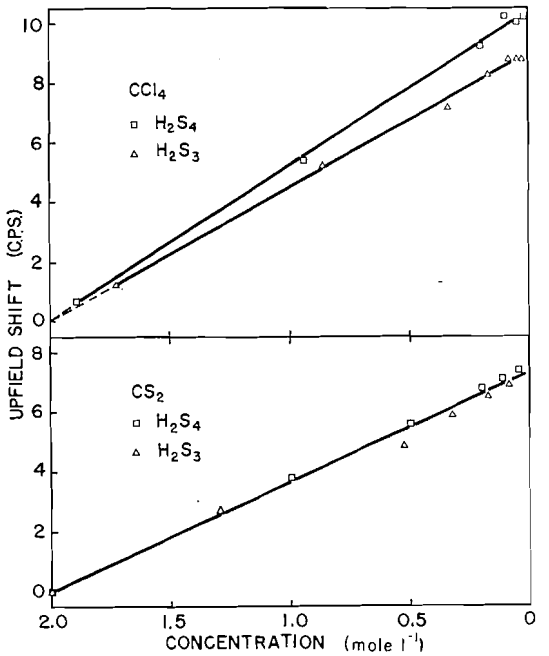

FIG. 1. Chemical shifts of sulfane proton signals as a function of concentration and solvent. Note: where necessary, the lines were extrapolated to a common base of 2 mole l^{-1}.

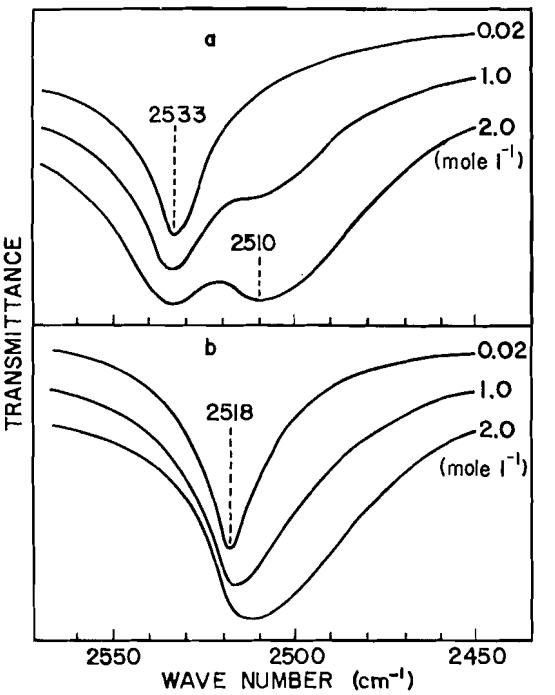

FIG. 2. SH-absorption bands of sulfanes (H_2S_3 and higher).

Concentration Effects

The effect of concentration upon the sulfane signal position is shown in Fig. 1. Upon dilution of a 2 *M* solution of H_2S_3 in CCl_4 with CCl_4, the H_2S_3 signal moved upfield by 8.8 ± 0.4 c.p.s. Comparatively, the H_2S_4 signal under the same conditions moved upfield by 10.0 ± 0.4 c.p.s. In CS_2 solution, however, the effect of dilution on the sulfane signal positions appears, within the experimental accuracy, to be the same for H_2S_3 and H_2S_4.

Figure 2 shows the effect of dilution on the shape and position of the S–H stretching absorption band of sulfanes. It should be noted that individually resolved peaks are not observed in the infrared for S–H stretching frequencies for each sulfane. In 2 *M* CCl_4 solutions, three SH-absorption bands were observed at 2596 (not shown in Fig. 2), 2533, and 2510 cm^{-1}, regardless of the composition of the sulfane mixture. The weak band at 2596 cm^{-1} originated from small amounts of H_2S dissolved in CCl_4. Upon dilution, the 2510 cm^{-1} band gradually became weaker and finally disappeared completely. In 2 *M* CS_2 solutions, apart from the H_2S absorption band at 2584 cm^{-1}, only one major absorption band was observed at comparatively lower wave numbers (2513 cm^{-1}). Upon dilution with CS_2, the bandwidth decreased and the absorption maximum shifted from 2513 to 2518 cm^{-1}. As in CCl_4 solution, the composition of the sulfane mixture had no effect on the position and appearance of the SH-absorption bands.

Temperature Effect

Decreasing temperature shifted the sulfane proton signal positions towards lower fields (Table II). The effect of lowering the temperature from +35 to −25 °C in CCl_4 solution is greater than in CS_2. Unfortunately, at −25 °C the n.m.r.

TABLE II

Chemical shift of sulfane proton signals as a function of solvent and temperature in 1 *M* solution

	Downfield shift in c.p.s. for $\Delta t = -60°$	
Sulfane	CCl_4	CS_2
H_2S_3	3.6±1	1.9±0.5
H_2S_4	4.0±1	2.5±0.5

Can. J. Chem. Downloaded from www.nrcresearchpress.com by 210.87.254.5 on 09/05/12
For personal use only.

Can. J. Chem. Downloaded from www.nrcresearchpress.com by 210.87.254.5 on 09/05/12
For personal use only.

resolution is poor and shift differences between signals of different sulfanes, if present at all, are difficult to establish. It appears, however, that the signal of H_2S_3 was affected less by the 60° temperature drop than the H_2S_4 signal.

Discussion

Intramolecular Hydrogen Bonding in Sulfanes

Evidence for preferential intramolecular hydrogen bonding in H_2S_3 is presented in Fig. 1. The upfield shift observed on dilution of H_2S_4 in CCl_4 is significantly greater than that for H_2S_3. As proton signals of solely intermolecularly hydrogen bonded species are shifted towards higher fields upon extended dilution, and proton signals of intramolecularly hydrogen bonded species are much less affected by a change of concentration (6), it appears that the hydrogen atoms of H_2S_3 are involved in both intermolecular and intramolecular hydrogen bonding, the latter of which will reduce the upfield shift of the H_2S_3 signals upon dilution relative to H_2S_4. In CS_2 solutions this effect is reduced below the limits of detection by the dilution method, presumably because CS_2 interacts with H_2S_3, thus interfering with its intramolecularly hydrogen bonded state by equilibrium [1]:

$$[1] \qquad H_2S_3(\text{intra}) + CS_2 \rightleftharpoons H_2S_3\cdots CS_2 \rightleftharpoons H_2S_3(\text{free}) + CS_2$$

This does not imply, however, that *all* intramolecular hydrogen bonding is removed in CS_2 solution since the H_2S_3 n.m.r. signal is still found at an abnormally low field in this solvent.

As the proton lifetime in any of the three sites, as given by equilibrium [1], is smaller than the reciprocal frequency differences between the sites, only one proton signal for each sulfane is observed, the position of which is in response to the time-averaged state of the equilibrium.

Intermolecular Interactions of Sulfanes

The observed downfield shift accompanying reduction in temperature (Table II) supports the argument of increased solute–solvent hydrogen bonding. A greater *increase* in hydrogen bonding with reduction of temperature would be expected in CCl_4, as opposed to CS_2, since a significant amount of sulfane/CS_2 bonding will already exist at room temperature. Despite the apparent difference in temperature dependence between H_2S_3 and H_2S_4, the uncertainties in the values preclude drawing any significant conclusions from the data.

Confirming results for the relative strength of the sulfane–solvent interactions were obtained by the infrared analysis (Fig. 2). In samples of high dilution, intermolecular interactions will be minimized. The SH-absorption band in very dilute solutions, therefore, originates from the absorption of solvated monomeric sulfanes. The SH-absorption band in dilute CCl_4 solutions was found at 2533 cm^{-1}, as compared with 2518 cm^{-1} in CS_2 solution, suggesting a stronger intermolecular sulfane–solvent interaction in CS_2 than in CCl_4. Recently, the SH-absorption band for the higher sulfanes in molten sulfur as solvent was reported to be at 2498 cm^{-1} (7). As the SH-absorption band for sulfanes is lowest in liquid sulfur, the sulfane–solvent interaction is strongest in this solvent, as might be expected.

For a given solvent, decreasing sulfane concentration was found to shift the n.m.r. signals of the sulfanes towards higher field positions (Fig. 1) suggesting a breakdown of sulfane–sulfane hydrogen bonding interactions.

The breakdown of these intermolecular hydrogen bonds upon dilution is most strikingly demonstrated by the infrared analysis. Sulfanes in concentrated CCl_4 solution exhibit two absorption bands in the SH-absorption region, the relative intensities of which are highly dependent on the concentration (Fig. 2). The gradual disappearance of the 2510 cm^{-1} band upon dilution must be due to the breakdown of intermolecular hydrogen bonds between the sulfanes. This band therefore may be assigned to the S–H stretching vibration of intermolecularly hydrogen bonded sulfanes. Comparatively, sulfanes in CS_2 exhibit only one broad absorption band at concentrations at which both monomeric and intermolecularly hydrogen bonded sulfanes exist. Apparently, in CS_2 solution, the SH-absorption bands of the monomeric and hydrogen bonded sulfanes overlap to such an extent that only one broad absorption band appears as a result. A complete analysis of the infrared and Raman spectra of H_2S_3 and H_2S_4, and of the valence force field calculations, is presently being carried out.

Experimental

Materials

Sulfane Mixtures

Two molar aqueous sodium tetrasulfide solutions were

acidified with diluted HCl, yielding a sulfane mixture of 0% H_2S_2, 18% H_2S_3, 33% H_2S_4, 17% H_2S_5, and 32% $H_2S_{\geqslant 6}$ (8). One molar solutions of these sulfane mixtures in CCl_4 and CS_2 were prepared for temperature studies.

H_2S_3 and H_2S_4 Solutions

Two molar solutions in CCl_4 and CS_2 were prepared by previously reported methods (8). Composition of the H_2S_3 solution (mole %): H_2S, 0; H_2S_2, 0; *H_2S_3, 88 ± 2*; H_2S_4, 6 ± 2; H_2S_5, 3.6 ± 0.5; and $H_2S_{\geqslant 6}$, 2.4 ± 0.5. Composition of the H_2S_4 solution (mole %): H_2S, 0; H_2S_2, 0; H_2S_3, 3 ± 2; *H_2S_4, 95 ± 2*; H_2S_5, 0; and $H_2S_{\geqslant 6}$, 2.0 ± 0.5. CCl_4 and CS_2: Fisher Scientific Co., spectrograde.

N.M.R. Analysis

A Varian A-60 high resolution spectrometer was used for n.m.r. analysis. For the studies of dilution series of sulfane solutions in the concentration range of 2 to 0.02 mole l^{-1}, the methyl proton signal of anisole was used as a secondary capillary reference standard and corrected to tetramethylsilane (TMS) = 10 p.p.m. scale. The spectra were run at a sweep time of 250 s using a sweep width of 500 and 100 c.p.s. The spectra of 1 *M* solutions of sulfane mixtures in CCl_4 and CS_2 were recorded at +35 ± 1 °C and −25 ± 1 °C with anisole as a secondary capillary reference standard. At 35 ± 1 °C, the spectra of these solutions were also taken with TMS as an internal reference standard.

Infrared Analysis

The infrared spectra of the S—H stretching vibration of sulfanes were recorded on a Beckman IR-7 infrared spectrophotometer in the 3000 to 2450 cm^{-1} range. The spectra were taken in KBr cells of 0.1 and 1.0 mm cell path. The spectra of highly dilute samples were taken in quartz cells of 50 mm cell path. Compensation for solvent absorption was provided.

Conclusions

N.m.r. and infrared spectroscopic examination of solutions of sulfanes in CS_2 and CCl_4 as a function of temperature and concentration clearly establishes the existence of hydrogen bonding in these systems. The experimental evidence points to the possibility of a special role for intramolecular hydrogen bonding in the particular case of H_2S_3.

1. P. PASCAL. Nouveau Traité de Chimie Minérale. Vol. I. Pt. 1. *Edited by* Masson and Cie. Paris. 1960. p. 493; Vol. XIII. Pt. 1. p. 501.
2. L. J. BELLAMY. The infrared spectra of complex molecules. John Wiley and Sons, Inc., New York. 1958. p. 351.
3. G. C. PIMENTEL and A. L. MCCLELLAN. The hydrogen bond. W. H. Freeman and Co., San Francisco. 1960. p. 201.
4. H. SCHMIDBAUR, M. SCHMIDT, and W. SIEBERT. Chem. Ber. **97**, 3374 (1964).
5. J. B. HYNE, E. MULLER, and T. K. WIEWIOROWSKI. J. Phys. Chem. **70**, 3733 (1966).
6. J. A. POPLE, W. G. SCHNEIDER, and H. J. BERNSTEIN. High resolution nuclear magnetic resonance. McGraw-Hill Book Co., Inc., New York. 1959. p. 414.
7. T. K. WIEWIOROWSKI and F. J. TOURO. J. Phys. Chem. **70**, 234 (1966).
8. E. MULLER and J. B. HYNE. Can. J. Chem. **46**, 2341 (1968).

Can. J. Chem. Downloaded from www.nrcresearchpress.com by 210.87.254.5 on 09/05/12
For personal use only.

Magnetic study of the hexachlororhodate(IV) ion

A. D. WESTLAND
Department of Chemistry, University of Ottawa, Ottawa, Canada
Received April 19, 1968

The magnetic susceptibilities and electron spin resonance spectra of solid solutions of cesium hexachlororhodate(IV) in a diamagnetic host lattice were examined over a range of temperatures. The Landé splitting parameter, g, was found to be 1.7545 ± 0.0005. This led to an orbital delocalization factor of 0.81 and a spin-orbit coupling parameter of 554 cm^{-1}. The susceptibility measurements failed to reveal any superexchange in the lattice but the electron spin resonance spectra gave some evidence for such coupling. Powder samples only were examined and these exhibited no hyperfine structure.

Canadian Journal of Chemistry, 46, 3591 (1968)

Can. J. Chem. Downloaded from www.nrcresearchpress.com by 210.87.254.40 on 09/05/12
For personal use only.

The electronic properties of hexachlororhodate(IV) have been the object of spectroscopic (1) and magnetochemical (2) studies. Considerable interest attaches to the spectroscopic studies because in electron transfer, only one state of the central ion plus one electron has low energy, viz. the filled subshell configuration t_{2g}^6. The charge transfer bands in $RhCl_6^{2-}$ occur at lower energies than in any other hexahalo complex of a transition metal. The magnetic properties too are especially amenable to interpretation (3).

Their magnetic susceptibility study led Feldman *et al.* (2) to conclude that there is a greater degree of π-bonding in $RhCl_6^{2-}$ than in $IrCl_6^{2-}$ and similarly, by their argument, one would conclude that the π-bonding in $RhCl_6^{2-}$ is greater than that in $RuCl_6^{2-}$. The contrast with $IrCl_6^{2-}$ is unexpected in view of the finding that there is strong π-bonding in K_2OsCl_6 while an examination of K_2RuCl_6 using a magnetic dilution technique failed to reveal similar evidence for strong π-bonding (4).

The technique referred to consists in following the change, if any, in molar susceptibility as the paramagnetic compound is diluted by an isomorphous, diamagnetic analogue. The evidence is indirect, based as it is upon an examination of the degree of superexchange which may occur between neighboring MCl_6^{2-} ions by means of the intermediary interaction of chlorine atoms on adjacent complex ions (5). If superexchange is observed, it follows that π-bonding is present. However, the absence of superexchange does not necessarily indicate that π-bonding is absent also: it may mean rather that there is simply no coupling between the chlorine atoms on adjacent anions. Feldman *et al.* (2) suggested that there is probably some superexchange interaction in Cs_2RhCl_6, but, as stated above, K_2RuCl_6 showed little if any such superexchange. The comparison of the third row analogues, K_2OsCl_6 and K_2IrCl_6 (6), showed that superexchange is marked in both compounds and especially so in the former. In order to determine whether there is some inconsistency in the properties of $RuCl_6^{2-}$ and $RhCl_6^{2-}$ respectively, it was decided to investigate Cs_2RhCl_6 further.

The investigation consisted in preparing mixed crystal systems $Cs_2(Rh,Pt)Cl_6$. The cesium salts were employed because Cs_2RhCl_6 was the only hexachloro compound of rhodium(IV) which Dwyer and Nyholm were able to prepare (7, 8) and even this was so unstable that it was not possible to obtain dry crystals without some reduction to Rh(III). Feldman *et al.* (2) did not record any such experience but reported acceptable rhodium and chlorine analyses of dry crystals. In our hands, however, the procedure for preparing Cs_2RhCl_6 did not yield a pure dry product, for determination of the oxidation state showed that upon drying, about one-third of the rhodium was reduced to Rh(III), in agreement with the findings of Dwyer and Nyholm (7).

Our most carefully prepared products possessed the same magnetic susceptibilities over a range of temperatures as those of Feldman *et al.* (2) so that we were disposed to doubt either the purity of the previous workers' product or our method of analysis for oxidation state. In order to be quite certain of our analyses, three independent titrimetric procedures were developed. These were devised with a view to accommodating the following exigencies:

(*a*) When Cs_2RhCl_6 is dissolved, chlorine is evolved and may be lost as gas.

Can. J. Chem. Downloaded from www.nrcresearchpress.com by 210.87.254.40 on 09/05/12
For personal use only.

(*b*) It seemed possible that there would be formation of some oxygen when Cs_2RhCl_6 reacts with water.

(*c*) The reducing agent must not be strong enough to reduce platinum when handling the mixed crystal samples.

Precautions designed to avoid error are described in the experimental section.

The three methods of analysis which were applicable to the cesium chlororhodate samples were as follows:

1. Reduction with Fe(II) ion followed by back titration with dichromate using an external indicator. Electrometric end-point detection with either platinum or gold electrodes was not satisfactory in the presence of rhodium(III).

2. Winkler's method for dissolved oxygen (9) was employed for the purpose of ascertaining whether any oxidizing power had been lost through formation of oxygen. In this method, a slurry of manganese(II) hydroxide in alkaline medium is the reducing agent. Upon acidifying the $Mn(OH)_3$ in the presence of iodide ion, iodine is liberated and this is titrated with thiosulfate.

3. Arsenious acid was used to reduce Rh(IV) to Rh(III). Platinum(IV) was not reduced. The excess of H_3AsO_3 was titrated with $KMnO_4$. This is the only method of the three which was applicable to $Cs_2(Rh,Pt)Cl_6$ solid solutions.

The three methods gave the same results when applied to a given sample of cesium chlororhodate. Different preparations gave slightly variable results. Analysis of highly dilute $Cs_2(Rh,Pt)Cl_6$ samples were considered to be uncertain because, after very prolonged treatment with H_3AsO_3, the samples were still faintly greenish in color. It should be pointed out that the solubility of samples which were very rich in Cs_2PtCl_6 were highly insoluble and the entrained rhodium was never entirely reduced. However, in the most dilute sample referred to below, reduction appeared to be at least 95% complete.

The magnetic susceptibilities of Cs_2RhCl_6 were determined by taking account of the partial reduction to Rh(III). The diamagnetic contribution of the reduced material was estimated using standard corrections (10) with the assumption that the Rh(III) compound was $Cs_2RhCl_5(H_2O)$.

The susceptibilities were measured in the range 88 to 298 °K. The electron spin resonance (e.s.r.) spectrum was obtained for the most dilute sample for which the susceptibility was determined and also for much more dilute samples of unknown rhodium(IV) concentration.

Results and Discussion

The most carefully prepared samples of cesium chlororhodate were found to consist of about 60 mole % Rh(IV) and to contain somewhat less chlorine than that required for Cs_2RhCl_6. Rh and Cl analyses were as follows.

Anal. Calcd. for Cs_2RhCl_6: Rh, 17.85; Cl, 36.56. Found: Rh, 17.7; Cl, 34.56, 35.06.

TABLE I

Magnetic susceptibility data for $RhCl_6^{2-}$. Molar susceptibilities × 10^3 are given for samples containing Rh(IV) in the following molar percentages: I, 59.7; II, 25.5; III, 7.9

Temperature (°K)	I	II	III
298	1.92	2.08	2.06
278	2.03	2.22	2.20
253	2.16	2.37	2.27
223	2.33	2.55	2.46
194	2.59	2.84	2.82
164	2.98	3.19	3.11
139	3.45	3.65	3.60
113	4.06	4.23	4.23
101	—	4.65	4.78
88	4.94	5.17	5.53

The corrected molar susceptibilities at various temperatures of a sample consisting of 59.7 mole % rhodium are listed in Table I. Similarly, susceptibilities of mixed crystal systems containing Cs_2PtCl_6 as a diluent are listed as well in columns headed by the mole percentage content of Rh(IV). The values for the 7.9 and 25.5% samples are only slightly greater than those for the 59.7% sample. The discrepancies are thus within the range of possible analytical error and cannot be considered as evidence for the uncoupling of superexchange interactions.

The Weiss constant θ in the susceptibility expression

$$\chi_M = C/(T + \theta) + A_p + A_d$$

where C is the Curie constant, T is temperature in °K, A_p is the temperature independent paramagnetism, and A_d is the diamagnetism, also gives an indication of superexchange. Positive

values of θ are related to the Heisenberg exchange parameter, J, by the expression

$$J = k\theta/3$$

where k is the Boltzman constant.

The parameters in the susceptibility expression can in principle be fitted by a least squares computer program. However, the parameters are so sensitive to the experimental data that this approach was discarded. Instead, the Landé splitting parameter, g, was obtained from e.s.r. spectra and the Curie constant evaluated from the relation

$$C = Ng^2\beta^2S(S + 1)/3k$$

The value found for g was 1.7545 ± 0.0005. A_d was taken as 218×10^{-6} c.g.s.u./mole. A fit of the remaining two parameters gave the values:

$$\theta = -28; A_p = 1.10 \times 10^{-3} \text{ c.g.s.u./mole}$$

The negative sign on θ is an indication that there is little, if any, superexchange. Moreover, the value of θ is not greatly affected upon dilution of the Cs_2RhCl_6—the value for the 7.9 mole % sample was −20°. In spite of this, there is some evidence of π-bonding between rhodium and chlorine as we shall proceed to show.

The expression

$$g = \frac{2}{3}(2k' + 1)$$

leads to the value 0.81 for the delocalization factor which compares well with the value 0.84 found (11, 12) for K_2IrCl_6 and $(NH_4)_2IrCl_6$. Since the delocalization factor k' is a measure of the probability of finding the unpaired electron about the metal atom, departure of k' from unity indicates that the electron spin is delocalized to some extent onto the ligands (13). This is generally believed to occur via dπ–pπ bonding.

On the other hand, no hyperfine structure was observed in the e.s.r. spectra, but as only powdered samples were examined, hyperfine structure would be very complex and difficult to resolve. It can be shown (11) that when the magnetic field direction makes an arbitrary angle with the axes of the $RhCl_6^{2-}$ group, each component of the doublet which should arise by interaction with the nucleus of ^{103}Rh should be split further into 19 components.

The most concentrated sample which was examined by e.s.r. spectrometry (7.9 mole % Rh(IV)) also showed a resonance indicating a free spin ($g = 2.0030$) which had an intensity of ~1/50 that of the main peak. The concentration of Rh(IV) in the more dilute samples was not determined owing to the unreliability of the analytical method with small concentrations of rhodium, but it was qualitatively evident that in the next, more dilute sample, the intensity of the weak resonance signal was ~1/100 that of the strong signal while in the most dilute sample, the weak signal could not be detected at all. We suggest that the weak resonance is due to spin interaction of nearest neighbor rhodium ions and represents transitions involving $S = 0$ and $S = 1$ states (14). The resonance line was asymmetric and appeared to consist of two lines lying less than 5 G apart. At 4 °K, the half-width of the weak, asymmetric signal was 15.5 G. The rapid weakening of the signal upon dilution may be ascribed to the sharp decrease in the probability of a given $RhCl_6^{2-}$ group having another $RhCl_6^{2-}$ group as one of its nearest anion neighbors.

It would be of interest to measure J for Cs_2RhCl_6, as was done for K_2IrCl_6 (13). We lacked the necessary equipment for obtaining e.s.r. spectra at various temperatures.

It appears that although spin delocalization onto the ligands is as great in $RhCl_6^{2-}$ as in $IrCl_6^{2-}$, the spin does not couple strongly with the spin on neighboring anions. The lattice of Cs_2RhCl_6 is expanded relative to K_2IrCl_6 because of the larger size of the cesium ion. This would have the effect of somewhat decreasing the exchange interaction. However, Johannesen and Candela (15) have investigated the effect of substituting cesium for smaller ions in hexachloroosmates and have found that the superexchange is diminished by a small amount only.

The behavior with respect to superexchange is similar to that of K_2RuCl_6. This suggests that superexchange is weak in compounds of the second row which have the K_2PtCl_6 structure, even though it is strong when the central atom is from the third transition row. In order to test the generality of this conclusion, we are currently examining the systems $K_2(Nb,Zr)Cl_6$ and $K_2(Ta,Zr)Cl_6$. Spin superexchange is detected in the e.s.r. experiments because this technique is extremely sensitive to the effect.

Can. J. Chem. Downloaded from www.nrcresearchpress.com by 210.87.254.40 on 09/05/12
For personal use only.

From the expression

$$A_p = N(2 + g)^2\beta^2/6\zeta$$

a value of 554 cm^{-1} is obtained for the effective spin-orbit coupling constant, ζ. This value is rather small compared with the free ion value of 1400 cm^{-1} for Ru^{4+}.

Experimental

Preparation of Samples

Cesium chlororhodate was prepared according to the procedure of Feldman *et al.* (2). Cesium chloroplatinate was prepared by precipitating the compound in the usual way and then treating the precipitate with the oxidizing wash solutions used in preparing Cs_2RhCl_6. This was done in order to ensure that the Cs_2PtCl_6 received treatment identical with that of the solid solutions. The solid solutions $Cs_2(Rh,Pt)Cl_6$ were prepared by coprecipitation from solutions containing variable relative amounts of chlororhodic and chloroplatinic acids. All preparations were green, varying from dark blue-green to a light leaf-green depending upon the concentration. X-ray powder photographs showed only a single set of lines characteristic of the structure type to which both of the compounds belong.

Analyses

The samples were placed in a small porcelain tray which was inserted into a nitrogen-filled vessel which contained the reducing solution. Upon closing the vessel, the tray was allowed to become immersed in the solution which was then stirred magnetically until the sample had either dissolved completely (rhodium-rich samples) or had acquired the yellow color of Cs_2PtCl_6 (platinum-rich samples). Reaction times of up to 4 h with the temperature maintained at 70 °C were permitted in order to ensure complete reduction. When 0.05 *N* Na_3AsO_3 was used as reductant, one drop of 0.002 *M* KIO_3 and 2 ml conc. HCl were added and the solution titrated with 0.05 *N* $KMnO_4$. A platinum electrode was employed, but it was not entirely satisfactory as an end-point detector. An external indicator ($Fe(phen)_3^{2+}$) was also used and these gave a more reliable detection of the end point.

Total rhodium and platinum were determined by X-ray fluorescence and chlorine by Volhard titration.

Magnetic Measurements

Susceptibilities were measured using a Gouy balance employing a field of 5200 G. The sample tube was suspended inside a copper jacket. The temperature of the jacket was controlled by a stream of cold gas produced by evaporation of liquid nitrogen from a Dewar vessel equipped with heaters which responded by negative feedback from a sensing thermocouple. The temperature was constant to within the sensitivity of the electronic control relay (Thermo Electric Co. type 80025).

The diamagnetic correction for the Cs_2PtCl_6 was our measured value, 208 $\times$ 10^{-6} c.g.s.u./mole.

E.s.r. spectra were obtained with a Varian V-4502 spectrometer with 100 kHz modulation. Spectra were measured at 77 and 4 °K. The strength of the magnetic field was obtained with a Varian F-8A proton fluxmeter.

Acknowledgments

The author wishes to express his appreciation to Dr. John Morton of the National Research Council of Canada for assistance with the e.s.r. spectra. Financial support from the National Research Council of Canada is also gratefully acknowledged.

1. C. K. Jørgensen. Mol. Phys. **4**, 231 (1961).
2. I. Feldman, R. S. Nyholm, and E. Watton. J. Chem. Soc. 4724 (1965).
3. A. H. Cooke, R. Lazenby, F. R. McKim, J. Owen, and W. P. Wolf. Proc. Roy. Soc. London, Ser. A, **250**, 97 (1959).
4. A. D. Westland. Can. J. Chem. **41**, 2692 (1963).
5. B. J. Judd. Proc. Roy. Soc. London, Ser. A, **250**, 110 (1959).
6. A. D. Westland and N. C. Bhiwandker. Can. J. Chem. **39**, 1284, 2353 (1961).
7. F. P. Dwyer and R. S. Nyholm. Nature, **160**, 502 (1947).
8. F. P. Dwyer, R. S. Nyholm, and L. E. Rogers. Proc. Roy. Soc. N. S. Wales, **81**, 267 (1947).
9. L. W. Winkler. Ber. **21**, 2843 (1888).
10. W. Klemm. Z. Anorg. Allgem. Chem. **244**, 377 (1940); **246**, 347 (1941).
11. J. H. E. Griffiths and J. Owen. Proc. Roy. Soc. London, Ser. A, **226**, 96 (1954).
12. K. W. H. Stevens. Proc. Roy. Soc. London, Ser. A, **219**, 542 (1953).
13. J. Owen. Proc. Roy. Soc. London, Ser. A, **227**, 183 (1955).
14. J. H. E. Griffiths, J. Owen, J. G. Park, and M. F. Partridge. Proc. Roy. Soc. London, Ser. A, **250**, 84 (1959).
15. R. B. Johannesen and G. A. Candela. Inorg. Chem. **2**, 67 (1963).

Can. J. Chem. Downloaded from www.nrcresearchpress.com by 210.87.254.40 on 09/05/12
For personal use only.

Can. J. Chem. Downloaded from www.nrcresearchpress.com by 210.87.254.6 on 09/05/12
For personal use only.

The chemical interpretation and the temperature dependence of the ^{14}N nuclear quadrupole resonance of aniline and several derivatives

C. T. YIM, M. A. WHITEHEAD, AND (IN PART) DONALD H. LO

Radiofrequency Spectroscopy Laboratory, Department of Chemistry, McGill University, Montreal 2, Quebec

Received November 10, 1967

The ^{14}N nuclear quadrupole resonance frequencies of aniline, *o*- and *p*-phenylene diamine, and *p*-chloro-, *p*-bromo-, and *p*-iodo-aniline were measured with a super-regenerative oscillator over a temperature range from 77 to 292 °K. The temperature dependence is analyzed. The chemical interpretation of the quadrupole coupling constants and asymmetry parameters is described.

Canadian Journal of Chemistry, **46**, 3595 (1968)

Introduction

Regenerative spectrometers (1, 2), using either magnetic field or frequency modulation (3, 4), have been used to measure ^{14}N nuclear quadrupole resonance (n.q.r.). The super-regenerative spectrometer has been used extensively to measure halogen n.q.r. (5–7); it has a greater sensitivity than the regenerative spectrometer, and the frequency modulation causes a smaller amplitude modulation. Consequently a super-regenerative spectrometer was used to measure the ^{14}N n.q.r. in aniline and several aniline derivatives. The ^{14}N n.q.r. frequencies in *p*-chloro- and *p*-bromo-aniline, and *p*-phenylene-diamine at 77 °K, have been measured with a regenerative spectrometer (8); these were remeasured with the super-regenerative spectrometer. The temperature dependence of the ^{14}N n.q.r. frequencies in aniline, *p*- and *o*-phenylene-diamine, *p*-iodo-, *p*-bromo-, and *p*-chloro-aniline was studied between 77 and 292 °K.

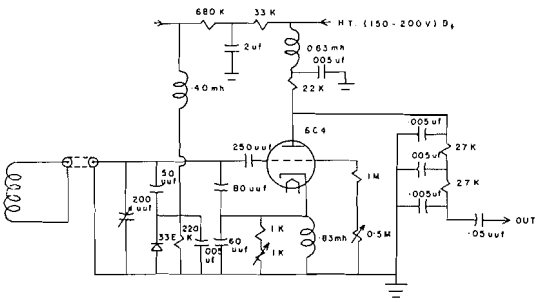

FIG. 1. Circuit diagram of the super-regenerative oscillator based on that of Narath, O'Sullivan, Robinson, and Simmons (9), but self-quenched. Modulation frequency 120 c.p.s. sine wave. Quench frequency 10–15 kc depending on the circuit parameters; thus in Fig. 2 the value was 13 kc.

Experimental

The super-regenerative spectrometer shown in Fig. 1 was self-quenched and frequency modulated sinusoidally (9). The signal was recorded using narrow band amplification and phase-sensitive detection (10, 11). The frequency sweep speed was 0.5 kc per min; the time constant was 8 s. The frequencies were determined using a calibrated BC 221 M frequency meter, standardized against the

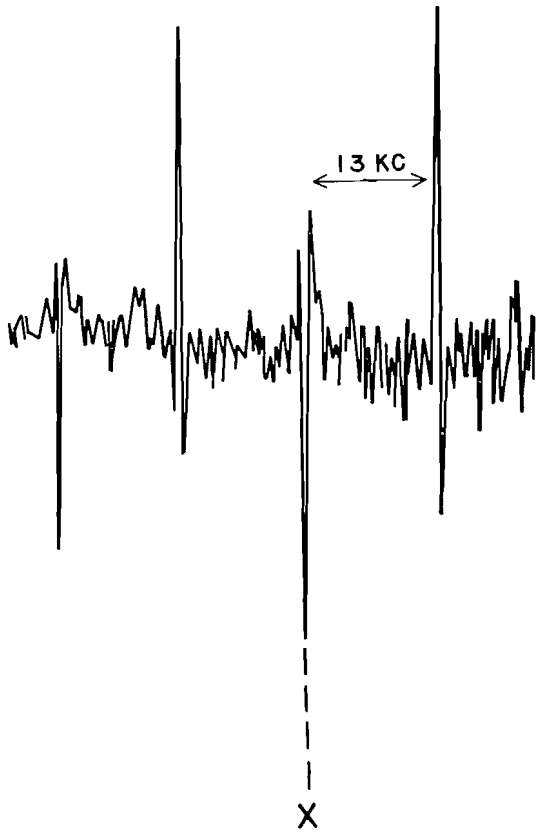

FIG. 2. ν_+ spectrum of *p*-chloro-aniline at 77 °K with a quench frequency of 13 kc.

Can. J. Chem. Downloaded from www.nrcresearchpress.com by 210.87.254.6 on 09/05/12
For personal use only.

WWV station frequency. The samples and resonance coil were immersed in liquid nitrogen or the appropriate slush (12) for low temperature measurements. All the samples were recrystallized from suitable solvents, and carefully melted into the sample tube, to avoid decomposition. Samples of 12, 18, or 40 cc were used depending on the signal strength and temperature. The recorded spectrum of the ν_+ line of *p*-chloroaniline at 292 °K is shown in Fig. 2; all the spectra were too weak to measure by oscilloscope display.

When a signal is recorded, the frequency of one line from the super-regenerative spectrometer coincides with the actual resonance frequency of the sample. Thus if the unknown signal is at (*a*) in Fig. 3(*i*) when the spectrometer sweeps through the signal, a spectrum such as Fig. 2 is obtained, since a super-regenerative spectrometer gives numerous side bands. One of the lines in the spectrum is selected as test line X (Fig. 2), and the spectrum is run through to the center of X. The spectrometer is then locked to this fixed frequency. The BC 221 M is tuned through this frequency to give the super-regenerative oscillator spectrum Fig. 3(*ii*) in which the fixed signal occurs as a side band. The quench frequency is then changed, a new BC 221 M spectrum obtained, and the n.q.r. signal frequency corresponds to the line (*a*) which does not shift. Each n.q.r. frequency was checked by fixing the frequencies of several different test lines X, in all cases the results were within the experimental error of ± 0.5 kc. This error is due to the difficulty of fixing the exact center of a line.

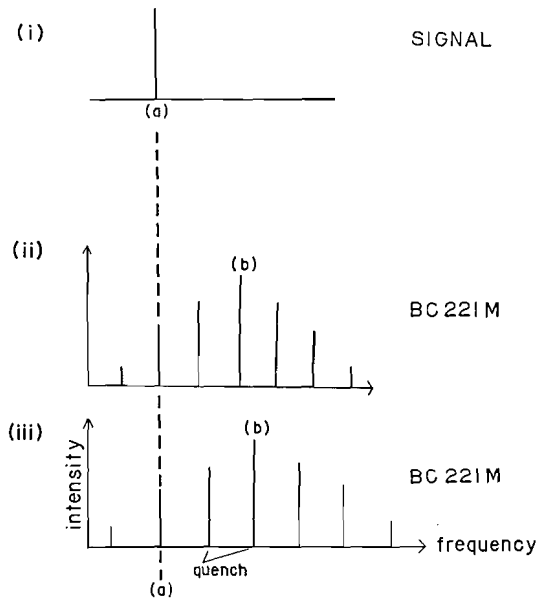

FIG. 3. The unknown signal frequency is at (*a*) in (*i*), the line spectrum is as Fig. 2, and X is the chosen line; (*ii*) shows the BC 221 M spectrum from sweeping through X; (*iii*) shows the BC 221 M spectrum at a different quench frequency; (*b*) marks the center line of the spectrum.

Since the method does not depend on the stability of the center band to varying quench frequency, it is possible to change the sensitivity of the spectrometer at a chosen quench frequency, by varying the various circuit parameters.

With B_+ at 250 V the voltages at the circumference of the coil and coil center were 4.0 and 2.5 V; at 200 V they were 3.0 and 2.0 V and at 150 V they were 2.0 and 1.5 V, respectively, with the 15 cc sample coil, of internal diameter 2.5 cm, wound from 18 gauge copper wire; the number of turns in the coil govern the coil's frequency.

Results and Discussion

1. The resonance frequencies, ν_+ and ν_-, the quadrupole coupling constants, e^2Qq/h, and the asymmetry parameters η, at 77 °K

These values are listed in Table I*a*.

The resonance frequencies ν_+ and ν_-, at various other temperatures are also given, and shown in Figs. 4, 5, and 6 for aniline, *p*-chloro- and *p*-bromo-aniline, and *o*-phenylene-diamine. The calculated coupling constants and asymmetry parameters are temperature dependent, but are given at 77 °K (Table I*a*); they are easily calculated for any other temperature using

$$[1a] \qquad e^2Qq/h = \tfrac{2}{3}(\nu_+ + \nu_-)$$

and

$$[1b] \qquad \nu_\pm = \frac{3e^2Qq}{4h}\left(1 \pm \frac{\eta}{3}\right)$$

respectively.

A strong piezoelectric effect occurs in *p*-iodoaniline below 195 °K (13, 14) so the resonance

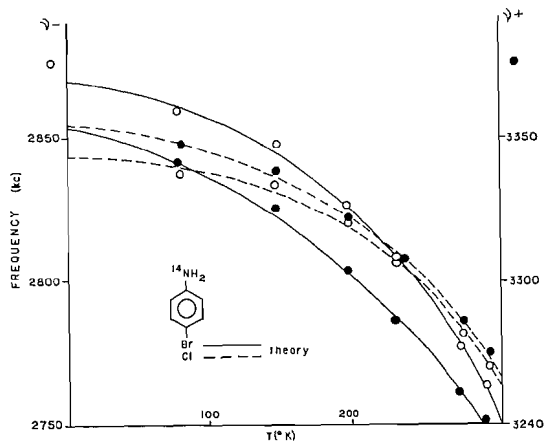

FIG. 4. The experimental points for the ν_+ and ν_- lines of *p*-chloro- and *p*-bromo-aniline, together with the calculated lines.

Note that the ν_- axis is calibrated on the left, and the ν_+ axis on the right.

TABLE I*a*

The ^{14}N n.q.r. frequencies ν, coupling constants e^2Qq/h and asymmetry parameters η, and the temperature dependence of the ν*

Molecule	e^2Qq/h (kc) at 77 °K	η (%) at 77 °K	Line	Frequency in kc ±0.5 kc at temperature (°K) 77	143	195	228	250	275	292
Aniline	3933	26.9	ν_+	3243.2	3234.5	3211.2	(210) (3201.7)	line vanished at 228 °K		
			ν'_+	3184.2	3176.2	3160.5	3146.0	3134.0		
			ν_-	2720.4	2716.0	2710.0	2704.3	2699.0		
			ν'_-	2650.0	2640.0	2618.0	2594.3	2578.0		
o-Phenylene-diamine	3773	33.1	ν_+	3150.6	3142.8	3134.0				3107.5
			ν'_+	3131.6	3121.5	3109.1				3074.0
			ν_-	2536.0	2533.8	2525.5				2500.0
			ν'_-	2497.3	2492.3	2484.2				2455.0
p-Phenylene-diamine	3910	26.4	ν_+	3190.5	Weak broad signals only					
			ν_-	2674.4						
p-Chloro-aniline	4116	24.3	ν_+	3337.5	3328.5	3311.5	3296.7		3275.0	3264.5
			ν_-	2836.5	2833.0	2819.8	2805.5		2780.7	2769.4
p-Bromo-aniline	4134	23.3	ν_+	3341.7	3325.5	3303.5	3286.0		3261.3	3351.1
			ν_-	2859.0	2848.2	2826.9	2808.0		2776.4	2763.7
p-Iodo-aniline	3766	33.1	ν_+			Piezoelectric effect				3136.0
			ν_-							2512.0

*Since $\nu_\pm = 3e^2Qq/4h\,(1 \pm \eta/3)$, the two lines ν_+ and ν_- coalesce when η is zero. The equations $e^2Qq/h = \frac{2}{3}(\nu_+ + \nu_-)$ and $(\eta/2)(e^2Qq/h) = \nu_+ - \nu_-$ allow e^2Qq/h to be calculated, with the average of $\nu_\pm$ and $\nu'_\pm$ used.
The frequency of *p*-iodo-aniline lies below that for *p*-bromo-aniline in contradiction to the predicted frequency in (8).

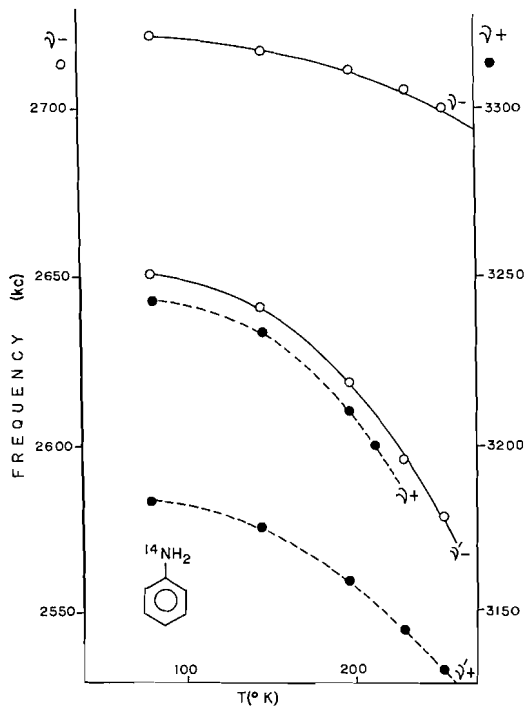

FIG. 5. The temperature dependence of the ν_+, ν'_+, ν_-, and ν'_- lines of aniline.
Note that the ν_- axis is calibrated on the left and the ν_+ axis on the right.

was only detected at 292 °K. The *p*-chloro- and *p*-bromo-aniline frequencies agree with those previously reported (8).

The signal line-width increased as the temperature decreased. While a super-regenerative oscillator cannot give absolute line-width measurement, it does give the right order of line-width (15). The line-width was not a function of the cooling procedure or rate, or of the time the sample was maintained at a given temperature;

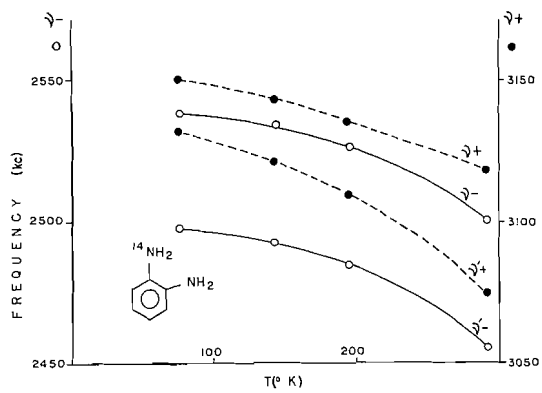

FIG. 6. The temperature dependence of the ν_+, ν'_+, ν_-, and ν'_- lines of *o*-phenylene-diamine.
Note that the ν_- axis is calibrated on the left and the ν_+ axis on the right.

Can. J. Chem. Downloaded from www.nrcresearchpress.com by 210.87.254.6 on 09/05/12
For personal use only.

Can. J. Chem. Downloaded from www.nrcresearchpress.com by 210.87.254.6 on 09/05/12
For personal use only.

therefore it is not due to crystal strain. The same phenomenon has been observed in NH_3 (16) and ethylene-diamine (17) and was attributed to magnetic dipole-broadening caused by the large proton magnetic moment (16, 17)[1].

TABLE I*b*

Some typical signal-to-noise ratios for *o*-phenylene-diamine, *p*-chloro- and *p*-bromo-aniline

Line	Sample volume (cc)	S/N for $B_+ = 150$ V at temperatures (°K) 77	196	292
o-Phenylene-diamine				
ν_+	18	4	7	10
	40	5	9	13
ν_-	18	0	6	13
	40	>1	7	17
p-Chloro-aniline				
ν_+	12	5	10	11
	40	7	16	17
ν_-	12	0	2	5
	40	>1	3	8
p-Bromo-aniline				
ν_+	40	9	9	9
ν_-	40	>1	3	8

The signal-to-noise ratio, S/N, decreased with decreasing temperature, except for the *p*-bromo-aniline ν_+ line in which S/N remained constant. The S/N are shown in Table I*b* for $\nu_\pm$ lines of *p*-chloro-aniline and *o*-phenylene-diamine at 77, 196, and 292 °K. The apparent decrease in S/N is partly due to line broadening.

The ν_+ line of aniline is a doublet up to 210 °K; at 228 °K the higher line vanishes; there was no phase change, and the lower ν_+ line and the ν_- doublet continued a smooth frequency change with increasing temperature.

To ensure that the decrease in S/N at 77 °K was not due to saturation effects, the measurements were carried out with a wide range of B_+. The S/N was constant for B_+ from 200 V to 125 V, below which it decreased markedly. Similar results were obtained by varying other circuit parameters. Measurements were carried out on 12, 15, 18, and 40 cc samples in several differently wound coils. The S/N of the ν_+ line increased with increased sample quantity, but still decreased by a factor of 10–15 at 77 °K; the ν_- line was enhanced sufficiently by the 40 cc sample to permit measurement at 77 °K. In view of the voltages involved in the coil it is not likely that saturation is responsible for the decrease in S/N. The S/N is actually improved by a large B_+ which causes larger coil voltages. However, the decrease in S/N with decreased temperature is important since, if common, it may prove a major obstacle to ^{14}N super-regenerative n.q.r.

2. *The ^{14}N n.q.r. temperature dependence of p-chloro- and p-bromo-aniline*

The principal axes of ^{14}N in *p-bromo*-aniline were established by a Zeeman study of a single crystal (8); the crystal structure is unknown. However, the crystal structure of *p-chloro*-aniline is known (18); the molecules are almost planar. Since chlorine and bromine are similar atoms, it can be assumed that the crystal structures and ^{14}N principal axes will be the same in *p*-bromo- and *p*-chloro-aniline. The temperature dependences of the ^{14}N n.q.r. frequencies can then be treated theoretically, although the assumption may cause minor errors.

Molecular torsional motions average the field gradient, thereby decreasing it with increasing temperature (19, 20). The ^{14}N n.q.r. frequencies and their temperature dependence are (21)

$$[2] \quad \nu_+ = \frac{3e^2Q}{4h} q\left\{\left(1 + \frac{\eta}{3}\right)(1 - 2\overline{\theta_x^2} - \overline{\theta_y^2}) - \frac{2}{3}\eta(\overline{\theta_z^2} - \overline{\theta_y^2})\right\}$$

and similarly for ν_-. The q and η are the stationary system values for the maximum field gradient component and the asymmetry parameter, and $\overline{\theta_x^2}$ etc. are the root-mean-squares of the angular displacements about three principal axes. Only if $\overline{\theta_z^2} \gg \overline{\theta_y^2}$ would the second term be large; the η values[2] in these substituted anilines are about 25%. Thermal data from X-ray crystallography (18) exclude this possibility in *p*-chloro-aniline; we assume this is also true in *p*-bromo-aniline. Therefore [2] becomes

$$[3] \quad \nu_+ = \nu_{+0}(1 - 2\overline{\theta_x^2} - \overline{\theta_y^2})$$

and similarly for ν_- with the coefficients reversed; $\nu_{\pm 0}$ are given by [1] and are the frequencies that would be observed in the absence of torsional

[1]This cause has been questioned, see ref. 48.

[2]The axes are: z perpendicular to ring, y along C—N bond, and x mutually perpendicular to z and y.

Can. J. Chem. Downloaded from www.nrcresearchpress.com by 210.87.254.6 on 09/05/12
For personal use only.

oscillations. The vibrational force constant is, quantum mechanically,

$$[4] \qquad K = 4\pi v^2 \theta$$

where θ is the moment of inertia, and v the torsional vibrational frequency, hence

$$[5] \quad \nu_+ = \nu_{+0}\left\{1 - \frac{h\nu_x}{K_x}\left[\coth\left(\frac{h\nu_x}{kT}\right)\right] - \frac{h\nu_y}{2K_y}\left[\coth\left(\frac{h\nu_y}{kT}\right)\right]\right\}$$

where x and y denote the field gradient axes; ν_- is similarly defined with x and y interchanged.

The terms $\nu_{\pm 0}$, v, and θ are temperature dependent under constant pressure (22, 23) but in a molecular crystal $\nu_{\pm 0}$ and θ are constants (24, 25) and only the volume dependence of v has to be considered. Thus

$$[6] \qquad v = v(T) = v(0)(1 - \alpha T)$$

where $v(0)$ is the vibrational frequency at an arbitrary zero of temperature and α an empirical constant particular to the axis considered (26); T is the temperature. The α accounts for the thermal expansion of the lattice, the anharmonicity in the torsional vibrations, and neglect of low frequency vibrational modes. Combining [5] and [6] gives

$$[7] \quad \nu_+ = \nu_{+0}\left\{1 - \left(\frac{h\nu_x(0)}{K_x(0)(1 - \alpha_x T)}\right) \cdot \left[\coth\left(\frac{h\nu_x(0)(1 - \alpha_x T)}{kT}\right)\right] - \left(\frac{h\nu_y(0)}{2K_y(0)(1 - \alpha_y T)}\right) \cdot \left[\coth\left(\frac{h\nu_y(0)(1 - \alpha_y T)}{kT}\right)\right]\right\}$$

and similarly for ν_-.

The θ were calculated from X-ray data (18) using average bond lengths (19). The McGill IBM 7044 computer was programmed for a least-square fit of the experimental ν_+ and ν_- against $\nu_{+0}, \nu_{-0}, \nu_x(0), \nu_y(0)\,\alpha_x$, and α_y; these parameters are listed in Table II. The standard deviation for both compounds is ± 2 kc. The torsional frequencies fall into the correct frequency region and in the correct order for the relative atomic weights, as can be seen by comparison with other torsional frequencies in Table II.

TABLE II

The theoretically calculated terms of [7]*

	Molecule	
Parameter	p-$ClC_6H_4NH_2$	p-$BrC_6H_4NH_2$
ν_{+0} (kc)	3351.1	3362.5
ν_{-0} (kc)	2850.3	2879.8
$\nu_x(0)$ (cm^{-1})	57.83	36.16
$\nu_y(0)$ (cm^{-1})	192.61	125.81
α_x (deg^{-1})	1.024×10^{-3}	4.622×10^{-4}
α_y (deg^{-1})	1.901×10^{-3}	1.548×10^{-3}

Comparable results

Molecule	Parameter	Value (cm^{-1} at 300 °K)	Reference
p-$Cl_2C_6H_4$	ν_z	94	28
	ν_x	54	
	ν_y	27	
$(CH_2)_6N_4$	ν	69.5 or 72	25
NH_3	ν_a	234	15
	ν_b	362	
ND_3	ν_a	213	15
	ν_b	260	
NF_3	ν_a	50	30
	ν_b	30	
C_2H_6	ν	275	29
C_2D_6	ν	200	29
CH_2Cl	ν	1355	29
p-$BrC_6H_4NH_2$	ν_{Br}	13.0	30

Molecule	Parameter	Value (deg^{-1})	Reference
$^{63}Cu_2O$	α	1.31×10^{-4}	31
$^{65}Cu_2O$	α	1.30×10^{-4}	31
$(CH_2)_6N_4$	α	3.5×10^{-4}	25

*$\nu_{\pm 0}$ are the quadrupole resonance frequencies at zero torsional vibration; $\nu_x(0)$ and $\nu_y(0)$ are the torsional vibrational frequencies at an arbitrary zero of temperature; α_x and α_y are empirical constants, and x and y are the field-gradient principal axes.

The temperature coefficients, α_x and α_y, are quite large but in the same region as those previously reported for $^{63}Cu_2O$, $^{65}Cu_2O$ (31), and $(CH_2)_6N_4$ (25). Thus the slope of any curve increases in the low temperature region.

The curves derived using these parameters are shown in Fig. 4, together with the experimental points, which deviate from the curves at the low temperature end. This may be due to ignoring v_z, which is present in p-dichloro-benzene (28). Including v_z would require $\overline{\theta_z^2}$ to be included in [3] and consequently θ and v_z in [4] through [7]. When a more extensive study of the temperature dependence is available, and the directions of the field-gradient principal axes are known together with the moments of inertia, a more comprehensive discussion will be possible.

Can. J. Chem. Downloaded from www.nrcresearchpress.com by 210.87.254.6 on 09/05/12
For personal use only.

3. The coupling constants and asymmetry parameters, e^2Qq/h and η for ^{14}N

Table I*a* shows that for ^{14}N:

(*a*) A smaller e^2Qq/h is associated with a larger η; the percentage change in η is five times that in e^2Qq/h: this is reasonable in view of the theoretical results for q_{aa}, q_{bb}, and q_{cc} (Table III) since a larger q_{aa} gives a larger e^2Qq/h and smaller η. The q_{aa}, q_{bb}, and q_{cc} are general expressions for any three mutually perpendicular q, such that $|q_{aa}| > |q_{bb}| > |q_{cc}|$. At any particular atom the q will be q_{xx}, q_{yy}, and q_{zz}, and the identification of the q_{aa}, etc., with the q_{xx}, etc., will be *particular to that atom* (Table III).

(*b*) The η and e^2Qq/h for *p*-iodo-aniline are anomalous; the values were calculated from the 292 °K frequencies, instead of the 77 °K frequencies, but the *p*-chloro- and *p*-bromo-aniline values at 292 °K are still higher for e^2Qq/h and lower for η than *p*-iodo-aniline. Hydrogen bonding between the $-NH_2$ and I, intermolecularly, would explain the large η and small e^2Qq/h, but the ^{127}I n.q.r. resonance at 261.14 mc does not support such an idea (27, 32).

(*c*) The e^2Qq/h and η for aniline (3933 kc; 26.9%) and *p*-phenylene-diamine (3910 kc; 26.4%) are surprisingly close in view of their different chemical properties. The e^2Qq/h and η of *o*-phenylene-diamine (3777 kc, 33.0%) are very different due perhaps to steric effects, or "direct field" effects between adjacent $-NH_2$ groups (33) which are absent in aniline and *p*-phenylene-diamine.

4. Theory

Preliminary calculations using the simple Hückel molecular orbital theory (34) and the extended Hückel method (35) led to our decision to analyze the results in terms of the bond electronegativity equalization method with Hückel molecular orbital π-bond treatment, BEEM-π (36).

BEEM-π is fully discussed elsewhere (40). The σ-orbitals in the molecule are treated by the bond electronegativity equalization method in which the orbital electronegativities as functions of their own occupancy and the occupancy of other orbitals on the same atom are equalized in a two centered bond (41–43). Thus the σ-core is changed from the free atom state, and this affects the σ-orbital parameters of the Hückel molecular orbital method, which change the charge density distributions, and alter the σ-orbital occupancies. Thus the σ and π orbitals are interrelated, and the procedure is taken to self-consistency for the σ and π orbitals (40).

The parameters in the BEEM-π calculations for the π-orbital are

$$[8] \qquad \alpha_x = \alpha_0 + h_x\beta_0$$

$$[9] \qquad \beta_{cx} = k_{cx}\beta_0 \qquad \text{i.e. } k_{CN} = 0.8$$

in which α is the coulomb integral and β the resonance integral, the subscripts x and 0 signifying the hetero-atom and the benzene carbon where $h_c = 0$ and $k_c = 1$, where $h_N = 1.5$, $k_{CN} = 0.8$, $h_{Cl} = 2.0$, and $k_{CCl} = 0.4$ (44). The σ-bond parameters were the usual valence state orbital electronegativities and their parameters (41).

BEEM-π has been successfully applied to predicting the ^{35}Cl n.q.r. frequencies in a series of conjugated molecules (40). In this paper it is applied to *p*-chloro-aniline.

The chlorine atom can be assumed to be in several different hybridized states. If it uses only *p*-orbitals in bonding it will be $sp_xp_yp_z$, if it is trigonally hybridized[3] (an extreme condition which is chemically unlikely) it will be tr.tr.tr.π, and if there is a certain percentage of s-character in the σ-orbital to the carbon atom in the ring, it will lie between these extreme positions. The results for *p*-chloro-aniline in Table III*c* demonstrate the sensitivity of the ^{35}Cl n.q.r. frequency to the hybridization of the ^{35}Cl. A pure p_σ orbital gives 50.75 Mc, a pure trigonal orbital gives 33.69 Mc, while 20% s-character in the σ-orbital gives 42.22 Mc. The respective asymmetry parameters are 2.5, 3.7, and 3.0% respectively. The experimental results are 34.15 Mc for the frequency and 6 $\pm$ 3% for the asymmetry parameter (37). Thus 28% s-character in the σ-orbital would predict the frequency, and presumably the asymmetry, exactly.

Since the BEEM-π theory is successful in predicting ^{35}Cl n.q.r. frequencies, it should be equally successful in predicting ^{14}N n.q.r. frequencies. However, at the ^{35}Cl atom the site axes coincide with the ring system axes, which in the planar molecule define the molecular axes; thus the only variable in the theory is the s-character of the chlorine σ-orbital.

[3]The nomenclature is discussed in refs. 49, 7, and 41–44.

Can. J. Chem. Downloaded from www.nrcresearchpress.com by 210.87.254.6 on 09/05/12
For personal use only.

This condition holds for the ^{35}Cl atom in *p*-chloro-aniline even when there is an angle of 25° 18′ between the π-orbital of the ^{14}N in the NH_2 group and the *z*-axis of the ring (38). The angle between the plane of the ring and the plane of the NH_2 unit is thus 39° 21′. Consequently BEEM-π calculations were repeated for such a non-planar *p*-chloro-aniline, in which the resonance integral β_{CN} was altered to its value for a 25° 18′ loss in overlap between the ^{14}N-π-orbital and the ring π-orbital. It is seen that the ^{35}Cl frequency and asymmetry parameter are quite *insensitive* to such changes.

At the ^{14}N atom on the other hand several variables can all affect the ^{14}N n.q.r. frequency and asymmetry parameter.

(a) The Hybridization at the Nitrogen

The actual σ-bond hybridization is unknown; thus the angle HNH for *p*-phenylene-diamine is 109° 4′ in CCl_4 solution (39) suggesting that the NH bonds are almost tetrahedral in hybridization (25% s-character) while the N—C bond will have 50% s-character in the ^{14}N σ-orbital. In the other molecules it is reported to be 112° for the angle HNH, so that the N—H σ-orbital has more s-character and the N—C σ-orbital less s-character than in *p*-phenylene-diamine. The exact hybridization governs the resolution into $sp_xp_yp_z$ occupancies, hence the values of q_{xx}, q_{yy}, and q_{zz} and consequently the e^2Qq/h and η, as seen above for ^{35}Cl, and as discussed by Das and Hahn (47). In all the BEEM-π calculations the ^{14}N is assumed to be *exactly* tr.tr.tr.π hybridized, and only the occupancy of these orbitals is considered as a variable.

(b) The Angle between the z-Axis of the Ring and the π Orbital of ^{14}N in the —NH_2 Group

The absence of X-ray data on the molecules makes it difficult to select the correct principal molecular axes and the site axes at the ^{14}N. In the BEEM-π calculations it is initially assumed that the molecular and site axes are the same; thus the molecule is planar and the results in Table III*a* are obtained. It will be noticed that the asymmetry parameters are about one tenth of the experimental and that e^2Qq_{at}/h is around −5.6 Mc, well below the predicted −7.4 Mc (45). Also the frequency

$$[10] \qquad \nu = (e^2Qq_{at}/h)q_{zz}$$

is experimentally in the order *p*-chloro-aniline > aniline > *p*-phenylene-diamine > *o*-phenylene-diamine. The BEEM-π planar molecule predicted order is *p*-phenylene-diamine > aniline > *p*-chloro-aniline > *o*-phenylene-diamine. The resonance integral β_{CN} is 0.80 in these calculations.

The angle between the molecular ring *z*-axis and the ^{14}N π-orbital in aniline is 25° 18′ (38). Thus if it is assumed that this angle is the same in *o*-phenylene-diamine, *p*-phenylene-diamine, and *p*-chloro-aniline, then BEEM-π calculations can be performed to give Table III*b*. The terms in this table are primed to signify that there is a 25° 18′ angle between the ^{14}N π-orbital and the π-orbital of the ring. It is immediately obvious that the theoretical asymmetry parameters η′ are now in the same region as the experimental (Table I), while the $e^2Qq'_{at}/h$ are all near the expected −7.4 Mc. An assumed angle slightly less than 25° 18′ for any of the molecules would bring η'_{theory} and η_{exp} into agreement, and e^2Qq_{at}/h nearer to −7.4 Mc. In Table III*b* the resonance integral β_{CN} is held at 0.80.

If the e^2Qq_{at}/h for ^{14}N were *absolutely* established as −7.4 Mc it would be possible to use it to find the angles needed to give η_{theory} in agreement with η_{exp} and to predict the frequency. However, the uncertainty in e^2Qq_{at}/h, and that discussed in (*a*), together with the choice of the resonance integral parameter β, make such calculations invalid.

In Table III*c* BEEM-π calculations are performed on *p*-chloro-aniline assuming a non-planar molecule and altering β_{CN} from 0.80, the value for a planar molecule, to 0.72 the value for an angle of 25° 18′, in the overlap expression, and for β = 0.62, an arbitrary decrease in β_{CN}. It is obvious that the ^{14}N η′ is quite insensitive to the change from 0.62 to 0.72 (both 40%) but sensitive to the change from 0.72 to 0.80 (40% to 30%). The $e^2Qq'_{at}/h$ is similarly sensitive to the change of β_{CN} from 0.80 to 0.72 (−8.37 and −7.71 Mc) but only slightly sensitive to the change from 0.72 to 0.62 (−7.71 to −7.35 Mc).

In Table III*b* the order of the predicted frequencies ν is *p*-phenylene-diamine > aniline > *p*-chloro-aniline > *o*-phenylene-diamine, the same order as for a planar molecule calculation. Either an angle change and/or a change in β_{CN} alters such an order. Thus in *p*-chloro-aniline with β_{CN} = 0.72, the value of $q_{zz}'(\pi)$ is 0.5339, predicting that *p*-chloro-aniline will have the highest n.q.r. frequency, in agreement with Table I*a*.

Can. J. Chem. Downloaded from www.nrcresearchpress.com by 210.87.254.6 on 09/05/12
For personal use only.

TABLE III

^{14}N and ^{35}Cl BEEM-π calculations of the electron densities and field gradients in aniline and several derivatives*

Define $\eta = \left|\frac{q_{bb} - q_{cc}}{q_{aa}}\right|$, and $\frac{e^2Qq}{h} = \frac{e^2Qq_{aa}}{h}$.

The maximum field gradient is chosen as $|q_{aa}| > |q_{bb}| > |q_{cc}|$.

For ^{14}N, $q_{aa} = q_{zz}$, the ^{14}N π-orbital; $q_{bb} = q_{xx}$, the ^{14}N p-orbital tangential to the benzene ring; $q_{cc} = q_{yy}$, the N^{14} p-orbital in the C—N bond.

For ^{35}Cl, $q_{aa} = q_{yy}$, the ^{35}Cl p-orbital in the C—Cl bond; $q_{bb} = q_{xx}$, the ^{35}Cl p-orbital tangential to the benzene ring; $q_{cc} = q_{zz}$, the ^{35}Cl π-orbital.

Full results for *p*-bromo-aniline and *p*-iodo-aniline are not shown as the necessary BEEM-π parameters for Br and I have not yet been completely established (40).

TABLE III*a*

^{14}N BEEM-π calculations on aniline and several substituted anilines*

Compound	$tr_1 = tr_2$	tr_3	$p_z(\pi)$	p_x	p_y	$q_{zz}(\pi)$	q_{xx}	q_{yy}	η (%)	e^2Qq_{at}/h
Aniline	1.1559	1.1297	1.8377	1.1559	1.1384	0.6905	−0.3321	−0.3584	3.80	−5.69
o-Phenylene-diamine	1.1562	1.1410	1.8259	1.1562	1.1461	0.6747	−0.3298	−0.3449	2.2	−5.60
p-Phenylene-diamine	1.1511	1.1339	1.8529	1.1511	1.1396	0.7075	−0.3451	−0.3624	2.4	−5.53
p-Chloro-aniline	1.1609	1.1179	1.8289	1.1609	1.1322	0.6823	−0.3627	−0.3197	6.3	−6.03

*^{14}N BEEM-π calculations on aniline and several substituted anilines assuming the molecules to be *planar*. The resonance integral β_{CN} is 0.80. The calculations are performed on a trigonally hybridized ^{14}N; $tr_1 = tr_2$ as these are bonded to H, tr_3 is bonded to C, and $p_z(\pi)$ is the lone pair orbital. The results are transformed to an s, p_x, p_y, and $p_z(\pi)$ basis set, and the field gradients q_{xx}, q_{yy}, and q_{zz} calculated from the p_x, p_y, and $p_z(\pi)$, since (47)

$$q_{zz} = p_z(\pi) - 1/2(p_y + p_x) \qquad \text{etc.}$$

The figures under columns 2 through 6 represent electron densities, or occupation numbers, those in columns 7 through 9 represent numbers by which the field gradient in the free atom must be multiplied to give the field gradient in the molecule (47). Thus

$$q_{mol} = q_{zz}q_{at} \qquad \text{etc.}$$

TABLE III*b*

^{14}N BEEM-π calculations on aniline and several substituted anilines*

Compound	$p'_z(\pi)$	p'_x	p'_y	$q'_{zz}(\pi)$	q'_{xx}	q'_{yy}	η′ (%)	$e^2Qq'_{at}/h$
Aniline	1.7100	1.1559	1.2662	0.4989	−0.3322	−0.1667	33	−7.88
o-Phenylene-diamine	1.7018	1.1562	1.2703	0.4885	−0.3292	−0.1587	35	−7.72
p-Phenylene-diamine	1.7227	1.1511	1.2699	0.5122	−0.3452	−0.1670	35	−7.63
p-Chloro-aniline	1.7017	1.1609	1.2595	0.4915	−0.3197	−0.1718	30	−8.37

*^{14}BEEM-π calculations on aniline and several substituted anilines assumed to have an angle 0 of 25° 18′ between the nitrogen lone pair axis and the *z*-axis of the benzene ring. The resonance integral β_{CN} is maintained at 0.80. The electron densities p′, and new field gradients q', are calculated using $p'_x = p_x$, $p'_y = p_y \cos 0 + p_z \sin 0$, and $p'_z = p_z \cos 0 + p_y \sin 0$.

TABLE III*c*

BEEM-π calculations on *p*-chloro-aniline*

(*i*) ^{35}Cl results for a fixed $\beta_{CN} = 0.80$ and variable hybridization

β_{CN}	Hybrid	$p_z(\pi)$	p_x	p_y	$q_{zz}(\pi)$	q_{xx}	q_{yy}	η (%)	ν Mc
0.80	tr.tr.tr.π	1.9848	2.000	1.3784	0.2956	0.3184	−0.6140	3.7	33.69
0.80	$p_xp_yp_z$	1.9848	2.000	1.0676	0.4510	0.4738	−0.9248	2.5	50.75
0.80	20% s in p_y	1.9848	2.000	1.2230	0.3733	0.3961	−0.7694	3.0	42.22

(*ii*) Variable β_{CN} and fixed hybridization

^{35}Cl		$p'_z(\pi)$	p'_x	p'_y	$q'_{zz}(\pi)$	q'_{xx}	q'_{yy}	η′ (%)	ν′ Mc
0.72	tr.tr.tr.π	1.9845	2.000	1.3901	0.2894	0.3127	−0.6022	3.9	33.04
0.62	tr.tr.tr.π	1.9841	2.000	1.3880	0.2901	0.3139	−0.6040	3.9	33.14
^{14}N		p'_x	$p'_z(\pi)$	p'_y	q'_{xx}	$q'_{zz}(\pi)$	q'_{yy}	η′ (%)	$e^2Qq'_{at}/h$
0.72	tr.tr.tr.π	1.2834	1.7454	1.1396	−0.3748	0.5339	−0.1591	40	−7.71
0.62	tr.tr.tr.π	1.2833	1.7685	1.1339	−0.3920	0.5599	−0.1679	40	−7.35

*(*i*) The table shows how the resonance frequency for ^{35}Cl is dependent on the hybridization of the chlorine orbitals. Two extreme cases tr.tr.tr.π and $sp_xp_yp_z$ are calculated, and a case with 20% s-character in the C—Cl σ bond (p_z).

(*ii*) With a fixed hybridization assumed for ^{35}Cl and ^{14}N the effect of changing the resonance integral β_{CN} is considered. The ^{35}Cl is, as expected, very insensitive to such a change, and so is the ^{14}N. Thus the calculations in Table III*b* are fairly reliable despite the use of an unaltered $\beta_{CN} = 0.80$, derived for planar molecules, in the non-planar molecule calculations.

Can. J. Chem. Downloaded from www.nrcresearchpress.com by 210.87.254.6 on 09/05/12
For personal use only.

(c) The Possible Twisting of the —NH_2 Group out of the Plane of the Ring

This would change both the site axes, now being at a solid angle to the molecular axes by θ for the angle between the z-axis of the ring and the ^{14}N π-orbital, and by ϕ for the angle between the x axis of the ring and the x axis of the ^{14}N. This would affect the values of q_{aa}, q_{bb}, and q_{cc} simply by the resolution of the orbital densities, and also the π-bonding to the ring and consequently the value of β_{CN}.

(d) Other Results

The results for *p*-bromo-aniline and *p*-iodo-aniline are not shown in detail in Table III due to the preliminary nature of their BEEM-π parameters (40). The *preliminary* results give $q_{aa}{}^{Br}$ as 0.4936 with η at 28% and $q_{aa}{}^{I}$ as 0.4497 with η at 40%. The predicted e^2Qq_{at}/h is 8.37 Mc as in *p*-chloro-aniline. The parameters in the Hückel part of the theory are derived relative to chlorine (44) and are of questionable validity (44) at $h_{Br} = 1.5$, $k_{CBr} = 0.3$, $h_1 = 1.2$, and $k_{Cl} = 0.15$.

5. Conclusion

In view of the uncertainty in the hybridization at the ^{14}N atom, the non-planarity angle θ, the twist angle ϕ, and the resonance integral β_{CN}, no definitive quantitative results can be expected. However, the value of e^2Qq_{at}'/h will not be changed by any of these factors to any significant extent and it can be concluded that e^2Qq_{at}/h cannot be far from -7.4 Mc (45). There is no justification for assuming it to be -14.0 Mc simply because it is more "appropriate" to some limited calculations (46).

It can be concluded that

(*i*) The ^{14}N n.q.r. frequencies and asymmetry parameters are explainable if the non-planarity of aniline and its derivatives is considered.

(*ii*) The BEEM-π theory gives a correct and consistent description of the conjugative effect through the π-system, of the inductive effect through the σ-system, and of the interaction between them. Such σ–π interaction is essential for any successful interpretation of the experimental results.

(*iii*) The e^2Qq_{at}/h for ^{14}N is approximately -7.4 Mc.

(*iv*) Further work awaits more detailed structural analysis.

(*v*) These results are sufficiently encouraging that work is at present under way to predict the ν precisely; it includes variations in the HNH angle, in θ and ϕ, as well as experimental measurements on 25 other substituted anilines over a wider temperature range. The β_{CN} parameters are being improved and BEEM-π parameters for Br and I verified.

Acknowledgments

This research was supported by the National Research Council of Canada. We wish to thank the Referee most sincerely for his advice and help. We wish to thank Dr. M. Kaplansky for useful discussions. C. T. Yim thanks McGill University for the award of University Graduate Fellowships (1966–1968); D. H. Lo thanks the NRCC for the award of a Studentship (1968–1969). We acknowledge the use of the McGill University IBM 7044 computer and time allotted.

1. R. V. Pound and W. D. Knight. Rev. Sci. Instr. **21**, 219 (1950).
2. F. N. H. Robinson. J. Sci. Instr. **36**, 481 (1959).
3. R. Livingston. Nuclear quadrupole resonance. *In* Methods of experimental physics. Vol. 3. 1962. p. 501.
4. G. A. Jeffrey and T. Sakurai. Application of NQR. *In* Progress in solid state chemistry. Vol. 1. 1964. p. 380.
5. A. H. Reddoch. J. Chem. Phys. **35**, 1085 (1961).
6. H. O. Hooper and P. J. Bray. J. Chem. Phys. **33**, 334 (1960).
7. M. A. Whitehead. Can. J. Chem. **42**, 1212 (1964).
8. M. Minematsu. J. Phys. Soc. Japan, **14**, 1030 (1959).
9. A. Narath, W. J. O'Sullivan, W. A. Robinson, and W. W. Simmons. Rev. Sci. Instr. **35**, 476 (1964).
10. R. Livingston. Ann. N.Y. Acad. Sci. **55**, 800 (1952).
11. C. Dean. Rev. Sci. Instr. **31**, 934 (1960).
12. M. Kaplansky and M. A. Whitehead. Can. J. Chem. **45**, 1669 (1967).
13. I. Tatsuzaki and M. M. Rodrigues. J. Chem. Phys. **44**, 2200 (1966).
14. E. A. C. Lucken and M. A. Whitehead. J. Chem. Soc. 2459 (1961).
15. K. Tsukada. J. Phys. Soc. Japan, **11**, 956 (1956).
16. S. S. Lehrer and C. T. O'Konski. J. Chem. Phys. **43**, 1941 (1965).
17. Y. Abe. J. Phys. Soc. Japan, **18**, 1804 (1963).
18. J. Trotter, S. H. Whitelaw, and T. Zobel. J. Chem. Soc. A, 353 (1966).
19. H. Bayer. Z. Physik. **130**, 227 (1951).
20. T. Kushida. J. Sci. Hiroshima Univ. Ser. A, **19**, 327 (1957).
21. D. H. Smith and R. M. Cotts. J. Chem. Phys. **41**, 2403 (1964).
22. T. Kushida, G. B. Benedek, and N. Bloembergen. Phys. Rev. **104**, 1364 (1956).
23. H. S. Gutowsky and G. A. Williams. Phys. Rev. **105**, 464 (1957).
24. R. J. C. Brown. J. Chem. Phys. **32**, 116 (1960).
25. G. A. Matzkanin, T. N. O'Neal, T. A. Scott, and P. J. Haigh. J. Chem. Phys. **44**, 4171 (1966).
26. I. Ichishima. J. Chem. Soc. Japan, Pure Chem. Sect. **71**, 607 (1950).

27. G. W. LUDWIG. J. Chem. Phys. **25**, 159 (1956).
28. B. D. SAKSENA. J. Chem. Phys. **18**, 1653 (1950).
29. G. HERZBERG. Molecular spectra and molecular structure. D. Van Nostrand Co. Inc., New York. 1966.
30. G. A. MATZKANIN, T. A. SCOTT, and P. J. HAIGH. J. Chem. Phys. **42**, 1646 (1965).
31. K. V. S. R. RAO and C. R. K. MURTY. Proc. Phys. Soc. London, **89**, 711 (1966).
32. J. HATTON and B. V. ROLLIN. Trans. Faraday Soc. **50**, 358 (1954).
33. E. S. GOULD. Mechanism and structure in organic chemistry. Holt, Rinehart and Winston Inc., New York. 1959. Chap. 7.
34. N. C. BAIRD and M. A. WHITEHEAD. Can. J. Chem. **44**, 1933 (1966).
35. J. M. SICHEL and M. A. WHITEHEAD. Theoret. Chim. Acta, **5**, 35 (1966).
36. R. J. BOYD, D. H. LO, and M. A. WHITEHEAD. Chem. Phys. Lett. **2**, 227 (1968).
37. H. C. MEAL. J. Chem. Phys. **24**, 1011 (1956).
38. D. T. CLARK and J. W. EMSLEY. Mol. Phys. **12**, 365 (1967).
39. D. G. LISTER and J. K. TYLER. Chem. Commun. 152 (1966).
40. M. KAPLANSKY and M. A. WHITEHEAD. Mol. Phys. **15**, 149 (1968).
41. M. A. WHITEHEAD, N. C. BAIRD, and M. KAPLANSKY. Theoret. Chim. Acta, **3**, 135 (1965).
42. N. C. BAIRD and M. A. WHITEHEAD. Theoret. Chim. Acta, **6**, 167 (1966).
43. N. C. BAIRD, J. M. SICHEL, and M. A. WHITEHEAD. Theoret. Chim. Acta, **11**, 38 1968.
44. N. C. BAIRD and M. A. WHITEHEAD. Can. J. Chem. **45**, 2059 (1967).
45. G. A. JEFFREY and T. SAKURAI. Progress in solid state chemistry. Vol. 1. The Pergammon Press, Ltd., Oxford. 1964.
46. D. W. DAVIES and W. C. MACKRODT. Chem. Commun. 1226 (1967).
47. T. P. DAS and E. L. HAHN. Nuclear quadrupole resonance spectroscopy. Academic Press, Inc., New York. 1959.
48. G. W. LEPPELMEIER and E. L. HAHN. Phys. Rev. **141**, 724 (1966).
49. J. HINZE, M. A. WHITEHEAD, and H. H. JAFFE. J. Am. Chem. Soc. **85**, 148 (1963).

Can. J. Chem. Downloaded from www.nrcresearchpress.com by 210.87.254.6 on 09/05/12
For personal use only.

Can. J. Chem. Downloaded from www.nrcresearchpress.com by 210.87.254.105 on 09/05/12
For personal use only.

Studies on metal hydroxy compounds. V. Heats of decomposition of zinc and cadmium halide (Cl,F) derivatives

P. RAMAMURTHY AND E. A. SECCO
Chemistry Department, St. Francis Xavier University, Antigonish, Nova Scotia

Received April 2, 1968

The heats of decomposition of the following hydroxy compounds are reported: $Zn(OH)_2$, Zn(OH)Cl, Zn(OH)F, $Cd(OH)_2$, Cd(OH)Cl, and Cd(OH)F.

Canadian Journal of Chemistry, 46, 3605 (1968)

Introduction

This communication is a part of a program of study on Zn and Cd hydroxyhalide compounds and reports on the heats of decomposition and the heats of formation of these compounds. Details of these decomposition reactions and analyses have already been reported (1, 2).

Experimental

All compounds used in this study were prepared in this laboratory using procedures already described (1, 2).

The heats of decomposition were determined using a duPont calorimeter cell (Cat. No. 900350), a plug-in module for the duPont DTA-900. The calorimeter cell follows design principles suggested by Boersma (3). Silver holders, or cups, for sample and reference are located in separate air cavities in a heating block. This construction provides for any heat developed during a reaction to be retained by the sample and its holder so that the resulting ΔH value is essentially independent of sample size, specific heat, and packing density.

The area of the decomposition peak in the thermogram was measured by planimetry. (A compensating polar planimeter, Gelman Instrument Co., Planimeter 39231, was used.) The peak is related to ΔH of the reaction by the equation:

$$\Delta H_{\text{mcal/mg}} = E\,\frac{A\Delta T_s T_s}{Ma}$$

where E is the calibration coefficient (mcal/°C min); A, peak area (in.^{2}); ΔT_s, y-axis sensitivity setting (°C/in.); T_s, x-axis sensitivity setting (°C/in.); M, mass of sample (mg); a, heating rate (°C/min). A calibration coefficient E curve versus peak temperature T was determined in the working temperature range 150–420 °C using substances with known heats of fusion, viz. In, Sn, Cd, and Zn, obtained from National Bureau of Standards (NBS) Circular No. 500.

Results and Discussion

The calorimetric results for decomposition are presented in Table I according to the following equations showing the onset and terminal temperatures:

[1] $\varepsilon\text{-}Zn(OH)_{2(c)} \xrightarrow{120\text{–}185\ ^\circ C} ZnO_{(c)} + H_2O_{(g)}$

[2] $\beta\text{-}Zn(OH)Cl_{(c)} \xrightarrow{245\text{–}330\ ^\circ C} ZnCl_{2(l)} + ZnO_{(c)} + H_2O_{(g)}$

[3] $Zn(OH)F_{(c)} \xrightarrow{350\text{–}480\ ^\circ C} ZnF_{2(c)} + ZnO_{(c)} + H_2O_{(g)}$

[4] $Cd(OH)_{2(c)} \xrightarrow{175\text{–}265\ ^\circ C} CdO_{(c)} + H_2O_{(g)}$

[5] $Cd(OH)Cl_{(c)} \xrightarrow{320\text{–}430\ ^\circ C} CdCl_{2(c)} + CdO_{(c)} + H_2O_{(g)}$

[6] $Cd(OH)F_{(c)} \xrightarrow{325\text{–}410\ ^\circ C} CdF_{2(c)} + CdO_{(c)} + H_2O_{(g)}$

The heats of fusion for bismuth metal, $AgNO_3$, and NH_4NO_3 were determined as internal checks on the reliability of the calorimeter cell and the method for calculating ΔH. The agreement between our value of ΔH_f^0 for $\varepsilon\text{-}Zn(OH)_2$ with the literature value further confirms the confidence of the calorimetric measurements.

The present ΔH_f^0 values were calculated using Kopp's rule approximation with $\Delta C_p^0 \approx 0$ in the equation:

$$\Delta H_T^0 = \Delta H_{298\ ^\circ K}^0 + \int_{298\ ^\circ K}^{T} \Delta C_p^0\, dT$$

because C_p^0 values for most compounds are unavailable to us. The sole case where the C_p^0 values were available was eq. [1] and here ΔC_p^0 was evaluated as -0.5 cal/deg mole which leads to a maximum correction of -0.08 kcal—an insignificant correction relative to the experimental

TABLE I

Heats of decomposition and values of ΔH_f^0

Compound	Heat of decomposition[a]		$-\Delta H_f^0$ (kcal/mole)	
	ΔH (kcal/mole of H_2O formed)	ΔH (kcal/mole of compound decomposed)	This work	Literature[b]
Bismuth (fusion)			2.643	2.640
NH_4NO_3 (fusion)			1.304	1.300
$AgNO_3$ (fusion)			2.722	2.752
$Zn(OH)_2$	11.60±0.35	11.60±0.35	154.35	153.74
Zn(OH)Cl[c]	11.08±0.16	5.54±0.08	126.52	—
Zn(OH)F[d]	9.26±0.66	4.63±0.33	167.46	—
$Cd(OH)_2$	12.10±0.01	12.10±0.01	126.20	128.08
Cd(OH)Cl	19.50±0.16	9.75±0.08	113.7	119.0
Cd(OH)F	18.00±0.06	9.00±0.03	149.75	—

[a]All determinations were done in duplicate except Cd(OH)Cl which was in triplicate. The ΔH values are given with their average deviations.
[b]Literature values cited for fusion are from NBS Circular No. 500 (1951), whereas all other values cited or used in our calculations are from NBS Technical Note 270–3 issued in January, 1968 by the United States Dept. of Commerce.
[c]Corrected for fusion endotherm of $ZnCl_2$ in decomposition doublet.
[d]Unable to correct for second endotherm in decomposition doublet. The actual ΔH value could be lower if the second endotherm is in fact associated with a process other than decomposition.

variations and thus justifying the Kopp's rule approximation.

The slight disparity between the ΔH_f^0 values for $Cd(OH)_2$ and Cd(OH)Cl from this work and the literature most probably resides in the purity of these compounds. In the case of $Cd(OH)_2$, the reported value of ΔH_f^0 is for a hydroxide prepared from $Cd(NO_3)_2$ and alkali (4). Detailed studies reported recently (5) showed that $Cd(OH)_2$ prepared from its salts and alkali is often admixed with basic salts. Likewise for Cd(OH)Cl, the possibility exists for the coprecipitation of higher hydroxyhalides.

The column of values for ΔH per mole of H_2O formed indicates a decreasing trend for the zinc derivatives and an increasing trend for the cadmium compounds. The slightly higher ΔH value for $Cd(OH)_2$ relative to $Zn(OH)_2$ suggests that the OH group might be more tightly bound in $Cd(OH)_2$. This suggestion is furthermore confirmed as the Cd—OH bond is strengthened considerably in the halide derivatives as evidenced by the significantly higher ΔH per mole of H_2O values observed for CdOHCl and CdOHF as contrasted with Zn—OH in ZnOHCl and ZnOHF.

The decomposition temperatures for the derivative compounds, on the other hand, are all higher relative to its parent hydroxide which arises primarily from increased separation of neighboring OH groups by interposition of the halogen substituent.

In summary, the presence of a halogen substituent, Cl or F, in zinc hydroxide, though effecting a higher decomposition temperature, in fact weakens the bonding between the OH group and the zinc cation, whereas, a parallel substitution in cadmium hydroxide strengthens the Cd—OH bond.

Acknowledgment

This research work has received generous support from the National Research Council of Canada.

1. O. K. Srivastava and E. A. Secco. Can. J. Chem. **45**, 579 (1967).
2. O. K. Srivastava and E. A. Secco. Can. J. Chem. **45**, 1375 (1967).
3. S. L. Boersma. J. Am. Ceram. Soc. **38**, 281 (1955).
4. R. Fricke and F. Blaschke. Z. Elektrochem. **46**, 46 (1940).
5. O. K. Srivastava and E. A. Secco. Can. J. Chem. **45**, 3203 (1967).

Can. J. Chem. Downloaded from www.nrcresearchpress.com by 210.87.254.105 on 09/05/12
For personal use only.

Polyatomic cations of the Group VIB elements. II. Compounds of the Se_4^{2+} cation

J. BARR, D. B. CRUMP, R. J. GILLESPIE, R. KAPOOR, AND P. K. UMMAT
Department of Chemistry, McMaster University, Hamilton, Ontario

Received May 16, 1968

The preparation and characterization of the compounds $Se_4(HS_2O_7)_2$, $Se_4S_4O_{13}$, $Se_4(SO_3F)_2$, and $Se_4(Sb_2F_{11})_2$ are described. All four compounds are shown to contain the Se_4^{2+} cation.

Canadian Journal of Chemistry, 46, 3607 (1968)

Can. J. Chem. Downloaded from www.nrcresearchpress.com by 210.87.254.105 on 09/05/12
For personal use only.

In part I of this series (1), the oxidation of selenium in fluorosulfuric acid, sulfuric acid, and oleum was shown to produce solutions containing the ions Se_4^{2+} and Se_8^{2+}, rather than the compound $SeSO_3$ as had previously been suggested (2). A yellow compound of the latter composition has been isolated from the reaction of selenium with sulfur trioxide (2), but in view of the results presented in part I, it seems probable that the formula $SeSO_3$ is not a good representation of this compound. This paper describes the preparation and characterization of solid compounds from the reaction of selenium with sulfur trioxide, disulfuric acid, and fluorosulfuric acid. It also seemed possible that the compound $Se(SbF_5)_2$ described by Aynsley, Peacock, and Robinson (3) might be related to the yellow $SeSO_3$ compound. Consequently, the reaction of selenium with antimony pentafluoride was investigated, although this gave a compound under our conditions with an analysis approximating to $SeSbF_5$.

Experimental

Preparation of the Compounds

Finely powdered selenium was dissolved in 65% oleum to give a solution about 6 *M* in selenium. The dark-green solution was heated at 50–55 °C until yellow-brown, then allowed to stand for several days. Orange, needle-like crystals (**1**) separated from the solution. These were filtered in a dry atmosphere, washed with a mixture of nitromethane and $S_2O_5F_2$ or with sulfur dioxide, and pumped dry at 50 °C.

A concentrated 4:1 $Se:S_2O_6F_2$ solution in fluorosulfuric acid was evaporated to dryness at 60–80 °C under vacuum, and the apparently dry solid further pumped for 24 h at 80 °C. The product was a bright-orange solid (**2**).

About 10 g of finely powdered selenium was dissolved in 15 g of freshly distilled sulfur trioxide at 0 °C. The green, viscous liquid changed to yellow with evolution of SO_2 over a period of 24 h, and a yellow solid separated. Excess SO_3 was removed by pumping to constant weight at room temperature. The product was a yellow, amorphous solid (**3**).

Powdered selenium was heated for 6 h at 100–140 °C with an excess of antimony pentafluoride to give a homogeneous yellow solution and a small amount of a white sublimate. On cooling the solution, a yellow crystalline solid separated. This was washed with SbF_5 and pumped dry at 140 °C for 36 h to give a bright-yellow powder (**4**).

All the compounds darken rapidly on exposure to moist air, and instantly decompose to red selenium when added to water. On heating in dry nitrogen, decomposition to black selenium without melting occurs below 200 °C. They dissolve immediately in sulfuric, disulfuric, and fluorosulfuric acids to produce yellow solutions.

Analysis

Selenium

Weighed quantities of each compound were decomposed with water and dissolved in the minimum volume of warm nitric acid. The diluted solution was warmed with an excess of hydrazine sulfate for 1 h, and the resulting grey selenium was filtered, dried, and weighed.

Sulfur

Weighed samples of **1**, **2**, and **3** were decomposed with a small volume of water in a sealed container and the selenium filtered from the solution. The sulfur in the filtrate from **1** or **3** was then determined gravimetrically as $BaSO_4$. The filtrate from **2** was made strongly acid, heated almost to boiling, and scrubbed with a current of air for 48 h. This ensures hydrolysis of fluorosulfate to sulfate and fluoride, and removal of the latter as HF. The sulfate was then determined gravimetrically.

Fluoride

Weighed samples of **2** and **4** were hydrolyzed with a slight excess of sodium hydroxide for 3 days at 100 °C in a sealed tube. After filtering off selenium, the fluoride in the filtrate was determined by potentiometric titration with standard lanthanum nitrate, using an Orion fluoride-ion-activity electrode as indicator (4).

Antimony

The method was adapted from that of Johnson and Newman (5). The Sb(V) from weighed samples of **4** was reduced with phosphorus and iodine, and the Sb(III) titrated with standard iodine solution, in the presence of boric acid to eliminate interference from fluoride ion (6).

Results

1. Se, 46.34, 46.88%; S, 19.24, 19.28%.

2. Se, 62.0, 62.5, 61.8%; S. 12.3, 12.3%; F, 7.0, 7.7%.

3. Se, 49.4, 48.6, 48.8, 49.4%; S, 20.2, 20.5, 19.4%.
4. Se, 27.06, 27.02%; Sb 38.65, 38.43%; F, 33.7, 34.10%.

Conductivity, Cryoscopy, and Absorption Spectra

The techniques used for studying solutions in sulfuric acid and fluorosulfuric acid were similar to those described in part I (1).

Nuclear Magnetic Resonance Measurements

The ^{19}F nuclear magnetic resonance (n.m.r.) spectra were recorded with a Varian Associates DP-60 spectrometer operating at 56.4 MHz.

Discussion

Table I shows the analyses expected for various compounds that might be formed under the experimental conditions. The analyses of **1** and **3** both correspond fairly closely to $SeSO_3$, but the analysis of **2**, obtained from fluorosulfuric acid solutions, clearly does not. The S:F ratio in **2** suggests strongly that fluorosulfate is present, and the analysis agrees well with the formula Se_2SO_3F. The analyses of both **1** and **3** are consistent with compounds of formulas $Se_4S_4O_{13}$ or $Se_2HS_2O_7$. As **1** and **2** were obtained from solutions known to contain Se_4^{2+} (1), it seems reasonable to formulate **2** as $Se_4(SO_3F)_2$ and **1** as $Se_4S_4O_{13}$ or $Se_4(HS_2O_7)_2$. The analysis of **4** is consistent with $Se_2Sb_2F_{11}$ or $SeSbF_6$, containing Se in the $+\frac{1}{2}$ and $+1$ oxidation states respectively.

The absorption spectra of **1** and **3** in sulfuric acid, and of **2** and **4** in fluorosulfuric acid, show in all cases the characteristic 410 mμ absorption of Se_4^{2+} (1), with the following values of extinction coefficients: **1**, 1940; **2**, 1970; **3**, 1820; **4**, 2170. In view of the value of extinction coefficient for Se_4^{2+} given in part I, it is clear that all four compounds give rise to Se_4^{2+} virtually quantitatively in solution. All four compounds, both in the solid state and in solution in sulfuric or fluorosulfuric acid, show a strong characteristic Raman line at ca. 328 cm^{-1}.[1] The solids thus contain the same selenium species, namely Se_4^{2+}, as the solutions.

TABLE I

Calculated analyses for possible compounds

Compound	Se (%)	S or Sb (%)	F (%)
$SeSO_3$	49.65	20.16	
Se_4SO_4	76.68	7.78	
$Se_4S_2O_7$	64.20	13.03	
$Se_4S_3O_{10}$	55.21	16.82	
$Se_4S_4O_{13}$	48.45	19.67	
$Se_2HS_2O_7$	47.13	19.14	
Se_2HSO_4	61.93	12.57	
Se_2SO_3F	61.45	12.48	7.40
$SeSbF_5$	26.70	41.17	32.12
Se_2SbF_6	40.12	30.93	28.96
$Se_2Sb_2F_{11}$	25.87	39.89	34.24
$SeSbF_6$	25.09	38.69	36.22

These results confirm the suggested formulation of **1** and **2** as given earlier, and demonstrate that both **3** and **4** are also compounds of Se_4^{2+}. Thus **3**, like **1**, could be either $Se_4S_4O_{13}$ or $Se_4(HS_2O_7)_2$, while a formula $Se_4(Sb_2F_{11})_2$ for **4** would be consistent with the analytical and other data.

Cryoscopic and Conductometric Measurements

Compounds **1** and **3**, which may be either $Se_4S_4O_{13}$ or $Se_4(HS_2O_7)_2$, would be expected to ionize in sulfuric acid according to one of the following equations:

$$Se_4(HS_2O_7)_2 = Se_4^{2+} + 2HS_2O_7^-$$

$$Se_4S_4O_{13} = Se_4^{2+} + 2HS_2O_7^- + H_2S_2O_7$$

It is not possible to distinguish easily between these two cases by direct conductometric or cryoscopic measurements in 100% sulfuric acid. They can, however, be readily distinguished by the effects on conductivity and freezing point of adding the compounds to aqueous sulfuric acid, since this results in reaction of the excess SO_3 with water according to the equations

$$Se_4(HS_2O_7)_2 + 2H_3O^+ + 2HSO_4^- = Se_4^{2+} + 2HSO_4^- + 2H_2SO_4$$

$$\Delta\nu = -0.25, \Delta\gamma = 0$$

$$Se_4S_4O_{13} + 3H_3O^+ + 3HSO_4^- = Se_4^{2+} + 2H_2SO_4 + 2HSO_4^-$$

$$\Delta\nu = -0.75, \Delta\gamma = -0.25$$

where $\Delta\nu$ and $\Delta\gamma$ are respectively, the change in the total number of solute particles and the change in the number of hydrogen sulfate ions produced in solution per g-atom of selenium.

Figure 1 shows the conductometric and cryoscopic measurements for compounds **1** and **3** in aqueous sulfuric acid. The values of $\Delta\nu = -0.25$, $\Delta\gamma = 0$ for compound **1** and $\Delta\nu = -0.75$, $\Delta\gamma = -0.25$ for **3** show clearly that **1** contains one excess SO_3 per two Se atoms, and can be formulated $Se_4(HS_2O_7)_2$, while **3** contains three excess SO_3 per four Se atoms and can be formulated $Se_4S_4O_{13}$.

The results of conductivity measurements on compound **2** in fluorosulfuric acid are shown in Table II. The value of $\gamma = 0.48$ shows that one fluorosulfate ion is produced per two selenium

[1]R. J. Gillespie and G. P. Pez. To be published.

Can. J. Chem. Downloaded from www.nrcresearchpress.com by 210.87.254.105 on 09/05/12
For personal use only.

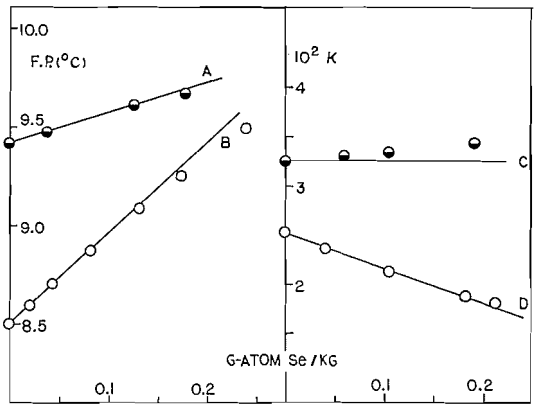

FIG. 1. Conductivities and freezing points of solutions of **1** and **3** in aqueous sulfuric acid: ◒, **1**; ○, **3**; A, $\Delta\nu = -0.25$; B, $\Delta\nu = -0.75$; C, $\Delta\gamma = 0$; D, $\Delta\gamma = -0.25$.

atoms, as would be expected from the formulation $Se_4(SO_3F)_2$.

The ^{19}F spectrum of a solution of **4** in HSO_3F had a single broad peak A at +162 p.p.m. (from HSO_3F) which may be assigned to SbF_6^-, a doublet B at 154 p.p.m., and a quintuplet C at 172 p.p.m. with a coupling constant of 103 Hz which may be assigned to the $SbF_5(SO_3F)^-$ anion (7). The relative areas of the peaks were A:B:C = 6:4:1 showing that the species SbF_6^- and $SbF_5(SO_3F)^-$ were present in equal amounts. It is known that SbF_5 forms the $SbF_5(SO_3F)^-$ anion in fluorosulfuric acid (7), hence compound **4** gives rise to equal amounts of SbF_6^- and SbF_5 in solution in fluorosulfuric acid and therefore presumably contains the $Sb_2F_{11}^-$ anion. The compound **4** is not very soluble in sulfur dioxide but at −80° the solution gave a weak ^{19}F spectrum of three peaks, a multiplet, a doublet of doublets, and a quintuplet essentially identical with that previously observed for the $Sb_2F_{11}^-$ ion in HF (8). The spectrum did not show any peak for the SbF_6^- ion or the SbF_5SO_2 complex. Thus the ^{19}F n.m.r. data confirm that the anion in **4** is $Sb_2F_{11}^-$ and that the compound may therefore be formulated as $Se_4(Sb_2F_{11})_2$.

TABLE II

Conductivity of solutions of compound II in HSO_3F (25 °C)

Concentration (g-atom Se/kg)	$10^3\kappa$	γ
0.01184	1.36	0.46
0.02968	3.39	0.49
0.05736	6.32	0.48
0.1095	11.42	0.48

Acknowledgment

We thank the National Research Council of Canada for financial support of this work.

1. J. BARR, R. J. GILLESPIE, R. KAPOOR, AND K. C. MALHOTRA. Can. J. Chem. **46**, 149 (1968).
2. E. DIVERS AND M. SHIMOSE. J. Chem. Soc. **43**, 329 (1883); **45**, 194, 201 (1884).
3. E. E. AYNSLEY, R. D. PEACOCK, and P. L. ROBINSON. Chem. Ind. London, 1117 (1951).
4. M. S. FRANT and J. W. ROSS. Science, **154**, 1553 (1966).
5. E. A. JOHNSON and E. J. NEWMAN. Analyst, **80**, 3631 (1955).
6. W. A. MAZEIKA and H. M. NEUMANN. Inorg. Chem. **5**, 309 (1966).
7. R. C. THOMPSON, J. BARR, R. J. GILLESPIE, J. B. MILNE, and R. A. ROTHENBURY. Inorg. Chem. **4**, 1641 (1965).
8. R. J. GILLESPIE and K. C. MOSS. J. Chem. Soc. A, 1170 (1966).

Ion–molecule reactions in methyl mercaptan and methyl-d_3 mercaptan

G. P. NAGY, J. C. J. THYNNE[1], AND A. G. HARRISON

Department of Chemistry, University of Toronto, Toronto 5, Ontario

Received May 28, 1968

The ion–molecule reactions occurring in CH_3SH and CD_3SH have been identified and rate constants measured for ions of 3.4 eV ion exit energy. The reaction $CD_3SH^+ + CD_3SH$ involves predominantly transfer of the mercaptyl hydrogen.

Canadian Journal of Chemistry, 46, 3609 (1968)

Recent studies (1–5) of the ion–molecule reactions of methyl alcohol have shown that both the molecule ion, CH_3OH^+, and the fragment ion, CH_2OH^+, react rapidly with neutral CH_3OH to produce the protonated molecule $CH_3OH_2^+$. Using CD_3OH it has been shown (1–4) that in the

[1]Permanent address: Department of Chemistry, University of Edinburgh, Edinburgh, Scotland.

Can. J. Chem. Downloaded from www.nrcresearchpress.com by 210.87.254.105 on 09/05/12
For personal use only.

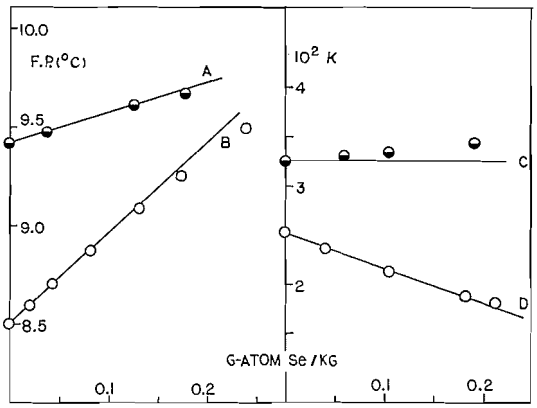

FIG. 1. Conductivities and freezing points of solutions of **1** and **3** in aqueous sulfuric acid: ◒, **1**; ○, **3**; A, $\Delta\nu = -0.25$; B, $\Delta\nu = -0.75$; C, $\Delta\gamma = 0$; D, $\Delta\gamma = -0.25$.

atoms, as would be expected from the formulation $Se_4(SO_3F)_2$.

The ^{19}F spectrum of a solution of **4** in HSO_3F had a single broad peak A at +162 p.p.m. (from HSO_3F) which may be assigned to SbF_6^-, a doublet B at 154 p.p.m., and a quintuplet C at 172 p.p.m. with a coupling constant of 103 Hz which may be assigned to the $SbF_5(SO_3F)^-$ anion (7). The relative areas of the peaks were A:B:C = 6:4:1 showing that the species SbF_6^- and $SbF_5(SO_3F)^-$ were present in equal amounts. It is known that SbF_5 forms the $SbF_5(SO_3F)^-$ anion in fluorosulfuric acid (7), hence compound **4** gives rise to equal amounts of SbF_6^- and SbF_5 in solution in fluorosulfuric acid and therefore presumably contains the $Sb_2F_{11}^-$ anion. The compound **4** is not very soluble in sulfur dioxide but at −80° the solution gave a weak ^{19}F spectrum of three peaks, a multiplet, a doublet of doublets, and a quintuplet essentially identical with that previously observed for the $Sb_2F_{11}^-$ ion in HF (8). The spectrum did not show any peak for the SbF_6^- ion or the SbF_5SO_2 complex. Thus the ^{19}F n.m.r. data confirm that the anion in **4** is $Sb_2F_{11}^-$ and that the compound may therefore be formulated as $Se_4(Sb_2F_{11})_2$.

TABLE II

Conductivity of solutions of compound II in HSO_3F (25 °C)

Concentration (g-atom Se/kg)	$10^3\kappa$	γ
0.01184	1.36	0.46
0.02968	3.39	0.49
0.05736	6.32	0.48
0.1095	11.42	0.48

Acknowledgment

We thank the National Research Council of Canada for financial support of this work.

1. J. BARR, R. J. GILLESPIE, R. KAPOOR, AND K. C. MALHOTRA. Can. J. Chem. **46**, 149 (1968).
2. E. DIVERS AND M. SHIMOSE. J. Chem. Soc. **43**, 329 (1883); **45**, 194, 201 (1884).
3. E. E. AYNSLEY, R. D. PEACOCK, and P. L. ROBINSON. Chem. Ind. London, 1117 (1951).
4. M. S. FRANT and J. W. ROSS. Science, **154**, 1553 (1966).
5. E. A. JOHNSON and E. J. NEWMAN. Analyst, **80**, 3631 (1955).
6. W. A. MAZEIKA and H. M. NEUMANN. Inorg. Chem. **5**, 309 (1966).
7. R. C. THOMPSON, J. BARR, R. J. GILLESPIE, J. B. MILNE, and R. A. ROTHENBURY. Inorg. Chem. **4**, 1641 (1965).
8. R. J. GILLESPIE and K. C. MOSS. J. Chem. Soc. A, 1170 (1966).

Ion–molecule reactions in methyl mercaptan and methyl-d_3 mercaptan

G. P. NAGY, J. C. J. THYNNE[1], AND A. G. HARRISON

Department of Chemistry, University of Toronto, Toronto 5, Ontario

Received May 28, 1968

The ion–molecule reactions occurring in CH_3SH and CD_3SH have been identified and rate constants measured for ions of 3.4 eV ion exit energy. The reaction $CD_3SH^+ + CD_3SH$ involves predominantly transfer of the mercaptyl hydrogen.

Canadian Journal of Chemistry, 46, 3609 (1968)

Recent studies (1–5) of the ion–molecule reactions of methyl alcohol have shown that both the molecule ion, CH_3OH^+, and the fragment ion, CH_2OH^+, react rapidly with neutral CH_3OH to produce the protonated molecule $CH_3OH_2^+$. Using CD_3OH it has been shown (1–4) that in the

[1]Permanent address: Department of Chemistry, University of Edinburgh, Edinburgh, Scotland.

Can. J. Chem. Downloaded from www.nrcresearchpress.com by 210.87.254.5 on 09/05/12
For personal use only.

Can. J. Chem. Downloaded from www.nrcresearchpress.com by 210.87.254.5 on 09/05/12
For personal use only.

reaction of the molecule ion the hydroxyl hydrogen is transferred approximately 2.5 times more readily than the methyl hydrogen, while in the reaction of CH_2OH^+ only the hydroxylic hydrogen is transferred. The present work reports a study of the related methyl mercaptan system to determine the reactions occurring and to determine the specificity of the hydrogens transferred.

Experimental

The reactions occurring, both in CH_3SH and CD_3SH, were identified from ratio plots (6) over a range of electron energies where only the molecule ion and fragment ion(s) formed by loss of a hydrogen (or deuterium) were significant primary ions. This work was carried out on the modified MS-2 instrument (7) at a source concentration of approximately 10^{13} molecules cm^{-3} and a constant repeller voltage corresponding to 3.4 eV ion exit energy.

Accurate rate constants for the reactions occurring were obtained from pressure plots. The mass spectrometer and the techniques employed have been described recently (5). All runs were carried out at 3.4 eV ion exit energy. The CH_3SH was obtained from Matheson Co. while the CD_3SH (1.9% CD_2HSH) was obtained from Merck, Sharp, and Dohme. Neither sample showed any detectable impurities.

Results and Discussion

Ion–Molecule Reactions in CH_3SH

Ratio plots at low energy showed the two reactions

[1] $CH_3SH^+ + CH_3SH \rightarrow CH_3SH_2^+ + CSH_3$

[2] $CSH_3^+ + CH_3SH \rightarrow CH_3SH_2^+ + CH_2S$

to be occurring with the relative rates $k_1/k_2 \approx 1.4 \pm 0.3$. No other products were detected. The ion written as CSH_3^+ is a mixture of the two structures CH_3S^+ and CH_2SH^+.

A typical pressure plot at 10 eV nominal electron energy and 3.4 eV ion exit energy is shown in Fig. 1. From the semi-logarithmic plots of the normalized primary ion intensities versus pressure we obtained as the average of four runs $k_1 = 11.9 \pm 0.6 \times 10^{-10}$ cm^3 $molecule^{-1}$ s^{-1} and $k_2 = 10.4 \pm 0.3 \times 10^{-10}$ cm^3 $molecule^{-1}$ s^{-1}.

Several pressure plots also were carried out at higher electron energies where CHS^+ was present as a primary ion. This ion was found to be reactive, having a disappearance rate constant of 7×10^{-10} cm^3 $molecule^{-1}$ s^{-1}. Although the products of the reaction were not positively identified there was some evidence that it reacted in part by charge transfer to produce CH_3SH^+.

Ion–Molecule Reactions in CD_3SH

The mass spectrum of CD_3SH shows both

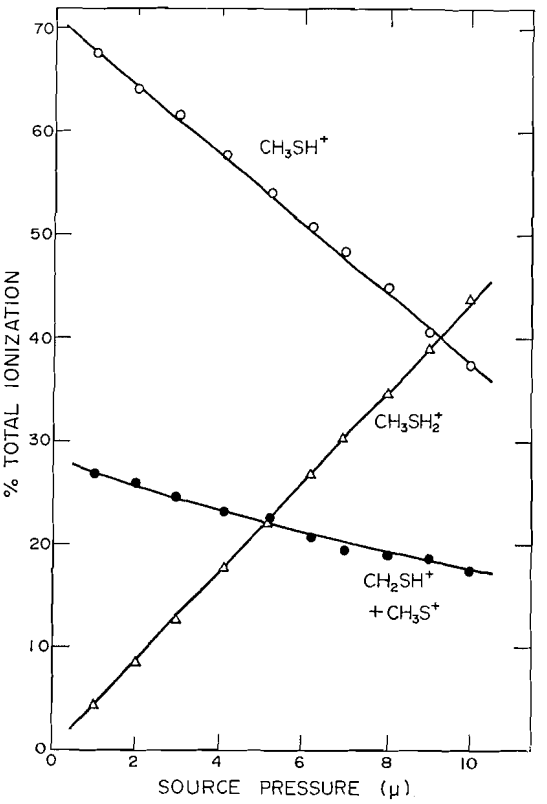

FIG. 1. Pressure plot CH_3SH, 10 eV nominal electron energy.

CD_3S^+ and CD_2SH^+ as fragment ions, the appearance potentials of the two ions being practically the same (8). Consequently it was not possible to work under conditions where only one fragment ion was present.

Using the modified MS-2 instrument at electron energies below the onset of fragment ion formation predominant formation of $CD_3SH_2^+$ was noted, the ratio $CD_3SH_2^+/CD_3SHD^+$ being approximately 15 ± 5. At higher electron energies both CD_3S^+ and CD_2SH^+ were significant reactive primary ions. CD_3S^+ can yield only CD_3SHD^+ while the results showed that CD_2SH^+ produced only $CD_3SH_2^+$.

Figure 2 shows a typical pressure plot for CD_3SH at 10 eV nominal electron energy and 3.4 eV ion exit energy. From four such runs we determined the following rate constants (units: cm^3 $molecule^{-1}$ s^{-1}).

[3] $CD_3SH^+ + CD_3SH \rightarrow CD_3SH_2^+ + CD_3S$
$\rightarrow CD_3SHD^+ + CD_2SH$

$$k_3 = 12.1 \pm 0.3 \times 10^{-10}$$

[4] $CD_2SH^+ + CD_3SH \rightarrow CD_3SH_2^+ + CD_2S$

$$k_4 = 8.0 \pm 0.6 \times 10^{-10}$$

[5] $CD_3S^+ + CD_3SH \rightarrow CD_3SHD^+ + CD_2S$

$$k_5 = 10.0 \pm 0.4 \times 10^{-10}$$

Pressure plots also were carried out at low electron energies, where only CD_3SH^+ was present as a primary ion, to determine the isotopic distribution of products from reaction [3]. Figure 3 shows a typical plot extending to 40 μ pressure. The initial yields show that 92% of the reaction produces $CD_3SH_2^+$ while 8% produces CD_3SHD^+. In addition the CD_3SHD^+ yield goes through a maximum and decreases with further increase in pressure. This is presumably due to the proton transfer reaction [6]

[6] $CD_3SHD^+ + CD_3SH \rightarrow CD_3SH_2^+ + CD_3SD$

similar to that observed in the CD_3OH system (3, 4). A small yield of the disolvated proton was observed at high pressures.

The above results indicate that in reaction [3] the mercaptyl hydrogen is transferred approximately 35 times more readily than the methyl hydrogen (allowing for the 3:1 ratio of available hydrogens). This is to be compared with the corresponding factor of 2.5 for the methyl alcohol system. A similar high reactivity of the mercaptyl hydrogen is also observed in hydrogen abstraction reactions by methyl radicals, where, with CH_3SH, abstraction of the mercaptyl hydrogen occurs much more rapidly than abstraction of a methyl hydrogen (9), while with methyl alcohol abstraction of the methyl hydrogen is the faster reaction (10).

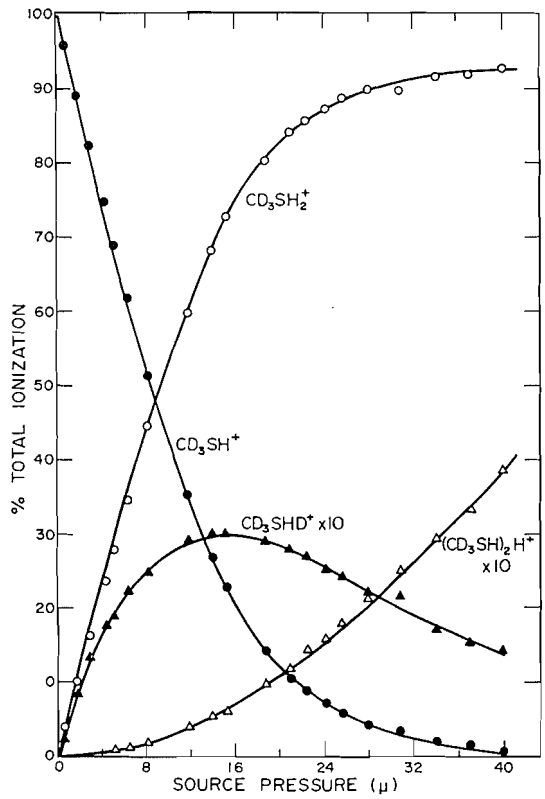

FIG. 2. Pressure plot CD_3SH, 10 eV nominal electron energy.

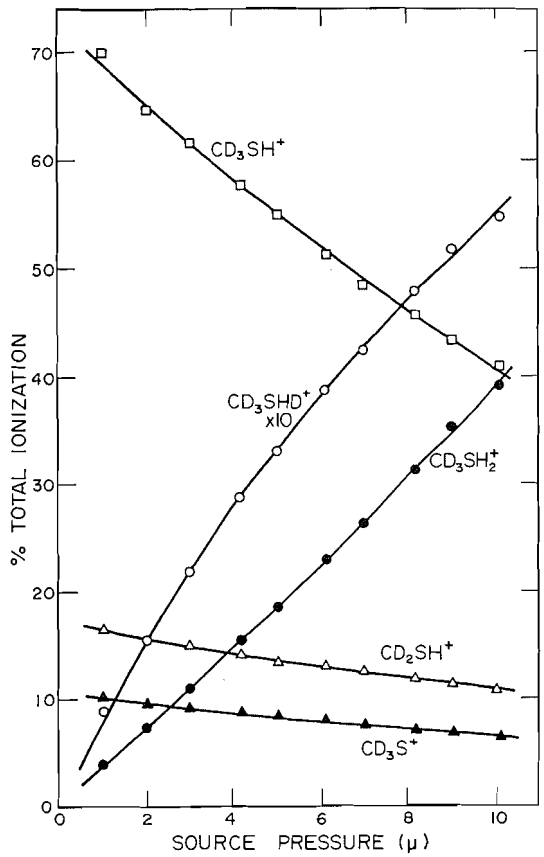

FIG. 3. Pressure plot CD_3SH, CD_3SH^+ only significant primary ion.

Acknowledgment

The authors are indebted to the National Research Council of Canada for financial support.

1. K. R. RYAN, L. W. SIECK, and J. H. FUTRELL. J. Chem. Phys. **41**, 111 (1964).
2. J. C. J. THYNNE, F. K. AMENU-KPODO, and A. G. HARRISON. Can. J. Chem. **44**, 1655 (1966).

Can. J. Chem. Downloaded from www.nrcresearchpress.com by 210.87.254.5 on 09/05/12
For personal use only.

3. L. W. SIECK, F. P. ABRAMSON, and J. H. FUTRELL. J. Chem. Phys. **45**, 2859 (1966).
4. D. J. HYATT, E. A. DODMAN, and M. J. HENCHMAN. Advan. Chem. Ser. **58**, 131 (1966).
5. S. K. GUPTA, E. G. JONES, A. G. HARRISON, and J. J. MYHER. Can. J. Chem. **45**, 3107 (1967).
6. T. W. SHANNON and A. G. HARRISON. J. Chem. Phys. **43**, 4201 (1965).
7. T. W. SHANNON, F. MEYER, and A. G. HARRISON. Can. J. Chem. **43**, 159 (1965).
8. B. G. KEYES and A. G. HARRISON. J. Am. Chem. Soc. In press.
9. G. GREIG and J. C. J. THYNNE. Trans. Faraday Soc. **62**, 379 (1966).
10. J. C. J. THYNNE and R. SHAW. Trans. Faraday Soc. **62**, 1 (1966).

Functionally substituted oligomeric stannoxanes

D. WAGNER[1], D. GERTNER, AND A. ZILKHA
Department of Organic Chemistry, The Hebrew University of Jerusalem, Jerusalem, Israel

Received June 10, 1968

The successive insertion of Bu_2SnO units into Sn—Cl, Sn—OOCR, Sn—OAr, and Sn—O—N(C=O)(C=O) bonds was found to lead to functionally substituted oligomeric stannoxanes.

Canadian Journal of Chemistry, 46, 3612 (1968)

The reactions of polymeric dialkyltin oxides, R_2SnO, and compounds of the type R'_3SnX (1, 2), R'_2SnX_2 (3), $R'SnX_3$ (1, 2), and SnX_4 (1) (X = halogen or acetate), in which distannoxanes of the general formula $X_{3-n}R'_nSnOSnR_2X$ (n = 3–0) are formed, were reported by Davies *et al.* In a preliminary note (4), the same author reported the synthesis of some polymeric stannoxanes. This communication prompts us to publish our results concerning some insertion reactions leading to the formation of functionally substituted oligomeric stannoxanes, wherein the reactions are carried out stepwise.

We found that tetrabutyl dichlorodistannoxane reacted readily with 1 mole of dibutyltin oxide in boiling toluene, the reaction product being hexabutyl dichlorotristannoxane

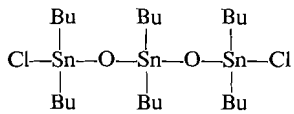

The end of the reaction is clearly indicated by the disappearance of the insoluble dibutyltin oxide. Adding an additional mole of the oxide and boiling for a short time resulted in the insertion of an additional Bu_2SnO unit into the molecule, producing octabutyl dichlorotetrastannoxane,

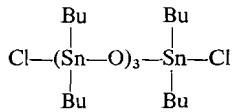

As the starting compound for these reactions contains a Sn—Cl bond as well as a Sn—O—Sn bond, it may react with Bu_2SnO as an organotin halide or as an organotin oxide. The end product will be the same by either path, so that no evidence concerning the site of insertion of the Bu_2SnO group can be deduced by the structure of the resulting reaction product. It was found that *bis*-tributyltin oxide, $R_3Sn—O—SnR_3$ (whose structure is very similar to that of tetrabutyl dichlorodistannoxane except that its two halogen atoms are replaced by alkyl groups), failed to react with dibutyltin oxide even on prolonged heating to high temperature. This fact suggests that in the reaction with the stannoxane the Sn—Cl bond is the active site and not the Sn—O one.

The tri- and tetra-stannoxanes are soft, low-melting solids which are easily soluble in organic solvents.

In analogy to the insertion reaction of dibutyltin oxide into Sn—Cl bonds, we tried to

[1]Part of a Ph.D. Thesis submitted by D. Wagner to the Senate of the Hebrew University of Jerusalem, September 1967.

Can. J. Chem. Downloaded from www.nrcresearchpress.com by 210.87.254.5 on 09/05/12
For personal use only.

3. L. W. SIECK, F. P. ABRAMSON, and J. H. FUTRELL. J. Chem. Phys. **45**, 2859 (1966).
4. D. J. HYATT, E. A. DODMAN, and M. J. HENCHMAN. Advan. Chem. Ser. **58**, 131 (1966).
5. S. K. GUPTA, E. G. JONES, A. G. HARRISON, and J. J. MYHER. Can. J. Chem. **45**, 3107 (1967).
6. T. W. SHANNON and A. G. HARRISON. J. Chem. Phys. **43**, 4201 (1965).
7. T. W. SHANNON, F. MEYER, and A. G. HARRISON. Can. J. Chem. **43**, 159 (1965).
8. B. G. KEYES and A. G. HARRISON. J. Am. Chem. Soc. In press.
9. G. GREIG and J. C. J. THYNNE. Trans. Faraday Soc. **62**, 379 (1966).
10. J. C. J. THYNNE and R. SHAW. Trans. Faraday Soc. **62**, 1 (1966).

Functionally substituted oligomeric stannoxanes

D. WAGNER[1], D. GERTNER, AND A. ZILKHA
Department of Organic Chemistry, The Hebrew University of Jerusalem, Jerusalem, Israel

Received June 10, 1968

The successive insertion of Bu_2SnO units into Sn—Cl, Sn—OOCR, Sn—OAr, and Sn—O—N(C=O)(C=O) bonds was found to lead to functionally substituted oligomeric stannoxanes.

Canadian Journal of Chemistry, 46, 3612 (1968)

The reactions of polymeric dialkyltin oxides, R_2SnO, and compounds of the type R'_3SnX (1, 2), R'_2SnX_2 (3), $R'SnX_3$ (1, 2), and SnX_4 (1) (X = halogen or acetate), in which distannoxanes of the general formula $X_{3-n}R'_nSnOSnR_2X$ (n = 3–0) are formed, were reported by Davies *et al.* In a preliminary note (4), the same author reported the synthesis of some polymeric stannoxanes. This communication prompts us to publish our results concerning some insertion reactions leading to the formation of functionally substituted oligomeric stannoxanes, wherein the reactions are carried out stepwise.

We found that tetrabutyl dichlorodistannoxane reacted readily with 1 mole of dibutyltin oxide in boiling toluene, the reaction product being hexabutyl dichlorotristannoxane

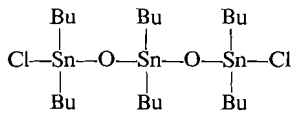

The end of the reaction is clearly indicated by the disappearance of the insoluble dibutyltin oxide. Adding an additional mole of the oxide and boiling for a short time resulted in the insertion of an additional Bu_2SnO unit into the molecule, producing octabutyl dichlorotetrastannoxane,

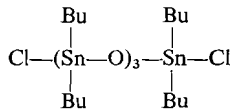

As the starting compound for these reactions contains a Sn—Cl bond as well as a Sn—O—Sn bond, it may react with Bu_2SnO as an organotin halide or as an organotin oxide. The end product will be the same by either path, so that no evidence concerning the site of insertion of the Bu_2SnO group can be deduced by the structure of the resulting reaction product. It was found that *bis*-tributyltin oxide, $R_3Sn—O—SnR_3$ (whose structure is very similar to that of tetrabutyl dichlorodistannoxane except that its two halogen atoms are replaced by alkyl groups), failed to react with dibutyltin oxide even on prolonged heating to high temperature. This fact suggests that in the reaction with the stannoxane the Sn—Cl bond is the active site and not the Sn—O one.

The tri- and tetra-stannoxanes are soft, low-melting solids which are easily soluble in organic solvents.

In analogy to the insertion reaction of dibutyltin oxide into Sn—Cl bonds, we tried to

[1]Part of a Ph.D. Thesis submitted by D. Wagner to the Senate of the Hebrew University of Jerusalem, September 1967.

Can. J. Chem. Downloaded from www.nrcresearchpress.com by 210.87.254.105 on 09/05/12
For personal use only.

Can. J. Chem. Downloaded from www.nrcresearchpress.com by 210.87.254.105 on 09/05/12
For personal use only.

TABLE I

Oligomeric stannoxanes

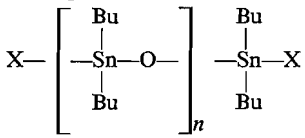

X	n	M.p. (°C)	Recrystallization from	Yield (%)	C (%) Calcd.	C (%) Found	H (%) Calcd.	H (%) Found	N (%) Calcd.	N (%) Found	Cl (%) Calcd.	Cl (%) Found	Sn (%) Calcd.	Sn (%) Found
Cl	2	104*	Heptane	73	35.96	36.06	6.79	6.58			8.84	7.03	44.42	44.20
Cl	3	102†	Heptane	86	36.58	36.55	6.91	6.58			6.75	6.84	45.19	45.70
p-$NO_2C_6H_4CO_2$	2	85	Heptane–benzene	90	42.93	43.10	5.88	5.60	2.64	2.43			33.50	33.60
o-$NO_2C_6H_4CO_2$	2	120	Heptane	96	42.93	42.60	5.88	6.00	2.64	2.50			33.50	33.10
p-$ClC_6H_4CO_2$	2	144–145	Toluene	94	43.80	43.94	6.00	6.21			6.81	6.64	34.18	33.90
$C_6H_5CONHCH_2CO_2$	2	140–141	Benzene–petroleum ether	89	46.40	46.15	6.49	6.71	2.58	2.47			32.76	32.50
Cl_2CHCO_2	2	124–125	Petroleum ether	46	34.08	34.29	5.72	5.70			14.37	14.8	36.09	35.90
p-$NO_2C_6H_4O$	2	171	Heptane	81	42.94	42.82	6.21	6.18	2.78	2.80			35.36	35.15
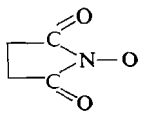	1	209–210	Hexane–benzene	92	40.60	40.74	6.25	6.07	3.95	3.97			33.43	33.40

*Literature (4), m.p. 89–90.
†Literature (4), m.p. 94–95.

insert the Bu_2SnO group into Sn—carboxylate bonds. In a previous paper (5) we described the preparation of organotin esters of the type

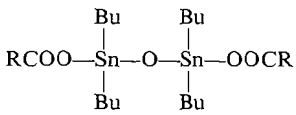

by an interfacial method, using tetrabutyl dichlorodistannoxane as starting material. Such esters were used in this study. It was found that the insertion reactions are fast and yielded the expected products. Thus, reacting tetrabutyl di-para-nitrobenzoyloxy distannoxane with 1 mole of dibutyltin oxide gave hexabutyl di-para-nitrobenzoyloxy tristannoxane.

We also found that organotin phenolates entered the insertion reaction, according to the equations

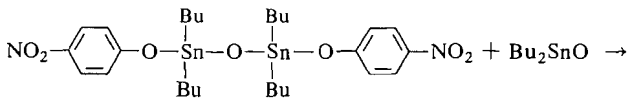

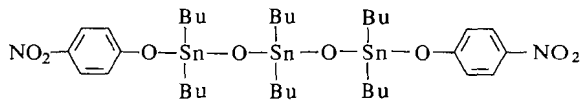

In the same manner the dibutyl tin ester of N-hydroxy succinimide entered the insertion reaction

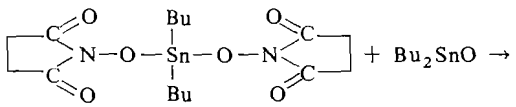

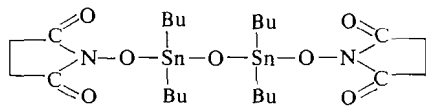

In contrast to the reactivity of tin–halogen, –carboxylate and –phenolate bonds, the tin–sulfur and tin–tin bonds were found to be unreactive in this insertion reaction.

Experimental

Melting points were determined on a Fisher–John apparatus and are uncorrected.

General Procedure for the Insertion Reactions

The insertion products were obtained by boiling dibutyltin oxide with 1 equivalent of organotin dichloride, dicarboxylate, diphenolate, or the N-hydroxy succinimide derivative in toluene. Upon clarification of the reaction mixture it was cooled, more dibutyltin oxide was added, and this process was repeated two or three times as required.

The compounds prepared are summarized in Table I.

1. A. G. Davies and P. G. Harrison. J. Organometal. Chem. Amsterdam, **7**, 13 (1967).
2. A. G. Davies and P. G. Harrison. J. Organometal. Chem. Amsterdam, **10**, 31 (1967).
3. D. L. Alleston, A. G. Davies, M. Hancock, and R. F. M. White. J. Chem. Soc. 5469 (1963).
4. A. G. Davies, P. G. Harrison, and P. R. Palan. J. Organometal. Chem. Amsterdam, **10**, 33 (1967).
5. M. Frankel, D. Gertner, D. Wagner, and A. Zilkha. J. Organometal. Chem. Amsterdam, **9**, 83 (1967).

Can. J. Chem. Downloaded from www.nrcresearchpress.com by 210.87.254.105 on 09/05/12
For personal use only.

Erratum: Effets ioniques spécifiques sur le taux de formation du ClO_2 par la réaction chlorure-chlorate

F. LENZI ET W. H. RAPSON
Department of Chemical Engineering and Applied Chemistry, University of Toronto, Toronto, Ontario

Reçu le 5 juillet 1968

(Ref.: Can. J. Chem. **46**, 979 (1968))

Canadian Journal of Chemistry, **46**, 3615 (1968)

Page 984, colonne gauche, éq. [7]: lire

$$\frac{2k_2k_3K^4[Cl^-]^2[ClO_3^-]^2[H^+.4H_2O]^4}{k_2'[Cl_2][H_2O]^{17} + k_3K[H^+.4H_2O][ClO_3^-][H_2O]^{12}}$$

au lieu de

$$\frac{2k_2k_3K^4[Cl^-]^2[ClO_3^-]^2}{k_2'[Cl_2][H_2O]^{17} + k_3K[H^+.4H_2O][ClO_3^-][H_2O]^{12}}$$

Page 984, colonne droite, ligne 10: lire 22.3 × 271 = 6032 au lieu de 22.4 × 230 = 5150.

Page 984, colonne droite, ligne 15: lire 6032 au lieu de 5150.

Can. J. Chem. Downloaded from www.nrcresearchpress.com by 210.87.254.6 on 09/05/12
For personal use only.

Can. J. Chem. Downloaded from www.nrcresearchpress.com by 210.87.254.105 on 09/05/12
For personal use only.

Canadian Journal of Chemistry

Published by THE NATIONAL RESEARCH COUNCIL OF CANADA

VOLUME 46 DECEMBER 1, 1968 NUMBER 23

Structure of pithecolobine. III. The synthesis of the 1,5- and 1,3-desoxypithecolobines

K. WIESNER, Z. VALENTA, D. E. ORR, V. LIEDE, AND G. KOHAN

Natural Product Research Center, University of New Brunswick, Fredericton, New Brunswick

Received June 17, 1968

The second communication of this series has shown that "pithecolobine" is a family of closely related analogues represented by the general formula **1**. In the present paper a crude semiquantitative estimate of the individual components is achieved by a combination of vapor-phase chromatography and chemical degradation.

The synthesis of the desoxypithecolobines **3***a* and **3***b* and their tetratosylates **11***a* and **11***b* is described. A comparison of these compounds with the corresponding "natural" mixtures by thin-layer chromatography in several systems, infrared, nuclear magnetic resonance, and mass spectrometry was found to support strongly the conclusions reached by the previous degradative work.

Canadian Journal of Chemistry, 46, 3617 (1968)

In the second communication (1) of this series we have shown that the "alkaloid pithecolobine" is in fact a mixture of homologues and analogues represented by the general formula **1**.

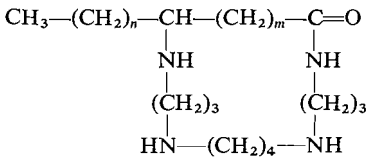

1 ($m + n = 9, 10, 11$)
1*a* ($m = 3, n = 6$)
1*b* ($m = 1, n = 8$)
1*c* ($m = 1, n = 10$)

In this mixture we have rigorously demonstrated the presence of **1***a* and we have shown that a significant proportion of compounds with $m = 1$ is present.

As a necessary prerequisite of the synthetic studies to be described in the sequel, we wished to have at least a semiquantitative estimate of the main components in the pithecolobine mixture.[1] It was possible to achieve such a crude analysis by vapor-phase chromatography (v.p.c.) of straight chain acids (in the form of their methyl esters) obtained from the Hofmann degradation of pithecolobine. We have shown in our second communication (1) that the Hofmann degradation of pithecolobine yields besides a mixture of neutral unsaturated amides, the lactone **2** by internal displacement. Hydrogenation and hydrolysis of the unsaturated amides gave *n*-dodecanoic acid contaminated by some *n*-tridecanoic and *n*-tetradecanoic acid. We have now determined quantitatively the proportions of these three acids in the mixture by v.p.c. of the methyl esters. The result was as follows: C-12 acid, 65%; C-13 acid, 4%; C-14 acid, 30%. The quantities of lactone **2** and unsaturated amides obtained in the experiment were 122 mg and 391 mg, respectively.

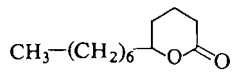

2

From these results it is clear that a minimum of 24% of the pithecolobines is compound **1***a* ($m = 3$, $n = 6$), a further 49% are other C-22 ($m + n = 9$) pithecolobines (including possibly some more **1***a* which did not yield the lactone **2**, but gave a normal Hofmann degradation); 3% are C-23 pithecolobines ($m + n = 10$), and

[1]Vapor-phase chromatography and other methods of separation on the alkaloids and their derivatives were repeatedly tried and failed.

23% are C-24 pithecolobines ($m + n = 11$). To get a further breakdown of the individual pithecolobine components, the neutral unsaturated amides were oxidized by permanganate–periodate in tertiary butanol. The fatty acids thus obtained were converted to methyl esters and analyzed by v.p.c. The result of this analysis is given in Table I.

TABLE I

Yield of straight chain acid from oxidation of unsaturated amides

Acid	Yield (%)
C_5	0
C_6	8
C_7	1
C_8	5
C_9	25
C_{10}	40
C_{11}	10
C_{12}	12

These results may now be simply interpreted as follows:

(a) There is only 6% of C-7 + C-8 acids. Consequently, most of the pithecolobine **1***a* degrades to lactone **2** rather than to the unsaturated amides.

(b) There is 22% of C-11 + C-12 acids. Most of these must be derived from the C-24 pithecolobine **1***c*.

(c) Finally, there is 65% of C-9 + C-10 acids.

Since the C-24 pithecolobines are mostly accounted for by the C-11 + C-12 acids and the amount of the C-23 pithecolobines is small, most of the C-9 + C-10 acids must be derived from the C-22 pithecolobine **1***b* ($m = 1, n = 8$).

If we neglect the possibility of yield differences in the various degradation pathways and take our data at face value, we may estimate the percentages of the three main pithecolobine components as follows: **1***a*, ($m = 3, n = 6$), 24–30%; **1***b*, ($m = 1$, $n = 8$), 40–49%; **1***c*, ($m = 1$, $n = 10$), 13.5–16.5%.

Even if we assume that the lowest numbers are correct, we see that compounds **1***a*, **1***b*, and **1***c* account for more than three-quarters of the pithecolobine mixture.

Since **1***a* and **1***b* are by far the most abundant components, we wished to synthesize the corresponding desoxypithecolobines and compare them with the "natural" desoxypithecolobine mixture.

We decided to synthesize first the desoxypithecolobine **3***a* which corresponds to the pithecolobine **1***a*.[2]

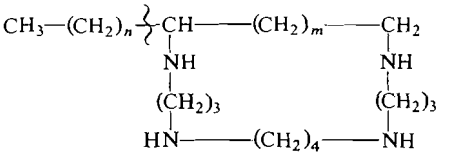

3*a* ($m = 3, n = 6$)
3*b* ($m = 1, n = 8$)
3*c* ($m = 1, n = 10$)

In this first approach, we have largely followed the work of Stetter and Roos (2) and our initial aim was thus the synthesis of the tetratosylate **11***a*. This work was reported in a preliminary paper (3) and it was accomplished as follows. Our starting material was 1,5-dibromododecane, previously described by Franke and Kroupa (4). We have, however, prepared this compound by a different and more convenient route.

Treatment of cyclopentanone with the Grignard reagent from 1-bromoheptane yielded the tertiary alcohol **4**. Dehydration of **4** with phosphorus pentoxide in benzene gave the olefin **5**, which was converted to the acid **6** by ozonolysis, followed by hydrogen peroxide oxidation. The acid was esterified with methanol and the methyl ester **7** was reduced with lithium aluminium hydride to 1,5-dihydroxydodecane. This last compound on treatment with fuming hydrobromic acid finally yielded the desired 1,5-dibromododecane **8**. The dibromide **8** was converted into 1,5-diazidododecane by treatment with sodium azide in diethylene glycol monomethyl ether. The diazide was not characterized, but immediately hydrogenated to the hygroscopic oily 1,5-diaminododecane. This material was finally tosylated to the ditosylate **9**. The dibromide **10** which was required as the second component of the synthesis was constructed as follows. The ditosylate of 1,4-diaminobutane was prepared in the usual manner and converted to (**10**) by treatment with 1,3-dibromopropane under the conditions recommended by Stetter and Roos (2)

[2]The reason for this was our initial belief that **1***a* is the major component of the pithecolobine mixture. This in turn was due to the comparatively good yield of lactone **2**, and the absence of the quantitative data reported in the present communication.

Can. J. Chem. Downloaded from www.nrcresearchpress.com by 210.87.254.105 on 09/05/12
For personal use only.

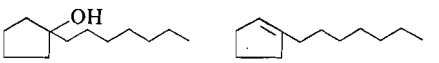

4 5

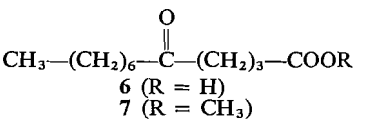

6 (R = H)
7 (R = CH_3)

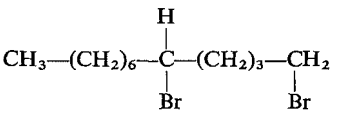

8

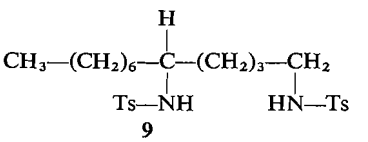

9

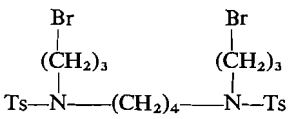

10

(see Experimental). The coupling of the disodium salt of **9** with compound **10** was performed in dimethyl formamide under high dilution. The product **11***a* was isolated in pure form by chromatography on alumina. It was a colorless

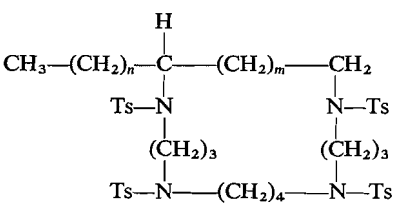

11*a* (m = 3, n = 6)
11*b* (m = 1, n = 8)

glass and the peak fraction showed a constant infrared (i.r.) spectrum on repeated chromatography and was homogeneous in thin-layer chromatography (t.l.c.).

Since the synthetic compound **11***a* resisted all detosylation attempts, we have prepared the tetratosylate of the "natural" desoxypithecolobine mixture and were able to show that both synthetic and "natural" material gave superimposable i.r. spectra in potassium bromide and chloroform. This finding certainly corroborates the structure of the pithecolobines in principle. However, at the same time it is clear that since the individual desoxypithecolobine components show insufficient differences in i.r. spectroscopy, this method of comparison has to be supplemented by others (*vide infra*).

Our next synthetic objective was the tetratosylate **11***b*, which we hoped to reach by methods completely analogous to those used for the tetratosylate **11***a*.

For this end, it was first necessary to synthesize 1,3-diaminododecane. After some difficulties experienced with more conventional approaches, the following route was found to be effective.[3] The ketonitrile **12** (5) was converted (6) by the action of hydroxylamine into the crystalline aminoisoxazole **13**. Catalytic hydrogenation of this last compound gave the amide **14** in quantitative yield. The reduction of **14** to the desired 1,3-diaminododecane **15** could not be accomplished by lithium aluminium hydride but it was achieved with an excellent result by the use of diborane (7).

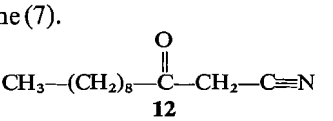

12

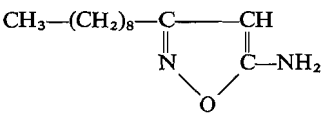

13

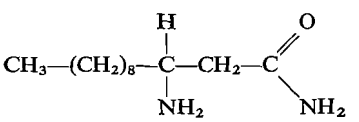

14

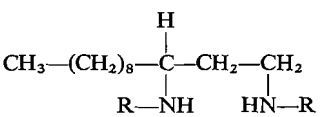

15 (R = H)
16 (R = Ts)

The tosylation of **15** to **16** and the subsequent synthesis of the tetratosylate **11***b* were uneventful and proceeded exactly as in the case of the tetratosylate **11***a*. The details may be found in the Experimental.

The i.r. spectrum of the synthetic tetratosylate

[3]This method is an application of a general procedure for the preparation of 1,3-diamines which has been worked out by two of the present authors (Z. V. and G. K.) and will be published in due course. To our surprise, no really acceptable and convenient route to these compounds was found in the literature.

Can. J. Chem. Downloaded from www.nrcresearchpress.com by 210.87.254.105 on 09/05/12
For personal use only.

11*b* was superimposable on the spectrum of the tosylated "natural" desoxypithecolobine mixture and of course also on the spectrum of the synthetic tetratosylate **11***a*. This was a clear proof that i.r. spectroscopy is not capable of distinguishing the fine details of ring size in the pithecolobine series.

Since all detosylation experiments on **11***a* and **11***b* resulted in complete failure, it was decided to design a new synthetic method which would yield directly the free desoxypithecolobines.

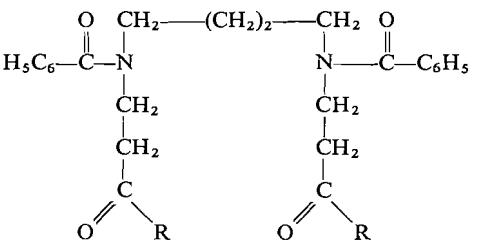

17 (R = —O—CH_2—CH_3)
18 (R = —OH)
19 (R = —Cl)

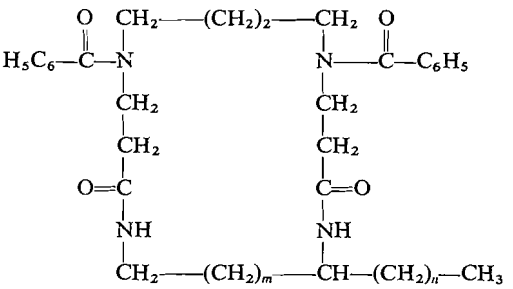

20 (*m* = 3, *n* = 6)
21 (*m* = 1, *n* = 8)

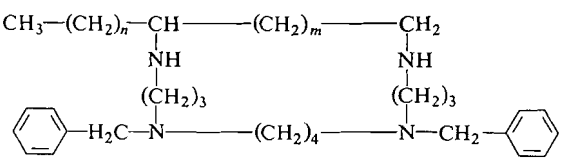

22 (*m* = 3, *n* = 6)
23 (*m* = 1, *n* = 8)

The basic idea of the new synthetic scheme was to synthesize the dichloride **19** and couple it under high dilution with 1,5- and 1,3-diaminododecane to the compounds **20** and **21**, respectively. These materials could be expected to yield the desoxypithecolobines **3***a* and **3***b* by reduction and hydrogenolysis.

The reaction of 1,4-diaminobutane with ethyl acrylate, followed by benzoylation of the product yielded the diester **17**, which was hydrolyzed to the crystalline diacid **18**. This last compound was then converted to the dichloride **19** by the action of thionyl chloride. The reaction of **19** with the two diamines (1,3- and 1,5-diaminododecanes) was performed under high dilution in carbon tetrachloride. The two tetramides **20** and **21**, thus obtained, were reduced to the dibenzyl desoxypithecolobines **22** and **23** by diborane and these last compounds were hydrogenolyzed to the desoxypithecolobines **3***a* and **3***b*. The two synthetic desoxypithecolobines were finally converted into the tetratosylates **11***a* and **11***b* and thus it was possible to interrelate the two synthetic series.

Infrared comparison of the desoxypithecolobines **3***a* and **3***b* in chloroform and carbon tetrachloride showed, as in the case of the tetratosylates **11***a* and **11***b*, complete superimposability of the spectra. It is thus not surprising that the i.r. spectra of both synthetic desoxypithecolobines were also superimposable on the corresponding spectrum of the "natural" desoxypithecolobine mixture. If the two main components of a mixture have identical spectra, then also the spectrum of the mixture itself must be identical with the spectra of the pure components. Next we have studied the synthetic and "natural" desoxypithecolobines and their tosylates by t.l.c. in several systems. The situation here is the same as in i.r. spectroscopy. Both in the case of the free desoxypithecolobines and their tosylates the two synthetic materials do not show significant differences from each other and from the "natural" mixture, which behaves as a single compound.

These studies, while clearly not possessing the rigorous validity of a confrontation between a pure synthetic and natural compound, nevertheless show that the "natural" desoxypithecolobine mixture possesses many physical characteristics which are identical with those of the pure synthetic components of known structure. Thus the conclusions drawn from our degradative work receive considerable synthetic support.

It now seemed desirable to find physical methods which would reveal some significant difference between the two synthetic compounds and the "natural" mixture. The first such method which revealed minor differences was nuclear magnetic resonance (n.m.r.) spectroscopy of the tetratosylates. The two synthetic tetratosylates differ by ring-size, i.e. by the number of hydrogens

Can. J. Chem. Downloaded from www.nrcresearchpress.com by 210.87.254.105 on 09/05/12
For personal use only.

Can. J. Chem. Downloaded from www.nrcresearchpress.com by 210.87.254.105 on 09/05/12
For personal use only.

situated inside the macrocycle. These hydrogens are subject (to put it in most general terms) to special shielding and deshielding influences which are quite different from those affecting the hydrogens of the side-chain. Thus, n.m.r. spectroscopy was expected to show some differences between **11***a* and **11***b*. The n.m.r. spectra revealed the following groups of hydrogens.

(a) A quadruplet (16 H) at τ 2.29, 2.43, 2.68, and 2.82 p.p.m. (aromatic hydrogens);

(b) A broad unresolved multiplet (15 H) centered at τ 7.00 p.p.m. (hydrogen unshielded by the four nitrogens);

(c) A singlet (1 2H) τ 7.6 p.p.m. (four aromatic methyl groups);

(d) A multiplet between τ 8.78 and 9.26 p.p.m. This group contains most of the aliphatic hydrogen including the *C*-methyl group and cannot be quantitatively separated from group *(e)*;

(e) A multiplet around τ 8.3–8.5 p.p.m. This group cannot be quantitatively separated from the preceding group *(d)* and contains a smaller part of the aliphatic hydrogens, subject to special unshielding influence, presumably inside the macrocycle.

It is only the precise shape of this last multiplet in which the two synthetic tosylates **11***a* and **11***b* differ. The shape of this group in the "natural" mixture lies in between, much closer to compound **11***b*. The remaining features of the spectra in all compounds are the same.

The closer resemblance of the "natural" tetratosylate to **11***b* is due not only to the greater concentration of this component in the "natural" mixture, but presumably also to the fact that the third most abundant component of the "natural" mixture (derived from the desoxypithecolobine **3***c*) contains the same macrocycle as compound **11***b*.

The second method which should reveal differences between the desoxypithecolobines **3***a* and **3***b* is mass spectrometry. The breaking of the side-chain on electron impact (indicated by the wavy line in **3**) should be important and it might differentiate between **3***a* and **3***b*. Again, the "natural" desoxypithecolobine mixture should resemble closely the synthetic desoxypithecolobine **3***b*, since the desoxypithecolobines **3***b* and **3***c* yield the same fragment by this type of fragmentation.

The mass spectra of the two synthetic samples **3***a* and **3***b* and "natural" desoxypithecolobine do not show a molecular ion, are extremely complicated and difficult to interpret. All three samples are very similar but *non-identical.* As expected, the spectrum of "natural" desoxypithecolobine is "almost identical" with the synthetic compound **3***b*.

Experimental

Vapor-phase Chromatography of Saturated Esters

The ether solutions of the saturated methyl esters were chromatographed on an SE30 column (25%) at 250 °C. The peaks of the individual components were identified by the addition of authentic samples. The percentage composition of the mixture was obtained by determining the area under each peak. (For tabulation of results see theoretical part.)

Permanganate–Periodate Oxidation of the Unsaturated Amides

One millimole of the unsaturated secondary amide mixture from the Hofmann degradation of pithecolobine **1** was dissolved in 6 ml of *t*-butyl alcohol and a few drops of water were added. Sodium metaperiodate (8 mmoles) was added in a 10% aqueous solution which has been adjusted by sodium carbonate to a pH of 7.5–7.8. Potassium permanganate (0.134 mmole) was then added in a 1% aqueous solution. Finally, approximately 2 ml of *t*-butyl alcohol were added and the mixture stirred for 5 h. After this time, 5 ml of water were added and the solution was made alkaline and exhaustively extracted, first with chloroform and then with ether. The aqueous alkaline layer was acidified with sulfuric acid and extracted with ether. The ether solution was concentrated to a small volume, esterified with diazomethane, dried, and further concentrated to a volume of 0.5 ml. This solution was analyzed by vapor-phase chromatography (v.p.c.) (*vide supra*).

Preparation of Compound ***4***

Normal heptyl bromide (268 g), dissolved in 600 ml of absolute ether, was added under nitrogen to 36 g of magnesium turnings. After 4 h of gentle reflux, the magnesium had dissolved and a slow addition of cyclopentanone (127 g) in 150 ml of absolute ether was started. The addition took 2 h and the solution was then heated under reflux for an additional 2 h. The reaction mixture was decomposed by pouring into an excess of aqueous ammonium chloride and exhaustively extracted with ether. The pure product was isolated by fractional distillation *in vacuo*. It was obtained in a yield of 161 g (67%) and it boiled at 114–115 °C (11 mm Hg).

Anal. Calcd. for $C_{12}H_{24}O$: C, 78.20; H, 13.13; O, 8.68. Found: C, 78.41; H, 12.69; O, 8.82.

Dehydration of ***4*** *to* ***5***

Compound (**4**) (160 g) was dissolved in 2 l of dry benzene and 500 g of phosphorus pentoxide were gradually added with stirring at room temperature. After 1 h ice water was added and the organic layer was washed with water and dried. The benzene was distilled off *in vacuo* and the residue was dissolved in petroleum ether

Can. J. Chem. Downloaded from www.nrcresearchpress.com by 210.87.254.105 on 09/05/12
For personal use only.

and filtered through 800 g of basic alumina. The petroleum ether was then distilled off and the product fractionated *in vacuo*. The olefin (**5**) was obtained in a yield of 139 g (95%) and it distilled at 132–133 °C (50 mm Hg).

Anal. Calcd. for $C_{12}H_{22}$: C, 86.66; H, 13.34. Found: C, 87.38; H, 13.63.

Preparation of 5-Ketododecanoic Acid (6)

Distilled 1-*n*-heptyl cyclopentene **5** (120 g) was dissolved in 1600 ml of ethyl acetate and the solution cooled to −70 °C. Ozone (6%) was bubbled through until the solution turned blue and ozone was no longer absorbed. After this most of the ethyl acetate was distilled off *in vacuo* at room temperature. The oily ozonide was dissolved in a mixture of the following composition: 750 ml glacial acetic acid, 500 ml water, 2 ml concentrated hydrochloric acid, and 360 ml 30% hydrogen peroxide. The resulting solution was stirred for 24 h after which the acidic material produced in the reaction was isolated in the usual manner. After recrystallization from ether, 94 g (61%) of the acid **6** were obtained. After several more crystallizations it melted at 69 °C.

Anal. Calcd. for $C_{12}H_{22}O_3$: C, 67.25; H, 10.34; O, 22.40. Found: C, 67.46; H, 9.93; O, 22.18.

Preparation of 1,5-Dodecane Diol

The acid **6** (94 g) was dissolved in 950 ml of absolute methanol containing 52 g of dry hydrogen chloride. The solution was refluxed for 1 h and the methyl ester **7** isolated in the usual manner and distilled. The middle fraction (62 g) boiled constantly at 114–118 °C (0.5 mm Hg). This material was reduced in dry ether with an excess (40 g) of lithium aluminium hydride. The product 1,5-dodecane diol was isolated in the usual manner and melted after crystallization at 45 °C. The yield of recrystallized material was 39 g (71%).

Anal. Calcd. for $C_{12}H_{26}O_2$: C, 71.24; H, 12.95; O, 15.82. Found: C, 71.08; H, 12.88; O, 16.24.

Preparation of 1,5-Dibromododecane (8)

Hydrobromic acid (48%, 100 ml) was saturated with hydrobromic acid gas and 20 g of 1,5-dodecane diol were added with stirring to this solution. The mixture was heated under reflux for 1 h after which it was diluted with water and extracted with ether. The dibromide **8** was isolated by distillation. The yield of constantly boiling material was 24.7 g (74%). The boiling point was 121–123 °C (0.7 mm Hg).

Anal. Calcd. for $C_{12}H_{24}Br_2$: C, 43.93; H, 7.38; Br, 48.71. Found: C, 45.69; H, 7.66; Br, 46.84.

Preparation of the Ditosylate 9

The dibromide **8** (24 g) was added to a solution of 1.368 g of sodium azide in water (34 ml) and diethylene glycol monomethyl ether (225 ml). The mixture was heated with stirring to 95 °C for 30 h. After this time it was diluted with water and the yellow diazide was extracted with ether. This material was hydrogenated in 700 ml of methanol with 700 mg of prehydrogenated platinum oxide. As no uptake of hydrogen is observable in this reaction the hydrogen was simply bubbled through the mixture for 24 h. The hygroscopic oily 1,5-diaminododecane was distilled and the fraction (9.24 g) boiling at 102–104 °C (10 mm Hg) was collected. It was immediately converted into the ditosylate **9**. For the tosylation the diamine (6.68 g) was suspended in 150 ml of water containing 2.68 g of sodium hydroxide. The suspension was vigorously stirred and 12.78 g of *p*-toluenesulfonyl chloride in 50 ml of ether were gradually added to it. The stirring was continued for 3 h. After this time the tosylate **9** was extracted with ether and purified by chromatography on alumina. The glassy ditosylate was obtained in a 94% yield. It was homogeneous in thin-layer chromatography (t.l.c.) and was sublimed for analysis in high vacuum at 200 °C.

Anal. Calcd. for $C_{26}H_{40}O_4N_2S_2$: C, 61.39; H, 7.93; O, 12.58; N, 5.50; S, 12.61. Found: C, 61.53; H, 7.93; O, 13.14; N, 4.96; S, 11.69.

Ditosyl-1,4-diaminobutane

The tosylation of 1,4-diaminobutane was performed exactly as described in the previous case. The yield of the product was 90%. It was recrystallized from methanol to a melting point 139–140 °C.

Anal. Calcd. for $C_{18}H_{24}O_4N_2S_2$: C, 54.52; H, 6.10; O, 16.14; N, 7.06; S, 16.17. Found: C, 54.35; H, 6.04; O, 15.82; N, 7.70; S, 15.89.

Preparation of the Dibromide 10

Ditosyl-1,4-diaminobutane (19.86 g) was added to a solution of 2.3 g of sodium in 75 ml of absolute methanol. The solution was refluxed for 30 min during which time the disodium salt precipitated. The methanol was removed *in vacuo* and the salt pulverized and dried *in vacuo* at 100 °C for 15 min. The salt was then suspended in dry dimethyl formamide and heated to 100 °C. At this point 30.3 g of 1,3-dibromopropane were added and the heating with vigorous stirring continued for 10 min. The reaction mixture was filtered, poured into water, and extracted with ether. The extract (41 g of yellow oil) was purified by chromatography on 800 g of neutral alumina. Benzene eluted crystalline material which after several crystallizations from chloroform–ether melted at 105 °C. The yield was 3.79 g of pure recrystallized compound **10**.

Anal. Calcd. for $C_{24}H_{34}O_4N_2S_2Br_2$: C, 45.15; H, 5.36; O, 10.02; N, 4.39; S, 10.04; Br, 25.03. Found: C, 44.63; H, 5.28; O, 10.42; N, 4.26; S, 9.98; Br, 25.32.

Preparation of the Tetratosyl Desoxypithecolobine 11a

The cyclization reaction was performed in a large round bottom flask containing 1000 ml of refluxing dimethyl formamide. To this flask were added at a very slow and equal rate the solutions *a* and *b* over a period of 30 h. Composition of solution *a*: 1.432 g of compound **10** in 160 ml of dimethyl formamide. Composition of solution *b*: 24 ml of absolute methanol, 100 mg of sodium, 1.136 g of compound **9**, 136 ml of dimethyl formamide. After the completion of the addition the reflux was continued for 3 h and then the reaction mixture was evaporated almost to dryness *in vacuo*. The residue was taken up in chloroform, washed with water, dried, and again evaporated to dryness. The yield was 2.65 g of brown oil. After chromatography on 80 g of neutral alumina 484 mg of a clear glass were obtained which was homogeneous in t.l.c. and had an infrared (i.r.) spectrum identical with "natural" desoxypithecolobine tetratosylate. This material was rechromatographed and the peak fraction of this new chromatogram did not show any difference either in i.r. or t.l.c. from either the bulk of

Can. J. Chem. Downloaded from www.nrcresearchpress.com by 210.87.254.105 on 09/05/12
For personal use only.

the material or from the "natural" tetratosylate. The material was a glass and could not be sublimed. It was consequently dried as a film deposited from carbon tetrachloride. The analysis for all the elements shows significant agreement. It shows that all of the oxygen, nitrogen, and sulfur, is in the form of sulfamido groups and that the ratio of these groups to carbon and hydrogen is the expected one. Since the compound is synthetic and from known elements, this ratio is sufficiently accurate to insure the correct molecular formula. A multiple of this formula is excluded by the approximate agreement of the molecular weight determination. Nuclear magnetic resonance (n.m.r.) spectroscopy (see theoretical part) corroborates quite accurately the correct ratios for various kinds of hydrogens. It is, in fact, in this case the most significant of all the analytical methods and has been used extensively besides i.r. spectroscopy and t.l.c. in the compounds prepared subsequently.

Anal. Calcd. for $C_{50}H_{72}O_8N_4S_4$ (mol. wt., 985): C, 60.94; H, 7.37; O, 12.99; N, 5.69; S, 13.03. Found (mol. wt. (osmometry in benzene) synthetic, 1032; "natural", 1045): C, 61.93; H, 8.11; O, 12.46; N, 5.61; S, 12.13.

Preparation of 2-Nonyl-4-amino-isoxazole (13)

The ketonitrile **12** (5) (20 g) was heated with hydroxylamine hydrochloride (21 g) and sodium acetate (41 g) in 450 ml of ethanol and 150 ml of water to 60 °C for 35 min. After this time the reaction mixture was poured into 2 l of water, extracted exhaustively with ether, and the isoxazole **13** recrystallized from petroleum ether to a melting point of 56 °C. The yield was 19.5 g (92.7%).

Anal. Calcd. for $C_{12}H_{22}N_2O$ (mol. wt., 210): C, 68.60; H, 10.50; N, 13.05; O, 7.57. Found (mol. wt., osmometry, 209): C, 68.60; H, 10.41; N, 13.31; O, 7.51.

Ultraviolet spectrum: λ_{max} 242 mμ (log ε 4.0).

Hydrogenation of the Isoxazole 13

Compound **13** (15 g) was hydrogenated in 100 ml of ethanol with 800 mg of prehydrogenated platinum oxide. Two moles of hydrogen were taken up overnight and the product **14** was recrystallized from chloroform–carbon tetrachloride to a melting point 124–128 °C; yield of recrystallized product 13.5 g (90%).

Anal. Calcd. for $C_{12}H_{26}N_2O$: C, 67.20; H, 12.10; N, 13.08. Found: C, 66.15; H, 11.62; N, 13.65.

Preparation of 1,3-Diaminododecane (15)

A solution of the amide **14** (10.5 g) in 150 ml of tetrahydrofuran was added dropwise with stirring to 200 ml of a 1 *M* solution of diborane in the same solvent. The whole operation was performed in a dry nitrogen atmosphere. When the addition was complete, the solution was refluxed for 3 h. After this time, the reaction mixture was evaporated to a small volume, an excess of absolute methanolic hydrochloric acid was added, and the precipitate which appeared was removed by filtration. The solution was then evaporated to dryness. The residue was dissolved in methanol and filtered through a column of Amberlite IR 400 in the OH^- form. The evaporation of the filtrate gave 7.6 g of 1,3-diaminododecane which was homogeneous in v.p.c. For characterization, it was converted into the crystalline diacetate by acetylation with acetic anhydride in pyridine. This derivative was recrystallized from carbon tetrachloride and melted at 128 °C.

Anal. Calcd. for $C_{16}H_{30}N_2O_2$ (mol. wt., 282): C, 68.04; H, 10.71; N, 9.92; O, 11.33. Found (mol. wt., osmometry, 280): C, 67.53; H, 11.55; N, 9.66; O, 11.51.

Preparation of the Ditosyl Derivative 16

The tosylation of **15** to **16** was performed in the same manner as the preparation of the ditosylate **9**. Compound **16** was obtained in a yield of 62%. It was a neutral glass homogeneous in several t.l.c. systems. The n.m.r. spectrum of this material was in quantitative agreement with the structure **16**.

Preparation of the Compound 11b

The coupling of **16** and **10** under high dilution to yield the tetratosyl desoxypithecolobine **11***b* was performed precisely as described above for the compound **11***a*. The quantities used were 420 mg of **16** and 540 mg of **10**. Extensive chromatography on two alumina columns followed by preparative t.l.c. on silica gel yielded 115 mg of glassy material, which was homogeneous in several t.l.c. systems and indistinguishable by t.l.c. from "natural" desoxypithecolobine tetratosylate. It had an i.r. spectrum identical both with the compound **11***a* and the "natural" tetratosylate. The n.m.r. spectrum of the product **11***b* was in quantitative agreement with the spectrum of the compound **11***a* (see theoretical part).

Preparation of the Diester 17

Ethyl acrylate (200 g) was added dropwise to a solution of 54 g of 1,4-diaminobutane in 500 ml of ether. The mixture was stirred overnight at room temperature. After this time it was cooled to 5 °C and 150 g of trimethylamine were added to it. A slow addition of 70 g of benzoyl chloride over the period of 1 h was now started and the mixture was allowed to stand for an additional hour. After this time 500 ml of ice water were added and the neutral reaction product isolated in the usual manner. The yield was 120 g (40%) of neutral material which surprisingly was homogeneous in t.l.c. It was immediately, without further purification, converted into the crystalline acid **18**.

Preparation of the Diacid 18

Compound **17** (100 g) was hydrolyzed for 1 h at 70 °C in 400 ml of 10% aqueous methanolic potassium hydroxide. The hydrolysis mixture was poured into 2 l of water and acidified with 20% hydrochloric acid to pH 2. After a period of standing the product **18** crystallized; it was filtered off and washed with water and finally recrystallized from methanol. The yield was 65 g (60%) and the pure product melted at 181–182 °C.

Anal. Calcd. for $C_{24}H_{28}N_2O_6$ (neutralization equivalent, 440): C, 65.44; H, 6.41; N, 6.36; O, 21.80. Found (neutralization equivalent, 436): C, 64.86; H, 6.52; N, 6.39; O, 22.29.

Preparation of the Dichloride 19

The acid **18** (6 g) was dissolved in 25 ml of thionyl chloride and the solution was stirred at 50 °C for 5 h. After this period, the thionyl chloride was evaporated *in vacuo*, the residue dissolved in dry carbon tetrachloride, evaporated to dryness *in vacuo*, and dried in high vacuum for several hours. The chloride **19** prepared in this way was used for the next step.

Desoxypithecolobine 3a

A solution of 1,5-diaminododecane (3 g) in 450 ml of carbon tetrachloride and a solution of the dichloride **19** (4.7 g) in the same volume of the same solvent were added in the course of 5 h to a vigorously stirred reaction vessel containing 1500 ml of carbon tetrachloride at room temperature. When the addition was completed, the stirring was continued for 8 h. The carbon tetrachloride was then evaporated *in vacuo*, the products dissolved in methanol and passed through a column of (*a*) Amberlite IR 400 in the OH^- form; (*b*) Dowex 50X in the H^+ form. The methanol was then evaporated to dryness yielding 1.8 g of a neutral light-brownish foam. This material (1 g) was dissolved in 50 ml of 1 *M* diborane in tetrahydrofuran and the solution was heated under reflux for 3 h. The tetrahydrofuran was evaporated and the residue was dissolved in saturated methanolic hydrochloric acid. A solid which separated was filtered off, the solution was evaporated to dryness and the basic products isolated in the usual manner. The yield was 600 mg of crude basic material. The crude bases were reconverted into the hydrochlorides and debenzylated by hydrogenation in ethanol with 150 mg of 10% palladium on charcoal for 18 h. The basic products were isolated in the usual manner. The yield was 300 mg of crude basic material. Thin-layer chromatography showed several spots, one of which had the same R_f value in several systems as "natural" desoxypithecolobine. Column chromatography on alumina and preparative t.l.c. on silica gel led to the isolation of 60 mg of compound (**3***a*) which was homogeneous in several systems of t.l.c. and showed an i.r. spectrum superimposable on the spectrum of "natural" desoxypithecolobine. For characterization, it was tosylated in the usual manner (*vide supra*). The product obtained in quantitative yield was identical by t.l.c. in several systems, i.r. in chloroform and carbon tetrachloride, and n.m.r. in deuterated chloroform with the previously synthesized compound **11***a*.

Desoxypithecolobine (3b)

The starting materials were 1,3-diaminododecane **15** and the dichloride **19**. The quantities, volumes and the entire procedure were the same as described for the preparation of compound **3***a*. The yield of pure **3***b* was 55 mg. For characterization, it was converted in quantitative yield into the independently synthesized tetratosylate **11***b*. Identity of the two tetratosylates was proved by t.l.c. in several systems, i.r., and n.m.r. spectroscopy.

Acknowledgment

We wish to thank the National Research Council of Canada for the continued support during the entire period of our pithecolobine studies.

1. K. Wiesner, D. M. MacDonald, C. Bankiewicz, and D. E. Orr. Can. J. Chem. **46**, 1881 (1968).
2. H. Stetter and E. E. Roos. Ber. **87**, 566 (1954).
3. K. Wiesner and D. E. Orr. Tetrahedron Letters, **16**, 11 (1960).
4. A. Franke and A. Kroupa. Monatsh. Chem. 347 (1930).
5. C. J. Eby and C. R. Hauser. J. Am. Chem. Soc. **79**, 723 (1957).
6. G. Shaw and G. Sugowdz. J. Chem. Soc. 665 (1954).
7. H. C. Brown and P. Heim. J. Am. Chem. Soc. **86**, 3566 (1964).

Can. J. Chem. Downloaded from www.nrcresearchpress.com by 210.87.254.105 on 09/05/12
For personal use only.

Can. J. Chem. Downloaded from www.nrcresearchpress.com by 210.87.254.6 on 09/05/12
For personal use only.

Studies in dehydrogenation of 6-methoxy-1-tetralone. Structure of a novel product formed with tetrachloro-1,2-benzoquinone

T. R. KASTURI AND T. ARUNACHALAM
Department of Organic Chemistry, Indian Institute of Science, Bangalore-12, India

Received April 30, 1968

Dehydrogenation of 6-methoxy-1-tetralone (**1**) using palladium–carbon (30%), palladium black, and quinones has been studied with a view to preparing 6-methoxy-1-naphthol (**3**). A novel addition product formed, during dehydrogenation of **1** with tetrachloro-1,2-benzoquinone, has been proved to be 2,2-(tetrachloro-*o*-phenylenedioxy)-3,4-dehydro-6-methoxy-1-tetralone (**5**). Bromination of **1** followed by dehydrobromination gave the naphthol **3** in excellent yield.

Canadian Journal of Chemistry, **46**, 3625 (1968)

In continuation of our effort (1) to prepare 6-methoxy-1-naphthol (**3**), which was required in connection with a projected synthesis of oxasteroids, in fairly good amount from 6-methoxy-1-tetralone (**1**), we undertook a detailed study of dehydrogenation of **1** with various dehydrogenating agents. This was necessary as the methods reported in the literature (2–4) for the preparation of **3** were not satisfactory and the yields reported were low. As reported earlier (1), our attempt to prepare **3** by treating **1** with potassium *t*-butoxide in *t*-butanol in an atmosphere of oxygen[1] failed to give **3**, but gave 2-hydroxy-6-methoxy-1,4-naphthaquinone (**2**) in very good yield. Subsequently, this was shown to be a simple and general method of preparation of 2-hydroxy-1,4-quinones (1, 6).

Initially, we studied the dehydrogenation of tetralone **1** using 30% palladized carbon around 280–300 °C for 2–3 h in an atmosphere of carbon dioxide and the naphthol **3** was obtained in 50–60% yield; however, on a larger scale, the yield was poor. The yields were also poor when palladium black in xylene or naphthalene was used (7). Hence, an alternative method has to be developed.

Quinones, such as chloranil (8), 2,3-dichloro-5,6-dicyanobenzoquinone (DDQ) (9) have been used for introducing double bonds in conjugation with a ketone or an α,β-unsaturated ketone. Initially, we tried the dehydrogenation of tetralone **1** with chloranil (10), but there was no formation of the naphthol **3**. When the more powerful dehydrogenating agent, tetrachloro-1,2-benzoquinone (**4**) (11) (1 mole) was used in xylene or benzene, again no naphthol **3**[2] was formed, but a greenish-yellow crystalline solid, m.p. 191–192 °C, could be isolated in 20% yield. When the above reaction was repeated using two moles of **4** for one mole of **1**, the yield of the solid could be increased to 30%. The solid showed λ_{max} at 220 (ε 53 500), 258 (ε 30 515), and 330 mμ (ε 9615) in the ultraviolet (u.v.) spectrum and ν_{max} at 1686 (conjugated C=O), 1597, 1572, 1497 (aromatic), 1250, 1215, 1163, 1149, 1131, 1070, 1025, and 909 cm^{-1} (probably due to 1,3-dioxole) (12) in the infrared (i.r.) spectrum. It showed positive test for the presence of chlorine and the elemental analyses corresponded to a molecular formula $C_{17}H_8O_4Cl_4$. The presence of three intense molecular ion peaks at *m/e* 416 (^{35}Cl), 418, and 420 in 3:4:2 ratio in the mass spectrum clearly indicated the presence of four chlorine atoms (13) besides confirming the above molecular formula. The solid, on pyrolysis at 200 °C at 1 mm, gave tetrachlorocatechol and a tar which could not be purified. The formation of tetrachlorocatechol proved beyond doubt that the aforementioned solid must be an addition product of tetralone **1** with the quinone **4**.[3]

The nuclear magnetic resonance (n.m.r.) spectrum of this "adduct"[4] showed the following signals; a sharp singlet with three proton intensity at δ 3.9 ($ArOCH_3$), a doublet with one proton

[1]N. A. J. Rogers and co-workers (5) have converted a Δ^2-cyclohexenone derivative to the corresponding phenol by the same reaction.

[2]Thin-layer chromatography was used for identification using an authentic sample of **3** as the reference compound.

[3]Our experience (14) with this quinone **4** in the dehydrogenation of abietic acid was helpful in arriving at the structure of this "adduct".

[4]This term has been used only for the sake of convenience while referring to it in the discussion though it is not a true adduct of **1** and **4**.

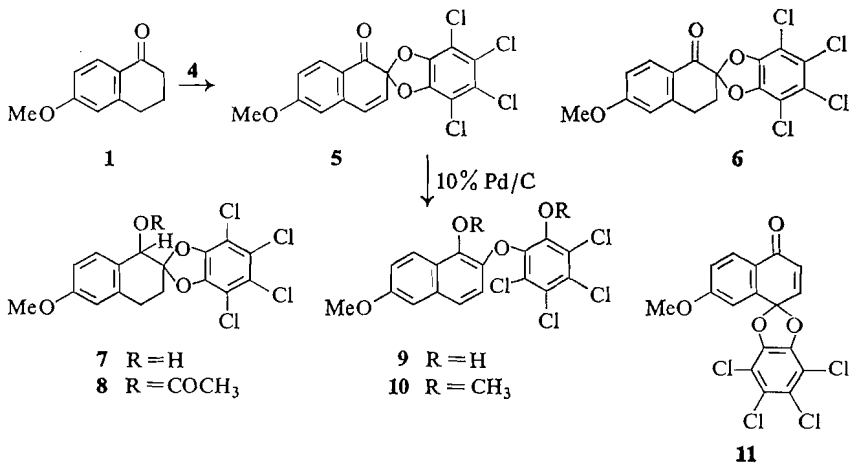

CHART I

intensity at δ 8.05 (J = 8.5 c.p.s.) (aromatic proton in *peri* position to the carbonyl group), a multiplet centered at δ 6.78 with two proton intensity (aromatic protons in *ortho* position to the methoxy group), a multiplet centered at δ 6.86 with one proton intensity (Ar—*CH*=CH—), and a doublet at δ 6.3 (J = 10 c.p.s.) with one proton intensity (Ar—CH=*CH*—). The above data indicated that the two carbonyl oxygen atoms of quinone moiety must be attached to a single carbon atom of tetralone **1** and the δ values of the two olefinic protons indicated the conjugation of the double bond with the phenyl ring. Therefore, the structure of the solid could be as represented in **5**.

Further proof in favor of structure **5** was arrived at as follows. The "adduct" **5**, on hydrogenation with 10% palladinized carbon in ethyl acetate, absorbed one mole of hydrogen and gave a mixture of a phenolic product, m.p. 188–189 °C (80%) and a ketone m.p. 208–209 °C (20%). When the hydrogenation was carried out with a little excess of catalyst, the aforementioned phenolic product was again formed in 80% yield, but none of the above ketone was obtained. Instead, an alcohol, m.p. 216–217 °C was obtained in 15–20% yield. The ketone exhibited λ_{max} at 217 (ε 51 860) and 306 mμ (ε 18 290) in the u.v. spectrum and in the i.r. spectrum it showed peaks at 1694 (conjugated C=O), 1607, 1493 cm^{-1} (aromatic). The elemental analyses corresponded to a molecular formula $C_{17}H_{10}O_4Cl_4$, which was supported by the presence of an intense molecular ion at *m/e* 418 (^{35}Cl) accompanied by peaks at *m/e* 420 and 422 in 3:4:2 ratio. In the n.m.r. spectrum of the ketone, signals due to the two olefinic protons found in the spectrum of "the adduct" **5**, disappeared; instead, two sets of triplets appeared around δ 3.22 and 2.68 due to the presence of two methylene groups adjacent to each other. The signal in the down field region (δ 3.22) could be assigned to the benzylic methylene. Further, the signals due to the following protons were also noticed in the above spectrum; a singlet at δ 3.87 ($ArOCH_3$), a doublet at δ 8.05 (J = 9 c.p.s.) (aromatic proton in *peri* position to the carbonyl), and a multiplet centered at δ 6.75 (2 aromatic protons on either side of the methoxyl group). These data indicated that this ketone must be the dihydro "adduct" **6**.

Unambiguous evidence for the structure of the "adduct" was obtained from the spectral data of the aforementioned alcohol, and its acetate which was prepared by treating the former with acetic anhydride in excess of pyridine. The i.r. spectrum of the alcohol showed peaks at 3610 (OH), and 1605 and 1497 cm^{-1} (aromatic) and it analyzed for $C_{17}H_{12}O_4Cl_4$. The acetate showed peaks in the i.r. spectrum at 1754 (acetate) 1613, 1587 (sh), and 1504 cm^{-1} (aromatic) and analyzed for $C_{19}H_{14}O_5Cl_4$. These data suggested structures **7** and **8** for the alcohol and its acetate respectively. If the structures **7** and **8** are correct for the alcohol and its acetate, the methine proton, attached to the carbon atom carrying the hydroxyl group in **7** and the acetate in **8**, should appear as a singlet in the n.m.r. spectrum as there are no protons to couple at the adjacent carbon atom. In fact, the

Can. J. Chem. Downloaded from www.nrcresearchpress.com by 210.87.254.6 on 09/05/12
For personal use only.

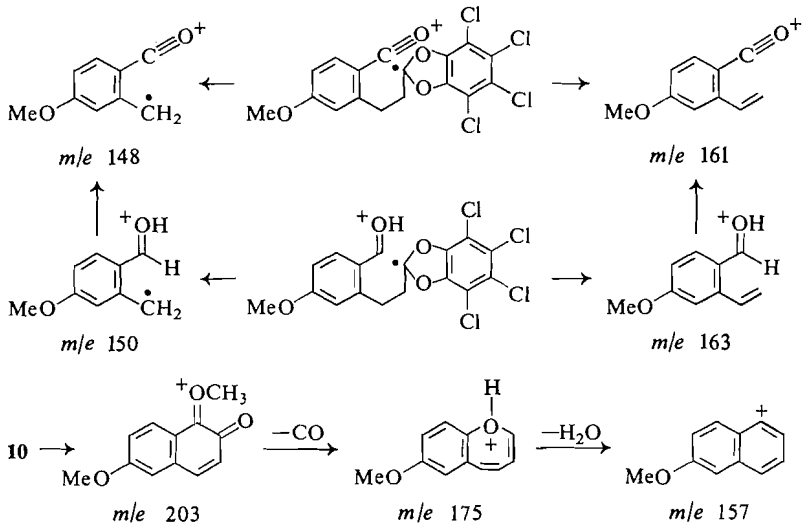

CHART II

n.m.r. spectrum[5] of the alcohol showed a singlet at δ 4.84 for the above methine proton (O*H* at δ 3.55, disappeared on shaking with D_2O), while that of the acetate, as expected, showed the signal for the methine proton in the downfield region at δ 6.2. These data clearly support the structures **7** and **8** for the alcohol and the acetate respectively. Since the alcohol **7** is obtained from the "adduct" by hydrogenation, the structure of the "adduct" should be **5** rather than **11**.

Additional support for the structure of the "adduct" could be obtained from the mass spectral fragmentation of these compounds (15) (Chart II). The presence of ions, at *m/e* 148 and 161 in **6**, at *m/e* 148, 150, 161, and 163 in **7**, and at *m/e* 157, 175, and 203 in **10**, clearly indicated that the tetrachloro-*o*-phenylenedioxy moiety, present in the "adduct", must be attached to the carbon atom α to the keto group as in **5** and not to the benzylic carbon atom as in **11**. Thus, all these data indicated that the "adduct" must be 2,2-(tetrachloro-*o*-phenylene dioxy)-3,4-dehydro-6-methoxy-1-tetralone (**5**).

The formation of the phenolic product in major amount during hydrogenation of the "adduct" **5** is an interesting observation. In the u.v. spectrum, this phenol showed λ_{max} at 220 (ε 42 840), 246 (ε 27 720), 286 (ε 2574), and 316 mμ (ε 4325) and in the presence of alkali it exhibited λ_{max} at 258 (ε 27 720) and 318 mμ (ε 6845). In the i.r. spectrum, it showed peaks at 3570 (free OH), 3460 (bonded OH), 1608, 1558, and 1515 cm^{-1} (aromatic) and analyzed for $C_{17}H_{10}O_4Cl_4$. The phenol could be methylated with dimethyl sulfate in the presence of anhydrous potassium carbonate in acetone to the corresponding methyl ether which analyzed for a molecular formula $C_{19}H_{14}O_4Cl_4$ which was again confirmed by the presence of intense molecular ion peaks at *m/e* 446 (^{35}Cl), 448 and 450 in 3:4:2 ratio in its mass spectrum. The n.m.r. spectrum of the methyl ether showed complete absence of methylene and methine protons, but showed three sharp singlets of three proton intensity at δ 4.11, 3.9, and 3.77 corresponding to three methoxyl groups attached to aromatic system. It also showed signals due to five aromatic protons, one of which appeared at δ 8.05 as a doublet (J = 9 c.p.s.) due to the proton at the *peri* position (with respect to methoxyl), which is deshielded by the methoxyl group (16). These data suggested structure **10** for the phenolic methyl ether and **9** for the parent phenol. The formation of the phenol **9** in major amount indicated that the hydrogenolysis of the "adduct" **5** took place preferably at the ketal function.

The "adduct" **5** is formed probably by the initial addition of the quinone **4** followed by dehydrogenation by another mole of quinone.

[5]Because of the poor solubility of **7** and **8** even in DMSO-d_6, good spectra could not be obtained.

Can. J. Chem. Downloaded from www.nrcresearchpress.com by 210.87.254.6 on 09/05/12
For personal use only.

Can. J. Chem. Downloaded from www.nrcresearchpress.com by 210.87.254.6 on 09/05/12
For personal use only.

If the dehydrogenation process is the first step then the naphthol **3** would have been formed.[6]

Finally, we tried to prepare the naphthol **3** by bromination of tetralone **1** followed by dehydrobromination. Bromination of tetralone **1**, carried out under normal conditions, viz., in acetic acid or carbon tetrachloride, gave a mixture of two products as shown by thin-layer chromatography. However, when the above reaction was carried out in ether containing a trace of hydrogen chloride (17), 2-bromo-6-methoxy-1-tetralone (**1***a*) was obtained exclusively in an excellent yield. The α-bromo ketone **1***a* was dehydrobrominated by refluxing in dimethyl formamide (DMF) with either calcium carbonate or a mixture of lithium bromide and lithium carbonate. With the latter reagent, the yield of 6-methoxy-1-naphthol (**3**) was as high as 80% and this method was finally chosen for large scale preparation.

Experimental

All melting points are uncorrected. The u.v. spectra were determined in ethanol on a Beckman DU spectrophotometer. The i.r. spectra were recorded in Nujol with a Perkin–Elmer model 137B infracord spectrophotometer. The n.m.r. spectra were taken in $CDCl_3$ (except those of 7 and **8** which were recorded in DMSO-d_6), at 60 Mc.p.s. using TMS as internal standard. The mass spectra were determined in an Atlas CH-4 spectrometer. The microanalyses were carried out by the CIBA research center, Bombay, India.

Dehydrogenation of 6-Methoxy-1-tetralone (1)

(a) With 30% Palladized Carbon

A mixture of 1.76 g of 6-methoxy-1-tetralone (18) and 0.88 g of 30% Pd/C was heated around 280–300 °C while a steady stream of dry carbon dioxide was passed through the system. When the evolution of hydrogen ceased (2 h), the mixture was cooled and repeatedly extracted with ether. The ether extract was washed with dilute sodium hydroxide; the alkali extract acidified with ice cold dilute hydrochloric acid to give the naphthol **3** as a gum which was again extracted with ether. Removal of solvent, after washing with water, afforded 1.05 g of crude naphthol **3** which was purified by passing through an alumina column followed by crystallization from 90% *n*-hexane/benzene to give 0.88 g of crystalline 6-methoxy-1-naphthol (**3**), m.p. 85 °C (lit. 85 °C (4)).

In a large scale experiment, the combined ether extract, obtained after washing with dilute alkali, was washed with water, the solvent removed, and the residue distilled under reduced pressure to afford 2-methoxynaphthalene, naphthalene, and the starting material.

(b) With Palladium Black

A mixture of 1.0 g of tetralone **1** and 0.2 g of palladium black (19) in 30 ml of xylene was refluxed for 24 h and after the removal of solvent *in vacuo*, the residue was extracted with ether and worked up as before to give 0.15 g of naphthol **3**.

(c) With Tetrachloro-1,2-benzoquinone (4) (11, 20)

A mixture of 1.76 g (0.01 *M*) of tetralone **1** and 5.92 g (0.02 *M*) of **4** in 40 ml of benzene was refluxed for 8 h. The solvent was removed *in vacuo* and the resulting gummy product was chromatographed over neutral alumina (120 g). Elution with pure *n*-hexane, and then with 90% *n*-hexane/benzene afforded the "adduct" **5** which was crystallized from benzene/hexane mixture as shining greenish-yellow crystals; yield 1.2 g, m.p. 191–192 °C (decomposed).

Anal. Calcd. for $C_{17}H_8O_4Cl_4$: C, 48.8; H, 1.91; Cl, 33.97. Found: C, 48.76; H, 2.04; Cl, 33.66.

Hydrogenation of the "Adduct" 5

(*a*) A solution of 1.00 g of the "adduct" **5** in 50 ml of dry ethyl acetate was hydrogenated in the presence of 10% palladized carbon. After 2–3 h, the solution had absorbed one mole of hydrogen and the greenish-yellow color had disappeared. After filtration of the catalyst, the solvent was removed and the residue was taken up in ether and washed with dilute sodium hydroxide solution followed by water. On concentration of the ether solution, the ketone **6** began crystallizing out, yield 0.18 g, m.p. 208–209 °C.

Anal. Calcd. for $C_{17}H_{10}O_4Cl_4$: C, 48.57; H, 2.40; Cl, 33.81. Found: C, 49.04; H, 2.84; Cl, 33.28.

The above alkali extract was acidified with dilute hydrochloric acid and the separated product was extracted with ether. The ether extract was washed with water and the removal of solvent gave a gummy product which on crystallization from chloroform/hexane furnished 0.7 g of the phenol **9**, m.p. 188–189 °C;

Anal. Calcd. for $C_{17}H_{10}O_4Cl_4$: C, 48.57; H, 2.40; Cl, 33.81. Found: C, 48.07; H, 2.81; Cl, 33.38.

Methyl ether **10**, m.p. 108–109 °C (from ethanol).

Anal. Calcd. for $C_{19}H_{14}O_4Cl_4$: C, 50.89; H, 3.08; Cl, 31.69. Found: C, 50.61; H, 3.42; Cl, 31.30.

(*b*) The above hydrogenation was repeated with 1.00 g of "adduct" **5** in the presence of 0.4 g of 10% palladium carbon for 4–5 h. The product was worked up as before. From the alkali extract, 0.75 g of phenol **9** was obtained. The neutral fraction, on crystallization from chloroform–hexane, gave 0.21 g of alcohol **7**, m.p. 216–217 °C.

Anal. Calcd. for $C_{17}H_{12}O_4Cl_4$: C, 48.58; H, 2.84; Cl, 33.65. Found: C, 49.11; H, 3.26; Cl, 33.20.

Acetyl derivative **7**, m.p. 238–240 °C (80% benzene/hexane).

Anal. Calcd. for $C_{19}H_{14}O_5Cl_4$: C, 49.35; H, 3.02; Cl, 30.60. Found: C, 49.81; H, 3.38; Cl, 30.40.

Bromination of 6-Methoxy-1-tetralone (1)

A solution of 6.4 g of analar bromine in 20 ml of carbon tetrachloride containing a few ml of dry ether was added dropwise (each drop was added only after the previous drop was completely decolorized) to a stirred solution of 7 g of tetralone **1** in 200 ml dry ether. The ether contained 2 ml of ethereal hydrogen chloride and was maintained at 0–5 °C throughout the addition. After

[6]*Note added in proof*:—Recent experiments have conclusively proved that the "adduct" is formed via the napthol **3**.

the complete addition of bromine, the reaction mixture was stirred for another 0.25 h and then water was added followed by ether. The ether layer was separated and washed with water. Removal of solvent afforded 10.1 g of gummy 2-bromo-6-methoxy-1-tetralone (**1***a*) and this material was used as such for the subsequent step. For analysis, a small amount of the above product was crystallized from *n*-hexane, m.p. 83 °C.

Anal. Calcd. for $C_{11}H_{11}O_2Br$: C, 51.80; H, 4.32; Br, 31.34. Found: C, 51.62; H, 4.35; Br, 31.30.

6-Methoxy-1-naphthol (3)

A solution of 10.1 g of the above α-bromoketone (**1***a*) in 200 ml of dimethyl formamide containing a mixture of 8 g of lithium bromide and 6 g of lithium carbonate was refluxed for 3 h in an atmosphere of nitrogen. The solvent was removed *in vacuo* and the residue treated with ice cold water followed by cold dilute hydrochloric acid. The separated gummy product was extracted with ether and washed with 10% sodium hydroxide solution. The alkali extract was acidified and again extracted with ether. Removal of ether afforded 5.85 g of crude naphthol **3** which was chromatographed over silica gel (120 g). Elution with *n*-hexane followed by 25% benzene/*n*-hexane mixture gave 4.95 g of 6-methoxy-1-naphthol (**3**), m.p. 85 °C (lit. 85 °C (4)).

Acknowledgments

We wish to thank Professor D. K. Banerjee, of this department, for his keen interest in this problem. We are grateful to Professor G. R. Pettit, Arizona State University, Tempe, U.S.A., for providing the nuclear magnetic resonance and mass spectra, to Professor T. R. Govindachari, CIBA Research Center, Bombay, for providing the microanalytical data, and nuclear magnetic resonance spectra of the alcohol **7** and its acetate **8**. We are also grateful to the authorities of the Indian Institute of Science, Bangalore and to the Department of Atomic Energy, Government of India, for the award of a predoctoral fellowship to one of us (T. A.).

1. T. R. KASTURI and T. ARUNACHALAM. Can. J. Chem. **44**, 1086 (1966).
2. A. J. SHAND and R. H. THOMSON. Tetrahedron, **19**, 1919 (1963).
3. G. SCHROETER. Ber. **63**, 1308 (1930).
4. R. J. W. BYRDE, D. F. DOWNING, and D. WOODCOCK. Biochem. J. **72**, 344 (1959).
5. K. CROWSHAW, R. C. NEWSTEAD, and N. A. J. ROGERS. Tetrahedron Letters, 2307 (1964).
6. A. C. BAILLIE and R. H. THOMSON. J. Chem. Soc. C, 2184 (1966).
7. E. MOSETTIG and H. M. DUVALL. J. Am. Chem. Soc. **59**, 367 (1937).
8. E. J. AGNELLO and G. D. LAUBACH. J. Am. Chem. Soc. **79**, 1257 (1957).
9. D. WALKER and J. D. HIEBERT. Chem. Rev. **67**, 153 (1967).
10. R. L. DATTA. J. Am. Chem. Soc. **36**, 1011 (1914). M. GALLOTI. Ann. chim. appl. **22**, 602 (1932); Chem. Abstr. **27**, 278 (1933).
11. R. A. RAPHAEL, E. C. TAYLOR, and H. WYNBERG. Advances in organic chemistry. Methods and results. Vol. II. Interscience Publishers, Inc., New York. 1960. p. 329.
12. KOJI NAKANISHI. Infrared absorption spectroscopy—practical. Holden-Day, Inc., New York. 1962. p. 36.
13. J. H. BEYNON. Mass spectrometry and its application to organic chemistry. Elsevier Publ. Co., Ltd., Amsterdam. 1960. p. 298.
14. T. R. KASTURI, E. RAGHAVAN, SUKH DEV, and D. K. BANERJEE. Tetrahedron, **22**, 745 (1966).
15. H. BUDZIKIEWICZ, C. DJERASSI, and H. B. WILLIAMS. Interpretation of mass spectra of organic compounds. Holden-Day, Inc., New York. 1964. p. 156 and 181.
16. A. ZWEIG, J. E. LANCASTER, and M. T. NEGLIA. Tetrahedron, **23**, 2577 (1967).
17. E. MOSETTIG and A. BURGER. J. Am. Chem. Soc. **57**, 2189 (1935).
18. G. STORK. J. Am. Chem. Soc. **69**, 576 (1947).
19. R. WILLSTATER and E. WALDSCHMIDT. Ber. **54**, 123 (1921).
20. C. L. JACKSON and R. D. MACLAURIN. Amer. Chem. J. **37**, 7 (1907).

Can. J. Chem. Downloaded from www.nrcresearchpress.com by 210.87.254.6 on 09/05/12
For personal use only.

Can. J. Chem. Downloaded from www.nrcresearchpress.com by 210.87.254.5 on 09/05/12
For personal use only.

Luciduline: a unique type of *Lycopodium* alkaloid

W. A. AYER, N. MASAKI,[1] AND D. S. NKUNIKA[2]
Department of Chemistry, University of Alberta, Edmonton, Alberta

Received June 5, 1968

The isolation and determination of the structure of luciduline, $C_{13}H_{21}ON$, an alkaloid present among the weak bases of *Lycopodium lucidulum* Michx, is described. Chemical and physical evidence which suggests structure **9** for luciduline is presented. An X-ray diffraction study on *O*-*p*-bromobenzoyldihydroluciduline confirmed this hypothesis and defined the stereochemistry of the methyl group at C-8. The complete structure of luciduline, including absolute configuration, is thus represented by **1**. A possible mode of biosynthesis of luciduline, which is a new type of *Lycopodium* alkaloid, is discussed. The mass spectra of luciduline and some of its derivatives are interpreted in terms of structure **1**.

Canadian Journal of Chemistry, 46, 3631 (1968)

In 1963 we described (1) the separation of the alkaloids of *Lycopodium lucidulum* into strong and weak bases and reported on the properties of some of the strong bases. From the weakly basic fraction we have isolated several alkaloids (2) including one, $C_{13}H_{21}ON$, for which we propose the name luciduline.[3] In this paper we report on the chemical and physical properties of luciduline and show that it has a structure, **1**, which is unique among the *Lycopodium* alkaloids known to date (4).

Luciduline is a colorless, somewhat unstable, oil which may be purified by evaporative distillation or by gas–liquid chromatography (g.l.c.). Its infrared (i.r.) spectrum shows pertinent absorption bands at 2780 (N—CH_3), 1690 (C=O), and 1400 (methylene adjacent to carbonyl) cm^{-1}. When luciduline is subjected to deuterium exchange (DCl–CH_3COOD, room temperature) two atoms of deuterium are incorporated. Luciduline-d_2 does not show absorption at 1400 cm^{-1} in the i.r. spectrum. Reduction of luciduline with sodium borohydride gives dihydroluciduline. The nuclear magnetic resonance (n.m.r.) spectrum of dihydroluciduline ($CDCl_3$ solution) shows a one-proton signal (multiplet, $w_{\frac{1}{2}} \simeq 23$ c.p.s.) at τ 6.05. This signal is shifted to τ 5.03 (multiplet, $w_{\frac{1}{2}} \simeq 24$ c.p.s.) in the n.m.r. spectrum of *O*-acetyldihydroluciduline (prepared by treatment of dihydroluciduline with acetic anhydride-pyridine). The n.m.r. spectrum of *O*-acetyldihydroluciduline-d_2, prepared from luciduline-d_2 by borohydride reduction followed by acetylation, shows a *doublet* ($J \simeq 4.5$ c.p.s.) at τ 4.98. The above facts, when taken together, show that luciduline contains a ketonic carbonyl group which is flanked on one side by a methylene group and on the other side by a methine carbon, and that enolization towards the methine carbon is not a favored process.

An examination of the n.m.r. spectra of luciduline (Figs. 1 and 2) and its simple derivatives in deuteriochloroform and in acetic acid-d_4 proved very informative. The spectra revealed the presence of a secondary *C*-methyl group (doublet at τ 9.15 ± 0.05) and confirmed the presence of an *N*-methyl group (singlet at τ 7.90 ± 0.05 in $CDCl_3$, shifted to τ 7.00 ± 0.05 in CD_3COOD (5)). Since luciduline and the derivatives mentioned thus far do not show N—H absorption in the i.r. and are resistant to *N*-acetylation, the *N*-methyl group is located on a fully substituted nitrogen. The n.m.r. spectrum of luciduline in $CDCl_3$ (Fig. 1) shows two partially overlapping low field one-proton quartets, one centered at τ 6.95 (J's $\simeq$ 16 and 11 c.p.s.) and one centered at τ 7.17 (J's $\simeq$ 13 and 4 c.p.s.). The signal centered at τ 6.95 is due to one of the protons of the methylene group α to the carbonyl since this signal is not present in the spectrum of luciduline-d_2. The larger coupling (16 c.p.s.) must be a *geminal* coupling (6) and the smaller (11 c.p.s.) an axial–axial coupling (assuming that we are dealing with a six-membered ring). The second proton of the methylene group is located in the

[1]On leave of absence from Kyoto University, Kyoto, Japan.

[2]Present address: Department of Chemistry, University of Zambia, Lusaka, Zambia.

[3]In 1946, Manske and Marion (3) reported the isolation of a compound $C_{13}H_{21}ON$ (alkaloid L. 21) from *L. lucidulum*. Although a direct comparison of alkaloid L.21 with luciduline has not been possible, the correspondence of the molecular formulas and of the melting points of the hydroperchlorates suggests that luciduline is identical with alkaloid L.21.

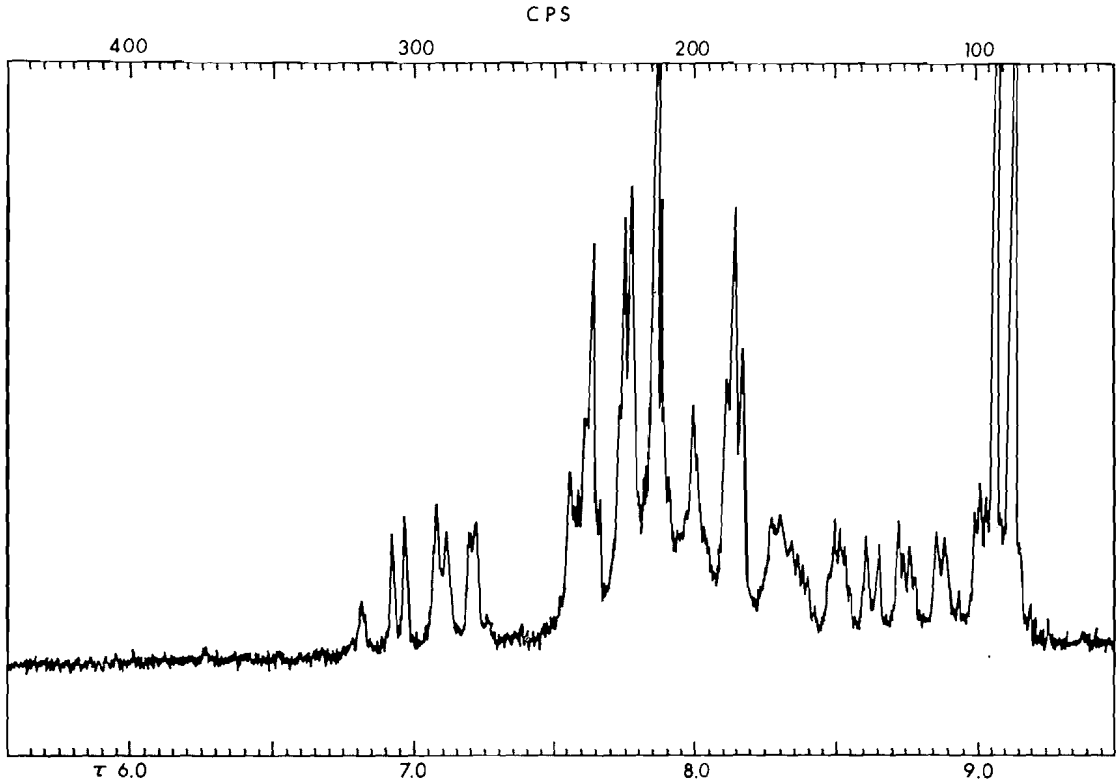

FIG. 1. Nuclear magnetic resonance spectrum (100 Mc.p.s.) of luciduline in deuteriochloroform.

region τ 7.7 as revealed by double-irradiation experiments and by a comparison of the spectrum of luciduline with that of luciduline-d_2. The environment of the carbonyl may thus be extended to part structure **2**.

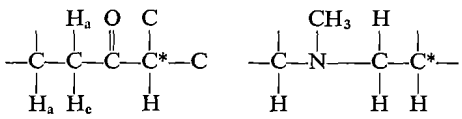

2

3

The low field region of the n.m.r. spectrum of luciduline in acetic acid-d_4 (Fig. 2) is informative as regards the environment of the nitrogen atom. The methylene proton responsible for the absorption at τ 6.95 in $CDCl_3$ has moved upfield since the spectrum of luciduline-d_2 is identical with that of luciduline in the region below τ 7.5. The region below τ 6.9 shows signals for three protons which are presumably on carbon atoms attached to the nitrogen. A methine proton appears as a broad singlet at 6.43 and methylene protons appear as a doublet at τ 6.20 (J = 13 c.p.s.) and a quartet at τ 6.67 (J's ≃ 13 and 4 c.p.s.). Spin–decoupling experiments confirmed that the latter two protons are mutually coupled, and the magnitude of the coupling constant (13 c.p.s.) is consistent with their geminal nature. The fact that one of these signals is further split suggests that

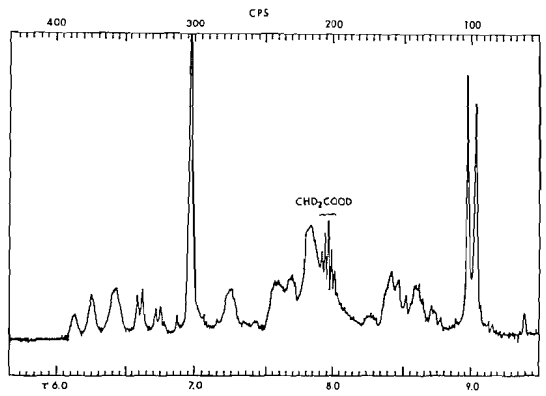

FIG. 2. Nuclear magnetic resonance spectrum (100 Mc.p.s.) of luciduline in acetic acid-d_4.

Can. J. Chem. Downloaded from www.nrcresearchpress.com by 210.87.254.5 on 09/05/12
For personal use only.

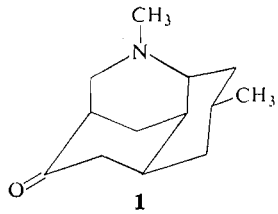

1

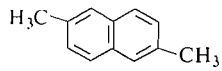

6

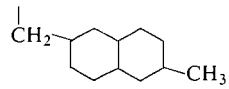

7

the adjacent carbon carries at least one hydrogen. The environment of the nitrogen may thus be represented as in **3**.

It was mentioned above that the proton geminal to the acetoxyl group in *O*-acetyldihydroluciduline-d_2, now represented as in **4**, appears as a doublet at τ 4.98 in the n.m.r. spectrum. The τ 6–7 region of the spectrum in acetic acid-d_4 is similar to that of luciduline, again showing the quartet (J's $\simeq$ 13 and 4 c.p.s.) at τ 6.80. Simultaneous irradiation at τ 7.87 causes the signal at

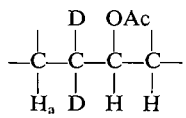

4

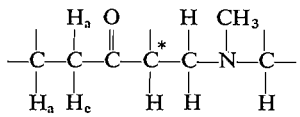

5

τ 4.98 to collapse to a singlet and the signal at τ 6.80 to collapse to a doublet, J = 13 c.p.s., suggesting that both are coupled to the same proton and thus that the starred carbons in **2** and **3** are one and the same, leading to part structure **5** for luciduline, where the hydrogen at C* is not readily exchangeable under enolizing conditions.

In order to gain further insight into the carbon skeleton of the alkaloid, luciduline was subjected to selenium dehydrogenation. 2,6-Dimethylnaphthalene (**6**) was isolated in good yield (>30%). A similar result was obtained using dihydroluciduline. The dehydrogenation product accounts for 12 of the 13 carbon atoms of luciduline, and assuming that it is the methyl group on nitrogen which is lost during the dehydrogenation it was tempting to consider that luciduline contained the carbon framework **7**. On the basis of the then favored biogenetic pathway for the *Lycopodium* alkaloids (7)[4] involving two 3,5,7-triketooctanoic acid chains the part structure **7** is readily accounted for as shown in Scheme 1.

Since in all the known *Lycopodium* alkaloids the nitrogen is attached to C-1 of one of the octanoic acid chains, and C-8 of one chain is always bonded to C-7 of the other chain (9) these features are retained in our "biogenetic structural hypothesis" shown in Scheme 1. Using this Scheme it is possible to arrive at a partial structure, **8**, which contains all the features of part structures **5** and **7**. In order to retain the features of **5** the final bond from the nitrogen has to be attached to one of the starred carbons in **8**. Attachment of the nitrogen to only one of these, starred carbon *a*, leads to a structure, **9**, which is essentially strain free, and this structure became our working hypothesis for the design of further experiments. It may be seen that structure **9** (=**9***a*) accounts for the observation that the methine proton adjacent to the carbonyl is not readily exchanged (bridgehead position) and for the fact that the axial proton at C-1 appears at abnormally low field in the n.m.r. spectrum (deshielded by the lone pair on nitrogen (10, 11)). The nitrogen atom in **9** is extremely hindered, which may account, at least in part, for the low basicity of the alkaloid. Attempts to form the methiodide, even under forcing conditions, were unsuccessful and luciduline was recovered unchanged after treatment with triethyloxonium fluoborate in methylene chloride.

The carbonyl stretching frequency in the i.r. spectrum of luciduline is rather low (1690 cm^{-1}) for a six-membered ketone. Since there is a severe non-bonded interaction between the nitrogen and the hydrogens on C-1 in structure **9** a possible explanation is that the carbonyl containing ring

[4]The structure was first tentatively assigned in August, 1966. The currently accepted biogenetic pathway (8) accounts equally well for the structure, as is discussed later.

Can. J. Chem. Downloaded from www.nrcresearchpress.com by 210.87.254.5 on 09/05/12
For personal use only.

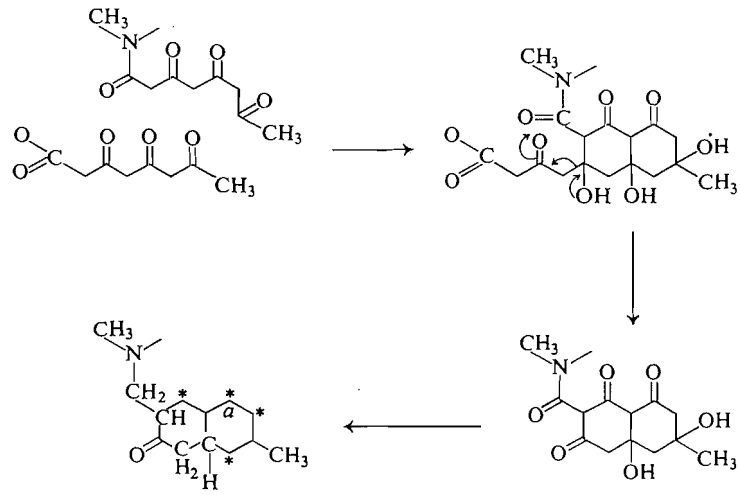

8 SCHEME 1

is distorted towards the half-chain with the consequent increase in the carbonyl bond angle causing the shift to lower frequency (12). A similar explanation has been used to explain the low carbonyl frequency in lycopodine (**10**)(13). An alternate structure, **11**, which accommodates part structure **6** and which could give rise to 2,6-dimethylnaphthalene by a simple rearrangement (arrows in **11**) might also explain the low carbonyl frequency, since cycloheptanones usually absorb at lower frequency than cyclohexanones.

Oxidation of luciduline with potassium permanganate in acetone provided, albeit in low yield, luciduline lactam (**12**) which showed carbonyl absorption at 1730 and 1640 cm^{-1}, assigned to the ketone and lactam groups respectively. The absorption of the ketonic carbonyl at higher frequency than in luciduline is, by analogy to other β-dicarbonyl systems (14), ascribed to its 1,3-relationship with another carbonyl group. The absorption of the lactam carbonyl at 1640 cm^{-1} indicates that the nitrogen is in a six- or larger-membered ring and thus luciduline does not have structure **11**. The n.m.r. spectrum of

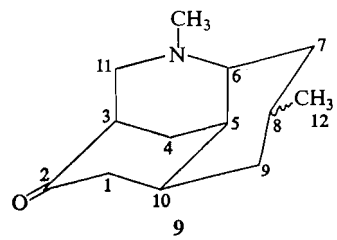

9

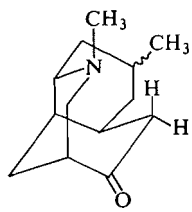

9a

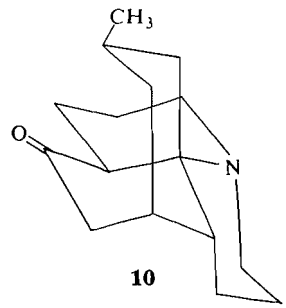

10

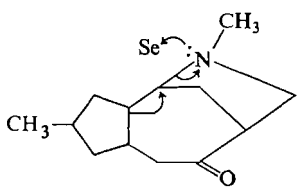

11

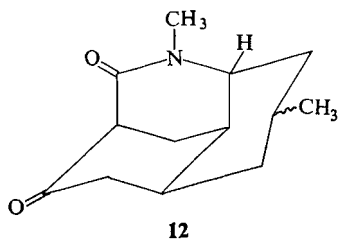

12

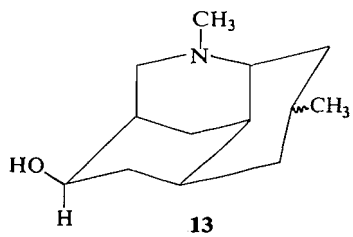

13

Can. J. Chem. Downloaded from www.nrcresearchpress.com by 210.87.254.5 on 09/05/12
For personal use only.

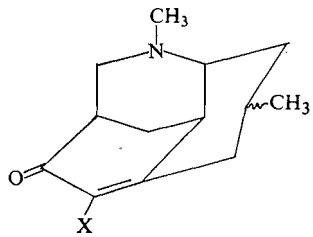

14, X = Br
15, X = OH
16, X = H

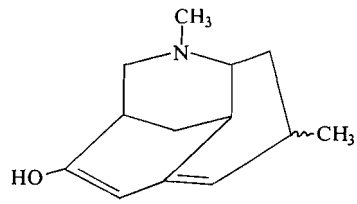

17

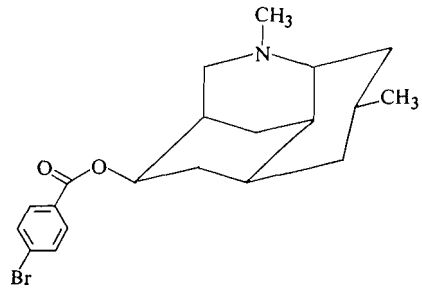

18

luciduline lactam (**12**) shows three low field signals, a one-proton quartet (J's $\simeq$ 3 and 6 c.p.s.) at τ 6.36, assigned to the proton on C-3, a complex multiplet at τ 6.72, assigned to the proton on C-6, and a three-proton singlet at τ 7.04 due to the *N*-methyl group. The signal for the axial proton on C-1 could no longer be observed in the region below τ 7.5. Attempts to bring about hydrolysis of the lactam and/or cleavage of the 1,3-dicarbonyl system were unsuccessful.

Several reactions designed to furnish information concerning the ketone containing ring were unsuccessful. We especially desired to open this ring, since we felt that dehydrogenation studies on the *seco* compound might furnish a recognizable quinoline derivative. Attempts to open the ring by Baeyer–Villiger oxidation and by photolysis were unsuccessful, and dihydroluciduline (**13**, the equatorial nature of the hydroxyl group is apparent from the n.m.r. data already quoted) proved resistant to dehydration with thionyl chloride in methylene chloride and with phosphorus oxychloride in pyridine. *O*-Acetyldihydroluciduline was recovered unchanged on pyrolysis at 300°. Bromination of luciduline hydrobromide with two equivalents of bromine in chloroform was more successful. A crystalline compound $C_{13}H_{18}NOBr$, corresponding to a bromodehydroluciduline, was obtained. The same bromodehydroluciduline was also obtained, but in poor yield, when only one equivalent of bromine was used in the reaction. On the basis of its spectral characteristics bromodehydroluciduline is assigned structure **14**.

The compound showed an absorption maximum at 263 mμ in the ultraviolet (calculated (15) 269 mμ), and at 1670 and 1603 cm^{-1} in the i.r. spectrum. The n.m.r. spectrum did not show absorption for an olefinic proton. The *N*-methyl signal appeared at τ 7.88 and the *C*-methyl doublet at τ 8.95. A complex series of peaks, corresponding to 4–5 protons appeared in the region τ 6.7–7.5. The chemical shift of the proton geminal to the *C*-methyl group, located by double irradiation, was τ 8.01, indicating that the methyl group is not allylic to the double bond. Ozonolysis as well as permanganate–periodate oxidation of **14** led to the formation of intractable mixtures. This route to ring-cleaved derivatives was therefore abandoned.

In an attempt to prepare the diosphenol **15**, luciduline was oxidized with selenium dioxide in dioxane. Instead of the diosphenol **15**, the dehydro compound **16** was obtained in about 50% yield. Dehydroluciduline (**16**) absorbs at 1668 and 1628 cm^{-1} in the i.r. spectrum. The n.m.r. spectrum showed a signal for an olefinic proton *as a sharp singlet* at τ 3.98. The failure to observe any long range coupling was somewhat disconcerting. Catalytic hydrogenation of dehydroluciduline over platinum afforded dihydroluciduline (**13**), indicating that no skeletal rearrangement had occurred during the oxidation. When a solution of dehydroluciduline in DCl–CH_3COOD was kept at room temperature for 60 h, conditions under which luciduline readily incorporated two atoms of deuterium, no exchange of hydrogen for deuterium occurred. Inspection of models indicates that the enolic form **17** of the ketone is very strained and thus the fact that no exchange occurs is not inconsistent with the proposed structure.

The mass spectra of dehydroluciduline (**16**) and bromodehydroluciduline (**14**) were informative. Each showed a prominent molecular ion and in each case the base peak resulted from the loss of the elements of propene from the molecular ion (confirmed in the case of **14** by high-resolution

Can. J. Chem. Downloaded from www.nrcresearchpress.com by 210.87.254.5 on 09/05/12
For personal use only.

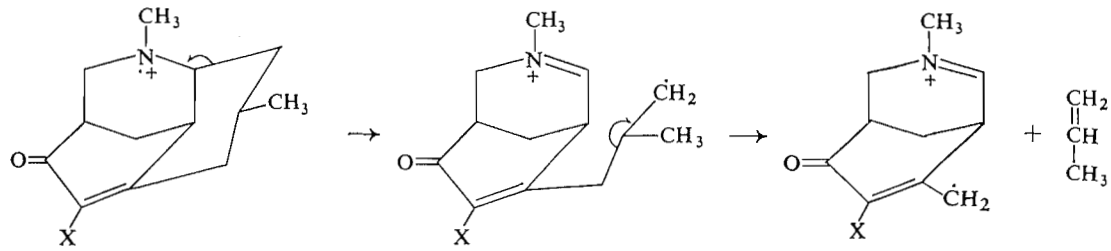

SCHEME 2

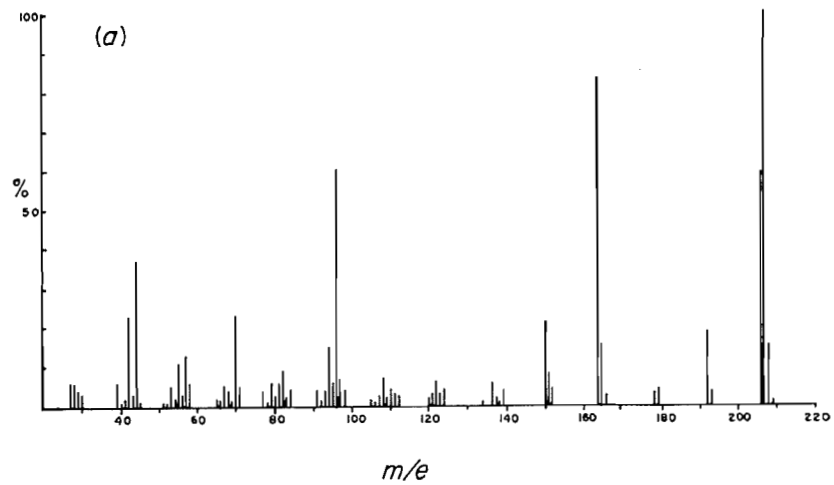

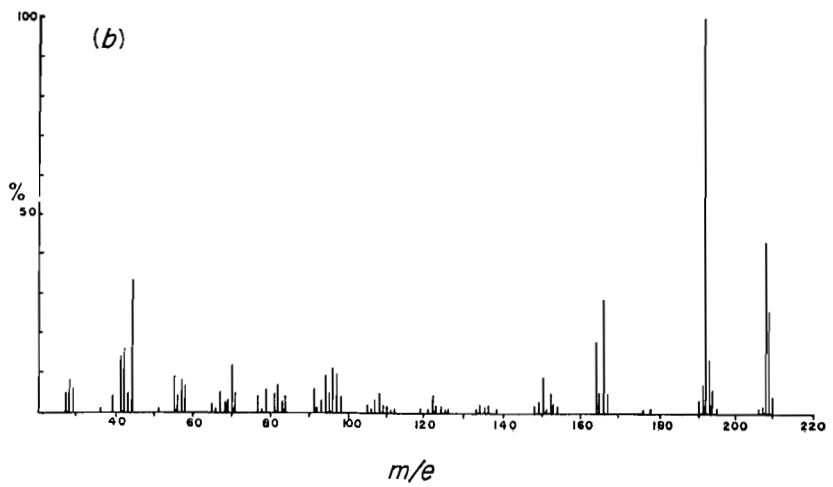

FIG. 3. Mass spectra of: (*a*) luciduline, (*b*) dihydroluciduline.

Can. J. Chem. Downloaded from www.nrcresearchpress.com by 210.87.254.5 on 09/05/12
For personal use only.

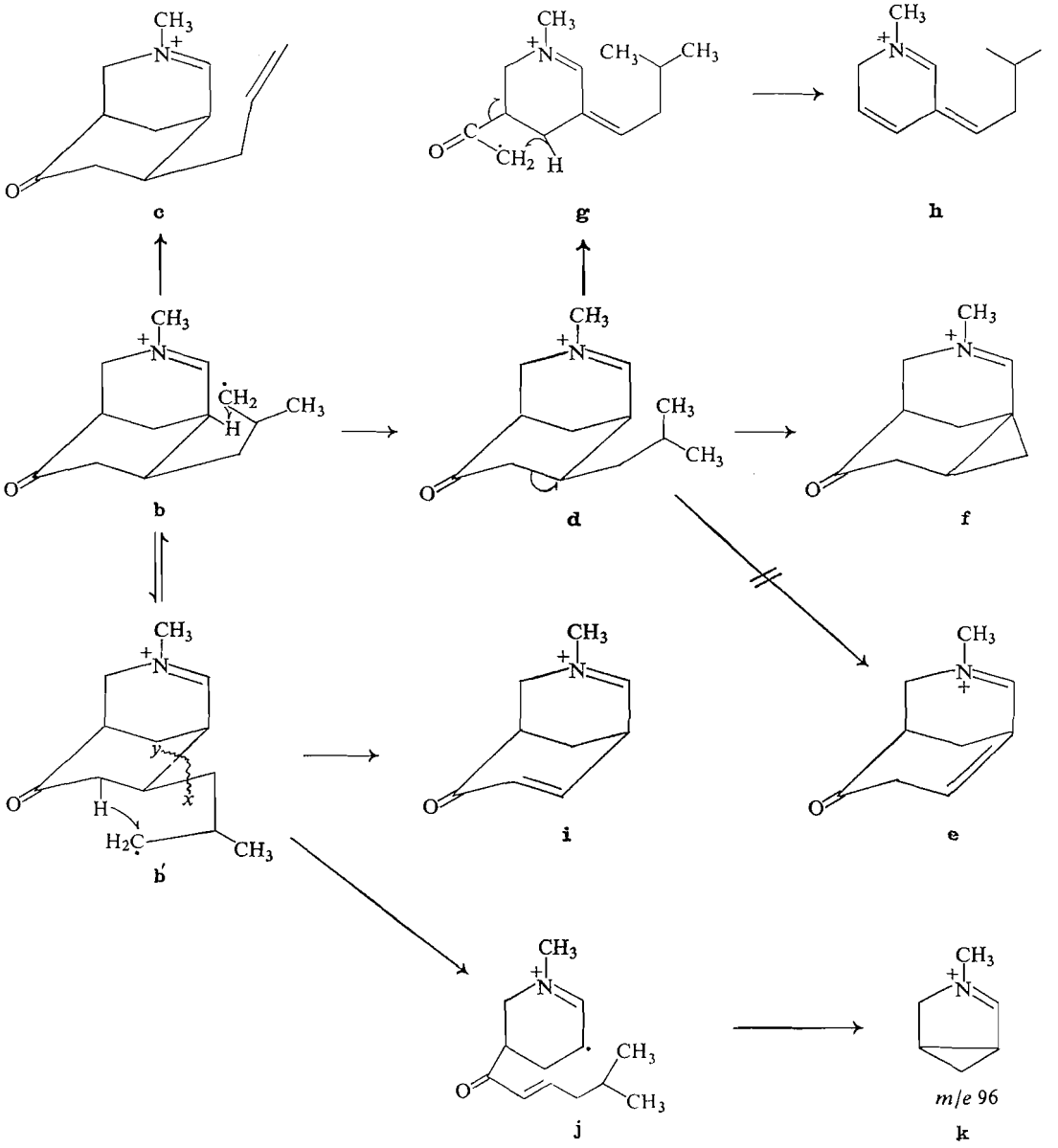

SCHEME 3

mass spectrometry and by the appearance of the appropriate metastable peak). Structures **14** and **16** readily account for this fragmentation as shown in Scheme 2.

α-Cleavage followed by elimination of propene leads to the resonance stabilized radical ion **a**. This fragmentation provides further indirect evidence for the position of the *C*-methyl group in the alkaloid.

The mass spectra of luciduline and dihydroluciduline (Fig. 3) are more complicated than those of the dehydro compounds, but may be interpreted in terms of the proposed structure. Luciduline has prominent peaks at *m/e* 207 (parent and base peak), 206 ($M^+ - 1$), 192 ($M^+ - CH_3$), 164, 150, 96, 70, and 44. The *m/e* 164 peak, which is the most intense peak other than the molecular ion is actually a doublet

Can. J. Chem. Downloaded from www.nrcresearchpress.com by 210.87.254.5 on 09/05/12
For personal use only.

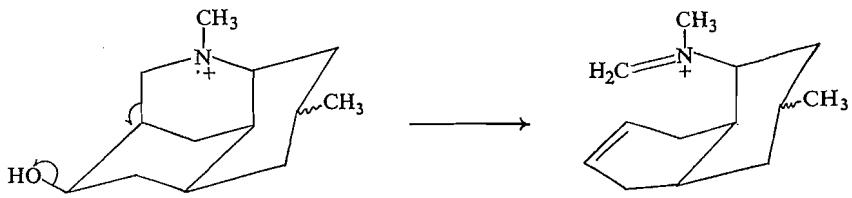

l m

(ca. 1:1) consisting of the ions $C_{11}H_{18}N^+$ and $C_{10}H_{14}NO^+$, and the peak at *m/e* 150 contains the ions $C_{10}H_{16}N^+$ and $C_9H_{12}NO^+$, mainly the latter, as shown by exact mass measurements. The composition of the *m/e* 96 ion is $C_6H_{10}N^+$ and the *m/e* 44 ion is $C_2H_6N^+$. A fragmentation pattern consistent with the spectrum is shown in Scheme 3. α-Cleavage leads to the ion **b** (= **b'**), which on loss of a methyl radical affords the ion **c** (*m/e* 192). Hydrogen rearrangement *via* a six-membered transition state may occur in two ways to give resonance stabilized ion-radicals (one or more of these processes may of course be concerted). Rearrangement as depicted by the fishhook in **b** gives ion-radical **d**. Loss of an isobutyl radical from **d**, the type of process normally encountered in cyclohexylamines (16), would in this case lead to an ion, **e**, in which there is a double bond at the bridgehead. More favored processes may involve the loss of an isopropyl radical to give an ion such as **f** ($C_{10}H_{14}NO^+$), or cleavage as indicated by the fishhook in **d** to furnish the ion **g**, which on loss of an acetyl radical (fishhooks in **g**) gives an ion $C_{11}H_{18}N^+$ (**h**). Hydrogen transfer as shown in **b'** could be accompanied by cleavage *x* to give ion **i** ($C_9H_{12}NO^+$) or cleavage *y* to ion **j**. Loss of the acyl radical from **j** leads to an ion $C_6H_{10}N^+$ (**k**). The formation of the ion *m/e* 44 ($CH_2{=}\overset{+}{N}H{-}CH_3$) from this type of compound is unexceptional (17).

The base peak in the mass spectrum of dihydroluciduline (Fig. 3) results from the loss of a hydroxyl radical from the molecular ion. This is consistent with the behavior of related 3-azabicyclo[3.3.1]nonanols (17) and may be represented as in **l** → **m**. The peak at *m/e* 164 may be attributed to ion **h** (Scheme 3) and that at *m/e* 166 to dihydro **f**. In agreement with these hypotheses is the finding that in the mass spectrum of dihydroluciduline-1,1-d_2, the *m/e* 192 peak shifts to 194, the *m/e* 166 peak shifts to 168, but the *m/e* 164 peak is not shifted.

The nature of the ring system in **9** defines the relative stereochemistry at all asymmetric centers except C-8. Luciduline displays a positive Cotton effect, due to the carbonyl chromophore, in its optical rotatory dispersion curve. Application of the Octant rule (18) leads to the prediction that **9** also represents the absolute configuration of luciduline, provided that **9** indeed represents the constitution of luciduline.

As the quantity of luciduline available to us was limited it was not possible to carry out further degradative studies and since the structural evidence obtained to this point, although con-

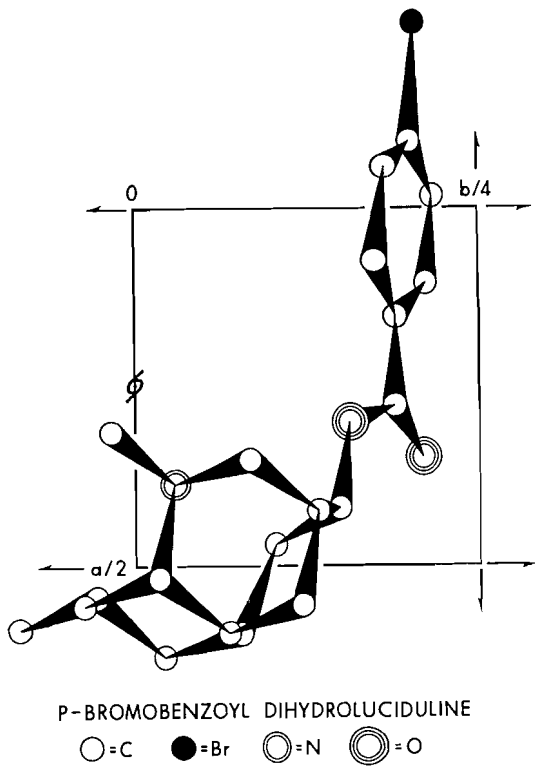

FIG. 4. Perspective drawing of a molecule of *p*-bromobenzoyldihydroluciduline.

Can. J. Chem. Downloaded from www.nrcresearchpress.com by 210.87.254.5 on 09/05/12
For personal use only.

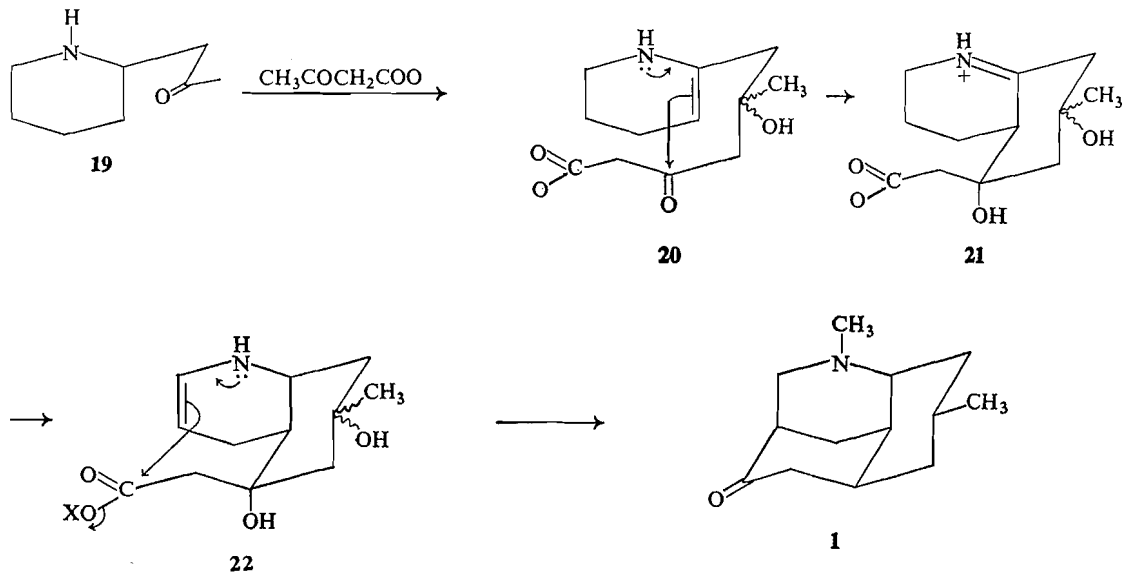

SCHEME 4

sistent with structure **9**, does not rigorously define every part of this unique alkaloid we set about to prepare a heavy atom derivative of luciduline for X-ray diffraction studies. *p*-Bromobenzoyldihydroluciduline crystallizes from ethanol in the orthorhombic space group $P2_12_12_1$ with four molecules in the unit cell of dimensions $a = 11.86$, $b = 23.70$, $c = 7.01$ Å; 1887 reflections from equiinclination Weissenberg photographs taken along the [*a*] and [*c*] axes with CuKα radiation were measured. The structure was solved by the heavy atom method and refined by full-matrix least squares methods to an *R*-factor of 9.9%.[5] The molecular structure so derived is shown in Fig. 4, where all the atoms in the asymmetric unit of the crystal, excluding hydrogen, are shown. The structure shown in Fig. 4 is also represented by **18**.

The result verifies the structure deduced by chemical methods and establishes the relative stereochemistry at C-8 in luciduline as shown in **1**. The absolute configuration shown in Fig. 4 (and in **18**) was determined from anomalous dispersion calculations using the observed differences in intensities of Bijvoet pairs of reflections in the Weissenberg photographs. It thus appears that the Octant rule is applicable in this case. The X-ray data also reveal that both rings A and C are distorted from the ideal chair toward the half-chair, presumably to relieve the non-bonded interaction between the nitrogen and the axial hydrogen at C-1. The interatomic distance between the nitrogen and C-1 when both rings are in the ideal chair form (as estimated from Drieding models) is 2.6 ± 0.1 Å. The actual distance as revealed by the X-ray data is 2.99 ± 0.02 Å. The C-2, C-1, C-10 bond angle is 115 ± 1° and the C-11, N, C-6 bond angle is 114 ± 1°.

It has recently been shown that lysine is a precursor of lycopodine (**10**) in the plant and a biosynthetic scheme in accord with the experimental results has been advanced (8).[6] The MacLean–Spenser hypothesis involves the condensation of two pelletierine (**19**) units, formed from lysine and acetoacetate. Condensation of pelletierine (**19**) with acetoacetate (Scheme 4, order of steps arbitrary) and oxidation to the enamine **20** followed by ring closure leads to the immonium salt **21**. Tautomerization to the enamine **22**, ring closure, *N*-methylation, and adjustment of the oxidation level leads to luciduline (1). It is thus apparent that as is the case for all other *Lycopodium* alkaloids of known structure the polyacetate hypothesis of Conroy (7) and the

[5]Full details of the X-ray analysis will be published separately.

[6]We wish to thank Professor D. B. MacLean for informing us of these results prior to publication. The biogenetic scheme shown for luciduline was first suggested, in more general form, by Professor MacLean.

Can. J. Chem. Downloaded from www.nrcresearchpress.com by 210.87.254.5 on 09/05/12
For personal use only.

MacLean–Spenser hypothesis (8) cannot be distinguished on the basis of structure alone.

Experimental

Infrared (i.r.) spectra were measured on a Perkin–Elmer model 441 or model 337 spectrophotometer and ultraviolet spectra on a Perkin–Elmer model 202 spectrophotometer. Nuclear magnetic resonance (n.m.r.) spectra were measured on a Varian HA-100 spectrometer. Internal tetramethylsilane was used as a standard. Optical rotatory dispersion spectra were determined on a Cary model 60 spectropolarimeter through the courtesy of Professor C. M. Kaye, Biochemistry Department, University of Alberta. Mass spectra were determined on an AEI MS-9 mass spectrometer. Alumina, unless otherwise specified, refers to basic alumina of activity II–III (Brockmann scale). Thin-layer chromatograms (t.l.c.), unless otherwise specified, were carried out on Alumina G (Research Specialties Co., Richmond, California) and were developed in an iodine chamber or with Dragendorff's reagent, the latter prepared according to the procedure described by Bobbitt (19). Skellysolve B refers to Skelly Oil Company light petroleum, b.p. 62–70°. Melting points were determined on a hot-stage and are uncorrected. Microanalyses were performed by C. Daessle, Montreal, and by Mrs. D. Mahlow of this department.

Isolation of Luciduline

Finely ground *Lycopodium lucidulum* Michx (5.1 kg), collected near Fredericton, New Brunswick, by Mr. M. A. Stillwell, was extracted for three days with methanol in a Soxhlet extractor. Most of the methanol was removed and the residue was digested with aqueous hydrochloric acid (6% by volume) and filtered. The insoluble portion was then digested with hydrochloric acid (10% by volume) and again filtered. The filtrates were combined and washed with ether, then basified to pH 10–11 with ammonium hydroxide and extracted with chloroform. Removal of the chloroform under reduced pressure gave the "crude alkaloids" (55.6 g). The "crude alkaloids" were dissolved in 10% hydrochloric acid and a saturated solution of disodium hydrogen phosphate was added until the solution was pH 6.5. This solution was extracted several times with methylene chloride. Evaporation of the solvent gave the "weak bases" (44 g). The pH of the aqueous solution was then raised to about 10 by the addition of ammonium hydroxide. Extraction with chloroform gave the "strong bases" (11.0 g). The weak bases (5.1 g) were subjected to one hundred funnel countercurrent distribution using chloroform (40 ml per tube) as the stationary phase and a saturated solution of potassium hydrogen tartarate (pH 3, 40 ml per tube) as the moving phase. Tubes 5 to 44 (total wt. 0.26 g) contained mainly one component (determined by t.l.c.), which was further purified by dry-column chromatography (20) over alumina, using ethyl acetate–ether (1:4) as the developing solvent. Luciduline showed an R_f value of about 0.9 under these conditions. The luciduline (0.07 g) was eluted from the adsorbent with chloroform and further purified by evaporative distillation (bath temperature 80–100°) under reduced pressure (0.5 mm). From 44 g of weak bases it was possible in this way to obtain about 0.5 g of luciduline. Luciduline is a colorless oil which becomes yellow on standing.

Anal. Calcd. for $C_{13}H_{21}NO$: mol. wt. 207.1623. Found: mol. wt. 207.1630 (high resolution mass spectrometry (h.r.m.s.)).

Infrared spectrum: $\nu_{max}(CHCl_3)$ 2780 (N—CH_3), 1690, and 1400 cm^{-1}.

Optical rotatory dispersion in ethanol (*c*, 0.283): $[\alpha]_{589}$ +10°, $[\alpha]_{308}$ +2400°, $[\alpha]_{268}$ −2860°.

Nuclear magnetic resonance spectra: see Figs. 1 and 2.

Mass spectrum: see Fig. 3. The high resolution measurements are as follows: *m/e* 164, 164.1439 (calcd. for $C_{11}H_{18}N$, 164.1439) and 164.1076 (calcd. for $C_{10}H_{14}NO$, 164.1075); *m/e* 150, 150.1281 (calcd. for $C_{10}H_{16}N$, 150.1282) and 150.0919 (calcd. for $C_9H_{12}NO$, 150.0919); *m/e* 96, 96.0810 (calcd. for $C_6H_{10}N$, 96.0813); *m/e* 44, 44.0500 (calcd. for C_2H_6N, 44.0504).

Luciduline shows no inflexion in its titration curve when titrated with sulfuric acid in 80% Methylcellosolve.

Dihydroluciduline

Luciduline (21 mg) was dissolved in ice-cold methanol (15 ml) and sodium borohydride (0.3 g) added. Analysis by t.l.c. indicated the reaction was complete in 3–4 min. The reaction mixture was diluted with water and extracted with chloroform. Evaporation of the chloroform gave dihydroluciduline (13 mg) as a colorless crystalline solid, m.p. 65–70°, which could not be induced to crystallize from a solvent and was further purified by sublimation under reduced pressure.

Anal. Calcd. for $C_{13}H_{23}ON$ (mol. wt., 209.1779): C, 74.59; H, 11.07; N, 6.69. Found (mol. wt., 209.1771 (h.r.m.s.)): C, 74.53; H, 10.93; N, 7.07. pK^*_{mcs} 7.7.

Infrared spectrum: $\nu_{max}(CHCl_3)$ 3603 (—OH, concentration independent), and 2780 (N—CH_3).

Nuclear magnetic resonance spectrum ($CDCl_3$): τ 6.05 (1H, multiplet, $w_{\frac{1}{2}}$ 23 c.p.s.), 7.86 (3H, singlet, shifted to 7.05 in CD_3COOD, N—CH_3), 9.14 (3H, doublet, splitting 7 c.p.s., CH—CH_3).

Mass spectrum: see Fig. 3; high resolution measurements indicate that the *m/e* 192 peak has the composition $C_{13}H_{22}N$, *m/e* 166 is $C_{10}H_{16}NO$, and *m/e* 164 is $C_{11}H_{18}N$.

O-Acetyldihydroluciduline

Dihydroluciduline (54 mg) was dissolved in a mixture of acetic anhydride (1 ml) and pyridine (0.5 ml) and kept at room temperature for 12 h. After workup, *O*-acetyldihydroluciduline was obtained as a colorless oil which was purified by evaporative distillation (100°/0.5 mm).

Anal. Calcd. for $C_{15}H_{25}O_2N$: mol. wt. 251.1885. Found: mol. wt. 251.1897 (h.r.m.s.).

Infrared spectrum: $\nu_{max}(CCl_4)$ 2779 (N—CH_3), 1733, and 1235 cm^{-1}. Nuclear magnetic resonance spectrum in $CDCl_3$: τ 5.03 (1H, multiplet, $w_{\frac{1}{2}}$ 24 c.p.s.), 6.93 (1H, doublet, splitting 11 c.p.s.), 7.92 and 7.98 (3H singlets, N—CH_3 and —$OCOCH_3$), and 9.17 (3H, doublet, splitting 7 c.p.s.).

Nuclear magnetic resonance spectrum in acetic acid-d_4: τ 4.98 (1H, multiplet, $w_{\frac{1}{2}}$ 23 c.p.s.), 6.08 (1H, doublet, J = 13.5 c.p.s., coupled to proton at 6.80), 6.60 (1H, broad singlet), 6.80 (quartet, J's = 13.5 (coupled to 6.08) and 3.5 c.p.s. (coupled to 7.87), 7.00 (3H, singlet), 7.94 (3H, singlet), and 9.04 (3H, doublet, splitting 6 c.p.s.).

Mass spectrum: *m/e* 251 (5), 250 (4), 208 (4), 192 (100), and 150 (4).

Luciduline-1,1-d_2

Freshly distilled luciduline (66 mg) was dissolved in a

Can. J. Chem. Downloaded from www.nrcresearchpress.com by 210.87.254.5 on 09/05/12
For personal use only.

Can. J. Chem. Downloaded from www.nrcresearchpress.com by 210.87.254.5 on 09/05/12
For personal use only.

5% solution of deuterium chloride in acetic acid-*O-d* (5 ml) and allowed to stand at room temperature for 5 days. The bulk of the solvent was removed under reduced pressure and a saturated solution (6 ml) of anhydrous potassium carbonate in deuterium oxide was added to the residue. Extraction with alcohol-free chloroform and evaporation of the solvent gave luciduline-1,1-d_2 (40 mg). To avoid exchange in the inlet system of the mass spectrometer, the deuterium analysis was performed on *O*-acetyldihydroluciduline-1,1-d_2, prepared as described below.

Infrared spectrum: ν_{max}($CHCl_3$) 2785, and 1690 cm^{-1}. The band present at 1400 cm^{-1} in luciduline was no longer apparent.

Nuclear magnetic resonance spectrum in $CDCl_3$: no signals below τ 7.0, τ 7.17 (1H, quartet, J's = 12 and 4 c.p.s.). The rest of the spectrum is similar to that of luciduline, except the intensity of the signal centered at τ 7.6 is diminished. The n.m.r. spectrum in acetic acid-d_4 is similar to that of undeuterated luciduline.

Dihydroluciduline-1,1-d_2

Luciduline-1,1-d_2 (40 mg) was dissolved in methanol-*O-d* (2 ml) and sodium borohydride was added to the cooled solution. After 2 h most of the solvent was removed and water was added. Extraction with chloroform gave dihydroluciduline-1,1-d_2 which was purified by sublimation.

Mass spectrum: *m/e* 212(6), 211(27), 210(44), 195(19), 194(100), 193(29), 168(26), 164(18), 150(12), 98(10), 70(10), and 44(18).

O-Acetyldihydroluciduline-1,1-d_2

Dihydroluciduline-1,1-d_2 (40 mg) was acetylated using acetic anhydride – pyridine in the usual manner and the product was purified as described for the undeuterated compound to give *O*-acetyldihydroluciduline-d_2 (35 mg) as a colorless oil.

Mass spectrum: *m/e* 253(5), 252(5), 195(20), 194(100), and 193(20). The large M-1 peak associated with the molecular ion made the peaks associated with the molecular ion unsuitable for the calculation of the percentage of deuteration (21). The calculation of the percentage of the various deuterated species was therefore done on the basis of the M-59 peak. The calculation indicated the presence of 84% of d_2, 14% of d, and 6% of d_3.

Nuclear magnetic resonance spectrum in $CDCl_3$: similar to the undeuterated compound except for the absence of a signal at τ 7.44 and the reduced multiplicity of the τ 5.03 signal. Nuclear magnetic resonance spectrum in acetic acid-d_4: τ 4.98 (1H, doublet, $J \simeq 4.5$ c.p.s.), the rest of the spectrum is similar to that of the undeuterated compound. Simultaneous irradiation of the τ 7.74 region collapses the τ 4.98 doublet to a singlet and the τ 6.81 quartet to a doublet ($J \simeq 13$ c.p.s.).

Dihydroluciduline-2-d_1

Luciduline (5 mg) in methanol (5 ml) was reduced with sodium borodeuteride (19 mg) in the usual manner. After workup, dihydroluciduline-2-d_1 (3 mg) was purified by sublimation.

Mass spectrum: *m/e* 210(30), 209(45), 194(16), 193(100), 192(18), 167(27), 164(19), 150(6), 96(11), 70(10), 57(11), and 44(56).

Selenium Dehydrogenation of Dihydroluciduline

Dihydroluciduline (25 mg) was mixed with selenium powder (200 mg) and heated in a sealed tube (sealed *in vacuo*) at 280–300° for 8 h. The dehydrogenation products were isolated by evaporative distillation directly from the reaction mixture. Gas–liquid chromatography (g.l.c.) showed the presence of two major components in the ratio 3:1 and four minor components. The major components were isolated by g.l.c. (Aerograph model A-90-P3 gas chromatograph, 10% QF-1 on Chromosorb W, 5 ft × ¼ in. column, 125°, helium flow rate 35 ml/min).

The major component (8 mg), retention time 8.7 min, was obtained as a colorless solid. Mass spectrum: *m/e* 156(100), 155(31), 141(55), and a metastable peak at 127.5 corresponding to 156 → 141. The exact mass of the molecular ion corresponded to $C_{12}H_{12}$ (Calcd: 156.0943. Found: 156.0940). The ultraviolet (u.v.), i.r., and mass spectra were identical with those of an authentic sample of 2,6-dimethylnaphthalene.

The other major product (3 mg), retention time 14.2 min, was obtained as an oil. Mass spectrum: *m/e* 170(100, shown to be $C_{13}H_{14}$ by h.r.m.s.), 169(19), and 155(52). Ultraviolet spectrum: λ_{max}(EtOH) 229, 280, 311, 317, 326 mμ. The u.v. spectrum and the mass spectrum suggest that this compound is a trimethylnaphthalene, but it has not been identified.

Selenium Dehydrogenation of Luciduline

Luciduline (30 mg) was mixed with selenium (100 mg) and heated in a sealed tube at 300–310° for 16 h. Direct sublimation of the dehydrogenation mixture (120°/5 mm) gave a solid (9 mg) which contained >90% of 2,6-dimethylnaphthalene as indicated by g.l.c. The i.r. spectrum of a sample purified by g.l.c. was identical with that of authentic 2,6-dimethylnaphthalene.

Bromination of Luciduline

Luciduline hydrobromide (0.43 g) was dissolved in chloroform (2 ml) and a solution of bromine (0.38 g) in chloroform (2.2 ml) added dropwise. The reaction mixture was kept at room temperature for 2 h. The solvent was removed under reduced pressure and excess aqueous sodium bicarbonate was added to the residue. Extraction with chloroform gave a colorless solid (0.12 g) which was purified by sublimation. Bromodehydroluciduline melts at 108–110°.

Anal. Calcd. for $C_{13}H_{18}ON^{81}Br$: mol. wt. 285.0549. Found: mol. wt. 285.0549.

Infrared spectrum: ν_{max}($CHCl_3$) 2770, 1670, and 1603 cm^{-1}.

Ultraviolet spectrum: λ_{max}(EtOH) 263 mμ (ε 7350).

Nuclear magnetic resonance spectrum ($CDCl_3$): τ 6.84 (1H, doublet, J = 7 c.p.s.), 7.10–7.46 (3H, multiplets), 7.88 (3H, singlet, N—CH_3), and 8.95 (3H, doublet, J = 7 c.p.s.).

Mass spectrum: *m/e* 285(59), 283(61), 243(98), 241(100), 205(17), 204(26), and 162(44). The peak at 243 analyzes for $C_{10}H_{12}NO^{81}Br$ (Calcd: 243.0083. Found: 243.0084).

Dehydroluciduline

Freshly sublimed selenium dioxide (100 mg) was dissolved in dioxane (5 ml) and luciduline (136 mg) was added. The solution was heated under reflux for 22 h, then cooled and the precipitated selenium filtered off. The dioxane was removed *in vacuo* and the dark brown

residue was dissolved in chloroform. The chloroform solution was washed with dilute aqueous sodium bicarbonate. The chloroform solution was then taken to dryness and the residue purified by evaporative distillation (150°, 0.5 mm). The *dehydroluciduline* thus obtained was a low melting solid.

Anal. Calcd. for $C_{13}H_{19}NO$: mol. wt. 205. Found: mol. wt. 205 (mass spectrometry).

Infrared spectrum: $\nu_{max}(CCl_4)$ 2780, 1668, and 1628 cm^{-1}. Ultraviolet spectrum: $\lambda_{max}(EtOH)$ 242 mμ (ε 10 600).

Nuclear magnetic resonance spectrum ($CDCl_3$): τ 3.95 (1H, singlet), 7.12 (1H, doublet (J = 7 c.p.s.) of triplets (J = 2.5 c.p.s.)), 7.86 (3H, singlet, N—CH_3), and 8.97 (3H, doublet, splitting 6 c.p.s.). Simultaneous irradiation at τ 8.0 causes the methyl doublet at 8.97 to collapse to a singlet.

Mass spectrum: *m/e* 205(61), 204(9), 190(5), 177(7), 163(100), and 162(16).

Luciduline Lactam

Luciduline (0.56 g) was dissolved in acetone and potassium permanganate (1.2 g) was added in portions over 4 h. The reaction mixture was diluted with 5% hydrochloric acid (50 ml) and continuously extracted with ether for 1½ days. Evaporation of the ether gave luciduline lactam (67 mg, single spot on t.l.c.). Further purification was effected by filtration through alumina followed by evaporative distillation. Basification of the aqueous layer and extraction with ether led to the recovery of 0.42 g of luciduline.

Luciduline lactam was obtained as an oil which partly solidified on standing at 0°.

Anal. Calcd. for $C_{13}H_{19}NO_2$: mol. wt. 221.1416. Found: mol. wt. 221.1413 (h.r.m.s.).

Infrared spectrum: $\nu_{max}(CHCl_3)$ 1730, and 1640 cm^{-1}.

Nuclear magnetic resonance spectrum ($CDCl_3$): τ 6.36 (1H, quartet, J's ≃ 3 and 6 c.p.s.), 6.72 (1H, multiplet), 7.04 (3H, singlet, N—CH_3), and 9.05 (3H, doublet, splitting 6 c.p.s.).

Mass spectrum: *m/e* 221(100), 193(35), 180(27), 178(25), 165(45), 151(34), 149(39), 136(22), 111(30), 110(80), 108(39), 95(37), 94(70), 68(35), 57(50), 55(71), and 41(78).

O-p-Bromobenzoyldihydroluciduline

p-Bromobenzoyl chloride was prepared by the method of Vogel (22).

A solution of dihydroluciduline (72 mg) in pyridine (3 ml) was added to a flask containing *p*-bromobenzoyl chloride (0.5 g) under nitrogen. The mixture was heated for 5 h in an oil bath kept at 120°. The reaction mixture was cooled and diluted with dilute hydrochloric acid. The acid solution was washed several times with ether, then made basic by the addition of ammonium hydroxide and extracted with chloroform. Removal of the chloroform left a solid which was recrystallized from 95% ethanol to give *O-p*-bromobenzoyldihydroluciduline (21 mg), m.p. 72–73°, density of crystals, 1.365 g/cm^3 (by flotation in aqueous potassium iodide).

Anal. Calcd. for $C_{20}H_{26}NO^{81}Br$: mol. wt. 391.1148. Found: mol. wt. 391.1153.

Infrared spectrum: $\nu_{max}(CHCl_3)$ 2780, 1715, 1600, and 1270 cm^{-1}.

Nuclear magnetic resonance spectrum ($CDCl_3$): τ 2.26 (4H, quartet, J = 8 c.p.s.), 4.80 (1H, multiplet, $w_{\frac{1}{2}}$ 24 c.p.s.), 7.82 (3H, N—CH_3), and 9.10 (3H, doublet, splitting 6 c.p.s.).

Mass spectrum: *m/e* 393(1), 392(1), 390(1),193 (14), 192(100), and 44(14).

Acknowledgments

We wish to thank the National Research Council of Canada for financial support and one of us (D.S.N.) thanks the Government of Zambia for a scholarship. We also wish to thank Dr. A. N. Hogg, Mrs. Judith Westwood, and Messrs. R. N. Swindlehurst, G. Bigam, and J. F. McCutcheon for their help in various phases of this work, and especially Professor David Hall for his help with the X-ray analysis.

1. W. A. Ayer, J. A. Berezowsky, and D. A. Law. Can. J. Chem. **41**, 649 (1963).
2. D. S. Nkunika. Ph.D. Thesis. University of Alberta, Edmonton, Alberta. 1967.
3. R. H. Manske and L. Marion. Can. J. Res. B, **24**, 57 (1946).
4. D. B. MacLean. *In* The alkaloids, chemistry and physiology. Vol. X. *Edited by* R. H. F. Manske. Academic Press, Inc., New York. 1968. pp. 305–382.
5. J. C. N. Ma and E. W. Warnhoff. Can. J. Chem. **43**, 1489 (1965).
6. D. H. Williams and I. Fleming. Spectroscopic methods in organic chemistry. McGraw-Hill Book Co., Inc., London. 1966. pp. 113–120.
7. H. Conroy. Tetrahedron Letters, **10**, 34 (1960).
8. R. N. Gupta, M. Castillo, D. B. MacLean, I. D. Spenser, and J. T. Wrobel. J. Am. Chem. Soc. **90**, 1360 (1968).
9. W. A. Ayer, J. K. Jenkins, S. Valverde-Lopez, and R. H. Burnell. Can. J. Chem. **45**, 433 (1967).
10. S. Yamaguchi, S. Okuda, and N. Nakagawa. Chem. and Pharm. Bull. Japan, **11**, 1465 (1963).
11. M. J. Robinson. Tetrahedron Letters, 1153 (1968).
12. P. von Schleyer and R. D. Nicholas. J. Am. Chem. Soc. **83**, 182 (1961).
13. W. A. Ayer and D. A. Law. Can. J. Chem. **40**, 2088 (1962).
14. G. Eglinton, J. Martin, and W. Parker. J. Chem. Soc. 1243 (1965).
15. A. I. Scott. Interpretation of the ultraviolet spectra of natural products. The Pergamon Press, Ltd., New York. 1964. p. 58.
16. H. Budzikiewicz, C. Djerassi, and D. H. Williams. Mass spectrometry of organic compounds. Holden-Day, San Francisco. 1967. pp. 307–309.
17. W. M. Bryant, A. L. Burlingame, H. O. House, C. G. Pitt, and B. A. Tefertiller. J. Org. Chem. **31**, 3120 (1966).
18. W. Moffit, R. B. Woodward, A. Moscowitz, W. Klyne, and C. Djerassi. J. Am. Chem. Soc. **83**, 3120 (1961).
19. J. M. Bobbitt. Thin-layer chromatography. Reinhold Publishing Corp., New York. 1963. p. 93.
20. B. Loev and K. M. Snader. Chem. and Ind. London, 15 (1965).
21. K. Biemann. Mass spectrometry. McGraw-Hill Book Co., Inc., New York. 1962. pp. 223–227.
22. A. I. Vogel. A textbook of practical organic chemistry. Longmans, Green & Co., Ltd., London. 1961. p. 262 and 792.

Can. J. Chem. Downloaded from www.nrcresearchpress.com by 210.87.254.5 on 09/05/12
For personal use only.

Synthèse de quelques dérivés du tétrahydro-4,5,6,7 benzothiazoline-$\Delta^{2\alpha}$-acétate d'éthyle[1]

RÉAL LALIBERTÉ, HILDA WARWICK ET GEORGES MÉDAWAR
Département de Chimie, Laboratoires de Recherche Ayerst, Montréal, Québec
Reçu le 4 juin 1968

On décrit la synthèse de quelques α-cyano tétrahydro benzothiazoline-$\Delta^{2\alpha}$-acétates d'éthyle en mentionnant certains intermédiaires. L'inertie chimique particulière à ce système est mise en évidence et certains résultats obtenus par traitement avec l'acide sulfurique sont mentionnés. On expose le choix qui y est fait d'une configuration particulière en établissant celle-ci à l'aide des spectres infrarouges et ultraviolets.

Some derivatives of α-cyano tetrahydro benzothiazoline-$\Delta^{2\alpha}$-acetic acid and their intermediates are described. The lack of reactivity of this class of compounds and products of treatment with concentrated sulfuric acid have been studied. Assignment of configuration was based on infrared and ultraviolet spectroscopic evidence.

Canadian Journal of Chemistry, 46, 3643 (1968)

Introduction

Certains acides acryliques polysubstitués (**3**) peuvent donner de nouveaux dérivés du tétrahydro-4,5,6,7 benzothiazoline-$\Delta^{2\alpha}$-acétate d'éthyle portant des substituants en positions α et 3. La séquence de réactions utilisée est générale et peut conduire à un nombre considérable de thiazolines polysubstituées (1). Ces produits présentent un intérêt appréciable en pharmacologie et plus particulièrement dans ce cas en parasitologie à cause des similitudes qu'ils présentent avec certains anthelmintiques nouveaux du type thiabendazole (2).

Synthèse

Les substances nouvelles décritent dans ce travail résultent de la réaction dans l'éthanol de la chloro-2 cyclohexanone avec un sel sodique d'un alkylamino-3 ou d'un arylamino-3 cyano-2 mercapto-3 acrylate d'éthyle (**3**). On prépare ce dernier produit (**3**) en faisant réagir dans l'éthanol le sel sodique du cyanoacétate d'éthyle avec un équivalent d'un isothiocyanate d'aryle ou d'alkyle. Un contact de 30 à 60 min à 25° suffit pour que la réaction soit complète. Cette addition, déjà décrite dans le cas des isothiocyanates d'aryle (3, 4), peut tout aussi bien se faire avec plusieurs isothiocyanates d'alkyle tel que l'isothiocyanate de méthyle mentionné dans cette publication: il suffit de chauffer un peu pour que l'addition s'effectue. Il faut cependant noter que les alkylamino-3 cyano-2 mercapto-3 acrylates d'éthyle (**4**, R = alkyle) obtenus après acidification sont moins stables que les arylamino-3 cyano-2 mercapto-3 acrylates d'éthyle (**4**, R = aryle) déjà décrits (3, 4). Cependant comme il n'est pas nécessaire de les isoler ceci ne présente aucune difficulté.

En faisant agir la chloro-2 cyclohexanone sur ce sel de sodium (**3**) on obtient après un reflux de quelques heures les alkyl-3 ou aryl-3 cyano-2 tétrahydro-4,5,6,7 benzothiazoline-$\Delta^{2\alpha}$-acétates d'éthyle (**7**). Lors de cette réaction il est difficile d'isoler les intermédiaires non cyclisés (**5**), mais l'utilisation de conditions douces permet d'isoler certaines hydroxybenzothiazolidines (**6**). Celles-ci perdent facilement une molécule d'eau par chauffage pour donner les benzothiazolines (**7**).

Configuration

Deux configurations de la molécule autour de la double liaison exocyclique sont possibles. Le groupe ester peut se trouver en position *cis* par rapport à l'amine comme en **9** ou en *trans* comme montré en **10**. Dans une publication récente Barnikow (5) décrit des produits de ce genre en choisissant la configuration *trans* et ceci sans le justifier, alors qu'une équipe japonaise (6) décrit des produits voisins en adoptant la configuration inverse. Ces derniers ont noté que la formation d'un pont hydrogène possible dans ce cas seulement a une influence marquée sur la position du carbonyle à l'infrarouge.

[1]Ce travail a reçu l'appui du Conseil National de Recherches du Canada.

Can. J. Chem. Downloaded from www.nrcresearchpress.com by 210.87.254.40 on 09/05/12
For personal use only.

Can. J. Chem. Downloaded from www.nrcresearchpress.com by 210.87.254.40 on 09/05/12
For personal use only.

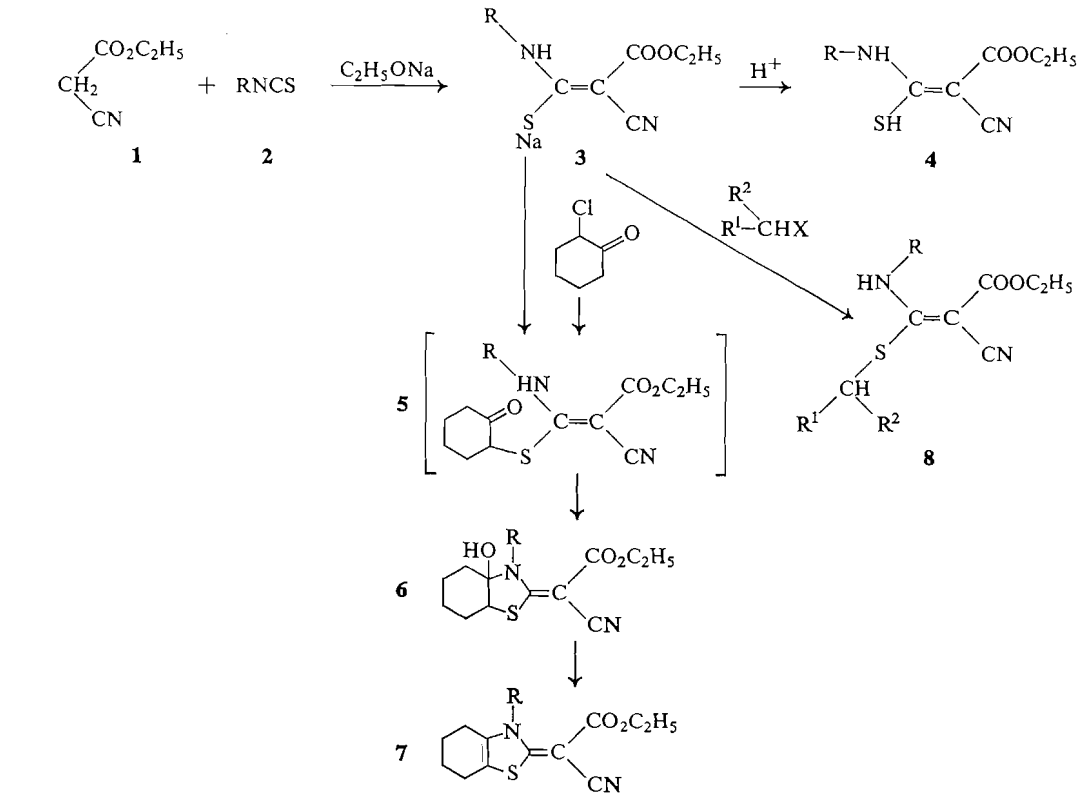

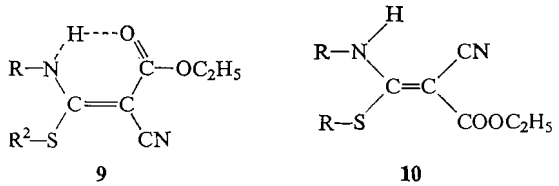

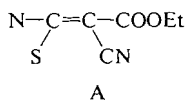

A

Nous préférons la configuration *cis* parce qu'elle explique mieux les spectres infrarouges et ultraviolets même si elle ne correspond pas à la configuration utilisée par Barnikow (5). Nous avons noté que les spectres infrarouges et ultraviolets des produits décrits ici dépendent de deux effets qu'il importe de bien distinguer: la configuration et la conjugaison. En dissociant ces deux effets de même sens et d'amplitude voisine nous pensons pouvoir établir avec une certitude satisfaisante la stéréochimie des substituants autour de la double liaison. En effet, on peut distinguer dans ces produits un système conjugué "A" représenté par les produits **3**, **4**, **6** et **8** et correspondant au chromophore A et un système plus conjugué représenté par le produit **7** et correspondant à la structure "B". En prenant pour acquis que la configuration de nos intermédiaires demeure constante au cours de la synthèse on peut déterminer celle-ci en examinant de près la position de la bande ester à l'infrarouge et la position du maximum à l'ultraviolet. Nous avons choisi comme terme de référence l'hydroxybenzothiazolidine (**6**) parce qu'elle appartient au système le moins conjugué "A" et qu'elle ne peut être stabilisée par la formation d'un pont hydrogène. A l'infrarouge

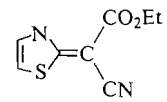

B

Can. J. Chem. Downloaded from www.nrcresearchpress.com by 210.87.254.40 on 09/05/12
For personal use only.

ces alcools montrent un signal carbonyle à 1680 cm^{-1} et à l'ultraviolet un maximum à 298 mμ. La déshydratation de ces hydroxythiazolidines (**6**) en thiazolines (**7**) diminue la fréquence du signal carbonyle d'environ 22 $cm^{-1} \pm 2$. En plus ce passage du système conjugué "A" au système plus conjugué "B" a un effet bathochrome d'environ 40 mμ: les thiazolines (**7**) ont un maximum à 340 ± 3.

Lorsqu'on compare à ces valeurs déjà mentionnées, les données infrarouge et ultraviolets de produits de type **8** il est possible de faire des observations intéressantes. Ces produits **8** correspondent au chromophore A et doivent ressembler, s'ils sont de configuration *trans*, aux hydroxythiazolidines (**6**) avec un signal carbonyle vers 1680 cm^{-1} avec un maximum vers 300 mμ. Or, nous avons constaté, ici aussi, une diminution importante de la fréquence du signal carbonyle; jusqu'à 1660 cm^{-1} avec un maximum à 323 mμ dans le cas du produit **8***b* ayant un groupe aniline en position 3 (**8**, R = C_6H_5) ou jusqu'à 1665 cm^{-1} avec un maximum 310 mμ dans le cas du produit **8***a* ayant un groupe methylamine en position 3 (**8**, R = CH_3). Ces différents maxima dépendent évidemment de la nature du substituant sur l'azote, cet effet devenant négligeable dans le cas des thiazolines **7***a*, **7***b*, et **7***c*. Le déplacement marqué du signal carbonyle ne s'explique alors que par la présence d'un pont hydrogène entre le NH et le carbonyle. Ceci implique évidemment que la configuration est *cis*.

Les produits de formule (**4**) existent sous la forme décrite ici c'est à dire d'amino mercapto acrylate d'éthyle que ce soit à l'état solide (Nujol) ou en solution dans le chloroforme. Nous n'avons décelé aucune trace du tautomère thioamide. Dans la réaction d'équilibre il ne semble pas y avoir d'inversion de configuration car nous avons obtenu la même thiazoline (**7**) en utilisant comme produit de départ le sel de sodium (**3**) ou en régénérant celui-ci à partir du mercaptan (**4**). La stabilisation qu'apporte la conjugaison du système et l'existence du pont hydrogène détermine la configuration de ces molécules.

L'examen de ces produits en résonance magnétique nucléaire n'a pas permis de détecter de preuve additionnelle pour confirmer ce choix. Il n'y a en effet pas de différence significative entre les hydrogènes α des produits **12** et **13**. Ils apparaissent à 280 Hz. On ne peut déceler d'effet à distance du phényle sur cet hydrogène, donc on ne peut déterminer la configuration des produits **12** et **13**. A cette exception près, nous acceptons donc la configuration *cis* comme étant la plus satisfaisante pour expliquer la spectroscopie de ces produits et nous ajouterons à ceci des arguments chimiques dans d'autres publications à venir.

Propriétés chimiques

L'acide sulfurique concentré à température ambiante transforme doucement le nitrile en amide (**11**). Un bref contact de cet amide (**11**) sur bain marie avec de l'acide sulfurique concentré provoque l'élimination complète de la fonction ester pour donner un tétrahydro-4,5,6,7 benzothiazoline-$\Delta^{2\alpha}$-acetamide (**12**). Une hydrolyse douce de l'amide (**11**) avec de l'acide sulfurique à 40% provoque l'élimination de la fonction carboxamide pour donner un tétrahydro-4,5,6,7 benzothiazoline-$\Delta^{2\alpha}$-acétate d'éthyle (**13**).

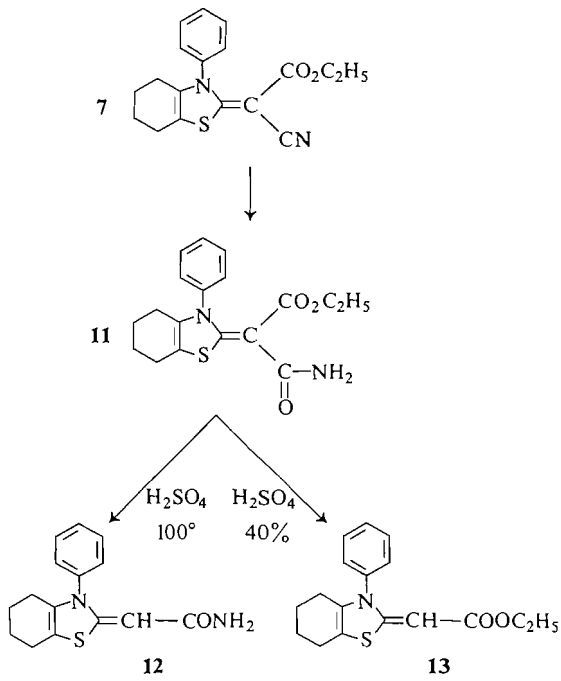

A part ces dégradations avec l'acide sulfurique les produits de formules **7** forment un système particulièrement stable (1). Le groupe ester en formant avec le reste de la molécule un système stabilisé par résonance est très peu réactif; il ne

Can. J. Chem. Downloaded from www.nrcresearchpress.com by 210.87.254.40 on 09/05/12
For personal use only.

se transforme pas en hydrazide par chauffage avec de l'hydrazine dans l'isopropanol, ni en amide par chauffage avec de la cyclohexylamine ou par contact avec de l'ammoniac dans l'éthanol à 30° pendant 6 jours. Les deux doubles liaisons forment aussi un système stable; elles résistent à l'hydrogène sous pression, à 75°, en présence de nickel de Raney. Ces molécules ne forment pas d'époxyde en présence de H_2O_2 30% dans l'acide acétique.

Cette faible réactivité nous a empêché d'utiliser ces produits comme intermédiaires dans la synthèse projetée d'analogues de la thiabenzadole. Ils ont cependant montré quelque activité contre *Trichomonas vaginalis*.

Partie expérimentale

Remarques générales

Les spectres infrarouges ont été obtenus à l'aide d'un spectrophotomètre Perkin–Elmer 225 (primes réseaux) en solution dans le chloroforme. Les spectres ultraviolets ont été mesurés dans l'éthanol avec un spectrophotomètre Perkin–Elmer 350. Les spectres de résonance magnétique nucléaire (r.m.n.) ont été enregistrés sur un appareil Varian A60-A en solution dans le chloroforme deutéré et en utilisant le tetramethylsilane comme référence interne, les positions étant exprimés en Hz. Les points de fusion ont été déterminés au microscope chauffant Reichert.

Sels de sodium d'arylamino-3 ou d'alkylamino-3 cyano-2 mercapto-3 acrylates d'éthyle

(a) Anilino-3 cyano-2 mercapto-3 acrylate d'éthyle 3a

On ajoute un équivalent de cyanoacétate d'éthyle à une solution refroidie de sodium (0.1 mole de sodium) dans 50 ml d'éthanol pur. On ajoute ensuite un équivalent d'isothiocyanate de phényle et après quelques minutes à froid on laisse reposer à température de la pièce la solution jaunâtre obtenue. Ceci donne après une heure une solution du sel de sodium de l'anilino-3 cyano-2 mercapto-3 acrylate d'éthyle qu'on peut utiliser tel quel pour le faire réagir avec la chloro-2 cyclohexanone.

(b) (Dichloro-3,4 anilino)-3 cyano-2 mercapto-3 acrylate d'éthyle 3b

On le prépare de la même façon que le produit **3***a* en utilisant de l'isothiocyanate de dichloro-3,4 phényle. La réaction est un peu exothermique et la solution devient jaune. Un contact de 30 min à température de la pièce suffit.

(c) Cyano-2 mercapto-3 methylamino-3 acrylate d'éthyle 3c

On le prépare de la même façon que le produit **3***a* en utilisant l'isothiocyanate de méthyle. La réaction est légèrement exothermique et la solution devient jaune. Un contact de 30 min à 50° est préférable dans ce cas.

Arylamino-3 et alkylamino-3 cyano-2 mercapto-3 acrylate d'éthyle

(a) Anilino-3 cyano-2 mercapto-3 acrylate d'éthyle 4a

On obtient ce mercaptan de la solution dans l'éthanol de son sel de sodium **3***a* après dilution avec 50 ml d'eau et acidification avec l'acide chlorhydrique. Il crystallise de l'éthanol. Le solide blanc jaunit à l'air comme l'a noté Ruhemann (3). Il fond à 116° (70%); γ_{max} NH, 3160; SH, 2575; CN, 2210; C=O 1657 cm^{-1}; λ_{max} 315 (ε 29 100) mμ.

Anal. Calc. pour $C_{12}H_{12}N_2O_2S$: C, 58.06; H, 4.84; N, 11.29; S, 12.91. Trouvé: C, 58.54; H, 4.99; N, 11.57; S, 12.93.

(b) (Dichloro-3,4 anilino)-3 cyano-2 mercapto-3 acrylate d'éthyle 4b

On l'obtient à partir de son sel de sodium **3***b* en diluant la solution dans l'éthanol avec un égal volume d'eau et en acidifiant avec de l'acide chlorhydrique. Il cristallise de l'éthanol et fond à 128–129° (60%); γ_{max} (Nujol) NH, 3170; SH, 2535; CN, 2200; C=O 1668 cm^{-1}; λ_{max} 325 (ε 30 900) mμ.

Anal. Calc. pour $C_{12}H_{10}Cl_2N_2O_2S$: C, 45.44; H, 3.18; N, 8.83. Trouvé: C, 45.56; H, 3.38; N, 9.05.

(c) Cyano-2 mercapto-3 méthylamino-3 acrylate d'éthyle 4c

On l'obtient à partir de son sel de sodium **3***c* de la façon suivante. Le solide obtenu par évaporation de l'éthanol est dissous dans l'eau et la solution est rendue acide avec l'acide chlorhydrique. L'huile obtenue cristallise lentement à froid. Le solide est repris de l'éthanol par addition d'eau et du benzène par addition d'éther de pétrole.

On obtient l'échantillon analytique par sublimation sous vide. Le solide blanc obtenu fond à 51–52° (60%); γ_{max} NH, 3110; SH, 2580; CN, 2200; C=O 1650 cm^{-1}; λ_{max} 295 (ε 27 000) mμ. Il est instable.

Anal. Calc. pour $C_7H_{10}N_2O_2S$: C, 45.16; H, 5.41; N, 15.05; S, 17.19. Trouvé: C, 44.86; H, 5.44; N, 14.80; S, 17.01.

α-Cyano hydroxy-3a phenyl-3 tétrahydro-4,5,6,7 benzothiazolidine-$\Delta^{2\alpha}$-acétate d'éthyle 6a

On l'obtient en ajoutant un équivalent de chloro-2 cyclohexanone à la solution du sel de sodium de l'anilino-3 cyano-2 mercapto-3 acrylate d'éthyle **3***a* en prenant soin de conserver la solution à 50° pendant 2 h. Après avoir évaporé le solvant doucement, le résidu est dissous dans le $CHCl_3$, lavé puis séché. L'évaporation laisse un solide blanc qu'on reprend rapidement du méthanol (85%). Il perd de l'eau par chauffage. γ OH, 3600 et 3400; CN, 2210; C=O 1680 bande intense à 1500 cm^{-1}; γ_{max} 298 (ε 15 900) mμ.

Anal. Calc. pour $C_{18}H_{20}N_2O_3S$: C, 62.78; H, 5.85; N, 8.14; S, 9.29. Trouvé: C, 62.63; H, 5.90; N, 8.20; S, 9.36.

α-Cyano (dichloro-3', 4' anilino)-3 hydroxy-3a, phenyl-3 tétrahydro-4,5,6,7 benzothiazolidine-$\Delta^{2\alpha}$-acétate d'éthyle 6b

On le prépare de la même façon que le produit précédent **6***a*. Il cristallise du benzène par addition d'hexane. Il fond à 164–165° (40%); γ OH, 3540 et 3350; CN, 2200; C=O 1680 bande intense à 1490 cm^{-1}; λ_{max} 298 (ε 16 000) mμ.

Anal. Calc. pour $C_{18}H_{18}Cl_2N_2O_3S$: C, 52.80; H, 4.39; N, 6.78; S, 7.76. Trouvé: C, 52.83; H, 4.59; N, 6.87; S, 7.53.

Can. J. Chem. Downloaded from www.nrcresearchpress.com by 210.87.254.40 on 09/05/12
For personal use only.

α-Cyano phényl-3 tétrahydro-4,5,6,7 benzothiazoline-$\Delta^{2\alpha}$-acétate d'éthyle 7a

On l'obtient en faisant réagir un équivalent de chloro-2 cyclohexanone avec la solution dans l'éthanol du sel de sodium de l'anilino-3 cyano-2 mercapto-3 acrylate d'éthyle **3***a*. Un reflux de 5 h suffit pour effectuer le couplage et la déshydratation de l'intermédiaire **6***a* que l'on n'isole pas. Après évaporation de l'éthanol, le résidu est dissous dans le chloroforme, lavé puis séché. L'évaporation donne un solide blanc qu'on cristallise du benzène par addition d'hexane et qu'on reprend rapidement du méthanol. Le produit fond a 194° (80%); CN, 2205; C=O 1659 bande intense à 1475 cm^{-1}, γ_{max} 338 (ε 26 200) mμ; r.m.n. CH_2 (7) 153, CH_2 (4) 118, $2CH_2$ (5 + 6) 108 Hz.

Anal. Calc. pour $C_{18}H_{18}N_2O_2S$: C, 66.24; H, 5.56; N, 8.56; S, 9.80. Trouvé: C, 66.16; H, 5.80; N, 8.38; S, 9.75.

α-Cyano (dichloro-3', 4' phényl)-3 tétrahydro-4,5,6,7 benzothiazoline-$\Delta^{2\alpha}$-acetate d'éthyle 7b

On l'obtient en faisant réagir un équivalent de chloro-2 cyclohexanone avec la solution dans l'éthanol du sel de sodium du (dichloro-3,4 anilino)-3 cyano-2 mercapto-3 acrylate d'éthyle **3***b*. Dans ce cas il faut garder sous reflux pendant 24 h pour que la déshydratation de l'intermédiaire **6***b* soit complète. On traite alors la solution comme décrit en **7***a*. Le produit blanc cristallise de l'éther, on peut le reprendre de l'acétone par addition d'eau. Il fond à 183° (50%); γ CN, 2200, C=O 1655 bande intense à 1470 cm^{-1}; λ_{max} 341 (ε 22 100) mμ; r.m.n. CH_2 (7) 154, CH_2 (4) 120, $2CH_2$ (5 + 6) 100 Hz.

Anal. Calc. pour $C_{18}H_{16}Cl_2N_2O_2S$: C, 54.69; H, 4.08; N, 7.09; S, 8.11. Trouvé: C, 54.39; H, 4.16; N, 7.25; S, 8.09.

α-Cyano méthyl-3 tétrahydro-4,5,6,7 benzothiazoline-$\Delta^{2\alpha}$-acétate d'éthyle 7c

Ce produit résulte de la réaction dans les conditions décrites en **7***a* de la chloro-2 cyclohexanone avec la solution dans l'éthanol du sel de sodium du cyano-2 mercapto-3 méthylamino-3 acrylate d'éthyle **3***c*. Le produit cristallise de l'éthanol et fond à 185° (50%); CN, 2200, C=O 1660 bande intense à 1500 cm^{-1}; λ_{max} 338 (ε 24 000) mμ; r.m.n. $2CH_2$ (4 + 7) à 150, $2CH_2$ (5 + 6) à 120 Hz.

Anal. Calc. pour $C_{13}H_{16}N_2O_2S$: C, 59.08; H, 6.10; N, 10.60; S, 12.11. Trouvé: C, 59.16; H, 6.34; N, 10.40; S, 12.31.

Benzylthio-3 cyano-2 méthylamino-3 acrylate d'éthyle 8a

On obtient ce produit en chauffant sous reflux pendant 3 h une solution dans 100 ml d'éthanol de 0.01 mole de chlorure de benzyle et de 0.01 mole du sel sodé du cyano-2, mercapto-3, méthylamino-3 acrylate d'éthyle **3***c*. L'huile obtenue après évaporation est reprise dans le chloroforme et lavée. Elle est passée sur gel de silice pour donner un solide que l'on reprend du méthanol additionné d'eau. Il fond à 62–63° (30); γ CN, 2205; C=O 1665 bande intense à 1575 cm^{-1}; λ_{max} 310 (ε 18 050); r.n.m. NH 590 Hz.

Anal. Calc. pour $C_{14}H_{16}N_2SO_2$: C, 60.86; H, 5.84; N, 10.14; S, 11.58. Trouvé: C, 61.02; H, 5.95; N, 10.40; S, 11.81.

Anilino-3 benzhydrylthio-3 cyano-2 acrylate d'éthyle 8b

On obtient ce produit en chauffant sous reflux pendant 20 h une solution dans 100 ml d'éthanol de 0.01 mole chlorure de benzhydryle et de 0.01 mole du sel sodé de l'anilino-3, cyano-2, mercapto-3 acrylate d'éthyle. Une évaporation donne un solide que l'on reprend dans le chloroforme pour le laver. Ce produit cristallise de l'éthanol et fond à 128–129° (35%); NH 3150, C=O 1660 bande intense à 1565; λ_{max} 323 (ε 21 950); r.m.n. NH 670 Hz.

Anal. Calc. pour $C_{25}H_{22}N_2O_2S$: C, 72.45; H, 5.35; N, 6.76; S, 7.72. Trouvé: C, 72.14; H, 5.49; N, 6.53; S, 7.68.

α-Carbamoyl phényl-3 tétrahydro-4,5,6,7 benzothiazoline-$\Delta^{2\alpha}$-acétate d'éthyle 11

Ce produit s'obtient en laissant 0.02 mole de α-cyano phenyl-3 tétrahydro-4,5,6,7 benzothiazoline-$\Delta^{2\alpha}$-acétate d'éthyle **7***a* en contact avec 15 ml d'acide sulfurique concentré à 25° pendant 4 jours. On verse la solution dans 150 ml d'un mélange eau et glace, et on neutralise avec de l'hydroxyde de sodium.

Une extraction avec du chloroforme suivie d'un lavage donne après évaporation une huile jaune qui cristallise par trituration avec de l'éther de pétrole. Le benzène donne un solide jaune fondant à 138–139° (70%); γ NH à 3530 et 3390, C=O 1650, C=O 1612, bande forte à 1555 cm^{-1}; λ_{max} 368 (ε 15 400); r.m.n. CH_2 (7) 155, CH_2 (4) 130, $2CH_2$ (5 + 6) 105 Hz.

Anal. Calc. pour $C_{18}H_{20}N_2O_3S$: C, 62.78; H, 5.85; N, 8.14; S, 9.30. Trouvé: C, 62.75; H, 6.09; N, 8.00; S, 9.27.

Phényl-3 tétrahydro-4,5,6,7 benzothiazoline-$\Delta^{2\alpha}$-acétamide 12

Ce produit résulte de l'action à 100° pendant 1 h de 15 ml d'acide sulfurique concentré sur l'α-carbamoyl phényl-3 tétrahydro-4,5,6,7 benzothiazoline-$\Delta^{2\alpha}$-acétate d'éthyle **11**. On verse la solution dans 150 ml d'un mélange d'eau et de glace et on neutralise avec de l'hydroxyde de sodium. Une extraction avec du chloroforme suivie d'un lavage donne après évaporation un solide qu'on reprend de l'acétone. Il fond à 230–231°; NH à 3500, 3420 et 3320, C=O 1632 bande intense à 1500 cm^{-1}; λ_{max} 345 (ε 20 400); r.m.n. CH_2 (7) 148, CH_2 (4) 115, $2CH_2$ (5 + 6) 105 H avec le NH_2 à 280 Hz.

Anal. Calc. pour $C_{15}H_{16}N_2OS$: C, 66.16; H, 5.92; N, 10.29; S, 11.08. Trouvé: C, 66.33; H, 5.96; N, 10.25; S, 11.19.

Phényl-3 tétrahydro-4,5,6,7 benzothiazoline-$\Delta^{2\alpha}$-acétate d'éthyle 13

Ce produit résulte de l'action de 30 ml d'acide sulfurique à 40% sur 0.02 mole de α-carbamoyl phényl-3 tétrahydro-4,5,6,7 benzothiazoline $\Delta^{2\alpha}$-acétate d'éthyle **11**.

Après 4 jours on traite la solution comme décrit en **11** pour obtenir un solide qui cristallise du benzène. Il fond à 153–154° (45%). Le produit sublime à 155° sous 0.1 mm C=O 1640 bande intense à 1520 cm^{-1}; λ_{max} 343 (ε 24 500) mμ; r.m.n. CH_2 (7) 150, CH_2 (4) 118, $2CH_2$ (5 + 6) 108 et H à 280 Hz.

Anal. Calc. pour $C_{17}H_{19}NO_2S$: C, 67.76; H, 6.36; N, 4.65; S, 10.62. Trouvé: C, 67.92; H, 6.60; N, 4.72; S, 10.85.

1. A. D. GRABENKO, L. N. KULAEVA, et P. PELKIS. Khim. Geterotsikl. Soedin. Akad. Nauk Latv. 364 (1966); cf. Chem. Abstr. **65**, 12190 *c* (1966).
2. P. E. THOMPSON. Ann. Rev. of Pharmacol. **7**, 77 (1967).
3. S. RUHEMANN. J. Chem. Soc. 93, 621 (1908).
4. A. D. GRABENKO, L. N. KULAEVA et P. PELKIS. Khim. Geterotsikl. Soedin. Akad. Nauk Latv. 698 (1965); cf. Chem. Abstr. **64**, 9702 *d* (1966).
5. G. BARNIKOW et H. NICLAS. Z. Chemie. **6**, 417 (1966).
6. K. ICHIMURA et M. OHTA. Bull. Chem. Soc. Japan, **40**, 2135 (1967).

Can. J. Chem. Downloaded from www.nrcresearchpress.com by 210.87.254.40 on 09/05/12
For personal use only.

Can. J. Chem. Downloaded from www.nrcresearchpress.com by 210.87.254.6 on 09/05/12
For personal use only.

Epoxides and *trans*-chlorohydrins of 3-methoxycyclopentene and their use in conformational studies in the cyclopentane system[1,2]

E. J. Langstaff and R. Y. Moir
Department of Chemistry, Queen's University, Kingston, Ontario

AND

R. A. B. Bannard and A. A. Casselman
Defence Chemical Biological and Radiation Laboratories, Ottawa, Canada

Received August 16, 1967

The stereoisomeric oxides of 3-methoxycyclopentene (**3** and **4**) and the four *trans*-chlorohydrins of the same olefin (**6–9**) were prepared by methods resembling those used previously in the cyclohexane system. Structure proofs were more difficult than in the cyclohexanes, but served to illustrate some interesting chemistry. Product ratios in the cleavage of each of the epoxides with hydrogen chloride were used to deduce the probable conformations of the four transition states, by comparing the results with those from the cyclohexane system. An unexpected outcome of the work was the new convincing evidence obtained for the intervention of chloronium ions in the addition of "hypochlorous acid" to the olefin.

Canadian Journal of Chemistry, 46, 3649 (1968)

For the past several years we have been interested in forming a reasonably accurate picture of the transition states involved in the formation and scission of the oxirane ring in the stereoisomeric oxides of 3-methoxycyclohexene (**1** and **2**) (1–8). Our approach has been that the model chosen for the transition state must explain both the relative rates of formation of the oxides from various halohydrins and the product ratios obtained in the scission of the oxides. In the present paper we report the synthesis of the corresponding compounds in the cyclopentane series and a study of the scission products of the epoxides (**3** and **4**). Kinetic studies of the rates of formation of the oxides will be reported later. From the comparison of the results in the two series, a clear picture emerges of the conformation of the transition states in the cyclopentane series.

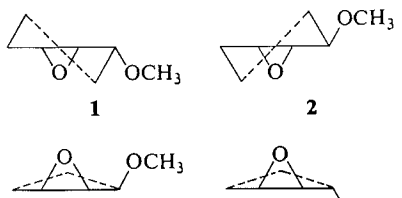

1 **2**

3 **4**

[1]Most of this work was presented at the National Meeting of the Chemical Institute of Canada, in Toronto, June 6, 1967.

[2]Discussion of recent related work has been added after the first submission.

Synthesis

Treatment of 3-methoxycyclopentene (**5***a*) (9) with chlorine and sodium carbonate in aqueous acetone (10) gave a mixture of chlorohydrins from which two (**6** and **7**) were readily separated in pure form by preparative gas–liquid chromatography (g.l.c.). The chlorohydrin **6** on treatment with aqueous alkali gave *cis*-3-methoxycyclopentene oxide (**3**), and the chlorohydrin **7** gave the isomeric *trans*-oxide (**4**). A mixture of the two

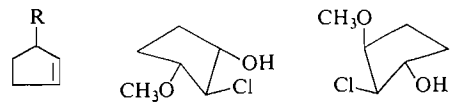

5*a*; R = OCH_3 **6** **7**
5*b*; R = OH
5*c*; R = Cl

oxides (**3** and **4**) was also obtained directly by the reaction of *meta*-chloroperbenzoic acid with the olefin, the *trans*-oxide predominating. Larger quantities of the oxides were prepared by the action of aqueous alkali either upon the crude chlorohydrin mixture obtained as above, or upon the mixture of bromohydrins resulting from the action of aqueous *N*-bromosuccinimide upon the olefin (**5***a*), just as in the cyclohexane series (1, 4). The resulting oxide mixtures were separated by preparative g.l.c., the *trans*-oxide being obtained in much larger yields, as in the other series.

Treatment of the *cis*-oxide (**3**) with a cold solution of hydrogen chloride in ether gave a

Can. J. Chem. Downloaded from www.nrcresearchpress.com by 210.87.254.6 on 09/05/12
For personal use only.

mixture from which the chlorohydrin **8** was obtained in good yield by preparative g.l.c. Its stereoisomer **9** was formed in very high yield as the only detectable product from the similar reaction of the *trans*-oxide (**4**). Thus all four *trans*-chlorohydrins of 3-methoxycyclopentene (**6–9**) had been obtained pure in amounts large enough for the kinetic studies.

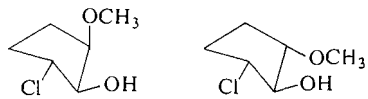

8 **9**

Proofs of Structure

The structures given above have been thoroughly verified in four different ways. One of these, the last to be accomplished, has already been published in another connection (19).[3] The other, earlier proofs remain separately valid, add independent support to that already given (19), and are interesting in respect to the chemistry of cyclopentane.

To begin with, analogies with the corresponding cyclohexane compounds (and the underlying theory) were used to predict the structures of the oxides and chlorohydrins of the present series. These predictions proved to be entirely correct. In both series, the *cis*-oxide has the higher boiling point and higher index of refraction, as could be expected for the more internally hindered, more compact, structure (12, 13). In both series, the order of elution (gas–liquid chromatography) of the four isomeric chlorohydrins was the same, in terms of the steric orientation of the substituents. In both series, the stereoisomeric oxides were opened with hydrogen chloride to give mainly the 1-chloro-2-hydroxy-3-methoxycyclanes (e.g. **8** and **9**), while the olefins reacted with "hypochlorous acid" to give mainly the 2-chloro-1-hydroxy-3-methoxycyclanes (e.g. **6** and **7**). This was to be expected if, as always observed previously, the polar effect of methoxy predominates over steric effects in the opening either of the oxirane ring or the chloronium ion ring (1, 2, 5–8, 14–16).

The next proof obtained relied upon contrasting the products obtained from 3-methoxycyclopentene (**5***a*), "active chlorine", and water with those from the olefin **5***b*, "active chlorine", and methanol. One would expect, by analogy with the reaction of aqueous *N*-chlorosuccinimide with olefins (7) and by the accepted theory of addition of halogens in methanol (17, 18) that methanolic *N*-chlorosuccinimide would attack an olefin to give methoxyl and chlorine adjacent and *trans* to each other. It therefore follows[4] that of the four chlorohydrins (**6–9**) only **6** could be produced by the action of methanolic *N*-chlorosuccinimide upon 3-hydroxycyclopentene (**5***b*), provided that no group wandering occurred due to neighbor participation. Careful consideration seemed to show that the only rearrangement to be expected was that involving the intermediate ion **10**; conceivably it might have reacted *via* the epoxide **11** (or its conjugate acid) to give **9**, a *trans*-chlorohydrin different from **6**, the only possibility in the absence of rearrangement. Fortunately **6** and **9** could easily be distinguished by nuclear magnetic resonance (n.m.r.) spectroscopy.

10 **11** **12**

The reaction was actually found to give one, and *only* one, of the *trans*-chlorohydrins of 3-methoxycyclopentene, and from its spectrum it was clearly **6** rather than **9**. Similarly, when the olefin **5***b* was treated with methanolic *N*-bromosuccinimide, and the product allowed to react with aqueous base, some *cis*-oxide (**3**) but no *trans*-oxide (**4**) was formed. From these observations the structures of both oxides and all four chlorohydrins followed (see below).

The third proof was simpler and more direct. The chlorohydrin thought to be **9** was dehalogenated by the method described previously (19) to give a methoxycyclopentanol (**12**) which proved to be identical with authentic *trans*-2-methoxycyclopentanol (20) made by the alkali-catalyzed methanolysis of cyclopentene oxide. This settled

[3]*Note added in proof*: The chlorohydrins (**6–9**) were each separately related to the 1,2- and 1,3-cyclopentanediols. We take this occasion to acknowledge the important work of Sable and Posternak (11) in establishing the configurations of some of the latter.

[4]Space does not permit a full outline of the argument. Analogy with the products obtained by an identical mode of addition of the elements of hypochlorous or hypobromous acids with 3-methoxycyclenes (6–8) would predict a low yield of **6**, because of the concurrent formation of *cis*-1,2-chlorohydrins or of 1,3-chlorohydrins. This does not spoil the proof since the formation of **7–8** is not possible. Fortunately also, none of the possible impurities in the 3-hydroxycyclopentene could lead to **6**.

Can. J. Chem. Downloaded from www.nrcresearchpress.com by 210.87.254.6 on 09/05/12
For personal use only.

the relative position and configuration of methoxyl and hydroxyl. The position and orientation of the chlorine (in **9**) followed from the conversion of the chlorohydrin by alkali to an epoxide (from which **9** could be regenerated with hydrogen chloride). The epoxide concerned could only have been the *trans*-isomer (**4**). (Its alternative formation from a peracid and olefin confirmed the presence of the epoxy-group, as did the presence in the infrared spectrum (21) of a band near 3040 cm^{-1}, absent in the chlorohydrin.) This same epoxide (**4**) could also be formed from another chlorohydrin, whose structure was therefore **7**. The structure **3** clearly belonged to the stereoisomeric epoxide, and the two remaining chlorohydrins, both of which gave **3** with aqueous alkali, must have been **6** and **8**. These two were finally distinguished by the n.m.r. spectra of their *p*-nitrobenzoates.[5]

In the *p*-nitrobenzoates of the chlorohydrins (**13–16**), the signal from H_x (geminal to the *p*-nitrobenzoxy group) was recognizable as the one farthest downfield (2, 7). Furthermore **15** and **16**

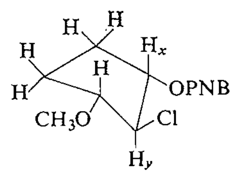

13

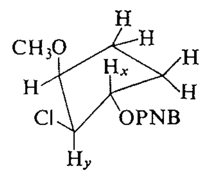

14

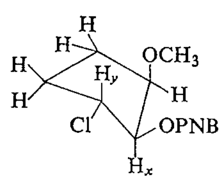

15

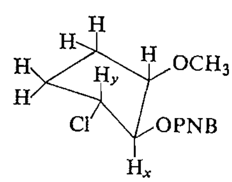

16

could be distinguished from **13** and **14** because the signal from H_x showed a much simpler coupling pattern for **15** and **16** than for the other pair. Similarly the signal from H_y showed a simpler pattern in **13** and **14** than in **15** and **16**, as expected from the number of adjacent hydrogens. Thus **6** and **8** could be distinguished through the spectra of their *p*-nitrobenzoates (**13** and **15**, respectively), and the proof was complete. However, unlike the situation for the analogous cyclohexane compounds (7), the coupling patterns of H_y in **13** and **14**, and of H_x in **15** and **16**, could not be used for a completely independent determination of all four structures.[5] The spectra are illustrated in Fig. 1.

Product Distribution in the Oxide Scissions with Hydrogen Chloride

In previous papers (1, 2, 5–8) we have set forth qualitatively the factors believed to influence the direction of oxide scission in the cyclohexane derivatives **1** and **2**. Briefly, if Y is the ratio of product yield from attack at position-1 to that from attack at position-2, and k_1 and k_2 the respective rate constants, then by the usual approximations of transition state theory:[6]

$$\ln Y = \ln \frac{k_1}{k_2} = \frac{\Delta^2 F^{\ddagger}}{RT}.$$

Here, however:

$$\Delta^2 F^{\ddagger} = F_2^{\ddagger} - F_1^{\ddagger}$$

where $F_2^{\ddagger}$ is the standard free energy of the transition state leading to scission at position-2, and $F_1^{\ddagger}$ that of the transition state leading to scission at position-1. (The energies of the common ground state and of the other participants cancel.) Presumably the transition states for oxide scission and formation are essentially identical,[7] and as will be shown in later papers, the kinetics

[5]Problems in the nuclear magnetic resonance spectroscopy of cyclopentane derivatives have been discussed by Professor Sable and his colleagues (16, 22, 23).

[6]The equations describe a particular case of the Curtin–Hammett Hypothesis (24). It is assumed that the conformational changes are relatively very fast, and that the product ratio is rate-controlled. The second assumption seems firmly based on the rather well-known chemistry of oxides (25) and is also supported by considerable evidence in the two series described here. In the cyclohexane series, the thermodynamically *less* stable product predominates in the scission of the *trans*-oxide. Furthermore, the product ratio does not vary appreciably when the nucleophile is changed from one giving a possibly reversible reaction (e.g. bromide or chloride) to one where reversibility is impossible (e.g. methoxide) (8). As will be shown later, yields and rates can be combined in a coherent system on this assumption. Less evidence is as yet available in the cyclopentane system, but aside from analogy, the fact that the kinetics of oxide closure show the same anomaly as the product ratio in oxide scission or chloronium ion scission seems to leave no doubt that rate control still applies in the new system.

[7]This seems a reasonable hypothesis for base-catalyzed scissions, strengthened in the cyclohexane work (8) by the observation that variations in the nucleophile caused little difference in the product ratios. It is of course not obvious that acid-catalyzed scissions have transition states similar geometrically to those for base-catalyzed scission, but the previously recorded observations (8) seem to make it clear that in the cyclohexane series, they do. The point has not yet been thoroughly verified in the cyclopentane series, but the regularities mentioned in footnote 6 seem to allow no other interpretation.

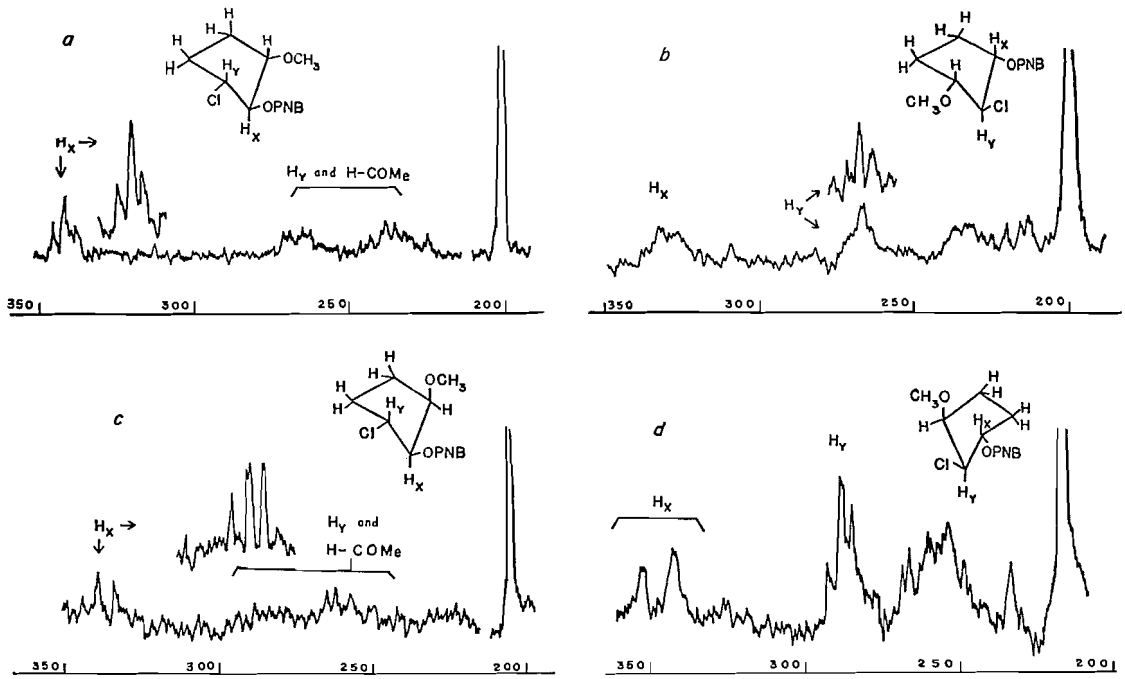

FIG. 1. Proton magnetic resonance spectra of the paranitrobenzoates of the *trans*-chlorohydrins of 3-methoxycyclopentene, taken at 60 MHz. Values on the scale are in Hz downfield from tetramethylsilane. (*a*) Compound **16**, in pyridine-d_5 at 47 °C. Inset: at slightly different conditions, and offset. The spectrum in chloroform-*d* at 40° is similar. (*b*) Compound **13**, in pyridine-d_5 at 47°. Inset is from an otherwise similar spectrum in chloroform-*d* solution at 40°. Peaks within 10 Hz to the left of methoxyl are spurious. (*c*) Compound **15**, in pyridine-d_5 at 74°. The inset was taken at slightly lower radio frequency field strength and spectrum amplitude, and is offset. The spectrum of a chloroform-*d* solution at 40° was similar. (*d*) Compound **14**, in pyridine-d_5 at 74°. At 47° in pyridine-d_5, and in chloroform-*d* at 40°, the signal from H_x was a long, rounded hump with many scarcely discernable, small peaks, and the signal from H_y, less clearly resolved than in Fig. 1, had the appearance of a triplet, but on a pedestal.

of oxide formation show that the transition state is much more like the chlorohydrins than the oxides. Thus ordinary conformational analysis may be brought to bear to explain both the rates of oxide formation and the product ratios from oxide scission. This has now been done in several series of cyclohexane compounds (8).

In the present cyclopentane series, as in the cyclohexane series, scission of either stereoisomeric oxide (**1** and **2**, or **3** and **4**) with hydrogen chloride gave mainly the 1-chloro compounds. This is attributed to an overriding inductive[8] effect of methoxyl. However, a striking difference appears in the minor products of scission of the two series. In the cyclohexane series, the *trans*-oxide (**2**) gave appreciable amounts of scission at position-2, while the *cis*-oxide (**1**) gave no detectable amounts of minor product. The cyclopentane derivatives were just the opposite in this respect, the *cis*-oxide (**3**), but not the *trans*-oxide (**4**), giving appreciable amounts of scission at position-2.

An explanation of this difference in conformational terms proved surprisingly demanding, and clearly led to one particular set of conformations, among the many available in the cyclopentane series (24), as most probable for the transition states. Preferred conformations in the cyclopentanes and in the presumably related furanoses have been discussed by Hall (26) by Bishop and Cooper (27), and by Tolbert *et al.* (16), and the probable conformations, as well as the ambiguities in deciding which are in fact occupied, have been well described. Our work differs some-

[8]The term is used in the widest sense, as before (8). Polar effects in the scission of cyclopentene oxides have been discussed by Sable and his colleagues (14–16), and in particular Tolbert *et al.* (16) observed a major and a minor product in the scission with aqueous acid of (3/4)-3,4-dihydroxycyclopentene oxide in a ratio much like those observed in the present series.

Can. J. Chem. Downloaded from www.nrcresearchpress.com by 210.87.254.6 on 09/05/12
For personal use only.

Can. J. Chem. Downloaded from www.nrcresearchpress.com by 210.87.254.6 on 09/05/12
For personal use only.

what from that reported previously. Nearly all the former discussions have been concerned with ground state conformations. In the present work, the conformations of transition states alone are at issue, as shown above, involving molecular geometries much more strained than would be allowable in the ground states. In the present work, ambiguity has been largely removed by the insistence that the explanation be consistent for the *complete set* of stereoisomers, and for the cyclohexane and cyclopentane series at the same time. It turned out that our set of compounds was just large enough for removal of the ambiguities. The following discussion has been based on a very thorough study of the models.

It appears that only the particular set of slightly distorted twist conformations **17–20** (charges and the state of protonation being omitted) provide an adequate basis for the explanation. Space does not permit a full explanation of how the many other possibilities were eliminated, but this will be obvious from the experimental results and from a study of the models, remembering that the carbon bearing the chlorine will approach sp^2 geometry, that the chlorine and oxirane oxygen need to be close to *trans*-diaxial geometry, and that torsional and close-approach interactions need to be minimized. Structures **17** and **18** represent transition states for the scissions of the *cis*-oxide (**3**); **19** and **20** for the *trans*-oxide (**4**). Structures **17** and **19** are for the "normal" scissions at position-1, structures **18** and **20** for the "abnormal" scission at position-2. Abnormal scission of the *cis*-oxide of the cyclohexane series (**1**) is relatively unfavorable because of the 1,3-diaxial methoxyl and oxygen; this effect[9] is absent in **18**, so that more abnormal scission would be expected in the cyclopentane series (as observed). A 1,3-diaxial-like interaction interferes with normal scission at position-1 of the *trans*-oxide in both series (e.g., in **19**); however, in the cyclopentane series (but not in the cyclohexanes) a still more serious interference occurs with abnormal scission. In **20** there is marked interference of a semi-eclipsing type between methoxyl and chlorine; the methoxyl cannot readily escape from this by distortion of the geometry, since it is trapped

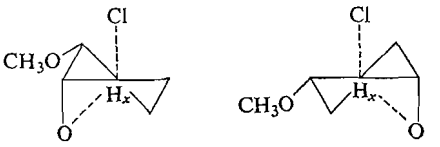

17

18

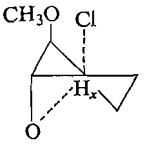

19

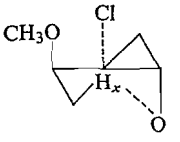

20

between the neighboring hydrogens. Escape into alternative conformations can only be had at the expense of almost eclipsing the four hydrogens on the unsubstituted carbons. Thus abnormal scission should be less favored in the *trans*-cyclopentane compound than in the cyclohexane, again as observed. This simple and elegant explanation, which arose entirely out of the present work, was also found to account for the relative rates of reaction of all four chlorohydrins with alkali, and their differences from the cyclohexane series. As will be shown in a later paper, all the factors mentioned above also appear clearly in the kinetics. Thus the suggested model has passed a very severe set of experimental tests.

One of the most interesting consequences of this analysis is the provision of strong evidence in favor of the chloronium ion as an intermediate in the formation of chlorohydrins from olefins. It is true that this is the currently accepted hypothesis, but as has been previously pointed out (17) the actual evidence is very slender.[10] In an earlier paper (7) we expressed our misgivings in that a free carbonium ion, electrostatically but not covalently held by a neighboring group, could at least as well explain our experimental results. Later (8) we showed that a comparison of

[9]Tolbert *et al.* (16) have drawn attention to this vital difference between the cyclohexanes and cyclopentanes in supporting a diaxial-dihydroxy conformation for an isopropylidene derivative in the latter series.

[10]Poutsma's review (28) appeared after the first submission of this paper. Fahey and Schubert (29) offered evidence for chloronium ion intervention in the structure of *olefinic* products. Poutsma (30) showed that in nonpolar solvents the rate of chlorination shows a lack of positional effects for alkyl groups. The evidence for bromonium ion participation is of course stronger (17). For series related to the present one, Hasegawa and Sable (31) have called attention to the analogy between oxide and bromonium ion scission in neighbor-participation reactions. Another analogy between oxides and bromonium ions had been previously pointed out by Bannard *et al.* (6).

Can. J. Chem. Downloaded from www.nrcresearchpress.com by 210.87.254.6 on 09/05/12
For personal use only.

the product ratios of chlorohydrin formation from olefin with those from oxide scissions showed parallels that suggested that three-membered rings were involved in both reactions. This parallel is now very much strengthened by the observation that the chlorohydrin yields from olefins show the same sort of differences between the cyclopentanes and cyclohexanes as do the oxide scissions. Thus in both series the predominant isomers are those (e.g., **6** and **7**) resulting from scission at position-1 of the chloronium ion, as expected from the large inductive effect of methoxyl. However, whereas some **9** is formed in the reaction of "hypochlorous acid" with **5***a*, i.e. corresponding to "abnormal" scission at position-2 of the *cis*-chloronium ion (**21**), none of the corresponding "abnormal" isomer could be detected in the cyclohexane series (7). Similarly, although no **8**, corresponding to "abnormal" scission of the *trans*-chloronium ion (**22**), could be detected in the present reaction, in the cyclohexane series the isomer representing

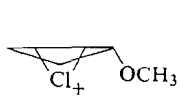

21

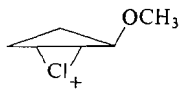

22

scission of the *trans*-chloronium ion at position-2 was formed in considerable amounts (7). It will be obvious that an analysis of the chloronium ion scissions similar to that done above for **17**–**20** of the epoxides (but with oxygen and chlorine exchanging roles as required) would lead to these observations as expected results, and that it would be difficult or impossible to explain them on the basis of any other currently favored mechanism.

Experimental

Infrared (i.r.) spectra were taken on a Perkin–Elmer model 21 spectrometer, repeatedly calibrated with polystyrene. Quoted comparisons are for spectra of chloroform solutions. The refractometer was calibrated with water at each use, and temperatures reported in its use are accurate to about ±0.1°. Proton resonance spectra (p.m.r.) were determined on a Varian A-60 instrument at 60 mHz, tetramethylsilane being used as the internal standard with each sample. All preparative gas–liquid chromatographic (g.l.c.) separations were performed with a Fisher Preparative Partitioner, using 6 ft × 1 in. glass columns filled with 10% Versamid 900 on Chromosorb. Analytical g.l.c. was performed on a Jarrell–Ash model 700, using an electron-affinity detector. Quantitative g.l.c. analyses are from uncorrected peak areas. All analytical samples of liquids were shown (with two exceptions as noted) to be homogeneous by g.l.c. on columns shown able to distinguish the corresponding isomers. Melting points were determined on a precision apparatus (32), with calibrated short stem thermometers totally immersed in the bath. Boiling points are uncorrected.

DL-*O-Methyl-2-cyclopenten-1-ol (3-Methoxycyclopentene) (5a)*

The method is that of Alder and Flock (9). Freshly prepared, undistilled 3-chlorocyclopentene (350 g, n_D^{25} 1.4740 uncorrected) (37) was added slowly over a period of about 80 min to a slurry of sodium bicarbonate (400 g) in methanol (1100 ml) which was kept at −10° and vigorously stirred during the addition. Stirring was continued an additional 2 h. Enough water was then added to bring about the formation of two layers. The lower layer was extracted with ether, the ether extract united with the upper layer, dried, and fractionally distilled. The fraction of b.p. 55–106° was washed twice with water, dried, and redistilled to give product, b.p. 106–108°, n_D^{25} 1.4362, in a yield of 183 g (53%), (lit. (9), 108°, n_D^{20} 1.4393). Analysis by g.l.c. showed the presence of about 1% of impurity.

Anal. Calcd. for $C_6H_{10}O$: C, 73.41; H, 10.28. Found: C, 73.51; H, 10.15.

In addition there was produced a rubber (8.6 g) and a high-boiling, evil-smelling liquid (15.9 g). At a reaction temperature of 20°, the rubber was the main product.

Reaction of 3-Methoxycyclopentene with "Hypochlorous Acid"

(*a*) The reaction with water and *N*-chlorosuccinimide, which gave excellent results with 3-methoxycyclohexene (7), and moderate yields with cyclopentene, gave only intractable tars with 3-methoxycyclopentene.

(*b*) The source of hypochlorous acid is that of Sumrell *et al.* (10). Water (100 ml), acetone (450 ml), sodium carbonate (25 g), and 3-methoxycyclopentene (42 g, n_D^{25} 1.4370) were rapidly stirred while chlorine was slowly bubbled into the solution for about 1 h, until a distinct second layer formed and further chlorine tended to lighten the dark color. (During a similar, larger preparation, the temperature rose from 23 to 42°, then fell.) The resulting bottom layer was extracted twice with 50 ml portions of ether. The ether extracts were united with the upper layer, dried, and distilled, three fractions being collected: (1) b.p. 30–48°/15 mm, n_D^{25} 1.4630, 3.4 g; (2) b.p. 48–105°/15 mm, n_D^{25} 1.4789, 23.2 g; and (3) b.p. 60–85°/0.03 mm, n_D^{25} 1.4842, 19.8 g. Analytical g.l.c. (10 ft column, neopentylglycol sebacate, 70°, 20 p.s.i.) showed for fraction (1), five peaks with retention times less than 10 min, for fraction (2) the same five peaks plus two new ones of much longer retention times, and for fraction (3), five initial peaks of much lower amplitude plus the same two peaks of fraction (2).

Two other preparations were made; each was partially separated by distillation as above (to facilitate the subsequent separation by g.l.c.). Preparative separation was then performed on material from all the runs at 100°/20 p.s.i. Material corresponding to the first five peaks above was collected as fraction (*a*), material corresponding to the first peak of long retention time as fraction (*b*),

TABLE I

Gas–liquid chromatography characteristics of the methoxychlorocyclopentanols

Compound	Retention time on column of: 10% NGS on Embacel*	10% Versamid-900 on Chromosorb P†	30% DEGS on Anakrom‡	10% S.E. on Fluoropak§
8	8.5	5	6.5	7.5
6	12.5	9	11	7.5
9	21.8	16.5	17.5	9
7	29.5	23	24	13

*6 ft × ¼ in. column, 70°, 20 p.s.i.
†45/60 mesh, 5 ft × 3/8 in. aluminium column, helium flow rate 300 ml/min.
‡60/70 mesh, 10 ft × 3/8 in. aluminium column, same flow rate.
§5 ft × 3/8 in. aluminium column, helium flow rate 150 ml/min.

and material corresponding to the second peak of long retention time as fraction (*c*). Approximately 15 g were collected in each of (*b*) and (*c*). Each fraction was distilled through a small column, kept 15 months, then redistilled successively from a Claisen flask and then in a Späth apparatus just before analysis and use in kinetic studies.

The total crude product from one of these later, larger preparations was vacuum distilled to give a complete "chlorohydrin" fraction, b.p. 50–80°/0.04 mm, yield 58.3%, and this unfractionated material was analyzed on a 6 ft × ¼ in. column packed with 10% neopentylglycol sebacate polymer on Embacel at 80° and 20 p.s.i. The peak areas (normalized to a total yield of 48%) suggested the following yields:

3-chloro-1-*O*-methyl-(1,3/2)-1,2-cyclopentanediol (**9**), 1.9%;
3-chloro-1-*O*-methyl-(1,2/3)-1,2-cyclopentanediol (**8**), absent;
2-chloro-1-*O*-methyl-(1,3/2)-1,3-cyclopentanediol (**6**), 15%;
2-chloro-1-*O*-methyl-(1,2/3)-1,3-cyclopentanediol (**7**), 10%; and
two unknown products (probably dichlorides), 12%.

Partial fractionation and preparative v.p.c. then followed as above.

DL-*2-Chloro-1-O-methyl-(1,3/2)-1,3-cyclopentanediol (6)*

Fraction (*b*) obtained just above was a clear colorless oil, b.p. 65–75°/0.01–0.02 mm, n_D^{25} 1.4748.

Anal. Calcd. for $C_6H_{11}O_2Cl$: C, 47.86; H, 7.36; Cl, 23.55. Found: C, 47.98; H, 7.33; Cl, 23.52.

The *p-nitrobenzoate* was obtained in a yield of 64% after three recrystallizations, m.p. 67.7–68.9°.

Anal. Calcd. for $C_{13}H_{14}O_5NCl$: C, 52.07; H, 4.71; N, 4.68; Cl, 11.84. Found: C, 52.11; H, 5.01; N, 4.71; Cl, 11.89.

The *2,4-dinitrobenzenesulfenate* was obtained in a yield of 60%, m.p. 96.9–98.2°.

Anal. Calcd. for $C_{12}H_{13}O_6N_2SCl$: C, 41.30; H, 3.76; S, 9.20. Found: C, 41.42, 41.50; H, 3.57, 3.63; S, 9.36, 9.43.

DL-*2-Chloro-1-O-methyl-(1,2/3)-1,3-cyclopentanediol (7)*

Fraction (*c*) was also obtained as a clear, colorless oil, b.p. 75–80°/0.01–0.02 mm, n_D^{25} 1.4815.

Anal. Calcd. for $C_6H_{11}O_2Cl$: C, 47.86; H, 7.36; Cl, 23.55. Found: C, 48.12; H, 7.27; Cl, 23.61.

The *p-nitrobenzoate* was obtained in a yield of 93% after one recrystallization, m.p. 63.5–64.6°.

Anal. Calcd. for $C_{13}H_{14}O_5NCl$: C, 52.07; H, 4.71; N, 4.68; Cl, 11.84. Found: C, 52.28; H, 4.88; N, 4.60; Cl, 11.81.

Gas–liquid chromatographic characteristics of the four stereoisomers are given in Table I. It will be observed that excellent separations of all four isomers are possible, and that the order of elution is the same on all columns tried.

DL-*2-Cyclopenten-1-ol (3-Hydroxycyclopentene) (5b)*

In our hands the method of Alder and Flock (9) was superior to that used by Bergstahler and Nordin (33) for the corresponding cyclohexene derivative. By the former method, crude 3-chlorocyclopentene (37) (240 g) was converted to crude 3-hydroxycyclopentene, b.p. 40–80°/14 mm, judged by g.l.c. to contain about 75% of the desired compound (retention time 5.3 min) as well as two impurities (retention times 1.9 and 8.5 min, respectively), the first impurity peak having about twice the area of the second. The i.r. spectrum showed a large hydroxyl absorption. Further purification was not practicable owing to the rapid decomposition of the material. Other runs showed a more complex set of impurity peaks, suggesting that decomposition in the flash evaporator might have been the source of some of them.

The *p-nitrobenzoate* after two recrystallizations from ethanol had m.p. 79.5–80.5°.

Anal. Calcd. for $C_{12}H_{11}O_4N$: C, 61.77; H, 4.76; N, 6.01. Found: C, 61.60; H, 4.82; N, 6.07.

Another run gave crude 3-hydroxycyclopentene approximately 85% pure by g.l.c. It was used in the preparations reported below.

The Stereoisomeric Oxides of 3-Methoxycyclopentene (3 and 4)

(*a*) A mixture of stereoisomeric chlorohydrins prepared as above from 3-methoxycyclopentene and "hypochlorous acid" was partially separated by fractional distillation. Each fraction was allowed to react, with stirring, with a slight excess of aqueous sodium hydroxide at 65° for a few min, until the oily layer moved to the top. Ethereal extracts of the acidified lower layers were united

Can. J. Chem. Downloaded from www.nrcresearchpress.com by 210.87.254.6 on 09/05/12
For personal use only.

Can. J. Chem. Downloaded from www.nrcresearchpress.com by 210.87.254.6 on 09/05/12
For personal use only.

with the top layers, dried, and fractionally distilled; this partial separation facilitated the next step. Preparative gas chromatography was carried on with manual programming between 100 and 130° and 20–28 p.s.i.; the traps were kept in a bath of dry ice and acetone. The final yields were 12.9 g (41%) of the *trans*-oxide (**4**) and 2.8 g (9%) of the *cis*-oxide (**3**) based on the original *olefin* used.

(*b*) A crude mixture of isomeric bromohydrins (157 g, approximately 70% yield) was obtained by the reaction of 3-methoxycyclopentene with *N*-bromosuccinimide and water in the same way described for the cyclohexene analogue (6). The mixture was allowed to react with a solution of sodium hydroxide (30 g) in water (250 ml) at room temperature, with vigorous stirring, until an upper layer appeared. This was removed, and the water layer allowed to react a further 15 min. After acidification, the water layer was extracted with five 50 ml portions of ether. Separation and isolation were achieved in the same way as described above. The final yield was 32.4 g of the *trans*-oxide (**4**) and 12.5 g of the *cis*-oxide (**3**), a total yield of 47.5%, based on the *olefin* used.

(*c*) A solution of *meta*-chloroperbenzoic acid (80 g) in anhydrous ether (350 ml) at −20° was treated with 3-methoxycyclopentene (43 g, 95–99% pure by g.l.c., the impurity being methanol). After being kept 3 days at −20°, the solution still showed (g.l.c.) much unreacted olefin. It was therefore allowed to warm up slowly. A vigorous reaction ensued with the evolution of heat. When this subsided, olefin was still present (g.l.c.), but after the mixture had been heated 1.5 h under reflux, only a trace of olefin remained. The excess peracid was destroyed by washing the solution with three 30 ml portions of 10% aqueous ferrous sulfate, then with three 30 ml portions of 10% aqueous sodium hydroxide, and finally with two portions of water. The ethereal layer was then dried and distilled *in vacuo*. Mixed oxides were obtained in a yield of 17.4 g (35%), the *cis*- and *trans*-oxides being present in the ratio 1:6, respectively, as judged by the peak areas in g.l.c. (The oxides were identified by peak enhancement using authentic samples.) All g.l.c. analyses were performed in a 4 ft × ¼ in. stainless steel column packed with 10% neopentylglycol sebacate on Embacel at 65–75° and 15–25 p.s.i.

(*d*) A mixture of *N*-bromosuccinimide (267 g) and methanol (600 ml) was brought to reflux temperature, and then freshly prepared 3-hydroxycyclopentene (crude, 85% pure by g.l.c., approximately 134 g judged by volume and g.l.c. analysis) (see above) was slowly added at such a rate that the mixture continued to boil. When the reaction had subsided, the solution was cooled, most of the methanol removed on the rotary evaporator, and the resulting oil filtered from the precipitated succinimide, and distilled. The distillate (b.p. 30–100°/0.3 mm) was dissolved in water. Aqueous sodium hydroxide was slowly added with vigorous stirring over about 20 min, until the mixture remained basic for 5 min. The mixture was then neutralized, the aqueous layer twice extracted with 50 ml portions of ether, the ether extract united with the upper layer, dried, and distilled to yield two fractions: (1) b.p. 60–72°/0.1 mm, 18.3 g; and (2) b.p. 72–100°/0.1 mm, 201.9 g. Analysis on a 6 ft × ¼ in. column filled with 10% neopentylglycol sebacate on Chromosorb, at 60° and 23 p.s.i., fraction (1) showed the following peaks: (*a*) a large peak, retention time 5.25 min (from cyclopentenone, see below), (*b*) a minor peak, retention time 9.00 min (unknown) and (*c*) a large peak, retention time 10.50 min, reinforced by the addition of authentic *cis*-oxide (**3**), whose retention time was the same. The retention time of authentic *trans*-oxide on the same column was 5.00 min. When authentic *trans*-oxide (**4**) was added to the sample, peak (*a*) was enlarged but the shape of the peak was changed, indicating two incompletely separated substances. Fraction (1) was separated on the Fisher Prep Partitioner, two major fractions being obtained: (*i*), corresponding to peak (*a*), was shown by the i.r. spectrum to be an unsaturated ketone. Some of the material (1.12 g, 99.5% pure by g.l.c.) was converted to its 2,4-dinitrophenylhydrazone, m.p. 167.2–168.4°. A twice crystallized sample was used for analysis. Its i.r. spectrum was identical to that of an authentic sample (34) of the 2,4-dinitrophenylhydrazone of Δ^2-cyclopentenone kindly given us by Dr. S. Wolfe and W. R. Pilgrim, and the mixture m.p. showed no depression.

Anal. Calcd. for $C_{11}H_{10}N_4O_4$: C, 50.36; H, 3.89; N, 21.38. Found: C, 50.67; H, 4.47; N, 21.07.

Fraction (*ii*), corresponding to peak (*c*) above, from the preparative v.p.c. was shown by retention time and peak enhancement on an analytical column, by refractive index, and by its i.r. spectrum to be identical to *cis*-3-methoxycyclopentene oxide (**3**) obtained from methods (*a*) and (*b*).

The large fraction (2) from the initial distillation showed on the same analytical column only one major peak with a retention time of 75 min. It gave no oxide on further treatment with base, and has not been further investigated.

(*e*) Pure 3-chloro-1-*O*-methyl-(1,3/2)-1,2-cyclopentanediol (3.00 g, n_D^{25} 1.4747) was stirred with a solution of sodium hydroxide (0.9 g) in water (10 ml) until all the oil had disappeared (about 10 min). The mixture was carefully neutralized with hydrochloric acid, and extracted with four 30 ml portions of ether. The dried ether extracts were distilled in the Späth apparatus to give 1.85 g (90%) of a clear colorless oil, whose i.r. spectrum was identica to that of pure *trans*-3-methoxycyclopentene oxide (**4**).

(*f*) Pure 2-chloro-1-*O*-methyl-(1,2/3)-1,3-cyclopentanediol (n_D^{25} 1.4815) was similarly treated and the product, isolated in the same way in 93% yield, also gave an i.r. spectrum identical to that of pure *trans*-3-methoxycyclopentene oxide (**4**).

(*g*) Pure 2-chloro-1-*O*-methyl-(1,3/2)-1,3-cyclopentanediol (n_D^{25} 1.4748), treated in the same way, gave an 88% yield of an oil whose i.r. spectrum was identical to that of the *cis*-3-methoxycyclopentene oxide (**3**) of the united sample below.

Corresponding purified fractions of the oxides from methods (*a*) and (*b*) were united.

DL-*2,3-Epoxy-1-O-methyl-(1|2,3)-1-cyclopentanol (trans-3-Methoxycyclopentene Oxide) (4)*

The united preparations mentioned above were obtained as a colorless liquid, b.p. 35–37°/9 mm, n_D^{25} 1.4400.

Anal. Calcd. for $C_6H_{10}O_2$: C, 63.11; H, 8.83. Found: C, 63.22, 63.20; H, 9.01, 9.10.

DL-*2,3-Epoxy-1-O-methyl-(1,2,3|)-1-cyclopentanol (cis-3-Methoxycyclopentene Oxide) (3)*

The united preparations above formed a colorless

Can. J. Chem. Downloaded from www.nrcresearchpress.com by 210.87.254.6 on 09/05/12
For personal use only.

liquid, b.p. 48–50°/9.0 mm, n_D^{25} 1.4468. However, the analytical sample was from preparation (*g*) above. It contained about 0.3% of an unknown impurity, not the *trans*-oxide. This sample was also used as the standard for the i.r. spectrum.

Anal. Calcd. for $C_6H_{10}O_2$: C, 63.11; H, 8.83. Found: C, 62.86; H, 8.86.

On a 6 ft × ¼ in. copper column packed with 10% butanediol succinate polymer on Embacel at 85° and 25 p.s.i., the *trans*-oxide (**4**) had a retention time of 6.0 min, and the *cis*-oxide (**3**) a retention time of 9.0 min.

DL-*3-Chloro-1-O-methyl-(1,3/2)-1,2-cyclopentanediol (9)*
Scission of the trans-Oxide with Hydrogen Chloride

A solution of pure *trans*-3-methoxycyclopentene oxide (27.5 g, n_D^{25} 1.4395) in anhydrous ether (50 ml) was cooled to −50°, saturated with dry hydrogen chloride, kept for 1 h at −50°, and then allowed to warm slowly to room temperature. Some hydrogen chloride was removed in a stream of air drawn through the solution, and the rest by five washings with water (325 ml in all) (200 ml more ether being added). The ether layer was dried and fractionally distilled through a small column to give three fractions: (1) b.p. up to 55°/0.02, very small amount; (2) 55–65°/0.02, 19.2 g; and (3) 65–155°/0.02 mm, nearly all at 155°, 5.1 g. Fraction (1) did not warrant further attention. Fraction (2) showed a single, sharp peak in the g.l.c., and fraction (3) the same peak plus a larger new peak of longer retention time. The n.m.r. spectrum of fraction (3) was almost identical to that of fraction (2), although its b.p. was considerably higher, suggesting that the former was a condensation product of the latter. Fraction (2) was a clear, colorless oil n_D^{25} 1.4747, b.p. 55–65°/0.02 mm.

Anal. Calcd. for $C_6H_{11}O_2Cl$: C, 47.86; H, 7.36; Cl, 23.55. Found: C, 47.83; H, 7.40; Cl, 23.45.

The *p-nitrobenzoate* was obtained in a yield of 72% after three recrystallizations, m.p. 68.0–69.2°.

Anal. Calcd. for $C_{13}H_{14}O_5NCl$: C, 52.07; H, 4.71; N, 4.68; Cl, 11.84. Found: C, 51.90, 52.10; H, 4.72, 4.87; N, 4.80, 4.63; Cl, 11.74, 11.67.

The presence of fraction (3) suggested trial of a more dilute reaction-mixture, and this succeeded. When the *trans*-oxide (**4**) (19.80 g) was allowed to react in ether (50 ml) and treated as before, only one compound was obtained, and in a yield of 24.93 g (95.9%). Careful analysis by g.l.c. under conditions known to be capable of separating all four chlorohydrins showed the presence only of the compound of the title.

DL-*3-Chloro-1-O-methyl-(1,2/3)-1,2-cyclopentanediol (8)*
Scission of the cis-Oxide with Hydrogen Chloride

A sample of *cis*-3-methoxycyclopentene oxide (11.87 g, containing 1.7% *trans*-oxide and 1.0% of unknown impurity by g.l.c.) was treated with ethereal hydrogen chloride as above. The total product was collected in one fraction (b.p. 35–85°/0.02 mm) in a yield of 14.10 g (90.5%). It was analyzed carefully by g.l.c. (6 ft × 1 in., neopentylglycol sebacate polymer 70°, 20 p.s.i.), giving the following peaks: (1) retention time 1.75 min, *trans*-oxide, trace; (2) retention time 3.50 min, *cis*-oxide, none; (3) retention times 5.40 and 6.80 min, impurities from oxide, traces; (4) retention time 8.5 min, 3-chloro-1-*O*-methyl-(1,2/3)-1,2-cyclopentanediol (**8**), relative area 4.8; (5) retention time 12.5 min, 2-chloro-1-*O*-methyl-(1,3/2)-1,3-cyclopentanediol (**6**), relative area 1.0; (6) retention time 21.8 min, 3-chloro-1-*O*-methyl-(1,3/2)-1,2-cyclopentanediol (**9**), trace; and (7) retention time 29.5 min, 2-chloro-1-*O*-methyl-(1,2/3)-1,3-cyclopentanediol (**7**), none. Authentic materials added for each of peaks (5), (6), and (7) gave exactly the retention times shown, and enhanced the corresponding product peaks for (5) and (6). Preparative g.l.c. was used to collect material corresponding to the two major peaks.

DL-*3-Chloro-1-O-methyl-(1,2/3)-1,2-cyclopentanediol (8)*

Material corresponding to peak (4) was twice distilled to give a clear, colorless oil, n_D^{25} 1.4720, b.p. 49–60°/0.02 mm.

Anal. Calcd. for $C_6H_{11}O_2Cl$: C, 47.86; H, 7.36; Cl, 23.55. Found: C, 47.91; H, 7.43; Cl, 23.58.

The *p-nitrobenzoate*, usually a gum, was obtained as a solid only with extraordinary difficulty, and was impossible to recrystallize. It was obtained in a yield of 12%, m.p. 37.5–39.5°.

Anal. Calcd. for $C_{13}H_{14}O_5NCl$: C, 52.07; H, 4.71; N, 4.68; Cl, 11.84. Found: C, 52.31; H, 4.62; N, 4.87; Cl, 10.53.

All the material corresponding to fraction (5) above was converted to its *p*-nitrobenzoate, yield (after two recrystallizations) 0.325 g or 55%, m.p. 68.9–69.7°. Mixture melting points with the *p*-nitrobenzoates of each of the four isomeric chlorohydrins gave a depression except with that of 2-chloro-1-*O*-methyl-(1,3/2)-1,3-cyclopentanediol (**6**), thus establishing its identity. It is important to note that neither isolated chlorohydrin could have arisen from the small amount of *trans*-oxide impurity in the *cis*-oxide used to produce them.

Reaction of Methanol and N-Chlorosuccinimide with 3-Hydroxycyclopentene

A mixture of *N*-chlorosuccinimide (200 g) and methanol (600 ml) was brought to reflux. Freshly prepared 3-hydroxycyclopentene (crude, about 85% pure by g.l.c., judged by volume and g.l.c. to contain about 126 g) was slowly added at such a rate as to maintain refluxing. After all the olefin had been added, the mixture was cooled, the methanol removed by evaporation, and the resulting oil (45.6 g) separated from the precipitated succinimide. Careful g.l.c. analysis (6 ft × ¼ in. stainless steel column, 10% neopentylglycol sebacate on Embacel, 60°, 20 p.s.i.) gave the following results (retention times in min, relative areas in %): (1) 17.0 min, 36.6%, unknown; (2) 25.5 min, 42.6%, unknown; (3) 32.5 min, none, 3-chloro-1-*O*-methyl-(1,2/3)-1,2-cyclopentanediol (**8**); (4) 39.0 min, 8.2%, unknown; (5) 58.75 min, 12.6%, 2-chloro-1-*O*-methyl-(1,3/2)-1,3-cyclopentanediol (**6**); (6) 68.5 min, none, 3-chloro-1-*O*-methyl-(1,3/2)-1,2-cyclopentanediol (**9**); and (7) more than 80 min, none, 2-chloro-1-*O*-methyl-(1,2/3)-1,3-cyclopentanediol (**7**). Peaks were identified by addition in succession of each of the four authentic *trans*-chlorohydrins of 3-methoxycyclopentene.

A preparative g.l.c. separation (100°, 20 p.s.i.) gave a very small amount of material corresponding to peak (5) just above. All of it was converted to the *p*-nitrobenzoate, m.p. 67.8–68.9° undepressed on admixture with the *p*-nitrobenzoate of authentic 2-chloro-1-*O*-methyl-(1,3/2)-1,3-cyclopentanediol (**6**) made from the reaction of 3-methoxycyclopentene with aqueous *N*-chlorosuccinimide.

Can. J. Chem. Downloaded from www.nrcresearchpress.com by 210.87.254.6 on 09/05/12
For personal use only.

DL-*trans-2-Bromocyclopentanol*

The compound was prepared by the action of aqueous *N*-bromosuccinimide upon cyclopentene following the general method of Guss and Rosenthal (35) as modified by Hawkins and Bannard (3) for the preparation of *trans*-2-bromocyclohexanol. The cyclopentene-*N*-bromosuccinimide reaction was much more exothermic than any of the olefin-*N*-bromosuccinimide reactions we have examined previously (3, 4) and efficient external cooling of the reaction vessel was necessary to prevent the loss of some of the cyclopentene. The product was obtained as a colorless oil, b.p. 83.5–85.0°/10 mm, n_D^{25} 1.5144, in 79% yield, (lit. (36), b.p. 92°/15 mm, n_D^{20} 1.5162).

1,2-Epoxycyclopentane (Cyclopentene Oxide)

This substance was prepared by the dropwise addition at 21–39° over a period of 15 min of aqueous sodium hydroxide (24.0 g in 60 ml of water) to a mechanically stirred mixture of *trans*-2-bromocyclopentanol (61.1 g) and water (20 ml). The oxide layer was decanted, and in view of the observations of Owen and Smith regarding the volatility of the oxide in ether (36), was dried over magnesium sulfate separately from the ether extract of the aqueous phase. (We did not experience the difficulty they encountered with emulsion formation in the preparation from the analogous chlorohydrin.) Separate distillations of the two fractions gave 25.6 g (81%) of a colorless, fragrant oil, b.p. 101–102°, n_D^{25} 1.4328, (lit. (36), b.p. 102°, n_D^{16} 1.4370).

DL-*1-O-Methyl-(1|2)-cyclopentanediol (**12**)*

(*a*) Cyclopentene oxide (12.6 g) was added to a solution made from sodium (1.0 g) in methanol (75 ml). The mixture, protected from moisture, was heated under reflux for 90 h. About 35 ml of methanol were then removed by distillation. The residue was cooled and neutralized with glacial acetic acid (2.6 g), and the precipitate collected and washed with ether. Fractional distillation of the combined filtrates gave 12.1 g (70%) of a colorless, mobile oil, b.p. 77°/10 mm, n_D^{25} 1.4518, (lit. (20), b.p. 175° n_D^{20} 1.4534.

(*b*) DL-3-Chloro-1-*O*-methyl-(1,3/2)-1,2-cyclopentanediol (**9**) (950 mg) on dechlorination in the manner described previously (15) furnished 697 mg (96%) of a colorless oil, n_D^{25} 1.4504, on distillation at 10 mm pressure from an air bath at 80–90°. Its i.r. spectrum was identical with that of the material from part (*a*).

Acknowledgments

Partial support of the work, and the grant of a Scholarship to one of us (E.J.L.), by the National Research Council of Canada is gratefully acknowledged. We thank Mr. J. Helie for performing some of the analyses reported here. Some of the experimental work was performed by Messrs. A. D. McKinnon, H. Johnston, and M. Little.

1. J. A. McRae, R. Y. Moir, J. W. Haynes, and L. G. Ripley. J. Org. Chem. **17**, 1621 (1952).
2. R. U. Lemieux, R. K. Kullnig, and R. Y. Moir. J. Am. Chem. Soc. **80**, 2237 (1958).
3. L. R. Hawkins and R. A. B. Bannard. Can. J. Chem. **36**, 220 (1958).
4. R. A. B. Bannard and L. R. Hawkins. Can. J. Chem. **36**, 1241 (1958).
5. R. A. B. Bannard and L. R. Hawkins. Can. J. Chem. **39**, 1530 (1961).
6. R. A. B. Bannard, A. A. Casselman, and L. R. Hawkins. Can. J. Chem. **43**, 2398 (1965).
7. E. U. Langstaff, E. Hamanaka, G. A. Neville, and R. Y. Moir. Can. J. Chem. **45**, 1907 (1967).
8. R. A. B. Bannard, A. A. Casselman, E. J. Langstaff, and R. Y. Moir. Can. J. Chem. **46**, 35 (1968).
9. K. Alder and F. H. Flock. Ber. **89**, 1732 (1956).
10. G. Sumrell, B. W. Wymann, R. G. Howell, and M. C. Harvey. Can. J. Chem. **42**, 2896 (1964).
11. H. Z. Sable and T. Posternak. Helv. Chim. Acta, **45**, 370 (1962).
12. N. L. Allinger. J. Org. Chem. **21**, 915 (1956).
13. R. B. Kelly. Can. J. Chem. **35**, 149 (1957).
14. J. A. Franks, B. Tolbert, R. Stein, and H. Z. Sable. J. Org. Chem. **30**, 1440 (1965).
15. A. Hasegawa and H. Z. Sable. J. Org. Chem. **31**, 4149 (1966).
16. B. Tolbert, R. Steyn, J. A. Franks, and H. Z. Sable. Carbohydrate Res. **5**, 62 (1967).
17. E. S. Gould. Mechanism and structure in organic chemistry. Henry Holt and Co., New York. 1959. p. 522.
18. R. U. Lemieux and B. Fraser-Reid. Can. J. Chem. **43**, 1460 (1965).
19. R. A. B. Bannard, A. A. Casselman, E. J. Langstaff, and R. Y. Moir. Can. J. Chem. **45**, 2605 (1967).
20. M. Mousseron and R. Granger. Compt. Rend. **205**, 327 (1937).
21. H. B. Henbest, G. D. Meakins, B. Nicholls, and K. J. Taylor. J. Chem. Soc. 1459 (1957).
22. H. Z. Sable, T. Anderson, B. Tolbert, and T. Posternak. Helv. Chim. Acta, **46**, 1157 (1963).
23. H. Z. Sable, W. M. Ritchey, and J. E. Nordlander. Carbohydrate Res. **1**, 10 (1965).
24. E. L. Eliel, N. L. Allinger, S. J. Angyal, and G. A. Morrison. Conformational analysis. Interscience Publishers, Inc., New York. 1965.
25. R. E. Parker and N. S. Isaacs. Chem. Rev. **59**, 737 (1959).
26. L. D. Hall. Chem. and Ind. London, 950 (1963).
27. C. T. Bishop and F. P. Cooper. Can. J. Chem. **41**, 2743 (1963).
28. M. L. Poutsma. Science, **157**, 997 (1967).
29. R. C. Fahey and C. Schubert. J. Am. Chem. Soc. **87**, 5172 (1965).
30. M. L. Poutsma. J. Am. Chem. Soc. **87**, 4285 (1965).
31. A. Hasegawa and H. Z. Sable. J. Org. Chem. **31**, 4161 (1966).
32. F. C. Merriam. Anal. Chem. **20**, 1246 (1948).
33. A. W. Bergstahler and I. C. Nordin. J. Am. Chem. Soc. **83**, 198 (1961).
34. M. Rosenblum. J. Am. Chem. Soc. **79**, 3179 (1957).
35. C. O. Guss and R. Rosenthal. J. Am. Chem. Soc. **77**, 2549 (1955).
36. L. N. Owen and P. N. Smith. J. Chem. Soc. 4026 (1952).
37. R. B. Moffett. Organic syntheses. Vol. 32. John Wiley and Sons, Inc., New York. 1952. p. 41.

Can. J. Chem. Downloaded from www.nrcresearchpress.com by 210.87.254.40 on 09/05/12
For personal use only.

Novel reaction of some 2-aminoheterocycles with acrylophenones

J. A. FINDLAY AND R. F. LANGLER
Department of Chemistry, University of New Brunswick, Fredericton, New Brunswick

AND

C. PODESVA AND K. VAGI
Delmar Chemicals Limited, LaSalle, Quebec

Received July 11, 1968

An unusual adduct is formed when 3-methylacrylophenone is treated with 2-aminothiazole. The structure of this product has been established as **4***a*. Similar adducts have been prepared from acrylophenones with other aminoheterocycles.

Canadian Journal of Chemistry, 46, 3659 (1968)

When 2-aminothiazole **1** is treated with 3-methylacrylophenone in refluxing ethanol a yellow crystalline product separates and is recovered in some 60% yield. Elemental analysis and mass spectral data show it to have the composition $C_{23}H_{21}O_2NS$. This formula suggests that the adduct results from condensation of two equivalents of 3-methylacrylophenone with one equivalent of 2-aminothiazole accompanied by loss of ammonia.

We have now assigned structure **4***a* to this novel adduct on the basis of chemical and spectroscopic evidence. The infrared spectrum shows strong absorption bands at 1675 and 1545 cm^{-1} in accord with phenone and enaminoketone functions, respectively. The ultraviolet spectrum displays maxima at 240 (ε, 19 000) and 365 mμ (ε, 24 000) in agreement with the chromophores in formulation **4***a*. The comparable chromophore of 3-anilinoacrylophenone has maxima at 242 (ε, 17 400) and 374 mμ (ε, 30 900) (1).

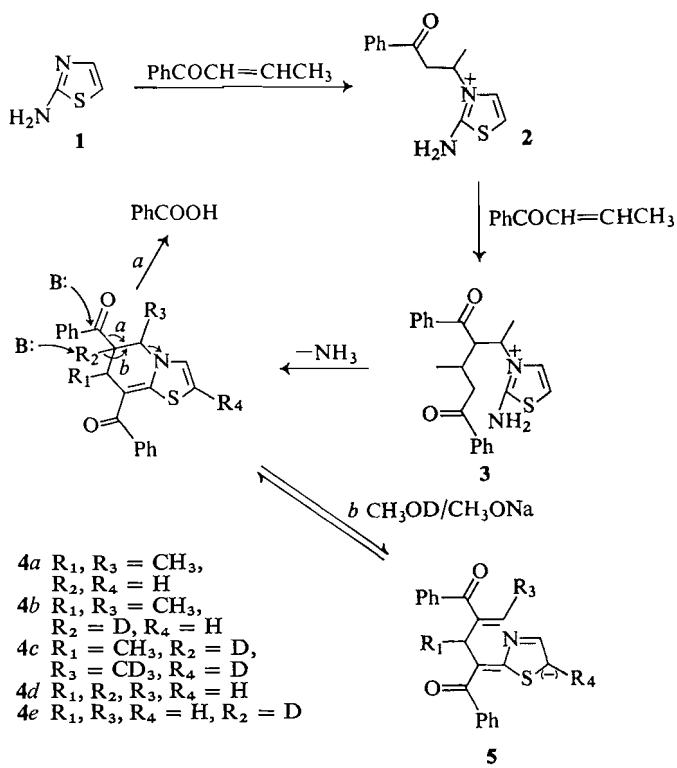

4*a* $R_1, R_3 = CH_3$, $R_2, R_4 = H$
4*b* $R_1, R_3 = CH_3$, $R_2 = D, R_4 = H$
4*c* $R_1 = CH_3, R_2 = D$, $R_3 = CD_3, R_4 = D$
4*d* $R_1, R_2, R_3, R_4 = H$
4*e* $R_1, R_3, R_4 = H, R_2 = D$

Can. J. Chem. Downloaded from www.nrcresearchpress.com by 210.87.254.40 on 09/05/12
For personal use only.

The adduct is readily reduced to a crystalline alcohol, $C_{23}H_{23}O_2NS$, by means of sodium borohydride in methanol. This product, formulated as **7***a*, displays the expected infrared bands at 3590 and 1542 cm^{-1} for the hydroxyl and enaminoketone absorptions. The ultraviolet spectrum shows λ_{max} 270 (ε, 2200) and λ_{max} 365 mμ (ε, 22 000) in agreement with the change in functionality in the reduction product. In the mass spectrum of this enaminoketone alcohol **7***a* abundant ions are present at M/*e* 270 (M − 107) and 105 corresponding to fragments resulting from fission of the benzyl alcohol and phenyl ketone groups, respectively. The mass spectrum of the adduct **4***a* displays abundant ions at M/*e* 270 (M − 105) and 105 compatible with fragmentations involving the phenylketone moieties.

The nuclear magnetic resonance (n.m.r.) spectrum of the adduct **4***a* shows multiple signals between τ 2.1 and 3.0 accounting for ten aromatic protons and the proton β to the sulfur atom. A doublet at τ 3.49 (J = 4.6 c.p.s.) accounts for the other thiazole ring proton.[1] A poorly resolved multiplet centered at τ 5.3 is assigned to the hydrogen α to the nitrogen atom while another broad signal centered at τ 6.4 accounts for the hydrogen α to the ketone and the allylic hydrogen. Methyl doublets appear at τ 8.43 (J = 6.9 c.p.s.) and 8.9 (J = 6.9 c.p.s.) the former being assigned to the group β to the nitrogen atom. When the adduct **4***a* is equilibrated with refluxing deuterated methanol, the n.m.r. spectrum of the product **4***b* clearly shows the exchange of one hydrogen and the mid-field region displays signals for only two protons and these appear as distinct quadruplets at τ 5.31 (J = 6.9 c.p.s.) and 6.40 (J = 6.9 c.p.s.). The remainder of the spectrum is identical with that of **4***a*. This result necessitates that at least one of the tertiary hydrogens, namely the one giving the n.m.r. signal at τ 5.31, must be situated β to the phenone carbonyl group.

Further clarification of the environment of the deuterium exchangeable hydrogen in adducts of the type **4***a* comes from the n.m.r. spectrum of the adduct prepared by reaction of acrylophenone[2] and 2-aminothiazole in refluxing ethanol. This yellow product, $C_{21}H_{17}O_2NS$, formulated as **4***d*, displays a complex multiplet between τ 5.6 and 6.5 (3 H) in its n.m.r. spectrum. A doublet at τ 7.0 (J = 7.0 c.p.s.) accounts for the other two non-aromatic protons. When **4***d* was subjected to treatment with refluxing methanol-*d* for 18 h the n.m.r. spectrum of the monodeuterated product displays in the mid-field region two singlets, one at τ 5.81 (2 H) and the other at τ 7.00 (2 H). It is evident from these results that the hydrogen α to the carbonyl group in **4***d* must also be α to both pairs of aliphatic hydrogens. The monodeuterated molecule is accordingly formulated as **4***e*. By analogy, the adduct **4***a* should have both methyl groups situated on carbons β to the phenone carbonyl.

The presence of an enaminoketone function in the adduct **4***a* was confirmed by its facile conversion into the enolacetate salt **6** using hot acetyl chloride. The labile salt readily separated from the solution as a white crystalline solid after several minutes of refluxing and it showed the expected infrared (1782, 1680, 1620 cm^{-1}) and ultraviolet (λ_{max} 244, ε, 24 000 and λ_{max} 324 mμ, ε 17 000) absorption bands (2). The enolacetate salt **6** was quantitatively converted back to **4***a* by treatment with aqueous methanol. A similar enolacetate salt was prepared from the enaminoketone alcohol **7***a*. This product features both enolacetate and acetate functions as evidenced by its infrared spectrum (1783, 1735 cm^{-1}). Treatment of this compound with aqueous methanol at room temperature furnished the enaminoketone acetate **7***b*.

It is known that cyclic enaminoketones are generally stable to hydrolysis with aqueous acid or base (2). The adduct **4***a*, however, was readily cleaved by heating with either strong acidic or basic solution. In either case a near quantitative yield of benzoic acid was recovered. There is little doubt that the benzoic acid comes from cleavage of the phenone rather than the enaminoketone group since, in the case of the former, rupture of the appropriate bond is facilitated by the β location of an electron deficient nitrogen atom. In accord with this is the finding that the enaminoketone alcohol **7***a* did not furnish any benzoic acid when treated under the same hydrolysis conditions. The base-catalyzed generation of benzoic acid from **4***a* can therefore be visualized as involving attack by hydroxide ion at the phenone carbonyl group with subsequent

[1]The corresponding proton in the n.m.r. spectrum of 2-aminothiazole appears at τ 3.56 (J = 4.6 c.p.s.).

[2]Acrylophenone was generated *in situ* from 3-dimethylaminopropiophenone hydrochloride.

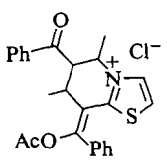

6

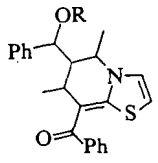

7*a* R = H
7*b* R = $COCH_3$

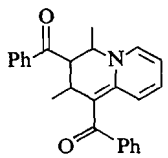

9

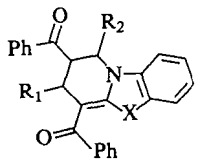

8*a* $R_1, R_2 = CH_3$, X = S
8*b* $R_1, R_2 = CH_3$, X = O
8*c* R_1, R_2 = H, X = S
8*d* R_1, R_2 = H, X = O

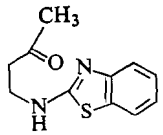

10

rupture of a carbon–carbon and a carbon–nitrogen bond as indicated by the arrows (*a*) in structure **4***a*. The amidic character of the nitrogen atom clearly assists these bond cleavages. The acid-catalyzed cleavage of **4***a* can be rationalized in a parallel way but involving prior protonation of the molecule.

A remarkable confirmation of the relationship of functional groups in the adduct **4***a* arises from its base-catalyzed equilibration with methanol-*d*. Prolonged treatment with methanol-*d* containing sodium methoxide gave a product which proved to be identical with **4***a* in all respects apart from the incorporation of five atoms of deuterium. This is quite evident from the mass spectrum which displays molecular ions of mass 380, 379, 378, 377, and 376 corresponding to molecules incorporating up to five heavy atoms. This conclusion is further substantiated by the n.m.r. spectrum of the polydeuterated product, which is similar to that of **4***b* but lacks the signal at τ 3.49 for the proton α to the sulfur atom. In addition a methyl doublet at τ 8.43 (J = 6.9 c.p.s.) integrates for only 2.3 hydrogens indicating that the methyl group α to the nitrogen has partially incorporated deuterium. It is noteworthy also that the quadruplet at τ 5.31 (J = 6.9 c.p.s.) while integrating for one proton, is poorly resolved due to partial deuteration of its neighboring methyl group. There is little doubt that the molecules incorporating five heavy atoms must possess structure **4***c* where R_2, R_3, and R_4 are fully deuterated. To account for this novel exchange reaction we postulate a reversible, base-catalyzed reverse Michael type opening of the six-membered ring leading to the resonance stabilized anion **5** which can permit deuterium exchange at the three sites. Support for this mechanism comes from the observation that the enaminoketone alcohol **7***a* exchanges only the hydroxyl hydrogen when subjected to prolonged equilibration with methanol-*d* and sodium methoxide.

In a cursory study of the scope of this novel reaction leading to **4***a* we have found that both 2-aminobenzothiazole and 2-aminobenzoxazole react readily with 3-methylacrylophenone giving products **8***a* and **8***b*, respectively. Yellow adducts prepared by the reaction of 2-aminothiazole, 2-aminobenzothiazole, and 2-aminobenzoxazole with β-diethylaminopropiophenone hydrochloride were reported in a previous communication (5). These compounds can now be formulated as **4***d*, **8***c*, and **8***d*, respectively.

Reaction of 2-aminobenzothiazole with methyl vinyl ketone in refluxing ethanol resulted in a moderate yield of the simple conjugate addition product **10**.

We have also prepared the enaminoketone **9**, in low yield, by appropriate reaction of 2-aminopyridine and 3-methylacrylophenone in hot ethanol. The structure of this and the other products mentioned above are adequately supported by spectroscopic and analytical data.

It is well known that amines react with acrylophenone giving conjugate addition products (3). Hurd and Hayao (4) have reported several cases where alkylation of the ring nitrogen occurs in reactions involving 2-aminothiazole and 2-aminopyridine. They have prepared 5,6-dihydrothiazolo [2,3*a*] pyridin-7-one by treatment of 2-aminothiazole with ethylacrylate thus demonstrating that conjugate addition utilizing the ring nitrogen atom of the 2-aminothiazole is a preferred pathway in that case. Accordingly the mode of formation of adducts of the type **4***a* can be rationalized by the sequence **1** → **4***a* which first involves conjugate addition of the heterocycle nitrogen to the α,β-unsaturated ketone leading to the resonance stabilized cation **2**. Abstraction of the hydrogen α to the carbonyl

Can. J. Chem. Downloaded from www.nrcresearchpress.com by 210.87.254.40 on 09/05/12
For personal use only.

group in **2** allows further condensation employing a second molecule of 3-methylacrylophenone. This affords an ion of the type **3** which is suitably disposed to undergo ring closure and elimination of ammonia giving the adduct **4***a*.

Experimental

General

The infrared spectra were recorded on a Perkin–Elmer model 237B spectrophotometer. The mass spectra were determined on a Hitachi Perkin–Elmer model RMU-6D spectrometer. The nuclear magnetic resonance (n.m.r.) spectra were recorded with a Varian 56.4 Mc.p.s. instrument and using tetramethylsilane as internal standard. A Kofler hot stage apparatus was employed to determine the melting points which are uncorrected.

Preparation of Adduct 4a

To a solution of 3-methylacrylophenone (9.7 g) in 95% ethanol (78 ml) was added 2-aminothiazole (3.3 g) and the mixture was refluxed for 18 h during which time an abundance of yellow crystals separated. The cooled mixture was filtered furnishing the yellow adduct **4***a* (5.6 g). Partial evaporation of solvent from the filtrate yielded another crop of crystalline adduct (0.8 g). Recrystallization from ethanol gave the pure adduct **4***a*, m p. 232–240 °C. Infrared bands were present ($CHCl_3$) at 1680 and 1545 cm^{-1}; λ_{max} (EtOH) were at 240 mμ (ε, 19 000) and 365 mμ (ε, 24 000). The n.m.r. spectrum showed signals at τ 2.1–3.0 (11 H), 3.49 (1 H), 5.3 (1 H), 6.4 (2 H), 8.43 (3 H), and 8.90 (3 H).

Anal. Calcd. for $C_{23}H_{21}NO_2S$: C, 73.60; H, 5.60; N, 3.73; O, 8.53; S, 8.53. Found: C, 73.58; H, 5.54; N, 3.61; O, 8.69; S, 8.65.

Preparation of Adducts 4d, 8a, 8b, 8c, and 8d

These were prepared in similar manner to the preparation of **4***a*. In each case the adduct gave correct analyses and the mass spectrum displayed the expected molecular ion. The infrared, ultraviolet, and n.m.r. spectra were unexceptional.

Preparation of Adduct 9

To a solution of 3-methylacrylophenone (646 mg) in 95% ethanol (20 ml) was added 2-aminopyridine (204 mg) and the mixture was refluxed for 6 h. The solution was then evaporated and taken up in methylene chloride and extracted with 5% hydrochloric acid solution. The organic layer was then dried over anhydrous magnesium sulfate and evaporated to dryness. The residue (160 mg) was taken up in hot ethanol and, after cooling, the yellow crystalline product **9** (50 mg), m.p. 206–214 °C separated. Recrystallization from ethanol did not improve the melting point. Infrared bands were present ($CHCl_3$) at 1685, 1645, 1590, and 1550 cm^{-1}; λ_{max} (EtOH) were at 245 (ε, 29 500), 280 (ε, 8900) and 350 mμ (ε, 5600). The n.m.r. spectrum showed signals τ 1.3–3.2 (14 H), 4.1 (1 H), 6.7 (2 H), 8.58 (3 H) and 8.81 (3 H). The mass spectrum displayed abundant ions at M/*e* 369, 354, 105, and 77.

Enaminoketone Alcohol 7a

A slurry consisting of sodium borohydride (120 mg) in dry methanol (35 ml) was added to the enaminoketone **4***a* (1 g) and the mixture was maintained at reflux temperature for 6 h. The bulk of the methanol was then distilled off and water (50 ml) was added. The aqueous mixture was treated with ether whereupon yellow crystals separated at the liquid interface. The crystals were collected and washed with ether furnishing enaminoketone alcohol **7***a* (763 mg), m.p. 254–259 °C. The infrared spectrum showed bands ($CHCl_3$) at 3590, 3300 and 1542 cm^{-1}; λ_{max} (EtOH) were at 270 (ε, 2200) and 365 mμ (ε, 22 000). The mass spectrum displayed ions at M/*e* 377, 362, 270, 105, and 77.

Anal. Calcd. for $C_{23}H_{23}NO_2S$: C, 73.21; H, 6.10; N, 3.71; O, 8.49; S, 8.49. Found: C, 72.87; H, 5.97; N, 3.57; O, 9.11; S, 7.83.

Equilibration of Enaminoketone 4a with Methanol-d

The adduct **4***a* (100 mg) was dissolved in methanol-*d* (10 ml) and the solution refluxed for 18 h. Partial evaporation of the solvent permitted crystallization of the deuterated product **4***b*, m.p. 232–240 °C, which showed no depression of melting point when admixed with **4***a*. Infrared and ultraviolet spectra confirmed identity with **4***a*. The n.m.r. spectrum showed signals at τ 2.1–3.0 (11 H), 3.50 (1 H), 5.31 (1 H), 6.40 (1 H), 8.43 (3 H), and 8.90 (3 H). The mass spectrum displayed a molecular ion M/*e* 376.

Equilibration of 4a with Methanol-d and Sodium Methoxide

To the enaminoketone **4***a* (100 mg) in methanol-*d* (20 ml) was added sodium (15 mg) and the solution was refluxed for 17 h. After partial evaporation of the solvent the yellow crystalline product **4***c* separated from the cooled solution and was filtered off and washed with methanol-*d*. Mixed melting point of this product with **4***a* showed no depression. Infrared and ultraviolet spectra confirmed identity with **4***a*. The mass spectrum displayed ions of M/*e* 380, 379, 378, 377 and 376. The n.m.r. spectrum showed signals at τ 2.1–3.0 (11 H), 5.31 (1 H), 6.40 (1 H), 8.43 (2.3 H), and 8.90 (3 H).

Enolacetate Salt 6

A solution of adduct **4***a* (100 mg) in freshly distilled acetyl chloride (10 ml) was refluxed for 5 min. A white crystalline solid (115 mg) separated from the hot solution and was filtered off and dried *in vacuo*. On heating this product **6** apparently decomposed at 140 °C to give **4***a*, m.p. 235–240 °C. The infrared spectrum of the enolacetate salt **6** showed bands at 1782, 1680, and 1620 cm^{-1} (no 1550 cm^{-1}); λ_{max} (CH_3CN) 244 (ε, 24 000) and 324 mμ (ε, 17 000). This product was quantitatively converted into **4***a* by treatment with 50% aqueous methanol at room temperature for 18 h.

Basic Hydrolysis of Adduct 4a

The adduct **4***a* (1 g) was treated with Claissen base (1600 ml) and the mixture refluxed for 24 h. Part of the methanol was evaporated and the aqueous solution extracted with three portions of chloroform. The aqueous layer was then acidified with dilute hydrochloric acid and extracted with chloroform. The chloroform extract was

Can. J. Chem. Downloaded from www.nrcresearchpress.com by 210.87.254.40 on 09/05/12
For personal use only.

dried over anhydrous magnesium sulfate and evaporated yielding a crystalline acid (201 mg), m.p. 120–123 °C, which was shown to be identical with authentic benzoic acid by mixture melting point and spectroscopic means.

Aminoketone ***10***

A solution of methyl vinyl ketone (3.5 g) and 2-aminobenzothiazole (3.75 g) in 95% ethanol (25 ml) was refluxed for 18 h. The cooled solution yielded a white crystalline solid **10** (1.3 g), m.p. 124–125 °C. The infrared spectrum showed bands ($CHCl_3$) at 3450, 1710, and 1605 cm^{-1}; λ_{max} (EtOH) 225 (ε, 16 400), 268 (ε, 7600) and 294 mμ (ε, 1650). The n.m.r. spectrum showed signals at τ 2.3–3.2 (4 H), 3.6 (1 H), 6.3 (2 H), 7.2 (2 H), and 7.94 (3 H).

Acknowledgment

This work was supported, in part, by a grant from the National Research Council of Canada.

1. K. Bowden, E. A. Braude, E. R. H. Jones, and B. C. L. Weedon. J. Chem. Soc. 45 (1946).
2. A. I. Meyers and Sujan Singh. Tetrahedron Letters, **52**, 5319 (1967).
3. I. Sestakora, V. Horak, and P. Zuman. Collection Czech. Chem. Commun. **31**, 3889 (1966).
4. C. D. Hurd and Shin Hayao. J. Am. Chem. Soc. **77**, 117 (1955).
5. C. Podesva and K. Vagi. Can. J. Chem. **44**, 1872 (1966).

Can. J. Chem. Downloaded from www.nrcresearchpress.com by 210.87.254.40 on 09/05/12
For personal use only.

Can. J. Chem. Downloaded from www.nrcresearchpress.com by 210.87.254.42 on 09/05/12
For personal use only.

Synthesis of 5*H*-dibenzo[*a*,*d*]cycloheptene-5-carboxylic acid and related compounds. 1,5-Hydride transfer to inductively destabilized carbonium ions

D. E. Horning and J. M. Muchowski[1]
Bristol Laboratories of Canada, Candiac, Quebec

Received May 16, 1968

The synthesis of 10,11-dihydro-5*H*-dibenzo[*a*,*d*]cycloheptene-5-carboxylic acid (**2**) and several derivatives of 5*H*-dibenzo[*a*,*d*]cycloheptene-5-carboxylic acid (**1**; *a–c*) from 5-hydroxy-10,11-dihydro-5*H*-dibenzo[*a*,*d*]cycloheptene-5-carboxylic acid and derivatives thereof (**3**; *a–c*) is described.

The *p*-toluenesulfonic acid-catalyzed elimination of water (at 110.6° in toluene) from the deuterated hydroxy ester (**3***b*; C-10, 11 d_2) resulted in the incorporation of deuterium at C-5 of the olefinic ester **1***b* with a K_H/K_D of 2.76. The large magnitude of this isotope effect indicated that the reaction proceeded *via* a rate-determining transannular 1,5-hydride transfer from one of the benzylic positions of **3***b* to the carbonium ion generated *alpha* to the methoxy-carbonyl group.

Canadian Journal of Chemistry, 46, 3665 (1968)

5*H*-Dibenzo[*a*,*d*]cycloheptene-5-carboxylic acid (**1***a*) and its 10,11-dihydro derivative (**2**) are intermediates of considerable importance for the synthesis of compounds of potential pharmacological interest (1, 2, and references therein). **1***a* and **2** are usually prepared by the acid-catalyzed hydrolysis of the appropriate nitriles (1–3), or by the carbonation (1–4) of some suitable organometallic reagent (usually the 5-lithio derivative). Unfortunately, the hydrolysis of the cyanide corresponding to **2** is not straightforward (ref. 5; but see refs. 1 and 2); mixtures of the carboxylic acid and the carboxamide, in which the latter generally predominates, are obtained irrespective of the hydrolysis medium employed.[1a] On the other hand, carbonation of 5-lithio-10,11-dihydro-5*H*-dibenzo[*a*,*d*]cycloheptene, prepared from the chloro compound by slight modification of the published procedure (2), consistently gave **2** in yields exceeding 85% (5). However, the application of similar processes to the preparation of **1***a* is reported (3) to be much less satisfactory.

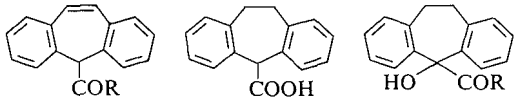

1 **2** **3**

a, R = OH
b, R = OCH_3
c, R = NR'_2

a, R = OH
b, R = OCH_3
c, R = NR'_2

We have found that the hydroxy acid (**3***a*), a high yield synthesis of which has been the subject of a recent patent application (6), is a convenient source of **1***a*, **2**, and various derivatives thereof. For example, hydrogenolysis of **3***a* in acetic acid containing perchloric acid produced **2**, while solvolysis in acetic acid containing *p*-toluenesulfonic acid provided **1***a*. In addition acid-catalyzed (*p*-toluenesulfonic acid monohydrate) azeotropic removal of water from the hydroxy acid or its methyl ester gave **1***a* and **1***b* respectively. Furthermore, crystallization from alcoholic hydrogen chloride of several of the analogous α-hydroxy-*N*,*N*-dialkylamides (**3***c*) proceeded with the loss of the elements of water to yield the *N*,*N*-dialkylamide derivatives (**1***c*) (7). In contrast, acid-catalyzed azeotropic water removal from 5-hydroxy-10,11-dihydro-5*H*-dibenzo[*a*,*d*]-cycloheptene gave little or no 5*H*-dibenzo[*a*,*d*]-cycloheptene.[2] It is also significant that numerous 5-hydroxy-5-alkyl-10,11-dihydrodibenzo[*a*,*d*]-cycloheptene derivatives are apparently converted exclusively to the 5-alkylidene compounds in a wide variety of acid-containing media (9).

There are two reasonable mechanisms by which the α-hydroxy carbonyl compounds (**3**) could give rise to derivatives of **1**, and both involve the formation of the carbonium ions **4**

[1]To whom enquiries concerning this paper should be addressed.

[1a]The carboxamide undergoes nitrous acid deamination in high yield (5).

[2]The major product in the complex mixture obtained was shown (5) by nuclear magnetic resonance spectroscopy to be 10,11-dihydro-5*H*-dibenzo[*a*,*d*]cycloheptene, and the corresponding olefin, if formed at all, was present in amounts undetectable by this method (< 5%). A small amount (ca. 7%) of the saturated 5,5′-dimer (8) could also be isolated. Mychajlyszyn and Protiva (8) report, however, that the above alcohol is converted to the olefin with hot concentrated hydrochloric acid, in about 20% yield.

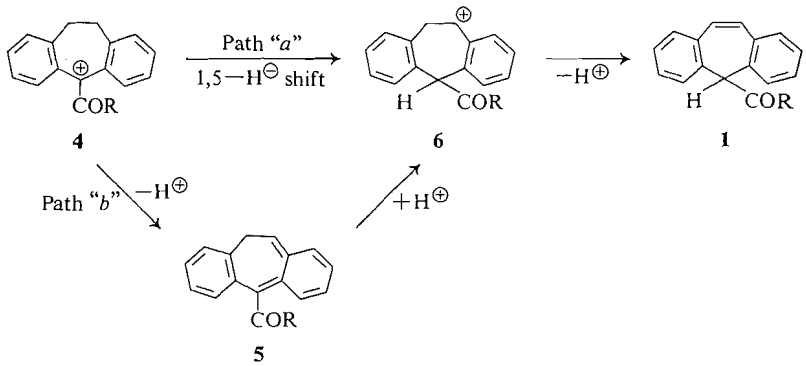

and **6** (not necessarily as discrete intermediates). One mechanism requires loss of a proton from **4** and reprotonation of the resulting *ortho*-quinonoid-type compound **5** (Path "*b*"), the other proceeds *via* a transannular 1,5-hydride shift (10, 11) from one of the benzylic positions to the highly reactive cationic center at C-5 (Path "*a*"); proton loss from **6** would then complete the sequence.

In principle, these two mechanisms should be distinguishable by experiments with isotopically labelled substrates. The acid-catalyzed azeotropic removal of water from the α-hydroxy ester (**3***b*) and its dideuterated analogue (93.8% d_2 at C-10, 11; for synthesis see below) was selected for study mainly because of the high product yield and the simplicity of the workup. When *O*-deuterated *p*-toluenesulfonic acid (mono D_2O) was used as the catalyst for the elimination of water from undeuterated **3***b*, integration of the nuclear magnetic resonance (n.m.r.) signal at δ 4.85 for the C-5 proton of **1***b* indicated that there was no detectable (<3%) deuterium incorporation at this position. This not only eliminated pathway "*b*" from consideration, but showed as well, that **1***b* did not undergo significant deuterium exchange (at C-5) under these conditions. A study of the elimination of water from the deuterated ester gave the results compiled in Table I.[3] The incorporation (0.255 ± 0.013 D) of deuterium at C-5 in **1***b* strongly supports mechanism "*a*" and the large deuterium isotope effect (2.76; corrected to 93.8% d_2) implicates the participation of the hydride transfer in the rate-determining step[4] (12). This effect has previously been sought in medium-membered ring systems (see pp. 124–130 in ref. 10 and p. 612 in ref. 11) wherein 1,5-hydride transfer to a carbonium ion is known to occur predominantly or exclusively, but K_H/K_D in those cases was always small. On the other hand a large deuterium isotope effect (1.8–2.6) has been observed (13) for intermolecular hydride transfer between the triphenylmethyl carbonium ion and 2-propanol-2*d* in sulfuric acid – water mixtures.

The great facility with which the hydride transfer occurs during the formation of **1***b* from **3***b* must be a consequence of an almost ideal geometry and a lack of other energetically favorable product forming routes. Dreiding models show that in the carbonium ion **4**, one of the four bridge hydrogens is always situated close to the positive center at C-5. The unique rate-determining nature of the hydride transfer must, at least in part, be due to the destabilizing effect of the methoxycarbonyl group on the carbonium ion. If this assumption is valid, one might expect to observe a large deuterium isotope effect whenever a transannular hydride transfer occurs to a carbonium ion bearing a strongly destabilizing α-substituent.

The hydride transfer mechanism may also play an important role in the hydrogenolysis of **3***a* since the olefinic acid (**1***a*) can be detected under conditions where its reduction is slow. For example, a 50% decrease in the concentration of perchloric acid resulted in the formation of an

[3]From the data given in columns 6 and 7 of Table I, it can be calculated that proton loss from **6** occurs with an apparent isotope effect of 1.44 ± 0.13 (corrected to 93.8% d_2). In the absence of mass spectral data concerning the abundance of those species containing d_0, d_1, and d_2 at C-10, 11 of **1***b*, we do not wish to comment on the significance of this value.

[4]It is assumed that the other 1,5-elimination reactions described herein proceed by the same mechanism. Experiments to ascertain the validity of this assumption are in progress.

Can. J. Chem. Downloaded from www.nrcresearchpress.com by 210.87.254.42 on 09/05/12
For personal use only.

TABLE I

Acid-catalyzed transformation of **3***b* to **1***b* at 110.6° in toluene. Deuterium distribution in **1***b* as determined by nuclear magnetic resonance spectroscopy*

Experiment number	Catalyst	C-5 H	C-5 D	K_H/K_D	C-10, 11 H	C-10, 11 D
1†	TSOH·H_2O‡	0.757±0.017§	0.243	3.13±0.29‖	0.775±0.035¶	1.225¶
2	TSOD·D_2O	0.758±0.014	0.242	3.13±0.24	0.791±0.021	1.209
3	TSOH·H_2O	0.739±0.010	0.261	2.84±0.15	0.823±0.018	1.177
4	TSOD·D_2O	0.725±0.007	0.275	2.64±0.09	0.772±0.020	1.228

*For the n.m.r. spectral parameters see Table II.
†See Table III for experimental details.
‡TSOH·H_2O = *p*-toluenesulfonic acid monohydrate; TSOD·D_2O = *O*-deuterated *p*-toluenesulfonic acid mono deuterium oxide.
§Average error in the integrated intensity.
‖Not corrected to 93.8% d_2 at C-10,11; average value K_H/K_D = 2.94 ± 0.20; K_H/K_D corrected to 93.8% d_2 = 2.76.
¶See footnote 3 in text.

approximately 1:1 mixture of **2** and **1***a* (as determined from the n.m.r. spectrum of the methyl esters obtained upon treatment of the crude product with excess ethereal diazomethane). A similar mixture was obtained from the hydroiodic acid red phosphorus reduction of **3***a*. In the light of this latter observation, it would be interesting to reexamine the product obtained (9) from the action of hydroiodic acid and red phosphorus on 5-hydroxy-5(2-pyridyl)-10, 11-dihydrodibenzo-[*a*,*d*]cycloheptene for the presence of olefinic compounds.

The 10,11-dideuterated hydroxy ester (**3***b*) was synthesized *via* the circuitous route indicated below. Catalytic reduction of the unsaturated ketone (**7**) with 2 moles of deuterium (we were unable to selectively reduce the olefinic function) gave a mixture of which the alcohol (**8**) was the main constituent. The alcohol was not rigorously purified, but instead it was oxidized with manganese dioxide to deuterated dibenzosuberone (**9**) and this ketone was then converted to the hydroxy acid according to the published (6) procedure. The acid was esterified with excess diazomethane in methanol–ether solution. The n.m.r. spectrum of this material indicated that, in addition to the expected deuterium incorporation at C-10, 11 (93.8% d_2), slight exchange of the aromatic hydrogens had occurred (the integrated intensity of the multiplet due to the 1,2,3 and 7,8,9 protons centered at δ 7.10 was about 6% low).

The direct conversion of **7** to **9** with dideuterodiimide could not be accomplished. The alcohol **10** was the only product obtained, and it was unaffected by an excess of the reducing agent. The diimide reduction of aldehydes and ketones to the corresponding alcohols is now known (14, 15), but we are unaware of any other instance where a carbonyl group is reduced in preference to an olefinic function.

Experimental

The melting points were determined in a Gallenkamp melting point apparatus and are not corrected. The nuclear magnetic resonance (n.m.r.) spectra were measured in deuteriochloroform with a Varian A-60 spectrometer. The infrared (i.r.) spectra were recorded with a Perkin–Elmer 237B grating spectrophotometer.

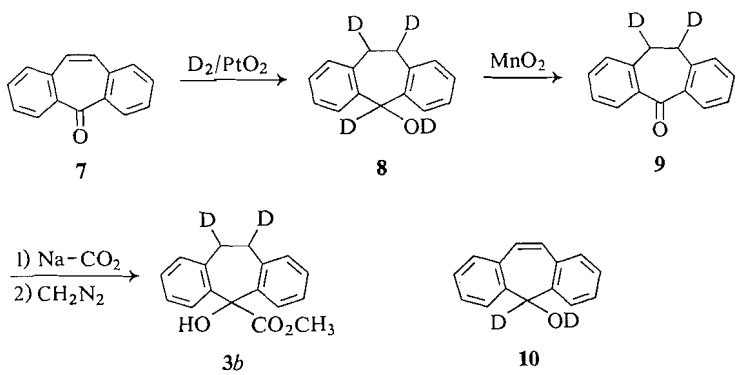

7 **8** **9**

3*b* **10**

Can. J. Chem. Downloaded from www.nrcresearchpress.com by 210.87.254.42 on 09/05/12
For personal use only.

TABLE II

Nuclear magnetic resonance spectra* of dibenzo[*a,d*]cycloheptene derivatives

Compound	Aromatic (4,6)	Aromatic (1,2,3:7,8,9)	Olefinic (C-10,11)	Methine (C-5)	Methylene (C-10,11)	OH	OCH_3
1*b*	7.33 (m)†		6.81 (s)	4.85 (s)	—	—	3.48 (s)
2 (methyl)‡ (ester)	7.17 (m)		—	4.77 (s)	3.06 (m)§	—	3.63 (s)
3*b*	7.65 (m)	7.10 (m)	—	—	3.07 (m)	3.92 (s)	3.60 (s)
7	8.15 (m)	7.43 (m)	6.87 (s)	—	—	—	—
9 (perhydro)	8.00 (m)	7.25 (m)	—	—	3.10 (s)	—	—

*Recorded in deuteriochloroform and expressed in p.p.m. (δ) from tetramethylsilane.
†m = multiplet; s = singlet.
‡The n.m.r. spectra of this and related compounds will be the subject of a future publication.
§This multiplet consists of at least 13 lines; see footnote ‡.

5*H*-Dibenzo[*a,d*]cycloheptene-5-one and dibenzosuberone were purchased from the Aldrich Chemical Company.

5-Hydroxy-10,11-dihydrodibenzo[a,d]cycloheptene-5-carboxylic Acid (3a)

This compound was prepared in 96% yield by carbonation of the sodium ketyl of dibenzosuberone (6). It had m.p. 210–215° (decomp.), with prior reddening [lit. (6), m.p. 170–190°].

The methyl ester, obtained by treatment of a methanol–ether solution of the acid with excess ethereal diazomethane, had m.p. 135–137° [lit. (6), m.p. 138–140°] when crystallized from cyclohexane.

The n.m.r. spectrum of this and other relevant compounds is given in Table II.

10,11-Dihydro-5H-dibenzo[a,d]cycloheptene-5-carboxylic Acid (2)

A mixture of the hydroxy acid (10.17 g, 40 mmoles) and 1.1 g of 10% palladium on charcoal in 200 ml of glacial acetic acid containing 8 ml of 60% perchloric acid, was hydrogenated at room temperature at an initial hydrogen pressure of 45 p.s.i.g. After 2 h the hydrogen absorption had become slow and after 2.5 h the reduction was stopped. Much of the product had crystallized and consequently the mixture was warmed to effect solution of the acid. The catalyst was removed by filtration through Celite, and the filtrate was concentrated to a small volume *in vacuo* (bath temperature, 40°). The residue was quantitatively transferred to a large Erlenmeyer flask with a little acetic acid, and the resultant was diluted with about 800 ml of ice-cold water. The crystalline solid was collected by filtration, washed well with ice-cold water, and dried *in vacuo*. The nicely crystalline solid, m.p. 215–217° [lit. (2), m.p. 220–221°], which weighed 7.71 g (80.8%) could be used without further purification.

The methyl ester was prepared by treatment of an ether solution of the acid with excess ethereal diazomethane. On crystallization from 1:1 cyclohexane – petroleum ether (b.p. 35–60°) a solid, m.p. 93.5–95° [lit. (16), m.p. 93–95°] was obtained. For analysis it was recrystallized from the same solvent system and then dried *in vacuo* at room temperature over phosphorus pentoxide for 24 h. The melting point remained unchanged.

Anal. Calcd. for $C_{17}H_{16}O_2$: C, 80.92; H, 6.39. Found: C, 81.19; H, 6.25.

5H-Dibenzo[a,d]cycloheptene-5-carboxylic Acid (1a)

A 250 ml round-bottomed flask fitted with a Dean–Stark water separator (prefilled with dry toluene), and containing the hydroxy acid (**3***a*, 1.271 g, 5 mmoles) and 254 mg of *p*-toluenesulfonic acid monohydrate in 125 ml of anhydrous toluene, was placed in a preheated heating mantle and brought rapidly to reflux temperature with magnetic stirring in a nitrogen atmosphere. After 1 h the solution was poured into an ice-cold sodium carbonate solution (100 g/l) and after thorough shaking the emulsion which resulted was broken by filtration. The aqueous phase was combined with a water extract of the organic phase. The basic solution was acidified with concentrated hydrochloric acid and the solid thus obtained was extracted into ethyl acetate. The extract was shaken with water, dried over sodium sulfate, and then concentrated *in vacuo*. The solid which remained (890 mg) was crystallized from 1:2 aqueous ethanol. The first crop of a beautiful, needle-shaped crystalline solid weighed 810 mg and had m.p. 239–241° [lit. (3), m.p. 241–242°]. Evaporation of the mother liquor and crystallization of the residue from the same solvent system (charcoal) gave an additional 39 mg of the product with m.p. 236–237°. The combined yield was 849 mg (71.9%).

This compound was also formed when a solution of the α-hydroxy carboxylic acid in glacial acetic acid containing *p*-toluenesulfonic acid monohydrate was heated at reflux temperature (0.5 h). The yield of product, m.p. 236–239°, was about 45%.

The methyl ester was prepared by treatment of a methanolic solution of the acid with excess ethereal diazomethane. The solid obtained on evaporation of the solvent was crystallized from cyclohexane to give a white, needle-shaped, crystalline material, m.p. 109–111°. For analysis it was twice recrystallized from 1:5 aqueous methanol, and then dried at room temperature *in vacuo* over phosphorus pentoxide for 15 h. It then had m.p. 111.5–113.5°.

Anal. Calcd. for $C_{17}H_{14}O_2$: C, 81.58; H, 5.64. Found: C, 81.50; H, 5.65.

Methyl-5H-dibenzo[a,d]cycloheptene-5-carboxylate (1b)

The hydroxy ester (**3***b*, 1.342 g, 5 mmoles), 268 mg of *p*-toluenesulfonic acid monohydrate, and 125 ml of dry

Can. J. Chem. Downloaded from www.nrcresearchpress.com by 210.87.254.42 on 09/05/12
For personal use only.

Can. J. Chem. Downloaded from www.nrcresearchpress.com by 210.87.254.42 on 09/05/12
For personal use only.

toluene in the apparatus described previously was rapidly heated to reflux with stirring in an atmosphere of nitrogen. After 1 h, the hot solution was poured onto ice-water, and after thorough shaking the organic phase was separated and combined with a toluene extract of the aqueous phase. The extract was shaken with sodium carbonate solution (100 g/l), then with water, and then it was dried over sodium sulfate. The solvent was then removed *in vacuo* leaving a crystalline solid (1.230 g) which was recrystallized from 1:5 aqueous methanol. A beautifully crystalline solid, m.p. 111.5–113.5° was obtained, identical in all respects to the methyl ester described in the previous experiment. It weighed 1.072 g. Evaporation of the mother liquor *in vacuo* gave a solid which on crystallization from the above solvent system (charcoal) yielded an additional 89 mg of product, m.p. 110.5–111.5°. The combined yield was 1.161 g or 92.8%.

Experiments with Deuterium Labelled Compounds

O-Deuterated p-Toluenesulfonic Acid (1 D_2O)

A mixture of *p*-toluenesulfonyl chloride (19.06 g) and 99.7% deuterium oxide (4.01 g, 3.63 ml) was heated to gentle reflux (protected from moisture with a calcium chloride drying tube). After 15 min an additional 3.63 ml of deuterium oxide were added. When a total of 1 h at reflux temperature had elapsed, the clear solution was cooled to room temperature, and then to 0° to effect crystallization of the sulfonic acid. Most of the excess deuterium oxide was removed *in vacuo* at 40°, the residue was twice washed by decantation with anhydrous benzene, heated for a few minutes *in vacuo* at 40° to remove any adhering benzene, and then dried *in vacuo* at room temperature over calcium chloride for 4 h. The white solid thus obtained had m.p. 95–100°, and was at least 99.2% *O*-deuterated *p*-toluenesulfonic acid mono deuterium oxide as shown by n.m.r.

Methyl-5-hydroxy-10,11-dihydrodibenzo[a,d]cycloheptene-5-carboxylate-10,11-d_2

The unsaturated ketone (7, 10.31 g, 50 mmoles) in ethyl acetate (150 ml) containing 300 mg of platinic oxide was reduced at room temperature (24°) and atmospheric pressure with deuterium gas (99.5 + mole % D_2). At the end of 2 h 40 min deuterium absorption had become slow (740 ml had been absorbed), consequently an additional 700 mg of the catalyst were added. At the end of a further 4.5 h a total of 2927 ml (111% of theoretical for 2 moles) of deuterium had been consumed and the reduction was stopped, even though deuterium absorption had not yet ceased. The catalyst was removed by filtration through Celite and the filtrate was evaporated *in vacuo*. The solid thus obtained was taken up in hot cyclohexane; on cooling, 5.82 g of the alcohol (**8**, m.p. 84–85°) crystallized from solution. Thin-layer chromatography (t.l.c.) on alumina indicated that at least two other components in addition to the required alcohol were present. The i.r. ($CHCl_3$) spectrum had weak bands at 2675 and 2150 cm^{-1}.

The mother liquor from the above crystallization was evaporated *in vacuo* to give 4.8 g of a complex mixture which contained ketonic material as shown by i.r. spectroscopy. Chromatography of this material on 200 g of neutral, activity II alumina (Fluka; benzene as elution solvent) gave a mobile oil which was evaporatively distilled at 130° (air bath temperature)/0.01 mm to give 2.44 g of deuterated dibenzosuberone which was contaminated with a hydrocarbon impurity as indicated by n.m.r. and t.l.c.

The crude alcohol (**8**) 4.82 g, dissolved in 500 ml of carbon tetrachloride, was stirred at room temperature with 50 g of activated manganese dioxide. At the end of 1 h t.l.c. indicated the absence of starting material. The mixture was filtered through Celite, the filtrate was evaporated *in vacuo*, and the oil thus obtained was evaporatively distilled at 125–135°/0.03 mm to give 4.27 g of fairly pure deuterated dibenzosuberone. Thin-layer chromatography indicated the presence of two minor impurities. The i.r. spectrum (liquid film) had bands at 2150 (w) and 1645 (s) cm^{-1}. Comparison of the integral for the aromatic hydrogens to that of the methylene hydrogens indicated that at least 85% of two deuterium atoms were at C-10, 11 (but see below).

The above ketone (3.15 g) was converted to the sodium ketyl and carbonated in the usual manner (6) to give 2.00 g of the beautifully crystalline hydroxy acid (m.p. ca. 215°, decomp.).

A methanol–ether solution of the hydroxy acid (1.580 g) was treated with excess ethereal diazomethane. After 1.5 h, the excess diazomethane was destroyed with a few drops of acetic acid. The ether solution was washed successively with 5% sodium carbonate solution, water, and saturated salt solution. The ether phase was dried over anhydrous sodium sulfate, and then evaporated *in vacuo*. The crystalline residue was recrystallized from cyclohexane to give 1.360 g of a product with m.p. 136–138° (mixture m.p. with undeuterated ester was undepressed). The i.r. spectrum (chloroform) had bands at 3575, 3490 (m), 2150 (w), and 1725 (s) cm^{-1}. Comparison of the integral for the protons of the methyl ester to that observed for the C-10,11 methylene protons, gave a value of 93.8 ± 1.0% d_2 at the latter positions. When hexamethyl benzene (2.22 p.p.m.) was used as an internal standard a value of 95.1% was obtained.

The integrated intensity for the aromatic protons was low. This was shown not to be a saturation effect by the constancy of the aromatic hydrogen: methyl ester integral ratio for various values of the r.f. field. Evidently, some exchange (0.5 ± 0.1 D; primarily at positions-1,2,3, and -7,8,9) of the aromatic hydrogens for deuterium had occurred during catalytic reduction of the unsaturated ketone.

Quantitative Examination of the Acid-Catalyzed Dehydration of Dideuterated and Undeuterated 3b

The following procedure was used throughout.

A 50 ml round-bottomed flask, containing 30 ml of anhydrous toluene and the specified quantities of catalyst and hydroxy ester (see Table III), was fitted with a Dean–Stark water separator (prefilled with dry toluene), and heated with stirring under reflux in an atmosphere of purified dry nitrogen for the indicated length of time. The reaction mixture was cooled briefly in an ice bath and then poured into an excess of ice-water. After vigorous shaking, the organic phase was separated and combined with a 10 ml toluene extract of the aqueous phase. The combined extracts were washed with two 10 ml portions of ice-cold water, dried over anhydrous sodium sulfate, and evaporated *in vacuo*. The yield of crude ester (**1***b*) thus

TABLE III

Acid-catalyzed dehydration of deuterated and undeuterated *3b*

Experiment number	Ester (mg)	Catalyst (mg)	Reaction time (h)	Melting point of product
1	*3b* d_2 270	TSOH:H_2O (54)	1	112.5–113.5*
2	*3b* d_2 270	TSOD:D_2O (54)	1	112 –114
3	*3b* d_2 150	TSOH:H_2O (30)	1	112 –114
4	*3b* d_2 150	TSOD:D_2O (30)	1	111.5–113.5
5	*3b* 268	TSOD:D_2O (54.6)	0.5	†
6	*3b* 268	TSOD:D_2O (54.6)	1	—

*After sublimation at 90°/0.001 mm. Undeuterated ester did not depress the melting point.
†Nuclear magnetic resonance spectra recorded on crude product; m.p. was not determined.

obtained was generally well over 90%. Inasmuch as the deuterium content did not change upon sublimation, the crude material from experiments 1–4 was sublimed at 90°/0.001 mm before n.m.r. analysis; this also served to remove a paramagnetic impurity which was sometimes present.

The n.m.r. spectra were all recorded at a concentration of ca. 75 mg of ester/0.4 ml of deuteriochloroform (containing tetramethylsilane). Four to eight integrations were made for each experiment. The results are compiled in Table I.

The proton content at C-5 could be measured with satisfactory accuracy. However, a small uncertainty in the integration (e.g. 2.2% in experiment number 1; see Table I) here, resulted in a maximum uncertainty of ±9% in the calculated deuterium isotope effect.

The measured values for the proton content at C-10,11 were subject to a somewhat greater error because of the close proximity of the aromatic hydrogens (e.g. a spinning side band of the aromatic hydrogen absorption had to be subtracted), and the necessity to subtract a small absorption due to the residual protium present in the commercial deuterated chloroform.

Acknowledgments

We thank Professor B. Belleau, University of Ottawa, for much helpful discussion of some of the mechanistic aspects of this paper, and Dr. T. Conway for his constructive criticism of this manuscript. The n.m.r. spectra were recorded by G. Lacasse whose efforts in this regard are gratefully acknowledged.

1. C. VAN DER STAAT, A. HAASJES, H. M. TERSTEEGE, and W. TH. NAUTA. Rec. Trav. Chim. **84**, 1466 (1965).
2. M. A. DAVIS, S. O. WINTHROP, J. STEWART, F. A. SUNAHARA, and F. HERR. J. Med. Chem. **6**, 251 (1963).
3. M. A. DAVIS, S. O. WINTHROP, R. A. THOMAS, F. HERR, M-P. CHAREST, and R. GAUDRY. J. Med. Chem. **7**, 88 (1964).
4. F. LEONARD and A. GAGNEUX. U.S. Patent No. 3,287,409 (1966). Chem. Abstr. **66**, 3582 (1966).
5. D. E. HORNING and J. M. MUCHOWSKI. Unpublished observations.
6. Neth. Appl. 6,513,732 (1966). Chem. Abstr. **65**, 15352 (1966).
7. J. CHAPUIS and R. FAESSLER. Unpublished observations; these laboratories.
8. V. MYCHAJLYSZYN and M. PROTIVA. Collection Czech. Chem. Commun. **24**, 3955 (1959).
9. S. O. WINTHROP, M. A. DAVIS, G. S. MEYERS, J. G. GAVIN, R. THOMAS, and R. BARBER. J. Org. Chem. **27**, 230 (1962).
10. A. C. COPE, M. M. MARTIN, and M. A. MCKERVEY. Quart. Rev. London, **20**, 119 (1966).
11. V. PRELOG and J. G. TRAYNHAM. Molecular rearrangements. Vol. 1. *Edited by* P. de Mayo. Interscience Publishers, Inc., New York. 1963. p. 593.
12. F. H. WESTHEIMER. Chem. Rev. **61**, 265 (1961).
13. P. D. BARTLETT and J. D. MCCOLLURN. J. Am. Chem. Soc. **78**, 1441 (1956).
14. E. E. VAN TAMELEN, M. DAVIS, and M. F. DEEM. Chem. Commun. 71 (1965).
15. D. C. CURRY, B. C. UFF, and N. D. WARD. J. Chem. Soc. C, 1120 (1967).
16. M. A. DAVIS, F. HERR, R. A. THOMAS, and M-P. CHAREST. J. Med. Chem. **10**, 627 (1967).

Can. J. Chem. Downloaded from www.nrcresearchpress.com by 210.87.254.42 on 09/05/12
For personal use only.

Can. J. Chem. Downloaded from www.nrcresearchpress.com by 210.87.254.5 on 09/05/12
For personal use only.

Fully fluorinated alkoxides. Part IV. Derivatives of perfluoropinacol[1]

M. ALLAN, A. F. JANZEN,[2] AND C. J. WILLIS
Department of Chemistry, University of Western Ontario, London, Ontario

Received June 25, 1968

The reductive dimerization of hexafluoroacetone, by reaction with sodium in a donor solvent, leads to the ionic disodium alkoxide of perfluoropinacol, a valuable intermediate for the preparation of pinacol derivatives. Cyclic alkoxides of silicon, germanium, tin, and boron are made by the reaction of this disodium alkoxide with various dihalides.

Reaction with thionyl chloride, sulfuryl chloride, or sulfur(II) chloride gives perfluoropinacol sulfite, sulfate, and *ortho*-sulfite respectively. The stereochemistry of the last compound is discussed.

Canadian Journal of Chemistry, 46, 3671 (1968)

In previous parts of this series, we have shown that ionic, fully fluorinated alkoxides of the heavier alkali metals may be prepared by the reaction of the anhydrous metal fluorides with various fluorinated carbonyl compounds in donor solvent. Trifluoromethoxides are given by carbonyl fluoride (1) while ethoxides and propoxides are given by trifluoroacetyl fluoride, heptafluoropropionyl fluoride, or hexafluoroacetone (2).

$$R_fCOF + MF \rightleftharpoons M^+[R_fCF_2O^-]$$

$$(CF_3)_2CO + MF \rightleftharpoons M^+[(CF_3)_2CFO^-]$$

(R_f = F, CF_3, or C_2F_5 M = K, Rb, or Cs)

In any ion made by a reaction of this type, there must always be at least one fluorine atom attached to the α-carbon atom, and we have suggested, as a result, that the alkoxide and the carbonyl compound are in equilibrium. The ready elimination of a fluoride ion limits the value of these ionic primary or secondary alkoxides as intermediates for the preparation of covalent derivatives. The reaction of trialkylchlorosilanes with the heptafluoroisopropoxide ion, for example, gives only trialkylfluorosilanes and hexafluoroacetone, rather than trialkylsilyl heptafluoroisopropoxides (2, 3).

A decomposition of this type would not be possible for covalent alkoxides derived from fluorinated tertiary alcohols, and there is no reason to suppose that such compounds would not be stable. Of the few fully fluorinated tertiary alcohols which have been reported, no alkoxide type derivatives appear to be known. The simplest example of this class of compound, perfluoro-*t*-butanol, was first reliably reported by Knunyants and Dyatkin (4), and by Filler and Schure (5); both of these accounts contain comments on earlier claims regarding this compound. Other known fluorinated tertiary alcohols include perfluoro(triphenyl)carbinol (6) and perfluoro(triethyl)carbinol (7).

More is known of the chemistry of the simplest fluorinated ditertiary alcohol, perfluoropinacol, first prepared by Middleton and Lindsey by the reaction of hexafluoroacetone with isopropyl alcohol (8). As expected, perfluoropinacol is considerably more stable than any primary or secondary fluorinated alcohol, and dissolves in water to give an acidic solution (pK_a = 5.95). Middleton and Lindsey attributed the high acidity to the formation of an anion stabilized by hydrogen bonding.

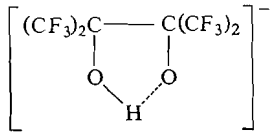

We have found that the solid ionic monosubstituted potassium derivative of perfluoropinacol, in which this ion is presumably present, may readily be obtained from aqueous solution. However, complete neutralization to give the dipotassium alkoxide, $K_2[(CF_3)_2CO \cdot CO(CF_3)_2]$, could not be achieved in aqueous solution because hydrolysis of the pinacol occurred on adding further base.

---

[1]Presented in part at the 50th Annual Conference of the Chemical Institute of Canada, Toronto, June 1967. For a preliminary communication, see M. Allan, A. F. Janzen, and C. J. Willis, Chem. Commun. 55 (1968). For part III, see M. Allan and C. J. Willis, J. Am. Chem. Soc. **90**, 5343 (1968).

[2]Present address: Department of Chemistry, University of Manitoba, Winnipeg, Manitoba.

Can. J. Chem. Downloaded from www.nrcresearchpress.com by 210.87.254.5 on 09/05/12
For personal use only.

An alternative route to the ionic, disubstituted alkoxides of perfluoropinacol is available through the reductive coupling of hexafluoroacetone with an alkali metal in non-aqueous donor solvent. Frye *et al.* (9) suggested the intermediacy of the dilithium alkoxide of perfluoropinacol in the reaction of dimethyldichlorosilane with hexafluoroacetone and lithium in tetrahydrofuran (THF). They did not, however,

$$2(CF_3)_2CO + 2\,Li + (CH_3)_2SiCl_2 \rightarrow$$

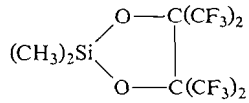

$$+ 2\,LiCl$$

attempt to isolate the alkoxide.

We have found that this reaction may be performed stepwise, the disodium alkoxide of perfluoropinacol being first prepared in a stable yellow solution in THF which gives, on evaporation, a stable white solid which appears to be a solvate of the alkoxide. The ready availability of this reactive intermediate opens up a simple route to the preparation of alkoxides and related derivatives of perfluoropinacol, and it is compounds of this type which will be described here.

In view of the known electrophilic nature of hexafluoroacetone, which we have discussed previously (10, 11), the first step in its reaction with sodium is presumably an electron transfer to give hexafluoroacetone ketyl, which would then dimerize.

$$(CF_3)_2CO + Na \xrightarrow{THF} (CF_3)_2CO^- + Na^+$$

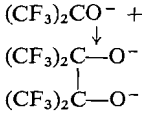

Strong support for such a mechanism is given by the recent report by Janzen and Gerlock (12) that hexafluoroacetone ketyl may exist as a stable radical in acetonitrile solution. The isoelectronic neutral radical, bis(trifluoromethyl)-nitroxide, has also been reported as a stable species (13).

The availability of the reactive solution of the disodium alkoxide provides a convenient route to alkoxides and esters of perfluoropinacol and, in particular, to the preparation of cyclic derivatives. Thus, the reaction of trimethylchlorosilane or dimethyldichlorosilane with the solution gave immediate reaction to precipitate sodium chloride and to give compounds **1** and **2** respectively.

$$(CH_3)_3SiOC(CF_3)_2C(CF_3)_2OSi(CH_3)_3$$

1

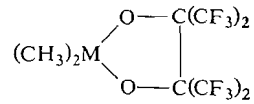

2, M = Si; **3**, M = Ge; **4**, M = Sn

Both **1** and **2** are known compounds, having been prepared by Frye *et al.* Compound **1** has also been prepared by us through the reaction of hexafluoroacetone with bis(trimethylsilyl)-mercury (10).

The analogous germanium and tin heterocycles, **3** and **4**, were readily prepared by the action of the disodium alkoxide on dimethyldichloro-germane or -stannane. The tin compound was significantly less volatile than the other two, but molecular weight measurements showed that, at least in solution, it was substantially monomeric.

A boron-containing heterocycle, **5**, was prepared by the reaction of phenylboron dichloride, while the complex borate, **6**, was made in aqueous solution by the reaction of sodium borate with perfluoropinacol.

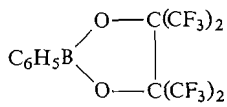

5

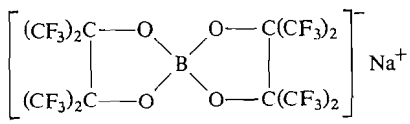

6

The analogous unfluorinated borate, derived from pinacol, may also be formed in aqueous solution (14).

The compounds described above were all stable under ordinary conditions of handling, and were resistant to acid hydrolysis. Compound **2**, for example, distilled unchanged from concentrated sulfuric acid at 150° when acid cleavage was attempted. Under aqueous basic conditions, however, rapid hydrolysis occurred.

Can. J. Chem. Downloaded from www.nrcresearchpress.com by 210.87.254.5 on 09/05/12
For personal use only.

Except in the complex borate, some part of this stability presumably comes from the p_π—p_π or p_π—d_π bonding from the two oxygen atoms to the other hetero-atom in the five-membered rings, since the four elements involved (Si, Ge, Sn, and B) may all act as acceptors.

Although π-bonding of this type would be less likely for a sulfur atom, it proved easy to incorporate sulfur into cyclic perfluoropinacol derivatives. The reaction of the disodium alkoxide of perfluoropinacol with thionyl chloride or with sulfuryl chloride gave respectively the cyclic sulfite, **7**, and sulfate, **8**.

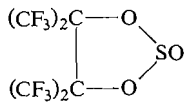

7

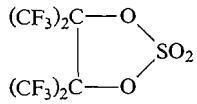

8

With sulfur(II) chloride, however, the reaction with the disodium alkoxide was more complex than a simple halogen replacement. A volatile crystalline product, m.p. 52°, was obtained, which was shown by analysis and mass spectroscopic examination to have the molecular formula $C_{12}F_{24}O_4S$. Although unexpected, this product may readily be characterized as perfluoropinacol *ortho*-sulfite, **9**, resulting from disproportionation of the sulfur(II) to sulfur(IV) and elementary sulfur.

A reaction of this type is not unprecedented for sulfur, since sulfur(IV) fluoride is best prepared by the reaction of sulfur(II) chloride with sodium fluoride in acetonitrile (15).

$$4\,NaF + 2\,SCl_2 \rightarrow SF_4 + S + 4\,NaCl$$

In both reactions, reaction of the chloride with an ionic salt in donor solvent leads to disproportionation and formation of a compound in which a sulfur(IV) atom is joined to four other atoms by single bonds. Perfluoropinacol *ortho*-sulfite, however, seems to be unique in having four oxygen atoms attached to sulfur(IV), since no reports of esters of the type $(RO)_4S$ have appeared. The stabilization of the system in the present case is presumably due to two factors; the electronegative nature of the ester group and the bicyclic structure of the compound.

The mass spectrum of the compound is given in Table I, and is entirely consistent with the structure given above.

TABLE I

Mass spectrum* of perfluoropinacol *ortho*-sulfite

Mass number	Intensity	Formula	Mass number	Intensity	Formula
677	0.5	$C_{12}F_{23}O_4S^+$	159	78	$C_4F_5O^+$
627	37	$C_{11}F_{21}O_4S^+$	150	3	$C_3F_6^+$
511	5	$C_9F_{17}O_3S^+$	147	9	$C_3F_5O_2^+$
364	19	$C_6F_{12}O_2S^+$	143	12	$C_4F_5^+$
311	1	$C_5F_9O_3S^+$	131	39	$C_3F_5^+$
300	6	$C_6F_{12}^+$	119	6	$C_2F_5^+$
281	5	$C_6F_{11}^+$	105	8	$C_4F_3^+$
247	15	$C_5F_9O^+$	97	403	CF_3CO^+
231	100	$C_5F_9^+$	93	9	$C_3F_3^+$
212	5	$C_6F_8^+$	69	850	CF_3^+
209	33	$C_5F_7O^+$	67	24	SOF^+
197	13	$C_4F_7O^+$	64	5	SO_2^+
181	36	$C_4F_7^+$	50	13	CF_2^+
178	6	$C_4F_6O^+$	48	25	SO^+
169	6	$C_3F_7^+$			

*Intensities are related to 100 for the peak at M = 231.

No peak corresponding to the molecular ion (M = 696) was seen, but five peaks above a mass of 310 corresponded to sulfur-containing fragments. Below mass 310 were a number of peaks given by fragments containing carbon, fluorine, and oxygen; the only other fragments containing sulfur were SO^+, SO_2^+, and SOF^+. The following scheme gives a rationalization for the structures and modes of formation of the heavier fragments.

The analogous tellurium compound, perfluoropinacol *ortho*-tellurite, was readily prepared by the reaction of the disodium alkoxide with tellurium tetrachloride. It was slightly less stable than the sulfite, undergoing slow hydrolysis in moist air.

The detailed configuration of perfluoropinacol *ortho*-sulfite is of some interest, since this compound presents an unusual opportunity for the study of the geometry of sulfur(IV). Previously

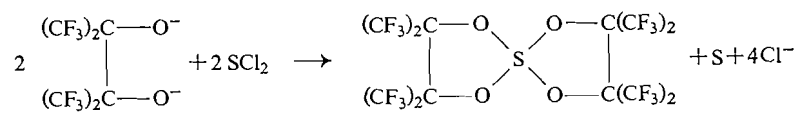

9

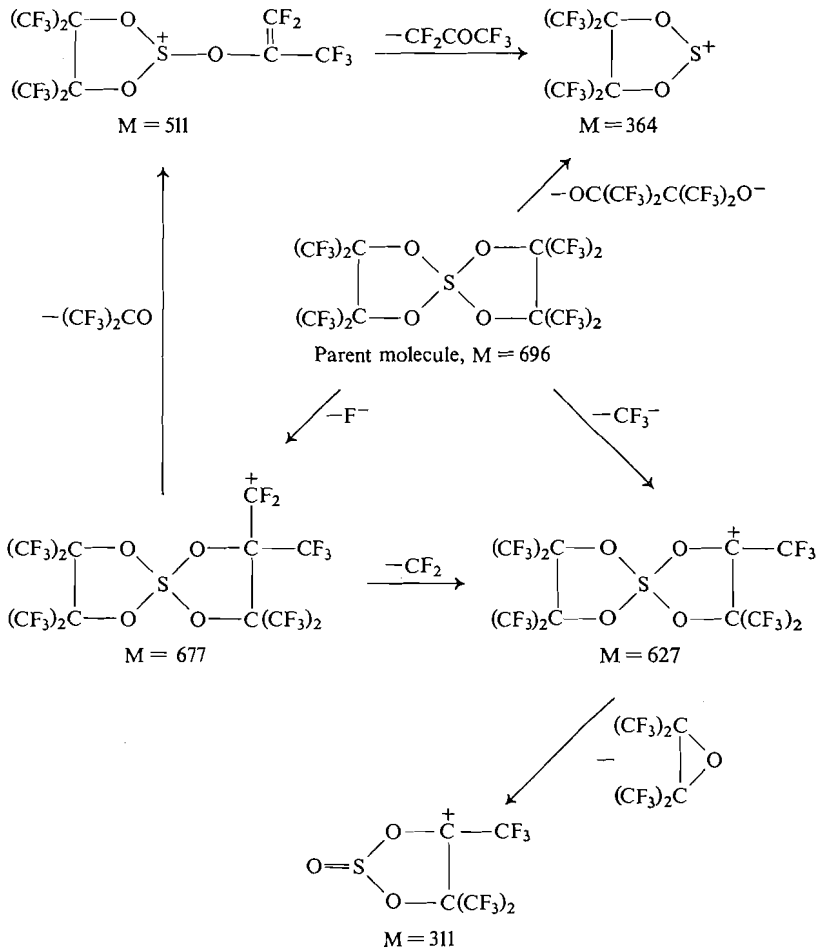

reported compounds in which a sulfur(IV) atom is linked by single bonds to four other atoms are restricted to sulfur tetrafluoride and its derivatives, and spectroscopic studies have established a trigonal bipyramid arrangement (including the non-bonding electron pair) for four atoms around sulfur. For sulfur tetrafluoride, infrared measurements showed that the molecule was of C_{2v} symmetry (16), while low-temperature fluorine nuclear magnetic resonance (n.m.r.) spectra showed the presence of two types of fluorine atoms (17).

No crystallographic determination of the structure of sulfur tetrafluoride has been reported, presumably because of the difficulty of working with such a volatile and reactive material. Perfluoropinacol *ortho*-sulfite, however, is unreactive and crystalline at room temperature, and a structural analysis by X-ray crystallography is therefore being undertaken.[3] Preliminary results show that the crystals, which have the external appearance of rectangular prisms, are tetragonal, with $a = 23.08$ Å and $c = 15.18$ Å. The space group is $I4_1/a$, with 16 molecules in the unit cell.

The four possible ways in which the oxygen atoms in the *ortho*-sulfite might be arranged about the sulfur atom are tetrahedral, square planar, trigonal bipyramidal, or tetragonal pyramidal. The first two, which would in any case be considered very unlikely for such an electronic arrangement at the sulfur atom, are eliminated by the appearance of the ^{19}F n.m.r. spectrum of the compound, which consists of

[3]By Dr. Kent Pullen of the University of Idaho.

Can. J. Chem. Downloaded from www.nrcresearchpress.com by 210.87.254.5 on 09/05/12
For personal use only.

Can. J. Chem. Downloaded from www.nrcresearchpress.com by 210.87.254.5 on 09/05/12
For personal use only.

two fairly broad absorptions of equal intensity at −10.5 and −12.2 p.p.m. from trifluoroacetic acid, the former peak showing partial resolution into a septet. This spectrum indicates the presence in the molecule of equal quantities of fluorine atoms in two different environments, a result which would not be obtained from either tetrahedral or square planar arrangements of the four oxygen atoms. The fluorine atoms are, however, divided into two environments if the steric influence of the non-bonding electron pair on the sulfur atom produces a tetragonal pyramid or trigonal bipyramid configuration. The two types of fluorine atom would be interconverted only by inversion of the entire molecule at the sulfur atom, and would therefore be expected to produce two n.m.r. signals. Further broadening of each signal would be expected from coupling within the twelve-spin system in each perfluoropinacol group. Presently available evidence, however, does not permit a decision to be made between the trigonal bipyramid or tetragonal pyramid models.

The ^{19}F n.m.r. spectrum of the analogous tellurium compound consists of only one signal, a singlet at −7.9 p.p.m., suggesting that all fluorine atoms in the molecule are equivalent. This is surprising, in view of the well-established trigonal bipyramidal structures of such other tellurium(IV) compounds as $TeCl_4$ (18). One explanation would be a rapid inversion of the molecule at the tellurium atom, but it is also possible that there is effectively a tetrahedral arrangement around the tellurium atom because the lone pair is not sterically active. There is precedent for such an effect in the stereochemistry of tellurium(IV), since the configuration of the ion $TeCl_6^{2-}$ has been shown by quadrupole resonance (19) and crystallographic study (20) to be octahedral.

A crystallographic examination of perfluoropinacol *ortho*-tellurite is being undertaken in an attempt to elucidate this point.

Experimental

CAUTION:—Perfluoropinacol has been reported to be extremely toxic (8). Due care should be exercized in handling this compound or its derivatives.

General

Volatile compounds were handled in a conventional vacuum system, to avoid contact with the atmosphere, and were separated by trap-to-trap condensation. Hexafluoroacetone was a redistilled commercial sample (Allied Chemical Co.) whose purity was checked by molecular weight determination and infrared spectroscopic examination. Tetrahydrofuran (THF) and 1,2-dimethoxyethane (glyme) were dried by refluxing over lithium tetrahydridoaluminate for 8 h under nitrogen, then stored and handled in the vacuum manifold.

Infrared spectra were determined on a Beckman IR-5A or IR-10 spectrophotometer. Nuclear magnetic resonance (n.m.r.) spectra were determined on Varian A-60 and DP-60 instruments, using 60 Mc.p.s. and 56.4 Mc.p.s. for proton and fluorine respectively. ^{19}F chemical shifts are all relative to trifluoroacetic acid (external). Microanalyses were performed by Alfred Bernhardt Laboratories, Mulheim (Ruhr), Germany.

Reaction of Hexafluoroacetone with Sodium

(i) In Tetrahydrofuran

Hexafluoroacetone (5.66 g, 34.1 mmole), sodium (0.80 g, 34.8 mmole), and THF (8 ml), in a sealed reaction tube (25 ml) in the absence of air, were shaken for 3 days at 25°. During this time the initially colorless solution became dark orange as the sodium was consumed, but no precipitate appeared. There was no apparent reaction when a similar mixture was kept for 3 days at −26° or −78°.

(ii) In Glyme

Hexafluoroacetone (7.82 g, 47.1 mmole), sodium (1.01 g, 43.9 mmole), and glyme (10 ml) in a sealed reaction tube (30 ml) in the absence of air were kept at −78° for 8 days, by which time all the sodium had dissolved to give a deep-red solution. There appeared to be no difference between the contents and properties of this solution and the THF solution, and the THF solution was used in all subsequent work.

The stability of the THF solutions prepared as above was briefly investigated. At −78°, it showed no change after keeping for several weeks. At 25°, the solutions appeared stable for at least 8 days, but after longer periods some decomposition was evident as solid material began to settle out. The rate of deposition of solid was variable, but an examination of the volatile compounds present after some time had elapsed showed only THF and hexafluoroacetone. Detailed analysis of the solid was not made, but it had an ionic fluoride content of about 4% (estimated as lead chloride fluoride).

When hexafluoroacetone was kept with sodium in a 1:2 molar ratio in THF at 25°, decomposition was much more rapid. The excess sodium reacted, giving a precipitate containing ionic fluoride, and the solution became extremely dark.

An attempt was made to prepare the disodium alkoxide in a pure state by complete removal of THF, but this was unsuccessful. After prolonged pumping at 25°, the solid still contained solvent (judged by its infrared spectrum). On heating *in vacuo*, some THF came off at 80°, together with decomposition products such as trifluoroacetyl fluoride, hexafluoroacetone, and carbon dioxide. Evolution of volatile products ceased when the temperature reached 200°, leaving a solid residue which appeared to be mainly sodium fluoride.

Preparation of Perfluoropinacol

Concentrated sulfuric acid was slowly added to a

Can. J. Chem. Downloaded from www.nrcresearchpress.com by 210.87.254.5 on 09/05/12
For personal use only.

solution of the disodium alkoxide in THF at 0°. Perfluoropinacol was evolved on gentle warming, and was identified by comparison of its infrared spectrum with that of known samples prepared by the reduction of hexafluoroacetone with isopropanol (8) or with triphenyl phosphite (21).

Potassium Hydrogen Perfluoropinacolate

Perfluoropinacol (5.0 g, 15 mmole) was dissolved in an aqueous solution of potassium carbonate (1.0 g, 7.3 mmole) and the solution evaporated to dryness *in vacuo*. The remaining white solid was recrystallized from water to give potassium hydrogen perfluoropinacolate (5.0 g, 13 mmole).

Anal. Calcd. for $C_6HF_{12}O_2K$: C, 19.4; H, 0.27; F, 61.3. Found: C, 19.6; H, 0.23; F, 61.4.

When further base was added, in an attempt to obtain the fully neutralized salt, the pH of the solution began to drift, and qualitative tests showed that fluoride ion was now present.

Reaction with Trimethylchlorosilane

To a solution of the disodium alkoxide (15 mmole, prepared as above), in THF at 25°, was added trimethylchlorosilane, (2.81 g, 26 mmole). Immediate reaction was apparent as a solid, identified as sodium chloride, precipitated. The liquid portion was removed under vacuum and distilled at reduced pressure to yield 1,2-bis(trimethylsiloxy)tetrakis(trifluoromethyl)ethane (3.7 g, 7.8 mmole, b.p. 99–100°/30 mm).

Anal. Calcd. for $C_{12}H_{18}F_{12}O_2Si_2$: C, 30.1; H, 3.79; F, 47.6. Found: C, 30.4; H, 3.61; F, 47.6.

Proton n.m.r. (neat) gave a single peak at −0.24 p.p.m. (internal TMS). Fluorine n.m.r. (carbon tetrachloride solution) showed a single peak at −10.7 p.p.m.

The same compound was readily produced when sodium, hexafluoroacetone, and trimethylchlorosilane were mixed in the appropriate proportions in THF.

Reaction with Dimethyldichlorosilane

To a solution of the disodium alkoxide (23 mmole) in THF at 25° was added dimethyldichlorosilane (4.2 g, 32 mmole). Immediate precipitation occurred, and fractionation of the volatile material gave a fraction boiling at 145–149° which was purified by vapor-phase chromatography (silicone column at 120°) to give 4,4,5,5-tetrakistrifluoromethyl-2,2-dimethyl-1,3-dioxa-2-silacyclopentane (4.5 g, 12 mmole).

Anal. Calcd. for $C_8H_6F_{12}O_2Si$: C, 24.6; H, 1.55; F, 58.4. Found: C, 25.0; H, 1.59; F, 58.4.

Proton n.m.r. gave a single peak at +0.89 p.p.m. (internal cyclohexane).

Reaction with Dimethylgermanium Dichloride

To a solution of the disodium alkoxide (5.4 mmole) in THF at 25° was added dimethylgermanium dichloride (0.80 g, 4.6 mmole). Immediate precipitation occurred, and the solution after filtration was evaporated to give a white solid. Purification by sublimation at 40°/10^{-3} mm yielded 4,4,5,5-tetrakistrifluoromethyl-2,2-dimethyl-1,3-dioxa-2-germacyclopentane, m.p. 69°.

Anal. Calcd. for $C_8H_6F_{12}O_2Ge$ (mol. wt., 435): C, 22.1; H, 1.4; F, 52.5. Found (mol. wt. (Rast) 419): C, 22.1; H, 1.4; F, 51.2.

Reaction with Dimethyltin Dichloride

To a solution of the disodium alkoxide (5.4 mmole) in THF at 25° was added dimethyltin dichloride (1.0 g, 4.6 mmole). Immediate precipitation occurred, and the solution after filtration was evaporated to give a white solid. The solid was redissolved in THF and crystallized by evaporation to give 4,4,5,5-tetrakistrifluoromethyl-2,2-dimethyl-1,3-dioxa-2-stannacyclopentane.

Anal. Calcd. for $C_8H_6F_{12}O_2Sn$ (mol. wt., 480): C, 19.9; H, 1.26; F, 47.4. Found (mol. wt. (Rast) 509): C, 19.1; H, 1.53; F, 47.6.

The solid did not appear to melt below 320° and did not sublime at 150°/10^{-3} mm.

Reaction with Phenylboron Dichloride

To a solution of the disodium alkoxide (23 mmole) in THF at 20° was added phenylboron dichloride (2.74 g, 17 mmole) in benzene (25 ml). Immediate precipitation occurred and fractionation of the volatile materials after 24 h gave 4,4,5,5-tetrakis(trifluoromethyl)-2-phenyl-1,3-dioxa-2-boracyclopentane (4.1 g, 9.9 mmole, b.p. 72–73°/30 mm).

Anal. Calcd. for $C_{12}H_5BF_{12}O_2$: C, 34.3; H, 1.20; F, 54.3. Found: C, 34.1; H, 1.22; F, 54.9.

The fluorine n.m.r spectrum (neat) showed a single absorption at −12.9 p.p.m.

Reaction of Perfluoropinacol with Sodium Borate

To a solution of sodium borate (0.39 g, 1.0 mmole) in hot water was added perfluoropinacol (6.0 g, 18.1 mmole). The solution was concentrated and then cooled, giving a colorless jelly. Crystallization from ethanol yielded sodium bis(perfluoropinacolato)borate.

Anal. Calcd. for $C_{12}F_{24}O_4BNa$: C, 20.6; F, 65.3; B, 1.54. Found: C, 20.6; F, 64.8; B, 1.49.

The fluorine n.m.r. spectrum (ethanol solution) showed a single peak at −7.87 p.p.m.

Reaction with Thionyl Chloride

To a solution of the disodium alkoxide (100 mmole) in THF at 25° was added thionyl chloride (11.2 g, 93 mmole). Immediate precipitation occurred and fractionation of the volatile material gave a fraction boiling at 120°/760 mm, identified as perfluoropinacol sulfite (15.0 g, 40.4 mmole).

Anal. Calcd. for $C_6F_{12}O_3S$: C, 19.0; F, 60.0; S, 8.43. Found: C, 19.1; F, 59.9; S, 8.32.

Reaction with Sulfuryl Chloride

To a solution of the disodium alkoxide (36.6 mmole) in THF at 25° was added sulfuryl chloride (4.1 g, 30 mmole). After 12 h the volatile material was fractionated, then distilled at atmospheric pressure to yield perfluoropinacol sulfate (2 g, 5.0 mmole, b.p. 120–122°).

Anal. Calcd. for $C_6F_{12}O_4S$: C, 18.2; F, 57.5; S, 8.09. Found: C, 18.3; F, 57.4; S, 7.93.

Reaction with Sulfur Dichloride

To a solution of the disodium alkoxide (6.7 mmole) in THF at 25° was added sulfur dichloride (1.74 g, 16.9 mmole). Immediate precipitation occurred. The reaction vessel was cooled to 0°, and the volatile material pumped out *in vacuo*. Sublimation of the residue *in vacuo* at 30° gave perfluoropinacol *ortho*-sulfite (0.42 g, 0.6 mmole, m.p. 51–53°).

TABLE II

Infrared absorption frequencies (cm^{-1})

Compound	Method by which spectrum taken	Spectral data†				
$(CH_3)_2Si(PFP)$*	Liquid film	1120 (s)	1003 (w)	952 (m)	887 (m)	742 (m)
$(CH_3)_2Ge(PFP)$	Liquid film	1104 (s)	997 (m)	950 (s)	879 (s)	750 (s)
$(CH_3)_2Sn(PFP)$	Nujol mull	1111 (m)	989 (m)	946 (s)	873 (s)	744 (s)
$C_6H_5B(PFP)$	Liquid film	1110 (s)	1007 (m)	954 (s)	889 (m)	747 (m)
$Na[B(PFP)_2]$	Nujol mull	1080 (s)	990 (m)	920 (m)	870 (m)	735 (m)
$(PFP)SO$	Liquid film	1081 (m)	997 (m)	954 (s)	877 (ms)	743 (s)
$(PFP)SO_2$	Liquid film	1080 (s)	1004 (w)	969 (s)	882 (m)	742 (m)
$(PFP)_2S$	Nujol mull	1111 (m)	1003 (ms)	969 (s)	886 (s)	750 (s)
$(PFP)_2Te$	Nujol mull	1112 (m)	992 (m)	941 (ms)	875 (m)	746 (s)

*(PFP) represents the perfluoropinacol group.
†(s) = strong, (m) = medium, (w) = weak.

Anal. Calcd. for $C_{12}F_{24}O_4S$: C, 20.7; F, 65.5. Found: C, 20.3; F, 64.8.

Fluorine n.m.r. (hexane solution) showed a pair of septets at −10.5 p.p.m. and −12.2 p.p.m.

Reaction with Tellurium Tetrachloride

To a solution of the disodium alkoxide (50 mmole) in THF at 25° was added tellurium tetrachloride (7.1 g, 26.3 mmole) in THF. Immediate precipitation occurred, and the mixture was filtered. After removal of the solvent, the residue was sublimed *in vacuo* overnight at 25° to give perfluoropinacol *ortho*-tellurite (3.1 g, 3.9 mmole, m.p. 84–86°).

Anal. Calcd. for $C_{12}F_{24}O_4Te$: C, 18.2; F, 57.6. Found: C, 18.0; F, 57.8.

The fluorine n.m.r. spectrum (THF solution) showed a single peak at −7.9 p.p.m.

Infrared Spectra

All the compounds prepared in this work had infrared spectra consistent with their proposed structures, the principle feature being strong absorption in the region 1100–1200 cm^{-1} associated with carbon–fluorine stretching frequencies. In the lower frequency region of the spectrum, however, certain similarities were present, all spectra showing absorptions near 1100, 1000, 950, 880, and 740 cm^{-1}, and we suggest that these are characteristic frequencies associated with the five-membered ring system derived from perfluoropinacol. Actual frequencies are given in Table II.

Acknowledgments

Financial assistance from the National Research Council of Canada is gratefully acknowledged. We also thank the Ontario Department of University Affairs for the award of a Graduate Fellowship (to A.F.J.).

1. M. E. Redwood and C. J. Willis. Can. J. Chem. **43**, 1893 (1965).
2. M. E. Redwood and C. J. Willis. Can. J. Chem. **45**, 389 (1967).
3. A. G. Pittman and D. L. Sharp. J. Org. Chem. **31**, 2316 (1966).
4. I. L. Knunyants and B. L. Dyatkin. Izv. Akad. Nauk SSSR, Ser. Khim. 923 (1964).
5. R. Filler and R. M. Schure. J. Org. Chem. **32**, 1217 (1967).
6. R. Filler, C.-S Wang, M. A. McKinney, and F. N. Miller. J. Am. Chem. Soc. **89**, 1026 (1967).
7. D. P. Graham and V. Weinmayr. J. Org. Chem. **31**, 957 (1966).
8. W. J. Middleton and R. V. Lindsey. J. Am. Chem. Soc. **86**, 4948 (1964).
9. C. L. Frye, R. M. Salinger, and T. J. Patin. J. Am. Chem. Soc. **88**, 2343 (1966).
10. A. F. Janzen, P. F. Rodesiler, and C. J. Willis. Chem. Commun. 672 (1966).
11. A. F. Janzen and C. J. Willis. Inorg. Chem. **6**, 1900 (1967).
12. E. G. Janzen and J. L. Gerlock. J. Phys. Chem. **71**, 4577 (1967).
13. W. D. Blackley and R. R. Reinhard. J. Am. Chem. Soc. **87**, 802 (1965).
14. J. Dale. J. Chem. Soc. 922 (1961).
15. C. W. Tullock, F. S. Fawcett, W. C. Smith, and D. D. Coffman. J. Am. Chem. Soc. **82**, 539 (1960).
16. R. E. Dodd, L. A. Woodward, and H. L. Roberts. Trans. Faraday Soc. **52**, 1052 (1956).
17. J. Bacon, R. J. Gillespie, and J. W. Quail. Can. J. Chem. **41**, 1016 (1963).
18. D. P. Stevenson and V. Schomaker. J. Am. Chem. Soc. **62**, 1267 (1940).
19. D. Nakamura, K. Ito, and M. Kubo. J. Am. Chem. Soc. **84**, 163 (1962).
20. G. Engel. Z. Krist. **90**, 341 (1935).
21. N. P. Gambaryan, Y. A. Cheburkov, and I. L. Knunyants. Izv. Akad. Nauk SSSR, Ser. Khim. 1526 (1964).

Can. J. Chem. Downloaded from www.nrcresearchpress.com by 210.87.254.5 on 09/05/12
For personal use only.

Can. J. Chem. Downloaded from www.nrcresearchpress.com by 210.87.254.6 on 09/05/12
For personal use only.

Lengthening of tetrose and pentose carbon chains by vinylation reactions

D. J. WALTON
Department of Biochemistry, Queen's University, Kingston, Ontario

Received July 9, 1968

Vinylation of 2,3:4,5-di-*O*-isopropylidene-*aldehydo*-D-arabinose gave a 1.3:1 mixture of 1,2:3,4-di-*O*-isopropylidene-6-heptene-L-*gulo* (and D-*manno*)-1,2,3,4,5-pentol (**1***a* and **2***a*). Successive ozonolysis and hydrolysis of the mixture of **1***a* and **2***a* gave D-glucose and D-mannose in a ratio of 1.4:1. Vinylation of 2,4-*O*-ethylidene-*aldehydo*-D-erythrose gave a 3.9:1 mixture of 1,3-*O*-ethylidene-5-hexene-L-*ribo* (and D-*lyxo*)-1,2,3,4-tetrol (**3***a* and **4***a*), which was degraded to form D-ribose and D-arabinose in a ratio of 4:1. The configuration of each of the *C*-vinyl compounds **1***a*, **2***a*, **3***a*, and **4***a* was assigned by degradation to the corresponding aldose.

Canadian Journal of Chemistry, **46**, 3679 (1968)

A report from this laboratory described a new method of lengthening aldose carbon chains, which involved vinylation of an *aldehydo* sugar, ozonolysis of the product, and removal of hydroxyl protecting groups (1). 2,3-*O*-Isopropylidene-D-glyceraldehyde was converted into D-threose and D-erythrose in this way. The method has now been applied successfully to two other *aldehydo* sugars. 2,3:4,5-Di-*O*-isopropylidene-*aldehydo*-D-arabinose gave D-glucose and D-mannose in a ratio of 1.4:1, and 2,4-*O*-ethylidene-*aldehydo*-D-erythrose gave D-ribose and D-arabinose in a ratio of 4:1.

Treatment of 2,3:4,5-di-*O*-isopropylidene-*aldehydo*-D-arabinose with vinylmagnesium chloride gave a product which was resolved by gas–liquid partition chromatography (g.l.p.c.) into two components, **A** and **B**, in the ratio of 1.3:1. The data obtained from elemental analysis, quantitative hydrogenation, and infrared spectroscopy were consistent with a di-*O*-isopropylidene-6-heptene-1,2,3,4,5-pentol structure. The formation of monoacetates with acetic anhydride indicated the presence of a single hydroxyl group. Ozonolysis and deketalization of pure component **A** gave D-glucose[1] with a small proportion of an arabinose. Component **A** (fast moving on g.l.p.c.) was therefore 1,2:3,4-di-*O*-isopropylidene-6-heptene-L-*gulo*-1,2,3,4,5-pentol (**1***a*). Similar degradation of component **B** (slow moving on g.l.p.c.) gave D-mannose,[1] with some arabinose. Hence component **B** was the D-*manno* epimer (**2***a*).

Similar methods were used to verify the structures of the 3-acetates (**1***b* and **2***b*), which were resolved by gas–liquid partition chromatography (g.l.p.c.) into a fast-flowing component, **C**, and a slow-flowing component **D**. Since components **C** and **D** were degraded to D-glucose[1] and D-mannose,[1] respectively, **C** was the L-*gulo* epimer (**1***b*) and **D** was the D-*manno* epimer (**2***b*).

Preliminary experiments in which **1***a* and **2***a* were ozonized in ethyl acetate, and then hydrogenated and deketalized, resulted in the formation of appreciable quantities of arabinose. Efforts were therefore directed to reducing the formation of this by-product. Since conditions which might lead to overozonation were avoided, arabinose formation appeared to be an example of "abnormal ozonolysis" of an allylic compound, involving the rearrangement of an alkene-ozone reaction intermediate (2). In this connection Young *et al.* (3) observed that allylic acetates were less prone to "abnormal ozonolysis" than their parent alcohols, while Milas and Nolan (4) claimed that some "abnormal ozonolyses" could be prevented by conducting ozonations in cold methanol. The mixture of **1***a* and **2***a*, and their acetates (**1***b* and **2***b*) were therefore ozonized under different conditions. The ozonation products were reduced and hydrolyzed to give aldose mixtures whose compositions were determined by gas–liquid partition chromatography. The results (Table I) showed that ozonations conducted in methanol at $-40°$ resulted in a degree of arabinose formation which was approximately a quarter of that observed when ethyl acetate was used. For any given solvent and temperature, there was no significant difference in the proportion of arabinose obtained from the alcohols (**1***a* and **2***a*) and their acetates (**1***b* and **2***b*).

Degradation of a larger sample of **1***a* and **2***a* gave a mixture of aldoses from which D-glucose

[1]Degradations of mixed epimers on a preparative scale gave only D-sugars. Aldoses formed for configurational assignment were therefore assumed to be D-enantiomers, although they were identified only by chromatography.

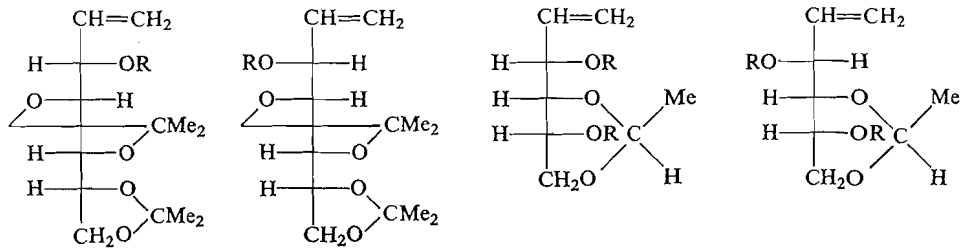

1 *a*, R = H
b, R = Ac

2 *a*, R = H
b, R = Ac

3 *a*, R = H
b, R = Ac

4 *a*, R = H
b, R = Ac

was isolated by preparative paper chromatography, and characterized as *N*-(*p*-nitrophenyl)-β-D-glucosylamine (5). Crystalline D-mannose was isolated from the mixture *via* its phenylhydrazone (6).

The work described so far parallels that of Horton and Tronchet (7), who obtained the L-enantiomers of **1***a* and **2***a* by ethynylation of 2,3:4,5-di-*O*-isopropylidene-*aldehydo*-L-arabinose, followed by Lindlar reduction of the product. These workers showed that the L-enantiomers of **1***a* and **2***a* could be degraded to glucose and arabinose, and mannose and arabinose, respectively, though the degradation reaction was not examined quantitatively.

The vinylation of 2,4-*O*-ethylidene-*aldehydo*-D-erythrose proceeded smoothly, in spite of the unprotected hydroxyl group, to give a product containing two components, **E** and **F**, in a ratio of 3.9:1. The structures **3***a* and **4***a* were verified by the methods used for **1***a* and **2***a*. Component **E** (fast moving on g.l.p.c.) was degraded to D-ribose[1] with a trace of erythrose, and was therefore 1,3-*O*-ethylidene-5-hexene-L-*ribo*-1,2,3,4-tetrol (**3***a*). Component **F** (slow moving on g.l.p.c.) which gave D-arabinose[1] with a trace of erythrose, was therefore the D-*lyxo* epimer (**4***a*).

The fast moving (g.l.p.c.) diacetate (component **G**) was the D-*lyxo* epimer (**4***b*) since it gave mainly D-arabinose[1] on degradation. The slow moving (g.l.p.c.) diacetate (component **H**) was the L-*ribo* epimer (**3***b*), as it was degraded to D-ribose.[1]

The mixture of **3***a* and **4***a* was degraded on a preparative scale, to give a mixture of ribose, arabinose, and erythrose in the proportions of 40:10:1. Crystalline D-ribose was isolated from the reaction mixture through the anilide – sodium sulfate complex (8) in 22% yield, based on 2,4-*O*-ethylidene-*aldehydo*-D-erythrose. A small sample of D-arabinose was isolated by preparative paper chromatography, and characterized by formation of the diphenylhydrazone (9).

It is apparent that the vinylation reaction can be used for lengthening the carbon chains of trioses, tetroses, and pentoses, with varying degrees of stereoselectivity. The degree of stereoselectivity (60%) for the vinylation of 2,4-*O*-ethylidene-*aldehydo*-D-erythrose was comparable to

TABLE I

Effect of ozonation solvent and temperature on proportions of aldoses formed by ozonolysis and hydrolysis

	Ozonation conditions				
Compounds*	Solvent	Temperature (°C)	Arabinose† (%)	Glucose† (%)	Mannose† (%)
1*a* and **2***a*	EtOAc	0	26	42	32
1*a* and **2***a*	EtOAc	−40	21	45	34
1*a* and **2***a*	MeOH	−40	6	54	40
1*b* and **2***b*	EtOAc	0	23	44	33
1*b* and **2***b*	EtOAc	−40	17	48	35
1*b* and **2***b*	MeOH	−40	5	53	42

*Each experiment was performed on an epimeric mixture.
†Proportions determined by gas–liquid chromatography of derived alditol acetates.

Can. J. Chem. Downloaded from www.nrcresearchpress.com by 210.87.254.6 on 09/05/12
For personal use only.

TABLE II

Operating conditions for gas–liquid partition chromatography

	Column 1	Column 2	Column 3	Column 4
Length (cm)	300	280	152	300
Internal diameter (mm)	1.55	1.55	1.55	7.90
Mesh size of Chromosorb W	80–100	80–100	80–100	60–80
Stationary phase	10% neopentylglycol sebacate	1.5% GEXF 1150* plus 1.5% ethylene glycol succinate*	10% neopentylglycol sebacate	10% neopentylglycol sebacate
Oven temperature (°C)	180–220†	180–220†	130–200	175
Rate of temperature increase (°C/min)	2	2	4	0
Hydrogen flow rate (ml/min)	50	20	40	—
Nitrogen flow rate (ml/min)	100	40	60	1800
Detector	Flame ionization	Flame ionization	Flame ionization	Thermal conductivity

*Two coated packings mixed in equal proportions.
†Isothermal operation after programming to 220°.

the values obtained in Kiliani cyanhydrin syntheses (10, 11), and was considerably higher than the values reported for vinylations (1, 13) and ethynylations (7, 12, 13) of *aldehydo* sugars.

Experimental

An Aerograph 1520 instrument was used for gas–liquid partition chromatography. The conditions of the columns are shown in Table II. Ratios of aldoses were determined by conversion into the corresponding alditol acetates according to Sjöström *et al.* (14), followed by chromatography on column 1. This method (14) was also used as an aid to the identification of aldoses by augmentation of peaks due to standard alditol acetates, when columns 1 and 2 were used. *C*-Vinyl compounds were separated on column 3. Their retention times are quoted relative to those of 1,2:5,6-di-*O*-isopropylidene-α-D-glucofuranose ($T_1 = 1.0$; retention time 16.6 min). Column 4 was used for preparative purposes.

Descending paper chromatography was performed on Whatman No. 1 paper. Chromatograms were developed with ethyl acetate – acetic acid – formic acid – water 18:3:1:4 (solvent *a*), or butan-1-ol – pyridine – water 5:3:2 (solvent *b*), or butan-1-ol – ethanol – water 3:1:1 (solvent *c*). The alkaline silver nitrate spray (15) was used.

The ozone generator used produced ozone at 0.55 mmole/min, with an oxygen flow rate of 400 ml/min.

Optical rotations were measured at 22°. Unless otherwise stated, no mutarotation was observed in the course of 1 h. Melting points are corrected.

For each quantitative hydrogenation a solution of the unsaturated substance (*ca.* 0.3 g) in ethanol (25 ml) was stirred under hydrogen (atmospheric pressure) in the presence of platinum oxide (15 mg). In all cases hydrogen absorption was complete in 10 min.

2,3:4,5-Di-*O*-isopropylidene-*aldehydo*-D-arabinose was prepared by periodate oxidation (16) of 1,2:3,4-di-*O*-isopropylidene-D-mannitol, and was distilled immediately before use. 2,4-*O*-Ethylidene-*aldehydo*-D-erythrose was prepared by periodate oxidation (17) of 4,6-*O*-ethylidene-D-glucose. Both *aldehydo* sugars were gas chromatographically pure.

Vinylmagnesium chloride in tetrahydrofuran was obtained from Peninsular ChemResearch, Gainesville, Florida.

"Fisher Certified" tetrahydrofuran, containing 0.025% of a stabilizer, was used for Grignard reactions.

*1,2;3,4-Di-O-isopropylidene-6-heptene-L-gulo (and D-manno)-1,2,3,4,5-pentol (**1a** and **2a**)*

A solution of 2,3:4,5-di-*O*-isopropylidene-*aldehydo*-D-arabinose (15.0 g, 0.065 mole) in 20 ml of tetrahydrofuran was added, over 15 min, to a solution (142 ml) of vinylmagnesium chloride (0.326 mole) in tetrahydrofuran, which was stirred under dry nitrogen. The addition resulted in a rise of temperature from 22 to 50°. The reaction mixture was stirred for 20 h at room temperature. Ether (12 ml) was added, and the mixture was cooled to 0°. Saturated ammonium chloride solution (70 ml) was added, keeping the temperature of the mixture below 15° with an ice-salt bath. The mixture was filtered, and the magnesium salts were washed with ether. The combined filtrate and washings were concentrated and the residue was distilled *in vacuo* using a vacuum-jacketed Vigreaux column (9 × 1.2 cm). A low-boiling fraction (0.2 g) was discarded. The product (10.8 g, 64%) was a colorless mobile liquid, b.p. 88–92° at 0.08 mm, $[\alpha]_D$ −3° (*c*, 4.0 in chloroform). Infrared spectrum (liquid film): 3470 (OH), 3070 (vinyl CH_2), 1860 (vinyl CH overtone), 1640 (vinyl C=C), 1365, 1375 (CMe_2 doublet), and 922 cm^{-1} (vinyl CH). Hydrogen absorption: 101% of theory.

Anal. Calcd. for $C_{13}H_{22}O_5$: C, 60.44; H, 8.59. Found: C, 60.69; H, 8.60.

Two peaks were recorded by gas–liquid partition chromatography: component **A**, T_1 0.514, and component **B**, T_1 0.590, in a ratio of areas of 1.3:1.

*Preparative Gas–Liquid Partition Chromatography of Compounds **1a** and **2a***

A solution of 1.5 g of the mixture of **1***a* and **2***a* in

Can. J. Chem. Downloaded from www.nrcresearchpress.com by 210.87.254.6 on 09/05/12
For personal use only.

Can. J. Chem. Downloaded from www.nrcresearchpress.com by 210.87.254.6 on 09/05/12
For personal use only.

chloroform (3.5 ml) was injected into column 4 in 80 μl portions. Component **A** (0.55 g), a liquid, $[\alpha]_D$ −21° (*c*, 4.1 in chloroform) was collected 9 min after each injection. Component **B** (0.37 g), also a liquid, $[\alpha]_D$ +23° (*c*, 3.5 in chloroform) was collected after 11.5 min. Analytical gas–liquid partition chromatography of each component showed that complete resolution had been achieved.

*1,2.3,4-Di-O-isopropylidene-6-heptene-*L*-gulo (and* D*-manno)-1,2,3,4,5-pentol 5-Acetate (**1b** and **2b**)*

The mixture of 2.0 g **1***a* and **2***a* was heated under reflux for 1.5 h with acetic anhydride (40 ml) and anhydrous sodium acetate (2 g). After the usual work-up procedure the product was obtained as a colorless, mobile liquid (1.8 g, 77%), b.p. 82–83° at 0.04 mm, $[\alpha]_D$ +9° (*c*, 3.6 in chloroform). Infrared spectrum (liquid film): no OH peak; peaks at 1740 (CO of OAc), 1640 (vinyl C=C), 1365, 1375 (CMe_2 doublet), and 1220 cm^{-1} (OAc). Hydrogen absorption: 98% of theory.

Anal. Calcd. for $C_{15}H_{24}O_6$: C, 59.98; H, 8.05. Found: C, 59.87; H, 8.16.

Gas–liquid partition chromatography gave two peaks: component **C**, T_l 0.576, and component **D**, T_l 0.631 in a ratio of areas of 1.6:1. Component **C**, isolated by preparative gas–liquid partition chromatography, had $[\alpha]_D$ +5° (*c*, 2.2 in chloroform), and component **D** had $[\alpha]_D$ +20° (*c*, 2.0 in chloroform). Both components were mobile liquids.

*Effect of Ozonation Solvent and Temperature on Proportions of Aldoses Formed by Ozonolysis and Hydrolysis of **1a** and **2a**, and **1b** and **2b***

Solutions were prepared containing the mixture (0.4 g) of **1***a* and **2***a*, or of **1***b* and **2***b* in 10 ml solvent (Table I). Each solution was maintained at the temperature shown in Table I while ozonized oxygen was bubbled through for 9 min, when the starting materials had just disappeared (gas–liquid partition chromatography). The products of ozonation were hydrogenated and hydrolyzed as described in the next paragraph. Paper chromatography in solvents *a* and *b* indicated that each final aqueous solution contained arabinose, glucose, and mannose. The proportions of these sugars (Table I) were determined by gas–liquid partition chromatography of their derived alditol acetates, using column 1.

D*-Glucose and* D*-Mannose from the Mixture of **1a** and **2a***

A solution of the Grignard reaction product (**1***a* and **2***a*, 2.2 g) in methanol (40 ml) was kept at −40° while ozonized oxygen was bubbled through for 35 min. Gas–liquid partition chromatography of the resulting solution showed the presence of traces of **1***a* and **2***a*. Nitrogen was bubbled through the solution while its temperature was brought to 0°, and the flow was continued for 10 min at 0°. Platinum oxide (60 mg) was added, and the solution at 0° was stirred under hydrogen at atmospheric pressure until gas absorption ceased. The solution, which gave a negative starch-iodide test, was filtered and concentrated to dryness. The resulting oil was heated on the steam bath for 2 h with 100 ml 0.2 *N* sulfuric acid, passed through Rexyn 203 (OH) resin, and concentrated to a small volume, which was then made up to 50 ml with water. This solution contained 590 mg glucose, 435 mg mannose, and 66 mg arabinose, based on a glucose oxidase estimation (18) of glucose, and on gas–liquid chromatographic determination of the proportions of the sugars.

Isolation of D*-Glucose*

One quarter of the solution of aldose was concentrated to *ca.* 0.5 ml and applied to two sheets of Whatman 3MM filter paper. After development with solvent *a*, glucose containing areas were eluted with water. Concentration of the eluate, followed by drying over P_2O_5, gave chromatographically pure D-glucose (90 mg) as a syrup, $[\alpha]_D$ +47° (*c*, 4.2 in water); lit. (2) $[\alpha]_D$ +52.7° (equilibrium value, in water). Treatment of a portion (60 mg) of the syrup with *p*-nitraniline according to the method of Weygand *et al.* (5) gave *N-(p-nitrophenyl)-*β*-*D*-glucosylamine* (84 mg, 84%), m.p. 183–185°, $[\alpha]_D$ −193 → −200° (*c*, 2.6 in pyridine) (20 h); lit. (5) m.p. 184°, $[\alpha]_D$ −192° → −202° (in pyridine).

Isolation of D*-Mannose*

The remaining three-quarters of the solution of aldose was concentrated to 14 ml. A solution of phenylhydrazine (540 mg) and acetic acid (3 drops) in water (2 ml) was added. The resulting mixture was treated by the method of Sowden and Schaffer (19) to give 460 mg of crude D-mannose phenylhydrazone, m.p. 186–190°. Cleavage with benzaldehyde according to Sowden and Fischer (20) gave a mannose containing syrup which was dissolved in hot methanol (0.3 ml). A mixture of methanol (0.6 ml) and 2-propanol (0.6 ml) was added. After cooling overnight crystalline D-mannose (210 mg) was obtained; m.p. 130–132°, $[\alpha]_D$ −3° → +14° (40 min) (*c*, 5.5 in water). The reported (21) constants for β-D-mannose are: m.p. 132°, $[\alpha]_D$ −17.0° → +14.2° (in water).

The *phenylhydrazone* (6) had m.p. 199–200°, $[\alpha]_D$ +27° (*c*, 2.2 in pyridine); lit. (6) m.p. 199–200°, $[\alpha]_D$ +26.3° (constant value over 1 h) (in pyridine).

*Degradation of Components **A**, **B**, **C**, and **D** for Configurational Assignment*

Ozonized oxygen was passed through a solution of each component (0.1 g) in methanol (10 ml) at −40° for 10 min. Hydrogenation and deketalization were carried out as described under the heading "D-Glucose and D-Mannose from the Mixture of **1***a* and **2***a*". The aldoses present in each final solution were identified by paper chromatography in solvents *a* and *b*, and by gas–liquid partition chromatography (columns 1 and 2) of the derived alditol acetates. The solutions obtained by treatment of components **A** and **C** each contained arabinose and glucose. Those obtained by treatment of components **B** and **D** each contained arabinose and mannose.

*1,3-O-Ethylidene-5-hexene-*L*-ribo (and* D*-lyxo)-1,2,3,4-tetrol (**3a** and **4a**)*

A mixture of compounds **3***a* and **4***a* was prepared by the addition of a solution of 2,4-*O*-ethylidene-*aldehydo*-D-erythrose (24.0 g, 0.164 mole) in tetrahydrofuran (30 ml) to a solution (430 ml) of vinylmagnesium chloride (0.988 mole) in tetrahydrofuran. The reaction conditions and the work-up procedure were similar to those used for the preparation of **1***a* and **2***a*. On distillation, an initial fraction (0.7 g) was collected, b.p. 42–80° at 0.08 mm, which contained by-products of low retention time. The

Can. J. Chem. Downloaded from www.nrcresearchpress.com by 210.87.254.6 on 09/05/12
For personal use only.

product (16.7 g, 58%) was a pale-yellow viscous liquid, b.p. 84–89° at 0.05 mm, $[\alpha]_D$ −21° (*c*, 3.7 in chloroform). Infrared spectrum (liquid film): 3500 (OH), 3070 (vinyl CH_2), 1860 (vinyl CH overtone), 1640 (vinyl C=C), and 930 cm^{-1} (vinyl CH). Hydrogen absorption: 98% of theory.

Anal. Calcd. for $C_8H_{14}O_4$: C, 55.16; H, 8.10. Found: C, 55.23; H, 7.81.

Gas–liquid partition chromatography showed the presence of two compounds: component **E**, T_l 0.660, and component **F**, T_l 0 728, in a ratio of 3.9:1. Component **E**, isolated by preparative gas–liquid partition chromatography, was a viscous liquid $[\alpha]_D$ −28.5° (*c*, 2.4 in chloroform). Component **F**, obtained in the same manner, crystallized spontaneously in the form of fine needles, m.p. 57–58°, $[\alpha]_D$ +6° (*c*, 2.3 in chloroform).

*1,3-O-Ethylidene-5-hexene-*L*-ribo (and* D*-lyxo)-1,2,3,4-tetrol 2,4-Diacetate (3b and 4b)*

Acetylation of 3.0 g of the mixture of **3***a* and **4***a* by the method described for **1***b* and **2***b* gave the mixed diacetates (**3***b* and **4***b*) as a colorless, mobile liquid (3.5 g, 79%), b.p. 95–97° at 0.2 mm, $[\alpha]_D$ −29° (*c*, 5.0 in chloroform). Infrared spectrum (liquid film): no OH peak; peaks at 1735 (CO of OAc), 1640 (vinyl C=C), and 1220 cm^{-1} (OAc). Hydrogen absorption: 102% of theory.

Anal. Calcd. for $C_{12}H_{18}O_6$: C, 55.80; H, 7.03. Found: C, 55.71; H, 7.15.

Two components were shown by gas–liquid partition chromatography: component **G**, T_l 0.495, and component **H**, T_l 0.548, in the proportions of 1:4.0. Component **G** had $[\alpha]_D$ −12° (*c*, 3.0 in chloroform), and component **H** had $[\alpha]_D$ −34° (*c*, 4.1 in chloroform).

D*-Ribose from the Mixture of 3a and 4a*

Ozonolysis of the mixture of **3***a* and **4***a* (1.48 g) was carried out in the manner described for ozonolysis of **1***a* and **2***a*. Subsequent treatment with sulfuric acid gave a final solution which contained ribose, arabinose, and erythrose in the proportions of 40:10:1. The complete process (ozonolysis and hydrolysis) was repeated on a second batch (1.48 g) of **3***a* and **4***a*. The volume of the combined aqueous solutions of aldoses was adjusted to 30 ml. Anhydrous sodium sulfate (2.52 g) was added, and the solution was adjusted to pH 4 with 0.2 *N* sulfuric acid. A solution of aniline (2 ml) in ethanol (14 ml) was added, and the solution was stirred for 2 h at room temperature, and for 18 h at 3°. The resulting precipitate was collected, and washed with ethanol. After drying *in vacuo* over phosphorus pentoxide, the *N-phenyl-*D*-ribosylamine–sodium sulfate complex* (8) weighed 3.36 g. After hydrolysis of the complex by the method of Berger *et al.* (22), the final aqueous solution was concentrated to dryness. The residue was extracted with warm ethanol and the solution was concentrated to a syrup. On storage in a desiccator (*in vacuo*, P_2O_5) overnight the syrup changed into a crystalline mass which was triturated with cold ethanol, collected, and dried; m.p. 77–80°, $[\alpha]_D$ −17° (*c*, 4.3 in water), yield 1.41 g. Recrystallization from ethanol gave chromatographically pure D-ribose (0.97 g; 22%, from 2,4-*O*-ethylidene-*aldehydo*-D-erythrose), m.p. 85–87°, $[\alpha]_D$ −20° (*c*, 4.0 in water); lit. (21) m.p. 84–86°, $[\alpha]_D$ −19.4° (in water). Treatment with *p*-bromophenylhydrazine gave D*-ribose p-bromophenylhydrazone*, which, after crystallization from 95% ethanol, had m.p. 166–167°, $[\alpha]_D$ +10° (*c*, 1.3 in ethanol);[2] lit. (23) m.p. 164–165°, $[\alpha]_D$ +10.3° (in ethanol).

D*-Arabinose from the Mixture of 3a and 4a*

Another batch (0.74 g) of the mixture of **3***a* and **4***a* was ozonolyzed and hydrolyzed as described above. The resulting mixture of aldoses was chromatographed on four sheets of Whatman 3MM paper, with solvent *c*. Elution of the appropriate areas gave a syrup of D-arabinose (63 mg) $[\alpha]_D$ −100° (*c*, 3.2 in water); lit. (2) $[\alpha]_D$ −105° (equilibrium value, in water). Treatment with 1,1-diphenylhydrazine hydrochloride (88 mg) and sodium acetate trihydrate (60 mg) by the method of Mandl and Neuberg (9) gave crude D*-arabinose diphenylhydrazone* (112 mg), m.p. 198–200°. Crystallization from 2-methoxyethanol gave pale-mauve needles, m.p. 206–207°, $[\alpha]_D$ −13° (*c*, 1.0 in pyridine);[2] lit. m.p. 206–207° (9). L-Arabinose diphenylhydrazone was reported (24) to have $[\alpha]_D$ +14.9° (in pyridine).

Degradation of Components E, F, G, and H for Configurational Assignment

A pure sample of each component was ozonolyzed and hydrolyzed as described for components **A**, **B**, **C**, and **D**. Under these conditions components **E** and **H** were each degraded to a mixture of ribose and erythrose. Components **F** and **G** were each degraded to a mixture of arabinose and erythrose.

Acknowledgment

The author wishes to thank the Medical Research Council of Canada for financial assistance during this work.

1. D. J. WALTON. Can. J. Chem. **45**, 2921 (1967).
2. P. S. BAILEY. Chem. Rev. **58**, 925 (1958).
3. W. G. YOUNG, A. C. MCKINNIS, I. D. WEBB, and J. D. ROBERTS. J. Am. Chem. Soc. **68**, 293 (1946).
4. N. A. MILAS and J. T. NOLAN. Advan. Chem. Ser. **27**, 136 (1959).
5. F. WEYGAND, W. PERKOW, and P. KUHNER. Ber. **84**, 594 (1951).
6. C. L. BUTLER and L. H. CRETCHER. J. Am. Chem. Soc. **53**, 4358 (1931).
7. D. HORTON and J. M. J. TRONCHET. Carbohydrate Res. **2**, 315 (1966).
8. L. BERGER and J. LEE. J. Org. Chem. **11**, 84 (1946).
9. I. MANDL and C. NEUBERG. Arch. Biochem. Biophys. **35**, 326 (1952).
10. H. S. ISBELL, J. V. KARABINOS, H. L. FRUSH, N. B. HOLT, A. SCHWEBEL, and T. T. GALKOWSKI. J. Res. Natl. Bur. Std. **48**, 163 (1952).
11. C. S. HUDSON. J. Am. Chem. Soc. **73**, 4498 (1951).
12. J. L. GODMAN, D. HORTON, and J. M. J. TRONCHET. Carbohydrate Res. 4, 392 (1967).
13. D. HORTON, J. B. HUGHES, and J. K. THOMSON. J. Org. Chem. **33**, 728 (1968).
14. E. SJÖSTRÖM, P. HAGLUND, and J. JANSON. Svensk Papperstid. **69**, 381 (1966).
15. W. E. TREVELYAN, D. P. PROCTOR, and J. S. HARRISON. Nature, **166**, 444 (1950).

[2]Heating was required to effect solution.

16. J. ENGLISH and P. H. GRISWALD. J. Am. Chem. Soc. **70**, 1390 (1948).
17. R. BAKER and D. J. MACDONALD. J. Am. Chem. Soc. **82**, 2301 (1960).
18. A. SAIFER and S. GERSTENFELD. J. Lab. Clin. Med. **51**, 448 (1958).
19. J. C. SOWDEN and R. SCHAFFER. J. Am. Chem. Soc. **74**, 499 (1952).
20. J. C. SOWDEN and H. O. L. FISCHER. J. Am. Chem. Soc. **60**, 1963 (1947).
21. J. STANĚK, M. ČERNÝ, J. KOCOUREK, and J. PACÁK. The Monosaccharides. Academic Press, Inc. New York. 1963. pp. 97–99.
22. L. BERGER, U. V. SOLMSSEN, F. LEONARD, E. WENIS, and J. LEE. J. Org. Chem. **11**, 91 (1946).
23. P. A. LEVENE and R. S. TIPSON. J. Biol. Chem. **115**, 731 (1936).
24. A. MÜTHERS and B. TOLLENS. Ber. **37**, 311 (1904).

Can. J. Chem. Downloaded from www.nrcresearchpress.com by 210.87.254.6 on 09/05/12
For personal use only.

Can. J. Chem. Downloaded from www.nrcresearchpress.com by 210.87.254.105 on 09/05/12
For personal use only.

Synthesis and spectra of some diarylidenecyclanones

P. G. FARRELL[1]
Department of Chemistry, Queen Elizabeth College, London, W.8, England

AND

B. A. READ
Department of Chemistry, Sir John Cass College, London, E.C.3, England

Received June 5, 1968

The synthesis and spectra (ultraviolet, infrared, and nuclear magnetic resonance) of some previously unknown 2,*n*-dibenzylidene and dicinnamylidenecyclanones where $n = 5$–10 are described. The spectra are in accord with the expected decrease in coplanarity of the conjugated groups with increasing ring size. *trans*-Ring hydrogen bonding may occur in 2,10-dibenzylidenecyclodecanone but no evidence is found for this effect in the parent cyclanone.

Canadian Journal of Chemistry, 46, 3685 (1968)

Introduction

The symmetrical diarylidene derivatives of α,α′-dimethylene ketones have been frequently used for characterization and identification (1) but there are few reports of such derivatives of the cyclic ketones $C_nH_{2n-2}O$ where $n > 7$. 2,8-Dibenzylidenecyclooctanone was reported as a liquid obtained from the dehydration of 2-benzylidene, 8-(α-hydroxybenzyl) cyclooctanone but no characteristics of this other than an analysis were recorded (2). Braude *et al.* (3, 4) have synthesized the monobenzylidene derivatives of the cyclanones with $n = 8$, 9, and 10 and also succeeded in isolating a small amount of a compound which they considered to be 2,10-dibenzylidenecyclodecanone. The monobenzylidene derivative of cyclopentadecanone has been reported but attempts to form the dibenzylidene compound were unsuccessful and yielded only starting materials (5, 6). We are unable to find any records of the corresponding cinnamylidene compounds or higher homologues.

Results

Alkaline condensation of cyclooctanone with benzaldehyde resulted initially in a yellow oil (c.f. (2)) which, after separation and solution in hot methanol, gave white crystals of the required product.

Our attempts to make 2,10-dibenzylidenecyclodecanone by a similar method to that employed by Braude and Gofton (4) resulted always in the isolation of a white crystalline solid differing in melting point and spectral properties from those reported by these authors for the compound. A molecular weight determination gave a mean value of 340 (theory 330). The nuclear magnetic resonance (n.m.r.) spectrum showed absorption bands whose positions and areas are in accord with those expected for dibenzylidenecyclodecanone (see Table I). Attempts to reduce this ketone or to make a 2,4-dinitrophenylhydrazone were unsuccessful, possibly due to the preferred "*O*-inside" conformation of cyclodecanones (7). (See (7) for a discussion of this terminology.) On attempted reduction the formation of a tetrahedral carbon atom from the carbonyl group is energetically unfavorable in this system (8), whereas steric factors may well mitigate against 2,4-dinitrophenylhydrazone formation.

Attempted syntheses of 2,15-dibenzylidenecyclopentadecanone resulted only in the rapid formation of a white solid, identified from its n.m.r. spectrum, analysis as 2-(α-hydroxybenzyl) cyclopentadecanone, which we were unable to dehydrate to the monobenzylidene compound. Reactions involving cinnamaldehyde yielded only starting materials, together with resinous materials from which no products were isolated.

Discussion

In Table I are shown the C=O and C=C stretching frequency values, together with the maximum electronic absorption wavelengths, for the dibenzylidene- and dicinnamylidenecyclanones ($n = 5$–10), and in Table II the chemical

[1]Author to whom correspondence should be addressed at Department of Chemistry, McGill University, Montreal 2, Quebec.

TABLE I

Spectroscopic data for dibenzylidene and dicinnamylidenecyclanones and related compounds

Ring size n	Cyclanone* $\nu_{C=O}$ (cm^{-1})	Dibenzylidene derivatives† $\nu_{C=O}$ (cm^{-1})	$\nu_{C=C}$ (cm^{-1})	λ_{max}(mμ), (ε)	Dicinnamylidene derivatives† $\nu_{C=O}$ (cm^{-1})	$\nu_{C=C}$ (cm^{-1})	λ_{max}(mμ), (ε)
5	1751	1691	1625	337(32,000)	1670	1617	380(58,000)
6	1718	1661	1610	315(25,000)	1650	1615	369(58,000)
7	1706	1663	1610	250(12,500); 289(25,000)	1655	1615	290(22,500); 335(52,000)
8	1704	1663	1610	250(14,500); 284(22,000)	1657	1613	290(47,000); 333(50,500)
9	1703	1661	1615	250(15,500); 280(22,000)	1644	1607	290(30,000); 330(50,000)
10	1705	1650	1610	250(13,500); 284(23,000)			
5E‡		1711	1616	303(35,000); 340(26,000)	1685	1607	353(70,000); 394(40,000)
Acetone	1720	1645	1620	331(35,800)§	1634	1608	376(54,900)§

*Values taken from ref. 12.
†Infrared measurements in KBr discs; u.v. measurements in *n*-hexane.
‡5E = cyclopent-3-ene-1-one.
§Values taken from R. N Beale, Nature, 178, 37 (1956).

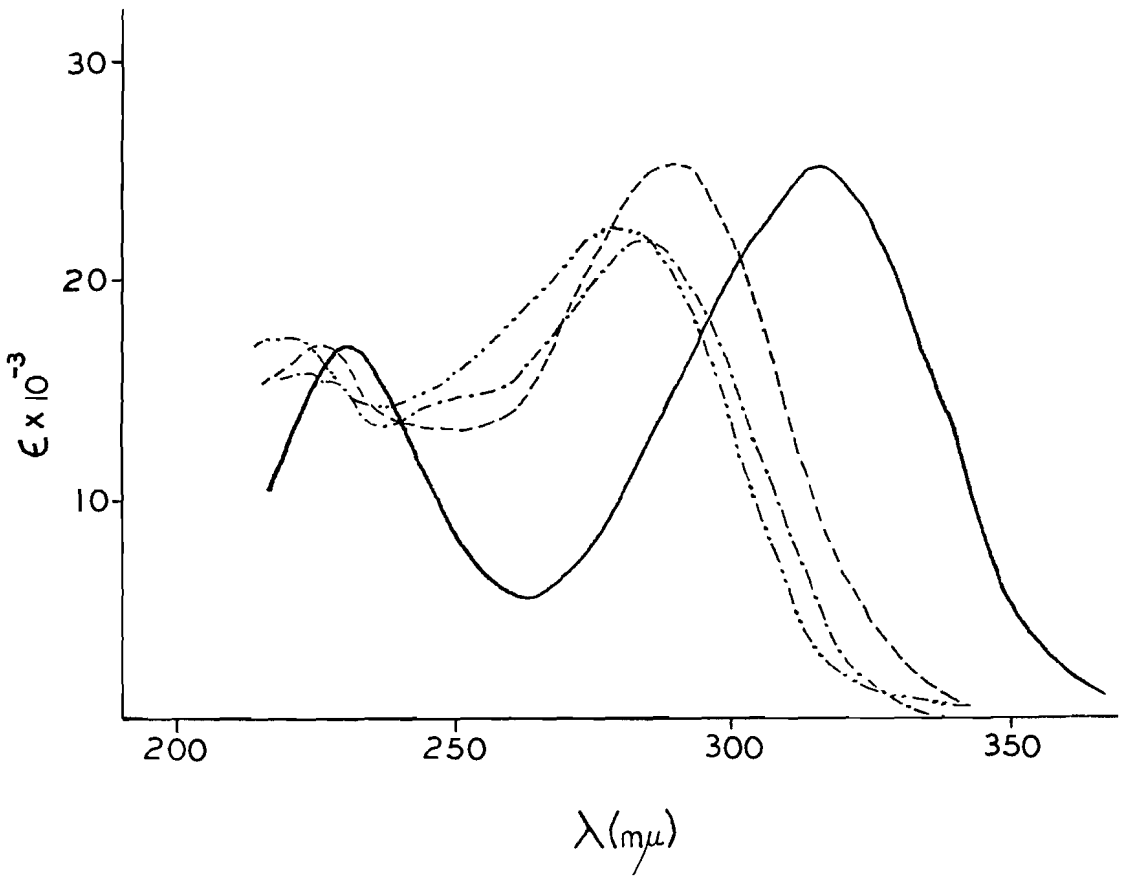

FIG. 1. The electronic spectra of —— 2,6-dibenzylidenecyclohexanone, ----- 2,7-dibenzylidenecycloheptanone, –·–·– 2,8-dibenzylidenecyclooctanone, and –··–··– 2,9-dibenzylidenecyclononanone measured in *n*-hexane solution.

Can. J. Chem. Downloaded from www.nrcresearchpress.com by 210.87.254.105 on 09/05/12
For personal use only.

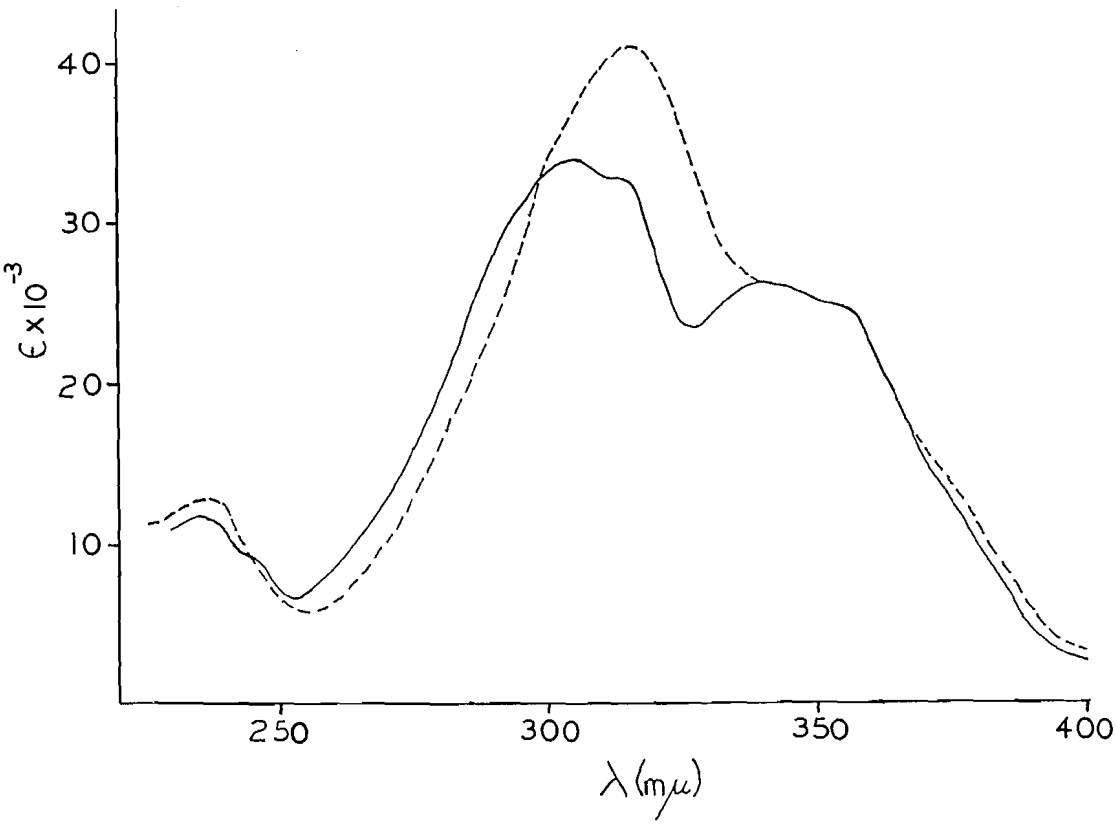

FIG. 2. The electronic spectrum of 2,5-dibenzylidenecyclopent-3-ene-1-one measured in —— *n*-hexane and ---- ethanol solutions.

shift values for the protons in the dibenzylidenecyclanones. The electronic spectra for some of the compounds are shown in Figs. 1 and 2.

The variation of the infrared C=O stretching frequencies of the cyclanones has been studied by various workers (9) who showed that the values reach a minimum when $n = 9$ and then rise with increasing n to approach the value for the open chain ketones (acetone = 1720 cm^{-1}). In the series studied here this frequency decreases for the small ring compounds, increases slightly for $n = 7$ and $n = 8$ and then decreases further. Values for the diarylideneacetone derivatives are lower than those for the cyclic analogues as would be expected. Although the differences are small they are consistent and the intensity variations of the long-wavelength electronic absorption bands are in qualitative accord with them. Such variations would be anticipated from the strain introduced into these systems by the two exocyclic C=C bonds. The high values for the cyclopent-3-enone derivatives reflect the increased '*s*' character of the carbonyl bond in these compounds, relative to the cyclopentanones, resulting from the more rigid geometrical requirements of the unsaturated-ring compounds.

It was suggested by Prelog (7) that some hydrogen bonding may exist in the medium-sized ring ketones between one or more of the intra-annular hydrogen atoms and the carbonyl group. This was considered as a possible reason for the lack of reactivity of cyclodecanone with respect to addition reactions but the effect of hydrogen bonding would lead to only small energy changes and could hardly be responsible entirely for the large rate changes observed. Sutherland (10) has suggested that evidence for hydrogen bonding of this type is found from the position of the first overtone of the C—H stretching vibration. If this is important one would expect that the

Can. J. Chem. Downloaded from www.nrcresearchpress.com by 210.87.254.105 on 09/05/12
For personal use only.

Can. J. Chem. Downloaded from www.nrcresearchpress.com by 210.87.254.105 on 09/05/12
For personal use only.

carbonyl stretching frequency of cyclodecanone would be lower than that of the preceding member of the series. In the case of 2,10-dibenzylidenecyclodecanone it is possible that the constraints imposed upon the system by the three trigonal carbon atoms are such that the molecule takes up a conformation in which the carbonyl oxygen is much nearer to the intraannular hydrogen atoms than in the parent ketone. Hydrogen bonding in this compound would explain the lower infrared absorption frequency and also the failure to reduce it or to form a 2,4-dinitrophenylhydrazone. In both of these reactions the reactant would have great difficulty in approaching the carbonyl group. Further the relative intensities of the C=C and C=O stretching absorptions for 2,10-dibenzylidenecyclodecanone do not obey the rule of Erskine and Waight (11). If no other factor were involved these absorptions should have very similar intensities as in 2,9-dibenzylidenecyclononanone, or the C=O intensity should be greater than the C=C intensity. Hydrogen bonding would reduce the intensity of the carbonyl vibration as is observed, and it would thus seem to be possible in this compound.

The influence of ring size upon the delocalization of the π electrons over the conjugated system is also illustrated in Table I, where it can be seen that the intense long-wavelength band in the electronic spectrum shifts to the blue with increasing n. The effect of increasing ring size is to twist part of the conjugated system until the *effective* conjugation extends over only one-half of the chromophore, i.e. the wavelength of maximum absorption approaches that of monobenzylideneacetone (278 mμ) (12). The long-wavelength band has its maximum value and intensity in the cyclopentanone derivatives and not in the expected cyclohexanone derivatives. This '5-membered ring effect' has been adduced by other workers as indicative of a greater degree of conjugation in these compounds (13). This enhancement of conjugation of the 5-membered ring compounds is also shown by comparison with the corresponding acetone derivatives (Table I).

The spectra of the 2,5-diarylidenecyclopentenones show two distinct bands at long wavelengths, only the lower wavelength band being sensitive to solvent changes and shifting to the blue with decreasing solvent polarity (Fig. 2). This may be explained by consideration of the two π-electron "pathways" within the molecule, i.e. the upper part of the molecule containing the exocyclic conjugation and the carbonyl group giving rise to a solvent sensitive band, and the lower part of the molecule corresponding to *cis*,-*cis*-1,6-diphenylhexatriene giving rise to a solvent independent band similar in shape and position to the long-wavelength band of all-*trans*-1,6-diphenylhexatriene. The decrease in intensity and smearing out of the fine structure on the long-wavelength band corresponding to that of all-*trans*-1,6-diphenylhexatriene results from the introduction of the central *cis*-linkage (14).

From a consideration of Table II it is of interest to note that the chemical shift for the methine protons of 2,6-dibenzylidenecyclohexanone occurs at lower field than that for any other cyclanone derivative. This would be anticipated if the formation of an all-*trans* planar conjugated system within the molecule is favored, the electron withdrawing influence of the carbonyl group thus being maximized.

TABLE II

^{1}H Chemical shifts of dibenzylidenecyclanones (relative to TMS)

Cyclanone ring size	Exocyclic methine proton τ (p.p.m.)	Ring protons α to C=C τ (p.p.m.)*	Remaining cyclanone ring protons τ (p.p.m.)*
5	2.40	6.90	—
6	2.20	7.10	8.24
7	2.70	7.34	8.06
8	2.96	7.23	8.28
9	3.09	7.25	8.40, 8.60
10	2.90	7.14	8.26, 8.53

*Centers of multiplets

For rings where $n > 7$ the non-equivalence of the ring protons, other than those α to the exocyclic double bond, is shown by the asymmetry and eventual splitting of the highest-field absorption. In the spectrum of 2,9-dibenzylidenecyclononanone the ring protons, other than those α to the C=C bonds, give rise to a broad band split into two parts, centered on $\tau = 8.40$ and $\tau = 8.60$, integration showing each part to be due to four protons. This non-equivalence is also shown in the spectrum of 2,10-dibenzylidenecyclodecanone where those ring protons give rise to bands at $\tau = 8.26$ and $\tau = 8.53$. The integration of these bands suggests that each is due to five protons, rather than one group of four

Can. J. Chem. Downloaded from www.nrcresearchpress.com by 210.87.254.105 on 09/05/12
For personal use only.

and one group of six protons. If the carbonyl group is hydrogen bonded to one of the six ring protons then this would be environmentally different from the remainder and its absorption could shift to lower field thus producing the observed spectrum which is equivalent to deshielding of one proton by the anisotropic carbonyl group. Again in agreement with previous arguments the n.m.r. spectrum of cyclodecanone does not support the idea of hydrogen bonding in this compound.

Experimental

General

Melting points were determined using a Koffler hot stage apparatus and are uncorrected.

All compounds were shown to be single substances using thin-layer chromatography.

Infrared spectra were measured on a Perkin–Elmer model 21 spectrometer. Ultraviolet/visible spectra were measured on a Cary 14 spectrometer. Nuclear magnetic resonance spectra were measured in deuteriochloroform on a Varian 100Mc.p.s. spectrometer equipped with a spin decoupler.

Molecular weights were determined in benzene using a 'Mechrolab Inc.' vapor pressure osmometer, average values of at least 3 determinations being taken.

The diarylidene ketones were all prepared in methanolic solution by the standard alkaline condensation procedure as used for the cyclanones where $n = 5$–7 (1). To minimize self-condensation of cinnamaldehyde in the presence of base it was found necessary to add the aldehyde slowly to the alkaline methanolic solution of the ketone, especially for 9- and 10-membered ring ketones. In most cases the yields were extremely low (1–2%) and have not been recorded owing to irreproducibility. Separation of the products was effected by column chromatography, followed by preparative thin-layer chromatography, on silica gel with benzene as eluent. The required product always had the highest R_f value. Some unchanged ketone was recovered in all cases, together with considerable amounts of intractable resinous materials. The dibenzylidene and dicinnamylidene derivatives of the 5-, 6-, and 7-membered ring ketones were prepared as described above (1) and had the melting points shown below. 2,5-Dibenzylidenecyclopentanone, pale-yellow needles (methanol), m.p. 189°. 2,6-Dibenzylidenecyclohexanone, yellow plates (methanol), m.p. 118–119°. 2,7-Dibenzylidenecycloheptanone, pale-yellow needles (methanol), m.p. 107°. 2,5-Dicinnamylidenecyclopentanone, yellow needles (trichloroethylene), m.p. 232–233°. 2,6-Dicinnamylidenecyclohexanone, yellow microcrystals (trichloroethylene), m.p. 181–182°. 2,7-Dicinnamylidenecycloheptanone, yellow microcrystals (trichloroethylene), m.p. 209°. 2,5-Dibenzylidenecyclopent-3-enone (15), lemon-yellow needles (trichloroethylene), m.p. 157°.

2,8-Dibenzylidenecyclooctanone (1)

A strong solution of potassium hydroxide (2 ml) in 1:1 methanol/water was added to a solution of cyclooctanone (3 g) together with excess freshly distilled benzaldehyde in a small volume of methanol. The mixture was warmed and then left to stand 1 h. On addition of water a yellow oil was deposited. This was separated from the solution and dissolved in the minimum volume of methanol. On cooling, white plate-like crystals of 2,8-dibenzylidenecyclooctanone were precipitated (1.75 g) which, on recrystallization from more methanol, had m.p. 111°. 2,4-Dinitrophenylhydrazone – deep red crystals from ethanol, m.p. 193–194°.

Anal. Calcd. for $C_{22}H_{22}O$ (mol.wt., 302): C, 87.40; H, 7.28; Found (mol.wt., 315): C, 87.49; H, 7.50.

2,9-Dibenzylidenecyclononanone was prepared by the general method described above for **1**, but the mixture was refluxed for 3 h, extracted with ether, dried, and chromatographed (benzene on silica gel). Recrystallization of the product from methanol gave white needles, m.p. 80°. 2,4-Dinitrophenylhydrazone – red crystals from ethanol, m.p. 154–155°.

Anal. Calcd. for $C_{23}H_{24}O$: C, 87.34; H, 7.59. Found: C, 87.13; H, 7.69.

2,10-Dibenzylidenecyclodecanone was also prepared as described for **1**. Recrystallization of the precipitated oil from pentane gave white plates, m.p. 108°.

Anal. Calcd. for $C_{24}H_{26}O$ (mol.wt., 330): C, 87.28; H, 7.88. Found (mol.wt., 340): C, 87.25; H, 7.82.

2-(α-Hydroxybenzyl) Cyclopentadecanone was obtained from the attempted preparation of the dibenzylidene derivative as described above for **1**. Recrystallization of the product from methanol gave white needles, m.p. 138°.

Anal. Calcd. for $C_{22}H_{34}O_2$: C, 80.00; H, 10.30. Found: C, 80.80; H, 10.45.

The infrared spectrum showed strong bands at 3360 and 1705 cm^{-1} attributable to the OH and CO stretching vibrations respectively, but no C=C stretching frequency was observable.

The ^1H nuclear magnetic resonance spectrum showed a doublet at $\tau = 7.15$, superimposed upon a triplet; a double doublet at $\tau = 5.28$; a multiplet centered on $\tau = 7.65$; a multiplet centered on $\tau = 8.75$ and a multiplet centered on $\tau = 2.70$. On deuteration the doublet at $\tau = 7.15$ disappears and the double doublet at $\tau = 5.28$ is resolved into one doublet. The integrated areas are in accord with the assigned structure.

2,8-Dicinnamylidenecyclooctanone (2)

Excess freshly distilled cinnamaldehyde, containing a little dissolved cyclooctanone, was added slowly, with stirring, to a solution of cyclooctanone (1 g) in methanol containing 1 ml of a strong solution of potassium hydroxide in 1:1 methanol/water solution. The mixture was allowed to stand for 4 h, any precipitated cinnamic acid filtered off, and the filtrate extracted with ether. Chromatography of the residue remaining after evaporation of the ether, using benzene on silica gel, yielded several products, that having the highest R_f being collected. Recrystallization from methanol of the solid obtained after removal of benzene gave yellow needles, m.p. 133°. 2,4-Dinitrophenylhydrazone – red crystals from ethanol, m.p. 145°.

Anal. Calcd. for $C_{26}H_{26}O$: C, 88.14; H, 7.35. Found: C, 88.00; H, 7.37.

2,9-Dicinnamylidenecyclononanone was prepared as described above for **2**, the mixture being allowed to

stand for 8 h. Recrystallization of the product from methanol gave pale-yellow needles, m.p. 147°. 2,4-Dinitrophenylhydrazone – red crystals from methanol, m.p. 140°.

Anal. Calcd. for $C_{27}H_{28}O$: C, 88.04; H, 7.66. Found: C, 88.30; H, 7.67.

2,5-Dicinnamylidenecyclopent-3-enone

This compound was prepared by the method described by Chapman and Pasto (15) for the dibenzylidene compound, using 2,5-dicinnamylidenecyclopentanone as starting material. The product was obtained as fine orange needles which, on recrystallization from trichloroethylene, had m.p. 228°. 2,4-Dinitrophenylhydrazone – black crystals from ethanol, m.p. 252°.

Anal. Calcd. for $C_{23}H_{18}O$: C, 89.52; H, 5.81. Found: C, 89.18; H, 6.00.

Acknowledgments

We are most grateful to Dr. E. C. Waight for the gift of samples of cyclononanone and cyclodecanone semicarbazone and to the Research Fund of the Chemical Society for a grant towards the purchase of chemicals. We also wish to thank the University of Saskatchewan for financial support and facilities for part of this work; Dr. A. S. Perlin and Mr. M. Mazurek of the Prairie Regional Laboratory, Saskatoon, for nuclear magnetic resonance facilities, and Sir John Cass College for financial support (to B.A.R.).

We are also grateful to the referees for helpful comments.

1. A. I. VOGEL. Practical organic chemistry. Longmans, Green & Co. Ltd. London. 1964. p. 345.
2. R. CORNUBERT, M. DEDEMO, R. JOLY, P. LOUIS, and A. STREBEL. Bull. Soc. Chim. France, **5** [5], 1490 (1938).
3. E. A. BRAUDE, W. F. FORBES, B. F. GOFTON, R. P. HOUGHTON, and E. S. WAIGHT. J. Chem. Soc. 4711 (1957).
4. E. A. BRAUDE and B. F. GOFTON. J. Chem. Soc. 4720 (1957).
5. R. POGGI and V. GUASTALLA. Gazz. Chim. Ital. **61**, 405 (1931).
6. L. RUZICKA, W. BRUGGER, C. F. SEIDEL, and H. SCHINZ. Helv. Chim. Acta, **11**, 496 (1928).
7. V. PRELOG. Pure Appl. Chem. **6**, 545 (1963).
8. H. C. BROWN and K. ICHIKAWA. Tetrahedron, **1**, 221 (1957).
9. TH. BÜRER and H. S. GÜNTHARD. Helv. Chim. Acta, **39**, 356 (1956).
10. G. B. B. M. SUTHERLAND. Discussions Faraday Soc. **1**, 274 (1950).
11. R. L. ERSKINE and E. S. WAIGHT. J. Chem. Soc. 3425 (1960).
12. R. E. LUTZ, C. R. BAUER, and R. H. JORDAN. J. Am. Chem. Soc. **72**, 4300 (1950).
13. S. V. TSUKERMAN, L. A. KUTULYA, and V. F. LAVRUSHIN. Zh. Obshch. Khim. **34**, 3597 (1964).
14. L. ZECHMEISTER and A. POLGAR. J. Am. Chem. Soc. **65**, 1522 (1943).
15. O. L. CHAPMAN and D. J. PASTO. J. Org. Chem. **24**, 120 (1959).

Can. J. Chem. Downloaded from www.nrcresearchpress.com by 210.87.254.105 on 09/05/12
For personal use only.

Synthesis of 6-chloro-9-(6′-deoxy-3′-*C*-methyl-2′,3′,4′-tri-*O*-methyl-β-D-allopyranosyl)purine: a branched-chain sugar nucleoside

G. B. HOWARTH, W. A. SZAREK, AND J. K. N. JONES
Department of Chemistry, Queen's University, Kingston, Ontario

Received June 13, 1968

The preparation of 6-deoxy-3-*C*-methyl-2,3,4-tri-*O*-methyl-D-allopyranose (**7**), a branched-chain sugar with the same constitution as nogalose from the antibiotic nogalamycin, is described. Condensation of the 1-*O*-acetyl derivative **8** with 6-chloropurine by the fusion method gave 6-chloro-9-(6′-deoxy-3′-*C*-methyl-2′,3′,4′-tri-*O*-methyl-β-D-allopyranosyl)purine (**9**), which to our knowledge is the first synthetic, purine nucleoside containing a branched-chain sugar with a pyranose ring.

Canadian Journal of Chemistry, 46, 3691 (1968)

Can. J. Chem. Downloaded from www.nrcresearchpress.com by 210.87.254.105 on 09/05/12
For personal use only.

Introduction

Some nucleosides of branched-chain sugars have been shown (1–3) to exhibit biological activity, an observation which has stimulated our interest in the chemical synthesis of nucleoside derivatives of this class of sugars. Very recently a new branched-chain sugar, which has been given the trivial name nogalose, was obtained (4) from nogalamycin, an antibiotic highly active against gram-positive bacteria and KB cells *in vitro*. The structure of nogalose, exclusive of stereochemistry, was shown to be that of a 6-deoxy-3-*C*-methyl-2,3,4-tri-*O*-methyl-aldohexopyranose. We report now the preparation of 6-deoxy-3-*C*-methyl-2,3,4-tri-*O*-methyl-D-allopyranose (**7**), a sugar with the same constitution as nogalose,[1] and its utilization in the synthesis of 6-chloro-9-(6′-deoxy-3′-*C*-methyl-2′,3′,4′-tri-*O*-methyl-β-D-allopyranosyl)purine (**9**) *via* the fusion method (5–7). Compound **9** is to our knowledge the first synthetic, purine nucleoside containing a branched-chain sugar with a pyranose ring.

Results and Discussion

Methyl 4,6-*O*-benzylidene-3-*C*-methyl-2-*O*-*p*-tolylsulfonyl-α-D-allopyranoside (**2**) has been prepared recently in this laboratory (8) by the addition of methylmagnesium iodide to methyl 4,6-*O*-benzylidene-2-*O*-*p*-tolylsulfonyl-α-D-*ribo*-hexopyranosid-3-ulose (**1**). Compound **2** was heated with sodium methoxide to give methyl 4,6-*O*-benzylidene-3-*C*-methyl-α-D-allopyranoside (**3**). This derivative has been obtained also in low yield as a side-product of the Grignard reaction. The benzylidene ring in compound **3** was opened by treatment with *N*-bromosuccinimide in boiling carbon tetrachloride (9) to give methyl 4-*O*-benzoyl-6-bromo-6-deoxy-3-*C*-methyl-α-D-allopyranoside (**4**). When compound **4** was heated with lithium aluminium hydride in tetrahydrofuran at reflux temperature, debromination and debenzoylation occurred to give an almost quantitative yield of the 6-deoxy triol **5**. Methylation of **5** with dimethyl sulfate and sodium hydroxide in tetrahydrofuran afforded methyl 6-deoxy-3-*C*-methyl-2,3,4-tri-*O*-methyl-α-D-allopyranoside (**6**), which was converted to the free sugar (**7**) by acid-catalyzed hydrolysis. A crystalline acetate (**8**) was obtained, and was assigned the β-D configuration by nuclear magnetic resonance (n.m.r.) spectroscopy.

Attempts to obtain a glycosyl halide derivative of **7** by some conventional procedures were unsuccessful. Treatment of either the glycoside **6** or the acetate **8** with hydrogen bromide in acetic acid or hydrogen chloride in methylene chloride resulted in the formation of tarry intractable materials.

Condensation of 1-*O*-acetyl-6-deoxy-3-*C*-methyl-2,3,4-tri-*O*-methyl-β-D-allopyranose (**8**) with 6-chloropurine was achieved by fusing an intimate mixture of the two compounds in the presence of a catalytic amount of *p*-toluenesulfonic acid or chloroacetic acid at 120° for 15 min. Fractionation of the crude product on silica gel afforded the pure branched-chain sugar nucleoside **9**. Assignment of the β-D anomeric configuration is based on the observation of a large spacing (9 Hz) of the doublet attributable

[1]The published physical properties of nogalose (4) are different from those of compound **7**, so the two compounds differ in configuration.

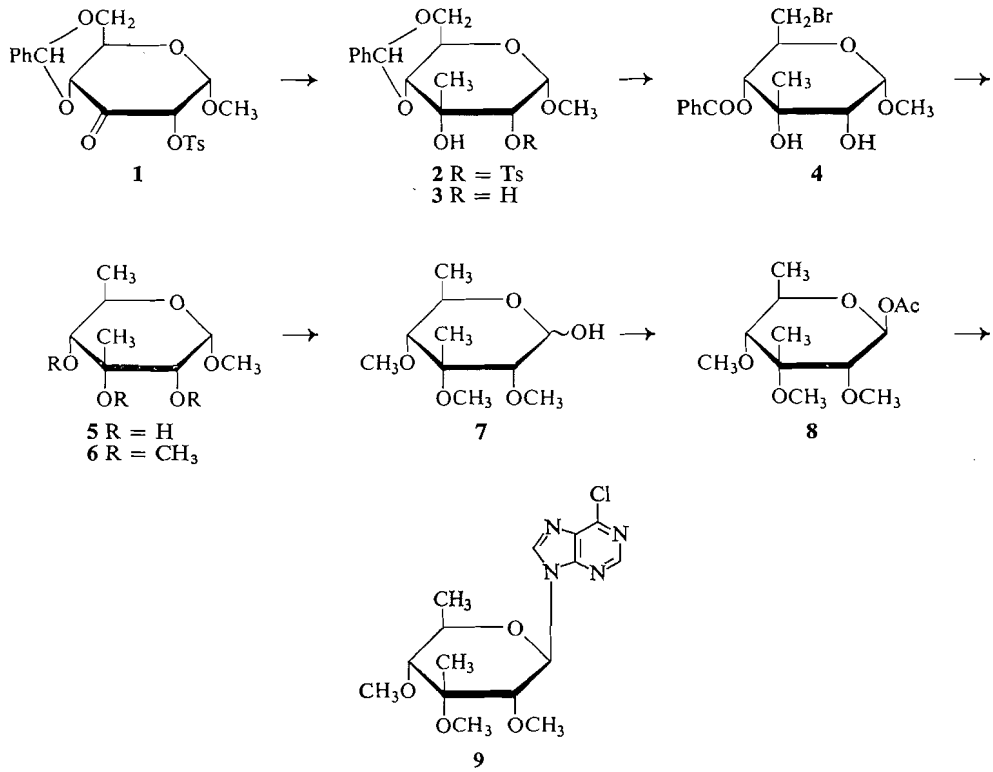

to H-1′ in the n.m.r. spectrum of **9**. The ultraviolet absorption, λ_{max} (Ethanol) 264 mμ (ε 10 000), is indicative of 9-substitution (10).

Experimental

Solutions were concentrated below 50° under reduced pressure. Melting points were determined on a Fisher–Johns melting point apparatus and are uncorrected. Optical rotations were measured with a Bendix ETL-NPL automatic polarimeter, type 143A, at 20 ± 2°. Infrared spectra were measured on a Beckman-IR5A spectrophotometer. Ultraviolet spectra were measured with a Unicam SP.800B spectrophotometer. Nuclear magnetic resonance (n.m.r.) spectra were determined at 60 MHz in chloroform-*d* and tetramethylsilane as internal standard. Paper chromatography was carried out by the descending method on Whatman No. 1 filter paper in the following solvent systems: 6:4:3 (v/v) butan-1-ol:pyridine:water (*a*); butan-1-ol saturated with water (*b*). The sugars were detected by spraying the chromatograms with a 1:1 mixture of vanillin (1% in ethanol) and perchloric acid (3% in water) and heating. Thin-layer chromatography (t.l.c.) was performed, unless otherwise stated, with Silica Gel G as the absorbent, and 2:3 ethyl acetate – petroleum ether (b.p. 60–80°) as the developing solvent. The developed plates were air dried, sprayed with 5% ethanolic sulfuric acid, and heated at about 150°. Gas–liquid chromatography was performed on an F and M, model 402, high-efficiency gas chromatograph employing a flame ionization detector. The conditions were as follows: column I, 5% (w/w) LAC-4R-886 polyester wax, supported on acid washed Chromosorb W (100–120 mesh), operated at 200° and a flow-rate setting of 3.0 at 30 p.s.i. of helium (50 ml/min); column II, 1% (w/w) Apiezon L supported on acid washed DMCS treated Chromosorb W (50–60 mesh), operated at 250° and a flow rate setting of 3.0 at 30 p.s.i. of helium (50 ml/min).

Methyl 4,6-O-Benzylidene-3-C-methyl-2-O-p-tolylsulfonyl-α-D-allopyranoside (2)

A solution of the ketone **1** (11) (4.4 g) in dry benzene (250 ml) was added dropwise to a stirred solution of methylmagnesium iodide (prepared from magnesium (5 g) and methyl iodide (17 ml)) in ether (250 ml) at 0°. After standing at room temperature overnight, the reaction mixture was poured into ammonium chloride solution, and the aqueous layer was extracted with chloroform. Concentration of the dried extracts yielded a syrup which crystallized from chloroform – petroleum ether (b.p. 60–80°). Recrystallization from this solvent mixture gave **2** as white plates (3.6 g, 80%), m.p. 138–139°, $[\alpha]_D$ +45° (*c*, 2.0 in chloroform); λ_{max} (KBr) 2.84 (OH), 6.24, 7.48, 8.49 (sulfonate), 13.2, 14.3 μm (Ph); n.m.r. data: τ 2.0–2.8 (9-proton multiplet, aromatic H's), τ 4.48 (1-proton singlet, benzylidene-methine H), τ 5.2 (1-proton doublet, $J_{1,2}$ 4 Hz, H-1), τ 6.67 (3-proton singlet, OMe), τ 7.58 (3-proton singlet, aromatic Me), τ 8.8 (3-proton singlet, C-3 Me).

Can. J. Chem. Downloaded from www.nrcresearchpress.com by 210.87.254.105 on 09/05/12
For personal use only.

Can. J. Chem. Downloaded from www.nrcresearchpress.com by 210.87.254.105 on 09/05/12
For personal use only.

Anal. Calcd. for $C_{22}H_{26}O_8S$: C, 58.7; H, 5.8; S, 7.1. Found: C, 58.7; H, 5.8; S, 7.3.

Methyl 4,6-O-Benzylidene-3-C-methyl-α-D-allopyranoside (3)

A solution of the sulfonate (**2**) (10 g) in dry methanol (200 ml) containing sodium (2 g) was heated at reflux temperature for 24 h. Thin-layer chromatography (t.l.c.) showed the presence of a compound with R_f 0.13, and the absence of starting material, R_f 0.37. The product was isolated in the usual manner, and obtained from chloroform – petroleum ether (b.p. 60–80°) in crystalline form (5.5 g, 82%), m.p. 210–212°, $[\alpha]_D$ +95° (*c*, 0.3 in chloroform); λ_{max} (Nujol) 2.9, 2.98 (OH), 13.2, 14.2 μm (Ph), no absorption attributable to sulfonate; n.m.r. data: τ 2.5–2.8 (5-proton multiplet, Ph), τ 4.42 (1-proton singlet, benzylidene-methine H), τ 5.24 (1-proton doublet, $J_{1,2}$ 4 Hz, H-1), τ 6.5 (3-proton singlet, OMe), τ 8.6 (3-proton singlet, C-3 Me).

Anal. Calcd. for $C_{15}H_{20}O_6$: C, 60.8; H, 6.8. Found: C, 60.7; H, 6.7.

Methyl 4-O-Benzoyl-6-bromo-6-deoxy-3-C-methyl-α-D-allopyranoside (4)

A solution of compound **3** (4 g) and *N*-bromosuccinimide (2.61 g) in carbon tetrachloride (350 ml) containing barium carbonate (12 g) was heated at reflux temperature with vigorous mechanical stirring for 1 h. The reaction mixture was filtered, and the filtrate concentrated to a pale-yellow syrup, which was chromatographed on silica gel with 2:3 ethyl acetate – petroleum ether (b.p. 60–80°) as eluent. Compound **4** was obtained as a homogeneous syrup (4.5 g, 88%); R_f 0.13 (t.l.c.); λ_{max} (Film) 5.8 (OBz), 6.21, 14.0 μm (Ph); n.m.r. data: τ 1.8–2.0, 2.45–2.75 (multiplets, 5 protons, Ph), τ 5.15 (1-proton doublet, $J_{1,2}$ 4 Hz, H-1), τ 6.5 (3-proton singlet, C-1 OMe), τ 8.75 (3-proton singlet, C-3 Me).

Anal. Calcd. for $C_{15}H_{19}O_6Br$: C, 48.0; H, 5.1; Br, 21.4. Found: C, 48.2; H, 5.0; Br, 21.6.

Methyl 6-Deoxy-3-C-methyl-α-D-allopyranoside (5)

A mixture of compound **4** (1.5 g) and lithium aluminium hydride (2 g) in tetrahydrofuran (100 ml) was heated at reflux temperature for 6 h. The product was isolated in the usual manner as a syrup which appeared to be predominantly one compound by t.l.c., R_f 0.3 (ethyl acetate). Compound **5** was obtained, by chromatography on silica gel with ethyl acetate as eluent, as a homogeneous syrup (0.710 g, 94%); λ_{max} (Film) 2.8–2.9 μm (OH), no absorption attributable to benzoate; n.m.r. data τ 5.3 (1-proton doublet, $J_{1,2}$ 4 Hz, H-1), τ 6.6 (3-proton singlet, C-1 OMe), τ 7.0 (1-proton doublet, $J_{4,5}$ 9 Hz, H-4), τ 8.7 (3-proton singlet, C-3 Me), τ 8.7 (3-proton doublet, *J* 6 Hz, C-5 Me).

Methyl 6-Deoxy-3-C-methyl-2,3,4-tri-O-methyl-α-D-allopyranoside (6)

Dimethyl sulfate (50 ml) was added dropwise with stirring to a slurry of **5** (2.8 g) and finely powdered sodium hydroxide (60 g) in tetrahydrofuran (200 ml). After the mixture was stirred at ambient temperature overnight, aqueous ammonia was added and the resulting solution extracted with chloroform. Concentration of the dried extracts afforded a mobile liquid, R_f 0.5 (t.l.c., ethyl acetate). Distillation gave an analytically pure product (2.5 g, 71%), b.p. 80–85° (0.05 mm), $[\alpha]_D$ +131° (*c*, 0.3 in chloroform); n.m.r. data: τ 5.28 (1-proton doublet, $J_{1,2}$ 4 Hz, H-1), τ 5.7–6.2 (1-proton multiplet, H-5), τ 6.5 (3-proton singlet, C-1 OMe), τ 6.6, 6.62 (6-proton and 3-proton singlets, C-2, C-3, and C-4 OMe's), τ 7.05 (1-proton doublet, $J_{2,1}$ 4 Hz, H-2), τ 7.49 (1-proton doublet, $J_{4,5}$ 9 Hz, H-4), τ 8.55 (3-proton singlet, C-3 Me), τ 8.74 (3-proton doublet, *J* 6 Hz, C-5 Me).

Anal. Calcd. for $C_{11}H_{22}O_5$: C, 56.5; H, 9.4. Found: C, 56.3; H, 9.4.

6-Deoxy-3-C-methyl-2,3,4-tri-O-methyl-D-allose (7)

A solution of the glycoside (0.5 g) in ethanol (3 ml) and 2 *N* hydrochloric acid (10 ml) was heated at 90° for 2 h. The solution was neutralized with Duolite A-4 (OH^-) ion-exchange resin and concentrated to a syrup (380 mg, 80%), $[\alpha]_D$ +28° (*c*, 2.6 in methanol); λ_{max} (Film) 2.9 μm (OH); n.m.r. data: τ 4.98 (1-proton doublet, $J_{1,2}$ 8 Hz, H-1), τ 5.7–6.2 (1-proton multiplet, H-5), τ 6.4, 6.5, 6.6 (3-proton singlets, C-2, C-3, and C-4 OMe's), τ 7.3 (1-proton doublet, $J_{2,1}$ 8 Hz, H-2), τ 7.4 (1-proton doublet, $J_{4,5}$ 9 Hz, H-4), τ 8.58 (3-proton singlet, C-3 Me), τ 8.74 (3-proton doublet, *J* 6 Hz, C-5 Me).

Paper chromatography of the free sugar showed it to be homogeneous with $R_{Rhamnose}$ 2.8 in solvent *a* and 2.98 in solvent *b* (pink spot which changed to a stable deep-blue on standing).

1-O-Acetyl-6-deoxy-3-C-methyl-2,3,4-tri-O-methyl-β-D-allose (8)

A solution of **7** (250 mg) in pyridine (3 ml) and acetic anhydride (2 ml) was heated at 90° for 15 min. The reaction was poured into water, and the product isolated in the usual manner. The crude crystalline product consisted of a 1:5 mixture of α and β anomers (n.m.r.). Pure β anomer was obtained by recrystallization from petroleum ether – pentane (210 mg, 70%), m.p. 88–89°, $[\alpha]_D$ −6° (*c*, 2.3 in ethyl acetate); λ_{max} (KBr) 5.70 μm (OAc); n.m.r. data: τ 4.1 (1-proton doublet, $J_{1,2}$ 8 Hz, H-1), τ 5.85–6.35 (1-proton multiplet, H-5), τ 6.47, 6.57 (6-proton and 3-proton singlets, C-2, C-3, and C-4 OMe's), τ 7.15 (1-proton doublet, $J_{2,1}$ 8 Hz, H-2), τ 7.4 (1-proton doublet, $J_{4,5}$ 9 Hz, H-4), τ 8.9 (3-proton singlet, OAc), τ 8.55 (3-proton singlet, C-3 Me), τ 8.74 (3-proton doublet, *J* 6 Hz, C-5 Me). Gas–liquid chromatography (column I) showed a single peak with a retention time of 0.46 relative to erythritol tetraacetate.

Anal. Calcd. for $C_{12}H_{22}O_6$: C, 55.0; H, 8.4. Found: C, 55.0; H, 8.5.

6-Chloro-9-(6'-deoxy-3'-C-methyl-2',3',4'-tri-O-methyl-β-D-allopyranosyl)purine (9)

A thoroughly ground mixture of compound **8** (25 mg), 6-chloropurine (16 mg), and a trace (ca. 0.5 mg) of *p*-toluenesulfonic acid was heated in an oil bath at 120°. When the mixture began to melt, it was put under vacuum (0.05 mm) and the heating continued at the same temperature for an additional 10 min. The black solid residue was extracted thoroughly with hot ethyl acetate and the extracts concentrated to a pale-yellow syrup (30 mg) after treatment with carbon. Thin-layer chromatography showed the presence of a predominant component with R_f 0.15, and several components present in smaller amounts. Preparative t.l.c. on silica gel, with 2:3 ethyl

acetate – petroleum ether (b.p. 60–80°) as the developing solvent, gave this component as a homogeneous glass (15 mg), R_f 0.55 (t.l.c., ethyl acetate); gas–liquid chromatography (column II) showed a single peak with a retention time of 1.8 min; $[\alpha]_D$ −25° (*c*, 0.1 in ethanol); λ_{max} (Film) 3.25 (aromatic C—H), 6.25, 6.4, 6.7 μm (purine ring); λ_{max} (Ethanol) 264 mμ (ε 10 000); n.m.r. data: τ 1.2, 1.7 (1-proton singlets, H-8 and H-2), τ 4.05 (1-proton doublet, $J_{1',2'}$ 9 Hz, H-1′), τ 5.7–6.1 (1-proton multiplet, H-5′), τ 6.26 (1-proton doublet, $J_{2',1'}$ 9 Hz, H-2′), τ 6.41, 6.48, 7.03 (3-proton singlets, C-2′, C-3′, and C-4′ OMe's), τ 7.06 (1-proton doublet, $J_{4',5'}$ 9 Hz, H-4′), τ 8.45 (3-proton singlet, C-3′ Me), τ 8.7 (3-proton doublet, *J* 6 Hz, C-5′ Me). Proton assignments were made with the aid of spin decoupling.

Anal. Calcd. for $C_{15}H_{21}O_4N_4Cl$: C, 50.6; H, 5.9; N, 15.7. Found: C, 50.7; H, 6.1; N, 15.4.

Acknowledgments

The authors thank the National Research Council of Canada for financial support of this research. Some of the nuclear magnetic resonance spectra were determined at the Royal Military College, Kingston, Ontario, and we are indebted to Dr. D. G. M. Diaper for the use of the spectrometer.

1. E. Walton, S. R. Jenkins, R. F. Nutt, M. Zimmerman, and F. W. Holly. J. Am. Chem. Soc. **88**, 4524 (1966).
2. R. F. Nutt and E. Walton. J. Med. Chem. **11**, 151 (1968).
3. R. F. Nutt, M. J. Dickinson, F. W. Holly, and E. Walton. J. Org. Chem. **33**, 1789 (1968).
4. P. F. Wiley, F. A. Mackellar, E. L. Caron, and R. B. Kelly. Tetrahedron Letters, No. 6, 663 (1968).
5. T. Sato, T. Simadate, and Y. Ishido. Nippon Kagaku Zasshi, **81**, 1440, 1442 (1960).
6. Y. Ishido and T. Sato. Bull. Chem. Soc. Japan, **34**, 347, 1374 (1961).
7. M. J. Robins, W. A. Bowles, and R. K. Robins. J. Am. Chem. Soc. **86**, 1251 (1964).
8. G. B. Howarth, W. A. Szarek, and J. K. N. Jones. To be published.
9. S. Hanessian. Carbohydrate Res. **2**, 86 (1966); Advan. Carbohydrate Chem. **21**, 143 (1966); G. B. Howarth, W. A. Szarek, and J. K. N. Jones. Carbohydrate Res. **7**, 284 (1968).
10. E. E. Leutzinger, W. A. Bowles, R. K. Robins, and L. B. Townsend. J. Am. Chem. Soc. **90**, 127 (1968).
11. B. R. Baker and D. H. Buss. J. Org. Chem. **30**, 2304 (1965).

Can. J. Chem. Downloaded from www.nrcresearchpress.com by 210.87.254.105 on 09/05/12
For personal use only.

Can. J. Chem. Downloaded from www.nrcresearchpress.com by 210.87.254.40 on 09/05/12
For personal use only.

Reaction of chromyl chloride with some olefins. II. The oxidation of tetraarylethylenes[1]

A. L. GATZKE[2] AND R. A. STAIRS[3]
Queen's University, Kingston, Ontario
AND
D. G. M. DIAPER
Royal Military College, Kingston, Ontario

Received July 16, 1968

Chromyl chloride oxidation of tetraphenylethylene results in a novel cyclization reaction giving 9,10-diphenylphenanthrene in high yield. Some cyclization between geminal phenyl groups and cleavage of the olefinic bond occurs as evidenced by the presence of fluorenone and benzophenone as minor products. Polynuclear hydrocarbons such as 1,1′-binaphthyl and *o*-terphenyl which can be cyclized by Lewis acids are unreactive towards chromyl chloride. The observation of rotation about the central bond of a substituted tetraphenylethylene and of retardation of cyclization by substituent chlorine suggest that the oxidative cyclization proceeds by initial electrophilic attack at the olefinic bond to give a carbonium ion.

Canadian Journal of Chemistry, 46, 3695 (1968)

Introduction

Our previous work (1) has shown that the main reaction of chromyl chloride with aliphatic and alicyclic olefins forming chlorohydrins is complicated by reactions involving vinylic and allylic hydrogens. To avoid these complications tetraphenylethylene was chosen as a model compound representing the symmetrically substituted double bond, free from vinylic and allylic hydrogens.

Mosher, Steffgen, and Lansbury (2) have made a detailed study of the chromyl acetate and chromic acid oxidation of tetraarylethylenes in acetic acid solution. These authors interpreted the formation of non-stereospecific epoxides and cyclic carbonates as a result of electrophilic attack of the chromium compound producing the carbonium ion **1**. This intermediate would be capable of free rotation about the central bond giving rise to the non-stereospecific products. These same workers found that chromyl chloride in acetic acid also oxidizes tetraphenylethylene to the epoxide along with what was believed to be the chlorohydrin. Again, substantial amounts of the epoxide were formed along with benzophenone, the major product, when potassium permanganate was used as oxidizing agent (2).

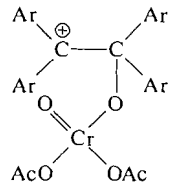

1

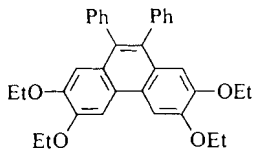

2

In contrast to this result, Gardent (3) observed a ring closure reaction giving the substituted phenanthrene **2** when 1,2-*bis*(3,4-diethoxyphenyl)-1,2-diphenylethylene was oxidized by potassium permanganate in acetic acid. Although Gardent did not offer a detailed mechanism for this reaction, he was of the opinion that the steric effect of the aryl rings and the electronic effect of the ethoxy groups combined to make the ring the favored position of attack.[4]

In this study we report the results of chromyl chloride oxidation of tetraarylethylenes in nonpolar media (carbon tetrachloride and carbon disulfide).

Results

The Reaction of Chromyl Chloride with Tetraphenylethylene

Chromyl chloride was found to react rapidly with tetraphenylethylene, **3**, in carbon tetrachloride solution at 0° to form a brown precipitate as observed with other olefins. The reaction is rapid even at −78°. After filtration, the

[1]For Part I see ref. 1.
[2]Taken in part from the Ph.D. Thesis of A. L. Gatzke submitted to Queen's University. Present address: The Dow Chemical Company, Midland, Michigan 48640.
[3]Present address: Department of Chemistry, Trent University, Peterborough, Ontario.

[4]*Note added in proof* :— C. D. Neuitzescu (22) found 9,10-diphenylphenanthrene to be a major product of the oxidation of 1,1,2,2-tetraphenylethanol by CrO_2Cl_2. It was presumed that dehydration produced oxidation. Experimental details were not given.

precipitate was hydrolyzed to give a surprisingly low yield (approximately 30%) of a yellow oil. The filtrate, which in previous experiments (1, 4) usually contained very little product, was then examined. Evaporation gave a 70% yield of 9,10-diphenylphenanthrene, **4**, m.p. and mixture m.p. 239°. This compound was characterized by elemental analysis, molecular weight determination, and infrared spectral comparison with an authentic sample.

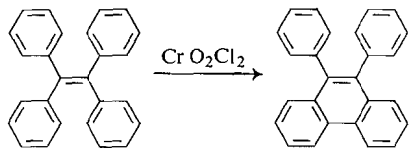

3 4

The conversion of a stilbene into a phenanthrene by oxidation with chromyl chloride is a new and unexpected reaction. Usually reaction between chromium(VI) and an olefin leads to oxidative addition or cleavage. This reaction is examined in more detail in order to define its scope and to gain some insight into its mechanism.

TABLE I

Reaction of tetraphenylethylene with varying molar ratios of chromyl chloride

Initial concentration (mmole)		Final concentration (mmole)			Ratio
3	CrO_2Cl_2	3	4	CrO_2Cl_2	CrO_2Cl_2 Consumed: 3 Consumed
3.00	3.08	1.32	1.21	—	1.79
3.00	6.16	—	1.95	0.26	1.96
3.00*	6.16	—	2.33		2.05

*Carbon disulfide solvent.

Determination of the Stoichiometry

Both the ultraviolet determination of residual tetraphenylethylene after reaction with varying molar ratios of chromyl chloride (Table I) and the calorimetric titration of the reaction according to the method of Stairs (5) (Fig. 1) showed that approximately two moles of chromyl chloride were required to consume one mole of tetraphenylethylene. This result might appear to require that chromium be reduced from (VI) to (V) since the oxidation is a net two electron change. However, iodometric titration of the reduced chromium species in the precipitate showed a net valence state of (IV), which is commonly observed for chromyl chloride oxidations in non-aqueous media. Examination of the minor

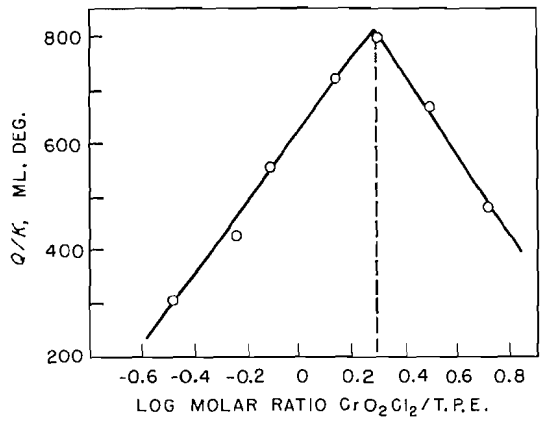

FIG. 1. Calorimetric titration of the reaction of chromyl chloride and tetraphenylethylene in carbon tetrachloride where Q = quantity of heat generated at constant total volume of reagent solutions (calories), and K = specific heat of carbon tetrachloride (0.32 cal. deg.$^{-1}$ mole^{-1}).

products showed the presence of minor quantities of more highly oxidized compounds such as benzophenone, fluorenone, and some highly colored compounds believed to be quinones. These products can account for the consumption of approximately one more mole of chromyl chloride.

It is possible that the observed stoichiometry results from a stepwise reduction of chromium(VI) to chromium(IV) where a chromium(V) intermediate is responsible for producing the minor products. When the reaction was carried out in the presence of an excess of toluene (a compound that reacts relatively slowly with chromyl chloride but may react more rapidly with a chromium(V) species), no induced oxidation of toluene occurred as determined from the yield of **4**. Unfortunately, this negative result is not very meaningful since the reactivity of toluene towards a chromium(V) intermediate is not known.

The Reaction of Chromyl Chloride with Other Aromatic Hydrocarbons

(a) 1,2-Dichlorotetraphenylethane

Since chromyl chloride is known to sometimes cause chlorination (6) and could be expected to show Lewis acid properties, and since 9,10-diphenylphenanthrene can be prepared by the action of stannic chloride on 1,2-dichlorotetraphenylethane (7), the behavior of chromyl chloride towards the chloro compound was investigated. Chromyl chloride was mixed with 1,2-

Can. J. Chem. Downloaded from www.nrcresearchpress.com by 210.87.254.40 on 09/05/12
For personal use only.

Can. J. Chem. Downloaded from www.nrcresearchpress.com by 210.87.254.40 on 09/05/12
For personal use only.

dichlorotetraphenylethane in carbon tetrachloride first at 0° then at 30° but no appreciable reaction occurred. The chloro compound was recovered in 90% yield and the portion that did react did not produce 9,10-diphenylphenanthrene. It was concluded that 1,2-dichlorotetraphenylethane is not an intermediate in the chromyl chloride oxidation of tetraphenylethylene.

(b) 1,1'-Binaphthyl, o-Terphenyl, and Hexaphenylbenzene

A combination of a Lewis acid and an oxidizing agent or a compound combining both these characteristics (as may be anticipated for chromyl chloride) will telomerize benzene and effect "peri" ring closures (8, 9). 1,1'-Binaphthyl and *o*-terphenyl are known to undergo ring closure under these conditions (10, 11). Both these compounds were largely unreactive towards chromyl chloride even after reaction times of two days. No perylene or triphenylene could be detected as products by color tests and ultraviolet spectroscopy. Hexaphenylbenzene is also unattacked by chromyl chloride at 0°. Under forcing conditions benzoic acid was the only product isolated.

(c) cis-Stilbene

The chromyl chloride oxidation of *trans*-stilbene is known to result mainly in cleavage to benzaldehyde (4). A ring closure to form phenanthrene must take place through a *cis* orientation of the rings. To ascertain whether the products were dependent on the isomerism, *cis*-stilbene was subjected to oxidation. The product obtained was mainly benzaldehyde and no phenanthrene or phenanthraquinone (the chromyl chloride oxidation product of phenanthrene) could be detected.

(d) trans-1,2-bis(p-Chlorophenyl)-1,2-diphenylethylene **5**

In order to observe whether an intermediate is formed in the oxidation which allows rotation around the central bond, the *trans*-dichloro substituted tetraarylethylene **5** was oxidized in the usual fashion.[5] The product was purified by column chromatography and recrystallization. The mass spectrum showed a molecular weight of 398 and the presence of two chlorine atoms per mole.

The infrared spectrum showed intense bands at 1010 cm^{-1} and 1090 cm^{-1} indicative of the *p*-chlorophenyl group. The band at 700 cm^{-1}, indicative of the phenyl group, was absent. On this basis the compound was assigned the structure **6**. It is believed some 10–20% of the isomers of **6** are present in the product before recrystallization as evidenced by a moderate intensity infrared band at 700 cm^{-1}, which disappeared on recrystallization.

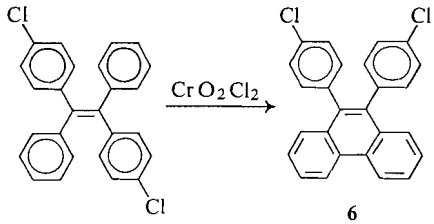

5 6

The nuclear magnetic resonance (n.m.r.) spectrum of recrystallized **6** showed three groups of aromatic proton signals. A multiplet with two major maxima at $\delta = 8.71$ and 8.82 p.p.m. was attributed to the two deshielded protons at positions -4 and -5. The A_2B_2 system of the chlorophenyl groups was upfield (because the rings were perpendicular to the phenanthrene plane) and centered at $\delta = 7.10$ p.p.m. Separation of the two major maxima of this system was 6 c.p.s. (*Cis*-1,2-*bis*(*p*-chlorophenyl)-1,2-diphenylethylene, the starting material, showed two peaks at $\delta = 7.02$ and 7.07 p.p.m., separated by only 2.5 c.p.s.; the larger ring current effect of the phenanthrene system caused the larger separation). Remaining aromatic protons, positions-1,2,3,6,7, and 8, showed as a multiplet at approximately $\delta = 7.5$ p.p.m.

The products of chromyl chloride oxidation of *cis* and *trans*-1,2-*bis*(*p*-chlorophenyl)-1,2-diphenylethylene in other experiments were chromatographed to free them from chromium containing products, starting material and ketones but not recrystallized. These products showed a similar aromatic proton n.m.r. pattern. In particular the profile of the downfield signals was very similar to that of purified **6**, and to that of 9,10-diphenylphenanthrene. Any significant quantity of impurities containing chlorine atoms

[5]Before this experiment could be interpreted it was necessary to assign the configurations of the two geometrically isomeric tetraarylethylenes. The dipole moments of both the high (m.p. 207°) and low (m.p. 151–155°, lit. 156–158°) melting isomers were measured, giving the values $\mu = 1.70$ D and $\mu = 3.24$ D, respectively. The high melting isomer has the low dipole moment, thus establishing it as the *trans* isomer. The low melting impure *cis* isomer contains about 20% of the *trans* isomer and consequently the true dipole moment should be somewhat higher than reported.

Can. J. Chem. Downloaded from www.nrcresearchpress.com by 210.87.254.40 on 09/05/12
For personal use only.

at positions -3 or -6 would greatly affect the splitting of such signals.

Discussion

This one-step stilbene to phenanthrene type cyclization is a simple and rapid method of preparation of 9,10-diarylphenanthrenes. The reaction appears limited to the tetraarylethylenes but the range of compounds investigated was not extensive.

The ortho positions of all aromatic nuclei of tetraphenylethylene are equivalent, therefore one might expect oxidative ring closure to lead successively to 9-benzhydrylidenefluorene and bifluorenylidene by reaction between geminal phenyls and successively to 9,10-diphenylphenanthrene (**4**) and dibenzo[*g*,*p*]chrysene by condensation of vicinal phenyls. The fact that (**4**) is the major product is explicable by conformational considerations. The conformation of tetraphenylethylene in which all four rings are coplanar with each other and with the sp^2 bonds of the ethylene system is energetically highly unfavorable because ortho hydrogen atoms interfere with each other. This interference is serious between geminal phenyls and less so, but still present between vicinal phenyls. The stable conformation, analogous to that of *trans* azobenzene, should have the rings more or less perpendicular to the major plane of the molecule. The upfield location of the n.m.r. peak, δ = 7.08 p.p.m., agrees with this hypothesis. When a pair of rings becomes oxidized, they are constrained into coplanarity and create an energy barrier to rotation of the other pair of rings into coplanarity. This is less serious when 9-benzhydrylidenefluorene is formed than when 9,10-diphenylphenanthrene is formed, moreover the geometry of the five-membered ring of the former relieves some of the steric strain. The latter is therefore less easily oxidized than the former. Both products of geminal phenyl oxidation, 9-benzhydrylidenefluorene and bifluorenylidene, have ethylenic double bonds and are susceptible to further oxidation to benzophenone and fluorenone; the double bond of 9,10-diphenylphenanthrene is part of the aromatic system and less susceptible to oxidative attack. Ring systems corresponding to the removal of more than four ortho protons of tetraphenylethylene have not yet been reported. A study of the oxidation of the *p*,*p*′-dichloro derivatives of tetraphenylethylene, discussed in detail below, showed that attack occurred mainly in the unchlorinated rings.

The results appear to be in best agreement with a mechanism involving initial electrophilic attack of chromyl chloride at the double bond to produce a carbonium ion similar to **1**. A portion of the positive charge rests at the *ortho* positions of the two aromatic rings directly attached to the carbonium ion center. The ring closure can now be effected by electrophilic attack by one of these *ortho* carbons on a vicinal or geminal aromatic ring leading to phenanthrene or fluorenylidene derivatives, respectively. Loss of a proton followed by a 1,4 elimination gives the products. The formation of 9,10-*bis*(*p*-chlorophenyl)-phenanthrene as the major product of the oxidation of *trans*-1,2-*bis*(*p*-chlorophenyl) 1,2-diphenylethylene establishes that rotation about the central bond can take place and that coupling involving an aromatic ring carrying a chlorine atom *meta* to the reaction site is not favored. Both observations taken together tend to support the carbonium ion mechanism. Further support for this mechanism comes from analogous ring closures reported in the literature. For example, both triphenylmethyl cation (12) and the pentaphenylcyclopentadienyl cation (13) undergo ring closure between adjacent phenyl groups. In addition, the formation of 9,10-diphenylphenanthrene from 1,2-dichlorotetraphenylethane catalyzed by stannic chloride (7) would intuitively be expected to proceed in a manner similar to that proposed for the chromyl chloride oxidation of tetraphenylethylene.

The failure of chromyl chloride to duplicate the aluminium trichloride ring closures of 1,1′-binaphthyl, hexaphenylbenzene, and *o*-terphenyl suggests that chromyl chloride does not attack the aromatic ring, or at least not in the same way as the Lewis acid.

A third mechanism for the oxidation that could be considered is an initial step involving the transfer of an electron from **3** to chromyl chloride giving a radical cation. Ring closure between adjacent phenyl groups followed by loss of a proton gives a radical which would be rapidly oxidized to the cation. Loss of a second proton from the cation gives the product. In order for a mechanism such as this to be valid, the radical cation must be capable of rapid rotation about the central double bond to account for the products from **5**. Although a reduced

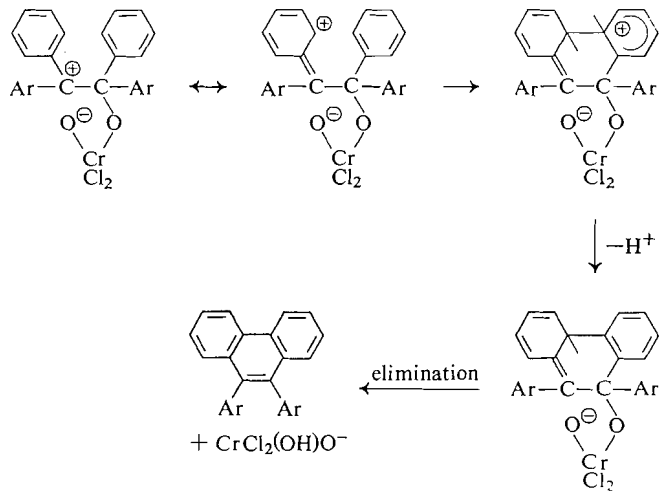

bond order is anticipated for this bond there is no information available that the rotational barrier is sufficiently low to allow rapid rotation on the reaction time scale. A mechanism involving electron transfer as the initial step has been proposed by Dewar, *et al.* (14) for the manganese(III) oxidation of some aromatic compounds. Under similar conditions the manganese(III) acetate oxidation of **3** was very slow giving mainly starting material and some benzophenone after one day at 100°.

Experimental

Materials

Tetraphenylethylene, **3**, was prepared by first converting benzophenone to benzpinacolone by the method of Bachmann (15), then following the procedure of Mosher, *et al.* (2), the ketone was reduced with lithium aluminium hydride and the resulting alcohol dehydrated to give the product, m.p. 223–224°. *cis* and *trans*-1,2-*bis*(*p*-Dichlorophenyl)-1,2-diphenylethylene was synthesized according to the method of Buckles and Meinhardt (16). The *trans* isomer had m.p. 205°, lit. m.p. 205° (2) after fractional crystallization from chloroform–ethanol. The *cis* isomer, m.p. 151–155°, lit. 156–158° (2), could not be completely freed of the *trans* isomer. Bifluorenylidene was synthesized from fluorene as described by Graebe and Stindt (17) and purified through its picrate complex, m.p. 186–187°. 1,2-Dichlorotetraphenylethane was prepared by chlorinating **3** according to the method of Norris, m.p. 180–182° (18). 1,1′-Binaphthyl and *o*-terphenyl were commercial products and were recrystallized before use. *cis*-Stilbene (Aldrich) was used as received.

Dipole moments were determined using a W-T-W "Dipolmeter" Type DM 01.

Reaction of Tetraphenylethylene with Chromyl Chloride

Tetraphenylethylene (4.0 g, 12 mmole) was dissolved in 200 ml of carbon tetrachloride and chromyl chloride (2.1 ml, 26 mmole) in 30 ml of carbon tetrachloride was added dropwise to the stirred solution. The temperature was maintained at 0–5° by means of an ice bath. The reaction mixture was let stir for 5 min after the addition was complete and the brown precipitate, which began to form on the addition of the first few drops of chromyl chloride, was filtered off under suction and washed with carbon tetrachloride. The filtrate was shaken with a 10% sodium bisulfite solution to remove the slight excess of chromyl chloride. Evaporation of the filtrate left a residue of 2.5 g of a material which when recrystallized from chloroform–ethanol (fine white needles) had m.p. 239–240°.

Characterization of 9,10-Diphenylphenanthrene

The product obtained from the filtrate was found not to contain chlorine as shown by a negative Beilstein test and by Schoeniger combustion analysis. The infrared spectrum showed a strong band at 725 cm^{-1} not present in the starting material and no absorption at the carbonyl or hydroxyl stretching frequencies. Osmometry gave a molecular weight of 360.

Anal. Calcd. for $C_{26}H_{18}$: C, 94.5; H, 5.5. Found: C, 94.3; H, 5.4.

An authentic sample of **4** was synthesized from 1,2-dichlorotetraphenylethane by reaction with stannic chloride using the method of Schoepfle and Ryan (7), m.p. 238–239°, lit. m.p. 239° (7). The infrared spectrum of authentic **4** was superimposable with that of the product from the chromyl chloride oxidation of **3**.

Characterization of the Products Obtained from the Brown Precipitate

The reaction of 10 g of tetraphenylethylene with 2 equivalents of chromyl chloride was carried out as outlined earlier. After filtering off with suction and washing with carbon tetrachloride, the brown precipitate was hydrolyzed by gradually stirring it into 400 ml of a 3% aqueous sodium bisulfite solution. The mixture was acidified with hydrochloric acid and extracted with two 100 ml portions of chloroform. The organic layer was washed with water and then extracted with 5% aqueous sodium bicarbonate.

Can. J. Chem. Downloaded from www.nrcresearchpress.com by 210.87.254.40 on 09/05/12
For personal use only.

Can. J. Chem. Downloaded from www.nrcresearchpress.com by 210.87.254.40 on 09/05/12
For personal use only.

Acidification of the bicarbonate layer followed by extraction with ether and evaporation of the dried ether extract yielded a dark colored residue weighing 0.1 g.

The residue from the chloroform extract (3.3 g) was chromatographed on silica gel (alumina was less satisfactory) using petroleum ether – benzene mixtures as eluent. The materials obtained are listed in their order of elution.

(a) 9,10-Diphenylphenanthrene (1.09 g, 33%)

In similar experiments it was found that the amount of this material could be reduced by more extensive washing of the precipitate. Identification was made by m.p. and infrared spectroscopy.

(b) A Mixture of Benzophenone and Fluorenone (0.76 g, 23%)

This mixture or the mixed 2,4-dinitrophenylhydrazones could not be separated by the usual techniques. Identification was established by comparison of the infrared and ultraviolet spectra with that of an authentic mixture. Quantitative infrared analysis showed the mixture was 20% fluorenone.

(c) An Orange Solid (0.85 g, 26%)

The melting point of this solid was 228–230°.

Anal.: Ash 19%; C, 66.9; H, 6.5; O, 7.5. Attempts to recrystallize this material were unsuccessful.

(d) Intractable Dark Tar (0.55 g, 16%)

Determination of the Stoichiometry

(a) Ultraviolet Determination of 3 and 4

After known weights of chromyl chloride and **3** were allowed to react in the usual way the filtrate was evaporated to dryness and the residue weighed. Appropriate aliquots of the residue dissolved in chloroform were evaporated to dryness in a volumetric flask, then redissolved in ethanol and the ultraviolet spectra determined. The weights of **3** and **4** were calculated from the absorbance at 257 mμ and 320 mμ using Vierordt's (19) method. The sum of the calculated weights was in good agreement with the measured weight of the residue showing no interfering impurities.

(b) Determination of Excess Chromyl Chloride

When chromyl chloride was used in excess, the filtrate was extracted with 1% sodium bisulfite to remove chromium. The aqueous extract was acidified and boiled to two-thirds of its original volume. The chromium was reoxidized with sodium peroxide and determined iodometrically after removing excess peroxide by boiling the acidified solution.

(c) Determination of the Average Oxidation State of Chromium in the Brown Precipitate

Chromyl chloride was allowed to react with a slight excess of **3** in carbon tetrachloride. The brown precipitate was hydrolyzed by the addition of 3% sodium hydroxide to the reaction mixture. Iodometric titration of the liberated chromate showed one equivalent of iodine produced per g-atom of chromium present. In a control experiment, iodometric titration of a mixture of a weighed amount of potassium dichromate dissolved in 3% sodium hydroxide and **3** and **4** dissolved in carbon tetrachloride showed three equivalents of iodine produced per g-atom of chromium present.

Reaction of Chromyl Chloride with 1,2-Dichloro-1,1,2,2-tetraphenylethane

1,2-Dichlorotetraphenylethane (2.0 g, 5.0 mmole) was suspended in 200 ml of carbon tetrachloride and chromyl chloride (1.5 ml, 10 mmole) in 50 ml of carbon tetrachloride was added to the stirred solution at 0°. After 2 h no appreciable reaction was noticed. The reaction temperature was raised to 30° for an additional 6 h. Filtration of the cooled reaction mixture led to the recovery of 1.8 g of the starting material. After extracting the filtrate with a 2% sodium bisulfite solution and evaporation of the carbon tetrachloride layer, no 9,10-diphenylphenanthrene could be detected by infrared spectroscopy of the residue.

Reaction of Chromyl Chloride with cis-Stilbene

cis-Stilbene (3.0 g, 17 mmole) was allowed to react with a carbon tetrachloride solution of chromyl chloride (1.5 ml, 18 mmole) in the usual manner. To the reaction mixture was added 150 ml of water containing 3 g of sodium bisulfite and 20 g of ice. The carbon tetrachloride layer was separated and the solvent removed. The product (viscous oil) was distilled under reduced pressure to give about 300 mg of benzaldehyde, b.p. 72°/10 mm, identified by its characteristic odor, positive Schiff test and infrared spectrum. The residue from the distillation was column chromatographed on alumina eluting with petroleum ether, petroleum ether – benzene, and finally benzene–ethanol. The various fractions obtained were examined for color, fluorescence under ultraviolet light, and for their infrared spectra. Phenanthrene or phenanthraquinone were not found among the products.

Reaction of Chromyl Chloride with 1,1'-Binaphthyl

1,1[1]-Binaphthyl (2.0 g, 7.9 mmole) was allowed to react with chromyl chloride (1.3 ml, 16 mmole) in the usual manner. An amorphous material (1.3 g) which had m.p. 95–105° when recrystallized from chloroform–ethanol was obtained from the filtrate. The infrared spectrum of this product was very similar to that of the starting material as was the ultraviolet spectrum.

The ultraviolet spectrum was quite different from that reported for perylene (20), and on treatment of a few milligrams of the product with concentrated sulfuric acid, the characteristic color produced by sulfuric acid and perylene was absent (21).

Reaction of Chromyl Chloride with o-Terphenyl

Chromyl chloride and *o*-terphenyl in carbon tetrachloride failed to undergo any appreciable reaction during two days at room temperature.

Reaction of Chromyl Chloride with Hexaphenylbenzene

Hexaphenylbenzene was prepared from diphenylacetylene using titanium tetrachloride and triisobutylaluminium. The hydrocarbon (1.0 g, 0.19 mmole) in dry carbon tetrachloride (100 ml) was treated with 0.5 g of chromyl chloride (6 mmoles) in carbon tetrachloride (50 ml) at room temperature. There was no precipitation. After one week in the dark at room temperature the solution was boiled, cooled, and shaken with excess of sodium bisulfite solution. After acidification, the water layer was extracted with ether. Solid acid (0.22 g) was obtained having an infrared spectrum similar to that of authentic benzoic acid.

Can. J. Chem. Downloaded from www.nrcresearchpress.com by 210.87.254.40 on 09/05/12
For personal use only.

Reaction of Chromyl Chloride with trans-1,2-bis-(p-Chlorophenyl)-1,2-Diphenylethylene (5)

Chromyl chloride (1.50 ml, 18.6 mmole) in 10 ml carbon tetrachloride was added over 10 min at 20° to **5** (5.0 g, 12.5 mmole) in 80 ml of carbon tetrachloride. After the addition was complete the reaction was let stir an additional 10 min, the mixture filtered, and the residue washed with 75 ml of ethanol-free chloroform. The organic layer was evaporated to give a residue of 3.75 g. This material (1.13 g) was chromatographed on silica gel initially using as eluent 10% benzene in hexane and finally increasing solvent polarity to 15:15:70 chloroform:benzene:hexane. The product was resolved into two main bands. The first band was identified as starting material through comparison of the infrared spectra (m.p. and m.m.p. 205°). A fraction comprising part of the second band was recrystallized twice from chloroform–ethanol giving a compound m.p. 255°. The mass spectrum showed this compound had a molecular weight of 398 and contained two chlorine atoms. The infrared spectrum showed sharp intense bands at 1010 and 1090 cm^{-1} (*p*-chlorophenyl) and no band at 700 cm^{-1} (phenyl). Infrared spectra of the crude fractions showed a moderate intensity band at 700 cm^{-1} which diminished in relative intensity with elution volume. Infrared bands associated exclusively with starting material and *p*-chlorobenzophenone were absent from these fractions. On this basis, the second chromatographic band is composed of **6** with some 10–20% of its isomers. The overall distribution of organic material from the reaction was as follows: recovered starting material, 28%; **6** and isomers, 48%; material associated with the brown precipitate, 26%.

Reaction of Chromyl Chloride with Bifluorenylidene

The addition of a solution of chromyl chloride (1.5 g, 18 mmole) in carbon tetrachloride (10 ml) to bifluorenylidene (3.0 g, 9 mmole) in carbon tetrachloride (75 ml) at room temperature resulted in the rapid formation of a brown precipitate. Work-up of the reaction mixture in the usual fashion followed by chromatography of the product on alumina gave fluorenone in 45% yield. Two other products in lower yield were not identified.

Reaction of Mn(III) Acetate with Tetraphenylethylene

Mn(III) acetate (1.6 g, 6.9 mmole) was allowed to react with **3** (1.0 g, 3.1 mmole) in glacial acetic acid at 100° for one day. The brown solution was evaporated to dryness and the residue dissolved in a mixture of chloroform and water. The infrared spectrum of the residue from the chloroform layer indicated the presence of mainly the starting material, **3**, and some benzophenone.

Mn(III) acetate and **3** failed to give any appreciable reaction in carbon tetrachloride or methylene chloride possibly because of the low solubility of the salt.

Acknowledgments

The financial support of the National Research Council of Canada and the Defence Research Board is gratefully acknowledged. We wish to thank Miss D. Androsoff, and Officer Cadets R. W. Brookes, R. G. W. Eberle, and R. H. Wall for technical assistance and also R. Kagel and L. Shadoff of the Chemical Physics Research Laboratory of The Dow Chemical Company for the infrared and mass spectral structure determinations of the isomeric 9,10-*bis*-(*p*-chlorophenyl) phenanthrenes.

1. R. A. STAIRS, D. G. M. DIAPER, and A. L. GATZKE. Can. J. Chem. **41**, 1059 (1963).
2. W. A. MOSHER, F. W. STEFFGEN, and P. T. LANSBURY. J. Org. Chem. **26**, 670 (1961).
3. J. GARDENT. Bull. Soc. Chim. France, 1049 (1962).
4. S. J. CRISTOL and K. R. EILAR. J. Am. Chem. Soc. **72**, 4353 (1950).
5. R. A. STAIRS. Can. J. Chem. **38**, 2028 (1960).
6. W. H. HARTFORD and M. DARRIN. Chem. Rev. **58**, 35 (1958).
7. C. S. SCHOEPFLE and J. D. RYAN. J. Am. Chem. Soc. **54**, 3687(1932).
8. P. KOVACIC and A. KYRIAKIS. Tetrahedron Letters, 467(1962).
9. P. KOVACIC and R. M. LANGE. J. Org. Chem. **28**, 968 (1963).
10. P. SCHOLL, C. SEER, and R. WEITZENBOCK. Ber. deut. chem. Ges. **43**, 2202 (1910).
11. C. F. H. ALLEN and F. P. PINGERT. J. Am. Chem. Soc. **64**, 1365 (1942).
12. R. A. BENKESER and W. SCHROEDER. J. Org. Chem. **23**, 1059 (1958).
13. R. BRESLOW and H. W. CHANG. J. Am. Chem. Soc. **83**, 3727 (1961).
14. P. J. ANDRULIS, M. J. S. DEWAR, R. DIETZ, and R. L. HUNT. J. Am. Chem. Soc. **88**, 5473 (1966).
15. W. E. BACHMANN. Organic syntheses. Coll. Vol. II. John Wiley and Sons, Inc., New York. 1943. p.71.
16. R. E. BUCKLES and N. A. MEINHARDT. J. Am. Chem. Soc. **74**, 1175 (1952).
17. C. GRAEBE and H. STINDT. Ann. Chem. **291** 2 (1896).
18. J. F. NORRIS. J. Am. Chem. Soc. **38**, 707 (1916).
19. A. E. GILLAM and E. S. STERN. An introduction to electronic absorption spectroscopy in organic chemistry. Edward Arnold and Co., London. 1954. p.186.
20. E. CLAR. Ber. 1 **65B**, 848 (1932).
21. W. CARRUTHERS and J. W. COOL. J. Chem. Soc. 2047 (1954).
22. C. D. NEUITZESCU. Bull. Soc. Chim. France, 1349 (1968).

Can. J. Chem. Downloaded from www.nrcresearchpress.com by 210.87.254.105 on 09/05/12
For personal use only.

Sur la réduction par $LiAlH_4$ de quelques dérivés de l'hydroxyméthylène-2 triméthyl-3,5,5 cyclohexanone

JEAN-CLAUDE RICHER ET WILLIAM A. MACDOUGALL[1]
Département de Chimie, Université de Montréal, B.P.6128, Montréal, Québec

Reçu le 8 mai 1968

La réduction des éthers *O*- et *S*-butyliques de l'hydroxyméthylène-2 triméthyl-3,5,5 cyclohexanone est examinée. La nature des produits de réduction obtenus après hydrolyse des complexes intermédiaires en milieu alcalin est comparée avec ceux provenant d'une hydrolyse effectuée en milieu acide.

Canadian Journal of Chemistry, 46, 3703 (1968)

Introduction

Alors que Schinz et ses collaborateurs (1, 2) ont suggéré que la réduction par $LiAlH_4$ d'éthers énoliques dérivés d'hydroxyméthylène-2 cyclohexanones suivie d'une hydrolyse des complexes intermédiaires par l'acide sulfurique conduit principalement aux aldéhydes α,β non-saturées, il a pu être mis en évidence dans plusieurs cas (3–6) que de telles réductions conduisent fréquemment à des additions 1,4 de l'hydrure sur l'éther énolique. Dans le cadre de ces travaux il nous apparaissait intéressant d'examiner la nature des produits obtenus lors de la réduction par $LiAlH_4$ d'éthers énoliques (**2***b* et *d*) dérivés de l'hydroxyméthylène-2 triméthyl-3,5,5 cyclohexanone (**2***a*). Les résultats obtenus au cours de cette étude font l'objet du présent travail. Les conclusions auxquelles nous arrivons sont comparées à celles rapportées par Vonderwahl et Schinz (2) pour la réduction par $LiAlH_4$ de l'éther énolique **2***c* très voisin de celui qui a été étudié dans le présent travail.

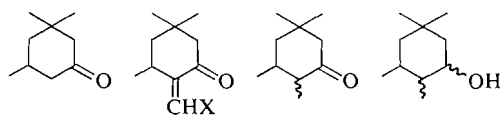

1 **2** **3** **4**

(*a*) X = OH
(*b*) X = OBu
(*c*) X = O*i*Bu
(*d*) X = SBu
(*e*) X = H

Résultats

L'hydroxyméthylène-2 triméthyl-3,5,5 cyclohexanone (**2***a*) est obtenue avec un rendement de 84% par formylation de la triméthyl-3,3,5 cyclohexanone (**1**) selon la méthode de Johnson et Posvic (7); les caractéristiques de ce produit sont conformes à celles déjà publiées (8). La conversion de l'hydroxyméthylène **2***a* en butoxyméthylène-2 triméthyl-3,5,5 cyclohexanone (**2***b*) est effectuée avec un rendement de 81% en suivant les indications de Seifert et Schinz (1) alors que la butylthiométhylène-2 triméthyl-3,5,5 cyclohexanone (**2***d*) est obtenue avec un rendement pratiquement quantitatif en utilisant la méthode de Ireland et Marshall (9). La structure de chacun de ces produits est confirmée par son spectre infrarouge et résonance magnétique nucléaire.

La désulfurisation du thioéther énolique **2***d* effectuée à l'aide du nickel de Raney selon les indications de Ireland et Marshall (9) conduit à un produit qui contiendrait d'après le spectre infra-rouge une forte proportion d'alcools **4** aux côtés de la cétone saturée **3**. L'oxydation de ce mélange brut par l'acide chromique selon la méthode de Brown (10) fournit la tétraméthyl-2,3,5,5 cyclohexanone (**3**) caractérisée sous forme de semicarbazone de p.f. 186–188°; considérant que Kasman et Wright (11) ont obtenu une tétraméthyl-2,3,5,5 cyclohexanone (**3**) qui, d'après son mode de formation, devrait être l'isomère *cis* et dont le p.f. de la semicarbazone est 143–145°, il peut être supposé que le produit que nous avons obtenu est l'isomère *trans*, le plus stable. Le chromatogramme en phase gazeuse de cette cétone montre toutefois la présence d'un autre produit, vraisemblablement l'isomère *cis* qui serait présent à 11%.

La réduction de la butoxyméthylène-2 triméthyl-3,5,5 cyclohexanone (**2***b*) par l'hydrure de lithium et d'aluminium suivant les indications de Vonderwahl et Schinz (2) conduit à un mélange réactionnel dont la composition a été déterminée par chromatographie en phase gazeuse. Ces résultats, rapportés dans le tableau I, indiquent

[1]Les résultats rapportés dans cette communication sont extraits, en partie, du mémoire soumis par M. W. A. MacDougall, à la Faculté des Sciences de l'Université de Montréal, Montréal, en vue de l'obtention du grade de Maître-ès-Sciences (avril 1966).

Can. J. Chem. Downloaded from www.nrcresearchpress.com by 210.87.254.105 on 09/05/12
For personal use only.

toutefois que l'aldéhyde attendu (**5**) est à peine le produit majoritaire dans le milieu réactionnel; le triméthyl-4,4,6 cyclohexène-1 carboxaldéhyde (**5**), est isolé par l'intermédiaire de sa semicarbazone de point de fusion 176–178°, similaire à ceux rapportés pour le même dérivé par Vonderwahl et Schinz (2) et par Ruzicka et ses collaborateurs (12). A la lueur des résultats indiqués dans le tableau I et sachant que la cétone saturée **3** peut provenir soit d'une addition 1,4 d'hydrure (4, 5) sur la méthylène-2 triméthyl-3,5,5 cyclohexanone (**2***e*) formée comme intermédiaire soit par réarrangement en milieu acide (4–6, 13) de l'alcool allylique **6***b*, retrouvé dans le milieu réactionnel, il s'avérait important de déterminer sans ambiguité la nature du précurseur des cétones saturées **3**.

TABLEAU I

Chromatographie en phase gazeuse des produits provenant de la réduction de **2***b* par $LiAlH_4$

Produits	t_R min	Pourcentage	
		Hydrolyse acide	Hydrolyse alcaline
3	15	18	6
4	18	9	4
5	22	56	1
6*b*	41	17	51
6*a*			38*

*Evalué par spectroscopie infra-rouge sur le mélange réactionnel brut.

Afin de vérifier si le traitement par l'acide sulfurique modifie considérablement la nature des produits obtenus, la réduction de l'éther énolique **2***b* par l'hydrure de lithium et d'aluminium a été reprise et les aluminates intermédiaires ont été décomposés en milieu alcalin au lieu d'en milieu acide. Les produits de la réaction ont été distillés sous vide: la fraction principale (36.6% du rendement théorique et p.e. 116–140°/15 mm) dont la composition, telle que déterminée par chromatographie en phase gazeuse, est résumée dans le tableau I contient principalement l'alcool allylique **6***b* isolé par l'intermédiaire de son *p*-nitrobenzoate de p.f. 92.5–93.5°; les propriétés spectrales (i.r. et r.m.n.) de l'autre fraction (23.4% du rendement théorique et p.e.: 132–134°/1.8 mm Hg) correspondent à celles attendues pour le butoxyméthylène-2 triméthyl-3,5,5 cyclohexanol (**6***a*). Le traitement de ce dernier intermédiaire par l'acide sulfurique concentré et de la glace pendant 1 h à −15° conduit avec un rendement de 70% au triméthyl-4,4,6 cyclohexène-1 carboxaldéhyde (**5**) caractérisé par l'intermédiaire de sa semicarbazone de p.f. 174.5–176.5°. Les résultats obtenus signifient donc que la réduction de **2***b* effectuée par une quantité équimoléculaire de $LiAlH_4$ conduit d'une part au complexe (environ 40% du total) résultant d'une addition 1,2 de l'hydrure sur le groupement carbonyle; sa décomposition en milieu alcalin permet d'isoler l'hydroxyéther **6***a*. D'autre part le traitement des intermédiaires en milieu alcalin permet de mettre en évidence la formation du méthylène-2 triméthyl-3,5,5 cyclohexanol (**6***b*) provenant d'une addition 1,4 de l'hydrure sur l'éther énolique **2***b* suivie d'une addition 1,2 de l'hydrure sur la méthylène-2 triméthyl-3,5,5 cyclohexanone (**2***e*) formée comme intermédiaire. Cette dernière observation permet de conclure que peu de tétraméthyl-2,3,5,5 cyclohexanone (**3**) est formée par addition 1,4 d'hydrure sur la cétone non-saturée **2***e*.

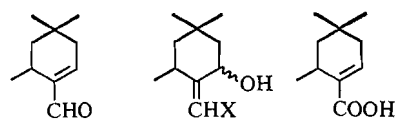

5 **6** **7**

(*a*) X = OBu
(*b*) X = H
(*c*) X = SBu

La réduction par $LiAlH_4$ de la butylthiométhylène-2 triméthyl-3,5,5 cyclohexanone (**2***d*) suivie par une décomposition alcaline des complexes intermédiaires conduit, avec un rendement de 69%, après distillation des produits de la réaction sous pression réduite, à un distillat contenant du soufre et dont le spectre infrarouge indique la présence d'alcools et de produits carbonylés; la composition du mélange réactionnel est résumée dans le tableau II. Une oxydation douce, par l'oxyde d'argent en milieu alcalin, effectuée sur ce mélange permet de transformer l'aldéhyde **5** en acide correspondant **7** et d'isoler une fraction neutre contenant le butylthiométhylène-2 triméthyl-3,5,5 cyclohexanol **6***c* pur à 78%. L'hydrolyse de cet hydroxythioéther **6***c* par l'acide chlorhydrique 10% à reflux, en suivant les indications de Ireland et Marshall (9), conduit avec un rendement de 95% à l'aldéhyde α,β non-saturé (**5**). Le fait que l'hydroxyéther-énolique **6***c* ne se soit pas décomposé par distillation indique que ce produit est relativement

Can. J. Chem. Downloaded from www.nrcresearchpress.com by 210.87.254.105 on 09/05/12
For personal use only.

stable à la chaleur et que la composition indiquée pour le mélange distillé de réduction reflète à peu de choses près la composition de ce mélange avant sa distillation. Les résultats rapportés dans le tableau II indiquent donc que la réduction par $LiAlH_4$ de la butylthiométhylène-2 triméthyl-3,5,5 cyclohexanone (**2***d*) conduit d'une façon prépondérante à une addition 1,2 de l'hydrure sur le groupement carbonyle (94% du total). Ce processus principal serait accompagné d'une faible quantité d'addition 1,4 d'hydrure sur le système conjugué; comme dans le cas précédent, la méthylène-2 triméthyl-3,5,5 cyclohexanone (**2***e*) formée comme intermédiaire serait réduite presque exclusivement par une addition 1,2 de l'hydrure sur le groupement carbonyle et donnerait naissance au méthylène-2 triméthyl-3,5,5 cyclohexanol (**6***b*) observé dans le milieu réactionnel.

TABLEAU II

Chromatographie en phase gazeuse des produits provenant de la réduction de **2***d* par $LiAlH_4$

Produits	t_R(min)*	%
5	7	64
6*b*	12	6
6*c*	28	30

*Analyse effectuée à 170° à l'aide d'une colonne de 2.5 m contenant du Polyester de Craig déposé à 15% sur du Chromosorb P (30–60).

Afin de vérifier les propos de Dreiding et Hartman (13) en ce qui regarde le réarrangement en milieu acide d'alcools allyliques cycliques, le méthylène-2 triméthyl-3,5,5 cyclohexanol (**6***b*) a été traité par l'acide sulfurique dilué à reflux pendant 3 h; le produit réactionnel brut analysé par chromatographie en phase gazeuse contient 83.3% de tétraméthyl-2,3,5,5 cyclohexanone (**3**) caractérisée par l'intermédiaire de sa semicarbazone. Ce résultat, en accord avec les observations précédentes (4–6, 13), confirme une fois de plus la généralité de la transformation d'α-méthylènecyclohexanols en méthylcétones correspondantes sous l'influence d'acides.

Les résultats obtenus au cours du présent travail peuvent être rationalisés à l'aide du mécanisme réactionnel proposé précédemment (4–6). Les proportions d'addition 1,4 sur les méthylènes-2 triméthyl-3,5,5 cyclohexanones substituées sont résumées dans le tableau III; pour fins de comparaison les résultats obtenus précédemment dans d'autres séries sont mis en regard. Il ressort de l'examen de ce tableau que les proportions d'additions 1,4 sur les éthers *S*-butyliques d'hydroxyméthylène-2 cyclanones sont toujours plus faibles que dans le cas des éthers *O*-butyliques correspondants. Cette observation présente beaucoup d'intérêt dans le domaine synthétique.

TABLEAU III

Pourcentages d'addition 1,4 d'hydrures sur des méthylène-2 cyclanones substituées

X=	OBu	SBu	H
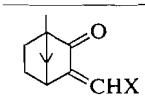	90–95*	23†	40†
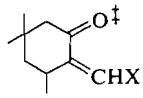	61§	6	7
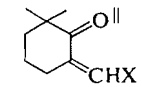	17	8	0

*Tiré de la référence 4.
†Tiré de la référence 5.
‡Présent travail.
§Valeur dérivée des résultats obtenus lors de la décomposition des complexes intermédiaires par hydrolyse alcaline.
||Tiré de la référence 6.

Partie expérimentale

Les spectres infra-rouges des produits ont été pris à l'état pur avec un spectrophotomètre Beckmann, modèle IR-8 à faisceau double. Les chromatographies en phase gazeuse ont été effectuées sur des appareils Burrell (Kromo-Tog K-2) et F & M (modèle 810) dans les conditions indiquées. Les spectres de résonance magnétique nucléaire ont été mesurés sur un spectromètre Varian, modèle A-60; les déplacements chimiques (δ) en parties par million (p.p.m.) sont exprimés par rapport au tétraméthylsilane comme étalon interne. Les spectres ultraviolets ont été pris dans l'éthanol 95% à l'aide d'un appareil Bausch & Lomb, modèle 505. Les indices de réfraction ont été mesurés sur un appareil Zeiss, N° 44061, et les points de fusion ont été pris à l'aide d'un appareil à microscope ("hot stage apparatus" de Reichert, Autriche). Les analyses élémentaires ont été effectuées au laboratoire du Dr. C. Daesslé, Montréal.

Ethers énoliques

Butoxyméthylène-2 triméthyl-3,5,5 cyclohexanone **2***b*

Une solution contenant 8.1 g (0.048 mole) de **2***a* (9), 7.1 g (0.096 mole) de butanol-1, et 100 mg d'acide *p*-toluène sulfonique dans 120 ml de benzène anhydre est chauffée à reflux et l'eau formée au cours de la réaction éliminée par distillation azéotropique. L'éther **2***b* (8.7 g, 81% du rendement théorique) est isolé à la manière habituelle et présente les caractéristiques suivantes: p.e.: 101–104°/0.6 mm Hg; n_D^{25}: 1.4778; i.r.: bandes fortes à

Can. J. Chem. Downloaded from www.nrcresearchpress.com by 210.87.254.105 on 09/05/12
For personal use only.

1665 cm^{-1} (carbonyle insaturé en α, β) et 1575 cm^{-1} (double liaison); r.m.n.: bandes à 4.00 p.p.m. —OCH_2— (triplet) et 7.30 p.p.m., proton vinylique.

Butylthiométhylène-2 triméthyl-3,5,5 cyclohexanone **2***d*

Suivant le même protocole expérimental, 16.2 g (0.1 mole) de **2***a* sont traités par 15.1 g (0.17 mole) de butanethiol-1 et conduisent à 23.8 g (rendement théorique) du thioéther **2***d* qui présente les caractéristiques suivantes: p.e.: 162–172°/3.5 mm Hg; n_D^{23}: 1.5195; i.r.: bandes fortes à 1665 cm^{-1} (carbonyle insaturé en α, β) et 1530 cm^{-1} (double liaison); r.m.n.: bandes à 2.8 p.p.m. —S—CH_2— et 6.85 et 7.45 p.p.m. protons vinyliques *trans* et *cis* par rapport au carbonyle adjacent.

Réduction des éthers énoliques; caractérisation des produits de référence

Tétraméthyl-2,3,5,5 cyclohexanone (3) et cyclohexanols **4**

Le traitement de 6.8 g du thioéther **2***d* par 26 g de nickel de Raney en solution éthanolique (9) conduit à 3.4 g (76% du rendement théorique) d'un produit dans le spectre i.r. duquel des bandes à 3480 cm^{-1} (alcool) et 1705 cm^{-1} (cétone saturée) sont présentes. La C.P.G. de cette fraction à 150° (débit d'hélium 28 ml/min) à l'aide d'une colonne de verre de 2.5 m contenant 15% de Polyester de Craig déposé sur du Chromosorb P 30–60 indique la présente de la cétone **3** (t_R 15 min) et des alcools **4** (t_R 18 min). L'oxydation de ce mélange par la méthode de Brown (10) conduit à 3.1 g (91% du rendement théorique) de la triméthyl-2,3,5,5 cyclohexanone (**4**) qui présente les caractéristiques suivantes: p.e.: 60–65°/11 mm Hg; n_D^{26}: 1.4583; i.r.: bande forte à 1705 cm^{-1} (cétone saturée); C.P.G.: (conditions décrites ci-haut) pics à t_R 11.1 min (89% du total) et t_R 19 min (11% du total et vraisemblablement la cétone *cis*. Ce produit ne disparaît pas lorsque soumis à une nouvelle oxydation). Le traitement de cette cétone par l'acétate de semicarbazide (14) conduit à une semicarbazone de p.f.: 186–188° (six recristallisations d'un mélange éthanol/eau);

Anal. calc. pour $C_{11}H_{21}N_3O$: N, 19.89. Trouvé: 19.93.

Réduction de l'éther **2***b selon les indications de Vonderwahl et Schinz (2)—Triméthyl-4,4,6 cyclohexène-1 carboxaldéhyde (5)*

La réduction (2) de 6.0 g (0.026 mole) de l'éther **2***b* par 1.0 g (0.025 mole) de $LiAlH_4$ est effectuée à reflux pendant 15 min; le mélange est ensuite refroidi à −15° et les complexes intermédiaires décomposés par additions successives de 3.75 ml d'eau, 15 g de glace pilée et 19 ml d'acide sulfurique concentré. Les produits de la réaction sont extraits à l'éther à la manière habituelle; leur distillation conduit à: la première fraction contenant 1 g (17% du rendement théorique) et de p.e.: 35–80°/17 mm Hg contient (d'après la C.P.G.) principalement du butanol-1; la deuxième fraction: 2.0 g (33% du rendement théorique), p.e.: 84–102°/16 mm Hg; n_D^{28}: 1.4696; u.v.: max 231 mμ et log 3.72; i.r.: bandes à 3450 cm^{-1} (hydroxyle), 2700 cm^{-1} (aldéhyde), 1675 cm^{-1} (carboxyle insaturé en α, β) a été analysé par C.P.G. (conditions décrites precédemment); le résultat de cette analyse apparaît dans le tableau I sous l'entête hydrolyse acide. Le traitement de ce mélange par l'acétate de semicarbazide (14) permet d'isoler l'aldéhyde **5** sous forme de semicarbazone de p.f.: 176.6–178° (litt. (12) p.f.: 176–177°).

Réduction de l'éther **2***b avec décomposition alcaline; Préparation et propriétés du butoxyméthylène-2 (6a) et du méthylène-2 (6b) triméthyl-3,5,5 cyclohexanol*

La réduction de 6.0 g (0.026 mole) de l'éther **2***b* par 1 g (0.025 mole) de $LiAlH_4$ est effectuée en suivant les indications décrites dans la section précédente. Les complexes intermédiaires sont décomposées par additions successives de 3.75 ml d'eau et de 100 ml de NaOH 10%. Les produits de la réaction sont extraits par l'éther à la manière habituelle et purifiés par distillation: la première fraction, 0.7 g et p.e.: 42–47/15.5 mm Hg consiste essentiellement en butanol-1; la deuxième fraction, 2.2 g (36.6% du rendement théorique) p.e.: 107–140°/15 mm Hg; n_D^{28}: 1.4638; i.r.: bandes à 3360 cm^{-1} (hydroxyle), 1640 cm^{-1} (double liaison) et 890 cm^{-1} (double liaison exocyclique) a été analysé par C.P.G. (conditions décrites précédemment); les résultats sont compilés dans le tableau I sous l'entête hydrolyse alcaline. Le traitement de cette fraction par le chlorure de *p*-nitrobenzoyle (14) conduit au *p*-nitrobenzoate de l'alcool **6***b*, p.f.: 92.5–93.5° (méthanol/eau); r.m.n.: 4.70 et 4.83 p.p.m. protons vinyliques; 5.58 p.p.m. proton carbinolique et 8.24 p.p.m. protons aromatiques.

La saponification de 4.4 g de ce dérivé conduit à 2.4 g (rendement théorique) de l'alcool **6***b* qui présente les caractéristiques suivantes: p.e.: 97.5–98.5°/10 mm Hg; n_D^{26}: 1.4750; i.r.: bandes à 3360 cm^{-1} (hydroxyle), 1640 cm^{-1} (double liaison) et 890 cm^{-1} (méthylène exocyclique); r.m.n.: 4.10 p.p.m. (proton carbinolique) 4.47 et 4.63 p.p.m. (protons éthyléniques). La troisième fraction, 1.4 g (23.4% du rendement théorique) p.e.: 132–134°/1.8 mm Hg; n_D^{29}: 1.4515; i.r.: bandes à 3530 cm^{-1} (hydroxyle), 1265 cm^{-1} et 1230 cm^{-1} (éther énolique) et 1050 cm^{-1} (éther); r.m.n.: 3.5 p.p.m. —O—CH_2— 4.3 p.p.m. (proton carbinolique) et 4.65 p.p.m. (proton vinylique) présente toutes les caractéristiques prévues pour l'hydroxyéther **6***a*.

Réduction de la butylthiométhylène-2 triméthyl-3,5,5 cyclohexanone (2d); préparation du butylthiométhylène-2 triméthyl-3,5,5 cyclohexanol (6c)

La réduction de 4.8 g (0.020 mole) de **2***d* par 3.2 g (0.080 mole) de $LiAlH_4$ dans l'éther anhydre en suivant les indications décrites dans la section précédente conduit à 3.3 g (69% du rendement théorique) d'un produit p.e.: 78–163°/6 mm Hg; n_D^{23}: 1.5081; i.r.: bandes à 3460 cm^{-1} (hydroxyle), 2700 cm^{-1} (aldéhyde), 1685 cm^{-1} (carbonyle conjugué) et 1630 cm^{-1} (double liaison).

L'analyse de ce produit par C.P.G. (tableau II) permet de remarquer la présence, en plus de l'alcool **6***b* et de l'aldéhyde **5** observés dans les milieux réactionnels précédents, d'un produit de temps de rétention beaucoup plus grand que ceux correspondant aux produits normaux. Une oxydation douce de 2 g de ce mélange par l'oxyde d'argent conduit après l'élimination de la portion acide à 0.3 g d'une fraction neutre de p.e.: 160°/13 mm Hg; n_D^{25}: 1.5104; et qui par fusion alcaline au sodium contient du soufre. En suivant les indications d'Ireland et Marshall (9) 0.3 g de cette fraction neutre est chauffé à reflux avec 1.5 ml d'HCl 10%, 5 ml d'éthanol sous agitation pendant 24 h. Le mélange extrait à la manière habituelle conduit à 0.2 g (67% de la quantité initiale) d'un liquide jaunâtre dont le spectre i.r. montre la présence des bandes caractéristiques de l'aldéhyde insaturé et pour lequel l'analyse par C.P.G. montre la présence d'un produit en prédominance (plus que 95%) ayant un temps de rétention

identique à celui de la triméthyl-4,6,6 cyclohexène-1 carboxaldéhyde.

Stabilité des intermédiaires en milieu acide

Traitement acide du butoxyméthylène-2 triméthyl-3,5,5 cyclohexanol (6a)

Le traitement de 3g d'éther **6a** pendant une heure par un mélange de 3 g de glace pilée et de 4ml d'acide sulfurique concentré maintenu à −15° conduit après extractions à l'éther à la manière habituelle à 2.1 g (70% du rendement théorique) de produits qui, par distillation, livrent le triméthyl-4,6,6 cyclohexène-1 carboxaldéhyde caractérisé sous forme de sa semicarbazone de p.f.: 176.5–178°.

Traitement acide du méthylène-2 triméthyl-3,5,5 cyclohexanol (6b)

En suivant les indications de Dreiding et Hartman (13), 1 g de l'alcool **6b** est chauffé à reflux, sous agitation, pendant trois heures, en présence de 50 ml de H_2SO_4 10%. Les produits (0.9 g, 90% du rendement théorique), isolés à la manière habituelle par extraction à l'éther, sont purifiés par distillation; la C.P.G. indique que la tétraméthyl-2,3,5,5 cyclohexanone (**3**) forme 83.3% du total. Cette cétone est caractérisée sous forme de semicarbazone de p.f.: 185–188.5°.

Remerciements

Les auteurs remercient vivement le Ministère de l'Education de la Province de Québec et le Conseil National de Recherches du Canada pour l'aide financière apportée sous forme de bourse d'étude et d'octrois de recherches.

1. P. SEIFERT et H. SCHINZ. Helv. Chim. Acta, **34**, 728 (1951).
2. R. VONDERWAHL et H. SCHINZ. Helv. Chim. Acta, **35**, 2368 (1952).
3. J. C. RICHER. Thèse de Doctorat. Faculté des Sciences, Université de Montréal (1958).
4. J. C. RICHER et R. CLARKE. Tetrahedron Letters, 935 (1964).
5. J. C. RICHER et C. LAMARRE. Can. J. Chem. **45**, 1581 (1967).
6. J. C. RICHER et J. M. HACHEY. Can. J. Chem. Sous presse.
7. W. S. JOHNSON et H. POSVIC. J. Am. Chem. Soc. **69**, 1361 (1947).
8. L. RUZICKA, H. SCHINZ et C. F. SEIDEL. Helv. Chim. Acta, **23**, 935 (1940).
9. R. E. IRELAND et J. A. MARSHALL. J. Org. Chem. **27**, 1615 (1962).
10. H. C. BROWN et C. P. CARG. J. Am. Chem. Soc. **83**, 2952 (1961).
11. S. KASMAN et C. F. WRIGHT. J. Org. Chem. **17**, 505 (1952).
12. L. RUZICKA, C. F. SEIDEL, H. SCHINZ et M. PFEIFFER. Helv. Chim. Acta, **31**, 422 (1948).
13. A. S. DREIDING et J. H. HARTMAN. J. Am. Chem. Soc. **78**, 1216 (1956).
14. G. PERRAULT. Mémoire de Maîtrise, Université de Montréal (1962).

Can. J. Chem. Downloaded from www.nrcresearchpress.com by 210.87.254.105 on 09/05/12
For personal use only.

Can. J. Chem. Downloaded from www.nrcresearchpress.com by 210.87.254.42 on 09/05/12
For personal use only.

Stéréochimie de l'époxydation du *tert*-butyl-3 cyclohexène

JEAN-CLAUDE RICHER ET CHRISTIAN FREPPEL
Département de Chimie, Université de Montréal, B.P. 6128, Montréal, Québec

Reçu le 2 juillet 1968

Le *tert*-butyl-3 cyclohexène, obtenu par pyrolyse de l'acétate du *tert*-butyl-2 cylcohexanol *cis*, a été transformé en époxyde et les résultats stéréochimiques sont présentés. L'ouverture de ces époxydes par l'hydrure double de lithium et d'aluminium ainsi que par le lithium dans l'éthylamine a aussi été examinée et les résultats obtenus sont discutés.

Canadian Journal of Chemistry, 46, 3709 (1968)

Introduction

A la suite de travaux (1–3) qui nous ont amené à examiner la stéréochimie, de la réaction d'époxydation de doubles liaisons faisant partie de cycles, il nous est apparu intéressant pour fins de comparaison d'examiner la stéréochimie de l'époxydation du *tert*-butyl-3 cyclohexène (**1**). Les résultats obtenus au cours de cette étude font l'objet de la présente communication.

Résultats et Discussion

L'alcène examiné (**1**) a été préparé pratiquement pur par pyrolyse (4, 5) de l'acétate (**2***b*) du *tert*-butyl-2 cyclohexanol-*cis*. Dans une réaction parallèle impliquant la pyrolyse d'un mélange des acétates (**2***b* et **3***b*) des *tert*-butyl-2 cyclohexanols, il a été observé que l'acétate dérivé de l'alcool *trans* (**3***a*) est pyrolysé plus rapidement que l'acétate dérivé de l'alcool *cis* (**2***a*); les résultats obtenus au cours de cette expérience ont aussi permis de confirmer l'observation de Hückel (4) concernant le fait que la pyrolyse de l'acétate **3***b* conduit à un mélange d'alcènes contenant principalement le *tert*-butyl-1 cyclohexène (**4**). Dans leur ensemble les résultats rapportés ici sont en accord avec la généralisation (6) selon laquelle la pyrolyse des acétates est une réaction concertée impliquant une "élimination *cis*" des éléments de l'acide acétique; le fait que la pyrolyse de l'acétate **3***b* soit plus rapide que celle de l'acétate **2***b* et qu'elle conduise à un mélange d'oléfines dans lequel le *tert*-butyl-1 cyclohexène (**4**) est en prédominance sur le produit (**1**) comportant la double liaison la moins substituée mérite toutefois quelques commentaires. Afin d'expliquer l'obtention préférentielle des oléfines les plus substituées au cours d'une *cis* élimination, Barton (7) a suggéré que ce fait pouvait être attribué à une énergie d'activation plus faible pour la rupture d'une liaison carbone–hydrogène tertiaire comparé à secondaire. Cope (8) a toutefois rapporté que la pyrolyse de l'oxyde de la *N*,*N*-diméthylmenthylamine (**7**) conduit à un mélange d'oléfines **8** et **9** dans lequel le produit résultant d'une élimination de l'hydrogène attaché au carbone tertiaire (conduisant à **9**) n'est pas prépondérant; une explication conformationnelle a été présentée pour rationaliser ces résultats. Quoique les observations rapportées ici pour la pyrolyse des acétates **2***b* et **3***b* ne soient pas en contradiction avec la suggestion de Barton, il semble qu'elles peuvent être mieux interprétées à l'aide d'une explication conformationnelle basée sur le concept de la déformabilité du noyau cyclohexanique (9–11). Alors qu'il est admis d'une manière générale que les substituants *cis* (axial–équatorial) ont la possibilité de se rapprocher l'un de l'autre, il apparait toutefois que dans le cas des groupes *tert*-butyle et acétoxyle de **2***b* une telle déformation serait énergiquement

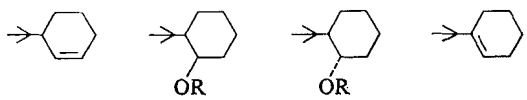

1 **2** **3** **4**

(*a*) R = H
(*b*) R = $OCOCH_3$

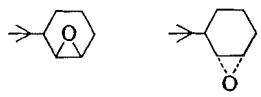

5 **6**

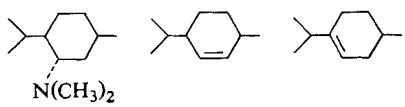

7 **8** **9**

TABLEAU I

Epoxydations du *tert*-butyl-3 cyclohexène (**1**)

Acide perbenzoïque	Conditions de réaction: Alcène mmoles	Peracide mmoles	Temps	Rendement brut	% époxyde *trans*
non-Substitué (12)	50	80	24 h à 80°	~50%	89%±2
p-Nitro (13)	14.4	21	2 h à reflux 18 h à temp. ambiante	85%	87%
m-Chloro (14)	14.4	21	48 h à 35°	75%	90%

peu rentable à cause des interactions supplémentaires qu'elle créerait entre les groupes; dans de telles conditions il est probable que l'angle de liaison entre le groupe acétoxyle en 1 et l'hydrogène équatorial en 6 sera normal. Par contre dans l'acétate **3***b* les groupes *tert*-butyle et acétoxyle sont dans la relation transdiéquatoriale qui leur permet de s'éloigner l'un de l'autre (angle de valence plus grand que 60°). Il est à noter que ce mouvement qui réduirait les interactions entre les substituants dans **3***b* aurait aussi comme effet de diminuer l'angle de valence—donc la distance—entre le groupe acétoxyle en position-1 et l'hydrogène tertiaire en position-2 permettant ainsi une élimination plus facile de l'acide acétique au cours d'un mécanisme cyclique; ces considérations permettraient de comprendre la facilité relative de pyrolyse de **3***b* vs. **2***b*. Afin de pouvoir rationaliser la formation d'une proportion de **4** plus grande que **1** lors de la pyrolyse de **3***b* il est essentiel de réaliser que la déformation préconisée plus haut pour cette molécule implique principalement la répulsion facile des groupes *tert*-butyle et acétoxyle en positions-1 et -2 mais ne provoque que des déformations d'angles de valence mineures entre le groupe acétoxyle en position-1 et les hydrogènes en position-6. D'après les considérations précédentes, il est possible de concevoir pourquoi l'élimination de l'acide acétique est rendue plus facile entre les positions-1 et -2—où les éléments à être éliminés sont rapprochés par une déformation de la molécule—que les positions-1 et -6 de **3***b*.

Le traitement de la tosylhydrazone (**12***b*) de la *tert*-butyl-2 cyclohexanone par le butyl-lithium (12) conduit aussi avec un excellent rendement à du *tert*-butyl-3 cyclohexène (**1**) d'une très haute pureté.

L'époxydation du *tert*-butyl-3 cyclohexène par divers peracides (13–15) conduit toujours à des mélanges d'époxydes contenant environ 12% de l'isomère *cis* (**5**) et 88% de l'isomère *trans* (**6**); les résultats obtenus sont résumés dans le tableau I. Chacun des époxydes a pu être obtenu à l'état pur par chromatographie en phase gazeuse préparative. Les résultats rapportés dans le tableau I et selon lesquels l'époxyde formé en quantités prépondérantes est l'isomère *trans* (**6**) suggèrent que l'effet principal affectant la stéréochimie de l'époxydation du *tert*-butyl-3 cyclohexène (**1**) est un facteur stérique attribuable à la présence du groupe *tert*-butyle qui—à cause d'une interaction 1:3 diaxiale (3, 16) entre un groupe méthyle du *tert*-butyle et le réactif—cache une face de la molécule et provoque les réactions d'époxydation vers la face opposée. Ces résultats démontrent une fois de plus l'influence des effets stériques sur cette réaction (17).

La réduction par le lithium dans l'éthylamine (18) d'un mélange 14/86 des époxydes **5** et **6** conduit à un mélange de *tert*-butylcyclohexanols contenant 14% de l'isomère 2-*cis* (**2***a*), 9% de l'isomère 2-*trans* (**3***a*) et 77% de l'isomère 3-*trans* (**11**). Ce résultat est en accord avec l'observation de Henbest (18) selon laquelle l'ouverture d'époxydes par le lithium dans l'éthylamine s'effectue presqu'exclusivement d'une façon *trans* et diaxiale selon la généralisation de Fürst et Plattner (19).

Les résultats obtenus lors de la réduction par $LiAlH_4$ de divers mélanges d'époxydes **5** et **6** sont consignés dans le tableau II. Ces résultats suggèrent que l'époxyde *cis* (**5**) conduit uniquement au *tert*-butyl-2 cyclohexanol-*cis* (**2***a*) par une ouverture *trans* diaxiale en accord avec les généralisations de Plattner (18). Si l'ouverture de l'époxyde *trans* (**6**) se faisait suivant ces normes sa réduction par $LiAlH_4$ conduirait uniquement au *tert*-butyl-3 cyclohexanol-*trans* (**11**); cette ouverture impliquerait toutefois une attaque de l'hydrure *cis* par rapport à un groupe *tert*-butyle sur la position adjacente. Les résultats obtenus

Can. J. Chem. Downloaded from www.nrcresearchpress.com by 210.87.254.42 on 09/05/12
For personal use only.

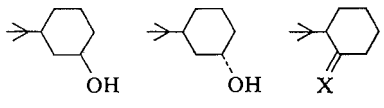

10 **11** **12**

(*a*) X = O
(*b*) X = N—NH—SO_2—C$_6$H$_4$—O—CH_3

au cours du présent travail—formation de 50% de **11**, 35% de **3***a* et 15% de **10**—sont toutefois en accord avec ceux obtenus par Rickborn et Lamke (20) lors de la réduction de l'époxyde *trans* du méthyl-3 cyclohexène et indiquent que l'état de transition menant à ce résultat est suffisamment élevé pour que seulement la moitié des molécules réagissent suivant ce processus. Le fait qu'il ne se forme pas de *tert*-butyl-2 cyclohexanol-*cis* (**2***a*) au cours de cette réaction implique que le *tert*-butyl-2 cyclohexanol-*trans* (**3***a*) formé ne provient pas d'une réduction de la *tert*-butyl-2 cyclohexanone (**12***a*) qui pourrait se former par réarrangement de l'époxyde (21) en présence d'un acide de Lewis; il est bien connu (22) en effet que la réduction de la *tert*-butyl-2 cyclohexanone (**12***a*) par l'hydrure double de lithium et d'aluminium conduit à un mélange équimoléculaire des deux *tert*-butyl-2 cyclohexanols (**2***a* et **3***a*). L'hypothèse qui permettrait le mieux d'expliquer la formation du *tert*-butyl-2 cyclohexanol-*trans* (**3***a*) serait le mécanisme alternatif—jugé le moins probable—proposé par Rickborn et Lamke (20) et impliquant la formation initiale d'un produit dans une conformation croisée. Cette proposition est basée sur l'hypothèse que s'il n'est pas impossible d'imaginer dans le cas examiné précédemment (20) qu'une portion de l'époxyde du méthyl-3 cyclohexène pourrait être réduite dans une conformation portant un substituant méthyle axial, il apparait peu plausible—même si Garbisch (23) a suggéré que plusieurs phenyl-1 cyclohexènes substitués en position 6 existent dans la conformation axiale—de concevoir qu'un groupe *tert*-butyle occupe une position axiale dans l'époxyde *trans* (**6**) du *tert*-butyl-3 cyclohexène. La présence du *tert*-butyl-3 cyclohexanol *cis* (**10**) peut être attribuée à la réduction par $LiAlH_4$ de *tert*-butyl-3 cyclohexanone formée par réarrangement de l'époxyde dans le milieu réactionnel.[1]

[1]La quantité de *tert*-butyl-3 cyclohexanol *trans* (**11**) qui pourrait se former suivant cette route est très faible puisque la réduction de la *tert*-butyl-3 cyclohexanone par $LiAlH_4$ conduit à 91% (24) de l'alcool *cis* (**10**).

TABLEAU II

Réductions, par $LiAlH_4$, de mélanges d'époxydes **5** et **6**

Composition des mélanges % *cis* (**5**)/% *trans* (**6**)	Composition des produits de réaction **2***a*	**11**	**3***a*	**10**
0/100	0	50	35	15
10/90	10	45	25	20
12/88	12	44	30	14
15/85	15	40	32	13

L'ensemble des résultats obtenus lors de ces réactions d'ouvertures d'époxydes permet de mettre en évidence l'influence des effets stériques sur ces réactions.

Partie expérimentale

*Tert-butyl-3 cyclohexène (**1**)*

Pyrolyses

*Pyrolyse de l'acétate **2b** du tert-butyl-2 cyclohexanol-cis*—La pyrolyse de 32 g d'acétate **2***b* est effectuée en l'ajoutant goutte à goutte (moins d'une goutte par seconde) dans un ballon contenant du verre pilé et maintenu à 450–500° au moyen d'un bain de sable. Les produits formés (20 g, 77% du rendement théorique) sont récupérés à la manière habituelle et analysés par chromatographie en phase gazeuse à 130° à l'aide d'une colonne de 12 pieds contenant du polyester de Craig (10%) absorbé sur du Chromosorb P (30–60); le mélange réactionnel serait formé de 14% d'acétate **2***b* qui n'a pas réagi, 6% de *tert*-butyl-1 cyclohexène (**4**) et 80% de *tert*-butyl-3 cyclohexène (**1**).

*Pyrolyse d'un mélange des acétates **2b** et **3b***—Un mélange 50/50 des acétates **2***b* et **3***b* (13 g) est traité en suivant les techniques expérimentales décrites dans la section précédente et conduit à 8 g (65% du rendement théorique) d'un produit qui d'après la c.p.g. dans les conditions décrites plus haut serait formé de 42% de *tert*-butyl-1 cyclohexène (**4**), 33% de *tert*-butyl-3 cyclohexène (**1**), 25% d'acétate **2***b* et moins que 1% d'acétate **3***b*.

*Par l'intermédiaire de la tosylhydrazone (**12b**) de la tert-butyl-2 cyclohexanone*

La tosylhydrazone (**12***b*) est obtenue quantitativement en faisant réagir, dans l'alcool absolu en présence d'une goutte d'acide chlorhydrique, un mélange équimoléculaire de tosylhydrazine et de *tert*-butyl-2 cyclohexanone (**12***a*) à reflux pendant 18 h. Le dérivé, recristallisé de l'éthanol absolu, fond à 146–147°. Son spectre de masse montre un pic parent à 322 alors que son spectre de résonance magnétique nucléaire (r.m.n.) présente des bandes à 0.85 ($C(CH_3)_3$) et 2.45 (—CH_3) p.p.m.

Can. J. Chem. Downloaded from www.nrcresearchpress.com by 210.87.254.42 on 09/05/12
For personal use only.

Réaction avec le butyl-lithium—Suivant la technique expérimentale de Shapiro et Heath (12), 37 g de tosylhydrazone (**12***b*) dans 200 ml d'éther anhydre est traité à 0° par 2 équivalents de butyl-lithium. Le mélange réactionnel hydrolysé au bout de 5 h est extrait à la manière habituelle et conduit à 15.7 g (99% du rendement théorique) de *tert*-butyl-3 cyclohexène (**1**) qui par chromatographie en phase gazeuse contiendrait moins de 1% de *tert*-butyl-1 cyclohexène (**4**).

Epoxydes (5 et 6)

Le traitement de 2 g de *tert*-butyl-3 cyclohexène en solution dans 20 ml de chlorure de méthylène par 4.0 g d'acide *p*-nitroperbenzoïque conduit à 1.9 g (85% du rendement théorique) d'époxydes (**5** et **6**) qui peuvent être analysés par c.p.g. à 140° en utilisant une colonne de cuivre de 10 pd. × ¼ po. contenant de l'hyprose à 10% déposé sur du Chromosorb P. Le traitement de 16 g (injections de 0.2 ml) de ces époxydes par c.p.g. préparative à 150° utilisant un appareil Varian Aérograph N° 705 à l'aide d'une colonne d'aluminium de 20 pd. × ⅜ po. contenant de l'hyprose à 20% sur Chromosorb P, il a été possible d'isoler 800 mg de l'époxyde *cis* (**5**) et 10 g d'époxyde *trans* (**6**) pur. Les caractéristiques de l'isomère *cis* (**5**) sont: p.e.: 170°/10 mm Hg; n_D^{23}: 1.4590; r.m.n.: groupe *tert*-butyl à 0.956 p.p.m. alors que les deux hydrogènes carbinoliques de l'époxyde apparaissent respectivement à 3.03 et 2.88 p.p.m.; le spectre de masse présente un pic moléculaire à 154. L'isomère *trans*: p.e.: 180°/15 mm Hg; n_D^{24}: 1.4581; spectre r.m.n.: groupe *tert*-butyl à 0.969 p.p.m. et les deux hydrogènes carbinoliques de l'époxyde apparaissent respectivement à 2.93 p.p.m. et 2.83 p.p.m.; le spectre de masse présente un pic parent à 154.

Les réductions des époxydes par l'hydrure double de lithium et d'aluminium ont été effectuées de façon standard (2). Les *tert*-butyl-2 (**2***a* et **3***a*) et *tert*-butyl-3 (**10** et **11**) cyclohexanols isomères nous étaient disponibles et les temps de rétention en c.p.g. de ces produits ainsi que ceux des époxydes (**5***a* et **6**) ont été déterminés à 175° avec un débit de gaz porteur de 35 ml/min à l'aide d'une colonne de cuivre de 10 pd. × ¼ po. renfermant 15% d'hyprose déposé sur du Chromosorb W (30–60). Dans ces conditions les temps de rétention sont les suivants: époxyde *cis* (**5**) 6.2; époxyde *trans* (**6**) 7.3; *tert*-butyl-2 cyclohexanol *cis* (**2***a*) 9.25; *tert*-butyl-2 cyclohexanol *trans* (**3***a*) 11; *tert*-butyl-3 cyclohexanol *trans* (**11**) 14.40 et *tert*-butyl-3 cyclohexanol *cis* (**10**) 18.40 min respectivement. Les produits de réduction des époxydes ont été identifiés par comparaison avec ces données et aussi par la méthode de superposition des pics.

Remerciement

Les auteurs remercient vivement le Conseil National de Recherches du Canada pour l'aide financière apportée sous forme d'octrois de recherches.

1. J. C. Richer et C. Gilardeau. Can. J. Chem. **43**, 3419 (1965).
2. J. C. Richer et P. Bélanger. Can. J. Chem. **44**, 2057 (1966).
3. J. C. Richer et C. Lamarre. Can. J. Chem. Sous presse.
4. W. Hückel et D. Rücker. Ann. Chem. **666**, 30 (1963).
5. D. J. Pasto et F. M. Klein. J. Org. Chem. **33**, 1468 (1968).
6. C. H. de Puy et R. W. King. Chem. Rev. **60**, 431 (1960).
7. D. H. R. Barton. J. Chem. Soc. 2174 (1949).
8. A. C. Cope et E. M. Acton. J. Am. Chem. Soc. **80**, 355 (1958).
9. M. Davis et O. Hassel. Acta Chem. Scand. **17**, 1181 (1963).
10. R. A. Wohl. Chimia Aurau, **18**, 219 (1964).
11. E. L. Eliel, S. H. Schroeter, T. J. Brett, F. J. Biros et J. C. Richer. J. Am. Chem. Soc. **88**, 3327 (1966).
12. R. H. Shapiro et M. J. Heath. J. Am. Chem. Soc. **89**, 5734 (1967).
13. A. Kergomard et J. Bijou. Bull. Soc. Chim. France, 486 (1956).
14. M. Vilkas. Bull. Soc. Chim. France, 1401 (1959).
15. B. M. Lynch et K. H. Pausacher. J. Chem. Soc. 1525 (1955).
16. J. C. Richer, L. A. Pilato et E. L. Eliel. Chem. Ind. London, 2007 (1961).
17. B. Rickborn et S. Y. Lwo. J. Org. Chem. **30**, 2212 (1965).
18. A. S. Hallsworth et H. B. Henbest. J. Chem. Soc. 4604 (1957).
19. A. Fürst et Pl. A. Plattner. Helv. Chim. Acta, **32**, 275 (1949).
20. B. Rickborn et W. E. Lamke. J. Org. Chem. **32**, 537 (1967).
21. B. Rickborn et J. Quartucci. J. Org. Chem. **29**, 2476 (1964).
22. H. L. Goering, R. L. Reeves et H. H. Espy. J. Am. Chem. Soc. **78**, 4926 (1956).
23. E. W. Garbisch, Jr. J. Org. Chem. **27**, 4249 (1962).
24. E. L. Eliel. Rec. Chem. Prog. **22**, 129 (1961).

Can. J. Chem. Downloaded from www.nrcresearchpress.com by 210.87.254.42 on 09/05/12
For personal use only.

Can. J. Chem. Downloaded from www.nrcresearchpress.com by 210.87.254.5 on 09/05/12
For personal use only.

Bicyclic analogues of cyclohexane-1,4-dione. I. Bicyclo[3·2·2]nonan-6,8-dione[1]

GORDON WOOD AND E. P. WOO[2]
Department of Chemistry, University of Windsor, Windsor, Ontario

Received June 7, 1968

Bicyclo[3·2·2]nonan-6,8-dione has been synthesized as an example of a molecule in which the cyclohexane-1,4-dione ring is constrained to non-chair forms. The synthesis includes the double decarboxylation of the corresponding bridgehead diacid. This reaction is consistent with a new formulation of Bredt's Rule. Conformational studies suggest that the title compound exists in solution as an equilibrium mixture of two twist forms.

Canadian Journal of Chemistry, 46, 3713 (1968)

Introduction

It is well known that cyclohexane and its derivatives exist predominantly in the chair form in which all the adjacent C—H and C—C bonds are staggered. The flexible (twist-boat) form is 5.3 kcal higher in energy, mainly as a result of the partial eclipse of four pairs of adjacent C—H bonds (two ethane units).

In cyclohexanone certain flexible forms with only one eclipsed ethane unit are possible (1, 2). The net effect of the carbonyl, then, is to reduce the energy difference between the flexible and the chair forms. Cyclohexane-1,4-dione, with two carbonyl groups, would be expected to have certain flexible forms of even lower energy. The energies (relative to the chair forms) of the flexible forms of cyclohexanone and cyclohexane-1,4-dione have been calculated by Allinger (2). The values calculated for cyclohexanone agree well with experimental data (2–4). The minimum values calculated for cyclohexane-1,4-dione are 1.8 kcal. Assuming reasonable values for the entropy difference between the chair and the flexible form it was concluded that the flexible form should be an important contributor, but that an unreasonably high entropy difference favoring the flexible form would be required for this latter to be the exclusive conformation (2). However, evidence from X-ray crystallography (5), Kerr constant measurement (6), and infrared and Raman spectroscopy (7) all support the exclusive preference for the flexible form.

In an attempt to clarify the conformational situation in cyclohexane-1,4-dione we have synthesized certain bicyclic analogues in which the additional bridge provides some constraint on the conformation of the dione ring. This paper describes the synthesis and some conformational studies of bicyclo[3·2·2]nonan-6,8-dione. This molecule lends itself to dipole moment studies since the two possible twist-boat forms have very different calculated moments. It may also prove useful as a precursor in the preparation of other disubstituted cyclohexanes locked in the twist conformation.

Mass spectra were obtained on several of the compounds prepared. Some evidence for a new fragmentation of diketals will be presented in a separate publication.

Results and Discussion

Synthesis of Bicyclo[3·2·2]nonan-6,8-dione

We chose alkylation of diethyl succinylsuccinate with 1,3-dibromopropane as entry to the bicyclo[3·2·2]nonane system (Scheme 1). The established procedure (8) for the synthesis of diethyl succinylsuccinate by condensation of two moles of diethyl succinate requires 3 to 4 days of reflux. We found that with sodium hydride in monoglyme the reaction time was shortened to 12 h with improved yield (75%). Heating the disodium salt of diethyl succinylsuccinate with 1,3-dibromopropane gave 50–55% yield of 1,5-dicarbethoxybicyclo[3·2·2]nonan-6,8-dione **2**, a substantial increase from the 30% yield reported by Guha (9). Acid hydrolysis of **2** afforded the corresponding diacid **3**.

When the diacid **3** was heated to a temperature slightly above its melting point (ca. 245°) for a

[1]Taken from the dissertation submitted by E. P. Woo in partial fulfillment of the requirements for the Ph.D. Degree from the University of Windsor, 1968.

[2]Holder of a Province of Ontario Fellowship 1965–1968.

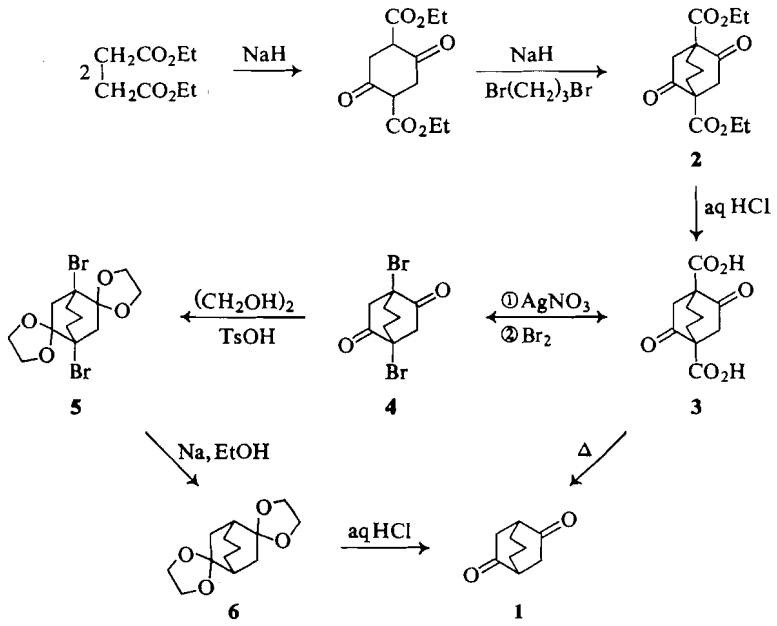

SCHEME 1

few minutes, a ketone was obtained. The same compound was obtained in 60–65% yield by refluxing **3** in triglyme for 3–5 h.[3] It was identified as **1** by the following data. It gives a disemicarbazone and has infrared (i.r.) absorption at 1725 cm^{-1} (C=O). Its nuclear magnetic resonance (n.m.r.) spectrum shows multiplets at 7.20 (2H), 7.37 (4H), and 8.20 (6H), which are assigned to the bridgehead protons, methylene protons *alpha* to carbonyl groups, and the six protons of the trimethylene bridge, respectively. Further proof of structure was accomplished by the synthesis of **1** through another pathway (Scheme 1). The diacid **3** was decarboxylated by the Hunsdiecker reaction to **4**. Conversion of **4** to the diketal **5** and subsequent hydrogenation afforded **6**. Acid hydrolysis of **6** gave a diketone identical to that obtained from thermal decarboxylation.

Conformations of Bicyclo[3·2·2]nonan-6,8-dione

Study of Drieding models suggests that there are two conformations of **1** which are free of angle strain (**1***a* and **1***b*). In both these forms the cyclohexane-1,4-dione ring is in a twisted boat. In one of these the carbonyl carbons lie in the same plane with the two carbons (C-5 and C-7) flanking one of them (**1***a*); in the other, one of the carbonyl carbons (C-8) lies on a plane with three (C-5, C-7, C-9) of the saturated carbons (**1***b*). Between these forms lies a form in which the cyclohexane-1,4-dione ring is in a stretched boat form and the cycloheptanone rings are pure boat and pure chair forms. This form has some angle strain (models) so that it will be populated only if the non-bonded interactions are considerably less than in the twist forms. Our qualitative estimation suggests that the non-bonded interactions are at least as bad in the chair–boat form and therefore we shall neglect this latter form. It should be noted that the trimethylene bridge is capable of a flipping motion, but this does not result in any additional conformations because of the symmetry of the molecule.

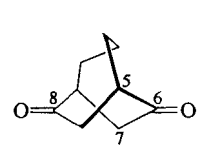

1*a*

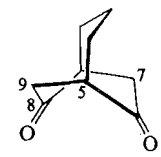

1*b*

[3]The ease of decarboxylation of **3** is not predicted by the **S** number formulation of Bredt's Rule. However, Wiseman (10) has proposed that **S** number is not as important as the ring size of *trans*-olefin formed. Our compound behaves in the manner predicted by this criterion.

Can. J. Chem. Downloaded from www.nrcresearchpress.com by 210.87.254.5 on 09/05/12
For personal use only.

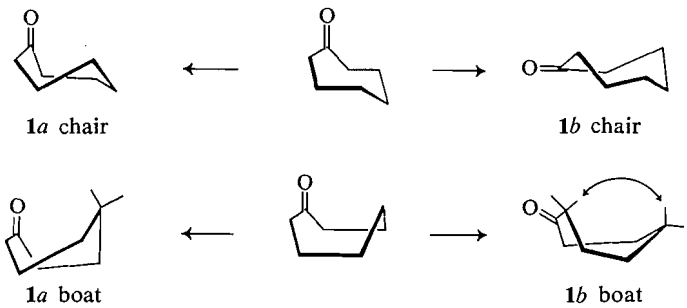

FIG. 1. The chair and boat rings of the cycloheptanone moieties of **1***a* and **1***b*.

Some indication that **1** may exist in solution as a mixture of **1***a* and **1***b* is derived from the i.r. spectra. There are a number of bands between 1100 and 1400 cm^{-1} which are characteristic of ketones. We have compared spectra obtained in the solid phase (KBr pellet) with those obtained in solution (CCl_4). In both spectra we find six major bands in this region (1095, 1120, 1210, 1250, 1300, and 1335 cm^{-1}), but the relative intensities are very different. The simplest interpretation of these results is that there is only one conformation present in the solid, but a mixture of conformations in solution.

TABLE I

Dipole moments of **1**

Solvent	μ (D)	Conformation (**1***a*:**1***b*)	$\Delta G°$ (**1***a*–**1***b*)
Benzene	1.39	89:11	1.2 kcal
Dioxan	1.81	82:18	0.9 kcal

Stronger evidence for the presence of more than one conformation in solution comes from dipole moment studies. We have determined the dipole moment of **1** in benzene and in dioxan solution at 20°. The moment of cyclohexane-1,4-dione was determined to be 1.25 D (benzene) by our method. This value agrees well with Allinger's result of 1.26 D at 18° (2). Our dipole moment results for **1** are presented in Table I. It will be noted that in both solvents the measured moment indicates significant amounts of each conformer[4] and further the proportion of the more polar **1***b* is greater in dioxan.[5] The 1 kcal free energy difference between **1***a* and **1***b* may be the result of an H–H non-bonded interaction in **1***b* (Fig. 1). Attempts to gain conformational evidence from variable temperature n.m.r. studies were unsuccessful. The spectrum of the diketone is constant over the temperature range studied (−99° to +164°).

Experimental

Mass spectral analyses were performed by Morgan and Schaffer Corporation, Montreal. Dipole moments were calculated according to the method of Moll and Lippert (12) from the dielectric constants determined with a Wissenschaftlich-Technische Werkstätten (Germany) Dipolemeter DMO1. Atom polarization was neglected throughout. Preparative gas–liquid chromatography (g.l.c.) columns were all of the same dimensions (8 ft × 0.5 in.) and packed with 10% silicone gum rubber SE-30 or LAC-728, on Diatoport W, 80–100 mesh. Microanalyses were performed by Midwest Microlab, Inc., Indianapolis, Indiana.

The structures of all compounds reported are in accord with their infrared (i.r.) and nuclear magnetic resonance (n.m.r.) spectra.

Diethyl Succinylsuccinate

Sodium hydride (0.2 mole, 9.6 g of 50% dispersion in mineral oil) was stirred in 80 ml of monoglyme (dried over sodium wire). *t*-Butyl alcohol (0.5 g) was added and the solution was heated at 60° until gas evolution ceased. Ethyl succinate (0.2 mole, 34.9 g) was added dropwise over a period of 0.5 h. After addition was complete, the viscous slurry was stirred and heated at 60–65° for 12 h. Sufficient cold 6 *N* sulfuric acid was added to acidify the solution. The solid material was filtered and washed with petroleum ether and water. Upon recrystallization from ethanol, 37 g (75%) yield of light-yellow solid was obtained, m.p. 125.5–126.5° (lit. (8) m.p. 126–127°).

[4]Calculated values of dipole moments for **1***a* and **1***b* were obtained by measurements of the carbonyl–carbonyl angle (ten measurements on two different models). The angles obtained (175° and 90°) and the carbonyl group moment (3.00 D) leads to values of 0 D and 4.2 D for **1***a* and **1***b*.

[5]In spite of its low bulk dielectric constant, dioxan behaves as a fairly polar solvent in the presence of polar solutes (11).

Can. J. Chem. Downloaded from www.nrcresearchpress.com by 210.87.254.5 on 09/05/12
For personal use only.

Can. J. Chem. Downloaded from www.nrcresearchpress.com by 210.87.254.5 on 09/05/12
For personal use only.

1,5-Dicarbethoxybicyclo[3·2·2]nonan-6,8-dione (2)

Sodium hydride (0.555 mole, 25 g of 53.5% dispersion) and diethyl succinylsuccinate (0.25 mole, 64 g) were added alternately in small portions to 500 ml of dry monoglyme. After all the reagents had been added, the slurry was heated at 100–110° for 3 h. Monoglyme was removed *in vacuo* and 710 ml of 1,3-dibromopropane (freshly distilled) and 90 ml of monoglyme were added. Heating was continued for 22 h. The mixture was filtered and the filtrate was steam distilled. The residue was allowed to cool with occasional shaking and crystallized from ethanol. The product was washed with 1% sodium hydroxide solution until the washing was no longer yellow. Subsequent washing with water, cold ethanol and petroleum ether, and recrystallization from ethanol gave 38.5 g (52%) of **2**, m.p. 130–132.5° (lit. (9) m.p. 132°).

1,5-Dicarboxybicyclo[3·2·2]nonan-6,8-dione (3)

The diester **2** was hydrolyzed by refluxing with 6 *N* hydrochloric acid for 8 h. Two recrystallizations from water gave an analytical sample, m.p. (decomp.) 245–247° (lit. (9) m.p. 238°).

Anal. Calcd. for $C_{11}H_{12}O_6$: C, 55.00; H, 5.04. Found: C, 54.88; H, 5.08.

1,5-Dibromobicyclo[3·2·2]nonan-6,8-dione (4)

A solution of the diacid **3** (5 mmoles, 1.2 g) in 20 ml of warm water was titrated to the end-point of phenolphthalein with 0.5 *N* sodium hydroxide, and treated with 20% silver nitrate solution. The precipitate was filtered and repeatedly washed with water, methanol, and ether. After drying in a vacuum desiccator for 24 h, the disilver salt was mixed with 35 ml of carbon tetrachloride (dried over P_2O_5). Bromine (0.011 mole, 1.76 g, distilled from P_2O_5) was added dropwise with vigorous stirring. The solution was slowly heated to boiling and refluxed for 8 h in the dark. The mixture was filtered and the filtrate distilled to give a residue which upon crystallization from a methanol–chloroform mixture gave 270 mg of **4**, m.p. 181–184°, 19% yield. An analytical sample was obtained by recrystallization from a chloroform – carbon tetrachloride mixture, m.p. 184.5–185.5°.

Anal. Calcd. for $C_9H_{10}O_2Br_2$: C, 34.88; H, 3.25; Br, 51.59. Found: C, 34.88; H, 3.45; Br, 51.61.

Diketal of 1,5-Dibromobicyclo[3·2·2]nonan-6,8-dione (5)

The diketal **5** was prepared by refluxing **4** (3.6 g, 11.6 mmoles) with 0.5 g of *p*-toluenesulfonic acid and 5 ml of ethylene glycol in 20 ml of benzene for 4 days. The benzene solution was washed with 5% sodium hydroxide and water. After removal of the solvent, the residue was crystallized from a hexane–ethanol mixture to give 3.47 g (75%) of **5**, m.p. 127–130°. Two more recrystallizations gave an analytical sample, m.p. 128.5–130°.

Anal. Calcd. for $C_{13}H_{18}O_4Br_2$: C, 39.22; H, 4.56; Br, 40.15. Found: C, 39.43; H, 4.54; Br, 39.96.

Diketal of Bicyclo[3·2·2]nonan-6,8-dione (6)

Sodium (6.8 g) was added in small pieces over a period of 2 h to a well-stirred solution of **5** (3.27 g, 8.2 mmoles) in 110 ml of absolute ethanol. Precipitation of sodium bromide was observed when about one-quarter of the sodium had been added. The solution was cooled and poured into 600 ml of water and was extracted with five 100-ml portions of 1:1 mixture of petroleum ether and ether. The solvents were removed after drying to give a yellow oil which solidified on standing. Preparative g.l.c. (silicone gum rubber) gave **6** in 53% yield, m.p. 63–64.2°.

Anal. Calcd. for $C_{13}H_{20}O_4$: C, 64.98; H, 8.39. Found: C, 65.17; H, 8.31.

Hydrolysis of 6

The diketal **6** (430 mg, 1.8 mmoles) and 6 ml of 1.2 *N* hydrochloric acid was refluxed for 7 h. The solution was poured onto 15 g of ice and extracted with methylene chloride. After washing with a 10% sodium bicarbonate solution and drying, the solvent was evaporated to give 290 mg (79%) of bicyclo[3·2·2]nonan-6,8-dione, **1**. The crude product was purified by sublimation (85°/5 mm) to give 215 mg of pure material, m.p. (sealed tube) 218–223°. This sample was shown to be pure by g.l.c. and thin-layer chromatography (t.l.c.) (silica gel). Multiple recrystallizations from various solvents and sublimations did not narrow its broad melting range.[6]

Anal. Calcd. for $C_9H_{12}O_2$: C, 71.10; H, 7.95. Found: C, 70.85; H, 7.86.

The disemicarbazone of **1** melts at 277.5–279°.

Anal. Calcd. for $C_{11}H_{18}O_2N_6$: C, 49.61; H, 6.81; N, 31.56. Found: C, 49.66; H, 7.00; N, 31.86.

Decarboxylation of 1,5-Dicarboxybicyclo[3·2·2]nonan-6,8-dione

(*a*) The diacid **3** (0.5 g) was placed in a sublimator which was quickly heated to 240–245° in an oil bath. The solid melted with evolution of gas and a light-yellow solid began to collect on the cold-finger. Reaction was complete after 15 min. Recrystallization from ether afforded 61 mg of impure **1**, m.p. (sealed tube) 194–212°. Purification was achieved by conversion of **1** to its diketal, **6**. A sample obtained this way is identical in every respect (i.r., n.m.r., g.l.c., and m.p.) to that obtained previously.

(*b*) A solution of **3** (24 g, 0.1 mole) and 300 ml of triglyme was refluxed for 5 h (temperature of the solution was 210–218°). Evolution of carbon dioxide was followed by the weight increase of the Ascarite tube. The reaction became very slow after 3 h of heating. At the end of 5 h, the weight of carbon dioxide generated indicated a conversion of 80% of diacid to **1**, while g.l.c. showed 81.5% yield. The triglyme solution was poured into 2.5 l of benzene and extracted with five 1-l portions of water. Benzene was removed after drying to give a heavy oil which upon treatment with pentane gave a crystalline solid and a gummy material. The solid was dissolved in methanol and filtered to remove the gummy material. Evaporation of methanol and recrystallization from a hexane–benzene mixture afforded 16.1 g of **1**. One sublimation gave 13.9 g (62%) of pure material.

Acknowledgments

The authors thank the National Research Council of Canada for their financial support of this work as well as for a grant towards the pur-

[6]Similar melting behavior was observed in tricyclo-[4·4·0·$0^{4,9}$] decan-3-one (13).

chase of a nuclear magnetic resonance spectrometer. We also thank Mr. David Hill for determining the infrared spectra and Mr. Maurice Miskow for assistance in measuring the dipole moments.

1. N. L. ALLINGER, J. ALLINGER, and M. A. DAROOGE. J. Am. Chem. Soc. **86**, 4061 (1964).
2. N. L. ALLINGER, H. M. BLATTER, L. A. FREIBERG, and F. M. KARKOWSKI. J. Am. Chem. Soc. **88**, 2999 (1966).
3. N. L. ALLINGER and H. M. BLATTER. J. Am. Chem. Soc. **83**, 994 (1961).
4. N. L. ALLINGER and F. M. KARKOWSKI. Tetrahedron Letters, 2171 (1965).
5. A. MOSSEL, C. ROMERS, and E. HAVINGA. Tetrahedron Letters, 1247 (1963).
6. C.-Y. CHEN and R. J. W. LEFEVRE. Australian J. Chem. **16**, 917 (1963).
7. N. L. ALLINGER and L. A. FREIBERG. J. Am. Chem. Soc. **83**, 5028 (1961).
8. C. R. HAUSER and B. E. HUDSON, JR. Org. Reactions, **1**, 283 (1942).
9. P. C. GUHA. Chem. Ber. **72**, 1359 (1939).
10. X. WISEMAN. J. Am. Chem. Soc. **89**, 5966 (1967).
11. M. B. LEDGER and P. SUPPAN. Spectrochim. Acta, **23**, 3007 (1967).
12. F. MOLL and E. LIPPERT. Z. Elektrochem. **58**, 853 (1954).
13. J. GAUTHIER and P. DESLONGCHAMPS. Can. J. Chem. **45**, 297 (1967).

Can. J. Chem. Downloaded from www.nrcresearchpress.com by 210.87.254.5 on 09/05/12
For personal use only.

Can. J. Chem. Downloaded from www.nrcresearchpress.com by 210.87.254.6 on 09/05/12
For personal use only.

On the lead tetraacetate and related oxidations of aromatic ketoximes[1]

M. M. FROJMOVIC[2] AND G. JUST
Department of Chemistry, McGill University, Montreal, Quebec

Received March 14, 1968

Fluorenone and benzophenone oxime react in glacial acetic acid with lead tetraacetate to give parent ketones, geminal dinitromethanes, iminyl ketal derivatives (9,9-difluorenylideniminoxylfluorene and 1,1-bis(diphenylmethylideniminoxyl)-diphenylmethane), and minor amounts of oxime *O*-acetate. Benzophenone nitrimine is also formed but only in the absence of oxygen. Side reactions due to nitric oxide, oxygen, and nitrogen dioxide take place. Separate studies with these oxidizing agents have therefore been conducted. The lead tetraacetate oxidation of these oximes in methylene chloride (or any other solvent) is complete with a half-mole equivalent of lead tetraacetate, is insensitive to molecular oxygen, and affords mainly parent ketone and ketazinemonoxides. No ketazine-bis-*N*-oxides, obtained from the ferricyanide oxidation of these oximes, are formed. The model oximes, benzil anti-monoxime, xanthone oxime, and indanone oxime have been studied in the light of these observations. Mechanisms involving iminoxyl radicals have been postulated for all reactions studied.

Canadian Journal of Chemistry, 46, 3719 (1968)

Introduction

It has been shown by electron spin resonance (e.s.r.) measurements that iminoxyl radicals formed by lead tetraacetate oxidations of bis-arylketoximes are very stable, with half lives ranging from 0.5 to 5.5 min (*1*). No reports have been published on the chemistry of these oxidations, except for the ferricyanide oxidation of benzophenone oxime (2), which gives benzophenone, benzophenone azine monoxide, and benzophenone anhydride *N*-oxide (**2***b*), probably better formulated as azine-bis-*N*-oxide (**3***b*). Similar oxidations of aliphatic ketoximes and substituted acetophenone oximes generate much shorter-lived radicals (1), with *gem*-nitrosoacetates generally produced as final products (3, 4); hindered and strained ketoximes generally lead to hydroxamic acids (5). In the following, the lead tetraacetate and related oxidations of fluorenone, benzophenone, xanthone, indanone, and benzil *anti*-monoxime (**1***a–e*) in glacial acetic acid and methylene chloride will be described.

The products obtained in these oxidations depended on the nature of the oxime and the oxidizing agent used, the solvent, the ratio of oxidizing agent to substrate and the presence of oxygen. Compounds isolated or detected were *gem*-dinitro compounds (**4**), iminylketals (**5**), azine monoxides (**6**) and bis-oxides (**3**), oxime-*O*-acetates (**7**), parent ketones, and a nitrimine (**8**). In order to simplify the discussion, structure proofs of products obtained will be first given.

Structure and Properties of Products

Gem-dinitro Compounds (4)

The molecular formula of 9,9-dinitrofluorene (**4**), $C_{13}H_8N_2O_4$, was confirmed by mass spectroscopy ($M^+ = 256$). Its ultraviolet (u.v.) spectrum showed maxima at 246 (ε 26 000) and 276 (ε 6800) mμ which are typical of the fluorenylidene skeleton. The infrared (i.r.) spectrum contained peaks at 1567 and 1350 cm^{-1}, characteristic of the NO_2-stretching vibrations. Although stable to acid, compound **4***a* decomposed with evolution of nitrous fumes and formation of fluorenone upon heating to its m.p. at 130°. Dinitrodiphenylmethane (**4***b*) and 1,1-dinitroindane (**4***d*) had similar chemical and spectroscopic properties.

Iminoxyl Ketals (5)

9,9-Difluorenylideniminoxylfluorene (**5***a*), $C_{39}H_{24}N_2O_2$, had a molecular weight of 597 (osmometry). Its i.r., u.v., and mass spectra (Table I) were consistent with the structure assigned. Hydrolysis of ketal **5***a* gave two equivalents of oxime and one equivalent of ketone. This ketal was synthesized in low yield by reaction of 9,9-dichlorofluorene with two equivalents of the sodium salt of fluorenone oxime in dimethyl sulfoxide. The analogous ketal **5***b*, derived from benzophenone, was characterized in a similar manner.

Fluorenone Azinemonoxide (6a)

Compound $C_{26}H_{16}N_2O$ had an u.v. (255 (ε 53 000) and 261 (ε 65 000) mμ) and an i.r.

---

[1]Abstracted from the Ph.D. thesis of M. M. Frojmovic. Present address: Department of Physiology, McGill University, Montreal, Quebec.

[2]Holder of a National Research Council of Canada Bursary, 1963–1964, and Studentships, 1964–1966.

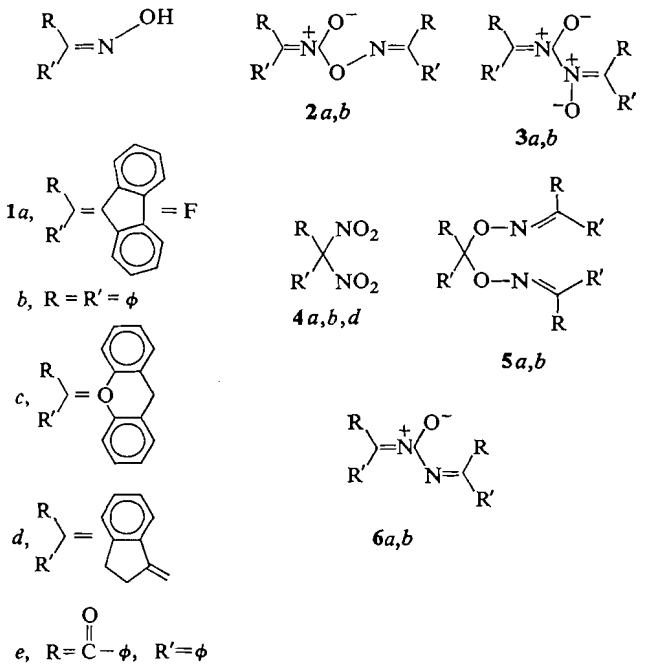

(1540 and 1268 cm^{-1}) spectrum consistent with the structure **6***a*. Its mass spectrum contained peaks at *m/e* 356 and 180 due to loss of oxygen and nitrogen, respectively (Table I). Reduction of **6***a* with triphenylphosphine gave fluorenonazine, which was independently synthesized by the autoxidation of fluorenone hydrazone in glacial acetic acid. Hydrolysis of **6***a* in glacial acetic acid containing concentrated hydrochloric acid gave fluorenone (63%) and 9-chlorofluorene (33%). The formation of 9-chlorofluorene is somewhat surprising since a similar hydrolysis of aldazine monoxides was reported (6) to give the corresponding aldehyde and primary acetate. 9-Diazofluorene, suspected to be the intermediate in the hydrolysis of **6***a*, gave 9-chlorofluorene in acetic acid – hydrochloric acid, and 9-fluorenyl acetate in pure acetic acid. Benzophenonazine-monoxide (**6***b*) had similar spectral and chemical properties. It was synthesized independently from benzophenone oxime and potassium ferricyanide (2).

Fluorenone Azine bis-N-Oxide (3a)

The compound $C_{26}H_{16}N_2O_2$ had i.r. and u.v. spectra similar to that of azine monoxide **6***a*. Acid hydrolysis gave a 1:1 mixture of fluorenone and its oxime. Pyrolysis gave fluorenone and the azinemonoxide **6***a*. These data do not permit differentiation of the azine bis-oxide structure **3***a* from the anhydride *N*-oxide structure **2***a*. The i.r. spectrum of **3***a* does not correspond to the published spectra of other oxime anhydride *N*-oxides and furoxans (7). The R_f value of **2***a* would be expected to be equal or less than that of azinemonoxide **6***a*. The observed R_f value was greater than that of **6***a*. The mass spectrum (Table II) showed a peak at M-16, while further fragmentation was strikingly similar to that of azinemonoxide **6***a*. Based on these criteria, structure **3***a* is preferred to **2***a*.

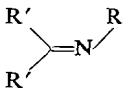

7, R = OAc
8, R′ = φ, R = NO_2

Benzophenone Nitrimine (8)

Compound $C_{13}H_{10}N_2O_2$ gave a mass spectrum consistent with the nitrimine structure **8**. Of note was the weak parent peak at mass 226 and the base peak at mass 30 (NO^+) which has been observed for other nitro compounds (8). Independent synthesis of **8** was effected from diazodiphenylmethane and nitric oxide (9).

Can. J. Chem. Downloaded from www.nrcresearchpress.com by 210.87.254.6 on 09/05/12
For personal use only.

TABLE I

Mass spectral data of fluorenone derivatives

Mass–charge ratio *m/e*	Relative Intensity				
	5*a*		**6***a*		**3***a*
	70 eV	10 eV	70 eV	12 eV	70 eV
358	7.3	4.2	0.3	0.9	1.0
357	*25.9*	*13.0*	1.7	6.4	2.7
356	9.0	3.0	6.2	20.0	4.4
355	4.0	0.6	*5.5*	*0.0*	*3.7*
328	11.6	4.0	2.4	1.3	1.9
327	*7.1*	*0.0*	*4.0*	*4.0*	*2.3*
180	51.2	100.0	78.2	70.0	100.0
179	*45.1*	*96.0*	*100.0*	*100.0*	*28.6*
Vapor temp. (°C)	200 (Direct)		250 (Indirect)		200 (Direct)
V_A	1750V		1750V		1750V
V_M	2400V		2000V		2000V

Mass Spectrometry of Fluorenone Derivatives

The data shown in Table I for the mass spectra of compounds **3***a*, **5***a*, and **6***a* indicate that loss of an aromatic radical constitutes an important if not predominating process in the fragmentation of these compounds. This process probably occurs through abstraction of a hydrogen radical by a departing fragmented radical, since no metastable peaks corresponding to M to M − 1 conversions were observed.

Product Distribution

The results of the oxidation of fluorenone oxime (**1***a*) and benzophenone oxime (**1***b*) under a variety of conditions are shown in Table II. Lead tetraacetate oxidations of these ketoximes in glacial acetic acid [entries 1, 2, and 9] led to products which could be independently formed by analogous reactions with molecular oxygen [6 and 11] and nitrogen dioxide [7, 8, and 12]. The corresponding oxidation in methylene chloride (representative of other solvents ranging from dimethyl sulfoxide to ether) led to different products whose distribution [3, 4, and 10] was now insensitive to oxygen and required only a half-mole equivalent of lead tetraacetate for complete reaction. It must be noted that the distinct difference described above was not reflected in the e.s.r. spectra of iminoxyl radicals, which, in the case of aromatic ketoximes, have been reported to be relatively solvent independent (10).

The products of oxidation of benzil-antimonoxime (**1***e*) were very different from those observed for the above bis-arylketoximes. The rapid (≪1 min) lead tetraacetate oxidation of **1***e* in glacial acetic acid was only slightly oxygen sensitive and gave mainly a single, uncharacterized compound with spectral properties similar to that of an azine dioxide (**3**). In addition, a minor amount of ketone (only in the presence of oxygen) and of oxime-*O*-acetate (**7**) was formed. The corresponding rapid oxidation in methylene chloride was O_2-insensitive, required only a half-mole equivalent of lead tetraacetate, and gave 50% of ketone as sole identifiable product. Finally, no autoxidation of oxime **1***e* took place.

Xanthone oxime (**1***c*) and indanone oxime (**1***d*) both behaved very similarly to aliphatic ketoximes (3–5). They underwent no autoxidation reactions. The lead tetraacetate oxidation of **1***d* in oxygen-free acetic acid led to 50% *gem*-nitrosoacetate and 50% parent ketone. All other lead tetraacetate oxidations of **1***c* and **1***d* in various solvents were insensitive to oxygen and led to parent ketone only. The nitrations of these oximes with NO_2, as described for **1***a* and **1***b*, led to 70% yield of a nitrated product similar to **4** and 8% yield of **4***d*, respectively.

Discussion

It is obvious from the above results that the oxidations of aromatic ketoximes do not proceed via a single pathway, and that, in addition to the primary oxidation step, many secondary reactions involving oxygen and nitrogen dioxide take place. Although by no means proved, the following schemes may account for the formation of various products described above.

Gem-dinitro Compounds

The most probable scheme for the formation of *gem*-dinitro compounds from the reaction of ketoximes with nitrogen dioxide may best be represented as shown in Scheme 1. A few reactions of this type have been described in the literature (11), but no mechanism has been given to describe in detail the course of the reaction.

Ionic reaction of dinitrogen tetroxide with fluorenone oxime was ruled out since the latter was inert to NO^+ (12). Dimerization between the iminoxyl radical and the NO_2 radical is expected to be very facile since the electronic and geometric properties of these two radicals have been reported to be strikingly similar (13). The above scheme will readily explain the formation

Can. J. Chem. Downloaded from www.nrcresearchpress.com by 210.87.254.6 on 09/05/12
For personal use only.

Can. J. Chem. Downloaded from www.nrcresearchpress.com by 210.87.254.6 on 09/05/12
For personal use only.

TABLE II

Oxidations of bis-aryl ketoximes

Substrate (S)	Oxidizing agent	Ratio S/O	Solvent	Atmosphere	Time (min)	Products (% yield) Dinitro **4**	Ketal **5**	Azine-monoxide **6**	Oxime-*O*-acetate 7	Nitrimine **8**	Ketone
F=NOH **1***a*	$Pb(OAc)_4$	1:1	HOAc	*a*)N_2	30	20	25	0	~5	0	25
				b)O_2	5	25	0	0	~5	0	> 50
	$Pb(OAc)_4$	1:½	HOAc	*a*)N_2	30	3	25	0	~5	0	20
				b)O_2	5	15	3	0	~5	0	> 50
	$Pb(OAc)_4$	1:½	CH_2Cl_2	O_2 *or* N_2	90	1	2	15	0	0	> 50
	$Pb(OAc)_4$	1:½	1% HOAc–CH_2Cl_2	N_2	25	2	2	15	0	0	> 50
	$K_3Fe(CN)_6$*	1:1.7	KOH–H_2O −5°	Air	60	0	<1	15	0	0	> 50
	O_2	*a*) saturated solution	HOAc	O_2	24 h	25	13	0	0	0	65
		b) O_2 blown through	HOAc	O_2	24 h	30	0	0	0	0	65
	NO_2	Excess	HOAc or CH_2Cl_2	NO_2	<1	95+	0	0	0	0	1
	NO_2	1:1	HOAc†	N_2	30	30	4	0	0	0	15
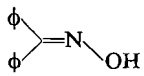 **1***b*	$Pb(OAc)_4$	1:1	HOAc	*a*)N_2	1	9	3	0	~5	11	60
				b)O_2	1	30	3	0	~5	0	60
	$Pb(OAc)_4$	1:½	CH_2Cl_2	O_2*or* N_2	1	0	0	35	~5	0	50
	O_2	Saturated solution	HOAc	O_2	24 h	30	0	0	0	0	70
	NO_2	Excess	HOAc or CH_2Cl_2	Air	1	77	0	0	0	0	15

*Azine dioxide 3 was obtained in 18% yield for reaction at −5°.
†Dropwise addition of $Pb(OAc)_4$ (50% oxime remained).

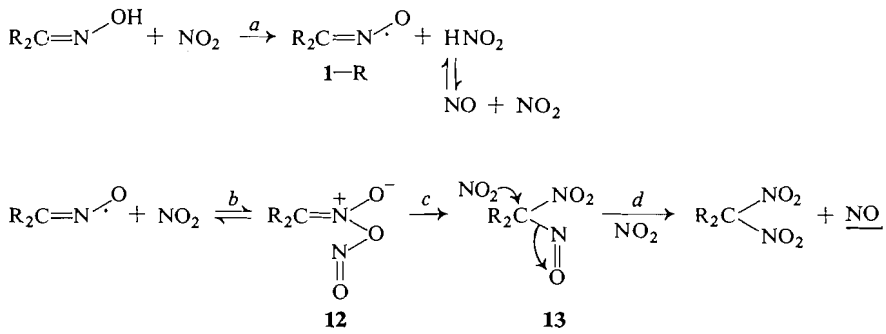

Scheme 1. *Gem*-dinitro compounds.

of pseudonitroles **13** reported for aliphatic ketoximes (14) and aromatic aldoximes (15). For bis-aryl-pseudonitroles (never detected), radical displacement of NO by NO_2 most likely occurs as shown in step (*d*) above. It should be noted that an intermediate similar to nitrito-nitrone **12** has previously been postulated (16, 17).

Auto-oxidations

Ionic reactions of organic compounds with oxygen have been reported (18). This type of mechanism may be ruled out since the sodium salt of fluorenone oxime was inert to oxygen. It is postulated that the auto-oxidation of fluorenone oxime is similar to the nitrogen dioxide oxidation depicted in Scheme 1. The iminoxyl radical initially formed can react with hydroperoxyl radicals to form ketone and nitrous acid. Nitrogen dioxide, generated from the latter, can then lead to *gem*-dinitro products (Scheme 1).

Auto-oxidations of the bis-aryl-ketoximes occurred *only* in glacial acetic acid and were totally quenched by catalytic amounts of water or acid. The latter phenomenon probably arises from the prohibitive activation energy required to form an iminoxyl radical whose unpaired electron cannot delocalize over both the iminoxyl oxygen and nitrogen (13).

Lead Tetraacetate Oxidations

Iminoxyl radicals produced in the lead tetraacetate oxidations of the oximes studied may recombine with lead triacetate and/or acetoxyl radicals to form *gem*-nitrosoacetates which, in the case of aromatic ketoximes, can be expected to decompose to parent ketone and nitric oxide (3). Nitric oxide was in fact isolated from the lead tetraacetate oxidation of fluorenone oxime in glacial acetic acid. Subsequent formation of *gem*-dinitro products (**4**) can proceed as shown in Scheme 1.

Iminyl Ketals (5)

These may be formed by Scheme 2 represented for the oxidation of fluorenone oxime. The *N*-nitroso-nitrone **14** may behave as a radical trap in analogy with the similar behavior of nitroso compounds (19).

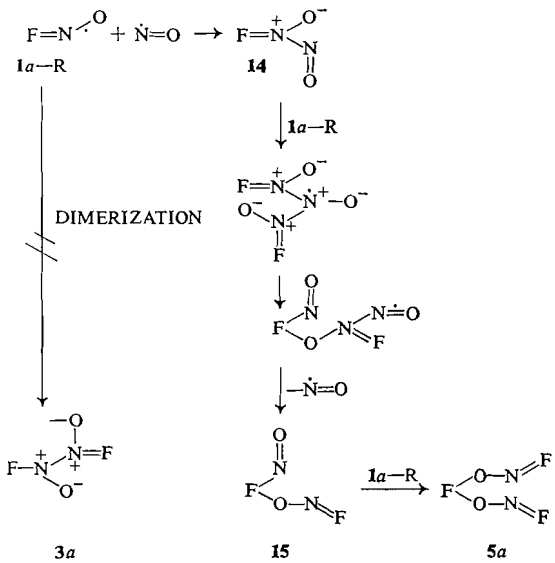

Scheme 2. Iminyl ketal formation.

Benzophenone Nitrimine (8)

The formation of benzophenone nitrimine probably occurred via reaction of the iminoxyl radical of benzophenone oxime with nitric oxide[3]

[3]Benzophenone oxime underwent rapid reaction with NO in glacial acetic acid to give unidentified products, while fluorenone oxime was inert.

Can. J. Chem. Downloaded from www.nrcresearchpress.com by 210.87.254.6 on 09/05/12
For personal use only.

Can. J. Chem. Downloaded from www.nrcresearchpress.com by 210.87.254.6 on 09/05/12
For personal use only.

which has independently been shown to lead to parent ketone and nitrimine **8** (9, 20).

Azine-bis-N-oxides (3)

These have been obtained only in ferricyanide oxidations of bis-arylketoximes and probably arose as shown in Scheme 3. The intermediate **16** has been proposed since similar radicals have been observed (21) in the oxidations of aromatic aldoximes which lead mainly to corresponding aldazine-bis-*N*-oxides (5, 7, 16). This intermediate **16** has not been observed in lead tetraacetate oxidations of bis-arylketoximes, nor has the expected product **3** been detected in these oxidations.

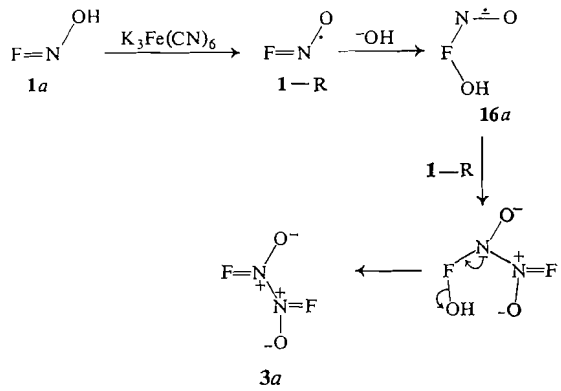

Scheme 3. Fluorenonazine-bis-*N*-oxide formation.

Azinemonoxide (6)

The formation is not understood. No intermediates, including azine-bis-*N*-oxides, were ever detected in the reactions leading to **6** [3, 5, and 10 in Table II], including those conducted at temperatures from −70° to room temperature.

Experimental

General

The lead tetraacetate used in all experiments was obtained from Fisher Scientific. It was crystallized from glacial acetic acid, filtered, covered with a sheet of polystyrene and briefly kept under vacuum. It was then dried in an Abderhalden (refluxing methanol and 0.1 mm pressure). This compound was stored in the dark *in vacuo* for a few days with no decomposition. Solvents were obtained oxygen-free by distilling them in a stream of helium. Mass spectra were taken on a Hitachi Perkin-Elmer RMU6D mass spectrometer by Morgan and Schaffer Corporation, Montreal. Low temperature infrared (i.r.) spectra were taken of solutions in 0.1 mm Amalgam FT cells (IRT-2) from Barnes Engineering Co.

Fluorenonazine-bis-N-oxide (3a)

Fluorenone oxime (2.34 g) and potassium hydroxide (680 mg) in ethanol (40 ml) were added (16 min) to a vigorously stirred solution of potassium ferricyanide (6.8 g) and potassium hydroxide (13.6 g) in distilled water (300 ml) kept at −3 to −7°. The resulting suspension was allowed to warm up overnight to give a red oily precipitate which was filtered. Addition of ether to the red oil gave 410 mg of light-yellow microcrystals of **3a**, m.p. 210° (decomposed). Two crystallizations from benzene–methylene chloride (7:1) gave an analytical sample of **3a** (70 mg), m.p. 212.5° (decomposed), ν_{KBr} 1620, 1520, and 1235 cm^{-1}.

Anal. Calcd. for $C_{26}H_{16}N_2O_2$: C, 80.4; H, 4.15; N, 7.21; O, 8.24. Found: C, 81.8; H, 3.18; N, 7.00; O, 8.08.

Oxidation Products from Fluorenone Oxime (1a)

9,9-Dinitrofluorene (4a)

Lead tetraacetate (1.4 g) in glacial acetic acid (3 ml) was added in 20 min to a stirred solution of **1a** (585 mg) in glacial acetic acid (25 ml). Reaction was complete at the end of the addition.[4] The insoluble lead diacetate was removed by filtration. Water was added to the filtrate to give a yellow precipitate which was dissolved in methylene chloride, washed with saline water and $NaHCO_3$ solution (5%), and dried ($MgSO_4$). Crystallization from hexane gave 150 mg of 9,9-dinitrofluorene (**4a**) as pale-yellow needles, m.p. 129.5–131° (decomposed, NO_2 evolved). Recrystallization gave an analytical sample with m.p. 131–133° (decomposed) (reported m.p. 130–131.5° (decomposed) (16)).

Anal. Calcd. for $C_{13}H_8NO_2$ (mol. wt., 256): C, 60.94; H, 3.15; N, 10.93; O, 24.98. Found (mol. wt., mass spectrometry, 256): C, 60.76; H, 3.53; N, 10.67; O, 25.20.

9,9-Difluorenylideniminoxylfluorene (5a)

(*i*) Lead tetraacetate (1.2 g) was added to glacial acetic acid (50 ml) which was purged with dry nitrogen for 1 h. To this vigorously stirred solution was added fluorenone oxime (1 g). After 4 h the suspension was filtered to give 290 mg of **5a**, slightly contaminated by **1a** (shown by thin-layer chromatography (t.l.c.)), m.p. 264.5–265.5 (decomposed). Three recrystallizations from methylene chloride – ethanol gave an analytical sample of **5a**, m.p. 267° (decomposed).

Anal. Calcd. for $C_{39}H_{24}N_2O_2$ (mol. wt., 552): C, 84.60; H, 4.34; N, 5.06; O, 5.78. Found (mol. wt., osmometric-$CHCl_3$, 597): C, 84.46; H, 4.26; N, 5.16; O, 5.96.

(*ii*) Fluorenone oxime (975 mg) was added to a solution of sodium hydride (480 mg of 50% NaH–oil suspension) in dimethyl sulfoxide. After 10 min, 9,9-dichlorofluorene, prepared according to ref. 22, was added. The solution was stirred overnight in a nitrogen atmosphere. Addition of water gave a precipitate which was filtered to give ketal **5a** (150 mg).

Fluorenonazinemonoxide (6a)

Lead tetraacetate (1.4 g) was added to a stirred solution of **1a** (1.17 g) in oxygen-free CH_2Cl_2 (200 ml). An opaque

[4]An aliquot (0.5 ml) was shaken with 0.1 *N* potassium iodide solution (2 drops). Addition of starch solution gave a purple color only when unreacted lead tetraacetate remained.

Can. J. Chem. Downloaded from www.nrcresearchpress.com by 210.87.254.6 on 09/05/12
For personal use only.

chocolate brown suspension immediately formed. After 4 h, lead acetate was removed by filtration. The CH_2Cl_2 filtrate was washed with water, dried and evaporated *in vacuo* to give a red oil (1.55 g). Elution on silica gel (30 g) with hexane followed by hexane–benzene (1:1) yielded ketal **5***a* (36 mg) and dinitro compound **4***a* (20 mg). Elution with benzene gave initial fractions containing azinemonoxide **6***a* and further fractions containing both the latter and starting oxime. Crystallizations of the initial benzene fractions from MetOH gave red rosettes of **6***a* (141 mg), homogeneous by t.l.c. A recrystallization from CH_2Cl_2–petroleum ether (90–120°) gave an analytic sample with m.p. 178°.

Anal Calcd. for $C_{26}H_{16}N_2O$: C, 83.85; H, 4.33; N, 7.52; O, 4.30. Found: C, 83.60; H, 4.43; N, 7.80; O, 4.38.

*Dinitrodiphenylmethane (**4b**), 1,1-bis(Diphenylmethylideniminoxyl)diphenylmethane (**5b**), and Benzophenone Nitrimine (**8**)*

Lead tetraacetate (4.48 g) was added to a rapidly stirred solution of benzophenone oxime (2 g), m.p. 143–144°, (lit. 142° (23)) in oxygen-free acetic acid in a nitrogen atmosphere. After 20 min, the reaction was complete.[4] The acetic acid solution was evaporated *in vacuo* at 30°. Methylene chloride (10 ml) was added, the lead acetate was filtered off, and the solution evaporated. The resulting oil (1.84 g) was crystallized from methanol at −10° overnight to give colorless flakes (60 mg). Two crystallizations from methanol – methylene chloride gave an analytic sample with m.p. 170.5–171.5°.

Anal. Calcd. for $C_{39}H_{30}N_2O_2$ (mol. wt., 558.6): C, 83.84; H, 5.41; N, 5.01; O, 5.73. Found (mol. wt., 547, osmometric-$CHCl_3$): C, 84.05; H, 4.93; N, 5.29; O, 6.07.

The mother liquor from the above reaction was evaporated. The yellow oil was dissolved in hexane and poured onto a column of silica gel (60 g). Elution with hexane–benzene (7:3) gave 226 mg of **6***b*, m.p. 78.5–79°, homogeneous by t.l.c. Crystallization from hexane gave an analytic sample of **6***b*, m.p. 80.5–81° (decomposed, 100° with NO_2 evolution).

Anal. Calcd. for $C_{13}H_{10}N_2O_4$ (mol. wt., 258.2): C, 60.46; H, 3.90; N, 10.85; O, 24.78. Found (mol. wt., 260, osmometric-$CHCl_3$): C, 60.22; H, 4.79; N, 10.60; O, 24.58.

Further elution with hexane–benzene gave crystals of compound **8** (245 mg), m.p. 62–66°, homogeneous by t.l.c. Crystallization from hexane gave an analytic sample of **8**, m.p. 70–71° (decomposed, 165° with NO_2 evolution), νNO_2/KBr 1540 and 1270 cm^{-1} (s).

Anal. Calcd. for $C_{39}H_{10}N_2O_2$ (mol. wt., 226): C, 69.01; H, 4.46; N, 13.48; O, 14.14. Found (mol. wt., 233, osmometric-$CHCl_3$): C, 69.15; H, 4.55; N, 12.37; O, 14.16.

Further elution with benzene afforded benzophenone (1.15 g) and elution with ether gave an oil (35 mg) probably corresponding to benzophenone oxime-*O*-acetate (**7***b*) (i.r. 1765 cm^{-1} and R_f value = that of **1***b*).

*Geminal Dinitromethanes (**4**)*

The following general method was used: methylene chloride (25 ml) was briefly purged with nitrogen dioxide to give a light brown solution. The oxime (ca. 100 mg) was added all at once to the stirred solution. Immediate reaction occurred. The light-green solution was evaporated at room temperature *in vacuo*. Work-up was continued as follows.

(*i*) 9,9-Dinitrofluorene (**4***a*) was obtained directly as pure crystals, m.p. 129.5–131°.

(*ii*) Pale-yellow crystals (174 mg) were obtained from oxime **1***b* (150 mg), treated as above, consisting of **4***b* and minor amounts of ketone. Crystallization from hexane gave pure **4***b* (115 mg), m.p. 79–79.5°.

(*iii*) The yellow oil (277 mg) obtained from indanone oxime (250 mg; prepared as in ref. 24) consisted mainly of indanone (t.l.c.). Elution on silica gel with hexane–benzene (1:1) gave a yellow oil (31 mg) whose i.r. spectrum in $CHCl_3$ contained bands characteristic of *gem*-dinitromethanes (1570 (s) and 1360 (m) cm^{-1}). These absorption bands and the R_f value indicated that this product was probably 1,1-dinitroindane (**4***d*).

Entries to Table II

The experimental runs were conducted as previously described. All solids used in the oxygen-free experiments were degassed in the reaction flask prior to reaction. In order to simplify analysis of crude reaction mixtures, the following graphical technique was used.

An aliquot was removed from the reaction mixture and analyzed by i.r. in 0.1 mm IRT cells. Bands at 3565, 1765, 1720, and 1570 cm^{-1} could be empirically related to the amounts of oxime, oxime-*O*-acetate, ketone, and azinemonoxide, respectively for the cases of **1***a* and **1***b*. Work-up led to actual isolation of the above compounds, except for oxime-*O*-acetates (**10**), which had R_f values identical to parent oximes. Actual amounts of products **10** were empirically calculated from i.r. and nuclear magnetic resonance (δ_{CDCl_3} 2.35 p.p.m.) spectra of the crude reaction mixtures.

Acknowledgments

This work was supported by the National Research Council of Canada and by Bristol Laboratories, Syracuse, New York.

1. B. C. Gilbert and R. O. C. Norman. J. Chem. Soc. B. No. 1, 86 (1966).
2. W. M. Lauer and W. S. Dyer. J. Am. Chem. Soc. **64**, 1453 (1942).
3. J. W. Lown. J. Chem. Soc. B. No. 5, 441 (1966).
4. D. C. Iffland and G. X. Criner. Chem. and Ind., London, 176 (1956).
5. K. Dahl and G. Just. Tetrahedron Letters, **22**, 2441 (1966).
6. L. Horner and W. Kirmse *et al.* Ber. **94**, 279 (1961).
7. H. Kropf and R. Lambeck. Ann. Chem. To be published.
8. J. Collin. Bull. Soc. Roy. Sci. Liege, **23**, 201 (1954).
9. L. Horner *et al.* Ber. **94**, 290 (1961).
10. B. C. Gilbert. Oxford University, England. Private communication.
11. J. Cane. Chem. Rev. **64**, 473 (1964). A. I. Titov. Tetrahedron, **19**, 557–580 (1963). L. I. Khmelnitski *et al.* Chem. Abstr. **55**, 19, 833*c* (1961).
12. O. Touster. Organic reactions. Vol. VII. John Wiley and Sons, Inc., New York. 1953. p. 349.
13. M. C. R. Symons. J. Chem. Soc. 1189 (1963); M. C. R. Symons. Advan. Phys. Org. Chem. **1**, 283 (1963).

14. R. SCHOLL. Ber. **21**, 506 (1888).
15. L. I. KHMELNITSKI *et al.* Chem. Abstr. **55**, 23, 389*c* (1961).
16. H. SCHECHTER and R. B. KAPLAN. J. Am. Chem. Soc. **83**, 3535 (1961).
17. O. L. CHAPMAN and D. C. HECKERT. J. Am. Chem. Soc. To be published.
18. G. A. RUSSELL. J. Chem. Educ. **36**, 111 (1959).
19. A. K. HOFFMAN, A. M. FELDMAN, and E. GELDBLUM. J. Am. Chem. Soc. **87**, 6461 (1964).
20. O. L. CHAPMAN and D. C. HECKERT. Chem. Commun. **8**, 242 (1966).
21. A. RASSAT *et al.* Bull. Soc. Chim. France, 1485, 1985 (1964).
22. F. J. MOORE and E. H. HUNTRESS. J. Am. Chem. Soc. **49**, 2618 (1927).
23. A. I. VOGEL. Practical organic chemistry. 3rd ed. Longmans, Green and Co., Inc., New York. 1961, p. 741.
24. W. UTERMARK and W. SCHICKE. Melting point tables of organic compounds. John Wiley and Sons, Inc., New York. 1963. pp. 719.

Can. J. Chem. Downloaded from www.nrcresearchpress.com by 210.87.254.6 on 09/05/12
For personal use only.

Absolute configurations of 13-hydroxydocosanoic and 17-hydroxyoctadecanoic acids[1]

A. P. TULLOCH
Prairie Regional Laboratory, National Research Council of Canada, Saskatoon, Saskatchewan
Received July 8, 1968

Methyl 13-D- and 13-L-hydroxydocosanoates have been synthesized from 9-D- and 9-L-hydroxyoctadecanoic acids. Comparison of these esters with the methyl ester of 13-hydroxydocosanoic acid, produced by *Candida bogoriensis*, shows that the natural product has the L-configuration. The known 2-D-octadecanol has been prepared from 17-hydroxyoctadecanoic acid, produced by *Torulopsis apicola*, showing that this acid also has the L-configuration. Most naturally occurring long-chain hydroxy acids, however, have the D-configuration.

Canadian Journal of Chemistry, 46, 3727 (1968)

The hydroxy fatty acids, 17-hydroxyoctadecanoic acid and 13-hydroxydocosanoic acid, have been isolated from extracellular sophorosides produced by the yeasts *Torulopsis apicola* (1) and *Candida bogoriensis* (2) respectively. Because the methyl esters of both hydroxy acids were dextrorotatory, even though the specific rotation of the C_{22} ester was very small, both were provisionally assigned the L-configuration. However, other long-chain hydroxy acids from plants and microorganisms all have the D-configuration: 12-D-hydroxyoctadecanoic acid is obtained by hydrogenation of ricinoleic acid from castor oil (3), 9-D-hydroxyoctadecanoic acid by hydrogenation of the hydroxy acid of *Strophanthus* seed oil (4, 5), and a hydroxy acid from *Coriaria nepalensis* seed oil yields 13-D-hydroxyoctadecanoic acid on hydrogenation (6). These conclusions have been extended by optical rotatory dispersion studies (7). The 10-hydroxyoctadecanoic acid, produced microbiologically from oleic acid, also has the D-configuration (5).

In view of these results it seemed advisable to confirm the configuration of the hydroxy acids from the yeasts. This was done by synthesis, by chain extension of both methyl 13-L- and 13-D-hydroxydocosanoates from 9-D-hydroxyoctadecanoate, the configuration of which is firmly established (4, 5, 7), and by converting 17-hydroxyoctadecanoic acid to 2-D-octadecanol. Chain extension of hydroxy acids of known configuration has been used previously to establish the configuration of new hydroxy acids (3, 4, 8).

Methyl 9-D-hydroxyoctadecanoate was obtained from hydrogenated oil of *Dimorphotheca aurantiaca* (9, 10). The specific rotation in methanol solution is shown in Table I and is very similar to that reported previously (5). It was more convenient, however, to record the rotation in chloroform solution since it was nearly twice as large and also because methyl 13-hydroxydocosanoate was very poorly soluble in methanol.

The 9-acetoxy acid was required for the next step, but acetylation of the hydroxy acid always gave the anhydride (cf. 11) which could not be hydrolyzed to the desired compound in reasonable yield. However, partial hydrolysis of the acetoxy methyl ester with one molar equivalent of sodium hydroxide gave the acetoxy acid. Anodic coupling of 9-D-acetoxyoctadecanoic acid with methyl hydrogen adipate gave, after deacetylation, methyl 13-D-hydroxydocosanoate which had a specific rotation opposite to that of the ester from the glycoside of *C. bogoriensis* (Table I). Also, admixture of the two esters gave the racemic ester which had been previously synthesized (2).

Next 9-L-hydroxyoctadecanoic acid was prepared from the *p*-toluenesulfonate of methyl 9-D-hydroxyoctadecanoate by treatment with sodium acetate. This method was described previously by Schroepfer and Bloch (5), but the intermediate tosylate was not characterized. The specific rotation of the methyl 9-L-hydroxyoctadecanoate (Table I) indicated that very little racemization had occurred during inversion, whereas Schroepfer and Bloch estimated that their product had an optical purity of 89%. Coupling of 9-L-acetoxyoctadecanoic acid with methyl hydrogen adipate gave methyl 13-L-hydroxydocosanoate indistinguishable from the natural ester. The specific rotation is shown in Table I.

[1]Issued as NRCC No. 10376.

TABLE I

Specific rotations of methyl 9-hydroxyoctadecanoates and 13-hydroxydocosanoates (±0.05°) at 25°

	Compound					
	9-D-Hydroxyoctadecanoate		9-L-Hydroxy-octadecanoate	13-D-Hydroxy-docosanoate	13-L-Hydroxy-docosanoate (Synthetic)	13-L-Hydroxy-docosanoate (Natural)
Wave-length (mμ)	Methanol (*c*, 11.1)	Chloroform (*c*, 10.4)	Chloroform (*c*, 11.3)	Chloroform (*c*, 10.1)	Chloroform (*c*, 8.3)	Chloroform (*c*, 9.3)
589	−0.22	−0.40	+0.37	−0.10	+0.11	+0.10
546	−0.24	−0.43	+0.50	−0.09	+0.14	+0.13
436	−0.38	−0.75	+0.80	−0.14	+0.20	+0.23
365	−0.58	−1.16	+1.22	−0.23	+0.27	+0.33

In assigning the configuration of 17-hydroxyoctadecanoic acid it was assumed that the ester group at the end of the chain would have little effect on the specific rotation and that it could be regarded as a 2-octadecanol (1) and would have the D-configuration since all dextrorotatory 2-alcohols have the D-configuration (12–14). The rules of nomenclature, however, require that the 17-hydroxy ester be named as an L-hydroxy compound.

Since the ester group might conceivably have had an effect on the rotation, the 17-hydroxy ester was converted to the 2-octadecanol. Also, 2-D-octadecanol has been previously isolated from the wax of tubercle bacteria (15). 17-Acetoxyoctadecanoic acid was prepared from the acetoxy ester and electrolyzed with acetic acid to give 2-D-octadecanol on hydrolysis. The specific rotations are shown in Table II; there is clearly very little difference between that of the 2-alcohol and that of the parent 17-hydroxy ester, so that the latter can be safely assigned the L-configuration. The considerably smaller, but still positive, rotation of the acetoxy ester is similar to the rotations of the acetates of homologous alcohols of shorter chain length (12).

The fact that hydroxy acids from yeast lipids have the opposite configuration to almost all of the others from natural sources may have some bearing on the biosynthesis of these compounds. 13-L-Hydroxyoctadecanoic acid has been prepared by reduction of the hydroperoxide obtained by the action of lipoxidase on linoleic acid (16). It seems unlikely, however, that dienoic acids would be involved in the biosynthesis of the yeast hydroxy acids. It is particularly unlikely in the case of 17-hydroxyoctadecanoic acid since unsaturated acids are always hydroxylated by *Torulopsis* at a position remote from the double bond (17).

Experimental

Specific rotations were measured at 25° in a 1-dm cell using a Perkin–Elmer model 141 Polarimeter. Nuclear magnetic resonance (n.m.r.) spectra were measured with carbon tetrachloride as solvent, using a Varian HA-100 spectrometer. Chemical shifts are in parts per million (p.p.m.) from tetramethylsilane (internal standard). Gas–liquid chromatography (g.l.c.) was carried out as described previously (18).

TABLE II

Specific rotations of methyl 17-L-hydroxyoctadecanoate and derived compounds in chloroform (±0.04 to ±0.06)

	Compound			
Wave-length (mμ)	Methyl 17-L-hydroxy-octadecanoate (*c*, 4.8)	Methyl 17-L-acetoxy-octadecanoate (*c*, 6.0)	17-L-Acetoxy-octadecanoic acid (*c*, 3.4)	2-D-Octadecanol (*c*, 4.2)
589	+3.6	+0.85	+1.02	+4.46
546	+4.3	+1.13	+0.91	+5.11
436	+6.9	+1.17	+0.85	+8.32
365	+10.6	+1.93	—	+12.56

Methyl 9-D-Hydroxyoctadecanoate

Oil of *Dimorphotheca auriantica* was kindly supplied by Dr. Glenn Fuller of the United States Department of Agriculture, Albany, California. The oil (60 g) was hydrogenated in glacial acetic acid using 10% palladium on charcoal as catalyst (10). Methyl esters (56 g) were obtained by refluxing the hydrogenated oil with 4% methanolic hydrogen chloride. Two crystallizations of the esters from hexane gave methyl 9-D-hydroxyoctadecanoate (16.7 g), m.p. 52.0–52.5° (lit. (7) gives 51.5–52.8°). Examination of the mother liquors by g.l.c. before and after acetylation (18) indicated that the oxygenated esters remaining in the oil consisted mainly of an oxo ester, probably methyl 9-oxooctadecanoate. The formation of oxo esters during hydrogenation of this and related compounds has been reported previously (10).

9-D-Acetoxyoctadecanoic Acid

The 9-hydroxy ester (4.8 g) was acetylated with acetic anhydride and the resulting acetoxy ester was distilled; yield (4.6 g); b.p. 145–155°/0.2 mm. The acetoxy ester (4.6 g) was allowed to stand for 24 h at room temperature in a mixture of aqueous sodium hydroxide (0.1 *N*, 129 ml) and acetone (300 ml) and then refluxed for 4 h. Most of the acetone was taken off, the solution acidified, and the product extracted with chloroform. Crystallization from hexane gave 9-D-acetoxyoctadecanoic acid (3.4 g), m.p. 34.5–35.5°. Nuclear magnetic resonance: CH_3, 0.88; CH_2, 1.28 (shoulder 1.32, cf. (19)); acetoxyl 1.96; α-CH_2, 2.29; H-9, 4.75 (multiplet).

Anal. Calcd. for $C_{20}H_{38}O_4$: C, 70.13; H, 11.18. Found: C, 70.31; H, 11.24.

Methyl 13-D-Hydroxydocosanoate

The 9-acetoxy acid (4.0 g) and methyl hydrogen adipate (4.3 g) were electrolyzed in a mixture of 0.022 *N* methanolic sodium methoxide (16 ml) and methanol (8 ml) until the solution was alkaline. The apparatus and conditions were those used by Greaves *et al.* (20) in their method B1. The solution was acidified with acetic acid, the methanol taken off, and the crude product refluxed with 4% methanolic hydrogen chloride. The reaction mixture was poured into water and the deacetylated product (5.8 g) was extracted with ether. Crystallization from methanol (50 ml) at 25° gave a white solid (1.4 g), m.p. 102–103° (probably 10,25-dihydroxytetratriacontane). After concentrating the filtrate to 25 ml and cooling to 0°, crude 13-hydroxydocosanoate (2.4 g) was obtained. This product was recrystallized from methanol and gave the ester (1.1 g), m.p. 65–66°. The ester was saponified and the acid obtained crystallized from acetone giving 13-hydroxydocosanoic acid (0.65 g), m.p. 85–86°. This acid was converted to the methyl ester with diazomethane and the ester crystallized from methanol to give pure methyl 13-D-hydroxydocosanoate (0.35 g), m.p. 69.5–70°.

Anal. Calcd. for $C_{23}H_{46}O_3$: C, 74.54; H, 12.51. Found: C, 74.60; H, 12.35.

A mixture of equal weights of the above D-ester and the ester isolated from *C. bogoriensis* (m.p. 70–70.5°) had m.p. 62.5–63°. After one crystallization from methanol this material had m.p. 62.5–63.5°. Racemic methyl 13-hydroxydocosanoate was previously found to have m.p. 63–63.5° (2). The infrared spectra (KBr disk) of the D-ester and the naturally occurring ester were indistinguishable. The spectra of the racemate obtained by mixing the two isomers and that obtained by synthesis (2) were also indistinguishable from each other, but differed from the spectra of the optically active isomers in the regions 1150–1225 and 1325–1375 cm^{-1}.

Methyl 9-L-Hydroxyoctadecanoate

A solution of methyl 9-D-hydroxyoctadecanoate (9.0 g) in dry pyridine (500 ml) was cooled to −15° and a solution of recrystallized *p*-toluenesulfonyl chloride (25 g) in pyridine (200 ml), also at −15°, was added. The mixture was kept at −15° for one week and at 0° for a further week. Water (250 ml) was cooled to +2° and added to the reaction mixture; after 4 h more water (1500 ml) was added and the product extracted with ether; the extract was washed 10 times with water and dried over sodium sulfate. The product obtained after removal of the ether was crystallized from hexane to give the *p*-toluenesulfonate of methyl 9-D-hydroxyoctadecanoate (9.1 g). The m.p. was 32° and $[\alpha]_D$ +1.35°, $[\alpha]_{546}$ +1.66°, $[\alpha]_{436}$ +2.93°, $[\alpha]_{365}$ +4.98° (*c*, 11.4 in chloroform).

Nuclear magnetic resonance: terminal CH_3, 0.88; CH_2, 1.25; α-CH_2, 2.20; CH_3 on aromatic ring, 2.44; OCH_3, 3.60; H-9, 4.46; aromatic protons, 7.26, 7.72 (doublets J = 8 c.p.s.).

Anal. Calcd. for $C_{26}H_{44}O_5S$: C, 66.68; H, 9.47. Found: C, 66.39; H, 9.32.

A solution of the *p*-toluenesulfonate (8.0 g) in acetic acid (120 ml) containing anhydrous sodium acetate (8.0 g) was heated at 60° for 18 h and then refluxed for 4 h. Acetic acid was taken off and the residue deacetylated with 4% methanolic hydrogen chloride. The crude product was chromatographed on silicic acid (Bio-Sil A, 100 g) when unsaturated by-products were eluted with hexane–ether (92:8). Elution with hexane–acetone (95:5) gave methyl 9-L-hydroxyoctadecanoate (3 g), m.p. 52–53°.

Anal. Calcd. for $C_{19}H_{38}O_3$: C, 72.56; H, 12.18. Found: C, 72.27; H, 11.97.

Methyl 13-L-Hydroxydocosanoate

Methyl 9-L-hydroxyoctadecanoate (3.0 g) was converted to the acetoxy acid (2.8 g) and electrolyzed with methyl hydrogen adipate (5.0 g) and the reaction mixture worked up as described in the preparation of methyl 13-D-hydroxydocosanoate. After purification methyl 13-L-hydroxydocosanoate (0.30 g) was obtained. The m.p. was 69–70° and was not depressed by admixture with an equal weight of the ester from the glycoside of *C. bogoriensis*. The infrared spectra of the synthetic and natural isomers were very similar.

Methyl 17-L-Hydroxyoctadecanoate

Crude esters (400 g) were prepared from the sophoroside as previously described (1) and crystallized three times from acetone (10% solution, charcoal); yield 95 g; m.p. 54.5–55.5°.

Methyl 17-L-Acetoxyoctadecanoate

The above hydroxy ester (10.5 g) was acetylated with acetic anhydride and pyridine at 100° for 2 h. After removal of the reagents the product was distilled, b.p./0.25 mm 168–172°, to give the acetate (11.1 g). A portion (2.1 g) was crystallized from hexane giving acetoxy ester (1.4 g) as large leaflets with m.p. 35–36°.

Anal. Calcd. for $C_{21}H_{40}O_4$: C, 70.74; H, 11.31. Found: C, 70.54; H, 11.09.

17-L-Acetoxyoctadecanoic Acid

Acetoxy ester (9.0 g) was hydrolyzed with 0.1 *N* aqueous sodium hydroxide (252 ml) in acetone (500 ml) and the product worked up as described in the preparation of 9-D-acetoxyoctadecanoic acid. Crystallization of the crude product from hexane first gave material (1.3 g) which appeared to be hydroxy acid and then the desired acetoxy acid (6.1 g), m.p. 53–54°.

Nuclear magnetic resonance: CH_3 (doublet), 1.15; CH_2, 1.25; acetoxyl, 1.93; α-CH_2, 2.28; H-17 (multiplet), 4.77.

Anal. Calcd. for $C_{20}H_{38}O_4$: C, 70.13; H, 11.18. Found: C, 70.31; H, 11.11.

2-D-Octadecanol

17-Acetoxyoctadecanoic acid (5.0 g) and acetic acid (5.1 g) were electrolyzed in a mixture of 0.022 *N* methanolic sodium methoxide solution (40 ml) and methanol (10 ml) for 5 h when the solution was alkaline. After working up as before the crude product was treated with warm methanol (25 ml) and the solution filtered from insoluble material (probably long chain diol). The product (1.2 g) crystallized at 10°. Recrystallization from ethyl acetate gave the pure alcohol (0.9 g); m.p. 54–55° (lit. (15) gives m.p. 56° and $[\alpha]_D^{25}$ +5.7°).

Nuclear magnetic resonance: terminal CH_3's, 0.88 (triplet) and 1.10 (doublet); CH_2, 1.26; H-2, 3.64 (multiplet).

Anal. Calcd. for: $C_{18}H_{38}O$: C, 79.87; H, 13.98. Found: C, 79.92; H, 14.16.

Acknowledgments

The author is indebted to Mr. L. L. Hoffman for experimental assistance, to Mr. M. Mazurek for nuclear magnetic resonance measurements, and to Mr. W. C. Haid for microanalyses and infrared measurements.

1. P. A. J. Gorin, J. F. T. Spencer, and A. P. Tulloch. Can. J. Chem. **39**, 846 (1961).
2. A. P. Tulloch, J. F. T. Spencer, and M. H. Deinema. Can. J. Chem. **46**, 345 (1968).
3. K. Serck-Hanssen. Chem. Ind. London, 1554 (1958).
4. C. D. Baker and F. D. Gunstone. J. Chem. Soc. 759 (1963).
5. G. J. Schroepfer and K. Bloch. J. Biol. Chem. **240**, 54 (1965).
6. W. H. Tallent, J. Harris, I. A. Wolff, and R. E. Lundin. Tetrahedron Letters, 4329 (1966).
7. T. H. Applewhite, R. G. Binder, and W. Gaffield. J. Org. Chem. **32**, 1173 (1967).
8. T. H. Applewhite. Tetrahedron Letters, 3391 (1965).
9. C. R. Smith, T. L. Wilson, E. H. Melvin, and I. A. Wolff. J. Am. Chem. Soc. **82**, 1417 (1960).
10. R. G. Powell, C. R. Smith, C. A. Glass, and I. A. Wolff. J. Org. Chem. **30**, 610 (1965).
11. A. P. Tulloch, A. Hill, and J. F. T. Spencer. Can. J. Chem. **46**, 3337 (1968).
12. R. H. Pickard and J. Kenyon. J. Chem. Soc. **105**, 830 (1914).
13. K. Serck-Hanssen, S. Ställberg-Stenhagen, and E. S. Stenhagen. Arkiv Kemi, **5**, 203 (1953).
14. J. A. Mills and W. Klyne. *In* Progress in stereochemistry. Vol. 1. *Edited by* W. Klyne. Butterworth and Co., London. 1954. p. 205.
15. M. C. Pangborn and R. J. Anderson. J. Am. Chem. Soc. **58**, 10 (1936).
16. M. Hamberg and B. Samuelsson. J. Biol. Chem. **242**, 5329 (1967).
17. A. P. Tulloch, J. F. T. Spencer, and P. A. J. Gorin. Can. J. Chem. **40**, 1326 (1962).
18. A. P. Tulloch. J. Am. Oil Chemists Soc. **41**, 833 (1964).
19. A. P. Tulloch. J. Am. Oil Chemists Soc. **43**, 670 (1966).
20. W. S. Greaves, R. P. Linstead, B. R. Shephard, S. L. S. Thomas, and B. C. L. Weedon. J. Chem. Soc. 3326 (1950).

Can. J. Chem. Downloaded from www.nrcresearchpress.com by 210.87.254.5 on 09/05/12
For personal use only.

Photo-addition of alkenes and alkynes to 3-carene-2,5-dione[1]

IAN W. J. STILL, M-H. KWAN, AND G. E. PALMER[2]
Department of Chemistry, University of Toronto, Toronto 5, Ontario

Received August 8, 1968

A number of photo-addition reactions have been carried out on the enedione system of 3-carene-2,5-dione by direct irradiation in the presence of a variety of alkenes and alkynes. Addition to the carbon–carbon double bond is by far the major pathway, and indeed in only one case is there evidence for formation of an oxetane ring. In the case of the unsymmetrical addends, the direction of addition which produces the cyclobutane or cyclobutene appears to be in accord with previous experiments on simpler systems.

Canadian Journal of Chemistry, 46, 3731 (1968)

Introduction

The photochemical addition of olefins to simple conjugated ketones such as 2-cyclohexenone has been extensively investigated (1, 2). Recent work (3, 4) has been concerned with the photo-addition of olefins to more complex conjugated molecules, incorporating for example a *p*-quinonoid structure. Relatively little has appeared in the literature on the corresponding photo-addition of alkynes to conjugated carbonyl compounds although Pappas and Pappas (5), and Pappas and Portnoy (6) recently reported the successful formation of cyclobutene adducts from methoxy-*p*-benzoquinone and various substituted acetylenes.

The present paper describes some photochemical additions to a system intermediate in complexity between the simple enones and the quinones. We have used as our substrate the 1,4-enedione system of 3-carene-2,5-dione (**1**), while our addends have consisted of a variety of cyclic and acyclic alkenes. We have attempted to determine whether cyclobutane formation, by addition of the olefin to the C=C of the enedione (path *a*), or oxetane formation, by addition to the C=O group (path *b*), would be preferred in such a system. For completeness, we have also investigated a small number of alkynes as addends in this study.

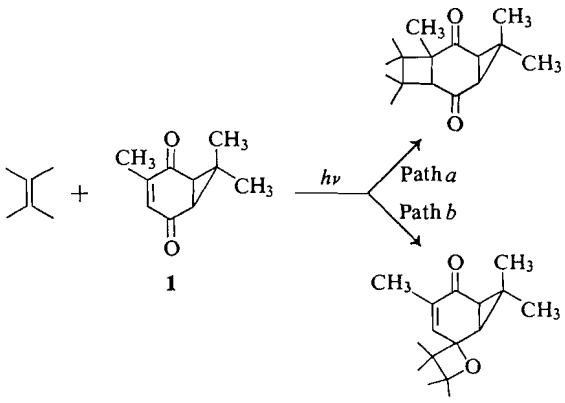

1

Results and Discussion

All the photochemical reactions were carried out in quartz vessels using a 125-W medium-pressure mercury arc lamp[3] as the light source. The solvents used were degassed by prior boiling and cooling under nitrogen and all reactions were carried out under nitrogen. With the exception of the norbornene photo-addition—an extremely slow reaction in any circumstances—no photosensitizer was required, and we normally used at least a 5-fold excess of the alkene or alkyne, in benzene as solvent. In a few cases, indicated in Table I and Table II, the alkene served as both reactant and solvent.

In all the cases we have examined, with the exception of the cyclohexene addition, the photo-addition has taken place exclusively at the C=C bond of 3-carene-2,5-dione, i.e. by path *a*. Even in the exceptional case, the oxetane addition product is very much the minor product of the reaction. (This particular reaction will be discussed in more detail later.) The structures of the photo-adducts have been established by elemental analysis and by the usual spectroscopic techniques. The spectral details of individual products appear in the Experimental section but

[1]Presented in part at the 51st Annual Conference of the Chemical Institute of Canada, Vancouver, June 3–5, 1968.

[2]Present address: Prince of Wales College, Charlottetown, Prince Edward Island.

[3]Engelhard Hanovia Lamps, Bath Road, Slough, England.

Can. J. Chem. Downloaded from www.nrcresearchpress.com by 210.87.254.5 on 09/05/12
For personal use only.

certain general points may be mentioned here. The mass spectra, for example, afforded molecular ions in all cases, but the base peak usually appeared at *m/e* 164, (3-carene-2,5-dione ion–radical), indicating that retro-addition is a major disintegration pathway. Infrared spectroscopy, in addition to its use in the identification of products, was also invaluable as a means of following the progress of a reaction, the CO band of 3-carene-2,5-dione at 1665 cm^{-1} being replaced by the saturated CO band at about 1685 cm^{-1} in the adducts.

It was assumed from the presence of liquids, or of solids melting over a wide range, in Tables I–III, that the adducts were possibly mixtures of stereoisomers in some cases. No attempts have been made to assign the stereochemistry at the cyclobutane ring junctions, although inspection of the appropriate Dreiding models will usually indicate possible preferences in particular cases. In addition, we assume that the fusion of the cyclobutane ring to the carane system is *cis*-, because in none of the adducts we have examined have we been able to obtain any evidence for base-catalyzed epimerization of *trans*-fused to *cis*-fused adducts such as were observed by Corey *et al.* (2).

TABLE I

Results of alkene addition*

Addend	Time of irradiation (h)	Yield† (%)	Melting point °C
1-Hexene	9‡	80	Liquid
Tetramethylethylene	66§	47	Liquid
Tetrachloroethylene	46§	—	—
Vinyl acetate	95§	58	Liquid
Methyl vinyl ether	23§	100	Liquid
Ethyl vinyl ether	17‡	100	Liquid
Acrylonitrile	22‡	98	177–178
Isoprene	29‡	39 51	116–117 Liquid

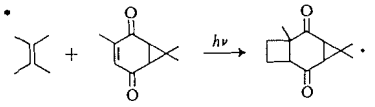

†Chromatographically pure.
‡Addend as solvent (0.5–1% carenedione).
§Solution, in benzene, with 5–10 molar equivalents of alkene.

The data in Table I are obtained from the photo-addition of acyclic alkenes to 3-carene-2,5-dione. In the case of tetrachloroethylene, no reaction at all could be observed. On the other hand, unsymmetrical alkenes with electron-donating substituents (e.g. ethyl vinyl ether) and with electron-withdrawing substituents (e.g. acrylonitrile) reacted almost equally rapidly. In the case of the vinyl ether adducts **2**, both products, obtained in quantitative yield, were very high-boiling liquids and attempted distillation resulted in apparent thermal reversal of the addition, with the regeneration of some 3-carene-2,5-dione. As a result, satisfactory analytical data could not be obtained for these compounds. The appearance of molecular ions at *m/e* 222 and 236 in the respective mass spectra, however, along with the infrared and nuclear magnetic resonance (n.m.r.) data on undistilled material, confirmed the presence of the expected 1:1 cyclobutane adducts. It is tempting to speculate that the unusually facile thermal reversal of the addition takes place via a dipolar intermediate as shown (the alternative location of the ether

TABLE II

Results of cycloalkene addition*

Addend	Time of irradiation† (h)	Yield‡ (%)	Melting point °C
Cyclopentene	95§	43§	70–72
Cyclohexene	26	65‖	93–102
Cycloheptene	77	85	67–68
Cycloöctene	36	80	78–85
Norbornene	290¶	40	129–130

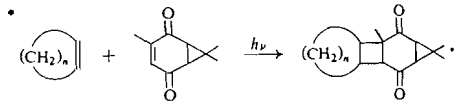

†Solutions of carenedione (0.5–1.0%) in the alkene as solvent.
‡Chromatographically pure.
§Irradiation in benzene with 8 molar equivalents of alkene.
‖Minor product (10%) believed to be oxetane.
¶Irradiation in benzene with 6 molar equivalents of alkene and 0.1 molar equivalents of acetophenone.

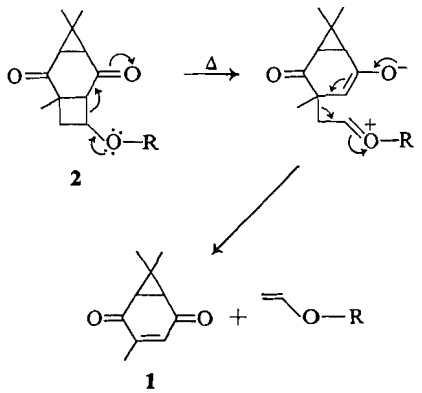

2

1

Can. J. Chem. Downloaded from www.nrcresearchpress.com by 210.87.254.5 on 09/05/12
For personal use only.

function is not ruled out, but it would still be located β- to a carbonyl group).

Although we regard the gross structure in each case as being the normal cyclobutane type adduct, the products obtained from the photo-addition reactions with 1-hexene, vinyl acetate, and isoprene (one isomer) were also liquids, and this fact together with the complexity of the n.m.r. spectra suggest that we may have mixtures of stereoisomers or even of positional isomers (*3a, b*) in these cases. Additional confirmation of the structures of the liquid products from 1-hexene and tetramethylethylene was afforded by the preparation of the crystalline monoxime **4** and bis-oxime **5** respectively, each of which has physical properties in accord with the expected structures.

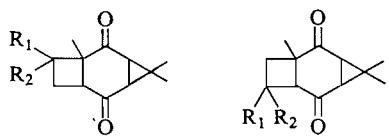

3a *3b*

$R_1 = H, R_2 = n\text{-}C_4H_9$
$R_1 = H, R_2 = OAc$
$R_1 = CH_3, R_2 = -CH{=}CH_2$

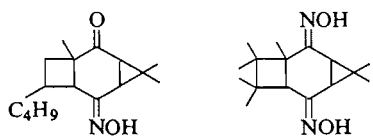

4 **5**

The sharp-melting solid adducts from the reactions with acrylonitrile and isoprene have been assigned the gross structures **6** and **7**, largely on the basis of the following argument. Corey and his co-workers (2) established that a 2-methyl substituent on the basic cyclohexenone chromophore greatly diminished the rate of the photo-reaction (relative to that of 2-cyclohexenone itself), whereas the substitution of a 3-methyl group for hydrogen caused no significant rate retardation. Furthermore, with isobutylene and 3-methyl-2-cyclohexenone the *only* cyclobutane addition product obtained was **8**, in sharp contrast to the direction of addition of isobutylene to 2-cyclohexenone itself. If we now make the somewhat oversimplifying assumption that our enedione system is in fact made up of two enone components, of which the 3-methyl enone will be much the more reactive, and that reaction takes place by addition of excited state ketone to ground state olefin, then the direction of addition predicted will be that shown schematically below.

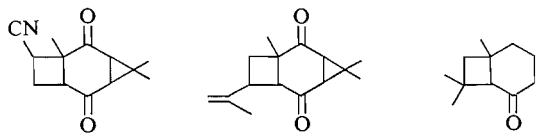

6 **7** **8**

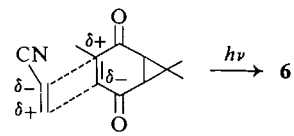

Ground state Excited state

Supporting evidence on this point from the n.m.r. is limited by the complexity of the relevant regions of the spectra. Of the two isoprene adducts (Table I), however, we can assign a structure such as **7** to the solid adduct because of the characteristic allylic methyl group singlet at τ 8.40 and the appearance of only two vinyl protons at τ 5.1 and 5.4. As we have already mentioned, the n.m.r. spectrum of the liquid product from isoprene photo-addition is much more complex, even in the methyl region of the spectrum, but reveals three vinyl protons between τ 4.0 and 5.4 and no allylic methyl group signal. The n.m.r. evidence from the alkyne photo-additions provides much stronger support for the structure assigned to the unsymmetrical (ethyl propiolate) adduct in that series, and we will return to this point later.

No problems regarding direction of addition arise with the cycloalkene series of adducts represented in Table II. It would appear from the table that the even-membered cycloalkenes undergo more rapid photo-addition than the odd-membered, although the data obtained are insufficient to enable us to speculate on possible reasons for this variation. In addition, the wide melting point range of the cyclohexene and cyclooctene adducts indicates the probability of more than one configuration being present (*syn–syn*, *anti–anti*, *syn–anti*, and *anti–syn* forms are possible, even with all *-cis* ring junctions). The presence of a sensitizer during the formation of

the norbornene photo-adduct may have no significance, since a prior reaction without sensitizer, and in which no significant amount of product was isolated, was stopped after only 90 h.

TABLE III

Results of alkyne addition*

Addend	Time of irradiation† (h)	Yield‡ (%)	Melting point °C
Acetylene	50	11§	95–96
Ethyl propiolate	94	59‖	Liquid
Diethyl acetylene-dicarboxylate	53	23	61–62

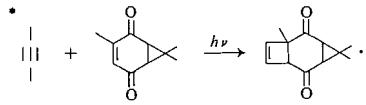

†1% solutions of carenedione in benzene with a large excess of alkyne.
‡Chromatographically pure.
§13% recovery of carenedione.
‖35% recovery of carenedione.

The minor isomeric product (10% yield) in the cyclohexene case was assigned the oxetane structure **9** on the basis of the spectral data (see Experimental section). One-proton signals in the n.m.r. at τ 4.04 and 4.90 were attributed to protons H_B and H_C respectively, while a three-proton signal at τ 8.02 was attributed to the allylic methyl. In addition to the carbonyl band at 1685 cm^{-1}, a medium intensity band appeared in the infrared at 1620 cm^{-1}, due to the C=C

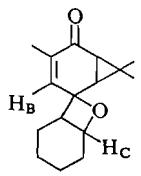

9

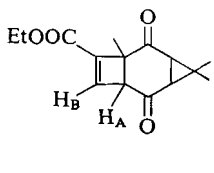

10

double bond. The mass spectral molecular weight of 246 was in accordance with the expected 1:1 adduct, but the strong peak at *m/e* 164, which appeared in the mass spectra of all the other photo-adducts and has been assigned to the formation of the carenedione radical–ion by retro-addition, was not present.

In Table III are listed the results of photo-additions carried out with alkynes. In all these cases, reactions were carried out in benzene as the solvent, with a large excess (> 10-fold) of the alkyne present. In the only unsymmetrical photo-addition in this series, we have assigned structure **10** to the ethyl propiolate adduct, by extending the argument already used to predict the outcome of the acrylonitrile addition, and also on the basis of the n.m.r. evidence (see also Experimental section).

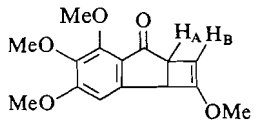

11

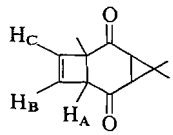

12

The vinylic proton (H_B) appeared as a doublet (J = 1.8 Hz) at τ 3.33 and the bridgehead proton (H_A) also appeared as a doublet (J = 1.8 Hz) at τ 6.95. This value for the vicinal coupling constant in such a situation agrees very closely with the value of 1.3 Hz reported very recently by Forbes *et al.* (7) for J_{AB} in compound **11**. In the acetylene adduct itself **12**, the bridgehead proton H_A appears at an almost identical value, τ 6.92. If, in the unsymmetrical adduct, the ester group rather than a proton, were vicinal to H_A, one would have expected a noticeable deshielding effect, such as is produced in the adduct **13** from diethyl acetylenedicarboxylate and 3-carene-2,5-dione. Here the cyclobutene ring bridgehead proton must have an ester group adjacent, and accordingly appears as a singlet at τ 6.65. Analysis of the ABC system in the acetylene adduct **12** by the exact method (8), (9) led to coupling constants of J_{AC} = 1.0 Hz, J_{AB} = 1.4 Hz, and J_{BC} = 2.6 Hz. (J_{AB} and J_{AC} are opposite in sign.)

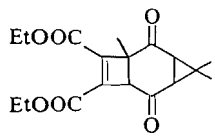

13

Further photochemical investigations in this area are continuing, particularly, from the standpoint of photodimerization of the 3-carene-2,5-dione used as a substrate in the present study.

Experimental

Infrared spectra were recorded in CCl_4 or $CHCl_3$ on a Perkin–Elmer model 237B grating spectrometer, and the ultraviolet spectra on a Unicam SP 800 recording spec-

Can. J. Chem. Downloaded from www.nrcresearchpress.com by 210.87.254.5 on 09/05/12
For personal use only.

Can. J. Chem. Downloaded from www.nrcresearchpress.com by 210.87.254.5 on 09/05/12
For personal use only.

trophotometer. Nuclear magnetic resonance spectra were obtained on Varian A-60 or HA-100 instruments, with tetramethylsilane as internal standard. Mass spectra were measured on the AEI MS-902 machine, and elemental analyses were carried out by Dr. C. Daesslé, Montreal, and by Mr. A. B. Gygli, Toronto. Column chromatography was performed on Davison Chemical Grade 923 100–200 mesh Silica Gel. All melting points are uncorrected.

3-Carene-2,5-dione (1)

This compound was prepared by deoximation of 3-carene-2,5-dione-2-oxime (10), utilizing a sodium nitrite/acetic acid procedure (11). The pale-yellow crystals had m.p 90–92° on sublimation (lit. m.p. (10), 93–94°) and the 60 MHz n.m.r. spectrum (CCl_4) had signals at τ 8.64 (6H), 8.07 (3H), and 7.80 (2H), and 3.62 (1H).

Photo-addition of 1-Hexene to 3-Carene-2,5-dione

A 0.5% solution of 3-carene-2,5-dione in freshly distilled 1-hexene was irradiated in a quartz vessel for 9 h under nitrogen, using the 125W medium-pressure mercury arc referred to earlier. Aliquots were withdrawn at regular intervals and the infrared spectra recorded. The reaction was considered complete when almost all of the conjugated carbonyl band had disappeared, to be replaced by a nonconjugated carbonyl peak. Chromatography on silica of the crude product obtained on evaporation of the excess alkene led to the isolation of an oil (80%), b.p. 124°/0.3 mm, on elution with 4% ether in benzene. The infrared spectrum showed a strong carbonyl band at 1688 cm^{-1} and no olefinic absorption. The n.m.r. spectrum (CCl_4) had signals at τ 8.95–9.2 (3H, terminal CH_3), 8.79, 8.75, 8.68 (all 3H, s, methyl protons), 8.40–8.95 (6H, methylene protons), 7.88 (2H, cyclopropyl bridgehead), 7.40–7.95 (4H, cyclobutyl protons).

Anal. Calcd. for $C_{16}H_{24}O_2$: C, 77.41; H, 9.68. Found: C, 77.21; H, 9.77.

The dioxime was prepared by the standard hydroxylamine hydrochloride – pyridine procedure and had m.p. 238° (aqueous ethanol).

Anal. Calcd. for $C_{16}H_{26}N_2O_2$: C, 69.07; H, 9.35; N, 10.07. Found: C, 68.98; H, 9.42; N, 9.98.

Adduct from Tetramethylethylene

A 3% solution of 3-carene-2,5-dione in benzene was irradiated for 66 h under nitrogen, in the presence of 6 molar equivalents of redistilled tetramethylethylene. Chromatography of the product on silica yielded the cycloadduct as an oil (47%) on elution with 10% ether in benzene. The infrared spectrum showed a strong carbonyl band at 1687 cm^{-1}. The n.m.r. spectrum (CCl_4) showed τ 8.7–9.1 (seven singlets, each 3H), 8.0 (2H), and 7.7 (1H).

The oil was not distilled, but was converted directly to the mono-oxime by standard procedures. This compound had m.p. 169–171°, on recrystallization from cyclohexane. The mass spectrum revealed a peak at *m/e* 263, in accord with the formula $C_{16}H_{25}NO_2$.

Anal. Calcd. for $C_{16}H_{25}NO_2$: C, 73.00; H, 9.50; N, 5.32. Found: C, 72.93; H, 9.48; N, 5.45.

Adduct from Vinyl Acetate

A 4% solution of 3-carene-2,5-dione in benzene was irradiated in benzene solution for 95 h, with 3 molar equivalents of vinyl acetate. Chromatography of the crude product on silica led to the isolation of an oil (58%), by elution with 20% ether in benzene. The adduct showed infrared carbonyl bands at 1745 (OAc), and 1684 (CO) cm^{-1}. The n.m.r. spectrum (CCl_4) revealed signals at τ 8.50–8.85 (three singlets, each 3H), 8.04 (3H, s), 7.83 (2H, s), 7.0–7.8 (3H, m), and 5.0–5.3 (1H, m).

Photo-addition of Methyl Vinyl Ether to 3-Carene-2,5-dione

Methyl vinyl ether was passed continuously into a 1% solution of carenedione in benzene, and the solution was irradiated for 23 h. Chromatography on silica gel and elution with 20% ether in benzene gave a quantitative yield of the photo-adduct as a pale-yellow oil, b.p. 100°/0.1 mm. The oil deepened in color during this process due to apparent retroaddition (see Discussion) and the regeneration of 3-carene-2,5-dione. (It was estimated from the intensity of the shoulder in the ultraviolet spectrum (CH_3OH) at 240 nm that as much as 25–30% retroaddition had occurred.) As a result, no satisfactory elemental analysis could be obtained. The infrared spectrum of the undistilled eluate after chromatography, however, revealed the expected peak at 1680 cm^{-1}, while the n.m.r. spectrum (CCl_4) had τ 8.96 (3H, s), 8.88 (3H, s), 8.66 (3H, s), 8.1 (2H, m), 7.3 (2H, m), 6.72 (1H, t), 6.61 (3H, s), and 4.8 (1H, m) in general agreement with expectation for the cyclobutane type adduct. The mass spectrum showed a peak at *m/e* 222, in agreement with the formula $C_{13}H_{18}O_3$.

Photo-addition of Ethyl Vinyl Ether to 3-Carene-2,5-dione

A 1% solution of carenedione in freshly distilled ethyl vinyl ether was irradiated for 17 h. Chromatography of the crude product on silica gel and elution with 7–10% ether in benzene gave the photo-adduct as a yellow oil (100%), b.p. 117°/0.7 mm. The same decomposition problems were encountered on distillation as for the methyl analogue above, and once again no satisfactory elemental analysis was obtained. The infrared spectrum, however, again revealed the expected saturated carbonyl band at 1680 cm^{-1}, while the n.m.r. spectrum (CCl_4) had τ 8.98 (3H, s), 8.91 (3H, s), 8.83 (3H, s), 8.72 (3H, s,) 8.15 (2H, s), 7.96 (2H, s), 7.46 (1H, m), 6.1–6.8 (2H, m), and 4.8 (1H, m). The mass spectrum revealed a molecular ion at *m/e* 236 in agreement with the formula $C_{14}H_{20}O_3$.

Photo-addition of Isoprene (2-Methyl-1,3-butadiene) to 3-Carene-2,5-dione

A 2% solution of carenedione in isoprene was irradiated under the usual conditions for 29 h. Chromatography on silica gel yielded the fractions *a* and *b* described below. Fraction *a* was a white crystalline solid (39%), m.p. 116–117° (pentane), obtained on elution with 4–7% ether in benzene. The infrared spectrum revealed bands at 1680 (saturated CO), 1647 (C=C) and 890 (C=CH_2) cm^{-1}. The n.m.r. spectrum (CCl_4) had τ 8.88 (3H, s), 8.74 (3H, s), 8.65 (3H, s), 8.40 (3H, s), 7.3–8.0 (5H, envelope), 6.9–7.2 (1H, m), 5.40 (1H, s), and 5.11 (1H, quartet). The mass spectrum revealed a molecular ion at *m/e* 232, and the ultraviolet spectrum (MeOH) had λ_{max} 212 nm (ε6900); 295 nm (ε120).

Anal. Calcd. for $C_{15}H_{20}O_2$: C, 77.59; H, 8.62. Found: C, 77.69; H, 8.66.

Can. J. Chem. Downloaded from www.nrcresearchpress.com by 210.87.254.5 on 09/05/12
For personal use only.

Fraction *b* was eluted with 7% ether in benzene and was a yellow oil (51%), b.p. 87–89°/0.1 mm; n_D^{25} 1.5126. The infrared spectrum showed bands at 1688 (saturated CO), 1654 (C=C), 995 (—CH=CH_2), and 915 (—CH=CH_2) cm^{-1}, while the n.m.r. spectrum (CCl_4) had τ 8.6–9.0 (12H, complex), 7.2–8.4 (5H, envelope), 4.8–5.4 (2H, m) and 3.9–4.4 (1H, m). The mass spectrum revealed a molecular ion at *m/e* 232, while the ultraviolet spectrum (MeOH) showed λ_{max} 210 nm (ε 6700), and 293 nm (ε 150).

Anal. Calcd. for $C_{15}H_{20}O_2$: C, 77.59; H, 8.62. Found: C, 77.25; H, 8.57.

Adduct from Acrylonitrile

A 1% solution of 3-carene-2,5-dione in acrylonitrile was irradiated for 22 h. The dark-yellow oil obtained on evaporation was chromatographed on silica. Elution with 10–15% ether in benzene gave a small amount (<2%) of recovered carenedione. Continued elution with 20–50% ether in benzene gave a white solid (98%), m.p. 177–178° on recrystallization from ethyl acetate/light petroleum (b.p. 60–70°). The infrared spectrum revealed the expected bands at 2240 (CN) and 1680 (CO) cm^{-1}, and the n.m.r. ($CDCl_3$) revealed peaks at τ 8.69 (3H, s), 8.66 (3H, s), 8.46 (3H, s), 7.52 (2H, d, J = 2.2 Hz), 7.1–7.4 (3H, envelope) and 6.95–7.05 (1H, m). Mass spectral analysis confirmed the expected molecular weight of 217.

Anal. Calcd. for $C_{13}H_{15}NO_2$: C, 71.88; H, 6.91; N, 6.45. Found: C, 72.04; H, 7.11; N, 6.37.

Adduct from Cyclopentene

A 4% solution of 3-carene-2,5-dione in benzene was irradiated with 8 molar equivalents of cyclopentene for 95 h. Chromatography of the crude product on silica gel and elution with 8% ether in benzene afforded the photo-adduct as a white crystalline solid (43%), m.p. 70–72° (pentane). The infrared spectrum showed the usual carbonyl band at 1688 cm^{-1}, and no olefinic peaks. The n.m.r. spectrum (CCl_4) showed signals at τ 8.93 (3H, s), 8.85 (3H, s), 8.65 (3H, s), 8.0–8.5 (6H, envelope), 7.9 (2H, s), 7.8 (1H, d, J = 9.5 Hz) and 7.0–7.5 (2H, envelope).

Anal. Calcd. for $C_{15}H_{20}O_2$: C, 77.55; H, 8.68. Found: C, 77.41; H, 8.84.

Photo-addition of Cyclohexene to 3-Carene-2,5-dione

A 0.5% solution of carenedione in cyclohexene was irradiated for 26 h under the usual conditions. Chromatography on silica permitted us to separate two fractions, *a* and *b*.

Fraction *a* was eluted with 3% ether in benzene and afforded white crystals (10%), m.p. 84–85°, on recrystallization from hexane. The infrared spectrum showed a strong band at 1688 (CO), with a shoulder at 1705, and a medium intensity band at 1620 (C=C) cm^{-1}. The ultraviolet spectrum (MeOH) showed λ_{max} 221 nm (ε 6000) and 300 nm (ε 190), while the n.m.r. spectrum (CCl_4) had signals at τ 8.83 (3H. s), 8.70 (3H, s), 8.1–9.0 (10H, envelope), 8.02 (3H, s), 7.13 (1H, d, J = 6.5 Hz), 4.90 (1H, d, $J \sim 2$ Hz) and 4.04 (1H, *d*, $J \sim 2$ Hz). The mass spectrum showed a molecular ion at *m/e* 246, but no major peak at *m/e* 164, such as was present in all the cyclobutane type adducts.

Anal. Calcd. for $C_{16}H_{22}O_2$: C, 78.01; H, 9.00. Found: C, 77.87; H, 8.96.

Fraction *b*, a white solid (65%) m.p. 93–102° (hexane) was obtained by elution with 5–10% ether in benzene. This product has a band in the infrared at 1688 cm^{-1} and λ_{max}(MeOH) 275 nm (ε 200). The n.m.r. spectrum (CCl_4) had signals at τ 8.68–8.81 (9H, m), 8.0–8.7 (8H, envelope), 7.7–8.1 (3H, m), and 7.25–7.60 (2H, m). The mass spectrum provided confirmation of the expected molecular weight of 246.

Anal. Calcd. for $C_{16}H_{22}O_2$: C, 78.01; H, 9.00. Found: C, 77.88; H, 8.90.

Adduct from Cycloheptene

A 1% solution of 3-carene-2,5-dione in cycloheptene was irradiated for 77 h. Chromatography afforded the photo-adduct as a white solid (85%), m.p. 67–68° (pentane–hexane), on elution with 8–15% ether in benzene. The infrared spectrum showed a band at 1675 (CO) cm^{-1} and the n.m.r. (CCl_4) had signals at τ 8.88 (3H, s), 8.82 (3H, s), 8.66 (3H, s), 8.05–8.6 (10H, envelope), 7.98 (2H, d, J = 4 Hz), 7.80 (1H, d, J = 4.5 Hz) and 7.4–7.7 (2H, m). The mass spectrum showed a peak at *m/e* 260, indicative of the molecular formula $C_{17}H_{24}O_2$.

Anal. Calcd. for $C_{17}H_{24}O_2$: C, 78.45; H, 9.23. Found: C, 78.03; H, 9.01.

Adduct from Cycloöctene

A 1% solution of 3-carene-2,5-dione in cycloöctene was irradiated for 36 h. After chromatography on silica, a colorless oil was obtained on elution with 6–15% ether in benzene. The liquid solidified on cooling in dry ice – methanol to a white solid (80%), which was best purified by sublimation and had m.p. 78–85°. The infrared spectrum revealed a strong band at 1675 cm^{-1}, while the n.m.r. spectrum (CCl_4) had signals at τ 8.94 (3H, s), 8.84 (3H, s), 8.67 (3H, s), 8.05–8.6 (12H, envelope), 8.07 (1H, s), 8.01 (1H, s), 7.94 (1H, s), and 7.5–7.8 (2H, envelope). The mass spectrum confirmed the expected molecular weight of 274.

Anal. Calcd. for $C_{18}H_{26}O_2$: C, 78.83; H, 9.49. Found: C, 78.70; H, 9.46.

Photo-addition of Norbornene to 3-Carene-2,5-dione

A 1% solution of carenedione in benzene was irradiated under the usual conditions in the presence of 6 molar equivalents of norbornene and 0.1 molar equivalents of acetophenone as sensitizer. Chromatography on silica afforded the adduct as a white crystalline solid (40%), m.p. 129–130° (hexane), on elution with 2% ether in benzene. The product had the usual band in the infrared at 1688 cm^{-1}, while the n.m.r. spectrum (CCl_4) had signals at τ 8.77 (6H, s), 8.68 (3H, s), 8.15–9.10 (6H, envelope), 7.90 (2H, s), and 7.5–7.9 (5H, m). The mass spectrum showed a molecular ion at *m/e* 258, in agreement with the formula $C_{17}H_{22}O_2$.

Anal. Calcd. for $C_{17}H_{22}O_2$: C, 79.03; H, 8.58. Found: C, 78.87; H, 8.49.

Photo-addition of Acetylene to 3-Carene-2,5-dione

Acetylene was passed continuously through a 1% solution of carenedione in benzene and irradiation was continued for 50 h. Chromatography on silica and elution with 4% ether in benzene gave recovered carenedione (13%), closely followed by a white solid (11%),

m.p. 95–96° on sublimation, which appeared to be the photo-adduct. The infrared spectrum revealed the expected saturated ketone band at 1690 cm^{-1} while the ultraviolet spectrum (MeOH) showed only weak absorption [λ_{max} 281 nm (ε 280)] above 210 nm. The n.m.r. spectrum (CCl_4) had signals at τ 8.82 (3H, s), 8.68 (3H, s), 8.64 (3H, s), 8.06 (2H, s), 6.91 (1H, m) and 3.9 (2H, m). The mass spectrum showed a molecular ion at *m/e* 190, in agreement with the expected 1:1 adduct.

Anal. Calcd. for $C_{12}H_{14}O_2$: C, 75.78; H, 7.37. Found: C, 75.54; H, 7.36.

Adduct from Ethyl Propiolate

A 1% solution of 3-carene-2,5-dione in benzene containing 5 molar equivalents of ethyl propiolate was irradiated for 94 h. Chromatography on silica led to the isolation of the adduct as a colorless oil (59%), on elution with 10% ether in benzene. (An earlier fraction may have been a small amount of the ethyl ester of cycloöctatetraene carboxylic acid arising from photo-addition of the alkyne to solvent benzene.) The carenedione adduct had infrared bands at 1730 (ester), 1695 (ketone), and 1615 (conjugated alkene) cm^{-1}. The n.m.r. spectrum (CCl_4) revealed signals at τ 8.90 (3H, s), 8.72 (3H, t, J = 7.0 Hz), 8.70 (3H, s), 8.57 (3H, s), 8.08 (2H, AB quartet, J = 6.0 Hz), 6.95 (1H, d, J = 1.8 Hz), 5.87 (2H, q, J = 7.0 Hz) and 3.33 (1H, d, J = 1.8 Hz).

Anal. Calcd. for $C_{15}H_{18}O_4$: C, 68.71; H, 6.87. Found: C, 68.41; H, 6.95.

Adduct from Diethyl Acetylenedicarboxylate

A 1% solution of 3-carene-2,5-dione in benzene was irradiated for 53 h with 4 molar equivalents of the alkyne. Chromatography on silica afforded the photo-adduct as a white crystalline solid (23%), m.p. 61–62° (aqueous methanol). The infrared spectrum revealed bands at 1735 (ester), 1695 (ketone), and 1650 (alkene) cm^{-1}, while the n.m.r. spectrum (CCl_4) had peaks at τ 8.90 (3H, s), 8.68 (6H, t, J = 7.0 Hz), 8.67 (3H, s), 8.51 (3H, s), 7.99 (2H, s), 6.65 (1H, s) and 5.74 (4H, q, J = 7.0 Hz). The mass spectral molecular weight of 334 was in agreement with that expected.

Anal. Calcd. for $C_{18}H_{22}O_6$: C, 64.65; H, 6.63. Found: C, 64.62; H, 6.28.

Attempt to Epimerize the Isoprene Photo-adduct (7) by Base Catalysis

The following procedure is typical of a number of attempts, all of them unsuccessful, to find evidence for base-catalyzed epimerization of our cyclobutane photo-adducts, and is based on the procedure employed in a similar situation by Yates *et al.* (12). The photo-adduct (33 mg) was refluxed in a solution of sodium (0.5 g) in methanol (25 ml) for 3 h under nitrogen. After careful neutralization with acetic acid and dilution with water a white solid (25 mg) was obtained, m.p. 117–118° before and after admixture with the starting adduct. The infrared spectrum was essentially indistinguishable from that of the starting material.

Acknowledgments

It is a pleasure to record our thanks to Dr. W. F. Reynolds of this department for valuable discussions concerning the n.m.r. spectra. We wish also to thank the National Research Council of Canada for financial assistance.

1. P. E. Eaton. Accounts of chemical research, **1**, 50 (1968).
2. E. J. Corey, J. D. Bass, R. LeMahieu, and R. B. Mitra. J. Am. Chem. Soc. **86**, 5570 (1964).
3. J. A. Barltrop and B. Hesp. J. Chem. Soc. 5182 (1965).
4. C. H. Krauch and S. Farid. Tetrahedron Letters, No. 39, 4783 (1966).
5. S. P. Pappas and B. C. Pappas. Tetrahedron Letters, No. 17, 1597 (1967).
6. S. P. Pappas and N. A. Portnoy. J. Org. Chem. **33**, 2200 (1968).
7. E. J. Forbes, J. Griffiths, and R. A. Ripley. J. Chem. Soc. C, 1149 (1968).
8. S. Castellano and J. S. Waugh. J. Chem. Phys. **34**, 295 (1961).
9. J. R. Cavanaugh. J. Chem. Phys. **39**, 2378 (1963).
10. E. J. Corey and H. J. Burke. J. Am. Chem. Soc. **78**, 174 (1956).
11. G. L. Buchanan, R. A. Raphael, and I. W. J. Still. J. Chem. Soc. 4372 (1963).
12. P. Yates, S. N. Ege, G. Büchi, and D. Knutsen. Can. J. Chem. **45**, 2927 (1967).

Can. J. Chem. Downloaded from www.nrcresearchpress.com by 210.87.254.5 on 09/05/12
For personal use only.

Can. J. Chem. Downloaded from www.nrcresearchpress.com by 210.87.254.42 on 09/05/12
For personal use only.

Methyl 2-hydroxy-4-methoxy-6-phenylbenzoate and methyl 2-hydroxy-6-methoxy-4-phenylbenzoate: reassignment of a structure[1]

T. Trefor Howarth and Thomas M. Harris[2]
Department of Chemistry, Vanderbilt University, Nashville, Tennessee 37203

Received July 15, 1968

Methyl 2-hydroxy-4-methoxy-6-phenylbenzoate (*3b*) was synthesized by treatment of methyl 6-phenyl-β-resorcylate (*3a*) with diazomethane. 5-Phenylresorcinol (**8**) was carboxylated in a Kolbe–Schmitt reaction to give γ-resorcylic acid *7b*. Treatment of *7b* with diazomethane gave a mixture of the corresponding dihydroxy ester *7c*, monomethoxy ester *7a*, and dimethoxy ester *7d*. Evidence is presented that the structure of a compound obtained by Douglas and Money from base treatment of phenyl dipyrone **1** is *7a* rather than the previously assigned *3b*. A mechanistic proposal is presented.

Canadian Journal of Chemistry, 46, 3739 (1968)

Douglas and Money recently reported that treatment of phenyl dipyrone **1** with 1*M* methanolic potassium hydroxide for 16 h at room temperature afforded a mixture from which esters **2***a*, **3***a*, and **3***b* were isolated in 13.6, 8.7, and 2.8% yield, respectively (1). The structural assignments were made on the basis of elemental analyses and infrared (i.r.), ultraviolet (u.v.), nuclear magnetic resonance (n.m.r.), and mass spectra. Diester **2***a* undoubtedly arises by methoxide attack at the two carbonyl groups (*a* and *b*) of **1** and aldol cyclization of the intermediate triketo diester **4***a*. β-Resorcylic ester **3***a* might reasonably be formed by methoxide attack at *a* and hydroxide attack at *b*. The resulting triketo ester–acid **4***b* would be expected to decarboxylate to give triketo ester **5***a*, which has been previously shown to undergo aldol cyclization to form **3***a* under the above conditions (2).

The formation of methoxy ester **3***b* cannot be explained by such simple processes since formation of the required intermediate 5-methoxy ester **6***a* requires methoxide attack at both *a* and *c* of **1**, as well as hydrolytic cleavage of the other ring. Methoxide attack at either *a* or *c* precludes subsequent attack at the other one. Thus, either the minor component must arise by a more complex process than do **2***a* or **3***a*,[3] or the structure **3***b* was incorrectly assigned.[4]

Our attention was attracted to this problem when, during investigations of biogenetic-type syntheses of phenols in this laboratory [see (2)], treatment of methyl 6-phenyl-β-resorcylate (**3***a*) with diazomethane was shown to give two monomethylation products. On the basis of steric considerations and by analogy with other methylation reactions (5) the major product was assigned structure **3***b*. The i.r. and n.m.r. spectra supported this assignment; the stretching frequency (1645 cm^{-1}) of the carbonyl group and the chemical shift ($\tau = -1.3$) of the hydroxyl proton indicated that the hydroxyl group was hydrogen bound to the carbomethoxy group. The other monomethylation product (**3***c*)[5] was present in trace amounts and was detected by thin-layer chromatography (t.l.c.). The melting

---

[1]Supported by research grant GM-12848 from the National Institutes of Health, United States Public Health Service.

[2]Alfred P. Sloan Fellow and Career Development Awardee, K3-GM-27013, of the National Institutes of Health, United States Public Health Service.

[3]One such process would involve methoxide attack at *c* to give carboxylic acid **i** followed by rearrangement to anhydride **ii**. Subsequent methanolysis, decarboxylation, and cyclization would give ester **3***b*. However, we are not aware of a satisfactory precedent for the conversion of **i** to **ii**.

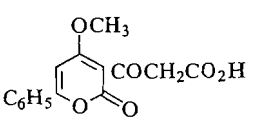

i

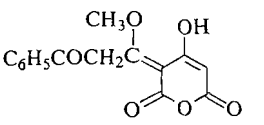

ii

[4]The same criticism applies to methoxy esters **iii** and **iv**, which have been obtained by similar reactions of complex pyrones with methoxide ion (3, 4).

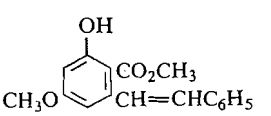

iii

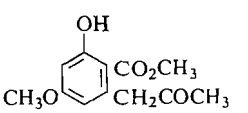

iv

[5]Monomethoxy ester **3***c* was identified by t.l.c. comparison with an authentic sample which had been prepared by aldol cyclization of the appropriate enol ether of triketo ester **5***a*. This reaction will be reported elsewhere.

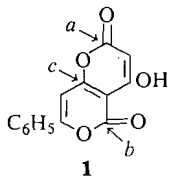

1

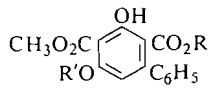

2*a*, R = CH_3, R′ = H
b, R = H, R′ = CH_3

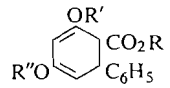

3*a*, R = CH_3, R′ = H, R″ = H
b, R = CH_3, R′ = H, R″ = CH_3
c, R = CH_3, R′ = CH_3, R″ = H
d, R = H, R′ = H, R″ = H

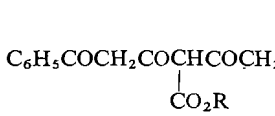

4*a*, R = CH_3
b, R = H

5*a*, R = CH_3
b, R = H

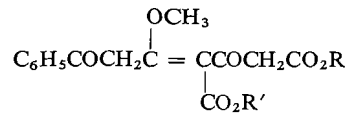

6*a*, R = CH_3, R′ = H
b, R = H, R′ = CH_3

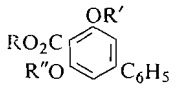

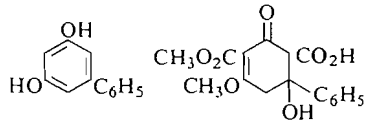

7*a*, R = CH_3, R′ = H, R″ = CH_3
b, R = H, R′ = H, R″ = H
c, R = CH_3, R′ = H, R″ = H
d, R = CH_3, R′ = CH_3, R″ = CH_3

8 **9**

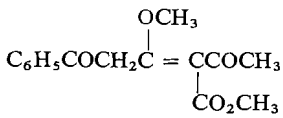

10

point of **3***b* obtained from the diazomethane reaction was 7° higher than that reported by Douglas and Money (1). Also, the spectra of this material differed from those reported by Douglas and Money for their compound (see Table I). It was concluded, therefore, that the structure of their compound was incorrectly assigned. A possible alternative structural assignment for their compound is **7***a*; the hydroxyl group of **7***a* could participate in hydrogen bonding similar to that in **3***b*, and the two compounds would be expected to have similar spectral characteristics.

Verification of the above structural assignment was accomplished by unambiguous synthesis of **7***a*. Thermal decarboxylation of 6-phenyl-β-resorcylic acid (**3***d*) gave 5-phenylresorcinol (**8**) which was carboxylated with carbon dioxide and potassium bicarbonate by a modified Kolbe–Schmitt reaction in satisfactory yield. The carboxylation product was assigned structure **7***b* by analogy with the carboxylation of orcinol (6). In addition, the n.m.r. spectrum showed that the two aromatic protons of the phenolic ring were chemically equivalent, thereby indicating the symmetrical arrangement of the substituents [cf. the corresponding protons in isomeric acid **3***d* are non-equivalent]. Methylation of acid **7***b* using excess diazomethane gave a mixture of three methyl esters as a colorless oil and trituration with ether effected crystallization of dihydroxy ester **7***c*. The mother liquors were subjected to chromatography on silicic acid. The first fraction contained a mixture of monomethoxy ester **7***a* and dihydroxy ester **7***c*, and partial separation was achieved by preparative thin-layer chromatography to give monomethoxy ester **7***a*. The material had the same melting point as the material obtained by Douglas and Money. Spectral characteristics of **7***a* are shown in Table I and are in good agreement with those quoted by these workers (1), and it is concluded that their product was in fact **7***a*. The second fraction eluted from the column contained dimethoxy ester **7***d*. The chemical

Can. J. Chem. Downloaded from www.nrcresearchpress.com by 210.87.254.42 on 09/05/12
For personal use only.

TABLE I

Melting points and spectral data of monomethoxy esters

Compound	Melting point	Infrared,* cm^{-1}	Ultraviolet†, mμ (log ε)	Nuclear magnetic resonance‡ τ
3*b*§	110–111°	1645, 1600, 1568	302 (3.75), 261 (4.04), 224 (4.45)	6.56 (s, 3), 6.20 (s, 3), 3.65 (d, 1, J = 2 Hz), 3.50 (d, 1, J = 2 Hz), 2.7 (m, 5), −1.3 (s, 1)
7*a*‖	102–104°	1638, 1606, 1549, 1496	323 (sh; 3.33), 276 (4.30), 220 (sh; 4.34)	6.04 (s, 3), 6.00 (s, 3), 3.33 (d, 1, J = 2 Hz), 3.12 (d, 1, J = 2 Hz), 2.5 (m, 5), −1.63 (s, 1)
Compound described by Douglas and Money (1)	103–104°	1650, 1610, 1560, 1500	325 (sh; 3.38), 277 (4.28), 220 (sh; 4.35)	6.13 (s, 3), 6.09 (s, 3), 3.43 (d, 1, J = 2 Hz), 3.20 (d, 1, J = 2 Hz), 2.58 (m, 5), −1.54 (s, 1)

*Nujol mulls.
†Solutions in 95% ethanol.
‡Solutions in deuteriochloroform.
§Prepared by treatment of **3***a* with diazomethane.
‖Prepared by treatment of **7***b* with diazomethane.

equivalence of the aromatic protons in the phenolic rings of esters **7***c* and **7***d*, as illustrated by the n.m.r. spectra, substantiates the symmetry of these compounds and of the parent acid **7***b*.

A reasonable pathway for formation of **7***a* from phenyl dipyrone **1** would involve methoxide attack at *b* and *c* to give **6***b*. Aldol cyclization of **6***b* could then be envisaged to give hydroxy acid **9** which, after dehydration and concomitant decarboxylation, would afford **7***a*. Two alternative pathways, *viz.* **9** → **2***b* → **7***a* and **6***b* → **10** → **7***a*, appear less likely. Neither **2***b* nor **6***b* would be expected to decarboxylate under the conditions employed by Douglas and Money (1).[6]

Experimental[7]

Methylation of Methyl 6-phenyl-β-resorcylate (3a)

Ester **3***a* (40 mg) (2) was treated with diazomethane (10 equivalents) in ether (100 ml) and left at room temperature for 20 h. Evaporation of the solvent *in vacuo* gave a pale-yellow oil which was shown by thin-layer chromatography (t.l.c.) to contain methyl 2-hydroxy-4-methoxy-6-phenylbenzoate (**3***b*), ester **3***a*, and a trace amount of methyl 4-hydroxy-2-methoxy-6-phenylbenzoate (**3***c*).[5] The oil was subjected to chromatography on silicic acid eluting with ether–hexane mixtures. Elution with ether–hexane (1:9) gave **3***b* as minute prisms (20.5 mg, 48%), m.p. 107–108° and 110–111° after recrystallization from chloroform–hexane.

Anal. Calcd. for $C_{15}H_{14}O_4$ (mol. wt., 258): C, 69.76; H, 5.46. Found (mol. wt., (Mass spectroscopy)[8] 258): C, 69.93; H, 5.67.

Further elution with ether–hexane (1:4) gave starting ester **3***a* (15.5 mg, 39%).

5-Phenylresorcinol (8)

6-Phenyl-β-resorcylic acid (**3***d*, 948 mg) (2) was heated at 160° for 1.5 h. The oil was sublimed at 130°/0.07 mm to give 590 mg (77%) of **8**, m.p. 158–158.5° [lit. m.p. 157–158° (7)].

4-Phenyl-γ-resorcylic Acid (7b)

5-Phenylresorcinol (190 mg), potassium bicarbonate (400 mg), glycerol (1.2 g), and solid carbon dioxide were heated in a stainless steel bomb at 150° (1000 p.s.i. autogenous pressure) for 16 h with stirring (magnetic stirrer). The mixture was cooled, diluted with water, and acidified with dilute hydrochloric acid. The solid was extracted with ether, dried ($MgSO_4$), and the ether was evaporated *in vacuo* to give 210 mg (89%) of **7***b* as minute prisms, m.p. 181–184° (decomp.). Recrystallization from ether and sublimation at 120°/0.05 mm raised the melting point to 189–191° (decomp.); i.r. (KBr) 1605 and 1545 cm^{-1}; n.m.r. (Et_2O) τ 3.72 (s, 2), 3.0 (m, 5).

Anal. Calcd. for $C_{13}H_{10}O_4$: C, 67.82; H, 4.38. Found: C, 67.81; H, 4.39.

[6]The proposed pathway is consistent with unpublished experiments carried out in this laboratory with triketo acid **5***b*. Treatment of this acid with 2 *M* potassium hydroxide afforded the corresponding undehydrated aldol cyclization product as its dianion, which was slowly converted to 5-phenylresorcinol (**8**). Evidently dehydration and decarboxylation occurred simultaneously: there was no evidence that resorcylic acid **3***d* was an intermediate. Moreover, decarboxylation of the triketo acid was not observed.

[7]All melting points were taken with a Thomas–Hoover apparatus in unsealed capillaries. Elemental analyses were performed by Galbraith Laboratories, Inc., Knoxville, Tennessee. Infrared and ultraviolet spectra were obtained with Beckman IR-10 and Cary 14 spectrophotometers, respectively. Nuclear magnetic resonance spectra were obtained with a Varian A-60 spectrometer. Tetramethylsilane (τ = 10.0) was employed as an internal standard.

[8]We wish to thank Mr. A. H. Struck and Mrs. D. Franks for recording the mass spectrum on a Hitachi RMU-6 single focusing mass spectrometer.

Can. J. Chem. Downloaded from www.nrcresearchpress.com by 210.87.254.42 on 09/05/12
For personal use only.

Methylation of 7b

Acid *7b* (192 mg) was added to a solution of diazomethane (ca. 0.28 g, 7 equivalents) in ether (40 ml) and the solution was set aside at room temperature for 18 h. The solvent was removed *in vacuo* and the residual oil was triturated with ether to give methyl 2,6-dihydroxy-4-phenylbenzoate (*7c*, 30 mg, 13%), m.p. 145–150°. Sublimation at 85–95°/0.03 mm raised the melting point to 151–153°; u.v. (95% EtOH) 333 mμ (log ε 3.52), 280 (4.40), and 220 (sh., 4.33); i.r. (Nujol) 1664, 1632, and 1543 cm^{-1}; n.m.r. ($CDCl_3$) τ 5.89 (s, 3), 3.19 (s, 2), 2.5 (m, 5), 0.25 (s, 2).

Anal. Calcd. for $C_{14}H_{12}O_4$: C, 68.85; H, 4.95. Found: C, 68.85; H, 5.18.

The mother liquors were evaporated and fractionated on silicic acid. Elution with mixtures of ether:hexane gave initially an oil (79 mg) which was shown to contain two compounds. Nuclear magnetic resonance indicated the presence of *7c* and *7a* in a ratio of ca. 0.7:1. The mixture was partially separated using preparative t.l.c. to give *7a*, m.p. 102–104°; mass spectrum *m/e* (rel. intensity) 258 (40), 226 (100), 198 (15), 183 (20), 155 (13), 139 (8), 127 (16), 115 (12), metastables (transitions) 174 (226 → 198), 169 (198 → 183), 131 (183 → 155), 104 (155 → 127).[9]

[9]We wish to thank Drs. W. Goodlett and J. C. Gilland, Jr. for recording this spectrum on a CEC 21-110B mass spectrometer.

Further elution of the silicic acid afforded methyl 2,6-dimethoxy-4-phenylbenzoate (*7d*) as a colorless oil (76 mg, 34%) which slowly crystallized. Recrystallization from chloroform–hexane and sublimation at 100°/0.01 mm gave minute prisms; m.p. 130–130.5°; u.v. (95% EtOH) 263 mμ (log ε 4.28); i.r. (Nujol) 1728, 1585, and 1565 cm^{-1}; n.m.r. ($CDCl_3$) τ 6.14 (s, 6), 6.09 (s, 3), 3.27 (s, 2), 2.52 (m, 5).

Anal. Calcd. for $C_{16}H_{16}O_4$: C, 70.58; H, 5.92. Found: C, 70.54; H, 5.89.

1. J. L. Douglas and T. Money. Can. J. Chem. **45**, 1990 (1967).
2. T. M. Harris and R. L. Carney. J. Am. Chem. Soc. **89**, 6734 (1967).
3. J. L. Douglas and T. Money. Tetrahedron, **23**, 3545 (1967).
4. T. Money, F. W. Comer, G. R. B. Webster, I. G. Wright, and A. I. Scott. Tetrahedron, **23**, 3435 (1967).
5. R. H. Thomson. Biochemistry of phenolic compounds. *Edited by* J. B. Harborne. Chap.1. 1964. Academic Press, Inc., New York.
6. A. S. Lindsey and H. Jeskey. Chem. Rev. **57**, 583 (1957).
7. C. M. Suter and P. G. Smith. J. Am. Chem. Soc. **61**, 166 (1939).

Can. J. Chem. Downloaded from www.nrcresearchpress.com by 210.87.254.42 on 09/05/12
For personal use only.

Can. J. Chem. Downloaded from www.nrcresearchpress.com by 210.87.254.105 on 09/05/12
For personal use only.

Gas–liquid chromatography of terpenes. Part XVII. The volatile oil of the leaves of *Juniperus virginiana* L.[1]

A. R. VINUTHA[2] AND E. VON RUDLOFF

Prairie Regional Laboratory, National Research Council of Canada, Saskatoon, Saskatchewan

Received June 3, 1968

The leaf oil of the red juniper was found to contain mainly sabinene, as well as limonene, α-pinene, γ-terpinene, terpinolene, 3-carene, myrcene, 4-terpinenol, citronellol, elemol, γ-, α-, and β-eudesmol, the aromatic ethers estragole, safrole, methyl eugenol, and elemicin. Another aromatic ether, methyl vinyl anisole, was isolated which has not been found previously in essential oils. The acetates **1** and **2** obtained previously in two related juniper leaf oils were present and the first has been identified as elemol acetate. Small amounts of α-thujene, *p*-cymene, linalool, and δ-cadinene were also identified.

Quantitative aspects were studied with a view of future chemosystematic investigations. The error in duplicate runs was 0.1% for well-resolved peaks, but the absolute error, as determined by use of internal standards, was larger. Leaf oils of different trees from Texas and Ontario were found to give wide quantitative variations of the individual components.

Canadian Journal of Chemistry, 46, 3743 (1968)

Introduction

In continuation of the systematic analysis of the volatile oils of North American conifers by gas–liquid chromatography (g.l.c.), the leaf oil of the red juniper, *Juniperus virginiana* L. (erroneously called red cedar) was investigated. This is one of the most widely distributed North American juniper species, ranging from southern Ontario in the north to Texas in the south, and from the Atlantic coast to the plains in the west. The introgression and possible hybridization with neighboring western juniper species, including *J. horizontalis* Moench., *J. scopulorum* Sarg., and *J. ashei* Buchholz was studied by Fassett (1) and Hall (2). The volatile oil of the wood of the red juniper is the commercial cedar wood oil (3, 4), which was analyzed in detail by Runeberg (5) and is a major source of cedrene and cedrol (3, 6). In contrast, the leaf oil does not appear to have been investigated to any extent; Guenther (3) quoted only two very early references relating to incomplete work.

The current study was also designed to provide data for a chemosystematic investigation of the introgression of *J. virginiana* and *J. ashei* (7) in addition to giving a more modern chemical analysis. Particular attention was paid to reproducible quantitative and qualitative (retention) data. In the previous paper of this series the detailed analysis of the leaf oil of *J. ashei* was described (8), and it was shown that by employing an electronic digital integrator, the areas of well-resolved major peaks could be determined with a precision of 0.1%. In this study, more attention was paid to the minor or partially resolved components, as well as the use of internal standards to test the internal normalization method. Furthermore, a number of leaf samples of *J. virginiana* from different locations were analyzed to determine possible variation within or between populations.

Experimental

The gas–liquid chromatographic (g.l.c.) analyses were carried out with an F & M model 500 instrument (linear temperature programming, thermal conductivity detector; F & M Scientific Instruments Inc.) and a unit of conventional design (isothermal operation). Integration and summation of the area under the peaks was achieved by means of an Aerograph model 471 digital integrator, the instrumental error being less than 0.1% on full scale recorder (1 mV) deflection with no base line drift. An Aerograph model A-700 gas chromatograph (Wilkens Instrument and Research Inc.) was used for preparative g.l.c. Helium was used as carrier gas in all experiments and the flow rates were determined by the soap bubble method. Retention times were measured from the time of injection to the initial emergence of the peaks (9). The packing of the g.l.c. columns was prepared by the tray method and columns were packed by means of mild mechanical vibration. The liquid phases employed in the columns were polyethylene glycol (PEG) (Carbowax 20M, 5% on Aeropak 30, 70–80 mesh, 5% and 15% on Gaschrom P, 60–80 mesh), silicone gum polymer (SE-30) (5% on silanized Anakron ABS, 70–80 mesh, 15% on Gaschrom P, 60–80 mesh), fluorinated silicone polymer (QF-1) (5% on Anakron ABS and 15% on Gaschrom P), ethylene glycol *bis*-propionitrile (EGPN) (15% on Gaschrom P) and C-modified polyphenyl ether (MCS-562)

[1]Issued as NRCC No. 10391.
[2]NRCC Postdoctorate Fellow 1967–1968.

Can. J. Chem. Downloaded from www.nrcresearchpress.com by 210.87.254.105 on 09/05/12
For personal use only.

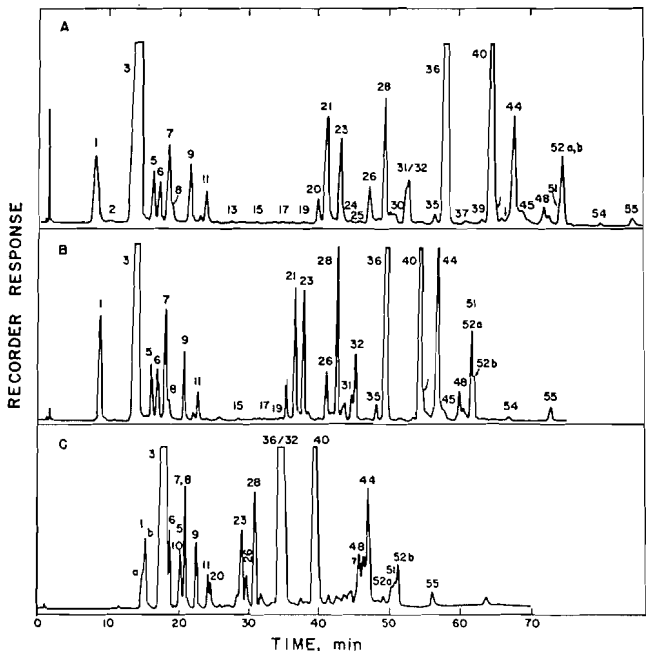

FIG. 1. Gas chromatograms of the leaf oil of *Juniperus virginiana* L. (large batch from Texas) (PTGC: 50° to 215° at 2.9°/min; 350 × 0.4 cm O.D. columns). A: 5% polyethylene glycol 20M on Gas Chrom. P. (60–80 mesh); B: 5% polyethylene glycol on Aeropak 30 (70–80 mesh); C: 5% SE-30 Silicone gum on Anakrom ABS (60–70 mesh).

(10) (15% on Gaschrom P). The 5% columns were used for analytical runs (90–120 ml He/min) whereas the more heavily loaded columns were employed in preparative work (40–70 ml He/min).

Figure 1 shows the trace obtained with the oil from Texas, using the 5% PEG columns (350 × 0.4 cm O.D.) at 50° programmed at 2.9°/min to 215°, the final temperature being held until the last peak had been eluted; *a*) with Gaschrom P and *b*) with Aeropak 30 as support. The peak numbering used throughout this study is the sequence of elution under conditions (*a*), which are those employed previously (7, 8). The purity of individual components was determined on this column as well as on the other columns where necessary. Figure 1*c* shows the chromatogram as obtained on the 5% SE-30 column at 50° programmed at 2.9°/min to 215°.

Individual components were trapped at the exit of the gas chromatographs by hand collection in teflon tubes (externally cooled with ice or solid carbon dioxide) or in the special collection flasks of the Aerograph A-700 unit. Infrared spectra of the purified components were recorded as films on sodium chloride plates using a Perkin–Elmer model 21 double beam spectrophotometer. Fractions which were submitted to nuclear magnetic resonance (n.m.r.) analysis were collected directly in carbon tetrachloride (0.5 ml). The n.m.r. spectra were recorded with the aid of a Varian HA-100 (100 Hz) spectrometer, using tetramethylsilane as internal standard. The signals are reported as p.p.m.

Plant Material and Recovery of the Volatile Oil

Most of the foliage from *J. virginiana* L. (identified by Prof. B. L. Turner, Department of Botany, University of Texas, Austin) was collected near Austin, Texas, during November 1966, and this was steam-distilled at the University of Texas the following day. The distillate was extracted with methylene chloride and, after drying, the solvent was removed by distillation; yield 1.15% (based on fresh weight of foliage), $[\alpha]_D^{22}$ +31.3° (*c*, 11.2; $CHCl_3$), n_D^{22} 1.4973. Smaller leaf samples (15 to 30 g each) were also collected from several trees in the same area. Two larger batches (4–5 kg) of foliage were also collected from two trees located near St. Williams, southern Ontario, (collected and identified by Prof. E. Jörgensen, Faculty of Forestry, University of Toronto, Ontario) and these were shipped to Saskatoon for steam-distillation; yield of volatile oil 0.22 and 0.15%, $[\alpha]_D^{22}$ +47.4° and +60.17°, n_D^{22} 1.4858 and 1.4810 respectively. Considering the low yield, it is likely that loss of oil occurred during transport. Several small leaf samples were also collected in the same areas from different trees. Small scale distillation was carried out in the apparatus described previously (11). Since complete removal of solvent from small oil samples (less than 1 g) cannot be achieved without substantial loss of oil (11), the evaporation of solvent was stopped when about 10% solvent remained. Hence, physical constants of these small leaf oil samples were not determined. The yields were in the 1 to 2% range.

Can. J. Chem. Downloaded from www.nrcresearchpress.com by 210.87.254.105 on 09/05/12
For personal use only.

Prefractionation

Aliquots (10.0 g) of the oil were chromatographed on modified silicic acid (120 g) as described previously (8, 12, 13). Elution with petrol (Skellysolve F, b.p. 40–50°; 500 ml) gave an impure hydrocarbon fraction I (4.0 g), elution with methylene chloride (400 ml) a mid-fraction II (3.5 g), and elution with methanol (400 ml) a polar fraction III (2.5 g). The latter fraction was rechromatographed on a fresh batch of silicic acid (35 g) and elution with methylene chloride and methanol (200 ml each) gave fraction III*a* (1.2 g) and III*b* (1.3 g) respectively.

In subsequent work, it was found that fraction I contained, in addition to the terpene hydrocarbons, several percent of the aromatic ethers. These could be removed to a large extent by rechromatography on the silicic acid column, but decomposition (especially peak 21) was encountered and the fraction was used as such for preparative g.l.c.

Individual Components

a) Hydrocarbons

The hydrocarbon fraction I was separated into individual peaks (multiple injections of 20 μl mixture) on a 200 × 0.6 cm O.D. MCS-562 polyphenyl ether column (100°, 40 ml He/min). Peaks 1*a* and *b* (see Fig. 1*c*) could not be collected separately since the partial resolution obtained in analytical runs (less than 1 μl aliquots) was lost in preparative work. The mixture had infrared (i.r.) and nuclear magnetic resonance (n.m.r.) spectra closely resembling those of α-pinene. However, the small signals at 0.68, 0.90–0.98, 1.12 and 1.45 p.p.m. indicated that a small amount of α-thujene may be present. This is in agreement with the retention data obtained in analytical runs on the PEG, EGPN, MCS-562 and SE-30 columns. All other major peaks of this fraction were obtained virtually pure and identified as sabinene (peak 3) ($[\alpha]_D$ +75.4°), 3-carene (peak 5), myrcene (peak 6), limonene (peak 7) ($[\alpha]_D$ +8.8°), γ-terpinene (peak 9), *p*-cymene (peak 10), and terpinolene (peak 11) by comparison of the spectra with those of the authentic compounds. The trace components 4 and 8 could not be separated from sabinene and limonene respectively. Retention data suggest that peak 8 is either β-phellandrene or 1:8-cineole. Since the latter oxide is usually removed from the hydrocarbons in the prefractionation (8, 12, 13) the presence of β-phellandrene in peak 8 is very likely. The retention data of the trace peak 2 are in agreement with those of camphene.

The higher boiling components in fraction I were fractionated on an SE-30 column (300 × 0.4 cm, 50 to 220° at 2.9°/min) when estragole (peak 26), methyl vinyl anisole (peak 28), safrole (peak 36), and δ-cadinene (peak 29) were isolated and identified by comparison of spectral data (see also below).

b) Mid-fraction II

Gas–liquid chromatography of fraction II showed it contained mainly peaks 26, 28, 36, and 40, as well as smaller amounts of peaks 3, 9, 11, 17, 20, 21, 22, 23, 35, 39, 44 (or 43; decomposition?), 48, 49, 52 and 54. Of these only peaks 23, 26, 28, 36, 40 and 52 were collected in sufficient amounts (SE-30 or PEG columns) to permit rigorous identification. Comparison of spectral data with those of authentic specimens showed peaks 23, 26, 36, 40 and 52 to be 4-terpinenol ($[\alpha]_D$ +6.3°), estragole, safrole, methyl eugenol, and elemicin, respectively. The i.r. spectrum of component 28 indicated it to be a new compound, and it was obtained reasonably pure after refractionation on the PEG column.

Anal. Calcd. for $C_{10}H_{12}O$: C, 81.04; H, 8.16. Found: C, 80.83; H, 8.09.

The i.r. spectrum (3080 (w), 2940 (multiplet) (s), 1632 (m), 1595 (s), 1575 (s), 1508 (m), 1465 (s), 1435 (s), 1405 (m), 1287 (s), 1260 (s), 1190 (m), 1178 (m), 1095–1075 (doublet) (s), 1055 (m), 985 (s), 905 (s), 770 (s), and 740 (s) cm^{-1}) indicated the compound to be an aromatic vinyl ether with a substitution pattern similar to that of safrole. The various signals of the n.m.r. spectrum are shown in Table III*a*. Hydrogenation of component 28 with platinum catalyst resulted in the consumption of one mole of hydrogen per mole. The n.m.r. signals of the product are shown in Table III*b*.

c) Fraction IIIa

This fraction was composed mainly of peaks 20, 23, 30, 31, 36, 40, 44, 51, and 52. Crude fractions were obtained by preparative g.l.c. on either 15% PEG or SE-30 (180 × 0.9 cm O.D.) columns. Refractionation gave linalool (peak 20), 4-terpinenol (peak 23), citronellol (peak 30), safrole (peak 36), methyl eugenol (peak 40), elemol (peak 44), and a mixture of α- and β-eudesmol (peaks 51 and 52*b*). Some elemicin (peak 52*a*) appeared to be present in the eudesmol fraction (i.r. spectrum). The safrole fraction contained a ketone (i.r. spectrum, 1705 cm^{-1}), but this component could not be obtained in sufficient amount to permit identification. The retention time of this ketone (PEG column) is higher than that of carvone, pulegone, or piperitone. Similarly, the methyl eugenol fraction was found to contain a hydroxy ketone (i.r. spectrum, 3500 cm^{-1}, 1725 cm^{-1}). The elemol fraction was found to be contaminated with an aromatic compound (i.r. spectrum, 1505 cm^{-1}).

d) Fraction IIIb

Fraction III*b* solidified on standing and was found to be composed mainly of elemol (peak 44). It was purified by preparative g.l.c., and the spectra agreed with those of the authentic specimen; $[\alpha]_D^{23}$ −11.0° (*c*, 2.1; $CHCl_3$). In addition to elemol, small amounts of γ-eudesmol (peak 48), α- and β-eudesmol (peaks 51 and 52*b*), and of peak 55 were isolated. Component 55 had an i.r. spectrum which is similar to that of acetate **2** isolated from the leaf oil of *Juniperus horizontalis* Moench (14) and *J. scopulorum* Sarg. (13) (designated peak 41). The n.m.r. spectrum of this compound contained a 3-proton signal at 1.99 p.p.m. confirming the presence of an acetoxy group. Three proton signals were also recorded near 1.09 (doublet, —$CHCH_3$), 1.14 (singlet C—CH_3) and near 1.68 (broad singlet, C=C—CH_3) and less well-defined single proton signals near 4.56, 4.78, and 4.92 p.p.m. (doublet, —CH=C). As with most terpenes, the methylene proton signals in the 1.0–1.8 p.p.m. range were not amenable to interpretation. Neither the n.m.r. nor the i.r. spectra could be correlated with that of known terpene acetates.

Component 45 appeared to decompose during fractionation. Its properties are very similar to that of acetate **1** of *J. horizontalis* (13) and *J. scopulorum* (14) and this could now be shown to be elemol acetate. Elemol was

TABLE I

Percentage composition of the leaf oil of the red juniper from different populations in Texas and Ontario

Peak* No.	Compound†	Texas‡					Ontario§			
		A‖	1	2	3	4	1	2	3	4
1	α-Pinene	3.2	1.3	0.6	1.4	1.2	1.1	11.5	1.2	0.8
2	α-Thujene (Camphene)	0.1	—	—	—	—	0.1	Trace	0.1	0.1
3	Sabinene	29.6	16.3	8.4	20.0	15.0	9.2	3.8	9.9	3.7
4	Unidentified	0.1	0.1	0.1	0.4	Trace	—	—	0.1	0.5
5	3-Carene	1.6	0.8	0.5	1.3	1.3	0.4	1.0	0.6	0.7
6	Myrcene	1.3	0.5	0.5	0.8	0.4	0.3	0.1	0.3	0.1
7	Limonene	2.9	0.9	2.0	2.9	2.3	17.8	19.8	15.3	33.5
8	(β-Phellandrene)	0.3	0.5	0.3	0.2	0.1	0.2	0.1	0.3	0.2
9	γ-Terpinene	2.0	1.4	1.3	2.1	1.3	0.7	0.3	0.9	0.2
10	*p*-Cymene	0.2	Trace	Trace	Trace	Trace	Trace	Trace	Trace	Trace
11	Terpinolene	0.8	0.5	0.4	0.7	0.4	0.4	0.4	0.5	0.3
12	Unidentified	Trace	Trace	Trace					Trace	
13	Unidentified	0.1	—	—	—	Trace	Trace	—	Trace	Trace
14	Unidentified	Trace	—	—	—	—	0.1	0.1	Trace	Trace
15	(Fenchone)	Trace	—	—	—	—	—	Trace	0.1	Trace
16	(Thujone)	Trace	—	—	—	—	0.2	—	0.1	Trace
17	(Isothujone)	Trace	0.3	0.2	0.4	0.1	Trace	0.1	0.1	
18	Unidentified	Trace	—	Trace	Trace	—	—	—	Trace	
19	(Camphor)	Trace	—	—	—	—	—	—	0.7	
20	Linalool	0.7	1.2	0.4	1.0	0.4	0.3	0.6	0.9	0.1
21	Methyl citronellate + unknown¶	4.5¶	2.3	4.5	2.5	1.2	9.3	2.0	6.6	1.7
22	(Bornyl acetate)	Trace	0.1	0.1	0.1	0.2	Trace	0.1	1.3	0.6
23	4-Terpinenol	3.0	4.0	3.6	6.0	3.3	1.8	0.9	2.8	0.3
24	Unidentified	0.1	Trace	0.1	0.1	Trace	Trace	Trace	0.4	0.2
25	Unidentified	0.1		Trace	Trace		Trace	Trace	0.1	Trace
26	Estragole	1.3	0.2	1.1	1.1	0.4	0.1	0.6	0.2	0.2
27	(Borneol)	0.2	0.1	0.1	0.1	0.1	0.2	Trace	0.1	0.1
28	Methyl vinyl anisole	4.0	6.1	Trace	Trace	4.8	0.3	0.1	0.2	0.8
29	δ-Cadinene	0.3	0.1	0.2	0.1	0.1	0.2	0.3	0.3	0.2
30	Unidentified	0.3	0.1	0.2	0.1	0.1	Trace	0.4	0.3	0.9
31	Citronellol	1.1	1.6	1.4	2.4	0.9	0.5	1.0	Trace	1.0
32		1.3					1.0	2.2	1.7	4.8
33	(Nerol)	Trace	—	—	—	—	Trace	Trace	0.1	0.1
34	Unidentified	Trace	—	—	—	—	Trace	0.1	Trace	
35	(Geraniol)	0.3	0.3	0.2	Trace	0.4	0.1	Trace	0.2	0.1
36	Safrole (+ C=O)	18.7	18.7	17.5	5.4	18.9	Trace	1.5	9.6	
37	Aliph. alcohol	0.1	—	Trace	Trace	—	0.2	0.1	0.2	0.2
38	Unidentified	Trace	—	Trace	Trace	—	0.1	Trace		0.1
39	Unidentified	0.2	0.1	0.2	0.1	—	0.2	0.1	0.2	0.2
40	Methyl eugenol	12.1	11.8	9.0	7.3	3.9	Trace	0.7	2.9	Trace
41	(C=O; —OH)	0.2	2.9	0.6	0.3	2.4	0.2	0.3	0.6	0.4
42	Unidentified	0.2	0.4	0.5	0.1	0.1	1.3	0.8	0.6	1.4
43	? Decomposition	0.1	0.2	18.6	16.3	15.3	22.8	8.1	23.8	22.9
44	Elemol	4.7¶	7.6							
45	Elemol acetate	0.5¶	2.5	5.1	7.4	7.5	8.5	3.2	1.4	0.5
46	Unidentified	Trace	0.1	0.1	Trace	0.2	Trace	0.9	Trace	0.2
47	Unidentified	Trace	0.3				Trace	Trace	—	—
48	γ-Eudesmol	0.8	1.2	3.2	1.9	2.3	2.7	2.2	2.7	4.8
49	Aromatic compound	0.3	0.6	1.3	0.6	0.8	1.4	2.0	1.1	3.3
50	Unidentified	Trace	0.1	0.1	Trace	0.1	Trace	0.1	Trace	0.2
51a	α-Eudesmol	1.0**	8.5	11.8	8.9	9.8	7.0	7.3	7.6	12.3
51b	Elemicin	1.0**								
52	β-Eudesmol	0.8								
53	Unidentified	0.1	0.1	0.1	Trace	Trace	0.1	0.2	0.1	0.2
54	Unidentified	Trace	Trace	Trace	—	—	—	Trace	Trace	Trace
55	Acetate **2**	0.4	6.0	5.7	7.5	3.7	6.5	4.5	3.1	2.2

*In the sequence of elution from the 5% PEG column (45° to 215°, 2.9°/min).
†Names in parentheses are tentatively identified components.
‡Collected 20 miles west of Austin (near Bastrop).
§Collected near St. Williams, Southern Ontario.
‖Large batch.
¶These components decompose.
**Approximate value (±0.2%).

Can. J. Chem. Downloaded from www.nrcresearchpress.com by 210.87.254.105 on 09/05/12
For personal use only.

Can. J. Chem. Downloaded from www.nrcresearchpress.com by 210.87.254.105 on 09/05/12
For personal use only.

acetylated under mild conditions (acetic anhydride – pyridine at room temperatures for two weeks) and a mixture of elemol and elemol acetate was obtained. Separation by g.l.c. (PEG column) gave impure elemol acetate, which had a similar i.r. spectrum and retention times as acetate **1**. In all experiments decomposition (as deduced from peak shape) was appreciable.

Attempts to isolate peaks 21, 32, and the unidentified trace components met with difficulties owing to extensive decomposition, poor resolution, or paucity of material. Peak 21 has the retention time of methyl citronellate (16) which is a rather stable ester. An attempt was, therefore, made to collect peak 21 directly without prefractionation. The yield was lower than expected, indicating once again that decomposition took place. The i.r. and n.m.r. spectra showed some similarity with those of methyl citronellate, but a major impurity was present. Attempts to isolate this impurity failed owing to further decomposition.

Results and Discussion

Figure 1*a* shows the chromatogram of the leaf oil of the red juniper as obtained with the 5% PEG column under standard conditions (8, 12). Although the separation appeared to be satisfactory, closer inspection showed poor resolution between peaks 7 and 8, 31 and 32, 40 and 41, 43, 44 and 45 (this may be owing to decomposition of elemol and elemol acetate), peak 49 and 50, as well as 51 and 52. When Aeropak 30 (70–80 mesh) was used as solid support instead of Gaschrom P (60–80 mesh), this column under the same conditions gave the chromatogram as shown in Fig. 1*b*. Not only were all the peaks slightly sharper, but the total analysis time was reduced by about 10 min and the separation between peaks 7 and 8, 31 and 32, as well as 40 and 41 was slightly better. Peaks 51 and 52 appear to be reversed, but subsequent isolation showed that a third component was present (see Table I). When the new solid support was used with SE-30 as the liquid phase no improvement or changes in resolution were obtained, but again a slightly lower analysis time was possible. In fact, with the SE-30 columns a program of 4°/min from 55 to 220° gave the same degree of resolution as shown in Fig. 1*c*. Although some peak resolutions were better on SE-30, notably between peaks 1*a* and 1*b*, and peaks 51, 52*a*, and 52*b*, the overall fractionation of this oil was better on the PEG column and this column was, therefore, used in the quantitative experiments.

The quantitative composition of the leaf oil of the red juniper from Texas is shown in Table I (column *a*). This was determined in duplicate runs, when a precision of 0.1% for all well-resolved, stable components was obtained. Even those present in less than 0.5% amount were integrated with a precision of 0.1%. Larger errors must be assumed for the poorly resolved or decomposing peaks (especially peaks 45 to 53). To test the internal normalization method (15), various reference compounds were added to the oil (from 5 to 20% of the weight of oil). With *n*-paraffins (C-8 to C-20) rather variable results were obtained. Since olefins and branched paraffins give a different detector (katharometer) response than the *n*-paraffins (15), correction factors have to be employed and make the quantitation procedure cumbersome. When fenchone and safrole were added, reproducible results were obtained (see Table II), and these indicated that summation of the area under the peaks of all oil constituents was about 1% low. The response of the detector towards several monoterpenes and safrole was found to be virtually the same. Hence, this low result can be explained best by assuming that losses during g.l.c. owing to decomposition occurred. This is most reasonable when one considers the difficulties encountered in identifying the labile components 21, 45, and 55 (see below). When cedrol was added (see Table II*c*) the recorded quantity was almost the weight percentage. However, in comparison with fenchone and safrole, the response was low. Hence, sesquiterpenes may require a correction factor. The optimum quantitative reproducibility was obtained when 1 to 5 μl of oil were chromatographed. With larger aliquots peak broadening resulted in poorer resolution of the individual components, whereas smaller aliquots gave lower peak areas, which in turn resulted in the errors owing to baseline correction being more pronounced. With aliquots of 1 to 3 μl, a reproducibility of 0.1% for all peaks that are well resolved is possible. This degree of precision could not be obtained when the data from two different columns (PEG and SE-30) were compared. It is possible that the shift in retention of some minor components into major ones caused this larger error (up to 0.3%), but a different response when different columns are used cannot be ruled out. This aspect, as well as the response of individual terpenes to both thermal conductivity and flame ionization detectors is being studied in more detail. The reproducibility obtained and overall accuracy is entirely sufficient for chemosystematic and other comparative studies.

TABLE II

Percentage composition of the red juniper leaf oil with added internal standards

	Weight (mg)	% calcd.	% found*
a)			
Leaf oil	141.87	88.41	87.5
Fenchone	18.60	11.59	12.5
b)			
Leaf oil	109.76	90.50	89.9†
Safrole	11.54	9.50	10.1†
c)			
Leaf oil	654.38	95.04	94.9
Cedrol	34.12	4.96	5.1

*Triplicate determinations (±0.1%) using 3–5 μl aliquots.
†Calculated with the content of safrole in the oil before addition as 18.7% (see Table I).

Isolation and comparison of spectra confirmed the identity of the known constituents listed in Table I. The amount of α-thujene determined in peak 1 is subject to a large error. Whereas g.l.c. analysis on the SE-30, EGPN, and PPE columns indicated a ratio of α-thujene to α-pinene of about 1 to 2, the n.m.r. spectrum of the collected mixed fraction indicated that less thujene was present. Possibly, α-thujene is condensed less efficiently than α-pinene in the collection procedure. All the other major monoterpene hydrocarbons were recorded and collected satisfactorily, except that the overlap between limonene (peak 7) and β-phellandrene (peak 8) introduced a larger error. On keeping the leaf oil in the dark and at low temperature (near 0 °C) for several weeks, a drop in the amounts of γ-terpinene (peak 9) and terpinolene (peak 11) and a corresponding rise in that of *p*-cymene (peak 10) was noted. Also, the amount of peak 21 decreased and acetate **2** (peak 55) was changed to a new peak of longer retention time. The new compound may be the same compound as peak 42 of the leaf oil of *J. horizontalis* (14).

The major oxygenated terpenes and aromatic ethers were also readily identified, linalool (peak 20), 4-terpinenol (peak 23), estragole (peak 26), methyl vinyl anisole (peak 28, see below), citronellol (peak 31), safrole (peak 36), methyl eugenol (peak 40), and elemol (peak 44) being obtained in a fairly pure state. γ-Eudesmol (peak 48) was not obtained pure and α- and β-eudesmol (peaks 51 and 52*b*) were isolated as a mixture. The prefractionation procedure on modified silicic acid was inefficient owing to the presence of the many aromatic ethers. However, the aromatic ethers could be separated from oxygenated terpenes by g.l.c. on two different columns (PEG and SE-30). Peak 21 has the retention characteristics of methyl citronellate (13, 14, 16), but is far more labile than this methyl ester. An attempt was made to isolate this constituent directly by g.l.c. without prefractionation, but recovery was poor and impure material was collected. The spectral evidence indicates that a minor portion is methyl citronellate.

The identity of methyl vinyl anisole (peak 28) was established by interpretation of its i.r. and n.m.r. spectra, as well as those of its hydrogenation product. The i.r. spectrum indicated an aromatic ether with a vinyl group and possibly a 1,3,4 substitution pattern (as in safrole). The elementary analysis was in agreement with $C_{10}H_{12}O$ and hence the compound is isomeric with estragole. The n.m.r. spectrum (see Table III*a*) confirmed the presence of a vinyl and a methoxy group, and contained a signal for a methyl group attached to the aromatic ring. The assignment of the vinyl (signals *c*, *d*, and *e*) and aromatic (signals *f* and *g*) protons was confirmed by the spin decoupling technique. However, no conclusions as to the substitution order could be drawn. The n.m.r. spectrum of the dihydro derivative (see Table II*b*) not only confirmed the presence of a vinyl group in the parent compound, by virtue of the ethyl group signals, but showed a chemical shift of the methyl signal (signal *b*) from 2.34 to 2.05 p.p.m., whereas that of the methoxy group remained virtually unchanged. Hence, the methyl group appears to be adjacent to the vinyl group and component 28 is most likely *m*-methyl-*p*-vinyl anisole (1-methyl-2-vinyl 5-methoxy benzene). Spin decoupling experiments showed that the conjugated single proton of the vinyl group (signal *e*) in the parent compound was coupled with one aromatic proton (signal *f*) and that the three aromatic protons were coupled with each other. In the dihydro compound the signals caused by the three aromatic protons were again complex, but the triplet of the parent compound (signal *g*) showed no chemical shift, whereas the major peaks of signal *f* appeared further upfield (shift from 6.62–6.71 to 6.49–6.63 p.p.m.). Hence, it appears that the triplet is generated by an isolated proton which is not located adjacent to the vinyl group. This lends support to component 28 being 3-methyl-4-vinyl anisole. The presence of this

Can. J. Chem. Downloaded from www.nrcresearchpress.com by 210.87.254.105 on 09/05/12
For personal use only.

TABLE III

Nuclear magnetic resonance signals and assignments of component 28 and its hydrogenation product

Signal type	Number of protons	Chemical shift (p.p.m.)	Assignment
a Component 28			
a Singlet	3	2.34	Ph—CH_3
b Singlet	3	3.79	Ph—OCH_3
c Quartet	1	~5.38	Ph—CH=C(H)(H)
d Quartet	1	~5.52	
e Multiplet	1	6.50–6.80	Ph—CH=CH_2
f Multiplet	2	6.50–6.80	Aromatic H
g Triplet	1	6.96	Aromatic H
b Hydrogenation product			
a Triplet	3	1.05	—CH_2—CH_3
b Singlet	3	2.05	Ph—CH_3
c Quartet	2	2.62	Ph—CH_2—CH_3
d Singlet	3	3.76	Ph—O—CH_3
e Multiplet	2	6.49–6.82	Aromatic H
f Triplet	1	7.00	Aromatic H

vinyl compound raises interesting possibilities as to its biosynthesis in *Juniperus virginiana* L. If one assumes that the aromatic ethers are derived via the phenyl propanoid pathway, then a methyl migration from the side-chain of estragol to the aromatic nucleus would account for the formation of methyl vinyl anisole. Alternatively, it may be derived by an entirely different pathway. It is also noteworthy that all the other aromatic ethers contain allylic side-chains and that the "iso"-compounds with a propenyl side chain are not present in detectable amounts. The large variation in the quantity of these aromatic components (see Table I) in different oil samples may have a bearing on the high degree of variability in the percentage composition of the leaf oil of red juniper from one tree to another, even within the same population.

Component 55 had the same i.r. spectrum as that of acetate **2** isolated previously from the leaf oils of *Juniperus horizontalis* (13). The n.m.r. spectrum (see Experimental) permitted conclusions only as to the number of methyl substituents and double bonds, but the basic structure of this sesquiterpenoid acetate could not be established. Attempts to isolate larger amounts for chemical investigations (e.g. dehydrogenation) invariably resulted in mixtures being obtained. Subsequently it was found that storage of the oil in the dark resulted in a change to a peak of longer retention time (peak 42 of the leaf oil of *Juniperus scopulorum* (14)). Hence, acetate **2** is of a rather labile nature and a different method of isolation must be sought.

It is noteworthy that whereas the wood oil of the red juniper was found to consist mainly of α-cedrene, thujopsene, cuparene, a (+)-curcumene, cedrol and widdrol (5, 6), these sesquiterpenes were not isolated from the leaf oil. These compounds may, of course, be present in trace amounts. However, the absence of major amounts indicates clearly a distinct difference in the biosynthesis of terpenes in the wood and in the leaves. This is of considerable importance for taxonomic (chemosystematic) applications.

The similarity of most of the components of the leaf oil of *Juniperus virginiana* L. and those found in that of *J. horizontalis* (Moench) (13) and *J. scopulorum* Sarg. (14), indicates a close phylogenetic relationship. If the quantitative differences were constant within the different populations of these species, chemosystematic studies could be carried out fairly readily. However, quantitative analysis of a number of leaf oil samples of *J. virginiana* from Texas and Ontario (see Table I) indicates that a wide quantitative variation is to be found in the leaf oil of this species. The overlap of range and possible introgression of *J. virginiana* and *J. ashei* Buchholz is of considerable taxonomic interest

Can. J. Chem. Downloaded from www.nrcresearchpress.com by 210.87.254.105 on 09/05/12
For personal use only.

(2). Comparison of the chemical composition of the leaf oils of these two species shows that the latter contains the typical terpenes of the family Pinaceae rather than those of the family Cupressaceae (to which the junipers belong). This difference in chemical constituents makes a study of the possible introgression of these two species feasible. Early results (7) indicate that in the overlap which occurs near Austin, Texas, no hybridization appears to occur and that the taxonomic evaluation must be re-examined. These chemosystematic aspects are being studied further by us.

Acknowledgments

We wish to thank Prof. B. L. Turner and Prof. E. Jörgensen for their help in collecting and identifying the plant material; Mr. R. Irving for the large scale steam distillation; Mr. M. Granat for technical assistance; and Mr. M. Mazurek and Mr. W. C. Haid for recording the spectra and microanalysis.

1. N. C. FASSETT. Bull. Torry Botan. Club, **71**, 410, 475 (1944); **72**, 42, 379, 480 (1945).
2. M. T. HALL. Annals of the Missouri Botanical Garden, **39**(1), 1 (1952); Evolution, **6**, 347 (1952).
3. E. GUENTHER. The essential oils. Vol. VI. D. van Nostrand Co., Inc., New York. 1952. p. 353–364.
4. R. HEGNAUER. Chemotaxonomie der pflanzen. Vol. VI. Brikenhäuser, Basel & Stuttgard. 1962. p. 284–287.
5. J. RUNEBERG. Acta Chem. Scand. **14**, 1288 (1960).
6. A. S. DUBENCHIEK. Perfumery Ess. Oil Record, **46**, 298 (1955).
7. R. IRVING, B. L. TURNER, and E. VON RUDLOFF. Annual Meeting Am. Inst. Biol. Sci., College Station, Texas. August 27–September 1, 1967.
8. E. VON RUDLOFF. Can. J. Chem. **46**, 619 (1968).
9. E. VON RUDLOFF. Can. J. Chem. **39**, 1190 (1961).
10. K. MCHUGH. Monsanto Co., St. Louis, Missouri.
11. E. VON RUDLOFF. Can. J. Botany, **45**, 891 (1967).
12. E. VON RUDLOFF. Phytochem. **5**, 331 (1966).
13. E. VON RUDLOFF and F. M. COUCHMAN. Can. J. Chem. **42**, 1890 (1964).
14. F. M. COUCHMAN and E. VON RUDLOFF. Can. J. Chem. **43**, 1017 (1965).
15. H. P. BURCHFIELD and E. E. STORRS. *In* Biochemical applications of gas chromatography. Academic Press, Inc., New York. 1962. p. 114–124.
16. E. VON RUDLOFF. Can. J. Chem. **41**, 2876 (1963).

Can. J. Chem. Downloaded from www.nrcresearchpress.com by 210.87.254.105 on 09/05/12
For personal use only.

Can. J. Chem. Downloaded from www.nrcresearchpress.com by 210.87.254.5 on 09/05/12
For personal use only.

Reaction of 1,2:5,6-di-*O*-isopropylidene-3-*O*-*p*-nitrophenylsulfonyl (and 3-*O*-*p*-tolylsulfonyl) α-D-glucofuranose with tetramethylammonium hydroxide in methyl sulfoxide

ALEX ROSENTHAL AND L. NGUYEN[1]

Department of Chemistry, University of British Columbia, Vancouver, British Columbia

Received July 15, 1968

Treatment of 1,2:5,6-di-*O*-isopropylidene-3-*O*-*p*-tolylsulfonyl-α-D-glucofuranose with tetramethylammonium hydroxide in methyl sulfoxide gave 1,2:5,6-di-*O*-isopropylidene-α-D-glucofuranose in 89% yield. Under similar conditions, the 3-*O*-*p*-nitrobenzenesulfonate ester of 1,2:5,6-di-*O*-isopropylidene-α-D-glucofuranose **1**, gave 3-*O*-[*p*-(3-deoxy-1,2:5,6-di-*O*-isopropylidene-α-D-glucofuranose-3-yl)oxyphenylsulfonyl]-1,2:5,6-di-*O*-isopropylidene-α-D-gluocofuranose **2**, and 1,2:5,6-di-*O*-isopropylidene-3-*O*-*p*-nitrophenyl-α-D-glucofuranose **3**. A discussion of the probable mechanism of this reaction is based on a study of the products obtained by application of the same reaction to ethyl *p*-nitrobenzenesulfonate.

Canadian Journal of Chemistry, **46**, 3751 (1968)

The synthesis of 3-deoxy-1,2:5,6-di-*O*-isopropylidene-α-D-erythro-hex-3-enose has posed a problem of considerable difficulty. Employment of potassium hydroxide as base to effect elimination of *p*-toluenesulfonic acid from 1,2:5,6-di-*O*-isopropylidene-3-*O*-*p*-tolylsulfonyl-α-D-glucofuranose led to low, variable yields of unsaturated sugar (1, 2). Some success toward finding a better method of elimination of *p*-toluenesulfonic acid from sulfonate esters of model alcohols was attained by using potassium *t*-butoxide in methyl sulfoxide (3). Because the *p*-nitrobenzenesulfonate is known to be a better leaving group than the *p*-toluenesulfonate (4), other workers (5) have used the former sulfonate ester in their studies but have found that ethers, in addition to olefins, are produced. From studies on the sulfonate esters of natural products, it has been shown that the product is also dependent on the nature of the sulfonate and on its conformation. Thus, cholestan-3β-ol-3-meslyate afforded cholestan-3β-ol and an olefin in 86% and 4% yields, respectively, whereas cholestan-3β-ol-3*p*-toluenesulfonate gave mainly an olefin. When the epimeric form of the latter (namely, the 3α-*p*-toluenesulfonate) was used then the yield of olefin was reduced to 68% (6). Utilization of potassium hydrogen carbonate or of collidine as base has resulted in the conversion of sulfonate esters of steroidal compounds into mixtures of alcohols, ketones, and unsaturated compounds (7, 8). The present work arose from an attempt to find a better method of synthesizing 1,2:5,6-di-*O*-isopropylidene-α-D-erythro-hex-3-enose. It was considered that use of a more powerful base, for example, tetramethylammonium hydroxide (TMAH) in methyl sulfoxide (DMSO) (9), might allow the elimination reaction to be carried out at room temperature. It was envisaged that the unsaturated sugar could subsequently be extracted with petroleum ether or chloroform from the reaction mixture.

When 1,2:5,6-di-*O*-isopropylidene-3-*O*-*p*-tolylsulfonyl-α-D-glucofuranose was allowed to react with aqueous TMAH (25%) in DMSO at room temperature for 3 days, the starting material was hydrolyzed to yield 1,2:5,6-di-*O*-isopropylidene-α-D-glucofuranose in 89% yield. Treatment of 1,2:5,6-di-*O*-isopropylidene-3-*O*-*p*-nitrophenylsulfonyl-α-D-glucofuranose **1** with tetramethylammonium hydroxide in methyl sulfoxide at room temperature for 2 days gave, after work-up, a mixture of three crystalline compounds. The major crystalline product **2**, isolated in 54% yield, showed absorption in the infrared characteristic of the sulfonyl (1190 and 1380 cm^{-1}) and no absorption for a nitro group. Its mass spectrum gave a peak at *m/e* 643. Because isopropylidene derivatives of carbohydrates are known to lose a methyl group during their initial mass breakdown (10, 11), therefore, the molecular weight of **2** was 658. This molecular weight suggested strongly that compound **2** was a dimer of **1** in which a *p*-nitrophenylsulfonyl and a nitro group were eliminated from 2 molecules of **1**. Elemental analysis of **2** agreed with the molecular constitution $C_{30}H_{42}O_{14}S$. The dimeric structure of **2** was confirmed by cleaving **2** with sodium

[1]Née Benzing.

Can. J. Chem. Downloaded from www.nrcresearchpress.com by 210.87.254.5 on 09/05/12
For personal use only.

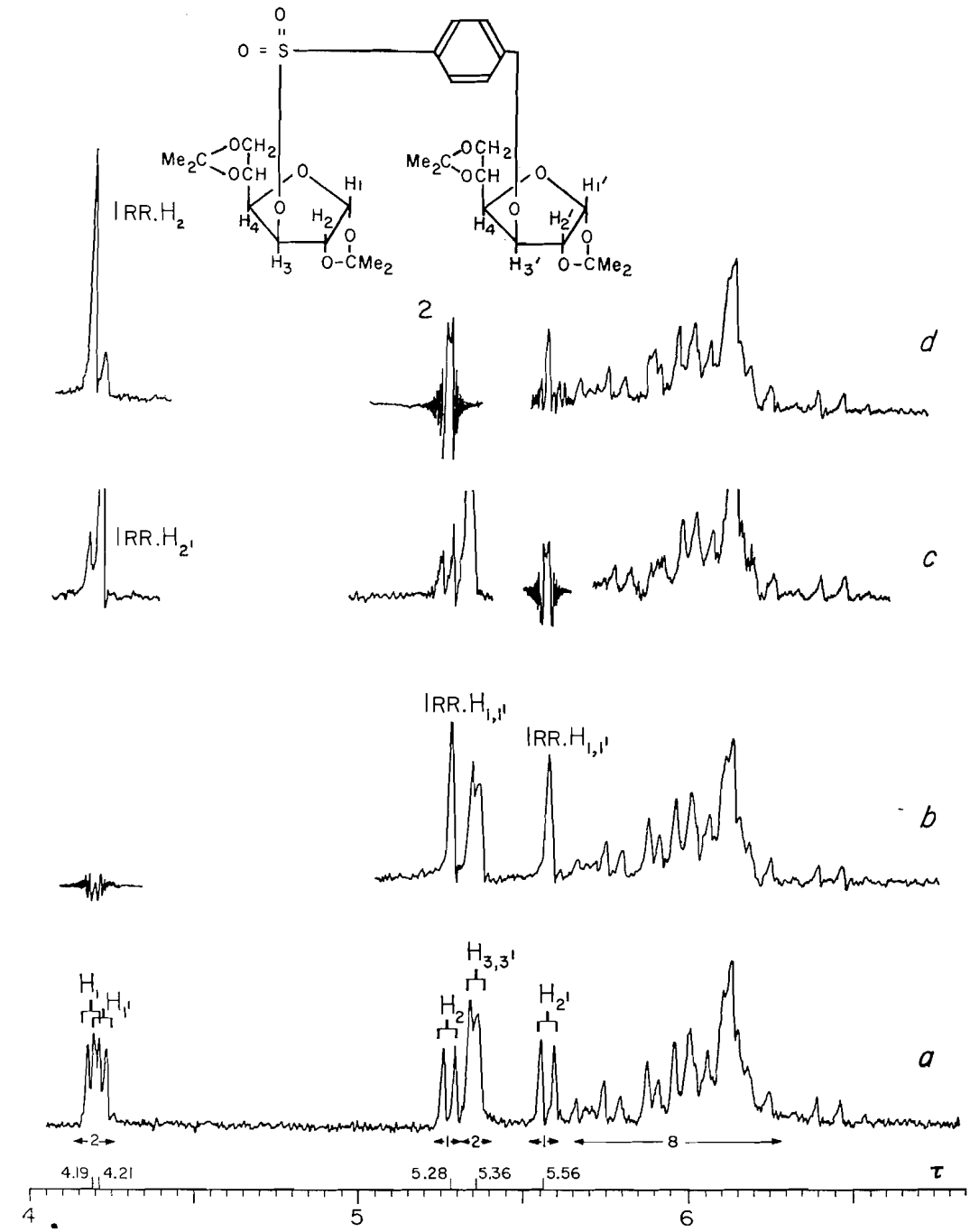

FIG. 1. The proton magnetic resonance spectrum of **2** in CCl_4 as solvent. [(*a*) at 100 MHz; (*b*) at 100 MHz, H-1 and H-1′ protons irradiated; (*c*) at 100 MHz, H-2′ proton irradiated; (*d*) at 100 MHz, H-2 proton irradiated.]

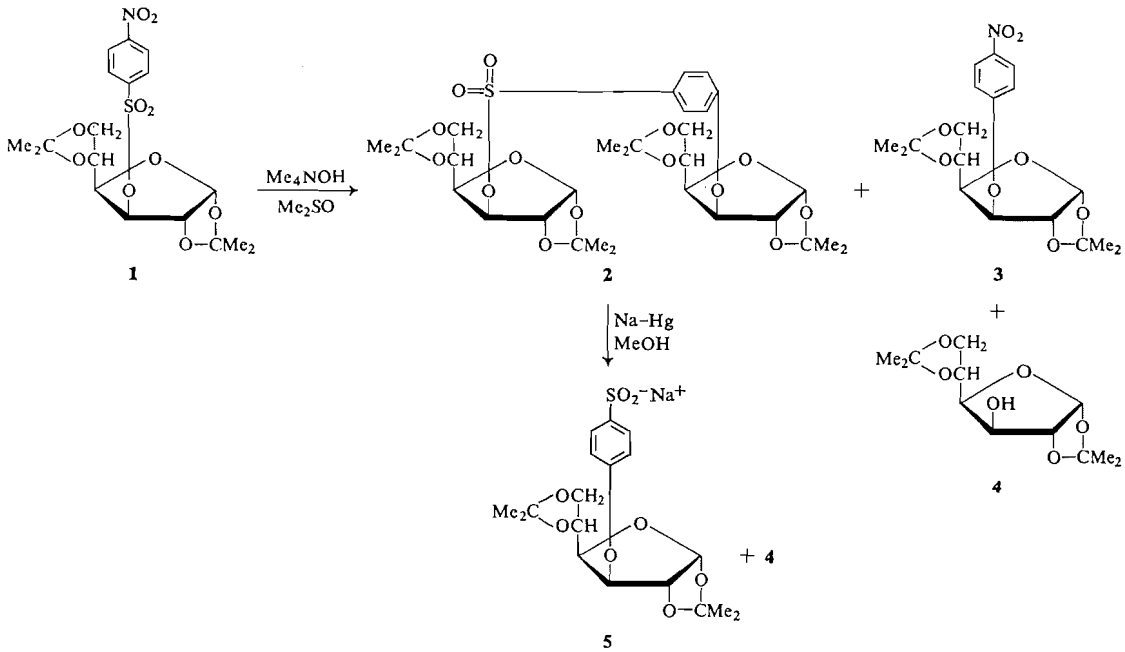

amalgam. 1,2:5,6-Di-*O*-isopropylidene-α-D-glucofuranose (identical to an authentic sample) was obtained in almost quantitative yield. The second fragment **5** was a water-soluble crystalline substance. Its nuclear magnetic resonance (n.m.r.) showed two doublets at τ 2.43 and 2.91 (relative area 4), typical of the A_2B_2 pattern of aromatic protons. A doublet at τ 3.96 (relative area 1) was assigned to the anomeric hydrogen. Signals for H-2, H-3, H-4, and H-5 could not be assigned because of the interference with the lock signal of the HOD peak. Compound **5** was assumed tentatively to be *p*(3-deoxy-1,2:5,6-di-*O*-isopropylidene-α-D-glucofuranose-3-yl)oxybenzenesulfinic acid, sodium salt.

The partial nuclear magnetic resonance spectrum of **2** (shown in Fig. 1) corroborated the dimeric structure of **2** and also permitted an easy assignment of the configuration of C-3 of each of the furanose moieties of **2**. Eight clearly defined peaks occurred at about τ 8.6 (equal to 24 protons) that are undoubtedly due to the 8 methyl groups. Two doublets at τ 1.98 and 2.80 were assigned to the 4 aromatic protons (gave the typical A_2B_2 pattern of aromatic protons). The two pairs of doublets at τ 4.19 ($J_{1,2}$ = 3.5 Hz) and 4.21 ($J_{1',2'}$ = 3.7 Hz) (see Fig. 1*a*) were assigned to H-1 and H-1′ on the basis of the fact that the doublet of 1,2:5,6-di-*O*-isopropylidene-α-D-glucofuranose at τ 4.22 has a $J_{1,2}$ = 3.5 Hz. Irradiation of **2** at τ 5.56 and 5.28 led to a collapse of the two pairs of doublets at τ 4.2 (Fig. 1*c* and *d*). When **2** was irradiated at τ 4.2, then the doublets at τ 5.28 and 5.56 collapsed to singlets (Fig. 1*b*). Since the H-2 signals of 1,2:5,6-di-*O*-isopropylidene-α-D-glucofuranose occurs at τ 5.6, whereas the H-2 signal of the 3-*O*-tosylate derivative occurs at τ 5.28, therefore, the doublets at 5.28 and 5.56 are those of H-2 and H-2′, respectively. The configuration of C-3 of each furanose moiety of the dimer was deduced on the following evidence. H-2 and H-2′ signals occurring as two doublets show no measurable coupling between H-2 and H-3, H-2′ and H-3′. Since H-2 of 1,2:5,6-di-*O*-isopropylidene-α-D-glucofuranose gives a doublet (no measurable coupling between H-2 and H-3) whereas H-2 of 1,2-5,6:di-*O*-isopropylidene-α-D-allofuranose gives two pairs of doublets, therefore, each furanose moiety of **2** must have the D-*gluco*-configuration. From this evidence, it must follow that compound **2** is 3-*O*-[*p*-(3-deoxy-1,2:5,6-di-*O*-isopropylidene-α-D-glucofuranose-3-yl)oxyphenylsulfonyl]-1,2:5,6-di-*O*-isopropylidene-α-D-glucofuranose.

Compound **3**, obtained in 19% yield, showed absorption in its infrared spectrum characteristic

Can. J. Chem. Downloaded from www.nrcresearchpress.com by 210.87.254.5 on 09/05/12
For personal use only.

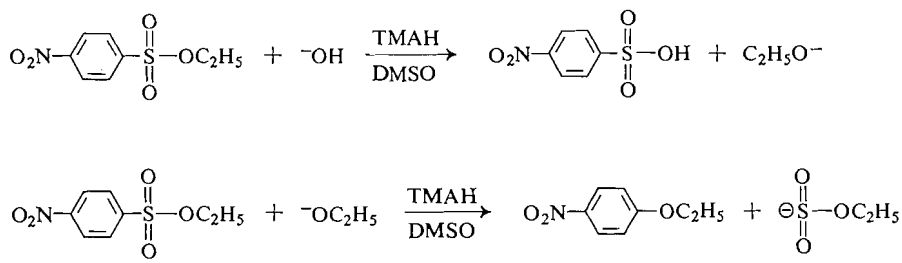

of a nitro group but none characteristic of a sulfonyl group. Its mass spectrum gave a peak at 366, thus establishing that **3** had a molecular weight of 381 (15 added to base peak to account for loss of a methyl group). The elemental analysis agreed with the molecular constitution $C_{18}H_{23}O_8N$. The n.m.r. spectrum of **3** exhibited two doublets at τ 1.79 and 2.98 (relative area 4) which is typical of an A_2B_2 pattern of aromatic protons, and a doublet at τ 4.23 (relative area 1), which was assigned to the anomeric hydrogen. The H-2 signal appears as a doublet at τ 5.57. C-3 was assigned the D-*gluco* configuration on the same basis as used for the assignment of C-3 of compound **2**. The signals for H-4, H-5, and H-6 are overlapping (relative area 4) and occur at τ 5.92. The four signals at τ 8.5, 8.65, 8.73, and 8.78 are due to the four isopropylidene methyl groups. On the basis of the aforementioned data, compound **3** is characterized as 1,2:5,6-di-*O*-isopropylidene-3-*O*-*p*-nitrophenyl-α-D-glucofuranose.

The remaining product **4**, obtained in 5% yield, was readily characterized as 1,2:5,6-di-*O*-isopropylidene-α-D-glucofuranose by direct comparison with an authentic sample.

In order to establish a mechanism for the reaction of the *p*-nitrobenzenesulfonate ester of 1,2:5,6-di-*O*-isopropylidene-α-D-glucofuranose with tetramethylammonium hydroxide in methyl sulfoxide, the sulfonates of model alcohols were subjected to similar treatment. Thus, treatment of the *p*-nitrobenzenesulfonate of ethyl alcohol afforded a mixture of at least four compounds. The two main components were the tetramethylammonium salt of *p*-nitrobenzenesulfonic acid and *p*-nitrophenetole isolated in 90 and about 5% yields, respectively (both substances were compared directly with authentic substances). Presumably, the hydroxide ion attacked the sulfur atom of the sulfonate liberating ethoxide ion. The latter ion probably then attacked the highly electron deficient carbon on the phenyl ring with expulsion of the ethoxysulfonyl group and consequent formation of *p*-nitrophenetole as shown below. The presence of a yellow substance (not characterized) in the reaction mixture probably indicated that a Meisenheimer type complex might have been formed during the reaction. This reaction thus closely parallels the well known reaction of 2,4,6-trinitroanisole with potassium ethoxide to give a yellow salt (Meisenheimer complex) which on acidification affords 2,4,6-trinitrophenetole.

The reaction of cyclohexyl *p*-nitrobenzenesulfonate with tetramethylammonium hydroxide in methyl sulfoxide also gave the tetramethylammonium salt of *p*-nitrobenzenesulfonic acid in almost quantitative yield.

A similar mechanism can be invoked to explain the formation of products **2**, **3**, and **4** from the 3-*O*-*p*-nitrobenzenesulfonate of 1,2:5,6-di-*O*-isopropylidene-α-D-glucofuranose. Obviously, a simple hydrolysis of **1** afforded 1,2:5,6-di-*O*-isopropylidene-α-D-glucofuranose (4). In the presence of methyl sulfoxide the 1,2:5,6-di-*O*-isopropylidene-α-D-glucofuranose 3-oxide ion of **4** might be expected to exhibit enhanced basicity, and, presumably, might be expected to be able to attack compound **1** at the carbon carrying the nitro group. This carbon would be positive in character due to the strong electron withdrawing effect of the sulfonyloxy group. The green to red-orange color of the solution during the reaction strongly indicates that a type of Meisenheimer complex was formed. Expulsion of the nitro group by the attacking 3-oxide ion of 1,2:5,6-di-*O*-isopropylidene-α-D-glucofuranose would then lead to the production of the dimer **2**. On the other hand, attack of the 3-oxide ion at the *p*-carbon on the aromatic ring (relative to the nitro group) of another molecule of **1** might also be

Can. J. Chem. Downloaded from www.nrcresearchpress.com by 210.87.254.5 on 09/05/12
For personal use only.

Can. J. Chem. Downloaded from www.nrcresearchpress.com by 210.87.254.5 on 09/05/12
For personal use only.

expected to lead to expulsion of the 1,2:5,6-di-*O*-isopropylidene-α-D-glucofuranose-3-*O*-sulfonyl group with consequent formation of **3**.

Experimental

All melting points are uncorrected. Microanalyses were performed by the Microanalytical Laboratory, University of British Columbia. Infrared spectra were recorded with a Perkin–Elmer model 137 spectrophotometer. Nuclear magnetic resonance (n.m.r.) spectra were obtained with a Varian HA-100 spectrometer. Unless otherwise stated the samples were dissolved in carbon tetrachloride with tetramethylsilane ($\tau = 10.0$) as the internal standard. The molecular weights were determined by mass spectroscopy using an A.E.I.-M.S.9 spectrometer.

Thin-layer chromatography (t.l.c.) was performed with Silica Gel G (E. Merck, Darmstadt, Germany) on plates activated at 110° and then air-dried. The developing solvent was 99:1 benzene–methanol and indication was effected with iodine vapors or sulfuric acid – water (1:1 by volume).

Methyl sulfoxide was purified by shaking it for 2 days over calcium hydride and then distilling it under reduced pressure.

Reaction of 1,2:5,6-Di-O-isopropylidene-3-O-p-tolylsulfonyl-α-D-glucofuranose with Tetramethylammonium Hydroxide in Methyl Sulfoxide to yield 1,2:5,6-Di-O-isopropylidene-α-D-glucofuranose

1,2:5,6-Di-*O*-isopropyldiene-3-*O*-*p*-tolylsulfonyl-α-D-glucofuranose (1.3 g) was allowed to react with 1.5 ml of a 25% aqueous solution of tetramethylammonium hydroxide in 20 ml of methyl sulfoxide for 3 days at room temperature. An amount of 40 ml of water was then added to the reaction mixture. The mixture was extracted three times with 60 ml of chloroform. The combined chloroform extracts were washed with water, dried over anhydrous sodium sulfate, and then evaporated under reduced pressure to yield 0.7 g (89%) of crystalline material which was recrystallized from petroleum ether (b.p. 65–110°), m.p. 110° (0.6 g), $[\alpha]_D^{22}$ −19° (*c*, 3.5 acetone). The mixed m.p. of this substance and authentic 1,2:5,6-di-*O*-isopropylidene-α-D-glucofuranose was 109–110°. The optical rotation of authentic 1,2:5,6-di-*O*-isopropylidene-α-D-glucofuranose is −19°.

Reaction of 1,2:5,6-Di-O-isopropylidene-3-O-p-nitrophenylsulfonyl-α-D-glucofuranose (1) with Tetramethylammonium Hydroxide in Methyl Sulfoxide to yield 3-O-[p-(3-Deoxy-1,2:5,6-di-O-isopropylidene-α-D-glucofuranose-3-yl-oxyphenylsulfonyl]-1,2:5,6-di-O-isopropylidene-α-D-glucofuranose (2) and 1,2:5,6-Di-O-isopropylidene-3-O-p-nitrophenyl-α-D-glucofuranose (3)

To a solution of 1,2:5,6-di-*O*-isopropylidene-3-*O*-*p*-nitrophenylsulfonyl-α-D-glucofuranose (10 g (12)) in 40 ml of methyl sulfoxide was added 10 ml of a 25% aqueous solution of tetramethylammonium hydroxide. The reaction mixture, kept at room temperature for 2 days, gradually changed in color from green to orange-red. The crystalline compound **2** that separated was removed by filtration, washed with water, dried, and then recrystallized from petroleum ether (b.p. 30–60°), yield 4 g (54%), m.p. 93–94°, $[\alpha]_D^{22}$ −78° (*c*, 2, chloroform), R_f 0.3 (benzene:methanol 99:1 v/v) $\lambda_{max}(CCl_4)$ 1470 and 1315 cm^{-1} (O—SO_2—); $\tau(CDCl_3)$ 1.98, 2.80 (4H, aromatic), 4.19 (1-H, doublet, $J_{1,2}$ 3.5 Hz), 4.21 (1′-H, doublet, $J_{1',2'}$ 3.7 Hz), 5.28 (1-H, doublet $J_{2,1}$ 3.5 Hz, due to H-2), 5.56 (1-H, doublet, $J_{2',1'}$ 3.7 Hz, due to H-2′), 5.36 (2-H, doublet, $J_{3,4}$ and $J_{3',4'}$ 3.0 Hz, due to H-3 and H-3′), 8.34 (24-H, 8 peaks due to CH_3). The partial n.m.r. of **2** is shown in Fig. 1. Mass spectroscopy: 643, 585, 527, 502 (molecular weight found by adding 15 to 643).

Anal. Calcd. for $C_{30}H_{42}O_{14}S$ (mol. wt., 658.73): C, 54.70; H, 6.43; S, 4.87. Found (mol. wt., 658): C, 54.42; H, 6.33; S, 5.08; N, 0.0.

The mother liquor of the above reaction mixture was poured into an equal volume of water and the solution then extracted 3 times with 100 ml aliquots of chloroform. The combined chloroform extracts were dried with anhydrous sodium sulfate, and subsequently evaporated under vacuum. The residue was extracted with 100 ml of petroleum ether (b.p. 30–60°). The extract was evaporated under reduced pressure affording a solid **4**, yield 0.32 g, which was recrystallized from petroleum ether (b.p. 30–60°), m.p. 109–110°; mixed m.p. with an authentic sample of 1,2:5,6-di-*O*-isopropylidene-α-D-glucofuranose (13) was 109–110°.

Characterization of Product 3

The oil remaining after the petroleum ether extraction of the residue was a mixture of compounds **2** and **3**. This mixture was separated by preparative thin-layer chromatography. Product **3** (1.2 g (10%)), was recrystallized from petroleum ether (b.p. 30–60°), m.p. 136–137°, $[\alpha]_D^{22}$ −52° (*c*, 2, chloroform), R_f 0.75, $\nu_{max}(CCl_4)$ 1540 cm^{-1} (NO_2), $\tau(CDCl_3)$, 1.79 and 2.96 (4-H, 2 doublets), 4.23 (1-H, $J_{1,2}$ 4 Hz, due to H-1), 5.35 (1-H, doublet, $J_{3,4}$ 3.0 Hz, due to H-3), 5.57 (1-H, doublet, $J_{2,1}$ 4.0 Hz, due to H-2), 8.50, 8.65, 8.73, 8.78 (12-H. due to 4-CH_3). Mass spectroscopy: *m/e* 366, 351, 336, 308, 266, 248.

Anal. Calcd. for $C_{18}H_{23}O_8N$ (mol. wt., 381.39): C, 56.68; H, 6.07; N, 3.67. Found (mol. wt., 381 (15 added to parent *m/e* peak)): C, 56.35; H, 6.66; N, 3.90; S, 0.0.

Reductive Cleavage of 2 using Sodium Amalgam (14)

To a solution of 100 mg of 2 in 6 ml of absolute methanol, was added 1.6 g of sodium amalgam. After the reaction mixture was stirred for 14 h at room temperature, it was worked-up according to a known procedure (14). The white residue obtained after evaporation of the final ether extract showed by t.l.c. (using 100% isopropyl alcohol as developer) two major products and one minor one. Elution of each zone of the preparative t.l.c. plates with ethanol:water 1:1 v/v gave a quantitative yield of **4** (30 mg), and **5** (43 mg). Fraction 4 was recrystallized from petroleum ether, m.p. 109–110°; mixed m.p. with authentic sample of 1,2:5,6-di-*O*-isopropylidene-α-D-glucofuranose, 109–110°. Product **5**, m.p. 190–191°, R_f 0.30 (100% isopropyl alcohol) was water soluble. $\tau(D_2O)$ 2.43, 2.91 (2 doublets, due to 4 aromatic protons, 3.98 (1-H, $J_{1,2}$ 4.0 Hz, due to H-1), 8.55 (12-H, triplet, due to 4-CH_3), $[\alpha]_D^{22} = -19°$ (*c*, 0.4 in water). Compound **5** had a trace of an impurity which could not be removed and was not analyzed.

Reaction of Ethyl p-Nitrobenzenesufolnate with Tetramethylammonium Hydroxide in Methyl Sulfoxide to yield Tetramethylammonium p-Nitrobenzenesulfonate and p-Nitrophenetole

To a solution of 1 g of ethyl *p*-nitrobenzene sulfonate (4) in 8 ml of methyl sulfoxide was added 1.7 g of 25% aqueous tetramethylammonium hydroxide. After the reaction mixture was left standing at room temperature for 5 h, the crystals (0.50 g) were removed by filtration, and then recrystallized from petroleum ether (b.p. 60–90°), m.p. 283–284°, R_f 0.80 on alumina (benzene:methanol, 75:25), $\tau(CDCl_3)$, 1.44 (4-H, quartet, due to aromatic protons), 6.46 (12-H, triplet, due to 4-CH_3).

The mother liquor was poured into an equal volume of water and then extracted three times with chloroform. The remaining water – methyl sulfoxide mixture was evaporated under reduced pressure. The remaining residue (0.450 g), had a m.p. of 283–284° and was identical to the crystals which precipitated from the reaction mixture. The over-all yield of tetramethylammonium *p*-nitrobenzenesulfonate was 80%.

Anal. Calcd. for $C_{10}H_{16}NO_5S$: C, 43.46; H, 5.90; N, 10.13. Found: C, 43.84; H, 5.94; N, 10.32.

The chloroform extract was dried with sodium sulfate and then evaporated under reduced pressure. The residual oil (0.070 g) was purified by alumina preparative t.l.c. (benzene – petroleum ether (30–60°) (60–40 v/v)) to give crystalline (m.p. 56–57°) material. $\tau(CDCl_3)$, 1.85, 3.13 (2 doublets due to 4 aromatic H), 5.92 (2 protons, quartet), 8.55 (3 protons, triplet). The n.m.r. spectrum and m.p. of an authentic sample of *p*-nitrophenetole were identical to those of the substance obtained from the above chromatographic separation.

Reaction of Cyclohexyl p-Nitrobenzenesulfonate with Tetramethylammonium Hydroxide in Methyl Sulfoxide

Cyclohexyl *p*-nitrobenzenesulfonate was allowed to react with tetramethylammonium hydroxide in methyl sulfoxide as described in the preceding section. Work-up of the reaction mixture gave an almost quantitative yield of tetramethylammonium *p*-nitrobenzenesulfonate.

Acknowledgment

This work was supported by the National Research Council of Canada. The author (L.N.) gratefully acknowledges a National Research Council of Canada studentship (1965–1968).

1. F. Weygand and H. Wolz. Chem. Ber. **85**, 256 (1952).
2. J. Prokop and D H. Murray. J. Pharm. Sci. **54**, 359 (1965).
3. C. H. Snyder. Chem. Ind. (London), 121 (1963).
4. M. S. Morgan and L. H. Cretcher. J. Am. Chem. Soc. **70**, 375 (1948).
5. C. H. Snyder and A. R. Soto. J. Org. Chem. **29**, 742 (1964).
6. F. C. Chang. Tetrahedron Letters, No. 6, 306 (1964).
7. F. X. Jarreau, B. Tchoubar, and R. Goutarel. Bull. Soc. Chim. France, 887 (1962).
8. D. N. Jones and M. A. Saeed. J. Chem. Soc. 4657 (1963).
9. D. Dolman and R. Stewart. Can. J. Chem. **45**, 911 (1967).
10. D. C. De Jongh and K. Biemann. J. Am. Chem. Soc. **86**, 67 (1964).
11. N. K. Kochetkov and O. S. Chizhov. Advan. Carbohydrate Chem. **21**, 39 (1966).
12. K. Freudenberg and O. Ivers. Chem. Ber. **55**, 929 (1922).
13. W. L. Glen, G. S. Myers, and G. A. Grant. J. Chem. Soc. 2568 (1951).
14. P. A. Levene and J. Compton. J. Biol. Chem. **116**, 189 (1936).

Can. J. Chem. Downloaded from www.nrcresearchpress.com by 210.87.254.5 on 09/05/12
For personal use only.

Can. J. Chem. Downloaded from www.nrcresearchpress.com by 210.87.254.40 on 09/05/12
For personal use only.

Reactions of sulfenyl chlorides and their derivatives. III.[1] The reaction of 2,4-dinitrobenzenesulfenyl chloride with *cis,cis*-1,5-cyclooctadiene

GEORGE H. SCHMID
Department of Chemistry, University of Toronto, Toronto 5, Ontario

Received May 6, 1968

The reaction of 2,4-dinitrobenzenesulfenyl chloride with *cis,cis*-1,5-cyclooctadiene forms a normal 1,2 addition product without ring closure to a bicyclic product. This result indicates that an open carbonium ion is not involved at any stage in the reaction mechanism of the addition of sulfenyl halides to symmetrical alkenes.

Canadian Journal of Chemistry, **46**, 3757 (1968)

The mechanism of the addition of sulfenyl halides to olefins has been postulated (1–3) to involve the formation of an episulfonium ion intermediate such as **1** followed by S_N2 ring opening by chloride ion in the product determining step.

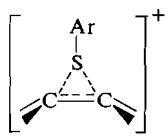

1

Recently Jacobs *et al.* (4) have pointed out that the experimental results might also be explained by a mechanism involving an episulfonium ion that would open to a carbonium ion before the product determining step. While this mechanism might be expected in the addition of sulfenyl halides to olefins such as diene, allene, and styrene systems in which the incipient carbonium ion would be of increased stability, it cannot be ruled out *a priori* for the addition to a symmetrical alkene.

To test this possibility, the addition of 2,4-dinitrobenzenesulfenyl chloride to the symmetrical olefin *cis,cis*-1,5-cyclooctadiene was carried out. Because of the conformation of this diene, the two double bonds are very close together. If the addition involves an episulfonium ion intermediate in which, as postulated (3), there is little charge at C-1 and C-2 of the ion, then the expected product would be the 1,2-adduct **2**. However, if considerable charge were generated during the addition on C-2, it would be expected that the double bond would interact with the cationic center to form bicyclic products. The ability of a suitably placed carbon–carbon double bond to take part in ring closure reactions is well known. Examples include the formation of norbornyl acetate from the acetolysis of 2-(Δ^3-cyclopentyl) ethyl *p*-nitrobenzenesulfonate (5, 6) and the formation of compounds having the bicyclo-[3·3·0]octane ring system from the acetolysis of 4-cycloocten-1-yl *p*-bromobenzenesulfonate (7). Similar ring closure reactions have been reported in electrophilic addition reactions with *cis,cis*-1,5-cyclooctadiene (8, 9) and *cis,cis*-3,8-cyclodecadiene-1,1,6,6-tetracarboxylate (10).

In contrast to these findings, the addition of 2,4-dinitrobenzenesulfenyl chloride to *cis,cis*-1,5-cyclooctadiene in chloroform as solvent forms a monoadduct **2** without ring closure in 96% yield. The structure of the product is based on analytical data and particularly the nuclear magnetic resonance (n.m.r.) spectrum which shows two vinyl protons at δ 5.78, a methine proton α to chlorine at δ 4.45, and a methine proton α to sulfur at δ 4.10.

The experimental results reported here indicate that the additions of sulfenyl halides to symmetrical alkenes do not involve an open carbonium ion before the product determining step. Rather the evidence is consistent with a mechanism in which the transition state leading to products resembles the episulfonium ion intermediate.

Experimental

All melting points and boiling points are uncorrected. Infrared spectra were recorded on a Perkin–Elmer model 237B spectrophotometer. Nuclear magnetic resonance

[1]For part II, see ref. 1.

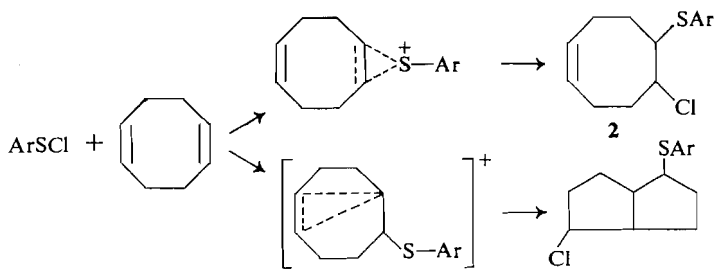

spectra were measured on a Varian Associates A-60 spectrometer as approximately 10% w/v solution in deuteriochloroform and chemical shifts are reported in p.p.m. downfield from TMS as internal standard.

Microanalysis was carried out by A. B. Gygli Microanalysis Laboratory, Toronto, Ontario.

2,4-Dinitrobenzenesulfenyl Chloride

This was prepared according to the method of Lawson and Kharasch (11) and purified by recrystallization from carbon tetrachloride, m.p. 96–97°; lit. m.p. 97–98° (11).

Chloroform

This was cleaned by washing commercial grade solvent with concentrated sulfuric acid and then with water. The solvent was dried over anhydrous $MgSO_4$ and then distilled.

2-Chloro-1-(2',4'-dinitrophenylthio)cyclooctene-5

A solution of 4.70 g (0.020 mole) of 2,4-dinitrobenzenesulfenyl chloride and 2.50 g (0.023 mole) of *cis,cis*-1,5-cyclooctadiene (obtained from Matheson, Coleman, and Bell Company, Inc.) in 250 ml of $CHCl_3$ was allowed to stand at room temperature until a starch iodide test was negative. The solvent was removed in a stream of dry air and the solid was recrystallized from 95% ethanol to give 6.90 g of product, m.p. 113.5–114.5°. ν_{max} (KBr): 1590 cm^{-1} (C=C). Nuclear magnetic resonance: δ 5.78 (2H, vinyl protons); δ 4.45 (1H, CHCl); δ 4.10 (1H, CHSAr); δ 1.88–2.83 (8H, CH_2).

Anal. Calcd. for $C_{14}H_{15}SClN_2O_4$: C, 49.05; H, 4.41; S, 9.35; Cl, 10.34. Found: C, 49.10; H, 4.35; S, 9.31; Cl, 10.45.

Acknowledgment

Financial support by the National Research Council of Canada is gratefully acknowledged.

1. G. H. Schmid and M. Heinola. J. Am. Chem. Soc. **90**, 3466 (1968).
2. N. Kharasch. *In* Organic sulfur compounds. Vol. I. *Edited by* N. Kharasch. The Pergamon Press, Ltd., London. 1961. Chap. 32.
3. W. H. Mueller and P. E. Butler. J. Am. Chem. Soc. **88**, 2866 (1966).
4. T. L. Jacobs, R. Macomber, and D. Zunker. J. Am. Chem. Soc. **89**, 7001 (1967).
5. R. G. Lawton. J. Am. Chem. Soc. **83**, 2399 (1961).
6. P. D. Bartlett and S. Bank. J. Am. Chem. Soc. **83**, 2591 (1961).
7. A. C. Cope and P. E. Peterson. J. Am. Chem. Soc. **81**, 1643 (1959).
8. I. Tabushi, K. Fjuita, and R. Oda. Tetrahedron Letters, 3815 (1967).
9. R. K. Sharma, B. A. Shoulders, and P. D. Gardner. Chem. and Ind. London, 2087 (1962).
10. R. M. Gipson, H. W. Guin, S. H. Simonsen, C. G. Skinner, and W. Shive. J. Am. Chem. Soc. **88**, 5366 (1966).
11. D. D Lawson and N. Kharasch. J. Org. Chem. **24**, 858 (1959).

Second order Beckmann rearrangement of norcamphor oxime

George H. Schmid and Patrick H. Fitzgerald[1]

Department of Chemistry, University of Toronto, Toronto 5, Ontario

Received June 24, 1968

The product of the second order Beckmann rearrangement of norcamphor oxime is not Δ^3-cyclopentenylacetonitrile but rather a mixture of Δ^2- and Δ^3-cyclopentenylacetonitrile.

Canadian Journal of Chemistry, **46**, 3758 (1968)

In the search for a direct and simple route to Δ^3-cyclopentenylacetonitrile, it was noted that Hall (1) reported a 30% yield of a nitrile as the product of the second order Beckmann rearrangement of norcamphor oxime. While Hall did not completely identify the nitrile, Roberts and Caserio (2) have indicated that this compound is Δ^3-cyclopentenylacetonitrile.

The Beckmann rearrangement of norcamphor oxime was, therefore, carried out according to the method of Hall. The nitrile was separated from

[1]Holder of a Province of Ontario Government Fellowship, 1967–1968.

Can. J. Chem. Downloaded from www.nrcresearchpress.com by 210.87.254.40 on 09/05/12
For personal use only.

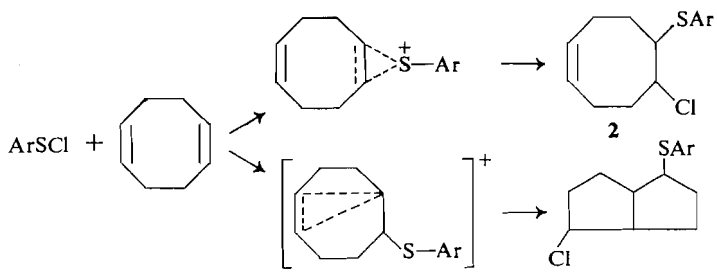

spectra were measured on a Varian Associates A-60 spectrometer as approximately 10% w/v solution in deuteriochloroform and chemical shifts are reported in p.p.m. downfield from TMS as internal standard.

Microanalysis was carried out by A. B. Gygli Microanalysis Laboratory, Toronto, Ontario.

2,4-Dinitrobenzenesulfenyl Chloride

This was prepared according to the method of Lawson and Kharasch (11) and purified by recrystallization from carbon tetrachloride, m.p. 96–97°; lit. m.p. 97–98° (11).

Chloroform

This was cleaned by washing commercial grade solvent with concentrated sulfuric acid and then with water. The solvent was dried over anhydrous $MgSO_4$ and then distilled.

2-Chloro-1-(2',4'-dinitrophenylthio)cyclooctene-5

A solution of 4.70 g (0.020 mole) of 2,4-dinitrobenzenesulfenyl chloride and 2.50 g (0.023 mole) of *cis,cis*-1,5-cyclooctadiene (obtained from Matheson, Coleman, and Bell Company, Inc.) in 250 ml of $CHCl_3$ was allowed to stand at room temperature until a starch iodide test was negative. The solvent was removed in a stream of dry air and the solid was recrystallized from 95% ethanol to give 6.90 g of product, m.p. 113.5–114.5°. ν_{max} (KBr): 1590 cm^{-1} (C=C). Nuclear magnetic resonance: δ 5.78 (2H, vinyl protons); δ 4.45 (1H, CHCl); δ 4.10 (1H, CHSAr); δ 1.88–2.83 (8H, CH_2).

Anal. Calcd. for $C_{14}H_{15}SClN_2O_4$: C, 49.05; H, 4.41; S, 9.35; Cl, 10.34. Found: C, 49.10; H, 4.35; S, 9.31; Cl, 10.45.

Acknowledgment

Financial support by the National Research Council of Canada is gratefully acknowledged.

1. G. H. Schmid and M. Heinola. J. Am. Chem. Soc. **90**, 3466 (1968).
2. N. Kharasch. *In* Organic sulfur compounds. Vol. I. *Edited by* N. Kharasch. The Pergamon Press, Ltd., London. 1961. Chap. 32.
3. W. H. Mueller and P. E. Butler. J. Am. Chem. Soc. **88**, 2866 (1966).
4. T. L. Jacobs, R. Macomber, and D. Zunker. J. Am. Chem. Soc. **89**, 7001 (1967).
5. R. G. Lawton. J. Am. Chem. Soc. **83**, 2399 (1961).
6. P. D. Bartlett and S. Bank. J. Am. Chem. Soc. **83**, 2591 (1961).
7. A. C. Cope and P. E. Peterson. J. Am. Chem. Soc. **81**, 1643 (1959).
8. I. Tabushi, K. Fjuita, and R. Oda. Tetrahedron Letters, 3815 (1967).
9. R. K. Sharma, B. A. Shoulders, and P. D. Gardner. Chem. and Ind. London, 2087 (1962).
10. R. M. Gipson, H. W. Guin, S. H. Simonsen, C. G. Skinner, and W. Shive. J. Am. Chem. Soc. **88**, 5366 (1966).
11. D. D Lawson and N. Kharasch. J. Org. Chem. **24**, 858 (1959).

Second order Beckmann rearrangement of norcamphor oxime

George H. Schmid and Patrick H. Fitzgerald[1]

Department of Chemistry, University of Toronto, Toronto 5, Ontario

Received June 24, 1968

The product of the second order Beckmann rearrangement of norcamphor oxime is not Δ^3-cyclopentenylacetonitrile but rather a mixture of Δ^2- and Δ^3-cyclopentenylacetonitrile.

Canadian Journal of Chemistry, **46**, 3758 (1968)

In the search for a direct and simple route to Δ^3-cyclopentenylacetonitrile, it was noted that Hall (1) reported a 30% yield of a nitrile as the product of the second order Beckmann rearrangement of norcamphor oxime. While Hall did not completely identify the nitrile, Roberts and Caserio (2) have indicated that this compound is Δ^3-cyclopentenylacetonitrile.

The Beckmann rearrangement of norcamphor oxime was, therefore, carried out according to the method of Hall. The nitrile was separated from

[1]Holder of a Province of Ontario Government Fellowship, 1967–1968.

Can. J. Chem. Downloaded from www.nrcresearchpress.com by 210.87.254.40 on 09/05/12
For personal use only.

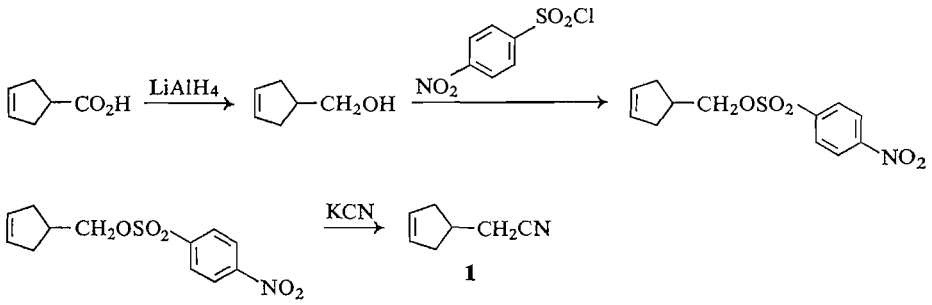

1

CHART 1

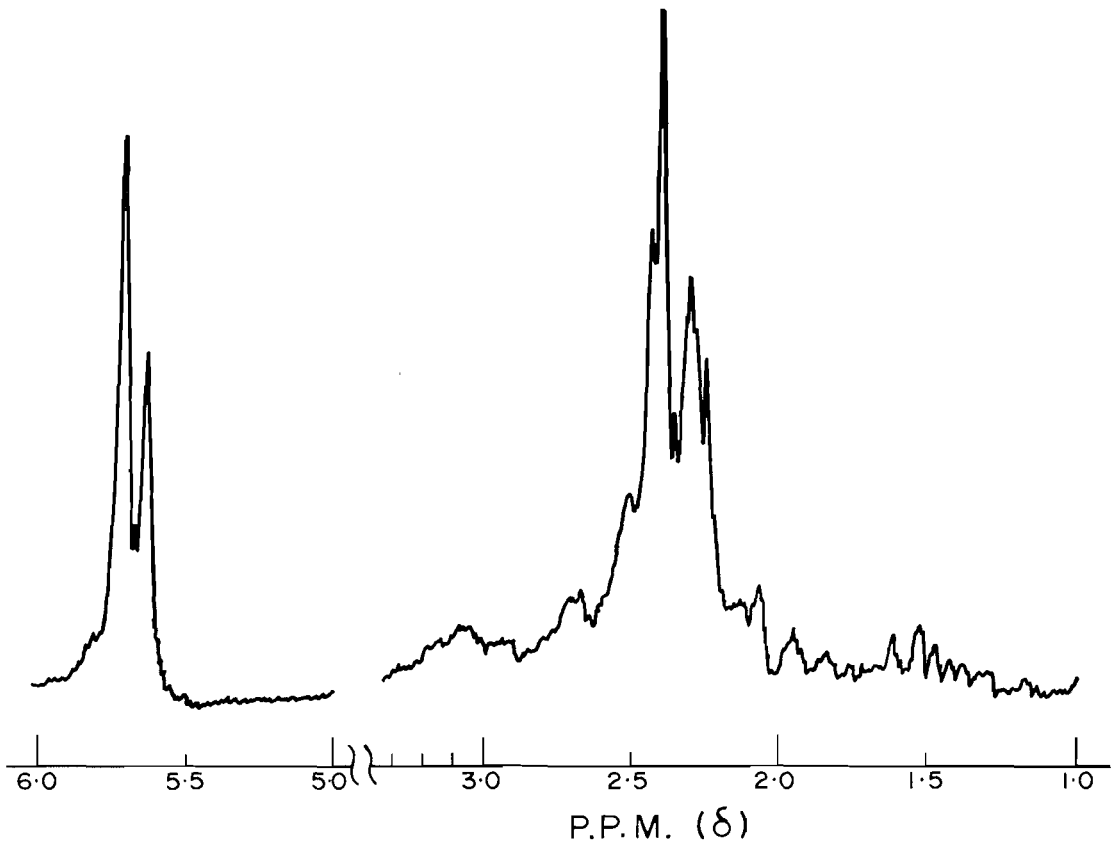

FIG. 1. The nuclear magnetic resonance spectrum of the hydrolysis product of the Beckmann rearrangement product.

the lactam by distillation and its nuclear magnetic resonance (n.m.r.) spectrum compared to that of an authentic sample of Δ^3-cyclopentenylacetonitrile prepared by the alternate synthesis outlined in Chart 1.

The n.m.r. spectrum of the nitrile prepared by the Beckmann rearrangement shows complex multiplets in the regions δ 5.60–5.90 and δ 1.50–2.00 which are absent in the spectrum of **1**. On this basis it seemed possible that the product was a mixture of the isomeric Δ^2- and Δ^3-cyclopentenylacetonitriles. Attempts to separate the mixture by vapor-phase chromatography (v.p.c.) were unsuccessful. Since both the Δ^2- and Δ^3-cyclopentenylacetic acids were available from independent sources, it was decided to hydrolyze the mixture of nitriles.

The n.m.r. spectrum of the hydrolysis product

Can. J. Chem. Downloaded from www.nrcresearchpress.com by 210.87.254.40 on 09/05/12
For personal use only.

Can. J. Chem. Downloaded from www.nrcresearchpress.com by 210.87.254.40 on 09/05/12
For personal use only.

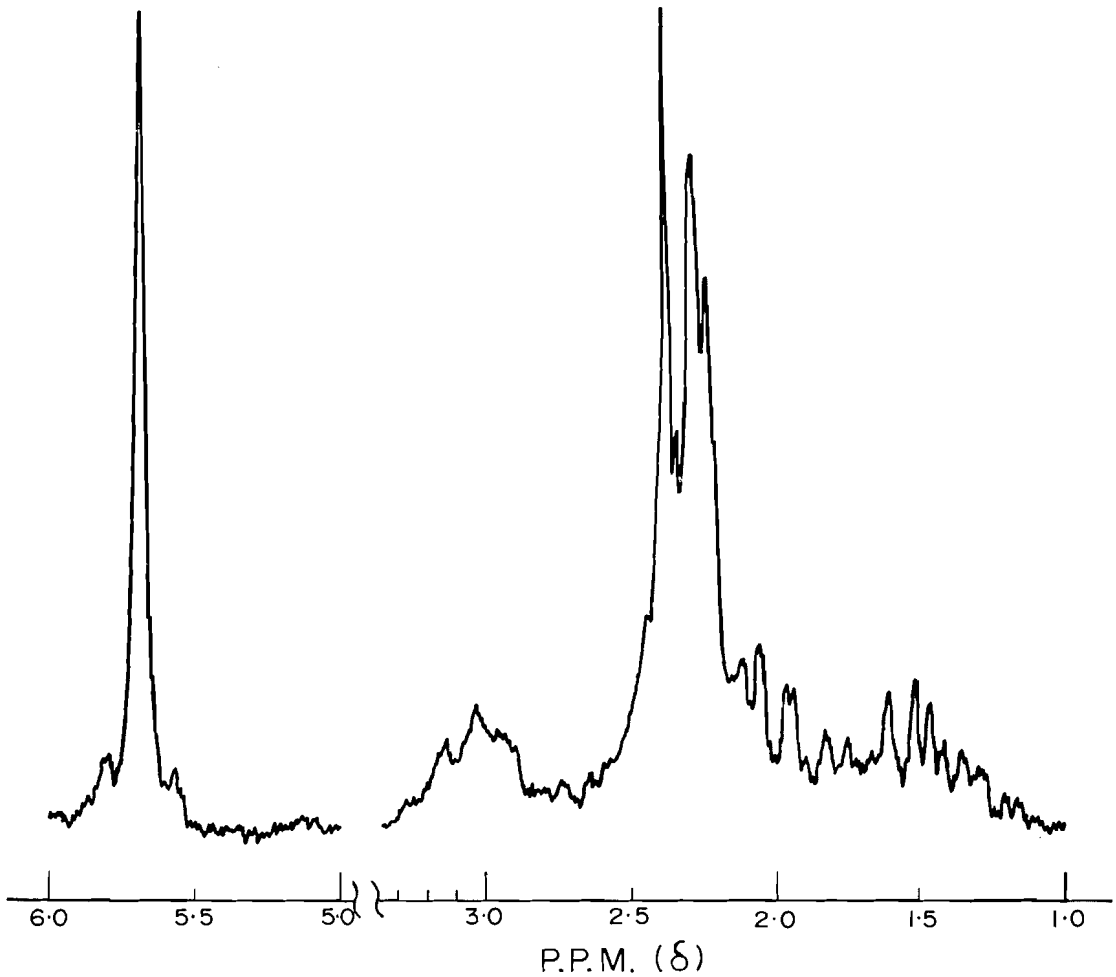

FIG. 2. The nuclear magnetic resonance spectrum of Δ^2-cyclopentenylacetic acid.

is shown in Fig. 1 while Figs. 2 and 3 show the n.m.r. spectra of pure samples of Δ^2- and Δ^3-cyclopentenylacetic acid, respectively. The spectra of the Δ^2- and Δ^3-isomers differ in two important respects. The vinyl protons of the Δ^2-isomer are further downfield than the Δ^3-isomer and the Δ^2-isomer has several peaks in the δ 1.2–1.7 region that are absent in the Δ^3-isomer. These are characteristic differences in the n.m.r. spectra of Δ^2- and Δ^3-cyclopentenyl derivatives.[2]

The hydrolysis product clearly is a mixture of Δ^2- and Δ^3-cyclopentenylacetic acid. Control experiments have established that the acids are stable under the basic hydrolysis conditions used to prepare them from the corresponding nitriles. Therefore on the basis of the products of hydrolysis the product of the second order Beckmann rearrangement is a mixture of Δ^2- and Δ^3-cyclopentenylacetonitrile in the ratio of 2:1.

Experimental

All boiling points are uncorrected. Infrared spectra were recorded on a Perkin–Elmer model 237B spectrophotometer. Nuclear magnetic resonance (n.m.r.) spectra were measured on a Varian Associates A-60 spectrometer. Samples were measured as approximately 10% w/v solutions in the solvents indicated and chemical shifts are reported in p.p.m. downfield from TMS as internal standard.

Microanalysis was carried out by A. B. Gygli, Microanalysis Laboratory, Toronto, Ontario.

Δ^3-Cyclopentenylcarboxylic Acid

This was prepared according to the method of Schmid

[2]G. H. Schmid and P. H. Fitzgerald. Unpublished observation.

Can. J. Chem. Downloaded from www.nrcresearchpress.com by 210.87.254.40 on 09/05/12
For personal use only.

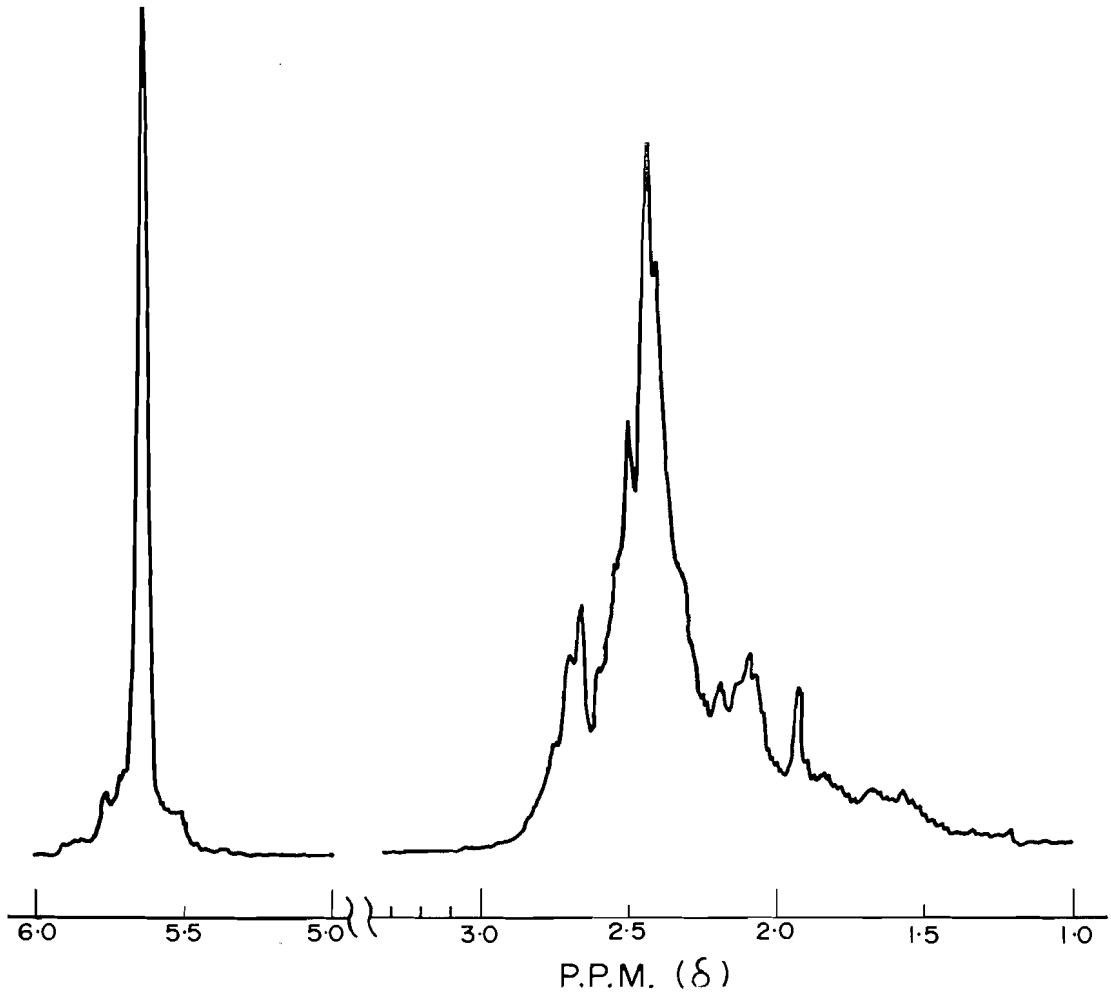

FIG. 3. The nuclear magnetic resonance spectrum of Δ^3-cyclopentenylacetic acid.

and Wolkoff (3), b.p. 118–121°/20 mm Hg (ref. (6), b.p. 83–85°/2 mm Hg).

Nuclear magnetic resonance δ (neat): singlets at 5.70 p.p.m. (vinyl, 2H) and 10.53 p.p.m. (—OH, 1H); and a complex multiplet at 2.73 p.p.m. (methylene and methine protons, 5H).

Δ^3-Cyclopentenylmethanol

This was prepared in a 41% yield from Δ^3-cyclopentenylcarboxylic acid by treatment with a 25% molar excess of ethereal lithium aluminium hydride, b.p. 66°/10 mm Hg (lit. (4), b.p. 98–99°/57 mm Hg).

Infrared $\lambda_{max}(CCl_4)$: 2.75 (O—H); 3.00 (broad, O—H); 9.31, 9.64, 10.58, 10.71 μ.

Nuclear magnetic resonance δ (neat): singlets at 5.60 p.p.m. (vinyl, 2H) and 5.22 p.p.m. (hydroxyl, 1H) doublet at 3.45 p.p.m. (CH_2O, J = 6.5 Hz) and a complex multiplet at 2.74–1.77 p.p.m. (methylene and methine, 5H).

Δ^3-Cyclopentenylmethyl p-Nitrobenzenesulfonate

This was prepared according to the method of Tipson (5), m.p. 69–70°.

Infrared $\lambda_{max}(CCl_4)$: 6.54 μ and 7.40 μ (asymmetric and symmetric NO_2 stretch respectively), 7.30 μ (S=O), 8.42 μ (S=O), 10.37 μ, 10.49 μ.

Nuclear magnetic resonance δ ($CDCl_3$): singlet at 5.55 p.p.m. (vinyl, 2H); doublet at 4.00 p.p.m. (CH_2O, 2H) complex multiplet at 2.63–1.50 p.p.m. (methylene and methine, 5H); a quartet at 8.18 p.p.m. (aromatic, 4H).

Anal. Calcd. for $C_{12}H_{13}O_5NS$: C, 50.84; H, 4.62; N, 4.94. Found: C, 50.98; H, 4.59; N, 5.00.

Δ^3-Cyclopentenylacetonitrile

To a solution of 6.5 g (0.100 mole) of KCN in 100 ml of dimethyl sulfoxide,[3] contained in a 300 ml flask equipped with thermometer, condenser, and magnetic stirring bar, was added dropwise a solution of 18.0 g of Δ^3-cyclopentenylmethyl *p*-nitrobenzenesulfonate in 70 ml of DMSO. During the addition, the temperature did not rise above 40 °C and the solution turned a deep

[3]Caution: Solution is extremely toxic and will penetrate skin and, possibly, thin rubber gloves. Contact can be fatal.

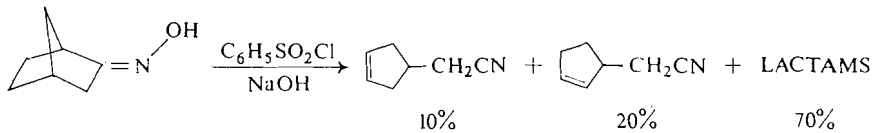

purple. After stirring the solution overnight at room temperature, the solution was poured carefully into about 450 ml of water. This solution was extracted with four 100 ml portions of ether and the ether extracts combined and washed with four 100 ml portions of water to remove DMSO. The ether was then concentrated on the rotary evaporator and 4 g of crude brown liquid were obtained. Distillation gave 2.4 g (35%) of a clear, foul-smelling liquid; b.p. 68–69°/11 mm Hg.

Infrared $\lambda_{max}(CCl_4)$: 3.25 μ, 3.40 μ, 3.50 μ, 4.44 μ (C≡N); 7.50 μ, 7.40 μ.

Nuclear magnetic resonance δ (CCl_4): singlet at 5.66 p.p.m. (vinyl, 2H); a complex multiplet at 2.00–3.00 p.p.m. (methylene and methine, 7H).

Δ^3-Cyclopentenylacetic Acid

This was prepared according to the procedure of Bartlett (6), b.p. 141–145°/47 mm Hg (ref. (6), b.p. 120°/20 mm Hg).

The Beckmann Rearrangement

This was carried out according to the method of Hall (1), b.p. 69–71°/11 mm Hg (ref. (1), b.p. 150–185°/23 mm Hg).

Hydrolysis of Nitriles

To a solution of 20 ml of 2.5 *M* NaOH was added 0.5 g of the nitrile mixture. The mixture was heated at reflux for 2 h, cooled, and made acidic with a 10% HCl solution. The reaction mixture was extracted with three 30 ml portions of ether. The ether extracts were combined, dried over $MgSO_4$ and the ether removed on a rotary evaporator. The n.m.r. spectrum was taken in CCl_4.

Control Reaction

A 1 g sample of a mixture of the acids containing 46% Δ^2- and 54% Δ^3-cyclopentenylacetic acids by weight was prepared. An n.m.r. spectrum of the mixture showed 45% Δ^2- and 55% Δ^3-cyclopentenylacetic acids. After subjecting the mixture to the hydrolysis and work-up conditions used above, the n.m.r. of the mixture showed 45% Δ^2- and 55% Δ^3-cyclopentenylacetic acids.

Acknowledgment

Financial support by the National Research Council of Canada is gratefully acknowledged.

1. H. K. Hall, Jr. J. Am. Chem. Soc. **82**, 1209 (1960).
2. J. D. Roberts and M. C. Caserio. Basic principles of organic chemistry. W. A. Benjamin, Inc., New York. 1965. p. 658.
3. G. H. Schmid and A. W. Wolkoff. J. Org. Chem. **32**, 254 (1967).
4. J. Meinwald, P. G. Gassman, and J. K. Crandell. J. Org. Chem. **27**, 3366 (1962).
5. R. S. Tipson. J. Org. Chem. **9**, 238 (1944).
6. P. D. Bartlett, S. Bank, R. J. Crawford, and G. H. Schmid. J. Am. Chem. Soc. **87**, 1288 (1965).

Can. J. Chem. Downloaded from www.nrcresearchpress.com by 210.87.254.40 on 09/05/12
For personal use only.

Détermination d'un équilibre conformationnel par résonance magnétique nucléaire de polyesters

Guy Perrault

Centre Canadien de Recherches et de Perfectionnement des Armes, Québec, Québec

Reçu le 18 mars 1968

La conformation du groupe hydroxy-2 propyl dans les polysébacates de la méthyl-*N* bis-(hydroxy-2 propyl)amine et de la méthyl-*N*(hydroxy-2 éthyl, hydroxy-2 propyl)amine a été étudiée par spectroscopie de résonance magnétique nucléaire.

The conformation of the 2-hydroxypropyl group in the polysebacates of the *N*-methyl bis-(2-hydroxypropyl)-amine and the *N*-methyl (2-hydroxyethyl, 2-hydroxypropyl)-amine has been studied by nuclear magnetic resonance spectroscopy.

Canadian Journal of Chemistry, 46, 3762 (1968)

Introduction

La spectroscopie de résonance magnétique nucléaire (r.m.n.) a déjà été utilisée pour étudier des équilibres conformationnels (1–3). La plupart du temps, ces spectres sont mesurés à des températures très basses afin de ralentir les rotations autour des liaisons.

Durant une étude sur les polymères, un cas spécial s'est présenté où il était possible de mesurer la différence d'énergie entre deux conformations gauches en ralentissant la rotation autour d'une liaison par formation d'un polymère.

Deux produits ont été étudiés de cette façon:

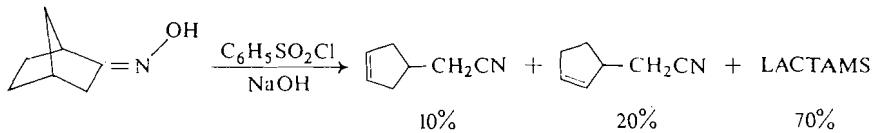

purple. After stirring the solution overnight at room temperature, the solution was poured carefully into about 450 ml of water. This solution was extracted with four 100 ml portions of ether and the ether extracts combined and washed with four 100 ml portions of water to remove DMSO. The ether was then concentrated on the rotary evaporator and 4 g of crude brown liquid were obtained. Distillation gave 2.4 g (35%) of a clear, foul-smelling liquid; b.p. 68–69°/11 mm Hg.

Infrared $\lambda_{max}(CCl_4)$: 3.25 μ, 3.40 μ, 3.50 μ, 4.44 μ (C≡N); 7.50 μ, 7.40 μ.

Nuclear magnetic resonance δ (CCl_4): singlet at 5.66 p.p.m. (vinyl, 2H); a complex multiplet at 2.00–3.00 p.p.m. (methylene and methine, 7H).

Δ^3-Cyclopentenylacetic Acid

This was prepared according to the procedure of Bartlett (6), b.p. 141–145°/47 mm Hg (ref. (6), b.p. 120°/20 mm Hg).

The Beckmann Rearrangement

This was carried out according to the method of Hall (1), b.p. 69–71°/11 mm Hg (ref. (1), b.p. 150–185°/23 mm Hg).

Hydrolysis of Nitriles

To a solution of 20 ml of 2.5 *M* NaOH was added 0.5 g of the nitrile mixture. The mixture was heated at reflux for 2 h, cooled, and made acidic with a 10% HCl solution. The reaction mixture was extracted with three 30 ml portions of ether. The ether extracts were combined, dried over $MgSO_4$ and the ether removed on a rotary evaporator. The n.m.r. spectrum was taken in CCl_4.

Control Reaction

A 1 g sample of a mixture of the acids containing 46% Δ^2- and 54% Δ^3-cyclopentenylacetic acids by weight was prepared. An n.m.r. spectrum of the mixture showed 45% Δ^2- and 55% Δ^3-cyclopentenylacetic acids. After subjecting the mixture to the hydrolysis and work-up conditions used above, the n.m.r. of the mixture showed 45% Δ^2- and 55% Δ^3-cyclopentenylacetic acids.

Acknowledgment

Financial support by the National Research Council of Canada is gratefully acknowledged.

1. H. K. Hall, Jr. J. Am. Chem. Soc. **82**, 1209 (1960).
2. J. D. Roberts and M. C. Caserio. Basic principles of organic chemistry. W. A. Benjamin, Inc., New York. 1965. p. 658.
3. G. H. Schmid and A. W. Wolkoff. J. Org. Chem. **32**, 254 (1967).
4. J. Meinwald, P. G. Gassman, and J. K. Crandell. J. Org. Chem. **27**, 3366 (1962).
5. R. S. Tipson. J. Org. Chem. **9**, 238 (1944).
6. P. D. Bartlett, S. Bank, R. J. Crawford, and G. H. Schmid. J. Am. Chem. Soc. **87**, 1288 (1965).

Can. J. Chem. Downloaded from www.nrcresearchpress.com by 210.87.254.40 on 09/05/12
For personal use only.

Détermination d'un équilibre conformationnel par résonance magnétique nucléaire de polyesters

Guy Perrault

Centre Canadien de Recherches et de Perfectionnement des Armes, Québec, Québec

Reçu le 18 mars 1968

La conformation du groupe hydroxy-2 propyl dans les polysébacates de la méthyl-*N* bis-(hydroxy-2 propyl)amine et de la méthyl-*N*(hydroxy-2 éthyl, hydroxy-2 propyl)amine a été étudiée par spectroscopie de résonance magnétique nucléaire.

The conformation of the 2-hydroxypropyl group in the polysebacates of the *N*-methyl bis-(2-hydroxypropyl)-amine and the *N*-methyl (2-hydroxyethyl, 2-hydroxypropyl)-amine has been studied by nuclear magnetic resonance spectroscopy.

Canadian Journal of Chemistry, 46, 3762 (1968)

Introduction

La spectroscopie de résonance magnétique nucléaire (r.m.n.) a déjà été utilisée pour étudier des équilibres conformationnels (1–3). La plupart du temps, ces spectres sont mesurés à des températures très basses afin de ralentir les rotations autour des liaisons.

Durant une étude sur les polymères, un cas spécial s'est présenté où il était possible de mesurer la différence d'énergie entre deux conformations gauches en ralentissant la rotation autour d'une liaison par formation d'un polymère.

Deux produits ont été étudiés de cette façon:

Can. J. Chem. Downloaded from www.nrcresearchpress.com by 210.87.254.40 on 09/05/12
For personal use only.

la méthyl-*N* bis-(hydroxy-2 propyl)amine (1,2) et la méthyl-*N*(hydroxy-2 éthyl, hydroxy-2 propyl)amine (4).

Les conformations gauches de la liaison en α, β de l'azote sont représentées. La conformation C

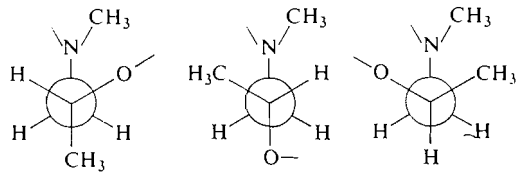

A B C

étant défavorisée énergétiquement, l'équilibre conformationnel peut être simplifié, aux erreurs expérimentales près, à un équilibre entre les conformères A et B. Or, dans chacun de ces conformères, le méthyle (CH_3) en β de l'azote se trouve dans un entourage magnétique différent. Cet équilibre (A ⇌ B) peut donc être mesuré si la rotation autour de la liaison C—C est ralentie. La préparation d'un polysébacate permet d'obtenir ce résultat.

Partie expérimentale

La préparation et les caractéristiques du produit **2** ont été publiés (4).

Le diol azoté **1** a été préparé de la même façon et distillé à 77–78 °C sous 0.7 mm, n_D^{27} = 1.4469 (88–96 °C 10.8 mm (5) et n_D^{21} = 1.4472 (6)).

Les spectres r.m.n. ont été enregistrés sur un appareil Varian A-60 calibré pour la température selon l'espacement entre les pics du méthanol et de l'éthylèneglycol. Les mesures ont été faites sur des solutions à 20% de polyester dans le CCl_4 en utilisant 0.5% de $(CH_3)_4Si$ comme standard interne.

Les polysébacates ont été préparés en vrac en faisant réagir 1.3 mole de diol azoté sur une mole d'acide sébacique. Le mélange est maintenu à 175 °C avec barbotage d'azote durant 4 h. Il est ensuite chauffé à 175 °C sous vide (≃0.1 mm) durant 4 h additionnelles. Le polysébacate de méthyl-*N* bis-(hydroxy-2 propyl)-amine (1,3) donne un poids moléculaire de 1870 par analyse des groupements terminaux (7). Le polysébacate de **2** a un poids moléculaire de 1790.

$CH_3N(CH_2CHOHCH_3)_2$

1

$HOCH_2CH_2N(CH_3)CH_2CHOHCH_3$

2

Résultats

A la Fig. 1, le spectre r.m.n. du méthyl-*N* bis-(hydroxy-2 propyl)amine (1) est reproduit partiellement. Le méthyle sur le carbinol donne, tel qu'attendu, un doublet centré à 1.09 p.p.m. plus bas que le $(CH_3)_4Si$, et manifeste une constante de couplage de 6 c.p.s. Le méthyl-*N*(hydroxy-2 éthyl, hydroxy-2 propyl)amine (2) montre le même doublet à la même position.

Par contre, le polysébacate du méthyl-*N* bis-(hydroxy-2 propyl)amine (1) montre deux doublets qui sont reproduits à la Fig. 1 avec les méthylènes de l'acide sébacique. Le premier de ces doublets est centré à 1.09 p.p.m. plus bas que le $(CH_3)_4Si$, et le second à 1.18 p.p.m. Dans les deux cas, la constante de couplage est de 6 c.p.s.

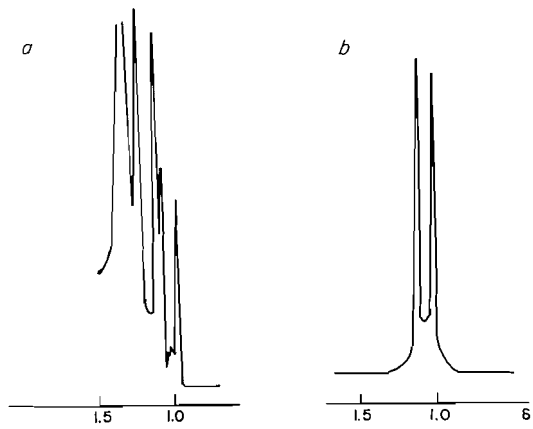

FIG. 1. Spectres résonance magnétique nucléaire à 30 °C: (*a*) 20% polysébacate de **1** dans CCl_4; (*b*) méthyl-*N* bis-(hydroxy-2 propyl)amine (**1**).

Il était difficile cependant d'évaluer la proportion de chaque conformère par l'aire sous les pics à cause de la superposition des doublets. Le postulat a donc été posé que la proportion des deux conformères pouvait être évaluée en mesurant la hauteur de chacun des premiers pics des doublets, soit respectivement la hauteur du pic à 0.99 p.p.m. et celle du pic à 1.13 p.p.m. Les pourcentages du conformère le plus stable aux différentes températures sont rapportés au Tableau I. Ces valeurs sont reproductibles à ±0.5%.

A partir de ces valeurs, les ΔH et ΔS ont été calculés à la façon usuelle (8). Ils sont compilés au Tableau II. D'après un article récent (9) il est plausible, vu la marge de température utilisée et la précision des mesures, de prévoir une erreur de 5–10% sur le ΔH et de 1 cal/° mole sur le ΔS.

Discussion

Le polysébacate de méthyl-*N*(hydroxy-2 éthyl, hydroxy-2 propyl) amine (2) donne un ΔH de −0.9 kcal/mole et un ΔS de 1.0 cal/° mole (cf. Tableau II) pour l'équilibre A ⇌ B. Dans le

TABLEAU I

Pourcentage du conformère le plus stable

Température (°C)	Polysébacate de méthyl-*N* (hydroxy-2 éthyl, hydroxy-2 propyl)amine	Polysébacate de méthyl-*N* bis-(hydroxy-2 propyl)amine
50	65.4	72.5
30	68.4	73.7
10	72.3	75.3
0		77.5
−10	77.0	

polysébacate du méthyl-*N* bis-(hydroxy-2 propyl)amine (1), le ΔH obtenu est de −1.6 kcal/mole et le ΔS de 3.7 cal/° mole. Cependant, les deux substituants hydroxy-2 propyles sur l'azote participent à cet équilibre de sorte que les valeurs thermodynamiques d'interaction pour un seul de ces substituants seraient de −0.8 kcal/mole pour le ΔH et de 1.8 cal/° mole pour le ΔS.

Plusieurs problèmes se posent à ce point. Quel est le conformère le plus stable? A quoi est due la différence entre les pourcentages du conformère le plus stable, obtenus pour les deux polysébacates à une même température et est-ce que les différences entre les ΔH et les ΔS pour les deux produits confirment une interaction intramoléculaire? Et finalement, est-ce que l'équilibre observé avec les polysébacates est représentatif de l'équilibre conformationnel dans les diols monomériques initiaux?

En premier lieu, le doublet à 1.09 p.p.m. peut être attribué au conformère B, où les hydrogènes du méthyle gauche par rapport à l'azote doivent apparaître à un champ plus fort à cause de l'effet d'écran de la paire d'électrons libres sur l'azote. Le conformère le plus stable serait donc le conformère A (Fig. 1) avec le méthyle en *trans* par rapport à l'azote. Ceci semble plausible si on se réfère aux résultats obtenus en série alicyclique quant aux équilibres conformationnels impliquant un méthyle et un hydroxyle (10).

D'autre part, une seule des mesures du Tableau I pourrait impliquer qu'une interaction intramoléculaire vient influencer l'équilibre entre les deux interactions gauches. Cette hypothèse paraît d'ailleurs plausible à l'examen des modèles de Dreiden, ou des représentations de Newman, où il apparaît que certaines conformations peuvent augmenter l'énergie interne de la molécule lorsqu'il y a deux substituants hydroxyl-2 propyles adjacents sur l'azote. Toutefois, cet effet ne se fait sentir que très légèrement sur le ΔH et le

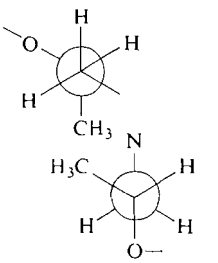

ΔS. Si ces interactions intramoléculaires existent, elles sont de l'ordre de 0.1 kcal/mole en ΔH et de 0.8 cal/° mole en ΔS, ce qui est trop près de l'erreur expérimentale pour tirer une conclusion.

Finalement, il faut souligner que les valeurs thermodynamiques obtenues avec les polysébacates ne s'appliquent pas directement à l'équilibre conformationnel dans les diols monomériques initiaux. En effet, les diols azotés **1** et **2** peuvent former des liaisons hydrogènes intramoléculaires qui vont influencer la position de

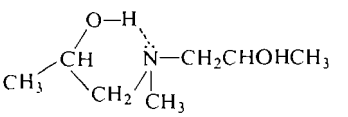

l'équilibre. Or, si les liaisons hydrogènes augmentent de façon notable le pourcentage de conformère C qui avait été négligé dans les polysébacates, ses hydrogènes méthyliques viendront se superposer à ceux du conformère B.

L'équilibre dans les diols azotés peut être évalué en comparant la position du doublet des hydrogènes méthyliques aux positions des deux doublets des polysébacates, tel qu'il a été proposé en série alicyclique (11). Alors, avec les deux produits **1** et **2**, le résultat est le même, soit 65% de conformère A à 30 °C.

Remerciements

Tous mes remerciements s'adressent à Mlle M. Talbot et à Yves Giguère pour leur collaboration technique, de même qu'à M. Bédard qui nous a aidé à solutionner les problèmes que suscitent l'appareil de résonance magnétique nucléaire.

1. J. A. POPLE, W. G. SCHNEIDER, et H. J. BERNSTEIN. High resolution nuclear magnetic resonance. McGraw-Hill Book Co., Inc., New York.
2. J. W. EMSLEY, J. FEENEY, et L. H. SUTCLIFFE. High resolution nuclear magnetic resonance spectroscopy. The Pergamon Press, Ltd., London.
3. L. W. REEVES. Advanced physical organic chemistry. 5th ed. Vol. 3. Gold, 1965. p. 186–269.

Can. J. Chem. Downloaded from www.nrcresearchpress.com by 210.87.254.40 on 09/05/12
For personal use only.

4. G. PERRAULT. Can. J. Chem. **45**, 1063 (1967).
5. H. J. BARBER et K. GAIMSTER. J. Pharm. Pharmacol. **3**, 663 (1951).
6. W. E. HANBY et H. N. RYDON. J. Chem. Soc. 513 (1947).
7. V. V. KORSHAK et S. V. VINOGRADOVA. Polyesters. The Pergamon Press, Ltd., London. p. 185.
8. S. GLASSTONE. The elements of physical chemistry. D. Van Nostrand Company, Inc., New York.
9. J. E. LEFFLER. J. Org. Chem. **31**, 533 (1966).
10. E. L. ELIEL et M. H. GIANNI. Tetrahedron Letters, 97 (1962).
11. J. SIPOS, J. KRUPICKA, M. TICHY, et J. SICHER. Collection Czech. Chem. Commun. **27**, 2079 (1962).

Structure of bisnorquassin

J. A. FINDLAY[1]
Department of Chemistry, University of New Brunswick, Fredericton, New Brunswick
AND
D. T. CROPP
Millhaven Fibres Ltd., Kingston, Ontario

Received June 14, 1968

Structure **2***a* has been deduced for bisnorquassin, a remarkable product of demethylation of the bitter principle quassin **1***a* from *Quassia amara*.

Canadian Journal of Chemistry, **46**, 3765 (1968)

The complete structure and relative stereochemistry of quassin, $C_{22}H_{28}O_6$, a bitter principle from *Quassia amara*, was established as **1***a*[2] by Valenta and co-workers (1). Bisnorquassin, $C_{20}H_{24}O_6$, was prepared by Robertson *et al.* by treatment of either quassin or norquassin **1***b* with a warm mixture of concentrated hydrochloric and acetic acids (2, 3). It was apparent from these early studies that bisnorquassin was not a simple bis-demethylated quassin in view of its ultraviolet spectrum which indicated an extended system of conjugation.

The ultraviolet absorption spectrum of bisnorquassin (λ_{max} 312 mμ, ε 18 800 in alcohol, λ_{max} 384, ε 48 100 in alcoholic alkali) closely resembles that of cholest-5-ene-3,7-dione (λ_{max} 320, ε 24 300 in alcohol, λ_{max} 392, ε 62 200 in alcoholic alkali) (4). There exists only one possibility for the inclusion of this type of chromophore in an unrearranged quassin skeleton, namely as in **2***a* where the lactone carbonyl group is part of the system of extended conjugation.[3] The formation of bisnorquassin **2***a* from quassin **1***a* or norquassin **1***b* can be readily understood via normal demethylation followed by acid-catalyzed enolization, double-bond migration, and hemiketal formation. One possible pathway is indicated in the figure.

The functionality of **2***a* is adequately supported by infrared and chemical data. The infrared spectrum ($CHCl_3$) of bisnorquassin displays bands at 3500, 3250 (OH), 1720 (six-membered ketone), 1700, 1660, and 1580 cm^{-1} (conjugated enol lactone).

Robertson and co-workers (3) reported the transformation of bisnorquassin into monomethyl, dimethyl, methyl acetyl, and diacetyl derivatives demonstrating the presence of two hydroxyl groups. In addition, the dimethyl derivative, formulated now as **2***c*, was converted into both an oxime and a 2,4-dinitrophenylhydrazone establishing the presence of a carbonyl group. Bisnorquassin can be converted into both

[1]The authors have independently deduced the structure **2***a* for bisnorquassin.

[2]The absolute configuration of quassin has not yet been determined. The structures in this article are drawn to conform with the established absolute configuration of the structurally related terpenoids simarolide (5) and chapparin (6).

[3]In view of the preferred direction of enolization of β ketolactones bisnorquassin and derivatives are represented with enol lactone features; however, the tautomeric arrangement in which the lactone carbonyl is enolized cannot be completely excluded.

Can. J. Chem. Downloaded from www.nrcresearchpress.com by 210.87.254.40 on 09/05/12
For personal use only.

4. G. PERRAULT. Can. J. Chem. **45**, 1063 (1967).
5. H. J. BARBER et K. GAIMSTER. J. Pharm. Pharmacol. **3**, 663 (1951).
6. W. E. HANBY et H. N. RYDON. J. Chem. Soc. 513 (1947).
7. V. V. KORSHAK et S. V. VINOGRADOVA. Polyesters. The Pergamon Press, Ltd., London. p. 185.
8. S. GLASSTONE. The elements of physical chemistry. D. Van Nostrand Company, Inc., New York.
9. J. E. LEFFLER. J. Org. Chem. **31**, 533 (1966).
10. E. L. ELIEL et M. H. GIANNI. Tetrahedron Letters, 97 (1962).
11. J. SIPOS, J. KRUPICKA, M. TICHY, et J. SICHER. Collection Czech. Chem. Commun. **27**, 2079 (1962).

Structure of bisnorquassin

J. A. FINDLAY[1]
Department of Chemistry, University of New Brunswick, Fredericton, New Brunswick

AND

D. T. CROPP
Millhaven Fibres Ltd., Kingston, Ontario

Received June 14, 1968

Structure **2***a* has been deduced for bisnorquassin, a remarkable product of demethylation of the bitter principle quassin **1***a* from *Quassia amara*.

Canadian Journal of Chemistry, **46**, 3765 (1968)

The complete structure and relative stereochemistry of quassin, $C_{22}H_{28}O_6$, a bitter principle from *Quassia amara*, was established as **1***a*[2] by Valenta and co-workers (1). Bisnorquassin, $C_{20}H_{24}O_6$, was prepared by Robertson *et al.* by treatment of either quassin or norquassin **1***b* with a warm mixture of concentrated hydrochloric and acetic acids (2, 3). It was apparent from these early studies that bisnorquassin was not a simple bis-demethylated quassin in view of its ultraviolet spectrum which indicated an extended system of conjugation.

The ultraviolet absorption spectrum of bisnorquassin (λ_{max} 312 mμ, ε 18 800 in alcohol, λ_{max} 384, ε 48 100 in alcoholic alkali) closely resembles that of cholest-5-ene-3,7-dione (λ_{max} 320, ε 24 300 in alcohol, λ_{max} 392, ε 62 200 in alcoholic alkali) (4). There exists only one possibility for the inclusion of this type of chromophore in an unrearranged quassin skeleton, namely as in **2***a* where the lactone carbonyl group is part of the system of extended conjugation.[3] The formation of bisnorquassin **2***a* from quassin **1***a* or norquassin **1***b* can be readily understood via normal demethylation followed by acid-catalyzed enolization, double-bond migration, and hemiketal formation. One possible pathway is indicated in the figure.

The functionality of **2***a* is adequately supported by infrared and chemical data. The infrared spectrum ($CHCl_3$) of bisnorquassin displays bands at 3500, 3250 (OH), 1720 (six-membered ketone), 1700, 1660, and 1580 cm^{-1} (conjugated enol lactone).

Robertson and co-workers (3) reported the transformation of bisnorquassin into monomethyl, dimethyl, methyl acetyl, and diacetyl derivatives demonstrating the presence of two hydroxyl groups. In addition, the dimethyl derivative, formulated now as **2***c*, was converted into both an oxime and a 2,4-dinitrophenylhydrazone establishing the presence of a carbonyl group. Bisnorquassin can be converted into both

[1]The authors have independently deduced the structure **2***a* for bisnorquassin.

[2]The absolute configuration of quassin has not yet been determined. The structures in this article are drawn to conform with the established absolute configuration of the structurally related terpenoids simarolide (5) and chapparin (6).

[3]In view of the preferred direction of enolization of β ketolactones bisnorquassin and derivatives are represented with enol lactone features; however, the tautomeric arrangement in which the lactone carbonyl is enolized cannot be completely excluded.

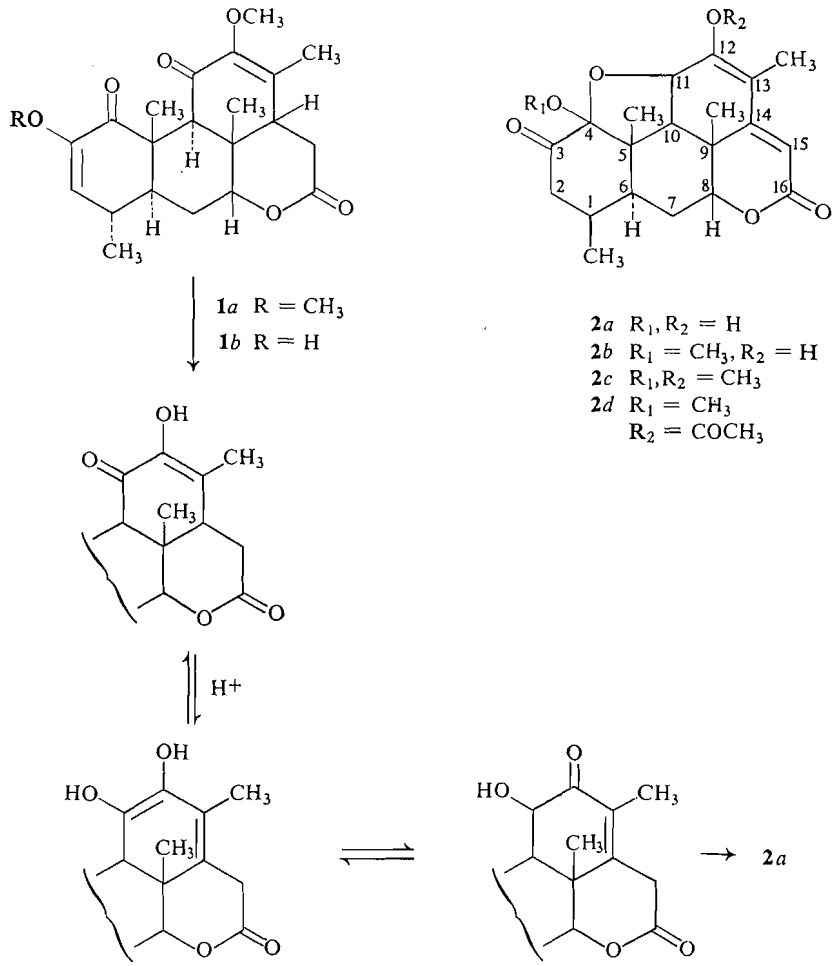

monomethyl and dimethyl derivatives by the action of alkaline dimethyl sulfate. These compounds were named β-*O*-methylbisnorquassin and β-*O*,*O*-dimethylbisnorquassin by Robertson's group. The ultraviolet spectrum of β-*O*-methylbisnorquassin (λ_{max} 314, ε 19 200 in alcohol, λ_{max} 389, ε 48 900 in alcoholic alkali) is nearly identical with the spectrum of bisnorquassin. Since this monomethyl derivative undergoes anion formation in basic medium it can be formulated as **2***b*. Acetylation of **2***b* with acetic anhydride furnishes an acetate formulated as **2***d*. The ultraviolet spectrum of this β-*O*-methylbisnorquassin acetate (λ_{max} 277, ε 15 800) is quite comparable with the absorption curve of 3-acetoxycholesta-3,5-diene-7-one (λ_{max} 282, ε 22 500) (4) in accord with structure **2***d*.

Conversion of β-*O*-methylbisnorquassin **2***b* into β-*O*,*O*-dimethylbisnorquassin **2***c* can be accomplished by treatment with diazomethane. The ultraviolet spectrum of **2***c* (λ_{max} 313, ε 19 500 in alcohol) does not undergo any substantial change on addition of alkali in agreement with the chromophore in **2***c*. The structure of β-*O*,*O*-dimethylbisnorquassin **2***c* is confirmed in detail by the nuclear magnetic resonance spectrum which displays a singlet (1 H) at τ 4.2 ($C_{15}H$), a doublet (1 H) at τ 5.05 (J = 9 c.p.s.) ($C_{11}H$), a triplet (1 H) at τ 5.45 (J = 8 c.p.s.) (C_8H), and a doublet (1 H) at τ 7.52 (J = 9 c.p.s.) ($C_{10}H$) partly superimposed on a poorly resolved multiplet (2 H) the main body of which appears at τ 7.75 (C_2H's). The methyl ether hydrogens give rise to two sharp singlets (3 H each) at τ 6.05 and 6.54. A singlet (3 H) at τ 8.1 is assigned to the methyl group at C_{13} while two sharp singlets (3 H each)

at τ 8.65 and 8.99 and a doublet at τ 9.09 account for the three other methyl groups. The remaining hydrogens give rise to signals in the region τ 7.9–8.5. The pattern of the high-field signals resembles the same region in the spectrum of quassin (1).

From the above data it is clear that the hydrogens at C-10 and C-11 must be *trans* antiparallel to account for the observed coupling constant of 9 c.p.s. In view of the complex nature of the bisnorquassin molecule and the fact that centers C-1, C-4, and C-10 are all potentially epimerizable during the course of its formation, the stereochemistry of this remarkable demethylation product of quassin offers an interesting and separate challenge. Experiments to establish the configuration of centers C-1, C-4, C-10, and C-11 are currently in progress.

Acknowledgment

One of us (J.A.F.) is grateful to Professor Z. Valenta for bringing the bisnorquassin problem to his attention and for stimulating discussions of the subject.

1. Z. Valenta, A. H. Gray, D. E. Orr, S. Papadopoulos, and C. Podesva. Tetrahedron, **18**, 1433 (1962); Z. Valenta, S. Papadopoulos, and C. Podesva. Tetrahedron, **15**, 100 (1961).
2. E. London, Alexander Robertson, and H. Worthington. J. Chem. Soc. 3431 (1950).
3. K. R. Hansen, D. B. Jaquiss, J. A. Lamberton, Alexander Robertson, and W. E. Savige. J. Chem. Soc. 4238 (1954).
4. C. W. Greenhalgh, H. B. Henbest, and E. R. H. Jones. J. Chem. Soc. 2375 (1952).
5. W. A. C. Brown and G. A. Sim. Proc. Chem. Soc. 293 (1964).
6. T. R. Hollands, P. De Mayo, M. Nisbet, and P. Crabbé. Can. J. Chem. **43**, 3008 (1965).

Preparation of 15-hydroxypentadecanoic acid by means of condensation reaction via β-ketosulfoxide

H. Nozaki, T. Mori, and M. Kawanisi

Department of Industrial Chemistry, Kyoto University, Kyoto, Japan

Received July 8, 1968

Basic condensation of 1,12-dodecanolide with methylsulfinylcarbanion ($DMSO^-$) gives a β-ketosulfoxide **2** which is ethoxycarbonylmethylated and the product is converted to 15-hydroxypentadecanoic acid (**6**) in a 46% overall yield based on the lactone. Another β-ketosulfoxide **9** is prepared by condensation of methyl 10-undecenoate with $DMSO^-$ and is subjected to the Michael condensation with methyl acrylate. Treatment of the adduct gives 14-pentadecenoic acid (**13**) in a 38% overall yield based on the undecenoate.

Canadian Journal of Chemistry, 46, 3767 (1968)

The present paper is concerned with two novel preparations of linear C-15 acids related to Exaltolide (1,15-pentadecanolide) as summarized in the flow-sheet. The starting materials are either 1,12-dodecanolide (**1**) (1) or methyl 10-undecenoate (**8**) and the key steps utilize the recently developed condensation reactions involving β-ketosulfoxide (2) such as **3** and **9**.

The reaction of **1** with $DMSO^-$ proceeded smoothly in dimethyl sulfoxide (DMSO)–tetrahydrofuran (THF) (1:1) solution to give **2**, which was then acetylated to **3**. Condensation of **3** with ethyl bromoacetate by means of sodium hydride yielded **4** as an intractable oil. Desulfurization (2*a*) followed by saponification with potassium hydroxide gave crystalline acid **5** in a 62% yield based on **3**. The acid **5** was transformed into 15-hydroxypentadecanoic acid (**6**) by the Clemmensen reduction. Oxidation of **5** gave **7** which proved identical with a specimen prepared by ozonolysis of bicyclo[10·3·0]pentadec-1(12)-en-13-one (3).

Alternatively **8** was treated with $DMSO^-$ to give **9** as a crystalline solid. The absence of the shift of double bond was ascertained by the infrared (i.r.) and nuclear magnetic resonance (n.m.r.) spectra. Reaction of **9** with methyl acrylate occurred in ethereal solvents containing a catalytic amount of sodium hydride to give **10** as an oil, which was also immediately desulfurized to **11**. The ketoester **11** was obtained as a crystalline solid in a 72% yield based on **9**. To our best knowledge such Michael addition of a β-ketosulfoxide appears to be without precedent.

at τ 8.65 and 8.99 and a doublet at τ 9.09 account for the three other methyl groups. The remaining hydrogens give rise to signals in the region τ 7.9–8.5. The pattern of the high-field signals resembles the same region in the spectrum of quassin (1).

From the above data it is clear that the hydrogens at C-10 and C-11 must be *trans* antiparallel to account for the observed coupling constant of 9 c.p.s. In view of the complex nature of the bisnorquassin molecule and the fact that centers C-1, C-4, and C-10 are all potentially epimerizable during the course of its formation, the stereochemistry of this remarkable demethylation product of quassin offers an interesting and separate challenge. Experiments to establish the configuration of centers C-1, C-4, C-10, and C-11 are currently in progress.

Acknowledgment

One of us (J.A.F.) is grateful to Professor Z. Valenta for bringing the bisnorquassin problem to his attention and for stimulating discussions of the subject.

1. Z. Valenta, A. H. Gray, D. E. Orr, S. Papadopoulos, and C. Podesva. Tetrahedron, **18**, 1433 (1962); Z. Valenta, S. Papadopoulos, and C. Podesva. Tetrahedron, **15**, 100 (1961).
2. E. London, Alexander Robertson, and H. Worthington. J. Chem. Soc. 3431 (1950).
3. K. R. Hansen, D. B. Jaquiss, J. A. Lamberton, Alexander Robertson, and W. E. Savige. J. Chem. Soc. 4238 (1954).
4. C. W. Greenhalgh, H. B. Henbest, and E. R. H. Jones. J. Chem. Soc. 2375 (1952).
5. W. A. C. Brown and G. A. Sim. Proc. Chem. Soc. 293 (1964).
6. T. R. Hollands, P. De Mayo, M. Nisbet, and P. Crabbé. Can. J. Chem. **43**, 3008 (1965).

Preparation of 15-hydroxypentadecanoic acid by means of condensation reaction via β-ketosulfoxide

H. Nozaki, T. Mori, and M. Kawanisi

Department of Industrial Chemistry, Kyoto University, Kyoto, Japan

Received July 8, 1968

Basic condensation of 1,12-dodecanolide with methylsulfinylcarbanion ($DMSO^-$) gives a β-ketosulfoxide **2** which is ethoxycarbonylmethylated and the product is converted to 15-hydroxypentadecanoic acid (**6**) in a 46% overall yield based on the lactone. Another β-ketosulfoxide **9** is prepared by condensation of methyl 10-undecenoate with $DMSO^-$ and is subjected to the Michael condensation with methyl acrylate. Treatment of the adduct gives 14-pentadecenoic acid (**13**) in a 38% overall yield based on the undecenoate.

Canadian Journal of Chemistry, 46, 3767 (1968)

The present paper is concerned with two novel preparations of linear C-15 acids related to Exaltolide (1,15-pentadecanolide) as summarized in the flow-sheet. The starting materials are either 1,12-dodecanolide (**1**) (1) or methyl 10-undecenoate (**8**) and the key steps utilize the recently developed condensation reactions involving β-ketosulfoxide (2) such as **3** and **9**.

The reaction of **1** with $DMSO^-$ proceeded smoothly in dimethyl sulfoxide (DMSO)–tetrahydrofuran (THF) (1:1) solution to give **2**, which was then acetylated to **3**. Condensation of **3** with ethyl bromoacetate by means of sodium hydride yielded **4** as an intractable oil. Desulfurization (2*a*) followed by saponification with potassium hydroxide gave crystalline acid **5** in a 62% yield based on **3**. The acid **5** was transformed into 15-hydroxypentadecanoic acid (**6**) by the Clemmensen reduction. Oxidation of **5** gave **7** which proved identical with a specimen prepared by ozonolysis of bicyclo[10·3·0]pentadec-1(12)-en-13-one (3).

Alternatively **8** was treated with $DMSO^-$ to give **9** as a crystalline solid. The absence of the shift of double bond was ascertained by the infrared (i.r.) and nuclear magnetic resonance (n.m.r.) spectra. Reaction of **9** with methyl acrylate occurred in ethereal solvents containing a catalytic amount of sodium hydride to give **10** as an oil, which was also immediately desulfurized to **11**. The ketoester **11** was obtained as a crystalline solid in a 72% yield based on **9**. To our best knowledge such Michael addition of a β-ketosulfoxide appears to be without precedent.

Can. J. Chem. Downloaded from www.nrcresearchpress.com by 210.87.254.42 on 09/05/12
For personal use only.

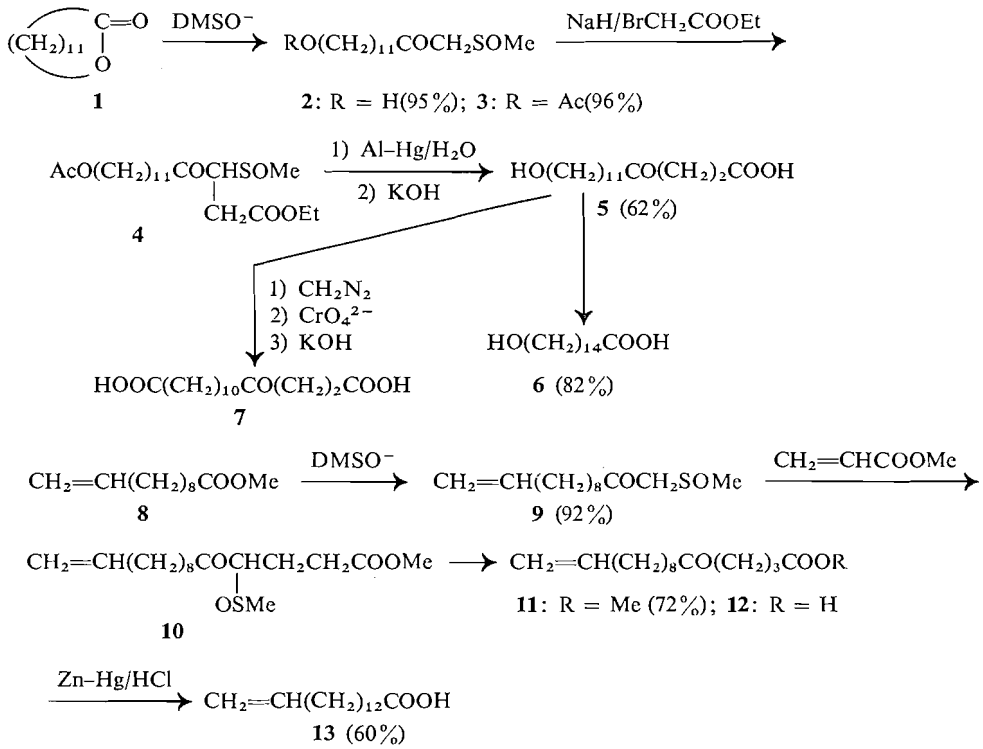

Saponification of **11** gives a known ketoacid **12** (4). Migration of the terminal double bond has been noticed in the case of the Wolff–Kishner reduction of a substance similar to **12** (5). Such rearrangement was observed also in the Clemmensen reduction of **12** to a considerable extent as evidenced by i.r. and n.m.r. spectra. Under carefully controlled conditions, however, the isomerization was reduced to a minimum and the isomer-free **13** was obtained in a 60% yield. The conversion of **13** to **6** is already known (6).

Experimental

All temperatures were uncorrected. Nuclear magnetic resonance (n.m.r.) spectra were obtained on a 60 Mc.p.s. instrument (JOEL C-60-H spectrometer) with $CDCl_3$ as the solvent and tetramethylsilane as the internal standard. The chemical shifts (δ) are reported in parts per million from tetramethylsilane. The multiplicity of signals was indicated in an abbreviated form: s, for singlet; d, for doublet; t, for triplet; and m, for multiplet, respectively.

Methyl 12-Hydroxydodecanoylmethyl Sulfoxide (2)

The $DMSO^-$ solution prepared from sodium hydride (12 g, 0.5 mole) and DMSO (250 ml) according to the published method (*2a*) was diluted with THF (250 ml) and was added with 1,12-dodecanolide (50 g, 0.25 mole) in the course of 0.5 h at 0° with stirring under nitrogen atmosphere. After stirring at room temperature for an additional 1 h, the reaction mixture was poured into ice-water (2 l). Neutralization with dilute hydrochloric acid gave **2** as white powdery precipitates which were collected, washed, and dried *in vacuo*. Recrystallization from benzene gave 65 g (95%) of pure **2** melting at 89°; infrared (i.r.) (Nujol): 3300 (OH), 1700 (C=O), 1020 cm^{-1} (S=O); n.m.r.: δ 3.78 s (2H), 3.60 t (2H), 2.70 s (3H), 2.60 t (2H), 2.92 s (1H), 1.8–1.1 m (18H).

Anal. Calcd. for $C_{14}H_{28}O_3S$: C, 60.8; H, 10.2. Found: C, 60.8; H, 10.2.

Methyl 12-Acetoxydodecanoylmethyl Sulfoxide (3)

To a solution of **2** (40 g) in pyridine (400 ml) acetic anhydride (160 g) was added gradually under stirring. The mixture was heated on a steam bath for 5 min and poured into ice-water (2 l). The precipitates were collected by filtration, washed, and dried *in vacuo*. Recrystallization of the dried material from THF gave 44 g (96%) of pure **3** melting at 76.5–78°; i.r.(Nujol): 1735, 1270 (OAc), 1700 (C=O), 1025, 1020 cm^{-1} (S=O).

Anal. Calcd. for $C_{16}H_{30}O_4S$: C, 60.4; H, 9.5. Found: C, 60.4; H, 9.3.

15-Hydroxy-4-oxopentadecanoic Acid (5)

A mixture of sodium hydride (1.2 g, 0.05 mole), DMSO (150 ml) and **3** (15.9 g, 0.05 mole) was stirred at room temperature under nitrogen atmosphere until evolution of hydrogen had subsided. To the resulting solution ethyl bromoacetate (8.4 g, 0.05 mole) was added and the mixture was stirred for an additional 0.5 h. Dilution with water followed by extraction with chloroform and eva-

Can. J. Chem. Downloaded from www.nrcresearchpress.com by 210.87.254.42 on 09/05/12
For personal use only.

Can. J. Chem. Downloaded from www.nrcresearchpress.com by 210.87.254.42 on 09/05/12
For personal use only.

poration of the solvent afforded an oily residue. To the residue dissolved in THF (100 ml) and water (80 ml) was added the $HgCl_2$-pretreated aluminium foil (13.5 g) (*2a*) under stirring at 50–60° and stirring was continued at the same temperature for 2 h, during which an additional amount of mixed solvent (THF:water = 1:1) was added successively in order to overcome the difficulty in stirring due to the formation of massive aluminium hydroxide. The supernatant THF solution was secured by decantation and the solid residue was washed repeatedly with chloroform. The combined organic solutions were washed with water and dried (Na_2SO_4). Upon evaporation of the solvent there was obtained a colorless residue which was dissolved in ethanol (100 ml) and 30% aqueous potassium hydroxide (40 ml). The mixture was heated under reflux for 5 h and diluted with water (100 ml). After washing with chloroform, the aqueous layer was acidified with dilute hydrochloric acid, and extracted with chloroform. Evaporation of the solvent followed by recrystallization from ethyl acetate gave 8.4 g (62%) of **5** melting at 103–104.5° (reported (7) m.p. 106–107°); i.r.(Nujol): 3600–2400 (COOH), 1710–1700 cm^{-1} (C=O, COOH).

Anal. Calcd. for $C_{15}H_{28}O_4$: C, 66.1; H, 10.4. Found: C, 66.3; H, 10.4.

15-Hydroxypentadecanoic Acid (6)

A mixture of zinc dust (50 g), mercuric chloride (5 g), concentrated hydrochloric acid (2.5 ml), and water (80 ml) was stirred for 5 min, and the aqueous layer was removed by decantation. The solid residue was mixed with acetic acid (100 ml), water (50 ml), and concentrated hydrochloric acid (50 ml). To this mixture **5** (5 g) was added and heated under reflux for 2 h. Heating and stirring were continued in the course of 6 h while concentrated hydrochloric acid was added at the rate of 5 ml per h. After cooling the reaction mixture was diluted with water and extracted with chloroform. Concentration of the extract gave a semisolid, which was dissolved in 30% aqueous potassium hydroxide (40 ml). The solution was heated on a steam bath for 2 h. After cooling and acidification the mixture was extracted with chloroform. Evaporation of the solvent and recrystallizations of the residue from benzene afforded 3.9 g (82%) of **6** melting at 87–88°. There was no depression of melting point of this product on the addition of the authentic specimen obtained by hydrolysis of Exaltolide. Comparison of the i.r. spectra of the two samples also confirmed their identity.

4-Oxopentadecanedioic Acid (7)

Methylation of **5** (1.86 g) by means of diazomethane in the usual manner afforded an ethereal solution of its methyl ester, to which a mixture of sodium dichromate dihydrate (1 g), concentrated sulfuric acid (0.9 g), and water (10 ml) was added and the whole mixture was stirred for 0.5 h at room temperature. After extraction with ether, an organic acid fraction was transferred into 30% aqueous potassium hydroxide. The solution was heated under reflux for 3 h, cooled, acidified with dilute hydrochloric acid, and extracted with ether. Evaporation of the solvent followed by recrystallization of the residue from benzene gave 0.47 g (24%) of **7**, melting at 121–122°. Mixture melting point showed no depression when admixed with the authentic specimen (3). The i.r. spectrum of **7** was completely superimposable with that of the authentic sample.

Methyl 10-Undecenoylmethyl Sulfoxide (9)

The $DMSO^-$ solution prepared from sodium hydride (16.8 g, 0.7 mole) and DMSO (350 ml) was diluted with THF (350 ml) and added with methyl 10-undecenoate (**8**) (69 g, 0.35 mole) in the course of 0.5 h at 0° with stirring under nitrogen atmosphere. Stirring was continued for an additional 0.5 h at room temperature, when the reaction mixture was poured into ice-water (2 l), acidified to pH 3–4 with dilute hydrochloric acid and extracted with chloroform. The organic layer was washed with water, dried (Na_2SO_4), and concentrated *in vacuo*. Recrystallization from ether afforded 79 g (92%) of **9** melting at 67–68°; i.r.(Nujol): 3080, 1645, 990, 910 (—CH=CH_2), 1700 (C=O) and 1020 cm^{-1} (S=O); n.m.r.: δ 6.0–5.5 m (1H), 5.3–4.8 m (2H), 3.75 s (2H), 2.70 s (3H), 2.60 t (2H), 2.3–1.8 m (2H), 1.8–1.1 m (12H).

Anal. Calcd. for $C_{13}H_{24}O_2S$: C, 63.9; H, 9.9. Found: C, 63.8; H, 9.8.

Methyl 5-Oxo-14-pentadecenoate (11)

To a mixture of sodium hydride (0.62 g, 0.026 mole), dioxane (80 ml) and **9** (61 g, 0.25 mole) methyl acrylate (22.4 g, 0.26 mole) was added in the course of 1.5 h with stirring at 45–50° under nitrogen atmosphere and stirring was continued for an additional 2 h. After standing overnight at room temperature the reaction mixture was neutralized with acetic acid (3 ml), diluted with water, and extracted with chloroform. Upon evaporation of the solvent there was obtained an oily material as a residue which was subsequently dissolved into the mixture of THF (500 ml) and water (400 ml). To this solution was added $HgCl_2$-pretreated aluminium foil (68 g). After stirring for 2 h with occasional addition of THF and water, the supernatant THF solution was separated by decantation. The precipitates were washed with benzene, and the combined organic solutions were washed with water, and dried (Na_2SO_4). Evaporation of the solvent followed by distillation *in vacuo* gave 48 g (72%) of **11** as a colorless low melting solid, b.p. 125–126°/0.18 mm Hg. Recrystallization from ether gave an analytically pure sample melting at 29–31°; i.r.(Nujol): 3100, 1650, 990, 910 (—CH=CH_2), 1740 (—$COOCH_3$), 1715 cm^{-1} (C=O); n.m.r.: δ 6.1–5.4 m (1H), 5.2–4.7 m (2H), 3.65 s (3H), 2.7–1.1 m (22H).

Anal. Calcd. for $C_{16}H_{28}O_3$: C, 71.6; H, 10.5. Found: C, 71.5; H, 10.7.

5-Oxo-14-pentadecenoic Acid (12)

Alkaline hydrolysis of methyl ester (**11**) in ethanol with aqueous potassium hydroxide in a usual manner gave **12** in a 95% yield. Recrystallizations from *n*-hexane afforded colorless crystals melting at 69–69.5° (reported (4) m.p. 68–68.5°); i.r.(Nujol): 3100, 1650, 990, 910 (—CH=CH_2), 3600–2400 (COOH), 1720–1700 cm^{-1} (C=O, COOH).

14-Pentadecenoic Acid (13)

To zinc dust (100 g) pretreated as described for the preparation of **6** was added acetic acid (400 ml), concentrated hydrochloric acid (100 ml) and **12** (30 g). The whole mixture was stirred at 70–80° for 1 h. Stirring was continued for an additional 4 h, during which

period concentrated hydrochloric acid was added at a rate of 25 ml per hour. After cooling the reaction mixture was diluted with water and extracted with benzene. The benzene solution was washed with water, dried (Na_2SO_4), and concentrated *in vacuo*. Recrystallization of the residual solid from aqueous ethanol gave 17 g of **13** (60%) melting at 49.0–49.5° (reported (8) m.p. 49.1–49.3°); i.r.(Nujol): 3100, 1650, 990, 910 (—CH=CH_2), 3600–2400, 1720–1700 cm^{-1} (COOH); n.m.r.: δ 6.0–5.4 m (1H), 5.2–4.7 m (2H), 2.5–1.1 m (24H).

Acknowledgment

The authors would like to thank Prof. Keiiti Sisido for his continued help and encouragement.

1. (*a*) H. Nozaki and R. Noyori. J. Org. Chem. **30**, 1652 (1965). (*b*) K. Kossiwig, W. Stumpf, and W. Kirchhof. Ann. Chem. Liebigs, **681**, 28 (1965).
2. (*a*) E. J. Corey and M. Chaykovsky. J. Am. Chem. Soc. **87**, 1345 (1965). (*b*) H. D. Becker, G. J. Mikol, and G. A. Russell. J. Am. Chem. Soc. **85**, 3410 (1963). (*c*) G. A. Russell and G. J. Mikol. J. Am. Chem. Soc. **88**, 5498 (1966). (*d*) E. J. Corey and M. Chaykovsky. J. Am. Chem. Soc. **86**, 1639 (1964). (*e*) P. G. Gassman and G. D. Richmond. J. Org. Chem. **31**, 2355 (1966). (*f*) J. B. Lee. Tetrahedron Letters, 5669 (1966).
3. H. Nozaki, T. Mori, R. Noyori, and M. Kawanisi. Can. J. Chem. **45**, 1804 (1967).
4. M. G. J. Beets and W. Meerburg. U. S. Pat. 2,820,805. Chem. Abstr. **52**, 10,160 (1958).
5. K. Sisido and M. Kawanisi. J. Org. Chem. **27**, 3722 (1962).
6. Y. Ookuni and M. Hirasawa. Japanese Pat. 238,216 (1957). N. V. Polak. Dutch Pat. 67,458 (1951). British Pat. 671,004 (1952).
7. T. Kariyone and H. Ageta. Yakugaku Zasshi. **77**, 764 (1957).
8. D. G. Bounds, R. P. Linstead, and B. C. L. Weedon. J. Chem. Soc. 2393 (1953).

Can. J. Chem. Downloaded from www.nrcresearchpress.com by 210.87.254.42 on 09/05/12
For personal use only.

Structure of β-mangostin

Peter Yates and H. B. Bhat
Lash Miller Chemical Laboratories, University of Toronto, Toronto, Ontario

Received July 5, 1968

β-Mangostin, a minor coloring matter of the dried latex of *Garcinia mangostana*, is shown to be 1,6-dihydroxy-3,7-dimethoxy-2,8-di-(3-methyl-2-butenyl)xanthone (**4**).

Canadian Journal of Chemistry, 46, 3770 (1968)

The fruit hulls, bark, and dried latex of *Garcinia mangostana* contain the yellow coloring matter mangostin, $C_{24}H_{26}O_6$, m.p. 182–183°, which has been shown to have structure **1** (1, 2). The dried latex is a particularly rich source, yielding 30–50% of mangostin (1, 3). During the course of the original work on the isolation of mangostin from the dried latex, Dragendorff (3) also isolated a minor yellow coloring matter (2%), m.p. 175.5°, which he named β-mangostin. This was considered to be isomeric with mangostin on the basis of elemental analytical data. On treatment with diazomethane it was found to give a methylation product identical with that obtained by similar treatment of mangostin, which is now known to be dimethylmangostin **2** (1). β-Mangostin was therefore considered to differ from mangostin only in respect to the interchange of a methoxyl and a hydroxyl group.

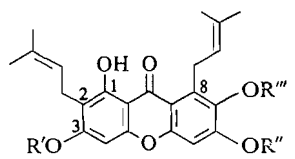

1 R′ = R″ = H; R‴ = CH_3
2 R′ = R″ = R‴ = CH_3
3 R′ = R″ = CH_3; R‴ = H
4 R′ = R‴ = CH_3; R″ = H
5 R′ = H; R″ = R‴ = CH_3

We have isolated from crude mangostin obtained from the dried latex (1) a minor constituent, m.p. 175–176°, which is considered to be the β-mangostin of Dragendorff. On the basis of mass spectral and elemental analytical data we assign to it the formula, $C_{25}H_{28}O_6$, a formulation which is in accord also with Dragendorff's elemental analytical data. Its formula thus differs from that of mangostin by a CH_2 unit.

period concentrated hydrochloric acid was added at a rate of 25 ml per hour. After cooling the reaction mixture was diluted with water and extracted with benzene. The benzene solution was washed with water, dried (Na_2SO_4), and concentrated *in vacuo*. Recrystallization of the residual solid from aqueous ethanol gave 17 g of **13** (60%) melting at 49.0–49.5° (reported (8) m.p. 49.1–49.3°); i.r.(Nujol): 3100, 1650, 990, 910 (—CH=CH_2), 3600–2400, 1720–1700 cm^{-1} (COOH); n.m.r.: δ 6.0–5.4 m (1H), 5.2–4.7 m (2H), 2.5–1.1 m (24H).

Acknowledgment

The authors would like to thank Prof. Keiiti Sisido for his continued help and encouragement.

1. (*a*) H. Nozaki and R. Noyori. J. Org. Chem. **30**, 1652 (1965). (*b*) K. Kossiwig, W. Stumpf, and W. Kirchhof. Ann. Chem. Liebigs, **681**, 28 (1965).
2. (*a*) E. J. Corey and M. Chaykovsky. J. Am. Chem. Soc. **87**, 1345 (1965). (*b*) H. D. Becker, G. J. Mikol, and G. A. Russell. J. Am. Chem. Soc. **85**, 3410 (1963). (*c*) G. A. Russell and G. J. Mikol. J. Am. Chem. Soc. **88**, 5498 (1966). (*d*) E. J. Corey and M. Chaykovsky. J. Am. Chem. Soc. **86**, 1639 (1964). (*e*) P. G. Gassman and G. D. Richmond. J. Org. Chem. **31**, 2355 (1966). (*f*) J. B. Lee. Tetrahedron Letters, 5669 (1966).
3. H. Nozaki, T. Mori, R. Noyori, and M. Kawanisi. Can. J. Chem. **45**, 1804 (1967).
4. M. G. J. Beets and W. Meerburg. U. S. Pat. 2,820,805. Chem. Abstr. **52**, 10,160 (1958).
5. K. Sisido and M. Kawanisi. J. Org. Chem. **27**, 3722 (1962).
6. Y. Ookuni and M. Hirasawa. Japanese Pat. 238,216 (1957). N. V. Polak. Dutch Pat. 67,458 (1951). British Pat. 671,004 (1952).
7. T. Kariyone and H. Ageta. Yakugaku Zasshi. **77**, 764 (1957).
8. D. G. Bounds, R. P. Linstead, and B. C. L. Weedon. J. Chem. Soc. 2393 (1953).

Structure of β-mangostin

Peter Yates and H. B. Bhat
Lash Miller Chemical Laboratories, University of Toronto, Toronto, Ontario

Received July 5, 1968

β-Mangostin, a minor coloring matter of the dried latex of *Garcinia mangostana*, is shown to be 1,6-dihydroxy-3,7-dimethoxy-2,8-di-(3-methyl-2-butenyl)xanthone (**4**).

Canadian Journal of Chemistry, 46, 3770 (1968)

The fruit hulls, bark, and dried latex of *Garcinia mangostana* contain the yellow coloring matter mangostin, $C_{24}H_{26}O_6$, m.p. 182–183°, which has been shown to have structure **1** (1, 2). The dried latex is a particularly rich source, yielding 30–50% of mangostin (1, 3). During the course of the original work on the isolation of mangostin from the dried latex, Dragendorff (3) also isolated a minor yellow coloring matter (2%), m.p. 175.5°, which he named β-mangostin. This was considered to be isomeric with mangostin on the basis of elemental analytical data. On treatment with diazomethane it was found to give a methylation product identical with that obtained by similar treatment of mangostin, which is now known to be dimethylmangostin **2** (1). β-Mangostin was therefore considered to differ from mangostin only in respect to the interchange of a methoxyl and a hydroxyl group.

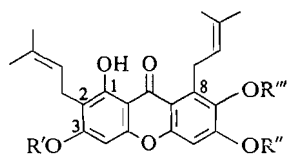

1 R′ = R″ = H; R‴ = CH_3
2 R′ = R″ = R‴ = CH_3
3 R′ = R″ = CH_3; R‴ = H
4 R′ = R‴ = CH_3; R″ = H
5 R′ = H; R″ = R‴ = CH_3

We have isolated from crude mangostin obtained from the dried latex (1) a minor constituent, m.p. 175–176°, which is considered to be the β-mangostin of Dragendorff. On the basis of mass spectral and elemental analytical data we assign to it the formula, $C_{25}H_{28}O_6$, a formulation which is in accord also with Dragendorff's elemental analytical data. Its formula thus differs from that of mangostin by a CH_2 unit.

Can. J. Chem. Downloaded from www.nrcresearchpress.com by 210.87.254.105 on 09/05/12
For personal use only.

Can. J. Chem. Downloaded from www.nrcresearchpress.com by 210.87.254.105 on 09/05/12
For personal use only.

We have confirmed that it can be converted by methylation to dimethylmangostin **2**; in the present instance this methylation was effected by treatment with dimethyl sulfate and potassium carbonate in acetone. These data require that β-mangostin have one of the structures **3**–**5**.

This conclusion is corroborated by spectroscopic data (see Experimental). Its infrared and ultraviolet spectra show the characteristic features of a xanthone with a free hydroxyl group at C-1 (1, 4). Its nuclear magnetic resonance spectrum resembles that of mangostin, but differs from it in showing two methoxyl proton signals instead of one.

Treatment of β-mangostin with anhydrous *p*-toluenesulfonic acid in boiling benzene for 30 min gave a single isomeric product, m.p. 281–282°, in low yield and led to the recovery of most of the starting material; longer heating resulted in an increased yield of the isomer. Methylation of the isomer with dimethyl sulfate and potassium carbonate in acetone gave a monomethyl derivative shown to be identical to **6**, the dimethyl derivative of 1-isomangostin (**7**) (2). The exclusive formation of a 1-isomangostin derivative here stands in contrast to the case of

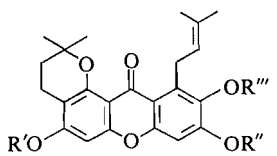

6 R′ = R″ = R‴ = CH_3
7 R′ = R″ = H; R‴ = CH_3
8 R′ = R‴ = CH_3; R″ = H

mangostin, where both 1- and 3-isomangostin derivatives are formed under similar conditions (2), corresponding to chroman ring formation involving attack of the free hydroxyl groups at C-1 and C-3 on the isopentenyl side chain at C-2. The exclusive formation of a 1-isomangostin derivative in the case of β-mangostin demonstrates that the C-3 substituent must be a methoxyl rather than a hydroxyl group. Further, the failure to observe the formation of any product in which the isopentenyl side chain at C-8 has undergone chroman ring formation demonstrates that the C-7 substituent must also be a methoxyl rather than a hydroxyl group. It follows that the structure of β-mangostin is **4** and that its isomerization product has structure **8**.[1]

Experimental

β-Mangostin (4)

Crude mangostin (25 g), isolated from the dried latex of *Garcinia mangostana* (1), was extracted in a Soxhlet apparatus with petroleum ether (b.p. 60–70°) for 5 days. The extract was allowed to stand at room temperature for 4 days, and the mangostin that crystallized was removed by filtration. The pale-yellow filtrate was stripped of solvent under reduced pressure, and the residue was crystallized from ethanol to give β-mangostin (0.12 g) as small lemon-yellow rods, m.p. 175–176° [lit. (3) m.p. 175.5°]; λ_{max} (CCl_4) 2.90, 3.5 (br), 6.07, 6.24 μ; λ_{max} (EtOH) (log ε) 245 (4.55), 258 (4.45), 317 (4.30), 356 mμ (4.10); δ ($CDCl_3$) 1.66 (6H), 1.78 and 1.80 (6H), 3.32 (2H, d, J = 7 Hz), 3.76 (3H, s), 3.84 (3H, s), 4.05 (2H d, $J \sim 7$ Hz), 5.20 (2H, m), 6.24 (1H, s), 6.37 (1H, br), 6.74 (1H, s), 13.38 (1H, s).

Anal. Calcd. for $C_{25}H_{28}O_6$: C, 70.74; H, 6.65. Found: C, 70.87; H, 6.67.

Methylation of β-Mangostin. Formation of Dimethylmangostin (2)

A solution of β-mangostin (15 mg) and dimethyl sulfate (0.05 ml) in acetone (8 ml) was boiled under reflux in the presence of anhydrous potassium carbonate (100 mg) for 6 h. The mixture was filtered, the filtrate was evaporated, and the residue was treated with water (10 ml); after 24 h the mixture was extracted with ether. The ethereal extract was washed with water, dried, and stripped of solvent. The residue was crystallized from ethanol to give dimethylmangostin (**2**), m.p. 123–124° [lit. (1) m.p. 123.3–123.8°], undepressed on admixture with an authentic sample (1); the infrared spectra of the two samples were superimposable.

Acid-catalyzed Cyclization of β-Mangostin. Formation of 8

p-Toluenesulfonic acid (12 mg) was dissolved in benzene (20 ml), 10 ml of the benzene was distilled, and β-mangostin (102 mg) was added. The solution was boiled under reflux for 30 min, diluted with ethyl acetate, washed with water, dried, and stripped of solvent. The residue was crystallized from acetone – petroleum ether to give colorless crystals (6 mg) of **8**, m.p. 281–282°. The mother liquor was stripped of solvent and the residue was recrystallized from ethanol to give unconsumed β-mangostin (70 mg), m.p. 175–176°.

Treatment of β-mangostin (45 mg) with *p*-toluenesulfonic acid (20 mg) in boiling benzene (7 ml) for 3 h and work-up as before gave a higher yield (20 mg) of **8**,

[1]The possibility that β-mangostin possesses a free C-3 or C-7 hydroxyl group, but preferential closure occurs at the C-1 hydroxyl group can clearly be excluded. Reaction of the chelated hydroxyl group at C-1 would be *slower* than that of unchelated hydroxyl groups at C-3 or C-7, as exemplified by the observation that the rates of conversion of β-mangostin and dimethylmangostin to cyclized products are considerably slower than the overall rate of cyclization of mangostin and that preferential cyclization at the C-3 hydroxyl group occurs in the case of mangostin.

m.p. 281–282°; λ_{max} (Nujol) 3.03, 6.06, 6.20 (sh), 6.24 μ; λ_{max} (EtOH) (log ε) 244 (4.53), 253 (sh, 4.47), 305 (4.32), 334 mμ (3.95).

Anal. Calcd. for $C_{25}H_{28}O_6$: C, 70.74, H, 6.82. Found: C, 70.48; H, 6.82.

Thin-layer chromatography of the crude reaction products failed to reveal the presence of any isomer of β-mangostin other than **8**.

*Methylation of **8**. Formation of Dimethyl-1-isomangostin (**6**)*

Compound **8** (6 mg) was methylated in acetone with dimethyl sulfate and potassium carbonate and the reaction mixture was worked up as in the methylation of β-mangostin above. The crude product was crystallized from cyclohexane to give dimethyl-1-isomangostin (**6**), m.p. 127–128°, undepressed on admixture with an authentic sample, m.p. 127–128° (2, 4): the infrared spectra of the two samples were superimposable.

Acknowledgment

The support of this research by the National Research Council of Canada is gratefully acknowledged.

1. P. YATES and G. H. STOUT. J. Am. Chem. Soc. **80**, 1691 (1958).
2. G. H. STOUT, M. M. KRAHN, P. YATES, and H. B. BHAT. Chem. Commun. 211 (1968).
3. O. DRAGENDORFF. Ann. **482**, 280 (1930).
4. P. YATES and A. AULT. Tetrahedron, **23**, 3307 (1967).

Can. J. Chem. Downloaded from www.nrcresearchpress.com by 210.87.254.105 on 09/05/12
For personal use only.

Can. J. Chem. Downloaded from www.nrcresearchpress.com by 210.87.254.105 on 09/05/12
For personal use only.

Canadian Journal of Chemistry

Published by The National Research Council of Canada

VOLUME 46 DECEMBER 15, 1968 NUMBER 24

Radiolysis of water vapor with fission fragments[1]

A. W. Boyd and O. A. Miller

Research Chemistry Branch, Chalk River Nuclear Laboratories, Atomic Energy of Canada Limited, Chalk River, Ontario

Received May 24, 1968

Water vapor, and mixtures of water vapor with radical and electron scavengers, have been irradiated with fission fragments at temperatures from 170 to 365 °C and densities from 1–50 mg/ml. The unimolecular hydrogen yield is the same as in γ-ray irradiations. In D_2O–C_6H_{12} mixtures the HD yield and HD/H_2 ratio are lower than in γ-ray irradiations and N_2O and SF_6 have little effect. The HD yield reaches a limiting value ($G(HD) \sim 4$) with increasing linear energy transfer suggesting that a fraction of the D atoms formed are hot.

Canadian Journal of Chemistry, **46**, 3773 (1968)

Introduction

The γ-ray radiolysis of mixtures of water vapor and a few mole percent of alkanes or alcohols gives a hydrogen yield of $G(H_2) \approx 8$ (molecules per 100 eV of absorbed dose) (1). This yield is reduced by ~ 3 G units by the addition of an electron scavenger such as SF_6 or N_2O (2, 3). The hydrogen yield from a mixture of water vapor (D_2O) and benzene is $G(D_2) \approx 0.5$ (4). These results are consistent with the following reactions

[1] $H_2O \rightarrow H_2O^*$ $\quad G(H_2O^*) \sim 5$

[2] $H_2O \rightarrow H_2O^+ + e$ $\quad G(H_2O^+) = G(e) \sim 3$

[3] $H_2O^* \rightarrow H + OH$

[4] $H_2O^* \rightarrow H_2 + O$ $\quad G(H_2) \sim 0.5$

[5] $H_2O^+ + H_2O \rightarrow H_3O^+ + OH$

[6] $H_3O^+ + e \rightarrow H + H_2O$

[7] $H + RH \rightarrow H_2 + R$ $\quad G(H_2) \sim 8$

[8] $H + C_6H_6 \rightarrow$ no H_2

[9] $e + SF_6$ (or N_2O) $+ H_3O^+ \rightarrow$ no H or H_2

The γ-ray radiolysis of pure water vapor results only in low steady state concentrations of hydrogen and hydrogen peroxide or oxygen. This is due to the disappearance of the products formed in reactions [10] and [11] by the back reactions [12] and [13]

[10] $H + H + M \rightarrow H_2 + M$

[11] $OH + OH + M \rightarrow H_2O_2 + M$

[12] $H + H_2O_2 \rightarrow H_2O + OH$

[13] $OH + H_2 \rightarrow H_2O + H$

The direct recombination of H and OH radicals is also possible as in reaction [14]

[14] $H + OH + M \rightarrow H_2O + M$

It is interesting to consider what would be the changes in yields in the irradiation of water vapor with high linear energy transfer (l.e.t.—the rate of energy loss per unit length of track) radiation. The unimolecular yield of hydrogen $G(H_2) \sim 0.5$ observed with the addition of radical scavengers should be the same. However high l.e.t. radiation may change the other yields in pure water vapor and in water vapor – alkane mixtures. This is because high l.e.t. will favor reactions [10], [11], and [14] over the back reactions [12] and [13] and the abstraction reaction [7]. This would lead to an increase in steady state product concentrations in pure water and a decrease in the H_2 yield in the alkane mixtures. Also it is expected that reaction [6] would be favored over reaction [9] so that the effect of electron scavengers will be reduced.

[1]Issued as A.E.C.L. 2744.

Can. J. Chem. Downloaded from www.nrcresearchpress.com by 210.87.254.105 on 09/05/12
For personal use only.

To obtain a l.e.t. of greater than 1 eV/Å in water vapor at a few atmospheres it is necessary to use heavy ions such as fission fragments. To determine if the above changes occur we have irradiated (1) water vapor, (2) mixtures of water vapor and radical scavengers, and (3) mixtures of water vapor and cyclohexane with and without electron scavengers. We used fission fragments and ^{60}Co γ rays at temperatures from 170–365 °C and densities from 1–50 mg/ml.

Experimental

The H_2O and D_2O (99.8% D) were triple distilled, preirradiated, and photolyzed. The C_6H_{12}, C_6H_6 (both Fisher Spectroanalyzed), N_2O (McDuff medical grade), NH_3, O_2, and SF_6 (Matheson C.P. grades) were used as received.

The quartz capsules used for the fission fragment irradiations are shown in Fig. 1. The ^{235}U was in the form of a coating of U_3O_8 on a quartz tube. This coating was made by painting on layers of uranyl nitrate dissolved in an alcohol – cellulose acetate mixture (5) and firing each layer at 750°.

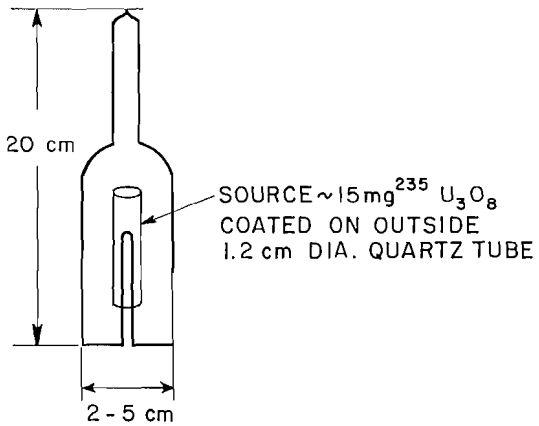

FIG. 1. Quartz cell for fission fragment irradiations of water vapor.

The uranium (93% ^{235}U) was the same as that used previously (6). The amount of U_3O_8 on the quartz tube was determined by weighing. The alpha particle activity was measured before each irradiation and corrections applied (less than 5%) for any loss of uranium from the source. These measurements were made with a windowless proportional alpha counter designed by the Counter Development Section at Chalk River Nuclear Laboratories.

Before filling, the capsules and the source were heated at 500 °C in air for several hours. The water and condensible gases were freed of permanent gases before sealing in the capsules.

The capsules were irradiated in a furnace in a 4 in. diameter horizontal hole in the NRX reactor. To obtain pressures above 10 atm. the quartz capsules were put in a welded stainless steel capsule containing enough water to give the saturated vapor. The temperature was measured by thermocouples inserted in the re-entrant hole in the capsules, or spot welded to the stainless steel. The thermal neutron flux in the sample was $\sim 1 \times 10^{12}$ n cm^{-2} s^{-1} and the γ-ray dose rate ~ 10 mW/g. The integrated thermal neutron flux in each sample was determined using cobalt monitors and the absorbed dose of reactor γ rays was calculated from the thermal neutron flux and previous measurements (7).

The total energy of the fission fragments was calculated from the weight of ^{235}U and the integrated thermal neutron flux. The fraction of the total energy of the fission fragments that escaped from the U_3O_8 and was absorbed by the water vapor was calculated from the following equation (8). This equation is derived assuming the loss of energy of the fission fragments is proportional to the square of the distance travelled.

$$\text{Fraction escaping} = 0.5\left[1 - 0.5\left(\frac{t}{R}\right)\right] - 0.33\left(\frac{t}{R}\right)^2 + \frac{t}{R}\ln\frac{t}{R}$$

where t is the thickness of the U_3O_8 and R the range of fission fragments in U_3O_8.

The diameter of the capsule was varied from 3.0 to 5.0 cm both to ensure that all the fission fragments were just stopped in the gas phase and that the absorbed dose from reactor γ rays was minimized.

The ^{60}Co γ-ray irradiations using the cells containing the ^{235}U sources, were done in a Gammacell-220. The absorbed dose was determined using the Fricke dosimeter and applying corrections for relative electron densities, stopping powers and self-shielding.

The dosimetry in the ^{60}Co γ-ray irradiations is estimated to be accurate to within $\pm 5\%$ and that in the fission fragment irradiations to be accurate to within $\pm 10\%$.

The volume of gas formed was measured using conventional vacuum line techniques. The H_2, HD, D_2, and nitrogen contents were determined by mass spectrometry.

Results

The irradiations can be divided into three groups: (1) pure water vapor, (2) water vapor with 1% benzene and water vapor with 0.5% NH_3 and 1% O_2, and (3) water vapor (H_2O and D_2O) with 5 mole % C_6H_{12}.

(1) Pure Water Vapor

Yields in pure water vapor are dependent upon the treatment of the irradiation vessel (1). Baxendale and Gilbert obtained $G(H_2) = 0.1$ for a dose of ~ 0.3 Mrads in a soft glass vessel cleaned and heated and evacuated at 116 °C. Values of $G(H_2)$ higher than this can be ascribed to addition or abstraction reactions of the radi-

Can. J. Chem. Downloaded from www.nrcresearchpress.com by 210.87.254.105 on 09/05/12
For personal use only.

TABLE I

Hydrogen yields from fission fragment irradiations of pure water vapor

Temperature (°C)	Density (mg/ml)	Absorbed dose (10^{19} eV)		$G(H_2)$
		Fission fragments	Reactor γ rays and fast neutrons	
157	0.8	—	8.9*	0.05
165	0.8	3.5	0.6	0.04
193	6	10.9	1.6	0.08
208	8.7	12.4	1.2	0.11
235	13	12.0	1.7	0.09
296	26	12.2	4.3	0.13
352	52	8.6	6.3	0.16

*^{60}Co γ-rays.

TABLE II

Hydrogen yields from fission fragment irradiations of water vapor with C_6H_6 or NH_3 and O_2

Composition	Temperature (°C)	Density (mg/ml)	Absorbed dose (10^{19} eV)		$G(H_2)$
			Fission fragments	Reactor γ rays and fast neutrons	
0.3 g H_2O 0.5% NH_3 1% O_2	247	7.7	12.3	2.2	0.41
0.3 g H_2O 0.5% NH_3 1% O_2	186	3	11.5	1.9	0.54
0.3 g H_2O 0.5% NH_3 1% O_2	250	13	10.2	1.8	0.34
0.3 g H_2O 0.04 g C_6H_6	186	3	11.3	2.0	0.68
0.3 g H_2O 0.04 g C_6H_6	251	7.7	9.9	1.8	0.80
0.3 g H_2O 0.04 g C_6H_6	250	13	7.4	1.2	0.66

cals with impurities thus preventing the back reactions [12] and [13].

The yields with fission fragments are given in Table I. As can be seen at the lowest densities the yield of H_2 is not significantly different from those in γ-ray irradiations showing that neither the higher l.e.t. nor the surface of the U_3O_8 reduce the radical yields enough to inhibit the back reactions.

The increase in the yields of H_2 at the higher densities may be due to an increase in the reactions [10] and [11] in the tracks of the fission fragments and a corresponding decrease in the H and OH escaping. As such they are only the difference between the combination reactions [10] and [11] and the back reactions [12] and [13].

(2) Water Vapor and C_6H_6, Water Vapor, and NH_3–O_2

Either C_6H_6 (4) or NH_3 and O_2 (9) will scavenge the hydrogen-forming radicals in water vapor. The hydrogen yields from fission fragment irradiation of these are given in Table II. As expected these yields are not significantly different from those in γ irradiations.

(3) Water Vapor and C_6H_{12}

The majority of the irradiations were done with mixtures of water (H_2O and D_2O) and 5 mole % cyclohexane with and without N_2O or SF_6. The results of these both for fission fragments and ^{60}Co γ rays are given in Table III (*a* and *b*).

There appears to be a reduction outside the

Can. J. Chem. Downloaded from www.nrcresearchpress.com by 210.87.254.105 on 09/05/12
For personal use only.

TABLE III

(*a*) Hydrogen yields from fission fragment irradiations of water vapor with *c*-C_6H_{12}

Composition	Temperature (°C)	Density (mg/ml)	Absorbed dose (10^{19} eV) Fission fragments	Reactor γ rays and fast neutrons	*G*(total hydrogen)	$G(H_2)$	$G(HD)$	$G(D_2)$	$G(N_2)$
0.11 g D_2O 0.023 g *c*-C_6H_{12}	169	1	47	0.8	6.5	1.1	5.1	0.3	
0.11 g D_2O 0.023 g *c*-C_6H_{12} 1 mole % N_2O	168	1	51	0.8	5.9	1.0	4.0	0.3	0.6
0.22 g D_2O 0.05 g *c*-C_6H_{12}	229	8.7	56	1.2	6.1	1.2	4.5	0.4	
0.22 g D_2O 0.05 g *c*-C_6H_{12} 1 mole % N_2O	230	8.7	62	1.4	5.7	1.4	4.0	0.3	1.2
0.22 g D_2O 0.05 g *c*-C_6H_{12} 1 mole % SF_6	240	8.7	30	0.7	5.4	1.4	3.7	0.3	
0.66 g D_2O 0.16 g *c*-C_6H_{12}	310	26	87	8.9	6.5	1.6	4.5	0.4	

(*b*) Hydrogen yields from ^{60}Co γ-ray irradiations of water vapor with *c*-C_6H_{12}

Composition	Temperature (°C)	Density (mg/ml)	Absorbed dose (10^{19} eV) ^{60}Co γ rays	*G*(total hydrogen)	$G(H_2)$	$G(HD)$	$G(D_2)$	$G(N_2)$
0.11 g D_2O 0.02 g *c*-C_6H_{12}	169	1	7.7	8.2	1.0	6.8	0.4	
0.11 g D_2O 0.023 g *c*-C_6H_{12} 1 mole % N_2O	169	1	5.8	6.0	1.0	4.5	0.5	4.0
0.1 g H_2O 0.031 g *c*-C_6H_{12}	170	2.5	9.0	8.3				
0.2 g H_2O 0.05 g *c*-C_6H_{12}	224	8.7	15.7	7.6				
0.1 g H_2O 0.031 g *c*-C_6H_{12}	230	2.5	7.9	8.6				
0.3 g H_2O 0.08 g *c*-C_6H_{12}	270	13	19	7.8				
1.2 g H_2O 0.31 g *c*-C_6H_{12}	364	52	87	8.0				

TABLE IV

Rate constants for radical and ion reactions

Reaction	Rate constant	References
$H + H + M \rightarrow H_2 + M$	$9.4\times10^{-33}\left(\frac{T}{300}\right)^{-0.6}$ cm^6 molecule^{-2} s^{-1}	(10, 11)
$OH + OH + M \rightarrow H_2O_2 + M$	3.3×10^{-30} cm^6 molecule^{-2} s^{-1}	(12)
$OH + OH \rightarrow H_2O + O$	$5\times10^{-12}\,T^{1/2}\exp\left(\frac{-1000}{T}\right)$ cm^3 molecule^{-1} s^{-1}	(13–16)
$H + OH + M \rightarrow H_2O + M$	$\sim3\times10^{-31}$ cm^6 molecule^{-2} s^{-1} $= (2\times9.4\times10^{-33}\times3.3\times10^{-30})^{\ddagger}$	
$H_2O^+ + H_2O \rightarrow H_3O^+ + OH$	8.5×10^{-10} cm^3 molecule^{-1} s^{-1}	(17)
$e + H_3O^+ \rightarrow H_2O + H$	2.4×10^{-7} cm^3 molecule^{-1} s^{-1}	(18, 19)
$H + C_6H_{12} \rightarrow H_2 + C_6H_{12}$	$2.5\times10^{-10}\exp\left(\frac{-8400}{RT}\right)$ cm^3 molecule^{-1} s^{-1}	(20)*
$e + N_2O \rightarrow N_2 + O^-$	4×10^{-13} cm^3 molecule^{-1} s^{-1}	(21)
$e + SF_6 \rightarrow SF_6$	4×10^{-7} cm^3 molecule^{-1} s^{-1}	(22)

*See B. deB. Darwent and R. Roberts (20) for $H + nC_4H_{10}$ and $H + n\text{-}C_3H_8$.

TABLE V

Calculated radical concentrations in fission fragment tracks in water vapor

Density (mg/ml)	Temperature[a] (°C)	c-C_6H_{12}[b] moles/l	l.e.t.[c] (eV/Å)	Radical pairs/cm of track[d]	Mean free path (Å)	Radical H or OH concentration (moles/l) for radius	
						10 MFP[e]	100 MFP[e]
1	116	2.8×10^{-3}	0.4	3.2×10^{6}	390	1.11×10^{-6}	1.11×10^{-8}
2	141	5.4×10^{-3}	0.8	6.4×10^{6}	203	8.22×10^{-6}	8.22×10^{-8}
4	169	1.08×10^{-2}	1.6	1.28×10^{7}	109	5.69×10^{-5}	5.69×10^{-7}
8	201	2.16×10^{-2}	3.2	2.56×10^{7}	58	4.02×10^{-4}	4.02×10^{-6}
12	222	3.2×10^{-2}	4.8	3.84×10^{7}	41	1.21×10^{-3}	1.21×10^{-5}
24	261	6.48×10^{-2}	9.6	7.68×10^{7}	23	7.7×10^{-3}	7.7×10^{-5}

[a]Minimum temperature required for pure water vapor.
[b]For 5 mole % of c-C_6H_{12} in H_2O.
[c]Assuming range of fission fragments in water vapor is 2 mg/cm².
[d]Assuming radical yield = 8.
[e]Radius of 10 MFP is equivalent to 10^2 collisions, 100 MFP to 10^4 collisions.

limits of error in the total hydrogen yield on going from γ rays to fission fragments with mixtures of water vapor and c-C_6H_{12}. The isotopic yields confirm this reduction.

At 169° for D_2O and 5 mole % C_6H_{12} the γ-ray values are $G(HD) = 6.8$ and $G(H_2) = 1.0$ so that $G(HD)/G(H_2) = 6.8$. These values are in good agreement with those of Johnson and Simic (3). At the same temperature the fission fragment values are $G(HD) = 5.1$, $G(H_2) = 1.1$, and $G(HD)/G(H_2) = 4.6$. Thus the ratio of these yields which is independent of dosimetry is reduced by a third in the fission fragment irradiations. There is an even more striking change in the mixtures of D_2O, C_6H_{12}, and N_2O. The addition of N_2O has little effect on the HD yield or the HD/H_2 yield ratio but the yield of N_2 is reduced from 4 with γ rays to 0.6 with fission fragments. The value of $G(HD)$ with fission fragments does not appear to change significantly at higher temperatures and pressures and SF_6 also has no effect.

It is interesting that the total hydrogen yield in the γ-ray irradiations of H_2O and C_6H_{12} at 364° and a density of 52 mg/ml is 8 while at 364° C and a density of 1 mg/ml Johnson and Simic (3) obtained $G(H_2) = 16$.

Discussion

The reduction in the yield of HD with fission fragments can clearly be seen to be a l.e.t. effect and can be explained by the favoring of reactions [10] and [14] over [15].

[10] $H + H + M \rightarrow H_2 + M$

[14] $H + OH + M \rightarrow H_2O + M$

[15] $H + C_6H_{12} \rightarrow H_2 + C_6H_{11}$

However, this favoring should result in a continuing decrease in the HD yield with increasing l.e.t. as shown by calculations based on the rate constants for these reactions and concentrations in the fission fragment tracks. The best available values of the rate constants are given in Table IV and the estimated concentrations in Table V.

Consider water vapor containing 5 mole % cyclohexane with a density of 8 mg/ml. As stated in Table V the number of radical pairs per cm of track is 2.56×10^7 for a radical yield of $G(H) = 8$ and a fission fragment range of 2 mg/cm². As these diffuse away from the track their concentration decreases and at a radius of 100 mean free paths it is 4×10^{-6} M. The ratio of rate of reaction [14] (which is much faster than [10]) to the rate of reaction [15] is equal to $(k_{14}[H][OH][H_2O])/(k_{15}[H][C_6H_{12}])$. At 100 mean free paths and a temperature of 230 °C this equals $[3 \times 10^{-31}(2.4 \times 10^{15})^2(2.7 \times 10^{20})]/[5.6 \times 10^{-14}(2.4 \times 10^{15})(1.35 \times 10^{19})] = 0.26$.

At 24 mg/ml and 100 mean free paths this ratio has increased from 0.26 to 1.3. Although there are large uncertainties in these ratios it appears that there is a reduction in $G(HD)$ at 8 mg/ml and that there should be a further reduction at 24 mg/ml since the ratio of rates increases by a factor of 5.

These considerations suggest that the "limiting" HD yield of ~ 4 results from hot H atoms, i.e. atoms that will react at comparable rates with C_6H_{12} molecules and radicals. This is approximately equal to the proposed yield from excited water molecules and it is possible that the H atoms which are formed directly are hot while those formed by neutralization are thermal.

Can. J. Chem. Downloaded from www.nrcresearchpress.com by 210.87.254.105 on 09/05/12
For personal use only.

The lack of effect of SF_6 on the HD yield is consistent with this interpretation. However, calculations of the competition between reaction [16] and reaction [6] ($e + H_3O^+$) are not conclusive.

$$[16] \qquad e + SF_6 \rightarrow SF_6^-$$

At 8 mg/ml and 10 mean free paths the ratio of reaction [16] to reaction [6] is $\sim 50{:}1$. This would imply that SF_6 does scavenge the electrons but since these reactions are faster than the collision frequencies they may be complete in less than 10 mean free paths.

The addition of N_2O fails to reduce the HD yield because reaction [17] does not compete effectively with reaction [6]

$$[17] \qquad e + N_2O \rightarrow N_2 + O^-$$

This is shown by the low yields of N_2 and the values in Tables IV and V. Even at 1 mg/ml reaction [6] is about 100 times faster than reaction [17] at 10 mean free paths from the fission fragment track.

Although the l.e.t. of fission fragments in gases is relatively high the marked inhomogeneity of the concentrations of transient species makes interpretation of the results difficult. Further studies of water vapor are being done with a high intensity pulsed source of electrons.

Acknowledgments

It is a pleasure to acknowledge many helpful discussions with Dr. C. Willis and the comments on our paper by Dr. R. S. Dixon.

1. J. H. Baxendale and G. P. Gilbert. Discussions Faraday Soc. **36**, 186 (1963).
2. J. H. Baxendale and G. P. Gilbert. Science, **144**, 1571 (1965).
3. G. R. A. Johnson and M. Simic. Nature, **212**, 1570 (1966).
4. J. H. Baxendale and G. P. Gilbert. J. Am. Chem. Soc. **86**, 516 (1964).
5. K. M. Glover and P. Burrell. J. Nucl. Energy, **1**, 214 (1955).
6. A. W. Boyd and H. W. Connor. Can. J. Chem. **42**, 1418 (1964).
7. A. W. Boyd, H. W. Connor, and J. J. Pieroni. Chalk River Nucl. Lab. Report AECL-2203 (1965).
8. G. Long. At. Energy Res. Estab. G. Brit. Report, AERE C/M 345 (1958).
9. A. R. Anderson, B. Knight, and J. Winter. Nature, **201**, 1026 (1964).
10. F. S. Larkin and B. A. Thrush. Symp. Combust. 10th Univ. Cambridge, Cambridge, Engl. 1964.
11. F. S. Larkin and B. A. Thrush. Discussions Faraday Soc. **37**, 112 (1964).
12. J. Caldwell and R. A. Back. Trans. Faraday Soc. **61**, 1939 (1965).
13. M. Nicolet. Discussions Faraday Soc. **37**, 7 (1964).
14. F. Kaufman. Ann. Geophys. **20**, 106 (1964).
15. F. Kaufman and F. P. Del Greco. Symp. Combust. 9th Cornell Univ. Ithaca, N.Y. 1962. **659** (1963).
16. F. P. Del Greco and F. Kaufman. Discussions Faraday Soc. **33**, 128 (1962).
17. A. G. Harrison, J. J. Myher, and J. C. J. Thynne. Advan. Chem. Ser. **58**, 150 (1966).
18. H. F. Calcote. 26th Meeting of AGARD Propulsion and Energetics Panel, Pisa, Italy, Sept. 1965. In press.
19. H. F. Calcote and D. E. Jensen. Advan. Chem. Ser. **58**, 291 (1966).
20. B. deB. Darwent and R. Roberts. Discussions Faraday Soc. **14**, 55 (1953).
21. J. M. Warman. Private communication.
22. B. M. Mahan and C. E. Young. J. Chem. Phys. **44**, 2192 (1966).

Can. J. Chem. Downloaded from www.nrcresearchpress.com by 210.87.254.105 on 09/05/12
For personal use only.

Can. J. Chem. Downloaded from www.nrcresearchpress.com by 210.87.254.5 on 09/05/12
For personal use only.

Coordination complexes of gallium(III) and indium(III) halides. III.[1] Complexes of gallium(III) halides with 2,2′-bipyridyl

A. J. CARTY
Department of Chemistry, University of Waterloo, Waterloo, Ontario

Received June 27, 1968

The new complexes $GaCl_3(bipy)$, $GaBr_3(bipy)_2MeCN$, $GaBr_3(bipy)_2$, $GaI_3(bipy)$, and the related compounds $[GaCl_2(bipy)_2]BF_4$, $[GaCl_2(bipy)_2]PF_6$, $[GaBr_2(bipy)_2]PF_6$ (bipy = 2,2′-bipyridyl) have been prepared and characterized. Conductivity and far-infrared measurements suggest the structures $[GaCl_2(bipy)_2][GaCl_4]$, $[GaBr_2(bipy)_2]Br$, and $[GaI_2(bipy)_2][GaI_4]$ for the trihalide adducts.

Canadian Journal of Chemistry, 46, 3779 (1968)

Introduction

Although there is now a considerable amount of structural evidence, particularly from far-infrared studies, to demonstrate that 1:1 adducts of gallium(III) halides with amines, ethers, sulfides, (2) and phosphines (1, 3) have monomeric, C_{3v} structures in the solid state, relatively little work has been carried out on 1:2 or 1:3 adducts or on complexes with bidentate ligands. This is in marked contrast to the analogous indium(III) and thallium(III) halide systems where several recent studies (4–8) have confirmed the existence of five and six coordinate indium and thallium in coordination complexes. Beattie and co-workers (9) have recently completed a vibrational analysis of the compound $GaCl_3(NMe_3)_2$ and concluded that the molecule has a D_{3h} trigonal bipyramidal structure. We know of no other structural studies on gallium trihalide addition compounds of coordination number greater than four. The work reported in this paper is part of a program designed to investigate and structurally characterize gallium trihalide complexes of higher coordination number.

Experimental

All reagents and solvents were commercially available. Gallium trihalides (99.99% purity) were purchased from Fluka A. G., Buchs, Switzerland in sealed ampoules and were subsequently handled under anhydrous conditions in a dry box or vacuum line. Anhydrous solvents were used in all preparations.

Reaction of 2,2′-Bipyridyl with Gallium Trichloride

A solution of gallium trichloride (1.76 g, 0.01 mole) in acetonitrile (15 ml) was added to 2,2′-bipyridyl (4.68 g, 0.03 mole) in acetonitrile (20 ml). Colorless crystals formed immediately. Even after several recrystallizations from acetonitrile this product corresponded most closely to $Ga_3Cl_6(bipy)_4$. Thus for two typical analyses,

Found: (*i*) C, 45.79; H, 4.33; N, 9.93; Cl, 20.48. (*ii*) C, 46.37; H, 3.93; N, 10.18; Cl, 20.07. Calcd. for $Ga_3Cl_6(bipy)_4$: C, 45.90; H, 3.06; N, 10.70; Cl, 20.36.

Changing the mole ratio ligand:halide did not appear to affect the course of the reaction.

On dissolving this compound in a 1:1 mixture of acetone and acetonitrile and allowing it to crystallize slowly, large colorless plates of $GaCl_3(bipy)$ were obtained. These were washed with ether and dried in vacuo. The same product was obtained by reacting gallium trichloride and 2,2′-bipyridyl in acetone.

Reaction of 2,2′-Bipyridyl with Gallium Tribromide

Treatment of an acetonitrile solution of the tribromide with 2,2′-bipyridyl using 1:3 mole ratios yielded crystals of $GaBr_3(bipy)_2MeCN$, which were recrystallized from acetonitrile and dried in vacuo. The presence of one molecule of acetonitrile in this compound was demonstrated by analysis and by infrared spectroscopy, $\nu(C{\equiv}N)$ of the nitrile appearing as a weak absorption at 2240 cm^{-1}.

An analogous reaction in acetone gave $GaBr_3(bipy)_2$ as colorless needles.

Reaction of 2,2′-Bipyridyl with Gallium Triiodide

Addition of 2,2′-bipyridyl (2.34 g, 0.015 mole) in acetonitrile (20 ml) to gallium triiodide (2.25 g, 0.005 mole) in the same solvent (20 ml) produced bright yellow crystals of a complex which analyzed as $GaI_3(bipy)$ after repeated recrystallization from acetonitrile. On standing in solution for some time decomposition occurred giving red products of high iodine content and variable composition.

In acetone, the same reaction produced a bright yellow precipitate which could not be recrystallized from acetone owing to its insolubility. The material was washed thoroughly with boiling benzene and dried in vacuo. Analysis indicated the composition to be intermediate between $GaI_3(bipy)_2$ and $GaI_3(bipy)_3$. This product was not investigated further.

$[GaCl_2(bipy)_2]BF_4$, $[GaCl_2(bipy)_2]PF_6$, and $[GaBr_2(bipy)_2]PF_6$

These compounds were prepared by refluxing stoichiometric quantities of sodium tetrafluoroborate or potassium hexafluorophosphate with the appropriate complex in acetonitrile. The precipitated sodium or

[1]For part II, see ref. 1.

TABLE I
Analytical data

Compound	%C Found	%C Calcd.	%H Found	%H Calcd.	%N Found	%N Calcd.	%X Found	%X Calcd.
$GaCl_3$(bipy) from acetonitrile	36.45	36.14	2.28	2.40	8.30	8.43	32.00	32.07
$GaCl_3$(bipy) from acetone	36.23	36.14	2.55	2.40	8.53	8.43	32.04	32.07
$GaBr_3(bipy)_2MeCN$	39.77	39.85	2.87	2.87	10.41	10.33	36.13	36.18
$GaBr_3(bipy)_2$	39.43	38.64	2.83	2.59	7.87	9.01	38.45	38.56
GaI_3(bipy)	19.80	19.79	1.37	1.33	4.63	4.62	62.82	62.74
$[GaCl_2(bipy)_2]BF_4$	44.20	44.50	3.12	2.99	10.09	10.39		
$[GaCl_2(bipy)_2]PF_6$	40.34	40.17	2.83	2.70	9.27	9.37		
$[GaBr_2(bipy)_2]PF_6$	35.27	34.97	2.24	2.35	8.09	8.16		

potassium halide was filtered off, the solution reduced in volume and allowed to crystallize. Recrystallization from acetonitrile afforded the pure complexes as pale yellow prisms.

Microanalyses

These were carried out by Alfred Bernhardt, Mulheim, Germany, and A. Gygli, Toronto. Analytical data for the complexes are shown in Table I.

Physical Measurements

Conductivities were measured at 23° in nitromethane. Infrared spectra were recorded as Nujol mulls between cesium iodide or polyethylene plates using Perkin–Elmer 225 and Beckmann IR 12 spectrometers.

Results and Discussion

Few coordination complexes of gallium(III) halides with bidentate ligands have been described in the literature. 1,2-Bis(diphenylphosphino)-ethane yields complexes of the type $(GaX_3)_2$-(diphos) (X = Cl, Br, I) (10), and 'o' phenylene bisdimethylarsine gives GaX_3(diars) (X = Br, I) and $(GaCl_3)_2$(diars) (11) with the trihalides, but the only reports involving bidentate nitrogen donors concern the compounds $[Ga(phen)_3]X_3$ (X = Cl, Br) (phen = 1,10-phenanthroline) (12). Dwyer, however, mentions briefly that the species $Ga(bipy)_3^{3+}$ exists in aqueous solutions containing gallium(III) salts and 2,2′-bipyridyl (unpublished observations, see ref. 13).

The present work shows that in nonaqueous solution, 2,2′-bipyridyl reacts with gallium(III) halides to yield the compounds $GaCl_3$(bipy), $GaBr_3(bipy)_2MeCN$, $GaBr_3(bipy)_2$, and GaI_3-(bipy). However, several features of the experimental work suggest that the reactions are complex in acetonitrile. The isolation of a compound analyzing as $Ga_3Cl_6(bipy)_4$ and the necessity for extensive recrystallization of the initial reaction products clearly testify to this. By contrast, in the analogous indium(III) system, the pure crystalline compounds $InX_3(bipy)_{1.5}$ are readily isolated from acetonitrile or ethanol (6, 14). This difference in behavior may be ascribed in part to the fact that gallium(III) chloride forms a well defined adduct with acetonitrile (15) whereas indium(III) chloride can be recovered unchanged from this solvent (16). It thus seems probable that in the systems GaX_3/MeCN/2,2′-bipyridyl there are several competing equilibria of the type

$$GaX_3(MeCN)_x + y(bipy) \rightleftarrows GaX_3(bipy)_y(MeCN)_{x-2y} + (MeCN)_{2y}$$
$$\updownarrow$$
$$GaX_3(bipy)_y + (MeCN)_{x-2y}$$

in solution. The compound crystallizing from solution will then depend on whether acetonitrile is completely or partly replaced from the gallium coordination sphere by 2,2′-bipyridyl and on the relative solubilities of the various complexes. In the weaker donor solvent acetone, the equilibria must lie well to the right since the pure adducts separate from solution. The absence of a stoichiometric adduct of gallium(III) iodide with 2,2′-bipyridyl in acetone is probably due to the precipitation of two different species $GaI_3(bipy)_y$ of similar solubility.

TABLE II
Molar conductivities in nitromethane at 23° and 10^{-3} *M*

Compound	Λ_M (ohm^{-1} cm^2 mole^{-1})
$GaCl_3$(bipy) from acetonitrile	39.35
$GaCl_3$(bipy) from acetone	42.29
$GaBr_3(bipy)_2MeCN$	79.82
$GaBr_3(bipy)_2$	77.85
GaI_3(bipy)	75.04
$[GaCl_2(bipy)_2]BF_4$	91.56
$[GaCl_2(bipy)_2]PF_6$	89.02
$[GaBr_2(bipy)_2]PF_6$	81.23

Can. J. Chem. Downloaded from www.nrcresearchpress.com by 210.87.254.5 on 09/05/12
For personal use only.

TABLE III

Far-infrared spectra (400–200 cm^{-1}) of gallium complexes*

Compound	ν* (cm^{-1})				
$GaCl_3$(bipy) from acetonitrile		374 (20)	305 (17)	273 (13)	251 (8)
$GaCl_3$(bipy) from acetone	373 (20)	306 (19)	268 (13)	254 (10)	
$[GaCl_2(bipy)_2]BF_4$	301 (20)	268 (16)	250 (10)		
$[GaCl_2(bipy)_2]PF_6$	304 (20)	270 (17)	252 (13)		
$GaBr_3(bipy)_2MeCN$	280 (20)	262 (8)	250 (17)	234 (10)	225 (11)
	220 (10)	206 (16)			
$GaBr_3(bipy)_2$	277 (17)	264 (15)	256 (14)	236 (16)	220 (20)
	208 (18)				
$[GaBr_2(bipy)_2]PF_6$	275 (20)	254 (17)	234 (20)	220 (18)	209 (18)
GaI_3(bipy)	272 (14)	250 (10)	224 (20)		

*Figures in brackets refer to the intensities of the bands. The strongest band in each spectrum is assigned an arbitrary intensity of 20 and other intensities measured relative to this.

Conductivities

Molar conductivities, calculated on the basis of a monomeric formulation are given in Table II. Typical values for 1:1 electrolytes in nitromethane are 80–120 ohm^{-1} cm^2. The results suggest an ionic dimer structure $[GaCl_2(bipy)_2][GaCl_4]$ for $GaCl_3$(bipy), an ionic monomer formulation $[GaBr_2(bipy)_2]Br$ for $GaBr_3(bipy)_2$, and for GaI_3(bipy) the structure $[GaI_2(bipy)]I$. The ionic tetrafluoroborate and hexafluorophosphate complexes all show Λ_M values at 10^{-3} *M* typical of 1:1 electrolytes.

Infrared Spectra

In the region 1700–650 cm^{-1} the spectra of the complexes are typical of the coordinated ligand (17). In particular, the out of plane ring hydrogen vibration at 756 cm^{-1} in the ligand is split into two strong bands in the complexes, one at ca. 730 cm^{-1} and the other at ca. 770 cm^{-1}. For $[GaCl_2(bipy)_2]BF_4$, $\nu_3(t_2)$ of the tetrahedral anion occurs at 1060 cm^{-1}, and for $[GaX_2(bipy)_2]PF_6$ (X = Cl, Br), $\nu_3(t_{1u})$ appears as a strong symmetrical band at 844 cm^{-1}.

2,2′-Bipyridyl has four absorption bands between 660 cm^{-1} and 400 cm^{-1} (5, 18, 19). The medium intensity band at 620 cm^{-1} moves 15–25 cm^{-1} to higher frequency on complexing and the 403 cm^{-1} band is resolved into two or three components in the complexes. Similar changes have been noted previously (5, 18, 19). A strong band at 560 cm^{-1} with shoulders at 540 and 546 cm^{-1} is presumably $\nu_4(t_{1u})$ of PF_6^- in $[GaX_2(bipy)_2]PF_6$ and $\nu_4(t_2)$ of BF_4^- in $[GaCl_2(bipy)_2]BF_4$ is at 541 cm^{-1}.

The ligand spectrum is free from absorption between 400–200 cm^{-1}. Bands occurring in this region are therefore due to metal–ligand skeletal stretching vibrations, although as Clark and Williams have recently pointed out (20) the possibility of the appearance of ligand vibrations activated by the crystal field cannot be entirely ruled out. In the absence of significant coupling the skeletal vibrations might be conveniently labelled metal–halogen or metal–nitrogen stretching modes. Before attempting to interpret the spectra, possible structures for the complexes must be considered. For a molecule of the type GaX_3(bipy) the most probable structures are **1**–**4**. For $GaBr_3(bipy)_2$ on the other hand the most obvious structure **5** may have a *cis* or *trans* octahedral cation. To a very low approximation the skeletal stretching modes can be considered in terms of symmetry coordinates. The number and types of metal–halogen ν(Ga—X) and metal nitrogen ν(Ga—N) stretching modes derived in this way are given in Table IV.

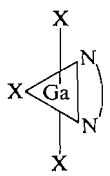

1

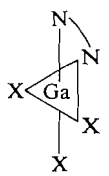

2

$[GaX_2(bipy)_2][GaX_4]$

3

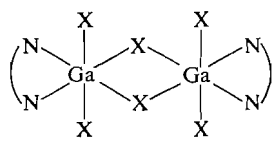

4

$[GaX_2(bipy)_2]X$

5

Can. J. Chem. Downloaded from www.nrcresearchpress.com by 210.87.254.5 on 09/05/12
For personal use only.

Can. J. Chem. Downloaded from www.nrcresearchpress.com by 210.87.254.5 on 09/05/12
For personal use only.

The far infrared spectrum of $GaCl_3(bipy)$ prepared from acetonitrile is identical with that from acetone and is characterized by two very strong bands at 306 and 373 cm^{-1}, a medium intensity band at 268 cm^{-1}, and a weak absorption at 254 cm^{-1} (Table III). The 306 and 373 cm^{-1} features must arise from ν(Ga—Cl) since they disappear in the bromide and iodide spectra (Fig. 1) but the two remaining bands are present in both $GaBr_3(bipy)_2$ and $GaI_3(bipy)$ thus suggesting that they are associated with metal–nitrogen stretching. On this basis it is unlikely that the halogen-bridged dimeric structure **4** is correct since two bridging ν(Ga—Cl) modes ($b_{2u} + b_{3u}$) and two terminal ν(Ga—Cl) modes ($b_{1u} + b_{3u}$) are predicted. By analogy with Ga_2Cl_6 (21) where the bridging modes ν_{17} and ν_{13} occur at 287 and 305 cm^{-1} and the terminal stretches ν_8 and ν_{16} at 453 and 389 cm^{-1} in the solid, four readily distinguishable bands are expected.

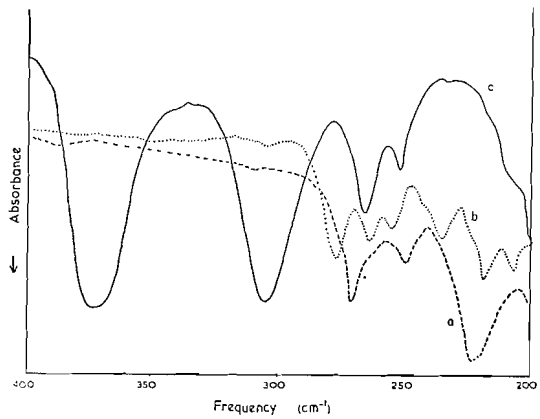

FIG. 1. Far-infrared spectra (400–200 cm^{-1}) of (*a*) $GaI_3(bipy)$, (*b*) $GaBr_3(bipy)_2$, (*c*) $GaCl_3(bipy)$.

The spectrum is most consistent with structure **3** in which the cation has a *trans* geometry. Thus two ν(Ga—Cl) modes are predicted, one (b_{1u}) from the cation and the other (t_2) from the anion $GaCl_4^-$. Moreover the t_2 ν(Ga—Cl) mode occurs at 372 cm^{-1} in $NMe_4[GaCl_4]$ and at 372 cm^{-1} in nitromethane solutions of several alkylammonium salts (22). We therefore assign the 373 cm^{-1} absorption as the t_2 mode of $GaCl_4^-$ and the 306 cm^{-1} absorption as the b_{1u} mode of a *trans* octahedral cation $[GaCl_2(bipy)_2]^+$. The two lower frequency features are then the expected ν(Ga—N) modes ($b_{2u} + b_{3u}$) of the cation. To confirm these assignments we have prepared the salts $[GaCl_2(bipy)_2]BF_4$ and $[GaCl_2(bipy)_2]PF_6$, and measured their far-infrared spectra. In both cases the spectra closely resemble that of $GaCl_3(bipy)$ except that the absorption due to the t_2 mode of the anion $GaCl_4^-$ is now missing (Fig. 2). Together with the Λ_M value, these results are excellent confirmation of the ionic dimer structure **3** for $GaCl_3(bipy)$. The assignments given above are the first reported ν(Ga—Cl) and ν(Ga—N) frequencies in an octahedral species.

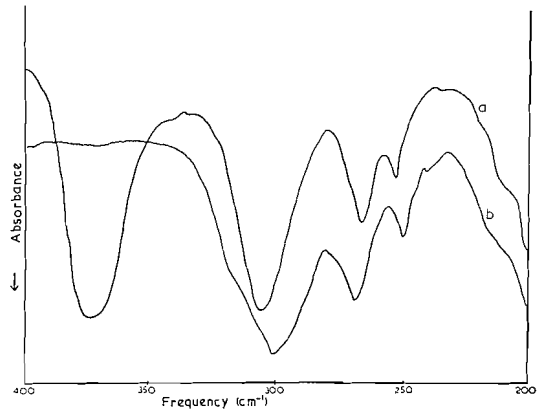

FIG. 2. Far-infrared spectra (400–200 cm^{-1}) of (*a*) $GaCl_3(bipy)$, (*b*) $[GaCl_2(bipy)_2]BF_4$.

For the bromide complex $GaBr_3(bipy)_2$ the most probable structure is $[GaBr_2(bipy)_2]Br$ in agreement with the observed 1:1 electrolyte behavior. The far-infrared spectrum however, is more complex than that of the chloride and six bands are readily distinguishable between 280 and 200 cm^{-1} (Fig. 1). Unfortunately, none of these can be unambiguously assigned as due to ν(Ga—Br) from their intensities alone but some idea of the expected position of ν(Ga—Br) can be obtained from the ratio ν(Ga—Br)/ν(Ga—Cl) ≈ 0.75 in octahedral complexes (23). Thus ν(Ga—Br) is expected at ca. 225 cm^{-1}. Comparison with the spectra of $GaCl_3(bipy)$ and $GaI_3(bipy)$ shows that the bands at ca. 275 and 250 cm^{-1} are present in all three spectra (Fig. 1), strongly suggesting that these are due to ν(Ga—N). Conversion to $[GaBr_2(bipy)_2]PF_6$ does not greatly affect the spectrum although a medium intensity band at 264 cm^{-1} is missing in the hexafluorophosphate salt and bands at 275, 245,

TABLE IV

Skeletal stretching modes for gallium complexes

Structure	Symmetry	ν(Ga—X)	ν(Ga—N)
GaX_3(bipy) Trigonal Bipyramidal	C_{2v}	$2a_1+b_1$	a_1+b_2
	C_s	$2a'+a''$	$a'+a''$
$[GaX_2(bipy)_2][GaX_4]$	Cation *cis* C_2	$a+b$	$2a+2b$
	Cation *trans* D_{2h}	b_{1u}	$b_{2u}+b_{3u}$
	Anion T_d	t_2	—
$Ga_2X_6(bipy)_2$	D_{2h}	$b_{2u}+b_{3u}$ (bridging) $b_{1u}+b_{3u}$ (terminal)	$b_{2u}+b_{3u}$

and 234 cm^{-1} are now more intense. We suggest in this case a *cis* cation. As shown in Table IV two ν(Ga—Br) $(a + b)$ modes and four ν(Ga—N) $(2a + 2b)$ modes are expected for C_2 symmetry, but it should be pointed out that since ν(Ga—Br) and ν(Ga—N) modes occur in the same spectral region, extensive coupling between modes of the same symmetry is expected. Labelling bands as ν(Ga—Br) or ν(Ga—N) may therefore be incorrect here. Nevertheless on the basis of frequency and intensity, the bands at 208 and 220 cm^{-1} may arise predominantly from gallium—bromine stretching. The spectrum of $GaBr_3(bipy)_2MeCN$ does not differ appreciably from that of $GaBr_3(bipy)_2$ in this region and the molecule of acetonitrile is probably present only as a molecule of solvation. Similar solvates have been reported in indium systems (6).

The infrared and conductivity data for GaI_3(bipy) are conflicting. A Λ_M value of 75.04 $ohm^{-1}\,cm^2$ is at the low end of the range expected for a 1:1 electrolyte and the structure $[Ga(bipy)I_2]I$ is suggested. Only three bands are distinguishable in the infrared at 272, 250, and 224 cm^{-1}. The 224 cm^{-1} absorption is very strong and remarkably similar in shape and intensity to the $\nu_3(t_2)$ mode of the GaI_4^- ion at 225 cm^{-1} in $Ph_3PMe[GaI_4]$ (1). Moreover the bands at higher frequency are present in $GaCl_3$(bipy) and $GaBr_3(bipy)_2$ and are characteristic of ν(Ga—N) of the cation $[GaX_2(bipy)_2]^+$. Also, ν(Ga—I) modes for a cation $[GaI_2(bipy)_2]^+$ are expected to be below 200 cm^{-1}, the limit of our instrumentation. Attempts to prepare a BF_4^- or PF_6^- salt in this case were unsuccessful; materials containing BF_4^- and PF_6^- could be obtained but microanalyses showed them to be mixtures. The infrared evidence although incomplete therefore favors $[GaI_2(bipy)_2][GaI_4]$. An explanation of the high molar conductivity may involve further dissociation of the complex $[GaI_2(bipy)_2][GaI_4]$ in nitromethane. Thus loss of one I^- ion from the cation would markedly increase the conductance of the solution. The instability of the cation in solution may also explain the difficulty experienced in preparing $[GaI_2(bipy)_2]BF_4$ and $[GaI_2(bipy)_2]PF_6$.

Acknowledgments

The author expresses his appreciation to Dr. J. M. W. Scott and Dr. E. Bullock of Memorial University of Newfoundland for the use of conductivity apparatus and a Perkin–Elmer 225 infrared spectrometer. Thanks are also due to Dr. A. Walker of Scarborough College, University of Toronto, for the use of the Beckmann IR 12 instrument. Continued support from the National Research Council of Canada is appreciated.

1. A. J. CARTY. Can. J. Chem. **45**, 3187 (1967).
2. N. N. GREENWOOD, T. S. SRIVASTAVA, and B. P. STRAUGHAN. J. Chem. Soc. A, 699 (1966).
3. A. BALLS, N. N. GREENWOOD, and B. P. STRAUGHAN. J. Chem. Soc. A, 753 (1968).
4. D. M. ADAMS, A. J. CARTY, P. CARTY, and D. G. TUCK. J. Chem. Soc. A, 162 (1968).
5. A. J. CARTY, S. J. PATEL, and D. G. TUCK. Can. J. Chem. (1968). In press.
6. R. A. WALTON. J. Chem. Soc. A, 1485 (1967).
7. R. A. WALTON. Inorg. Chem. **7**, 640 (1968).
8. M. J. TAYLOR. J. Chem. Soc. A, 1462 (1968).
9. I. R. BEATTIE, T. GILSON, and G. A. OZIN. J. Chem. Soc. A, 1092 (1968).
10. A. J. CARTY. Can. J. Chem. **45**, 345 (1967).
11. R. S. NYHOLM and K. ULM. J. Chem. Soc. 4199 (1965).
12. B. N. IVANOV-EMIN, L. A. NISELSON, YA. I. RABOVIK, and L. E. LARIONOVA. Russ. J. Inorg. Chem. English Transl. **5**, 583 (1961).
13. W. W. BRANDT, F. P. DWYER, and E. C. GYARFAS. Chem. Rev. **54**, 959 (1954).
14. A. J. CARTY and D. G. TUCK. J. Chem. Soc. A, 1081 (1966).

Can. J. Chem. Downloaded from www.nrcresearchpress.com by 210.87.254.5 on 09/05/12
For personal use only.

15. W. GERRARD, M. F. LAPPERT, and J. W. WALLIS. J. Chem. Soc. 2178 (1960).
16. B. F. G. JOHNSON and R. A. WALTON. Inorg. Chem. **5**, 49 (1966).
17. A. A. SCHILT and R. C. TAYLOR. J. Inorg. Nucl. Chem. **9**, 211 (1959).
18. R. J. H. CLARK. J. Chem. Soc. 1377 (1963).
19. J. R. FERRARO, L. J. BASILE, and D. L. KOVACIC. Inorg. Chem. **5**, 391 (1966).
20. R. J. H. CLARK and C. S. WILLIAMS. Spectrochim. Acta, **21**, 1861 (1965).
21. I. R. BEATTIE, T. GILSON, and P. COCKING. J. Chem. Soc. 702 (1967).
22. P. L. GOGGIN and T. G. BUICK. Chem. Commun. 290 (1967).
23. R. J. H. CLARK. Spectrochim. Acta, **21**, 955 (1965).

Can. J. Chem. Downloaded from www.nrcresearchpress.com by 210.87.254.5 on 09/05/12
For personal use only.

$H—N_3$ and $CH_3—N_3$ bond dissociation energies

MERVYN CHIANG[1] AND ROBERT WHEELER
Department of Chemistry, Queen's University, Kingston, Ontario
Received June 10, 1968

The thermal emission of negative azide ions from a heated filament operating in gases of both HN_3 and CH_3N_3 has been studied in a magnetron cell and the temperature variation of this current used to deduce the C—N bond dissociation energies in both molecules. Results indicate higher values than previous estimates. They are: $D_0(H—N_3) = 90 \pm 8$ kcal/mole and $D_0(CH_3—N_3) = 88 \pm 8$ kcal/mole at 0 °K.

Canadian Journal of Chemistry, 46, 3785 (1968)

Can. J. Chem. Downloaded from www.nrcresearchpress.com by 210.87.254.5 on 09/05/12
For personal use only.

Introduction

Thermal or photochemical decomposition of covalent azides occurs predominately through the breaking of $RN—N_2$ bonds (1, 2). In unimolecular dissociation this fission is favored even though spin conservation rules require decomposition to excited radicals, RN*. Bimolecular reaction between azide pairs would follow this path almost exclusively. The $RN—N_2$ bond is weak and the activation energy for a mechanism involving the fission of the complex at these bonds is probably extremely small. Heterogeneous dissociation is likely to proceed by the same N—N bond fission. Gaseous HN_3 striking a hot surface breaks into NH and N_2; slow decomposition to N_3 and H is very unlikely. Direct observation of the dissociation,

$$[1] \qquad RN_3 \xrightarrow{+D} R + N_3$$

is therefore difficult and the energy, D, is not available from spectroscopic data alone.

N_3 is not a stable radical. There is some evidence (3) for the production of N_3 in the photolysis of gaseous HN_3 but this is probably due to a secondary reaction of the imino radical NH with HN_3. In any event the concentrations produced are extremely small. In contrast, the ion N_3^- is quite stable; its existence in ionic salts and in various aqueous solutions attest to this. Direct measurement of the electron affinity, E, of the

$$[2] \qquad N_3 + e \xrightarrow{-E} N_3^-$$

azide radical is again difficult, if not impossible, because of the instability of the radical. There have been three indirect but independent methods thus far for estimating this energy (1, 2). Charge transfer spectra in solution yield two values. The ultraviolet peak at 2240 Å in the absorption of a sodium azide solution is interpreted as a transfer of an electron from N_3^- to the water molecule and this leads to a value of 67 ± 5 kcal/mole (4). Transfer of an electron from N_3^- to Fe(III) in ferric azide solutions with an absorption peak at 4600 Å suggests that E is as high as 73 ± 5 kcal/mole (5). Franklin, Dibeler, Reese, and Krauss (6) have carried out appearance potential measurements of the ionization and electron capture processes of HN_3 and CH_3N_3. They report a value for E at 72 kcal/mole. This includes an estimate of ΔH_f^0 for CH_3N_3 which is perhaps doubtful. Gray (2) has used their data, combining the appearance potentials of CH_3^+ and N_3^- with the ionization potential of CH_3 to place E at 69 ± 7 kcal/mole. Gray estimates the best average value from the three methods and places this at 70 ± 5 kcal/mole.

The value of D for reaction [1] has been calculated from fairly involved thermochemical cycles for a few covalent azides (1, 2, 5). This requires an estimate of $\Delta H_f^0(N_3)$, itself derived from the measured $E(N_3)$ and a calculated $\Delta H_f^0(N_3^-)$. A Born cycle using lattice energies of solid ionic azides appears to provide the most reliable calculation of $\Delta H_f^0(N_3^-)$. With a value of 105 kcal/mole estimated for $\Delta H_f^0(N_3)$, Evans, Yoffe, and Gray (1) report a value of $D = 85$ kcal/mole at 25 °C for the bond dissociation of $H—N_3$.

A more direct measurement of D might be obtained in the following way. Allowing that N_3^- is a much more stable entity than N_3, it should be possible to measure directly the energy required in the reaction

$$[3] \qquad RN_3 + e \xrightarrow{+D'} R + N_3^-$$

[1]Present address: Department of Chemistry, University of California, Berkeley, California, U.S.A.

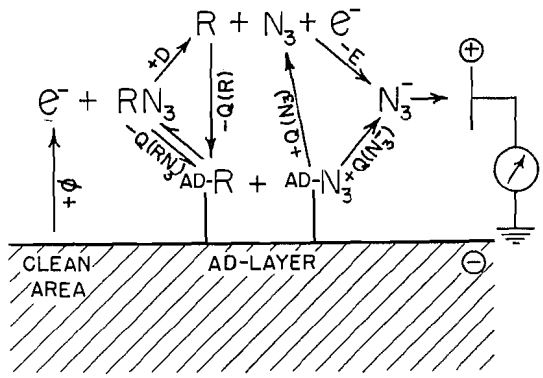

FIG. 1. Negative ion emission from a filament heated in a gas of RN_3.

Combining this with reactions [1] and [2] shows that $D = D' + E$. This in essence has been done in the ionization studies of HN_3 and CH_3N_3 by electron impact (6). However the abundance of N_3^- formed by resonance capture is small ($< 2.5\%$ of the total ion population) and moreover there is some concern that the particles possess excess kinetic energy. The data combined with $E = 70$ kcal/mole results in $D = 95$ kcal/mole for both the H—N_3 and CH_3—N_3 bond dissociations.

Figure 1 shows an alternative method for the same process; this is an application of Mayer's magnetron method for the measurement of electron affinities with Page's interpretation (7) of the events in the magnetron cell. Normally a gaseous azide striking a heated surface would break up via the weak RN—N_2 bond. In this case though, the surface is held at a negative potential and it acts as a ready source of electrons. The ions, N_3^-, have an excellent chance of forming by direct emission from the filament. The process assumed is this: a parent gas of RN_3 at low pressure sets up an adsorption–desorption equilibrium at the filament surface; desorption of N_3^- takes place from "patchy" adlayer areas which make up only a fractional coverage of the surface (this is assured by keeping the gas pressure of RN_3 low); these ions, as well as electrons emitted from "clean" surface areas are collected at a suitable positively charged electrode; the residue of ad-R remains adsorbed in a more or less mobile fractional layer. This mechanism is similar to reaction [3] with the exception that the fragment R remains adsorbed,

$$[4] \qquad RN_3 + e \xrightarrow{+D''} \text{ad-R} + N_3^-$$

From the various cycles it can be seen that it is equivalent to the sum of the following,

$$[1] \qquad RN_3 \xrightarrow{+D} R + N_3$$

$$[2] \qquad N_3 + e \xrightarrow{-E} N_3^-$$

$$[5] \qquad R \xrightarrow{-Q(R)} \text{ad-R}$$

with the condition

$$[6] \qquad D'' = D - Q(R) - E$$

E has already been discussed and is known to be 70 ± 5 kcal/mole. Q(R) at 0 °K is the binding energy of the adsorbed residue and data are available for a few simple molecules on metals, e.g. Q(H on W) = 75 kcal/mole (8), Q(CH_3 on W) = 47 kcal/mole (9). D'' can be determined by a measurement of the current ratios, electronic to ionic. This requires a separation of the two negative currents which can be effected by a deflection of the electrons in a weak magnetic field.

Experimental

The ionizing cell used in this study was a modified version of the elementary magnetron used in electron affinity and adsorption measurements (9). It was a glass vessel containing a heated tungsten wire filament, focusing and accelerating electrodes and an ion collector in linear array. The ion stream passed through the gap of an electromagnet. With the magnet turned off, the total negative current was collected at the anode and measured on a sensitive Keithly 610B electrometer calibrated by the maker. Switching on the electromagnet caused a deflection of the electrons off target and the negative ion current was determined. A conventional vacuum manifold system was employed to evacuate the magnetron and to allow the introduction of low pressures (10^{-3} Torr) of either HN_3 or CH_3N_3. These gas pressures, as measured on a Veeco cold cathode discharge gauge, were held constant during current measurements by cryoscopic traps or by a slow throughput of gas with a bleed to the backing pump. Current measurements were made at several filament temperatures usually starting at a region near 1450 °K and extending up to 1800 °K. These temperatures were determined at each current measurement first as brightness temperatures on a Leeds and Northrup optical pyrometer calibrated at the National Research Council, and later converted to true temperatures by an emissivity correction. The currents measured were recalculated as a ratio of electronic to negative ion currents i_e/i_1.

Page (7) has shown that this current ratio is given by the following expression under conditions whereby the adsorption–desorption processes of the parent RN_3 molecules are equilibrated at a fractional monolayer coverage of the filament,

Can. J. Chem. Downloaded from www.nrcresearchpress.com by 210.87.254.5 on 09/05/12
For personal use only.

Can. J. Chem. Downloaded from www.nrcresearchpress.com by 210.87.254.5 on 09/05/12
For personal use only.

$$[7] \quad i_e/i_i = \frac{CT^2}{P} \exp\{[-Q(RN_3) + Q(N_3^-) - \phi]/RT\}$$

P is the constant pressure of the gaseous RN_3, C is an emission constant, and ϕ is the normal electronic work function of the metal. From the cyclic relationships in Fig. 1, it is apparent that we can rewrite this in equivalent energy terms

$$[8] \quad i_e/i_i = \frac{CT^2}{P} \exp\{[D - Q(R) - E]/RT\}$$

$D'' = D - Q(R) - E$ was derived from the slope of a plot of $\log(i_e/i_i) - 2\log T$ against $1/T$.

Pure samples of HN_3 were prepared by the methods of Audrieth (10) while samples of CH_3N_3 were made by dropping dimethyl sulfate on an alkaline solution of sodium azide heated on a steam bath. These samples were dried over calcium chloride and redistilled for purification.

Results and Discussion

Figure 2 shows two representative plots, one for each gas. Both are quite linear over the temperature range studied. The slope of the HN_3 line corresponds to a value of $D'' = -64$ kcal/mole at an average $T = 1720$ °K, that of the CH_3N_3 line, -38 kcal/mole at an average $T = 1660$ °K. These energies can be recalculated to 0 °K using an assumed heat capacity change in reaction [4] of $-2R$ for HN_3 and $-2.5R$ for CH_3N_3. It is assumed in these calculations that the residual adlayer acts as a mobile two-dimensional gas held on the filament surface. Correction to 0 °K then leads to the values $D_0''(HN_3) = -57$ kcal/mole and $D_0''(CH_3N_3) = -30$ kcal/mole. The best average values of five HN_3 experiments and four CH_3N_3 experiments were $\langle D_0''(HN_3)\rangle = -55 \pm 3$ kcal/mole and $\langle D_0''(CH_3N_3)\rangle = -29 \pm 3$ kcal/mole.

Calculation of D for the H—N_3 and CH_3—N_3 bonds then follows with the insertion of $E(N_3) = 70$ kcal/mole, $Q(H \text{ on } W) = 75$ kcal/mole and $Q(CH_3 \text{ on } W) = 47$ kcal/mole in eq. [6]. The bond dissociation energies are $D_0(H—N_3) = 90 \pm 8$ kcal/mole and $D_0(CH_3—N_3) = 88 \pm 8$ kcal/mole at 0 °K.

Both of these results are higher than those in Gray's review. For H—$N_3 \rightarrow H + N_3$, ΔH (25 °C) $= 85 \pm 5$ kcal/mole is quoted. This value has been derived from an estimate of $\Delta H_f^0(N_3)$ requiring a fairly involved calculation from crystal lattice energies. The same review gives ΔH (25 °C) = 72 kcal/mole for the average bond dissociation energy of R—N_3 where R is an alkyl or substituted phenyl radical.

Calculated values of these two bond energies can be obtained by the empirical method of Neale (11) and Errede (12). The energy is written in terms of three factors,

$$[9] \quad D(X - Y) = \lambda\varepsilon(X)\varepsilon(Y)$$

the ε's being related to the electronegativities and ionization potentials of the two dissociated parts and λ is a constant determined by the type of bond formed. Using Neale's information, we derive $\varepsilon(H) = 1.32$, $\varepsilon(CH_3) = 1.08$, and $\varepsilon(N_3) = 0.91$. Also λ for the H—N_3 bond is assigned a value of 73 while that of CH_3—N_3, a value of 71, both in kcal/mole. These data calculate to $D(H—N_3) = 88$ and $D(CH_3—N_3) = 70$ kcal/mole. Agreement for HN_3 is good whereas our value for CH_3N_3 is much higher than this calculation which itself predicts a lower $D(CH_3—N_3)$ than Gray's average for the series.

Agreement of $D_0(H—N_3)$ is quite good and within the limits of error in these experiments. However, the high result for $D_0(CH_3—N_3)$ is perhaps surprising. At first sight, the similarity in the two measured values $D_0(H—N_3)$ and $D_0(CH_3—N_3)$ would lead one to suspect that we were in each case measuring an energy for a common dissociation mechanism. However, the slopes of the plots in Fig. 2 from which the D'' values are obtained are decidedly different. If

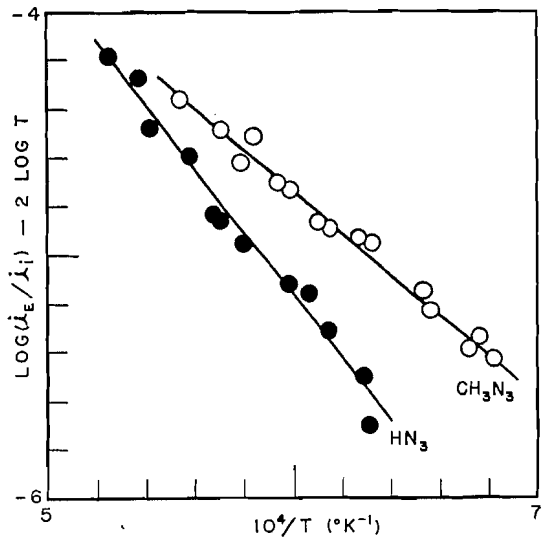

FIG. 2. Typical current ratio – inverse temperature plots for HN_3 and CH_3N_3.

$D_0(CH_3—N_3)$ is high, it must be because $Q(CH_3$ on W) is high or the negative CH_3N_3 slope is not steep enough. The former can only be true if CH_3N_3 in the magnetron cell produces different residues on the filament than CH_3NO_2, CH_3I, CH_3CH, and CH_3NH_2 (see ref. 8), or if it produces different negative ions than N_3^-. Whatever the final fate of the residual ad-CH_3, it is difficult to believe that it is any different here than in the other CH_3—X examples. Therefore some confidence can be placed in the value $Q(CH_3$ on W) = 47 kcal/mole used in this work.

The magnetron cell acts as a spectrometer with very low resolution. In its simplest form, it is only possible to distinguish electrons from heavy negative ions. The mass identity of the ion current is not established directly as a mass/charge ratio but diagnostically from the plausibility of the resulting energetic analysis. There are two facts to be considered here with regard to the nature of the ion emission. First in work with both HN_3 and CH_3N_3, considerable variation in the static pressure of the parent gas (100 times) does not alter the slope of the current ratio – temperature plots and hence the value of D'' is independent of pressure. Second, the electron affinities of all other species which might give rise to ions are known to be much lower than that of N_3 (13–15). Hence we can rule out NH_2^-, NH^-, N^-, CH_3^-, etc., as major contributors to the current. The only rational assumption then is that the emission in the CH_3N_3 work cannot be any different in nature from the experiments with HN_3 and moreover this emission is, in all probability, totally N_3^-.

The pertinent conclusion then is that $D_0(CH_3—N_3)$ is in fact greater than Gray's average and is just slightly less than $D_0(H—N_3)$. With $D_0(CH_3—N_3)$ placed at 88 ± 8 kcal/mole, the strength of the C—N bond in methyl azide is similar to that in methylamine (D = 80 to 91 kcal/mole (16)) and is much greater than the C—N strength in nitromethane (D = 54 kcal/mole (16)).

Acknowledgment

The authors are grateful to the National Research Council of Canada for a grant in support of this work.

1. B. L. Evans, A. D. Yoffe, and P. Gray. Chem. Rev. **59**, 515 (1959).
2. P. Gray. Quart. Rev. London, **17**, 446 (1963).
3. B. A. Thrush. Proc. Roy. Soc. London, Ser. A, **235**, 143 (1956).
4. A. Bonnemay and E. T. Verdier. Comp. Rend. **230**, 2300 (1950).
5. P. Gray and T. C. Waddington. Proc. Roy. Soc. London, Ser. A, **235**, 481 (1956).
6. J. L. Franklin, V. H. Dibeler, R. M. Reese, and M. Krauss. J. Am. Chem. Soc. **80**, 298 (1958).
7. F. M. Page. Trans. Faraday Soc. **56**, 1742 (1960); **59**, 1266 (1963).
8. G. Ehrlich. Trans. 8th Vacuum Symp. and 2nd Intern. Congr. Vol. 1. 1961. The Pergamon Press, Ltd., New York. 1962. p. 126.
9. B. Ritchie and R. Wheeler. J. Phys. Chem. **70**, 173 (1966).
10. L. F. Audrieth. Chem. Rev. **15**, 169 (1934).
11. R. S. Neale. J. Phys. Chem. **68**, 143 (1964).
12. L. A. Errede. J. Phys. Chem. **64**, 1031 (1960).
13. F. M. Page. Trans. Faraday Soc. **57**, 1254 (1961).
14. H. O. Pritchard. Chem. Rev. **52**, 529 (1953).
15. F. M. Page. Symp. Combust. 8th. Pasadena, Calif. (1960). The Williams and Wilkins Co., Baltimore, Maryland. 1962. p. 160.
16. T. L. Cottrell. The strengths of chemical bonds. 2nd ed. Butterworth and Co., London. 1958.

Can. J. Chem. Downloaded from www.nrcresearchpress.com by 210.87.254.5 on 09/05/12
For personal use only.

Can. J. Chem. Downloaded from www.nrcresearchpress.com by 210.87.254.6 on 09/05/12
For personal use only.

Photolysis of HBr at 77 °K

W. E. Falconer and W. A. Sunder
Bell Telephone Laboratories, Incorporated, Murray Hill, New Jersey

Received June 21, 1968

The photolysis of HBr has been studied at 77 °K. The photodecomposition of solid state HBr is an inefficient process which is strongly inhibited by a reaction product, probably Br atoms, or by added Br_2 or *trans*-butene-2. The results suggest H_2 is formed by abstraction from HBr by thermal H atoms, the activation energy for the abstraction being ~350 cal mole^{-1}. The photolysis of both pure HBr and HBr with added Br_2 or *trans*-butene-2 can be described by an absorber complex mechanism similar to that inferred by Hughes and Purnell in the photolysis of HI. The absorption tail of solid HBr extends beyond the gas phase absorption into the wavelength region in which trapped radicals are generated in HBr–olefin mixtures but where there is no H_2 evolution. The solid state absorption spectrum of Br_2 is contrasted with that of gaseous Br_2; an absorption peak is observed at 2725 Å which may be associated with $(Br_2)_n$ aglomerates.

Canadian Journal of Chemistry, 46, 3789 (1968)

Introduction

The photolysis of hydrogen halides at cryogenic temperatures has proved a convenient source of hydrogen atoms for reactions in solid matrices (1–9), complementing the gas–solid technique of Klein and Scheer (see ref. 10 and earlier references quoted therein). Frequently the investigations have been directed toward the spectroscopic study of selected products, and overall photochemical mechanisms have been of secondary interest. Hydrogen iodide has most often been used, presumably because of the increased quantum yield associated with a higher probability of H atoms with excess kinetic energy escaping the cage in which they are formed. Recently Hughes and Purnell (1) reported on the photolysis of HI in reactive matrices at 77 °K, emphasizing the mechanisms leading to the observed products.

A need exists for an improved understanding of the low temperature hydrogen bromide photolysis as it relates to the more extensively studied HI systems, to radiolysis of HBr in solid matrices (11), and to the controversy (3, 12, 13) over the identity of radicals whose electron spin resonance (e.s.r.) spectra were observed by Abell and Piette (12). The present paper bears on this understanding.

Experimental

Materials used were: *trans*-butene-2, Phillips research grade, stated purity 99.81%; Br_2, Baker analyzed reagent, stated purity 99.8%; HBr, Matheson, stated purity 99.8%; DBr, Merck, Sharp, and Dohme of Canada.

All were degassed and vacuum distilled prior to use. Infrared analysis showed traces of HCl as a contaminant in HBr. The isotopic composition of DBr was determined to be 97 atom % D by reacting aliquots with zinc pellets and analyzing the noncondensable gases by gas chromatography (see below) and by mass spectroscopy. The photodecomposition of this same DBr as a thin film at 77 °K confirmed this deuterium content.

Absorption spectra of solid films of HBr, Br_2, *trans*-butene-2, and various mixtures were determined between 1900 and 7000 Å with a Cary 14 spectrophotometer. Samples were sprayed in vacuum onto a lithium fluoride plate mounted in a copper frame connected to a cold finger cooled with liquid nitrogen. A small heater was also connected to the frame to anneal the deposited films and thus reduce strains and light scattering. For comparison, gas phase absorption spectra of the pure materials were also obtained on this same instrument.

The cell and Dewar arrangement in Fig. 1 was used for photolysis at 77 °K. Cell volume was 160 cm^3; internal diameter, 4.2 cm. Prior to irradiation, the required amounts of HBr, DBr, or *trans*-butene-2 were measured

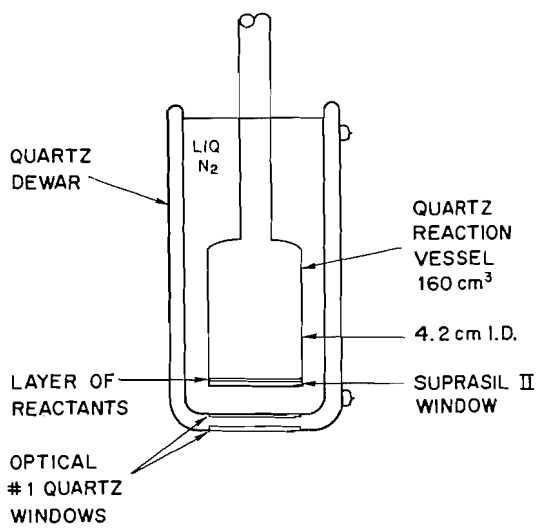

FIG. 1. Cryogenic photolysis apparatus.

Can. J. Chem. Downloaded from www.nrcresearchpress.com by 210.87.254.6 on 09/05/12
For personal use only.

manometrically in the cell itself, and then condensed into connected storage or mixing volumes. Br_2 pressures on the same volume were estimated by thermostatting a reservoir of liquid Br_2 in melting slushes of water (0 °C, P_{Br_2} = 67 Torr), carbon tetrachloride (−22.9°, 13 Torr), ethylene dichloride (−35.9°, 5.5 Torr), chlorobenzene (−45.5°, 2 Torr), 1-bromooctane (−55°, 0.7 Torr), chloroform (−63.8°, 0.22 Torr), 2-chloroethanol (−66.1°, 0.15 Torr), or ethylacetate (−83.9°, 0.015 Torr). Films of varying thickness and composition were deposited on the cell window. Assuming the density of HBr to be 2.81 g cm^{-3} and a uniform film on the cell window with no material on the cell walls, 100 Torr of HBr in the cell volume corresponds to a layer thickness of $\sim 1.8 \times 10^{-3}$ cm.

The technique for film deposition was found to be somewhat critical if nonuniformity or fissures were to be avoided and wall coating was to be minimized. The cell window was immersed 1–2 mm in liquid nitrogen for 60 s. A stopcock connecting the precooled cell with the premixed gas sample was cracked open until interference fringes began to develop on the window, and the sample was allowed to flow into the cell at this rate. The bulk of the sample condensed in 20–30 s, after which the stopcock was fully opened, and the cell was then immersed completely in liquid nitrogen. Good vacua ($\sim 10^{-6}$ Torr) were essential for satisfactory films. With system pressures of $\sim 10^{-5}$ Torr prior to deposition, the film would generally flake off the window during the photolysis. The deposited films were not annealed.

Distance from the cell window to the inner Dewar window was kept constant throughout the investigation. However, trial experiments demonstrated that increasing the thickness of the liquid nitrogen layer from ~0.5 to 1.5 in. caused negligible attenuation of the incident radiation.

Three light sources were used for irradiation: a Hanovia SH, medium pressure mercury arc, type 30 620; a Hanovia "Lo", low pressure mercury arc source, type 735 A-7 (the actinic radiation from this source was the 2537 Å mercury resonance line); and a Bausch and Lomb high intensity grating monochromator, with a 200 W Osram L-1 super-pressure mercury arc source and Reichoff d.c. power supply. The grating used was blazed at 2200 Å with a dispersion of 74 Å mm^{-1}. With the 3 mm exit slit used, the band passed was ~220 Å.

Products not condensable at 77 °K were collected with a Toepler pump, pumping in series with a small mercury diffusion pump through two traps packed with glass beads and immersed in liquid nitrogen. Gases were measured in a gas burette, usually after evaporating the irradiated film, but frequently both before and after. Samples could subsequently be taken for mass spectroscopic analysis, or in the case of DBr photolyses, the collected gases were injected directly into a gas chromatograph.

H_2, HD, and D_2 were separated at 77 °K by a 12 ft × 0.125 in. o.d. stainless steel column packed with 80/90 mesh activated alumina treated with ferric chloride according to the method of Shipman (14). The carrier gas was helium with a volume flow rate, measured at room temperature, of 130 cm^3 min^{-1}. After emerging from the column, the effluent hydrogen isotopes were oxidized to water by an 8 in. × 0.5 in. o.d. copper oxide furnace at ~565 °C. The resulting water was monitored by a thermal conductivity detector with type WX filaments, and the peak areas were integrated with a Varian model 475 digital integrator.

Results

Absorption Spectra

For solid *trans*-butene-2, only the absorption edge could be seen at wavelengths longer than 1900 Å. Very slight attenuation of the beam was observed between 3500 Å and 2050 Å, perhaps due to a long wavelength absorption tail, but more likely caused by beam scattering. At 2050 Å the optical density began to rise sharply, as would be expected from the gas phase absorption spectra (15).

The gas phase absorption of pure HBr agreed with published spectra (16); no significant absorption was observed at wavelengths above 2650–2700 Å. However, the solid phase absorption of pure HBr extended to 3600 Å, with a weak tail to ~4000 Å for films of undefined thickness but for which the optical density was about unity at 2050 Å. The absorption edge for a 1:1 mixture of HBr and *trans*-butene-2 was similar to that for HBr alone, but with less intense absorption in the 3000–3600 Å region, and no absorption beyond 3600 Å. These differences could be due in part to greater scattering from pure HBr films, as some difficulty was experienced in depositing films of HBr with no beam attenuation in the visible region. Annealing did not improve the relative transmission in the visible, nor did it sharpen the absorption bands for HBr, *trans*-butene-2, or Br_2. Mixtures were not annealed to prevent introducing uncertainties in their composition. Neither for pure HBr, pure *trans*-butene-2, nor for the 1:1 mixture were any additional absorption features observed below 7000 Å.

The features of the gas phase spectrum of Br_2, shown in Fig. 2*a*, are in agreement with published results (17, 18). In curve A, the high frequency part of the visible continuum is presumably due to the transition $^1\Pi_u \leftarrow {}^1\Sigma_g^+$, in which the $^1\Pi_u$ is an entirely repulsive state. The second feature in the visible absorption can be ascribed to the transition $^3\Pi_{0u^+} \leftarrow {}^1\Sigma_g^+$, with a long wavelength banded region which converges with an adjoining continuum at 5110 Å. The absorption at 2100 Å, curve B, coincides with that ascribed by Ogryzlo and Sanctuary (18) to the $(Br_2)_2$ double molecule. The pressure is comparable to that in their Fig. 1.

Can. J. Chem. Downloaded from www.nrcresearchpress.com by 210.87.254.6 on 09/05/12
For personal use only.

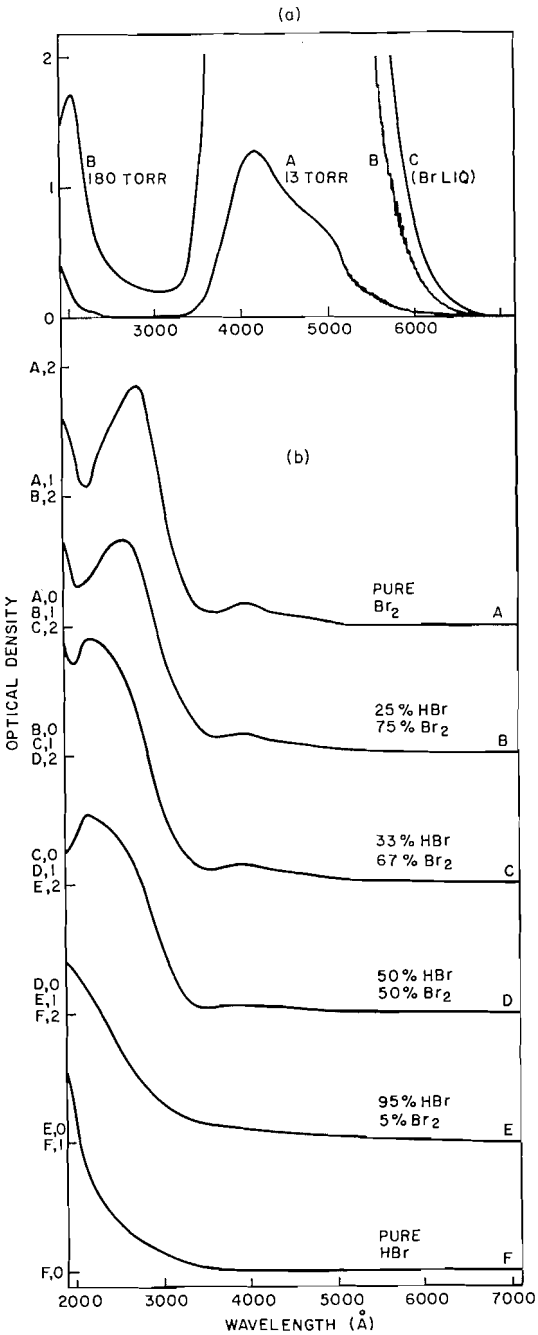

FIG. 2. Absorption spectra of Br_2 and Br_2–HBr mixtures. (*a*) Pure Br_2, gas and liquid phases: (A) 13 Torr gas, 10 cm path; (B) 180 Torr gas, 10 cm path; (C) liquid, 0.5 mm path. (*b*) Solid phase spectra: (A) pure Br_2; (B) 0.75 Br_2, 0.25 HBr; (C) 0.67 Br_2, 0.33 HBr; (D) 0.50 Br_2, 0.50 HBr; (E) 0.05 Br_2, 0.95 HBr; (F) pure HBr.

Also shown in Fig. 2*a* is an absorption edge for liquid Br_2, curve C. With the 0.5 mm path length used, the optical density was at all times greater than 2 below 5900 Å.

The spectrum of solid Br_2, Fig. 2*b*, is quite different from that of the gas. Two features observable in the visible are quite weak. If these correlate with the two transitions in the gas phase, they are shifted towards shorter wavelengths. A stronger two-component absorption with one maximum at 2725 Å and one at a shorter wavelength is apparent; this may be due to the associated Br_2 molecules, $(Br_2)_n$, such as are observed by X-ray diffraction in solid halogens. Clustering of Br_2 in organic matrices at 77 °K has been inferred from kinetic behavior by Iyer and Willard (19), who found that the clustering was reduced by complexing the Br_2 with additives such as alkyl halides at a concentration comparable to that of the Br_2.

When solid Br_2 was diluted with HBr, no new absorption peaks could be identified. The addition of HBr shifted the near ultraviolet (u.v.) absorption to shorter wavelengths, as can be seen by comparing the spectra in Fig. 2*b*. The most rapid change is when Br_2:HBr ratios are about 3:1 to 2:1. This shift may be associated with shortening of $(Br_2)_n$ chains, approaching the gas phase peak of $(Br_2)_2$ at 2100 Å. The film thicknesses in these traces are undoubtedly different; gas mixture was sprayed onto the LiF window until optical densities of 1.5–2.0 were attained for the absorption peak. The weak visible absorptions persist into the HBr-rich mixtures. In films which are predominately HBr, e.g., 5% Br_2 as shown in Fig. 2*b*, curve E, no structure is observed, but the absorption tail reaches into the visible beyond 5000 Å. As the Br_2 content of the film is further reduced, the spectrum approaches that of HBr alone, with a continuing decrease of the enhanced absorption tail. A contribution to the near u.v. absorption by an addition species, HBr_3 or $HBr{\cdot}Br_2$, cannot be ruled out, but no characteristic peaks are observed in the 3000–4000 Å region.

Photolysis of Pure HBr

Experiments in which the layer thickness of HBr was varied, using the SH light source unfiltered, showed that the actinic radiation incident on the cell was largely absorbed in a layer $\leqslant 2 \times 10^{-4}$ cm thick. Irradiation of this film for

Can. J. Chem. Downloaded from www.nrcresearchpress.com by 210.87.254.6 on 09/05/12
For personal use only.

3 h yielded 3.5 μmole of H_2. Increasing the layer thickness 70-fold to 1.4×10^{-2} cm increased the H_2 yield less than a factor of two to ~6 μmoles. The increase was approximately linear over this range. With the monochromator light source, this secondary increase in evolved H_2 with layer thickness was less pronounced, probably because wavelengths longer than 2660 Å were excluded.

No hydrogen was detected when Corning 0–53 or 1–69 filters with cutoffs at ~2800 Å were used in conjunction with the SH mercury source, even when layers of HBr 0.3 cm thick were irradiated extensively.

In Fig. 3, H_2 yields are plotted as a function of time of irradiation with the monochromator output centered at 2540 Å. These yields have been corrected for the steady degeneration of the L-1 lamps used in the monochromator light source, ~2% h^{-1}. Film thickness is constant, 3.6×10^{-3} cm. Based on uniform reaction throughout the film, ~0.25% of the HBr is photodecomposed with 65 h irradiation, corresponding to 0.5% consumption of HBr. However, 70% of the reaction occurs in the first 2×10^{-4} cm of the film, which in 65 h is 6.3% converted into products. The remaining bulk of the layer is ~0.15% converted. Figure 4 shows similar data obtained with the more intense, but less monochromatic, SH lamp source. Estimated initial slopes are shown in Figs. 3 and 4. Supporting data (not shown) have also been obtained with the mercury "Lo" light emitting at 2537 Å.

Approximate quantum yields were determined from the initial rates of H_2 generation. Incident

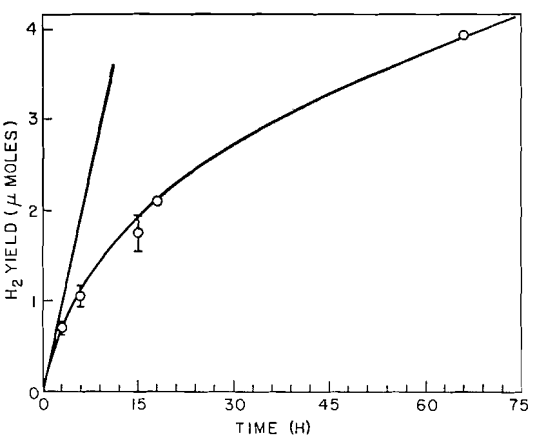

FIG. 3. H_2 yields vs time of photolysis for pure HBr using monochromator centered at 2540 Å as light source.

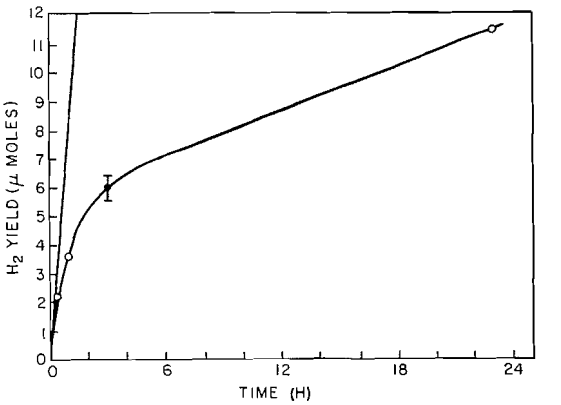

FIG. 4. H_2 yield vs time of photolysis for pure HBr using unfiltered SH lamp as light source.

fluxes, estimated from specifications provided by the manufacturers of the various light sources, were: SH lamp, 10^{17} quanta s^{-1}; mercury "Lo" lamp, 10^{16} quanta s^{-1}; and Bausch and Lomb monochromator centered at 2540 Å, 10^{16} quanta s^{-1}. The corresponding quantum yields, subject to considerable uncertainty, were respectively 1.3×10^{-2}, 4.6×10^{-3}, and 4.4×10^{-3}.

Photolysis of HBr with Added Br_2

The effect of added Br_2 on H_2 yields is shown in Fig. 5 for unfiltered SH and for monochromator 2540 Å irradiation. Despite careful mixing in the gas phase, Br_2 may not be dispersed uniformly throughout the HBr matrix, but may be present in aglomerates (19). Nevertheless, small quantities effectively suppress H_2 production in the photolysis. The absorption of actinic radiation by Br_2 when <1% is present should be small. Therefore, at this Br_2 level, the suppression in H_2 yield should not be due to the decrease in light entering the reactive system. Further attenuation by higher amounts of added Br_2 is in accord with competitive absorption by Br_2, with subsequent dissipation of energy without the generation of H_2.

For the unfiltered SH lamp, photolysis is principally in the first 2×10^{-4} cm of HBr, in which there are 5.2×10^{19} molecules of HBr and at 0.5% added Br_2, 2.6×10^{17} molecules of Br_2. With no additives, a total of 2.9×10^{18} molecules of H_2 would be generated in 2 h, corresponding to ~2×10^{18} molecules of H_2 in this primary reaction layer. This yield is reduced 20%, or ~4×10^{17} molecules, by 0.5% of added Br_2. This is equivalent to each Br_2 scavenging 1.5 H

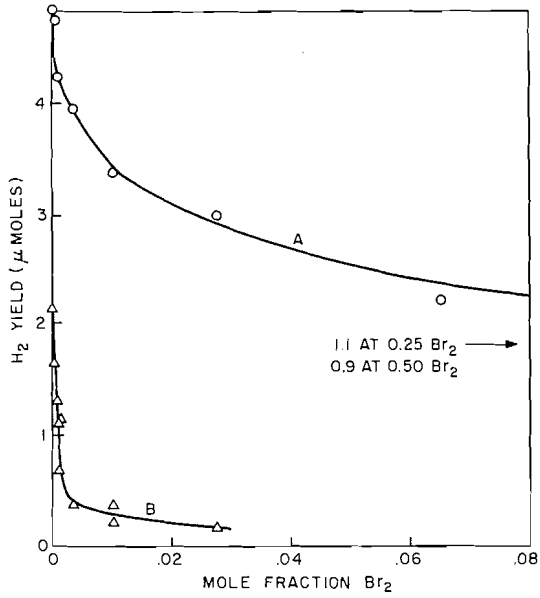

FIG. 5. H_2 yield vs concentration of added Br_2. Light sources: (A) unfiltered SH lamp, 2 h exposure, [HBr] = 200 Torr, (B) monochromator at 2540 Å, 18 h exposure, [HBr] = 200 Torr.

atoms, or each added Br atom scavenging almost one.

For 2540 Å monochromator irradiation, 1.3×10^{18} molecules of H_2 are produced overall in 18 h. If, analogously to the SH irradiation, 70% of reaction occurs in a region containing 5×10^{19} molecules of HBr, then 9×10^{17} molecules of H_2 will form in this layer in 18 h. Since H_2 yields are 80% suppressed by 0.25% or 1.3×10^{17} molecules of Br_2, each Br_2 molecule suppresses ~6 molecules of H_2 product. However, the rate of reaction is more than an order of magnitude lower when irradiation is with the less intense monochromator source.

Yields of H_2 were unaffected when a layer of Br_2 was deposited on top of a 2×10^{-3} cm layer of HBr. When a Br_2 layer was deposited below the HBr film, i.e. between the light source and the HBr, suppression of H_2 was virtually complete.

In an attempt to seed the HBr matrix with Br atoms prior to HBr photolysis, rather than or in addition to Br_2 molecules, mixtures of 0.1% Br_2 in HBr were pre-irradiated for several hours at 4025 Å at which wavelength solid Br_2 has a weak absorption but HBr is transparent. (Wavelengths below 6880 Å are sufficiently energetic to overcome the bond dissociation energy (20) of Br_2, D(Br—Br) = 45.46 kcal mole^{-1}.) For this mixture and 2540 Å monochromator irradiation, H_2 yields are suppressed ~50% by the added Br_2. No enhancement in this suppression was induced by the pre-irradiation.

Photolysis of HBr with Added Trans-butene-2

Trans-butene-2 absorbs radiation at 1942, 1973, and 2003 Å which was emitted by the SH arc and transmitted through ~10 cm of air. The resulting photodecomposition to yield H_2 and some methane was not detectable if a CS 9–54 filter with a 2300 Å cutoff was used with the SH lamp, or if irradiation was with the monochromator centered at 2540 Å.

Qualitatively, when *trans*-butene-2–HBr mixtures were irradiated with the full SH arc for 3 h, H_2 yields were suppressed by a factor of three for an equimolar mixture compared with pure HBr, but additional increases in olefin concentration had relatively little effect. When a layer of *trans*-butene-2 was deposited on top of a layer of HBr, the photolytic yield of H_2 was unaffected, whereas if the *trans*-butene-2 was below the HBr, the yield was reduced ~50%. These data obtained with the full SH arc were not corrected for the photolysis of olefin because of lack of understanding of this process, but part of the H_2 and all of the methane is undoubtedly formed by direct olefin photolysis. In similar photolyses with the monochromator light source, an eightfold decrease in H_2 yield could be obtained by addition of *trans*-butene-2.

In contrast to the absence of H_2 when pure HBr was photolyzed using 0–53 or 1–69 filters, intense e.s.r. spectra could be induced by brief irradiation of HBr–olefin mixtures using 1–69 filters, as was found previously by Abell and Piette (12). However, it must be remembered that the spin resonance technique is ~10^3 more sensitive than that of conventional gas analysis.

Little diffusion of H_2 to the gas volume above the film was observed, either for pure HBr, HBr–Br_2 mixtures, or HBr–*trans*-butene-2 mixtures. Even at *trans*-butene-2 to HBr ratios of 3:1, only ~10% of the collected H_2 was in the gas volume at the end of a 3 h photolysis. This apparent conflict with the observations of Hughes and Purnell (1) undoubtedly is due to differences in thickness of films used in the two sets of experiments; that used for the data in their Fig. 2 was ~2% of that used in the present study.

Can. J. Chem. Downloaded from www.nrcresearchpress.com by 210.87.254.6 on 09/05/12
For personal use only.

Can. J. Chem. Downloaded from www.nrcresearchpress.com by 210.87.254.6 on 09/05/12
For personal use only.

Photolysis of DBr

Yields of D_2 from DBr were ~20% less than corresponding H_2 yields from HBr when layers were irradiated with the unfiltered SH arc. However, when the shorter wavelengths were eliminated with a 9–54 filter, D_2 yields were only 35% of H_2 yields under identical conditions. Using the 2540 Å monochromator radiation, D_2 yields were 17% those of H_2.

Photolysis of DBr–Trans-butene-2 Mixtures

When equimolar DBr–*trans*-butene-2 mixtures are irradiated with the SH arc either unfiltered or with a CS 9–54 filter, extensive exchange occurs. For the filtered photolysis, the product is 70% H and 30% D atoms, statistically distributed between H_2, HD, and D_2. When equimolar cyclopentene–DBr mixtures were similarly photolyzed, 89% of the atoms were H, again with statistical distribution among the isomers. When DBr and *trans*-butene-2 were deposited in successive layers, the exchange was markedly inhibited. No exchange was observed with DBr the bottom layer; with DBr above the *trans*-butene-2 layer, ~20% of the atoms were H.

Discussion

The photolysis of HBr at 77 °K may most simply be described as

$$[1] \qquad HBr + h\nu \rightarrow HBr^*$$

$$[2] \qquad HBr^* + M \rightarrow HBr + M$$

$$[3] \qquad HBr^* \rightarrow H(^2S) + Br(^2P_{3/2})$$

where primary recombination is included in the deactivation step [2]. In the 2537 Å photolysis of HI mixtures, where 42 kcal mole^{-1} is available as excess energy, reactions have been correlated with both thermal and hot H atoms (3, 4). If H atoms are formed in the photolysis of HBr at 2537 Å by reaction [3], they could have 26 kcal mole^{-1} kinetic energy. Since hot H atoms show little discrimination toward reactions with small energy barriers, such hot atoms would be difficult to scavenge with reactive additives. Experimentally, however, H_2 yields are readily suppressed by added Br_2, or to a lesser extent, by *trans*-butene-2, suggesting that most or all of the H atoms are essentially at thermal equilibrium with the matrix. This behavior is compatible with a mechanism involving photodecomposition of complexes, as has been suggested for HI by Hughes and Purnell (1, 2),

$$[4] \qquad [HBr + HBr]_c + h\nu \rightarrow [HBr...H...Br]_c$$

$$[5] \qquad [HBr...H...Br]_c \rightarrow HBr + HBr$$

$$[6] \qquad [HBr...H...Br]_c \rightarrow H_2 + 2[Br]_c$$

$$[7] \qquad [HBr...H...Br]_c \rightarrow HBr + H + [Br]_c$$

where the dotted lines indicate complexes and the subscript c indicates caged or matrix restrained species. No evidence was found in the HBr solid spectra for new absorptions, such as charge transfer bands between 2000–7000 Å, suggesting that the cage restrained $[HBr + HBr]_c$ pair does not have additional absorption characteristics in the near u.v.–visible region. Reaction [5], which corresponds to deactivation without decomposition, must predominate in HBr photolysis at these wavelengths and reduce initial quantum yields for H_2 production to the low observed values, one or two orders of magnitude less than for HI photolyses (1, 4). Reaction [6] would be one source of H_2, and the thermal H atoms formed in reaction [7] could produce H_2 by reactions [8] or [9].

$$[8] \qquad H + H + M \rightarrow H_2 + M$$

$$[9] \qquad H + HBr \rightarrow H_2 + [Br]_c$$

Reaction [8] does not occur significantly in the gas phase between H atoms which have diffused through the matrix because little H_2 is present in the gas volume until the HBr film is melted. The low light intensities used, with corresponding low concentrations of H atoms, argue against reaction [8] being important in the solid, especially for the monochromator light source.

Figures 3 and 4 demonstrate that the rate of H_2 production is markedly reduced as photolysis proceeds, consistent with a reaction product inhibiting H_2 formation. Either Br or Br_2 are possible products which could cause this inhibition, but Br_2 is unlikely to be present in large concentrations because Br atoms will have very restricted motion at 77 °K in the HBr matrix and are therefore unlikely to combine. Trapped Br could scavenge H atoms from reaction [7]

$$[10] \qquad H + [Br]_c \rightarrow HBr$$

and thus prevent H_2 formation via [9]. Alternately, Br could form a complex $[HBr...Br]_c$ which may absorb strongly and dissipate energy more efficiently than reaction [5]. Although this process seems less probable than [10], especially in view of the relatively low concentrations of Br atoms available, energy could be transferred along HBr chains to a complex site (11).

Can. J. Chem. Downloaded from www.nrcresearchpress.com by 210.87.254.6 on 09/05/12
For personal use only.

With reactions [9] and [10] competing for thermal H atoms from reaction [7], and H_2 being generated in addition by reaction [6],

$$[11]\quad \frac{\partial[H_2]}{\partial t} = \Phi_6 I_a + \Phi_7 I_a \frac{k_9([HBr] - [Br])}{k_9([HBr] - [Br]) + k_{10}[Br]}$$

where I_a is the incident flux of actinic light. If uniform reaction throughout the first 5×10^{19} molecules of HBr is assumed, the data in Fig. 3 fit this expression when $\Phi_6 = 0$, $\Phi_7 = \Phi_I = 5 \times 10^{-3}$, and $k_9/k_{10} = 3 \times 10^{-2}$. The data from Fig. 4 when similarly treated yield $\Phi_6 = 0$, $\Phi_7 = \Phi_I = 1.3 \times 10^{-2}$, and $k_9/k_{10} \sim 0.1$. (Φ_I, Φ_6, and Φ_7 are the initial quantum yield, and the quantum yields of reactions [6] and [7], respectively.) The quantitative differences are probably due to the different spectral distributions of the light sources.

Uncertainties in the absolute values of the initial quantum yield Φ_I, which exist because of the rough estimates of incident flux, do not affect the conclusion that reaction [6] is unimportant in the HBr photolysis at wavelengths used. For a satisfactory fit to eq. [11], the data in Figs. 3 and 4 require Φ_6 to be zero, independent of the effective layer thickness, at least for effective HBr layers containing from 10^{19} to 2×10^{20} molecules, either uniformly reacted, or with a reaction gradient. Kinetically, reaction [6] corresponds to any hot H atom fraction of reaction [3]. If photodissociation is not via absorber complexes (reactions [4] to [7]), some alternate mechanism for generation of near thermal H atoms without a significant concentration of hot H atoms must be operative since the data do not support reaction on the first few collisions, but indicate more nearly thermalized species. One such mechanism might be

$$[12]\quad HBr^* \rightarrow H(^2S) + Br(^2P_{1/2})$$

where the excited atom $Br(^2P_{1/2})$ is ~ 10 kcal mole^{-1} above the ground state (21), and the excess kinetic energy available for the H atom would be reduced to 16 kcal mole^{-1}. Knowledge of the dissociating state of HBr could clarify this possibility. The corresponding reactions to [3] and [12] in the photodecomposition of HI at 2537 Å would leave 42 and 19 kcal mole^{-1} excess energy available for kinetic excitation of H atoms. The similarity in available excess energies for H atoms when dissociation is into electronically excited halogen atoms does not, however, explain the differences in observed behavior between HI and HBr photolysis. The photolyses with added reactants, particularly olefins, seem more consistent with absorber complexes. Furthermore, the higher value for Φ_I obtained with the unfiltered SH lamp which emitted more energetic photons appears to be associated with greater release of H atoms via reaction [7] or a similar path, rather than with greater abstraction probabilities of H atoms with excess kinetic energy. If dissociation were via reaction [12], the hotter H atoms formed at higher frequencies should be evidenced by an increasing Φ_6 which is not observed.

Unlike the values of Φ, the ratio k_9/k_{10} depends upon the assumed layer thickness, and decreases as the layer thickness increases. That is, it is dependent on the relative concentration of Br atoms, and since the effective reaction region cannot be closely defined, the data do not provide a good quantitative value for this ratio. However, it is clear that the majority of reaction is confined to a relatively thin film, containing $< 5 \times 10^{19}$ molecules of HBr, so that k_9/k_{10} is unlikely to be less than 3×10^{-2}, and 10^{-1} is probably a better estimate. If the frequency factors for reactions [9] and [10] are equal, e.g. if atom combination can occur on every spin-allowed encounter (one in every four) and H atom abstraction from HBr has a steric restriction of the same magnitude, then $E_9 - E_{10} \sim 350$ cal mole^{-1}. Since E_{10} is probably zero, or very small, $E_9 \sim 350$. By comparison, Sato (22) has calculated $E = 700$ cal mole^{-1} for H atom abstraction from HBr in the gas phase. A low activation energy for reaction [9] is anticipated from prior knowledge of related systems in the gas phase. For methyl radical abstraction of H from HBr, Fettis and Trotman-Dickenson (23) reported a 1.4 kcal mole^{-1} activation energy, based on zero activation energy for methyl radical reaction with iodine. Low activation energies have been found experimentally (24, 25) for the analogous reaction with HI. The value of $E_9 \sim 2000$ cal mole^{-1} used by Rumfeldt and Armstrong (26) is too high to be compatible with the present results.

The low quantum yields are evidence that most of the incident energy is degraded thermally after absorption by HBr; H_2 producing mechanisms

Can. J. Chem. Downloaded from www.nrcresearchpress.com by 210.87.254.6 on 09/05/12
For personal use only.

are relatively inefficient, and strongly self-inhibiting.

These effects appear to be even more pronounced in the photolysis of DBr. According to Bates *et al.* (16), the molecular absorption coefficient for DBr, measured in the gas phase, is only 1/3 that of HBr at frequencies of interest. Although in the present experiments the films are expected to be optically thick, except possibly on the long wavelength tail, nothing quantitative can be said about the relative quantum yields for HBr and DBr because the *ratio* of yields is strongly frequency dependent.

Although in the discussion of the photolysis of pure HBr it has been implicit that Br atoms are trapped and do not combine to form molecular Br_2, the latter is a possible product of the photolysis, especially at high conversions. Added Br_2 is very efficient in suppressing H_2 generation in the solid state photolysis of HBr. Again considering photolysis to proceed via absorber complexes, the following reactions may be significant in HBr–Br_2 mixtures, in addition to those for pure HBr. (The discussion pertains to low concentrations of Br_2 which do not significantly attenuate the actinic radiation and for which suppression is not simply due to Br_2 absorbing energy and dissipating it thermally.)

[13] $[Br_2 + HBr]_c + h\nu \rightarrow [Br_2...H...Br]_c$

[14] $[Br_2...H...Br]_c \rightarrow Br_2 + HBr$

[15] $[Br_2...H...Br]_c \rightarrow H + Br_2 + [Br]_c$

[16] $H + Br_2 \rightarrow HBr + Br$

If reactions [13] to [15] were not involved in the photolysis, H_2 yields would nevertheless be suppressed by reaction [16] intervening in the H_2 formation process. The sequence of reactions [4]–[7]–[16] yields two Br atoms, as does the sequence [4]–[7]–[9], so H_2 yields can be suppressed without reducing H atom scavenging by reaction [10]. However, Br_2 is unlikely to be a much more efficient interceptor of H atoms than Br atoms themselves. Even if E_{16} were zero, A_{16} is unlikely to be greater than $4A_{10}$, and k_{16}/k_9 would then be ~ 40. Then $\sim 2\%$ Br_2 would suppress H_2 by 50%. The data in Fig. 5 show that in fact Br_2 is much more effective than this in suppressing H_2 yields, which indicates that Br_2, in addition to removing H atoms when formed, also reduces the quantum yield for H atom production. This could be caused, of course, if Br_2 were absorbing strongly between 2000–3000 Å, but the absorption measurements show this is not the case for low Br_2 concentrations, e.g. $< 1\%$. Absorption by a Br_2–HBr caged pair might be much stronger than that of an HBr–HBr pair, but again the spectra show no evidence for this. Alternately, if energy were transferred from [HBr–HBr]* to Br_2–HBr, and if $k_{15}/k_{14} \ll k_7/k_5$, the result would be to degrade absorbed radiation into heat more efficiently in the presence of Br_2 and thus to inhibit the photolysis.

The layer experiments which show that Br_2 is ineffective when above the HBr film demonstrate that the diffusion range of H atoms is quite limited, in accordance with the conclusion that reaction [9] occurs on every ~ 50 encounters, even at 77 °K. Results of experiments in which the Br_2 layer is below the HBr film show that actinic radiation does not penetrate into the pure HBr region of the film, but is stopped in the Br_2 itself.

The observation that H_2 yields were unaffected by the pre-irradiation of 0.1% Br_2 mixtures in HBr suggests either that Br atoms and Br_2 molecules are equally effective scavengers or that cage restraint prevented Br atoms from being liberated during the pre-irradiation. Both suppositions are probably true, but the second most likely prevents the former from being put to the test.

The data show that *trans*-butene-2 also suppresses H_2 evolution in HBr photolyses at 77 °K. This behavior might be anticipated since H atom addition to olefins at cryogenic temperatures is well known (10, 27). However, the extent of H_2 reduction is perhaps larger than might be anticipated in view of the rapid reaction of H atoms with HBr itself. If the olefin is regarded simply as a chemical scavenger of H atoms from reaction [7], H atoms may either add to or abstract from the olefin,

[17] $H + CH_3CH{=}CHCH_3 \rightarrow CH_3CH_2\dot{C}HCH_3$

[18] $H + CH_3CH{=}CHCH_3 \rightarrow H_2 + \dot{C}H_2CH{=}CHCH_3$

[19] $H + CH_3CH{=}CHCH_3 \rightarrow H_2 + CH_3\dot{C}{=}CHCH_3$

Reactions [18] and [19] give H_2 as a product, and therefore would not give a net suppression of the yield. Furthermore, their activation energies are probably greater than that for addition, reaction [17]. Reaction [17] is also expected to

Can. J. Chem. Downloaded from www.nrcresearchpress.com by 210.87.254.6 on 09/05/12
For personal use only.

be activated with $E \geqslant 3$ kcal mole^{-1}, based on the gas phase data of Yang (28). Melville and Robb (29) have found that H atoms react with olefins at room temperature on every 10^3 to 10^4 encounters, which, with a 3 kcal mole^{-1} activation energy, makes addition at 77 °K very improbable relative to abstraction from HBr. Therefore, chemical scavenging of H atoms by olefins should be unimportant in the cryogenic photolysis of HBr. This conclusion would be consistent with the failure to observe spin resonance spectra of alkyl radicals following photolysis of HBr–olefin mixtures.

However, radical spectra are observed in *trans*-butene-2–HBr mixtures at wavelengths > 2800 Å where H_2 yields are negligible. Since D(H—Br) is 86.5 kcal mole^{-1} (20), corresponding to a wavelength of 3300 Å, sufficient energy is available for the dissociation. Furthermore, the absorption tail of solid HBr does extend through this spectral region. The radical spectra in the absence of H_2 generation suggests that photodecomposition occurs by way of absorber complexes.

[20] $[t\text{-B-2} + \text{HBr}]_c + h\nu \rightarrow [t\text{-B-2...H...Br}]_c$

[21] $[t\text{-B-2...H...Br}]_c \rightarrow t\text{-B-2} + \text{HBr}$

[22] $[t\text{-B-2...H...Br}]_c \rightarrow t\text{-B-2} + \text{H} + [\text{Br}]_c$

[23] $[t\text{-B-2...H...Br}]_c \rightarrow$ products involving t-B-2

The ineffectiveness of *trans*-butene-2 concentrations greater than 50 mole % in increasing H_2 suppression implies that HBr is intimately mixed with olefin. By the absorber complex mechanism, suppression of H_2 yields can occur by energy dissipation from an excited complex to the matrix. This requires that $(k_{21} + k_{23}) > k_{22}$, if reaction [23] is not a source of H_2, or otherwise, that $k_{21} > (k_{22} + k_{23})$. Reaction [23] seems to be a likely participant in the formation of trapped radicals in the photolysis of HBr–olefin mixtures and in the extensive isotopic scrambling found in DBr–*trans*-butene-2 photolyses.

The identification of the radicals formed when HBr–olefin mixtures are photolyzed is important in that it may bear on the hypothesized bridged bromoalkyly mechanism in the addition of HBr to double bonds. Abell and Piette (12) originally ascribed observed e.s.r. spectra to bridged bromoalkyl radicals, but Symons (13) has questioned this assignment because the spectra exhibit no g-value anisotropy or shift characteristic of halogenated species, and no hyperfine interaction with Br atoms is observed. Nor are H atoms from the HBr photodecomposition accounted for. If these H atoms were to abstract from olefins, allylic radicals would be formed, which, according to Symons, could give the observed e.s.r. spectra. However, one might anticipate that H atoms would react preferentially with HBr, even in the presence of considerable olefin concentration. In an attempt to clarify this point, DBr–*trans*-butene-2 mixtures were photolyzed in the expectation that if Symons' suggestion were correct, HD would be a product, but if all abstraction were from DBr, only D_2 would be formed. At the wavelengths used by Abell and Piette, intense radical spectra can be obtained, but no H_2 is evolved. At longer wavelengths, where H_2 can be collected, extensive exchange occurs so that this experiment does not provide a confirmation of Symons' postulate. However, photolysis of absorber complexes could nevertheless generate allylic radicals via reaction [23], or by reaction [24] following reaction [22],

[24] $[t\text{-B-2} + \text{Br}]_c \rightarrow \text{CH}_3\text{CH=CH}\dot{\text{C}}\text{H}_2 + \text{HBr}$

Conclusions

The evolution of H_2 from the solid phase photolysis of pure HBr is an inefficient process and is strongly inhibited by a product of the photolysis, probably Br atoms. Molecular Br_2 and *trans*-butene-2 are also effective in suppressing H_2 yields. The results suggest H_2 is formed by abstraction from HBr by thermal H atoms. This reaction has a low activation energy, ~350 cal mole^{-1}. The participation of hot H atoms is not indicated. The photolyses of both pure HBr and HBr with added Br_2 or *trans*-butene-2 can be described by an absorber complex mechanism similar to that inferred by Hughes and Purnell (1, 2) in the photolysis of HI.

Absorption spectra show that, in the solid state, the absorption tail of HBr extends into the wavelength region in which trapped radicals can be produced in HBr–olefin mixtures, but where no H_2 is observed. An absorption band in solid Br_2 at 2725 Å, not observed in the gas phase spectrum, may be associated with $(Br_2)_n$ aglomerates.

Acknowledgments

The authors are grateful to M. B. Robin and N. A. Kuebler for their advice and assistance in obtaining and interpreting the u.v.–visible spectra.

1. A. N. HUGHES and J. H. PURNELL. Trans. Faraday Soc. **62**, 156 (1966).
2. A. N. HUGHES and J. H. PURNELL. Nature, **210**, 255 (1966).
3. S. ADITYA and J. E. WILLARD. J. Am. Chem. Soc. **88**, 229 (1966).
4. J. R. NASH, R. R. WILLIAMS, JR., and W. H. HAMILL. J. Am. Chem. Soc. **82**, 5974 (1960).
5. E. L. COCHRAN, V. A. BOWERS, S. N. FONER, and C. K. JEN. Phys. Rev. Letters, **2**, 43 (1959).
6. G. E. EWING, W. E. THOMPSON, and G. C. PIMENTEL. J. Chem. Phys. **32**, 927 (1960).
7. F. J. ADRIAN, E. L. COCHRAN, and V. A. BOWERS. J. Chem. Phys. **36**, 1661 (1962).
8. E. L. COCHRAN, F. J. ADRIAN, and V. A. BOWERS. J. Chem. Phys. **40**, 213 (1964).
9. D. E. MILLIGAN and M. A. JACOX. J. Chem. Phys. **38**, 2816 (1963).
10. R. KLEIN and M. D. SCHEER. J. Phys. Chem. **67**, 1874 (1963).
11. R. C. RUMFELDT and D. A. ARMSTRONG. Can. J. Chem. **44**, 191 (1966).
12. P. I. ABELL and L. H. PIETTE. J. Am. Chem. Soc. **84**, 916 (1962).
13. M. C. R. SYMONS. J. Phys. Chem. **67**, 1566 (1963).
14. G. F. SHIPMAN. Anal. Chem. **34**, 877 (1962).
15. L. C. JONES, JR. and L. W. TAYLOR. Anal. Chem. **27**, 228 (1955).
16. J. R. BATES, J. O. HALFORD, and L. C. ANDERSON. J. Chem. Phys. **3**, 531 (1935).
17. J. G. CALVERT and J. N. PITTS, JR. Photochemistry. John Wiley and Sons, Inc., New York. 1966.
18. E. A. OGRYZLO and B. C. SANCTUARY. J. Phys. Chem. **69**, 4422 (1965).
19. R. M. IYER and J. E. WILLARD. J. Am. Chem. Soc. **88**, 4561 (1966).
20. T. L. COTTRELL. The strengths of chemical bonds. 2nd ed. Butterworths, London. 1958.
21. G. HERZBERG. Spectra of diatomic molecules. 2nd ed. D. Van Nostrand Co., Inc., Princeton, New Jersey. 1950.
22. S. SATO. J. Chem. Phys. **23**, 2465 (1955).
23. G. C. FETTIS and A. F. TROTMAN-DICKENSON. J. Chem. Soc. 3037 (1961).
24. S. W. BENSON. The foundations of chemical kinetics. McGraw-Hill Book Co., Inc., London. 1960.
25. J. H. SULLIVAN. J. Chem. Phys. **36**, 1927 (1962); **39**, 3001 (1963).
26. R. C. RUMFELDT and D. A. ARMSTRONG. J. Phys. Chem. **68**, 761 (1964).
27. A. N. HUGHES and J. H. PURNELL. Trans. Faraday Soc. **61**, 1 (1965).
28. K. YANG. J. Am. Chem. Soc. **84**, 3795 (1962).
29. H. W. MELVILLE and J. C. ROBB. Proc. Roy. Soc. London, Ser. A, **202**, 181 (1950).

Can. J. Chem. Downloaded from www.nrcresearchpress.com by 210.87.254.6 on 09/05/12
For personal use only.

Can. J. Chem. Downloaded from www.nrcresearchpress.com by 210.87.254.5 on 09/05/12
For personal use only.

Nuclear magnetic resonance studies of ketone.BF_3 complexes. II. The boron trifluoride catalyzed condensation of acetone

R. J. Gillespie and J. S. Hartman[1]
Department of Chemistry, McMaster University, Hamilton, Ontario
Received May 23, 1968

A detailed study of the reactions of the acetone.BF_3 complex in excess acetone has been carried out by ^{19}F nuclear magnetic resonance (n.m.r.) spectroscopy. It is shown that rapid reversible fluorine exchange processes occur in solution, in addition to the slower aldol condensation–dehydration reaction. Two of the new ^{19}F absorptions which appear during the reaction are shown to arise from BF_3 complexes of donors which are formed by condensation and dehydration of acetone. The rate of the aldol condensation reaction is shown to fall off markedly as an increasing proportion of the BF_3 becomes complexed with water; thus BF_3 catalysis of the reaction appears to depend on the existence of a ketone–BF_3 donor–acceptor bond. ^1H and ^{19}F n.m.r. studies of the acetone.BF_3 complex in methylene chloride throw some light on the apparent greatly decreased reactivity of the complex in this solvent. Evidence is presented for the reversibility of the first step of the condensation reaction.

Canadian Journal of Chemistry, 46, 3799 (1968)

Introduction

It has long been known that simple ketones form well-defined 1:1 adducts with boron trifluoride (1). Our recent nuclear magnetic resonance (n.m.r.) studies have shown that these adducts in methylene chloride solution undergo two distinct rapid reversible reactions, namely breaking and re-forming of the donor–acceptor bond and fluorine exchange among boron atoms (see part I of this series, ref. 2). There have been conflicting reports concerning the stability of the ketone.BF_3 complexes. The crystalline donor–acceptor adduct acetone.BF_3 has variously been reported to be stable to 50° (3) and to decompose above 0° with formation of a dark polymeric material and hydration products of BF_3 (4). The high reactivity of the complexed ketones apparently results from their ability to undergo aldol condensation reactions catalyzed by the Lewis acid. Under the mild influence of aqueous protonic acids, dimerization and dehydration of acetone yields mesityl oxide (**1**). Lewis acids such as $ZnCl_2$ allow condensation of an additional molecule of acetone, followed by dehydration to yield phorone (**2**). A strong Lewis acid such as BF_3 can evidently cause further condensation reactions. **1** and **2** are susceptible to further aldol-type condensation involving the γ-methyl groups because of the conjugated system linking them to the carbonyl group; thus many different complex structures of higher molecular weights might be built up.

$CH_3\overset{O}{\overset{\|}{C}}CH{=}C(CH_3)_2$ **1**

$(CH_3)_2C{=}CH\overset{O}{\overset{\|}{C}}CH{=}C(CH_3)_2$ **2**

In our previous n.m.r. study of ketone.BF_3 complexes in methylene chloride solution (2), we observed that even after heating dilute solutions of the acetone.BF_3 complex at 100° for short periods there was very little color change in the solution; the absence of extensive reaction was confirmed by the occurrence of only slight changes in the n.m.r. spectra. This behavior contrasts with that of the crystalline acetone.BF_3 complex, and of solutions of BF_3 in excess acetone, in both of which cases the formation of colored materials was found to be fairly rapid at room temperature. In the present work the reaction of solutions of acetone.BF_3 has been investigated by ^{19}F and ^1H n.m.r. spectroscopy, with a view to explaining the different behavior observed in acetone and in methylene chloride solvents.

Results and Discussion

Acetone.BF_3 in Excess Acetone

Approximately 1 *M* solutions of boron trifluoride in acetone, which were initially colorless, darkened through yellow and straw color to dark brown on standing for 2 h at room temperature. On further standing the liquid became black and opaque.

Room temperature ^{19}F spectra of a 1.2 *M* solution of BF_3 in acetone, prepared at low temperatures, are shown in Fig. 1. Our previous

[1]Present address: Department of Chemistry, Brock University, St. Catharines, Ontario.

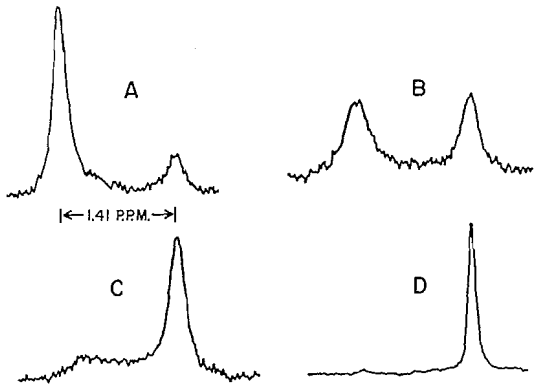

FIG. 1. Room temperature ^{19}F spectra of a 1.2 *M* solution of BF_3 in acetone. Reaction times at room temperature: (A), 4 min, colorless solution; (B), 14 min, pale yellow solution; (C), 34 min, orange solution; (D), 108 min, dark brown solution.

studies (2) have shown that only the 1:1 complex forms, and that in the presence of excess ketone the amount of non-complexed BF_3 present is negligible and should not have any effect on the n.m.r. spectrum; thus we might expect a single ^{19}F resonance arising from the acetone.BF_3 complex. However, spectrum A, obtained as soon as possible after warming the fresh solution to room temperature, contained two peaks. Spectra B–D show the gradual disappearance of one of the peaks and the increasing intensity of the second high-field peak over a period of 2 h. The high-field peak became sharper as the low-field peak disappeared. The growth of the high-field peak is not directly related to the darkening of the solution since the spectrum shows that almost half of the fluorine was incorporated in the new species after 14 min, when the solution still had only a pale yellow color. Darkening of the solution continued when changes in the ^{19}F spectrum were no longer apparent. The new peak did not become significantly sharper than shown in D even after the sample was allowed to stand at room temperature for several days.

The peaks of Fig. 1 are broad and not completely separated, suggesting that rapid reversible chemical exchange occurs (5). Evidence for this is provided by the temperature dependence of the ^{19}F spectrum of a 1.5 *M* solution of BF_3 in acetone, which had been allowed to react for 1 h at 22° (Fig. 2). Two well-separated peaks were obtained below room temperature, and at much lower temperatures further fine structure appeared. Below 0° the temperature-dependence of the spectrum was reversible; above 0° there was a tendency for the condensation reaction to proceed, so that changes in relative peak areas

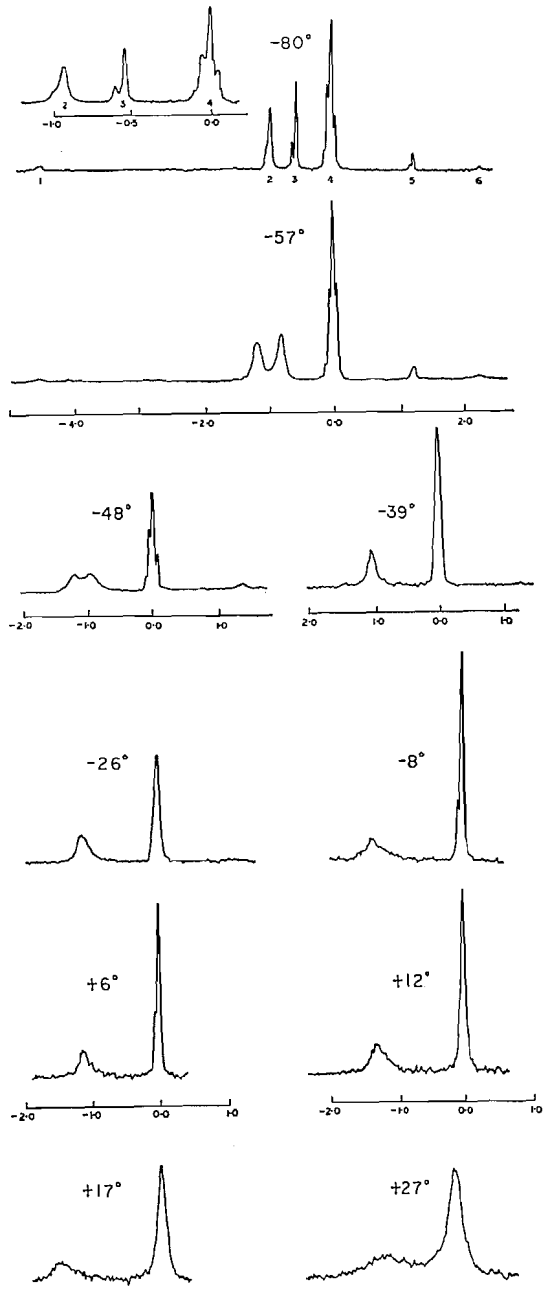

FIG. 2. ^{19}F spectra at various temperatures of a 1.5 *M* solution of BF_3 in acetone after standing for 1 h at 22°. Calibration is in p.p.m. from peak 4.

Can. J. Chem. Downloaded from www.nrcresearchpress.com by 210.87.254.5 on 09/05/12
For personal use only.

Can. J. Chem. Downloaded from www.nrcresearchpress.com by 210.87.254.5 on 09/05/12
For personal use only.

were observed after the sample had been warmed to a higher temperature. It is evident from the spectrum of the complex at $-80°$ that a number of different fluorine-containing species are present in solution. All of the observed peaks occur in a quite narrow region of the total fluorine spectrum, corresponding to the usual range for fluorine on tetrahedral boron (6), and thus would appear to arise from complexes of BF_3 with different donor molecules. The collapse of the low temperature peaks as the temperature is raised probably results from a rapid reversible exchange of BF_3 molecules among the different donor species; other cases of exchange averaging of ^{19}F peaks arising from different BF_3 complexes have been reported (7–9). The BF_3 exchange processes which occur in the present case are discussed later in this paper.

In order to obtain spectra of solutions of BF_3 in acetone containing essentially no decomposition products, samples were prepared and sealed off on a high-vacuum system and liquefied without warming above $-40°$. Such samples, which could be stored at $-78°$ for a month with no decomposition, gave low-temperature ($-80°$) spectra very similar to those obtained in methylene chloride solutions of acetone and BF_3 with acetone present in excess (2). The only large absorption, which arises from acetone.BF_3, was split by a ^{10}B–^{11}B isotope shift into a doublet of relative areas 1:4 and relative chemical shift 0.066 p.p.m. In addition a very small multiplet was present at 0.78 p.p.m. to higher field, with skewed quartet fine structure arising from two overlapping triplets of relative intensities about 1:4 which showed that it arises from $H_2O.BF_3$ (10); this was confirmed by studies involving isotopically substituted samples, similar to those described previously (10). The $H_2O.BF_3$, which is present in fresh samples, is apparently formed from a trace of water in the solvent acetone in spite of the drying procedures used.

The peaks due to acetone.BF_3 and $H_2O.BF_3$ which are seen in spectra of fresh solutions can also be identified in the more complex spectra of partially reacted solutions. Figure 3 illustrates that the reaction at room temperature can be monitored by the changes in appearance of the ^{19}F spectrum at $-80°$. The acetone.BF_3 peak, initially very large, diminishes throughout the reaction. The peak at higher field with skewed quartet fine structure, which arises from $H_2O.BF_3$,

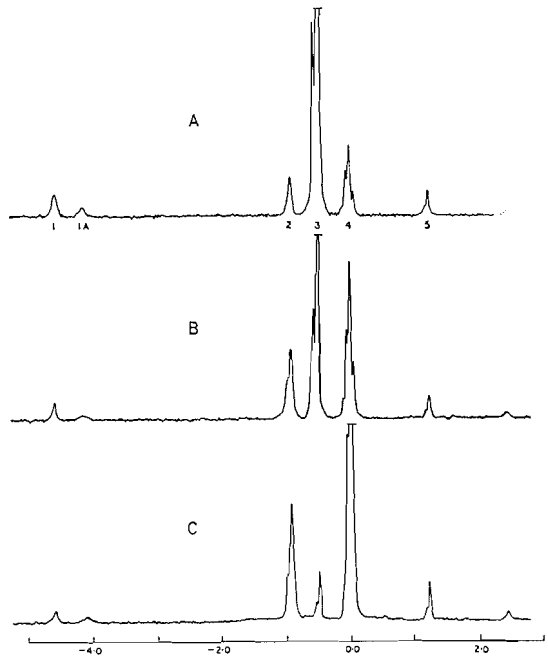

FIG. 3. ^{19}F spectra at $-80°$ of a 1.1 *M* solution of BF_3 in acetone after reaction at room temperature for (A), 7 min; (B), 22 min; (C), 102 min. Calibration is in p.p.m. from peak 4.

gains in relative intensity throughout the reaction; hence $H_2O.BF_3$ is the major fluorine-containing reaction product. Thus water is formed in the reaction, and complexes with BF_3 as it forms.

For convenience in the following discussion the low-temperature peaks are numbered from low to high field as in the $-80°$ spectra of Figs. 2 and 3. A similar pattern of peaks was observed in all of the samples studied, including a number of isotopically substituted samples. In some of the samples a new peak, not visible in the $-80°$ spectrum of Fig. 2, was observed at quite low field; this peak is labelled 1A. ^{19}F chemical shifts at $-80°$, in p.p.m. from peak 4 which from its skewed quartet fine structure is assigned to $H_2O.BF_3$, are given in Table I for the samples studied. The relative chemical shifts were almost constant in all of the samples at this temperature. It is of interest that in deuterated samples the shifts from $D_2O.BF_3$ differed by -0.19 ± 0.05 p.p.m. from the shifts with respect to $H_2O.BF_3$ in the non-deuterated samples. This is probably due chiefly to a high field shift of $D_2O.BF_3$ with respect to $H_2O.BF_3$, which might result from

TABLE I

^{19}F chemical shifts in solutions of BF_3 in acetone at $-80°$, after reaction at room temperature for 20–60 min

BF_3 (moles/l at $-80°$)	Isotopic substitution	Chemical shifts (p.p.m. from $H_2O.BF_3$*)						
		1	1A	2	3	4	5	6
1.5	—	−4.50	—	−0.93	−0.51	0	1.29	2.58
1.1	—	−4.59	−4.08	−0.95	−0.54	0	1.33	2.42
1.2	^{10}B	−4.56	−4.00	−0.89	−0.50	0	1.28	2.44
1.6	50% ^{10}B, 50% ^{11}B	−4.55	−4.05	−0.93	−0.50	0	1.28	2.46
0.9†	—	−4.59	−4.13	−0.91	−0.50	0	1.24	2.44
1.1	deuterated	−4.70	−4.32	−1.14	−0.72	0	1.07	—
1.0	deuterated	−4.69	−4.27	−1.13	−0.73	0	1.14	—
Average shifts of non-deuterated samples		−4.56	−4.06	−0.92	−0.51	0	1.28	2.47
Average shifts of deuterated samples		−4.70	−4.30	−1.14	−0.72	0	1.10	—
Change of chemical shift on deuteration		−0.14	−0.24	−0.22	−0.21	—	−0.14	—

*146.6 p.p.m. to high field of trichlorofluoromethane.
†Also contains mesityl oxide, 0.5 *M*.

differences in the vibrational amplitude of the hydrogen and deuterium atoms (ref. 11, p. 875), or alternatively from greater donor ability of D_2O with respect to H_2O.

Some of the peaks in the $-80°$ spectra would be expected to arise from BF_3 complexes of donors formed in the acetone condensation reaction, in addition to water. The most likely donor would seem to be the primary product of the consensation–dehydration reaction, mesityl oxide (**1**); higher ketones such as phorone (**2**) might be present as well. A solution of mesityl oxide (0.6 *M*) and BF_3 (0.9 *M*) in acetone yielded a ^{19}F spectrum at $-80°$ containing two large peaks of relative chemical shift 0.44 p.p.m., and a few very small peaks. Figure 4 shows the spectrum A at a high power level so that the small peaks are visible. A comparison of the relative chemical shifts of all the peaks present yielded a pattern very similar to that observed in partially decomposed samples of BF_3 in acetone (Table I), and indicated that the two large peaks correspond to peaks 2 and 3. This assignment of peaks was confirmed by the presence of skewed quartet fine structure on the small peak corresponding to peak 4. Since peak 3 arises from acetone.BF_3, the other large peak, peak 2, must arise from (mesityl oxide).BF_3. To obtain further evidence supporting this assignment of peaks, room temperature decomposition of the sample was allowed to proceed for 25 min. In the resulting $-80°$ spectrum B, the expected diminution of peak 3 and growth of peak 4 was observed. Most of the decrease in the initial large peaks was at the expense of the acetone.BF_3 peak. This indicates that acetone forms a weaker BF_3 complex than

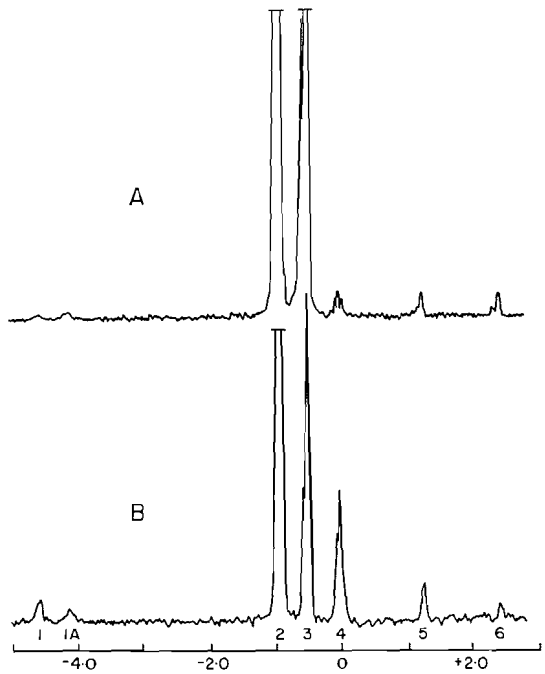

FIG. 4. ^{19}F spectra at $-80°$ of a solution of mesityl oxide (0.6 *M*) and BF_3 (0.9 *M*) in acetone, calibrated in p.p.m. from peak 4. (A), freshly prepared solution, high power level; (B), after 25 min of reaction at 22°, normal power level.

Can. J. Chem. Downloaded from www.nrcresearchpress.com by 210.87.254.5 on 09/05/12
For personal use only.

Can. J. Chem. Downloaded from www.nrcresearchpress.com by 210.87.254.5 on 09/05/12
For personal use only.

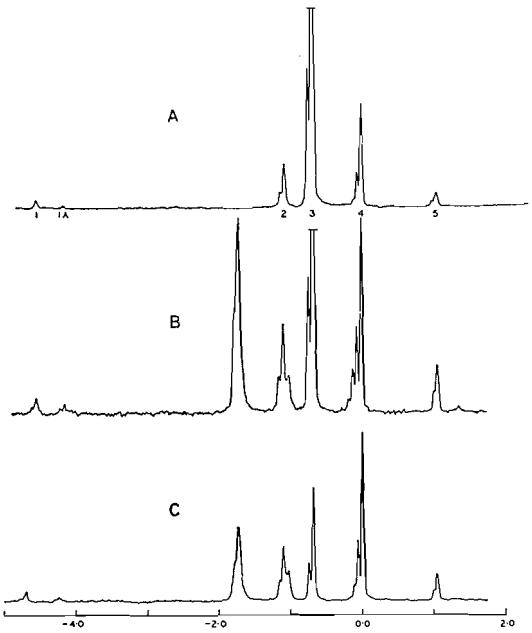

FIG. 5. ^{19}F spectra at $-80°$ of a 1.0 *M* solution of BF_3 in acetone-d_6, after 12 min of reaction at 22°. (A), before addition of phorone; (B), immediately after addition of phorone; (C), after a further 21 min of reaction at 22°. The spectra are calibrated in p.p.m. from peak 4.

mesityl oxide; as water is formed and competes successfully for BF_3, it removes BF_3 chiefly from the acetone complex.

The low-temperature ^{19}F spectrum of a partially reacted solution of BF_3 in acetone-d_6 is shown in Fig. 5, spectrum A. Addition of a small amount of purified phorone gave the spectrum B at $-80°$. A new large peak, 1.74 p.p.m. to low field of $D_2O.BF_3$ in a region of the spectrum which had previously been clear, is assigned to the phorone.BF_3 complex. A few new impurity peaks are also present. Since none of the usual set of ^{19}F peaks corresponds to the phorone.BF_3 peak, it appears that phorone is not produced in significant amounts in the condensation reaction. The large size of the phorone.BF_3 peak which results from the addition of only a small amount of phorone shows that phorone, like mesityl oxide, can displace acetone from its complex. The possibility remains that phorone might be produced in the condensation reaction but is more reactive than the other ketones in further condensation, so that its concentration would never become large enough to give an observable ^{19}F peak. To investigate this possibility, the solution was allowed to react at room temperature (22°) for 21 min; it then gave spectrum C at $-80°$. Comparison of the relative peak areas in B and C shows the expected increase in intensity of peak 4, with a marked decrease in the intensities of the phorone.BF_3 and acetone.BF_3 peaks; the (mesityl oxide).BF_3 peak was not seriously affected. Thus phorone reacts more rapidly than mesityl oxide, and we cannot therefore exclude the possibility of its formation and rapid further reaction.

The remaining peaks have not been identified. However, proof that all the peaks arise from fluorine on boron is obtained from spectra of partially reacted solutions containing isotopically substituted BF_3. Figure 6 shows the low-temperature spectra of partially decomposed solutions of $^{10}BF_3$, and of almost equimolar $^{10}BF_3$ and $^{11}BF_3$, in acetone. The usual pattern of peaks was obtained in both solutions. The $^{10}BF_3$ solution yielded sharp singlets for all peaks except peak 4 (a triplet). The solution of almost equimolar $^{10}BF_3$ and $^{11}BF_3$ yielded a spectrum with all peaks split into doublets except peak 4 (a quartet). In the latter spectrum the almost equal size of the F-on-^{10}B and F-on-^{11}B peaks allowed the isotope splitting to be detected even on small or somewhat broadened peaks. The presence of

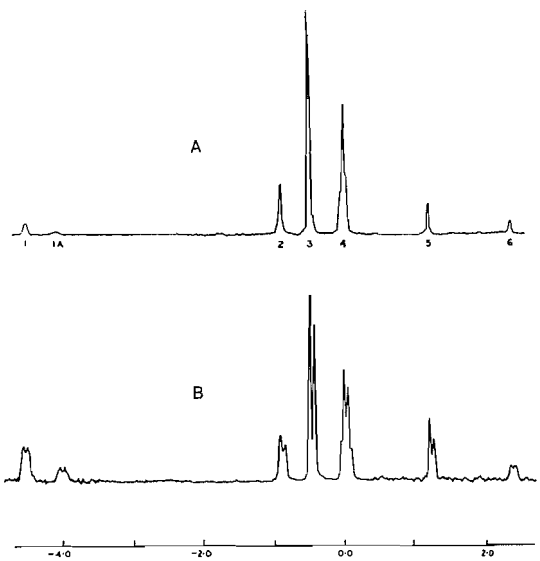

FIG. 6. ^{19}F spectra at $-80°$ of solutions of BF_3 in acetone, after 25 min of reaction at 22°. (A), $^{10}BF_3$; (B), $^{10}BF_3$:$^{11}BF_3$ = 53:47; peaks 1, 1A, 5, and 6 in (B) were obtained at a high power level.

Can. J. Chem. Downloaded from www.nrcresearchpress.com by 210.87.254.5 on 09/05/12
For personal use only.

the isotope splitting on all of the peaks proves that they all arise from fluorine bonded to boron. The triplet and quartet fine structure obtained for peak 4 using $^{10}BF_3$ and $^{10}BF_3/^{11}BF_3$ respectively show that it is due to $H_2O.BF_3$ (10).

There are a number of reasons for believing that all the peaks arise from BF_3 complexes rather than from other species having fluorine bonded to boron, such as RBF_2 or $ROBF_2$ or complexes of these. Chemical shift data (ref. 11, p. 946) appear to exclude species such as RBF_2, but not complexes of such species. However, the rapid exchange of fluorine among all of the species but $H_2O.BF_3$ at low temperatures, as shown by the collapse of the ^{19}F peaks, seems much more in keeping with breaking and reforming of donor–acceptor bonds than with the occurrence of disproportionation reactions. Also, no other ^{19}F peaks have been observed which could arise from the fluorine which would have been split off as fluoride ion or alkyl fluoride. In addition, spectrum B in Fig. 6 can be considered to be made up of two separate spectra like A offset by 0.066 p.p.m. The isotope shifts are very similar on all peaks and are considerably different from the value of 0.050 p.p.m. found for the tetrafluoroborate ion (12). The considerable change of 0.016 p.p.m. with a change of donor from fluorine to oxygen suggests a dependence of the isotope shift on the donor atom, and similar changes in magnitude might be expected in species such as RBF_2 or complexes of these. The similarity of all the isotope shifts in the partially reacted solution of BF_3 in acetone suggests that all the peaks arise from complexes of BF_3 with oxygen donors.

It appears that peaks 1A and 6 do not arise from the BF_3-catalyzed condensation–dehydration reaction. They are present in some but not all of the samples studied, and when present have different peak areas in otherwise similar samples. The areas of these peaks do not appear to vary greatly as the reaction proceeds. Peaks 1A and 6 apparently arise from trace Lewis base impurities in the solvent, which are able to displace acetone from its BF_3 complex and thus become noticeable in the ^{19}F spectrum although their concentrations are probably very low.

Peaks 1 and 5 probably arise, like peaks 2 and 4, from BF_3 complexes of Lewis bases which are formed in the aldol condensation reaction. These could be ketones of higher molecular weights and with longer conjugated systems than mesityl oxide. The absence of phorone in the reaction mixture suggests favored formation or greater stability of linearly conjugated rather than cross-conjugated systems. Other possible structures for the donors giving rise to these peaks cannot be excluded, however. Acid-catalyzed rearrangement of mesityl oxide is known to yield an equilibrium mixture containing 9% of the non-conjugated isomer 4-methyl-4-pentene-2-one (13). Acid-catalyzed rearrangement of phorone also yields non-conjugated isomers (14). The enol forms of the ketones, and the β-hydroxy acids which would result if condensation occurs faster than dehydration, could also be present in significant amounts, and since alcohols are generally better Lewis bases than ketones (15) these species should complex preferentially. The presence of such species could thus account for the unidentified ^{19}F peaks.

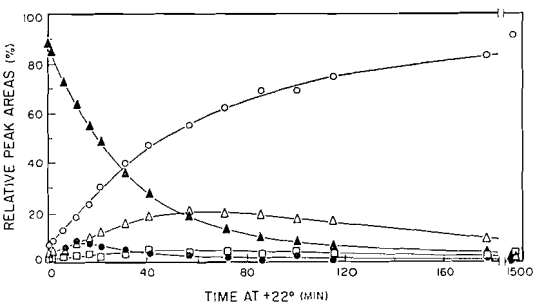

FIG. 7. Plot of the changes in relative areas of the ^{19}F peaks at −80° of the 1.1 *M* sample (Fig. 3) with reaction time at 22°. ● Peak 1, △ Peak 2, ▲ Peak 3, ○ Peak 4, □ Peak 5.

Figure 7 is a plot of the changes in relative area of the −80° ^{19}F peaks of the 1.1 *M* sample against reaction time at 22°. It confirms that peak 3 arises from the initial species and peak 4 from the final fluorine-containing product. It is clear from the plot that the relative area of peak 2 varies in such a way that it can be assigned to an intermediate fluorine-containing product. The later diminution of this peak, shown to arise from (mesityl oxide).BF_3, need not be due to a decrease in the amount of mesityl oxide in solution. Instead, the additional water produced in the continuing condensation–dehydration reaction apparently competes successfully with the organic donors for the limited amount of BF_3 available,

Can. J. Chem. Downloaded from www.nrcresearchpress.com by 210.87.254.5 on 09/05/12
For personal use only.

so that eventually the $H_2O.BF_3$ peak is the only major peak. Peaks 1 and 5 also appear to arise from intermediate products of the reaction, but because of their small size and the resulting difficulty in determining their areas accurately this is not certain.

The n.m.r. spectra can be used to assign an order of relative donor–acceptor bond strengths to the different complexes found in solution. This is most clearly shown by a comparison of the fluorine and proton spectra of solutions of BF_3 in acetone which had been allowed to react at room temperature for an hour or more. The proton spectrum of such a solution still consists mainly of the solvent acetone peak. The very different appearance of the fluorine spectrum, with the $H_2O.BF_3$ peak predominant, shows that water can displace acetone from its BF_3 complex. A similar comparison of relative fluorine and proton peak areas shows that mesityl oxide can largely displace acetone from its complex. The greater donor strength of mesityl oxide appears to be the result of the conjugated unsaturated system which should assist in making electronic charge available on the carbonyl oxygen for donation to BF_3.

Since there appear to be no proton peaks which can be assigned to the donors postulated to be present as impurities, such donor species would appear to be present only in trace amounts. Thus they would have to be stronger donors than mesityl oxide or acetone in order that they be able to displace enough of the major species from their complexes that (trace impurity).BF_3 peaks be visible in the ^{19}F spectrum. The fact that the relative areas of these peaks do not change as markedly with time as do those of acetone.BF_3 and (mesityl oxide).BF_3 is a further indication that these peaks arise from complexes of donors rather stronger than the ketones. Thus the donor–acceptor bond strengths are estimated to increase in the order acetone.BF_3 < (mesityl oxide).BF_3 < (trace impurity).BF_3 < $H_2O.BF_3$.

The skewed quartet structure of peak 4 remained present throughout the time of reaction represented by the curves of Fig. 7. However, this structure, arising from proton–fluorine coupling in $H_2O.BF_3$ superimposed on an isotope shift, later collapsed; after 24 h the peak had only an isotope shift of 0.066 p.p.m. We have previously shown (10) that the fine structure due to proton–fluorine coupling is present only when there is no appreciable amount of uncomplexed water in solution. The collapse of the fine structure, apparently because of a rapid proton exchange between free and complexed water, should thus occur when sufficient water has been produced that $[H_2O] > [BF_3]$. Since the fine structure survives over the time of reaction included in the curves of Fig. 7, it is apparent that, in the early stages of the reaction, essentially all the water becomes complexed as it forms and thus the rate of increase of the $H_2O.BF_3$ peak provides a measure of the rate of the dehydration reaction. If, as is probable, the dehydration reaction follows closely the ketone condensation reaction, then the rate of growth of the $H_2O.BF_3$ peak should give a measure of the rate of the ketone condensation reaction. Thus it is of interest that the rate of increase of this peak falls off as the peak becomes larger; this indicates a falling off of the rate of the condensation reaction. Since proton spectra show that a very large excess of acetone remains, the decrease in rate cannot be attributed to a significant decrease in the amount of acetone available. Instead, it seems necessary to attribute this effect to a decrease in the effectiveness of BF_3 as a catalyst. This would result if an essential condition for the condensation reaction to occur is the existence of a donor–acceptor bond between BF_3 and a ketone carbonyl group. As the reaction proceeds, the water formed complexes preferentially with the BF_3, so that the amount of ketone.BF_3 decreases; hence the rate of further reaction decreases. The catalytic effect of BF_3 is thus due to its ability to form a complex with the carbonyl group.

Most proton acids, including $H_2O.BF_3$ (10), are not strong enough to protonate acetone, a very weak base, so that the "proton complex" of acetone, which might react in a similar fashion to the BF_3 complex, is not formed. However, very strong acids such as anhydrous sulfuric acid are able to protonate acetone (16). The protonated acetone so formed is apparently quite reactive towards excess free acetone; addition of a small amount of oleum to anhydrous acetone is found to cause decomposition at room temperature similar to that caused by BF_3, yielding organic products of similar color and odor. This provides further evidence that the decomposition is dependent on electron pair donation by acetone to a strong Lewis acid such as BF_3 or the proton in the presence of excess acetone.

Can. J. Chem. Downloaded from www.nrcresearchpress.com by 210.87.254.5 on 09/05/12
For personal use only.

Fluorine Exchange

In addition to the condensation reaction, other reactions occur in solution at rates which are several orders of magnitude greater. The collapse of the low-temperature peaks as the temperature is raised (Fig. 2) is apparently caused by rapid reversible chemical exchange reactions, exchanging fluorine among the different complexes. By analogy with our previous studies (2), the exchange would be expected to take place by the breaking and re-forming of donor–acceptor bonds, with a resulting rapid rearrangement of the BF_3 molecules among the different donor species. The collapse of the peaks seems consistent with a scheme of fluorine exchange in which BF_3 exchanges readily among all the donor molecules except H_2O. Because of the survival of peak 4 to much higher temperatures than the other peaks, it seems necessary to assume that the donor–acceptor bond lifetime of $H_2O.BF_3$ is much greater than that of the other species. Since all of the other peaks, which apparently arise from BF_3 complexes with organic donors, collapse in the same temperature range we assume as a first approximation that they have equal donor–acceptor bond lifetimes. Our previous studies of ketone.BF_3 complexes in methylene chloride solution (2) led to the similar conclusion that fluorine exchange between $H_2O.BF_3$ and ketone.BF_3 species is much slower than BF_3 exchange among ketone donor molecules; it was also demonstrated by the collapse of the $^{10}B-^{11}B$ isotope shift at high temperatures that at least part of the fluorine exchange between $H_2O.BF_3$ and ketone.BF_3 arises from fluorine exchange among different boron atoms rather than from breaking and re-forming of the boron–oxygen donor–acceptor bond. Similar fluorine exchange among boron atoms would seem reasonable in acetone solution as well, but this would not affect the accessible part of the coalescence pattern; the high-temperature spectra which would be required to demonstrate fluorine exchange between boron atoms could not be obtained because the aldol condensation reaction is very rapid at high temperatures in acetone solution.

Further evidence for our postulate that fluorine in $H_2O.BF_3$ is less labile than fluorine in the other complexes was obtained by the calculation of theoretical spectra for chemical exchange among six chemically shifted sites. A computer program based on the full line-shape expressions summarized by Abragam (17) was used for the calculations. Theoretical spectra were calculated for various values of the bond lifetimes, according to our assumption of equal donor–acceptor bond lifetimes and equal probabilities of mutual exchange among all of the species other than $H_2O.BF_3$. These were compared with the experimental spectra; comparison led to better trial values of the lifetimes, so that calculated spectra were eventually obtained which closely resembled the observed spectra. By this trial-and-error method of choosing bond lifetimes and visually matching calculated and experimental spectra, it was possible to obtain the qualitative agreement shown in Fig. 8. In our calculations we made no allowance for the isotope shift or additional fine structure which do not seriously affect the overall spectral shape. To obtain the agreement shown in Fig. 8 it was necessary to assume that the donor–acceptor bond lifetime of $H_2O.BF_3$ is three orders of magnitude greater than that of the other species; spectra calculated on the assumption of equal donor–acceptor bond lifetimes for

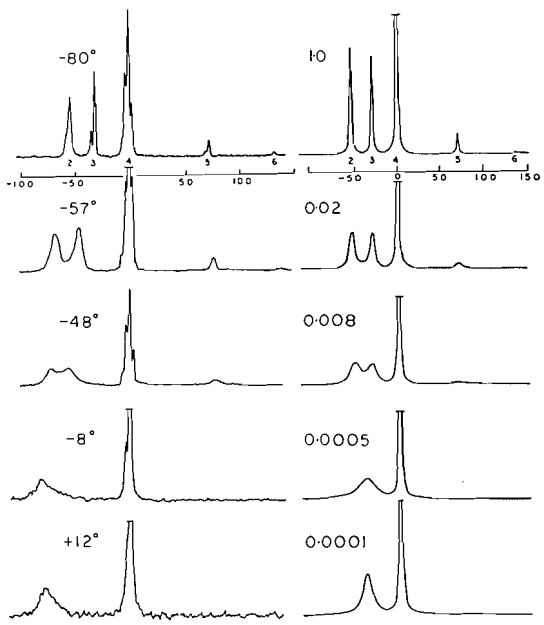

FIG. 8. Computer fit of some of the ^{19}F spectra of Fig. 2. The calculations assume equal donor–acceptor bond lifetimes, given (in seconds) on the spectra, for all of the complexes except $H_2O.BF_3$. The donor–acceptor bond of $H_2O.BF_3$, which gives rise to peak 4, is assumed to have a lifetime 1000 times greater. The spectra are calibrated in Hz from peak 4.

Can. J. Chem. Downloaded from www.nrcresearchpress.com by 210.87.254.5 on 09/05/12
For personal use only.

all species including $H_2O.BF_3$ were not similar to the observed spectra.

Our matching of theoretical and experimental spectra of chemical exchange yields only limited and qualitative information about exchange rates. The changes in shape of the spectrum are not sufficiently pronounced to allow all six donor–acceptor bond lifetimes to be determined. Also the relative chemical shifts used in the calculations, determined at low temperatures, apparently do not remain constant over the range of temperatures. This is shown clearly in Fig. 8 by the discrepancy in peak separations between calculated and observed spectra at the higher temperatures; this discrepancy is not believed to have too great an effect on the signal shape. Another factor limiting us to qualitative deductions is that the calculations must assume a mechanism of exchange. We assumed that exchange occurs between two molecules of complex, with equal probabilities of exchange for all pairs of complex molecules which come together in solution, except when $H_2O.BF_3$ is involved. Exchange between two molecules of complex has been reported to occur in systems of ether.BF_3 complexes, but in competition with another mechanism (8). Although the assumption of equal donor–acceptor bond lifetimes for all species but $H_2O.BF_3$ gave good qualitative agreement for the spectra of one sample, as shown in Fig. 8, this was not the case for a second sample, in which peak 6 was much larger (3.1% of the total peak area, compared with considerably less than 1% in the first sample). In this sample, peak 6 was found to remain separate to a higher temperature than was predicted from calculations based on the above assumption. Presumably this effect was not observed in the previous sample because of the very small size of the peak. In order to obtain agreement of calculated and observed spectra in this sample it was necessary to assume that the donor–acceptor bond lifetime of the peak 6 species is intermediate between those of $H_2O.BF_3$ and of the ketone.BF_3 species. The fairly good fit shown in Fig. 9 was obtained for the ratio of bond lifetimes

$$\text{ketone.}BF_3\text{:peak 6 species:}H_2O.BF_3 = 1:20:1000$$

The intermediate bond lifetime of the species giving rise to peak 6 suggests an intermediate donor–acceptor bond strength. This lends weight

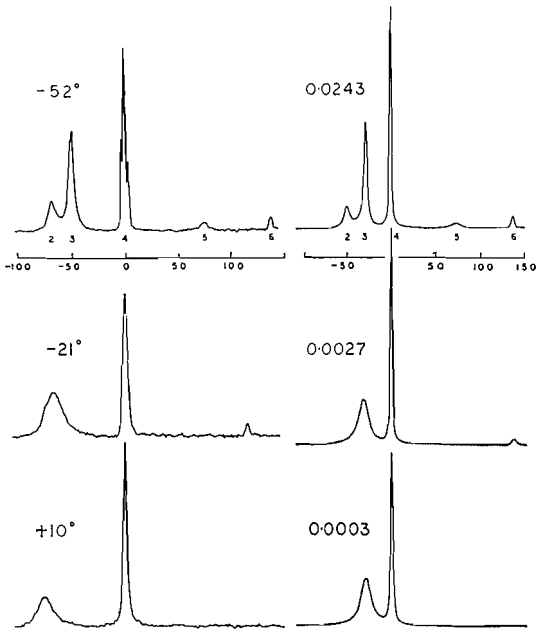

FIG. 9. Computer fit of some ^{19}F spectra of a partially decomposed 1.2 *M* solution of $^{10}BF_3$ in acetone. The calculations assume equal donor–acceptor bond lifetimes, given (in seconds) on the spectra, for the complexes giving rise to peaks 1, 2, 3, and 5. The complex giving rise to peak 6 is assumed to have a lifetime 20 times greater; $H_2O.BF_3$ giving rise to peak 4, is assumed to have a lifetime 1000 times greater. The spectra are calibrated in Hz from peak 4.

to the proposal made above that peak 6 arises from the complex of a Lewis base impurity which has sufficient base strength to displace the ketones from their complexes.

Acetone.BF_3 in Methylene Chloride

None of the dilute solutions of acetone.BF_3 in methylene chloride studied in our previous work (2) showed pronounced changes in color such as were observed when acetone was the solvent. However, in solutions in which [acetone] > [BF_3] a pale yellow color appeared on standing for a few hours at room temperature, which did not darken much more even after reaction for an hour at 100°. The color change is dependent on the relative proportions of acetone and BF_3 since it did not occur in solutions in which [acetone] < [BF_3].

^{19}F spectra of acetone.BF_3 solutions in methylene chloride did not change noticeably after the solutions had been allowed to stand at room temperature or above (2). However, proton

Can. J. Chem. Downloaded from www.nrcresearchpress.com by 210.87.254.5 on 09/05/12
For personal use only.

spectra showed slight changes which provide evidence of a chemical reaction, apparently related to the slight color change. In solutions in which [acetone] > [BF_3], very small new peaks appeared on standing, two of them unsymmetrically situated on either side of the acetone peak, and others at about 6.5 and 11.2 δ. Further standing at room temperature seemed to have no further effect on the proton spectrum. Even standing for 1 h at 100°, which resulted in a slight darkening of the color, did not significantly increase the size of the small peaks near the acetone peak or the peak at 6.5 δ. However, the peak at 11.2 δ gained in intensity, and some new small peaks appeared at high field. In contrast, in spectra of solutions in which [acetone] < [BF_3] no new peaks appeared near the acetone peak or at 6.5 or 10–12 δ after standing for several hours at room temperature. In solutions containing considerable excess BF_3 which had been allowed to stand at room temperature for several days, a doublet centered at 0.23 δ, with a splitting of 7.4 ± 0.3 Hz, appeared in the proton spectrum and became larger on further standing. Since the observed pattern agrees closely with that reported for trimethylsilyl fluoride (0.20 δ, J = 7.48 Hz (18)) it appears that a methyl group has been split off from the tetramethylsilane (TMS) present as an internal reference[2]. Since the same doublet was obtained under similar conditions from a solution containing phenol instead of acetone, it does not arise from any reaction of the ketone. No peak arising from the second product of this reaction, presumably methylboron difluoride, was identified. The stability of acetone when excess BF_3 is present is analogous to the known stability of protonated ketones when dissolved in an excess of a strong proton acid such as sulfuric acid (16).

Our observation of the stability of acetone.BF_3 in the presence of excess BF_3, but of some reaction when the acetone is in excess, suggests an explanation of the conflicting reports in the literature concerning the stability of the crystalline acetone.BF_3 complex (3, 4). It seems likely that the complex is stable only under conditions of rigorous exclusion of free acetone, and of water which would form free acetone by displacement from the complex.

Proton chemical shifts of mesityl oxide and (mesityl oxide).BF_3 at −80° are given in Table II. Room temperature shifts are very similar to these. On the n.m.r. time scale BF_3 exchange was found to be rapid at room temperature but slow at −80°, as for the saturated ketones studied previously (2). In the Table the methyl peaks are tentatively assigned on the basis of their complexation shifts, the α-methyl peak being expected to show a greater shift than the two γ-methyl peaks[3]. The methyl chemical shifts in the Table cover the range 1.90 to 2.70 δ, which includes practically the entire range of chemical shifts expected (2) for mixtures of acetone and acetone.BF_3. Thus small amounts of mesityl oxide, if present in methylene chloride solutions of acetone and BF_3, should give rise to small peaks near the acetone peak. Normally in solutions in which [acetone] > [BF_3] and which have been allowed to stand at room temperature, two small peaks of relative chemical shift 0.42 p.p.m. are visible, one on each side of the acetone peak. This shift is in agreement with the separation of the outermost two methyl peaks of (mesityl oxide).BF_3; presumably the central methyl peak is obscured by the large acetone peak. The small peak at 6.5 δ corresponds to the olefinic α-proton peak of (mesityl oxide).BF_3, and provides further evidence for the presence of mesityl oxide. The low-field peak at 10–12 δ has been assigned to $H_2O.BF_3$ on the basis of the fine structure observed in a few samples (2).

Thus small amounts of mesityl oxide and water are formed from acetone in the presence of BF_3 in methylene chloride solution. A number of factors might contribute to the decreased reactivity of acetone in the presence of BF_3 when dissolved in methylene chloride rather than acetone. The absence of a large excess of free acetone would be expected to slow the reaction somewhat, but not to the extent observed. However, if there is an equilibrium between acetone and mesityl oxide –

[2]The reaction of TMS with BF_3 is analogous to its reaction with strong proton acids such as concentrated sulfuric acid (19). and emphasizes that TMS must be used with caution as an internal standard in highly acidic mixtures containing either proton acids or Lewis acids.

[3]The complexation shifts of the γ-methyl peaks, which are two-thirds as large as those of the α-methyl and olefinic α-proton peaks, are much greater than would be expected if charge donation were due entirely to an inductive effect (2). This indicates delocalization of charge along the conjugated system by a mesomeric effect, in accord with the greater donor strength of mesityl oxide with respect to acetone which was reported earlier in this paper.

TABLE II

Proton chemical shifts of mesityl oxide and mesityl oxide – BF_3 at −80° in methylene chloride

	Chemical shifts (δ)*			
	olefinic α-proton	α-methyl	γ-methyl	
Mesityl oxide	6.14	2.18	2.14	1.90
(mesityl oxide).BF_3	6.64	2.70	2.44	2.26
Complexation shift to low field (p.p.m.)	0.50	0.52	0.30	0.36

*p.p.m. to low field of internal TMS.

water, the presence of a large excess of free acetone, as when acetone is the solvent, might be required to give large amounts of the condensation products. Also the reaction products, especially the highly polar $H_2O.BF_3$, could be less well solvated in methylene chloride; this could decrease the equilibrium constant for the formation of condensation products and thus shift the equilibrium still further towards acetone. Another possibility might be poorer solvation of the transition state of the reaction; this could raise the activation energy and greatly decrease the rate of reaction.

Detailed studies have not been carried out to determine the cause of the slowing of the reaction in methylene chloride. However, some preliminary experiments indicate that the BF_3-catalyzed condensation of acetone is a reversible reaction. A solution of mesityl oxide (1.6 *M*), water (0.4 *M*), and BF_3 (1.1 *M*) in methylene chloride, initially colorless, gave a room-temperature proton spectrum having the expected three peaks in the methyl region. After a week at room temperature, during which the solution had discolored to a dark brown, the methyl region of the room temperature spectrum contained an additional peak (Fig. 10, spectrum A). Spectra B and C show the methyl region after the sample was heated at 100° for short periods; a fairly rapid disappearance of the mesityl oxide is evident. It seems reasonable to assume that the large sharp peak at 2.55 δ, which appears during the reaction, arises from acetone; it is difficult to think of any other reaction product which could give rise to a proton spectrum consisting of a single sharp peak in the methyl region. The shift of this peak to lower field on reaction of the sample at 100° (Fig. 10) is in accord with the expected behavior of a peak due to acetone. In this sample, in which [mesityl oxide] + [water] > [BF_3], the first acetone to form would not be able to displace much of the stronger bases water and mesityl oxide from their complexes and should give a proton resonance not far from the position of free acetone, 2.14 δ. However, reaction to give more acetone would eventually have to consume complexed mesityl oxide and water; BF_3 would be displaced as these stronger donors are consumed and would complex with the weaker donor, acetone, which is formed. Thus a peak due to acetone should show the observed shift to lower field as it gains in intensity, since it is a

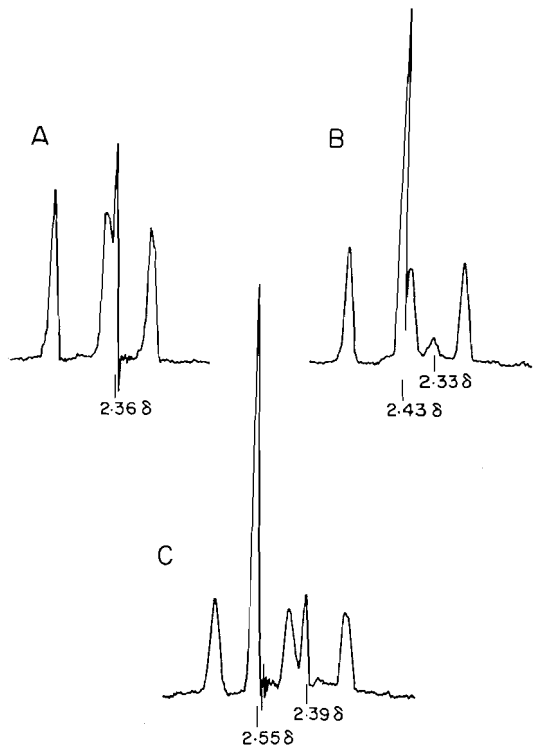

FIG. 10. Room temperature proton spectra (methyl region) of a solution of mesityl oxide, water, and BF_3 in methylene chloride. Reaction times: (A) one week at room temperature; (B) one week at room temperature and 10 min at 100°; (C) one week at room temperature and 25 min at 100°.

Can. J. Chem. Downloaded from www.nrcresearchpress.com by 210.87.254.5 on 09/05/12
For personal use only.

TABLE III

Room temperature proton chemical shifts in methylene chloride solutions after reaction at 100°

Solute	Time at 100° (min)	Chemical shifts (δ)*							
Acetone and BF_3	60	11.23	6.47	2.64		2.42 (sh)	2.36	2.22	(1.70 etc.)†
Mesityl oxide, water, and BF_3	25	*10.43*†	*6.53*	*2.66*	*2.55*	*2.44*	2.39	2.25	(1.67 etc.)†

*p.p.m. to low field of internal TMS. Peaks present initially are printed in italics.
†A number of small peaks appear at higher field.

weighted average of peaks arising from free and complexed acetone and the relative proportion of complexed acetone should be increasing. This assignment was confirmed as follows. A similar solution (mesityl oxide, 1.5 *M*; water, 0.3 *M*; BF_3, 1.2 *M*) gave a similar small sharp peak in the "ketone methyl" region after standing for a few days at room temperature. The addition of small amounts of acetone to the sample caused this peak to increase greatly in size and to shift to higher field, eventually to 2.23 δ, as is expected if the peak is a weighted average of peaks arising from free and complexed acetone.

Extensive reaction to give a range of higher condensation products occurs in the methylene chloride solutions of mesityl oxide – water – BF_3, in addition to the apparent reversion to acetone. This is indicated by the appearance of a dark brown color on standing at room temperature for a few days. It is shown more clearly by the appearance of broad irregular proton resonances to high field of the "ketone methyl" region. These increased quite rapidly in size at high temperatures; after 25 min at 100° they had a total area about equal to the total area of the peaks in the "ketone methyl" region. The condensation reaction is considerably less rapid in the methylene chloride solutions of acetone–BF_3 studied, since very little color change was observed, and the new peaks in the proton spectrum remained fairly small, after an hour at 100°. However, similar reactions appear to be taking place in both cases, involving reversible BF_3-catalyzed interconversions among acetone, mesityl oxide – water, and higher condensation products. This can be illustrated by comparison of the proton chemical shifts, after reaction at 100°, of solutions of acetone and BF_3, and of mesityl oxide, water, and BF_3, in methylene chloride, as shown in Table III. Exact correspondences in room temperature chemical shifts are not to be expected since these values are weighted averages of the shifts of free and complexed species, the relative proportions of which vary from sample to sample. Nevertheless the similarities in the patterns are significant, especially since the two samples initially had no species in common except BF_3, TMS, and methylene chloride. The following simplified reaction scheme may be useful in explaining the results:

$$[1] \qquad 2(\text{acetone}) \overset{BF_3}{\rightleftharpoons} \text{mesityl oxide} + \text{water}$$

$$\text{mesityl oxide} + \text{acetone} \overset{BF_3}{\rightleftharpoons} \text{higher condensation products} + \text{water}$$

If the first equilibrium strongly favors acetone, the mesityl oxide concentration would never become large in solutions of acetone and BF_3; also the reverse aldol reaction to give acetone would be expected to occur to a considerable extent in solutions of mesityl oxide, water, and BF_3, as is observed.

It would be unwise to attempt to make further deductions from the proton spectra of the mesityl oxide – water – BF_3 solutions, especially because the fluorine spectra of these solutions have not been explained. Four peaks are present in the fluorine-on-tetrahedral boron region in freshly prepared samples, instead of the two peaks expected for (mesityl oxide).BF_3 and $H_2O.BF_3$, and the relative peak areas vary in an unexplained manner among samples. It seems possible that some of the peaks arise from disproportionation of $H_2O.BF_3$ to give species such as BF_4^- and $BF_2(H_2O)_2^+$; a similar disproportionation affects the ^{19}F spectrum of $H_2O.BF_3$ in aqueous solution (7). Further studies of these solutions would be of interest.

Conclusion

Our detailed studies of the early stages of the boron trifluoride catalyzed reaction of acetone suggest the application of n.m.r. spectroscopy to the investigation of catalysis by boron trifluoride and other Lewis acid fluorides in systems of more

Can. J. Chem. Downloaded from www.nrcresearchpress.com by 210.87.254.5 on 09/05/12
For personal use only.

interest to the synthetic chemist. Fluorine magnetic resonance seems especially useful because it can be used to detect and identify very small amounts of complexed species in solution, and thus may prove to be of value in detecting intermediate reaction products the concentrations of which never become large.

Experimental

The purification of most of the chemicals, the technique of sample preparation, and the n.m.r. spectrometer have been described previously (2, 10). Proton chemical shifts (δ) are given in p.p.m. to low-field of internal tetramethylsilane. Practical grade mesityl oxide was dried over calcium chloride and magnesium sulfate, and fractionated; the fraction of boiling range 128.5–128.6° was taken and was allowed to stand overnight over Linde 4A molecular sieves before use. Practical grade phorone was purified by vacuum sublimation onto a cold finger cooled by dry ice to give pale yellow needles which could be stored unchanged at 10°. Warming of the crystals to room temperature (29°) gave a pale yellow liquid.

An IBM 7040 computer was used for the calculation of spectral shapes resulting from various rates of chemical exchange of magnetic nuclei among six non-equivalent sites. Matching of experimental and calculated spectra was done visually to give an approximation to the rates of exchange at various temperatures.

Acknowledgments

We wish to thank the National Research Council of Canada and the United States Air Force Office of Scientific Research for financial support of this work and the Department of University Affairs, Province of Ontario, for the award of an Ontario Graduate Fellowship (to J. S. H.).

1. F. LANDOLPH. Compt. Rend. **86**, 1463 (1878). D. R. MARTIN and J. M. CANNON. *In* Friedel–Crafts and related reactions. Vol. 1. *Edited by* G. A. Olah. Interscience Publishers, Inc., New York. 1963. Chap. 6.
2. R. J. GILLESPIE and J. S. HARTMAN. Can. J. Chem. **46**, 2147 (1968).
3. A. V. TOPCHIEV, S. V. ZAVGORODNII, and Y. M. PAUSHKIN. Boron trifluoride and its compounds as catalysts in organic chemistry. The Pergamon Press, Ltd., London. 1959. p. 76.
4. R. LOMBARD and J. P. STEPHAN. Bull. Soc. Chim. France, 1369 (1957).
5. J. A. POPLE, W. G. SCHNEIDER, and H. J. BERNSTEIN. High-resolution nuclear magnetic resonance. McGraw-Hill Book Co., Inc., New York. 1959. Chap. 10.
6. S. BROWSTEIN, A. M. EASTHAM, and G. A. LATREMOUILLE. J. Phys. Chem. **67**, 1028 (1963).
7. P. DIEHL. Helv. Phys. Acta, **31**, 685 (1958). R. A. OGG and P. DIEHL. J. Inorg. Nucl. Chem. **8**, 468 (1957).
8. A. C. RUTENBERG, A. A. PALKO, and J. S. DRURY. J. Am. Chem. Soc. **85**, 2702 (1963); J. Phys. Chem. **68**, 976 (1964). A. C. RUTENBERG and A. A. PALKO. J. Phys. Chem. **69**, 527 (1965).
9. R. A. CRAIG and R. E. RICHARDS. Trans. Faraday Soc. **59**, 1962 (1963).
10. R. J. GILLESPIE and J. S. HARTMAN. Can. J. Chem. **45**, 859 (1967).
11. J. W. EMSLEY, J. FEENEY, and L. H. SUTCLIFFE. High-resolution nuclear magnetic resonance spectroscopy. Vol. 2. The Pergamon Press, Ltd., Oxford. 1965.
12. K. KUHLMANN and D. M. GRANT. J. Phys. Chem. **68**, 3208 (1964). R. J. GILLESPIE and J. S. HARTMAN. J. Chem. Phys. **45**, 2712 (1966).
13. F. H. STROSS, J. M. MONGER, and H. DEV. FINCH. J. Am. Chem. Soc. **69**, 1627 (1947).
14. E. C. CRAVEN and W. R. WARD. J. Appl. Chem. **10**, 18 (1960).
15. N. N. GREENWOOD and R. L. MARTIN. Quart. Rev. London, **8**, 1 (1954).
16. R. J. GILLESPIE and J. A. LEISTEN. Quart. Rev. London, **8**, 40 (1954).
17. A. ABRAGAM. The principles of nuclear magnetism. The Clarendon Press, Oxford. 1961. Chap. 10.
18. H. SCHMIDBAUR. J. Am. Chem. Soc. **85**, 2336 (1963).
19. R. E. REAVILL. J. Chem. Soc. 519 (1964).

Can. J. Chem. Downloaded from www.nrcresearchpress.com by 210.87.254.5 on 09/05/12
For personal use only.

Can. J. Chem. Downloaded from www.nrcresearchpress.com by 210.87.254.40 on 09/05/12
For personal use only.

Evidence for the existence of an electric field effect from the vinyl proton magnetic resonance spectra of 4-substituted styrenes

G. K. HAMER[1] AND W. F. REYNOLDS
Department of Chemistry, University of Toronto, Toronto 5, Ontario

Received May 3, 1968

Vinyl proton chemical shifts of styrene and six 4-substituted styrenes have been determined at infinite dilution in cyclohexane. It is shown that changes in the chemical shift difference of the β protons, $\Delta(\delta_C - \delta_B)$ can be accounted for by electric field effects. Reasonable values of the constant in the Buckingham equation of $(-3.11 \pm 0.50) \times 10^{-12}$ and $(-4.77 \pm 0.83) \times 10^{-12}$ are obtained from two different types of field effect calculations. Residual chemical shift changes for β protons after correction for electric field effects can be explained in terms of mesomeric and possibly inductive mechanisms. α-Proton chemical shift values cannot be satisfactorily rationalized. Small concentration effects are noted, usually resulting in high field shifts with increasing concentration. Previous results are reexamined in order to resolve a conflict in the literature.

Canadian Journal of Chemistry, 46, 3813 (1968)

Introduction

The question of whether substituent effects other than mesomeric effects are transmitted through bonds (inductive effects) or through space (electric field effects) is still under investigation, largely by measurements of acid dissociation constants (1–4). However, Buckingham has derived an equation (5), $\Delta\delta = AE_z + BE^2$, which allows one to predict the change in proton chemical shifts, $\Delta\delta$, due to intra- and intermolecular electric fields. In the case of neutral molecules, the change in proton chemical shift due to an electric field is predicted to be very nearly proportional to the strength of the electric field along the X—H bond axis, E_z, since the second term is negligible (6, 7). Buckingham's equation has been tested by Zürcher (6, 7) using a variety of substituted steroids. The agreement between calculated and experimental chemical shifts is generally very good.

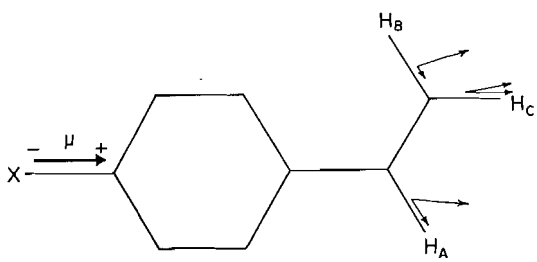

FIG. 1. Labelling of vinyl protons and electric field components due to a polar substituent in a 4-substituted styrene.

As part of a continuing interest in the mechanism of transmission of substituent effects to side chains of substituted aromatic compounds (8, 9), it was considered desirable to further test Buckingham's equation in a system of this type. The compounds chosen were 4-substituted styrenes. Due to the geometry of these compounds (see Fig. 1), one would expect considerably different components of the electric field (due to the polar C—X group) along the C—H_B and C—H_C bond axes and consequently considerably different electric field effects upon these protons.

When this investigation was started, there were three sets of chemical shift data for the vinyl protons of substituted styrenes. Measurements had been carried out for concentrated solutions (20 wt. %) in CCl_4 (10), moderately concentrated solutions (10 mole %) in $CDCl_3$ (11), and over a range of concentrations (extrapolated to infinite dilution) in acetone (12). From the results in acetone it had been concluded that there was no evidence for the existence of an electric field effect. However, the available data could all be significantly affected by dilution effects and/or effects due to solvent polarity. Since the electric field effect should be quite small, we considered that it was necessary to accurately determine the chemical shifts for the vinyl protons at infinite dilution in an inert solvent. After this investigation had started, the possibility of ambiguity in the interpretation of the available results was confirmed when a further publication appeared, claiming that the results for vinyl proton chemical shifts in CCl_4 could be interpreted largely in terms of electric

[1]Holder of an NRCC Studentship, 1967–68.

Can. J. Chem. Downloaded from www.nrcresearchpress.com by 210.87.254.40 on 09/05/12
For personal use only.

field effects and π-electron density changes at the β carbon (13).

In view of the disagreement in the literature (12, 13), it was decided to limit this investigation to a series of substituted styrenes for which relatively large field effects might be expected. Only 4-substituted styrenes were chosen since the interpretation of the results for 3-substituted styrenes would be complicated by the existence of two planar conformers (13) with possibly different populations.

In this paper it is shown that changes in the chemical shift difference between B and C protons of 4-substituted styrenes can be accounted for by an electric field effect but not by any other single substituent effect. Previous results are reexamined and it is shown that the chemical shift data for styrenes in CCl_4 (10) and $CDCl_3$ (11) show evidence of electric field effects while in acetone (12) these effects are largely obscured, apparently by specific solvent effects.

Experimental

The styrenes used in this investigation were commercially available. Liquid styrenes were distilled just before use under reduced N_2 pressure (20 mm Hg). 4-Nitrostyrene and 4-iodostyrene were purified by evaporation on to a cold finger at 0.5 mm pressure. Fisher A.C.S. grade cyclohexane was fractionally distilled from sodium in a nitrogen atmosphere and stored over Linde type 5A molecular sieve until used. Three or more solutions (1–5 mole % of styrene in cyclohexane) were prepared in each case. Spectra were recorded on a Varian HA-100 spectrometer operating in frequency sweep mode at a probe temperature of 30 °C. The spectrometer was locked on to the solvent peak. Spectral peak positions relative to the solvent peak were determined by measuring frequency differences between the manual (lock) oscillator and sweep oscillator. Frequencies were measured to ±0.02 Hz using a Hewlett–Packard 5245 electronic counter in period average mode. Measurements were repeated at least six times for each peak, sweeping alternately in opposite directions at a sweep rate of 0.05 Hz/s. The proton chemical shift of tetramethylsilane relative to cyclohexane was measured for a range of concentrations in order to determine styrene proton chemical shifts relative to tetramethylsilane at infinite dilution.

Results

Vinyl proton spectra were initially analyzed as ABC spectra by the exact method (14), using the computer program EXAN. As previously observed (11), the best fit between calculated and observed spectral intensities was found for the solution with positive vicinal and geminal coupling constants. The spectrum of 4-fluorostyrene was complicated by H_B–F^{19} and H_C–F^{19} coupling. In this case the repeated spacings (14) in the ABCX spectrum were determined, assuming first order splitting by F^{19}, and the spectrum was analyzed as an ABC spectrum.

Spectral parameters were further refined in each case by carrying out an iterative ABC or ABCX spectral analysis, using the computer program LAOCN3. Changes in spectral parameters were smaller than the experimental error in each case.

Infinite dilution chemical shifts were determined by least squares fitting, assuming linear dilution curves. In the case of styrene, there was deviation from linearity for the most concentrated solution (see Fig. 2). Consequently the data from this solution were not included in the least squares fitting process. In all other cases, dilution shifts were linear within experimental error and three concentrations were sufficient. Typical dilution curves are shown in Fig. 3.

Experimental data for infinite dilution vinyl proton chemical shifts relative to tetramethylsilane at infinite dilution in cyclohexane are given

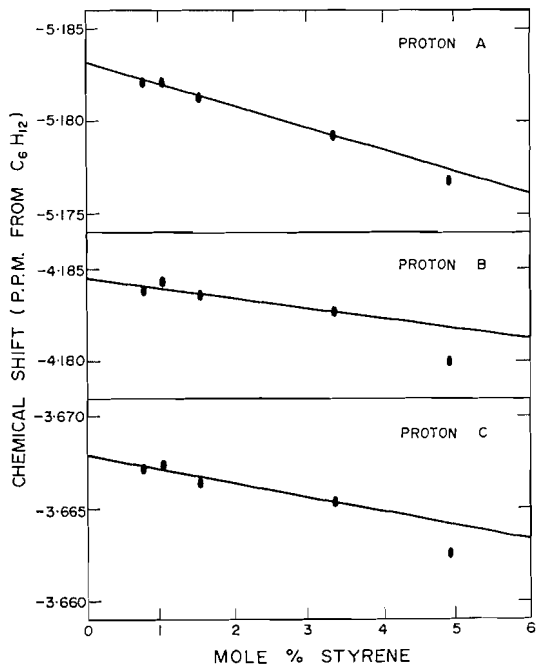

FIG. 2. Plot of vinyl proton chemical shifts for styrene (in p.p.m. relative to internal cyclohexane) versus concentration in mole %.

TABLE I

Vinyl proton chemical shift data for 4-substituted styrenes in p.p.m. relative to tetramethylsilane, both at infinite dilution in cyclohexane

Substituent	δ_A*	δ_B	δ_C	$(\delta_C - \delta_B)$
H	−6.6270±0.0001	−5.6283±0.0003	−5.1116±0.0002	+0.5167
F	−6.5895±0.0003	−5.5503±0.0007	−5.0993±0.0004	+0.4510
Cl	−6.5802±0.0005	−5.6101±0.0003	−5.1450±0.0004	+0.4651
Br	−6.5657±0.0002	−5.6281±0.0004	−5.1556±0.0001	+0.4725
I	−6.5479±0.0004	−5.6398±0.0002	−5.1471±0.0003	+0.4927
OCH_3	−6.5593±0.0006	−5.4800±0.0008	−4.9848±0.0007	+0.4952
NO_2	−6.6995±0.0005	−5.8050±0.0003	−5.3610±0.0006	+0.4439

*Defined as $\delta = (H - H_{reference})/H \times 10^6$.

in Table I. Chemical shift data were converted relative to tetramethylsilane by adding a constant factor of −1.4438 p.p.m., the experimentally determined chemical shift of cyclohexane relative to tetramethylsilane at infinite dilution. Standard deviations for measurements of individual peaks never exceeded 0.05 Hz. Consequently it is estimated that experimental chemical shifts are accurate to within this error. Quoted error limits for infinite dilution chemical shifts are standard deviations (15) of the intercepts of the least squares plots. It is estimated that chemical shift differences are accurate to within 0.1 Hz. Chemical shift differences for B and C protons were independently determined by plotting $(\delta_C - \delta_B)$ versus concentration and extrapolating to infinite dilution. The plots were generally better than those for the individual proton chemical shifts. The extrapolated chemical shift differences by the two techniques agreed to within 0.01 Hz in each case.

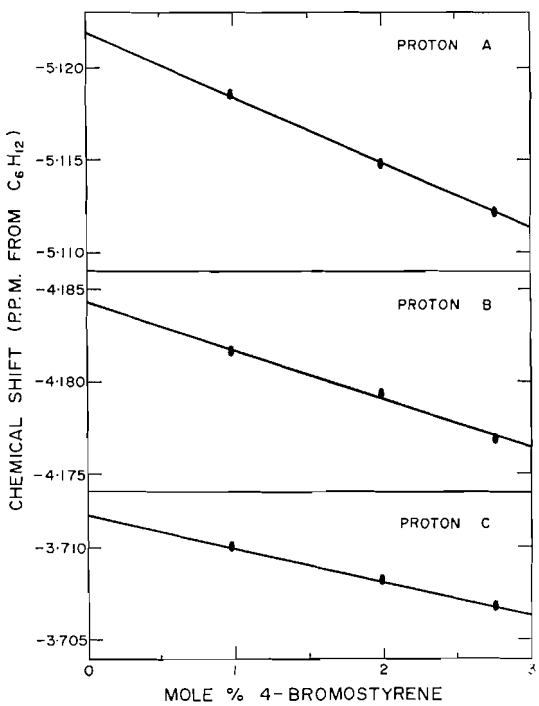

FIG. 3. Plot of vinyl proton chemical shifts for 4-bromostyrene (in p.p.m. relative to internal cyclohexane) versus concentration in mole %.

Discussion

(a) β-Proton Chemical Shifts

Protons B and C should be equally affected by any inductive mechanism since they are an equal number of bonds removed from the substituent. Similarly any mesomeric interaction involving a substituent in the 4 position should affect both protons nearly equally since the main effect will be due to changes in π-electron density at the β carbon[2]. Consequently changes in the difference in chemical shift between B and C protons

[2]A referee has disputed this assumption stating that he believes that the mesomeric interaction will not affect both protons equally. He offers in support of this contention the fact that the *cis* and *trans* coupling constants are different in these systems. We do not believe his assumption since it is inconsistent with our results. First, there is absolutely no correlation between chemical shift differences $(\delta_C - \delta_B)$ and the expected mesomeric effects of the substituents; e.g., $(\delta_C - \delta_B)$ is less for the fluoro and nitro derivatives than for styrene even though these substituents have opposite mesomeric effects. Secondly, according to the reverse of the referee's arguments, one would expect significant changes in the *cis* and *trans* vinyl proton coupling constants if the changes in $(\delta_C - \delta_B)$ were due to different mesomeric effects upon these protons. In actual fact, these coupling constants are constant within experimental error (see Table II). Consequently, we conclude that any effect of the sort suggested by the referee is negligible compared to other effects.

Can. J. Chem. Downloaded from www.nrcresearchpress.com by 210.87.254.40 on 09/05/12
For personal use only.

TABLE II

Vinyl proton coupling constants (Hz)

Substituent	J_{AB}	J_{AC}	J_{BC}
H	17.56	10.90	1.09
F*	17.56	10.93	0.90
Cl	17.56	10.89	0.87
Br	17.55	10.89	0.87
I	17.56	10.89	0.89
OCH_3	17.55	10.89	1.12
NO_2	17.57	10.93	0.58

*$J_{AF} \approx 0, J_{BF} = 0.57, J_{CF} = 0.72$.

should be a sensitive measure of through space effects.

^{13}C chemical shift data for substituted styrenes indicate that deviations from coplanarity of the phenyl and vinyl groups only occur when there are bulky substituents in one or both of the ortho positions (16). Therefore, it is assumed that all styrenes which have been investigated are planar and that ring current effects upon vinyl protons do not vary from compound to compound. Consequently the only through space effects which must be considered are the effect of the anisotropic magnetic susceptibility of the C—X bond and the effect of the electric field of the C—X bond dipole. Experimental and calculated chemical shift differences are given in Table III.

For axially symmetric C—X bonds, the effect of anisotropic magnetic susceptibility is given (17) by the equation

$$\Delta\delta = (\chi_{\parallel} - \chi_{\perp})(1 - 3\cos^2\theta)/3R^3$$

For halogens it is believed that $\Delta\chi$ is negative (18, 19). Therefore, both B and C protons should be shielded and $\delta_C - \delta_B$ should decrease, as observed. However, $|\Delta\chi|$ increases from F to I (18, 19). Consequently $\Delta(\delta_C - \delta_B)$ should be greatest for I. Clearly the observed changes in $\delta_C - \delta_B$ for 4-halostyrenes cannot be explained solely in terms of the anisotropic effects of the C—halogen bonds. In fact, the agreement between experiment and field effect calculations is made worse by the inclusion of an anisotropic correction. Consequently, it must be concluded that there is no evidence for an anisotropic effect for the C—halogen bond in this system. Zürcher reached a similar conclusion (6, 7). It has also

TABLE III

Experimental and calculated chemical shift differences for 4-substituted styrenes

Substituent		Chemical shift differences (p.p.m.) Experimental	Anisotropic effect†	Electric field effect	Dipole moment
H	$\Delta(\delta_C-\delta_B)$	0	—	—	−0.3
F	$\Delta(\delta_C-\delta_B)$	−0.0657	+1.85	−0.0485	1.51
	$\Delta\delta_A$	+0.0375	−6.17	−0.0482	
	$\Delta\delta_B$	+0.0780	−5.23	+0.0048	
	$\Delta\delta_C$	+0.0123	−3.38	−0.0437	
Cl	$\Delta(\delta_C-\delta_B)$	−0.0516	+1.72	−0.0470	1.56
	$\Delta\delta_A$	+0.0468	−5.57	−0.0450	
	$\Delta\delta_B$	+0.0182	−4.83	+0.0052	
	$\Delta\delta_C$	−0.0334	−3.11	−0.0417	
Br	$\Delta(\delta_C-\delta_B)$	−0.0442	+1.67	−0.0440	1.48
	$\Delta\delta_A$	+0.0613	−5.37	−0.0416	
	$\Delta\delta_B$	+0.0002	−4.68	+0.0050	
	$\Delta\delta_C$	−0.0440	−3.01	−0.0389	
I	$\Delta(\delta_C-\delta_B)$	−0.0240	+1.60	−0.0384	1.29
	$\Delta\delta_A$	+0.0791	−5.10	−0.0358	
	$\Delta\delta_B$	−0.0115	−4.50	+0.0046	
	$\Delta\delta_C$	−0.0355	−2.90	−0.0337	
OCH_3	$\Delta(\delta_C-\delta_B)$	−0.0214	—	−0.0194	0.473*
	$\Delta\delta_A$	+0.0677	—	−0.0185	
	$\Delta\delta_B$	+0.1483	—	+0.0022	
	$\Delta\delta_C$	+0.1268	—	−0.0172	
NO_2	$\Delta(\delta_C-\delta_B)$	−0.0738	—	−0.0772	2.95
	$\Delta\delta_A$	−0.0725	—	+0.0711	
	$\Delta\delta_B$	−0.1767	—	+0.0096	
	$\Delta\delta_C$	−0.2494	—	−0.0676	

*Component along φ—O bond for the resultant of two C—O bond dipole moments and a methyl group moment.
†In units of 10^3 $\Delta\chi$, $\Delta\chi$ = anisotropic magnetic susceptibility of C—X bond per mole.

Can. J. Chem. Downloaded from www.nrcresearchpress.com by 210.87.254.40 on 09/05/12
For personal use only.

Can. J. Chem. Downloaded from www.nrcresearchpress.com by 210.87.254.40 on 09/05/12
For personal use only.

recently been claimed that apparent anisotropic effects for C—F and C—Cl bonds are really largely due to electric field and inductive effects (20). Very little is known about the anisotropic effects of the other substituents. The one available estimate of the anisotropic effect of the NO_2 group (21) indicates that there should be very little effect upon vinyl protons.

There are two methods for carrying out electric field calculations. Buckingham (5) and, apparently, Zürcher calculate E_z at the proton in question while Musher (22) has argued that E_z should be determined at a point half way along the X—H bond. Both types of calculations have been carried out, using a computer program written for this purpose. Typical values of bond angles and bond lengths (23) were chosen. Aliphatic bond dipole moments (24) were used in order to eliminate mesomeric effects from the calculation. For styrene and 4-halostyrenes, the bond dipole was considered to be a point dipole located half way along the C—X bond. Assumed locations of the dipoles for the 4-methoxy and 4-nitro groups are shown in Fig. 4. Calculations were carried out for both C—H and C—X bonds and the electric field difference, ΔE_z (where $\Delta E_z \equiv E_z$ (C—X) $- E_z$ (C—H)), was determined for each vinyl proton.

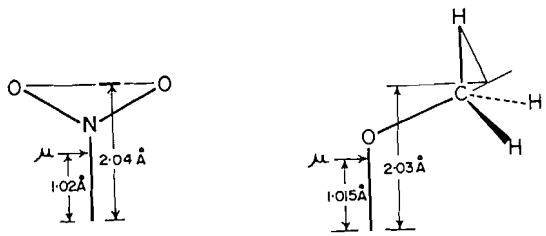

FIG. 4. Assumed locations of point dipoles in 4-nitro and 4-methoxy groups.

If $\Delta(\delta_C - \delta_B)$ is solely the result of electric field effects, then the slope of a plot of ΔE_z(C) $-$ ΔE_z(B) versus either $(\delta_C - \delta_B)$ or $\Delta(\delta_C - \delta_B)$ should give a reasonable value for A, the constant of the Buckingham equation. For the calculation of E_z at a point half way along the C—H bond, $A = -3.11 \times 10^{-12}$ (see Fig. 5). This is in excellent agreement with the theoretical value of -3.1×10^{-12} and the experimental "best value" of -2.9×10^{-12} (22). For the calculation of E_z at the proton, $A = -4.77 \times 10^{-12}$. This agrees closely with the experimental

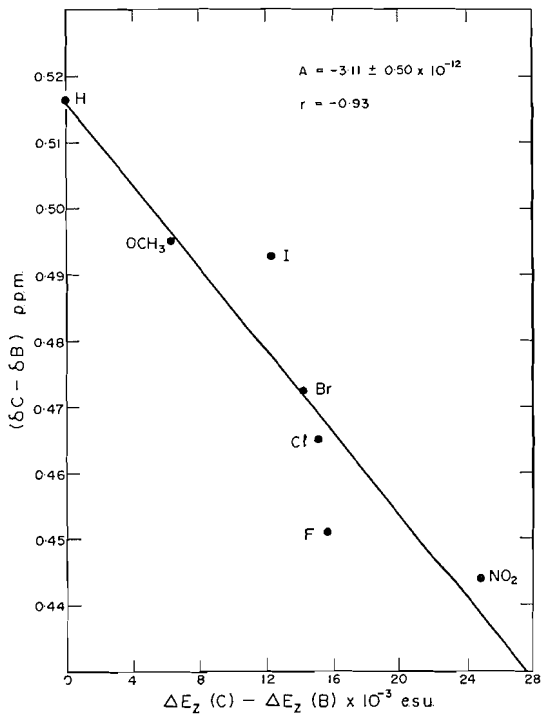

FIG. 5. Plot of chemical shift difference for β protons versus difference of changes in electric field at β protons upon replacement of the 4 proton with a polar substituent.

value of -4.5×10^{-12} obtained by Zürcher (6, 7). It is impossible to determine from these results which type of calculation is better. Calculated values for $\Delta(\delta_C - \delta_B)$ are given in Table III. The agreement between experimental and calculated values is good although minor deviations occur for F and I. It may be significant that the points for the halogens essentially lie on a straight line. This possibly indicates that there is an additional substituent effect due to the halogens (presumably acting through space). It would be tempting to assume that this is an anisotropic magnetic susceptibility effect. However, this appears improbable since the deviations are in the wrong direction. It is clear from this and results discussed in part (*b*) that substituent effects for halogens are not completely understood.

In spite of the deviations noted above, the generally good agreement between calculated and observed chemical shift differences and the reasonable values for A strongly suggest that the observed changes in $(\delta_C - \delta_B)$ can be explained

Can. J. Chem. Downloaded from www.nrcresearchpress.com by 210.87.254.40 on 09/05/12
For personal use only.

in terms of electric field effects. No other single substituent effect could explain the results. It could be argued that this agreement is accidental and arises from a fortuitous combination of effects. It would be difficult to prove or disprove this contention by considering our results in isolation. However, Zürcher, from chemical shift measurements of a large number of compounds which are unrelated to ours, has also concluded that the chemical shifts can be explained in terms of electric field effects (6, 7). The chance of accidental agreement in both cases would appear to be slight. Consequently, although we cannot claim to have proven beyond doubt the existence of electric field effects, we feel that our results are significant since they provide further evidence that electric field effects may be an important factor contributing to proton chemical shifts.

Agreement for $\Delta\delta_C$ and $\Delta\delta_B$ is generally poor. This is presumably due to inductive and/or mesomeric interactions which affect both protons nearly equally. Estimates of the magnitudes of these effects have been obtained by subtracting the average electric field effects from the average chemical shift changes (see Table IV). The results for 4-iodostyrene and 4-bromostyrene indicate that inductive effects may be present. The residual chemical shift changes for other substituted styrenes are largely due to mesomeric effects since they correlate reasonably well with calculated π-electron densities (13, 25) and with ^{13}C chemical shifts (16) for β-carbon atoms in substituted styrenes. The agreement between $\Delta(\delta_C - \delta_B)$ and the electric field calculations are particularly encouraging in view of the great range of mesomeric effects in the compounds which were investigated.

No correction has been made for reaction field effects (5). According to reaction field theory, the changes in chemical shift for the vinyl protons of 4-substituted styrenes with increasing solvent dielectric constant should be $-0.5X$, $+0.5X$, and $-X$ for A, B, and C protons respectively. X depends upon solvent dielectric constant and upon the dipole moment, size, and polarizability of the solute (5) and probably upon solute shape (26). Comparison of our results with those in acetone (12) (see part (*e*)) shows that the pattern of solvent shifts is completely unrelated to that predicted by reaction field theory. Buckingham's theory of the reaction field effect has been criticized (27, 28) although in one of the cases the criticism may not be justified (29). In the absence of any evidence to the contrary, it is assumed that solvent effects are minimal for the vinyl protons of styrenes in cyclohexane.

TABLE IV

Estimated chemical shifts for β protons (in p.p.m.) due to inductive and mesomeric effects

	$(\Delta\delta_B + \Delta\delta_C)/2$		
Substituent	Experimental	Electric field	Difference
F	+0.0452	−0.0194	+0.0646
Cl	−0.0076	−0.0199	+0.0123
Br	−0.0221	−0.0170	−0.0051
I	−0.0235	−0.0145	−0.0090
OCH_3	+0.1376	−0.0075	+0.1451
NO_2	−0.2131	−0.0290	−0.1841

(b) α-Proton Chemical Shifts

Just as in the case of the individual β-proton chemical shifts, the α-proton chemical shift data can be explained only by considering inductive and mesomeric effects as well as electric field and anisotropic effects. In the case of 4-halostyrenes, it is difficult to explain the results with any combination of the four effects. High field shifts ranging from 0.038 p.p.m. for 4-fluorostyrene to 0.078 p.p.m. for 4-iodostyrene are noted. Previous workers have also reported difficulties in explaining α-proton chemical shifts in halostyrenes (11, 13).

The high field shifts are similar to those noted for the *meta* protons in halobenzenes (30, 31). These shifts have apparently never been explained although it has been shown conclusively that they cannot be attributed to anisotropic magnetic susceptibility effects (32).

(c) Coupling Constants

The vicinal coupling constants (see Table II) are amazingly constant. Since it seems most unlikely that this agreement is accidental, this is a reassuring indication of the accuracy of the measurements. In the case of styrene, the agreement with the vicinal coupling constants reported by Gurudata *et al.* (11) is much better than with those reported by Snyder (33).

Geminal coupling constants are much more sensitive to substituent effects. As previously noted (11), they correlate reasonably well with Hammett σ constants. However, they also cor-

Can. J. Chem. Downloaded from www.nrcresearchpress.com by 210.87.254.40 on 09/05/12
For personal use only.

relate at least as well with calculated electric field differences. The possibility that the trend in coupling constants is due to intramolecular electric field effects cannot be excluded.

(d) Concentration Effects

Slopes of the plots of chemical shift versus concentration are given in Table V. Concentration effects are generally small. However, certain trends can be distinguished in the case of 4-halostyrenes. With increasing polarizability of the substituent, there is apparently an increasing tendency for solute molecules to form collision complexes in a stacked configuration. This is indicated by the increase in chemical shift of the vinyl protons with increasing concentration. The changes are greatest for the protons closest to the ring, as would be expected if the high field shifts are due to the ring current of the adjacent solute molecule.

TABLE V

Slopes of plots of vinyl proton chemical shifts (in p.p.m.) versus styrene concentration (in mole %)

	Slope (p.p.m./mole %) × 10^3		
Substituent	A	B	C
H	+1.17	+0.53	+0.75
F	+2.25	+1.04	+1.20
Cl	+2.96	+2.10	+1.39
Br	+3.54	+2.62	+1.80
I	+3.85	+2.37	+1.17
OCH_3	+0.70	−0.43	−0.65
NO_2	+0.98	−2.07	−0.71

(e) Comparison with Previous Results

The vinyl proton chemical shifts in acetone are to low field of those in cyclohexane by 0.09 to 0.25 p.p.m. The difference decreases in the order A > B > C. Low field shifts of 0.04 to 0.12 p.p.m. are found in $CDCl_3$ relative to cyclohexane but in this case the shifts are in the order C > B > A. These results can be rationalized in terms of solvent–solute hydrogen bonding, and concentration effects in the case of $CDCl_3$ solutions.

The results in CCl_4 are similar to those in cyclohexane. Shifts of +0.03 to −0.02, −0.02 to −0.06, and −0.02 to −0.07 p.p.m. are noted for A, B, and C protons respectively. Since the concentrations in CCl_4 range from 15 to 30 mole %, one might reasonably expect high shifts of as much as 0.1 p.p.m. due to concentration effects. However, these high field shifts may be cancelled by low field shifts, possibly due to induced dipole – induced dipole solvent–solute interactions. Low field shifts of 0.15 p.p.m. have been noted for polar solutes in CCl_4 relative to cyclohexane (34, 35).

Values of $(\delta_C - \delta_B)$ for 4-substituted styrenes are given in Table VI. Trends in $(\delta_C - \delta_B)$ which can be attributed to electric field effects are noted for CCl_4 and $CDCl_3$ solutions. Any specific solvent effects which may be present do not obscure these trends. Reasonable values for $(\delta_C - \delta_B)$ are also obtained for the 3-substituted styrenes which have been previously investigated.

It has been claimed that styrene proton chemical shift data in acetone show no evidence of electric field effects (12). δ_C was plotted versus δ_B and a straight line of unit slope was obtained. However, this technique is insensitive in systems such as styrenes where mesomeric interactions

TABLE VI

Comparison of values of $(\delta_C - \delta_B)$ for 4-substituted styrenes from this and previous investigations

	$(\delta_C - \delta_B)$*			
Substituent	This study	Ref. 10	Ref. 11	Ref. 12
H	0.517	0.500	0.505	0.562
4-F	0.451	—	—	—
4-Cl	0.465	0.442	0.449	0.528
4-Br	0.473	0.448	0.451	—
4-I	0.493	—	—	—
4-OCH_3	0.495	0.475	0.486	0.540
4-NO_2	0.444	0.438	0.427	0.538
4-CH_3	—	0.503	0.512	0.558
4-$N(CH_3)_2$	—	—	0.519	—
3,4-diCl	—	0.438	0.412	—

*In parts per million.

Can. J. Chem. Downloaded from www.nrcresearchpress.com by 210.87.254.40 on 09/05/12
For personal use only.

may be more important than field effects. The values of $(\delta_C - \delta_B)$ do show evidence of electric field effects although the trend is partially obscured, presumably by specific solvent effects. In particular, the change in $(\delta_C - \delta_B)$ in going from styrene to 4-nitrostyrene is much smaller in acetone than in the other solvents. Consequently, this previous failure to observe an electric field effect is not surprising.

On the other hand, the claim that vinyl proton chemical shift data for substituted styrenes can be correlated with calculated π-electron densities and electric field calculations (13), is, on the basis of our results, correct. In spite of the high styrene concentrations in CCl_4, and perhaps fortuitously, the results in the two solvents are very similar.

Conclusions

1. Changes in the chemical shift difference between β protons, $\Delta(\delta_C - \delta_B)$ in 4-substituted styrenes can be explained in terms of electric field effects. Reasonable values are obtained for *A*, the constant in the Buckingham equation.

2. There is no evidence for anisotropic magnetic susceptibility and reaction field effects upon β protons.

3. Residual chemical shifts of β protons after correction for electric field effects can be accounted for in terms of mesomeric interactions and possibly inductive effects.

4. α-Proton shifts for 4-halostyrenes cannot be explained by any reasonable combination of electric field, inductive, mesomeric, and magnetic anisotropy effects.

Acknowledgments

Financial support from the National Research Council of Canada and from the Department of University Affairs of the Province of Ontario is gratefully acknowledged.

1. J. D. Roberts and W. T. Moreland. J. Am. Chem. Soc. **75**, 2167 (1953).
2. R. Golden and L. M. Stock. J. Am. Chem. Soc. **88**, 5928 (1966).
3. C. F. Wilcox and C. Leung. J. Am. Chem. Soc. **90**, 336 (1968).
4. K. Bowden and D. C. Parkin. Chem. Commun. 76 (1968).
5. A. D. Buckingham. Can. J. Chem. **38**, 300 (1960).
6. R. F. Zürcher. *In* Nuclear magnetic resonance in chemistry. Academic Press, Inc., New York. 1965. p. 45.
7. R. F. Zürcher. *In* Progress in nuclear magnetic resonance spectroscopy. Vol. 2. The Pergamon Press, Ltd., New York. 1967.
8. T. Yonemoto, W. F. Reynolds, H. M. Hutton, and T. Schaefer. Can. J. Chem. **43**, 2668 (1965).
9. S. H. Marcus, W. F. Reynolds, and S. I. Miller. J. Org. Chem. **31**, 1872 (1966).
10. J. E. Dubois, J. A. Miller, and J. Doucet. J. Chim. Phys. **63**, 1283 (1966).
11. Gurudata, J. B. Stothers, and J. D. Talman. Can. J. Chem. **45**, 731 (1967).
12. T. A. Wittstruck and E. N. Trachtenberg. J. Am. Chem. Soc. **89**, 3803 (1967).
13. J. E. Dubois and J. P. Doucet. Bull. Chim. Soc. France, 1145 (1967).
14. (*a*) S. Castellano and J. S. Waugh. J. Chem. Phys. **35**, 1900 (1961); (*b*) J. R. Cavanaugh. J. Chem. Phys. **39**, 2378 (1963).
15. H. D. Young. Statistical treatment of experimental data. McGraw-Hill Book Co., Inc., New York. 1962.
16. K. S. Dhami and J. B. Stothers. Can. J. Chem. **43**, 510 (1965).
17. H. M. McConnell. J. Chem. Phys. **27**, 226 (1957).
18. J. H. Goldstein and G. S. Reddy. J. Chem. Phys. **36**, 2644 (1962).
19. R. S. Drago and N. A. Matwiyoff. J. Organometal. Chem. Amsterdam, **3**, 62 (1965).
20. J. Homer and D. Callaghan. J. Chem. Soc. **A**, 518 (1968).
21. I. Yamaguchi. Mol. Phys. **6**, 105 (1963).
22. J. I. Musher. J. Chem. Phys. **37**, 34 (1962).
23. Tables of interatomic distances and configuration in molecules and ions. Chem. Soc. London, Spec. Publ. 11. 1958.
24. L. E. Sutton. *In* Determination of organic structures by physical methods. Vol. 1. Academic Press, Inc., New York. 1965. Chap. 9.
25. F. W. Wehrli, E. Pretsch, and W. Simon. Helv. Chim. Acta, **50**, 2189 (1967).
26. P. Diehl and R. Freeman. Mol. Phys. **4**, 39 (1961).
27. J. K. Becconsall and P. Hampson. Mol. Phys. **10**, 23 (1965).
28. P. Laszlo and J. I. Musher. J. Chem. Phys. **41**, 3906 (1964).
29. Y. Pan and J. B. Stothers. Can. J. Chem. **45**, 2943 (1967).
30. H. Spiesecke and W. G. Schneider. J. Chem. Phys. **35**, 731 (1961).
31. S. Castellano, R. Kostelnik, and C. Sun. Tetrahedron Letters, 4635 (1967).
32. (*a*) J. S. Martin. Ph.D. Thesis. Columbia University, New York. 1962. (*b*) J. S. Martin and B. P. Dailey. J. Chem. Phys. **39**, 1722 (1963).
33. E. I. Snyder. J. Am. Chem. Soc. **88**, 1155 (1966).
34. T. Matsuo. Can. J. Chem. **45**, 1829 (1967).
35. I. D. Kuntz and M. D. Johnston. J. Am. Chem. Soc. **89**, 6008 (1967).

Can. J. Chem. Downloaded from www.nrcresearchpress.com by 210.87.254.5 on 09/05/12
For personal use only.

Complexes mixtes de la sérine et de l'arginine

JULIUS ISRAELI ET MARIA CECCHETTI
Département de Chimie, Université de Montréal, Montréal, Québec

Reçu le 13 mars 1968

Les nitrilotriacétates métalliques réagissent avec la sérine et avec l'arginine pour former des complexes mixtes qui contiennent le métal, le nitrilotriacétate et un acide aminé dans la proportion 1:1:1.
On a déterminé la constante de formation de ces complexes mixtes.

Canadian Journal of Chemistry, 46, 3821 (1968)

Introduction

Dans la synthèse et l'hydrolyse des peptides et protéines il se forme un complexe mixte entre une métalloenzyme et un acide aminé. Les nitrilotriacétates métalliques peuvent être comparés avec les métalloenzymes. Une étude des complexes mixtes formés par la réaction des nitrilotriacétates métalliques avec les divers acides aminés peut expliquer la spécificité de quelques cations dans la synthèse et l'hydrolyse des peptides et protéines.

La réaction de la glycine avec les nitrilotriacétates métalliques a été étudié auparavant par Israeli (1) et par Jacobs et Margerum (2). Perrin *et al.* (3) a étudié récemment quelques complexes mixtes de la sérine.

Dans ce travail nous avons étudié la réaction des nitrilotriacétates métalliques (MeX) avec la sérine L(+) et avec l'arginine L(+).

Partie expérimentale

Nous avons utilisé des solutions des perchlorates métalliques qui ont été étalonnées par des méthodes complexométriques (4, 5).

Le pH est mesuré avec un "pH mètre Radiometer 26" et l'électrode de calomel est reliée à la solution par un pont Fisher 13-639-55 remplie d'une solution de $NaNO_3$ 0.5 *M*. Le pH mètre est calibré de manière à donner directement la concentration des ion H^+ (6).

Les titrations potentiométriques sont effectuées a une force ionique de 0.1 maintenue constante par $NaClO_4$. La température est fixée à 25 °C.

Résultats

La Fig. 1 représente la titration d'un mélange équimoléculaire de perchlorate de cuivre, nitrilotriacétate disodique et de sérine.

Soit a le nombre des moles de base ajoutée pour 1 mole de métal. Sur la Fig. 1 on voit qu'il y a deux points d'inflexion situés respectivement à $a = 1$ et $a = 2$.

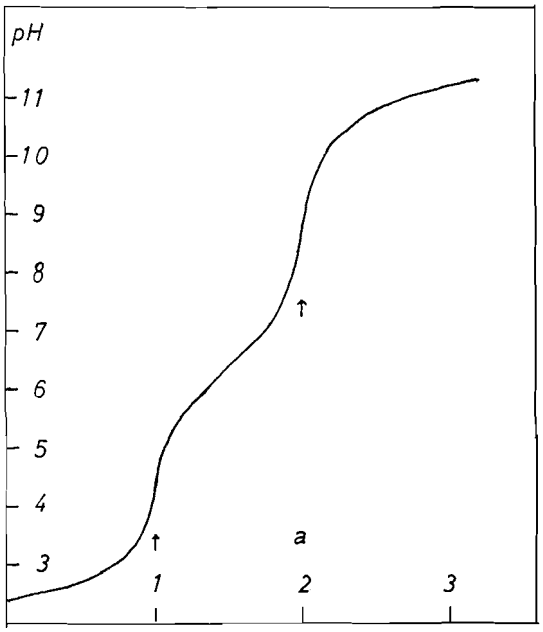

FIG. 1. Titration par la soude d'un mélange contenant perchlorate de cuivre 0.01 *M* en présence de nitrilotriacétate disodique 0.01 *M* et de sérine 0.01 *M*. La force ionique de la solution est maintenue à 0.1 avec l'aide du $NaClO_4$. a représente le nombre des moles de base ajoutée pour 1 mole de métal.

Jusqu'à $a = 1$ on titre le proton qui est libéré par le nitrilotriacétate disodique et on forme le complexe simple MeX.

Entre $a = 1$ et $a = 2$ on titre le proton qui provient de l'acide aminé et en cette région se forme le complexe mixte MeXL. En conclusion le complexe simple et le complexe mixte se forment suivant deux étapes distinctes et bien séparées. Des résultats similaires sont observés avec Ni(II), Co(II), Mn(II), Zn(II), Pb(II).

Quand on remplace la sérine par la monohydrochlorure d'arginine on observe aussi deux points d'inflexion situés respectivement à $a = 1$ et $a = 2$.

Can. J. Chem. Downloaded from www.nrcresearchpress.com by 210.87.254.5 on 09/05/12
For personal use only.

Entre $a = 1$ et $a = 2$, on titre le proton lié au groupement amino ($K_a = 9.34 \times 10^{-10}$) car le proton lié au groupement guanidino est moins labile ($K_a = 3.31 \times 10^{-13}$). En conclusion, le groupement guanidino n'intervient pas dans la formation des complexes mixtes. Pour cette raison, pour simplifier les calculs nous admettons que la monohydrochlorure d'arginine est un acide de la forme HL, le proton étant lié au groupement amino de l'arginine. Avec cette notation H_2L représente une molécule de monohydrochlorure d'arginine qui contient un proton supplémentaire lié au groupement carboxyle.

Dans le cas du Cu(II), Ni(II) et Co(II) on a étudié également la composition des complexes mixtes par la méthode des variations continues (7, 8). Sur la Fig. 2 on montre les résultats obtenus pour le système cuivre–nitrilotriacétate–arginine.

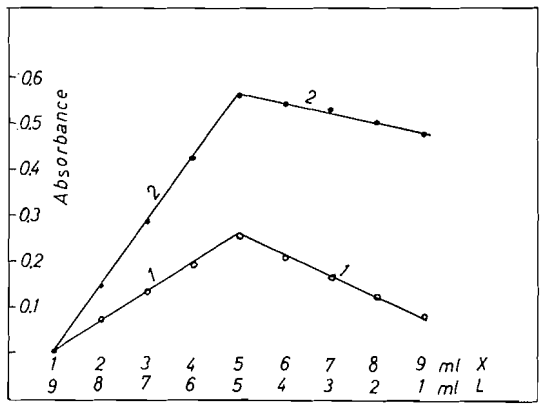

FIG. 2. Curbes des variations continues pour le système Cu(II), nitrilotriacétate (X) et arginine (L). Compostion de la solution: 5 ml Cu 0.1 M + X ml 0.1 M + (10 − X)ml L 0.1 M + 35 ml H_2O pH = 9. La curbe 1 a été mesuré a 610 mμ et la curbe 2 a été mesuré à 850 mμ.

On voit clairement sur la Fig. 2 que le complexe mixte contient cuivre, nitrilotriacétate et arginine dans la proportion 1:1:1.

Pour calculer la constante de formation des complexes mixtes nous nous servons de la portion de la courbe de titrage située entre $a = 1$ et $a = 2$ et on utilise les équations suivantes (9):

$$[1] \quad C_{Me} = C_L = C_X$$

$$[2] \quad C_{Me} = |Me| + |MeX| + |MeXL| \simeq |MeX| + |MeXL|$$

$$[3] \quad C_L = C_{Me} = |H_2L| + |HL| + |L| + |MeXL|$$

$$[4] \quad (2 - a)C_{Me} = 2|H_2L| + |HL| + |H| - |OH|$$

$$[5] \quad K_f = \frac{|MeXL|}{|MeX||L|}$$

$$[6] \quad K_1 = \frac{|H||L|}{|HL|}; \qquad K_{12} = \frac{|H||HL|}{|H_2L|}$$

Dans ces équations K_1 désigne la constante de dissociation du groupement amino protoné et K_{12} désigne la constante de dissociation du carboxyle protoné. D'autre part l'éq. [4] donne la concentration du proton titrable à chaque point de la courbe situé entre $a = 1$ et $a = 2$.

Nous avons redéterminé K_1 et K_{12} et nous trouvons (10): pour la sérine $K_1 = 9.65 \times 10^{-10}$ et $K_{12} = 6.05 \times 10^{-3}$; pour l'arginine $K_1 = 9.34 \times 10^{-10}$ et $K_{12} = 7.76 \times 10^{-3}$.

Ces équations de base conduisent aux équations suivantes:

$$[7] \quad |L| = \frac{(2 - a)C_{Me} - |H| + |OH|}{\frac{|H|}{K_1} + \frac{2|H|^2}{K_1K_{12}}}$$

$$[8] \quad K_f|L| + 1 = \frac{C_{Me}}{|L|\left\{1 + \frac{|H|}{K_1} + \frac{|H|^2}{K_1K_{12}}\right\}} = y$$

Le graphique de y en fonction de $|L|$ donne une droite dont la pente est égale à K_f et dont l'ordonnée à l'origine est 1.

Le calcul de K_f est représenté graphiquement sur la Fig. 3 pour le système cobalt–nitrilotriacétate–arginine.

Nous voulons mentionner que nous obtenons toujours la même constante K_f quand $C_{Me} = C_L = C_X$ varie entre 4×10^{-3} et 2×10^{-2} mole/l.

Le Tableau I donne les constantes de formation des complexes mixtes.

Discussion

Sur le Tableau I on voit que la constante de formation de ces complexes mixtes suit la série de stabilité de Irving et Williams (11).

Il n'y a pas grande différence entre les constantes de formation des complexes mixtes de la sérine et celles de l'arginine. Ces constantes sont très proches de celles trouvées pour les complexes mixtes de la glycine (1). Les constantes de formation K_f de ces complexes mixtes sont très proches car les K_1 et K_{12} d'acides aminés corre-

Can. J. Chem. Downloaded from www.nrcresearchpress.com by 210.87.254.5 on 09/05/12
For personal use only.

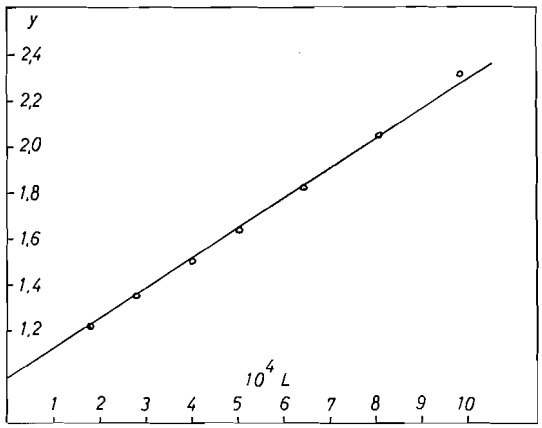

FIG. 3. Calcul graphique du K_f pour le système cobalt–nitrilotriacétate–arginine.

TABLEAU I

Constantes de formation des complexes mixtes MeXL

	Log K_f		
Me	L = sérine	L = arginine	L = glycine
Cu(II)	5.01±0.02	5.22±0.03	5.44±0.02
Ni(II)	4.14±0.02	4.20±0.02	4.41±0.01
Co(II)	3.18±0.03	3.13±0.03	
Zn(II)	3.18±0.03	3.28±0.03	
Mn(II)	1.28±0.05	1.94±0.04	
Pb(II)	1.15±0.05	1.58±0.04	

spondants sont très peu différents. On peut doc conclure que la constante de formation de ces complexes mixtes est déterminé principalement par les groupes amino et carboxyle de l'acide aminé et l'autre partie de l'acide aminé n'a pas grande influence.

L'acide aminé se comporte comme un coordinat bidenté. En formant le complexe mixte avec le nitrilotriacétate métallique l'hexacoordination du métal est facilité.

La constante de stabilité global du complexe mixte K_s est évidemment, égale à $K_{MeX} \cdot K_f$. Si K_1 représente la constante de formation du complexe MeL, nous trouvons la relation empirique suivante:

$$[9] \qquad \log K_s = \alpha \log K_{MeX} \cdot K_1 + C$$

La Fig. 4 nous explicite cette relation pour les complexes mixtes de l'arginine.

Les constantes K_{MeX} et K_1 furent empruntées à la litérature (10). Cette relation empirique est également vérifiée pour d'autres complexes mixtes[1].

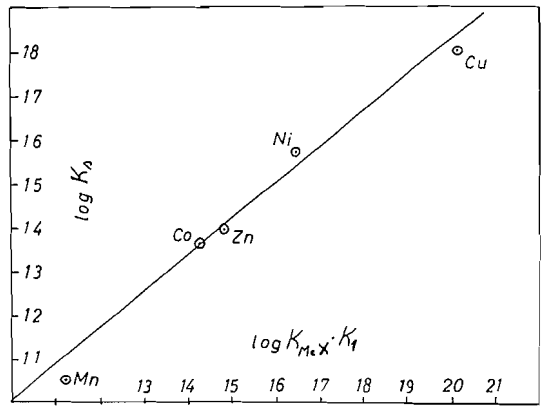

FIG. 4. Log K_s en fonction du log $K_{MeX} \cdot K_1$ pour les complexes mixtes de l'arginine.

Pour expliquer cette relation empirique on doit supposer que l'énergie libre du complexe mixte ΔG_m est lié a l'énergie libre des complexes simples par la relation:

$$[10] \qquad \Delta G_m = \alpha(\Delta G_{MeX} + \Delta G_{ML}) + b$$

Le terme constant b de l'éq. [10] représente un interaction électrostatique constante. Grâce à la Fig. 4 on détermine une valeur d'α égale à 0.85.

Remerciements

L'un de nous (J.I.) remercie le Conseil National de Recherches du Canada pour l'octroi d'une subvention de recherche qui a permis également le stage postdoctoral du docteur M.C. au Canada.

1. J. ISRAELI. Can. J. Chem. **41**, 2710 (1963).
2. N. E. JACOBS et D. W. MARGERUM. Inorg. Chem. **6**, 2038 (1967).
3. D. D. PERRIN, I. G. SAYCE et V. S. SHARMA. J. Chem. Soc. A, 1755 (1967).
4. H. FLASCHKA. EDTA titrations. The Pergamon Press, Ltd., London. 1959.
5. F. J. WELCHER. The analytical use of EDTA. D. Van Nostrand Co., Inc., Toronto. 1958.
6. K. S. RAJAN et A. E. MARTELL. J. Inorg. Nucl. Chem. **26**, 789 (1964).
7. P. JOB. Ann. Chim. Paris, **9**, 113 (1928).
8. K. O. WATKINS et M. JONES. J. Inorg. Nucl. Chem. **24**, 809 (1962).
9. A. E. MARTELL et S. CHABEREK. J. Am. Chem. Soc. **74**, 5053 (1952).
10. Stability constants. The Chemical Society, London. 1964.
11. H. IRVING et R. J. P. WILLIAMS. J. Chem. Soc. 3192 (1953).

[1]J. Israeli. Résultats non publiés.

Can. J. Chem. Downloaded from www.nrcresearchpress.com by 210.87.254.105 on 09/05/12
For personal use only.

Etude potentiométrique de la réaction du glycylglycine avec les nitrilotriacétates métalliques

JULIUS ISRAELI ET MARIA CECCHETTI
Département de Chimie, Université de Montréal, Montréal, Québec

Reçu le 2 mai 1968

La glycylglycine (HL) réagit avec les nitrilotriacétates métalliques (MeX) et forme avec eux des complexes mixtes dont la formule est MeXL. On a déterminé par potentiométrie la constante de formation de ces complexes mixtes. Ces complexes mixtes en milieu plus basique s'hydrolisent et forment des complexes hydroxylés dont la formule est MeXLOH.

Canadian Journal of Chemistry, 46, 3825 (1968)

Nous avons étudié récemment la réaction des acides aminés avec les nitrilotriacétates métalliques (1–4). Comme suite de ce travail, nous nous sommes proposés d'étudier la réaction de la glycylglycine avec des nitrilotriacétates métalliques.

Les complexes simples de la glycylglycine ont été beaucoup étudiées et la bibliographie des travaux publiés jusqu'à 1960 est donné par la réf. 5. Les complexes simples du cuivre(II) avec la glycylglycine ont été étudiés de nouveau récemment par Kim et Martell (6) et par Sheinblatt et Becker (7). Martell a montré que dans certaines conditions la glycylglycine se comporte comme un ligand bidenté.

Partie expérimentale

Nous avons utilisé des solutions de perchlorates métalliques étalonnées par des méthodes complexométriques (8, 9).

L'électrode de calomel du pH mètre "Radiometer Model 26" est reliée à la solution à titrer par un pont Fischer 13-639-55 remplie de $NaNO_3$ 0.5 *M* et le pH mètre est calibré de façon à donner directement la concentration analytique des ions H^+ (2–4, 10), quand on utilise l'électrode de verre comme électrode indicatrice.

La force ionique de la solution à titrer est fixée à 0.1 par $NaClO_4$ et la température de la solution est maintenue à 25 °C.

Résultats

Sur la Fig. 1 nous montrons le titrage d'un mélange équimoléculaire de perchlorate de nickel(II), de nitrilotriacétate disodique et de glycylglycine.

Si a représente le nombre de moles de soude ajoutée pour 1 mole de métal de transition, on observe sur la Fig. 1 qu'il y a deux points d'inflexion situés respectivement à $a = 1$ et à $a = 2$. On a observé aussi deux points d'inflexion situés respectivement à $a = 1$ et $a = 2$ quand on

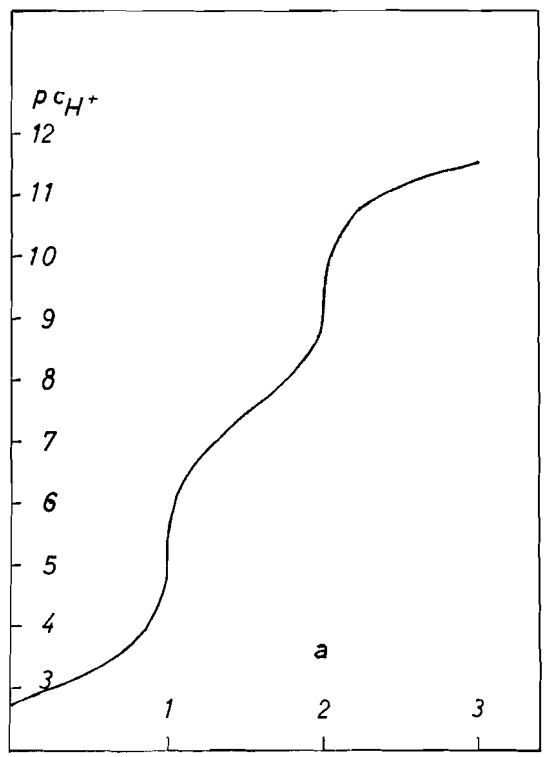

FIG. 1. Titration par la soude d'un mélange contenant du perchlorate de nickel 0.01 *M* en présence du nitrilotriacétate disodique 0.01 *M* et de glycylglycine 0.01 *M*. a représente le nombre de moles de soude ajoutée pour 1 mole de nickel. La force ionique de la solution est maintenue à 0.1 à l'aide de $NaNO_3$.

remplace le nickel(II) par des métaux comme le cuivre(II), le cobalt(II), le manganèse(II) ou le zinc(II). Dans le cas du Mn(II), après le deuxième point d'inflexion, il se forme un précipité d'hydroxyde de manganèse(II).

Jusqu'à $a = 1$ on titre le proton du nitrilotriacétate disodique et on forme le complexe simple

Can. J. Chem. Downloaded from www.nrcresearchpress.com by 210.87.254.105 on 09/05/12
For personal use only.

$[MeX]^-$. Entre $a = 1$ et $a = 2$ on titre le proton du glycylglycine (LH) et on forme le complexe mixte $[MeXL]^-$. Cette partie de la courbe est plus basse que la courbe que l'on obtient quand on titre la même quantité de glycylglycine seule.

On voit donc que le complexe simple $[MeX]^-$ et le complexe mixte $[MeXL]^{2-}$ se forment suivant deux étapes bien séparées et bien distinctes.

Pour calculer la constante de formation K_f du complexe mixte nous utilisons la partie de la courbe située entre $a = 1$ et $a = 2$ et d'après la méthode de Schwarzenbach *et al.* (11) et Kim et Martell (6) les équations suivantes sont valables dans cette région de titrage:

$$[1] \quad T_{Me} = |MeX| + |MeXL|$$

$$[2] \quad T_{Me} = T_L = |H_2L| + |HL| + |L| + |MeXL|$$

$$[3] \quad (2 - a)T_{Me} = 2|H_2L| + |HL| + |H| - |OH|$$

$$[4] \quad K_1 = \frac{|H||L|}{|HL|} \qquad K_{12} = \frac{|H||HL|}{|H_2L|}$$

$$[5] \quad K_f = \frac{|MeXL|}{|MeX||L|}$$

Nous avons redéterminé K_1 et K_{12} et nous trouvons: $K_1 = 5.75 \times 10^{-9}$, $K_{12} = 6.76 \times 10^{-4}$. Ces valeurs se comparent bien avec les valeurs données dans la littérature (5). De l'éq. [3] on tire

$$[6] \quad |L| = \frac{(2 - a)T_{Me} - |H| + |OH|}{\left\{\frac{|H|}{K_1} + \frac{2|H|^2}{K_1K_{12}}\right\}}$$

En combinant les éqs. [1], [2] et [5] on obtient:

$$[7] \quad K_f|L| + 1 = \frac{T_{Me}}{L\left\{1 + \frac{|H|}{K_1} + \frac{|H|^2}{K_1K_{12}}\right\}} = y$$

Donc, un graphique de y en fonction de $|L|$ donne une droite dont la pente est K_f et dont l'ordonnée à l'origine est 1.

La constante K_f calculée par nous est indépendente de la concentration initiale de réactifs $T_{Me} = T_L = T_X$ qui a varié entre 4×10^{-3} et 2×10^{-2} mole/l. Dans le Tableau I nous donnons la constante K_f pour les métaux étudiés.

TABLEAU I

Constante de formation K_f des complexes MeXL

Me	Log K_f
Cu(II)	3.43 ± 0.05
Ni(II)	3.04 ± 0.04
Zn(II)	2.28 ± 0.05
Co(II)	2.08 ± 0.03
Mn(II)	2.08 ± 0.08

La constante de stabilité globale du complexe mixte K_s est évidemment égale à $K_{MeX} \cdot K_f$, ici K_{MeX} étant la constante de formation du complexe MeX.

Si K_L représente la constante de formation du complexe 1:1 du métal avec la glycylglycine nous trouvons la relation empirique:

$$\log K_s = \alpha \log K_{MeX} \cdot K_L + \text{constante}$$

Dans nos travaux antérieures nous avons trouvé une relation identique pour les complexes mixtes dérivant de la réaction des acides aminés avec les nitrilotriacétates métalliques. Dans la Fig. 2 nous montrons la variation de log K_s en fonction de log $K_{MeX} \cdot K_L$. De la Fig. 2 on tire que la valeur expérimentale de α est d'environ 0.67.

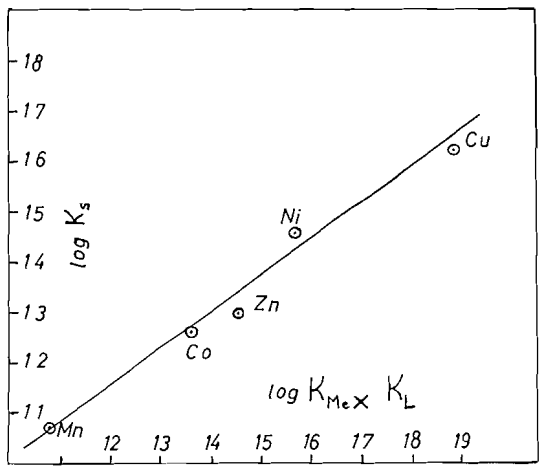

FIG. 2. Log K_s en fonction du log $K_{MeX} \cdot K_L$.

Après $a = 2$, on peut expliquer l'allure de la courbe de titrage en supposant la réaction suivante:

$$[8] \quad MeXL^{2-} + H_2O \rightleftarrows MeXLOH^{3-} + H^+$$

La constante d'équilibre de cette réaction est définie par l'expression:

Can. J. Chem. Downloaded from www.nrcresearchpress.com by 210.87.254.105 on 09/05/12
For personal use only.

$$[9] \qquad K_h^{MeXL} = \frac{|H||MeXLOH|}{|MeXL|}$$

Pour calculer K_h^{MeXL} nous utilisons les équations suivantes:

$$[10] \quad (a-2)T_{Me} = |MeXLOH| + |OH| - |H|$$

$$[11] \quad T_{Me} = |MeX| + |MeXL| + |MeXLOH|$$

$$[12] \quad T_L = T_{Me} = |MeXL| + |MeXLOH| + |L|$$

Avec l'aide de l'éq. [10] on trouve aisément la valeur de MeXLOH. En retranchant l'éq. [11] de l'éq. [12] on obtient:

$$[13] \qquad |MeX| = |L|$$

L'éq. [12] donne:

$$[14] \quad K_f|MeX|^2 + |MeX| + |MeXLOH| - T_{Me} = 0$$

En utilisant ces équations, on peut calculer aisément K_h^{MeXL}.

Le Tableau II donne la valeur de K_h^{MeXL} pour les métaux étudiés.

TABLEAU II

La valeur de la constante $K_h^{MeXL} = |H|\,|MeXLOH|/|MeXL|$

Me	$-\log K_h^{MeXL}$
Cu(II)	9.79±0.03
Zn(II)	10.20±0.10
Co(II)	10.80±0.10
Ni(II)	11.30±0.10

Schwarzenbach et Beidermann (12) a signalé la réaction de hydroxylation des nitrilotriacétates métalliques et il a donné seulement des valeurs approximatives pour la constante K_h^{MeX}. Pour déterminer à nouveau K_h^{MeX} nous titrons par la soude un mélange équimoléculaire de perchlorate métallique et de nitrilotriacétate disodique et pour les calculs nous utilisons la partie de la courbe située après $a = 1$. Dans ces calculs les équations suivantes sont utilisées:

$$[15] \quad K_h^{MeX} = \frac{|H||MeXOH|}{|MeX|}$$

$$[16] \quad T_{Me} = |MeX| + |MeXOH|$$

$$[17] \quad (a-1)T_{Me} = |MeXOH| + |OH| - |H|$$

Dans le Tableau III nous donnons les valeurs du K_h^{MeX}.

TABLEAU III

La valeur de la constante $K_h^{MeX} = |H|\,|MeXOH|/|MeX|$

Me	$-\log K_h^{MeX}$
Cu(II)	9.14±0.02
Zn(II)	10.06±0.03
Co(II)	10.80±0.03
Ni(II)	10.86±0.04

Discussion

Le nitrilotriacétate étant un ligand tétradenté, dans les complexes MeX il y a encore deux places libres qui peuvent être occupées par un ligand bidenté.

Les complexes mixtes MeXL se forment dans la région dans laquelle on titre le proton lié au groupement amino du glycylglycine et pour cette raison il nous semble que le groupement amino est lié au métal.

Nous voulons mentionner que la constante de formation du $[NiXL]^{2-}$ est trois fois plus grande que la constante de formation du $[NiXNH_3]^-$ (Jacobs et Margerum (13) a trouvé $\log K_f = 2.54 \pm 0.04$ pour le nickel–nitrilotriacétate–ammoniac). Ce fait nous indique que le glycylglycinate forme un chélate avec le nitrilotriacétate métallique probablement par le groupe amino et par le groupe peptidique. Malheureusement, ce travail ne nous permet pas de préciser si le métal est lié à l'azote ou à l'oxygène peptidique.

Après $a = 2$, on peut expliquer la courbe de titrage de deux façons: ou bien on neutralise l'hydrogène peptidique ou bien on brise la liaison entre le métal et le groupe peptidique et on forme en même temps une nouvelle liaison entre le métal et un groupe OH^-. Nous préférons cette dernière hypothèse pour les raisons suivantes:

(*a*) Au pH qui correspond à $a > 2$, il y a hydroxylation du MeX et des complexes du métal avec la glycylglycine.

(*b*) Les constantes K_h^{MeXLOH} sont très voisines des constantes K_h^{MeXOH}.

Nous voulons mentionner que les constantes de formation des complexes hydroxylés sont données par les équations suivantes:

$$[18] \quad K_f^{MeXOH} = \frac{|MeXOH|}{|MeX||OH|} = \frac{K_h^{MeX}}{K_W}$$

$$[19]\quad K_f^{MeXLOH} = \frac{|MeXLOH|}{|MeXL||OH|} = \frac{K_h^{MeXL}}{K_W}$$

La petite différence qui existe entre K_h^{MeXL} et K_h^{MeX} nous indique que la liaison entre le métal et le groupe peptidique est très faible.

Remerciements

L'un de nous (J.I.) remercie le Conseil National de Recherches du Canada pour l'octroi d'une subvention de recherche qui a permis également le stage postdoctoral du Dr. M.C. au Canada.

1. J. ISRAELI. Can. J. Chem. **41**, 2710 (1963).
2. J. ISRAELI et M. CECCHETTI. J. Inorg. Nucl. Chem. Sous presse.
3. J. ISRAELI et M. CECCHETTI. Can. J. Chem. Sous presse.
4. J. ISRAELI et M. CECCHETTI. Talanta. Sous presse.
5. L. G. SILLEN et A. E. MARTELL. Stability constants. Special Publication No. 17. The Chemical Society, London. 1964. p. 430.
6. M. K. KIM et A. E. MARTELL. Biochemistry, **3**, 1169 (1964).
7. M. SHEINBLATT et E. D. BECKER. J. Biol. Chem. **242**, 3159 (1964).
8. H. FLASCHKA. EDTA titrations. The Pergamon Press, Ltd., London. 1959.
9. F. J. WELCHER. The analytical use of EDTA. D. Van Nostrand, Co., Inc., Toronto. 1958.
10. K. S. RAJAN et A. E. MARTELL. J. Inorg. Nucl. Chem. **26**, 789 (1964).
11. G. SCHWARZENBACH, A. WILLI et O. R. BACH. Helv. Chim. Acta, **30**, 1303 (1947).
12. G. SCHWARZENBACH et W. BEIDERMANN. Helv. Chim. Acta, **31**, 331 (1948).
13. N. E. JACOBS et D. MARGERUM. Inorg. Chem. **11**, 2040 (1967).

Can. J. Chem. Downloaded from www.nrcresearchpress.com by 210.87.254.105 on 09/05/12
For personal use only.

Can. J. Chem. Downloaded from www.nrcresearchpress.com by 210.87.254.40 on 09/05/12
For personal use only.

Pyrochlores. IV. Crystallographic and Mössbauer studies of A_2FeSbO_7 pyrochlores[1]

OSVALD KNOP AND FRANÇOIS BRISSE[2]
Department of Chemistry, Dalhousie University, Halifax, Nova Scotia

AND

R. E. MEADS AND J. BAINBRIDGE
Department of Physics, University of Exeter, Exeter, England

Received May 14, 1968

The lattice parameters and the quadrupole splittings of the room-temperature Mössbauer spectra of the cubic A_2FeSbO_7 pyrochlores (A = Sm, Eu, Gd, Tb, Y, Er, Lu) have been found to vary linearly with the Templeton–Dauben radii of the A^{3+} ions. The variation of the quadrupole splitting can be correlated with the positional parameter of the majority oxygen atom, $x(O_2)$, which determines the degree of distortion of the BO_6 octahedron in cubic $A_2B_2O_7$ pyrochlores. An increase of 0.1 Å in $r(A^{3+})$ corresponds to a decrease of ca. 0.20 mm/s in the quadrupole splitting in the A_2FeSbO_7 series, and to an estimated increase of ca. 0.005 in $x(O_2)$. The isomer shift and quadrupole splitting at room temperature are typical of Fe^{3+} (high spin) in octahedral coordination of relatively high distortion. Y_2FeSbO_7 at 4.2 °K was found to exhibit magnetic order with a hyperfine magnetic field of approximately 400 kOe. An attempt to prepare a cubic La_2FeSbO_7 pyrochlore by the standard procedure was not successful.

Canadian Journal of Chemistry, 46, 3829 (1968)

Cubic phases A_2FeSbO_7 (A = Pr, Nd, Sm, Eu, Gd, Tb, Dy, Ho, Er, Yb, and Y) formed by firing mixtures of A_2O_3 and $FeSbO_4$ at 1300 °C have been shown by Montmory and Bertaut (1) to be of the pyrochlore type. As part of our systematic investigation of the crystal chemistry of the pyrochlores we have reexamined the Sm, Eu, Gd, Tb, Er, and Y compounds, for which we were able to confirm Montmory and Bertaut's findings, and added another member, Lu_2FeSbO_7, to the series.

The lattice parameters of these pyrochlores (Table I) gave a satisfactory straight line when plotted against the Templeton–Dauben radii of A^{3+} (Fig. 1). The break at Nd, which appears in a similar plot based on the lattice parameters of ref. 1 and Goldschmidt's radii (1), does not correspond to reality; it reflects the lack of internal consistency of Goldschmidt's set of $r(A^{3+})$ (cf. ref. 2). A similar observation applies to the corresponding plots for $A_2Ru_2O_7$ and $A_2Ir_2O_7$ (1).

From the radius-ratio criterion (2, 3) one would not expect $A_2^{3+}B_2^{4+}O_7$ compounds with $r(A^{3+}):r(B^{4+})$ greater than 1.61 (Ahrens) or 1.55 ("improved" radii; refs. 2 and 3) to be cubic pyrochlores. La_2FeSbO_7 has a radius ratio of 1.81 (Ahrens) or 1.62 ("improved") and would thus qualify only marginally as a member of the above series. Indeed, the X-ray powder pattern of this preparation was quite different from the pyrochlore pattern. Lines of the orthorhombic $LaFeO_3$ perovskite predominated, but there were other lines as well.

The degree of distortion of the BO_6 octahedra in the 3–4 pyrochlore structure increases with the decreasing value of the positional parameter of the majority oxygen atom, $x(O_2)$ (4). In turn $x(O_2)$, in $A_2Sn_2O_7$ (2) and $A_2Ti_2O_7$ (5) pyrochlores, has been shown to increase with the increasing ionic radius of A^{3+}, so that the smaller the A^{3+} ion the more distorted the BO_6 octahedron.

A similar relationship would be expected to hold in the A_2FeSbO_7 series. Its validity could, of course, be established by detailed crystal-structure analysis. However, since these compounds contain iron, they are suitable for investigation by Mössbauer spectroscopy, and it was of interest to see whether the distortion of the octahedra could be detected and followed from the quadrupole splitting in the spectra.

In Mössbauer spectra of Fe^{3+} (high spin) in octahedral environments the isomer shift, relative to metallic iron, is commonly found to be in the range +0.3 to +0.5 mm/s. Quadrupole splittings are found to be in the range zero to

[1]For Part III see ref. 2.
[2]Present address: Division of Pure Chemistry, National Research Council of Canada, Ottawa, Canada.

TABLE I

Unit-cell dimensions and Mössbauer parameters of A_2FeSbO_7 pyrochlores at room temperature

A	Preparation	a_0 (Å)	Isomer shift (±0.02 mm/s)	Quadrupole splitting (±0.005 mm/s)	Line width (±0.01 mm/s) Γ_1	Γ_2
La	Standard plus 1300 °C/36 h	Not *P*				
Sm	Standard	10.3389±15	+0.38	0.759	0.37	0.37
Eu	Standard plus 1300 °C/36 h	10.3051±20	+0.38	0.790	0.34	0.35
Gd	Standard	10.2914±11	+0.38	0.801	0.43	0.44
Tb	Standard plus 1300 °C/36 h*	10.2669±20	+0.36	0.848	0.38	0.38
Y	Standard	10.2122±11	$+0.36_5$	0.919	0.35	0.36_5
Er	Standard	10.1914±7	+0.36	0.925	0.34	0.34
Lu	Standard	10.1375±7				

*The commercial brown "Tb_4O_7" of accurately known Tb content (5) was used in the preparation.

1.0 mm/s, the value zero corresponding to the case of an undistorted environment. The isomer shift for tetrahedrally coordinated Fe^{3+} is usually about 0.15 mm/s. The isomer shift for Fe^{2+} is generally found to be in the range

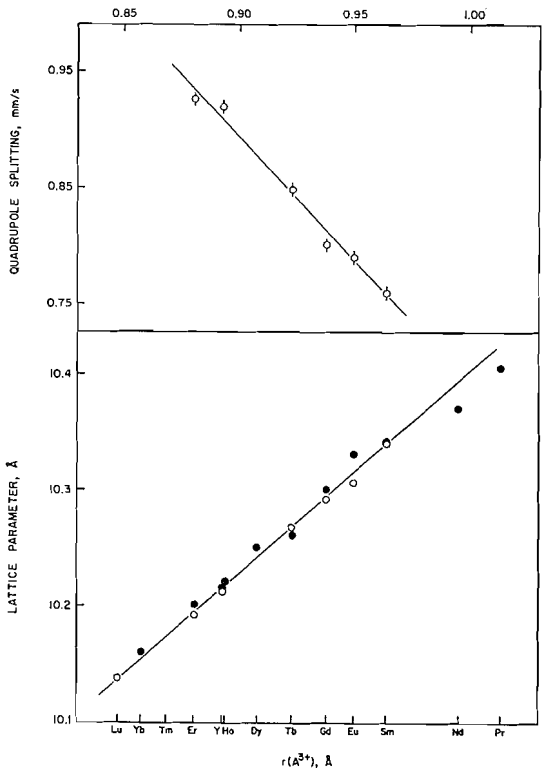

FIG. 1. (*Bottom*) Dependence of the lattice parameters of A_2FeSbO_7 pyrochlores on the ionic radii of A^{3+} (Templeton–Dauben). Full circles, Montmory and Bertaut (1); open circles, present work. (*Top*) Variation of the quadrupole splitting of ^{57}Fe in A_2FeSbO_7 pyrochlores with $r(A^{3+})$.

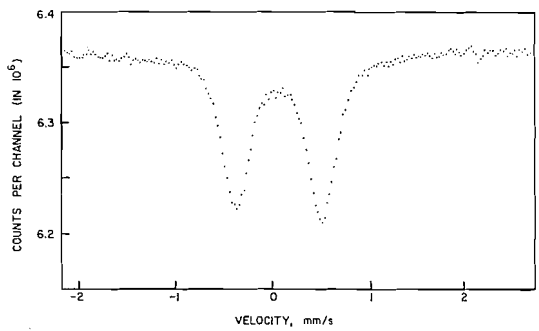

FIG. 2. Mössbauer spectrum of Y_2FeSbO_7 at room temperature. The zero of velocity refers to the center of ^{57}Fe calibration spectrum. The left-hand absorption line is Γ_1.

+1.0 to +1.3 mm/s and the quadrupole splittings 2.0 to 3.0 mm/s. A Mössbauer spectrum typical of the six A_2FeSbO_7 compounds examined by this method is shown in Fig. 2, and the results of measurements at room temperature on five lanthanon phases appear in Table I. The isomer shifts and quadrupole splittings were clearly characteristic of Fe^{3+} (high spin) in octahedral coordination of relatively high distortion. The isomer shift at room temperature was essentially the same for all the compounds[3], but the quadrupole splitting in the five lanthanon phases increased from Sm to Er (Table I). When plotted against Templeton–Dauben's $r(A^{3+})$ the variation was linear (Fig. 1). Least-squares fitting of the data yields the result

[3]Although the isomer shift at room temperature (Table I) seems to decrease with decreasing ionic radius of A^{3+} and thus to indicate progressive decrease of the s electron density at the Fe nuclei, in view of the experimental uncertainty this trend cannot be considered as significant. In any event it is very small.

Can. J. Chem. Downloaded from www.nrcresearchpress.com by 210.87.254.40 on 09/05/12
For personal use only.

TABLE II

Temperature dependence of isomer shift, quadrupole splitting, and line widths of Y_2FeSbO_7 and Gd_2FeSbO_7

T (°K)	Isomer shift (mm/s)	Quadrupole splitting (mm/s)	Line width (mm/s) Γ_1	Line width (mm/s) Γ_2
		Y_2FeSbO_7		
18.2	+0.48	0.923	0.42	0.45
42.6	+0.48	0.930	0.40	0.40
78.0	+0.47	0.946	0.37	0.37
95.3	+0.47	0.920	0.40	0.41
96.2	$+0.47_5$	0.918	0.39	0.42
143.8	+0.44	0.920	0.39_5	0.39
169.9	$+0.44_5$	0.913	0.39	0.39
225.7	+0.37	0.920	0.36	0.38
294	+0.35	0.920	0.33	0.35
295.3	+0.38	0.918	0.37_5	0.38
302.1	+0.36	0.926	0.37_5	0.37_5
		Gd_2FeSbO_7		
25.4	$+0.49\pm0.04$	0.77 ± 0.04	0.74 ± 0.08	0.65 ± 0.08
109.4	+0.48	0.815	0.46	0.48
294	+0.38	0.801	0.43	0.44

$$\text{quadrupole splitting} = -(2.12 \pm 0.13)\, r(A^{3+}) + (2.80 \pm 0.12)$$

This indicates a progressive increase in the distortion of the FeO_6 octahedron with decreasing $r(A^{3+})$, which is just what one would expect by analogy with the titanates and stannates.

The quadrupole splitting for Y_2FeSbO_7, when plotted against Geller's value of $r(Y^{3+})$, 0.893 Å (2), fits in very well with the values for the lanthanons (Fig. 1). This confirms the conclusion reached for the titanates and stannates, viz. the distortion of the BO_6 octahedron in the pyrochlore structure is governed by the size rather than the particular chemistry of the Y^{3+} ion as distinct from the trivalent lanthanons.

Assuming that for no distortion the splitting would be zero, the $r(A^{3+})$ required for a regular FeO_6 octahedron would have to be about 1.32 Å. This is far in excess of the size limit of A^{3+} for cubic A_2FeSbO_7 pyrochlores, which appears to be between La and Pr, and of course there are no trivalent ions of that size. The distortion is thus an inevitable feature of the structure of these compounds.

The room-temperature line widths showed fairly considerable differences from compound to compound (Table I). They were particularly large for Gd_2FeSbO_7. The line widths for the only two compounds investigated so far at low temperatures, Y_2FeSbO_7 and Gd_2FeSbO_7, *increased* significantly as the temperature was lowered from 300 to 4.2 °K (Table II). The reason for these effects is not at all clear. Possible explanations of the line broadening on cooling might be sought in structure imperfections whose effect makes itself increasingly felt as the temperature is lowered or, less likely, in electron-spin relaxation effects leading to unresolved magnetic hyperfine structure. The line widths may also be affected by the state of order of Fe and Sb in the B sites.

As would be expected for Fe^{3+} sites, the quadrupole splitting in the Y and Gd compounds was essentially temperature independent, but the isomer shifts increased by some 25–30% when the temperature dropped from ambient to the vicinity of 20 °K (Table II). The temperature variation of the isomer shift of Y_2FeSbO_7 is consistent with the view that it is due to second-order Doppler effect, the material having a Debye temperature of the order of 450 °K.

No magnetic ordering occurred at room temperature in any of the six pyrochlores. In the Y and Gd phases no ordering was observed above 20 °K. However, Y_2FeSbO_7 at 4.2 °K was found to exhibit magnetic order with a hyperfine magnetic field of approximately 400 kOe.[4] The spectrum is probably not a simple six-line one. Further investigation of the low-temperature

[4]The analogous Y_2CrSbO_7 pyrochlore has been found by Bongers and Van Meurs (6) to be ferromagnetic with an asymptotic Curie temperature of 15 °K.

Can. J. Chem. Downloaded from www.nrcresearchpress.com by 210.87.254.40 on 09/05/12
For personal use only.

Can. J. Chem. Downloaded from www.nrcresearchpress.com by 210.87.254.40 on 09/05/12
For personal use only.

spectra in ^{57}Fe-enriched samples and a detailed study of possible order on the B sublattice are under way (R. E. Meads, J. Bainbridge, O. Knop, and C. Ayasse. To be published).

The present results show that in detecting structural trends such as the progressive distortion of the FeO_6 octahedra, Mössbauer spectroscopy, where applicable, has a distinct advantage over detailed crystal-structure analysis. It is much simpler and less time consuming, and there are no practical difficulties of the kind encountered in X-ray diffraction, e.g. the desirability of having suitable single crystals or, in powder diffractometry, the heavy background scattering from some of the lanthanon titanates (Sm, Gd), which seriously impairs experimental accuracy when CuKα radiation is used (2). Once a correlation of the quadrupole splitting with $x(O_2)$ has been obtained for a particular isostructural series (e.g. the $A_2FeM^VO_7$ pyrochlores), the degree of distortion of the octahedron can be estimated simply and directly from the Mössbauer spectrum. An increase of 0.1 Å in $r(A^{3+})$ corresponds, in the $A_2Sn_2O_7$ and $A_2Ti_2O_7$ series (2, 5), to an increase of ca. 0.005 in $x(O_2)$ and, on the other hand, to a decrease of ca. 0.20 mm/s in the quadrupole splitting in the intermediate A_2FeSbO_7 series. The experimental uncertainty of the present determination of the quadrupole splitting on unenriched material, $\pm$0.005 mm/s, would thus correspond to an uncertainty of ca. $\pm$0.0001 in $x(O_2)$. This is better than a typical standard deviation resulting from a least-squares refinement of a 3–4 pyrochlore structure from good powder diffractometer data.

Experimental

The compounds were prepared by firing pressed pellets of intimate mixtures of freshly calcined A_2O_3 of at least 99.9% purity (Lindsay Chemical Division, American Potash and Chemical Corporation) and $FeSbO_4$, with intermediate grinding and pressing as required. The standard firing schedule was 900 °C/12 h, 1000 °C/24 h, 1100 °C/10 h, 1300 °C/10 h, 1300 °C/10 h, followed by cooling in the furnace. The progress of the reaction was followed by X-ray powder diffraction.

The rutile-type $FeSbO_4$ was prepared by firing intimately mixed powders of reagent-grade Fe_2O_3 and Sb_2O_3 in air. Its unit-cell dimensions were $a_0 = 4.635 \pm 2$ Å, $c_0 = 3.0715 \pm 10$ Å, as compared with 4.632 and 3.017 Å (converted from kX) of ref. 7.

For details of the lattice parameter determination ref. 4 may be consulted. The wavelengths used were CuKα_1 = 1.540562 Å, CuKα_2 = 1.544398 Å.

For Mössbauer spectroscopy the unenriched powder specimens were mounted in acrylic resin disks $\frac{1}{2}$ in. in diameter, containing ca. 25 mg/cm^2 of pyrochlore. The ^{57}Co source, originally 10 mCi in strength diffused in palladium, was purchased from the Radiochemical Centre, Amersham, Bucks. A typical room-temperature metallic-iron calibration spectrum gave a line width of ca. 0.30 mm/s. The γ-ray detector consisted of a 1 in. diameter disk, 0.015 in. thick, of NaI(Tl) mounted on a photomultiplier tube. The Mössbauer spectrometer was of the constant-acceleration type incorporating an electromechanical transducer synchronized to a 400 channel Intertechnique SA40B analyzer operating in the time mode. The constant-acceleration drive system has been recently reported (8).

The isomer shifts are expressed relative to metallic iron. The uncertainties in the isomer shifts, quadrupole splittings, and line widths are given in Table I and apply to all measurements except that of Gd_2FeSbO_7 at 25.4 °K.

Acknowledgment

This work has been supported in part by a grant from the National Research Council of Canada to the first-named author.

1. M.-C. Montmory and F. Bertaut. Compt. Rend. **252**, 4171 (1961).
2. F. Brisse and O. Knop. Can. J. Chem. **46**, 859 (1968).
3. O. Knop and F. Brisse. To be published.
4. O. Knop, F. Brisse, L. Castelliz, and Sutarno. Can. J. Chem. **43**, 2812 (1965).
5. O. Knop, F. Brisse, and L. Castelliz. Can. J. Chem. To be published.
6. P. F. Bongers and E. R. Van Meurs. J. Appl. Phys. **38**, 944 (1967).
7. K. Brandt. Arkiv Kemi Mineral. Geol. **17A**, No. 15 (1943).
8. P. E. Clark, A. W. Nichol, and J. S. Carlow. J. Sci. Instr. **44**, 1001 (1967).

Can. J. Chem. Downloaded from www.nrcresearchpress.com by 210.87.254.42 on 09/05/12
For personal use only.

Reactions of alkyl free radicals with 4-vinylcyclohexene[1]

J. Reid Shelton[2] and Earl E. Borchert[3]
Department of Chemistry, Case Western Reserve University, Cleveland, Ohio 44106

Received April 18, 1968

Tertiary alkyl and cyanoalkyl free radicals prepared from *t*-butyl peroxypivalate and azobisisobutyronitrile were reacted with 4-vinylcyclohexene (**1**) for comparison with results previously obtained in the reaction of certain alkyl, alkoxy, peroxy, and thiyl radicals with this model olefin. The $(CH_3)_3C\cdot$ and $(CH_3)_2(CN)C\cdot$ radicals (like thiyl but in contrast to *t*-butoxy and *t*-butyl peroxy radicals) added to the vinyl double bond with subsequent abstraction of hydrogen by the resulting secondary alkyl radicals to give RH adducts along with higher molecular weight material.

Vinylcyclohexenyl radicals formed by hydrogen abstraction from **1** reacted mainly by coupling to form dehydro dimers. They also formed substituted products by coupling with cyanoisopropyl radicals, but not with *t*-butyl radicals. The presence of both stabilized and unstabilized alkyl radicals of both secondary and tertiary types in these reactions with **1** permitted the observation of differences in the relative tendencies of these types of radicals to participate in addition, hydrogen abstraction, disproportionation, and coupling reactions. The observed effect of temperature (60 and 90°) on product distribution, together with estimated bond dissociation energies, suggest that the addition of cyanoisopropyl radicals to **1** is a reversible process.

Canadian Journal of Chemistry, 46, 3833 (1968)

Introduction

This study of the reaction of alkyl radicals with 4-vinylcyclohexene (**1**) is part of a continuing investigation of the reaction of various types of free radicals with selected olefins (2–5). Thiyl radicals generated by photolysis of either diphenyl disulfide or dibenzyl disulfide add readily to the vinylic double bond of **1** (4), but *t*-butoxy and *t*-butyl peroxy radicals do not add to either the *cis* internal or vinyl unsaturation present in this olefin. The alkoxy and peroxy radicals react preferentially by abstraction of hydrogen from the allylic methylene groups, with the 6-position favored over the more hindered 3-position (2, 5). Oxy radicals formed in the autoxidation of **1** react similarly, and contrary to the first report (6), no more than 12% of the products are derived from abstraction of the tertiary allylic hydrogen in the 4-position (7)[4].

This is consistent with calculations using the relative reactivities of tertiary allylic and cyclic secondary allylic hydrogens from Walling and Thaler's study of the reaction of *t*-butyl hypochlorite with various model olefins (8).

Since methyl radicals (derived from *t*-butyl peracetate along with *t*-butoxy radical) and secondary alkyl radicals (obtained by addition of thiyl or other radicals to the vinyl group of **1**) gave evidence of both hydrogen abstraction and addition reactions with **1** (3, 4), it was desired to extend the study to include other alkyl radicals. Tertiary alkyl radicals were selected to permit comparison with the tertiary alkoxy and peroxy radicals previously studied. Two sources of alkyl radicals were used: 2,2′-azobisisobutyronitrile (AIBN) which yields cyanoisopropyl radical (1-cyano-1-methylethyl) by thermal or photolytic decomposition (9), and *t*-butyl peroxypivalate (TBPP) which undergoes cleavage of the O—O and C—C bonds with formation of *t*-butyl and *t*-butoxy radicals plus carbon dioxide (10).

The reactions of **1** with free radicals from both of these sources were investigated at 60° and, in the case of AIBN, also at 90°. The reaction mixtures obtained by heating for a period corresponding to five half-lives were analyzed by gas–liquid partition chromatography (g.l.p.c.) to determine the yields of products. Removal of excess of **1** and the volatile products by evaporation at reduced pressure left a viscous residue. The identity of the products and the nature of the residue were established in each case by spectroscopic and other analytical methods.

Results and Discussion

Decomposition of Azobisisobutyronitrile in 4-Vinylcyclohexene (1)

The cyanoisopropyl radicals formed by the decomposition of AIBN may undergo coupling or disproportionation reactions, as illustrated in

[1]This work was supported by the Goodyear Tire and Rubber Company, Akron, Ohio, as part of a continuing study of the reactions of free radicals with olefins.

[2](*a*) For recent related papers see ref. 1. (*b*) On leave 1967–68 at the University of Leiden, The Netherlands.

[3]Taken from the Ph.D. thesis of E. E. Borchert. Present address: Ferro Chemical Corp., Bedford, Ohio.

[4]This result was also found independently by Shelton and Gilde (unpublished work).

Can. J. Chem. Downloaded from www.nrcresearchpress.com by 210.87.254.42 on 09/05/12
For personal use only.

Fig. 1, either within the solvent cage or after diffusion (9). Since the cyanoisopropyl radical is known to disproportionate in other systems (11, 12), methacrylonitrile would also be expected. It was not found in the reaction mixture, but this can be explained on the basis that it would be readily polymerized in the presence of a free radical initiator. The residue showed infrared absorptions for both the cyano group and an internal double bond. Absorptions due to the vinyl group were very weak. The insoluble portion of the residue remaining after extraction with petroleum ether appeared to be mainly a copolymer of **1** and methacrylonitrile which gave an analysis for nitrogen and an average molecular weight corresponding to approximately 2.5 cyanoisopropyl units combined with 3.3 monomer units of **1**. A copolymer independently prepared by reaction of **1** with methacrylonitrile exhibited similar infrared absorptions.

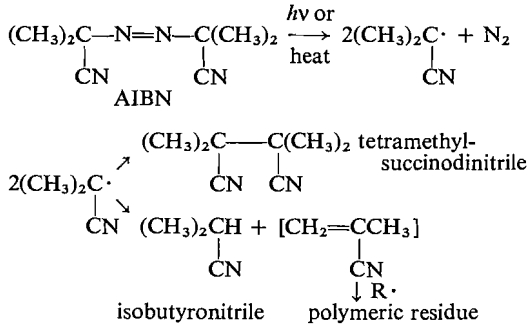

FIG. 1. Products from decomposition of azobisisobutyronitrile.

Figure 2 illustrates the probable reaction scheme leading to products derived from the olefin. If the addition of cyanoisopropyl radical to the double bond is reversible, a temperature increase would be expected to favor dissociation of the intermediate radical to regenerate the cyanoisopropyl radical. This is consistent with the somewhat larger yield of tetramethylsuccinodinitrile at 90° compared to 60°[5].

The reversibility of the addition reaction in this case is a reasonable postulate from the standpoint of energy since the formation of a stabilized radical and a double bond could compensate for the energy needed to break the C—C bond. The bond dissociation energy, DH^0, for RCH_2CH_2—$C(CH_3)_2CN$ can be estimated to be about 67 kcal per mole, since the value for CH_3—$C(CH_3)_2CN$ is 70 kcal (13), and replacement of CH_3 by C_2H_5 usually lowers DH^0 by approximately 3 kcal. The presence of an unpaired electron in the β position lowers the bond dissociation energy by 60–65 kcal (13), so the energy requirement for breaking the bond in the radical $RCHCH_2$—$C(CH_3)_2CN$ should be quite small.

The tendency to reverse the addition process at the higher temperature would also decrease the availability of the intermediate radical (which can either abstract hydrogen from **1** or initiate polymerization) and thus account for the decreased yield of both the product of addition and copolymer residue at 90°, as shown in Table I.

The increase in substituted products at the higher temperature can be explained also by increased availability of the cyanoisopropyl radicals. This increased coupling with vinylcyclohexenyl radicals would also diminish the self-coupling of vinylcyclohexenyl radicals leading to the observed decrease in yield of dehydro dimers at 90°. The product designated as dehydro dimers consists of a mixture of position isomers in which products derived from the 6-isomer predominate along with significant amounts of dimers derived from radicals localized in the 1- and 3-positions, plus some dimer formed by addition of cyclohexenyl radicals to **1** (5). The substituted products would be expected by analogy to consist of a similar mixture of isomers since they are obtained by coupling with a comparable mixture of isomeric vinylcyclohexenyl radicals.

Comparable runs were also made at 60° with twice the volume of olefin to observe any effect

TABLE I

Yield of products from reaction of AIBN with 4-vinylcyclohexene (**1**)*

Product	Yield 60°	Yield 90°
Tetramethylsuccinodinitrile	51%†	57%†
Isobutyronitrile	7%	7%
Product of addition	25%	17%
Substituted products	7%	10%
Dehydro dimers	7.5%	4%
Copolymer residue	9.5 g	7.6 g

*0.10 mole of AIBN in 200 ml of **1**.
†Based on AIBN.

[5]A corresponding increase in the 7% isobutyronitrile formed by disproportionation would be within the limits of reproducibility and thus would not be observable.

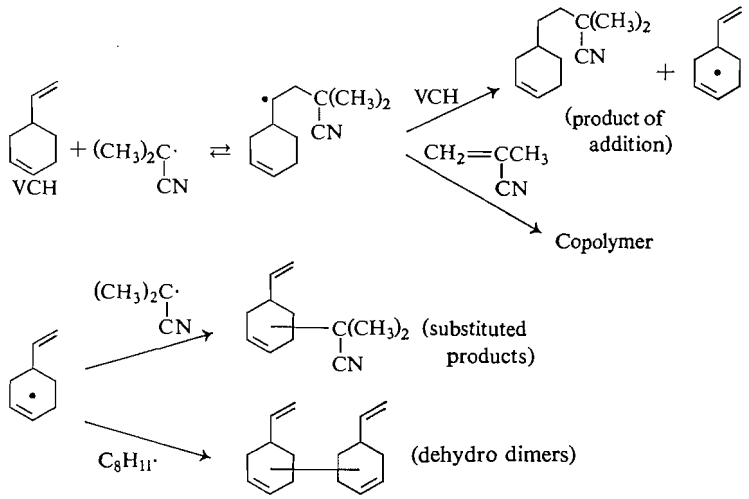

FIG. 2. Reaction of radicals from AIBN with 4-vinylcyclohexene.

of dilution. The only significant change was a small increase in polymer formation, consistent with less coupling and more addition of radicals to **1**, and an increase in dimer yield which can be explained similarly by increased addition of vinylcyclohexenyl radicals to **1**.

Photolysis of the reaction mixture at 60° with ultraviolet light resulted in a more rapid consumption of AIBN, but there were no significant changes in the relative amounts of the products as reported in Table I for the thermal reaction at the same temperature.

The yields of identified products in Table I account for 90% of the cyanoisopropyl radicals available from AIBN. The remaining 10% is evidently present in the residue, in part as initiating radical, and also as methacrylonitrile units in a low molecular weight copolymer.

According to the reaction sequence of Fig. 2, the sum of the yield of substituted products plus one-half the yield of dehydro dimers should equal the yield of the product of addition. The observed yields at both 60 and 90° do account on this basis for 90% of the vinylcyclohexenyl radicals formed, and utilization of these radicals in initiation and termination reactions in the formation of polymer would account for the remainder.

Decomposition of t-Butyl Peroxypivalate in 4-Vinylcyclohexene

The perester (TBPP) was heated at 60° in excess **1** for 5 half-lives employing the same ratio of reactants and procedures used for the AIBN reactions. The observed products and the relative yields (based on perester) are shown in Table II. No products of reaction with pivaloxy radicals were found, consistent with Bartlett's observation that this perester decomposes to yield *t*-butyl and *t*-butoxy radicals plus carbon dioxide (10). The *t*-butoxy radicals abstract hydrogen from **1** to form *t*-butyl alcohol and vinylcyclohexenyl radicals which react mainly by coupling to form dehydro dimers. Only traces of acetone were observed in the reaction mixture, indicating little fragmentation of the *t*-butoxy radical at 60° when abstractable hydrogen is available. Alcohol formation and carbon dioxide evolution were measured, and repeated determinations have shown yields of 95% or more for both.

The *t*-butyl radicals react mainly by addition to **1**, as shown in Fig. 3, followed by hydrogen

TABLE II

Yield of products from reaction of TBPP with 4-vinylcyclohexene (**1**)*

Products	Yield
Product of addition	25%†
Dehydro dimers	20%
Isobutylene	22%
Isobutane	7%
Polymeric residue	5.2 g

*0.10 mole of TBPP in 200 ml of **1**, temperature = 60°.
†Based on perester.

Can. J. Chem. Downloaded from www.nrcresearchpress.com by 210.87.254.42 on 09/05/12
For personal use only.

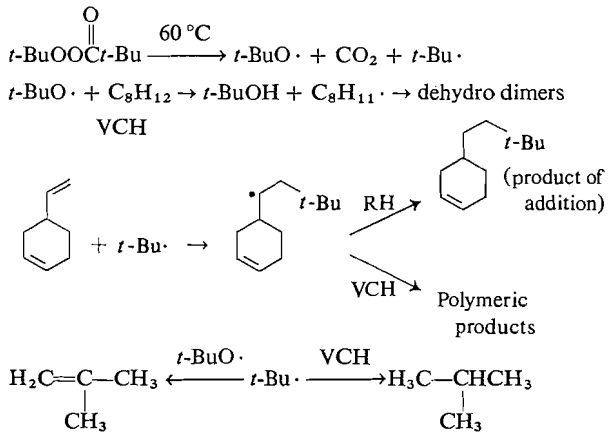

FIG. 3. Reaction of *t*-butyl peroxypivalate with 4-vinylcyclohexene.

abstraction by the intermediate radical to form RH adduct. The adduct radical may alternatively add to additional molecules of **1** to form polymeric products. Methyl radicals derived from *t*-butyl peracetate have been observed to react similarly with **1**, both by abstraction of hydrogen and by addition to the vinyl group (3).

The presence of both isobutylene and isobutane in the reaction mixture suggests the disproportionation of *t*-butyl radical. However, the absence of detectable amounts of coupling products, either with vinylcyclohexenyl radicals or with another *t*-butyl radical, suggests that these products may be formed in other ways. Disproportionation and coupling of alkyl radicals normally occur together in a ratio which is nearly independent of temperature. The ratio k_d/k_c observed for *t*-butyl radicals formed in the liquid phase by photolysis of pivaldehyde was 4.3 (14). Hydrogen abstraction by *t*-butyl from the aldehyde was also observed with the formation at 57° of 2.4 times as much isobutane by abstraction as by disproportionation. Thus, an analogous abstraction of hydrogen from **1** could account for the 7% of isobutane reported in Table II. If it is assumed that the larger number of abstractable hydrogens (four cyclic secondary allylic and one tertiary allylic) in **1** at least compensate for the possible greater reactivity of the hydrogen on the carbonyl group of pivaldehyde, no more than 2 to 3% of disproportionation products would be expected, and the amount of coupling product formed would be too small to measure.

The formation of three times as much isobutylene as isobutane shows that another radical species must be abstracting hydrogen from *t*-butyl radicals. Since *t*-butoxy and *t*-butyl radicals are formed together with an elimination of CO_2 from the perester, transfer of hydrogen to the alkoxy radical could readily account for the observed yield of isobutylene[6]. Radicals, which do not react in this way are evidently trapped by reaction with **1** either by hydrogen abstraction to form *t*-butyl alcohol and isobutane or, in the case of *t*-butyl, by addition to form RH adduct and higher molecular weight products. Thus the combined yield of isobutane and isobutylene accounts for nearly 30% of the *t*-butyl radicals with little or no contribution of self-disproportionation.

The nonvolatile residue isolated from the reaction mixture showed characteristic infrared absorptions for the *t*-butyl group and for both types of unsaturation of **1**. Partial separation of the polymeric material by solvent extraction produced one component which showed no vinyl absorption. The presence of isobutylene as a reaction product and the smaller yield of residue (compared to the AIBN reaction) show that it is not polymerized as readily as the methacrylonitrile. However, since products other than polymer account for only 54% of the *t*-butyl radicals, it is evident that the remainder must be consumed

[6]The formation of excess olefin by transfer of hydrogen to *t*-butoxy radical has been suggested in a comparable case (10).

Can. J. Chem. Downloaded from www.nrcresearchpress.com by 210.87.254.42 on 09/05/12
For personal use only.

Can. J. Chem. Downloaded from www.nrcresearchpress.com by 210.87.254.42 on 09/05/12
For personal use only.

not only in the initiation, but also in the polymerization of much of the isobutylene formed from these radicals. Formation of polyisobutylene in the thermolysis of TBPP in chlorobenzene has been observed previously (10).

The observed average molecular weight (380) corresponds to one *t*-butyl group combined with two vinylcyclohexene units and an average of two units of isobutylene. These observations are consistent with initiation mainly by addition of *t*-butyl groups to **1** (as in Fig. 3) with propagation by combination with additional molecules of **1** or isobutylene, and termination by hydrogen abstraction in analogy to the formation of the RH adduct. Initiation of some polymer formation by addition of vinylcyclohexenyl radicals to **1**, or some termination by coupling with such radicals, would account for the observed vinyl absorption.

Comparison of the Observed Behaviors

The tertiary alkyl radicals, cyanoisopropyl, and *t*-butyl both add to the vinyl unsaturation of **1** to form RH adducts and some polymeric products. The preference for addition rather than hydrogen abstraction is analogous to the behavior of thiyl radicals, and in contrast to the behavior of *t*-butoxy and *t*-butyl peroxy radicals which preferentially abstract hydrogen from **1**. Cyanoisopropyl radicals also undergo disproportionation in part, but the expected methacrylonitrile is consumed in the formation of copolymer with **1**. Little or no self-disproportionation of *t*-butyl radicals occurs although both isobutane (formed by hydrogen abstraction from **1**) and isobutylene (formed by the transfer of hydrogen to *t*-butoxy radicals) are found as reaction products.

Free radicals stabilized by delocalization of the unpaired electron, as in the cyanoisopropyl radical and the allylic free radicals derived by abstraction of hydrogen from **1**, are less reactive in both addition and hydrogen abstraction reactions. Consequently, they are more likely to undergo coupling reactions. Dimers and cross coupling products are thus obtained along with the products resulting from addition. No coupling with *t*-butyl radicals was observed.

Unstabilized alkyl radicals such as methyl, secondary alkyl radicals resulting from additions to the vinyl group of **1**, and the *t*-butyl radical, are able to abstract hydrogen from **1**, and also react by addition to form higher molecular weight products. The addition of these radicals to **1** would be expected to be irreversible at the temperatures used in this study. However, the addition of cyanoisopropyl radical to **1** appears to be reversible, as is also observed with thiyl radicals (4, 15).

Experimental

The 4-vinylcyclohexene (**1**) was either a Philips Petroleum (99 mole% minimum purity) or the Cities Service (99.8 weight % pure) product. Inhibitors and/or hydroperoxides were removed by passing the liquid through an alumina column just prior to use (16). The azobisisobutronitrile (AIBN) obtained from the Aldrich Chemical Company was purified by recrystallization from methanol and stored at −20°. The methacrylonitrile obtained from the Borden Chemical Company was passed through an alumina column just prior to use.

The *t*-butyl peroxypivalate (TBPP) obtained from the Lucidol Division of Wallace and Tiernan as a 75% solution (Lupersol 11) in mineral spirits was stored at −20° until used. The solution assayed 75.8% using the procedure supplied by Lucidol.

Decomposition of AIBN in 1

In all reactions 16.4 g (0.10 mole) of AIBN was added to the desired amount of **1** (either 200 or 400 ml) in a flask equipped with a magnetic stirring bar and reflux condenser. The weight of the flask and stirring bar were recorded prior to admitting the reactants. The reaction flask was purged with nitrogen and placed in a constant temperature bath with a positive pressure of nitrogen maintained during the reaction. The heating was continued for a period of 5 half-lives, corresponding to 104 h at 60° and 95 min at 90° (17). The AIBN was not completely dissolved in 200 ml of **1** at the lower temperature, but the reaction mixture became homogeneous after 13 h.

A photolytic decomposition was carried out for comparison at the lower temperature using a special pyrex flask to accommodate the General Electric H 100-A4 ultraviolet lamp. It was necessary to remove the outer envelope of the bulb so that it would fit within the well in the apparatus and still allow enough clearance for removing the heat emitted by the lamp with a stream of air. The only significant effect of photolysis was a more rapid disappearance of undissolved AIBN.

Method of Analysis of Reaction Mixtures

The weight of the contents of the flask was determined after the reaction was terminated and the mixture was then analyzed immediately by g.l.p.c. Samples of the homogeneous solutions were injected into an F and M model 500 chromatograph and the areas of the emerging product peaks were determined with a planimeter. A 1/4 in. × 12 ft column of silicone grease on Chromosorb W was used. The temperature was programed from 100 to 235° to effect the best separation of the components with a helium flow rate of 30 ml per min on the column and 15 ml per min on the detector. The pure materials used for calibration were either commercially available samples

Can. J. Chem. Downloaded from www.nrcresearchpress.com by 210.87.254.42 on 09/05/12
For personal use only.

or material previously trapped from the chromatograph. The total weight of product formed in the reaction mixture was obtained by multiplying the amount present in the injected sample by the ratio of the total weight to the weight of sample injected. Each reaction mixture was analyzed several times and average values were used to calculate the yields (based on AIBN or TBPP) which are rounded off in Tables I and II to the nearest 0.5%, consistent with the reproducibility of the data.

Characterization of Products

Pure materials were trapped from the gas chromatograph using a silicone grease preparative column 3/8 in. diameter by 15 ft long. Materials obtained in this way were used for infrared spectra, elemental analysis, molecular weight determination, and other operations necessary to their identification.

Product of Addition

The infrared spectrum indicated the presence of the internal double bond (3030, 660 cm^{-1}), and the cyanoisopropyl group (2240, 1390, 1375 cm^{-1}) with no absorptions characteristic of the vinyl group (915, 995 cm^{-1}).

Anal. Calcd. for $C_{12}H_{19}N$ (mol. wt. 177): C, 81.3; H, 10.9; N, 7.90. Found[7] (mol. wt. 176): C, 81.4; H, 10.9; N, 8.09. n_D^{25}, 1.4666.

A 0.96 mmole sample was hydrogenated over reduced platinum oxide (Adams' catalyst) in 30 ml of 95% ethanol. It absorbed 1.00 mmole of hydrogen.

A sample was aromatized by heating at 305° with selenium. The infrared spectrum showed that a monosubstituted aromatic ring was present (1600, 1500, 758, 705 cm^{-1}), as well as the cyanoisopropyl group.

Substituted Product

The infrared spectrum indicated the presence of both internal and vinyl double bonds and the cyanoisopropyl group.

Anal. Calcd. for $C_{12}H_{17}N$: C, 82.2; H, 9.78; N, 7.99. Found: C, 82.1; H, 9.85; N, 8.25.

A solution of 0.4 ml of this product in 10 ml of toluene together with 0.5 g of 5% palladium on charcoal was stirred under reflux for 24 h. This reaction, when carried out with **1**, yields ethylbenzene and ethylcyclohexane (18).

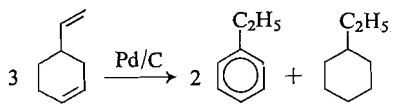

A gas chromatogram of either of these reaction mixtures confirmed that about twice as much of the aromatic as the saturated component was formed. In the reaction with the substituted product the aromatic peak was trapped and its infrared spectrum taken. Absorptions were observed for the aromatic C—H (3090, 320 cm^{-1}), the cyano group (2240 cm^{-1}), the aromatic ring (1600, 1500 cm^{-1}), and for a 1,3-disubstituted aromatic (800, 710 cm^{-1}).

Vinylcyclohexene Dehydro Dimer

The infrared spectrum showed strong absorptions for internal and vinyl double bonds, and was identical with spectra of this material obtained previously in this laboratory (2, 5).

Anal. Calcd. for $C_{16}H_{22}$ (mol. wt. 214): C, 89.6; H, 10.3. Found (mol. wt. 212): C, 89.5; H, 10.4. n_D^{26}, 1.5181; b.p. 82°/0.23 mm.

Hydrogenation over Adams' catalyst in glacial acetic acid of 0.31 mmole required 1.20 mmole of hydrogen (4 moles hydrogen per mole of dehydro dimer).

Isobutronitrile

Identification was made by comparing its infrared spectrum and its retention time on the gas chromatograph with an authentic sample.

Tetramethylsuccinodinitrile

Identification was made by examination of its infrared spectrum and its m.p. (165–167°). The literature gives m.p. 167–167.5° (11).

Copolymer Residue

Most of the volatile products were removed from the reaction mixture at aspirator pressure and 30–40°. The remaining liquid (25 ml) was placed in the bulb of a modified retort and heated at 60° and 0.03–0.05 mm mercury until no more distillate was collected in a second bulb immersed in dry ice – acetone. The residue remaining was a very viscous yellow to brown material readily soluble in benzene and somewhat soluble in 95% ethanol. Its infrared spectrum indicated the presence of cyanoisopropyl (2240, 1390, and 1375 cm^{-1}) and strong absorption for the internal double bond (3030 and 660 cm^{-1}). Absorptions due to the vinyl group (915 and 995 cm^{-1}) were very weak.

Analysis by thin layer chromatography (t.l.c.) was carried out using Brinkmann silica-gel G as the adsorbant. The chromatogram (developed with benzene followed by immersing the plate in vapors of iodine) contained three well-defined spots and a band with unmoved material remaining at the base point. A plate prepared with known samples of addition product, substituted product, and dehydro dimer indicated that the materials being eluted from the residue were traces of these previously characterized materials.

Extraction of the residue with petroleum ether (30–60°) left a hard brown substance which dissolved in benzene and showed only one spot at the base point of the t.l.c. chromatogram. The average molecular weight of the petroleum ether insoluble portion determined on a Mechrolab model 301A osmometer was 520 g/mole, and elemental analysis showed 6.61% N. These values correspond to 2.5 methacrylonitrile units and 3.3 units of **1** per mole of polymer in the residue after the removal of the petroleum ether soluble portion.

Formation of a copolymer of methacrylonitrile and **1** under comparable reaction conditions was demonstrated by dissolving 6.7 g (0.1 mole) methacrylonitrile in 108 g (1 mole) of **1** and adding 0.7 g of Lupersol 11 initiator. The reaction mixture was purged with nitrogen and kept at 60° for 21 h under a positive pressure of nitrogen. A brown-colored residue which separated from the reaction mixture gave absorptions in the infrared characteristic of the cyanoisopropyl group and the internal double bond of **1**.

Decomposition of t-Butyl Peroxypivalate in 1

In a flask fitted with a magnetic stirring bar and reflux condenser, was placed 200 ml of **1** and 23.2 g Lupersol 11.

[7]Elemental analyses and molecular weight determinations were done by Schwarzkopf, Microanalytical Laboratory, Woodside, N.Y.

This represents 0.10 mole of TBPP in the mineral spirits solution. The flask was purged with nitrogen and immersed in the 60° bath for 25 h which represent 5 half-lives (10), under a positive pressure of nitrogen.

A g.l.p.c. analysis was made on the reaction mixture in the same way as for the AIBN reaction mixtures except that the temperature program was altered as required to obtain good separation of the components. Pure products for comparison and calibration were either commercially available or were trapped from the gas chromatograph.

Product of Addition

The infrared spectrum contained absorptions for the *t*-butyl group (1395, 1365 cm^{-1}) and the internal double bond of **1** (3030, 660 cm^{-1}). Absorptions at 915 and 995 cm^{-1} characteristic of the vinyl group were absent.

Anal. Calcd. for $C_{12}H_{22}$ (mol. wt. 166): C, 86.7; H, 13.3. Found (mol. wt. 170): C, 87.1; H, 13.2. n_D^{26}: 1.4520; b.p.: 76° (0.8 mm).

The RH adduct was hydrogenated over Adams' catalyst in 30 ml of glacial acetic acid. The sample weighed 81.3 mg (0.49 mmole) and took up 0.49 mmole of hydrogen.

t-Butyl Alcohol

Identification was made on the basis of a comparison of the infrared spectrum and the g.l.p.c. retention time with that of an authentic sample.

Residue

The residue obtained in the same manner as described for the AIBN reaction weighed 5.2 g. The average molecular weight determined on a Mechrolab Model 301A osometer was 380 g/mole. Infrared analysis showed the presence of internal unsaturation (3030, 660 cm^{-1}), vinyl unsaturation (915, 995 cm^{-1}), and the *t*-butyl group (1395, 1365 cm^{-1}). Partial separation by solvent extraction produced a fraction which gave no vinyl absorption. A t.l.c. chromatogram indicated that the residue also contained traces of dehydro dimer.

Determination of Carbon Dioxide, Isobutane, and Isobutylene

The yields of carbon dioxide, isobutane, and isobutylene formed in the decomposition of a known amount of perester were determined by decomposing 0.10 mole of TBPP for a period of 10 h or 2 half-lives (10), and trapping the gas emitted. The carbon dioxide was absorbed in an ascarite train and the isobutane and isobutylene were collected in a liquid nitrogen trap. The frozen gases were warmed and their total volume measured by displacement of a brine solution. The relative amounts of each gas was then determined by g.l.p.c. The quantitative evolution of carbon dioxide had been established previously (10).

1. J. R. SHELTON, L. W. HAYNES, C. K. LIANG, J. F. GORMISH, P. L. SAMUEL, and P. KOVACIC. Can. J. Chem. **46**, 1149 (1968). J. R. SHELTON, C. K. LIANG, and P. KOVACIC. J. Am. Chem. Soc. **90**, 354 (1968). J. R. SHELTON and C. W. UZELMEIER. J. Am. Chem. Soc. **88**, 5222 (1966).
2. J. R. SHELTON and J. N. HENDERSON. J. Org. Chem. **26**, 2185 (1961). J. R. SHELTON and A. E. CHAMP. J. Org. Chem. **28**, 1393 (1963).
3. J. R. SHELTON and H. G. GILDE. J. Org. Chem. **29**, 482 (1964).
4. J. R. SHELTON and A. E. CHAMP. J. Org. Chem. **30**, 4183 (1965).
5. J. R. SHELTON and J. F. SIUDA. J. Org. Chem. **31**, 2028 (1966).
6. W. F. BRILL. J. Org. Chem. **24**, 257 (1959).
7. W. J. FARRISSEY, JR. J. Org. Chem. **29**, 391 (1964).
8. C. WALLING and W. THALER. J. Am. Chem. Soc. **83**, 3877 (1961).
9. G. S. HAMMOND, J. N. SEN, and C. E. BOOZER. J. Am. Chem. Soc. **77**, 3244 (1955). G. S. HAMMOND, C. H. S. WU, O. D. TRAPP, J. WARKENTIN, and R. T. KEYS. J. Am. Chem. Soc. **82**, 5394 (1960).
10. P. D. BARTLETT and R. R. HIATT. J. Am. Chem. Soc. **80**, 1398 (1958). P. D. BARTLETT and D. M. SIMONS. J. Am. Chem. Soc. **82**, 1753 (1960).
11. A. F. BICKEL and W. A. WATERS. Rec. Trav. Chim. **69**, 1490 (1950).
12. J. C. BEVINGTON. J. Chem. Soc. 3707 (1954).
13. J. A. KERR. Chem. Rev. **66**, 465 (1966).
14. R. N. BIRRELL and A. F. TROTMAN-DICKENSON. J. Chem. Soc. 4218 (1960).
15. C. WALLING. Free radicals in solution. John Wiley and Sons, Inc., New York. 1957. p. 322.
16. W. DASLER and C. D. BAUER. Ind. Eng. Chem. Anal. Ed. **18**, 52 (1946).
17. Bulletin by DuPont. Vazo vinyl polymerization catalyst. p. 10.
18. S. R. SERGUIENKO. Compt. rend. acad. sci. U.R.S.S. **26**, 73 (1940); Chem. Abstr. **34**, 5418 (1940).

Can. J. Chem. Downloaded from www.nrcresearchpress.com by 210.87.254.42 on 09/05/12
For personal use only.

Can. J. Chem. Downloaded from www.nrcresearchpress.com by 210.87.254.42 on 09/05/12
For personal use only.

Studies of the oxide surfaces at the liquid–solid interface. Part II.[1] Fe oxides

SYED M. AHMED[2] AND DIMITRY MAKSIMOV[3]
Department of Energy, Mines and Resources, Mines Branch, Ottawa, Canada

Received October 19, 1967[4,5]

The double layer on hematite and magnetite in KNO_3, $NaClO_4$, and KCl solutions has been investigated by studying the equilibrium distribution of the potential determining ions (H^+ and OH^-) at the interface as a function of their electrochemical potentials. Data have been obtained on the pH_s of the zero point of charge (5.3 and 6.4 for hematite and magnetite, respectively, in 0.001 *M* KNO_3 solution), the surface charge densities, $q^{\pm}$, and the differential capacities $C(\pm)$ of the double layer.

For hematite, the q^+ values in NO_3^- and ClO_4^- solutions are due to chemisorption of H^+ on the surface, with NO_3^- and ClO_4^- showing no tendency for specific adsorption. In KCl solutions, high values of q^+ were obtained, depending on Cl^- concentration that are attributed to the replacement of the surface–OH groups by Cl^- (specific adsorption). Magnetite (a semiconductor) shows anomalous behavior with respect to H^+ adsorption.

The negative charge on the two oxides originates from acidic dissociation of the surface–OH groups which is followed by adsorption of K^+ on the surface. At high values of q^-, K^+ ions are specifically adsorbed on the surface-metal atoms through an O^{2-} bridge.

Canadian Journal of Chemistry, 46, 3841 (1968)

Introduction

The oxide–solution interface has been investigated earlier (1–4) by studying the equilibrium distribution of potential-determining ions (H^+, OH^-) at the interface in the absence of an applied electric field. From a thermodynamic analysis of the resultant data, by analogy with other reversible (e.g. AgI (5–7)) and polarizable interfaces, information has been obtained on the double-layer characteristics and the nature of ion–surface interactions. Some information can also be obtained from this work on the behavior of oxide electrodes (8–10). The present work on coarse and crystalline samples of Fe_2O_3 (specular hematite) and Fe_3O_4 (magnetite) of known surface areas is an extension of the previous work carried out on a series of oxides, SiO_2, ZrO_2, ThO_2 (1, 11), SnO_2, and TiO_2 (11, 12), in different electrolyte solutions.

Experimental

Materials

Naturally occurring samples of specular hematite and magnetite were supplied, respectively, by the Quebec Cartier Mining Co. and the Geological Survey of Canada. These samples were crushed and screened and a middle fraction of hematite was collected on a high-intensity Jones wet magnetic separator, rejecting the highly magnetic and non-magnetic portions. In a similar magnetic separation, the most magnetic portion was collected for magnetite. The material, in $-150 + 200$ mesh size (~ 0.1 mm), was leached with hot, 10% HCl to dissolve the slimes that usually adhere to the surface. The resultant material was washed free of HCl, deslimed (1), and stored in conductivity water. The materials were at least 99% pure, the major impurity being SiO_2 whose interference is assumed to be negligible on the basis of the previous work (1); the trace impurities were Mg, Cu, and Al. The crystals of specular hematite (Fe_2O_3) possessed several smooth, lustrous planes, which, when uncontaminated, showed some degree of native hydrophobicity (13) around the neutral pH_s, as tested by a flotation method (14). Specular hematite has an hexagonal structure, is weakly magnetic, and the co-ordination of Fe^{3+} is 6. Magnetite (Fe^{2+}-$Fe^{3+}{}_2O_4$), which belongs to the spinel group of oxides, is hexoctahedral where Fe^{2+} and Fe^{3+} are in 4 and 6 co-ordination states respectively. It is highly magnetic and is a semiconductor. The surfaces of magnetite were dull metallic in appearance and hydrophilic when tested by a bubble contact method (14).

Method

Except where mentioned, the experimental procedure was the same as described earlier (1). The pH_s of the solution before and after adding the oxides was followed at intervals of 2 min usually and 1 min near the zero point of charge (z.p.c.). Fresh samples of oxide and solutions were used for each point on the charge-density plots. The time to reach equilibrium (Fig. 1) between the solution and the oxide in each experiment (1) did not exceed 2 min (at high and low pH_s) to 6 min (at intermediate values of pH_s). Under these experimental conditions, no dissolved iron could be detected, at any pH_s, by standard colorimetric methods (sensitivity 1 μmole/l)

---

[1]For Part I, see ref. 1.
[2]Research Scientist, Mineral Sciences Division, Mines Branch, Department of Energy, Mines and Resources, Ottawa, Canada.
[3]Visiting Scientist, Skochinski Mining Institute, Moscow, U.S.S.R.
[4]Revision received July 31, 1968.
[5]Crown copyright reserved.

Can. J. Chem. Downloaded from www.nrcresearchpress.com by 210.87.254.42 on 09/05/12
For personal use only.

whereas, about 10^{-5} mole/l of Fe was found to dissolve if the material was stirred in solutions for 1 h near the z.p.c. Calibration curves of pH_s against the molar concentrations of HNO_3, HCl, and $HClO_4$ in solutions of KNO_3, KCl, and $NaClO_4$, respectively, of 0.001, 0.1, and 1 *M* concentrations, were obtained by potentiometric titrations. Similar calibration curves were also obtained for KOH in KNO_3 solutions. These curves were used in calculating the charge densities, $q^{\pm}$, from the measured values of $\Delta a_{H^+/OH^-}$ (1). The calomel electrode was separated from the KNO_3 solutions by means of a saturated KNO_3 solution bridge through a fiber junction. For the $NaClO_4$ solutions, a solution bridge consisting of KNO_3 and $NaNO_3$ in the molar ratio of 1:7 was used (ref. 5, p. 773). The liquid-junction potentials in both the cases are small. As the calibration curves of pH_s against H^+/OH^- concentration were obtained separately for each ionic strength under constant conditions of electrode combinations, small shifts may arise in the potential scale on increasing the ionic strength, but the calculations of charge densities should remain unaffected. The total shifts in the half-cell potential, as measured by the glass electrode, on increasing the ionic strength from 0.001 to 0.1 *M* and 1 *M* were also determined and taken into account where necessary.

The individual ionic activity coefficients used in the thermodynamic treatment in Part I (1) of this series are usually replaced at a final stage by the mean activity coefficients. This subject has been discussed in detail by Grahame (15).

The specific surface areas were determined (16) by the standard Kr gas-adsorption method. They were 800 cm^2/g for magnetite and 451 and 308 cm^2/g for the two samples of hematite. These surface areas were determined on samples that had been given a blank stirring treatment in water under the same conditions as used in the experiment, so that any increase in surface area due to slime formation was also taken into account. Recrystallized (A.R.) KNO_3, $NaClO_4$, or KCl were used to adjust the ionic strength of the solution and KOH and HNO_3, $HClO_4$, or HCl were used, as necessary, for adjusting the pH_s.

Results

Addition of hematite and magnetite to solutions of $pH_s >$ their respective z.p.c., resulted in a decrease in pH_s, whereas, below their respective z.p.c. the pH_s increased. The resultant surfaces, therefore, acquire a negative charge in the former region of pH_s and a positive charge in the latter. In general, this behavior is similar to that of other oxides studied (1, 11, 12). The variation of pH_s with time before and after adding the oxides to the electrolyte solutions was also studied. In a typical measurement (Fig. 1), it is seen that almost all the change in pH_s occurred in the first few minutes after the addition of the oxide to the solution. These changes in pH_s are attributed to the primary equilibrium between the oxide surfaces and H^+ and OH^- and

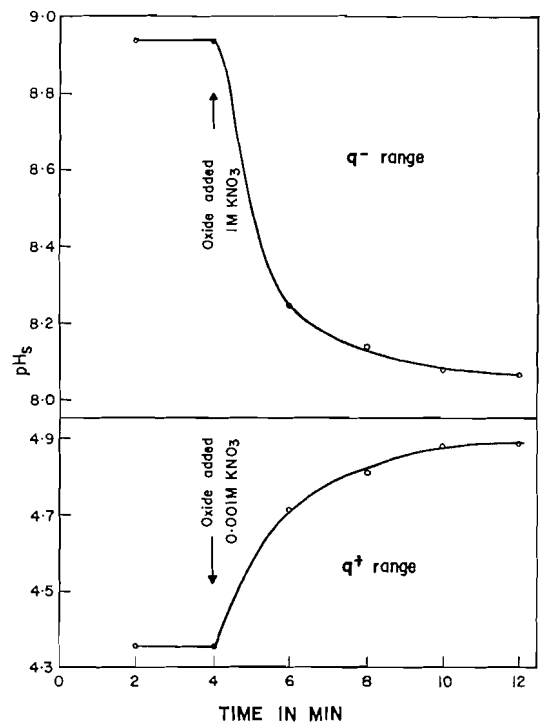

FIG. 1. Variation of pH_s with time before and after adding the oxide to the electrolyte solution.

the surface-charge densities ($q^{\pm}$) were calculated as before (1). The later changes in pH_s are so slow that the initial equilibrium between the surface and the potential determining ions may be taken as practically complete in a few minutes. The validity of the above assumptions can be checked by comparing with theory (15, 17) the experimental values obtained for the surface-charge densities and for the minimum differential capacity of the double layer at the z.p.c., and with the results obtained for other solid–solution interfaces (17). These values, as seen later, are of the expected order of magnitude regardless of the material and the surface area used. The slow changes in pH_s are attributed to secondary effects such as slime formation, solubility of the material, dissociation, and complex formation of the dissolved species, adsorption of the resultant complexes on the surface and also precipitation. Such reactions of iron oxide with electrolyte solutions have been known to continue for days (18).

The $q^{\pm}$ values for hematite and magnetite in KNO_3 solutions are shown as a function of final

Can. J. Chem. Downloaded from www.nrcresearchpress.com by 210.87.254.42 on 09/05/12
For personal use only.

pH_s and potential relative to the z.p.c., in Figs. 2 and 4 respectively. The values of q^+ on hematite in $NaClO_4$ and KCl solutions are shown plotted against the final pH_s in Fig. 3A and B respectively. It is seen in these figures that the values of $q^{\pm}$ increase in magnitude with the increasing half-cell potential ($\pm$) of the oxide electrode, relative to the z.p.c. In NO_3^- (Fig. 2) and ClO_4^- (Fig. 3A) solutions the positive charge densities are found to be almost independent of the respective anionic concentrations and depend mainly on a_{H^+}. A slight increase in the magnitude of q^+ of hematite (Fig. 2) on increasing the concentration of KNO_3 from 0.001 and 0.1 *M* to 1 *M* appears to be due to the effect of increased ionic strength on a_{H^+} and due to compression of the diffuse double layer. Similar behavior was also found to occur with $NaClO_4$ solutions where the q^+ values in 0.001 *M* solution were slightly lower than in 0.1 and 1 *M* $NaClO_4$ solutions (not shown in Fig. 3A). In a similar study carried out recently (11, 12), the q^+ values of SnO_2 in NO_3^- solutions and of TiO_2 in NO_3^- and Cl^- solutions were found to be practically independent of the anion concentration and depended mainly on a_{H^+}. In KCl solutions, however (Fig. 3B), a definite and substantial increase in the q^+ values of hematite occurs on increasing the Cl^- concentration at any given pH_s. SnO_2 surfaces have also been found (11, 12) to behave similarly in Cl^- solutions.

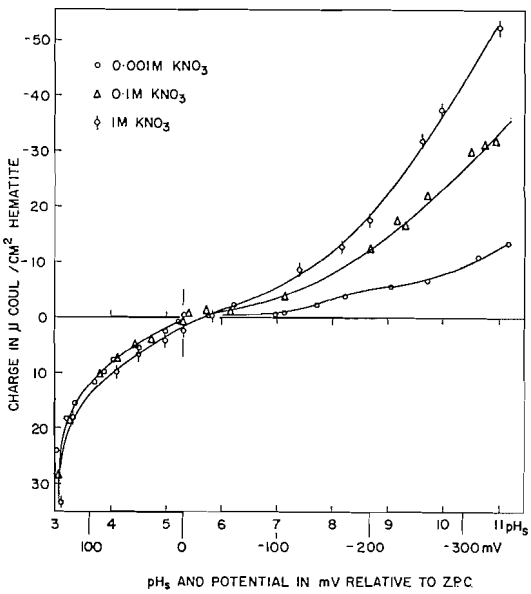

FIG. 2. Variation in charge density ($q^{\pm}$) on hematite with final pH_s and potential difference relative to the z.p.c. Indifferent electrolyte is KNO_3.

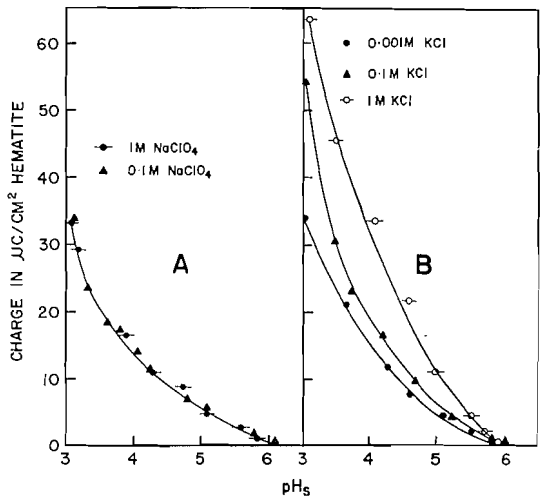

FIG. 3. Variation in charge density (q^+) on hematite with final pH_s in: A, $NaClO_4$ solutions; B, KCl solutions.

For the magnetite samples (Fig. 4), comparatively high values of q^+ were obtained in KNO_3 solutions and also q^+ slightly decreased in magnitude with increasing concentrations of KNO_3 in solution. The magnetite samples under investigation were found to be strongly magnetic and n-type semiconductors. Similar work, on magnetite samples of different origin, gave very low values of q^+. The behavior of magnetite in the q^+ region, therefore, is inconsistent with the general behavior of the oxides investigated and will not be discussed further, until more detailed investigations are performed.

It was also considered probable that the surfaces might have been dehydrated on evacuating the samples (a water aspirator was used at room temperature (1)) and this might interfere with the results. Hence, a set of experiments was carried out where the oxide samples were taken freshly out of water and the excess water was filtered out under suction in an atmosphere of argon. The resultant moist material (water = 2.5% by wt. oxide) was used for subsequent work. The same variation in q^+ with respect to ionic strength was obtained, as mentioned above, and we feel confident that this behavior is reproducible. The q^+ values (Figs. 2–4) were obtained on moist

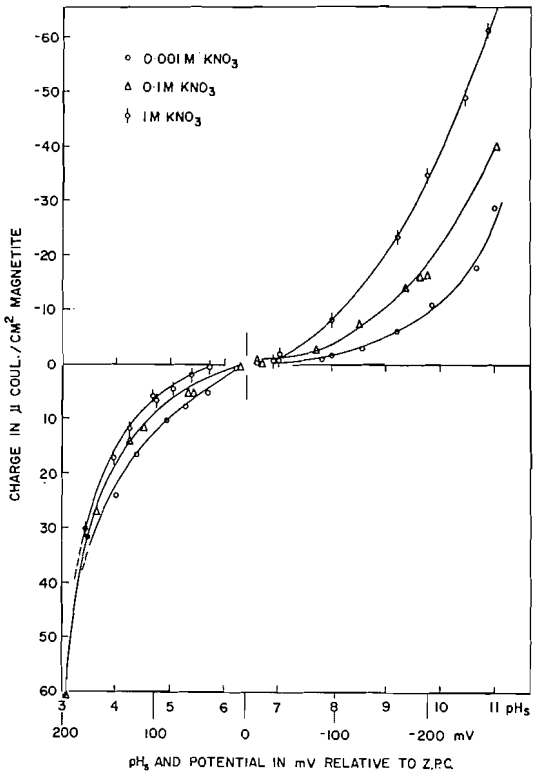

FIG. 4. Variation in charge density ($q^{\pm}$) on magnetite with final pH_s and potential relative to the z.p.c. Indifferent electrolyte is KNO_3.

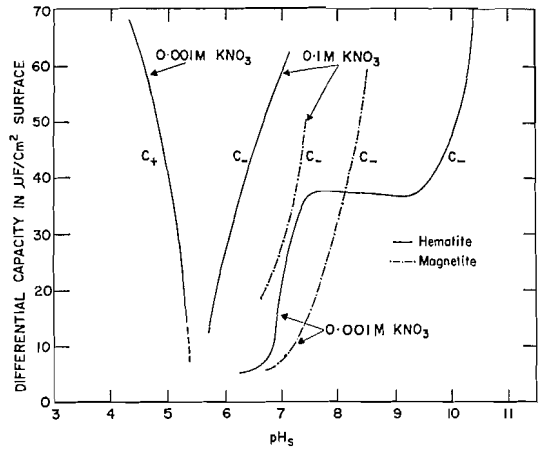

FIG. 5. Variation in the differential capacity of the double layer on hematite and magnetite ($C(-)$ only) with pH_s. Indifferent electrolyte is KNO_3.

samples of oxides except for a few points near the z.p.c. This behavior of q^+ with respect to the ionic strength of the solution may be different for precipitated iron oxide (2, 3) or slimes, and may even be masked if excess of dissolved iron is present in solution.

The differential capacity $C(\pm)$ of the entire double layer was obtained by graphical differentiation of the smoothed charge-density plots of Figs. 2 and 4. The resultant $C(\pm)$ curves obtained for hematite and magnetite in 0.001 and 0.1 M KNO_3 solutions are shown plotted against pH_s in Fig. 5. The $C(+)$ values for magnetite have not been included, but they were considerably higher than theoretically expected (15, 17) for non-specific adsorption of ions on the surface. The interfacial energy of the double layer on oxides obtained by the graphical integration (1) of the charge-density plots of Figs. 2 and 4 were similar to those obtained earlier for other oxides (1, 11, 12) and are not reported here.

Discussion

The Zero Point of Charge

The z.p.c. of hematite in 0.001, 0.1, and 1 M KNO_3 solutions were found to occur at pH_s 5.3 ± 0.05, 5.4 ± 0.05, and 5.7 ± 0.1, respectively. On increasing the concentration of KNO_3 in a blank solution from 0.001 to 1 M, the glass electrode measured a decrease in pH_s of 0.30 ± 0.05 units in the vicinity of the z.p.c., although this effect was negligible below $pH_s = 4$. The z.p.c. of solid surfaces is known (15, 17) to shift towards a more positive or a more negative potential when cations or anions, respectively, are specifically adsorbed on the surface. However, the observed shifts in the z.p.c. of the oxide to a higher pH_s, on increasing the ionic strength of the solution, is to compensate for the above-mentioned change in the cell potential and does not seem to indicate specific adsorption of NO_3^- on the oxide surfaces to a noticeable degree. In ClO_4^- (Fig. 3A) and Cl^- solutions (Fig. 3B) the z.p.c. of hematite occurred at pH_s equals 6. The z.p.c. of magnetite in 0.001 M KNO_3 solution was found to occur at pH_s equals 6.4 ± 0.1 and was somewhat smeared at higher ionic strengths of the solution. The present values for the z.p.c. of iron oxides are for the primary equilibrium (Fig. 1, first few minutes) that occurs between the oxide surfaces and the potential determining ions (H^+ and OH^-) in the presence of K^+, NO_3^-, etc., in solutions that are practically free of the dissolved iron complexes. Hence, the pH_s values

Can. J. Chem. Downloaded from www.nrcresearchpress.com by 210.87.254.42 on 09/05/12
For personal use only.

Can. J. Chem. Downloaded from www.nrcresearchpress.com by 210.87.254.42 on 09/05/12
For personal use only.

reported here for the z.p.c. of iron oxides are in close agreement with some of the values obtained on similar samples by streaming potential methods (19) where mostly fresh solutions, free of dissolved iron complexes, are in contact with the surfaces. However, if the oxides are allowed to equilibrate with solutions for several hours (15 h) (2, 20, 21) the solutions become saturated with the dissolved complexes that may also be adsorbed on the surfaces or be precipitated. Under such conditions, the experimental z.p.c. of oxides should occur at the same pH_s as the isoelectric point (i.e.p.) of the soluble complexes. Thus, Parks and De Bruyn (2) found that the z.p.c. of precipitated iron oxide under slow conditions of equilibria occurs at the same pH_s (8.5) as the i.e.p. of the soluble complexes of iron. Specular hematite, obtained from the same source as in the present work, has also been examined by others (20) under slow conditions of equilibria and a pH_s of 8.5 has been reported for the z.p.c. A similar coincidence of the z.p.c. of TiO_2 surfaces with the i.e.p. of titanium complexes has also been reported (21). It is evident from the above considerations that the z.p.c. of oxide surfaces, under primary equilibrium with H^+ and OH^-, is usually quite different from the i.e.p. of the corresponding dissolved complexes in solution. Hence, the experimental z.p.c. of oxides will depend mainly on the oxide–solution equilibria under investigation and the concentration of the dissolved complexes in solution. The adsorption of metal complexes on solids would itself shift the z.p.c. considerably. Thus, for hematite, depending on the experimental conditions, the z.p.c. may vary from an initial pH_s of 5.3 to a final pH_s 8.5. In addition, the z.p.c. of different forms of iron oxide, as reviewed by Parks (22), also depends on the oxide composition, crystalline form and size, and method of surface preparation.

The Primary Oxide–Solution Equilibria and the Surface Charge

The negative surface charge on oxides in solutions of $pH_s >$ z.p.c. is attributed (1) to the acidic dissociation of the surface OH groups which is followed by adsorption of K^+ on the oxides. The q^- values of hematite and magnetite increase with increasing pH_s as well as K^+ concentration (Figs. 2, 4). This behavior is common to all the oxides (1, 11, 12) investigated.

The q^+ values of hematite, however, depend on a_{H^+} as well as on the nature of anions present in solution. In NO_3^- and ClO_4^- solutions (Figs. 2 and 3A), these q^+ values are almost independent of the anion concentration within the experimental errors. The positive surface charge under these conditions is attributed, mainly, to the chemisorption of H^+ on the neutral surface as the a_{H^+} in solution is increased with respect to the z.p.c. This is schematically shown below

$$\left[\text{>Fe(H}_2\text{O)(OH)}_2\right] \underset{OH^-}{\overset{H^+}{\rightleftharpoons}} \left[\text{>Fe(H}_2\text{O)}_2\text{(OH)}\right]^+ \text{ etc.}$$

neutral, aquo-complex at the z.p.c.

where only 3 of the 6 co-ordination numbers of Fe^{3+}, including 2 valence states, are assumed to be exposed to the solution. In the above reaction, NO_3^- and ClO_4^- do not replace the surface–OH groups. In terms of the double-layer theories (15, 17), it means that these anions are not specifically adsorbed on the surface and stay at the outer Helmholtz plane and in the diffuse double layer. Under these conditions, the anions exert only a small, indirect influence on the q^+ values by changing a_{H^+} and by compressing the double layer, when the salt concentration is raised. From the double-layer theories (23, 24), the q^+ values in the absence of specific adsorption of anions increase only by 2 $\mu C/cm^2$ on increasing the 1–1 electrolyte concentration from 0.001 to 1 M, for a change of 100 mV in the double layer potential. This is in agreement with the q^+ values of hematite obtained in 0.001, 0.1, and 1 M KNO_3 solutions (Fig. 2). In general, the expected variations in q^+ with increasing anion concentration are small in the absence of specific adsorption of anions and lie within the experimental errors of the present work. Hence, under the above conditions, the oxide electrode is reversible to H^+ (8) mainly and the q^+ values depend mainly on a_{H^+}. Compared to the above behavior, the q^+ values (apparent) of hematite in KCl solutions (Fig. 3B) are found to increase not only with a_{H^+} but also substantially with a_{Cl^-}. This increase in q^+ (apparent) with a_{Cl^-}, at a given pH_s, is attributed to the replacement of the surface OH groups by Cl^- (more OH^- liberated), as shown below schematically

$$\left[\text{>Fe(H}_2\text{O)(OH)}_2\right] \underset{OH^-}{\overset{H^+,\ Cl^-}{\rightleftharpoons}} \left[\text{>Fe(H}_2\text{O)}_2{}^{2+}\text{Cl}^-\right]^+ + OH^-$$

chloro-complex

In terms of the double-layer theories (15, 17, 24), Cl^- in the above reaction is specifically adsorbed on the surface. Such specific adsorption of anions on polarized, anodic surfaces of solids is known to result in high values of q^+ depending on the anion concentration.

The differential capacity (Fig. 5) and the interfacial-energy variations (not reported) with pH_s are similar to those of other oxides studied (1, 11). The high values of the differential capacity, $C(+)$, in the q^+ region of hematite in KNO_3 and $KClO_4$ solutions may be attributed to the chemisorption of H^+ on the surface.

The $C(-)$ curves in Fig. 4 show a plateau for hematite between pH_s 7.5–9.5 ($C(-) = 30$–40 $\mu F/cm^2$) followed by a steep rise in $C(-)$. The steep rise in $C(-)$, at $pH_s > 9.5$, is similar to that obtained for quartz and ZrO_2 (1) in the q^- region and is most probably due to the specific adsorption of cations to the metal atoms of the surface through chemisorbed O^{2-} bridge, as discussed earlier (1). The plateaux probably correspond to the characteristic "hump" in the C curves of the polarized Hg surfaces (15, 17, 24) except that in this work the hump has been smoothed in the graphical differentiation of the q^- curves. The hump has been attributed (25) to two opposing effects, the specific adsorption of ions and dielectric saturation. If the specific adsorption of ions is intense, e.g. I^- on Hg (15, 17), the hump is found to be masked. In the case of magnetite, the intense specific adsorption of ions appears to have masked the effects which give rise to such humps.

Acknowledgments

The authors would like to thank the Quebec Cartier Mining Company, Canada, for providing the specular hematite. One of us (D.M.) is grateful to the Mines Branch, Department of Energy, Mines and Resources, Ottawa, for providing the research facilities.

1. S. M. Ahmed. Can. J. Chem. **44**, 1663, 2769 (1966).
2. G. A. Parks and P. L. De Bruyn. J. Phys. Chem. **66**, 967 (1962).
3. G. Y. Onoda, Jr. and P. L. De Bruyn. Surface Sci. **4**, 48 (1966).
4. J. A. Yopps and D. W. Fuerstenau. J. Colloid Sci. **19**, 61 (1964).
5. E. L. Mackor. Rec. Trav. Chim. **70**, 663 (1951); **70**, 747 (1951); **70**, 763 (1951).
6. J. Th. G. Overbeek. Symposium, Electrochemical Constants, Nat. Bur. Std. U.S., Circ. No. 524, 213 (1953).
7. J. Lyklema and J. Th. G. Overbeek. J. Colloid Sci. **16**, 595 (1961).
8. G. Kortüm and J. O'M. Bockris. Text book of electrochemistry. Vol. 1. Elsevier Publ. Co., London. 1951. p. 293.
9. D. J. G. Ives and G. J. Janz. Reference electrodes, theory and practice. Academic Press, Inc., New York. 1961. p. 322.
10. J. T. Stock, W. C. Purdy, and L. M. Garcia. Chem. Rev. **58**, 611 (1958).
11. S. M. Ahmed and D. Maksimov. Department of Energy, Mines and Resources, Mines Branch, Ottawa. Research Report R196. 1968.
12. S. M. Ahmed and D. Maksimov. J. Colloid Interface Sci. In press.
13. A. M. Gaudin, H. L. Miaw, and H. R. Spedden. Proceedings, Second International Congress of Surface Activity. Vol. III. Butterworth Scientific Publications, London. 1957. p. 202.
14. A. M. Gaudin. Flotation. 2nd ed. McGraw-Hill Book Co., Inc., New York. 1958. p. 147, p. 418.
15. D. C. Grahame. Chem. Rev. **41**, 441 (1947).
16. S. M. Ahmed. Department of Energy, Mines and Resources, Mines Branch, Ottawa, Technical Bulletin TB 84. 1966.
17. M. A. V. Devanathan and B. V. K. S. R. A. Tilak. Chem. Rev. **65**, 635 (1965).
18. G. Biedermann and J. T. Chow. Acta Chem. Scand. **20**, 1376 (1966).
19. A. S. Joy, D. Watson, and R. W. G. Cropton. Trans. AIME, **229**, 5 (1964).
20. G. W. Smith and T. Salman. Can. Met. Quart. **5**, 93 (1966).
21. G. W. Smith and T. Salman. Can. Met. Quart. **6**, 167 (1967).
22. G. A. Parks. Chem. Rev. **65**, 177 (1965).
23. C. D. Russell. J. Electroanal. Chem. **6**, 486 (1963).
24. P. Delahay. Double layer and electrode kinetics. Interscience Publishers, Inc., New York. 1965. p. 17–80.
25. J. R. Macdonald and C. A. Barlow, Jr. J. Chem. Phys. **36**, 3062 (1962).

Can. J. Chem. Downloaded from www.nrcresearchpress.com by 210.87.254.42 on 09/05/12
For personal use only.

Electron spin resonance of fluorine-substituted nitro-aromatic anion radicals

P. H. H. FISCHER AND H. ZIMMERMANN
Max-Planck-Institut, Jahnstrasse 29, Heidelberg, Germany

Received May 13, 1968

Electron spin resonance spectra have been observed for anion radicals derived from 2-fluoro-nitrobenzene, 3-fluoro-nitrobenzene, 2,4-difluoro-nitrobenzene, 2,5-difluoro-nitrobenzene, 4-fluoro-2-nitrophenol, 2-fluoro-6-nitrophenol, and 3-fluoro-6-nitrophenol. All radicals were generated electrolytically in dimethoxyethane/acetonitrile solution, acetonitrile, or dimethylformamide. The radicals are generally quite stable with the exception of those from 2-fluoro-6-nitrophenol and 3-fluoro-6-nitrophenol, the latter decaying with a half-life of approximately 6 min. All spectra can be interpreted completely, and coupling constants are assigned by comparison to related compounds and consistency arguments.

Canadian Journal of Chemistry, 46, 3847 (1968)

Can. J. Chem. Downloaded from www.nrcresearchpress.com by 210.87.254.6 on 09/05/12
For personal use only.

Introduction

Several fluorine containing radicals have been investigated by electron spin resonance (e.s.r.) techniques. Amongst these are the fluoranil semiquinone (1), monofluorinated nitrobenzene radicals (2–5), *p*-fluoro-acetophenone (6), 2,7-difluoro-fluorenone (7), and recently some highly fluorinated nitro and nitroso radicals (8). By means of fluorine nuclear resonance investigations (9) on nickel chelate complexes it has been shown that electron delocalization occurs between fluorine and neighboring carbon, conclusions also reached by e.s.r. crystal studies on monofluoroacetamide (10) and trifluoroacetamide (11).

Initially it was assumed that the fluorine splitting a_F could be represented by an equation similar to the McConnell equation, namely $a_F = Q\rho^{\pi}_C$, that is, the fluorine coupling constant would be determined by the π electron spin density on the adjacent carbon atom. It was, however, shown for ^{13}C and ^{14}N, that for many electron atoms a more complex form to express the coupling constants is required, so that for fluorine also we should expect an equation of the type

$$a_F = (S_i + Q_{FC})\rho^{\pi}_F + Q_{CF}\rho^{\pi}_C$$

where the Q's and the ρ^{π}'s are the so called spin-polarization parameters and spin densities, and S_i would take into account any contributions from 1s and/or lone-pair electrons. Possibly non-diagonal elements should also be considered.

Several attempts at estimation of these Q's have been made (4, 8–10), but a set of values applicable to a larger group of fluorinated aromatic radicals is as yet not available. In an effort to determine these parameters we have measured the e.s.r. spectra of a large number of fluorine containing radicals, including some previously recorded. The anion radicals of *o*- and *m*-fluoro-nitrobenzene, for instance, have been rerecorded in aprotic solvents to exclude strong solvation effects as could be found in aqueous systems (5). The samples chosen had to obey the following criteria: they should not be too large and unsymmetric so as to allow a complete interpretation of the spectra, and more important, they must, in addition to the fluorine nuclei, contain aromatic protons to allow a check of the spin density calculations used in the elucidation of the spin-polarization parameters (12).

Below are the results obtained for the above-mentioned nitro-aromatic anion radicals.

Experimental

2,4-Dinitrofluorobenzene (puriss.), 2-fluoro-6-nitrophenol (purum), 3-fluoro-6-nitrophenol (purum), and 4-fluoro-2-nitrophenol (purum) were obtained from Fluka AG/Switzerland. 1,3-Dinitro-4,6-difluoro-benzene, melting point 72–74 °C, was purchased from Aldrich Chemical Co./U.S.A. 2-Fluoro-nitrobenzene, 2,4-difluoro-nitrobenzene, and 2,5-difluoro-nitrobenzene were available from Koch-Light Laboratories/England, while 3-fluoro-nitrobenzene came from Schuchardt AG/Germany. 1-Fluoro-4-nitronaphthalene was obtained from Ega Chemie/Germany, *o*-nitrophenol was Merck reagent grade, and 2,3,4,5-tetrafluoro-nitrobenzene came from K. and K. Laboratories/U.S.A. 2,3,4,6-Tetrafluoro-nitrobenzene was prepared by the method of Finger *et al.* (13) from 1,2,3,5-tetrafluoro-benzene. All purchased substances were used without further purification. The three fluorinated nitrophenols and *o*-nitrophenol were converted to the corresponding OD analogues by steam distillation of the respective compound with a 100-fold excess of 99.9% D_2O. Deuteration was in excess of 99% as proved by nuclear magnetic resonance spectra.

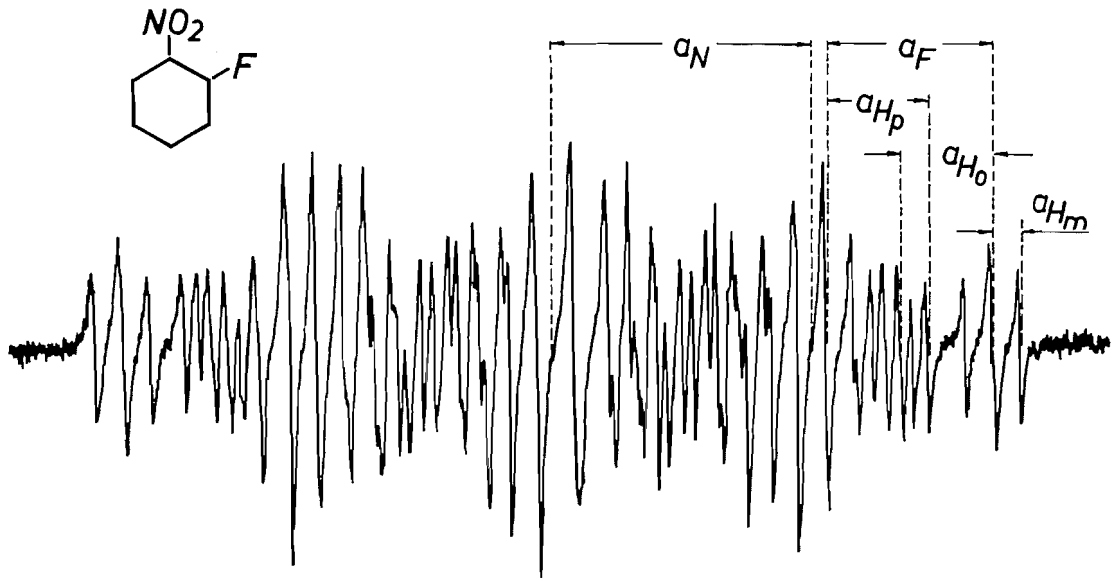

FIG. 1. Electron spin resonance spectrum of 2-fluoro-nitrobenzene anion radical.

The solvents employed were acetonitrile, dimethylformamide, and dimethoxyethane. Acetonitrile, Merck Uvasol grade, was made oxygenfree by repeated freezing, pumping, and thawing, and stored on a vacuum rack over calcium hydride to remove traces of water. Dimethylformamide, also Merck Uvasol grade, was distilled from anhydrous potassium carbonate and made oxygenfree in the same manner. Dimethoxyethane, Merck lab. grade, was stored on the vacuum rack over sodium and anthracene.

As supporting electrolyte we used tetra-*n*-propylammonium-perchlorate prepared according to Geske and Maki's procedure (14).

All radicals were generated by reduction at a platinum wire cathode in a vacuum electrolytic cell described elsewhere (15).

The spectra were recorded with a conventional Varian V-4500 e.s.r. spectrometer, using 100 kHz modulation of the magnetic field produced by a 6 in. magnet. The field was monitored with an AEG magnetometer.

Results

2-Fluoro-nitrobenzene

When a 10^{-3} *M* solution of *o*-fluoro-nitrobenzene in a mixture of dimethoxyethane (75%) and acetonitrile (25%) is reduced, a reddish-brown solution exhibiting the hyperfine pattern shown in Fig. 1 results. The spectrum consists of 62 resolved lines with indications of others. If all coupling constants are different and all lines resolved, a maximum number of $3 \cdot 2^5 = 96$ lines is possible. The outside three lines on each side of the spectrum are nearly in the intensity ratio 1:2:1, the center line showing slight asymmetry in each case. Within the linewidth, which is ~ 0.18 G, two spin 1/2 coupling constants are identical and a maximum number of 72 lines is possible. The spectrum can be analyzed in terms of the following splitting constants: $a_N = 9.81$, $a_1 = 6.36$, $a_2 = 4.01$, $a_3 = 3.47$, and $2 \cdot a_4 = 1.01$ G.

3-Fluoro-nitrobenzene

Reduction of a 10^{-3} *M* solution of *m*-fluoro-nitrobenzene in dimethoxyethane/acetonitrile (3:1) yields a brown solution which exhibits the e.s.r. spectrum shown in Fig. 2. It consists of 80 of the 96 theoretically possible lines, the remaining 16 being hidden by overlap with other lines. Linewidths are 0.18 G. The spectrum can be unambiguously explained with the coupling constants: $a_N = 9.23$, $a_1 = 3.91$, $a_2 = 3.37$, $a_3 = 3.16$, $a_4 = 2.92$, and $a_5 = 1.01$ G.

2,4-Difluoro-nitrobenzene

Electrolytic reduction of a 10^{-3} *M* solution of this compound in dimethoxyethane/acetonitrile in 3 to 1 ratio, results in a brown solution which shows the 50 line e.s.r. spectrum reproduced in Fig. 3. As in the case of the *o*-fluoro-nitrobenzene anion radical, a triplet structure in the intensity ratio 1:2:1 and splitting of 1.11 G, limits the maximum number of lines to 72. Analysis of the

Can. J. Chem. Downloaded from www.nrcresearchpress.com by 210.87.254.6 on 09/05/12
For personal use only.

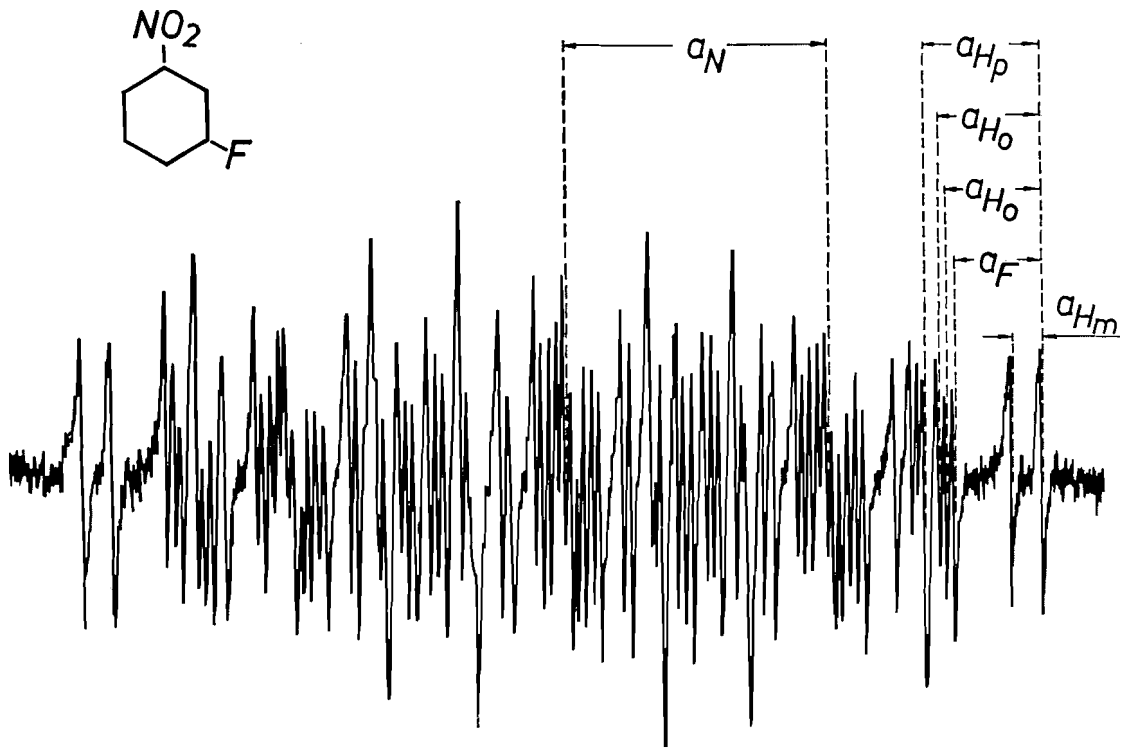

FIG. 2. Electron spin resonance spectrum of 3-fluoro-nitrobenzene anion radical.

spectrum is possible with the following coupling constants: $a_N = 9.81$, $a_1 = 8.59$, $a_2 = 6.40$, $a_3 = 3.63$, and $2 \cdot a_4 = 1.11$ G.

2,5-Difluoro-nitrobenzene

When a 10^{-3} *M* solution of this substance in an acetonitrile/dimethoxyethane mixture (1:3) is electrolyzed, a reddish-brown solution results and shows the well resolved spectrum reproduced in Fig. 4. It shows 78 of the theoretically possible 96 lines and is interpretable with the following coupling constants: $a_N = 8.44$, $a_1 = 6.24$, $a_2 = 4.19$, $a_3 = 3.57$, $a_4 = 3.03$, and $a_5 = 0.92$ G. The linewidths of well resolved lines towards the outside of the spectrum are, as for the other anions, 0.18 G peak to peak.

2-Nitrophenol and 2-Nitrophenol-H[2]

The parent compound of the three fluorinated nitrophenols investigated in the present paper is *o*-nitrophenol. The anion radical of this compound has been investigated by Nordio *et al.* (16), who interpret a 45 line spectrum in terms of three coupling constants: a_N, a_H(ortho) = a_H(para), and $2 \cdot a_H$(meta) = a_H(hydroxyl). We generated a radical species from *o*-nitrophenol in a mixture of dimethoxyethane and acetonitrile, the e.s.r. spectrum of which resembled in general that published by Nordio *et al.* However, in contrast to the 45 lines obtained by these authors, our spectrum exhibited 57 resolved lines. The spectrum can be adequately interpreted with the following coupling constants: $a_N = 12.21$, $2 \cdot a_1 = 3.63$, $a_2 = 1.08$, and $2 \cdot a_3 = 0.50$ G. The splitting constants are similar to those obtained previously with the exception of one constant, which we obtain as 1.08 G, and which the above authors do not quote. With our coupling constants the line positions are accurately reproduced, though intensities do vary from the theoretically calculated ones. This may have several reasons, the most obvious one being the fact that the coupling constants of 3.63 and 0.50 G for two equivalent protons each, may be composed of two slightly differing splittings, i.e. the respective sites do not exhibit an exactly degenerate coupling. Secondly, one coupling constant is

Can. J. Chem. Downloaded from www.nrcresearchpress.com by 210.87.254.6 on 09/05/12
For personal use only.

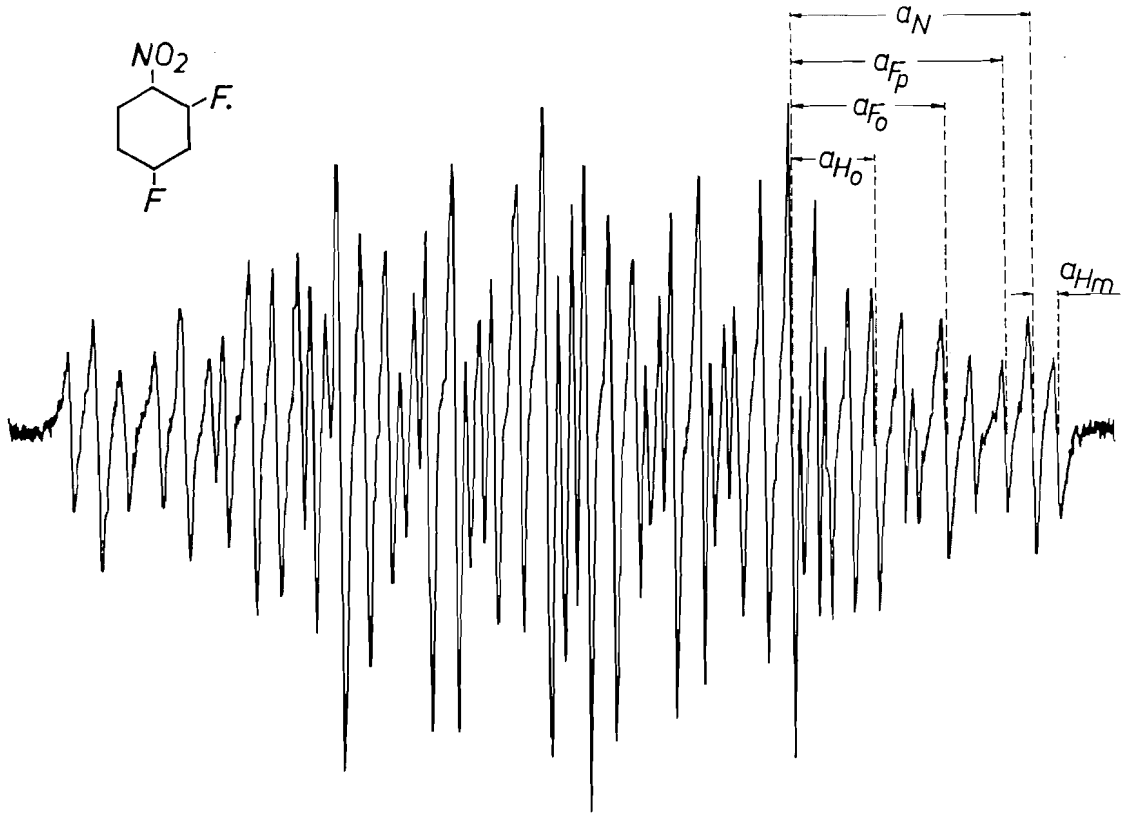

FIG. 3. Electron spin resonance spectrum of 2,4-difluoro-nitrobenzene anion radical.

very nearly twice the size of another, and thirdly, odd linewidth effects, so particular to nitro radicals and already observed and discussed in diverse papers, may be playing a role.

The species deuterated in the hydroxyl position yielded a well resolved spectrum of 36 lines and was easily interpreted in terms of four coupling constants. As for the undeuterated species the splitting due to two spin $I = 1/2$ nuclei (3.54 G) was degenerate within the linewidth. Of great importance is the fact that the degenerate coupling of 0.50 G in the undeuterated species is no longer observed, proving that not two ring protons, rather one ring proton and the hydroxyl proton give rise to the 0.50 G coupling constant.

4-Fluoro-2-nitrophenol and 4-Fluoro-2-nitrophenol-H[2]

When a 10^{-3} M solution of 4-fluoro-2-nitrophenol in a dimethoxyethane/acetonitrile mixture (3:1) is reduced, a yellow solution results showing the e.s.r. spectrum reproduced in Fig. 5. The spectrum consists of 10 groups of lines, 72 altogether. If all nuclei are non-equivalent and if the phenolic proton is not lost as in 4-nitrophenol (17), during electrolysis of which the acidic proton is dissociated and the spectrum of the dianion radical is observed, a maximum of 96 lines is to be expected. As the two outside groups consist of 3 lines in the intensity ratio of 1:2:1 exactly, two spin 1/2 coupling constants must be identical, and a maximum number of 72 lines is possible. This is the exact number of lines observed and we attribute our spectrum as being due to the anion radical of the compound being investigated. This is also in agreement with results obtained by us and by Nordio *et al.* (16) on non-fluorinated *o*-nitrophenol. When compared to a 4-nitrophenol, the OH proton is probably hindered from being easily dissociated by an internal hydrogen bond to the neighboring NO_2 group. The spectrum can be perfectly analyzed with the coupling constants $a_N = 11.08$, $a_1 = 3.89$, $a_2 = 3.51$, $a_3 = 2.74$, and $2 \cdot a_4 = 0.50$ G. The radical

Can. J. Chem. Downloaded from www.nrcresearchpress.com by 210.87.254.6 on 09/05/12
For personal use only.

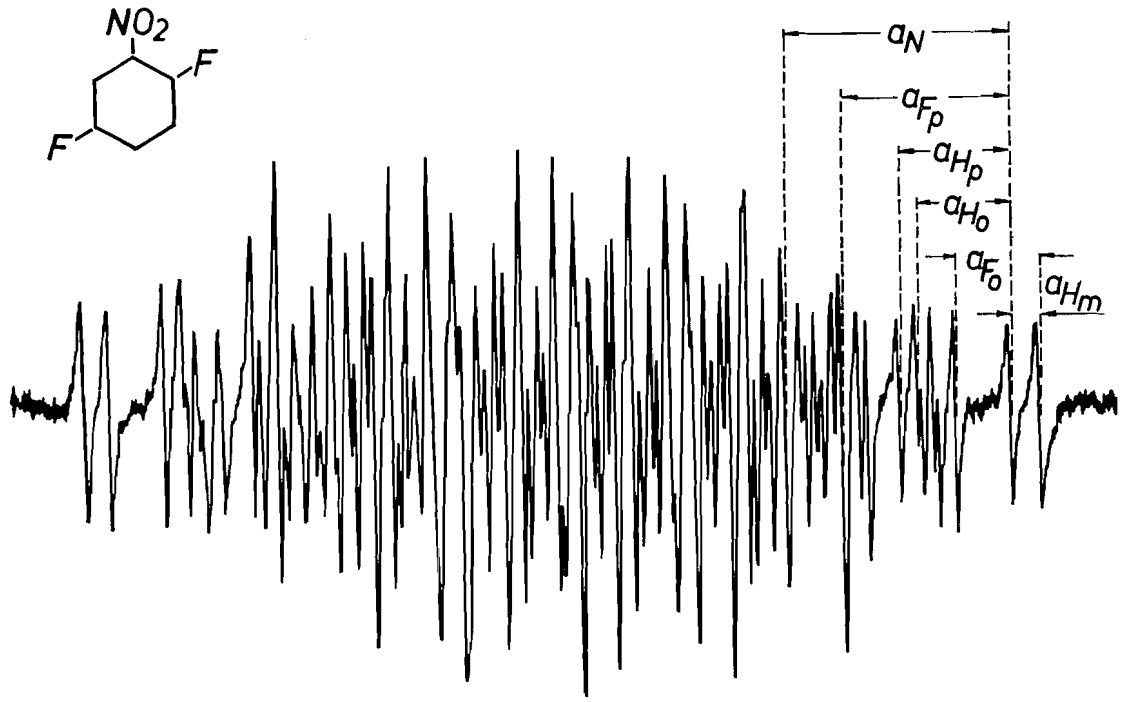

FIG. 4. Electron spin resonance spectrum of 2,5-difluoro-nitrobenzene anion radical.

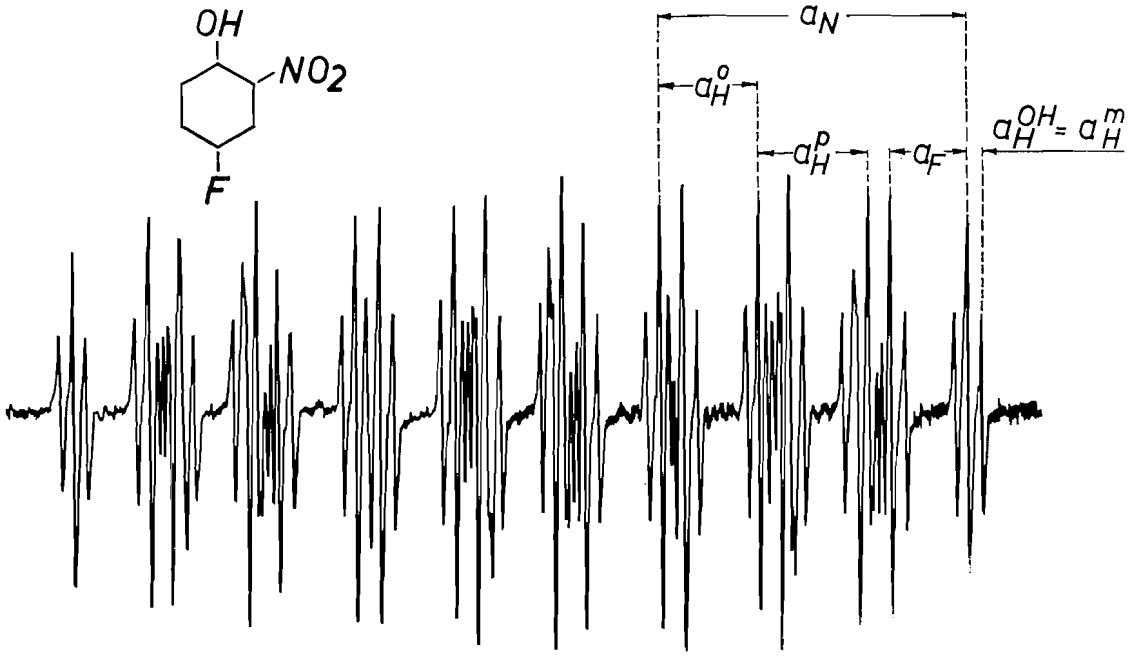

FIG. 5. Electron spin resonance spectrum of 4-fluoro-2-nitrophenol anion radical.

Can. J. Chem. Downloaded from www.nrcresearchpress.com by 210.87.254.6 on 09/05/12
For personal use only.

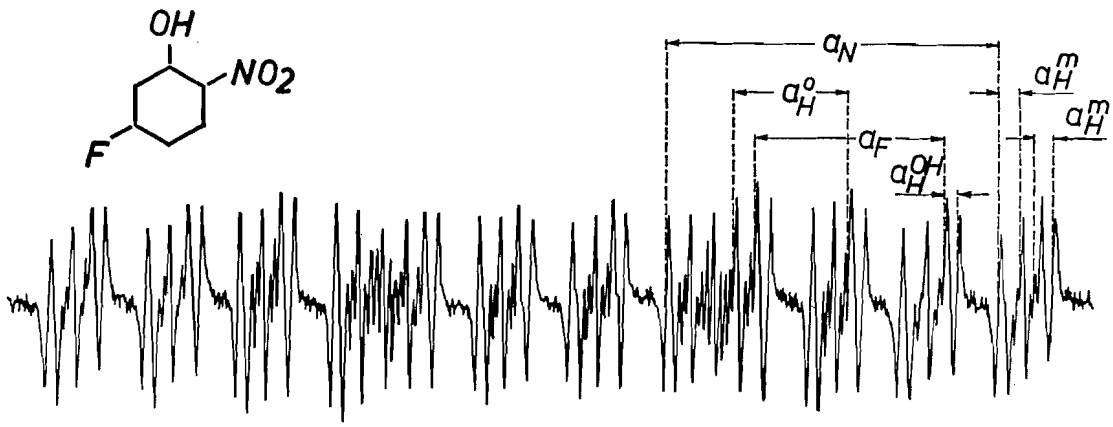

FIG. 6. Electron spin resonance spectrum of 3-fluoro-6-nitrophenol anion radical.

is very stable and can be monitored over periods of hours.

The corresponding radical having an OD substituent instead of OH, yielded a spectrum composed of 42 lines, 36 of which were of equal intensity and 6 of which showed a relative intensity twice that of the others. Obviously an accidental superposition of twice six lines is observed, and all 48 lines expected from the radical, if no deuterium splitting is found, are present. The spectrum may be perfectly analyzed with coupling constants very similar to those of the undeuterated species. Of importance is again the fact that the 1:2:1 triplet due to two protons in the non-deuterated species is replaced by a 1:1 intensity doublet of almost identical splitting. This proves that the OH proton and one ring proton exhibit a degenerate coupling constant, definitely not two protons of the aromatic ring. Secondly, a coupling constant of 0.50 G can be definitely assigned to the OH proton in 4-fluoro-2-nitrophenol.

3-Fluoro-6-nitrophenol and 3-Fluoro-6-nitrophenol-H[2]

When we reduced a solution of 3-fluoro-6-nitrophenol in a 75% dimethoxyethane and 25% acetonitrile mixture, a yellowish solution giving an only moderately stable spectrum was obtained. By increasing acetonitrile to approximately 75%, we found that the radical could be stabilized sufficiently for a spectrum to be recorded. The spectrum thus obtained is shown in Fig. 6. It consists of exactly 96 lines, the maximum number to be expected if all splittings are non-degenerate and all lines resolved. The spectrum is interpreted in terms of the following coupling constants: $a_N = 12.68$, $a_1 = 7.21$, $a_2 = 3.78$, $a_3 = 0.87$, $a_4 = 0.73$, and $a_5 = 0.52$ G. As the maximum number of possible lines is actually observed, we must, as in the two previous cases, be dealing with the monoanion radical.

Deuteration of the hydroxyl group resulted in a simplified spectrum of 36 lines instead of the possible 48 lines, as one coupling constant of 7.48 G is almost exactly twice another coupling of 3.67 G. The smallest coupling of 0.52 G could be definitely shown to be absent, and is thus attributable to the phenolic proton.

2-Fluoro-6-nitrophenol and 2-Fluoro-6-nitrophenol-H[2]

The radical derived from this species proved to be the most elusive of the four nitrophenol anions. When a 10^{-3} M solution of 2-fluoro-6-nitrophenol in a mixture of 25% dimethoxyethane and 75% acetonitrile was reduced, a yellow coloration resulted, and the e.s.r. spectrum shown in Fig. 7 was observed. The spectrum consists of 60 lines of nearly equal intensity and was stable for only 15 to 20 min. To obtain better resolution, slower scanning speeds were required and the spectrum was recorded in segments. Under these conditions up to 30 additional lines could be observed. In any case, we are dealing with a species giving rise to a spectrum of more than 48 lines, so that here also the dianion radical can be excluded as paramagnetic species. The spectrum is interpreted in

Can. J. Chem. Downloaded from www.nrcresearchpress.com by 210.87.254.6 on 09/05/12
For personal use only.

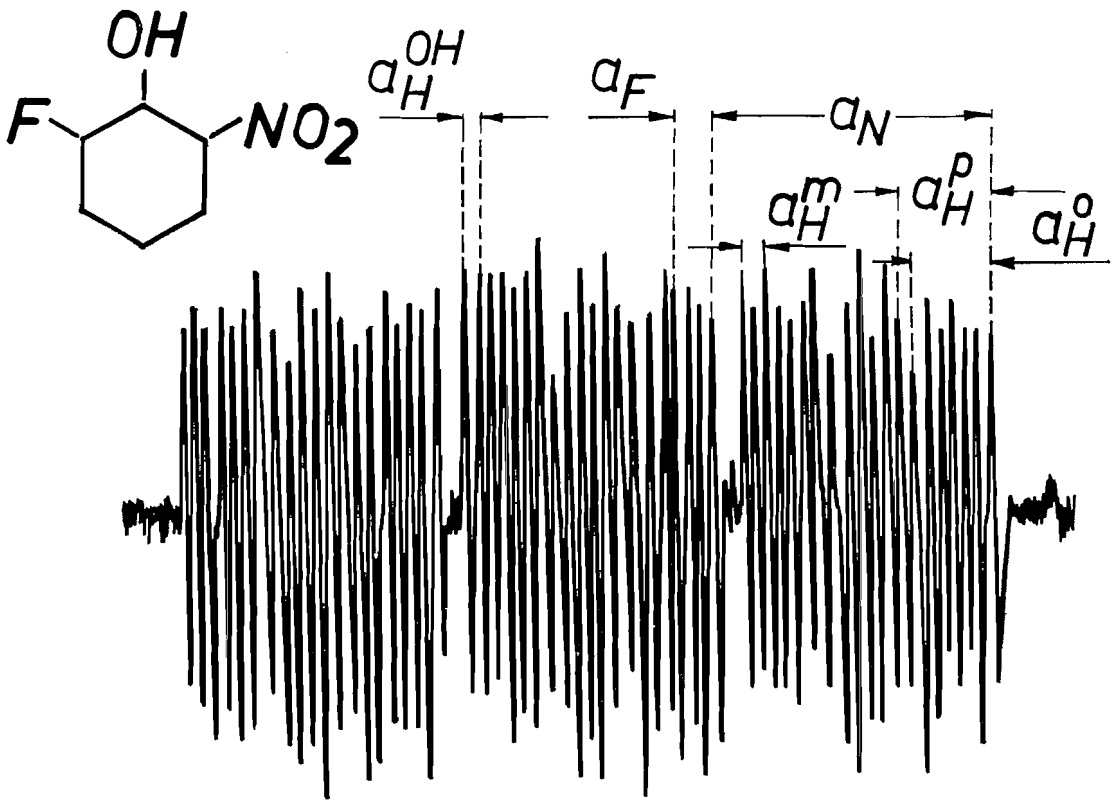

FIG. 7. Electron spin resonance spectrum of 2-fluoro-6-nitrophenol anion radical.

terms of the following coupling constants: $a_N = 11.71$, $a_1 = 3.97$, $a_2 = 3.50$, $a_3 = 1.63$, $a_4 = 1.04$, and $a_5 = 0.57$ G.

Reduction of a solution of 2-fluoro-6-nitrophenol-H[2] under identical conditions gave a much simplified spectrum of almost identical coupling constants a_N and a_1 to a_4. It indicated very clearly that the smallest splitting of 0.57 G was absent, and the latter must consequently be due to the OH proton.

Other Substances

Reduction of a 10^{-3} *M* solution of 2,4-dinitrofluorobenzene yielded a reddish-brown solution exhibiting a complex e.s.r. spectrum. The signal was quite stable and consists of at least 90 resolved lines. If all coupling constants are non-equivalent and all lines resolved, then a total number of 144 lines is theoretically possible, and it is obvious from the number of lines and intensities that considerable overlapping must occur. An anomaly in this spectrum appears to be the small overall width. The splitting extends only over 16.04 G, whereas the *m*-dinitrobenzene anion radical shows an overall splitting of roughly 30 G, which, through the fluorine substitution of one of the largest coupling protons in position 1, we would expect to be increased by approximately 4–5 G. Analysis of the spectrum in terms of meaningful coupling constants was not possible. At a potential 0.2 V more negative, a second species with a completely different e.s.r. spectrum of 42 lines divided into 6 groups, could be generated. Its identity is not known.

Although brown coloration was also observed when a solution of 1,3-dinitro-4,6-difluorobenzene in various solvents such as acetonitrile, acetonitrile/dimethoxyethane, dimethylformamide, or dimethylsulfoxide, was reduced at the first half-wave potential, no e.s.r. signal could be observed.

Both 2,3,4,5-tetrafluoro-nitrobenzene and 2,3,4,6-tetrafluoro-nitrobenzene gave, upon reduction, reddish solutions yielding strong, but

Can. J. Chem. Downloaded from www.nrcresearchpress.com by 210.87.254.6 on 09/05/12
For personal use only.

Can. J. Chem. Downloaded from www.nrcresearchpress.com by 210.87.254.6 on 09/05/12
For personal use only.

continuously changing e.s.r. spectra. The color changed rapidly from red to brown and no resonances could then be detected. The anion radicals, if they are the species giving rise to the e.s.r. spectra, appear to be quite unstable, at least under the present conditions. Brown and Williams (8) have attempted to prepare the anion radical of pentafluoronitrobenzene without success. It appears likely that nucleophilic attack on highly fluorinated anion radicals may be held responsible (18).

Discussion

Assignment of Coupling Constants and Spin Densities

If sufficiently accurate spin-polarization parameters are available, then the analysis of e.s.r. spectra can yield valuable information regarding the π electron spin density distribution of organic radicals. The reverse process, the semiempirical evaluation of spin-polarization parameters requires knowledge of assigned coupling constants and knowledge of spin densities, calculated via molecular orbital methods for instance. A detailed calculation of electron spin density distribution in fluorinated radicals is to be presented elsewhere (12). In the present discussion an attempt at assigning the experimentally measured coupling constants to specific nuclei will be made, employing internal consistency of assignment, comparison to non-fluorinated species, in our case nitrobenzene and *o*-nitrophenol anion radicals, and experimental knowledge of spin distribution behavior in benzene-like anion radicals possessing a single, strongly electron withdrawing substituent.

In the spectrum of the anion of 2-fluoro-nitrobenzene the triplet structure towards the wings of the spectrum is in the approximate ratio of 1:2:1, and assignment of the 1.01 G coupling to the meta protons (referred to the nitro group) seems very reasonable. The coupling of 9.81 G is assigned to the nitrogen nucleus, the 6.36 G splitting to the fluorine nucleus. Of the two remaining coupling constants of 3.47 and 4.01 G, the larger is assigned to the splitting from the para proton, the smaller to the ortho proton.

The spectrum of the anion of 3-fluoro-nitrobenzene shows a smallest spin 1/2 splitting of 1.01 G, which can, with reasonable certainty, be assigned to the proton in position 5. The coupling of 9.23 G can be unambiguously assigned to the ^{14}N nucleus. Of the remaining four coupling constants it appears reasonable to assign the largest coupling of 3.91 G to the para position proton, the couplings of 3.16 and 3.37 G to the two remaining ortho position protons, and the 2.92 G splitting to the ^{19}F nucleus. The assignment of coupling constants in this manner agrees with the ordering of splittings of Carrington *et al.* (5). Further confidence in the above assignment is given by the work of Kaplan *et al.* (4) on the anion radical of 3,5-difluoro-nitrobenzene.

For the anion of 2,4-difluoro-nitrobenzene, the splitting of 9.81 G may be assigned to ^{14}N. A triplet in the approximate ratio of 1:2:1 and splitting of 1.11 G arises from hyperfine interaction with two nearly equivalent meta protons. If no completely anomalous behavior is exhibited by this radical, and there is no reason to suspect this, then the smallest coupling of 3.63 G is to be assigned to the ortho proton. Of the two remaining splittings, a preferable choice of assignments is a_F(para) = 8.58 and a_F(ortho) = 6.40 G.

In the 2,5-difluoro-nitrobenzene anion the nitrogen splitting of 8.44 G can be assigned positively. A coupling of 0.92 G is with reasonable certainty due to the single meta position proton, whereas the largest of the remaining splittings, of 6.24 G, may be safely assumed to be due to the fluorine substituent in position 2. The coupling of 4.19 G is very similar to the coupling of 4.05 G for the para proton of the nitrobenzene anion and the ratio of a_F/a_H of 3.97, were it the fluorine splitting, would be considerably larger than ratios usually observed. On this basis, assignment to the para proton seems very reasonable. For identical reasons the coupling of 3.57 G is assigned to the hyperfine interaction with the proton ortho to the nitro group. The remaining coupling of 3.03 G must then be due to the fluorine nucleus.

The non-fluorinated parent compound of the three fluorinated nitrophenols investigated is ortho nitrophenol. In the spectrum of its anion, only the 12.21 G splitting is unambiguously assignable to the ^{14}N nucleus. From a study of the spectrum of the hydroxyl-deuterated species, a coupling constant of 0.50 G is assigned to the hydroxyl proton with certainty, whereas all other splitting constants remain unassignable on the basis of experimental data alone. If we consider the nitrophenol as a substituted nitrobenzene, however, assignment of the 3.63 G coupling to protons in positions ortho and para

TABLE I

Coupling constants in fluorinated nitrobenzene anions

Radical	Coupling constants at position [a]					
	2	3	4	5	6	N
Nitrobenzene[b]	3.35	1.06	4.05	1.06	3.35	9.57
2-Fluoro-nitrobenzene	6.36[c]	1.01	4.01	1.01	3.47	9.82
3-Fluoro-nitrobenzene	3.37[d]	2.92[c]	3.91	1.01	3.16[d]	9.23
4-Fluoro-nitrobenzene[b]	3.52	1.14	8.61[c]	1.14	3.52	9.95
2,4-Difluoro-nitrobenzene	6.40[c]	1.11	8.59[c]	1.11	3.63	9.81
2,5-Difluoro-nitrobenzene	6.24[c]	0.92	4.19	3.03[c]	3.57	8.44
3,5-Difluoro-nitrobenzene[b]	3.26	2.73[c]	3.98	2.73[c]	3.26	8.10
2-Nitrophenol	3.63	1.08	3.63	0.50	0.50	12.21
4-Fluoro-2-nitrophenol	3.51	2.74[c]	3.89	0.50	0.50	11.08
6-Fluoro-2-nitrophenol	3.50	1.05	3.97	1.63[c]	0.57	11.71
5-Fluoro-2-nitrophenol	3.78	0.87[d]	7.21[c]	0.73[d]	0.52	12.68

[a] NO_2 group in position 1, OH group in position 5.
[b] Work cited from ref. 4.
[c] Fluorine coupling constant.
[d] Assignments could be reversed.

to the nitro group is indicated. The remaining two coupling constants of 1.08 and 0.50 G are due to the two meta protons.

In the anion radical of 4-fluoro-2-nitrophenol, the coupling of 11.08 G is due to the nitrogen nucleus. From deuteration of the OH group, the splitting of this proton can be positively assigned as 0.50 G. Again treating this fluorinated nitrophenol anion as a substituted nitrobenzene anion, the couplings of 3.89 and 3.51 G are assignable to para and ortho position protons, respectively. These coupling constants are quite similar in size and their assignment could well be reversed. The coupling constant of 2.74 G is assigned to the fluorine substituent in the 3 position, the 0.50 G coupling to the position 5 proton. The fluorine substitution also sheds some light on the assignment of coupling constants in the nitrophenol anion. Were the 0.50 G splitting in this latter species due to the position 3 proton, a ratio of a_F to a_H of 5.5 would result, a value larger by a factor of 2 than the commonly observed a_F/a_H ratios. If, on the other hand, the coupling of 1.08 G is assigned to the proton in ring position 3, the ratio a_F/a_H is 2.54, a value commonly found and expected.

In the anion radical of 3-fluoro-6-nitrophenol, the coupling constant of 12.68 G is due to the ^{14}N nucleus and the coupling of 0.52 G to the hydroxyl proton on the basis of deuteration results. There is further little ambiguity in assigning the large splitting of 7.21 G to the fluorine nucleus para to the nitro group, and the coupling of 3.78 G to the ortho proton. The two remaining a_H are similar in size and are due to the two meta protons. An assignment cannot be made.

As for the other nitrophenols, only the ^{14}N splitting of 11.71 G and the OH proton coupling of 0.57 G are assignable on the basis of experimental evidence in the spectrum of the 2-fluoro-6-nitrophenol anion. Two coupling constants, $a_1 = 3.97$ and $a_2 = 3.50$ G, are considerably larger than the remaining splittings and are very likely due to the para and ortho position protons. The remaining couplings of 1.04 and 1.63 G are due to the position 5 fluorine nucleus and the meta proton. To preserve internal consistency amongst all of the fluorinated anion radicals, the 1.63 G splitting must be assigned to the fluorine nucleus.

Table I summarizes all coupling constants, including those of the anions of nitrobenzene, 4-fluoro-nitrobenzene, and 3,5-difluoro-nitrobenzene (4).

As can be seen, the above set of coupling constants presents a fully consistent set of assignments, although the splittings are not in all cases assigned by experimental evidence.

Fluorine Coupling Constants

In the fluorine containing radicals investigated to date, a ratio of the fluorine splitting to the corresponding proton splitting in the similar, but non-fluorinated species, was generally found to be in the vicinity of 2.5. An exception here is the 2,7-difluoro-fluorenone ketyl (7), in which a ratio of 37.0 is indicated, if the splitting constant assignments are correct. Based on the assignment

Can. J. Chem. Downloaded from www.nrcresearchpress.com by 210.87.254.6 on 09/05/12
For personal use only.

of coupling constants as presented in Table I, the following ratios of a_F to a_H are obtained:

TABLE II

Ratio of a_F to a_H in fluorinated nitrobenzene anions

Radical anion of	a_F	a_H	a_F/a_H
2-Fluoro-nitrobenzene	6.36	3.35	1.90
3-Fluoro-nitrobenzene	2.92	1.06	2.75
4-Fluoro-nitrobenzene	8.61	4.05	2.13
2,4-Difluoro-nitrobenzene	$6.40_{(2)}$	3.35	1.91
	$8.59_{(4)}$	4.05	2.12
2,5-Difluoro-nitrobenzene	$6.24_{(2)}$	3.35	1.86
	$3.03_{(5)}$	1.06	2.86
3,5-Difluoro-nitrobenzene	2.73	1.06	2.58
4-Fluoro-2-nitrophenol	2.74	1.08	2.54
6-Fluoro-2-nitrophenol	1.63	0.50	3.26
5-Fluoro-2-nitrophenol	7.21	3.63	1.99

The ratios vary from 1.86 to 3.26, and all compounds show what is considered a normal a_F/a_H ratio. It is to be noted that for fluorine substituents in ortho and para position to the nitro group, the tendency for a_F/a_H is towards smaller values; for meta substituted fluorines the ratio is on the high side of the range. It is considered possible that this trend of showing low and high a_F to a_H ratios, depending on whether meta or ortho/para substitution has taken place, is due to changes in the C—F bonding character, more precisely, to changes in the π electron (i.e. double bond) character in the C—F fragment, as shown by the relative insensitivity of the remaining coupling constants to fluorine substitution.

Conclusions

The electrolytic reduction of several mono- and di-fluorinated nitrobenzenes takes place via one-electron addition to yield the corresponding anion radicals. *O*-nitrophenol and three fluorinated *o*-nitrophenols react upon polarographic reduction to yield mono-negative radicals, in contrast to say *p*-nitrophenol, in which the OH proton is dissociated and the e.s.r. spectrum of the di-negative radical is observed. The species are all reasonably stable and yield well resolved spectra which may be fully analyzed. The assignment of coupling constants is in some cases determined by symmetry and by deuteration results. Other coupling constants are assigned by comparison with related species and experimental knowledge of behavior of splittings in radicals of the benzene type and having a single, strongly electron-withdrawing substituent. Using these two aids, a completely internally consistent set of assignments for the compounds investigated can be made, as seen in Table I. For all systems investigated the ratios of a_F to a_H cluster around the value 2.5, with a tendency to lower ratios if fluorine is substituted in ortho or para position to the electron-withdrawing group, to higher values if the fluorine is meta substituted. Highly fluorinated nitrobenzenes do not form anion radicals easily.

Acknowledgment

We thank Professor Dr. K. H. Hausser for his continued interest during the course of this work.

1. P. H. Anderson, P. J. Frank, and H. S. Gutowski. J. Chem. Phys. **32**, 196 (1960).
2. A. H. Maki and D. H. Geske. J. Am. Chem. Soc. **83**, 1852 (1961).
3. P. B. Ayscough, F. P. Sargent, and R. Wilson. J. Chem. Soc. 5418 (1963).
4. M. Kaplan, J. R. Bolton, and G. K. Fraenkel. J. Chem. Phys. **42**, 955 (1965).
5. A. Carrington, A. Hudson, and H. C. Longuet-Higgins. Mol. Phys. **9**, 377 (1965). A. Carrington, A. Hudson, and G. R. Luckhurst. Proc. Roy. Soc. Ser. A, **284**, 382 (1965).
6. P. H. Rieger and G. K. Fraenkel. J. Chem. Phys. **37**, 2811 (1962). N. Steinberger and G. K. Fraenkel. J. Chem. Phys. **40**, 723 (1964).
7. R. Dehl and G. K. Fraenkel. J. Chem. Phys. **39**, 1793 (1963).
8. J. K. Brown and W. G. Williams. Trans. Faraday Soc. **64**, 298 (1968).
9. D. R. Eaton, A. D. Josey, W. D. Philips, and R. E. Benson. Mol. Phys. **5**, 407 (1962). D. R. Eaton, A. D. Josey, W. D. Philips, R. E. Benson, and T. L. Cairns. J. Am. Chem. Soc. **84**, 4100 (1962).
10. R. J. Cook, J. R. Rowlands, and D. H. Whiffen. Mol. Phys. **7**, 31 (1963).
11. R. J. Lontz and W. Gordy. J. Chem. Phys. **37**, 1357 (1962).
12. P. H. H. Fischer. To be published.
13. G. C. Finger, F. H. Reed, and R. E. Oesterling. J. Am. Chem. Soc. **73**, 152 (1950).
14. D. H. Geske and A. H. Maki. J. Am. Chem. Soc. **82**, 2671 (1960).
15. P. H. H. Fischer and C. A. McDowell. Mol. Phys. **8**, 357 (1964).
16. P. L. Nordio, M. V. Pavan, and C. Corvajy. Trans. Faraday Soc. **60**, 1985 (1964).
17. P. H. Rieger and G. K. Fraenkel. J. Chem. Phys. **39**, 609 (1963).
18. J. C. Tatlow. Endeavour, **22**, 89 (1963).

Can. J. Chem. Downloaded from www.nrcresearchpress.com by 210.87.254.6 on 09/05/12
For personal use only.

Can. J. Chem. Downloaded from www.nrcresearchpress.com by 210.87.254.40 on 09/05/12
For personal use only.

Kinetics of formation of ethylene oxide hydrate. Part I. Experimental method and congruent solutions[1]

D. N. GLEW AND M. L. HAGGETT
Exploratory Research Laboratory, Dow Chemical of Canada, Limited, Sarnia, Ontario

Received June 17, 1968

A dilatometer was constructed for studying the formation of ethylene oxide hydrate. In unstirred, congruent solutions heat transfer appeared to be the significant rate-controlling factor. Initial hydrate formation rates were independent of stirring at speeds greater than approximately 100 r.p.m. Magnetic stirring was inadequate due to hydrate build-up on the walls of the dilatometer bulb. Mechanical stirring eliminated this build-up and gave satisfactory results.

Canadian Journal of Chemistry, **46**, 3857 (1968)

Introduction

Most studies that have been made of the rates and rate-determining factors of the formation of clathrate gas hydrates have been concerned with water-insoluble hydrate formers, e.g. propane (1), methyl bromide (2), and rare gases (3). However, some saturated cyclic ethers, which are miscible with water in all proportions, also form hydrates (4, 5). Pinder (6) has studied the kinetics of formation of tetrahydrofuran hydrate from solutions of incongruent melting points. He concluded that the rates were diffusion controlled. Ethylene oxide (EO) also forms a hydrate (5, 7, 8) but no previous investigation has been made of its rates of formation.

The freezing point diagram for EO–water mixtures has been determined by several workers (7–9). According to experiments in this laboratory (9), there is a eutectic point at -2.1 °C at 2.0 mole % EO and a maximum freezing point (congruent) at 11.1 °C at 12.7 mole % EO. Lippert *et al.* (4) determined that the EO hydrate is not isomorphous with chloroform hydrate, i.e. it is not a structure II hydrate (10). Structure determinations from X-ray powder photographs (5) and from single crystals (11) showed it to be a structure I hydrate with a lattice constant of 12.0 Å. The EO molecules were considered to be hindered axial rotors, and a limiting formula of $2M.6C_2H_4O.46H_2O$, where $M \equiv EO, O_2$, or N_2 was suggested (11). The variable composition of this hydrate was demonstrated from density measurements (12) and a formula $C_2H_4O.6.89H_2O$ was obtained at the congruent point.

In a study of the formation of EO hydrate in polyacrylamide gel (13), it was shown that the maximum amount of hydrate was formed at approximately 26 wt. % EO, i.e. when H_2O:EO = 6.95:1 (moles). This is the congruent composition and is the expected result since it is the only solution composition at which the amount of hydrate formed is independent of the temperature of formation. It has been reported (8) that crystals several mm in size could be formed at approximately 10 °C.

Ethylene oxide was chosen as the hydrate former because of its ready availability, its complete miscibility with water, and the high freezing point of the hydrate at the congruent composition. For the reason, that the amount of hydrate formed is independent of the applied supercooling, we decided to investigate the kinetics of hydrate formation initially from solutions of congruent composition. Since the densities of the solution and crystals are different but invariant at constant temperature, a dilatometric method was used. This method had the advantages

1. Several kinetic runs could be made on a solution by simply melting the crystals at the end of a run.
2. Air could be excluded from the system.
3. An air–liquid interface could be avoided (in preliminary experiments, nucleation often occurred prematurely at the air interface).
4. Since EO is highly volatile, a closed system was necessary to prevent its loss.

We have also measured rates of hydrate formation from solutions with compositions below the congruent EO concentration (water-rich) and compositions above congruent concentration (EO-rich).

Attempts were made to study the effects of various salts on the rate of hydrate formation.

[1]Contribution No. 164.

However, as will be discussed later, complications arose which prevented reproducible results being obtained.

Experimental

(a) Materials

Ethylene Oxide

99.998 mole % EO was selected from the material produced by Dow Chemical of Canada, Limited.

Water

Laboratory distilled water was twice redistilled, once from alkaline permanganate and once from dilute phosphoric acid. Its conductivity was less than 4×10^{-7} ohm^{-1}

Mercury

After filtering, mercury was washed for a few days with 10% KOH solution, then with water, 2% HNO_3 solution, and water again. Finally, it was vacuum distilled.

Sodium chloride, ammonium chloride, and sodium nitrate solutions (0.46 *M*) were prepared directly from Fisher certified reagents; 0.24 *M* sodium perchlorate solution was prepared directly from Fisher laboratory chemical.

(b) Apparatus

The dilatometer is shown in Fig. 1. Lower case letters refer to Nupro (Nuclear Products Co., Ohio, U.S.A.) series BG bellows valves with 1/4 in. Swagelok (Crawford Fitting Co., Ohio, U.S.A.) fittings. Numbers indicate high vacuum stopcocks.

The inverted conical vessel A, for degassing water, is connected to the apparatus via a joint so that, when rotated through 180°, liquid runs into the 100 ml burette C. The cylindrical glass vessel B, for degassing EO, is sealed with a Swagelok plug and connected to the apparatus by a short length of 1/4 in. outer diameter (o.d.) nylon pressure tubing (Polypenco Inc., Penna., U.S.A.). An in-line filter (Nupro series F, 7 μ nominal size) is incorporated at H before the 50 ml burette D. Mixing vessel E, containing a glass-covered stirring bar, is connected to the dilatometer bulb F through a flexible coil and stainless steel – glass seal S (O. H. Johns Glass Co., Toronto, Ontario). Dilatometer stem M is a 50 cm length of 1.5 mm inner diameter (i.d.) precision-bore capillary tubing. The mercury reservoir J is connected to the apparatus at h by 1/8 in. nylon tubing. Similarly, the 1 ml pipette with reservoir at K is joined at stopcock 2 by 1/8 in. nylon pressure tubing.

Stirring of the contents of dilatometer bulb F was achieved using a magnetic stirring bar and three solenoids (14). These solenoids G were made by closely winding two layers of No. 20 B and S gauge shellaced copper wire onto soft-iron rods approximately 6 in. in length and 1 cm diameter. They were encased in glass tubing, wiring being led in through tygon tubing attached to the glass enclosures. The three solenoids were arranged symmetrically about the dilatometer bulb which contained a teflon-covered stirring bar only slightly shorter than the internal diameter of the bulb. The solenoids are energized in turn either via a commutator (14) or, as in our case, by a cam operating three micro switches. The required d.c. power was produced from the a.c. mains via a rectifier giving 4 A at 4 V.

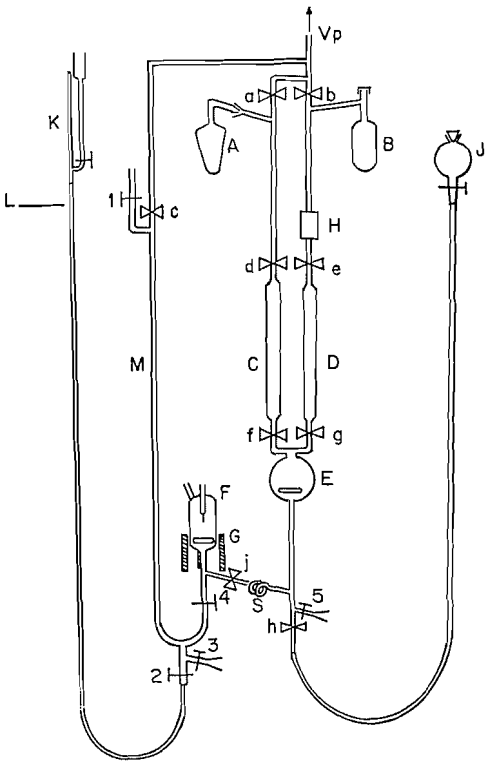

FIG. 1. Dilatometer and filling equipment.

Details of the dilatometer bulb are shown in Fig. 2. Sealed into the top is a 1/8 in. Kovar–glass seal which is silver soldered at the metal end. Also at the top is a side-arm, sealed at the bulb, down which liquid nitrogen could be added. The bulb is joined at the bottom to approximately 4 cm of 1 cm i.d. precision bore tubing. The bulb volume 78.5 ml was calibrated to mark X.

We observed (*vide infra*) that hydrate growth inevitably stopped the magnetic stirring bar with congruent solutions, so that a new dilatometer bulb was required in which the walls were kept free from hydrate build-up. The dilatometer bulb shown in Fig. 3 was constructed for this purpose. The stirring arrangement consists of an

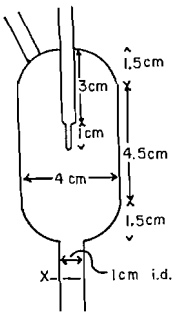

FIG. 2. Magnetically stirred dilatometer bulb.

Can. J. Chem. Downloaded from www.nrcresearchpress.com by 210.87.254.40 on 09/05/12
For personal use only.

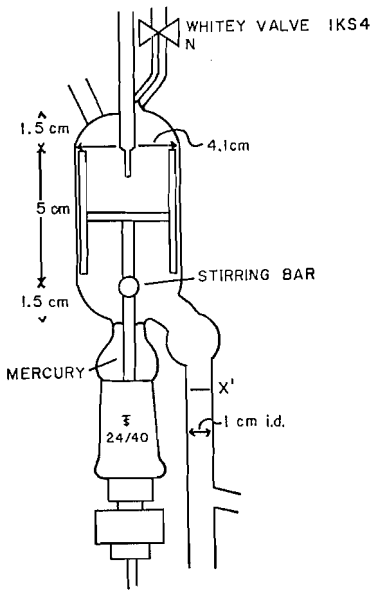

FIG. 3. Mechanically stirred dilatometer bulb.

inverted Stir-O-Vac (Labline Instruments Inc., Ill., U.S.A., Cat. No. 1280) unit with an additional seal at the shaft provided by mercury. The commercial cruciform impellor was replaced by an H-shaped stirrer, the vertical arms of which swept very close to the walls of the bulb. A metal stirring bar was also attached to the shaft. The bulb volume, calibrated to mark X′, was 96.7 ml.

The complete apparatus (Fig. 1) was fixed to a metal rack which could be immersed in a large thermostat up to level L. The thermostat had Lucite (polymethyl methacrylate) windows on two sides, one for illumination and the other for reading the mercury level in M with a cathetometer. Cooling to the thermostat was supplied by continuously circulating refrigerant from an auxiliary Forma bath (Forma Scientific Inc., Ohio, U.S.A.) through a copper coil. A Bayley temperature controller (Bayley Instrument Co., Calif., U.S.A., model 251) provided variable power to a heating coil in the thermostat. Through the center of both coils was positioned the shaft, carrying two propellors, of a Lightnin (Greey Mixing Equipment Ltd., Toronto, Ontario) portable mixer which vigorously circulated the ethylene glycol – water thermostat fluid. During a crystallization experiment of 4–8 h duration, the temperature of the thermostat was constant to ± 0.002 °C.

The temperature inside the dilatometer bulb was determined to 0.005 °C by a calibrated, single junction copper–constantan thermocouple positioned inside the Kovar seal. The reference junction was soldered at the end of another Kovar seal which was placed in a hole drilled in a stainless steel cylinder suspended in the thermostat. The temperature of the thermostat was determined to 0.001 °C using a calibrated Tinsley (H. Tinsley and Co. Ltd., London, England) platinum resistance thermometer, standardized at the triple point of water, with a Leeds and Northrup Mueller bridge, (Leeds and Northrup, Canada, Ltd., Toronto, Ontario, Cat. No. 8069-B) type G-2. Both outputs from the thermocouple and resistance thermometer were amplified by Keithley (Keithley Instruments Inc., Ohio, U.S.A.) nanovoltmeters, model 148, and displayed on a Moseley (F. L. Moseley Co., Calif., U.S.A.) two-pen, strip-chart recorder, model 7100B. The recorder had an event marker which was activated by a conveniently positioned switch.

(c) Method

The nylon tubing joining K to stopcock 2 and J to valve h are kept permanently filled with mercury.

The apparatus is connected at Vp to the vacuum line and evacuated to better than 10^{-4} Torr. Vessel A, containing approximately 120 ml of water previously filtered through a 7 μ Nupro filter, was then connected. The water was freeze degassed at least 5 times, then run in to almost fill burette C. Mercury from reservoir J was allowed to fill the apparatus to the closed stopcock 5, valve j, and to the bottom of bulb E. After attaining temperature equilibrium, the required volume of water was measured into bulb E via f.

Approximately 45 ml of ethylene oxide was measured from a pre-cooled syringe into vessel B, which was cooled in an acetone – dry ice mixture. After sealing the vessel, the cooling mixture was replaced by liquid nitrogen and the ethylene oxide freeze degassed as for the water. By bending the nylon tubing the degassed liquid was run through the filter H into burette D from which, after reaching the thermostat temperature, the required volume was run into the water in vessel E. Mixing was accelerated by agitating the spin bar in E with a magnet.

Mercury from K was admitted to the U-tube filling to the upper end of dilatometer stem M and to just above stopcock 4 which was then closed. The mercury in bulb E was then almost completely removed via stopcock 5. Valve j was opened and the dilatometer bulb F almost filled with the ethylene oxide – water mixture, the bulb F being cooled periodically with ice-cold water. With F almost full, j was closed, h opened, and mercury allowed to rise as far as j which was then reopened. The mercury ran into the tubing below F pushing the solution above it. When there was only a very small vapor space remaining in F above the solution, j was closed and stopcocks 1 and 4 opened, so that mercury from M pushed the solution to completely fill F. The mercury meniscus was finally situated close to the calibration mark X. The position of the meniscus with respect to X was determined using the cathetometer; the volume of the solution could thus be calculated.

Filling of the vessel shown in Fig. 3 was essentially the same except that, since the vessel would not hold a high vacuum, pressure was quickly applied above the solution in E and the liquid pushed into the vessel until it was completely filled to a point above the Whitey (Whitey Research Tool Co., Calif., U.S.A.) valve N, having expelled all air. The process of filling with mercury to a point near the calibration mark X′ was followed after which valve N was closed.

Since the mercury level in M falls during a crystallization, the pressure on the solution changes and, consequently, its volume. The effect of pressure on a solution was determined by first arranging the mercury level near

Can. J. Chem. Downloaded from www.nrcresearchpress.com by 210.87.254.40 on 09/05/12
For personal use only.

Can. J. Chem. Downloaded from www.nrcresearchpress.com by 210.87.254.40 on 09/05/12
For personal use only.

the top of M and evacuating the space above the meniscus, the level of which was noted. Stopcock 1 was then opened to the atmosphere and the new (lower) mercury level read. The volume change for 1 atm pressure change was thus calculated. Assuming a linear change of meniscus level with applied pressure, as determined by Hepler, Stokes, and Stokes (15) for dilute aqueous electrolyte solutions, the change in volume for intermediate changes in pressure could be interpolated.

Cubical coefficients of thermal expansion of the solutions were also required. These were obtained at atmospheric pressure by measuring the change in volume as the temperature was raised by small increments over approximately 1 °C. The mercury level in M was initially arranged to be slightly lower than the meniscus level below the solution in F.

A crystallization experiment was carried out by first supercooling the solution to the thermostat temperature. A small volume of liquid nitrogen was poured down the side-arm of F to initiate nucleation and, if required, the stirrer immediately started. The decrease of the mercury level in M was measured at intervals, the event marker on the recorder being activated each time a reading was taken. The temperature inside the bulb was also continuously recorded. When the mercury level reached the bottom of M, stopcock 2 could be opened, from above the thermostat liquid L, and a measured volume of mercury admitted from the pipette K to refill M. The crystallization was then followed further.

Results

(a) General Observations

Before describing our results, we must establish satisfactory units for the rates of hydrate formation. A simple moles hydrate time^{-1} is insufficient since, obviously, the rate of formation will depend on the quantity of solution from which crystals are growing. Initially, since the volume of the solutions used with the magnetically stirred vessel, was approximately constant ($\pm 5\%$), comparisons were made with rates expressed as moles time^{-1}. The rate constants appeared to increase as the EO concentration was increased. However, if the rates are recalculated as moles time^{-1} (mole EO)$^{-1}$, then the constants decrease as EO increases. This ambiguity arises whenever the rates are expressed as a function of one component of the solution. Volume is completely inadequate since it depends on temperature (note Pinder's (6) units).

We have finally decided to express our rates of hydrate formation as mole hydrate time^{-1} (g soln.)$^{-1}$, where the solution is the starting mixture in the dilatometer before crystallization begins. For a given volume of solution at constant temperature, the mass of the solution varies only approximately 12% in the range 0–100% EO. Other units may be used and sufficient information is given in the Tables for their calculation if required.

The initial supercooling of a solution ΔT_0 is defined as the difference between the hydrate freezing point of the solution T_f^0 and the thermostat temperature T_b. The supercooling is the difference between the solution freezing point T_f and the thermostat temperature T_b. T_{obs} is the solution temperature determined by the dilatometer thermocouple.

The results for rates of hydrate formation for congruent solutions containing 12.7 mole % EO (EO.6.89 H_2O) of freezing point $T_f^0 = 11.12$ °C are now described; the tabulated results are given in Part III[2]. Results for incongruent solutions are described in Part II together with the numerical interpretation of the results for stirred, congruent solutions.

(b) Magnetically Stirred Vessel

Using the magnetically stirred dilatometer the following observations were made on crystallizations from congruent solutions.

With no stirring, there are two distinct regions of supercooling in which the mode of hydrate formation differs greatly. When the initial supercooling ΔT_0 is less than 1.4 °C, hydrate formation is extremely slow and the hydrate grows predominantly from the area on the wall where nucleation was induced. Large compact crystals grow in this region. If $\Delta T_0 \ll 1.4$ °C, the crystals agglomerate into a compact mass with some flat faces appearing at the solid–solution interface. As $\Delta T_0 \rightarrow 1.4$, fern-like crystals (or dendrites) begin to appear from the compact mass and grow along the vessel wall.

With $\Delta T_0 > 1.4$, at nucleation a thin layer of hydrate forms almost instantaneously around the entire dilatometer wall and gradually thickens to a transparent crust.

In Fig. 4 are shown curves obtained at various supercoolings in the absence of stirring. The shape of the hydrate formation curves changes as the supercooling is increased. At small super-

[2]Photocopies of Part III may be obtained free of charge, upon request, from: Depository of Unpublished Data, National Science Library, National Research Council of Canada, Ottawa, Canada.

CUN stands for congruent, unstirred solutions, CMA stands for congruent, magnetically-stirred solutions, SUM stands for summary of results, and CME stands for congruent, mechanically-stirred solutions.

Can. J. Chem. Downloaded from www.nrcresearchpress.com by 210.87.254.40 on 09/05/12
For personal use only.

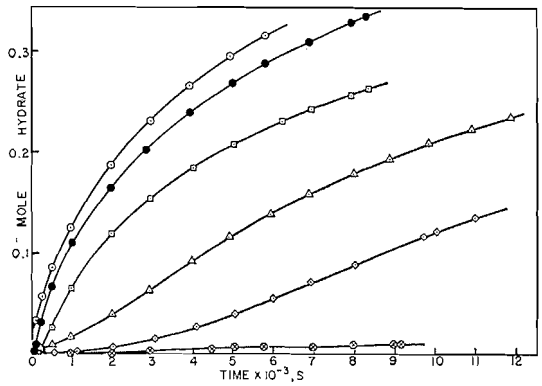

FIG. 4. Moles hydrate formed with time for congruent, unstirred solutions. Run number, supercooling ΔT_0 (°C): ⊗, CUN6, 0.60; ◇, CUN1, 0.93; △, CUN4, 1.47; ⊡, CUN2, 2.12; ●, CUN5, 2.65; ⊙, CUN3, 3.18.

coolings they are sigmoid indicating autocatalysis. As the supercooling increases, the initial acceleratory period becomes shorter, disappearing completely at $\Delta T_0 > 3$ °C.

In stirred solutions, a "slush", of many small fern-like crystals, forms at induced nucleation. Simultaneously, the mercury meniscus in M rapidly falls for a few seconds, slows briefly, and then decreases steadily. Gradually, hydrate builds up on the walls of the dilatometer bulb and this thickening layer of solid eventually stops the rotation of the stirring bar. Sometimes the layer was completely transparent appearing to be a single crystal; at other times it was very "grainy", appearing like a mosaic. The layer thickened until the solution had completely solidified.

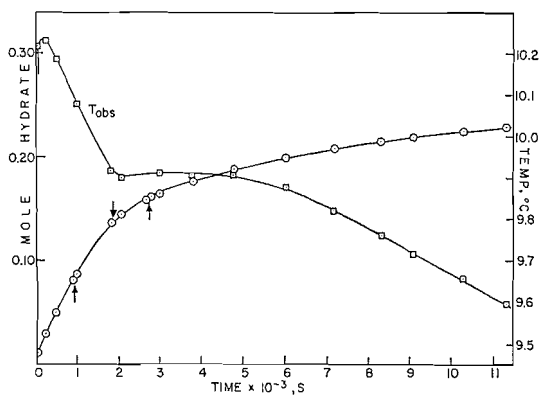

FIG. 5. Moles hydrate formed (⊙) and dilatometer temperature (⊡) versus time curves for run CMA6 at 320 r.p.m. and $\Delta T_0 = 2.12$.

Also, at nucleation, the temperature inside the bulb increased very rapidly to a maximum and then irregularly decreased more slowly as hydrate formed. Figure 5 shows this behavior and also two other features. The arrow at ~1800 s shows where the stirring ceased. The other two arrows show the points at which the capillary tube M was refilled with mercury; here the pressure on the solution increased rapidly from atmospheric to atmospheric plus ~ 50 cm Hg, but no discontinuities in the hydrate formation curve were observed. The rate of hydrate formation is independent of pressure in this small range.

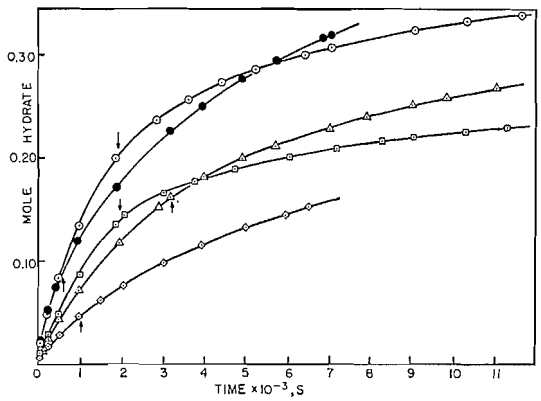

FIG. 6. Moles hydrate formed with time for solutions of congruent composition magnetically stirred at 320 r.p.m. Run number, supercooling ΔT_0: ◇, CMA2, 0.96; △, CMA9, 1.47; ⊡, CMA6, 2.12; ●, CMA11, 2.64; ⊙, CMA10, 3.19.

In Fig. 6 are shown hydrate formation curves obtained for various supercoolings with stirring speed 320 r.p.m. There appears to be a regular variation of rate with supercooling while the stirring is taking place but when stirring ceases, as indicated by the arrows in Fig. 6, the rate curves become unpredictable and cross over.

Neglecting the rapid nucleation process, the initial rates were estimated from the smooth portions of the curves extrapolated to zero time.

The effect of stirring on the initial rate of hydrate formation is shown in Fig. 7 for various supercoolings. Above approximately 100 r.p.m. the rates are independent of the stirring speed at all supercoolings. Also the rate with no stirring approaches that with stirring as the supercooling is increased. These results show that, above 100 r.p.m. under our experimental conditions, diffusion is not an important factor controlling EO

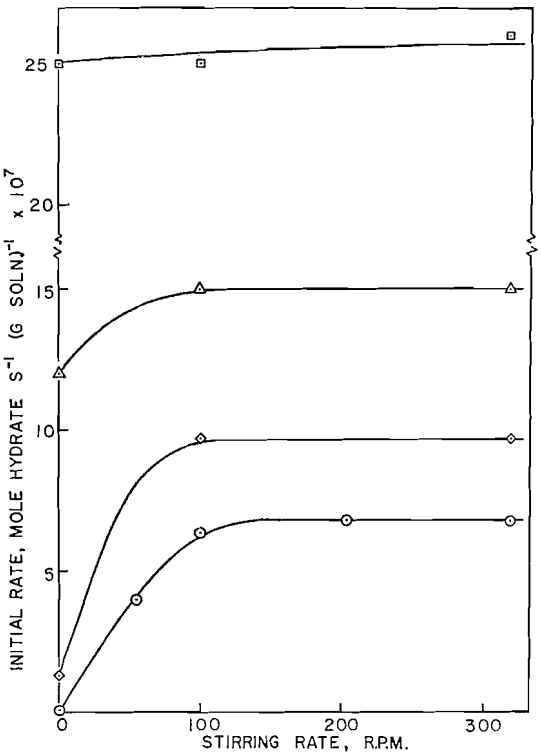

FIG. 7. Variation of initial rates of hydrate formation with stirring speed for congruent, magnetically stirred solutions. Run, supercooling ΔT_0: ⊙, 0.94; ◇, 1.47; △, 2.12; ⊡, 3.18.

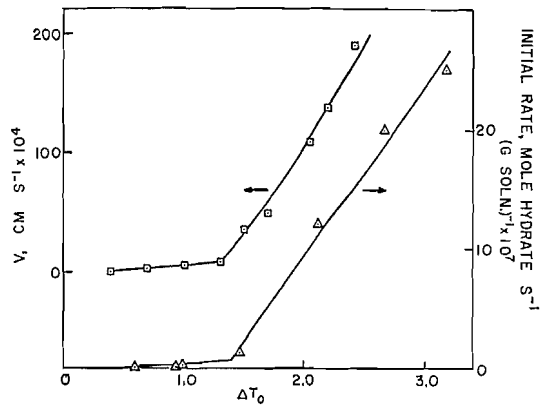

FIG. 8. Variation of rates of hydrate formation with supercooling ΔT_0 for unstirred solutions. △, initial rates in dilatometer; ⊡, rates in capillary tubing.

hydrate formation. This independence of rate on agitation above a certain minimum is similar to that observed for the growth of ice (16), and of ethylene diamine tartrate (17), sodium thiosulfate (18), sucrose (19), and $CuSO_4.5H_2O$ (20) from their supersaturated solutions.

In Fig. 8 we have plotted the initial rates against the supercooling ΔT_0 for runs with no stirring. On the same graph are plotted the results of preliminary experiments in which the linear velocity of crystallization V along narrow bore glass tubing (4 mm o.d., 2 mm i.d.) was measured (Part III, Table SUM1)[2]. The two curves are seen to be of similar form.

In the capillary growth experiments, it was observed that at $\Delta T_0 < 1.3$ °C, the growth front was uniform and compact, whereas at $\Delta T_0 > 1.3$ °C, the front became unstable and dendritic growth occurred. For aqueous solutions of heteropolar substances, Yamamoto (21) found similar growth rates above which skeletal rather than compact forms were produced. At $\Delta T_0 > 1.3$ °C, our results obtained in capillaries conform to a $(\Delta T)^2$ law, but those obtained in the dilatometer are more consistent with a ΔT growth law.

Dendritic growth in melts generally occurs when large latent heats must be rapidly dissipated (22) during crystallization, for which it has been shown that crystal growth rates are proportional to $(\Delta T)^2$ for non-convective steady state conditions (23). The $(\Delta T)^2$ law is obeyed approximately for crystallization of ice (2, 16, 24–26) and tin (27). When convection becomes significant, crystal growth rates for ice (2) showed a dependence on $(\Delta T)^{1.5}$, the exponent having fallen away from the ideal value of 2. Our capillary results are consistent with rate control by heat conduction away from the crystal, whereas convective heat transfer is significant in the unstirred dilatometer.

With $\Delta T_0 < 1.3$ °C, the rates are extremely slow. This is the range in which compact crystals with well-defined faces are formed. Also, there is a small range of supercooling, below 0.4 °C, in which we were unable to detect any hydrate growth.

The results at constant stirring speeds are shown in Fig. 9 (Part III, Table SUM2)[2]; the slope of the line is 7.6×10^{-7} mole s^{-1} deg^{-1} (g soln.)$^{-1}$. The solid circle represents an experiment (Part III, Table CMA14)[2] in which the dilatometer solution volume was 63 ml, being made deliberately smaller than the usual 74 ml approximately. In this experiment the mercury–solution interface was in the dilatometer bulb itself, giving a much larger area of contact between the solution and mercury. The linear dependence of rate on ΔT_0 will be discussed in Part II.

Can. J. Chem. Downloaded from www.nrcresearchpress.com by 210.87.254.40 on 09/05/12
For personal use only.

Can. J. Chem. Downloaded from www.nrcresearchpress.com by 210.87.254.40 on 09/05/12
For personal use only.

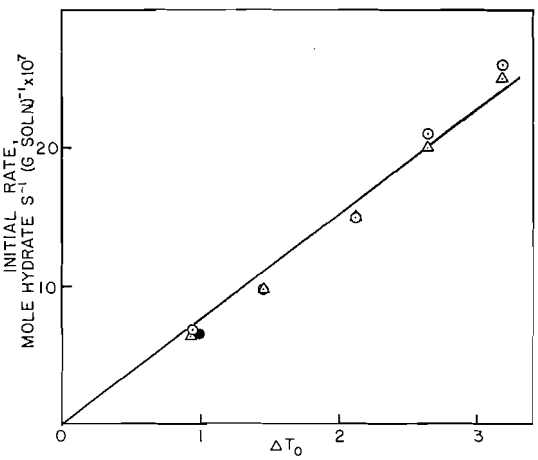

FIG. 9. Variation of initial rates of hydrate formation with supercooling ΔT_0 at high magnetic stirring rates: ⊙, 320 r.p.m.; ●, 320 r.p.m., small volume; △, 100 r.p.m.

(c) Mechanically Stirred Vessel

According to results obtained for incongruent solutions reported in Part II, the rate of hydrate formation in congruent solutions is predicted by eq. [15] to be constant for a fixed thermostat temperature T_b. However, this rate law cannot be expected to hold for complete solidification of a solution since the effectiveness of the stirrer changes with the proportion of solid to liquid.

Our results for congruent solutions have indicated progressively falling rates of hydrate formation which were partially due to the thickening layer of hydrate on the walls of the dilatometer bulb. To avoid this hydrate build up, the mechanically stirred dilatometer vessel shown in Fig. 3 was used. This did not keep the walls completely free of hydrate but limited its thickness to less than 1 mm. At the top of the vessel above the stirrer, the hydrate layer grew to greater thickness.

The results of these experiments are reported in full elsewhere (Part III, Table CME1–7 and SUM3)[2]. It was noticeable in some runs, particularly at small supercoolings, that crystals grew slowly at first on the stainless steel stirring bar. At some point, copious nucleation occurred throughout the solution, the rate of hydrate formation increased to an approximately constant value for some time and then started to decrease (e.g. Part III, Table CME3)[2]. In those runs where the induced nucleation immediately produced many small crystals in the solution, the rate very quickly reached a constant value. Simultaneously, the temperature rose to a constant value (±0.01 °C) and later fluctuated; this behavior is shown in Figs. 10 and 11 (Part III, Table CME5)[2].

The constant initial rates of formation and the corresponding average constant temperatures for

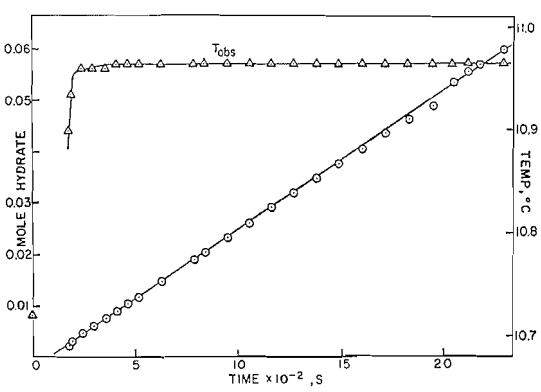

FIG. 10. Moles hydrate formed (⊙) and solution temperature (△) versus time curves for the initial stage of run CME5 in the mechanically stirred dilatometer. Stirring speed 220 r.p.m. and $\Delta T_0 = 0.39$.

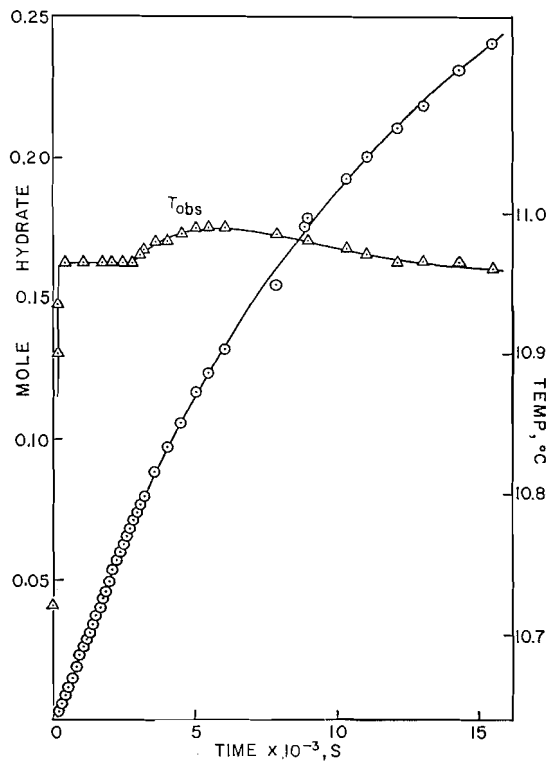

FIG. 11. Complete results of run CME5; experimental conditions as for Fig. 10.

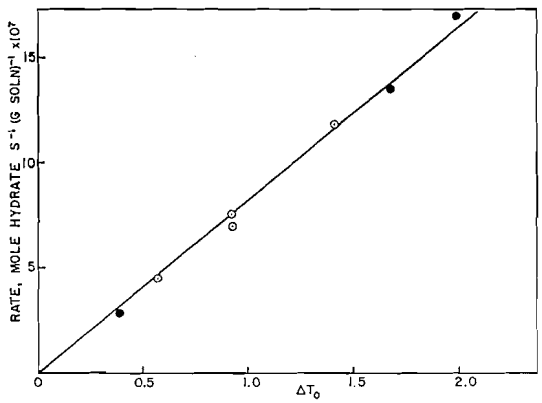

FIG. 12. Variation of initial rates of hydrate formation with supercooling ΔT_0 at high mechanical stirring rates: ⊙, 175 r.p.m.; ●, 220 r.p.m.

these runs are given in Part III, Table SUM3[2] and are plotted against ΔT_0 in Fig. 12; ΔT_0 was limited to 2° by spontaneous nucleation on the metallic stirrer. The slope of the regression line is 8.2×10^{-7} mole s^{-1} deg^{-1} (g soln.)$^{-1}$ for the mechanically stirred dilatometer which compares with the value 7.6×10^{-7} for the magnetically stirred vessel. Detailed discussion of these results is given at the end of Part II.

(d) Salt Solutions

In the presence of salts (0.24–0.46 *M* with respect to the water), initial hydrate formation rates in stirred congruent solutions were of the same order of magnitude as those without salt at the same supercooling. Under identical conditions, successive crystallizations from the same EO–water–salt solution gave irreproducible rate curves which indicated accelerated EO decomposition. Freshly-prepared solutions had pH ~ 6, and whereas after crystallizing several times (~ 6) the sodium perchlorate solution showed no pH change, the sodium chloride solution became more alkaline with pH ⩾ 10.

Appendix

Method of Converting the Observed Decrease in Volume to Moles of Hydrate Formed in Solutions of Congruent Composition

Initially the EO–water solution has a volume V_0. At time t, let X mole EO and RX mole water have combined to form hydrate and let the slurry temperature have increased from the thermostat temperature T_b to T_{obs}, (T in °C).

Then, V_s, volume of solution at T_{obs} is

$$V_s = \left\{\frac{(n_A - RX)M_A + (n_B - X)M_B}{\rho_s}\right\} \cdot (1 + \alpha\Delta T)$$

where n_A = moles of water initially,
n_B = moles of EO initially,
M_A = molecular weight of water,
M_B = molecular weight of EO,
ρ_s = density of solution at T_b,
α = coefficient of cubical expansion of solution, and
$\Delta T = T_{obs} - T_b$.

Volume of hydrate, V_h, at T_{obs} is

$$V_h = \left\{\frac{RXM_A + XM_B}{\rho_h}\right\}(1 + \beta\Delta T),$$

where ρ_h = density of hydrate at T_b,
β = coefficient of cubical expansion of hydrate, and
R = water:EO mole ratio in the hydrate.

Defining

$$\Delta V = V_0 - (V_s + V_h)$$

$$\Delta V = \frac{n_AM_A + n_BM_B}{\rho_s} - \left\{\frac{(n_A - RX)M_A + (n_B - X)M_B}{\rho_s}\right\}(1 + \alpha\Delta T) - \left\{\frac{RXM_A + XM_B}{\rho_h}\right\}(1 + \beta\Delta T)$$

Simplifying and solving for X, the number of moles of hydrate formed, gives

$$X = \frac{\frac{\Delta V + \alpha\Delta T}{\rho_s}\{n_AM_A + n_BM_B\}}{\{RM_A + M_B\}\left\{\frac{(1 + \alpha\Delta T)}{\rho_s} - \frac{(1 + \beta\Delta T)}{\rho_h}\right\}}$$

For a given run, (α/ρ_s) $(n_AM_A + n_BM_B)$ is a constant; also $(RM_A + M_B)$ is constant with $R = 6.89$. Over the small temperature range investigated $\rho_h = 1.06954$ g ml^{-1} and $\beta = 91.3 \times 10^{-5}$ deg^{-1} were assumed constant (12). Solution densities (g ml^{-1}) were calculated from

$$\rho_s = 0.997249 - 0.0005867\ t$$

Can. J. Chem. Downloaded from www.nrcresearchpress.com by 210.87.254.40 on 09/05/12
For personal use only.

with t in °C (9). The solution cubical expansion coefficients measured were

Temperature range (°C)	Mole % EO	$\alpha \times 10^5$ (deg^{-1})
7.4–8.8	5.62	30.5
10.7–11.1	12.67	56.7
7.4–8.5	34.03	98.9

1. KOPPERS COMPANY, INC. The Koppers hydrate process for saline water conversion experimental and engineering studies. Office of Saline Water, U.S. Dept. of Interior, Progress Reports Nos. 90, 125. 1964.
2. A. J. BARDUHN, S. L. COLTEN, R. FERNANDEZ, and J. B. PANGBORN. Studies on ice crystal growth rates and hydrate kinetics. Syracuse Univ. Res. Inst., Office of Saline Water, U.S. Dept. of Interior, Progress Report No. 230. 1966.
3. R. M. BARRER and D. J. RUZICKA. Trans. Faraday Soc. **58**, 2262 (1962); R. M. BARRER and A. V. J. EDGE. Proc. Roy. Soc. London, Ser. A, **300**, 1 (1967).
4. E. L. LIPPERT, H. A. PALMER, and F. F. BLANKENSHIP. Proc. Oklahoma Acad. Sci. **31**, 115 (1950).
5. M. VON STACKELBERG and B. MEUTHEN. Z. Elektrochem. **62**, 130 (1958).
6. K. L. PINDER. Can. J. Chem. Eng. **43**, 271 (1965).
7. O. MAASS and E. H. BOOMER. J. Am. Chem. Soc. **44**, 1709 (1922).
8. A. MAZZUCCHELLI and R. ARMENANTE. Gazz. Chim. Ital. **52**, 344 (1922).
9. D. N. GLEW and N. S. RATH. Unpublished experiments.
10. W. F. CLAUSSEN. J. Chem. Phys. **19**, 259 (1951); **19**, 662 1951; **19**, 1425 (1951).
11. R. K. MCMULLAN and G. A. JEFFREY. J. Chem. Phys. **42**, 2725 (1965).
12. D. N. GLEW and N. S. RATH. J. Chem. Phys. **44**, 1710 (1966).
13. G. VAN HULLE, O. FENNEMA, and W. D. POWRIE. Cryobiology, **2**, 246 (1966).
14. A. N. C. BENNETT. J. Phys. Chem. **31**, 890 (1927).
15. L. G. HEPLER, J. M. STOKES, and R. H. STOKES. Trans. Faraday Soc. **61**, 20 (1965).
16. J. FARRAR and W. S. HAMILTON. Nucleation and growth of ice crystals. Office of Saline Water, U.S. Dept. of Interior, Progress Report No. 127. 1965.
17. A. H. BOOTH and H. E. BUCKLEY. Can. J. Chem. **33**, 1155 (1955).
18. J. M. COULSON and J. F. RICHARDSON. Chemical engineering. Vol. 2. McGraw-Hill Book Co., Inc., New York. 1955. p. 817.
19. A. VAN HOOK. Ind. Eng. Chem. **37**, 782 (1945).
20. W. L. MCCABE and R. P. STEVENS. Chem. Eng. Prog. **47**, 168 (1951).
21. T. YAMAMOTO. Sci. Papers Inst. Phys. Chem. Res. Tokyo, **35**, 228 (1939).
22. R. VOGEL. Z. Anorg. Allgem. Chem. **116**, 21 (1921).
23. D. TURNBULL. J. Phys. Chem. **66**, 609 (1962).
24. W. B. HILLIG and D. TURNBULL. J. Chem. Phys. **24**, 914 (1956).
25. C. S. LINDENMEYER, G. T. ORROK, K. A. JACKSON, and B. CHALMERS. J. Chem. Phys. **27**, 822 (1957).
26. C. S. LINDENMEYER and B. CHALMERS. J. Chem. Phys. **45**, 2807 (1966).
27. A. ROSENBERG and W. C. WINEGARD. Acta Met. **2**, 342 (1954).

Can. J. Chem. Downloaded from www.nrcresearchpress.com by 210.87.254.40 on 09/05/12
For personal use only.

Kinetics of formation of ethylene oxide hydrate. Part II. Incongruent solutions and discussion[1]

D. N. GLEW AND M. L. HAGGETT
Exploratory Research Laboratory, Dow Chemical of Canada, Limited, Sarnia, Ontario
Received June 17, 1968

Equations were developed to describe the experimental rates of formation of ethylene oxide hydrate from stirred, incongruent solutions. Heat conduction through the walls of the dilatometer bulb was rate-controlling. Results for congruent solutions were consistent with these equations during the early stages of hydrate growth.

Canadian Journal of Chemistry, 46, 3867 (1968)

Can. J. Chem. Downloaded from www.nrcresearchpress.com by 210.87.254.105 on 09/05/12
For personal use only.

General observations

In Part I the kinetics of hydrate formation from congruent solutions were described. Experiments on incongruent solutions using the magnetically stirred dilatometer were conducted (*a*) in the water-rich region on solutions containing 5.62 mole % ethylene oxide (EO) which forms a hydrate of formula EO.7.05 H_2O at freezing point $T_f^0 = 8.02$ °C, and (*b*) in EO-rich solutions containing 34.03 mole % EO which forms a hydrate of formula identical to that in congruent solutions, EO.6.89 H_2O, at freezing point $T_f^0 = 8.04$ °C (1, 2). The tabulated results are given in Part III[2].

The behavior of EO hydrate formation from stirred incongruent solutions was entirely different from that in congruent solutions. The crystals appeared as small spheres (3), up to about 1 mm in diameter, and did not stick to the glass walls, so that all experiments on incongruent solutions were made in the magnetically stirred dilatometer. Hydrate formation decreased steadily with time and eventually ceased altogether as shown by the results in Fig. 1 for the water-rich region (*a*). Correspondingly, the solution temperature rose rapidly to a sharp maximum, then decreased back to the thermostat temperature. Figure 2 shows this behavior together with the equilibrium freezing points of the solution of changing composition.

At constant thermostat temperature, the rates of hydrate formation are practically identical at stirring rates of 100 r.p.m. or greater, as shown in Fig. 1 by the identical hydrate formation rate curves for run WMA4[2] at 100 r.p.m. and WMA5 at 320 r.p.m.

Dependence of hydrate formation rate on $(T_{obs} - T_b)$

(a) Water-Rich Solutions

Results in water-rich solutions revealed that, after the maximum temperature increase, there was a direct proportionality between the rate of hydrate formation and the difference of the solution and thermostat temperatures, $(T_{obs} - T_b)$: the data are plotted accordingly in Fig. 3 (Part III, Table WMA1-12)[2].

This dependence is consistent with the rate of hydrate formation depending on the rate of heat conduction through the glass walls of the dilatometer bulb. Accordingly, we derive an expression for this process and compare our experimental results with this expression. Assume the simplest possible temperature profile through the wall as follows:

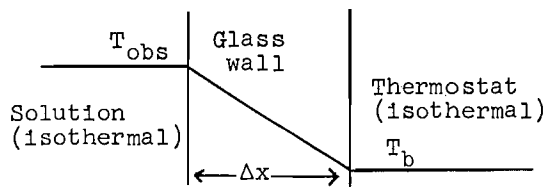

By Fourier's law of heat conduction, the rate of heat flow Q out of the dilatometer is given by

$$[1] \qquad Q = \frac{\lambda_g A}{\Delta x}(T_{obs} - T_b)$$

[1]Contribution No. 165.
[2]Photocopies of Part III may be obtained free of charge, upon request, from: Depository of Unpublished data, National Science Library, National Research Council of Canada, Ottawa, Canada.
WMA stands for water-rich, magnetically stirred solution, EMA stands for EO-rich, magnetically stirred solution, and SUM stands for summary of results.

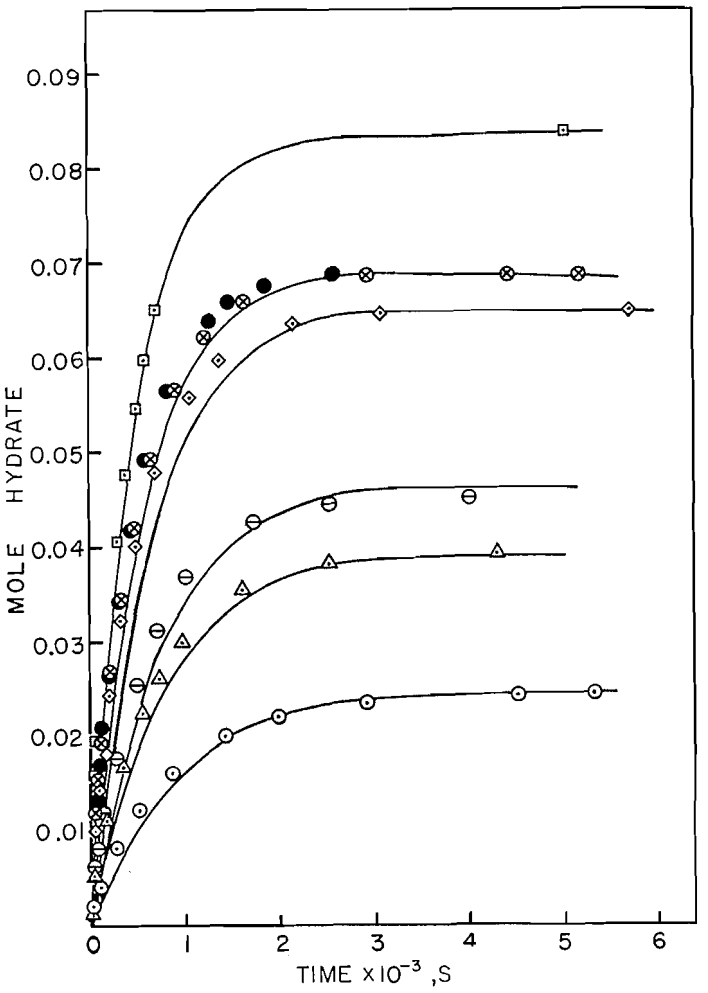

FIG. 1. Moles of hydrate formed versus time for water-rich solutions at high magnetic stirring rates. Run number, supercooling ΔT_0: ⊙, WMA9, 0.46; △, WMA10, 0.79; ⊖, WMA1, 1.07; ◇, WMA8, 1.58; ⊗, WMA4, ●, WMA5, 1.84; □, WMA12, 2.25.

where

λ_g = thermal conductivity of pyrex glass,
Δx = wall thickness, and
A = dilatometer bulb wall area.

During the initial heat evolution from hydrate formation, part of the heat is used in raising the temperature of the solution and dilatometer bulb, and the remainder is conducted to the thermostat, so that

$$[2] \qquad \frac{L}{W}\frac{dm}{dt} = \frac{c_p}{W}\frac{d(\Delta T)}{dt} + \frac{\lambda_g A}{W\Delta x}(\Delta T)$$

where

m = mole of hydrate formed (1 mole of hydrate ≡ 1 mole of EO + R moles H_2O; $R \sim 7$),
$\frac{dm}{dt}$ = rate of hydrate formation in mole s^{-1},
W = weight of solution in g,
L = latent heat per mole of hydrate,
c_p = heat capacity of total system, and
$\Delta T = T_{obs} - T_b$.

If $(c_p/W)[d(\Delta T)/dt]$ is comparatively small and can be neglected, then the rate of hydrate formation is given by

$$[3] \qquad \frac{1}{W}\frac{dm}{dt} \simeq k_1(T_{obs} - T_b)$$

Can. J. Chem. Downloaded from www.nrcresearchpress.com by 210.87.254.105 on 09/05/12
For personal use only.

Can. J. Chem. Downloaded from www.nrcresearchpress.com by 210.87.254.105 on 09/05/12
For personal use only.

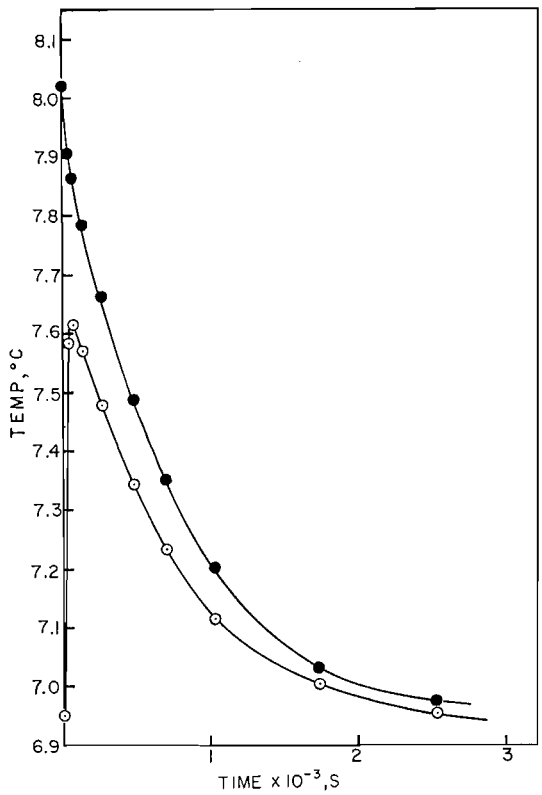

FIG. 2. Solution temperature, ⊙, and equilibrium freezing point, ●, versus time curves for water-rich run WMA1 at 320 r.p.m. and $\Delta T_0 = 1.07$.

where $k_1 = \lambda_g A/LW\Delta x$ is the heat transfer reaction velocity constant, which is found to be rate limiting in all experiments.

Numerical evaluation of $\lambda_g A/LW\Delta x$ for the magnetically stirred dilatometer (Part I, Fig. 2) gives 10.5×10^{-7} mole s^{-1} deg^{-1} (g soln.)$^{-1}$, assuming that the bulb is a cylinder with spherical caps having the dimensions shown.

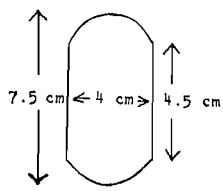

The bulb holds 76.6 g water-rich solution, has a wall area A of 94 cm^2, a wall thickness Δx of 0.25 cm, and is constructed of pyrex glass of thermal conductivity λ_g of 2.6×10^{-3} cal cm^{-1} deg^{-1} s^{-1} (4). The latent heat of hydrate formation L is 12 130 cal (mole hydrate)$^{-1}$ (5).

Experimental evaluation of k_1 gives 9.5×10^{-7} mole s^{-1} deg^{-1} (g soln.)$^{-1}$ determined from the dependence of $(1/W)(dm/dt)$ on $(T_{obs} - T_b)$ by least squares analysis of the data in Fig. 3. The agreement between experimental and calculated values is good and supports a rate of incongruent hydrate formation limited by heat transfer only.

(b) Ethylene Oxide-Rich Solutions

Similar results were observed for the EO-rich solution measurements (Part III, Table EMA1–4)[2]. Figure 4 shows hydrate formation rate curves and in Fig. 5 the results are plotted according to eq. [3].

Numerical evaluation of $\lambda_g A/LW\Delta x$ gives 11.2×10^{-7} mole s^{-1} deg^{-1} (g soln.)$^{-1}$ with $W = 73.7$ g and $L = 11\,850$ cal $mole^{-1}$ (5), and values of the other constants as before. Least squares evaluation of the experimental measurements according to eq. [3] gives a k_1 value of 10.7×10^{-7} mole s^{-1} deg^{-1} (g soln.)$^{-1}$, again in good agreement with conduction theory.

Dependence of hydrate formation rate on $(T_f - T_{obs})$

We have already established a proportionality between the EO hydrate formation rate and $(T_{obs} - T_b)$. However, the actual driving force for crystallization is the difference between the solution freezing point and the temperature at the crystal surface (or the equivalent concentration difference). This crystal temperature is unknown and is extremely difficult to measure. But it is possible (6) to relate crystal growth to the difference between the freezing point and the bulk solution temperature as follows.

Let the temperature of the crystal surface be T_c, the solution freezing point T_f ($T_f > T_c$ (7)), and the bulk temperature T_{obs} ($T_c > T_{obs}$ (8)). Assume that there is a laminar film of liquid of thickness δ around the crystal as shown:

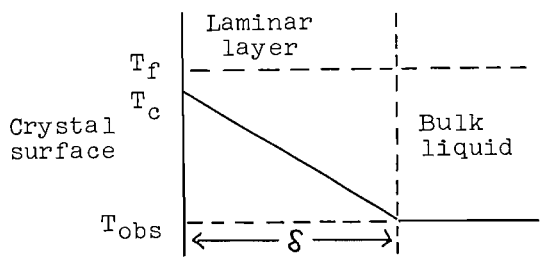

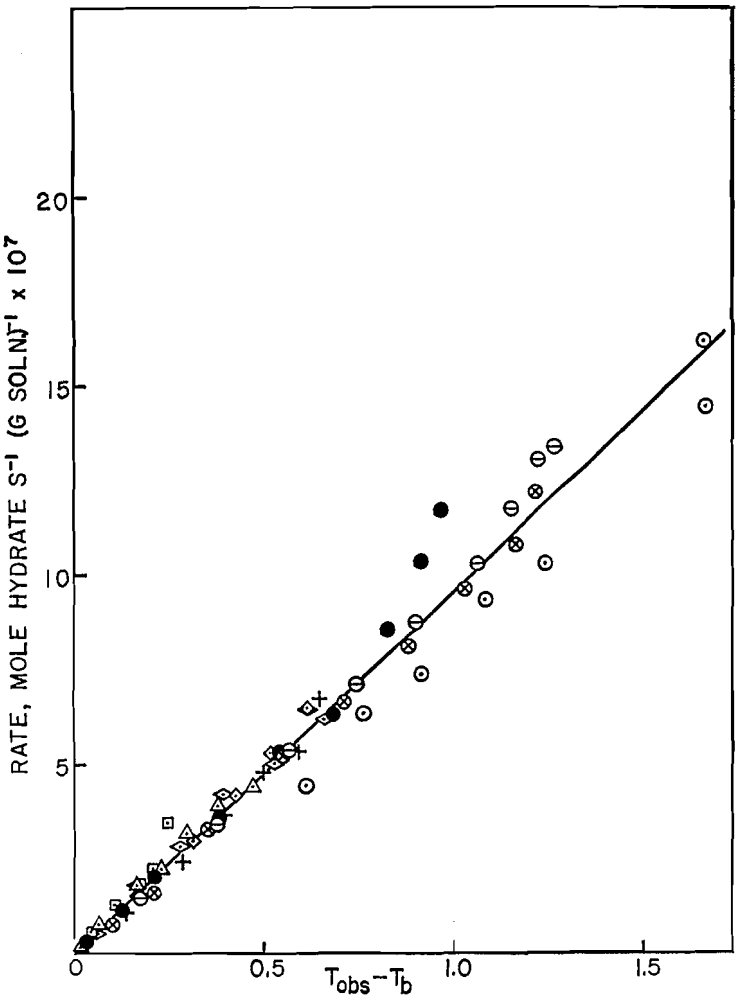

FIG. 3. Plot of instantaneous rate of hydrate formation $(1/W)(dm/dt)$ against the instantaneous solution cooling differential $(T_{obs} - T_b)$ for water-rich experiments. Run: ◈, WMA1; ◇, WMA2; +, WMA3; ⊗, WMA4; ⊖, WMA5; ●, WMA8; ⊡, WMA9; △, WMA10; ⊙, WMA12.

Neglecting the heat taken up by the crystal, in the steady state heat is continuously transferred to the solution at a rate given by

$$[4] \qquad Q = \frac{\lambda_h C}{\delta}(T_c - T_{obs})$$

where

λ_h = thermal conductivity of the laminar layer,
δ = the layer thickness, and
C = surface area of crystal.

Also,

$$[5] \qquad \frac{Q}{W} = \frac{L}{W}\frac{dm}{dt}$$

so that elimination of Q from eqs. [4] and [5] gives

$$[6] \qquad \frac{1}{W}\frac{dm}{dt} = \frac{\lambda_h C}{LW\delta}(T_c - T_{obs})$$

Assuming that the crystal growth at the surface follows a linear dependence on $(T_f - T_c)$, the relation

$$[7] \qquad \frac{1}{W}\frac{dm}{dt} = \frac{K}{W}(T_f - T_c)$$

defining a rate constant K is obtained.

Can. J. Chem. Downloaded from www.nrcresearchpress.com by 210.87.254.105 on 09/05/12
For personal use only.

Can. J. Chem. Downloaded from www.nrcresearchpress.com by 210.87.254.105 on 09/05/12
For personal use only.

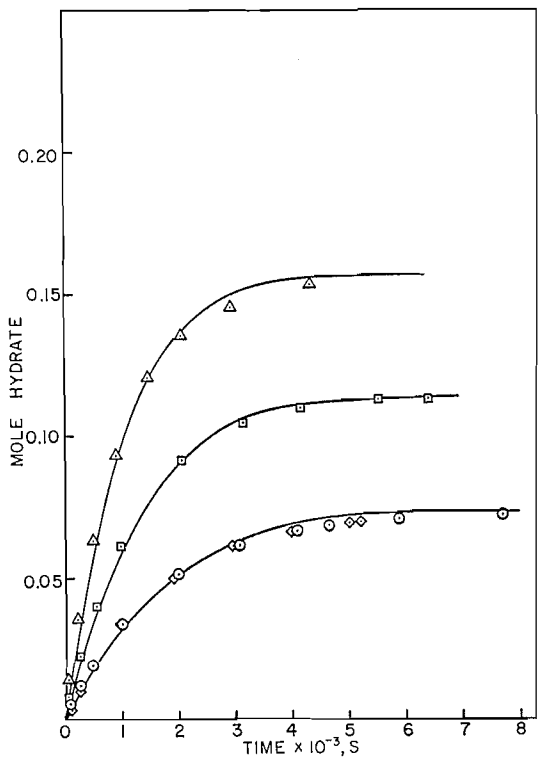

FIG. 4. Moles of hydrate formed versus time for EO-rich solutions at high magnetic stirring rates. Run, supercooling ΔT_0: ◇, EMA1, 0.57; ⊙, EMA2, 0.60; ⊡, EMA3, 1.11; △, EMA4, 1.86.

Eliminating T_c from eqs. [6] and [7] gives the rate of hydrate crystallization,

$$[8] \quad \frac{1}{W}\frac{dm}{dt} = \frac{1}{(W/K + W\delta L/\lambda_h C)}(T_f - T_{obs}) = k_2(T_f - T_{obs})$$

in which k_2 is a composite reaction velocity constant appropriate to steps other than heat transfer through the dilatometer walls.

(a) Water-Rich Solutions

The results of applying eq. [8] to the hydrate formation rates in the water-rich region are shown in Fig. 6. The values of the slopes k_{2w} are given in Table I. Although k_{2w} is seen to vary from (2.3–5.8) $\times 10^{-6}$ mole s^{-1} deg^{-1} (g soln.)$^{-1}$ it generally retains a constant value in each experiment. We have no explanation of the variation between experiments but incline to the mean $k_{2w} = 2.5 \times 10^{-6}$ mole s^{-1} deg^{-1} (g soln.)$^{-1}$ of the 5 lowest values which were obtained in freshly-prepared solutions.

TABLE I

Values of k_{2w} in water-rich region

Run	$k_{2w} \times 10^6$
WMA12	5.8
WMA5	4.4
WMA10	3.6
WMA4	3.7
WMA8	2.8
WMA9	2.3
WMA1	2.6
WMA2	2.6
WMA3	2.4

(b) Ethylene Oxide-Rich Solutions

The plot of hydrate formation rate against $(T_f - T_{obs})$ in EO-rich solutions is shown in

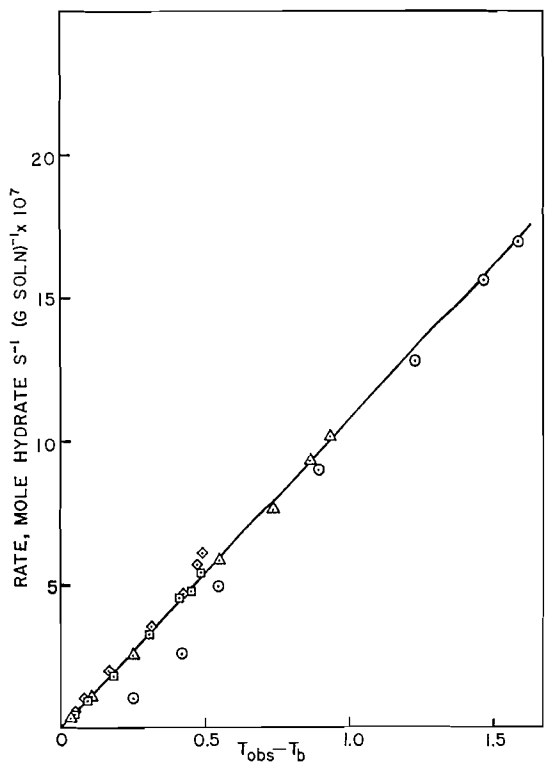

FIG. 5. Plot of instantaneous rate of hydrate formation $(1/W)(dm/dt)$ against the instantaneous solution temperature differential $(T_{obs} - T_b)$ for EO-rich experiments. Run: ◇, EMA1; ⊡, EMA2; △, EMA3; ⊙, EMA4.

Can. J. Chem. Downloaded from www.nrcresearchpress.com by 210.87.254.105 on 09/05/12
For personal use only.

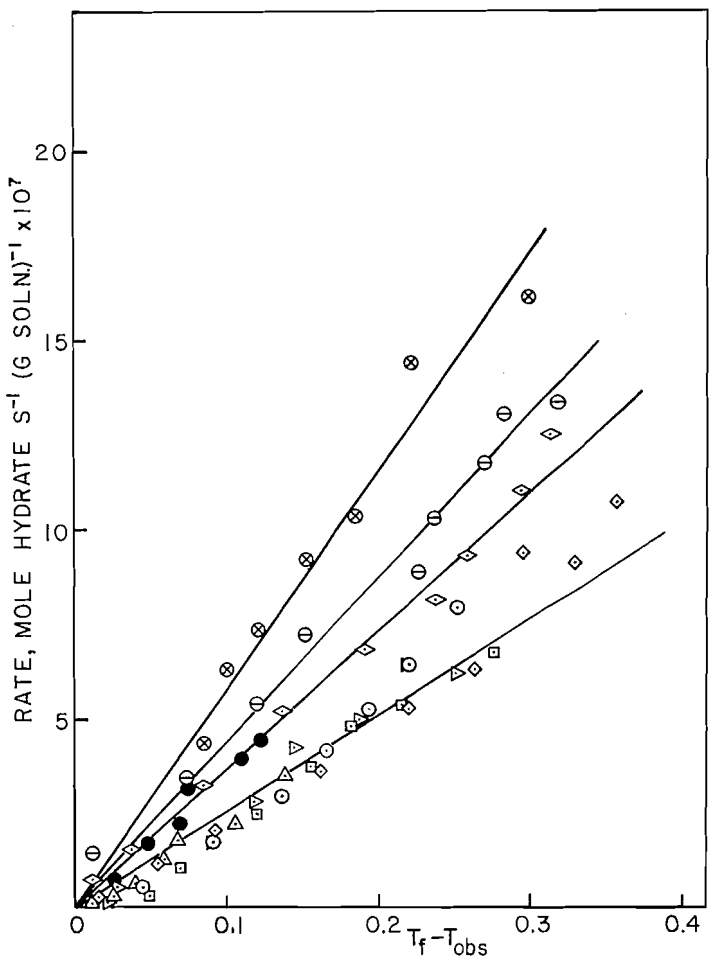

FIG. 6. Plot of instantaneous rate of hydrate formation $(1/W)(dm/dt)$ against the instantaneous $(T_f - T_{obs})$ for water-rich solutions. Run: ▷, WMA1; ⊙, WMA2; ⊡, WMA3; ⋄, WMA4; ⊖, WMA5; ◇, WMA8; △, WMA9; ●, WMA10; ⊗, WMA12.

Fig. 7. All points fall around a single straight line of slope $k_{2e} = 9.9 \times 10^{-6}$ mole s^{-1} deg^{-1} (g soln.)$^{-1}$.

Discussion

It may at first appear surprising that plots of rate against $(T_f - T_{obs})$ are linear at all, since, presumably K and λ_h both vary with absolute temperature, and also the area C varies as the crystals grow. We do not know what kind of crystallization process the coefficient K represents but if, for example, it involves a diffusion mechanism (9) then the scatter of our results over the small experimental temperature range would mask any temperature dependence of K (10). Similarly, changes of thermal conductivity of, for example, water would be hidden. In stirred and unstirred studies (6) of growth of benzophenone and salol, it was observed that the heat transfer coefficients were constant.

Barrer and Ruzicka (11) observed constant rates of argon uptake while growing the tetrahydrofuran–argon double hydrate; they have discussed the variation of δ with increasing crystal size. Nancollas and Purdie (12) also point out that in many systems the effective growth area

Can. J. Chem. Downloaded from www.nrcresearchpress.com by 210.87.254.105 on 09/05/12
For personal use only.

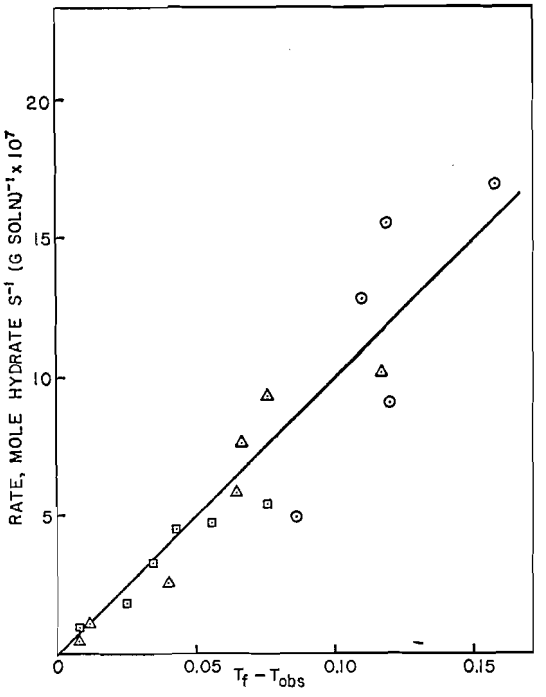

FIG. 7. Plot of instantaneous rate of hydrate formation $(1/W)(dm/dt)$ against the instantaneous $(T_f - T_{obs})$ for EO-rich solutions. Run: □, EMA2; △, EMA3; ⊙, EMA4.

of crystals becomes constant even though they continue to increase in size.

Prediction of Rate Curves

For water-rich and EO-rich solutions, we now have two equations of the form:

$$[3] \qquad \frac{1}{W}\frac{dm}{dt} = k_1(T_{obs} - T_b)$$

$$[8] \qquad \frac{1}{W}\frac{dm}{dt} = k_2(T_f - T_{obs})$$

where

$$k_1 = \frac{\lambda_g A}{LW\Delta x}$$

and

$$k_2 = \frac{1}{W/K + \delta LW/\lambda_h C}$$

from which T_{obs} can be eliminated to give

$$[9] \qquad \frac{1}{W}\frac{dm}{dt} = \frac{k_1 k_2}{k_1 + k_2}(T_f - T_b)$$

which is useful for predicting rates of hydrate formation when the solution freezing point is known.

From the hydrate freezing point curve (1) for water-rich solutions with $T_f^0 = 8.02$ °C in the region $0\ °C \leqslant T_f^0 - T_f \leqslant 2.15\ °C$, we obtain the empirical relationship

$$[10] \qquad \frac{m}{W} = k_3 \log[1 + k_4(T_f^0 - T_f)]$$

with $k_3 = 24.92 \times 10^{-4}$ and $k_4 = 0.735$. Substituting for T_f in eq. [9] and integrating gives

$$[11] \qquad \log\left[\frac{\exp(m/k_5 W)}{1 - K_1 \exp(m/k_5 W)}\right] = \frac{k_{1w}k_{2w}t}{K_1 k_3 k_4(k_{1w} + k_{2w})} - \log(1 - K_1)$$

with

$K_1 = 1/(1 + k_4(T_f^0 - T_b))$,
$k_{1w} = 9.5 \times 10^{-7}$ (Fig. 3),
$k_{2w} = 2.5 \times 10^{-6}$ (Fig. 6),
$k_5 = k_3/2.303 = 1.082 \times 10^{-3}$,

which expresses mole of hydrate formed m as a function of time t for water-rich solutions.

Similarly for EO-rich solutions with $T_f^0 = 8.04$ °C in the region $0\ °C \leqslant T_f^0 - T_f \leqslant 2.04\ °C$ we have the relation

$$[12] \qquad \frac{m}{W} = k_6 \log[1 + k_7(T_f^0 - T_f)]$$

with $k_6 = 39.20 \times 10^{-4}$ and $k_7 = 1.43$. Substituting for T_f in eq. [9] and integrating gives

$$[13] \qquad \log\left[\frac{\exp(m/k_8 W)}{1 - K_2 \exp(m/k_8 W)}\right] = \frac{k_{1e}k_{2e}t}{K_2 k_6 k_7(k_{1e} + k_{2e})} - \log(1 - K_2)$$

with

$K_2 = 1/(1 + k_7(T_f^0 - T_b))$,
$k_{1e} = 10.7 \times 10^{-7}$ (Fig. 5),
$k_{2e} = 9.9 \times 10^{-6}$ (Fig. 7),
$k_8 = k_6/2.303 = 1.702 \times 10^{-3}$,

which expresses the moles of hydrate formed m as a function of time t for EO-rich solutions.

The predicted rate curves for the water-rich region are shown by the solid lines in Fig. 1 evaluated from eq. [11]; for the EO-rich region those in Fig. 4 are given by eq. [13].

It is noticeable, particularly for the water-rich solutions, that the calculated curves consistently

Can. J. Chem. Downloaded from www.nrcresearchpress.com by 210.87.254.105 on 09/05/12
For personal use only.

fall below the experimental points during the early part of a crystallization but approach the points as the reaction reaches completion. We have investigated this behavior and find that the assumption for eq. [3]

$$\frac{c_p}{LW} \cdot \frac{d(T_{obs} - T_b)}{dt} \ll \frac{\lambda_g A}{LW\Delta x}(T_{obs} - T_b)$$

while true after the maximum temperature increase, is incorrect during the initial part of a reaction, when the slurry temperature is increasing. We demonstrate the closer fit of the curves to the experimental points taking the full eq. [2] with eqs. [8] and [10] from which we obtain

$$[14] \quad m = k_3 W \log\left[1 + \frac{k_4}{k_2}\left\{(T_f^0 - T_{obs}) - \frac{\lambda_g A}{LW\Delta x}(T_{obs} - T_b) - \frac{c_p}{LW}\frac{d(T_{obs} - T_b)}{dt}\right\}\right]$$

expressing m as a function of T_{obs} and dT_{obs}/dt.

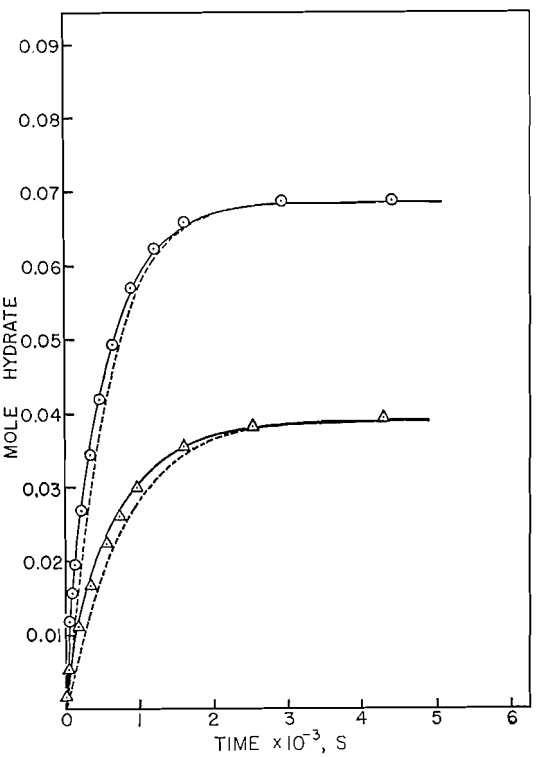

FIG. 8. Comparison of experimental points with calculated curves: - - - - using the approximate integrated eq. [11]; —— using the exact differential eq. [14]. For water-rich run: △, WMA10; ⊙, WMA4.

A value for c_p was estimated as 82 ± 20 cal deg^{-1} using eq. [2] at $t = 0$ where $(T_{obs} - T_b) = 0$ and

$$c_p = \frac{L(dm/dt)_{t\to 0}}{[d(T_{obs} - T_b)/dt]_{t\to 0}}$$

The solid lines for the two curves in Fig. 8 are calculated from eq. [14] and the dashed lines from eq. [11]; the better fit of the solid curves to the data is apparent.

To predict hydrate formation rates, approximate values of m may be obtained explicitly from eq. [11] for water-rich solutions or eq. [13] for EO-rich solutions. Better approximations for m are given for water-rich solutions by eq. [14] which requires the knowledge of T_{obs} as a function of time t.

Interpretation of results for congruent solutions of Part I

The results shown in Fig. 9 (Part III, Table SUM2)[2] and Fig. 12 (Part III, Table SUM3)[2] of Part I for stirred congruent solutions can now be interpreted.

Using our treatment for incongruent solutions according to eq. [9] we are now able to treat congruent solutions replacing T_f by the constant T_f^0 to give

$$[15] \quad \frac{1}{W}\frac{dm}{dt} = K_c(T_f^0 - T_b)$$

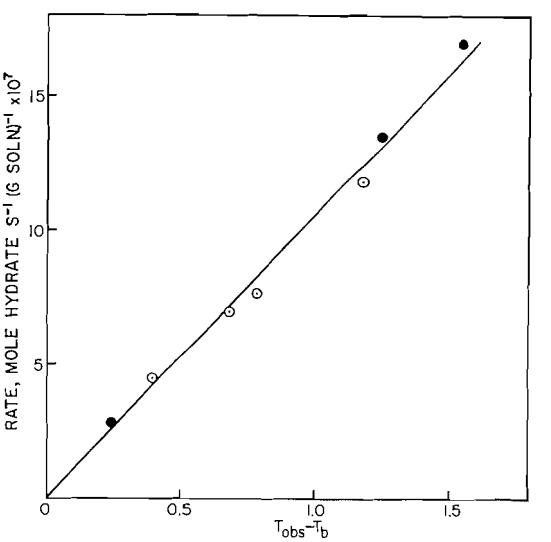

FIG. 9. Variation of initial rates of hydrate formation with $(T_{obs} - T_b)$ at high mechanical stirring rates: ⊙, 175 r.p.m.; ●, 220 r.p.m.

Can. J. Chem. Downloaded from www.nrcresearchpress.com by 210.87.254.105 on 09/05/12
For personal use only.

in which K_c is the composite first order velocity constant. The results of Fig. 12 (Part I) for the mechanically stirred dilatometer in eq. [15] give a least squares $K_c = 8.2 \times 10^{-7}$ mole deg^{-1} s^{-1} (g soln.)$^{-1}$; according to our analysis K_c is given by

$$[16] \qquad K_c = \frac{k_{1c}k_{2c}}{k_{1c} + k_{2c}}$$

where k_{1c} is the heat transfer velocity constant $\lambda_g A/LW\Delta x$ and is the coefficient of the rate dependence on $(T_{obs} - T_b)$, and k_{2c} is the coefficient of the rate dependence on $(T_f^0 - T_{obs})$.

To evaluate k_{1c} the results (Part III, Table SUM3)[2] are plotted according to

$$\frac{1}{W}\frac{dm}{dt} = k_{1c}(T_{obs} - T_b)$$

in Fig. 9 (Part II) giving a least squares $k_{1c} = 10.5 \times 10^{-7}$ mole deg^{-1} s^{-1} (g soln.)$^{-1}$ for the heat transfer velocity constant.

Due to the shape of this vessel (Part I, Fig. 3), it is difficult to estimate a reliable value for the surface area; as an equivalent we have taken the simplified shape with the measured dimensions,

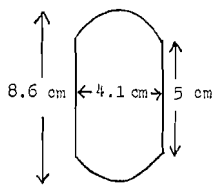

$A = \sim 111$ cm^2,
$W = \sim 90$ g,
$\lambda_g = 2.6 \times 10^{-3}$ cal cm^{-1} deg^{-1} s^{-1},
$\Delta x = 0.25$ cm,
$L = 11\,850$ cal mole^{-1} (5);
which give a calculated value for the heat transfer velocity constant $\lambda_g A/LW\Delta x$ of 11.0×10^{-7} mole s^{-1} deg^{-1} (g soln.)$^{-1}$, in agreement with the experimental value above.

To evaluate k_{2c} the results (Part III, Table SUM3)[2] are plotted according to

$$\frac{1}{W}\frac{dm}{dt} = k_{2c}(T_f^0 - T_{obs})$$

in Fig. 10 giving a least squares $k_{2c} = 35.4 \times 10^{-7}$ mole s^{-1} deg^{-1} (g soln.)$^{-1}$.

Using our values of k_{1c} and k_{2c} in eq. [16] we obtain $K_c = 8.1 \times 10^{-7}$ mole s^{-1} deg^{-1} (g soln.)$^{-1}$, which is in agreement with that 8.2×10^{-7} mole s^{-1} deg^{-1} (g soln.)$^{-1}$ from direct application of eq. [15] to the measurements. This excellent agreement shows that the behavior of our congruent solutions is kinetically comparable with that of incongruent solutions and gives, further, a posteriori support for our kinetic analysis.

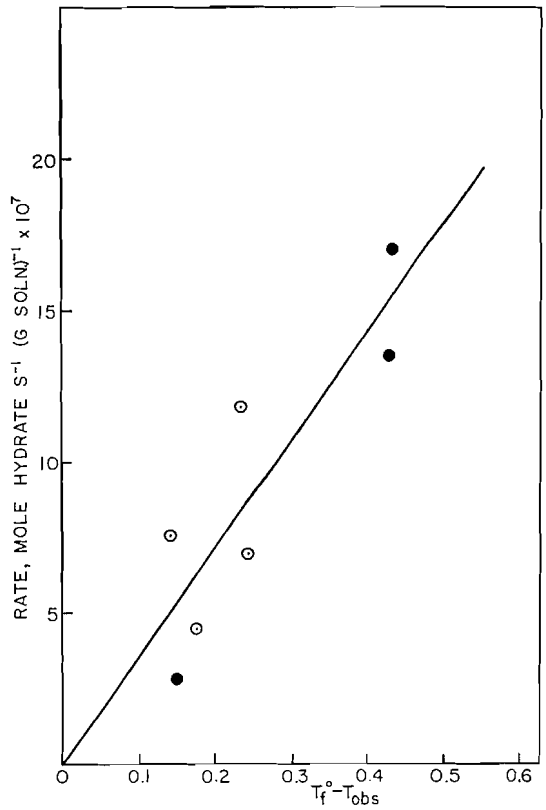

FIG. 10. Variation of initial rates of hydrate formation with $(T_f^\circ - T_{obs})$ at high mechanical stirring rates: ⊙, 175 r.p.m.; ●, 220 r.p.m.

Using a similar analysis for congruent solutions in the magnetically stirred vessel, we find that the slope of the line in Fig. 9 (Part I) is given by the least squares $K_c = 7.6 \times 10^{-7}$ mole s^{-1} deg^{-1} (g soln.)$^{-1}$ from eq. [15]. For the magnetically stirred reaction vessel we have the heat transfer velocity constant $k_{1c} = 10.7 \times 10^{-7}$ mole s^{-1} deg^{-1} (g soln.)$^{-1}$ derived from experiments on EO-rich solutions. We take the value of k_{2c} for the magnetically stirred vessel as that $k_{2c} = 35.4 \times 10^{-7}$ mole s^{-1} deg^{-1} (g soln.)$^{-1}$ for the mechanically stirred vessel, since both

Can. J. Chem. Downloaded from www.nrcresearchpress.com by 210.87.254.105 on 09/05/12
For personal use only.

velocity constants refer to the same process of uniform slurry growth in congruent solutions. Substituting these k_{1c} and k_{2c}° values in eq. [16] gives $K_c = 8.2 \times 10^{-7}$ mole s^{-1} deg^{-1} (g soln.)$^{-1}$, in agreement with the experimental value 7.6×10^{-7} obtained directly. Agreement between the kinetic constants observed in mechanically and magnetically stirred vessels confirms our analysis of EO hydrate growth limited by heat transfer from the slurry.

Conclusion

In summary, it has been concluded that the formation of EO hydrate in our experimental system can be described by 3 consecutive reactions:

[17] $\mathrm{EO} + \mathrm{RH_2O} \xrightarrow{k_{2a}} \mathrm{EO(H_2O)_R} + Q$ surface

[18] Q surface $\xrightarrow{k_{2b}} Q$ bulk

[19] Q bulk $\xrightarrow{k_1} Q$ thermostat

where Q represents the heat produced by the hydrate crystallization,

$$k_1 = \frac{\lambda_g A}{LW\Delta x}$$

$$k_{2a} = \frac{K}{W}$$

$$k_{2b} = \frac{\lambda_h C}{LW\delta}$$

and

$$k_2 = \frac{1}{1/k_{2a} + 1/k_{2b}}$$

Under all our experimental conditions in stirred reactions, it has been found that

$$k_1 \ll \frac{1}{1/k_{2a} + 1/k_{2b}}$$

and, therefore, heat transfer by conduction through the glass walls of the dilatometer bulb is the controlling step in the hydrate formation.

The values of the composite constant k_2 given below increase as the EO concentration increases. Estimations (13) of the temperature and concentration gradients, needed to transport heat from, and mass to, the growing crystals indicate they are very small when stirring at 320 r.p.m. This supports our previous conclusion that these are not significant rate-controlling steps in our system. The variation of k_2 therefore appears to reflect a variation of k_{2a} with EO concentration, i.e. $k_{2a} \ll k_{2b}$. As this constant itself probably represents a combination of rate constants for several steps, such as nucleation, surface reaction, we cannot ascribe the variation of k_2 unambiguously.

Solution composition wt. % EO	$k_2 \times 10^7$ mole s^{-1} deg^{-1} (g soln.)$^{-1}$
5.62	25
12.67	35
34.03	99

In congruent solutions using the mechanically driven stirrer, hydrate formation rates for various ΔT_0 were constant for some time but later decreased. The rates must then be controlled by a process other than heat conduction through the dilatometer walls. Such a process could be heat transfer from crystal to bulk liquid when the population of crystals per unit volume of solution becomes large and laminar layers around the crystals overlap.

Appendix

Method of Converting the Observed Decrease in Volume to the Mole of Hydrate Formed in Solutions of Incongruent Composition

Several experiments, at different supercoolings, were allowed to go to completion i.e. until hydrate formation ceased. The total volume decrease was measured. After correcting for changes in pressure, the volume decrease was plotted against the mole of hydrate formed which was calculated as follows

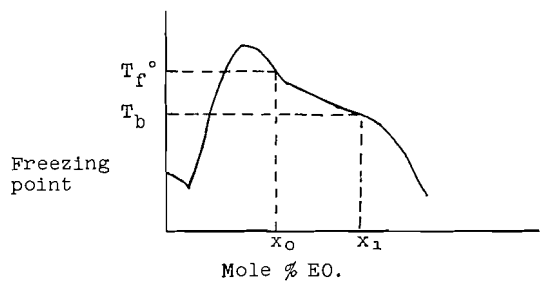

Let the prepared solution have composition x_0 mole % EO and initial freezing point T_f^0. Also, let the thermostat temperature be T_b. With hydrate formation, the solution freezing point decreases asymptotically to T_b and the composi-

tion changes to x_1 mole % EO. Per 100 moles of solution, let X moles of hydrate of composition $H_2O:EO = R:1$ be formed between x_0 and x_1. Then the solution at T_b °C will contain $(x_0 - X)$ mole EO and $(100 - x_0 - RX)$ mole water, so that

$$\frac{x_0 - X}{100 - x_0 - RX} = \frac{x_1}{100 - x_1}$$

whence

$$X = \frac{100(x_1 - x_0)}{x_1(R + 1) - 100}$$

This amount of hydrate X is formed from x_0 mole EO, so that for n_B mole EO in the dilatometer the amount of hydrate formed is Xn_B/x_0.

R was taken as 7.05 in water-rich solutions and 6.89 in EO-rich solutions (2).

A calibration curve of mole hydrate against volume decrease was constructed. Intermediate volume changes, after correcting for temperature changes within the dilatometer, were interpolated from this graph. At the conclusion of this work, sufficient data became available (14) to calculate the volume decrease on crystallization of hydrate from EO-water mixtures; agreement to within $3\frac{1}{2}$% between experimental and calculated values of ΔV was obtained when this comparison was done for run EMA3[2].

1. D. N. GLEW and N. S. RATH. Unpublished experiments.
2. D. N. GLEW and N. S. RATH. J. Chem. Phys. **44**, 1710 (1966).
3. R. K. MCMULLAN and G. A. JEFFREY. J. Chem. Phys. **42**, 2725 (1965).
4. E. H. RATCLIFFE. *In* Handbook of chemistry and physics. 47th ed. *Edited by* R. C. Weast. Chemical Rubber Co., Cleveland, Ohio. 1966.
5. E. W. PHILIPS. Private communication.
6. J. B. MORRIS and R. F. STRICKLAND-CONSTABLE. Trans. Faraday Soc. **50**, 1378 (1954).
7. H. POLLATSCHEK. Z. phys. Chem. **142A**, 289 (1929).
8. M. H. R. J. PLUSJÉ. Discussions Faraday Soc. **5**, 183 (1949); S. H. BRANSOM and W. J. DUNNING. Discussions Faraday Soc. **5**, 96 (1949).
9. D. TURNBULL. J. Phys. Chem. **66**, 609 (1962).
10. J. H. WANG. J. Am. Chem. Soc. **73**, 4181 (1951).
11. R. M. BARRER and D. J. RUZICKA. Trans. Faraday Soc. **58**, 2262 (1962).
12. G. H. NANCOLLAS and N. PURDIE. Quart. Rev. London, **18**, 1 (1964).
13. J. L. DUDA. Private communication.
14. D. N. GLEW, H. D. MAK, and N. S. RATH. Can. J. Chem. **45**, 3059 (1967).

Can. J. Chem. Downloaded from www.nrcresearchpress.com by 210.87.254.105 on 09/05/12
For personal use only.

Can. J. Chem. Downloaded from www.nrcresearchpress.com by 210.87.254.105 on 09/05/12
For personal use only.

Metal–acetylene complexes. II.[1] Acetylene complexes of nickel, palladium, and platinum

E. O. GREAVES, C. J. L. LOCK, AND P. M. MAITLIS[2]
Chemistry Department, McMaster University, Hamilton, Ontario

Received April 22, 1968

The preparations of complexes of the type $L_2M(RC_2R')$ (where L = Ph_3P, M = Ni, Pd, Pt, R = R′ = CF_3; L = Ph_3P, M = Ni, Pt, R = R′ = Ph, and R = Ph, R′ = Me; L = Ph_3P, M = Pd, Pt, R = R′ = COOMe; and R = R′ = CF_3, M = Pd, Pt, L = *n*-Bu_3P, Me_2PhP) are described. From their nuclear magnetic resonance spectra these complexes appear to be approximately planar in solution. The $\nu_{C\equiv C}$ observed in their infrared spectra indicate strong bonding of the acetylene to the metal.

A new approach to the bonding in metal–acetylene complexes is proposed which can be extended to other π-complexes and which allows some predictions to be made.

Canadian Journal of Chemistry, 46, 3879 (1968)

Introduction

Some years ago Chatt and his co-workers reported the preparation and some properties of two types of platinum–acetylene complexes, $RC_2R'PtCl_2L$, (**1**) [where L was Cl^- or an amine] and $(Ph_3P)_2PtRC_2R'$ (**2**) (1–3). Simple mono- or di-alkyl or -aryl acetylenes did not form complexes of type (**1**) but reacted further to give products which were not characterized. Only acetylenes bearing at least one very bulky alkyl group, for example, —CMe_3, —CMe_2OH or —CMe_2OMe, formed this type of complex.

From a study of the infrared spectra of the complexes (**1**) Chatt *et al.* (1–3) deduced that the acetylenes were relatively weakly bonded to the metal, their criterion being $\Delta\nu_{C\equiv C}$ ($\nu_{C\equiv C}$(free acetylene) − $\nu_{C\equiv C}$(complexed acetylene)). In most disubstituted acetylenes $\nu_{C\equiv C}$ occurs between 2190 and 2260 cm^{-1} (1), in these complexes it varied from about 1994 to about 2046 cm^{-1} The decrease in frequency observed, of about 200 cm^{-1}, was therefore comparable to that observed on complexing olefins to Pt(II) in complexes such as Zeise's salt, $KPtC_2H_4Cl_3$ (~ 150 cm^{-1}). The relatively small $\Delta\nu_{C\equiv C}$ and the low intensity of the $\nu_{C\equiv C}$ band in the complexes of symmetrical acetylenes appeared to indicate rather weak bonding to the metal with only a small distortion of the acetylene from its uncomplexed geometry. Hence a structure was proposed for these complexes similar to that of Zeise's salt, with the acetylene perpendicular to the coordination plane. This conclusion was recently verified by the publication in a preliminary communication by Owston *et al.* (4) of the crystal structure of $(Bu^tC_2Bu^t)PtCl_2$-$(NH_2C_6H_4CH_3$-*p*), which was found to have a geometry similar to that of the olefin complex $(C_2H_4)PtCl_2(HNMe_2)$, (**5**).

The second type of complex, (**2**), investigated by Chatt *et al.* (1–3) showed a strong band at ~ 1800 cm^{-1} in the infrared spectrum which was ascribed to $\nu_{C\equiv C}$ of the acetylene coordinated to the metal. $\Delta\nu_{C\equiv C}$ was much larger here and Chatt *et al.* suggested (*a*), that the bonding of the acetylene to the metal (formally Pt(0)) was much stronger in (**2**) and (*b*), that in (**2**) the acetylene was coplanar (or nearly so) with the two P atoms and the Pt. This prediction was also recently shown to be correct by the determination of the crystal structure of $(Ph_3P)_2Pt(PhC_2Ph)$ by Grim *et al.* (6).

Wilke and Herrmann (7) briefly mentioned, but with a complete absence of details, the preparation of the analogous nickel complexes, $(Ph_3P)_2Ni(RC_2R)$, where R = Ph or Me; and Wilkinson *et al.* have described $(Ph_3P)_2Pt$-$(CF_3C_2CF_3)$ (8).

During the past few years we have been very interested in the reactions of acetylenes with various noble metal compounds, particularly palladium chloride (9, 10), since a variety of interesting and as yet quite unexplained reactions occur under very simple conditions. One obvious path by which this particular problem could be attacked was by the preparation and study of complexes analogous to (**1**), i.e., $acPdCl_2L$ which

[1]Parts of this work have appeared as preliminary communications, see refs. 41 and 42. Reference 41 is regarded as part I of this series.

[2]Fellow of the Alfred P. Sloan Foundation and author to whom any correspondence should be addressed.

TABLE I

$\nu_{C\equiv C}$ for complexes prepared in this paper

Complex	$\nu_{C\equiv C}$ (cm^{-1})		
	M=Ni	M=Pd	M=Pt
$(Ph_3P)_2M(PhC_2Ph)$	1800	—	1768, 1740
$(Ph_3P)_2M(PhC_2Me)$	1795	—	1756
$(Ph_3P)_2M(MeOOCC_2COOMe)$	—	1845, 1830 (sh)	1782, 1765 (sh)
$(Ph_3P)_2M(CF_3C_2CF_3)$	1790	1838, 1811	1775
$(PhMe_2P)_2M(CF_3C_2CF_3)$	—	1837, 1800	1767
$(n\text{-}Bu_3P)_2M(CF_3C_2CF_3)$	—	1837, 1795	1758

can be expected to be important in the first stage of these reactions. Despite a number of attempts, however, we have not yet succeeded in isolating and characterizing such a complex unambiguously.

However, since complexes of type (**2**) were known for nickel and platinum, it was reasonable to suppose that they could also be made for palladium. We therefore set out with the intention first, of synthesizing a range of complexes of the type $(R_3P)_2M(R'C{\equiv}CR'')$, secondly of comparing their physical properties, and thirdly of investigating their reactions, especially with a view to understanding typical metal-catalyzed reactions of acetylenes such as hydrogenation, polymerization, etc. In this paper we describe the preparation and some of the properties of such complexes.

Results

Three nickel, four palladium, and six platinum complexes of the type $(R_3P)_2M(R'C{\equiv}CR'')$ have been prepared (Table I). The hexafluoro-2-butyne complexes $(Ph_3P)_2M(CF_3C_2CF_3)$, (M = Ni, Pd, and Pt) were, however, the only ones where it was possible to prepare the whole series.

Nickel Complexes

The acetylenebis(triphenylphosphine)nickel complexes (**5**) were prepared by reaction of ethylenebis(triphenylphosphine)nickel (**4**) with the appropriate acetylene. Ethylenebis(triphenylphosphine)nickel was prepared by a modification of the procedure of Wilke and Herrmann (7) in which the more readily available triethylaluminium was substituted for diethylaluminium ethoxide. Care was taken to wash the ethylene complex (**4**) thoroughly with ether before adding an acetylene, otherwise polymerization, especially in the case of hexafluoro-2-butyne, was found to occur.

The yellow crystalline diphenyl- and methylphenylacetylene complexes (**5***a*) and (**5***b*) were very air sensitive and too unstable for elemental analyses. They were characterized by their infrared and nuclear magnetic resonance n.m.r. spectra, which were very similar to those of the analogous, and fully characterized platinum complexes. Attempts to prepare the dimethyl acetylenedicarboxylate complex gave an unidentified amorphous yellow compound. However, hexafluoro-2-butyne gave the more stable bright yellow crystalline complex (**5***c*). In the solid, this changed color (to a pale green) only after exposure to air for several hours. In solution, however, it decomposed rapidly and an osmometric molecular weight measurement was not possible.

Attempts to prepare acetylenebis(trialkylphosphine)nickel complexes were all unsuccessful. The previously reported ethylenebis(tri-*n*-butylphosphine)nickel (7) was obtained as an air sensitive oil. With acetylenes this gave gums or oils which could not be crystallized or purified without decomposition. The relatively stable ethylenebis(tricyclohexylphosphine)nickel gave a gum with hexafluoro-2-butyne, and trimerized diphenylacetylene to hexaphenylbenzene.

$$\underset{\mathbf{3}}{[Ni(acac)_2]_3} + Et_3Al + PPh_3 + C_2H_4 \rightarrow \underset{\mathbf{4}}{(Ph_3P)_2Ni(C_2H_4)}$$

$$\underset{\mathbf{4}}{(Ph_3P)_2Ni(C_2H_4)} + RC{\equiv}CR' \rightarrow (Ph_3P)_2Ni(RC_2R')$$

5*a*, R = R′ = Ph
5*b*, R = Ph, R′ = Me
5*c*, R = R′ = CF_3

Palladium Complexes

Acetylenebis(triphenylphosphine)palladium complexes could not be prepared by a method analogous to that used in the preparation of the nickel complexes; addition of small amounts of triethylaluminium to bis(acetylacetonato)palla-

Can. J. Chem. Downloaded from www.nrcresearchpress.com by 210.87.254.105 on 09/05/12
For personal use only.

Can. J. Chem. Downloaded from www.nrcresearchpress.com by 210.87.254.105 on 09/05/12
For personal use only.

dium and triphenylphosphine (mole ratio 1:2) gave tetrakis(triphenylphosphine)palladium (**6**). Further addition of triethylaluminium caused the deposition of metallic palladium.

Attempts to prepare the complexes by the hydrazine reduction of dichlorobis(triphenylphosphine)palladium in the presence of the acetylene, which was successful for the platinum complexes (**2**), here led to the precipitation of palladium or the formation of gums. By analogy with the platinum complexes, a plausible intermediate in the reaction is $(Ph_3P)_2Pd$.

Some acetylenes bearing electronegative substituents (—CF_3 or —COOMe) replaced two molecules of triphenylphosphine in tetrakis(triphenylphosphine)palladium (**6**) to give the acetylene complexes (**7**). Other acetylenes (e.g. PhC≡CPh, PhC≡CMe, and *p*-$NO_2C_6H_4C{\equiv}CC_6H_4$*p*-$NO_2$) did not give isolable complexes. Tetrakis(triphenylphosphine)palladium was conveniently prepared by triethylaluminium reduction of bis(acetylacetonato)palladium (**11**) in the presence of excess triphenylphosphine. A plausible intermediate in this reaction is a thermally unstable diethylpalladium complex, $[(Ph_3P)_2PdEt_2]$.

$$Pd(acac)_2 + Et_3Al + PPh_3 \rightarrow [(Ph_3P)_2PdEt_2] \xrightarrow{-Et} [(Ph_3P)_2Pd] \xrightarrow{PPh_3} (Ph_3P)_4Pd$$
$$\mathbf{6}$$

$$(Ph_3P)_4Pd + RC{\equiv}CR \rightarrow (Ph_3P)_2Pd(RC_2R) + 2Ph_3P$$
$$\mathbf{6} \qquad \mathbf{7a},\ R = CF_3;\ \mathbf{7b},\ R = COOMe$$

The analogous complexes $(n\text{-}Bu_3P)_2Pd(CF_3C_2CF_3)$, (**8**), and $(Me_2PhP)_2Pd(CF_3C_2CF_3)$, (**9**), were prepared by addition of the acetylene to the hydrazine reduction product of $(R_3P)_2PdCl_2$ in the presence of excess R_3P. The probable intermediate, $(R_3P)_4Pd$, was not isolated.

Platinum Complexes

The general method used by Chatt *et al.* (3) for the preparation of the platinum complexes (**2**), has been described by Allen and Cook (12). This involves the addition of the acetylene to the hydrazine reduction product of *cis*-dichlorobis(triphenylphosphine)platinum. Dobinson *et al.* (13) have indicated that the reduction may be thought of as going via the following reaction path

$$(Ph_3P)_2PtCl_2 + N_2H_4 + EtOH \rightarrow [(Ph_3P)_2PtN_2H.]_2^{2+}2Cl^- \xrightarrow{N_2H_4} (Ph_3P)_2PtH.Cl$$
$$\xrightarrow{N_2H_4} (Ph_3P)_2Pt \xrightarrow{RC{\equiv}CR'} (Ph_3P)_2Pt(RC_2R') \xleftarrow{RC{\equiv}CR'} (Ph_3P)_4Pt$$
$$\mathbf{2a},\ R = R' = Ph;\ \mathbf{2b},\ R = R' = CF_3;\ \mathbf{2c},\ R = R' = COOMe;\ \mathbf{2d},\ R = Ph,\ R' = Me \qquad \mathbf{10}$$

The complexes (**2***a*, **2***b*, **2***d*) were prepared by this method. As for the palladium complex (**6**), acetylenes bearing electron-withdrawing substituents (CF_3, COOMe) replaced two molecules of triphenylphosphine in tetrakis(triphenylphosphine)platinum (**10**); (**2***b*) and (**2***c*) were prepared this way. We also attempted to prepare the complexes $(Bu_3P)_2Pt(CF_3C_2CF_3)$ (**11**) and $(PhMe_2P)_2Pt(CF_3C_2CF_3)$ (**12**) by the hydrazine reduction method from the appropriate dichlorobis(tert-phosphine)platinum. However, only uncharacterizable red oils were obtained. These complexes were successfully prepared by reducing K_2PtCl_4 with ethanolic KOH in the presence of an excess of the appropriate phosphine, and adding the acetylene to the reduction product, presumably $(R_3P)_4Pt$.

Spectra

The infrared spectra of the complexes prepared have been measured, and in each case they exhibited a band in the region 1740–1845 cm^{-1} which is ascribed to $\nu_{C\equiv C}$ of the coordinated acetylene. In some cases this band was split; the reason for this is not understood. These values are presented in Table I; Table II also gives the values of $\nu_{C\equiv C}$ obtained by other authors for a variety of hexafluoro-2-butyne metal complexes.

The proton magnetic resonance (p.m.r.) spectra of the complexes $(Ph_3P)_2M(PhC_2Ph)$ (M = Ni, Pt), showed only a complex resonance at ca. 2.5 τ due to phenyl protons. The 60 Mc p.m.r. spectrum of methylphenylacetylenebis(triphenylphosphine)platinum (**2***d*) both in benzene and in chloroform solution at 34° showed a

TABLE II

$\nu_{C\equiv C}$ for some hexafluoro-2-butyne metal complexes

Compound	$\nu_{C\equiv C}$ (cm^{-1})	$\Delta\nu_{C\equiv C}$ (cm^{-1})	Reference
$CF_3C{\equiv}CCF_3$	2300 (Raman)	—	38
$C_5H_5Mn(CO)_2{\cdot}C_4F_6$	1919[a]	381	8
$(Ph_3P)_2RhCl{\cdot}C_4F_6$	1917[b]	383	20
$(Ph_3P)_2Pd{\cdot}C_4F_6$	1811, 1838[a]	475	*d*
$(PhMe_2P)Pd{\cdot}C_4F_6$	1800, 1837[a]	482	*d*
$(n\text{-}Bu_3P)_2Pd{\cdot}C_4F_6$	1795, 1837[a]	484	*d*
$(C_5H_5)_2V{\cdot}C_4F_6$	1800	500	39
$(Ph_3P)_2Ni{\cdot}C_4F_6$	1790[c]	510	*d*
$(Ph_3P)_2Pt{\cdot}C_4F_6$	1775[a]	525	8, *d*
$(Ph_3P)_2IrCO{\cdot}Cl{\cdot}C_4F_6$	1773[b]	527	19
$(PhMe_2P)_2Pt{\cdot}C_4F_6$	1767[a]	533	*d*
$(n\text{-}Bu_3P)_2Pt{\cdot}C_4F_6$	1758[a]	542	*d*

[a]Solution; [b]Nujol mull; [c]KBr disc; [d]this paper.

multiplet at 2.7 τ (phenyl protons), and a doublet centered at 7.88 τ due to methyl protons coupling with a phosphorus (J_{P-H} 6.2 c.p.s.). Two pairs of satellite peaks due to coupling of the methyl protons with ^{195}Pt (I = 1/2, 34% abundance) were also observed (J_{Pt-H} 41.5 c.p.s.). The 100 Mc spectrum in chloroform – methylene chloride solution at 22.5° showed the same coupling constants, but in addition, the resonances noted above were further split into symmetrical doublets due to coupling with the second phosphorus ($J_{P'-H}$ ca. 1.2 c.p.s.). Since it is generally agreed that *trans*-coupling in octahedral or square-planar complexes is larger than *cis*-coupling (14), the larger, J_{P-H}, is assigned to coupling with the *trans*-phosphorus, and the smaller, $J_{P'-H}$, to coupling with the *cis*-phosphorus.

The spectrum of (**2***d*) in chloroform was complicated by the slow appearance of a new singlet at 7.99 τ; this was shown to be free methylphenylacetylene. By carrying out the reaction on a larger scale for 48 h at 25°, a yellow crystalline precipitate of chloro(dichloromethyl)-bis(triphenylphosphine)platinum (**13**) was obtained.

$$(Ph_3P)_2Pt(PhC_2Me) + CHCl_3 \rightarrow (Ph_3P)_2Pt(CHCl_2)Cl + PhC_2Me$$

13

Similar examples of electrophilic attack on tetrakis(triphenylphosphine)platinum (**10**) by alkyl and acyl halides

e.g. $(Ph_3P)_4Pt + MeBr \rightarrow (Ph_3P)_2PtMe.Br + 2PPh_3$

have been reported by Cook and Jauhal (15). They interpreted their reactions as proceeding via primary dissociation of the phosphine complex (**10**), possibly to $(PPh_3)_2Pt$, which has itself been found to react with alkyl halides in the above manner (16). In our case however, the p.m.r. spectrum of (**2***d*) in benzene does not show any peak attributable to free methylphenyl-acetylene, so that we conclude that the equilibrium

$$(Ph_3P)_2Pt(PhC_2Me) \rightleftharpoons (Ph_3P)_2Pt + PhC_2Me$$

lies well over to the left hand side. Furthermore, our observation of both *cis*- and *trans*- P—H coupling in (**2***d*) makes it very unlikely that the rate of the dissociation is fast, since this would imply a fast backreaction and consequent rapid exchange of the acetylene.

The 60 Mc p.m.r. spectrum of methylphenyl-acetylenebis(triphenylphosphine)nickel (**5***c*) was similar to that of (**2***d*); the methyl protons were observed as a symmetrical doublet centered at 7.86 τ (J_{P-H} 4.5 c.p.s.) due to coupling with the *trans*-phosphorus and again each resonance appeared to be further split into a symmetrical doublet ($J_{P'-H}$ ca. 1 c.p.s.) due to coupling with the *cis*-phosphorus.

The ^{19}F n.m.r. spectra of $(Ph_3P)_2M(CF_3C_2\text{-}CF_3)$ (M = Ni, Pd, and Pt) were also measured. The spectrum of hexafluoro-2-butynebis(tri-phenylphosphine)platinum (**2***b*) in benzene at 30° showed a doublet centered at 10.4 p.p.m. on the low-field side of benzotrifluoride due to fluorine–phosphorus coupling (J_{P-F} 10.2 c.p.s.). Two pairs of satellite peaks due to coupling of the fluorines with ^{195}Pt were also observed (J_{Pt-F} 64 c.p.s.). The n.m.r. spectrum of (**2***b*) was

Can. J. Chem. Downloaded from www.nrcresearchpress.com by 210.87.254.105 on 09/05/12
For personal use only.

Can. J. Chem. Downloaded from www.nrcresearchpress.com by 210.87.254.105 on 09/05/12
For personal use only.

also run in methylene chloride at 30° (J_{P-F} 10.3 c.p.s., J_{Pt-F} 66 c.p.s.); the coupling constants did not change on cooling this solution to −60 °C, nor were the peaks further split.

The spectrum of hexafluoro-2-butynebis(triphenylphosphine)nickel (**5***c*) in benzene at 30 °C showed only a doublet centered at 10.6 p.p.m. on the low-field side of benzotrifluoride due to coupling with ^{31}P (J_{P-F} 6.1 c.p.s.). Similarly the analogous palladium complex (**7***a*) showed a doublet centered at 10.7 p.p.m. from benzotrifluoride (J_{P-F} 11.2 c.p.s.).

The ^{19}F n.m.r. spectrum of hexafluoro-2-butynebis(tri-*n*-butyl-phosphine)platinum (**11**) showed a doublet centered at 8.8 p.p.m. on the low-field side of benzotrifluoride (J_{P-F} 10.8 c.p.s.), with two pairs of satellite peaks due to ^{195}Pt—F coupling (J_{Pt-F} 67 c.p.s.).

In view of the magnitude of these P—F couplings they are assigned to coupling with the *trans*-phosphorus; *cis*-P—F couplings could not be detected.

The p.m.r. spectra of the palladium and platinum dimethyl acetylenedicarboxylate complexes (**7***b*) and (**2***c*) in deuterochloroform showed multiplets at 2.9 τ due to the phenyl protons and singlets at 6.80 τ (Pd) and 6.75 τ (Pt) due to the ester methyl protons. No coupling, either to platinum or to the phosphines, was observed.

Discussion

Structures of the Complexes

The p.m.r. spectra of the methylphenylacetylenebis(triphenylphosphine)-nickel and -platinum complexes (**5***b*) and (**2***c*) show coupling of the methyl protons to both the *trans*- and the *cis*-phosphines; hence these molecules must be planar or nearly so. The magnitude of the smaller (*cis*-) coupling in (**2***c*) implies that the rate of rotation of the acetylene about the Pt–acetylene axis is very slow (less than 1.2 s^{-1}) and that this process has a high activation energy barrier (17). By contrast, the hexafluoro-2-butyne complexes (**5***c*), (**7***a*), (**2***b*), and (**11**) showed only coupling to the *trans*-phosphines; this was also observed by Wilkinson *et al.* for (**2***b*) (8). Our inability to observe *cis*- coupling here is puzzling especially since the *trans*- P—H coupling is smaller than the P—F coupling. However, this result still implies a planar or near-planar structure for the two phosphorus atoms, the metal, and the acetylenic carbons. If, for example, the acetylene were at right angles to the plane of the metal and the phosphorus atoms or were rotating rapidly about the metal–acetylene axis, then coupling of the fluorines to two equivalent phosphorus atoms would be observed, and the ^{19}F resonance would appear as a triplet.

We are thus able to say that the structures of these acetylene complexes in solution are very similar to the structures in the solid state; Glanville *et al.* (6) have shown that $(Ph_3P)_2Pt(PhC_2Ph)$ (**2***a*) has the two P atoms, the Pt, and one acetylenic carbon in a plane, with the acetylenic CC bond making an angle of 14° with this plane.

Bonding in the Complexes

Chatt *et al.* (3) have suggested that the bonding of acetylenes to platinum might be described in two ways, (**14**) and (**15**).

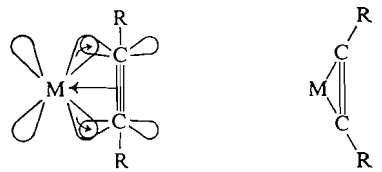

14 **15**

The structure (**14**) implies that bonding is caused by donation of acetylene π electron density into an empty p- or d-orbital of the metal and back-donation of electron density from a filled metal d (or dp-hybrid) orbital to an acetylene π* orbital.

The structure (**15**) implies that the electron density in the acetylene has been reorganized to give an arrangement close to that for an olefin, and that the resulting two unpaired electrons combine with two unpaired electrons on the metal to give two "σ" bonds between the acetylene and the metal in a "metallacyclopropene" ring.

This argument was based on the values of $\Delta\nu_{C\equiv C}$ found in the complexes (**1**) and (**2**) respectively. The smaller value of $\Delta\nu_{C\equiv C}$, found in (**1**), was taken to imply weaker bonding of the acetylene to the metal, less distortion of the acetylenic geometry from linear, and a shorter acetylenic CC bond. It was also assumed that the acetylene was bonded perpendicular to the coordination plane of the metal. The larger value of $\Delta\nu_{C\equiv C}$, found in (**2**), was taken to imply a stronger bonding of the acetylene to the metal, greater

Can. J. Chem. Downloaded from www.nrcresearchpress.com by 210.87.254.105 on 09/05/12
For personal use only.

distortion of the acetylene from linear, and a longer acetylenic CC bond. If it is assumed that two Pt—C σ bonds are formed in (**2**), the metal is then in the +2 oxidation state and hence would probably be square-planar with the acetylene taking up two coordination positions in the plane.

In a later paper Chatt (18) explicitly pointed out the possibility of there existing a series of complexes in which a gradual transition occurred between bonding of types **14** and **15**. He also pointed out that the essential difference between the two types was due to the electron-releasing or -withdrawing character of the group R on the acetylenes.

Later workers extended these suggestions to other acetylene–metal complexes. However, they hardened the distinctions between the two types of bonding, and implied that two different structures and two different types of bonding were in fact possible. Parshall and Jones (19), for example, noted that $\nu_{C\equiv C}$ in $(Ph_3P)_2IrCO.Cl(CF_3C_2CF_3)$ (**16**) occurred at 1773 cm^{-1}, between $\nu_{C\equiv C}$ for

$CF_3C{=}CCF_3$ (1715 cm^{-1})
$CF_2{-}CF_2$

and

$CF_3C{=}C.CF_3$ (1820 cm^{-1})
CF_2

as might be expected if the iridium in (**16**) were part of a metallacyclopropene ring. Mays and Wilkinson (20) suggested that the bonding in $C_5H_5Mn(CO)_2(CF_3C_2CF_3)$ was described by (**14**) whereas in $(Ph_3P)_2RhCl(CF_3C_2CF_3)$ it was of type (**15**).

Support for these two descriptions also comes from the recent X-ray crystal structures of $(Ph_3P)_2Pt(PhC_2Ph)$ (6) which is apparently a type (**15**) complex, and $(Bu^tC_2Bu^t)PtCl_2$(*p*-toluidine) (4) which is apparently a type (**14**) complex.

Collman and Kang (21) summarized the position in 1967, "At the present time it is an unsettled question whether the two bond types (i.e. **14** and **15**) represent energy minima and could be found in valence tautomerism or whether these are extreme descriptions of a gradual transformation". These authors inclined towards the second viewpoint on the basis of their results using different acetylenes bonded to rhodium and iridium. As is shown in Table I, when values of $\nu_{C\equiv C}$ for the same acetylene bonded to different metals (or to the same metal with different ligands), are compared, a similar gradation is observed.

Although the two descriptions are pictorially attractive, we feel that the observations can be interpreted completely and more usefully using only one model. Similar conclusions, but of less generality, have recently been arrived at by Pannatoni *et al.* (22) and by McGinnety and Ibers (23) for olefin complexes.

In this interpretation only Chatt's first model is needed; an electron density distribution of the type shown in the so-called "σ bonded" model then arises naturally as one point in a continuous range of bond types. The factors determining whether any significant bond is formed are (*i*) that orbitals of the same symmetry exist on the metal and the acetylene, (*ii*) that significant overlap of the orbitals occurs, (*iii*) that the energy of the two orbitals used is similar. We assume that the first two conditions are fulfilled; simple group theory arguments show that (*i*) is true and (*ii*) seems to be well-accepted by other workers in discussing bonding of this type.

Point (*iii*) is of most interest because we feel that this factor, namely the relative energies of the acetylene π and π* orbitals and the metal s, p, and d orbitals, is most important in deciding the bonding. To obtain an accurate value of the relative energy of the orbitals in the acetylene and the remaining metal complex fragment is not possible, but one can get approximate estimates for the acetylene and the free metal ions. If the energy of the ion and the separated electron is defined as zero then the two π levels in acetylene are at $-92\,000$ cm^{-1} and the two π* levels are at $-33\,700$ cm^{-1} (24). The bonding s, p, and d levels in platinum and palladium are estimated to be: Pt^0, $-34\,000$ to $-74\,000$ cm^{-1}; Pt^+, $-87\,000$ to $-150\,000$ cm^{-1}; Pd^0, $-24\,000$ to $-67\,000$ cm^{-1}; Pd^+, $-84\,000$ to $-157\,000$ cm^{-1}; Pd^{2+}, $-148\,000$ to $-266\,000$ cm^{-1} (25). This data shows that the energy levels for a non-charged metal atom are expected to lie roughly midway between the acetylene π and π* levels and that as electron density is removed from the metal, the charge is increased and the metal levels fall below those of the acetylene.

Using such a simple picture, one may draw up a general diagram of the type shown (Fig. 1). In this, we may consider the relative position of the

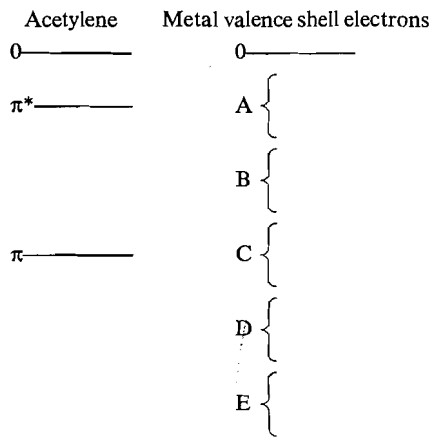

FIG. 1. Energy levels.

metal bonding orbitals (s, p, and d) as compared to π and π* orbitals on the acetylene.

Five different situations can reasonably be postulated to occur, A–E. In case A, the metal orbitals lie as high as or above the π* orbitals on the acetylene; in B, the metal orbitals lie between the π and π* orbitals; in C, the metal orbitals are of the same energy as the π orbitals; while in D, the metal orbitals lie below the π orbitals, but are still sufficiently close in energy for a chemically significant bond to be formed. In the fifth case, E, the metal orbitals lie a long way below the acetylene orbitals and no bond is formed.

We may now consider what will happen when we attempt to write bonding and antibonding orbitals using these two sets. In case A, bonding orbitals formed from the metal orbitals and the acetylene π orbitals will have mostly acetylene character, and the antibonding orbitals metal character. As a result, there will be very little transfer of electron density from the acetylene to the metal. However, the bonding and antibonding orbitals formed from the metal and acetylene π* orbitals will both have large amounts of metal and acetylene character and hence "back-donation" of electron density from the metal to the acetylene should be large. The CC bond order will be more than in case B, and the distortion of the acetylene will be somewhat less since it resembles $C_2H_2^-$ rather than the excited state of acetylene (26).

In case B, where the orbitals of the metal lie between the acetylene π and π* orbitals, we may write molecular orbitals combining metal orbitals with both π and π* orbitals so that all orbitals, both bonding and antibonding, will have considerable acetylene and metal character. As a result, there will be significant transfer of electron density from the acetylene π orbitals to the area between the acetylene and the metal and there will also be significant back-bonding from the metal into the π* orbitals of the acetylene. We can expect the metal–acetylene bond order to be very high. Since electron density is effectively being taken from the π and fed into the π* orbitals of the acetylene we would expect the acetylene to assume the shape of the excited state of acetylene. The first excited state is *trans*-bent at about $-50\,000\ cm^{-1}$. However, calculations have shown that there is a *cis*-bent excited state lying at about $-33\,000\ cm^{-1}$ (24, 27) and this is the energy value we have assumed for the π* orbitals, since it is known that the acetylene adopts a *cis*-bent configuration in the complexes. It has been shown that the following parameters are consistent with the observed spectra of free acetylene in the excited *trans*-bent state, ∠HCC = 120°, there is an increase in the CC bond length of 0.18 Å and a corresponding drop in the "C≡C stretch" of about $900\ cm^{-1}$. The calculations of Kroto and Santry (27) predict a value of 142° for ∠HCC in the *cis*-bent state.

In case C, the π orbitals of the acetylene are of the same energy as the metal valence orbitals and bonding will occur; both bonding and antibonding combinations will have considerable amounts of acetylene and metal character. Bonding will be fairly strong since both π orbitals on the acetylene may bond[3], and there will be considerable sharing of the acetylene π electron density between the acetylene and the metal. There is a considerable energy difference between the acetylene π* orbitals and metal orbitals of the correct symmetry, and so interaction between these two will be weak and back-donation of density from the metal to the acetylene π* orbitals will not be large. Therefore the significant part of the bonding will be donation of electron density from the acetylene to the metal.

Case D is also interesting since we postulate that there will be weak interaction between the

[3]It is conventionally assumed that only one π orbital of the acetylene will bond to one metal. However, the possibility that the other π orbital, at right angles to this one, may also have significant overlap with suitable metal orbitals cannot be ignored and may contribute significantly to the total stabilization energy[5].

Can. J. Chem. Downloaded from www.nrcresearchpress.com by 210.87.254.105 on 09/05/12
For personal use only.

Can. J. Chem. Downloaded from www.nrcresearchpress.com by 210.87.254.105 on 09/05/12
For personal use only.

metal and the acetylene. Thus the bonding orbital will have mostly metal character and the antibonding orbital will have mostly acetylene character. As a result the pair of electrons originally on the acetylene will be transferred to the metal, with an effective positive charge being left on the acetylene. It should be difficult to isolate compounds of this type since the bonding will be only dative and hence weak.

In the fifth case E, the orbitals are of such disparate energies that no significant bond is formed.

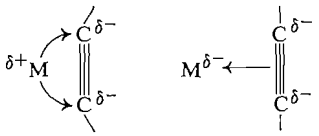

A D

The four cases A–D therefore represent points on a continuum of bond types, the extremes of which may be pictorially depicted as shown. In the limiting case, complexes of type A would be expected to be stabilized by metals in very low oxidation states carrying electron-donating ligands, and by acetylenes bearing electron-withdrawing substituents[4]. Other important characteristics of such complexes include low C≡C bond orders (and hence low $\nu_{C\equiv C}$) and high reactivity towards electrophilic reagents (X^+) at the acetylenic carbons. This description of the bonding in A is somewhat analogous to that implied by structure (**15**) with two M—C σ bonds.

In contrast, complexes whose limiting case is D are expected to be formed by metals in higher oxidation states carrying electronegative ligands and by electron-donating substituents on the acetylene[4]. It is expected that these complexes would be weak and would be susceptible to nucleophilic attack (X^-) at the acetylenic carbons.

It is probable that no complexes can exist which actually correspond to these two extremes. However, the two types of platinum–acetylene complexes known can be described using A and D as models.

The bonding in complexes $RC_2R'PtCl_2L$ (**1**) is closer to D, the metal is in the Pt(II) state but the charge on the metal will not be as great as +2 and we postulate that this complex represents our case C. Chatt discovered that complexes of this type were only stable when at least one substituent (R) was a bulky alkyl group (such as *t*-butyl) and that the acetylene was not greatly perturbed on complexing. This is shown by the low $\Delta\nu_{C\equiv C}$ observed and also from the recent crystal structure of $(Bu^tC_2Bu^t)PtCl_2NH_2C_7H_7$ where $\angle Bu^tCC$ is 165°.

The bonding in L_2MRC_2R' on the other hand is probably closer to the other extreme and we feel is best described by B. The larger $\Delta\nu_{C\equiv C}$ observed for complexes of this type is in agreement with this as are our results that for a given metal $\nu_{C\equiv C}$ is decreased by electron-withdrawing groups (R and R′) and by electron-donating ligands (Table I). For $L_2Pt(CF_3C_2CF_3)$ the order of increasing $\nu_{C\equiv C}$ is $L = Ph_3P < PhMe_2P < n\text{-}Bu_3P$, the expected Lewis basicities of these ligands. The preliminary X-ray crystal structure of $(Ph_3P)_2Pt(PhC_2Ph)$ is also in agreement with this since it shows an appreciable lengthening of the C≡C bond and a large distortion from linearity of the acetylene. The angle PhCC (140°) is in excellent agreement with that predicted for the excited *cis*-bent state of acetylene (27).

Simple symmetry arguments show that the maximum overlap of possible bonding orbitals occurs both in (**1**) and (**2**) when the acetylene is either (*a*) in the coordination plane[5] (case (*i*), π_z with dsp^2, π^*_z with d_{xz}; case (*ii*), π_z with sp^2, π^*_z with d_{xz}) or (*b*), at 90° to it (case (*i*), π_z with dsp^2, π^*_z with d_{yz}; case (*ii*), π_z with sp^2, π^*_z with d_{yz}). It can easily be shown that overlap is poorer when the acetylene makes an angle other than 0 or 90° with the coordination plane.

Either arrangement should therefore be possible for both (**1**) and (**2**). The acetylene is probably constrained to the perpendicular arrangement (*b*) in (**1**) as otherwise the halogen to acetylenic carbon distance would be much less

[4]This argument can also be expressed in terms of electron-withdrawing substituents on the acetylene raising the energies of the π and π* states while electron-releasing substituents lower them.

[5]All these molecules are of C_{2v} or C_2 symmetry. The following conventions are adopted here: the *z* direction is the C_2 axis; the *x* direction is in the plane of the metal and the ligands (other than the acetylene) and perpendicular to *z*; and the *y* direction is orthogonal to *x* and *z*. The π and π* orbitals in the acetylene will be labelled π_n and π^*_n where *n* is the axis perpendicular to the nodal plane.

In addition to the overlap of π_z and π^*_z with the metal orbitals the other acetylenic orbitals π_x and π^*_x (or π_y and π^*_y) will also be able to combine with metal orbitals as follows: arrangement (*b*) cases (*i*) and (*ii*): π_x with d_{xz} or p_x, π^*_x with d_{xz}.

Can. J. Chem. Downloaded from www.nrcresearchpress.com by 210.87.254.105 on 09/05/12
For personal use only.

than the van der Waals contact distance. The near-planar arrangement found in complexes (**2**) may also be caused by steric effects; until full details of the crystal structure are available, however, their importance cannot be assessed. On electronic grounds, the planar arrangement (*a*) would be favored. The M—P σ bonds in (**2**) will involve interaction with the d_{xz} orbital; since this is filled in (**2**), a d^{10} complex, this would result in a destabilization of d_{xz} were it not for the stabilization which this orbital achieves by interaction with the acetylenic π^*_z. Additional stabilization by interaction of π_y and p_y is also possible. Neither of these additional stabilizations can occur in the perpendicular arrangement (*b*)[6].

Very similar arguments can be used to describe the bonding in other types of π complexes, particularly of olefins where the electronic states are very similar to those described here. Thus, two types of platinum–olefin complexes are also known, $(Ph_3P)_2PtC_2(CN)_4$ and $K^+C_2H_4PtCl^-{}_3$.

Few reactions of the first type of olefin complex are known. However, as expected, olefin complexes of the latter type are very susceptible to nucleophilic attack[7],

$$[C_2H_4PdCl_2]_2 + 2OH^- \rightarrow 2CH_3CHO + 2Pd + 2Cl^- + 2HCl$$

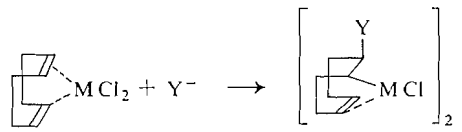

M = Pd, Pt,
Y = OR, CHXCOOR etc.

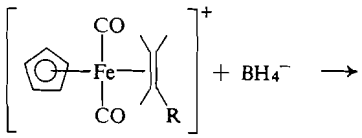

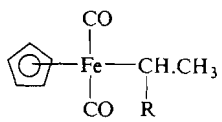

[6]The recently determined crystal structure of $(Ph_3P)_2Ni(C_2H_4)$ (**4**) indicates the presence of strong steric interaction between the ethylenic carbons and the phosphorus atoms (28, 29). Despite this, the complex is still very nearly planar. The small distortion from planarity observed (12°) is presumably due to this. By analogy, the distortion observed in the structures of $(Ph_3P)_2Pt(PhC_2Ph)$ and $[(Ph_3P)_2PtC_2(CN)_4]$ are of similar origin. The forces holding the olefin or acetylene coplanar in these compounds must be very strong indeed.

[7]See refs. 30–32 for the three equations followed.

The Hg(II)-catalyzed hydration of acetylenes may well also proceed by primary nucleophilic attack by H_2O on a Hg(II)–acetylene complex (33). An interesting contrast also exists in the reactivity of cyclobutadiene complexes of d^8 metals which may well be related to the above ideas. Thus complexes of the type $[R_4C_4PdBr_2]_2$ readily undergo nucleophilic attack (to give $[(R_4C_4X)PdBr]_2$) while $R_4C_4Fe(CO)_3$ complexes appear inert to these reactions. However, $H_4C_4Fe(CO)_3$ readily undergoes electrophilic substitution reactions (34).

Just how widely these ideas can be extended is not at present certain but they seem likely to be a useful guideline in predicting stabilities and reactivities of some organometallic π complexes.

Stabilities of the Complexes

On the basis of the foregoing discussion, it seems reasonable to assume that for a series of closely related and structurally similar complexes, $\Delta\nu_{C\equiv C}$ can be used as an indication of the comparative acetylene CC bond orders. The larger $\Delta\nu_{C\equiv C}$, the stronger the bonding of the acetylene to the metal and hence the greater the thermodynamic stability of the complex. For complexes $(R_3P)_2M(R'C_2R'')$ we have shown that for a constant metal M, the effect on $\Delta\nu_{C\equiv C}$ of changes in R, R′, and R″ are as expected. We were also able to investigate the change in $\Delta\nu_{C\equiv C}$ for one series of complexes, $(Ph_3P)_2M(CF_3C_2CF_3)$, with change in M. This gave the rather surprising result (Table I) that the stability of the complexes decreased in the order Pt > Ni > Pd, an order quite different to that generally accepted for the relative stabilities of M—C σ bonds in $(R_3P)_2MR'_2$ which is Pt > Pd > Ni (35).

The reason for this difference in relative stability is not clear, but two points should be made. (1) This reinforces the argument that no true M—C σ bonds are present in the acetylene complexes. (2) Other evidence suggests this order of stability may be quite general for π complexes of transition metals. For example, Bennett *et al.* found that for the complexes (**16**) $\Delta\nu_{C\equiv C}$ decreased in the order M = W > Cr > Mo (36).

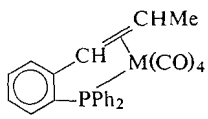

16

17

TABLE III

Analyses of $(R_3P)_2M(ac)$ complexes

Complex	Found C	H	F	P	Mol. wt.	Calcd. C	H	F	P	Mol. wt.
$(Ph_3P)_2NiC_4F_6$ (**5***c*)	64.56	4.07	15.36	8.24	—	64.44	4.06	15.30	8.31	—
$(Ph_3P)_2PdC_4F_6$ (**7***a*)	60.29	3.76	14.88	7.82	770	60.59	3.82	14.37	7.81	793
$(Me_2PhP)_2PdC_4F_6$ (**9**)	43.97	4.08	21.11	11.31	—	44.10	4.07	20.92	11.37	—
$(Bu_3P)_2PdC_4F_6$ (**8**)	49.83	8.04	17.05	—	—	49.96	8.09	16.94	—	—
$(Ph_3P)_2Pd(MeOOC.C)_2$ (**7***b*)	64.71	4.87	—	8.62	763	65.25	4.69	—	8.01	773
$(Ph_3P)_2Pt(PhC_2Me)$ (**2***d*)	64.68	4.74	—	7.61	—	64.73	4.59	—	7.42	—
$(Ph_3P)_2Pt(MeOOC.C)_2$ (**2***c*)	58.00	4.19	—	7.71	852	58.51	4.21	—	7.19	862
$(Bu_3P)_2Pt.C_4F_6$ (**11**)	44.06	7.17	15.31	8.31	764	44.30	7.14	14.95	8.13	762
$(Me_2PhP)_2PtC_4F_6$ (**12**)	37.51	3.73	18.09	9.66	—	37.92	3.50	18.00	9.78	—

Description of the Bonding

In order to facilitate rational consideration of the bonding in these complexes we have proposed writing the formula as shown in **17** (37).

Experimental

Reactions involving air-sensitive compounds were carried out in heavy-walled centrifuge tubes of 30 ml or 40 ml capacity, sealed with butyl-rubber cap liners and crimped bottle caps, the latter having two $\frac{1}{8}$ in. diameter holes drilled in them to accommodate syringe needles. Liquids were introduced and removed by a "Luer-Lok" hypodermic syringe, stopcock, and Gauge 20 6 in. needle assembly. Gases were introduced and removed by Gauge 20 needles fitted with rubber-hose connectors. Solutions were stirred magnetically using 15 mm micro Teflon-coated stirring bars, and solids were separated by centrifuging the tubes in a hand-driven centrifuge. Solids were isolated by removing the liquor with a syringe.

Reagent grade benzene, hexane, toluene, and diethyl-ether were all sodium-dried and saturated with nitrogen before use. Matheson ethylene (C.P. Grade) was used without further purification. Nitrogen (Purified Grade) was deoxygenated by passage through a vanadium(II) solution and then dried by concentrated sulfuric acid and anhydrous silica gel. Triethylaluminium was purchased from Texas Alkyls Inc. as a 10% solution in *n*-hexane and was used as received.

Infrared spectra were measured on a Perkin–Elmer 521 spectrophotometer, 60 Mc p.m.r. spectra on a Varian A-60 spectrometer, 100 Mc p.m.r. spectra on a Varian HR-100 (kindly determined by Professor W. T. Reynolds, of the University of Toronto) and ^{19}F n.m.r. spectra on a Varian H-60 spectrometer. Air-sensitive samples were made up under nitrogen. Tetramethylsilane or benzene were used as internal standards for p.m.r. spectra and benzotrifluoride for ^{19}F n.m.r. spectra.

Molecular weights were determined osmometrically in chloroform on a Mechrolab osmometer. Analytical data on the complexes are given in Table III.

Melting points were determined in evacuated capillaries.

Ethylenebis(triphenylphosphine)nickel (4)

Particular care was taken to exclude air from all solvents and apparatus used in the preparation of these complexes. Bis(acetylacetonato)nickel (11) was dried for 24 h at 110°/0.1 mm.

Bis(acetylacetonato)nickel (**3**) (1.0 g, 3.9 mmoles), and triphenylphosphine (2.0 g, 7.6 mmoles) were dissolved in ether (10 ml) and the green solution saturated with ethylene at 0°. To this stirred solution was then added an excess of triethylaluminium (7 ml of a 10% solution in hexane) over a period of 30 min; a vigorous effervescence occurred, the solution became brown, then yellow, and after 1 h yellow crystals began to form. Stirring was continued at 0° for 24 h, and the yellow crystalline material was then separated from the red liquor, washed three times with ethylene-saturated ether, and finally dried under a rapid stream of ethylene to give 2.02 g (85%) of yellow ethylenebis(triphenylphosphine)nickel (**4**).

Diphenylacetylenebis(triphenylphosphine)nickel (5a)

To 15 ml of benzene containing 2.0 g (3.3 mmoles) of ethylenebis(triphenylphosphine)nickel was added a solution of diphenylacetylene (0.90 g, 5 mmoles) in 5 ml of benzene. A steady evolution of gas occurred. After stirring at 25° for 30 min, 15 ml of *n*-hexane was added, the solution cooled to 10°, and the yellow crystalline diphenylacetylenebis(triphenylphosphine)nickel (**5***a*), isolated in 80% yield. The product was moderately stable at room temperature under nitrogen, but was immediately decolorized upon contact with air. It was too unstable for an analysis to be made. However, the close similarity of its infrared spectrum to that of diphenylacetylenebis(triphenylphosphine)platinum supported its identification as diphenylacetylenebis(triphenylphosphine)nickel.

Methylphenylacetylenebis(triphenylphosphine)nickel (5b)

This was prepared in a manner analogous to the above, but substituting methylphenylacetylene (0.70 g, 6 mmoles) for diphenylacetylene. The yellow crystalline complex (**5***b*) which was obtained in 80% yield was moderately stable at 25° under nitrogen, but was rapidly decolorized by air. The compound was too unstable for an analysis to be made, but the close similarity of its infrared and n.m.r. spectra to those of methylphenylacetylenebis(tri-

Can. J. Chem. Downloaded from www.nrcresearchpress.com by 210.87.254.105 on 09/05/12
For personal use only.

Can. J. Chem. Downloaded from www.nrcresearchpress.com by 210.87.254.105 on 09/05/12
For personal use only.

phenylphosphine)platinum again indicated that the product was methylphenylacetylenebis(triphenylphosphine)-nickel.

Hexafluoro-2-butynebis(triphenylphosphine)nickel (5c)

Hexafluoro-2-butyne (ca. 4 g) was condensed into a trap at −78°. The liquid was allowed to warm up and the gas then passed into a vigorously stirred solution 2.2 g (3.6 mmoles) of ethylenebis(triphenylphosphine)-nickel in 20 ml of benzene at 25°. A rapid evolution of gas occurred, and yellow crystals began to form after 10 min. Crystallization was completed by the addition of 15 ml of *n*-hexane and cooling to 10°. The crystals were separated from the liquor and recrystallized from methylene chloride – methanol to give 1.3 g (48%) of yellow hexafluoro-2-butynebis(triphenylphosphine)nickel (**5c**), m.p. 221–222° (decomp.).

Tetrakis(triphenylphosphine)palladium (6)

The preparation and recrystallization of all palladium complexes was carried out in an atmosphere of nitrogen.

Method (a)

To a stirred suspension of *trans*-dichlorobis(triphenylphosphine)palladium (0.7 g, 1 mmole) in 30 ml of ethanol and triphenylphosphine (0.52 g, 2 mmoles) at 40°, was added 2 ml of anhydrous hydrazine. The pale cream suspension slowly became light green in color, and after stirring for 45 min, the mixture was cooled and 0.9 g (80%) of the product, tetrakis(triphenylphosphine)-palladium, isolated under nitrogen, m.p. 190–195° (decomp.).

Method (b)

A solution of bis(acetylacetonato)palladium (11) (0.92 g, 3 mmoles) and triphenylphosphine (3.2 g, 12 mmoles) in 15 ml of ether was cooled to 0°. A 10% solution of triethylaluminium (7 ml) in hexane was added, and the mixture stirred for 3 h. The yellow solid was then separated and washed three times with ether to give 3.1 g (90%) of pale yellow crystals of tetrakis(triphenylphosphine)palladium, m.p. 194–196° (decomp.).

This was the method generally used for the preparation of this complex.

Hexafluoro-2-butynebis(triphenylphosphine)palladium (7a)

Tetrakis(triphenylphosphine)palladium (**6**) (1.05 g, 1 mmole) and hexafluoro-2-butyne (ca. 5 g) in 20 ml of methylene chloride were stirred for 30 min at 25° under a −78° reflux condenser. Methanol (15 ml) was then added to the pale yellow solution, and the methylene chloride removed on a rotary evaporator to give a grey precipitate. This was recrystallized from methylene chloride – methanol and washed with a little ether to give 0.4 g (50%) of colorless crystals of hexafluoro-2-butynebis(triphenylphosphine)palladium (**7a**), m.p. 194–195° (decomp.).

Dimethylacetylenedicarboxylatebis(triphenylphosphine)-palladium (7b)

This was prepared in a manner analogous to the above, but substituting dimethylacetylenedicarboxylate (0.84 g, 6 mmoles) for hexafluoro-2-butyne. Recrystallization from methylene chloride – methanol gave the white crystalline complex (**7b**) (0.45 g, 58%), m.p. 195–196° (decomp.). In the solid, the product slowly turned yellow on exposure to air; more rapid decomposition occurred in solution.

Hexafluoro-2-butynebis(tri-n-butylphosphine)palladium (8)

Hydrazine (2 ml) in 5 ml of ethanol was added to a solution of *trans*-dichlorobis(tri-*n*-butylphosphine)palladium (0 59 g, 1 mmole) and tributylphosphine (0.40 g, 2 mmoles) in 20 ml of ethanol. A gas was evolved and the yellow color of the solution became less intense. The solution was allowed to cool to 25°, hexafluoro-2-butyne (ca. 5 g) passed into it, and stirring continued under a −78° reflux condenser for 1 h. Water (15 ml) was then added, and after the solution had been standing at 0° for 24 h, the product (**8**) was obtained as white crystals (0.37 g, 55%), m.p. 34–36° (decomp.).

Hexafluoro-2-butynebis(dimethylphenylphosphine)-palladium (9)

This was prepared in a manner analogous to the above, but substituting *trans*-dichlorobis(dimethylphenylphosphine)palladium (0.45 g, 1 mmole) for *trans*-dichlorobis-(tri-*n*-butylphosphine)palladium and dimethylphenylphosphine (0.28 g, 2 mmoles) for tributylphosphine. The crude product was crystallized, with difficulty, from aqueous methanol to give white crystals of (**9**) (0.090 g, 16%), m.p. 118–119° (decomp.).

Diphenylacetylenebis(triphenylphosphine)platinum (2a)

All platinum complexes were prepared under nitrogen, but the subsequent workup was performed in open vessels.

A solution of hydrazine (2 ml) in 5 ml of ethanol was added to a stirred suspension of *cis*-dichlorobis(triphenylphosphine)platinum (0.79 g, 1 mmole) in 15 ml of ethanol at 45°. A gas was evolved and the suspension dissolved to give an intense yellow solution, from which yellow crystals rapidly separated. After stirring for 30 min, an ethanolic solution of diphenylacetylene (0.72 g, 4 mmoles) was added. A further evolution of gas occurred, and the yellow suspension dissolved to give a pale yellow solution. Water (50 ml) was added, and the solution allowed to stand for 12 h at 0°. The white crystals which had formed were filtered off, washed with a little aqueous ethanol, and recrystallized from 95% ethanol to give the white crystalline product (0.52 g, 58%), m.p. 161–164° (decomp.), identical to that of an authentic sample provided by Dr. C. D. Cook of University of Toronto.

Methylphenylacetylenebis(triphenylphosphine)platinum (2d)

This was prepared in a manner analogous to the above but substituting methylphenylacetylene (0.70 g, 6 mmoles) for diphenylacetylene. Recrystallization from methylene chloride – methanol under nitrogen, gave the cream colored crystalline product (0.70 g, 84%), m.p. 176–178° (decomp.), with a color change from cream to red at 153–155°.

Hexafluoro-2-butynebis(triphenylphosphine)platinum (2b)

Method (a)

A solution of 2 ml of hydrazine in 5 ml of ethanol was added to 15 ml of a stirred ethanolic suspension of *cis*-dichlorobis(triphenylphosphine)platinum (0.79 g, 1 mmole) at 45°. After 30 min, the solution was cooled to 25°

Can. J. Chem. Downloaded from www.nrcresearchpress.com by 210.87.254.105 on 09/05/12
For personal use only.

and the yellow crystals which had formed were isolated and dissolved in benzene (20 ml) under nitrogen. Hexafluoro-2-butyne (ca. 5 g) was added and the solution stirred at 25° under a −78° reflux condenser for 4 h. *n*-Hexane (10 ml) was added and the white solid filtered off. Recrystallization from methylene chloride – methanol gave 0.48 g (54%) of the white crystalline product, m.p. 212–214° (lit. (8) 215–216°).

Method (b)

Hexafluoro-2-butynebis(triphenylphosphine)platinum was also prepared (in 60% yield) in a manner analogous to that used to prepare hexafluoro-2-butynebis(triphenylphosphine)palladium, but using tetrakis(triphenylphosphine)platinum (**10**) (35) instead of tetrakis(triphenylphosphine)palladium (**6**).

Dimethylacetylenedicarboxylatebis(triphenylphosphine)-platinum (2c)

This was prepared in a manner analogous to method (*b*) above, but substituting dimethylacetylenedicarboxylate (0.57 g, 4 mmoles) for hexafluoro-2-butyne. The grey solid obtained from the reaction was recrystallized from methylene chloride – methanol to give the white crystalline complex (**2c**) (0.50 g, 58%), m.p. 188–190° (decomp.).

Hexafluoro-2-butynebis(tri-n-butylphosphine)platinum (11)

A solution of 0.42 g (1 mmole) of potassium tetrachloroplatinate(II) in 5 ml of water was added to a solution of 0.112 g (2 mmoles) of potassium hydroxide and 1.01 g (5 mmoles) of tri-*n*-butylphosphine in 5 ml of ethanol. The solution was stirred at 25° for 30 min, a small quantity of metallic platinum was filtered off under nitrogen, the solution was transferred to a flask fitted with a −78° reflux condenser, and hexafluoro-2-butyne (ca. 5 g) was passed into it. After stirring for 4 h water (10 ml) was added to give a fine white crystalline precipitate. Recrystallization from aqueous methanol gave 0.23 g (30%) of white crystals of hexafluoro-2-butynebis(tri-*n*-butylphosphine)platinum, m.p. 53–54° (decomp.). Hexafluoro-2-butynebis(dimethylphenylphosphine)platinum, m.p. 141–142° was prepared in a similar manner in 6% yield.

Chloro(dichloromethyl)bis(triphenylphosphine)platinum (13)

A benzene solution of 0.42 g (0.5 mmole) of methylphenylacetylenebis(triphenylphosphine)platinum and 1.5 g (8 mmoles) of chloroform was stirred at 25° for 48 h under nitrogen. A yellow crystalline precipitate formed slowly which was filtered off and shown to be chloro(dichloromethyl)bis(triphenylphosphine)platinum (**13**) (0.28 g, 68%), m.p. 248–266°.

Anal. Calcd. for $C_{37}H_{31}Cl_3P_2Pt$: C, 53.60; H, 3.76; Cl, 12.83; P, 7.47. Found: C, 53.48; H, 3.74; Cl, 12.40; P, 7.45.

Acknowledgments

We thank the National Research Council of Canada for supporting this work, Johnson, Matthey, and Mallory for the loan of palladium and platinum compounds, and M and T Chemicals for gifts of phosphines. We should also like to express our appreciation to Drs. R. J. Gillespie and R. A. Bell for their help in interpreting the n.m.r. spectra, and to Professor R. Mason for helpful discussion.

1. J. Chatt, L. A. Duncanson, and R. G. Guy. Chem. Ind. London, 430 (1959). J. Chem. Soc. 827 (1961).
2. J. Chatt, R. G. Guy, L. A. Duncanson, and D. T. Thompson. J. Chem. Soc. 5170 (1963).
3. J. Chatt, G. A. Rowe, and A. A. Williams. Proc. Chem. Soc. 208 (1957).
4. G. R. Davies, W. Hewertson, R. H. B. Mais, and P. G. Owston. Chem. Commun. 423 (1967).
5. R. R. H. Alderman, P. G. Owston, and J. M. Rowe. Acta Cryst. **13**, 149 (1960).
6. J. O. Glanville, J. M. Stewart, and S. O. Grim. J. Organometal. Chem. Amsterdam, **7**, 9 (1967).
7. G. Wilke and G. Herrmann. Angew. Chem. **74**, 693 (1962).
8. J. L. Boston, S. O. Grim, and G. Wilkinson. J. Chem. Soc. 3468 (1963).
9. A. T. Blonquist and P. M. Maitlis. J. Am. Chem. Soc. **84**, 2329 (1962).
10. P. M. Maitlis, D. Pollock, M. L. Games, and W. J. Pryde. Can. J. Chem. **43**, 470 (1965).
11. R. G. Charles and M. A. Pawlikowski. J. Phys. Chem. **62**, 440 (1958).
12. A. D. Allen and C. D. Cook. Can. J. Chem. **42**, 1063 (1964).
13. G. C. Dobinson, R. Mason, G. B. Robertson, R. Ugo, F. Conti, D. Morelli, S. Cenini, and F. Bonati. Chem. Commun. 739 (1967).
14. J. M. Jenkins and B. L. Shaw. Proc. Chem. Soc. 279 (1963); J. A. Osborn, F. H. Jardine, J. F. Young, and G. Wilkinson. J. Chem. Soc. A, 1711 (1966).
15. C. D. Cook and G. S. Jauhal. Can. J. Chem. **45**, 301 (1967).
16. R. Ugo, F. Cariati, and G. Lamonica. Chem. Commun. 868 (1966).
17. J. W. Emsley, J. Feeney, and L. H. Sutcliffe. High resolution N.M.R. spectroscopy. Vol. 1. The Pergamon Press, Ltd., Oxford. 1965. p. 488.
18. J. Chatt. Chimica inorganica. Accad. Nazl. Lincei, Roma. 1961. p. 113.
19. G. W. Parshall and F. N. Jones. J. Am. Chem. Soc. **87**, 5356 (1965).
20. M. J. Mays and G. Wilkinson. J. Chem. Soc. 6629 (1965).
21. J. P. Collman and J. W. Kang. J. Am. Chem. Soc. **89**, 844 (1967).
22. C. Pannatoni, G. Bombieri, V. Belluco, and W. H. Baddley. J. Am. Chem. Soc. **90**, 798 (1968).
23. J. A. McGinnety and J. A. Ibers. Chem. Commun. 235 (1968).
24. H. Howard and G. W. King. Can. J. Chem. **37**, 700 (1959).
25. C. E. Moore. Atomic energy levels. Natl. Bur. Stds. Circ. 467. Washington D.C. 1952.
26. A. C. Blizzard and D. P. Santry. J. Am. Chem. Soc. **90**, 5749 (1968).
27. H. W. Kroto and D. P. Santry. J. Chem. Phys. **47**, 792 (1967).
28. W. Dreissis and H. Dietrich. Acta Cryst. **B24**, 108 (1968).
29. C. D. Cook, C. H. Koo, S. C. Nyburg, and M. T. Shiomi. Chem. Commun. 426 (1967).
30. A. Aguilo. Advan. Organometal. Chem. **5**, 321 (1967).

31. J. CHATT, L. M. VALLARINO, and L. M. VENANZI. J. Chem. Soc. 2496, 3413 (1957).
32. M. L. H. GREEN and P. L. I. NAGY. J. Organometal. Chem. Amsterdam, **1**, 58 (1963).
33. F. BASOLO and R. G. PEARSON. Mechanisms of inorganic reactions. 2nd ed. John Wiley and Sons, Inc., New York. 1967. p. 600.
34. P. M. MAITLIS. Advan. Organometal. Chem. **4**, 130, 140 (1966).
35. J. CHATT. Record Chem. Progr. Kresge-Hooker Sci. Lib. **21**, 147 (1960).
36. M. A. BENNETT, L. V. INTERRANTE, and R. S. NYHOLM. Z. Naturforsch. **20***b*, 633 (1965).
37. E. O. GREAVES and P. M. MAITLIS. J. Organometal. Chem. Amsterdam, **6**, 104 (1966).
38. F. A. MILLER and R. P. BAUMANN. J. Chem. Phys. **22**, 1544 (1954).
39. R. TSUMURA and N. HAGIHARA. Bull. Chem. Soc. Japan, **38**, 861 (1965).
40. L. MALATESTA and C. CARIELLO. J. Chem. Soc. 2328 (1958).
41. E. O. GREAVES and P. M. MAITLIS. J. Organometal. Chem. Amsterdam, **6**, 104 (1966).
42. E. O. GREAVES, R. BRUCE, and P. M. MAITLIS. Chem. Commun. 860 (1967).

Can. J. Chem. Downloaded from www.nrcresearchpress.com by 210.87.254.105 on 09/05/12
For personal use only.

Physical nature of the chemical bond. III. A quasi-optimized l.c.G.t.o.-m.o.-s.c.f. wavefunction for the neon hydride ion

J. B. MOFFAT
Department of Chemistry, University of Waterloo, Waterloo, Ontario
Received June 19, 1968

Quasi-optimized wavefunctions for the neon hydride positive ion (NeH^+) have been obtained for various sizes of basis sets of Gaussian orbitals. The effect of varying the size of basis set and the exponents has been examined.

Canadian Journal of Chemistry, 46, 3893 (1968)

Can. J. Chem. Downloaded from www.nrcresearchpress.com by 210.87.254.6 on 09/05/12
For personal use only.

Previous reports (1) of the research in quantum chemistry in this laboratory have been largely concerned with studies of nitriles. Particular attention has been given to various means for obtaining wavefunctions for nitrile molecules, both large and small. Recently the work has turned toward an analysis of the nature of the nitrile bond (2). This has been done for various reasons, some of which have been discussed previously (2). However, an additional purpose for such analysis rests on the potential applicability of such methods to the testing of the accuracy of wavefunctions. The previous paper in the present series (3) was concerned with the helium hydride positive ion. The present report on the neon hydride positive ion provides another set of wavefunctions covering a range of accuracy for the next largest molecule in the inert gas hydride ion series.

The present paper is intended to provide wavefunctions for later testing as a function of the size of basis set. The molecule NeH^+ was chosen because of its relationship to the HeH^+ molecule, and for the secondary reason that very few quantum chemical calculations on NeH^+ have been reported in the literature. No previous calculations on NeH^+ with Gaussian orbitals have been found.

It is well known that calculations with Slater orbitals require smaller basis sets than those with Gaussian orbitals to achieve the same accuracy of results. Substantial efforts have been made to either circumvent or at least diminish this problem with Gaussian orbitals. Clementi (4), using a method of contracted basis sets of Gaussian orbitals, has studied a number of large molecules, including pyrrole, pyridine, and pyrazine. The alternative approach with Gaussian orbitals has been to perform calculations on large molecules using basis sets which are relatively small, at least from the standpoint of number of functions per number of electrons. Moskowitz and co-workers (5) have applied this technique to ethylene and benzene. Of course, it is assumed that these wavefunctions, built from small numbers of basis functions, will represent most of the molecular properties reasonably well.

It appeared to be of interest to determine to what extent some optimization of exponents could improve these wavefunctions obtained with small basis sets. The technique of optimization used here, which is being called "quasi-optimization", involves two variables, the value of the smallest exponent in either or both of the S and P type functions, and the multiplicative factor which operated to generate the remainder of the particular set of exponents. The assumption was thus made that the exponents in any given S or P series form a geometrical progression. The advantage of this simplification was of course, that optimization by means of varying each exponent, one at a time, was avoided. In its place, the statement of the value of the initial exponent and the multiplicative factor was sufficient to define the entire set of exponents. It is not claimed that this technique is as satisfactory as the more laborious one, but rather that what may be referred to as a "quasi-optimized" function is hopefully produced in a minimum of calculations. Further it seemed reasonable to test both the effect of optimizing the smaller basis and the method of optimizing itself, on molecules small enough so that reasonably accurate results could be obtained with larger basis sets for comparison purposes. There is surprisingly little work reported in the literature on the consequences of optimizing wavefunctions of smaller basis sets of Gaussian orbitals.

TABLE I

Recent calculations on the ground $^1\Sigma$ state of NeH^+

Method	R_e (a.u.)	$-E$ (a.u.)	k (10^5 dyne cm^{-1})	Reference
Modified Platt electrostatic model	1.53	—	5.52	8
United atom	2.33	127.5703	0.17	7
Two-center Hartree–Fock–Roothaan	1.83	128.6284	5.29	6
Self consistent field Gaussian orbitals	1.90	128.6029	—	Present work

Finally, it was hoped that at some later time semi-empirical correlations between the best exponent values for various molecules might be obtained which would be capable of extrapolation to other molecules not originally considered.

The first observation of rare-gas hydride ions was made in mass spectrometers. Because of their short lifetime it is of some interest to obtain accurate wavefunctions for these ions.

The most accurate calculation on NeH^+ appears to be that of Peyerimhoff (6) who obtained a Hartree–Fock–Roothaan wavefunction using a basis set of 24 Slater-type orbitals (S.t.o.) centered on the nuclei. More recently, Banyard and Sutton (7) performed a united-atom (u.a.) calculation on NeH^+ but their results were disappointingly poor, although interesting from the standpoint of providing information on the u.a. method. The only other report of theoretical work on NeH^+ is that of Moran and Friedmann (8) using Platt's electrostatic model. A summary of the results of these previous workers together with the best value obtained in the present work is given in Table I.

Method

The Gaussian basis set calculations have been performed using the Roothaan self-consistent-field (s.c.f.) method (9) as described previously (1). A brief survey of earlier work involving Gaussian basis sets has been given (1) and need not be repeated here. The basis sets employed in the present work contained S- and P_q-type Gaussian functions, of the form $N \exp(-\alpha r^2)$ and $Nq \exp(-\alpha r^2)$, respectively, where q may be x, y, or z. The bond in NeH^+ was taken to be directed along the x-axis with the neon atom at the origin. Internuclear distances between 1.45 and 2.00 bohr were employed in the present work, so as to cover the range of values for R_e found by most of the previous workers, although the united atom work mentioned earlier had predicted a value of 2.33. The number of S, P_x, P_y, and P_z functions of neon are denoted by the first four figures, respectively, those of hydrogen by the second four figures, respectively, in the labelling used with the tables. The basis sets contained 2, 4, 9, 11, 17, 21, 31, 37, or 41 functions, but most of the work was done with the last three sizes mentioned. Two variables were employed in the quasi-optimization technique, the value of the smallest exponent in either or both of the S and P type functions, and the multiplicative factor which was used to generate the remainder of the particular set of exponents. Only the exponents for neon were varied. The exponents employed for hydrogen were those of Reeves (10).

Results and Discussion

Approximately 100 calculations were performed on the positive neon hydride molecular ion. Only the results for the largest three basis sets are reported here. Other results may be obtained from the author. All calculations have been iterated to an accuracy of 10^{-4} hartree. Table II lists the values of the initial exponents and the multiplicative factors used in the present work. Table III shows the calculated values of electronic energy for the three largest basis sets used and for various sets of exponents.

Table III shows that the basis set of 31 functions (9555/4300) is the smallest set, of those basis sets employed, which yields a reasonably good energy value. The 31 function set appears to yield a minimum energy at $R = 1.90$ bohr, as do the 37 function and 41 function sets, in contrast with the results found earlier for HeH^+ using Gaussian functions (3), where the value of R_e appeared to depend on the size of basis set.

Table III further illustrates, at least for $R = 1.90$ bohr, that the exponents labelled NeS12, NeP4, produced the lowest energy values with the 37-function set (9555/4333). These exponents are those which were used by Huzinaga (11) in calculations on neon with a similarly sized basis set. Exponents NeS10, NeP3 are those employed by Harrison (12) in his earlier work on neon with a basis set consisting of 9s and 5p functions. With Harrison's exponents, the present 37-function set yields an energy value approximately 0.02 hartree higher than with Huzinaga's exponents, for NeH^+ at $R = 1.90$ bohr. Approx-

Can. J. Chem. Downloaded from www.nrcresearchpress.com by 210.87.254.6 on 09/05/12
For personal use only.

Can. J. Chem. Downloaded from www.nrcresearchpress.com by 210.87.254.6 on 09/05/12
For personal use only.

TABLE II

Neon atom exponents

S exponents			P exponents		
Exponent set number	Initial exponent	Multiplying factor	Exponent set number	Initial exponent	Multiplying factor
NeS1	0.0280	3.143	NeP1	0.0160	3.438
NeS2	0.3000	3.000	NeP2	0.2567	3.059
NeS3	0.3000	4.000	NeP3	0.3300	3.455
NeS4	0.3500	3.000	NeP4	0.3444	3.493
NeS5	0.4000	3.000	NeP5	0.3500	3.500
NeS6	0.4000	3.200	NeP6	0.3500	4.000
NeS7	0.4000	4.000	NeP7	0.4000	3.500
NeS8	0.4063	3.054	NeP8	0.4000	4.000
NeS9	0.4200	3.200	NeP9	0.5000	3.470
NeS10	0.4400	3.182	NeP10	0.5780	5.173
NeS11	0.4400	4.000			
NeS12	0.4468	3.338			
NeS13	0.4500	3.500			
NeS14	0.4600	3.000			
NeS15	0.4710	3.949			
NeS16	0.5000	3.000			
NeS17	0.5000	3.160			

TABLE III

Effect of changes of exponents on the total energy of NeH^+ at various interatomic distances and for various basis sets of Gaussian functions

Size of basis set	Exponent set numbers	−Total energy (hartree) at interatomic distance of						
		1.70	1.80	1.83	1.85	1.87	1.90	2.00
31	NeS10, NeP3	128.5577	128.5641	128.5652	—	—	128.5664	128.5660
37	NeS10, NeP3	128.5616	128.5677	128.5686	—	—	128.5696	128.5688
37	NeS11, NeP4	—	—	—	—	—	128.5179	—
37	NeS12, NeP4	128.5791	128.5850	128.5860	—	—	128.5870	128.5864
37	NeS12, NeP5	—	—	—	—	—	128.5838	—
37	NeS12, NeP6	—	—	—	—	—	128.5622	—
37	NeS12, NeP7	—	—	—	—	—	128.5834	—
37	NeS12, NeP8	—	—	—	—	—	128.5608	—
37	NeS13, NeP4	—	—	—	—	—	128.5715	—
37	NeS14, NeP4	—	—	—	—	—	128.5671	—
37	NeS16, NeP4	—	—	—	—	—	128.5700	—
41	NeS3, NeP2	—	—	—	—	—	128.5439	—
41	NeS4, NeP2	—	—	—	—	128.5949	—	—
41	NeS5, NeP2	—	—	—	—	—	128.5960	—
41	NeS6, NeP2	—	—	—	—	—	128.5950	—
41	NeS7, NeP2	—	—	—	—	—	128.5343	—
41	NeS8, NeP2	128.5943	—	128.6017	128.6022	128.6026	128.6029	128.6023
41	NeS9, NeP2	—	—	—	—	—	128.5953	—

imately the same energy difference exists between the results of Harrison (12) and of Huzinaga (11) for neon using the same size of basis set.

The lowest value of energy for NeH^+ found in the present work is −128.6029 hartree at $R = 1.90$ bohr. This was obtained with the 41-function set (10,666/4333). This is 0.0255 hartree above Peyerimhoff's lowest value which was found at $R = 1.83$ bohr. Of those sets of exponents tested with the 41-function set, Huzinaga's (11) exponents again yielded the "best" value. Of course, in all the present work it is not impossible that

Can. J. Chem. Downloaded from www.nrcresearchpress.com by 210.87.254.6 on 09/05/12
For personal use only.

TABLE IV

Gaussian orbital wavefunction for the ground state of NeH^+ ($1\sigma^2 2\sigma^2 3\sigma^2 1\Pi^4$, $^1\Sigma^+$) at $R = 1.90$ bohr*

Basis function	$C_{1\sigma,K}$	$C_{2\sigma,K}$	$C_{3\sigma,K}$	$C_{1\pi,K}$
Ne: S	0.003952	−0.370895	−0.149500	
S	−0.007854	−0.633112	−0.088610	
S	0.057669	−0.099096	−0.031476	
S	0.376341	0.185006	0.034468	
S	0.422150	0.133542	0.020678	
S	0.212098	0.054920	0.009280	
S	0.070125	0.016971	0.002676	
S	0.017321	0.004073	0.000674	
S	0.003236	0.000757	0.000121	
S	0.000409	0.000095	0.000016	
Ne: P	0.000524	0.002737	0.096627	0.168479
P	0.000167	−0.049357	0.396839	0.436800
P	−0.000122	−0.026625	0.337615	0.374614
P	0.000598	−0.013651	0.178005	0.199314
P	0.000541	−0.003947	0.052681	0.058407
P	0.000055	−0.000634	0.007950	0.008841
H: S	−0.000713	0.003151	0.016074	
S	−0.000595	−0.047194	0.217689	
S	0.000153	−0.028828	0.067007	
S	−0.000035	−0.003586	0.009179	
H: P	−0.000125	0.004022	−0.008562	0.004410
P	0.000334	−0.010506	0.029674	−0.010135
P	0.000480	0.016884	−0.073126	0.031993

*Obtained with a basis set of 41 functions.

TABLE V

Orbital energies for the ground state of NeH^+ as obtained with various sets of Gaussian orbitals and as compared with those from the work of Peyerimhoff (6) ($R = 1.83$ bohr)

	Orbital energies (hartree)			
	Number of Gaussian orbitals			Number of Slater orbitals (6)
	31	37	41	24
1σ	−33.3511	−33.3629	−33.3583	−33.33881
2σ	−2.5096	−2.5127	−2.5098	−2.49750
3σ	−1.4566	−1.4610	−1.4591	−1.45857
1π	−1.3880	−1.3935	−1.3916	−1.38468
Sigma-Pi gap	0.0686	0.0675	0.0675	0.07389
Pi-Pi* gap[a]	1.1291	1.1370	1.1354	
Total energy	−128.5652	−128.5860	−128.6017	−128.62836

[a]Pi* refers to the first unoccupied Pi orbital.

only relative minima have been found. However, it is believed, based on the energy values obtained, that this is not likely.

Table IV shows the molecular orbital coefficients found for the Gaussian wavefunction at $R = 1.90$ bohr with the 41-function set. Comparison of these with those found by Huzinaga (11) for the neon atom shows a marked similarity, as would be expected.

Table V illustrates the change in orbital energies with increasing size of basis set and compares the orbital energies obtained with Gaussian functions with those found by Peyerimhoff (6) using Slater functions. The separation between σ and π orbitals together with the separation between the occupied and unoccupied π orbitals is also shown. It is readily seen that the sigma–pi gap found with any of the Gaussian sets differs substantially

from that found with the Slater set by Peyerimhoff. This results, of course, from the relatively large difference in π orbital energies for Gaussian and Slater sets.

Table VI illustrates variation of the distance of the center of negative charge from the neon nucleus with R for the 41-function set. Again a substantial difference exists between the Gaussian value and the Slater value, at least for $R = 1.83$ bohr.

TABLE VI

Distance x of the center of negative charge from the Ne-nucleus for different internuclear distance R

R (bohr)	Basis set of 41 G.t.o.	Basis set of 24 S.t.o. (6)
1.70	0.05093	—
1.83	0.05137	0.0604
1.85	0.05136	—
1.87	0.05135	—
1.90	0.05129	—
2.00	0.05138	—

In conclusion, the best Gaussian wavefunctions for NeH^+ obtained in this work were calculated using a 41-function set and the exponents from the earlier work of Huzinaga (11) on neon. It is apparently possible to represent the wavefunction adequately using a 31-function basis set.

Acknowledgments

The generous cooperation of the Computing Center at the University of Waterloo and the financial assistance of the National Research Council of Canada are gratefully acknowledged. The technical assistance of L. Scott is greatly appreciated.

1. See, for example, J. B. MOFFAT and R. J. COLLENS. Can. J. Chem. **45**, 655 (1967), and references therein.
2. J. B. MOFFAT and H. E. POPKIE. Int. J. Quantum Chem. **11**, 565 (1968).
3. J. B. MOFFAT. Theoret. Chim. Acta, **10**, 447 (1968).
4. E. CLEMENTI. J. Chem. Phys. **46**, 4725 (1967); **46**, 4731 (1967); **46**, 4737 (1967).
5. J. M. SCHULMAN and J. W. MOSKOWITZ. J. Chem. Phys. **47**, 3491 (1967); **43**, 3287 (1965); J. W. MOSKOWITZ and M. C. HARRISON. J. Chem. Phys. **42**, 1726 (1965); J. M. SCHULMAN, J. W. MOSKOWITZ, and C. HOLLISTER. J. Chem. Phys. **46**, 2759 (1967).
6. S. PEYERIMHOFF. J. Chem. Phys. **43**, 998 (1965).
7. K. E. BANYARD and A. SUTTON. J. Chem. Phys. **46**, 2143 (1967).
8. T. F. MORAN and L. FRIEDMAN. J. Chem. Phys. **40**, 860 (1964).
9. C. C. J. ROOTHAAN. Rev. Mod. Phys. **23**, 69 (1951).
10. C. M. REEVES. J. Chem. Phys. **39**, 1 (1963).
11. S. HUZINAGA. J. Chem. Phys. **42**, 1293 (1965).
12. M. C. HARRISON. J. Chem. Phys. **41**, 495 (1964).

Can. J. Chem. Downloaded from www.nrcresearchpress.com by 210.87.254.6 on 09/05/12
For personal use only.

Diffusive and convective flow in a hydrogen-atom flow system

PHILIP B. RUDNICK AND SIDNEY TOBY
School of Chemistry, Rutgers, The State University, New Brunswick, New Jersey 08903
Received April 10, 1968

Diffusive and convective flow was studied in a hydrogen-atom flow system using an isothermal calorimetric detector. By varying detector area, total pressure, and linear flow rate, the importance of axial diffusion in the system was investigated. Under conditions of predominantly diffusive flow, signal–distance plots were independent of flow rate. When convective flow predominated, concentration–time plots were independent of flow rate. The efficiency of a detector was clearly dependent on its surface area within wide limits, but diffusion gradients produced by the presence of even large detectors did not appear to be important.

Canadian Journal of Chemistry, 46, 3899 (1968)

Can. J. Chem. Downloaded from www.nrcresearchpress.com by 210.87.254.40 on 09/05/12
For personal use only.

Introduction

The equation describing the flow and recombination of atoms in a flow system (1) is

$$[1] \qquad D\nabla^2 c - V_f(\partial c/\partial x) - \sum^n k_n c^n = 0$$

where D is the interdiffusion coefficient, V_f is the convective flow rate, x is the axial distance, and k_n is the rate constant of order n. The atom concentration c is often measured by the use of an isothermal calorimetric detector (2–5). Wise and co-workers (6, 7) have discussed the effects of diffusion and detector perturbation. However, diffusion effects are often assumed to be negligible, even for H-atom systems (8–10).

There does not appear to be in the literature any systematic attempt to measure directly the relative contributions of mass and diffusive flow in an atom flow system other than some isolated experiments of Shaw (11) and of Wood, Mills, and Wise (12). The present work describes experiments in which pressure and flow rate were systematically varied. The data presented are insufficiently precise for detailed evaluation of kinetic recombination constants, but the results clearly delineate regions of predominantly diffusive and convective flow. The conditions for which diffusion is negligible in an H-atom system represent an upper limit for all comparable systems of recombining atoms. To study probe effect, a series of isothermal detectors of different surface areas with a wide range of calibrated efficiencies was used. Since in the limit of an infinitely small probe there is no perturbation, a comparison with larger probes should indicate the extent of probe perturbation.

Experimental criteria

We neglect radial concentration gradients (to be discussed later). For hydrogen at 300 °K for small $[H]/[H_2]$ the interdiffusion coefficient as given by Weissman and Mason (13) reduces to $D = a/[H_2]$, where $a = 1.58 \times 10^3$ cm^2 Torr s^{-1} with $[H_2]$ in Torr. Equation [1] then takes the form

$$[2] \qquad \frac{a}{[H_2]}\frac{d^2[H]}{dx^2} - V_f\frac{d[H]}{dx} = \sum^n k_n[H]^n$$

There are two limiting cases. At low pressures and flow rates, the diffusive term predominates. Experimentally this is shown by plotting detector signal (in W) against axial distance for a series of varying flow rates. For any given value of detector signal the axial decay should be independent of V_f. At sufficiently high pressures and flow rates, the convective term predominates. We then plot atom concentration [proportional to signal/V_f under conditions of convective flow (14)] against time at varying flow rates. For any given value of atom concentration, the decay rate should be independent of V_f.

Apparatus

A Welch 1397B pump was connected to a flow system provided with inlet needle valves and an exit bellows valve. Experiments were conducted at pressures in the range 0.1–10 Torr and linear flow rates of 200–1500 cm s^{-1}. The thermostatted reactor tube was kept at 25° and used with either G. E. Dri-Film SC77 or a sleeve of thin-walled Teflon tubing as a wall poison. The latter gave more reproducible results.

Two grades of hydrogen were used, Linde Commercial (99.8% minimum purity) and Matheson Ultra Pure (99.999% minimum purity). The gases were passed through a DeOxo purifier and a silica-gel trap at −196°. Pressure was measured with a triple-scale McLeod gauge (range 10^{-5}–7.5 Torr) or with an RGI float-type vacuum gauge (range 0–10 Torr) which could be connected to the system at various points. Between runs the static system pressure was reduced to $< 10^{-6}$ Torr by use of a mercury diffusion pump. The hydrogen dissociator consisted

Can. J. Chem. Downloaded from www.nrcresearchpress.com by 210.87.254.40 on 09/05/12
For personal use only.

either of a tungsten filament or the microwave cavity of a Raytheon Microtherm generator operating at 2.45 GHz. Dissociation of the hydrogen was limited to ~5% or less. Measurements were made with 4 different reaction chambers with respective lengths of 25, 65, 100, and 120 cm and all with a radius of 1.1 cm. A tightly wound coil of platinum wire, approximately 32 ga., serving as one arm of a Wheatstone bridge (located outside) was moved along the reaction chamber by means of a poisoned support. The platinum coil was used as an isothermal calorimetric detector (15). Detector efficiencies were checked by mounting a second detector immediately downstream from the other.

When a tungsten filament was used as a dissociator, appreciable heat was carried down to the detector at high flow rates and pressures, as shown by blanks using helium and nitrogen as the carrier gas. A heat-transfer correction was made assuming He and H_2 behaved similarly. The corrections were always less than 10% and could be reduced further by increasing the dissociator–detector distance or by reducing the dissociator filament temperature.

Results

Detector Efficiency

For a given H-atom concentration the detector response was found to decrease with detector temperature below 190 °C. Above this temperature the output was constant up to at least 400°, the highest temperature studied. Detector temperatures were therefore kept at 200°.

A series of detectors with surface areas in the range 0.1–10 cm^2 was employed consisting of spirals of platinum wire up to 160 cm long. Two large detectors, one immediately downstream from the other, were independently connected to the outside power supply. Signal measurements were made on both simultaneously in a H-atom stream, at various pressures and flow rates. The assumption was made that all of the atoms recombine on the combination of detectors so that the total signal of both front and rear detectors corresponded to the total atom flux. The efficiency, ϕ, of the front detector was then taken to be the ratio of its signal to the total signal and this ratio was found to be independent of flow rate and pressure. ϕ was measured for a variety of detectors and the results are plotted as a function of detector surface area in Fig. 1.

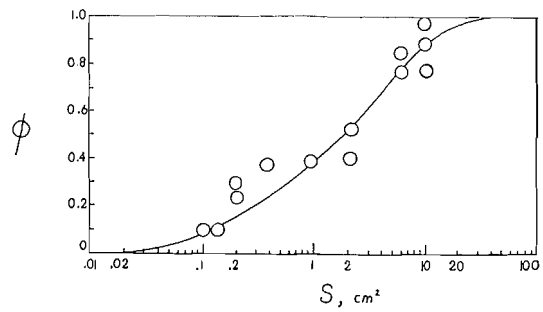

FIG. 1. Detector efficiency ϕ as a function of detector surface area S.

Effect of Pressure and Flow Rate on Decay Plots

Experiments at varying pressure and flow rate were performed and the results are given as diffusive plots (signal, in W, vs. distance) in Figs. 2A, C, E, and convective plots ([H] vs. time) in Figs. 2B, D, F. At 0.8 Torr the diffusive plot is independent of flow rate, the convective plot is not. Conversely, at 3.1 Torr the gradient of the convective plot is independent of flow rate, but the diffusive plot shows dependence on flow rate. Similar data, omitted for brevity, were also obtained at 5.4, 7.3, and 9.9 Torr and these results also showed predominantly convective flow. Results at 1.4 Torr shown in Figs. 2C, D represent an intermediate case where diffusive and convective flow are comparable.

Effect of Other Variables on Diffusion

Data in Fig. 2 were obtained using an efficient detector ($\phi = 0.81$). A series of experiments was performed with an inefficient detector ($\phi = 0.15$) and representative results at 0.8 and 5.4 Torr are shown in Figs. 3A, B. Although a much smaller signal was obtained, the diffusive and convective plots remained similar to those obtained with detectors of higher efficiency. Altogether a variety of detectors with efficiencies ranging from 0.04 to 0.96 were used. As a further check on the effect of the magnitude of an atom sink on the profile, some detectors were wired with copper just behind the platinum detector. It was found that in predominantly convective regions detector efficiency had no effect, while in predominantly diffusive regions a small effect on the decay plots was noted.

Runs in which ultra-pure rather than commercial grade hydrogen was used showed a decrease in atom concentration by about a factor of 5. This caused appreciably more scatter in the decay curves. However, whether diffusive or convective, flow obtained was found to be independent of gas purity (16).

Discussion

Detector Efficiency ϕ

A criticism of the use of a solid catalytic

Can. J. Chem. Downloaded from www.nrcresearchpress.com by 210.87.254.40 on 09/05/12
For personal use only.

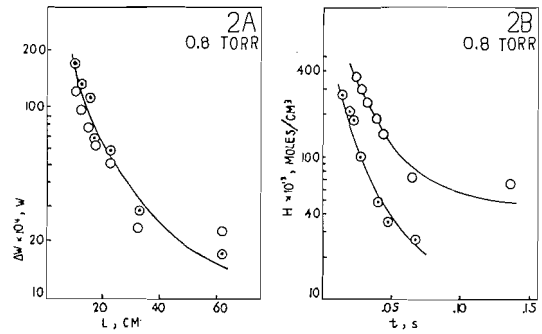

FIG. 2A, B. Atom decay plots at 0.8 Torr, $\phi = 0.81$. 2A diffusive plot, 2B convective plot. Flow rates: ○, 470 cm s^{-1}; ⊙, 900 cm s^{-1}.

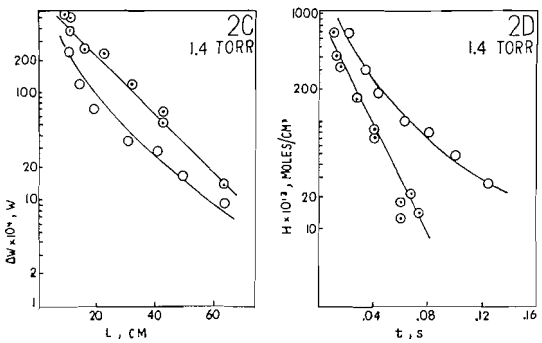

FIG. 2C, D. Atom decay plots at 1.4 Torr, $\phi = 0.81$. 2C diffusive plot, 2D convective plot. Flow rates: ○, 500 cm s^{-1}; ⊙, 1040 cm s^{-1}.

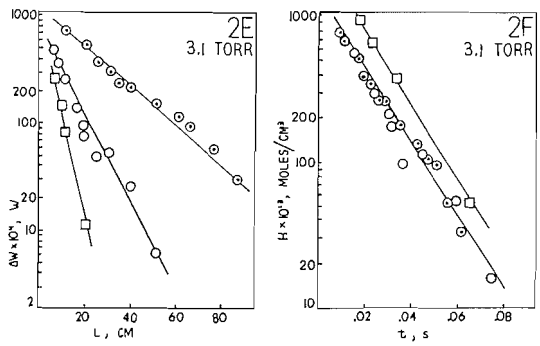

FIG. 2E, F. Atom decay plots at 3.1 Torr, $\phi = 0.81$. 2E diffusive plot, 2F convective plot. Flow rates: □, 340 cm s^{-1}; ○, 690 cm s^{-1}; ⊙, 1380 cm s^{-1}.

surface to measure absolute atom concentrations was made by Wood, Mills, and Wise (12) who found only a fraction of the energy of atom recombination to be accommodated by the catalyst. This leads to the possibility that a calorimetric detector could be completely efficient

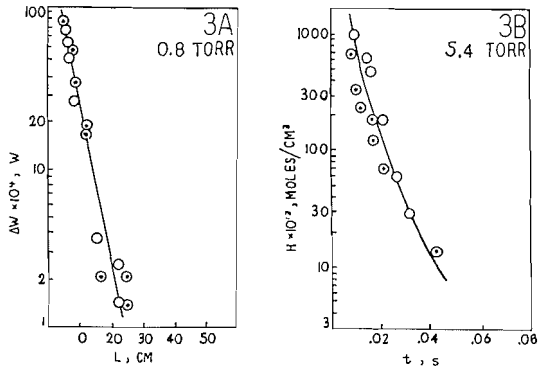

FIG. 3A, B. Atom decay plots with inefficient detector, $\phi = 0.15$. 3A diffusive plot at 0.8 Torr, flow rates: ○, 500 cm s^{-1}; ⊙, 850 cm s^{-1}. 3B convective plot at 5.4 Torr, flow rates: ○, 690 cm s^{-1}; ⊙, 1500 cm s^{-1}.

in recombining atoms but only partially efficient in detecting them. However, if the desorbing molecules leave the surface energetically excited, some of this excess energy should be transferred by collision with a second detector placed behind the first one. We found that if the surface area of the first detector was made sufficiently large, no energy was found to be transferred to the second one. Therefore, a sufficiently large detector must be completely efficient in both recombining atoms and in accommodating them. The fall-off in detector signal with decreasing detector surface area shown in Fig. 1 may reflect both incomplete recombination and incomplete accommodation (17). In the limit of an infinitely small detector, atom removal and any perturbation by the detector would vanish.

The assumption of negligible radial concentration gradients is valid if radial diffusion is sufficiently rapid to wipe out gradients caused by wall recombination. Under conditions of predominantly heterogeneous recombination (i.e. at low pressures) the condition for negligible radial gradients is given by (18)

$$[3] \qquad \gamma \ll 4RD/\bar{v}L^2 \quad \text{and} \quad \gamma' \ll 4D/\bar{v}L$$

where γ and γ' are the wall and detector recombination coefficients, $\bar{v}$ is the mean atomic velocity, and L is the distance from the atom source to detector[1]. At higher pressures these

[1]A somewhat different criterion, based on a less rigorous analysis, has been given by W. Smith. See ref. 22.

gradients are unimportant because of the increased number of homogeneous collisions (1).

An efficient catalytic probe used as a detector will set up an axial diffusion gradient the importance of which has been disputed (1, 2, 19). An approximate criterion for negligible probe effect has been given (20, 21) as

$$[4] \qquad D/LV_f \ll 1$$

If we take $L_{min} = 10$ cm as the smallest distance, the maximum values of D/LV_f are given in Table I. Thus the diffusion effects seen in Figs. 2 and 3 are presumably not due to the presence of the detector, except perhaps at the smallest values of L.

TABLE I

Test of criterion for axial diffusion due to probe

p (Torr)	V_f (cm/s)	$D/L_{min}V_f$
0.8	900	0.19
	470	0.37
1.4	1000	0.10
	500	0.20
3.0	1400	0.033
	690	0.068
	340	0.14
5.0	1500	0.019
	750	0.037
	350	0.080
10.0	1500	0.009
	750	0.019
	400	0.035

The relative unimportance of the detector is consistent with the calculations of Wise *et al.* Figure 5 of ref. 1 shows that under typical operating conditions, an increase in γ' by a factor of 100 increases the fall-off rate from $[H]/[H_0] = 1$ to $[H]/[H]_0 = 0.2$ by a factor of only 1.2.

Acknowledgments

We are grateful to the U.S. Army Research Office (Durham) for support of this work. We thank Dr. Lorne Elias of the National Aeronautical Establishment, Ottawa, for helpful criticism.

1. H. Wise and C. M. Ablow. J. Chem. Phys. **35**, 10 (1961).
2. B. J. Wood and H. Wise. J. Phys. Chem. **65**, 1976 (1961).
3. H. A. Kazmi, R. J. Diefendorf, and D. J. Le Roy. Can. J. Chem. **41**, 690 (1963).
4. J. E. Morgan and H. I. Schiff. Can. J. Chem. **41**, 903 (1963).
5. J. E. Morgan and H. I. Schiff. J. Chem. Phys. **38**, 2631 (1963).
6. H. Wise, C. M. Ablow, and D. J. Schott. J. Chem. Phys. **39**, 2063 (1963).
7. H. Wise, C. M. Ablow, and K. M. Sancier. J. Chem. Phys. **41**, 3569 (1964).
8. T. Marshall. Phys. Fluids, **5**, 743 (1962).
9. C. Kretchmer and H. Petersen. J. Chem. Phys. **39**, 1772 (1963).
10. F. Larkin and B. Thrush. Discussions Faraday Soc. **37**, 112 (1964).
11. T. M. Shaw. Studies of microwave gas discharges. General Electric Microwave Laboratory, Palo Alto, Calif., Report TISR-58ELM115. 1958.
12. B. Wood, J. Mills, and H. Wise. J. Phys. Chem. **67**, 1462 (1963).
13. S. Weissman and E. A. Mason. J. Chem. Phys. **36**, 794 (1962).
14. W. Schulz and D. J. Le Roy. Can. J. Chem. **40**, 2413 (1962).
15. E. Tollefson and D. J. Le Roy. J. Chem. Phys. **16**. 1057 (1948).
16. P. R. Rony and D. N. Hanson. J. Chem. Phys. **44**, 2536 (1966).
17. C. M. Ablow, H. Wise, and H. Motz. J. Chem. Phys. **43**, 10 (1965).
18. H. Wise and B. J. Wood. Advan. At. Mol. Phys. **3**, 309 (1967).
19. L. Elias, E. A. Ogryzlo, and H. I. Schiff. Can. J. Chem. **37**, 1680 (1960).
20. H. Smallwood. J. Am. Chem. Soc. **56**, 1542 (1934).
21. P. R. Rony. Lawrence Radiation Lab Rept. UCRL-16050. April, 1965.
22. W. Smith. J. Chem. Phys. **11**, 110 (1943).

Can. J. Chem. Downloaded from www.nrcresearchpress.com by 210.87.254.40 on 09/05/12
For personal use only.

The transmission of polar effects. Part VII.[1] A proton magnetic resonance spectra study of substituted mesitylenes, durenes, anthracenes, and triptycenes

KEITH BOWDEN, J. G. IRVING, AND M. J. PRICE

Department of Chemistry, The University of Essex, Wivenhoe Park, Colchester, Essex, England

Received February 16, 1968

The chemical shifts of the ring protons in a series of monosubstituted mesitylenes and durenes, and of the 10-protons of a series of 9-substituted triptycenes and anthracenes have been measured in dimethyl sulfoxide, acetone, 2-methoxyethanol, and carbon tetrachloride. The solvent dependence of the substituent chemical shifts has been analyzed by linear free energy relations. The systems all show similar dependence which increases with increasing dielectric constant of the solvent. This does not result from the field effect being transmitted through the medium, but appears to arise from the formation of a hydrogen-bonded interaction between the solvent and the hydrogen of the solute. The substituent chemical shifts appear to arise from contributions from substituent field, resonance, magnetic anisotropy, and solvent effects.

Canadian Journal of Chemistry, 46, 3903 (1968)

Can. J. Chem. Downloaded from www.nrcresearchpress.com by 210.87.254.42 on 09/05/12
For personal use only.

Introduction

Recently, many studies have attempted to relate the chemical shifts to properties of the substituents causing them (1–4). The chemical shift, δ, of a proton, relative to that in the unsubstituted compound, can be considered to consist of several additive factors, as shown below

$$[1] \qquad \delta = \delta_I + \delta_R + \delta_F + \delta_M + \delta_{solv.}$$

The factors are those due to the inductive (δ_I), resonance (δ_R), electric field (δ_F), magnetic (δ_M), and solvent ($\delta_{solv.}$) effects. Particular theories of the substituent chemical shift have been advanced in terms of the electric field (5, 6) and magnetic anisotropy (7, 8) effects. For an electric field, the substituent field effect at the proton, E, is a function of the substituent dipole, μ, the distance between the dipole and the proton, r, and the angle, θ, between the dipole and r, as shown in eq. [2].

$$[2] \qquad E = \frac{\mu(1 + 3\cos^2\theta)^{\frac{1}{2}}}{r^3}$$

The shielding, σ_E, arising from this field has been related by Buckingham (5) to the electric field by the eq. [3], where φ is the angle between the C—H bond and the vector E.

$$[3] \qquad \sigma_E = -10^{-12}E(2\cos\phi + 10^{-6}E)$$

A similar relation has been suggested by Musher (6). An anisotropic magnetic field has been shown by McConnell (7) to be approximated by the eq. [4], where the shielding, σ_M, is related to the anisotropy in the magnetic susceptibility of the gth bond, $\Delta\chi_g$, the distance between the proton and that bond, r_g, and the angle between r_g and the bond axis, θ_g.

$$[4] \qquad \sigma_M = \Sigma_g\left[\Delta\chi_g \frac{(1 - 3\cos\theta_g)}{3r_g^3}\right]$$

Solvent effects on the chemical shifts have contributions (9–14) from the bulk magnetic susceptibility of the medium (δ_B), the van der Waals interactions (δ_W), the magnetic anisotropy of the solvent (δ_A), and the solvent reaction field effect (δ_{ES}), as shown in eq. [5]

$$[5] \qquad \delta_{solv.} = \delta_B + \delta_W + \delta_A + \delta_{ES}$$

Specific local effects such as hydrogen-bonding to the solvent will strongly influence the chemical shift (14). In considering the substituent chemical shifts in large molecules at non-proximate positions only δ_{ES} and specific local effects can be considered to be important. The local solvent reaction field treatment of Buckingham (5) implicitly includes dependence on the medium as shown in eq. [6]

$$[6] \qquad R \propto \frac{\varepsilon - 1}{2\varepsilon + 2.5}$$

where ε represents the dielectric constant of the medium and R the reaction field.

Recent studies of solvent induced chemical shift (15) have shown the limitations of the reaction field theory. Specific solvent–solute complex formation has been suggested as being particularly suitable for aromatic solvents but has an analogy in hydrogen-bonding for non-aromatic solvents.

[1]For Part VI, see ref. 62.

Can. J. Chem. Downloaded from www.nrcresearchpress.com by 210.87.254.42 on 09/05/12
For personal use only.

Many attempts have been made to correlate chemical shifts of protons with Hammett substituent constants σ (16–20), with varying degrees of success. These constants express the polar effect of the substituent relative to hydrogen and are the sum of the "inductive" and resonance effects (21). The "inductive" effect probably originates from a field effect (22). A recent study (23) of substituted styrenes and ethylbenzenes has concluded that inductive and resonance effects are of greatest importance.

It was considered that a study of the substituent chemical shifts in model systems, and their solvent dependence, would give important information about the factors which control chemical shifts. This would then enable an evaluation of their use in assessing the transmission of polar substituent effects. The model systems selected for this study are those of fixed and known geometry, together with simplicity of spectra. These are the ring protons of substituted durenes (**1**) and mesitylenes (**2**), the 10-proton of 9-substituted anthracenes (**3**), and the 10-proton of 9-substituted triptycenes (**4**).

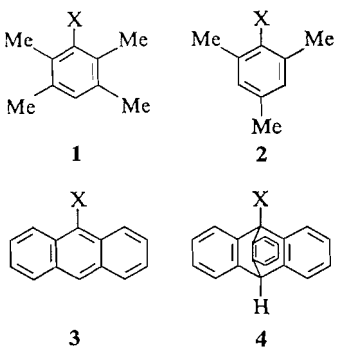

1 **2** **3** **4**

Previously, very complete studies have been made of substituted mesitylenes in cyclohexane (24), together with very limited studies of durenes and mesitylenes in carbon tetrachloride (25), and of triptycenes in tetrahydrofuran (26).

Experimental

Materials

Mesitylene, 1,2,3,5-tetramethylbenzene, 2,4,6-trimethylacetophenone, 2,4,6-trimethylaniline, 2,4,6-trimethylphenol, 2,4,6-trimethylbenzaldehyde, and 2,4,6-trimethylbenzoic acid were obtained commercially. Nitromesitylene was prepared by nitration of mesitylene by fuming nitric acid in acetic acid (27). Mesitylene was chlorinated, using an anhydrous ferric chloride catalyst, to give chloromesitylene (28). Bromomesitylene was synthesized by bromination of mesitylene in carbon tetrachloride (29). Esterification of 2,4,6-trimethylbenzoic acid with diazomethane in ether gave the methyl ester (30).

Durene, pentamethylbenzene, and 2,3,5,6-tetramethylphenol were obtained commercially. Durene was nitrated to give dinitrodurene (31), which was reduced with sodium sulfide to nitroaminodurene (32). The diazonium salt, prepared from nitroaminodurene, was reduced with hypophosphorus acid to give nitrodurene (33). Aminodurene was prepared by the reduction of nitrodurene with zinc and acetic acid (34). Friedel–Craft acylation of durene gave 2,3,5,6-tetramethylacetophenone (35). Bromodurene was prepared by bromination of durene with bromine in carbon tetrachloride (36). The chlorination of durene using an iodine catalyst gave chlorodurene (37). The carboxylation of the Grignard compound obtained from bromodurene gave 2,3,5,6-tetramethylbenzoic acid, which was esterified with diazomethane in ether to form the methyl ester (38).

Anthracene, 9-methylanthracene, 9-acetylanthracene, and 9-anthraldehyde were obtained commercially. Nitration of anthracene with concentrated nitric acid in acetic acid gave 9-nitroanthracene (39). 9-Bromoanthracene was prepared by bromination of anthracene (40) and gave, on treatment with phenyl lithium and carboxylation, 9-anthroic acid (41). Methyl 9-anthroate was obtained by esterification of the acid by the action of trifluoroacetic anhydride and methanol (42). The reaction of anthrone with phenyl magnesium bromide gave 9-phenylanthracene (43).

The triptycenes were synthesized from the corresponding 9-substituted anthracenes by the addition of benzyne. The benzyne was generated by a modification of the method of Friedman and Logullo (44). A solution of anthranilic acid (15 g, 0.109 mole) in acetone (50 ml) was added over a period of 1 to 4 h to a refluxing mixture of the substituted anthracene (e.g. 9-nitroanthracene; 6.5 g, 0.0292 mole) in dichloromethane (50 ml) and isoamyl nitrite (13.5 g, 0.115 mole). The solution was then evaporated in a rotary evaporator to form a dark oil. This oil was dissolved in a minimum amount of dry benzene and eluted on an alumina chromatographic column with benzene. The first fraction was, in all cases, the triptycene and the second fraction was the unreacted anthracene. The triptycene could be purified by treatment with maleic anhydride and then a base, or by N-ethylmaleimide and

TABLE I

Physical properties of triptycenes

9-Substituent	Melting points (°C) This study	Literature	Reference
H	249–250	247–248	45
Me	255–257	253–254	45
Ph*	274–275	—	
Br	246–247	246–248	45
COMe†	210–211	—	
NO_2	244	241–243	45

*Anal. Calcd. for $C_{26}H_{18}$: C, 94.55; H, 5.55. Found: C, 94.99; H, 5.54.

†Anal. Calcd. for $C_{22}H_{16}O$: C, 89.17; H, 5.42; O, 5.41. Found: C, 89.36; H, 5.49; O, 5.43.

TABLE II

Chemical shifts of proton in substituted mesitylenes, durenes, and anthracenes

	Chemical shifts* of											
	Mesitylenes in				Durenes in				Anthracenes in			
Substituent	DMSO	MCS	Acetone	CTC	DMSO	MCS	Acetone	CTC	DMSO	MCS	Acetone	CTC
H	6.78	6.73	6.77	6.68	6.89	6.84	6.88	6.77	8.58	8.48	8.52	8.39
Me	6.78	6.74	6.79	6.69	6.79	6.74	6.79	6.68	8.49	8.35	8.42	8.23
NH_2	6.64	6.66	6.65	6.61	6.33	6.31	6.32	6.29	—	—	—	—
OH	6.71	6.70	6.73	6.66	6.50	6.48	6.50	6.46	—	—	—	—
Cl	6.99	6.86	6.91	6.80	6.95	6.90	6.93	6.78	—	—	—	—
Br	7.01	6.88	6.93	6.82	6.98	6.92	6.94	6.83	8.74	8.58	8.59	8.40
CHO	6.96	6.91	6.92	6.81	—	—	—	—	9.03	8.85	8.82	8.58
CO_2Me	6.90	6.85	6.89	6.76	7.05	6.98	7.00	6.88	8.81	8.68	8.70	8.46
COMe	6.86	6.80	6.85	6.73	7.00	6.95	6.98	6.85	8.73	8.61	8.63	8.42
NO_2	7.11	7.04	7.08	6.88	7.21	7.13	7.16	6.98	9.04	8.85	8.89	8.59
Ph	—	—	—	—	—	—	—	—	8.70	8.58	8.59	8.41

*Chemical shifts are accurate to ±0.01 p.p.m. relative to TMS.
Solvents: DMSO, dimethyl sulfoxide; MCS, 2-methoxyethanol; CTC, carbon tetrachloride.

then chromatography over alumina. After recrystallization from methylcyclohexane, the triptycenes were obtained as colorless solids whose physical properties are shown in Table I. The yields of triptycenes varied from between 25 to 50%, and the recovery of unreacted anthracenes between 60 to 30%.

The samples used for measurements were fractionally distilled or recrystallized to constant melting points. The physical constants of these samples were identical or close to those in the literature, except 9-methyltriptycene whose calculated and found elemental analyses were in good agreement. The elemental analysis for 9-phenyltriptycene was rather less satisfactory. The solvents, dimethyl sulfoxide and 2-methoxyethanol, were purified in the manner previously described (46). Acetone and carbon tetrachloride were "Analar" grade and were dried over 5 Å molecular sieves before use.

Nuclear Magnetic Resonance Measurements

A Varian A60-A nuclear magnetic resonance (n.m.r.) spectrometer operating at 60 Mc/s was used to obtain the spectra. These were measured as 0.1 *M* solutions in dimethyl sulfoxide, 2-methoxyethanol, acetone, and carbon tetrachloride containing 2% tetramethylsilane (TMS) as an internal standard. No significant shifts were noted on further dilution. A number of duplicate runs were made for each measurement. The uncertainty in peak position was considered to be ±0.5 c.p.s., relative to TMS. The spectra were calibrated by means of a Varian Associates standard and the calibration was checked at convenient and regular intervals. Standard instrument conditions were used throughout the measurements.

Results and Discussion

The chemical shifts of the selected protons of the durenes, mesitylenes, anthracenes, and triptycenes in the four solvents are shown in Tables II and III.

As stated previously, many attempts have been made to correlate substituent chemical shifts using linear free energy relations, especially the Hammett equation (16–20). Fair correlations have been made between substituent chemical shifts for the proton para to the substituent in benzene (16), while the correlation fails badly for the protons meta to the substituent in benzene (19). However, for mesitylenes, durenes, and anthracenes, substituents such as the nitro group will be extensively deconjugated with the aromatic ring. Studies on 4-substituted 3,5-dimethylbenzoic acids (47) and 9-substituted 10-anthroic acids (48, 49) enable the calculation of "effective" σ values which should be applicable to studies of substituted durenes and anthracenes. These "effective" σ values are calculated by dividing the observed ΔpK_a values for substituents such as the nitro group by the reaction constant obtained

TABLE III

Chemical shifts of proton in substituted triptycenes

	Chemical shifts* in			
Substituent	DMSO	MCS	Acetone	CTC
H	5.63	5.50	5.61	5.29
Me	5.64	5.50	5.59	5.29
Br	5.78	5.60	5.75	5.31
CO_2Me	5.69	5.52	5.64	5.29
COMe	5.67	5.51	5.61	5.24
NO_2	5.82	5.64	5.76	5.29
Ph	5.72	5.56	5.64	5.29

*Chemical shifts are accurate to ±0.01 p.p.m. relative to TMS. For abbreviations of solvents, see footnote of Table II.

Can. J. Chem. Downloaded from www.nrcresearchpress.com by 210.87.254.42 on 09/05/12
For personal use only.

Can. J. Chem. Downloaded from www.nrcresearchpress.com by 210.87.254.42 on 09/05/12
For personal use only.

from the unaffected substituents such as the halogeno groups. These values are shown in Table IV and the correlations for the chemical shifts in dimethyl sulfoxide in Table V. The correlations are only fair. In particular the chemical shift for the acetyl group appears to be too low and for the phenyl group appears to be too high to have resulted from the polar effect of the substituent as measured by the σ value. The failure of the correlation of the chemical shift of mesitylenes with meta-σ values has been ascribed to magnetic anisotropy effects at these positions (50). The acetyl and phenyl groups could have significant magnetic anisotropy effects also at the paraposition.

TABLE IV
Substituent constants

Substituent (R)	σ	σ_I (RCH_2)†
H	0.0	0.0
Me	−0.170	−0.03
NH_2	−0.63*	—
OH	−0.37	—
Cl	0.227	—
Br	0.232	0.47
CHO	0.19*	—
CO_2Me	0.32*	0.35_5
COMe	0.36*	0.29_5
NO_2	0.67*	0.73
Ph	0.00*	0.11_5

*"Effective" σ value (47–49).
†σ_I values used are those previously used (46) or those derived from reliable pK_a values of substituted acetic acids in water at 25° (51, 49).

Aliphatic substituent constants are required to correlate the effect of 9-substituents for triptycenes, where both proton and substituent are bonded to saturated carbon atoms. The parallel constants σ_I (46, 51) and σ^* (52) are available. The correlation with σ_I is shown in Table V for dimethyl sulfoxide as solvent and is only fair. The acetyl and phenyl groups show the same divergencies as shown in the durene and anthracene series. Both of these substituents have substantial magnetic anisotropy contributions (53, 54). It is very likely that this effect opposes the polar contribution for the acetyl group and augments that of the phenyl group.

Specific interactions between the substituents and solvents must be considered. The substituents and solvents have been chosen to avoid this. However, the hydroxy and amino groups are prone to this behavior (55) and the results for these groups must be treated with reserve.

TABLE V
Linear free energy correlations for chemical shifts in dimethyl sulfoxide

System	Reaction constants	δ_0* (p.p.m.)	r†	n‡
1,4-Durene	0.67 (ρ)	6.81	0.975	9
9,10-Anthracene	0.58 (ρ)	8.65	0.778	8
9,10-Triptycene	0.23 (ρ_I)	5.64	0.888	7

*δ_0 is the calculated chemical shift for hydrogen.
†r is the correlation coefficient.
‡n is the number of substituents studied.

The degree of success obtained for the durenes and anthracenes seems to indicate that, like para-substituted benzenes (16), the electron densities at these positions are more directly affected by the substituent polar effect (50). The mesitylenes and meta-substituted benzenes are less strongly affected by the substituent polar effect and magnetic anisotropy effects intervene (50). The partial success of the triptycene correlation indicates a small and not very significant substituent polar effect through systems not directly π-bonded. This is in accord with the recent studies of substituent effects on fluorine chemical shifts in saturated systems (56).

In the absence of very satisfactory correlations with substituent constants, it is necessary to suggest another method of analyzing the results in different solvents. Thus, the results have been analyzed by taking the chemical shift in dimethyl sulfoxide (DMSO), δ^{DMSO}, as a standard *for each system*. The chemical shifts in the other solvents have been correlated with these values, as shown in Table VI. The correlations are very good[2] and give the susceptibilities, γ, of these systems to the solvent effect, relative to that in dimethyl sulfoxide. However, the significance of these linear free energy relations is limited by their derivation and their scope. In spite of this, consideration of these γ values shows that the effect of the solvents for each series is almost the same and falls in the order:

dimethyl sulfoxide > acetone
$\approx$ 2-methoxyethanol > carbon tetrachloride

This is the opposite order to that expected if the effect was due to the field effect of the substituents (see Table VII). The transmission of the substituent field effect would increase as the di-

[2]The sole exception is the triptycene series in carbon tetrachloride where the shifts were very small.

TABLE VI

γ values for various systems*

System	Solvent	γ	δ_0 (p.p.m.)	r	n
Durene	DMSO	1.00	—	—	9
	Acetone	0.94	−0.01	0.999	9
	MCS	0.92	0.00	1.000	9
	CTC	0.79	−0.02	0.997	9
Mesitylene	DMSO	1.00	—	—	10
	Acetone	0.80	0.01	0.983	10
	MCS	0.73	0.02	0.969	10
	CTC	0.58	0.01	0.994	10
Anthracene	DMSO	1.00	—	—	8
	Acetone	0.78	−0.02	0.985	8
	MCS	0.87	−0.02	0.992	8
	CTC	0.56	−0.06	0.959	8
Triptycene	DMSO	1.00	—	—	7
	Acetone	0.93	−0.02	0.962	7
	MCS	0.77	−0.01	0.988	7
	CTC	0.61	−0.01	0.452	7

*δ_0 is the calculated chemical shift for hydrogen; r is the correlation coefficient; n is the number of substituents studied. For abbreviations of solvents, see footnote of Table II.

TABLE VII

Solvent parameters

Solvent	ε*	$\frac{\varepsilon - 1}{2\varepsilon + 2.5}$
Dimethyl sulfoxide	48.9†	0.177
Acetone	20.5‡	0.435
2-Methoxyethanol	15.95§	0.448
Carbon tetrachloride	2.23‡	0.478

*Literature values (61), ε = dielectric constant.
†Value at 20°.
‡Value at 25°.
§Value at 30°.

electric constant of the medium falls. The dielectric constants, as shown in Table VII, decrease as γ decreases. The function proposed by Buckingham (5) does not account for the results found in this study.

The order of the susceptibility of the systems to substituent effects can be understood if the protons are interacting with the solvent by means of hydrogen-bonded interactions (14). These will vary in strength with the ability of the hydrogen-bond acceptor and will decrease in strength in the order (57):

dimethyl sulfoxide ≫ acetone
> 2-methoxyethanol ≫ carbon tetrachloride

The carbon–hydrogen bond will be polarized in accord with the strength of the hydrogen bond (5).

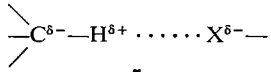

5

The chemical shift of the hydrogen will have increased susceptibility to the polar effect of the substituent as the carbon–hydrogen bond becomes more polarized.

A number of fluorine n.m.r. studies of substituted fluoroaromatics have been made in a number of solvents (55, 58–60). Considerable differences occur in the interpretation of these results. It would appear that the effect of solvents on the fluorine chemical shifts are not interpretable in terms of a field effect (60), but are better expressed in terms of specific interactions between solute and solvent (55). The results of Wittstruck and Trachtenberg (23) are in general agreement with those presented here. The latter workers have deduced that the "net effect of field effects is insignificantly small". The possibility that electric and magnetic field effects cancel in their system remains. The present study has shown that the magnetic field effect of some substituents persists at remote positions. Wittstruck and Trachtenberg emphasize that chemical shifts can be used to evaluate conjugation. Our study shows that difficulties may arise from the intervention of other effects and stresses the importance of considering specific solvent interactions in elucidating the origin of chemical shifts. The conclusion of Dewar and Takeuchi (50) that "proton chemical shifts cannot be interpreted in terms of 'normal' substituent theory" seems amply justified.

Our conclusion from this study is that hydrogen n.m.r. shifts are not a good probe for studying the polar effects of substituents. Chemical shifts arise from complex causes. These causes are not always the same or are not governed in the same way as those affecting substituent effects on chemical reactivity.

1. J. N. Shoolery. J. Chem. Phys. **21**, 1899 (1953).
2. B. P. Dailey and J. N. Shoolery. J. Am. Chem. Soc. **77**, 3977 (1955).
3. A. A. Bothner-By and C. Naar-Colin. J. Am. Chem. Soc. **80**, 1728 (1958).
4. S. Reddy, J. H. Goldstein, and L. Mandell. J. Am. Chem. Soc. **83**, 1300 (1961).
5. A. D. Buckingham. Can. J. Chem. **38**, 300 (1960).
6. J. I. Musher. J. Chem. Phys. **37**, 34 (1962).
7. H. M. McConnell. J. Chem. Phys. **27**, 226 (1957).
8. J. A. Pople. Proc. Roy. Soc. London, Ser. A, **239**, 541, 550 (1957).
9. A. D. Buckingham, T. Schaefer, and W. G. Schneider. J. Chem. Phys. **32**, 1227 (1960).

Can. J. Chem. Downloaded from www.nrcresearchpress.com by 210.87.254.42 on 09/05/12
For personal use only.

10. J. K. BECCONSALL and P. HAMPSON. Mol. Phys. **10**, 21 (1965).
11. P. DE MONTGOLFIER. J. Chim. Phys. **64**, 639 (1967).
12. N. LUMBROSO, T. K. WU, and B. P. DAILEY. J. Phys. Chem. **67**, 2469 (1963).
13. G. KATOWYCZ and T. SCHAEFER. Can. J. Chem. **45**, 1093 (1967).
14. T. SCHAEFER and W. G. SCHNEIDER. J. Chem. Phys. **32**, 1218 (1960).
15. I. D. KUNTZ and M. D. JOHNSTON. J. Am. Chem. Soc. **89**, 6008 (1967).
16. H. SPIESECKE and W. G. SCHNEIDER. J. Chem. Phys. **35**, 731 (1961).
17. T. SCHAEFER and W. G. SCHNEIDER. Can. J. Chem. **41**, 966 (1963).
18. P. DIEHL. Helv. Chim. Acta, **44**, 829 (1961).
19. F. LANGENBUCHER, E. D. SCHMID, and R. MECKE. J. Chem. Phys. **39**, 1901 (1963).
20. S. H. MARCUS, W. F. REYNOLDS, and S. I. MILLER. J. Org. Chem. **31**, 1872 (1966).
21. R. W. TAFT and I. C. LEWIS. J. Am. Chem. Soc. **80**, 2436 (1958); **81**, 5343 (1959).
22. M. J. S. DEWAR and P. J. GRISDALE. J. Am. Chem. Soc. **84**, 3539, 3548 (1962).
23. T. A. WITTSTRUCK and E. N. TRACHTENBERG. J. Am. Chem. Soc. **89**, 3803 (1967).
24. W. A. GIBBONS and V. M. S. GIL. Mol. Phys. **9**, 167 (1965).
25. E. BULLOCK. Can. J. Chem. **41**, 711 (1963).
26. W. THEILACKER, K. ALBRECHT, and H. UFFMANN. Chem. Ber. **98**, 428 (1965).
27. G. POWELL and F. R. JOHNSON. Org. Syn. **14**, 68 (1934).
28. *cf.* F. BROWN, J. M. A. DE BRYNE, and P. GROSS. J. Am. Chem. Soc. **56**, 1291 (1934).
29. L. I. SMITH. Org. Syn. **11**, 24 (1931).
30. H. PECKMANN. Ber. **31**, 501 (1898).
31. R. H. BIRTLES and G. C. HAMPSON. J. Chem. Soc. 10 (1937).
32. C. E. INGHAM and G. C. HAMPSON. J. Chem. Soc. 981 (1939).
33. G. ILLUMINATI. J. Am. Chem. Soc. **74**, 4951 (1952).
34. R. WILLSTATTER and H. KUBLI. Ber. **42**, 4159 (1909).
35. L. I. SMITH and C. GUSS. J. Am. Chem. Soc. **59**, 804 (1937).
36. L. I. SMITH and C. L. MOYLE. J. Am. Chem. Soc. **55**, 1676 (1933).
37. A. TOHL. Ber. **25**, 1523 (1892).
38. L. I. SMITH and J. J. ROSENBAUM. J. Am. Chem. Soc. **73**, 3843 (1951).
39. C. E. BRAUN, C. D. COOK, C. MERRITT, and J. E. ROUSSEAU. Org. Syn. **31**, 77 (1951).
40. O. L. WRIGHT and L. E. MURA. J. Chem. Ed. **43**, 150 (1966).
41. B. M. MIKHAILOV and V. P. BRONOVITSKAYA. J. Gen. Chem. USSR, Eng. Transl. **22**, 195 (1952).
42. R. C. PARISH and L. M. STOCK. J. Org. Chem. **30**, 927 (1965).
43. J. W. COOK. J. Chem. Soc. 2160 (1926).
44. L. FRIEDMAN and F. M. LOGULLO. J. Am. Chem. Soc. **85**, 1549 (1963).
45. W. THEILACKER, U. BERGER-BROSE, and K. H. BEYER. Chem. Ber. **93**, 1658 (1960).
46. K. BOWDEN, M. HARDY, and D. C. PARKIN. Can. J. Chem. **46**, 2929 (1968).
47. J. P. SCHAEFER and T. J. MIRAGLIA. J. Am. Chem. Soc. **86**, 64 (1964).
48. R. O. C. NORMAN and P. D. RALPH. J. Chem. Soc. 2221 (1961).
49. K. BOWDEN and D. C. PARKIN. Can. J. Chem., in press, and some unpublished studies.
50. M. J. S. DEWAR and Y. TAKEUCHI. J. Am. Chem. Soc. **89**, 390 (1967).
51. M. CHARTON. J. Org. Chem. **29**, 1222 (1964).
52. R. W. TAFT. *In* Steric effects in organic chemistry. *Edited by* M. S. Newman. John Wiley and Sons, Inc., New York. 1956. Chap. 13.
53. R. F. ZURCHER. *In* Progress in nuclear magnetic resonance spectroscopy. *Edited by* J. W. Emsley, J. Feeney, and L. H. Sutcliffe. The Pergamon Press, Ltd., Oxford. 1967. p. 259.
54. G. J. KARABATSOS, G. C. SONNICHSEN, N. HSI, and D. J. FENOGLIO. J. Am. Chem. Soc. **89**, 5067 (1967).
55. R. W. TAFT, E. PRICE, I. R. FOX, I. C. LEWIS, K. K. ANDERSEN, and G. T. DAVIS. J. Am. Chem. Soc. **85**, 709 (1963); **85**, 3146 (1963).
56. M. J. S. DEWAR and T. G. SQUIRES. J. Am. Chem. Soc. **90**, 210 (1968). G. L. ANDERSON and L. M. STOCK. J. Am. Chem. Soc. **90**, 212 (1968).
57. F. TAKAHASHI and N. C. LI. J. Am. Chem. Soc. **88**, 117 (1966); and references therein.
58. R. W. TAFT and L. D. MCKEEVER. J. Am. Chem. Soc. **87**, 2489 (1965).
59. M. J. S. DEWAR and A. P. MARCHAND. J. Am. Chem. Soc. **88**, 3318 (1966).
60. W. ADCOCK and M. J. S. DEWAR. J. Am. Chem. Soc. **89**, 379 (1967).
61. C. REICHARDT. Angew. Chem. Intern. Ed. Engl. **4**, 29 (1965).
62. K. BOWDEN and G. E. MANSER. Can. J. Chem. **46**, 2941 (1968).

Can. J. Chem. Downloaded from www.nrcresearchpress.com by 210.87.254.42 on 09/05/12
For personal use only.

Can. J. Chem. Downloaded from www.nrcresearchpress.com by 210.87.254.105 on 09/05/12
For personal use only.

The transmission of polar effects. Part VIII.[1] Esterification with diazodiphenylmethane and the ionization of ortho-substituted *trans*-cinnamic, phenoxyacetic, 3-phenylpropionic, *cis*- and *trans*-α-phenylcinnamic acids

KEITH BOWDEN AND D. C. PARKIN
Department of Chemistry, The University of Essex, Wivenhoe Park, Colchester, Essex, England

Received February 16, 1968

The rate coefficients for the esterification with diazodiphenylmethane in ethanol at 30° and the pK_a values at 25° of a number of ortho-substituted *trans*-cinnamic, phenoxyacetic, 3-phenylpropionic, ortho-, meta-, and para-substituted *cis*- and *trans*-α-phenylcinnamic acids have been determined. The effects of substitution have been assessed by a Hammett-type correlation. A comparison of the transmission of the polar effects of ortho and meta/para substituents indicates the prime importance of the field effect, augmented where possible by a π-inductive effect. A reversed dipolar substituent field effect has been detected for the *cis*-ortho-substituted cinnamic acids.

Canadian Journal of Chemistry, 46, 3909 (1968)

Introduction

In a search for model systems to distinguish between the inductive and field effects (1, 2), a previous analysis (3) suggested that for certain reaction and substituents, the polar effect of ortho-substituents in benzoic acids is transmitted approximately twice as efficiently as that of meta/para-substituents. A very simple test presents itself. If the field effect is the main means of transmission, the ratio will decrease and approach unity as the substituted phenyl group becomes more distant from the reaction site. This is due to the field effect varying with $\cos\theta/r^2$ for a point dipole (4), where r is the distance from the dipole and the reaction site and θ is the angle between r and the dipole. However, if an inductive effect is mainly responsible, the ratio will remain the same. This is because the inductive effect decreases by a factor ε for each intervening link (2, 5).

In this study, the reactivities of a series of ortho-substituted *trans*-cinnamic, phenoxyacetic, 3-phenylpropionic, *cis*- and *trans*-α-phenylcinnamic acids in their ionization and their reaction with diazodiphenylmethane in ethanol have been studied, together with the meta/para-substituted α-phenylcinnamic acids. The ortho-substituted systems have been correlated by a Hammett-type equation and compared with the corresponding meta/para-substituted systems. Charton has previously correlated a number of reactions of ortho-substituted systems using para-σ values (6). Other workers (7, 8) have attempted correlations using polar substituent constants obtained from a separation of polar and steric effects. In the ortho-substituted benzoic system, this treatment has been criticized (9). An interesting and earlier attempt to use a similar model system to test the inductive and field theories of the propagation of substituent effects was made by Roberts and Carboni (10). This study of phenylpropiolic acids has since been extended (11). The latter analysis enabled the estimation of a series of ortho-σ values. Both of these studies have been interpreted in terms of a field effect.

Previous studies by Hogeveen (12) and ourselves (3, 9) have indicated the importance of dipolar substituent effects in 3-substituted acrylic acids. Hogeveen (12) noted a possible specific direct field effect for certain *ortho*-substituted *cis*-cinnamic acids. This was probably related to the observation of a reversed dipolar substituent field effect demonstrated recently by Golden and Stock (13).

Results and Discussion

The rate coefficients for the esterification of the acids with diazodiphenylmethane in ethanol at 30.0° are shown in Tables I and II. In Tables III and IV the pK_a values of the acids in water or 80% w/w 2-methoxyethanol–water are shown.

[1]For Part VII, see preceding paper. A preliminary account of certain aspects of this study has appeared in Chem. Commun. 75 (1968).

Can. J. Chem. Downloaded from www.nrcresearchpress.com by 210.87.254.105 on 09/05/12
For personal use only.

TABLE I

Rate coefficients for the esterification with diazodiphenylmethane of the ortho-substituted acids in ethanol at 30.0°

		Rate coefficients k*				
	Substituent	*trans*-Cinnamic	Phenoxyacetic	3-Phenyl-propionic	*trans*-α-Phenyl-cinnamic	*cis*-α-Phenyl-cinnamic
1	H	1.04†	6.03†	0.716†	0.997	9.82
2	Me	1.04	5.30	0.705	1.22	7.52
3	F	1.21	7.40	0.811	1.47	10.2
4	Cl	1.28	7.55	0.817	1.50	10.6
5	Br	1.27	7.46	0.815	1.53	10.9
6	NO_2	1.64	10.0	1.08	1.99	9.59
7	OMe	0.733	5.46	0.539	0.791	6.97
8	OH	0.594	12.1	0.670	—	—

*The rate coefficients, k (l mole^{-1} min^{-1}), are reproducible to ±3% or better and are the mean of at least two determinations.
†Previous workers found k for *trans*-cinnamic acid to be 0.972 (14); phenoxyacetic, 6.60, 6.25 (14, 15); and 3-phenylpropionic acid, 0.735, 0.740 (14, 15).

TABLE II

Rate coefficients for the esterification with diazodiphenylmethane of meta- and para-substituted α-phenylcinnamic acids in ethanol at 30.0°

		Rate coefficients, k*	
	Substituent	*trans*	*cis*
1	H	0.997	9.82
2	*m*-Cl	1.58	—
3	*m*-Br	1.65	—
4	*m*-NO_2	2.24	—
5	*p*-OMe	0.809	9.02
6	*p*-Me	0.927	8.36
7	*p*-Cl	1.31	12.0
8	*p*-NO_2	2.83	15.8

*See footnote of Table I.

The results have been analyzed by a similar method to that previously used for ortho-substituted benzoic acids (3, 18). The Hammett equation was used with para-σ" values (19). These values are most applicable to the present insulated or partially insulated systems, and this scale was used in our previous analysis of meta/para-substitution in similar systems (2). A value of 0.530 is used for the ortho-nitro group to allow for steric deconjugation by the proximate link (18) and a σ" value of 0.168 for the insulated ortho- or para-fluoro substituent (20). The results of these correlations are shown in Table V. The ortho-hydroxy group was excluded from the correlations because of its anomalous behavior (to be discussed later).

The correlations, shown in Table V, vary from very good to satisfactory (21), except for the *cis*-ortho-substituted α-phenylcinnamic acid system. The α-phenylcinnamic acids show interesting discrepancies and are discussed in detail separately. The available data for phenylpropiolic acids (10, 11) have been analyzed in the

TABLE III

pK_a values of the ortho-substituted acids in water or 80% w/w 2-methoxyethanol–water (80% MCS) at 25°

		pK_a* values of				
	Substituent	*trans*-Cinnamic in water	Phenoxyacetic in water	3-Phenyl-propionic in water	*trans*-α-Phenyl-cinnamic in 80% MCS	*cis*-α-Phenyl-cinnamic in 80% MCS
1	H	4.44†	3.17†	4.66†	7.00	5.59
2	Me	4.50†	3.23†	4.66†	6.74	5.94
3	F	4.28	3.09†	4.60	6.82	5.55
4	Cl	4.23†	3.05†	4.58†	6.86	5.57
5	Br	4.23	3.12†	4.58	6.80	5.64
6	NO_2	4.15†	2.90†	4.50†	6.64	5.48
7	OMe	4.46†	3.23†	4.80†	7.30	5.90
8	OH	4.61†	3.02	4.75	—	—

*Mean of at least two determinations; reproducible to ±0.01$_5$ (water) or ±0.03 (80% MCS).
†Literature values from ref. 16.

TABLE IV

pK_a values of the meta- and para-substituted cinnamic acids in 80% w/w 2-methoxyethanol–water at 25°

	Substituent	pK_a*		
		trans-α-Phenyl	*cis*-α-Phenyl	*trans*
1	H	7.00	5.59	6.61†
2	*m*-Cl	6.62	—	6.36
3	*m*-Br	6.64	—	6.38
4	*m*-NO_2	6.29	—	6.09
5	*p*-OMe	7.23	5.71	—
6	*p*-Me	6.99	5.73	—
7	*p*-Cl	6.66	5.36	—
8	*p*-NO_2	6.33	5.08	6.03

*See footnote of Table III.
†Previous workers found pK_a for *trans*-cinnamic acid to be 6.68 (17).

same way and the results are also shown in Table V.

In Table VI the reaction constants for ortho and for meta/para-substitution are compared. The ratio of the reaction constants, $\rho^{ortho}/\rho^{meta/para}$, for the dimethylene, oxymethylene, and *trans*-ethylene links are all very much less than those for the benzoic systems, as shown in Table VI. These former systems have an average ratio of $1.3 \pm 0.1_5$, compared to 2.2 ± 0.2 for the benzoic system. The reduction in this ratio indicates that the polar substituent effect is mainly transmitted by a field effect. As has been stated in the Introduction, an inductive effect would not have altered the ratio. The field effect can be augmented by a π-inductive effect in appropriate cases. The reaction constants for either type of substitution or reaction are always in the order

trans-cinnamic > phenoxyacetic > 3-phenylpropionic

In the first two systems, the π-inductive effect probably causes this increase in transmission and only operates efficiently when the reaction site and substituent are linked by a continuous π-electron system. Similar conclusions arise from the analysis of the phenylpropiolic acids.

α-*Phenylcinnamic Acids*

The transmission of polar effects for *cis*- or *trans*-meta/para-substituted α-phenylcinnamic acids is quite normal. The ionization of *cis*-cinnamic acids has been studied (22, 23) since

TABLE V

Hammett reaction constants

System	Reaction	ρ	log k_0	r*	n†	Substituents
3-(ortho-Substituted phenyl)propionic	Ionization in water, 25°	0.258	4.64	0.982	6	1–6
	DDM esterification, 30°	0.277	−0.138	0.955	6	1–6
ortho-Substituted phenoxyacetic	Ionization in water, 25°	0.475	3.18	0.969	7	1–7
	DDM esterification, 30°	0.410	0.781	0.994	7	1–7
trans-ortho-Substituted cinnamic	Ionization in water, 25°	0.564	4.40	0.969	7	1–7
	DDM esterification, 30°	0.412	0.001	0.950	7	1–7
trans-ortho-Substituted α-phenylcinnamic	Ionization in 80% MCS, 25°	0.651	6.98	0.968	5	1,3–6
	DDM esterification, 30°	0.536	0.036	0.959	5	1,3–6
cis-ortho-Substituted α-phenylcinnamic	Ionization in 80% MCS, 25°	0.188	5.61	0.616	5	1,3–6
	DDM esterification, 30°	−0.021	1.014	0.177	5	1,3–6
trans-meta/para-Substituted α-phenylcinnamic	Ionization in 80% MCS, 25°	0.917	6.98	0.967	8	1–8
		0.883	6.98	0.950	5	1,5–8
	DDM esterification, 30°	0.540	−0.001	0.991	8	1–8
		0.570	0.000	0.992	5	1,5–8
cis-meta/para-Substituted α-phenylcinnamic	Ionization in 80% MCS, 25°	0.716	5.61	0.986	5	1,5–8
	DDM esterification, 30°	0.291	0.984	0.985	5	1,5–8
trans-meta/para-Substituted cinnamic	Ionization in 80% MCS, 25°	0.743	6.63	0.993	5	1–4,8
ortho-Substituted-phenylpropiolic	Ionization in 50% ethanol, 25°	0.240	3.55	0.801	5	—
	DDM esterification, 30°	0.330	0.308	0.960	5	—
meta/para-Substituted-phenylpropiolic	Ionization in 50% ethanol, 25°	0.434	3.58	0.960	9	—
	DDM esterification, 30°	0.327	0.295	0.916	9	—

*r is the correlation coefficient.
†n is the number of substituents studied.

Can. J. Chem. Downloaded from www.nrcresearchpress.com by 210.87.254.105 on 09/05/12
For personal use only.

TABLE VI
Reaction constant ratios

System	Reaction	$\rho^{meta/para}$	ρ^{ortho}	$\rho^{ortho}/\rho^{meta/para}$
Benzoic	Ionization in water, 25°	1.00	2.39	2.4
	DDM esterification, 30°	0.94	1.89	2.0
3-Phenylpropionic	Ionization in water, 25°	0.24	0.26	1.1
	DDM esterification, 30°	0.22	0.28	1.3
Phenoxyacetic	Ionization in water, 25°	0.34	0.48	1.4
	DDM esterification, 30°	0.25	0.41	1.6
trans-Cinnamic	Ionization in water, 25°	0.42	0.56	1.3
	DDM esterification, 30°	0.42	0.41	1.0
Phenylpropiolic	Ionization in 50% ethanol, 25°	0.43	0.24	0.6
	DDM esterification, 30°	0.33	0.33	1.0

our earlier review (2). These results show that the transmission is comparable for *cis*- and *trans*-cinnamic acids, with the lower value occurring for the *cis*-system for comparable substitution. In the α-phenylcinnamic system studied here, transmission is more efficient in the *trans*- than in the *cis*-system. It is very important to note the large acid-strengthening effect observed for the *cis*-acids, which amounts to about 1.4 pK_a units and 1.0 log k units for the unsubstituted acid. This is due to the steric effect of the *cis*-3-phenyl group deconjugating the carboxylic acid group (24). Catalin models of the α-phenylcinnamic acids show that, in the *cis*-acids, both phenyl groups assist in deconjugating the carboxylic acid group, and that, in the *trans*-acids, both phenyl groups mutually interact and do not affect the carboxylic acid group.

The *trans*-ortho-substituted α-phenylcinnamic acids present a reasonably similar picture to those ortho systems already discussed. The acid-strengthening substituents, such as the halogeno and nitro groups, operate normally. However, the *cis*-ortho-substituted α-phenylcinnamic acids show almost no effect on substituting with the usual acid-strengthening groups. This small reversal or greatly diminished substituent effect has been previously observed in isolated cases for *cis*-ortho-substituted cinnamic acids (25, 12). This is considered to arise from a reversed dipolar substituent field effect (13, 26). Catalin models show that in favorable conformations of the *cis*-cinnamic acids the ortho-substituent can be very close to the reaction site (**1**). The substituent effect is normally characterized by that end of the dipole embedded in the molecule. The proximate position of the "negative" end of the dipole allows its field effect to effectively oppose

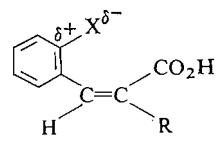

1

or even reverse the normal substituent effect[2]. This discussion depends on the suitable conformations of the ortho-acids. This seems more likely than any other effect which will adequately explain the results[3].

[2]This explanation appears to be preferable to that of a competition between opposing direct field and inductive effects suggested by Hogeveen (12).

[3]Since the preliminary account of some of these results (26), Dewar (32) has commented on them and offered an alternative interpretation of the results for the *cis*-ortho-substituted α-phenylcinnamic acids. This consists of an acid-weakening caused by hydrogen-bonding stabilizing the acids relative to their conjugate bases. *No* relevant *experimental evidence* appears in Dewar's contribution. In fact, all the evidence available at this time indicates that hydrogen-bonding of this type is extremely unlikely and does not occur for *ortho*-substituted benzoic and similar acids. The evidence is detailed in a similar note to Part X of this series. Dewar also comments on the "sterically unfavorable orientation" (shown above as **1**) and describes a more favorable geometry which is in fact identical with **1**. The latter surely must be a mistake as a probably more favorable geometry exists where the substituent is *cis–trans* to the carboxylic acid (*not cis–cis* as in **1**). The possibility, however, remains that dipole–dipole interactions make conformations similar to **1** more stable. Both our interpretation and that of Hogeveen (12) require this or a similar conformation and appear to be the only reasonable explanations offered. Dewar was apparently unaware of both the studies of Hogeveen (12) and our previous investigations (3, 9) which all indicate the importance of normal transmissive routes for dipolar substituent effects. Roberts and Carboni (10) were probably the first to visualize the possibility of reversed dipolar substituent effects in their study of phenylpropiolic acids. Another possible indication may be in the somewhat dissimilar behavior of the meta- and para-substituted *cis*-cinnamic acids (22).

Can. J. Chem. Downloaded from www.nrcresearchpress.com by 210.87.254.105 on 09/05/12
For personal use only.

TABLE VII
Previously unreported acids

Acid	m.p. (°C)	Analysis calcd. for	% Composition Calcd. C	H	Halogen	Found C	H	Halogen
3-(*o*-Fluorophenyl)propionic	82	$C_9H_9O_2F$	64.3	5.36	11.3	63.4	5.34	11.1
trans-o-Methyl-α-phenylcinnamic	164	$C_{16}H_{14}O_2$	80.7	5.88	—	80.1	6.00	—
trans-o-Fluoro-α-phenylcinnamic	178	$C_{15}H_{11}O_2F$	74.4	4.54	7.85	74.1	4.58	7.80
cis-o-Methyl-α-phenylcinnamic	131	$C_{16}H_{14}O_2$	80.7	5.88	—	80.8	5.94	—
cis-o-Fluoro-α-phenylcinnamic	108	$C_{15}H_{11}O_2F$	74.4	4.54	7.85	74.1	4.58	7.67
cis-o-Chloro-α-phenylcinnamic	152	$C_{15}H_{11}O_2Cl$	69.6	4.25	13.7	69.1	4.27	13.5
cis-o-Bromo-α-phenylcinnamic	148	$C_{15}H_{11}O_2Br$	59.4	3.63	26.4	59.0	3.68	26.6
cis-p-Methyl-α-phenylcinnamic	97–99	$C_{16}H_{14}O_2$	80.7	5.88	—	80.2	6.03	—
cis-p-Chloro-α-phenylcinnamic	132–133	$C_{15}H_{11}O_2Cl$	69.6	4.25	13.7	69.6	4.28	13.6

The rather odd acid-strengthening effect of the ortho-methyl group in the *trans*-acids has close similarities to results found for related systems (12, 27), but has no simple explanation.

Ortho-Hydroxy Groups

This substituent has been excluded from these correlations. It is strongly acid-strengthening in phenoxyacetic acid, strongly acid-weakening in *trans*-cinnamic acid, and mildly acid-weakening in 3-phenylpropionic acid. The para-hydroxy group is always strongly acid-weakening (21). The opposite effect shown by the ortho-hydroxy group in salicylic acid has been attributed to the occurrence of a hydrogen-bonded stabilization of the anion (18). Such an effect is structurally impossible for *trans*-ortho-hydroxycinnamic acid, c.f. the *cis*-isomer spontaneously cyclizes to form coumarin (28). It appears that the ortho-hydroxyphenoxyacetic acid anion has a hydrogen-bonded anion (**2**). This might also occur to some extent for 3-

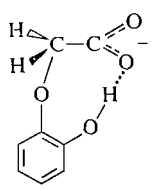

2

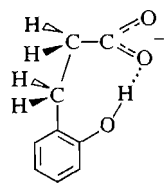

3

(ortho-hydroxyphenyl)propionic acid. However, steric interactions in the necessarily eclipsed conformations of the dimethylene link apparently inhibit the formation of the hydrogen-bonded anion (**3**).

The ortho-methoxyl groups, like the para-isomers (19), are not well behaved. This is believed to be due to the important electron-releasing resonance effect being almost completely thwarted in the isolated systems, particularly the 3-phenylpropionic acids.

This study emphasizes and reinforces our conviction that the field effect is of great importance in the transmission of polar effects. It is important to note that in handling the effects of the ortho-substituents it has been necessary to make a number of convenient assumptions. Though these reduce the certainty of the reaction constants obtained, they do not alter the significance of the results themselves.

Experimental

Materials

The 3-phenylpropionic, phenoxyacetic, and *trans*-cinnamic acids were commercial samples or were prepared by standard routes. The α-phenylcinnamic acids were prepared by the method of Ketcham and Jambotkar (29). The *cis*-isomers were given in poor yields by this method and the appropriate *trans*-isomer was isomerized by ultraviolet light according to a method used for converting *trans*- to *cis*-cinnamic acids (23). In our hands, this method gave samples of *cis*-ortho-substituted cinnamic acids containing the *trans*-isomers, detected by a nuclear magnetic resonance (n.m.r.) analysis, which could not be separated on a sufficient scale to make a study of these *cis*-acids. All the acids studied were recrystallized to constant melting points (m.p.) which were identical with, or very close to, those recorded in the literature. The equivalent weight of each acid was determined by titration, and was found to be within 1% of the calculated value. The m.p. and elemental analyses of previously unreported acids are given in Table VII. The stereochemistry of the α-phenylcinnamic acids was confirmed by p.m.r. spectral measurements. The β-hydrogen in *cis*-cinnamic acids occurs at a higher τ value than in *trans*-cinnamic

Can. J. Chem. Downloaded from www.nrcresearchpress.com by 210.87.254.105 on 09/05/12
For personal use only.

acids, in agreement with the studies of Rappe (30). A 10% solution of the acid in dimethyl sulfoxide, containing 2% tetramethylsilane (TMS) as an internal standard, was measured with a Varian A60-A n.m.r. spectrometer operating at 60 Mc/s under standard instrument conditions. The spectral shifts are given in Table VIII. These shifts are comparable to those recently recorded for cinnamic acids (31). No isomer impurities were observed in the purified acids, i.e. they were at least 98% pure isomer.

TABLE VIII

Proton magnetic resonance spectral shifts for β hydrogen of α-phenylcinnamic acids

	τ (p.p.m.)	
Substituent	*trans*	*cis*
H	2.20	2.97
o-Me	2.04	2.97
o-F	2.08	2.90
o-Cl	2.06	2.87
o-Br	2.12	2.87
o-NO_2	1.95	2.60
o-OMe	1.93	2.88
m-Cl	2.22	—
m-Br	2.23	—
m-NO_2	2.13	—
p-Me	2.22	2.98
p-OMe	2.23	3.11
p-Cl	2.18	2.93
p-NO_2	2.14	2.90

Other reagents for the kinetic and equilibrium measurements were prepared as previously stated and had similar physical constants (15).

Measurements

Rate Coefficients for Diazodiphenylmethane Reaction

These have been determined, at 30° (±0.05), spectrophotometrically as described previously (15), using a 10-fold excess acid concentration (0.06 *M*).

pK_a Values

These were determined, at 25° (±0.1), by potentiometric methods as described previously (3, 15). Ionization constants in water were only measured for acids for which reliable values were not available, as indicated in Table III.

1. M. J. S. DEWAR and P. J. GRISDALE. J. Am. Chem. Soc. **84**, 3539 (1962); **84**, 3548 (1962).
2. K. BOWDEN. Can. J. Chem. **41**, 2781 (1963).
3. K. BOWDEN. Can. J. Chem. **43**, 3354 (1965).
4. J. G. KIRKWOOD and F. H. WESTHEIMER. J. Chem. Phys. **6**, 506 (1938).
5. J. C. MCGOWAN. J. Appl. Chem. London, **10**, 312 (1960).
6. M. CHARTON. Can. J. Chem. **38**, 2493 (1960).
7. R. W. TAFT. *In* Steric effects in organic chemistry. *Edited by* M. S. Newman. John Wiley and Sons, Inc., New York. 1956. Chap. 13.
8. A. C. FARTHING and B. NAM. *In* Steric effects in conjugated systems. *Edited by* G. W. Gray. Butterworths, London. 1958. p. 131.
9. K. BOWDEN. Can. J. Chem. **44**, 661 (1966).
10. J. D. ROBERTS and R. A. CARBONI. J. Am. Chem. Soc. 77, 5554 (1955).
11. I. J. SOLOMON and R. FILLER. J. Am. Chem. Soc. **85**, 3492 (1963).
12. H. HOGEVEEN. Rec. Trav. Chim. **83**, 815, 829, 836 (1964).
13. R. GOLDEN and L. M. STOCK. J. Am. Chem. Soc. **88**, 5928 (1966).
14. K. BOWDEN, N. B. CHAPMAN, and J. SHORTER. Can. J. Chem. **42**, 1979 (1964).
15. K. BOWDEN, M. HARDY, and D. C. PARKIN. Can. J. Chem. **46**, 2929 (1968).
16. G. KORTUM, W. VOGEL, and K. ANDRUSSOW. Pure Appl. Chem. **1**, 190 (1960).
17. W. SIMON *et al.* Zusammenstellung von scheinbaren Dissoziation-konstanten im Losungsmittelsystem Methylcellosolve/Wasser. Vol. 1. Juris-Verlog, Zurich. 1959.
18. K. BOWDEN and G. E. MANSER. Can. J. Chem. **46**, 2941 (1968).
19. H. VAN BEKKUM, P. E. VERKADE, and B. M. WEPSTER. Rec. Trav. Chim. **78**, 815 (1959).
20. Reference 19, p. 833. Footnote.
21. H. H. JAFFE. Chem. Rev. **53**, 191 (1953).
22. R. FUCHS and J. J. BLOOMFIELD. J. Org. Chem. **31**, 3423 (1966).
23. V. I. ZDANOVICH, Z. N. PARNES, and D. N. KURSANOV. Proc. Acad. Sci. USSR, **165**, 1112 (1965).
24. G. S. HAMMOND. *In* Steric effects in organic chemistry. *Edited by* M. S. Newman. John Wiley and Sons, Inc., New York. 1956. Chap. 9.
25. M. BETTI and E. LUCCHI. Mem. Accad. Sci. Ist. Bologna, Classe Sci. Fis. Sez. Sci. Nat. **6**, 37 (1939).
26. K. BOWDEN and D. C. PARKIN. Chem. Commun. 75 (1968).
27. H. C. BROWN, D. H. MCDANIEL, and O. HAFLIGER. *In* Determination of organic structures by physical methods. Vol. 1. *Edited by* E. A. Braude and F. C. Nachrod. Academic Press, Inc., New York. 1955. Chap. 14.
28. K. BOWDEN, M. J. HANSON, and G. R. TAYLOR. J. Chem. Soc. B, 174 (1968).
29. R. KETCHAM and D. JAMBOTKAR. J. Org. Chem. **28**, 1034 (1963).
30. C. RAPPE. Acta Chem. Scand. **18**, 818 (1964).
31. T. A. WITTSTRUCK and E. N. TRACHTENBERG. J. Am. Chem. Soc. **89**, 3803 (1967).
32. M. J. S. DEWAR. Chem. Commun. 547 (1968).

Can. J. Chem. Downloaded from www.nrcresearchpress.com by 210.87.254.105 on 09/05/12
For personal use only.

Can. J. Chem. Downloaded from www.nrcresearchpress.com by 210.87.254.42 on 09/05/12
For personal use only.

Mechanism of decarboxylation of substituted salicylic acids. II. Kinetics and ^{13}C-carboxyl kinetic isotope effects in nitrobenzene–quinoline mixtures

A. N. BOURNS
Department of Chemistry, McMaster University, Hamilton, Ontario

AND

J. BUCCINI, G. E. DUNN, AND W. RODEWALD
Department of Chemistry, University of Manitoba, Winnipeg 19, Manitoba

Received August 13, 1968

The decarboxylation of 4-methylsalicylic acid in dilute solutions of quinoline in nitrobenzene at 200 °C is first order with respect to the salicylic acid and first order with respect to quinoline. The pseudo-first-order rate constant reaches a maximum at 0.25 *M* quinoline, then decreases as the quinoline concentration increases. The ^{13}C-carboxyl kinetic isotope effect, $100(k_{12}/k_{13} - 1)$, is 2.2% in pure quinoline and 0.7% in 0.02 *M* quinoline. It is therefore concluded that the mechanism proposed in Part I of this series involves three steps: ionization of the salicylic acid to a quinolinium salicylate ion pair, reversible protonation by quinolinium ion of the salicylate ion at carbon 1 of the aromatic ring, and loss of carbon dioxide from the protonated salicylate ion. In dilute quinoline solution the second step is slow, while in pure quinoline the third step becomes rate determining.

Canadian Journal of Chemistry, **46**, 3915 (1968)

In Part I of this series (1) it was proposed that a number of 4- and 5-substituted salicylic acids decarboxylate in quinoline solution by the following mechanism

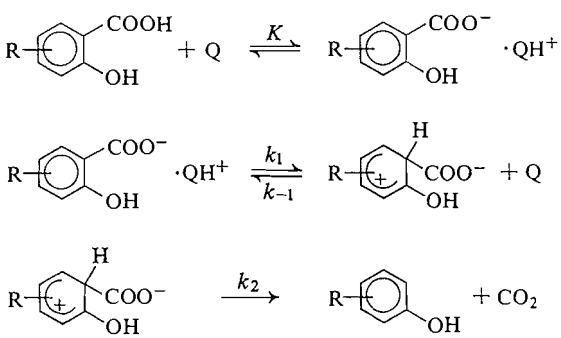

This mechanism was designed to account for 3 major experimental observations. (*a*) Although the decarboxylation in nitrobenzene solution is second order with respect to salicylic acid, in quinoline it is first order, so that the quinoline must be a reactant in the decarboxylation. (*b*) Most 4- and 5-substituents have little effect on the rate, so that their influence on one process (step 1) must be cancelled by that on another (step 2). (*c*) The rate is sharply increased by those substituents for which σ^+ (applicable to step 2) is distinctly more negative than σ (applicable to step 1), so that for these substituents cancellation is not complete.

The evidence did not permit a decision as to whether steps 2 and 3 are sequential, as shown, or concerted. It was, therefore, the object of the present investigation to study the kinetics of decarboxylation and the ^{13}C-carboxyl kinetic isotope effect in the "inert" solvent nitrobenzene.

Experimental

The apparatus and method used to follow the kinetics of the reaction have been described previously (1), as have the methods of sample collection and calculation of the isotope effects (2).

Results and Discussion

The decarboxylation of salicylic acid has been shown to be second order with respect to the acid in nitrobenzene solution (1). However, in nitrobenzene containing quinoline the decarboxylation of 4-methylsalicylic acid is now found to be first order with respect to the acid to more than 3 half lives, even when the concentration of the acid is in considerable excess over that of the quinoline. This, of course, is in agreement with the proposed mechanism since, according to it,

TABLE I

Rates of decarboxylation of 4-methylsalicylic acid in nitrobenzene–quinoline mixtures at 200 °C

Acid, M*	Quinoline, M*	$k_{obs} \times 10^4$ s^{-1}	$k_{calcd} \times 10^2$ l mole^{-1} s^{-1}
0.086	4.85×10^{-3}	0.955 ± 0.036	1.97
0.154	5.35×10^{-3}	0.982 ± 0.006	1.84
0.147	7.58×10^{-3}	1.44 ± 0.20	1.90
0.140	9.98×10^{-3}	1.91 ± 0.01	1.92
0.144	1.26×10^{-2}	2.37 ± 0.02	1.88
0.146	1.99×10^{-2}	3.56 ± 0.02	1.79
0.154	2.69×10^{-2}	4.61 ± 0.05	1.71
0.149	5.87×10^{-2}	7.93 ± 0.09	1.35
0.144	1.35×10^{-1}	10.00 ± 1.47	0.74
0.183	2.45×10^{-1}	12.63 ± 0.15	0.52
0.135	4.46×10^{-1}	10.25 ± 0.14	0.23
0.123	8.00×10^{-1}	8.95 ± 0.07	0.11
0.132	1.61	6.81 ± 0.08	0.04
0.165	1.61	7.14 ± 0.11	0.04
0.155	pure (~8 M)	3.60 ± 0.07	0.006

*Concentrations at 200 °C for all runs except the last are calculated on the assumption that the densities of the solutions are the same as that of nitrobenzene ($d_4^{200} = 1.023$).

quinoline is not consumed but rather acts as a catalyst.

However, the first-order rate constant varies with the concentration of quinoline, as shown in Table I, and up to about 0.025 M quinoline, the reaction is first order with respect to quinoline. In that range the second-order constant k_{calcd} (column 4, Table I), for the rate law

$$\frac{d[CO_2]}{dt} = k[\text{acid}][\text{quinoline}]$$

averages (1.86 ± .08) × 10^{-2} l mole^{-1} s^{-1} at 200 °C. The much smaller rate constant, 2×10^{-4} l mole^{-1} s^{-1}, found previously (1) for the decarboxylation of salicylic acid in pure nitrobenzene according to the rate law

$$\frac{d[CO_2]}{dt} = k[\text{acid}]^2$$

accounts for the fact that no significant decarboxylation of 4-methylsalicylic acid occurred in the absence of quinoline during the time required for any of the runs shown in Table I.

The observed first order with respect to quinoline in concentrations up to 0.025 M shows that, in this concentration range, the reverse of step 2 in the proposed mechanism is not important. Such would be the case if step 2 were the slow step in the three-step mechanism shown, or if the protonation of step 2 and the decarboxylation of step 3 were concerted processes — that is, in a two-step mechanism where the dipolar species is a transition state rather than an intermediate.

For the two-step mechanism the observed rate constant would be given by

$$k_{obs} = k_1 \frac{K[Q]}{K[Q] + 1}$$

so that at low [Q] the reaction would be first order with respect to quinoline. In principle, k_{obs} should level off to k_1 at high [Q] but, since K is likely to be much less than 1, and the maximum possible value for [Q] is about 8 M, this levelling off is almost certainly unattainable.

If a steady state is assumed for the concentration of the dipolar intermediate in the three-step mechanism, its rate expression is

$$k_{obs} = \frac{k_1 k_2}{k_{-1}[Q] + k_2} \cdot \frac{K[Q]}{K[Q] + 1}$$

Once again at low [Q] the reaction will be first order with respect to quinoline. However, it is quite conceivable that $k_{-1}[Q] \gg k_2$ at attainable values of [Q] and, therefore, that the [Q] in the numerator of the rate law would be cancelled by a [Q] in the denominator. At high [Q], k_{obs} would then decrease with increasing [Q]. That is, the protonation of step 2 would be rate-controlling at low [Q], but the decarboxylation of step 3 would become rate-controlling at high [Q].

Table I shows that k_{obs} does, in fact, reach a maximum at about 0.25 M quinoline and then

Can. J. Chem. Downloaded from www.nrcresearchpress.com by 210.87.254.42 on 09/05/12
For personal use only.

TABLE II

C-isotope effect in the decarboxylation of 4-methylsalicylic acid

Solvent	Temperature (°C)	Acid (mg)	Reaction time (min)	f*	R†	$100\left(\frac{k_{12}}{k_{13}} - 1\right)$
Quinoline	207.7	33.47	540	0.9932	0.010685	
Quinoline	207.5	34.30	540	0.9911	0.010692	
Quinoline	207.7	367.33	9	0.2044	0.010487	2.19
Quinoline	195.7	374.80	8	0.09331	0.010467	2.24
Quinoline	195.7	359.32	8	0.08350	0.010471	2.19
0.0200 M quinoline in $C_6H_5NO_2$	194.3	397.08	8	0.08364	0.010618	0.69
,,	193.3	382.24	8	0.07336	0.010612	0.76

*f = molcs CO_2/moles acid.
†$R = {}^{13}CO_2/{}^{12}CO_2$.

decreases as [Q] increases. The kinetic evidence, therefore, strongly favors the three-step mechanism over the two-step one. It is not conclusive, however. Increasing the concentration of quinoline in the nitrobenzene–quinoline mixtures will have a solvent as well as a kinetic effect. Both mechanisms involve the formation of highly polar intermediates and transition states from neutral reactants, and nitrobenzene ($\varepsilon^{200} \sim 20$) is no doubt a better solvent for such polar species than is quinoline ($\varepsilon^{200} \sim 5$). It is therefore possible, although perhaps not very probable, that the decrease in rate at high quinoline concentrations could be accommodated by the two-step mechanism through a combination of the levelling tendency previously mentioned and the solvent effect.

It should be possible to distinguish between the two-step and three-step mechanisms by means of the kinetic isotope effect on carbon–carbon bond breaking. In the two-step mechanism, where protonation and decarboxylation are concerted, carbon–carbon bond breaking is always part of the rate-determining step, so there should be a carboxyl carbon isotope effect at all quinoline concentrations. However, in the three-step mechanism k_2, the rate constant for carbon–carbon bond breaking, cancels out of the rate expression in the region of [Q] where the reaction is first order with respect to quinoline, but not at higher values of [Q]. There should, therefore, be a carbon isotope effect at high values of [Q] but not at low ones.

Table II shows that the ^{13}C-carboxyl kinetic isotope effect decreases from 2.2% when the solvent is pure quinoline to 0.7% when it is 0.02 M quinoline in nitrobenzene. This makes it evident that protonation and decarboxylation are not concerted processes and that the two-step mechanism can not be correct. All the kinetic and isotopic evidence is readily accommodated by the three-step mechanism shown at the beginning of this paper and it is therefore the preferred mechanism.

Protonation and decarboxylation of aromatic carboxylate ions have previously been shown to be sequential rather than concerted when 4-hydroxysalicylic (3) and 4-methoxyanthranilic acids (2, 4) decarboxylate in aqueous solution. The general similarity of the mechanisms for decarboxylation of aromatic acids in water and quinoline is very striking.

Acknowledgments

The authors are grateful to the National Research Council of Canada for financial support, to Shell Oil (Canada) for a fellowship, and to Mr. Jan Monster for the mass-spectrometric measurements.

1. G. E. DUNN, E. G. JANZEN, and W. RODEWALD. Can. J. Chem. **46**, 2905 (1968).
2. G. E. DUNN and J. BUCCINI. Can. J. Chem. **46**, 563 (1968).
3. K. R. LYNN and A. N. BOURNS. Chem. Ind. London, 782 (1963).
4. G. E. DUNN, P. LEGGATE, and I. E. SCHEFFLER. Can. J. Chem. **43**, 3080 (1965).

Can. J. Chem. Downloaded from www.nrcresearchpress.com by 210.87.254.42 on 09/05/12
For personal use only.

A method for the calculation of surface and interfacial tensions from the shape of pendent drops

H. LOMAS
Department of Organic Chemistry, Ontario Research Foundation, Sheridan Park, Ontario

Received August 8, 1968

A classical capillary equation is applied to the shape of the portion of a pendent drop on the opposite side to the source, and the interfacial tension is calculated by the use of a simple computer program.

Canadian Journal of Chemistry, 46, 3918 (1968)

Can. J. Chem. Downloaded from www.nrcresearchpress.com by 210.87.254.6 on 09/05/12
For personal use only.

Methods used for the determination of surface and interfacial tensions include drop weight (1), drop pressure (2), and the shape of sessile drops (3–5). A more convenient method involves the shape of pendent drops (6–8), with calculations based on data-derived or semi-empirical equations.

In the pendent-drop methods described in the literature, measurements are taken from the portion of the drop near the capillary tip, the nature of which affects the shape of the drop. The calculations proposed in the present work are based on the shape of the profile of the drop on the opposite side to the tip. The x and y coordinates of this curve are given by the classical capillary equations (9)

$$[1] \qquad x = b\left(\frac{2}{k} - k\right)F(k, \phi) - \frac{2b}{k}E(k, \phi)$$

$$[2] \qquad y = -\frac{2b}{k}(1 - k^2 \sin^2 \phi)^{\frac{1}{2}}$$

$$[3] \qquad b^2 = \frac{T}{g\rho}$$

$$[4] \qquad \phi = \tfrac{1}{2}\pi + \tfrac{1}{2}\psi$$

$F(k, \phi)$ and $E(k, \phi)$ are the first and second order elliptic integrals respectively, k is the modulus, T is the surface tension in dynes/cm, ρ is the density differential, and ψ is the angle of the interface to the horizontal in radians. A computer program was written enabling families of curves to be plotted (e.g. Fig. 1) for different values of k.

The maximum horizontal radius (R_1) and the distance between this and the point where the tangent to the curve is horizontal (R_2) may readily be measured. These dimensions are also given by the differences between the values of x and of y when ψ is $\pi/2$ and π. Equations [1] and [2] then become:

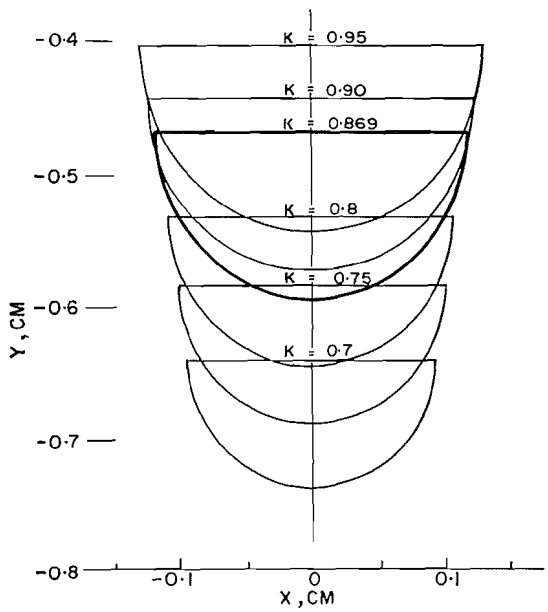

FIG. 1. Families of curves calculated from the capillary equations with a drop profile superimposed in heavy outline.

$$[5] \qquad R_1 = b\left[\left(\frac{2}{k} - k\right)F\left(k, \frac{\pi}{4}\right) - \frac{2}{k}E\left(k, \frac{\pi}{4}\right)\right]$$

$$[6] \qquad R_2 = b\left[\frac{2}{k}\left(1 - k^2 \sin^2 \frac{\pi}{4}\right)^{\frac{1}{2}} - \frac{2}{k}\right]$$

since $\sin \frac{3\pi}{4} = \sin \frac{\pi}{4}$

It will be seen from these equations that k is only dependent upon R_1/R_2 and that once k is known b can be easily calculated.

A modification of the computer program was written to solve the two equations for k and b.

The surface tension is then given from eq. [3] by

$$T = b^2 g\rho \qquad [7]$$

The method described by Andreas, Hauser, and Tucker (6) is suitable for the measurement of drop dimensions. Drops should be of such a size that the ratio $R_1/R_2 > 0.9096$ (corresponding to $k = 1$). Profiles of drops were found to correspond exactly to the calculated curves, and one such profile is shown in heavy outline in Fig. 1.

This method is particularly applicable to measurements at high or low temperatures, at very low interfacial tension (e.g. when there is a tendency for spontaneous emulsification), and for measuring the effect of ageing of the surface. Equations may also be derived for the case when $R_1/R_2 < 0.9096$ and for the profile near the tip which may have an inflection in the curve (8), but the system described above is simpler.

Copies of the computer program written in BASIC are available on request from the author.

Acknowledgments

The author is grateful to Mr. E. Remedios for assistance in writing the programs. The work was made possible by funds received from the Province of Ontario through the Department of Trade and Development.

1. ARNOLD WEISSBERGER. Techniques of organic chemistry. Vol. I. Physical methods. Part I. Interscience Publishers, Inc., New York. 1959. pp. 774–786.
2. A. FERGUSON and P. E. DOWSON. Trans. Faraday Soc. **17**, 384 (1922).
3. D. N. STAICOPOLUS. J. Colloid Sci. **17**, 439 (1962).
4. D. N. STAICOPOLUS. J. Colloid Sci. **18**, 793 (1963).
5. D. N. STAICOPOLUS. J. Colloid Interface Sci. **23**(3), 453 (1967).
6. J. M. ANDREAS, E. A. HAUSER, and W. B. TUCKER. J. Phys. Chem. **42**, 1001 (1938).
7. S. FORDHAM. Proc. Roy. Soc. London, Ser. A, **194**, 1 (1948).
8. MARVIN D. MISAK. J. Colloid Interface Sci. **27**(1), 141 (1968).
9. HORACE LAMB. Statics. University Press, Cambridge. 1928. p. 279.

Estimation of the cohesive energy density of a polymer from critical opalescence measurements

J. M. G. COWIE

Department of Chemistry, University of Essex, Wivenhoe Park, Colchester, Essex, England

Received June 12, 1968

It has been demonstrated recently by Koningsveld that the concentration dependence of the solvent–polymer interaction parameter cannot be neglected in certain systems. By considering this effect in the polystyrene–cyclohexane system it has been possible to calculate a value for the entropy parameter ψ. Estimation of the cohesive energy density (c.e.d.) of polystyrene using this corrected ψ gave a result in good agreement with values of the c.e.d. obtained from other sources.

Canadian Journal of Chemistry, **46**, 3919 (1968)

In a recent publication, Eskin and Nesterov (1) outlined a method of calculating the cohesive energy density of a polymer from measurements of the critical opalescence temperature. Briefly, they related the partial molar heat of mixing $\overline{\Delta H_c}$ at the critical temperature to the solubility parameter δ, by

$$\overline{\Delta H_c} = (\delta_1 - \delta_2)^2 \phi_2^2 V_1 \qquad [1]$$

where 1 and 2 represent the solvent and polymer respectively, ϕ is the volume fraction, V the molar volume, and the cohesive energy density $= (\delta)^2$. Substitution of $\overline{\Delta H_c} = R\theta\psi\phi_2^2$ (using the Flory nomenclature) then gave

$$(\delta_2)^2 = \left[\delta_1 - \left(\frac{R\theta\psi}{V_1}\right)^{\frac{1}{2}}\right]^2 \qquad [2]$$

where θ is the theta temperature, R is the gas constant, and ψ, the entropy parameter, is obtained from a plot of the critical temperature $(T_C)^{-1}$ against $M^{-\frac{1}{2}}$, in the usual manner (2). Although reasonably good agreement was obtained, using eq. [2], for certain systems, a value of $\delta_2 = 5.9$ (cal/cc)$^{\frac{1}{2}}$ was calculated for

Can. J. Chem. Downloaded from www.nrcresearchpress.com by 210.87.254.6 on 09/05/12
For personal use only.

The surface tension is then given from eq. [3] by

$$[7] \qquad T = b^2 g\rho$$

The method described by Andreas, Hauser, and Tucker (6) is suitable for the measurement of drop dimensions. Drops should be of such a size that the ratio $R_1/R_2 > 0.9096$ (corresponding to $k = 1$). Profiles of drops were found to correspond exactly to the calculated curves, and one such profile is shown in heavy outline in Fig. 1.

This method is particularly applicable to measurements at high or low temperatures, at very low interfacial tension (e.g. when there is a tendency for spontaneous emulsification), and for measuring the effect of ageing of the surface. Equations may also be derived for the case when $R_1/R_2 < 0.9096$ and for the profile near the tip which may have an inflection in the curve (8), but the system described above is simpler.

Copies of the computer program written in BASIC are available on request from the author.

Acknowledgments

The author is grateful to Mr. E. Remedios for assistance in writing the programs. The work was made possible by funds received from the Province of Ontario through the Department of Trade and Development.

1. ARNOLD WEISSBERGER. Techniques of organic chemistry. Vol. I. Physical methods. Part I. Interscience Publishers, Inc., New York. 1959. pp. 774–786.
2. A. FERGUSON and P. E. DOWSON. Trans. Faraday Soc. **17**, 384 (1922).
3. D. N. STAICOPOLUS. J. Colloid Sci. **17**, 439 (1962).
4. D. N. STAICOPOLUS. J. Colloid Sci. **18**, 793 (1963).
5. D. N. STAICOPOLUS. J. Colloid Interface Sci. **23**(3), 453 (1967).
6. J. M. ANDREAS, E. A. HAUSER, and W. B. TUCKER. J. Phys. Chem. **42**, 1001 (1938).
7. S. FORDHAM. Proc. Roy. Soc. London, Ser. A, **194**, 1 (1948).
8. MARVIN D. MISAK. J. Colloid Interface Sci. **27**(1), 141 (1968).
9. HORACE LAMB. Statics. University Press, Cambridge. 1928. p. 279.

Estimation of the cohesive energy density of a polymer from critical opalescence measurements

J. M. G. COWIE

Department of Chemistry, University of Essex, Wivenhoe Park, Colchester, Essex, England

Received June 12, 1968

It has been demonstrated recently by Koningsveld that the concentration dependence of the solvent–polymer interaction parameter cannot be neglected in certain systems. By considering this effect in the polystyrene–cyclohexane system it has been possible to calculate a value for the entropy parameter ψ. Estimation of the cohesive energy density (c.e.d.) of polystyrene using this corrected ψ gave a result in good agreement with values of the c.e.d. obtained from other sources.

Canadian Journal of Chemistry, **46**, 3919 (1968)

In a recent publication, Eskin and Nesterov (1) outlined a method of calculating the cohesive energy density of a polymer from measurements of the critical opalescence temperature. Briefly, they related the partial molar heat of mixing $\overline{\Delta H_c}$ at the critical temperature to the solubility parameter δ, by

$$[1] \qquad \overline{\Delta H_c} = (\delta_1 - \delta_2)^2 \phi_2^2 V_1$$

where 1 and 2 represent the solvent and polymer respectively, ϕ is the volume fraction, V the molar volume, and the cohesive energy density $= (\delta)^2$. Substitution of $\overline{\Delta H_c} = R\theta\psi\phi_2^2$ (using the Flory nomenclature) then gave

$$[2] \qquad (\delta_2)^2 = \left[\delta_1 - \left(\frac{R\theta\psi}{V_1}\right)^{\frac{1}{2}}\right]^2$$

where θ is the theta temperature, R is the gas constant, and ψ, the entropy parameter, is obtained from a plot of the critical temperature $(T_C)^{-1}$ against $M^{-\frac{1}{2}}$, in the usual manner (2). Although reasonably good agreement was obtained, using eq. [2], for certain systems, a value of $\delta_2 = 5.9$ (cal/cc)$^{\frac{1}{2}}$ was calculated for

Can. J. Chem. Downloaded from www.nrcresearchpress.com by 210.87.254.40 on 09/05/12
For personal use only.

Can. J. Chem. Downloaded from www.nrcresearchpress.com by 210.87.254.40 on 09/05/12
For personal use only.

polystyrene in cyclohexane. This is considerably lower than the previously published results (3, 4) which vary between 8.6 and 9.2 $(cal/cc)^{\frac{1}{2}}$.

Inspection of the equations shows that the low value is obtained for polystyrene in cyclohexane because $\delta_1 < \delta_2$. Equation [2] should in fact be expressed in the general form

$$[3] \qquad (\delta_2)^2 = \left[\delta_1 \pm \left(\frac{R\theta\psi}{V_1}\right)^{\frac{1}{2}}\right]^2$$

thus allowing both roots to be considered.

Application of eq. [3] to the polystyrene–cyclohexane system yields the alternative value of $\delta_2 \sim 10.6$ $(cal/cc)^{\frac{1}{2}}$, which is now somewhat higher than the generally accepted value. The reason for this can be found in the magnitude of ψ calculated from critical opalescence measurements, which has been reported as 1.056 (5) and 0.93 (6), both considerably higher than the values obtained from other dilute solution studies (7–10). The calculation of ψ from critical solution data is based on the assumption that the interaction parameter χ is independent of both concentration and sample heterogeneity, but Koningsveld and Staverman (11) and others (12) have shown that this is not necessarily true. The concentration dependence of χ has also been demonstrated experimentally (9, 13), and obviously this behavior should be considered when dealing with critical opalescence measurements.

Thus the free energy parameter depends on the experimental variables and in certain instances the solution properties can be accounted for by assuming a g function linear in ϕ (11), then

$$[4] \qquad g = (g_0 - g_1) + 2g_1\phi_2$$

(where Koningsveld's nomenclature has now been introduced, i.e. $g = \chi$, and will be used from now on). The critical conditions which follow from these assumptions are given by Koningsveld and Staverman (11) as

$$[5] \qquad 6g_1\phi_c^2 = \frac{\phi_c^2}{(1-\phi_c)^2} - \frac{m_z}{m_w}$$

and

$$[6] \qquad 2(g_0 - g_1) = \frac{1}{m_w\phi_c} + \frac{[1 - 6g_1\phi_c(1-\phi_c)]}{(1-\phi_c)}$$

where m_w and m_z are the weight and z-average relative chain lengths of a polymer component and can be related in a general manner to the polymer molecular weight M by

$$[7] \qquad m = \frac{\bar{v}_2}{V_1} M$$

Here $\bar{v}_2$ is the partial specific volume of the polymer. Manipulation of eq. [5] gives

$$[8] \qquad \phi_c = \frac{m_z^{\frac{1}{2}}}{m_w} \cdot \frac{1}{(1-6g_1)^{\frac{1}{2}}}$$

while eq. [6] can be recast as

$$[9] \qquad (g_0 - g_1) = \tfrac{1}{2} + \frac{1}{2m_w\phi_c} + \frac{\phi_c(1-6g_1)}{2}$$

The temperature dependence of g must now be considered and it can be written in the usually accepted form (Koningsveld's nomenclature)

$$[10] \qquad g = g_{0.1} + \frac{g_{0.2}}{T}$$

which is valid for both dilute and concentrated solutions. This may also be expressed in terms of the Flory theory as

$$[11] \qquad g = \tfrac{1}{2} + \psi\theta\left(\frac{1}{T_c} - \frac{1}{\theta}\right)$$

Examination of the data reported by Rehage and Palmer (13) suggests that the concentration dependent part of g is temperature independent and so one can write

$$[12] \qquad (g_0 - g_1) = \tfrac{1}{2} + \psi\theta\left(\frac{1}{T_c} - \frac{1}{\theta}\right)$$

Substitution of eqs. [8] and [9] in eq. [12] followed by rearrangement leads to

$$[13] \qquad \frac{1}{T_c} = \frac{1}{\theta} + \frac{(1-6g_1)^{\frac{1}{2}}}{2\psi\theta}\left\{\frac{m_w + m_z}{m_z^{\frac{1}{2}} m_w}\right\}$$

which for a monodisperse polymer reduces to

$$[14] \qquad \frac{1}{T_c} = \frac{1}{\theta} + \frac{(1-6g_1)^{\frac{1}{2}}}{\psi\theta} \cdot \frac{1}{m^{\frac{1}{2}}}$$

for critical conditions.

Experimental evidence for the concentration dependence of g in the polystyrene–cyclohexane system has been provided by Krigbaum and Geymer (9) who found that

$$[15] \qquad g = 0.5 + 0.33\phi_2$$

was valid up to $\phi_2 \sim 0.3$, at the theta temperature. This allows g_1 to be estimated as 0.165 and computation of ψ from eq. [14] gives 0.106 from the Flory–Schultz (5) data and 0.093 from that of Debye and his co-workers (6). Debye used sharp fractions of anionically polymerized polystyrene which reduces the heterogeneity correction to less than 1% but no correction can be applied to the Flory–Schultz data as the molecular weight distribution of each sample is unknown.

The solubility parameter for polystyrene may be recalculated using the new values of ψ, and $\delta_2 \sim 9.0$ (cal/cc)$^{\frac{1}{2}}$ is obtained which is now in good agreement with the published values. Thus for this particular system, the corrections introduced in eq. [14] lead to acceptable values of ψ and δ, but it should be stressed that this will not necessarily be valid for all systems. Hence for the polyethylene – diphenyl ether pair, g has been observed (11) to be concentration independent and in that case eq. [14], with $g_1 = 0$, reduces to the original Flory relation (2). Similarly, if g_1 was observed to be temperature dependent for any system, eq. [14] would assume a different form from that reported here.

1. V. E. Eskin and A. E. Nesterov. Vysokomolekul. Soedin. **8**, 1051 (1966).
2. P. J. Flory. Principles of polymer chemistry. Cornell Univ. Press, Ithaca, N.Y. 1953.
3. J. Brandrup and E. H. Immergut. Polymer handbook. Interscience Publishers, Inc., New York. 1966.
4. K. W. Suh and D. H. Clarke. J. Polymer Sci. **A1**, **5**, 1671 (1967).
5. A. R. Schultz and P. J. Flory. J. Am. Chem. Soc. **74**, 4760 (1952).
6. P. Debye, H. Coll, and D. Woermann. J. Chem. Phys. **33**, 1746 (1960).
7. G. V. Schulz and H. Hellfritz. Z. Elektrochem. **57**, 835 (1953).
8. H. J. Cantow. Z. Physik. Chem. Frankfurt, **7**, 58 (1956).
9. W. R. Krigbaum and D. O. Geymer. J. Am. Chem. Soc. **81**, 1859 (1959).
10. T. A. Orofino and J. W. Mickey. J. Chem. Phys. **38**, 2512 (1963).
11. R. Koningsveld and A. J. Staverman. J. Polymer Sci. **A2**, **6**, 325 (1968).
12. E. D. Holly. J. Polymer Sci. **B2**, 541 (1964) and M. L. Huggins. J. Am. Chem. Soc. **86**, 3535 (1964).
13. G. Rehage and H. J. Palmer. To be published.

Studies on trifluoroacetoxygermanes

N. K. Hota and C. J. Willis

Department of Chemistry, University of Western Ontario, London, Ontario

Received June 28, 1968

The synthesis of various trifluoroacetoxygermanes has been achieved, including $Ge(OCOCF_3)_4$, $CH_3Ge(OCOCF_3)_3$, $(CH_3)_2Ge(OCOCF_3)_2$, and $CF_3Ge(OCOCF_3)_3$. These do not decarboxylate to trifluoromethyl germanium compounds, but some of them react with silver trifluoroacetate to form complex trifluoroacetoxygermanates such as $Ag_2[Ge(OCOCF_3)_6]$, $Ag_2[CH_3Ge(OCOCF_3)_5]$, and $Ag_2[CF_3Ge(OCOCF_3)_5]$.

The preparation and properties of trimethyl(trifluoromethyl)germane, $(CH_3)_3GeCF_3$, are described; differences between it and the analogous tin compound are noted.

Canadian Journal of Chemistry, 46, 3921 (1968)

The work of Sartori and Weidenbruch has led to the preparation of tetrakis(trifluoroacetates), $(CF_3COO)_4M$, of several Group IV metals. The reaction of the appropriate tetrachloride with trifluoroacetic acid was successful for silicon, titanium, zirconium, and thorium (1), while reaction of the tetrachlorides with mercury(II) trifluoroacetate was used for germanium and tin (2).

Our interest in these compounds, particularly that of germanium, stemmed from the possibility of using them as intermediates in the preparation of trifluoromethyl derivatives through decarboxylation reactions. Cullen and Walker (3) have shown that the decarboxylation of dimethyl(trifluoroacetoxy)arsine, $(CH_3)_2AsOCOCF_3$, readily gives dimethyl(trifluoromethyl)arsine, while Emeléus and Dunn (4) have isolated bis(trifluoromethyl)selenide from the reaction of silver trifluoroacetate with selenium. However, attempts to carry out the same type of reaction with phosphorus, sulfur, and mercury were unsuccessful (5).

We have found that the reaction of germanium(IV) chloride with silver trifluoroacetate is a convenient preparative route to tetrakis(trifluoroacetoxy)germane. Thermal decomposition,

Can. J. Chem. Downloaded from www.nrcresearchpress.com by 210.87.254.40 on 09/05/12
For personal use only.

was valid up to $\phi_2 \sim 0.3$, at the theta temperature. This allows g_1 to be estimated as 0.165 and computation of ψ from eq. [14] gives 0.106 from the Flory–Schultz (5) data and 0.093 from that of Debye and his co-workers (6). Debye used sharp fractions of anionically polymerized polystyrene which reduces the heterogeneity correction to less than 1% but no correction can be applied to the Flory–Schultz data as the molecular weight distribution of each sample is unknown.

The solubility parameter for polystyrene may be recalculated using the new values of ψ, and $\delta_2 \sim 9.0$ (cal/cc)$^{\frac{1}{2}}$ is obtained which is now in good agreement with the published values. Thus for this particular system, the corrections introduced in eq. [14] lead to acceptable values of ψ and δ, but it should be stressed that this will not necessarily be valid for all systems. Hence for the polyethylene – diphenyl ether pair, g has been observed (11) to be concentration independent and in that case eq. [14], with $g_1 = 0$, reduces to the original Flory relation (2). Similarly, if g_1 was observed to be temperature dependent for any system, eq. [14] would assume a different form from that reported here.

1. V. E. Eskin and A. E. Nesterov. Vysokomolekul. Soedin. **8**, 1051 (1966).
2. P. J. Flory. Principles of polymer chemistry. Cornell Univ. Press, Ithaca, N.Y. 1953.
3. J. Brandrup and E. H. Immergut. Polymer handbook. Interscience Publishers, Inc., New York. 1966.
4. K. W. Suh and D. H. Clarke. J. Polymer Sci. **A1**, **5**, 1671 (1967).
5. A. R. Schultz and P. J. Flory. J. Am. Chem. Soc. **74**, 4760 (1952).
6. P. Debye, H. Coll, and D. Woermann. J. Chem. Phys. **33**, 1746 (1960).
7. G. V. Schulz and H. Hellfritz. Z. Elektrochem. **57**, 835 (1953).
8. H. J. Cantow. Z. Physik. Chem. Frankfurt, **7**, 58 (1956).
9. W. R. Krigbaum and D. O. Geymer. J. Am. Chem. Soc. **81**, 1859 (1959).
10. T. A. Orofino and J. W. Mickey. J. Chem. Phys. **38**, 2512 (1963).
11. R. Koningsveld and A. J. Staverman. J. Polymer Sci. **A2**, **6**, 325 (1968).
12. E. D. Holly. J. Polymer Sci. **B2**, 541 (1964) and M. L. Huggins. J. Am. Chem. Soc. **86**, 3535 (1964).
13. G. Rehage and H. J. Palmer. To be published.

Studies on trifluoroacetoxygermanes

N. K. Hota and C. J. Willis

Department of Chemistry, University of Western Ontario, London, Ontario

Received June 28, 1968

The synthesis of various trifluoroacetoxygermanes has been achieved, including $Ge(OCOCF_3)_4$, $CH_3Ge(OCOCF_3)_3$, $(CH_3)_2Ge(OCOCF_3)_2$, and $CF_3Ge(OCOCF_3)_3$. These do not decarboxylate to trifluoromethyl germanium compounds, but some of them react with silver trifluoroacetate to form complex trifluoroacetoxygermanates such as $Ag_2[Ge(OCOCF_3)_6]$, $Ag_2[CH_3Ge(OCOCF_3)_5]$, and $Ag_2[CF_3Ge(OCOCF_3)_5]$.

The preparation and properties of trimethyl(trifluoromethyl)germane, $(CH_3)_3GeCF_3$, are described; differences between it and the analogous tin compound are noted.

Canadian Journal of Chemistry, 46, 3921 (1968)

The work of Sartori and Weidenbruch has led to the preparation of tetrakis(trifluoroacetates), $(CF_3COO)_4M$, of several Group IV metals. The reaction of the appropriate tetrachloride with trifluoroacetic acid was successful for silicon, titanium, zirconium, and thorium (1), while reaction of the tetrachlorides with mercury(II) trifluoroacetate was used for germanium and tin (2).

Our interest in these compounds, particularly that of germanium, stemmed from the possibility of using them as intermediates in the preparation of trifluoromethyl derivatives through decarboxylation reactions. Cullen and Walker (3) have shown that the decarboxylation of dimethyl(trifluoroacetoxy)arsine, $(CH_3)_2AsOCOCF_3$, readily gives dimethyl(trifluoromethyl)arsine, while Emeléus and Dunn (4) have isolated bis(trifluoromethyl)selenide from the reaction of silver trifluoroacetate with selenium. However, attempts to carry out the same type of reaction with phosphorus, sulfur, and mercury were unsuccessful (5).

We have found that the reaction of germanium(IV) chloride with silver trifluoroacetate is a convenient preparative route to tetrakis(trifluoroacetoxy)germane. Thermal decomposition,

Can. J. Chem. Downloaded from www.nrcresearchpress.com by 210.87.254.6 on 09/05/12
For personal use only.

Can. J. Chem. Downloaded from www.nrcresearchpress.com by 210.87.254.6 on 09/05/12
For personal use only.

however, did not lead to the formation of any trifluoromethyl germanium compound, but to such decomposition products as trifluoroacetic anhydride and trifluoroacetyl fluoride.

In an attempt to find other germanium compounds which offer promise of successful decarboxylation, we have prepared methyltris(trifluoroacetoxy)germane, $CH_3Ge(OCOCF_3)_3$, dimethylbis(trifluoroacetoxy)germane, $(CH_3)_2Ge(OCOCF_3)_2$, and trifluoromethyltris(trifluoroacetoxy)germane, $CF_3Ge(OCOCF_3)_3$, by the reaction of silver trifluoroacetate with the appropriate chlorogermane. In no case, however, did thermal decomposition lead to a trifluoromethyl germanium compound.

The failure of these decarboxylation reactions is presumably due to the marginal difference in thermal stability between the desired products and the starting materials. It was necessary to heat the trifluoroacetoxy germanium compounds above 220° to obtain decomposition, and known trifluoromethyl germanium compounds undergo slow breakdown under these conditions.

The decarboxylation of trimethyl(trifluoroacetoxy)germane, $(CH_3)_3GeOCOCF_3$, a known compound (6), was not attempted, since the product, trimethyl(trifluoromethyl)germane was readily available from the methylation of trifluoromethyltrichlorogermane.

An investigation was made of the ability of the trifluoroacetoxy derivatives prepared to form complexes with further trifluoroacetate ions. It was found that silver trifluoroacetate gave silver hexakis(trifluoroacetoxy)germanate, $Ag_2[Ge(OCOCF_3)_6]$, silver methylpentakis(trifluoroacetoxy)germanate, $Ag_2[CH_3Ge(OCOCF_3)_5]$, and silver trifluoromethylpentakis(trifluoroacetoxy)-germanate, $Ag_2[CF_3Ge(OCOCF_3)_5]$, by reaction with the appropriate trifluoroacetoxy compound, but no addition occurred with silicon tetrakis(trifluoroacetate) or with dimethylbis(trifluoroacetoxy)germane. With the former compound, it is presumably the smaller size of the silicon atom which prevents the coordination of two further trifluoroacetate ions, while in the latter case the substitution of methyl groups for the more electronegative trifluoroacetoxy groups has lessened the acceptor power of the germanium atom.

Sartori and Weidenbruch (2) note the progressive trend to lower frequency of the C=O stretching infrared absorption band as the ionic character of the compound increases from $Si(OCOCF_3)_4$ ($\nu = 1815\ cm^{-1}$) to $Sn(OCOCF_3)_4$ ($\nu = 1750\ cm^{-1}$). We find a similar trend in the series $Ge(OCOCF_3)_4$ ($\nu = 1800\ cm^{-1}$), $CH_3Ge(OCOCF_3)_3$ ($\nu = 1770\ cm^{-1}$), and $(CH_3)_2Ge(OCOCF_3)_2$ ($\nu = 1755\ cm^{-1}$). For the compound $(CH_3)_3Ge(OCOCF_3)$, the C=O absorption frequency has been reported at $1750\ cm^{-1}$ (6), so the trend is again to lower frequency as the substitution of methyl for trifluoroacetoxy groups increases the polarity of the bonds to remaining trifluoroacetoxy groups.

The compound trimethyl(trifluoromethyl)germane, $(CH_3)_3GeCF_3$, was found to have properties considerably different from those of its tin analogue. The two outstanding features of the chemistry of the latter compound are its ready elimination of difluorocarbene to give trimethyltin fluoride (7), and its reaction with boron trifluoride to give trimethyltin trifluoromethylfluoroborate, $(CH_3)_3Sn^+[CF_3BF_3]^-$, by heterolytic cleavage of the trifluoromethyl group (8).

The germanium analogue did not undergo either of these reactions. Its thermal stability was much greater than that of the tin compound, and it was recovered unchanged after heating at 185° for 48 h. Slight decomposition occurred at 235° in 24 h and extensive breakdown at 275°, but the products did not include compounds such as tetrafluoroethylene or perfluorocyclopropane, suggesting that difluorocarbene was not formed. This difference in behavior may be explained by the known difference in structure between trimethyltin fluoride, a fluorine-bridged polymeric solid (9), and trimethylfluorogermane, a monomeric gas. It is presumably the favorable lattice energy of formation of the former which provides the driving force for the difluorocarbene elimination.

No reaction occurred between boron trifluoride and trimethyl(trifluoromethyl)germane, whereas reaction with the tin compound occurs at once on mixing. This difference may be explained by the much readier formation of an ionic solid with the trimethyltin cation than the trimethylgermanium cation, associated with the more electropositive nature of tin, and the greater initial polarization of bond from the metal atom to the trifluoromethyl group.

Experimental

General

A conventional vacuum system was used for handling volatile materials in the absence of air and for separating volatile products by trap-to-trap condensation. Infrared

Can. J. Chem. Downloaded from www.nrcresearchpress.com by 210.87.254.6 on 09/05/12
For personal use only.

spectra were recorded on Beckman IR-5 and IR-10 spectrophotometers. Microanalyses were performed by Alfred Bernhardt Laboratories, Mulheim (Ruhr), Germany, except for silver and germanium, which were estimated by conventional gravimetric procedures as the chloride and the sulfide respectively.

Silver trifluoroacetate was prepared by dissolving silver carbonate in aqueous trifluoroacetic acid and evaporating to dryness. It was finely powdered and kept in vacuo over phosphorus(V) oxide in the absence of light.

Reaction of Germanium Tetrachloride with Silver Trifluoroacetate

Germanium tetrachloride (8.5 g, 40 mmoles) was condensed onto silver trifluoroacetate (42 g, 190 mmoles) in an evacuated Carius tube (100 ml). The tube was sealed and allowed to warm to 20°, when an exothermic reaction was apparent. After keeping at 20° for 4 h, the tube was opened and volatile products removed and distilled to give tetrakis(trifluoroacetoxy)germane (20 g, 38 mmoles), with boiling point (b.p.) 140–141°/760 mm.

Anal. Calcd. for $C_8F_{12}GeO_8$: C, 18.3; F, 43.5; Ge, 13.8. Found: C, 17.8; F, 43.6; Ge, 13.2.

Reaction of Methyltrichlorogermane with Silver Trifluoroacetate

Methyltri-iodogermane was prepared by the reaction of methyl iodide with germanium(II) iodide (10) and converted to the trichloride by reaction with excess anhydrous silver chloride at 110° for 1 h in a sealed tube.

Reaction of methyltrichlorogermane (4.4 g, 22 mmoles) with silver trifluoroacetate (20 g, 90 mmoles), using the procedure described above for germanium tetrachloride, gave methyltris(trifluoroacetoxy)germane (9.0 g, 20 mmoles) with b.p. 167°/760 mm.

Anal. Calcd. for $C_7H_3F_9GeO_6$: C, 19.7; H, 0.71; F, 40.1. Found: C, 19.3; H, 0.87; F, 40.4.

Reaction of Dimethyldichlorogermane with Silver Trifluoroacetate

Dimethyldichlorogermane (3.7 g, 21 mmoles, supplied by Alfa Inorganics Inc., Beverley, Mass.) reacted with silver trifluoroacetate (20 g, 90 mmoles), under conditions similar to those described above, to yield dimethylbis(trifluoroacetoxy)germane (6.4 g, 19 mmoles) with b.p. 167°/755 mm.

Anal. Calcd. for $C_6H_6F_6GeO_4$: C, 21.9; H, 1.83; F, 34.7. Found: C, 21.9; H, 1.70; F, 34.8.

Reaction of Trifluoromethyltrichlorogermane with Silver Trifluoroacetate

Trifluoromethyltrichlorogermane was prepared by the method of Clark and Willis (11) and a sample (2.5 g, 10 mmoles) allowed to react with silver trifluoroacetate (9.0 g, 40 mmoles) under conditions similar to those described above. Fractionation gave trifluoromethyltris(trifluoroacetoxy)germane (4.8 g, 8.2 mmoles) with b.p. 120°/758 mm.

Anal. Calcd. for $C_7F_{12}GeO_6$: C, 17.5; F, 47.4; Ge, 15.3. Found: C, 17.7; F, 47.3; Ge, 14.8.

Thermal Decompositions

Studies on the thermal decomposition of the above compounds were carried out by heating samples in sealed tubes, in the absence of air, to 240° for 24 h. Methyltris(trifluoroacetoxy)germane was recovered unchanged, but the other compounds underwent extensive decomposition to give trifluoroacetic anhydride, trifluoroacetyl chloride, carbon dioxide, and silicon tetrafluoride. In each case a solid residue remained which appeared to be mainly germanium(IV) oxide.

Formation of Complex Trifluoroacetoxygermanates

The trifluoroacetoxy derivatives described above did not react with solid silver trifluoroacetate, as is shown by their recovery in high yield from an excess of that compound in their preparations. The various complex trifluoroacetoxygermanates were made by reacting the trifluoroacetoxy germanium compound in a ratio of 1:1.9 with a solution of silver trifluoroacetate in benzene in a sealed tube under anhydrous conditions. Removal of all volatile material left the complex silver salts as white or pale-yellow light-sensitive solids. In this way were prepared:

Silver Hexakis(trifluoroacetoxy)germanate(IV)

Anal. Calcd. for $C_{12}F_{18}GeO_{12}Ag_2$: C, 14.8; F, 35.4; Ag, 22.3. Found: C, 15.3; F, 35.4; Ag, 21.8.

Silver Methylpentakis(trifluoroacetoxy)germanate(IV)

Anal. Calcd. for $C_{11}H_3F_{15}GeO_{10}Ag_2$: C, 15.2; H, 0.35; F, 32.8. Found: C, 15.0; H, 0.30; F, 32.6.

Silver Trifluoromethylpentakis(trifluoroacetoxy)-germanate(IV)

Anal. Calcd. for $C_{11}F_{18}GeO_{10}Ag_2$: C, 14.3; F, 37.0. Found: C, 14.1; F, 36.7.

When tetrakis(trifluoroacetoxy)silane or dimethylbis-(trifluoroacetoxy)germane were mixed with benzene solutions of silver trifluoroacetate no reaction occurred, and removal of volatile materials left unchanged silver trifluoroacetate.

Trimethyltrifluoromethylgermane

In a typical preparation, trifluoromethyltrichlorogermane (1.65 g, 6.7 mmoles) and dimethylzinc (1.0 g, 11 mmoles) prepared by the method previously described (12) were condensed into an evacuated Carius tube (50 ml) which was sealed and allowed to warm to 20°, when a vigorous reaction, accompanied by precipitation of solid, was apparent. [CAUTION: the reaction of dimethylzinc with chlorogermanes may proceed with explosive violence on occasions, and should not be attempted on a large scale.]

Fractionation of volatile products gave a trace of unreacted dimethylzinc and trimethyltrifluoromethylgermane (1.2 g, 6.5 mmoles) with b.p. 71°/760 mm.

Anal. Calcd. for $C_4H_9F_3Ge$: mol. wt., 187. C, 25.7; H, 4.83; F, 30.6. Found: mol. wt. (gas density), 187. C, 25.9; H, 4.90; F, 30.9.

Principal infrared absorptions (vapor phase) were at 3080(w), 3010(m), 2940(m), 2840(w), 1420(m), 1255(m), 1185(vs), 1155(s), 1125(m), 1085(vs), 835(s), 760(m), and 610(s) cm^{-1}. The ^{19}F nuclear magnetic resonance spectrum (carbon tetrachloride solution) gave a sharp singlet at +61.6 p.p.m. from CCl_3F (internal).

Thermal decomposition of trimethyltrifluoromethylgermane was carried out by heating small samples (0.5 g) in Carius tubes in the absence of air. Quantitative recovery was made after 48 h at 185° and over 95% recovery after 24 h at 235°, with a trace of fluoroform as the only decomposition product. After 12 h at 275° none of the

germane was recovered, and volatile decomposition products included fluoroform, silicon tetrafluoride, and unidentified non-condensible gas.

In an attempt to obtain a reaction with boron trifluoride, trimethyltrifluoromethylgermane (0.4 g), and boron trifluoride (0.18 g) were kept in solution in carbon tetrachloride (1.5 ml) in a sealed tube (20 ml) for 24 h at 20°. No reaction was apparent, and fractionation of the contents of the tube gave quantitative recovery of unreacted boron trifluoride.

Acknowledgments

We thank the National Research Council of Canada for financial assistance and the Germanium Research Council for gifts of germanium compounds.

1. P. SARTORI and M. WEIDENBRUCH. Angew. Chem. **76**, 376 (1964).
2. P. SARTORI and M. WEIDENBRUCH. Angew. Chem. Intern. Ed. Engl. **4**, 1079 (1965).
3. W. R. CULLEN and L. G. WALKER. Can. J. Chem. **38**, 472 (1960).
4. H. J. EMELÉUS and M. J. DUNN. J. Inorg. Nucl. Chem. **27**, 752 (1965).
5. R. N. HASZELDINE. J. Chem. Soc. 584 (1961). H. J. EMELÉUS and R. N. HASZELDINE. J. Chem. Soc. 2953 (1949). G. A. R. BRANDT, H. J. EMELÉUS, and R. N. HASZELDINE. J. Chem. Soc. 2198 (1952).
6. R. H. FISH and H. G. KUIVALA. J. Org. Chem. **31**, 2445 (1966).
7. H. C. CLARK and C. J. WILLIS. J. Am. Chem. Soc. **82**, 1888 (1960).
8. R. D. CHAMBERS, H. C. CLARK, and C. J. WILLIS. J. Am. Chem. Soc. **82**, 5298 (1960).
9. H. C. CLARK, R. J. O'BRIEN, and J. TROTTER. J. Chem. Soc. 2332 (1964).
10. E. A. FLOOD, K. L. GODFREY, and L. S. FOSTER. Inorg. Syn. **3**, 64 (1950).
11. H. C. CLARK and C. J. WILLIS. J. Am. Chem. Soc. **84**, 898 (1962).
12. N. K. HOTA and C. J. WILLIS. J. Organometal. Chem. Amsterdam, **9**, 169 (1967).

Role of polynuclear species in the processes following nuclear transformations in solids

A. G. MADDOCK AND K. E. COLLINS

Department of Chemistry, The State University of New York at Buffalo, Buffalo, New York 14214

Received June 19, 1968

The hypothesis that recoil atoms from nuclear transformations have a high probability of forming polynuclear complexes in ionic solids is shown to correlate a wide variety of experimental observations.

Canadian Journal of Chemistry, **46**, 3924 (1968)

It is well established that in most nuclear reactions, including the radiative thermal neutron capture reaction, more than 99% of the events rupture the molecule in which the atom undergoing the transformation was initially bound. The products found on radiochemical analysis of the irradiated solid are commonly less complex in structure than the target material and are often those predicted from the fragments produced by molecular disruption. When the radionuclide *M is produced by nuclear transformation in an ionic solid containing a complex ion, $ML_6^{m\pm}$, and a chemically inert co-ion, an aqueous solution of the solid commonly gives the radioactive *M in a cationic form, $*M^{q+}$, the parent form, $*ML_6^{m\pm}$, and, perhaps, as aquated ions of the type $*ML_n(H_2O)_{6-n}^{r\pm}$. Redox reactions involving reduction of M also occur. As was first pointed out by Libby (1), such results can be explained by supposing the mechanical recoil following individual nuclear events leads to the stripping of varying numbers of ligand groups, up to *n*. The rupture of the M—L bonds can take place in two ways: to yield M^+ and L^- with the preservation of the original oxidation state of M, or to yield M and L, with reduction of M. The annealing reactions which can commonly be effected in the irradiated solid can then be interpreted as a recombination of the *M-containing fragments with either its original partners, in the case of small mechanical recoil when the partners are not greatly separated, or by recombination with L fragments generated from inactive $ML_6^{m\pm}$ units toward the end of the recoil track of the *M containing fragment in the lattice. This model has survived nearly intact since first proposed by Libby (1), although it has recently been shown that electronic processes involving point defects in the lattice are also important in annealing reactions (2, 3).

Can. J. Chem. Downloaded from www.nrcresearchpress.com by 210.87.254.6 on 09/05/12
For personal use only.

germane was recovered, and volatile decomposition products included fluoroform, silicon tetrafluoride, and unidentified non-condensible gas.

In an attempt to obtain a reaction with boron trifluoride, trimethyltrifluoromethylgermane (0.4 g), and boron trifluoride (0.18 g) were kept in solution in carbon tetrachloride (1.5 ml) in a sealed tube (20 ml) for 24 h at 20°. No reaction was apparent, and fractionation of the contents of the tube gave quantitative recovery of unreacted boron trifluoride.

Acknowledgments

We thank the National Research Council of Canada for financial assistance and the Germanium Research Council for gifts of germanium compounds.

1. P. SARTORI and M. WEIDENBRUCH. Angew. Chem. **76**, 376 (1964).
2. P. SARTORI and M. WEIDENBRUCH. Angew. Chem. Intern. Ed. Engl. **4**, 1079 (1965).
3. W. R. CULLEN and L. G. WALKER. Can. J. Chem. **38**, 472 (1960).
4. H. J. EMELÉUS and M. J. DUNN. J. Inorg. Nucl. Chem. **27**, 752 (1965).
5. R. N. HASZELDINE. J. Chem. Soc. 584 (1961). H. J. EMELÉUS and R. N. HASZELDINE. J. Chem. Soc. 2953 (1949). G. A. R. BRANDT, H. J. EMELÉUS, and R. N. HASZELDINE. J. Chem. Soc. 2198 (1952).
6. R. H. FISH and H. G. KUIVALA. J. Org. Chem. **31**, 2445 (1966).
7. H. C. CLARK and C. J. WILLIS. J. Am. Chem. Soc. **82**, 1888 (1960).
8. R. D. CHAMBERS, H. C. CLARK, and C. J. WILLIS. J. Am. Chem. Soc. **82**, 5298 (1960).
9. H. C. CLARK, R. J. O'BRIEN, and J. TROTTER. J. Chem. Soc. 2332 (1964).
10. E. A. FLOOD, K. L. GODFREY, and L. S. FOSTER. Inorg. Syn. **3**, 64 (1950).
11. H. C. CLARK and C. J. WILLIS. J. Am. Chem. Soc. **84**, 898 (1962).
12. N. K. HOTA and C. J. WILLIS. J. Organometal. Chem. Amsterdam, **9**, 169 (1967).

Role of polynuclear species in the processes following nuclear transformations in solids

A. G. MADDOCK AND K. E. COLLINS

Department of Chemistry, The State University of New York at Buffalo, Buffalo, New York 14214

Received June 19, 1968

The hypothesis that recoil atoms from nuclear transformations have a high probability of forming polynuclear complexes in ionic solids is shown to correlate a wide variety of experimental observations.

Canadian Journal of Chemistry, **46**, 3924 (1968)

It is well established that in most nuclear reactions, including the radiative thermal neutron capture reaction, more than 99% of the events rupture the molecule in which the atom undergoing the transformation was initially bound. The products found on radiochemical analysis of the irradiated solid are commonly less complex in structure than the target material and are often those predicted from the fragments produced by molecular disruption. When the radionuclide *M is produced by nuclear transformation in an ionic solid containing a complex ion, $ML_6^{m\pm}$, and a chemically inert co-ion, an aqueous solution of the solid commonly gives the radioactive *M in a cationic form, $*M^{q+}$, the parent form, $*ML_6^{m\pm}$, and, perhaps, as aquated ions of the type $*ML_n(H_2O)_{6-n}^{r\pm}$. Redox reactions involving reduction of M also occur. As was first pointed out by Libby (1), such results can be explained by supposing the mechanical recoil following individual nuclear events leads to the stripping of varying numbers of ligand groups, up to *n*. The rupture of the M—L bonds can take place in two ways: to yield M^+ and L^- with the preservation of the original oxidation state of M, or to yield M and L, with reduction of M. The annealing reactions which can commonly be effected in the irradiated solid can then be interpreted as a recombination of the *M-containing fragments with either its original partners, in the case of small mechanical recoil when the partners are not greatly separated, or by recombination with L fragments generated from inactive $ML_6^{m\pm}$ units toward the end of the recoil track of the *M containing fragment in the lattice. This model has survived nearly intact since first proposed by Libby (1), although it has recently been shown that electronic processes involving point defects in the lattice are also important in annealing reactions (2, 3).

Can. J. Chem. Downloaded from www.nrcresearchpress.com by 210.87.254.5 on 09/05/12
For personal use only.

Can. J. Chem. Downloaded from www.nrcresearchpress.com by 210.87.254.5 on 09/05/12
For personal use only.

It seems justifiable to question the likelihood of this model. In the case of hard ionic solids, if L is an atom, such as halogen or oxygen, the structure of the compound can be approximated by a close packed array of L, with M and the co-ion occupying appropriate sites in the lattice. Even if L is not monatomic, this is a good approximation to the lattice. The fragment containing M will therefore come to rest, after most events, in close proximity to $ML_6^{m\pm}$ units. Hence, if the ligand group L can act as a bridging group, and both oxygen and the halogens can fulfil this function, one might expect a very appreciable proportion of the recoiling fragments to yield polynuclear species.

Thus, we might write

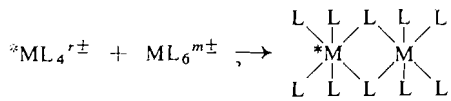

In these polynuclear products, the two M atoms may or may not be in the same oxidation state.

It is, of course, not suggested that all the radioactive atoms end up in polynuclear species. The lattice can certainly accommodate a proportion of mononuclear fragments. Recent results on the radiolysis of solids suggest that even single crystals can accommodate about 10^{19} radical fragments per g mole before recombination and other reactions prevent further build up (4).

However, it is important to consider how far experimental evidence supports the proposed model involving a polynuclear recoil species, in contrast to the monatomic species, and to what extent the polynuclear species can facilitate an interpretation of the post-irradiation behavior of these systems.

First, one must recognize that many of the polynuclear species formed in a crystal in this way will be unstable in solution and therefore may not survive for direct analytical detection. There are, however, some systems, such as the phosphates, where the chemical properties permit survival. The experimental data for phosphates show that polynuclear species play a very important part; as much as 50% of the ^{32}P can appear in polynuclear forms (5, 6). Both P^{V}—O—P^{V} and P^{III}—O—P^{V} dinuclear species are formed. It seems reasonable to suggest that the unusual feature of the phosphate system is not that polynuclear species are formed, but that they are stable upon solution of the irradiated salt in water. The chromate system is another in which polynuclear species have been reported (7, 8). Up to 20% of the recoil (7) ^{51}Cr appears upon analysis as dinuclear or polynuclear chromium(III) species. Perhaps even more significant is the formation of polymeric products containing the Mo—O—Cr unit when ^{51}Cr is introduced into sodium molybdate by ion implantation (8). In other systems, the evidence is less direct, but suggestive nevertheless. For example, in the chloroiridate system, paper electrophoretic analysis reveals more products than can be accounted for even by assigning peaks to all the possible isomers in the $IrCl_n(H_2O)_{6-n}$ series (9). These extra species tend to disappear, yielding increased amounts of the several mononuclear entities, when solutions of the irradiated salt are aged prior to electrophoresis (9). This evidence is also strongly suggestive of polynuclear products.

Second, even if the polynuclear species produced in the lattice are unstable in solution, it might be predicted that the products found on dissolution will depend upon the composition of the solvent and upon such conditions of dissolution as pH and temperature. For example, a

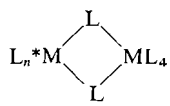

unit may, in principle, react in one of three different ways, if it does not survive as such. Thus, upon dissolution it may yield the following sets of products:

[*i*] $L_n{*}MS_2 + ML_6$

[*ii*] $L_n{*}ML_2 + S_2ML_4$

[*iii*] $L_n{*}MLS + SLML_4$

where S represents a solvent molecule. Which path is chosen will depend on the exact conditions of analysis of the irradiated salt. Further, if the solvent is a solution containing a potential ligand, A (for example, OH^-), still further products can appear.

Cobalt complexes seem particularly susceptible to the effect of changing solvent. The appearance of different products or a change in the observed product ratio with a change from an aqueous to a nonaqueous solvent system has been reported for such diverse complexes as hexamminecobalt(III) nitrate (10), potassium trisoxalatocobaltate (10), cobalt(III) acetylacetonate (10, 11), and several other cobalt complexes (10, 12). The effects on

Can. J. Chem. Downloaded from www.nrcresearchpress.com by 210.87.254.5 on 09/05/12
For personal use only.

product distribution of changing the pH of the aqueous solution have been reported for the cobalt complexes (10, 13) and for several oxyanion systems (14, 15). These data can be convincingly interpreted in terms of the reactions of polynuclear species such as outlined above.

Thirdly, it is expected that the radioactive polynuclear products may play a very important part in annealing processes. Such processes will arise from either, or both, a redox reaction affecting the polynuclear complex and/or a rearrangement of ligand units within the complex. The redox step may either involve electron transfer between the bridged M atoms or between the complex and other entities in the lattice, leading to oxidation of the complex.

There is, indeed, one system in which there is clear evidence for the above model. Andersen and Sørensen (8) have noted that in the chromate system, the appearance of chromate through annealing in the lower temperature range is paralleled by the disappearance of one or more of the polynuclear chromium(III) species. This finding has recently been confirmed in these laboratories where it has also been found that monomeric radioactive chromic ions incorporated into chromate by co-crystallization appear upon analysis, to a substantial extent as a dimeric chromium(III) species, even though the concentration of $^{51}Cr^{III}$ in the initial solution was very small (16).

Additional evidence for the proposed polynuclear species comes from other annealing experiments. Recent work has confirmed the reality of transfer annealing in some of the simpler systems in which the effects of nuclear changes have been studied (17, 18). For example, radioiodine introduced into calcium iodate crystals by co-crystallization (17) and radiochromic ions introduced into potassium chromate, either by implantation (8) or co-crystallization (18) seem to be able to attain the form of the host species by a thermal reaction, which is effectively the same as the corresponding recoil atom annealing process. The polynuclear model accounts for such similarity very easily. However, at the present time, there does not seem to be sufficient evidence to say whether annealing processes in the solid are accompanied by break-up of the polynuclear entity or simply by its transformation by ligand transfer and redox reactions, with formation of the observed mononuclear species upon solution for analysis.

Lastly, it has been observed on a number of occasions that the phase changes accompanying hydration or dehydration of irradiated crystals usually lead to reformation of the radioactive target substance (19–21). It has been suggested that this annealing might arise from recombination of fragments accompanying movement in the lattice during the phase change. However, it has also been observed that further thermal annealing is still possible after one or even two such hydration–dehydration steps have taken place.

In the proposed model, the recombination accompanying the phase change may still arise from recombination involving the mononuclear fragments, but the phase change could be expected to leave the polynuclear species largely unchanged and these may still be available for subsequent thermal annealing.

The above points suggest that the role of polynuclear complexes in the solid state chemistry of recoil atoms may be of considerable importance. They also indicate several ways in which experimental tests of the proposed model can be made.

Acknowledgment

One of the authors (A.G.M.) is indebted to the State University of New York at Buffalo and the New York State Science and Technology Foundation for a visiting professorship.

1. W. F. LIBBY. J. Am. Chem. Soc. **62**, 1930 (1940).
2. T. ANDERSEN, H. E. LUNDAGER MADSEN, and K. OLESEN. Trans. Faraday Soc. **62**, 2409 (1966).
3. A. G. MADDOCK, F. E. TRELOAR, and J. I. VARGAS. Trans. Faraday Soc. **59**, 924 (1963).
4. J. CUNNINGHAM. J. Phys. Chem. **67**, 1772 (1963).
5. R. F. CLARIDGE and A. G. MADDOCK. Trans. Faraday Soc. **59**, 935 (1963).
6. G. HARBOTTLE and L. LINDNER. *In* Chemical effects of nuclear transformations. Proc. I.A.E.A. Conference. Vol. 1. Vienna, 1961. p. 485.
7. P. GÜTLICH and G. HARBOTTLE. Radiochim. Acta, **5**, 70 (1966).
8. T. ANDERSEN and G. SØRENSEN. Trans. Faraday Soc. **62**, 3427 (1966).
9. J. M. PEIXOTO CABRAL and A. G. MADDOCK. J. Inorg. Nucl. Chem. **29**, 1825 (1967).
10. G. L. STUCKY. Ph.D. Thesis, Kansas State University, Kansas. 1967. (v. Dissertation Abstr. **28**, 1845B (1968).)
11. J. SHANKAR, K. S. VENKATESWARLU, and M. LAL. *In* Chemical effects of nuclear transformations. Proc. I.A.E.A. Conference. Vol. 1. Vienna, 1961. p. 309.
12. H. E. RAUCHER and G. HARBOTTLE. J. Inorg. Nucl. Chem. **4**, 155 (1957).
13. J. SHANKAR and R. SHANKER. J. Univ. Bombay Sci. 1960/61, **29**, Parts 3 and 5, No. 48/49, p. 63.
14. D. J. APERS and G. HARBOTTLE. Radiochim. Acta, **1**, 188 (1963).

15. J. H. GREEN, G. HARBOTTLE, and A. G. MADDOCK. Trans. Faraday Soc. **49**, 1413 (1953).
16. R. E. ACKERHALT and K. E. COLLINS. To be published.
17. S. KAUCIC and M. VLATKOVIC. Croatica Chem. Acta, **35**, 305 (1963).
18. C. H. COLLINS, K. E. COLLINS, Y. F. GHOOS, and D. J. APERS. Radiochim. Acta, **4**, 211 (1965).
19. H. MULLER. *In* Chemical effects of nuclear transformations. Proc. I.A.E.A. Conference. Vol. 1. Vienna, 1961. p. 521.
20. J. R. BOLTON and K. J. MCCALLUM. Can. J. Chem. **35**, 761 (1957).
21. J. SHANKAR, A. NATH, and S. P. VAISH. Radiochim. Acta, **3**, 162 (1965).

Can. J. Chem. Downloaded from www.nrcresearchpress.com by 210.87.254.5 on 09/05/12
For personal use only.

On sulfenium ions in 100% sulfuric acid

E. A. ROBINSON AND S. A. A. ZAIDI
Lash Miller Chemical Laboratories and Erindale College, University of Toronto, Toronto 5, Ontario

Received May 3, 1968

Cryoscopic and conductimetric measurements on solutions of 2:4 dinitrobenzene sulfenyl chloride in 100% H_2SO_4 and dilute oleum are found to be more consistent with simple protonation of the sulfenyl chloride rather than with sulfenium ion formation as previously reported by Kharasch and co-workers (1) in 99% H_2SO_4.

Canadian Journal of Chemistry, 46, 3927 (1968)

Some years ago Kharasch and co-workers (1) claimed that 2:4 dinitrobenzene sulfenyl chloride **1** reacts with sulfuric acid to give the sulfenium ion **2**:

[1] $R—S—Cl + H_2SO_4 \leftrightharpoons R—S^+ + HCl + HSO_4^-$

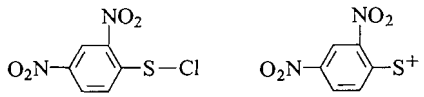

1 **2**

They observed that **1** gives a stable bright red solution in sulfuric acid and freezing point depressions corresponding to a van't Hoff *i-factor* between 1.6 and 2.6. It was claimed that hydrogen chloride is slowly evolved, that the red color migrates to the cathode on electrolysis of the solutions, and that its intensity is repressed by addition of a base or dry HCl. When the solutions were poured onto ice some of the original compound was recovered.

In view of our recent observation that HCl reacts with sulfuric acid (2), ionization according to eq. [1] would be expected to go substantially to completion in 100% H_2SO_4, in which case a cryoscopic ν-factor close to 5 would be expected.

[2] $R—S—Cl + 3H_2SO_4 = R—S^+ + HSO_3Cl + H_3O^+ + 2HSO_4^-$

Thus the nature of the red solutions formed when 2:4 dinitrobenzene sulfenyl chloride dissolves in sulfuric acid seemed worthy of reinvestigation since sulfenium ions have been claimed to be important reaction intermediates (3).

Results and Discussion

The results of our studies on solutions of **1** in 100% H_2SO_4 are shown in Table I. Cryoscopy

TABLE I

Cryoscopic and conductimetric measurements on solutions of 2:4 dinitrobenzene sulfenyl chloride in 100% H_2SO_4

m	f.p. (°C)	ν
.02	10.205	1.72
.03	10.125	1.70
.04	10.046	1.65
.05	9.970	1.60
.06	9.888	1.57
.07	9.800	1.56
.08	9.722	1.52

ω*	$\kappa \times 10^2$ (Ω^{-1} cm^{-1})	γ	K_b†
.02	1.066	0.56	[0.030]
.03	1.091	0.52	[0.029]
.04	1.119	0.48	0.025
.05	1.148	0.44	0.024
.06	1.176	0.42	0.024
.07	1.203	0.40	0.024
.08	1.232	0.38	0.024
			Mean 0.024

*ω = moles per kg of solution.
†$K_b = [(RSCl)H^+][HSO_4^-]/[RSCl]$(moles kg^{-1}).

15. J. H. GREEN, G. HARBOTTLE, and A. G. MADDOCK. Trans. Faraday Soc. **49**, 1413 (1953).
16. R. E. ACKERHALT and K. E. COLLINS. To be published.
17. S. KAUCIC and M. VLATKOVIC. Croatica Chem. Acta, **35**, 305 (1963).
18. C. H. COLLINS, K. E. COLLINS, Y. F. GHOOS, and D. J. APERS. Radiochim. Acta, **4**, 211 (1965).
19. H. MULLER. *In* Chemical effects of nuclear transformations. Proc. I.A.E.A. Conference. Vol. 1. Vienna, 1961. p. 521.
20. J. R. BOLTON and K. J. MCCALLUM. Can. J. Chem. **35**, 761 (1957).
21. J. SHANKAR, A. NATH, and S. P. VAISH. Radiochim. Acta, **3**, 162 (1965).

Can. J. Chem. Downloaded from www.nrcresearchpress.com by 210.87.254.5 on 09/05/12
For personal use only.

On sulfenium ions in 100% sulfuric acid

E. A. ROBINSON AND S. A. A. ZAIDI
Lash Miller Chemical Laboratories and Erindale College, University of Toronto, Toronto 5, Ontario

Received May 3, 1968

Cryoscopic and conductimetric measurements on solutions of 2:4 dinitrobenzene sulfenyl chloride in 100% H_2SO_4 and dilute oleum are found to be more consistent with simple protonation of the sulfenyl chloride rather than with sulfenium ion formation as previously reported by Kharasch and co-workers (1) in 99% H_2SO_4.

Canadian Journal of Chemistry, 46, 3927 (1968)

Some years ago Kharasch and co-workers (1) claimed that 2:4 dinitrobenzene sulfenyl chloride **1** reacts with sulfuric acid to give the sulfenium ion **2**:

[1] $R—S—Cl + H_2SO_4 \leftrightharpoons R—S^+ + HCl + HSO_4^-$

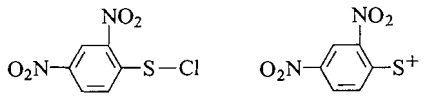

1 **2**

They observed that **1** gives a stable bright red solution in sulfuric acid and freezing point depressions corresponding to a van't Hoff *i-factor* between 1.6 and 2.6. It was claimed that hydrogen chloride is slowly evolved, that the red color migrates to the cathode on electrolysis of the solutions, and that its intensity is repressed by addition of a base or dry HCl. When the solutions were poured onto ice some of the original compound was recovered.

In view of our recent observation that HCl reacts with sulfuric acid (2), ionization according to eq. [1] would be expected to go substantially to completion in 100% H_2SO_4, in which case a cryoscopic ν-factor close to 5 would be expected.

[2] $R—S—Cl + 3H_2SO_4 = R—S^+ + HSO_3Cl + H_3O^+ + 2HSO_4^-$

Thus the nature of the red solutions formed when 2:4 dinitrobenzene sulfenyl chloride dissolves in sulfuric acid seemed worthy of reinvestigation since sulfenium ions have been claimed to be important reaction intermediates (3).

Results and Discussion

The results of our studies on solutions of **1** in 100% H_2SO_4 are shown in Table I. Cryoscopy

TABLE I

Cryoscopic and conductimetric measurements on solutions of 2:4 dinitrobenzene sulfenyl chloride in 100% H_2SO_4

m	f.p. (°C)	ν
.02	10.205	1.72
.03	10.125	1.70
.04	10.046	1.65
.05	9.970	1.60
.06	9.888	1.57
.07	9.800	1.56
.08	9.722	1.52

ω*	$\kappa \times 10^2$ (Ω^{-1} cm^{-1})	γ	K_b†
.02	1.066	0.56	[0.030]
.03	1.091	0.52	[0.029]
.04	1.119	0.48	0.025
.05	1.148	0.44	0.024
.06	1.176	0.42	0.024
.07	1.203	0.40	0.024
.08	1.232	0.38	0.024
			Mean 0.024

*ω = moles per kg of solution.
†$K_b = [(RSCl)H^+][HSO_4^-]/[RSCl]$(moles kg^{-1}).

gives a ν-factor which changes from 1.7 to 1.5 over the concentration range 0.02 to 0.08*m* while electrical conductivity measurements in 100% H_2SO_4 show that the number of hydrogen sulfate ions produced per molecule of solute (γ) changes from 0.6 to 0.4 over the same concentration range.

To a good approximation $\nu - \gamma = 1$, consistent with the simple incomplete protonation of **1** in sulfuric acid:

$$[3]\quad \mathrm{R{-}S{-}Cl} + \mathrm{H_2SO_4} \leftrightharpoons \mathrm{R{-}\overset{\overset{\mathrm{H}}{|}}{\underset{+}{S}}{-}Cl} + \mathrm{HSO_4^-}$$

$$m(1-\alpha) \qquad \alpha m \qquad \alpha m$$

$$\nu = 1 + \alpha;\ \gamma = \alpha;\ \nu - \gamma = 1$$

The behavior of **1** as a simple base might be anticipated in view of Gillespie and Passerini's observation (4) that 4,4′-dinitrodiphenyl sulfide behaves as a base in sulfuric acid.

In order to confirm reaction according to eq. [3] a titration with 0.1*m* oleum was carried out (5). A conductivity minimum was observed at *b*/*a* (the ratio of the number of moles of base added at the minimum to the initial number of moles of disulfuric acid) = 1.15, consistent with the behavior of **1** as a weak base with a basic dissociation constant K_b[1] of 0.02 moles kg^{-1} (5). Calculation of a K_b value from the results in 100% H_2SO_4 gave a value of 0.024 moles kg^{-1} (Table I).

If **1** had ionized to give a sulfenium ion according to eq. [3] the conductivity minimum in a titration with 0.1*m* oleum would be expected to occur at $b/a = 0.36$ (2).

With regard to Kharasch's observations (1), the migration of the red color to the cathode would also be consistent with the presence of a red protonated species $(RSCl)H^+$; addition of a base or dry HCl produces HSO_4^- which would repress the ionization of the weak base, and some sulfenyl chloride would be expected to be recovered when the solutions are poured onto ice.

The only apparent discrepancy between our observations in 100% H_2SO_4 and those of Kharasch (1) in 99% acid is with respect to the evolution of HCl. In 100% acid the quantity of HCl evolved over several days is very small, while in aqueous acid the evolution of HCl was apparently significant (1).

Thus sulfenium ion formation seems unlikely in 100% H_2SO_4 but cannot be definitely ruled out in 99% H_2SO_4

$$[4]\quad \mathrm{R{-}S{-}Cl} + \mathrm{H_2SO_4} \leftrightharpoons \mathrm{R{-}S^+} + \mathrm{HCl} + \mathrm{HSO_4^-} \qquad 1 < \nu < 3$$

although in the light of the above results this reaction seems unlikely.

In other media, however, sulfenium ions may be important. For example, the reaction of 2:4 dinitrobenzene sulfenyl chloride with silver perchlorate to precipitate silver chloride with the formation of a bright red solution, and the Friedel–Crafts reactions of sulfenyl chlorides have been explained in this way (3).

Experimental

Cryoscopic and conductimetric measurements and the treatment of the data obtained have been described previously (6).

2:4 Dinitrobenzene sulfenyl chloride was prepared according to the method of Lawson and Kharasch (7) by the reaction between the corresponding disulfide and sulfenyl chloride. The yellow crystals were recrystallized from carbon tetrachloride, m.p. 97.5–97.8 °C (8).

Acknowledgments

Professor Normal Kharasch is thanked for useful discussion, and the National Research Council of Canada and the Research Board of the University of Toronto are thanked for generous financial assistance.

1. N. Kharasch, C. M. Buess, and W. King. J. Am. Chem. Soc. **75**, 6035 (1953).
2. R. J. Gillespie and E. A. Robinson. J. Am. Chem. Soc. **87**, 2428 (1965).
3. N. Kharasch. Sulfenium ions and sulfenyl compounds. *In* Organic sulfur compounds. *Edited by* N. Kharasch. The Pergamon Press, Ltd., London. 1961. pp. 375–396.
4. R. J. Gillespie and R. C. Passerini. J. Chem. Soc. 3850 (1956).
5. R. H. Flowers, R. J. Gillespie, and E. A. Robinson. Can. J. Chem. **38**, 1363 (1960).
6. R. J. Gillespie and E. A. Robinson. Sulfuric acid. *In* Non-aqueous solvent systems. *Edited by* T. C. Waddington. Academic Press, Inc., London. 1965. pp. 117–210.
7. D. D. Lawson and N. Kharasch. J. Org. Chem. **24**, 858 (1959).
8. R. A. Turner and R. Connor. J. Am. Chem. Soc. **69**, 1009 (1947).

[1] $K_b = [(RSCl)H^+][HSO_4^-]/[RSCl]$.

Can. J. Chem. Downloaded from www.nrcresearchpress.com by 210.87.254.5 on 09/05/12
For personal use only.